Supplementary Figures

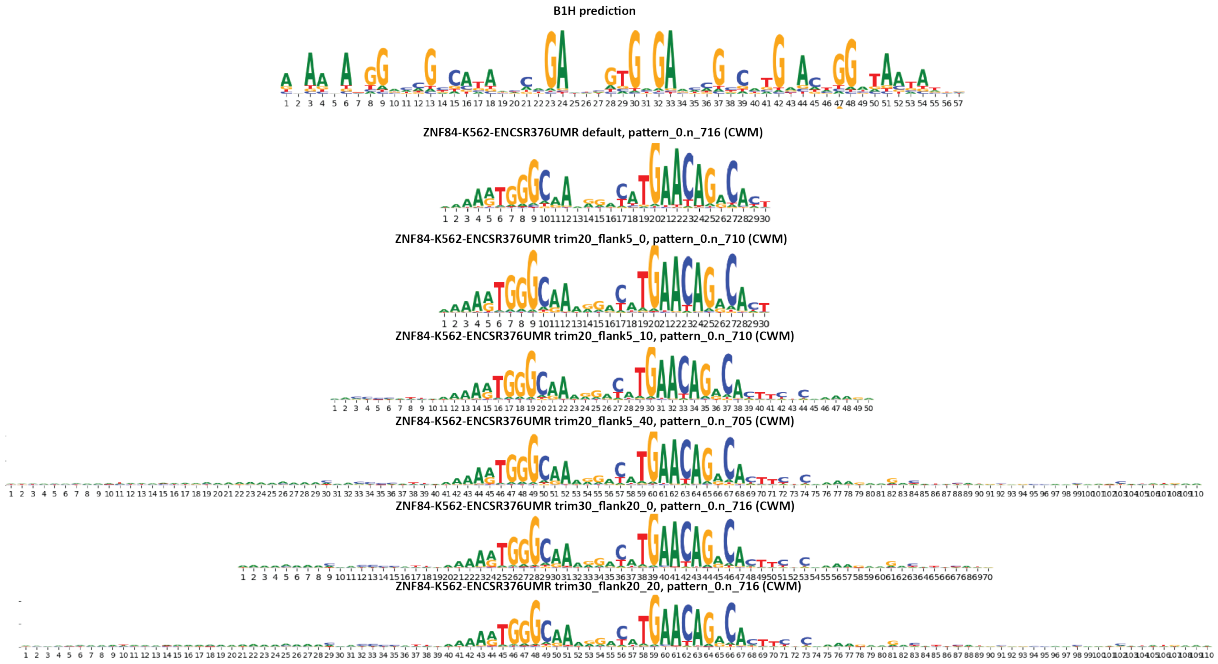

Supplementary Figure 1: Effect of TF-MoDISco settings on motif discovery.. Shown are motifs defined using different trim/flank TF-MoDISco settings (see the Methods section for details) for the ZNF84 transcription factor in K562 cells (ENCODE ID ENCSR376UMR).

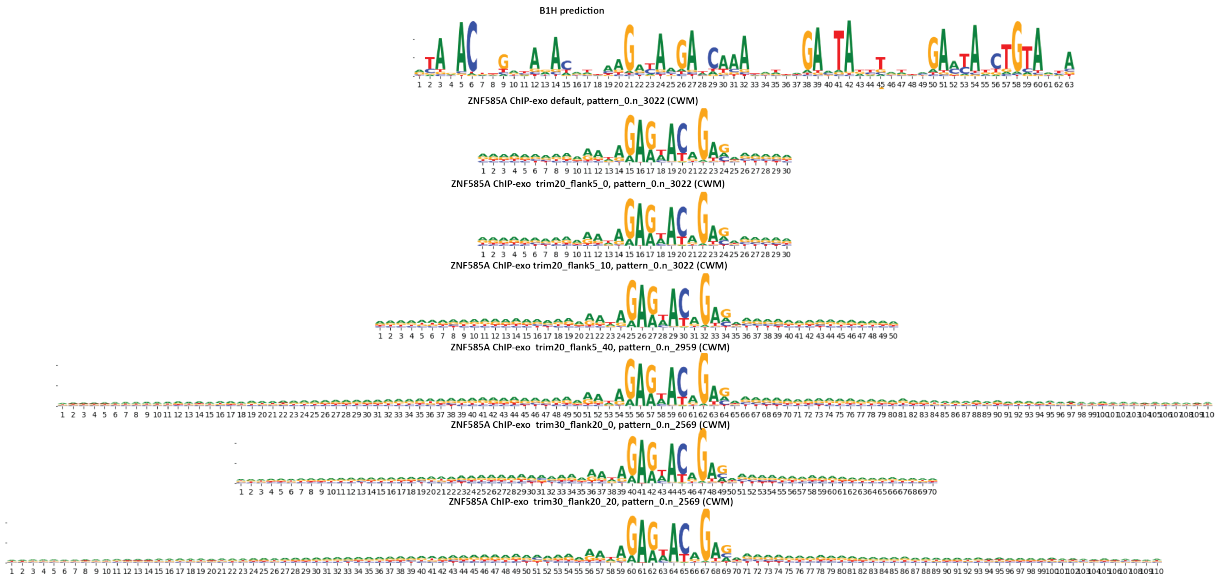

Supplementary Figure 2: Effect of TF-MoDISco settings on motif discovery.. Shown are motifs defined using different trim/flank TF-MoDISco settings (see the Methods section for details) for the ZNF585A transcription factor (ChIP-exo dataset).



Supplementary Figure 3: Effect of TF-MoDISco settings on motif discovery.. Shown are motifs defined using different trim/flank TF-MoDISco settings (see the Methods section for details) for the ZNF600 transcription factor in HEK293 cells (ENCODE ID ENCSR017QBI).

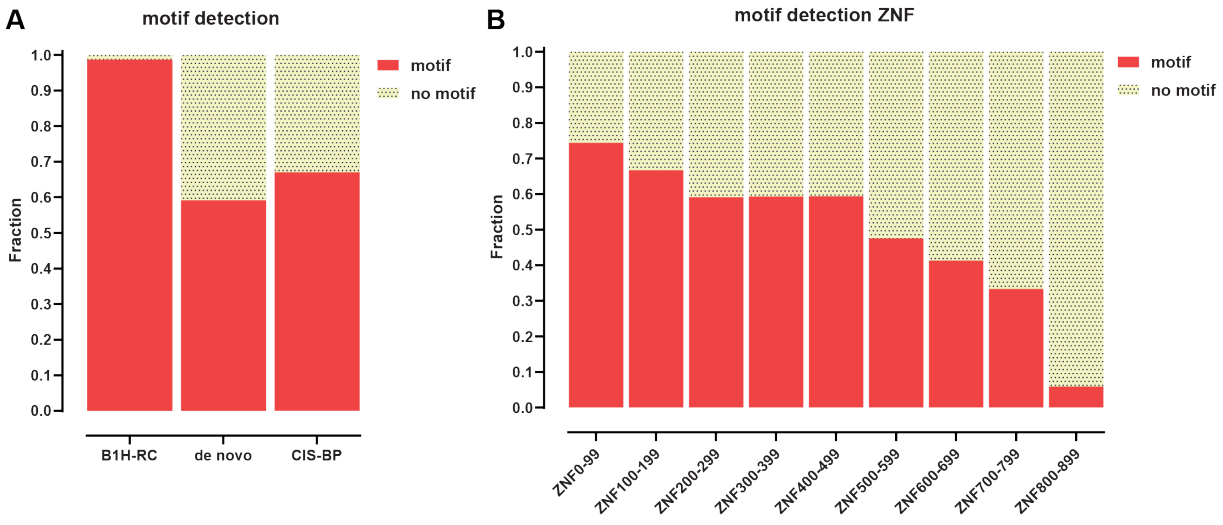

Supplementary Figure 4: Summary of motif detection. (A) All ZNF TFs; (B) "ZNF" C2H2 TFs only, split by ZNF number.

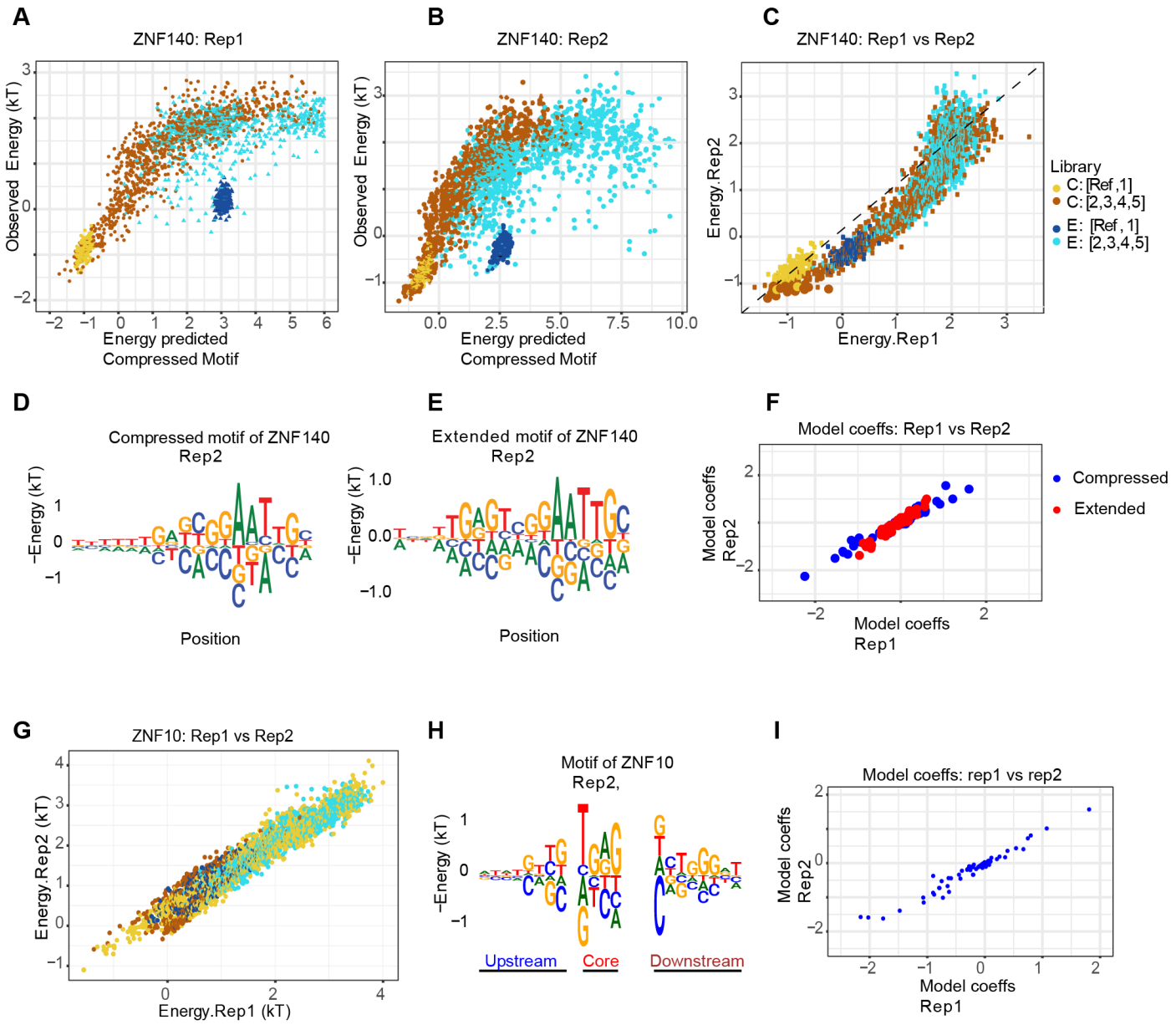

Supplementary Figure 5: High replicate concordance in ZNF140 and ZNF10 Spec-seq experiments. (A) Observed and predicted energies for ZNF140 (Rep1); (B) Observed and predicted energies for ZNF140 (Rep2); (C) Replicate concordance for observed energies; (D) Spec-seq logo for the ZNF140 "compressed" motif (Rep2); (E) Spec-seq logo for the ZNF140 "extended" motif (Rep2); (F) High replicate correlation of ZNF140 PEM model weights; (G) High replicate concordance of ZNF10 level energies (H) PEM logo for ZNF10 (Rep2); (I) High replicate correlation of ZNF10 PEM model weights.

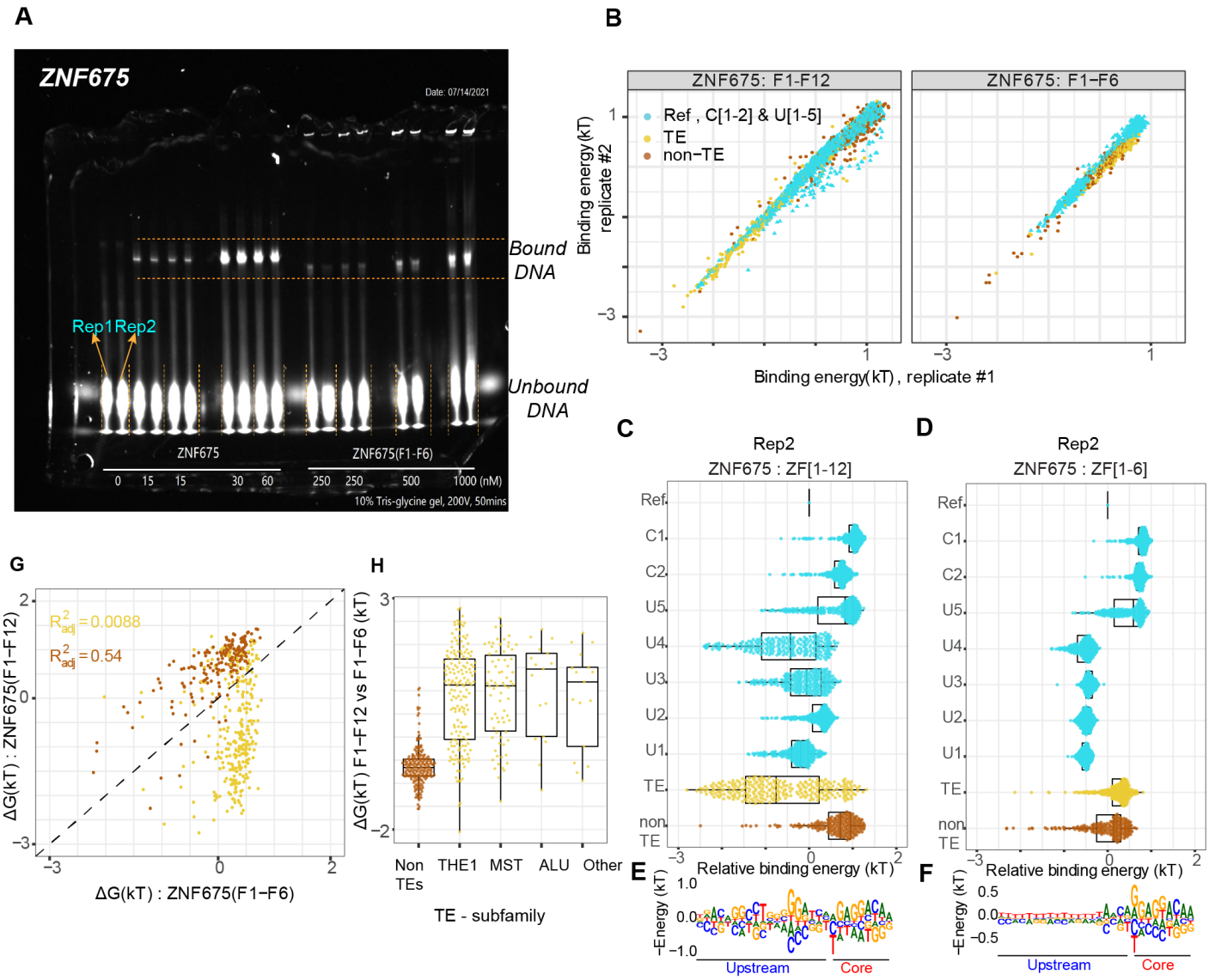

Supplementary Figure 6: ZNF675 Spec-seq results. (A) Gel-shift image for ZNF675 Spec-seq for both ZNF675(F1-F11) and ZNF675(F1-F6); (B) High Spec-seq replicate-level concordance for both ZNF675 ZF[1-11] and ZNF675 ZF[1-6]; (C,D) Full Spec-seq energy distribution across all libraries for ZNF675 ZF[1-11]) and ZNF675 ZF[1-6] (replicate 2); (E,F) Spec-seq derived PEMs for ZNF675 ZF[1-11] and ZNF675 ZF[1-6]; (G) Free energy difference of TE versus non-TE sites across both ZNF675 constructs; (H) Comparing the difference in binding affinity over the two replicates (ZF[1-11] and ZF[1-6]) for TE sites and non-TE sites.

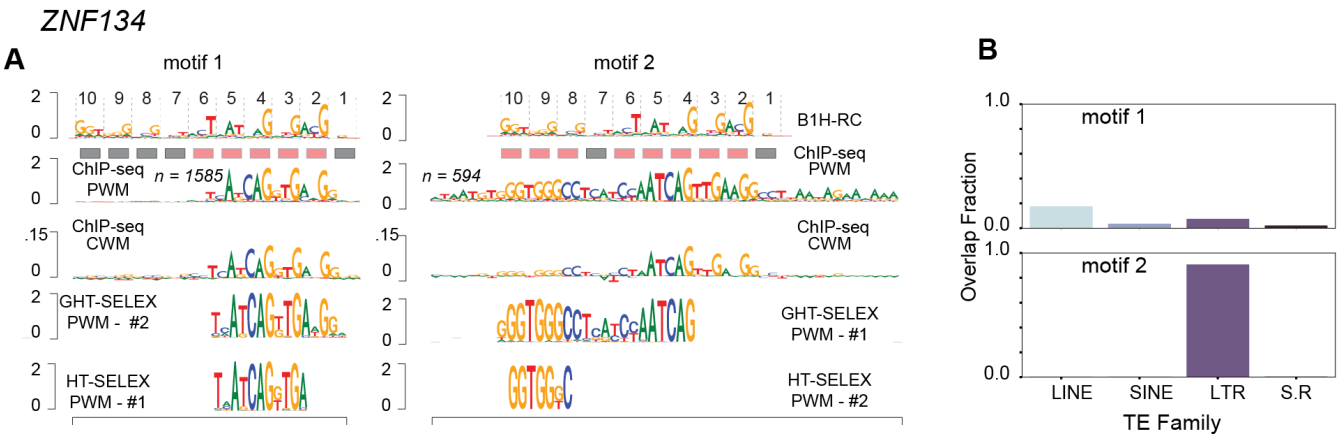

Supplementary Figure 7: ZNF134 exhibits upstream ZF preference when binding TE sequences. (A) Comparing motifs derived from various experimental measurements: B1H recognition code (top row), ChIP-seq PWM , ChIP-seq CWM, GHT-SELEX PWM, HT-SELEX PWM; for both motif 1 and motif; (B) Motif1 is enriched specifically within LTR elements.

Motifs and other dataset properties for each ZNF ChIP/ChIP-exo dataset

The following section contains detailed descriptions of each ZNF ChIP/ChIP-exo dataset and characteristics of the motifs discovered from it and/or associated previously with the TF in question.

All such figures follow the same format:

(A) Annotated GENCODE transcript/protein isoforms and their domain composition;
(B) Forward- and reverse-strand read distribution over all ChIP peaks (ranked by peak strength);
(C) Distribution of ChIP peaks over chromHMM states;
(D) Distribution of ChIP peaks over repetitive elements;
(E) GREAT enrichment of ChIP peaks;
(F) CIS-BP motif, B1H-RC sequence preference prediction, and de novo discovered TF-MoDISco motifs (aligned to the B1H-RC prediction);
(G) Aggregate DNase-seq cut sites (footprint) profiles for each de novo discovered motif (shown are both footprint profiles over all motifs in the genome and over only motifs found in called peaks);
(H) Aggregate PhastCons conservation scores (100-way and 30-way mammalian) over all genome-wide and within-peaks-only instances for each de novo discovered motif;
(I) Aggregate PhyloP conservation scores (100-way and 30-way mammalian) over all genome-wide and within-peaks-only instances for each de novo discovered motif.

Note that panels (G, H, and I) may not be present if no motif was discovered de novo for a given dataset.

Each TF/dataset can be directly accessed through clickable links in the following list:

Supplementary Figure 8: AEBP2 HEK293 ENCSR769JRS
Supplementary Figure 9: BCL11A GM12878 ENCSR000BHA
Supplementary Figure 10: BCL11A GM12878 ENCSR000BHA subpatterns
Supplementary Figure 11: BCL11A H1 ENCSR000BIP
Supplementary Figure 12: BCL11A H1 ENCSR000BIP subpatterns
Supplementary Figure 13: BCL11A H1 ENCSR000BMJ
Supplementary Figure 14: BCL11A HEK293 ENCSR021DJC
Supplementary Figure 15: BCL6B HEK293 ENCSR673SGK
Supplementary Figure 16: BCL6B HEK293 ENCSR673SGK subpatterns
Supplementary Figure 17: BCL6 HepG2 ENCSR759BDG
Supplementary Figure 18: BCL6 HepG2 ENCSR759BDG subpatterns
Supplementary Figure 19: BCL6 K562 ENCSR802AHH
Supplementary Figure 20: BCL6 K562 ENCSR802AHH subpatterns
Supplementary Figure 21: CTCFL K562 ENCSR000BNK
Supplementary Figure 22: CTCFL K562 ENCSR000BNK subpatterns
Supplementary Figure 23: DZIP1 HepG2 ENCSR895KNN
Supplementary Figure 24: E4F1 GM12878 ENCSR439WAF
Supplementary Figure 25: E4F1 K562 ENCSR003GUC
Supplementary Figure 26: E4F1 K562 ENCSR003GUC subpatterns
Supplementary Figure 27: E4F1 K562 ENCSR731LHZ
Supplementary Figure 28: E4F1 K562 ENCSR731LHZ subpatterns
Supplementary Figure 29: E4F1 MCF-7 ENCSR841YWU
Supplementary Figure 30: E4F1 MCF-7 ENCSR841YWU subpatterns
Supplementary Figure 31: EGR2 HEK293 ENCSR919CZU
Supplementary Figure 32: EGR2 HEK293 ENCSR919CZU subpatterns
Supplementary Figure 33: EGR2 HEK293 Hughes GR models EGR2
Supplementary Figure 34: FEZF1 HEK293 Hughes GR models FEZF1
Supplementary Figure 35: FEZF1 HEK293 Hughes GR models FEZF1 subpatterns
Supplementary Figure 36: GFI1B HEK293 ENCSR445PDR
Supplementary Figure 37: GFI1B HEK293 ENCSR445PDR subpatterns
Supplementary Figure 38: GFI1 HEK293 ENCSR445PDR
Supplementary Figure 39: GFI1 HEK293 ENCSR445PDR subpatterns
Supplementary Figure 40: GFI1 HepG2 ENCSR849FVL
Supplementary Figure 41: GFI1 HepG2 ENCSR849FVL subpatterns

Supplementary Figure 42: GLI2 HEK293 ENCSR978EQY
Supplementary Figure 43: GLI4 HEK293 ENCSR211PZO
Supplementary Figure 44: GLI4 HEK293 ENCSR211PZO subpatterns
Supplementary Figure 45: GLI4 HEK293 Hughes GR models GLI4
Supplementary Figure 46: GLI4 HepG2 ENCSR502YME
Supplementary Figure 47: GLIS1 HEK293 ENCSR482BBZ
Supplementary Figure 48: GLIS1 HEK293 ENCSR482BBZ subpatterns
Supplementary Figure 49: GLIS2 HEK293 ENCSR535DIA
Supplementary Figure 50: GLIS2 HEK293 ENCSR535DIA subpatterns
Supplementary Figure 51: GTF3A HepG2 ENCSR220AQM
Supplementary Figure 52: GZF1 HepG2 ENCSR479WQX
Supplementary Figure 53: GZF1 HepG2 ENCSR479WQX subpatterns
Supplementary Figure 54: HIC1 HEK293 ENCSR803GYT
Supplementary Figure 55: HIC1 HEK293 ENCSR803GYT subpatterns
Supplementary Figure 56: HINFP HepG2 ENCSR621PAN
Supplementary Figure 57: HINFP HepG2 ENCSR621PAN subpatterns
Supplementary Figure 58: HINFP K562 ENCSR619GFP
Supplementary Figure 59: HINFP K562 ENCSR619GFP subpatterns
Supplementary Figure 60: HIVEP1 HepG2 ENCSR697WMX
Supplementary Figure 61: HIVEP1 HepG2 ENCSR697WMX subpatterns
Supplementary Figure 62: HIVEP1 K562 ENCSR947PJZ
Supplementary Figure 63: HIVEP1 K562 ENCSR947PJZ subpatterns
Supplementary Figure 64: HKR1 HEK293 ChipExo models HKR1
Supplementary Figure 65: HKR1 HEK293 ChipExo models HKR1 subpatterns
Supplementary Figure 66: IKZF1 GM12878 ENCSR000EUJ
Supplementary Figure 67: IKZF1 GM12878 ENCSR000EUJ subpatterns
Supplementary Figure 68: IKZF1 GM12878 ENCSR441VHN
Supplementary Figure 69: IKZF1 GM12878 ENCSR441VHN subpatterns
Supplementary Figure 70: IKZF1 GM12878 ENCSR874AFU
Supplementary Figure 71: IKZF1 GM12878 ENCSR874AFU subpatterns
Supplementary Figure 72: IKZF1 HepG2 ENCSR278JQG
Supplementary Figure 73: IKZF1 K562 ENCSR395HWC
Supplementary Figure 74: IKZF1 K562 ENCSR395HWC subpatterns
Supplementary Figure 75: IKZF1 K562 ENCSR948VFL
Supplementary Figure 76: IKZF1 K562 ENCSR948VFL subpatterns
Supplementary Figure 77: IKZF2 GM12878 ENCSR680UQE
Supplementary Figure 78: IKZF2 GM12878 ENCSR680UQE subpatterns
Supplementary Figure 79: IKZF2 GM12878 ENCSR822AHX
Supplementary Figure 80: IKZF2 GM12878 ENCSR822AHX subpatterns
Supplementary Figure 81: IKZF3 HEK293 ENCSR304AMN
Supplementary Figure 82: IKZF3 HEK293 ENCSR304AMN subpatterns
Supplementary Figure 83: IKZF3 HEK293 Hughes GR models IKZF3
Supplementary Figure 84: IKZF3 HEK293 Hughes GR models IKZF3 subpatterns
Supplementary Figure 85: IKZF4 HepG2 ENCSR799DUB
Supplementary Figure 86: IKZF5 HepG2 ENCSR210HBN
Supplementary Figure 87: IKZF5 HepG2 ENCSR210HBN subpatterns
Supplementary Figure 88: INSM2 HEK293 ENCSR382GSF
Supplementary Figure 89: INSM2 HEK293 ENCSR382GSF subpatterns
Supplementary Figure 90: KLF10 HEK293 ENCSR006GAQ
Supplementary Figure 91: KLF10 HEK293 ENCSR006GAQ subpatterns
Supplementary Figure 92: KLF10 HEK293 Hughes NB models KLF10
Supplementary Figure 93: KLF10 K562 ENCSR121SPB
Supplementary Figure 94: KLF12 HEK293 Hughes GR models KLF12
Supplementary Figure 95: KLF12 HEK293 Hughes GR models KLF12 subpatterns
Supplementary Figure 96: KLF12 HepG2 ENCSR552YWL
Supplementary Figure 97: KLF12 HepG2 ENCSR552YWL subpatterns

Supplementary Figure 98: KLF13 HepG2 ENCSR756SZU
Supplementary Figure 99: KLF13 HepG2 ENCSR756SZU subpatterns
Supplementary Figure 100: KLF13 K562 ENCSR608HVP
Supplementary Figure 101: KLF13 K562 ENCSR608HVP subpatterns
Supplementary Figure 102: KLF14 HEK293 Hughes NB models KLF14
Supplementary Figure 103: KLF14 HEK293 Hughes NB models KLF14 subpatterns
Supplementary Figure 104: KLF15 HepG2 ENCSR860ONE
Supplementary Figure 105: KLF15 HepG2 ENCSR860ONE subpatterns
Supplementary Figure 106: KLF16 HEK293 ENCSR397DQC
Supplementary Figure 107: KLF16 HEK293 ENCSR397DQC subpatterns
Supplementary Figure 108: KLF16 HepG2 ENCSR009KLQ
Supplementary Figure 109: KLF16 HepG2 ENCSR009KLQ subpatterns
Supplementary Figure 110: KLF16 HepG2 ENCSR913KJZ
Supplementary Figure 111: KLF16 K562 ENCSR760UVO
Supplementary Figure 112: KLF16 K562 ENCSR760UVO subpatterns
Supplementary Figure 113: KLF17 HEK293 ENCSR065WUF
Supplementary Figure 114: KLF17 HEK293 ENCSR065WUF subpatterns
Supplementary Figure 115: KLF1 HEK293 ENCSR006GAQ
Supplementary Figure 116: KLF1 HEK293 ENCSR006GAQ subpatterns
Supplementary Figure 117: KLF1 K562 ENCSR550HCT
Supplementary Figure 118: KLF1 K562 ENCSR550HCT subpatterns
Supplementary Figure 119: KLF4 MCF-7 ENCSR265WJC
Supplementary Figure 120: KLF4 MCF-7 ENCSR265WJC subpatterns
Supplementary Figure 121: KLF6 HepG2 ENCSR757EKM
Supplementary Figure 122: KLF6 HepG2 ENCSR757EKM subpatterns
Supplementary Figure 123: KLF6 K562 ENCSR297CGF
Supplementary Figure 124: KLF6 K562 ENCSR297CGF subpatterns
Supplementary Figure 125: KLF7 HEK293 ENCSR604VWJ
Supplementary Figure 126: KLF7 HEK293 ENCSR604VWJ subpatterns
Supplementary Figure 127: KLF7 HEK293 Hughes GR models KLF7
Supplementary Figure 128: KLF8 HEK293 ENCSR635NOQ
Supplementary Figure 129: KLF8 HEK293 ENCSR635NOQ subpatterns
Supplementary Figure 130: KLF9 HEK293 ENCSR076EZB
Supplementary Figure 131: KLF9 HEK293 ENCSR076EZB subpatterns
Supplementary Figure 132: KLF9 HepG2 ENCSR938ETG
Supplementary Figure 133: KLF9 HepG2 ENCSR938ETG subpatterns
Supplementary Figure 134: KLF9 MCF-7 ENCSR125ZYC
Supplementary Figure 135: KLF9 MCF-7 ENCSR125ZYC subpatterns
Supplementary Figure 136: MAZ A549 ENCSR636YLV
Supplementary Figure 137: MAZ A549 ENCSR636YLV subpatterns
Supplementary Figure 138: MAZ GM12878 ENCSR000DZA
Supplementary Figure 139: MAZ GM12878 ENCSR000DZA subpatterns
Supplementary Figure 140: MAZ GM12878 ENCSR903MVU
Supplementary Figure 141: MAZ GM12878 ENCSR903MVU subpatterns
Supplementary Figure 142: MAZ HEK293 ENCSR290SSQ
Supplementary Figure 143: MAZ HEK293 ENCSR290SSQ subpatterns
Supplementary Figure 144: MAZ HeLa-S3 ENCSR000ECL
Supplementary Figure 145: MAZ HeLa-S3 ENCSR000ECL subpatterns
Supplementary Figure 146: MAZ HepG2 ENCSR000EDN
Supplementary Figure 147: MAZ HepG2 ENCSR000EDN subpatterns
Supplementary Figure 148: MAZ HepG2 ENCSR700PNE
Supplementary Figure 149: MAZ HepG2 ENCSR700PNE subpatterns
Supplementary Figure 150: MAZ IMR-90 ENCSR000EFF
Supplementary Figure 151: MAZ IMR-90 ENCSR000EFF subpatterns
Supplementary Figure 152: MAZ K562 ENCSR000EFX
Supplementary Figure 153: MAZ K562 ENCSR000EFX subpatterns

Supplementary Figure 154: MAZ K562 ENCSR163IUV
Supplementary Figure 155: MAZ K562 ENCSR163IUV subpatterns
Supplementary Figure 156: MAZ K562 ENCSR643JRH
Supplementary Figure 157: MAZ K562 ENCSR643JRH subpatterns
Supplementary Figure 158: MAZ MCF-7 ENCSR288IJC
Supplementary Figure 159: MAZ MCF-7 ENCSR288IJC subpatterns
Supplementary Figure 160: MTF1 HepG2 ENCSR194NVP
Supplementary Figure 161: MTF1 HepG2 ENCSR194NVP subpatterns
Supplementary Figure 162: MTF1 K562 ENCSR849LXI
Supplementary Figure 163: MTF1 K562 ENCSR849LXI subpatterns
Supplementary Figure 164: MYNN HEK293 ENCSR707BNG
Supplementary Figure 165: MYNN HEK293 ENCSR707BNG subpatterns
Supplementary Figure 166: MYNN HEK293 Hughes GR models MYNN
Supplementary Figure 167: MYNN HEK293 Hughes GR models MYNN subpatterns
Supplementary Figure 168: MYNN HepG2 ENCSR398TMP
Supplementary Figure 169: MYNN K562 ENCSR307YJU
Supplementary Figure 170: MYNN K562 ENCSR737LTZ
Supplementary Figure 171: MYNN K562 ENCSR737LTZ subpatterns
Supplementary Figure 172: MYNN K562 ENCSR992KLV
Supplementary Figure 173: MZF1 HEK293 ENCSR298QUH
Supplementary Figure 174: MZF1 HEK293 ENCSR298QUH subpatterns
Supplementary Figure 175: MZF1 HEK293 Hughes GR models MZF1
Supplementary Figure 176: MZF1 HEK293 Hughes NB models MZF1
Supplementary Figure 177: MZF1 HEK293 Hughes NB models MZF1 subpatterns
Supplementary Figure 178: MZF1 HepG2 ENCSR384YOP
Supplementary Figure 179: OSR2 HEK293 ENCSR324LTM
Supplementary Figure 180: OVOL1 MCF-7 ENCSR829WBA
Supplementary Figure 181: OVOL1 MCF-7 ENCSR829WBA subpatterns
Supplementary Figure 182: OVOL3 HEK293 ENCSR768LIO
Supplementary Figure 183: PATZ1 HEK293 ENCSR966ULI
Supplementary Figure 184: PATZ1 HEK293 ENCSR966ULI subpatterns
Supplementary Figure 185: PATZ1 HEK293 Hughes GR models PATZ1
Supplementary Figure 186: PATZ1 HEK293 Hughes GR models PATZ1 subpatterns
Supplementary Figure 187: PATZ1 HepG2 ENCSR658YLN
Supplementary Figure 188: PATZ1 HepG2 ENCSR658YLN subpatterns
Supplementary Figure 189: PATZ1 K562 ENCSR549PVK
Supplementary Figure 190: PATZ1 SK-N-SH ENCSR969AIM
Supplementary Figure 191: PATZ1 SK-N-SH ENCSR969AIM subpatterns
Supplementary Figure 192: PRDM10 HEK293 ENCSR223TAV
Supplementary Figure 193: PRDM10 HEK293 ENCSR223TAV subpatterns
Supplementary Figure 194: PRDM10 HepG2 ENCSR289PSX
Supplementary Figure 195: PRDM10 HepG2 ENCSR289PSX subpatterns
Supplementary Figure 196: PRDM10 K562 ENCSR120MPG
Supplementary Figure 197: PRDM10 K562 ENCSR120MPG subpatterns
Supplementary Figure 198: PRDM15 GM12878 ENCSR748SQL
Supplementary Figure 199: PRDM15 HepG2 ENCSR011INW
Supplementary Figure 200: PRDM15 HepG2 ENCSR011INW subpatterns
Supplementary Figure 201: PRDM15 WTC11 ENCSR092DCD
Supplementary Figure 202: PRDM15 WTC11 ENCSR092DCD subpatterns
Supplementary Figure 203: PRDM1 A549 ENCSR977FEF
Supplementary Figure 204: PRDM1 A549 ENCSR977FEF subpatterns
Supplementary Figure 205: PRDM1 HEK293 ENCSR098YLE
Supplementary Figure 206: PRDM1 HEK293 ENCSR098YLE subpatterns
Supplementary Figure 207: PRDM1 HEK293 Hughes GR models PRDM1
Supplementary Figure 208: PRDM1 HEK293 Hughes GR models PRDM1 subpatterns
Supplementary Figure 209: PRDM1 HeLa-S3 ENCSR000ECY

Supplementary Figure 210: PRDM2 HEK293 ENCSR714LYA
Supplementary Figure 211: PRDM4 HEK293 ENCSR443MVV
Supplementary Figure 212: PRDM4 HEK293 ENCSR443MVV subpatterns
Supplementary Figure 213: PRDM4 HepG2 ENCSR130NZQ
Supplementary Figure 214: PRDM4 HepG2 ENCSR130NZQ subpatterns
Supplementary Figure 215: PRDM6 HEK293 ENCSR892QHR
Supplementary Figure 216: PRDM6 HEK293 ENCSR892QHR subpatterns
Supplementary Figure 217: PRDM9 HEK293 ChipExo models PRDM9
Supplementary Figure 218: PRDM9 HEK293 ChipExo models PRDM9 subpatterns
Supplementary Figure 219: RBAK HEK293 ENCSR441UBA
Supplementary Figure 220: RBAK HEK293 ENCSR441UBA subpatterns
Supplementary Figure 221: RBAK HEK293 ChipExo models RBAK
Supplementary Figure 222: RBAK HepG2 ENCSR144NTH
Supplementary Figure 223: RBAK HepG2 ENCSR144NTH subpatterns
Supplementary Figure 224: REPIN1 HEK293 ENCSR146NLL
Supplementary Figure 225: REPIN1 HepG2 ENCSR893BAO
Supplementary Figure 226: REST GM12878 ENCSR000BGF
Supplementary Figure 227: REST GM12878 ENCSR000BGF subpatterns
Supplementary Figure 228: REST GM12878 ENCSR000BQS
Supplementary Figure 229: REST GM12878 ENCSR000BQS subpatterns
Supplementary Figure 230: REST H1 ENCSR000BHM
Supplementary Figure 231: REST H1 ENCSR000BHM subpatterns
Supplementary Figure 232: REST HCT116 ENCSR000BVI
Supplementary Figure 233: REST HCT116 ENCSR000BVI subpatterns
Supplementary Figure 234: REST HEK293 ENCSR896UBV
Supplementary Figure 235: REST HEK293 ENCSR896UBV subpatterns
Supplementary Figure 236: REST HepG2 ENCSR000BJL
Supplementary Figure 237: REST HepG2 ENCSR000BJL subpatterns
Supplementary Figure 238: REST HepG2 ENCSR000BOT
Supplementary Figure 239: REST HepG2 ENCSR000BOT subpatterns
Supplementary Figure 240: REST Ishikawa ENCSR000BUU
Supplementary Figure 241: REST Ishikawa ENCSR000BUU subpatterns
Supplementary Figure 242: REST K562 ENCSR000ATM
Supplementary Figure 243: REST K562 ENCSR000ATM subpatterns
Supplementary Figure 244: REST K562 ENCSR000BMW
Supplementary Figure 245: REST K562 ENCSR000BMW subpatterns
Supplementary Figure 246: REST K562 ENCSR054JMQ
Supplementary Figure 247: REST K562 ENCSR054JMQ subpatterns
Supplementary Figure 248: REST K562 ENCSR137ZMQ
Supplementary Figure 249: REST K562 ENCSR137ZMQ subpatterns
Supplementary Figure 250: REST liver ENCSR893QWP
Supplementary Figure 251: REST liver ENCSR893QWP subpatterns
Supplementary Figure 252: REST MCF-7 ENCSR000BSP
Supplementary Figure 253: REST MCF-7 ENCSR000BSP subpatterns
Supplementary Figure 254: REST neural cell ENCSR000BTV
Supplementary Figure 255: REST neural cell ENCSR000BTV subpatterns
Supplementary Figure 256: REST Panc1 ENCSR000BJO
Supplementary Figure 257: REST Panc1 ENCSR000BJO subpatterns
Supplementary Figure 258: REST Panc1 ENCSR000BPK
Supplementary Figure 259: REST Panc1 ENCSR000BPK subpatterns
Supplementary Figure 260: REST Panc1 ENCSR000BUP
Supplementary Figure 261: REST Panc1 ENCSR000BUP subpatterns
Supplementary Figure 262: REST PFSK-1 ENCSR000BOX
Supplementary Figure 263: REST PFSK 1 ENCSR000BOX subpatterns
Supplementary Figure 264: RLF K562 ENCSR718SDE
Supplementary Figure 265: RREB1 HepG2 ENCSR180MUU

Supplementary Figure 266: RREB1 HepG2 ENCSR180MUU subpatterns
Supplementary Figure 267: RREB1 K562 ENCSR250WFW
Supplementary Figure 268: RREB1 K562 ENCSR250WFW subpatterns
Supplementary Figure 269: SALL2 HEK293 ENCSR044FMM
Supplementary Figure 270: SALL2 HepG2 ENCSR062TDX
Supplementary Figure 271: SCRT1 HEK293 ENCSR605MGM
Supplementary Figure 272: SCRT2 HEK293 ENCSR338DGO
Supplementary Figure 273: SCRT2 HEK293 ENCSR338DGO subpatterns
Supplementary Figure 274: SP1 A549 ENCSR000BPE
Supplementary Figure 275: SP1 A549 ENCSR000BPE subpatterns
Supplementary Figure 276: SP1 GM12878 ENCSR000BHK
Supplementary Figure 277: SP1 GM12878 ENCSR000BHK subpatterns
Supplementary Figure 278: SP1 H1 ENCSR000BIR
Supplementary Figure 279: SP1 HCT116 ENCSR000BSF
Supplementary Figure 280: SP1 HCT116 ENCSR000BSF subpatterns
Supplementary Figure 281: SP1 HEK293T ENCSR906PEI
Supplementary Figure 282: SP1 HEK293T ENCSR906PEI subpatterns
Supplementary Figure 283: SP1 HepG2 ENCSR000BJX
Supplementary Figure 284: SP1 HepG2 ENCSR000BJX subpatterns
Supplementary Figure 285: SP1 HepG2 ENCSR334KIQ
Supplementary Figure 286: SP1 HepG2 ENCSR460YAM
Supplementary Figure 287: SP1 HepG2 ENCSR460YAM subpatterns
Supplementary Figure 288: SP1 K562 ENCSR000BKO
Supplementary Figure 289: SP1 K562 ENCSR000BKO subpatterns
Supplementary Figure 290: SP1 K562 ENCSR372IML
Supplementary Figure 291: SP1 K562 ENCSR372IML subpatterns
Supplementary Figure 292: SP1 liver ENCSR085IXF
Supplementary Figure 293: SP1 liver ENCSR085IXF subpatterns
Supplementary Figure 294: SP1 liver ENCSR386YIH
Supplementary Figure 295: SP1 liver ENCSR386YIH subpatterns
Supplementary Figure 296: SP1 MCF-7 ENCSR729LGA
Supplementary Figure 297: SP1 MCF-7 ENCSR729LGA subpatterns
Supplementary Figure 298: SP1 WTC11 ENCSR583CGO
Supplementary Figure 299: SP1 WTC11 ENCSR583CGO subpatterns
Supplementary Figure 300: SP2 H1 ENCSR000BQG
Supplementary Figure 301: SP2 HEK293 ENCSR807LQP
Supplementary Figure 302: SP2 HEK293 ENCSR807LQP subpatterns
Supplementary Figure 303: SP2 HepG2 ENCSR000BOU
Supplementary Figure 304: SP2 HepG2 ENCSR946RZN
Supplementary Figure 305: SP2 K562 ENCSR000BNL
Supplementary Figure 306: SP3 HEK293 ENCSR141PZA
Supplementary Figure 307: SP3 HEK293 ENCSR141PZA subpatterns
Supplementary Figure 308: SP4 H1 ENCSR000BQV
Supplementary Figure 309: SP4 H1 ENCSR000BQV subpatterns
Supplementary Figure 310: SP4 HepG2 ENCSR642PQK
Supplementary Figure 311: SP4 HepG2 ENCSR642PQK subpatterns
Supplementary Figure 312: SP5 HepG2 ENCSR019NPF
Supplementary Figure 313: SP5 HepG2 ENCSR019NPF subpatterns
Supplementary Figure 314: TRERF1 WTC11 ENCSR547WSB
Supplementary Figure 315: TRERF1 WTC11 ENCSR547WSB subpatterns
Supplementary Figure 316: TSHZ1 HEK293 ENCSR958JPH
Supplementary Figure 317: TSHZ1 HEK293 ENCSR958JPH subpatterns
Supplementary Figure 318: TSHZ1 K562 ENCSR958JPH
Supplementary Figure 319: TSHZ1 K562 ENCSR958JPH subpatterns
Supplementary Figure 320: WIZ HepG2 ENCSR434ZNS
Supplementary Figure 321: WT1 HEK293 ENCSR966PJJ

Supplementary Figure 322: WT1 HEK293 ENCSR966PJJ subpatterns
Supplementary Figure 323: YY1 A549 ENCSR000BPM
Supplementary Figure 324: YY1 A549 ENCSR000BPM subpatterns
Supplementary Figure 325: YY1 GM12878 ENCSR000BNP
Supplementary Figure 326: YY1 GM12878 ENCSR000BNP subpatterns
Supplementary Figure 327: YY1 GM12878 ENCSR000EUM
Supplementary Figure 328: YY1 GM12878 ENCSR000EUM subpatterns
Supplementary Figure 329: YY1 GM12891 ENCSR000BKJ
Supplementary Figure 330: YY1 GM12891 ENCSR000BKJ subpatterns
Supplementary Figure 331: YY1 GM12892 ENCSR000BLT
Supplementary Figure 332: YY1 GM12892 ENCSR000BLT subpatterns
Supplementary Figure 333: YY1 H1 ENCSR000BKD
Supplementary Figure 334: YY1 H1 ENCSR000BKD subpatterns
Supplementary Figure 335: YY1 HCT116 ENCSR000BNX
Supplementary Figure 336: YY1 HCT116 ENCSR000BNX subpatterns
Supplementary Figure 337: YY1 HEK293 ENCSR859RAO
Supplementary Figure 338: YY1 HEK293 ENCSR859RAO subpatterns
Supplementary Figure 339: YY1 HEK293 Hughes NB models YY1
Supplementary Figure 340: YY1 HepG2 ENCSR000BNT
Supplementary Figure 341: YY1 HepG2 ENCSR000BNT subpatterns
Supplementary Figure 342: YY1 Ishikawa ENCSR000BSY
Supplementary Figure 343: YY1 Ishikawa ENCSR000BSY subpatterns
Supplementary Figure 344: YY1 K562 ENCSR000BKU
Supplementary Figure 345: YY1 K562 ENCSR000BKU subpatterns
Supplementary Figure 346: YY1 K562 ENCSR000BMH
Supplementary Figure 347: YY1 K562 ENCSR000BMH subpatterns
Supplementary Figure 348: YY1 K562 ENCSR000EWF
Supplementary Figure 349: YY1 K562 ENCSR000EWF subpatterns
Supplementary Figure 350: YY1 liver ENCSR382MOM
Supplementary Figure 351: YY1 liver ENCSR382MOM subpatterns
Supplementary Figure 352: YY1 liver ENCSR994YLZ
Supplementary Figure 353: YY1 liver ENCSR994YLZ subpatterns
Supplementary Figure 354: YY1 NT2 D1 ENCSR000EXG
Supplementary Figure 355: YY1 NT2 D1 ENCSR000EXG subpatterns
Supplementary Figure 356: YY1 SK-N-SH ENCSR000BLZ
Supplementary Figure 357: YY1 SK-N-SH ENCSR000BLZ subpatterns
Supplementary Figure 358: YY1 SK-N-SH ENCSR000BSM
Supplementary Figure 359: YY1 SK-N-SH ENCSR000BSM subpatterns
Supplementary Figure 360: YY2 HEK293 ENCSR692HSE
Supplementary Figure 361: YY2 HEK293 ENCSR692HSE subpatterns
Supplementary Figure 362: ZBED1 GM12878 ENCSR207PFI
Supplementary Figure 363: ZBED1 GM12878 ENCSR207PFI subpatterns
Supplementary Figure 364: ZBED1 K562 ENCSR286PCG
Supplementary Figure 365: ZBED1 K562 ENCSR286PCG subpatterns
Supplementary Figure 366: ZBED4 HepG2 ENCSR409PMR
Supplementary Figure 367: ZBED4 HepG2 ENCSR409PMR subpatterns
Supplementary Figure 368: ZBED5 HepG2 ENCSR656SIB
Supplementary Figure 369: ZBED5 HepG2 ENCSR656SIB subpatterns
Supplementary Figure 370: ZBTB10 HEK293 ENCSR004PLU
Supplementary Figure 371: ZBTB10 HEK293 ENCSR004PLU subpatterns
Supplementary Figure 372: ZBTB10 HepG2 ENCSR959COF
Supplementary Figure 373: ZBTB10 HepG2 ENCSR959COF subpatterns
Supplementary Figure 374: ZBTB11 GM12878 ENCSR057DTZ
Supplementary Figure 375: ZBTB11 GM12878 ENCSR057DTZ subpatterns
Supplementary Figure 376: ZBTB11 HEK293 ENCSR882ZTS
Supplementary Figure 377: ZBTB11 HEK293 ENCSR882ZTS subpatterns

Supplementary Figure 378: ZBTB11 K562 ENCSR331GDC
Supplementary Figure 379: ZBTB11 K562 ENCSR331GDC subpatterns
Supplementary Figure 380: ZBTB11 K562 ENCSR468DVP
Supplementary Figure 381: ZBTB11 K562 ENCSR468DVP subpatterns
Supplementary Figure 382: ZBTB11 K562 ENCSR706BJO
Supplementary Figure 383: ZBTB11 K562 ENCSR706BJO subpatterns
Supplementary Figure 384: ZBTB11 K562 ENCSR985OYK
Supplementary Figure 385: ZBTB11 K562 ENCSR985OYK subpatterns
Supplementary Figure 386: ZBTB11 MCF-7 ENCSR155VDK
Supplementary Figure 387: ZBTB11 MCF-7 ENCSR155VDK subpatterns
Supplementary Figure 388: ZBTB12 HEK293 ENCSR543KOA
Supplementary Figure 389: ZBTB12 HEK293 ENCSR543KOA subpatterns
Supplementary Figure 390: ZBTB12 HEK293 Hughes NB models ZBTB12
Supplementary Figure 391: ZBTB12 K562 ENCSR172OSX
Supplementary Figure 392: ZBTB12 K562 ENCSR172OSX subpatterns
Supplementary Figure 393: ZBTB14 HEK293 Hughes GR models ZBTB14
Supplementary Figure 394: ZBTB14 HEK293 Hughes GR models ZBTB14 subpatterns
Supplementary Figure 395: ZBTB14 HepG2 ENCSR532WFC
Supplementary Figure 396: ZBTB14 HepG2 ENCSR532WFC subpatterns
Supplementary Figure 397: ZBTB17 HEK293 ENCSR631WAA
Supplementary Figure 398: ZBTB17 HEK293 ENCSR631WAA subpatterns
Supplementary Figure 399: ZBTB17 K562 ENCSR026KKZ
Supplementary Figure 400: ZBTB18 HEK293 Hughes NB models ZBTB18
Supplementary Figure 401: ZBTB18 HEK293 Hughes GR models ZBTB18
Supplementary Figure 402: ZBTB18 HEK293 Hughes GR models ZBTB18 subpatterns
Supplementary Figure 403: ZBTB1 HEK293 ENCSR927UJQ
Supplementary Figure 404: ZBTB1 HepG2 ENCSR331HWO
Supplementary Figure 405: ZBTB1 K562 ENCSR166BAY
Supplementary Figure 406: ZBTB1 MCF-7 ENCSR309ELI
Supplementary Figure 407: ZBTB20 HEK293 ENCSR460MBI
Supplementary Figure 408: ZBTB20 HEK293 ENCSR460MBI subpatterns
Supplementary Figure 409: ZBTB20 HepG2 ENCSR392TWV
Supplementary Figure 410: ZBTB21 HEK293 ENCSR321MSF
Supplementary Figure 411: ZBTB21 HepG2 ENCSR549PAU
Supplementary Figure 412: ZBTB21 WTC11 ENCSR962BEI
Supplementary Figure 413: ZBTB24 HepG2 ENCSR396XDF
Supplementary Figure 414: ZBTB24 HepG2 ENCSR396XDF subpatterns
Supplementary Figure 415: ZBTB25 HepG2 ENCSR485OYR
Supplementary Figure 416: ZBTB25 HepG2 ENCSR485OYR subpatterns
Supplementary Figure 417: ZBTB26 HEK293 ENCSR229DYF
Supplementary Figure 418: ZBTB26 HEK293 Hughes GR models ZBTB26
Supplementary Figure 419: ZBTB26 HEK293 Hughes GR models ZBTB26 subpatterns
Supplementary Figure 420: ZBTB26 HepG2 ENCSR184SVO
Supplementary Figure 421: ZBTB26 HepG2 ENCSR184SVO subpatterns
Supplementary Figure 422: ZBTB26 K562 ENCSR115HLM
Supplementary Figure 423: ZBTB2 HepG2 ENCSR175MIA
Supplementary Figure 424: ZBTB2 HepG2 ENCSR175MIA subpatterns
Supplementary Figure 425: ZBTB2 K562 ENCSR230PTV
Supplementary Figure 426: ZBTB2 K562 ENCSR230PTV subpatterns
Supplementary Figure 427: ZBTB33 A549 ENCSR000BPZ
Supplementary Figure 428: ZBTB33 A549 ENCSR000BPZ subpatterns
Supplementary Figure 429: ZBTB33 GM12878 ENCSR000BHC
Supplementary Figure 430: ZBTB33 GM12878 ENCSR000BHC subpatterns
Supplementary Figure 431: ZBTB33 GM12878 ENCSR542FLV
Supplementary Figure 432: ZBTB33 GM12878 ENCSR542FLV subpatterns
Supplementary Figure 433: ZBTB33 HCT116 ENCSR000BNY

Supplementary Figure 434: ZBTB33 HCT116 ENCSR000BNY subpatterns
Supplementary Figure 435: ZBTB33 HepG2 ENCSR000BHR
Supplementary Figure 436: ZBTB33 HepG2 ENCSR000BHR subpatterns
Supplementary Figure 437: ZBTB33 HepG2 ENCSR000BNA
Supplementary Figure 438: ZBTB33 HepG2 ENCSR000BNA subpatterns
Supplementary Figure 439: ZBTB33 HepG2 ENCSR421DAO
Supplementary Figure 440: ZBTB33 HepG2 ENCSR421DAO subpatterns
Supplementary Figure 441: ZBTB33 K562 ENCSR000BKF
Supplementary Figure 442: ZBTB33 K562 ENCSR000BKF subpatterns
Supplementary Figure 443: ZBTB33 K562 ENCSR876GXA
Supplementary Figure 444: ZBTB33 K562 ENCSR876GXA subpatterns
Supplementary Figure 445: ZBTB33 K562 ENCSR955LXM
Supplementary Figure 446: ZBTB33 K562 ENCSR955LXM subpatterns
Supplementary Figure 447: ZBTB33 liver ENCSR345YWJ
Supplementary Figure 448: ZBTB33 liver ENCSR345YWJ subpatterns
Supplementary Figure 449: ZBTB33 liver ENCSR516HUP
Supplementary Figure 450: ZBTB33 liver ENCSR516HUP subpatterns
Supplementary Figure 451: ZBTB33 MCF-7 ENCSR231YFE
Supplementary Figure 452: ZBTB33 MCF-7 ENCSR231YFE subpatterns
Supplementary Figure 453: ZBTB33 SK-N-SH ENCSR000BTS
Supplementary Figure 454: ZBTB33 SK-N-SH ENCSR000BTS subpatterns
Supplementary Figure 455: ZBTB33 WTC11 ENCSR943MQH
Supplementary Figure 456: ZBTB33 WTC11 ENCSR943MQH subpatterns
Supplementary Figure 457: ZBTB37 HepG2 ENCSR775YXE
Supplementary Figure 458: ZBTB37 HepG2 ENCSR775YXE subpatterns
Supplementary Figure 459: ZBTB39 HepG2 ENCSR087NSZ
Supplementary Figure 460: ZBTB3 HepG2 ENCSR481AIK
Supplementary Figure 461: ZBTB40 GM12878 ENCSR189YYK
Supplementary Figure 462: ZBTB40 GM12878 ENCSR189YYK subpatterns
Supplementary Figure 463: ZBTB40 HepG2 ENCSR200AWS
Supplementary Figure 464: ZBTB40 HepG2 ENCSR200AWS subpatterns
Supplementary Figure 465: ZBTB40 HepG2 ENCSR525YFS
Supplementary Figure 466: ZBTB40 HepG2 ENCSR525YFS subpatterns
Supplementary Figure 467: ZBTB40 K562 ENCSR158RYZ
Supplementary Figure 468: ZBTB40 K562 ENCSR158RYZ subpatterns
Supplementary Figure 469: ZBTB40 K562 ENCSR237VLT
Supplementary Figure 470: ZBTB40 K562 ENCSR237VLT subpatterns
Supplementary Figure 471: ZBTB40 K562 ENCSR579YNY
Supplementary Figure 472: ZBTB40 K562 ENCSR579YNY subpatterns
Supplementary Figure 473: ZBTB40 MCF-7 ENCSR318LVG
Supplementary Figure 474: ZBTB40 MCF-7 ENCSR318LVG subpatterns
Supplementary Figure 475: ZBTB42 HEK293 Hughes GR models ZBTB42
Supplementary Figure 476: ZBTB42 HEK293 Hughes GR models ZBTB42 subpatterns
Supplementary Figure 477: ZBTB42 HepG2 ENCSR232AAR
Supplementary Figure 478: ZBTB42 HepG2 ENCSR232AAR subpatterns
Supplementary Figure 479: ZBTB43 HepG2 ENCSR173USN
Supplementary Figure 480: ZBTB43 HepG2 ENCSR173USN subpatterns
Supplementary Figure 481: ZBTB43 K562 ENCSR800KMQ
Supplementary Figure 482: ZBTB43 WTC11 ENCSR199PXS
Supplementary Figure 483: ZBTB43 WTC11 ENCSR199PXS subpatterns
Supplementary Figure 484: ZBTB44 HEK293 ENCSR076STQ
Supplementary Figure 485: ZBTB44 HEK293 ENCSR076STQ subpatterns
Supplementary Figure 486: ZBTB44 HepG2 ENCSR269MEF
Supplementary Figure 487: ZBTB46 HepG2 ENCSR931SYA
Supplementary Figure 488: ZBTB48 HEK293 ENCSR781EQJ
Supplementary Figure 489: ZBTB48 HEK293 ENCSR781EQJ subpatterns

Supplementary Figure 490: ZBTB48 HEK293 Hughes GR models ZBTB48
Supplementary Figure 491: ZBTB49 HEK293 ENCSR924GRG
Supplementary Figure 492: ZBTB49 HepG2 ENCSR803IYP
Supplementary Figure 493: ZBTB49 HepG2 ENCSR803IYP subpatterns
Supplementary Figure 494: ZBTB49 K562 ENCSR249VFB
Supplementary Figure 495: ZBTB4 GM12878 ENCSR691IQB
Supplementary Figure 496: ZBTB4 HepG2 ENCSR479PRL
Supplementary Figure 497: ZBTB5 K562 ENCSR389PWB
Supplementary Figure 498: ZBTB5 K562 ENCSR389PWB subpatterns
Supplementary Figure 499: ZBTB5 K562 ENCSR786OQY
Supplementary Figure 500: ZBTB5 K562 ENCSR786OQY subpatterns
Supplementary Figure 501: ZBTB6 HEK293 ENCSR619OUC
Supplementary Figure 502: ZBTB6 HEK293 ENCSR619OUC subpatterns
Supplementary Figure 503: ZBTB7A HEK293 ENCSR773REP
Supplementary Figure 504: ZBTB7A HEK293 ENCSR773REP subpatterns
Supplementary Figure 505: ZBTB7A HepG2 ENCSR000BQA
Supplementary Figure 506: ZBTB7A HepG2 ENCSR000BQA subpatterns
Supplementary Figure 507: ZBTB7A HepG2 ENCSR850YDX
Supplementary Figure 508: ZBTB7A HepG2 ENCSR850YDX subpatterns
Supplementary Figure 509: ZBTB7A Ishikawa ENCSR000BSZ
Supplementary Figure 510: ZBTB7A Ishikawa ENCSR000BSZ subpatterns
Supplementary Figure 511: ZBTB7A K562 ENCSR000BME
Supplementary Figure 512: ZBTB7A K562 ENCSR000BME subpatterns
Supplementary Figure 513: ZBTB7B HepG2 ENCSR322ULL
Supplementary Figure 514: ZBTB7B HepG2 ENCSR322ULL subpatterns
Supplementary Figure 515: ZBTB7B MCF-7 ENCSR277BXW
Supplementary Figure 516: ZBTB8A HEK293 ENCSR481FEC
Supplementary Figure 517: ZBTB8A HEK293 ENCSR481FEC subpatterns
Supplementary Figure 518: ZBTB8A HepG2 ENCSR625XAV
Supplementary Figure 519: ZBTB8A K562 ENCSR283ZNI
Supplementary Figure 520: ZBTB9 K562 ENCSR536CBU
Supplementary Figure 521: ZBTB9 K562 ENCSR536CBU subpatterns
Supplementary Figure 522: ZC3H8 HepG2 ENCSR734CRN
Supplementary Figure 523: ZC3H8 HepG2 ENCSR734CRN subpatterns
Supplementary Figure 524: ZC3H8 K562 ENCSR143CEO
Supplementary Figure 525: ZC3H8 K562 ENCSR494PWZ
Supplementary Figure 526: ZC3H8 K562 ENCSR494PWZ subpatterns
Supplementary Figure 527: ZEB1 bipolar neuron ENCSR418KUS
Supplementary Figure 528: ZEB1 bipolar neuron ENCSR418KUS subpatterns
Supplementary Figure 529: ZEB1 GM12878 ENCSR000BND
Supplementary Figure 530: ZEB1 GM12878 ENCSR000BND subpatterns
Supplementary Figure 531: ZEB1 HEK293 ENCSR909HMT
Supplementary Figure 532: ZEB1 HEK293 ENCSR909HMT subpatterns
Supplementary Figure 533: ZEB1 HepG2 ENCSR000BVN
Supplementary Figure 534: ZEB1 HepG2 ENCSR000BVN subpatterns
Supplementary Figure 535: ZEB2 HEK293 ENCSR417VWF
Supplementary Figure 536: ZEB2 HEK293 ENCSR417VWF subpatterns
Supplementary Figure 537: ZEB2 K562 ENCSR004GKA
Supplementary Figure 538: ZEB2 K562 ENCSR004GKA subpatterns
Supplementary Figure 539: ZEB2 K562 ENCSR322CFO
Supplementary Figure 540: ZEB2 K562 ENCSR322CFO subpatterns
Supplementary Figure 541: ZFAT HepG2 ENCSR409DYM
Supplementary Figure 542: ZFAT HepG2 ENCSR409DYM subpatterns
Supplementary Figure 543: ZFHX2 HEK293 ENCSR632SIM
Supplementary Figure 544: ZFHX2 HEK293 ENCSR632SIM subpatterns
Supplementary Figure 545: ZFHX3 HepG2 ENCSR879RGN

Supplementary Figure 546: ZFHX3 HepG2 ENCSR879RGN subpatterns
Supplementary Figure 547: ZFP14 HEK293 ChipExo models ZFP14
Supplementary Figure 548: ZFP14 HEK293 ChipExo models ZFP14 subpatterns
Supplementary Figure 549: ZFP14 HepG2 ENCSR620DBD
Supplementary Figure 550: ZFP1 HEK293 ChipExo models ZFP1
Supplementary Figure 551: ZFP1 HepG2 ENCSR586DEH
Supplementary Figure 552: ZFP1 HepG2 ENCSR586DEH subpatterns
Supplementary Figure 553: ZFP1 K562 ENCSR617POJ
Supplementary Figure 554: ZFP1 K562 ENCSR617POJ subpatterns
Supplementary Figure 555: ZFP28 HEK293 Hughes GR models ZFP28
Supplementary Figure 556: ZFP28 HEK293 Hughes GR models ZFP28 subpatterns
Supplementary Figure 557: ZFP30 K562 ENCSR279OXE
Supplementary Figure 558: ZFP30 SK-N-SH ENCSR376QPI
Supplementary Figure 559: ZFP30 SK-N-SH ENCSR376QPI subpatterns
Supplementary Figure 560: ZFP37 HEK293 ENCSR365GRX
Supplementary Figure 561: ZFP37 HepG2 ENCSR505LJT
Supplementary Figure 562: ZFP37 HepG2 ENCSR505LJT subpatterns
Supplementary Figure 563: ZFP3 HEK293 ENCSR134QIE
Supplementary Figure 564: ZFP3 HEK293 ENCSR134QIE subpatterns
Supplementary Figure 565: ZFP3 HEK293 Hughes NB models ZFP3
Supplementary Figure 566: ZFP3 HEK293 Hughes NB models ZFP3 subpatterns
Supplementary Figure 567: ZFP3 SK-N-SH ENCSR581GUY
Supplementary Figure 568: ZFP3 SK-N-SH ENCSR581GUY subpatterns
Supplementary Figure 569: ZFP41 HEK293 ENCSR348ONY
Supplementary Figure 570: ZFP41 HepG2 ENCSR731UPJ
Supplementary Figure 571: ZFP41 HepG2 ENCSR731UPJ subpatterns
Supplementary Figure 572: ZFP42 HEK293 Hughes GR models ZFP42
Supplementary Figure 573: ZFP42 HEK293 Hughes GR models ZFP42 subpatterns
Supplementary Figure 574: ZFP62 HepG2 ENCSR495RMN
Supplementary Figure 575: ZFP62 HepG2 ENCSR495RMN subpatterns
Supplementary Figure 576: ZFP64 HepG2 ENCSR487CPI
Supplementary Figure 577: ZFP64 HepG2 ENCSR487CPI subpatterns
Supplementary Figure 578: ZFP69B HEK293 ENCSR381VYR
Supplementary Figure 579: ZFP69B HEK293 ENCSR381VYR subpatterns
Supplementary Figure 580: ZFP69B HEK293 ChipExo models ZFP69B
Supplementary Figure 581: ZFP69B HEK293 ChipExo models ZFP69B subpatterns
Supplementary Figure 582: ZFP69 HEK293 ChipExo models ZFP69
Supplementary Figure 583: ZFP69 HEK293 ChipExo models ZFP69 subpatterns
Supplementary Figure 584: ZFP82 HEK293 Hughes GR models ZFP82
Supplementary Figure 585: ZFP82 HEK293 Hughes GR models ZFP82 subpatterns
Supplementary Figure 586: ZFP82 HepG2 ENCSR196FSX
Supplementary Figure 587: ZFP90 HEK293 ChipExo models ZFP90
Supplementary Figure 588: ZFP90 HepG2 ENCSR377GZS
Supplementary Figure 589: ZFP90 HepG2 ENCSR377GZS subpatterns
Supplementary Figure 590: ZFP91 HepG2 ENCSR678KUJ
Supplementary Figure 591: ZFP91 HepG2 ENCSR678KUJ subpatterns
Supplementary Figure 592: ZFP91 K562 ENCSR201DCF
Supplementary Figure 593: ZFP91 K562 ENCSR201DCF subpatterns
Supplementary Figure 594: ZFP91 K562 ENCSR898XMH
Supplementary Figure 595: ZFP91 K562 ENCSR898XMH subpatterns
Supplementary Figure 596: ZFX 22Rv1 ENCSR246MLJ
Supplementary Figure 597: ZFX C4 2B ENCSR027UFT
Supplementary Figure 598: ZFX C4 2B ENCSR027UFT subpatterns
Supplementary Figure 599: ZFX HCT116 ENCSR503GVO
Supplementary Figure 600: ZFX HCT116 ENCSR503GVO subpatterns
Supplementary Figure 601: ZFX HEK293T ENCSR218GSN

Supplementary Figure 602: ZFX HEK293T ENCSR218GSN subpatterns
Supplementary Figure 603: ZFX HepG2 ENCSR266HHO
Supplementary Figure 604: ZFX HepG2 ENCSR266HHO subpatterns
Supplementary Figure 605: ZFX K562 ENCSR628DJK
Supplementary Figure 606: ZFX K562 ENCSR628DJK subpatterns
Supplementary Figure 607: ZFX K562 ENCSR920ASP
Supplementary Figure 608: ZFX K562 ENCSR920ASP subpatterns
Supplementary Figure 609: ZFX MCF-7 ENCSR435OQD
Supplementary Figure 610: ZFX MCF-7 ENCSR435OQD subpatterns
Supplementary Figure 611: ZFY HepG2 ENCSR949OEV
Supplementary Figure 612: ZFY HepG2 ENCSR949OEV subpatterns
Supplementary Figure 613: ZHX1 HeLa-S3 ENCSR887MXT
Supplementary Figure 614: ZHX1 HeLa-S3 ENCSR887MXT subpatterns
Supplementary Figure 615: ZHX1 HepG2 ENCSR978DQT
Supplementary Figure 616: ZHX1 HepG2 ENCSR978DQT subpatterns
Supplementary Figure 617: ZHX1 K562 ENCSR557RVF
Supplementary Figure 618: ZHX1 K562 ENCSR557RVF subpatterns
Supplementary Figure 619: ZHX2 HepG2 ENCSR401VBM
Supplementary Figure 620: ZHX2 HepG2 ENCSR401VBM subpatterns
Supplementary Figure 621: ZHX2 HepG2 ENCSR407BEZ
Supplementary Figure 622: ZHX2 HepG2 ENCSR407BEZ subpatterns
Supplementary Figure 623: ZHX2 MCF-7 ENCSR876UYH
Supplementary Figure 624: ZHX2 MCF-7 ENCSR876UYH subpatterns
Supplementary Figure 625: ZHX3 HepG2 ENCSR367KYL
Supplementary Figure 626: ZHX3 HepG2 ENCSR367KYL subpatterns
Supplementary Figure 627: ZIC2 HEK293 ENCSR728MWW
Supplementary Figure 628: ZIC2 HEK293 ENCSR728MWW subpatterns
Supplementary Figure 629: ZIC2 HEK293 Hughes NB models ZIC2
Supplementary Figure 630: ZIK1 HEK293 ChipExo models ZIK1
Supplementary Figure 631: ZIK1 HepG2 ENCSR862VDD
Supplementary Figure 632: ZIK1 HepG2 ENCSR862VDD subpatterns
Supplementary Figure 633: ZKSCAN1 HeLa-S3 ENCSR000ECJ
Supplementary Figure 634: ZKSCAN1 HeLa-S3 ENCSR000ECJ subpatterns
Supplementary Figure 635: ZKSCAN1 HepG2 ENCSR157CAU
Supplementary Figure 636: ZKSCAN1 HepG2 ENCSR157CAU subpatterns
Supplementary Figure 637: ZKSCAN1 K562 ENCSR882ERE
Supplementary Figure 638: ZKSCAN1 K562 ENCSR882ERE subpatterns
Supplementary Figure 639: ZKSCAN1 MCF-7 ENCSR449UFF
Supplementary Figure 640: ZKSCAN1 MCF-7 ENCSR449UFF subpatterns
Supplementary Figure 641: ZKSCAN2 HEK293 ChipExo models ZKSCAN2
Supplementary Figure 642: ZKSCAN3 HEK293 ChipExo models ZKSCAN3
Supplementary Figure 643: ZKSCAN3 K562 ENCSR199HGP
Supplementary Figure 644: ZKSCAN5 HEK293 ChipExo models ZKSCAN5
Supplementary Figure 645: ZKSCAN5 HEK293 ChipExo models ZKSCAN5 subpatterns
Supplementary Figure 646: ZKSCAN5 HepG2 ENCSR159BTO
Supplementary Figure 647: ZKSCAN5 HepG2 ENCSR159BTO subpatterns
Supplementary Figure 648: ZKSCAN8 HepG2 ENCSR808FFI
Supplementary Figure 649: ZKSCAN8 HepG2 ENCSR808FFI subpatterns
Supplementary Figure 650: ZKSCAN8 K562 ENCSR448UKK
Supplementary Figure 651: ZKSCAN8 K562 ENCSR448UKK subpatterns
Supplementary Figure 652: ZKSCAN8 K562 ENCSR755CRA
Supplementary Figure 653: ZKSCAN8 K562 ENCSR755CRA subpatterns
Supplementary Figure 654: ZKSCAN8 WTC11 ENCSR115QIT
Supplementary Figure 655: ZKSCAN8 WTC11 ENCSR115QIT subpatterns
Supplementary Figure 656: ZMAT4 WTC11 ENCSR807VQT
Supplementary Figure 657: ZMAT5 HepG2 ENCSR215XSZ

Supplementary Figure 658: ZMYM2 HepG2 ENCSR066EWR
Supplementary Figure 659: ZMYM2 HepG2 ENCSR066EWR subpatterns
Supplementary Figure 660: ZNF100 HEK293 ChipExo models ZNF100
Supplementary Figure 661: ZNF100 HEK293 ChipExo models ZNF100 subpatterns
Supplementary Figure 662: ZNF101 HEK293 ChipExo models ZNF101
Supplementary Figure 663: ZNF101 HepG2 ENCSR519QYU
Supplementary Figure 664: ZNF10 HEK293 ENCSR019WUS
Supplementary Figure 665: ZNF10 HEK293 ENCSR019WUS subpatterns
Supplementary Figure 666: ZNF10 HEK293 ChipExo models ZNF10
Supplementary Figure 667: ZNF10 HEK293 ChipExo models ZNF10 subpatterns
Supplementary Figure 668: ZNF10 HepG2 ENCSR009LIA
Supplementary Figure 669: ZNF112 HEK293 ENCSR751PNN
Supplementary Figure 670: ZNF112 HEK293 ENCSR751PNN subpatterns
Supplementary Figure 671: ZNF114 GM23338 ENCSR555KFE
Supplementary Figure 672: ZNF114 HEK293 ENCSR985MYI
Supplementary Figure 673: ZNF114 HEK293 ChipExo models ZNF114
Supplementary Figure 674: ZNF121 HEK293 ENCSR224QDY
Supplementary Figure 675: ZNF121 HEK293 ENCSR224QDY subpatterns
Supplementary Figure 676: ZNF121 HepG2 ENCSR945QEW
Supplementary Figure 677: ZNF121 HepG2 ENCSR945QEW subpatterns
Supplementary Figure 678: ZNF121 K562 ENCSR799URB
Supplementary Figure 679: ZNF121 K562 ENCSR799URB subpatterns
Supplementary Figure 680: ZNF121 WTC11 ENCSR203PCF
Supplementary Figure 681: ZNF121 WTC11 ENCSR203PCF subpatterns
Supplementary Figure 682: ZNF124 HEK293 ChipExo models ZNF124
Supplementary Figure 683: ZNF124 HEK293 ChipExo models ZNF124 subpatterns
Supplementary Figure 684: ZNF124 HepG2 ENCSR357YPP
Supplementary Figure 685: ZNF124 HepG2 ENCSR357YPP subpatterns
Supplementary Figure 686: ZNF124 K562 ENCSR124YFA
Supplementary Figure 687: ZNF12 HEK293 ChipExo models ZNF12
Supplementary Figure 688: ZNF12 HepG2 ENCSR711KBM
Supplementary Figure 689: ZNF12 HepG2 ENCSR711KBM subpatterns
Supplementary Figure 690: ZNF12 K562 ENCSR041YBR
Supplementary Figure 691: ZNF12 K562 ENCSR041YBR subpatterns
Supplementary Figure 692: ZNF132 HEK293 ENCSR138RCE
Supplementary Figure 693: ZNF132 HEK293 ChipExo models ZNF132
Supplementary Figure 694: ZNF132 HEK293 ChipExo models ZNF132 subpatterns
Supplementary Figure 695: ZNF133 HEK293 ENCSR283MWQ
Supplementary Figure 696: ZNF133 HEK293 ENCSR283MWQ subpatterns
Supplementary Figure 697: ZNF133 HEK293 ChipExo models ZNF133
Supplementary Figure 698: ZNF133 HEK293 ChipExo models ZNF133 subpatterns
Supplementary Figure 699: ZNF133 K562 ENCSR619UPN
Supplementary Figure 700: ZNF133 K562 ENCSR619UPN subpatterns
Supplementary Figure 701: ZNF134 HEK293 Hughes GR models ZNF134
Supplementary Figure 702: ZNF134 HEK293 Hughes GR models ZNF134 subpatterns
Supplementary Figure 703: ZNF134 K562 ENCSR553NTC
Supplementary Figure 704: ZNF134 K562 ENCSR553NTC subpatterns
Supplementary Figure 705: ZNF135 HEK293 ChipExo models ZNF135
Supplementary Figure 706: ZNF135 HEK293 ChipExo models ZNF135 subpatterns
Supplementary Figure 707: ZNF136 HEK293 Hughes NB models ZNF136
Supplementary Figure 708: ZNF136 HEK293 ChipExo models ZNF136
Supplementary Figure 709: ZNF136 HEK293 ChipExo models ZNF136 subpatterns
Supplementary Figure 710: ZNF138 HEK293 ENCSR551KAP
Supplementary Figure 711: ZNF138 HepG2 ENCSR910MUD
Supplementary Figure 712: ZNF138 WTC11 ENCSR373KKV
Supplementary Figure 713: ZNF140 HEK293 ENCSR464KFG

Supplementary Figure 714: ZNF140 HEK293 ENCSR464KFG subpatterns
Supplementary Figure 715: ZNF140 HEK293 Hughes GR models ZNF140
Supplementary Figure 716: ZNF140 HEK293 Hughes GR models ZNF140 subpatterns
Supplementary Figure 717: ZNF140 K562 ENCSR377HQG
Supplementary Figure 718: ZNF140 K562 ENCSR377HQG subpatterns
Supplementary Figure 719: ZNF141 HEK293 ChipExo models ZNF141
Supplementary Figure 720: ZNF141 HEK293 ChipExo models ZNF141 subpatterns
Supplementary Figure 721: ZNF142 HepG2 ENCSR512ECF
Supplementary Figure 722: ZNF142 HepG2 ENCSR512ECF subpatterns
Supplementary Figure 723: ZNF143 GM12878 ENCSR000DZL
Supplementary Figure 724: ZNF143 GM12878 ENCSR000DZL subpatterns
Supplementary Figure 725: ZNF143 GM12878 ENCSR936XTK
Supplementary Figure 726: ZNF143 GM12878 ENCSR936XTK subpatterns
Supplementary Figure 727: ZNF143 H1 ENCSR000EBW
Supplementary Figure 728: ZNF143 H1 ENCSR000EBW subpatterns
Supplementary Figure 729: ZNF143 HeLa-S3 ENCSR000ECO
Supplementary Figure 730: ZNF143 HeLa-S3 ENCSR000ECO subpatterns
Supplementary Figure 731: ZNF143 HepG2 ENCSR080UEM
Supplementary Figure 732: ZNF143 HepG2 ENCSR080UEM subpatterns
Supplementary Figure 733: ZNF143 K562 ENCSR000EGP
Supplementary Figure 734: ZNF143 K562 ENCSR000EGP subpatterns
Supplementary Figure 735: ZNF143 K562 ENCSR427WZJ
Supplementary Figure 736: ZNF143 K562 ENCSR427WZJ subpatterns
Supplementary Figure 737: ZNF143 WTC11 ENCSR063FUV
Supplementary Figure 738: ZNF143 WTC11 ENCSR063FUV subpatterns
Supplementary Figure 739: ZNF146 HEK293 ENCSR689YFA
Supplementary Figure 740: ZNF146 HEK293 ENCSR689YFA subpatterns
Supplementary Figure 741: ZNF146 HEK293 Hughes GR models ZNF146
Supplementary Figure 742: ZNF146 HEK293 Hughes GR models ZNF146 subpatterns
Supplementary Figure 743: ZNF146 HepG2 ENCSR957LTN
Supplementary Figure 744: ZNF146 HepG2 ENCSR957LTN subpatterns
Supplementary Figure 745: ZNF146 K562 ENCSR713IFY
Supplementary Figure 746: ZNF146 K562 ENCSR713IFY subpatterns
Supplementary Figure 747: ZNF148 HEK293 ENCSR736ZKL
Supplementary Figure 748: ZNF148 K562 ENCSR018MSO
Supplementary Figure 749: ZNF148 K562 ENCSR018MSO subpatterns
Supplementary Figure 750: ZNF154 HEK293 ChipExo models ZNF154
Supplementary Figure 751: ZNF155 HEK293 ENCSR801BWR
Supplementary Figure 752: ZNF157 HEK293 ENCSR564YYW
Supplementary Figure 753: ZNF157 HEK293 ENCSR564YYW subpatterns
Supplementary Figure 754: ZNF157 HEK293 ChipExo models ZNF157
Supplementary Figure 755: ZNF157 HEK293 ChipExo models ZNF157 subpatterns
Supplementary Figure 756: ZNF160 HepG2 ENCSR917SSX
Supplementary Figure 757: ZNF160 HepG2 ENCSR917SSX subpatterns
Supplementary Figure 758: ZNF165 K562 ENCSR172XJS
Supplementary Figure 759: ZNF165 K562 ENCSR172XJS subpatterns
Supplementary Figure 760: ZNF169 HEK293 ENCSR661AXW
Supplementary Figure 761: ZNF169 HEK293 ChipExo models ZNF169
Supplementary Figure 762: ZNF16 HEK293 ENCSR093HXE
Supplementary Figure 763: ZNF16 HEK293 ENCSR093HXE subpatterns
Supplementary Figure 764: ZNF174 HEK293 ENCSR516VQK
Supplementary Figure 765: ZNF174 K562 ENCSR056VYW
Supplementary Figure 766: ZNF175 HEK293 ENCSR103GAK
Supplementary Figure 767: ZNF175 K562 ENCSR011PEI
Supplementary Figure 768: ZNF175 K562 ENCSR011PEI subpatterns
Supplementary Figure 769: ZNF17 HEK293 ChipExo models ZNF17

Supplementary Figure 770: ZNF17 HEK293 ChipExo models ZNF17 subpatterns
Supplementary Figure 771: ZNF17 HepG2 ENCSR075BAS
Supplementary Figure 772: ZNF17 HepG2 ENCSR075BAS subpatterns
Supplementary Figure 773: ZNF180 HEK293 ChipExo models ZNF180
Supplementary Figure 774: ZNF180 HEK293 ChipExo models ZNF180 subpatterns
Supplementary Figure 775: ZNF180 HepG2 ENCSR298DSB
Supplementary Figure 776: ZNF181 HEK293 ChipExo models ZNF181
Supplementary Figure 777: ZNF181 HepG2 ENCSR115LFG
Supplementary Figure 778: ZNF182 HEK293 ChipExo models ZNF182
Supplementary Figure 779: ZNF182 HEK293 ChipExo models ZNF182 subpatterns
Supplementary Figure 780: ZNF184 HEK293 ENCSR020UPN
Supplementary Figure 781: ZNF184 HEK293 ENCSR020UPN subpatterns
Supplementary Figure 782: ZNF184 HEK293 ChipExo models ZNF184
Supplementary Figure 783: ZNF184 K562 ENCSR526HRN
Supplementary Figure 784: ZNF184 K562 ENCSR526HRN subpatterns
Supplementary Figure 785: ZNF184 K562 ENCSR546IHU
Supplementary Figure 786: ZNF184 K562 ENCSR546IHU subpatterns
Supplementary Figure 787: ZNF184 K562 ENCSR621ATC
Supplementary Figure 788: ZNF184 K562 ENCSR621ATC subpatterns
Supplementary Figure 789: ZNF184 WTC11 ENCSR640STN
Supplementary Figure 790: ZNF184 WTC11 ENCSR640STN subpatterns
Supplementary Figure 791: ZNF189 HEK293 ENCSR163RYW
Supplementary Figure 792: ZNF189 HEK293 ENCSR163RYW subpatterns
Supplementary Figure 793: ZNF189 HEK293 Hughes NB models ZNF189
Supplementary Figure 794: ZNF189 HEK293 Hughes NB models ZNF189 subpatterns
Supplementary Figure 795: ZNF189 HEK293 ChipExo models ZNF189
Supplementary Figure 796: ZNF189 HEK293 ChipExo models ZNF189 subpatterns
Supplementary Figure 797: ZNF18 HEK293 ENCSR977HTH
Supplementary Figure 798: ZNF18 HEK293 ENCSR977HTH subpatterns
Supplementary Figure 799: ZNF18 HEK293 ChipExo models ZNF18
Supplementary Figure 800: ZNF18 HEK293 ChipExo models ZNF18 subpatterns
Supplementary Figure 801: ZNF18 HEK293 Hughes GR models ZNF18
Supplementary Figure 802: ZNF18 HEK293 Hughes GR models ZNF18 subpatterns
Supplementary Figure 803: ZNF18 HepG2 ENCSR553ZJQ
Supplementary Figure 804: ZNF18 HepG2 ENCSR553ZJQ subpatterns
Supplementary Figure 805: ZNF197 HEK293 ChipExo models ZNF197
Supplementary Figure 806: ZNF197 K562 ENCSR580IAO
Supplementary Figure 807: ZNF197 K562 ENCSR580IAO subpatterns
Supplementary Figure 808: ZNF19 HEK293 ENCSR811JJM
Supplementary Figure 809: ZNF19 HEK293 ChipExo models ZNF19
Supplementary Figure 810: ZNF200 HEK293 Hughes NB models ZNF200
Supplementary Figure 811: ZNF202 HEK293 ENCSR996FYT
Supplementary Figure 812: ZNF202 HEK293 ChipExo models ZNF202
Supplementary Figure 813: ZNF202 HEK293 ChipExo models ZNF202 subpatterns
Supplementary Figure 814: ZNF205 HEK293 ChipExo models ZNF205
Supplementary Figure 815: ZNF205 HEK293 ChipExo models ZNF205 subpatterns
Supplementary Figure 816: ZNF205 HepG2 ENCSR157CEN
Supplementary Figure 817: ZNF205 HepG2 ENCSR157CEN subpatterns
Supplementary Figure 818: ZNF20 HepG2 ENCSR720PDY
Supplementary Figure 819: ZNF211 HEK293 ENCSR365DQH
Supplementary Figure 820: ZNF211 HEK293 ENCSR365DQH subpatterns
Supplementary Figure 821: ZNF211 HEK293 ChipExo models ZNF211
Supplementary Figure 822: ZNF211 HEK293 ChipExo models ZNF211 subpatterns
Supplementary Figure 823: ZNF212 HEK293 ChipExo models ZNF212
Supplementary Figure 824: ZNF212 K562 ENCSR002ZGC
Supplementary Figure 825: ZNF212 K562 ENCSR002ZGC subpatterns

Supplementary Figure 826: ZNF213 HEK293 Hughes GR models ZNF213
Supplementary Figure 827: ZNF214 HEK293 ENCSR993DED
Supplementary Figure 828: ZNF214 HEK293 ENCSR993DED subpatterns
Supplementary Figure 829: ZNF214 HEK293 ChipExo models ZNF214
Supplementary Figure 830: ZNF215 K562 ENCSR699RWG
Supplementary Figure 831: ZNF215 K562 ENCSR699RWG subpatterns
Supplementary Figure 832: ZNF217 GM12878 ENCSR764CZW
Supplementary Figure 833: ZNF217 GM12878 ENCSR764CZW subpatterns
Supplementary Figure 834: ZNF217 HepG2 ENCSR055FQB
Supplementary Figure 835: ZNF217 HepG2 ENCSR055FQB subpatterns
Supplementary Figure 836: ZNF217 K562 ENCSR841GLE
Supplementary Figure 837: ZNF217 MCF-7 ENCSR000EWU
Supplementary Figure 838: ZNF217 MCF-7 ENCSR000EWU subpatterns
Supplementary Figure 839: ZNF217 MCF-7 ENCSR465XQW
Supplementary Figure 840: ZNF217 MCF-7 ENCSR465XQW subpatterns
Supplementary Figure 841: ZNF217 MCF-7 ENCSR912ATU
Supplementary Figure 842: ZNF217 MCF-7 ENCSR912ATU subpatterns
Supplementary Figure 843: ZNF219 HepG2 ENCSR243BPI
Supplementary Figure 844: ZNF219 HepG2 ENCSR243BPI subpatterns
Supplementary Figure 845: ZNF221 HEK293 ENCSR194BBY
Supplementary Figure 846: ZNF221 HEK293 ENCSR194BBY subpatterns
Supplementary Figure 847: ZNF221 HepG2 ENCSR347HAM
Supplementary Figure 848: ZNF222 HEK293 ChipExo models ZNF222
Supplementary Figure 849: ZNF223 HEK293 ENCSR906PCS
Supplementary Figure 850: ZNF223 HEK293 ENCSR906PCS subpatterns
Supplementary Figure 851: ZNF223 HEK293 ChipExo models ZNF223
Supplementary Figure 852: ZNF224 HEK293 ChipExo models ZNF224
Supplementary Figure 853: ZNF224 HEK293 ChipExo models ZNF224 subpatterns
Supplementary Figure 854: ZNF224 HepG2 ENCSR886VSY
Supplementary Figure 855: ZNF224 K562 ENCSR409PXW
Supplementary Figure 856: ZNF225 HEK293 ChipExo models ZNF225
Supplementary Figure 857: ZNF225 HepG2 ENCSR075PWK
Supplementary Figure 858: ZNF227 MCF-7 ENCSR877UJB
Supplementary Figure 859: ZNF22 HEK293 Hughes GR models ZNF22
Supplementary Figure 860: ZNF230 HepG2 ENCSR087HFN
Supplementary Figure 861: ZNF232 HepG2 ENCSR837GLU
Supplementary Figure 862: ZNF232 HepG2 ENCSR837GLU subpatterns
Supplementary Figure 863: ZNF232 K562 ENCSR360ECJ
Supplementary Figure 864: ZNF232 K562 ENCSR360ECJ subpatterns
Supplementary Figure 865: ZNF232 WTC11 ENCSR034IND
Supplementary Figure 866: ZNF232 WTC11 ENCSR034IND subpatterns
Supplementary Figure 867: ZNF234 HepG2 ENCSR800ASH
Supplementary Figure 868: ZNF235 HEK293 ChipExo models ZNF235
Supplementary Figure 869: ZNF235 HepG2 ENCSR924KZA
Supplementary Figure 870: ZNF235 HepG2 ENCSR924KZA subpatterns
Supplementary Figure 871: ZNF239 HEK293 ENCSR440COG
Supplementary Figure 872: ZNF239 HEK293 ENCSR440COG subpatterns
Supplementary Figure 873: ZNF239 K562 ENCSR606KTL
Supplementary Figure 874: ZNF239 K562 ENCSR606KTL subpatterns
Supplementary Figure 875: ZNF23 HEK293 ENCSR679KXF
Supplementary Figure 876: ZNF23 HEK293 ENCSR679KXF subpatterns
Supplementary Figure 877: ZNF23 K562 ENCSR898IDK
Supplementary Figure 878: ZNF23 K562 ENCSR898IDK subpatterns
Supplementary Figure 879: ZNF248 HEK293 ENCSR338SEM
Supplementary Figure 880: ZNF248 HEK293 ENCSR338SEM subpatterns
Supplementary Figure 881: ZNF248 HEK293 ChipExo models ZNF248

Supplementary Figure 882: ZNF248 HEK293 ChipExo models ZNF248 subpatterns
Supplementary Figure 883: ZNF24 GM12878 ENCSR072PWP
Supplementary Figure 884: ZNF24 GM12878 ENCSR072PWP subpatterns
Supplementary Figure 885: ZNF24 HEK293 ENCSR984MDV
Supplementary Figure 886: ZNF24 HEK293 ENCSR984MDV subpatterns
Supplementary Figure 887: ZNF24 HepG2 ENCSR362NWP
Supplementary Figure 888: ZNF24 HepG2 ENCSR362NWP subpatterns
Supplementary Figure 889: ZNF24 HepG2 ENCSR791AGT
Supplementary Figure 890: ZNF24 HepG2 ENCSR791AGT subpatterns
Supplementary Figure 891: ZNF24 K562 ENCSR099NCH
Supplementary Figure 892: ZNF24 K562 ENCSR099NCH subpatterns
Supplementary Figure 893: ZNF24 K562 ENCSR117WTM
Supplementary Figure 894: ZNF24 K562 ENCSR117WTM subpatterns
Supplementary Figure 895: ZNF24 K562 ENCSR385AHH
Supplementary Figure 896: ZNF24 K562 ENCSR385AHH subpatterns
Supplementary Figure 897: ZNF24 K562 ENCSR695EQB
Supplementary Figure 898: ZNF24 K562 ENCSR695EQB subpatterns
Supplementary Figure 899: ZNF24 MCF-7 ENCSR503VTG
Supplementary Figure 900: ZNF24 MCF-7 ENCSR503VTG subpatterns
Supplementary Figure 901: ZNF250 HEK293 Hughes GR models ZNF250
Supplementary Figure 902: ZNF250 HEK293 Hughes GR models ZNF250 subpatterns
Supplementary Figure 903: ZNF250 HEK293 Hughes NB models ZNF250
Supplementary Figure 904: ZNF250 HEK293 Hughes NB models ZNF250 subpatterns
Supplementary Figure 905: ZNF251 HepG2 ENCSR605KVV
Supplementary Figure 906: ZNF253 HepG2 ENCSR569GKR
Supplementary Figure 907: ZNF253 K562 ENCSR271RRH
Supplementary Figure 908: ZNF254 HEK293 ChipExo models ZNF254
Supplementary Figure 909: ZNF254 HEK293 ChipExo models ZNF254 subpatterns
Supplementary Figure 910: ZNF256 HepG2 ENCSR563JME
Supplementary Figure 911: ZNF256 HepG2 ENCSR563JME subpatterns
Supplementary Figure 912: ZNF257 HEK293 Hughes GR models ZNF257
Supplementary Figure 913: ZNF257 HEK293 Hughes GR models ZNF257 subpatterns
Supplementary Figure 914: ZNF257 K562 ENCSR492FKD
Supplementary Figure 915: ZNF257 K562 ENCSR492FKD subpatterns
Supplementary Figure 916: ZNF25 HepG2 ENCSR384SQB
Supplementary Figure 917: ZNF260 HEK293 Hughes GR models ZNF260
Supplementary Figure 918: ZNF260 HEK293 Hughes GR models ZNF260 subpatterns
Supplementary Figure 919: ZNF260 HepG2 ENCSR024ZIS
Supplementary Figure 920: ZNF260 HepG2 ENCSR024ZIS subpatterns
Supplementary Figure 921: ZNF263 HEK293 ENCSR000EVD
Supplementary Figure 922: ZNF263 HEK293 ENCSR000EVD subpatterns
Supplementary Figure 923: ZNF263 HEK293 ChipExo models ZNF263
Supplementary Figure 924: ZNF263 HEK293 ChipExo models ZNF263 subpatterns
Supplementary Figure 925: ZNF263 HepG2 ENCSR313MMD
Supplementary Figure 926: ZNF263 HepG2 ENCSR313MMD subpatterns
Supplementary Figure 927: ZNF263 K562 ENCSR000EWN
Supplementary Figure 928: ZNF263 K562 ENCSR000EWN subpatterns
Supplementary Figure 929: ZNF263 K562 ENCSR845GGY
Supplementary Figure 930: ZNF263 K562 ENCSR845GGY subpatterns
Supplementary Figure 931: ZNF263 WTC11 ENCSR156JWW
Supplementary Figure 932: ZNF263 WTC11 ENCSR156JWW subpatterns
Supplementary Figure 933: ZNF264 HEK293 Hughes NB models ZNF264
Supplementary Figure 934: ZNF264 HEK293 Hughes NB models ZNF264 subpatterns
Supplementary Figure 935: ZNF264 HEK293 Hughes GR models ZNF264
Supplementary Figure 936: ZNF264 HEK293 Hughes GR models ZNF264 subpatterns
Supplementary Figure 937: ZNF264 HEK293 ChipExo models ZNF264

Supplementary Figure 938: ZNF264 HepG2 ENCSR248BVU
Supplementary Figure 939: ZNF264 HepG2 ENCSR248BVU subpatterns
Supplementary Figure 940: ZNF266 HEK293 ENCSR466VYP
Supplementary Figure 941: ZNF266 HEK293 ENCSR466VYP subpatterns
Supplementary Figure 942: ZNF266 HEK293 ChipExo models ZNF266
Supplementary Figure 943: ZNF266 HEK293 ChipExo models ZNF266 subpatterns
Supplementary Figure 944: ZNF267 HEK293 ChipExo models ZNF267
Supplementary Figure 945: ZNF267 HEK293 ChipExo models ZNF267 subpatterns
Supplementary Figure 946: ZNF26 HEK293 ENCSR028EGI
Supplementary Figure 947: ZNF26 HEK293 ENCSR028EGI subpatterns
Supplementary Figure 948: ZNF26 HEK293 ChipExo models ZNF26
Supplementary Figure 949: ZNF26 HEK293 ChipExo models ZNF26 subpatterns
Supplementary Figure 950: ZNF273 HEK293 Hughes NB models ZNF273
Supplementary Figure 951: ZNF273 HEK293 ChipExo models ZNF273
Supplementary Figure 952: ZNF273 HEK293 ChipExo models ZNF273 subpatterns
Supplementary Figure 953: ZNF274 GM08714 ENCSR000EUI
Supplementary Figure 954: ZNF274 GM08714 ENCSR000EUI subpatterns
Supplementary Figure 955: ZNF274 GM12878 ENCSR000EUK
Supplementary Figure 956: ZNF274 H1 ENCSR000EUN
Supplementary Figure 957: ZNF274 H1 ENCSR000EUN subpatterns
Supplementary Figure 958: ZNF274 HCT116 ENCSR101FJM
Supplementary Figure 959: ZNF274 HCT116 ENCSR101FJM subpatterns
Supplementary Figure 960: ZNF274 HEK293 ENCSR000FCI
Supplementary Figure 961: ZNF274 HEK293 ENCSR178QVJ
Supplementary Figure 962: ZNF274 HEK293 ENCSR178QVJ subpatterns
Supplementary Figure 963: ZNF274 HEK293 ChipExo models ZNF274
Supplementary Figure 964: ZNF274 HeLa-S3 ENCSR000EVG
Supplementary Figure 965: ZNF274 HepG2 ENCSR000EVR
Supplementary Figure 966: ZNF274 HepG2 ENCSR871VNN
Supplementary Figure 967: ZNF274 K562 ENCSR000EVX
Supplementary Figure 968: ZNF274 K562 ENCSR000EVX subpatterns
Supplementary Figure 969: ZNF274 K562 ENCSR000EWE
Supplementary Figure 970: ZNF274 NT2 D1 ENCSR000EWY
Supplementary Figure 971: ZNF274 NT2 D1 ENCSR000EWY subpatterns
Supplementary Figure 972: ZNF275 HepG2 ENCSR590BHJ
Supplementary Figure 973: ZNF276 HepG2 ENCSR076KLJ
Supplementary Figure 974: ZNF277 K562 ENCSR358PJI
Supplementary Figure 975: ZNF277 K562 ENCSR358PJI subpatterns
Supplementary Figure 976: ZNF280A HEK293 Hughes GR models ZNF280A
Supplementary Figure 977: ZNF280A HEK293 Hughes GR models ZNF280A subpatterns
Supplementary Figure 978: ZNF280A K562 ENCSR370NFS
Supplementary Figure 979: ZNF280B HepG2 ENCSR940EZR
Supplementary Figure 980: ZNF280B K562 ENCSR775FSH
Supplementary Figure 981: ZNF280C HEK293 ENCSR076KZW
Supplementary Figure 982: ZNF280D HEK293 ENCSR451CYX
Supplementary Figure 983: ZNF280D HEK293 ENCSR451CYX subpatterns
Supplementary Figure 984: ZNF280D HepG2 ENCSR233FJO
Supplementary Figure 985: ZNF280D HepG2 ENCSR233FJO subpatterns
Supplementary Figure 986: ZNF281 HEK293 Hughes GR models ZNF281
Supplementary Figure 987: ZNF281 HEK293 Hughes GR models ZNF281 subpatterns
Supplementary Figure 988: ZNF281 HepG2 ENCSR403MJY
Supplementary Figure 989: ZNF281 HepG2 ENCSR403MJY subpatterns
Supplementary Figure 990: ZNF281 K562 ENCSR214EKV
Supplementary Figure 991: ZNF281 K562 ENCSR214EKV subpatterns
Supplementary Figure 992: ZNF281 WTC11 ENCSR032DGZ
Supplementary Figure 993: ZNF281 WTC11 ENCSR032DGZ subpatterns

Supplementary Figure 994: ZNF282 HEK293 ChipExo models ZNF282
Supplementary Figure 995: ZNF282 HEK293 ChipExo models ZNF282 subpatterns
Supplementary Figure 996: ZNF282 HepG2 ENCSR752NDX
Supplementary Figure 997: ZNF282 K562 ENCSR229KXQ
Supplementary Figure 998: ZNF282 K562 ENCSR742TMU
Supplementary Figure 999: ZNF282 K562 ENCSR742TMU subpatterns
Supplementary Figure 1000: ZNF283 HEK293 ChipExo models ZNF283
Supplementary Figure 1001: ZNF283 HEK293 ChipExo models ZNF283 subpatterns
Supplementary Figure 1002: ZNF284 HEK293 ChipExo models ZNF284
Supplementary Figure 1003: ZNF284 HEK293 ChipExo models ZNF284 subpatterns
Supplementary Figure 1004: ZNF287 HEK293 ChipExo models ZNF287
Supplementary Figure 1005: ZNF287 HEK293 ChipExo models ZNF287 subpatterns
Supplementary Figure 1006: ZNF28 HEK293 ChipExo models ZNF28
Supplementary Figure 1007: ZNF28 HEK293 ChipExo models ZNF28 subpatterns
Supplementary Figure 1008: ZNF292 HEK293 ENCSR228PGT
Supplementary Figure 1009: ZNF292 HepG2 ENCSR853BYT
Supplementary Figure 1010: ZNF292 HepG2 ENCSR853BYT subpatterns
Supplementary Figure 1011: ZNF296 HepG2 ENCSR862LJQ
Supplementary Figure 1012: ZNF296 HepG2 ENCSR862LJQ subpatterns
Supplementary Figure 1013: ZNF2 HEK293 ENCSR011CKE
Supplementary Figure 1014: ZNF2 HEK293 ENCSR011CKE subpatterns
Supplementary Figure 1015: ZNF2 HEK293 ChipExo models ZNF2
Supplementary Figure 1016: ZNF300 HEK293 ChipExo models ZNF300
Supplementary Figure 1017: ZNF302 A549 ENCSR590IHT
Supplementary Figure 1018: ZNF302 HEK293 ENCSR513MGG
Supplementary Figure 1019: ZNF302 HEK293 ChipExo models ZNF302
Supplementary Figure 1020: ZNF304 HEK293 ChipExo models ZNF304
Supplementary Figure 1021: ZNF304 HEK293 ChipExo models ZNF304 subpatterns
Supplementary Figure 1022: ZNF30 HEK293 Hughes GR models ZNF30
Supplementary Figure 1023: ZNF30 HEK293 Hughes GR models ZNF30 subpatterns
Supplementary Figure 1024: ZNF30 HEK293 ChipExo models ZNF30
Supplementary Figure 1025: ZNF30 HepG2 ENCSR891KNP
Supplementary Figure 1026: ZNF311 HEK293 ENCSR096LSN
Supplementary Figure 1027: ZNF311 HEK293 ChipExo models ZNF311
Supplementary Figure 1028: ZNF311 K562 ENCSR388ZRV
Supplementary Figure 1029: ZNF311 K562 ENCSR388ZRV subpatterns
Supplementary Figure 1030: ZNF316 K562 ENCSR167KBO
Supplementary Figure 1031: ZNF316 K562 ENCSR167KBO subpatterns
Supplementary Figure 1032: ZNF316 K562 ENCSR200JYP
Supplementary Figure 1033: ZNF316 K562 ENCSR200JYP subpatterns
Supplementary Figure 1034: ZNF317 HEK293 Hughes NB models ZNF317
Supplementary Figure 1035: ZNF317 HEK293 Hughes NB models ZNF317 subpatterns
Supplementary Figure 1036: ZNF317 HEK293 ChipExo models ZNF317
Supplementary Figure 1037: ZNF317 HEK293 ChipExo models ZNF317 subpatterns
Supplementary Figure 1038: ZNF317 HepG2 ENCSR016OHL
Supplementary Figure 1039: ZNF317 HepG2 ENCSR016OHL subpatterns
Supplementary Figure 1040: ZNF317 K562 ENCSR976MXN
Supplementary Figure 1041: ZNF317 K562 ENCSR976MXN subpatterns
Supplementary Figure 1042: ZNF317 WTC11 ENCSR795KRU
Supplementary Figure 1043: ZNF317 WTC11 ENCSR795KRU subpatterns
Supplementary Figure 1044: ZNF318 HepG2 ENCSR832PID
Supplementary Figure 1045: ZNF318 K562 ENCSR334HSW
Supplementary Figure 1046: ZNF318 K562 ENCSR352BJL
Supplementary Figure 1047: ZNF319 K562 ENCSR231PDA
Supplementary Figure 1048: ZNF319 K562 ENCSR231PDA subpatterns
Supplementary Figure 1049: ZNF320 HEK293 Hughes GR models ZNF320

Supplementary Figure 1050: ZNF320 HEK293 Hughes GR models ZNF320 subpatterns
Supplementary Figure 1051: ZNF320 HEK293 ChipExo models ZNF320
Supplementary Figure 1052: ZNF320 HEK293 ChipExo models ZNF320 subpatterns
Supplementary Figure 1053: ZNF322 HEK293 Hughes GR models ZNF322
Supplementary Figure 1054: ZNF324 HEK293 ENCSR768HOH
Supplementary Figure 1055: ZNF324 HEK293 ENCSR768HOH subpatterns
Supplementary Figure 1056: ZNF324 HEK293 ChipExo models ZNF324
Supplementary Figure 1057: ZNF324 HEK293 Hughes GR models ZNF324
Supplementary Figure 1058: ZNF324 K562 ENCSR712KVZ
Supplementary Figure 1059: ZNF324 K562 ENCSR712KVZ subpatterns
Supplementary Figure 1060: ZNF329 HEK293 Hughes GR models ZNF329
Supplementary Figure 1061: ZNF329 HEK293 Hughes GR models ZNF329 subpatterns
Supplementary Figure 1062: ZNF329 HepG2 ENCSR681KXT
Supplementary Figure 1063: ZNF329 HepG2 ENCSR681KXT subpatterns
Supplementary Figure 1064: ZNF331 GM23338 ENCSR918LRB
Supplementary Figure 1065: ZNF331 GM23338 ENCSR918LRB subpatterns
Supplementary Figure 1066: ZNF331 HEK293 Hughes GR models ZNF331
Supplementary Figure 1067: ZNF331 HEK293 Hughes GR models ZNF331 subpatterns
Supplementary Figure 1068: ZNF331 HEK293 ChipExo models ZNF331
Supplementary Figure 1069: ZNF331 HEK293 ChipExo models ZNF331 subpatterns
Supplementary Figure 1070: ZNF331 HepG2 ENCSR369TCR
Supplementary Figure 1071: ZNF331 HepG2 ENCSR369TCR subpatterns
Supplementary Figure 1072: ZNF331 MCF-7 ENCSR860XVO
Supplementary Figure 1073: ZNF331 MCF-7 ENCSR860XVO subpatterns
Supplementary Figure 1074: ZNF333 HEK293 ChipExo models ZNF333
Supplementary Figure 1075: ZNF333 HEK293 ChipExo models ZNF333 subpatterns
Supplementary Figure 1076: ZNF333 HepG2 ENCSR505UNL
Supplementary Figure 1077: ZNF334 HEK293 ChipExo models ZNF334
Supplementary Figure 1078: ZNF337 HEK293 ChipExo models ZNF337
Supplementary Figure 1079: ZNF337 HEK293 ChipExo models ZNF337 subpatterns
Supplementary Figure 1080: ZNF337 HepG2 ENCSR759KXQ
Supplementary Figure 1081: ZNF337 HepG2 ENCSR759KXQ subpatterns
Supplementary Figure 1082: ZNF33A HEK293 ChipExo models ZNF33A
Supplementary Figure 1083: ZNF33A HEK293 ChipExo models ZNF33A subpatterns
Supplementary Figure 1084: ZNF33A HepG2 ENCSR110BYN
Supplementary Figure 1085: ZNF33A HepG2 ENCSR110BYN subpatterns
Supplementary Figure 1086: ZNF33B HEK293 ChipExo models ZNF33B
Supplementary Figure 1087: ZNF33B HepG2 ENCSR052FXA
Supplementary Figure 1088: ZNF33B HepG2 ENCSR052FXA subpatterns
Supplementary Figure 1089: ZNF341 HEK293 ENCSR185FOY
Supplementary Figure 1090: ZNF341 HEK293 ENCSR185FOY subpatterns
Supplementary Figure 1091: ZNF341 HEK293 Hughes GR models ZNF341
Supplementary Figure 1092: ZNF341 HEK293 Hughes GR models ZNF341 subpatterns
Supplementary Figure 1093: ZNF343 HEK293 ChipExo models ZNF343
Supplementary Figure 1094: ZNF343 HEK293 ChipExo models ZNF343 subpatterns
Supplementary Figure 1095: ZNF343 HepG2 ENCSR938VRO
Supplementary Figure 1096: ZNF347 K562 ENCSR590FLL
Supplementary Figure 1097: ZNF347 K562 ENCSR590FLL subpatterns
Supplementary Figure 1098: ZNF34 HEK293 ENCSR727PIC
Supplementary Figure 1099: ZNF34 HEK293 ENCSR727PIC subpatterns
Supplementary Figure 1100: ZNF34 HEK293 Hughes GR models ZNF34
Supplementary Figure 1101: ZNF34 HepG2 ENCSR904JEY
Supplementary Figure 1102: ZNF350 HEK293 ENCSR854ORP
Supplementary Figure 1103: ZNF350 HEK293 ENCSR854ORP subpatterns
Supplementary Figure 1104: ZNF350 HEK293 Hughes GR models ZNF350
Supplementary Figure 1105: ZNF350 HEK293 Hughes GR models ZNF350 subpatterns

Supplementary Figure 1106: ZNF350 HepG2 ENCSR842SRB
Supplementary Figure 1107: ZNF354A HEK293 Hughes GR models ZNF354A
Supplementary Figure 1108: ZNF354A HEK293 ChipExo models ZNF354A
Supplementary Figure 1109: ZNF354A HEK293 ChipExo models ZNF354A subpatterns
Supplementary Figure 1110: ZNF354B HEK293 ChipExo models ZNF354B
Supplementary Figure 1111: ZNF354B HepG2 ENCSR124QQJ
Supplementary Figure 1112: ZNF354B K562 ENCSR044IXA
Supplementary Figure 1113: ZNF354B K562 ENCSR044IXA subpatterns
Supplementary Figure 1114: ZNF354B K562 ENCSR674SCQ
Supplementary Figure 1115: ZNF354B K562 ENCSR674SCQ subpatterns
Supplementary Figure 1116: ZNF354C HEK293 ENCSR289NSN
Supplementary Figure 1117: ZNF354C K562 ENCSR506SSQ
Supplementary Figure 1118: ZNF35 HEK293 Hughes NB models ZNF35
Supplementary Figure 1119: ZNF35 HEK293 Hughes NB models ZNF35 subpatterns
Supplementary Figure 1120: ZNF35 HEK293 Hughes GR models ZNF35
Supplementary Figure 1121: ZNF35 HEK293 Hughes GR models ZNF35 subpatterns
Supplementary Figure 1122: ZNF367 HepG2 ENCSR048WVW
Supplementary Figure 1123: ZNF367 HepG2 ENCSR048WVW subpatterns
Supplementary Figure 1124: ZNF37A HEK293 ENCSR371LLY
Supplementary Figure 1125: ZNF37A HEK293 ENCSR371LLY subpatterns
Supplementary Figure 1126: ZNF37A HEK293 Hughes GR models ZNF37A
Supplementary Figure 1127: ZNF37A HEK293 Hughes GR models ZNF37A subpatterns
Supplementary Figure 1128: ZNF382 HEK293 Hughes NB models ZNF382
Supplementary Figure 1129: ZNF382 HEK293 Hughes NB models ZNF382 subpatterns
Supplementary Figure 1130: ZNF382 HepG2 ENCSR014HQD
Supplementary Figure 1131: ZNF383 HEK293 ChipExo models ZNF383
Supplementary Figure 1132: ZNF383 HEK293 ChipExo models ZNF383 subpatterns
Supplementary Figure 1133: ZNF383 HepG2 ENCSR264LQX
Supplementary Figure 1134: ZNF384 HEK293 Hughes GR models ZNF384
Supplementary Figure 1135: ZNF384 HepG2 ENCSR101FJU
Supplementary Figure 1136: ZNF384 HepG2 ENCSR101FJU subpatterns
Supplementary Figure 1137: ZNF391 HEK293 ENCSR210MET
Supplementary Figure 1138: ZNF394 HEK293 ENCSR125DNC
Supplementary Figure 1139: ZNF394 HEK293 ENCSR125DNC subpatterns
Supplementary Figure 1140: ZNF395 K562 ENCSR462QZZ
Supplementary Figure 1141: ZNF395 K562 ENCSR462QZZ subpatterns
Supplementary Figure 1142: ZNF396 WTC11 ENCSR422ODX
Supplementary Figure 1143: ZNF397 K562 ENCSR508EEX
Supplementary Figure 1144: ZNF397 K562 ENCSR508EEX subpatterns
Supplementary Figure 1145: ZNF398 HEK293 ENCSR676ZEF
Supplementary Figure 1146: ZNF398 HEK293 ENCSR676ZEF subpatterns
Supplementary Figure 1147: ZNF398 HEK293 ChipExo models ZNF398
Supplementary Figure 1148: ZNF398 K562 ENCSR948JND
Supplementary Figure 1149: ZNF398 K562 ENCSR948JND subpatterns
Supplementary Figure 1150: ZNF3 HEK293 ChipExo models ZNF3
Supplementary Figure 1151: ZNF3 HepG2 ENCSR182QWU
Supplementary Figure 1152: ZNF3 HepG2 ENCSR182QWU subpatterns
Supplementary Figure 1153: ZNF3 K562 ENCSR195QFV
Supplementary Figure 1154: ZNF3 K562 ENCSR934RJP
Supplementary Figure 1155: ZNF3 K562 ENCSR934RJP subpatterns
Supplementary Figure 1156: ZNF404 HEK293 ENCSR669GUM
Supplementary Figure 1157: ZNF407 HepG2 ENCSR005WGY
Supplementary Figure 1158: ZNF407 K562 ENCSR011NOZ
Supplementary Figure 1159: ZNF407 K562 ENCSR011NOZ subpatterns
Supplementary Figure 1160: ZNF407 K562 ENCSR439OCL
Supplementary Figure 1161: ZNF407 K562 ENCSR439OCL subpatterns

Supplementary Figure 1162: ZNF408 K562 ENCSR758PLU
Supplementary Figure 1163: ZNF414 HepG2 ENCSR224NQI
Supplementary Figure 1164: ZNF414 HepG2 ENCSR224NQI subpatterns
Supplementary Figure 1165: ZNF415 HEK293 Hughes NB models ZNF415
Supplementary Figure 1166: ZNF416 HEK293 ENCSR604CNJ
Supplementary Figure 1167: ZNF416 HEK293 ENCSR604CNJ subpatterns
Supplementary Figure 1168: ZNF416 WTC11 ENCSR288NNJ
Supplementary Figure 1169: ZNF417 HEK293 ChipExo models ZNF417
Supplementary Figure 1170: ZNF418 HEK293 Hughes GR models ZNF418
Supplementary Figure 1171: ZNF418 HEK293 Hughes GR models ZNF418 subpatterns
Supplementary Figure 1172: ZNF418 HEK293 ChipExo models ZNF418
Supplementary Figure 1173: ZNF418 HEK293 ChipExo models ZNF418 subpatterns
Supplementary Figure 1174: ZNF419 HEK293 ChipExo models ZNF419
Supplementary Figure 1175: ZNF41 HEK293 Hughes NB models ZNF41
Supplementary Figure 1176: ZNF41 HEK293 Hughes GR models ZNF41
Supplementary Figure 1177: ZNF41 HEK293 Hughes GR models ZNF41 subpatterns
Supplementary Figure 1178: ZNF41 K562 ENCSR235PYI
Supplementary Figure 1179: ZNF41 K562 ENCSR235PYI subpatterns
Supplementary Figure 1180: ZNF423 HEK293 ENCSR477OJI
Supplementary Figure 1181: ZNF423 HEK293 ENCSR477OJI subpatterns
Supplementary Figure 1182: ZNF423 WTC11 ENCSR413CVQ
Supplementary Figure 1183: ZNF423 WTC11 ENCSR413CVQ subpatterns
Supplementary Figure 1184: ZNF425 HEK293 ChipExo models ZNF425
Supplementary Figure 1185: ZNF425 HEK293 ChipExo models ZNF425 subpatterns
Supplementary Figure 1186: ZNF425 WTC11 ENCSR717QWW
Supplementary Figure 1187: ZNF426 HEK293 ENCSR224NFP
Supplementary Figure 1188: ZNF426 HEK293 ENCSR224NFP subpatterns
Supplementary Figure 1189: ZNF429 HEK293 ChipExo models ZNF429
Supplementary Figure 1190: ZNF429 HEK293 ChipExo models ZNF429 subpatterns
Supplementary Figure 1191: ZNF430 HEK293 ChipExo models ZNF430
Supplementary Figure 1192: ZNF430 HEK293 ChipExo models ZNF430 subpatterns
Supplementary Figure 1193: ZNF430 HepG2 ENCSR618END
Supplementary Figure 1194: ZNF430 HepG2 ENCSR618END subpatterns
Supplementary Figure 1195: ZNF431 HEK293 ChipExo models ZNF431
Supplementary Figure 1196: ZNF431 HepG2 ENCSR204ALX
Supplementary Figure 1197: ZNF431 HepG2 ENCSR204ALX subpatterns
Supplementary Figure 1198: ZNF431 K562 ENCSR609ZLF
Supplementary Figure 1199: ZNF431 K562 ENCSR609ZLF subpatterns
Supplementary Figure 1200: ZNF432 HEK293 ChipExo models ZNF432
Supplementary Figure 1201: ZNF432 HEK293 ChipExo models ZNF432 subpatterns
Supplementary Figure 1202: ZNF432 HepG2 ENCSR043VRG
Supplementary Figure 1203: ZNF433 HEK293 ENCSR586BRJ
Supplementary Figure 1204: ZNF433 HEK293 ENCSR586BRJ subpatterns
Supplementary Figure 1205: ZNF433 HEK293 ChipExo models ZNF433
Supplementary Figure 1206: ZNF433 HEK293 ChipExo models ZNF433 subpatterns
Supplementary Figure 1207: ZNF436 HEK293 Hughes GR models ZNF436
Supplementary Figure 1208: ZNF436 HEK293 Hughes GR models ZNF436 subpatterns
Supplementary Figure 1209: ZNF436 K562 ENCSR335SUD
Supplementary Figure 1210: ZNF436 K562 ENCSR335SUD subpatterns
Supplementary Figure 1211: ZNF439 HEK293 ChipExo models ZNF439
Supplementary Figure 1212: ZNF440 HEK293 ChipExo models ZNF440
Supplementary Figure 1213: ZNF440 HEK293 ChipExo models ZNF440 subpatterns
Supplementary Figure 1214: ZNF441 HEK293 ChipExo models ZNF441
Supplementary Figure 1215: ZNF441 HEK293 ChipExo models ZNF441 subpatterns
Supplementary Figure 1216: ZNF441 HepG2 ENCSR673GDQ
Supplementary Figure 1217: ZNF441 HepG2 ENCSR673GDQ subpatterns

Supplementary Figure 1218: ZNF442 HEK293 ChipExo models ZNF442
Supplementary Figure 1219: ZNF443 HEK293 ChipExo models ZNF443
Supplementary Figure 1220: ZNF444 K562 ENCSR164RIC
Supplementary Figure 1221: ZNF444 K562 ENCSR164RIC subpatterns
Supplementary Figure 1222: ZNF444 MCF-7 ENCSR038XIA
Supplementary Figure 1223: ZNF444 MCF-7 ENCSR038XIA subpatterns
Supplementary Figure 1224: ZNF445 HEK293 ChipExo models ZNF445
Supplementary Figure 1225: ZNF445 K562 ENCSR883UGG
Supplementary Figure 1226: ZNF445 K562 ENCSR883UGG subpatterns
Supplementary Figure 1227: ZNF446 HepG2 ENCSR839AJZ
Supplementary Figure 1228: ZNF449 HEK293 ENCSR738SLS
Supplementary Figure 1229: ZNF449 HEK293 ENCSR738SLS subpatterns
Supplementary Figure 1230: ZNF449 HEK293 Hughes GR models ZNF449
Supplementary Figure 1231: ZNF449 HEK293 Hughes GR models ZNF449 subpatterns
Supplementary Figure 1232: ZNF449 K562 ENCSR659YWQ
Supplementary Figure 1233: ZNF449 K562 ENCSR659YWQ subpatterns
Supplementary Figure 1234: ZNF44 HEK293 ChipExo models ZNF44
Supplementary Figure 1235: ZNF44 HepG2 ENCSR914HPP
Supplementary Figure 1236: ZNF454 HEK293 Hughes NB models ZNF454
Supplementary Figure 1237: ZNF454 HEK293 ChipExo models ZNF454
Supplementary Figure 1238: ZNF454 HEK293 ChipExo models ZNF454 subpatterns
Supplementary Figure 1239: ZNF45 HEK293 Hughes NB models ZNF45
Supplementary Figure 1240: ZNF45 HEK293 Hughes NB models ZNF45 subpatterns
Supplementary Figure 1241: ZNF45 HEK293 ChipExo models ZNF45
Supplementary Figure 1242: ZNF460 HEK293 ChipExo models ZNF460
Supplementary Figure 1243: ZNF460 HEK293 ChipExo models ZNF460 subpatterns
Supplementary Figure 1244: ZNF460 HepG2 ENCSR261UIH
Supplementary Figure 1245: ZNF460 HepG2 ENCSR261UIH subpatterns
Supplementary Figure 1246: ZNF462 GM23338 ENCSR334UWP
Supplementary Figure 1247: ZNF462 GM23338 ENCSR334UWP subpatterns
Supplementary Figure 1248: ZNF468 HEK293 ChipExo models ZNF468
Supplementary Figure 1249: ZNF468 HEK293 ChipExo models ZNF468 subpatterns
Supplementary Figure 1250: ZNF468 HepG2 ENCSR613YQN
Supplementary Figure 1251: ZNF473 HEK293 ENCSR567XAM
Supplementary Figure 1252: ZNF480 HEK293 ChipExo models ZNF480
Supplementary Figure 1253: ZNF480 HEK293 ChipExo models ZNF480 subpatterns
Supplementary Figure 1254: ZNF483 HEK293 ChipExo models ZNF483
Supplementary Figure 1255: ZNF483 HEK293 ChipExo models ZNF483 subpatterns
Supplementary Figure 1256: ZNF483 HepG2 ENCSR436PIH
Supplementary Figure 1257: ZNF484 HEK293 ChipExo models ZNF484
Supplementary Figure 1258: ZNF484 HEK293 ChipExo models ZNF484 subpatterns
Supplementary Figure 1259: ZNF484 HepG2 ENCSR471VAY
Supplementary Figure 1260: ZNF484 HepG2 ENCSR471VAY subpatterns
Supplementary Figure 1261: ZNF485 HEK293 ChipExo models ZNF485
Supplementary Figure 1262: ZNF485 HEK293 ChipExo models ZNF485 subpatterns
Supplementary Figure 1263: ZNF485 HepG2 ENCSR574UJE
Supplementary Figure 1264: ZNF486 HEK293 ChipExo models ZNF486
Supplementary Figure 1265: ZNF487 HEK293 ChipExo models ZNF487
Supplementary Figure 1266: ZNF488 HEK293 ENCSR363XBR
Supplementary Figure 1267: ZNF48 HEK293 ENCSR517DDU
Supplementary Figure 1268: ZNF48 HepG2 ENCSR415AEB
Supplementary Figure 1269: ZNF48 HepG2 ENCSR415AEB subpatterns
Supplementary Figure 1270: ZNF490 HepG2 ENCSR542PZA
Supplementary Figure 1271: ZNF490 HepG2 ENCSR542PZA subpatterns
Supplementary Figure 1272: ZNF492 HEK293 ChipExo models ZNF492
Supplementary Figure 1273: ZNF496 HEK293 ChipExo models ZNF496

Supplementary Figure 1274: ZNF496 HepG2 ENCSR828TVO
Supplementary Figure 1275: ZNF501 HEK293 ENCSR461ZJT
Supplementary Figure 1276: ZNF501 HepG2 ENCSR227PHM
Supplementary Figure 1277: ZNF502 HEK293 Hughes GR models ZNF502
Supplementary Figure 1278: ZNF502 HEK293 Hughes GR models ZNF502 subpatterns
Supplementary Figure 1279: ZNF503 HepG2 ENCSR998YJI
Supplementary Figure 1280: ZNF506 HEK293 ChipExo models ZNF506
Supplementary Figure 1281: ZNF506 HEK293 ChipExo models ZNF506 subpatterns
Supplementary Figure 1282: ZNF507 K562 ENCSR577KQD
Supplementary Figure 1283: ZNF507 K562 ENCSR577KQD subpatterns
Supplementary Figure 1284: ZNF507 K562 ENCSR598TIR
Supplementary Figure 1285: ZNF507 K562 ENCSR598TIR subpatterns
Supplementary Figure 1286: ZNF507 MCF-7 ENCSR419ODQ
Supplementary Figure 1287: ZNF510 HEK293 ENCSR595FAO
Supplementary Figure 1288: ZNF510 HEK293 ENCSR595FAO subpatterns
Supplementary Figure 1289: ZNF510 HepG2 ENCSR695SLS
Supplementary Figure 1290: ZNF511 HepG2 ENCSR372JXR
Supplementary Figure 1291: ZNF511 K562 ENCSR652OGX
Supplementary Figure 1292: ZNF512B HepG2 ENCSR801SNX
Supplementary Figure 1293: ZNF512B MCF-7 ENCSR555DCF
Supplementary Figure 1294: ZNF512B MCF-7 ENCSR761LRR
Supplementary Figure 1295: ZNF512 HepG2 ENCSR264SRY
Supplementary Figure 1296: ZNF512 K562 ENCSR591CCL
Supplementary Figure 1297: ZNF512 K562 ENCSR591CCL subpatterns
Supplementary Figure 1298: ZNF512 K562 ENCSR696URR
Supplementary Figure 1299: ZNF512 K562 ENCSR696URR subpatterns
Supplementary Figure 1300: ZNF512 WTC11 ENCSR634WRC
Supplementary Figure 1301: ZNF512 WTC11 ENCSR634WRC subpatterns
Supplementary Figure 1302: ZNF513 HEK293 ENCSR503DPC
Supplementary Figure 1303: ZNF513 HEK293 ENCSR503DPC subpatterns
Supplementary Figure 1304: ZNF513 HepG2 ENCSR171KUL
Supplementary Figure 1305: ZNF514 HEK293 ENCSR897RVP
Supplementary Figure 1306: ZNF518A HEK293 ENCSR159GFL
Supplementary Figure 1307: ZNF518B K562 ENCSR597CHL
Supplementary Figure 1308: ZNF519 HEK293 Hughes NB models ZNF519
Supplementary Figure 1309: ZNF519 HEK293 Hughes NB models ZNF519 subpatterns
Supplementary Figure 1310: ZNF521 HEK293 ENCSR665KYH
Supplementary Figure 1311: ZNF524 HEK293 Hughes GR models ZNF524
Supplementary Figure 1312: ZNF524 HEK293 Hughes GR models ZNF524 subpatterns
Supplementary Figure 1313: ZNF525 HEK293 ChipExo models ZNF525
Supplementary Figure 1314: ZNF526 HepG2 ENCSR608XRC
Supplementary Figure 1315: ZNF527 HEK293 ChipExo models ZNF527
Supplementary Figure 1316: ZNF527 HepG2 ENCSR656RTA
Supplementary Figure 1317: ZNF528 HEK293 Hughes GR models ZNF528
Supplementary Figure 1318: ZNF528 HEK293 Hughes NB models ZNF528
Supplementary Figure 1319: ZNF528 HEK293 Hughes NB models ZNF528 subpatterns
Supplementary Figure 1320: ZNF528 HEK293 ChipExo models ZNF528
Supplementary Figure 1321: ZNF528 HEK293 ChipExo models ZNF528 subpatterns
Supplementary Figure 1322: ZNF529 HEK293 ENCSR754SOI
Supplementary Figure 1323: ZNF529 HEK293 ENCSR754SOI subpatterns
Supplementary Figure 1324: ZNF529 HEK293 ChipExo models ZNF529
Supplementary Figure 1325: ZNF530 HEK293 ENCSR701RXW
Supplementary Figure 1326: ZNF530 HEK293 ENCSR701RXW subpatterns
Supplementary Figure 1327: ZNF530 HEK293 ChipExo models ZNF530
Supplementary Figure 1328: ZNF530 HEK293 ChipExo models ZNF530 subpatterns
Supplementary Figure 1329: ZNF530 HepG2 ENCSR013DKM

Supplementary Figure 1330: ZNF530 HepG2 ENCSR013DKM subpatterns
Supplementary Figure 1331: ZNF532 WTC11 ENCSR444BFV
Supplementary Figure 1332: ZNF532 WTC11 ENCSR444BFV subpatterns
Supplementary Figure 1333: ZNF540 HEK293 ChipExo models ZNF540
Supplementary Figure 1334: ZNF543 HEK293 ChipExo models ZNF543
Supplementary Figure 1335: ZNF543 HEK293 ChipExo models ZNF543 subpatterns
Supplementary Figure 1336: ZNF543 HepG2 ENCSR584DEL
Supplementary Figure 1337: ZNF543 HepG2 ENCSR584DEL subpatterns
Supplementary Figure 1338: ZNF544 HEK293 ENCSR167XFW
Supplementary Figure 1339: ZNF546 HepG2 ENCSR782WWY
Supplementary Figure 1340: ZNF546 HepG2 ENCSR782WWY subpatterns
Supplementary Figure 1341: ZNF547 HEK293 ENCSR909TSW
Supplementary Figure 1342: ZNF547 HEK293 ENCSR909TSW subpatterns
Supplementary Figure 1343: ZNF547 HEK293 Hughes GR models ZNF547
Supplementary Figure 1344: ZNF547 HEK293 Hughes GR models ZNF547 subpatterns
Supplementary Figure 1345: ZNF547 HEK293 ChipExo models ZNF547
Supplementary Figure 1346: ZNF547 HepG2 ENCSR964ZJC
Supplementary Figure 1347: ZNF548 HEK293 ENCSR892ZTO
Supplementary Figure 1348: ZNF548 HEK293 ENCSR892ZTO subpatterns
Supplementary Figure 1349: ZNF548 HEK293 ChipExo models ZNF548
Supplementary Figure 1350: ZNF548 HepG2 ENCSR756UNW
Supplementary Figure 1351: ZNF549 HEK293 ENCSR185QFX
Supplementary Figure 1352: ZNF549 HEK293 ENCSR185QFX subpatterns
Supplementary Figure 1353: ZNF549 HEK293 Hughes GR models ZNF549
Supplementary Figure 1354: ZNF549 HEK293 Hughes GR models ZNF549 subpatterns
Supplementary Figure 1355: ZNF549 HEK293 ChipExo models ZNF549
Supplementary Figure 1356: ZNF549 HEK293 ChipExo models ZNF549 subpatterns
Supplementary Figure 1357: ZNF549 HepG2 ENCSR545ACM
Supplementary Figure 1358: ZNF549 HepG2 ENCSR545ACM subpatterns
Supplementary Figure 1359: ZNF550 HEK293 ChipExo models ZNF550
Supplementary Figure 1360: ZNF550 HepG2 ENCSR198BHH
Supplementary Figure 1361: ZNF551 K562 ENCSR451UQX
Supplementary Figure 1362: ZNF552 HEK293 ChipExo models ZNF552
Supplementary Figure 1363: ZNF552 HepG2 ENCSR448RAP
Supplementary Figure 1364: ZNF552 HepG2 ENCSR448RAP subpatterns
Supplementary Figure 1365: ZNF554 HEK293 Hughes GR models ZNF554
Supplementary Figure 1366: ZNF554 HEK293 Hughes GR models ZNF554 subpatterns
Supplementary Figure 1367: ZNF555 HEK293 ENCSR767XSF
Supplementary Figure 1368: ZNF555 HEK293 ChipExo models ZNF555
Supplementary Figure 1369: ZNF555 HEK293 ChipExo models ZNF555 subpatterns
Supplementary Figure 1370: ZNF556 HepG2 ENCSR644WQN
Supplementary Figure 1371: ZNF557 HEK293 ChipExo models ZNF557
Supplementary Figure 1372: ZNF557 HepG2 ENCSR325VYA
Supplementary Figure 1373: ZNF557 HepG2 ENCSR325VYA subpatterns
Supplementary Figure 1374: ZNF558 HEK293 ENCSR447ZTA
Supplementary Figure 1375: ZNF558 HEK293 ENCSR447ZTA subpatterns
Supplementary Figure 1376: ZNF558 HEK293 ChipExo models ZNF558
Supplementary Figure 1377: ZNF558 HEK293 ChipExo models ZNF558 subpatterns
Supplementary Figure 1378: ZNF558 HepG2 ENCSR154YWK
Supplementary Figure 1379: ZNF558 HepG2 ENCSR154YWK subpatterns
Supplementary Figure 1380: ZNF560 HEK293 ENCSR538RDA
Supplementary Figure 1381: ZNF561 HEK293 ENCSR125ULS
Supplementary Figure 1382: ZNF561 HEK293 ChipExo models ZNF561
Supplementary Figure 1383: ZNF561 HEK293 ChipExo models ZNF561 subpatterns
Supplementary Figure 1384: ZNF561 K562 ENCSR350GZC
Supplementary Figure 1385: ZNF561 K562 ENCSR350GZC subpatterns

Supplementary Figure 1386: ZNF562 HEK293 ChipExo models ZNF562
Supplementary Figure 1387: ZNF562 HEK293 ChipExo models ZNF562 subpatterns
Supplementary Figure 1388: ZNF562 HepG2 ENCSR727IJD
Supplementary Figure 1389: ZNF562 HepG2 ENCSR727IJD subpatterns
Supplementary Figure 1390: ZNF563 HEK293 Hughes GR models ZNF563
Supplementary Figure 1391: ZNF563 HEK293 Hughes GR models ZNF563 subpatterns
Supplementary Figure 1392: ZNF563 HepG2 ENCSR977FRK
Supplementary Figure 1393: ZNF564 HEK293 ChipExo models ZNF564
Supplementary Figure 1394: ZNF564 HEK293 ChipExo models ZNF564 subpatterns
Supplementary Figure 1395: ZNF564 HepG2 ENCSR397EOT
Supplementary Figure 1396: ZNF564 HepG2 ENCSR397EOT subpatterns
Supplementary Figure 1397: ZNF565 HEK293 ChipExo models ZNF565
Supplementary Figure 1398: ZNF565 HEK293 ChipExo models ZNF565 subpatterns
Supplementary Figure 1399: ZNF565 SK-N-SH ENCSR754ALX
Supplementary Figure 1400: ZNF565 SK-N-SH ENCSR754ALX subpatterns
Supplementary Figure 1401: ZNF566 HEK293 ChipExo models ZNF566
Supplementary Figure 1402: ZNF566 HEK293 ChipExo models ZNF566 subpatterns
Supplementary Figure 1403: ZNF567 HEK293 ChipExo models ZNF567
Supplementary Figure 1404: ZNF567 HEK293 ChipExo models ZNF567 subpatterns
Supplementary Figure 1405: ZNF567 HepG2 ENCSR231NMZ
Supplementary Figure 1406: ZNF569 HepG2 ENCSR225SLE
Supplementary Figure 1407: ZNF570 HEK293 ChipExo models ZNF570
Supplementary Figure 1408: ZNF570 HepG2 ENCSR055ZIA
Supplementary Figure 1409: ZNF571 HEK293 ENCSR421QXA
Supplementary Figure 1410: ZNF571 HEK293 ChipExo models ZNF571
Supplementary Figure 1411: ZNF571 HepG2 ENCSR697CNF
Supplementary Figure 1412: ZNF572 HepG2 ENCSR663CTC
Supplementary Figure 1413: ZNF573 HEK293 ChipExo models ZNF573
Supplementary Figure 1414: ZNF573 HEK293 ChipExo models ZNF573 subpatterns
Supplementary Figure 1415: ZNF574 HEK293 Hughes NB models ZNF574
Supplementary Figure 1416: ZNF574 HEK293 Hughes NB models ZNF574 subpatterns
Supplementary Figure 1417: ZNF574 HEK293 Hughes GR models ZNF574
Supplementary Figure 1418: ZNF574 HEK293 Hughes GR models ZNF574 subpatterns
Supplementary Figure 1419: ZNF574 HepG2 ENCSR886YJI
Supplementary Figure 1420: ZNF574 HepG2 ENCSR886YJI subpatterns
Supplementary Figure 1421: ZNF574 MCF-7 ENCSR402JAC
Supplementary Figure 1422: ZNF574 MCF-7 ENCSR402JAC subpatterns
Supplementary Figure 1423: ZNF576 HepG2 ENCSR253HUM
Supplementary Figure 1424: ZNF576 HepG2 ENCSR253HUM subpatterns
Supplementary Figure 1425: ZNF577 HepG2 ENCSR436RQS
Supplementary Figure 1426: ZNF57 K562 ENCSR918EFA
Supplementary Figure 1427: ZNF57 K562 ENCSR918EFA subpatterns
Supplementary Figure 1428: ZNF580 HEK293 ENCSR668HOP
Supplementary Figure 1429: ZNF580 HEK293 ENCSR668HOP subpatterns
Supplementary Figure 1430: ZNF580 HepG2 ENCSR173CTF
Supplementary Figure 1431: ZNF580 HepG2 ENCSR173CTF subpatterns
Supplementary Figure 1432: ZNF582 HEK293 ChipExo models ZNF582
Supplementary Figure 1433: ZNF582 HEK293 Hughes GR models ZNF582
Supplementary Figure 1434: ZNF582 HEK293 Hughes GR models ZNF582 subpatterns
Supplementary Figure 1435: ZNF583 K562 ENCSR775EQV
Supplementary Figure 1436: ZNF583 K562 ENCSR775EQV subpatterns
Supplementary Figure 1437: ZNF584 HEK293 ChipExo models ZNF584
Supplementary Figure 1438: ZNF584 HEK293 ChipExo models ZNF584 subpatterns
Supplementary Figure 1439: ZNF584 K562 ENCSR149ZBI
Supplementary Figure 1440: ZNF584 K562 ENCSR149ZBI subpatterns
Supplementary Figure 1441: ZNF585A HEK293 ChipExo models ZNF585A

Supplementary Figure 1442: ZNF585B HEK293 ENCSR011XCI
Supplementary Figure 1443: ZNF585B HEK293 ENCSR011XCI subpatterns
Supplementary Figure 1444: ZNF586 HEK293 Hughes GR models ZNF586
Supplementary Figure 1445: ZNF586 HEK293 Hughes GR models ZNF586 subpatterns
Supplementary Figure 1446: ZNF586 K562 ENCSR236JZN
Supplementary Figure 1447: ZNF586 K562 ENCSR236JZN subpatterns
Supplementary Figure 1448: ZNF587 HEK293 ChipExo models ZNF587
Supplementary Figure 1449: ZNF587 HEK293 ChipExo models ZNF587 subpatterns
Supplementary Figure 1450: ZNF589 HepG2 ENCSR827ZGB
Supplementary Figure 1451: ZNF589 HepG2 ENCSR827ZGB subpatterns
Supplementary Figure 1452: ZNF589 K562 ENCSR603XLW
Supplementary Figure 1453: ZNF589 K562 ENCSR603XLW subpatterns
Supplementary Figure 1454: ZNF592 GM12878 ENCSR173ZVL
Supplementary Figure 1455: ZNF592 K562 ENCSR249BHQ
Supplementary Figure 1456: ZNF592 MCF-7 ENCSR028NUR
Supplementary Figure 1457: ZNF592 MCF-7 ENCSR701AQS
Supplementary Figure 1458: ZNF594 HEK293 Hughes GR models ZNF594
Supplementary Figure 1459: ZNF596 HEK293 ENCSR344SBD
Supplementary Figure 1460: ZNF596 HEK293 ENCSR344SBD subpatterns
Supplementary Figure 1461: ZNF596 HEK293 Hughes GR models ZNF596
Supplementary Figure 1462: ZNF597 HepG2 ENCSR669PVF
Supplementary Figure 1463: ZNF597 HepG2 ENCSR669PVF subpatterns
Supplementary Figure 1464: ZNF600 HEK293 ENCSR017QBI
Supplementary Figure 1465: ZNF600 HEK293 ENCSR017QBI subpatterns
Supplementary Figure 1466: ZNF605 HEK293 ChipExo models ZNF605
Supplementary Figure 1467: ZNF605 HEK293 ChipExo models ZNF605 subpatterns
Supplementary Figure 1468: ZNF605 HepG2 ENCSR903JFF
Supplementary Figure 1469: ZNF605 HepG2 ENCSR903JFF subpatterns
Supplementary Figure 1470: ZNF607 HepG2 ENCSR788SXN
Supplementary Figure 1471: ZNF607 HepG2 ENCSR788SXN subpatterns
Supplementary Figure 1472: ZNF608 HepG2 ENCSR277VXX
Supplementary Figure 1473: ZNF608 SK-N-SH ENCSR837YGS
Supplementary Figure 1474: ZNF609 HepG2 ENCSR407BPU
Supplementary Figure 1475: ZNF609 K562 ENCSR940PYZ
Supplementary Figure 1476: ZNF610 HEK293 ENCSR691TXI
Supplementary Figure 1477: ZNF610 HEK293 ENCSR691TXI subpatterns
Supplementary Figure 1478: ZNF610 HEK293 Hughes GR models ZNF610
Supplementary Figure 1479: ZNF610 HEK293 Hughes GR models ZNF610 subpatterns
Supplementary Figure 1480: ZNF610 HEK293 ChipExo models ZNF610
Supplementary Figure 1481: ZNF610 HEK293 ChipExo models ZNF610 subpatterns
Supplementary Figure 1482: ZNF611 HEK293 ChipExo models ZNF611
Supplementary Figure 1483: ZNF611 HEK293 ChipExo models ZNF611 subpatterns
Supplementary Figure 1484: ZNF613 HEK293 ChipExo models ZNF613
Supplementary Figure 1485: ZNF613 HEK293 ChipExo models ZNF613 subpatterns
Supplementary Figure 1486: ZNF614 HEK293 ChipExo models ZNF614
Supplementary Figure 1487: ZNF614 HepG2 ENCSR011CIR
Supplementary Figure 1488: ZNF614 HepG2 ENCSR011CIR subpatterns
Supplementary Figure 1489: ZNF615 HEK293 ChipExo models ZNF615
Supplementary Figure 1490: ZNF615 HepG2 ENCSR286LPH
Supplementary Figure 1491: ZNF616 HEK293 ChipExo models ZNF616
Supplementary Figure 1492: ZNF616 HEK293 ChipExo models ZNF616 subpatterns
Supplementary Figure 1493: ZNF616 HepG2 ENCSR654PQY
Supplementary Figure 1494: ZNF619 HEK293 ChipExo models ZNF619
Supplementary Figure 1495: ZNF619 HepG2 ENCSR613RDS
Supplementary Figure 1496: ZNF620 HEK293 ChipExo models ZNF620
Supplementary Figure 1497: ZNF621 HEK293 ENCSR858FAN

Supplementary Figure 1498: ZNF621 HEK293 ChipExo models ZNF621
Supplementary Figure 1499: ZNF621 HEK293 Hughes NB models ZNF621
Supplementary Figure 1500: ZNF621 HEK293 Hughes NB models ZNF621 subpatterns
Supplementary Figure 1501: ZNF623 HEK293 ENCSR022IZK
Supplementary Figure 1502: ZNF623 HEK293 ENCSR022IZK subpatterns
Supplementary Figure 1503: ZNF624 A549 ENCSR419VVI
Supplementary Figure 1504: ZNF624 A549 ENCSR419VVI subpatterns
Supplementary Figure 1505: ZNF624 HEK293 ENCSR878DES
Supplementary Figure 1506: ZNF626 HEK293 ENCSR588MQZ
Supplementary Figure 1507: ZNF626 HEK293 ENCSR588MQZ subpatterns
Supplementary Figure 1508: ZNF626 HEK293 ChipExo models ZNF626
Supplementary Figure 1509: ZNF627 HEK293 ChipExo models ZNF627
Supplementary Figure 1510: ZNF627 HEK293 ChipExo models ZNF627 subpatterns
Supplementary Figure 1511: ZNF629 HEK293 ENCSR351NON
Supplementary Figure 1512: ZNF629 HepG2 ENCSR363ASY
Supplementary Figure 1513: ZNF629 HepG2 ENCSR363ASY subpatterns
Supplementary Figure 1514: ZNF639 HEK293 ENCSR080CST
Supplementary Figure 1515: ZNF639 HepG2 ENCSR665UFC
Supplementary Figure 1516: ZNF639 HepG2 ENCSR665UFC subpatterns
Supplementary Figure 1517: ZNF639 K562 ENCSR258PSN
Supplementary Figure 1518: ZNF639 K562 ENCSR258PSN subpatterns
Supplementary Figure 1519: ZNF639 K562 ENCSR497VFH
Supplementary Figure 1520: ZNF639 K562 ENCSR845BCL
Supplementary Figure 1521: ZNF639 K562 ENCSR845BCL subpatterns
Supplementary Figure 1522: ZNF639 K562 ENCSR949NVY
Supplementary Figure 1523: ZNF641 HEK293 ChipExo models ZNF641
Supplementary Figure 1524: ZNF641 HEK293 ChipExo models ZNF641 subpatterns
Supplementary Figure 1525: ZNF644 HepG2 ENCSR578CXC
Supplementary Figure 1526: ZNF644 K562 ENCSR729HVR
Supplementary Figure 1527: ZNF644 K562 ENCSR729HVR subpatterns
Supplementary Figure 1528: ZNF646 HepG2 ENCSR488ZNK
Supplementary Figure 1529: ZNF646 HepG2 ENCSR488ZNK subpatterns
Supplementary Figure 1530: ZNF649 HEK293 ChipExo models ZNF649
Supplementary Figure 1531: ZNF649 HEK293 ChipExo models ZNF649 subpatterns
Supplementary Figure 1532: ZNF652 HepG2 ENCSR502GAX
Supplementary Figure 1533: ZNF652 HepG2 ENCSR502GAX subpatterns
Supplementary Figure 1534: ZNF654 HEK293 ENCSR504VDV
Supplementary Figure 1535: ZNF655 K562 ENCSR568YNC
Supplementary Figure 1536: ZNF658 HEK293 ENCSR762DQP
Supplementary Figure 1537: ZNF658 HEK293 ENCSR762DQP subpatterns
Supplementary Figure 1538: ZNF660 HEK293 ENCSR283DOU
Supplementary Figure 1539: ZNF660 HepG2 ENCSR902AMJ
Supplementary Figure 1540: ZNF662 HEK293 ChipExo models ZNF662
Supplementary Figure 1541: ZNF662 HEK293 ChipExo models ZNF662 subpatterns
Supplementary Figure 1542: ZNF664 HEK293 ENCSR714LZQ
Supplementary Figure 1543: ZNF664 HEK293 ENCSR714LZQ subpatterns
Supplementary Figure 1544: ZNF667 HEK293 ChipExo models ZNF667
Supplementary Figure 1545: ZNF668 K562 ENCSR682AAS
Supplementary Figure 1546: ZNF668 K562 ENCSR682AAS subpatterns
Supplementary Figure 1547: ZNF669 HEK293 Hughes NB models ZNF669
Supplementary Figure 1548: ZNF669 HEK293 Hughes NB models ZNF669 subpatterns
Supplementary Figure 1549: ZNF669 HEK293 ChipExo models ZNF669
Supplementary Figure 1550: ZNF669 HEK293 ChipExo models ZNF669 subpatterns
Supplementary Figure 1551: ZNF669 HEK293 Hughes GR models ZNF669
Supplementary Figure 1552: ZNF669 HEK293 Hughes GR models ZNF669 subpatterns
Supplementary Figure 1553: ZNF670 HEK293 ENCSR233MWH

Supplementary Figure 1554: ZNF670 HepG2 ENCSR699ZES
Supplementary Figure 1555: ZNF671 HEK293 ChipExo models ZNF671
Supplementary Figure 1556: ZNF671 HEK293 ChipExo models ZNF671 subpatterns
Supplementary Figure 1557: ZNF671 WTC11 ENCSR260GQA
Supplementary Figure 1558: ZNF672 HepG2 ENCSR263YXJ
Supplementary Figure 1559: ZNF674 HEK293 ChipExo models ZNF674
Supplementary Figure 1560: ZNF674 HEK293 ChipExo models ZNF674 subpatterns
Supplementary Figure 1561: ZNF674 HepG2 ENCSR171BKT
Supplementary Figure 1562: ZNF675 HEK293 Hughes NB models ZNF675
Supplementary Figure 1563: ZNF675 HEK293 Hughes NB models ZNF675 subpatterns
Supplementary Figure 1564: ZNF675 HEK293 ChipExo models ZNF675
Supplementary Figure 1565: ZNF675 HEK293 ChipExo models ZNF675 subpatterns
Supplementary Figure 1566: ZNF677 HEK293 ENCSR279KDC
Supplementary Figure 1567: ZNF677 HEK293 ENCSR279KDC subpatterns
Supplementary Figure 1568: ZNF677 HEK293 Hughes GR models ZNF677
Supplementary Figure 1569: ZNF678 HepG2 ENCSR946PKH
Supplementary Figure 1570: ZNF680 HEK293 ENCSR307CKC
Supplementary Figure 1571: ZNF680 HEK293 ENCSR307CKC subpatterns
Supplementary Figure 1572: ZNF680 HEK293 Hughes GR models ZNF680
Supplementary Figure 1573: ZNF680 HEK293 Hughes GR models ZNF680 subpatterns
Supplementary Figure 1574: ZNF681 HEK293 ChipExo models ZNF681
Supplementary Figure 1575: ZNF681 HEK293 ChipExo models ZNF681 subpatterns
Supplementary Figure 1576: ZNF682 HEK293 ChipExo models ZNF682
Supplementary Figure 1577: ZNF682 HEK293 ChipExo models ZNF682 subpatterns
Supplementary Figure 1578: ZNF684 HEK293 Hughes NB models ZNF684
Supplementary Figure 1579: ZNF684 HEK293 Hughes NB models ZNF684 subpatterns
Supplementary Figure 1580: ZNF684 HEK293 ChipExo models ZNF684
Supplementary Figure 1581: ZNF684 HEK293 ChipExo models ZNF684 subpatterns
Supplementary Figure 1582: ZNF687 GM12878 ENCSR859FDL
Supplementary Figure 1583: ZNF687 GM12878 ENCSR859FDL subpatterns
Supplementary Figure 1584: ZNF687 HepG2 ENCSR647PSR
Supplementary Figure 1585: ZNF687 MCF-7 ENCSR899BKM
Supplementary Figure 1586: ZNF691 HepG2 ENCSR130ZAR
Supplementary Figure 1587: ZNF691 HepG2 ENCSR130ZAR subpatterns
Supplementary Figure 1588: ZNF692 HEK293 ENCSR418MKG
Supplementary Figure 1589: ZNF692 HEK293 ENCSR418MKG subpatterns
Supplementary Figure 1590: ZNF692 HEK293 Hughes NB models ZNF692
Supplementary Figure 1591: ZNF692 HEK293 Hughes NB models ZNF692 subpatterns
Supplementary Figure 1592: ZNF695 HEK293 ChipExo models ZNF695
Supplementary Figure 1593: ZNF695 HEK293 ChipExo models ZNF695 subpatterns
Supplementary Figure 1594: ZNF695 K562 ENCSR187RGF
Supplementary Figure 1595: ZNF695 K562 ENCSR187RGF subpatterns
Supplementary Figure 1596: ZNF696 K562 ENCSR276RQG
Supplementary Figure 1597: ZNF697 HepG2 ENCSR734WFB
Supplementary Figure 1598: ZNF697 HepG2 ENCSR734WFB subpatterns
Supplementary Figure 1599: ZNF699 K562 ENCSR303SHG
Supplementary Figure 1600: ZNF69 HEK293 ChipExo models ZNF69
Supplementary Figure 1601: ZNF700 K562 ENCSR959BQO
Supplementary Figure 1602: ZNF700 K562 ENCSR959BQO subpatterns
Supplementary Figure 1603: ZNF701 HEK293 ENCSR547TGL
Supplementary Figure 1604: ZNF701 HEK293 ChipExo models ZNF701
Supplementary Figure 1605: ZNF701 HEK293 ChipExo models ZNF701 subpatterns
Supplementary Figure 1606: ZNF703 HepG2 ENCSR400JHG
Supplementary Figure 1607: ZNF704 HEK293 ENCSR194KWL
Supplementary Figure 1608: ZNF704 HEK293 ENCSR194KWL subpatterns
Supplementary Figure 1609: ZNF704 HepG2 ENCSR523RGJ

Supplementary Figure 1610: ZNF705G HEK293 ChipExo models ZNF705G
Supplementary Figure 1611: ZNF705G HEK293 ChipExo models ZNF705G subpatterns
Supplementary Figure 1612: ZNF707 HEK293 ENCSR854IPI
Supplementary Figure 1613: ZNF707 HEK293 ENCSR854IPI subpatterns
Supplementary Figure 1614: ZNF707 HEK293 ChipExo models ZNF707
Supplementary Figure 1615: ZNF707 HEK293 ChipExo models ZNF707 subpatterns
Supplementary Figure 1616: ZNF707 HepG2 ENCSR017XHZ
Supplementary Figure 1617: ZNF707 HepG2 ENCSR017XHZ subpatterns
Supplementary Figure 1618: ZNF707 K562 ENCSR077TKJ
Supplementary Figure 1619: ZNF707 K562 ENCSR077TKJ subpatterns
Supplementary Figure 1620: ZNF708 HEK293 Hughes GR models ZNF708
Supplementary Figure 1621: ZNF708 HEK293 Hughes GR models ZNF708 subpatterns
Supplementary Figure 1622: ZNF708 HEK293 ChipExo models ZNF708
Supplementary Figure 1623: ZNF708 HEK293 ChipExo models ZNF708 subpatterns
Supplementary Figure 1624: ZNF709 HepG2 ENCSR984IXF
Supplementary Figure 1625: ZNF709 HepG2 ENCSR984IXF subpatterns
Supplementary Figure 1626: ZNF70 SK-N-SH ENCSR207GYC
Supplementary Figure 1627: ZNF70 SK-N-SH ENCSR207GYC subpatterns
Supplementary Figure 1628: ZNF710 HepG2 ENCSR670UEX
Supplementary Figure 1629: ZNF710 HepG2 ENCSR670UEX subpatterns
Supplementary Figure 1630: ZNF713 HepG2 ENCSR513NBU
Supplementary Figure 1631: ZNF714 HEK293 ChipExo models ZNF714
Supplementary Figure 1632: ZNF716 HEK293 ChipExo models ZNF716
Supplementary Figure 1633: ZNF716 HEK293 ChipExo models ZNF716 subpatterns
Supplementary Figure 1634: ZNF717 K562 ENCSR987KYK
Supplementary Figure 1635: ZNF717 K562 ENCSR987KYK subpatterns
Supplementary Figure 1636: ZNF71 HEK293 Hughes NB models ZNF71
Supplementary Figure 1637: ZNF71 HEK293 Hughes NB models ZNF71 subpatterns
Supplementary Figure 1638: ZNF720 HepG2 ENCSR643XPG
Supplementary Figure 1639: ZNF720 HepG2 ENCSR643XPG subpatterns
Supplementary Figure 1640: ZNF730 HEK293 ChipExo models ZNF730
Supplementary Figure 1641: ZNF730 HEK293 ChipExo models ZNF730 subpatterns
Supplementary Figure 1642: ZNF736 HEK293 ChipExo models ZNF736
Supplementary Figure 1643: ZNF736 HEK293 ChipExo models ZNF736 subpatterns
Supplementary Figure 1644: ZNF737 HepG2 ENCSR127IHN
Supplementary Figure 1645: ZNF740 HepG2 ENCSR755ZAY
Supplementary Figure 1646: ZNF740 HepG2 ENCSR755ZAY subpatterns
Supplementary Figure 1647: ZNF740 K562 ENCSR427XYP
Supplementary Figure 1648: ZNF740 K562 ENCSR427XYP subpatterns
Supplementary Figure 1649: ZNF740 K562 ENCSR532EMP
Supplementary Figure 1650: ZNF740 K562 ENCSR532EMP subpatterns
Supplementary Figure 1651: ZNF740 K562 ENCSR737UST
Supplementary Figure 1652: ZNF740 K562 ENCSR737UST subpatterns
Supplementary Figure 1653: ZNF746 HepG2 ENCSR591MYB
Supplementary Figure 1654: ZNF746 HepG2 ENCSR591MYB subpatterns
Supplementary Figure 1655: ZNF747 HEK293 ENCSR497IAS
Supplementary Figure 1656: ZNF747 HepG2 ENCSR155IXY
Supplementary Figure 1657: ZNF749 HEK293 ChipExo models ZNF749
Supplementary Figure 1658: ZNF749 HepG2 ENCSR125MLR
Supplementary Figure 1659: ZNF74 HEK293 ChipExo models ZNF74
Supplementary Figure 1660: ZNF75A K562 ENCSR099MNR
Supplementary Figure 1661: ZNF75A K562 ENCSR099MNR subpatterns
Supplementary Figure 1662: ZNF75D HEK293 ChipExo models ZNF75D
Supplementary Figure 1663: ZNF75D HEK293 ChipExo models ZNF75D subpatterns
Supplementary Figure 1664: ZNF75D HepG2 ENCSR693TYT
Supplementary Figure 1665: ZNF761 HepG2 ENCSR622AMZ

Supplementary Figure 1666: ZNF764 HEK293 ChipExo models ZNF764
Supplementary Figure 1667: ZNF764 K562 ENCSR023OOE
Supplementary Figure 1668: ZNF765 HEK293 ChipExo models ZNF765
Supplementary Figure 1669: ZNF765 HEK293 ChipExo models ZNF765 subpatterns
Supplementary Figure 1670: ZNF766 HEK293 ChipExo models ZNF766
Supplementary Figure 1671: ZNF766 HEK293 ChipExo models ZNF766 subpatterns
Supplementary Figure 1672: ZNF766 HepG2 ENCSR869RSW
Supplementary Figure 1673: ZNF766 K562 ENCSR194IJN
Supplementary Figure 1674: ZNF768 HEK293 ENCSR070HWF
Supplementary Figure 1675: ZNF768 HEK293 ENCSR070HWF subpatterns
Supplementary Figure 1676: ZNF768 HEK293 Hughes GR models ZNF768
Supplementary Figure 1677: ZNF768 HEK293 Hughes GR models ZNF768 subpatterns
Supplementary Figure 1678: ZNF768 HepG2 ENCSR181ABP
Supplementary Figure 1679: ZNF768 HepG2 ENCSR181ABP subpatterns
Supplementary Figure 1680: ZNF76 HEK293 ENCSR072LQF
Supplementary Figure 1681: ZNF76 HEK293 ENCSR072LQF subpatterns
Supplementary Figure 1682: ZNF76 HEK293 Hughes GR models ZNF76
Supplementary Figure 1683: ZNF76 HEK293 Hughes GR models ZNF76 subpatterns
Supplementary Figure 1684: ZNF76 K562 ENCSR257AFV
Supplementary Figure 1685: ZNF76 K562 ENCSR257AFV subpatterns
Supplementary Figure 1686: ZNF770 HEK293 ENCSR242BGR
Supplementary Figure 1687: ZNF770 HEK293 ENCSR242BGR subpatterns
Supplementary Figure 1688: ZNF770 HepG2 ENCSR510GKB
Supplementary Figure 1689: ZNF770 HepG2 ENCSR510GKB subpatterns
Supplementary Figure 1690: ZNF772 HepG2 ENCSR248WAU
Supplementary Figure 1691: ZNF773 HepG2 ENCSR029ARE
Supplementary Figure 1692: ZNF773 HepG2 ENCSR029ARE subpatterns
Supplementary Figure 1693: ZNF775 HepG2 ENCSR856QJP
Supplementary Figure 1694: ZNF775 HepG2 ENCSR856QJP subpatterns
Supplementary Figure 1695: ZNF776 HEK293 ENCSR274LVQ
Supplementary Figure 1696: ZNF776 HEK293 ChipExo models ZNF776
Supplementary Figure 1697: ZNF776 HEK293 ChipExo models ZNF776 subpatterns
Supplementary Figure 1698: ZNF776 HepG2 ENCSR704ENT
Supplementary Figure 1699: ZNF777 HEK293 ENCSR295BIP
Supplementary Figure 1700: ZNF777 HEK293 ENCSR295BIP subpatterns
Supplementary Figure 1701: ZNF777 HEK293 ChipExo models ZNF777
Supplementary Figure 1702: ZNF777 HepG2 ENCSR068ZQR
Supplementary Figure 1703: ZNF777 HepG2 ENCSR068ZQR subpatterns
Supplementary Figure 1704: ZNF778 HEK293 Hughes GR models ZNF778
Supplementary Figure 1705: ZNF778 HEK293 Hughes GR models ZNF778 subpatterns
Supplementary Figure 1706: ZNF778 HEK293 ChipExo models ZNF778
Supplementary Figure 1707: ZNF778 HEK293 ChipExo models ZNF778 subpatterns
Supplementary Figure 1708: ZNF778 HepG2 ENCSR141ELR
Supplementary Figure 1709: ZNF778 HepG2 ENCSR141ELR subpatterns
Supplementary Figure 1710: ZNF778 K562 ENCSR110JLQ
Supplementary Figure 1711: ZNF77 HEK293 ChipExo models ZNF77
Supplementary Figure 1712: ZNF77 K562 ENCSR844MAB
Supplementary Figure 1713: ZNF780A HEK293 ChipExo models ZNF780A
Supplementary Figure 1714: ZNF780A HEK293 ChipExo models ZNF780A subpatterns
Supplementary Figure 1715: ZNF780A HepG2 ENCSR095JQV
Supplementary Figure 1716: ZNF780A K562 ENCSR214PDW
Supplementary Figure 1717: ZNF781 HepG2 ENCSR517HGZ
Supplementary Figure 1718: ZNF782 HEK293 ChipExo models ZNF782
Supplementary Figure 1719: ZNF782 HepG2 ENCSR198RHC
Supplementary Figure 1720: ZNF783 HEK293 ChipExo models ZNF783
Supplementary Figure 1721: ZNF783 HEK293 ChipExo models ZNF783 subpatterns

Supplementary Figure 1722: ZNF784 HEK293 Hughes GR models ZNF784
Supplementary Figure 1723: ZNF784 HepG2 ENCSR082QGT
Supplementary Figure 1724: ZNF785 HEK293 ENCSR950ACO
Supplementary Figure 1725: ZNF785 HEK293 ChipExo models ZNF785
Supplementary Figure 1726: ZNF785 K562 ENCSR222TVA
Supplementary Figure 1727: ZNF786 HEK293 ChipExo models ZNF786
Supplementary Figure 1728: ZNF786 HEK293 ChipExo models ZNF786 subpatterns
Supplementary Figure 1729: ZNF786 HepG2 ENCSR206BVQ
Supplementary Figure 1730: ZNF789 HEK293 ChipExo models ZNF789
Supplementary Figure 1731: ZNF789 HEK293 ChipExo models ZNF789 subpatterns
Supplementary Figure 1732: ZNF790 HEK293 ChipExo models ZNF790
Supplementary Figure 1733: ZNF790 HepG2 ENCSR117XJA
Supplementary Figure 1734: ZNF791 HEK293 ENCSR775HFF
Supplementary Figure 1735: ZNF791 HEK293 ENCSR775HFF subpatterns
Supplementary Figure 1736: ZNF791 HEK293 ChipExo models ZNF791
Supplementary Figure 1737: ZNF792 HEK293 ENCSR679STZ
Supplementary Figure 1738: ZNF792 HEK293 ENCSR679STZ subpatterns
Supplementary Figure 1739: ZNF792 HEK293 ChipExo models ZNF792
Supplementary Figure 1740: ZNF792 HEK293 ChipExo models ZNF792 subpatterns
Supplementary Figure 1741: ZNF792 HepG2 ENCSR396SOH
Supplementary Figure 1742: ZNF799 HEK293 ChipExo models ZNF799
Supplementary Figure 1743: ZNF799 HEK293 ChipExo models ZNF799 subpatterns
Supplementary Figure 1744: ZNF79 HEK293 ChipExo models ZNF79
Supplementary Figure 1745: ZNF79 K562 ENCSR995FUM
Supplementary Figure 1746: ZNF79 K562 ENCSR995FUM subpatterns
Supplementary Figure 1747: ZNF7 HEK293 ChipExo models ZNF7
Supplementary Figure 1748: ZNF7 HepG2 ENCSR553QMC
Supplementary Figure 1749: ZNF7 HepG2 ENCSR553QMC subpatterns
Supplementary Figure 1750: ZNF7 K562 ENCSR454SCH
Supplementary Figure 1751: ZNF7 K562 ENCSR454SCH subpatterns
Supplementary Figure 1752: ZNF805 HEK293 ChipExo models ZNF805
Supplementary Figure 1753: ZNF805 HEK293 ChipExo models ZNF805 subpatterns
Supplementary Figure 1754: ZNF808 HEK293 ChipExo models ZNF808
Supplementary Figure 1755: ZNF808 HEK293 ChipExo models ZNF808 subpatterns
Supplementary Figure 1756: ZNF816 HEK293 ChipExo models ZNF816
Supplementary Figure 1757: ZNF816 HEK293 ChipExo models ZNF816 subpatterns
Supplementary Figure 1758: ZNF816 HEK293 Hughes GR models ZNF816
Supplementary Figure 1759: ZNF816 HEK293 Hughes GR models ZNF816 subpatterns
Supplementary Figure 1760: ZNF816 HepG2 ENCSR905BNO
Supplementary Figure 1761: ZNF81 HEK293 ChipExo models ZNF81
Supplementary Figure 1762: ZNF81 HEK293 ChipExo models ZNF81 subpatterns
Supplementary Figure 1763: ZNF823 HEK293 ChipExo models ZNF823
Supplementary Figure 1764: ZNF823 HEK293 ChipExo models ZNF823 subpatterns
Supplementary Figure 1765: ZNF827 HepG2 ENCSR148FHD
Supplementary Figure 1766: ZNF837 HEK293 ENCSR711UOA
Supplementary Figure 1767: ZNF839 HepG2 ENCSR540LPD
Supplementary Figure 1768: ZNF83 HepG2 ENCSR263XFO
Supplementary Figure 1769: ZNF83 K562 ENCSR257XVY
Supplementary Figure 1770: ZNF83 K562 ENCSR257XVY subpatterns
Supplementary Figure 1771: ZNF843 HEK293 ENCSR502KPJ
Supplementary Figure 1772: ZNF843 HEK293 ENCSR502KPJ subpatterns
Supplementary Figure 1773: ZNF846 HEK293 ChipExo models ZNF846
Supplementary Figure 1774: ZNF84 HEK293 ChipExo models ZNF84
Supplementary Figure 1775: ZNF84 HEK293 ChipExo models ZNF84 subpatterns
Supplementary Figure 1776: ZNF84 K562 ENCSR376UMR
Supplementary Figure 1777: ZNF84 K562 ENCSR376UMR subpatterns

Supplementary Figure 1778: ZNF850 HepG2 ENCSR756CJS
Supplementary Figure 1779: ZNF85 HEK293 ChipExo models ZNF85
Supplementary Figure 1780: ZNF85 HEK293 Hughes GR models ZNF85
Supplementary Figure 1781: ZNF85 HEK293 Hughes GR models ZNF85 subpatterns
Supplementary Figure 1782: ZNF860 HEK293 ChipExo models ZNF860
Supplementary Figure 1783: ZNF865 HepG2 ENCSR891KPP
Supplementary Figure 1784: ZNF878 HepG2 ENCSR907PAR
Supplementary Figure 1785: ZNF879 HEK293 ChipExo models ZNF879
Supplementary Figure 1786: ZNF879 HepG2 ENCSR073OBD
Supplementary Figure 1787: ZNF880 HEK293 ChipExo models ZNF880
Supplementary Figure 1788: ZNF883 HepG2 ENCSR882YYL
Supplementary Figure 1789: ZNF891 HepG2 ENCSR020CLV
Supplementary Figure 1790: ZNF8 HEK293 Hughes GR models ZNF8
Supplementary Figure 1791: ZNF8 MCF-7 ENCSR785UCD
Supplementary Figure 1792: ZNF8 SK-N-SH ENCSR325QLX
Supplementary Figure 1793: ZNF8 SK-N-SH ENCSR325QLX subpatterns
Supplementary Figure 1794: ZSCAN12 HepG2 ENCSR574YRZ
Supplementary Figure 1795: ZSCAN12 HepG2 ENCSR574YRZ subpatterns
Supplementary Figure 1796: ZSCAN16 HEK293 ENCSR864VJE
Supplementary Figure 1797: ZSCAN16 HEK293 ENCSR864VJE subpatterns
Supplementary Figure 1798: ZSCAN18 HEK293 ENCSR721QZV
Supplementary Figure 1799: ZSCAN18 WTC11 ENCSR499FDW
Supplementary Figure 1800: ZSCAN18 WTC11 ENCSR499FDW subpatterns
Supplementary Figure 1801: ZSCAN20 A549 ENCSR548FLW
Supplementary Figure 1802: ZSCAN20 A549 ENCSR548FLW subpatterns
Supplementary Figure 1803: ZSCAN20 HepG2 ENCSR169JRW
Supplementary Figure 1804: ZSCAN20 HepG2 ENCSR169JRW subpatterns
Supplementary Figure 1805: ZSCAN21 HEK293 ENCSR253CKN
Supplementary Figure 1806: ZSCAN21 HEK293 ENCSR253CKN subpatterns
Supplementary Figure 1807: ZSCAN21 HepG2 ENCSR210DDA
Supplementary Figure 1808: ZSCAN22 HEK293 Hughes NB models ZSCAN22
Supplementary Figure 1809: ZSCAN22 HEK293 Hughes NB models ZSCAN22 subpatterns
Supplementary Figure 1810: ZSCAN22 HEK293 Hughes GR models ZSCAN22
Supplementary Figure 1811: ZSCAN22 HEK293 Hughes GR models ZSCAN22 subpatterns
Supplementary Figure 1812: ZSCAN22 HepG2 ENCSR050KWL
Supplementary Figure 1813: ZSCAN22 HepG2 ENCSR050KWL subpatterns
Supplementary Figure 1814: ZSCAN23 HEK293 ENCSR705ASR
Supplementary Figure 1815: ZSCAN23 HEK293 ENCSR705ASR subpatterns
Supplementary Figure 1816: ZSCAN25 HepG2 ENCSR037LQB
Supplementary Figure 1817: ZSCAN25 HepG2 ENCSR037LQB subpatterns
Supplementary Figure 1818: ZSCAN26 HEK293 ENCSR501NSC
Supplementary Figure 1819: ZSCAN29 GM12878 ENCSR412YGM
Supplementary Figure 1820: ZSCAN29 GM12878 ENCSR412YGM subpatterns
Supplementary Figure 1821: ZSCAN29 HepG2 ENCSR422VAG
Supplementary Figure 1822: ZSCAN29 K562 ENCSR175SZH
Supplementary Figure 1823: ZSCAN29 K562 ENCSR175SZH subpatterns
Supplementary Figure 1824: ZSCAN29 K562 ENCSR635EXI
Supplementary Figure 1825: ZSCAN29 K562 ENCSR635EXI subpatterns
Supplementary Figure 1826: ZSCAN30 HEK293 ENCSR768VNZ
Supplementary Figure 1827: ZSCAN30 HEK293 ENCSR768VNZ subpatterns
Supplementary Figure 1828: ZSCAN30 HepG2 ENCSR795CKZ
Supplementary Figure 1829: ZSCAN31 HEK293 Hughes NB models ZSCAN31
Supplementary Figure 1830: ZSCAN31 HEK293 Hughes NB models ZSCAN31 subpatterns
Supplementary Figure 1831: ZSCAN31 HEK293 Hughes GR models ZSCAN31
Supplementary Figure 1832: ZSCAN31 HEK293 Hughes GR models ZSCAN31 subpatterns
Supplementary Figure 1833: ZSCAN31 HepG2 ENCSR493VBX

Supplementary Figure 1834: ZSCAN32 K562 ENCSR870YEN
Supplementary Figure 1835: ZSCAN32 K562 ENCSR870YEN subpatterns
Supplementary Figure 1836: ZSCAN4 HEK293 ENCSR211GNP
Supplementary Figure 1837: ZSCAN4 HEK293 ENCSR211GNP subpatterns
Supplementary Figure 1838: ZSCAN5A HEK293 ENCSR357QJR
Supplementary Figure 1839: ZSCAN5A HepG2 ENCSR216GKQ
Supplementary Figure 1840: ZSCAN5C HEK293 ENCSR731AGO
Supplementary Figure 1841: ZSCAN5C HEK293 ENCSR731AGO subpatterns
Supplementary Figure 1842: ZSCAN5C HEK293 Hughes GR models ZSCAN5C subpatterns
Supplementary Figure 1843: ZSCAN5C HEK293 Hughes GR models ZSCAN5C
Supplementary Figure 1844: ZSCAN9 HepG2 ENCSR712FAM
Supplementary Figure 1845: ZSCAN9 HepG2 ENCSR712FAM subpatterns
Supplementary Figure 1846: ZXDB HEK293 ENCSR559IOZ
Supplementary Figure 1847: ZXDC HepG2 ENCSR347PUQ

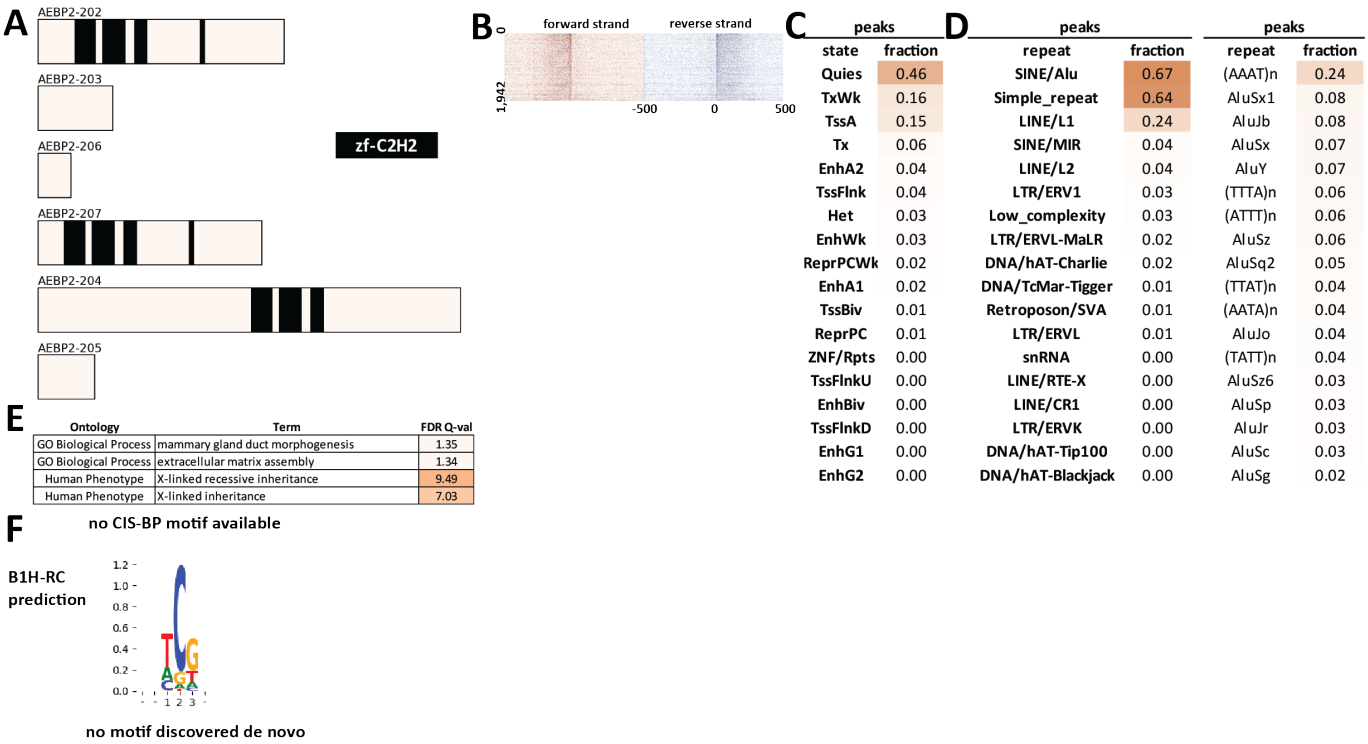

Supplementary Figure 8: Properties and genomic distribution of motifs identified for the AEBP2 transcription factor in HEK293 (accession ENCSR769JRS).

A

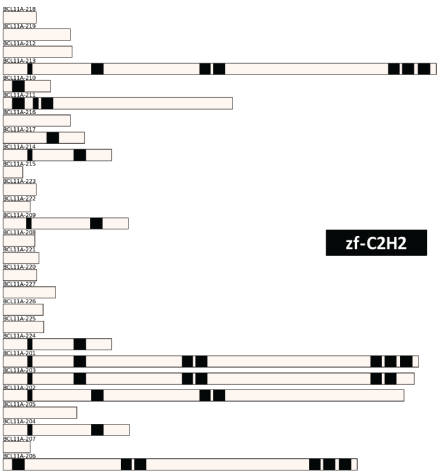

B

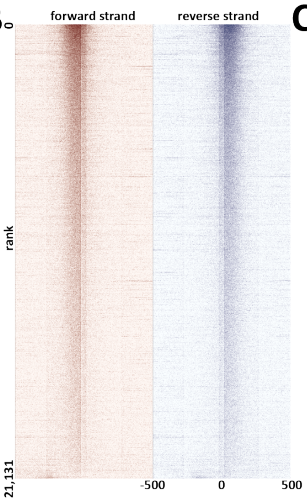

C

peaks	
state	fraction
EnhWk	0.30
EnhA1	0.27
TssA	0.14
EnhA2	0.13
Quies	0.09
TssFlnkU	0.07
TxWk	0.04
TssFlnk	0.04
TssFlnkD	0.03
ReprPCWk	0.02
EnhG1	0.01
Het	0.01
EnhG2	0.01
ZNF/Rpts	0.01
Tx	0.00
EnhBiv	0.00
ReprPC	0.00
TssBiv	0.00

D

peaks		peaks	
repeat	fraction	repeat	fraction
SINE/MIR	0.09	MIRb	0.03
LINE/L1	0.09	MIR	0.02
SINE/Alu	0.07	L2a	0.02
LINE/L2	0.07	L2c	0.02
Simple_repeat	0.06	MIR3	0.02
LTR/ERVL-MaLR	0.05	MIRc	0.02
DNA/hAT-Charlie	0.04	L2b	0.02
LTR/ERV1	0.03	L2	0.01
LTR/ERVL	0.03	L3	0.01
DNA/TcMar-Tigger	0.02	AluJb	0.01
LINE/CR1	0.01	AluSx1	0.01
Low_complexity	0.01	MER5A	0.01
DNA/hAT-Tip100	0.00	AluSx	0.01
DNA/hAT-Blackjack	0.00	AluSz	0.01
LTR/Gypsy	0.00	L1MB7	0.01
LINE/RTE-BovB	0.00	MER5B	0.00
LINE/RTE-X	0.00	AluY	0.00
DNA/TcMar-Mariner	0.00	AluJo	0.00

E

Ontology	Term	FDR Q-val
GO Biological Process	lymphocyte activation	133.20
GO Biological Process	leukocyte cell-cell adhesion	97.30
GO Biological Process	lymphocyte differentiation	97.28
GO Biological Process	leukocyte aggregation	95.41
GO Biological Process	lymphocyte aggregation	87.41
GO Biological Process	T cell activation	85.99
GO Biological Process	positive regulation of leukocyte cell-cell adhesion	85.44
GO Biological Process	adaptive immune response	83.00
GO Biological Process	regulation of adaptive immune response	70.45
GO Biological Process	regulation of B cell activation	66.06
GO Biological Process	regulation of lymphocyte differentiation	64.31
GO Biological Process	positive regulation of leukocyte differentiation	63.92
GO Biological Process	antigen receptor-mediated signaling pathway	63.43
GO Biological Process	cellular response to biotic stimulus	61.67
GO Biological Process	cellular response to molecule of bacterial origin	60.97
GO Biological Process	T cell differentiation	60.00
GO Biological Process	regulation of leukocyte mediated immunity	59.18
GO Biological Process	cellular response to lipopolysaccharide	58.73
GO Biological Process	regulation of intrinsic apoptotic signaling pathway	55.87
GO Biological Process	interferon-gamma-mediated signaling pathway	55.74
Human Phenotype	Abnormality of lymphocytes	48.71
Human Phenotype	Decreased antibody level in blood	41.27
Human Phenotype	Abnormal immunoglobulin level	41.25
Human Phenotype	Abnormality of B cell physiology	41.09
Human Phenotype	Abnormality of the lymph nodes	21.29
Human Phenotype	Abnormality of cells of the lymphoid lineage	19.55
Human Phenotype	Lymphadenopathy	17.99
Human Phenotype	Recurrent upper respiratory tract infections	16.65
Human Phenotype	Lymphopenia	15.10
Human Phenotype	IgG deficiency	13.43

F

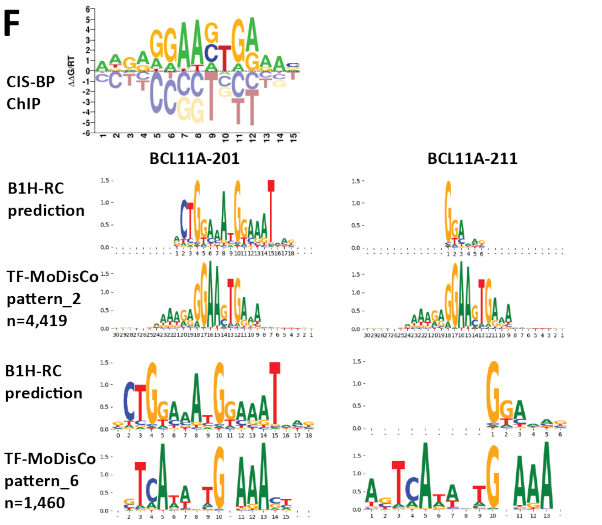

G

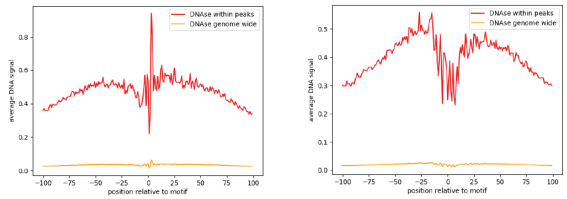

H

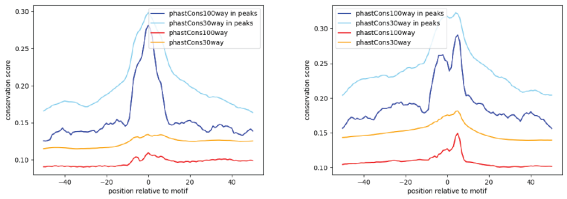

I

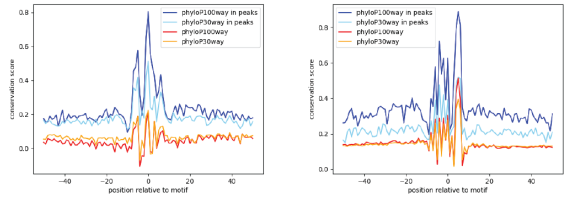

Supplementary Figure 9: Properties and genomic distribution of motifs identified for the BCL11A transcription factor in GM12878 (accession ENCSR000BHA).

TF-MoDisCO pattern_2 n=4419, CWM

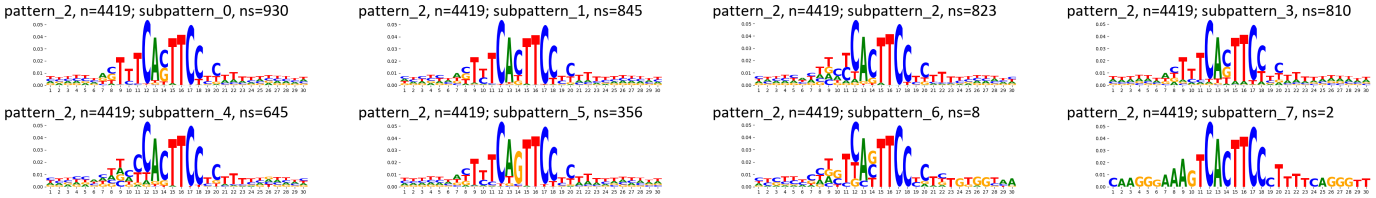

TF-MoDisCO pattern_2 n=4419, PWM

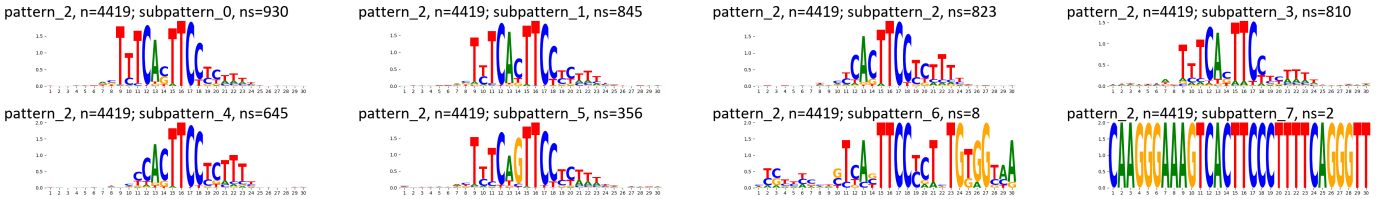

TF-MoDisCO pattern_6 n=1460, CWM

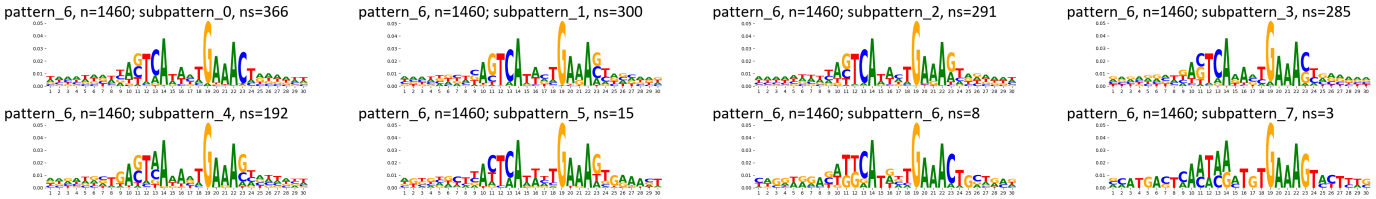

TF-MoDisCO pattern_6 n=1460, PWM

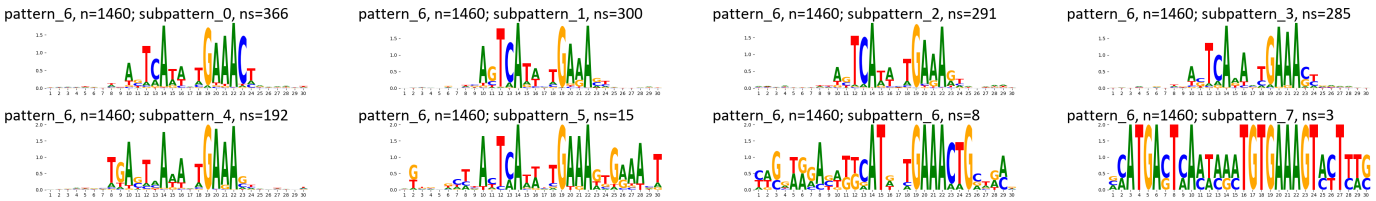

Supplementary Figure 10: TF-MoDisCO subpatterns for the BCL11A transcription factor in GM12878 (accession ENCSR000BHA).

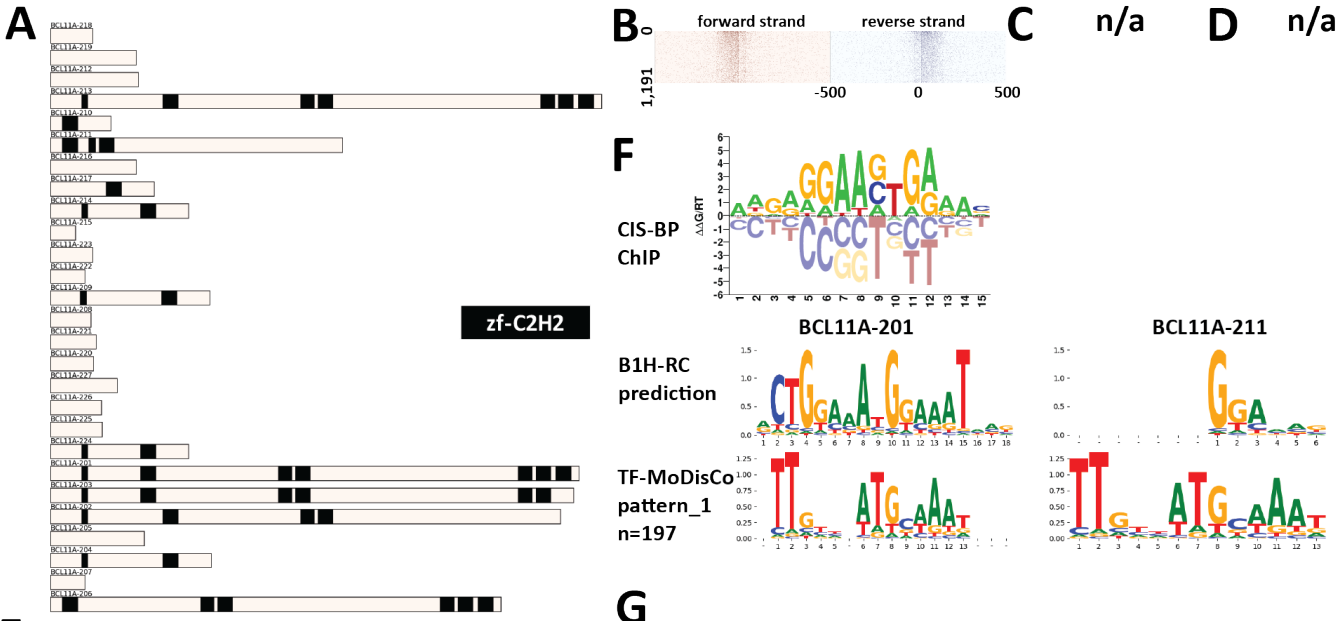

E

Ontology	Term	FDR Q-val
GO Biological Process	axis specification	4.74
GO Biological Process	neural tube development	3.69
GO Biological Process	tube formation	3.35
GO Biological Process	neural tube formation	3.25
GO Biological Process	anterior/posterior axis specification	3.25
GO Biological Process	gastrulation	3.21
GO Biological Process	regulation of glomerular mesangial cell proliferation	3.22
GO Biological Process	primary neural tube formation	3.06
GO Biological Process	endoderm development	3.04
GO Biological Process	regulation of cell proliferation involved in kidney development	2.80
GO Biological Process	cardiac septum morphogenesis	2.79
GO Biological Process	segmentation	2.78
GO Biological Process	formation of primary germ layer	2.73
GO Biological Process	lens morphogenesis in camera-type eye	2.72
GO Biological Process	mesoderm development	2.55
GO Biological Process	pituitary gland development	2.54
GO Biological Process	neural tube closure	2.54
GO Biological Process	epithelial tube formation	2.50
GO Biological Process	cell proliferation involved in kidney development	2.45
GO Biological Process	embryonic epithelial tube formation	2.43
Human Phenotype	Abnormality of the pituitary gland	3.63
Human Phenotype	Abnormality of the hypothalamus-pituitary axis	3.77
Human Phenotype	Microphthalmia	3.81
Human Phenotype	Hypoplastic male external genitalia	3.79
Human Phenotype	Anterior pituitary dysgenesis	3.61
Human Phenotype	Abnormality of globe size	3.61
Human Phenotype	External genital hypoplasia	3.65
Human Phenotype	Intrahepatic cholestasis	3.68
Human Phenotype	Abnormality of the anterior pituitary	3.28
Human Phenotype	Micropenis	3.28
Human Phenotype	Hypoplasia of penis	3.17
Human Phenotype	Anophthalmia	3.02
Human Phenotype	Cleft upper lip	2.99
Human Phenotype	Malar flattening	2.92
Human Phenotype	Abnormality of malar bones	2.84
Human Phenotype	Cleft lip	2.67
Human Phenotype	Hemivertebrae	2.61
Human Phenotype	Coloboma	2.56
Human Phenotype	Anterior pituitary hypoplasia	2.49
Human Phenotype	Upslanted palpebral fissure	2.42

Supplementary Figure 11: Properties and genomic distribution of motifs identified for the BCL11A transcription factor in H1 (accession ENCSR000BIP).

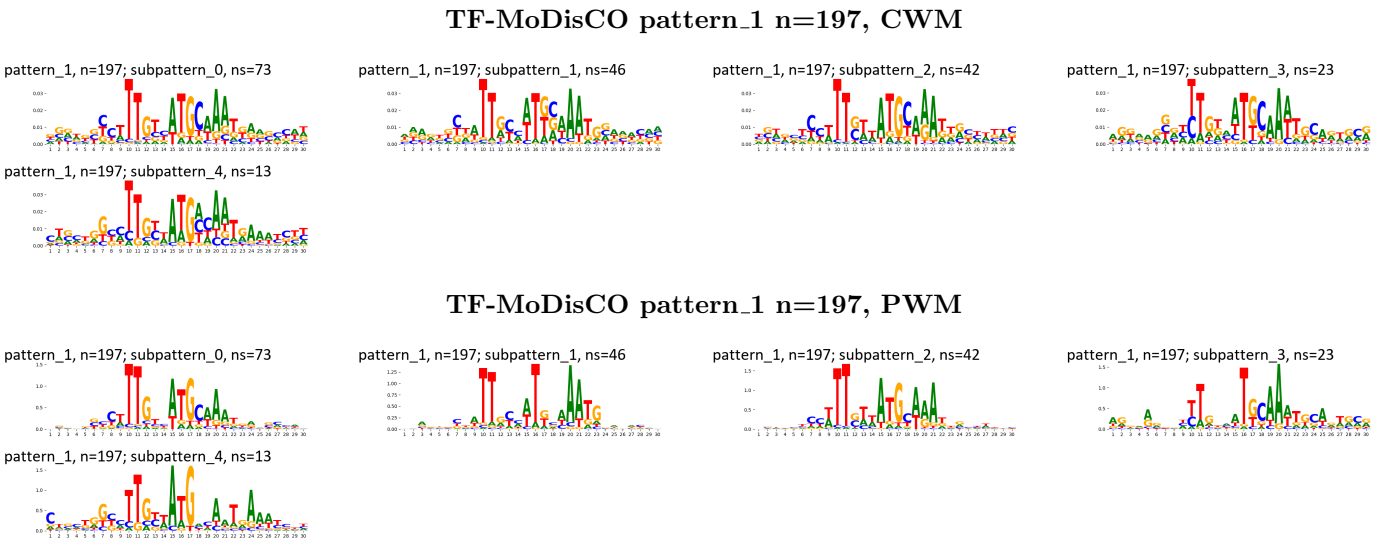

Supplementary Figure 12: TF-MoDisCO subpatterns for the BCL11A transcription factor in H1 (accession ENCSR000BIP).

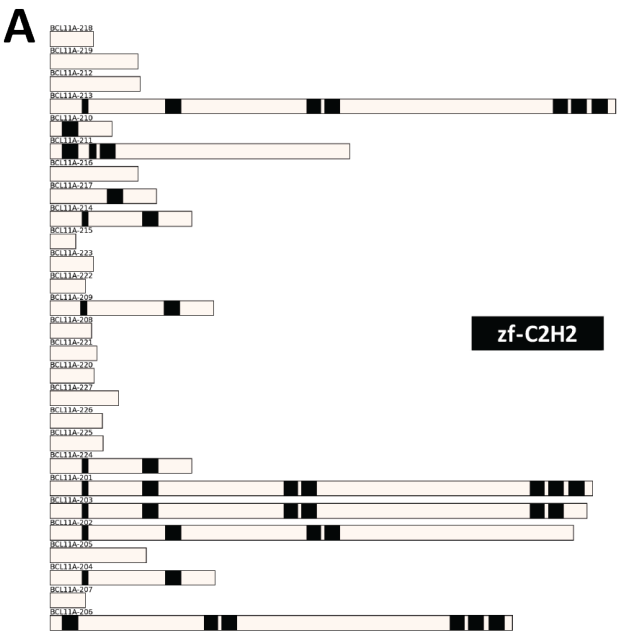

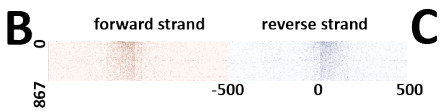

C n/a

D n/a

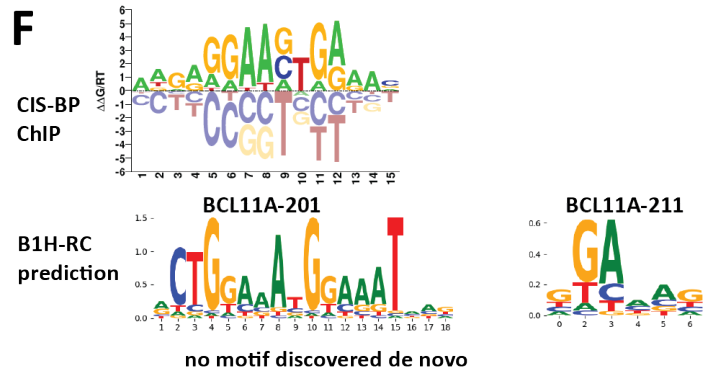

Ontology	Term	FDR Q-val
GO Biological Process	axis specification	3.27
GO Biological Process	regulation of gastrulation	2.87
GO Biological Process	regulation of retina development in camera-type eye	2.81
GO Biological Process	regulation of neural precursor cell proliferation	2.60
GO Biological Process	stem cell proliferation	2.04
GO Biological Process	regulation of neural retina development	1.92
GO Biological Process	regulation of histone H3-K9 methylation	1.90
GO Biological Process	miRNA metabolic process	1.88
GO Biological Process	regulation of embryonic development	1.85
GO Biological Process	anterior/posterior axis specification	1.83
GO Biological Process	T cell mediated cytotoxicity	1.69
GO Biological Process	gene silencing by RNA	1.65
GO Biological Process	positive regulation of embryonic development	1.43
GO Biological Process	regulation of stem cell proliferation	1.43
GO Biological Process	regulation of neuroblast proliferation	1.31
Human Phenotype	Holoprosencephaly	2.76
Human Phenotype	Abnormality of the pituitary gland	2.72
Human Phenotype	Abnormality of the hypothalamus-pituitary axis	2.66
Human Phenotype	Malar flattening	2.45
Human Phenotype	Abnormality of the anterior pituitary	2.47
Human Phenotype	Abnormality of malar bones	2.40
Human Phenotype	Incomplete penetrance	2.29
Human Phenotype	Abnormal localization of kidney	2.21
Human Phenotype	Cleft upper lip	2.16
Human Phenotype	Abnormality of thrombocytes	2.03
Human Phenotype	Coloboma	2.03
Human Phenotype	Hypoplastic facial bones	2.02
Human Phenotype	Cleft lip	1.97
Human Phenotype	Abnormal visual electrophysiology	1.96
Human Phenotype	Abnormality of the scapula	1.96
Human Phenotype	Thrombocytopenia	1.93
Human Phenotype	Absent nasal septal cartilage	1.89
Human Phenotype	Median cleft lip and palate	1.89
Human Phenotype	Abnormality of the nasal skeleton	1.89
Human Phenotype	Abnormality of the chin	1.86

Supplementary Figure 13: Properties and genomic distribution of motifs identified for the BCL11A transcription factor in H1 (accession ENCSR000BMJ).

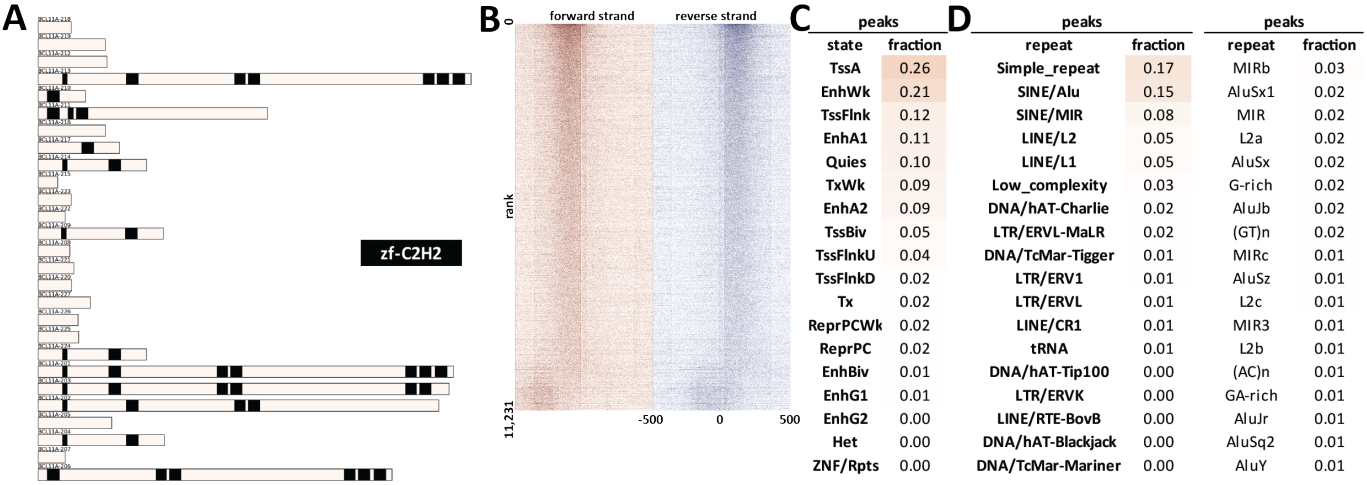

C

peaks	
state	fraction
TssA	0.26
EnhWk	0.21
TssFlnk	0.12
EnhA1	0.11
Quies	0.10
TxWk	0.09
EnhA2	0.09
TssBiv	0.05
TssFlnkU	0.04
TssFlnkD	0.02
Tx	0.02
ReprPCWk	0.02
ReprPC	0.02
EnhBiv	0.01
EnhG1	0.01
EnhG2	0.00
Het	0.00
ZNF/Rpts	0.00

D

peaks		peaks	
repeat	fraction	repeat	fraction
Simple_repeat	0.17	MIRb	0.03
SINE/Alu	0.15	AluSx1	0.02
SINE/MIR	0.08	MIR	0.02
LINE/L2	0.05	L2a	0.02
LINE/L1	0.05	AluSx	0.02
Low_complexity	0.03	G-rich	0.02
DNA/hAT-Charlie	0.02	AluJb	0.02
LTR/ERVL-MaLR	0.02	(GT)n	0.02
DNA/TcMar-Tigger	0.01	MIRc	0.01
LTR/ERV1	0.01	AluSz	0.01
LTR/ERVL	0.01	L2c	0.01
LINE/CR1	0.01	MIR3	0.01
tRNA	0.01	L2b	0.01
DNA/hAT-Tip100	0.00	(AC)n	0.01
LTR/ERVK	0.00	GA-rich	0.01
LINE/RTE-BovB	0.00	AluJr	0.01
DNA/hAT-Blackjack	0.00	AluSq2	0.01
DNA/TcMar-Mariner	0.00	AluY	0.01

E

Ontology	Term	FDR Q-val
GO Biological Process	mRNA transcription	16.80
GO Biological Process	heterochromatin organization	16.54
GO Biological Process	adherens junction assembly	11.89
GO Biological Process	purine ribonucleoside biosynthetic process	11.76
GO Biological Process	regulation of pri-miRNA transcription from RNA polymerase II promoter	10.96
GO Biological Process	trachea cartilage development	9.10
GO Biological Process	positive regulation of pri-miRNA transcription from RNA polymerase II promoter	8.67
GO Biological Process	cellular response to epidermal growth factor stimulus	8.34
GO Biological Process	regulation of mammary gland epithelial cell proliferation	7.36
GO Biological Process	AMP biosynthetic process	7.16
GO Biological Process	cytoplasmic microtubule organization	6.89
GO Biological Process	placenta blood vessel development	6.70
GO Biological Process	parasympathetic nervous system development	6.69
GO Biological Process	histone H3 acetylation	6.57
GO Biological Process	membrane raft assembly	6.55
GO Biological Process	cell-substrate junction assembly	6.52
GO Biological Process	histone H4-K5 acetylation	6.44
GO Biological Process	histone H4-K8 acetylation	6.44
GO Biological Process	positive regulation of transcription from RNA polymerase II promoter in response to stress	6.41
GO Biological Process	preganglionic parasympathetic fiber development	5.83
Human Phenotype	Enlarged thorax	3.97

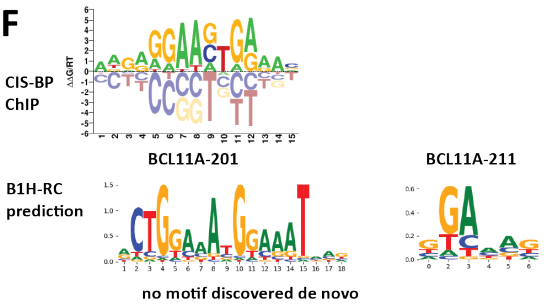

Supplementary Figure 14: Properties and genomic distribution of motifs identified for the BCL11A transcription factor in HEK293 (accession ENCSR021DJC).

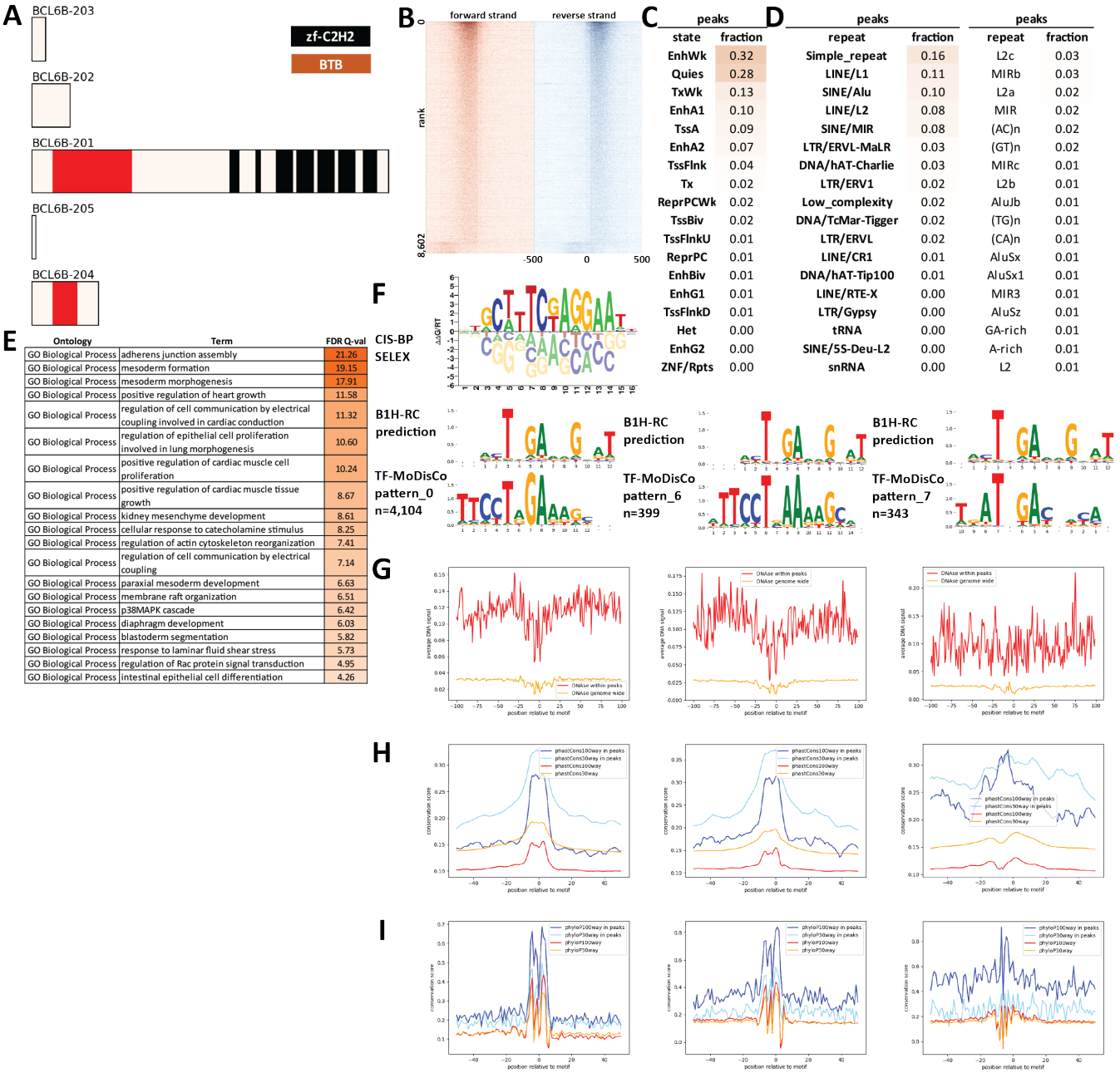

Supplementary Figure 15: Properties and genomic distribution of motifs identified for the BCL6B transcription factor in HEK293 (accession ENCSR673SGK).

TF-MoDisCO pattern_0 n=4104, CWM

pattern_0, n=4104; subpattern_0, ns=997

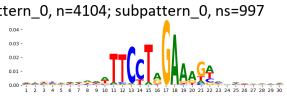

pattern_0, n=4104; subpattern_1, ns=986

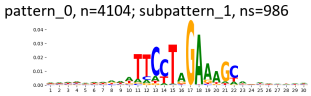

pattern_0, n=4104; subpattern_10, ns=9

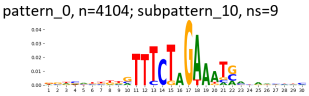

pattern_0, n=4104; subpattern_11, ns=5

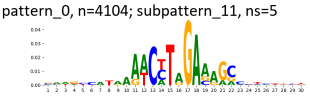

pattern_0, n=4104; subpattern_12, ns=3

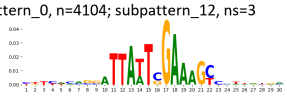

pattern_0, n=4104; subpattern_2, ns=908

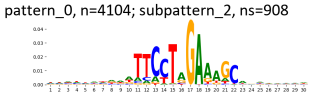

pattern_0, n=4104; subpattern_3, ns=825

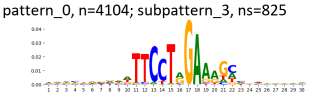

pattern_0, n=4104; subpattern_4, ns=141

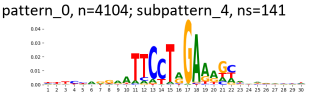

pattern_0, n=4104; subpattern_5, ns=88

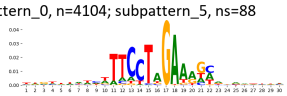

pattern_0, n=4104; subpattern_6, ns=50

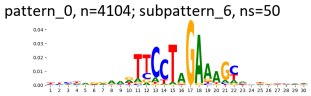

pattern_0, n=4104; subpattern_7, ns=48

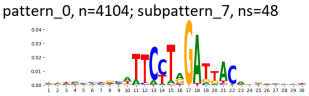

pattern_0, n=4104; subpattern_8, ns=22

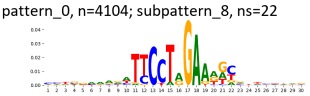

pattern_0, n=4104; subpattern_9, ns=22

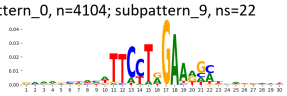

TF-MoDisCO pattern_0 n=4104, PWM

pattern_0, n=4104; subpattern_0, ns=997

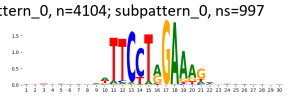

pattern_0, n=4104; subpattern_1, ns=986

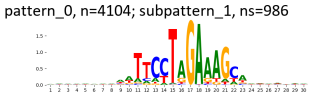

pattern_0, n=4104; subpattern_10, ns=9

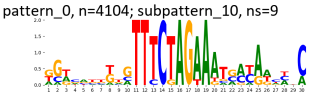

pattern_0, n=4104; subpattern_11, ns=5

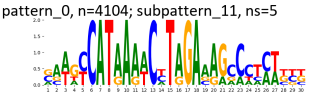

pattern_0, n=4104; subpattern_12, ns=3

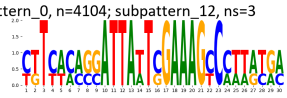

pattern_0, n=4104; subpattern_2, ns=908

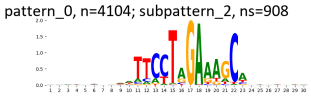

pattern_0, n=4104; subpattern_3, ns=825

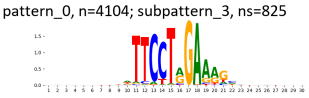

pattern_0, n=4104; subpattern_4, ns=141

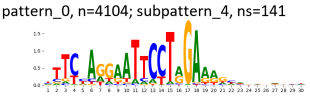

pattern_0, n=4104; subpattern_5, ns=88

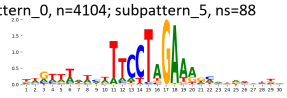

pattern_0, n=4104; subpattern_6, ns=50

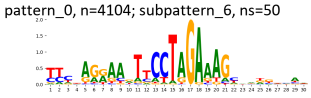

pattern_0, n=4104; subpattern_7, ns=48

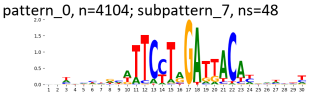

pattern_0, n=4104; subpattern_8, ns=22

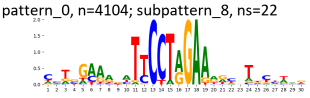

pattern_0, n=4104; subpattern_9, ns=22

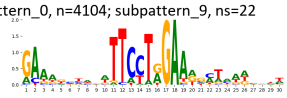

TF-MoDisCO pattern_6 n=399, CWM

pattern_6, n=399; subpattern_0, ns=147

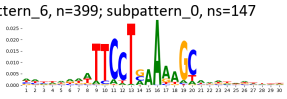

pattern_6, n=399; subpattern_1, ns=140

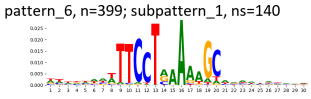

pattern_6, n=399; subpattern_2, ns=44

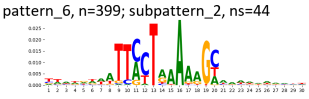

pattern_6, n=399; subpattern_3, ns=35

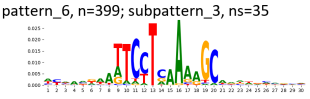

pattern_6, n=399; subpattern_4, ns=33

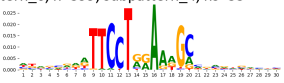

TF-MoDisCO pattern_6 n=399, PWM

pattern_6, n=399; subpattern_0, ns=147

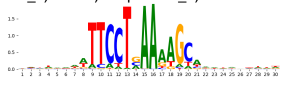

pattern_6, n=399; subpattern_1, ns=140

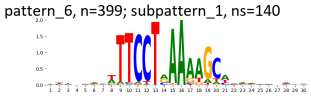

pattern_6, n=399; subpattern_2, ns=44

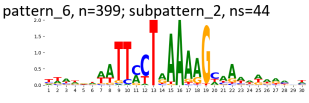

pattern_6, n=399; subpattern_3, ns=35

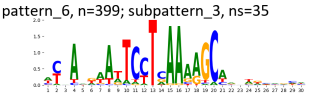

pattern_6, n=399; subpattern_4, ns=33

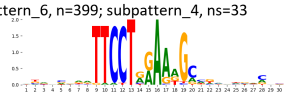

TF-MoDisCO pattern_7 n=343, CWM

pattern_7, n=343; subpattern_0, ns=98

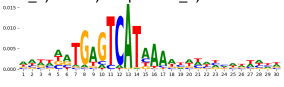

pattern_7, n=343; subpattern_1, ns=63

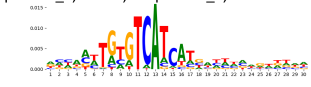

pattern_7, n=343; subpattern_2, ns=50

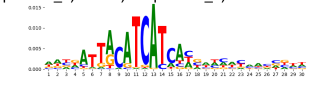

pattern_7, n=343; subpattern_3, ns=50

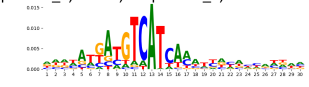

pattern_7, n=343; subpattern_4, ns=36

pattern_7, n=343; subpattern_5, ns=27

pattern_7, n=343; subpattern_6, ns=19

TF-MoDisCO pattern_7 n=343, PWM

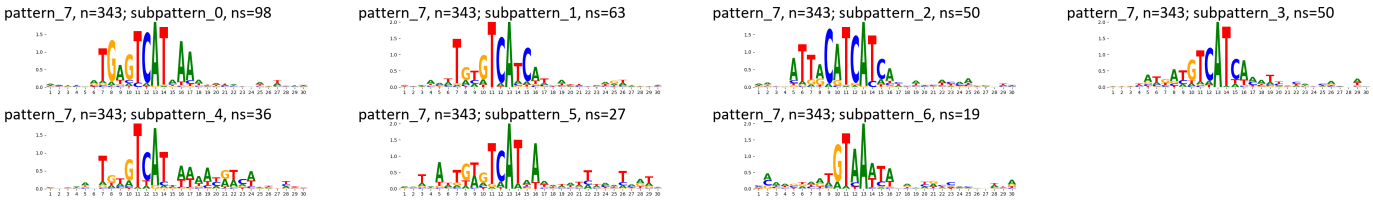

Supplementary Figure 16: TF-MoDisCO subpatterns for the BCL6B transcription factor in HEK293 (accession ENCSR673SGK).

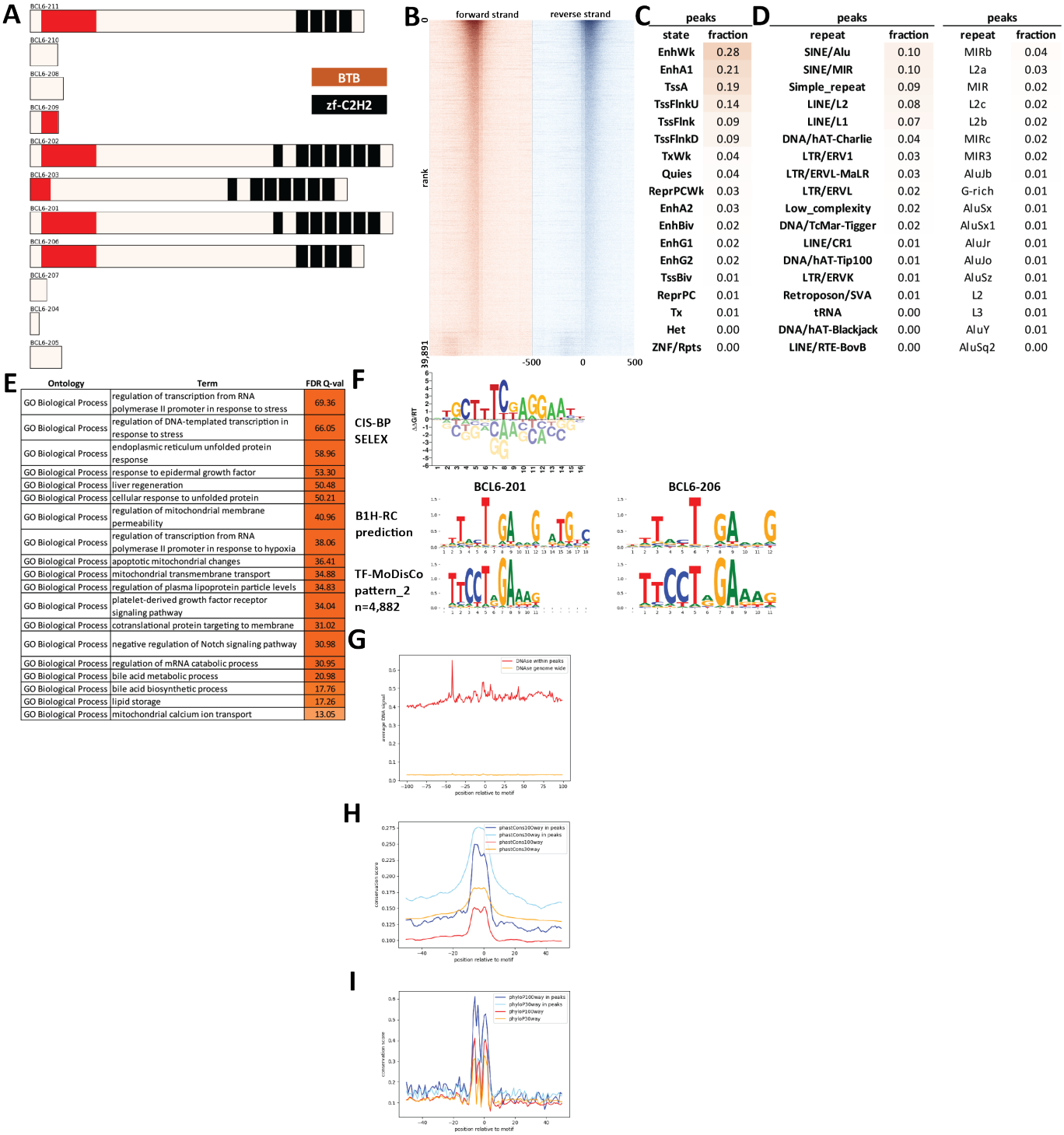

Supplementary Figure 17: Properties and genomic distribution of motifs identified for the BCL6 transcription factor in HepG2 (accession ENCSR759BDG).

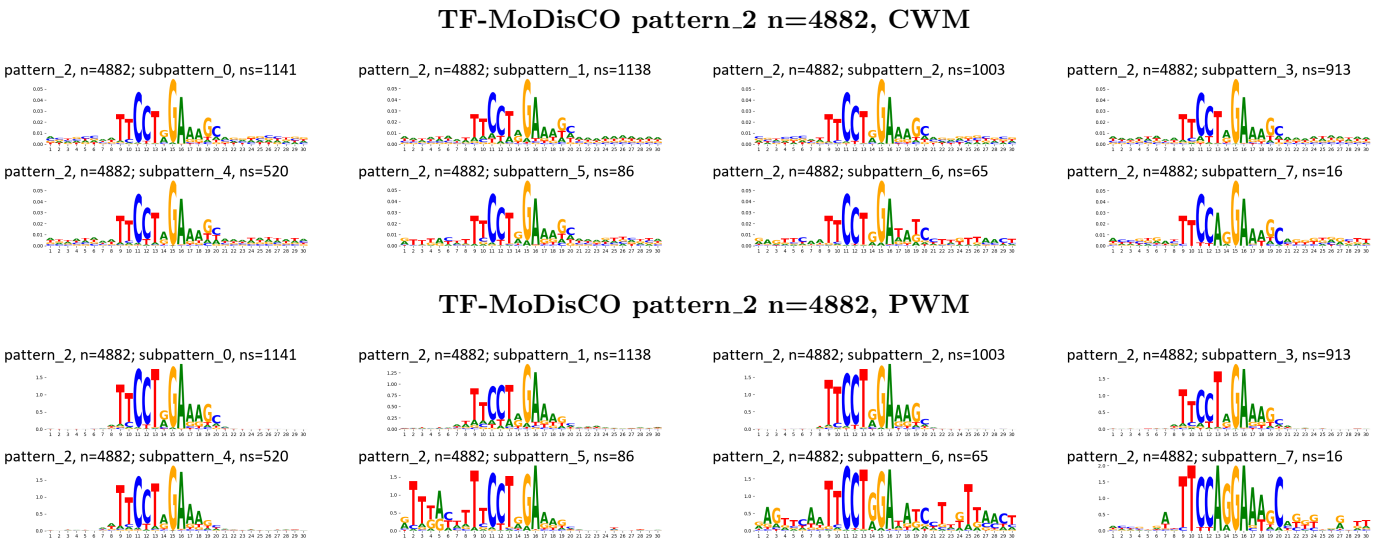

Supplementary Figure 18: TF-MoDisCO subpatterns for the BCL6 transcription factor in HepG2 (accession ENCSR759BDG).

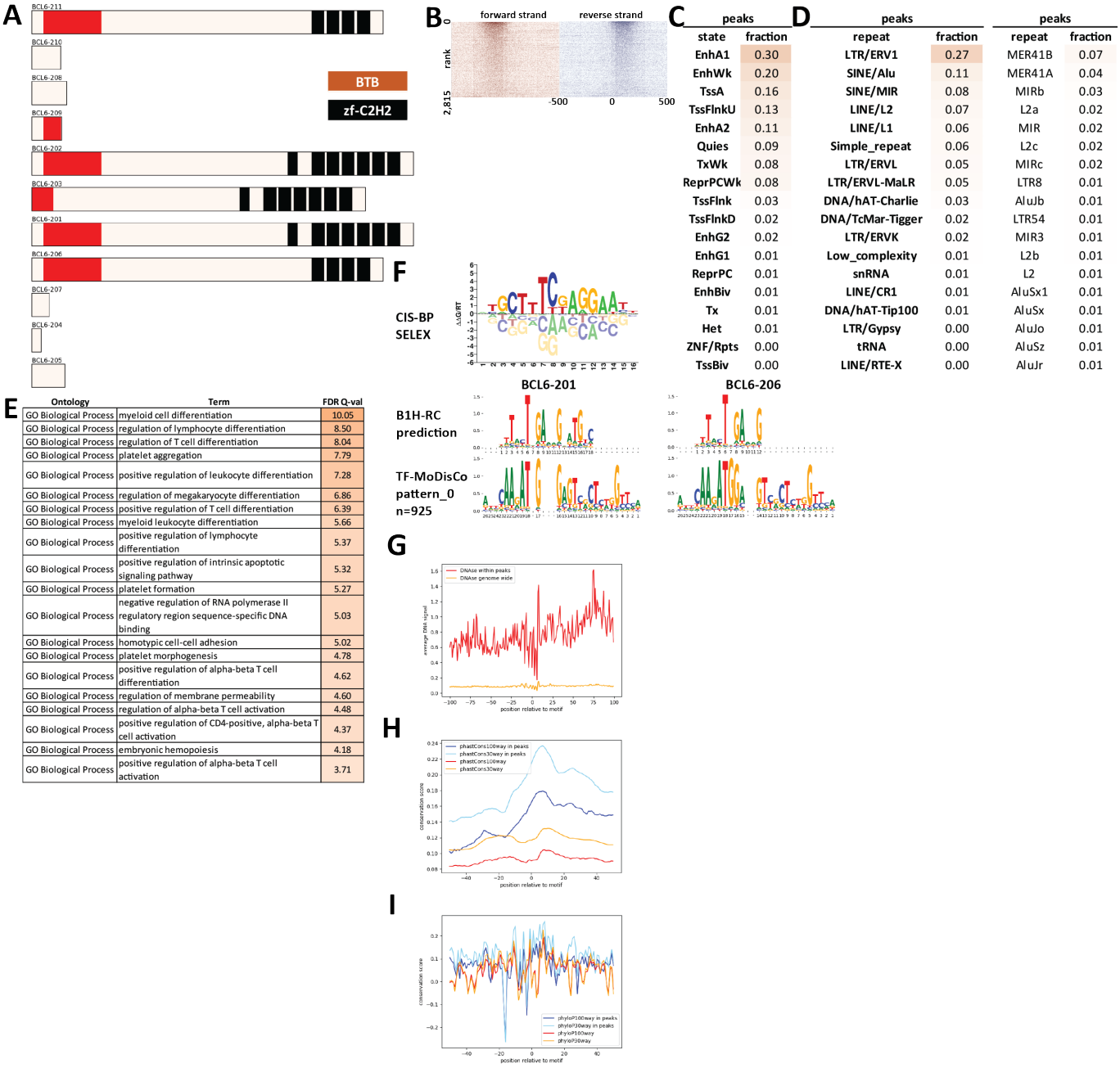

Supplementary Figure 19: Properties and genomic distribution of motifs identified for the BCL6 transcription factor in K562 (accession ENCSR802AHH).

TF-MoDisCO pattern_0 n=925, CWM

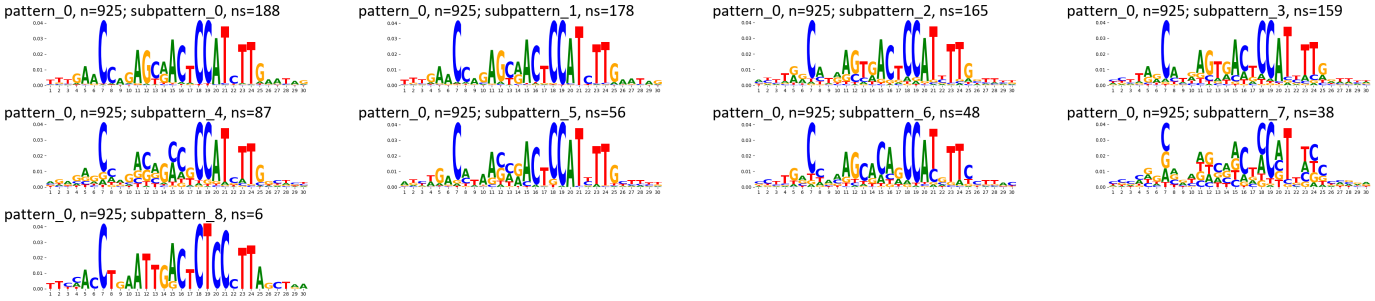

TF-MoDisCO pattern_0 n=925, PWM

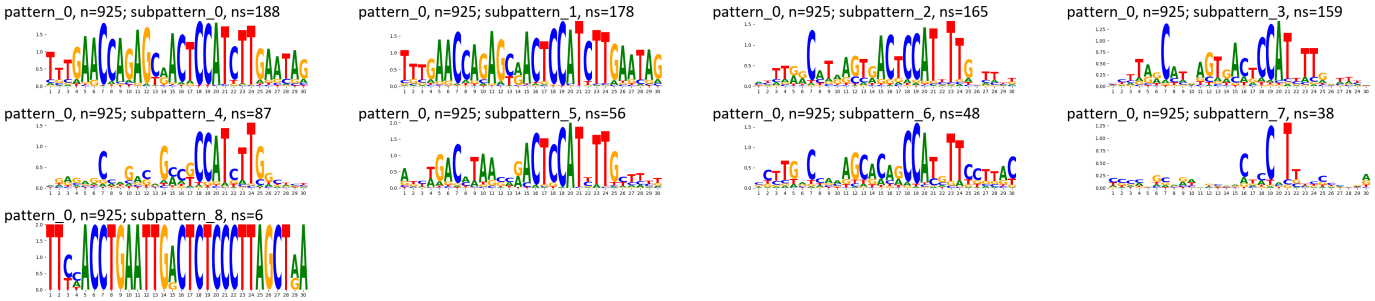

Supplementary Figure 20: TF-MoDisCO subpatterns for the BCL6 transcription factor in K562 (accession ENCSR802AHH).

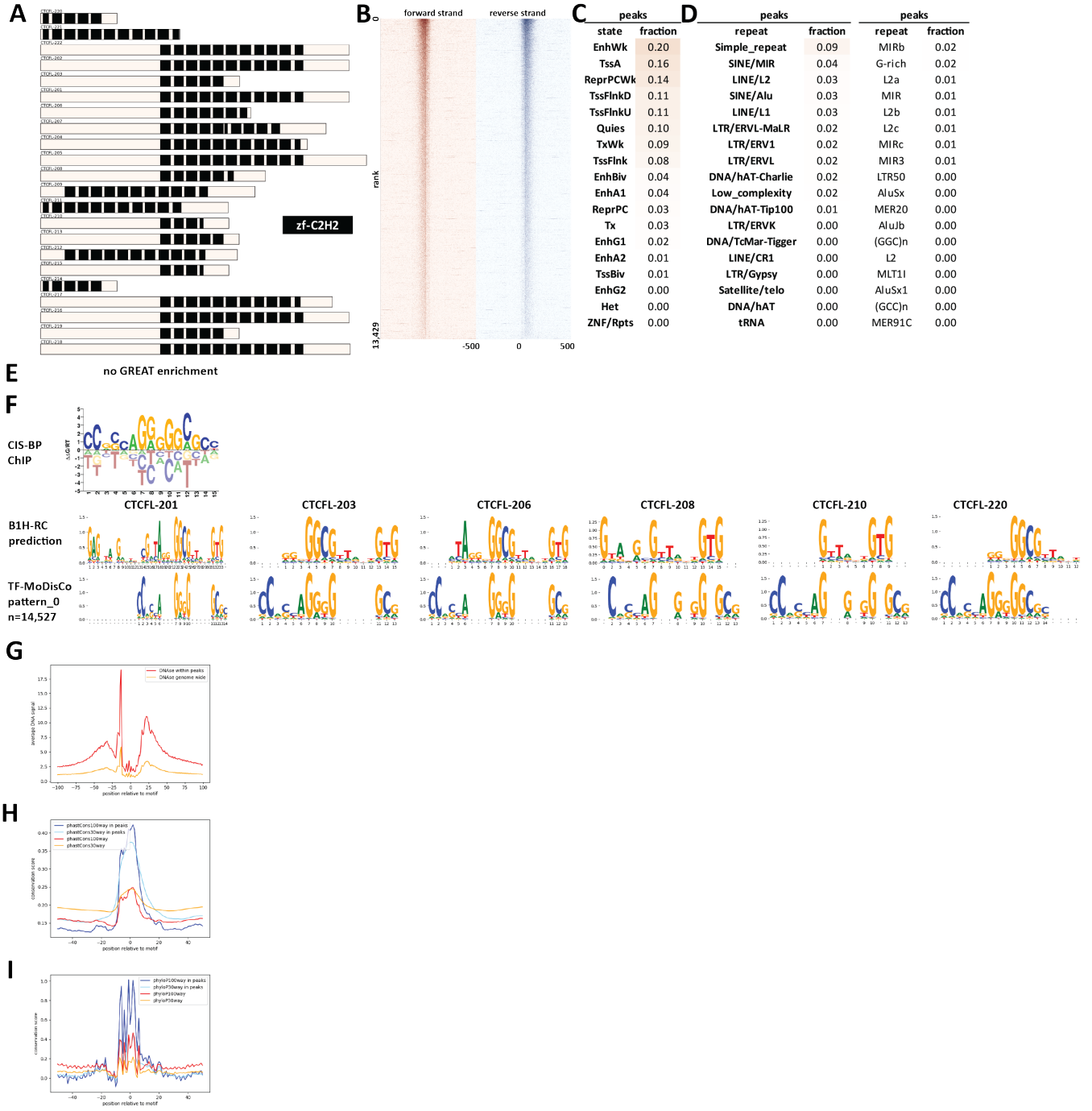

Supplementary Figure 21: Properties and genomic distribution of motifs identified for the CTCFL transcription factor in K562 (accession ENCSR000BNK).

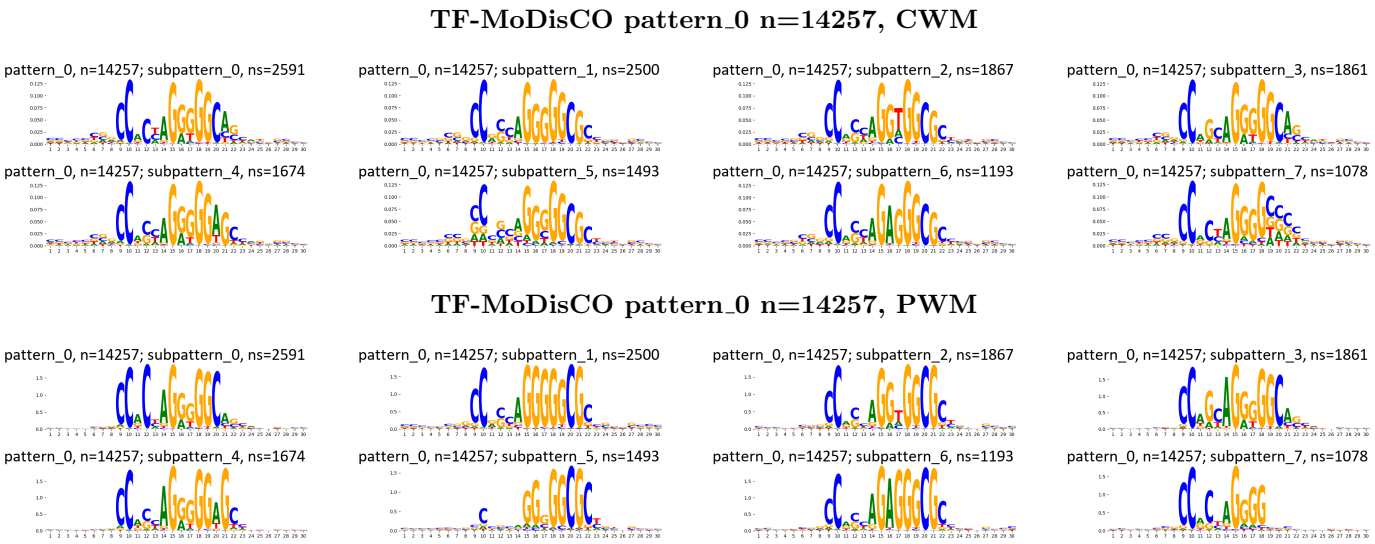

Supplementary Figure 22: TF-MoDisCO subpatterns for the CTCFL transcription factor in K562 (accession ENCSR000BNK).

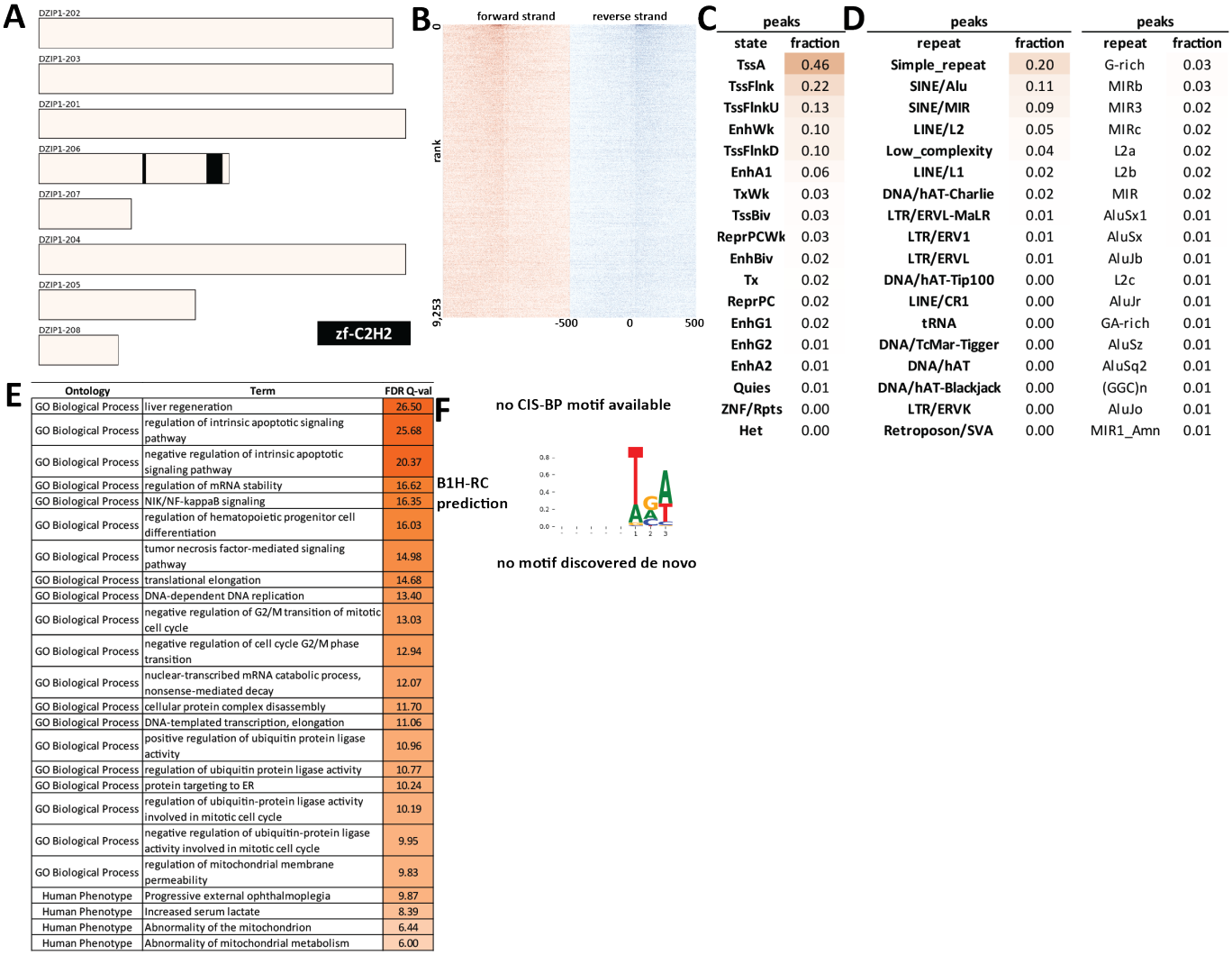

Supplementary Figure 23: Properties and genomic distribution of motifs identified for the DZIP1 transcription factor in HepG2 (accession ENCSR895KNN).

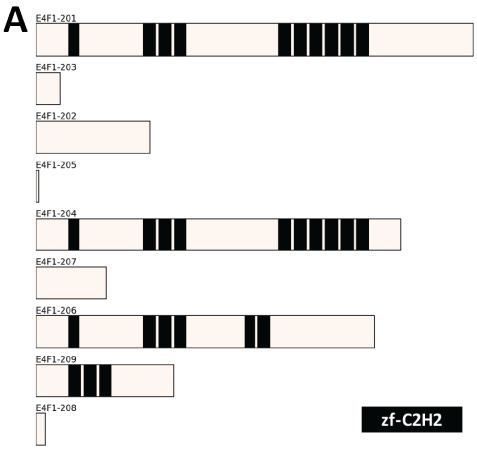

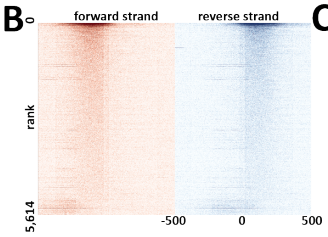

C

peaks	
state	fraction
TssA	0.68
TssFlnk	0.31
EnhA1	0.06
EnhA2	0.06
TssFlnkU	0.05
Quies	0.05
EnhWk	0.04
TxWk	0.03
ReprPCWk	0.02
TssFlnkD	0.02
Het	0.00
ZNF/Rpts	0.00
Tx	0.00
ReprPC	0.00
EnhG2	0.00
TssBiv	0.00
EnhG1	0.00
EnhBiv	0.00

D

peaks		peaks	
repeat	fraction	repeat	fraction
Simple_repeat	0.21	G-rich	0.02
SINE/Alu	0.09	GA-rich	0.02
Low_complexity	0.04	MIRb	0.01
SINE/MIR	0.04	AluSx1	0.01
LINE/L2	0.03	(GT)n	0.01
LINE/L1	0.02	AluSx	0.01
LTR/ERV1	0.01	L2a	0.01
LTR/ERVL-MaLR	0.01	(AC)n	0.01
DNA/hAT-Charlie	0.01	(CA)n	0.01
LTR/ERVL	0.01	MIRc	0.01
DNA/TcMar-Tigger	0.00	L2b	0.01
LINE/CR1	0.00	(TG)n	0.01
tRNA	0.00	AluJb	0.01
DNA/hAT-Tip100	0.00	MIR3	0.01
snRNA	0.00	AluY	0.01
LTR/Gypsy	0.00	MIR	0.01
LTR/ERVK	0.00	AluSz	0.01
DNA/hAT-Blackjack	0.00	L2c	0.01

E

Ontology	Term	FDR Q-val
GO Biological Process	RNA processing	64.87
GO Biological Process	ncRNA metabolic process	59.89
GO Biological Process	ncRNA processing	48.68
GO Biological Process	ribonucleoprotein complex biogenesis	47.69
GO Biological Process	ribosome biogenesis	46.31
GO Biological Process	rRNA processing	41.82
GO Biological Process	rRNA metabolic process	41.75
GO Biological Process	RNA splicing, via transesterification reactions	30.96
GO Biological Process	mRNA splicing, via spliceosome	30.43
GO Biological Process	translation	28.27
GO Biological Process	nuclear-transcribed mRNA catabolic process, nonsense-mediated decay	27.70
GO Biological Process	viral gene expression	25.85
GO Biological Process	multi-organism metabolic process	25.86
GO Biological Process	nuclear-transcribed mRNA catabolic process	25.84
GO Biological Process	RNA catabolic process	25.63
GO Biological Process	mRNA catabolic process	25.48
GO Biological Process	peptide biosynthetic process	24.31
GO Biological Process	translational initiation	23.99
GO Biological Process	protein targeting to ER	23.19
GO Biological Process	viral transcription	22.68
Human Phenotype	Increased serum lactate	13.38
Human Phenotype	Abnormal CSF metabolite level	9.68
Human Phenotype	Abnormal CNS myelination	9.59
Human Phenotype	Increased CSF lactate	9.02
Human Phenotype	Exercise intolerance	8.96
Human Phenotype	Lactic acidosis	8.96
Human Phenotype	Leukodystrophy	6.58
Human Phenotype	Abnormality of the mitochondrion	6.55
Human Phenotype	Abnormality of mitochondrial metabolism	5.77
Human Phenotype	Decreased activity of mitochondrial respiratory chain	4.02
Human Phenotype	Abnormal mitochondria in muscle tissue	3.79
Human Phenotype	CNS hypomyelination	3.73
Human Phenotype	Progressive microcephaly	2.83
Human Phenotype	Infantile encephalopathy	1.86

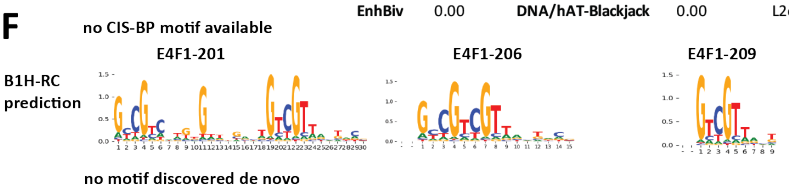

Supplementary Figure 24: Properties and genomic distribution of motifs identified for the E4F1 transcription factor in GM12878 (accession ENCSR439WAF).

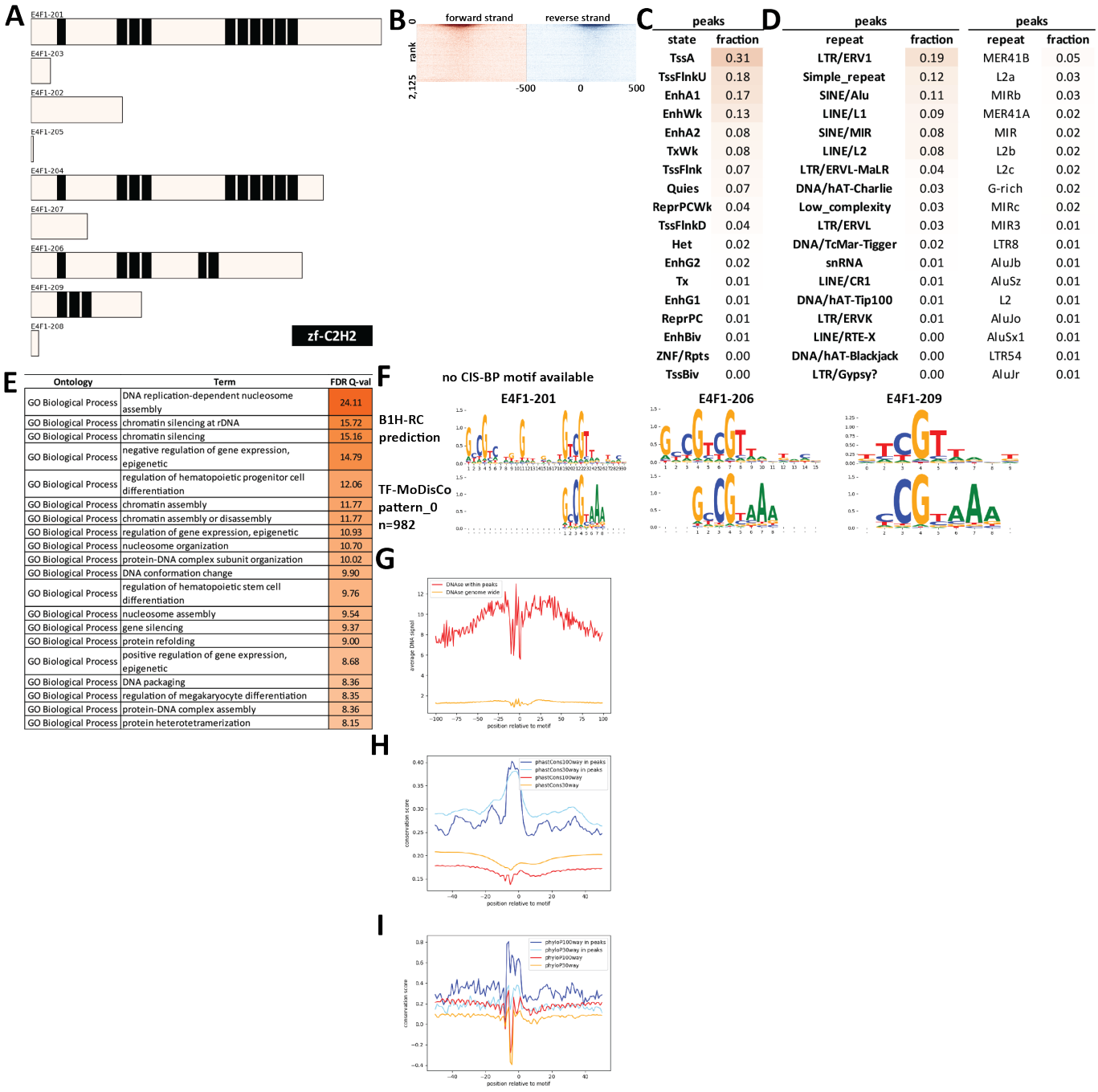

peaks		peaks		peaks	
state	fraction	repeat	fraction	repeat	fraction
TssA	0.31	LTR/ERV1	0.19	MER41B	0.05
TssFlnkU	0.18	Simple_repeat	0.12	L2a	0.03
EnhA1	0.17	SINE/Alu	0.11	MIRb	0.03
EnhWk	0.13	LINE/L1	0.09	MER41A	0.02
EnhA2	0.08	SINE/MIR	0.08	MIR	0.02
TxWk	0.08	LINE/L2	0.08	L2b	0.02
TssFlnk	0.07	LTR/ERVL-MaLR	0.04	L2c	0.02
Quies	0.07	DNA/hAT-Charlie	0.03	G-rich	0.02
ReprPCWk	0.04	Low_complexity	0.03	MIRc	0.02
TssFlnkD	0.04	LTR/ERVL	0.03	MIR3	0.01
Het	0.02	DNA/TcMar-Tigger	0.02	LTR8	0.01
EnhG2	0.02	snRNA	0.01	AluJb	0.01
Tx	0.01	LINE/CR1	0.01	AluSz	0.01
EnhG1	0.01	DNA/hAT-Tip100	0.01	L2	0.01
ReprPC	0.01	LTR/ERVK	0.01	AluJo	0.01
EnhBiv	0.01	LINE/RTE-X	0.00	AluSx1	0.01
ZNF/Rpts	0.00	DNA/hAT-Blackjack	0.00	LTR54	0.01
TssBiv	0.00	LTR/Gypsy?	0.00	AluJr	0.01

Ontology	Term	FDR Q-val
GO Biological Process	DNA replication-dependent nucleosome assembly	24.11
GO Biological Process	chromatin silencing at rDNA	15.72
GO Biological Process	chromatin silencing	15.16
GO Biological Process	negative regulation of gene expression, epigenetic	14.79
GO Biological Process	regulation of hematopoietic progenitor cell differentiation	12.06
GO Biological Process	chromatin assembly	11.77
GO Biological Process	chromatin assembly or disassembly	11.77
GO Biological Process	regulation of gene expression, epigenetic	10.93
GO Biological Process	nucleosome organization	10.70
GO Biological Process	protein-DNA complex subunit organization	10.02
GO Biological Process	DNA conformation change	9.90
GO Biological Process	regulation of hematopoietic stem cell differentiation	9.76
GO Biological Process	nucleosome assembly	9.54
GO Biological Process	gene silencing	9.37
GO Biological Process	protein refolding	9.00
GO Biological Process	positive regulation of gene expression, epigenetic	8.68
GO Biological Process	DNA packaging	8.36
GO Biological Process	regulation of megakaryocyte differentiation	8.35
GO Biological Process	protein-DNA complex assembly	8.36
GO Biological Process	protein heterotetramerization	8.15

Supplementary Figure 25: Properties and genomic distribution of motifs identified for the E4F1 transcription factor in K562 (accession ENCSR003GUC).

TF-MoDisCO pattern_0 n=982, CWM

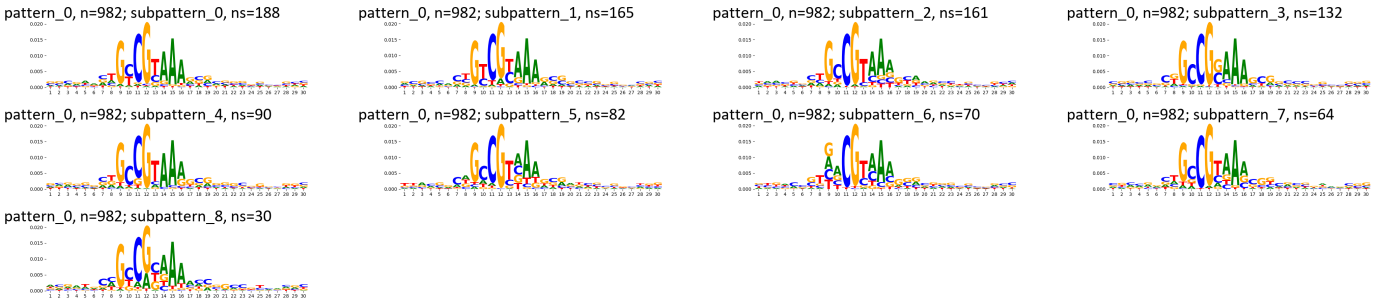

TF-MoDisCO pattern_0 n=982, PWM

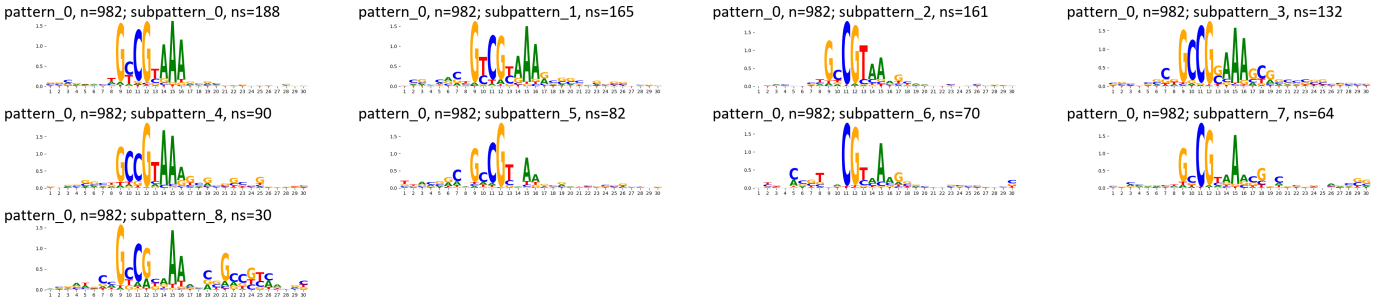

Supplementary Figure 26: TF-MoDisCO subpatterns for the E4F1 transcription factor in K562 (accession ENCSR003GUC).

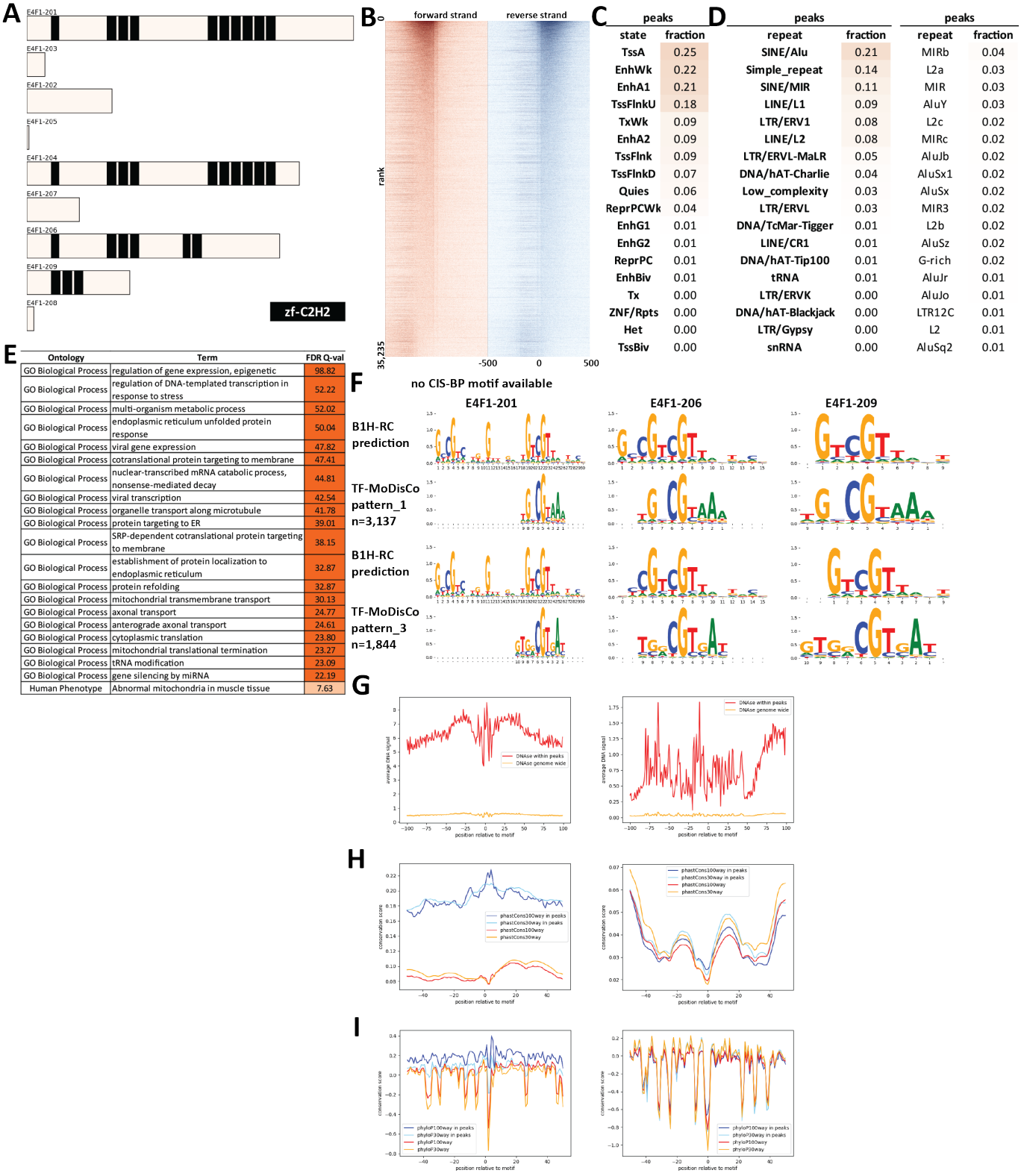

Supplementary Figure 27: Properties and genomic distribution of motifs identified for the E4F1 transcription factor in K562 (accession ENCSR731LHZ).

TF-MoDisCO pattern_1 n=3137, CWM

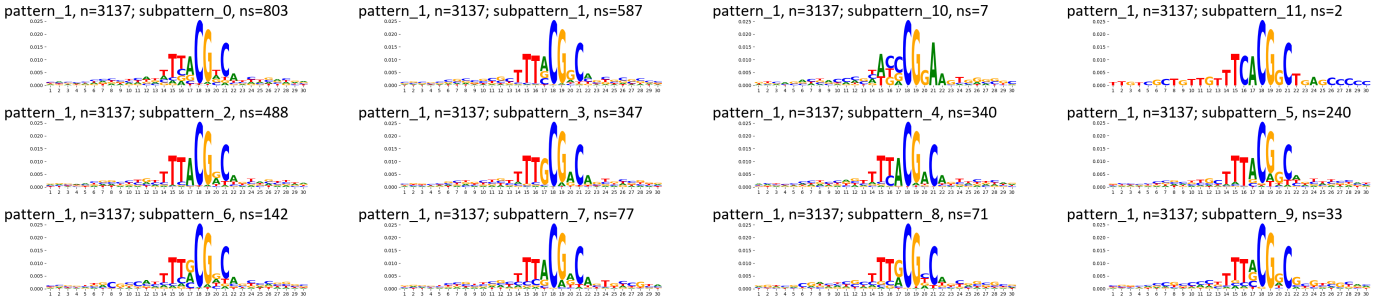

TF-MoDisCO pattern_1 n=3137, PWM

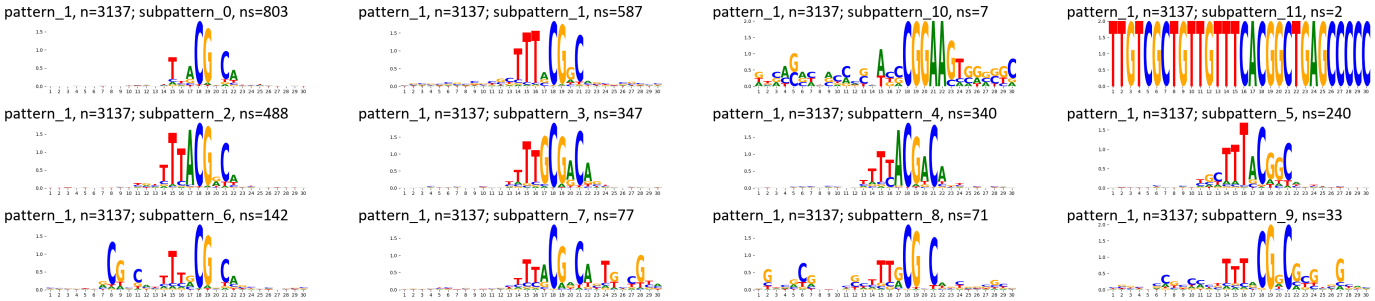

TF-MoDisCO pattern_3 n=1844, CWM

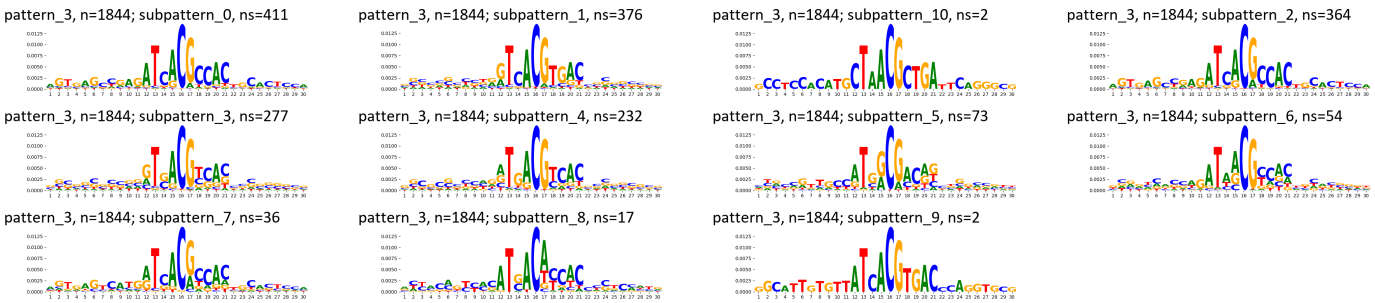

TF-MoDisCO pattern_3 n=1844, PWM

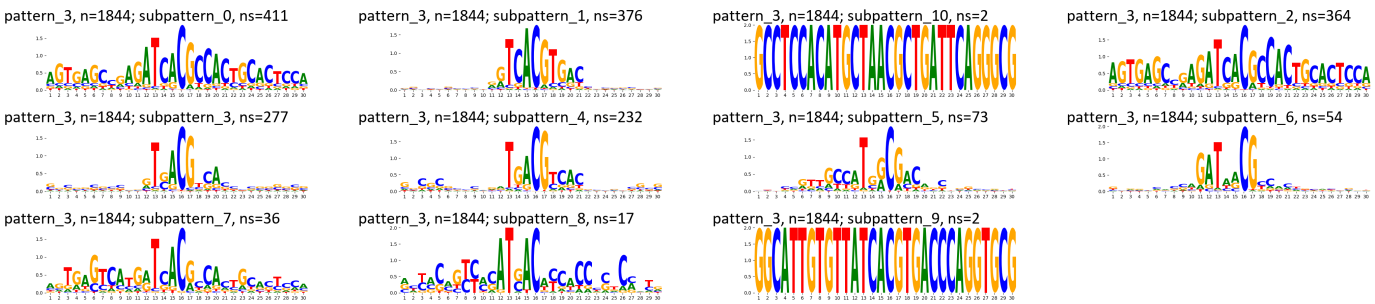

Supplementary Figure 28: TF-MoDisCO subpatterns for the E4F1 transcription factor in K562 (accession ENCSR731LHZ).

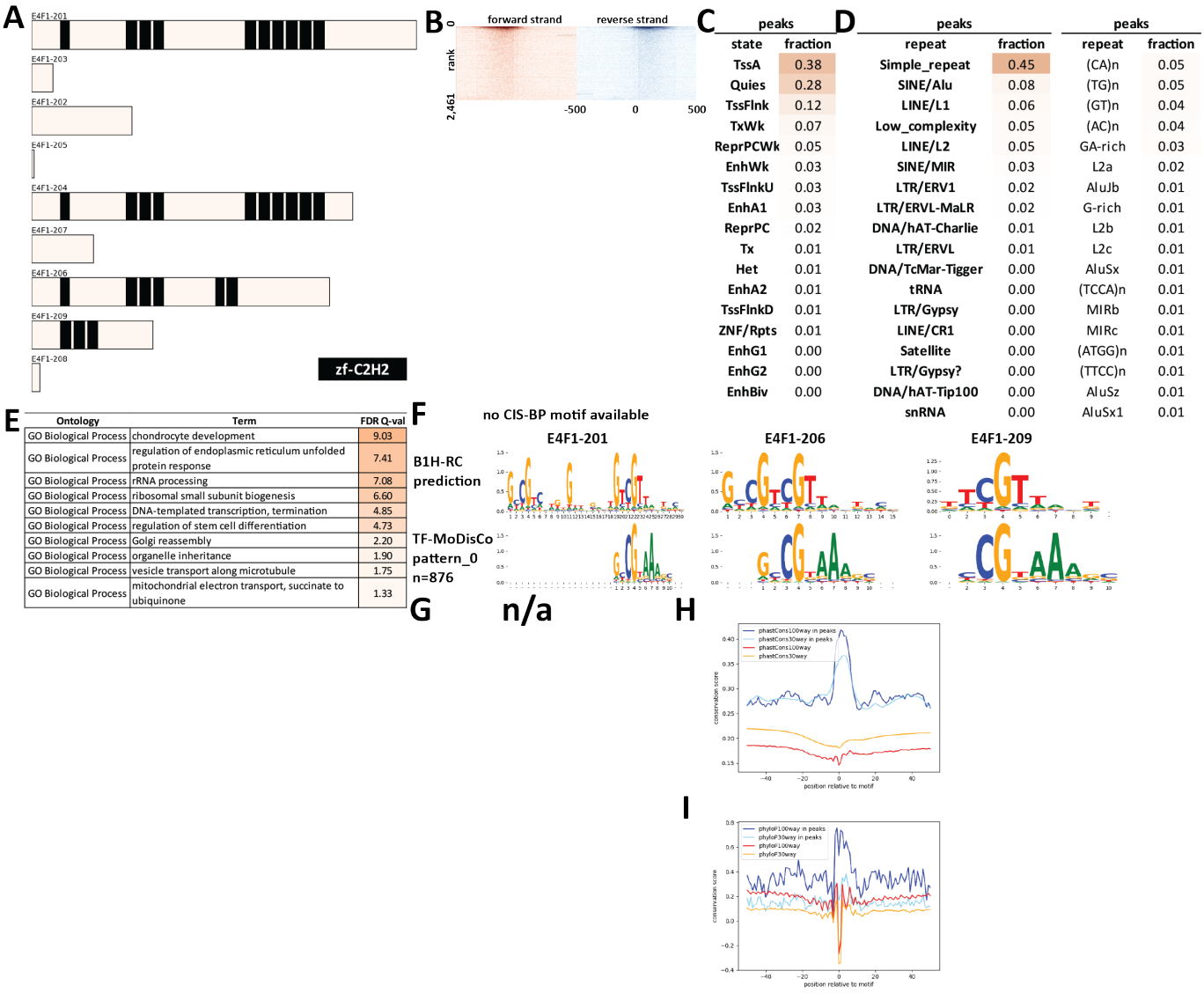

Supplementary Figure 29: Properties and genomic distribution of motifs identified for the E4F1 transcription factor in MCF-7 (accession ENCSR841YWU).

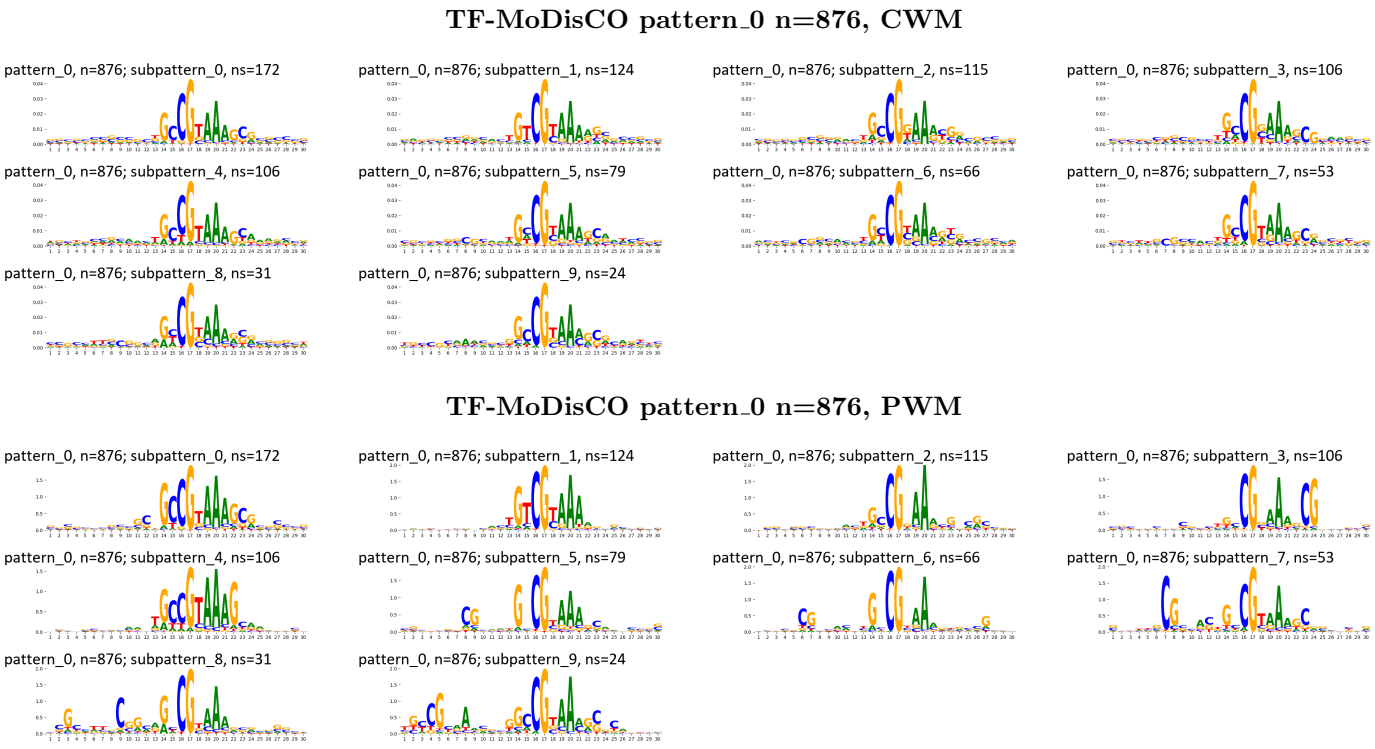

Supplementary Figure 30: TF-MoDisCO subpatterns for the E4F1 transcription factor in MCF-7 (accession ENCSR841YWU).

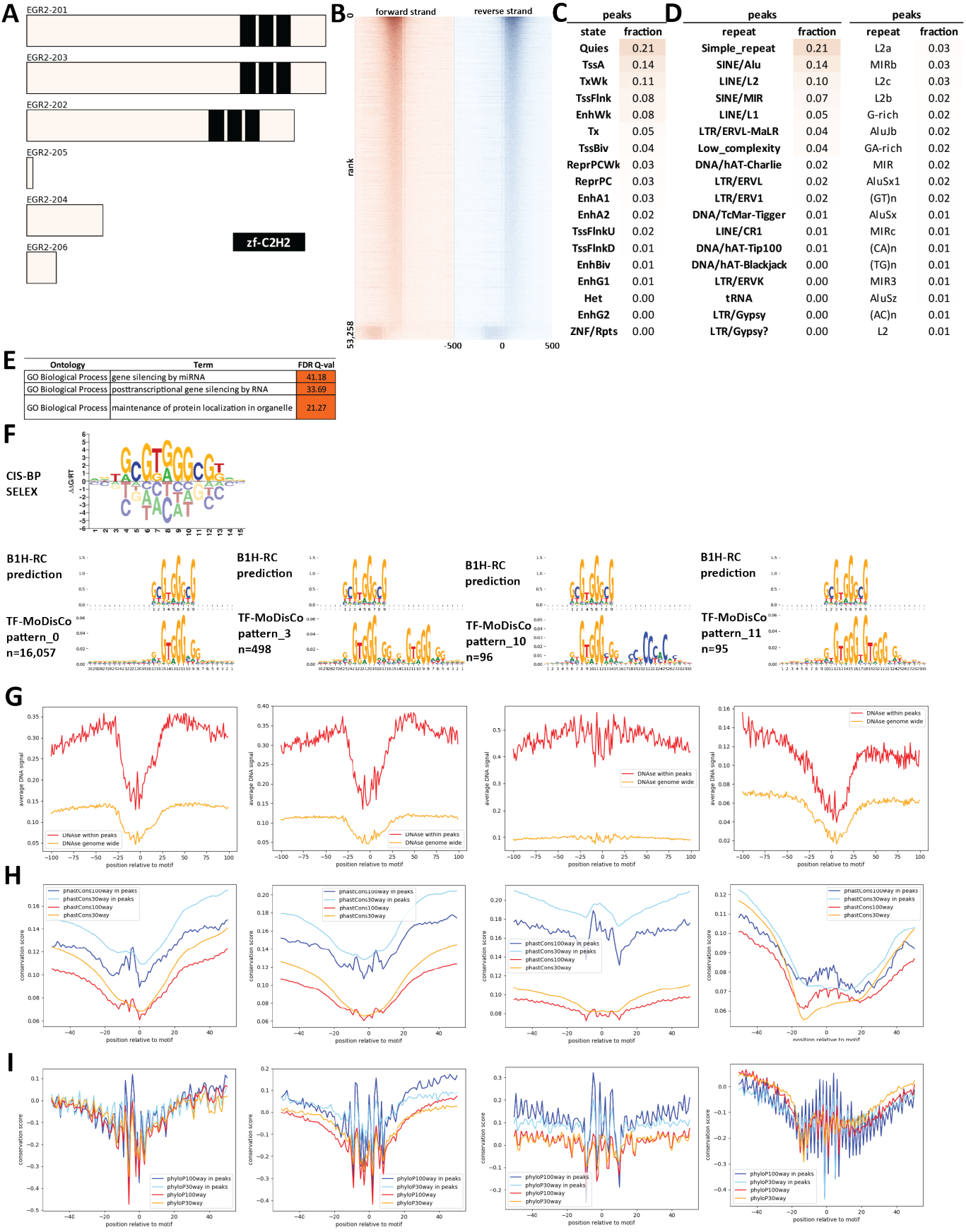

peaks	
state	fraction
Quies	0.21
TssA	0.14
TxWk	0.11
TssFlnk	0.08
EnhWk	0.08
Tx	0.05
TssBiv	0.04
ReprPCWk	0.03
ReprPC	0.03
EnhA1	0.03
EnhA2	0.02
TssFlnkU	0.02
TssFlnkD	0.01
EnhBiv	0.01
EnhG1	0.01
Het	0.00
EnhG2	0.00
ZNF/Rpts	0.00

peaks		peaks	
repeat	fraction	repeat	fraction
Simple_repeat	0.21	L2a	0.03
SINE/Alu	0.14	MIRb	0.03
LINE/L2	0.10	L2c	0.03
SINE/MIR	0.07	L2b	0.02
LINE/L1	0.05	G-rich	0.02
LTR/ERVL-MaLR	0.04	AluJb	0.02
Low_complexity	0.04	GA-rich	0.02
DNA/hAT-Charlie	0.02	MIR	0.02
LTR/ERVL	0.02	AluSx1	0.02
LTR/ERV1	0.02	(GT)n	0.02
DNA/TcMar-Tigger	0.01	AluSx	0.01
LINE/CR1	0.01	MIRc	0.01
DNA/hAT-Tip100	0.01	(CA)n	0.01
DNA/hAT-Blackjack	0.00	(TG)n	0.01
LTR/ERVK	0.00	MIR3	0.01
tRNA	0.00	AluSz	0.01
LTR/Gypsy	0.00	(AC)n	0.01
LTR/Gypsy?	0.00	L2	0.01

Ontology	Term	FDR Q-val
GO Biological Process	gene silencing by miRNA	41.18
GO Biological Process	posttranscriptional gene silencing by RNA	33.69
GO Biological Process	maintenance of protein localization in organelle	21.27

Supplementary Figure 31: Properties and genomic distribution of motifs identified for the EGR2 transcription factor in HEK293 (accession ENCSR919CZU).

TF-MoDisCO pattern_0 n=16057, CWM

pattern_0, n=16057; subpattern_0, ns=1975

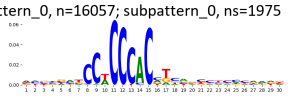

pattern_0, n=16057; subpattern_1, ns=1968

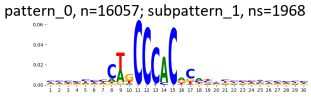

pattern_0, n=16057; subpattern_10, ns=641

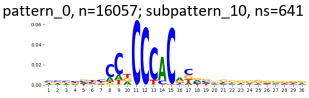

pattern_0, n=16057; subpattern_11, ns=510

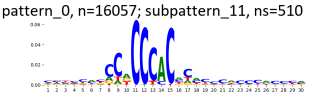

pattern_0, n=16057; subpattern_12, ns=391

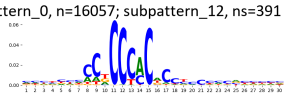

pattern_0, n=16057; subpattern_13, ns=375

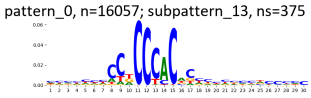

pattern_0, n=16057; subpattern_14, ns=266

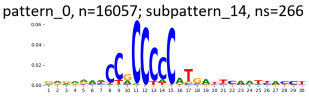

pattern_0, n=16057; subpattern_2, ns=1928

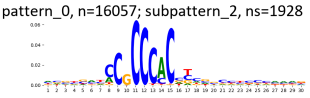

pattern_0, n=16057; subpattern_3, ns=1791

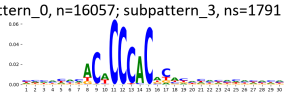

pattern_0, n=16057; subpattern_4, ns=1667

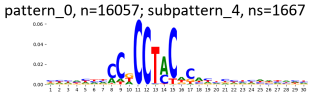

pattern_0, n=16057; subpattern_5, ns=1296

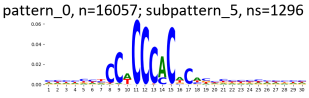

pattern_0, n=16057; subpattern_6, ns=872

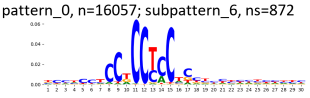

pattern_0, n=16057; subpattern_7, ns=855

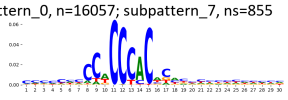

pattern_0, n=16057; subpattern_8, ns=846

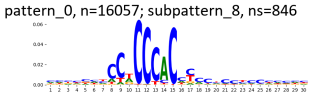

pattern_0, n=16057; subpattern_9, ns=676

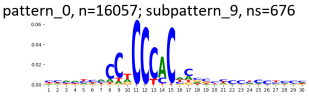

TF-MoDisCO pattern_0 n=16057, PWM

pattern_0, n=16057; subpattern_0, ns=1975

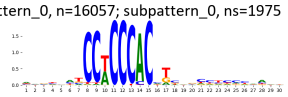

pattern_0, n=16057; subpattern_1, ns=1968

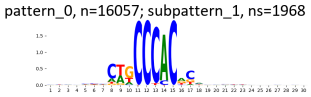

pattern_0, n=16057; subpattern_10, ns=641

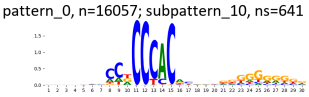

pattern_0, n=16057; subpattern_11, ns=510

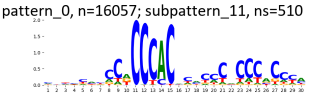

pattern_0, n=16057; subpattern_12, ns=391

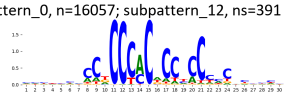

pattern_0, n=16057; subpattern_13, ns=375

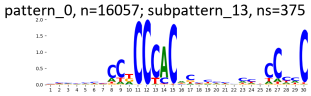

pattern_0, n=16057; subpattern_14, ns=266

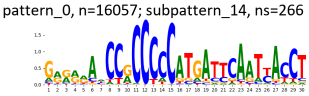

pattern_0, n=16057; subpattern_2, ns=1928

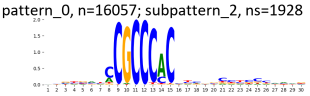

pattern_0, n=16057; subpattern_3, ns=1791

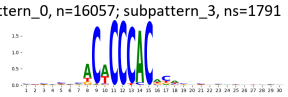

pattern_0, n=16057; subpattern_4, ns=1667

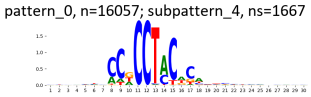

pattern_0, n=16057; subpattern_5, ns=1296

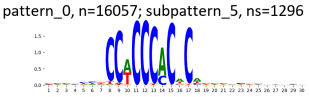

pattern_0, n=16057; subpattern_6, ns=872

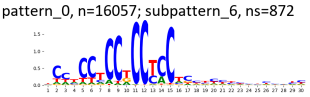

pattern_0, n=16057; subpattern_7, ns=855

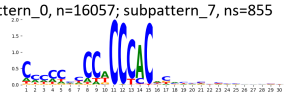

pattern_0, n=16057; subpattern_8, ns=846

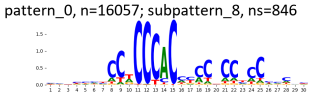

pattern_0, n=16057; subpattern_9, ns=676

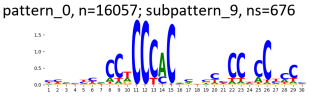

TF-MoDisCO pattern_10 n=96, CWM

pattern_10, n=96; subpattern_0, ns=28

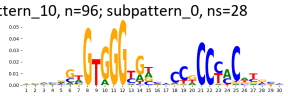

pattern_10, n=96; subpattern_1, ns=27

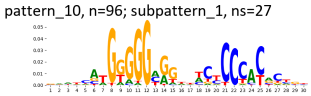

pattern_10, n=96; subpattern_2, ns=18

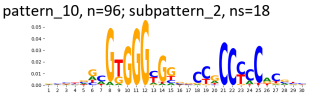

pattern_10, n=96; subpattern_3, ns=13

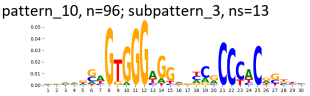

pattern_10, n=96; subpattern_4, ns=10

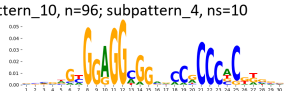

TF-MoDisCO pattern_10 n=96, PWM

pattern_10, n=96; subpattern_0, ns=28

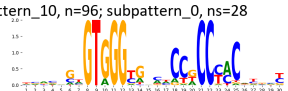

pattern_10, n=96; subpattern_1, ns=27

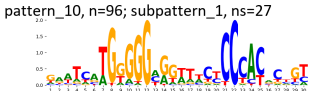

pattern_10, n=96; subpattern_2, ns=18

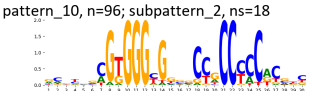

pattern_10, n=96; subpattern_3, ns=13

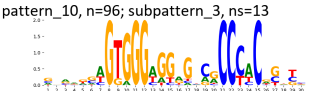

pattern_10, n=96; subpattern_4, ns=10

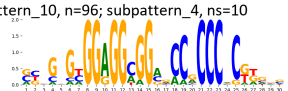

TF-MoDisCO pattern_11 n=95, CWM

pattern_11, n=95; subpattern_0, ns=35

pattern_11, n=95; subpattern_1, ns=35

pattern_11, n=95; subpattern_2, ns=25

TF-MoDisCO pattern_11 n=95, PWM

pattern_11, n=95; subpattern_0, ns=35

pattern_11, n=95; subpattern_1, ns=35

pattern_11, n=95; subpattern_2, ns=25

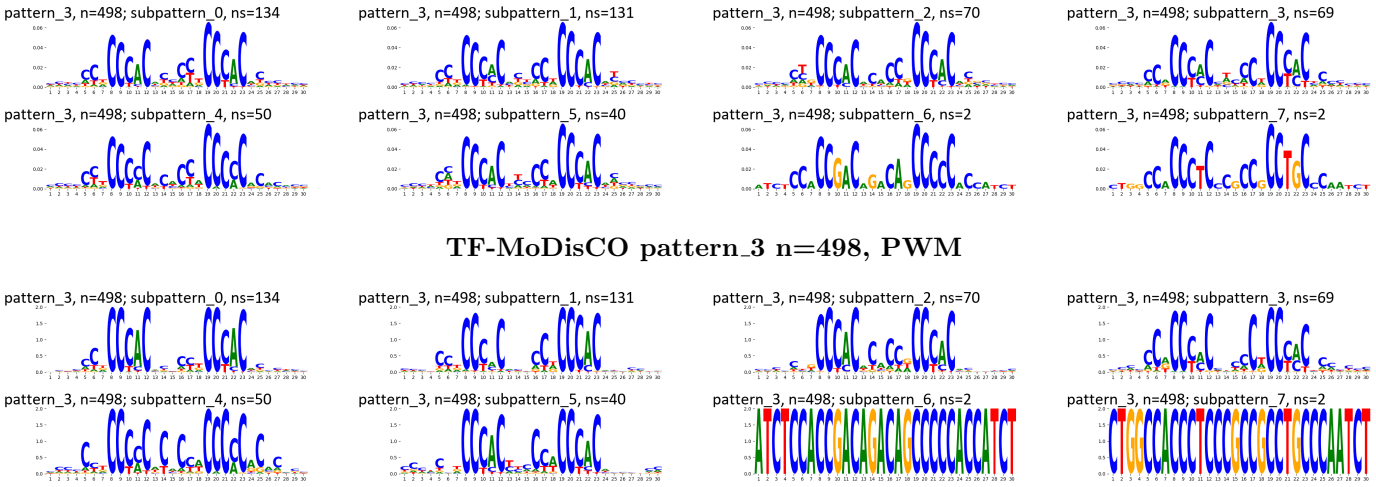

Supplementary Figure 32: TF-MoDisCO subpatterns for the EGR2 transcription factor in HEK293 (accession ENCSR919CZU).

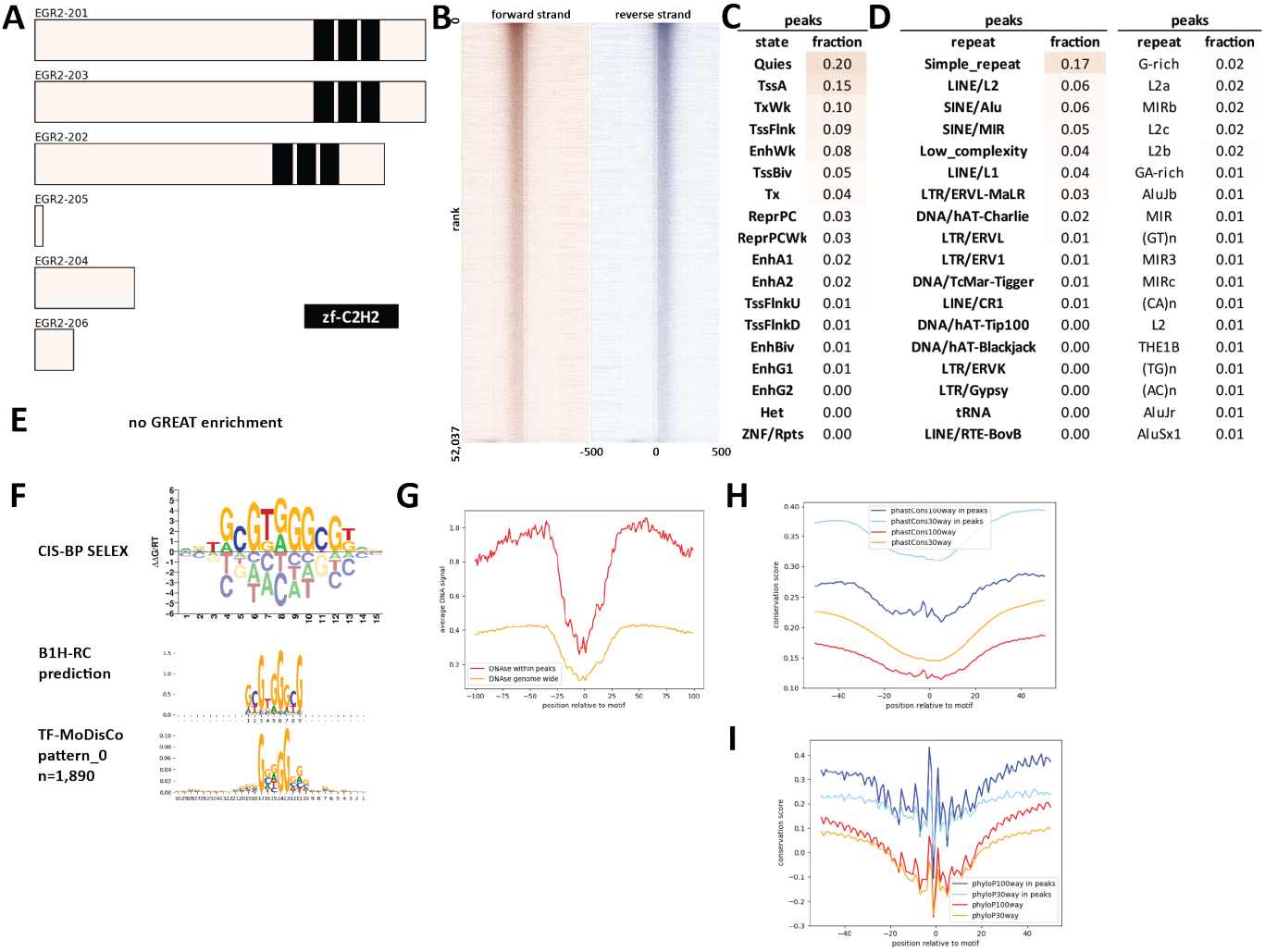

Supplementary Figure 33: Properties and genomic distribution of motifs identified for the EGR2 transcription factor in HEK293 (accession Hughes GR models).

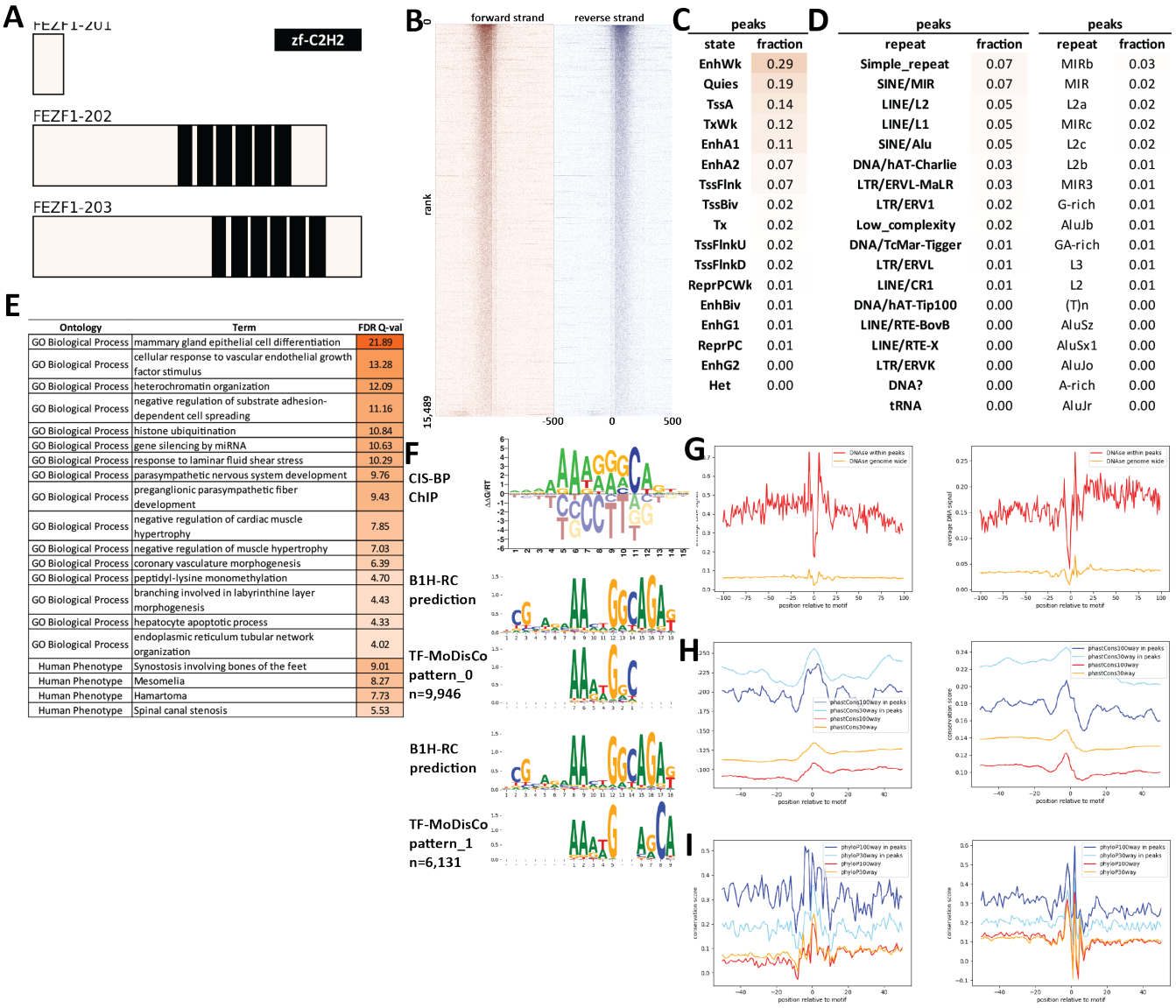

C

peaks	
state	fraction
EnhWk	0.29
Quies	0.19
TssA	0.14
TxWk	0.12
EnhA1	0.11
EnhA2	0.07
TssFlnk	0.07
TssBiv	0.02
Tx	0.02
TssFlnkU	0.02
TssFlnkD	0.02
ReprPCWk	0.01
EnhBiv	0.01
EnhG1	0.01
ReprPC	0.01
EnhG2	0.00
Het	0.00

D

peaks		peaks	
repeat	fraction	repeat	fraction
Simple_repeat	0.07	MIRb	0.03
SINE/MIR	0.07	MIR	0.02
LINE/L2	0.05	L2a	0.02
LINE/L1	0.05	MIRc	0.02
SINE/Alu	0.05	L2c	0.02
DNA/hAT-Charlie	0.03	L2b	0.01
LTR/ERVL-MaLR	0.03	MIR3	0.01
LTR/ERV1	0.02	G-rich	0.01
Low_complexity	0.02	AluJb	0.01
DNA/TcMar-Tigger	0.01	GA-rich	0.01
LTR/ERVL	0.01	L3	0.01
LINE/CR1	0.01	L2	0.01
DNA/hAT-Tip100	0.00	(T)n	0.00
LINE/RTE-BovB	0.00	AluSz	0.00
LINE/RTE-X	0.00	AluSx1	0.00
LTR/ERVK	0.00	AluJo	0.00
DNA?	0.00	A-rich	0.00
tRNA	0.00	AluJr	0.00

E

Ontology	Term	FDR Q-val
GO Biological Process	mammary gland epithelial cell differentiation	21.89
GO Biological Process	cellular response to vascular endothelial growth factor stimulus	13.28
GO Biological Process	heterochromatin organization	12.09
GO Biological Process	negative regulation of substrate adhesion-dependent cell spreading	11.16
GO Biological Process	histone ubiquitination	10.84
GO Biological Process	gene silencing by miRNA	10.63
GO Biological Process	response to laminar fluid shear stress	10.29
GO Biological Process	parasympathetic nervous system development	9.76
GO Biological Process	preganglionic parasympathetic fiber development	9.43
GO Biological Process	negative regulation of cardiac muscle hypertrophy	7.85
GO Biological Process	negative regulation of muscle hypertrophy	7.03
GO Biological Process	coronary vasculature morphogenesis	6.39
GO Biological Process	peptidyl-lysine monomethylation	4.70
GO Biological Process	branching involved in labyrinthine layer morphogenesis	4.43
GO Biological Process	hepatocyte apoptotic process	4.33
GO Biological Process	endoplasmic reticulum tubular network organization	4.02
Human Phenotype	Synostosis involving bones of the feet	9.01
Human Phenotype	Mesomelia	8.27
Human Phenotype	Hamartoma	7.73
Human Phenotype	Spinal canal stenosis	5.53

Supplementary Figure 34: Properties and genomic distribution of motifs identified for the FEZF1 transcription factor in HEK293 (accession Hughes GR models).

TF-MoDisCO pattern_0 n=9946, CWM

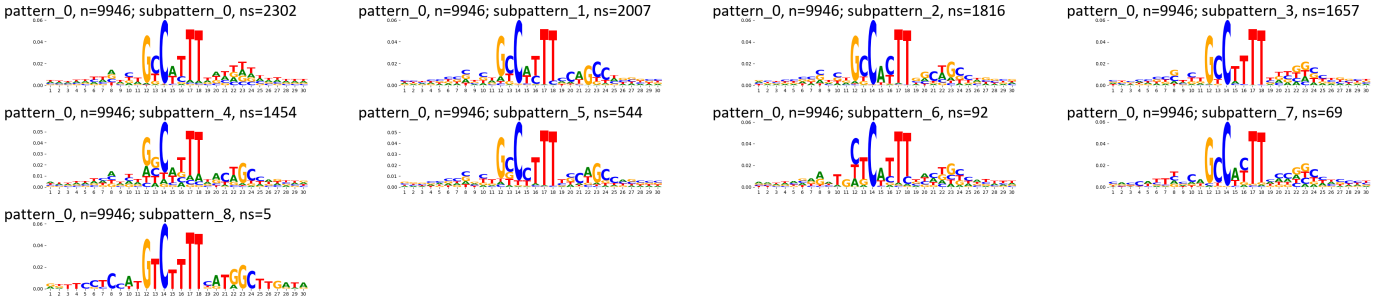

TF-MoDisCO pattern_0 n=9946, PWM

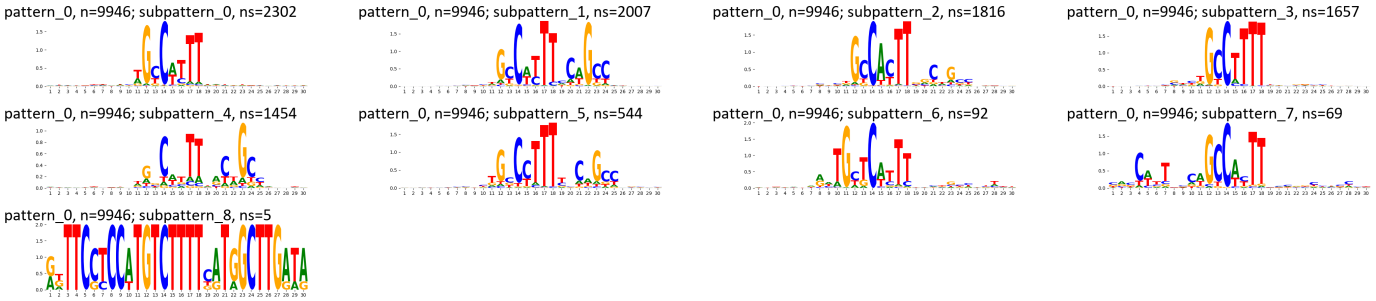

TF-MoDisCO pattern_1 n=6131, CWM

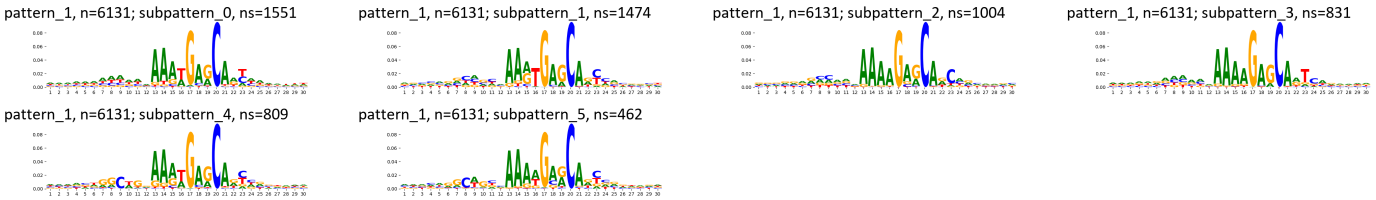

TF-MoDisCO pattern_1 n=6131, PWM

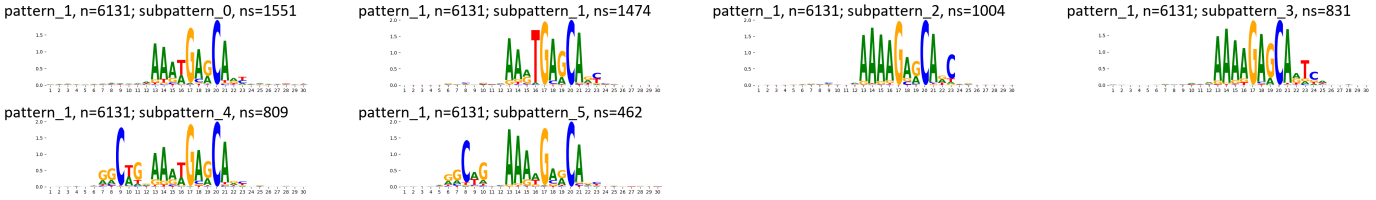

Supplementary Figure 35: TF-MoDisCO subpatterns for the FEZF1 transcription factor in HEK293 (accession Hughes GR models).

A

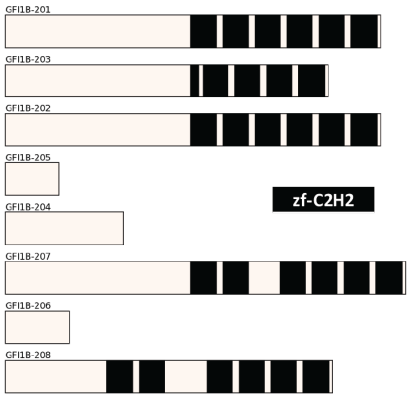

B

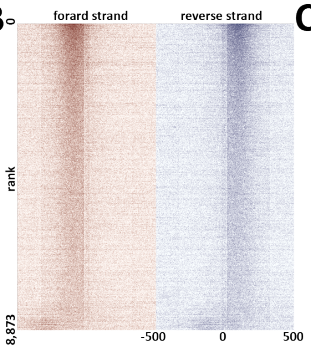

C

peaks	
state	fraction
EnhWk	0.28
Quies	0.18
TssA	0.17
EnhA1	0.13
TxWk	0.11
EnhA2	0.10
TssFlnk	0.07
TssFlnkU	0.02
TssBiv	0.02
Tx	0.02
TssFlnkD	0.02
EnhBiv	0.02
ReprPCWk	0.01
EnhG1	0.01
ReprPC	0.01
Het	0.00
EnhG2	0.00
ZNF/Rpts	0.00

D

peaks		peaks	
repeat	fraction	repeat	fraction
SINE/Alu	0.23	(AAAT)n	0.03
Simple_repeat	0.17	MIRb	0.03
SINE/MIR	0.08	AluJb	0.03
LINE/L1	0.06	AluSx	0.03
LINE/L2	0.06	AluSx1	0.03
DNA/hAT-Charlie	0.03	AluSz	0.02
LTR/ERVL-MaLR	0.02	MIR	0.02
LTR/ERV1	0.02	L2a	0.02
Low_complexity	0.02	L2c	0.02
DNA/TcMar-Tigger	0.02	AluJr	0.02
LTR/ERVL	0.01	AluY	0.02
tRNA	0.01	AluJo	0.01
LINE/CR1	0.01	MIRc	0.01
DNA/hAT-Tip100	0.00	L2b	0.01
snRNA	0.00	MIR3	0.01
LINE/RTE-X	0.00	(GT)n	0.01
LTR/ERVK	0.00	AluSz6	0.01
DNA/hAT-Blackjack	0.00	AluSq2	0.01

E

Ontology	Term	FDR Q-val
GO Biological Process	adherens junction assembly	17.34
GO Biological Process	mammary gland epithelial cell differentiation	15.49
GO Biological Process	mesoderm formation	14.92
GO Biological Process	positive regulation of epithelial to mesenchymal transition	14.05
GO Biological Process	interferon-gamma secretion	12.50
GO Biological Process	DNA damage response, detection of DNA damage	10.15
GO Biological Process	thyroid gland development	9.49
GO Biological Process	positive regulation of stem cell differentiation	9.46
GO Biological Process	metanephric mesenchyme development	8.59
GO Biological Process	response to laminar fluid shear stress	8.54
GO Biological Process	positive regulation of mesonephros development	8.39
GO Biological Process	membrane raft assembly	8.12
GO Biological Process	kidney mesenchyme development	7.69
GO Biological Process	mesodermal cell differentiation	7.69
GO Biological Process	diaphragm development	7.56
GO Biological Process	cell proliferation in hindbrain	6.67
GO Biological Process	negative regulation of cyclin-dependent protein serine/threonine kinase activity	6.67
GO Biological Process	membrane raft organization	6.52
GO Biological Process	smooth muscle tissue development	6.49
GO Biological Process	cerebellar granule cell precursor proliferation	6.36
Human Phenotype	Abnormal localization of kidney	9.27
Human Phenotype	Ectopic kidney	5.85
Human Phenotype	Cutis marmorata	5.39
Human Phenotype	Pancreatic islet-cell hyperplasia	4.74
Human Phenotype	Abnormality of the pancreatic islet cells	4.68
Human Phenotype	Absent or minimally ossified vertebral bodies	2.40

F

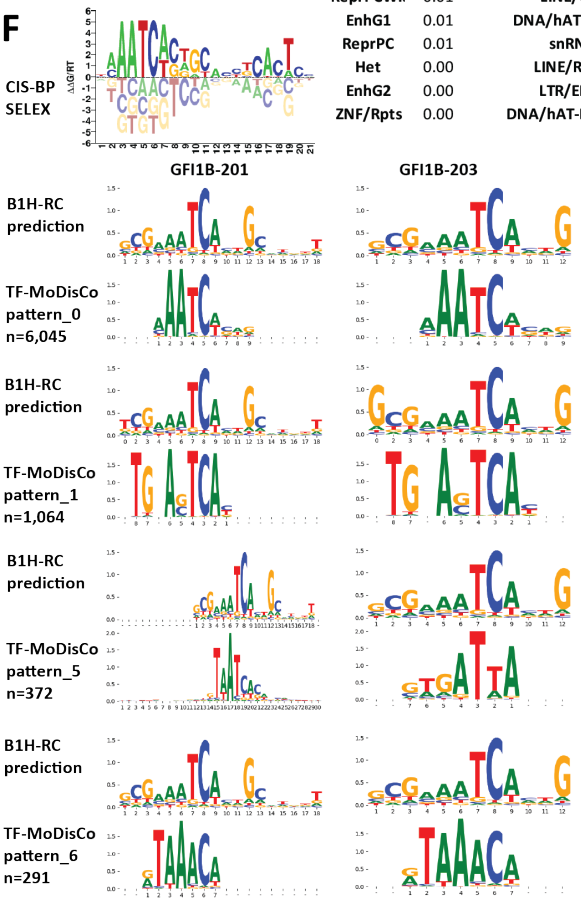

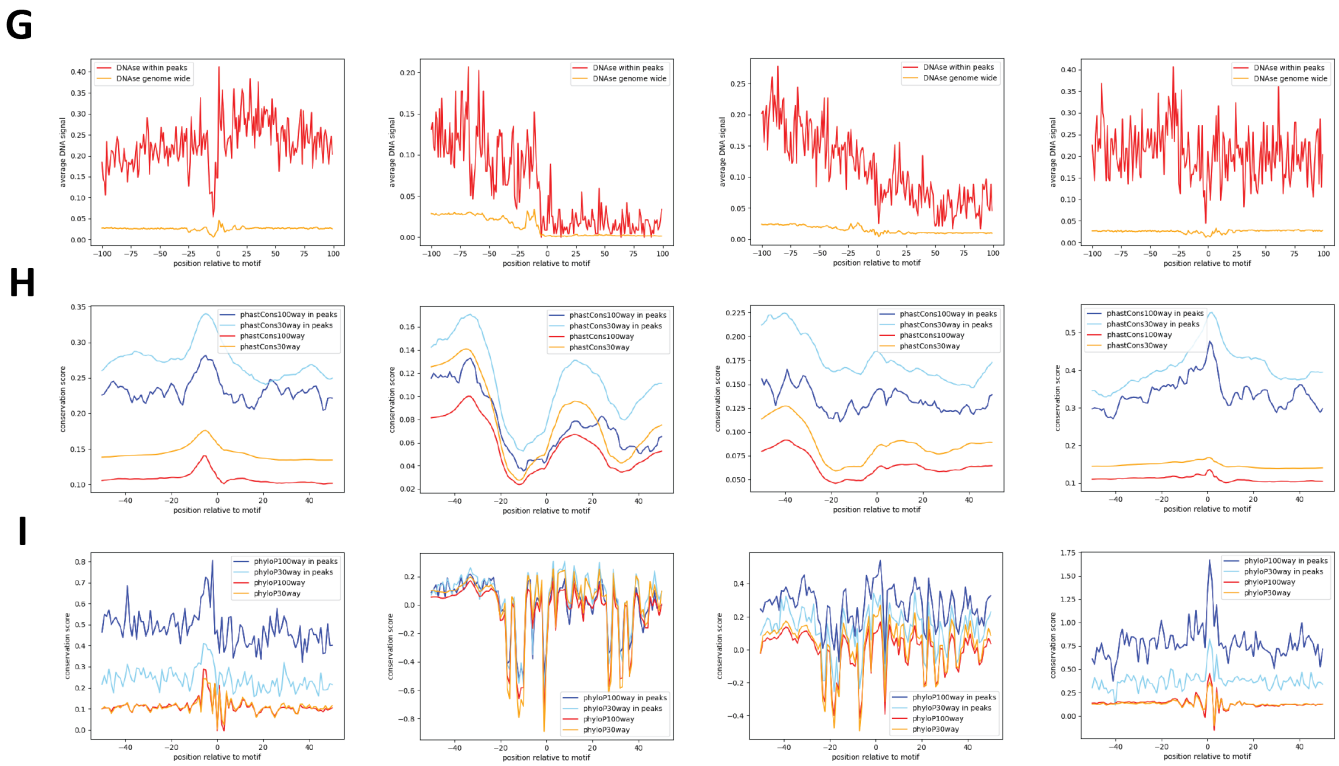

Supplementary Figure 36: Properties and genomic distribution of motifs identified for the GFI1B transcription factor in HEK293 (accession ENCSR445PDR).

TF-MoDisCO pattern_0 n=6045, CWM

pattern_0, n=6045; subpattern_0, ns=1478

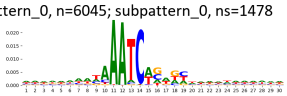

pattern_0, n=6045; subpattern_1, ns=1267

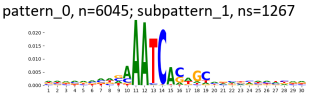

pattern_0, n=6045; subpattern_10, ns=68

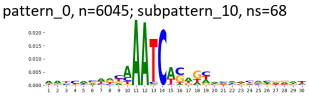

pattern_0, n=6045; subpattern_2, ns=1176

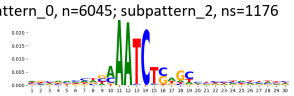

pattern_0, n=6045; subpattern_3, ns=849

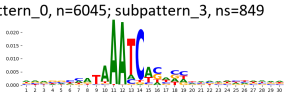

pattern_0, n=6045; subpattern_4, ns=305

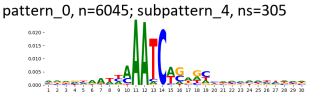

pattern_0, n=6045; subpattern_5, ns=236

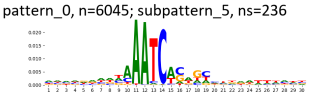

pattern_0, n=6045; subpattern_6, ns=216

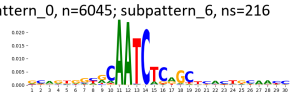

pattern_0, n=6045; subpattern_7, ns=178

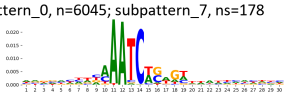

pattern_0, n=6045; subpattern_8, ns=175

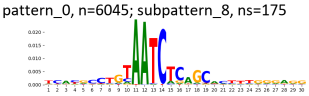

pattern_0, n=6045; subpattern_9, ns=97

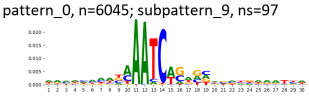

TF-MoDisCO pattern_0 n=6045, PWM

pattern_0, n=6045; subpattern_0, ns=1478

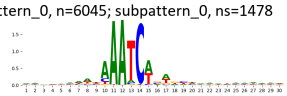

pattern_0, n=6045; subpattern_1, ns=1267

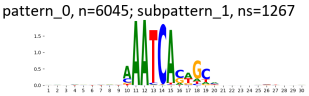

pattern_0, n=6045; subpattern_10, ns=68

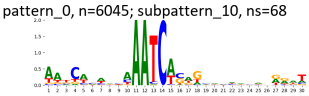

pattern_0, n=6045; subpattern_2, ns=1176

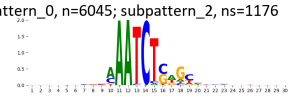

pattern_0, n=6045; subpattern_3, ns=849

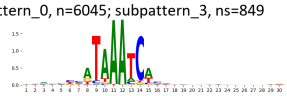

pattern_0, n=6045; subpattern_4, ns=305

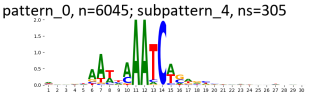

pattern_0, n=6045; subpattern_5, ns=236

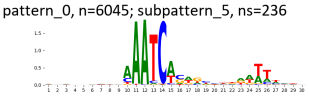

pattern_0, n=6045; subpattern_6, ns=216

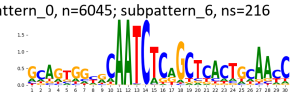

pattern_0, n=6045; subpattern_7, ns=178

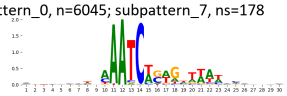

pattern_0, n=6045; subpattern_8, ns=175

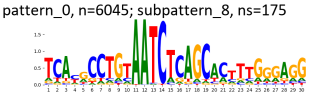

pattern_0, n=6045; subpattern_9, ns=97

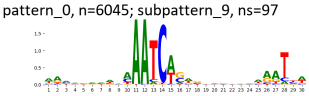

TF-MoDisCO pattern_1 n=1064, CWM

pattern_1, n=1064; subpattern_0, ns=363

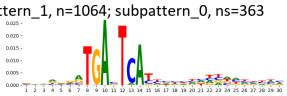

pattern_1, n=1064; subpattern_1, ns=250

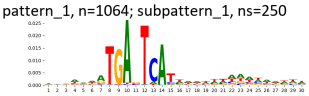

pattern_1, n=1064; subpattern_2, ns=218

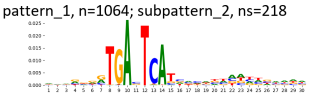

pattern_1, n=1064; subpattern_3, ns=173

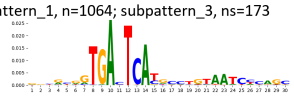

pattern_1, n=1064; subpattern_4, ns=21

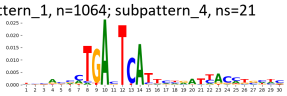

pattern_1, n=1064; subpattern_5, ns=15

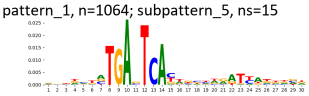

pattern_1, n=1064; subpattern_6, ns=12

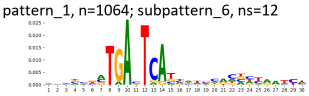

pattern_1, n=1064; subpattern_7, ns=12

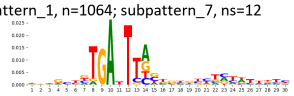

TF-MoDisCO pattern_1 n=1064, PWM

pattern_1, n=1064; subpattern_0, ns=363

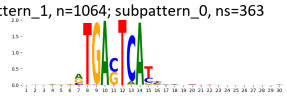

pattern_1, n=1064; subpattern_1, ns=250

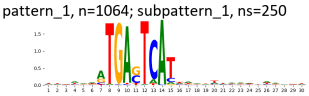

pattern_1, n=1064; subpattern_2, ns=218

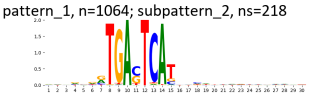

pattern_1, n=1064; subpattern_3, ns=173

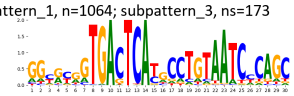

pattern_1, n=1064; subpattern_4, ns=21

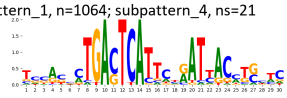

pattern_1, n=1064; subpattern_5, ns=15

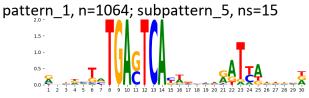

pattern_1, n=1064; subpattern_6, ns=12

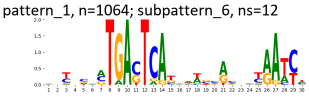

pattern_1, n=1064; subpattern_7, ns=12

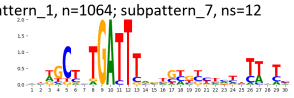

TF-MoDisCO pattern_5 n=372, CWM

pattern_5, n=372; subpattern_0, ns=81

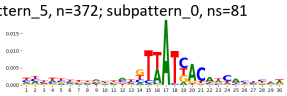

pattern_5, n=372; subpattern_1, ns=78

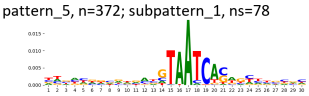

pattern_5, n=372; subpattern_2, ns=69

pattern_5, n=372; subpattern_3, ns=63

pattern_5, n=372; subpattern_4, ns=32

pattern_5, n=372; subpattern_5, ns=25

pattern_5, n=372; subpattern_6, ns=20

pattern_5, n=372; subpattern_7, ns=2

pattern_5, n=372; subpattern_8, ns=2

TF-MoDisCO pattern_5 n=372, PWM

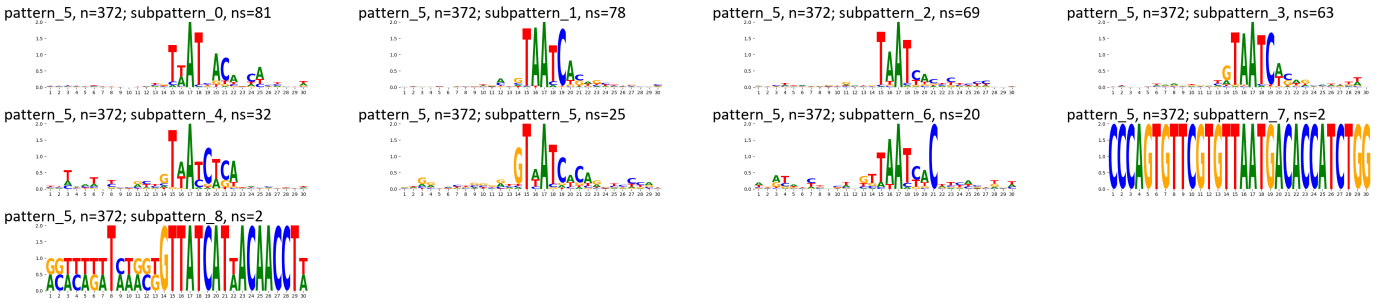

TF-MoDisCO pattern_6 n=291, CWM

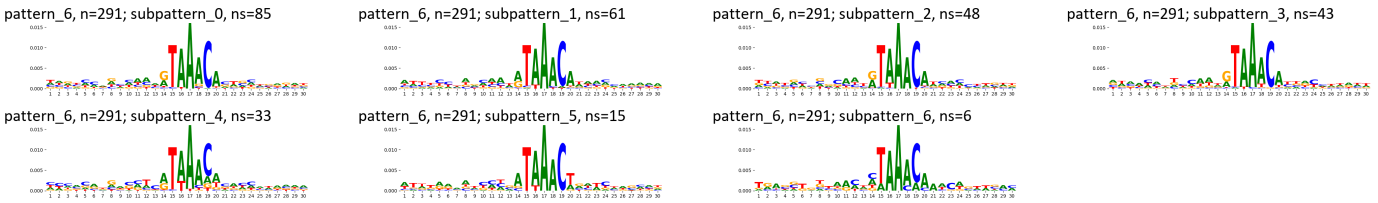

TF-MoDisCO pattern_6 n=291, PWM

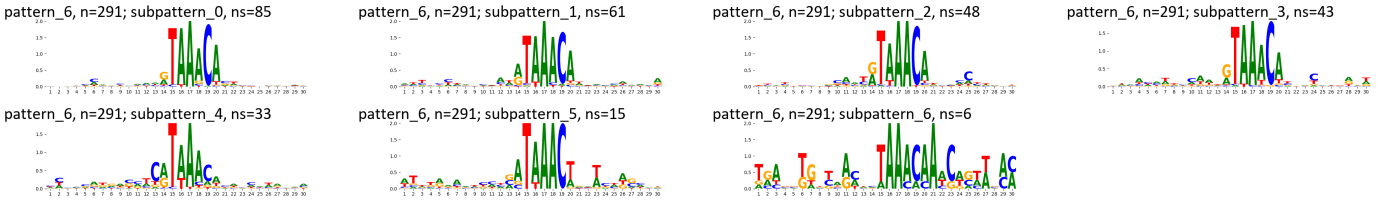

Supplementary Figure 37: TF-MoDisCO subpatterns for the GFI1B transcription factor in HEK293 (accession ENCSR445PDR).

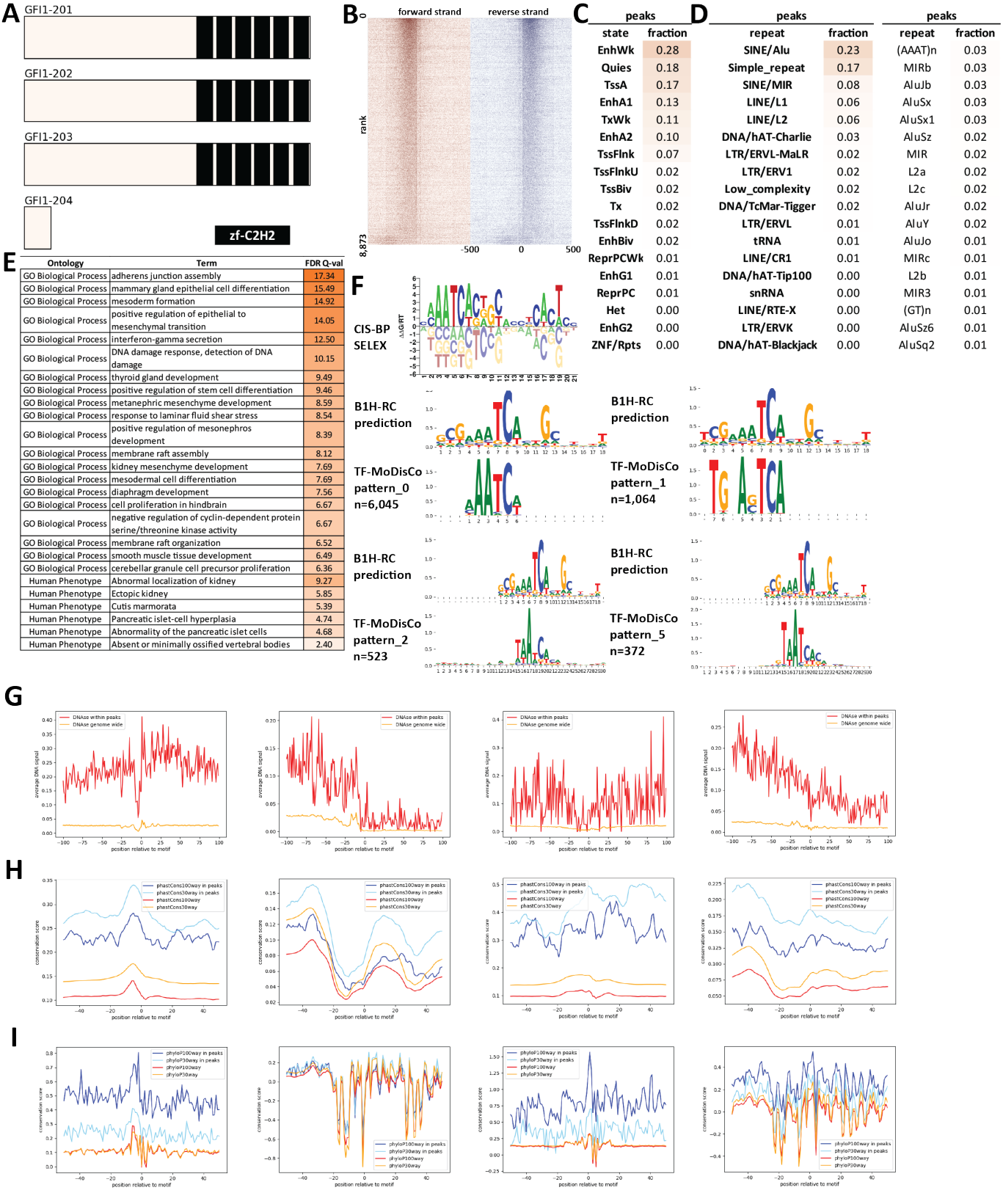

Supplementary Figure 38: Properties and genomic distribution of motifs identified for the GFI1 transcription factor in HEK293 (accession ENCSR445PDR).

TF-MoDisCO pattern_0 n=6045, CWM

pattern_0, n=6045; subpattern_0, ns=1478

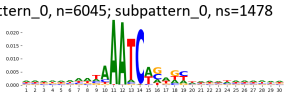

pattern_0, n=6045; subpattern_1, ns=1267

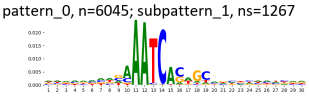

pattern_0, n=6045; subpattern_10, ns=68

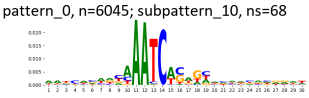

pattern_0, n=6045; subpattern_2, ns=1176

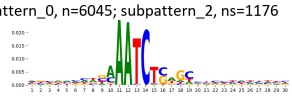

pattern_0, n=6045; subpattern_3, ns=849

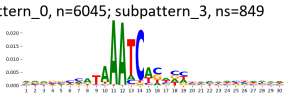

pattern_0, n=6045; subpattern_4, ns=305

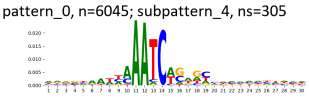

pattern_0, n=6045; subpattern_5, ns=236

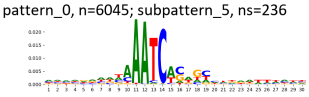

pattern_0, n=6045; subpattern_6, ns=216

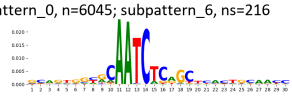

pattern_0, n=6045; subpattern_7, ns=178

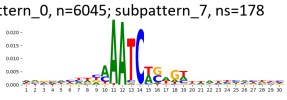

pattern_0, n=6045; subpattern_8, ns=175

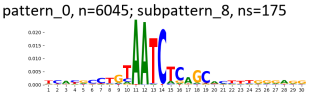

pattern_0, n=6045; subpattern_9, ns=97

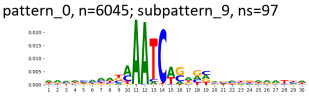

TF-MoDisCO pattern_0 n=6045, PWM

pattern_0, n=6045; subpattern_0, ns=1478

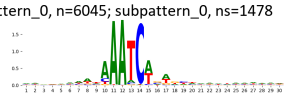

pattern_0, n=6045; subpattern_1, ns=1267

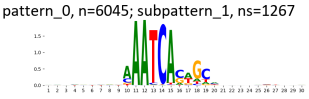

pattern_0, n=6045; subpattern_10, ns=68

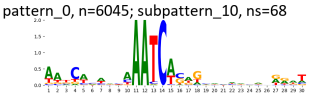

pattern_0, n=6045; subpattern_2, ns=1176

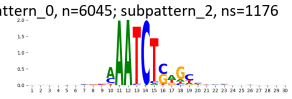

pattern_0, n=6045; subpattern_3, ns=849

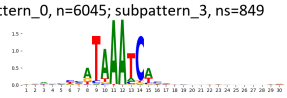

pattern_0, n=6045; subpattern_4, ns=305

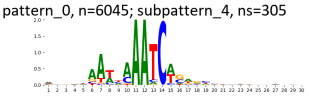

pattern_0, n=6045; subpattern_5, ns=236

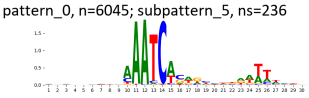

pattern_0, n=6045; subpattern_6, ns=216

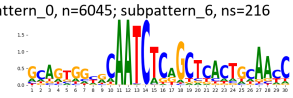

pattern_0, n=6045; subpattern_7, ns=178

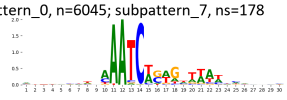

pattern_0, n=6045; subpattern_8, ns=175

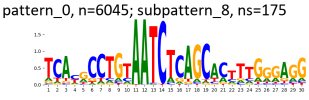

pattern_0, n=6045; subpattern_9, ns=97

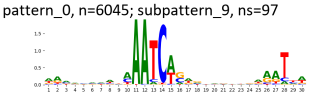

TF-MoDisCO pattern_1 n=1064, CWM

pattern_1, n=1064; subpattern_0, ns=363

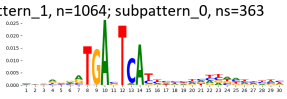

pattern_1, n=1064; subpattern_1, ns=250

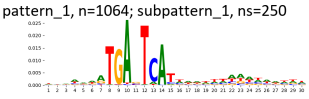

pattern_1, n=1064; subpattern_2, ns=218

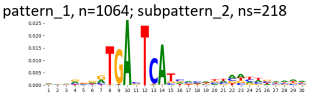

pattern_1, n=1064; subpattern_3, ns=173

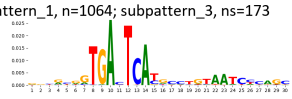

pattern_1, n=1064; subpattern_4, ns=21

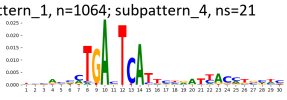

pattern_1, n=1064; subpattern_5, ns=15

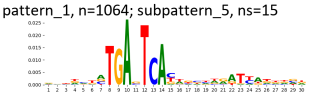

pattern_1, n=1064; subpattern_6, ns=12

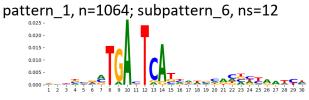

pattern_1, n=1064; subpattern_7, ns=12

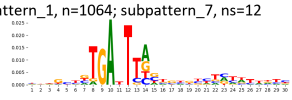

TF-MoDisCO pattern_1 n=1064, PWM

pattern_1, n=1064; subpattern_0, ns=363

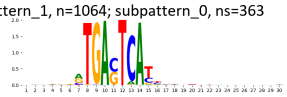

pattern_1, n=1064; subpattern_1, ns=250

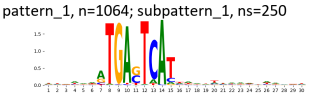

pattern_1, n=1064; subpattern_2, ns=218

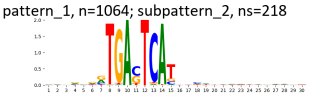

pattern_1, n=1064; subpattern_3, ns=173

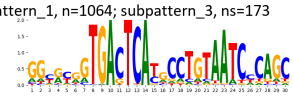

pattern_1, n=1064; subpattern_4, ns=21

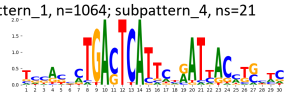

pattern_1, n=1064; subpattern_5, ns=15

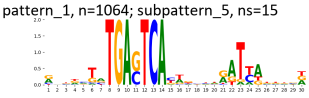

pattern_1, n=1064; subpattern_6, ns=12

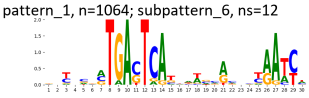

pattern_1, n=1064; subpattern_7, ns=12

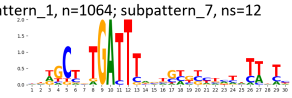

TF-MoDisCO pattern_2 n=523, CWM

pattern_2, n=523; subpattern_0, ns=121

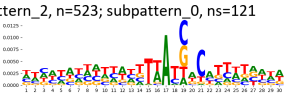

pattern_2, n=523; subpattern_1, ns=93

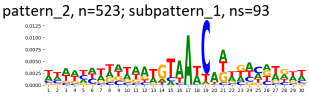

pattern_2, n=523; subpattern_2, ns=90

pattern_2, n=523; subpattern_3, ns=66

pattern_2, n=523; subpattern_4, ns=52

pattern_2, n=523; subpattern_5, ns=40

pattern_2, n=523; subpattern_6, ns=33

pattern_2, n=523; subpattern_7, ns=28

TF-MoDisCO pattern_2 n=523, PWM

pattern_2, n=523; subpattern_0, ns=121

pattern_2, n=523; subpattern_1, ns=93

pattern_2, n=523; subpattern_2, ns=90

pattern_2, n=523; subpattern_3, ns=66

pattern_2, n=523; subpattern_4, ns=52

pattern_2, n=523; subpattern_5, ns=40

pattern_2, n=523; subpattern_6, ns=33

pattern_2, n=523; subpattern_7, ns=28

TF-MoDisCO pattern_5 n=372, CWM

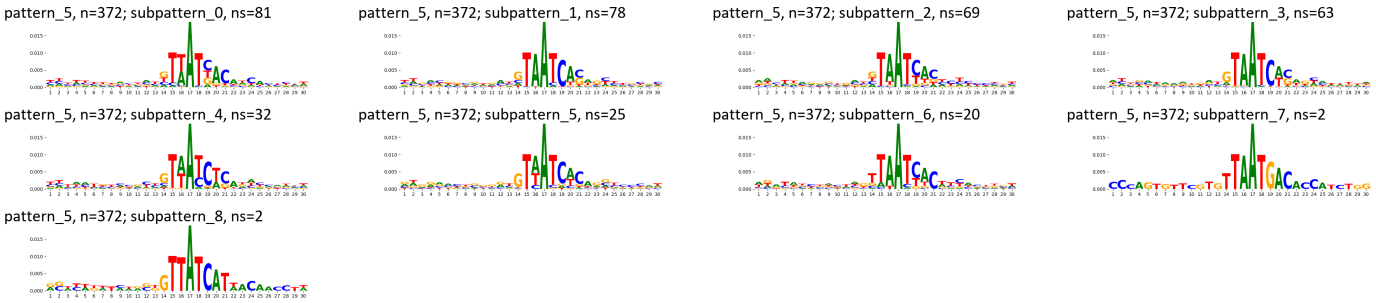

TF-MoDisCO pattern_5 n=372, PWM

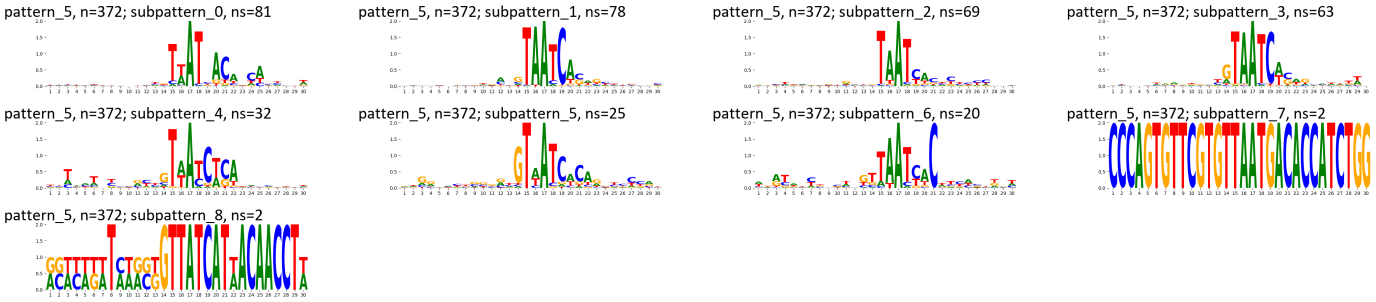

Supplementary Figure 39: TF-MoDisCO subpatterns for the GFI1 transcription factor in HEK293 (accession ENCSR445PDR).

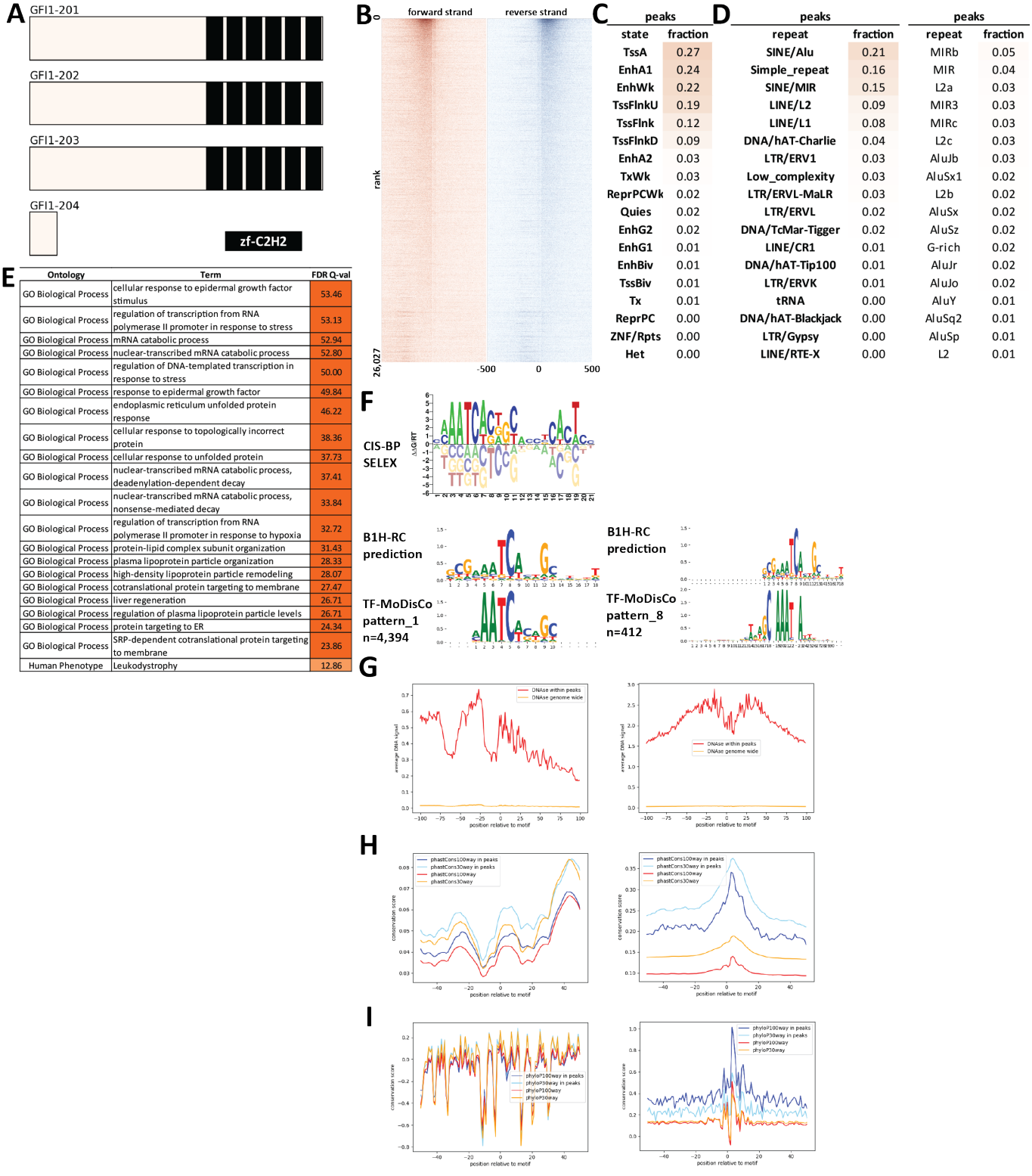

Supplementary Figure 40: Properties and genomic distribution of motifs identified for the GFI1 transcription factor in HepG2 (accession ENCSR849FVL).

TF-MoDisCO pattern_1 n=4394, CWM

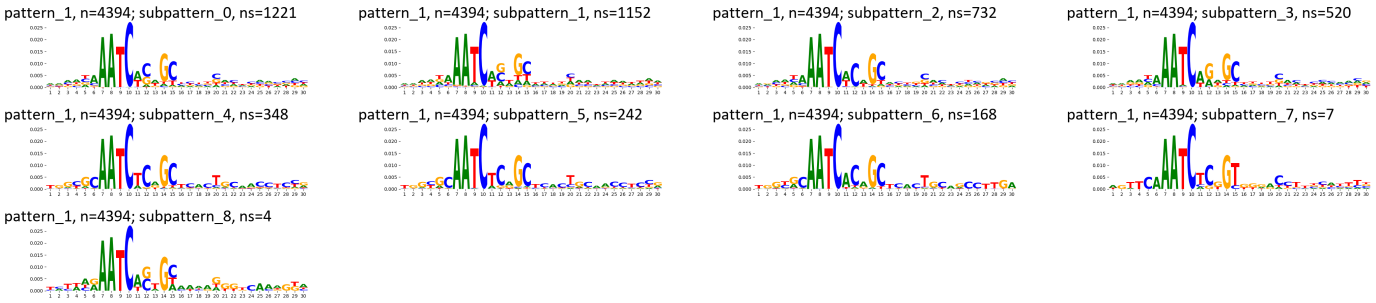

TF-MoDisCO pattern_1 n=4394, PWM

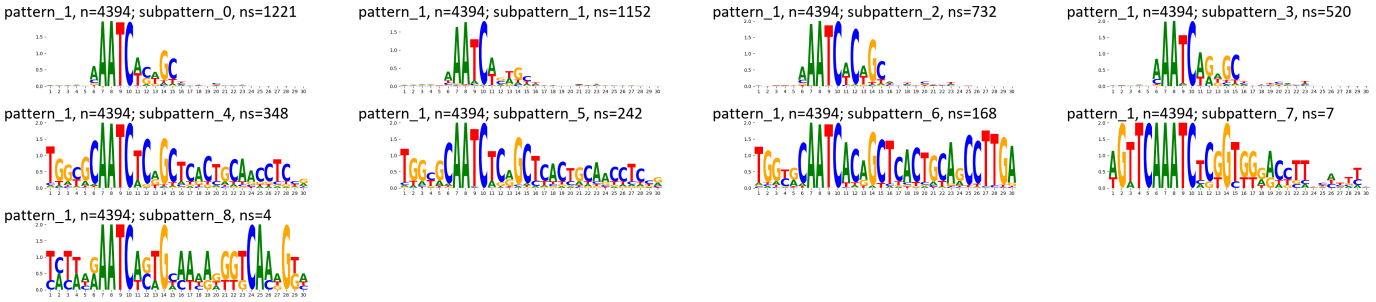

TF-MoDisCO pattern_8 n=412, CWM

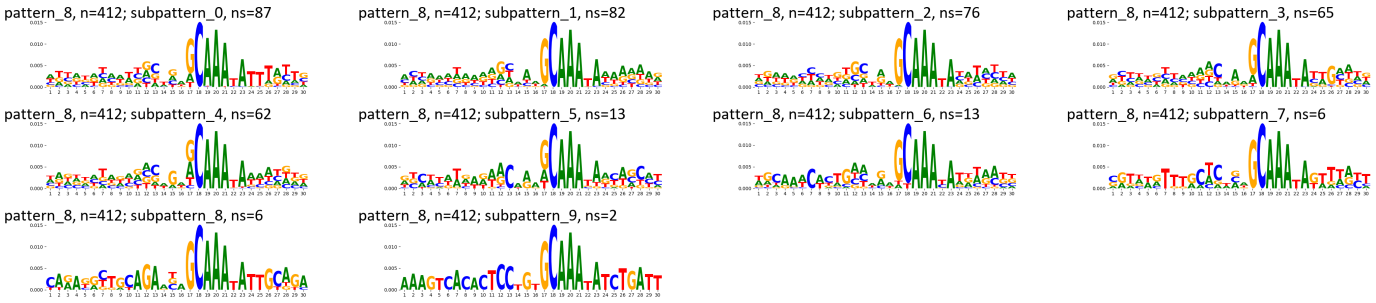

TF-MoDisCO pattern_8 n=412, PWM

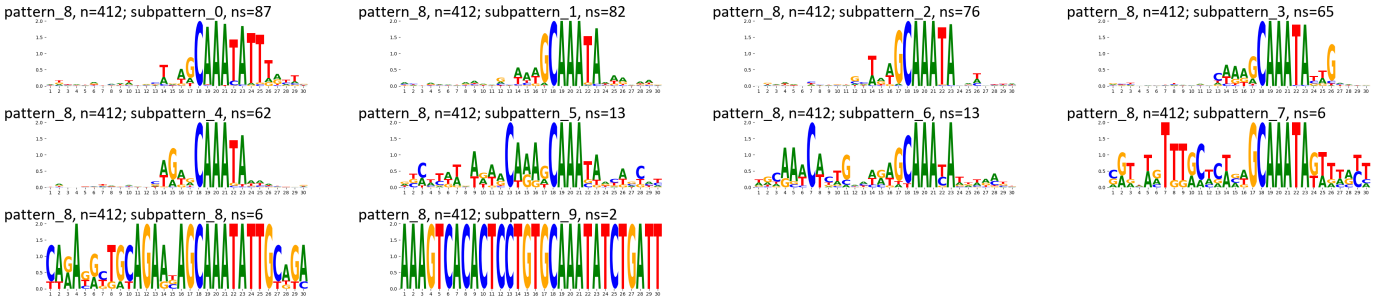

Supplementary Figure 41: TF-MoDisCO subpatterns for the GFI1 transcription factor in HepG2 (accession ENCSR849FVL).

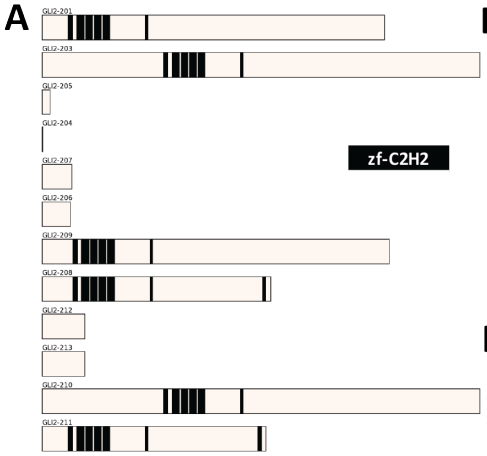

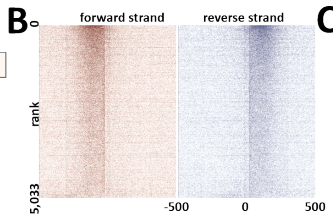

C

peaks	
state	fraction
EnhWk	0.35
Quies	0.22
EnhA1	0.16
EnhA2	0.15
TxWk	0.12
TssA	0.05
Tx	0.02
TssFlnk	0.02
EnhBiv	0.01
ReprPCWk	0.01
TssBiv	0.01
TssFlnkU	0.01
EnhG1	0.01
TssFlnkD	0.01
ReprPC	0.01
Het	0.01
EnhG2	0.00
ZNF/Rpts	0.00

D

peaks		peaks	
repeat	fraction	repeat	fraction
SINE/Alu	0.27	(AAAT)n	0.07
Simple_repeat	0.20	MIRb	0.04
SINE/MIR	0.09	AluSx1	0.03
LINE/L1	0.09	AluSx	0.03
LINE/L2	0.05	MIR	0.03
DNA/hAT-Charlie	0.03	AluJb	0.03
LTR/ERVL-MaLR	0.02	AluY	0.03
DNA/TcMar-Tigger	0.02	AluSz	0.02
LTR/ERV1	0.02	L2c	0.02
LTR/ERVL	0.01	(ATTT)n	0.02
LINE/CR1	0.01	L2a	0.02
Low_complexity	0.01	AluJr	0.02
tRNA	0.01	(TTTA)n	0.02
DNA?	0.00	(TTAT)n	0.02
DNA/hAT-Tip100	0.00	AluJo	0.02
LINE/RTE-X	0.00	MIRc	0.02
Unknown	0.00	AluSq2	0.01
LINE/RTE-BovB	0.00	AluSz6	0.01

E

Ontology	Term	FDR Q-val
GO Biological Process	mesoderm formation	28.48
GO Biological Process	mesoderm morphogenesis	27.64
GO Biological Process	anterior/posterior pattern specification	25.55
GO Biological Process	mesoderm development	23.87
GO Biological Process	formation of primary germ layer	20.27
GO Biological Process	gastrulation	19.17
GO Biological Process	segmentation	18.57
GO Biological Process	mammary gland epithelium development	15.60
GO Biological Process	outflow tract morphogenesis	14.23
GO Biological Process	mammary gland epithelial cell differentiation	13.40
GO Biological Process	positive regulation of stem cell differentiation	13.08
GO Biological Process	somitogenesis	12.73
GO Biological Process	outflow tract septum morphogenesis	12.63
GO Biological Process	cardiac septum morphogenesis	12.19
GO Biological Process	positive regulation of epithelial to mesenchymal transition	11.21
GO Biological Process	positive regulation of mesonephros development	10.17
GO Biological Process	positive regulation of stress fiber assembly	9.86
GO Biological Process	embryonic pattern specification	9.30
GO Biological Process	preganglionic parasympathetic fiber development	8.96
GO Biological Process	parasympathetic nervous system development	8.95
Human Phenotype	Reduced number of teeth	13.27
Human Phenotype	Abnormal number of teeth	12.17
Human Phenotype	Hypodontia	10.64
Human Phenotype	Vaginal atresia	6.87
Human Phenotype	Poor speech	6.11
Human Phenotype	Abnormality of the vagina	6.08
Human Phenotype	Renal dysplasia	4.97
Human Phenotype	Abnormality of the choanae	4.73
Human Phenotype	Abnormality of the lacrimal duct	4.25
Human Phenotype	Intestinal malrotation	3.85
Human Phenotype	Abnormality of the nasolacrimal system	3.84
Human Phenotype	Mixed hearing impairment	3.06
Human Phenotype	Lacrimal duct aplasia	2.13
Human Phenotype	Resting tremor	1.88

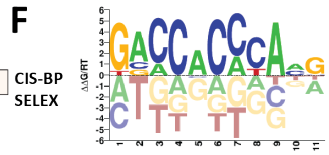

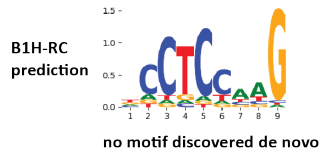

Supplementary Figure 42: Properties and genomic distribution of motifs identified for the GLI2 transcription factor in HEK293 (accession ENCSR978EQY).

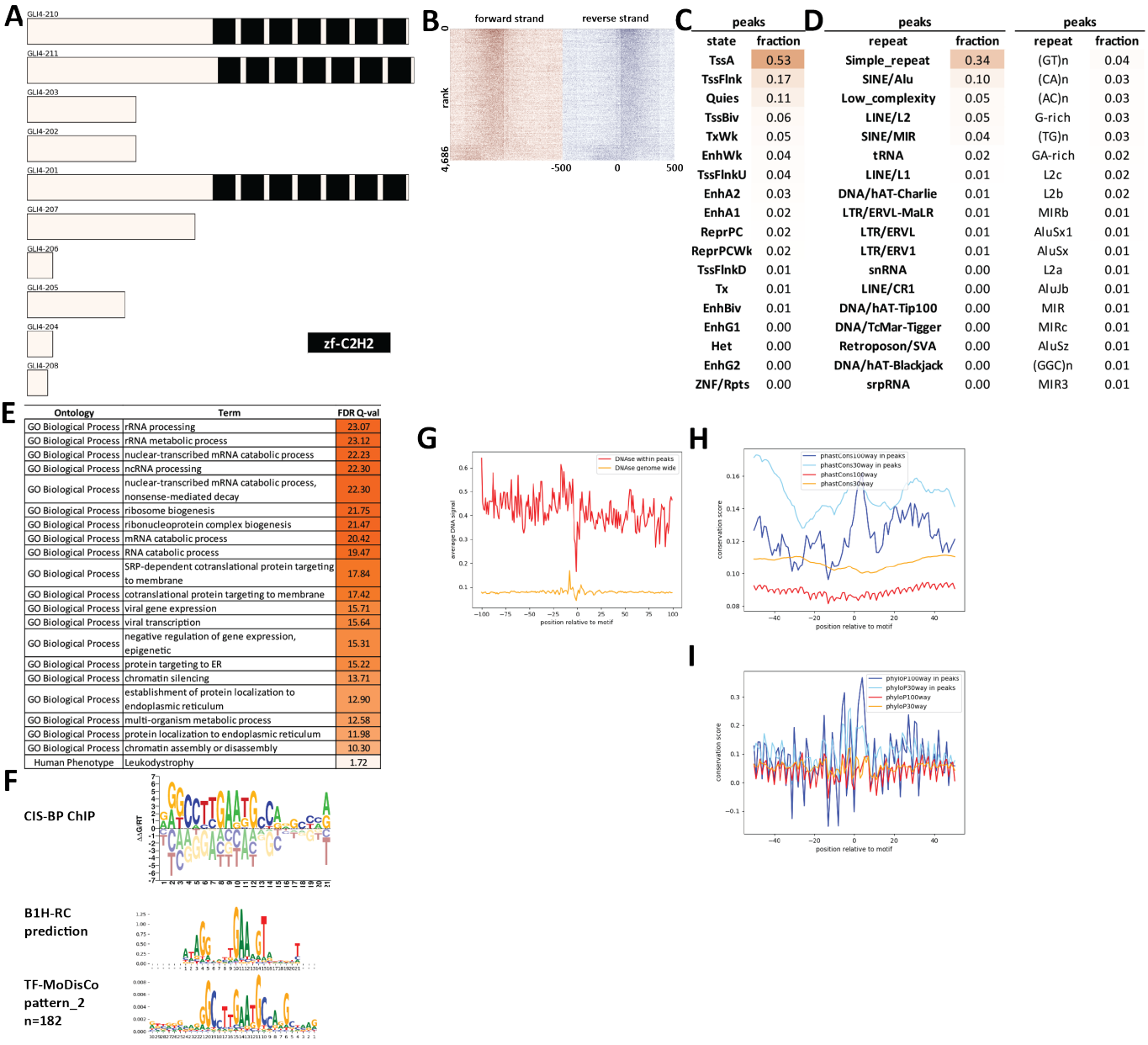

C

peaks	
state	fraction
TssA	0.53
TssFlnk	0.17
Quies	0.11
TssBiv	0.06
TxWk	0.05
EnhWk	0.04
TssFlnkU	0.04
EnhA2	0.03
EnhA1	0.02
ReprPC	0.02
ReprPCWk	0.02
TssFlnkD	0.01
Tx	0.01
EnhBiv	0.01
EnhG1	0.00
Het	0.00
EnhG2	0.00
ZNF/Rpts	0.00

D

peaks		peaks	
repeat	fraction	repeat	fraction
Simple_repeat	0.34	(GT)n	0.04
SINE/Alu	0.10	(CA)n	0.03
Low_complexity	0.05	(AC)n	0.03
LINE/L2	0.05	G-rich	0.03
SINE/MIR	0.04	(TG)n	0.03
tRNA	0.02	GA-rich	0.02
LINE/L1	0.01	L2c	0.02
DNA/hAT-Charlie	0.01	L2b	0.02
LTR/ERVL-MaLR	0.01	MIRb	0.01
LTR/ERVL	0.01	AluSx1	0.01
LTR/ERV1	0.01	AluSx	0.01
snRNA	0.00	L2a	0.01
LINE/CR1	0.00	AluJb	0.01
DNA/hAT-Tip100	0.00	MIR	0.01
DNA/TcMar-Tigger	0.00	MIRc	0.01
Retroposon/SVA	0.00	AluSz	0.01
DNA/hAT-Blackjack	0.00	(GGC)n	0.01
srpRNA	0.00	MIR3	0.01

E

Ontology	Term	FDR Q-val
GO Biological Process	rRNA processing	23.07
GO Biological Process	rRNA metabolic process	23.12
GO Biological Process	nuclear-transcribed mRNA catabolic process	22.23
GO Biological Process	ncRNA processing	22.30
GO Biological Process	nuclear-transcribed mRNA catabolic process, nonsense-mediated decay	22.30
GO Biological Process	ribosome biogenesis	21.75
GO Biological Process	ribonucleoprotein complex biogenesis	21.47
GO Biological Process	mRNA catabolic process	20.42
GO Biological Process	RNA catabolic process	19.47
GO Biological Process	SRP-dependent cotranslational protein targeting to membrane	17.84
GO Biological Process	cotranslational protein targeting to membrane	17.42
GO Biological Process	viral gene expression	15.71
GO Biological Process	viral transcription	15.64
GO Biological Process	negative regulation of gene expression, epigenetic	15.31
GO Biological Process	protein targeting to ER	15.22
GO Biological Process	chromatin silencing	13.71
GO Biological Process	establishment of protein localization to endoplasmic reticulum	12.90
GO Biological Process	multi-organism metabolic process	12.58
GO Biological Process	protein localization to endoplasmic reticulum	11.98
GO Biological Process	chromatin assembly or disassembly	10.30
Human Phenotype	Leukodystrophy	1.72

Supplementary Figure 43: Properties and genomic distribution of motifs identified for the GLI4 transcription factor in HEK293 (accession ENCSR211PZO).

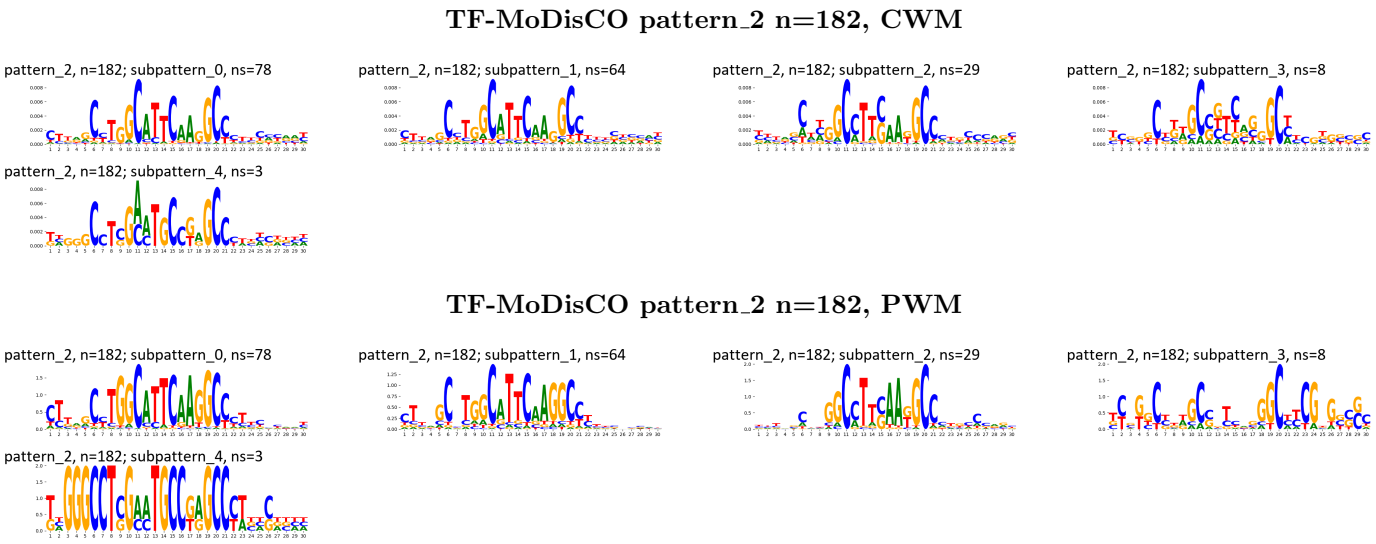

Supplementary Figure 44: TF-MoDisCO subpatterns for the GLI4 transcription factor in HEK293 (accession ENCSR211PZO).

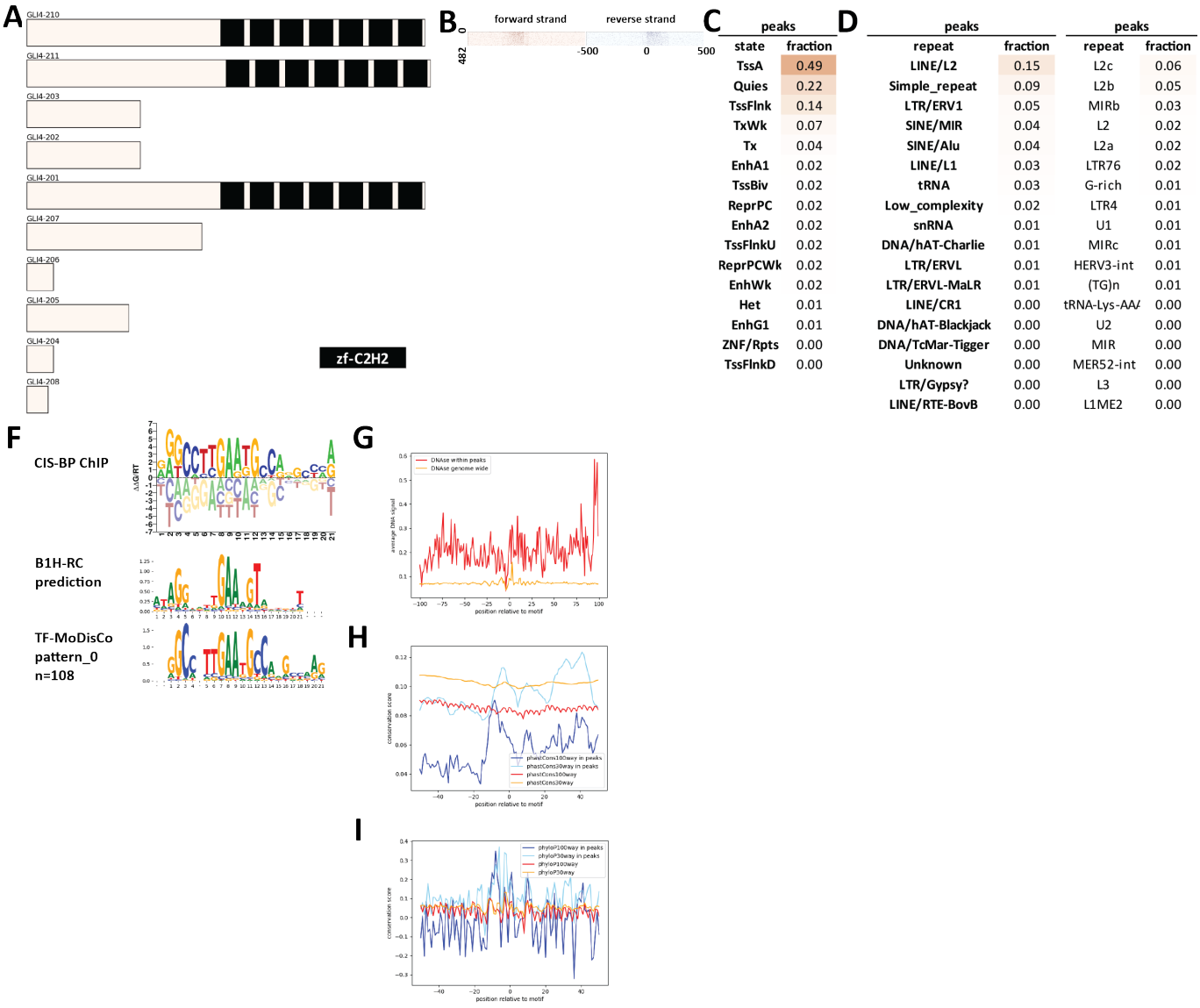

Supplementary Figure 45: Properties and genomic distribution of motifs identified for the GLI4 transcription factor in HEK298 (accession Hughes GR models).

A

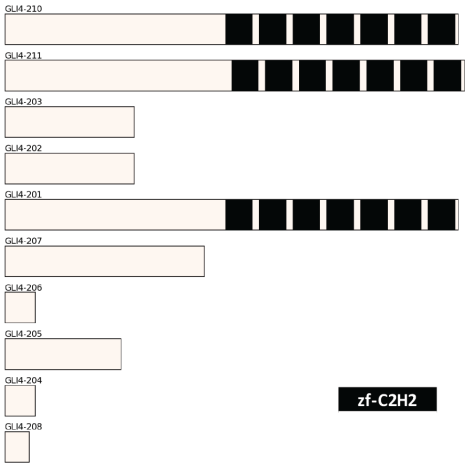

B

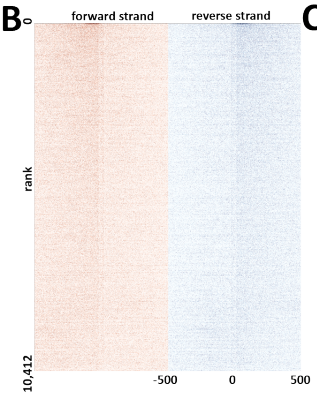

C

peaks	
state	fraction
TssA	0.47
TssFlnk	0.22
TssFlnkU	0.18
EnhWk	0.11
EnhA1	0.10
TssFlnkD	0.10
TssBiv	0.02
TxWk	0.02
ReprPCWk	0.02
EnhG2	0.02
EnhA2	0.01
EnhBiv	0.01
EnhG1	0.01
Quies	0.01
ReprPC	0.01
Tx	0.00
ZNF/Rpts	0.00

D

peaks		peaks	
repeat	fraction	repeat	fraction
Simple_repeat	0.20	MIRb	0.04
SINE/MIR	0.12	G-rich	0.03
SINE/Alu	0.12	MIR3	0.03
LINE/L2	0.07	MIR	0.03
Low_complexity	0.04	L2a	0.02
LINE/L1	0.03	MIRc	0.02
DNA/hAT-Charlie	0.03	L2b	0.02
LTR/ERV1	0.02	L2c	0.02
LTR/ERVL-MaLR	0.02	AluJb	0.02
LTR/ERVL	0.01	AluSx1	0.01
LINE/CR1	0.01	AluSx	0.01
DNA/hAT-Tip100	0.00	AluSz	0.01
DNA/TcMar-Tigger	0.00	AluJr	0.01
tRNA	0.00	AluJo	0.01
LTR/ERVK	0.00	GA-rich	0.01
DNA/hAT	0.00	(GGC)n	0.01
Satellite	0.00	L2	0.01
LINE/RTE-BovB	0.00	AluSq2	0.01

E

Ontology	Term	FDR Q-val
GO Biological Process	regulation of transcription from RNA polymerase II promoter in response to stress	37.47
GO Biological Process	regulation of DNA-templated transcription in response to stress	31.51
GO Biological Process	mRNA catabolic process	27.06
GO Biological Process	RNA catabolic process	27.03
GO Biological Process	nuclear-transcribed mRNA catabolic process	26.81
GO Biological Process	nuclear-transcribed mRNA catabolic process, nonsense-mediated decay	21.47
GO Biological Process	regulation of transcription from RNA polymerase II promoter in response to hypoxia	20.99
GO Biological Process	RNA phosphodiester bond hydrolysis	18.76
GO Biological Process	protein targeting to ER	16.97
GO Biological Process	viral gene expression	16.69
GO Biological Process	ribonucleoprotein complex export from nucleus	16.37
GO Biological Process	ribonucleoprotein complex localization	15.79
GO Biological Process	protein localization to endoplasmic reticulum	15.13
GO Biological Process	negative regulation of intrinsic apoptotic signaling pathway	15.13
GO Biological Process	establishment of protein localization to endoplasmic reticulum	15.03
GO Biological Process	viral transcription	14.99
GO Biological Process	regulation of telomere maintenance	14.97
GO Biological Process	multi-organism metabolic process	14.27
GO Biological Process	nuclear-transcribed mRNA catabolic process, deadenylation-dependent decay	13.35
GO Biological Process	regulation of ubiquitin-protein ligase activity involved in mitotic cell cycle	13.22
Human Phenotype	Increased serum lactate	10.39
Human Phenotype	Ependymoma	2.31

F

CIS-BP ChIP

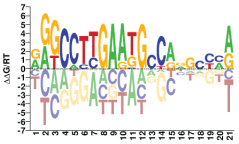

no motifs discovered de novo

Supplementary Figure 46: Properties and genomic distribution of motifs identified for the GLI4 transcription factor in HepG2 (accession ENCSR502YME).

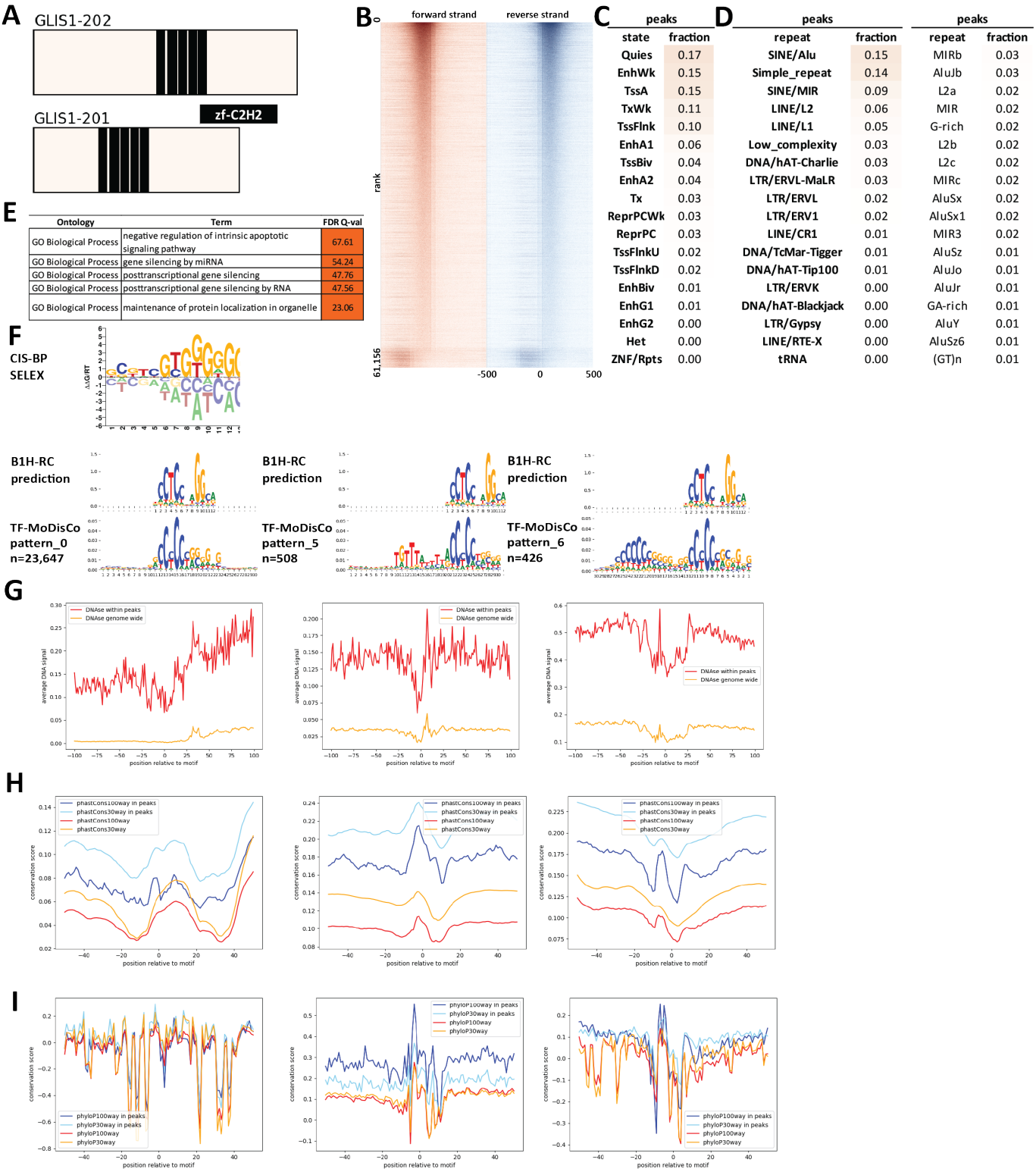

Supplementary Figure 47: Properties and genomic distribution of motifs identified for the GLIS1 transcription factor in HEK293 (accession ENCSR482BBZ).

TF-MoDisCO pattern_0 n=23647, CWM

pattern_0, n=23647; subpattern_0, ns=4941

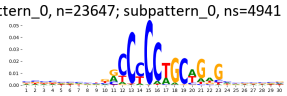

pattern_0, n=23647; subpattern_1, ns=4305

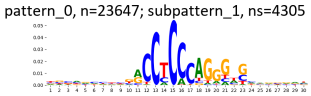

pattern_0, n=23647; subpattern_10, ns=396

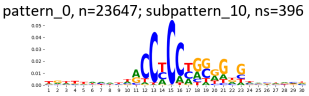

pattern_0, n=23647; subpattern_11, ns=94

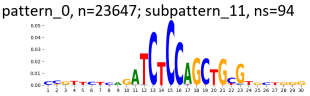

pattern_0, n=23647; subpattern_12, ns=30

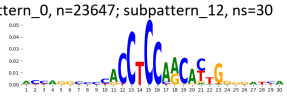

pattern_0, n=23647; subpattern_13, ns=24

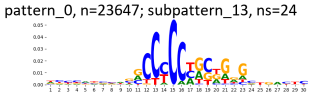

pattern_0, n=23647; subpattern_2, ns=3195

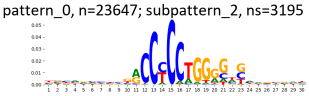

pattern_0, n=23647; subpattern_3, ns=2939

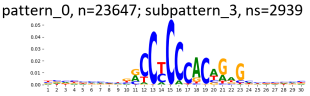

pattern_0, n=23647; subpattern_4, ns=2081

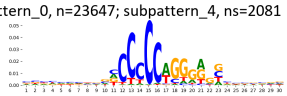

pattern_0, n=23647; subpattern_5, ns=1727

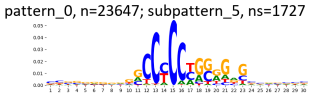

pattern_0, n=23647; subpattern_6, ns=1535

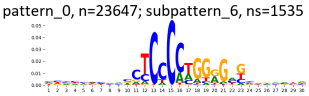

pattern_0, n=23647; subpattern_7, ns=864

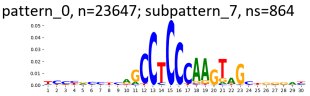

pattern_0, n=23647; subpattern_8, ns=759

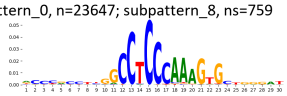

pattern_0, n=23647; subpattern_9, ns=757

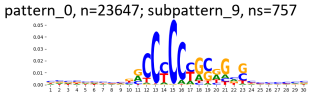

TF-MoDisCO pattern_0 n=23647, PWM

pattern_0, n=23647; subpattern_0, ns=4941

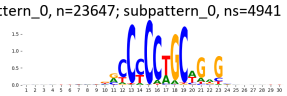

pattern_0, n=23647; subpattern_1, ns=4305

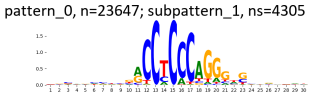

pattern_0, n=23647; subpattern_10, ns=396

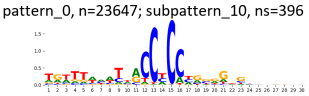

pattern_0, n=23647; subpattern_11, ns=94

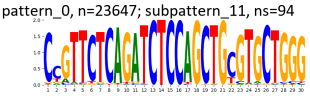

pattern_0, n=23647; subpattern_12, ns=30

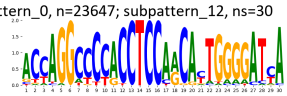

pattern_0, n=23647; subpattern_13, ns=24

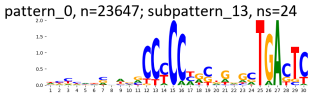

pattern_0, n=23647; subpattern_2, ns=3195

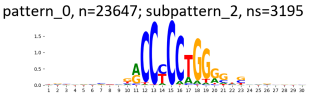

pattern_0, n=23647; subpattern_3, ns=2939

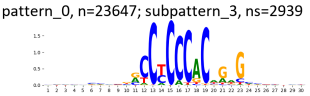

pattern_0, n=23647; subpattern_4, ns=2081

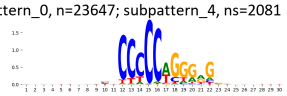

pattern_0, n=23647; subpattern_5, ns=1727

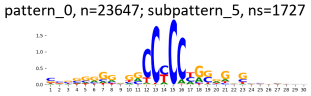

pattern_0, n=23647; subpattern_6, ns=1535

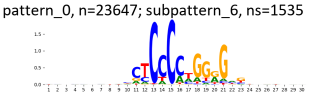

pattern_0, n=23647; subpattern_7, ns=864

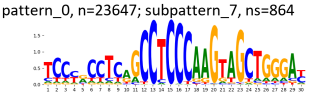

pattern_0, n=23647; subpattern_8, ns=759

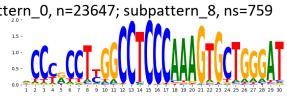

pattern_0, n=23647; subpattern_9, ns=757

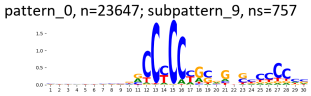

TF-MoDisCO pattern_5 n=508, CWM

pattern_5, n=508; subpattern_0, ns=128

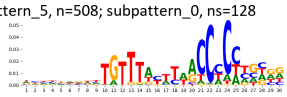

pattern_5, n=508; subpattern_1, ns=115

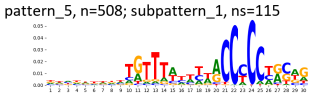

pattern_5, n=508; subpattern_2, ns=110

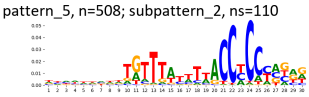

pattern_5, n=508; subpattern_3, ns=53

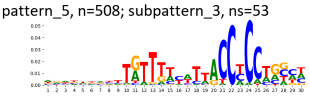

pattern_5, n=508; subpattern_4, ns=42

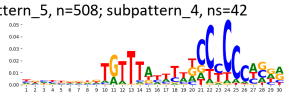

pattern_5, n=508; subpattern_5, ns=27

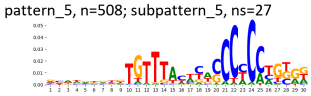

pattern_5, n=508; subpattern_6, ns=21

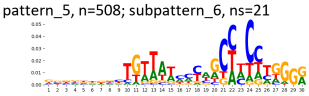

pattern_5, n=508; subpattern_7, ns=12

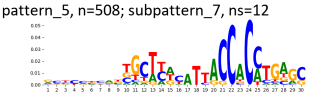

TF-MoDisCO pattern_5 n=508, PWM

pattern_5, n=508; subpattern_0, ns=128

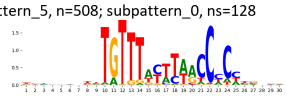

pattern_5, n=508; subpattern_1, ns=115

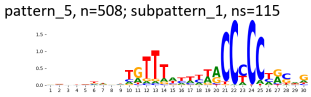

pattern_5, n=508; subpattern_2, ns=110

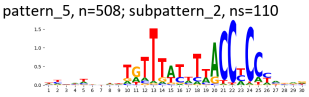

pattern_5, n=508; subpattern_3, ns=53

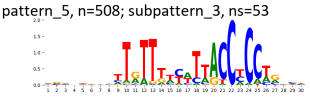

pattern_5, n=508; subpattern_4, ns=42

pattern_5, n=508; subpattern_5, ns=27

pattern_5, n=508; subpattern_6, ns=21

pattern_5, n=508; subpattern_7, ns=12

TF-MoDisCO pattern_6 n=426, CWM

pattern_6, n=426; subpattern_0, ns=124

pattern_6, n=426; subpattern_1, ns=100

pattern_6, n=426; subpattern_2, ns=74

pattern_6, n=426; subpattern_3, ns=61

pattern_6, n=426; subpattern_4, ns=50

pattern_6, n=426; subpattern_5, ns=17

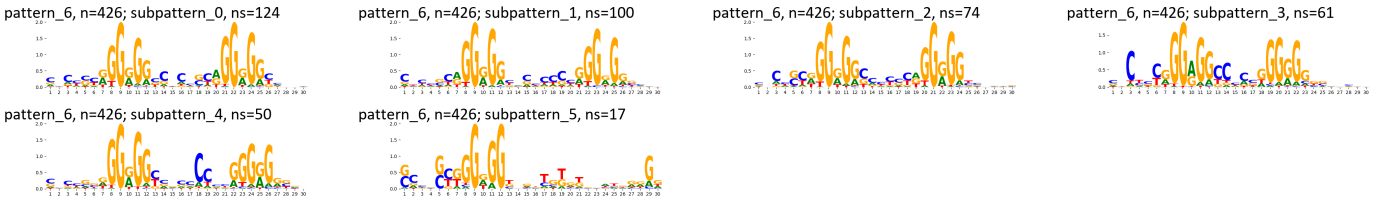

Supplementary Figure 48: TF-MoDisCO subpatterns for the GLIS1 transcription factor in HEK293 (accession ENCSR482BBZ).

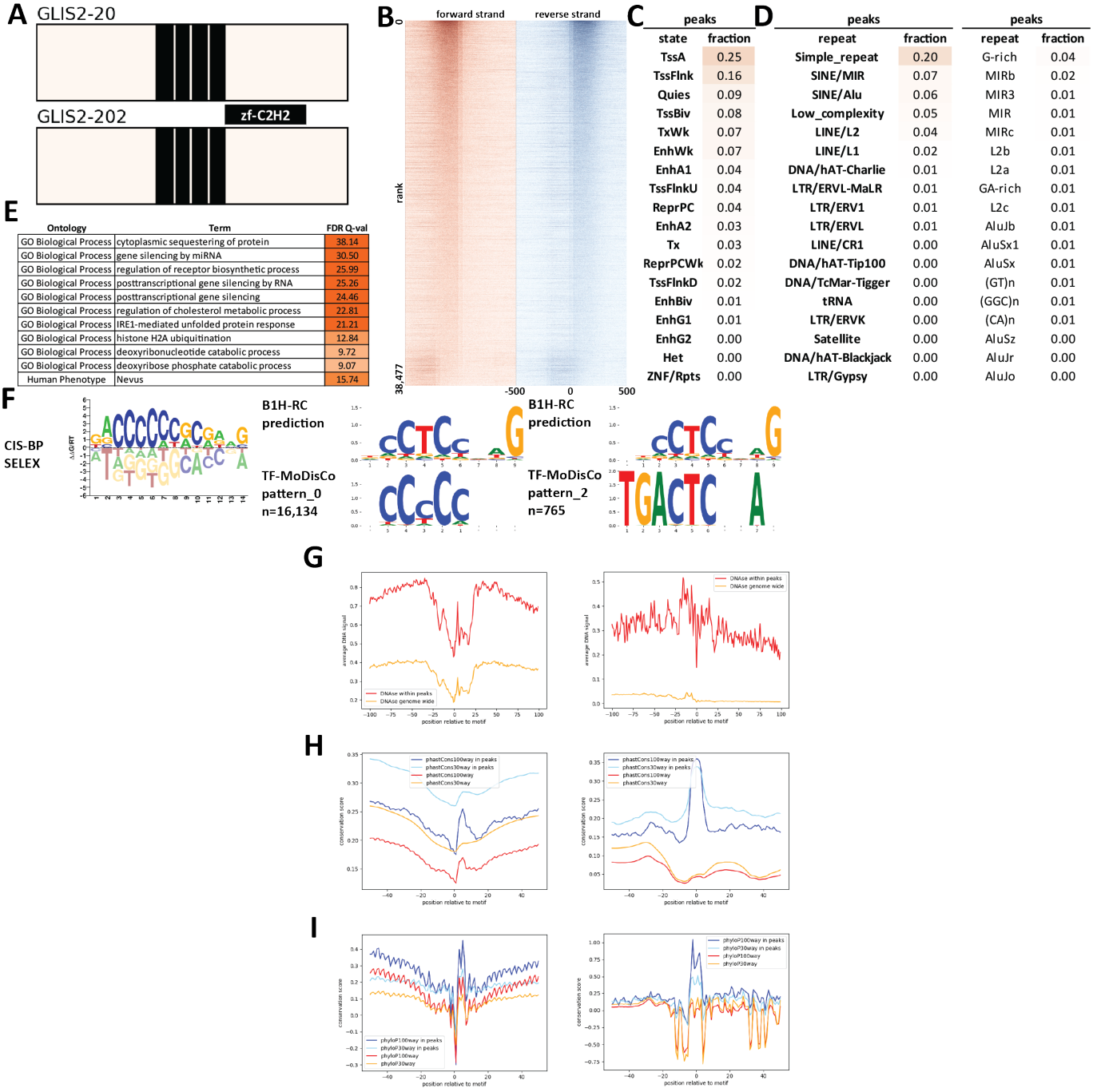

Supplementary Figure 49: Properties and genomic distribution of motifs identified for the GLIS2 transcription factor in HEK293 (accession ENCSR535DIA).

TF-MoDisCO pattern_0 n=16134, CWM

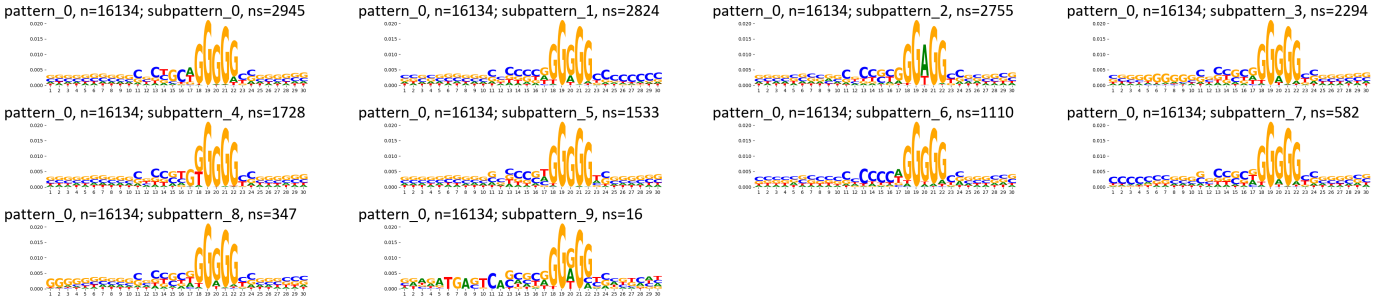

TF-MoDisCO pattern_0 n=16134, PWM

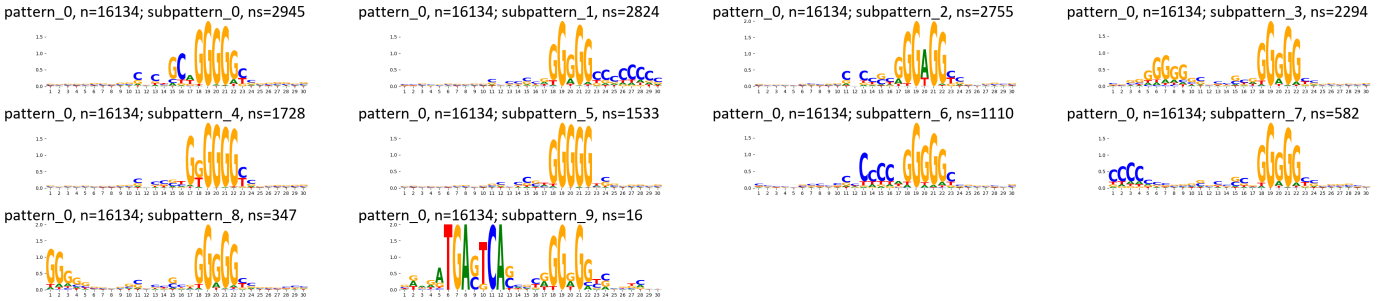

TF-MoDisCO pattern_2 n=765, CWM

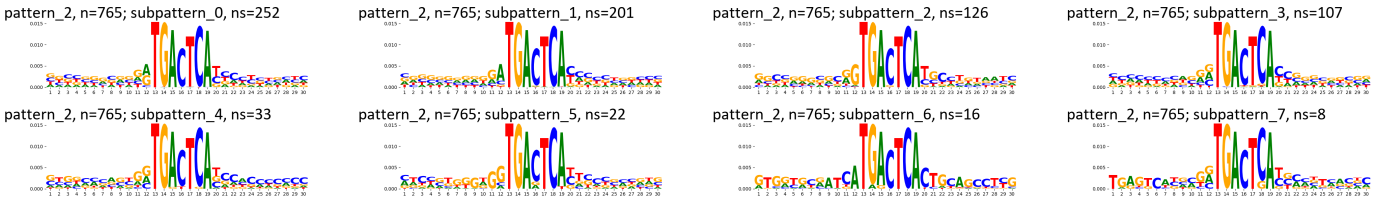

TF-MoDisCO pattern_2 n=765, PWM

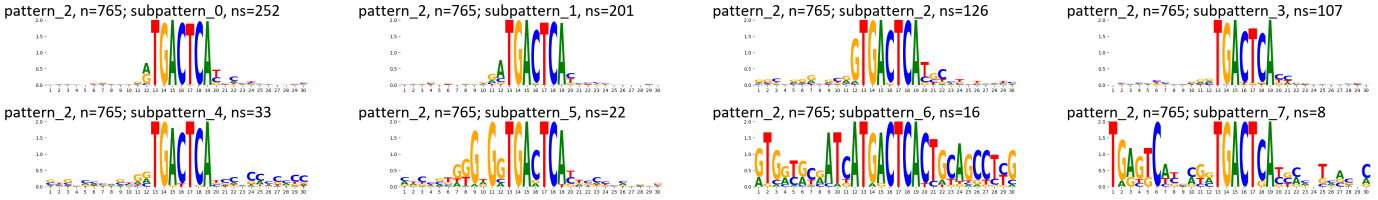

Supplementary Figure 50: TF-MoDisCO subpatterns for the GLIS2 transcription factor in HEK293 (accession ENCSR535DIA).

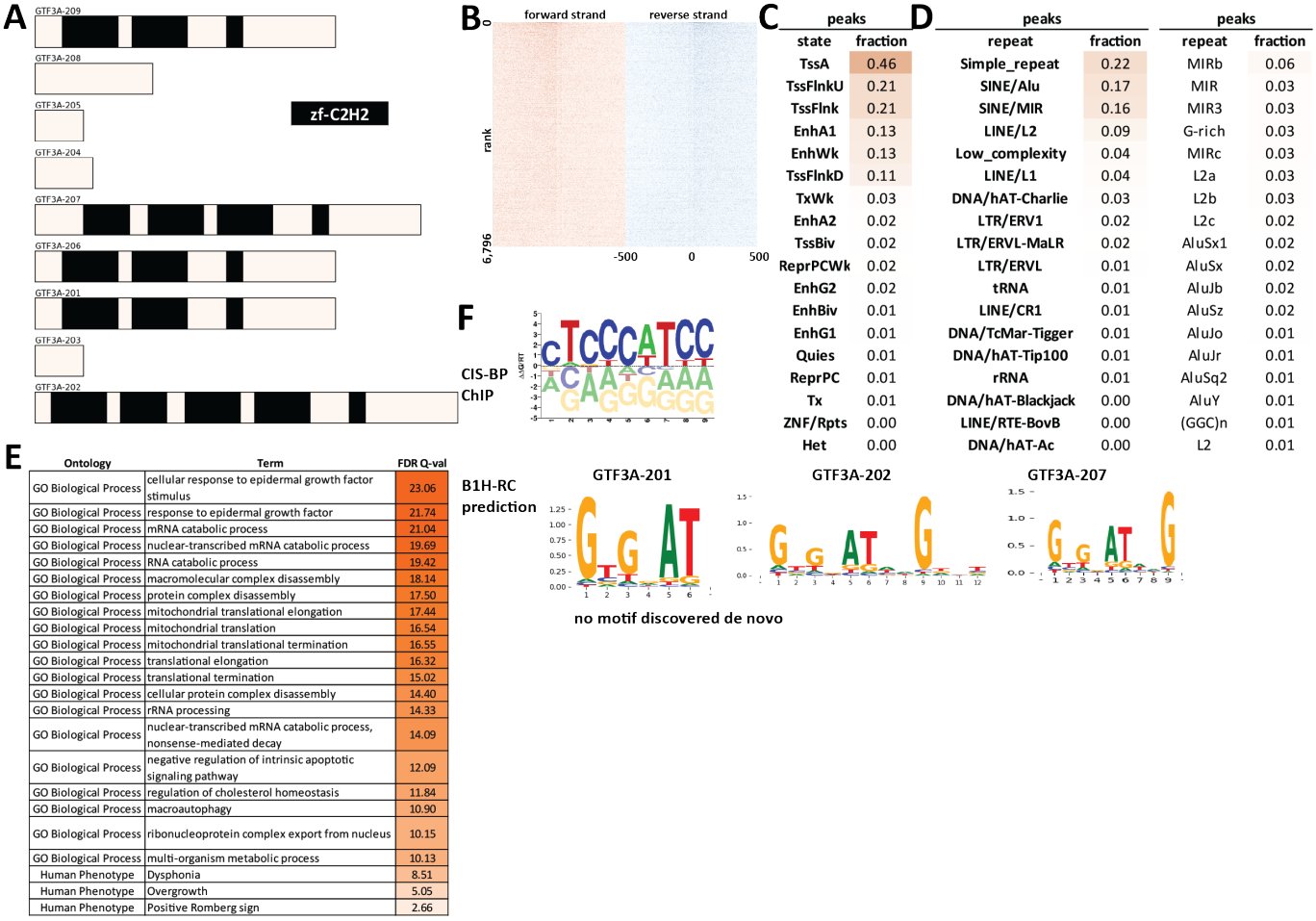

Supplementary Figure 51: Properties and genomic distribution of motifs identified for the GTF3A transcription factor in HepG2 (accession ENCSR220AQM).

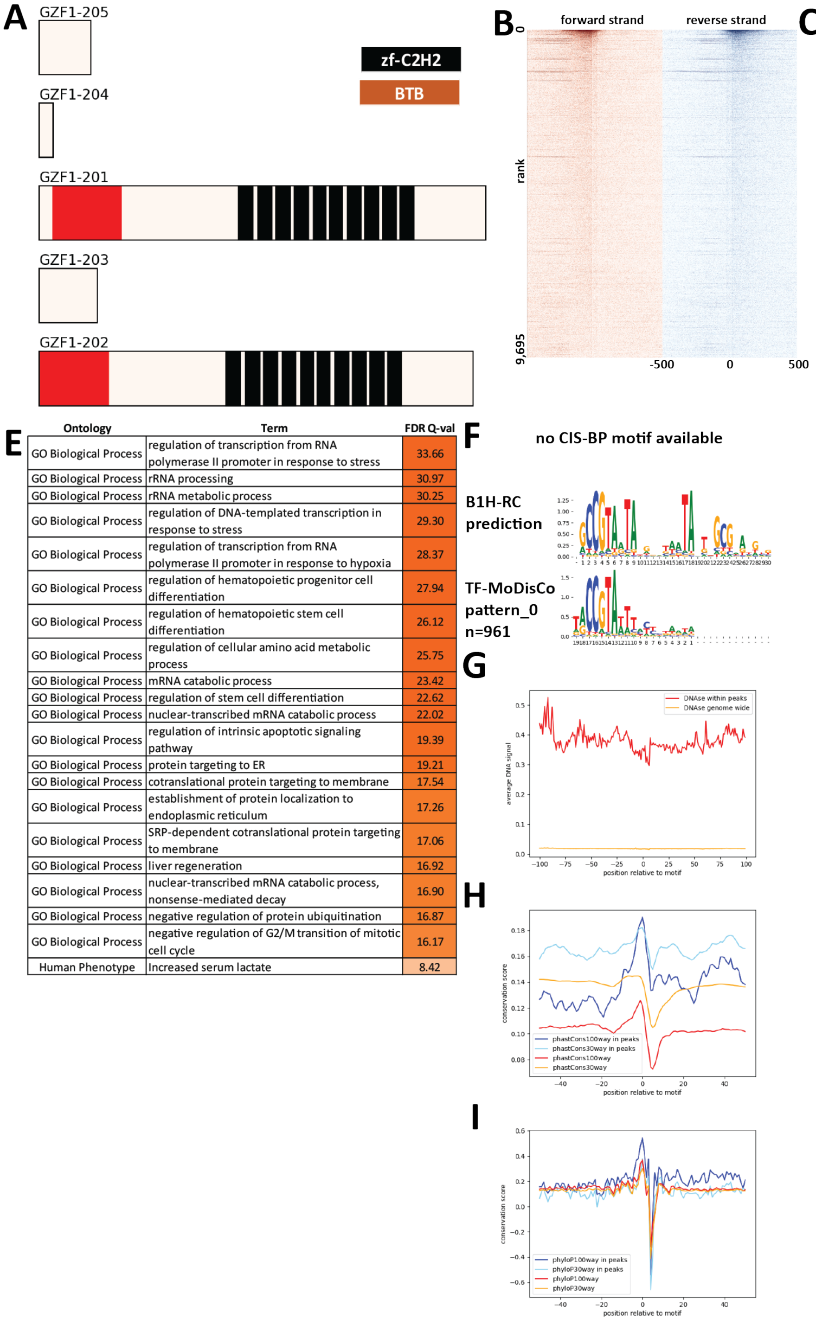

C

peaks	
state	fraction
TssA	0.44
TssFlnkU	0.21
TssFlnk	0.19
EnhA1	0.13
EnhWk	0.11
TssFlnkD	0.10
ReprPCWk	0.03
TxWk	0.02
EnhA2	0.02
TssBiv	0.02
Quies	0.02
EnhG2	0.01
EnhBiv	0.01
ReprPC	0.01
EnhG1	0.01
Tx	0.00
Het	0.00
ZNF/Rpts	0.00

D

peaks		peaks	
repeat	fraction	repeat	fraction
Simple_repeat	0.19	MIRb	0.04
SINE/Alu	0.14	G-rich	0.03
SINE/MIR	0.13	MIR	0.03
LINE/L2	0.07	MIR3	0.03
LINE/L1	0.05	L2a	0.03
Low_complexity	0.04	MIRc	0.02
DNA/hAT-Charlie	0.03	L2c	0.02
LTR/ERVL-MaLR	0.02	L2b	0.02
LTR/ERV1	0.02	AluJb	0.02
LTR/ERVL	0.01	AluSx1	0.01
DNA/TcMar-Tigger	0.01	AluSx	0.01
LINE/CR1	0.01	AluSz	0.01
tRNA	0.01	AluJr	0.01
DNA/hAT-Tip100	0.01	AluJo	0.01
LTR/ERVK	0.00	AluY	0.01
DNA/hAT-Blackjack	0.00	GA-rich	0.01
snRNA	0.00	L2	0.01
LTR/Gypsy	0.00	AluSq2	0.01

E

Ontology	Term	FDR Q-val
GO Biological Process	regulation of transcription from RNA polymerase II promoter in response to stress	33.66
GO Biological Process	rRNA processing	30.97
GO Biological Process	rRNA metabolic process	30.25
GO Biological Process	regulation of DNA-templated transcription in response to stress	29.30
GO Biological Process	regulation of transcription from RNA polymerase II promoter in response to hypoxia	28.37
GO Biological Process	regulation of hematopoietic progenitor cell differentiation	27.94
GO Biological Process	regulation of hematopoietic stem cell differentiation	26.12
GO Biological Process	regulation of cellular amino acid metabolic process	25.75
GO Biological Process	mRNA catabolic process	23.42
GO Biological Process	regulation of stem cell differentiation	22.62
GO Biological Process	nuclear-transcribed mRNA catabolic process	22.02
GO Biological Process	regulation of intrinsic apoptotic signaling pathway	19.39
GO Biological Process	protein targeting to ER	19.21
GO Biological Process	cotranslational protein targeting to membrane	17.54
GO Biological Process	establishment of protein localization to endoplasmic reticulum	17.26
GO Biological Process	SRP-dependent cotranslational protein targeting to membrane	17.06
GO Biological Process	liver regeneration	16.92
GO Biological Process	nuclear-transcribed mRNA catabolic process, nonsense-mediated decay	16.90
GO Biological Process	negative regulation of protein ubiquitination	16.87
GO Biological Process	negative regulation of G2/M transition of mitotic cell cycle	16.17
Human Phenotype	Increased serum lactate	8.42

Supplementary Figure 52: Properties and genomic distribution of motifs identified for the GZF1 transcription factor in HepG2 (accession ENCSR479WQX).

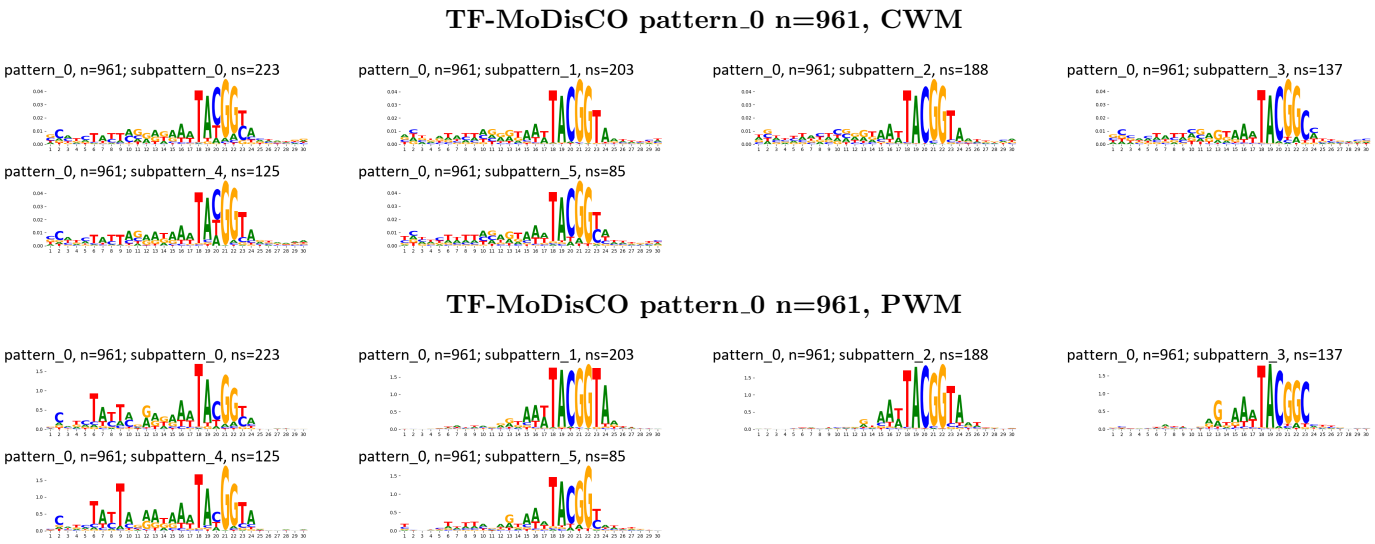

Supplementary Figure 53: TF-MoDisCO subpatterns for the GZF1 transcription factor in HepG2 (accession ENCSR479WQX).

A

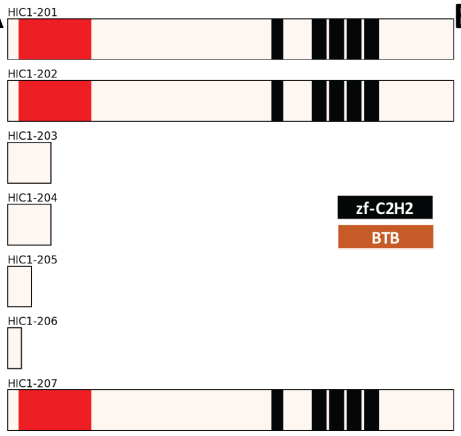

B

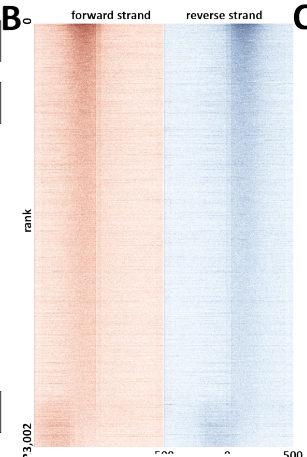

C

peaks	
state	fraction
TssA	0.24
EnhWk	0.16
Quies	0.14
TssFlnk	0.13
TxWk	0.10
EnhA1	0.07
TssBiv	0.06
EnhA2	0.06
TssFlnkU	0.04
Tx	0.04
ReprPC	0.03
TssFlnkD	0.02
ReprPCWk	0.02
EnhG1	0.01
EnhBiv	0.01
EnhG2	0.00
Het	0.00
ZNF/Rpts	0.00

D

peaks		peaks	
repeat	fraction	repeat	fraction
Simple_repeat	0.18	MIRb	0.03
SINE/Alu	0.12	G-rich	0.02
SINE/MIR	0.09	MIR	0.02
LINE/L2	0.06	L2a	0.02
LINE/L1	0.04	L2c	0.02
Low_complexity	0.04	MIRc	0.02
DNA/hAT-Charlie	0.02	L2b	0.02
LTR/ERVL-MaLR	0.02	AluSx1	0.02
LTR/ERV1	0.02	MIR3	0.01
DNA/TcMar-Tigger	0.01	AluSx	0.01
LTR/ERVL	0.01	AluJb	0.01
LINE/CR1	0.01	(GT)n	0.01
DNA/hAT-Tip100	0.00	AluSz	0.01
tRNA	0.00	(AC)n	0.01
LTR/ERVK	0.00	GA-rich	0.01
LINE/RTE-BovB	0.00	(TG)n	0.01
LINE/RTE-X	0.00	AluJr	0.01
LTR/Gypsy	0.00	(CA)n	0.01

E

Ontology	Term	FDR Q-val
GO Biological Process	cellular response to arsenic-containing substance	16.45
GO Biological Process	response to arsenic-containing substance	16.39
GO Biological Process	pyrimidine deoxyribonucleotide catabolic process	14.99
GO Biological Process	pyrimidine nucleotide catabolic process	14.30
GO Biological Process	positive regulation of mRNA catabolic process	10.23
GO Biological Process	positive regulation of mitochondrial membrane permeability	8.53
GO Biological Process	pyrimidine deoxyribonucleotide metabolic process	7.85
GO Biological Process	mitochondrial outer membrane permeabilization involved in programmed cell death	7.81
GO Biological Process	mitochondrion transport along microtubule	7.81
GO Biological Process	positive regulation of membrane permeability	7.61
GO Biological Process	regulation of Rac protein signal transduction	6.42
Human Phenotype	Trigonocephaly	17.58
Human Phenotype	Abnormality of subcutaneous fat tissue	10.52
Human Phenotype	Aplasia/hypoplasia of the femur	9.92
Human Phenotype	Distal upper limb amyotrophy	7.16
Human Phenotype	Lipomatous tumor	4.72

F

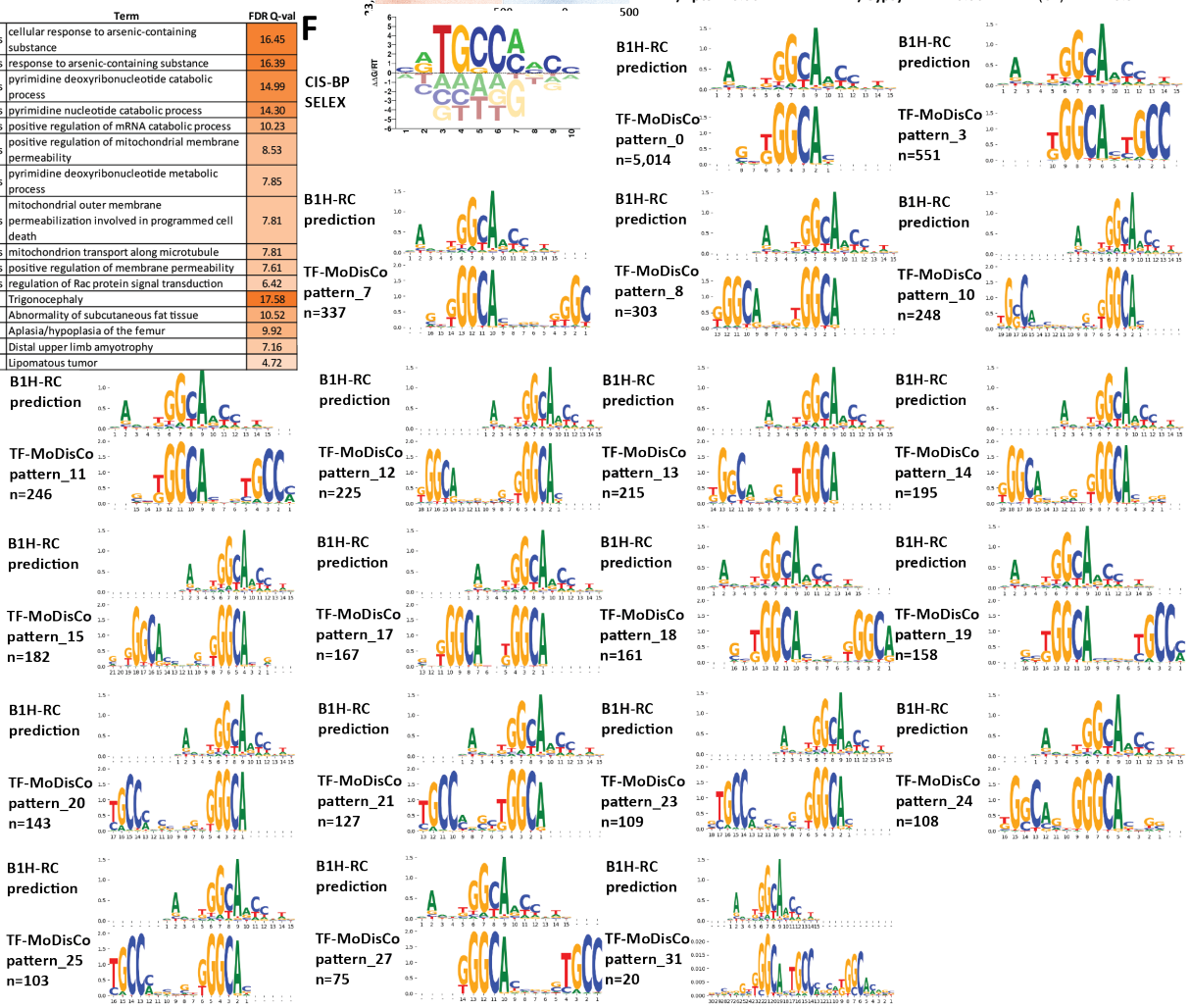

G

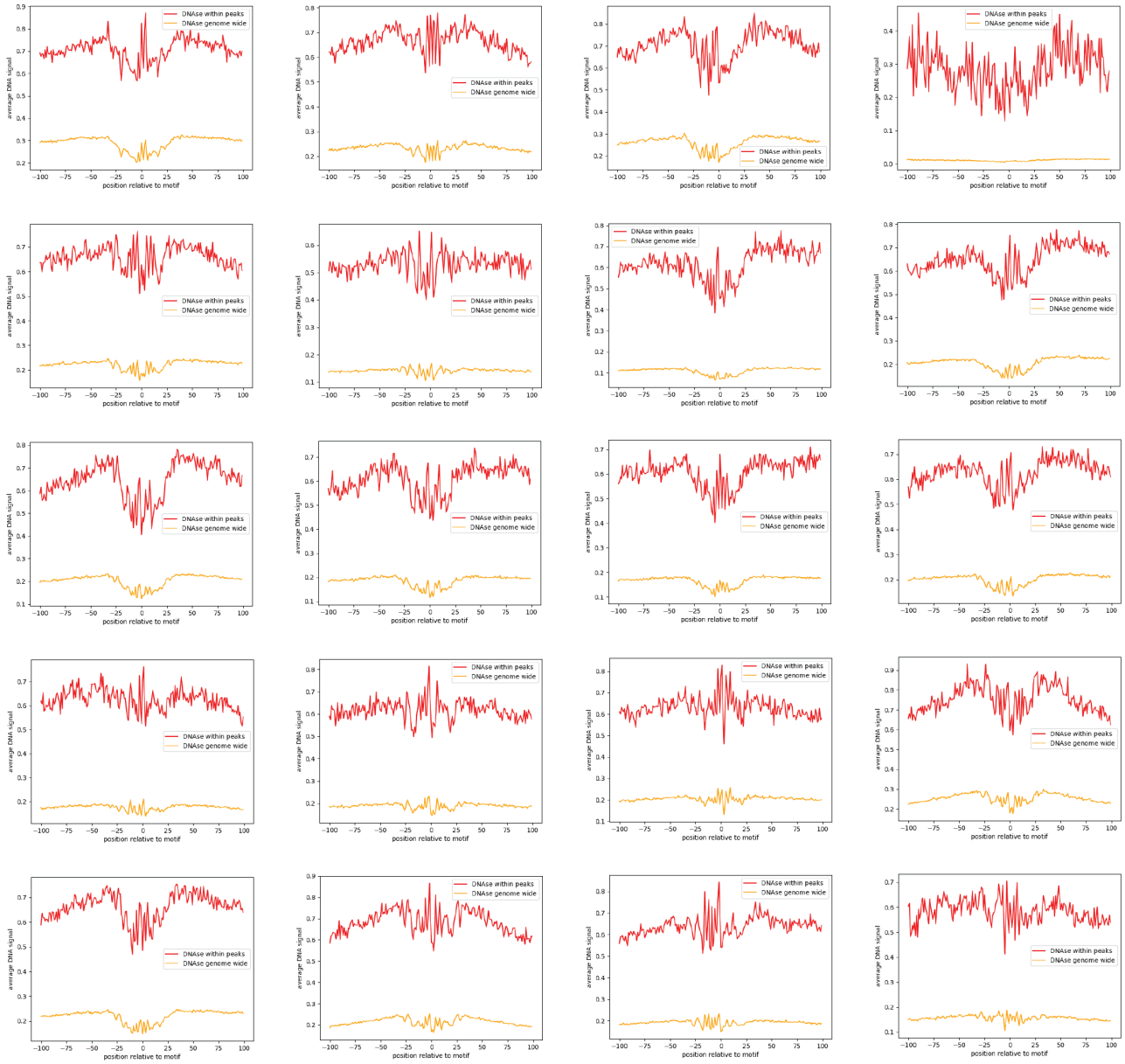
DNAse within peaks
DNAse genome wide
average DNA signal
position relative to motif

H


phastCons100way in peaks
phastCons30way in peaks
phastCons100way
phastCons30way
conservation score
position relative to motif

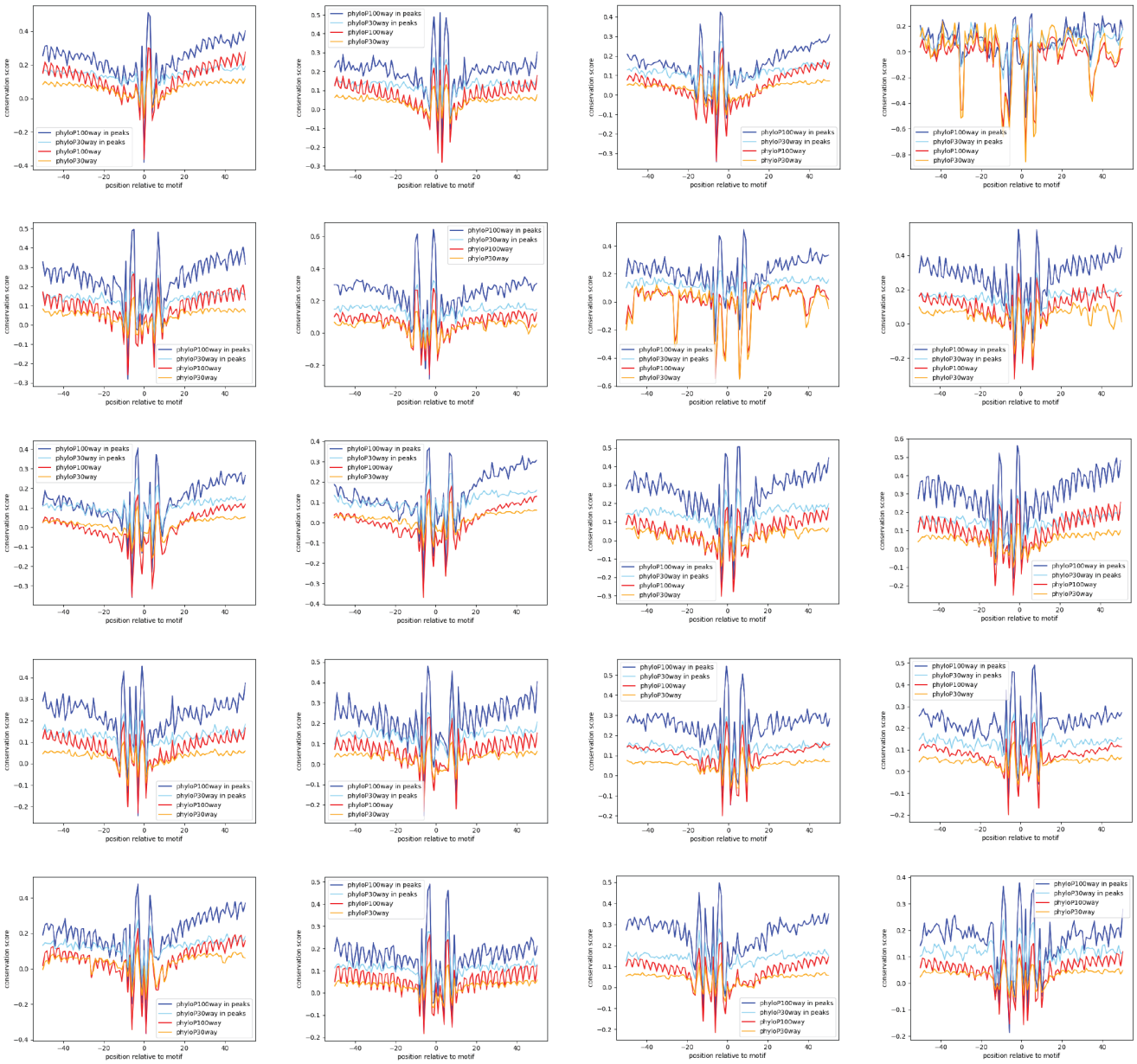

Supplementary Figure 54: Properties and genomic distribution of motifs identified for the HIC1 transcription factor in HEK293 (accession ENCSR803GYT).

TF-MoDisCO pattern_0 n=5014, CWM

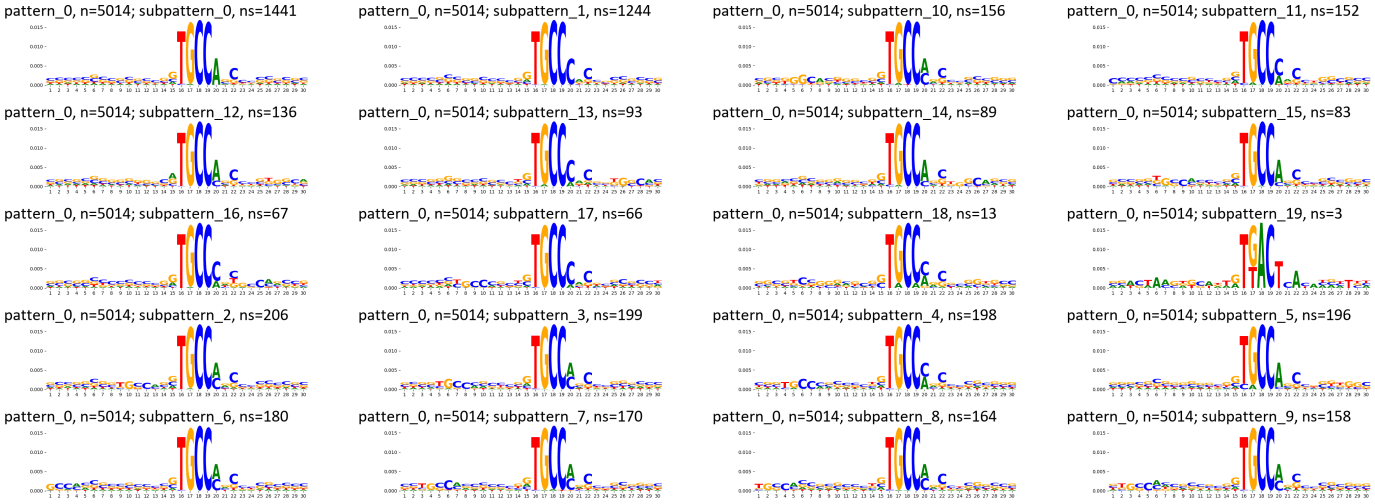

TF-MoDisCO pattern_0 n=5014, PWM

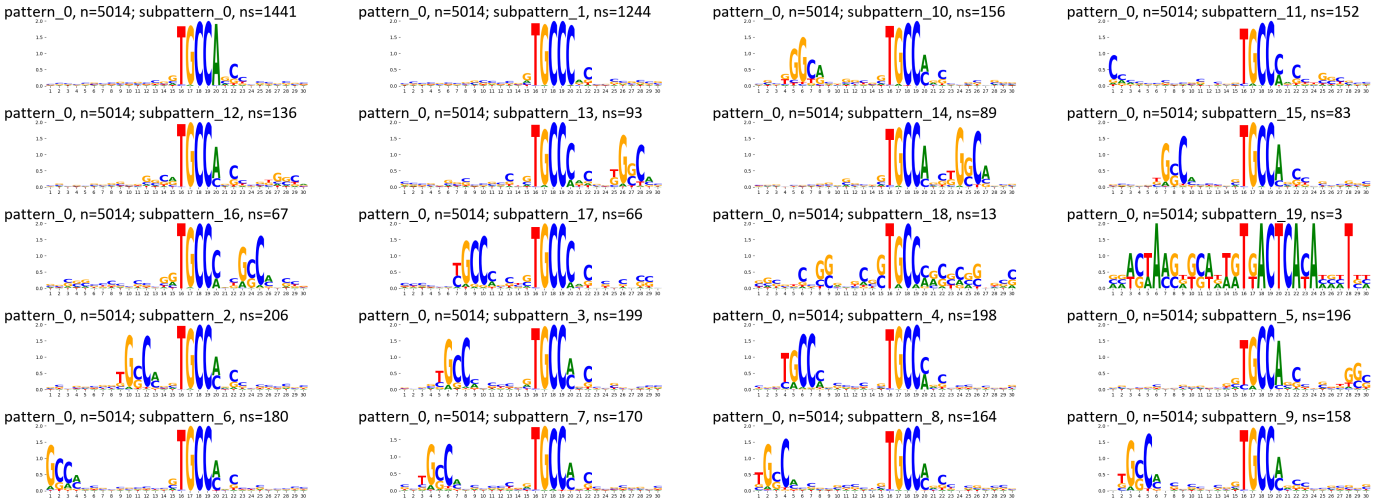

TF-MoDisCO pattern_10 n=248, CWM

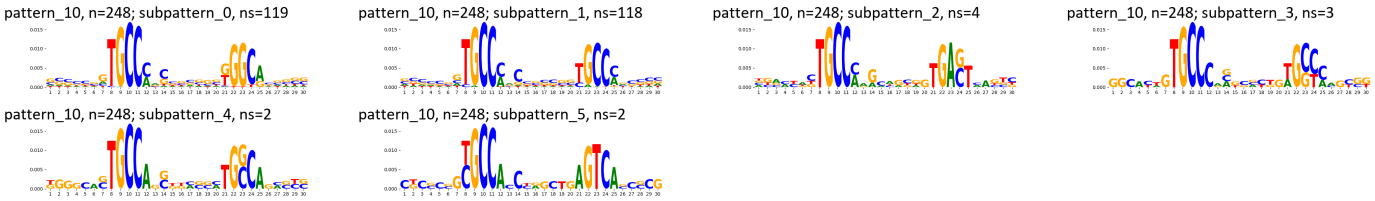

TF-MoDisCO pattern_10 n=248, PWM

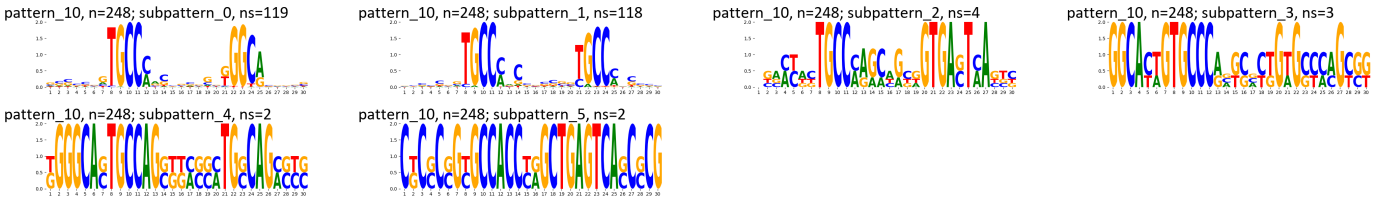

TF-MoDisCO pattern_11 n=246, CWM

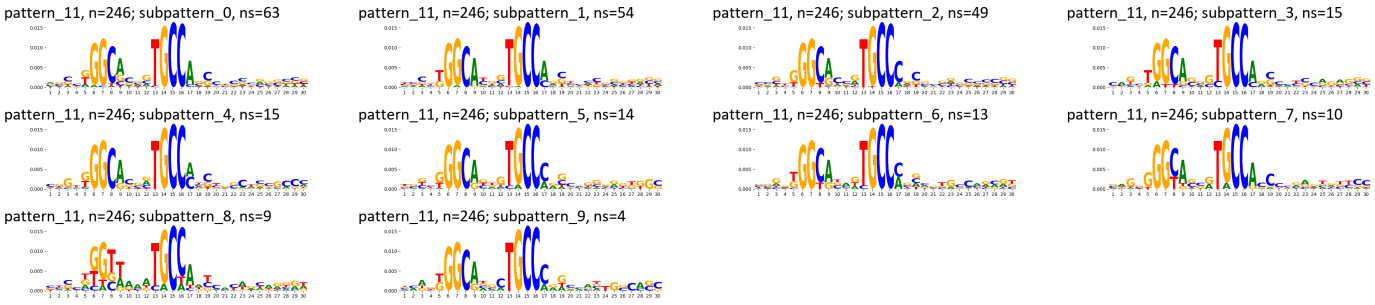

TF-MoDiSCO pattern_11 n=246, PWM

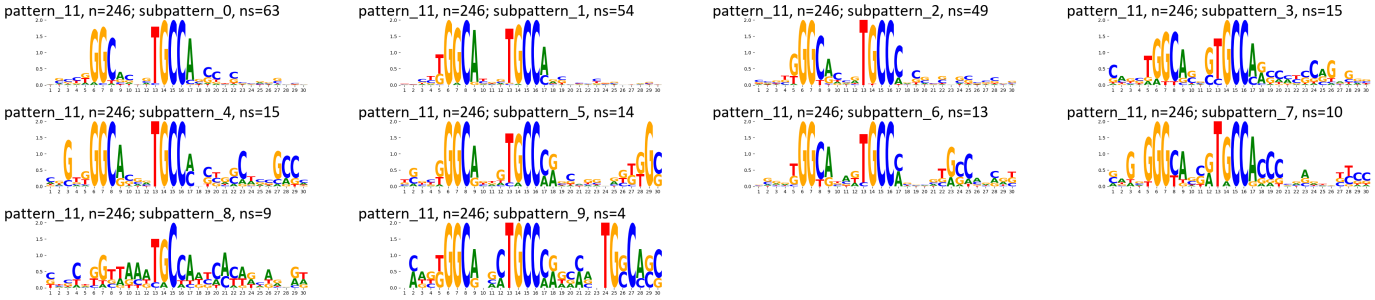

TF-MoDiSCO pattern_12 n=225, CWM

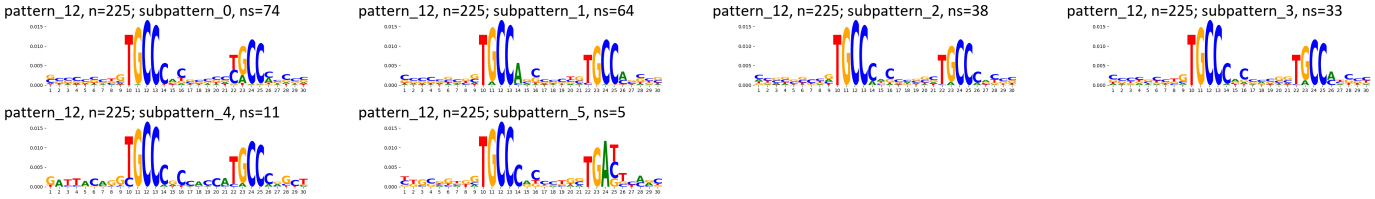

TF-MoDiSCO pattern_12 n=225, PWM

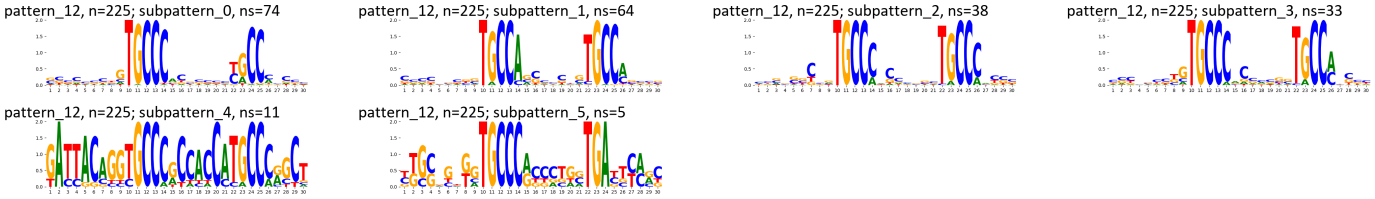

TF-MoDiSCO pattern_13 n=215, CWM

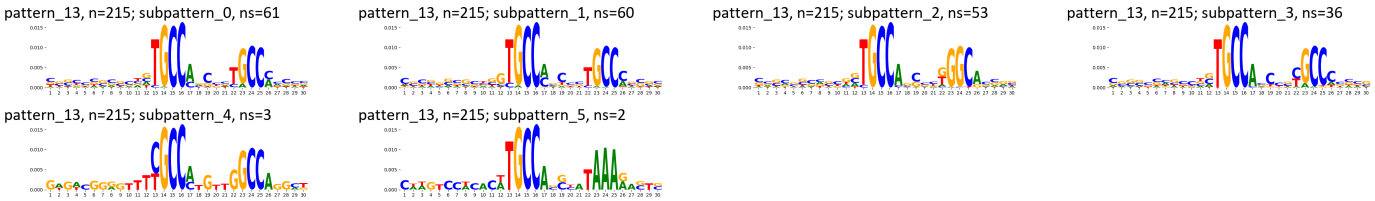

TF-MoDiSCO pattern_13 n=215, PWM

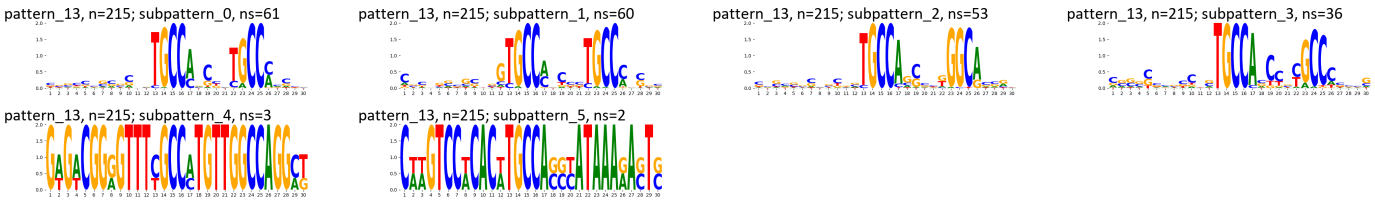

TF-MoDisCO pattern_14 n=195, CWM

pattern_14, n=195; subpattern_0, ns=46

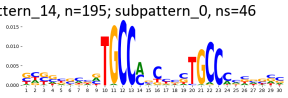

pattern_14, n=195; subpattern_1, ns=42

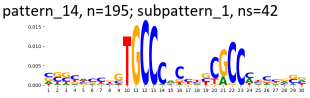

pattern_14, n=195; subpattern_2, ns=34

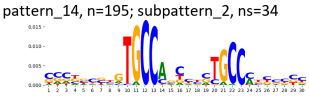

pattern_14, n=195; subpattern_3, ns=20

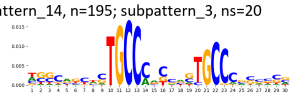

pattern_14, n=195; subpattern_4, ns=18

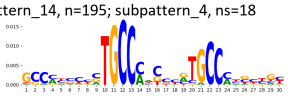

pattern_14, n=195; subpattern_5, ns=16

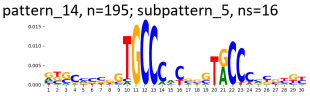

pattern_14, n=195; subpattern_6, ns=12

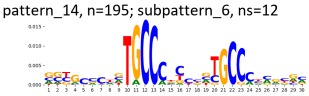

pattern_14, n=195; subpattern_7, ns=7

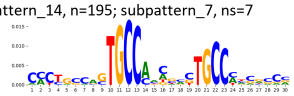

TF-MoDisCO pattern_14 n=195, PWM

pattern_14, n=195; subpattern_0, ns=46

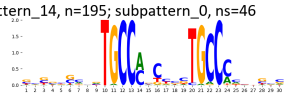

pattern_14, n=195; subpattern_1, ns=42

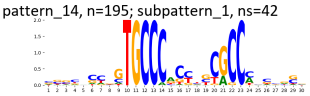

pattern_14, n=195; subpattern_2, ns=34

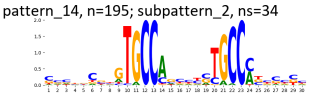

pattern_14, n=195; subpattern_3, ns=20

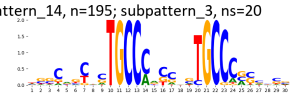

pattern_14, n=195; subpattern_4, ns=18

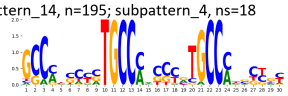

pattern_14, n=195; subpattern_5, ns=16

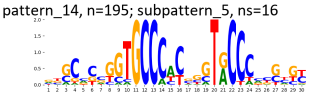

pattern_14, n=195; subpattern_6, ns=12

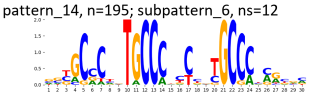

pattern_14, n=195; subpattern_7, ns=7

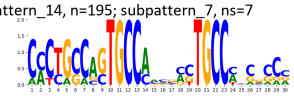

TF-MoDisCO pattern_15 n=182, CWM

pattern_15, n=182; subpattern_0, ns=53

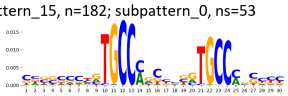

pattern_15, n=182; subpattern_1, ns=53

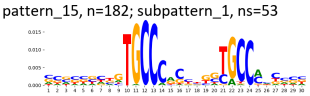

pattern_15, n=182; subpattern_2, ns=24

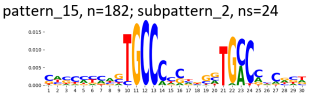

pattern_15, n=182; subpattern_3, ns=14

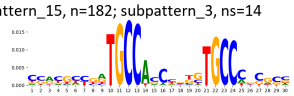

pattern_15, n=182; subpattern_4, ns=13

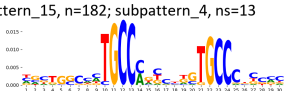

pattern_15, n=182; subpattern_5, ns=10

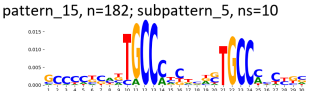

pattern_15, n=182; subpattern_6, ns=6

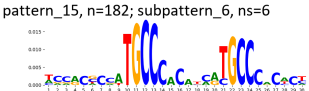

pattern_15, n=182; subpattern_7, ns=5

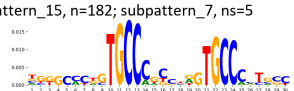

pattern_15, n=182; subpattern_8, ns=4

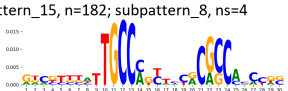

TF-MoDisCO pattern_15 n=182, PWM

pattern_15, n=182; subpattern_0, ns=53

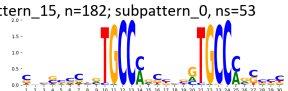

pattern_15, n=182; subpattern_1, ns=53

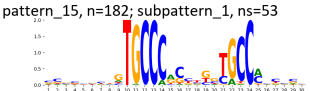

pattern_15, n=182; subpattern_2, ns=24

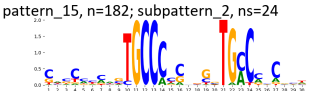

pattern_15, n=182; subpattern_3, ns=14

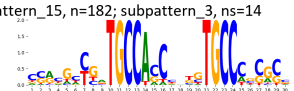

pattern_15, n=182; subpattern_4, ns=13

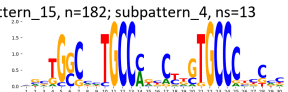

pattern_15, n=182; subpattern_5, ns=10

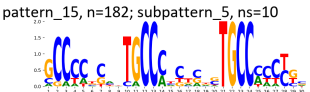

pattern_15, n=182; subpattern_6, ns=6

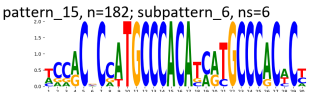

pattern_15, n=182; subpattern_7, ns=5

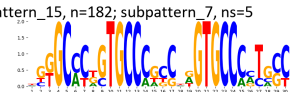

pattern_15, n=182; subpattern_8, ns=4

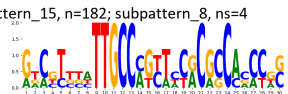

TF-MoDisCO pattern_17 n=167, CWM

pattern_17, n=167; subpattern_0, ns=40

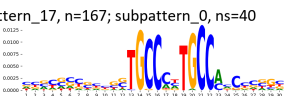

pattern_17, n=167; subpattern_1, ns=37

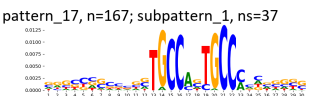

pattern_17, n=167; subpattern_2, ns=31

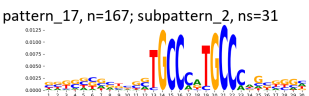

pattern_17, n=167; subpattern_3, ns=19

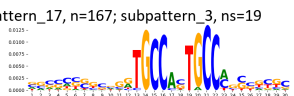

pattern_17, n=167; subpattern_4, ns=14

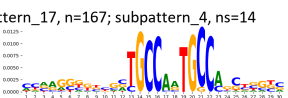

pattern_17, n=167; subpattern_5, ns=11

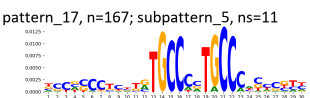

pattern_17, n=167; subpattern_6, ns=8

pattern_17, n=167; subpattern_7, ns=7

TF-MoDisCO pattern_17 n=167, PWM

pattern_17, n=167; subpattern_0, ns=40

pattern_17, n=167; subpattern_1, ns=37

pattern_17, n=167; subpattern_2, ns=31

pattern_17, n=167; subpattern_3, ns=19

pattern_17, n=167; subpattern_4, ns=14

pattern_17, n=167; subpattern_5, ns=11

pattern_17, n=167; subpattern_6, ns=8

pattern_17, n=167; subpattern_7, ns=7

TF-MoDisCO pattern_18 n=161, CWM

pattern_18, n=161; subpattern_0, ns=42

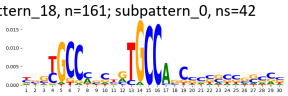

pattern_18, n=161; subpattern_1, ns=40

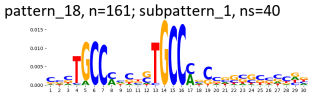

pattern_18, n=161; subpattern_2, ns=34

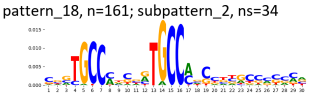

pattern_18, n=161; subpattern_3, ns=23

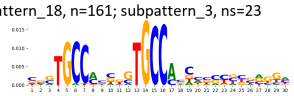

pattern_18, n=161; subpattern_4, ns=17

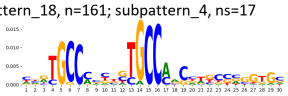

pattern_18, n=161; subpattern_5, ns=5

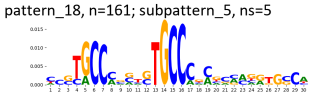

TF-MoDisCO pattern_18 n=161, PWM

pattern_18, n=161; subpattern_0, ns=42

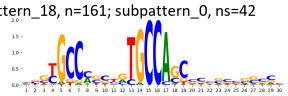

pattern_18, n=161; subpattern_1, ns=40

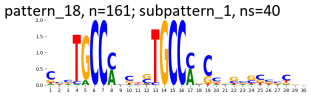

pattern_18, n=161; subpattern_2, ns=34

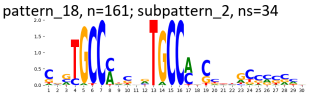

pattern_18, n=161; subpattern_3, ns=23

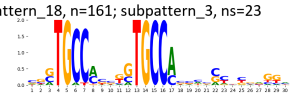

pattern_18, n=161; subpattern_4, ns=17

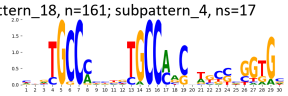

pattern_18, n=161; subpattern_5, ns=5

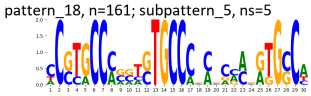

TF-MoDisCO pattern_19 n=158, CWM

pattern_19, n=158; subpattern_0, ns=49

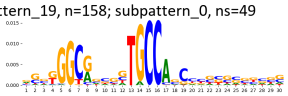

pattern_19, n=158; subpattern_1, ns=43

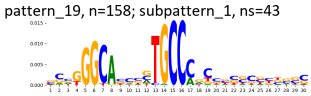

pattern_19, n=158; subpattern_2, ns=36

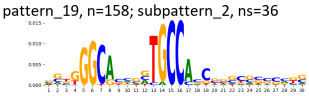

pattern_19, n=158; subpattern_3, ns=26

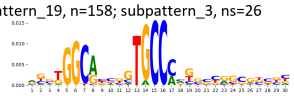

pattern_19, n=158; subpattern_4, ns=2

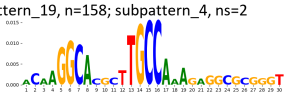

pattern_19, n=158; subpattern_5, ns=2

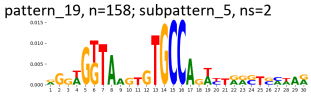

TF-MoDisCO pattern_19 n=158, PWM

pattern_19, n=158; subpattern_0, ns=49

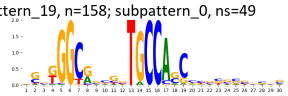

pattern_19, n=158; subpattern_1, ns=43

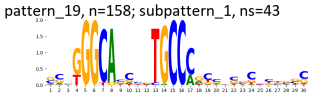

pattern_19, n=158; subpattern_2, ns=36

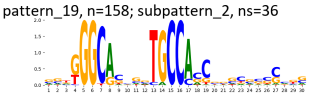

pattern_19, n=158; subpattern_3, ns=26

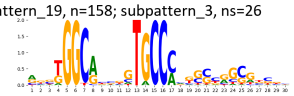

pattern_19, n=158; subpattern_4, ns=2

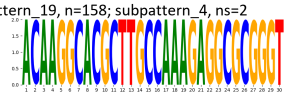

pattern_19, n=158; subpattern_5, ns=2

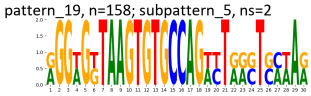

TF-MoDisCO pattern_20 n=143, CWM

pattern_20, n=143; subpattern_0, ns=51

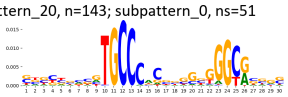

pattern_20, n=143; subpattern_1, ns=40

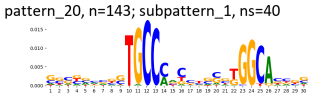

pattern_20, n=143; subpattern_2, ns=32

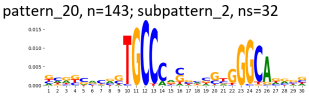

pattern_20, n=143; subpattern_3, ns=14

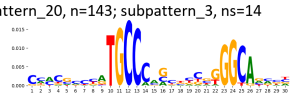

pattern_20, n=143; subpattern_4, ns=2

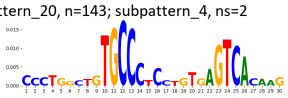

pattern_20, n=143; subpattern_5, ns=2

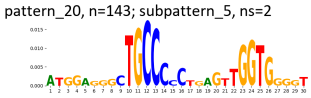

pattern_20, n=143; subpattern_6, ns=2

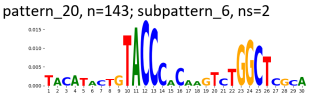

TF-MoDisCO pattern_20 n=143, PWM

pattern_20, n=143; subpattern_0, ns=51

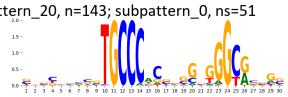

pattern_20, n=143; subpattern_1, ns=40

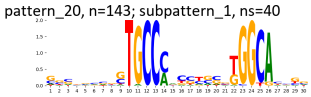

pattern_20, n=143; subpattern_2, ns=32

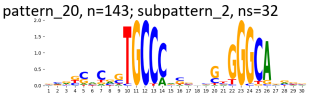

pattern_20, n=143; subpattern_3, ns=14

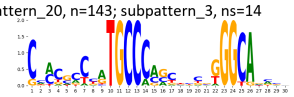

pattern_20, n=143; subpattern_4, ns=2

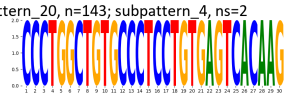

pattern_20, n=143; subpattern_5, ns=2

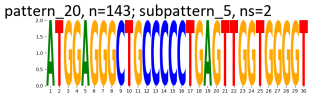

pattern_20, n=143; subpattern_6, ns=2

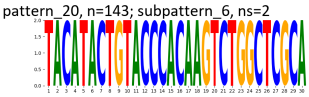

TF-MoDisCO pattern_21 n=127, CWM

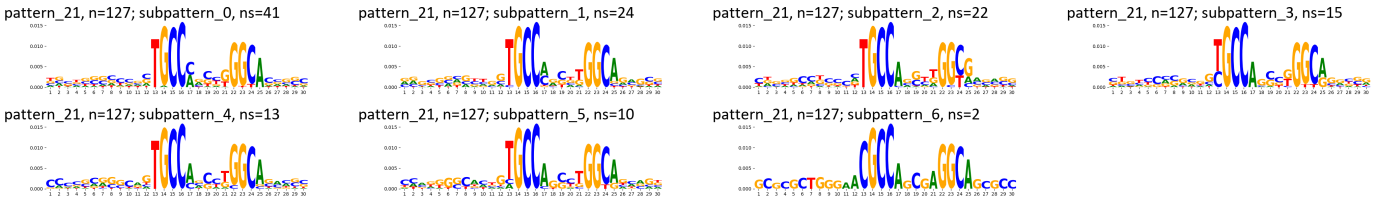

TF-MoDisCO pattern_21 n=127, PWM

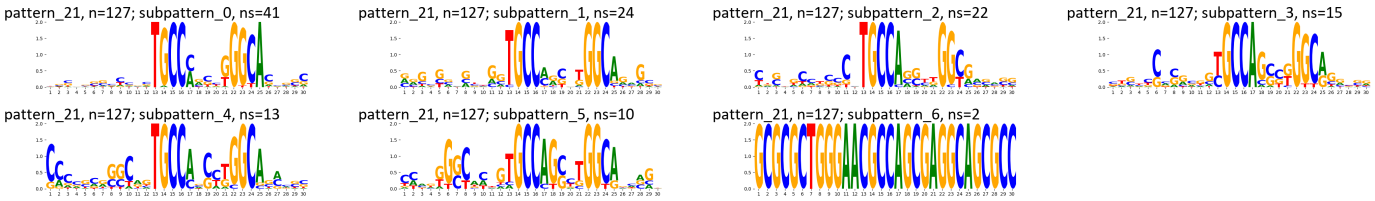

TF-MoDisCO pattern_23 n=109, CWM



TF-MoDisCO pattern_23 n=109, PWM



TF-MoDisCO pattern_24 n=108, CWM

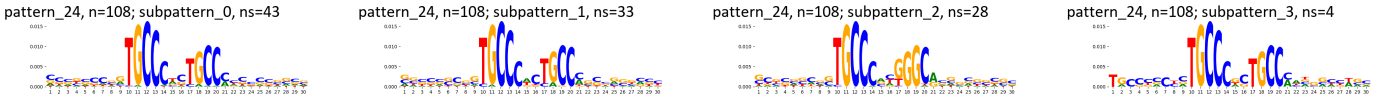

TF-MoDisCO pattern_24 n=108, PWM

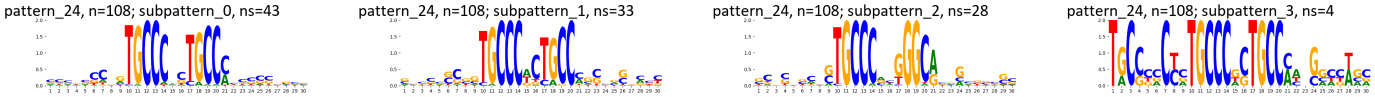

TF-MoDisCO pattern_25 n=103, CWM

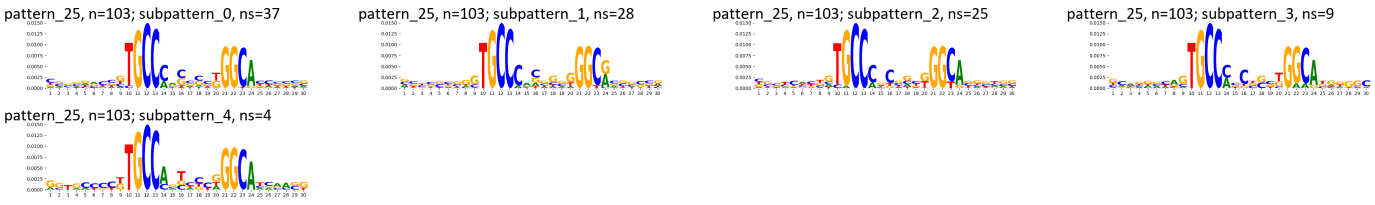

TF-MoDisCO pattern_25 n=103, PWM

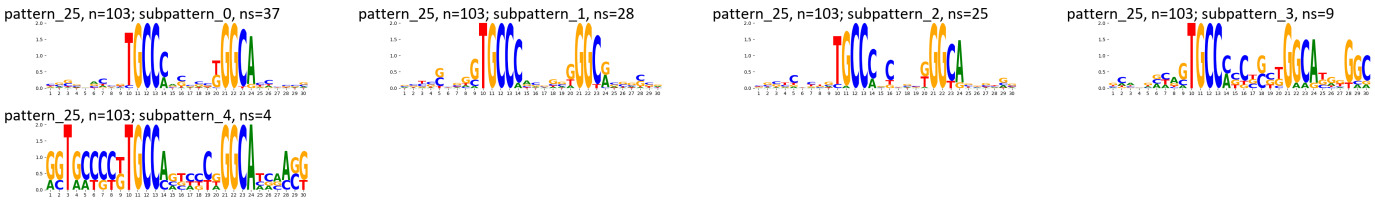

TF-MoDisCO pattern_27 n=75, CWM

pattern_27, n=75; subpattern_0, ns=23

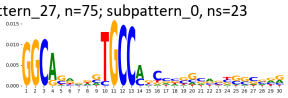

pattern_27, n=75; subpattern_1, ns=21

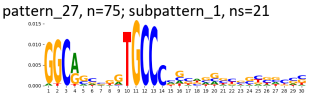

pattern_27, n=75; subpattern_2, ns=17

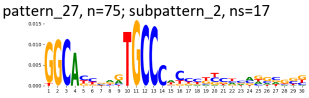

pattern_27, n=75; subpattern_3, ns=14

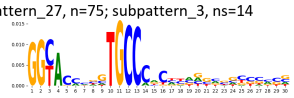

TF-MoDisCO pattern_27 n=75, PWM

pattern_27, n=75; subpattern_0, ns=23

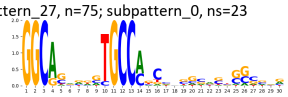

pattern_27, n=75; subpattern_1, ns=21

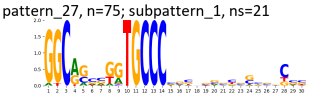

pattern_27, n=75; subpattern_2, ns=17

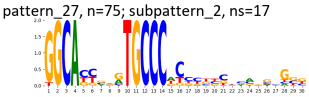

pattern_27, n=75; subpattern_3, ns=14

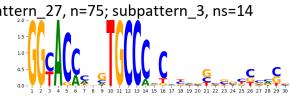

TF-MoDisCO pattern_3 n=551, CWM

pattern_3, n=551; subpattern_0, ns=136

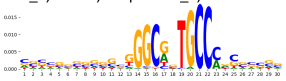

pattern_3, n=551; subpattern_1, ns=134

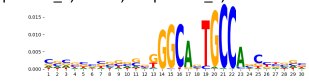

pattern_3, n=551; subpattern_2, ns=98

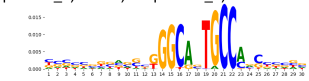

pattern_3, n=551; subpattern_3, ns=48

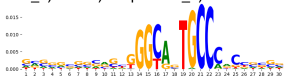

pattern_3, n=551; subpattern_4, ns=44

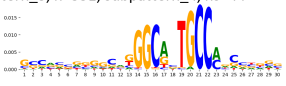

pattern_3, n=551; subpattern_5, ns=37

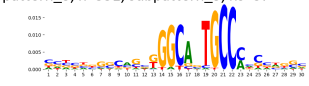

pattern_3, n=551; subpattern_6, ns=31

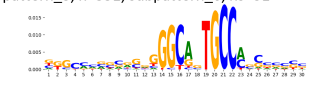

pattern_3, n=551; subpattern_7, ns=16

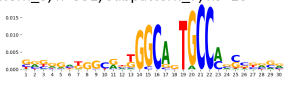

pattern_3, n=551; subpattern_8, ns=5

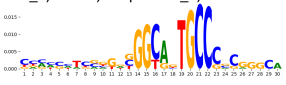

pattern_3, n=551; subpattern_9, ns=2

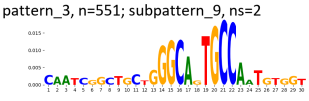

TF-MoDisCO pattern_3 n=551, PWM

pattern_3, n=551; subpattern_0, ns=136

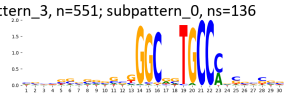

pattern_3, n=551; subpattern_1, ns=134

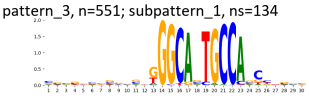

pattern_3, n=551; subpattern_2, ns=98

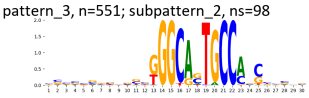

pattern_3, n=551; subpattern_3, ns=48

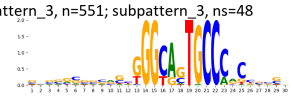

pattern_3, n=551; subpattern_4, ns=44

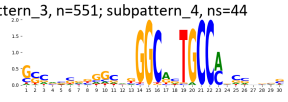

pattern_3, n=551; subpattern_5, ns=37

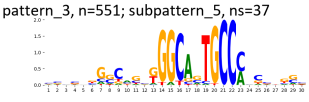

pattern_3, n=551; subpattern_6, ns=31

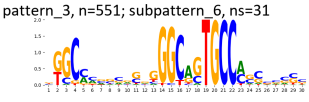

pattern_3, n=551; subpattern_7, ns=16

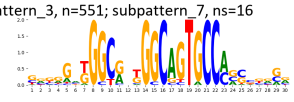

pattern_3, n=551; subpattern_8, ns=5

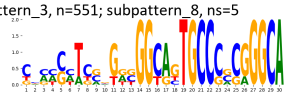

pattern_3, n=551; subpattern_9, ns=2

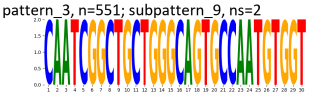

TF-MoDisCO pattern_31 n=20, CWM

pattern_31, n=20; subpattern_0, ns=20

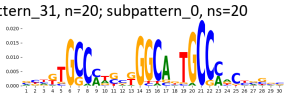

TF-MoDisCO pattern_31 n=20, PWM

pattern_31, n=20; subpattern_0, ns=20

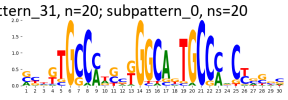

TF-MoDisCO pattern_7 n=337, CWM

pattern_7, n=337; subpattern_0, ns=96

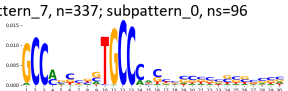

pattern_7, n=337; subpattern_1, ns=86

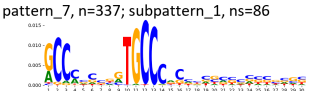

pattern_7, n=337; subpattern_2, ns=73

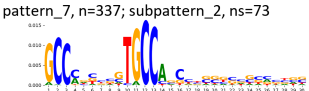

pattern_7, n=337; subpattern_3, ns=70

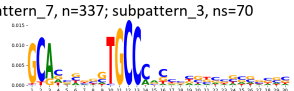

pattern_7, n=337; subpattern_4, ns=7

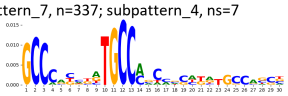

pattern_7, n=337; subpattern_5, ns=3

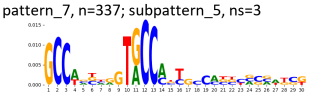

pattern_7, n=337; subpattern_6, ns=2

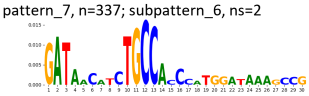

TF-MoDisCO pattern_7 n=337, PWM

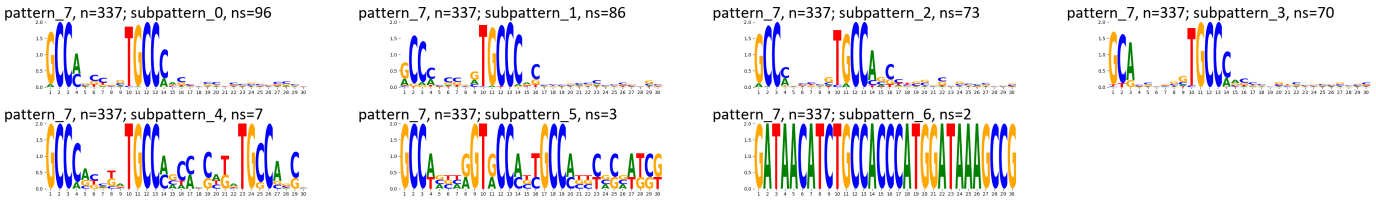

TF-MoDisCO pattern_8 n=303, CWM

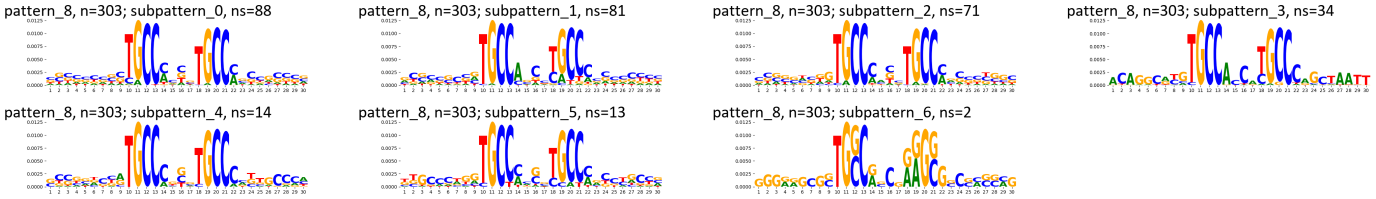

TF-MoDisCO pattern_8 n=303, PWM

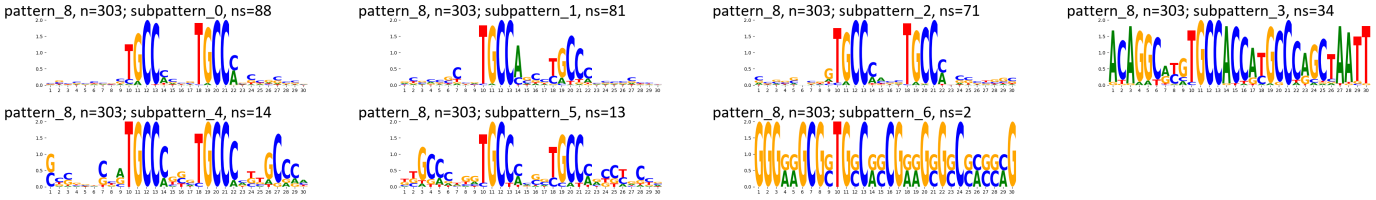

Supplementary Figure 55: TF-MoDisCO subpatterns for the HIC1 transcription factor in HEK293 (accession ENCSR803GYT).

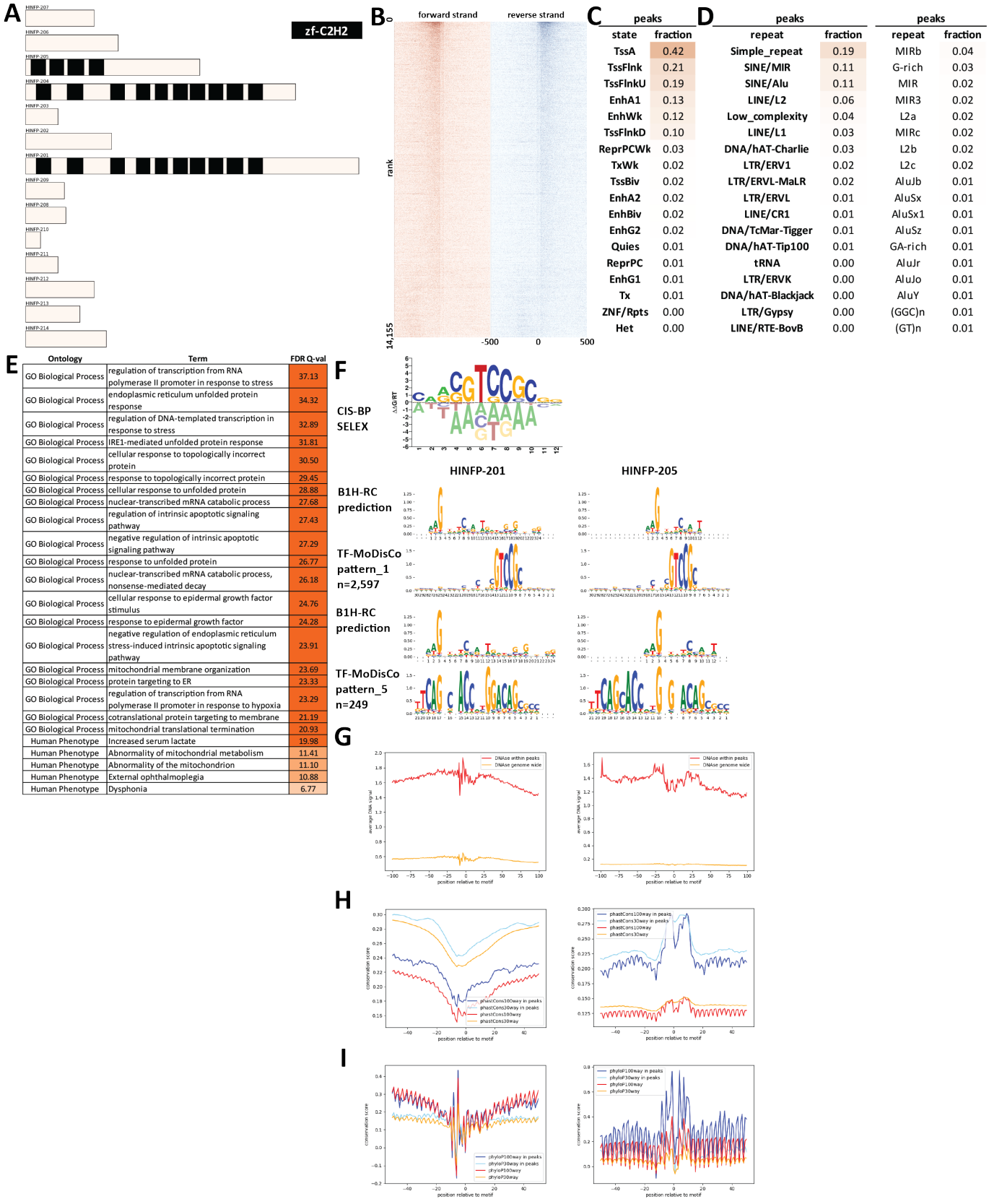

C

peaks	
state	fraction
TssA	0.42
TssFlnk	0.21
TssFlnkU	0.19
EnhA1	0.13
EnhWk	0.12
TssFlnkD	0.10
ReprPCWk	0.03
TxWk	0.02
TssBiv	0.02
EnhA2	0.02
EnhBiv	0.02
EnhG2	0.02
Quies	0.01
ReprPC	0.01
EnhG1	0.01
Tx	0.01
ZNF/Rpts	0.00
Het	0.00

D

peaks		peaks	
repeat	fraction	repeat	fraction
Simple_repeat	0.19	MIRb	0.04
SINE/MIR	0.11	G-rich	0.03
SINE/Alu	0.11	MIR	0.02
LINE/L2	0.06	MIR3	0.02
Low_complexity	0.04	L2a	0.02
LINE/L1	0.03	MIRc	0.02
DNA/hAT-Charlie	0.03	L2b	0.02
LTR/ERV1	0.02	L2c	0.02
LTR/ERVL-MaLR	0.02	AluJb	0.01
LTR/ERVL	0.01	AluSx	0.01
LINE/CR1	0.01	AluSx1	0.01
DNA/TcMar-Tigger	0.01	AluSz	0.01
DNA/hAT-Tip100	0.01	GA-rich	0.01
tRNA	0.00	AluJr	0.01
LTR/ERVK	0.00	AluJo	0.01
DNA/hAT-Blackjack	0.00	AluY	0.01
LTR/Gypsy	0.00	(GGC)n	0.01
LINE/RTE-BovB	0.00	(GT)n	0.01

E

Ontology	Term	FDR Q-val
GO Biological Process	regulation of transcription from RNA polymerase II promoter in response to stress	37.13
GO Biological Process	endoplasmic reticulum unfolded protein response	34.32
GO Biological Process	regulation of DNA-templated transcription in response to stress	32.89
GO Biological Process	IRE1-mediated unfolded protein response	31.81
GO Biological Process	cellular response to topologically incorrect protein	30.50
GO Biological Process	response to topologically incorrect protein	29.45
GO Biological Process	cellular response to unfolded protein	28.88
GO Biological Process	nuclear-transcribed mRNA catabolic process	27.68
GO Biological Process	regulation of intrinsic apoptotic signaling pathway	27.43
GO Biological Process	negative regulation of intrinsic apoptotic signaling pathway	27.29
GO Biological Process	response to unfolded protein	26.77
GO Biological Process	nuclear-transcribed mRNA catabolic process, nonsense-mediated decay	26.18
GO Biological Process	cellular response to epidermal growth factor stimulus	24.76
GO Biological Process	response to epidermal growth factor	24.28
GO Biological Process	negative regulation of endoplasmic reticulum stress-induced intrinsic apoptotic signaling pathway	23.91
GO Biological Process	mitochondrial membrane organization	23.69
GO Biological Process	protein targeting to ER	23.33
GO Biological Process	regulation of transcription from RNA polymerase II promoter in response to hypoxia	23.29
GO Biological Process	cotranslational protein targeting to membrane	21.19
GO Biological Process	mitochondrial translational termination	20.93
Human Phenotype	Increased serum lactate	19.98
Human Phenotype	Abnormality of mitochondrial metabolism	11.41
Human Phenotype	Abnormality of the mitochondrion	11.10
Human Phenotype	External ophthalmoplegia	10.88
Human Phenotype	Dysphonia	6.77

Supplementary Figure 56: Properties and genomic distribution of motifs identified for the HINFP transcription factor in HepG2 (accession ENCSR621PAN).

TF-MoDisCO pattern_1 n=2597, CWM

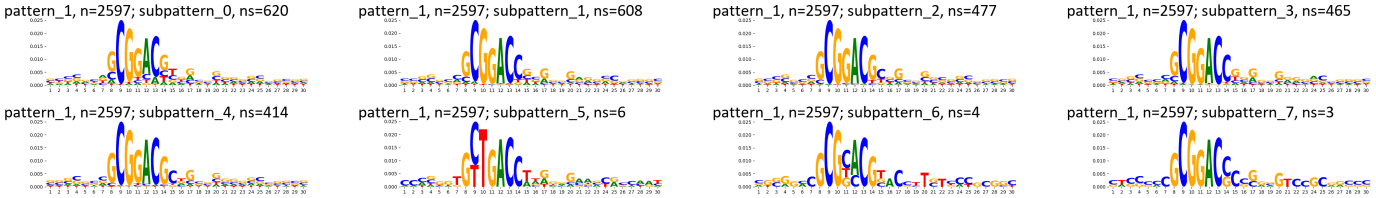

TF-MoDisCO pattern_1 n=2597, PWM

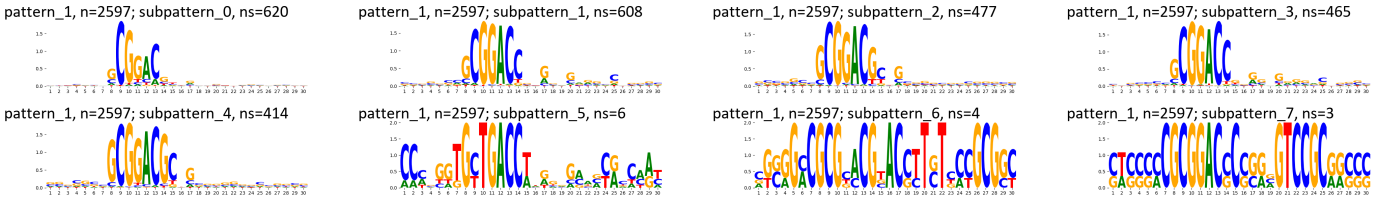

TF-MoDisCO pattern_5 n=249, CWM

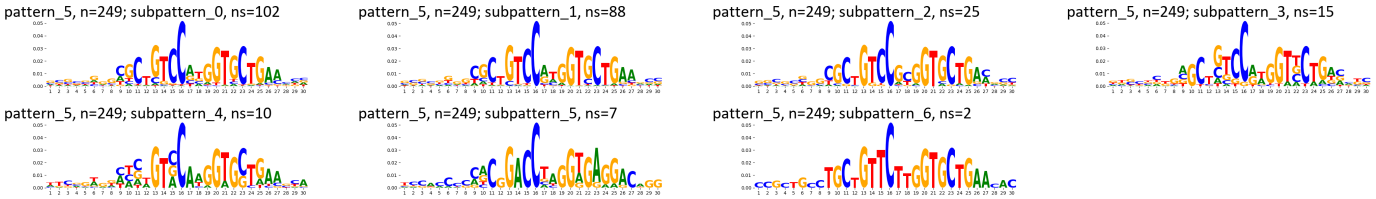

TF-MoDisCO pattern_5 n=249, PWM

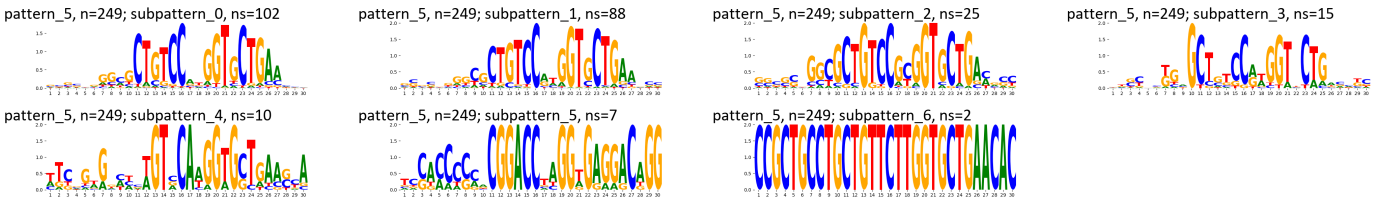

Supplementary Figure 57: TF-MoDisCO subpatterns for the HINFP transcription factor in HepG2 (accession ENCSR621PAN).



Supplementary Figure 58: Properties and genomic distribution of motifs identified for the HINFP transcription factor in K562 (accession ENCSR619GFP).

TF-MoDisCO pattern_0 n=1553, CWM

pattern_0, n=1553; subpattern_0, ns=338

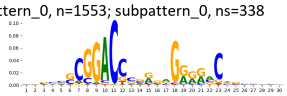

pattern_0, n=1553; subpattern_1, ns=290

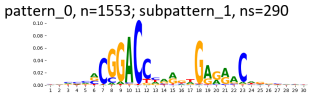

pattern_0, n=1553; subpattern_2, ns=262

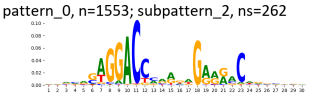

pattern_0, n=1553; subpattern_3, ns=229

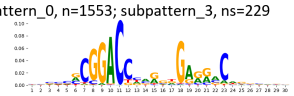

pattern_0, n=1553; subpattern_4, ns=220

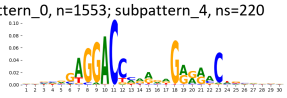

pattern_0, n=1553; subpattern_5, ns=202

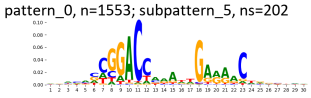

pattern_0, n=1553; subpattern_6, ns=8

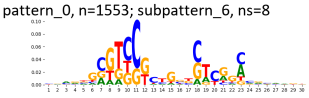

pattern_0, n=1553; subpattern_7, ns=4

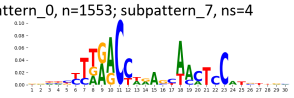

TF-MoDisCO pattern_0 n=1553, PWM

pattern_0, n=1553; subpattern_0, ns=338

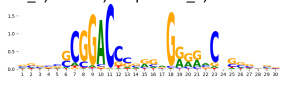

pattern_0, n=1553; subpattern_1, ns=290

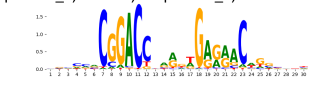

pattern_0, n=1553; subpattern_2, ns=262

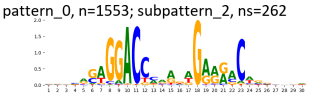

pattern_0, n=1553; subpattern_3, ns=229

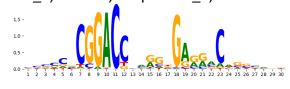

pattern_0, n=1553; subpattern_4, ns=220

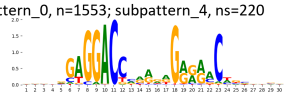

pattern_0, n=1553; subpattern_5, ns=202

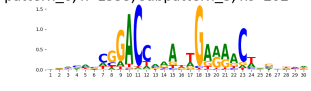

pattern_0, n=1553; subpattern_6, ns=8



pattern_0, n=1553; subpattern_7, ns=4

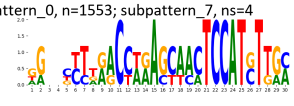

TF-MoDisCO pattern_1 n=1193, CWM

pattern_1, n=1193; subpattern_0, ns=228

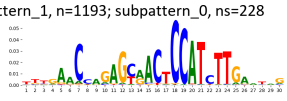

pattern_1, n=1193; subpattern_1, ns=224

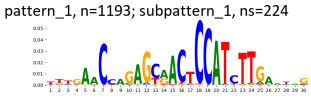

pattern_1, n=1193; subpattern_2, ns=200

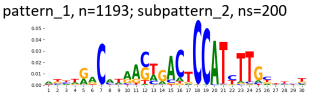

pattern_1, n=1193; subpattern_3, ns=153

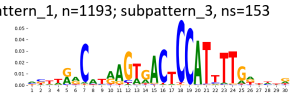

pattern_1, n=1193; subpattern_4, ns=130

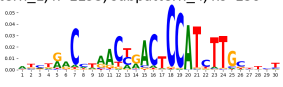

pattern_1, n=1193; subpattern_5, ns=105

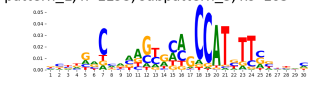

pattern_1, n=1193; subpattern_6, ns=85

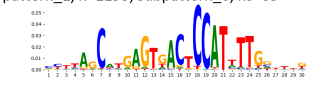

pattern_1, n=1193; subpattern_7, ns=68

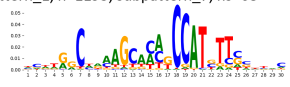

TF-MoDisCO pattern_1 n=1193, PWM

pattern_1, n=1193; subpattern_0, ns=228

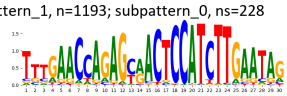

pattern_1, n=1193; subpattern_1, ns=224

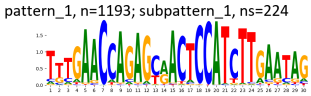

pattern_1, n=1193; subpattern_2, ns=200

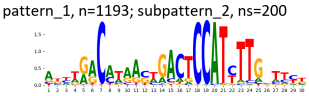

pattern_1, n=1193; subpattern_3, ns=153

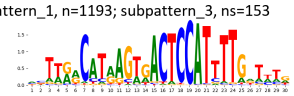

pattern_1, n=1193; subpattern_4, ns=130

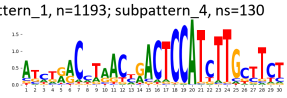

pattern_1, n=1193; subpattern_5, ns=105

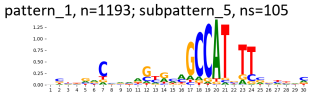

pattern_1, n=1193; subpattern_6, ns=85

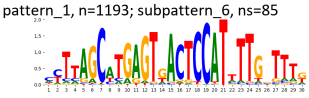

pattern_1, n=1193; subpattern_7, ns=68

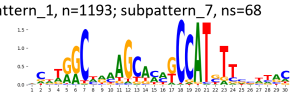

TF-MoDisCO pattern_2 n=1179, CWM

pattern_2, n=1179; subpattern_0, ns=242

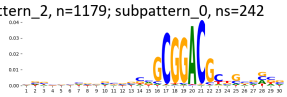

pattern_2, n=1179; subpattern_1, ns=224

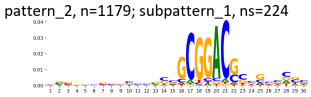

pattern_2, n=1179; subpattern_2, ns=212

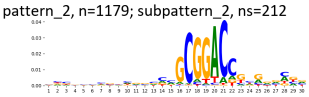

pattern_2, n=1179; subpattern_3, ns=202

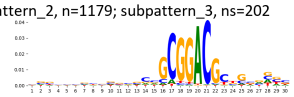

pattern_2, n=1179; subpattern_4, ns=199

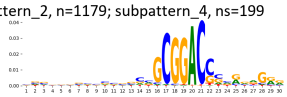

pattern_2, n=1179; subpattern_5, ns=86

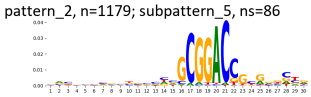

pattern_2, n=1179; subpattern_6, ns=14

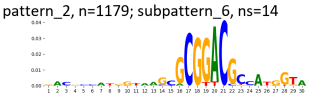

TF-MoDisCO pattern_2 n=1179, PWM

pattern_2, n=1179; subpattern_0, ns=242

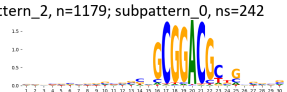

pattern_2, n=1179; subpattern_1, ns=224

pattern_2, n=1179; subpattern_2, ns=212

pattern_2, n=1179; subpattern_3, ns=202

pattern_2, n=1179; subpattern_4, ns=199

pattern_2, n=1179; subpattern_5, ns=86

pattern_2, n=1179; subpattern_6, ns=14

Supplementary Figure 59: TF-MoDisCO subpatterns for the HINFP transcription factor in K562 (accession ENCSR619GFP).

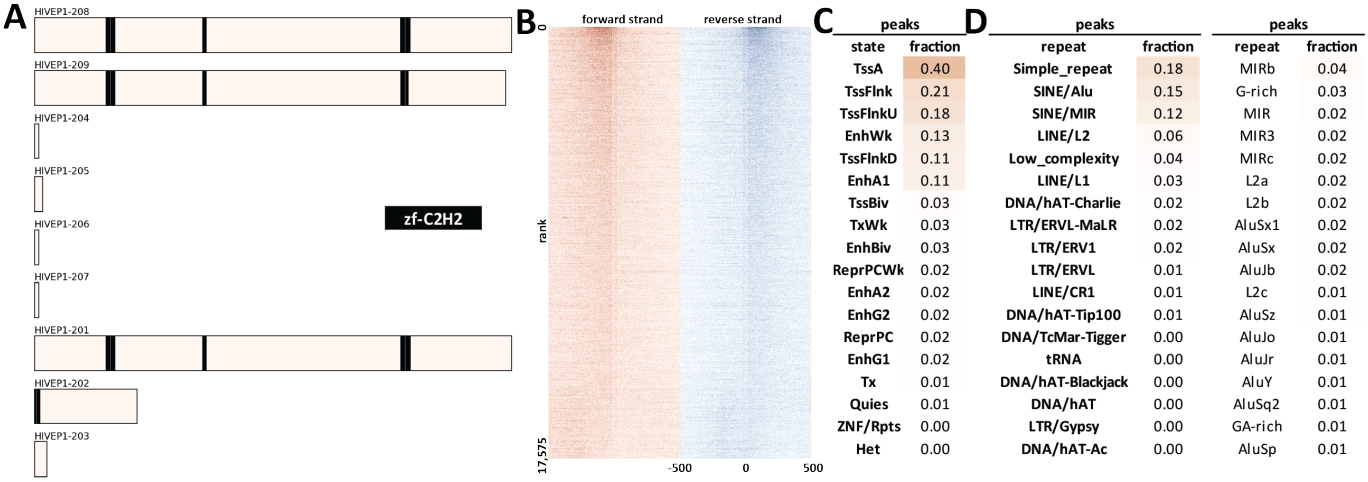

C

peaks

state	fraction
TssA	0.40
TssFlnk	0.21
TssFlnkU	0.18
EnhWk	0.13
TssFlnkD	0.11
EnhA1	0.11
TssBiv	0.03
TxWk	0.03
EnhBiv	0.03
ReprPCWk	0.02
EnhA2	0.02
EnhG2	0.02
ReprPC	0.02
EnhG1	0.02
Tx	0.01
Quies	0.01
ZNF/Rpts	0.00
Het	0.00

D

peaks

repeat	fraction
Simple_repeat	0.18
SINE/Alu	0.15
SINE/MIR	0.12
LINE/L2	0.06
Low_complexity	0.04
LINE/L1	0.03
DNA/hAT-Charlie	0.02
LTR/ERVL-MaLR	0.02
LTR/ERV1	0.02
LTR/ERVL	0.01
LINE/CR1	0.01
DNA/hAT-Tip100	0.01
DNA/TcMar-Tigger	0.00
tRNA	0.00
DNA/hAT-Blackjack	0.00
DNA/hAT	0.00
LTR/Gypsy	0.00
DNA/hAT-Ac	0.00

peaks

repeat	fraction
MIRb	0.04
G-rich	0.03
MIR	0.02
MIR3	0.02
MIRc	0.02
L2a	0.02
L2b	0.02
AluSx1	0.02
AluSx	0.02
AluJb	0.02
L2c	0.01
AluSz	0.01
AluJo	0.01
AluJr	0.01
AluY	0.01
AluSq2	0.01
GA-rich	0.01
AluSp	0.01

E

Ontology	Term	FDR Q-val
GO Biological Process	regulation of transcription from RNA polymerase II promoter in response to stress	49.68
GO Biological Process	regulation of intrinsic apoptotic signaling pathway	47.97
GO Biological Process	endoplasmic reticulum unfolded protein response	45.56
GO Biological Process	IRE1-mediated unfolded protein response	44.66
GO Biological Process	regulation of DNA-templated transcription in response to stress	44.28
GO Biological Process	positive regulation of transcription from RNA polymerase II promoter in response to endoplasmic reticulum stress	43.24
GO Biological Process	positive regulation of transcription from RNA polymerase II promoter in response to stress	42.33
GO Biological Process	cellular response to topologically incorrect protein	41.39
GO Biological Process	liver regeneration	40.53
GO Biological Process	cellular response to unfolded protein	38.76
GO Biological Process	negative regulation of intrinsic apoptotic signaling pathway	35.04
GO Biological Process	response to topologically incorrect protein	34.49
GO Biological Process	nuclear-transcribed mRNA catabolic process	34.21
GO Biological Process	response to unfolded protein	31.82
GO Biological Process	response to cadmium ion	31.58
GO Biological Process	nuclear-transcribed mRNA catabolic process, nonsense-mediated decay	28.61
GO Biological Process	regulation of transcription from RNA polymerase II promoter in response to hypoxia	27.47
GO Biological Process	regulation of endoplasmic reticulum unfolded protein response	27.33
GO Biological Process	protein targeting to ER	26.79
GO Biological Process	viral gene expression	22.85
Human Phenotype	Increased serum lactate	18.86
Human Phenotype	Exercise intolerance	16.07
Human Phenotype	External ophthalmoplegia	11.77
Human Phenotype	Abnormal CSF metabolite level	9.84
Human Phenotype	Increased CSF lactate	9.64
Human Phenotype	Abnormal activity of mitochondrial respiratory chain	3.53

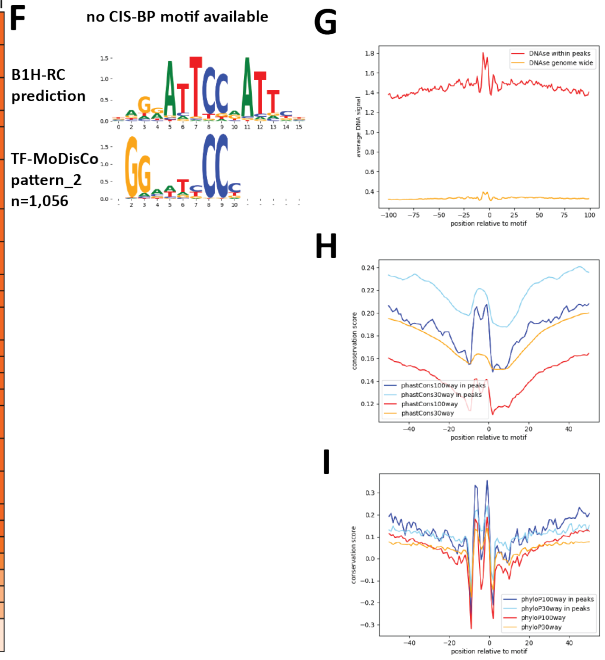

Supplementary Figure 60: Properties and genomic distribution of motifs identified for the HIVEP1 transcription factor in HepG2 (accession ENCSR697WMX).

TF-MoDisCO pattern_2 n=1056, CWM

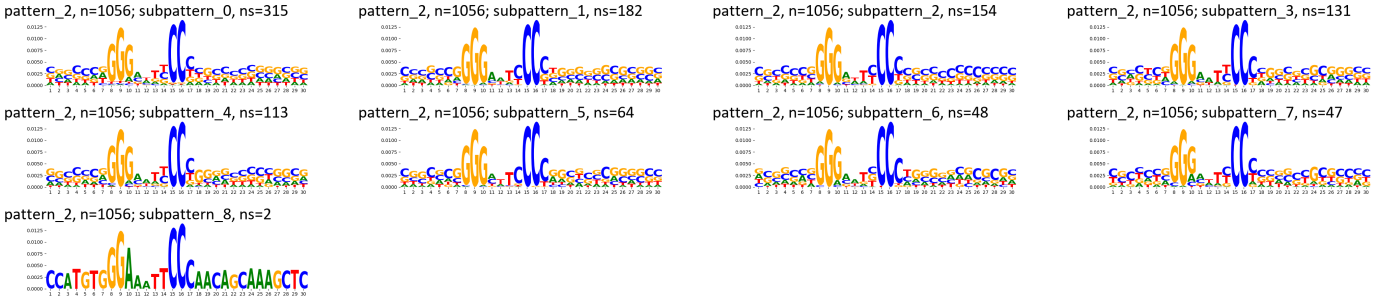

TF-MoDisCO pattern_2 n=1056, PWM

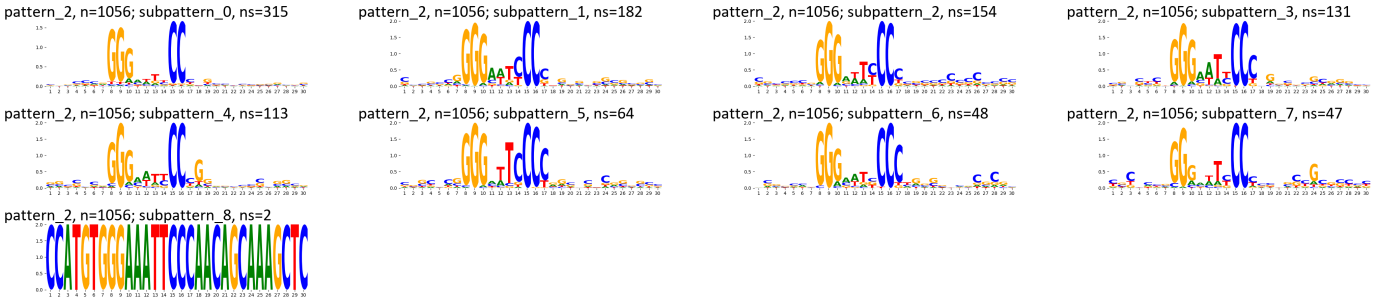

Supplementary Figure 61: TF-MoDisCO subpatterns for the HIVEP1 transcription factor in HepG2 (accession ENCSR697WMX).



C

peaks	
state	fraction
TssA	0.25
EnhA1	0.24
TssFlnkU	0.22
EnhWk	0.17
EnhA2	0.07
TxWk	0.06
Quies	0.06
TssFlnkD	0.05
TssFlnk	0.05
ReprPCWk	0.04
EnhG2	0.01
ReprPC	0.01
EnhG1	0.01
EnhBiv	0.01
Tx	0.01
TssBiv	0.00
Het	0.00
ZNF/Rpts	0.00

D

peaks		peaks	
repeat	fraction	repeat	fraction
LTR/ERV1	0.18	MER41B	0.04
SINE/Alu	0.09	MER41A	0.03
Simple_repeat	0.08	MIRb	0.02
SINE/MIR	0.07	L2a	0.02
LINE/L2	0.05	MIRc	0.02
LINE/L1	0.04	MIR3	0.02
LTR/ERVL	0.04	MIR	0.02
LTR/ERVL-MaLR	0.04	L2c	0.01
DNA/hAT-Charlie	0.02	LTR8	0.01
Low_complexity	0.02	AluJb	0.01
LTR/ERVK	0.01	G-rich	0.01
LINE/CR1	0.01	L2b	0.01
DNA/TcMar-Tigger	0.01	LTR54	0.01
snRNA	0.01	AluSx1	0.01
DNA/hAT-Tip100	0.00	AluJo	0.01
tRNA	0.00	AluSx	0.01
LTR/Gypsy	0.00	AluSz	0.01
DNA/hAT-Blackjack	0.00	L2	0.01

E

Ontology	Term	FDR Q-val
GO Biological Process	blood coagulation	18.71
GO Biological Process	coagulation	18.67
GO Biological Process	production of molecular mediator of immune response	13.61
GO Biological Process	platelet activation	12.75
GO Biological Process	platelet-derived growth factor receptor signaling pathway	12.63
GO Biological Process	cellular response to dexamethasone stimulus	11.70
GO Biological Process	regulation of intrinsic apoptotic signaling pathway	10.31
GO Biological Process	response to dexamethasone	8.97
GO Biological Process	chromatin assembly or disassembly	8.60
GO Biological Process	cellular response to glucocorticoid stimulus	8.09
GO Biological Process	cellular response to corticosteroid stimulus	7.85
GO Biological Process	positive regulation of neuron death	7.40
GO Biological Process	face development	7.15
GO Biological Process	placenta blood vessel development	6.95
GO Biological Process	regulation of endoplasmic reticulum stress-induced intrinsic apoptotic signaling pathway	6.08
GO Biological Process	face morphogenesis	6.04
GO Biological Process	head morphogenesis	5.99
GO Biological Process	positive regulation of intrinsic apoptotic signaling pathway	4.79
GO Biological Process	negative regulation of transcription from RNA polymerase II promoter in response to stress	4.32
GO Biological Process	preganglionic parasympathetic fiber development	4.02

Supplementary Figure 62: Properties and genomic distribution of motifs identified for the HIVEP1 transcription factor in K562 (accession ENCSR947PJZ).

TF-MoDisCO pattern_0 n=990, CWM

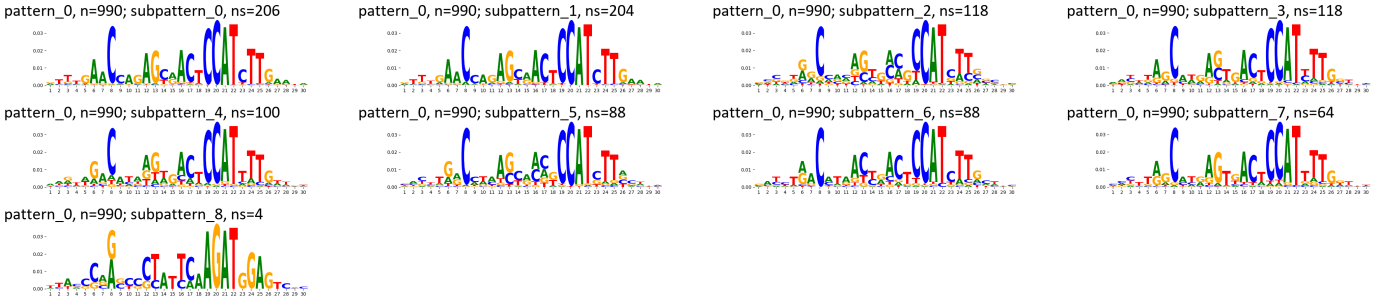

TF-MoDisCO pattern_0 n=990, PWM

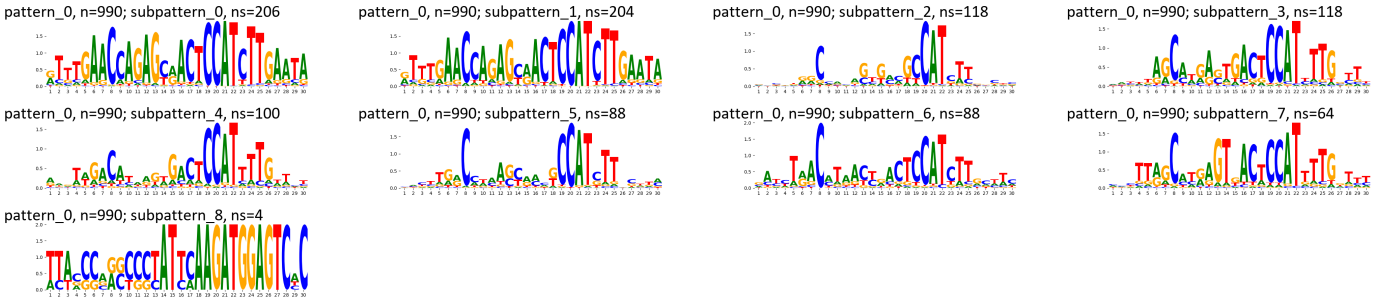

TF-MoDisCO pattern_1 n=317, CWM

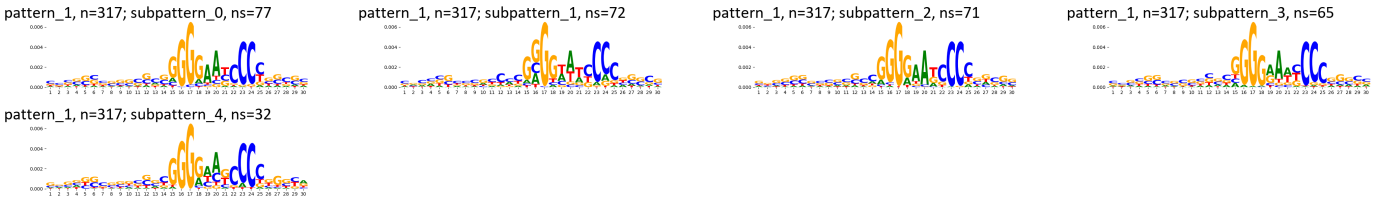

TF-MoDisCO pattern_1 n=317, PWM

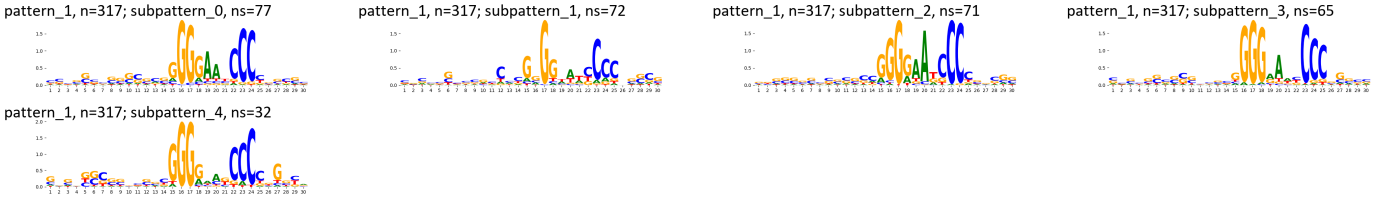

Supplementary Figure 63: TF-MoDisCO subpatterns for the HIVEP1 transcription factor in K562 (accession ENCSR947PJZ).

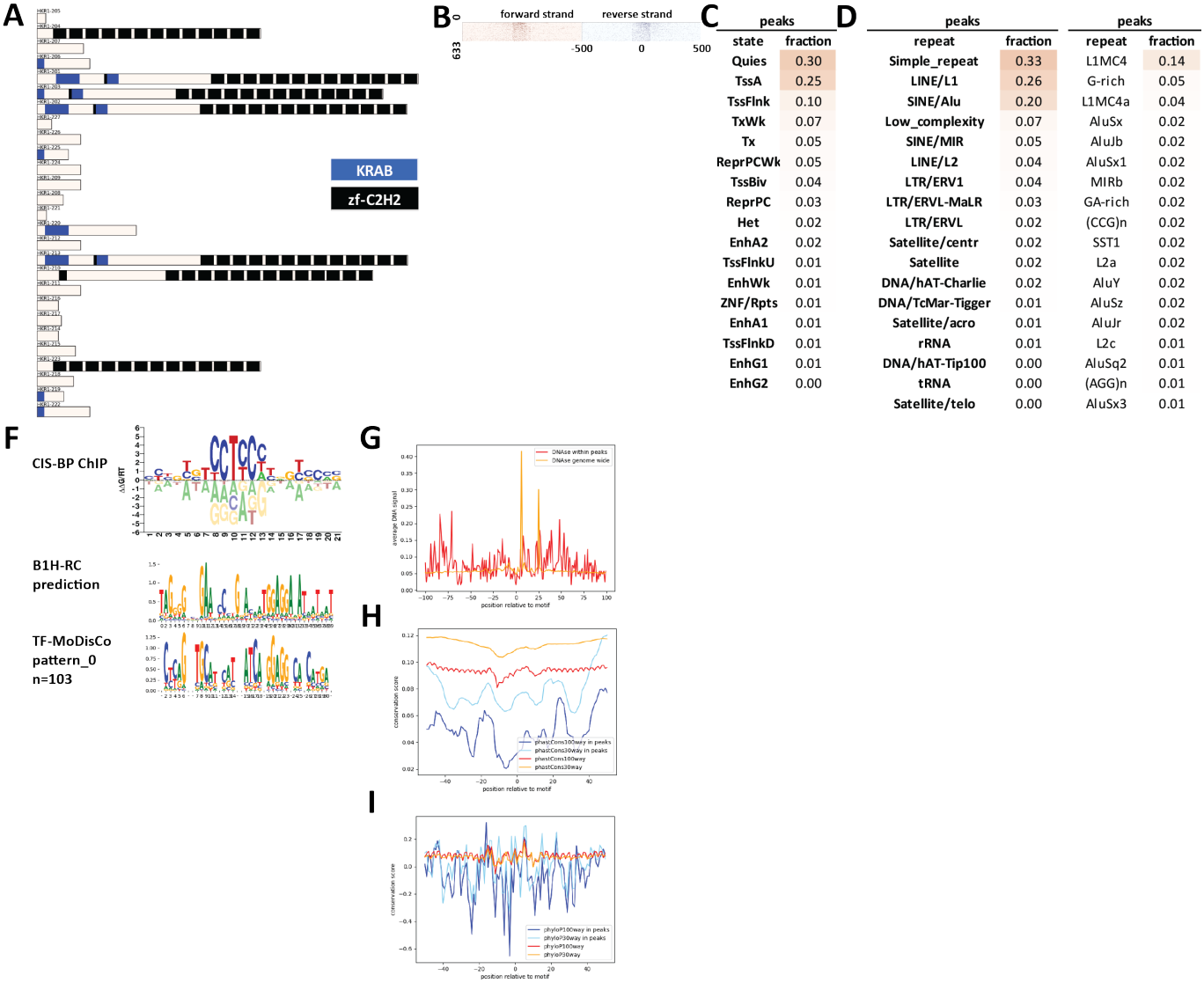

Supplementary Figure 64: Properties and genomic distribution of motifs identified for the HKR1 transcription factor in HEK293 (accession ChipExo models).

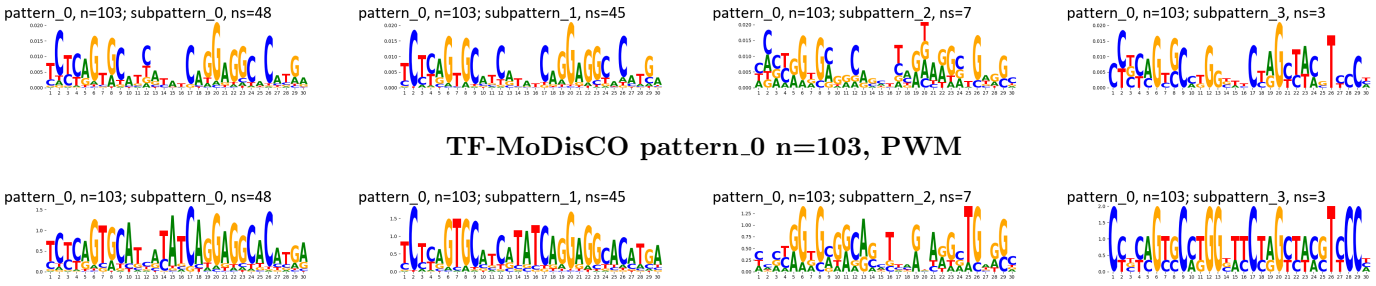

Supplementary Figure 65: TF-MoDisCO subpatterns for the HKR1 transcription factor in HEK293 (accession ChipExo models).

A

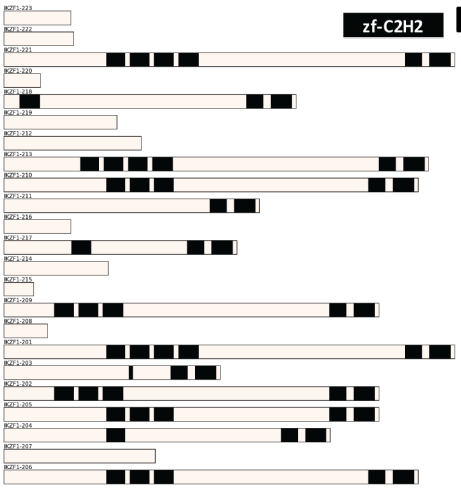

B

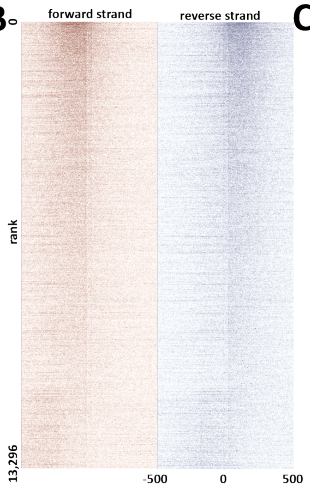

C

peaks

state	fraction
EnhA1	0.36
EnhWk	0.30
TssFlnkU	0.14
EnhA2	0.14
TssA	0.11
Quies	0.07
TxWk	0.05
TssFlnkD	0.04
TssFlnk	0.02
ReprPCWk	0.01
EnhG2	0.01
EnhG1	0.01
Het	0.01
ZNF/Rpts	0.01
Tx	0.00
EnhBiv	0.00
ReprPC	0.00
TssBiv	0.00

D

peaks

repeat	fraction	repeat	fraction
SINE/Alu	0.18	MIRb	0.06
SINE/MIR	0.15	L2a	0.04
LINE/L1	0.13	MIR	0.03
Simple_repeat	0.12	L2c	0.03
LINE/L2	0.11	MIR3	0.03
LTR/ERVL-MaLR	0.06	MIRc	0.03
DNA/hAT-Charlie	0.06	L2b	0.03
LTR/ERV1	0.03	AluSx	0.02
LTR/ERVL	0.03	AluSx1	0.02
Low_complexity	0.02	AluJb	0.02
LINE/CR1	0.02	AluSz	0.02
DNA/TcMar-Tigger	0.02	L3	0.01
DNA/hAT-Tip100	0.01	L2	0.01
DNA/hAT-Blackjack	0.00	AluJo	0.01
LINE/RTE-X	0.00	AluJr	0.01
LTR/Gypsy	0.00	(T)n	0.01
DNA/TcMar-Mariner	0.00	A-rich	0.01
LINE/RTE-BovB	0.00	MER5A	0.01

E

Ontology	Term	FDR Q-val
GO Biological Process	positive regulation of immune system process	198.35
GO Biological Process	regulation of immune response	169.99
GO Biological Process	leukocyte activation	169.16
GO Biological Process	response to external biotic stimulus	140.19
GO Biological Process	response to other organism	139.03
GO Biological Process	regulation of cytokine production	133.31
GO Biological Process	regulation of leukocyte activation	125.59
GO Biological Process	regulation of cell activation	123.73
GO Biological Process	lymphocyte activation	121.40
GO Biological Process	regulation of lymphocyte activation	120.58
GO Biological Process	adaptive immune response	112.39
GO Biological Process	positive regulation of cell activation	109.81
GO Biological Process	cytokine-mediated signaling pathway	109.58
GO Biological Process	positive regulation of immune response	109.39
GO Biological Process	positive regulation of leukocyte activation	105.54
GO Biological Process	regulation of innate immune response	100.69
GO Biological Process	positive regulation of cytokine production	97.83
GO Biological Process	positive regulation of lymphocyte activation	97.12
GO Biological Process	leukocyte differentiation	97.01
GO Biological Process	regulation of T cell activation	93.41
Human Phenotype	Abnormality of leukocytes	53.63
Human Phenotype	Abnormality of lymphocytes	48.94
Human Phenotype	Abnormality of B cell physiology	37.79
Human Phenotype	Abnormality of bone marrow cell morphology	37.04
Human Phenotype	Abnormal leukocyte count	36.81
Human Phenotype	Abnormal immunoglobulin level	36.74
Human Phenotype	Abnormality of cells of the lymphoid lineage	32.19
Human Phenotype	Decreased antibody level in blood	31.85
Human Phenotype	Inflammatory abnormality of the skin	28.52
Human Phenotype	Abnormality of the lymph nodes	26.88
Human Phenotype	Lymphadenopathy	23.73
Human Phenotype	Leukopenia	22.82
Human Phenotype	Lymphopenia	22.43

F

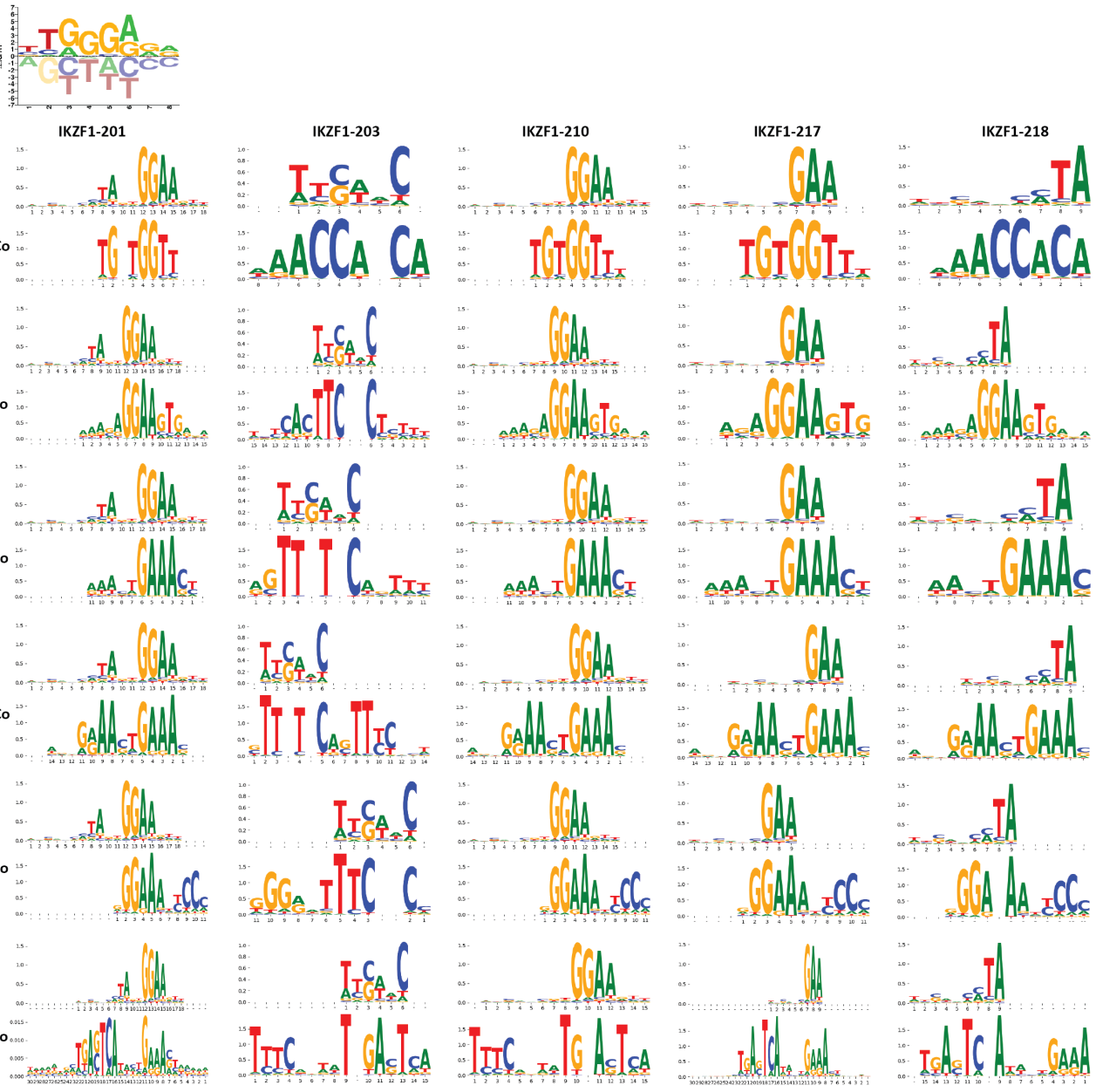
CIS-BP misc
IKZF1-201
IKZF1-203
IKZF1-210
IKZF1-217
IKZF1-218
B1H-RC prediction
TF-MoDisCo pattern_0 n=3,075
B1H-RC prediction
TF-MoDisCo pattern_1 n=2,259
B1H-RC prediction
TF-MoDisCo pattern_3 n=1,623
B1H-RC prediction
TF-MoDisCo pattern_4 n=1,306
B1H-RC prediction
TF-MoDisCo pattern_5 n=666
B1H-RC prediction
TF-MoDisCo pattern_6 n=448

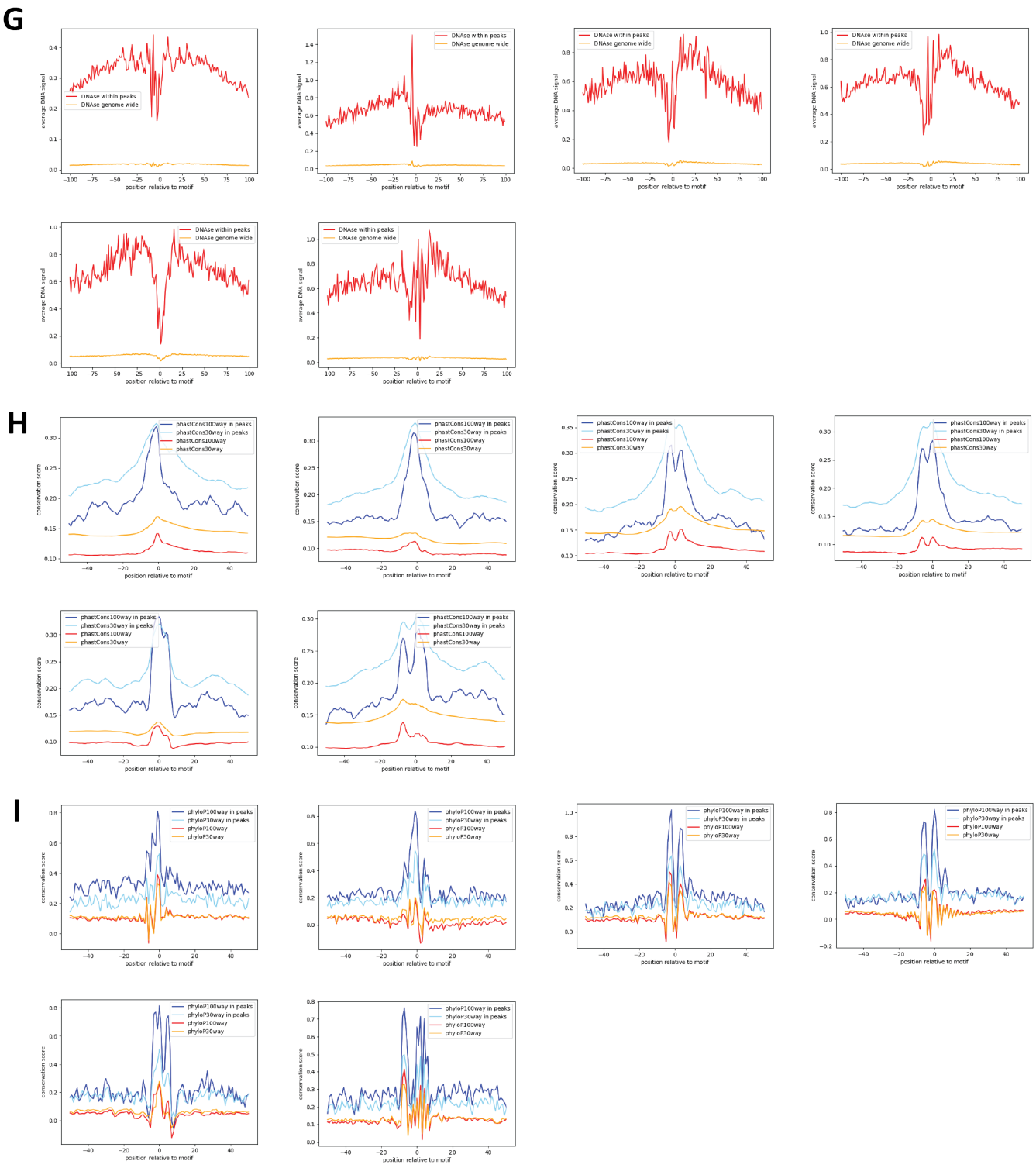

Supplementary Figure 66: Properties and genomic distribution of motifs identified for the IKZF1 transcription factor in GM12878 (accession ENCSR000EUJ).

TF-MoDisCO pattern_0 n=3075, CWM

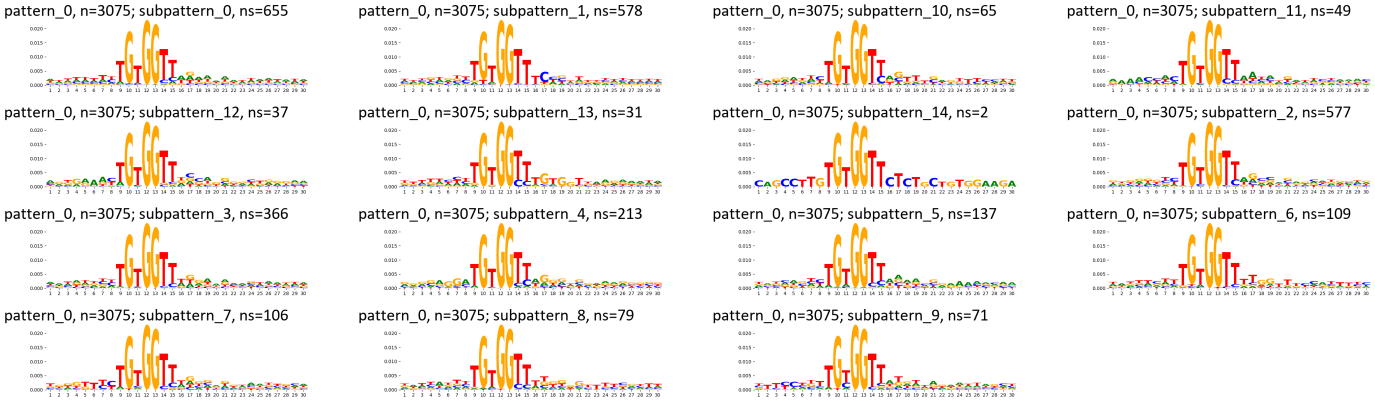

TF-MoDisCO pattern_0 n=3075, PWM

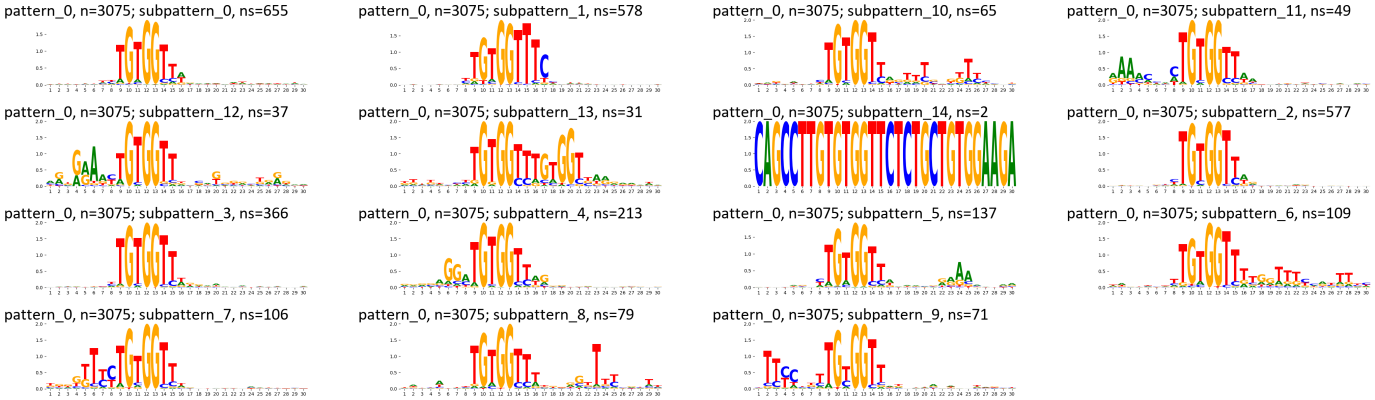

TF-MoDisCO pattern_1 n=2259, CWM

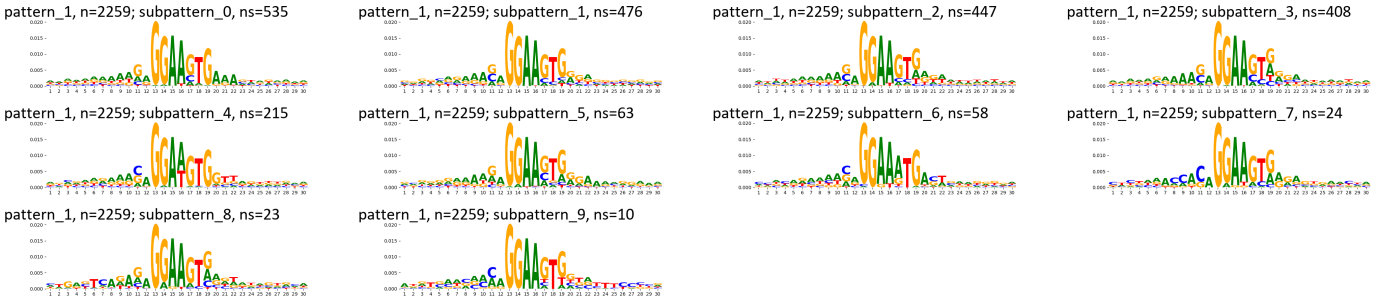

TF-MoDisCO pattern_1 n=2259, PWM

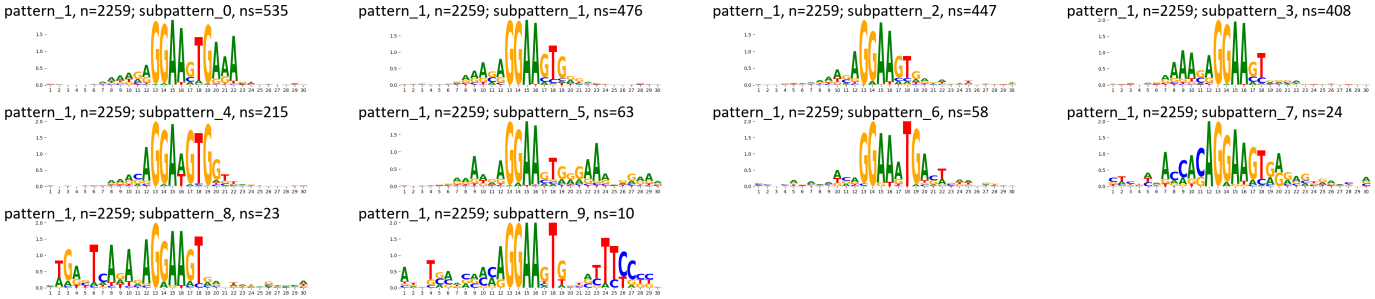

TF-MoDisCO pattern_3 n=1623, CWM

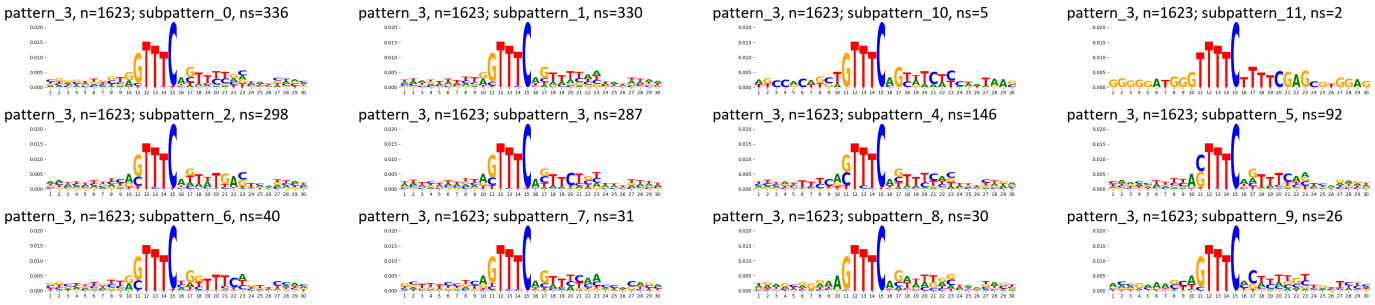

TF-MoDisCO pattern_3 n=1623, PWM

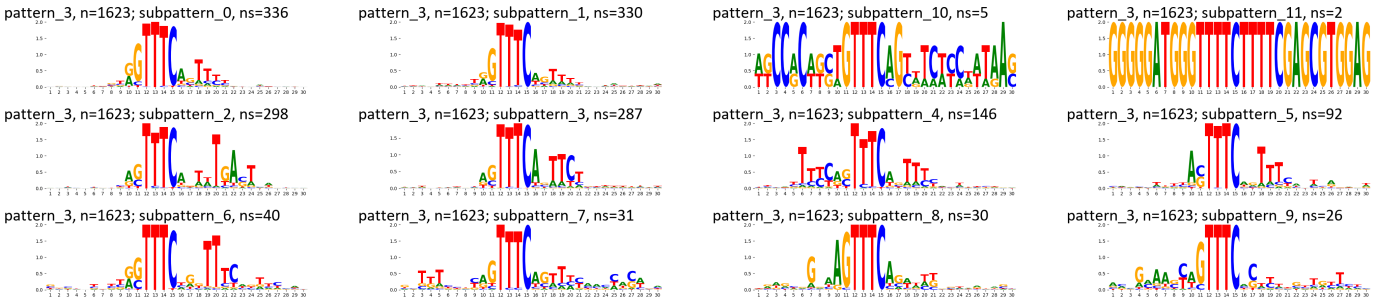

TF-MoDisCO pattern_4 n=1306, CWM

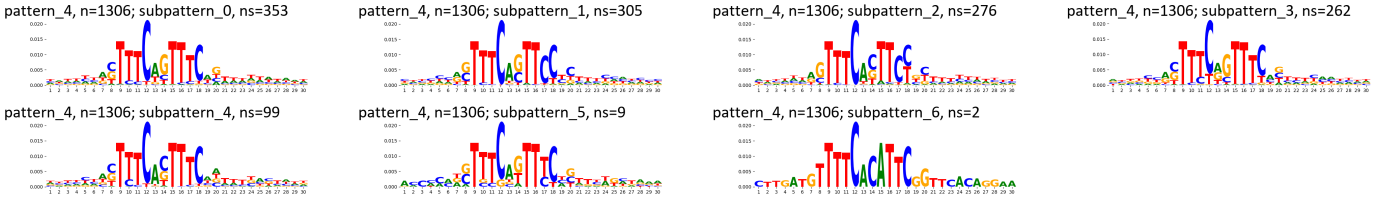

TF-MoDisCO pattern_4 n=1306, PWM

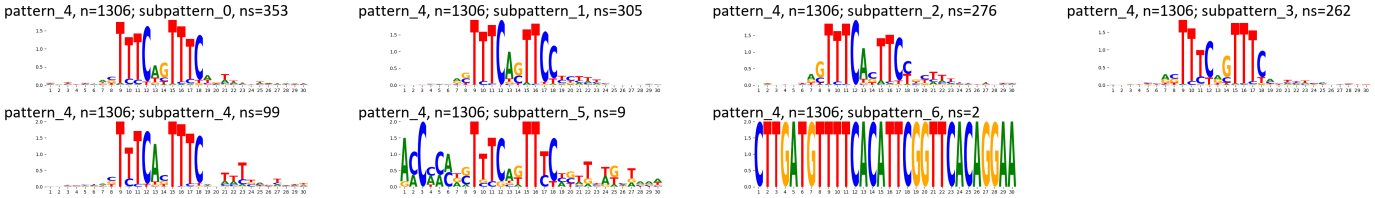

TF-MoDisCO pattern_5 n=666, CWM

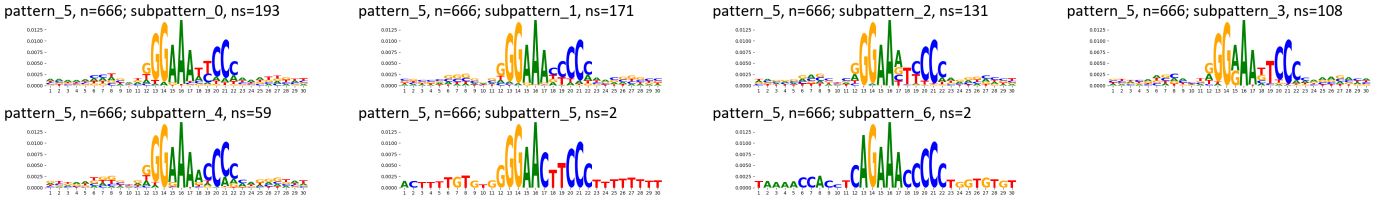

TF-MoDisCO pattern_5 n=666, PWM

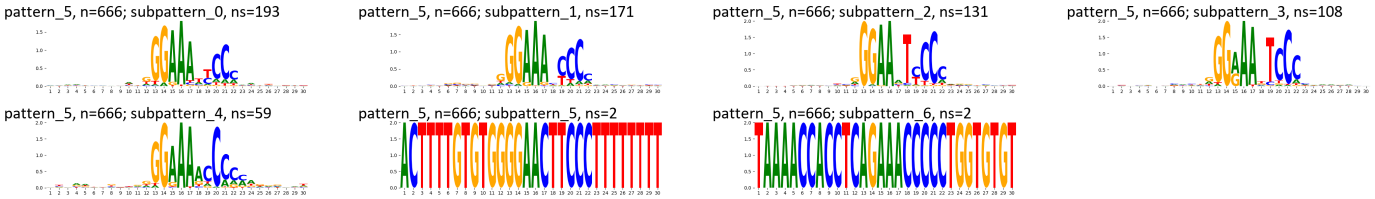

TF-MoDisCO pattern_6 n=448, CWM

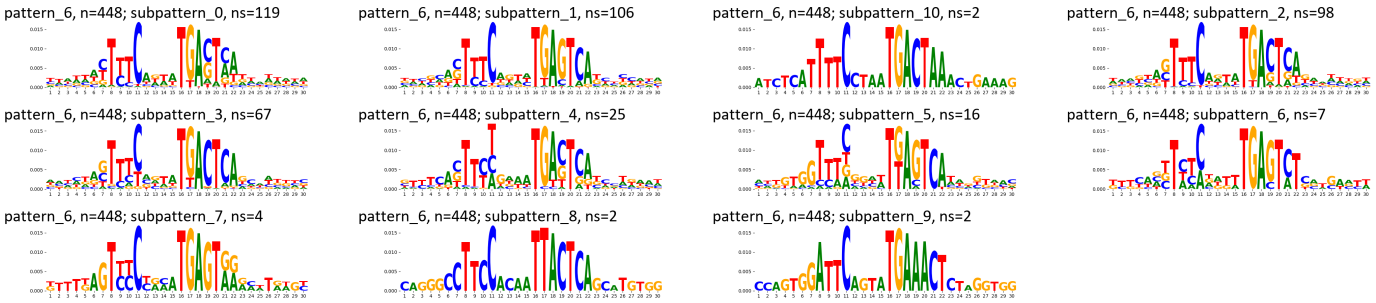

TF-MoDisCO pattern_6 n=448, PWM

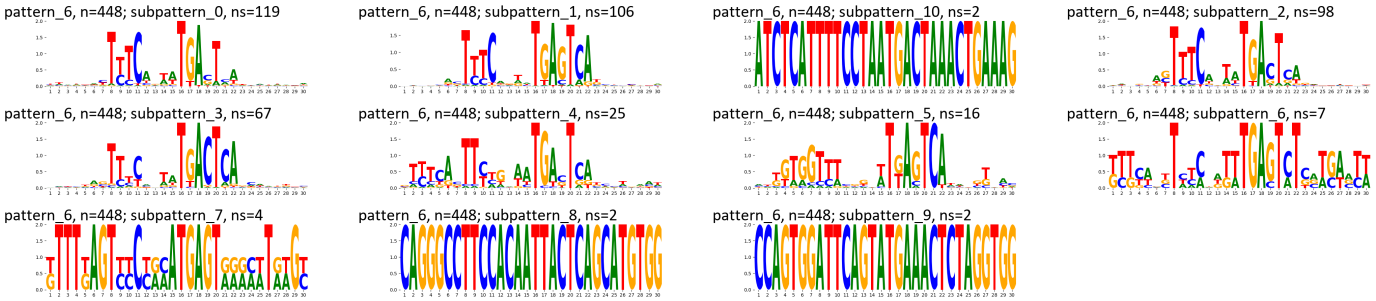

Supplementary Figure 67: TF-MoDisCO subpatterns for the IKZF1 transcription factor in GM12878 (accession ENCSR000EUJ).

A

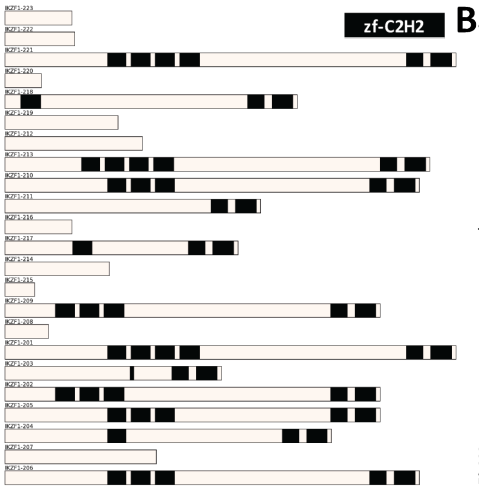

B

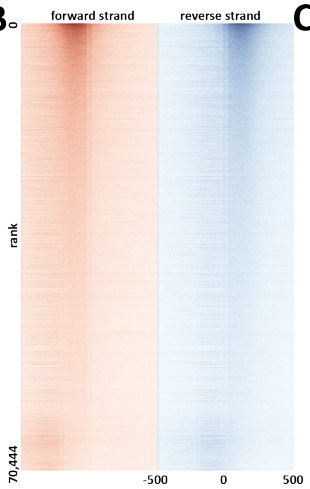

C

peaks	
state	fraction
EnhWk	0.22
TssA	0.19
EnhA1	0.16
TssFlnk	0.12
Quies	0.08
TssFlnkU	0.08
EnhA2	0.07
TxWk	0.06
TssFlnkD	0.05
ReprPCWk	0.04
EnhG1	0.01
EnhG2	0.01
ReprPC	0.01
TssBiv	0.01
Het	0.01
EnhBiv	0.01
ZNF/Rpts	0.01
Tx	0.01

D

peaks		peaks	
repeat	fraction	repeat	fraction
Simple_repeat	0.17	MIRb	0.05
SINE/Alu	0.14	MIR	0.03
SINE/MIR	0.12	L2a	0.03
LINE/L1	0.08	MIR3	0.02
LINE/L2	0.08	MIRc	0.02
LTR/ERVL-MaLR	0.04	L2c	0.02
DNA/hAT-Charlie	0.04	G-rich	0.02
Low_complexity	0.04	L2b	0.02
LTR/ERV1	0.03	AluSx	0.02
LTR/ERVL	0.03	AluSx1	0.02
DNA/TcMar-Tigger	0.01	AluJb	0.02
LINE/CR1	0.01	AluSz	0.01
DNA/hAT-Tip100	0.01	L2	0.01
DNA/hAT-Blackjack	0.00	AluJr	0.01
LTR/Gypsy	0.00	AluY	0.01
tRNA	0.00	GA-rich	0.01
LTR/ERVK	0.00	AluJo	0.01
LINE/RTE-BovB	0.00	L3	0.01

E

Ontology	Term	FDR Q-val
GO Biological Process	tumor necrosis factor-mediated signaling pathway	114.38
GO Biological Process	interferon-gamma-mediated signaling pathway	106.66
GO Biological Process	intrinsic apoptotic signaling pathway in response to DNA damage	103.83
GO Biological Process	cellular response to interferon-gamma	103.26
GO Biological Process	regulation of type I interferon production	95.36
GO Biological Process	negative regulation of type I interferon production	77.71
GO Biological Process	positive regulation of cytokine biosynthetic process	74.01
GO Biological Process	positive regulation of intrinsic apoptotic signaling pathway	61.76
GO Biological Process	regulation of mitochondrial outer membrane permeabilization involved in apoptotic signaling pathway	47.77
GO Biological Process	positive regulation of mitochondrial outer membrane permeabilization involved in apoptotic signaling pathway	46.77
GO Biological Process	liver regeneration	35.63
Human Phenotype	Decreased antibody level in blood	81.09

F

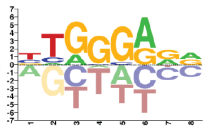

CIS-BP misc

	IKZF1-201	IKZF1-203	IKZF1-210	IKZF1-217	IKZF1-218
B1H-RC prediction	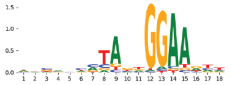		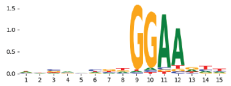	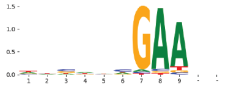	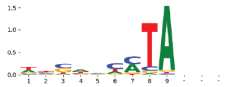
TF-MoDisCo pattern_1 n=5,934	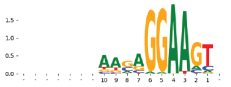		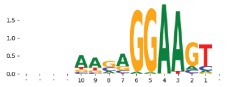		
B1H-RC prediction	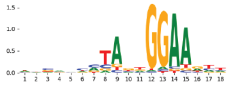		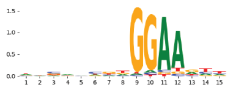	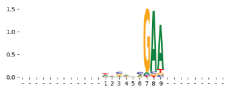	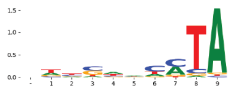
TF-MoDisCo pattern_3 n=4,718			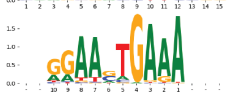	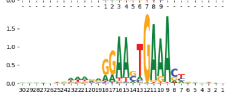	
B1H-RC prediction	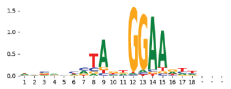		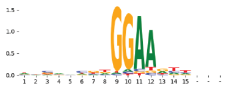		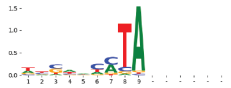
TF-MoDisCo pattern_4 n=3,502		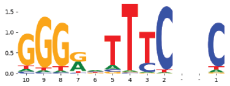			
B1H-RC prediction	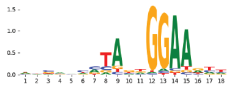	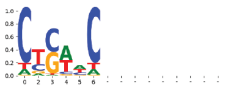	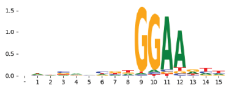	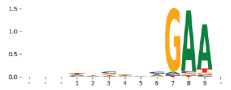	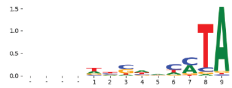
TF-MoDisCo pattern_7 n=792	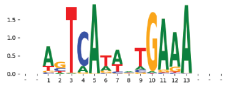	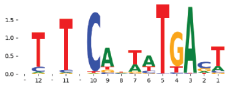	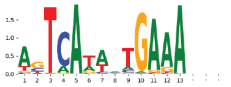	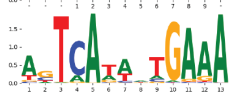	
B1H-RC prediction					
TF-MoDisCo pattern_8 n=553					
B1H-RC prediction					
TF-MoDisCo pattern_9 n=414					
B1H-RC prediction					
TF-MoDisCo pattern_16 n=156					

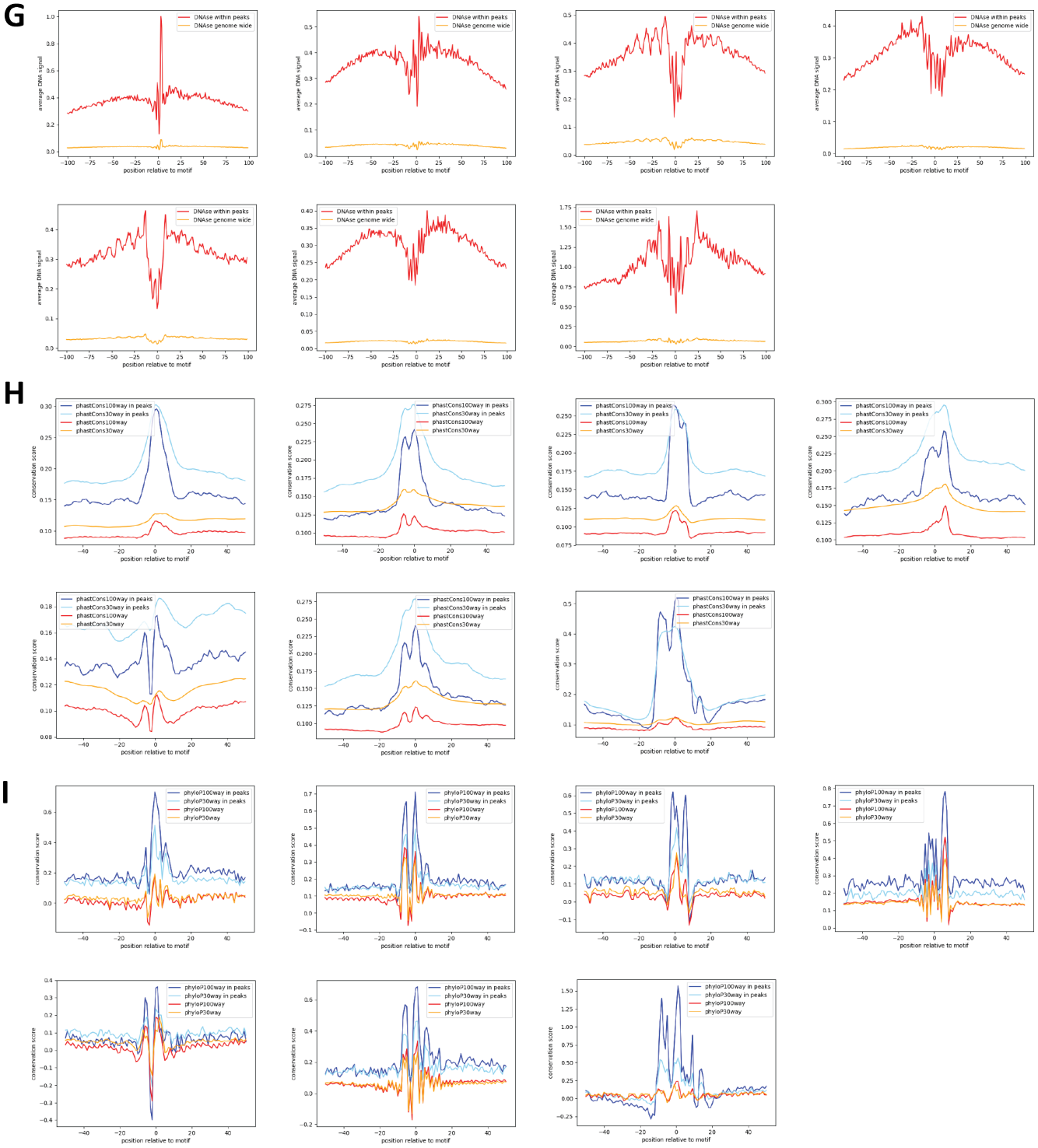

Supplementary Figure 68: Properties and genomic distribution of motifs identified for the IKZF1 transcription factor in GM12878 (accession ENCSR441VHN).

TF-MoDisCO pattern_1 n=5934, CWM

pattern_1, n=5934; subpattern_0, ns=1149

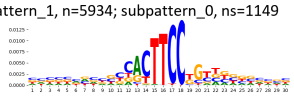

pattern_1, n=5934; subpattern_1, ns=1071

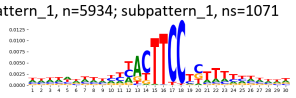

pattern_1, n=5934; subpattern_10, ns=30

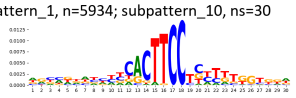

pattern_1, n=5934; subpattern_11, ns=3

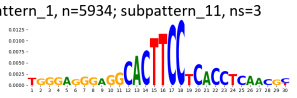

pattern_1, n=5934; subpattern_12, ns=2

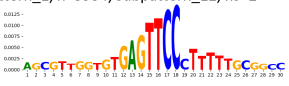

pattern_1, n=5934; subpattern_13, ns=2

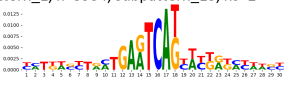

pattern_1, n=5934; subpattern_14, ns=2

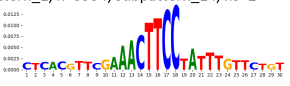

pattern_1, n=5934; subpattern_2, ns=1065

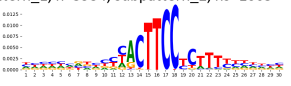

pattern_1, n=5934; subpattern_3, ns=907

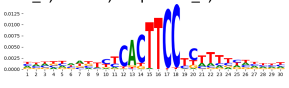

pattern_1, n=5934; subpattern_4, ns=611

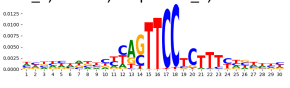

pattern_1, n=5934; subpattern_5, ns=591

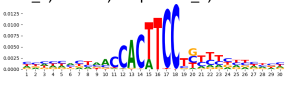

pattern_1, n=5934; subpattern_6, ns=239

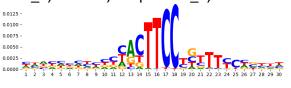

pattern_1, n=5934; subpattern_7, ns=103

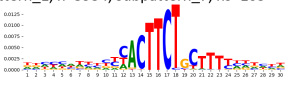

pattern_1, n=5934; subpattern_8, ns=102

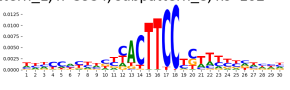

pattern_1, n=5934; subpattern_9, ns=57

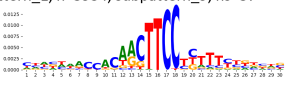

TF-MoDisCO pattern_1 n=5934, PWM

pattern_1, n=5934; subpattern_0, ns=1149

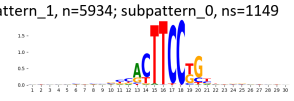

pattern_1, n=5934; subpattern_1, ns=1071

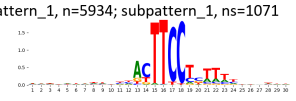

pattern_1, n=5934; subpattern_10, ns=30

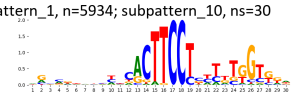

pattern_1, n=5934; subpattern_11, ns=3

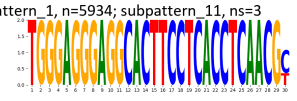

pattern_1, n=5934; subpattern_12, ns=2

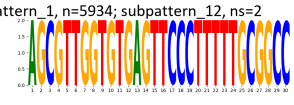

pattern_1, n=5934; subpattern_13, ns=2

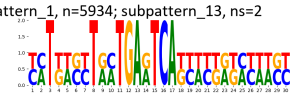

pattern_1, n=5934; subpattern_14, ns=2

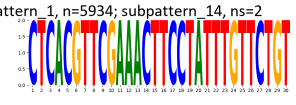

pattern_1, n=5934; subpattern_2, ns=1065

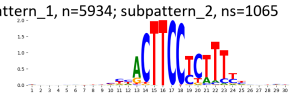

pattern_1, n=5934; subpattern_3, ns=907

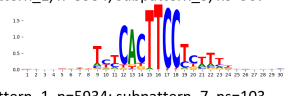

pattern_1, n=5934; subpattern_4, ns=611

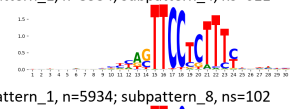

pattern_1, n=5934; subpattern_5, ns=591

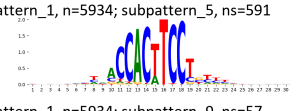

pattern_1, n=5934; subpattern_6, ns=239

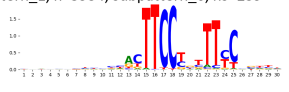

pattern_1, n=5934; subpattern_7, ns=103

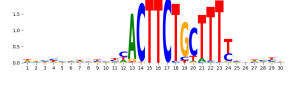

pattern_1, n=5934; subpattern_8, ns=102

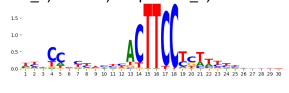

pattern_1, n=5934; subpattern_9, ns=57

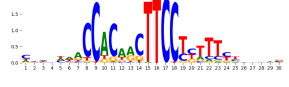

TF-MoDisCO pattern_16 n=156, CWM

pattern_16, n=156; subpattern_0, ns=61

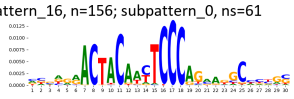

pattern_16, n=156; subpattern_1, ns=60

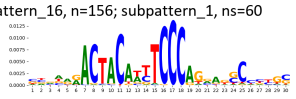

pattern_16, n=156; subpattern_2, ns=22

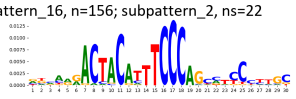

pattern_16, n=156; subpattern_3, ns=10

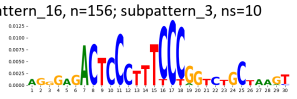

pattern_16, n=156; subpattern_4, ns=3

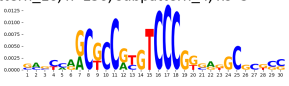

TF-MoDisCO pattern_16 n=156, PWM

pattern_16, n=156; subpattern_0, ns=61

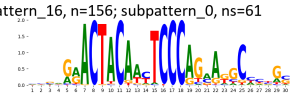

pattern_16, n=156; subpattern_1, ns=60

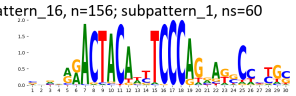

pattern_16, n=156; subpattern_2, ns=22

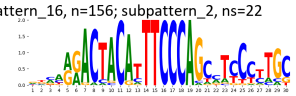

pattern_16, n=156; subpattern_3, ns=10

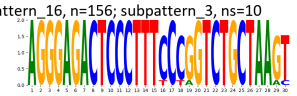

pattern_16, n=156; subpattern_4, ns=3

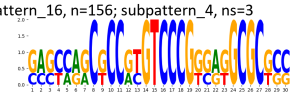

TF-MoDisCO pattern_3 n=4718, CWM

pattern_3, n=4718; subpattern_0, ns=1053

pattern_3, n=4718; subpattern_1, ns=731

pattern_3, n=4718; subpattern_2, ns=605

pattern_3, n=4718; subpattern_3, ns=604

pattern_3, n=4718; subpattern_4, ns=599

pattern_3, n=4718; subpattern_5, ns=532

pattern_3, n=4718; subpattern_6, ns=508

pattern_3, n=4718; subpattern_7, ns=62

pattern_3, n=4718; subpattern_8, ns=24

TF-MoDisCO pattern_3 n=4718, PWM

pattern_3, n=4718; subpattern_0, ns=1053

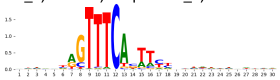

pattern_3, n=4718; subpattern_1, ns=731

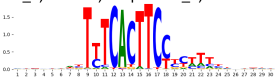

pattern_3, n=4718; subpattern_2, ns=605

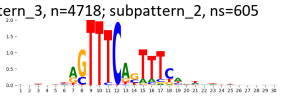

pattern_3, n=4718; subpattern_3, ns=604

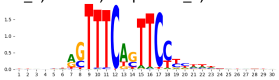

pattern_3, n=4718; subpattern_4, ns=599

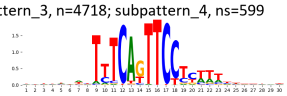

pattern_3, n=4718; subpattern_5, ns=532

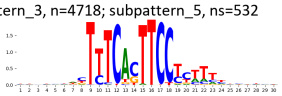

pattern_3, n=4718; subpattern_6, ns=508

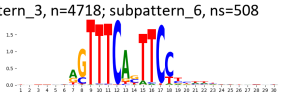

pattern_3, n=4718; subpattern_7, ns=62

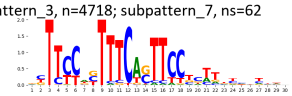

pattern_3, n=4718; subpattern_8, ns=24

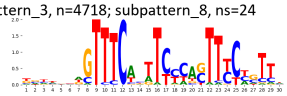

TF-MoDisCO pattern_4 n=3502, CWM

pattern_4, n=3502; subpattern_0, ns=627

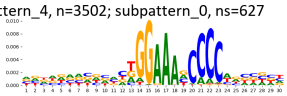

pattern_4, n=3502; subpattern_1, ns=622

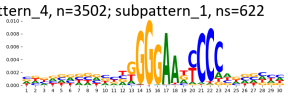

pattern_4, n=3502; subpattern_10, ns=6

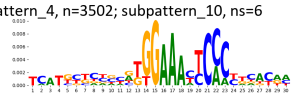

pattern_4, n=3502; subpattern_2, ns=560

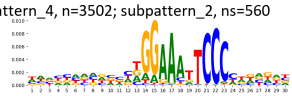

pattern_4, n=3502; subpattern_3, ns=471

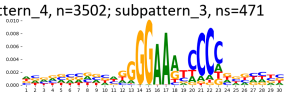

pattern_4, n=3502; subpattern_4, ns=469

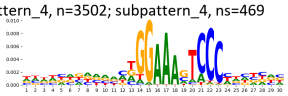

pattern_4, n=3502; subpattern_5, ns=375

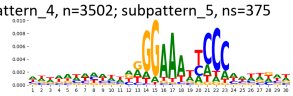

pattern_4, n=3502; subpattern_6, ns=239

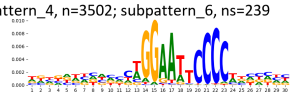

pattern_4, n=3502; subpattern_7, ns=91

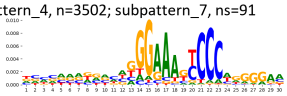

pattern_4, n=3502; subpattern_8, ns=23

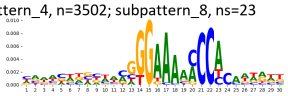

pattern_4, n=3502; subpattern_9, ns=19

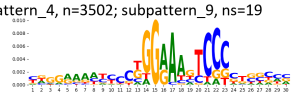

TF-MoDisCO pattern_4 n=3502, PWM

pattern_4, n=3502; subpattern_0, ns=627

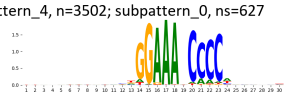

pattern_4, n=3502; subpattern_1, ns=622

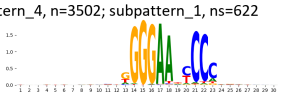

pattern_4, n=3502; subpattern_10, ns=6

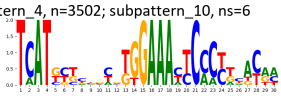

pattern_4, n=3502; subpattern_2, ns=560

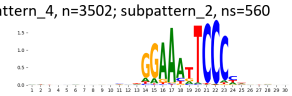

pattern_4, n=3502; subpattern_3, ns=471

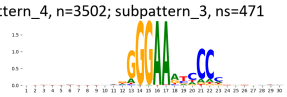

pattern_4, n=3502; subpattern_4, ns=469

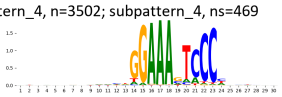

pattern_4, n=3502; subpattern_5, ns=375

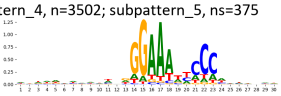

pattern_4, n=3502; subpattern_6, ns=239

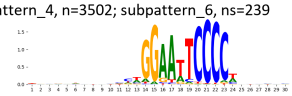

pattern_4, n=3502; subpattern_7, ns=91

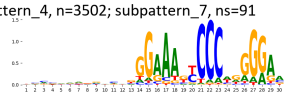

pattern_4, n=3502; subpattern_8, ns=23

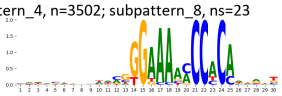

pattern_4, n=3502; subpattern_9, ns=19

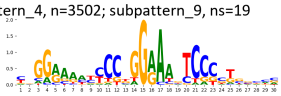

TF-MoDisCO pattern_7 n=792, CWM

pattern_7, n=792; subpattern_0, ns=207

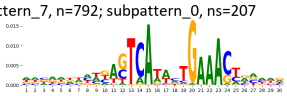

pattern_7, n=792; subpattern_1, ns=203

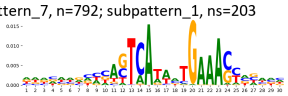

pattern_7, n=792; subpattern_2, ns=168

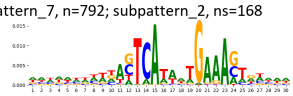

pattern_7, n=792; subpattern_3, ns=138

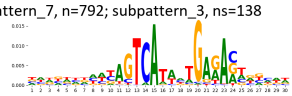

pattern_7, n=792; subpattern_4, ns=65

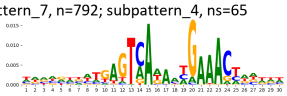

pattern_7, n=792; subpattern_5, ns=6

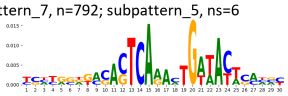

pattern_7, n=792; subpattern_6, ns=3

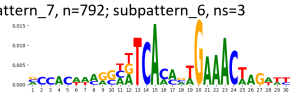

pattern_7, n=792; subpattern_7, ns=2

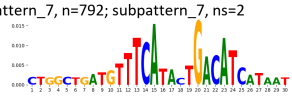

TF-MoDisCO pattern_7 n=792, PWM

pattern_7, n=792; subpattern_0, ns=207

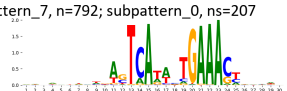

pattern_7, n=792; subpattern_1, ns=203

pattern_7, n=792; subpattern_2, ns=168

pattern_7, n=792; subpattern_3, ns=138

pattern_7, n=792; subpattern_4, ns=65

pattern_7, n=792; subpattern_5, ns=6

pattern_7, n=792; subpattern_6, ns=3

pattern_7, n=792; subpattern_7, ns=2

TF-MoDisCO pattern_8 n=553, CWM

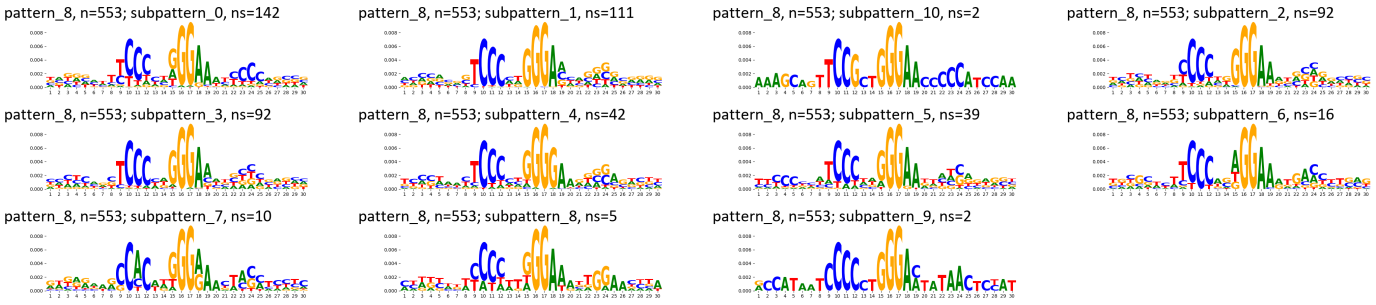

TF-MoDisCO pattern_8 n=553, PWM

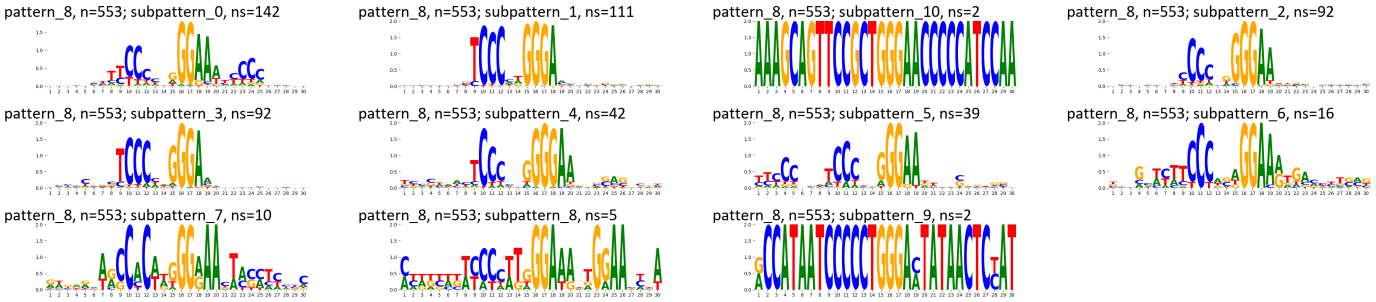

TF-MoDisCO pattern_9 n=414, CWM

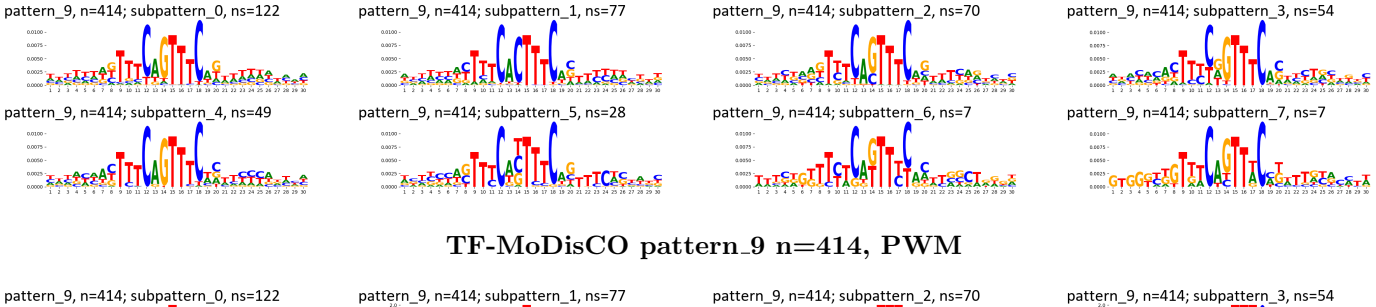

TF-MoDisCO pattern_9 n=414, PWM

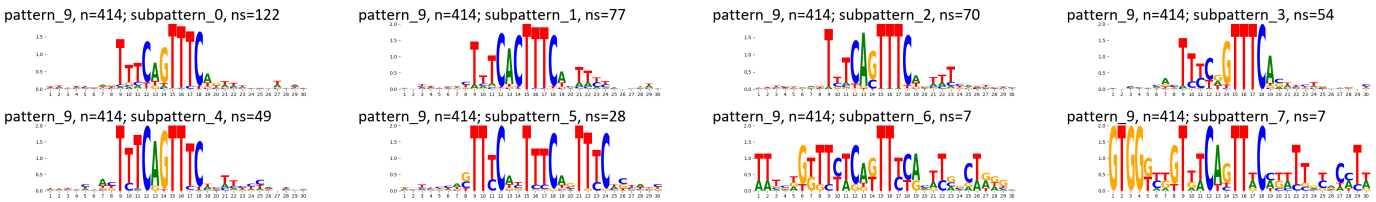

Supplementary Figure 69: TF-MoDisCO subpatterns for the IKZF1 transcription factor in GM12878 (accession ENCSR441VHN).

A

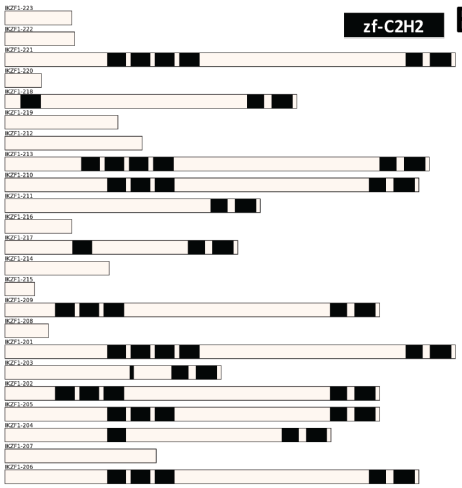

B

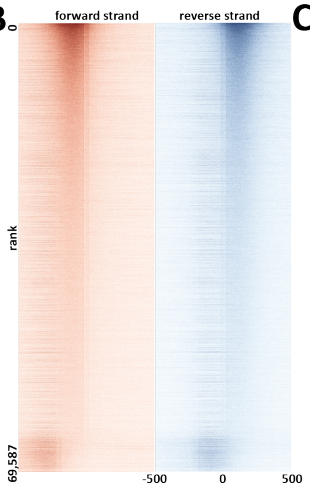

C

peaks	
state	fraction
EnhWk	0.26
EnhA1	0.18
TssA	0.15
Quies	0.10
TssFlnkU	0.08
TssFlnk	0.08
EnhA2	0.08
TxWk	0.07
TssFlnkD	0.04
ReprPCWk	0.04
EnhG1	0.01
Het	0.01
EnhG2	0.01
ZNF/Rpts	0.01
Tx	0.01
EnhBiv	0.00
ReprPC	0.00
TssBiv	0.00

D

peaks		peaks	
repeat	fraction	repeat	fraction
SINE/Alu	0.18	MIRb	0.05
SINE/MIR	0.13	L2a	0.03
Simple_repeat	0.13	MIR	0.03
LINE/L1	0.11	L2c	0.03
LINE/L2	0.09	MIR3	0.02
LTR/ERVL-MaLR	0.05	MIRc	0.02
DNA/hAT-Charlie	0.04	L2b	0.02
LTR/ERV1	0.04	AluSx1	0.02
LTR/ERVL	0.03	AluSx	0.02
Low_complexity	0.03	AluJb	0.02
DNA/TcMar-Tigger	0.02	AluSz	0.02
LINE/CR1	0.01	L2	0.01
DNA/hAT-Tip100	0.01	AluY	0.01
DNA/hAT-Blackjack	0.00	AluJr	0.01
LTR/Gypsy	0.00	AluJo	0.01
LTR/ERVK	0.00	GA-rich	0.01
LINE/RTE-X	0.00	AluSq2	0.01
tRNA	0.00	L3	0.01

E

Ontology	Term	FDR Q-val
GO Biological Process	regulation of adaptive immune response	141.12
GO Biological Process	interferon-gamma-mediated signaling pathway	125.58
GO Biological Process	cellular response to interferon-gamma	124.03
GO Biological Process	response to interferon-gamma	117.93
GO Biological Process	regulation of type I interferon production	102.93
GO Biological Process	tumor necrosis factor-mediated signaling pathway	101.26
GO Biological Process	intrinsic apoptotic signaling pathway in response to DNA damage	88.25
GO Biological Process	B cell receptor signaling pathway	85.52
GO Biological Process	regulation of B cell proliferation	78.55
GO Biological Process	regulation of toll-like receptor signaling pathway	66.77
GO Biological Process	nucleotide-binding domain, leucine rich repeat containing receptor signaling pathway	62.24
GO Biological Process	interleukin-12-mediated signaling pathway	57.73
GO Biological Process	nucleotide-binding oligomerization domain containing signaling pathway	55.63
GO Biological Process	response to interleukin-12	54.36
GO Biological Process	cytoplasmic pattern recognition receptor signaling pathway	51.34
GO Biological Process	negative regulation of adaptive immune response	50.33
GO Biological Process	liver regeneration	44.95
GO Biological Process	T cell differentiation involved in immune response	40.87
GO Biological Process	alpha-beta T cell differentiation involved in immune response	40.61
GO Biological Process	MyD88-independent toll-like receptor signaling pathway	40.30
Human Phenotype	Abnormality of lymphocytes	122.91
Human Phenotype	Decreased antibody level in blood	94.75
Human Phenotype	Abnormality of the lymph nodes	59.34

F

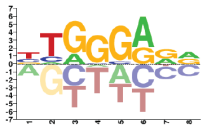

CIS-BP misc

	IKZF1-201	IKZF1-203	IKZF1-210	IKZF1-217	IKZF1-218
B1H-RC prediction	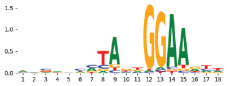		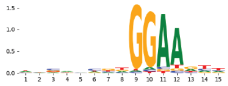	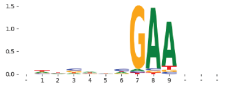	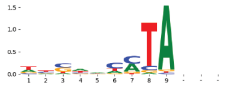
TF-MoDisCo pattern_1 n=5,916	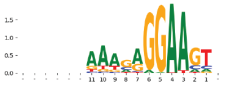		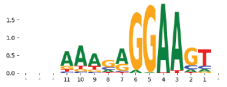	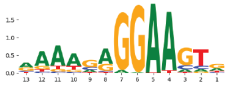	
B1H-RC prediction	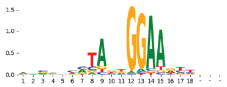		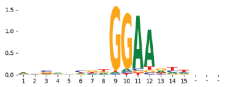		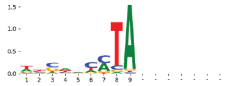
TF-MoDisCo pattern_3 n=3,936			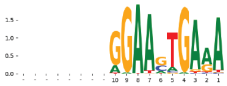		
B1H-RC prediction	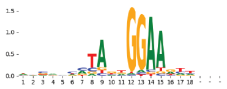				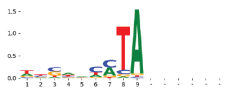
TF-MoDisCo pattern_4 n=3,838	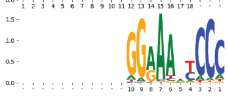	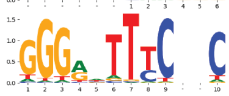	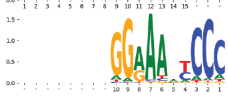		
B1H-RC prediction	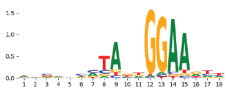		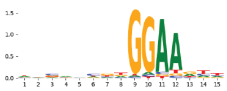		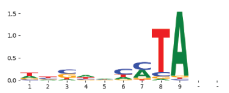
TF-MoDisCo pattern_5 n=3,745	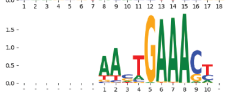	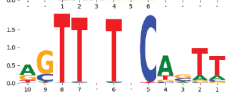	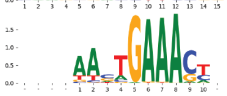		
B1H-RC prediction					
TF-MoDisCo pattern_6 n=966					
B1H-RC prediction					
TF-MoDisCo pattern_7 n=932					

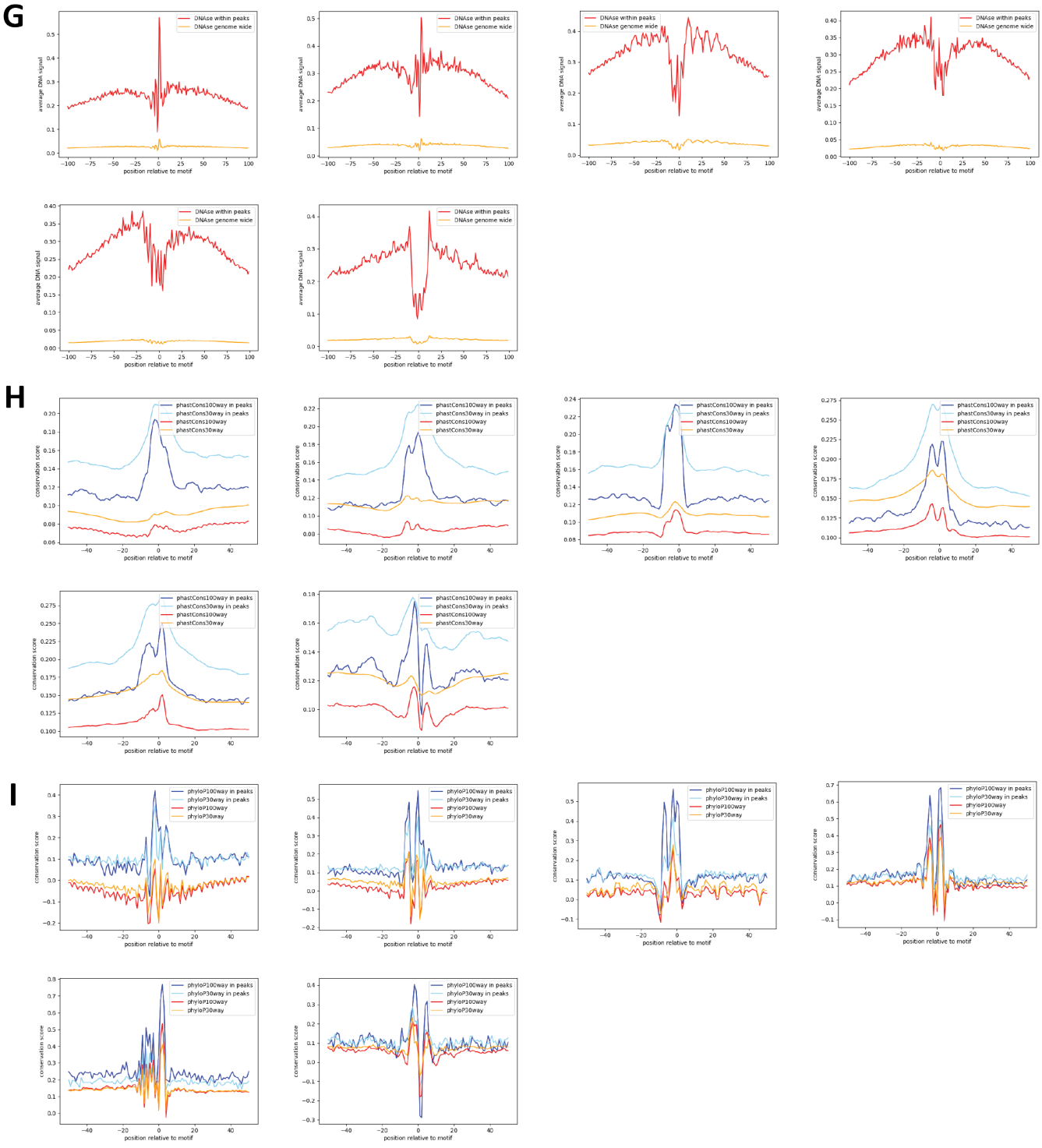

Supplementary Figure 70: Properties and genomic distribution of motifs identified for the IKZF1 transcription factor in GM12878 (accession ENCSR874AFU).

TF-MoDisCO pattern_1 n=5916, CWM

pattern_1, n=5916; subpattern_0, ns=1201

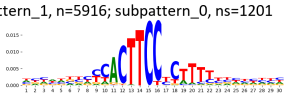

pattern_1, n=5916; subpattern_1, ns=1095

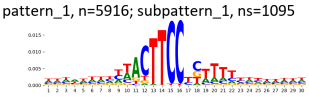

pattern_1, n=5916; subpattern_2, ns=1017

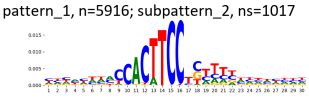

pattern_1, n=5916; subpattern_3, ns=720

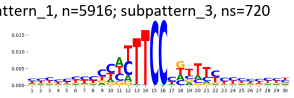

pattern_1, n=5916; subpattern_4, ns=712

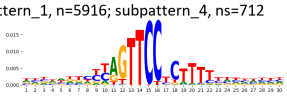

pattern_1, n=5916; subpattern_5, ns=588

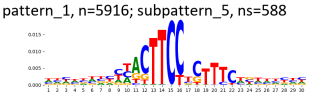

pattern_1, n=5916; subpattern_6, ns=402

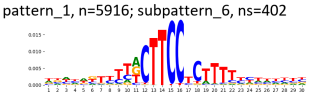

pattern_1, n=5916; subpattern_7, ns=110

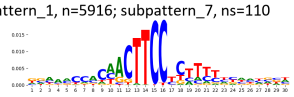

pattern_1, n=5916; subpattern_8, ns=66

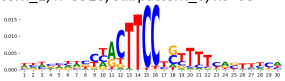

pattern_1, n=5916; subpattern_9, ns=5

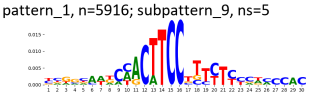

TF-MoDisCO pattern_1 n=5916, PWM

pattern_1, n=5916; subpattern_0, ns=1201

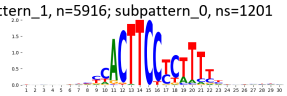

pattern_1, n=5916; subpattern_1, ns=1095

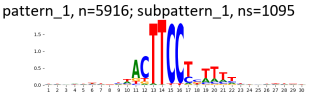

pattern_1, n=5916; subpattern_2, ns=1017

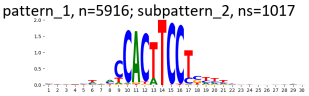

pattern_1, n=5916; subpattern_3, ns=720

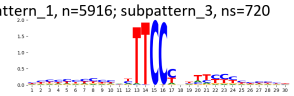

pattern_1, n=5916; subpattern_4, ns=712

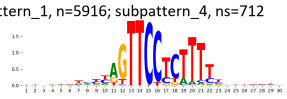

pattern_1, n=5916; subpattern_5, ns=588

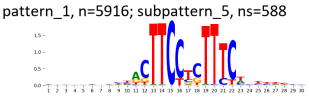

pattern_1, n=5916; subpattern_6, ns=402

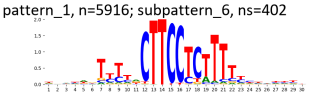

pattern_1, n=5916; subpattern_7, ns=110

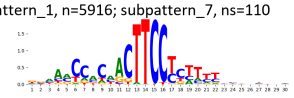

pattern_1, n=5916; subpattern_8, ns=66

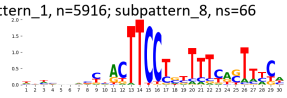

pattern_1, n=5916; subpattern_9, ns=5

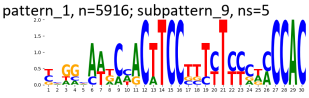

TF-MoDisCO pattern_3 n=3936, CWM

pattern_3, n=3936; subpattern_0, ns=661

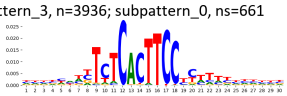

pattern_3, n=3936; subpattern_1, ns=600

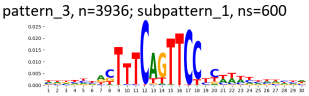

pattern_3, n=3936; subpattern_2, ns=584

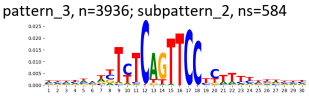

pattern_3, n=3936; subpattern_3, ns=546

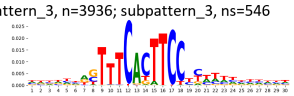

pattern_3, n=3936; subpattern_4, ns=489

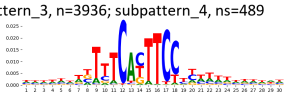

pattern_3, n=3936; subpattern_5, ns=432

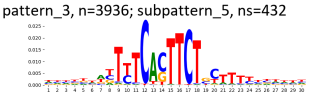

pattern_3, n=3936; subpattern_6, ns=406

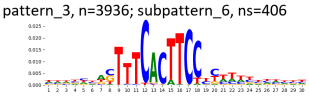

pattern_3, n=3936; subpattern_7, ns=193

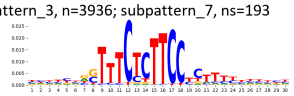

pattern_3, n=3936; subpattern_8, ns=25

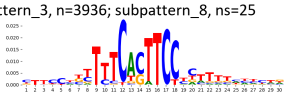

TF-MoDisCO pattern_3 n=3936, PWM

pattern_3, n=3936; subpattern_0, ns=661

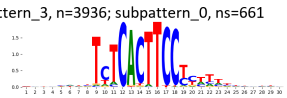

pattern_3, n=3936; subpattern_1, ns=600

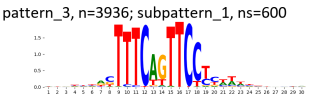

pattern_3, n=3936; subpattern_2, ns=584

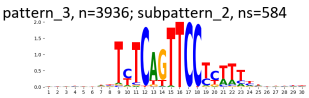

pattern_3, n=3936; subpattern_3, ns=546

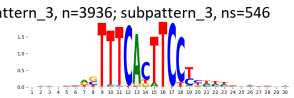

pattern_3, n=3936; subpattern_4, ns=489

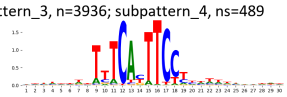

pattern_3, n=3936; subpattern_5, ns=432

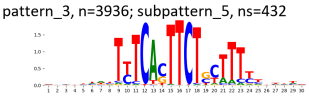

pattern_3, n=3936; subpattern_6, ns=406

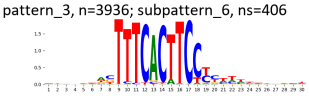

pattern_3, n=3936; subpattern_7, ns=193

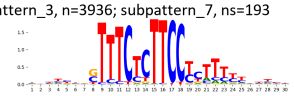

pattern_3, n=3936; subpattern_8, ns=25

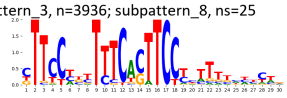

TF-MoDisCO pattern_4 n=3838, CWM

pattern_4, n=3838; subpattern_0, ns=890

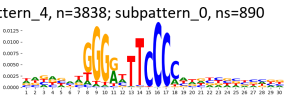

pattern_4, n=3838; subpattern_1, ns=833

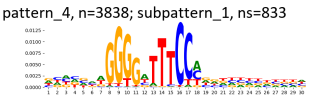

pattern_4, n=3838; subpattern_2, ns=683

pattern_4, n=3838; subpattern_3, ns=682

pattern_4, n=3838; subpattern_4, ns=615

pattern_4, n=3838; subpattern_5, ns=85

pattern_4, n=3838; subpattern_6, ns=43

pattern_4, n=3838; subpattern_7, ns=5

pattern_4, n=3838; subpattern_8, ns=2

TF-MoDisCO pattern_4 n=3838, PWM

pattern_4, n=3838; subpattern_0, ns=890

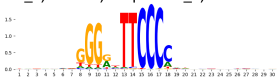

pattern_4, n=3838; subpattern_1, ns=833

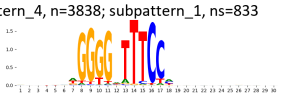

pattern_4, n=3838; subpattern_2, ns=683

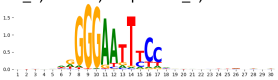

pattern_4, n=3838; subpattern_3, ns=682

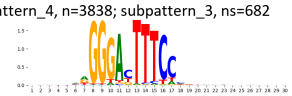

pattern_4, n=3838; subpattern_4, ns=615

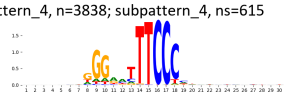

pattern_4, n=3838; subpattern_5, ns=85

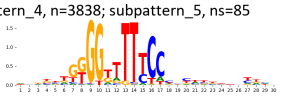

pattern_4, n=3838; subpattern_6, ns=43

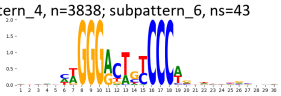

pattern_4, n=3838; subpattern_7, ns=5

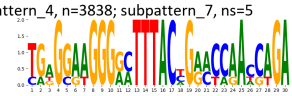

pattern_4, n=3838; subpattern_8, ns=2

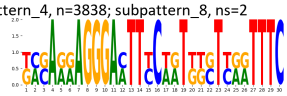

TF-MoDisCO pattern_5 n=3745, CWM

pattern_5, n=3745; subpattern_0, ns=843

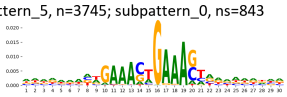

pattern_5, n=3745; subpattern_1, ns=818

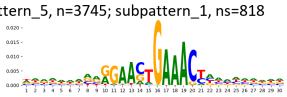

pattern_5, n=3745; subpattern_2, ns=768

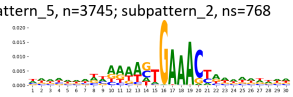

pattern_5, n=3745; subpattern_3, ns=533

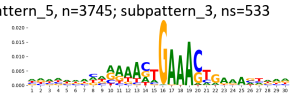

pattern_5, n=3745; subpattern_4, ns=514

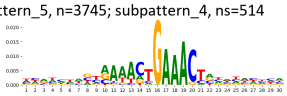

pattern_5, n=3745; subpattern_5, ns=201

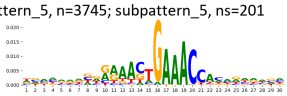

pattern_5, n=3745; subpattern_6, ns=48

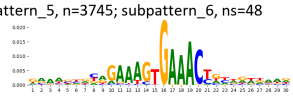

pattern_5, n=3745; subpattern_7, ns=15

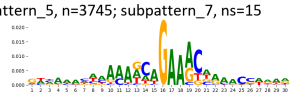

pattern_5, n=3745; subpattern_8, ns=5

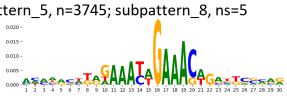

TF-MoDisCO pattern_5 n=3745, PWM

pattern_5, n=3745; subpattern_0, ns=843

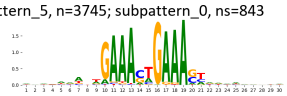

pattern_5, n=3745; subpattern_1, ns=818

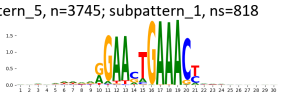

pattern_5, n=3745; subpattern_2, ns=768

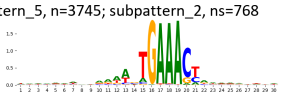

pattern_5, n=3745; subpattern_3, ns=533

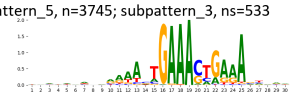

pattern_5, n=3745; subpattern_4, ns=514

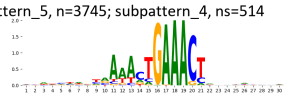

pattern_5, n=3745; subpattern_5, ns=201

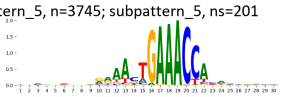

pattern_5, n=3745; subpattern_6, ns=48

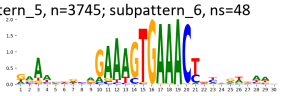

pattern_5, n=3745; subpattern_7, ns=15

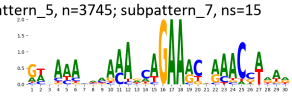

pattern_5, n=3745; subpattern_8, ns=5

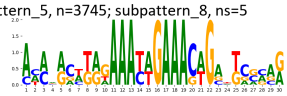

TF-MoDisCO pattern_6 n=966, CWM

pattern_6, n=966; subpattern_0, ns=188

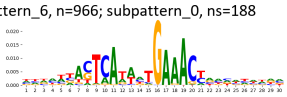

pattern_6, n=966; subpattern_1, ns=185

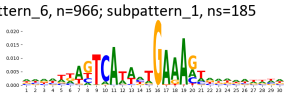

pattern_6, n=966; subpattern_2, ns=169

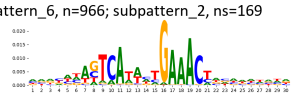

pattern_6, n=966; subpattern_3, ns=146

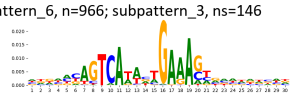

pattern_6, n=966; subpattern_4, ns=146

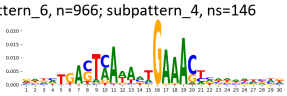

pattern_6, n=966; subpattern_5, ns=117

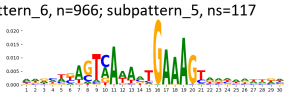

pattern_6, n=966; subpattern_6, ns=15

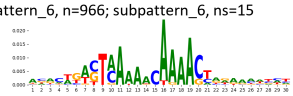

TF-MoDisCO pattern_6 n=966, PWM

pattern_6, n=966; subpattern_0, ns=188

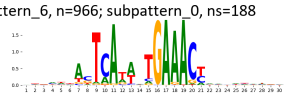

pattern_6, n=966; subpattern_1, ns=185

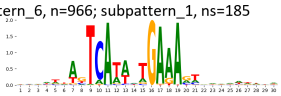

pattern_6, n=966; subpattern_2, ns=169

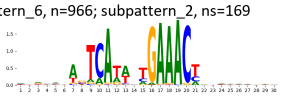

pattern_6, n=966; subpattern_3, ns=146

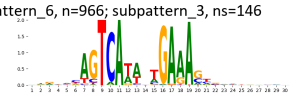

pattern_6, n=966; subpattern_4, ns=146

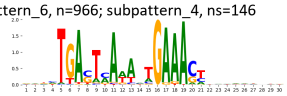

pattern_6, n=966; subpattern_5, ns=117

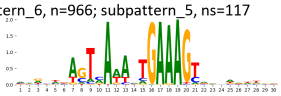

pattern_6, n=966; subpattern_6, ns=15

TF-MoDisCO pattern_7 n=932, CWM

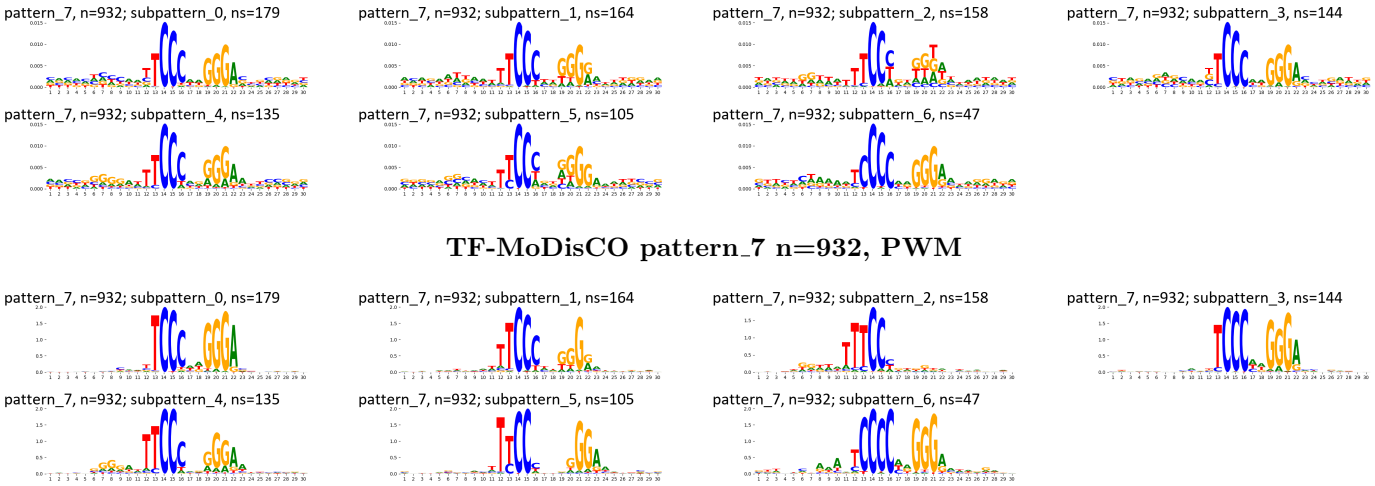

Supplementary Figure 71: TF-MoDisCO subpatterns for the IKZF1 transcription factor in GM12878 (accession ENCSR874AFU).

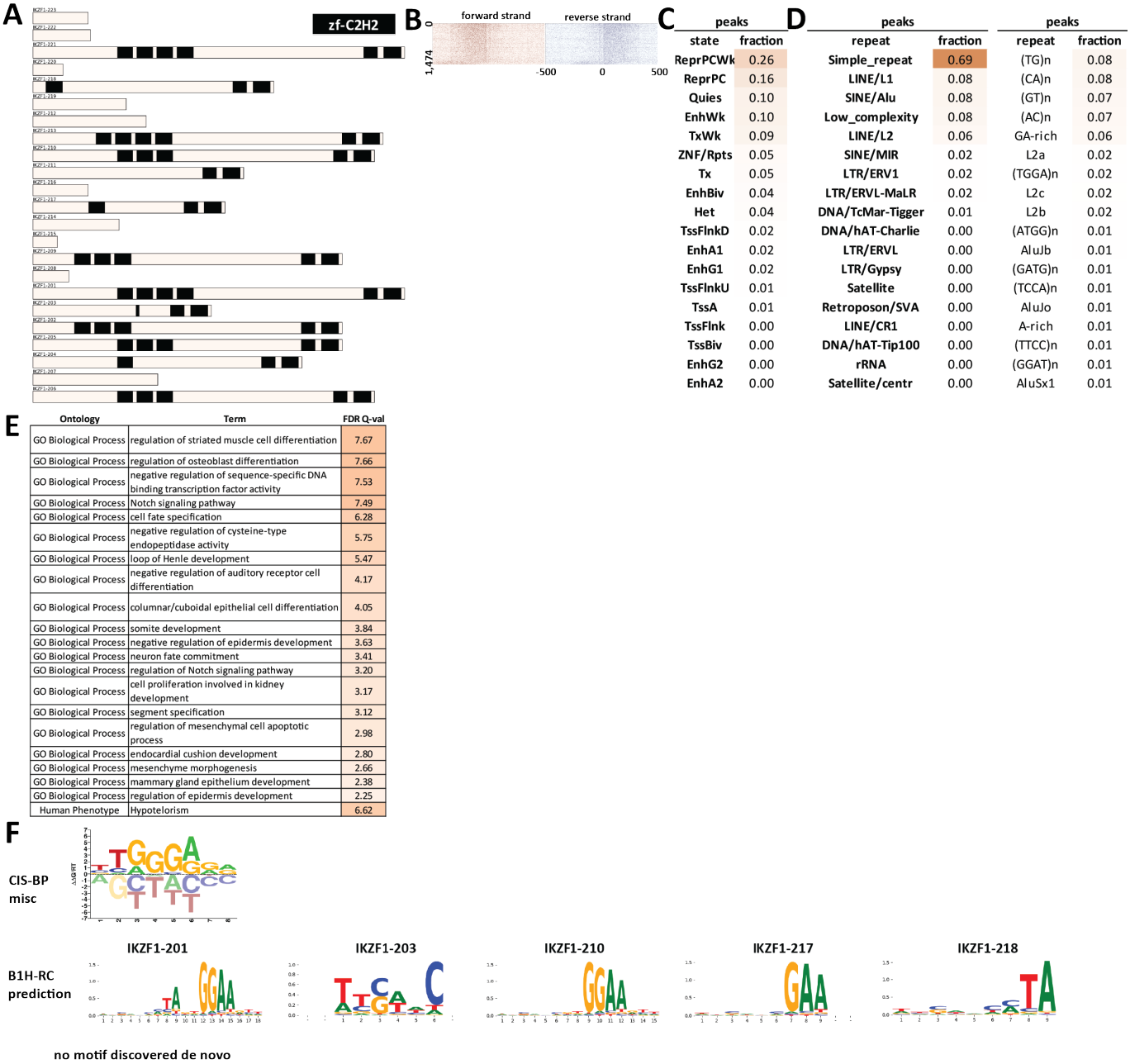

Supplementary Figure 72: Properties and genomic distribution of motifs identified for the IKZF1 transcription factor in HepG2 (accession ENCSR278JQG).

A

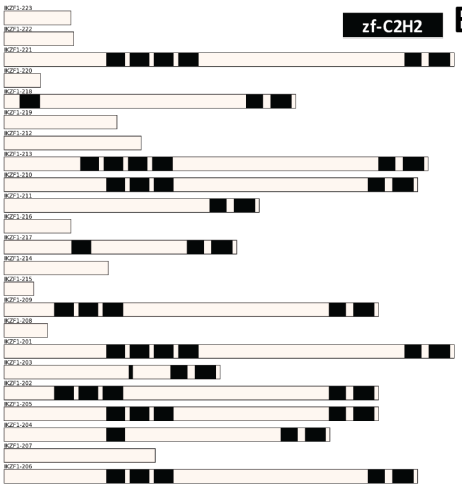

B

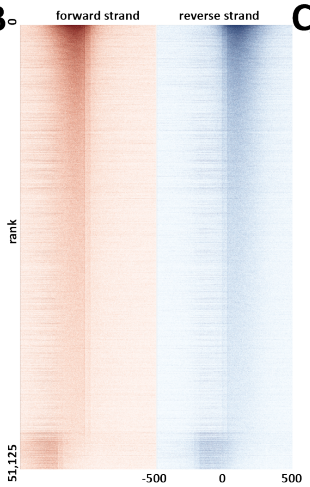

C

peaks	
state	fraction
EnhWk	0.30
EnhA1	0.16
TxWk	0.13
TssA	0.11
Quies	0.10
TssFlnkU	0.09
ReprPCWk	0.07
EnhA2	0.05
TssFlnkD	0.05
TssFlnk	0.04
ReprPC	0.02
EnhG1	0.02
EnhBiv	0.02
EnhG2	0.01
Tx	0.01
TssBiv	0.00
Het	0.00
ZNF/Rpts	0.00

D

peaks		peaks	
repeat	fraction	repeat	fraction
SINE/Alu	0.18	MIRb	0.04
LINE/L2	0.12	L2a	0.04
SINE/MIR	0.11	L2c	0.03
Simple_repeat	0.11	L2b	0.03
LINE/L1	0.10	MIR	0.02
LTR/ERV1	0.06	MIR3	0.02
LTR/ERVL-MaLR	0.06	MIRc	0.02
DNA/hAT-Charlie	0.03	AluSx1	0.02
LTR/ERVL	0.03	AluJb	0.02
Low_complexity	0.03	L2	0.02
LINE/CR1	0.02	AluSx	0.02
DNA/TcMar-Tigger	0.01	AluSz	0.02
DNA/hAT-Tip100	0.01	GA-rich	0.01
LTR/ERVK	0.01	AluJo	0.01
tRNA	0.00	AluJr	0.01
LTR/Gypsy	0.00	AluY	0.01
DNA/hAT-Blackjack	0.00	L3	0.01
LINE/RTE-X	0.00	AluSq2	0.01

E

Ontology	Term	FDR Q-val
GO Biological Process	erythrocyte homeostasis	66.75
GO Biological Process	erythrocyte differentiation	59.43
GO Biological Process	regulation of CD4-positive, alpha-beta T cell differentiation	47.58
GO Biological Process	positive regulation of intrinsic apoptotic signaling pathway	36.88
GO Biological Process	negative regulation of extrinsic apoptotic signaling pathway via death domain receptors	30.13
GO Biological Process	actin nucleation	25.71
GO Biological Process	positive regulation of neutrophil migration	23.36
GO Biological Process	regulation of membrane protein ectodomain proteolysis	20.09
GO Biological Process	mismatch repair	16.50
Human Phenotype	Hematological neoplasm	60.91
Human Phenotype	Leukemia	31.94

F

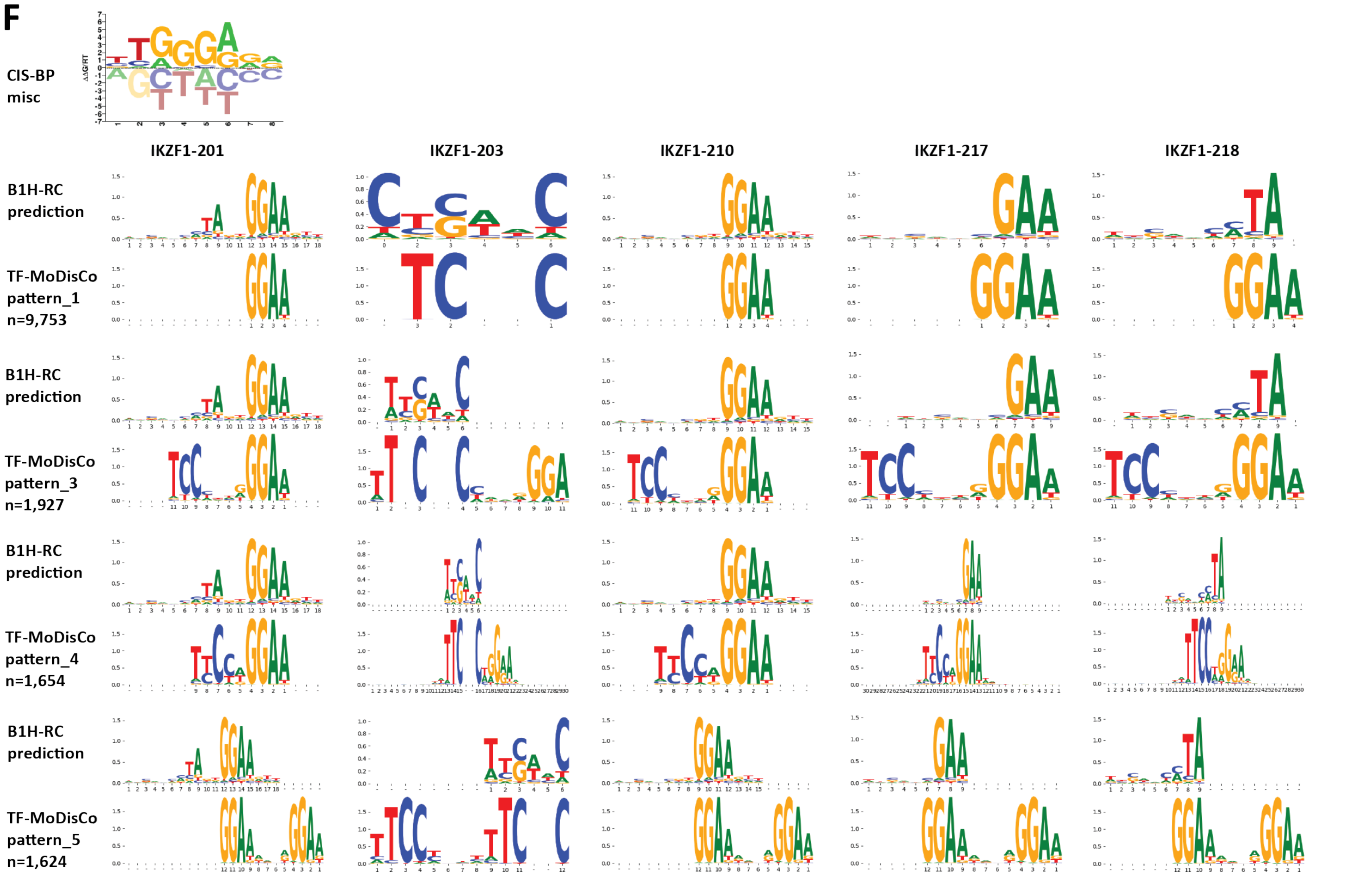

F

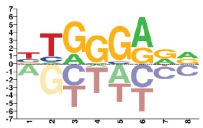

CIS-BP misc

	IKZF1-201	IKZF1-203	IKZF1-210	IKZF1-217	IKZF1-218
B1H-RC prediction					
TF-MoDisCo pattern_6 n=1,570					
B1H-RC prediction					
TF-MoDisCo pattern_7 n=1,509					
B1H-RC prediction					
TF-MoDisCo pattern_8 n=1,310					
B1H-RC prediction					
TF-MoDisCo pattern_9 n=1,215					
B1H-RC prediction					
TF-MoDisCo pattern_10 n=1,041					
B1H-RC prediction					
TF-MoDisCo pattern_12 n=507					
B1H-RC prediction					
TF-MoDisCo pattern_13 n=398					
B1H-RC prediction					
TF-MoDisCo pattern_14 n=276					
B1H-RC prediction					
TF-MoDisCo pattern_15 n=243					

F

CIS-BP misc

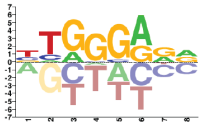

	IKZF1-201	IKZF1-203	IKZF1-210	IKZF1-217	IKZF1-218
B1H-RC prediction	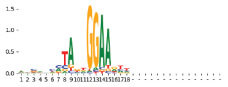	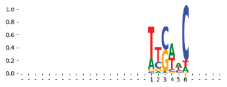	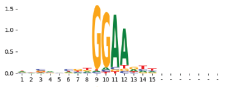		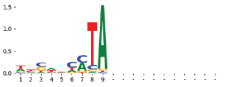
TF-MoDisCo pattern_16 n=209	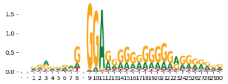	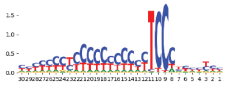	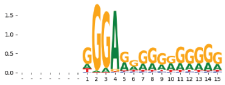	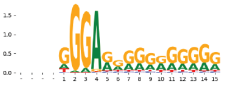	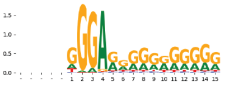
B1H-RC prediction	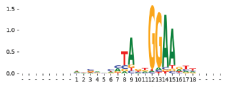	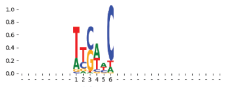	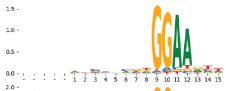	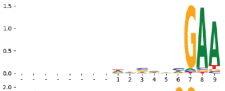	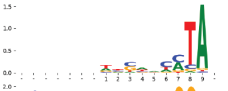
TF-MoDisCo pattern_17 n=203	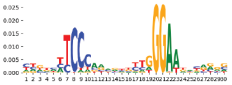	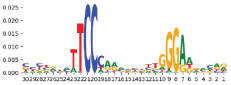	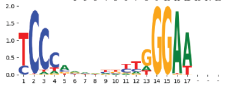	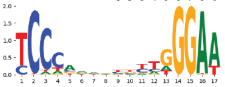	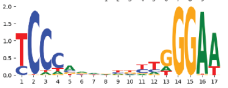

G

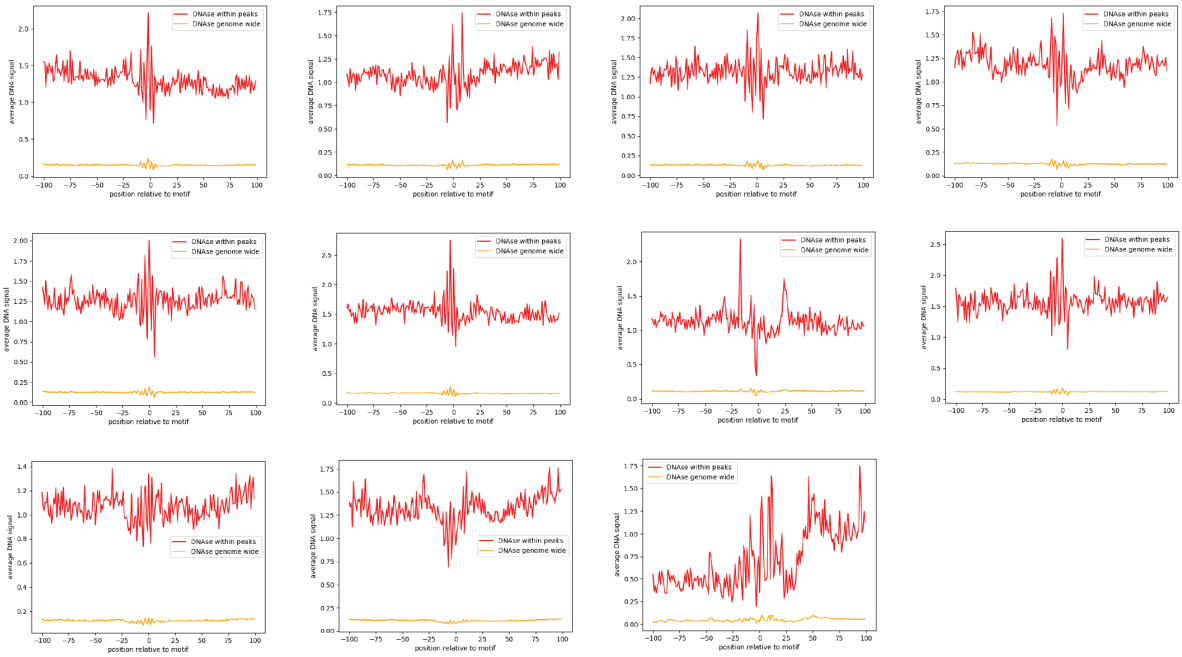

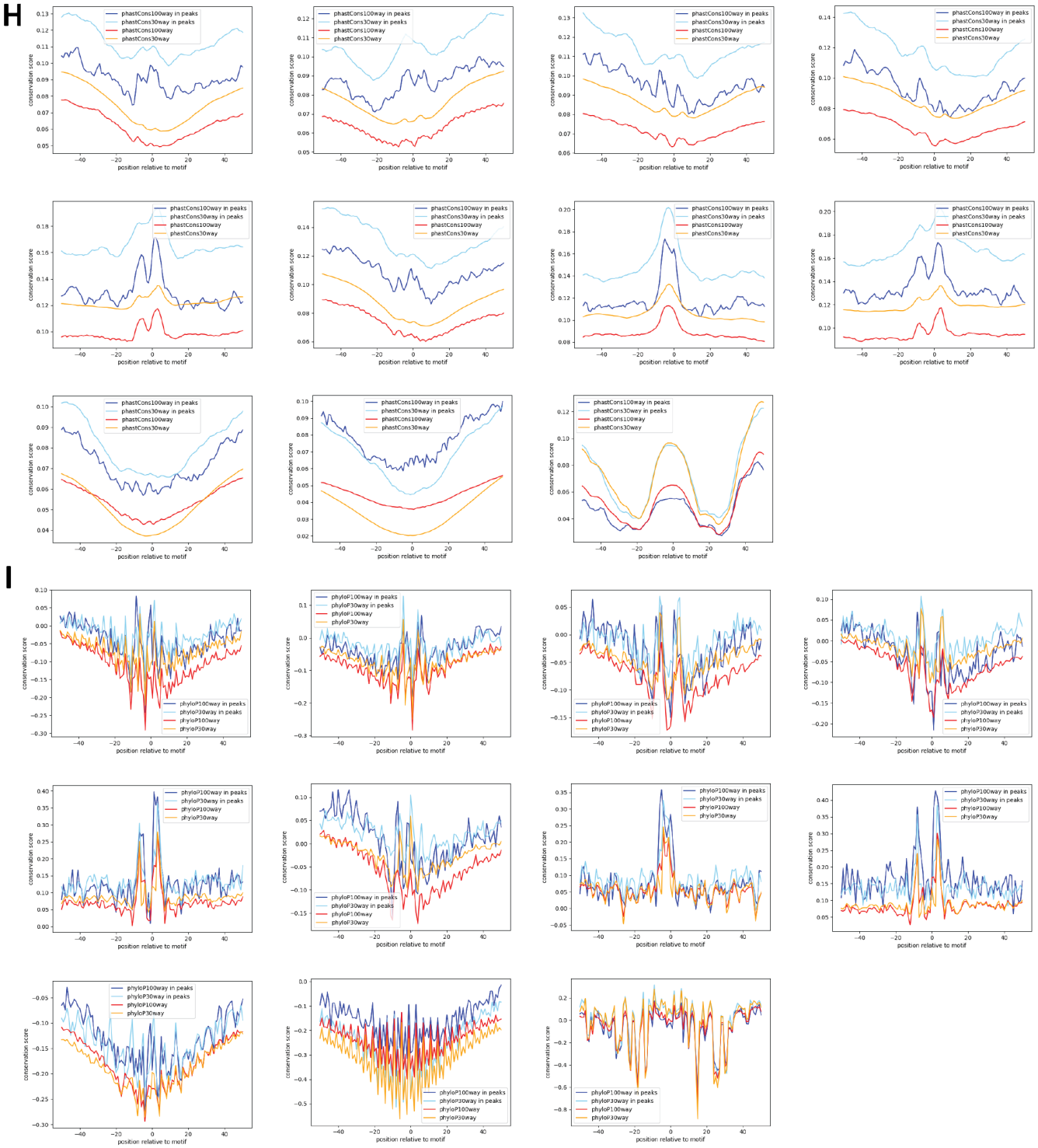

Supplementary Figure 73: Properties and genomic distribution of motifs identified for the IKZF1 transcription factor in K562 (accession ENCSR395HWC).

TF-MoDisCO pattern_0 n=9753, CWM

pattern_0, n=9753; subpattern_0, ns=1798

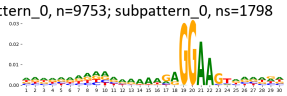

pattern_0, n=9753; subpattern_1, ns=1610

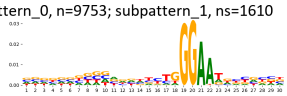

pattern_0, n=9753; subpattern_10, ns=367

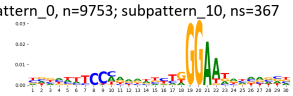

pattern_0, n=9753; subpattern_11, ns=257

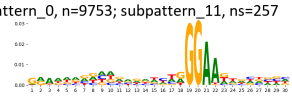

pattern_0, n=9753; subpattern_12, ns=208

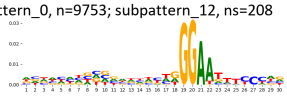

pattern_0, n=9753; subpattern_13, ns=177

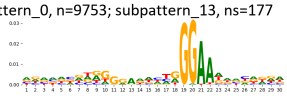

pattern_0, n=9753; subpattern_2, ns=1360

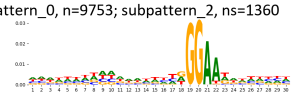

pattern_0, n=9753; subpattern_3, ns=1093

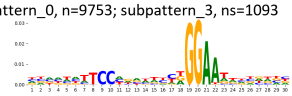

pattern_0, n=9753; subpattern_4, ns=651

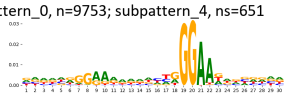

pattern_0, n=9753; subpattern_5, ns=510

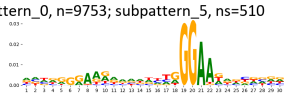

pattern_0, n=9753; subpattern_6, ns=476

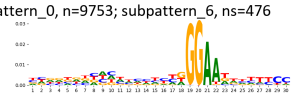

pattern_0, n=9753; subpattern_7, ns=469

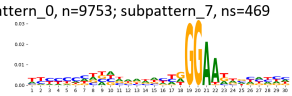

pattern_0, n=9753; subpattern_8, ns=406

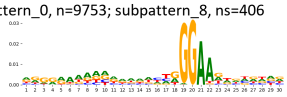

pattern_0, n=9753; subpattern_9, ns=371

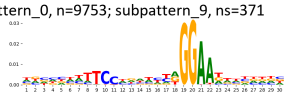

TF-MoDisCO pattern_0 n=9753, PWM

pattern_0, n=9753; subpattern_0, ns=1798

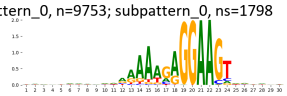

pattern_0, n=9753; subpattern_1, ns=1610

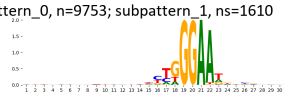

pattern_0, n=9753; subpattern_10, ns=367

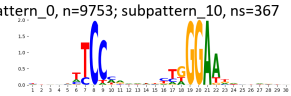

pattern_0, n=9753; subpattern_11, ns=257

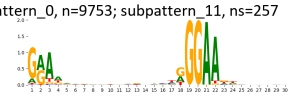

pattern_0, n=9753; subpattern_12, ns=208

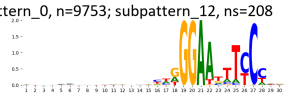

pattern_0, n=9753; subpattern_13, ns=177

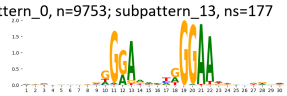

pattern_0, n=9753; subpattern_2, ns=1360

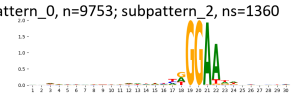

pattern_0, n=9753; subpattern_3, ns=1093

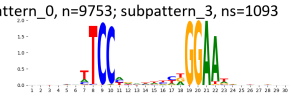

pattern_0, n=9753; subpattern_4, ns=651

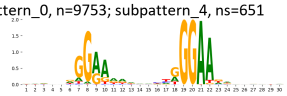

pattern_0, n=9753; subpattern_5, ns=510

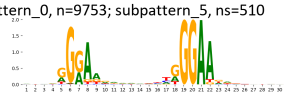

pattern_0, n=9753; subpattern_6, ns=476

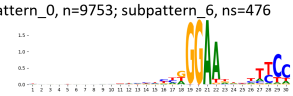

pattern_0, n=9753; subpattern_7, ns=469

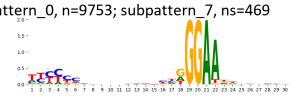

pattern_0, n=9753; subpattern_8, ns=406

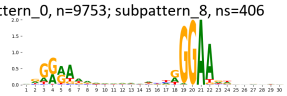

pattern_0, n=9753; subpattern_9, ns=371

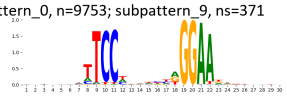

TF-MoDisCO pattern_10 n=1041, CWM

pattern_10, n=1041; subpattern_0, ns=326

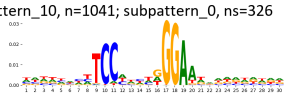

pattern_10, n=1041; subpattern_1, ns=292

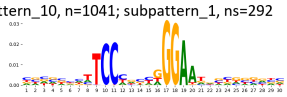

pattern_10, n=1041; subpattern_2, ns=178

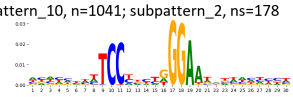

pattern_10, n=1041; subpattern_3, ns=113

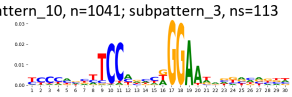

pattern_10, n=1041; subpattern_4, ns=40

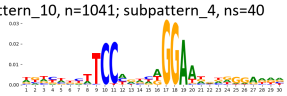

pattern_10, n=1041; subpattern_5, ns=38

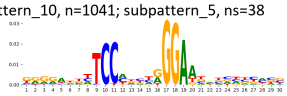

pattern_10, n=1041; subpattern_6, ns=27

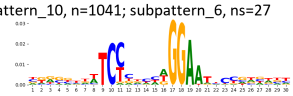

pattern_10, n=1041; subpattern_7, ns=27

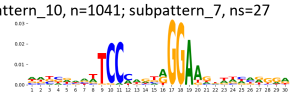

TF-MoDisCO pattern_10 n=1041, PWM

pattern_10, n=1041; subpattern_0, ns=326

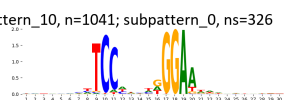

pattern_10, n=1041; subpattern_1, ns=292

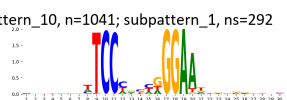

pattern_10, n=1041; subpattern_2, ns=178

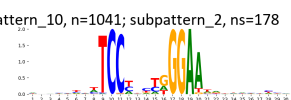

pattern_10, n=1041; subpattern_3, ns=113

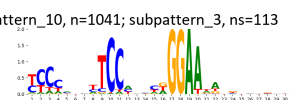

pattern_10, n=1041; subpattern_4, ns=40

pattern_10, n=1041; subpattern_5, ns=38

pattern_10, n=1041; subpattern_6, ns=27

pattern_10, n=1041; subpattern_7, ns=27

TF-MoDisCO pattern_12 n=507, CWM

pattern_12, n=507; subpattern_0, ns=138

pattern_12, n=507; subpattern_1, ns=121

pattern_12, n=507; subpattern_2, ns=119

pattern_12, n=507; subpattern_3, ns=105

pattern_12, n=507; subpattern_4, ns=24

TF-MoDisCO pattern_12 n=507, PWM

pattern_12, n=507; subpattern_0, ns=138

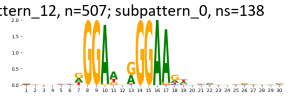

pattern_12, n=507; subpattern_1, ns=121

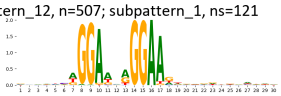

pattern_12, n=507; subpattern_2, ns=119

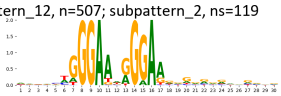

pattern_12, n=507; subpattern_3, ns=105

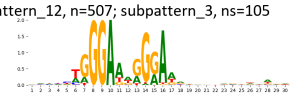

pattern_12, n=507; subpattern_4, ns=24

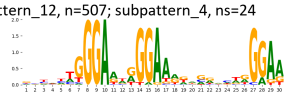

TF-MoDisCO pattern_13 n=398, CWM

pattern_13, n=398; subpattern_0, ns=116

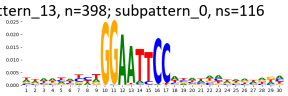

pattern_13, n=398; subpattern_1, ns=114

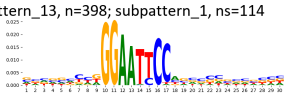

pattern_13, n=398; subpattern_2, ns=46

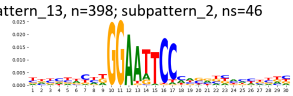

pattern_13, n=398; subpattern_3, ns=28

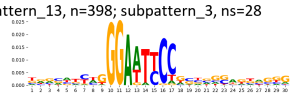

pattern_13, n=398; subpattern_4, ns=26

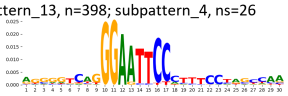

pattern_13, n=398; subpattern_5, ns=25

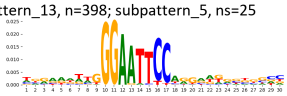

pattern_13, n=398; subpattern_6, ns=25

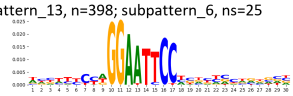

pattern_13, n=398; subpattern_7, ns=18

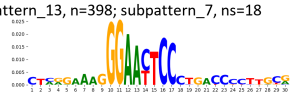

TF-MoDisCO pattern_13 n=398, PWM

pattern_13, n=398; subpattern_0, ns=116

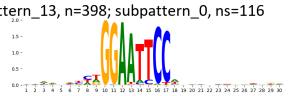

pattern_13, n=398; subpattern_1, ns=114

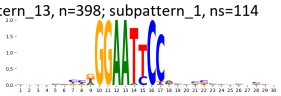

pattern_13, n=398; subpattern_2, ns=46

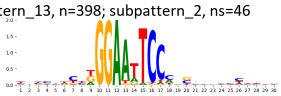

pattern_13, n=398; subpattern_3, ns=28

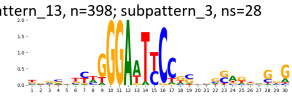

pattern_13, n=398; subpattern_4, ns=26

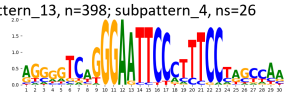

pattern_13, n=398; subpattern_5, ns=25

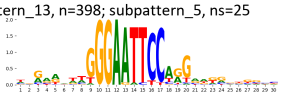

pattern_13, n=398; subpattern_6, ns=25

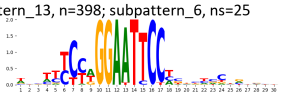

pattern_13, n=398; subpattern_7, ns=18

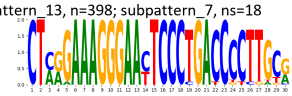

TF-MoDisCO pattern_14 n=276, CWM

pattern_14, n=276; subpattern_0, ns=95

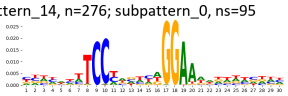

pattern_14, n=276; subpattern_1, ns=94

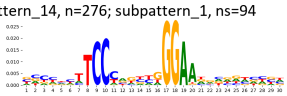

pattern_14, n=276; subpattern_2, ns=62

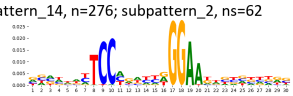

pattern_14, n=276; subpattern_3, ns=17

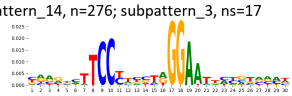

pattern_14, n=276; subpattern_4, ns=6

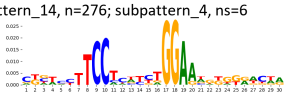

pattern_14, n=276; subpattern_5, ns=2

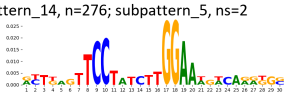

TF-MoDisCO pattern_14 n=276, PWM

pattern_14, n=276; subpattern_0, ns=95

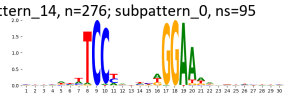

pattern_14, n=276; subpattern_1, ns=94

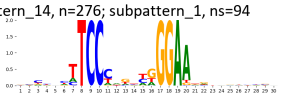

pattern_14, n=276; subpattern_2, ns=62

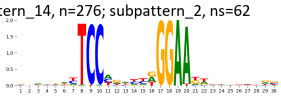

pattern_14, n=276; subpattern_3, ns=17

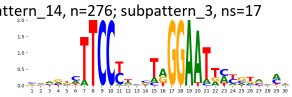

pattern_14, n=276; subpattern_4, ns=6

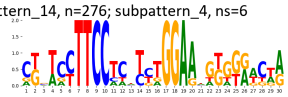

pattern_14, n=276; subpattern_5, ns=2

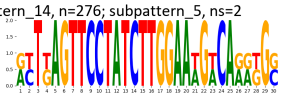

TF-MoDisCO pattern_15 n=243, CWM

pattern_15, n=243; subpattern_0, ns=75

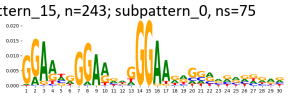

pattern_15, n=243; subpattern_1, ns=63

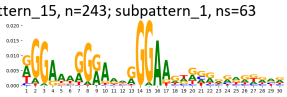

pattern_15, n=243; subpattern_2, ns=50

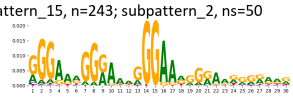

pattern_15, n=243; subpattern_3, ns=40

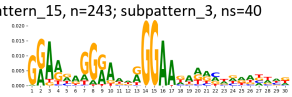

pattern_15, n=243; subpattern_4, ns=11

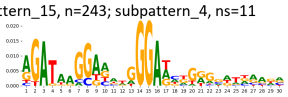

pattern_15, n=243; subpattern_5, ns=4

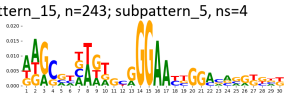

TF-MoDisCO pattern_15 n=243, PWM

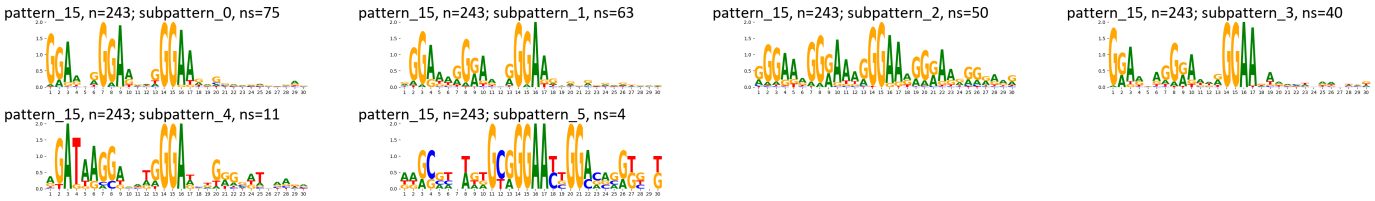

TF-MoDiSCO pattern_16 n=209, CWM

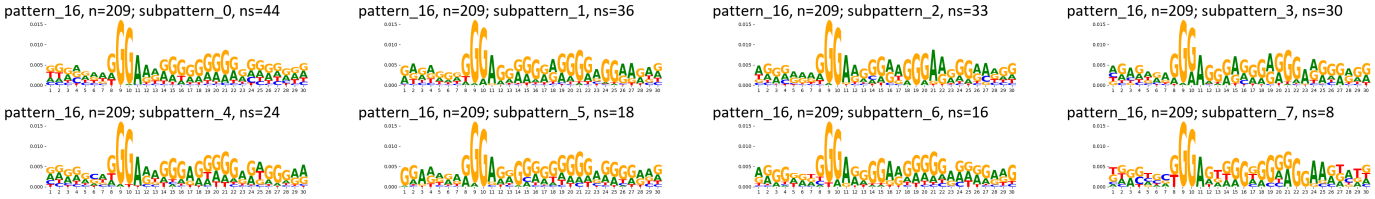

TF-MoDiSCO pattern_16 n=209, PWM

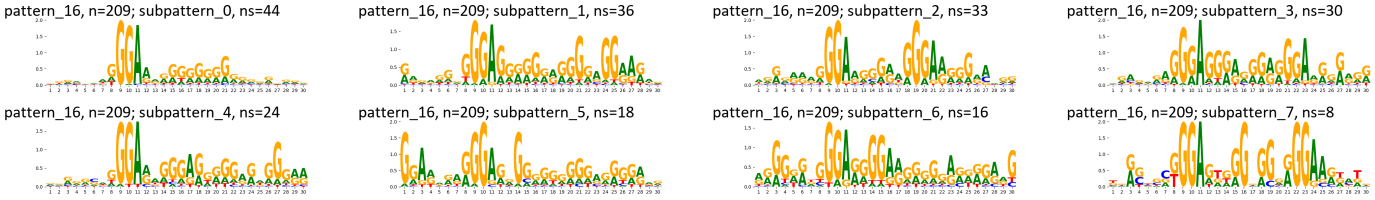

TF-MoDiSCO pattern_17 n=203, CWM

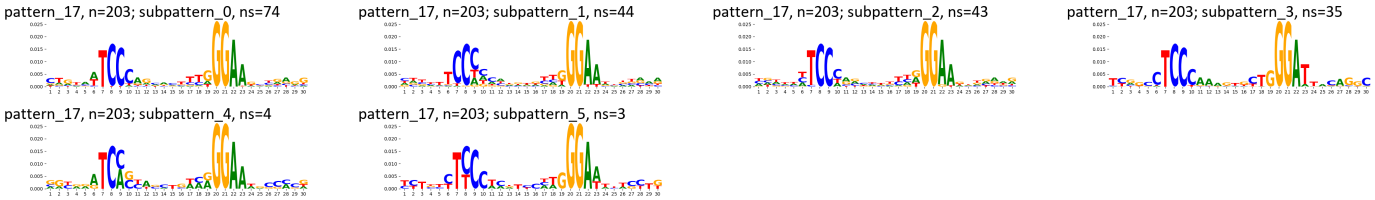

TF-MoDiSCO pattern_17 n=203, PWM

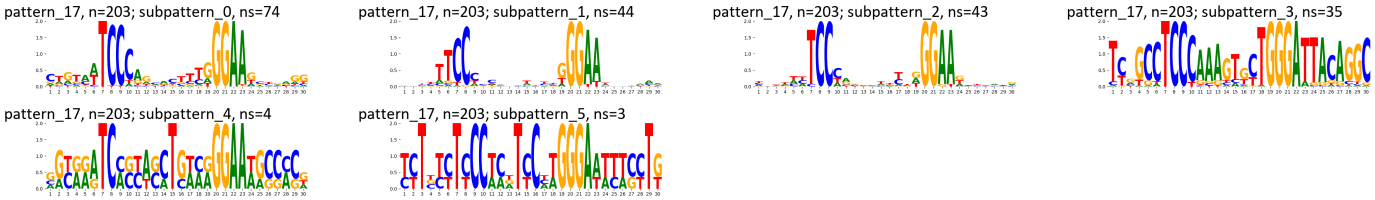

TF-MoDiSCO pattern_3 n=1927, CWM

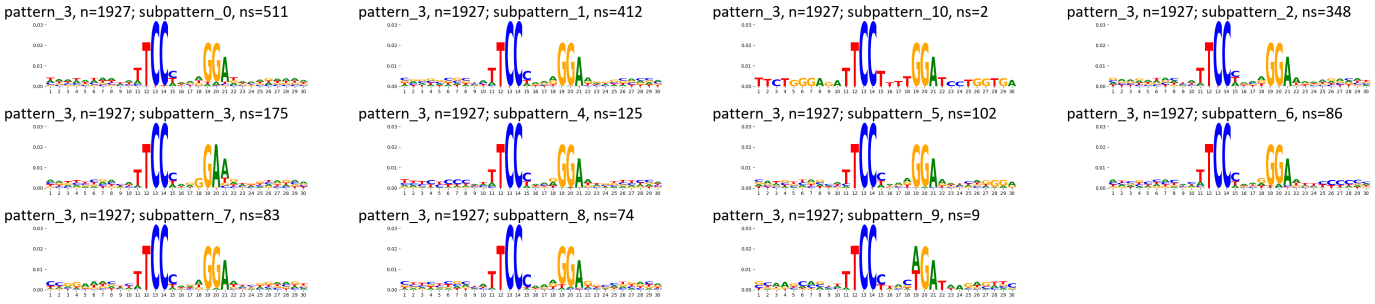

TF-MoDiSCO pattern_3 n=1927, PWM

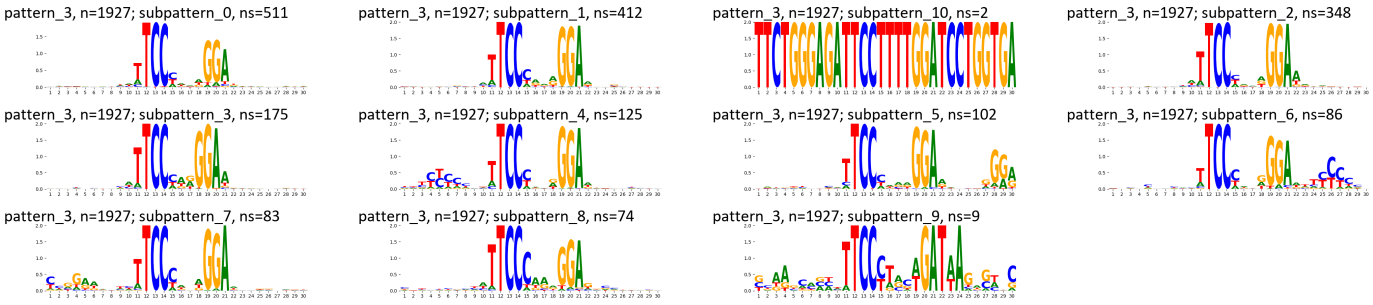

TF-MoDiSCO pattern_4 n=1654, CWM

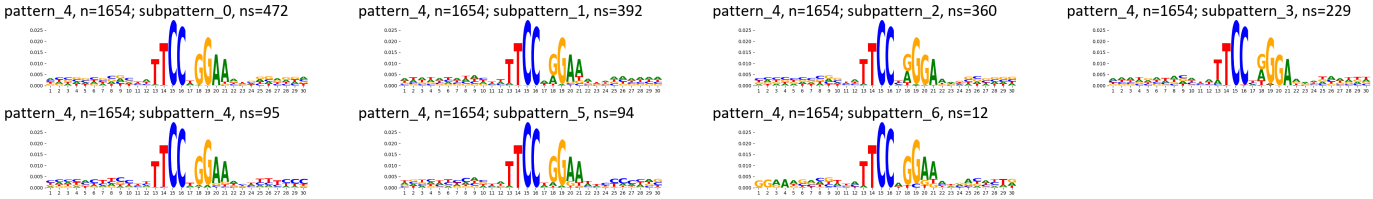

TF-MoDiSCO pattern_4 n=1654, PWM

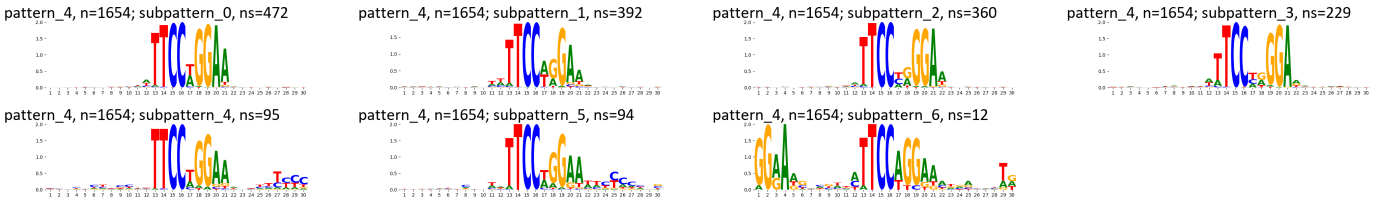

TF-MoDiSCO pattern_5 n=1624, CWM

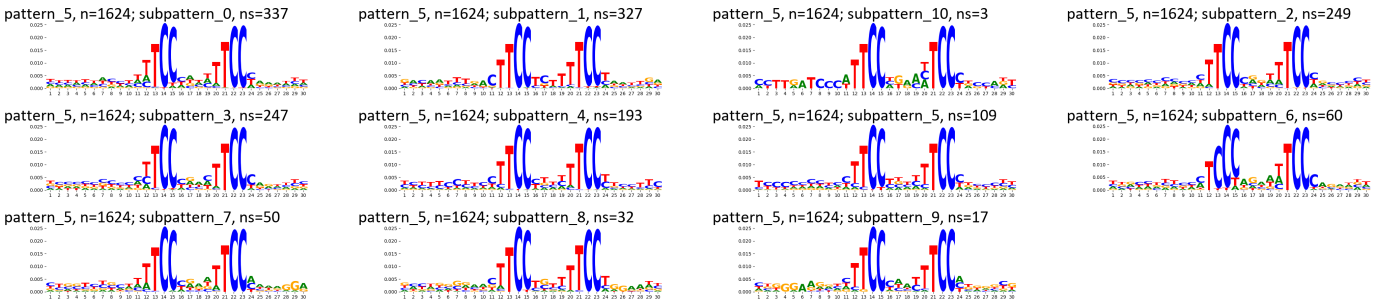

TF-MoDiSCO pattern_5 n=1624, PWM

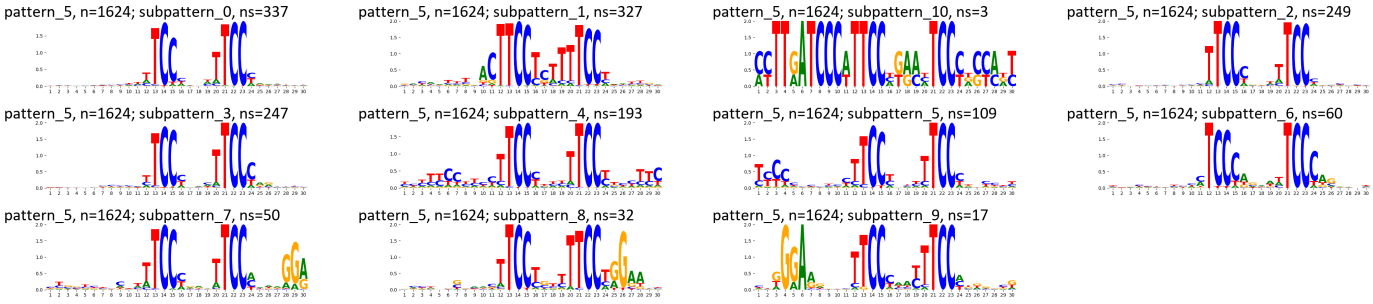

TF-MoDiSCO pattern_6 n=1570, CWM

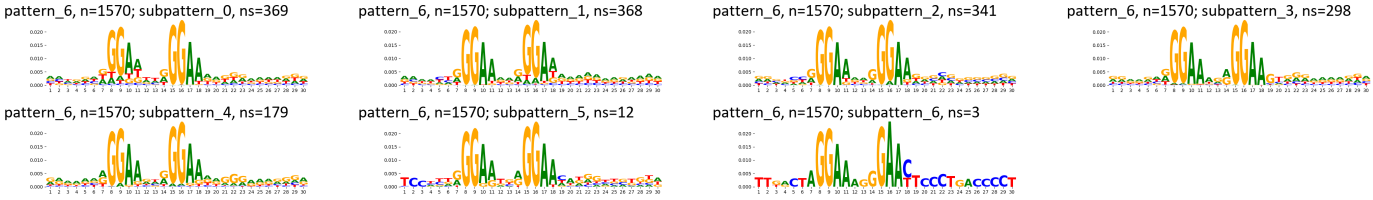

TF-MoDisCO pattern_6 n=1570, PWM

pattern_6, n=1570; subpattern_0, ns=369

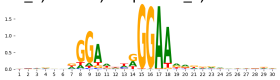

pattern_6, n=1570; subpattern_1, ns=368

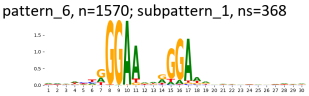

pattern_6, n=1570; subpattern_2, ns=341

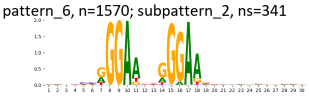

pattern_6, n=1570; subpattern_3, ns=298

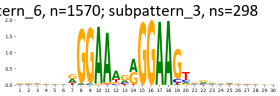

pattern_6, n=1570; subpattern_4, ns=179

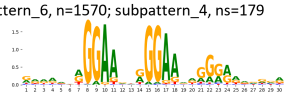

pattern_6, n=1570; subpattern_5, ns=12

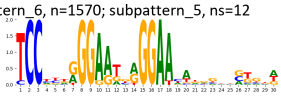

pattern_6, n=1570; subpattern_6, ns=3

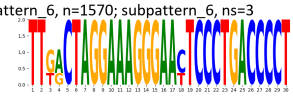

TF-MoDisCO pattern_7 n=1509, CWM

pattern_7, n=1509; subpattern_0, ns=377

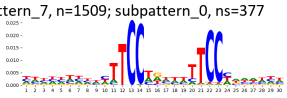

pattern_7, n=1509; subpattern_1, ns=350

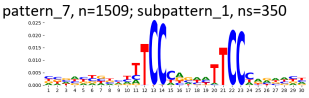

pattern_7, n=1509; subpattern_2, ns=238

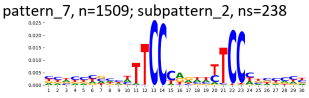

pattern_7, n=1509; subpattern_3, ns=231

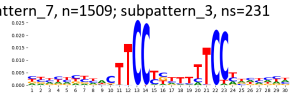

pattern_7, n=1509; subpattern_4, ns=134

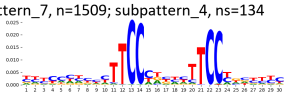

pattern_7, n=1509; subpattern_5, ns=82

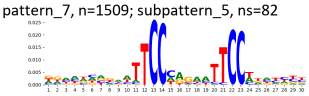

pattern_7, n=1509; subpattern_6, ns=50

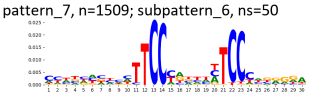

pattern_7, n=1509; subpattern_7, ns=47

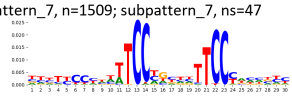

TF-MoDisCO pattern_7 n=1509, PWM

pattern_7, n=1509; subpattern_0, ns=377

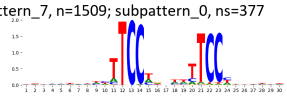

pattern_7, n=1509; subpattern_1, ns=350

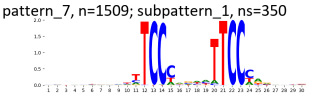

pattern_7, n=1509; subpattern_2, ns=238

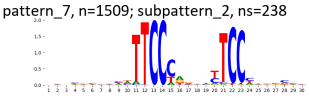

pattern_7, n=1509; subpattern_3, ns=231

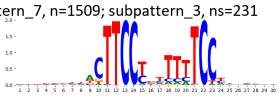

pattern_7, n=1509; subpattern_4, ns=134

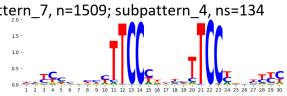

pattern_7, n=1509; subpattern_5, ns=82

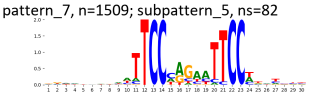

pattern_7, n=1509; subpattern_6, ns=50

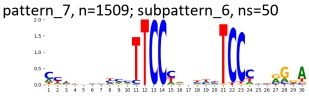

pattern_7, n=1509; subpattern_7, ns=47

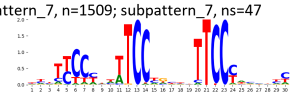

TF-MoDisCO pattern_8 n=1310, CWM

pattern_8, n=1310; subpattern_0, ns=318

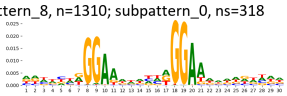

pattern_8, n=1310; subpattern_1, ns=267

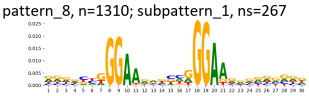

pattern_8, n=1310; subpattern_10, ns=14

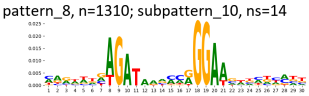

pattern_8, n=1310; subpattern_2, ns=210

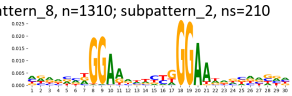

pattern_8, n=1310; subpattern_3, ns=174

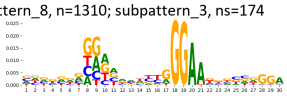

pattern_8, n=1310; subpattern_4, ns=116

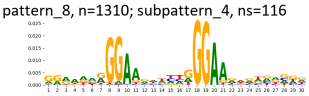

pattern_8, n=1310; subpattern_5, ns=71

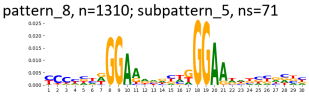

pattern_8, n=1310; subpattern_6, ns=56

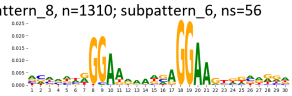

pattern_8, n=1310; subpattern_7, ns=35

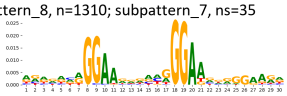

pattern_8, n=1310; subpattern_8, ns=33

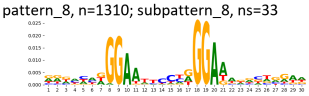

pattern_8, n=1310; subpattern_9, ns=16

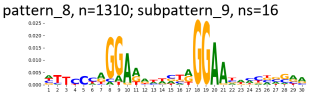

TF-MoDisCO pattern_8 n=1310, PWM

pattern_8, n=1310; subpattern_0, ns=318

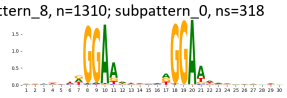

pattern_8, n=1310; subpattern_1, ns=267

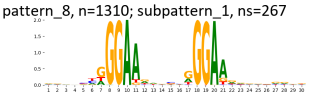

pattern_8, n=1310; subpattern_10, ns=14

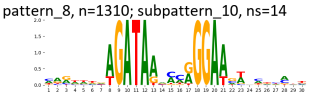

pattern_8, n=1310; subpattern_2, ns=210

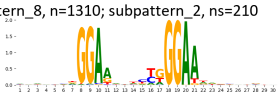

pattern_8, n=1310; subpattern_3, ns=174

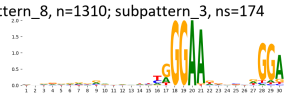

pattern_8, n=1310; subpattern_4, ns=116

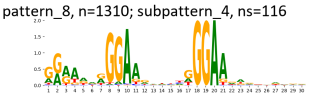

pattern_8, n=1310; subpattern_5, ns=71

pattern_8, n=1310; subpattern_6, ns=56

pattern_8, n=1310; subpattern_7, ns=35

pattern_8, n=1310; subpattern_8, ns=33

pattern_8, n=1310; subpattern_9, ns=16

TF-MoDisCO pattern_9 n=1215, CWM

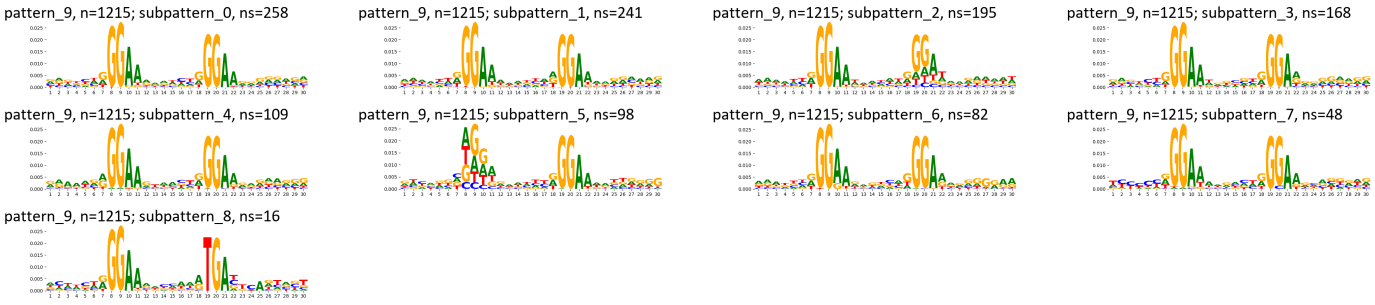

TF-MoDisCO pattern_9 n=1215, PWM

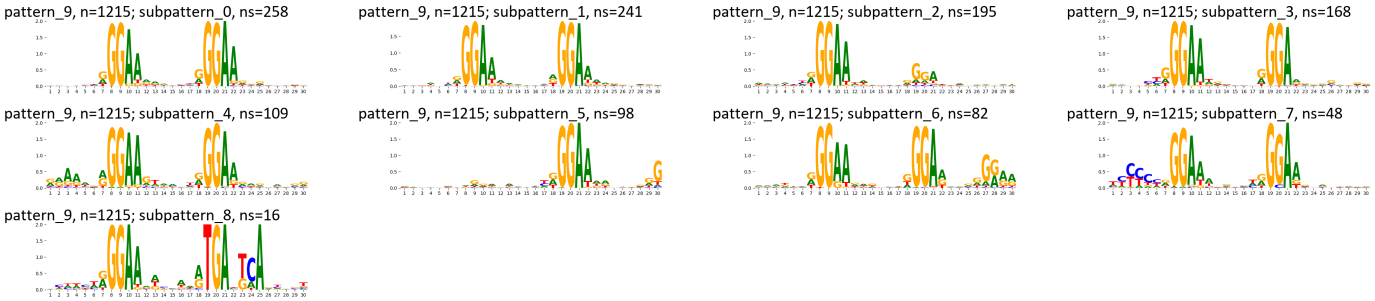

Supplementary Figure 74: TF-MoDisCO subpatterns for the IKZF1 transcription factor in K562 (accession ENCSR395HWC).

A

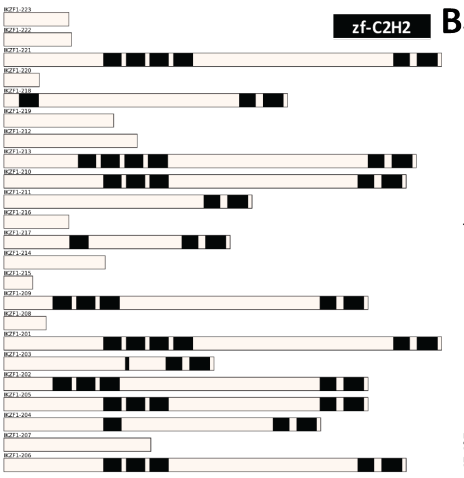

B

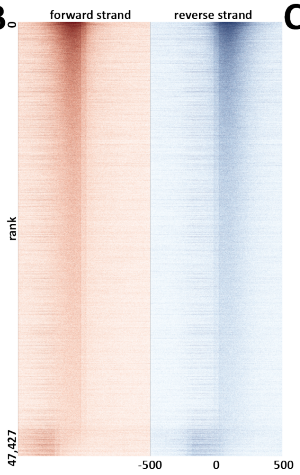

C

peaks	
state	fraction
EnhWk	0.30
EnhA1	0.17
TssA	0.14
TxWk	0.13
TssFlnkU	0.12
Quies	0.07
TssFlnkD	0.06
EnhA2	0.06
ReprPCWk	0.05
TssFlnk	0.05
EnhG1	0.02
ReprPC	0.02
EnhBiv	0.01
EnhG2	0.01
Tx	0.01
Het	0.00
ZNF/Rpts	0.00
TssBiv	0.00

D

peaks		peaks	
repeat	fraction	repeat	fraction
SINE/Alu	0.21	L2a	0.04
Simple_repeat	0.15	MIRb	0.04
LINE/L2	0.12	L2c	0.03
SINE/MIR	0.10	L2b	0.03
LINE/L1	0.08	MIR	0.02
LTR/ERV1	0.06	AluSx1	0.02
LTR/ERVL-MaLR	0.05	AluJb	0.02
Low_complexity	0.04	AluSx	0.02
DNA/hAT-Charlie	0.03	GA-rich	0.02
LTR/ERVL	0.03	MIR3	0.02
LINE/CR1	0.01	AluSz	0.02
DNA/TcMar-Tigger	0.01	MIRc	0.02
DNA/hAT-Tip100	0.01	L2	0.02
LTR/ERVK	0.01	AluY	0.02
tRNA	0.00	AluJo	0.01
Retroposon/SVA	0.00	AluJr	0.01
LTR/Gypsy	0.00	G-rich	0.01
DNA/hAT-Blackjack	0.00	AluSq2	0.01

E

Ontology	Term	FDR Q-val
GO Biological Process	regulation of gene expression, epigenetic	159.82
GO Biological Process	regulation of intrinsic apoptotic signaling pathway	99.82
GO Biological Process	regulation of DNA-templated transcription in response to stress	97.21
GO Biological Process	endoplasmic reticulum unfolded protein response	93.83
GO Biological Process	cellular response to topologically incorrect protein	86.08
GO Biological Process	cellular response to unfolded protein	81.08
GO Biological Process	regulation of mitochondrial membrane permeability	71.86
GO Biological Process	platelet aggregation	69.22
GO Biological Process	erythrocyte homeostasis	59.54
GO Biological Process	erythrocyte differentiation	52.50
GO Biological Process	positive regulation of mRNA metabolic process	50.34
GO Biological Process	cotranslational protein targeting to membrane	48.31
GO Biological Process	nuclear-transcribed mRNA catabolic process, nonsense-mediated decay	46.57
GO Biological Process	regulation of mitochondrial outer membrane permeabilization involved in apoptotic signaling pathway	42.40
GO Biological Process	SRP-dependent cotranslational protein targeting to membrane	37.34
GO Biological Process	gene silencing by miRNA	35.25
GO Biological Process	positive regulation of intrinsic apoptotic signaling pathway	31.21
GO Biological Process	negative regulation of response to endoplasmic reticulum stress	28.32
GO Biological Process	mismatch repair	21.88
Human Phenotype	Gastrointestinal hemorrhage	24.58

F

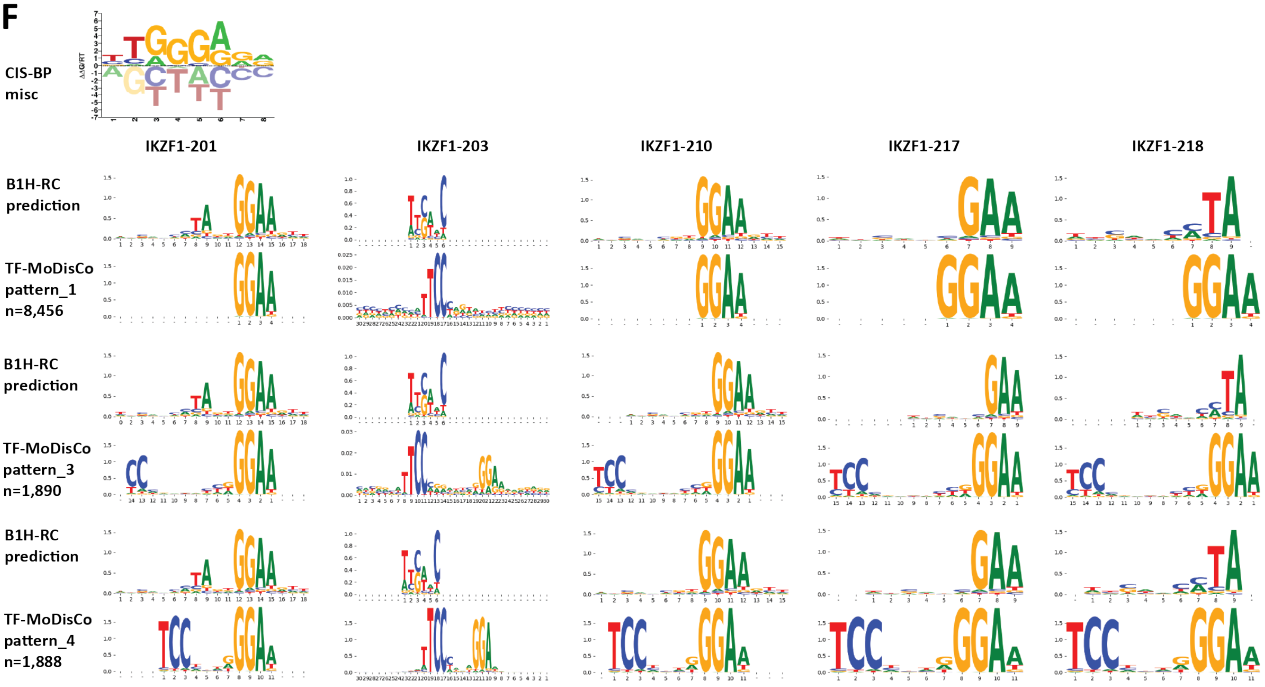

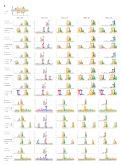

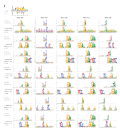

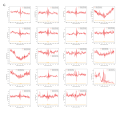

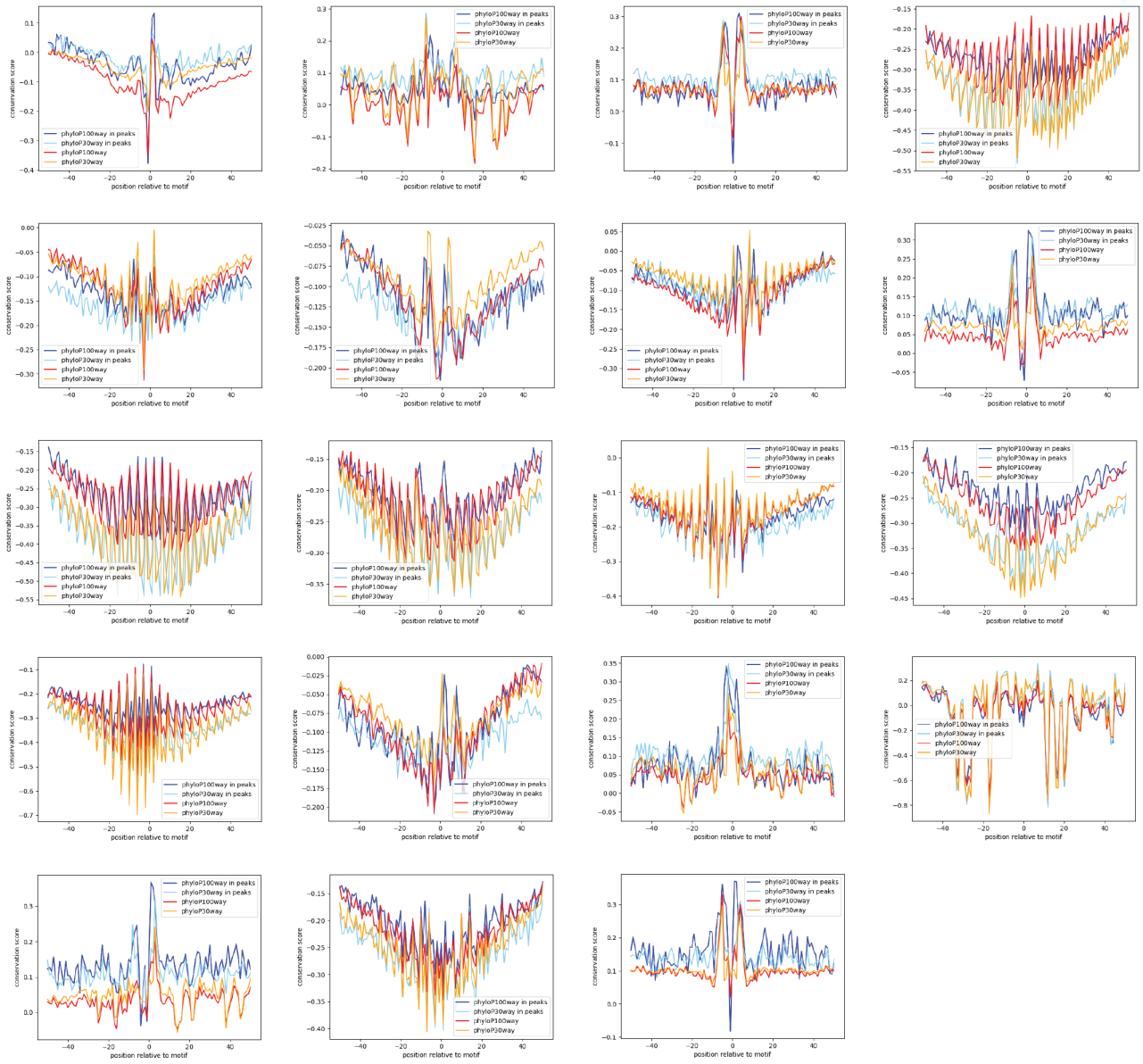

Supplementary Figure 75: Properties and genomic distribution of motifs identified for the IKZF1 transcription factor in K562 (accession ENCSR948VFL).

TF-MoDisCO pattern_1 n=8456, CWM

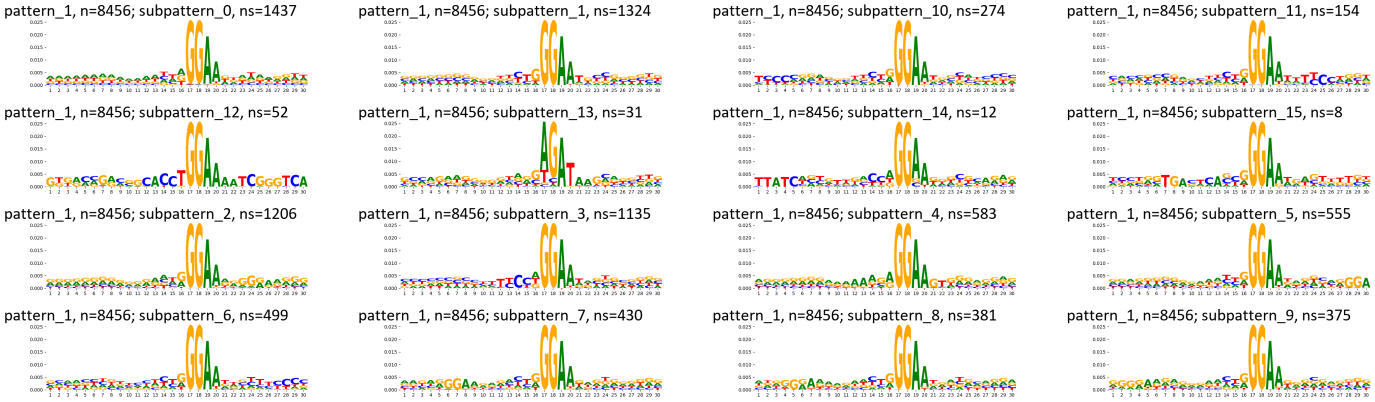

TF-MoDisCO pattern_1 n=8456, PWM

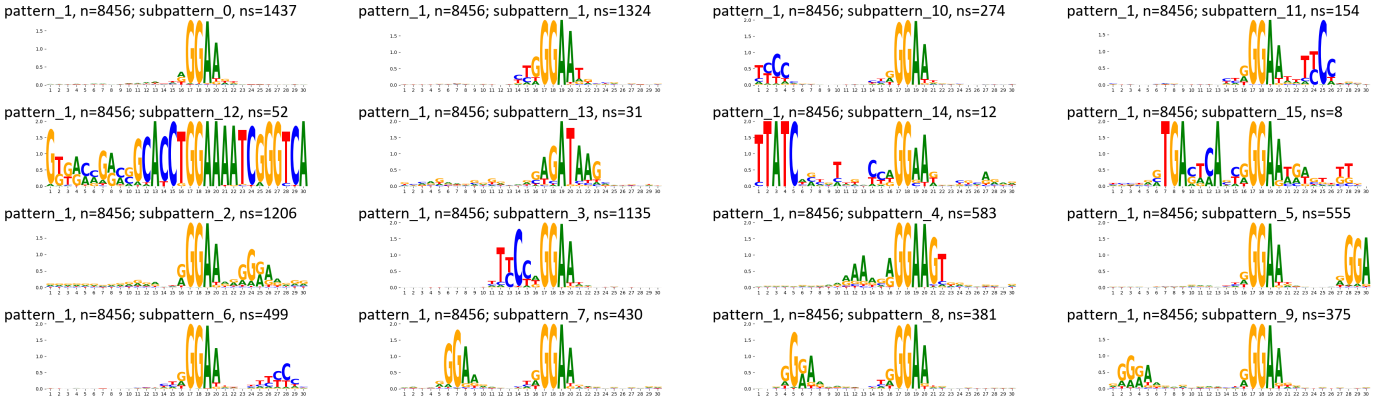

TF-MoDisCO pattern_10 n=882, CWM

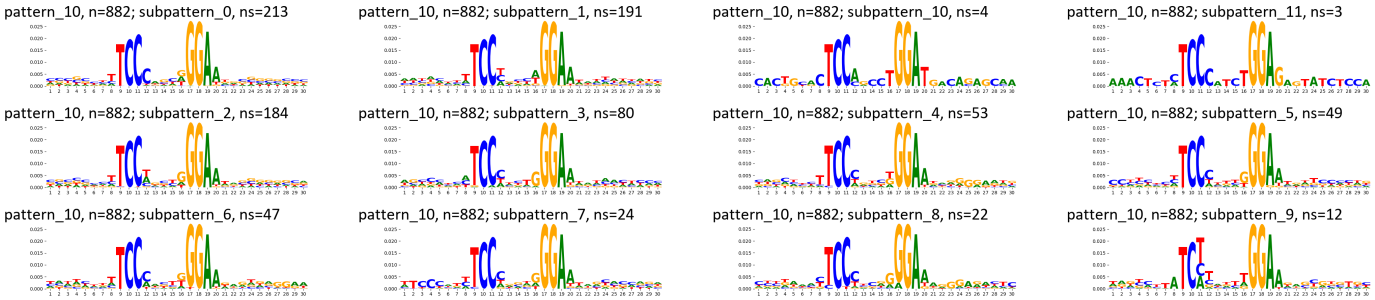

TF-MoDisCO pattern_10 n=882, PWM

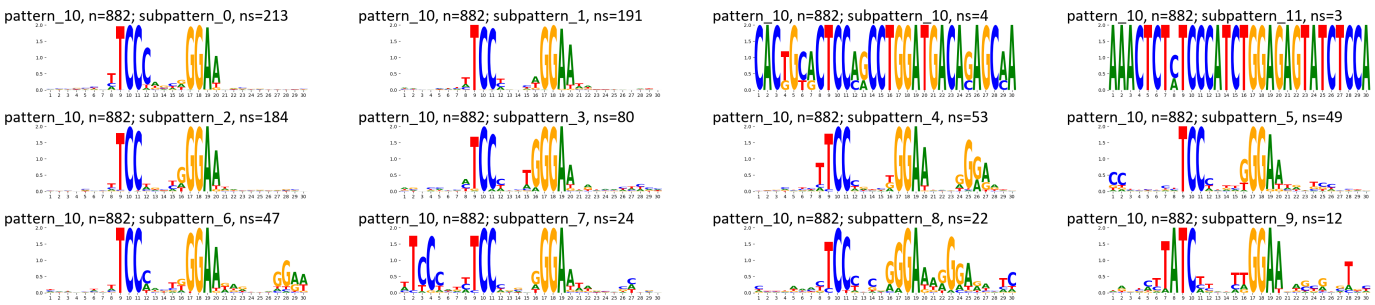

TF-MoDisCO pattern_11 n=633, CWM

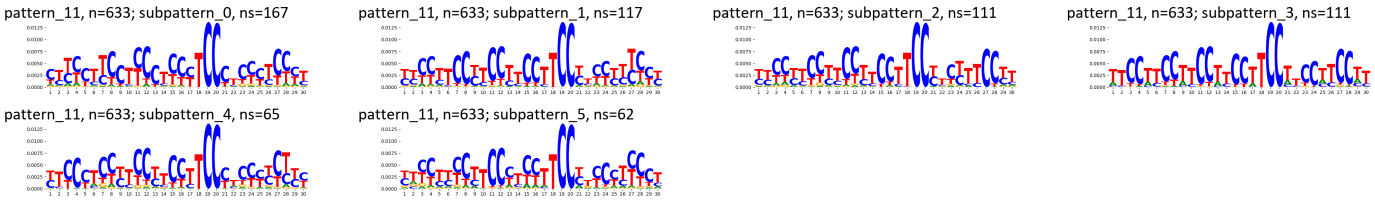

TF-MoDisCO pattern_11 n=633, PWM

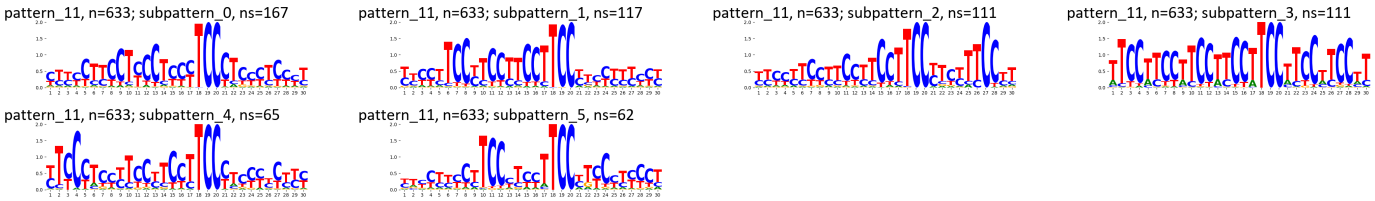

TF-MoDisCO pattern_12 n=592, CWM

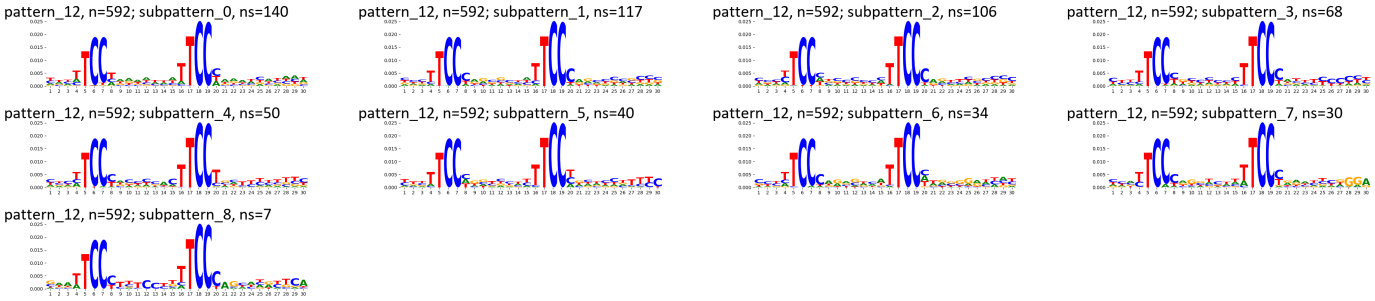

TF-MoDisCO pattern_12 n=592, PWM

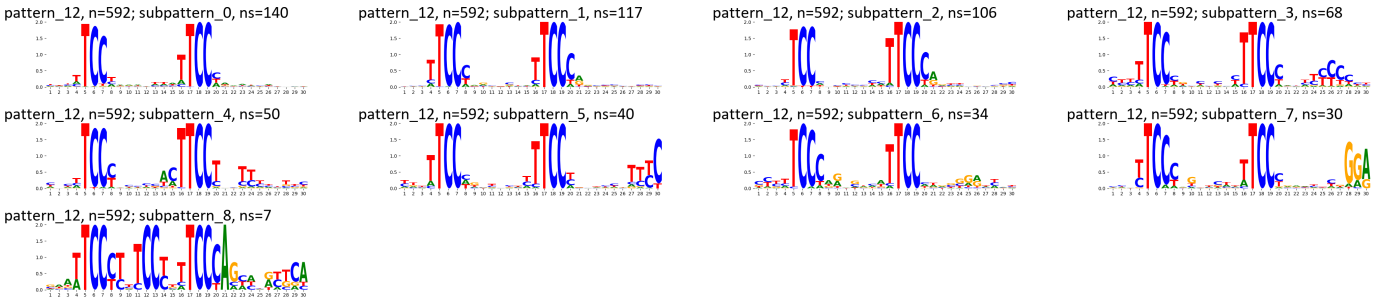

TF-MoDisCO pattern_13 n=500, CWM

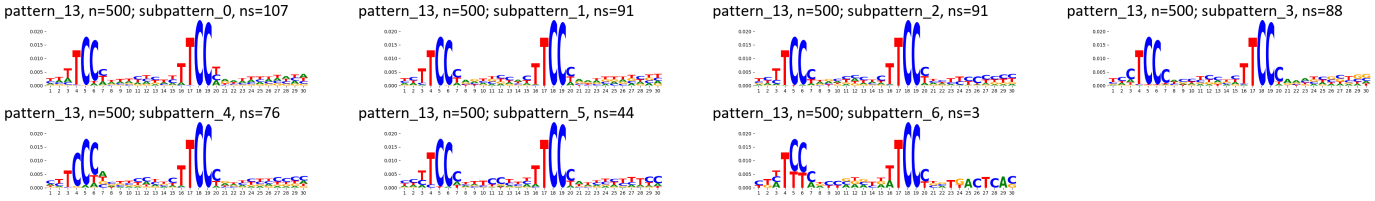

TF-MoDisCO pattern_13 n=500, PWM

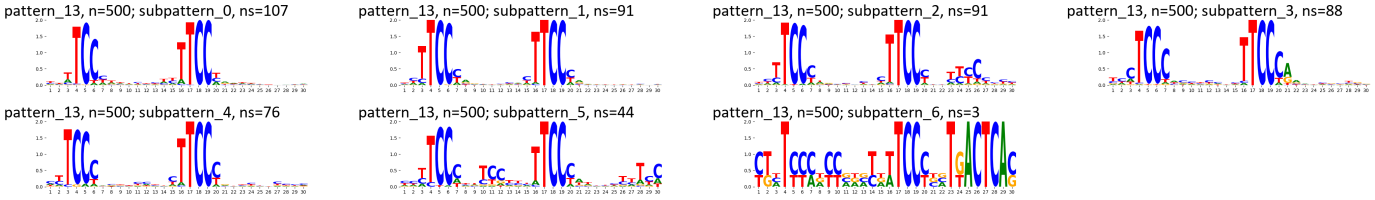

TF-MoDisCO pattern_14 n=468, CWM

pattern_14, n=468; subpattern_0, ns=89

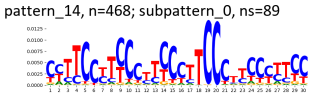

pattern_14, n=468; subpattern_1, ns=83

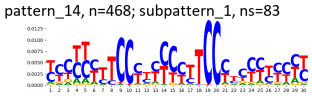

pattern_14, n=468; subpattern_2, ns=77

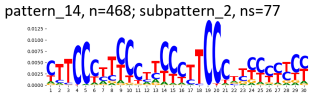

pattern_14, n=468; subpattern_3, ns=67

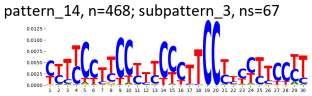

pattern_14, n=468; subpattern_4, ns=54

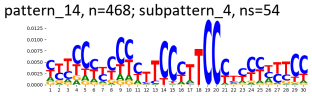

pattern_14, n=468; subpattern_5, ns=49

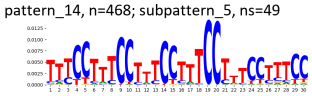

pattern_14, n=468; subpattern_6, ns=47

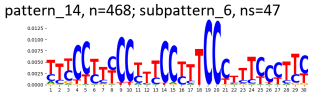

pattern_14, n=468; subpattern_7, ns=2

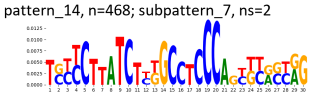

TF-MoDisCO pattern_14 n=468, PWM

pattern_14, n=468; subpattern_0, ns=89

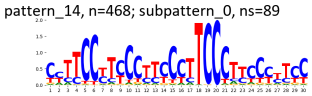

pattern_14, n=468; subpattern_1, ns=83

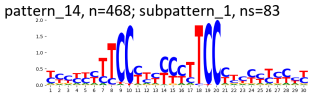

pattern_14, n=468; subpattern_2, ns=77

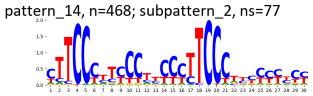

pattern_14, n=468; subpattern_3, ns=67

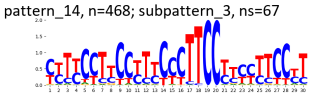

pattern_14, n=468; subpattern_4, ns=54

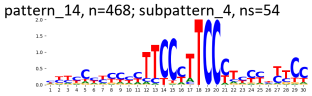

pattern_14, n=468; subpattern_5, ns=49

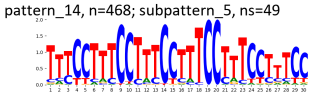

pattern_14, n=468; subpattern_6, ns=47

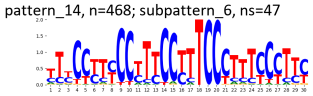

pattern_14, n=468; subpattern_7, ns=2

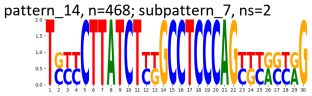

TF-MoDisCO pattern_15 n=423, CWM

pattern_15, n=423; subpattern_0, ns=98

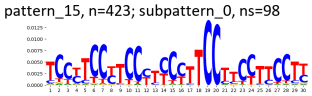

pattern_15, n=423; subpattern_1, ns=86

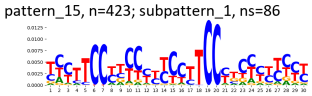

pattern_15, n=423; subpattern_2, ns=79

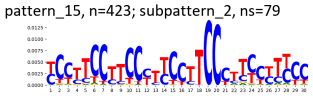

pattern_15, n=423; subpattern_3, ns=69

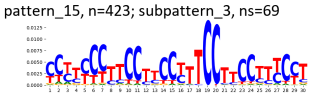

pattern_15, n=423; subpattern_4, ns=57

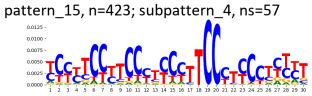

pattern_15, n=423; subpattern_5, ns=34

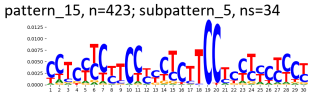

TF-MoDisCO pattern_15 n=423, PWM

pattern_15, n=423; subpattern_0, ns=98

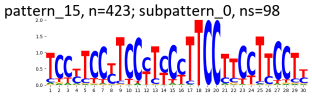

pattern_15, n=423; subpattern_1, ns=86

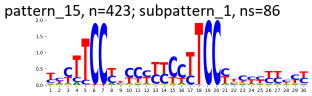

pattern_15, n=423; subpattern_2, ns=79

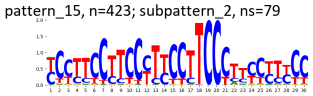

pattern_15, n=423; subpattern_3, ns=69

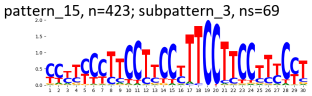

pattern_15, n=423; subpattern_4, ns=57

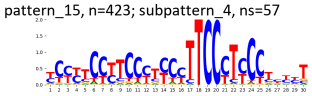

pattern_15, n=423; subpattern_5, ns=34

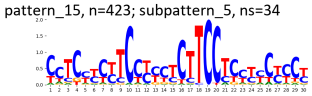

TF-MoDisCO pattern_16 n=367, CWM

pattern_16, n=367; subpattern_0, ns=81

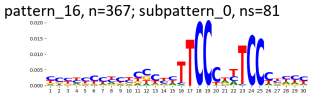

pattern_16, n=367; subpattern_1, ns=80

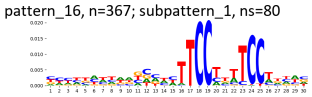

pattern_16, n=367; subpattern_2, ns=70

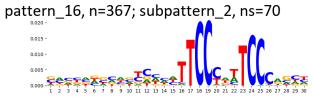

pattern_16, n=367; subpattern_3, ns=61

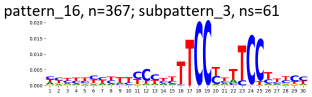

pattern_16, n=367; subpattern_4, ns=33

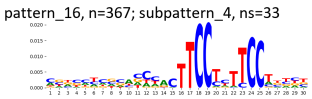

pattern_16, n=367; subpattern_5, ns=33

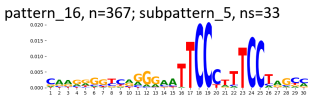

pattern_16, n=367; subpattern_6, ns=9

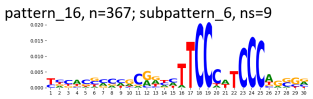

TF-MoDisCO pattern_16 n=367, PWM

pattern_16, n=367; subpattern_0, ns=81

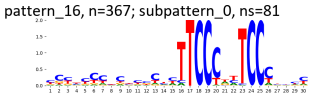

pattern_16, n=367; subpattern_1, ns=80

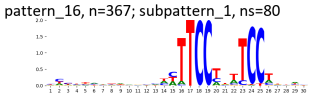

pattern_16, n=367; subpattern_2, ns=70

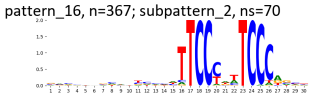

pattern_16, n=367; subpattern_3, ns=61

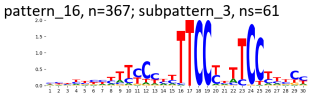

pattern_16, n=367; subpattern_4, ns=33

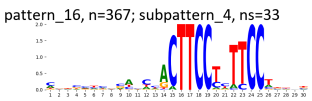

pattern_16, n=367; subpattern_5, ns=33

pattern_16, n=367; subpattern_6, ns=9

TF-MoDisCO pattern_18 n=256, CWM

pattern_18, n=256; subpattern_0, ns=82

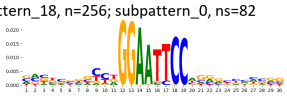

pattern_18, n=256; subpattern_1, ns=61

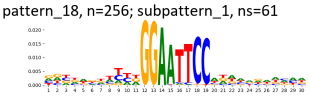

pattern_18, n=256; subpattern_2, ns=48

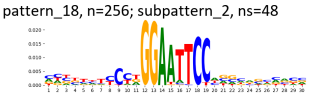

pattern_18, n=256; subpattern_3, ns=26

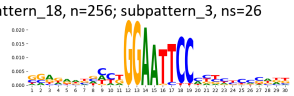

pattern_18, n=256; subpattern_4, ns=26

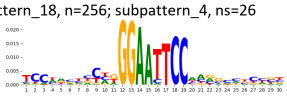

pattern_18, n=256; subpattern_5, ns=9

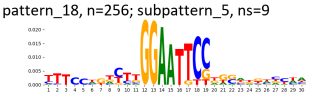

pattern_18, n=256; subpattern_6, ns=2

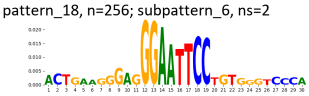

pattern_18, n=256; subpattern_7, ns=2

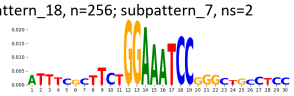

TF-MoDisCO pattern_18 n=256, PWM

pattern_18, n=256; subpattern_0, ns=82

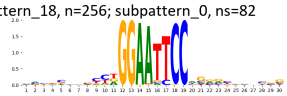

pattern_18, n=256; subpattern_1, ns=61

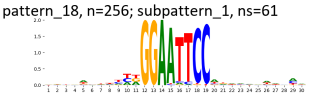

pattern_18, n=256; subpattern_2, ns=48

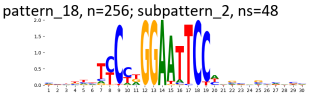

pattern_18, n=256; subpattern_3, ns=26

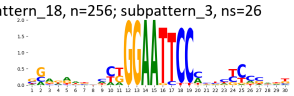

pattern_18, n=256; subpattern_4, ns=26

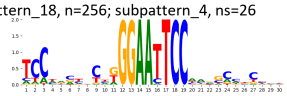

pattern_18, n=256; subpattern_5, ns=9

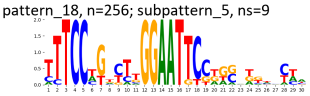

pattern_18, n=256; subpattern_6, ns=2

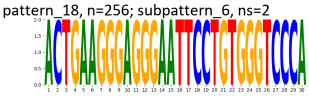

pattern_18, n=256; subpattern_7, ns=2

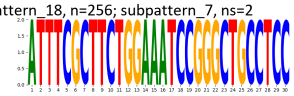

TF-MoDisCO pattern_20 n=240, CWM

pattern_20, n=240; subpattern_0, ns=85

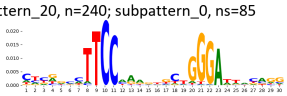

pattern_20, n=240; subpattern_1, ns=80

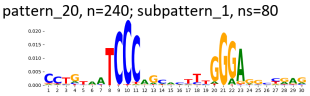

pattern_20, n=240; subpattern_2, ns=48

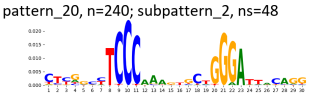

pattern_20, n=240; subpattern_3, ns=25

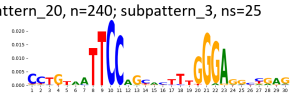

pattern_20, n=240; subpattern_4, ns=2

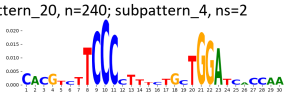

TF-MoDisCO pattern_20 n=240, PWM

pattern_20, n=240; subpattern_0, ns=85

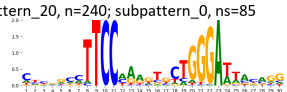

pattern_20, n=240; subpattern_1, ns=80

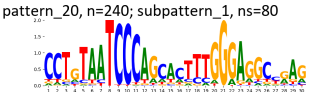

pattern_20, n=240; subpattern_2, ns=48

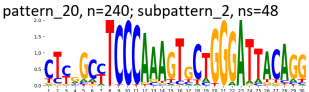

pattern_20, n=240; subpattern_3, ns=25

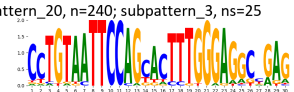

pattern_20, n=240; subpattern_4, ns=2

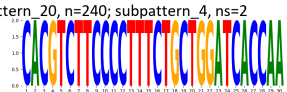

TF-MoDisCO pattern_21 n=185, CWM

pattern_21, n=185; subpattern_0, ns=65

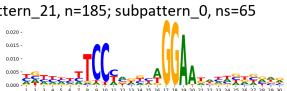

pattern_21, n=185; subpattern_1, ns=37

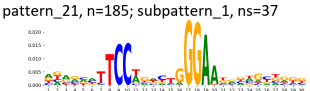

pattern_21, n=185; subpattern_2, ns=36

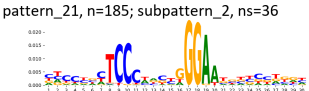

pattern_21, n=185; subpattern_3, ns=36

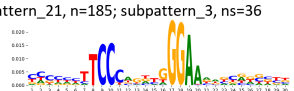

pattern_21, n=185; subpattern_4, ns=7

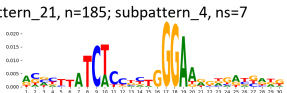

pattern_21, n=185; subpattern_5, ns=4

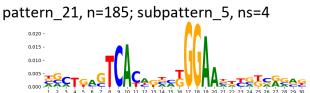

TF-MoDisCO pattern_21 n=185, PWM

pattern_21, n=185; subpattern_0, ns=65

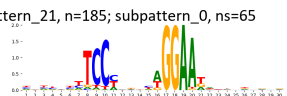

pattern_21, n=185; subpattern_1, ns=37

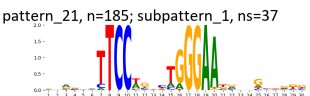

pattern_21, n=185; subpattern_2, ns=36

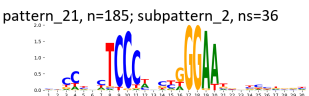

pattern_21, n=185; subpattern_3, ns=36

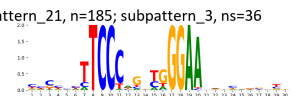

pattern_21, n=185; subpattern_4, ns=7

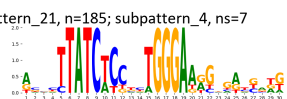

pattern_21, n=185; subpattern_5, ns=4

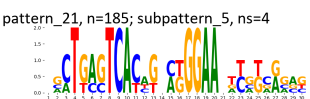

TF-MoDisCO pattern_22 n=144, CWM

pattern_22, n=144; subpattern_0, ns=42



pattern_22, n=144; subpattern_1, ns=34

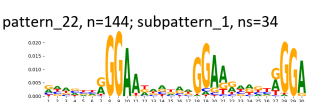

pattern_22, n=144; subpattern_2, ns=28

pattern_22, n=144; subpattern_3, ns=28

pattern_22, n=144; subpattern_4, ns=7

pattern_22, n=144; subpattern_5, ns=5

TF-MoDisCO pattern_22 n=144, PWM

pattern_22, n=144; subpattern_0, ns=42

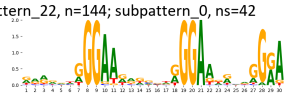

pattern_22, n=144; subpattern_1, ns=34

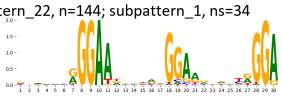

pattern_22, n=144; subpattern_2, ns=28

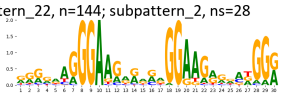

pattern_22, n=144; subpattern_3, ns=28

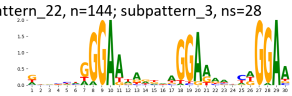

pattern_22, n=144; subpattern_4, ns=7

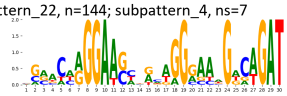

pattern_22, n=144; subpattern_5, ns=5

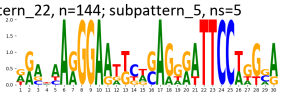

TF-MoDisCO pattern_23 n=124, CWM

pattern_23, n=124; subpattern_0, ns=47

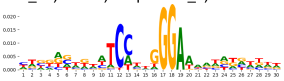

pattern_23, n=124; subpattern_1, ns=45

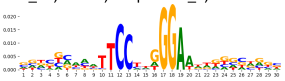

pattern_23, n=124; subpattern_2, ns=22

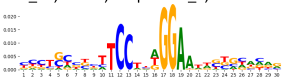

pattern_23, n=124; subpattern_3, ns=10

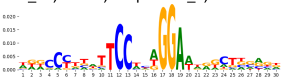

TF-MoDisCO pattern_23 n=124, PWM

pattern_23, n=124; subpattern_0, ns=47

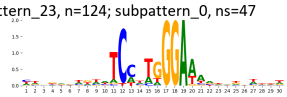

pattern_23, n=124; subpattern_1, ns=45

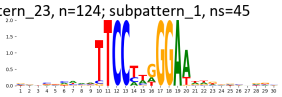

pattern_23, n=124; subpattern_2, ns=22

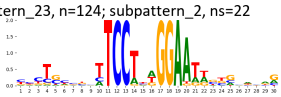

pattern_23, n=124; subpattern_3, ns=10

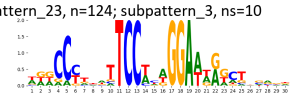

TF-MoDisCO pattern_3 n=1890, CWM

pattern_3, n=1890; subpattern_0, ns=351

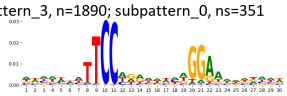

pattern_3, n=1890; subpattern_1, ns=321

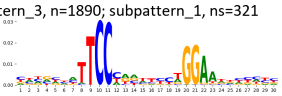

pattern_3, n=1890; subpattern_2, ns=315

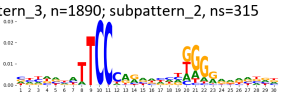

pattern_3, n=1890; subpattern_3, ns=311

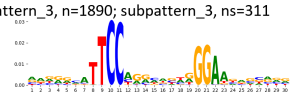

pattern_3, n=1890; subpattern_4, ns=249

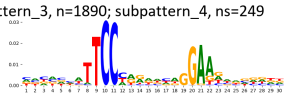

pattern_3, n=1890; subpattern_5, ns=108

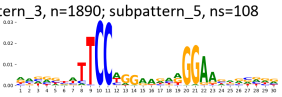

pattern_3, n=1890; subpattern_6, ns=103

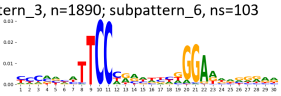

pattern_3, n=1890; subpattern_7, ns=82

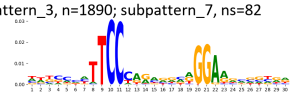

pattern_3, n=1890; subpattern_8, ns=50

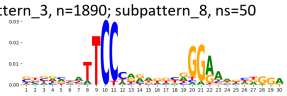

TF-MoDisCO pattern_3 n=1890, PWM

pattern_3, n=1890; subpattern_0, ns=351

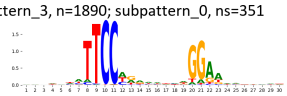

pattern_3, n=1890; subpattern_1, ns=321

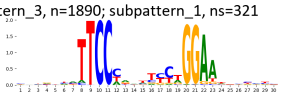

pattern_3, n=1890; subpattern_2, ns=315

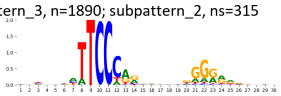

pattern_3, n=1890; subpattern_3, ns=311

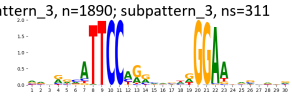

pattern_3, n=1890; subpattern_4, ns=249

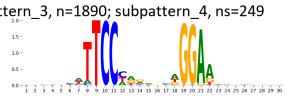

pattern_3, n=1890; subpattern_5, ns=108

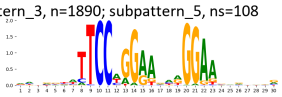

pattern_3, n=1890; subpattern_6, ns=103

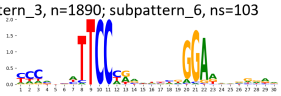

pattern_3, n=1890; subpattern_7, ns=82

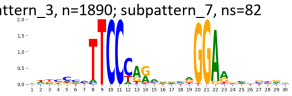

pattern_3, n=1890; subpattern_8, ns=50

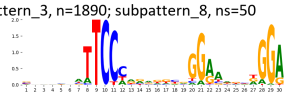

TF-MoDisCO pattern_4 n=1888, CWM

pattern_4, n=1888; subpattern_0, ns=482

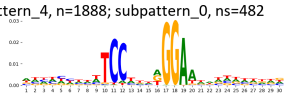

pattern_4, n=1888; subpattern_1, ns=375

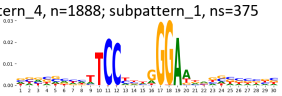

pattern_4, n=1888; subpattern_10, ns=6

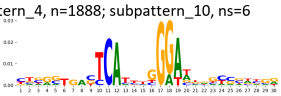

pattern_4, n=1888; subpattern_11, ns=4

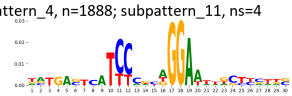

pattern_4, n=1888; subpattern_2, ns=300

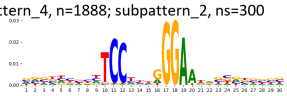

pattern_4, n=1888; subpattern_3, ns=187

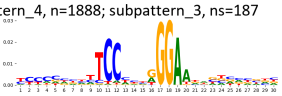

pattern_4, n=1888; subpattern_4, ns=168

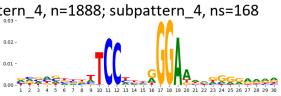

pattern_4, n=1888; subpattern_5, ns=83

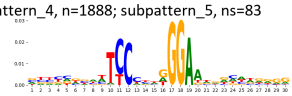

pattern_4, n=1888; subpattern_6, ns=78

pattern_4, n=1888; subpattern_7, ns=78

pattern_4, n=1888; subpattern_8, ns=77

pattern_4, n=1888; subpattern_9, ns=50

TF-MoDisCO pattern_4 n=1888, PWM

pattern_4, n=1888; subpattern_0, ns=482

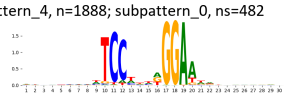

pattern_4, n=1888; subpattern_1, ns=375

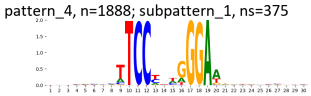

pattern_4, n=1888; subpattern_10, ns=6

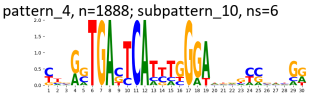

pattern_4, n=1888; subpattern_11, ns=4

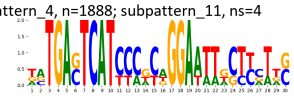

pattern_4, n=1888; subpattern_2, ns=300

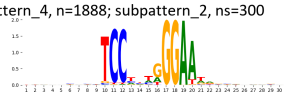

pattern_4, n=1888; subpattern_3, ns=187

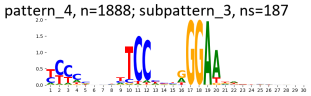

pattern_4, n=1888; subpattern_4, ns=168

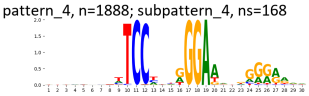

pattern_4, n=1888; subpattern_5, ns=83

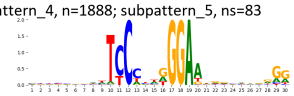

pattern_4, n=1888; subpattern_6, ns=78

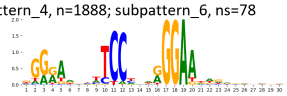

pattern_4, n=1888; subpattern_7, ns=78

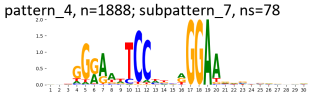

pattern_4, n=1888; subpattern_8, ns=77

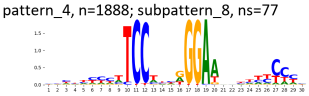

pattern_4, n=1888; subpattern_9, ns=50

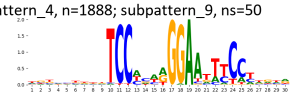

TF-MoDisCO pattern_5 n=1710, CWM

pattern_5, n=1710; subpattern_0, ns=347

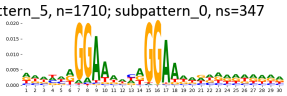

pattern_5, n=1710; subpattern_1, ns=317

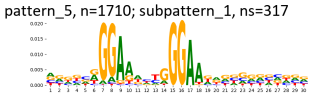

pattern_5, n=1710; subpattern_2, ns=312

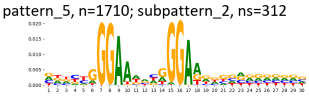

pattern_5, n=1710; subpattern_3, ns=304

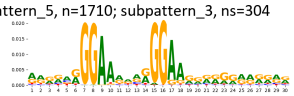

pattern_5, n=1710; subpattern_4, ns=172

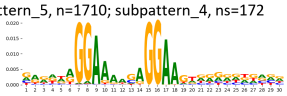

pattern_5, n=1710; subpattern_5, ns=157

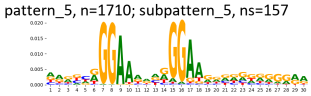

pattern_5, n=1710; subpattern_6, ns=99

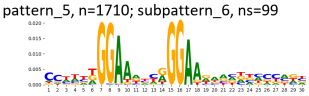

pattern_5, n=1710; subpattern_7, ns=2

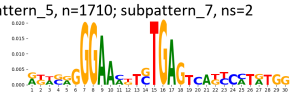

TF-MoDisCO pattern_5 n=1710, PWM

pattern_5, n=1710; subpattern_0, ns=347

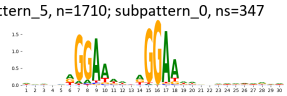

pattern_5, n=1710; subpattern_1, ns=317

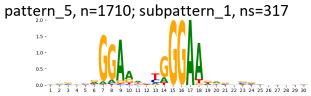

pattern_5, n=1710; subpattern_2, ns=312

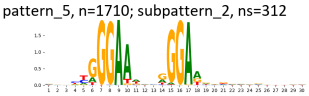

pattern_5, n=1710; subpattern_3, ns=304

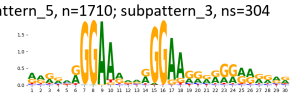

pattern_5, n=1710; subpattern_4, ns=172

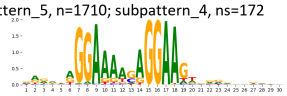

pattern_5, n=1710; subpattern_5, ns=157

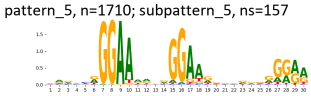

pattern_5, n=1710; subpattern_6, ns=99

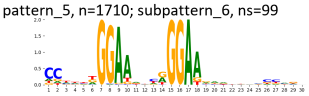

pattern_5, n=1710; subpattern_7, ns=2

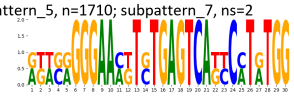

TF-MoDisCO pattern_6 n=1619, CWM

pattern_6, n=1619; subpattern_0, ns=356

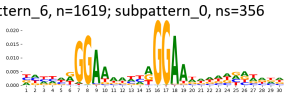

pattern_6, n=1619; subpattern_1, ns=316

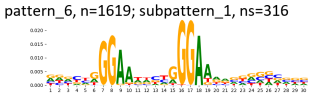

pattern_6, n=1619; subpattern_2, ns=300

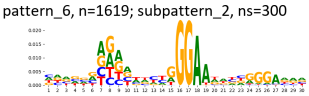

pattern_6, n=1619; subpattern_3, ns=243

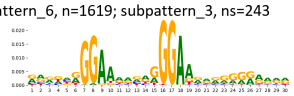

pattern_6, n=1619; subpattern_4, ns=210

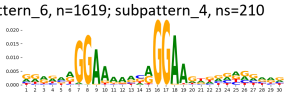

pattern_6, n=1619; subpattern_5, ns=174

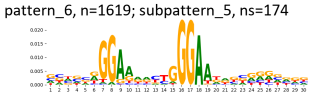

pattern_6, n=1619; subpattern_6, ns=20

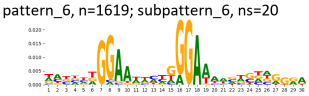

TF-MoDisCO pattern_6 n=1619, PWM

pattern_6, n=1619; subpattern_0, ns=356

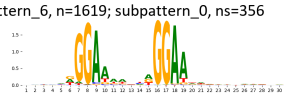

pattern_6, n=1619; subpattern_1, ns=316

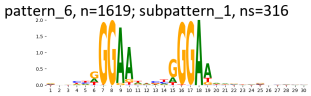

pattern_6, n=1619; subpattern_2, ns=300

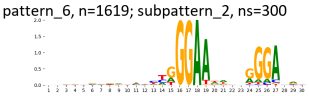

pattern_6, n=1619; subpattern_3, ns=243

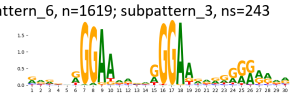

pattern_6, n=1619; subpattern_4, ns=210

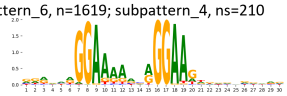

pattern_6, n=1619; subpattern_5, ns=174

pattern_6, n=1619; subpattern_6, ns=20

TF-MoDisCO pattern_8 n=1051, CWM

pattern_8, n=1051; subpattern_0, ns=263

pattern_8, n=1051; subpattern_1, ns=222

pattern_8, n=1051; subpattern_2, ns=187

pattern_8, n=1051; subpattern_3, ns=143

pattern_8, n=1051; subpattern_4, ns=109

pattern_8, n=1051; subpattern_5, ns=89

pattern_8, n=1051; subpattern_6, ns=28

pattern_8, n=1051; subpattern_7, ns=7

pattern_8, n=1051; subpattern_8, ns=3

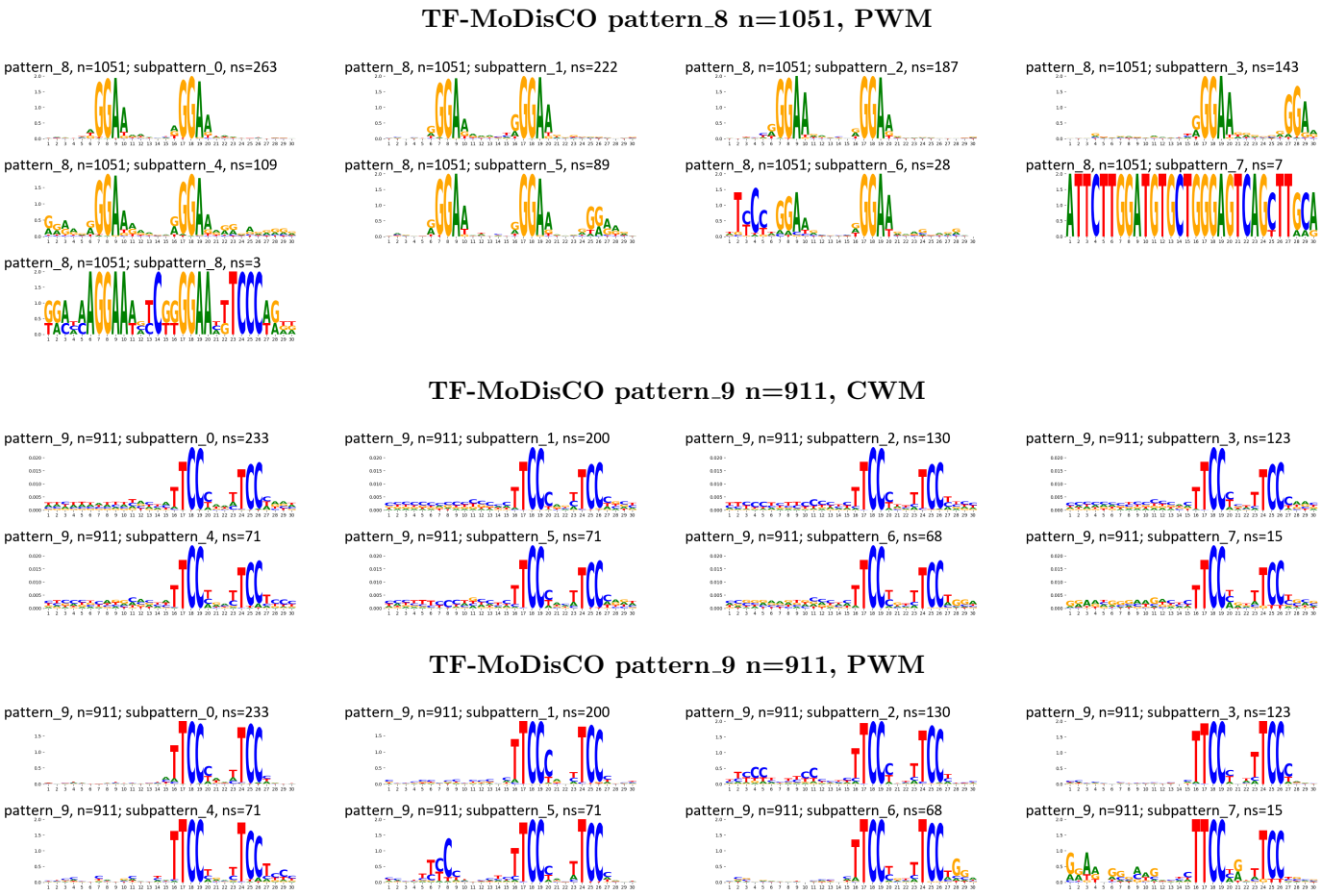

Supplementary Figure 76: TF-MoDisCO subpatterns for the IKZF1 transcription factor in K562 (accession ENCSR948VFL).

A

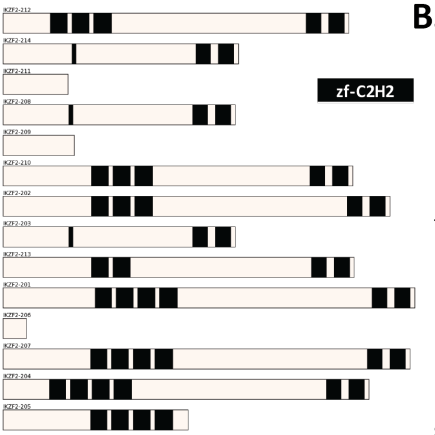

B

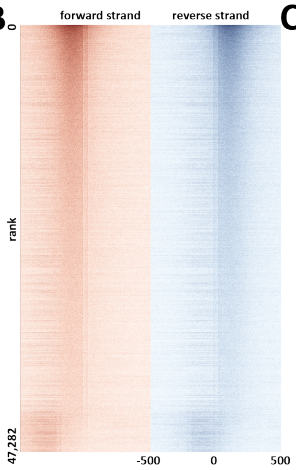

C

peaks	
state	fraction
EnhWk	0.28
EnhA1	0.23
TssA	0.17
TssFlnkU	0.10
Quies	0.09
EnhA2	0.09
TssFlnk	0.08
TxWk	0.07
TssFlnkD	0.05
ReprPCWk	0.03
EnhG1	0.01
EnhG2	0.01
Het	0.01
ZNF/Rpts	0.01
Tx	0.00
EnhBiv	0.00
TssBiv	0.00
ReprPC	0.00

D

peaks		peaks	
repeat	fraction	repeat	fraction
SINE/Alu	0.17	MIRb	0.05
Simple_repeat	0.13	L2a	0.03
SINE/MIR	0.13	MIR	0.03
LINE/L1	0.11	L2c	0.03
LINE/L2	0.09	MIR3	0.02
LTR/ERVL-MaLR	0.05	MIRc	0.02
DNA/hAT-Charlie	0.05	L2b	0.02
LTR/ERV1	0.04	AluSx1	0.02
Low_complexity	0.03	AluJb	0.02
LTR/ERVL	0.03	AluSx	0.02
DNA/TcMar-Tigger	0.02	AluSz	0.02
LINE/CR1	0.01	L2	0.01
DNA/hAT-Tip100	0.01	AluJr	0.01
DNA/hAT-Blackjack	0.00	AluJo	0.01
LTR/Gypsy	0.00	AluY	0.01
tRNA	0.00	L3	0.01
LINE/RTE-X	0.00	GA-rich	0.01
LTR/ERVK	0.00	AluSq2	0.01

E

Ontology	Term	FDR Q-val
GO Biological Process	adaptive immune response	165.09
GO Biological Process	regulation of adaptive immune response	107.45
GO Biological Process	regulation of B cell activation	104.43
GO Biological Process	cellular response to interferon-gamma	101.65
GO Biological Process	interferon-gamma-mediated signaling pathway	101.63
GO Biological Process	response to interferon-gamma	99.41
GO Biological Process	tumor necrosis factor-mediated signaling pathway	90.60
GO Biological Process	regulation of antigen receptor-mediated signaling pathway	86.17
GO Biological Process	defense response to virus	84.70
GO Biological Process	regulation of adaptive immune response based on somatic recombination of immune receptors built from immunoglobulin superfamily domains	82.61
GO Biological Process	intrinsic apoptotic signaling pathway in response to DNA damage	76.13
GO Biological Process	regulation of B cell proliferation	74.91
GO Biological Process	regulation of type I interferon production	74.27
GO Biological Process	T cell costimulation	70.46
GO Biological Process	lymphocyte costimulation	70.20
GO Biological Process	leukocyte homeostasis	66.07
GO Biological Process	T cell activation involved in immune response	58.86
GO Biological Process	Fc receptor mediated stimulatory signaling pathway	55.27
GO Biological Process	positive regulation of cytokine biosynthetic process	55.27
GO Biological Process	positive regulation of intrinsic apoptotic signaling pathway	53.61
Human Phenotype	Abnormality of lymphocytes	104.26
Human Phenotype	Decreased antibody level in blood	77.08
Human Phenotype	Abnormality of the lymph nodes	58.75
Human Phenotype	Lymphadenopathy	54.41
Human Phenotype	Abnormality of cells of the lymphoid lineage	45.70
Human Phenotype	Lymphopenia	35.25

F no CIS-BP motif available

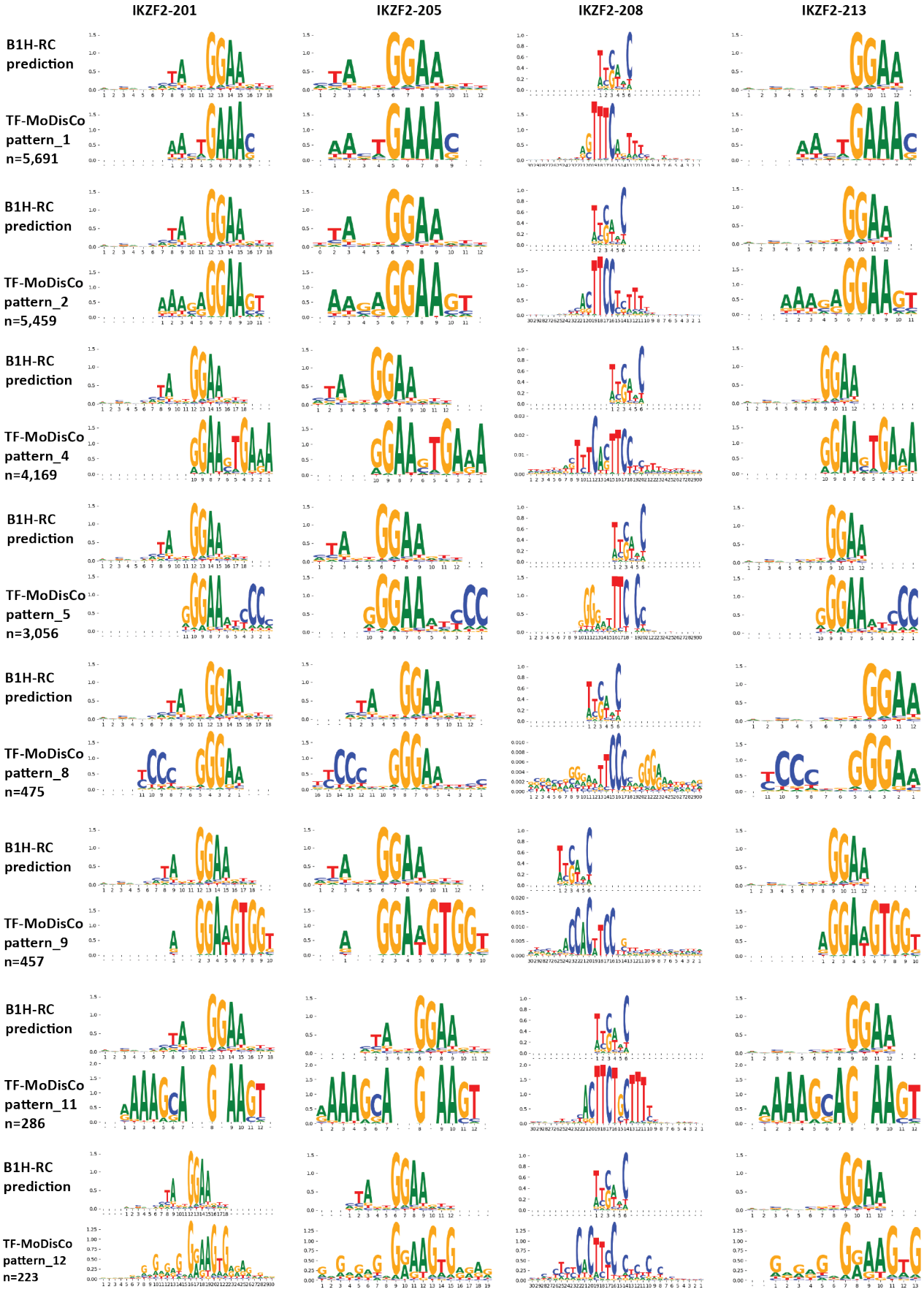

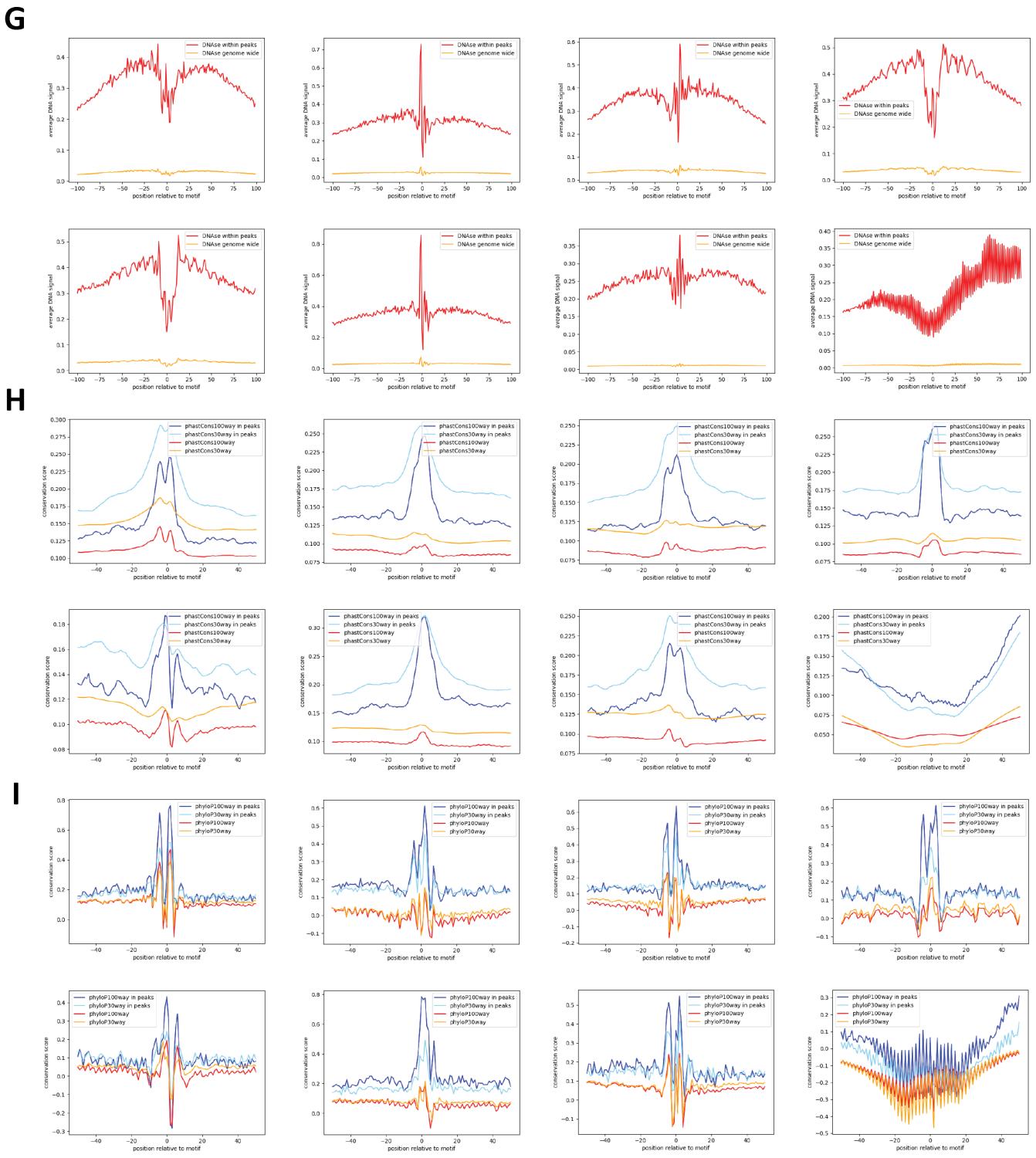

Supplementary Figure 77: Properties and genomic distribution of motifs identified for the IKZF2 transcription factor in GM12878 (accession ENCSR680UQE).

TF-MoDisCO pattern_1 n=5691, CWM

pattern_1, n=5691; subpattern_0, ns=1175

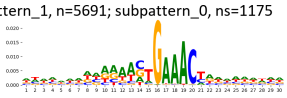

pattern_1, n=5691; subpattern_1, ns=1119

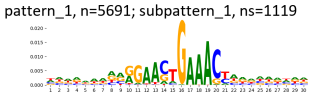

pattern_1, n=5691; subpattern_2, ns=997

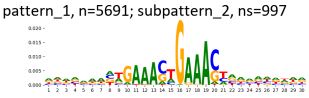

pattern_1, n=5691; subpattern_3, ns=923

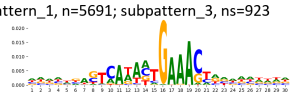

pattern_1, n=5691; subpattern_4, ns=718

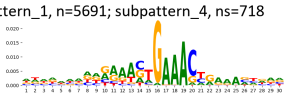

pattern_1, n=5691; subpattern_5, ns=486

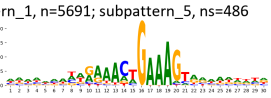

pattern_1, n=5691; subpattern_6, ns=189

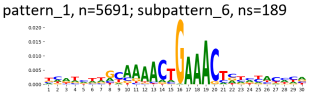

pattern_1, n=5691; subpattern_7, ns=82

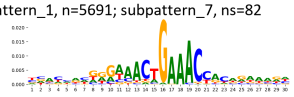

pattern_1, n=5691; subpattern_8, ns=2

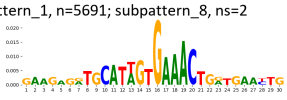

TF-MoDisCO pattern_1 n=5691, PWM

pattern_1, n=5691; subpattern_0, ns=1175

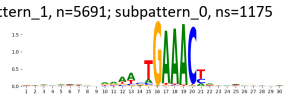

pattern_1, n=5691; subpattern_1, ns=1119

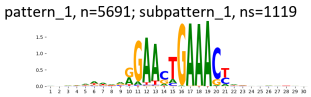

pattern_1, n=5691; subpattern_2, ns=997

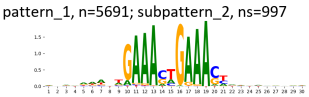

pattern_1, n=5691; subpattern_3, ns=923

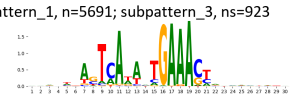

pattern_1, n=5691; subpattern_4, ns=718

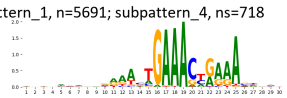

pattern_1, n=5691; subpattern_5, ns=486

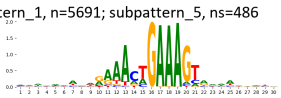

pattern_1, n=5691; subpattern_6, ns=189

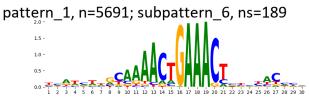

pattern_1, n=5691; subpattern_7, ns=82

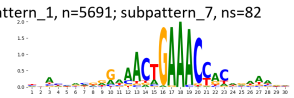

pattern_1, n=5691; subpattern_8, ns=2

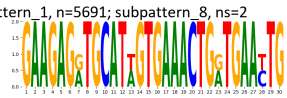

TF-MoDisCO pattern_11 n=286, CWM

pattern_11, n=286; subpattern_0, ns=75

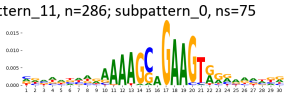

pattern_11, n=286; subpattern_1, ns=70

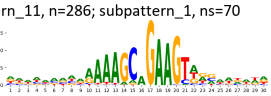

pattern_11, n=286; subpattern_2, ns=49

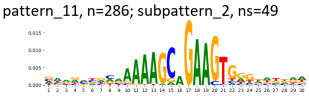

pattern_11, n=286; subpattern_3, ns=44

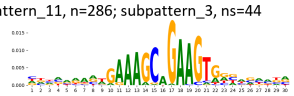

pattern_11, n=286; subpattern_4, ns=23

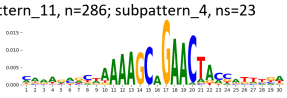

pattern_11, n=286; subpattern_5, ns=23

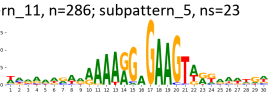

pattern_11, n=286; subpattern_6, ns=2

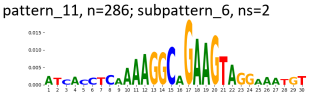

TF-MoDisCO pattern_11 n=286, PWM

pattern_11, n=286; subpattern_0, ns=75

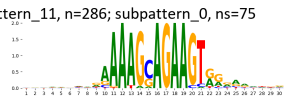

pattern_11, n=286; subpattern_1, ns=70

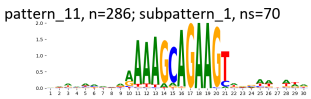

pattern_11, n=286; subpattern_2, ns=49

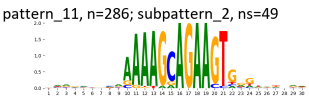

pattern_11, n=286; subpattern_3, ns=44

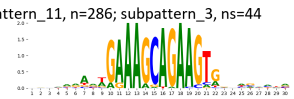

pattern_11, n=286; subpattern_4, ns=23

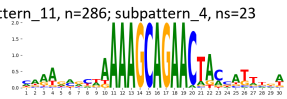

pattern_11, n=286; subpattern_5, ns=23

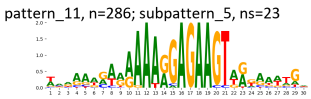

pattern_11, n=286; subpattern_6, ns=2

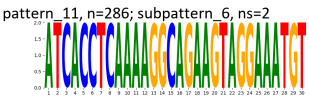

TF-MoDisCO pattern_12 n=223, CWM

pattern_12, n=223; subpattern_0, ns=59

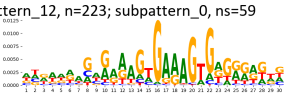

pattern_12, n=223; subpattern_1, ns=56

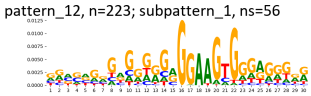

pattern_12, n=223; subpattern_2, ns=43

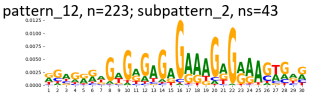

pattern_12, n=223; subpattern_3, ns=35

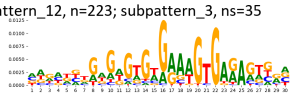

pattern_12, n=223; subpattern_4, ns=30

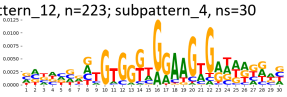

TF-MoDisCO pattern_12 n=223, PWM

pattern_12, n=223; subpattern_0, ns=59

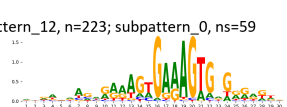

pattern_12, n=223; subpattern_1, ns=56

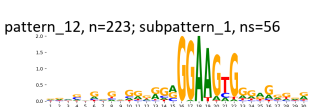

pattern_12, n=223; subpattern_2, ns=43

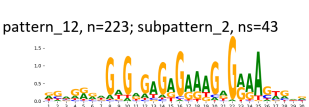

pattern_12, n=223; subpattern_3, ns=35

pattern_12, n=223; subpattern_4, ns=30

TF-MoDisCO pattern_2 n=5459, CWM

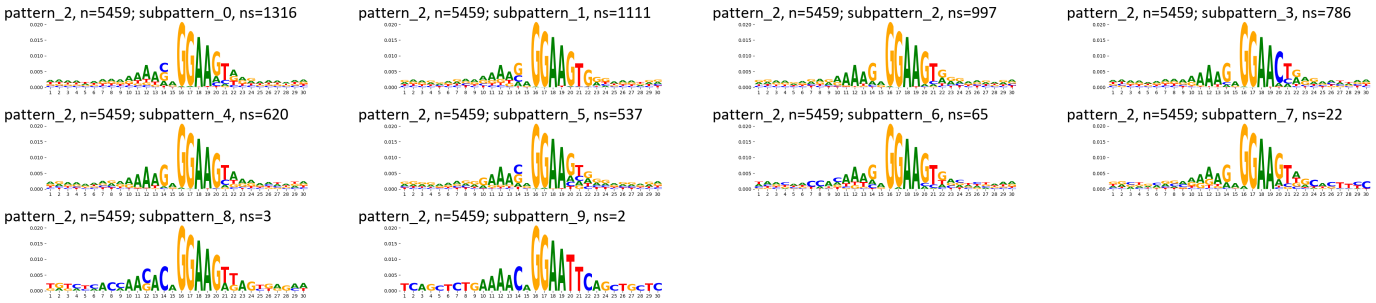

TF-MoDisCO pattern_2 n=5459, PWM

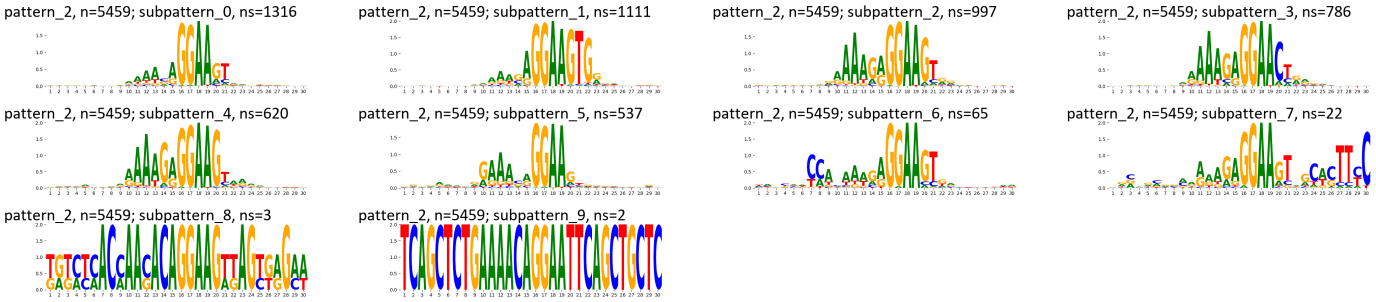

TF-MoDisCO pattern_4 n=4169, CWM

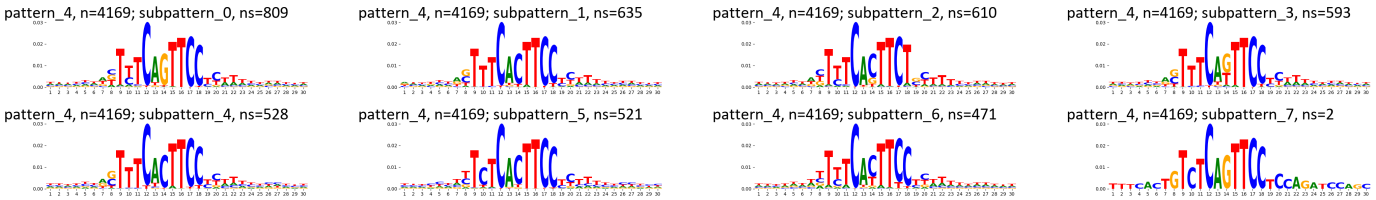

TF-MoDisCO pattern_4 n=4169, PWM

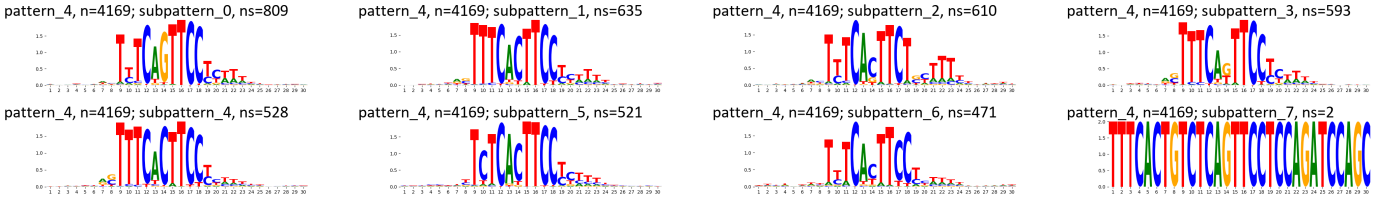

TF-MoDisCO pattern_5 n=3056, CWM

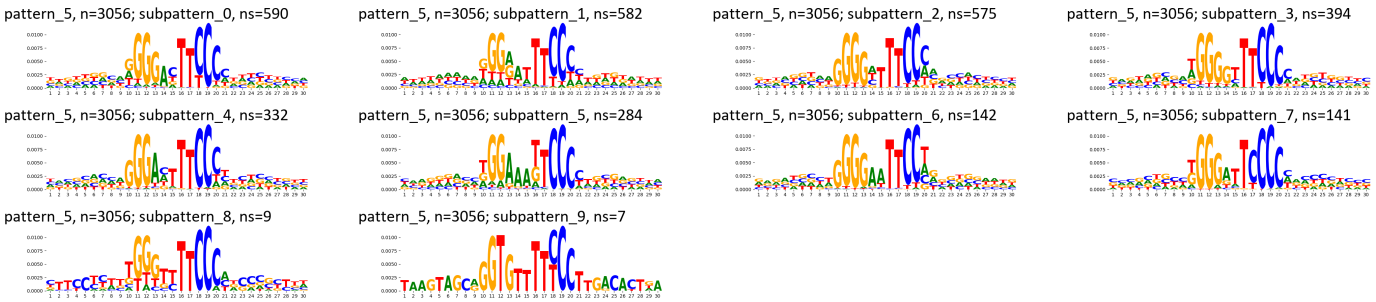

TF-MoDisCO pattern_5 n=3056, PWM

pattern_5, n=3056; subpattern_0, ns=590

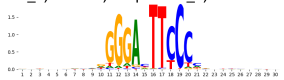

pattern_5, n=3056; subpattern_1, ns=582

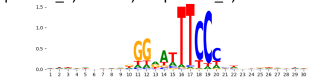

pattern_5, n=3056; subpattern_2, ns=575

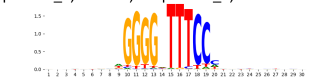

pattern_5, n=3056; subpattern_3, ns=394

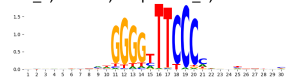

pattern_5, n=3056; subpattern_4, ns=332

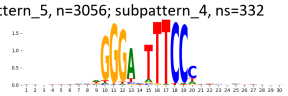

pattern_5, n=3056; subpattern_5, ns=284

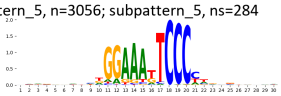

pattern_5, n=3056; subpattern_6, ns=142

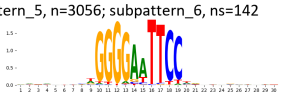

pattern_5, n=3056; subpattern_7, ns=141

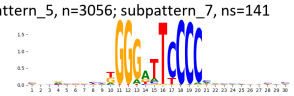

pattern_5, n=3056; subpattern_8, ns=9

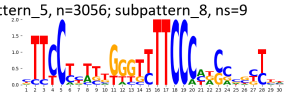

pattern_5, n=3056; subpattern_9, ns=7

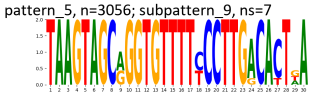

TF-MoDisCO pattern_8 n=475, CWM

pattern_8, n=475; subpattern_0, ns=124

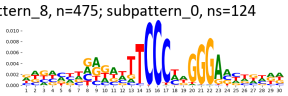

pattern_8, n=475; subpattern_1, ns=108

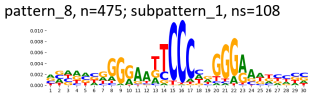

pattern_8, n=475; subpattern_2, ns=78

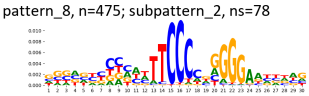

pattern_8, n=475; subpattern_3, ns=75

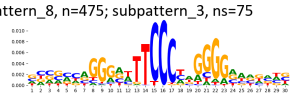

pattern_8, n=475; subpattern_4, ns=51

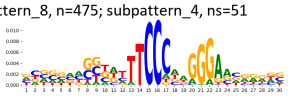

pattern_8, n=475; subpattern_5, ns=29

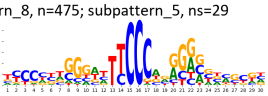

pattern_8, n=475; subpattern_6, ns=4

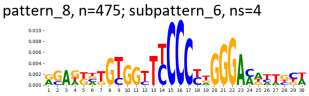

pattern_8, n=475; subpattern_7, ns=4

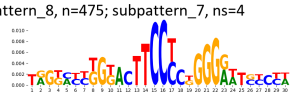

pattern_8, n=475; subpattern_8, ns=2

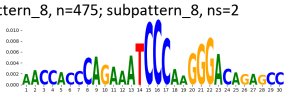

TF-MoDisCO pattern_8 n=475, PWM

pattern_8, n=475; subpattern_0, ns=124

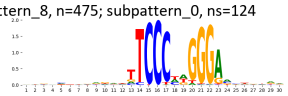

pattern_8, n=475; subpattern_1, ns=108

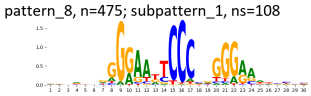

pattern_8, n=475; subpattern_2, ns=78

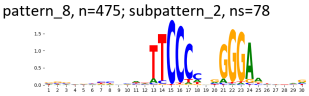

pattern_8, n=475; subpattern_3, ns=75

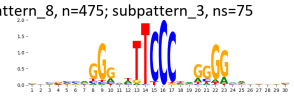

pattern_8, n=475; subpattern_4, ns=51

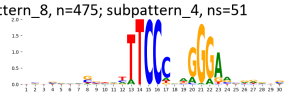

pattern_8, n=475; subpattern_5, ns=29

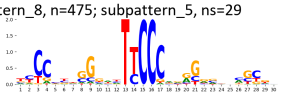

pattern_8, n=475; subpattern_6, ns=4

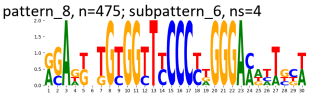

pattern_8, n=475; subpattern_7, ns=4

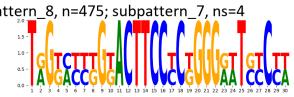

pattern_8, n=475; subpattern_8, ns=2

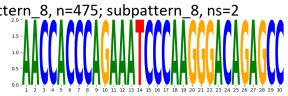

TF-MoDisCO pattern_9 n=457, CWM

pattern_9, n=457; subpattern_0, ns=134

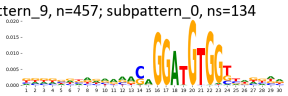

pattern_9, n=457; subpattern_1, ns=96

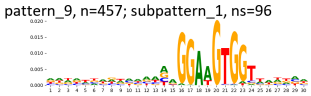

pattern_9, n=457; subpattern_2, ns=82

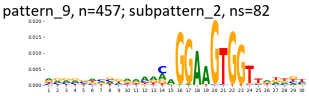

pattern_9, n=457; subpattern_3, ns=72

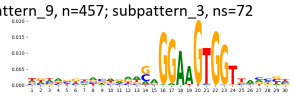

pattern_9, n=457; subpattern_4, ns=58

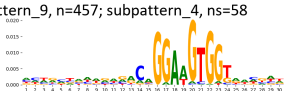

pattern_9, n=457; subpattern_5, ns=13

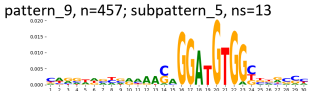

pattern_9, n=457; subpattern_6, ns=2



TF-MoDisCO pattern_9 n=457, PWM

pattern_9, n=457; subpattern_0, ns=134

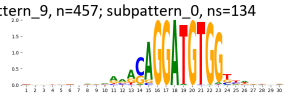

pattern_9, n=457; subpattern_1, ns=96

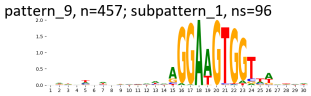

pattern_9, n=457; subpattern_2, ns=82

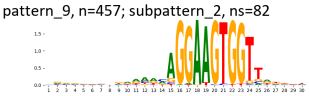

pattern_9, n=457; subpattern_3, ns=72

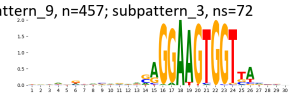

pattern_9, n=457; subpattern_4, ns=58

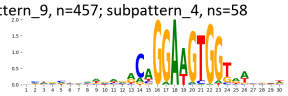

pattern_9, n=457; subpattern_5, ns=13

pattern_9, n=457; subpattern_6, ns=2

Supplementary Figure 78: TF-MoDisCO subpatterns for the IKZF2 transcription factor in GM12878 (accession ENCSR680UQE).

A

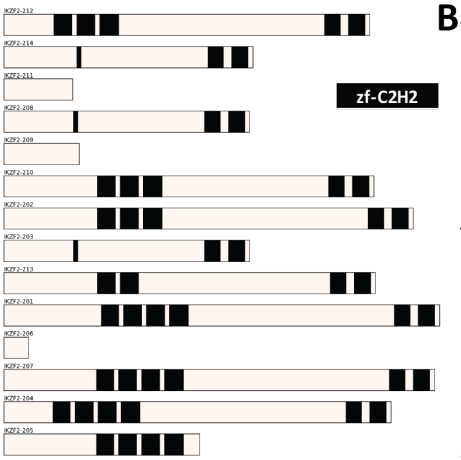

B

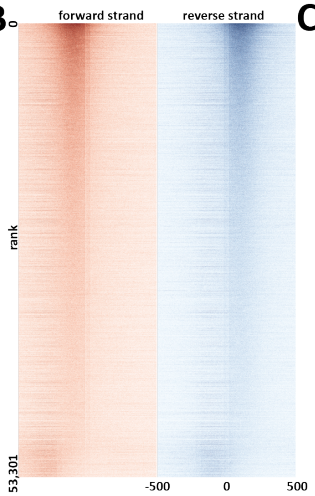

C

peaks	
state	fraction
EnhWk	0.28
EnhA1	0.22
TssA	0.17
Quies	0.10
TssFlnkU	0.10
EnhA2	0.09
TssFlnk	0.09
TxWk	0.08
TssFlnkD	0.05
ReprPCWk	0.03
EnhG1	0.01
Het	0.01
EnhG2	0.01
ZNF/Rpts	0.01
Tx	0.00
EnhBiv	0.00
TssBiv	0.00
ReprPC	0.00

D

peaks		peaks	
repeat	fraction	repeat	fraction
SINE/Alu	0.20	MIRb	0.05
Simple_repeat	0.15	MIR	0.03
SINE/MIR	0.14	L2a	0.03
LINE/L1	0.12	L2c	0.03
LINE/L2	0.10	MIR3	0.03
LTR/ERVL-MaLR	0.05	MIRc	0.03
DNA/hAT-Charlie	0.05	L2b	0.02
LTR/ERV1	0.04	AluSx1	0.02
Low_complexity	0.03	AluJb	0.02
LTR/ERVL	0.03	AluSx	0.02
DNA/TcMar-Tigger	0.02	AluSz	0.02
LINE/CR1	0.02	L2	0.01
DNA/hAT-Tip100	0.01	AluY	0.01
DNA/hAT-Blackjack	0.00	AluJr	0.01
LTR/Gypsy	0.00	AluJo	0.01
tRNA	0.00	AluSq2	0.01
LTR/ERVK	0.00	G-rich	0.01
DNA/TcMar-Mariner	0.00	(AC)n	0.01

E

Ontology	Term	FDR Q-val
GO Biological Process	regulation of adaptive immune response	125.67
GO Biological Process	regulation of B cell activation	116.16
GO Biological Process	interferon-gamma-mediated signaling pathway	97.49
GO Biological Process	tumor necrosis factor-mediated signaling pathway	95.76
GO Biological Process	cellular response to interferon-gamma	92.69
GO Biological Process	response to interferon-gamma	90.67
GO Biological Process	regulation of type I interferon production	84.93
GO Biological Process	regulation of antigen receptor-mediated signaling pathway	81.91
GO Biological Process	intrinsic apoptotic signaling pathway in response to DNA damage	72.22
GO Biological Process	lymphocyte costimulation	70.95
GO Biological Process	T cell costimulation	70.60
GO Biological Process	Fc receptor mediated stimulatory signaling pathway	61.94
GO Biological Process	positive regulation of intrinsic apoptotic signaling pathway	61.92
GO Biological Process	negative regulation of type I interferon production	59.46
GO Biological Process	interleukin-12-mediated signaling pathway	54.64
GO Biological Process	regulation of defense response to virus	53.71
GO Biological Process	response to interleukin-12	52.05
GO Biological Process	nucleotide-binding domain, leucine rich repeat containing receptor signaling pathway	50.66
GO Biological Process	nucleotide-binding oligomerization domain containing signaling pathway	47.75
GO Biological Process	lipopolysaccharide-mediated signaling pathway	47.16
Human Phenotype	Abnormality of lymphocytes	106.86
Human Phenotype	Abnormality of the lymph nodes	50.63
Human Phenotype	Lymphadenopathy	46.13

F no CIS-BP motif available

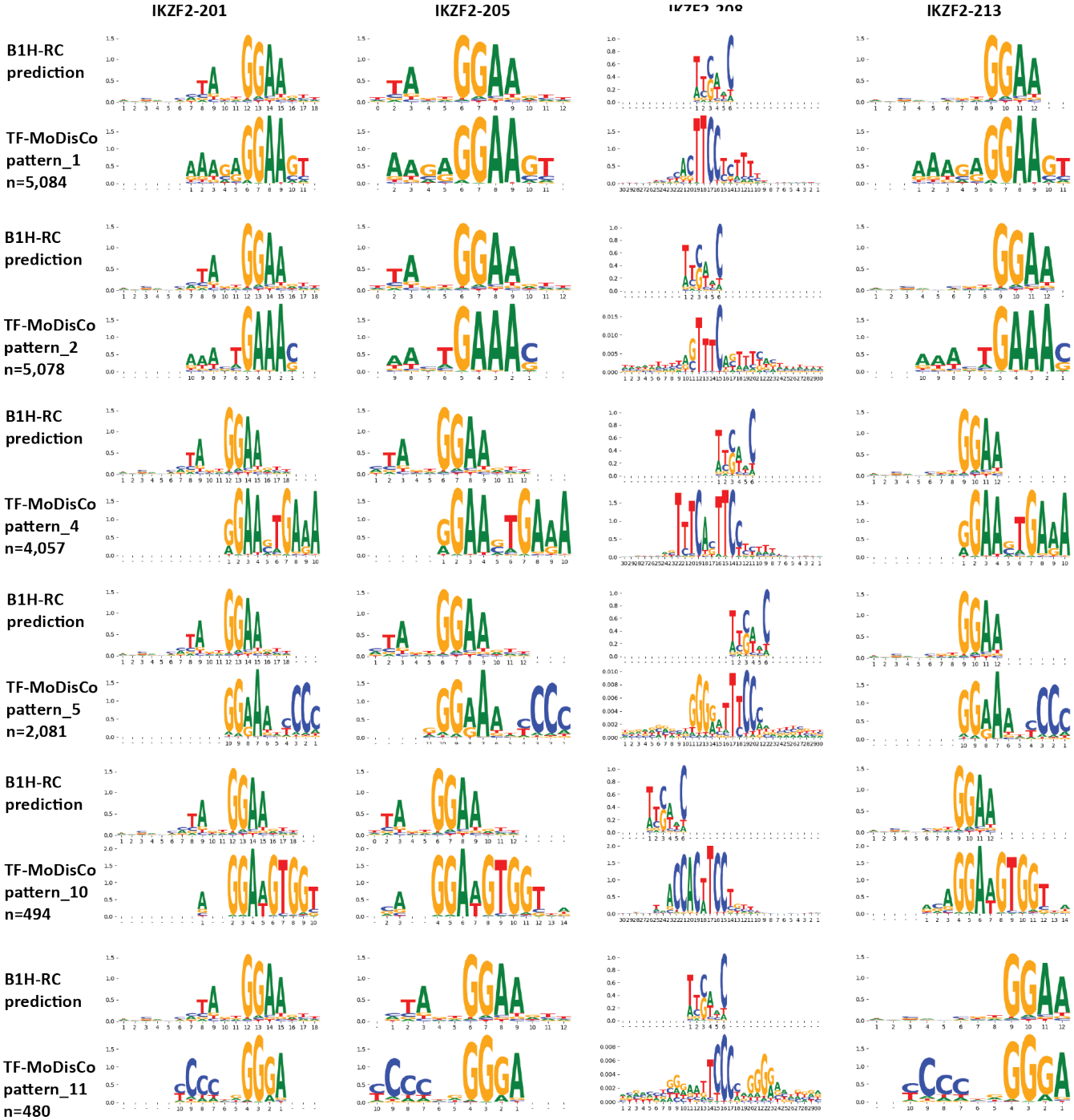

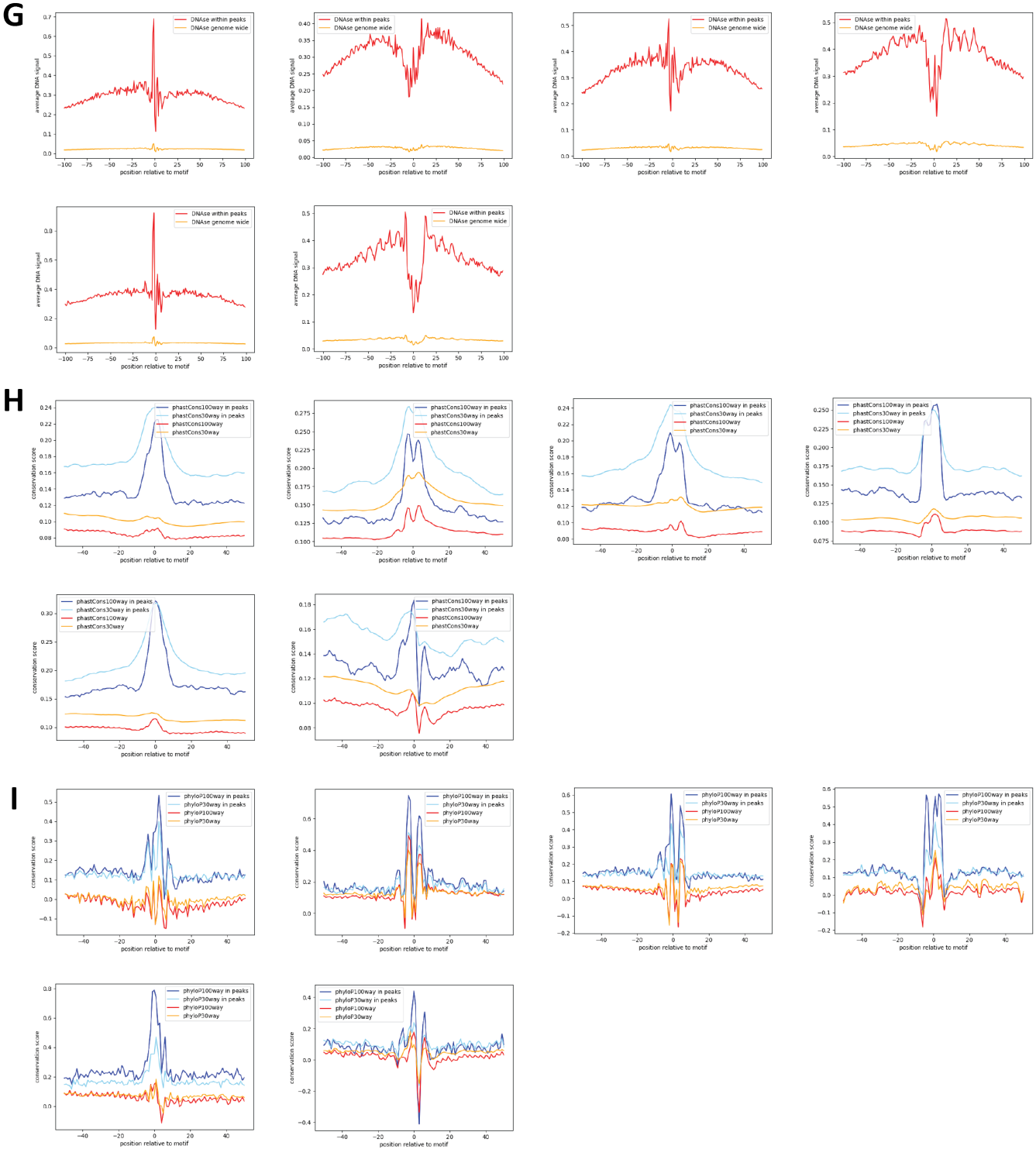

Supplementary Figure 79: Properties and genomic distribution of motifs identified for the IKZF2 transcription factor in GM12878 (accession ENCSR822AHX).

TF-MoDisCO pattern_1 n=5084, CWM

pattern_1, n=5084; subpattern_0, ns=952

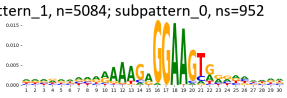

pattern_1, n=5084; subpattern_1, ns=949

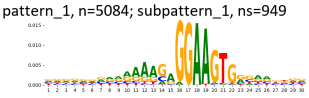

pattern_1, n=5084; subpattern_10, ns=3

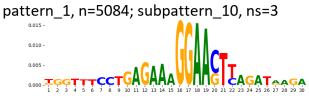

pattern_1, n=5084; subpattern_11, ns=3

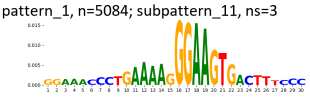

pattern_1, n=5084; subpattern_2, ns=732

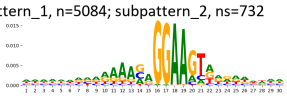

pattern_1, n=5084; subpattern_3, ns=652

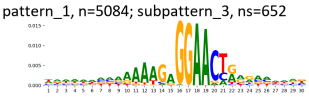

pattern_1, n=5084; subpattern_4, ns=510

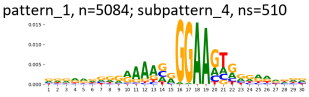

pattern_1, n=5084; subpattern_5, ns=502

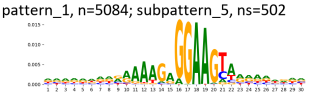

pattern_1, n=5084; subpattern_6, ns=407

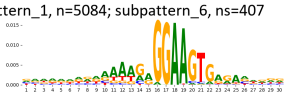

pattern_1, n=5084; subpattern_7, ns=293

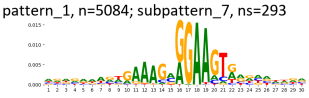

pattern_1, n=5084; subpattern_8, ns=45

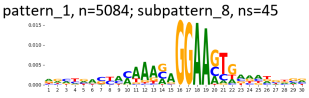

pattern_1, n=5084; subpattern_9, ns=36

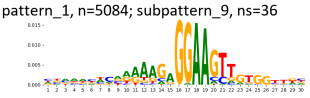

TF-MoDisCO pattern_1 n=5084, PWM

pattern_1, n=5084; subpattern_0, ns=952

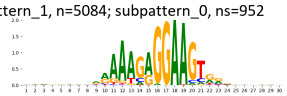

pattern_1, n=5084; subpattern_1, ns=949

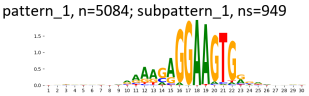

pattern_1, n=5084; subpattern_10, ns=3

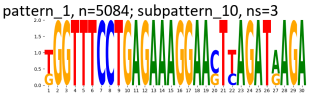

pattern_1, n=5084; subpattern_11, ns=3

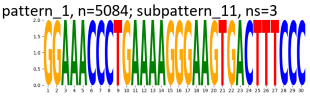

pattern_1, n=5084; subpattern_2, ns=732

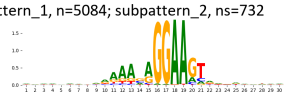

pattern_1, n=5084; subpattern_3, ns=652

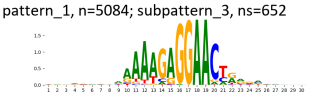

pattern_1, n=5084; subpattern_4, ns=510

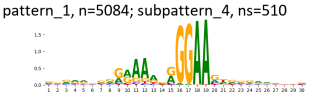

pattern_1, n=5084; subpattern_5, ns=502

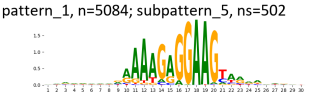

pattern_1, n=5084; subpattern_6, ns=407

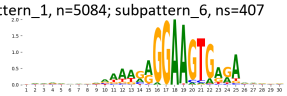

pattern_1, n=5084; subpattern_7, ns=293

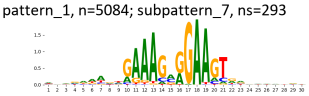

pattern_1, n=5084; subpattern_8, ns=45

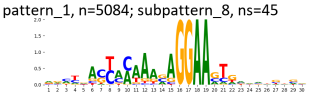

pattern_1, n=5084; subpattern_9, ns=36

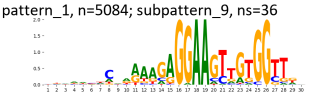

TF-MoDisCO pattern_10 n=494, CWM

pattern_10, n=494; subpattern_0, ns=163

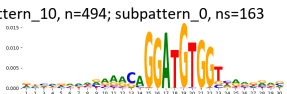

pattern_10, n=494; subpattern_1, ns=134

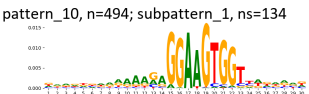

pattern_10, n=494; subpattern_2, ns=97

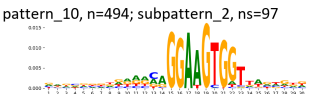

pattern_10, n=494; subpattern_3, ns=75

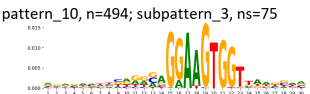

pattern_10, n=494; subpattern_4, ns=21

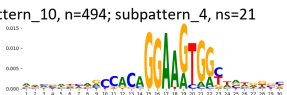

pattern_10, n=494; subpattern_5, ns=2

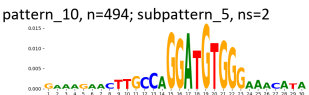

pattern_10, n=494; subpattern_6, ns=2

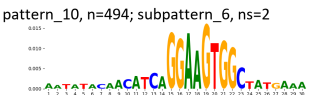

TF-MoDisCO pattern_10 n=494, PWM

pattern_10, n=494; subpattern_0, ns=163

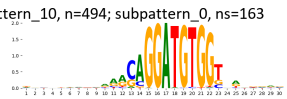

pattern_10, n=494; subpattern_1, ns=134

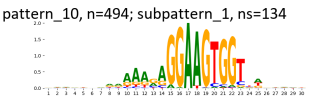

pattern_10, n=494; subpattern_2, ns=97

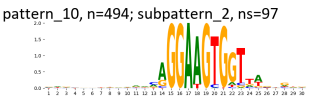

pattern_10, n=494; subpattern_3, ns=75

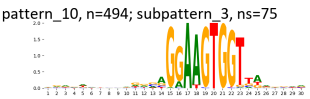

pattern_10, n=494; subpattern_4, ns=21

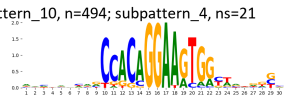

pattern_10, n=494; subpattern_5, ns=2

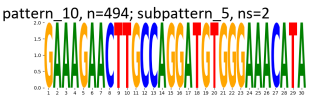

pattern_10, n=494; subpattern_6, ns=2

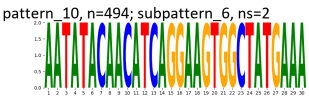

TF-MoDisCO pattern_11 n=480, CWM

pattern_11, n=480; subpattern_0, ns=139

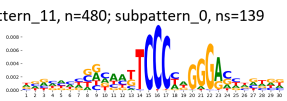

pattern_11, n=480; subpattern_1, ns=115

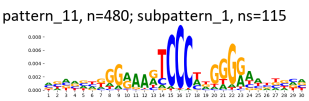

pattern_11, n=480; subpattern_2, ns=106

pattern_11, n=480; subpattern_3, ns=72

pattern_11, n=480; subpattern_4, ns=48

TF-MoDisCO pattern_11 n=480, PWM

pattern_11, n=480; subpattern_0, ns=139

pattern_11, n=480; subpattern_1, ns=115

pattern_11, n=480; subpattern_2, ns=106

pattern_11, n=480; subpattern_3, ns=72

pattern_11, n=480; subpattern_4, ns=48

TF-MoDisCO pattern_2 n=5078, CWM

pattern_2, n=5078; subpattern_0, ns=1015

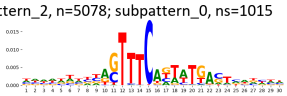

pattern_2, n=5078; subpattern_1, ns=865

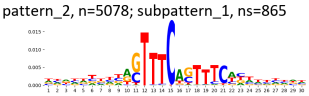

pattern_2, n=5078; subpattern_2, ns=787

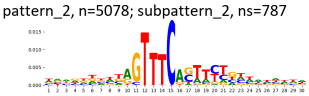

pattern_2, n=5078; subpattern_3, ns=748

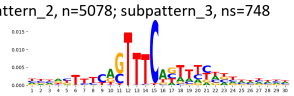

pattern_2, n=5078; subpattern_4, ns=717

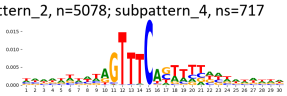

pattern_2, n=5078; subpattern_5, ns=524

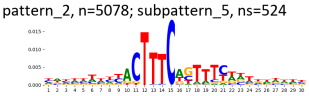

pattern_2, n=5078; subpattern_6, ns=358

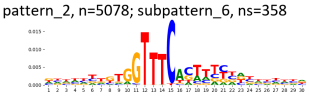

pattern_2, n=5078; subpattern_7, ns=59

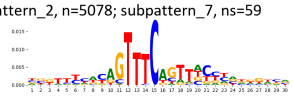

pattern_2, n=5078; subpattern_8, ns=5

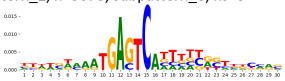

TF-MoDisCO pattern_2 n=5078, PWM

pattern_2, n=5078; subpattern_0, ns=1015

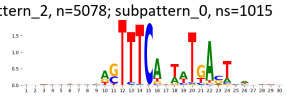

pattern_2, n=5078; subpattern_1, ns=865

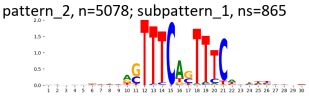

pattern_2, n=5078; subpattern_2, ns=787

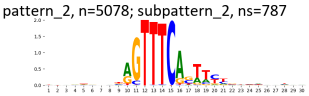

pattern_2, n=5078; subpattern_3, ns=748

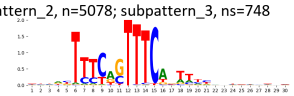

pattern_2, n=5078; subpattern_4, ns=717

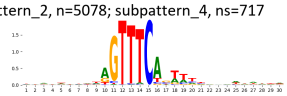

pattern_2, n=5078; subpattern_5, ns=524

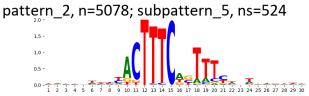

pattern_2, n=5078; subpattern_6, ns=358

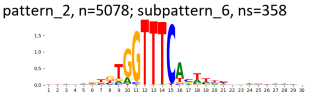

pattern_2, n=5078; subpattern_7, ns=59

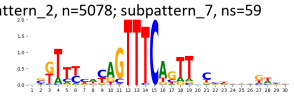

pattern_2, n=5078; subpattern_8, ns=5

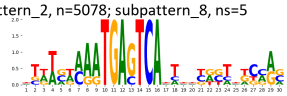

TF-MoDisCO pattern_4 n=4057, CWM

pattern_4, n=4057; subpattern_0, ns=667

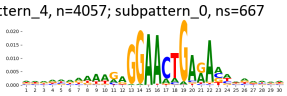

pattern_4, n=4057; subpattern_1, ns=651

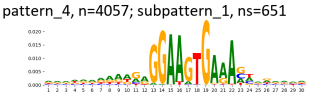

pattern_4, n=4057; subpattern_2, ns=632

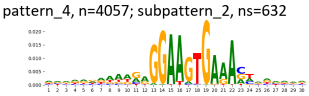

pattern_4, n=4057; subpattern_3, ns=559

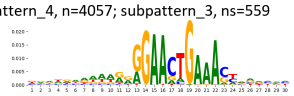

pattern_4, n=4057; subpattern_4, ns=534

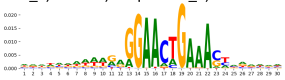

pattern_4, n=4057; subpattern_5, ns=436

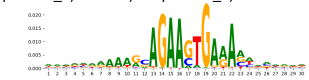

pattern_4, n=4057; subpattern_6, ns=420

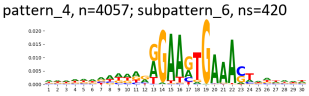

pattern_4, n=4057; subpattern_7, ns=126

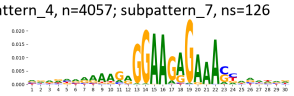

pattern_4, n=4057; subpattern_8, ns=32

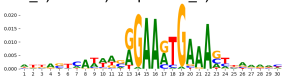

TF-MoDisCO pattern_4 n=4057, PWM

pattern_4, n=4057; subpattern_0, ns=667

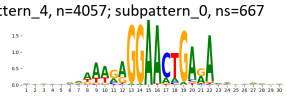

pattern_4, n=4057; subpattern_1, ns=651

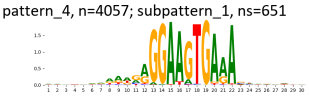

pattern_4, n=4057; subpattern_2, ns=632

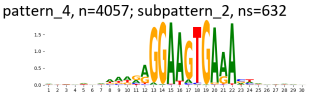

pattern_4, n=4057; subpattern_3, ns=559

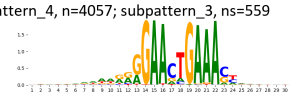

pattern_4, n=4057; subpattern_4, ns=534

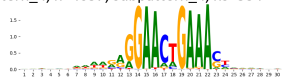

pattern_4, n=4057; subpattern_5, ns=436

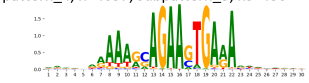

pattern_4, n=4057; subpattern_6, ns=420

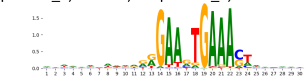

pattern_4, n=4057; subpattern_7, ns=126

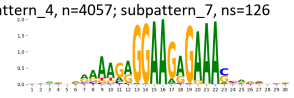

pattern_4, n=4057; subpattern_8, ns=32

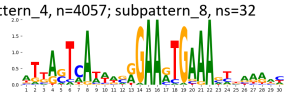

TF-MoDisCO pattern_5 n=2801, CWM

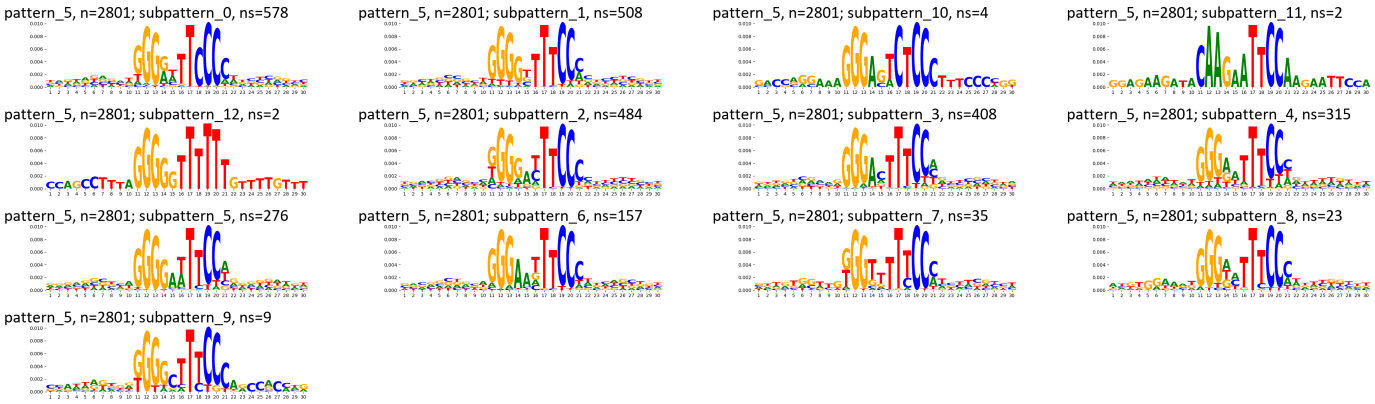

TF-MoDisCO pattern_5 n=2801, PWM

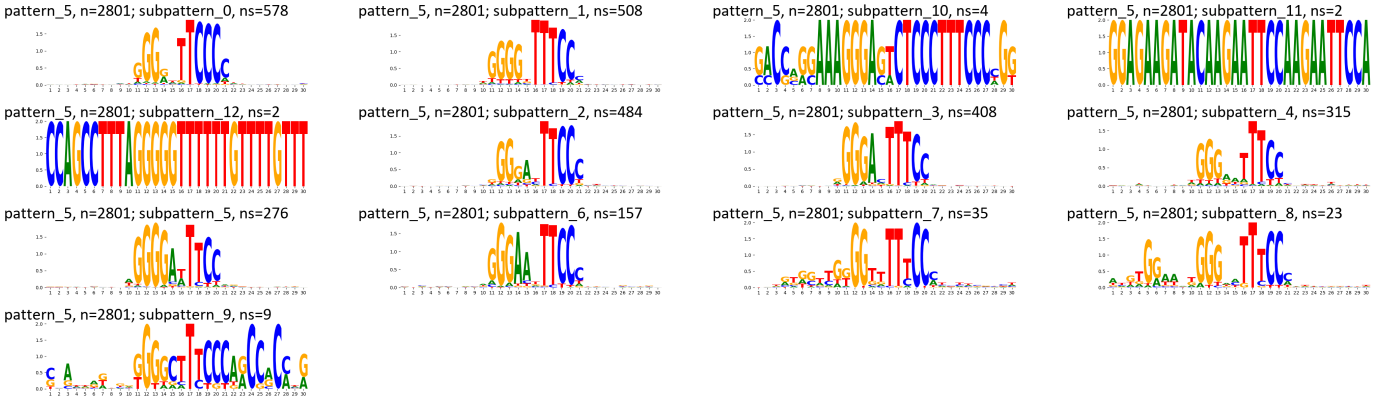

Supplementary Figure 80: TF-MoDisCO subpatterns for the IKZF2 transcription factor in GM12878 (accession ENCSR822AHX).

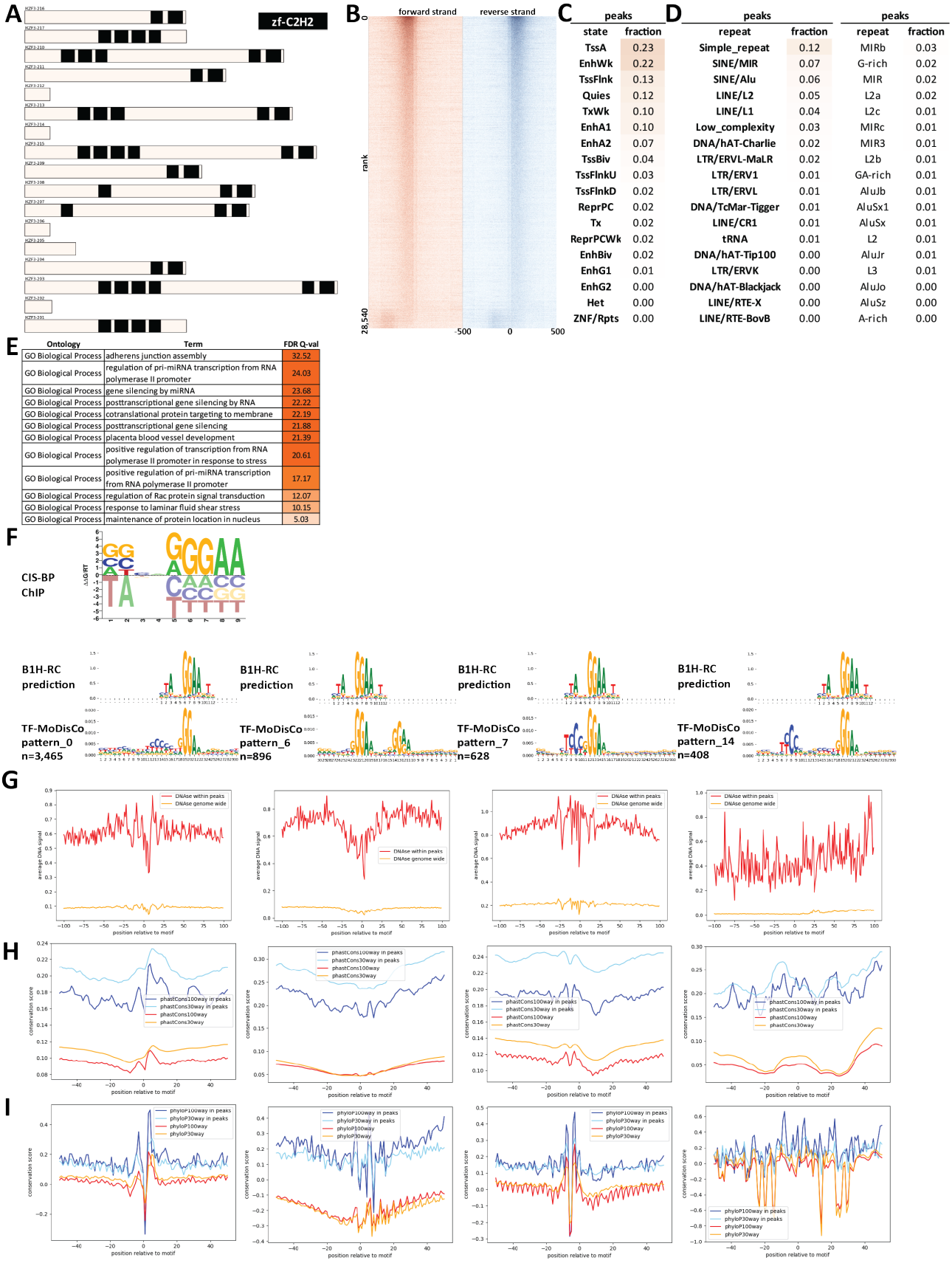

Supplementary Figure 81: Properties and genomic distribution of motifs identified for the IKZF3 transcription factor in HEK293 (accession ENCSR304AMN).

TF-MoDisCO pattern_0 n=3465, CWM

pattern_0, n=3465; subpattern_0, ns=866

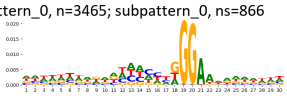

pattern_0, n=3465; subpattern_1, ns=545

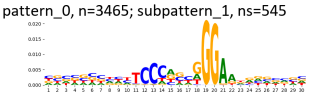

pattern_0, n=3465; subpattern_10, ns=18

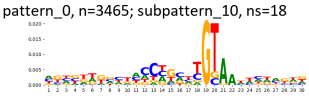

pattern_0, n=3465; subpattern_2, ns=413

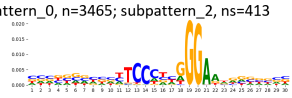

pattern_0, n=3465; subpattern_3, ns=349

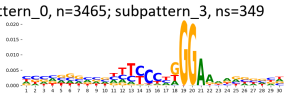

pattern_0, n=3465; subpattern_4, ns=333

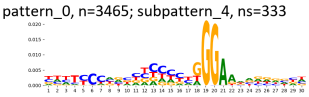

pattern_0, n=3465; subpattern_5, ns=281

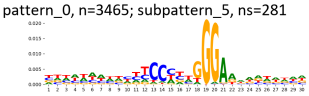

pattern_0, n=3465; subpattern_6, ns=225

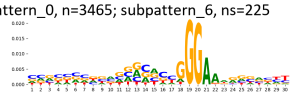

pattern_0, n=3465; subpattern_7, ns=223

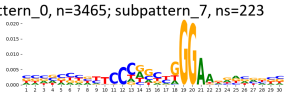

pattern_0, n=3465; subpattern_8, ns=136

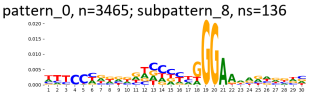

pattern_0, n=3465; subpattern_9, ns=76

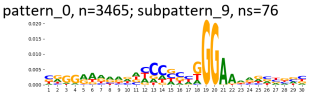

TF-MoDisCO pattern_0 n=3465, PWM

pattern_0, n=3465; subpattern_0, ns=866

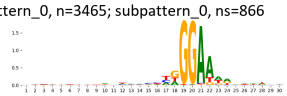

pattern_0, n=3465; subpattern_1, ns=545

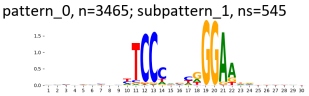

pattern_0, n=3465; subpattern_10, ns=18

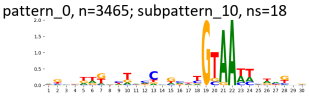

pattern_0, n=3465; subpattern_2, ns=413

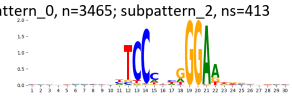

pattern_0, n=3465; subpattern_3, ns=349

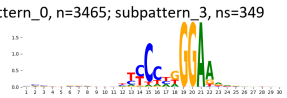

pattern_0, n=3465; subpattern_4, ns=333

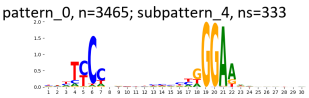

pattern_0, n=3465; subpattern_5, ns=281

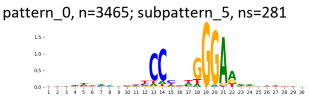

pattern_0, n=3465; subpattern_6, ns=225

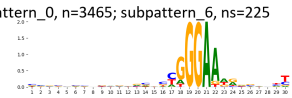

pattern_0, n=3465; subpattern_7, ns=223

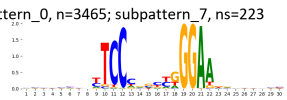

pattern_0, n=3465; subpattern_8, ns=136

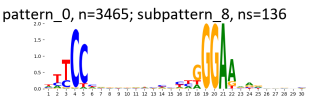

pattern_0, n=3465; subpattern_9, ns=76

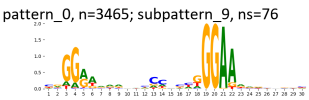

TF-MoDisCO pattern_14 n=408, CWM

pattern_14, n=408; subpattern_0, ns=118

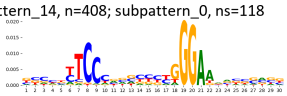

pattern_14, n=408; subpattern_1, ns=115

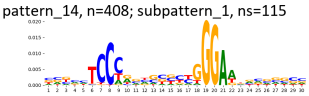

pattern_14, n=408; subpattern_2, ns=70

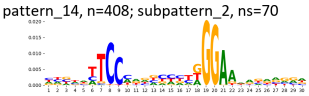

pattern_14, n=408; subpattern_3, ns=60

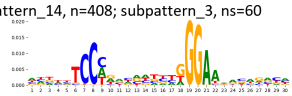

pattern_14, n=408; subpattern_4, ns=29

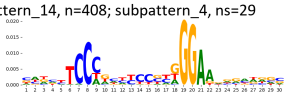

pattern_14, n=408; subpattern_5, ns=9

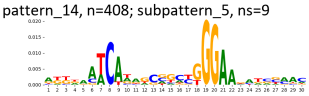

pattern_14, n=408; subpattern_6, ns=7

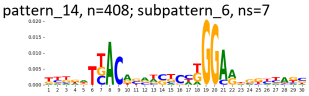

TF-MoDisCO pattern_14 n=408, PWM

pattern_14, n=408; subpattern_0, ns=118

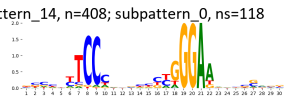

pattern_14, n=408; subpattern_1, ns=115

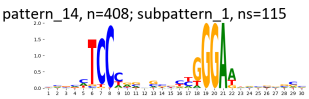

pattern_14, n=408; subpattern_2, ns=70

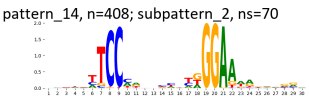

pattern_14, n=408; subpattern_3, ns=60

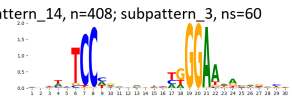

pattern_14, n=408; subpattern_4, ns=29

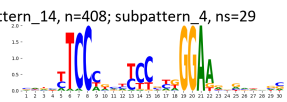

pattern_14, n=408; subpattern_5, ns=9

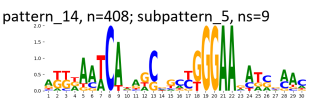

pattern_14, n=408; subpattern_6, ns=7

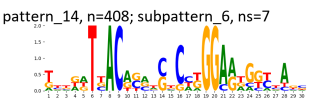

TF-MoDisCO pattern_6 n=896, CWM

pattern_6, n=896; subpattern_0, ns=298

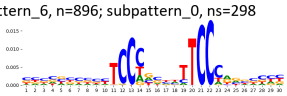

pattern_6, n=896; subpattern_1, ns=242

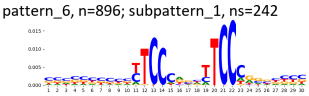

pattern_6, n=896; subpattern_2, ns=229

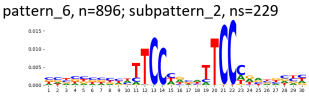

pattern_6, n=896; subpattern_3, ns=68

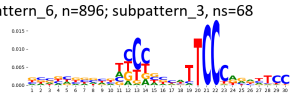

pattern_6, n=896; subpattern_4, ns=48

pattern_6, n=896; subpattern_5, ns=9

pattern_6, n=896; subpattern_6, ns=2

TF-MoDisCO pattern_6 n=896, PWM

pattern_6, n=896; subpattern_0, ns=298

pattern_6, n=896; subpattern_1, ns=242

pattern_6, n=896; subpattern_2, ns=229

pattern_6, n=896; subpattern_3, ns=68

pattern_6, n=896; subpattern_4, ns=48

pattern_6, n=896; subpattern_5, ns=9

pattern_6, n=896; subpattern_6, ns=2

TF-MoDisCO pattern_7 n=628, CWM

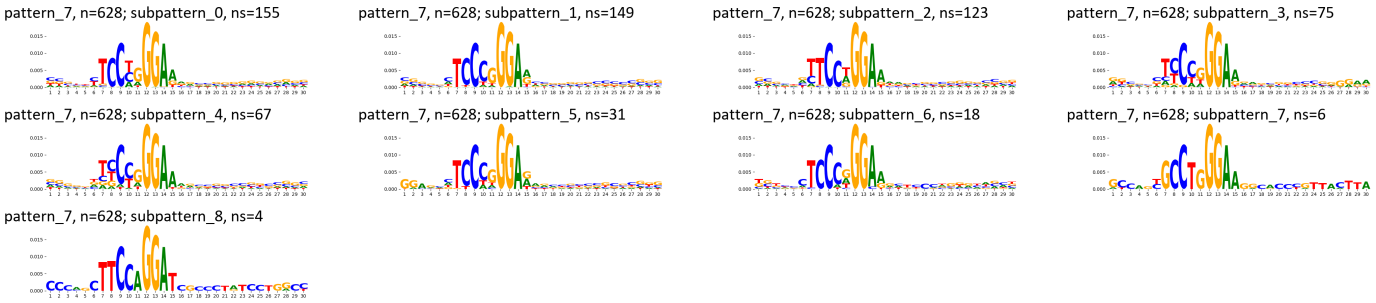

TF-MoDisCO pattern_7 n=628, PWM

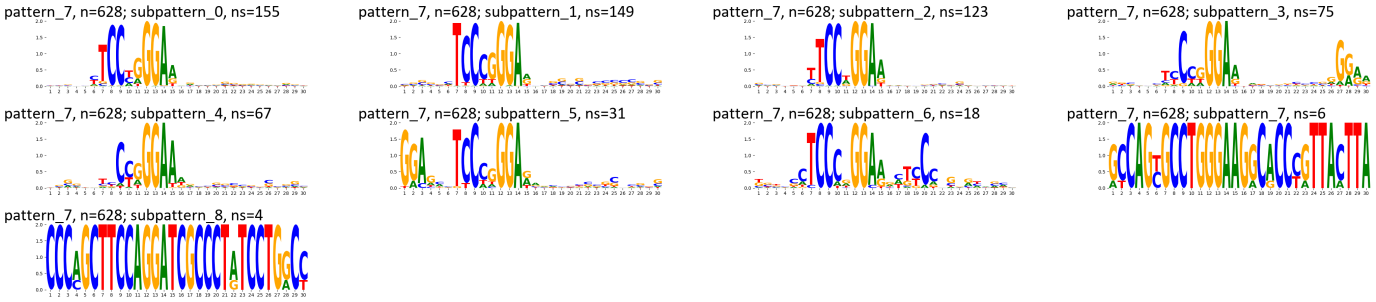

Supplementary Figure 82: TF-MoDisCO subpatterns for the IKZF3 transcription factor in HEK293 (accession ENCSR304AMN).

A



B

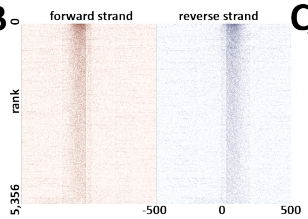

C

peaks	
state	fraction
TssA	0.38
TssFlnk	0.14
EnhWk	0.12
Quies	0.10
EnhA1	0.10
EnhA2	0.07
TxWk	0.06
TssBiv	0.04
TssFlnkU	0.04
ReprPCWk	0.02
TssFlnkD	0.02
EnhBiv	0.01
ReprPC	0.01
Tx	0.01
EnhG1	0.01
EnhG2	0.00
ZNF/Rpts	0.00
Het	0.00

D

peaks		peaks	
repeat	fraction	repeat	fraction
Simple_repeat	0.09	G-rich	0.02
SINE/MIR	0.04	MIRb	0.01
SINE/Alu	0.03	GA-rich	0.01
Low_complexity	0.03	L2a	0.01
LINE/L2	0.03	MIRc	0.01
LINE/L1	0.02	L2c	0.01
LTR/ERVL-MaLR	0.01	MIR3	0.01
LTR/ERV1	0.01	L2b	0.01
DNA/hAT-Charlie	0.01	MIR	0.01
LTR/ERVL	0.01	L2	0.00
tRNA	0.01	AluJr	0.00
DNA/TcMar-Tigger	0.01	AluJb	0.00
LINE/CR1	0.00	AluSx1	0.00
DNA/hAT-Tip100	0.00	(GGC)n	0.00
LTR/ERVK	0.00	AluJo	0.00
snRNA	0.00	L3	0.00
LINE/RTE-BovB	0.00	AluSx	0.00
SINE/5S-Deu-L2	0.00	(CCT)n	0.00

E

Ontology	Term	FDR Q-val
GO Biological Process	positive regulation of transcription from RNA polymerase II promoter in response to stress	8.58
GO Biological Process	heterochromatin organization	8.30
GO Biological Process	platelet formation	5.16
GO Biological Process	histone H4 acetylation	4.99
GO Biological Process	regulation of telomere capping	4.67
GO Biological Process	axonal transport	4.46
GO Biological Process	regulation of homotypic cell-cell adhesion	4.40
GO Biological Process	negative regulation of cyclin-dependent protein kinase activity	4.19
GO Biological Process	axo-dendritic transport	3.87
GO Biological Process	negative regulation of cyclin-dependent protein serine/threonine kinase activity	3.84
GO Biological Process	blood vessel endothelial cell migration	3.71
GO Biological Process	regulation of pri-miRNA transcription from RNA polymerase II promoter	3.40
GO Biological Process	maintenance of protein localization in organelle	3.39
GO Biological Process	lung vasculature development	3.35
GO Biological Process	positive regulation of telomere capping	2.82
GO Biological Process	placenta blood vessel development	2.69
GO Biological Process	maternal placenta development	2.51
GO Biological Process	histone H2A acetylation	2.41
GO Biological Process	cellular response to arsenic-containing substance	2.35
GO Biological Process	negative regulation of pri-miRNA transcription from RNA polymerase II promoter	1.93
Human Phenotype	Trigonocephaly	1.95

F

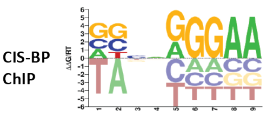

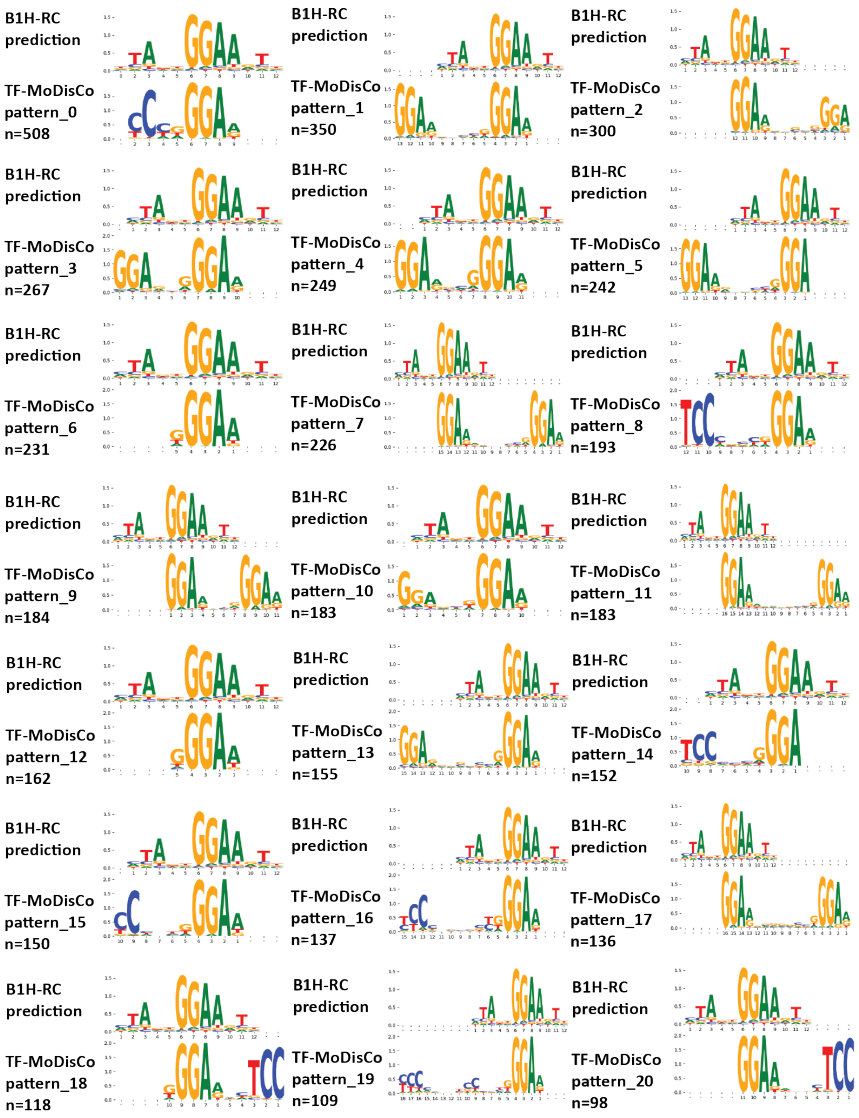

G

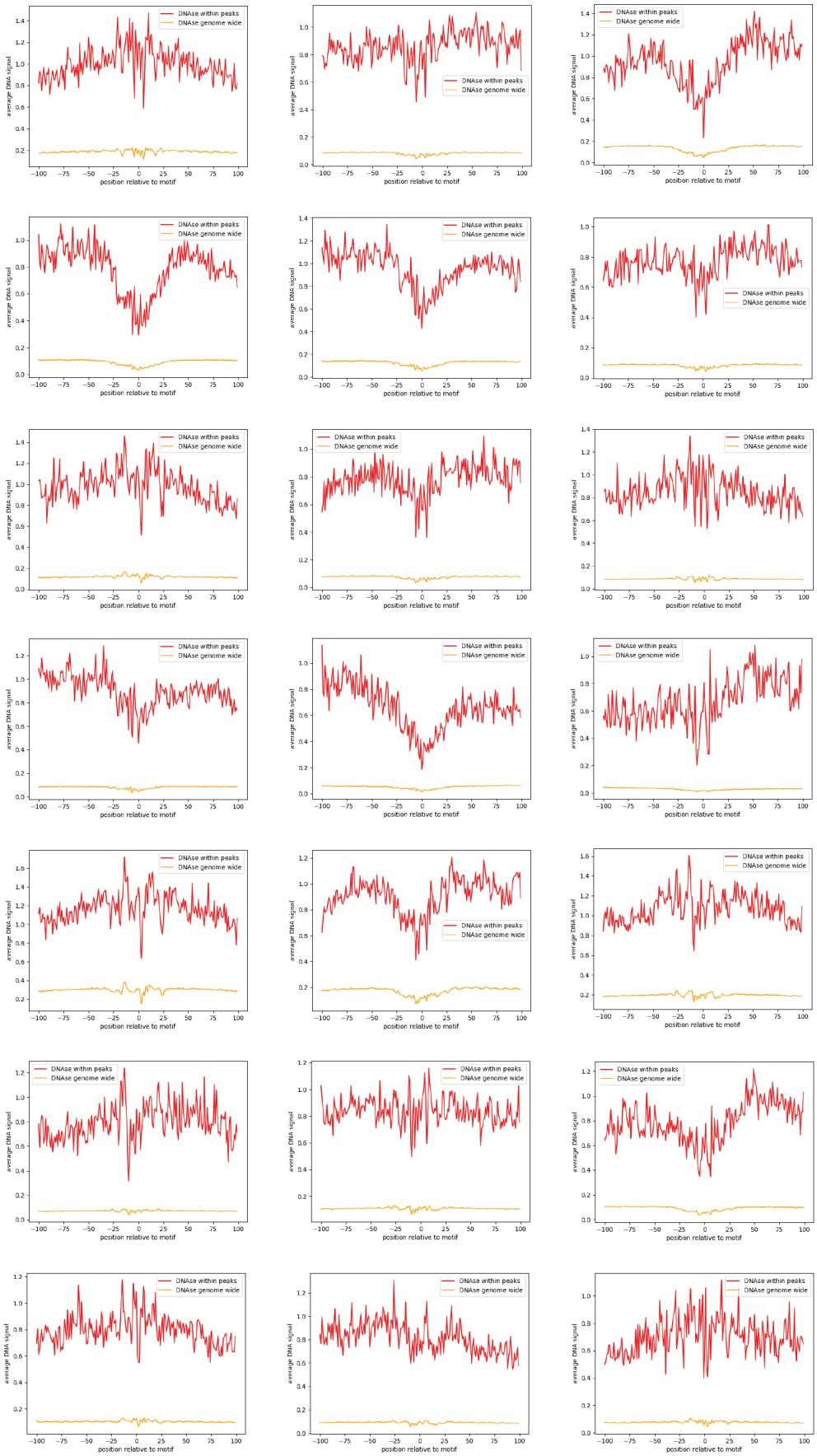
DNAse within peaks
DNAse genome wide
average DNA signal
position relative to motif

H

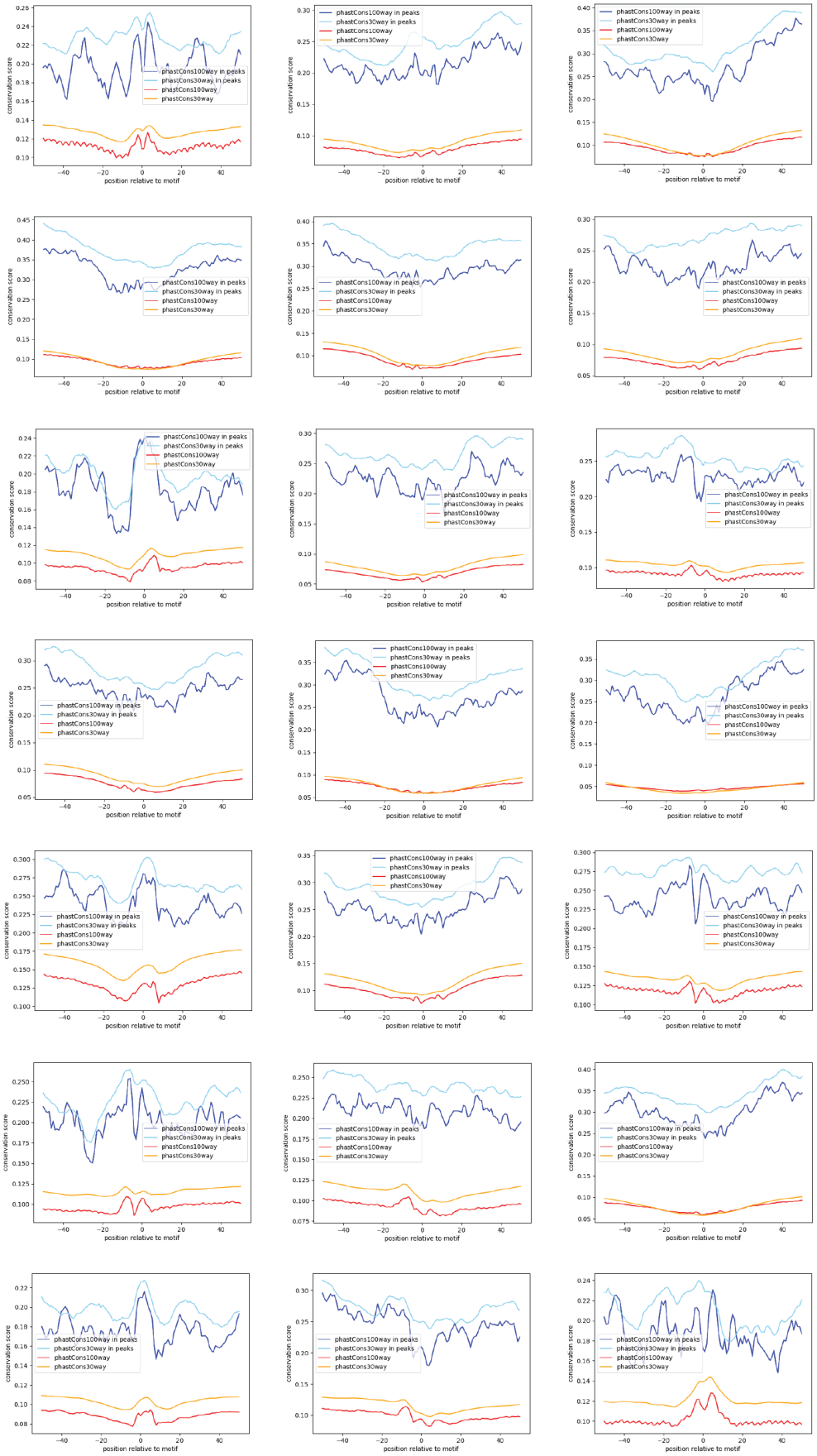
phastCons100way in peaks
phastCons30way in peaks
phastCons100way
phastCons30way
conservation score
position relative to motif

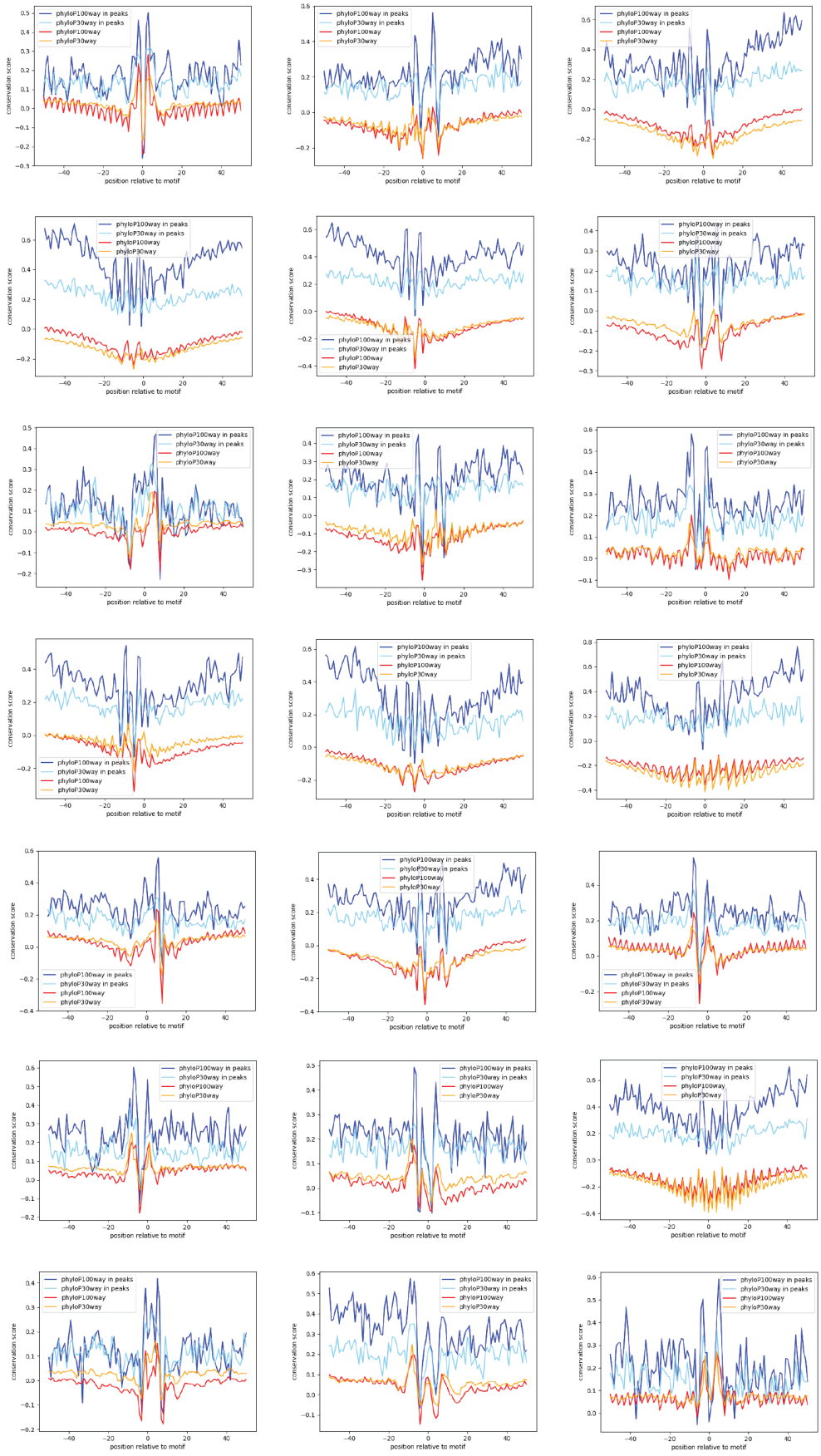

Supplementary Figure 83: Properties and genomic distribution of motifs identified for the IKZF3 tran-

TF-MoDisCO pattern_0 n=508, CWM

pattern_0, n=508; subpattern_0, ns=146

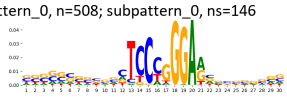

pattern_0, n=508; subpattern_1, ns=106

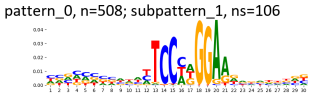

pattern_0, n=508; subpattern_2, ns=93

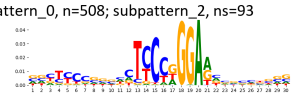

pattern_0, n=508; subpattern_3, ns=70

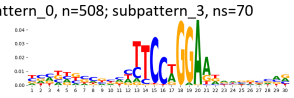

pattern_0, n=508; subpattern_4, ns=69

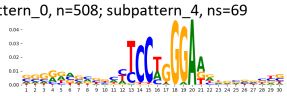

pattern_0, n=508; subpattern_5, ns=24

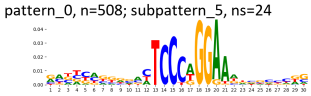

TF-MoDisCO pattern_0 n=508, PWM

pattern_0, n=508; subpattern_0, ns=146

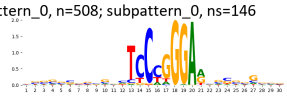

pattern_0, n=508; subpattern_1, ns=106

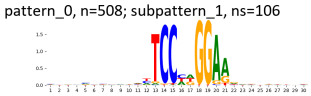

pattern_0, n=508; subpattern_2, ns=93

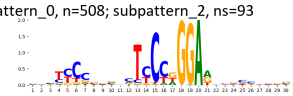

pattern_0, n=508; subpattern_3, ns=70

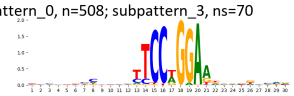

pattern_0, n=508; subpattern_4, ns=69

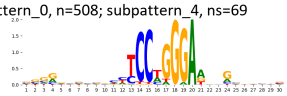

pattern_0, n=508; subpattern_5, ns=24

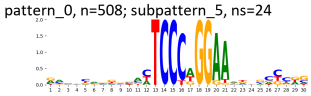

TF-MoDisCO pattern_1 n=350, CWM

pattern_1, n=350; subpattern_0, ns=130

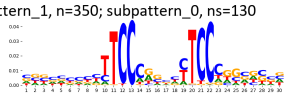

pattern_1, n=350; subpattern_1, ns=94

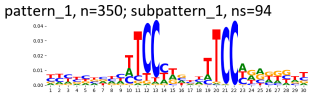

pattern_1, n=350; subpattern_2, ns=55

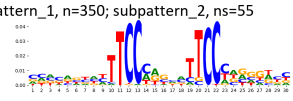

pattern_1, n=350; subpattern_3, ns=40

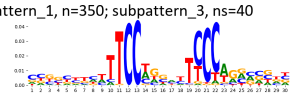

pattern_1, n=350; subpattern_4, ns=31

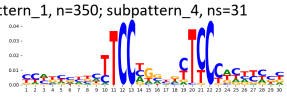

TF-MoDisCO pattern_1 n=350, PWM

pattern_1, n=350; subpattern_0, ns=130

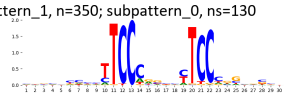

pattern_1, n=350; subpattern_1, ns=94

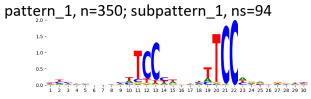

pattern_1, n=350; subpattern_2, ns=55

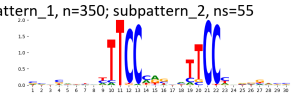

pattern_1, n=350; subpattern_3, ns=40

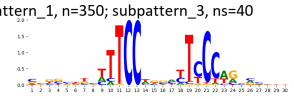

pattern_1, n=350; subpattern_4, ns=31

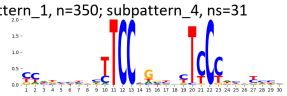

TF-MoDisCO pattern_10 n=183, CWM

pattern_10, n=183; subpattern_0, ns=54

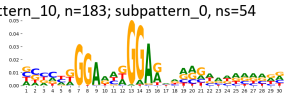

pattern_10, n=183; subpattern_1, ns=51

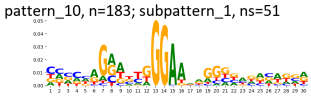

pattern_10, n=183; subpattern_2, ns=31

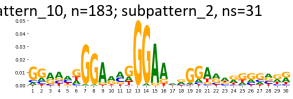

pattern_10, n=183; subpattern_3, ns=29

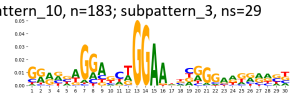

pattern_10, n=183; subpattern_4, ns=10

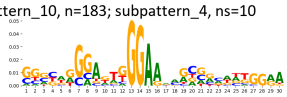

pattern_10, n=183; subpattern_5, ns=8

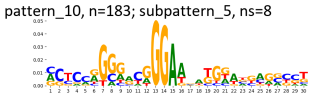

TF-MoDisCO pattern_10 n=183, PWM

pattern_10, n=183; subpattern_0, ns=54

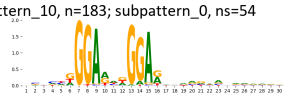

pattern_10, n=183; subpattern_1, ns=51

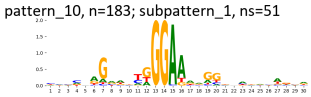

pattern_10, n=183; subpattern_2, ns=31

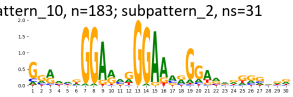

pattern_10, n=183; subpattern_3, ns=29

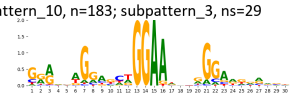

pattern_10, n=183; subpattern_4, ns=10

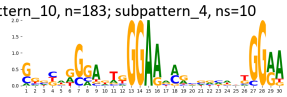

pattern_10, n=183; subpattern_5, ns=8

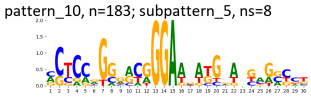

TF-MoDisCO pattern_11 n=183, CWM

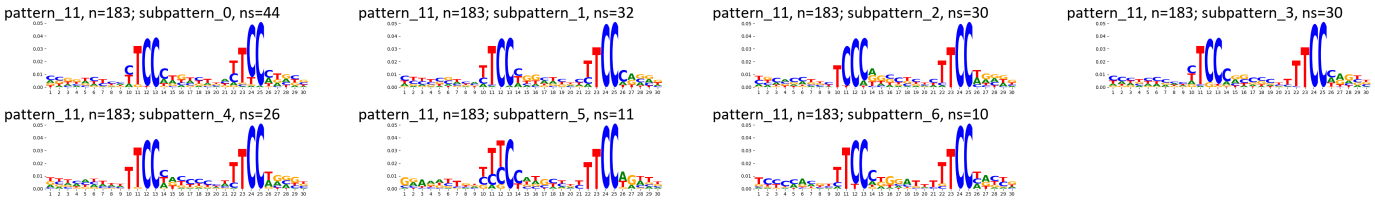

TF-MoDisCO pattern_11 n=183, PWM

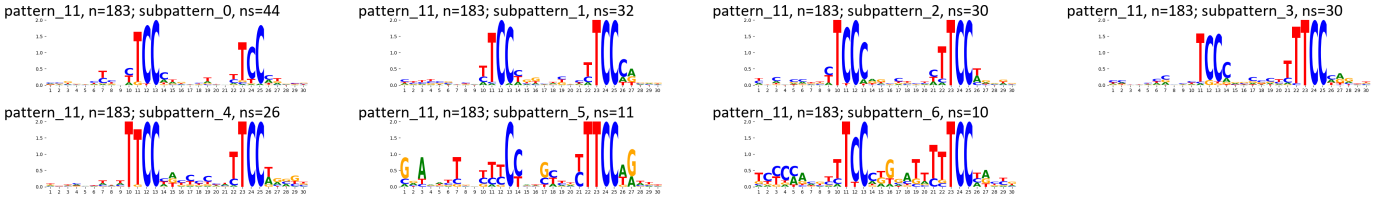

TF-MoDisCO pattern_12 n=162, CWM

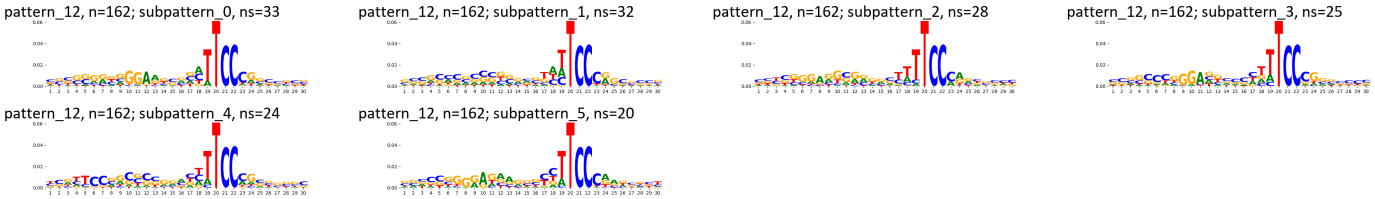

TF-MoDisCO pattern_12 n=162, PWM

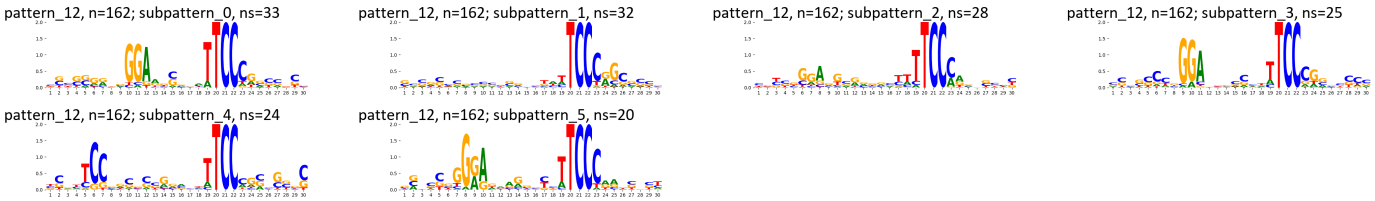

TF-MoDisCO pattern_13 n=155, CWM

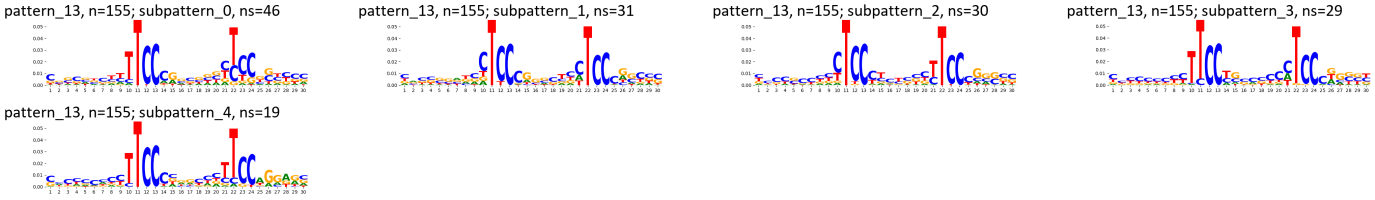

TF-MoDisCO pattern_13 n=155, PWM

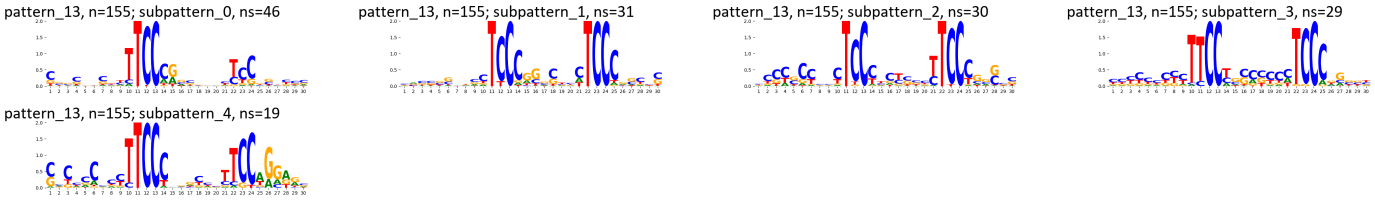

TF-MoDisCO pattern_14 n=152, CWM

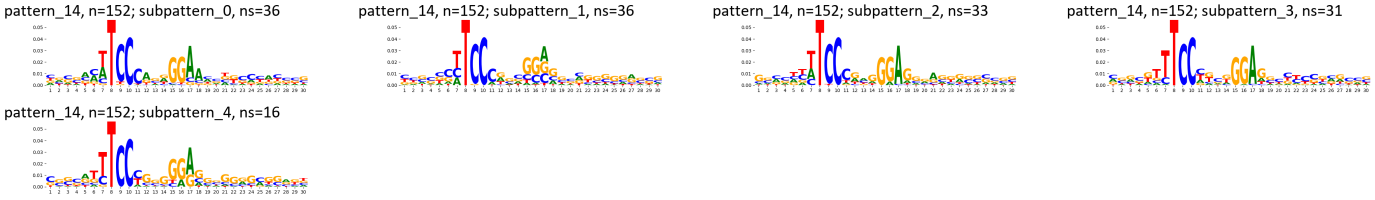

TF-MoDisCO pattern_14 n=152, PWM

pattern_14, n=152; subpattern_0, ns=36

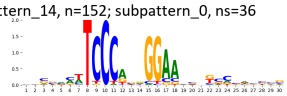

pattern_14, n=152; subpattern_1, ns=36

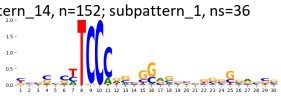

pattern_14, n=152; subpattern_2, ns=33

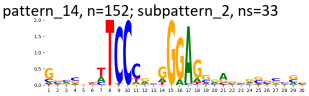

pattern_14, n=152; subpattern_3, ns=31

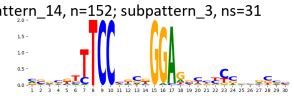

pattern_14, n=152; subpattern_4, ns=16

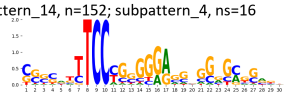

TF-MoDisCO pattern_15 n=150, CWM

pattern_15, n=150; subpattern_0, ns=31

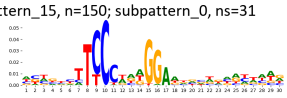

pattern_15, n=150; subpattern_1, ns=30

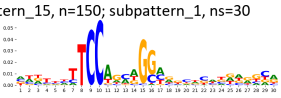

pattern_15, n=150; subpattern_2, ns=27

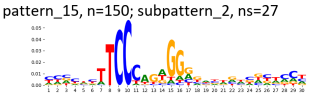

pattern_15, n=150; subpattern_3, ns=24

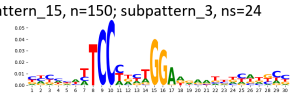

pattern_15, n=150; subpattern_4, ns=23

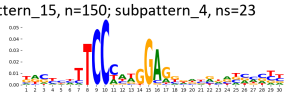

pattern_15, n=150; subpattern_5, ns=15

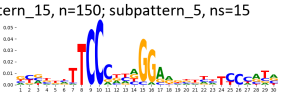

TF-MoDisCO pattern_15 n=150, PWM

pattern_15, n=150; subpattern_0, ns=31

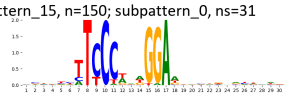

pattern_15, n=150; subpattern_1, ns=30

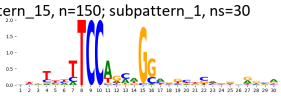

pattern_15, n=150; subpattern_2, ns=27

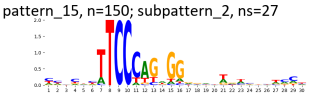

pattern_15, n=150; subpattern_3, ns=24

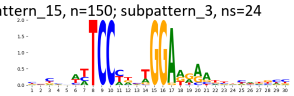

pattern_15, n=150; subpattern_4, ns=23

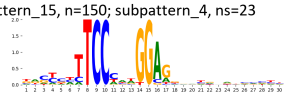

pattern_15, n=150; subpattern_5, ns=15

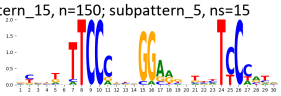

TF-MoDisCO pattern_16 n=137, CWM

pattern_16, n=137; subpattern_0, ns=32

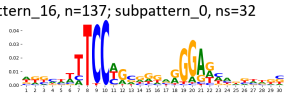

pattern_16, n=137; subpattern_1, ns=31

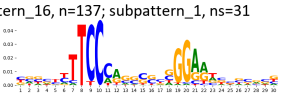

pattern_16, n=137; subpattern_2, ns=30

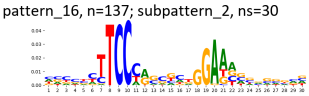

pattern_16, n=137; subpattern_3, ns=29

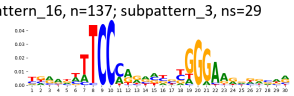

pattern_16, n=137; subpattern_4, ns=15

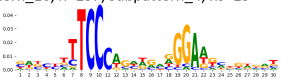

TF-MoDisCO pattern_16 n=137, PWM

pattern_16, n=137; subpattern_0, ns=32

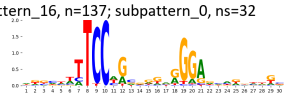

pattern_16, n=137; subpattern_1, ns=31

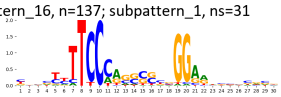

pattern_16, n=137; subpattern_2, ns=30

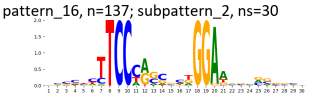

pattern_16, n=137; subpattern_3, ns=29

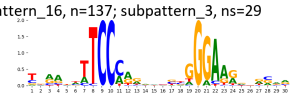

pattern_16, n=137; subpattern_4, ns=15

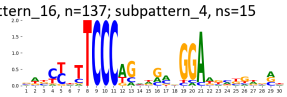

TF-MoDisCO pattern_17 n=136, CWM

pattern_17, n=136; subpattern_0, ns=37

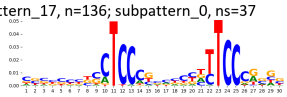

pattern_17, n=136; subpattern_1, ns=33

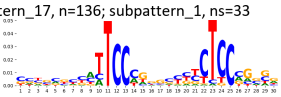

pattern_17, n=136; subpattern_2, ns=25

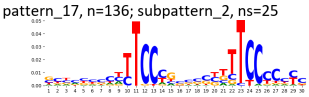

pattern_17, n=136; subpattern_3, ns=18

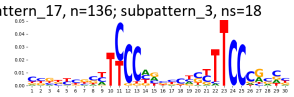

pattern_17, n=136; subpattern_4, ns=17

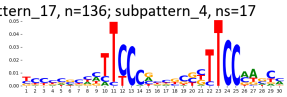

pattern_17, n=136; subpattern_5, ns=6

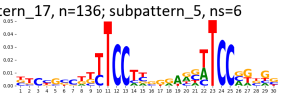

TF-MoDisCO pattern_17 n=136, PWM

pattern_17, n=136; subpattern_0, ns=37

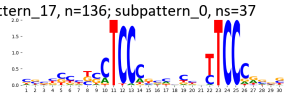

pattern_17, n=136; subpattern_1, ns=33

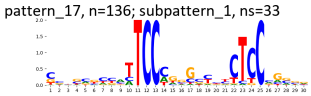

pattern_17, n=136; subpattern_2, ns=25

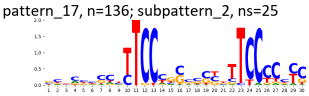

pattern_17, n=136; subpattern_3, ns=18

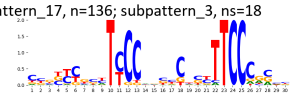

pattern_17, n=136; subpattern_4, ns=17

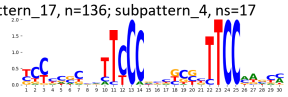

pattern_17, n=136; subpattern_5, ns=6

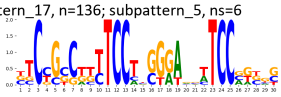

TF-MoDisCO pattern_18 n=118, CWM

pattern_18, n=118; subpattern_0, ns=47

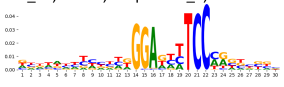

pattern_18, n=118; subpattern_1, ns=38

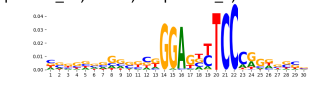

pattern_18, n=118; subpattern_2, ns=21

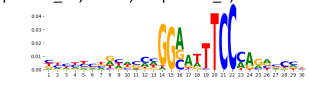

pattern_18, n=118; subpattern_3, ns=12

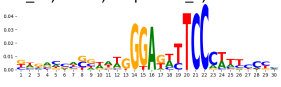

TF-MoDisCO pattern_18 n=118, PWM

pattern_18, n=118; subpattern_0, ns=47

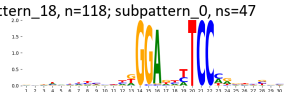

pattern_18, n=118; subpattern_1, ns=38

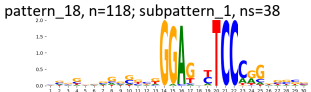

pattern_18, n=118; subpattern_2, ns=21

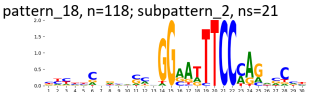

pattern_18, n=118; subpattern_3, ns=12

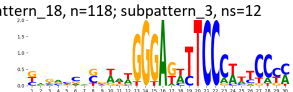

TF-MoDisCO pattern_19 n=109, CWM

pattern_19, n=109; subpattern_0, ns=43

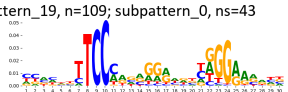

pattern_19, n=109; subpattern_1, ns=23

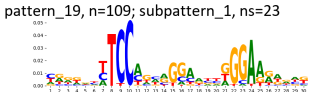

pattern_19, n=109; subpattern_2, ns=22

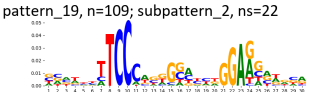

pattern_19, n=109; subpattern_3, ns=21

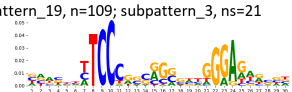

TF-MoDisCO pattern_19 n=109, PWM

pattern_19, n=109; subpattern_0, ns=43

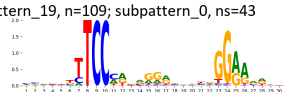

pattern_19, n=109; subpattern_1, ns=23

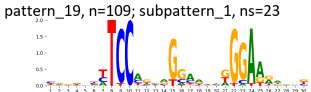

pattern_19, n=109; subpattern_2, ns=22

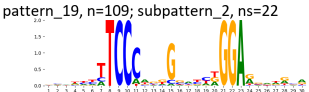

pattern_19, n=109; subpattern_3, ns=21

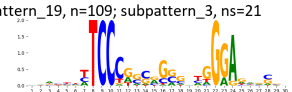

TF-MoDisCO pattern_2 n=300, CWM

pattern_2, n=300; subpattern_0, ns=99

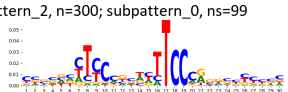

pattern_2, n=300; subpattern_1, ns=69

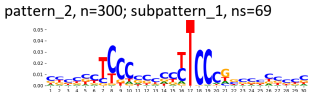

pattern_2, n=300; subpattern_2, ns=59

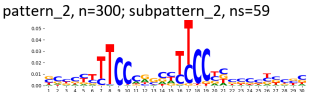

pattern_2, n=300; subpattern_3, ns=41

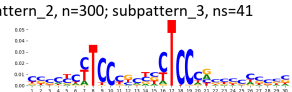

pattern_2, n=300; subpattern_4, ns=32

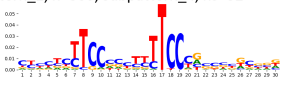

TF-MoDisCO pattern_2 n=300, PWM

pattern_2, n=300; subpattern_0, ns=99

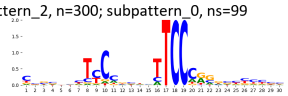

pattern_2, n=300; subpattern_1, ns=69

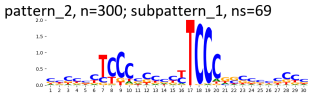

pattern_2, n=300; subpattern_2, ns=59

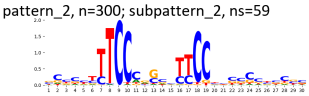

pattern_2, n=300; subpattern_3, ns=41

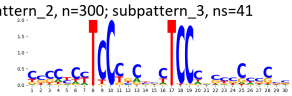

pattern_2, n=300; subpattern_4, ns=32

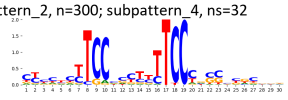

TF-MoDisCO pattern_20 n=98, CWM

pattern_20, n=98; subpattern_0, ns=43

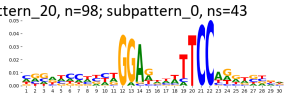

pattern_20, n=98; subpattern_1, ns=42

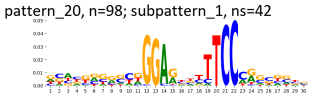

pattern_20, n=98; subpattern_2, ns=13

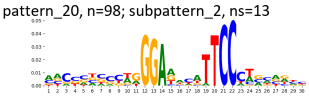

TF-MoDisCO pattern_20 n=98, PWM

pattern_20, n=98; subpattern_0, ns=43

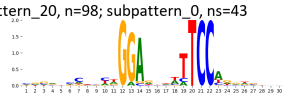

pattern_20, n=98; subpattern_1, ns=42

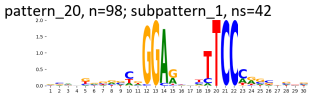

pattern_20, n=98; subpattern_2, ns=13

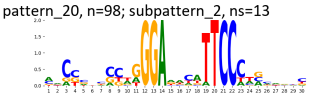

TF-MoDisCO pattern_3 n=267, CWM

pattern_3, n=267; subpattern_0, ns=57

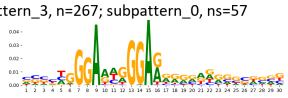

pattern_3, n=267; subpattern_1, ns=56

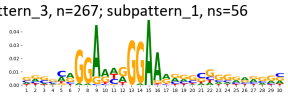

pattern_3, n=267; subpattern_2, ns=55

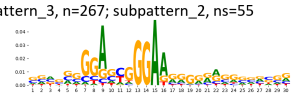

pattern_3, n=267; subpattern_3, ns=38

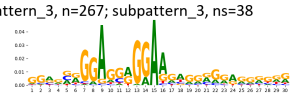

pattern_3, n=267; subpattern_4, ns=36

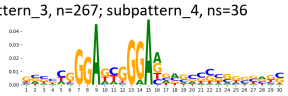

pattern_3, n=267; subpattern_5, ns=25

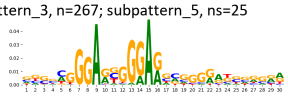

TF-MoDisCO pattern_3 n=267, PWM

pattern_3, n=267; subpattern_0, ns=57

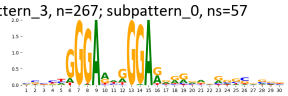

pattern_3, n=267; subpattern_1, ns=56

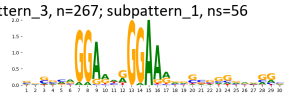

pattern_3, n=267; subpattern_2, ns=55

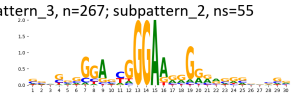

pattern_3, n=267; subpattern_3, ns=38

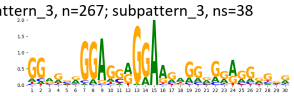

pattern_3, n=267; subpattern_4, ns=36

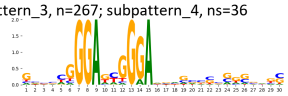

pattern_3, n=267; subpattern_5, ns=25

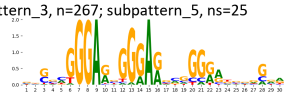

TF-MoDisCO pattern_4 n=249, CWM

pattern_4, n=249; subpattern_0, ns=55

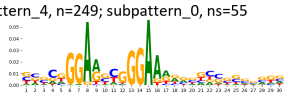

pattern_4, n=249; subpattern_1, ns=46

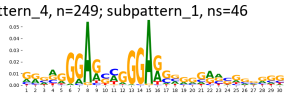

pattern_4, n=249; subpattern_2, ns=37

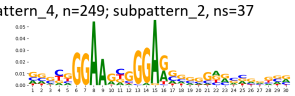

pattern_4, n=249; subpattern_3, ns=36

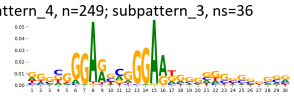

pattern_4, n=249; subpattern_4, ns=35

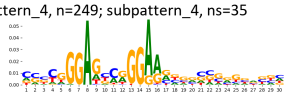

pattern_4, n=249; subpattern_5, ns=19

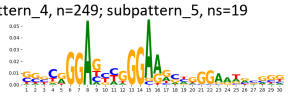

pattern_4, n=249; subpattern_6, ns=18

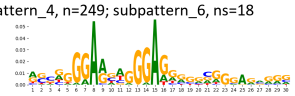

pattern_4, n=249; subpattern_7, ns=3

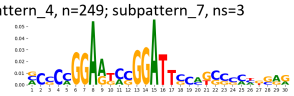

TF-MoDisCO pattern_4 n=249, PWM

pattern_4, n=249; subpattern_0, ns=55

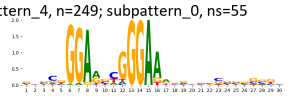

pattern_4, n=249; subpattern_1, ns=46

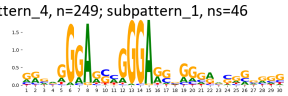

pattern_4, n=249; subpattern_2, ns=37

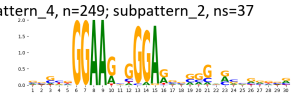

pattern_4, n=249; subpattern_3, ns=36

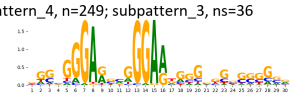

pattern_4, n=249; subpattern_4, ns=35

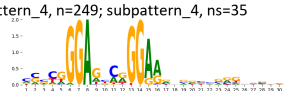

pattern_4, n=249; subpattern_5, ns=19

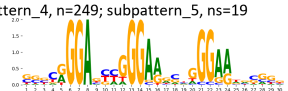

pattern_4, n=249; subpattern_6, ns=18

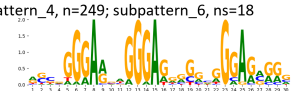

pattern_4, n=249; subpattern_7, ns=3

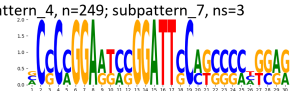

TF-MoDisCO pattern_5 n=242, CWM

pattern_5, n=242; subpattern_0, ns=89

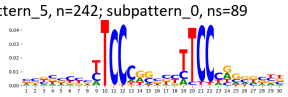

pattern_5, n=242; subpattern_1, ns=54

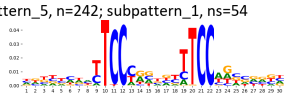

pattern_5, n=242; subpattern_2, ns=50

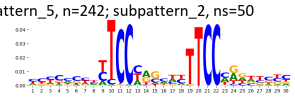

pattern_5, n=242; subpattern_3, ns=40

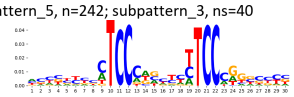

pattern_5, n=242; subpattern_4, ns=9

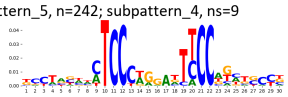

TF-MoDisCO pattern_5 n=242, PWM

pattern_5, n=242; subpattern_0, ns=89

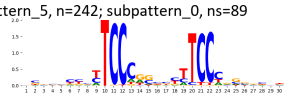

pattern_5, n=242; subpattern_1, ns=54

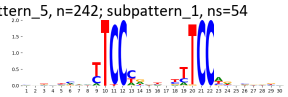

pattern_5, n=242; subpattern_2, ns=50

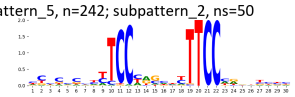

pattern_5, n=242; subpattern_3, ns=40

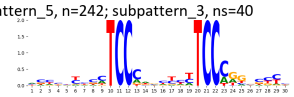

pattern_5, n=242; subpattern_4, ns=9

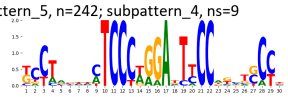

TF-MoDisCO pattern_6 n=231, CWM

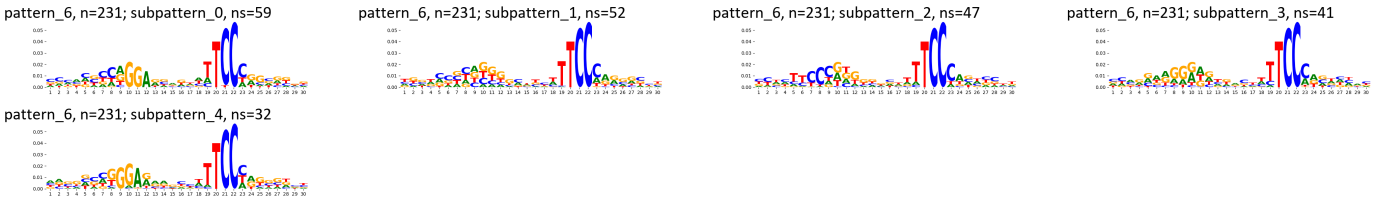

TF-MoDisCO pattern_6 n=231, PWM

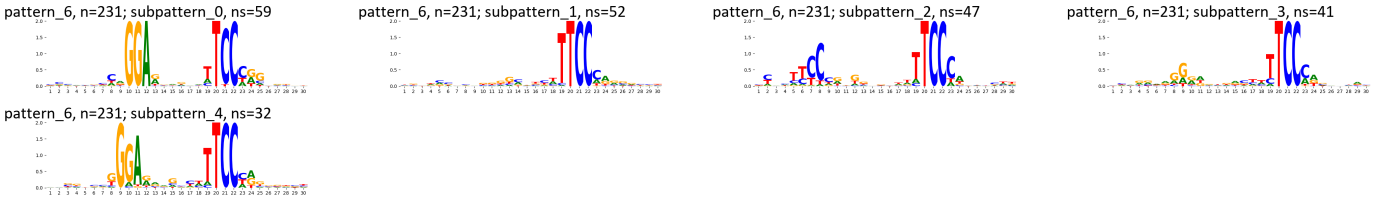

TF-MoDisCO pattern_7 n=226, CWM

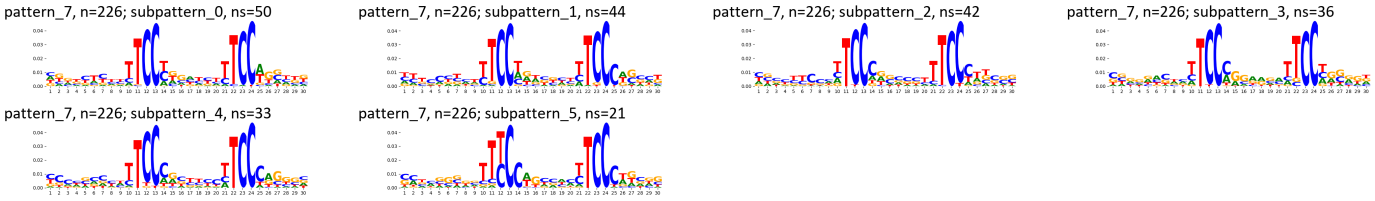

TF-MoDisCO pattern_7 n=226, PWM

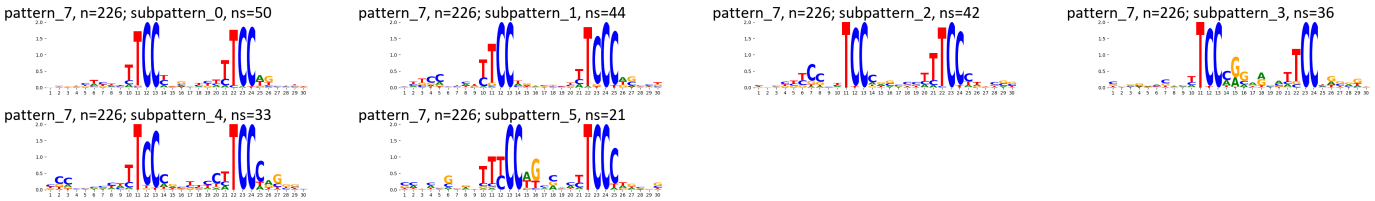

TF-MoDisCO pattern_8 n=193, CWM

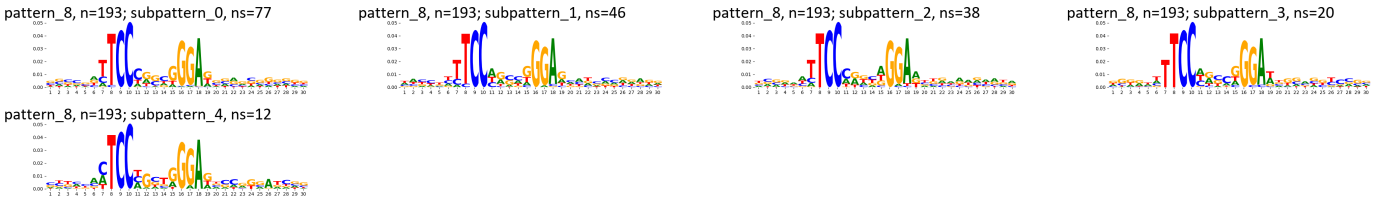

TF-MoDisCO pattern_8 n=193, PWM

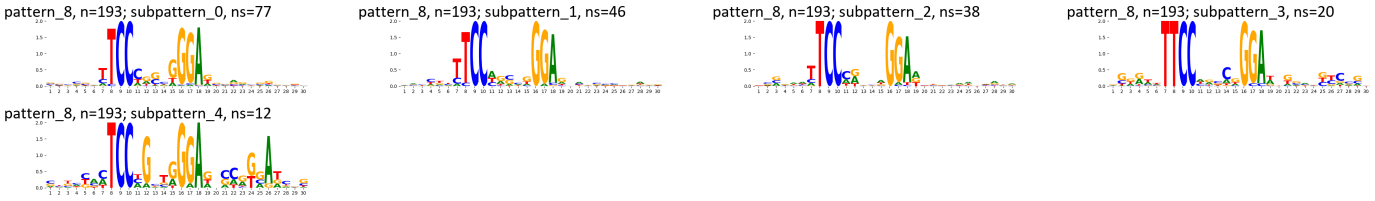

TF-MoDisCO pattern_9 n=184, CWM

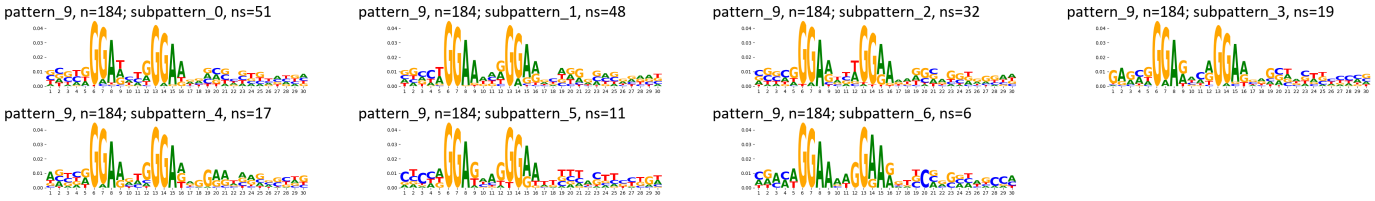

TF-MoDisCO pattern_9 n=184, PWM

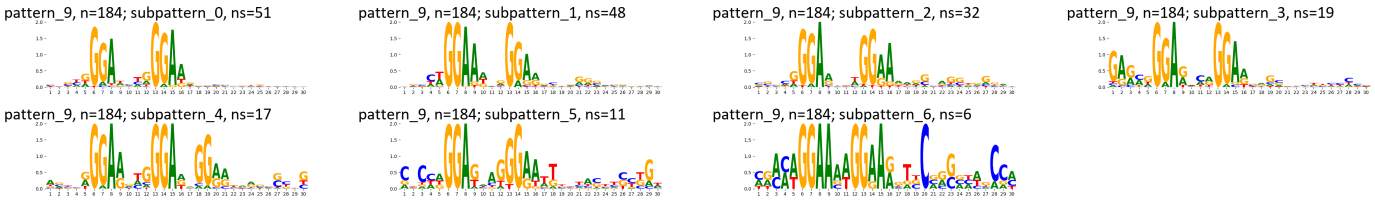

Supplementary Figure 84: TF-MoDisCO subpatterns for the IKZF3 transcription factor in HEK293 (accession Hughes GR models).

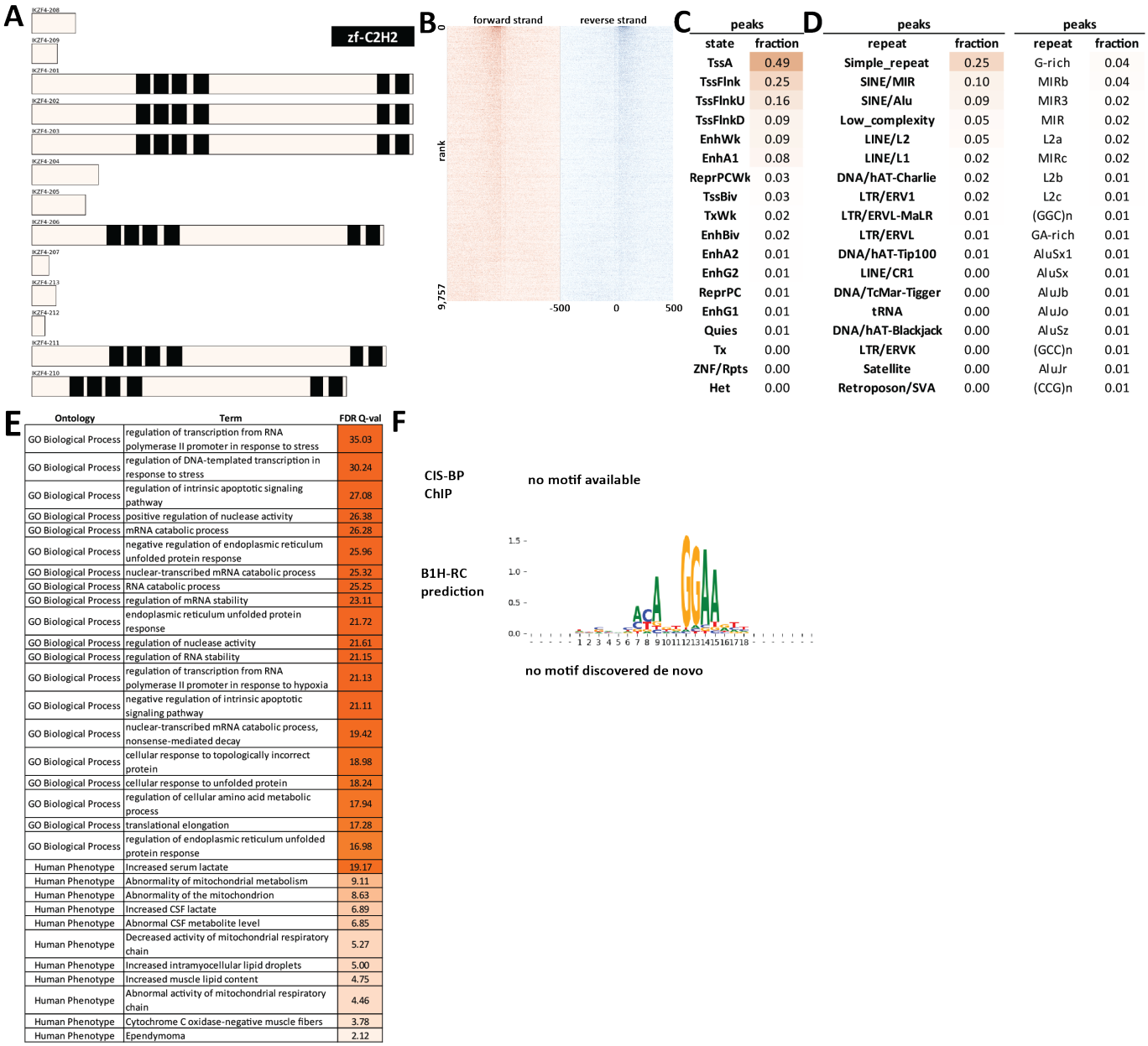

C

peaks	
state	fraction
TssA	0.49
TssFlnk	0.25
TssFlnkU	0.16
TssFlnkD	0.09
EnhWk	0.09
EnhA1	0.08
ReprPCWk	0.03
TssBiv	0.03
TxWk	0.02
EnhBiv	0.02
EnhA2	0.01
EnhG2	0.01
ReprPC	0.01
EnhG1	0.01
Quies	0.01
Tx	0.00
ZNF/Rpts	0.00
Het	0.00

D

peaks		peaks	
repeat	fraction	repeat	fraction
Simple_repeat	0.25	G-rich	0.04
SINE/MIR	0.10	MIRb	0.04
SINE/Alu	0.09	MIR3	0.02
Low_complexity	0.05	MIR	0.02
LINE/L2	0.05	L2a	0.02
LINE/L1	0.02	MIRc	0.02
DNA/hAT-Charlie	0.02	L2b	0.01
LTR/ERV1	0.02	L2c	0.01
LTR/ERVL-MaLR	0.01	(GGC)n	0.01
LTR/ERVL	0.01	GA-rich	0.01
DNA/hAT-Tip100	0.01	AluSx1	0.01
LINE/CR1	0.00	AluSx	0.01
DNA/TcMar-Tigger	0.00	AluJb	0.01
tRNA	0.00	AluJo	0.01
DNA/hAT-Blackjack	0.00	AluSz	0.01
LTR/ERVK	0.00	(GCC)n	0.01
Satellite	0.00	AluJr	0.01
Retroposon/SVA	0.00	(CCG)n	0.01

E

Ontology	Term	FDR Q-val
GO Biological Process	regulation of transcription from RNA polymerase II promoter in response to stress	35.03
GO Biological Process	regulation of DNA-templated transcription in response to stress	30.24
GO Biological Process	regulation of intrinsic apoptotic signaling pathway	27.08
GO Biological Process	positive regulation of nuclease activity	26.38
GO Biological Process	mRNA catabolic process	26.28
GO Biological Process	negative regulation of endoplasmic reticulum unfolded protein response	25.96
GO Biological Process	nuclear-transcribed mRNA catabolic process	25.32
GO Biological Process	RNA catabolic process	25.25
GO Biological Process	regulation of mRNA stability	23.11
GO Biological Process	endoplasmic reticulum unfolded protein response	21.72
GO Biological Process	regulation of nuclease activity	21.61
GO Biological Process	regulation of RNA stability	21.15
GO Biological Process	regulation of transcription from RNA polymerase II promoter in response to hypoxia	21.13
GO Biological Process	negative regulation of intrinsic apoptotic signaling pathway	21.11
GO Biological Process	nuclear-transcribed mRNA catabolic process, nonsense-mediated decay	19.42
GO Biological Process	cellular response to topologically incorrect protein	18.98
GO Biological Process	cellular response to unfolded protein	18.24
GO Biological Process	regulation of cellular amino acid metabolic process	17.94
GO Biological Process	translational elongation	17.28
GO Biological Process	regulation of endoplasmic reticulum unfolded protein response	16.98
Human Phenotype	Increased serum lactate	19.17
Human Phenotype	Abnormality of mitochondrial metabolism	9.11
Human Phenotype	Abnormality of the mitochondrion	8.63
Human Phenotype	Increased CSF lactate	6.89
Human Phenotype	Abnormal CSF metabolite level	6.85
Human Phenotype	Decreased activity of mitochondrial respiratory chain	5.27
Human Phenotype	Increased intramyocellular lipid droplets	5.00
Human Phenotype	Increased muscle lipid content	4.75
Human Phenotype	Abnormal activity of mitochondrial respiratory chain	4.46
Human Phenotype	Cytochrome C oxidase-negative muscle fibers	3.78
Human Phenotype	Ependymoma	2.12

Supplementary Figure 85: Properties and genomic distribution of motifs identified for the IKZF4 transcription factor in HepG2 (accession ENCSR799DUB).

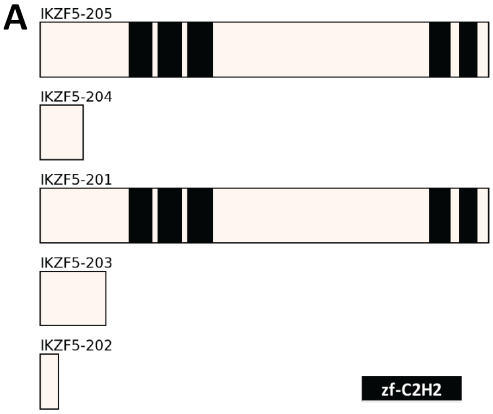

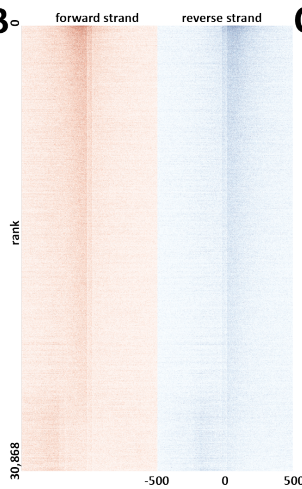

C

peaks	
state	fraction
TssA	0.29
EnhA1	0.20
EnhWk	0.19
TssFlnkU	0.17
TssFlnk	0.15
TssFlnkD	0.10
TxWk	0.03
ReprPCWk	0.03
EnhA2	0.03
EnhBiv	0.02
TssBiv	0.02
EnhG2	0.02
Quies	0.01
EnhG1	0.01
ReprPC	0.01
Tx	0.01
ZNF/Rpts	0.00
Het	0.00

D

peaks		peaks	
repeat	fraction	repeat	fraction
SINE/Alu	0.15	MIRb	0.04
Simple_repeat	0.14	L2a	0.03
SINE/MIR	0.12	MIR	0.03
LINE/L2	0.08	L2c	0.02
LINE/L1	0.06	MIRc	0.02
DNA/hAT-Charlie	0.03	MIR3	0.02
Low_complexity	0.03	L2b	0.02
LTR/ERV1	0.03	G-rich	0.02
LTR/ERVL-MaLR	0.02	AluJb	0.02
LTR/ERVL	0.02	AluSx	0.02
DNA/TcMar-Tigger	0.01	AluSx1	0.01
DNA/hAT-Tip100	0.01	AluJr	0.01
LINE/CR1	0.01	AluSz	0.01
tRNA	0.01	AluJo	0.01
LTR/ERVK	0.01	AluY	0.01
DNA/hAT-Blackjack	0.00	AluSq2	0.01
LTR/Gypsy	0.00	GA-rich	0.01
LINE/RTE-BovB	0.00	L2	0.01

E

Ontology	Term	FDR Q-val
GO Biological Process	regulation of transcription from RNA polymerase II promoter in response to stress	71.68
GO Biological Process	regulation of DNA-templated transcription in response to stress	67.31
GO Biological Process	regulation of intrinsic apoptotic signaling pathway	60.33
GO Biological Process	nuclear-transcribed mRNA catabolic process	60.25
GO Biological Process	endoplasmic reticulum unfolded protein response	57.21
GO Biological Process	negative regulation of intrinsic apoptotic signaling pathway	53.59
GO Biological Process	cellular response to topologically incorrect protein	48.42
GO Biological Process	positive regulation of transcription from RNA polymerase II promoter in response to stress	48.01
GO Biological Process	cellular response to unfolded protein	47.77
GO Biological Process	IRE1-mediated unfolded protein response	46.87
GO Biological Process	nuclear-transcribed mRNA catabolic process, nonsense-mediated decay	46.32
GO Biological Process	regulation of necrotic cell death	39.78
GO Biological Process	liver regeneration	39.04
GO Biological Process	regulation of transcription from RNA polymerase II promoter in response to hypoxia	38.11
GO Biological Process	regulation of mitochondrial membrane permeability	35.66
GO Biological Process	cotranslational protein targeting to membrane	33.50
GO Biological Process	translational elongation	32.86
GO Biological Process	viral gene expression	31.29
GO Biological Process	mitochondrial transmembrane transport	30.39
GO Biological Process	mitochondrial translational termination	30.03
Human Phenotype	Abnormality of transition element cation homeostasis	23.04
Human Phenotype	Abnormal CSF metabolite level	22.54
Human Phenotype	Increased CSF lactate	17.27

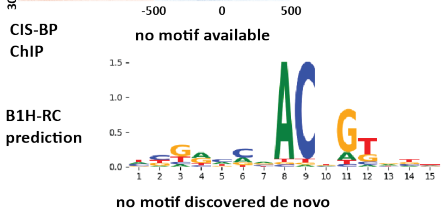

Supplementary Figure 86: Properties and genomic distribution of motifs identified for the IKZF5 transcription factor in HepG2 (accession ENCSR210HBN).

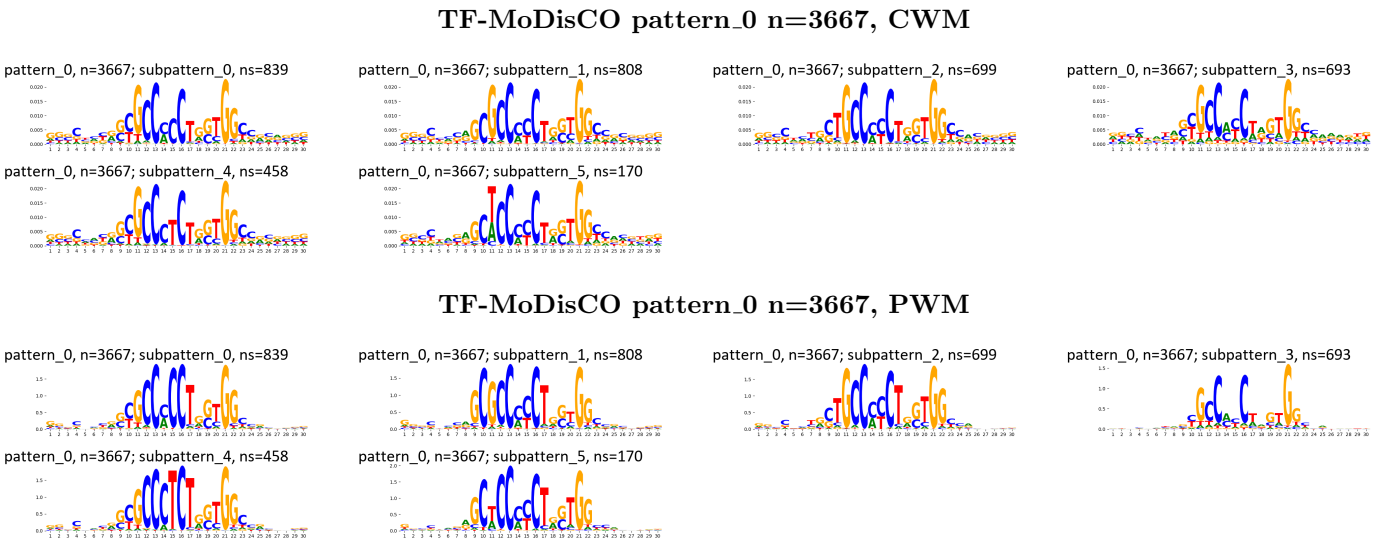

Supplementary Figure 87: TF-MoDisCO subpatterns for the IKZF5 transcription factor in HepG2 (accession ENCSR210HBN).

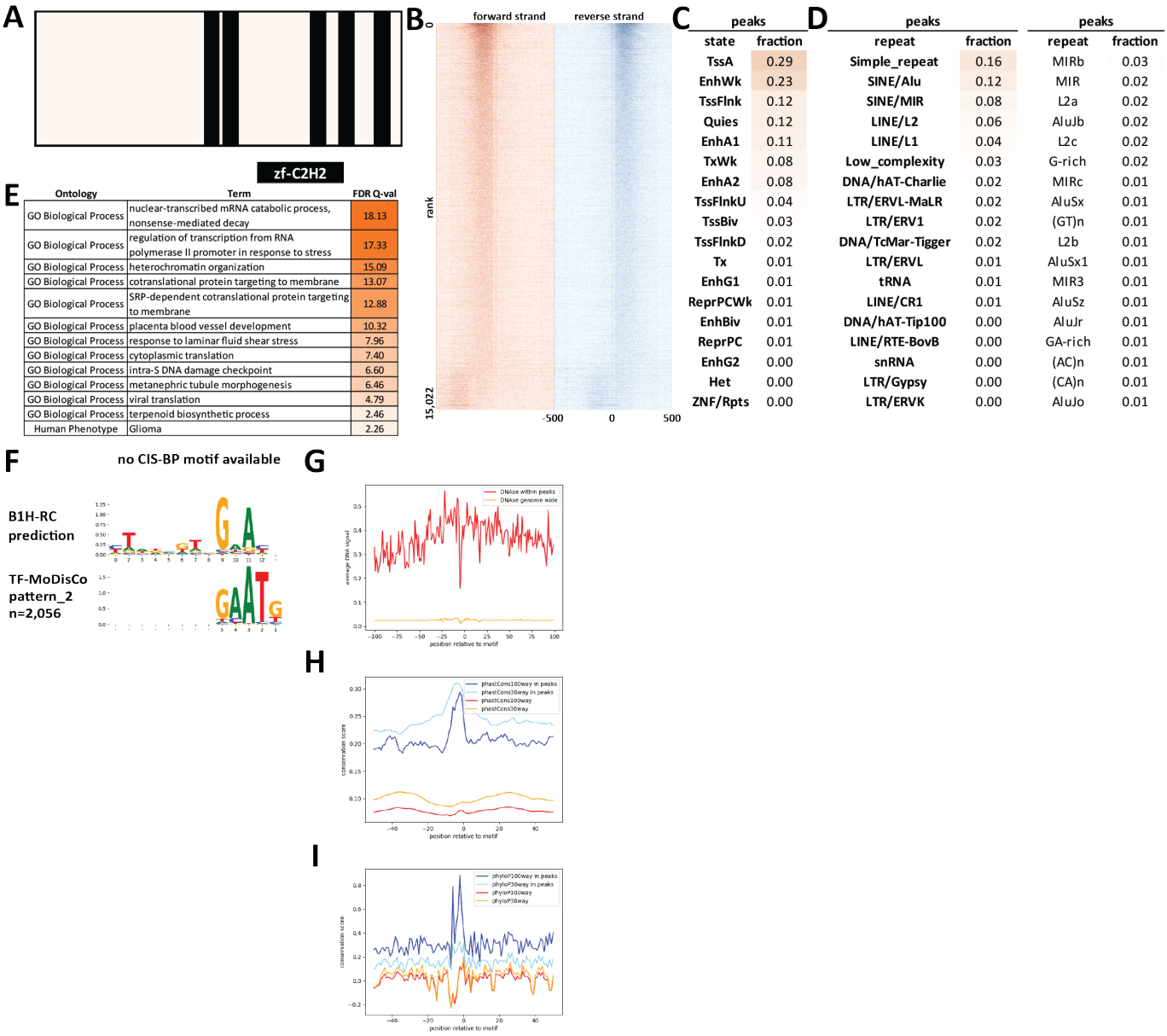

Supplementary Figure 88: Properties and genomic distribution of motifs identified for the INSM2 transcription factor in HEK293 (accession ENCSR382GSF).

TF-MoDisCO pattern_2 n=2026, CWM

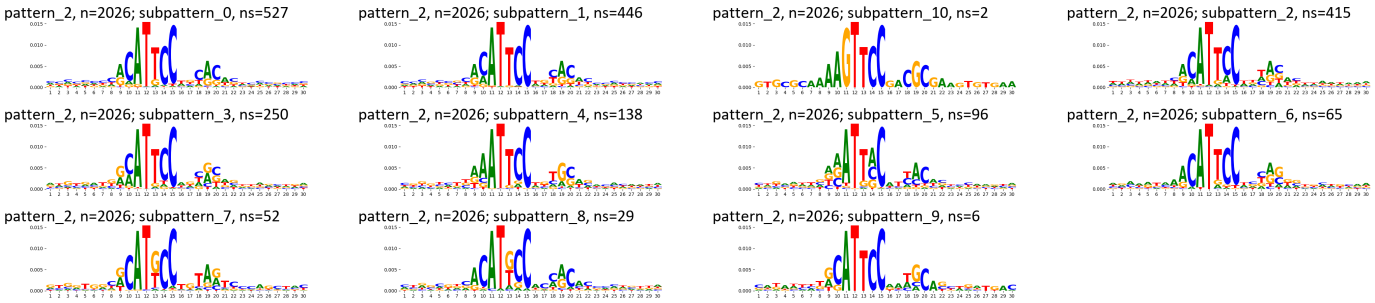

TF-MoDisCO pattern_2 n=2026, PWM

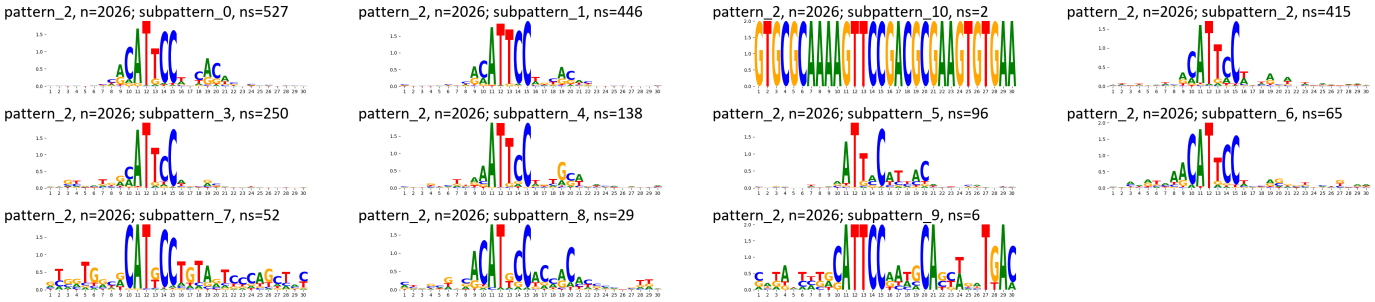

Supplementary Figure 89: TF-MoDisCO subpatterns for the INSM2 transcription factor in HEK293 (accession ENCSR382GSF).

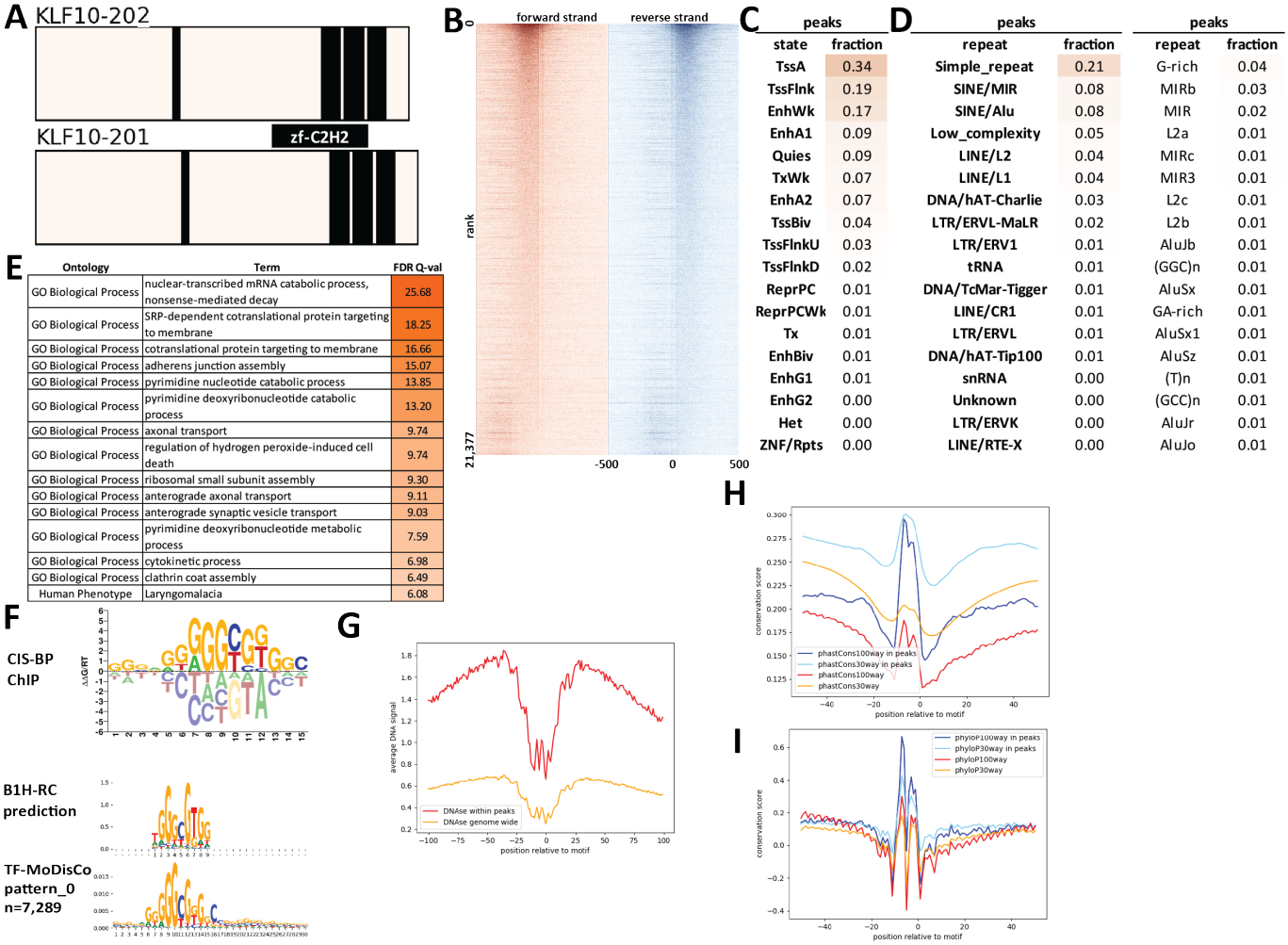

Supplementary Figure 90: Properties and genomic distribution of motifs identified for the KLF10 transcription factor in HEK293 (accession ENCSR006GAQ).

TF-MoDisCO pattern_0 n=7289, CWM

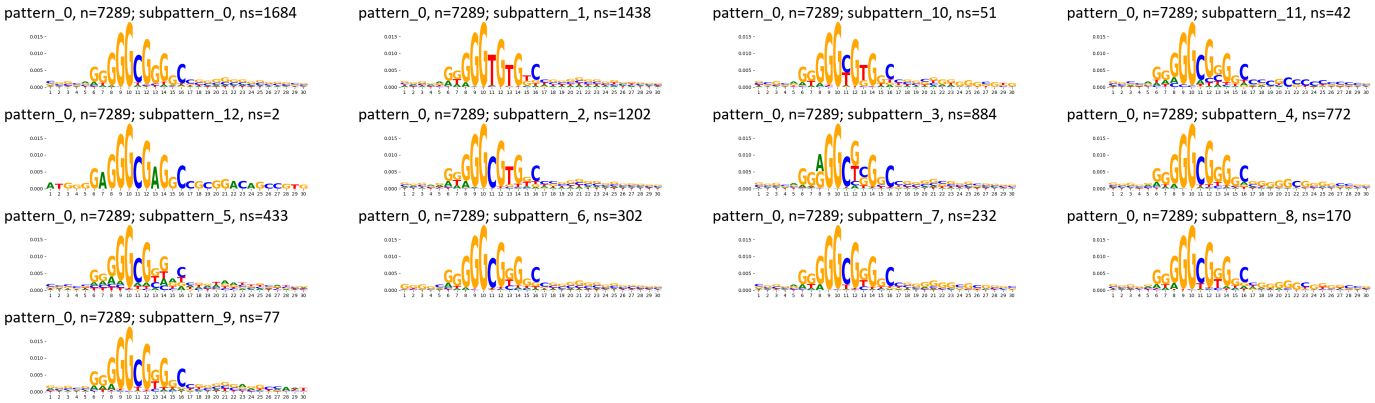

TF-MoDisCO pattern_0 n=7289, PWM

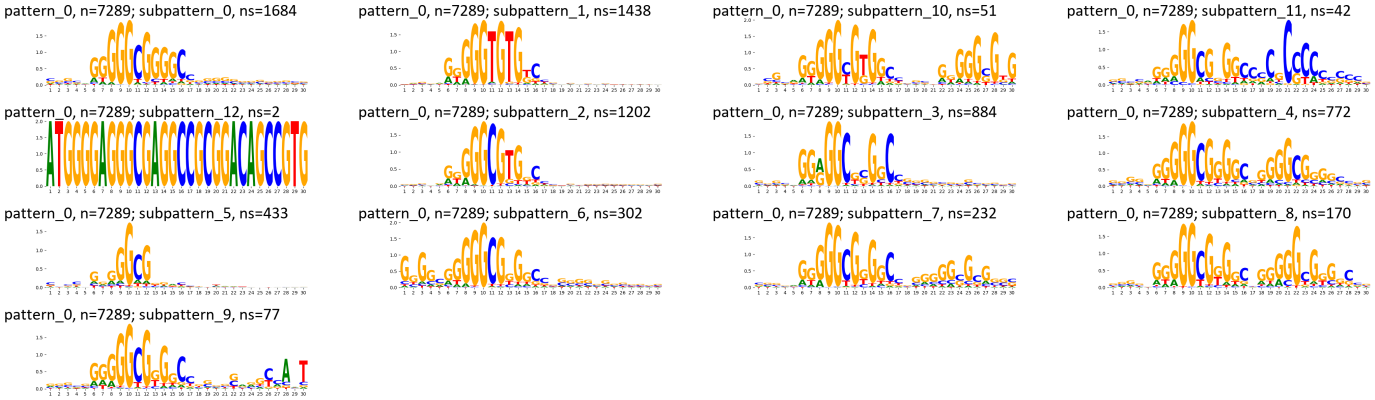

Supplementary Figure 91: TF-MoDisCO subpatterns for the KLF10 transcription factor in HEK293 (accession ENCSR006GAQ).

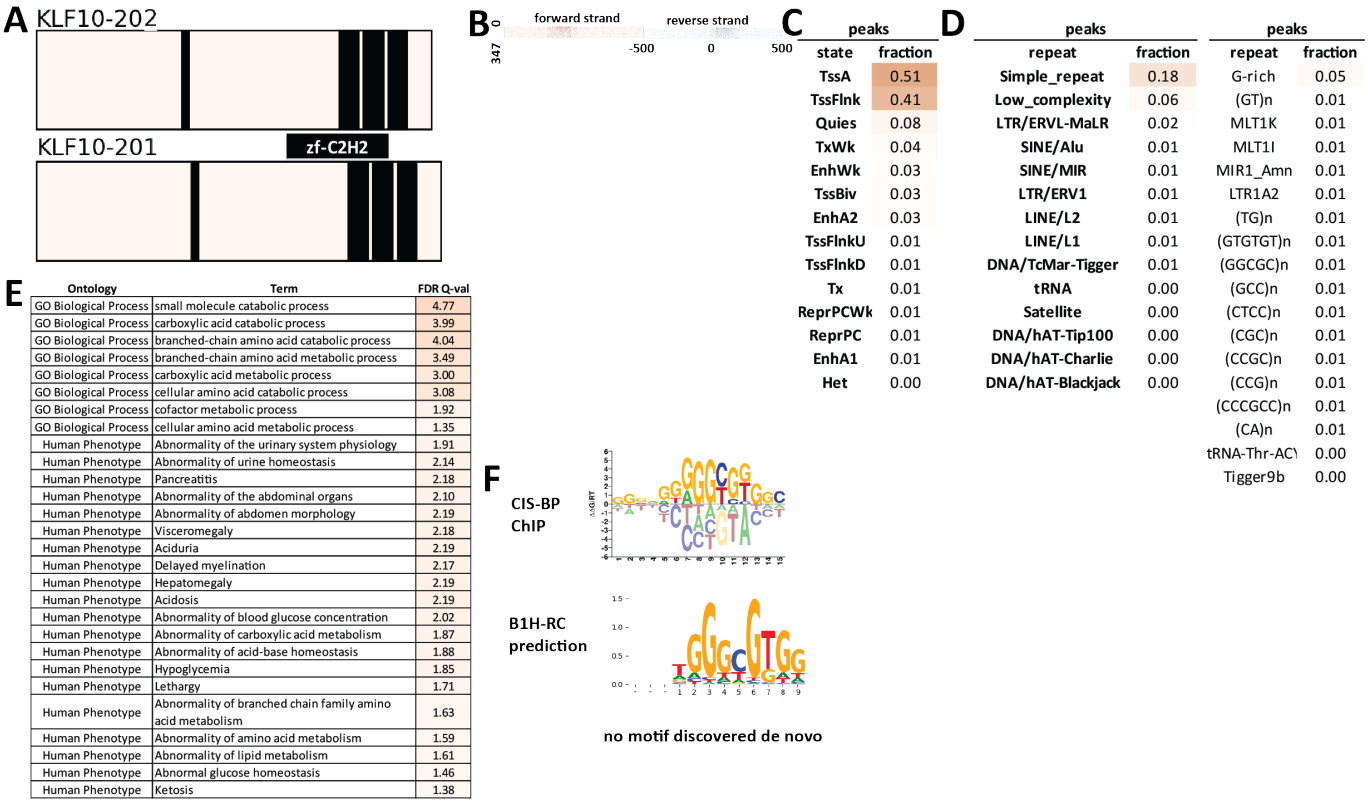

Supplementary Figure 92: Properties and genomic distribution of motifs identified for the KLF10 transcription factor in HEK293 (accession Hughes NB models).

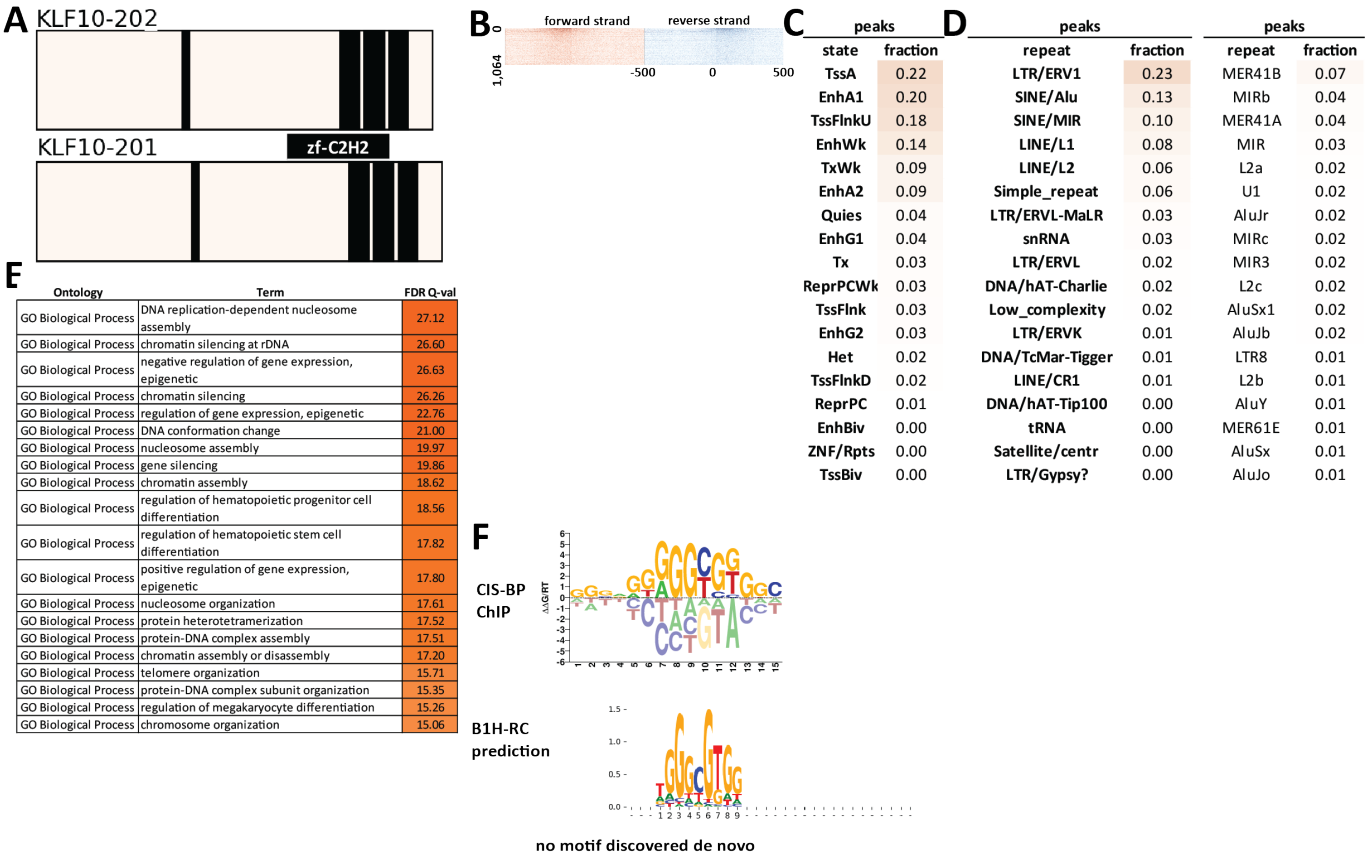

Supplementary Figure 93: Properties and genomic distribution of motifs identified for the KLF10 transcription factor in K562 (accession ENCSR121SPB).

A

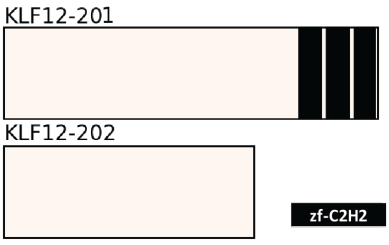

B

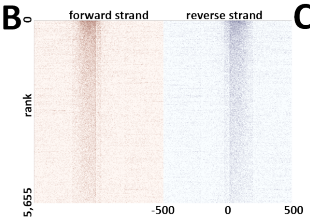

C

peaks	
state	fraction
TssA	0.54
TssFlnk	0.31
TssBiv	0.06
Quies	0.05
TxWk	0.04
EnhWk	0.02
EnhA2	0.02
ReprPC	0.02
Tx	0.02
TssFlnkU	0.02
ReprPCWk	0.01
TssFlnkD	0.01
EnhA1	0.01
EnhBiv	0.00
EnhG1	0.00
EnhG2	0.00
Het	0.00
ZNF/Rpts	0.00

D

peaks		peaks	
repeat	fraction	repeat	fraction
Simple_repeat	0.22	G-rich	0.06
Low_complexity	0.07	(GCCCC)n	0.01
SINE/MIR	0.01	GA-rich	0.01
SINE/Alu	0.01	(GGCGG)n	0.01
LINE/L2	0.01	(CCGCC)n	0.01
LINE/L1	0.00	(GGC)n	0.01
LTR/ERV1	0.00	(CCCGC)n	0.01
DNA/hAT-Charlie	0.00	MIRb	0.00
LTR/ERVL-MaLR	0.00	(CGCCC)n	0.00
DNA/hAT-Tip100	0.00	(CCCCG)n	0.00
tRNA	0.00	(GCG)n	0.00
LTR/ERVL	0.00	(GCC)n	0.00
DNA/TcMar-Tigger	0.00	L2a	0.00
Satellite	0.00	(CGG)n	0.00
LINE/CR1	0.00	L2b	0.00
LTR/Gypsy	0.00	(CGC)n	0.00
DNA/hAT-Blackjack	0.00	(CCG)n	0.00
rRNA	0.00	MIR3	0.00

E

Ontology	Term	FDR Q-val
GO Biological Process	cellular component disassembly involved in execution phase of apoptosis	3.93
GO Biological Process	regulation of mitochondrial membrane permeability	3.89
GO Biological Process	virion assembly	3.64
GO Biological Process	posttranscriptional gene silencing	3.38
GO Biological Process	posttranscriptional gene silencing by RNA	3.26
GO Biological Process	gene silencing by miRNA	3.25
GO Biological Process	interleukin-12-mediated signaling pathway	3.19
GO Biological Process	positive regulation of mitochondrial outer membrane permeabilization involved in apoptotic signaling pathway	3.12
GO Biological Process	translesion synthesis	3.00
GO Biological Process	regulation of cholesterol metabolic process	2.96
GO Biological Process	regulation of mitochondrial outer membrane permeabilization involved in apoptotic signaling pathway	2.86
GO Biological Process	production of miRNAs involved in gene silencing by miRNA	2.75
GO Biological Process	apoptotic DNA fragmentation	2.38
GO Biological Process	establishment of Golgi localization	2.28
GO Biological Process	production of small RNA involved in gene silencing by RNA	2.04
GO Biological Process	DNA catabolic process, endonucleolytic	1.99
GO Biological Process	nucleotide-excision repair, DNA gap filling	1.37

F

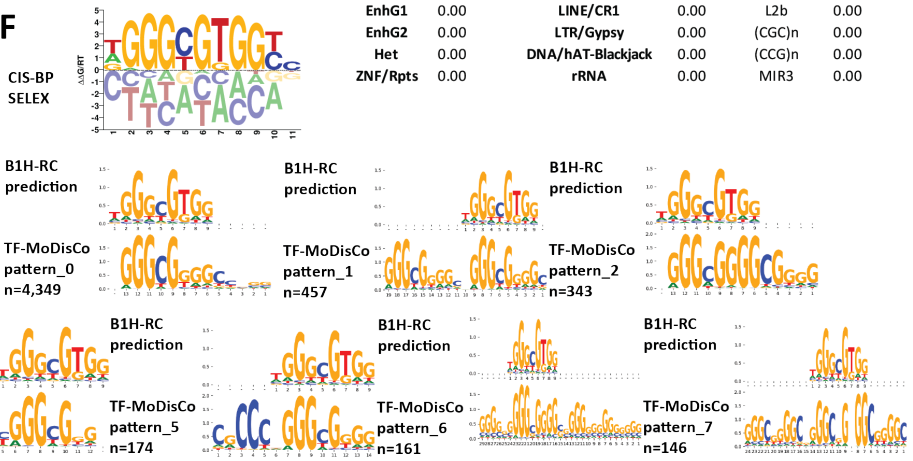

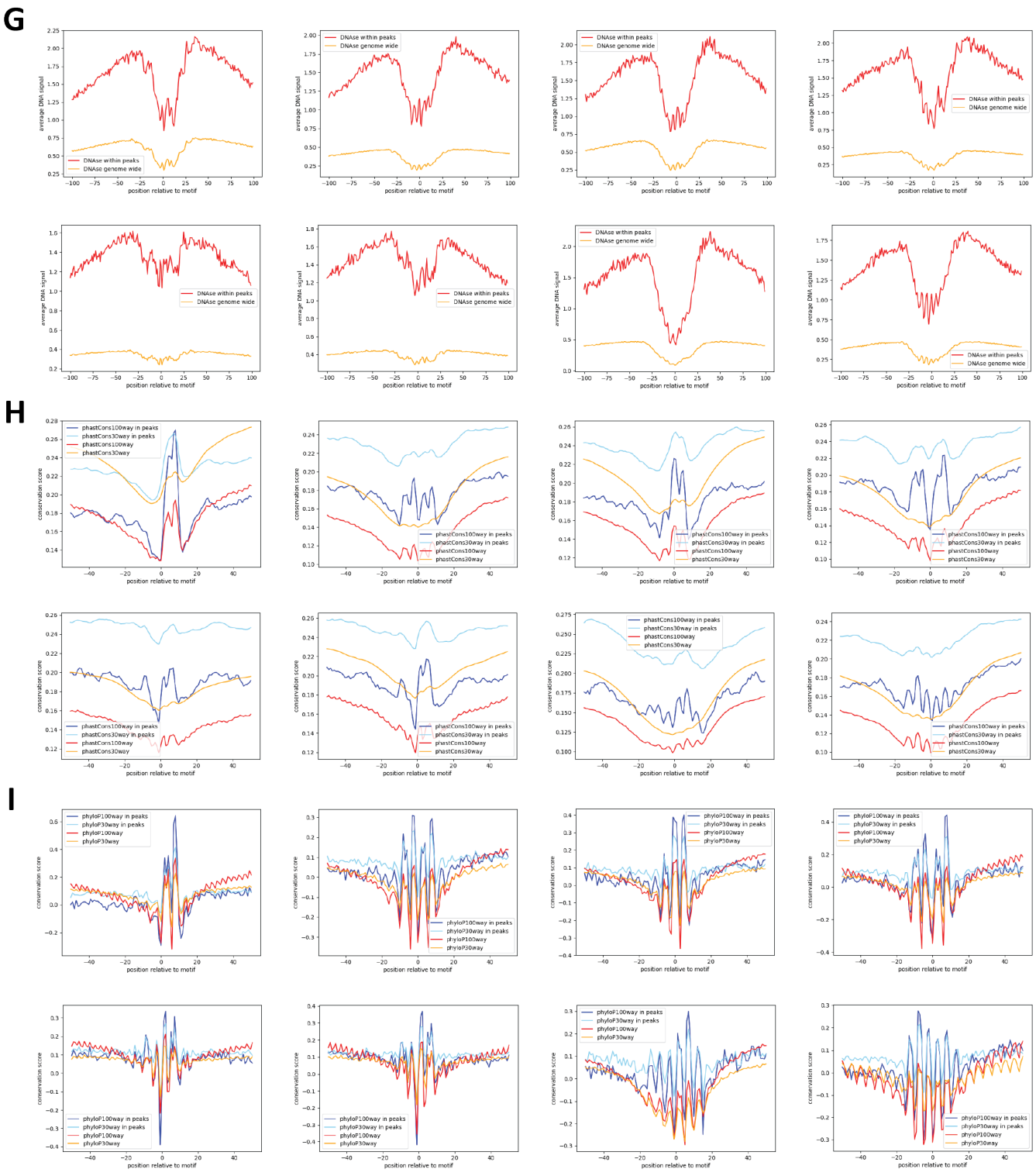

Supplementary Figure 94: Properties and genomic distribution of motifs identified for the KLF12 transcription factor in HEK293 (accession Hughes GR models).

TF-MoDisCO pattern_0 n=4349, CWM

pattern_0, n=4349; subpattern_0, ns=759

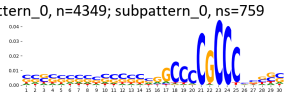

pattern_0, n=4349; subpattern_1, ns=642

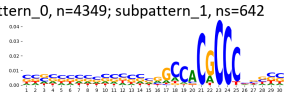

pattern_0, n=4349; subpattern_10, ns=138

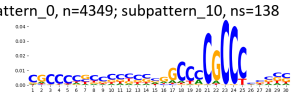

pattern_0, n=4349; subpattern_11, ns=110

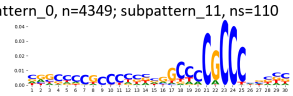

pattern_0, n=4349; subpattern_12, ns=73

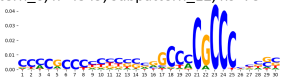

pattern_0, n=4349; subpattern_13, ns=68

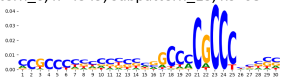

pattern_0, n=4349; subpattern_14, ns=64

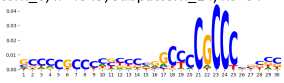

pattern_0, n=4349; subpattern_15, ns=54

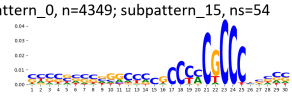

pattern_0, n=4349; subpattern_16, ns=47

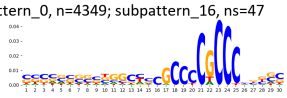

pattern_0, n=4349; subpattern_17, ns=33

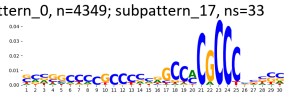

pattern_0, n=4349; subpattern_2, ns=564

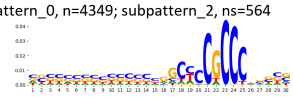

pattern_0, n=4349; subpattern_3, ns=381

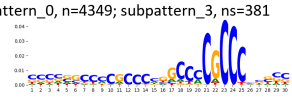

pattern_0, n=4349; subpattern_4, ns=337

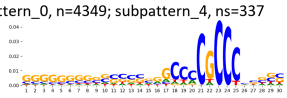

pattern_0, n=4349; subpattern_5, ns=242

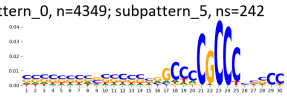

pattern_0, n=4349; subpattern_6, ns=235

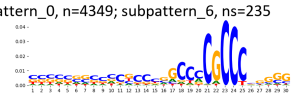

pattern_0, n=4349; subpattern_7, ns=219

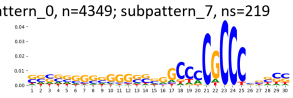

pattern_0, n=4349; subpattern_8, ns=217

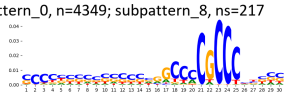

pattern_0, n=4349; subpattern_9, ns=166

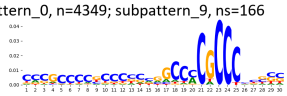

TF-MoDisCO pattern_0 n=4349, PWM

pattern_0, n=4349; subpattern_0, ns=759

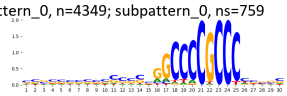

pattern_0, n=4349; subpattern_1, ns=642

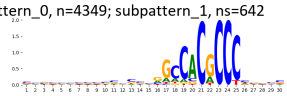

pattern_0, n=4349; subpattern_10, ns=138

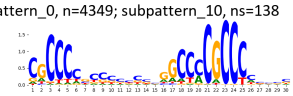

pattern_0, n=4349; subpattern_11, ns=110

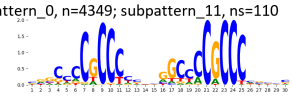

pattern_0, n=4349; subpattern_12, ns=73

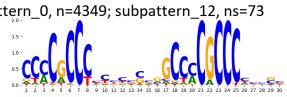

pattern_0, n=4349; subpattern_13, ns=68

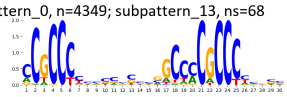

pattern_0, n=4349; subpattern_14, ns=64

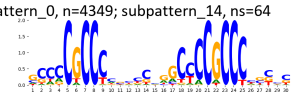

pattern_0, n=4349; subpattern_15, ns=54

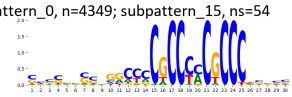

pattern_0, n=4349; subpattern_16, ns=47

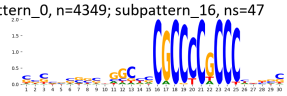

pattern_0, n=4349; subpattern_17, ns=33

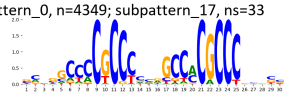

pattern_0, n=4349; subpattern_2, ns=564

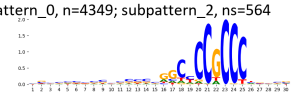

pattern_0, n=4349; subpattern_3, ns=381

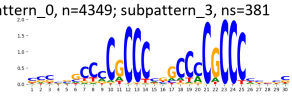

pattern_0, n=4349; subpattern_4, ns=337

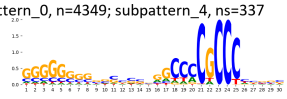

pattern_0, n=4349; subpattern_5, ns=242

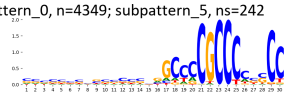

pattern_0, n=4349; subpattern_6, ns=235

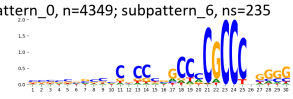

pattern_0, n=4349; subpattern_7, ns=219

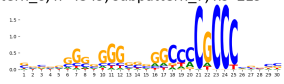

pattern_0, n=4349; subpattern_8, ns=217

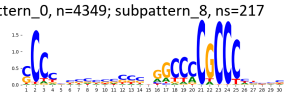

pattern_0, n=4349; subpattern_9, ns=166

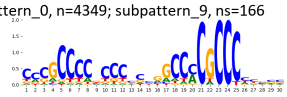

TF-MoDisCO pattern_1 n=457, CWM

pattern_1, n=457; subpattern_0, ns=123

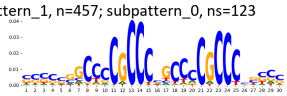

pattern_1, n=457; subpattern_1, ns=108

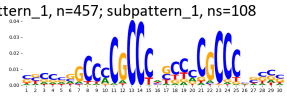

pattern_1, n=457; subpattern_2, ns=98

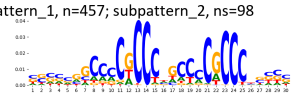

pattern_1, n=457; subpattern_3, ns=58

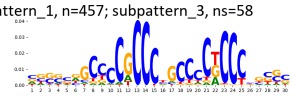

pattern_1, n=457; subpattern_4, ns=42

pattern_1, n=457; subpattern_5, ns=23

pattern_1, n=457; subpattern_6, ns=5

TF-MoDisCO pattern_1 n=457, PWM

pattern_1, n=457; subpattern_0, ns=123

pattern_1, n=457; subpattern_1, ns=108

pattern_1, n=457; subpattern_2, ns=98

pattern_1, n=457; subpattern_3, ns=58

pattern_1, n=457; subpattern_4, ns=42

pattern_1, n=457; subpattern_5, ns=23

pattern_1, n=457; subpattern_6, ns=5

TF-MoDisCO pattern_2 n=343, CWM

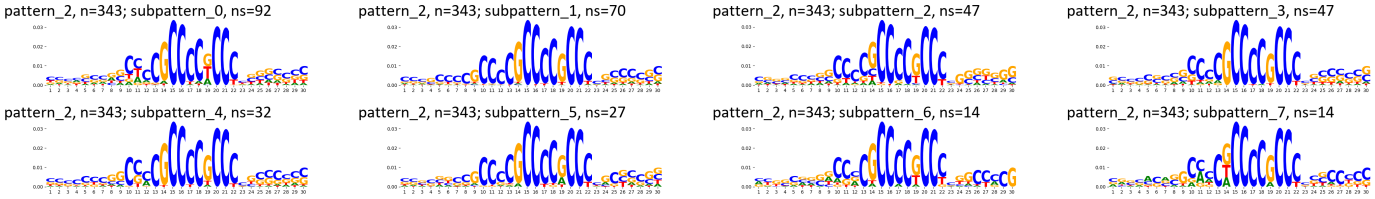

TF-MoDisCO pattern_2 n=343, PWM

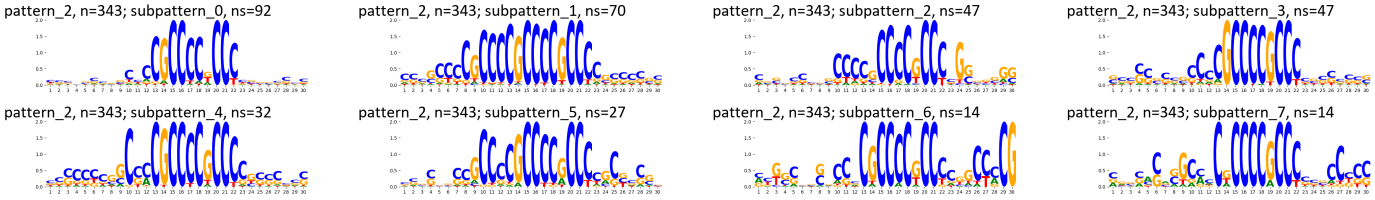

TF-MoDisCO pattern_3 n=285, CWM

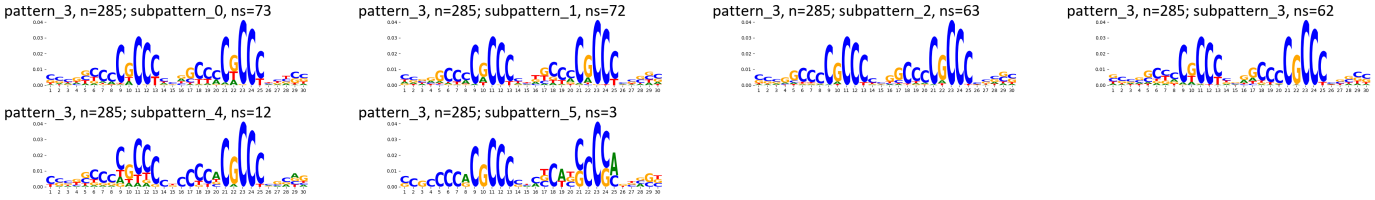

TF-MoDisCO pattern_3 n=285, PWM

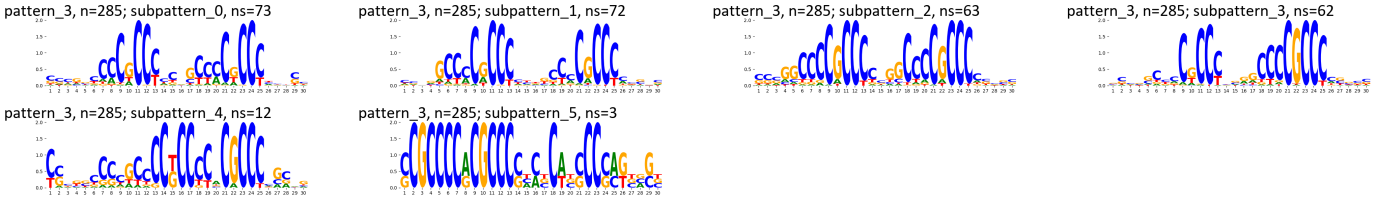

TF-MoDisCO pattern_4 n=275, CWM

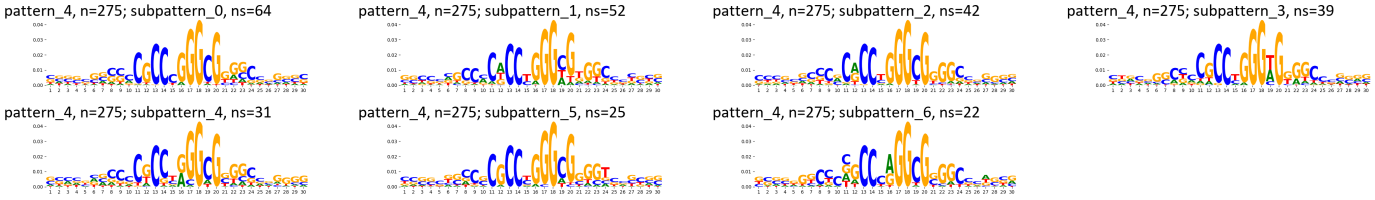

TF-MoDisCO pattern_4 n=275, PWM

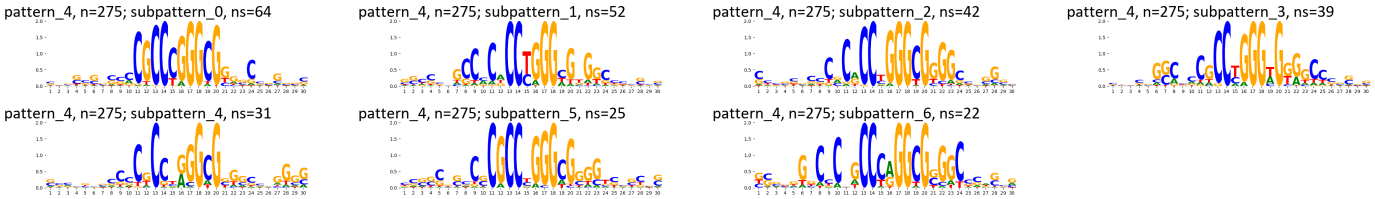

TF-MoDisCO pattern_5 n=174, CWM

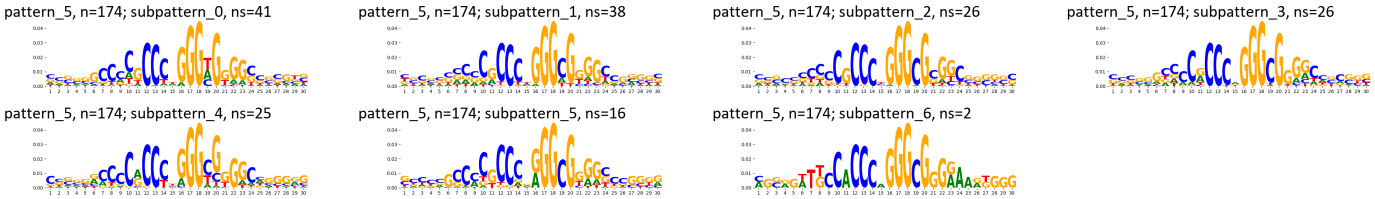

TF-MoDisCO pattern_5 n=174, PWM

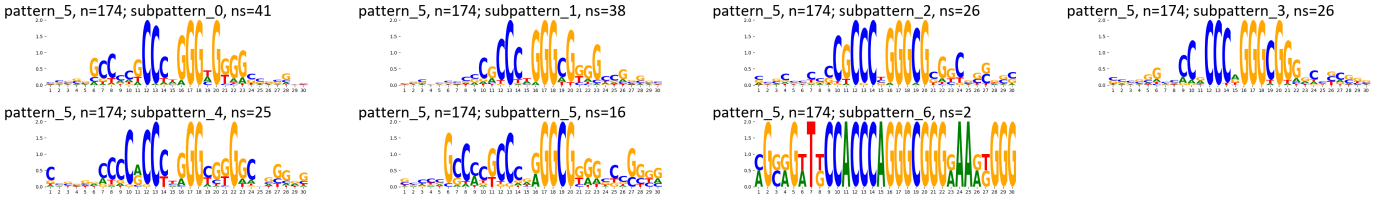

TF-MoDisCO pattern_6 n=161, CWM

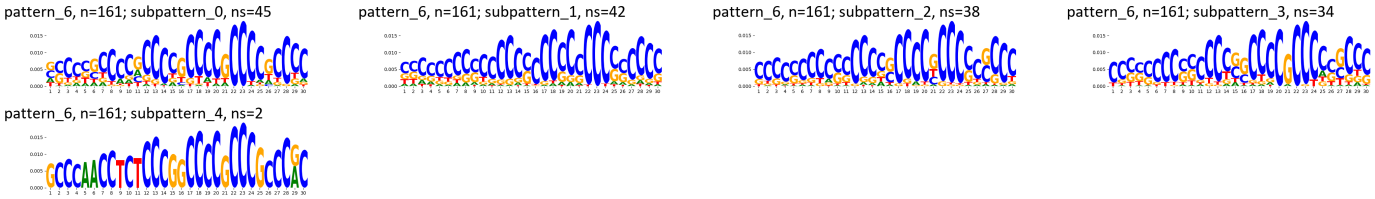

TF-MoDisCO pattern_6 n=161, PWM

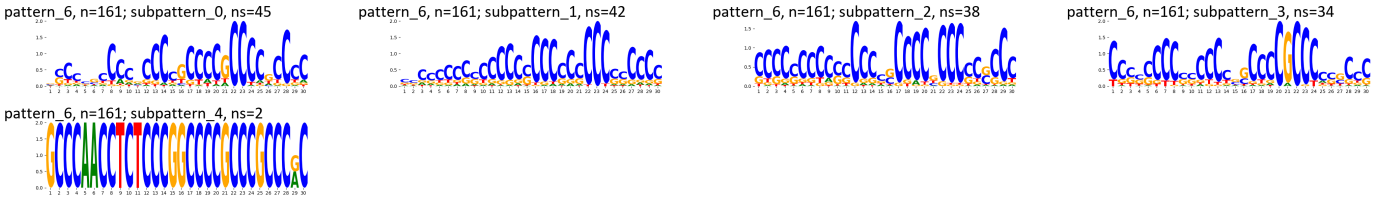

TF-MoDisCO pattern_7 n=146, CWM

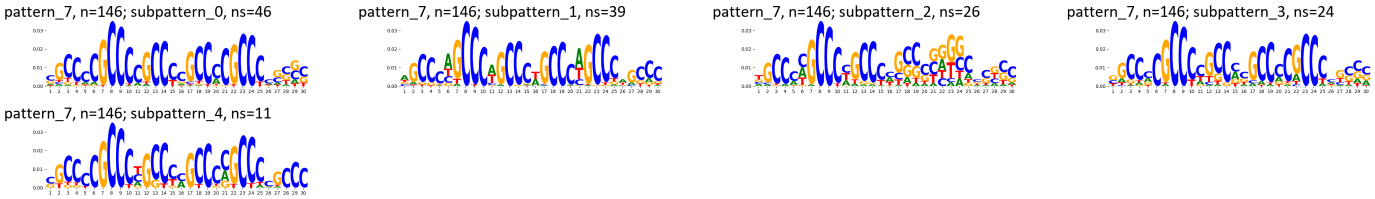

TF-MoDisCO pattern_7 n=146, PWM

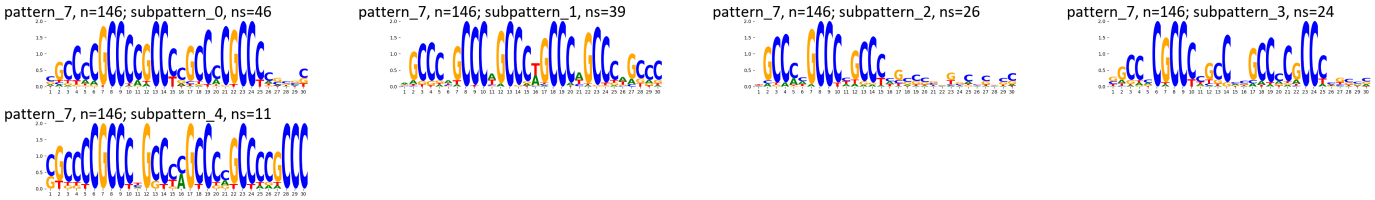

Supplementary Figure 95: TF-MoDisCO subpatterns for the KLF12 transcription factor in HEK293 (accession Hughes GR models).

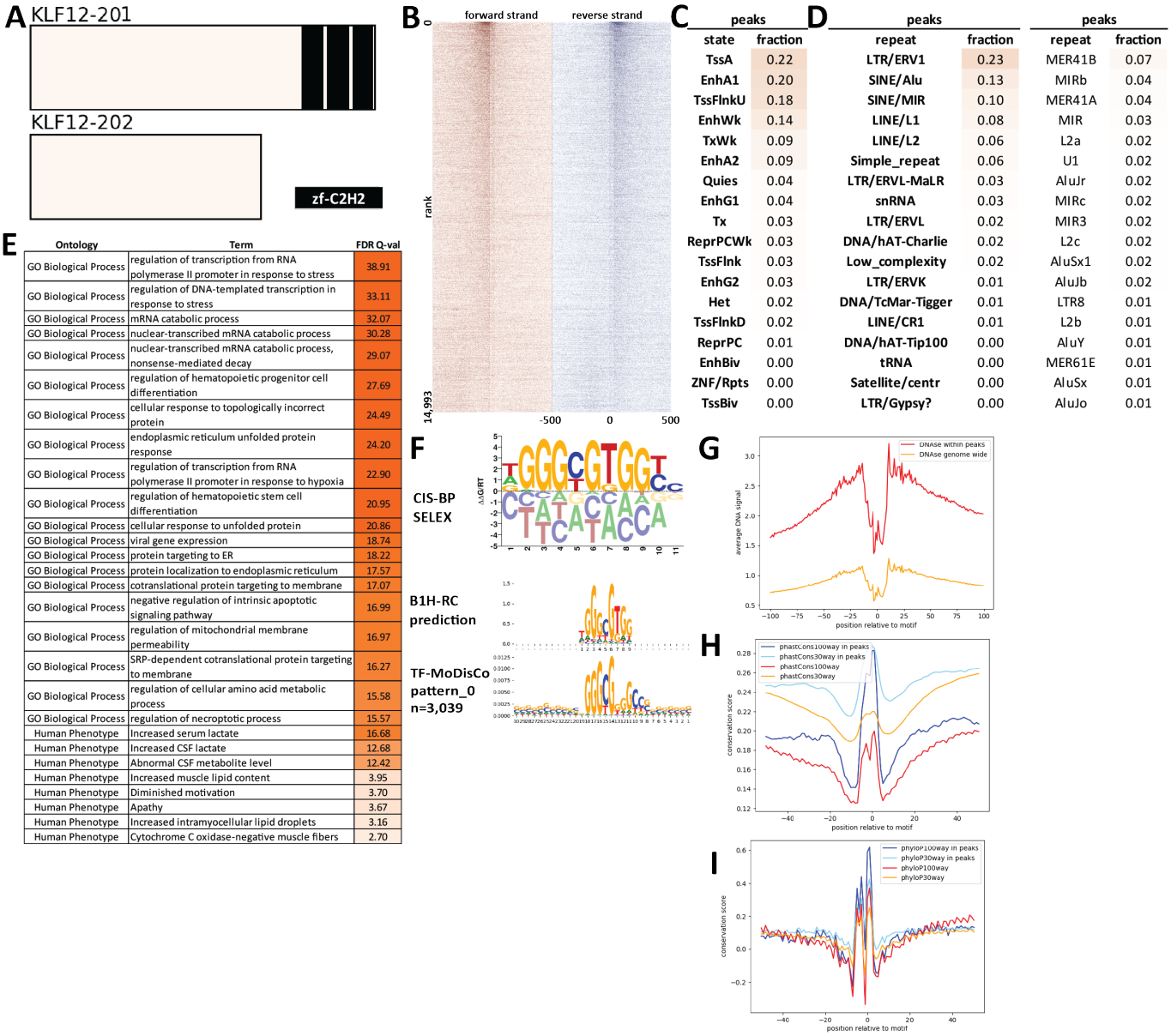

Supplementary Figure 96: Properties and genomic distribution of motifs identified for the KLF12 transcription factor in HepG2 (accession ENCSR552YWL).

TF-MoDisCO pattern_0 n=3039, CWM

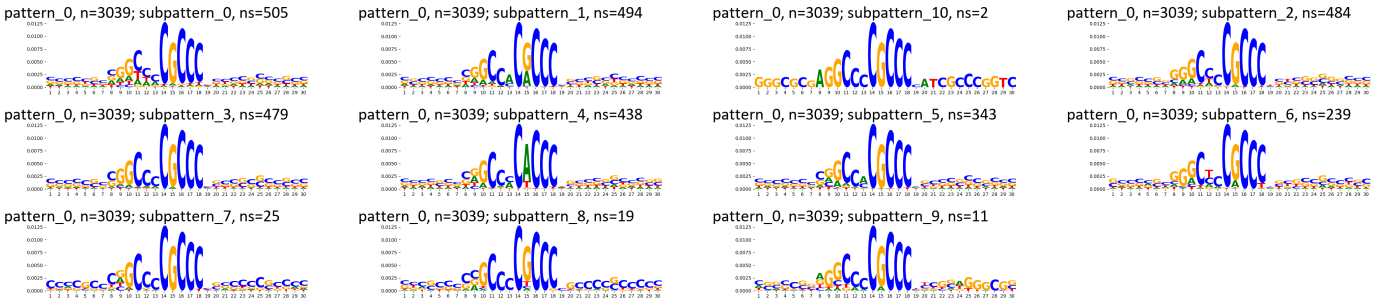

TF-MoDisCO pattern_0 n=3039, PWM

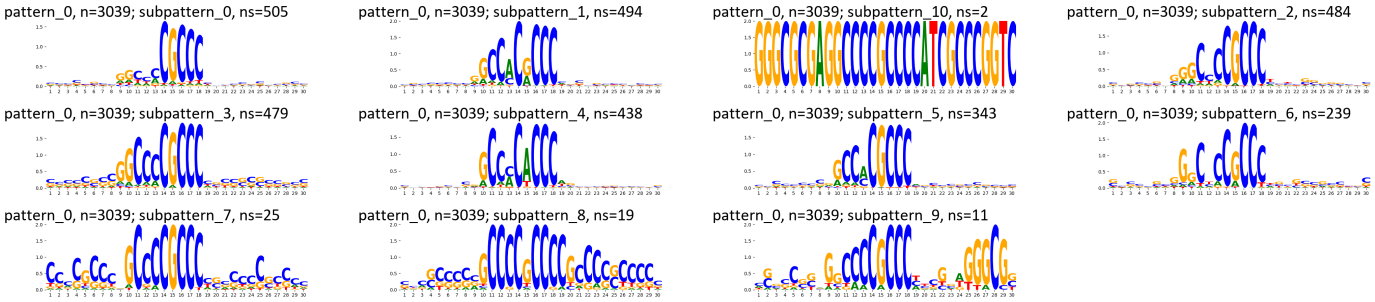

Supplementary Figure 97: TF-MoDisCO subpatterns for the KLF12 transcription factor in HepG2 (accession ENCSR552YWL).

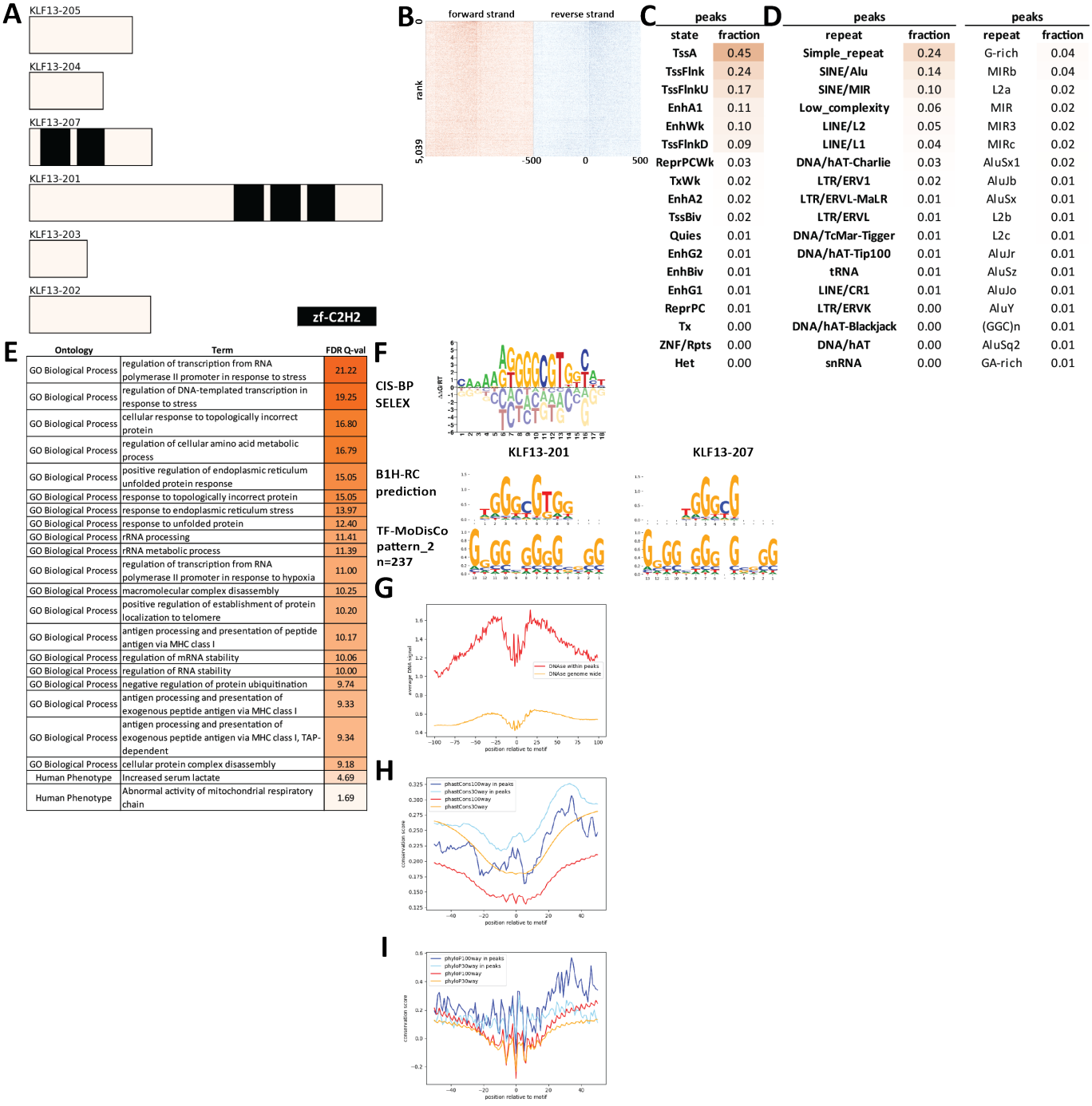

Supplementary Figure 98: Properties and genomic distribution of motifs identified for the KLF13 transcription factor in HepG2 (accession ENCSR756SZU).

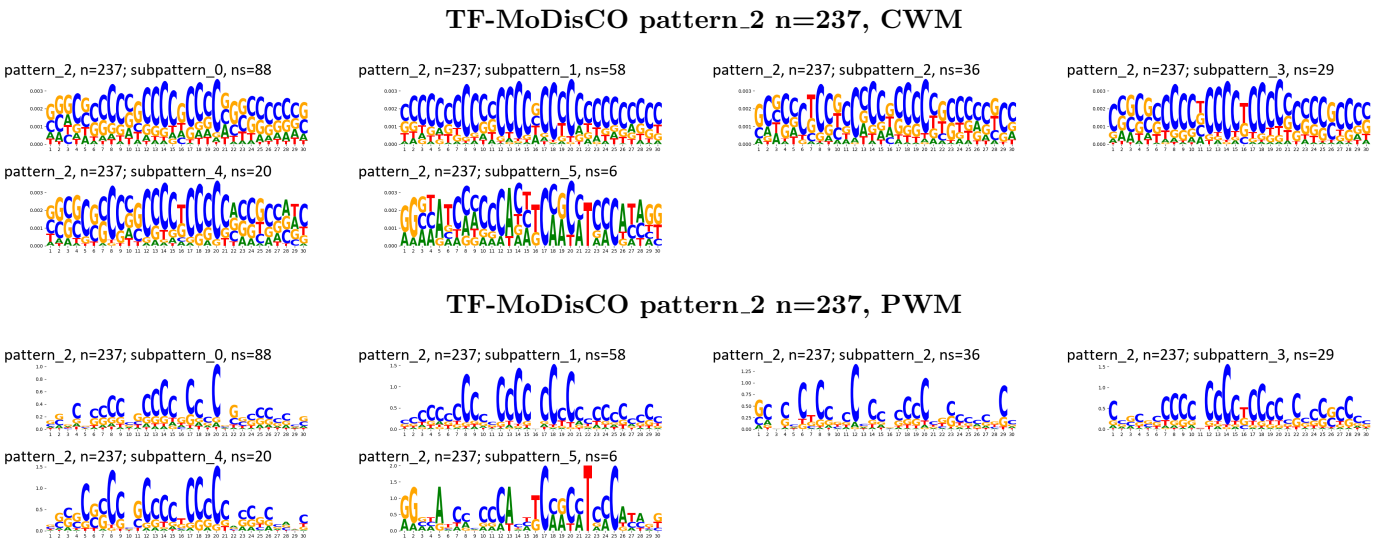

Supplementary Figure 99: TF-MoDisCO subpatterns for the KLF13 transcription factor in HepG2 (accession ENCSR756SZU).

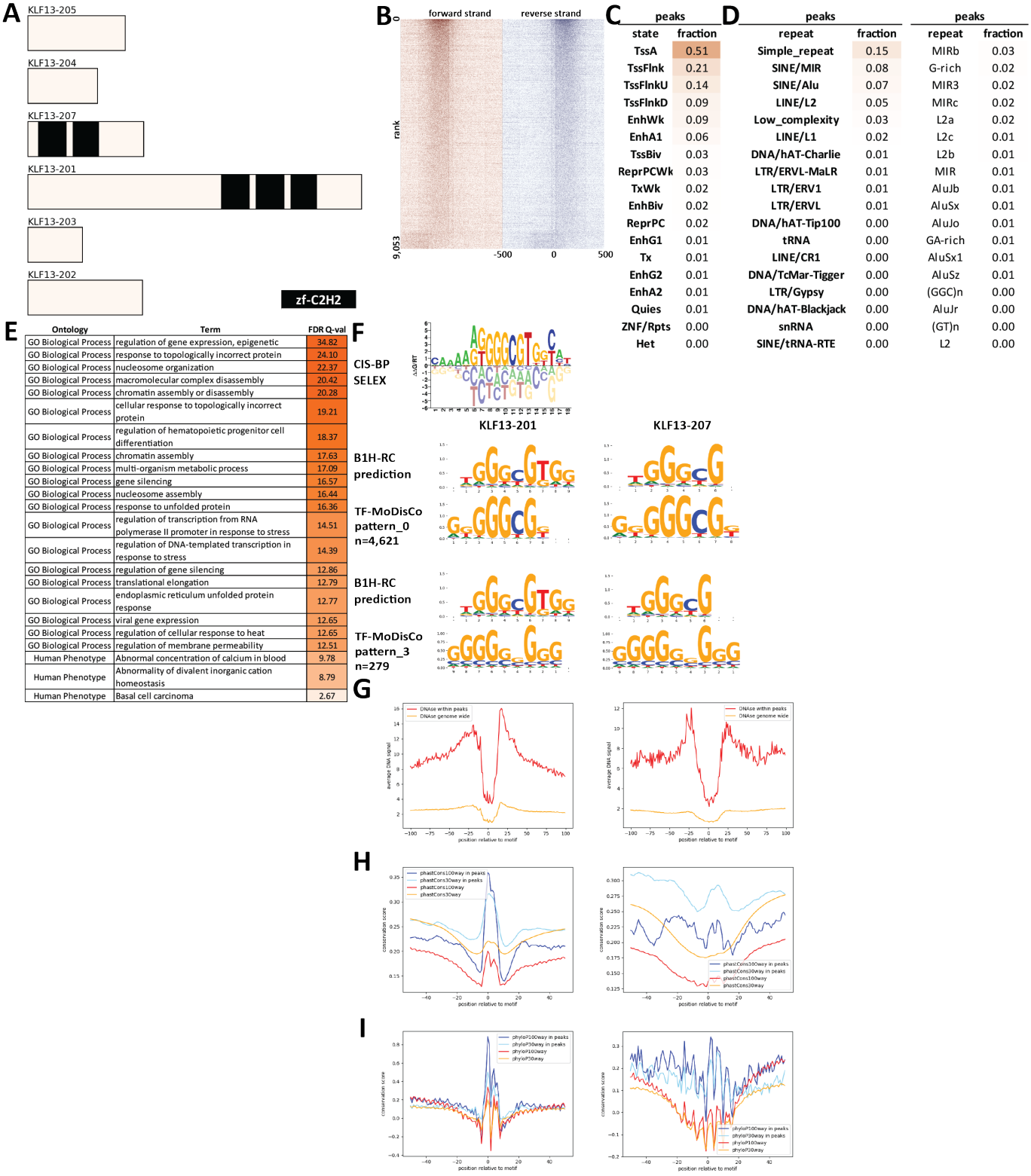

Supplementary Figure 100: Properties and genomic distribution of motifs identified for the KLF13 transcription factor in K562 (accession ENCSR608HVP).

TF-MoDisCO pattern_0 n=4621, CWM

pattern_0, n=4621; subpattern_0, ns=1002

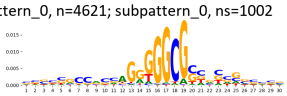

pattern_0, n=4621; subpattern_1, ns=939

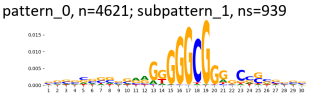

pattern_0, n=4621; subpattern_2, ns=906

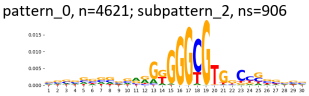

pattern_0, n=4621; subpattern_3, ns=893

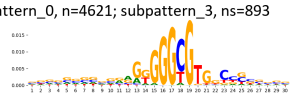

pattern_0, n=4621; subpattern_4, ns=822

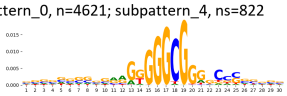

pattern_0, n=4621; subpattern_5, ns=52

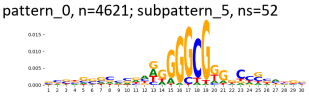

pattern_0, n=4621; subpattern_6, ns=3

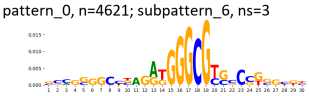

pattern_0, n=4621; subpattern_7, ns=2

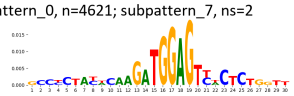

pattern_0, n=4621; subpattern_8, ns=2

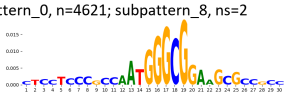

TF-MoDisCO pattern_0 n=4621, PWM

pattern_0, n=4621; subpattern_0, ns=1002

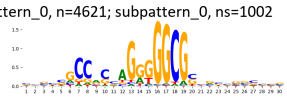

pattern_0, n=4621; subpattern_1, ns=939

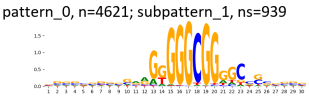

pattern_0, n=4621; subpattern_2, ns=906

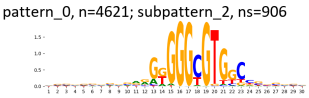

pattern_0, n=4621; subpattern_3, ns=893

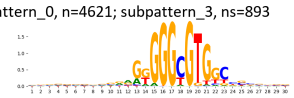

pattern_0, n=4621; subpattern_4, ns=822

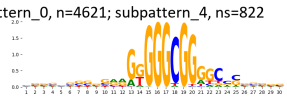

pattern_0, n=4621; subpattern_5, ns=52

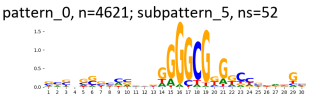

pattern_0, n=4621; subpattern_6, ns=3

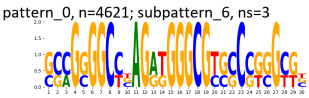

pattern_0, n=4621; subpattern_7, ns=2

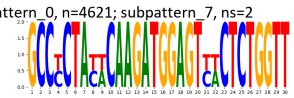

pattern_0, n=4621; subpattern_8, ns=2

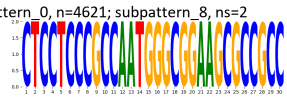

TF-MoDisCO pattern_3 n=279, CWM

pattern_3, n=279; subpattern_0, ns=113

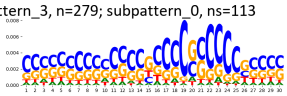

pattern_3, n=279; subpattern_1, ns=106

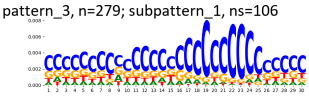

pattern_3, n=279; subpattern_2, ns=49

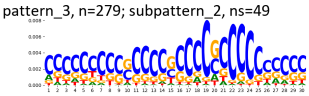

pattern_3, n=279; subpattern_3, ns=6

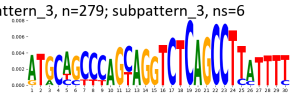

pattern_3, n=279; subpattern_4, ns=3

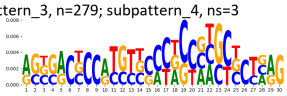

pattern_3, n=279; subpattern_5, ns=2

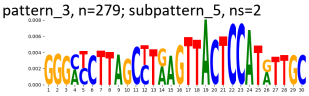

TF-MoDisCO pattern_3 n=279, PWM

pattern_3, n=279; subpattern_0, ns=113

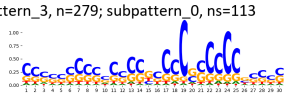

pattern_3, n=279; subpattern_1, ns=106

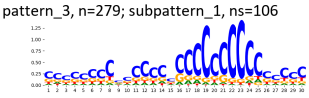

pattern_3, n=279; subpattern_2, ns=49

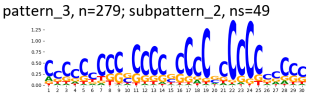

pattern_3, n=279; subpattern_3, ns=6

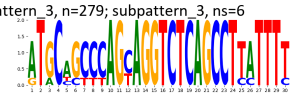

pattern_3, n=279; subpattern_4, ns=3

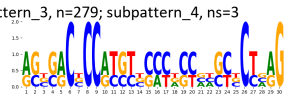

pattern_3, n=279; subpattern_5, ns=2

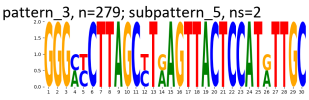

Supplementary Figure 101: TF-MoDisCO subpatterns for the KLF13 transcription factor in K562 (accession ENCSR608HVP).

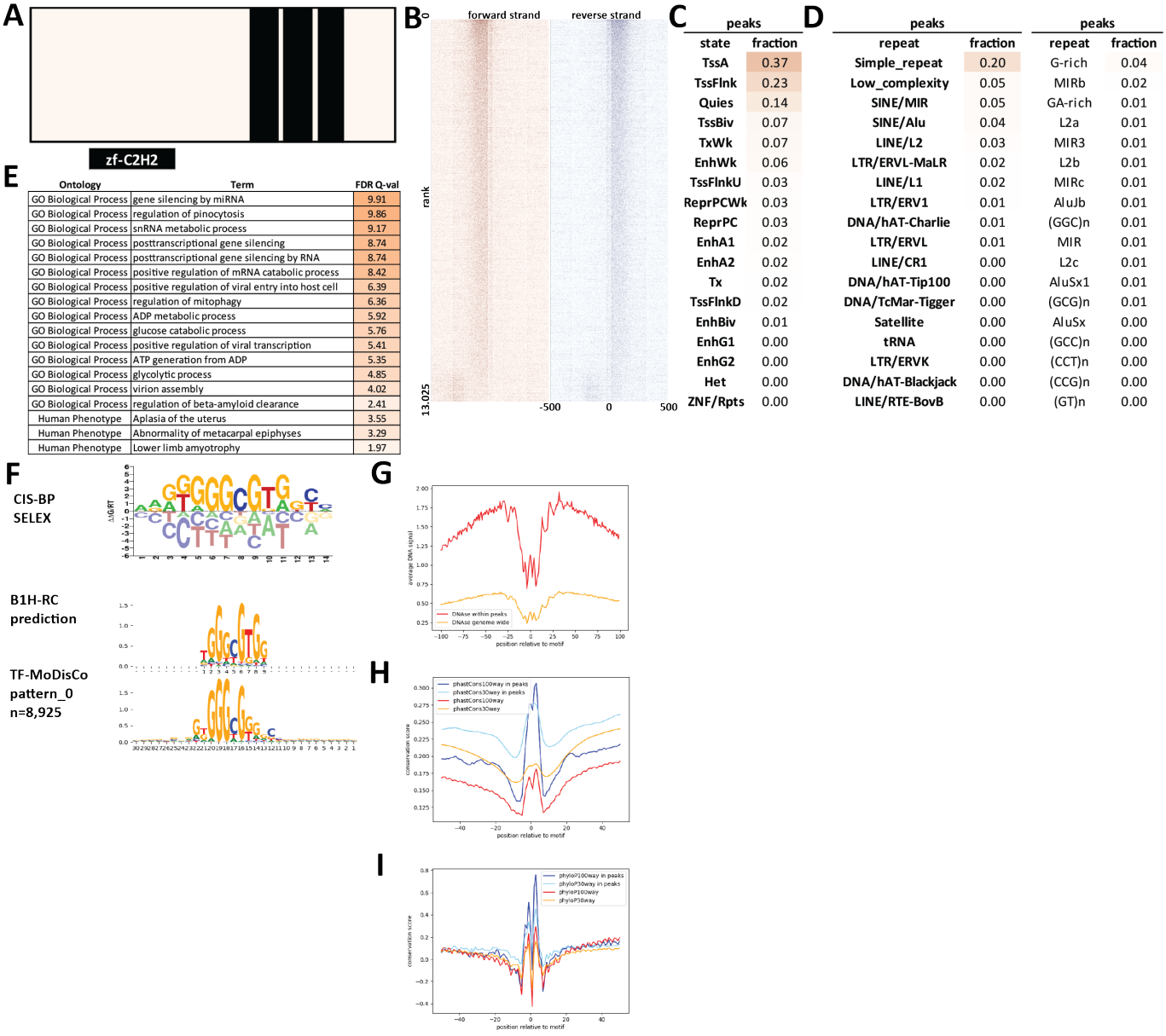

Supplementary Figure 102: Properties and genomic distribution of motifs identified for the KLF14 transcription factor in HEK293 (accession Hughes NB models).

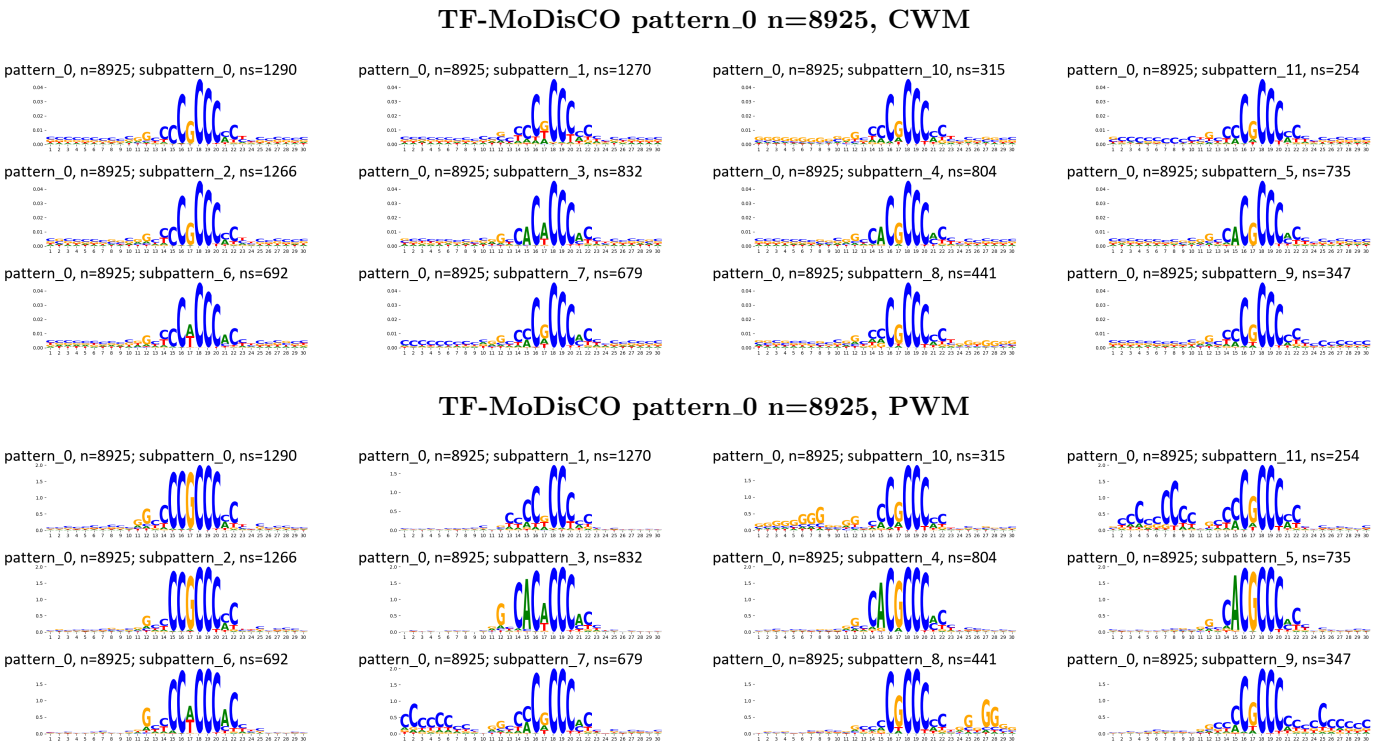

Supplementary Figure 103: TF-MoDisCO subpatterns for the KLF14 transcription factor in HEK293 (accession Hughes NB models).

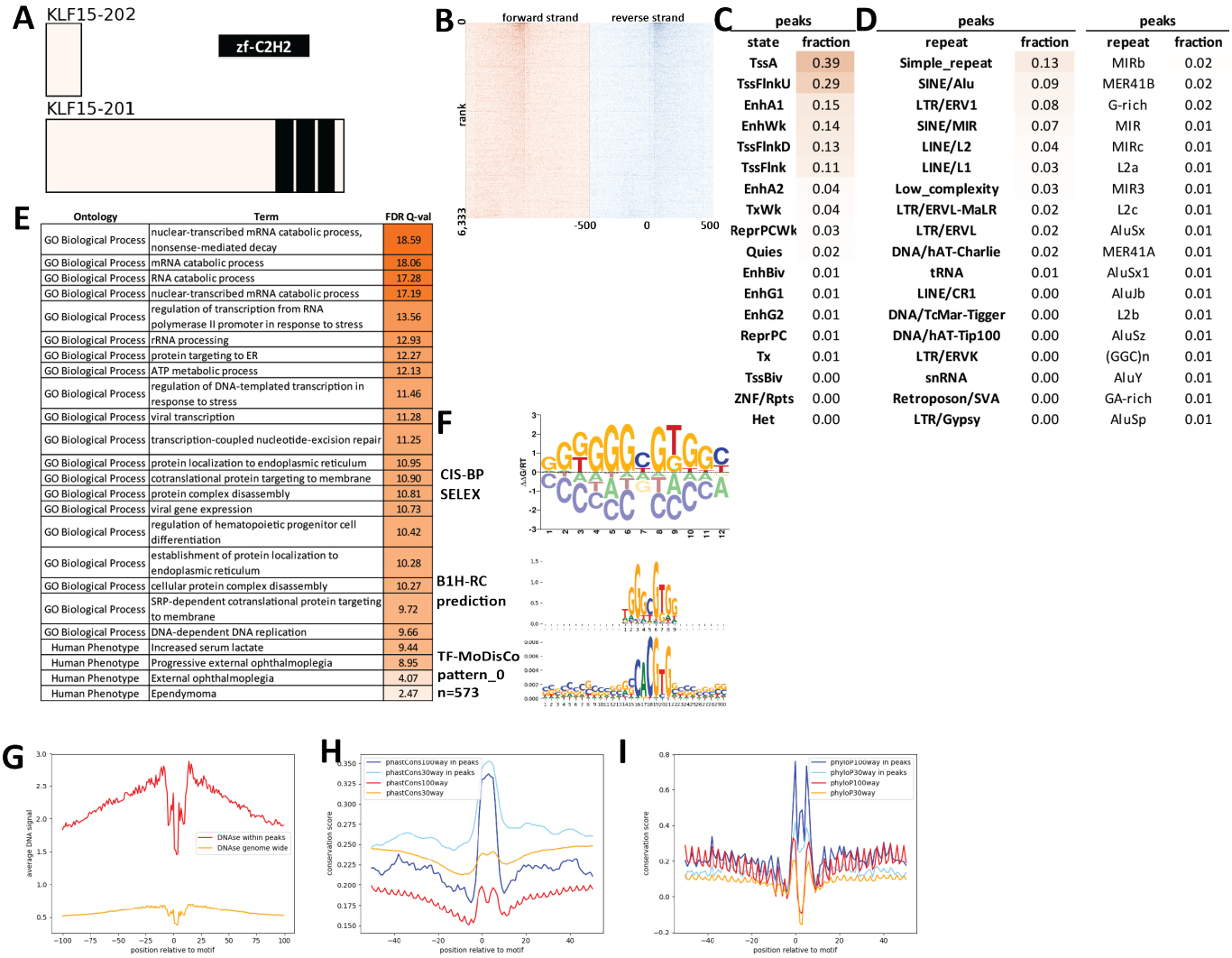

Supplementary Figure 104: Properties and genomic distribution of motifs identified for the KLF15 transcription factor in HepG2 (accession ENCSR860ONE).

TF-MoDisCO pattern_0 n=573, CWM

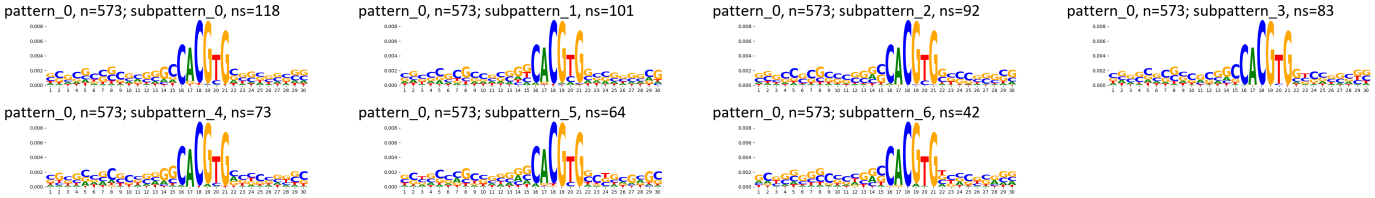

TF-MoDisCO pattern_0 n=573, PWM

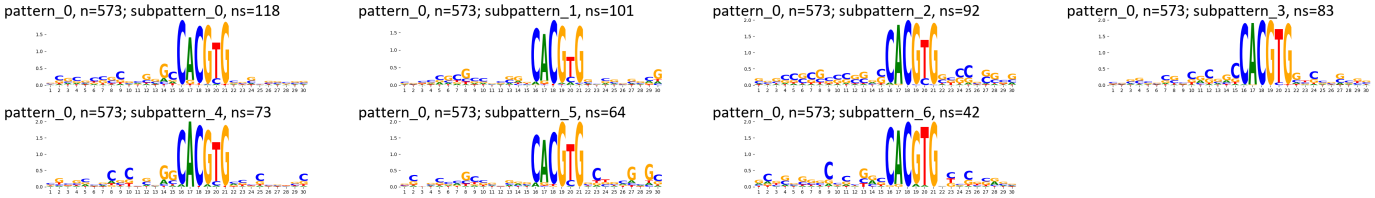

TF-MoDisCO pattern_1 n=357, CWM



TF-MoDisCO pattern_1 n=357, PWM

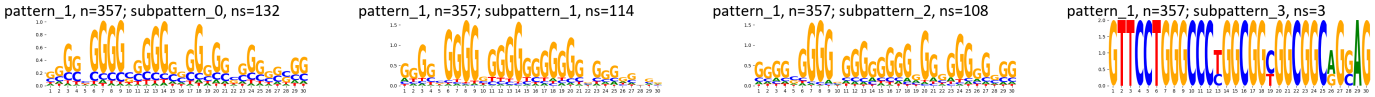

TF-MoDisCO pattern_4 n=255, CWM

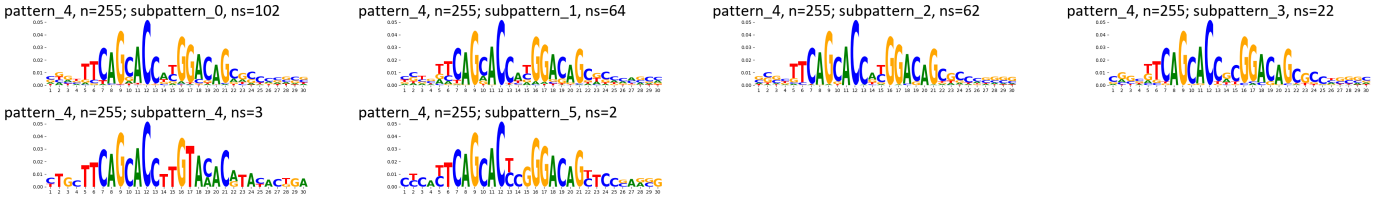

TF-MoDisCO pattern_4 n=255, PWM

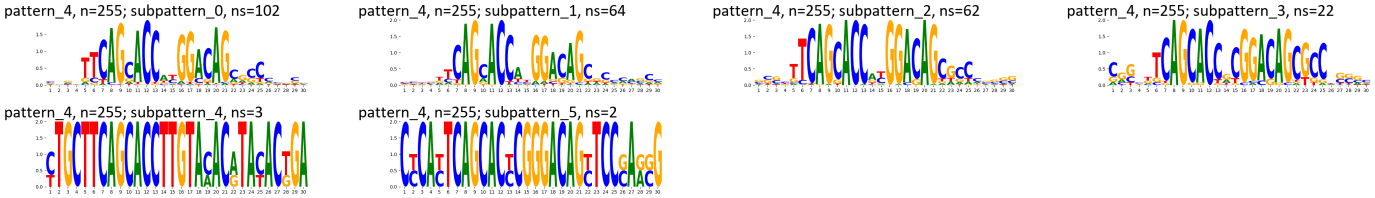

Supplementary Figure 105: TF-MoDisCO subpatterns for the KLF15 transcription factor in HepG2 (accession ENCSR860ONE).

A

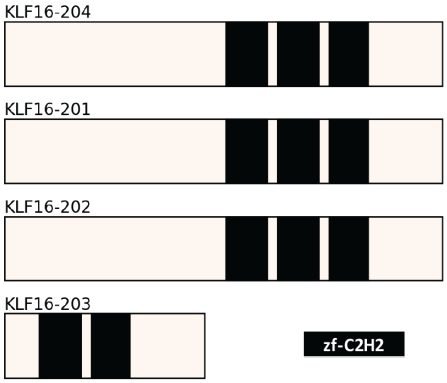

B

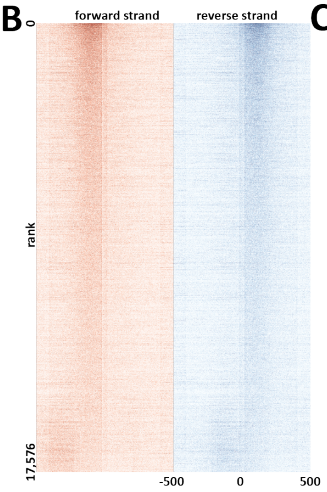

C

peaks	
state	fraction
TssA	0.57
TssFlnk	0.25
TssFlnkU	0.13
TssFlnkD	0.07
EnhA1	0.05
EnhWk	0.04
ReprPCWk	0.03
TssBiv	0.02
EnhA2	0.02
TxWk	0.01
EnhBiv	0.01
Quies	0.01
ReprPC	0.01
EnhG2	0.01
EnhG1	0.00
Tx	0.00
ZNF/Rpts	0.00
Het	0.00

D

peaks		peaks	
repeat	fraction	repeat	fraction
Simple_repeat	0.19	G-rich	0.03
SINE/Alu	0.06	MIRb	0.02
SINE/MIR	0.06	L2a	0.01
Low_complexity	0.04	MIR3	0.01
LINE/L2	0.04	MIRc	0.01
LINE/L1	0.01	MIR	0.01
DNA/hAT-Charlie	0.01	L2b	0.01
LTR/ERV1	0.01	L2c	0.01
tRNA	0.01	GA-rich	0.01
LTR/ERVL-MaLR	0.00	(GGC)n	0.01
LTR/ERVL	0.00	AluSx1	0.01
LINE/CR1	0.00	AluJb	0.01
DNA/hAT-Tip100	0.00	(CCG)n	0.01
DNA/TcMar-Tigger	0.00	AluSx	0.01
snRNA	0.00	(GCC)n	0.01
DNA/hAT	0.00	AluSz	0.01
LTR/ERVK	0.00	(GCG)n	0.00
DNA/hAT-Blackjack	0.00	(CGC)n	0.00

E

Ontology	Term	FDR Q-val
GO Biological Process	nuclear-transcribed mRNA catabolic process, nonsense-mediated decay	23.91
GO Biological Process	regulation of transcription from RNA polymerase II promoter in response to stress	23.92
GO Biological Process	viral gene expression	18.03
GO Biological Process	negative regulation of ubiquitin-protein transferase activity	16.92
GO Biological Process	SRP-dependent cotranslational protein targeting to membrane	16.46
GO Biological Process	cotranslational protein targeting to membrane	15.94
GO Biological Process	positive regulation of transcription from RNA polymerase II promoter in response to endoplasmic reticulum stress	13.89
GO Biological Process	protein targeting to ER	13.38
GO Biological Process	maintenance of protein localization in organelle	11.59
GO Biological Process	termination of RNA polymerase II transcription	11.39
GO Biological Process	positive regulation of transcription from RNA polymerase II promoter in response to stress	11.32
GO Biological Process	mitochondrial translational termination	11.03
GO Biological Process	mitochondrial translational elongation	10.91
GO Biological Process	IRE1-mediated unfolded protein response	10.25
GO Biological Process	gene silencing by miRNA	9.33
GO Biological Process	positive regulation of DNA-templated transcription, elongation	8.51
GO Biological Process	negative regulation of cyclin-dependent protein serine/threonine kinase activity	8.47
GO Biological Process	'de novo' protein folding	8.05
GO Biological Process	negative regulation of cyclin-dependent protein kinase activity	7.78
GO Biological Process	cytoplasmic translation	7.62
Human Phenotype	Exercise intolerance	8.03
Human Phenotype	Increased CSF lactate	6.90
Human Phenotype	Abnormality of renal resorption	4.38
Human Phenotype	Abnormality of glycolysis	3.88

F

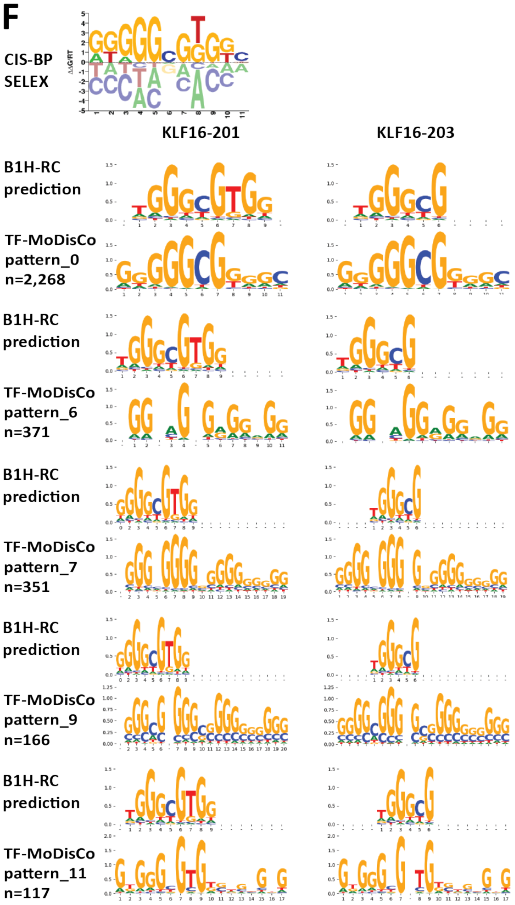

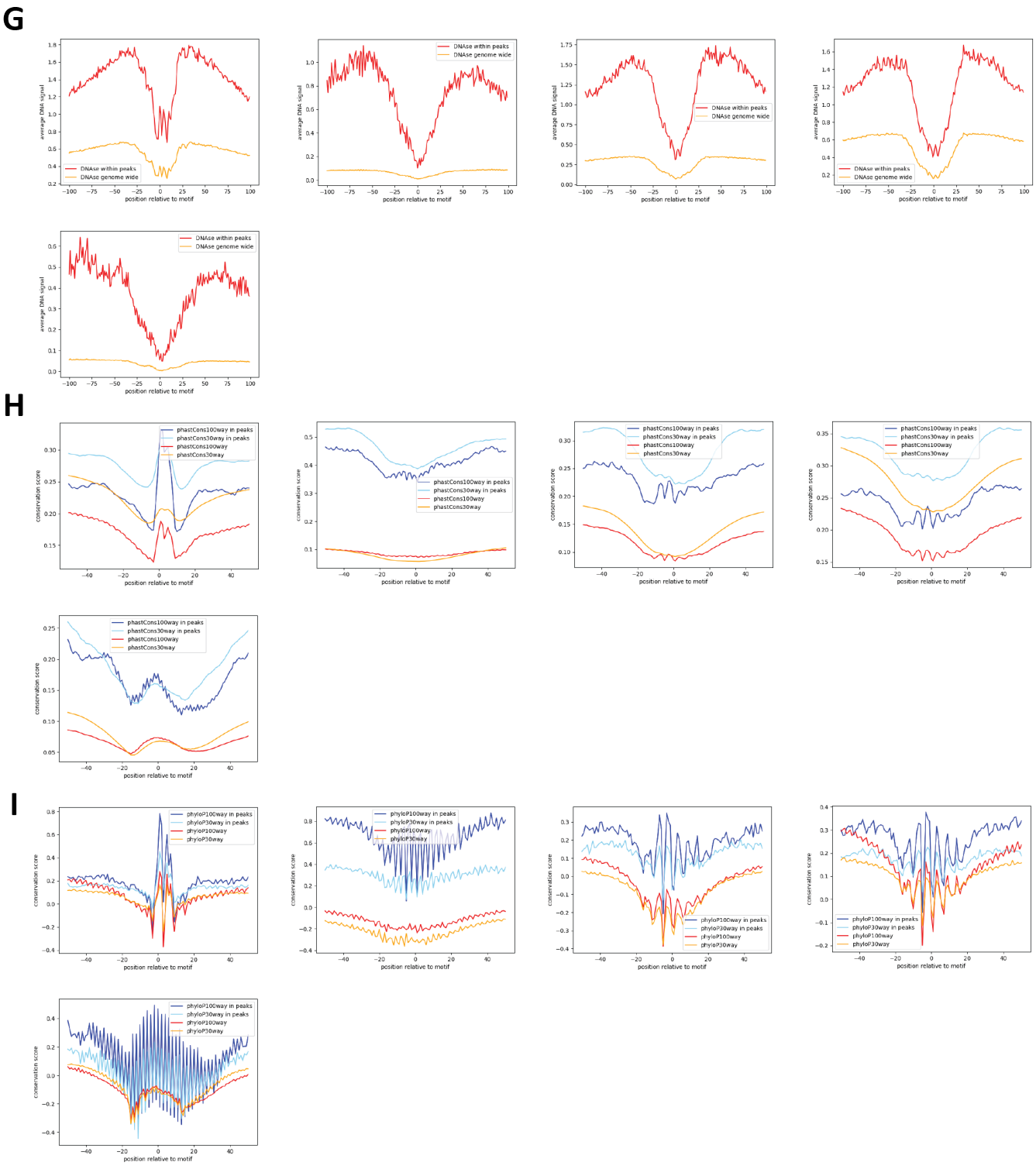

Supplementary Figure 106: Properties and genomic distribution of motifs identified for the KLF16 transcription factor in HEK293 (accession ENCSR397DQC).

TF-MoDisCO pattern_0 n=2268, CWM

pattern_0, n=2268; subpattern_0, ns=492

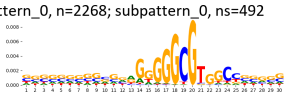

pattern_0, n=2268; subpattern_1, ns=447

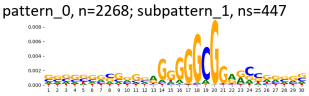

pattern_0, n=2268; subpattern_10, ns=2

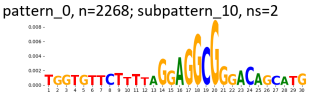

pattern_0, n=2268; subpattern_2, ns=440

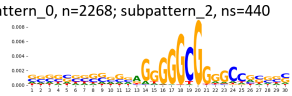

pattern_0, n=2268; subpattern_3, ns=267

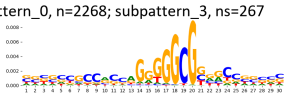

pattern_0, n=2268; subpattern_4, ns=262

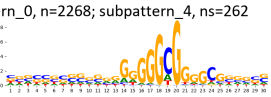

pattern_0, n=2268; subpattern_5, ns=133

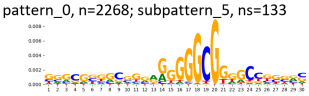

pattern_0, n=2268; subpattern_6, ns=73

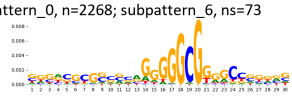

pattern_0, n=2268; subpattern_7, ns=64

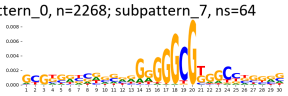

pattern_0, n=2268; subpattern_8, ns=49

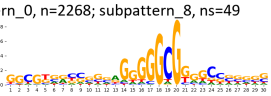

pattern_0, n=2268; subpattern_9, ns=39

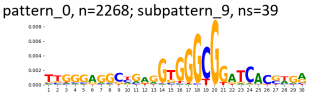

TF-MoDisCO pattern_0 n=2268, PWM

pattern_0, n=2268; subpattern_0, ns=492

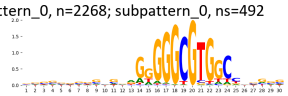

pattern_0, n=2268; subpattern_1, ns=447

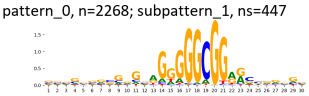

pattern_0, n=2268; subpattern_10, ns=2

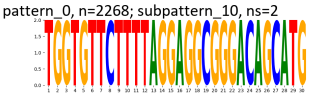

pattern_0, n=2268; subpattern_2, ns=440

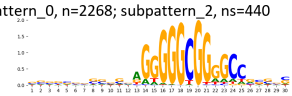

pattern_0, n=2268; subpattern_3, ns=267

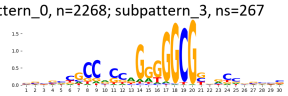

pattern_0, n=2268; subpattern_4, ns=262

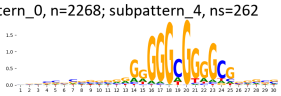

pattern_0, n=2268; subpattern_5, ns=133

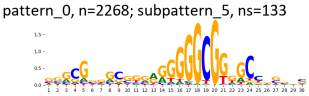

pattern_0, n=2268; subpattern_6, ns=73

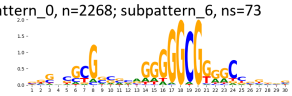

pattern_0, n=2268; subpattern_7, ns=64

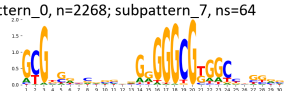

pattern_0, n=2268; subpattern_8, ns=49

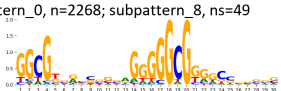

pattern_0, n=2268; subpattern_9, ns=39

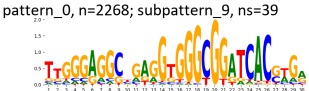

TF-MoDisCO pattern_11 n=117, CWM

pattern_11, n=117; subpattern_0, ns=39

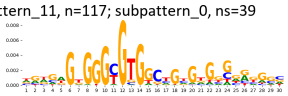

pattern_11, n=117; subpattern_1, ns=32

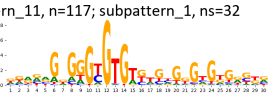

pattern_11, n=117; subpattern_2, ns=28

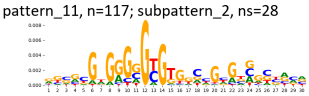

pattern_11, n=117; subpattern_3, ns=14

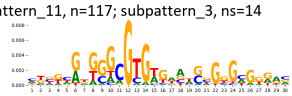

pattern_11, n=117; subpattern_4, ns=4

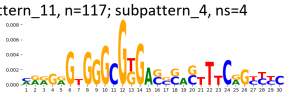

TF-MoDisCO pattern_11 n=117, PWM

pattern_11, n=117; subpattern_0, ns=39

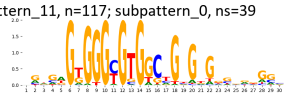

pattern_11, n=117; subpattern_1, ns=32

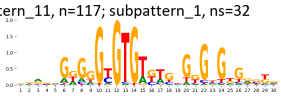

pattern_11, n=117; subpattern_2, ns=28

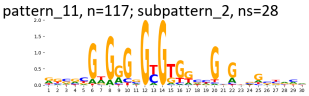

pattern_11, n=117; subpattern_3, ns=14

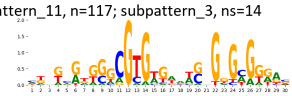

pattern_11, n=117; subpattern_4, ns=4

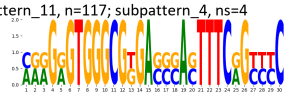

TF-MoDisCO pattern_6 n=371, CWM

pattern_6, n=371; subpattern_0, ns=86

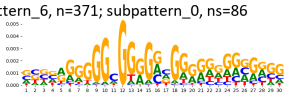

pattern_6, n=371; subpattern_1, ns=66

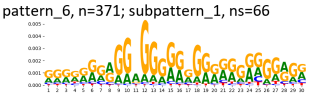

pattern_6, n=371; subpattern_2, ns=53

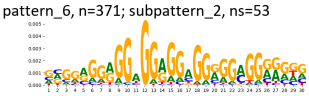

pattern_6, n=371; subpattern_3, ns=39

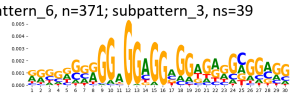

pattern_6, n=371; subpattern_4, ns=35

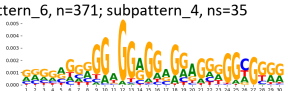

pattern_6, n=371; subpattern_5, ns=34

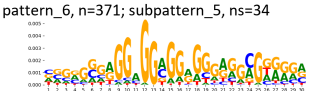

pattern_6, n=371; subpattern_6, ns=31

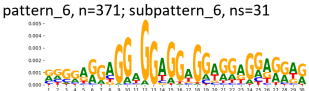

pattern_6, n=371; subpattern_7, ns=27

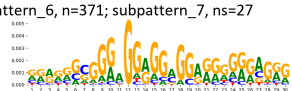

TF-MoDisCO pattern_6 n=371, PWM

pattern_6, n=371; subpattern_0, ns=86

pattern_6, n=371; subpattern_1, ns=66

pattern_6, n=371; subpattern_2, ns=53

pattern_6, n=371; subpattern_3, ns=39

pattern_6, n=371; subpattern_4, ns=35

pattern_6, n=371; subpattern_5, ns=34

pattern_6, n=371; subpattern_6, ns=31

pattern_6, n=371; subpattern_7, ns=27

TF-MoDisCO pattern_7 n=351, CWM

pattern_7, n=351; subpattern_0, ns=89

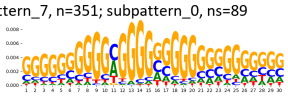

pattern_7, n=351; subpattern_1, ns=87

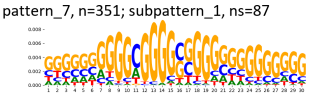

pattern_7, n=351; subpattern_2, ns=59

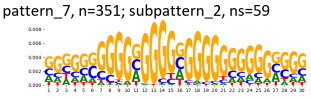

pattern_7, n=351; subpattern_3, ns=59

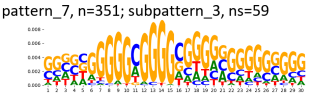

pattern_7, n=351; subpattern_4, ns=48

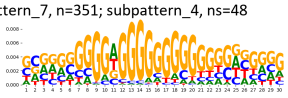

pattern_7, n=351; subpattern_5, ns=9

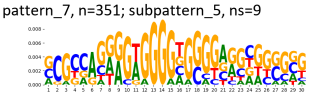

TF-MoDisCO pattern_7 n=351, PWM

pattern_7, n=351; subpattern_0, ns=89

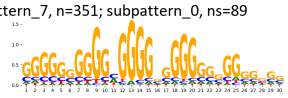

pattern_7, n=351; subpattern_1, ns=87

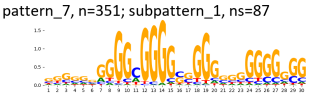

pattern_7, n=351; subpattern_2, ns=59

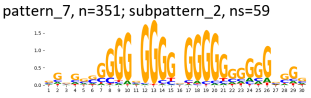

pattern_7, n=351; subpattern_3, ns=59

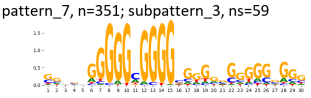

pattern_7, n=351; subpattern_4, ns=48

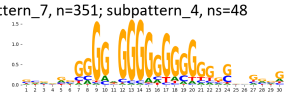

pattern_7, n=351; subpattern_5, ns=9

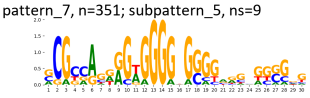

TF-MoDisCO pattern_9 n=166, CWM

pattern_9, n=166; subpattern_0, ns=45

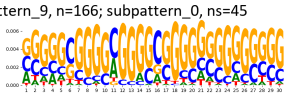

pattern_9, n=166; subpattern_1, ns=41

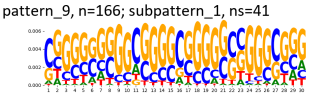

pattern_9, n=166; subpattern_2, ns=28

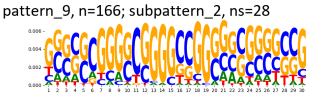

pattern_9, n=166; subpattern_3, ns=25

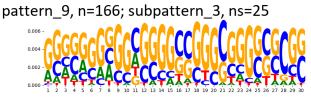

pattern_9, n=166; subpattern_4, ns=15

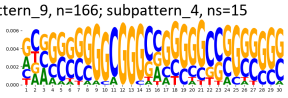

pattern_9, n=166; subpattern_5, ns=12

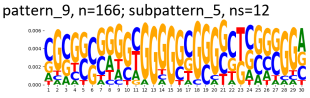

TF-MoDisCO pattern_9 n=166, PWM

pattern_9, n=166; subpattern_0, ns=45

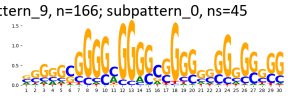

pattern_9, n=166; subpattern_1, ns=41

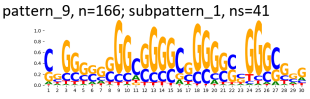

pattern_9, n=166; subpattern_2, ns=28

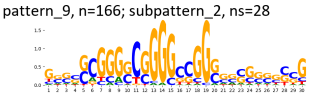

pattern_9, n=166; subpattern_3, ns=25

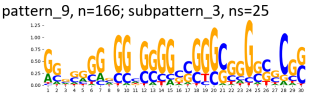

pattern_9, n=166; subpattern_4, ns=15

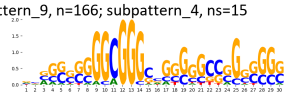

pattern_9, n=166; subpattern_5, ns=12

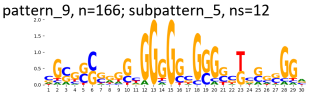

Supplementary Figure 107: TF-MoDisCO subpatterns for the KLF16 transcription factor in HEK293 (accession ENCSR397DQC).

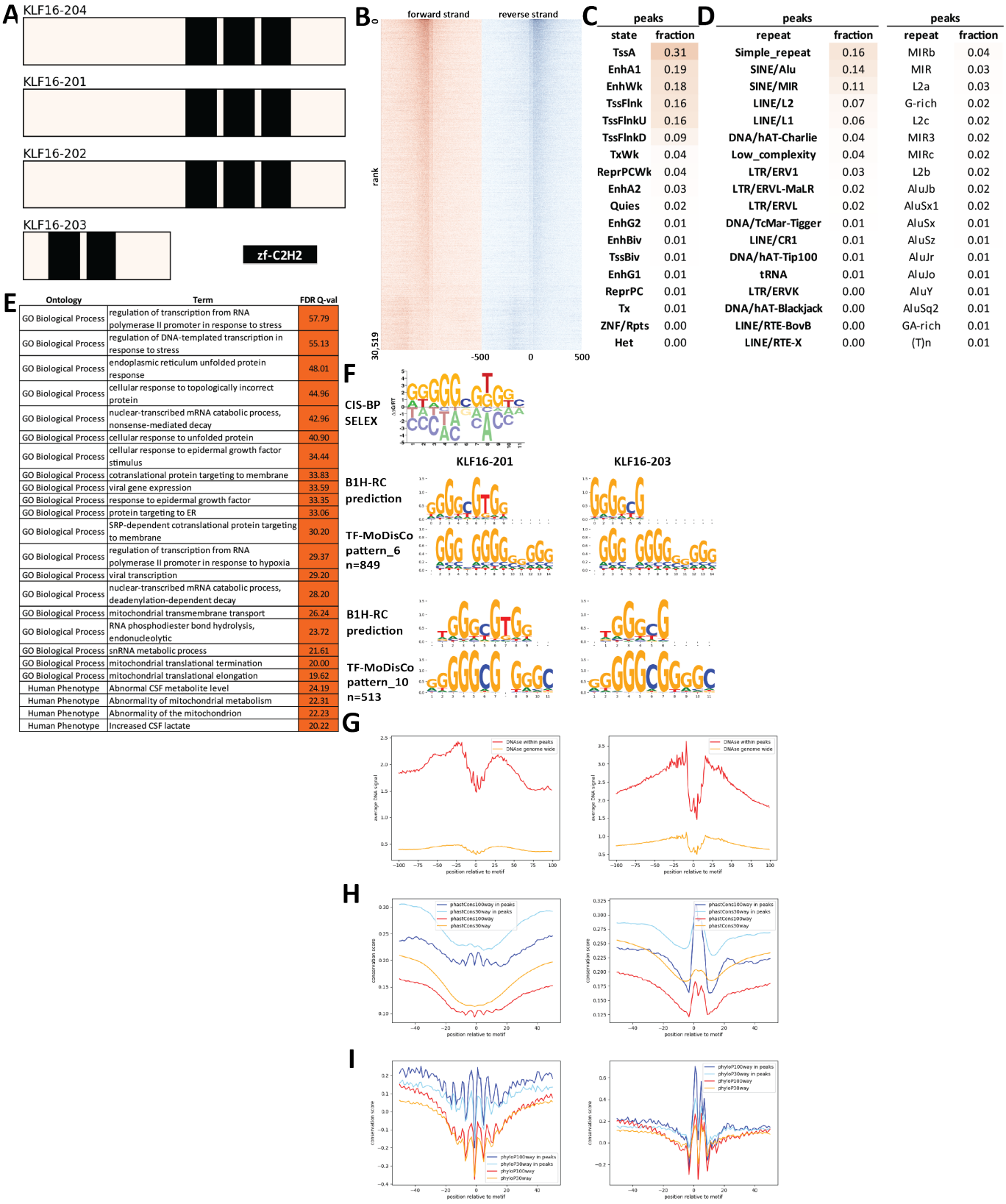

Supplementary Figure 108: Properties and genomic distribution of motifs identified for the KLF16 transcription factor in HepG2 (accession ENCSR009KLQ).

TF-MoDisCO pattern_10 n=513, CWM

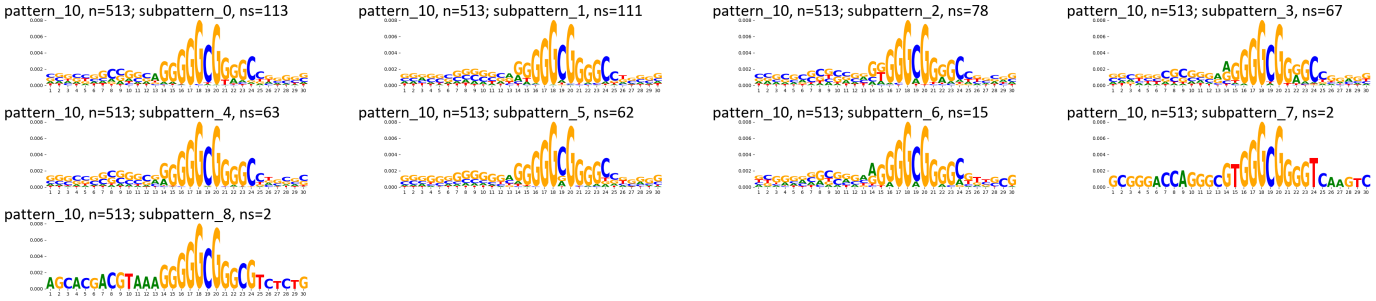

TF-MoDisCO pattern_10 n=513, PWM

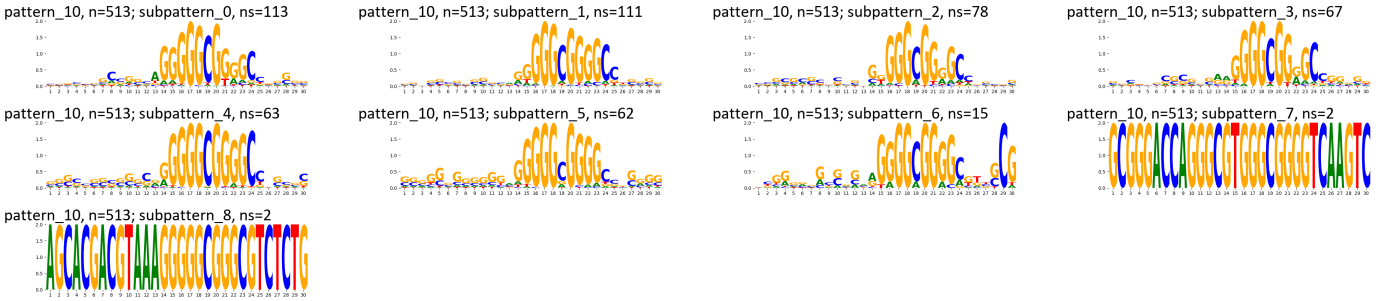

TF-MoDisCO pattern_6 n=849, CWM

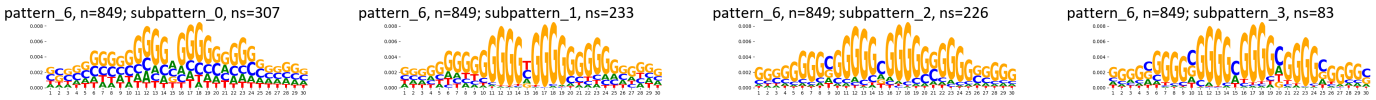

TF-MoDisCO pattern_6 n=849, PWM

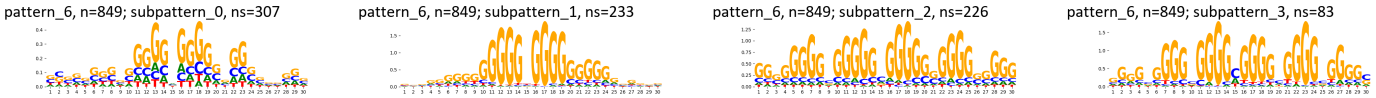

Supplementary Figure 109: TF-MoDisCO subpatterns for the KLF16 transcription factor in HepG2 (accession ENCSR009KLQ).

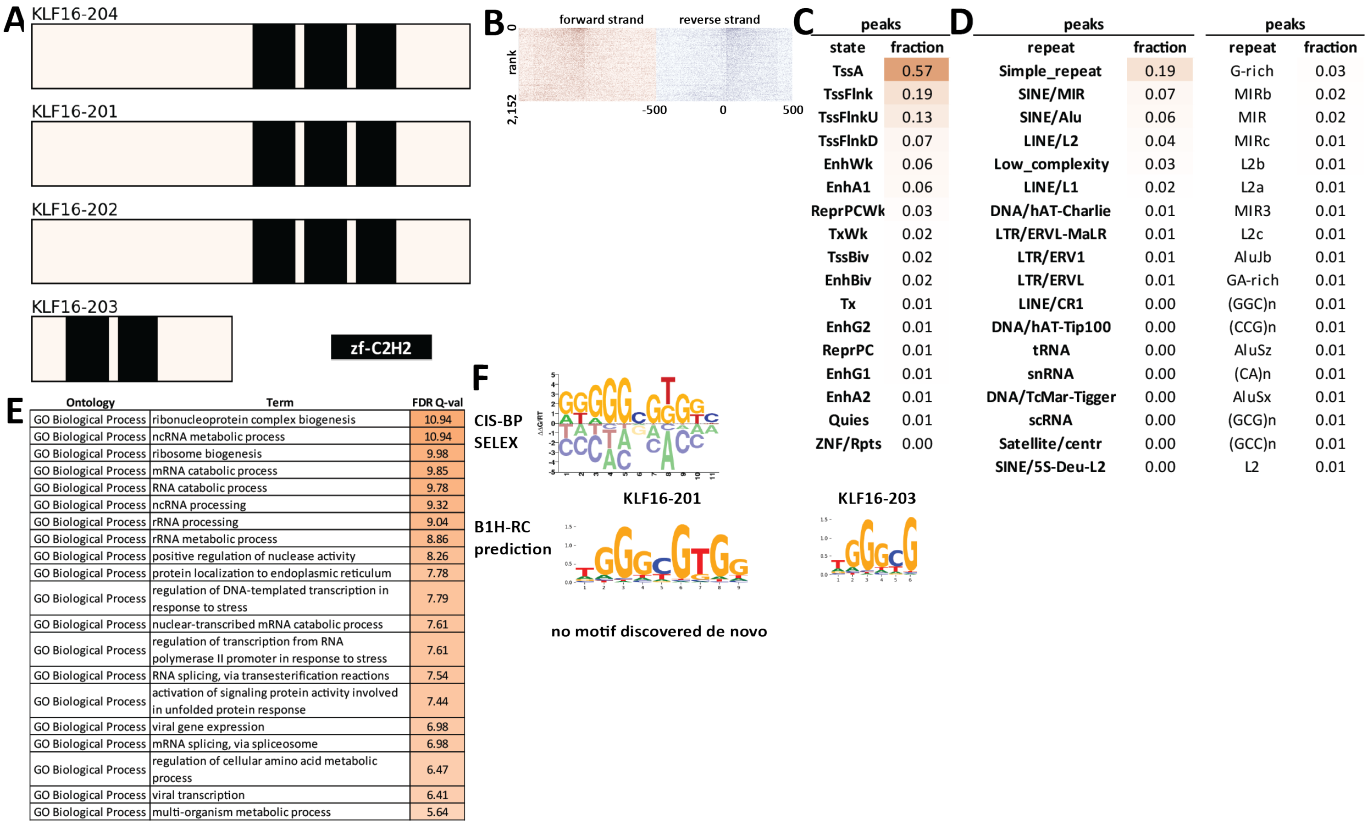

Supplementary Figure 110: Properties and genomic distribution of motifs identified for the KLF16 transcription factor in HepG2 (accession ENCSR913KJZ).

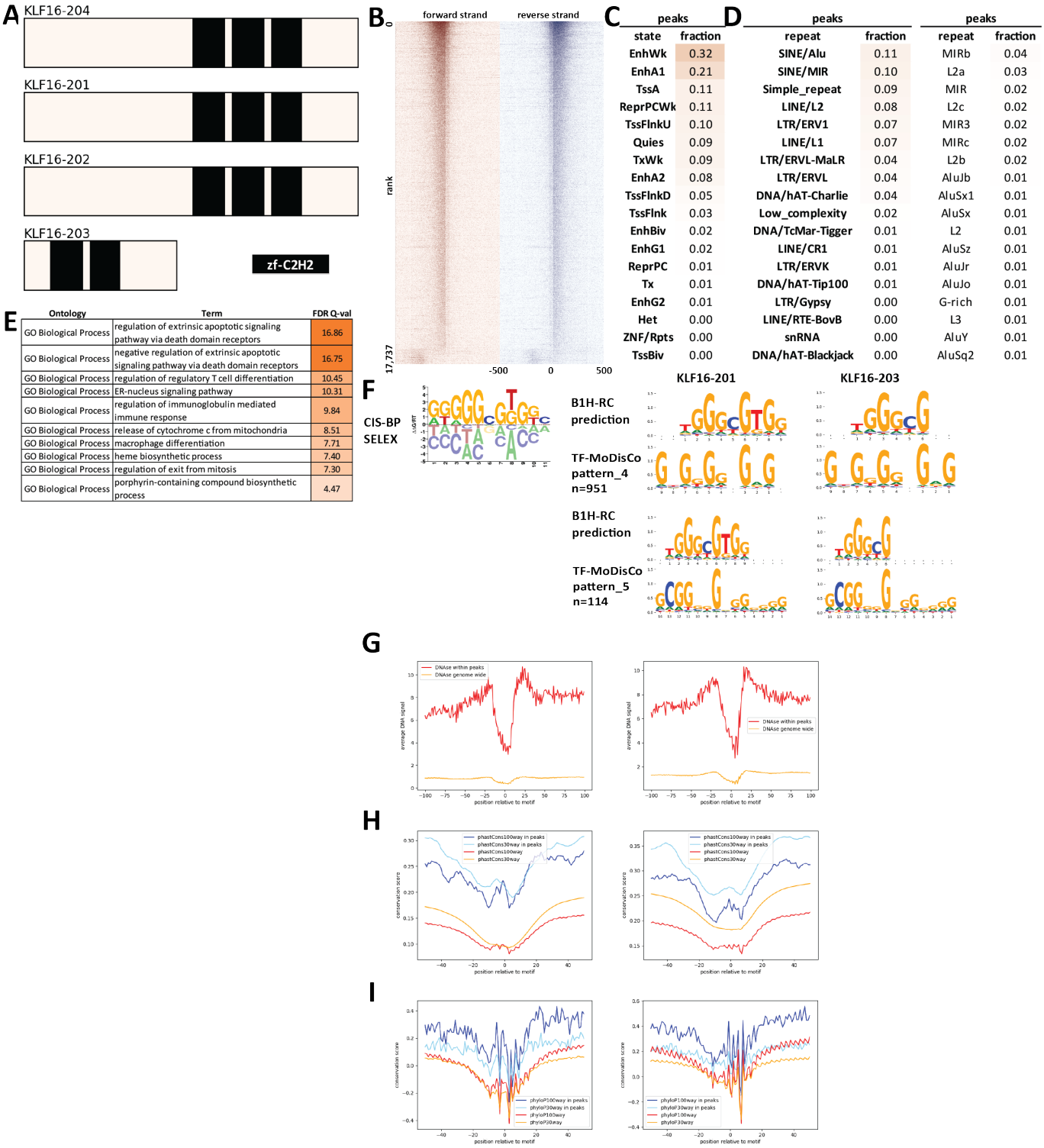

Supplementary Figure 111: Properties and genomic distribution of motifs identified for the KLF16 transcription factor in K562 (accession ENCSR760UVO).

TF-MoDisCO pattern_4 n=951, CWM

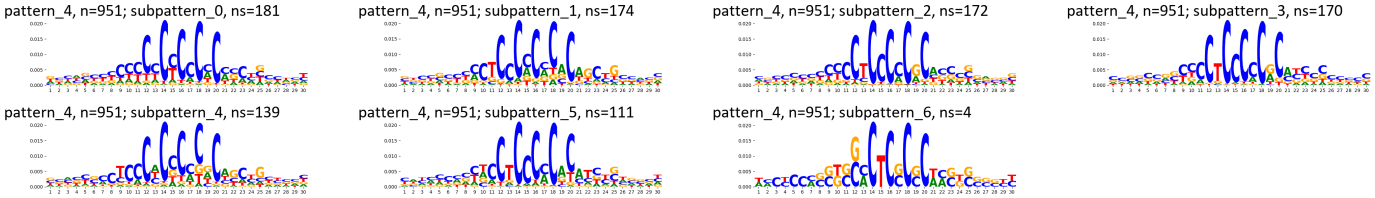

TF-MoDisCO pattern_4 n=951, PWM

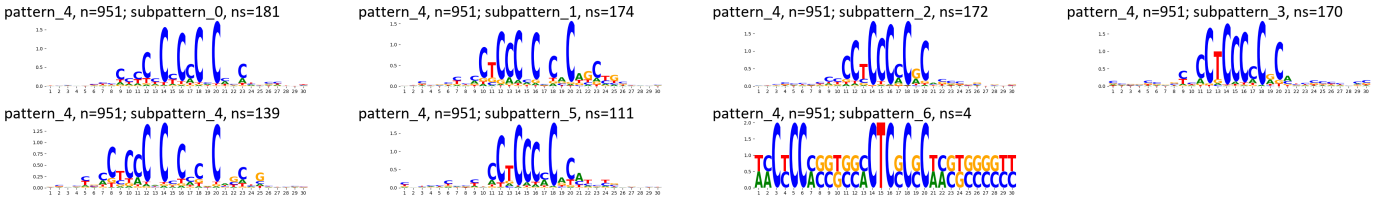

TF-MoDisCO pattern_5 n=114, CWM

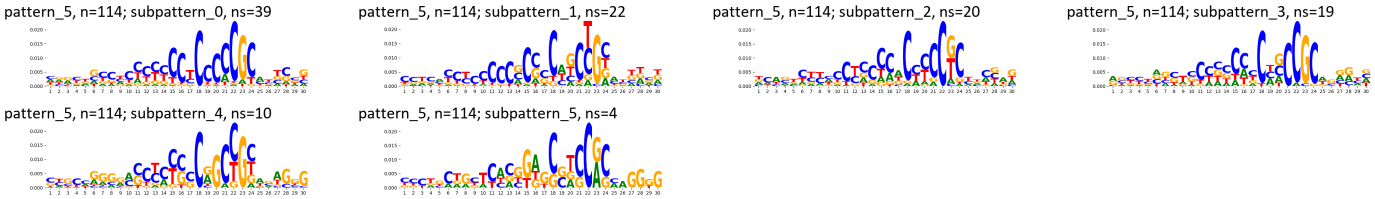

TF-MoDisCO pattern_5 n=114, PWM

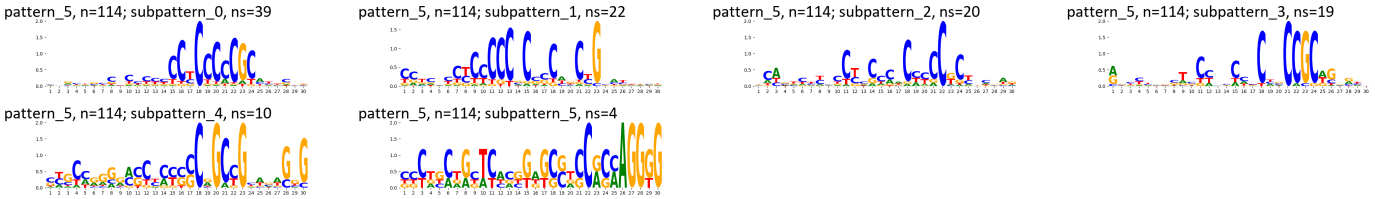

Supplementary Figure 112: TF-MoDisCO subpatterns for the KLF16 transcription factor in K562 (accession ENCSR760UVO).

A

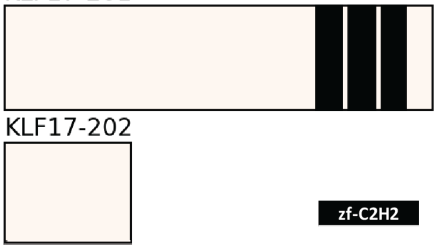

B

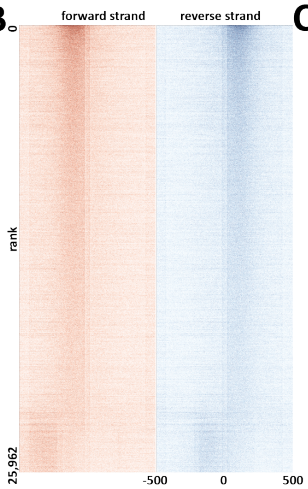

C

peaks	
state	fraction
TssA	0.27
TssFlnk	0.15
Quies	0.13
EnhWk	0.12
TxWk	0.09
EnhA1	0.06
TssBiv	0.05
EnhA2	0.05
TssFlnkU	0.04
ReprPCWk	0.03
ReprPC	0.02
Tx	0.02
TssFlnkD	0.02
EnhBiv	0.01
EnhG1	0.01
EnhG2	0.00
Het	0.00
ZNF/Rpts	0.00

D

peaks		peaks	
repeat	fraction	repeat	fraction
Simple_repeat	0.18	MIRb	0.03
SINE/Alu	0.11	G-rich	0.03
SINE/MIR	0.08	L2a	0.02
LINE/L2	0.06	MIR	0.02
Low_complexity	0.04	L2b	0.02
LINE/L1	0.03	MIRc	0.02
LTR/ERVL-MaLR	0.02	L2c	0.02
DNA/hAT-Charlie	0.02	MIR3	0.02
LTR/ERV1	0.01	GA-rich	0.01
LTR/ERVL	0.01	AluJb	0.01
tRNA	0.01	AluSx	0.01
LINE/CR1	0.01	AluSx1	0.01
DNA/TcMar-Tigger	0.01	(GT)n	0.01
DNA/hAT-Tip100	0.00	AluSz	0.01
LTR/ERVK	0.00	AluJr	0.01
LTR/Gypsy	0.00	AluJo	0.01
snRNA	0.00	(AC)n	0.01
DNA/hAT-Blackjack	0.00	(CA)n	0.01

E

Ontology	Term	FDR Q-val
GO Biological Process	regulation of intrinsic apoptotic signaling pathway	50.02
GO Biological Process	nuclear-transcribed mRNA catabolic process, nonsense-mediated decay	46.02
GO Biological Process	viral gene expression	39.61
GO Biological Process	negative regulation of intrinsic apoptotic signaling pathway	37.15
GO Biological Process	SRP-dependent cotranslational protein targeting to membrane	36.49
GO Biological Process	multi-organism metabolic process	35.13
GO Biological Process	cotranslational protein targeting to membrane	34.21
GO Biological Process	regulation of transcription from RNA polymerase II promoter in response to stress	32.90
GO Biological Process	viral transcription	32.47
GO Biological Process	protein targeting to ER	31.71
GO Biological Process	regulation of mitochondrial membrane permeability	28.67
GO Biological Process	positive regulation of release of cytochrome c from mitochondria	27.10
GO Biological Process	establishment of protein localization to endoplasmic reticulum	26.90
GO Biological Process	translational elongation	24.77
GO Biological Process	cellular protein complex localization	23.47
GO Biological Process	heterochromatin organization	22.21
GO Biological Process	gene silencing by miRNA	22.11
GO Biological Process	positive regulation of transcription from RNA polymerase II promoter in response to stress	22.07
GO Biological Process	intrinsic apoptotic signaling pathway in response to DNA damage	21.24
GO Biological Process	posttranscriptional gene silencing by RNA	20.68
Human Phenotype	Onion bulb formation	9.33
Human Phenotype	Abnormal ovarian morphology	7.46

F

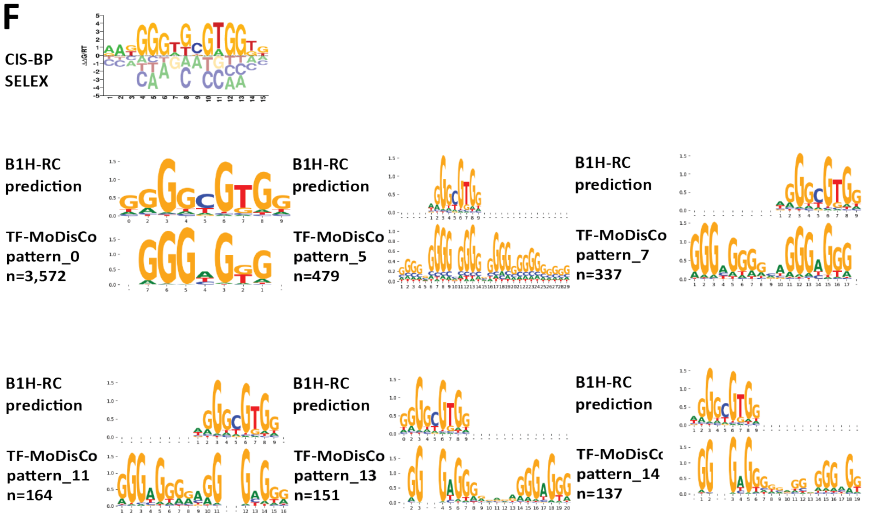

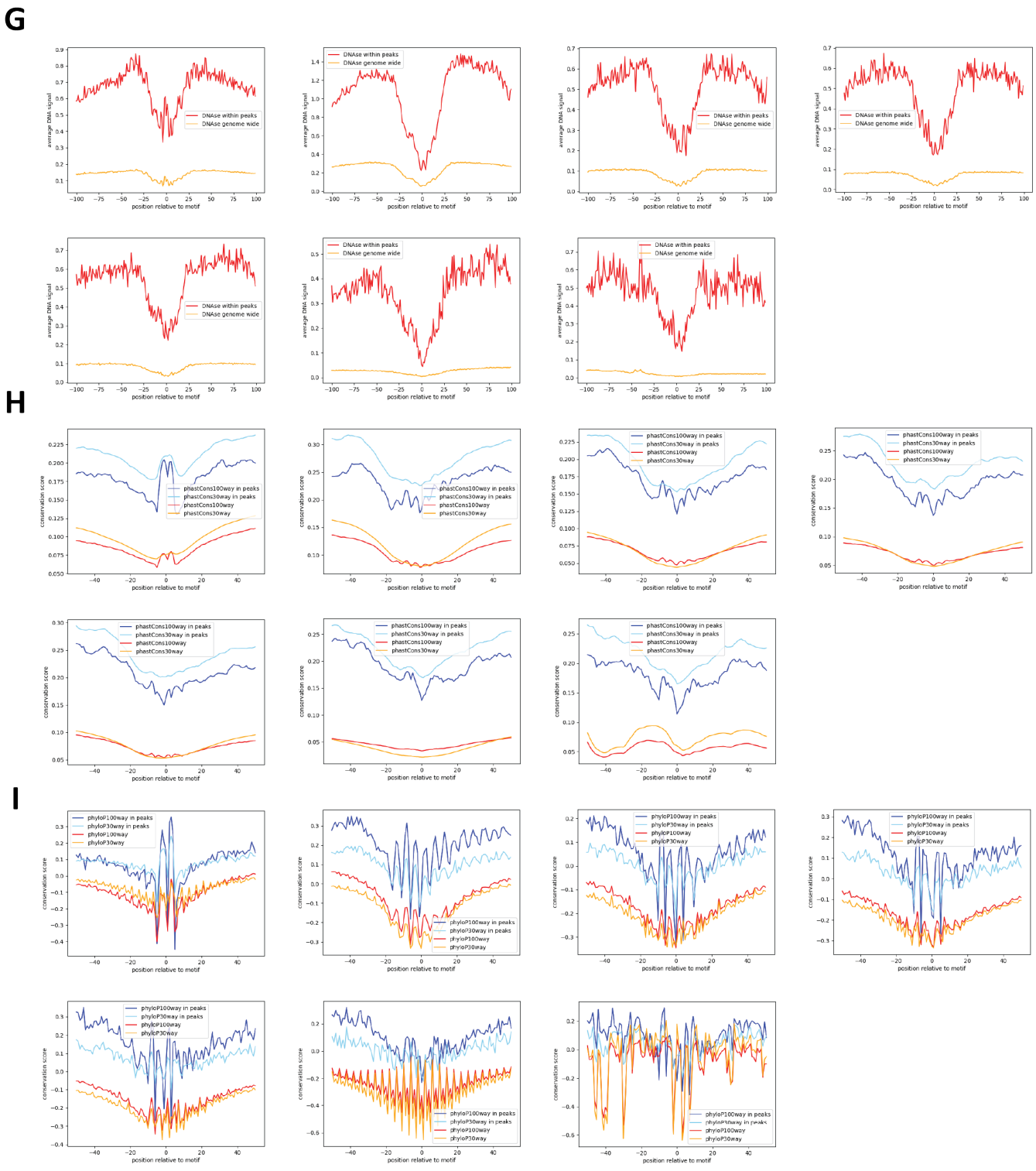

Supplementary Figure 113: Properties and genomic distribution of motifs identified for the KLF17 transcription factor in HEK293 (accession ENCSR065WUF).

TF-MoDisCO pattern_0 n=3572, CWM

pattern_0, n=3572; subpattern_0, ns=844

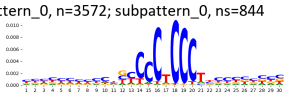

pattern_0, n=3572; subpattern_1, ns=637

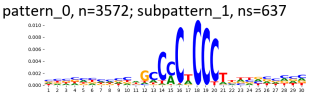

pattern_0, n=3572; subpattern_10, ns=62

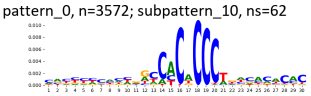

pattern_0, n=3572; subpattern_11, ns=50

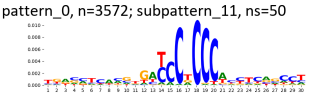

pattern_0, n=3572; subpattern_12, ns=8

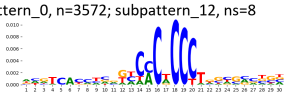

pattern_0, n=3572; subpattern_2, ns=550

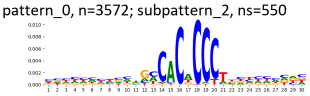

pattern_0, n=3572; subpattern_3, ns=370

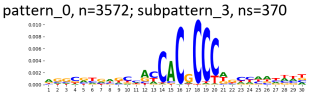

pattern_0, n=3572; subpattern_4, ns=266

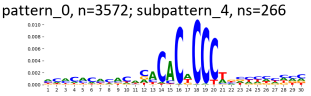

pattern_0, n=3572; subpattern_5, ns=229

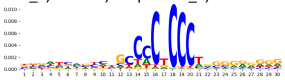

pattern_0, n=3572; subpattern_6, ns=222

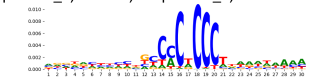

pattern_0, n=3572; subpattern_7, ns=168

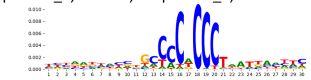

pattern_0, n=3572; subpattern_8, ns=88

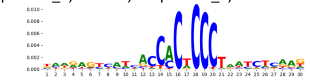

pattern_0, n=3572; subpattern_9, ns=78

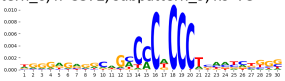

TF-MoDisCO pattern_0 n=3572, PWM

pattern_0, n=3572; subpattern_0, ns=844

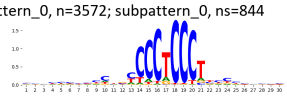

pattern_0, n=3572; subpattern_1, ns=637

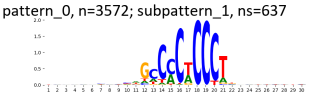

pattern_0, n=3572; subpattern_10, ns=62

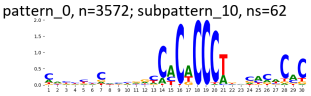

pattern_0, n=3572; subpattern_11, ns=50

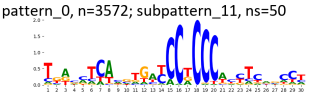

pattern_0, n=3572; subpattern_12, ns=8

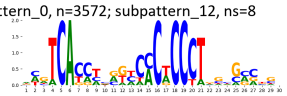

pattern_0, n=3572; subpattern_2, ns=550

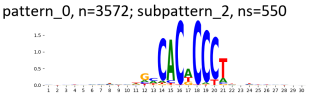

pattern_0, n=3572; subpattern_3, ns=370

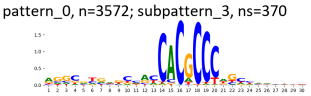

pattern_0, n=3572; subpattern_4, ns=266

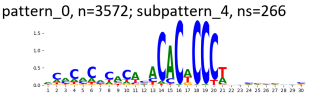

pattern_0, n=3572; subpattern_5, ns=229

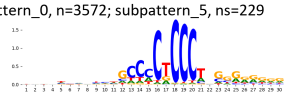

pattern_0, n=3572; subpattern_6, ns=222

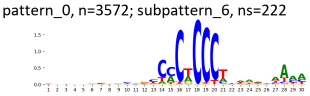

pattern_0, n=3572; subpattern_7, ns=168

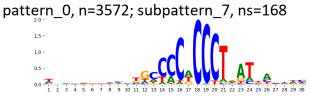

pattern_0, n=3572; subpattern_8, ns=88

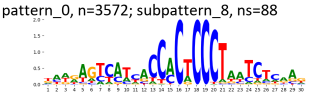

pattern_0, n=3572; subpattern_9, ns=78

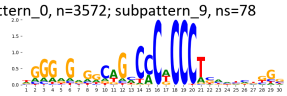

TF-MoDisCO pattern_11 n=164, CWM

pattern_11, n=164; subpattern_0, ns=37

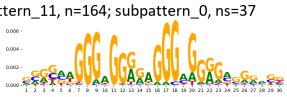

pattern_11, n=164; subpattern_1, ns=36

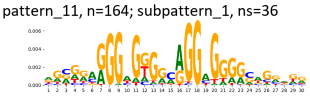

pattern_11, n=164; subpattern_2, ns=28

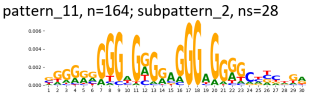

pattern_11, n=164; subpattern_3, ns=28

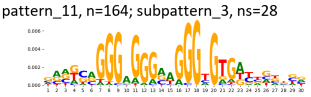

pattern_11, n=164; subpattern_4, ns=19

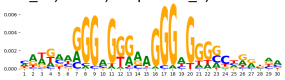

pattern_11, n=164; subpattern_5, ns=16

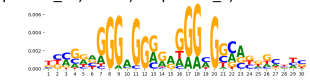

TF-MoDisCO pattern_11 n=164, PWM

pattern_11, n=164; subpattern_0, ns=37

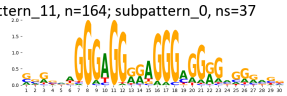

pattern_11, n=164; subpattern_1, ns=36

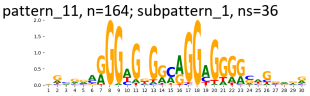

pattern_11, n=164; subpattern_2, ns=28

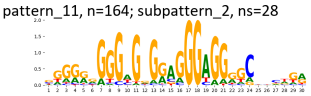

pattern_11, n=164; subpattern_3, ns=28

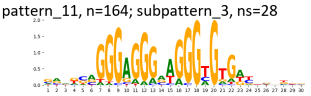

pattern_11, n=164; subpattern_4, ns=19

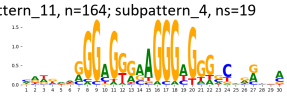

pattern_11, n=164; subpattern_5, ns=16

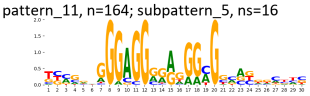

TF-MoDisCO pattern_13 n=151, CWM

pattern_13, n=151; subpattern_0, ns=58

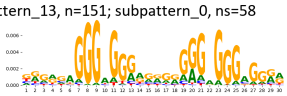

pattern_13, n=151; subpattern_1, ns=57

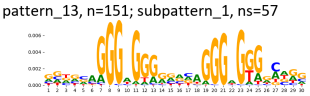

pattern_13, n=151; subpattern_2, ns=32

pattern_13, n=151; subpattern_3, ns=2

pattern_13, n=151; subpattern_4, ns=2

TF-MoDisCO pattern_13 n=151, PWM

pattern_13, n=151; subpattern_0, ns=58

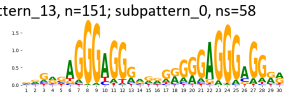

pattern_13, n=151; subpattern_1, ns=57

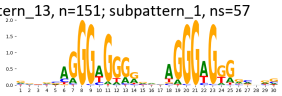

pattern_13, n=151; subpattern_2, ns=32

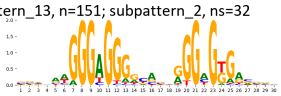

pattern_13, n=151; subpattern_3, ns=2

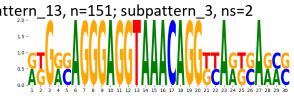

pattern_13, n=151; subpattern_4, ns=2

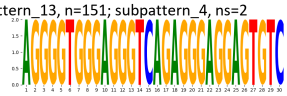

TF-MoDisCO pattern_14 n=137, CWM

pattern_14, n=137; subpattern_0, ns=27

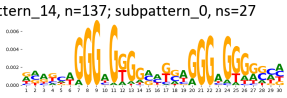

pattern_14, n=137; subpattern_1, ns=27

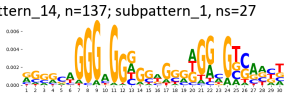

pattern_14, n=137; subpattern_2, ns=27

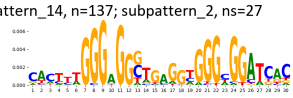

pattern_14, n=137; subpattern_3, ns=26

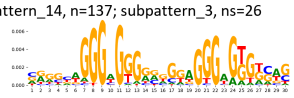

pattern_14, n=137; subpattern_4, ns=22

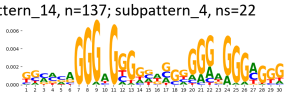

pattern_14, n=137; subpattern_5, ns=8

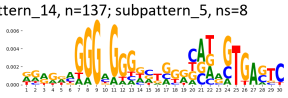

TF-MoDisCO pattern_14 n=137, PWM

pattern_14, n=137; subpattern_0, ns=27

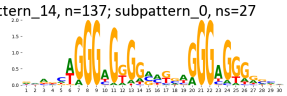

pattern_14, n=137; subpattern_1, ns=27

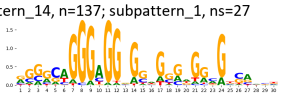

pattern_14, n=137; subpattern_2, ns=27

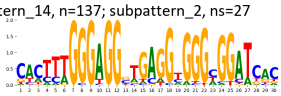

pattern_14, n=137; subpattern_3, ns=26

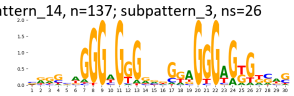

pattern_14, n=137; subpattern_4, ns=22

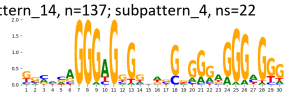

pattern_14, n=137; subpattern_5, ns=8

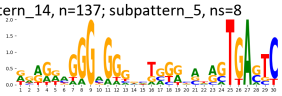

TF-MoDisCO pattern_5 n=479, CWM

pattern_5, n=479; subpattern_0, ns=164

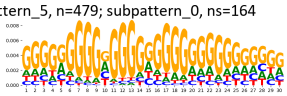

pattern_5, n=479; subpattern_1, ns=129

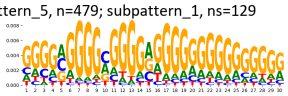

pattern_5, n=479; subpattern_2, ns=92

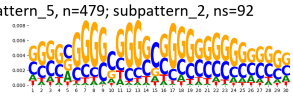

pattern_5, n=479; subpattern_3, ns=89

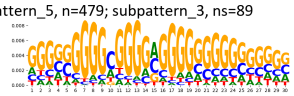

pattern_5, n=479; subpattern_4, ns=3

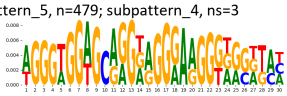

pattern_5, n=479; subpattern_5, ns=2

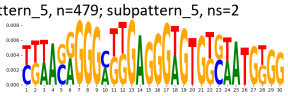

TF-MoDisCO pattern_5 n=479, PWM

pattern_5, n=479; subpattern_0, ns=164

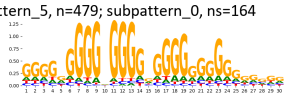

pattern_5, n=479; subpattern_1, ns=129

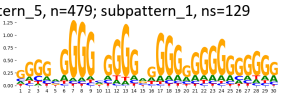

pattern_5, n=479; subpattern_2, ns=92

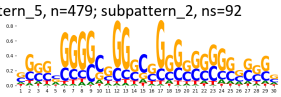

pattern_5, n=479; subpattern_3, ns=89

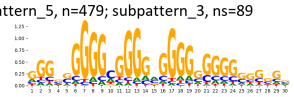

pattern_5, n=479; subpattern_4, ns=3

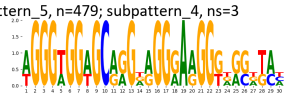

pattern_5, n=479; subpattern_5, ns=2

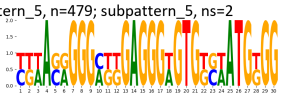

TF-MoDisCO pattern_7 n=337, CWM

pattern_7, n=337; subpattern_0, ns=103

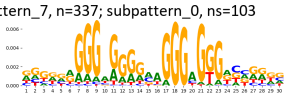

pattern_7, n=337; subpattern_1, ns=90

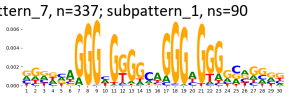

pattern_7, n=337; subpattern_2, ns=64

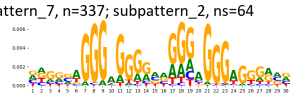

pattern_7, n=337; subpattern_3, ns=54

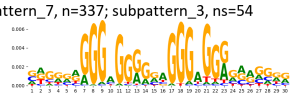

pattern_7, n=337; subpattern_4, ns=11

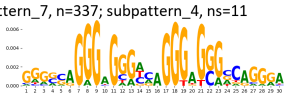

pattern_7, n=337; subpattern_5, ns=6

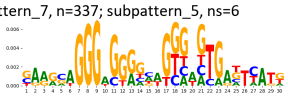

pattern_7, n=337; subpattern_6, ns=6

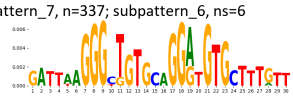

pattern_7, n=337; subpattern_7, ns=3

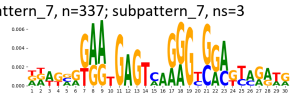

TF-MoDisCO pattern_7 n=337, PWM

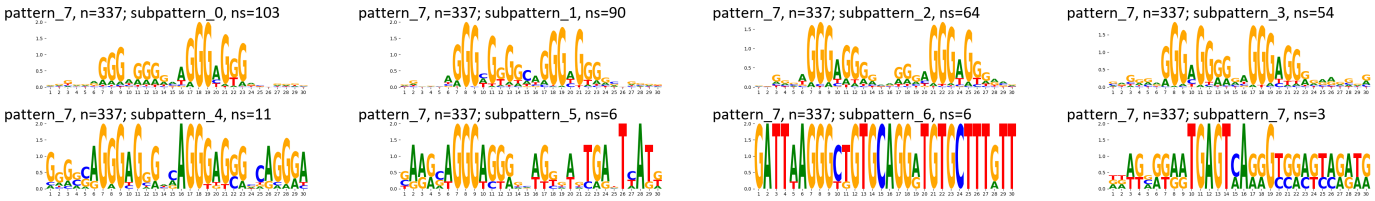

TF-MoDisCO pattern_9 n=188, CWM

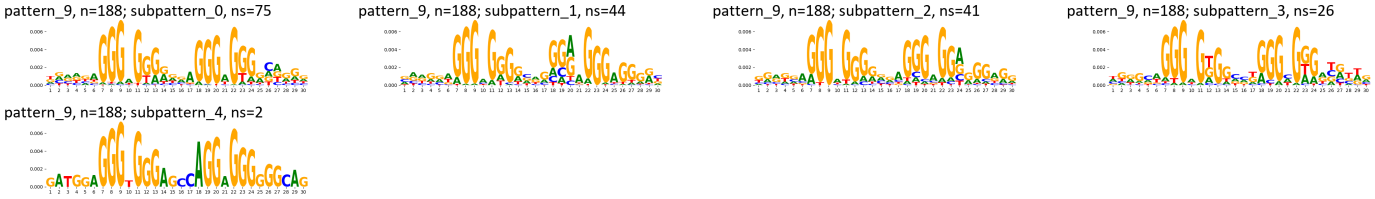

TF-MoDisCO pattern_9 n=188, PWM

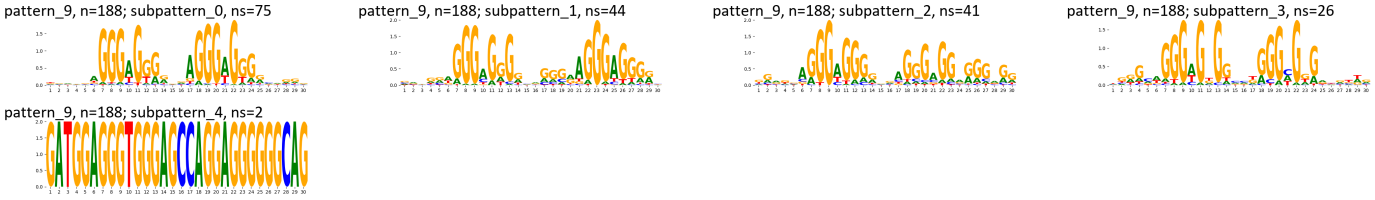

Supplementary Figure 114: TF-MoDisCO subpatterns for the KLF17 transcription factor in HEK293 (accession ENCSR065WUF).

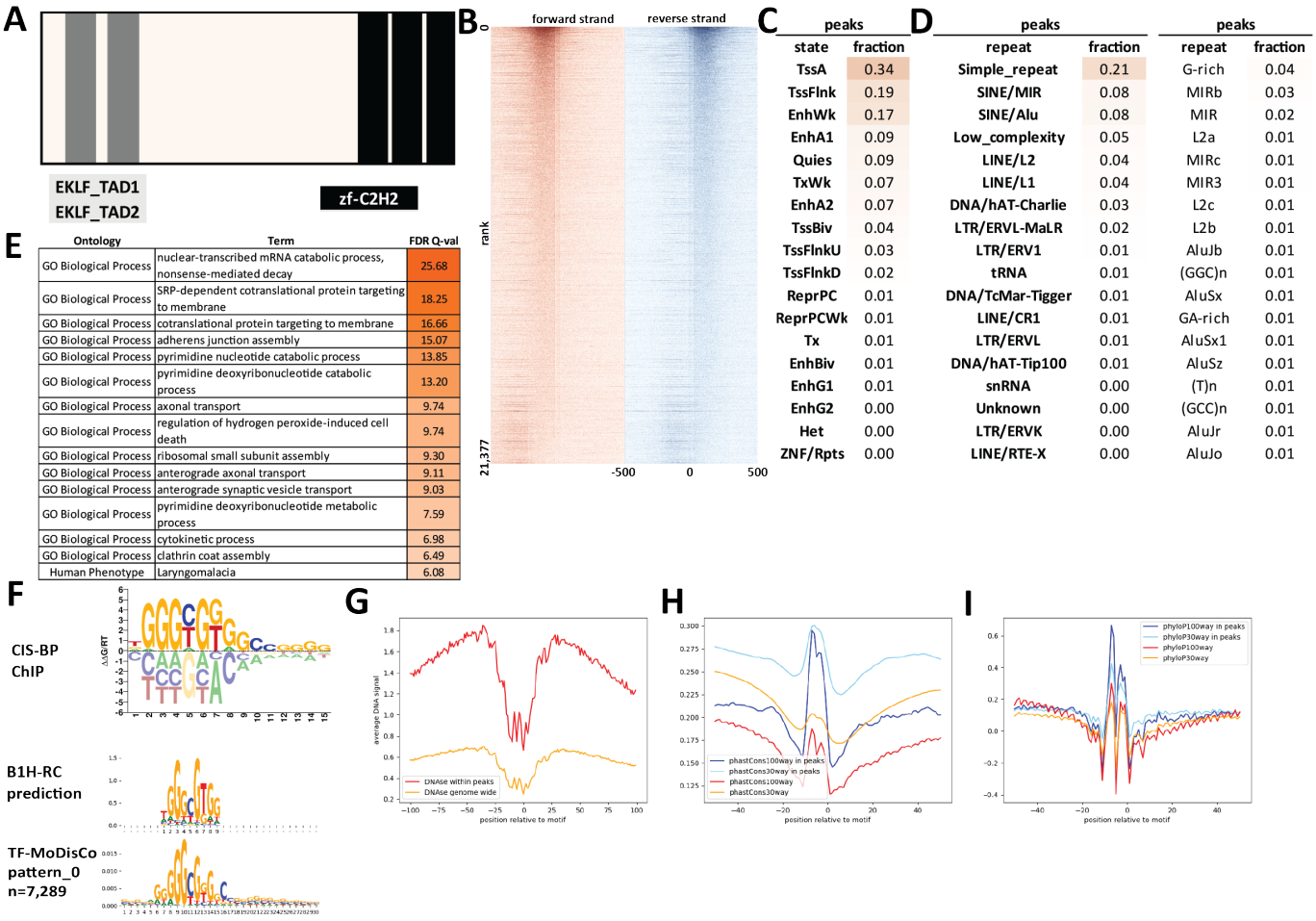

C

peaks	
state	fraction
TssA	0.34
TssFlnk	0.19
EnhWk	0.17
EnhA1	0.09
Quies	0.09
TxWk	0.07
EnhA2	0.07
TssBiv	0.04
TssFlnkU	0.03
TssFlnkD	0.02
ReprPC	0.01
ReprPCWk	0.01
Tx	0.01
EnhBiv	0.01
EnhG1	0.01
EnhG2	0.00
Het	0.00
ZNF/Rpts	0.00

D

peaks		peaks	
repeat	fraction	repeat	fraction
Simple_repeat	0.21	G-rich	0.04
SINE/MIR	0.08	MIRb	0.03
SINE/Alu	0.08	MIR	0.02
Low_complexity	0.05	L2a	0.01
LINE/L2	0.04	MIRc	0.01
LINE/L1	0.04	MIR3	0.01
DNA/hAT-Charlie	0.03	L2c	0.01
LTR/ERVL-MaLR	0.02	L2b	0.01
LTR/ERV1	0.01	AluJb	0.01
tRNA	0.01	(GGC)n	0.01
DNA/TcMar-Tigger	0.01	AluSx	0.01
LINE/CR1	0.01	GA-rich	0.01
LTR/ERVL	0.01	AluSx1	0.01
DNA/hAT-Tip100	0.01	AluSz	0.01
snRNA	0.00	(T)n	0.01
Unknown	0.00	(GCC)n	0.01
LTR/ERVK	0.00	AluJr	0.01
LINE/RTE-X	0.00	AluJo	0.01

E

Ontology	Term	FDR Q-val
GO Biological Process	nuclear-transcribed mRNA catabolic process, nonsense-mediated decay	25.68
GO Biological Process	SRP-dependent cotranslational protein targeting to membrane	18.25
GO Biological Process	cotranslational protein targeting to membrane	16.66
GO Biological Process	adherens junction assembly	15.07
GO Biological Process	pyrimidine nucleotide catabolic process	13.85
GO Biological Process	pyrimidine deoxyribonucleotide catabolic process	13.20
GO Biological Process	axonal transport	9.74
GO Biological Process	regulation of hydrogen peroxide-induced cell death	9.74
GO Biological Process	ribosomal small subunit assembly	9.30
GO Biological Process	anterograde axonal transport	9.11
GO Biological Process	anterograde synaptic vesicle transport	9.03
GO Biological Process	pyrimidine deoxyribonucleotide metabolic process	7.59
GO Biological Process	cytokinetic process	6.98
GO Biological Process	clathrin coat assembly	6.49
Human Phenotype	Laryngomalacia	6.08

Supplementary Figure 115: Properties and genomic distribution of motifs identified for the KLF1 transcription factor in HEK293 (accession ENCSR006GAQ).

TF-MoDisCO pattern_0 n=7289, CWM

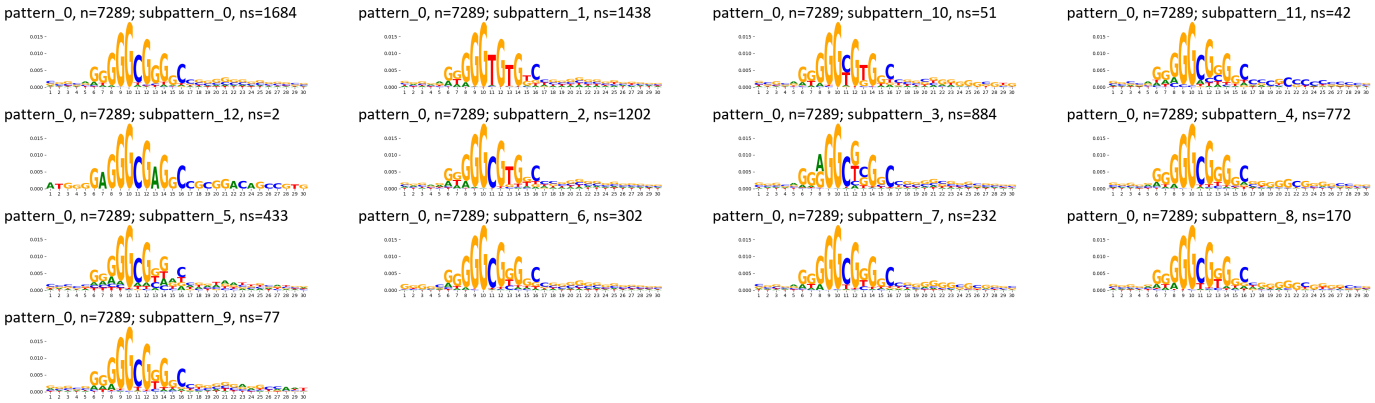

TF-MoDisCO pattern_0 n=7289, PWM

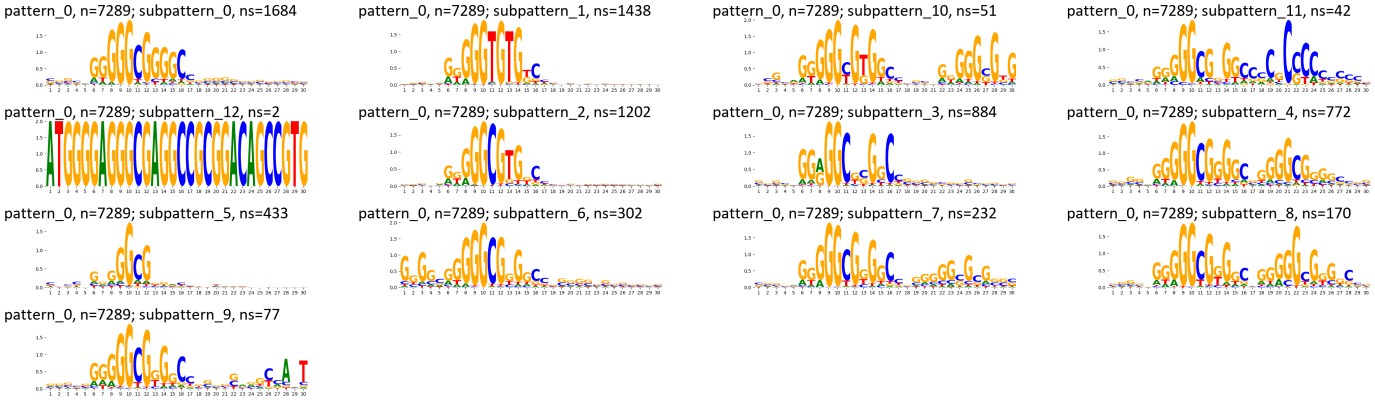

Supplementary Figure 116: TF-MoDisCO subpatterns for the KLF1 transcription factor in HEK293 (accession ENCSR006GAQ).

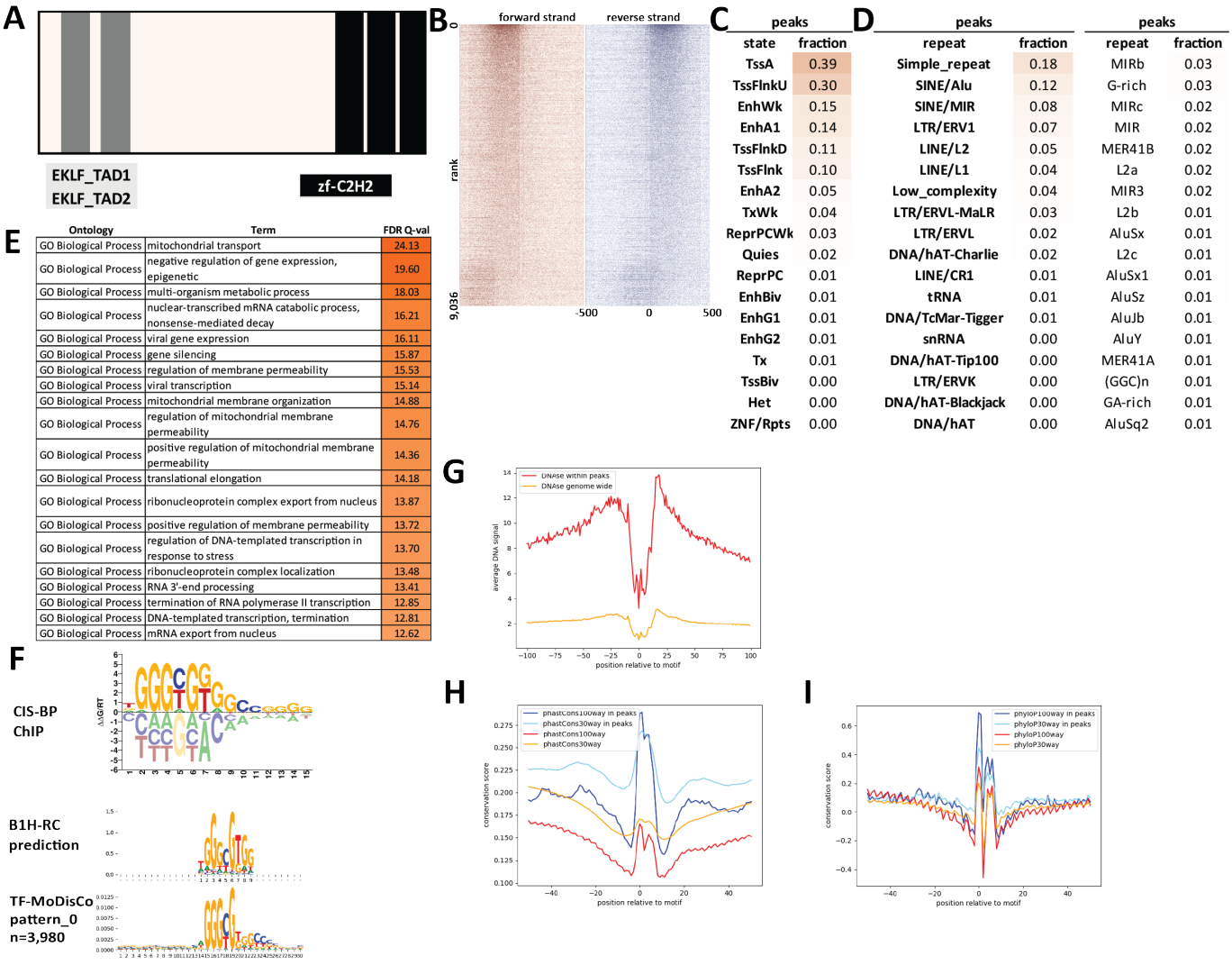

C

peaks	
state	fraction
TssA	0.39
TssFlnkU	0.30
EnhWk	0.15
EnhA1	0.14
TssFlnkD	0.11
TssFlnk	0.10
EnhA2	0.05
TxWk	0.04
ReprPCWk	0.03
Quies	0.02
ReprPC	0.01
EnhBiv	0.01
EnhG1	0.01
EnhG2	0.01
Tx	0.01
TssBiv	0.00
Het	0.00
ZNF/Rpts	0.00

D

peaks		peaks	
repeat	fraction	repeat	fraction
Simple_repeat	0.18	MIRb	0.03
SINE/Alu	0.12	G-rich	0.03
SINE/MIR	0.08	MIRc	0.02
LTR/ERV1	0.07	MIR	0.02
LINE/L2	0.05	MER41B	0.02
LINE/L1	0.04	L2a	0.02
Low_complexity	0.04	MIR3	0.02
LTR/ERVL-MaLR	0.03	L2b	0.01
LTR/ERVL	0.02	AluSx	0.01
DNA/hAT-Charlie	0.02	L2c	0.01
LINE/CR1	0.01	AluSx1	0.01
tRNA	0.01	AluSz	0.01
DNA/TcMar-Tigger	0.01	AluJb	0.01
snRNA	0.00	AluY	0.01
DNA/hAT-Tip100	0.00	MER41A	0.01
LTR/ERVK	0.00	(GGC)n	0.01
DNA/hAT-Blackjack	0.00	GA-rich	0.01
DNA/hAT	0.00	AluSq2	0.01

E

Ontology	Term	FDR Q-val
GO Biological Process	mitochondrial transport	24.13
GO Biological Process	negative regulation of gene expression, epigenetic	19.60
GO Biological Process	multi-organism metabolic process	18.03
GO Biological Process	nuclear-transcribed mRNA catabolic process, nonsense-mediated decay	16.21
GO Biological Process	viral gene expression	16.11
GO Biological Process	gene silencing	15.87
GO Biological Process	regulation of membrane permeability	15.53
GO Biological Process	viral transcription	15.14
GO Biological Process	mitochondrial membrane organization	14.88
GO Biological Process	regulation of mitochondrial membrane permeability	14.76
GO Biological Process	positive regulation of mitochondrial membrane permeability	14.36
GO Biological Process	translational elongation	14.18
GO Biological Process	ribonucleoprotein complex export from nucleus	13.87
GO Biological Process	positive regulation of membrane permeability	13.72
GO Biological Process	regulation of DNA-templated transcription in response to stress	13.70
GO Biological Process	ribonucleoprotein complex localization	13.48
GO Biological Process	RNA 3'-end processing	13.41
GO Biological Process	termination of RNA polymerase II transcription	12.85
GO Biological Process	DNA-templated transcription, termination	12.81
GO Biological Process	mRNA export from nucleus	12.62

Supplementary Figure 117: Properties and genomic distribution of motifs identified for the KLF1 transcription factor in K562 (accession ENCSR550HCT).

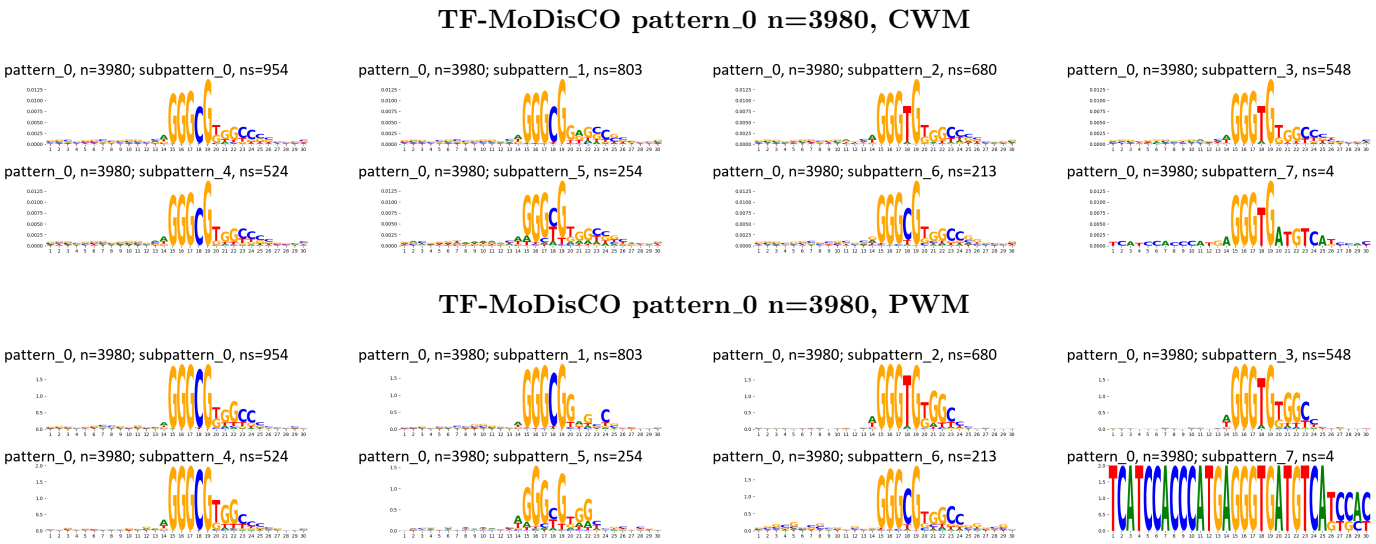

Supplementary Figure 118: TF-MoDisCO subpatterns for the KLF1 transcription factor in K562 (accession ENCSR550HCT).

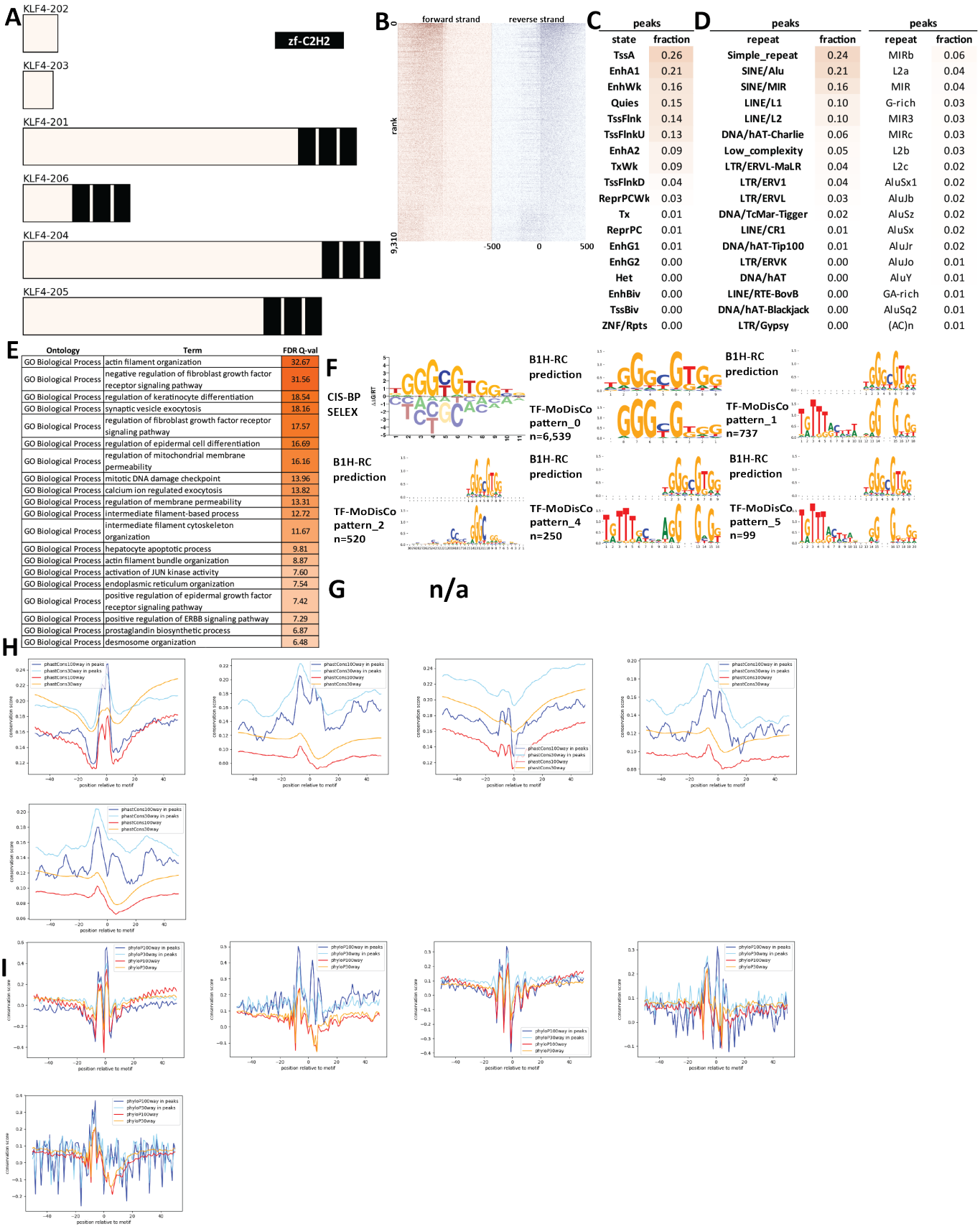

peaks	
state	fraction
TssA	0.26
EnhA1	0.21
EnhWk	0.16
Quies	0.15
TssFlnk	0.14
TssFlnkU	0.13
EnhA2	0.09
TxWk	0.09
TssFlnkD	0.04
ReprPCWk	0.03
Tx	0.01
ReprPC	0.01
EnhG1	0.01
EnhG2	0.00
Het	0.00
EnhBiv	0.00
TssBiv	0.00
ZNF/Rpts	0.00

peaks	
repeat	fraction
Simple_repeat	0.24
SINE/Alu	0.21
SINE/MIR	0.16
LINE/L1	0.10
LINE/L2	0.10
DNA/hAT-Charlie	0.06
Low_complexity	0.05
LTR/ERVL-MaLR	0.04
LTR/ERV1	0.04
LTR/ERVL	0.03
DNA/TcMar-Tigger	0.02
LINE/CR1	0.01
DNA/hAT-Tip100	0.01
LTR/ERVK	0.00
DNA/hAT	0.00
LINE/RTE-BovB	0.00
DNA/hAT-Blackjack	0.00
LTR/Gypsy	0.00

peaks	
repeat	fraction
MIRb	0.06
L2a	0.04
MIR	0.04
G-rich	0.03
MIR3	0.03
MIRc	0.03
L2b	0.03
L2c	0.02
AluSx1	0.02
AluJb	0.02
AluSz	0.02
AluSx	0.02
AluJr	0.02
AluJo	0.01
AluY	0.01
GA-rich	0.01
AluSq2	0.01
(AC)n	0.01

Ontology	Term	FDR Q-val
GO Biological Process	actin filament organization	32.67
GO Biological Process	negative regulation of fibroblast growth factor receptor signaling pathway	31.56
GO Biological Process	regulation of keratinocyte differentiation	18.54
GO Biological Process	synaptic vesicle exocytosis	18.16
GO Biological Process	regulation of fibroblast growth factor receptor signaling pathway	17.57
GO Biological Process	regulation of epidermal cell differentiation	16.69
GO Biological Process	regulation of mitochondrial membrane permeability	16.16
GO Biological Process	mitotic DNA damage checkpoint	13.96
GO Biological Process	calcium ion regulated exocytosis	13.82
GO Biological Process	regulation of membrane permeability	13.31
GO Biological Process	intermediate filament-based process	12.72
GO Biological Process	intermediate filament cytoskeleton organization	11.67
GO Biological Process	hepatocyte apoptotic process	9.81
GO Biological Process	actin filament bundle organization	8.87
GO Biological Process	activation of JUN kinase activity	7.60
GO Biological Process	endoplasmic reticulum organization	7.54
GO Biological Process	positive regulation of epidermal growth factor receptor signaling pathway	7.42
GO Biological Process	positive regulation of ERBB signaling pathway	7.29
GO Biological Process	prostaglandin biosynthetic process	6.87
GO Biological Process	desmosome organization	6.48

Supplementary Figure 119: Properties and genomic distribution of motifs identified for the KLF4 transcription factor in MCF-7 (accession ENCSR265WJC).

TF-MoDisCO pattern_0 n=6539, CWM

pattern_0, n=6539; subpattern_0, ns=1415

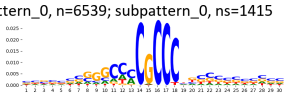

pattern_0, n=6539; subpattern_1, ns=1185

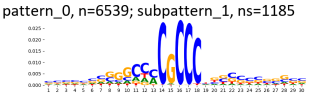

pattern_0, n=6539; subpattern_10, ns=31

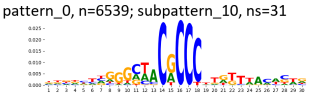

pattern_0, n=6539; subpattern_11, ns=13

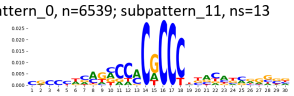

pattern_0, n=6539; subpattern_12, ns=2

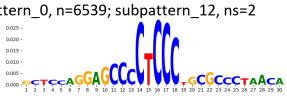

pattern_0, n=6539; subpattern_13, ns=2

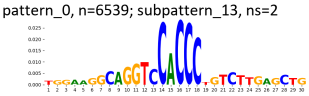

pattern_0, n=6539; subpattern_2, ns=1153

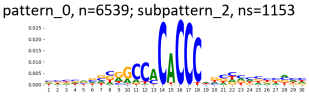

pattern_0, n=6539; subpattern_3, ns=1136

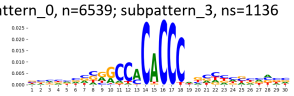

pattern_0, n=6539; subpattern_4, ns=1083

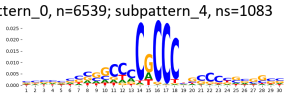

pattern_0, n=6539; subpattern_5, ns=223

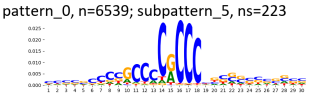

pattern_0, n=6539; subpattern_6, ns=109

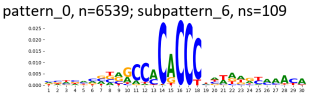

pattern_0, n=6539; subpattern_7, ns=89

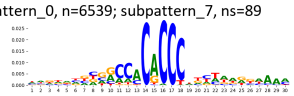

pattern_0, n=6539; subpattern_8, ns=57

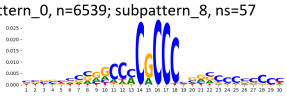

pattern_0, n=6539; subpattern_9, ns=41

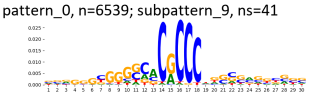

TF-MoDisCO pattern_0 n=6539, PWM

pattern_0, n=6539; subpattern_0, ns=1415

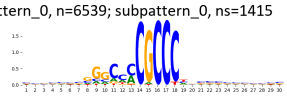

pattern_0, n=6539; subpattern_1, ns=1185

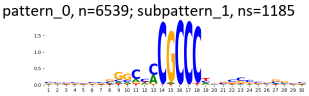

pattern_0, n=6539; subpattern_10, ns=31

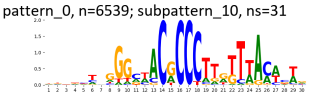

pattern_0, n=6539; subpattern_11, ns=13

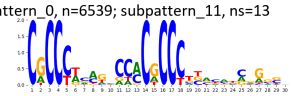

pattern_0, n=6539; subpattern_12, ns=2

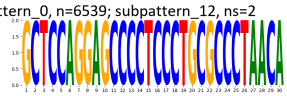

pattern_0, n=6539; subpattern_13, ns=2

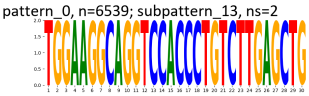

pattern_0, n=6539; subpattern_2, ns=1153

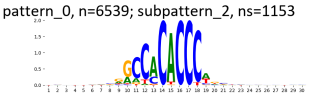

pattern_0, n=6539; subpattern_3, ns=1136

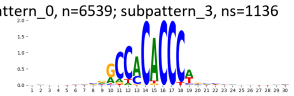

pattern_0, n=6539; subpattern_4, ns=1083

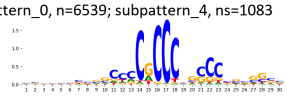

pattern_0, n=6539; subpattern_5, ns=223

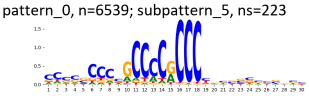

pattern_0, n=6539; subpattern_6, ns=109

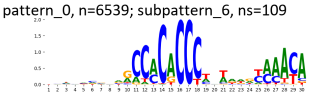

pattern_0, n=6539; subpattern_7, ns=89

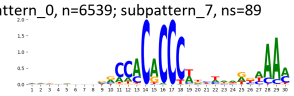

pattern_0, n=6539; subpattern_8, ns=57

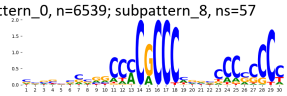

pattern_0, n=6539; subpattern_9, ns=41

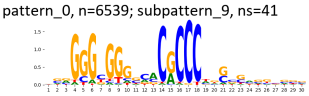

TF-MoDisCO pattern_1 n=737, CWM

pattern_1, n=737; subpattern_0, ns=255

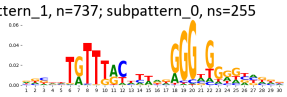

pattern_1, n=737; subpattern_1, ns=184

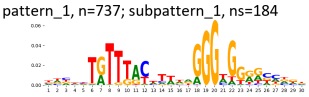

pattern_1, n=737; subpattern_2, ns=164

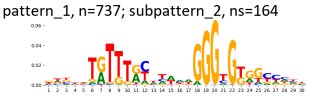

pattern_1, n=737; subpattern_3, ns=122

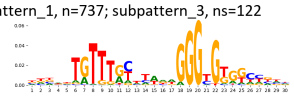

pattern_1, n=737; subpattern_4, ns=10

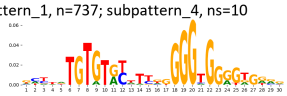

pattern_1, n=737; subpattern_5, ns=2

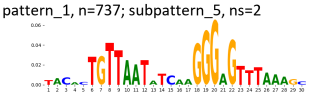

TF-MoDisCO pattern_1 n=737, PWM

pattern_1, n=737; subpattern_0, ns=255

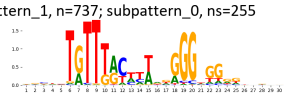

pattern_1, n=737; subpattern_1, ns=184

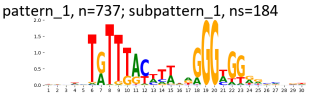

pattern_1, n=737; subpattern_2, ns=164

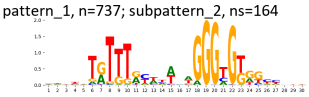

pattern_1, n=737; subpattern_3, ns=122

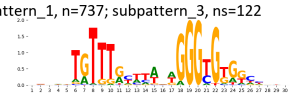

pattern_1, n=737; subpattern_4, ns=10

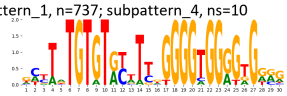

pattern_1, n=737; subpattern_5, ns=2

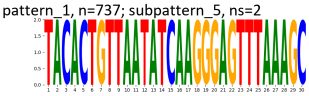

TF-MoDisCO pattern_2 n=520, CWM

pattern_2, n=520; subpattern_0, ns=158

pattern_2, n=520; subpattern_1, ns=124

pattern_2, n=520; subpattern_2, ns=82

pattern_2, n=520; subpattern_3, ns=73

pattern_2, n=520; subpattern_4, ns=69

pattern_2, n=520; subpattern_5, ns=9

pattern_2, n=520; subpattern_6, ns=5

TF-MoDisCO pattern_2 n=520, PWM

pattern_2, n=520; subpattern_0, ns=158

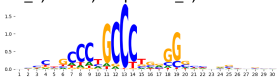

pattern_2, n=520; subpattern_1, ns=124

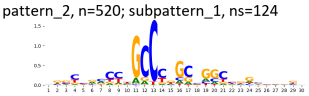

pattern_2, n=520; subpattern_2, ns=82

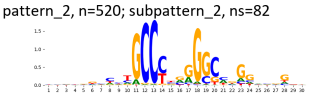

pattern_2, n=520; subpattern_3, ns=73

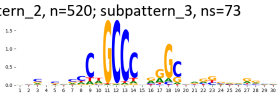

pattern_2, n=520; subpattern_4, ns=69

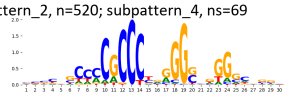

pattern_2, n=520; subpattern_5, ns=9

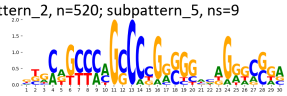

pattern_2, n=520; subpattern_6, ns=5

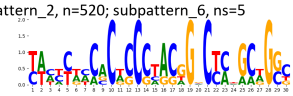

TF-MoDisCO pattern_4 n=250, CWM

pattern_4, n=250; subpattern_0, ns=63

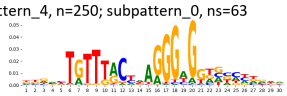

pattern_4, n=250; subpattern_1, ns=61

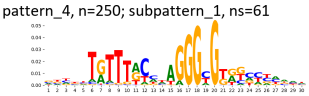

pattern_4, n=250; subpattern_2, ns=58

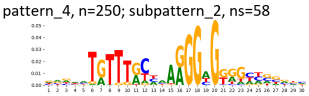

pattern_4, n=250; subpattern_3, ns=43

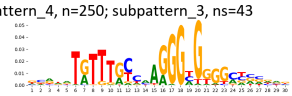

pattern_4, n=250; subpattern_4, ns=10

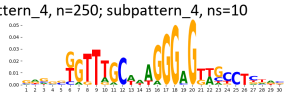

pattern_4, n=250; subpattern_5, ns=9

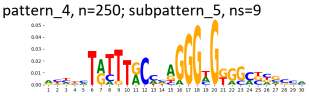

pattern_4, n=250; subpattern_6, ns=4

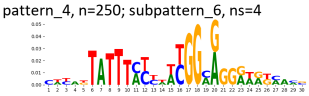

pattern_4, n=250; subpattern_7, ns=2

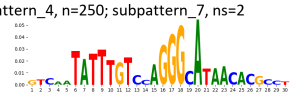

TF-MoDisCO pattern_4 n=250, PWM

pattern_4, n=250; subpattern_0, ns=63

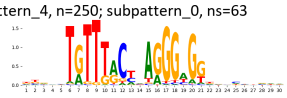

pattern_4, n=250; subpattern_1, ns=61

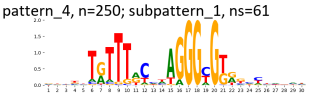

pattern_4, n=250; subpattern_2, ns=58

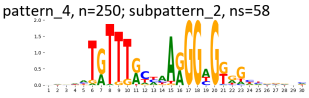

pattern_4, n=250; subpattern_3, ns=43

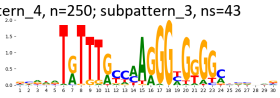

pattern_4, n=250; subpattern_4, ns=10

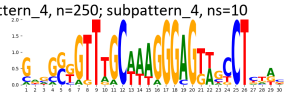

pattern_4, n=250; subpattern_5, ns=9

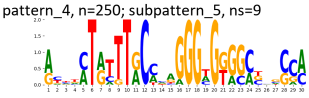

pattern_4, n=250; subpattern_6, ns=4

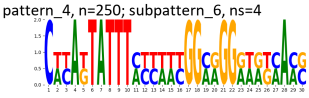

pattern_4, n=250; subpattern_7, ns=2

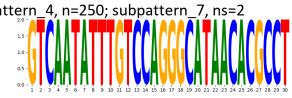

TF-MoDisCO pattern_5 n=99, CWM

pattern_5, n=99; subpattern_0, ns=42

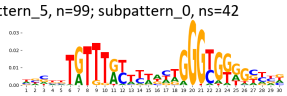

pattern_5, n=99; subpattern_1, ns=39

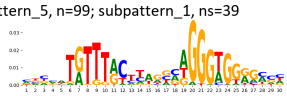

pattern_5, n=99; subpattern_2, ns=11

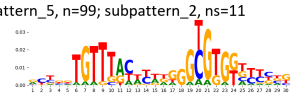

pattern_5, n=99; subpattern_3, ns=5

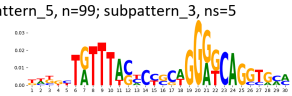

pattern_5, n=99; subpattern_4, ns=2

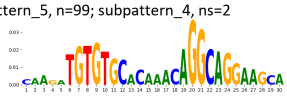

TF-MoDisCO pattern_5 n=99, PWM

pattern_5, n=99; subpattern_0, ns=42

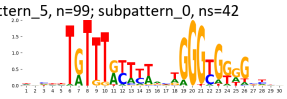

pattern_5, n=99; subpattern_1, ns=39

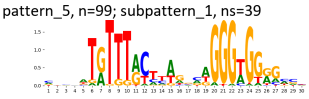

pattern_5, n=99; subpattern_2, ns=11

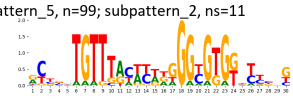

pattern_5, n=99; subpattern_3, ns=5

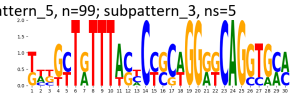

pattern_5, n=99; subpattern_4, ns=2

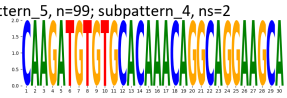

Supplementary Figure 120: TF-MoDisCO subpatterns for the KLF4 transcription factor in MCF-7 (accession ENCSR265WJC).

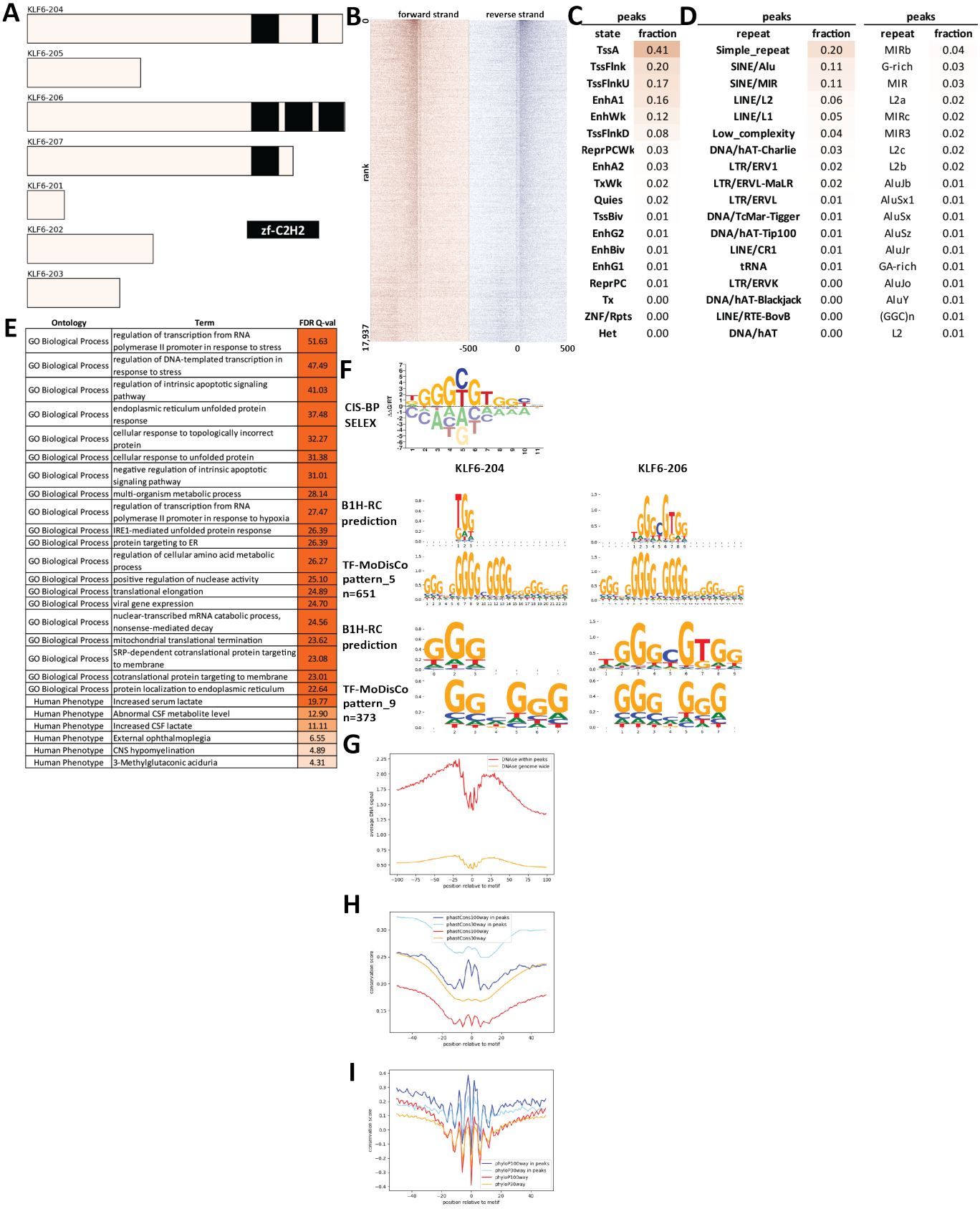

Supplementary Figure 121: Properties and genomic distribution of motifs identified for the KLF6 transcription factor in HepG2 (accession ENCSR757EKM).

TF-MoDisCO pattern_5 n=651, CWM

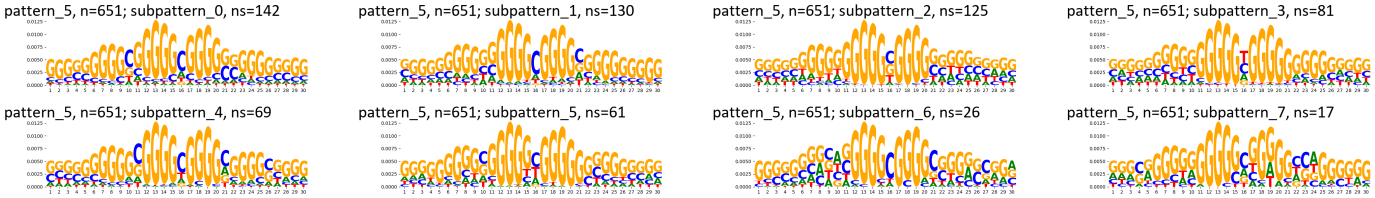

TF-MoDisCO pattern_5 n=651, PWM

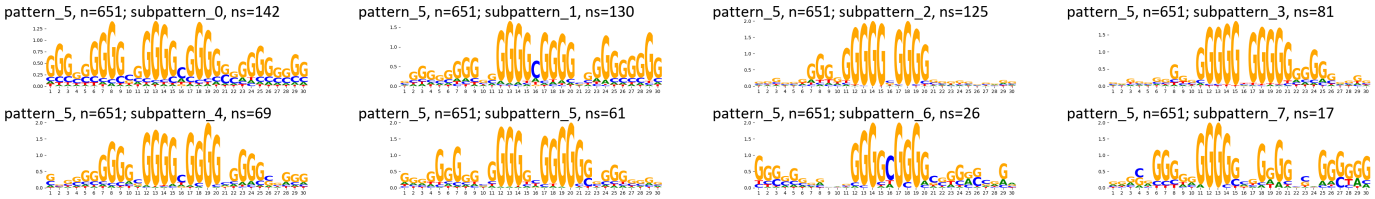

TF-MoDisCO pattern_9 n=373, CWM

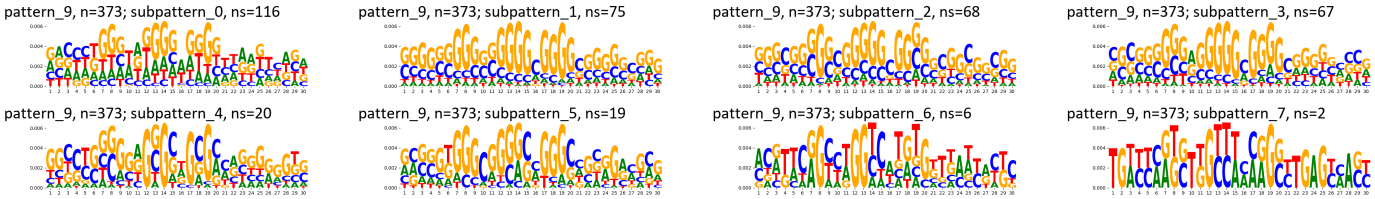

TF-MoDisCO pattern_9 n=373, PWM

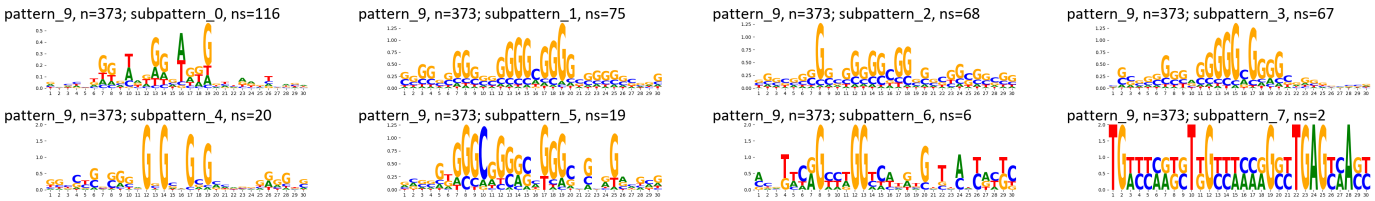

Supplementary Figure 122: TF-MoDisCO subpatterns for the KLF6 transcription factor in HepG2 (accession ENCSR757EKM).

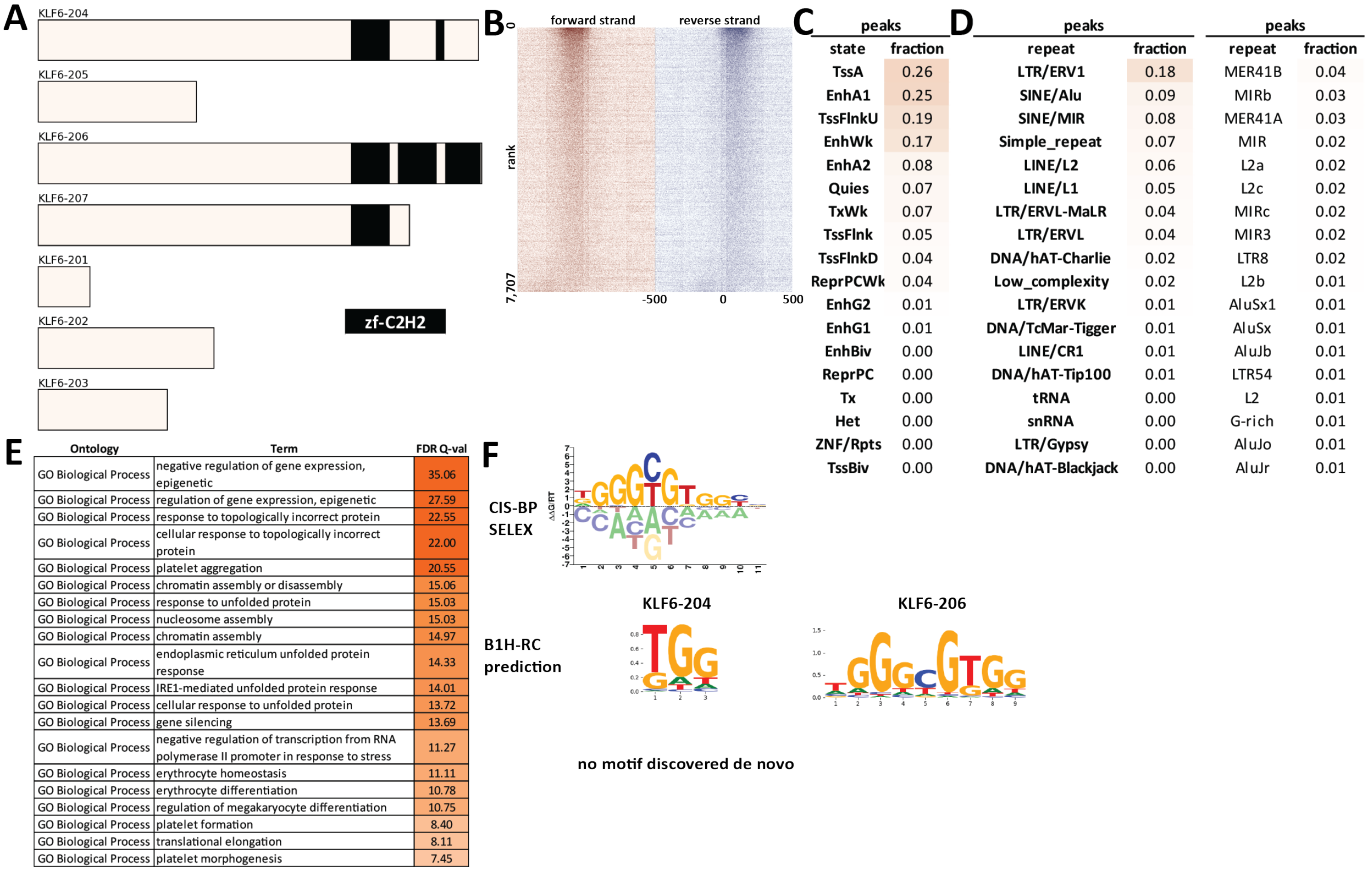

Supplementary Figure 123: Properties and genomic distribution of motifs identified for the KLF6 transcription factor in K562 (accession ENCSR297CGF).

TF-MoDisCO pattern_0 n=1660, CWM

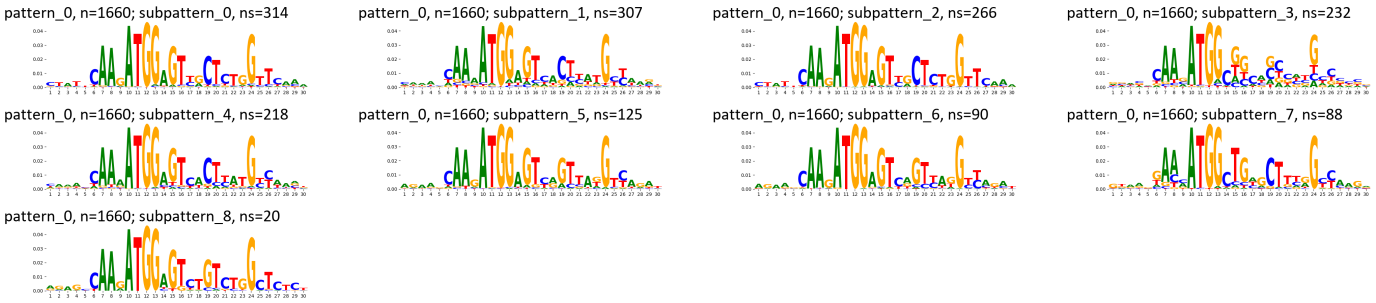

TF-MoDisCO pattern_0 n=1660, PWM

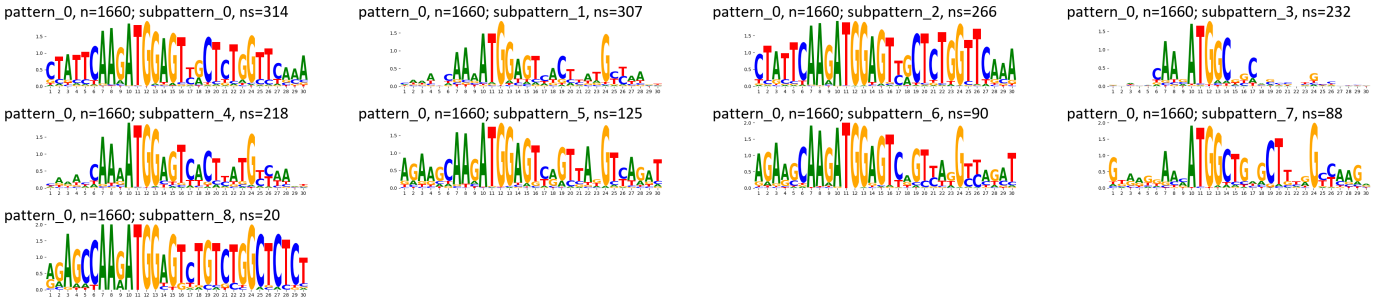

Supplementary Figure 124: TF-MoDisCO subpatterns for the KLF6 transcription factor in K562 (accession ENCSR297CGF).

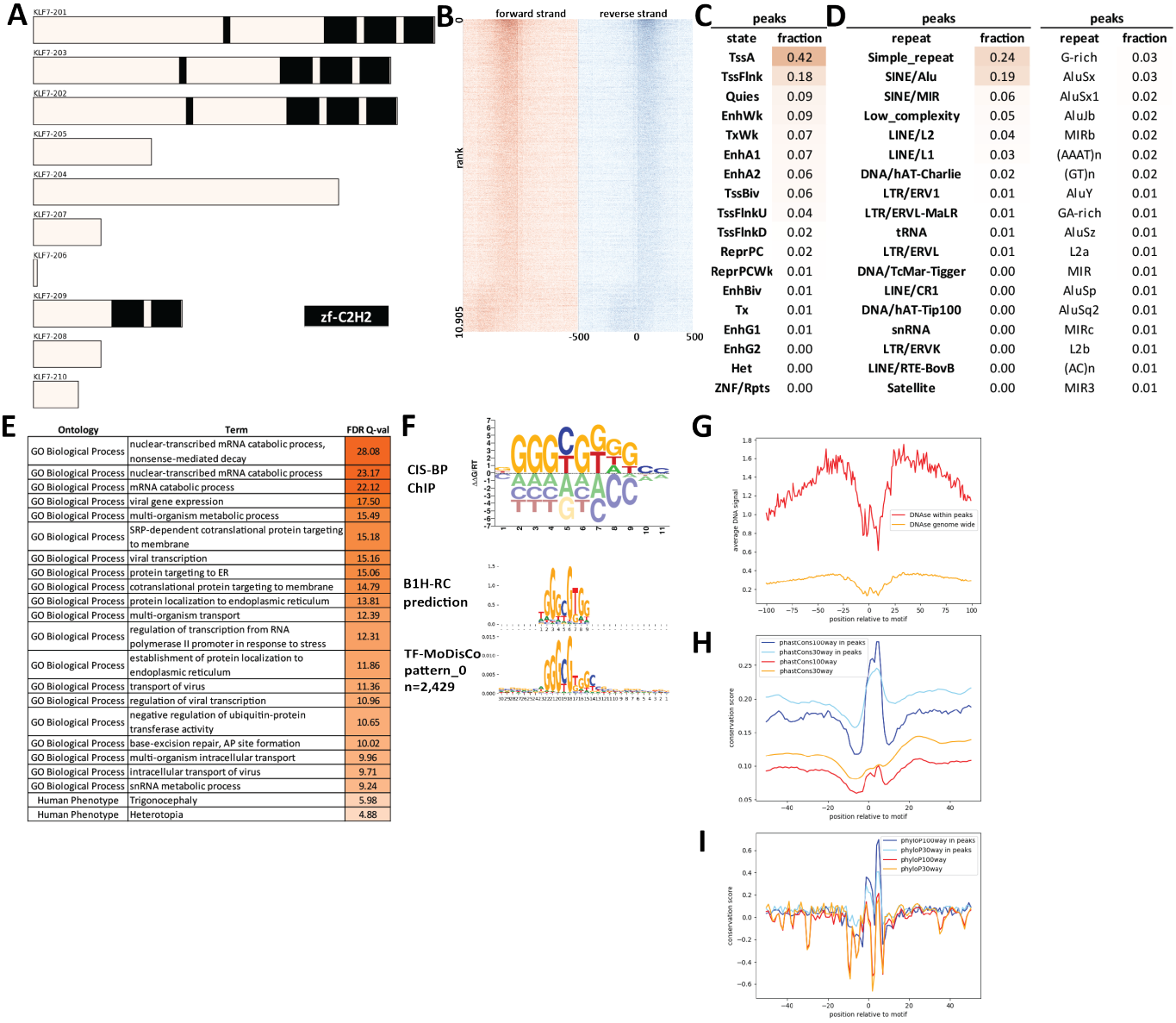

Supplementary Figure 125: Properties and genomic distribution of motifs identified for the KLF7 transcription factor in HEK293 (accession ENCSR604VWJ).

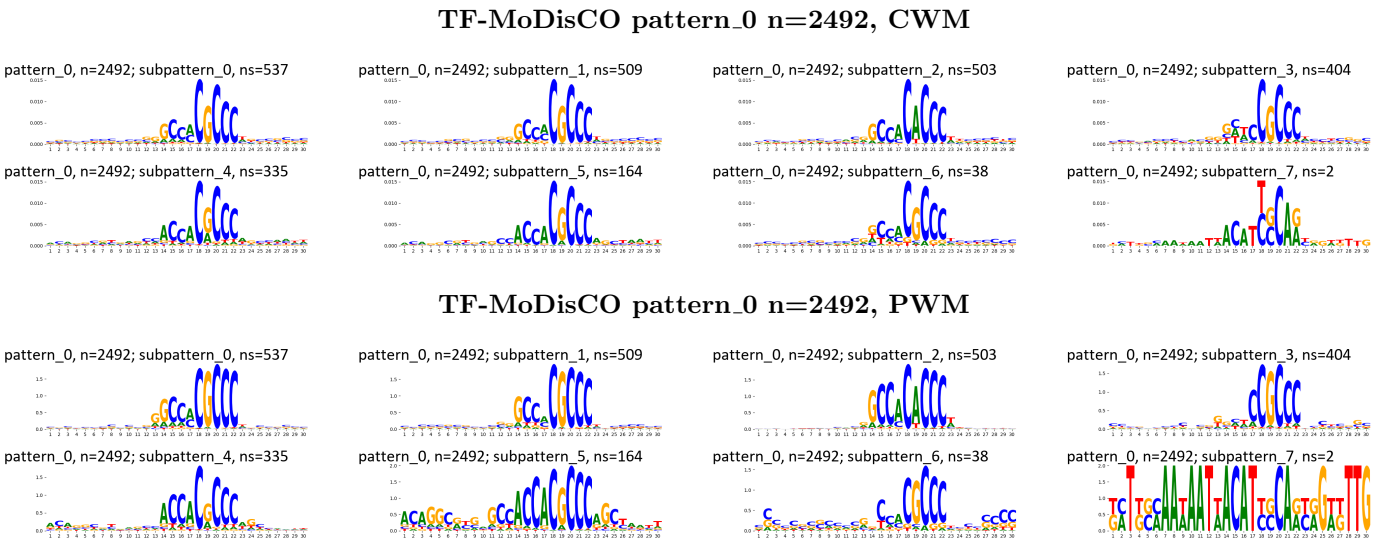

Supplementary Figure 126: TF-MoDisCO subpatterns for the KLF7 transcription factor in HEK293 (accession ENCSR604VWJ).

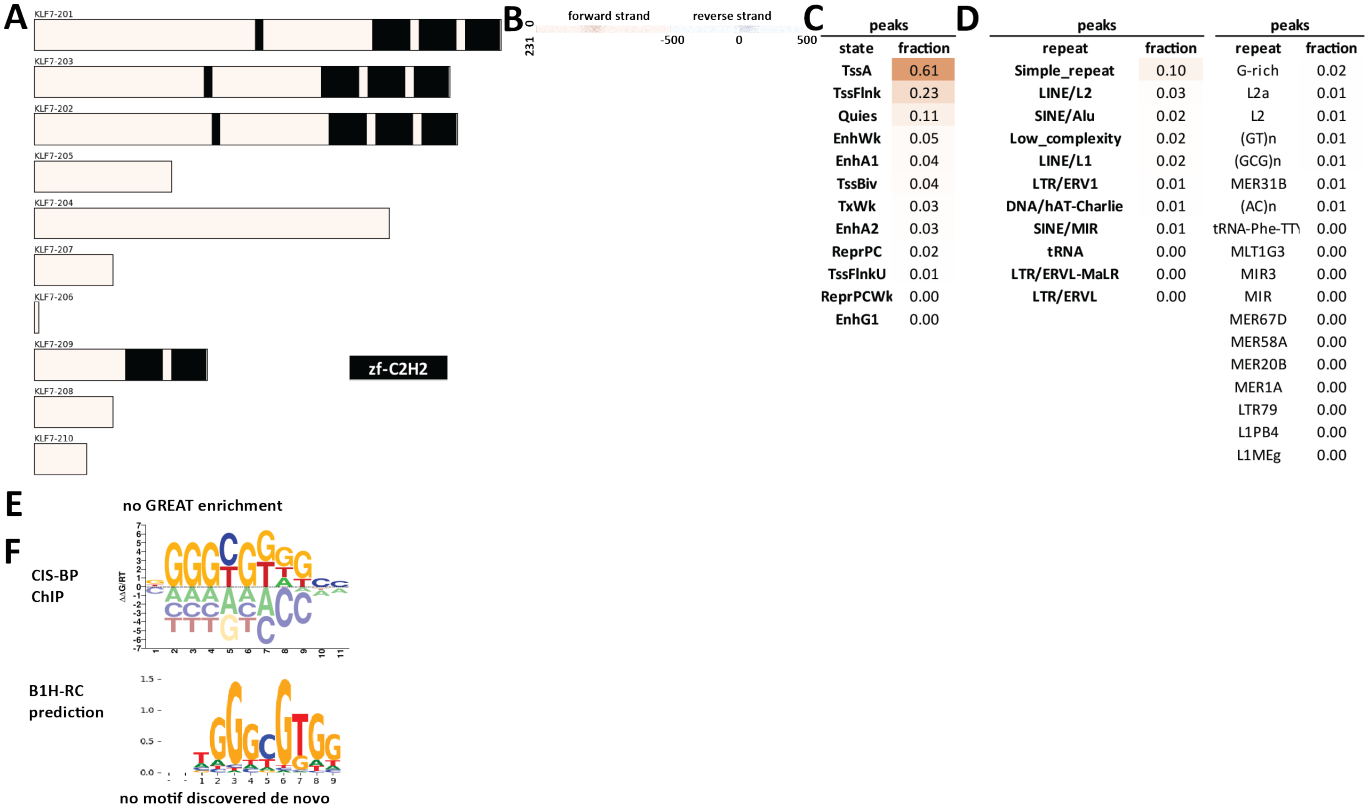

Supplementary Figure 127: Properties and genomic distribution of motifs identified for the KLF7 transcription factor in HEK293 (accession Hughes GR models).

A

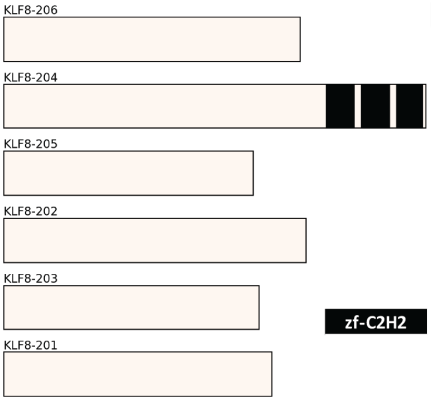

B

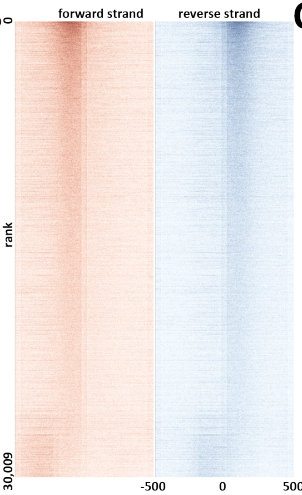

C

peaks	
state	fraction
TssA	0.31
TssFlnk	0.18
EnhWk	0.12
Quies	0.10
TxWk	0.07
EnhA1	0.06
TssBiv	0.05
EnhA2	0.05
TssFlnkU	0.03
Tx	0.02
ReprPC	0.02
TssFlnkD	0.02
ReprPCWk	0.02
EnhBiv	0.01
EnhG1	0.01
Het	0.00
EnhG2	0.00
ZNF/Rpts	0.00

D

peaks		peaks	
repeat	fraction	repeat	fraction
Simple_repeat	0.22	G-rich	0.03
SINE/Alu	0.12	MIRb	0.03
SINE/MIR	0.07	MIR	0.02
Low_complexity	0.05	L2a	0.02
LINE/L2	0.04	AluSx	0.01
LINE/L1	0.04	AluSx1	0.01
LTR/ERVL-MaLR	0.02	GA-rich	0.01
DNA/hAT-Charlie	0.02	L2c	0.01
LTR/ERV1	0.01	MIRc	0.01
LTR/ERVL	0.01	MIR3	0.01
DNA/TcMar-Tigger	0.01	AluJb	0.01
tRNA	0.01	L2b	0.01
LINE/CR1	0.01	(GT)n	0.01
DNA/hAT-Tip100	0.00	AluY	0.01
LTR/ERVK	0.00	AluSz	0.01
snRNA	0.00	AluJr	0.01
LINE/RTE-BovB	0.00	AluJo	0.01
DNA/hAT-Blackjack	0.00	(AC)n	0.01

E

Ontology	Term	FDR Q-val
GO Biological Process	nuclear-transcribed mRNA catabolic process, nonsense-mediated decay	29.02
GO Biological Process	cytoplasmic sequestering of protein	27.09
GO Biological Process	SRP-dependent cotranslational protein targeting to membrane	22.45
GO Biological Process	positive regulation of viral transcription	14.70
GO Biological Process	mismatch repair	14.03
GO Biological Process	global genome nucleotide-excision repair	10.88
GO Biological Process	nucleotide-excision repair, DNA damage recognition	8.37
GO Biological Process	deoxyribose phosphate catabolic process	5.91
GO Biological Process	deoxyribonucleotide catabolic process	5.90

F

no CIS-BP motif available

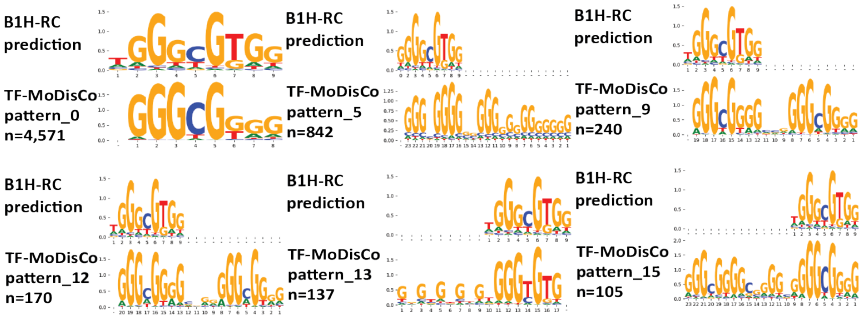

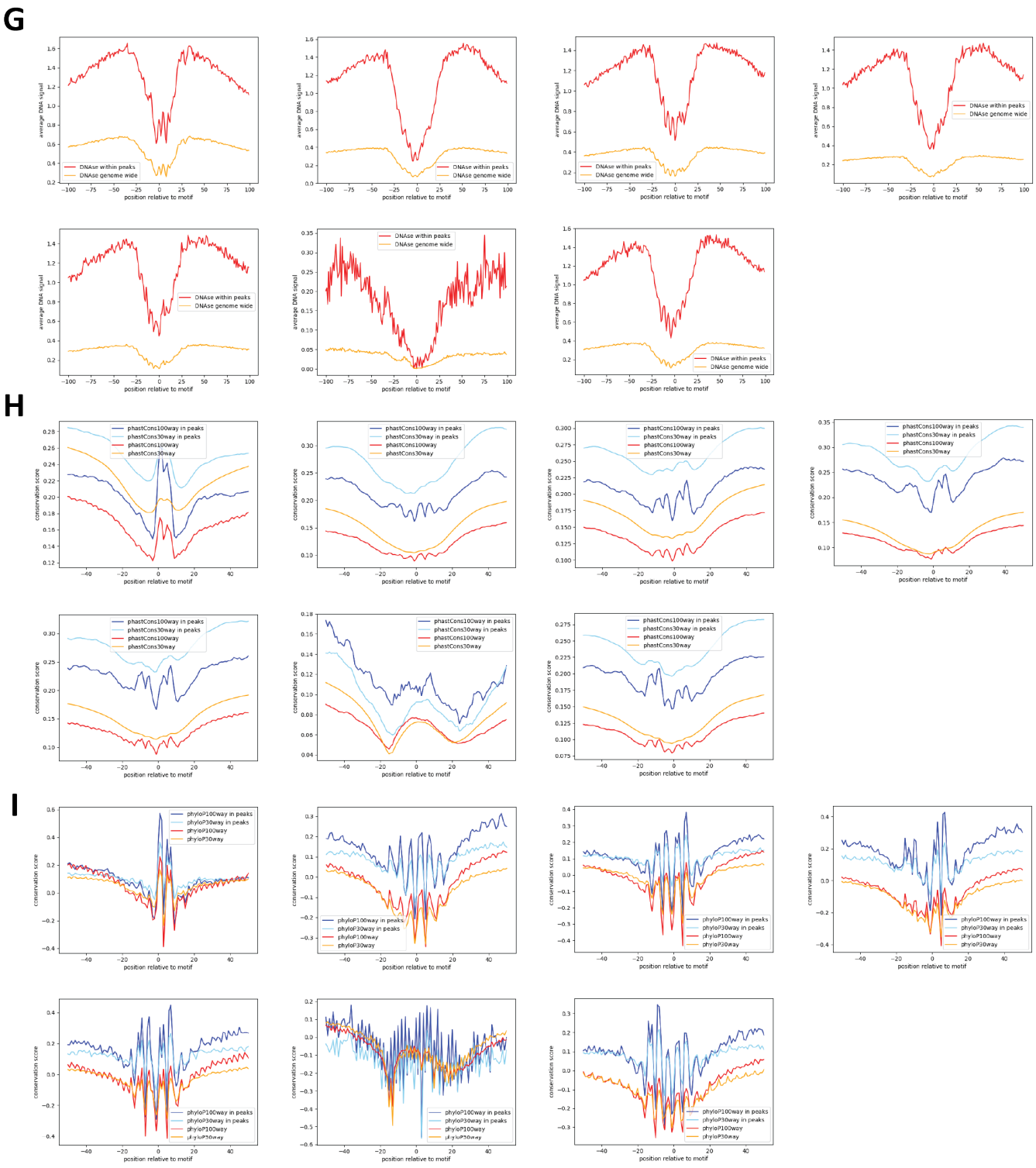

Supplementary Figure 128: Properties and genomic distribution of motifs identified for the KLF8 transcription factor in HEK293 (accession ENCSR635NOQ).

TF-MoDisCO pattern_0 n=4571, CWM

pattern_0, n=4571; subpattern_0, ns=1004

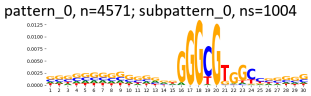

pattern_0, n=4571; subpattern_1, ns=796

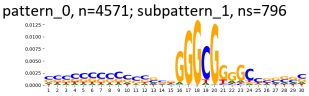

pattern_0, n=4571; subpattern_10, ns=163

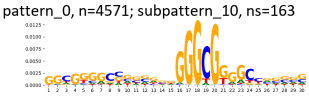

pattern_0, n=4571; subpattern_11, ns=156

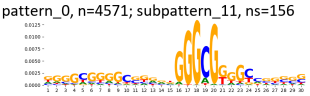

pattern_0, n=4571; subpattern_12, ns=102

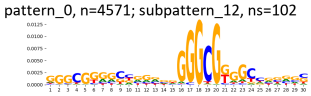

pattern_0, n=4571; subpattern_13, ns=72

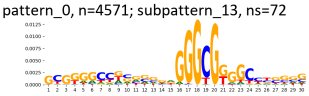

pattern_0, n=4571; subpattern_14, ns=30

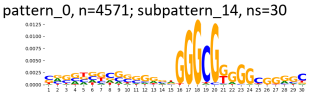

pattern_0, n=4571; subpattern_15, ns=2

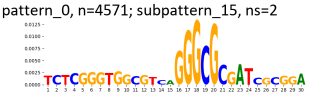

pattern_0, n=4571; subpattern_2, ns=671

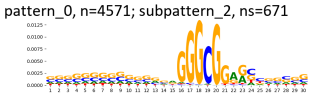

pattern_0, n=4571; subpattern_3, ns=317

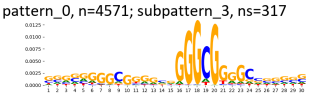

pattern_0, n=4571; subpattern_4, ns=312

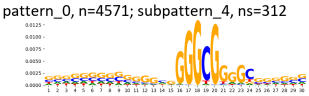

pattern_0, n=4571; subpattern_5, ns=206

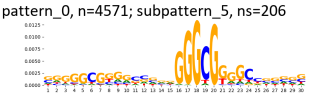

pattern_0, n=4571; subpattern_6, ns=202

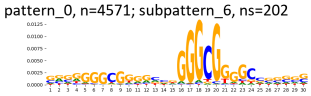

pattern_0, n=4571; subpattern_7, ns=187

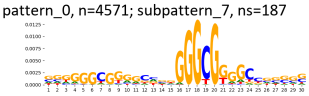

pattern_0, n=4571; subpattern_8, ns=179

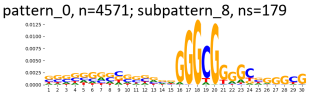

pattern_0, n=4571; subpattern_9, ns=172

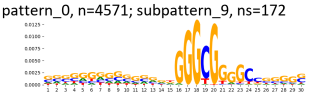

TF-MoDisCO pattern_0 n=4571, PWM

pattern_0, n=4571; subpattern_0, ns=1004

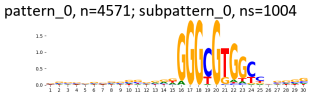

pattern_0, n=4571; subpattern_1, ns=796

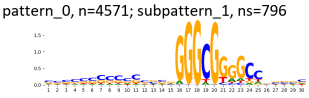

pattern_0, n=4571; subpattern_10, ns=163

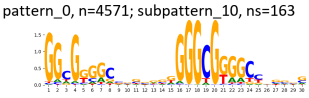

pattern_0, n=4571; subpattern_11, ns=156

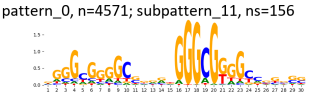

pattern_0, n=4571; subpattern_12, ns=102

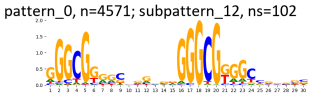

pattern_0, n=4571; subpattern_13, ns=72

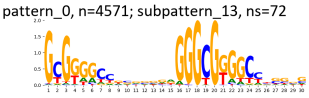

pattern_0, n=4571; subpattern_14, ns=30

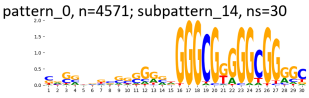

pattern_0, n=4571; subpattern_15, ns=2

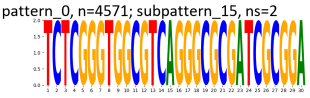

pattern_0, n=4571; subpattern_2, ns=671

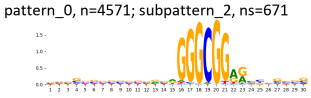

pattern_0, n=4571; subpattern_3, ns=317

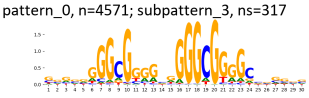

pattern_0, n=4571; subpattern_4, ns=312

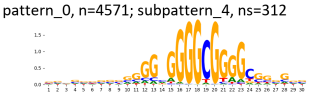

pattern_0, n=4571; subpattern_5, ns=206

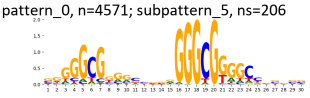

pattern_0, n=4571; subpattern_6, ns=202

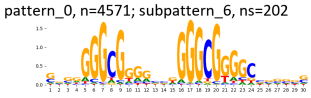

pattern_0, n=4571; subpattern_7, ns=187

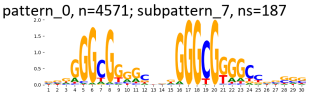

pattern_0, n=4571; subpattern_8, ns=179

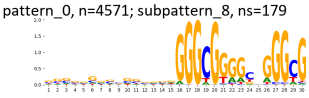

pattern_0, n=4571; subpattern_9, ns=172

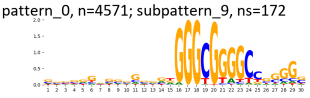

TF-MoDisCO pattern_10 n=217, CWM

pattern_10, n=217; subpattern_0, ns=60

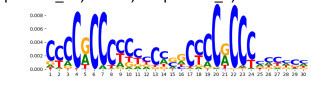

pattern_10, n=217; subpattern_1, ns=56

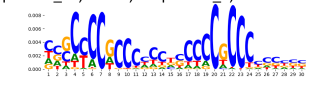

pattern_10, n=217; subpattern_2, ns=36

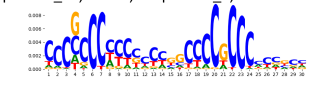

pattern_10, n=217; subpattern_3, ns=22

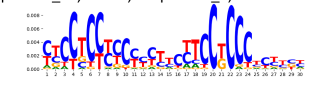

pattern_10, n=217; subpattern_4, ns=20

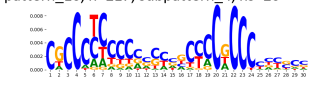

pattern_10, n=217; subpattern_5, ns=13

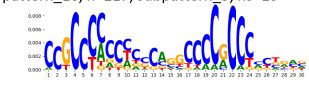

pattern_10, n=217; subpattern_6, ns=10



TF-MoDisCO pattern_10 n=217, PWM

pattern_10, n=217; subpattern_0, ns=60

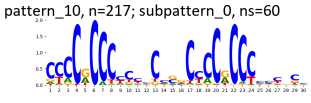

pattern_10, n=217; subpattern_1, ns=56

pattern_10, n=217; subpattern_2, ns=36

pattern_10, n=217; subpattern_3, ns=22

pattern_10, n=217; subpattern_4, ns=20

pattern_10, n=217; subpattern_5, ns=13

pattern_10, n=217; subpattern_6, ns=10

TF-MoDisCO pattern_12 n=170, CWM

pattern_12, n=170; subpattern_0, ns=40

pattern_12, n=170; subpattern_1, ns=29

pattern_12, n=170; subpattern_2, ns=29

pattern_12, n=170; subpattern_3, ns=26

pattern_12, n=170; subpattern_4, ns=23

pattern_12, n=170; subpattern_5, ns=18

pattern_12, n=170; subpattern_6, ns=5

TF-MoDisCO pattern_12 n=170, PWM

pattern_12, n=170; subpattern_0, ns=40

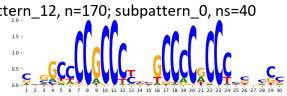

pattern_12, n=170; subpattern_1, ns=29

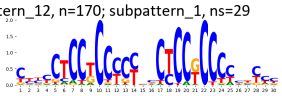

pattern_12, n=170; subpattern_2, ns=29

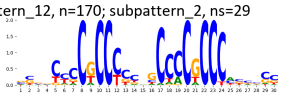

pattern_12, n=170; subpattern_3, ns=26

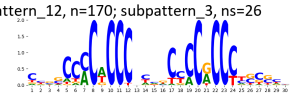

pattern_12, n=170; subpattern_4, ns=23

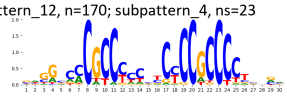

pattern_12, n=170; subpattern_5, ns=18

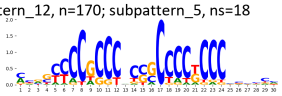

pattern_12, n=170; subpattern_6, ns=5

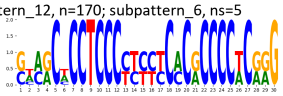

TF-MoDisCO pattern_13 n=137, CWM

pattern_13, n=137; subpattern_0, ns=38

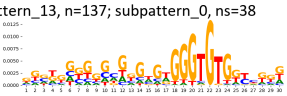

pattern_13, n=137; subpattern_1, ns=35

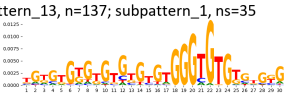

pattern_13, n=137; subpattern_2, ns=20

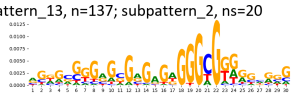

pattern_13, n=137; subpattern_3, ns=17

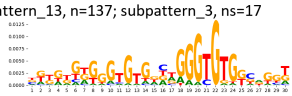

pattern_13, n=137; subpattern_4, ns=15

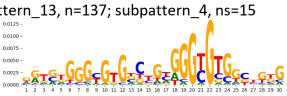

pattern_13, n=137; subpattern_5, ns=12

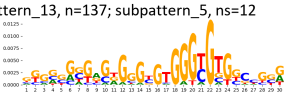

TF-MoDisCO pattern_13 n=137, PWM

pattern_13, n=137; subpattern_0, ns=38

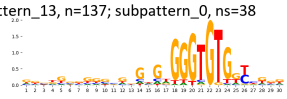

pattern_13, n=137; subpattern_1, ns=35

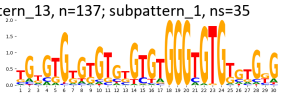

pattern_13, n=137; subpattern_2, ns=20

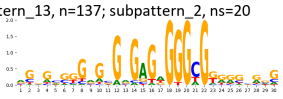

pattern_13, n=137; subpattern_3, ns=17

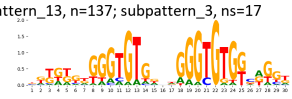

pattern_13, n=137; subpattern_4, ns=15

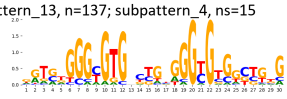

pattern_13, n=137; subpattern_5, ns=12

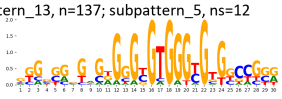

TF-MoDisCO pattern_15 n=105, CWM

pattern_15, n=105; subpattern_0, ns=34

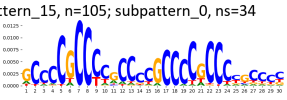

pattern_15, n=105; subpattern_1, ns=33

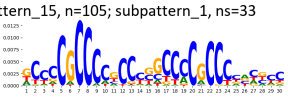

pattern_15, n=105; subpattern_2, ns=21

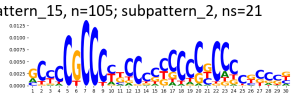

pattern_15, n=105; subpattern_3, ns=17

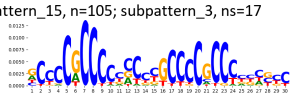

TF-MoDisCO pattern_15 n=105, PWM

pattern_15, n=105; subpattern_0, ns=34

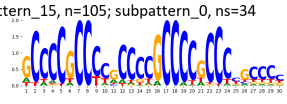

pattern_15, n=105; subpattern_1, ns=33

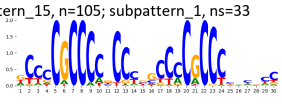

pattern_15, n=105; subpattern_2, ns=21

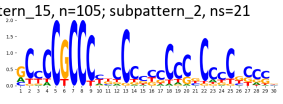

pattern_15, n=105; subpattern_3, ns=17

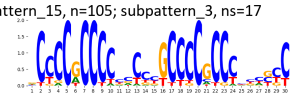

TF-MoDisCO pattern_5 n=842, CWM

pattern_5, n=842; subpattern_0, ns=193

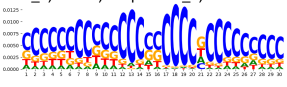

pattern_5, n=842; subpattern_1, ns=186

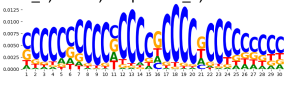

pattern_5, n=842; subpattern_2, ns=174

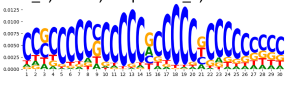

pattern_5, n=842; subpattern_3, ns=166

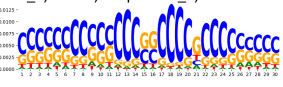

pattern_5, n=842; subpattern_4, ns=101

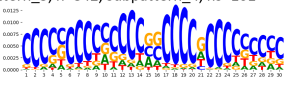

pattern_5, n=842; subpattern_5, ns=10



pattern_5, n=842; subpattern_6, ns=10



pattern_5, n=842; subpattern_7, ns=2

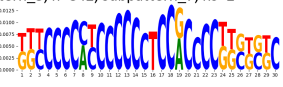

TF-MoDisCO pattern_5 n=842, PWM

pattern_5, n=842; subpattern_0, ns=193

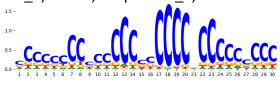

pattern_5, n=842; subpattern_1, ns=186

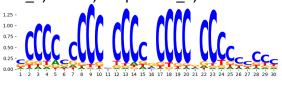

pattern_5, n=842; subpattern_2, ns=174

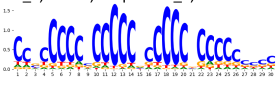

pattern_5, n=842; subpattern_3, ns=166



pattern_5, n=842; subpattern_4, ns=101

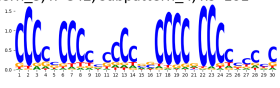

pattern_5, n=842; subpattern_5, ns=10

pattern_5, n=842; subpattern_6, ns=10

pattern_5, n=842; subpattern_7, ns=2

TF-MoDisCO pattern_9 n=240, CWM

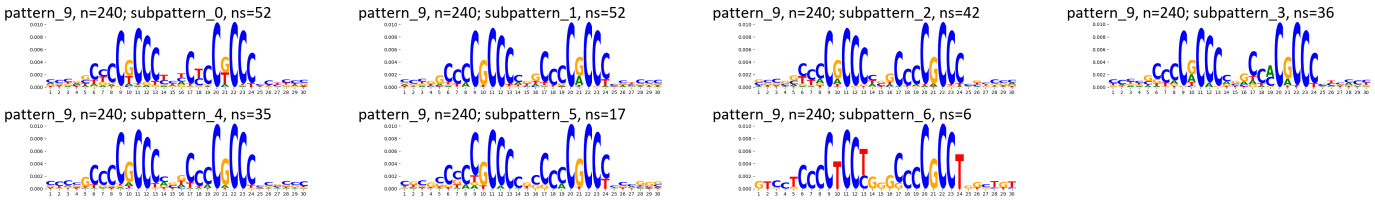

TF-MoDisCO pattern_9 n=240, PWM

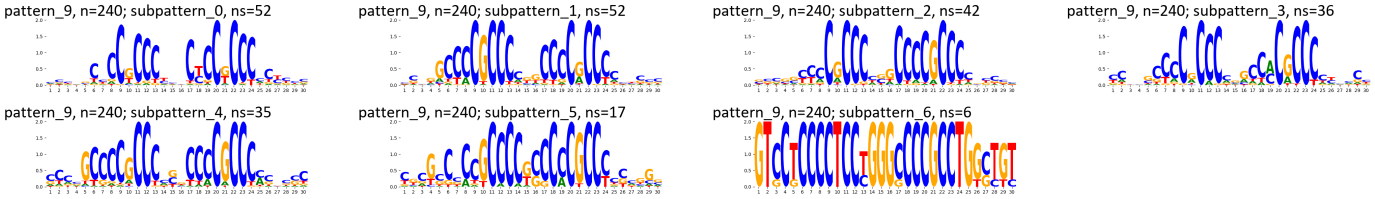

Supplementary Figure 129: TF-MoDisCO subpatterns for the KLF8 transcription factor in HEK293 (accession ENCSR635NOQ).

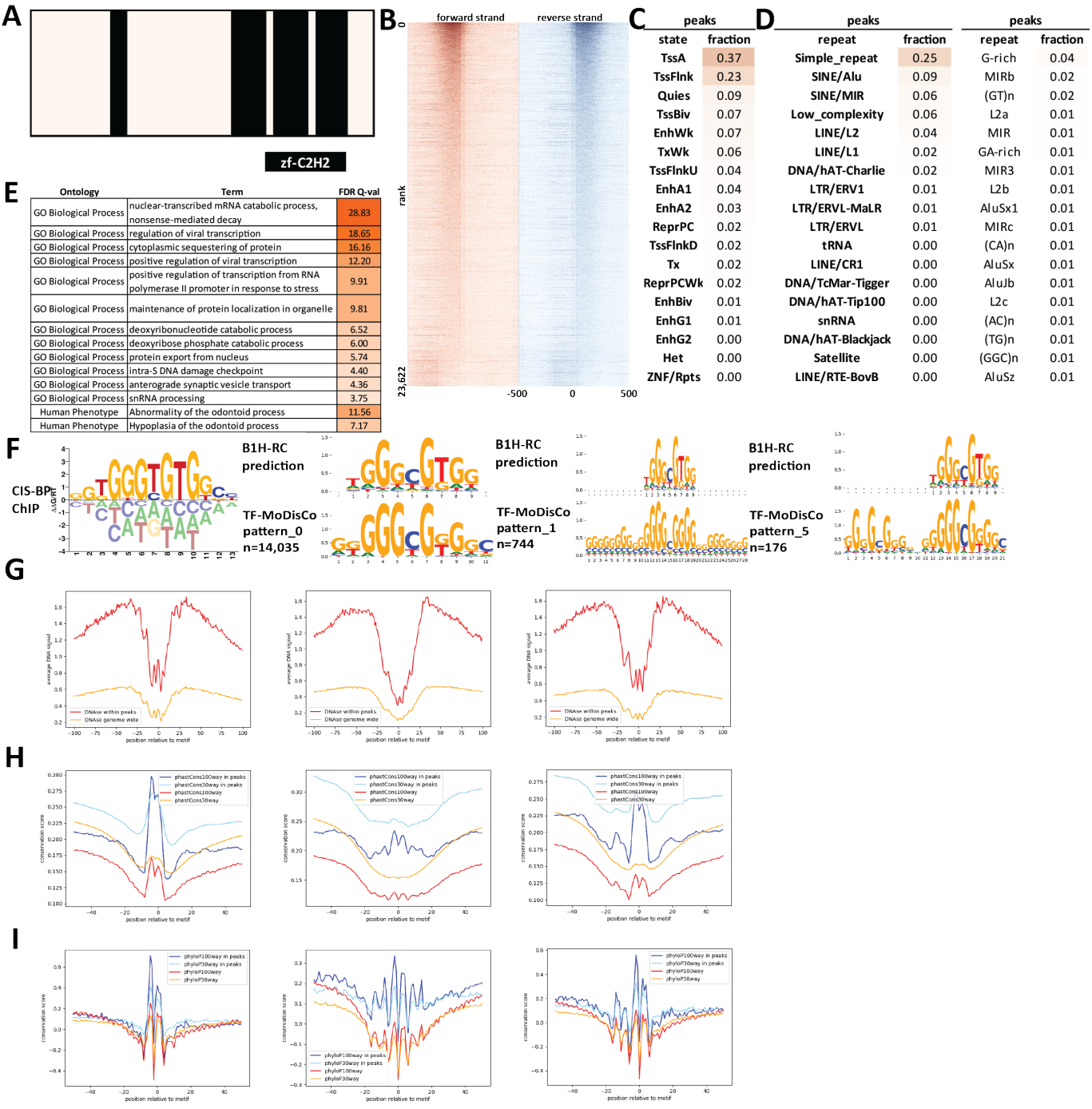

Supplementary Figure 130: Properties and genomic distribution of motifs identified for the KLF9 transcription factor in HEK293 (accession ENCSR076EZB).

TF-MoDisCO pattern_0 n=14035, CWM

pattern_0, n=14035; subpattern_0, ns=2745

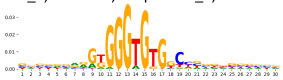

pattern_0, n=14035; subpattern_1, ns=2227

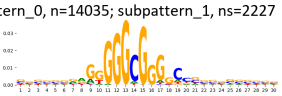

pattern_0, n=14035; subpattern_10, ns=250

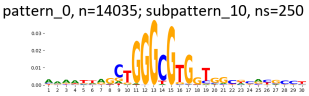

pattern_0, n=14035; subpattern_11, ns=239

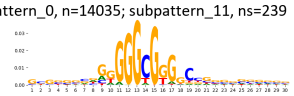

pattern_0, n=14035; subpattern_2, ns=1924

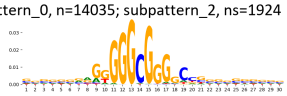

pattern_0, n=14035; subpattern_3, ns=1516

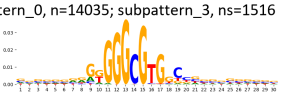

pattern_0, n=14035; subpattern_4, ns=1405

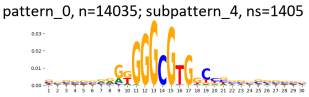

pattern_0, n=14035; subpattern_5, ns=1028

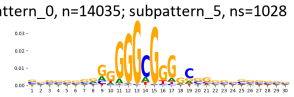

pattern_0, n=14035; subpattern_6, ns=911

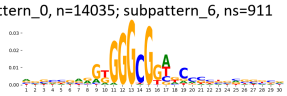

pattern_0, n=14035; subpattern_7, ns=674

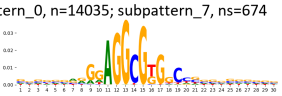

pattern_0, n=14035; subpattern_8, ns=570

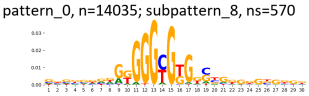

pattern_0, n=14035; subpattern_9, ns=546

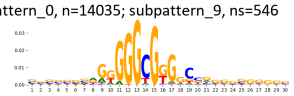

TF-MoDisCO pattern_0 n=14035, PWM

pattern_0, n=14035; subpattern_0, ns=2745

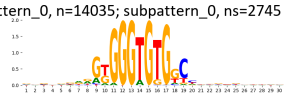

pattern_0, n=14035; subpattern_1, ns=2227

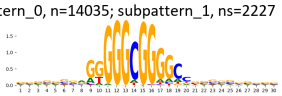

pattern_0, n=14035; subpattern_10, ns=250

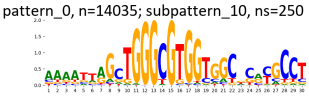

pattern_0, n=14035; subpattern_11, ns=239

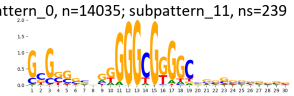

pattern_0, n=14035; subpattern_2, ns=1924

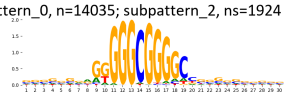

pattern_0, n=14035; subpattern_3, ns=1516

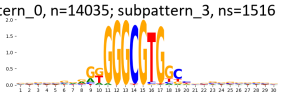

pattern_0, n=14035; subpattern_4, ns=1405

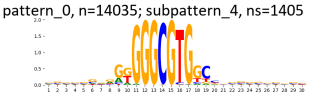

pattern_0, n=14035; subpattern_5, ns=1028

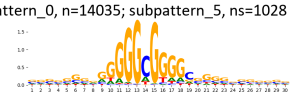

pattern_0, n=14035; subpattern_6, ns=911

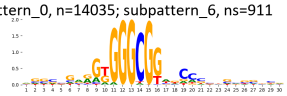

pattern_0, n=14035; subpattern_7, ns=674

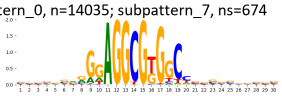

pattern_0, n=14035; subpattern_8, ns=570

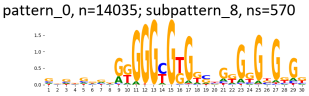

pattern_0, n=14035; subpattern_9, ns=546

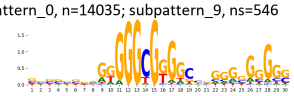

TF-MoDisCO pattern_1 n=744, CWM

pattern_1, n=744; subpattern_0, ns=244

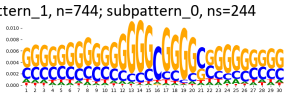

pattern_1, n=744; subpattern_1, ns=193

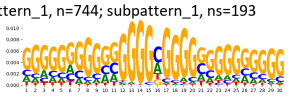

pattern_1, n=744; subpattern_2, ns=162

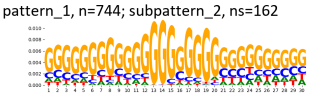

pattern_1, n=744; subpattern_3, ns=82

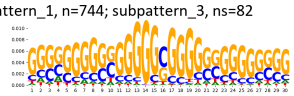

pattern_1, n=744; subpattern_4, ns=53

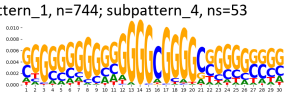

pattern_1, n=744; subpattern_5, ns=6

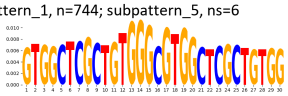

pattern_1, n=744; subpattern_6, ns=4

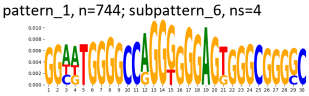

TF-MoDisCO pattern_1 n=744, PWM

pattern_1, n=744; subpattern_0, ns=244

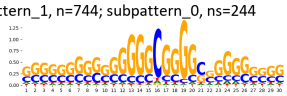

pattern_1, n=744; subpattern_1, ns=193

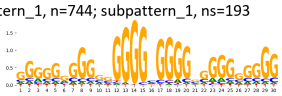

pattern_1, n=744; subpattern_2, ns=162

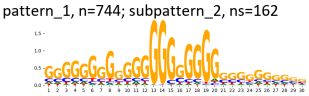

pattern_1, n=744; subpattern_3, ns=82

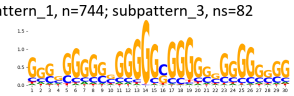

pattern_1, n=744; subpattern_4, ns=53

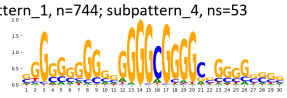

pattern_1, n=744; subpattern_5, ns=6

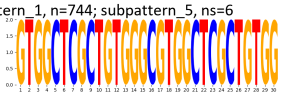

pattern_1, n=744; subpattern_6, ns=4

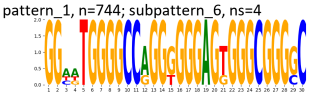

TF-MoDisCO pattern_5 n=176, CWM

pattern_5, n=176; subpattern_0, ns=50

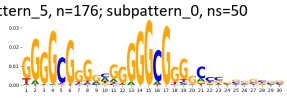

pattern_5, n=176; subpattern_1, ns=49

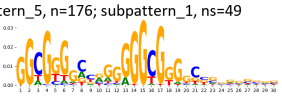

pattern_5, n=176; subpattern_2, ns=48

pattern_5, n=176; subpattern_3, ns=15

pattern_5, n=176; subpattern_4, ns=14

TF-MoDisCO pattern_5 n=176, PWM

pattern_5, n=176; subpattern_0, ns=50

pattern_5, n=176; subpattern_1, ns=49

pattern_5, n=176; subpattern_2, ns=48

pattern_5, n=176; subpattern_3, ns=15

pattern_5, n=176; subpattern_4, ns=14

Supplementary Figure 131: TF-MoDisCO subpatterns for the KLF9 transcription factor in HEK293 (accession ENCSR076EZB).

A

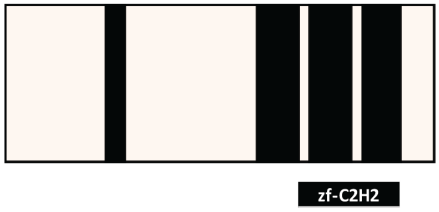

B

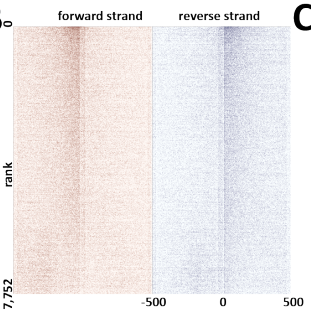

C

peaks	
state	fraction
TssA	0.47
TssFlnkU	0.22
TssFlnk	0.19
EnhA1	0.17
EnhWk	0.09
TssFlnkD	0.08
EnhA2	0.03
ReprPCWk	0.02
TxWk	0.02
EnhG2	0.01
Quies	0.01
TssBiv	0.01
EnhBiv	0.01
EnhG1	0.01
ReprPC	0.00
Tx	0.00
ZNF/Rpts	0.00

D

peaks		peaks	
repeat	fraction	repeat	fraction
Simple_repeat	0.15	MIRb	0.04
SINE/MIR	0.10	G-rich	0.02
SINE/Alu	0.10	L2a	0.02
LINE/L2	0.07	MIR	0.02
LINE/L1	0.04	L2c	0.02
Low_complexity	0.03	MIRc	0.02
DNA/hAT-Charlie	0.02	L2b	0.02
LTR/ERV1	0.02	MIR3	0.02
LTR/ERVL-MaLR	0.01	AluJb	0.01
LTR/ERVL	0.01	AluSx1	0.01
LINE/CR1	0.01	AluSx	0.01
tRNA	0.01	AluSz	0.01
DNA/TcMar-Tigger	0.01	AluJr	0.01
DNA/hAT-Tip100	0.01	AluJo	0.01
snRNA	0.00	L2	0.01
LTR/ERVK	0.00	GA-rich	0.01
LINE/RTE-BovB	0.00	(GGC)n	0.01
DNA/hAT-Blackjack	0.00	AluY	0.01

E

Ontology	Term	FDR Q-val
GO Biological Process	mitochondrion organization	46.37
GO Biological Process	nuclear-transcribed mRNA catabolic process	29.45
GO Biological Process	mRNA catabolic process	29.26
GO Biological Process	ncRNA processing	27.58
GO Biological Process	RNA catabolic process	26.83
GO Biological Process	nuclear-transcribed mRNA catabolic process, nonsense-mediated decay	26.22
GO Biological Process	rRNA processing	24.93
GO Biological Process	rRNA metabolic process	24.62
GO Biological Process	IRE1-mediated unfolded protein response	23.92
GO Biological Process	endoplasmic reticulum unfolded protein response	21.36
GO Biological Process	regulation of DNA-templated transcription in response to stress	21.25
GO Biological Process	cellular response to topologically incorrect protein	19.96
GO Biological Process	response to topologically incorrect protein	18.90
GO Biological Process	cellular response to unfolded protein	18.76
GO Biological Process	response to unfolded protein	17.15
GO Biological Process	macromolecular complex disassembly	16.70
GO Biological Process	multi-organism metabolic process	16.05
GO Biological Process	mitochondrial translation	15.26
GO Biological Process	liver regeneration	15.21
GO Biological Process	viral gene expression	14.99
Human Phenotype	Progressive external ophthalmoplegia	11.41
Human Phenotype	Increased serum lactate	8.80
Human Phenotype	Abnormality of mitochondrial metabolism	7.93
Human Phenotype	Abnormal CSF metabolite level	7.62
Human Phenotype	Increased CSF lactate	7.25
Human Phenotype	External ophthalmoplegia	5.85
Human Phenotype	Basal cell carcinoma	2.06
Human Phenotype	Increased serum pyruvate	1.87
Human Phenotype	Abnormality of glycolysis	1.87
Human Phenotype	Atrophy/Degeneration affecting the brainstem	1.53

F

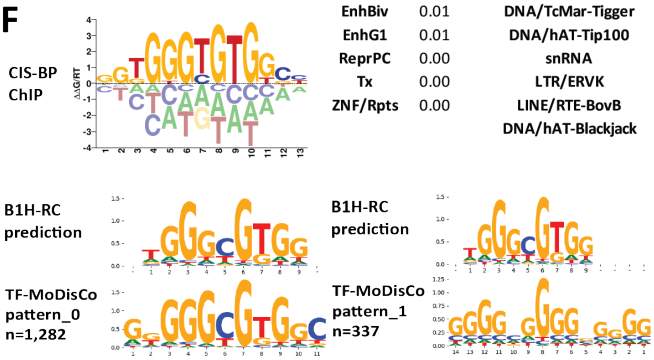

G

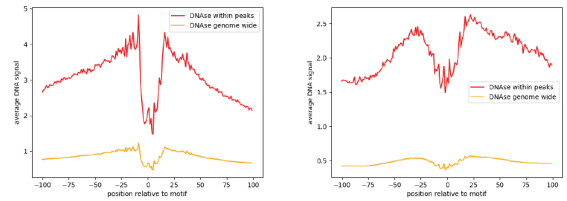

H

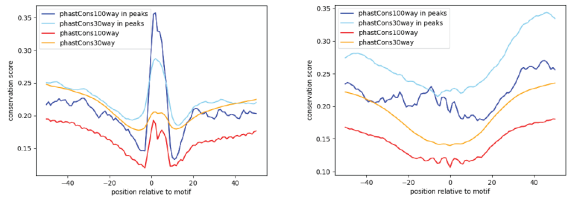

I

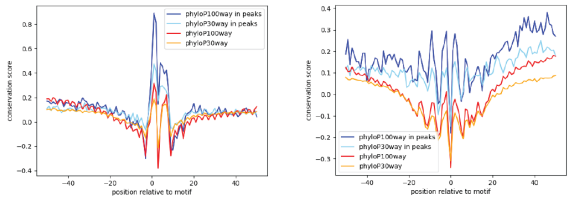

Supplementary Figure 132: Properties and genomic distribution of motifs identified for the KLF9 transcription factor in HepG2 (accession ENCSR938ETG).

TF-MoDisCO pattern_0 n=1282, CWM

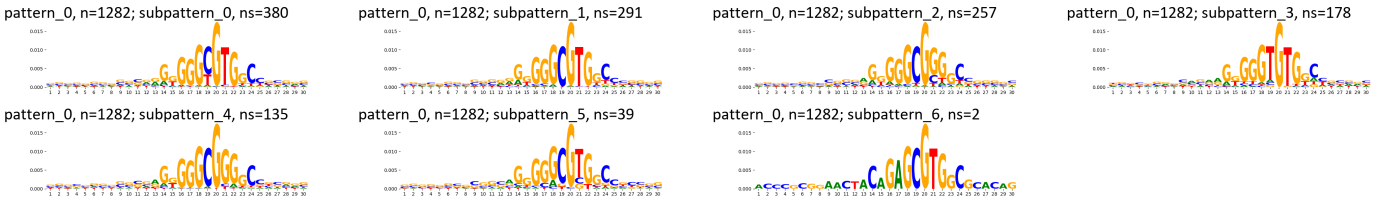

TF-MoDisCO pattern_0 n=1282, PWM

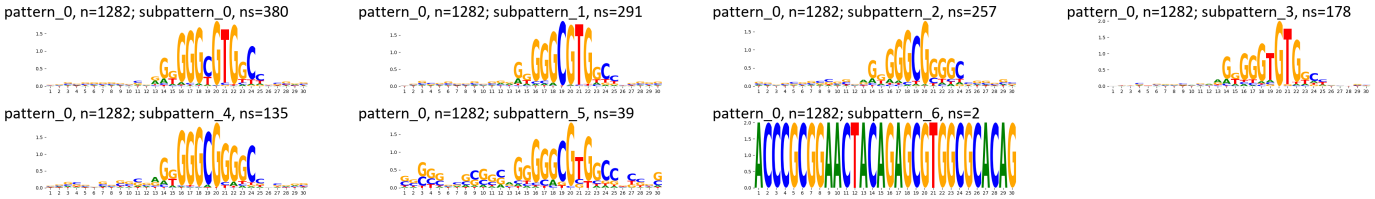

TF-MoDisCO pattern_1 n=337, CWM

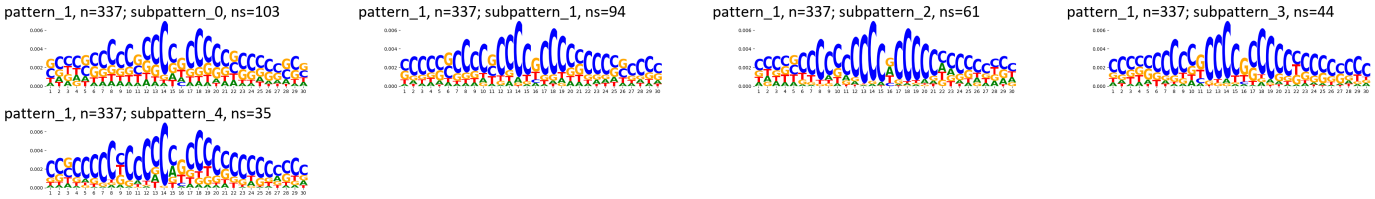

TF-MoDisCO pattern_1 n=337, PWM

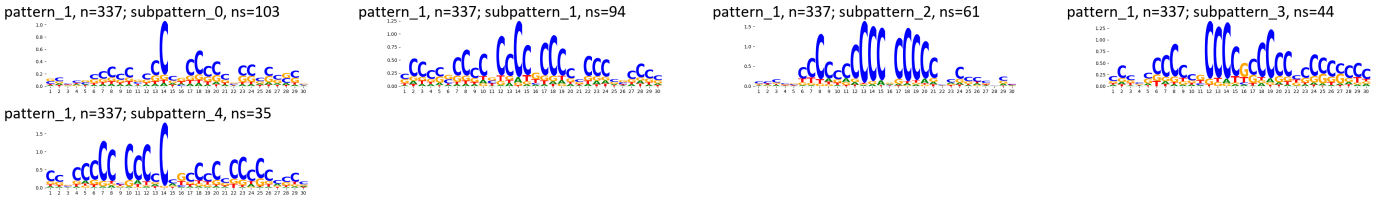

Supplementary Figure 133: TF-MoDisCO subpatterns for the KLF9 transcription factor in HepG2 (accession ENCSR938ETG).

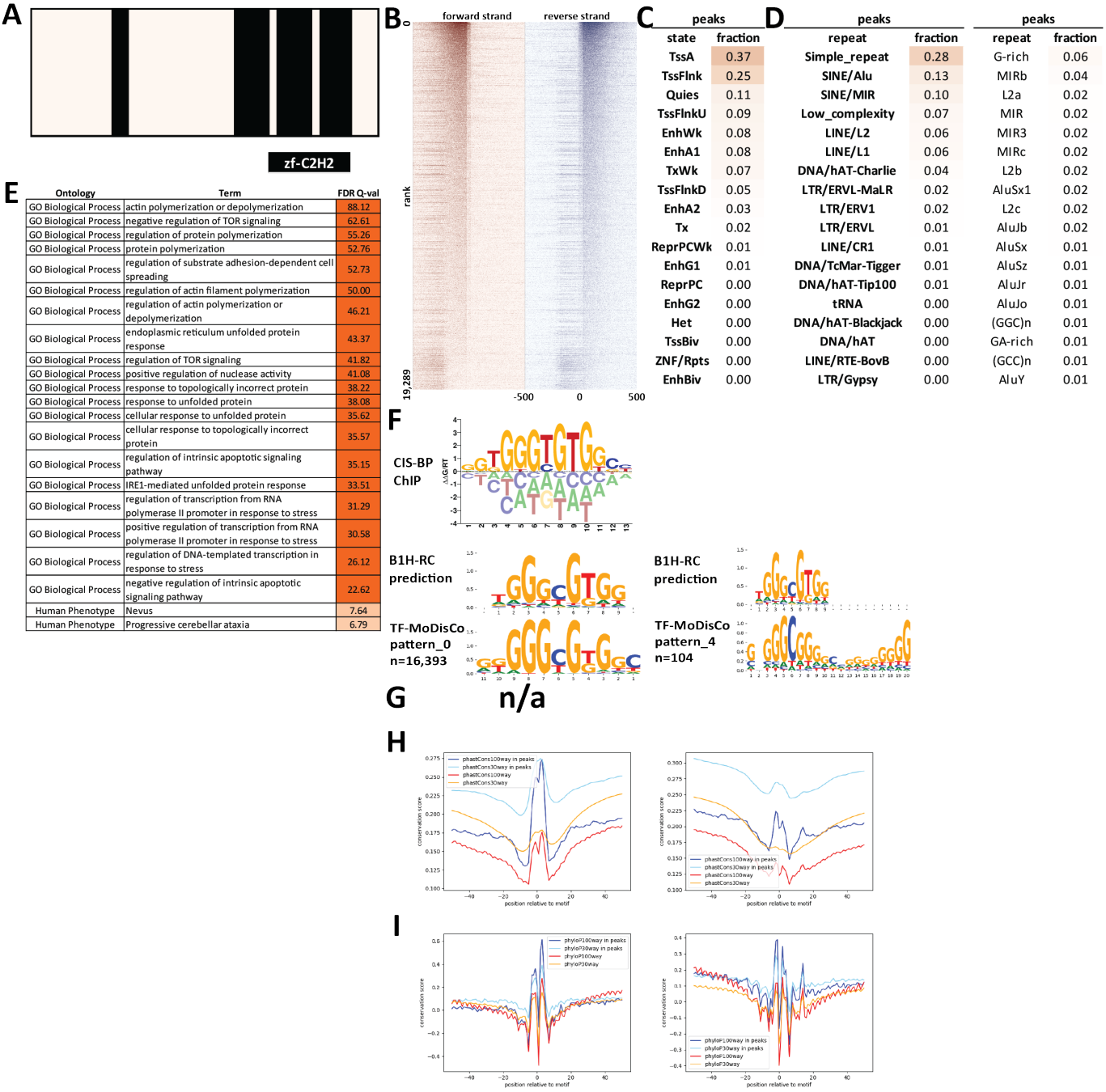

Supplementary Figure 134: Properties and genomic distribution of motifs identified for the KLF9 transcription factor in MCF-7 (accession ENCSR125ZYC).

TF-MoDisCO pattern_0 n=16393, CWM

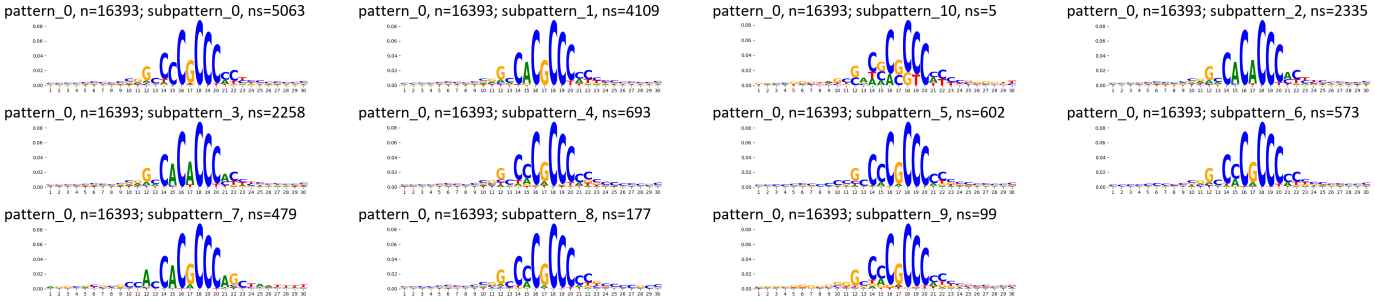

TF-MoDisCO pattern_0 n=16393, PWM

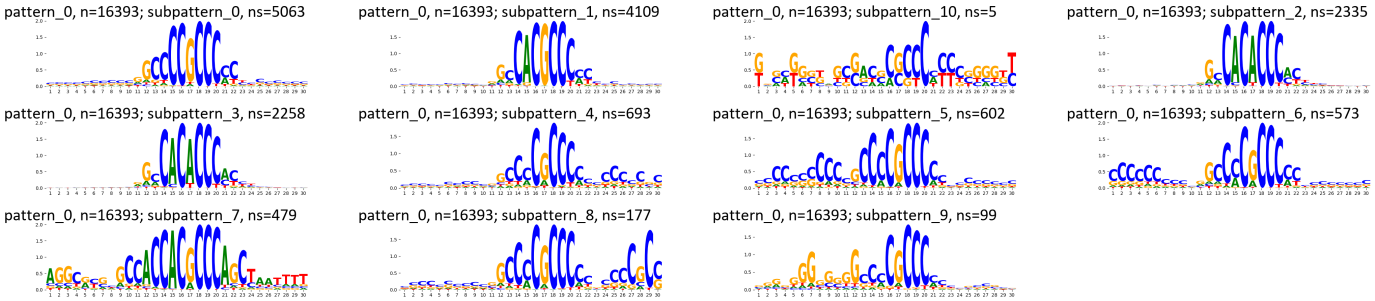

TF-MoDisCO pattern_4 n=104, CWM

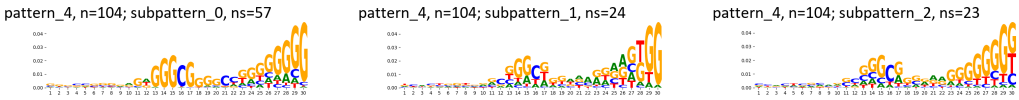

TF-MoDisCO pattern_4 n=104, PWM

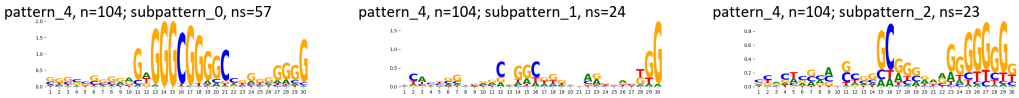

Supplementary Figure 135: TF-MoDisCO subpatterns for the KLF9 transcription factor in MCF-7 (accession ENCSR125ZYC).

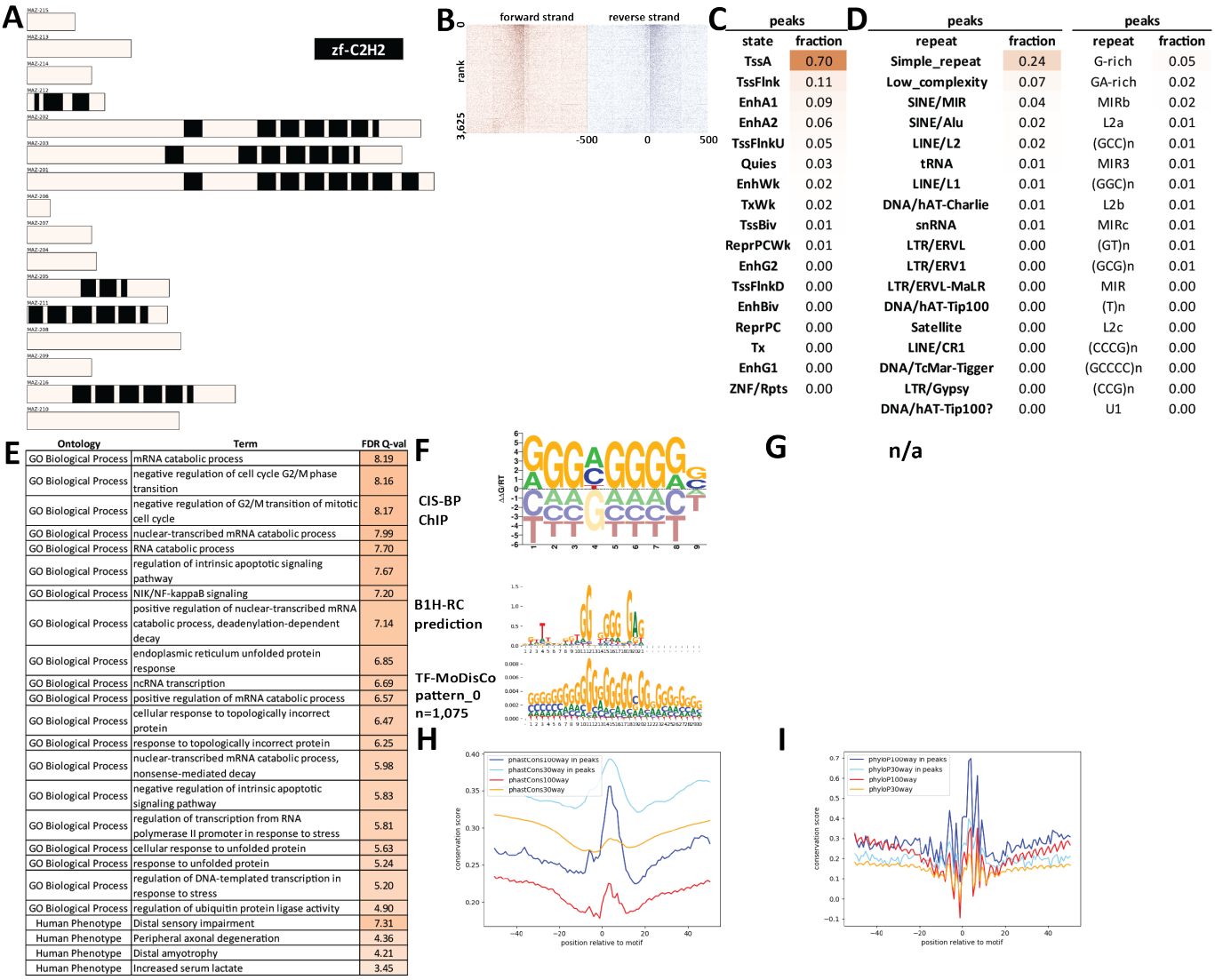

Supplementary Figure 136: Properties and genomic distribution of motifs identified for the MAZ transcription factor in A549 (accession ENCSR636YLV).

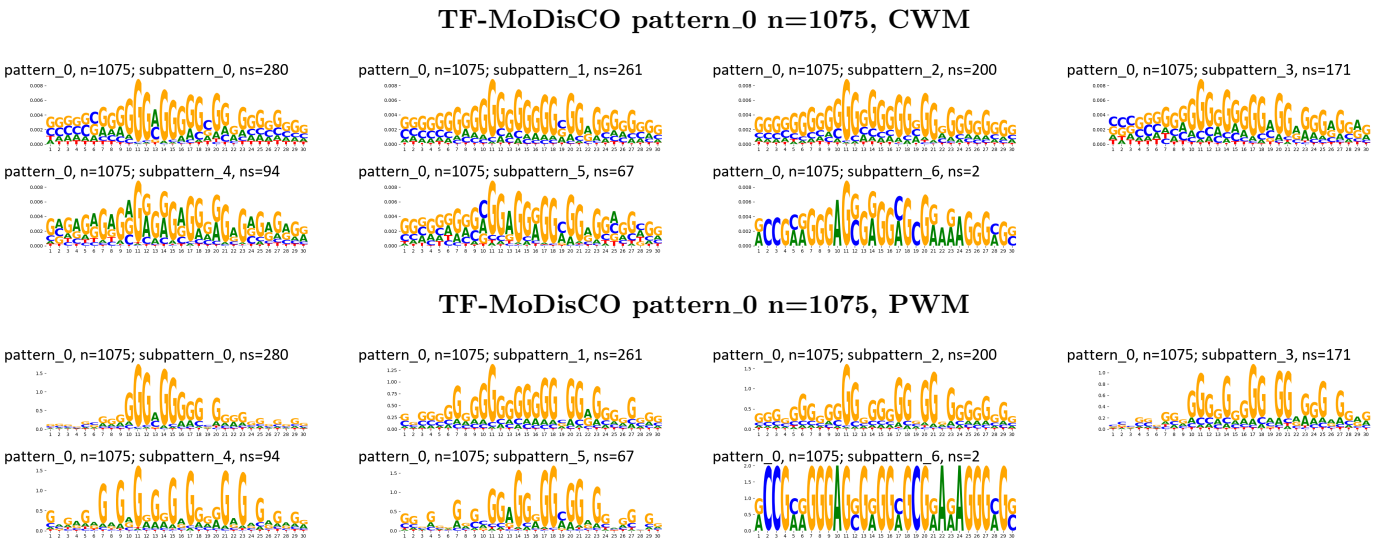

Supplementary Figure 137: TF-MoDisCO subpatterns for the MAZ transcription factor in A549 (accession ENCSR636YLV).

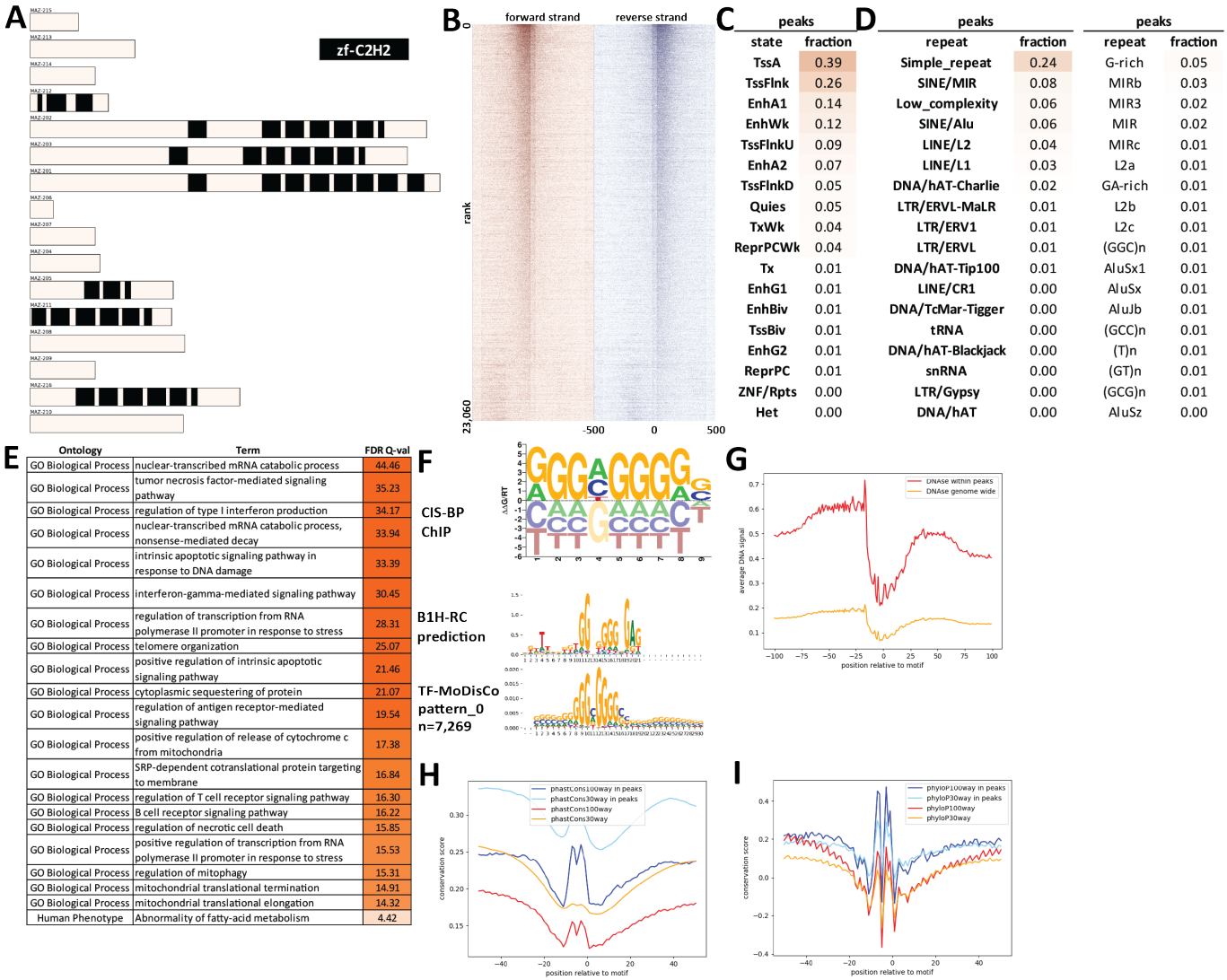

Supplementary Figure 138: Properties and genomic distribution of motifs identified for the MAZ transcription factor in GM12878 (accession ENCSR000DZA).

TF-MoDisCO pattern_0 n=7269, CWM

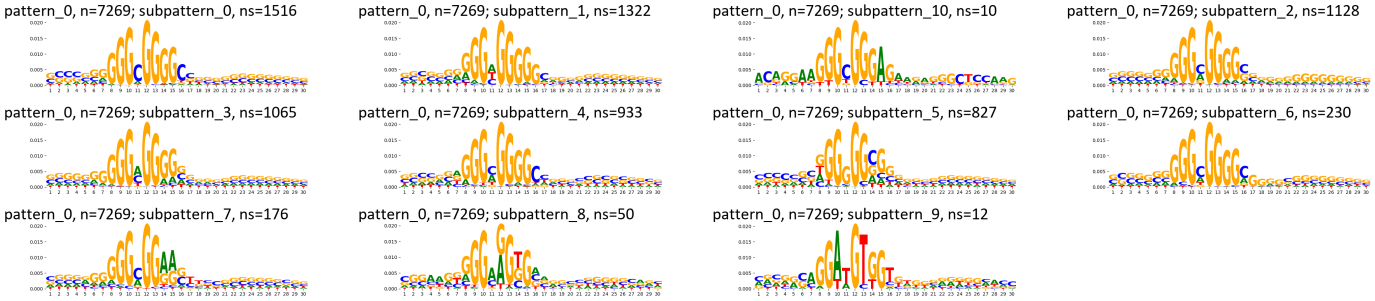

TF-MoDisCO pattern_0 n=7269, PWM

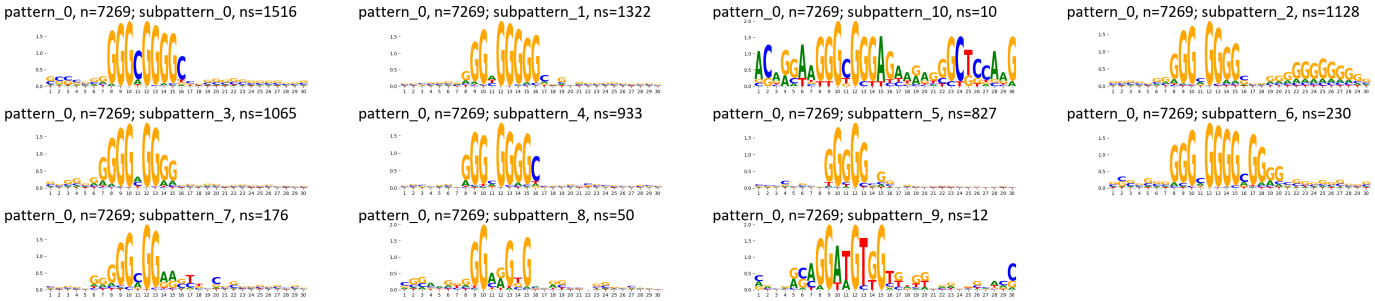

Supplementary Figure 139: TF-MoDisCO subpatterns for the MAZ transcription factor in GM12878 (accession ENCSR000DZA).

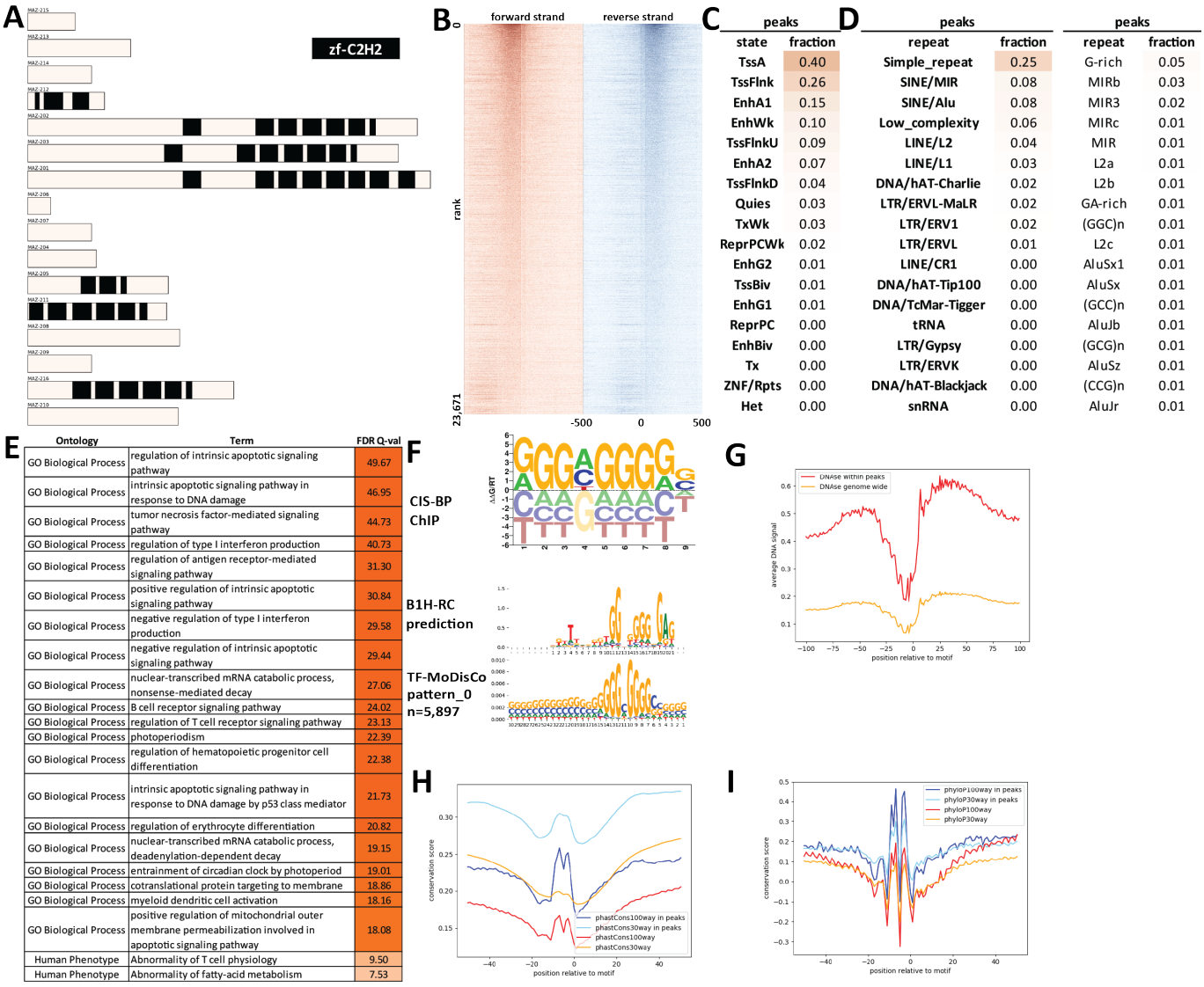

C

peaks	
state	fraction
TssA	0.40
TssFlnk	0.26
EnhA1	0.15
EnhWk	0.10
TssFlnkU	0.09
EnhA2	0.07
TssFlnkD	0.04
Quies	0.03
TxWk	0.03
ReprPCWk	0.02
EnhG2	0.01
TssBiv	0.01
EnhG1	0.01
ReprPC	0.00
EnhBiv	0.00
Tx	0.00
ZNF/Rpts	0.00
Het	0.00

D

peaks		peaks	
repeat	fraction	repeat	fraction
Simple_repeat	0.25	G-rich	0.05
SINE/MIR	0.08	MIRb	0.03
SINE/Alu	0.08	MIR3	0.02
Low_complexity	0.06	MIRc	0.01
LINE/L2	0.04	MIR	0.01
LINE/L1	0.03	L2a	0.01
DNA/hAT-Charlie	0.02	L2b	0.01
LTR/ERVL-MaLR	0.02	GA-rich	0.01
LTR/ERV1	0.02	(GGC)n	0.01
LTR/ERVL	0.01	L2c	0.01
LINE/CR1	0.00	AluSx1	0.01
DNA/hAT-Tip100	0.00	AluSx	0.01
DNA/TcMar-Tigger	0.00	(GCC)n	0.01
tRNA	0.00	AluJb	0.01
LTR/Gypsy	0.00	(GCG)n	0.01
LTR/ERVK	0.00	AluSz	0.01
DNA/hAT-Blackjack	0.00	(CCG)n	0.01
snRNA	0.00	AluJr	0.01

E

Ontology	Term	FDR Q-val
GO Biological Process	regulation of intrinsic apoptotic signaling pathway	49.67
GO Biological Process	intrinsic apoptotic signaling pathway in response to DNA damage	46.95
GO Biological Process	tumor necrosis factor-mediated signaling pathway	44.73
GO Biological Process	regulation of type I interferon production	40.73
GO Biological Process	regulation of antigen receptor-mediated signaling pathway	31.30
GO Biological Process	positive regulation of intrinsic apoptotic signaling pathway	30.84
GO Biological Process	negative regulation of type I interferon production	29.58
GO Biological Process	negative regulation of intrinsic apoptotic signaling pathway	29.44
GO Biological Process	nuclear-transcribed mRNA catabolic process, nonsense-mediated decay	27.06
GO Biological Process	B cell receptor signaling pathway	24.02
GO Biological Process	regulation of T cell receptor signaling pathway	23.13
GO Biological Process	photoperiodism	22.39
GO Biological Process	regulation of hematopoietic progenitor cell differentiation	22.38
GO Biological Process	intrinsic apoptotic signaling pathway in response to DNA damage by p53 class mediator	21.73
GO Biological Process	regulation of erythrocyte differentiation	20.82
GO Biological Process	nuclear-transcribed mRNA catabolic process, deadenylation-dependent decay	19.15
GO Biological Process	entrainment of circadian clock by photoperiod	19.01
GO Biological Process	cotranslational protein targeting to membrane	18.86
GO Biological Process	myeloid dendritic cell activation	18.16
GO Biological Process	positive regulation of mitochondrial outer membrane permeabilization involved in apoptotic signaling pathway	18.08
Human Phenotype	Abnormality of T cell physiology	9.50
Human Phenotype	Abnormality of fatty-acid metabolism	7.53

Supplementary Figure 140: Properties and genomic distribution of motifs identified for the MAZ transcription factor in GM12878 (accession ENCSR903MVU).

TF-MoDisCO pattern_0 n=5897, CWM

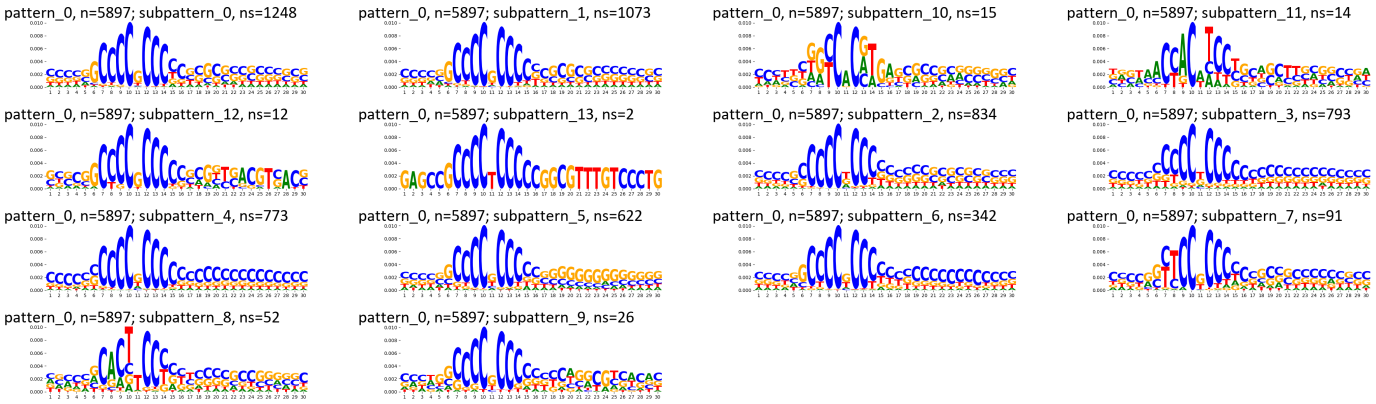

TF-MoDisCO pattern_0 n=5897, PWM

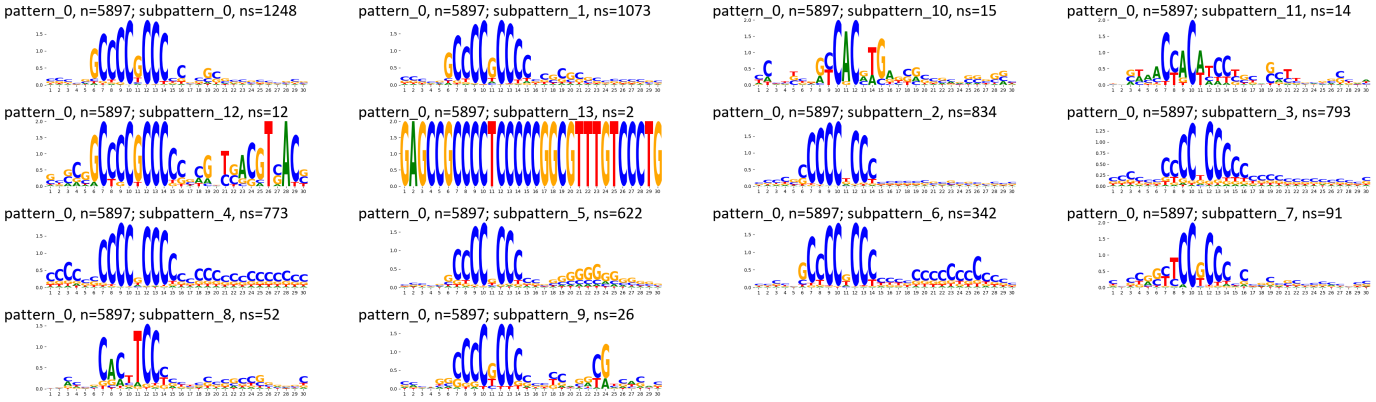

Supplementary Figure 141: TF-MoDisCO subpatterns for the MAZ transcription factor in GM12878 (accession ENCSR903MVU).

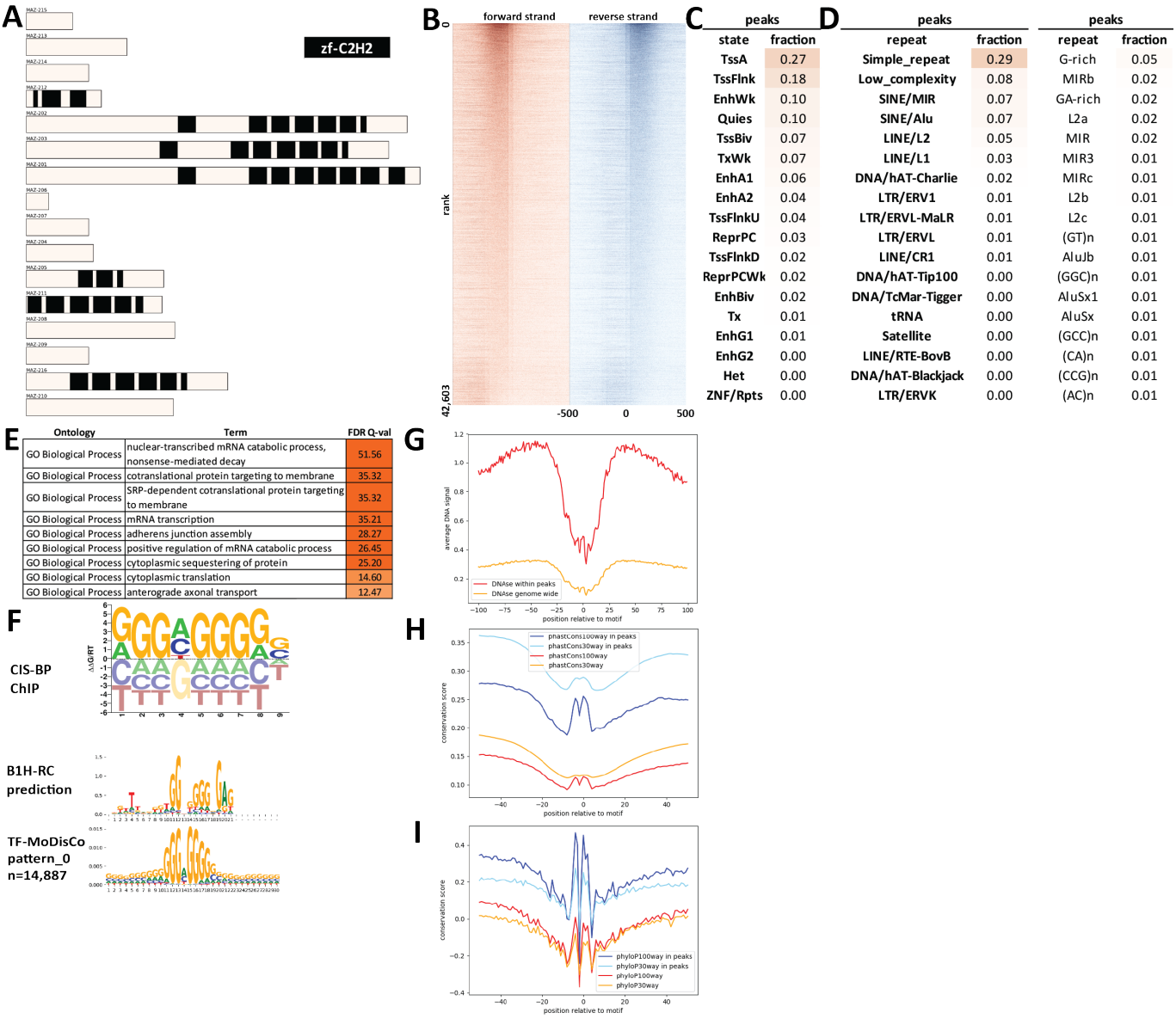

Supplementary Figure 142: Properties and genomic distribution of motifs identified for the MAZ transcription factor in HEK293 (accession ENCSR290SSQ).

TF-MoDisCO pattern_0 n=14887, CWM

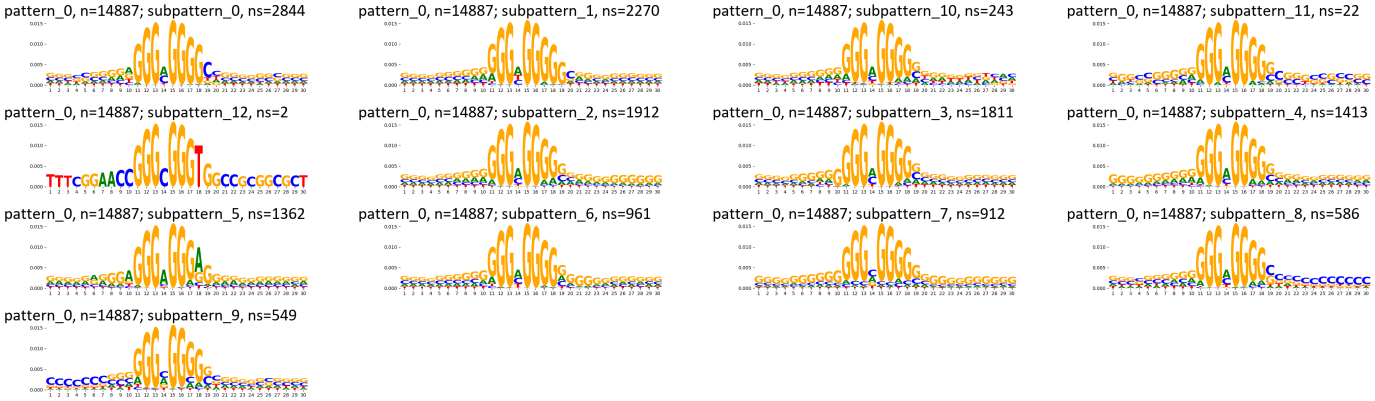

TF-MoDisCO pattern_0 n=14887, PWM

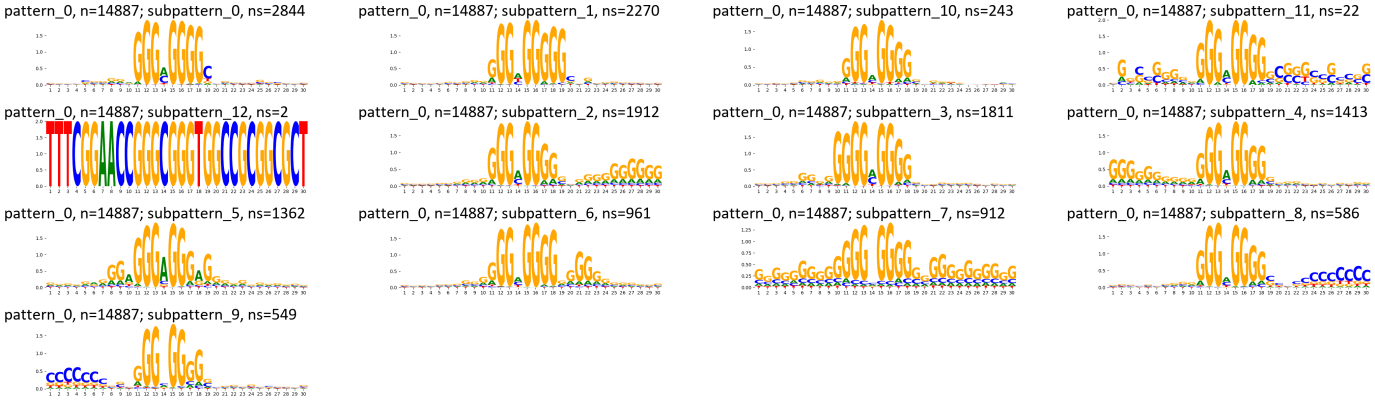

Supplementary Figure 143: TF-MoDisCO subpatterns for the MAZ transcription factor in HEK293 (accession ENCSR290SSQ).

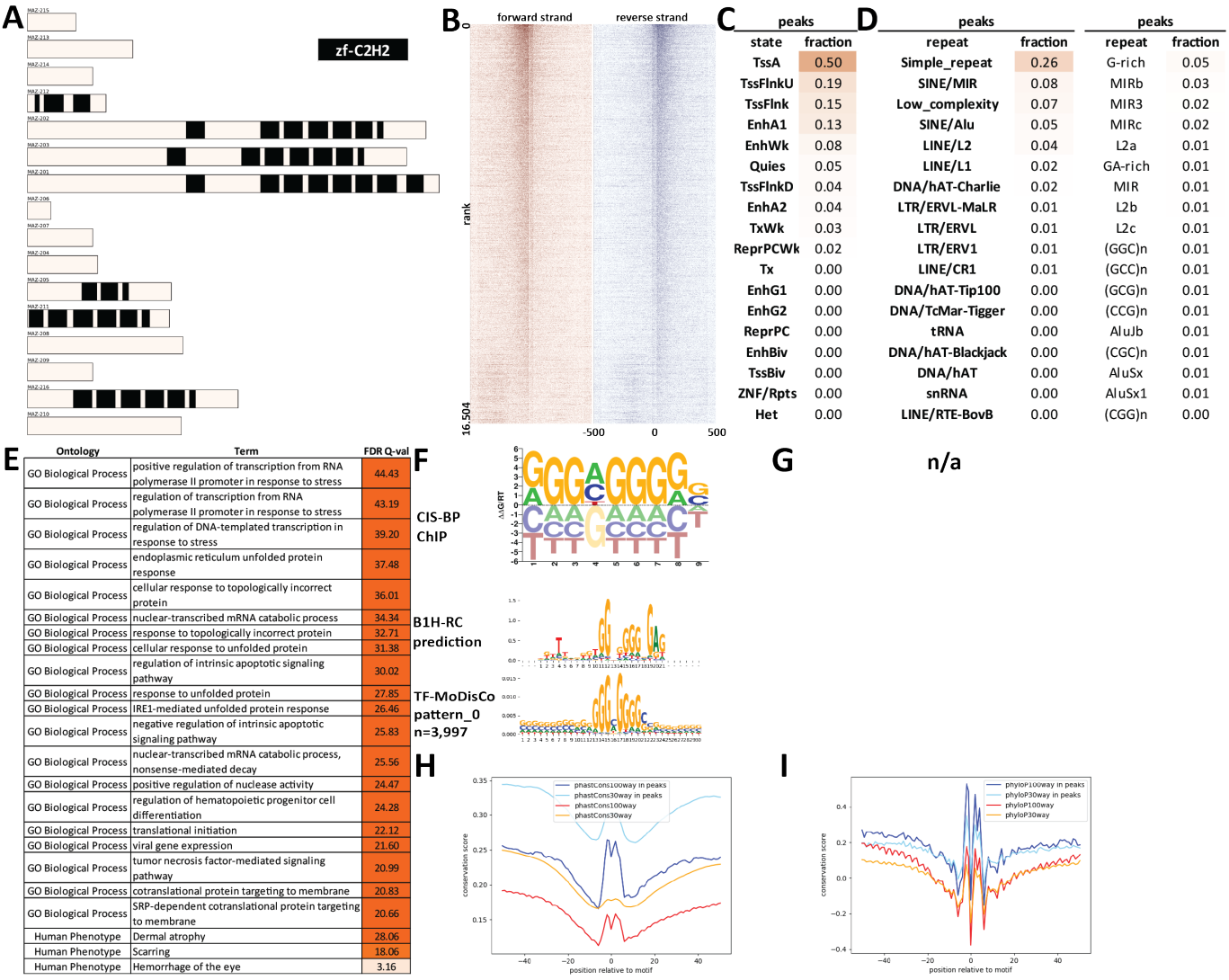

Supplementary Figure 144: Properties and genomic distribution of motifs identified for the MAZ transcription factor in HeLa-S3 (accession ENCSR000ECL).

TF-MoDisCO pattern_0 n=3997, CWM

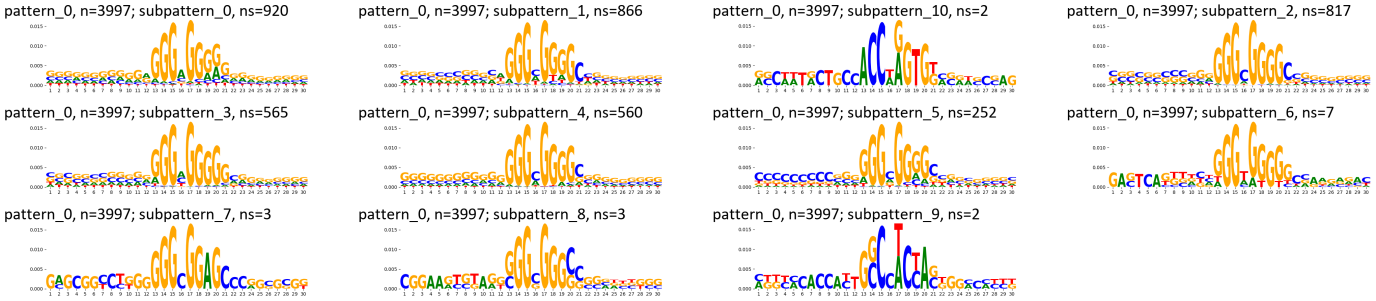

TF-MoDisCO pattern_0 n=3997, PWM

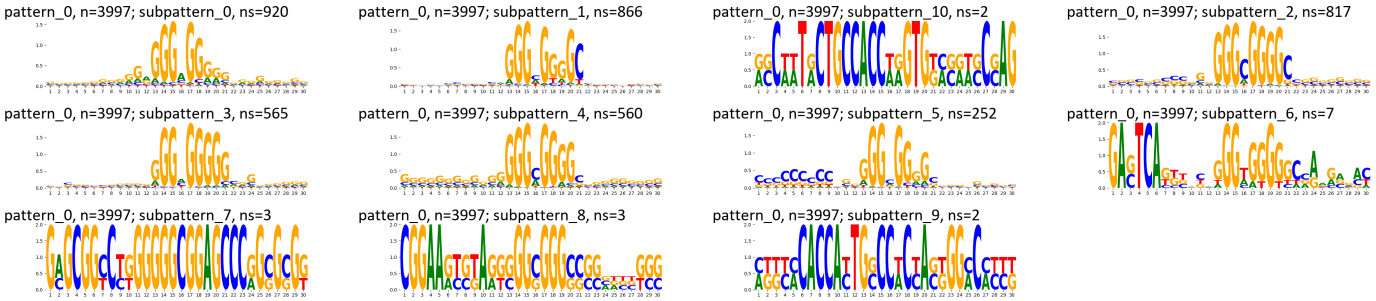

Supplementary Figure 145: TF-MoDisCO subpatterns for the MAZ transcription factor in HeLa-S3 (accession ENCSR000ECL).

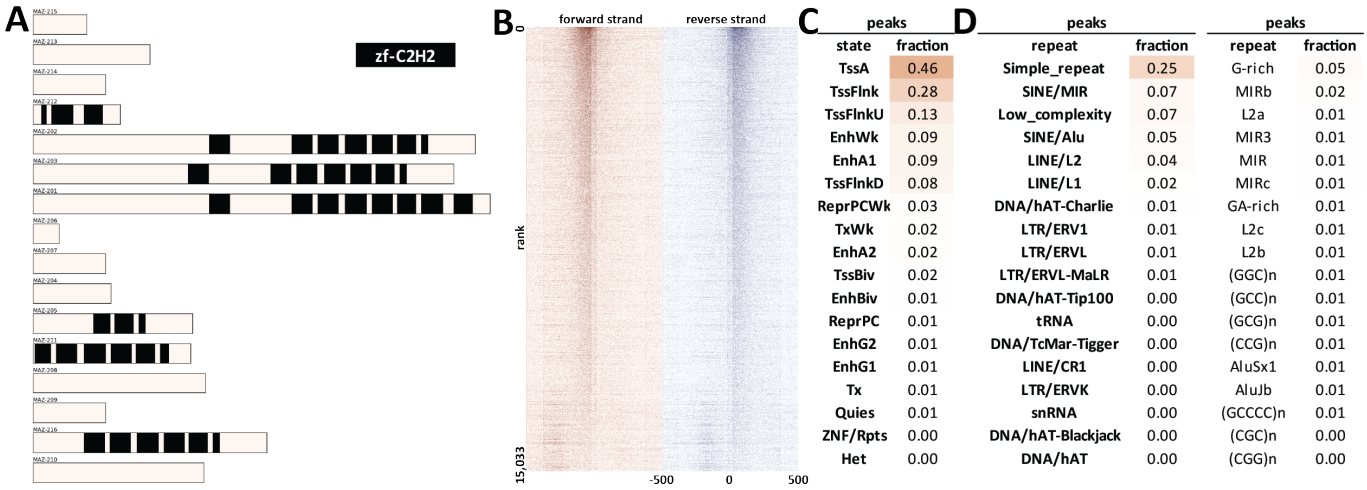

C

peaks	
state	fraction
TssA	0.46
TssFlnk	0.28
TssFlnkU	0.13
EnhWk	0.09
EnhA1	0.09
TssFlnkD	0.08
ReprPCWk	0.03
TxWk	0.02
EnhA2	0.02
TssBiv	0.02
EnhBiv	0.01
ReprPC	0.01
EnhG2	0.01
EnhG1	0.01
Tx	0.01
Quies	0.01
ZNF/Rpts	0.00
Het	0.00

D

peaks		peaks	
repeat	fraction	repeat	fraction
Simple_repeat	0.25	G-rich	0.05
SINE/MIR	0.07	MIRb	0.02
Low_complexity	0.07	L2a	0.01
SINE/Alu	0.05	MIR3	0.01
LINE/L2	0.04	MIR	0.01
LINE/L1	0.02	MIRc	0.01
DNA/hAT-Charlie	0.01	GA-rich	0.01
LTR/ERV1	0.01	L2c	0.01
LTR/ERVL	0.01	L2b	0.01
LTR/ERVL-MaLR	0.01	(GGC)n	0.01
DNA/hAT-Tip100	0.00	(GCC)n	0.01
tRNA	0.00	(GCG)n	0.01
DNA/TcMar-Tigger	0.00	(CCG)n	0.01
LINE/CR1	0.00	AluSx1	0.01
LTR/ERVK	0.00	AluJb	0.01
snRNA	0.00	(GCCCC)n	0.01
DNA/hAT-Blackjack	0.00	(CGC)n	0.00
DNA/hAT	0.00	(CGG)n	0.00

E

Ontology	Term	FDR Q-val
GO Biological Process	cellular response to topologically incorrect protein	46.25
GO Biological Process	endoplasmic reticulum unfolded protein response	46.40
GO Biological Process	response to topologically incorrect protein	44.46
GO Biological Process	IRE1-mediated unfolded protein response	42.71
GO Biological Process	cellular response to unfolded protein	41.05
GO Biological Process	response to unfolded protein	38.31
GO Biological Process	regulation of intrinsic apoptotic signaling pathway	37.74
GO Biological Process	regulation of transcription from RNA polymerase II promoter in response to stress	33.22
GO Biological Process	negative regulation of intrinsic apoptotic signaling pathway	30.45
GO Biological Process	regulation of DNA-templated transcription in response to stress	30.04
GO Biological Process	regulation of endoplasmic reticulum stress-induced intrinsic apoptotic signaling pathway	18.59
GO Biological Process	translational elongation	17.45
GO Biological Process	regulation of endoplasmic reticulum unfolded protein response	17.22
GO Biological Process	DNA-templated transcription, elongation	15.09
GO Biological Process	regulation of transcription from RNA polymerase II promoter in response to hypoxia	14.30
GO Biological Process	mitochondrial translational termination	13.78
GO Biological Process	negative regulation of response to endoplasmic reticulum stress	13.38
GO Biological Process	mitochondrial translational elongation	13.24
GO Biological Process	regulation of pri-miRNA transcription from RNA polymerase II promoter	12.88
GO Biological Process	mitochondrial translation	12.52
Human Phenotype	Aplasia/Hypoplasia involving the femoral head and neck	6.82
Human Phenotype	Short femoral neck	6.28
Human Phenotype	External ophthalmoplegia	5.98
Human Phenotype	Diminished motivation	5.92
Human Phenotype	Apathy	5.91
Human Phenotype	Aplasia/hypoplasia of the femur	5.52
Human Phenotype	Supranuclear gaze palsy	3.04
Human Phenotype	Death in childhood	2.99

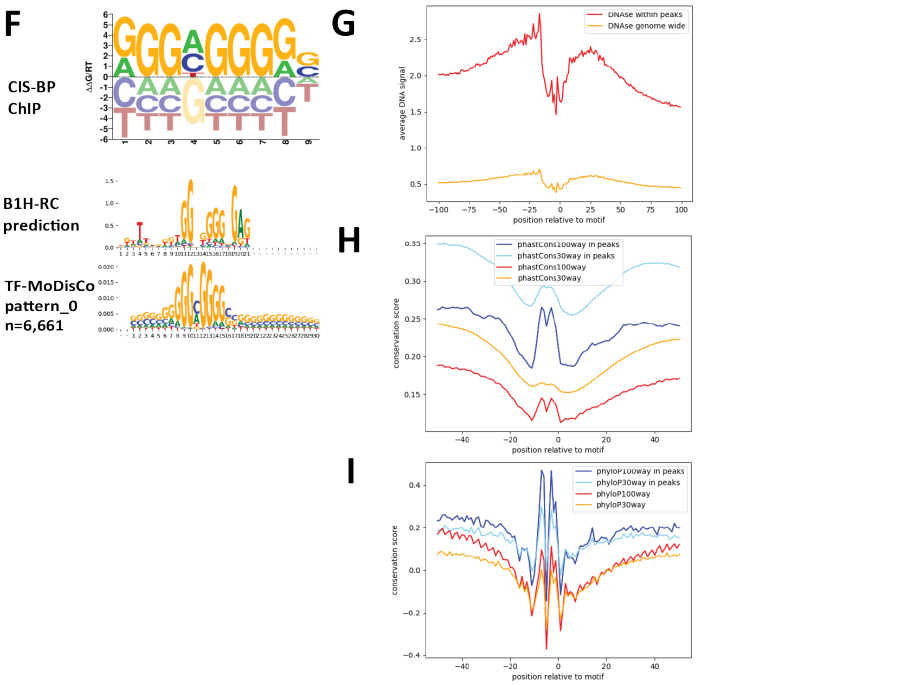

Supplementary Figure 146: Properties and genomic distribution of motifs identified for the MAZ transcription factor in HepG2 (accession ENCSR000EDN).

TF-MoDisCO pattern_0 n=6611, CWM

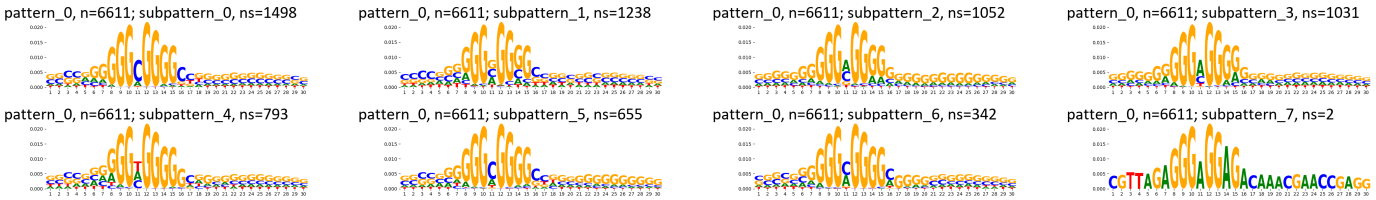

TF-MoDisCO pattern_0 n=6611, PWM

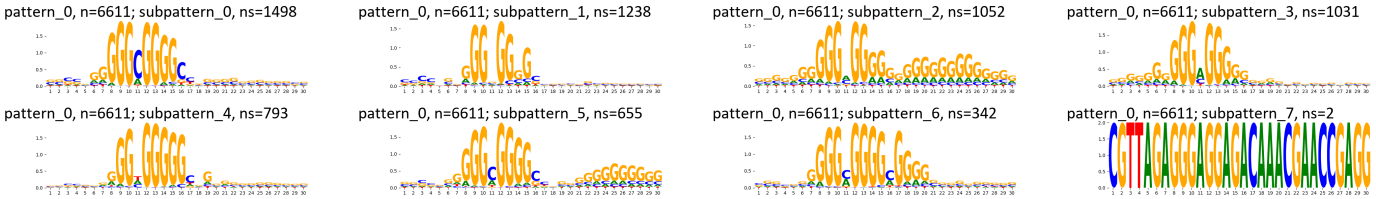

TF-MoDisCO pattern_1 n=1764, CWM

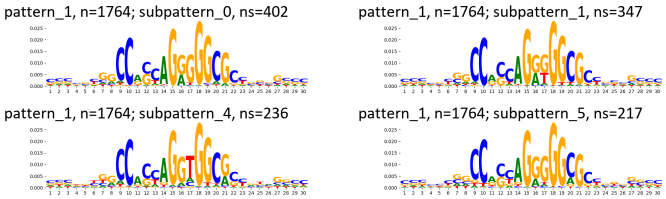

TF-MoDisCO pattern_1 n=1764, PWM

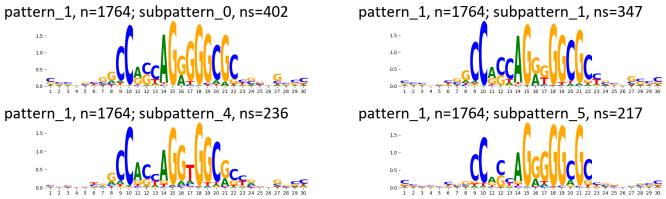

Supplementary Figure 147: TF-MoDisCO subpatterns for the MAZ transcription factor in HepG2 (accession ENCSR000EDN).

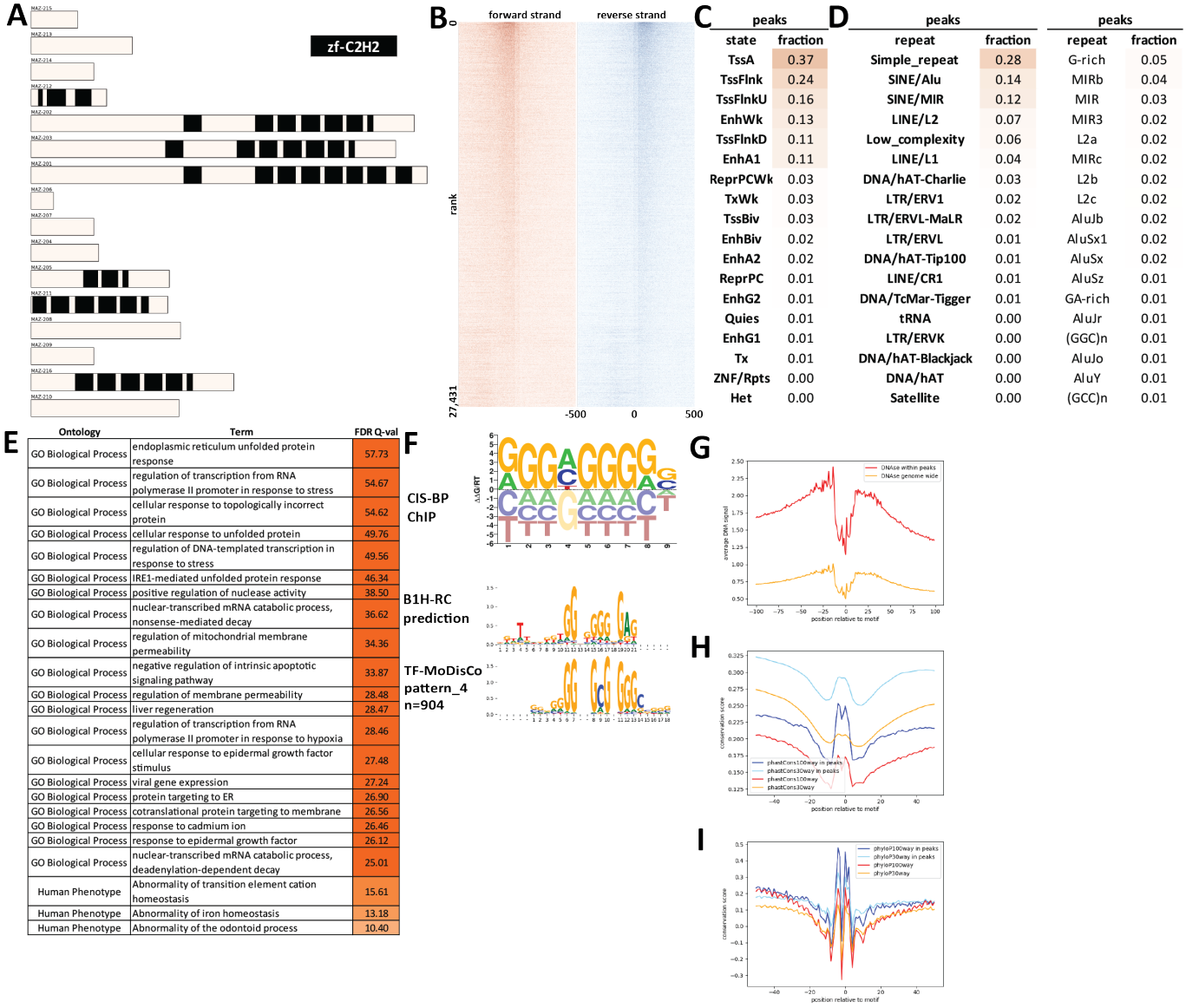

Supplementary Figure 148: Properties and genomic distribution of motifs identified for the MAZ transcription factor in HepG2 (accession ENCSR700PNE).

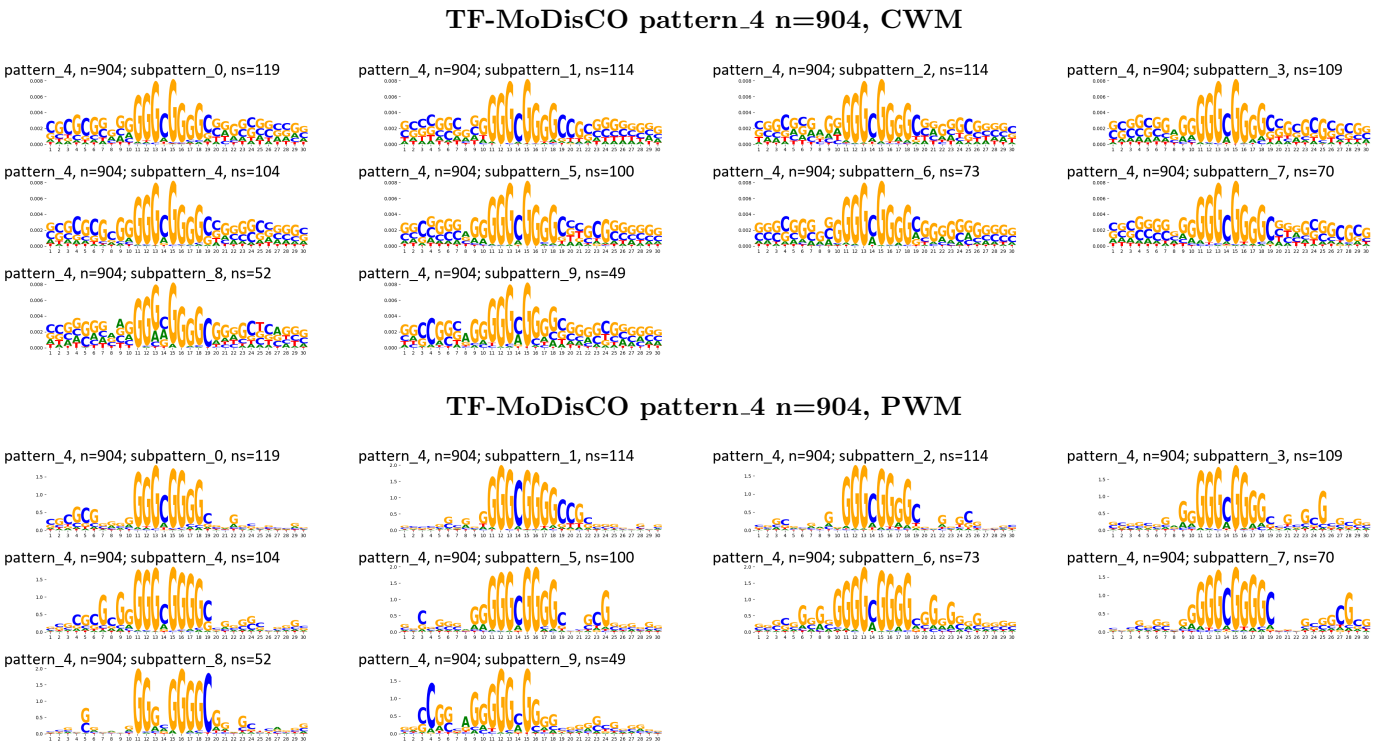

Supplementary Figure 149: TF-MoDisCO subpatterns for the MAZ transcription factor in HepG2 (accession ENCSR700PNE).

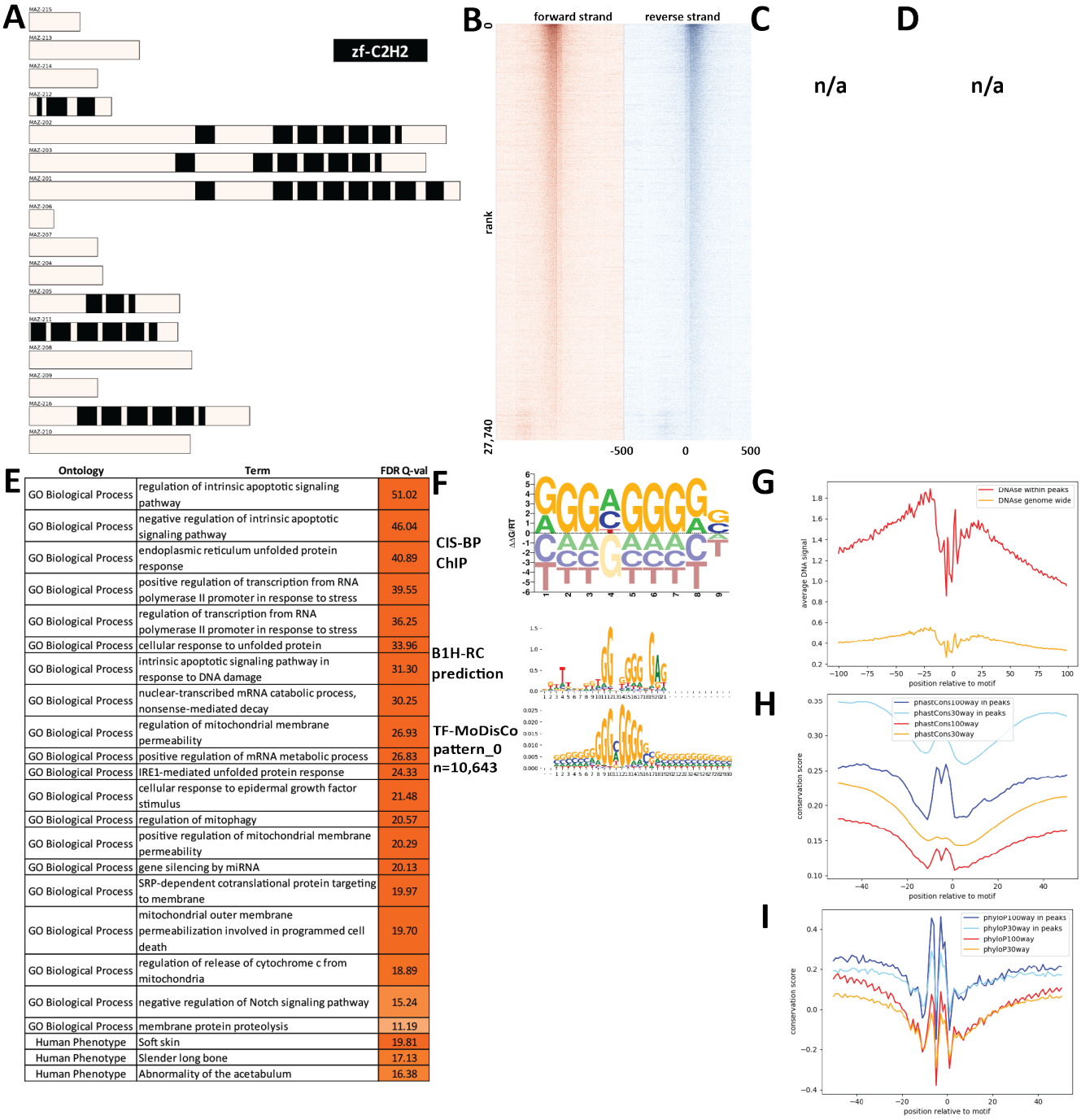

Ontology	Term	FDR Q-val
GO Biological Process	regulation of intrinsic apoptotic signaling pathway	51.02
GO Biological Process	negative regulation of intrinsic apoptotic signaling pathway	46.04
GO Biological Process	endoplasmic reticulum unfolded protein response	40.89
GO Biological Process	positive regulation of transcription from RNA polymerase II promoter in response to stress	39.55
GO Biological Process	regulation of transcription from RNA polymerase II promoter in response to stress	36.25
GO Biological Process	cellular response to unfolded protein	33.96
GO Biological Process	intrinsic apoptotic signaling pathway in response to DNA damage	31.30
GO Biological Process	nuclear-transcribed mRNA catabolic process, nonsense-mediated decay	30.25
GO Biological Process	regulation of mitochondrial membrane permeability	26.93
GO Biological Process	positive regulation of mRNA metabolic process	26.83
GO Biological Process	IRE1-mediated unfolded protein response	24.33
GO Biological Process	cellular response to epidermal growth factor stimulus	21.48
GO Biological Process	regulation of mitophagy	20.57
GO Biological Process	positive regulation of mitochondrial membrane permeability	20.29
GO Biological Process	gene silencing by miRNA	20.13
GO Biological Process	SRP-dependent cotranslational protein targeting to membrane	19.97
GO Biological Process	mitochondrial outer membrane permeabilization involved in programmed cell death	19.70
GO Biological Process	regulation of release of cytochrome c from mitochondria	18.89
GO Biological Process	negative regulation of Notch signaling pathway	15.24
GO Biological Process	membrane protein proteolysis	11.19
Human Phenotype	Soft skin	19.81
Human Phenotype	Slender long bone	17.13
Human Phenotype	Abnormality of the acetabulum	16.38

Supplementary Figure 150: Properties and genomic distribution of motifs identified for the MAZ transcription factor in IMR-90 (accession ENCSR000EFF).

TF-MoDisCO pattern_0 n=10643, CWM

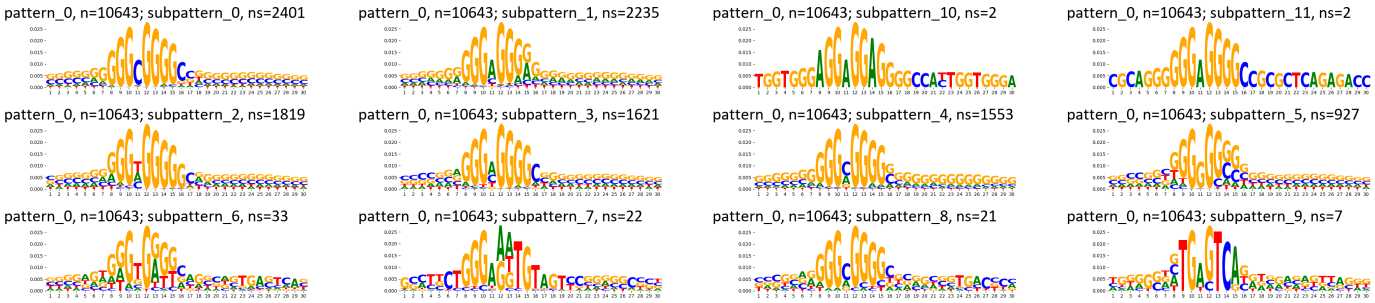

TF-MoDisCO pattern_0 n=10643, PWM

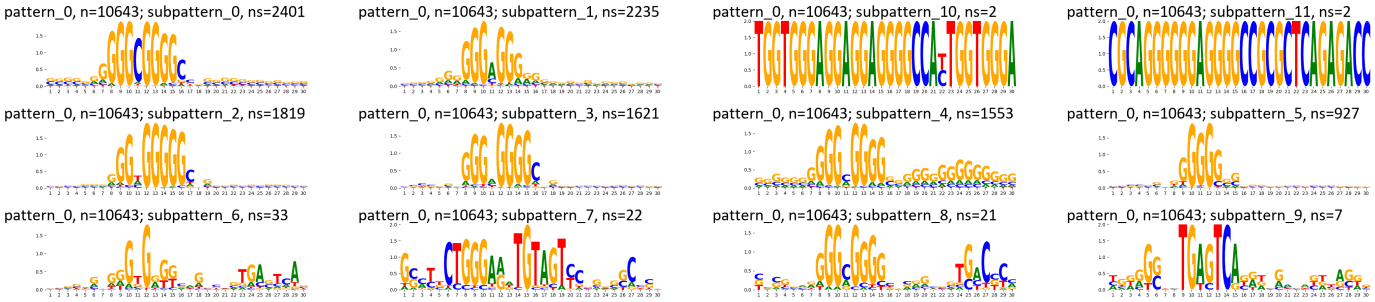

Supplementary Figure 151: TF-MoDisCO subpatterns for the MAZ transcription factor in IMR-90 (accession ENCSR000EFF).

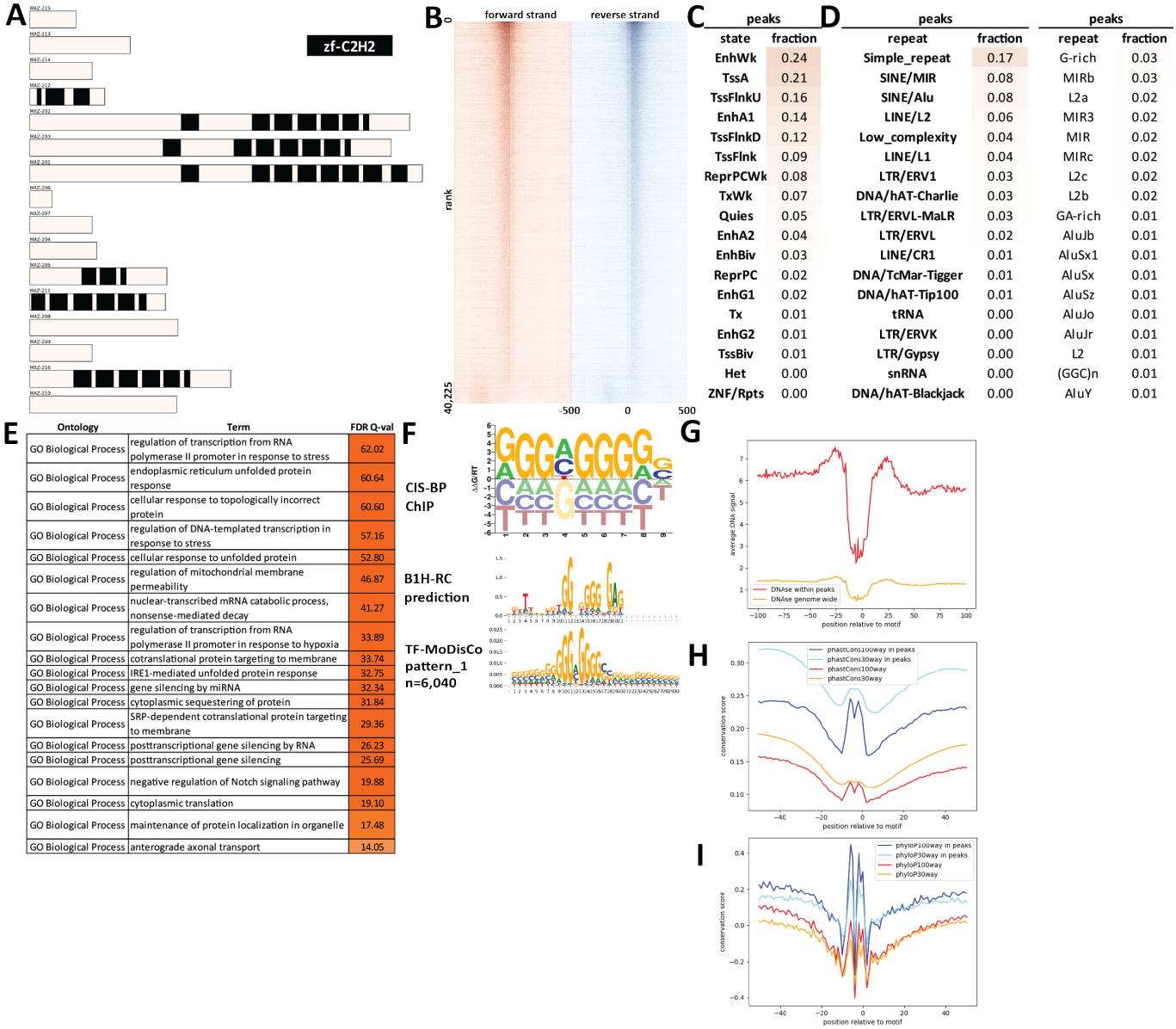

peaks	
state	fraction
EnhWk	0.24
TssA	0.21
TssFlnkU	0.16
EnhA1	0.14
TssFlnkD	0.12
TssFlnk	0.09
ReprPCWk	0.08
TxWk	0.07
Quies	0.05
EnhA2	0.04
EnhBiv	0.03
ReprPC	0.02
EnhG1	0.02
Tx	0.01
EnhG2	0.01
TssBiv	0.01
Het	0.00
ZNF/Rpts	0.00

peaks		peaks	
repeat	fraction	repeat	fraction
Simple_repeat	0.17	G-rich	0.03
SINE/MIR	0.08	MIRb	0.03
SINE/Alu	0.08	L2a	0.02
LINE/L2	0.06	MIR3	0.02
Low_complexity	0.04	MIR	0.02
LINE/L1	0.04	MIRc	0.02
LTR/ERV1	0.03	L2c	0.02
DNA/hAT-Charlie	0.03	L2b	0.02
LTR/ERVL-MaLR	0.03	GA-rich	0.01
LTR/ERVL	0.02	AluJb	0.01
LINE/CR1	0.01	AluSx1	0.01
DNA/TcMar-Tigger	0.01	AluSx	0.01
DNA/hAT-Tip100	0.01	AluSz	0.01
tRNA	0.00	AluJo	0.01
LTR/ERVK	0.00	AluJr	0.01
LTR/Gypsy	0.00	L2	0.01
snRNA	0.00	(GGC)n	0.01
DNA/hAT-Blackjack	0.00	AluY	0.01

Ontology	Term	FDR Q-val
GO Biological Process	regulation of transcription from RNA polymerase II promoter in response to stress	62.02
GO Biological Process	endoplasmic reticulum unfolded protein response	60.64
GO Biological Process	cellular response to topologically incorrect protein	60.60
GO Biological Process	regulation of DNA-templated transcription in response to stress	57.16
GO Biological Process	cellular response to unfolded protein	52.80
GO Biological Process	regulation of mitochondrial membrane permeability	46.87
GO Biological Process	nuclear-transcribed mRNA catabolic process, nonsense-mediated decay	41.27
GO Biological Process	regulation of transcription from RNA polymerase II promoter in response to hypoxia	33.89
GO Biological Process	cotranslational protein targeting to membrane	33.74
GO Biological Process	IRE1-mediated unfolded protein response	32.75
GO Biological Process	gene silencing by miRNA	32.34
GO Biological Process	cytoplasmic sequestering of protein	31.84
GO Biological Process	SRP-dependent cotranslational protein targeting to membrane	29.36
GO Biological Process	posttranscriptional gene silencing by RNA	26.23
GO Biological Process	posttranscriptional gene silencing	25.69
GO Biological Process	negative regulation of Notch signaling pathway	19.88
GO Biological Process	cytoplasmic translation	19.10
GO Biological Process	maintenance of protein localization in organelle	17.48
GO Biological Process	anterograde axonal transport	14.05

Supplementary Figure 152: Properties and genomic distribution of motifs identified for the MAZ transcription factor in K562 (accession ENCSR000EFX).

TF-MoDisCO pattern_1 n=6040, CWM

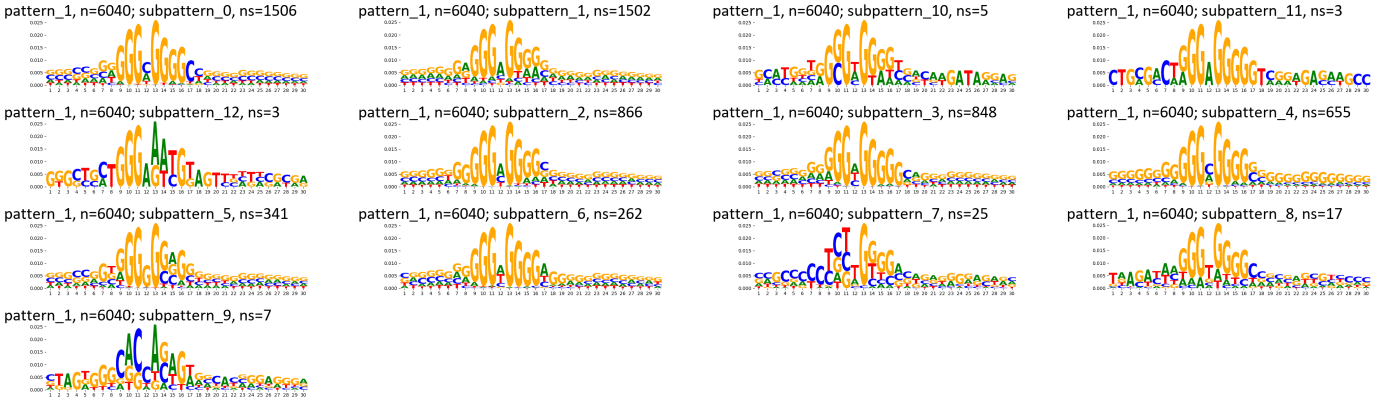

TF-MoDisCO pattern_1 n=6040, PWM

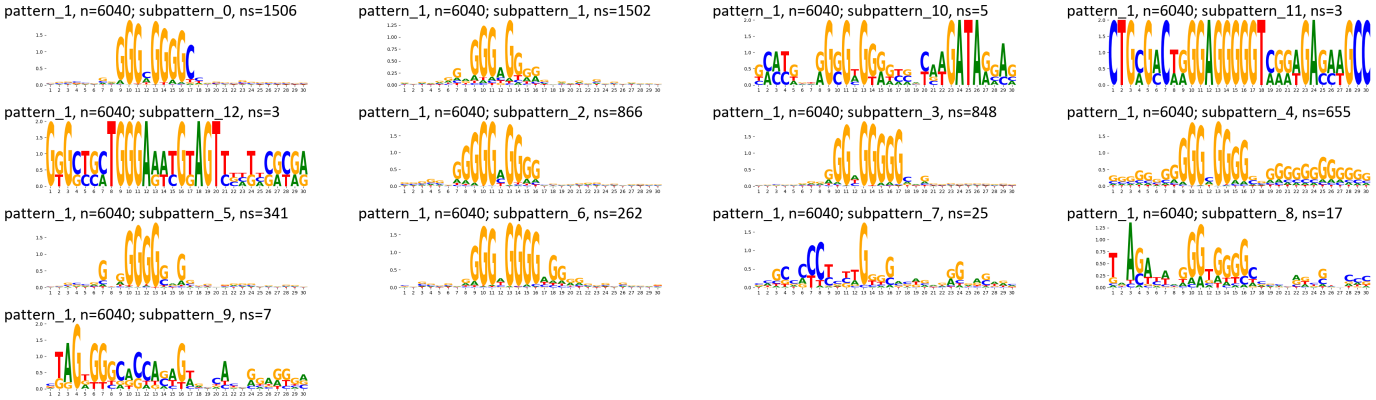

Supplementary Figure 153: TF-MoDisCO subpatterns for the MAZ transcription factor in K562 (accession ENCSR000EFX).

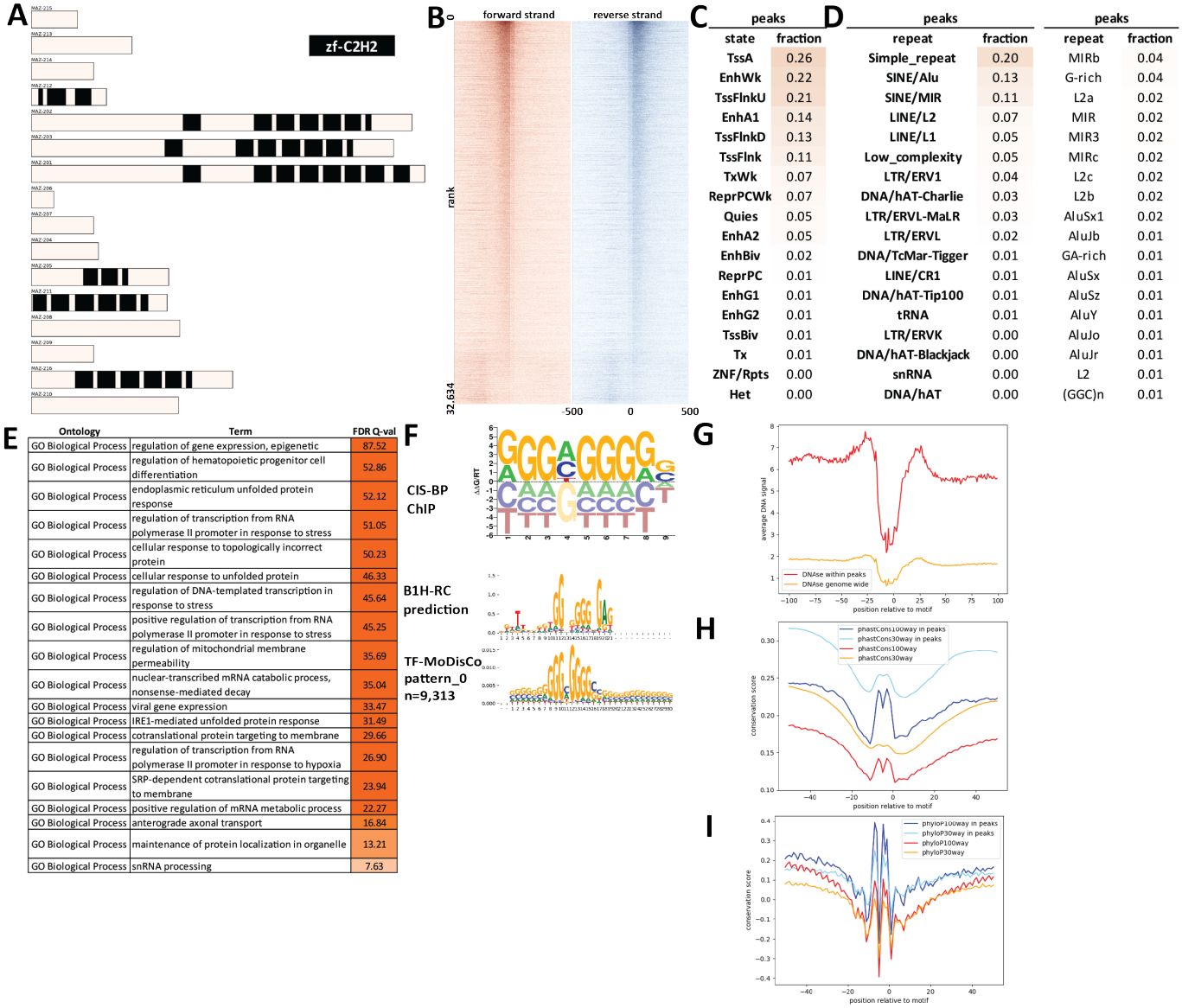

Supplementary Figure 154: Properties and genomic distribution of motifs identified for the MAZ transcription factor in K562 (accession ENCSR163IUV).

TF-MoDisCO pattern_0 n=9313, CWM

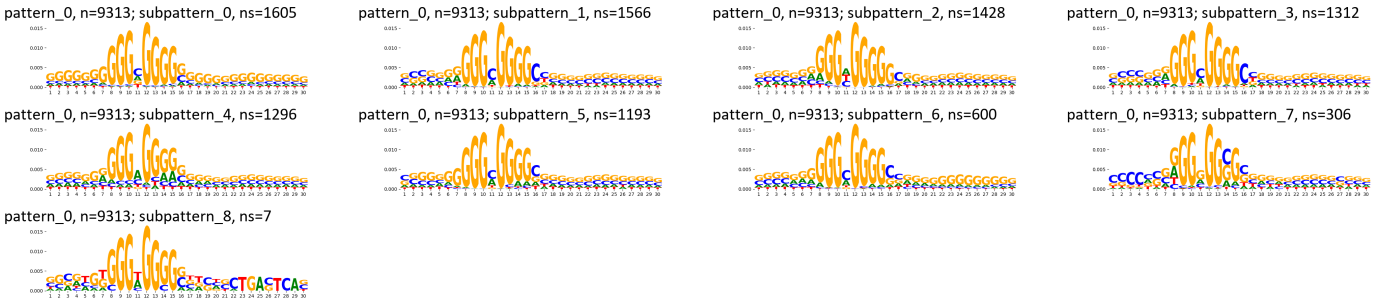

TF-MoDisCO pattern_0 n=9313, PWM

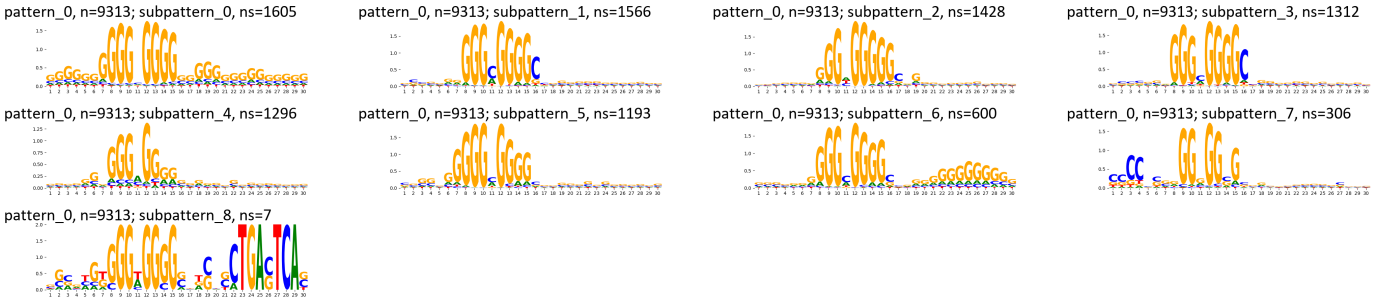

Supplementary Figure 155: TF-MoDisCO subpatterns for the MAZ transcription factor in K562 (accession ENCSR163IUV).

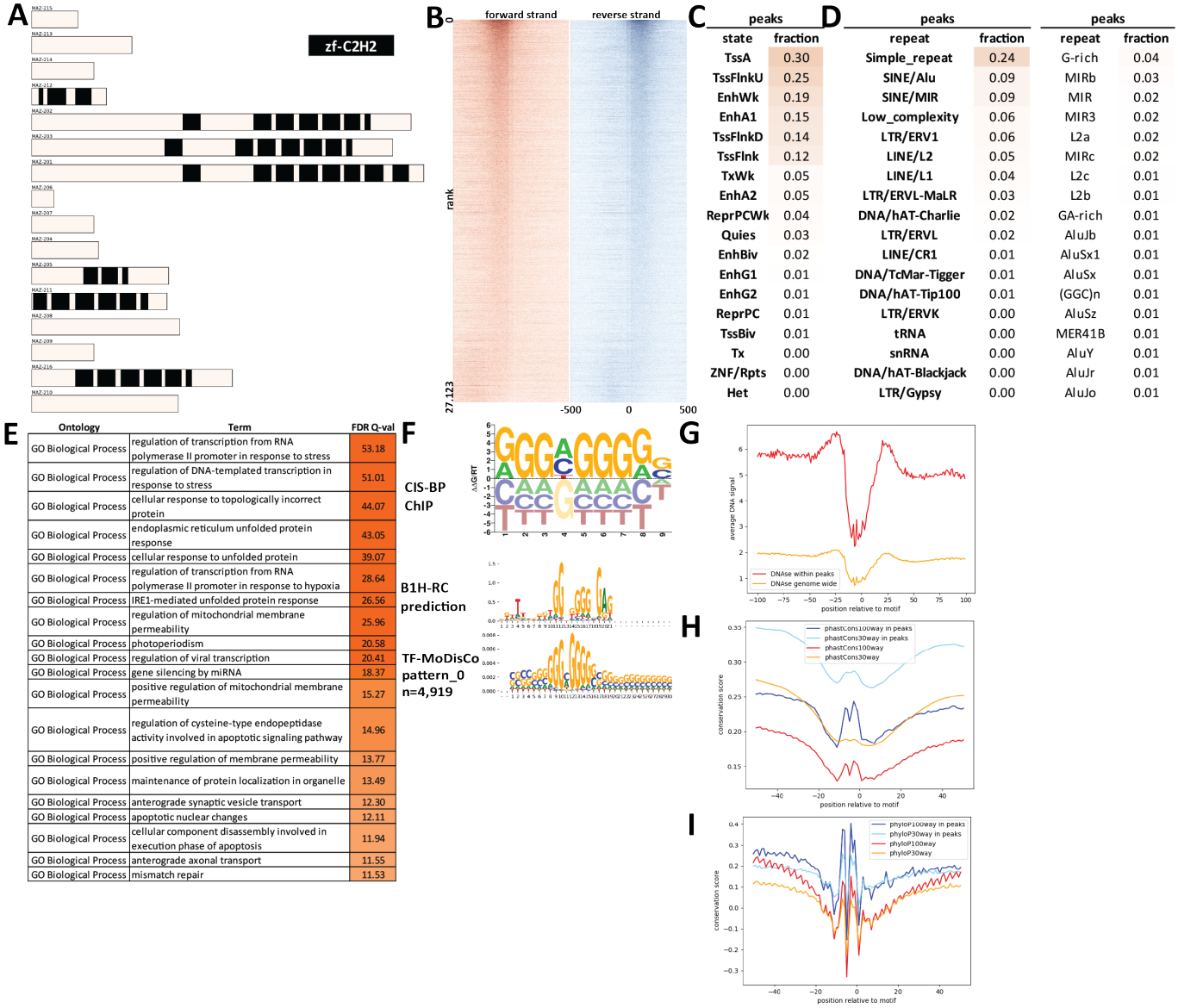

Supplementary Figure 156: Properties and genomic distribution of motifs identified for the MAZ transcription factor in K562 (accession ENCSR643JRH).

TF-MoDisCO pattern_0 n=4919, CWM

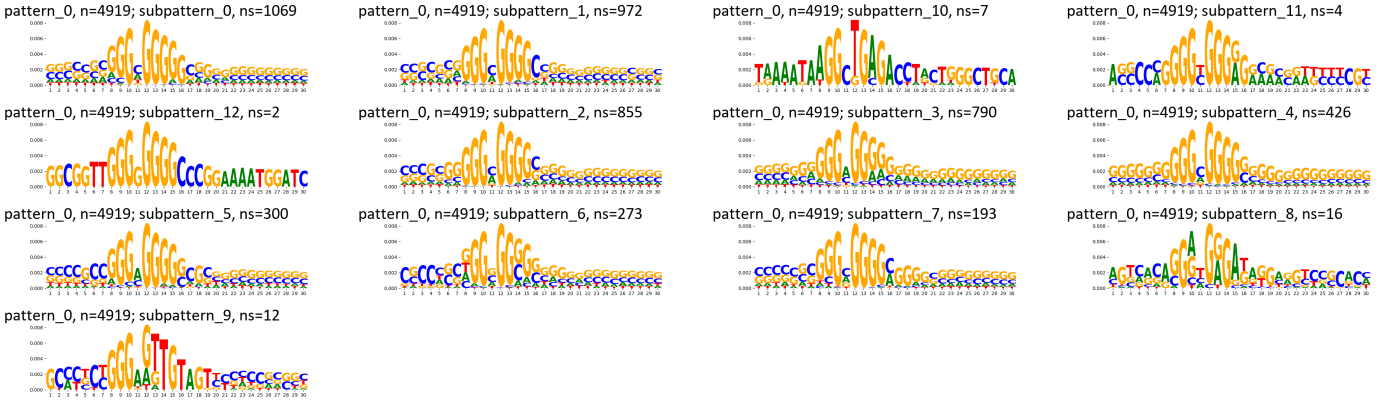

TF-MoDisCO pattern_0 n=4919, PWM

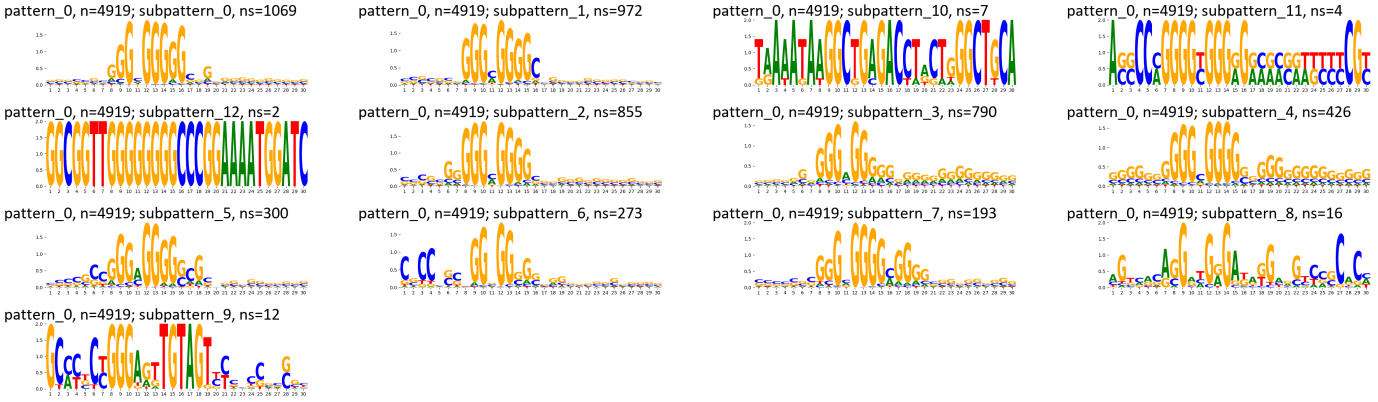

Supplementary Figure 157: TF-MoDisCO subpatterns for the MAZ transcription factor in K562 (accession ENCSR643JRH).

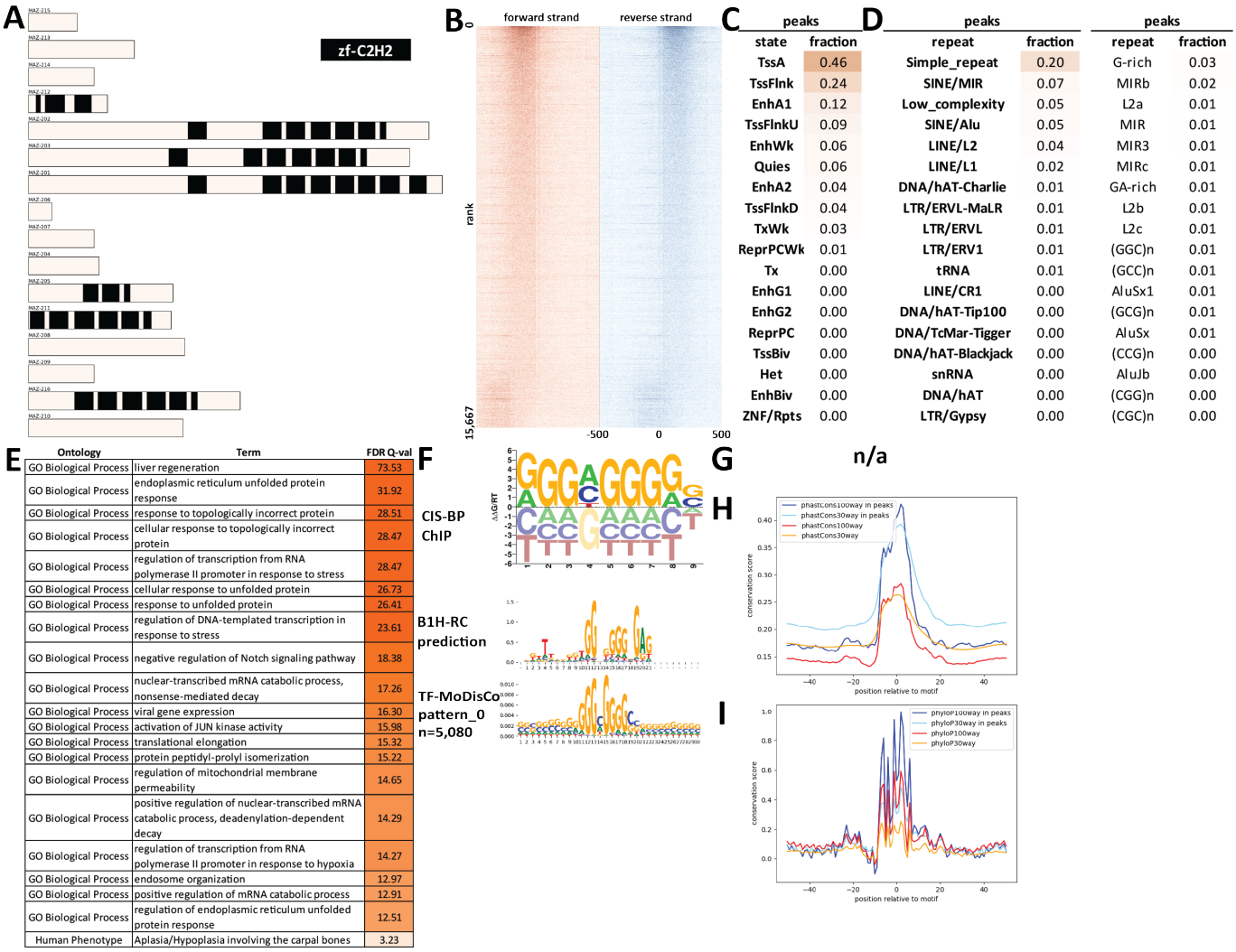

Supplementary Figure 158: Properties and genomic distribution of motifs identified for the MAZ transcription factor in MCF-7 (accession ENCSR288IJC).

TF-MoDisCO pattern_0 n=5080, CWM

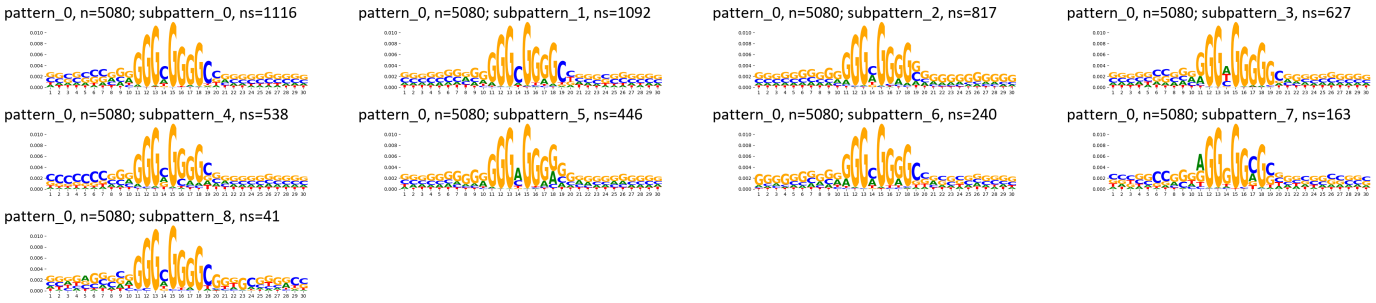

TF-MoDisCO pattern_0 n=5080, PWM

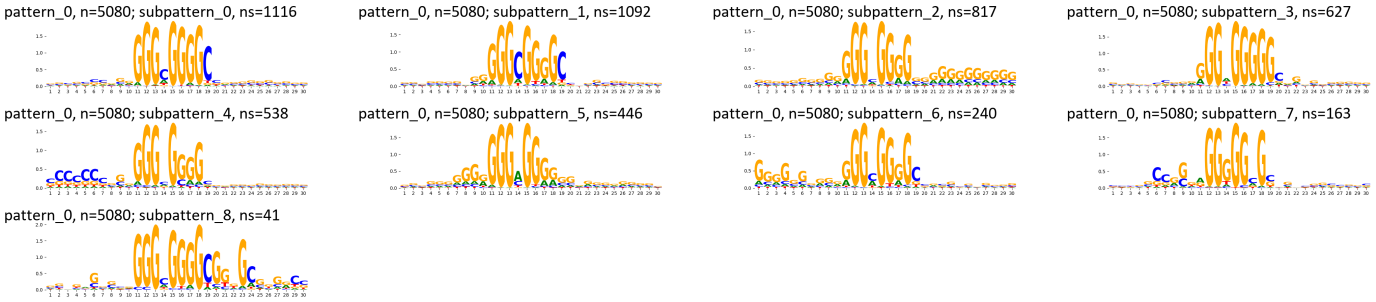

Supplementary Figure 159: TF-MoDisCO subpatterns for the MAZ transcription factor in MCF-7 (accession ENCSR288IJC).

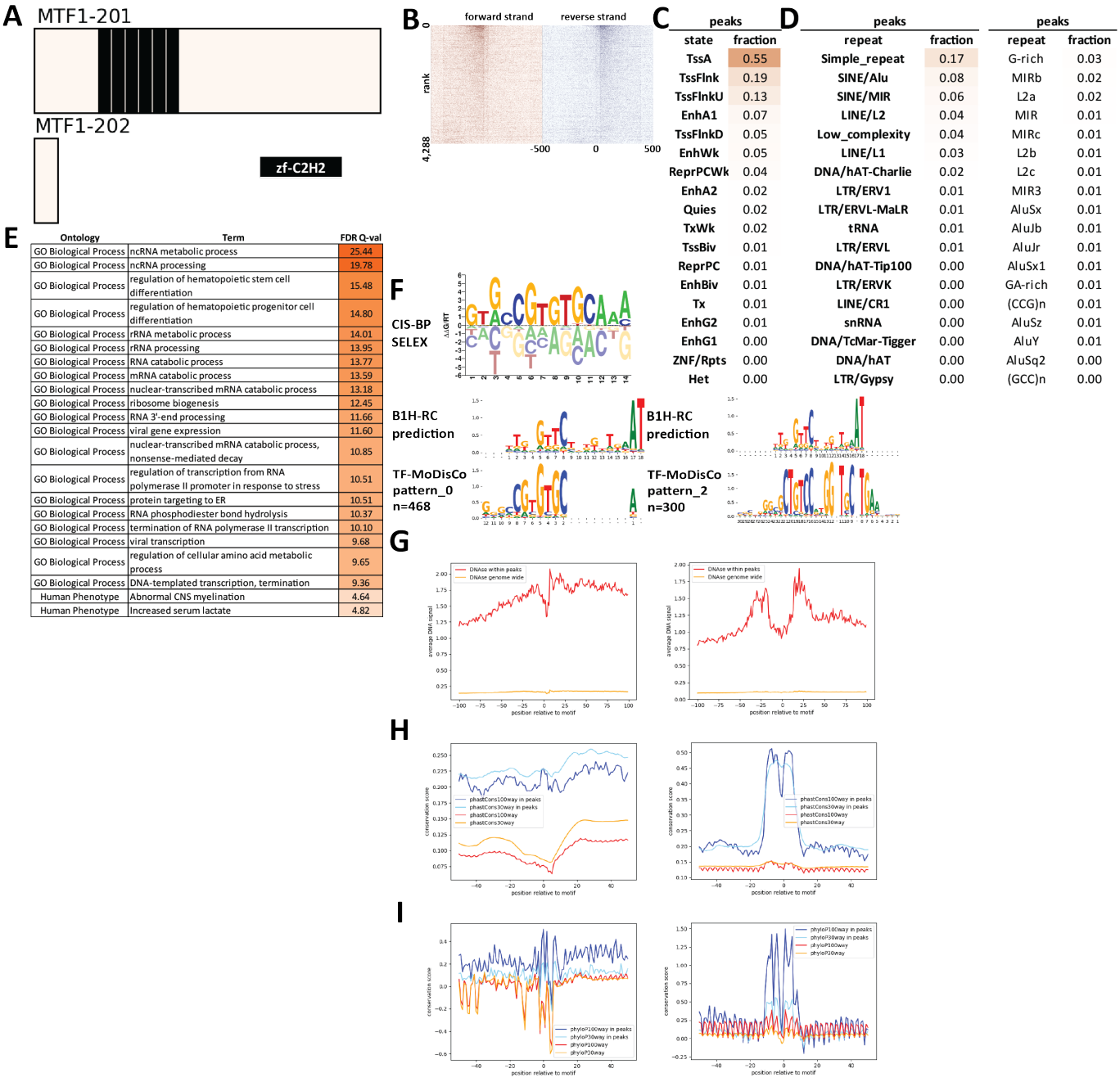

Supplementary Figure 160: Properties and genomic distribution of motifs identified for the MTF1 transcription factor in HepG2 (accession ENCSR194NVP).

TF-MoDisCO pattern_0 n=468, CWM

pattern_0, n=468; subpattern_0, ns=116

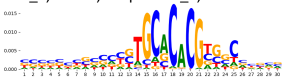

pattern_0, n=468; subpattern_1, ns=109

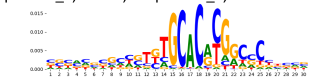

pattern_0, n=468; subpattern_2, ns=106

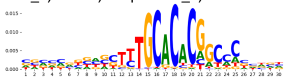

pattern_0, n=468; subpattern_3, ns=81

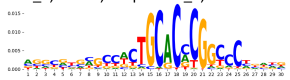

pattern_0, n=468; subpattern_4, ns=56

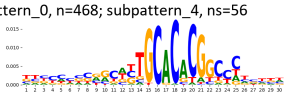

TF-MoDisCO pattern_0 n=468, PWM

pattern_0, n=468; subpattern_0, ns=116

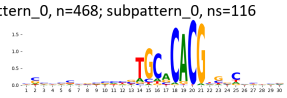

pattern_0, n=468; subpattern_1, ns=109

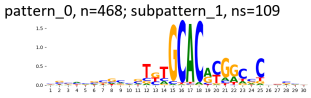

pattern_0, n=468; subpattern_2, ns=106

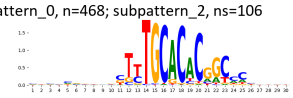

pattern_0, n=468; subpattern_3, ns=81

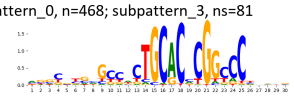

pattern_0, n=468; subpattern_4, ns=56

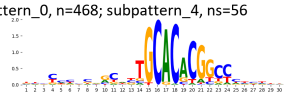

TF-MoDisCO pattern_2 n=300, CWM

pattern_2, n=300; subpattern_0, ns=137

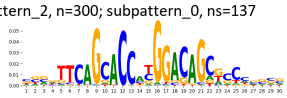

pattern_2, n=300; subpattern_1, ns=135

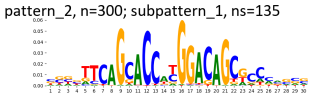

pattern_2, n=300; subpattern_2, ns=28

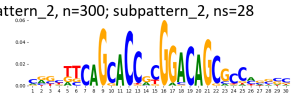

TF-MoDisCO pattern_2 n=300, PWM

pattern_2, n=300; subpattern_0, ns=137

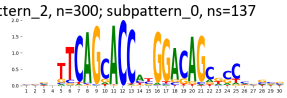

pattern_2, n=300; subpattern_1, ns=135

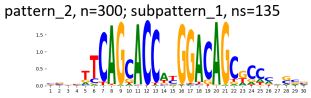

pattern_2, n=300; subpattern_2, ns=28

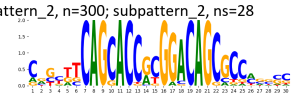

Supplementary Figure 161: TF-MoDisCO subpatterns for the MTF1 transcription factor in HepG2 (accession ENCSR194NVP).

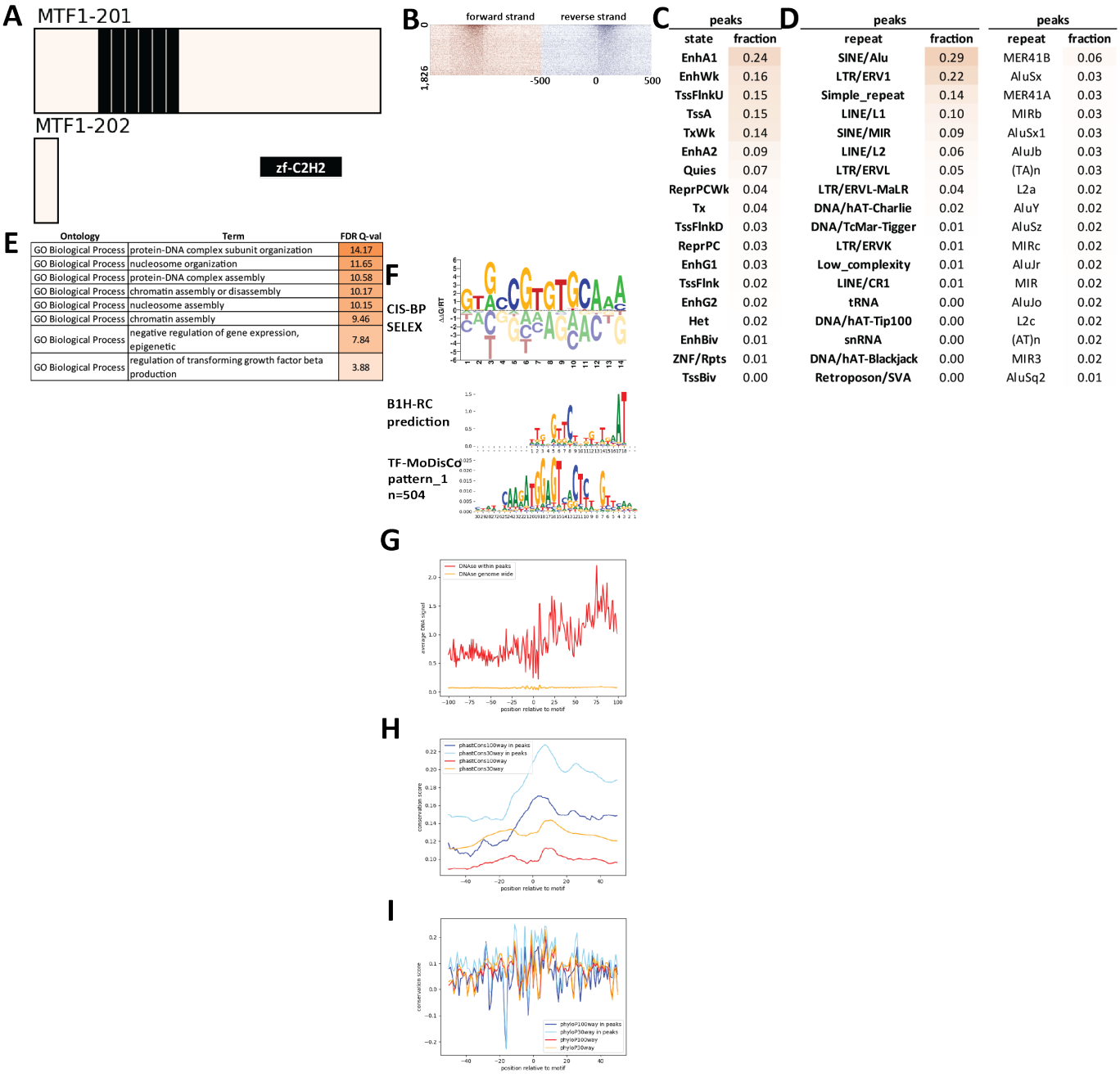

Supplementary Figure 162: Properties and genomic distribution of motifs identified for the MTF1 transcription factor in K562 (accession ENCSR849LXI).

TF-MoDisCO pattern_1 n=504, CWM

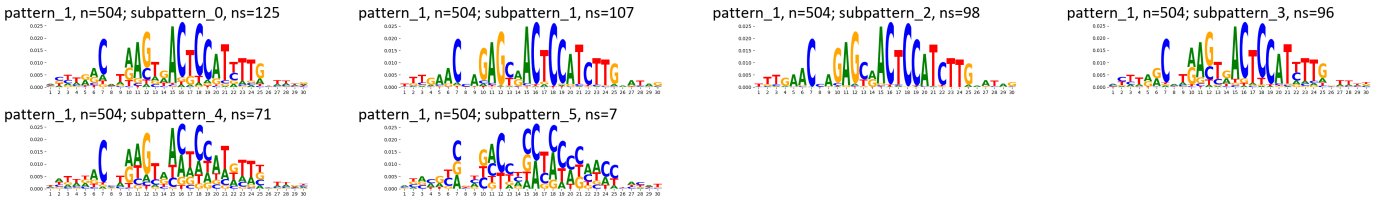

TF-MoDisCO pattern_1 n=504, PWM

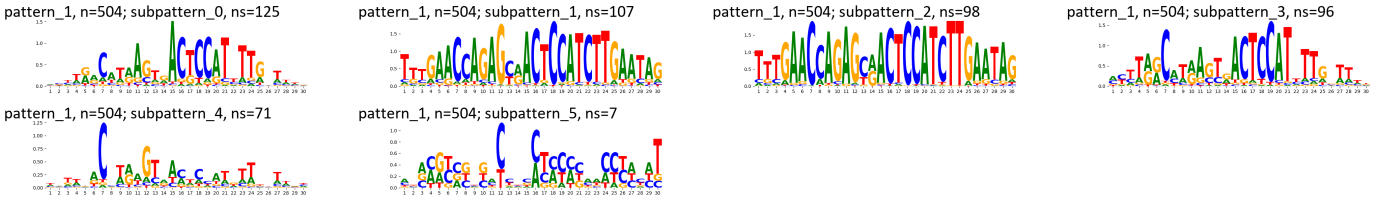

Supplementary Figure 163: TF-MoDisCO subpatterns for the MTF1 transcription factor in K562 (accession ENCSR849LXI).

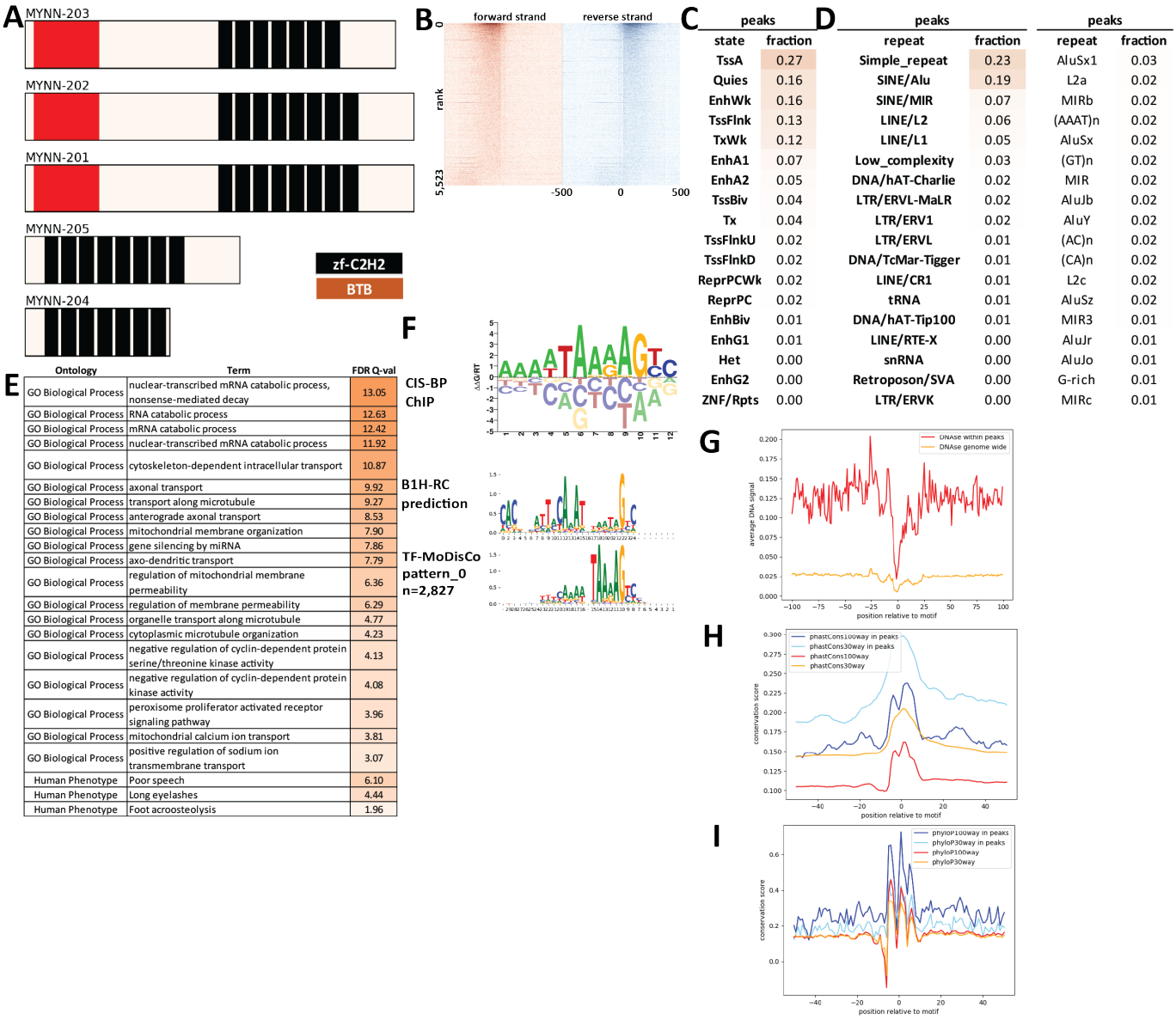

Supplementary Figure 164: Properties and genomic distribution of motifs identified for the MYNN transcription factor in HEK293 (accession ENCSR707BNG).

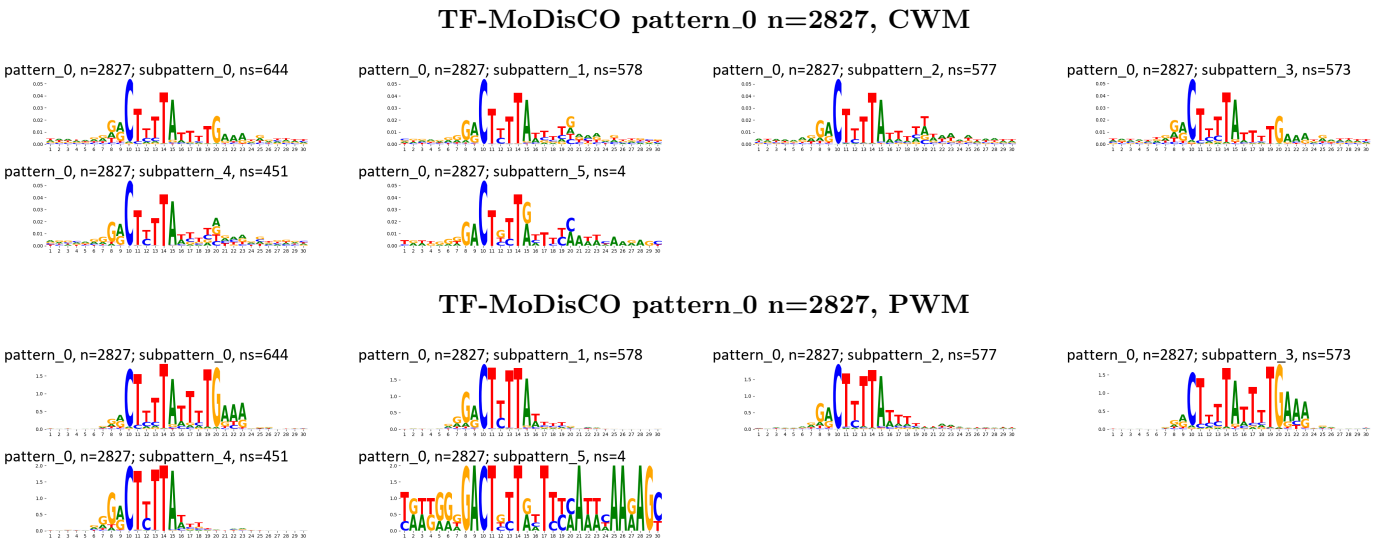

Supplementary Figure 165: TF-MoDisCO subpatterns for the MYNN transcription factor in HEK293 (accession ENCSR707BNG).

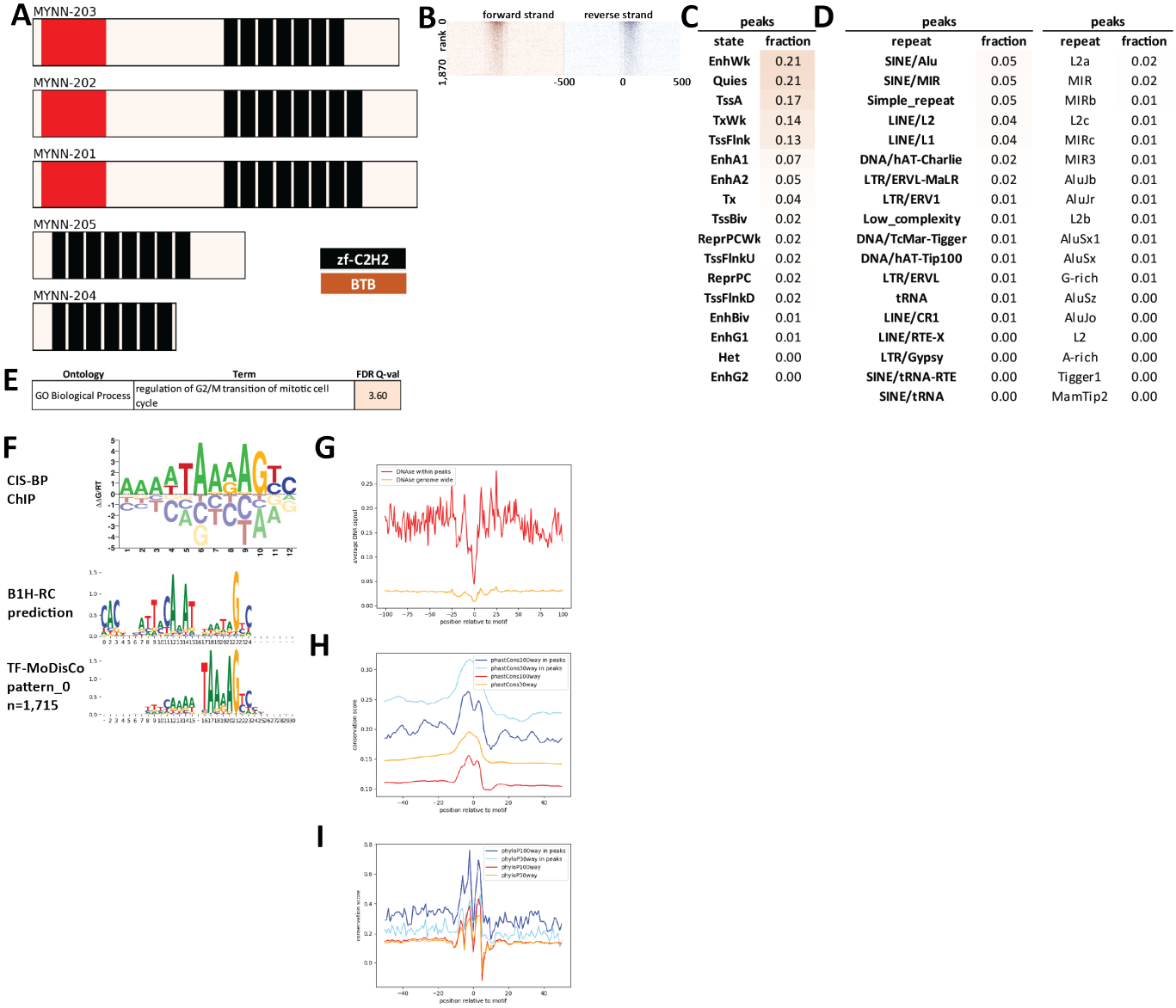

Supplementary Figure 166: Properties and genomic distribution of motifs identified for the MYNN transcription factor in HEK293 (accession Hughes GR models).

TF-MoDisCO pattern_0 n=1715, CWM

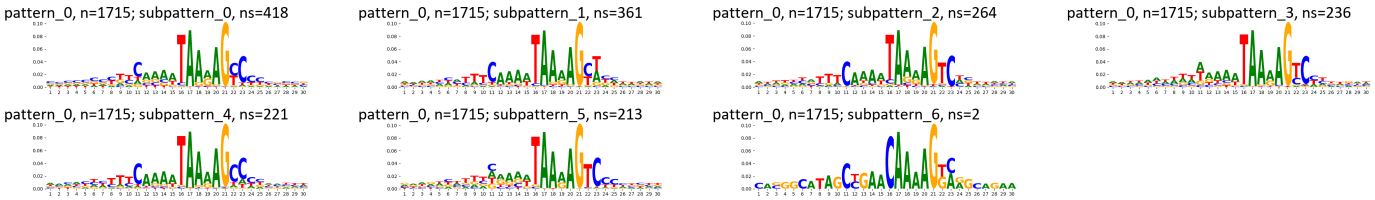

TF-MoDisCO pattern_0 n=1715, PWM

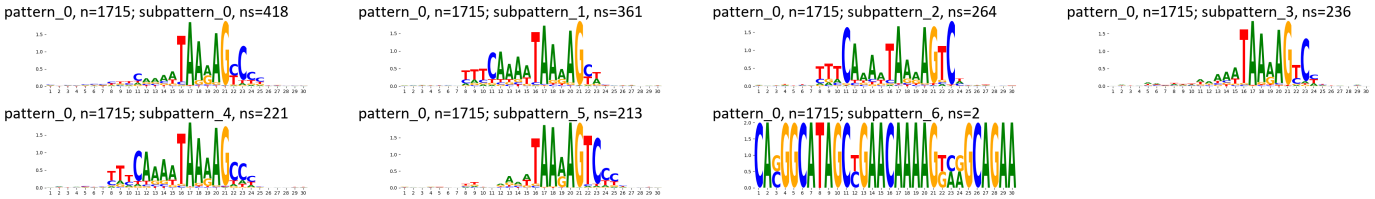

Supplementary Figure 167: TF-MoDisCO subpatterns for the MYNN transcription factor in HEK293 (accession Hughes GR models).

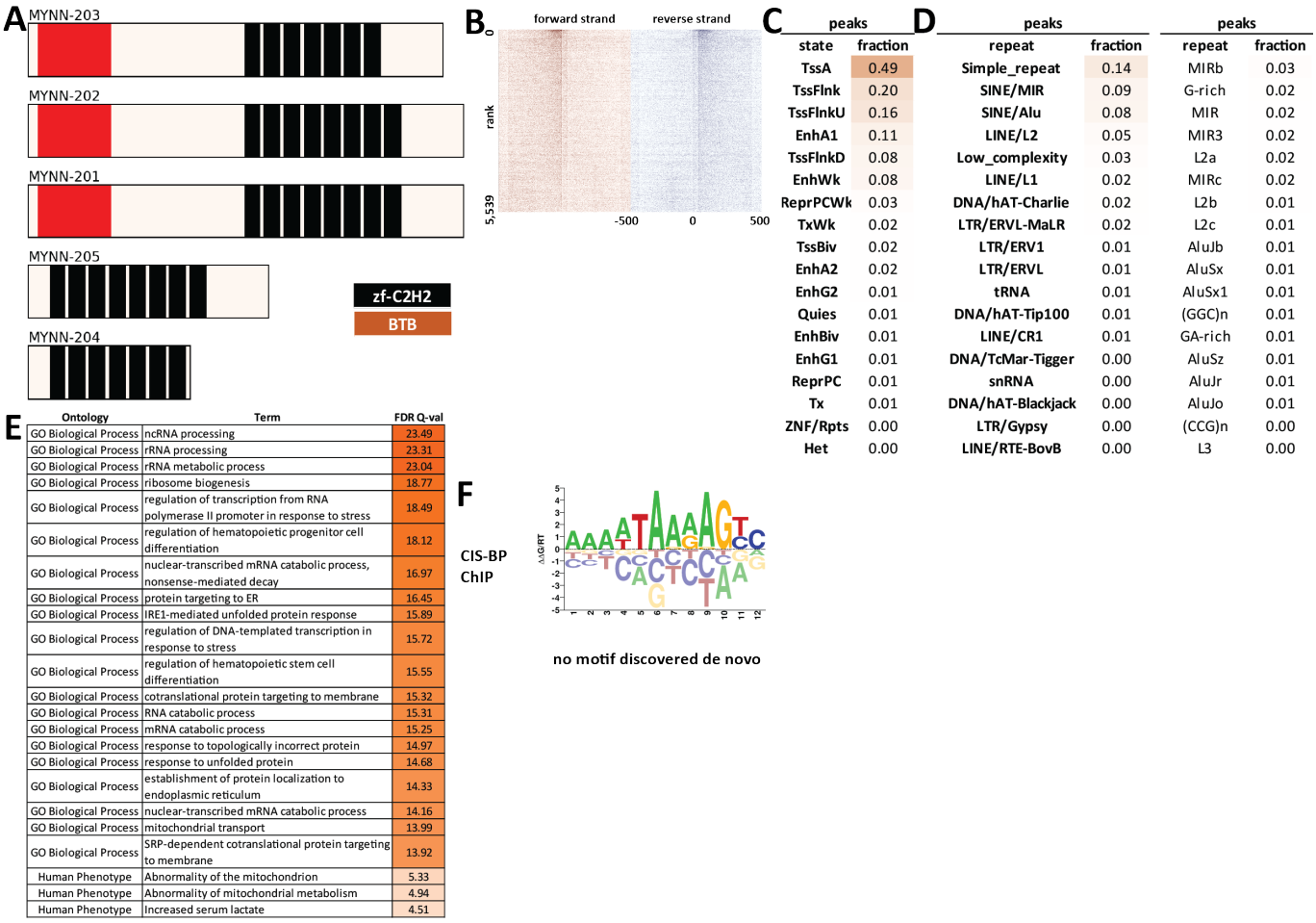

C

peaks	
state	fraction
TssA	0.49
TssFlnk	0.20
TssFlnkU	0.16
EnhA1	0.11
TssFlnkD	0.08
EnhWk	0.08
ReprPCWk	0.03
TxWk	0.02
TssBiv	0.02
EnhA2	0.02
EnhG2	0.01
Quies	0.01
EnhBiv	0.01
EnhG1	0.01
ReprPC	0.01
Tx	0.01
ZNF/Rpts	0.00
Het	0.00

D

peaks		peaks	
repeat	fraction	repeat	fraction
Simple_repeat	0.14	MIRb	0.03
SINE/MIR	0.09	G-rich	0.02
SINE/Alu	0.08	MIR	0.02
LINE/L2	0.05	MIR3	0.02
Low_complexity	0.03	L2a	0.02
LINE/L1	0.02	MIRc	0.02
DNA/hAT-Charlie	0.02	L2b	0.01
LTR/ERVL-MaLR	0.02	L2c	0.01
LTR/ERV1	0.01	AluJb	0.01
LTR/ERVL	0.01	AluSx	0.01
tRNA	0.01	AluSx1	0.01
DNA/hAT-Tip100	0.01	(GGC)n	0.01
LINE/CR1	0.01	GA-rich	0.01
DNA/TcMar-Tigger	0.00	AluSz	0.01
snRNA	0.00	AluJr	0.01
DNA/hAT-Blackjack	0.00	AluJo	0.01
LTR/Gypsy	0.00	(CCG)n	0.00
LINE/RTE-BovB	0.00	L3	0.00

E

Ontology	Term	FDR Q-val
GO Biological Process	ncRNA processing	23.49
GO Biological Process	rRNA processing	23.31
GO Biological Process	rRNA metabolic process	23.04
GO Biological Process	ribosome biogenesis	18.77
GO Biological Process	regulation of transcription from RNA polymerase II promoter in response to stress	18.49
GO Biological Process	regulation of hematopoietic progenitor cell differentiation	18.12
GO Biological Process	nuclear-transcribed mRNA catabolic process, nonsense-mediated decay	16.97
GO Biological Process	protein targeting to ER	16.45
GO Biological Process	IRE1-mediated unfolded protein response	15.89
GO Biological Process	regulation of DNA-templated transcription in response to stress	15.72
GO Biological Process	regulation of hematopoietic stem cell differentiation	15.55
GO Biological Process	cotranslational protein targeting to membrane	15.32
GO Biological Process	RNA catabolic process	15.31
GO Biological Process	mRNA catabolic process	15.25
GO Biological Process	response to topologically incorrect protein	14.97
GO Biological Process	response to unfolded protein	14.68
GO Biological Process	establishment of protein localization to endoplasmic reticulum	14.33
GO Biological Process	nuclear-transcribed mRNA catabolic process	14.16
GO Biological Process	mitochondrial transport	13.99
GO Biological Process	SRP-dependent cotranslational protein targeting to membrane	13.92
Human Phenotype	Abnormality of the mitochondrion	5.33
Human Phenotype	Abnormality of mitochondrial metabolism	4.94
Human Phenotype	Increased serum lactate	4.51

Supplementary Figure 168: Properties and genomic distribution of motifs identified for the MYNN transcription factor in HepG2 (accession ENCSR398TMP).

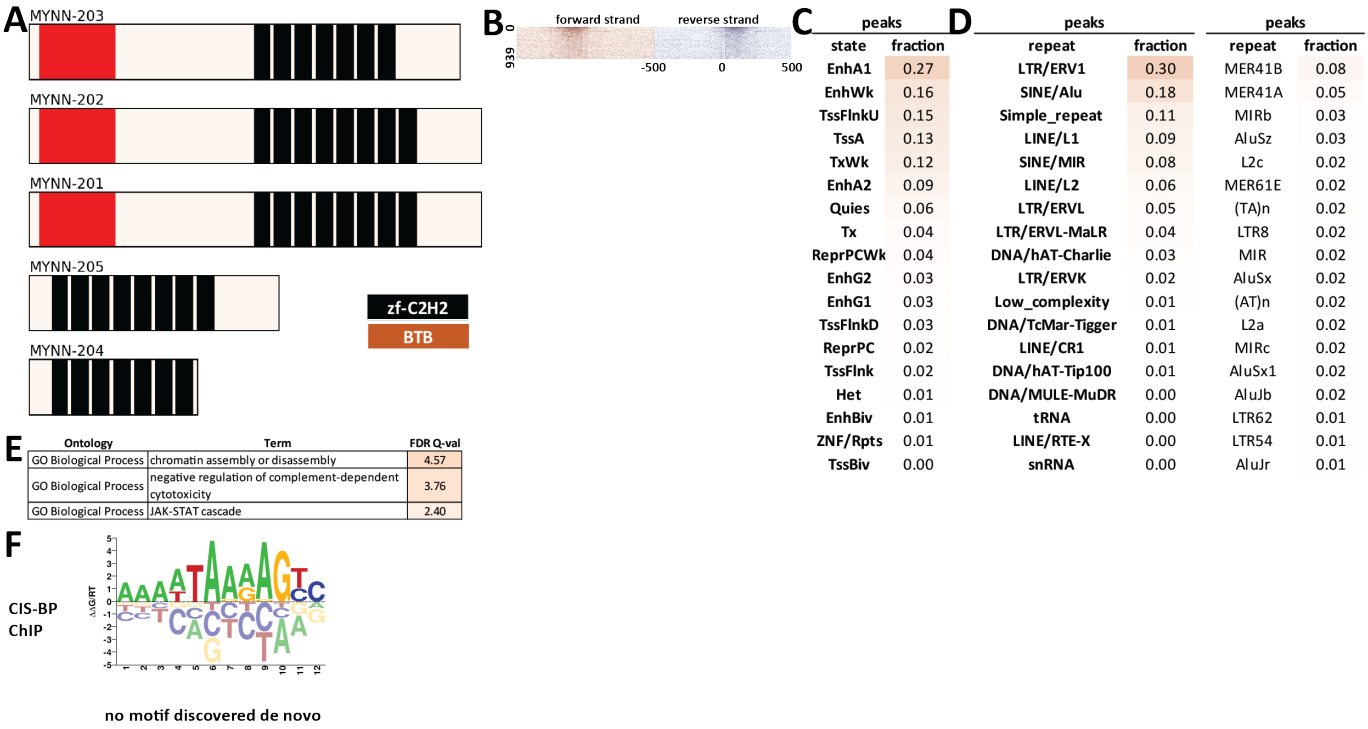

Supplementary Figure 169: Properties and genomic distribution of motifs identified for the MYNN transcription factor in K562 (accession ENCSR307YJU).

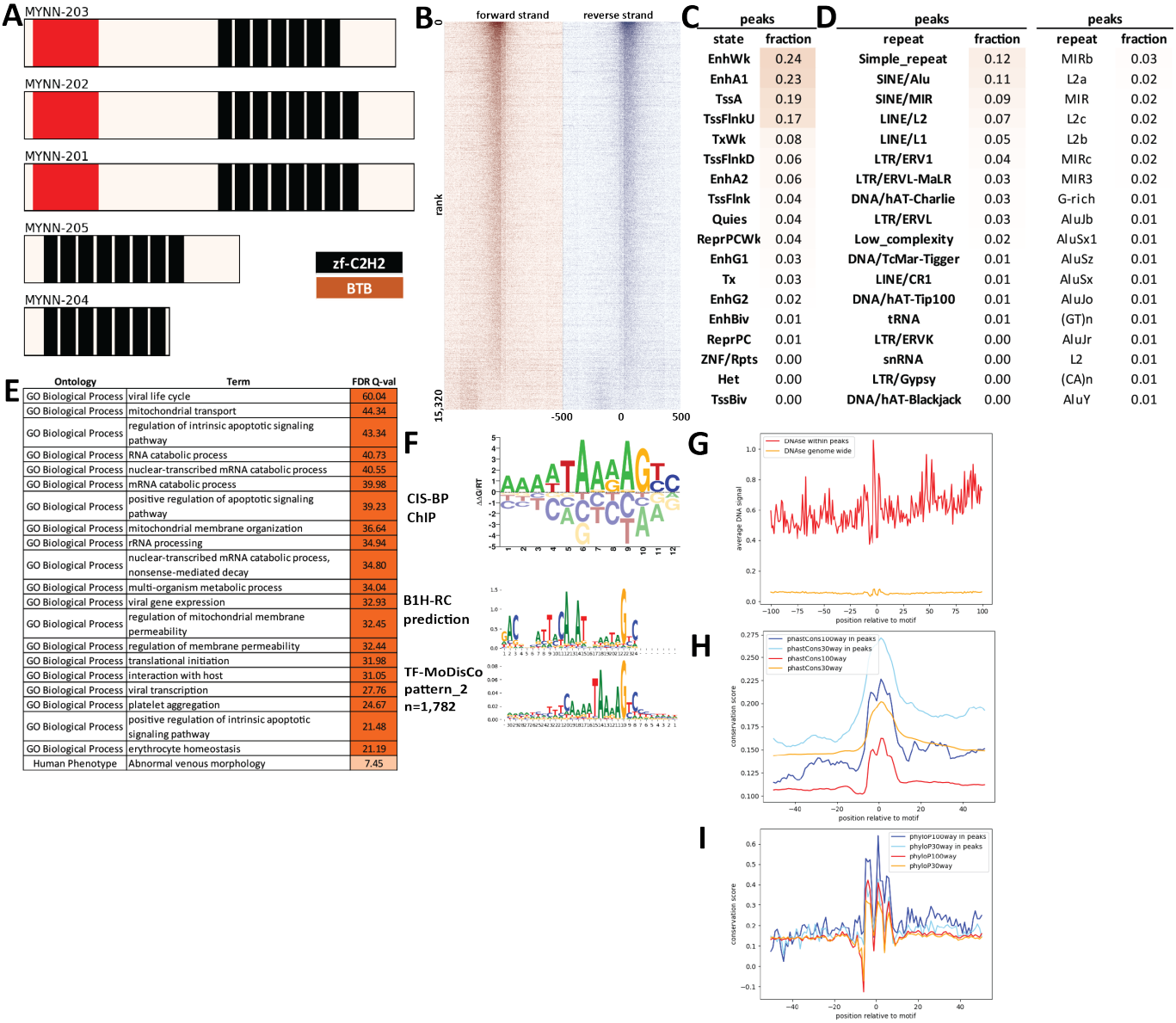

C

peaks	
state	fraction
EnhWk	0.24
EnhA1	0.23
TssA	0.19
TssFlnkU	0.17
TxWk	0.08
TssFlnkD	0.06
EnhA2	0.06
TssFlnk	0.04
Quies	0.04
ReprPCWk	0.04
EnhG1	0.03
Tx	0.03
EnhG2	0.02
EnhBiv	0.01
ReprPC	0.01
ZNF/Rpts	0.00
Het	0.00
TssBiv	0.00

D

peaks		peaks	
repeat	fraction	repeat	fraction
Simple_repeat	0.12	MIRb	0.03
SINE/Alu	0.11	L2a	0.02
SINE/MIR	0.09	MIR	0.02
LINE/L2	0.07	L2c	0.02
LINE/L1	0.05	L2b	0.02
LTR/ERV1	0.04	MIRc	0.02
LTR/ERVL-MaLR	0.03	MIR3	0.02
DNA/hAT-Charlie	0.03	G-rich	0.01
LTR/ERVL	0.03	AluJb	0.01
Low_complexity	0.02	AluSx1	0.01
DNA/TcMar-Tigger	0.01	AluSz	0.01
LINE/CR1	0.01	AluSx	0.01
DNA/hAT-Tip100	0.01	AluJo	0.01
tRNA	0.01	(GT)n	0.01
LTR/ERVK	0.00	AluJr	0.01
snRNA	0.00	L2	0.01
LTR/Gypsy	0.00	(CA)n	0.01
DNA/hAT-Blackjack	0.00	AluY	0.01

E

Ontology	Term	FDR Q-val
GO Biological Process	viral life cycle	60.04
GO Biological Process	mitochondrial transport	44.34
GO Biological Process	regulation of intrinsic apoptotic signaling pathway	43.34
GO Biological Process	RNA catabolic process	40.73
GO Biological Process	nuclear-transcribed mRNA catabolic process	40.55
GO Biological Process	mRNA catabolic process	39.98
GO Biological Process	positive regulation of apoptotic signaling pathway	39.23
GO Biological Process	mitochondrial membrane organization	36.64
GO Biological Process	rRNA processing	34.94
GO Biological Process	nuclear-transcribed mRNA catabolic process, nonsense-mediated decay	34.80
GO Biological Process	multi-organism metabolic process	34.04
GO Biological Process	viral gene expression	32.93
GO Biological Process	regulation of mitochondrial membrane permeability	32.45
GO Biological Process	regulation of membrane permeability	32.44
GO Biological Process	translational initiation	31.98
GO Biological Process	interaction with host	31.05
GO Biological Process	viral transcription	27.76
GO Biological Process	platelet aggregation	24.67
GO Biological Process	positive regulation of intrinsic apoptotic signaling pathway	21.48
GO Biological Process	erythrocyte homeostasis	21.19
Human Phenotype	Abnormal venous morphology	7.45

Supplementary Figure 170: Properties and genomic distribution of motifs identified for the MYNN transcription factor in K562 (accession ENCSR737LTZ).

TF-MoDisCO pattern_2 n=1782, CWM

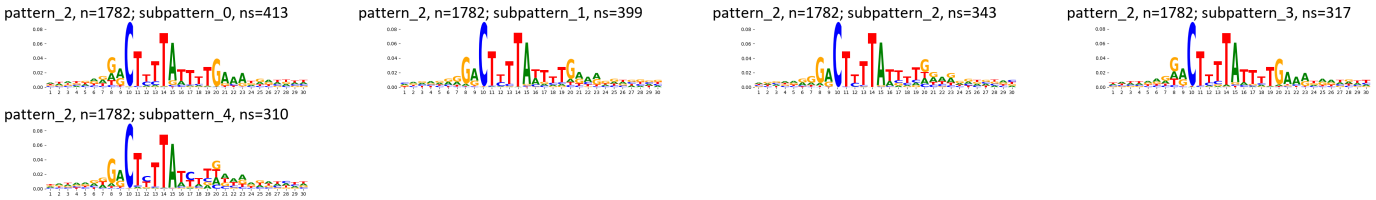

TF-MoDisCO pattern_2 n=1782, PWM

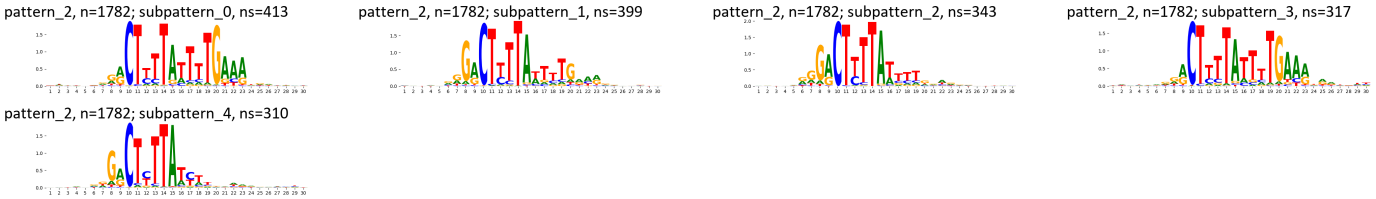

Supplementary Figure 171: TF-MoDisCO subpatterns for the MYNN transcription factor in K562 (accession ENCSR737LTZ).

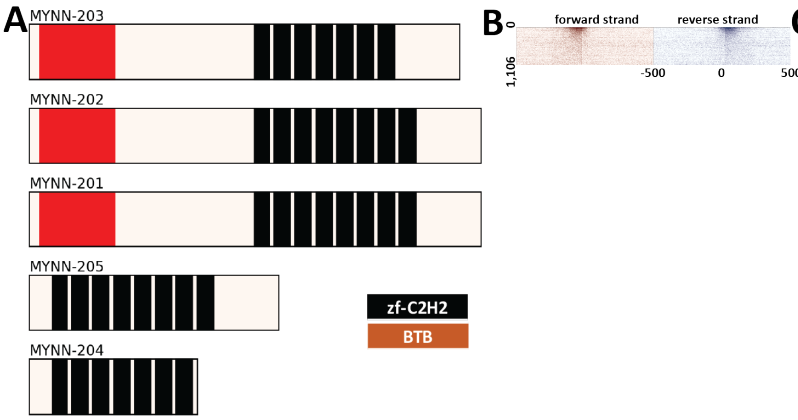

C

peaks	
state	fraction
ReprPCWk	0.17
EnhWk	0.14
ReprPC	0.13
Quies	0.10
TssA	0.08
TxWk	0.07
TssFlnkD	0.07
TssFlnkU	0.05
Tx	0.04
EnhBiv	0.04
Het	0.04
TssFlnk	0.03
EnhG1	0.03
EnhA1	0.03
EnhA2	0.01
ZNF/Rpts	0.01
TssBiv	0.01
EnhG2	0.00

D

peaks		peaks	
repeat	fraction	repeat	fraction
SINE/Alu	0.14	L2a	0.03
LINE/L1	0.07	AluJb	0.02
LINE/L2	0.06	MIRb	0.02
Simple_repeat	0.05	L2c	0.01
SINE/MIR	0.05	AluY	0.01
LTR/ERVL-MaLR	0.04	AluSz	0.01
LTR/ERV1	0.04	AluJo	0.01
DNA/hAT-Charlie	0.03	MIR3	0.01
LTR/ERVL	0.03	AluSx	0.01
Low_complexity	0.01	L2	0.01
DNA/TcMar-Tigger	0.01	AluSx1	0.01
DNA/hAT-Tip100	0.01	L2b	0.01
LINE/CR1	0.00	AluSz6	0.01
DNA/hAT-Blackjack	0.00	AluJr	0.01
tRNA	0.00	MIR	0.01
srpRNA	0.00	AluSp	0.01
Unknown	0.00	MIRc	0.01
Satellite/telo	0.00	G-rich	0.01

E

no functional enrichment (GREAT)

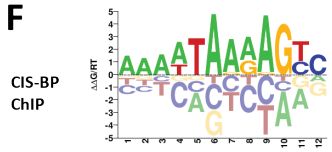

no motif discovered de novo

Supplementary Figure 172: Properties and genomic distribution of motifs identified for the MYNN transcription factor in K562 (accession ENCSR992KLV).

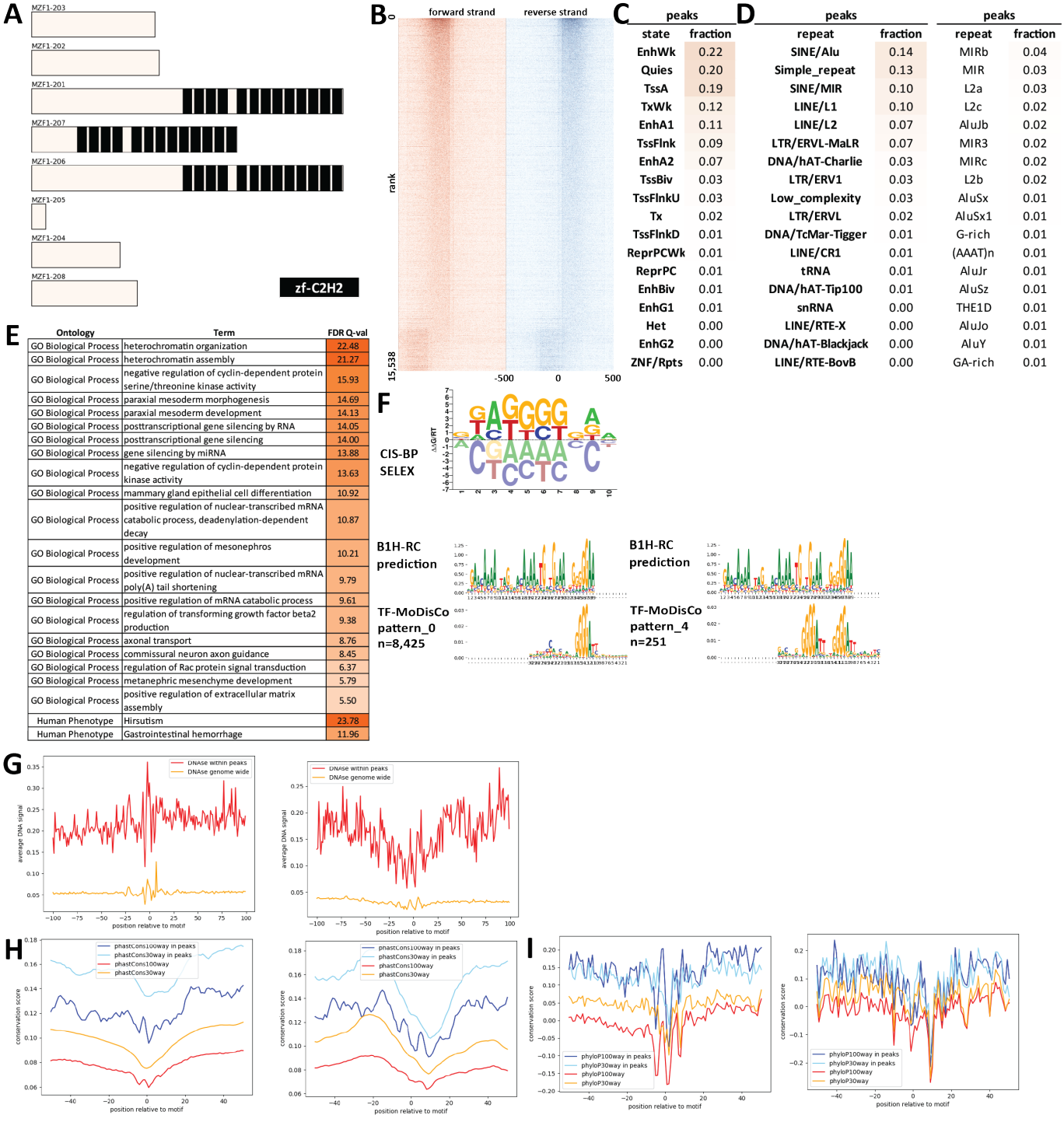

Supplementary Figure 173: Properties and genomic distribution of motifs identified for the MZF1 transcription factor in HEK293 (accession ENCSR298QUH).

TF-MoDisCO pattern_0 n=8425, CWM

pattern_0, n=8425; subpattern_0, ns=2171

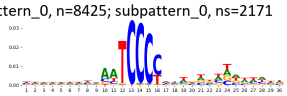

pattern_0, n=8425; subpattern_1, ns=1731

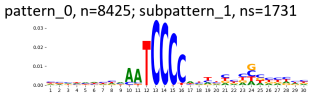

pattern_0, n=8425; subpattern_10, ns=122

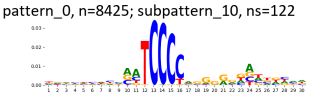

pattern_0, n=8425; subpattern_11, ns=65

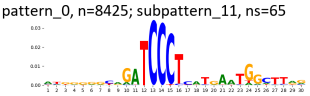

pattern_0, n=8425; subpattern_12, ns=2

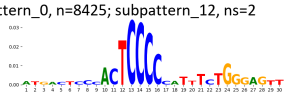

pattern_0, n=8425; subpattern_13, ns=2

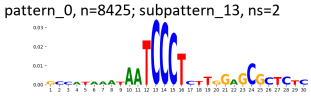

pattern_0, n=8425; subpattern_2, ns=1100

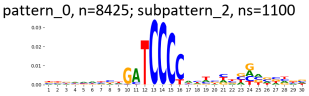

pattern_0, n=8425; subpattern_3, ns=1041

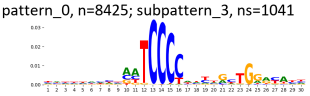

pattern_0, n=8425; subpattern_4, ns=1019

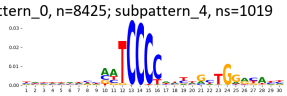

pattern_0, n=8425; subpattern_5, ns=351

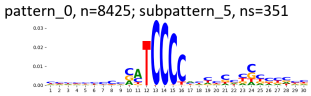

pattern_0, n=8425; subpattern_6, ns=303

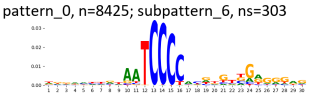

pattern_0, n=8425; subpattern_7, ns=196

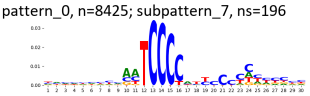

pattern_0, n=8425; subpattern_8, ns=195

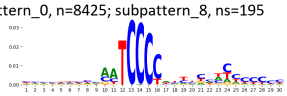

pattern_0, n=8425; subpattern_9, ns=127

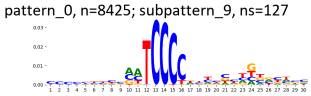

TF-MoDisCO pattern_0 n=8425, PWM

pattern_0, n=8425; subpattern_0, ns=2171

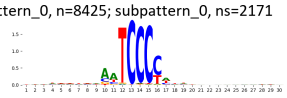

pattern_0, n=8425; subpattern_1, ns=1731

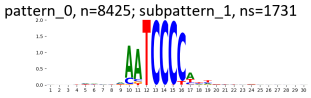

pattern_0, n=8425; subpattern_10, ns=122

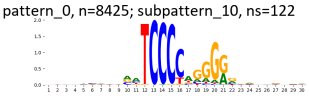

pattern_0, n=8425; subpattern_11, ns=65

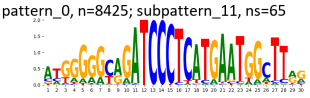

pattern_0, n=8425; subpattern_12, ns=2

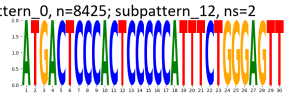

pattern_0, n=8425; subpattern_13, ns=2

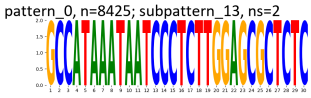

pattern_0, n=8425; subpattern_2, ns=1100

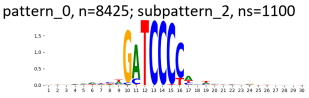

pattern_0, n=8425; subpattern_3, ns=1041

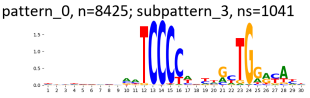

pattern_0, n=8425; subpattern_4, ns=1019

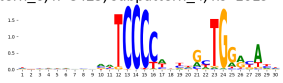

pattern_0, n=8425; subpattern_5, ns=351

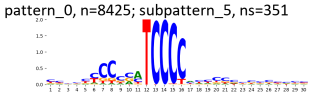

pattern_0, n=8425; subpattern_6, ns=303

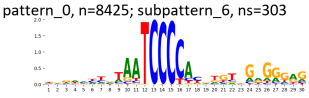

pattern_0, n=8425; subpattern_7, ns=196

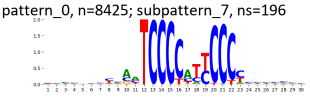

pattern_0, n=8425; subpattern_8, ns=195

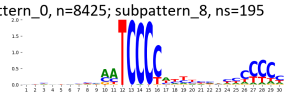

pattern_0, n=8425; subpattern_9, ns=127

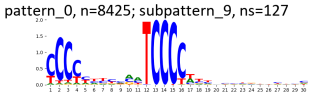

TF-MoDisCO pattern_4 n=251, CWM

pattern_4, n=251; subpattern_0, ns=79

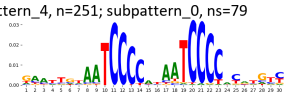

pattern_4, n=251; subpattern_1, ns=61

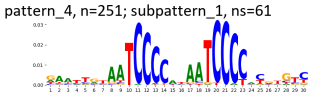

pattern_4, n=251; subpattern_2, ns=43

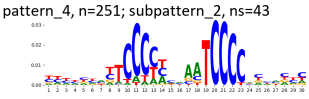

pattern_4, n=251; subpattern_3, ns=34

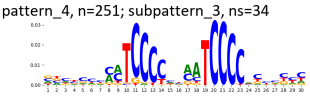

pattern_4, n=251; subpattern_4, ns=12

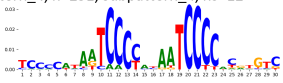

pattern_4, n=251; subpattern_5, ns=8

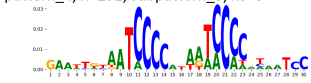

pattern_4, n=251; subpattern_6, ns=6

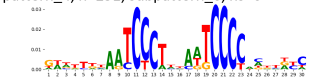

pattern_4, n=251; subpattern_7, ns=4

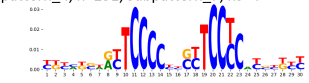

pattern_4, n=251; subpattern_8, ns=4

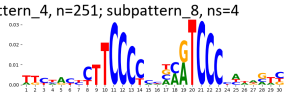

TF-MoDisCO pattern_4 n=251, PWM

pattern_4, n=251; subpattern_0, ns=79

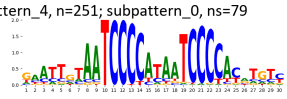

pattern_4, n=251; subpattern_1, ns=61

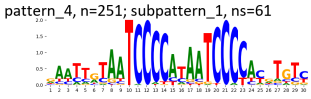

pattern_4, n=251; subpattern_2, ns=43

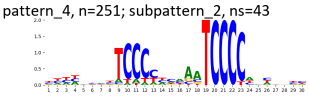

pattern_4, n=251; subpattern_3, ns=34

pattern_4, n=251; subpattern_4, ns=12

pattern_4, n=251; subpattern_5, ns=8

pattern_4, n=251; subpattern_6, ns=6

pattern_4, n=251; subpattern_7, ns=4

pattern_4, n=251; subpattern_8, ns=4

Supplementary Figure 174: TF-MoDisCO subpatterns for the MZF1 transcription factor in HEK293 (accession ENCSR298QUH).

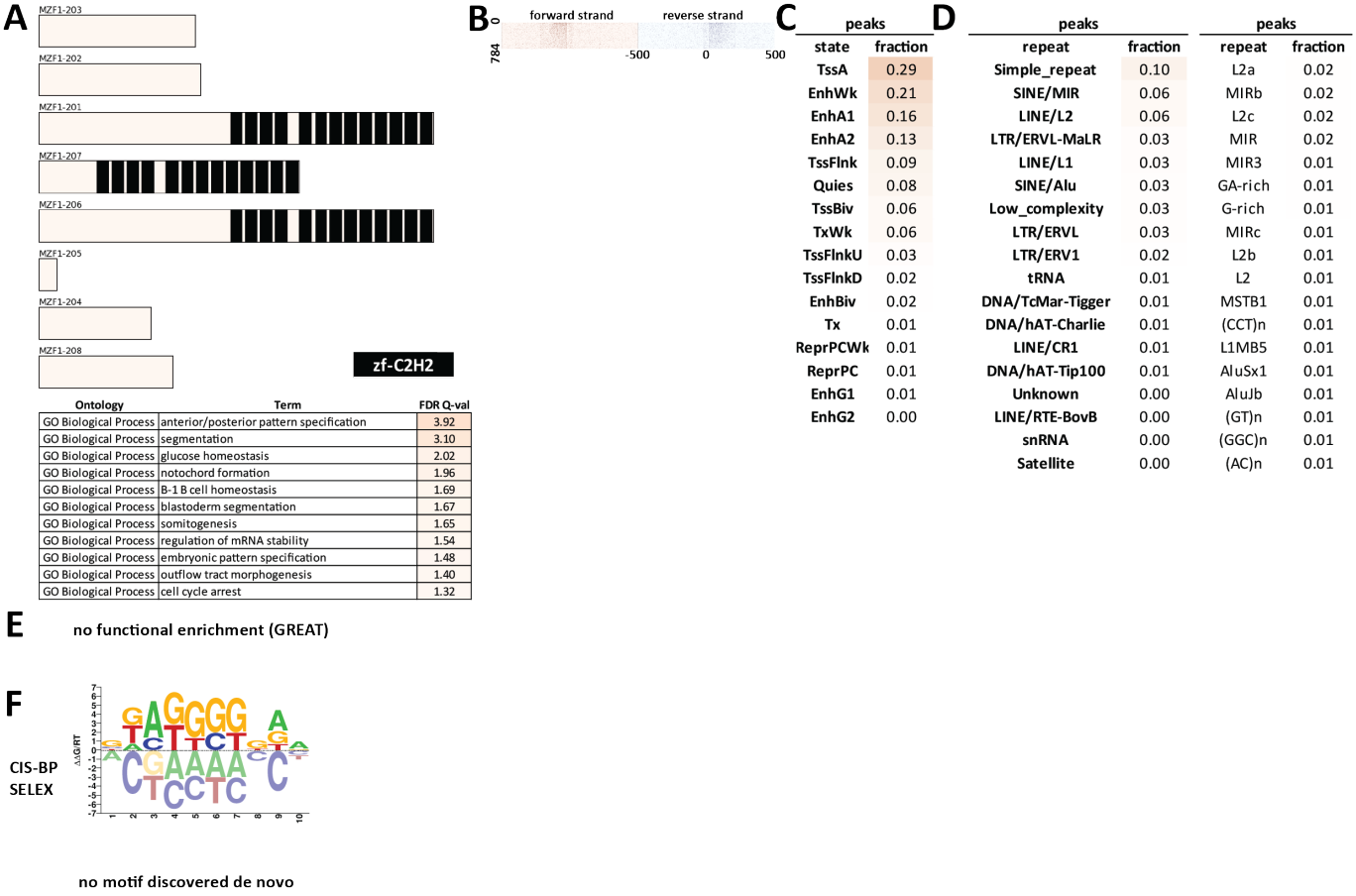

Ontology	Term	FDR Q-val
GO Biological Process	anterior/posterior pattern specification	3.92
GO Biological Process	segmentation	3.10
GO Biological Process	glucose homeostasis	2.02
GO Biological Process	notochord formation	1.96
GO Biological Process	B-1 B cell homeostasis	1.69
GO Biological Process	blastoderm segmentation	1.67
GO Biological Process	somitogenesis	1.65
GO Biological Process	regulation of mRNA stability	1.54
GO Biological Process	embryonic pattern specification	1.48
GO Biological Process	outflow tract morphogenesis	1.40
GO Biological Process	cell cycle arrest	1.32

peaks	
state	fraction
TssA	0.29
EnhWk	0.21
EnhA1	0.16
EnhA2	0.13
TssFlnk	0.09
Quies	0.08
TssBiv	0.06
TxWk	0.06
TssFlnkU	0.03
TssFlnkD	0.02
EnhBiv	0.02
Tx	0.01
ReprPCWk	0.01
ReprPC	0.01
EnhG1	0.01
EnhG2	0.00

peaks		peaks	
repeat	fraction	repeat	fraction
Simple_repeat	0.10	L2a	0.02
SINE/MIR	0.06	MIRb	0.02
LINE/L2	0.06	L2c	0.02
LTR/ERVL-MaLR	0.03	MIR	0.02
LINE/L1	0.03	MIR3	0.01
SINE/Alu	0.03	GA-rich	0.01
Low_complexity	0.03	G-rich	0.01
LTR/ERVL	0.03	MIRc	0.01
LTR/ERV1	0.02	L2b	0.01
tRNA	0.01	L2	0.01
DNA/TcMar-Tigger	0.01	MSTB1	0.01
DNA/hAT-Charlie	0.01	(CCT)n	0.01
LINE/CR1	0.01	L1MB5	0.01
DNA/hAT-Tip100	0.01	AluSx1	0.01
Unknown	0.00	AluJb	0.01
LINE/RTE-BovB	0.00	(GT)n	0.01
snRNA	0.00	(GGC)n	0.01
Satellite	0.00	(AC)n	0.01

Supplementary Figure 175: Properties and genomic distribution of motifs identified for the MZF1 transcription factor in HEK293 (accession Hughes GR models).

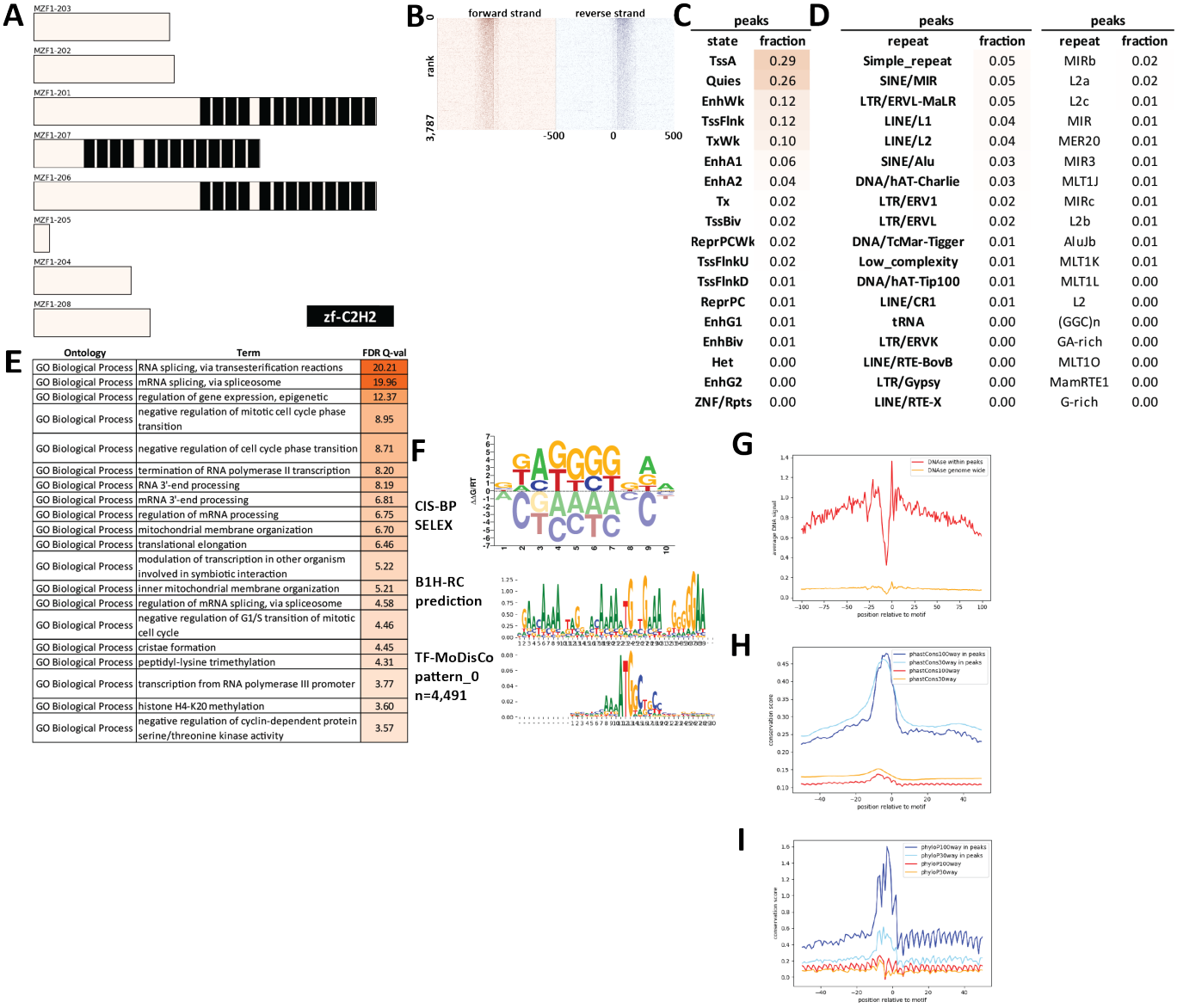

Supplementary Figure 176: Properties and genomic distribution of motifs identified for the MZF1 transcription factor in HEK293 (accession Hughes NB models).

TF-MoDisCO pattern_0 n=4491, CWM

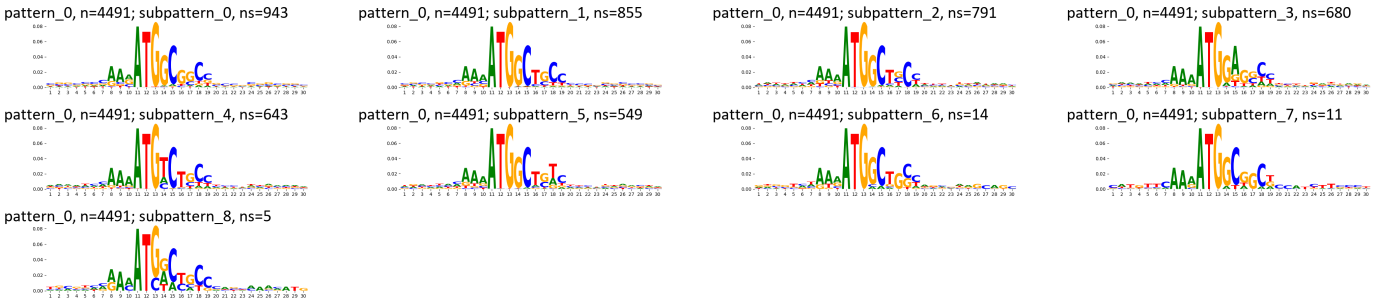

TF-MoDisCO pattern_0 n=4491, PWM

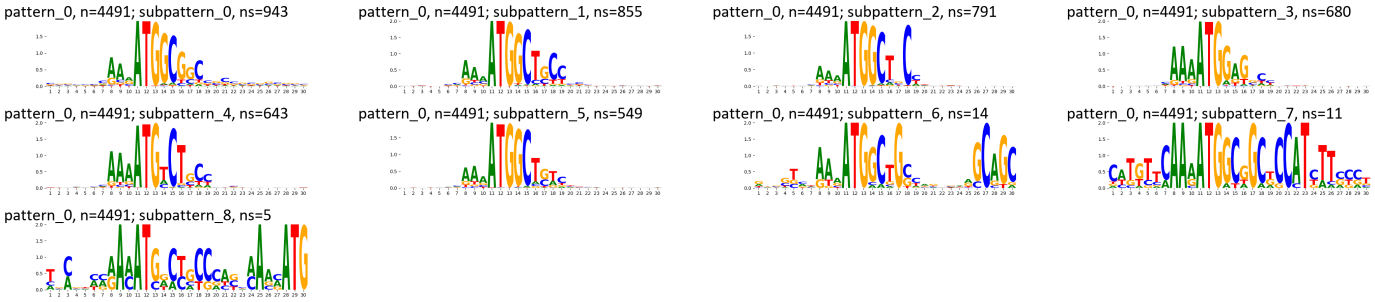

Supplementary Figure 177: TF-MoDisCO subpatterns for the MZF1 transcription factor in HEK293 (accession Hughes NB models).

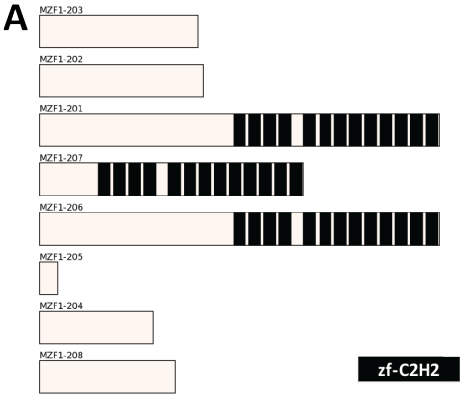

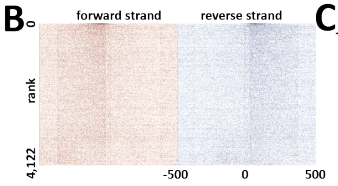

C

peaks	
state	fraction
TssA	0.46
TssFlnkU	0.18
TssFlnk	0.15
EnhA1	0.11
TssFlnkD	0.10
EnhWk	0.09
TssBiv	0.02
ReprPCWk	0.02
EnhG2	0.02
EnhBiv	0.02
EnhA2	0.02
TxWk	0.01
EnhG1	0.01
Tx	0.01
ReprPC	0.01
Quies	0.00
ZNF/Rpts	0.00

D

peaks		peaks	
repeat	fraction	repeat	fraction
Simple_repeat	0.12	MIRb	0.03
SINE/MIR	0.10	L2a	0.02
SINE/Alu	0.08	MIR	0.02
LINE/L2	0.05	MIR3	0.02
Low_complexity	0.03	G-rich	0.02
LINE/L1	0.02	L2b	0.02
DNA/hAT-Charlie	0.02	MIRc	0.02
LTR/ERVL-MaLR	0.01	L2c	0.01
LTR/ERV1	0.01	AluSx	0.01
LTR/ERVL	0.01	AluSx1	0.01
tRNA	0.01	AluSz	0.01
DNA/hAT-Tip100	0.01	AluJb	0.01
LINE/CR1	0.00	AluJo	0.01
DNA/TcMar-Tigger	0.00	AluJr	0.01
DNA/hAT-Blackjack	0.00	GA-rich	0.01
DNA/hAT	0.00	MIR1_Amn	0.01
DNA/hAT-Ac	0.00	L2	0.01
LTR/ERVK	0.00	(GT)n	0.01

E

Ontology	Term	FDR Q-val
GO Biological Process	platelet-derived growth factor receptor signaling pathway	14.27
GO Biological Process	nuclear-transcribed mRNA catabolic process, nonsense-mediated decay	12.86
GO Biological Process	rRNA processing	12.01
GO Biological Process	rRNA metabolic process	11.46
GO Biological Process	nuclear-transcribed mRNA catabolic process	10.91
GO Biological Process	RNA catabolic process	10.38
GO Biological Process	mRNA catabolic process	10.20
GO Biological Process	cotranslational protein targeting to membrane	10.03
GO Biological Process	SRP-dependent cotranslational protein targeting to membrane	9.67
GO Biological Process	protein targeting to ER	9.24
GO Biological Process	regulation of protein ubiquitination involved in ubiquitin-dependent protein catabolic process	8.40
GO Biological Process	PERK-mediated unfolded protein response	8.15
GO Biological Process	establishment of protein localization to endoplasmic reticulum	8.09
GO Biological Process	protein targeting to membrane	7.38
GO Biological Process	response to epidermal growth factor	7.32
GO Biological Process	protein complex disassembly	6.94
GO Biological Process	protein localization to endoplasmic reticulum	6.85
GO Biological Process	multi-organism metabolic process	6.37
GO Biological Process	cellular protein complex disassembly	6.34
GO Biological Process	translational termination	5.97

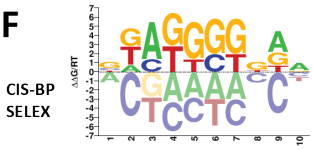

no motif discovered de novo

Supplementary Figure 178: Properties and genomic distribution of motifs identified for the MZF1 transcription factor in HepG2 (accession ENCSR384YOP).

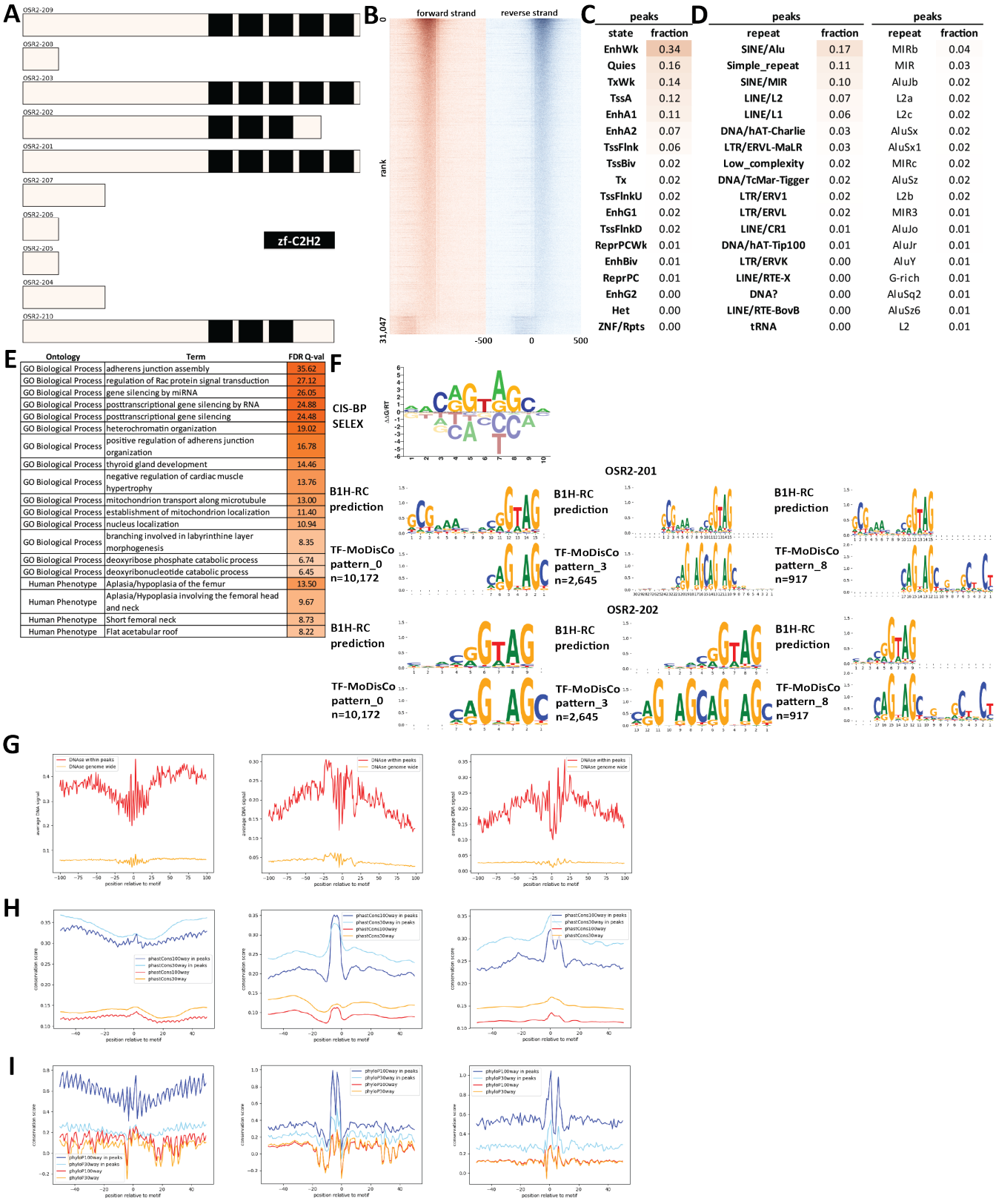

Supplementary Figure 179: Properties and genomic distribution of motifs identified for the OSR2 transcription factor in HEK293 (accession ENCSR324LTM).

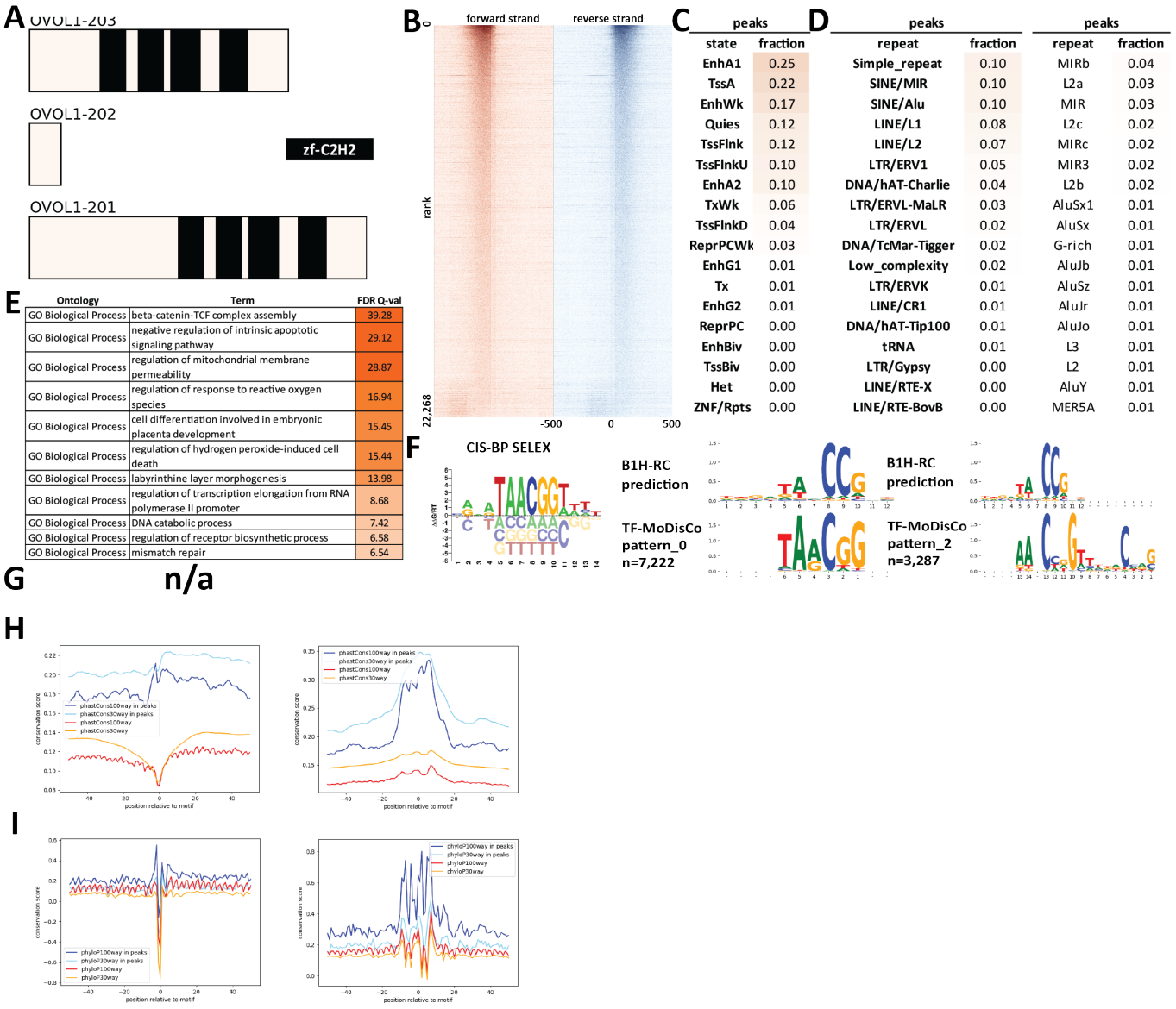

peaks	
state	fraction
EnhA1	0.25
TssA	0.22
EnhWk	0.17
Quies	0.12
TssFlnk	0.12
TssFlnkU	0.10
EnhA2	0.10
TxWk	0.06
TssFlnkD	0.04
ReprPCWk	0.03
EnhG1	0.01
Tx	0.01
EnhG2	0.01
ReprPC	0.00
EnhBiv	0.00
TssBiv	0.00
Het	0.00
ZNF/Rpts	0.00

peaks	
repeat	fraction
Simple_repeat	0.10
SINE/MIR	0.10
SINE/Alu	0.10
LINE/L1	0.08
LINE/L2	0.07
LTR/ERV1	0.05
DNA/hAT-Charlie	0.04
LTR/ERVL-MaLR	0.03
LTR/ERVL	0.02
DNA/TcMar-Tigger	0.02
Low_complexity	0.02
LTR/ERVK	0.01
LINE/CR1	0.01
DNA/hAT-Tip100	0.01
tRNA	0.01
LTR/Gypsy	0.00
LINE/RTE-X	0.00
LINE/RTE-BovB	0.00

peaks	
repeat	fraction
MIRb	0.04
L2a	0.03
MIR	0.03
L2c	0.02
MIRc	0.02
MIR3	0.02
L2b	0.02
AluSx1	0.01
AluSx	0.01
G-rich	0.01
AluJb	0.01
AluSz	0.01
AluJr	0.01
AluJo	0.01
L3	0.01
L2	0.01
AluY	0.01
MER5A	0.01

Ontology	Term	FDR Q-val
GO Biological Process	beta-catenin-TCF complex assembly	39.28
GO Biological Process	negative regulation of intrinsic apoptotic signaling pathway	29.12
GO Biological Process	regulation of mitochondrial membrane permeability	28.87
GO Biological Process	regulation of response to reactive oxygen species	16.94
GO Biological Process	cell differentiation involved in embryonic placenta development	15.45
GO Biological Process	regulation of hydrogen peroxide-induced cell death	15.44
GO Biological Process	labyrinthine layer morphogenesis	13.98
GO Biological Process	regulation of transcription elongation from RNA polymerase II promoter	8.68
GO Biological Process	DNA catabolic process	7.42
GO Biological Process	regulation of receptor biosynthetic process	6.58
GO Biological Process	mismatch repair	6.54

Supplementary Figure 180: Properties and genomic distribution of motifs identified for the OVOL1 transcription factor in MCF-7 (accession ENCSR829WBA).

TF-MoDisCO pattern_0 n=7222, CWM

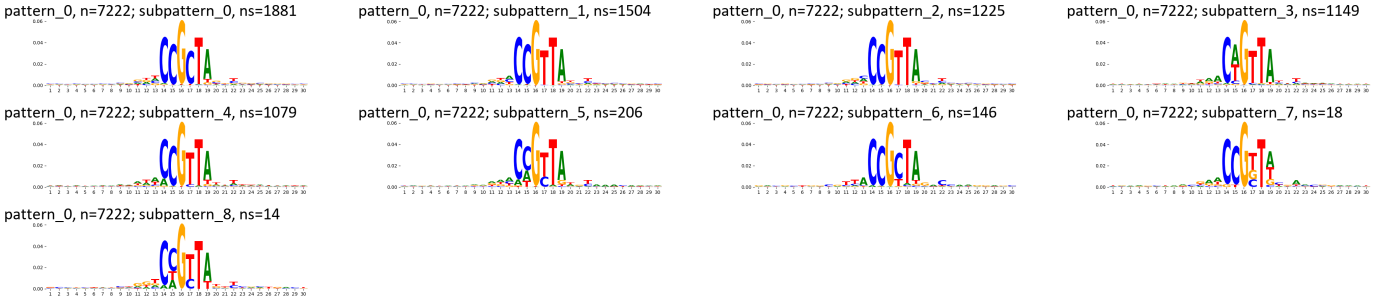

TF-MoDisCO pattern_0 n=7222, PWM

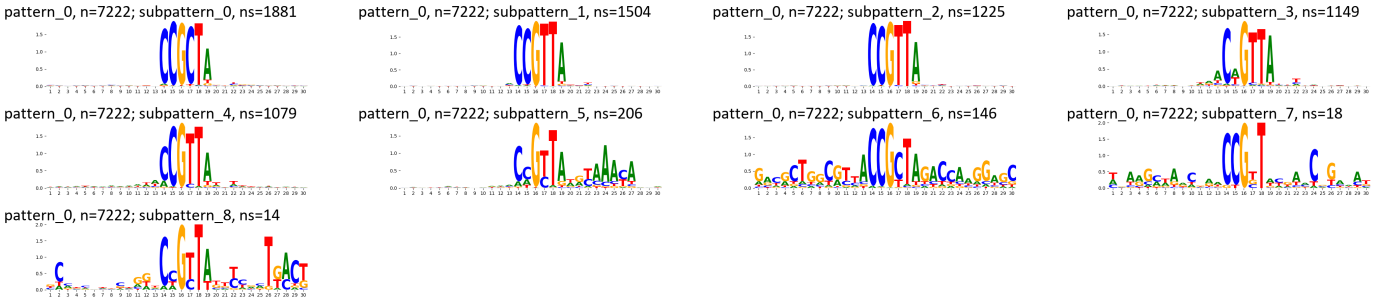

TF-MoDisCO pattern_2 n=3287, CWM

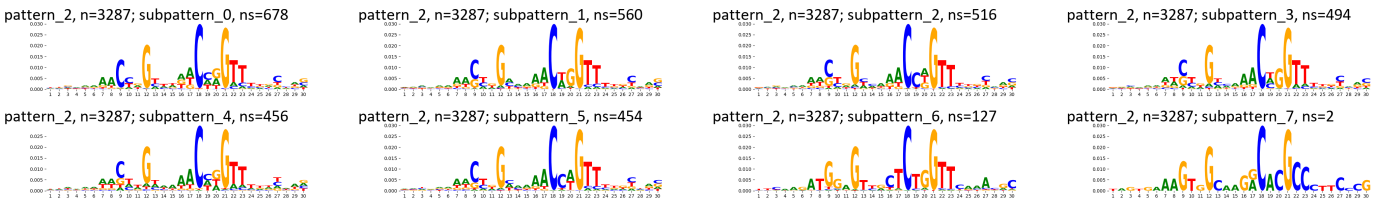

TF-MoDisCO pattern_2 n=3287, PWM

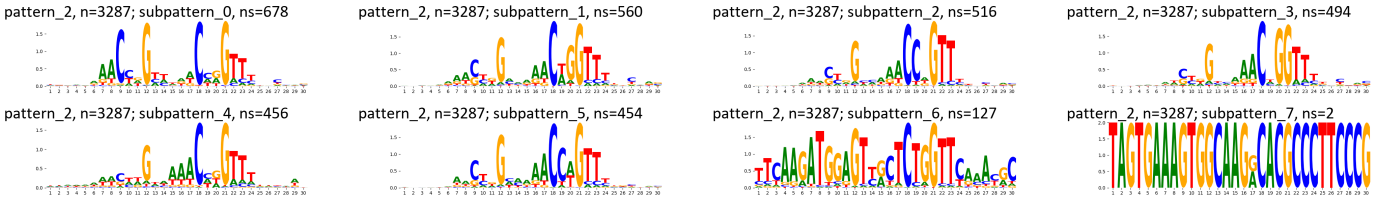

Supplementary Figure 181: TF-MoDisCO subpatterns for the OVOL1 transcription factor in MCF-7 (accession ENCSR829WBA).

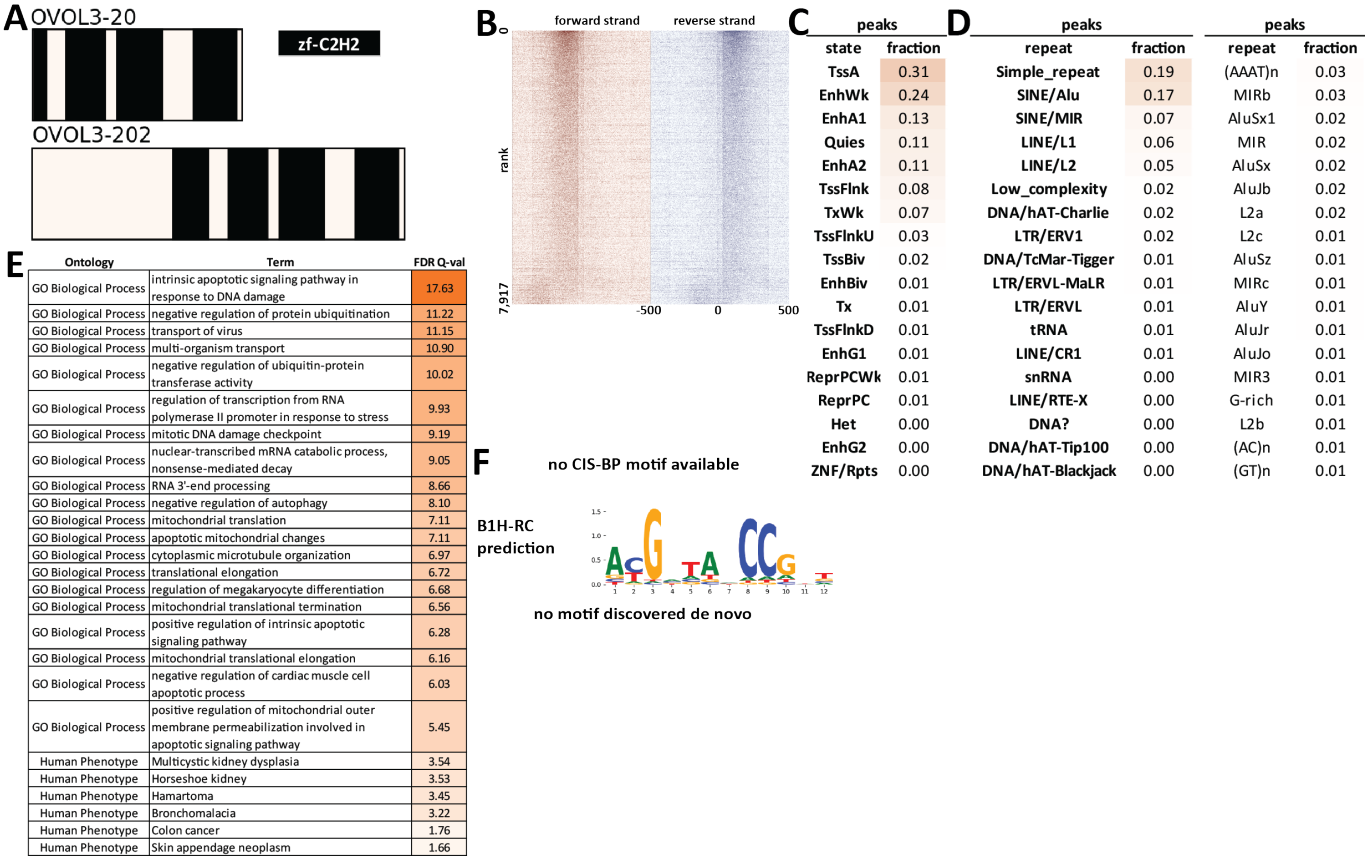

Supplementary Figure 182: Properties and genomic distribution of motifs identified for the OVOL3 transcription factor in HEK293 (accession ENCSR768LIO).

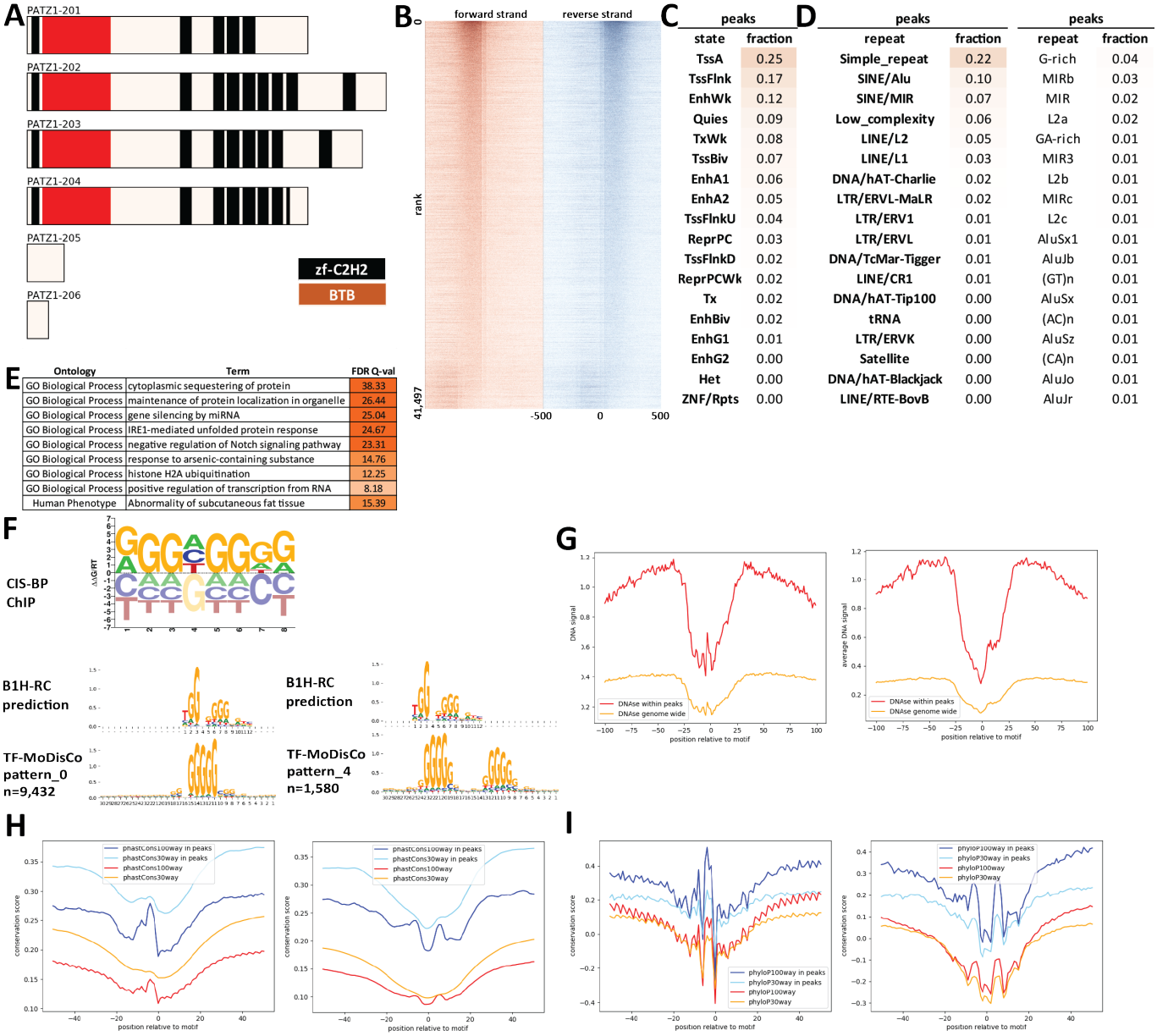

Supplementary Figure 183: Properties and genomic distribution of motifs identified for the PATZ1 transcription factor in HEK293 (accession ENCSR966ULI).

TF-MoDisCO pattern_0 n=9432, CWM

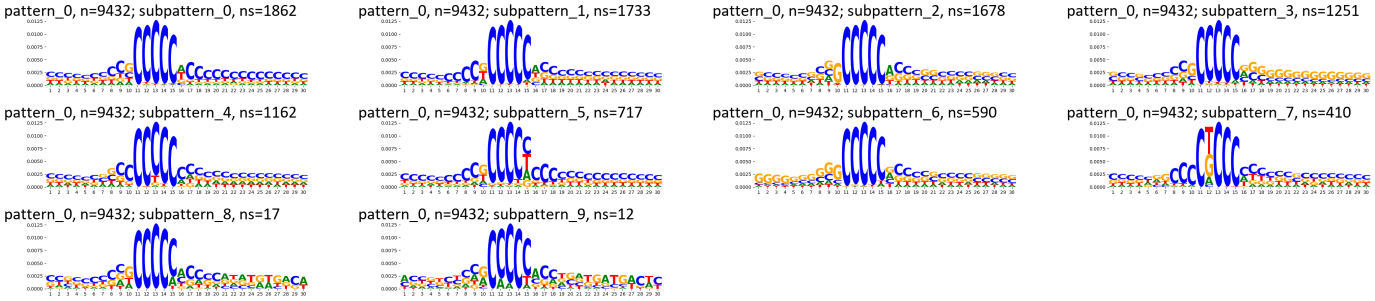

TF-MoDisCO pattern_0 n=9432, PWM

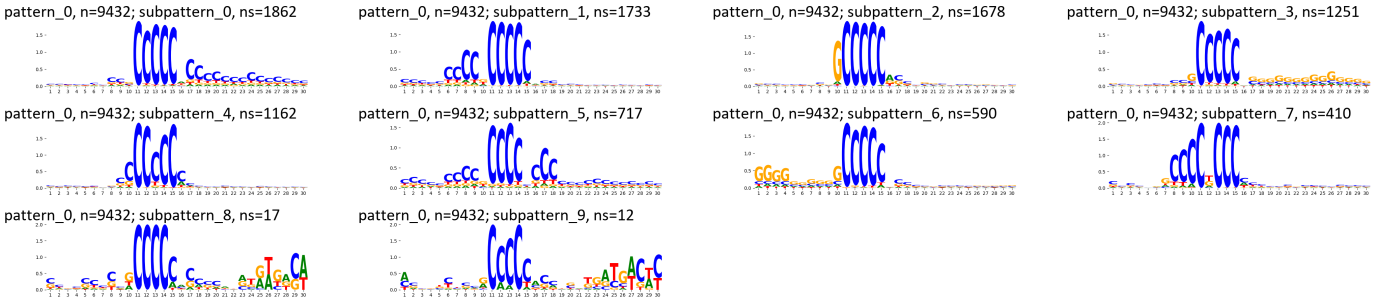

TF-MoDisCO pattern_4 n=1580, CWM

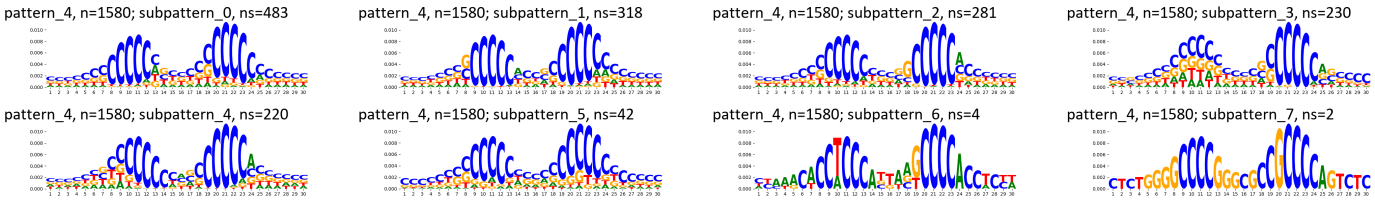

TF-MoDisCO pattern_4 n=1580, PWM

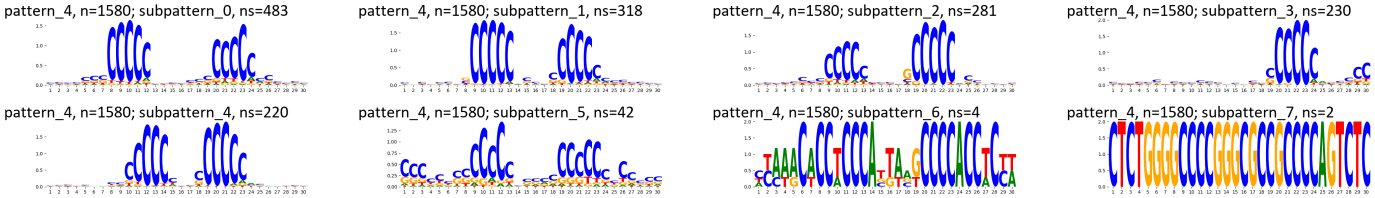

Supplementary Figure 184: TF-MoDisCO subpatterns for the PATZ1 transcription factor in HEK293 (accession ENCSR966ULI).

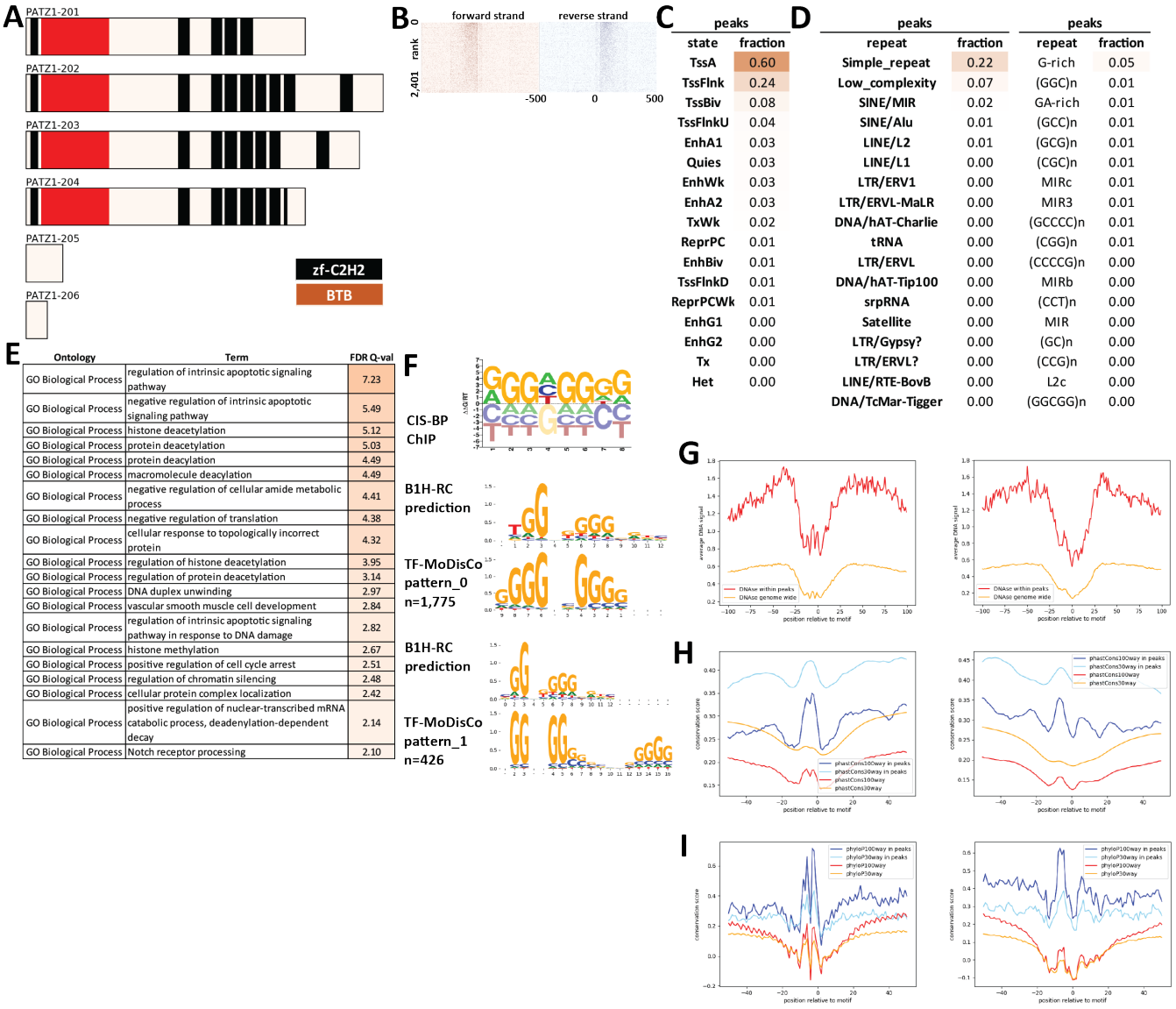

Supplementary Figure 185: Properties and genomic distribution of motifs identified for the PATZ1 transcription factor in HEK293 (accession Hughes GR models).

TF-MoDisCO pattern_0 n=1775, CWM

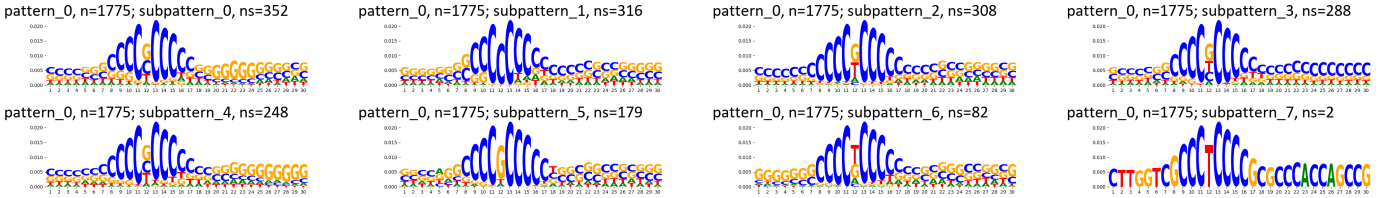

TF-MoDisCO pattern_0 n=1775, PWM

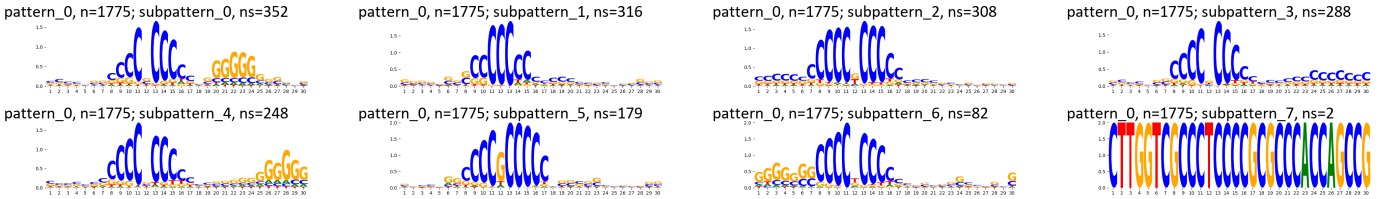

TF-MoDisCO pattern_1 n=426, CWM

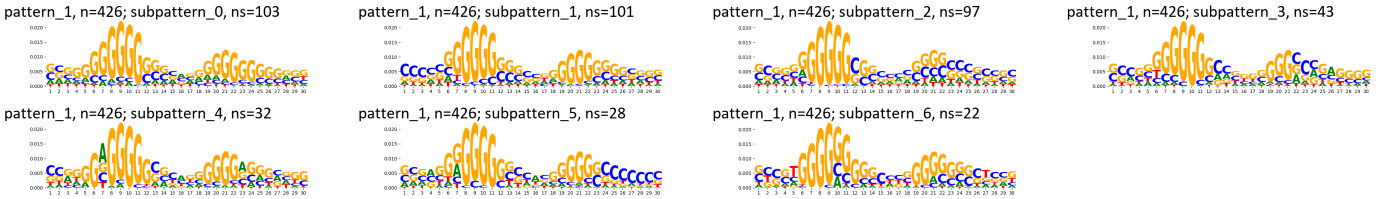

TF-MoDisCO pattern_1 n=426, PWM

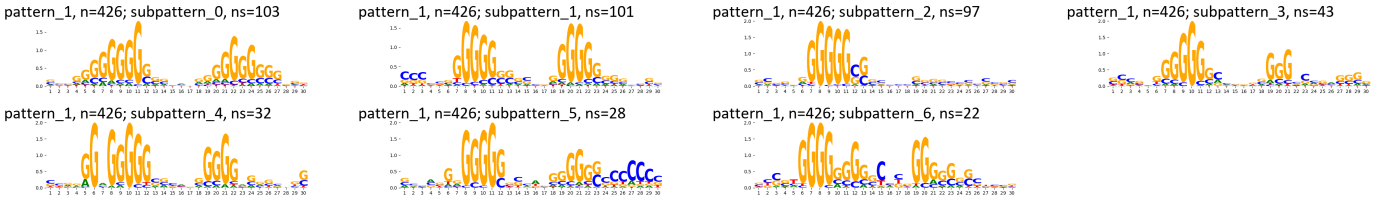

Supplementary Figure 186: TF-MoDisCO subpatterns for the PATZ1 transcription factor in HEK293 (accession Hughes GR models).

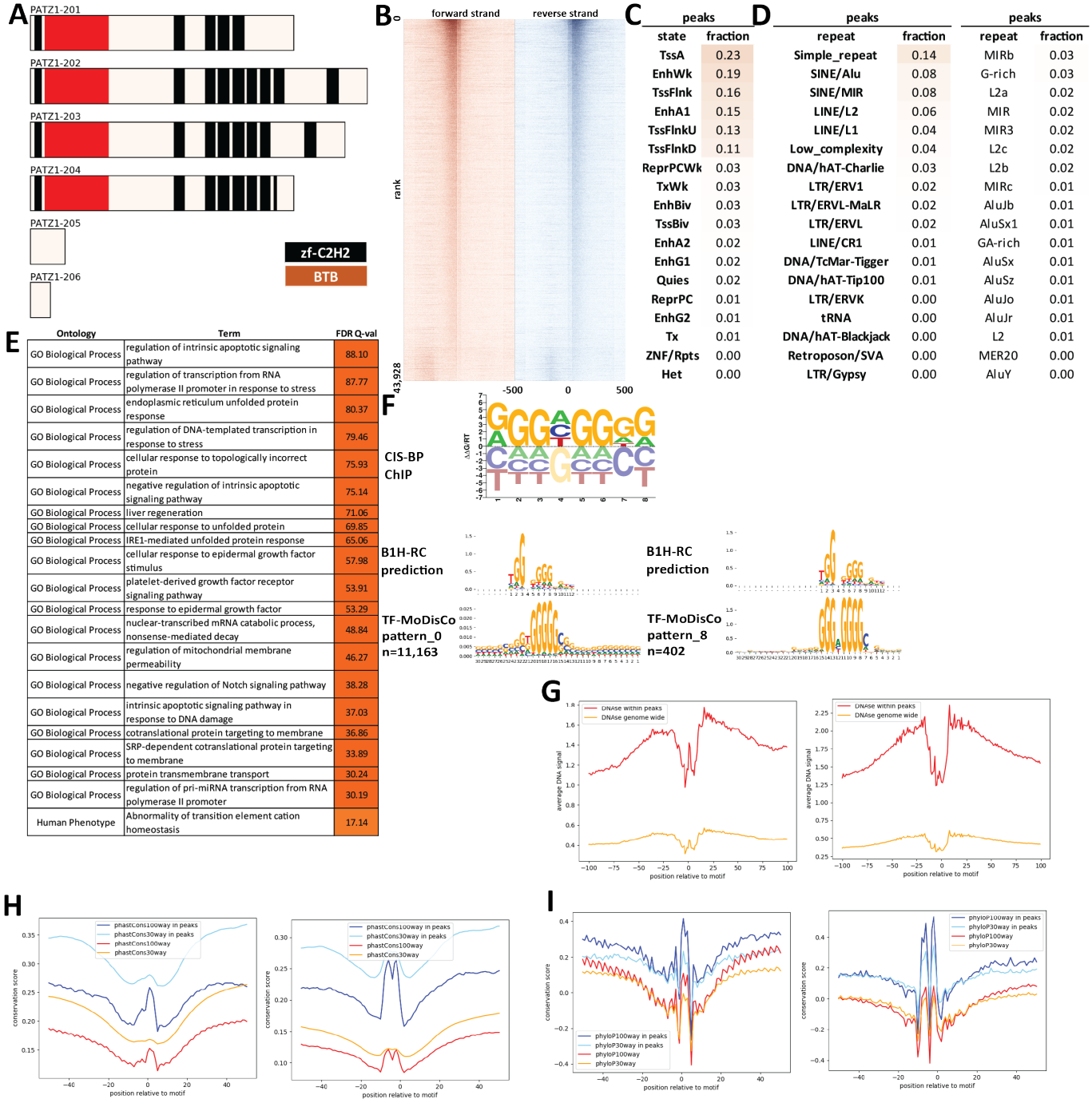

Supplementary Figure 187: Properties and genomic distribution of motifs identified for the PATZ1 transcription factor in HepG2 (accession ENCSR658YLN).

TF-MoDisCO pattern_0 n=11163, CWM

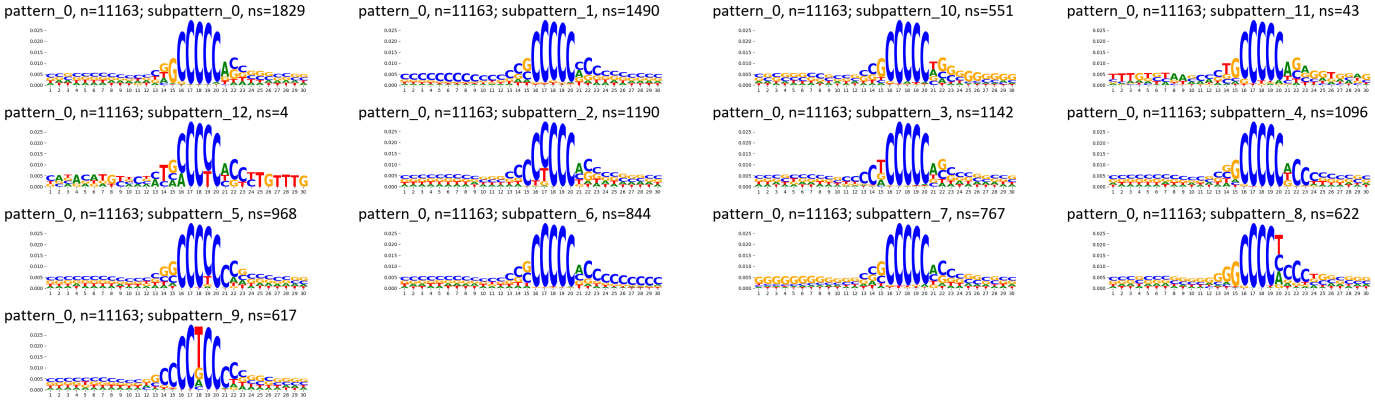

TF-MoDisCO pattern_0 n=11163, PWM

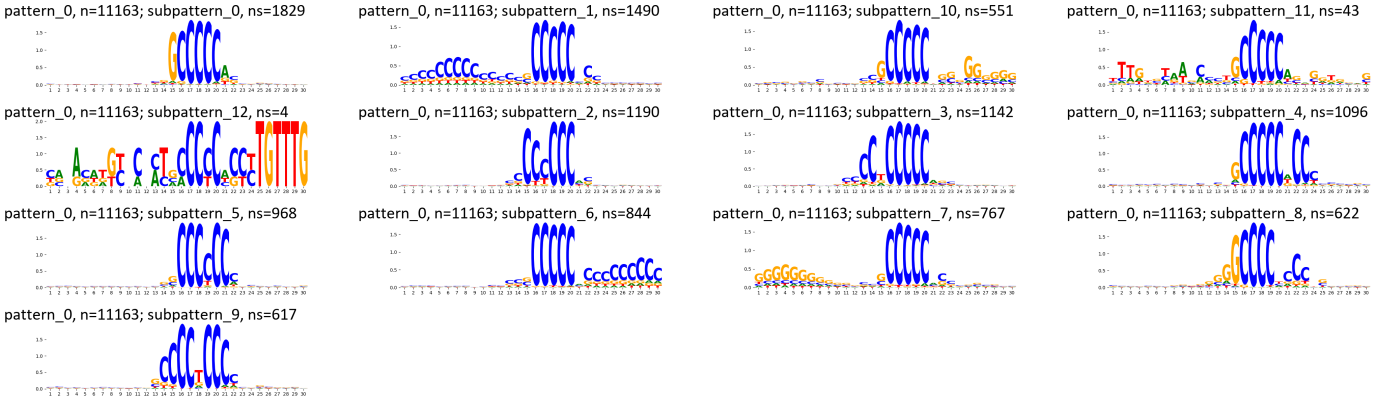

TF-MoDisCO pattern_8 n=402, CWM

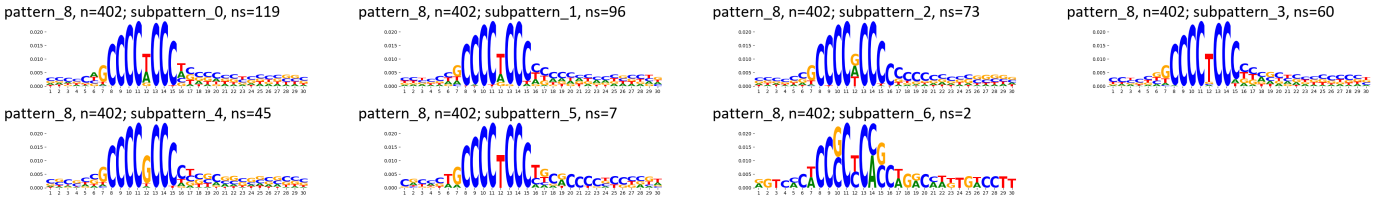

TF-MoDisCO pattern_8 n=402, PWM

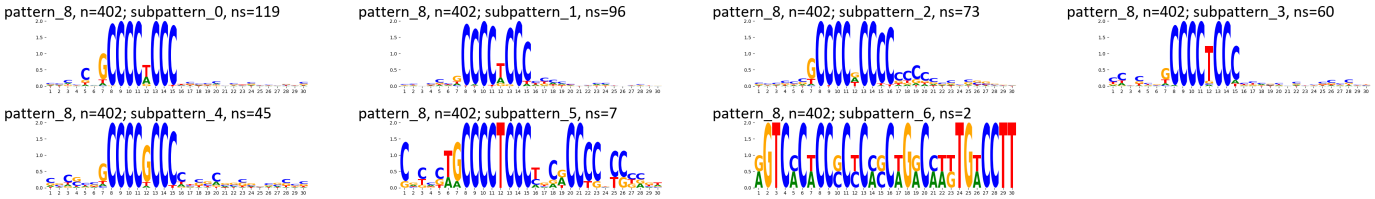

Supplementary Figure 188: TF-MoDisCO subpatterns for the PATZ1 transcription factor in HepG2 (accession ENCSR658YLN).

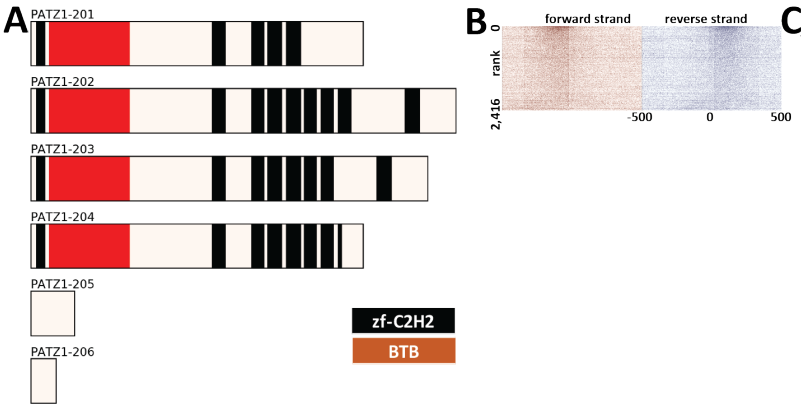

C

peaks	
state	fraction
TssA	0.27
EnhA1	0.23
TssFlnkU	0.22
EnhWk	0.15
EnhA2	0.09
TxWk	0.07
Quies	0.06
ReprPCWk	0.04
TssFlnk	0.04
TssFlnkD	0.03
EnhG2	0.02
EnhG1	0.02
Tx	0.01
EnhBiv	0.01
ReprPC	0.01
ZNF/Rpts	0.00
Het	0.00
TssBiv	0.00

D

peaks		peaks	
repeat	fraction	repeat	fraction
LTR/ERV1	0.21	MER41B	0.06
SINE/Alu	0.11	MIRb	0.04
SINE/MIR	0.10	MER41A	0.03
Simple_repeat	0.08	L2a	0.02
LINE/L2	0.07	MIR	0.02
LINE/L1	0.04	MIRc	0.02
LTR/ERVL	0.04	L2c	0.02
LTR/ERVL-MaLR	0.04	MIR3	0.02
DNA/hAT-Charlie	0.03	LTR8	0.02
snRNA	0.01	L2	0.01
Low_complexity	0.01	L2b	0.01
DNA/TcMar-Tigger	0.01	LTR54	0.01
LINE/CR1	0.01	AluJb	0.01
tRNA	0.01	AluJr	0.01
LTR/ERVK	0.01	AluSz	0.01
DNA/hAT-Tip100	0.01	U1	0.01
LTR/Gypsy	0.00	AluY	0.01
LINE/RTE-BovB	0.00	AluSx1	0.01

E

Ontology	Term	FDR Q-val
GO Biological Process	DNA replication-dependent nucleosome assembly	19.87
GO Biological Process	negative regulation of gene expression, epigenetic	19.48
GO Biological Process	regulation of hematopoietic progenitor cell differentiation	19.21
GO Biological Process	regulation of hematopoietic stem cell differentiation	18.36
GO Biological Process	negative regulation of megakaryocyte differentiation	17.35
GO Biological Process	regulation of gene expression, epigenetic	17.11
GO Biological Process	regulation of transcription from RNA polymerase II promoter in response to stress	17.02
GO Biological Process	regulation of DNA-templated transcription in response to stress	16.71
GO Biological Process	chromatin silencing at rDNA	14.70
GO Biological Process	chromatin assembly	12.74
GO Biological Process	protein-DNA complex subunit organization	12.70
GO Biological Process	chromatin assembly or disassembly	12.48
GO Biological Process	nucleosome organization	12.44
GO Biological Process	chromatin silencing	12.26
GO Biological Process	nucleosome assembly	12.18
GO Biological Process	protein-DNA complex assembly	11.73
GO Biological Process	regulation of megakaryocyte differentiation	11.69
GO Biological Process	DNA conformation change	10.97
GO Biological Process	blood coagulation	10.33
GO Biological Process	coagulation	10.31

F

CIS-BP ChIP

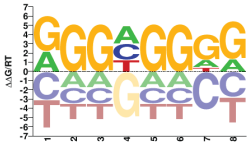

no motif discovered de novo

Supplementary Figure 189: Properties and genomic distribution of motifs identified for the PATZ1 transcription factor in K562 (accession ENCSR549PVK).

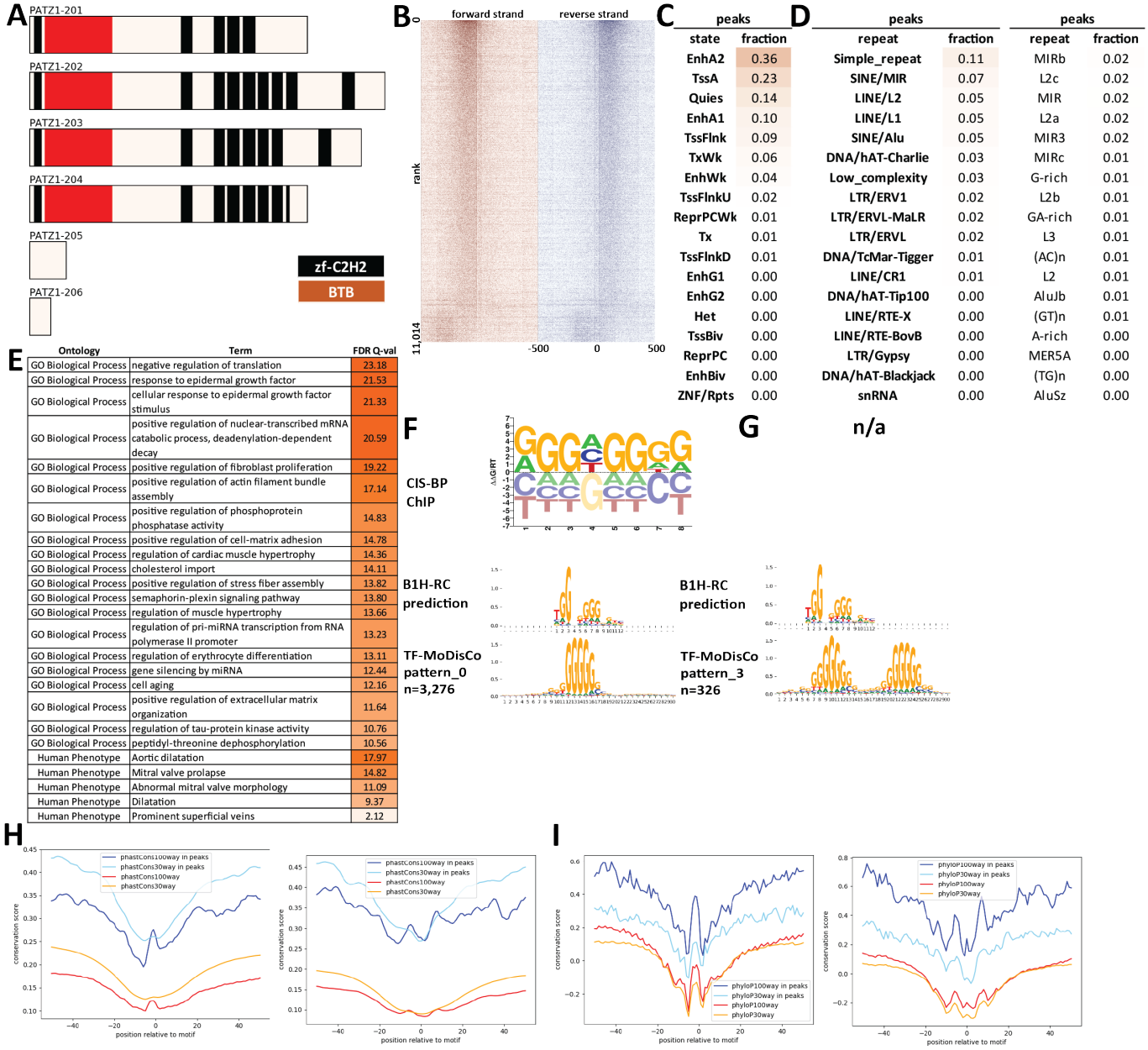

Supplementary Figure 190: Properties and genomic distribution of motifs identified for the PATZ1 transcription factor in SK-N-SH (accession ENCSR969AIM).

TF-MoDisCO pattern_0 n=3276, CWM

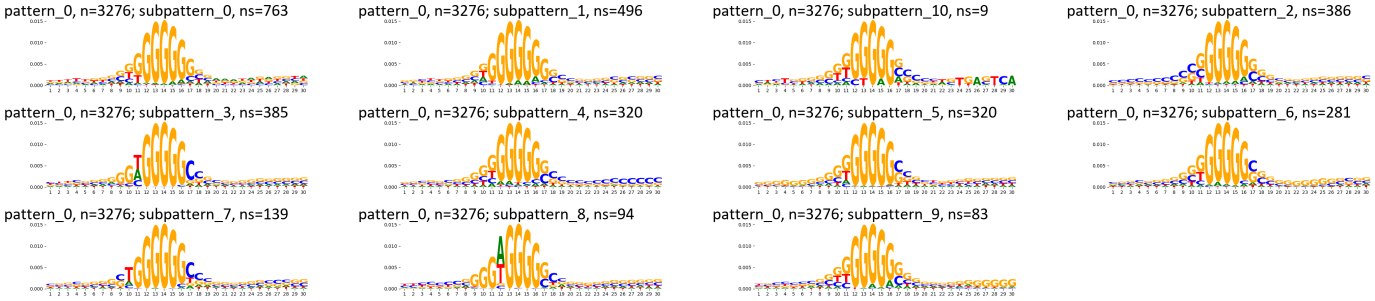

TF-MoDisCO pattern_0 n=3276, PWM

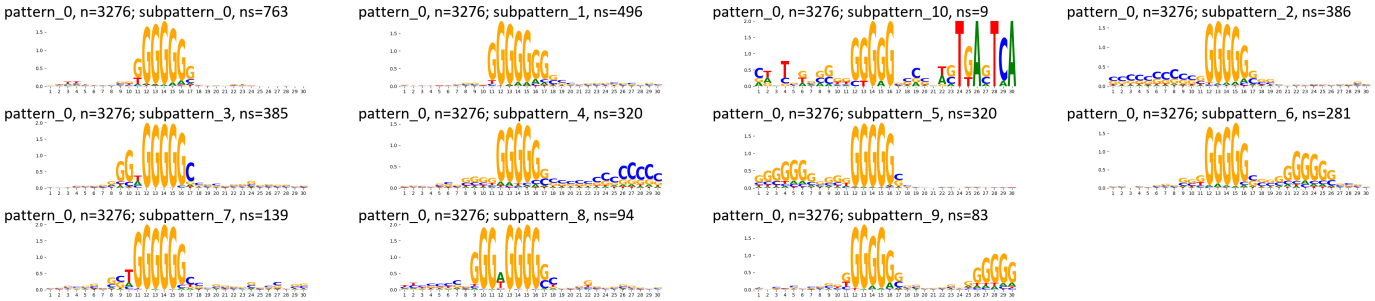

TF-MoDisCO pattern_3 n=324, CWM

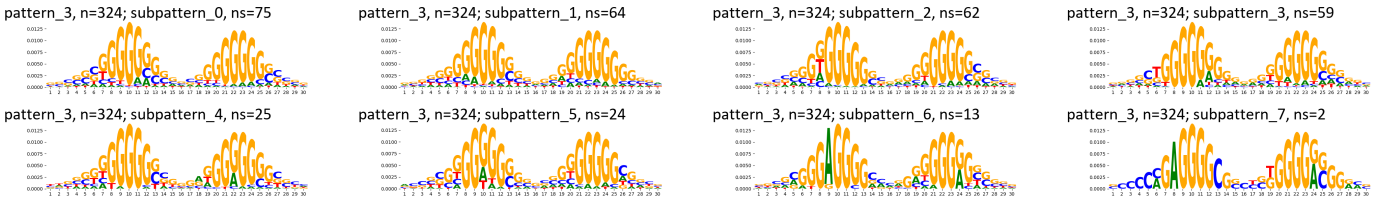

TF-MoDisCO pattern_3 n=324, PWM

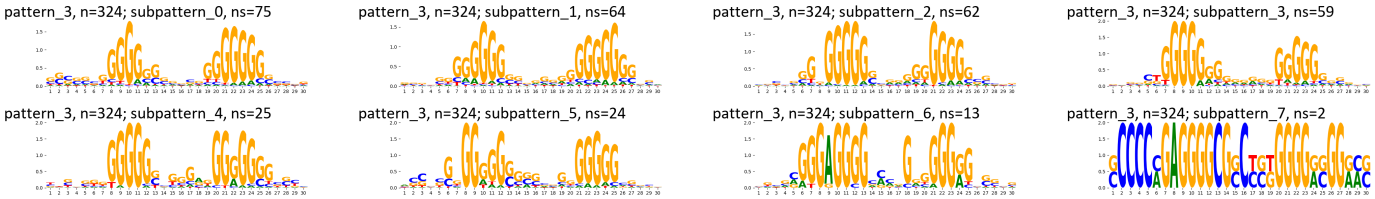

Supplementary Figure 191: TF-MoDisCO subpatterns for the PATZ1 transcription factor in SK-N-SH (accession ENCSR969AIM).

A

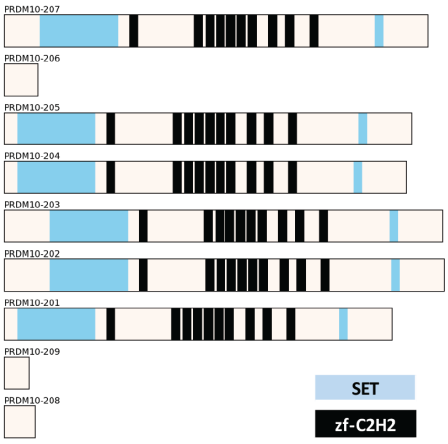

B

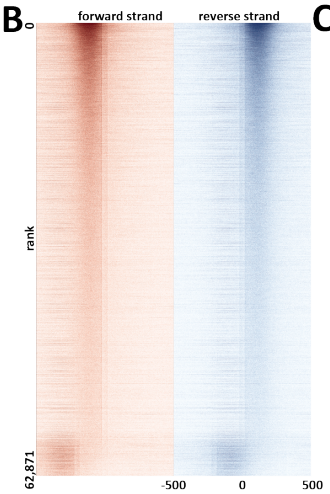

C

peaks	
state	fraction
Quies	0.18
EnhWk	0.17
TssA	0.15
TxWk	0.13
TssFlnk	0.11
EnhA1	0.06
EnhA2	0.04
TssBiv	0.03
Tx	0.03
TssFlnkU	0.03
ReprPCWk	0.02
ReprPC	0.02
TssFlnkD	0.02
EnhBiv	0.01
EnhG1	0.01
EnhG2	0.00
Het	0.00
ZNF/Rpts	0.00

D

peaks		peaks	
repeat	fraction	repeat	fraction
SINE/Alu	0.22	MIRb	0.03
Simple_repeat	0.14	L2a	0.03
SINE/MIR	0.09	AluJb	0.03
LINE/L2	0.08	AluSx1	0.03
LINE/L1	0.07	AluSx	0.03
LTR/ERVL-MaLR	0.04	L2c	0.02
DNA/hAT-Charlie	0.03	MIR	0.02
Low_complexity	0.03	AluSz	0.02
LTR/ERV1	0.02	AluY	0.02
LTR/ERVL	0.02	L2b	0.02
DNA/TcMar-Tigger	0.02	MIR3	0.02
LINE/CR1	0.01	MIRc	0.02
DNA/hAT-Tip100	0.01	G-rich	0.02
tRNA	0.00	AluJo	0.01
DNA/hAT-Blackjack	0.00	AluJr	0.01
LTR/Gypsy	0.00	AluSq2	0.01
LTR/ERVK	0.00	GA-rich	0.01
LINE/RTE-BovB	0.00	AluSz6	0.01

E

Ontology	Term	FDR Q-val
GO Biological Process	regulation of transcription from RNA polymerase II promoter in response to stress	95.41
GO Biological Process	regulation of DNA-templated transcription in response to stress	87.36
GO Biological Process	nuclear-transcribed mRNA catabolic process, nonsense-mediated decay	69.40
GO Biological Process	regulation of transcription from RNA polymerase II promoter in response to hypoxia	55.65
GO Biological Process	posttranscriptional gene silencing	47.93
GO Biological Process	posttranscriptional gene silencing by RNA	47.11
GO Biological Process	gene silencing by miRNA	46.68
GO Biological Process	cytoplasmic sequestering of protein	28.70

F

no CIS-BP motif available

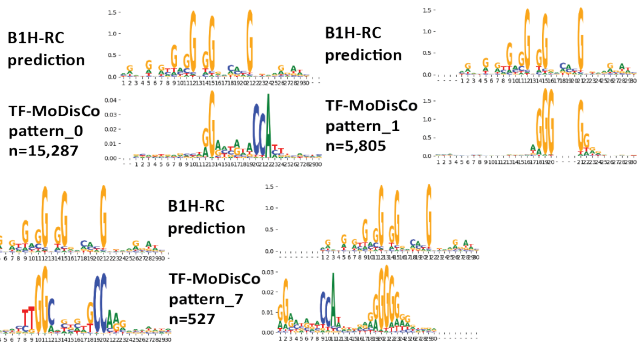

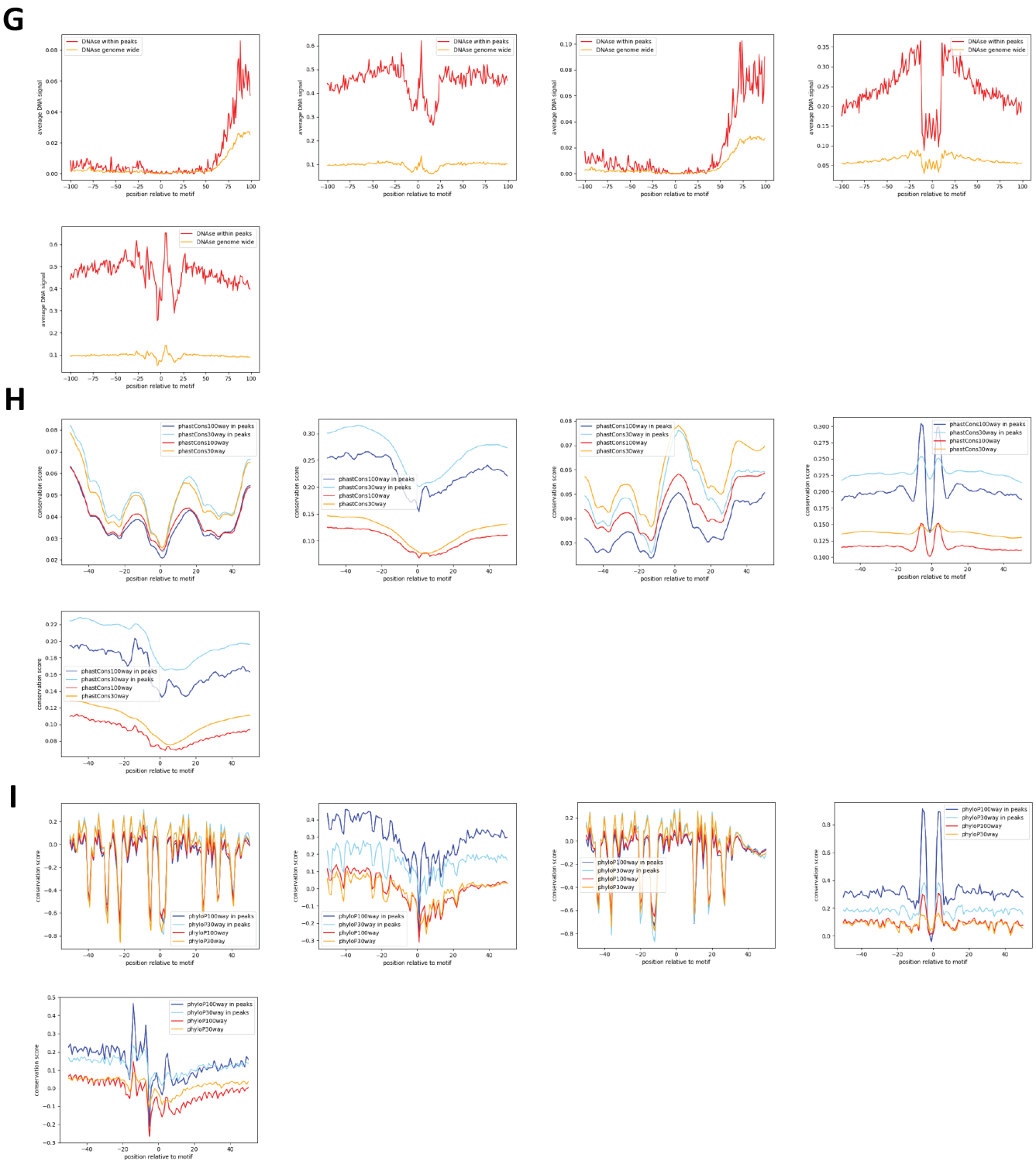

Supplementary Figure 192: Properties and genomic distribution of motifs identified for the PRDM10 transcription factor in HEK293 (accession ENCSR223TAV).

TF-MoDisCO pattern_0 n=15287, CWM

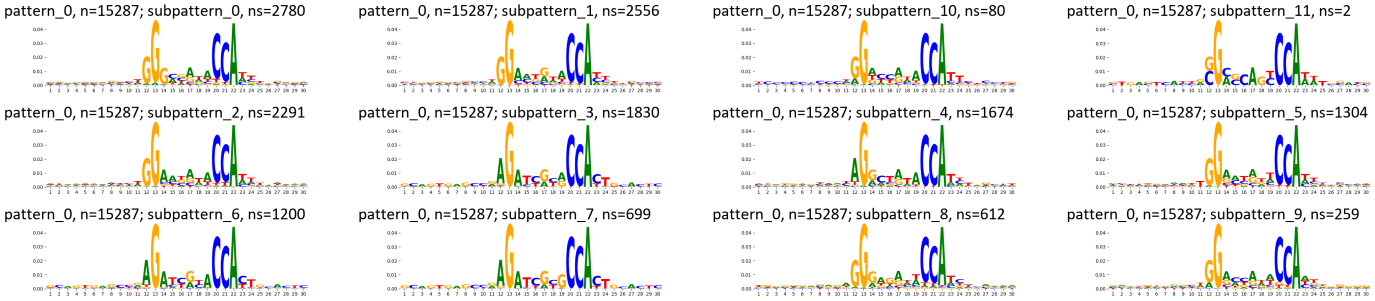

TF-MoDisCO pattern_0 n=15287, PWM

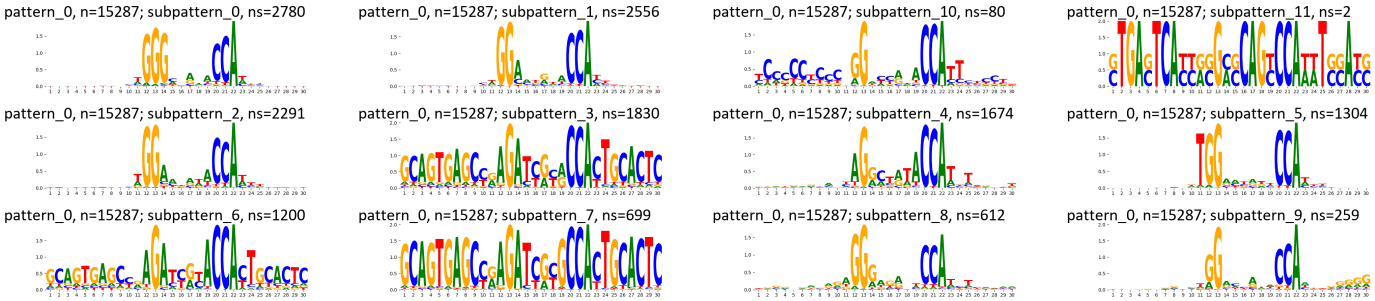

TF-MoDisCO pattern_1 n=5805, CWM

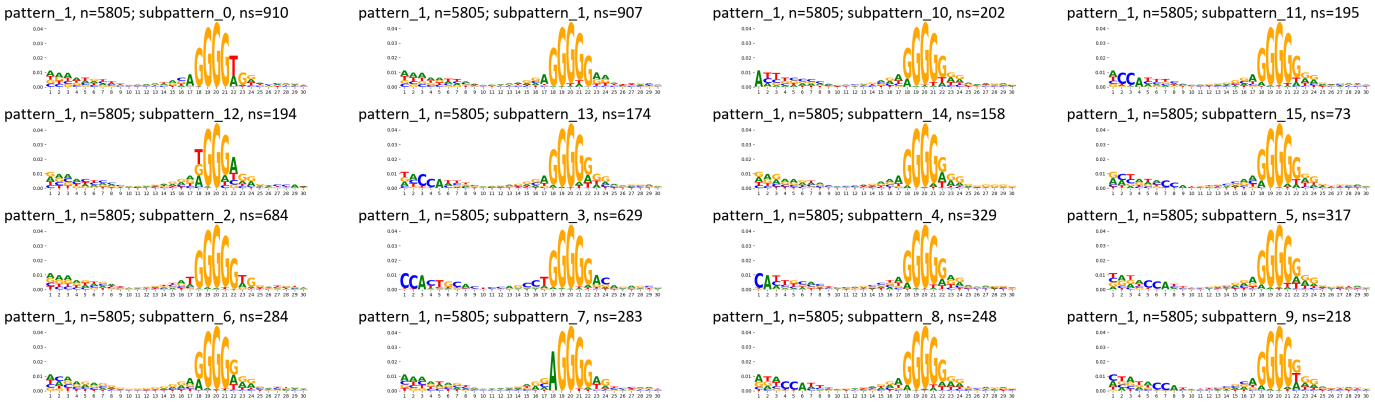

TF-MoDisCO pattern_1 n=5805, PWM

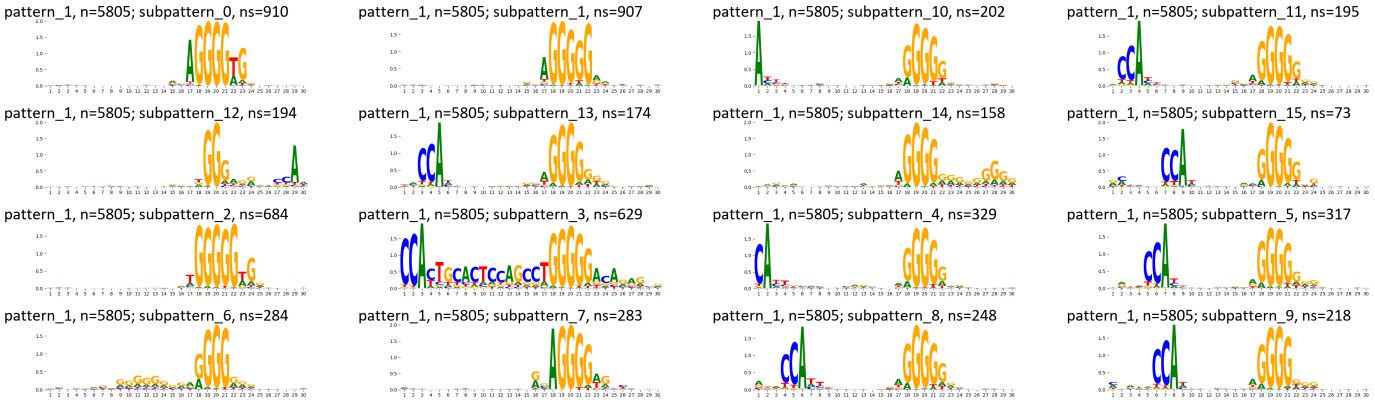

TF-MoDisCO pattern_3 n=812, CWM

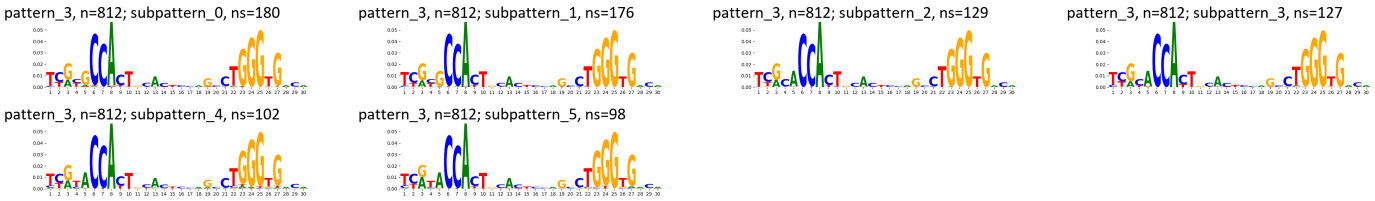

TF-MoDisCO pattern_3 n=812, PWM

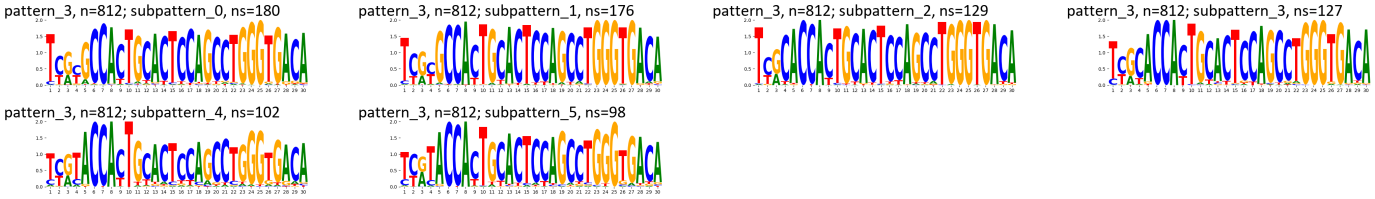

TF-MoDisCO pattern_4 n=739, CWM

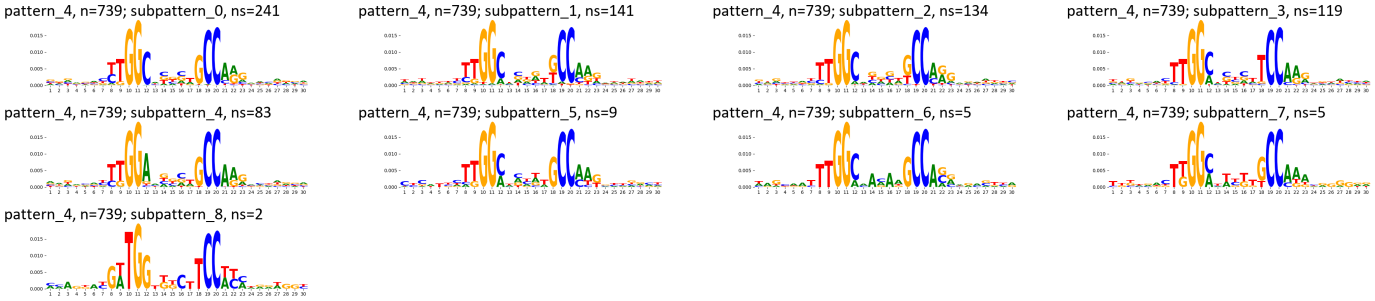

TF-MoDisCO pattern_4 n=739, PWM

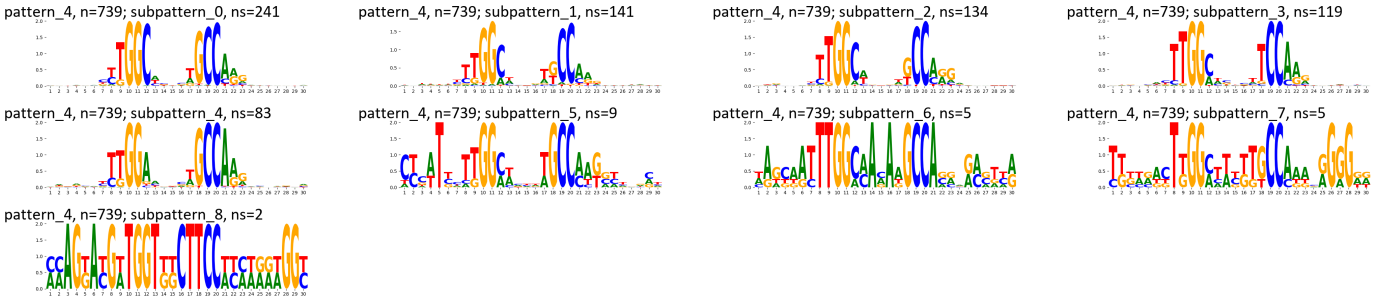

TF-MoDisCO pattern_7 n=527, CWM

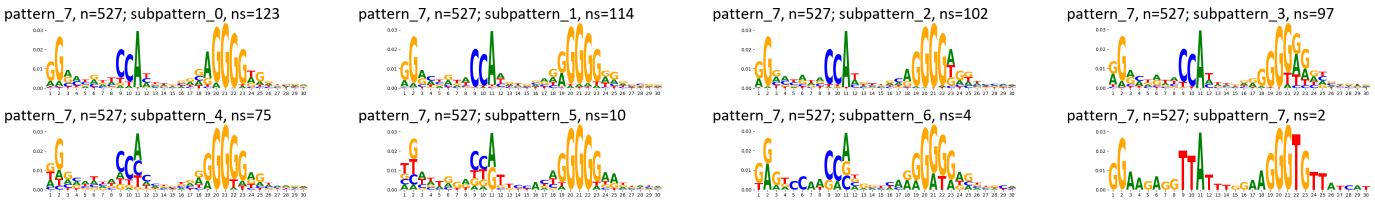

TF-MoDisCO pattern_7 n=527, PWM

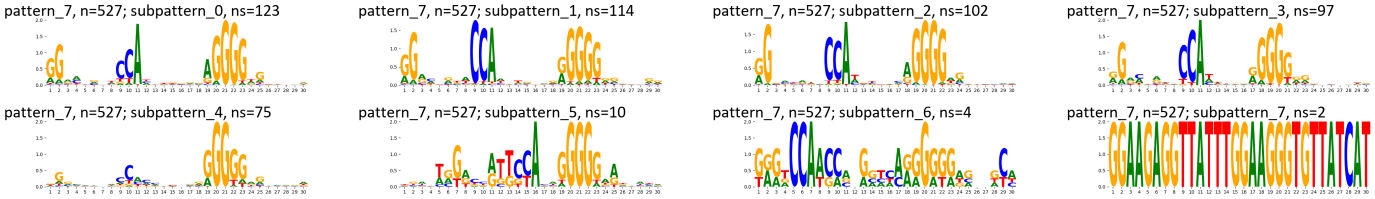

Supplementary Figure 193: TF-MoDisCO subpatterns for the PRDM10 transcription factor in HEK293 (accession ENCSR223TAV).

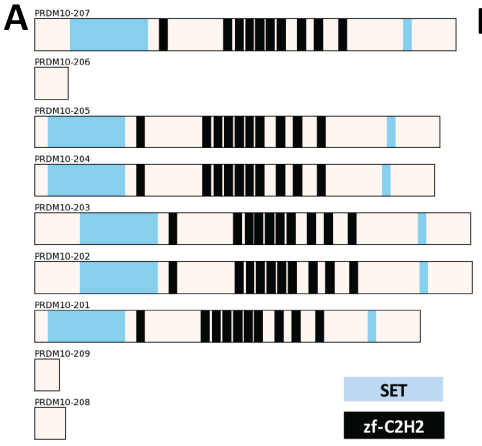

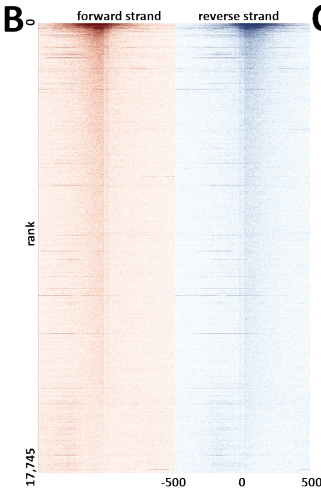

C

peaks	
state	fraction
TssA	0.33
EnhA1	0.21
TssFlnkU	0.20
EnhWk	0.17
TssFlnk	0.15
TssFlnkD	0.10
EnhA2	0.03
TxWk	0.03
ReprPCWk	0.03
EnhG2	0.02
EnhBiv	0.02
Quies	0.02
TssBiv	0.01
EnhG1	0.01
ReprPC	0.01
Tx	0.00
Het	0.00
ZNF/Rpts	0.00

D

peaks		peaks	
repeat	fraction	repeat	fraction
SINE/Alu	0.14	MIRb	0.04
Simple_repeat	0.13	L2a	0.03
SINE/MIR	0.12	MIR	0.03
LINE/L2	0.08	MIR3	0.02
LINE/L1	0.05	L2b	0.02
DNA/hAT-Charlie	0.03	L2c	0.02
Low_complexity	0.03	G-rich	0.02
LTR/ERV1	0.03	MIRc	0.02
LTR/ERVL-MaLR	0.02	AluJb	0.02
LTR/ERVL	0.02	AluSx	0.02
DNA/TcMar-Tigger	0.01	AluSx1	0.02
LINE/CR1	0.01	AluSz	0.01
DNA/hAT-Tip100	0.01	AluJr	0.01
tRNA	0.01	AluJo	0.01
LTR/ERVK	0.00	AluY	0.01
DNA/hAT-Blackjack	0.00	GA-rich	0.01
LINE/RTE-BovB	0.00	AluSq2	0.01
LTR/Gypsy	0.00	L2	0.01

E

Ontology	Term	FDR Q-val
GO Biological Process	regulation of transcription from RNA polymerase II promoter in response to stress	67.49
GO Biological Process	regulation of DNA-templated transcription in response to stress	62.32
GO Biological Process	endoplasmic reticulum unfolded protein response	54.06
GO Biological Process	liver regeneration	49.69
GO Biological Process	response to topologically incorrect protein	48.11
GO Biological Process	cellular response to topologically incorrect protein	47.35
GO Biological Process	cellular response to unfolded protein	46.86
GO Biological Process	response to unfolded protein	45.92
GO Biological Process	IRE1-mediated unfolded protein response	43.92
GO Biological Process	regulation of intrinsic apoptotic signaling pathway	42.11
GO Biological Process	mRNA catabolic process	37.15
GO Biological Process	nuclear-transcribed mRNA catabolic process	36.47
GO Biological Process	cellular response to epidermal growth factor stimulus	33.83
GO Biological Process	protein targeting to ER	32.45
GO Biological Process	nuclear-transcribed mRNA catabolic process, nonsense-mediated decay	28.70
GO Biological Process	establishment of protein localization to endoplasmic reticulum	27.99
GO Biological Process	cotranslational protein targeting to membrane	27.66
GO Biological Process	multi-organism metabolic process	26.98
GO Biological Process	protein localization to endoplasmic reticulum	25.50
GO Biological Process	SRP-dependent cotranslational protein targeting to membrane	24.65
Human Phenotype	Death in infancy	11.90
Human Phenotype	Abnormality of mitochondrial metabolism	11.88
Human Phenotype	Abnormality of the mitochondrion	11.74
Human Phenotype	Hypergonadotropic hypogonadism	10.27
Human Phenotype	Increased serum ferritin	10.09
Human Phenotype	CNS hypomyelination	7.47

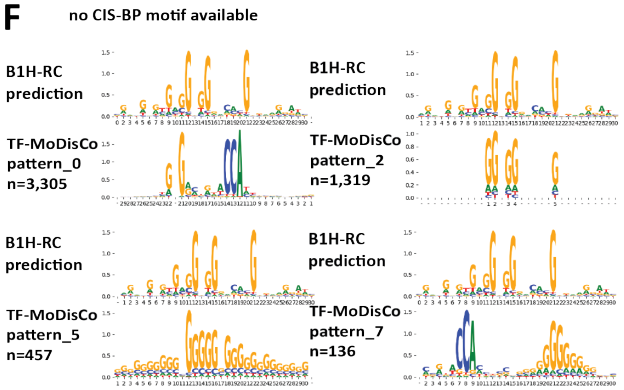

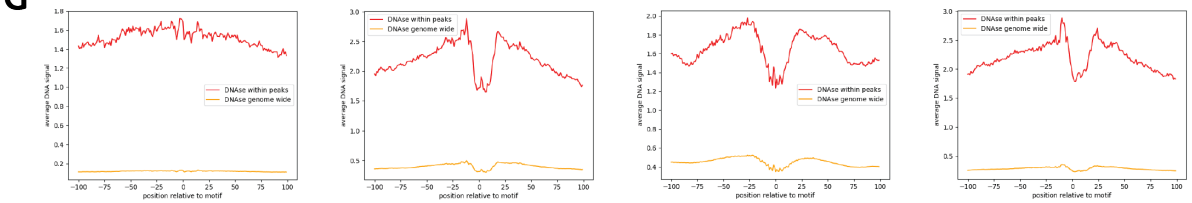

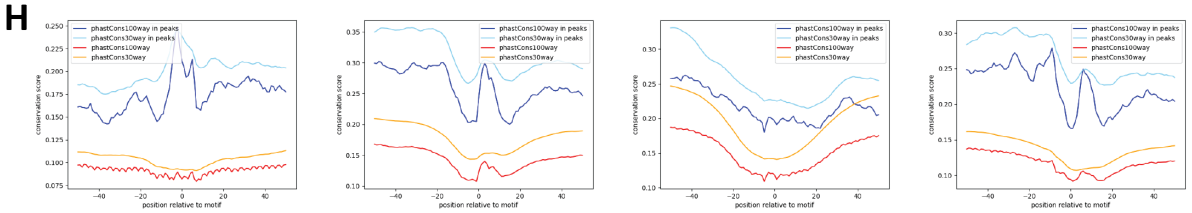

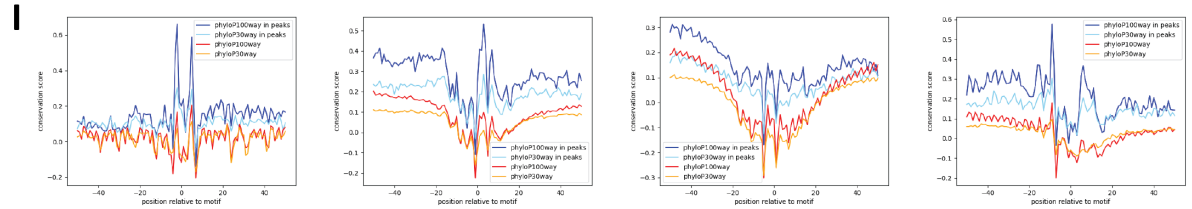

Supplementary Figure 194: Properties and genomic distribution of motifs identified for the PRDM10 transcription factor in HepG2 (accession ENCSR289PSX).

TF-MoDisCO pattern_0 n=3305, CWM

pattern_0, n=3305; subpattern_0, ns=970

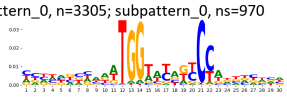

pattern_0, n=3305; subpattern_1, ns=805

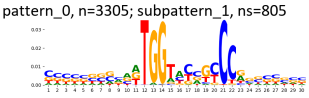

pattern_0, n=3305; subpattern_2, ns=607

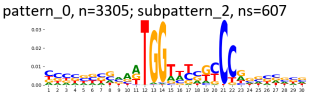

pattern_0, n=3305; subpattern_3, ns=576

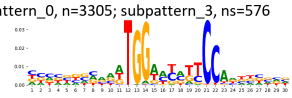

pattern_0, n=3305; subpattern_4, ns=179

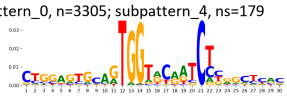

pattern_0, n=3305; subpattern_5, ns=159

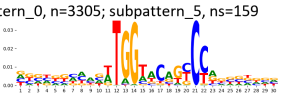

pattern_0, n=3305; subpattern_6, ns=5

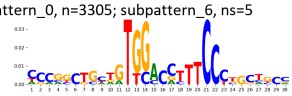

pattern_0, n=3305; subpattern_7, ns=2

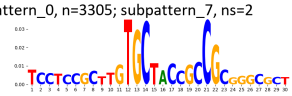

pattern_0, n=3305; subpattern_8, ns=2

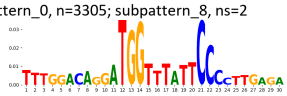

TF-MoDisCO pattern_0 n=3305, PWM

pattern_0, n=3305; subpattern_0, ns=970

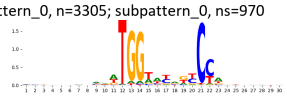

pattern_0, n=3305; subpattern_1, ns=805

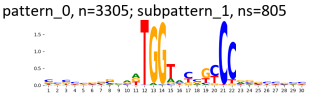

pattern_0, n=3305; subpattern_2, ns=607

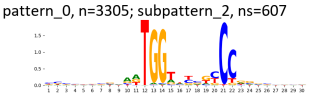

pattern_0, n=3305; subpattern_3, ns=576

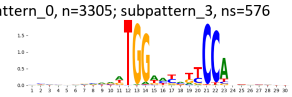

pattern_0, n=3305; subpattern_4, ns=179

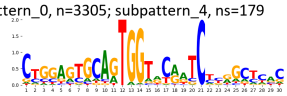

pattern_0, n=3305; subpattern_5, ns=159

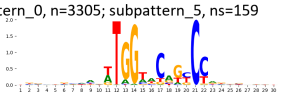

pattern_0, n=3305; subpattern_6, ns=5

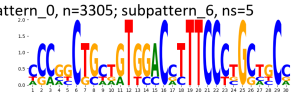

pattern_0, n=3305; subpattern_7, ns=2

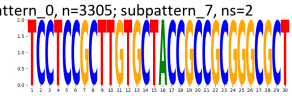

pattern_0, n=3305; subpattern_8, ns=2

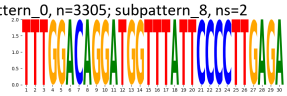

TF-MoDisCO pattern_2 n=1319, CWM

pattern_2, n=1319; subpattern_0, ns=416

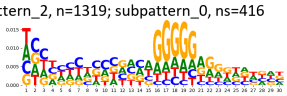

pattern_2, n=1319; subpattern_1, ns=298

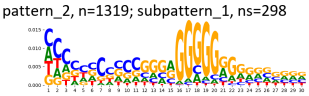

pattern_2, n=1319; subpattern_2, ns=248

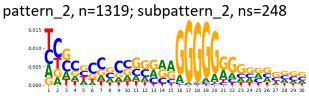

pattern_2, n=1319; subpattern_3, ns=124

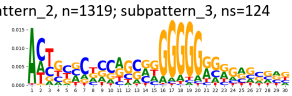

pattern_2, n=1319; subpattern_4, ns=79

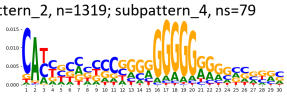

pattern_2, n=1319; subpattern_5, ns=78

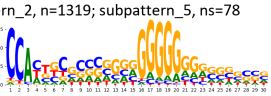

pattern_2, n=1319; subpattern_6, ns=66

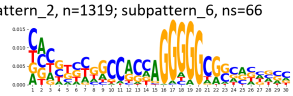

pattern_2, n=1319; subpattern_7, ns=10

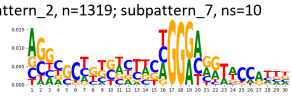

TF-MoDisCO pattern_2 n=1319, PWM

pattern_2, n=1319; subpattern_0, ns=416

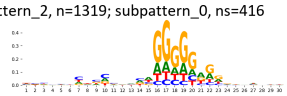

pattern_2, n=1319; subpattern_1, ns=298

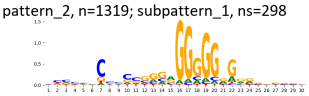

pattern_2, n=1319; subpattern_2, ns=248

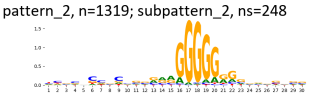

pattern_2, n=1319; subpattern_3, ns=124

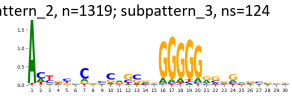

pattern_2, n=1319; subpattern_4, ns=79

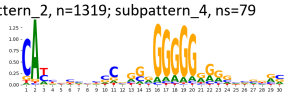

pattern_2, n=1319; subpattern_5, ns=78

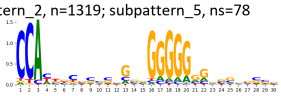

pattern_2, n=1319; subpattern_6, ns=66

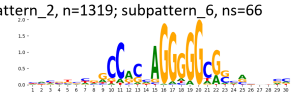

pattern_2, n=1319; subpattern_7, ns=10

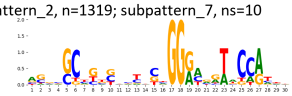

TF-MoDisCO pattern_5 n=457, CWM

pattern_5, n=457; subpattern_0, ns=154

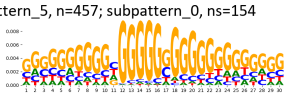

pattern_5, n=457; subpattern_1, ns=121

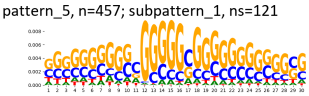

pattern_5, n=457; subpattern_2, ns=103

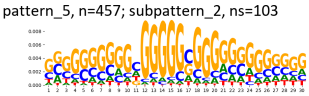

pattern_5, n=457; subpattern_3, ns=61

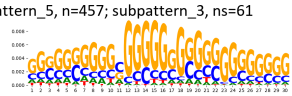

pattern_5, n=457; subpattern_4, ns=18

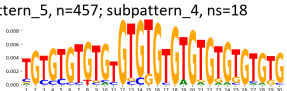

TF-MoDisCO pattern_5 n=457, PWM

pattern_5, n=457; subpattern_0, ns=154

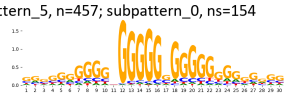

pattern_5, n=457; subpattern_1, ns=121

pattern_5, n=457; subpattern_2, ns=103

pattern_5, n=457; subpattern_3, ns=61

pattern_5, n=457; subpattern_4, ns=18

TF-MoDisCO pattern_7 n=136, CWM

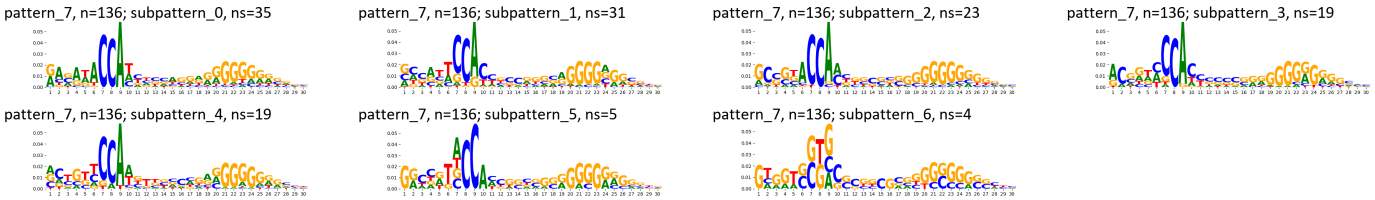

TF-MoDisCO pattern_7 n=136, PWM

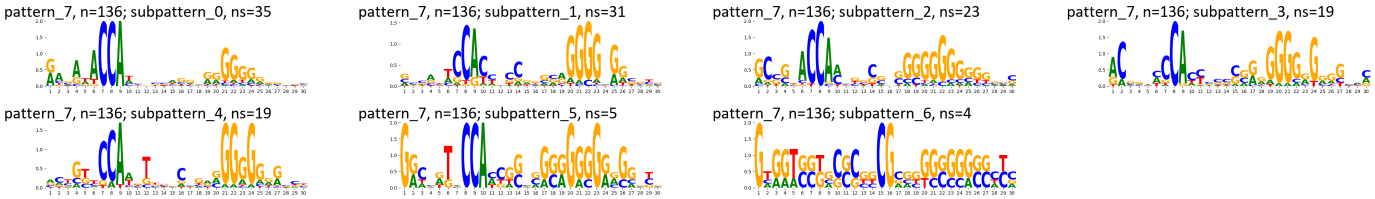

Supplementary Figure 195: TF-MoDisCO subpatterns for the PRDM10 transcription factor in HepG2 (accession ENCSR289PSX).

A

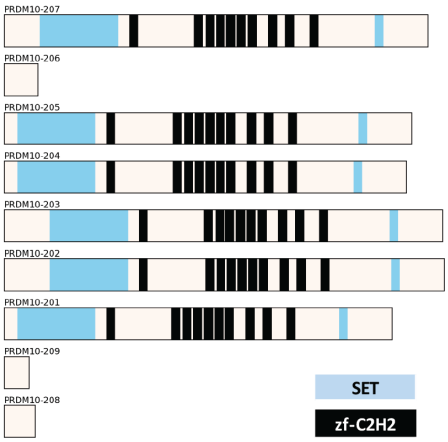

B

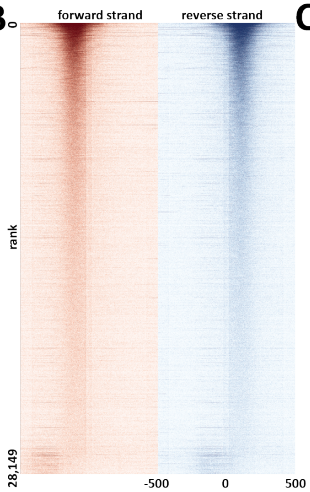

C

peaks	
state	fraction
EnhWk	0.22
TssA	0.21
EnhA1	0.16
TssFlnkU	0.16
TxWk	0.11
Quies	0.10
ReprPCWk	0.08
TssFlnkD	0.07
TssFlnk	0.07
EnhA2	0.05
ReprPC	0.03
EnhG1	0.02
EnhBiv	0.01
Tx	0.01
EnhG2	0.01
TssBiv	0.00
Het	0.00
ZNF/Rpts	0.00

D

peaks		peaks	
repeat	fraction	repeat	fraction
SINE/Alu	0.25	AluY	0.04
Simple_repeat	0.12	MIRb	0.03
SINE/MIR	0.09	L2a	0.03
LINE/L2	0.09	AluSx1	0.03
LINE/L1	0.08	AluSx	0.03
LTR/ERVL-MaLR	0.06	L2c	0.03
LTR/ERV1	0.06	AluJb	0.02
DNA/hAT-Charlie	0.03	AluSz	0.02
LTR/ERVL	0.03	MIR	0.02
Low_complexity	0.03	L2b	0.02
DNA/TcMar-Tigger	0.02	MIR3	0.02
LINE/CR1	0.01	MIRc	0.02
DNA/hAT-Tip100	0.01	AluSq2	0.01
tRNA	0.00	G-rich	0.01
LTR/ERVK	0.00	AluJo	0.01
DNA/hAT-Blackjack	0.00	AluJr	0.01
LTR/Gypsy	0.00	L2	0.01
snRNA	0.00	AluSz6	0.01

E

Ontology	Term	FDR Q-val
GO Biological Process	regulation of gene expression, epigenetic	85.29
GO Biological Process	response to topologically incorrect protein	52.60
GO Biological Process	endoplasmic reticulum unfolded protein response	52.23
GO Biological Process	cellular response to topologically incorrect protein	49.21
GO Biological Process	response to unfolded protein	49.19
GO Biological Process	regulation of hematopoietic progenitor cell differentiation	49.07
GO Biological Process	cellular response to unfolded protein	46.98
GO Biological Process	regulation of transcription from RNA polymerase II promoter in response to stress	43.77
GO Biological Process	regulation of DNA-templated transcription in response to stress	43.11
GO Biological Process	regulation of hematopoietic stem cell differentiation	42.84
GO Biological Process	multi-organism metabolic process	38.15
GO Biological Process	nuclear-transcribed mRNA catabolic process, nonsense-mediated decay	37.49
GO Biological Process	viral gene expression	31.23
GO Biological Process	mRNA transcription	27.96
GO Biological Process	regulation of mitochondrial membrane permeability	26.80
GO Biological Process	mRNA transcription from RNA polymerase II promoter	24.70
GO Biological Process	interleukin-12-mediated signaling pathway	20.92
GO Biological Process	regulation of cellular amino acid metabolic process	14.49

F

no CIS-BP motif available

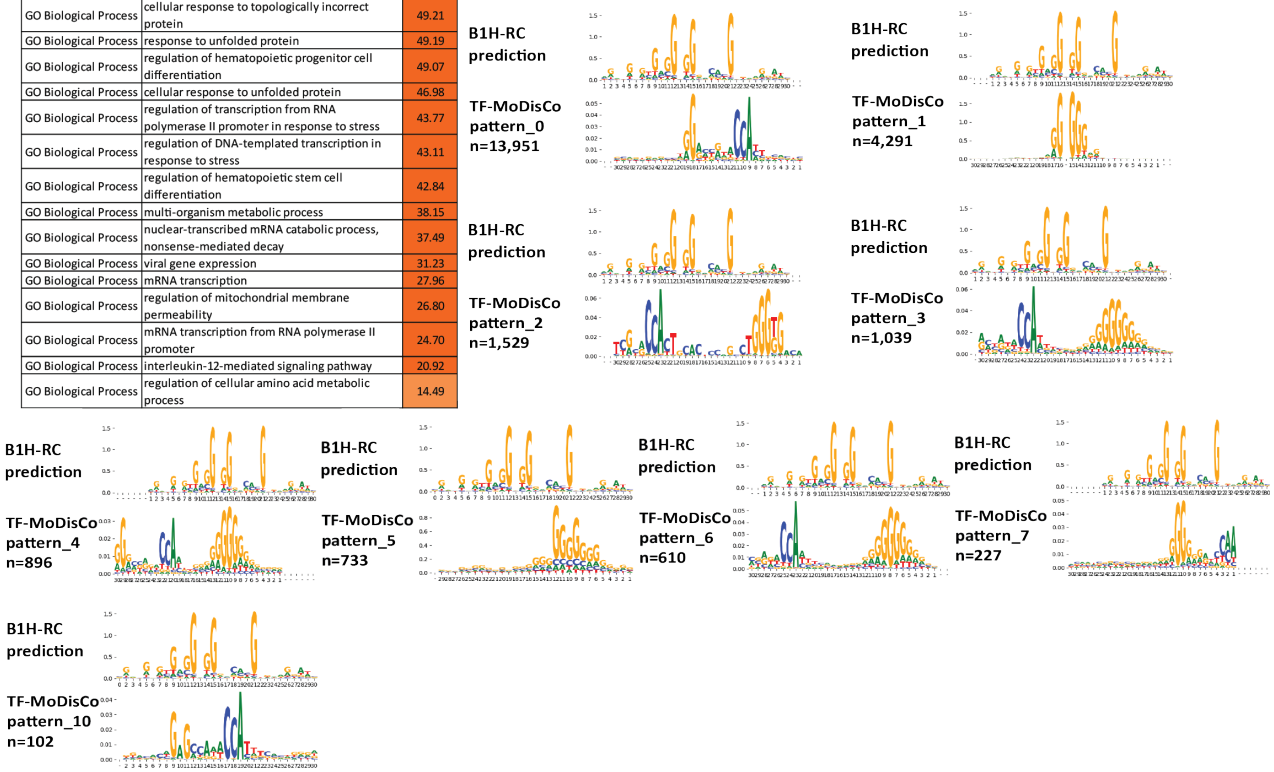

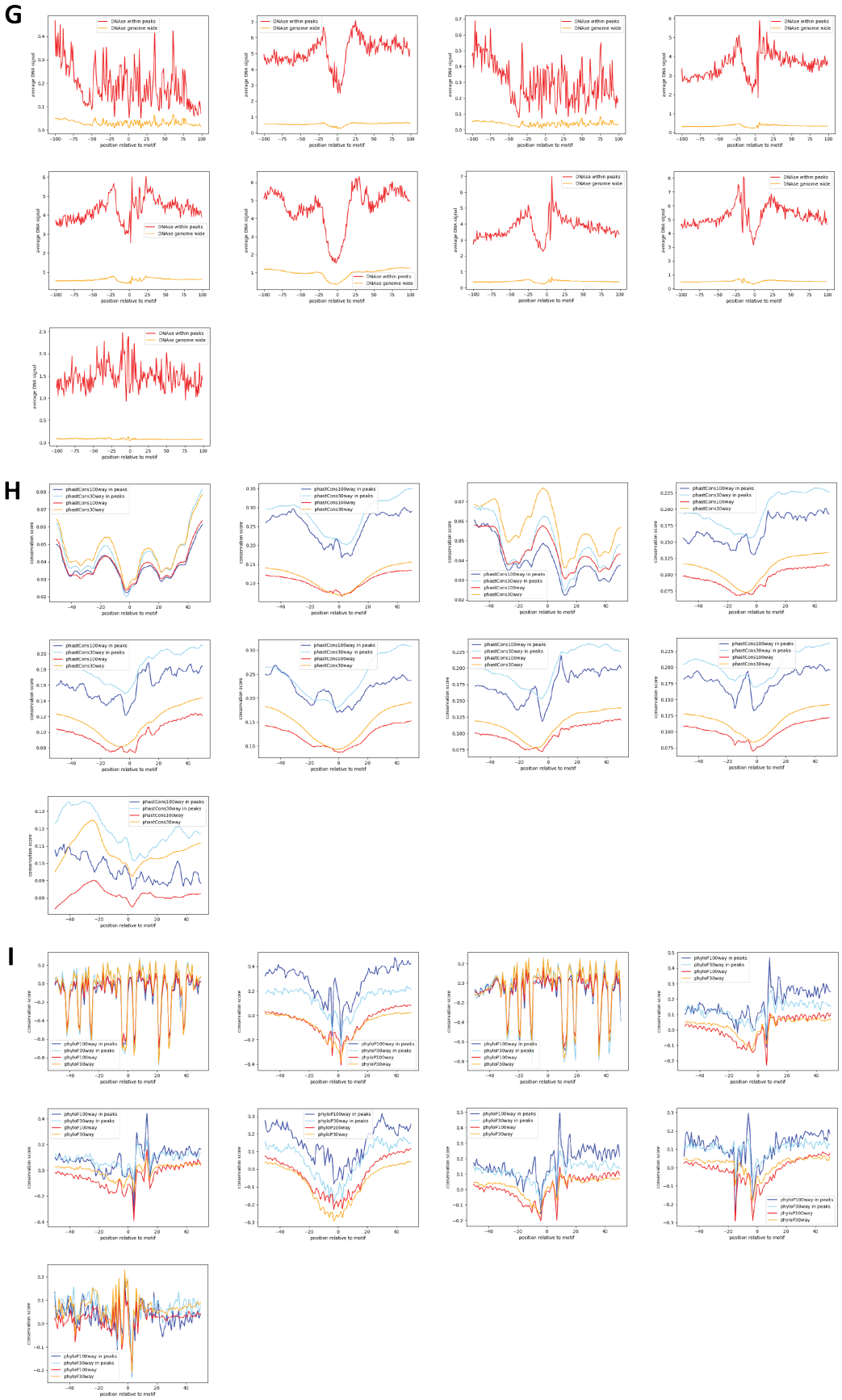

Supplementary Figure 196: Properties and genomic distribution of motifs identified for the PRDM10 transcription factor in K562 (accession ENCSR120MPG).

TF-MoDisCO pattern_0 n=13951, CWM

pattern_0, n=13951; subpattern_0, ns=2755

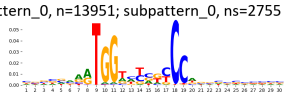

pattern_0, n=13951; subpattern_1, ns=2439

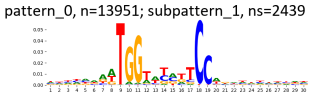

pattern_0, n=13951; subpattern_10, ns=5

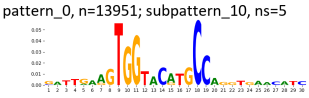

pattern_0, n=13951; subpattern_2, ns=1641

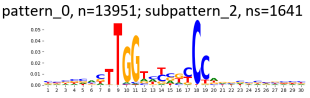

pattern_0, n=13951; subpattern_3, ns=1452

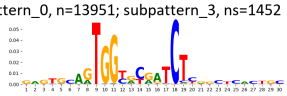

pattern_0, n=13951; subpattern_4, ns=1415

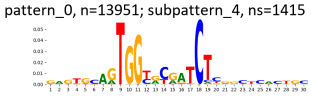

pattern_0, n=13951; subpattern_5, ns=1342

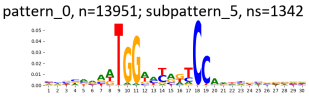

pattern_0, n=13951; subpattern_6, ns=1321

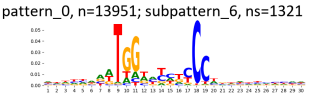

pattern_0, n=13951; subpattern_7, ns=1257

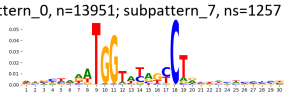

pattern_0, n=13951; subpattern_8, ns=308

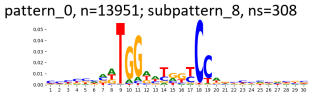

pattern_0, n=13951; subpattern_9, ns=16

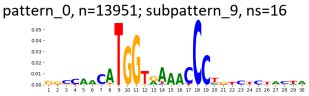

TF-MoDisCO pattern_0 n=13951, PWM

pattern_0, n=13951; subpattern_0, ns=2755

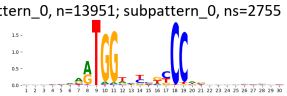

pattern_0, n=13951; subpattern_1, ns=2439

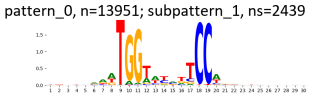

pattern_0, n=13951; subpattern_10, ns=5

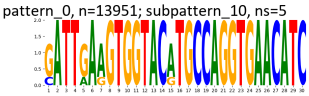

pattern_0, n=13951; subpattern_2, ns=1641

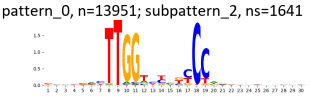

pattern_0, n=13951; subpattern_3, ns=1452

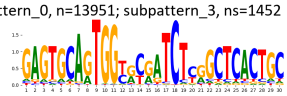

pattern_0, n=13951; subpattern_4, ns=1415

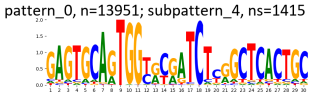

pattern_0, n=13951; subpattern_5, ns=1342

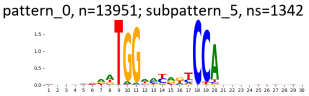

pattern_0, n=13951; subpattern_6, ns=1321

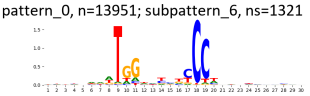

pattern_0, n=13951; subpattern_7, ns=1257

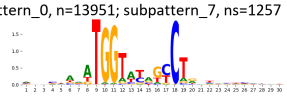

pattern_0, n=13951; subpattern_8, ns=308

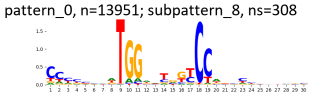

pattern_0, n=13951; subpattern_9, ns=16

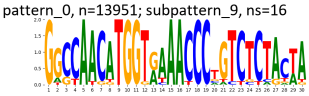

TF-MoDisCO pattern_1 n=4291, CWM

pattern_1, n=4291; subpattern_0, ns=799

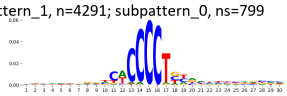

pattern_1, n=4291; subpattern_1, ns=794

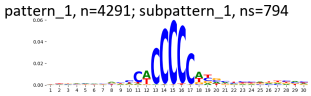

pattern_1, n=4291; subpattern_2, ns=683

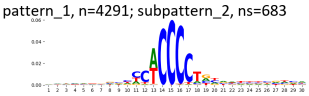

pattern_1, n=4291; subpattern_3, ns=600

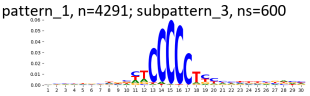

pattern_1, n=4291; subpattern_4, ns=477

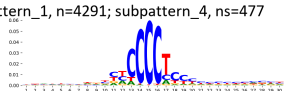

pattern_1, n=4291; subpattern_5, ns=461

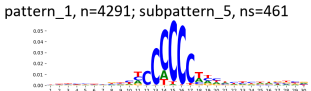

pattern_1, n=4291; subpattern_6, ns=352

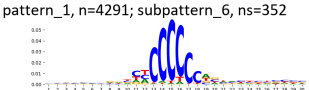

pattern_1, n=4291; subpattern_7, ns=105

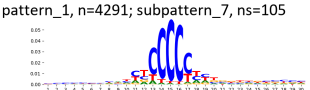

pattern_1, n=4291; subpattern_8, ns=20

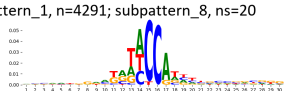

TF-MoDisCO pattern_1 n=4291, PWM

pattern_1, n=4291; subpattern_0, ns=799

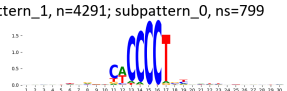

pattern_1, n=4291; subpattern_1, ns=794

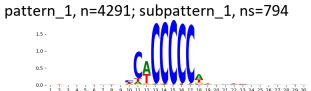

pattern_1, n=4291; subpattern_2, ns=683

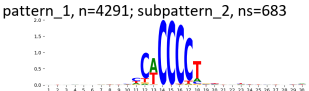

pattern_1, n=4291; subpattern_3, ns=600

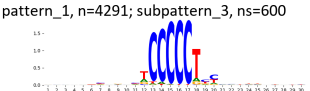

pattern_1, n=4291; subpattern_4, ns=477

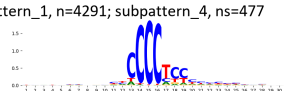

pattern_1, n=4291; subpattern_5, ns=461

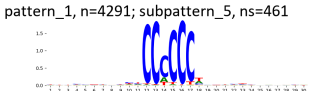

pattern_1, n=4291; subpattern_6, ns=352

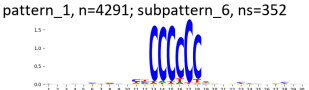

pattern_1, n=4291; subpattern_7, ns=105

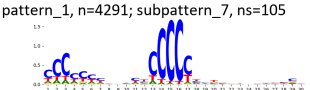

pattern_1, n=4291; subpattern_8, ns=20

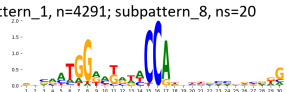

TF-MoDisCO pattern_10 n=102, CWM

pattern_10, n=102; subpattern_0, ns=38

pattern_10, n=102; subpattern_1, ns=26

pattern_10, n=102; subpattern_2, ns=22

pattern_10, n=102; subpattern_3, ns=16

TF-MoDisCO pattern_10 n=102, PWM

pattern_10, n=102; subpattern_0, ns=38

pattern_10, n=102; subpattern_1, ns=26

pattern_10, n=102; subpattern_2, ns=22

pattern_10, n=102; subpattern_3, ns=16

TF-MoDisCO pattern_2 n=1529, CWM

pattern_2, n=1529; subpattern_0, ns=356

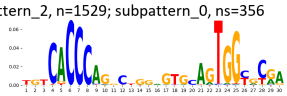

pattern_2, n=1529; subpattern_1, ns=304

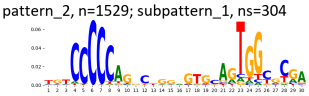

pattern_2, n=1529; subpattern_2, ns=273

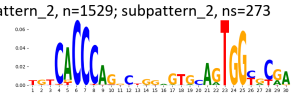

pattern_2, n=1529; subpattern_3, ns=247

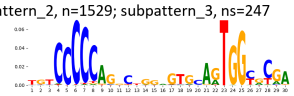

pattern_2, n=1529; subpattern_4, ns=217

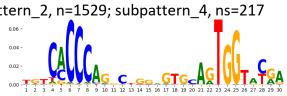

pattern_2, n=1529; subpattern_5, ns=132

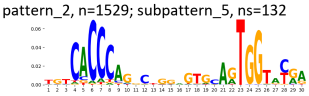

TF-MoDisCO pattern_2 n=1529, PWM

pattern_2, n=1529; subpattern_0, ns=356

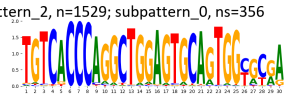

pattern_2, n=1529; subpattern_1, ns=304

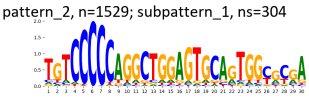

pattern_2, n=1529; subpattern_2, ns=273

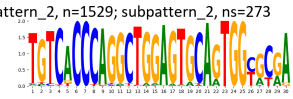

pattern_2, n=1529; subpattern_3, ns=247

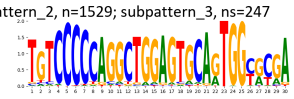

pattern_2, n=1529; subpattern_4, ns=217

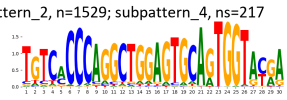

pattern_2, n=1529; subpattern_5, ns=132

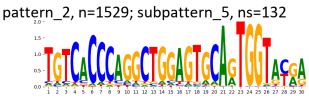

TF-MoDisCO pattern_3 n=1039, CWM

pattern_3, n=1039; subpattern_0, ns=264

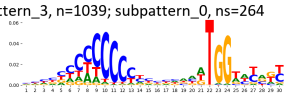

pattern_3, n=1039; subpattern_1, ns=253

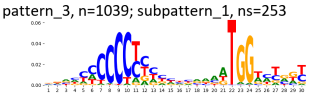

pattern_3, n=1039; subpattern_2, ns=175

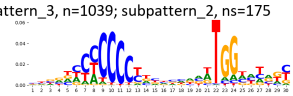

pattern_3, n=1039; subpattern_3, ns=158

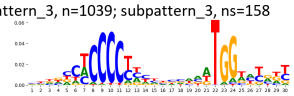

pattern_3, n=1039; subpattern_4, ns=130

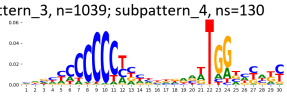

pattern_3, n=1039; subpattern_5, ns=29

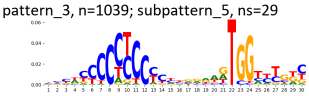

pattern_3, n=1039; subpattern_6, ns=16

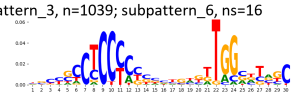

pattern_3, n=1039; subpattern_7, ns=14

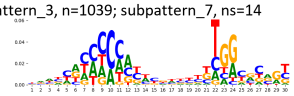

TF-MoDisCO pattern_3 n=1039, PWM

pattern_3, n=1039; subpattern_0, ns=264

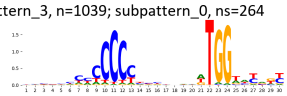

pattern_3, n=1039; subpattern_1, ns=253

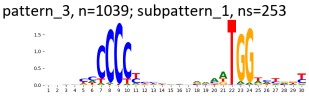

pattern_3, n=1039; subpattern_2, ns=175

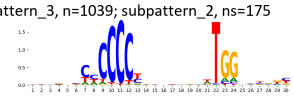

pattern_3, n=1039; subpattern_3, ns=158

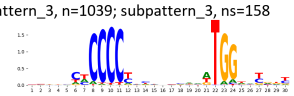

pattern_3, n=1039; subpattern_4, ns=130

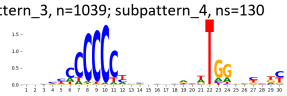

pattern_3, n=1039; subpattern_5, ns=29

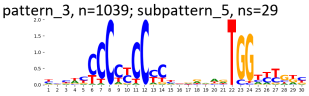

pattern_3, n=1039; subpattern_6, ns=16

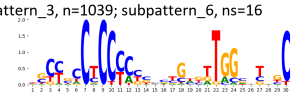

pattern_3, n=1039; subpattern_7, ns=14

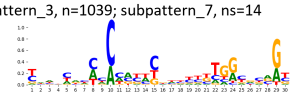

TF-MoDisCO pattern_4 n=896, CWM

pattern_4, n=896; subpattern_0, ns=201

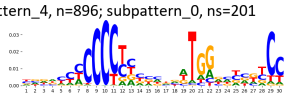

pattern_4, n=896; subpattern_1, ns=199

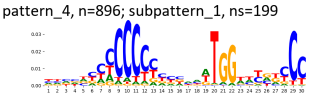

pattern_4, n=896; subpattern_2, ns=198

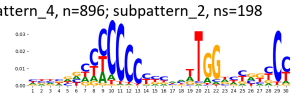

pattern_4, n=896; subpattern_3, ns=122

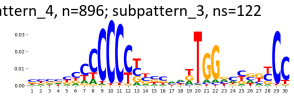

pattern_4, n=896; subpattern_4, ns=110

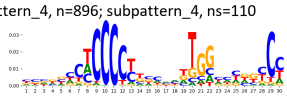

pattern_4, n=896; subpattern_5, ns=59

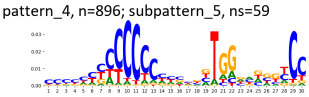

pattern_4, n=896; subpattern_6, ns=5

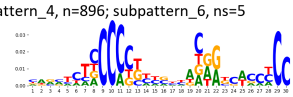

pattern_4, n=896; subpattern_7, ns=2

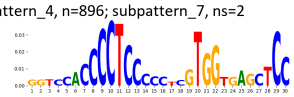

TF-MoDisCO pattern_4 n=896, PWM

pattern_4, n=896; subpattern_0, ns=201

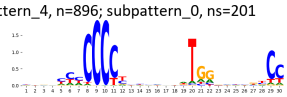

pattern_4, n=896; subpattern_1, ns=199

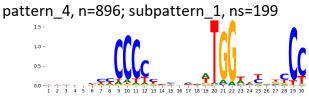

pattern_4, n=896; subpattern_2, ns=198

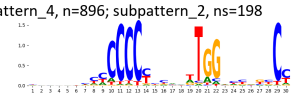

pattern_4, n=896; subpattern_3, ns=122

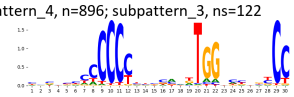

pattern_4, n=896; subpattern_4, ns=110

pattern_4, n=896; subpattern_5, ns=59

pattern_4, n=896; subpattern_6, ns=5

pattern_4, n=896; subpattern_7, ns=2

TF-MoDisCO pattern_5 n=733, CWM

pattern_5, n=733; subpattern_0, ns=217

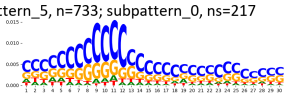

pattern_5, n=733; subpattern_1, ns=194

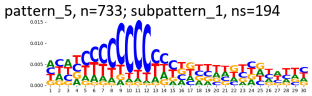

pattern_5, n=733; subpattern_2, ns=135

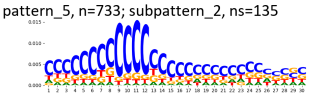

pattern_5, n=733; subpattern_3, ns=78

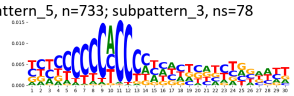

pattern_5, n=733; subpattern_4, ns=39

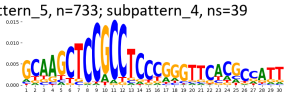

pattern_5, n=733; subpattern_5, ns=32

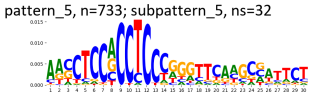

pattern_5, n=733; subpattern_6, ns=28

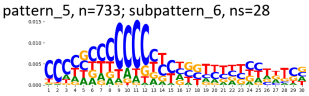

pattern_5, n=733; subpattern_7, ns=7

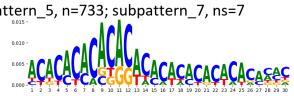

pattern_5, n=733; subpattern_8, ns=3

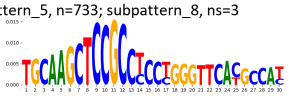

TF-MoDisCO pattern_5 n=733, PWM

pattern_5, n=733; subpattern_0, ns=217

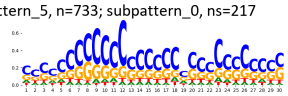

pattern_5, n=733; subpattern_1, ns=194

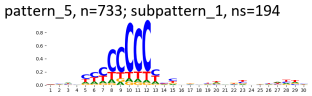

pattern_5, n=733; subpattern_2, ns=135

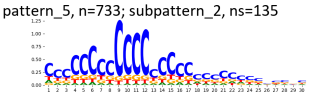

pattern_5, n=733; subpattern_3, ns=78

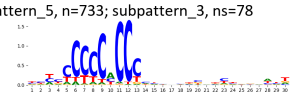

pattern_5, n=733; subpattern_4, ns=39

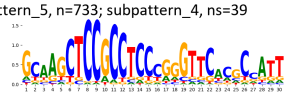

pattern_5, n=733; subpattern_5, ns=32

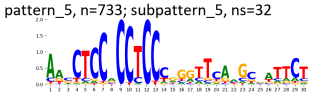

pattern_5, n=733; subpattern_6, ns=28

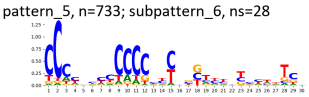

pattern_5, n=733; subpattern_7, ns=7

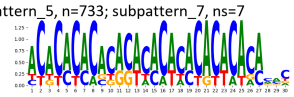

pattern_5, n=733; subpattern_8, ns=3

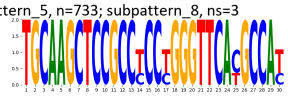

TF-MoDisCO pattern_6 n=610, CWM

pattern_6, n=610; subpattern_0, ns=167

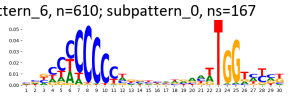

pattern_6, n=610; subpattern_1, ns=128

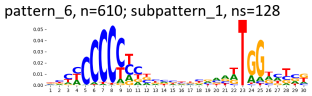

pattern_6, n=610; subpattern_2, ns=126

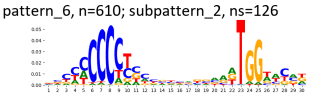

pattern_6, n=610; subpattern_3, ns=101

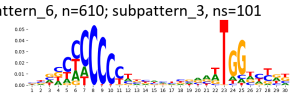

pattern_6, n=610; subpattern_4, ns=88

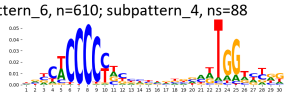

TF-MoDisCO pattern_6 n=610, PWM

pattern_6, n=610; subpattern_0, ns=167

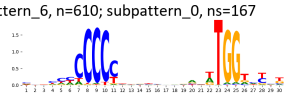

pattern_6, n=610; subpattern_1, ns=128

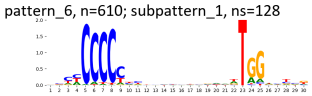

pattern_6, n=610; subpattern_2, ns=126

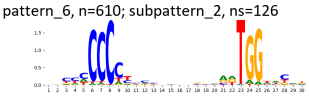

pattern_6, n=610; subpattern_3, ns=101

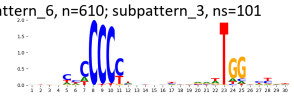

pattern_6, n=610; subpattern_4, ns=88

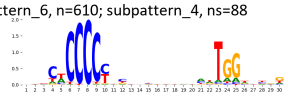

TF-MoDisCO pattern_7 n=227, CWM

pattern_7, n=227; subpattern_0, ns=67

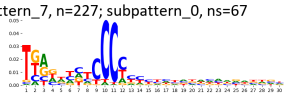

pattern_7, n=227; subpattern_1, ns=67

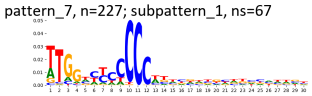

pattern_7, n=227; subpattern_2, ns=48

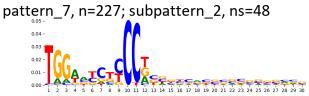

pattern_7, n=227; subpattern_3, ns=33

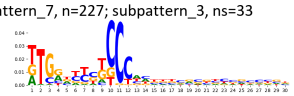

pattern_7, n=227; subpattern_4, ns=12

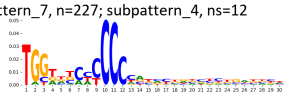

TF-MoDisCO pattern_7 n=227, PWM

pattern_7, n=227; subpattern_0, ns=67

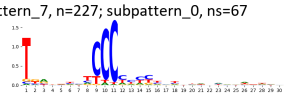

pattern_7, n=227; subpattern_1, ns=67

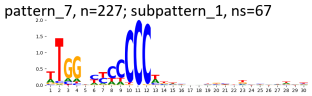

pattern_7, n=227; subpattern_2, ns=48

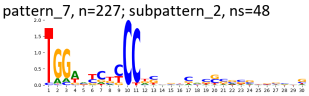

pattern_7, n=227; subpattern_3, ns=33

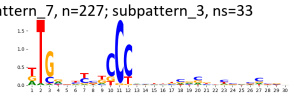

pattern_7, n=227; subpattern_4, ns=12

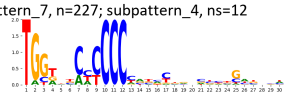

Supplementary Figure 197: TF-MoDisCO subpatterns for the PRDM10 transcription factor in K562 (accession ENCSR120MPG).

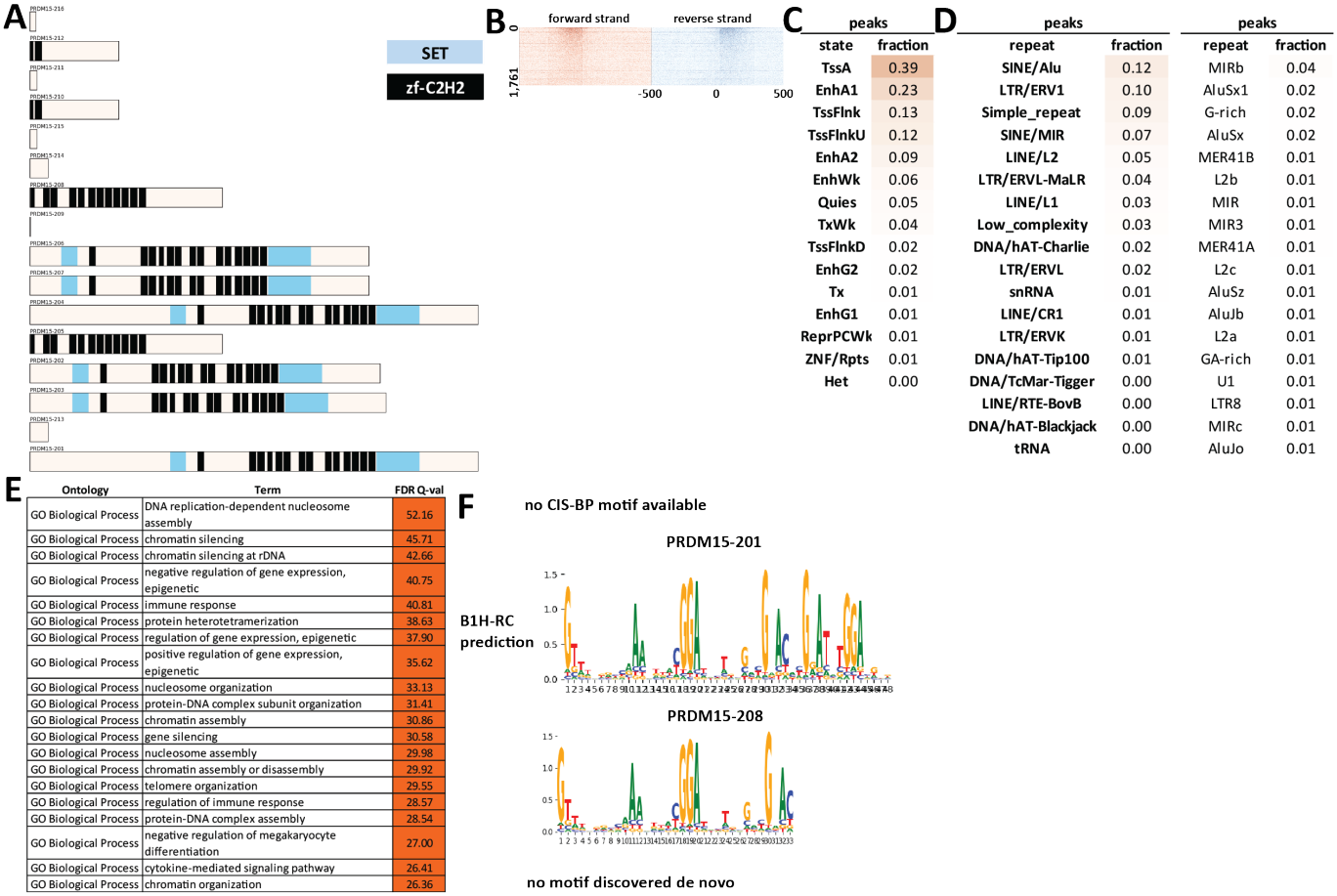

Supplementary Figure 198: Properties and genomic distribution of motifs identified for the PRDM15 transcription factor in GM12878 (accession ENCSR748SQL).

A

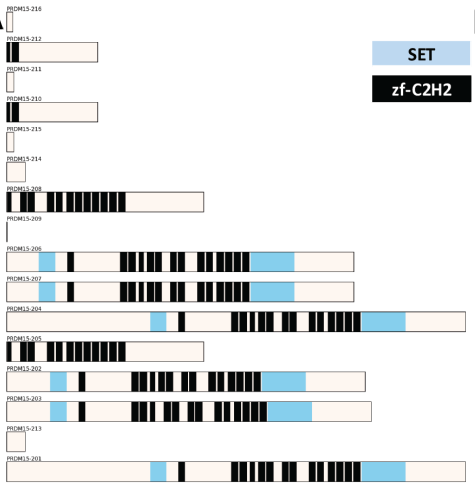

B

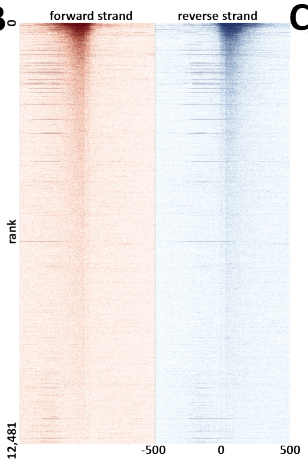

C

peaks	
state	fraction
TssA	0.40
TssFlnk	0.20
TssFlnkU	0.15
EnhWk	0.12
EnhA1	0.11
TssFlnkD	0.09
ReprPCWk	0.04
TxWk	0.03
Quies	0.03
TssBiv	0.02
EnhA2	0.02
ReprPC	0.02
EnhBiv	0.02
EnhG1	0.01
EnhG2	0.01
Tx	0.01
ZNF/Rpts	0.00
Het	0.00

D

peaks		peaks	
repeat	fraction	repeat	fraction
Simple_repeat	0.20	MIRb	0.04
SINE/MIR	0.11	G-rich	0.03
SINE/Alu	0.10	MIR	0.02
LINE/L2	0.06	L2a	0.02
Low_complexity	0.05	MIR3	0.02
LINE/L1	0.04	MIRc	0.02
DNA/hAT-Charlie	0.02	L2b	0.02
LTR/ERVL-MaLR	0.02	L2c	0.02
LTR/ERV1	0.02	AluSx1	0.01
LTR/ERVL	0.02	AluJb	0.01
DNA/TcMar-Tigger	0.01	AluSx	0.01
LINE/CR1	0.01	AluJr	0.01
DNA/hAT-Tip100	0.01	AluJo	0.01
tRNA	0.00	AluSz	0.01
DNA/hAT-Blackjack	0.00	GA-rich	0.01
LTR/ERVK	0.00	AluY	0.01
snRNA	0.00	(GGC)n	0.01
DNA/hAT	0.00	L2	0.01

E

Ontology	Term	FDR Q-val
GO Biological Process	regulation of transcription from RNA polymerase II promoter in response to stress	24.27
GO Biological Process	regulation of DNA-templated transcription in response to stress	22.31
GO Biological Process	regulation of transcription from RNA polymerase II promoter in response to hypoxia	18.56
GO Biological Process	mitochondrial membrane organization	18.48
GO Biological Process	mitochondrial transmembrane transport	15.55
GO Biological Process	negative regulation of intrinsic apoptotic signaling pathway	15.49
GO Biological Process	nuclear-transcribed mRNA catabolic process, deadenylation-dependent decay	14.21
GO Biological Process	regulation of mitochondrial membrane permeability	12.78
GO Biological Process	regulation of cholesterol metabolic process	11.58
GO Biological Process	intrinsic apoptotic signaling pathway in response to DNA damage	11.44
GO Biological Process	protein transmembrane transport	11.25
GO Biological Process	negative regulation of cyclin-dependent protein kinase activity	11.20
GO Biological Process	protein targeting to mitochondrion	10.49
GO Biological Process	regulation of cholesterol biosynthetic process	9.94
GO Biological Process	establishment of protein localization to mitochondrion	9.42
GO Biological Process	intracellular protein transmembrane transport	9.17
GO Biological Process	gene silencing by miRNA	8.65
GO Biological Process	cellular protein complex localization	6.32
GO Biological Process	regulation of mitochondrial translation	5.16
GO Biological Process	regulation of receptor catabolic process	4.72

F

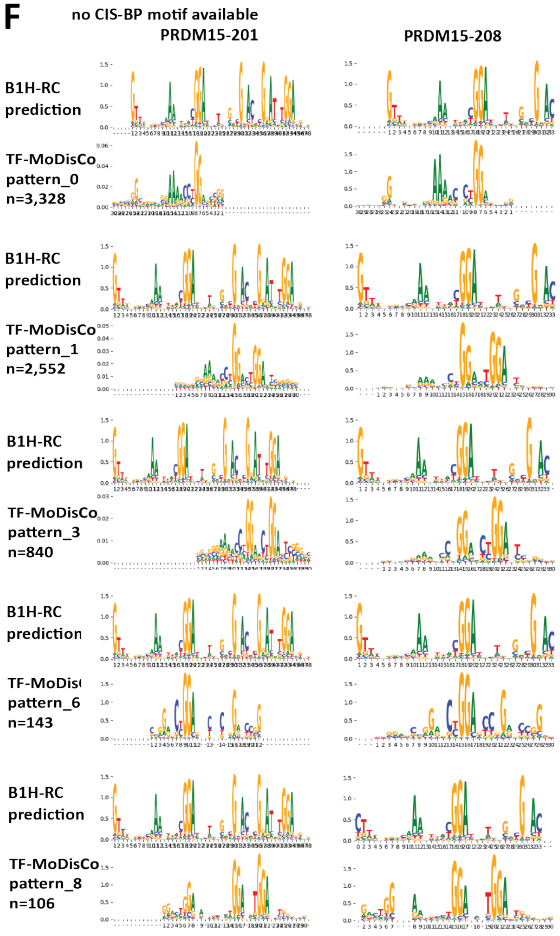

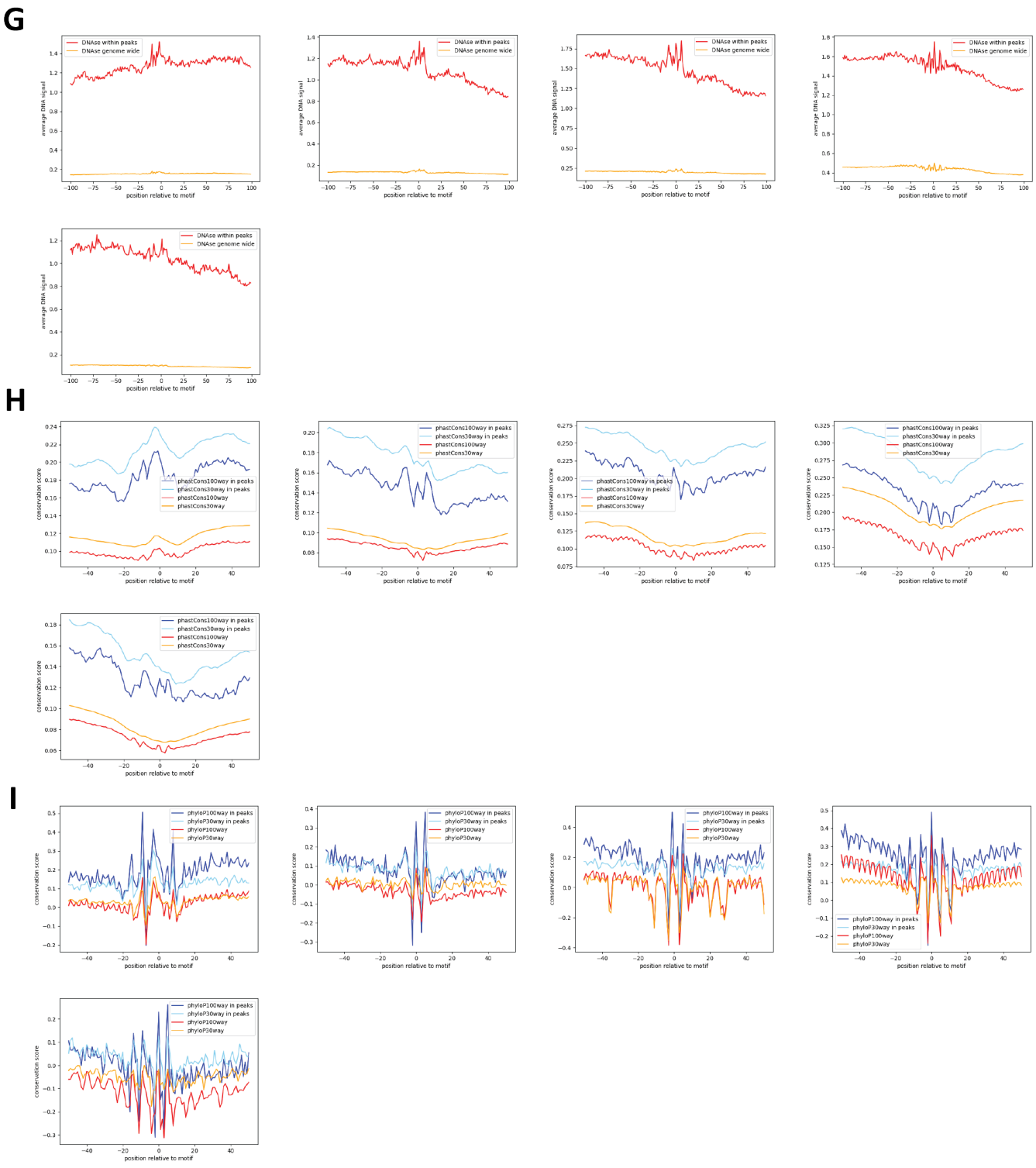

Supplementary Figure 199: Properties and genomic distribution of motifs identified for the PRDM15 transcription factor in HepG2 (accession ENCSR011INW).

TF-MoDisCO pattern_0 n=3328, CWM

pattern_0, n=3328; subpattern_0, ns=696

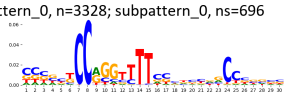

pattern_0, n=3328; subpattern_1, ns=646

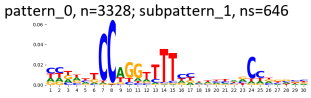

pattern_0, n=3328; subpattern_2, ns=620

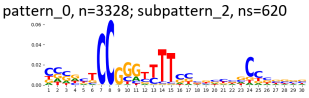

pattern_0, n=3328; subpattern_3, ns=368

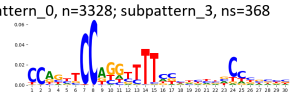

pattern_0, n=3328; subpattern_4, ns=361

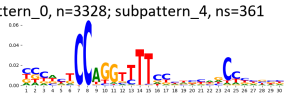

pattern_0, n=3328; subpattern_5, ns=269

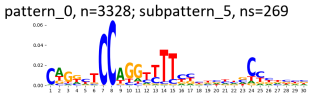

pattern_0, n=3328; subpattern_6, ns=179

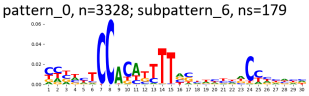

pattern_0, n=3328; subpattern_7, ns=113

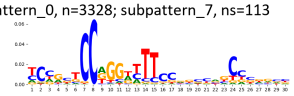

pattern_0, n=3328; subpattern_8, ns=76

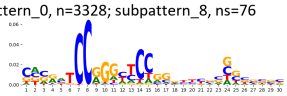

TF-MoDisCO pattern_0 n=3328, PWM

pattern_0, n=3328; subpattern_0, ns=696

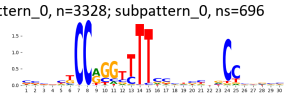

pattern_0, n=3328; subpattern_1, ns=646

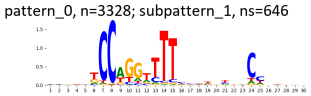

pattern_0, n=3328; subpattern_2, ns=620

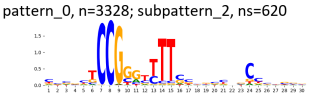

pattern_0, n=3328; subpattern_3, ns=368

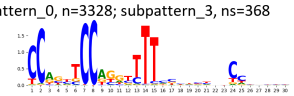

pattern_0, n=3328; subpattern_4, ns=361

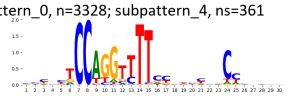

pattern_0, n=3328; subpattern_5, ns=269

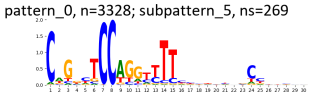

pattern_0, n=3328; subpattern_6, ns=179

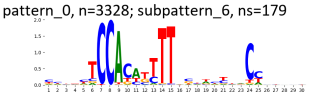

pattern_0, n=3328; subpattern_7, ns=113

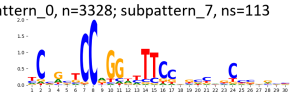

pattern_0, n=3328; subpattern_8, ns=76

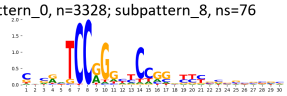

TF-MoDisCO pattern_1 n=2552, CWM

pattern_1, n=2552; subpattern_0, ns=636

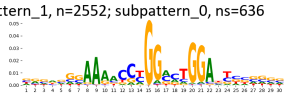

pattern_1, n=2552; subpattern_1, ns=505

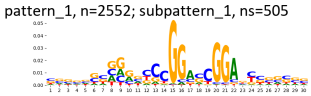

pattern_1, n=2552; subpattern_2, ns=487

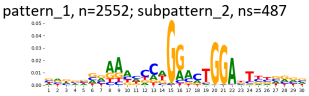

pattern_1, n=2552; subpattern_3, ns=332

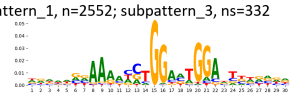

pattern_1, n=2552; subpattern_4, ns=330

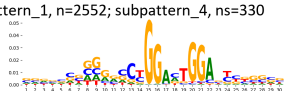

pattern_1, n=2552; subpattern_5, ns=262

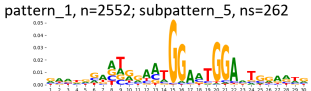

TF-MoDisCO pattern_1 n=2552, PWM

pattern_1, n=2552; subpattern_0, ns=636

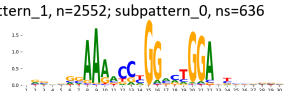

pattern_1, n=2552; subpattern_1, ns=505

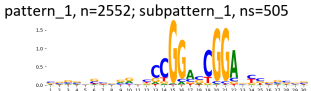

pattern_1, n=2552; subpattern_2, ns=487

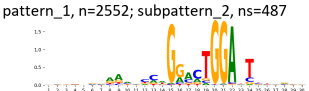

pattern_1, n=2552; subpattern_3, ns=332

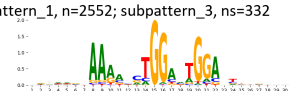

pattern_1, n=2552; subpattern_4, ns=330

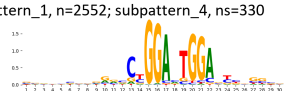

pattern_1, n=2552; subpattern_5, ns=262

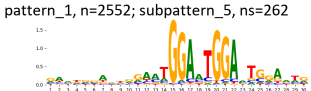

TF-MoDisCO pattern_3 n=840, CWM

pattern_3, n=840; subpattern_0, ns=216

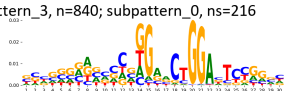

pattern_3, n=840; subpattern_1, ns=178

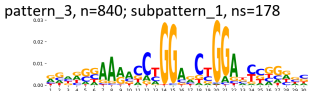

pattern_3, n=840; subpattern_2, ns=131

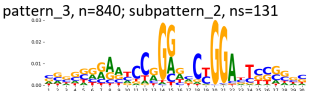

pattern_3, n=840; subpattern_3, ns=117

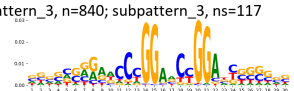

pattern_3, n=840; subpattern_4, ns=101

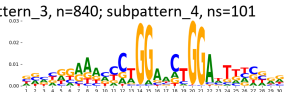

pattern_3, n=840; subpattern_5, ns=90

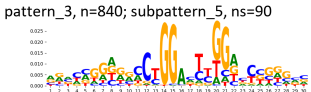

pattern_3, n=840; subpattern_6, ns=4

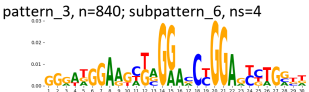

pattern_3, n=840; subpattern_7, ns=3

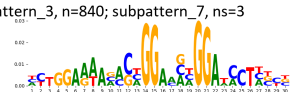

TF-MoDisCO pattern_3 n=840, PWM

pattern_3, n=840; subpattern_0, ns=216

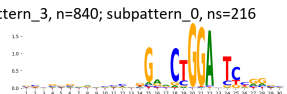

pattern_3, n=840; subpattern_1, ns=178

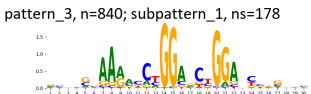

pattern_3, n=840; subpattern_2, ns=131

pattern_3, n=840; subpattern_3, ns=117

pattern_3, n=840; subpattern_4, ns=101

pattern_3, n=840; subpattern_5, ns=90

pattern_3, n=840; subpattern_6, ns=4

pattern_3, n=840; subpattern_7, ns=3

TF-MoDisCO pattern_6 n=153, CWM

pattern_6, n=153; subpattern_0, ns=46

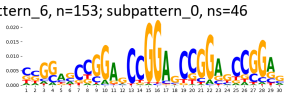

pattern_6, n=153; subpattern_1, ns=45

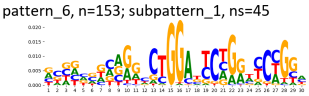

pattern_6, n=153; subpattern_2, ns=30

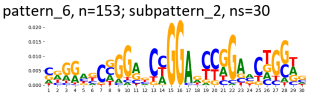

pattern_6, n=153; subpattern_3, ns=25

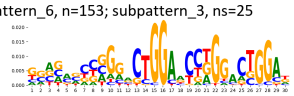

pattern_6, n=153; subpattern_4, ns=7

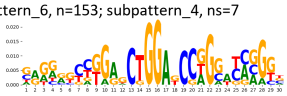

TF-MoDisCO pattern_6 n=153, PWM

pattern_6, n=153; subpattern_0, ns=46

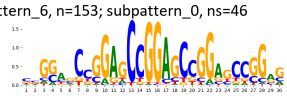

pattern_6, n=153; subpattern_1, ns=45

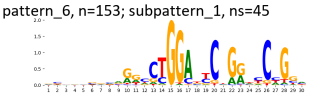

pattern_6, n=153; subpattern_2, ns=30

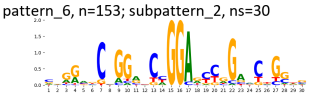

pattern_6, n=153; subpattern_3, ns=25

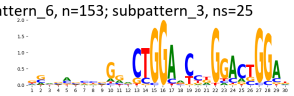

pattern_6, n=153; subpattern_4, ns=7

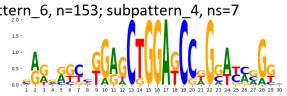

TF-MoDisCO pattern_8 n=106, CWM

pattern_8, n=106; subpattern_0, ns=24

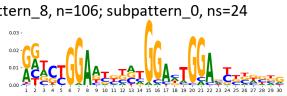

pattern_8, n=106; subpattern_1, ns=22

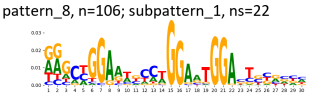

pattern_8, n=106; subpattern_2, ns=20

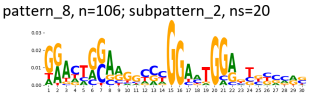

pattern_8, n=106; subpattern_3, ns=20

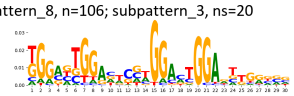

pattern_8, n=106; subpattern_4, ns=13

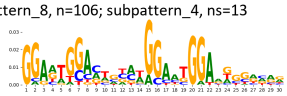

pattern_8, n=106; subpattern_5, ns=7

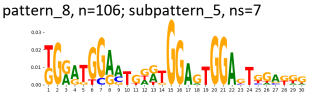

TF-MoDisCO pattern_8 n=106, PWM

pattern_8, n=106; subpattern_0, ns=24

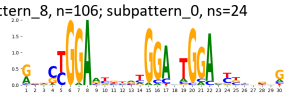

pattern_8, n=106; subpattern_1, ns=22

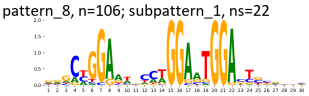

pattern_8, n=106; subpattern_2, ns=20

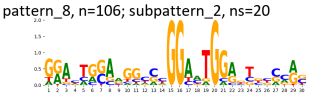

pattern_8, n=106; subpattern_3, ns=20

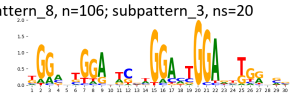

pattern_8, n=106; subpattern_4, ns=13

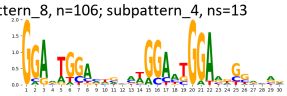

pattern_8, n=106; subpattern_5, ns=7

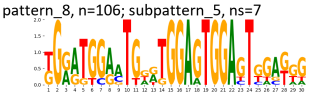

Supplementary Figure 200: TF-MoDisCO subpatterns for the PRDM15 transcription factor in HepG2 (accession ENCSR011INW).

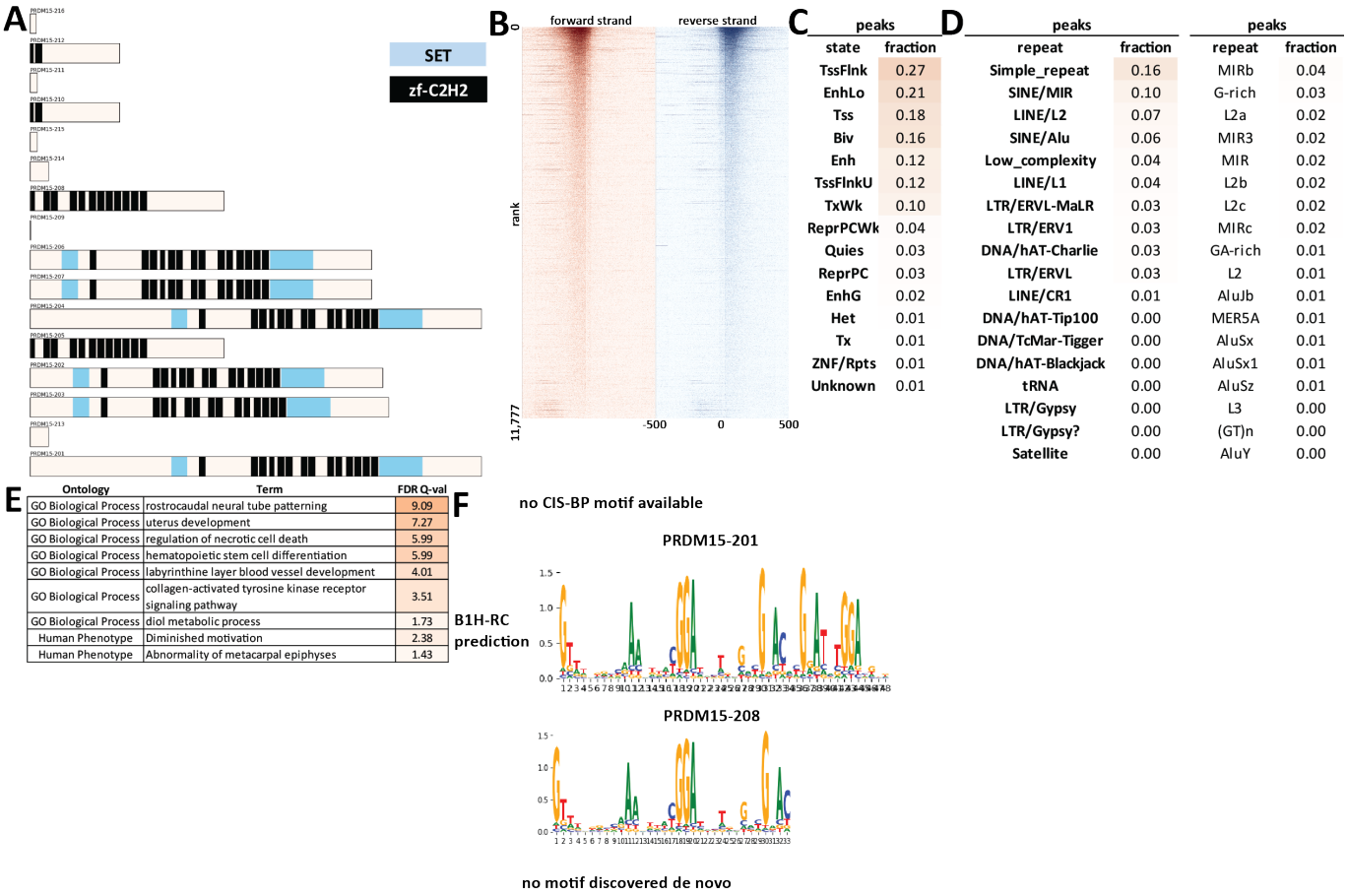

Supplementary Figure 201: Properties and genomic distribution of motifs identified for the PRDM15 transcription factor in WTC11 (accession ENCSR092DCD).

TF-MoDisCO pattern_0 n=5352, CWM

pattern_0, n=5352; subpattern_0, ns=1684

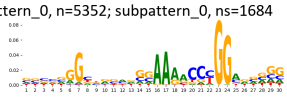

pattern_0, n=5352; subpattern_1, ns=1019

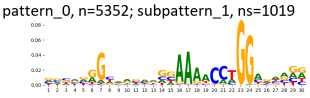

pattern_0, n=5352; subpattern_10, ns=2

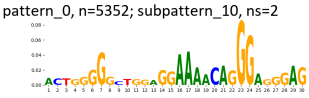

pattern_0, n=5352; subpattern_11, ns=2

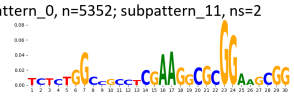

pattern_0, n=5352; subpattern_2, ns=1010

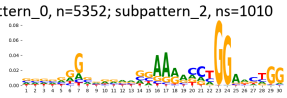

pattern_0, n=5352; subpattern_3, ns=802

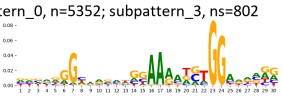

pattern_0, n=5352; subpattern_4, ns=582

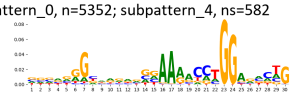

pattern_0, n=5352; subpattern_5, ns=128

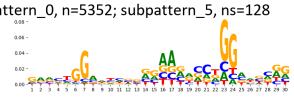

pattern_0, n=5352; subpattern_6, ns=63

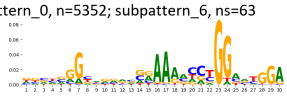

pattern_0, n=5352; subpattern_7, ns=53

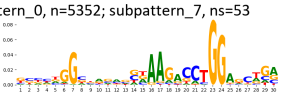

pattern_0, n=5352; subpattern_8, ns=4

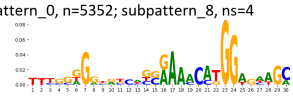

pattern_0, n=5352; subpattern_9, ns=3

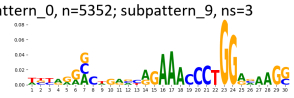

TF-MoDisCO pattern_0 n=5352, PWM

pattern_0, n=5352; subpattern_0, ns=1684

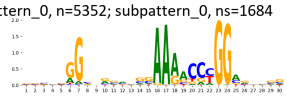

pattern_0, n=5352; subpattern_1, ns=1019

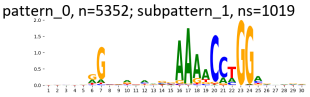

pattern_0, n=5352; subpattern_10, ns=2

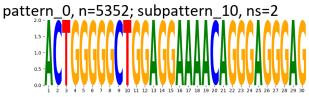

pattern_0, n=5352; subpattern_11, ns=2

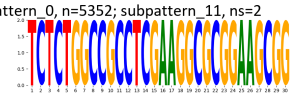

pattern_0, n=5352; subpattern_2, ns=1010

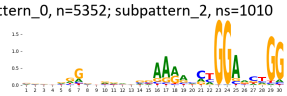

pattern_0, n=5352; subpattern_3, ns=802

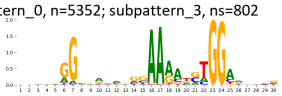

pattern_0, n=5352; subpattern_4, ns=582

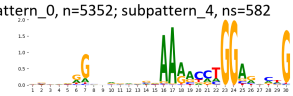

pattern_0, n=5352; subpattern_5, ns=128

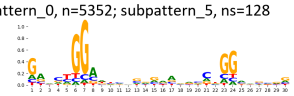

pattern_0, n=5352; subpattern_6, ns=63

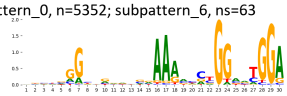

pattern_0, n=5352; subpattern_7, ns=53

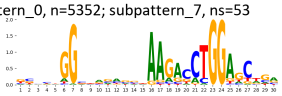

pattern_0, n=5352; subpattern_8, ns=4

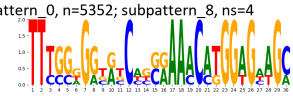

pattern_0, n=5352; subpattern_9, ns=3

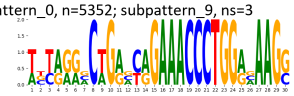

TF-MoDisCO pattern_1 n=2129, CWM

pattern_1, n=2129; subpattern_0, ns=478

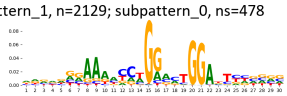

pattern_1, n=2129; subpattern_1, ns=471

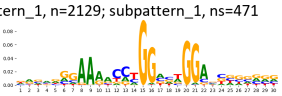

pattern_1, n=2129; subpattern_2, ns=439

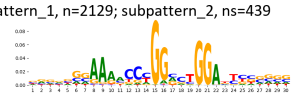

pattern_1, n=2129; subpattern_3, ns=384

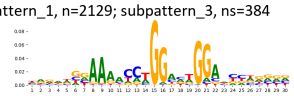

pattern_1, n=2129; subpattern_4, ns=331

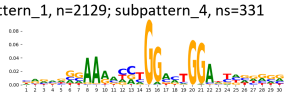

pattern_1, n=2129; subpattern_5, ns=21

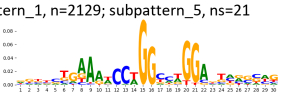

pattern_1, n=2129; subpattern_6, ns=3

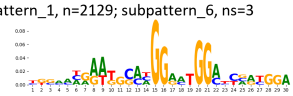

pattern_1, n=2129; subpattern_7, ns=2

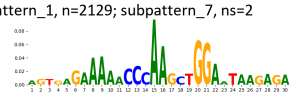

TF-MoDisCO pattern_1 n=2129, PWM

pattern_1, n=2129; subpattern_0, ns=478

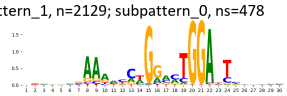

pattern_1, n=2129; subpattern_1, ns=471

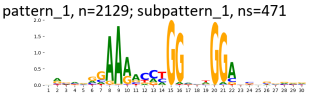

pattern_1, n=2129; subpattern_2, ns=439

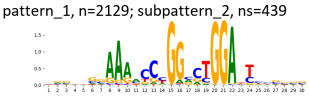

pattern_1, n=2129; subpattern_3, ns=384

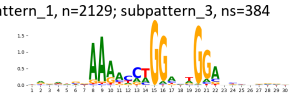

pattern_1, n=2129; subpattern_4, ns=331

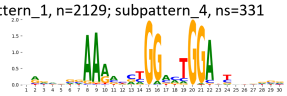

pattern_1, n=2129; subpattern_5, ns=21

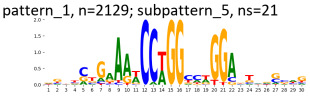

pattern_1, n=2129; subpattern_6, ns=3

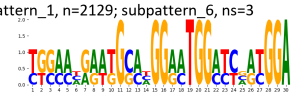

pattern_1, n=2129; subpattern_7, ns=2

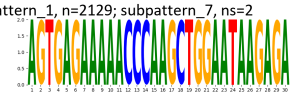

TF-MoDisCO pattern_2 n=1916, CWM

pattern_2, n=1916; subpattern_0, ns=430

pattern_2, n=1916; subpattern_1, ns=388

pattern_2, n=1916; subpattern_2, ns=339

pattern_2, n=1916; subpattern_3, ns=275

pattern_2, n=1916; subpattern_4, ns=221

pattern_2, n=1916; subpattern_5, ns=148

pattern_2, n=1916; subpattern_6, ns=111

pattern_2, n=1916; subpattern_7, ns=4

TF-MoDisCO pattern_2 n=1916, PWM

pattern_2, n=1916; subpattern_0, ns=430

pattern_2, n=1916; subpattern_1, ns=388

pattern_2, n=1916; subpattern_2, ns=339

pattern_2, n=1916; subpattern_3, ns=275

pattern_2, n=1916; subpattern_4, ns=221

pattern_2, n=1916; subpattern_5, ns=148

pattern_2, n=1916; subpattern_6, ns=111

pattern_2, n=1916; subpattern_7, ns=4

TF-MoDisCO pattern_5 n=227, CWM

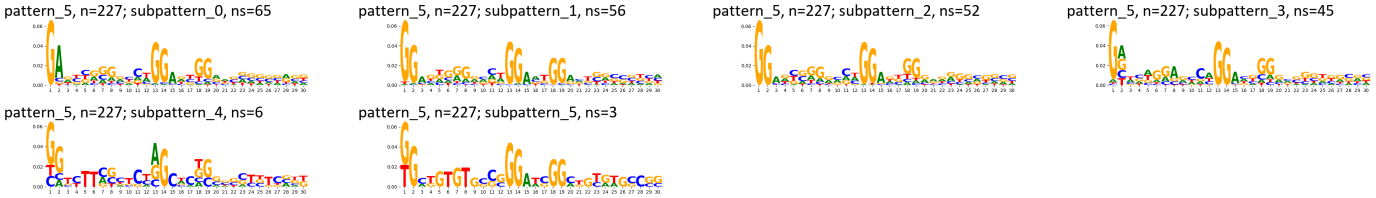

TF-MoDisCO pattern_5 n=227, PWM

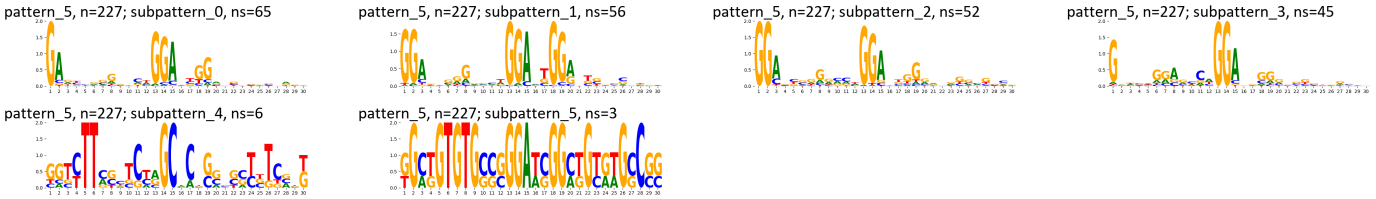

TF-MoDisCO pattern_7 n=114, CWM

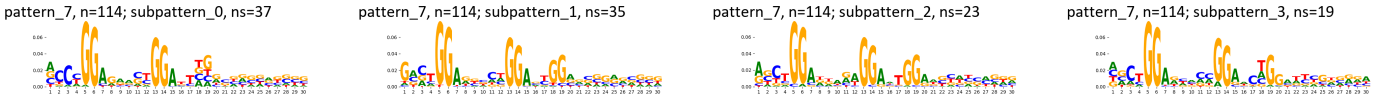

TF-MoDisCO pattern_7 n=114, PWM



Supplementary Figure 202: TF-MoDisCO subpatterns for the PRDM15 transcription factor in WTC11 (accession ENCSR092DCD).

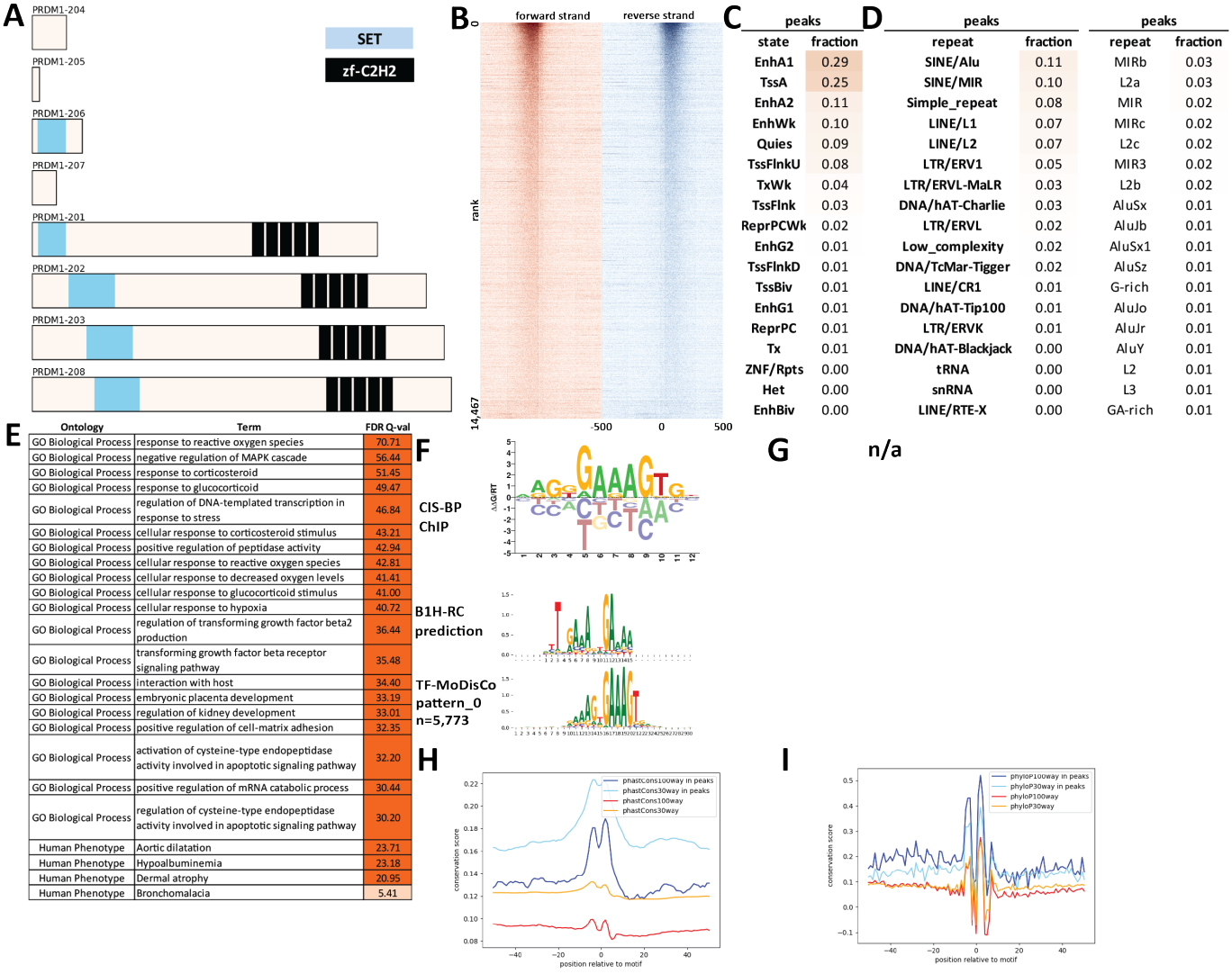

peaks	
state	fraction
EnhA1	0.29
TssA	0.25
EnhA2	0.11
EnhWk	0.10
Quies	0.09
TssFlnkU	0.08
TxWk	0.04
TssFlnk	0.03
ReprPCWk	0.02
EnhG2	0.01
TssFlnkD	0.01
TssBiv	0.01
EnhG1	0.01
ReprPC	0.01
Tx	0.01
ZNF/Rpts	0.00
Het	0.00
EnhBiv	0.00

peaks		peaks	
repeat	fraction	repeat	fraction
SINE/Alu	0.11	MIRb	0.03
SINE/MIR	0.10	L2a	0.03
Simple_repeat	0.08	MIR	0.02
LINE/L1	0.07	MIRc	0.02
LINE/L2	0.07	L2c	0.02
LTR/ERV1	0.05	MIR3	0.02
LTR/ERVL-MaLR	0.03	L2b	0.02
DNA/hAT-Charlie	0.03	AluSx	0.01
LTR/ERVL	0.02	AluJb	0.01
Low_complexity	0.02	AluSx1	0.01
DNA/TcMar-Tigger	0.02	AluSz	0.01
LINE/CR1	0.01	G-rich	0.01
DNA/hAT-Tip100	0.01	AluJo	0.01
LTR/ERVK	0.01	AluJr	0.01
DNA/hAT-Blackjack	0.00	AluY	0.01
tRNA	0.00	L2	0.01
snRNA	0.00	L3	0.01
LINE/RTE-X	0.00	GA-rich	0.01

Ontology	Term	FDR Q-val
GO Biological Process	response to reactive oxygen species	70.71
GO Biological Process	negative regulation of MAPK cascade	56.44
GO Biological Process	response to corticosteroid	51.45
GO Biological Process	response to glucocorticoid	49.47
GO Biological Process	regulation of DNA-templated transcription in response to stress	46.84
GO Biological Process	cellular response to corticosteroid stimulus	43.21
GO Biological Process	positive regulation of peptidase activity	42.94
GO Biological Process	cellular response to reactive oxygen species	42.81
GO Biological Process	cellular response to decreased oxygen levels	41.41
GO Biological Process	cellular response to glucocorticoid stimulus	41.00
GO Biological Process	cellular response to hypoxia	40.72
GO Biological Process	regulation of transforming growth factor beta2 production	36.44
GO Biological Process	transforming growth factor beta receptor signaling pathway	35.48
GO Biological Process	interaction with host	34.40
GO Biological Process	embryonic placenta development	33.19
GO Biological Process	regulation of kidney development	33.01
GO Biological Process	positive regulation of cell-matrix adhesion	32.35
GO Biological Process	activation of cysteine-type endopeptidase activity involved in apoptotic signaling pathway	32.20
GO Biological Process	positive regulation of mRNA catabolic process	30.44
GO Biological Process	regulation of cysteine-type endopeptidase activity involved in apoptotic signaling pathway	30.20
Human Phenotype	Aortic dilatation	23.71
Human Phenotype	Hypoalbuminemia	23.18
Human Phenotype	Dermal atrophy	20.95
Human Phenotype	Bronchomalacia	5.41

Supplementary Figure 203: Properties and genomic distribution of motifs identified for the PRDM1 transcription factor in A549 (accession ENCSR977FEF).

TF-MoDisCO pattern_0 n=5773, CWM

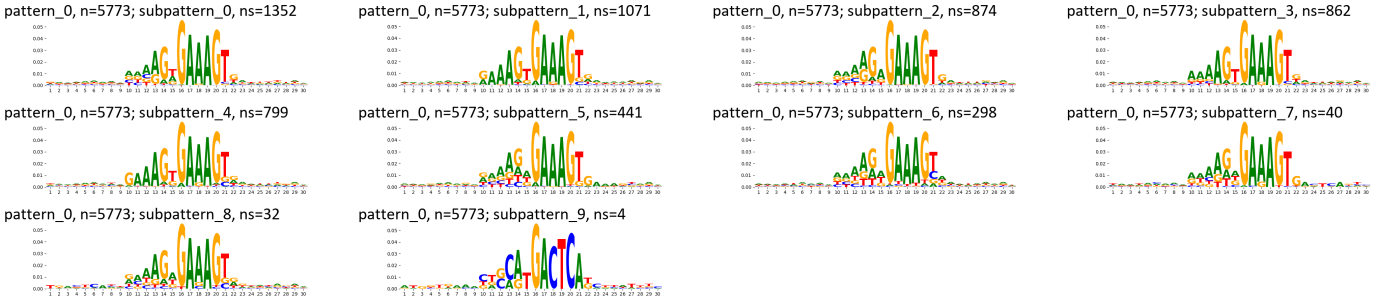

TF-MoDisCO pattern_0 n=5773, PWM

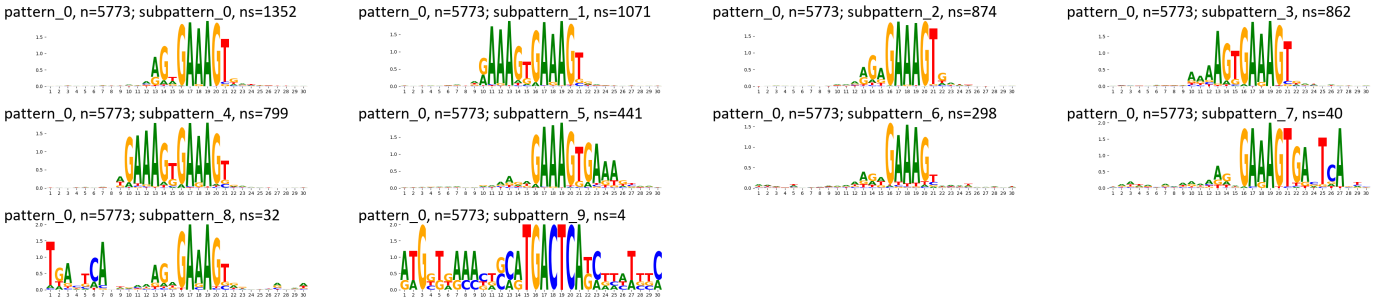

Supplementary Figure 204: TF-MoDisCO subpatterns for the PRDM1 transcription factor in A549 (accession ENCSR977FEF).

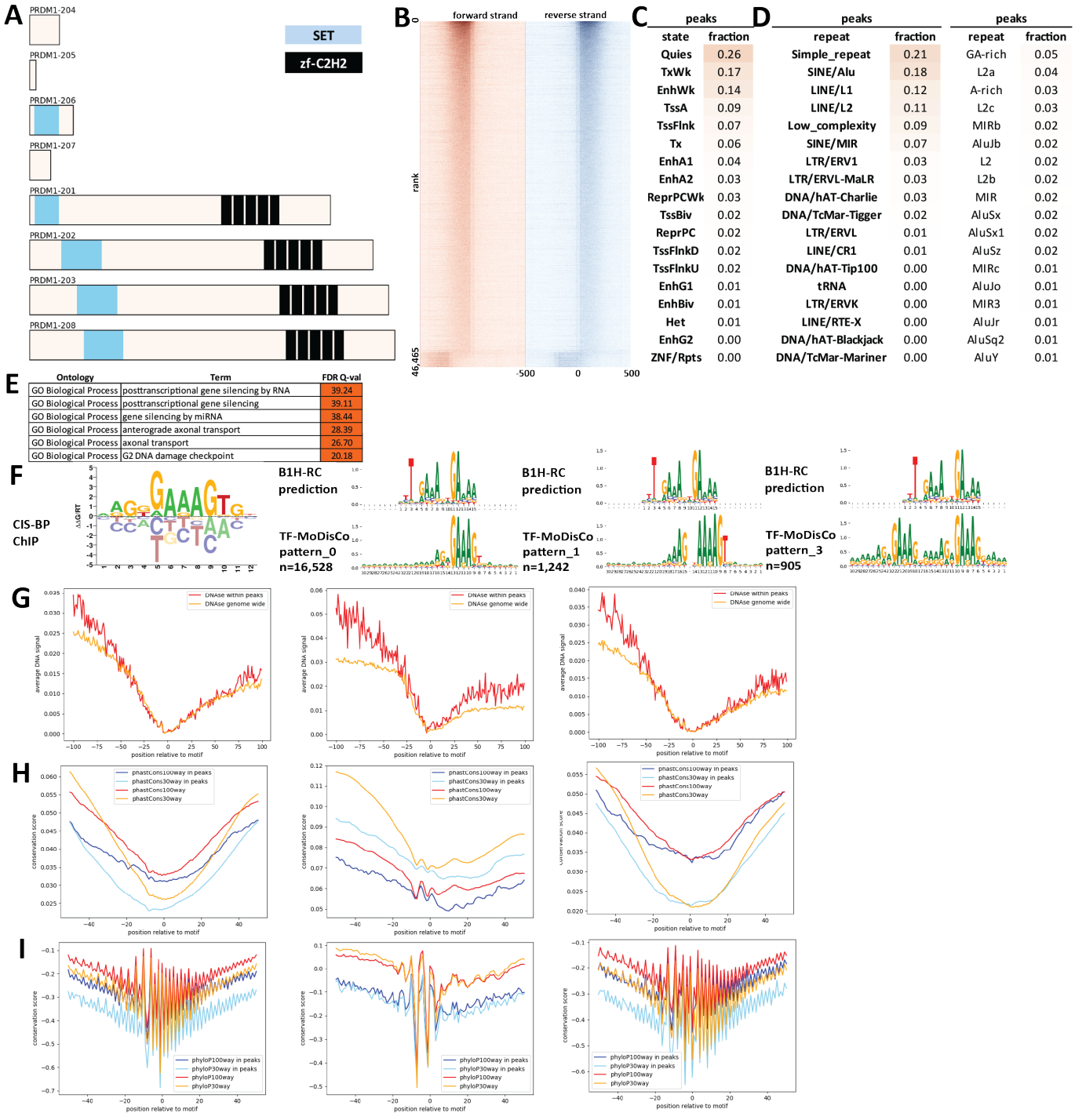

Supplementary Figure 205: Properties and genomic distribution of motifs identified for the PRDM1 transcription factor in HEK293 (accession ENCSR098YLE).

TF-MoDisCO pattern_0 n=16528, CWM

pattern_0, n=16528; subpattern_0, ns=2425

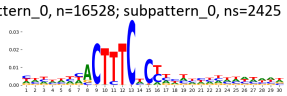

pattern_0, n=16528; subpattern_1, ns=1903

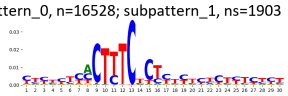

pattern_0, n=16528; subpattern_10, ns=563

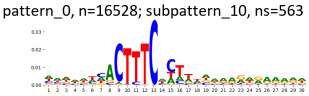

pattern_0, n=16528; subpattern_11, ns=556

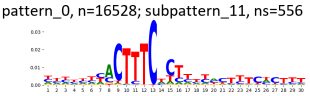

pattern_0, n=16528; subpattern_12, ns=340

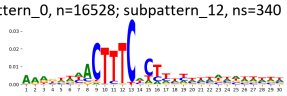

pattern_0, n=16528; subpattern_13, ns=307

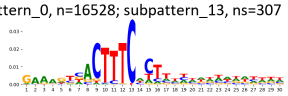

pattern_0, n=16528; subpattern_14, ns=290

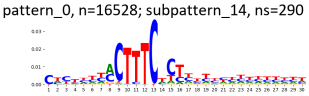

pattern_0, n=16528; subpattern_15, ns=120

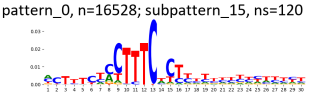

pattern_0, n=16528; subpattern_16, ns=15

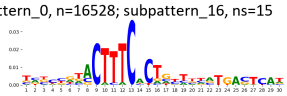

pattern_0, n=16528; subpattern_17, ns=6

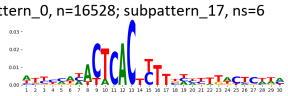

pattern_0, n=16528; subpattern_2, ns=1892

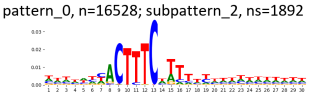

pattern_0, n=16528; subpattern_3, ns=1890

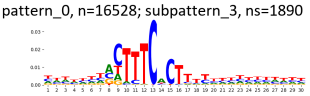

pattern_0, n=16528; subpattern_4, ns=1300

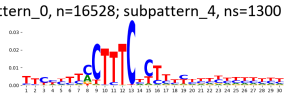

pattern_0, n=16528; subpattern_5, ns=1256

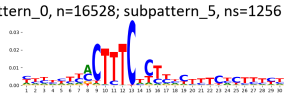

pattern_0, n=16528; subpattern_6, ns=1077

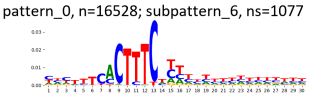

pattern_0, n=16528; subpattern_7, ns=931

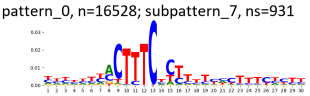

pattern_0, n=16528; subpattern_8, ns=912

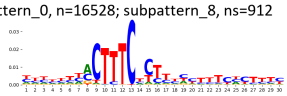

pattern_0, n=16528; subpattern_9, ns=745

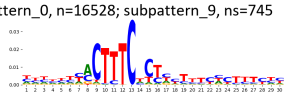

TF-MoDisCO pattern_0 n=16528, PWM

pattern_0, n=16528; subpattern_0, ns=2425

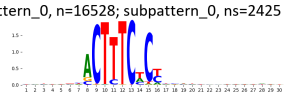

pattern_0, n=16528; subpattern_1, ns=1903

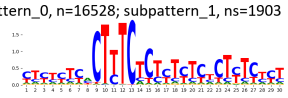

pattern_0, n=16528; subpattern_10, ns=563

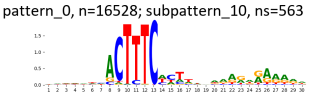

pattern_0, n=16528; subpattern_11, ns=556

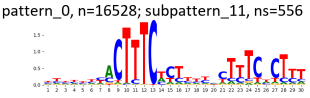

pattern_0, n=16528; subpattern_12, ns=340

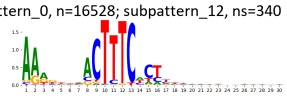

pattern_0, n=16528; subpattern_13, ns=307

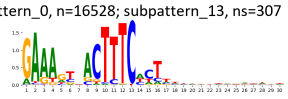

pattern_0, n=16528; subpattern_14, ns=290

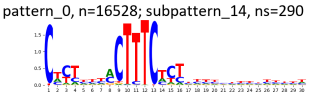

pattern_0, n=16528; subpattern_15, ns=120

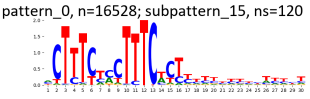

pattern_0, n=16528; subpattern_16, ns=15

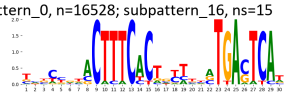

pattern_0, n=16528; subpattern_17, ns=6

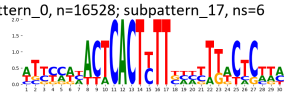

pattern_0, n=16528; subpattern_2, ns=1892

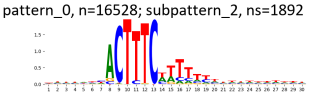

pattern_0, n=16528; subpattern_3, ns=1890

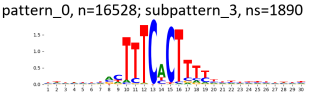

pattern_0, n=16528; subpattern_4, ns=1300

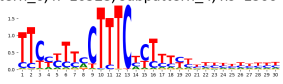

pattern_0, n=16528; subpattern_5, ns=1256

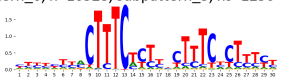

pattern_0, n=16528; subpattern_6, ns=1077

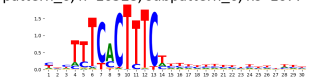

pattern_0, n=16528; subpattern_7, ns=931

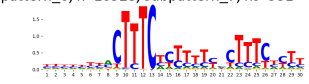

pattern_0, n=16528; subpattern_8, ns=912

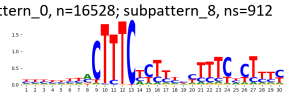

pattern_0, n=16528; subpattern_9, ns=745

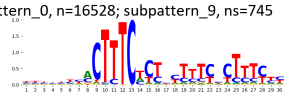

TF-MoDisCO pattern_1 n=1242, CWM

pattern_1, n=1242; subpattern_0, ns=280

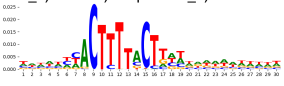

pattern_1, n=1242; subpattern_1, ns=270

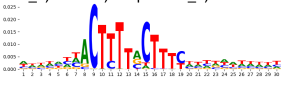

pattern_1, n=1242; subpattern_2, ns=193

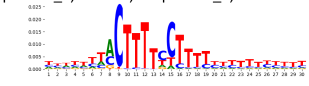

pattern_1, n=1242; subpattern_3, ns=188

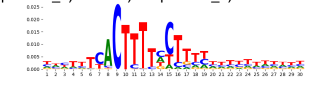

pattern_1, n=1242; subpattern_4, ns=112

pattern_1, n=1242; subpattern_5, ns=82

pattern_1, n=1242; subpattern_6, ns=67

pattern_1, n=1242; subpattern_7, ns=50

TF-MoDisCO pattern_1 n=1242, PWM

pattern_1, n=1242; subpattern_0, ns=280

pattern_1, n=1242; subpattern_1, ns=270

pattern_1, n=1242; subpattern_2, ns=193

pattern_1, n=1242; subpattern_3, ns=188

pattern_1, n=1242; subpattern_4, ns=112

pattern_1, n=1242; subpattern_5, ns=82

pattern_1, n=1242; subpattern_6, ns=67

pattern_1, n=1242; subpattern_7, ns=50

TF-MoDisCO pattern_3 n=905, CWM

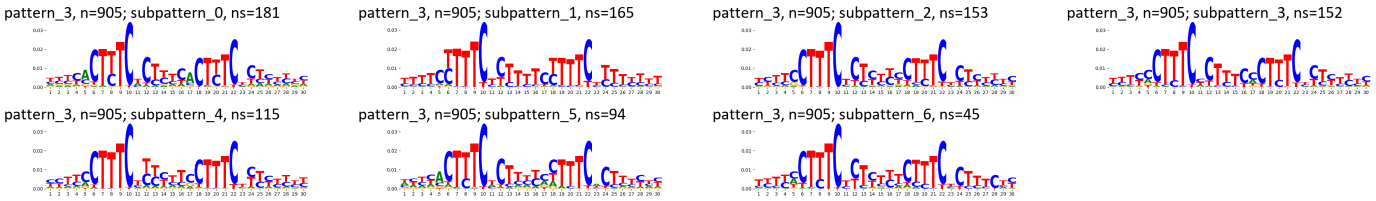

TF-MoDisCO pattern_3 n=905, PWM

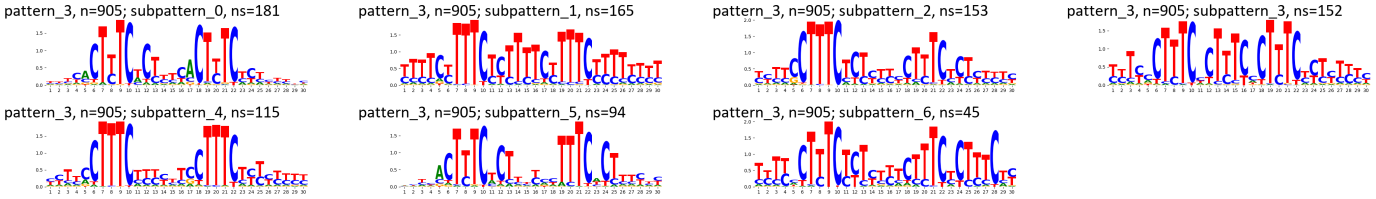

Supplementary Figure 206: TF-MoDisCO subpatterns for the PRDM1 transcription factor in HEK293 (accession ENCSR098YLE).

A

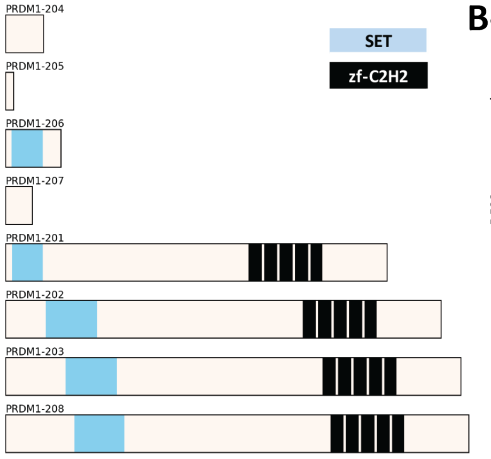

B

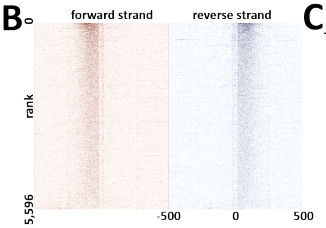

C

peaks	
state	fraction
Quies	0.28
TssA	0.16
TxWk	0.15
EnhWk	0.14
TssFlnk	0.09
Tx	0.06
EnhA1	0.05
TssBiv	0.04
EnhA2	0.03
ReprPC	0.03
TssFlnkU	0.02
TssFlnkD	0.02
ReprPCWk	0.02
EnhBiv	0.01
EnhG1	0.01
Het	0.00
EnhG2	0.00
ZNF/Rpts	0.00

D

peaks		peaks	
repeat	fraction	repeat	fraction
Simple_repeat	0.23	GA-rich	0.06
SINE/Alu	0.14	A-rich	0.04
Low_complexity	0.12	AluJb	0.02
LINE/L1	0.09	L2a	0.02
LINE/L2	0.06	MIRb	0.02
SINE/MIR	0.05	L2c	0.02
LTR/ERV1	0.03	AluJo	0.01
LTR/ERVL-MaLR	0.02	AluJr	0.01
DNA/hAT-Charlie	0.02	G-rich	0.01
DNA/TcMar-Tigger	0.02	AluSx1	0.01
LTR/ERVL	0.01	MIR3	0.01
LINE/CR1	0.01	MIR	0.01
DNA/hAT-Tip100	0.00	MIRc	0.01
tRNA	0.00	(TTTC)n	0.01
snRNA	0.00	L2	0.01
LTR/Gypsy	0.00	AluSx	0.01
LTR/ERVK	0.00	L2b	0.01
LINE/RTE-X	0.00	AluSz	0.01

E

Ontology	Term	FDR Q-val
GO Biological Process	thyroid gland development	8.87
GO Biological Process	maintenance of protein location in cell	6.10
GO Biological Process	positive regulation of stress fiber assembly	5.75
GO Biological Process	positive regulation of actin filament bundle assembly	5.25
GO Biological Process	organelle transport along microtubule	5.08
GO Biological Process	negative regulation of peptidyl-tyrosine phosphorylation	4.97
GO Biological Process	mesodermal cell differentiation	4.97
GO Biological Process	positive regulation of extrinsic apoptotic signaling pathway	4.71
GO Biological Process	positive regulation of extracellular matrix organization	4.65
GO Biological Process	regulation of transforming growth factor beta production	4.31
GO Biological Process	regulation of transforming growth factor beta2 production	4.24
GO Biological Process	response to laminar fluid shear stress	4.21
GO Biological Process	negative regulation of cardiac muscle hypertrophy in response to stress	3.96
GO Biological Process	heterochromatin assembly	3.60
GO Biological Process	peroxisome proliferator activated receptor signaling pathway	3.52
GO Biological Process	paraxial mesoderm development	3.01
GO Biological Process	paraxial mesoderm morphogenesis	2.83
GO Biological Process	hepatocyte apoptotic process	2.74
GO Biological Process	negative regulation of DNA replication	2.71
GO Biological Process	definitive hemopoiesis	2.58
Human Phenotype	Hirsutism	15.24
Human Phenotype	Coarctation of aorta	7.03
Human Phenotype	Hamartoma	6.73
Human Phenotype	Limb hypertonia	5.57
Human Phenotype	Adipose tissue loss	3.70
Human Phenotype	Short 4th metacarpal	3.12
Human Phenotype	Autoimmune thrombocytopenia	3.04
Human Phenotype	Rectal prolapse	1.80

F

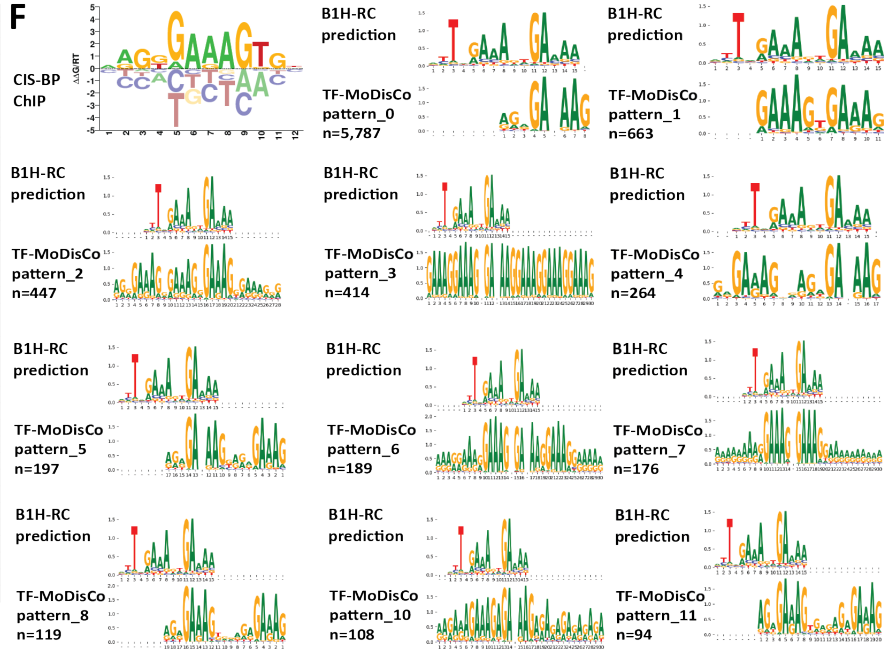

G

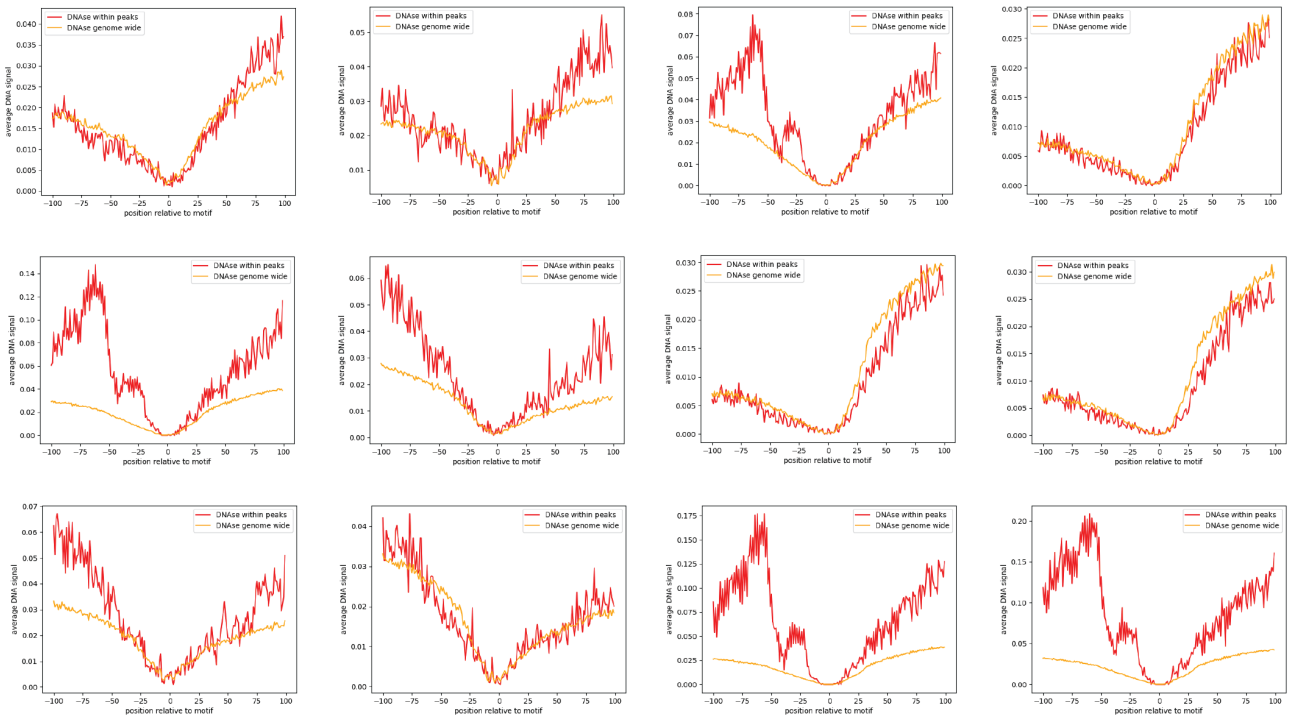
DNAse within peaks
DNAse genome wide
average DNA signal
position relative to motif

H

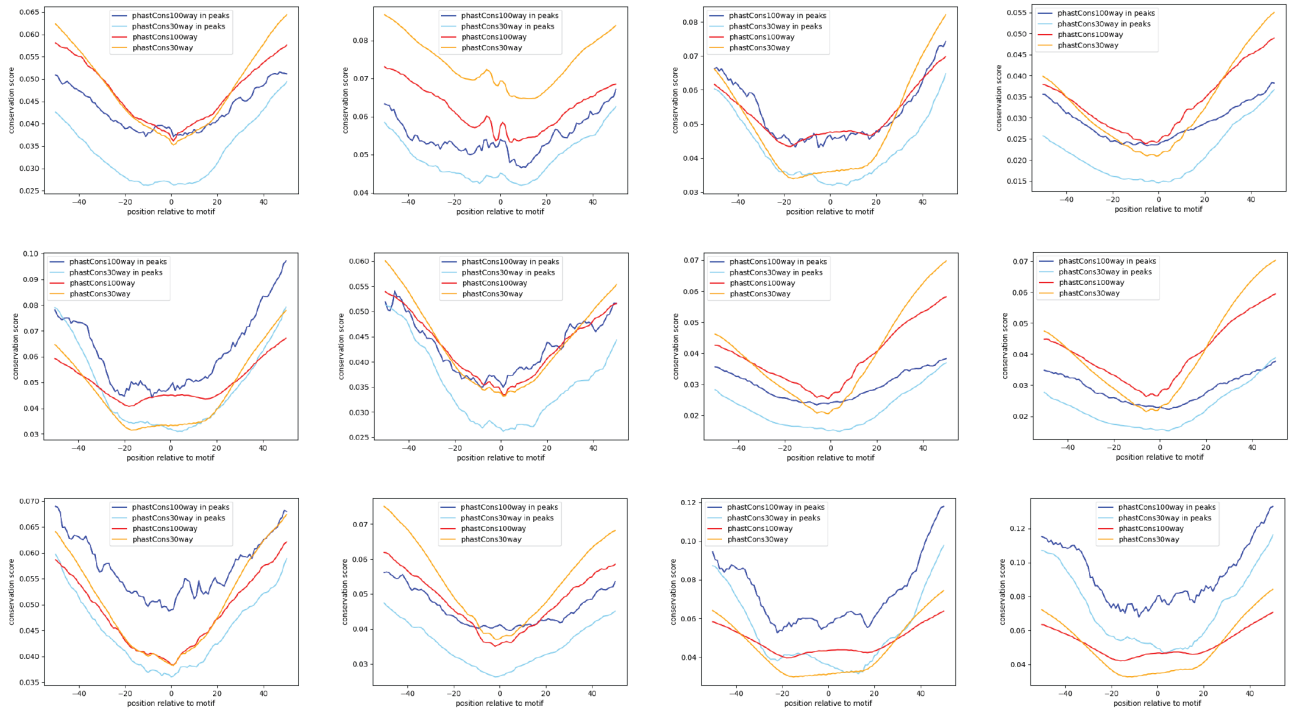
phastCons100way in peaks
phastCons30way in peaks
phastCons100way
phastCons30way
conservation score
position relative to motif

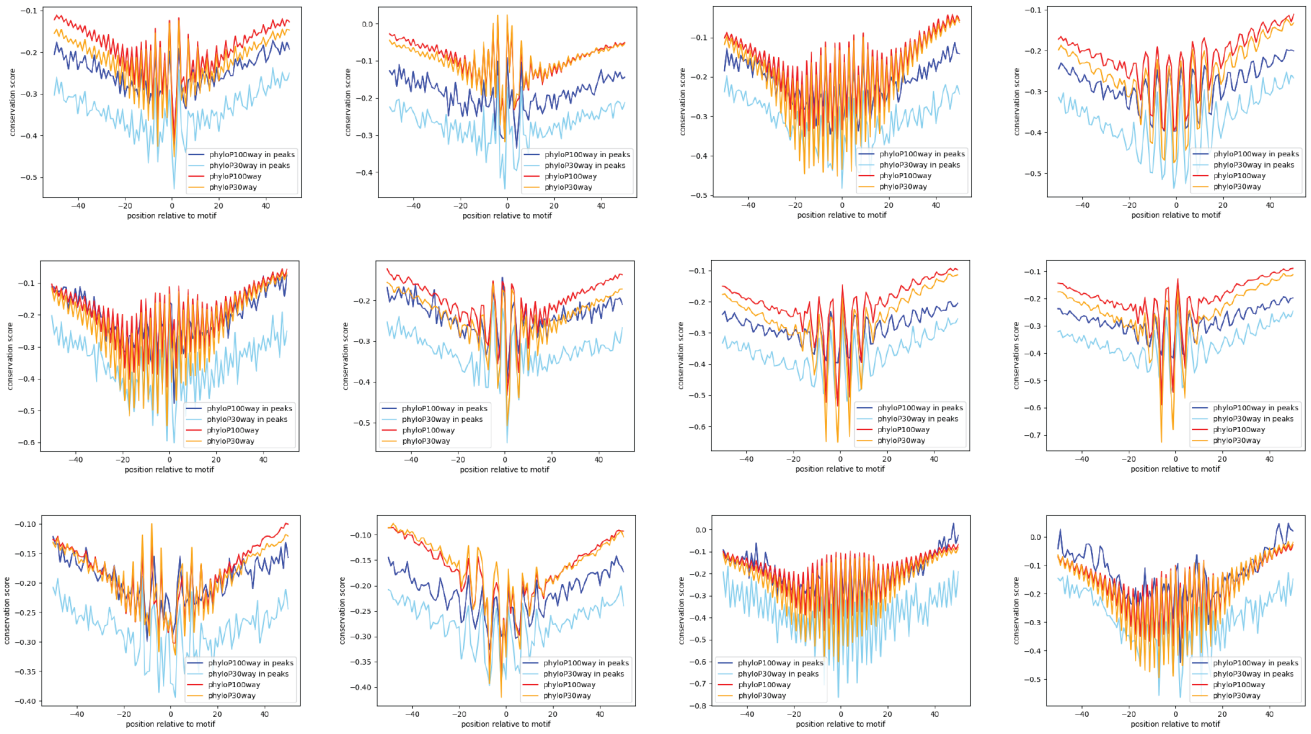

Supplementary Figure 207: Properties and genomic distribution of motifs identified for the PRDM1 transcription factor in HEK293 (accession Hughes GR models).

TF-MoDisCO pattern_0 n=5787, CWM

pattern_0, n=5787; subpattern_0, ns=1094

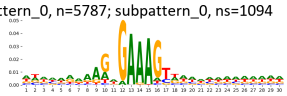

pattern_0, n=5787; subpattern_1, ns=736

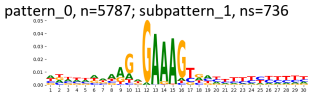

pattern_0, n=5787; subpattern_10, ns=165

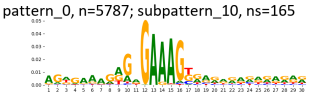

pattern_0, n=5787; subpattern_11, ns=148

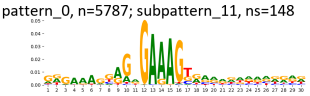

pattern_0, n=5787; subpattern_12, ns=131

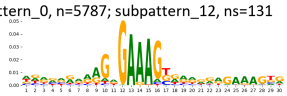

pattern_0, n=5787; subpattern_13, ns=61

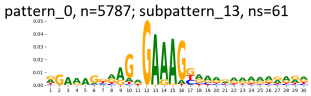

pattern_0, n=5787; subpattern_2, ns=666

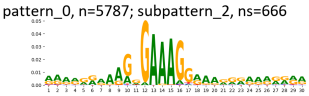

pattern_0, n=5787; subpattern_3, ns=647

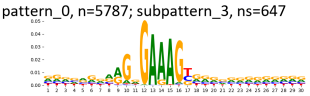

pattern_0, n=5787; subpattern_4, ns=579

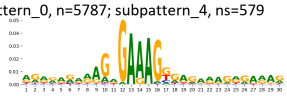

pattern_0, n=5787; subpattern_5, ns=413

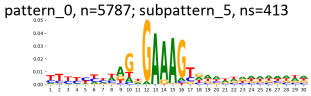

pattern_0, n=5787; subpattern_6, ns=335

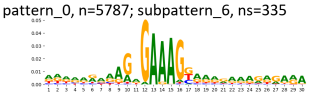

pattern_0, n=5787; subpattern_7, ns=321

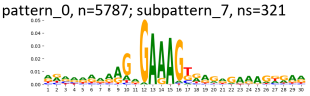

pattern_0, n=5787; subpattern_8, ns=271

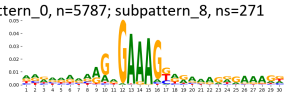

pattern_0, n=5787; subpattern_9, ns=220

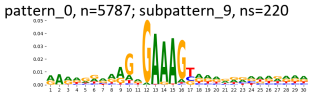

TF-MoDisCO pattern_0 n=5787, PWM

pattern_0, n=5787; subpattern_0, ns=1094

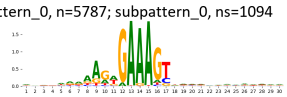

pattern_0, n=5787; subpattern_1, ns=736

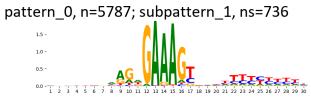

pattern_0, n=5787; subpattern_10, ns=165

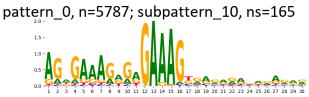

pattern_0, n=5787; subpattern_11, ns=148

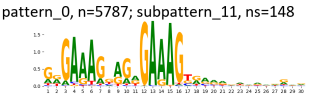

pattern_0, n=5787; subpattern_12, ns=131

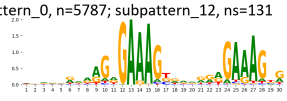

pattern_0, n=5787; subpattern_13, ns=61

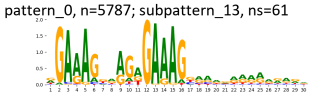

pattern_0, n=5787; subpattern_2, ns=666

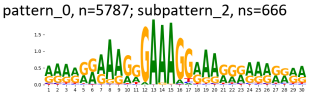

pattern_0, n=5787; subpattern_3, ns=647

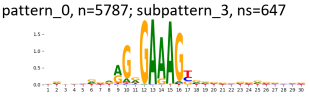

pattern_0, n=5787; subpattern_4, ns=579

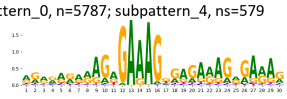

pattern_0, n=5787; subpattern_5, ns=413

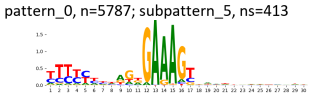

pattern_0, n=5787; subpattern_6, ns=335

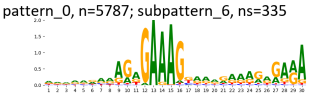

pattern_0, n=5787; subpattern_7, ns=321

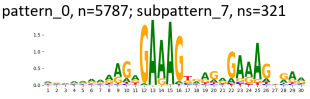

pattern_0, n=5787; subpattern_8, ns=271

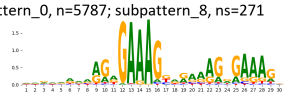

pattern_0, n=5787; subpattern_9, ns=220

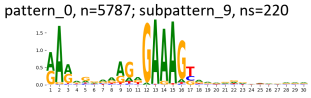

TF-MoDisCO pattern_1 n=663, CWM

pattern_1, n=663; subpattern_0, ns=163

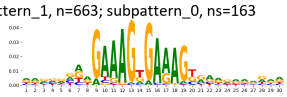

pattern_1, n=663; subpattern_1, ns=129

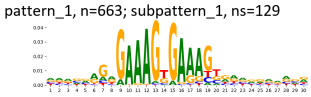

pattern_1, n=663; subpattern_2, ns=120

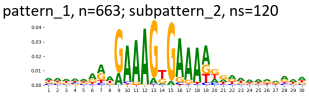

pattern_1, n=663; subpattern_3, ns=62

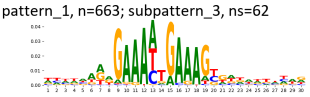

pattern_1, n=663; subpattern_4, ns=61

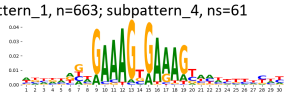

pattern_1, n=663; subpattern_5, ns=51

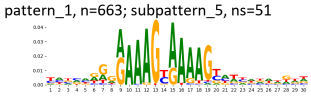

pattern_1, n=663; subpattern_6, ns=49

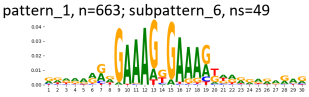

pattern_1, n=663; subpattern_7, ns=28

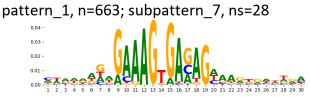

TF-MoDisCO pattern_1 n=663, PWM

pattern_1, n=663; subpattern_0, ns=163

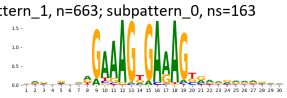

pattern_1, n=663; subpattern_1, ns=129

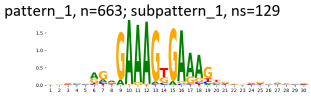

pattern_1, n=663; subpattern_2, ns=120

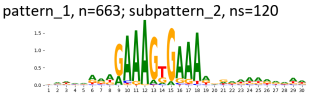

pattern_1, n=663; subpattern_3, ns=62

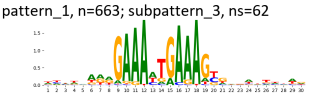

pattern_1, n=663; subpattern_4, ns=61

pattern_1, n=663; subpattern_5, ns=51

pattern_1, n=663; subpattern_6, ns=49

pattern_1, n=663; subpattern_7, ns=28

TF-MoDisCO pattern_10 n=108, CWM

pattern_10, n=108; subpattern_0, ns=32

pattern_10, n=108; subpattern_1, ns=27

pattern_10, n=108; subpattern_2, ns=26

pattern_10, n=108; subpattern_3, ns=23

TF-MoDisCO pattern_10 n=108, PWM

pattern_10, n=108; subpattern_0, ns=32

pattern_10, n=108; subpattern_1, ns=27

pattern_10, n=108; subpattern_2, ns=26

pattern_10, n=108; subpattern_3, ns=23

TF-MoDisCO pattern_11 n=94, CWM

pattern_11, n=94; subpattern_0, ns=31

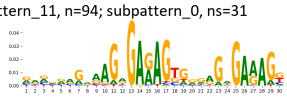

pattern_11, n=94; subpattern_1, ns=29

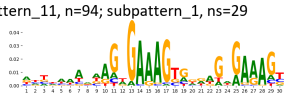

pattern_11, n=94; subpattern_2, ns=27

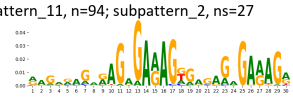

pattern_11, n=94; subpattern_3, ns=7

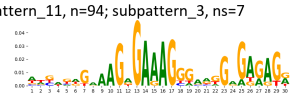

TF-MoDisCO pattern_11 n=94, PWM

pattern_11, n=94; subpattern_0, ns=31

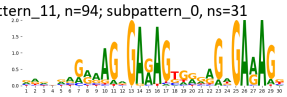

pattern_11, n=94; subpattern_1, ns=29

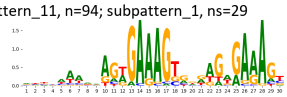

pattern_11, n=94; subpattern_2, ns=27

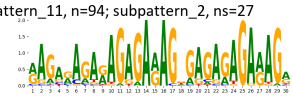

pattern_11, n=94; subpattern_3, ns=7

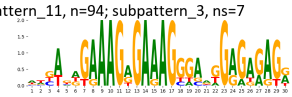

TF-MoDisCO pattern_2 n=447, CWM

pattern_2, n=447; subpattern_0, ns=144

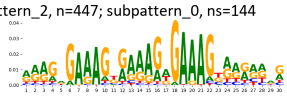

pattern_2, n=447; subpattern_1, ns=131

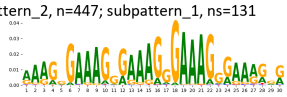

pattern_2, n=447; subpattern_2, ns=111

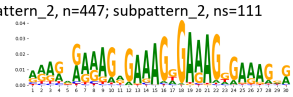

pattern_2, n=447; subpattern_3, ns=38

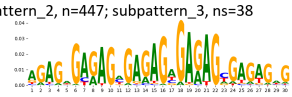

pattern_2, n=447; subpattern_4, ns=23

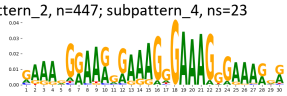

TF-MoDisCO pattern_2 n=447, PWM

pattern_2, n=447; subpattern_0, ns=144

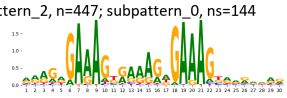

pattern_2, n=447; subpattern_1, ns=131

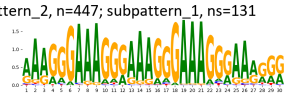

pattern_2, n=447; subpattern_2, ns=111

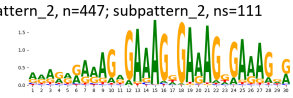

pattern_2, n=447; subpattern_3, ns=38

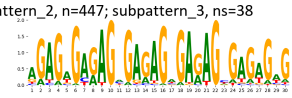

pattern_2, n=447; subpattern_4, ns=23

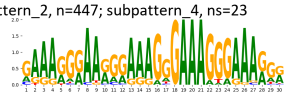

TF-MoDisCO pattern_3 n=414, CWM

pattern_3, n=414; subpattern_0, ns=133

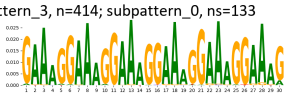

pattern_3, n=414; subpattern_1, ns=104

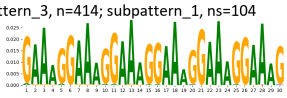

pattern_3, n=414; subpattern_2, ns=92

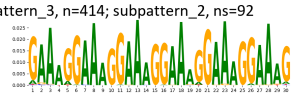

pattern_3, n=414; subpattern_3, ns=47

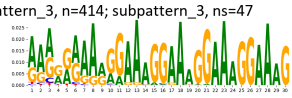

pattern_3, n=414; subpattern_4, ns=38

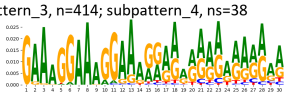

TF-MoDisCO pattern_3 n=414, PWM

pattern_3, n=414; subpattern_0, ns=133

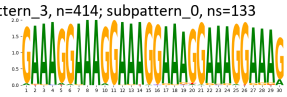

pattern_3, n=414; subpattern_1, ns=104

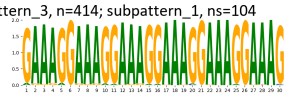

pattern_3, n=414; subpattern_2, ns=92

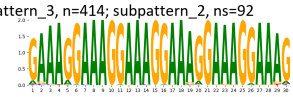

pattern_3, n=414; subpattern_3, ns=47

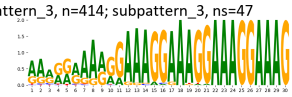

pattern_3, n=414; subpattern_4, ns=38

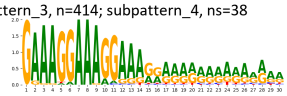

TF-MoDisCO pattern_4 n=264, CWM

pattern_4, n=264; subpattern_0, ns=70

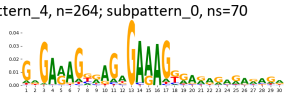

pattern_4, n=264; subpattern_1, ns=64

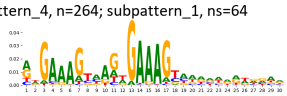

pattern_4, n=264; subpattern_2, ns=60

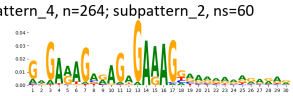

pattern_4, n=264; subpattern_3, ns=60

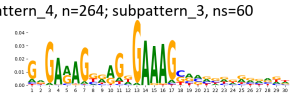

pattern_4, n=264; subpattern_4, ns=8

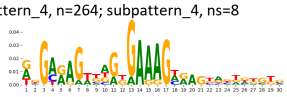

pattern_4, n=264; subpattern_5, ns=2

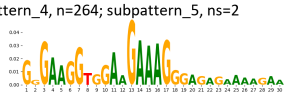

TF-MoDisCO pattern_4 n=264, PWM

pattern_4, n=264; subpattern_0, ns=70

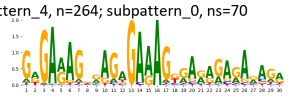

pattern_4, n=264; subpattern_1, ns=64

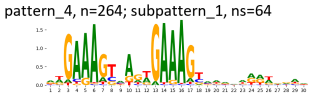

pattern_4, n=264; subpattern_2, ns=60

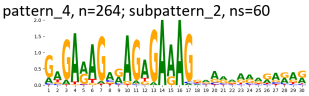

pattern_4, n=264; subpattern_3, ns=60

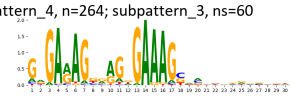

pattern_4, n=264; subpattern_4, ns=8

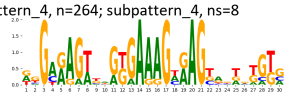

pattern_4, n=264; subpattern_5, ns=2

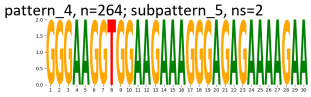

TF-MoDisCO pattern_5 n=197, CWM

pattern_5, n=197; subpattern_0, ns=50

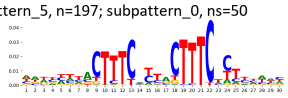

pattern_5, n=197; subpattern_1, ns=40

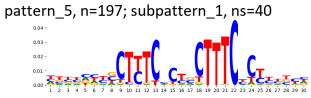

pattern_5, n=197; subpattern_2, ns=35

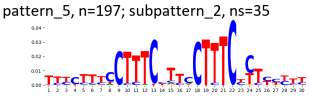

pattern_5, n=197; subpattern_3, ns=29

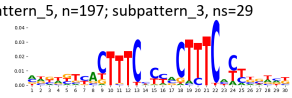

pattern_5, n=197; subpattern_4, ns=24

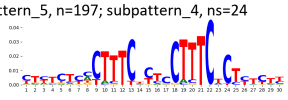

pattern_5, n=197; subpattern_5, ns=13

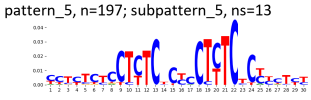

pattern_5, n=197; subpattern_6, ns=6

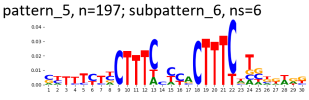

TF-MoDisCO pattern_5 n=197, PWM

pattern_5, n=197; subpattern_0, ns=50

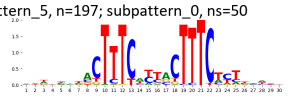

pattern_5, n=197; subpattern_1, ns=40

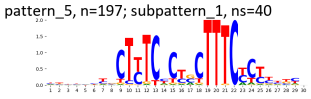

pattern_5, n=197; subpattern_2, ns=35

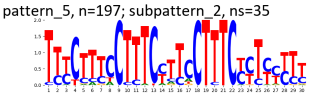

pattern_5, n=197; subpattern_3, ns=29

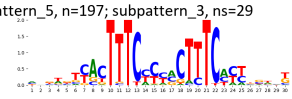

pattern_5, n=197; subpattern_4, ns=24

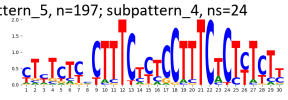

pattern_5, n=197; subpattern_5, ns=13

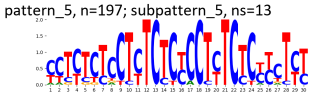

pattern_5, n=197; subpattern_6, ns=6

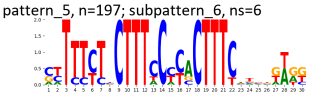

TF-MoDisCO pattern_6 n=189, CWM

pattern_6, n=189; subpattern_0, ns=46

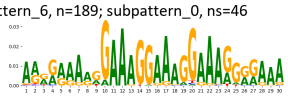

pattern_6, n=189; subpattern_1, ns=41

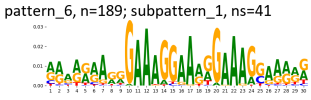

pattern_6, n=189; subpattern_2, ns=38

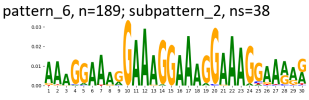

pattern_6, n=189; subpattern_3, ns=29

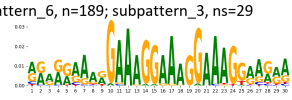

pattern_6, n=189; subpattern_4, ns=22

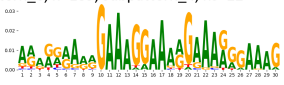

pattern_6, n=189; subpattern_5, ns=13

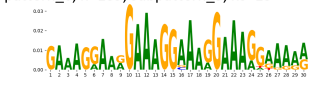

TF-MoDisCO pattern_6 n=189, PWM

pattern_6, n=189; subpattern_0, ns=46

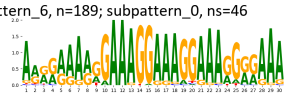

pattern_6, n=189; subpattern_1, ns=41

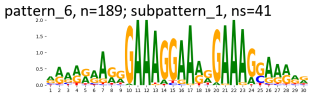

pattern_6, n=189; subpattern_2, ns=38

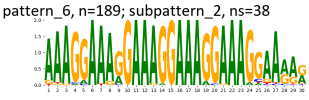

pattern_6, n=189; subpattern_3, ns=29

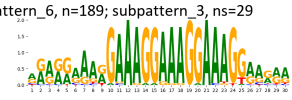

pattern_6, n=189; subpattern_4, ns=22

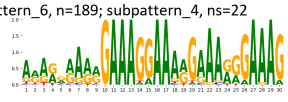

pattern_6, n=189; subpattern_5, ns=13

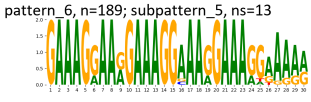

TF-MoDisCO pattern_7 n=176, CWM

pattern_7, n=176; subpattern_0, ns=52

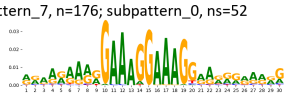

pattern_7, n=176; subpattern_1, ns=36

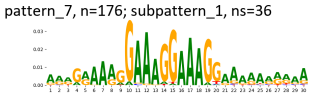

pattern_7, n=176; subpattern_2, ns=36

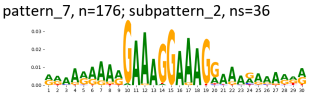

pattern_7, n=176; subpattern_3, ns=23

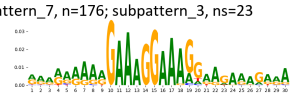

pattern_7, n=176; subpattern_4, ns=13

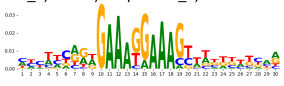

pattern_7, n=176; subpattern_5, ns=10

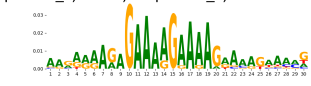

pattern_7, n=176; subpattern_6, ns=4

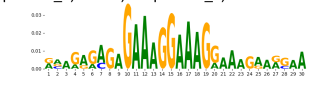

pattern_7, n=176; subpattern_7, ns=2

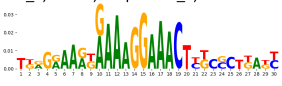

TF-MoDisCO pattern_7 n=176, PWM

pattern_7, n=176; subpattern_0, ns=52

pattern_7, n=176; subpattern_1, ns=36

pattern_7, n=176; subpattern_2, ns=36

pattern_7, n=176; subpattern_3, ns=23

pattern_7, n=176; subpattern_4, ns=13

pattern_7, n=176; subpattern_5, ns=10

pattern_7, n=176; subpattern_6, ns=4

pattern_7, n=176; subpattern_7, ns=2

TF-MoDisCO pattern_8 n=119, CWM

pattern_8, n=119; subpattern_0, ns=42

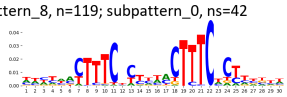

pattern_8, n=119; subpattern_1, ns=33

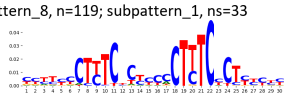

pattern_8, n=119; subpattern_2, ns=23

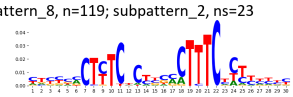

pattern_8, n=119; subpattern_3, ns=21

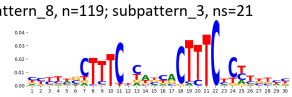

TF-MoDisCO pattern_8 n=119, PWM

pattern_8, n=119; subpattern_0, ns=42

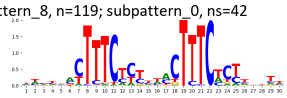

pattern_8, n=119; subpattern_1, ns=33

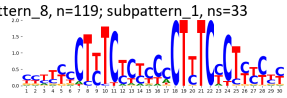

pattern_8, n=119; subpattern_2, ns=23

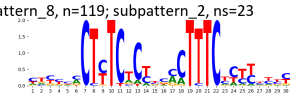

pattern_8, n=119; subpattern_3, ns=21

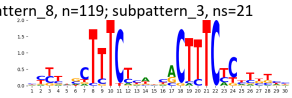

Supplementary Figure 208: TF-MoDisCO subpatterns for the PRDM1 transcription factor in HEK293 (accession Hughes GR models).

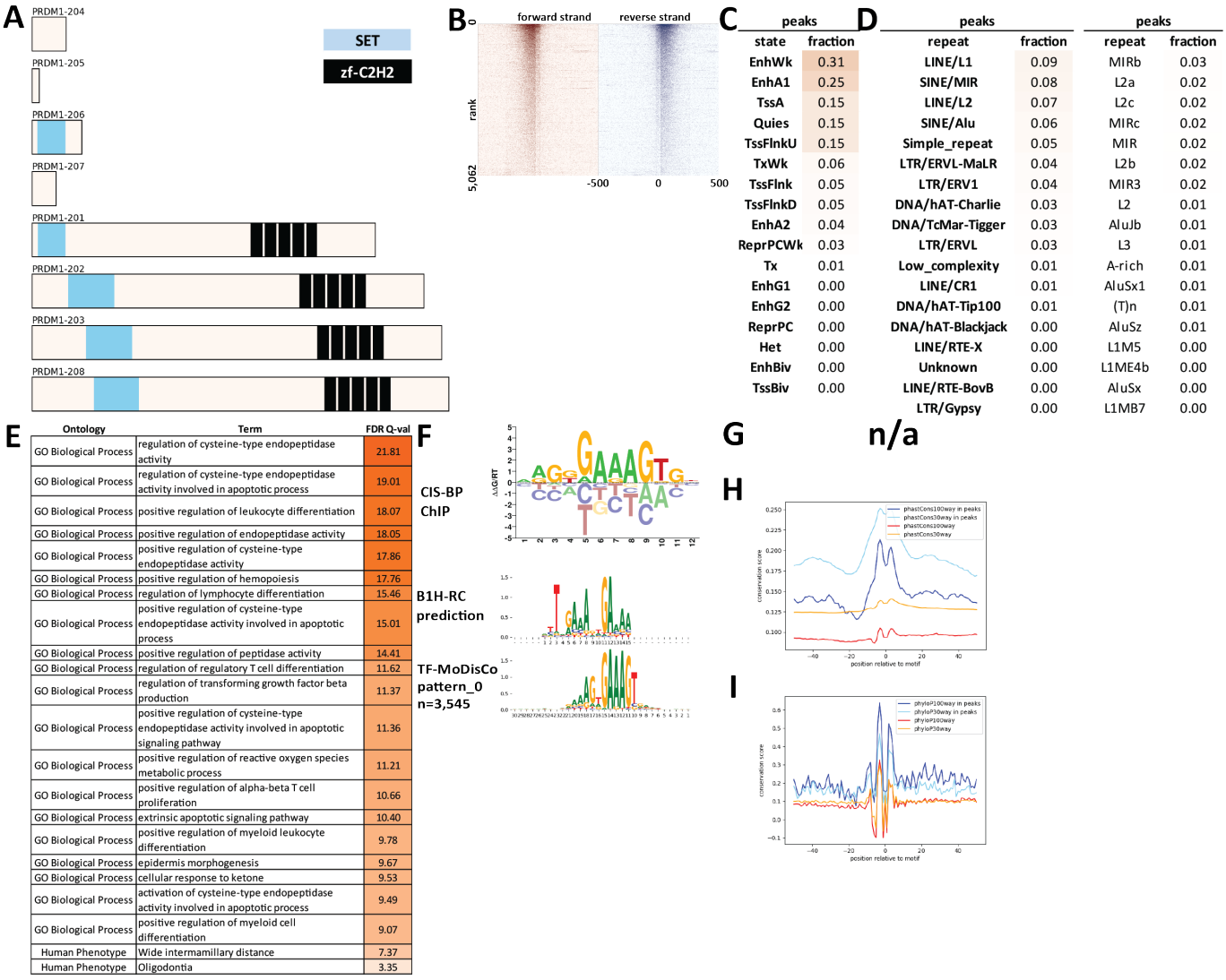

peaks	
state	fraction
EnhWk	0.31
EnhA1	0.25
TssA	0.15
Quies	0.15
TssFlnkU	0.15
TxWk	0.06
TssFlnk	0.05
TssFlnkD	0.05
EnhA2	0.04
ReprPCWk	0.03
Tx	0.01
EnhG1	0.00
EnhG2	0.00
ReprPC	0.00
Het	0.00
EnhBiv	0.00
TssBiv	0.00

peaks		peaks	
repeat	fraction	repeat	fraction
LINE/L1	0.09	MIRb	0.03
SINE/MIR	0.08	L2a	0.02
LINE/L2	0.07	L2c	0.02
SINE/Alu	0.06	MIRc	0.02
Simple_repeat	0.05	MIR	0.02
LTR/ERVL-MaLR	0.04	L2b	0.02
LTR/ERV1	0.04	MIR3	0.02
DNA/hAT-Charlie	0.03	L2	0.01
DNA/TcMar-Tigger	0.03	AluJb	0.01
LTR/ERVL	0.03	L3	0.01
Low_complexity	0.01	A-rich	0.01
LINE/CR1	0.01	AluSx1	0.01
DNA/hAT-Tip100	0.01	(T)n	0.01
DNA/hAT-Blackjack	0.00	AluSz	0.01
LINE/RTE-X	0.00	L1M5	0.00
Unknown	0.00	L1ME4b	0.00
LINE/RTE-BovB	0.00	AluSx	0.00
LTR/Gypsy	0.00	L1MB7	0.00

Ontology	Term	FDR Q-val
GO Biological Process	regulation of cysteine-type endopeptidase activity	21.81
GO Biological Process	regulation of cysteine-type endopeptidase activity involved in apoptotic process	19.01
GO Biological Process	positive regulation of leukocyte differentiation	18.07
GO Biological Process	positive regulation of endopeptidase activity	18.05
GO Biological Process	positive regulation of cysteine-type endopeptidase activity	17.86
GO Biological Process	positive regulation of hemopoiesis	17.76
GO Biological Process	regulation of lymphocyte differentiation	15.46
GO Biological Process	positive regulation of cysteine-type endopeptidase activity involved in apoptotic process	15.01
GO Biological Process	positive regulation of peptidase activity	14.41
GO Biological Process	regulation of regulatory T cell differentiation	11.62
GO Biological Process	regulation of transforming growth factor beta production	11.37
GO Biological Process	positive regulation of cysteine-type endopeptidase activity involved in apoptotic signaling pathway	11.36
GO Biological Process	positive regulation of reactive oxygen species metabolic process	11.21
GO Biological Process	positive regulation of alpha-beta T cell proliferation	10.66
GO Biological Process	extrinsic apoptotic signaling pathway	10.40
GO Biological Process	positive regulation of myeloid leukocyte differentiation	9.78
GO Biological Process	epidermis morphogenesis	9.67
GO Biological Process	cellular response to ketone	9.53
GO Biological Process	activation of cysteine-type endopeptidase activity involved in apoptotic process	9.49
GO Biological Process	positive regulation of myeloid cell differentiation	9.07
Human Phenotype	Wide intermamillary distance	7.37
Human Phenotype	Oligodontia	3.35

Supplementary Figure 209: Properties and genomic distribution of motifs identified for the PRDM1 transcription factor in HeLa-S3 (accession ENCSR000ECY).

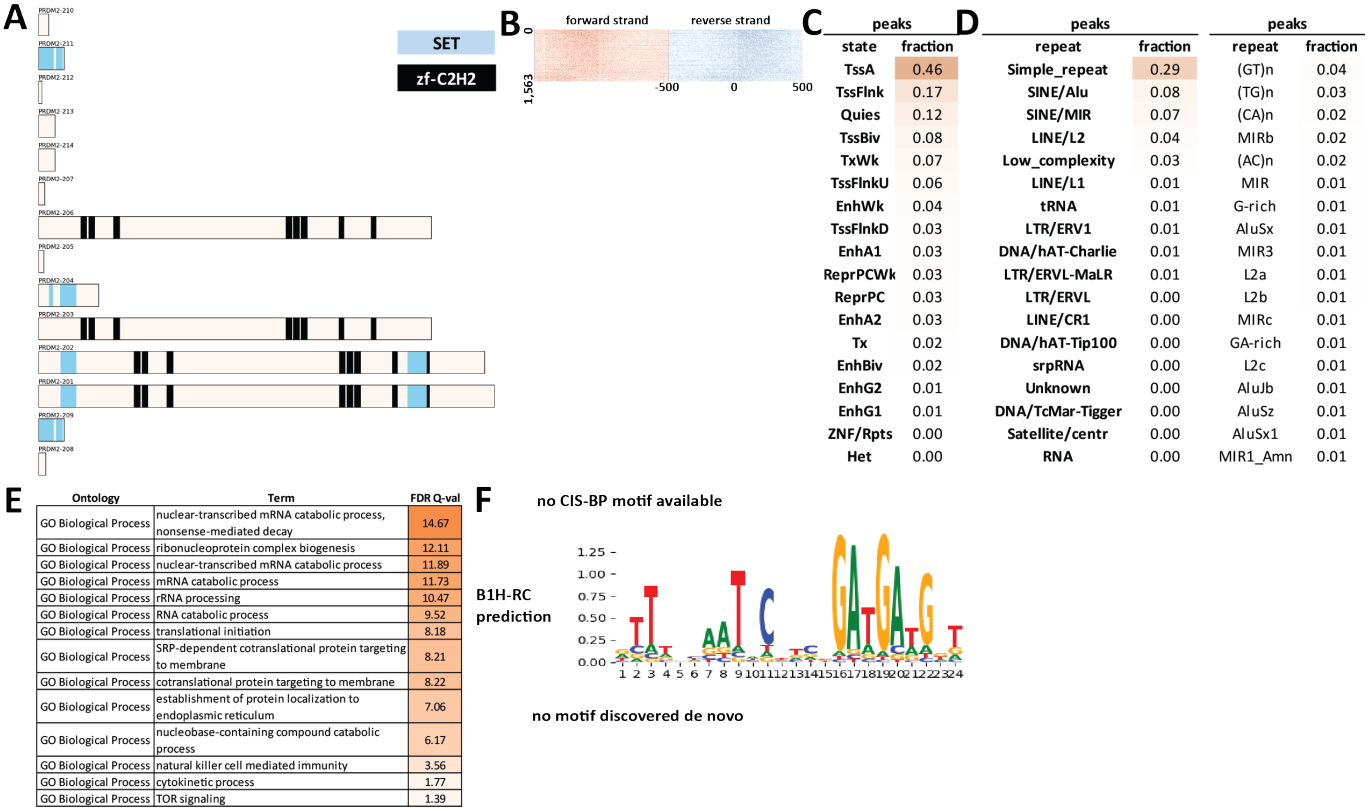

Supplementary Figure 210: Properties and genomic distribution of motifs identified for the PRDM2 transcription factor in HEK293 (accession ENCSR714LYA).

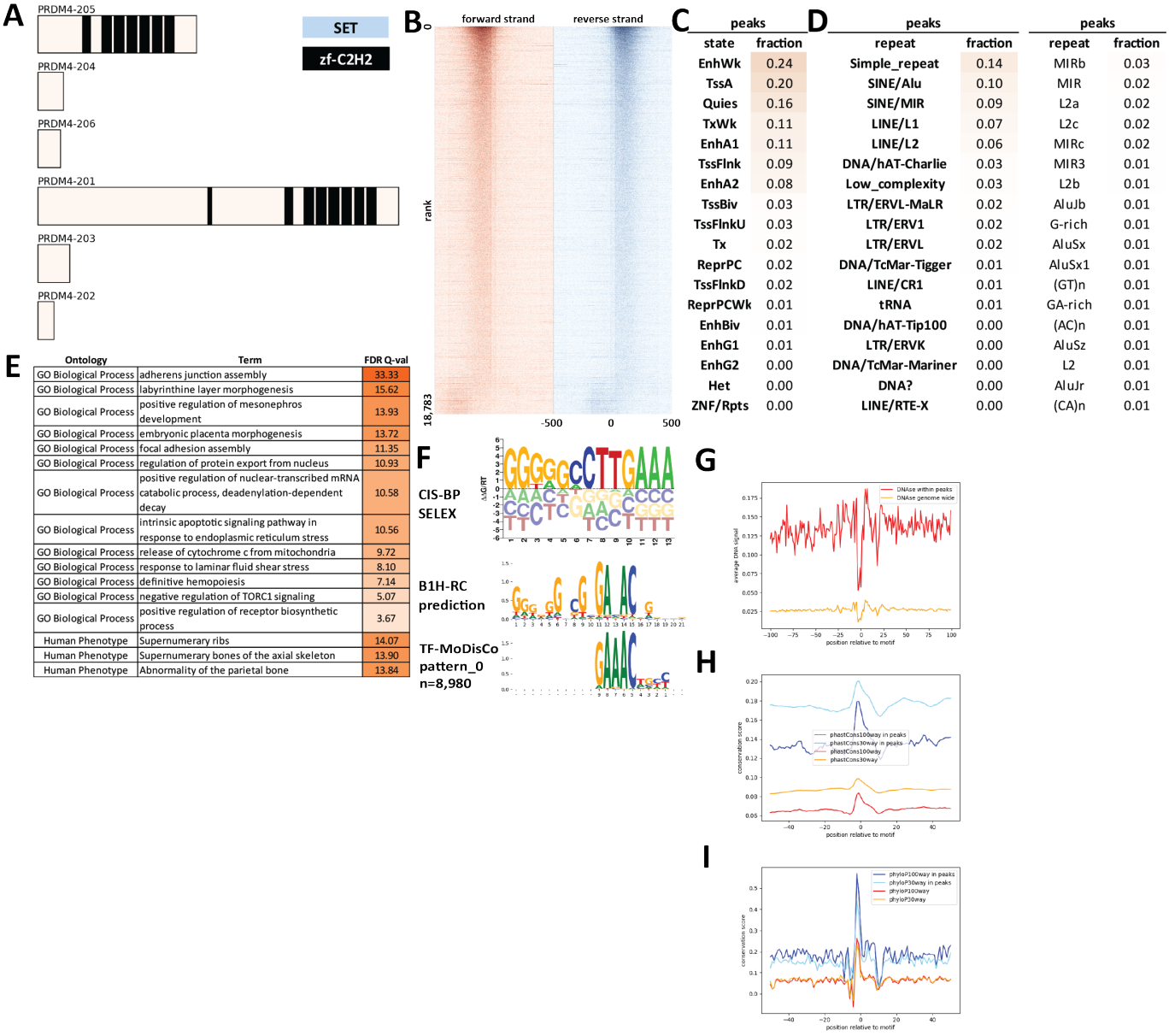

Supplementary Figure 211: Properties and genomic distribution of motifs identified for the PRDM4 transcription factor in HEK293 (accession ENCSR443MVV).

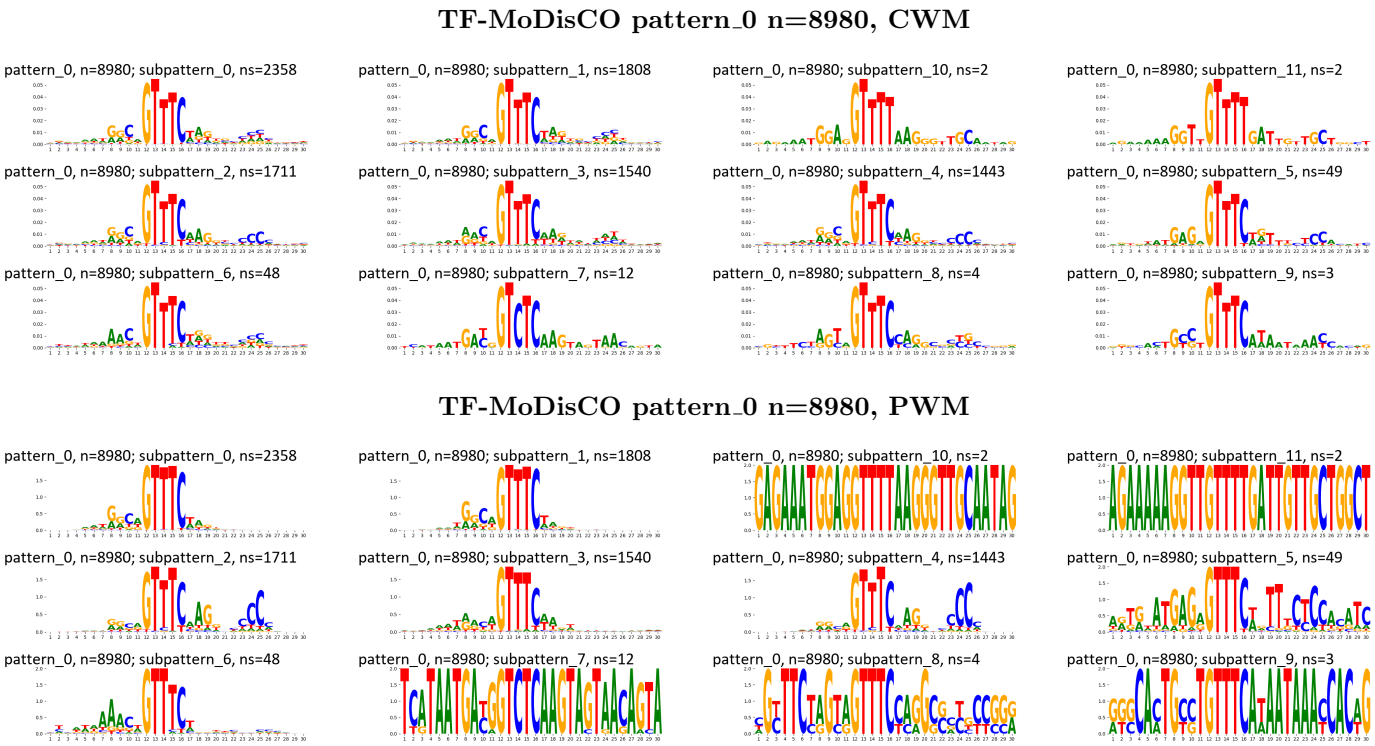

Supplementary Figure 212: TF-MoDisCO subpatterns for the PRDM4 transcription factor in HEK293 (accession ENCSR443MVV).

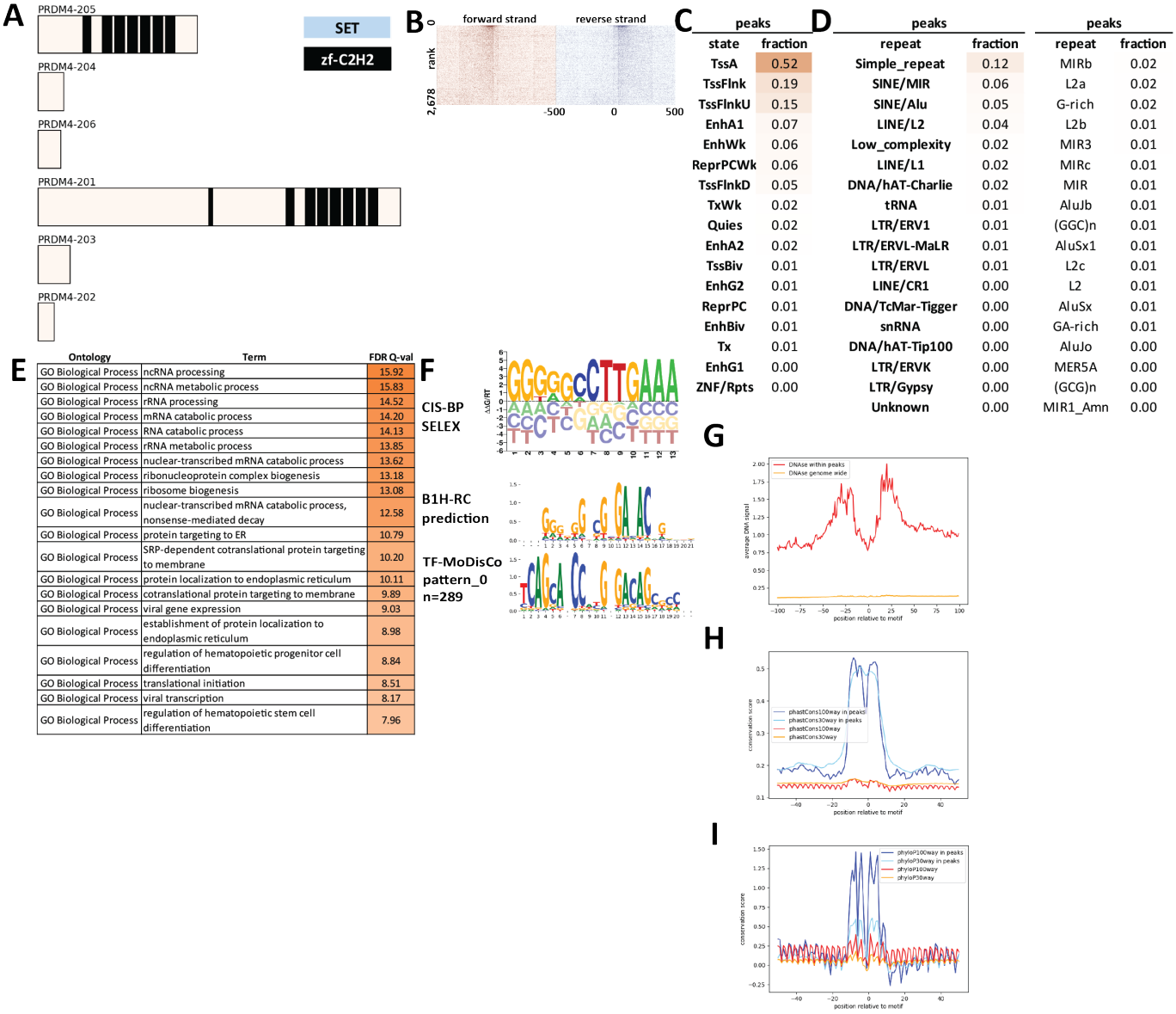

Supplementary Figure 213: Properties and genomic distribution of motifs identified for the PRDM4 transcription factor in HepG2 (accession ENCSR130NZQ).

TF-MoDisCO pattern_0 n=289, CWM

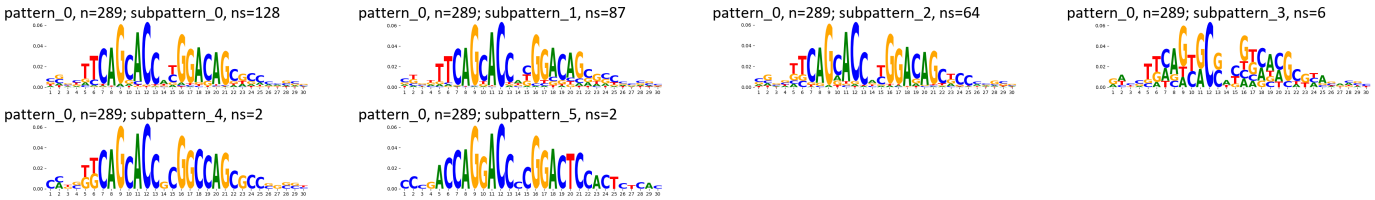

TF-MoDisCO pattern_0 n=289, PWM

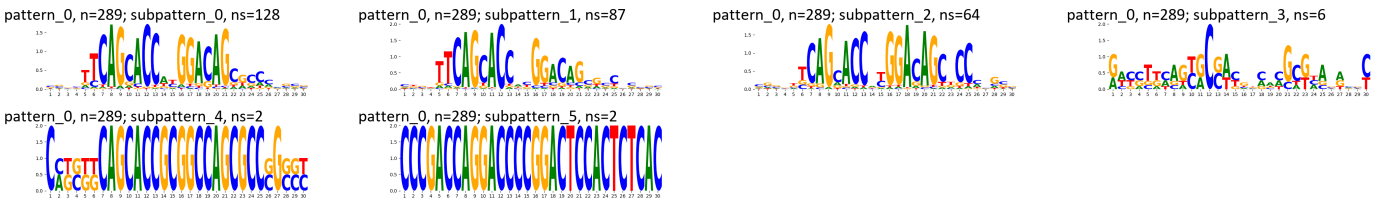

Supplementary Figure 214: TF-MoDisCO subpatterns for the PRDM4 transcription factor in HepG2 (accession ENCSR130NZQ).

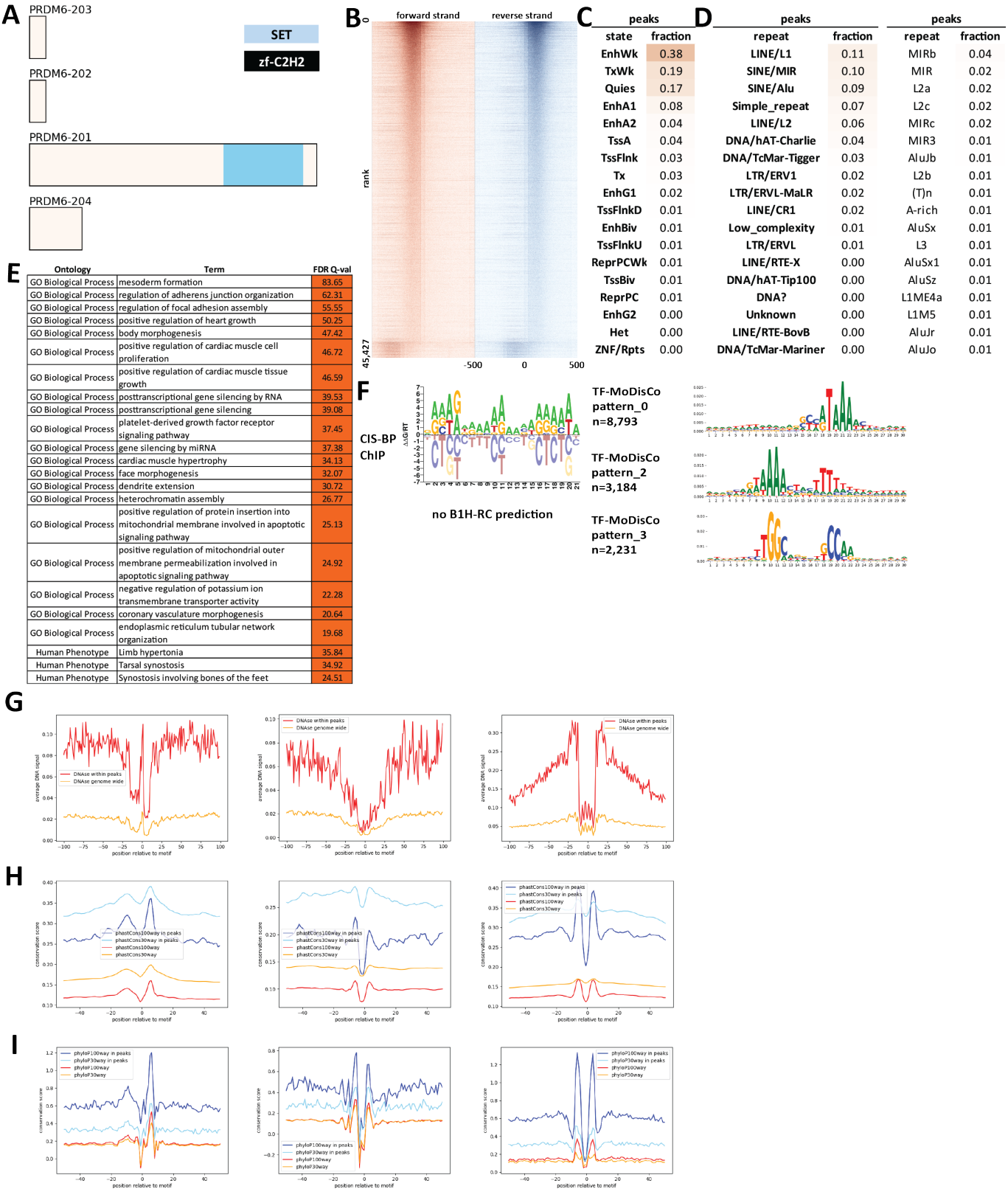

Supplementary Figure 215: Properties and genomic distribution of motifs identified for the PRDM6 transcription factor in HEK293 (accession ENCSR892QHR).

TF-MoDisCO pattern_0 n=8793, CWM

pattern_0, n=8793; subpattern_0, ns=1941

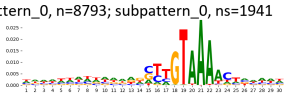

pattern_0, n=8793; subpattern_1, ns=1573

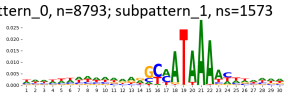

pattern_0, n=8793; subpattern_2, ns=1561

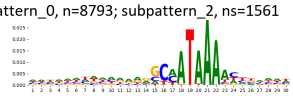

pattern_0, n=8793; subpattern_3, ns=936

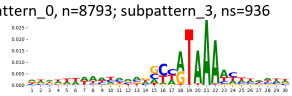

pattern_0, n=8793; subpattern_4, ns=882

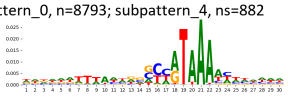

pattern_0, n=8793; subpattern_5, ns=837

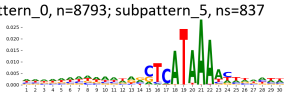

pattern_0, n=8793; subpattern_6, ns=743

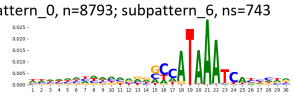

pattern_0, n=8793; subpattern_7, ns=320

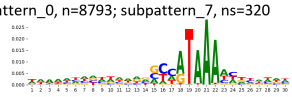

TF-MoDisCO pattern_0 n=8793, PWM

pattern_0, n=8793; subpattern_0, ns=1941

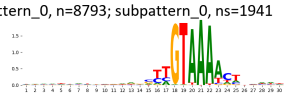

pattern_0, n=8793; subpattern_1, ns=1573

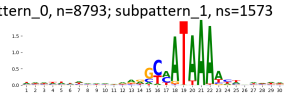

pattern_0, n=8793; subpattern_2, ns=1561

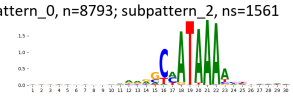

pattern_0, n=8793; subpattern_3, ns=936

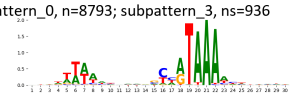

pattern_0, n=8793; subpattern_4, ns=882

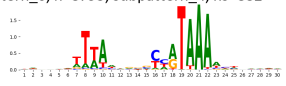

pattern_0, n=8793; subpattern_5, ns=837

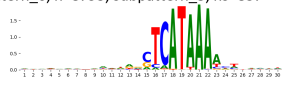

pattern_0, n=8793; subpattern_6, ns=743

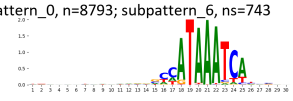

pattern_0, n=8793; subpattern_7, ns=320

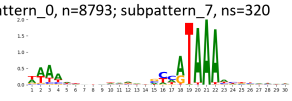

TF-MoDisCO pattern_2 n=3184, CWM

pattern_2, n=3184; subpattern_0, ns=745

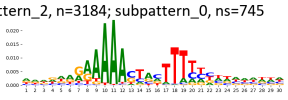

pattern_2, n=3184; subpattern_1, ns=593

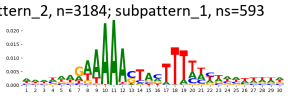

pattern_2, n=3184; subpattern_2, ns=518

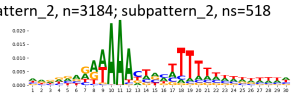

pattern_2, n=3184; subpattern_3, ns=428

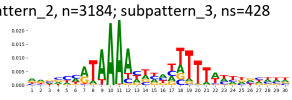

pattern_2, n=3184; subpattern_4, ns=334

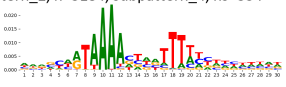

pattern_2, n=3184; subpattern_5, ns=206

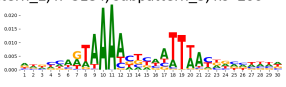

pattern_2, n=3184; subpattern_6, ns=202

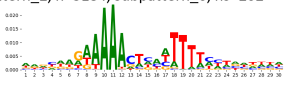

pattern_2, n=3184; subpattern_7, ns=158

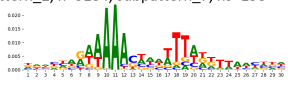

TF-MoDisCO pattern_2 n=3184, PWM

pattern_2, n=3184; subpattern_0, ns=745

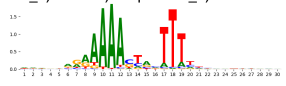

pattern_2, n=3184; subpattern_1, ns=593

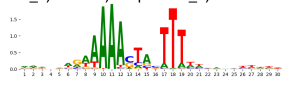

pattern_2, n=3184; subpattern_2, ns=518

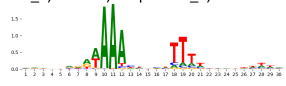

pattern_2, n=3184; subpattern_3, ns=428

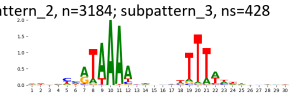

pattern_2, n=3184; subpattern_4, ns=334

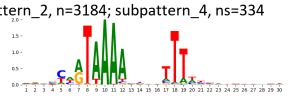

pattern_2, n=3184; subpattern_5, ns=206

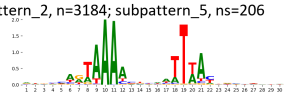

pattern_2, n=3184; subpattern_6, ns=202

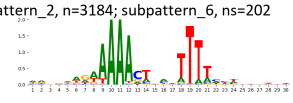

pattern_2, n=3184; subpattern_7, ns=158

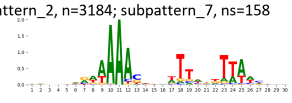

TF-MoDisCO pattern_3 n=2231, CWM

pattern_3, n=2231; subpattern_0, ns=520

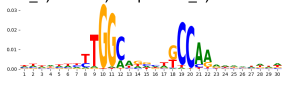

pattern_3, n=2231; subpattern_1, ns=403

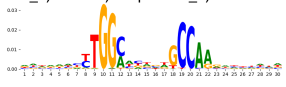

pattern_3, n=2231; subpattern_2, ns=297

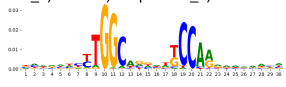

pattern_3, n=2231; subpattern_3, ns=278

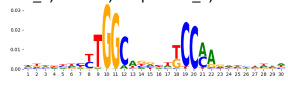

pattern_3, n=2231; subpattern_4, ns=241

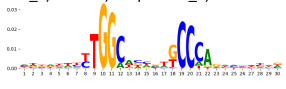

pattern_3, n=2231; subpattern_5, ns=228

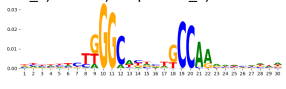

pattern_3, n=2231; subpattern_6, ns=187

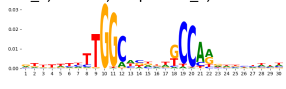

pattern_3, n=2231; subpattern_7, ns=75

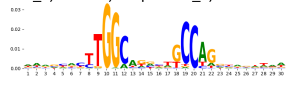

pattern_3, n=2231; subpattern_8, ns=2

TF-MoDisCO pattern_3 n=2231, PWM

pattern_3, n=2231; subpattern_0, ns=520

pattern_3, n=2231; subpattern_1, ns=403

pattern_3, n=2231; subpattern_2, ns=297

pattern_3, n=2231; subpattern_3, ns=278

pattern_3, n=2231; subpattern_4, ns=241

pattern_3, n=2231; subpattern_5, ns=228

pattern_3, n=2231; subpattern_6, ns=187

pattern_3, n=2231; subpattern_7, ns=75

pattern_3, n=2231; subpattern_8, ns=2

Supplementary Figure 216: TF-MoDisCO subpatterns for the PRDM6 transcription factor in HEK293 (accession ENCSR892QHR).

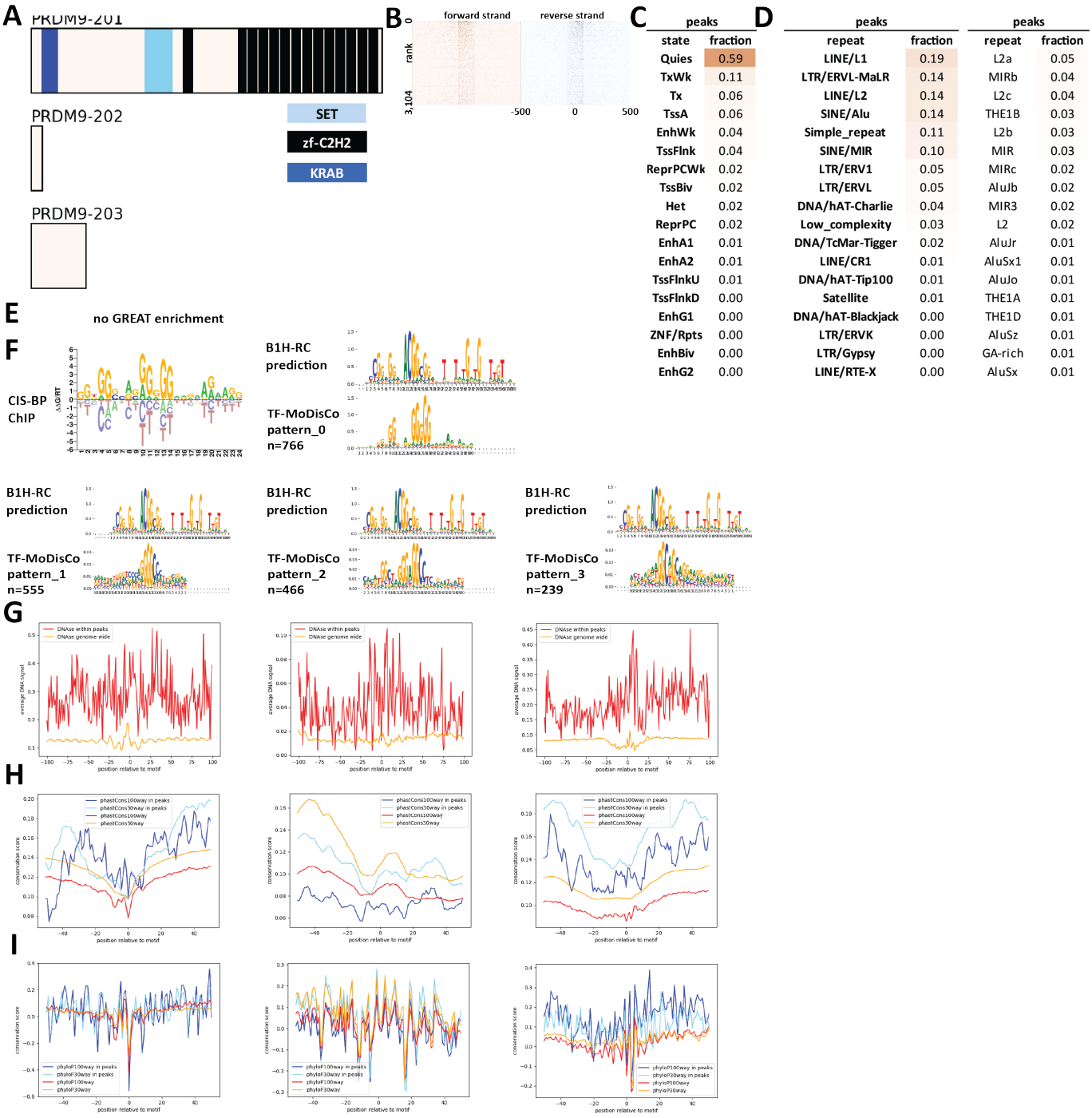

Supplementary Figure 217: Properties and genomic distribution of motifs identified for the PRDM9 transcription factor in HEK293 (accession ChipExo models).

TF-MoDisCO pattern_0 n=766, CWM

pattern_0, n=766; subpattern_0, ns=177

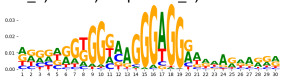

pattern_0, n=766; subpattern_1, ns=159

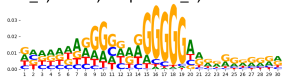

pattern_0, n=766; subpattern_2, ns=118

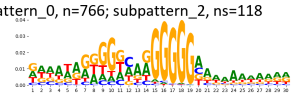

pattern_0, n=766; subpattern_3, ns=101

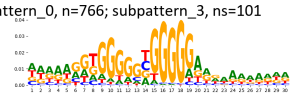

pattern_0, n=766; subpattern_4, ns=100

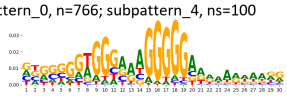

pattern_0, n=766; subpattern_5, ns=90

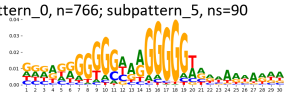

pattern_0, n=766; subpattern_6, ns=21

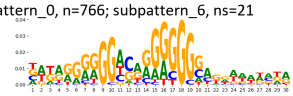

TF-MoDisCO pattern_0 n=766, PWM

pattern_0, n=766; subpattern_0, ns=177

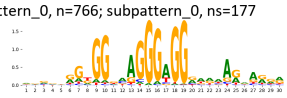

pattern_0, n=766; subpattern_1, ns=159

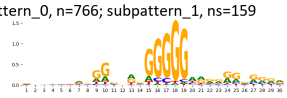

pattern_0, n=766; subpattern_2, ns=118

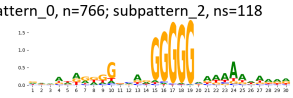

pattern_0, n=766; subpattern_3, ns=101

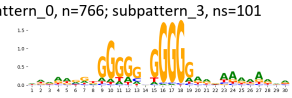

pattern_0, n=766; subpattern_4, ns=100

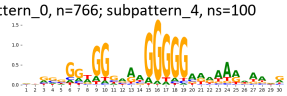

pattern_0, n=766; subpattern_5, ns=90

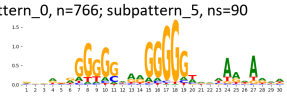

pattern_0, n=766; subpattern_6, ns=21

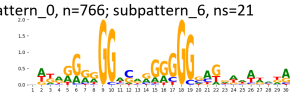

TF-MoDisCO pattern_1 n=555, CWM

pattern_1, n=555; subpattern_0, ns=116

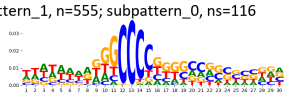

pattern_1, n=555; subpattern_1, ns=114

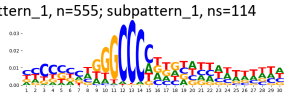

pattern_1, n=555; subpattern_2, ns=93

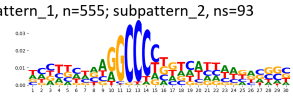

pattern_1, n=555; subpattern_3, ns=76

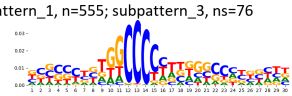

pattern_1, n=555; subpattern_4, ns=57

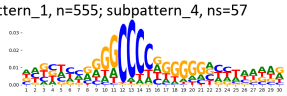

pattern_1, n=555; subpattern_5, ns=53

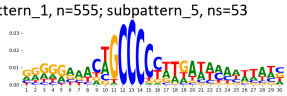

pattern_1, n=555; subpattern_6, ns=46

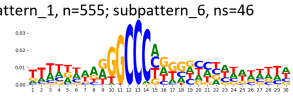

TF-MoDisCO pattern_1 n=555, PWM

pattern_1, n=555; subpattern_0, ns=116

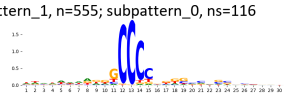

pattern_1, n=555; subpattern_1, ns=114

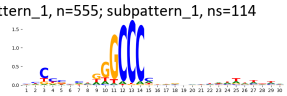

pattern_1, n=555; subpattern_2, ns=93

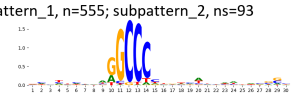

pattern_1, n=555; subpattern_3, ns=76

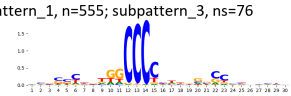

pattern_1, n=555; subpattern_4, ns=57

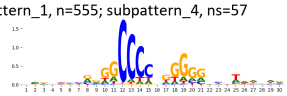

pattern_1, n=555; subpattern_5, ns=53

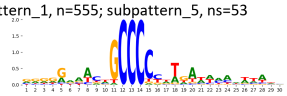

pattern_1, n=555; subpattern_6, ns=46

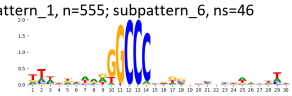

TF-MoDisCO pattern_2 n=466, CWM

pattern_2, n=466; subpattern_0, ns=100

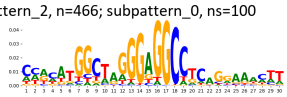

pattern_2, n=466; subpattern_1, ns=88

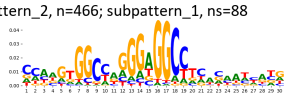

pattern_2, n=466; subpattern_2, ns=79

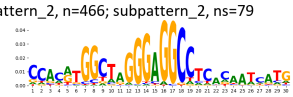

pattern_2, n=466; subpattern_3, ns=54

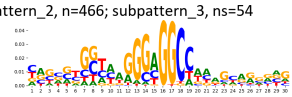

pattern_2, n=466; subpattern_4, ns=51

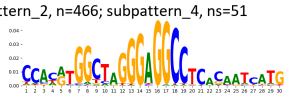

pattern_2, n=466; subpattern_5, ns=47

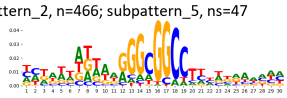

pattern_2, n=466; subpattern_6, ns=47

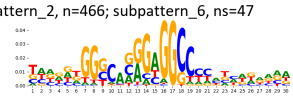

TF-MoDisCO pattern_2 n=466, PWM

pattern_2, n=466; subpattern_0, ns=100

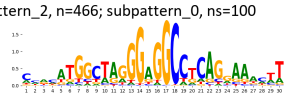

pattern_2, n=466; subpattern_1, ns=88

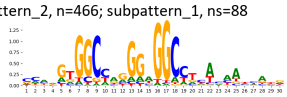

pattern_2, n=466; subpattern_2, ns=79

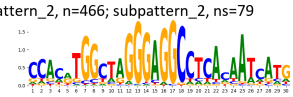

pattern_2, n=466; subpattern_3, ns=54

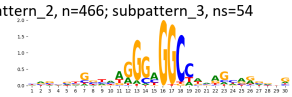

pattern_2, n=466; subpattern_4, ns=51

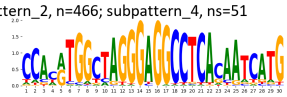

pattern_2, n=466; subpattern_5, ns=47

pattern_2, n=466; subpattern_6, ns=47

TF-MoDisCO pattern_3 n=239, CWM

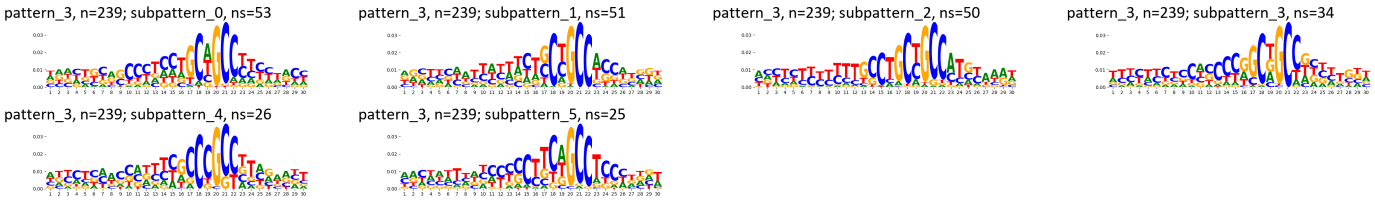

TF-MoDisCO pattern_3 n=239, PWM

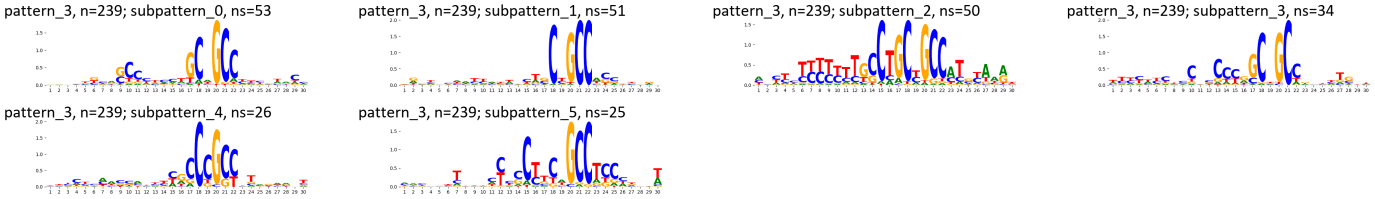

Supplementary Figure 218: TF-MoDisCO subpatterns for the PRDM9 transcription factor in HEK293 (accession ChipExo models).

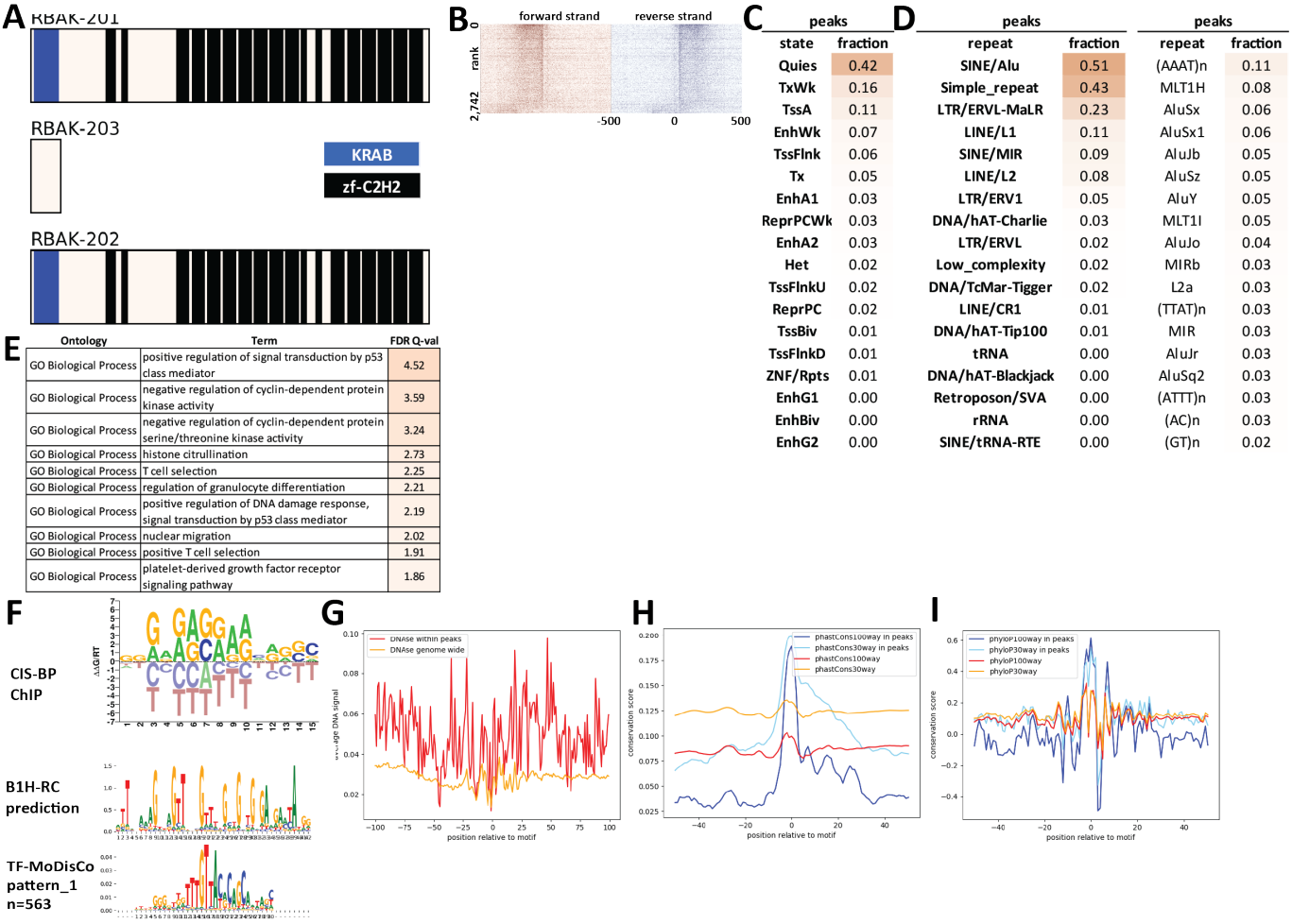

Supplementary Figure 219: Properties and genomic distribution of motifs identified for the RBAK transcription factor in HEK293 (accession ENCSR441UBA).

TF-MoDisCO pattern_1 n=563, CWM

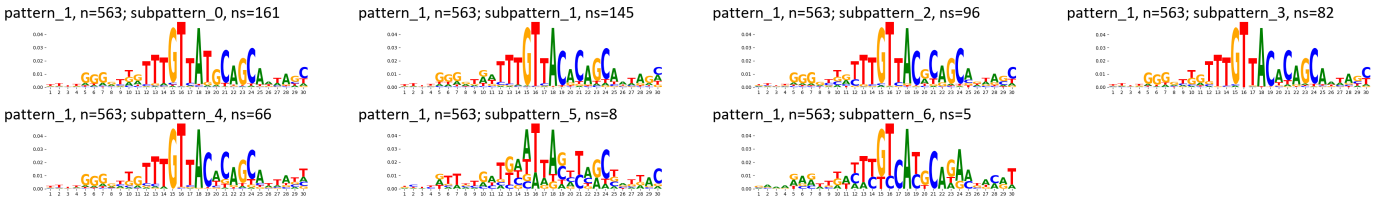

TF-MoDisCO pattern_1 n=563, PWM

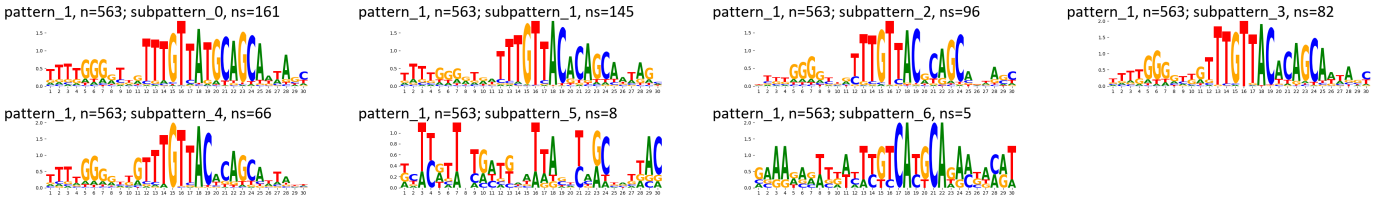

Supplementary Figure 220: TF-MoDisCO subpatterns for the RBAK transcription factor in HEK293 (accession ENCSR441UBA).

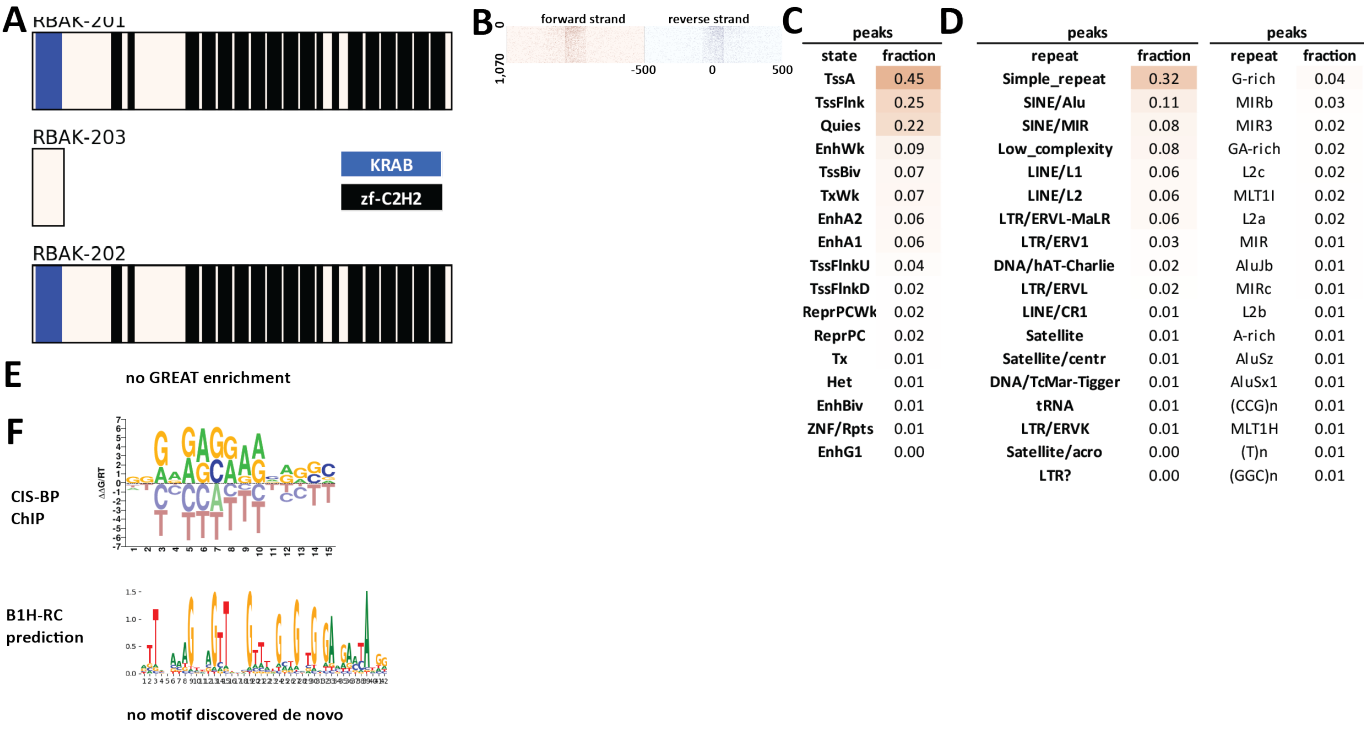

peaks	
state	fraction
TssA	0.45
TssFlnk	0.25
Quies	0.22
EnhWk	0.09
TssBiv	0.07
TxWk	0.07
EnhA2	0.06
EnhA1	0.06
TssFlnkU	0.04
TssFlnkD	0.02
ReprPCWk	0.02
ReprPC	0.02
Tx	0.01
Het	0.01
EnhBiv	0.01
ZNF/Rpts	0.01
EnhG1	0.00

peaks		peaks	
repeat	fraction	repeat	fraction
Simple_repeat	0.32	G-rich	0.04
SINE/Alu	0.11	MIRb	0.03
SINE/MIR	0.08	MIR3	0.02
Low_complexity	0.08	GA-rich	0.02
LINE/L1	0.06	L2c	0.02
LINE/L2	0.06	MLT1I	0.02
LTR/ERVL-MaLR	0.06	L2a	0.02
LTR/ERV1	0.03	MIR	0.01
DNA/hAT-Charlie	0.02	AluJb	0.01
LTR/ERVL	0.02	MIRc	0.01
LINE/CR1	0.01	L2b	0.01
Satellite	0.01	A-rich	0.01
Satellite/centr	0.01	AluSz	0.01
DNA/TcMar-Tigger	0.01	AluSx1	0.01
tRNA	0.01	(CCG)n	0.01
LTR/ERVK	0.01	MLT1H	0.01
Satellite/acro	0.00	(T)n	0.01
LTR?	0.00	(GGC)n	0.01

Supplementary Figure 221: Properties and genomic distribution of motifs identified for the RBAK transcription factor in HEK293 (accession ChipExo models).

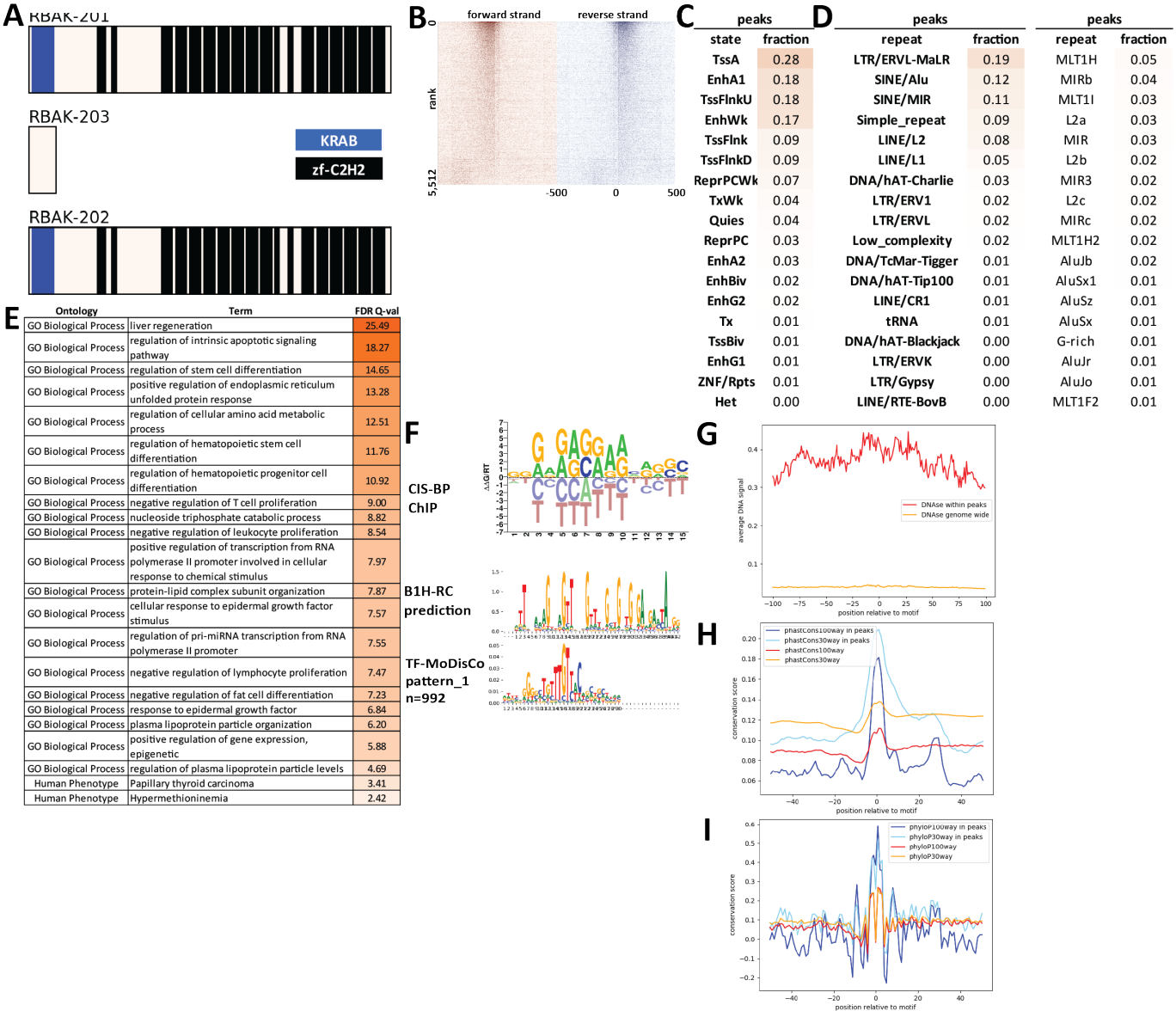

Supplementary Figure 222: Properties and genomic distribution of motifs identified for the RBAK transcription factor in HepG2 (accession ENCSR144NTH).

TF-MoDisCO pattern_1 n=992, CWM

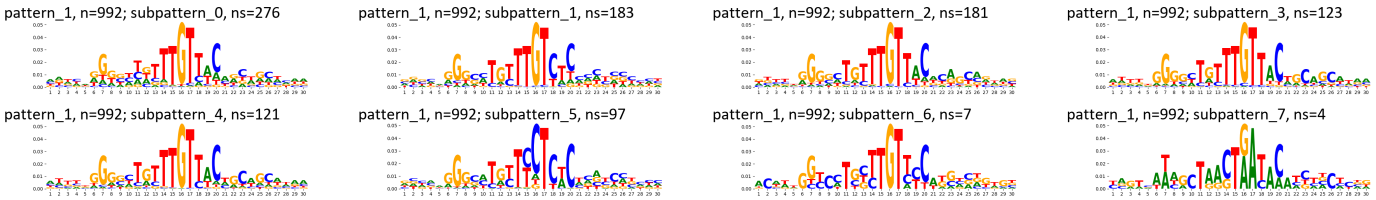

TF-MoDisCO pattern_1 n=992, PWM

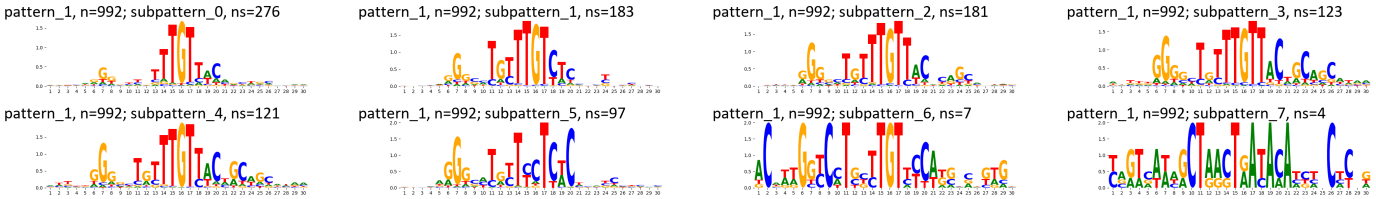

Supplementary Figure 223: TF-MoDisCO subpatterns for the RBAK transcription factor in HepG2 (accession ENCSR144NTH).

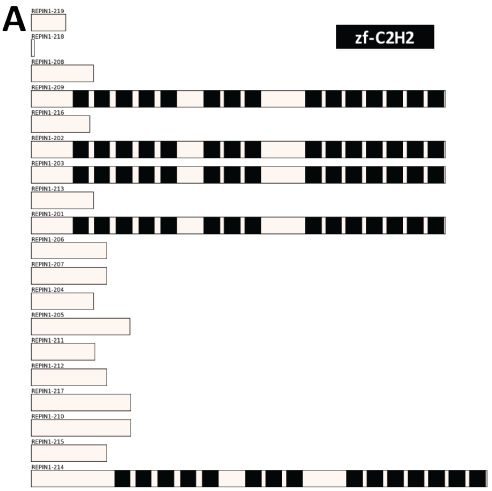

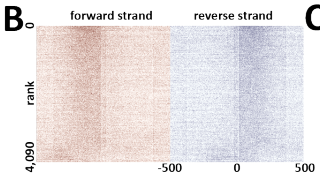

C

peaks	
state	fraction
TssA	0.53
TssFlnk	0.19
Quies	0.10
TxWk	0.07
EnhWk	0.06
TssBiv	0.05
TssFlnkU	0.04
EnhA1	0.04
EnhA2	0.03
TssFlnkD	0.02
ReprPCWk	0.01
Tx	0.01
ReprPC	0.01
EnhBiv	0.01
EnhG1	0.00
Het	0.00
EnhG2	0.00
ZNF/Rpts	0.00

D

peaks		peaks	
repeat	fraction	repeat	fraction
Simple_repeat	0.32	MIR	0.03
SINE/Alu	0.23	AluSx	0.03
SINE/MIR	0.08	AluSx1	0.03
Low_complexity	0.04	MIRb	0.03
LINE/L2	0.04	(AAT)n	0.03
LINE/L1	0.04	G-rich	0.02
tRNA	0.02	AluJb	0.02
DNA/hAT-Charlie	0.01	(GT)n	0.02
LTR/ERV1	0.01	AluSz	0.02
LTR/ERVL-MaLR	0.01	L2a	0.02
snRNA	0.01	AluY	0.02
LTR/ERVL	0.01	AluSq2	0.02
DNA/TcMar-Tigger	0.01	AluJr	0.01
LINE/CR1	0.00	(TTA)n	0.01
DNA/hAT-Tip100	0.00	GA-rich	0.01
Retroposon/SVA	0.00	(AC)n	0.01
LTR/ERVK	0.00	(TG)n	0.01
LINE/RTE-BovB	0.00	AluJo	0.01

E

Ontology	Term	FDR Q-val
GO Biological Process	nuclear-transcribed mRNA catabolic process, nonsense-mediated decay	27.81
GO Biological Process	ribonucleoprotein complex biogenesis	23.52
GO Biological Process	nuclear-transcribed mRNA catabolic process	22.45
GO Biological Process	ncRNA metabolic process	22.21
GO Biological Process	ncRNA processing	21.84
GO Biological Process	rRNA metabolic process	21.06
GO Biological Process	rRNA processing	21.03
GO Biological Process	mRNA catabolic process	20.64
GO Biological Process	ribosome biogenesis	19.49
GO Biological Process	RNA catabolic process	17.43
GO Biological Process	cotranslational protein targeting to membrane	17.28
GO Biological Process	SRP-dependent cotranslational protein targeting to membrane	16.98
GO Biological Process	protein localization to endoplasmic reticulum	15.61
GO Biological Process	protein targeting to ER	15.62
GO Biological Process	establishment of protein localization to endoplasmic reticulum	15.40
GO Biological Process	viral gene expression	14.67
GO Biological Process	multi-organism metabolic process	12.15
GO Biological Process	viral transcription	11.96
GO Biological Process	nucleic acid phosphodiester bond hydrolysis	11.58
GO Biological Process	protein targeting to membrane	11.05

F

no CIS-BP motif available

B1H-RC prediction

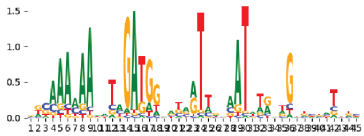

no motif discovered de novo

Supplementary Figure 224: Properties and genomic distribution of motifs identified for the REPIN1 transcription factor in HEK293 (accession ENCSR146NLL).

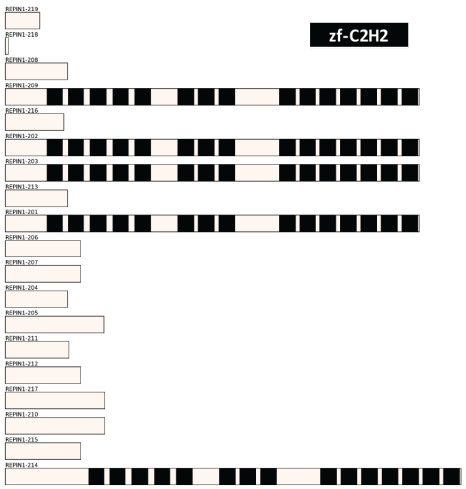

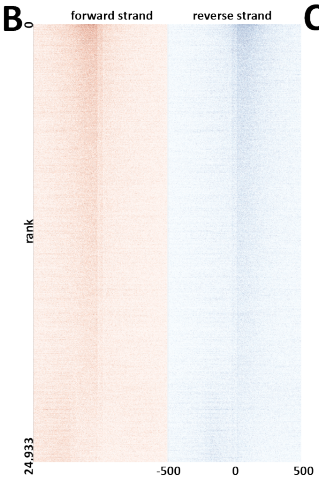

C

peaks	
state	fraction
TssA	0.33
TssFlnkU	0.19
EnhA1	0.18
EnhWk	0.18
TssFlnk	0.17
TssFlnkD	0.10
TxWk	0.04
ReprPCWk	0.03
EnhA2	0.03
Quies	0.02
TssBiv	0.02
EnhG2	0.02
EnhBiv	0.02
EnhG1	0.02
Tx	0.01
ReprPC	0.01
ZNF/Rpts	0.00
Het	0.00

D

peaks		peaks	
repeat	fraction	repeat	fraction
Simple_repeat	0.18	MIRb	0.05
SINE/Alu	0.16	MIR	0.03
SINE/MIR	0.14	L2a	0.03
LINE/L2	0.08	G-rich	0.02
LINE/L1	0.05	MIRc	0.02
Low_complexity	0.04	MIR3	0.02
DNA/hAT-Charlie	0.03	L2c	0.02
LTR/ERVL-MaLR	0.03	L2b	0.02
LTR/ERV1	0.03	AluJb	0.02
LTR/ERVL	0.02	AluSx	0.02
DNA/TcMar-Tigger	0.01	AluSx1	0.02
LINE/CR1	0.01	AluSz	0.01
DNA/hAT-Tip100	0.01	AluJr	0.01
tRNA	0.01	AluJo	0.01
LTR/ERVK	0.00	AluY	0.01
DNA/hAT-Blackjack	0.00	GA-rich	0.01
LTR/Gypsy	0.00	AluSq2	0.01
DNA/hAT	0.00	AluSp	0.01

E

Ontology	Term	FDR Q-val
GO Biological Process	regulation of transcription from RNA polymerase II promoter in response to stress	50.99
GO Biological Process	endoplasmic reticulum unfolded protein response	46.34
GO Biological Process	cellular response to topologically incorrect protein	46.27
GO Biological Process	response to topologically incorrect protein	46.26
GO Biological Process	regulation of DNA-templated transcription in response to stress	45.21
GO Biological Process	cellular response to unfolded protein	43.11
GO Biological Process	nuclear-transcribed mRNA catabolic process, nonsense-mediated decay	37.94
GO Biological Process	multi-organism metabolic process	36.25
GO Biological Process	cotranslational protein targeting to membrane	31.34
GO Biological Process	negative regulation of intrinsic apoptotic signaling pathway	31.24
GO Biological Process	viral gene expression	30.17
GO Biological Process	protein import into mitochondrial matrix	29.63
GO Biological Process	cellular response to epidermal growth factor stimulus	28.24
GO Biological Process	regulation of cholesterol metabolic process	28.07
GO Biological Process	protein targeting to ER	28.03
GO Biological Process	response to cadmium ion	27.91
GO Biological Process	SRP-dependent cotranslational protein targeting to membrane	27.45
GO Biological Process	mitochondrial transmembrane transport	27.35
GO Biological Process	response to epidermal growth factor	26.47
GO Biological Process	regulation of transcription from RNA polymerase II promoter in response to hypoxia	25.96
Human Phenotype	Increased serum lactate	24.80
Human Phenotype	Abnormal CSF metabolite level	22.18
Human Phenotype	Abnormality of mitochondrial metabolism	18.89
Human Phenotype	Abnormality of the mitochondrion	18.72
Human Phenotype	Increased CSF lactate	17.51
Human Phenotype	Exercise intolerance	12.97
Human Phenotype	Glycosuria	9.13
Human Phenotype	Progressive macrocephaly	5.20
Human Phenotype	Abnormal mitochondria in muscle tissue	4.97
Human Phenotype	Acute necrotizing encephalopathy	4.28
Human Phenotype	Increased muscle lipid content	4.21

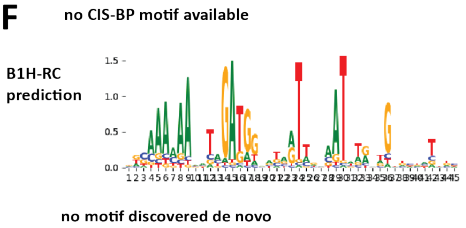

Supplementary Figure 225: Properties and genomic distribution of motifs identified for the REPIN1 transcription factor in HepG2 (accession ENCSR893BAO).

A

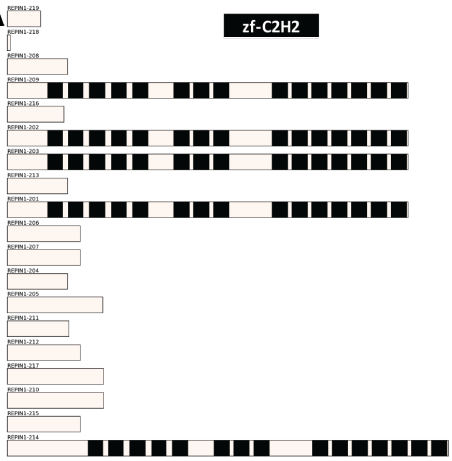

B

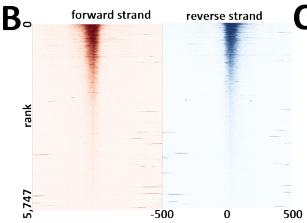

C

peaks	
state	fraction
ReprPCWk	0.23
Quies	0.22
TssA	0.17
TssFlnk	0.09
EnhWk	0.07
ReprPC	0.06
TxWk	0.06
EnhA1	0.03
Tx	0.02
Het	0.02
TssFlnkU	0.02
TssFlnkD	0.02
ZNF/Rpts	0.01
EnhA2	0.01
EnhBiv	0.01
EnhG1	0.01
TssBiv	0.01
EnhG2	0.00

D

peaks		peaks	
repeat	fraction	repeat	fraction
Simple_repeat	0.10	L2a	0.04
LINE/L2	0.09	MIRb	0.03
SINE/MIR	0.08	L2b	0.03
LINE/L1	0.04	L2c	0.02
SINE/Alu	0.03	MIR	0.02
DNA/hAT-Charlie	0.03	MIR3	0.01
LTR/ERVL-MaLR	0.02	G-rich	0.01
LTR/ERVL	0.02	MIRc	0.01
Low_complexity	0.02	L3	0.01
LINE/CR1	0.01	GA-rich	0.01
LTR/ERV1	0.01	LTR16E1	0.01
DNA/TcMar-Tigger	0.01	L2	0.01
DNA/hAT-Tip100	0.01	MER5A	0.00
Unknown	0.00	AluJb	0.00
LTR/Gypsy	0.00	(GGC)n	0.00
DNA/hAT	0.00	MER3	0.00
LINE/RTE-X	0.00	L1M1	0.00
DNA/hAT-Blackjack	0.00	AluJr	0.00

E

Ontology	Term	FDR Q-val
GO Biological Process	SRP-dependent cotranslational protein targeting to membrane	9.77
GO Biological Process	viral gene expression	9.77
GO Biological Process	protein targeting to ER	9.76
GO Biological Process	cotranslational protein targeting to membrane	9.20
GO Biological Process	nuclear-transcribed mRNA catabolic process, nonsense-mediated decay	8.62
GO Biological Process	establishment of protein localization to endoplasmic reticulum	7.97
GO Biological Process	viral transcription	7.93
GO Biological Process	multi-organism metabolic process	7.55
GO Biological Process	protein localization to endoplasmic reticulum	7.11
GO Biological Process	translational initiation	6.78
GO Biological Process	long-term memory	4.16
GO Biological Process	peptidyl-serine dephosphorylation	2.69
GO Biological Process	regulation of alpha-amino-3-hydroxy-5-methyl-4-isoxazole propionate selective glutamate receptor activity	2.41
GO Biological Process	antigen processing and presentation of endogenous antigen	1.80
GO Biological Process	negative regulation of catecholamine secretion	1.79
GO Biological Process	regulation of short-term neuronal synaptic plasticity	1.70
GO Biological Process	regulation of interleukin-12 secretion	1.51
GO Biological Process	cerebellar Purkinje cell-granule cell precursor cell signaling involved in regulation of granule cell precursor cell proliferation	1.44

F

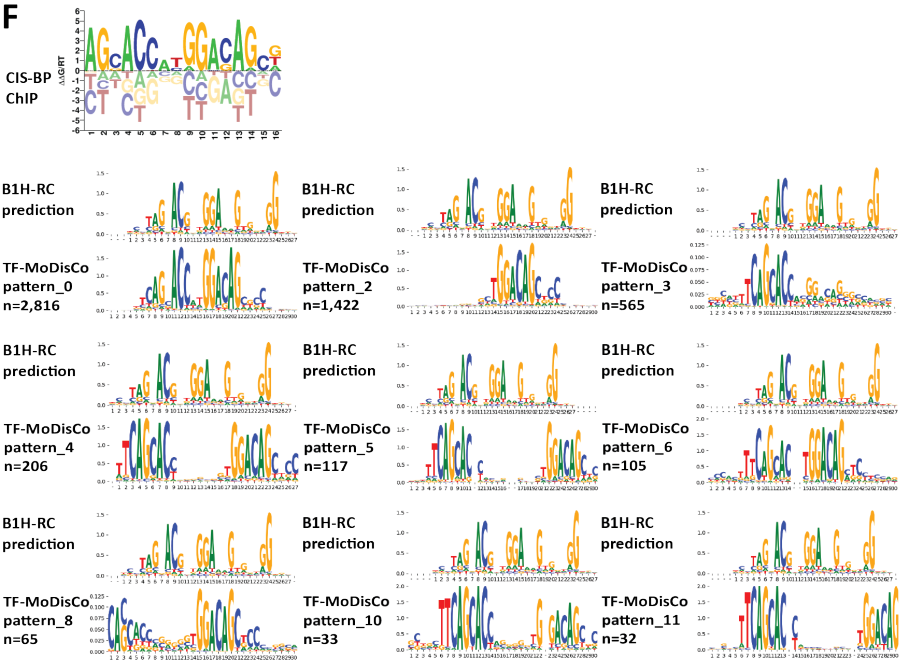

G

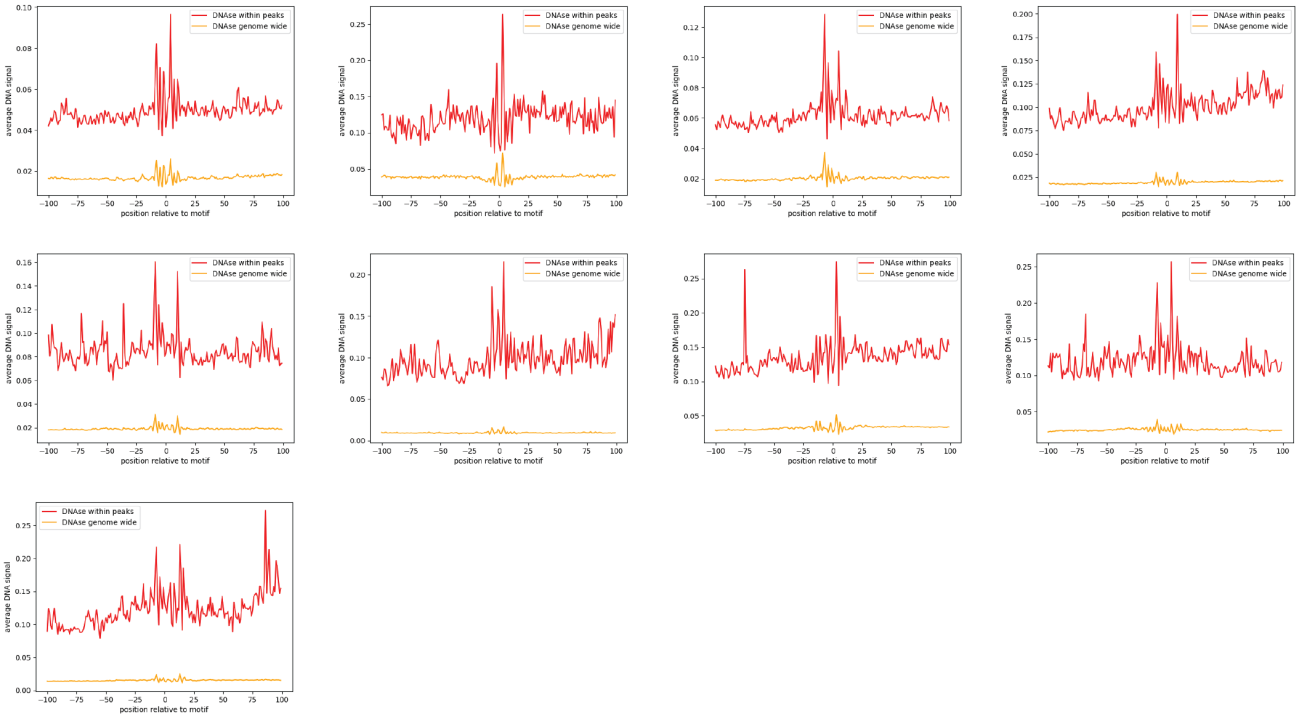
DNAse within peaks
DNAse genome wide
average DNA signal
position relative to motif

H

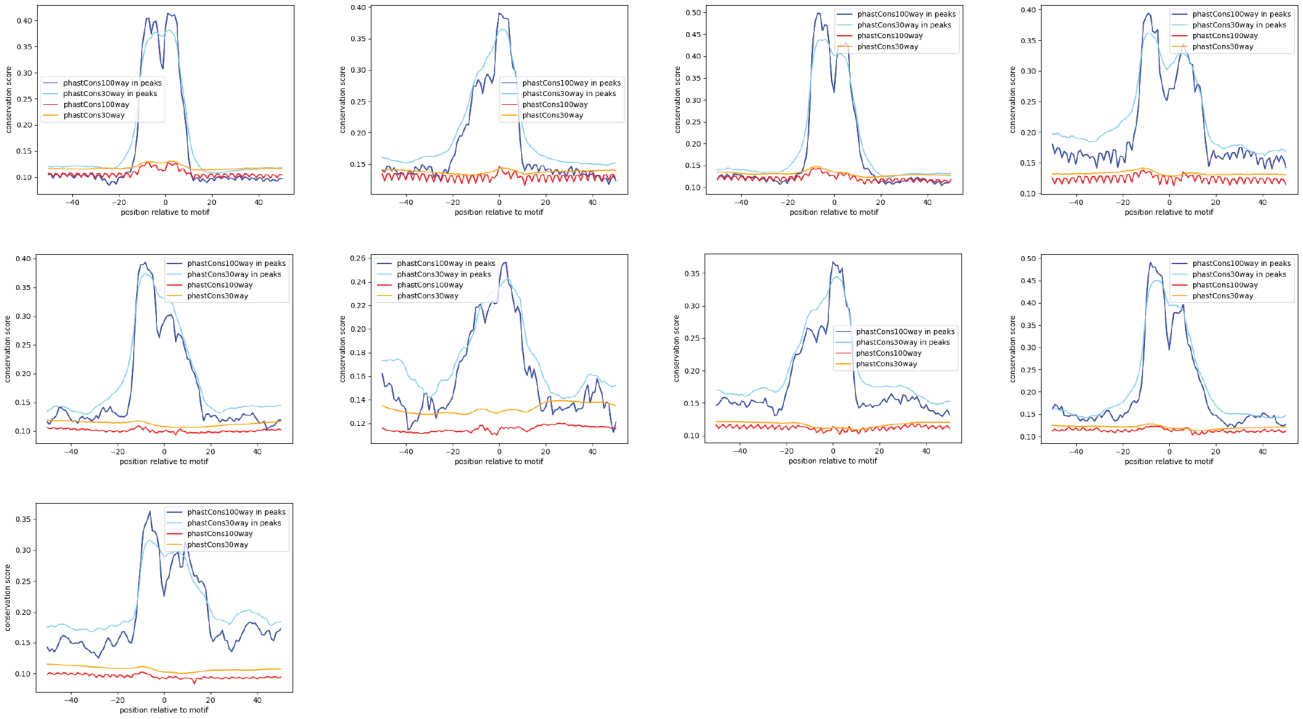
phastCons100way in peaks
phastCons30way in peaks
phastCons100way
phastCons30way
conservation score
position relative to motif

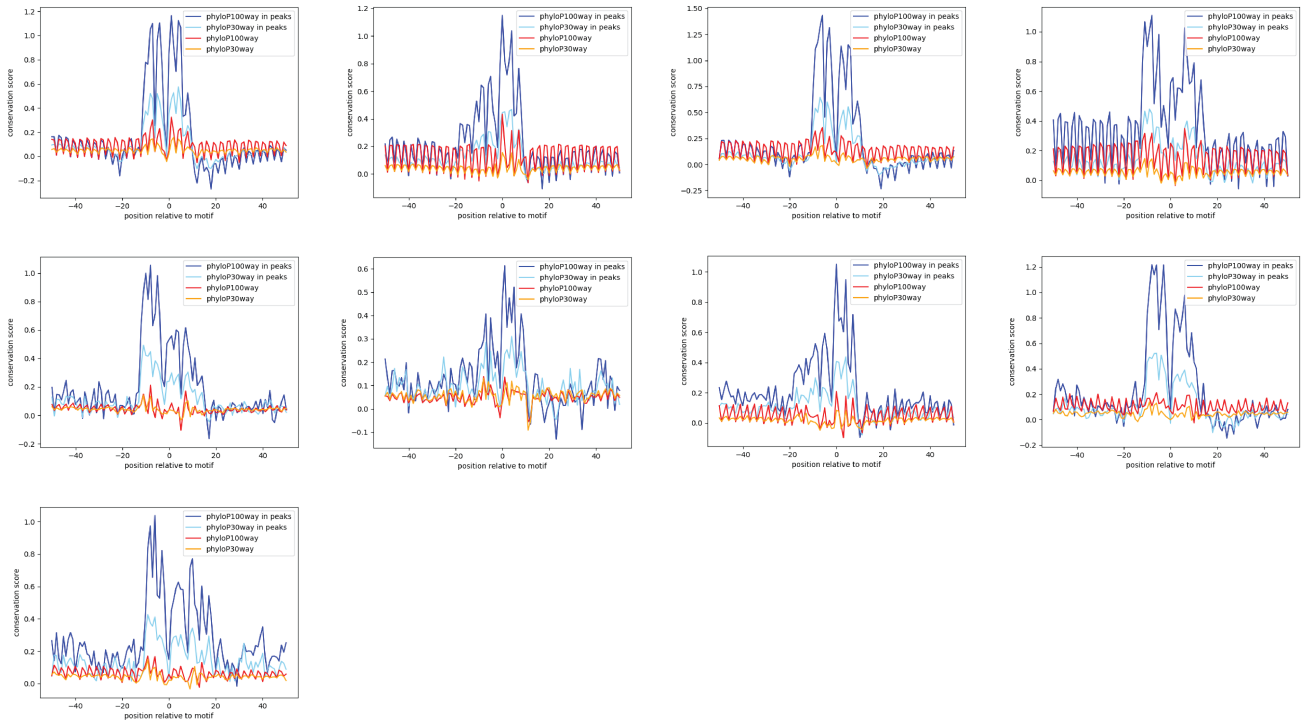

Supplementary Figure 226: Properties and genomic distribution of motifs identified for the REST transcription factor in GM12878 (accession ENCSR000BGF).

TF-MoDisCO pattern_0 n=2816, CWM

pattern_0, n=2816; subpattern_0, ns=611

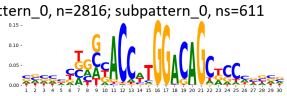

pattern_0, n=2816; subpattern_1, ns=442

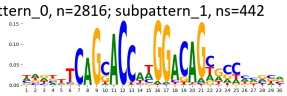

pattern_0, n=2816; subpattern_2, ns=435

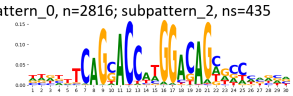

pattern_0, n=2816; subpattern_3, ns=342

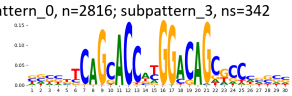

pattern_0, n=2816; subpattern_4, ns=332

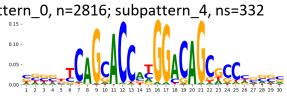

pattern_0, n=2816; subpattern_5, ns=329

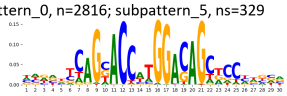

pattern_0, n=2816; subpattern_6, ns=325

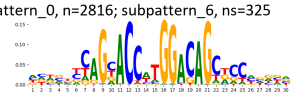

TF-MoDisCO pattern_0 n=2816, PWM

pattern_0, n=2816; subpattern_0, ns=611

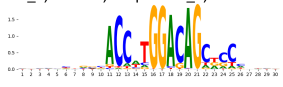

pattern_0, n=2816; subpattern_1, ns=442

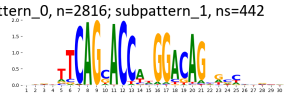

pattern_0, n=2816; subpattern_2, ns=435

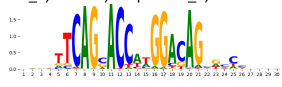

pattern_0, n=2816; subpattern_3, ns=342

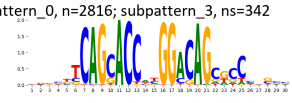

pattern_0, n=2816; subpattern_4, ns=332

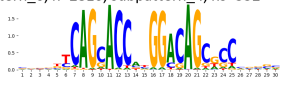

pattern_0, n=2816; subpattern_5, ns=329

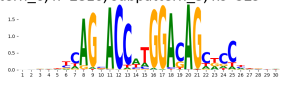

pattern_0, n=2816; subpattern_6, ns=325

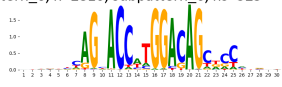

TF-MoDisCO pattern_10 n=33, CWM

pattern_10, n=33; subpattern_0, ns=33

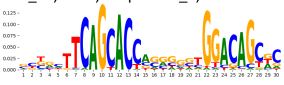

TF-MoDisCO pattern_10 n=33, PWM

pattern_10, n=33; subpattern_0, ns=33

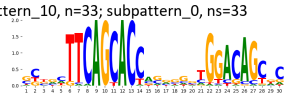

TF-MoDisCO pattern_11 n=32, CWM

pattern_11, n=32; subpattern_0, ns=32

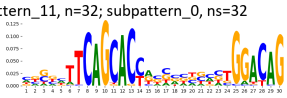

TF-MoDisCO pattern_11 n=32, PWM

pattern_11, n=32; subpattern_0, ns=32

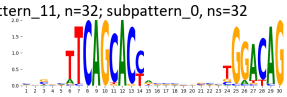

TF-MoDisCO pattern_2 n=1422, CWM

pattern_2, n=1422; subpattern_0, ns=312

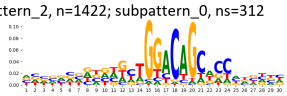

pattern_2, n=1422; subpattern_1, ns=224

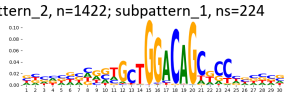

pattern_2, n=1422; subpattern_10, ns=7

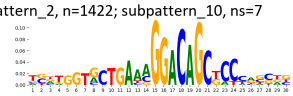

pattern_2, n=1422; subpattern_2, ns=222

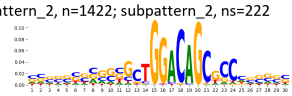

pattern_2, n=1422; subpattern_3, ns=195

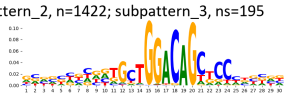

pattern_2, n=1422; subpattern_4, ns=175

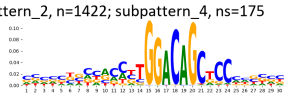

pattern_2, n=1422; subpattern_5, ns=117

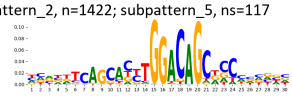

pattern_2, n=1422; subpattern_6, ns=102

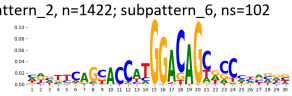

pattern_2, n=1422; subpattern_7, ns=36

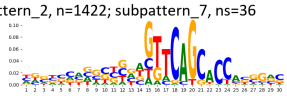

pattern_2, n=1422; subpattern_8, ns=22

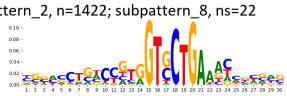

pattern_2, n=1422; subpattern_9, ns=10

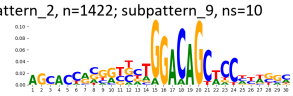

TF-MoDisCO pattern_2 n=1422, PWM

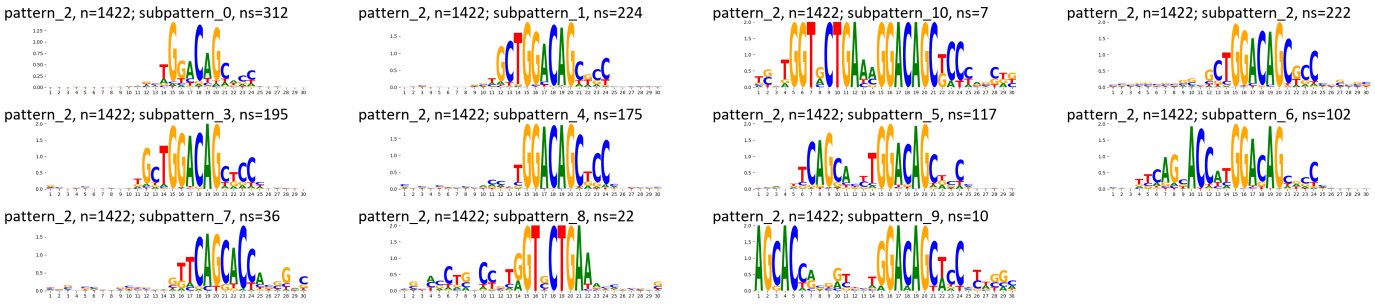

TF-MoDisCO pattern_3 n=565, CWM

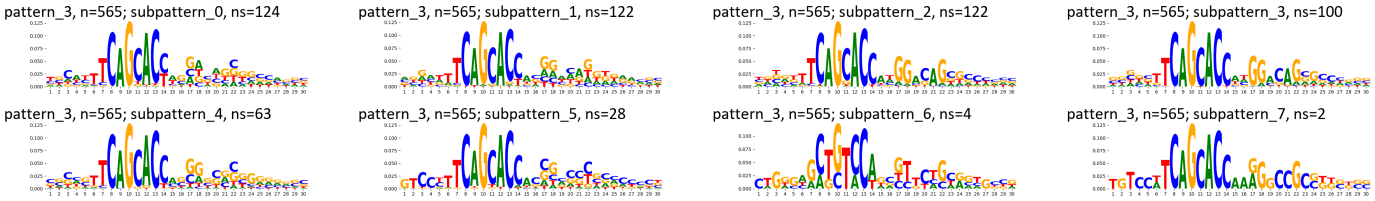

TF-MoDisCO pattern_3 n=565, PWM

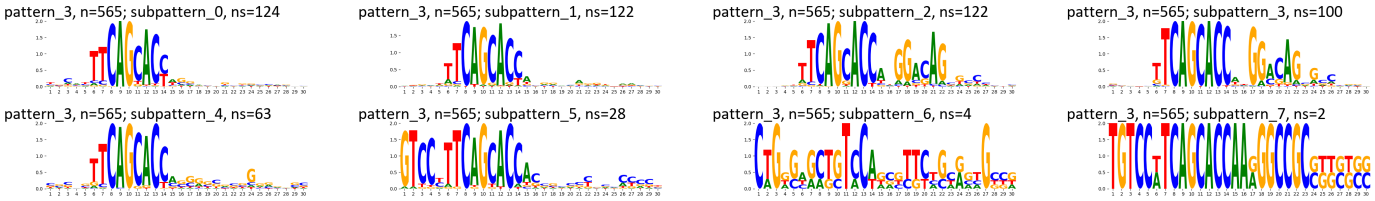

TF-MoDisCO pattern_4 n=206, CWM

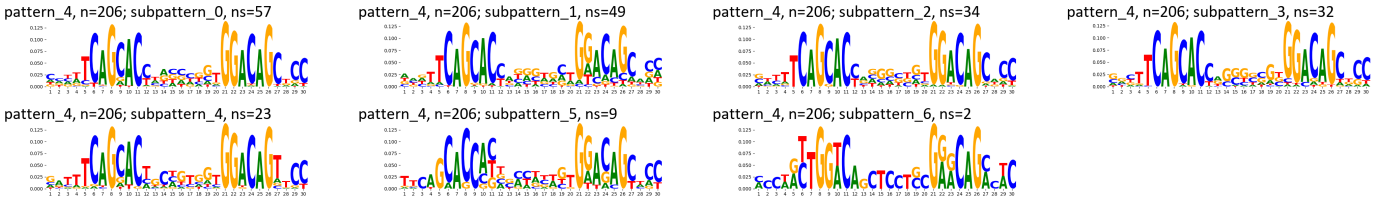

TF-MoDisCO pattern_4 n=206, PWM

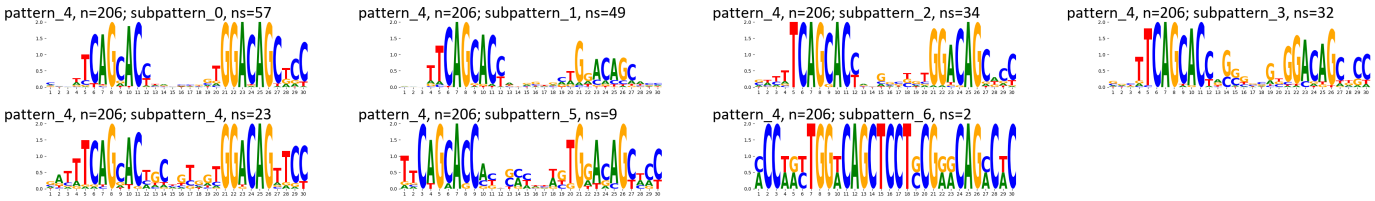

TF-MoDisCO pattern_5 n=117, CWM

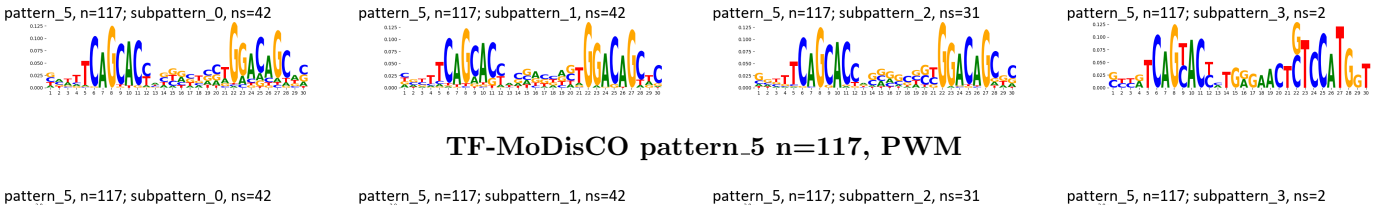

TF-MoDisCO pattern_5 n=117, PWM

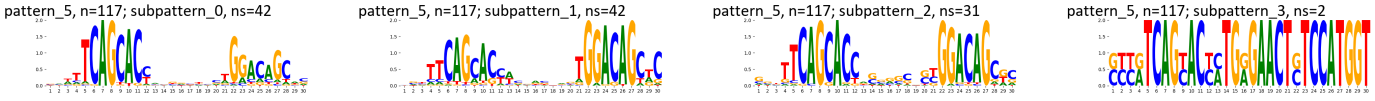

TF-MoDisCO pattern_6 n=105, CWM

pattern_6, n=105; subpattern_0, ns=33

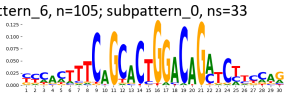

pattern_6, n=105; subpattern_1, ns=32

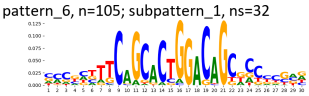

pattern_6, n=105; subpattern_2, ns=23

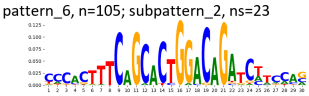

pattern_6, n=105; subpattern_3, ns=15

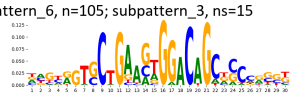

pattern_6, n=105; subpattern_4, ns=2

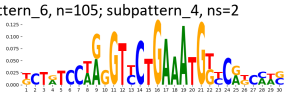

TF-MoDisCO pattern_6 n=105, PWM

pattern_6, n=105; subpattern_0, ns=33

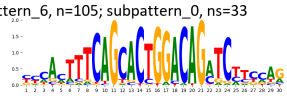

pattern_6, n=105; subpattern_1, ns=32

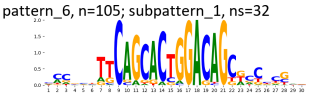

pattern_6, n=105; subpattern_2, ns=23

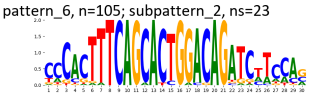

pattern_6, n=105; subpattern_3, ns=15

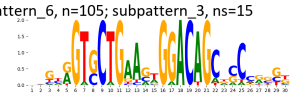

pattern_6, n=105; subpattern_4, ns=2

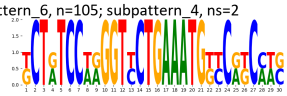

TF-MoDisCO pattern_8 n=65, CWM

pattern_8, n=65; subpattern_0, ns=32

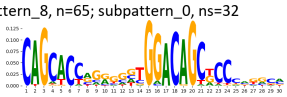

pattern_8, n=65; subpattern_1, ns=24

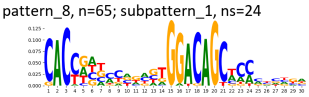

pattern_8, n=65; subpattern_2, ns=9

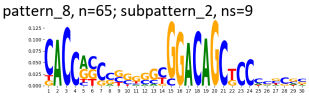

TF-MoDisCO pattern_8 n=65, PWM

pattern_8, n=65; subpattern_0, ns=32

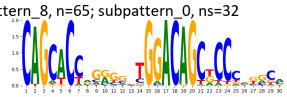

pattern_8, n=65; subpattern_1, ns=24

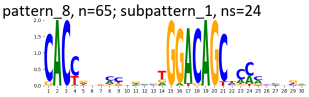

pattern_8, n=65; subpattern_2, ns=9

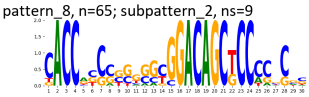

Supplementary Figure 227: TF-MoDisCO subpatterns for the REST transcription factor in GM12878 (accession ENCSR000BGF).

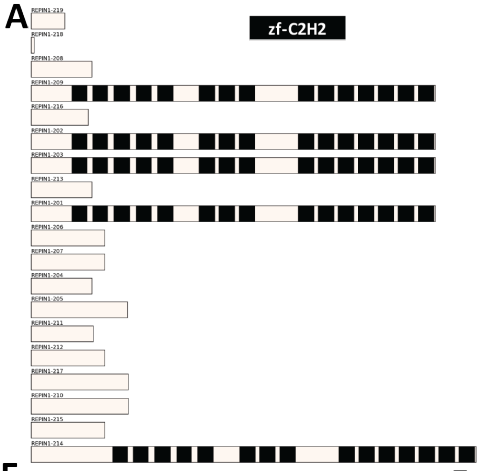

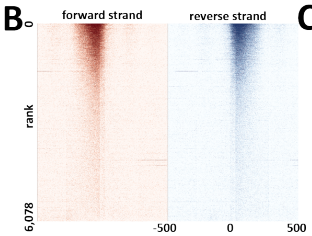

C

peaks	
state	fraction
TssA	0.29
Quies	0.18
ReprPCWk	0.17
TssFlnk	0.12
EnhA1	0.08
EnhWk	0.08
EnhA2	0.05
TxWk	0.04
ReprPC	0.04
TssFlnkU	0.04
Het	0.01
Tx	0.01
TssFlnkD	0.01
ZNF/Rpts	0.01
EnhG1	0.00
TssBiv	0.00
EnhBiv	0.00
EnhG2	0.00

D

peaks		peaks	
repeat	fraction	repeat	fraction
Simple_repeat	0.11	L2a	0.03
LINE/L2	0.08	MIRb	0.03
SINE/MIR	0.07	L2c	0.02
SINE/Alu	0.04	L2b	0.02
LINE/L1	0.04	MIR	0.02
DNA/hAT-Charlie	0.03	MIR3	0.01
LTR/ERVL-MaLR	0.02	G-rich	0.01
Low_complexity	0.02	MIRc	0.01
LTR/ERVL	0.02	L3	0.01
LINE/CR1	0.01	GA-rich	0.01
LTR/ERV1	0.01	L2	0.01
DNA/TcMar-Tigger	0.01	(GGC)n	0.01
DNA/hAT-Tip100	0.00	AluJb	0.00
snRNA	0.00	LTR16E1	0.00
Unknown	0.00	AluSx1	0.00
tRNA	0.00	MER5A	0.00
DNA/hAT-Blackjack	0.00	AluSx	0.00
LTR/Gypsy	0.00	AluJr	0.00

E

Ontology	Term	FDR Q-val
GO Biological Process	nuclear-transcribed mRNA catabolic process	12.84
GO Biological Process	nuclear-transcribed mRNA catabolic process, nonsense-mediated decay	11.76
GO Biological Process	mRNA catabolic process	11.40
GO Biological Process	SRP-dependent cotranslational protein targeting to membrane	11.27
GO Biological Process	viral gene expression	11.20
GO Biological Process	protein targeting to ER	10.64
GO Biological Process	viral transcription	10.26
GO Biological Process	cotranslational protein targeting to membrane	10.11
GO Biological Process	multi-organism metabolic process	9.92
GO Biological Process	translational initiation	9.80
GO Biological Process	establishment of protein localization to endoplasmic reticulum	8.94
GO Biological Process	protein localization to endoplasmic reticulum	8.41
GO Biological Process	ER-nucleus signaling pathway	4.41
GO Biological Process	negative regulation of endoplasmic reticulum unfolded protein response	1.45

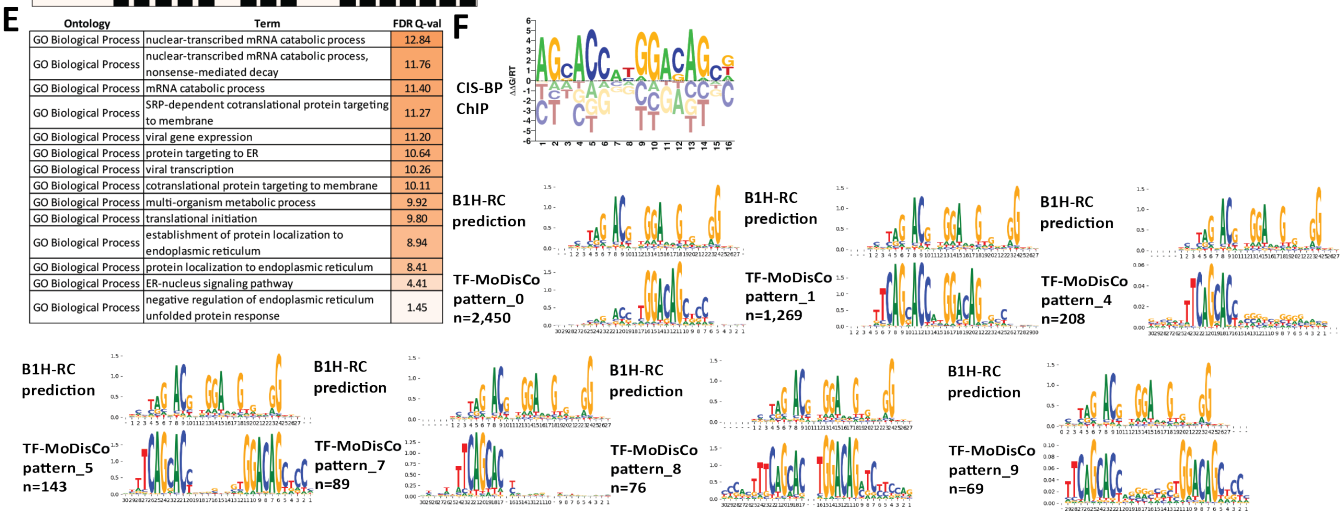

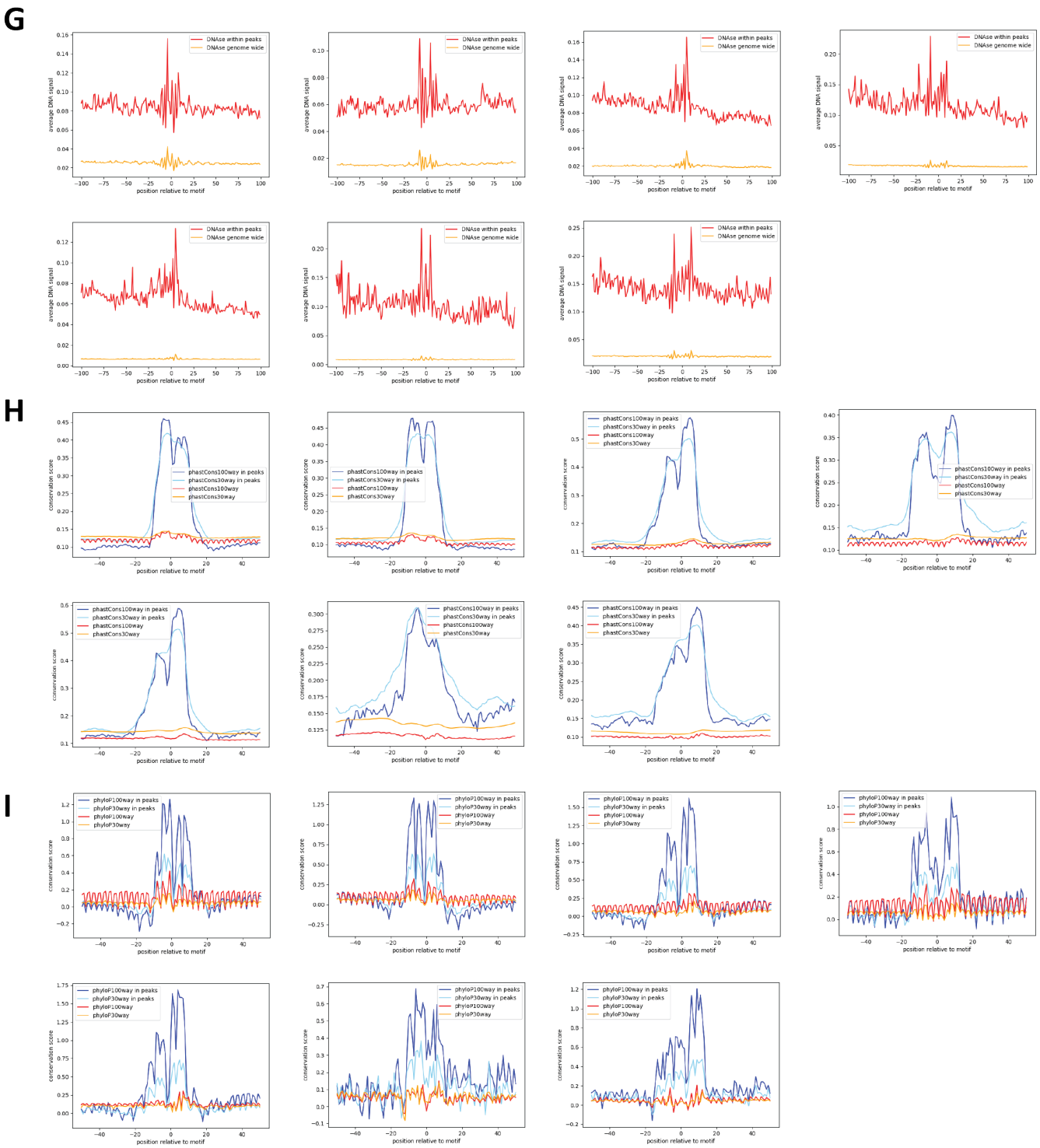

Supplementary Figure 228: Properties and genomic distribution of motifs identified for the REST transcription factor in GM12878 (accession ENCSR000BQS).

TF-MoDisCO pattern_0 n=2450, CWM

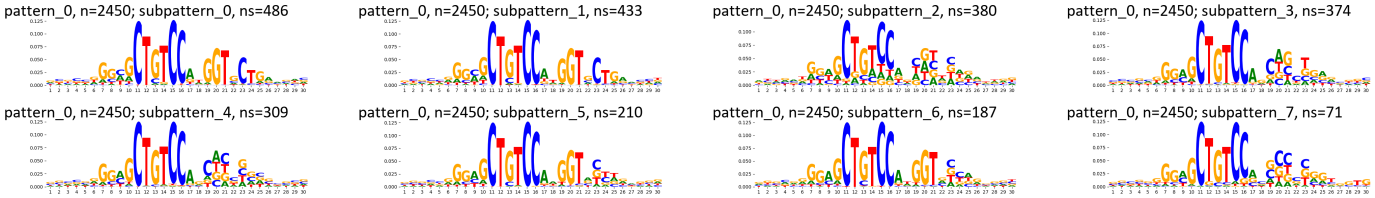

TF-MoDisCO pattern_0 n=2450, PWM

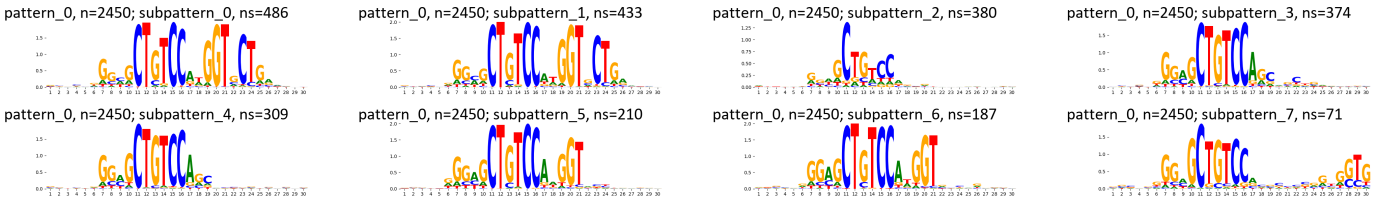

TF-MoDisCO pattern_1 n=1269, CWM

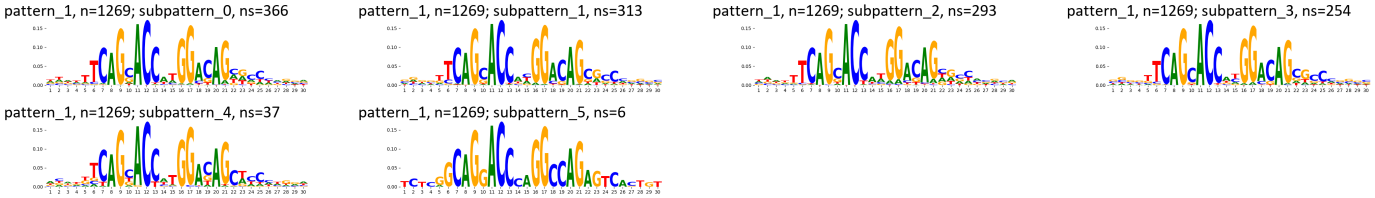

TF-MoDisCO pattern_1 n=1269, PWM

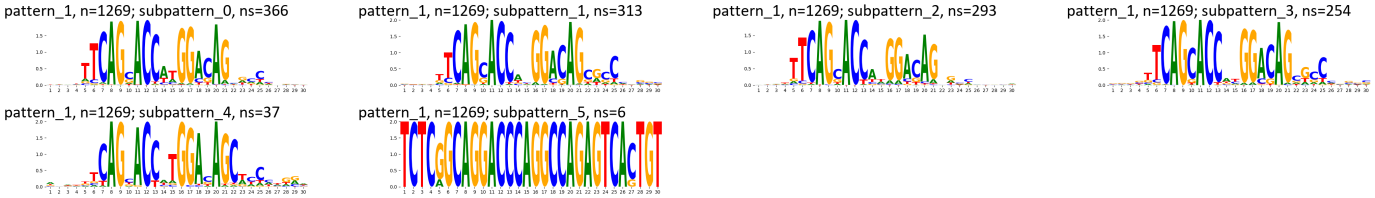

TF-MoDisCO pattern_4 n=208, CWM

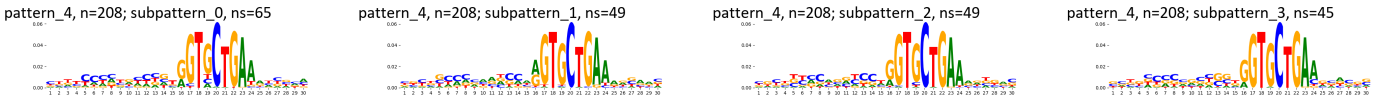

TF-MoDisCO pattern_4 n=208, PWM



TF-MoDisCO pattern_5 n=143, CWM

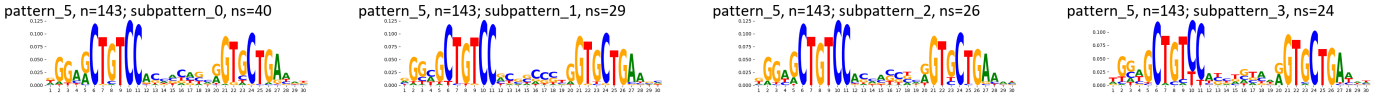

TF-MoDisCO pattern_5 n=143, PWM

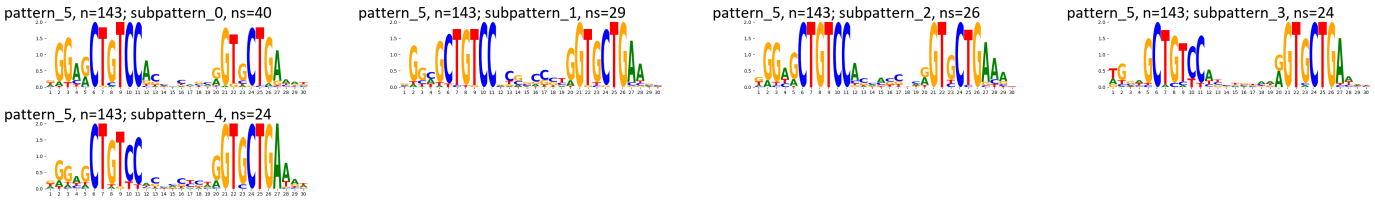

TF-MoDisCO pattern_7 n=89, CWM

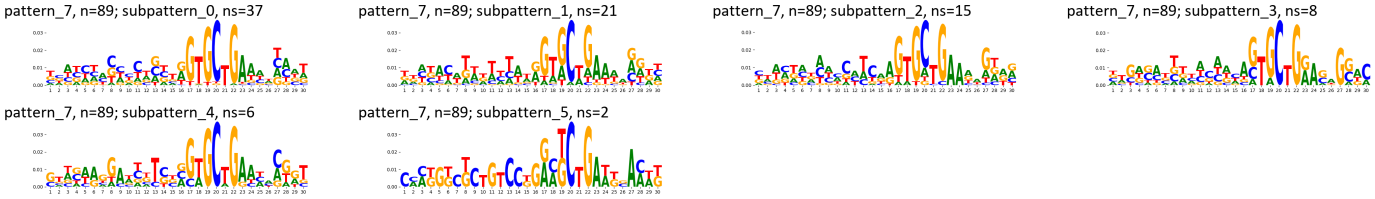

TF-MoDisCO pattern_7 n=89, PWM

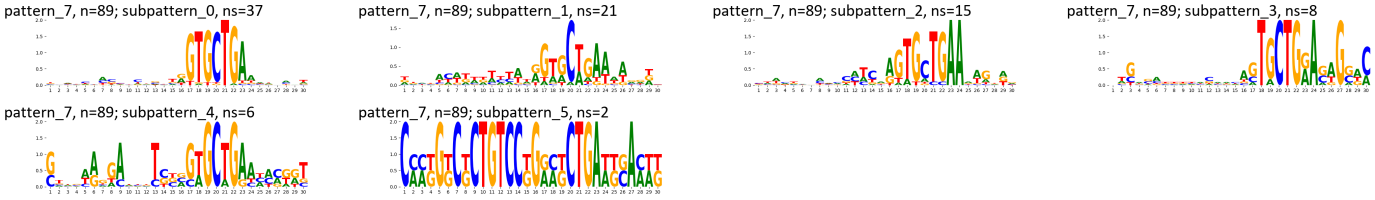

TF-MoDisCO pattern_8 n=76, CWM

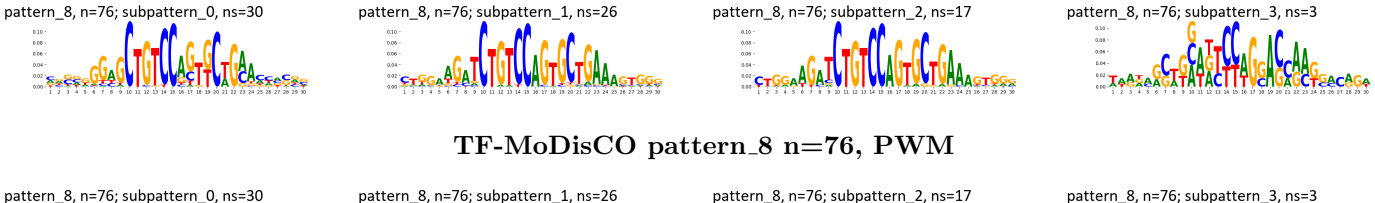

TF-MoDisCO pattern_8 n=76, PWM

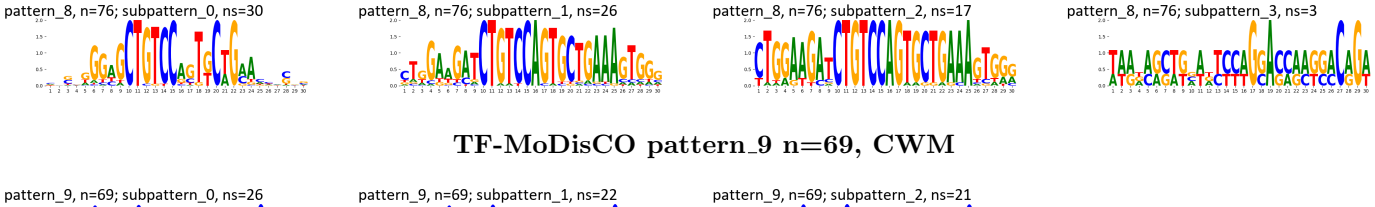

TF-MoDisCO pattern_9 n=69, CWM

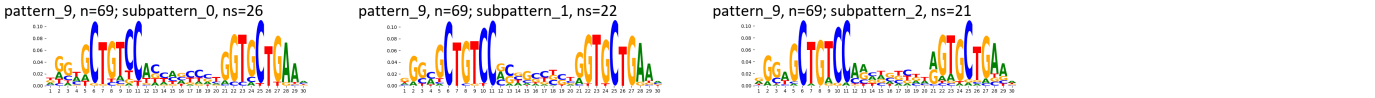

TF-MoDisCO pattern_9 n=69, PWM

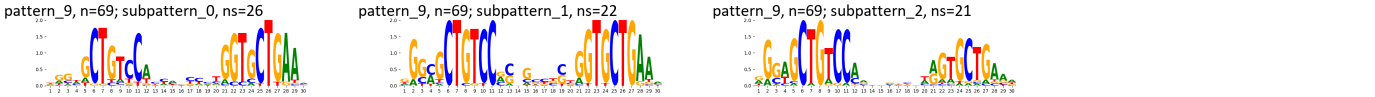

Supplementary Figure 229: TF-MoDisCO subpatterns for the REST transcription factor in GM12878 (accession ENCSR000BQS).

A

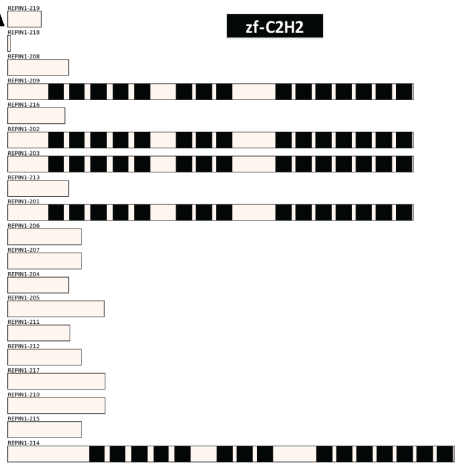

B

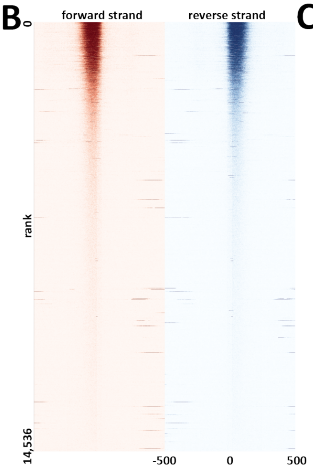

C

peaks	
state	fraction
Quies	0.43
TssA	0.11
ReprPCWk	0.10
TxWk	0.09
TssFlnk	0.07
EnhWk	0.04
EnhA1	0.02
Tx	0.02
TssFlnkU	0.01
ReprPC	0.01
TssFlnkD	0.01
Het	0.01
EnhA2	0.01
ZNF/Rpts	0.00
TssBiv	0.00
EnhG1	0.00
EnhBiv	0.00
EnhG2	0.00

D

peaks		peaks	
repeat	fraction	repeat	fraction
LINE/L2	0.09	L2a	0.04
SINE/MIR	0.08	MIRb	0.03
Simple_repeat	0.07	L2b	0.02
LINE/L1	0.06	MIR	0.02
SINE/Alu	0.05	L2c	0.02
DNA/hAT-Charlie	0.04	MIR3	0.02
LTR/ERVL-MaLR	0.03	MIRc	0.01
LTR/ERVL	0.03	L3	0.01
LTR/ERV1	0.03	G-rich	0.01
Low_complexity	0.02	L2	0.01
LINE/CR1	0.01	L1M1	0.01
DNA/TcMar-Tigger	0.01	GA-rich	0.01
DNA/hAT-Tip100	0.01	AluSx1	0.01
DNA/hAT-Blackjack	0.00	AluJb	0.01
LTR/ERVK	0.00	MER3	0.01
LTR/Gypsy	0.00	AluSx	0.00
DNA/hAT	0.00	MER5A	0.00
Unknown	0.00	AluSz	0.00

E

Ontology	Term	FDR Q-val
GO Biological Process	midbrain-hindbrain boundary development	2.85
GO Biological Process	negative regulation of endoplasmic reticulum unfolded protein response	2.55

F

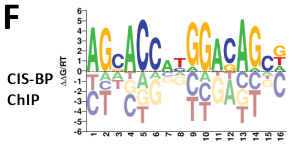

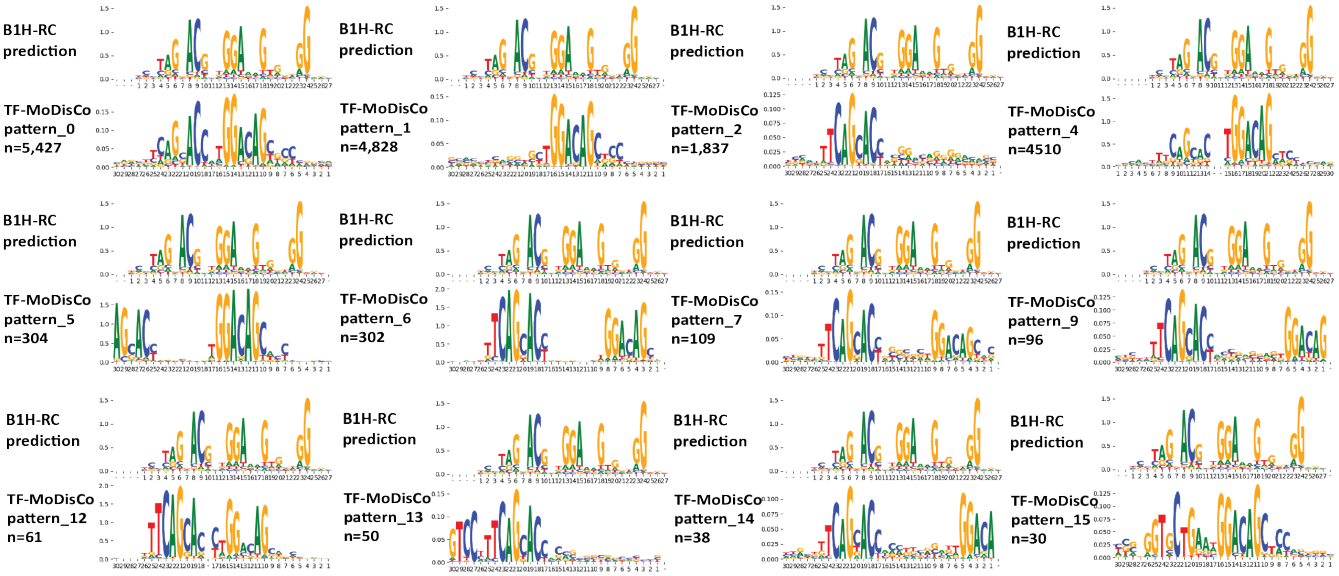

G

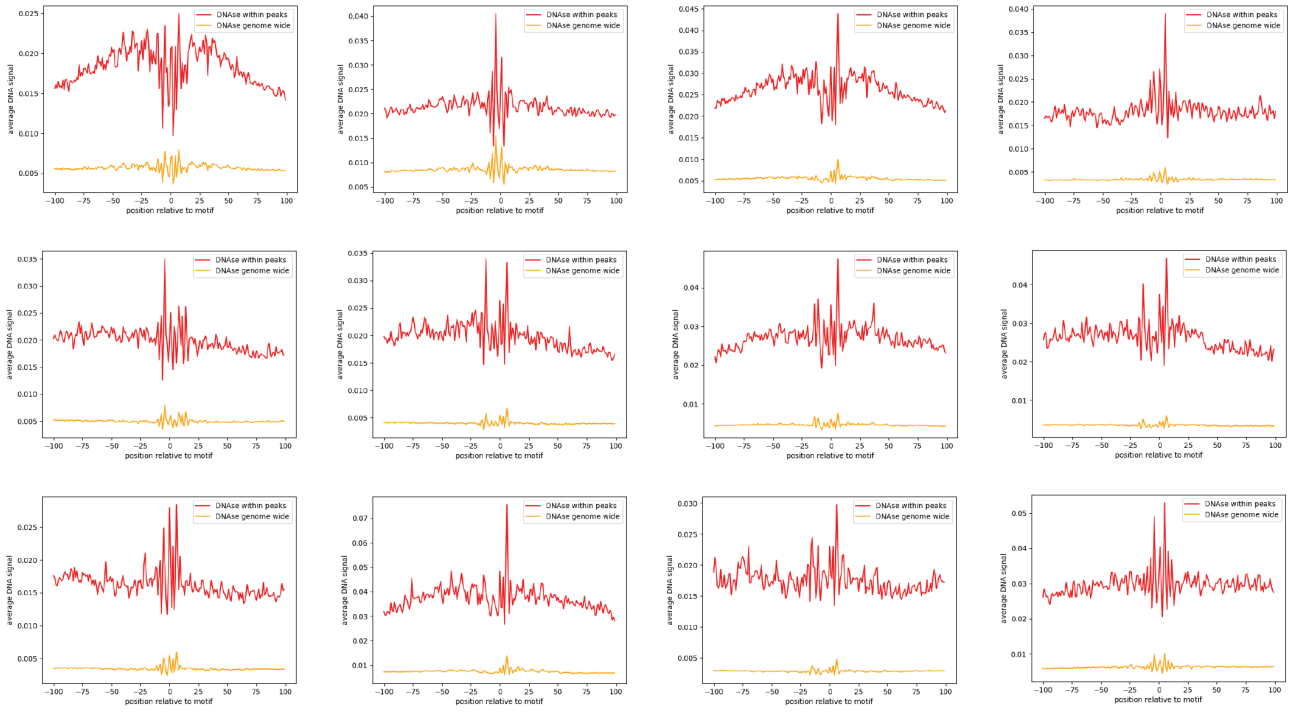
DNAse within peaks
DNAse genome wide
average DNA signal
position relative to motif

H

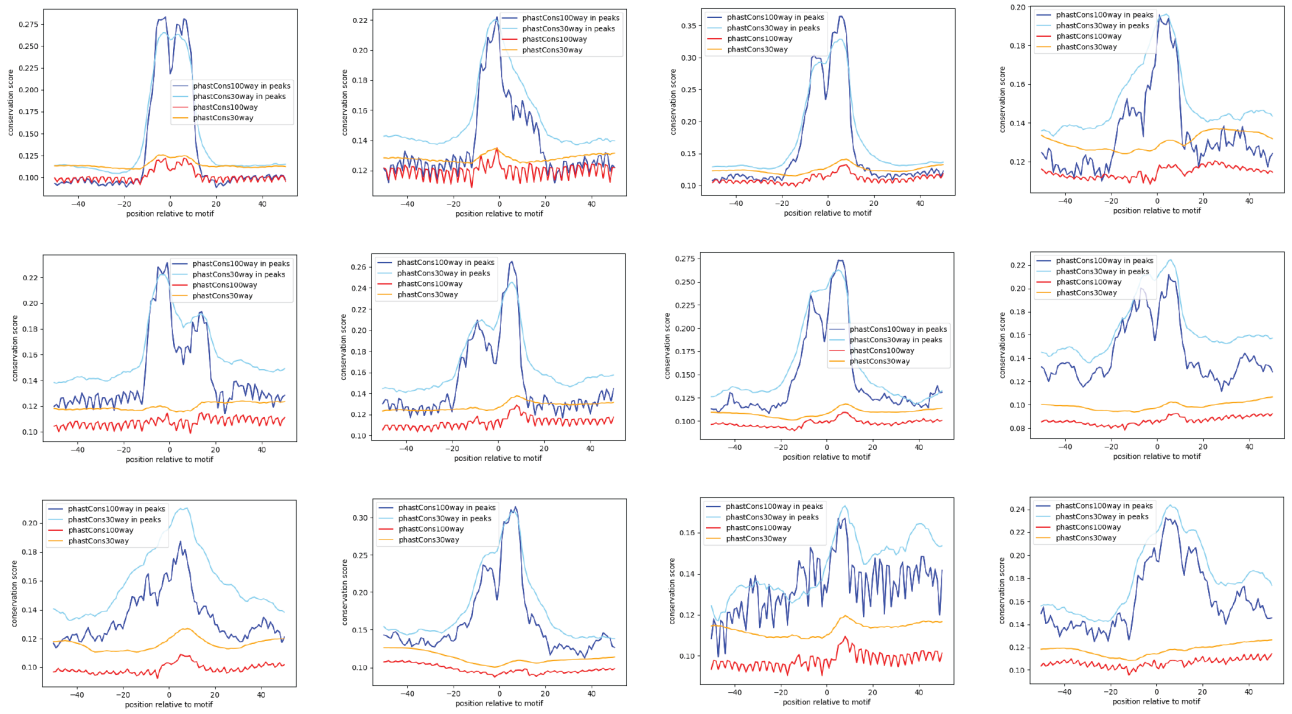
phastCons100way in peaks
phastCons30way in peaks
phastCons100way
phastCons30way
conservation score
position relative to motif

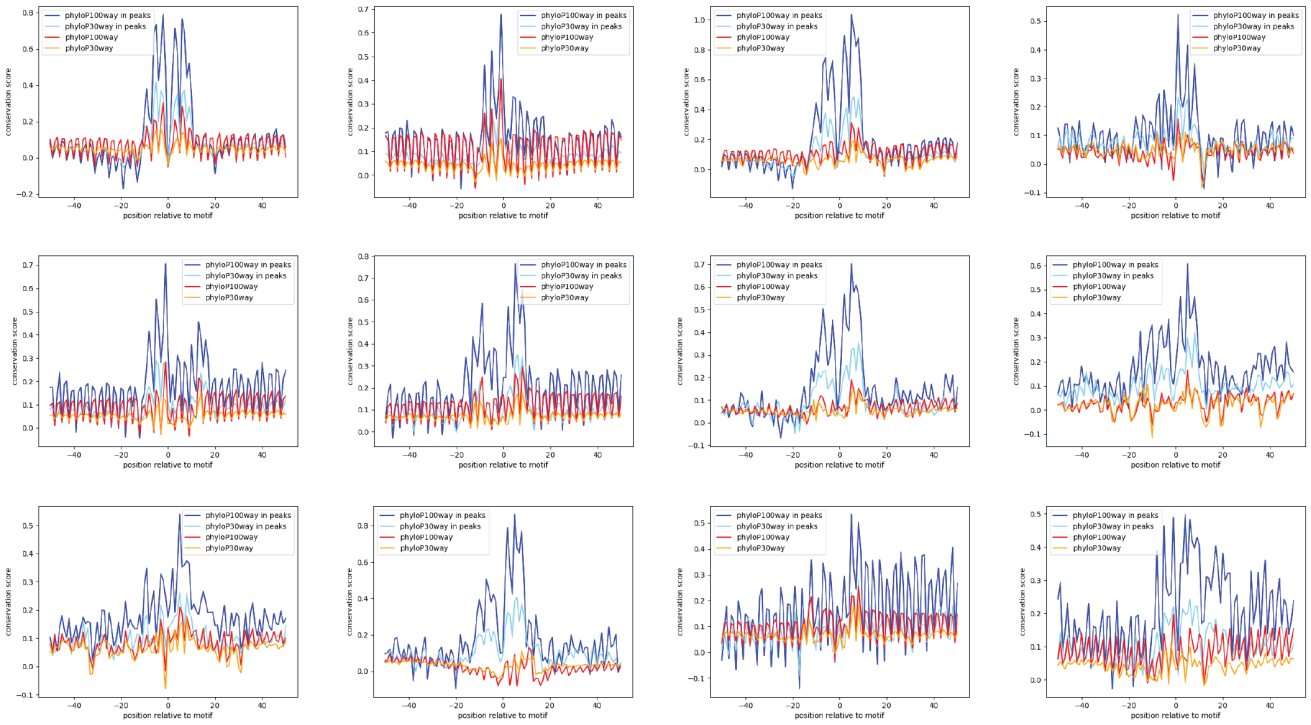

Supplementary Figure 230: Properties and genomic distribution of motifs identified for the REST transcription factor in H1 (accession ENCSR000BHM).

TF-MoDisCO pattern_0 n=5427, CWM

pattern_0, n=5427; subpattern_0, ns=1388

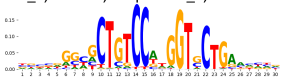

pattern_0, n=5427; subpattern_1, ns=1146

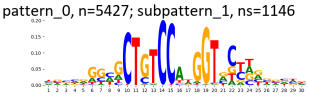

pattern_0, n=5427; subpattern_2, ns=1027

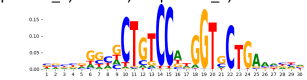

pattern_0, n=5427; subpattern_3, ns=891

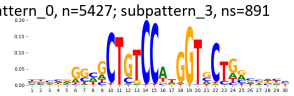

pattern_0, n=5427; subpattern_4, ns=801

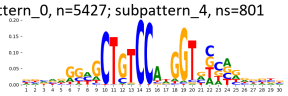

pattern_0, n=5427; subpattern_5, ns=170

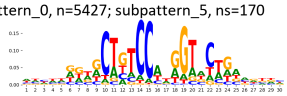

pattern_0, n=5427; subpattern_6, ns=4

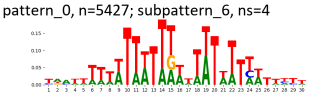

TF-MoDisCO pattern_0 n=5427, PWM

pattern_0, n=5427; subpattern_0, ns=1388

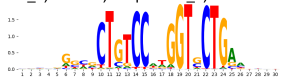

pattern_0, n=5427; subpattern_1, ns=1146

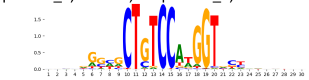

pattern_0, n=5427; subpattern_2, ns=1027

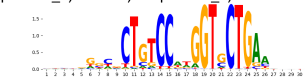

pattern_0, n=5427; subpattern_3, ns=891

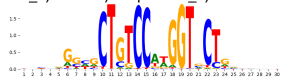

pattern_0, n=5427; subpattern_4, ns=801

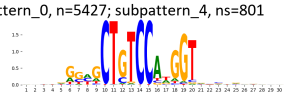

pattern_0, n=5427; subpattern_5, ns=170

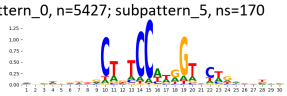

pattern_0, n=5427; subpattern_6, ns=4

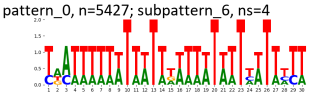

TF-MoDisCO pattern_1 n=4828, CWM

pattern_1, n=4828; subpattern_0, ns=892

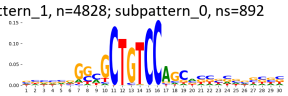

pattern_1, n=4828; subpattern_1, ns=850

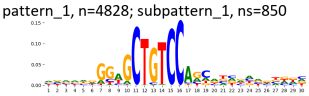

pattern_1, n=4828; subpattern_10, ns=19

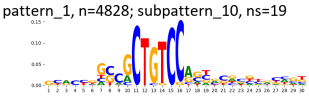

pattern_1, n=4828; subpattern_11, ns=9

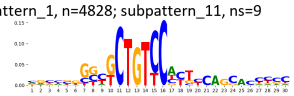

pattern_1, n=4828; subpattern_2, ns=777

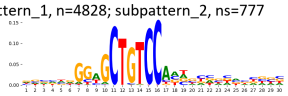

pattern_1, n=4828; subpattern_3, ns=734

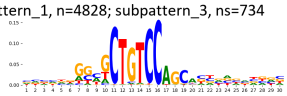

pattern_1, n=4828; subpattern_4, ns=479

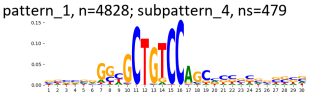

pattern_1, n=4828; subpattern_5, ns=471

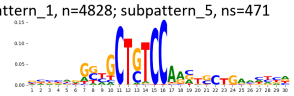

pattern_1, n=4828; subpattern_6, ns=222

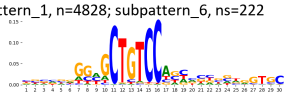

pattern_1, n=4828; subpattern_7, ns=199

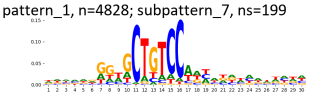

pattern_1, n=4828; subpattern_8, ns=150

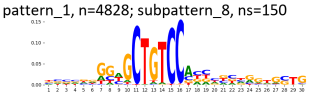

pattern_1, n=4828; subpattern_9, ns=26

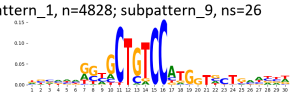

TF-MoDisCO pattern_1 n=4828, PWM

pattern_1, n=4828; subpattern_0, ns=892

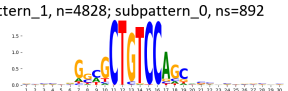

pattern_1, n=4828; subpattern_1, ns=850

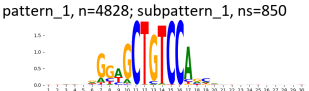

pattern_1, n=4828; subpattern_10, ns=19

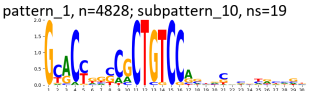

pattern_1, n=4828; subpattern_11, ns=9

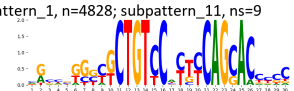

pattern_1, n=4828; subpattern_2, ns=777

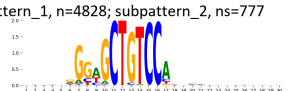

pattern_1, n=4828; subpattern_3, ns=734

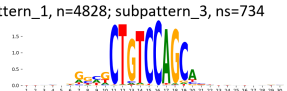

pattern_1, n=4828; subpattern_4, ns=479

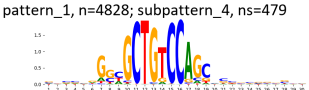

pattern_1, n=4828; subpattern_5, ns=471

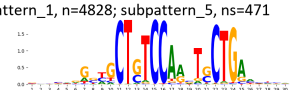

pattern_1, n=4828; subpattern_6, ns=222

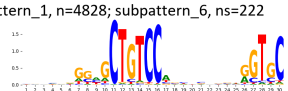

pattern_1, n=4828; subpattern_7, ns=199

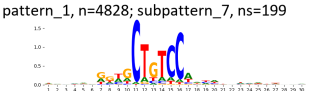

pattern_1, n=4828; subpattern_8, ns=150

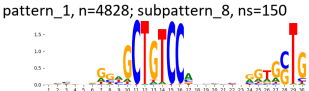

pattern_1, n=4828; subpattern_9, ns=26

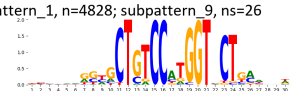

TF-MoDisCO pattern_12 n=61, CWM

pattern_12, n=61; subpattern_0, ns=24

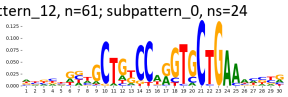

pattern_12, n=61; subpattern_1, ns=19

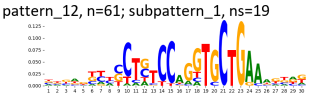

pattern_12, n=61; subpattern_2, ns=18

TF-MoDisCO pattern_12 n=61, PWM

pattern_12, n=61; subpattern_0, ns=24

pattern_12, n=61; subpattern_1, ns=19

pattern_12, n=61; subpattern_2, ns=18

TF-MoDisCO pattern_13 n=50, CWM

pattern_13, n=50; subpattern_0, ns=50

TF-MoDisCO pattern_13 n=50, PWM

pattern_13, n=50; subpattern_0, ns=50

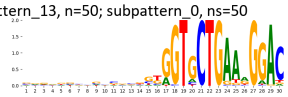

TF-MoDisCO pattern_14 n=38, CWM

pattern_14, n=38; subpattern_0, ns=38

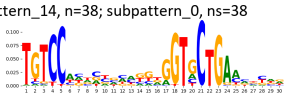

TF-MoDisCO pattern_14 n=38, PWM

pattern_14, n=38; subpattern_0, ns=38

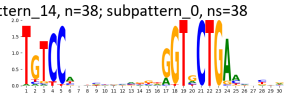

TF-MoDisCO pattern_15 n=30, CWM

pattern_15, n=30; subpattern_0, ns=30

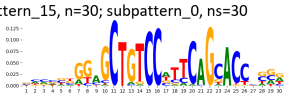

TF-MoDisCO pattern_15 n=30, PWM

pattern_15, n=30; subpattern_0, ns=30

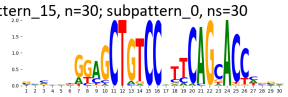

TF-MoDisCO pattern_2 n=1837, CWM

pattern_2, n=1837; subpattern_0, ns=469

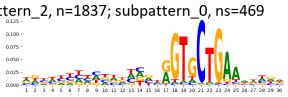

pattern_2, n=1837; subpattern_1, ns=414

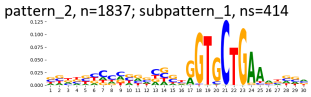

pattern_2, n=1837; subpattern_2, ns=366

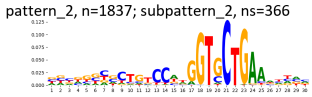

pattern_2, n=1837; subpattern_3, ns=313

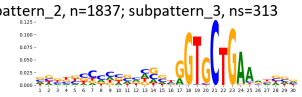

pattern_2, n=1837; subpattern_4, ns=233

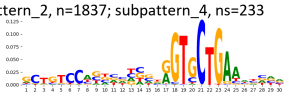

pattern_2, n=1837; subpattern_5, ns=30

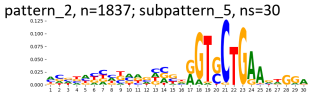

pattern_2, n=1837; subpattern_6, ns=12

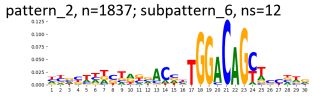

TF-MoDisCO pattern_2 n=1837, PWM

pattern_2, n=1837; subpattern_0, ns=469

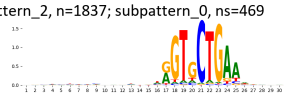

pattern_2, n=1837; subpattern_1, ns=414

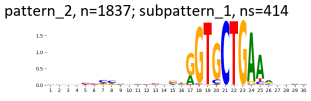

pattern_2, n=1837; subpattern_2, ns=366

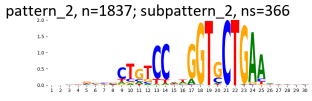

pattern_2, n=1837; subpattern_3, ns=313

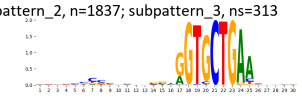

pattern_2, n=1837; subpattern_4, ns=233

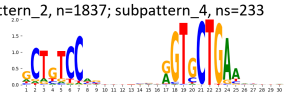

pattern_2, n=1837; subpattern_5, ns=30

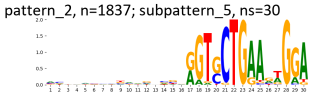

pattern_2, n=1837; subpattern_6, ns=12

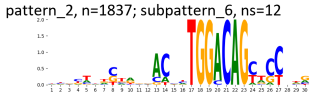

TF-MoDisCO pattern_4 n=510, CWM

pattern_4, n=510; subpattern_0, ns=159

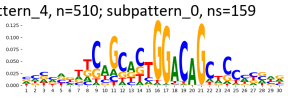

pattern_4, n=510; subpattern_1, ns=125

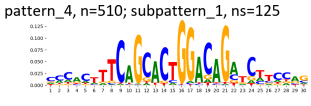

pattern_4, n=510; subpattern_2, ns=92

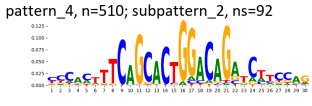

pattern_4, n=510; subpattern_3, ns=90

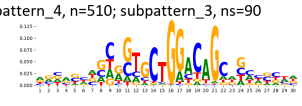

pattern_4, n=510; subpattern_4, ns=19

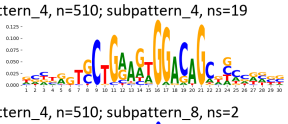

pattern_4, n=510; subpattern_5, ns=15

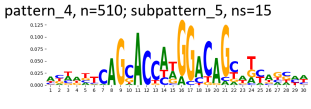

pattern_4, n=510; subpattern_6, ns=4

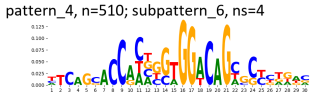

pattern_4, n=510; subpattern_7, ns=4

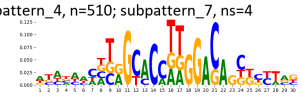

pattern_4, n=510; subpattern_8, ns=2



TF-MoDisCO pattern_4 n=510, PWM

pattern_4, n=510; subpattern_0, ns=159

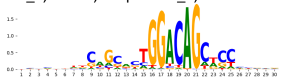

pattern_4, n=510; subpattern_1, ns=125

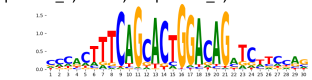

pattern_4, n=510; subpattern_2, ns=92

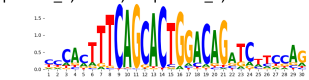

pattern_4, n=510; subpattern_3, ns=90

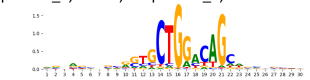

pattern_4, n=510; subpattern_4, ns=19

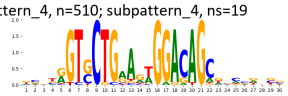

pattern_4, n=510; subpattern_5, ns=15

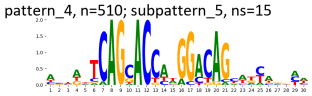

pattern_4, n=510; subpattern_6, ns=4

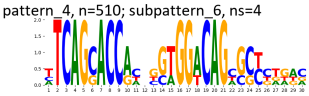

pattern_4, n=510; subpattern_7, ns=4

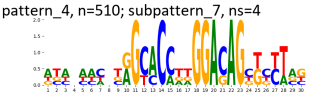

pattern_4, n=510; subpattern_8, ns=2

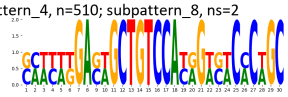

TF-MoDisCO pattern_5 n=304, CWM

pattern_5, n=304; subpattern_0, ns=79

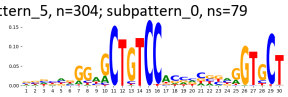

pattern_5, n=304; subpattern_1, ns=71

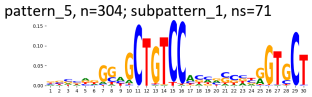

pattern_5, n=304; subpattern_2, ns=54

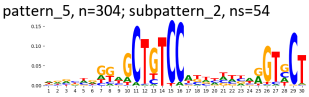

pattern_5, n=304; subpattern_3, ns=44

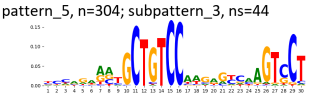

pattern_5, n=304; subpattern_4, ns=29

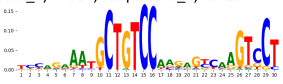

pattern_5, n=304; subpattern_5, ns=27

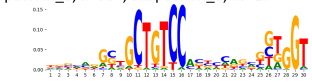

TF-MoDisCO pattern_5 n=304, PWM

pattern_5, n=304; subpattern_0, ns=79

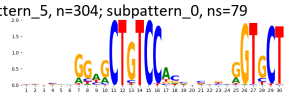

pattern_5, n=304; subpattern_1, ns=71

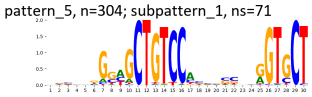

pattern_5, n=304; subpattern_2, ns=54

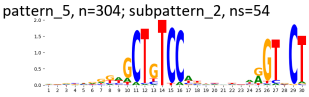

pattern_5, n=304; subpattern_3, ns=44

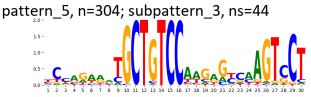

pattern_5, n=304; subpattern_4, ns=29

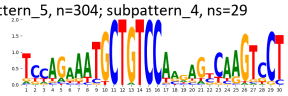

pattern_5, n=304; subpattern_5, ns=27

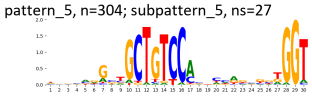

TF-MoDisCO pattern_6 n=302, CWM

pattern_6, n=302; subpattern_0, ns=102

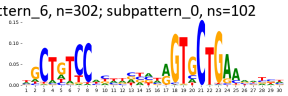

pattern_6, n=302; subpattern_1, ns=96

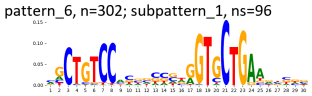

pattern_6, n=302; subpattern_2, ns=57

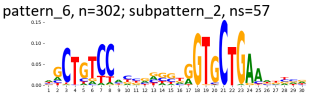

pattern_6, n=302; subpattern_3, ns=45

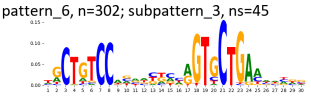

pattern_6, n=302; subpattern_4, ns=2

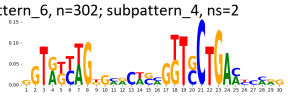

TF-MoDisCO pattern_6 n=302, PWM

pattern_6, n=302; subpattern_0, ns=102

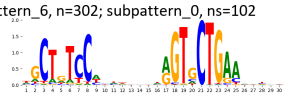

pattern_6, n=302; subpattern_1, ns=96

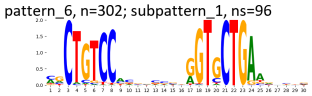

pattern_6, n=302; subpattern_2, ns=57

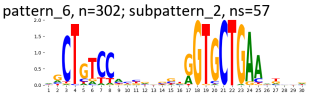

pattern_6, n=302; subpattern_3, ns=45

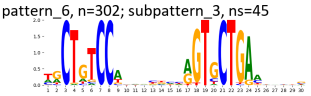

pattern_6, n=302; subpattern_4, ns=2

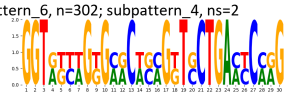

TF-MoDisCO pattern_7 n=109, CWM

pattern_7, n=109; subpattern_0, ns=35

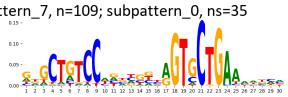

pattern_7, n=109; subpattern_1, ns=33

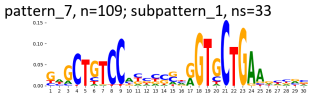

pattern_7, n=109; subpattern_2, ns=31

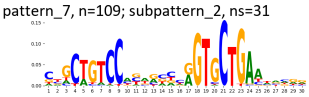

pattern_7, n=109; subpattern_3, ns=10

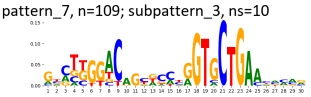

TF-MoDisCO pattern_7 n=109, PWM

pattern_7, n=109; subpattern_0, ns=35

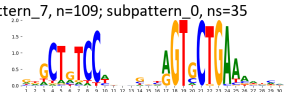

pattern_7, n=109; subpattern_1, ns=33

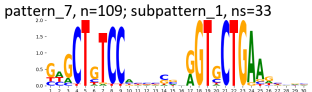

pattern_7, n=109; subpattern_2, ns=31

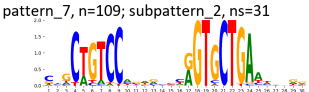

pattern_7, n=109; subpattern_3, ns=10

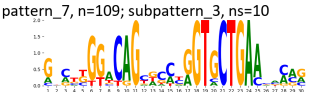

TF-MoDisCO pattern_9 n=96, CWM

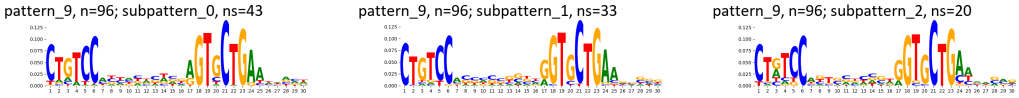

TF-MoDisCO pattern_9 n=96, PWM

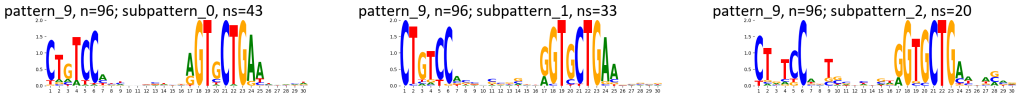

Supplementary Figure 231: TF-MoDisCO subpatterns for the REST transcription factor in H1 (accession ENCSR000BHM).



E

Ontology	Term	FDR Q-val
GO Biological Process	signal release	9.84
GO Biological Process	neurotransmitter secretion	8.29
GO Biological Process	regulation of cyclic nucleotide biosynthetic process	8.15
GO Biological Process	neurotransmitter transport	7.86
GO Biological Process	presynaptic process involved in chemical synaptic transmission	7.72
GO Biological Process	regulation of cAMP biosynthetic process	7.63
GO Biological Process	regulation of postsynaptic membrane potential	7.15
GO Biological Process	regulation of adenylate cyclase activity	6.60
GO Biological Process	regulation of cyclase activity	6.39
GO Biological Process	adenylate cyclase-activating G-protein coupled receptor signaling pathway	6.19
GO Biological Process	regulation of lyase activity	5.78
GO Biological Process	calcium ion regulated exocytosis	5.43
GO Biological Process	synaptic vesicle exocytosis	5.43
GO Biological Process	peptide hormone secretion	5.20
GO Biological Process	peptide secretion	5.16
GO Biological Process	positive regulation of cAMP metabolic process	5.00
GO Biological Process	positive regulation of cyclic nucleotide biosynthetic process	4.87
GO Biological Process	transmission of nerve impulse	4.71
GO Biological Process	positive regulation of cyclase activity	4.56
GO Biological Process	positive regulation of cAMP biosynthetic process	4.51

Supplementary Figure 232: Properties and genomic distribution of motifs identified for the REST transcription factor in HCT116 (accession ENCSR000BVI).

TF-MoDisCO pattern_0 n=2228, CWM

pattern_0, n=2228; subpattern_0, ns=519

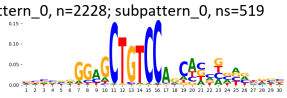

pattern_0, n=2228; subpattern_1, ns=467

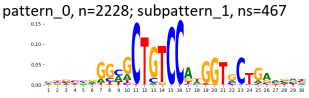

pattern_0, n=2228; subpattern_2, ns=409

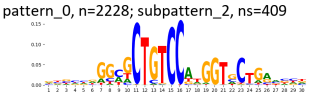

pattern_0, n=2228; subpattern_3, ns=371

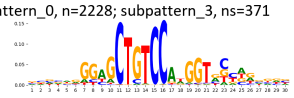

pattern_0, n=2228; subpattern_4, ns=159

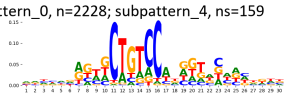

pattern_0, n=2228; subpattern_5, ns=130

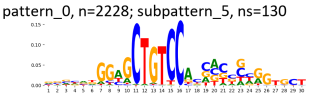

pattern_0, n=2228; subpattern_6, ns=91

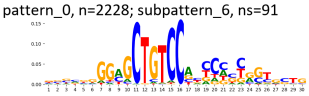

pattern_0, n=2228; subpattern_7, ns=53

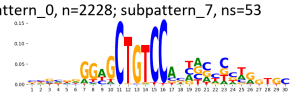

pattern_0, n=2228; subpattern_8, ns=29

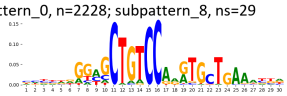

TF-MoDisCO pattern_0 n=2228, PWM

pattern_0, n=2228; subpattern_0, ns=519

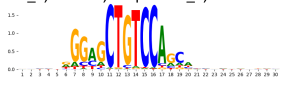

pattern_0, n=2228; subpattern_1, ns=467

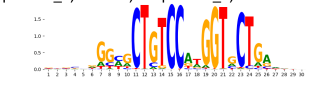

pattern_0, n=2228; subpattern_2, ns=409

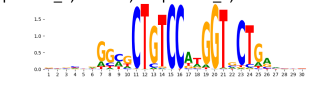

pattern_0, n=2228; subpattern_3, ns=371

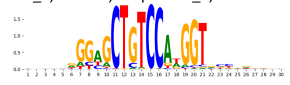

pattern_0, n=2228; subpattern_4, ns=159

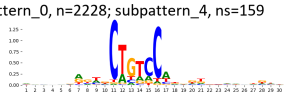

pattern_0, n=2228; subpattern_5, ns=130

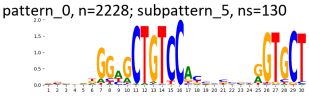

pattern_0, n=2228; subpattern_6, ns=91

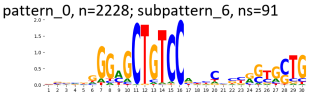

pattern_0, n=2228; subpattern_7, ns=53

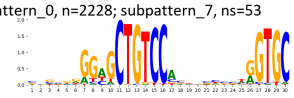

pattern_0, n=2228; subpattern_8, ns=29

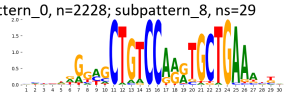

TF-MoDisCO pattern_1 n=1059, CWM

pattern_1, n=1059; subpattern_0, ns=287

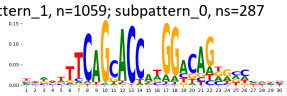

pattern_1, n=1059; subpattern_1, ns=272

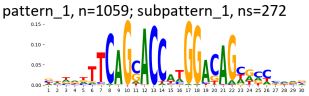

pattern_1, n=1059; subpattern_2, ns=182

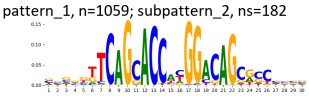

pattern_1, n=1059; subpattern_3, ns=157

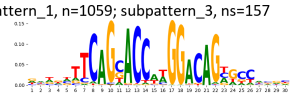

pattern_1, n=1059; subpattern_4, ns=98

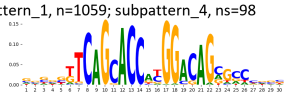

pattern_1, n=1059; subpattern_5, ns=63

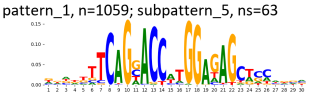

TF-MoDisCO pattern_1 n=1059, PWM

pattern_1, n=1059; subpattern_0, ns=287

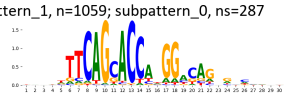

pattern_1, n=1059; subpattern_1, ns=272

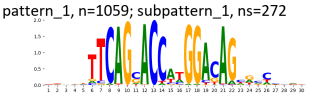

pattern_1, n=1059; subpattern_2, ns=182

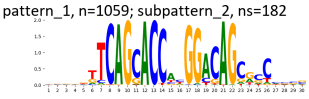

pattern_1, n=1059; subpattern_3, ns=157

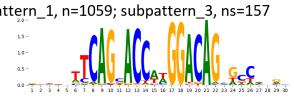

pattern_1, n=1059; subpattern_4, ns=98

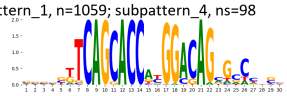

pattern_1, n=1059; subpattern_5, ns=63

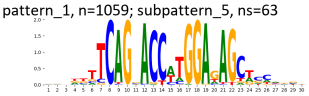

TF-MoDisCO pattern_2 n=183, CWM

pattern_2, n=183; subpattern_0, ns=60

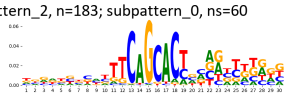

pattern_2, n=183; subpattern_1, ns=44

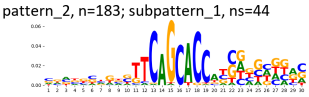

pattern_2, n=183; subpattern_2, ns=30

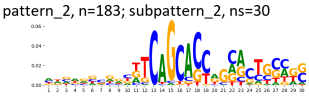

pattern_2, n=183; subpattern_3, ns=25

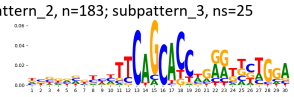

pattern_2, n=183; subpattern_4, ns=22

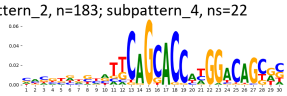

pattern_2, n=183; subpattern_5, ns=2

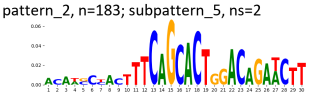

TF-MoDisCO pattern_2 n=183, PWM

pattern_2, n=183; subpattern_0, ns=60

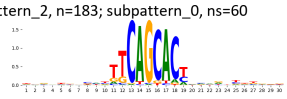

pattern_2, n=183; subpattern_1, ns=44

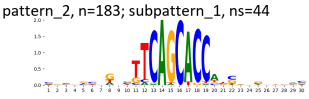

pattern_2, n=183; subpattern_2, ns=30

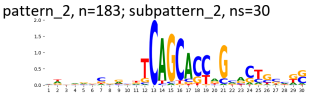

pattern_2, n=183; subpattern_3, ns=25

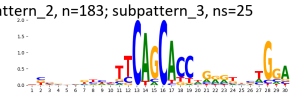

pattern_2, n=183; subpattern_4, ns=22

pattern_2, n=183; subpattern_5, ns=2

TF-MoDisCO pattern_5 n=114, CWM

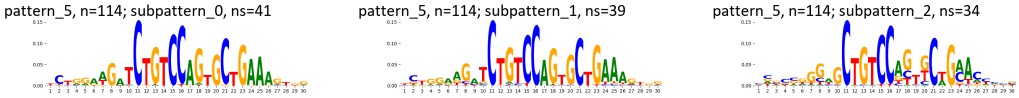

TF-MoDisCO pattern_5 n=114, PWM

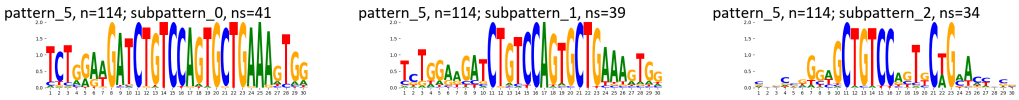

Supplementary Figure 233: TF-MoDisCO subpatterns for the REST transcription factor in HCT116 (accession ENCSR000BVI).

A

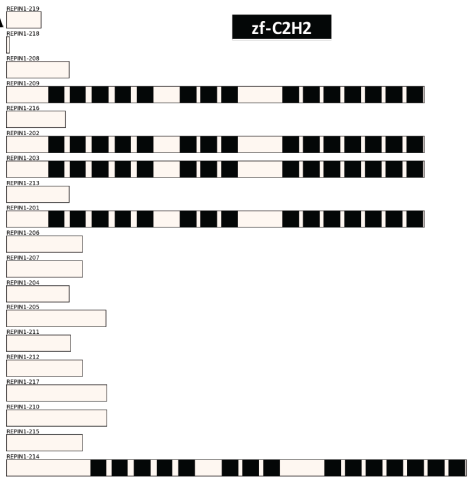

B

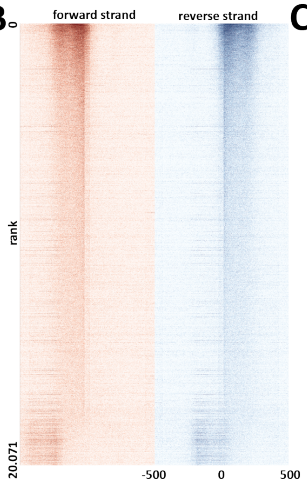

C

peaks	
state	fraction
Quies	0.32
TssA	0.20
TxWk	0.10
TssFlnk	0.09
EnhWk	0.06
TssBiv	0.04
Tx	0.04
ReprPCWk	0.03
ReprPC	0.03
EnhA1	0.02
EnhA2	0.02
TssFlnkU	0.02
TssFlnkD	0.01
EnhBiv	0.01
Het	0.01
EnhG1	0.00
EnhG2	0.00
ZNF/Rpts	0.00

D

peaks		peaks	
repeat	fraction	repeat	fraction
SINE/Alu	0.27	(AAAT)n	0.06
Simple_repeat	0.27	L2a	0.03
SINE/MIR	0.09	MIRb	0.03
LINE/L1	0.09	AluSx1	0.03
LINE/L2	0.08	AluY	0.03
DNA/hAT-Charlie	0.04	AluSx	0.03
LTR/ERVL-MaLR	0.03	AluJb	0.03
Low_complexity	0.03	MIR	0.02
LTR/ERVL	0.02	AluSz	0.02
LTR/ERV1	0.02	L2b	0.02
LINE/CR1	0.01	L2c	0.02
DNA/TcMar-Tigger	0.01	AluJo	0.02
tRNA	0.01	AluSq2	0.02
DNA/hAT-Tip100	0.01	MIR3	0.02
DNA/hAT-Blackjack	0.00	AluJr	0.02
Retroposon/SVA	0.00	(ATTT)n	0.01
LTR/Gypsy	0.00	(TTTA)n	0.01
LINE/RTE-X	0.00	MIRc	0.01

E

Ontology	Term	FDR Q-val
GO Biological Process	regulation of Rac protein signal transduction	5.64

F

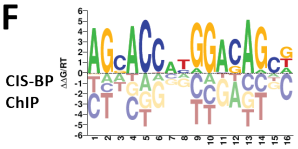

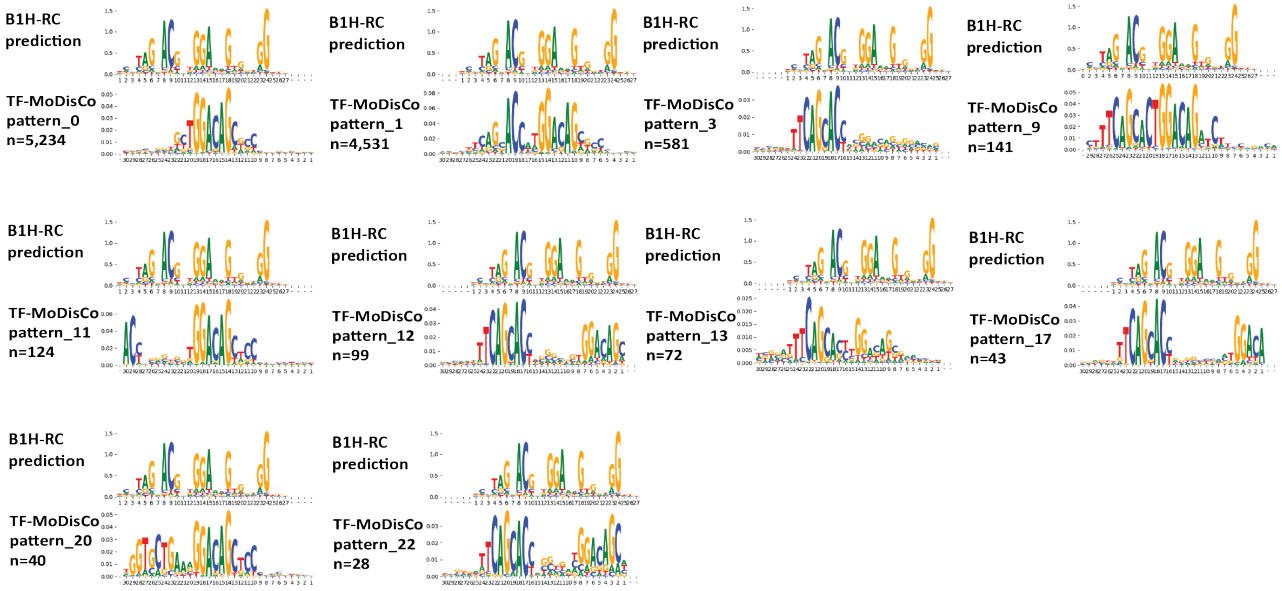

G

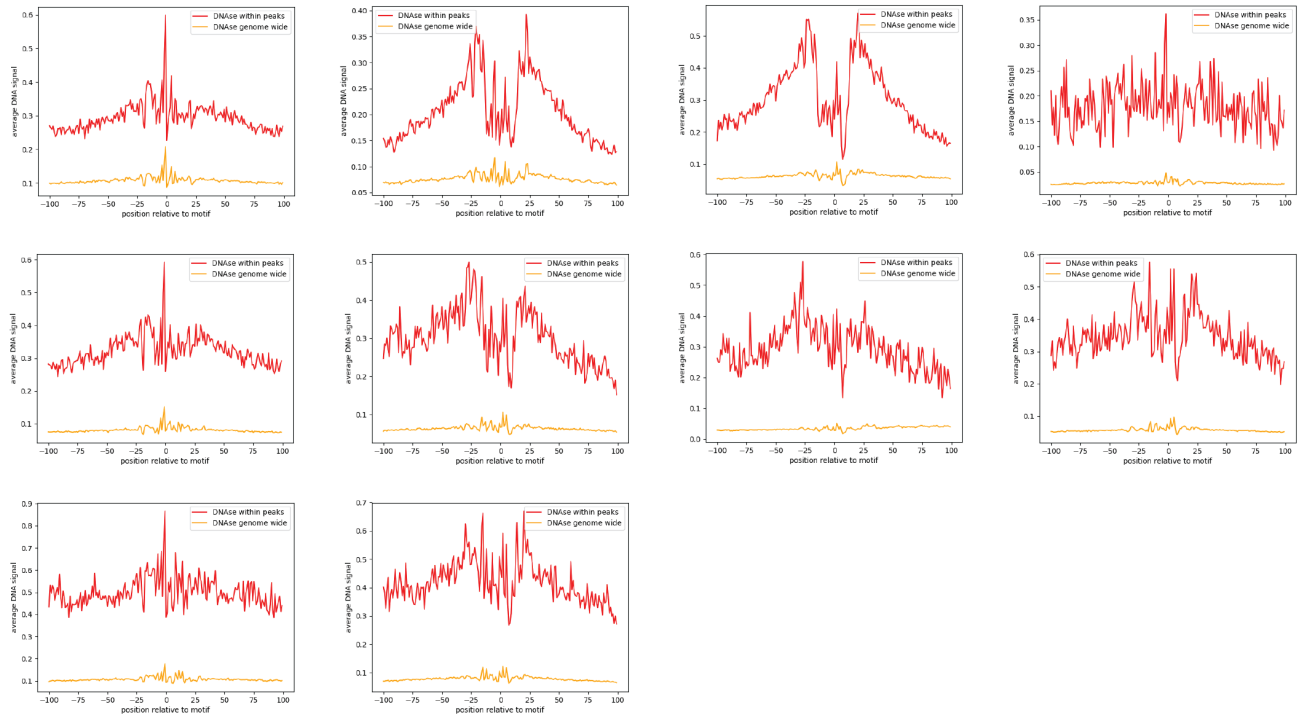
DNAse within peaks
DNAse genome wide
average DNA signal
position relative to motif

H

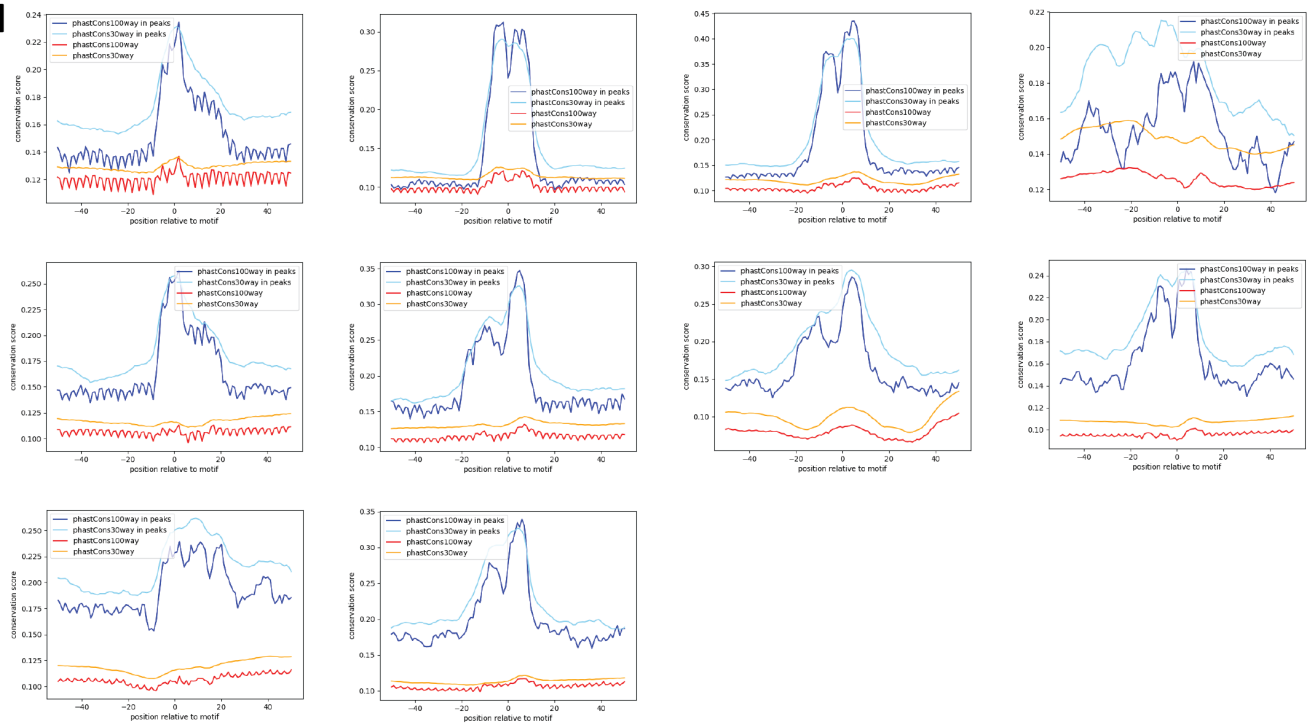
phastCons100way in peaks
phastCons30way in peaks
phastCons100way
phastCons30way
conservation score
position relative to motif

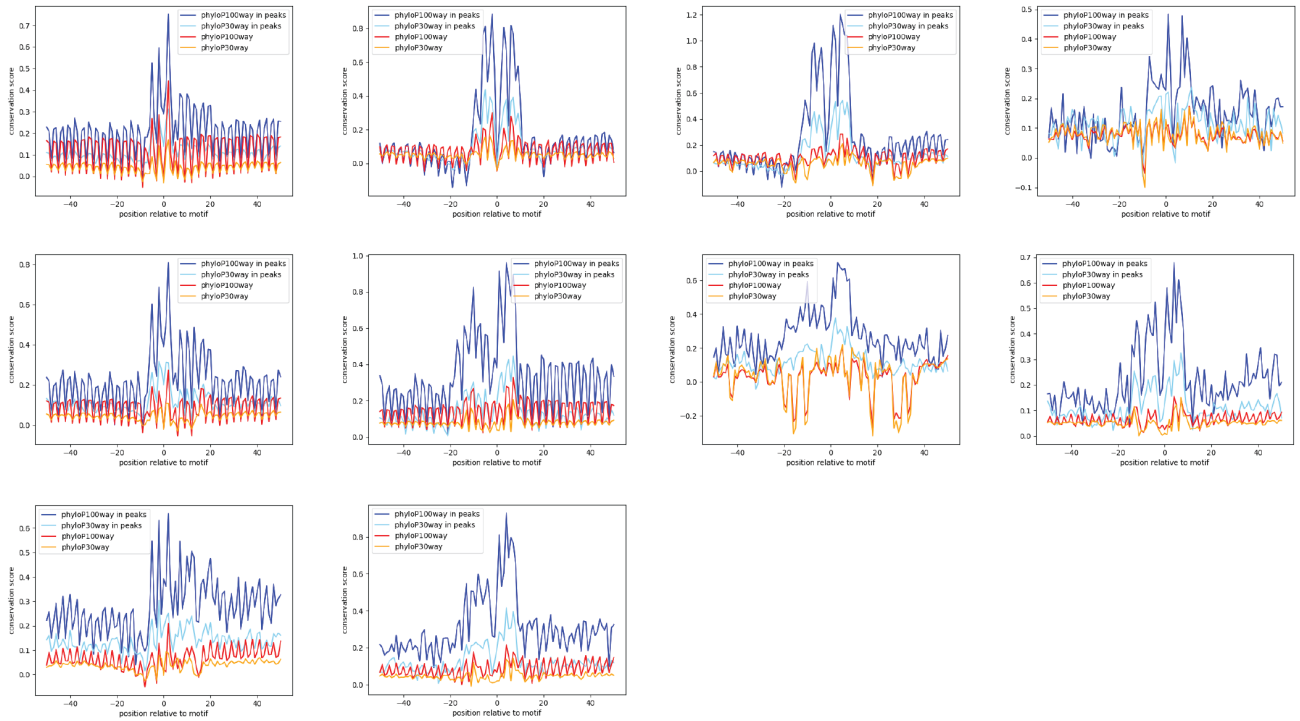

Supplementary Figure 234: Properties and genomic distribution of motifs identified for the REST transcription factor in HEK293 (accession ENCSR896UBV).

TF-MoDisCO pattern_0 n=5234, CWM

pattern_0, n=5234; subpattern_0, ns=998

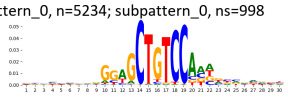

pattern_0, n=5234; subpattern_1, ns=842

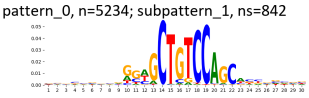

pattern_0, n=5234; subpattern_2, ns=781

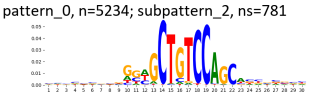

pattern_0, n=5234; subpattern_3, ns=741

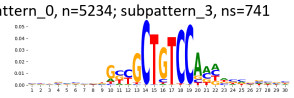

pattern_0, n=5234; subpattern_4, ns=609

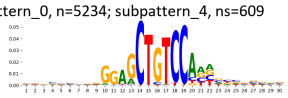

pattern_0, n=5234; subpattern_5, ns=409

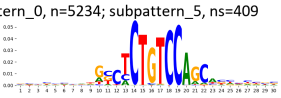

pattern_0, n=5234; subpattern_6, ns=377

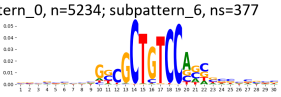

pattern_0, n=5234; subpattern_7, ns=286

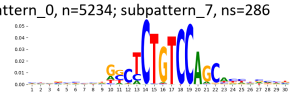

pattern_0, n=5234; subpattern_8, ns=113

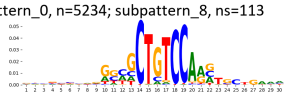

pattern_0, n=5234; subpattern_9, ns=78

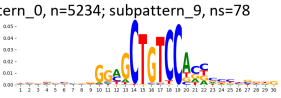

TF-MoDisCO pattern_0 n=5234, PWM

pattern_0, n=5234; subpattern_0, ns=998

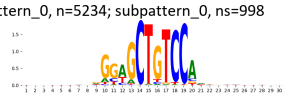

pattern_0, n=5234; subpattern_1, ns=842

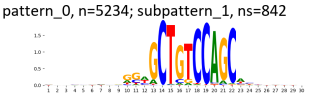

pattern_0, n=5234; subpattern_2, ns=781

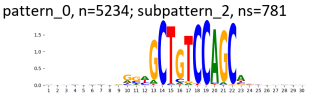

pattern_0, n=5234; subpattern_3, ns=741

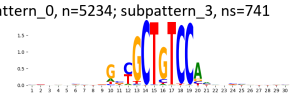

pattern_0, n=5234; subpattern_4, ns=609

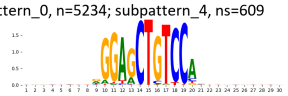

pattern_0, n=5234; subpattern_5, ns=409

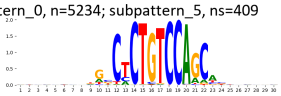

pattern_0, n=5234; subpattern_6, ns=377

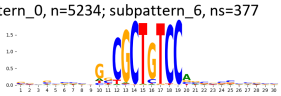

pattern_0, n=5234; subpattern_7, ns=286

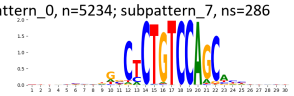

pattern_0, n=5234; subpattern_8, ns=113

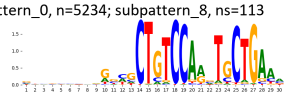

pattern_0, n=5234; subpattern_9, ns=78

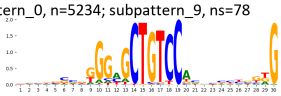

TF-MoDisCO pattern_1 n=4531, CWM

pattern_1, n=4531; subpattern_0, ns=1193

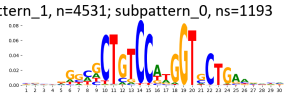

pattern_1, n=4531; subpattern_1, ns=1039

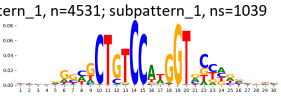

pattern_1, n=4531; subpattern_2, ns=671

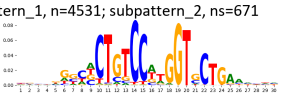

pattern_1, n=4531; subpattern_3, ns=586

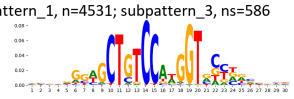

pattern_1, n=4531; subpattern_4, ns=521

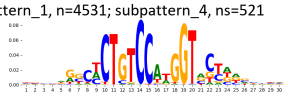

pattern_1, n=4531; subpattern_5, ns=517

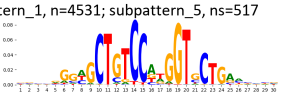

pattern_1, n=4531; subpattern_6, ns=4

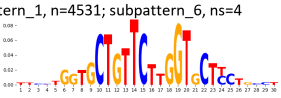

TF-MoDisCO pattern_1 n=4531, PWM

pattern_1, n=4531; subpattern_0, ns=1193

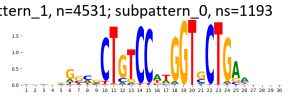

pattern_1, n=4531; subpattern_1, ns=1039

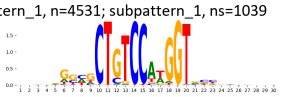

pattern_1, n=4531; subpattern_2, ns=671

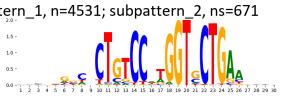

pattern_1, n=4531; subpattern_3, ns=586

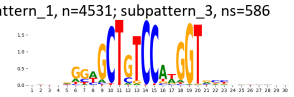

pattern_1, n=4531; subpattern_4, ns=521

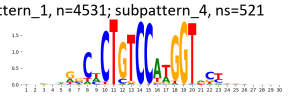

pattern_1, n=4531; subpattern_5, ns=517

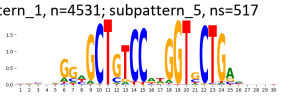

pattern_1, n=4531; subpattern_6, ns=4

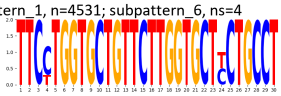

TF-MoDisCO pattern_11 n=124, CWM

pattern_11, n=124; subpattern_0, ns=32

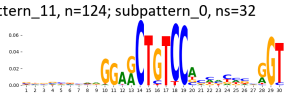

pattern_11, n=124; subpattern_1, ns=31

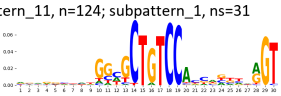

pattern_11, n=124; subpattern_2, ns=29

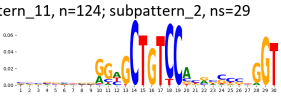

pattern_11, n=124; subpattern_3, ns=28

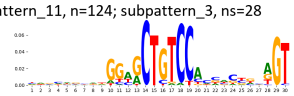

pattern_11, n=124; subpattern_4, ns=4

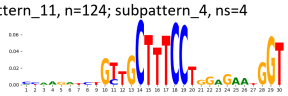

TF-MoDisCO pattern_11 n=124, PWM

pattern_11, n=124; subpattern_0, ns=32

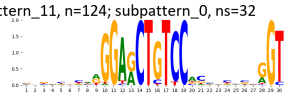

pattern_11, n=124; subpattern_1, ns=31

pattern_11, n=124; subpattern_2, ns=29

pattern_11, n=124; subpattern_3, ns=28

pattern_11, n=124; subpattern_4, ns=4

TF-MoDisCO pattern_12 n=99, CWM

pattern_12, n=99; subpattern_0, ns=36

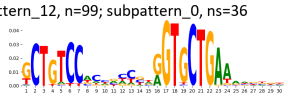

pattern_12, n=99; subpattern_1, ns=30

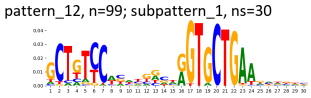

pattern_12, n=99; subpattern_2, ns=28

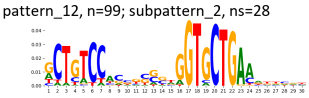

pattern_12, n=99; subpattern_3, ns=5

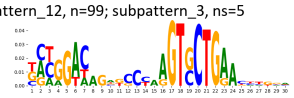

TF-MoDisCO pattern_12 n=99, PWM

pattern_12, n=99; subpattern_0, ns=36

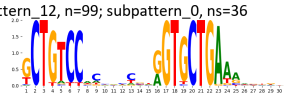

pattern_12, n=99; subpattern_1, ns=30

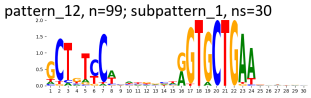

pattern_12, n=99; subpattern_2, ns=28

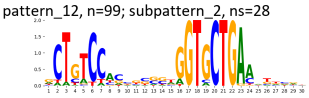

pattern_12, n=99; subpattern_3, ns=5

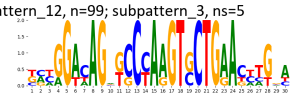

TF-MoDisCO pattern_13 n=72, CWM

pattern_13, n=72; subpattern_0, ns=26

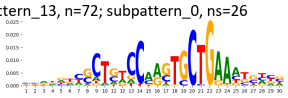

pattern_13, n=72; subpattern_1, ns=24

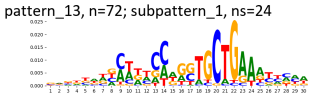

pattern_13, n=72; subpattern_2, ns=22

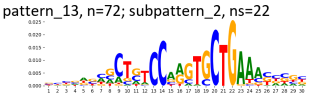

TF-MoDisCO pattern_13 n=72, PWM

pattern_13, n=72; subpattern_0, ns=26

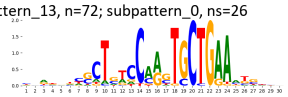

pattern_13, n=72; subpattern_1, ns=24

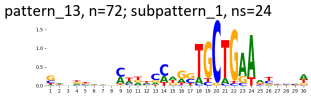

pattern_13, n=72; subpattern_2, ns=22

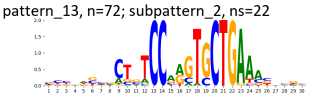

TF-MoDisCO pattern_17 n=43, CWM

pattern_17, n=43; subpattern_0, ns=43

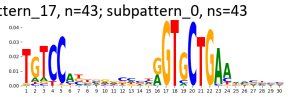

TF-MoDisCO pattern_17 n=43, PWM

pattern_17, n=43; subpattern_0, ns=43

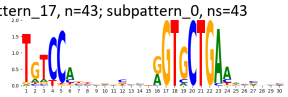

TF-MoDisCO pattern_20 n=40, CWM

pattern_20, n=40; subpattern_0, ns=40

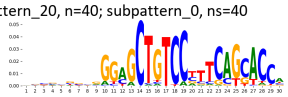

TF-MoDisCO pattern_20 n=40, PWM

pattern_20, n=40; subpattern_0, ns=40

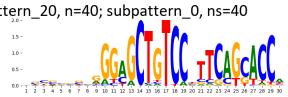

TF-MoDisCO pattern_22 n=28, CWM

pattern_22, n=28; subpattern_0, ns=28

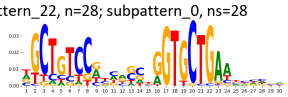

TF-MoDisCO pattern_22 n=28, PWM

pattern_22, n=28; subpattern_0, ns=28

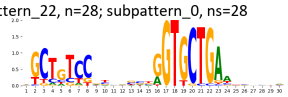

TF-MoDisCO pattern_3 n=581, CWM

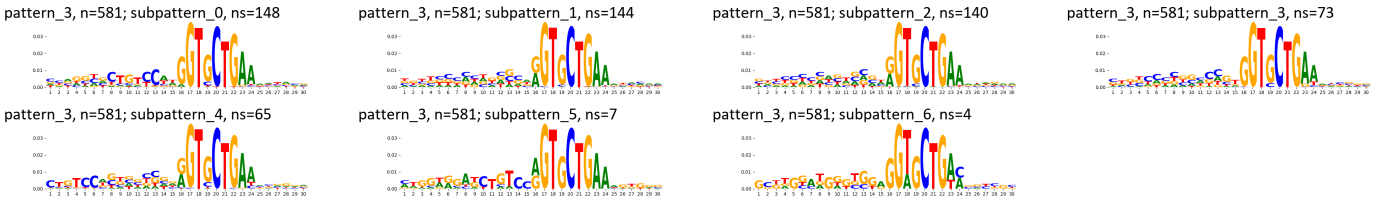

TF-MoDisCO pattern_3 n=581, PWM

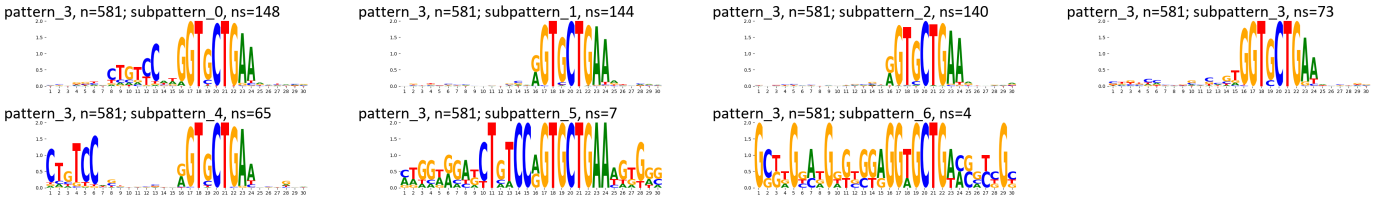

TF-MoDisCO pattern_9 n=141, CWM



TF-MoDisCO pattern_9 n=141, PWM

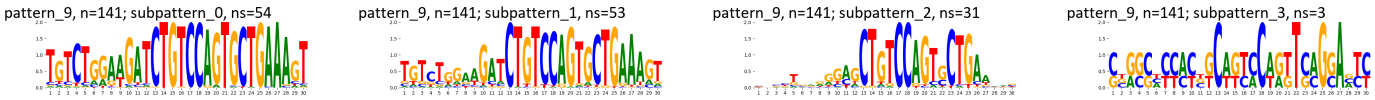

Supplementary Figure 235: TF-MoDisCO subpatterns for the REST transcription factor in HEK293 (accession ENCSR896UBV).

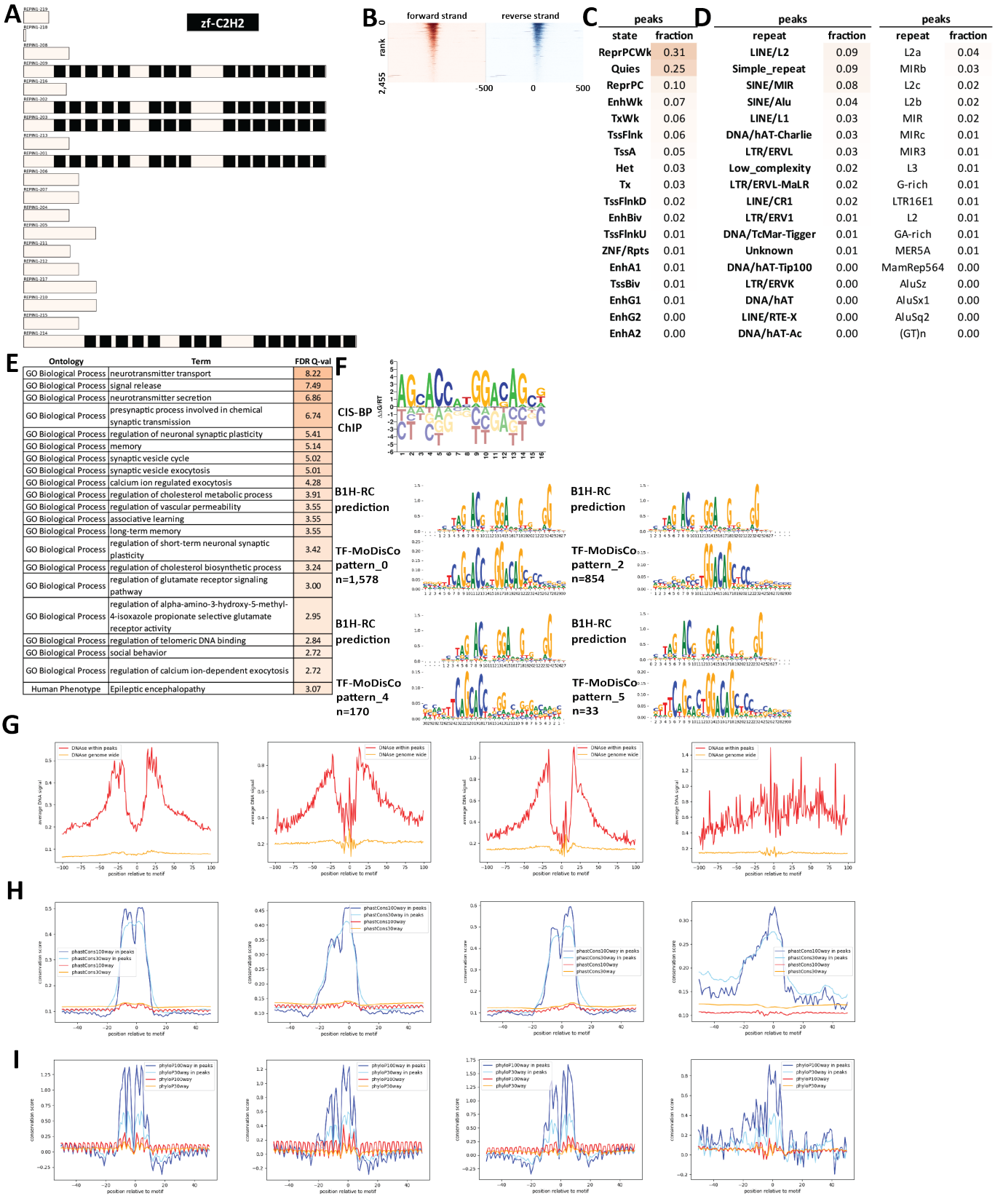

Supplementary Figure 236: Properties and genomic distribution of motifs identified for the REST transcription factor in HepG2 (accession ENCSR000BJL).

TF-MoDisCO pattern_0 n=1578, CWM

pattern_0, n=1578; subpattern_0, ns=317

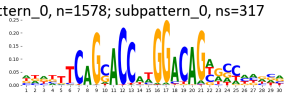

pattern_0, n=1578; subpattern_1, ns=295

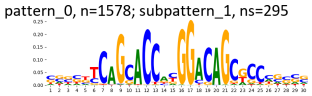

pattern_0, n=1578; subpattern_2, ns=237

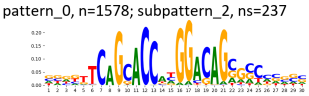

pattern_0, n=1578; subpattern_3, ns=221

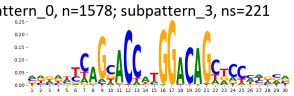

pattern_0, n=1578; subpattern_4, ns=180

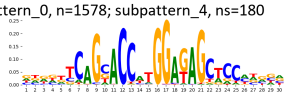

pattern_0, n=1578; subpattern_5, ns=175

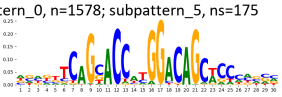

pattern_0, n=1578; subpattern_6, ns=153

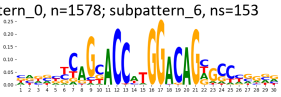

TF-MoDisCO pattern_0 n=1578, PWM

pattern_0, n=1578; subpattern_0, ns=317

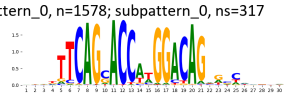

pattern_0, n=1578; subpattern_1, ns=295

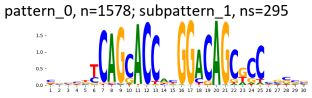

pattern_0, n=1578; subpattern_2, ns=237

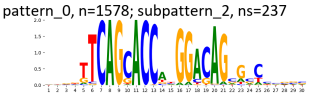

pattern_0, n=1578; subpattern_3, ns=221

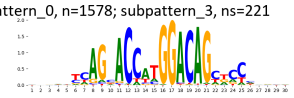

pattern_0, n=1578; subpattern_4, ns=180

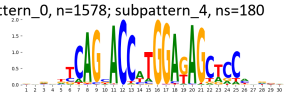

pattern_0, n=1578; subpattern_5, ns=175

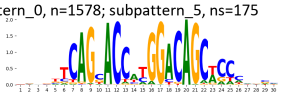

pattern_0, n=1578; subpattern_6, ns=153

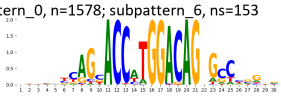

TF-MoDisCO pattern_2 n=854, CWM

pattern_2, n=854; subpattern_0, ns=233

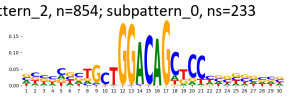

pattern_2, n=854; subpattern_1, ns=199

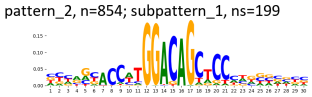

pattern_2, n=854; subpattern_2, ns=171

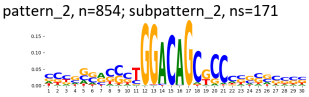

pattern_2, n=854; subpattern_3, ns=144

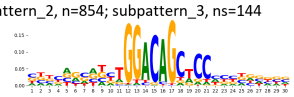

pattern_2, n=854; subpattern_4, ns=80

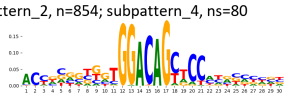

pattern_2, n=854; subpattern_5, ns=27

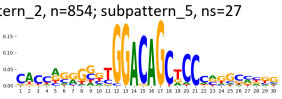

TF-MoDisCO pattern_2 n=854, PWM

pattern_2, n=854; subpattern_0, ns=233

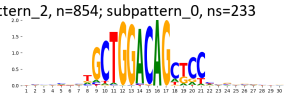

pattern_2, n=854; subpattern_1, ns=199

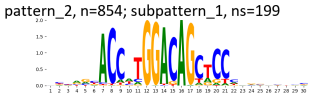

pattern_2, n=854; subpattern_2, ns=171

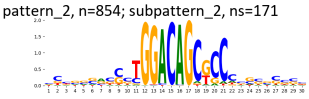

pattern_2, n=854; subpattern_3, ns=144

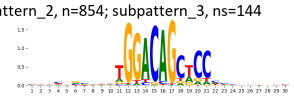

pattern_2, n=854; subpattern_4, ns=80

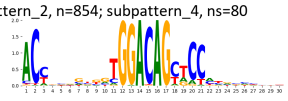

pattern_2, n=854; subpattern_5, ns=27

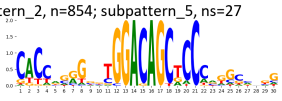

TF-MoDisCO pattern_4 n=170, CWM

pattern_4, n=170; subpattern_0, ns=43

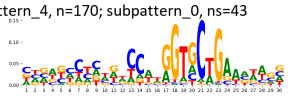

pattern_4, n=170; subpattern_1, ns=42

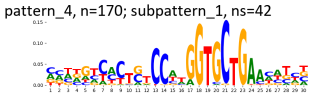

pattern_4, n=170; subpattern_2, ns=31

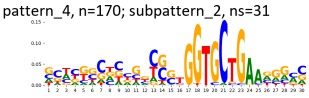

pattern_4, n=170; subpattern_3, ns=25

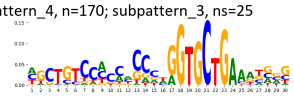

pattern_4, n=170; subpattern_4, ns=23

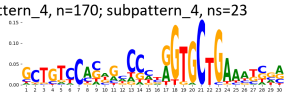

pattern_4, n=170; subpattern_5, ns=6

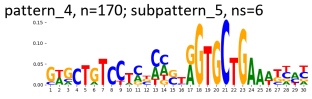

TF-MoDisCO pattern_4 n=170, PWM

pattern_4, n=170; subpattern_0, ns=43

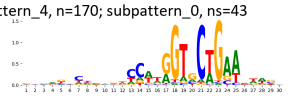

pattern_4, n=170; subpattern_1, ns=42

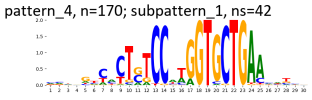

pattern_4, n=170; subpattern_2, ns=31

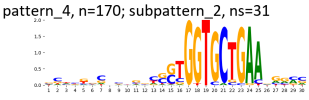

pattern_4, n=170; subpattern_3, ns=25

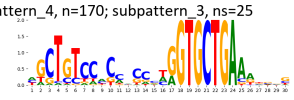

pattern_4, n=170; subpattern_4, ns=23

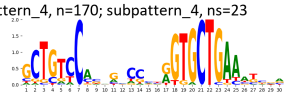

pattern_4, n=170; subpattern_5, ns=6

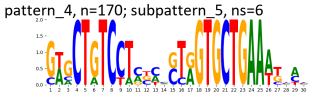

TF-MoDisCO pattern_5 n=33, CWM

pattern_5, n=33; subpattern_0, ns=33

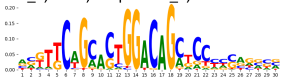

TF-MoDisCO pattern_5 n=33, PWM

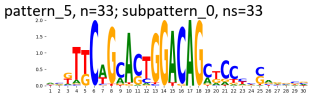

Supplementary Figure 237: TF-MoDisCO subpatterns for the REST transcription factor in HepG2 (accession ENCSR000BJL).

A

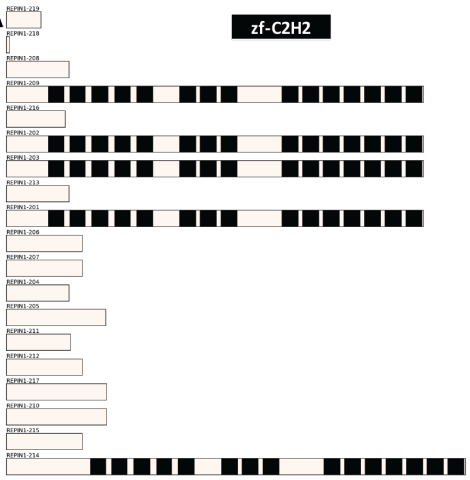

B

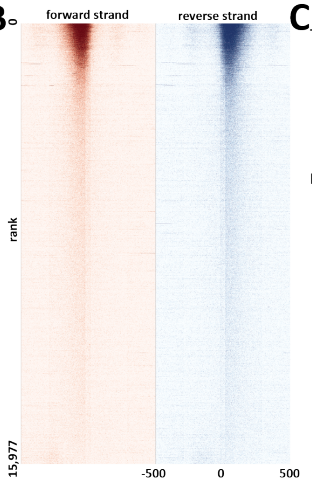

C

peaks	
state	fraction
TssA	0.34
EnhA1	0.17
TssFlnkU	0.14
TssFlnk	0.12
EnhWk	0.09
ReprPCWk	0.07
Quies	0.07
TssFlnkD	0.04
EnhA2	0.03
ReprPC	0.03
TxWk	0.02
EnhBiv	0.01
EnhG2	0.01
Het	0.01
Tx	0.01
TssBiv	0.01
EnhG1	0.00
ZNF/Rpts	0.00

D

peaks		peaks	
repeat	fraction	repeat	fraction
Simple_repeat	0.12	MIRb	0.03
SINE/MIR	0.08	L2a	0.03
LINE/L2	0.07	MIR	0.02
SINE/Alu	0.05	L2c	0.02
LINE/L1	0.04	L2b	0.02
DNA/hAT-Charlie	0.03	G-rich	0.02
Low_complexity	0.03	MIR3	0.01
LTR/ERV1	0.02	MIRc	0.01
LTR/ERVL	0.02	AluJb	0.01
LTR/ERVL-MaLR	0.02	L3	0.01
LINE/CR1	0.01	GA-rich	0.01
DNA/TcMar-Tigger	0.01	AluJr	0.01
DNA/hAT-Tip100	0.01	L2	0.01
tRNA	0.00	AluJo	0.01
LTR/ERVK	0.00	AluSx1	0.00
DNA/hAT-Blackjack	0.00	AluSx	0.00
LINE/RTE-BovB	0.00	(GGC)n	0.00
LTR/Gypsy	0.00	AluSz	0.00

E

Ontology	Term	FDR Q-val
GO Biological Process	regulation of transcription from RNA polymerase II promoter in response to stress	31.43
GO Biological Process	regulation of DNA-templated transcription in response to stress	30.54
GO Biological Process	multi-organism metabolic process	21.53
GO Biological Process	nuclear-transcribed mRNA catabolic process, nonsense-mediated decay	20.92
GO Biological Process	cotranslational protein targeting to membrane	20.14
GO Biological Process	protein targeting to ER	19.03
GO Biological Process	viral gene expression	19.01
GO Biological Process	regulation of transcription from RNA polymerase II promoter in response to hypoxia	19.00
GO Biological Process	SRP-dependent cotranslational protein targeting to membrane	18.78
GO Biological Process	endoplasmic reticulum unfolded protein response	18.08
GO Biological Process	viral transcription	16.04
GO Biological Process	regulation of cellular amino acid metabolic process	15.76
GO Biological Process	triglyceride homeostasis	15.69
GO Biological Process	establishment of protein localization to endoplasmic reticulum	14.86
GO Biological Process	plasma lipoprotein particle remodeling	13.61
GO Biological Process	regulation of plasma lipoprotein particle levels	13.46
GO Biological Process	snRNA metabolic process	11.64
GO Biological Process	cytoplasmic translation	10.91
GO Biological Process	mitochondrial translational termination	10.82
GO Biological Process	mitochondrial translational elongation	10.35
Human Phenotype	Abnormality of mitochondrial metabolism	11.29
Human Phenotype	Abnormality of the mitochondrion	10.91

F

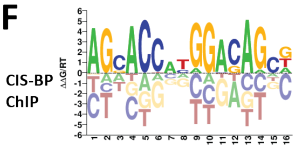

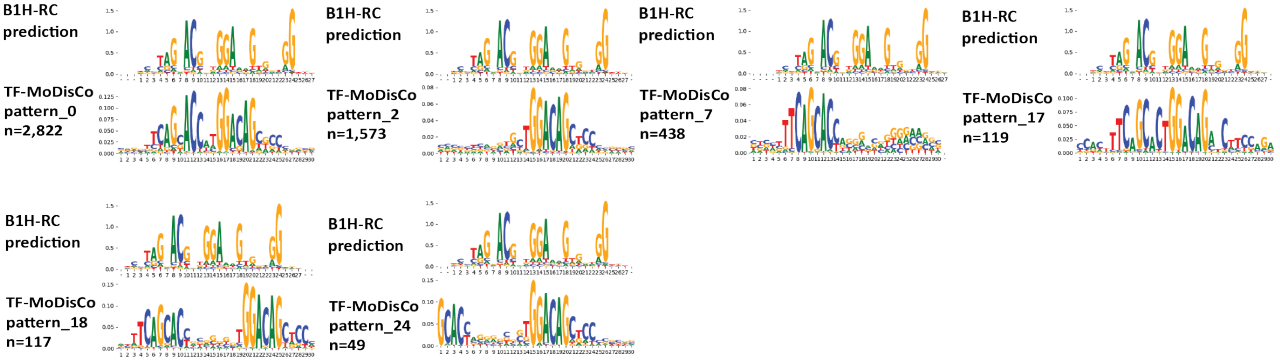

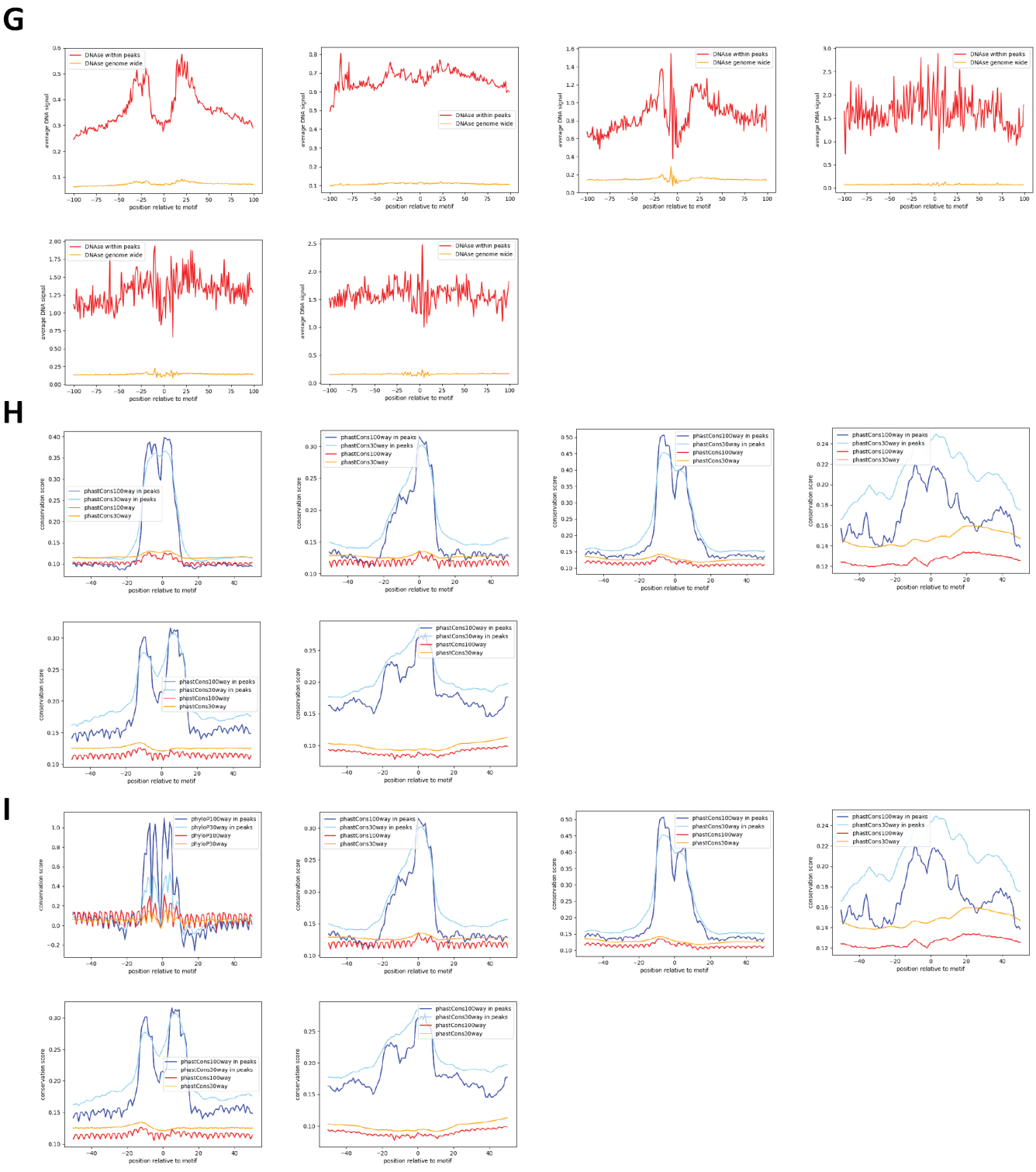

Supplementary Figure 238: Properties and genomic distribution of motifs identified for the REST transcription factor in HepG2 (accession ENCSR000BOT).

TF-MoDisCO pattern_0 n=2822, CWM

pattern_0, n=2822; subpattern_0, ns=754

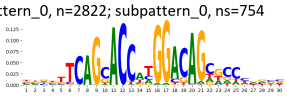

pattern_0, n=2822; subpattern_1, ns=584

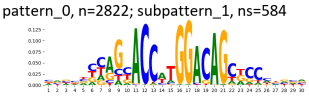

pattern_0, n=2822; subpattern_2, ns=409

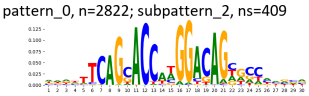

pattern_0, n=2822; subpattern_3, ns=357

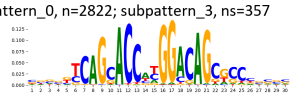

pattern_0, n=2822; subpattern_4, ns=333

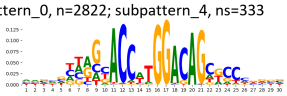

pattern_0, n=2822; subpattern_5, ns=235

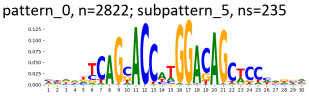

pattern_0, n=2822; subpattern_6, ns=150

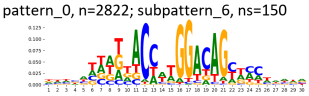

TF-MoDisCO pattern_0 n=2822, PWM

pattern_0, n=2822; subpattern_0, ns=754

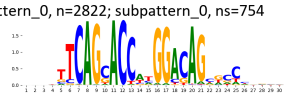

pattern_0, n=2822; subpattern_1, ns=584

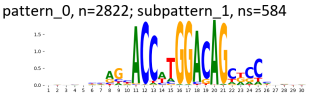

pattern_0, n=2822; subpattern_2, ns=409

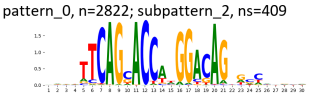

pattern_0, n=2822; subpattern_3, ns=357

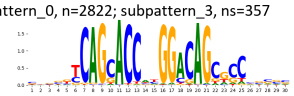

pattern_0, n=2822; subpattern_4, ns=333

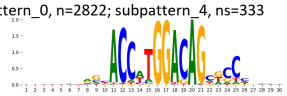

pattern_0, n=2822; subpattern_5, ns=235

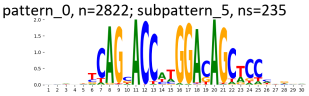

pattern_0, n=2822; subpattern_6, ns=150

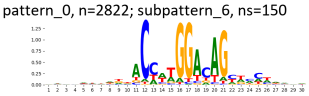

TF-MoDisCO pattern_17 n=119, CWM

pattern_17, n=119; subpattern_0, ns=53

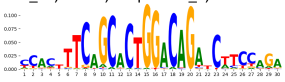

pattern_17, n=119; subpattern_1, ns=34

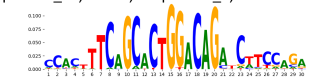

pattern_17, n=119; subpattern_2, ns=23

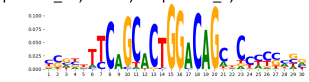

pattern_17, n=119; subpattern_3, ns=5

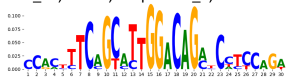

pattern_17, n=119; subpattern_4, ns=2

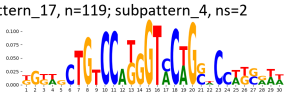

pattern_17, n=119; subpattern_5, ns=2

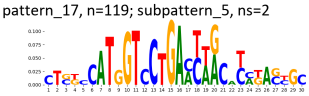

TF-MoDisCO pattern_17 n=119, PWM

pattern_17, n=119; subpattern_0, ns=53

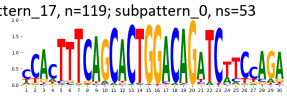

pattern_17, n=119; subpattern_1, ns=34

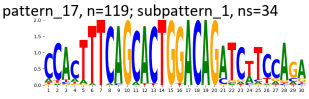

pattern_17, n=119; subpattern_2, ns=23

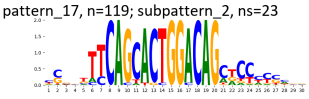

pattern_17, n=119; subpattern_3, ns=5

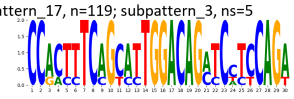

pattern_17, n=119; subpattern_4, ns=2

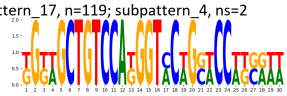

pattern_17, n=119; subpattern_5, ns=2

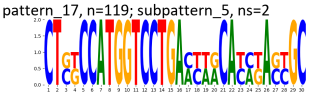

TF-MoDisCO pattern_18 n=117, CWM

pattern_18, n=117; subpattern_0, ns=26

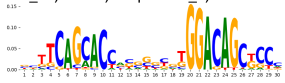

pattern_18, n=117; subpattern_1, ns=25

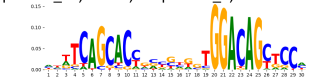

pattern_18, n=117; subpattern_2, ns=24

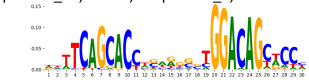

pattern_18, n=117; subpattern_3, ns=23

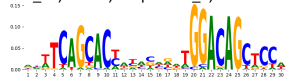

pattern_18, n=117; subpattern_4, ns=19

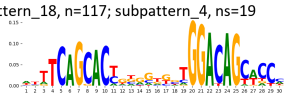

TF-MoDisCO pattern_18 n=117, PWM

pattern_18, n=117; subpattern_0, ns=26

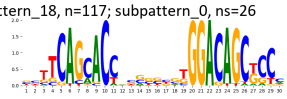

pattern_18, n=117; subpattern_1, ns=25

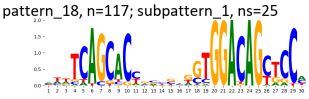

pattern_18, n=117; subpattern_2, ns=24

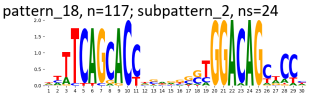

pattern_18, n=117; subpattern_3, ns=23

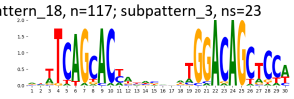

pattern_18, n=117; subpattern_4, ns=19

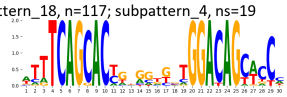

TF-MoDisCO pattern_2 n=1573, CWM

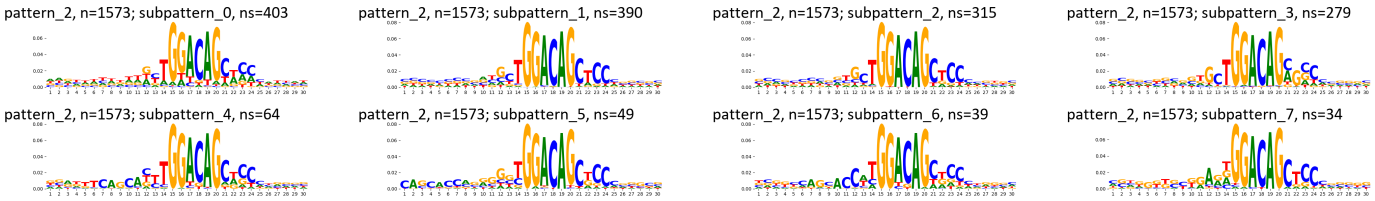

TF-MoDisCO pattern_2 n=1573, PWM

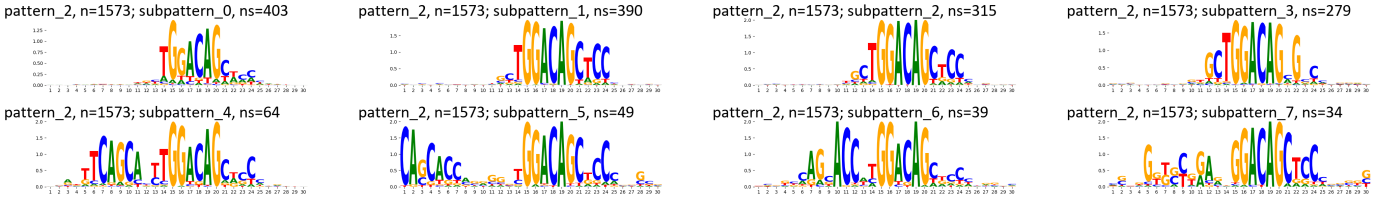

TF-MoDisCO pattern_24 n=49, CWM

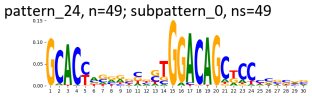

TF-MoDisCO pattern_24 n=49, PWM

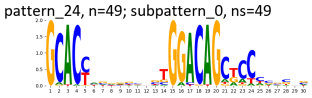

TF-MoDisCO pattern_7 n=438, CWM

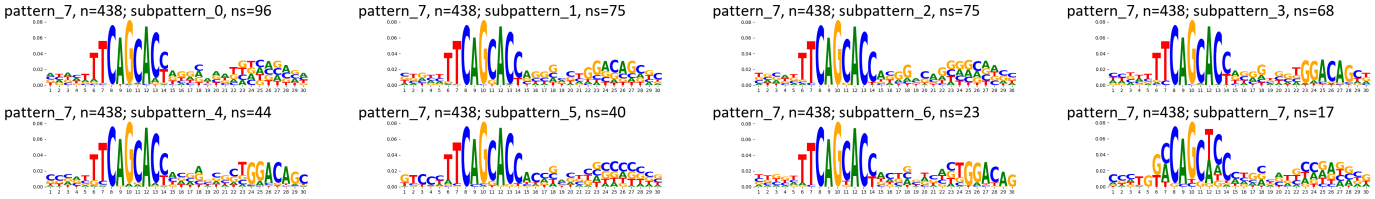

TF-MoDisCO pattern_7 n=438, PWM

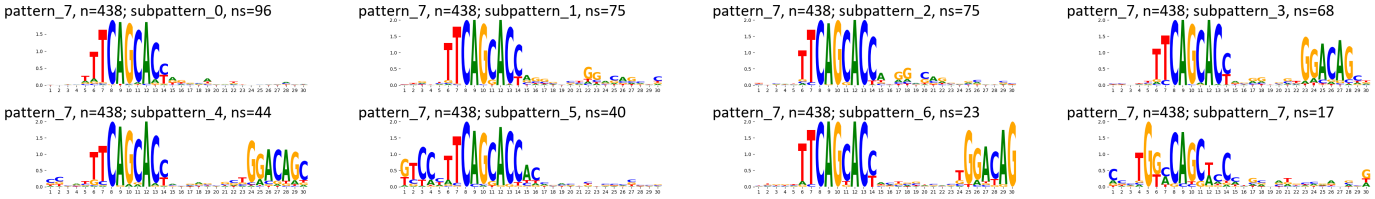

Supplementary Figure 239: TF-MoDisCO subpatterns for the REST transcription factor in HepG2 (accession ENCSR000BOT).

A

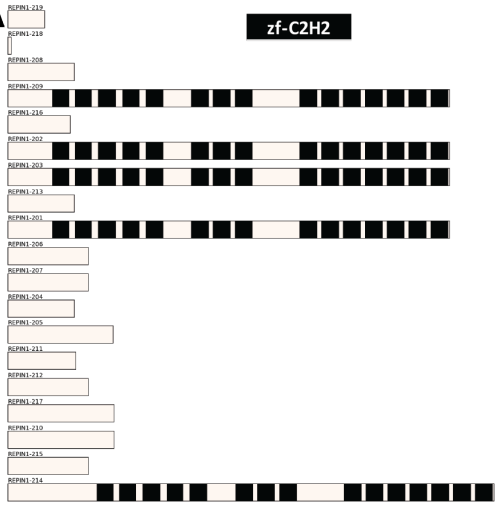

B

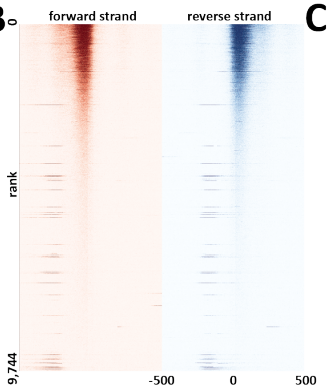

C n/a

D n/a

E

Ontology	Term	FDR Q-val
GO Biological Process	negative regulation of stem cell differentiation	4.96
GO Biological Process	protein-DNA complex disassembly	4.66
GO Biological Process	renal system process involved in regulation of blood volume	4.30
GO Biological Process	regulation of development, heterochronic	3.20
GO Biological Process	synapse maturation	1.87
GO Biological Process	regulation of type B pancreatic cell apoptotic process	1.70
GO Biological Process	positive regulation of epithelial cell differentiation involved in kidney development	1.37

F

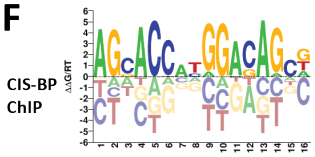

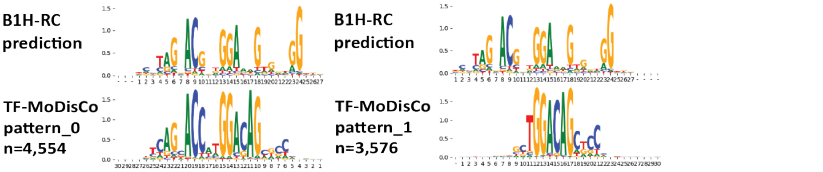

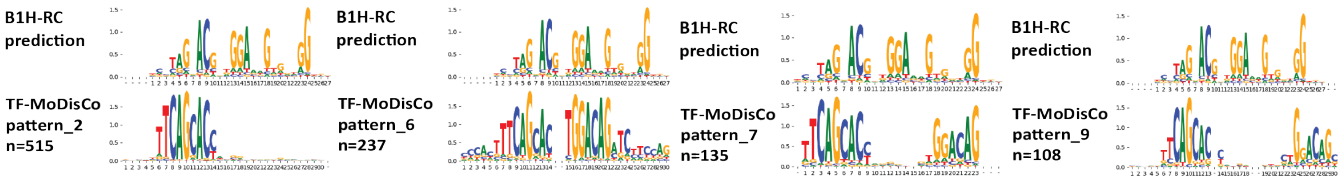

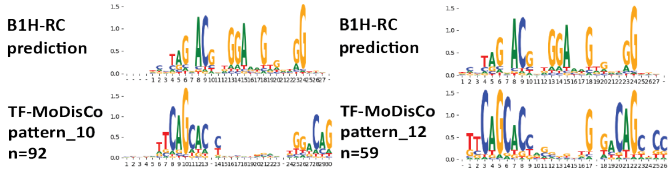

G n/a

H

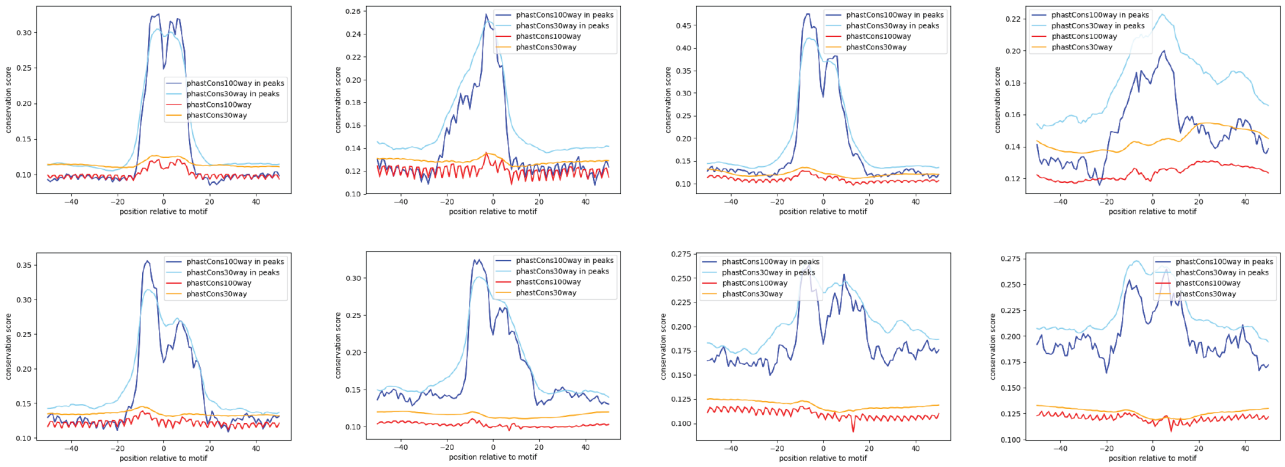

I

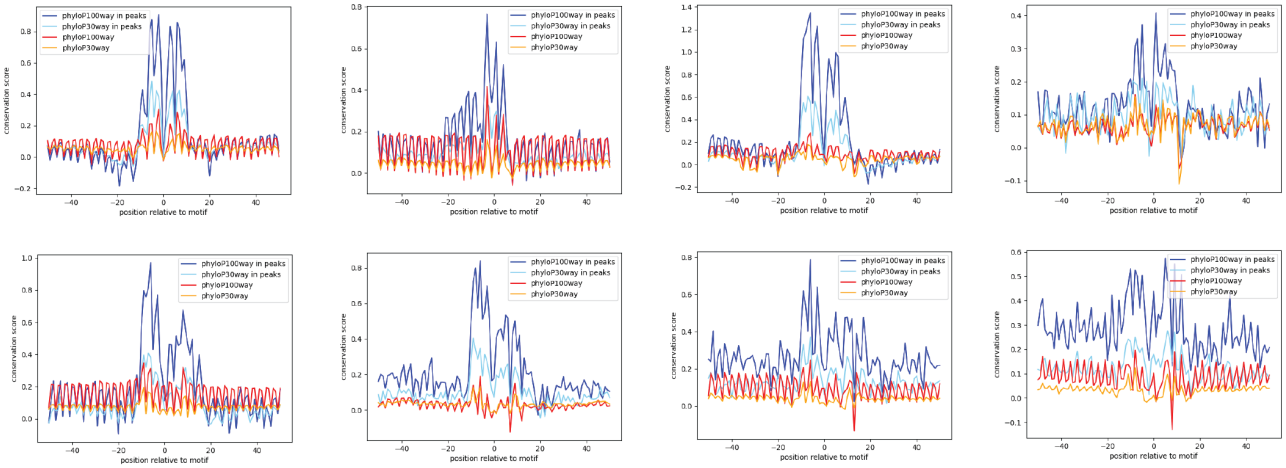

Supplementary Figure 240: Properties and genomic distribution of motifs identified for the REST transcription factor in Ishikawa (accession ENCSR000BUU).

TF-MoDisCO pattern_0 n=4554, CWM

pattern_0, n=4554; subpattern_0, ns=977

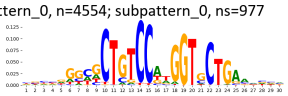

pattern_0, n=4554; subpattern_1, ns=776

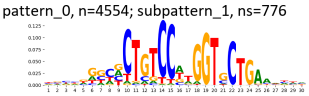

pattern_0, n=4554; subpattern_2, ns=754

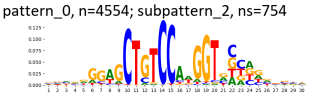

pattern_0, n=4554; subpattern_3, ns=646

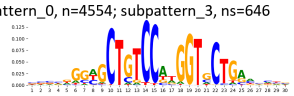

pattern_0, n=4554; subpattern_4, ns=631

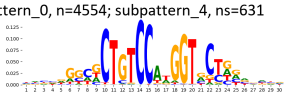

pattern_0, n=4554; subpattern_5, ns=551

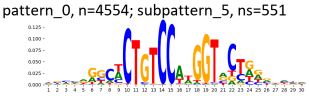

pattern_0, n=4554; subpattern_6, ns=155

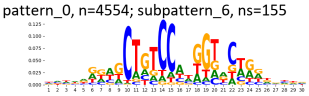

pattern_0, n=4554; subpattern_7, ns=64

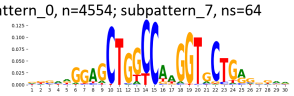

TF-MoDisCO pattern_0 n=4554, PWM

pattern_0, n=4554; subpattern_0, ns=977

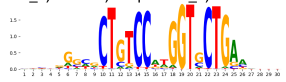

pattern_0, n=4554; subpattern_1, ns=776

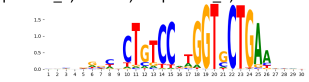

pattern_0, n=4554; subpattern_2, ns=754

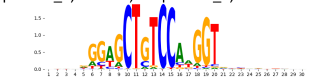

pattern_0, n=4554; subpattern_3, ns=646

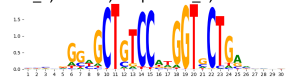

pattern_0, n=4554; subpattern_4, ns=631

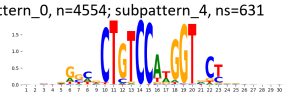

pattern_0, n=4554; subpattern_5, ns=551

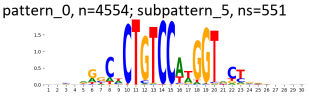

pattern_0, n=4554; subpattern_6, ns=155

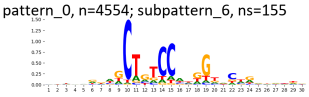

pattern_0, n=4554; subpattern_7, ns=64

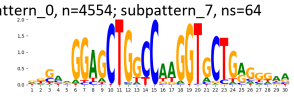

TF-MoDisCO pattern_1 n=3576, CWM

pattern_1, n=3576; subpattern_0, ns=640

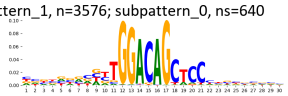

pattern_1, n=3576; subpattern_1, ns=567

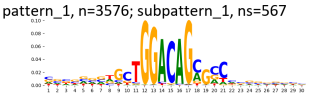

pattern_1, n=3576; subpattern_10, ns=28

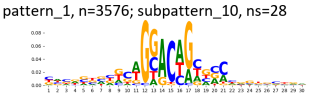

pattern_1, n=3576; subpattern_2, ns=564

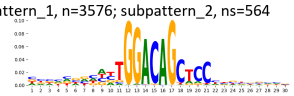

pattern_1, n=3576; subpattern_3, ns=475

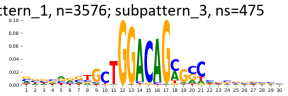

pattern_1, n=3576; subpattern_4, ns=425

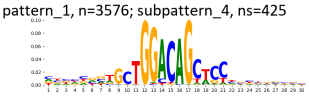

pattern_1, n=3576; subpattern_5, ns=371

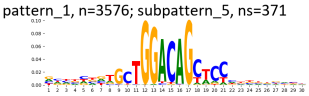

pattern_1, n=3576; subpattern_6, ns=201

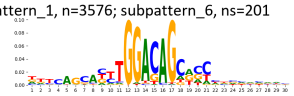

pattern_1, n=3576; subpattern_7, ns=132

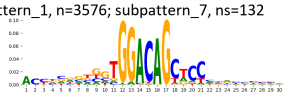

pattern_1, n=3576; subpattern_8, ns=107

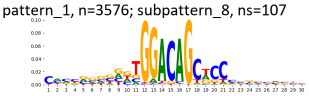

pattern_1, n=3576; subpattern_9, ns=66

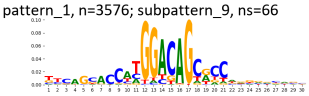

TF-MoDisCO pattern_1 n=3576, PWM

pattern_1, n=3576; subpattern_0, ns=640

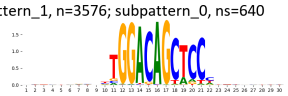

pattern_1, n=3576; subpattern_1, ns=567

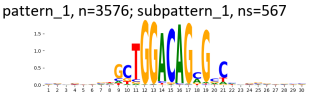

pattern_1, n=3576; subpattern_10, ns=28

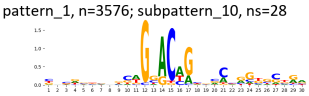

pattern_1, n=3576; subpattern_2, ns=564

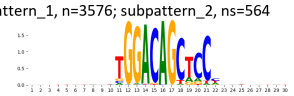

pattern_1, n=3576; subpattern_3, ns=475

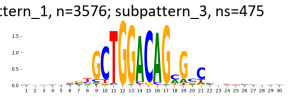

pattern_1, n=3576; subpattern_4, ns=425

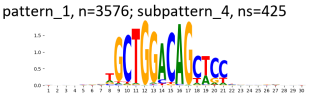

pattern_1, n=3576; subpattern_5, ns=371

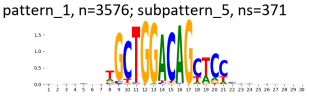

pattern_1, n=3576; subpattern_6, ns=201

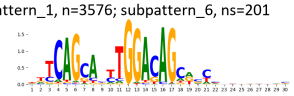

pattern_1, n=3576; subpattern_7, ns=132

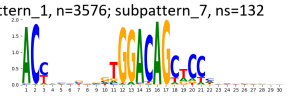

pattern_1, n=3576; subpattern_8, ns=107

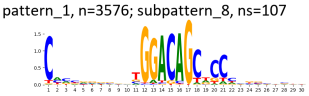

pattern_1, n=3576; subpattern_9, ns=66

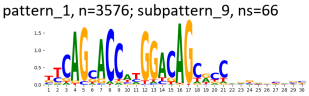

TF-MoDisCO pattern_10 n=92, CWM

pattern_10, n=92; subpattern_0, ns=54

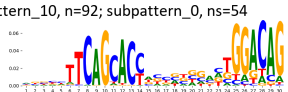

pattern_10, n=92; subpattern_1, ns=24

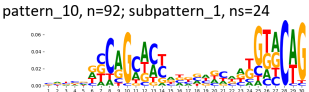

pattern_10, n=92; subpattern_2, ns=14

TF-MoDisCO pattern_10 n=92, PWM

pattern_10, n=92; subpattern_0, ns=54

pattern_10, n=92; subpattern_1, ns=24

pattern_10, n=92; subpattern_2, ns=14

TF-MoDisCO pattern_12 n=59, CWM

pattern_12, n=59; subpattern_0, ns=38

pattern_12, n=59; subpattern_1, ns=21

TF-MoDisCO pattern_12 n=59, PWM

pattern_12, n=59; subpattern_0, ns=38

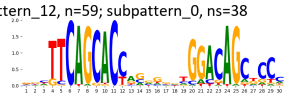

pattern_12, n=59; subpattern_1, ns=21

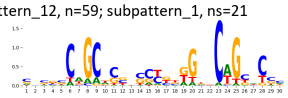

TF-MoDisCO pattern_2 n=515, CWM

pattern_2, n=515; subpattern_0, ns=107

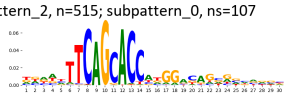

pattern_2, n=515; subpattern_1, ns=103

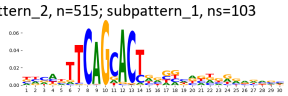

pattern_2, n=515; subpattern_2, ns=91

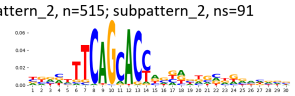

pattern_2, n=515; subpattern_3, ns=90

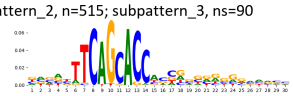

pattern_2, n=515; subpattern_4, ns=56

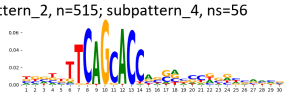

pattern_2, n=515; subpattern_5, ns=37

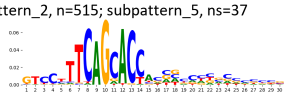

pattern_2, n=515; subpattern_6, ns=18

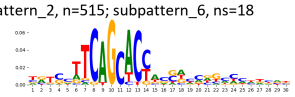

pattern_2, n=515; subpattern_7, ns=13

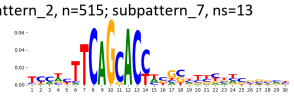

TF-MoDisCO pattern_2 n=515, PWM

pattern_2, n=515; subpattern_0, ns=107

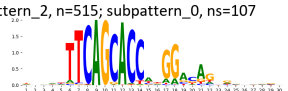

pattern_2, n=515; subpattern_1, ns=103

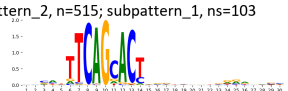

pattern_2, n=515; subpattern_2, ns=91

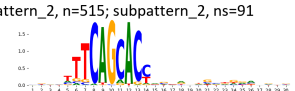

pattern_2, n=515; subpattern_3, ns=90

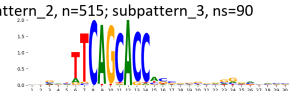

pattern_2, n=515; subpattern_4, ns=56

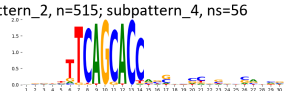

pattern_2, n=515; subpattern_5, ns=37

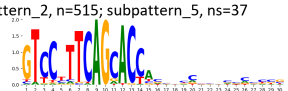

pattern_2, n=515; subpattern_6, ns=18

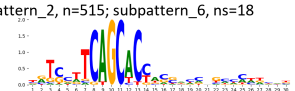

pattern_2, n=515; subpattern_7, ns=13

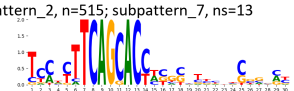

TF-MoDisCO pattern_6 n=237, CWM

pattern_6, n=237; subpattern_0, ns=69

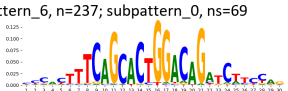

pattern_6, n=237; subpattern_1, ns=67

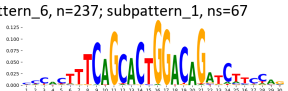

pattern_6, n=237; subpattern_2, ns=53

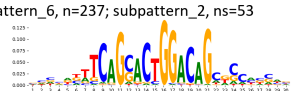

pattern_6, n=237; subpattern_3, ns=28

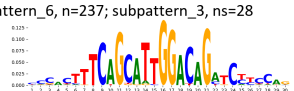

pattern_6, n=237; subpattern_4, ns=12

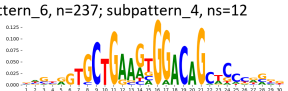

pattern_6, n=237; subpattern_5, ns=5



pattern_6, n=237; subpattern_6, ns=3

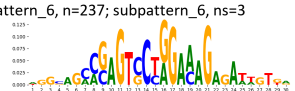

TF-MoDisCO pattern_6 n=237, PWM

pattern_6, n=237; subpattern_0, ns=69

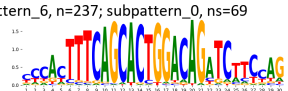

pattern_6, n=237; subpattern_1, ns=67

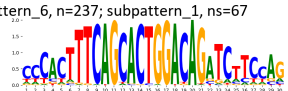

pattern_6, n=237; subpattern_2, ns=53

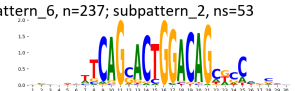

pattern_6, n=237; subpattern_3, ns=28

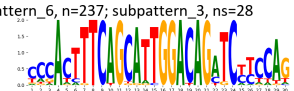

pattern_6, n=237; subpattern_4, ns=12

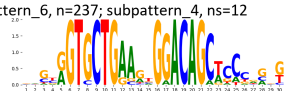

pattern_6, n=237; subpattern_5, ns=5

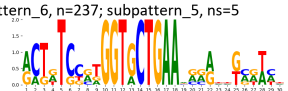

pattern_6, n=237; subpattern_6, ns=3

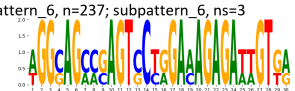

TF-MoDisCO pattern_7 n=135, CWM

pattern_7, n=135; subpattern_0, ns=39

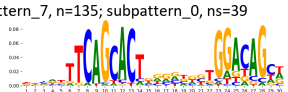

pattern_7, n=135; subpattern_1, ns=39

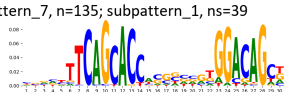

pattern_7, n=135; subpattern_2, ns=37

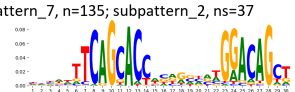

pattern_7, n=135; subpattern_3, ns=20

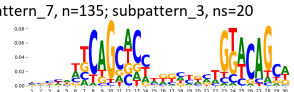

TF-MoDisCO pattern_7 n=135, PWM

pattern_7, n=135; subpattern_0, ns=39

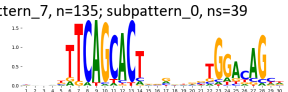

pattern_7, n=135; subpattern_1, ns=39

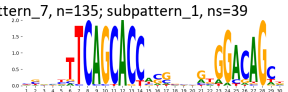

pattern_7, n=135; subpattern_2, ns=37

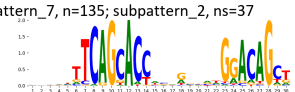

pattern_7, n=135; subpattern_3, ns=20

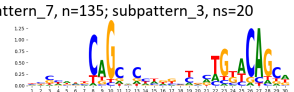

TF-MoDisCO pattern_8 n=108, CWM

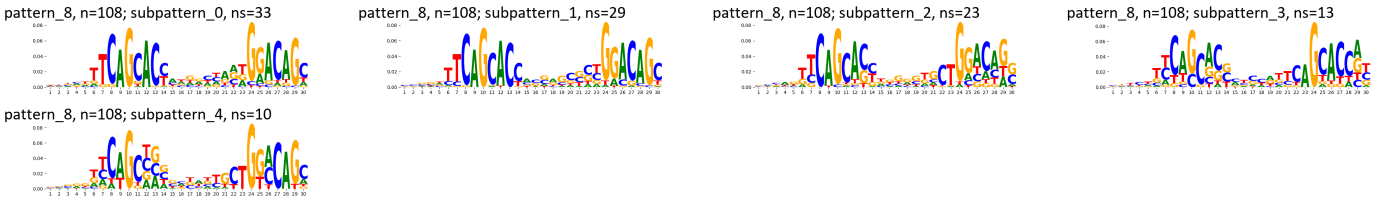

TF-MoDisCO pattern_8 n=108, PWM

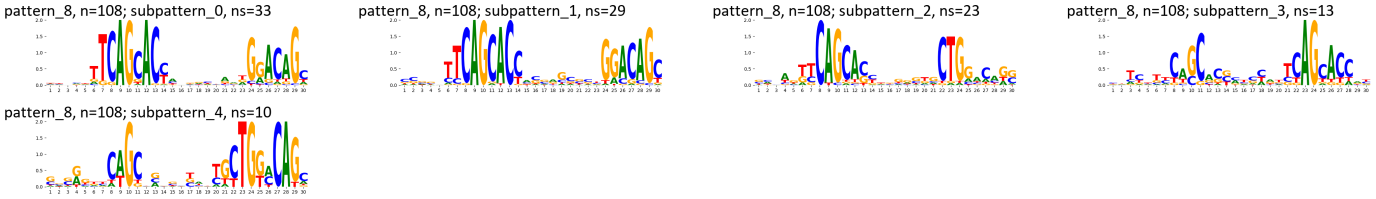

Supplementary Figure 241: TF-MoDisCO subpatterns for the REST transcription factor in Ishikawa (accession ENCSR000BUU).

A

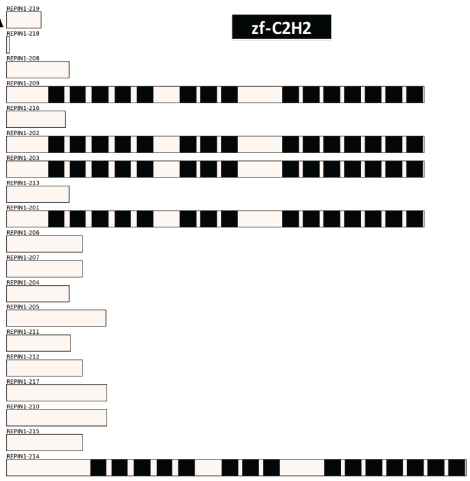

B

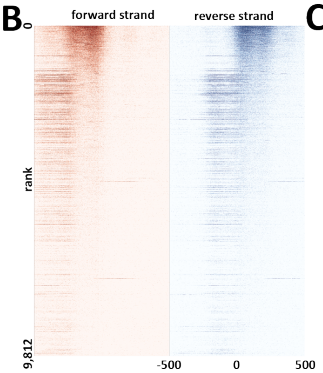

C

peaks	
state	fraction
TssA	0.17
ReprPCWk	0.15
Quies	0.15
EnhWk	0.10
TssFlnkU	0.09
ReprPC	0.07
TxWk	0.06
TssFlnk	0.05
TssFlnkD	0.05
EnhA1	0.04
EnhBiv	0.03
EnhA2	0.02
Tx	0.01
EnhG1	0.01
Het	0.01
EnhG2	0.00
TssBiv	0.00
ZNF/Rpts	0.00

D

peaks		peaks	
repeat	fraction	repeat	fraction
Simple_repeat	0.15	MIRb	0.06
SINE/MIR	0.14	L2a	0.05
SINE/Alu	0.13	MIR	0.04
LINE/L2	0.11	L2b	0.03
LTR/ERVL-MaLR	0.08	L2c	0.03
LINE/L1	0.08	MIR3	0.03
DNA/hAT-Charlie	0.04	MIRc	0.02
Low_complexity	0.03	G-rich	0.02
LTR/ERVL	0.03	AluJb	0.02
LTR/ERV1	0.02	AluSx	0.01
LINE/CR1	0.02	MSTA	0.01
DNA/TcMar-Tigger	0.01	AluSx1	0.01
DNA/hAT-Tip100	0.01	L3	0.01
Unknown	0.00	AluY	0.01
snRNA	0.00	AluSz	0.01
DNA/hAT	0.00	THE1D	0.01
tRNA	0.00	L2	0.01
LINE/RTE-BovB	0.00	AluJo	0.01

E

Ontology	Term	FDR Q-val
GO Biological Process	ER-nucleus signaling pathway	11.19
GO Biological Process	positive regulation of TOR signaling	9.44
GO Biological Process	negative regulation of muscle cell apoptotic process	5.37
GO Biological Process	regulation of alpha-amino-3-hydroxy-5-methyl-4-isoxazole propionate selective glutamate receptor activity	4.27
GO Biological Process	fat-soluble vitamin metabolic process	4.22
GO Biological Process	stress-induced premature senescence	1.67

F

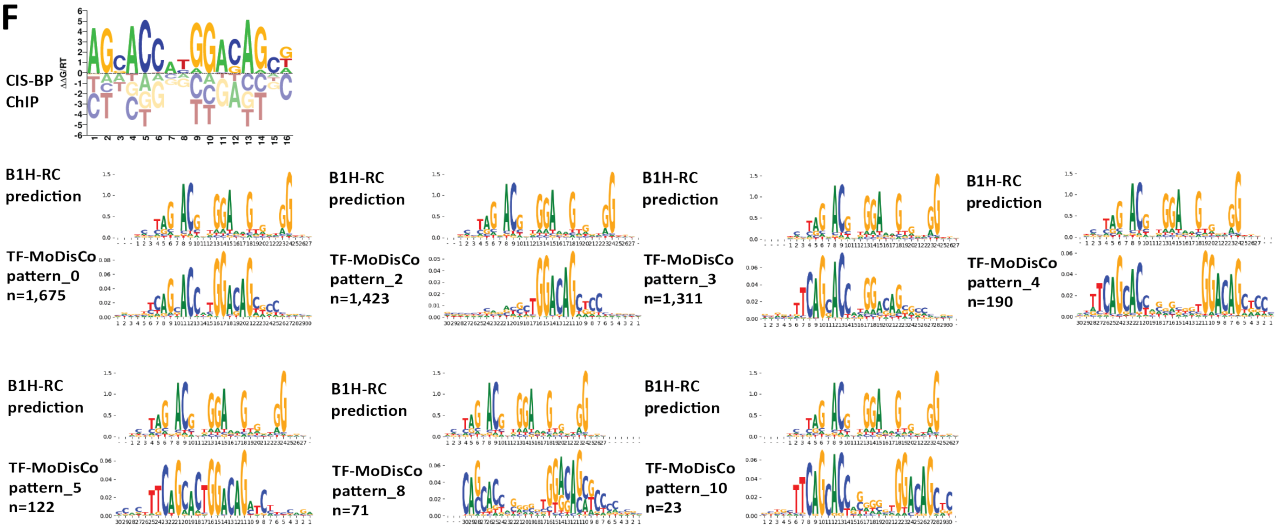

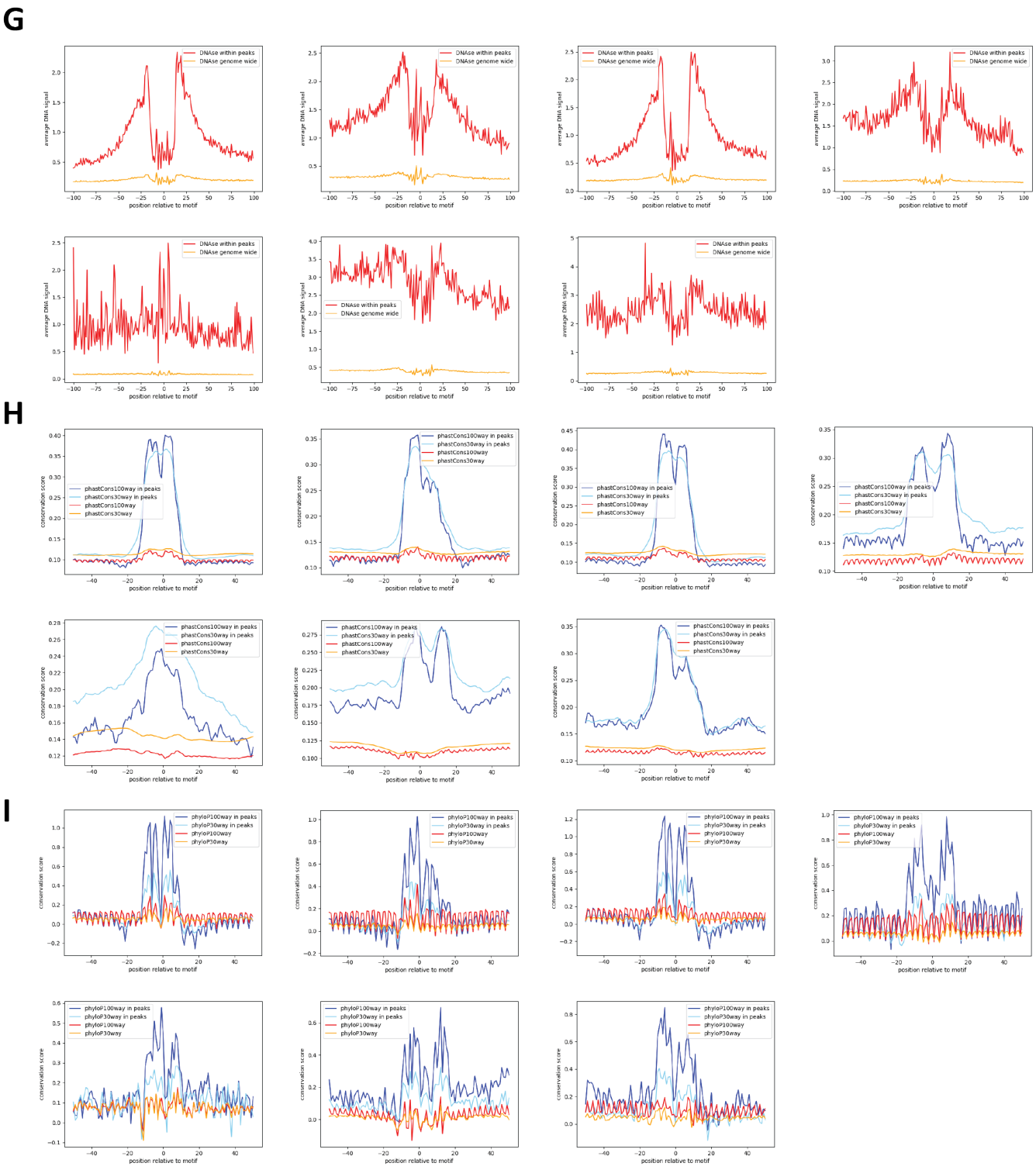

Supplementary Figure 242: Properties and genomic distribution of motifs identified for the REST transcription factor in K562 (accession ENCSR000ATM).

TF-MoDisCO pattern_0 n=1675, CWM

pattern_0, n=1675; subpattern_0, ns=454

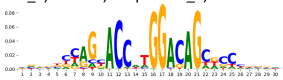

pattern_0, n=1675; subpattern_1, ns=442

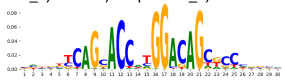

pattern_0, n=1675; subpattern_2, ns=362

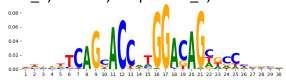

pattern_0, n=1675; subpattern_3, ns=241

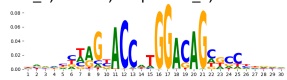

pattern_0, n=1675; subpattern_4, ns=173

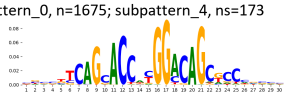

pattern_0, n=1675; subpattern_5, ns=3

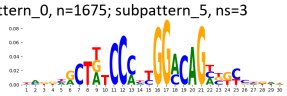

TF-MoDisCO pattern_0 n=1675, PWM

pattern_0, n=1675; subpattern_0, ns=454

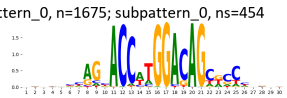

pattern_0, n=1675; subpattern_1, ns=442

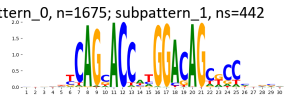

pattern_0, n=1675; subpattern_2, ns=362

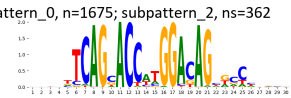

pattern_0, n=1675; subpattern_3, ns=241

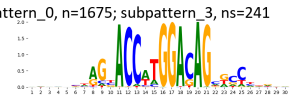

pattern_0, n=1675; subpattern_4, ns=173

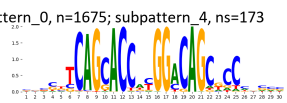

pattern_0, n=1675; subpattern_5, ns=3

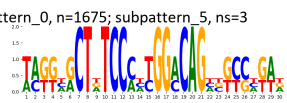

TF-MoDisCO pattern_10 n=23, CWM

pattern_10, n=23; subpattern_0, ns=23

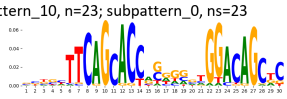

TF-MoDisCO pattern_10 n=23, PWM

pattern_10, n=23; subpattern_0, ns=23

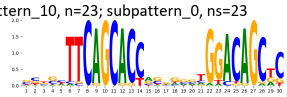

TF-MoDisCO pattern_2 n=1423, CWM

pattern_2, n=1423; subpattern_0, ns=537

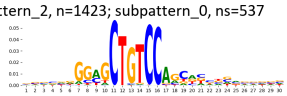

pattern_2, n=1423; subpattern_1, ns=308

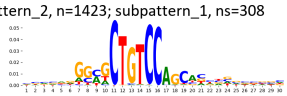

pattern_2, n=1423; subpattern_2, ns=263

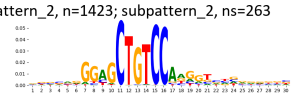

pattern_2, n=1423; subpattern_3, ns=171

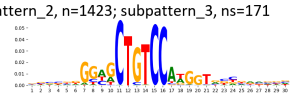

pattern_2, n=1423; subpattern_4, ns=103

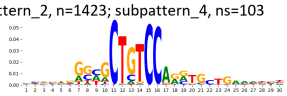

pattern_2, n=1423; subpattern_5, ns=31

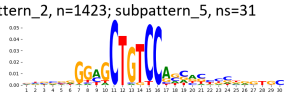

pattern_2, n=1423; subpattern_6, ns=4

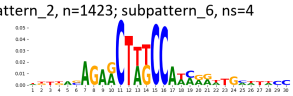

pattern_2, n=1423; subpattern_7, ns=4

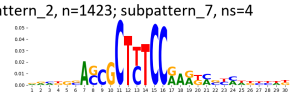

pattern_2, n=1423; subpattern_8, ns=2

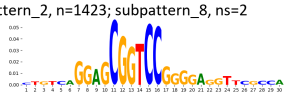

TF-MoDisCO pattern_2 n=1423, PWM

pattern_2, n=1423; subpattern_0, ns=537

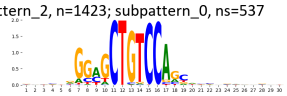

pattern_2, n=1423; subpattern_1, ns=308

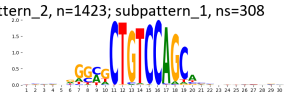

pattern_2, n=1423; subpattern_2, ns=263

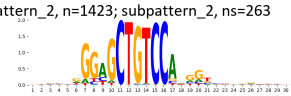

pattern_2, n=1423; subpattern_3, ns=171

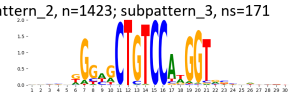

pattern_2, n=1423; subpattern_4, ns=103

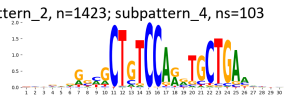

pattern_2, n=1423; subpattern_5, ns=31

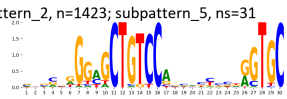

pattern_2, n=1423; subpattern_6, ns=4

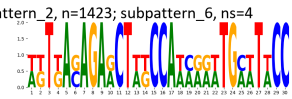

pattern_2, n=1423; subpattern_7, ns=4

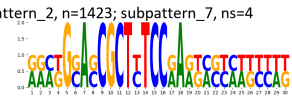

pattern_2, n=1423; subpattern_8, ns=2

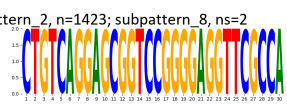

TF-MoDisCO pattern_3 n=1311, CWM

pattern_3, n=1311; subpattern_0, ns=450

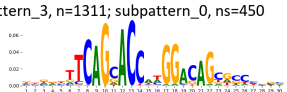

pattern_3, n=1311; subpattern_1, ns=320

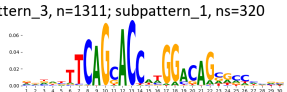

pattern_3, n=1311; subpattern_2, ns=288

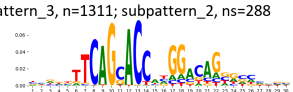

pattern_3, n=1311; subpattern_3, ns=253

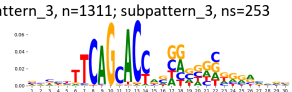

TF-MoDisCO pattern_3 n=1311, PWM

pattern_3, n=1311; subpattern_0, ns=450

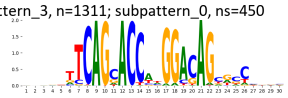

pattern_3, n=1311; subpattern_1, ns=320

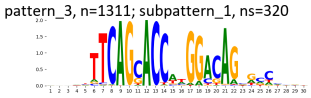

pattern_3, n=1311; subpattern_2, ns=288

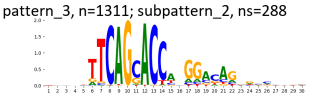

pattern_3, n=1311; subpattern_3, ns=253

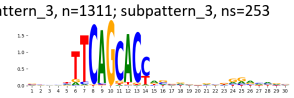

TF-MoDisCO pattern_4 n=190, CWM

pattern_4, n=190; subpattern_0, ns=61

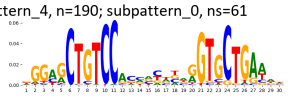

pattern_4, n=190; subpattern_1, ns=36

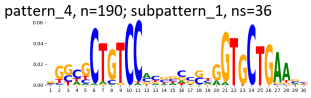

pattern_4, n=190; subpattern_2, ns=34

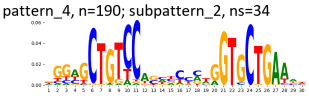

pattern_4, n=190; subpattern_3, ns=32

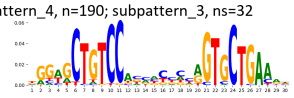

pattern_4, n=190; subpattern_4, ns=18

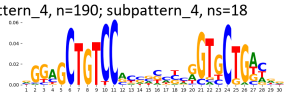

pattern_4, n=190; subpattern_5, ns=7

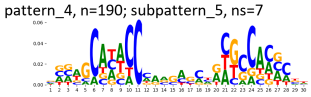

pattern_4, n=190; subpattern_6, ns=2

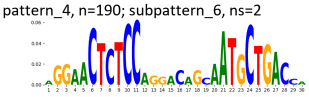

TF-MoDisCO pattern_4 n=190, PWM

pattern_4, n=190; subpattern_0, ns=61

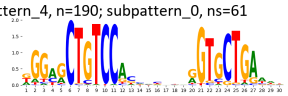

pattern_4, n=190; subpattern_1, ns=36

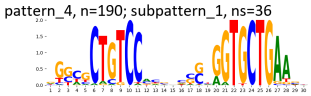

pattern_4, n=190; subpattern_2, ns=34

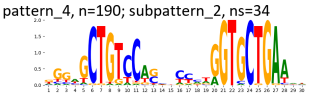

pattern_4, n=190; subpattern_3, ns=32

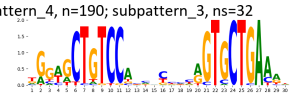

pattern_4, n=190; subpattern_4, ns=18

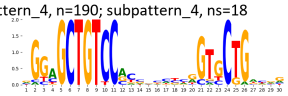

pattern_4, n=190; subpattern_5, ns=7

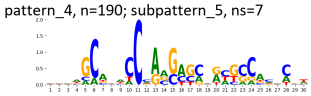

pattern_4, n=190; subpattern_6, ns=2

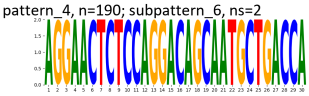

TF-MoDisCO pattern_5 n=122, CWM

pattern_5, n=122; subpattern_0, ns=46

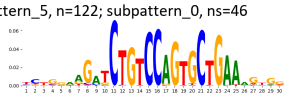

pattern_5, n=122; subpattern_1, ns=42

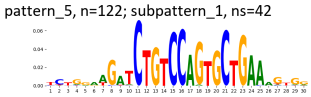

pattern_5, n=122; subpattern_2, ns=34

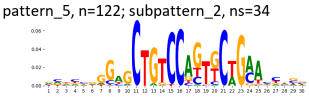

TF-MoDisCO pattern_5 n=122, PWM

pattern_5, n=122; subpattern_0, ns=46

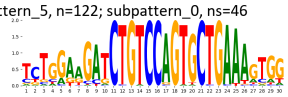

pattern_5, n=122; subpattern_1, ns=42

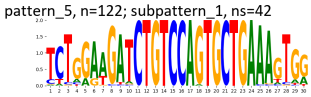

pattern_5, n=122; subpattern_2, ns=34

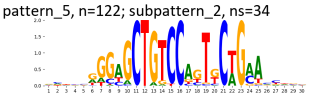

TF-MoDisCO pattern_8 n=71, CWM

pattern_8, n=71; subpattern_0, ns=29

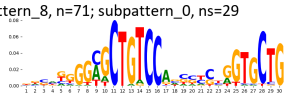

pattern_8, n=71; subpattern_1, ns=22

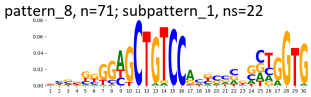

pattern_8, n=71; subpattern_2, ns=20

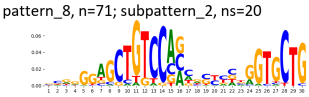

TF-MoDisCO pattern_8 n=71, PWM

pattern_8, n=71; subpattern_0, ns=29

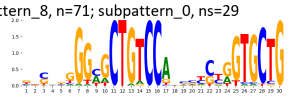

pattern_8, n=71; subpattern_1, ns=22

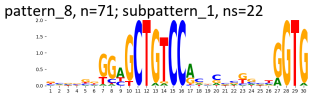

pattern_8, n=71; subpattern_2, ns=20

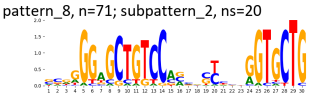

Supplementary Figure 243: TF-MoDisCO subpatterns for the REST transcription factor in K562 (accession ENCSR000ATM).

A

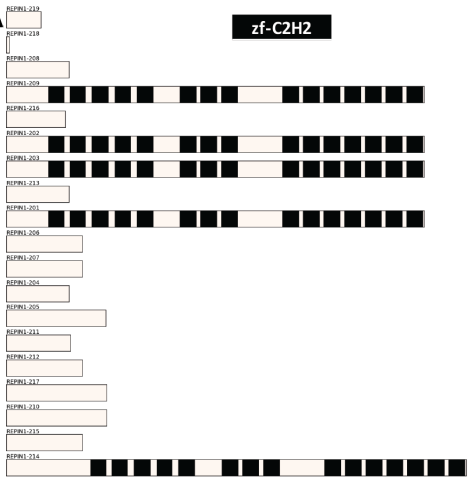

B

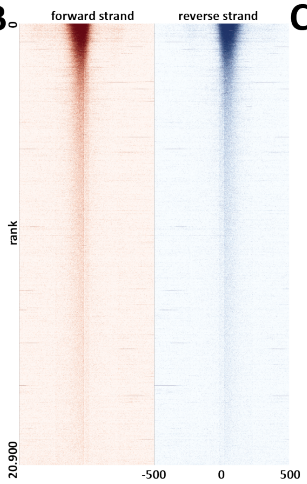

C

peaks	
state	fraction
TssA	0.21
EnhWk	0.18
EnhA1	0.17
TssFlnkU	0.14
Quies	0.09
ReprPCWk	0.08
EnhA2	0.06
TssFlnkD	0.06
TxWk	0.05
TssFlnk	0.05
ReprPC	0.04
EnhBiv	0.02
EnhG1	0.01
Tx	0.01
EnhG2	0.01
Het	0.00
TssBiv	0.00
ZNF/Rpts	0.00

D

peaks		peaks	
repeat	fraction	repeat	fraction
Simple_repeat	0.09	L2a	0.02
LINE/L2	0.07	MIRb	0.02
SINE/MIR	0.06	L2c	0.02
SINE/Alu	0.05	L2b	0.02
LINE/L1	0.04	MIR	0.01
LTR/ERV1	0.04	G-rich	0.01
LTR/ERVL-MaLR	0.03	MIR3	0.01
LTR/ERVL	0.02	MIRc	0.01
DNA/hAT-Charlie	0.02	AluJb	0.01
Low_complexity	0.02	L2	0.01
LINE/CR1	0.01	GA-rich	0.01
DNA/TcMar-Tigger	0.01	L3	0.01
LTR/ERVK	0.00	AluJr	0.01
DNA/hAT-Tip100	0.00	AluSx1	0.01
tRNA	0.00	AluSx	0.00
snRNA	0.00	AluSz	0.00
Unknown	0.00	AluJo	0.00
LINE/RTE-X	0.00	(GGC)n	0.00

E

Ontology	Term	FDR Q-val
GO Biological Process	endoplasmic reticulum unfolded protein response	38.13
GO Biological Process	cellular response to unfolded protein	32.34
GO Biological Process	cellular response to topologically incorrect protein	30.68
GO Biological Process	nuclear-transcribed mRNA catabolic process, nonsense-mediated decay	21.56
GO Biological Process	regulation of mitochondrial membrane permeability	18.85
GO Biological Process	IRE1-mediated unfolded protein response	18.05
GO Biological Process	cotranslational protein targeting to membrane	16.32
GO Biological Process	SRP-dependent cotranslational protein targeting to membrane	15.31
GO Biological Process	membrane protein proteolysis	8.77
GO Biological Process	mismatch repair	7.28

F

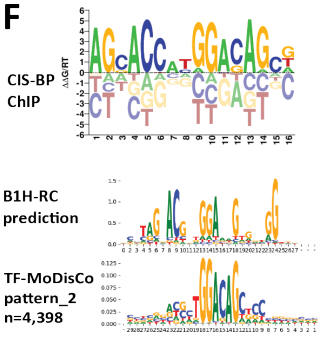

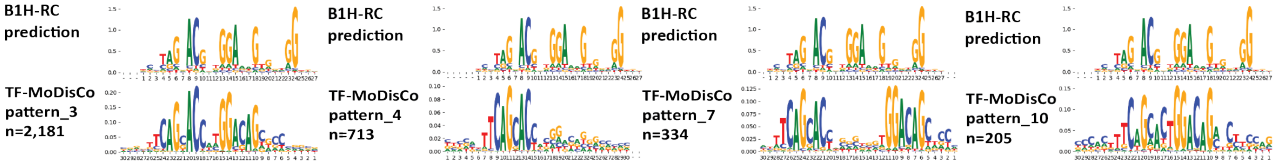

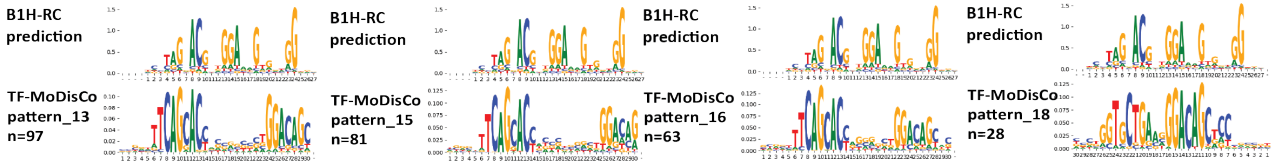

G

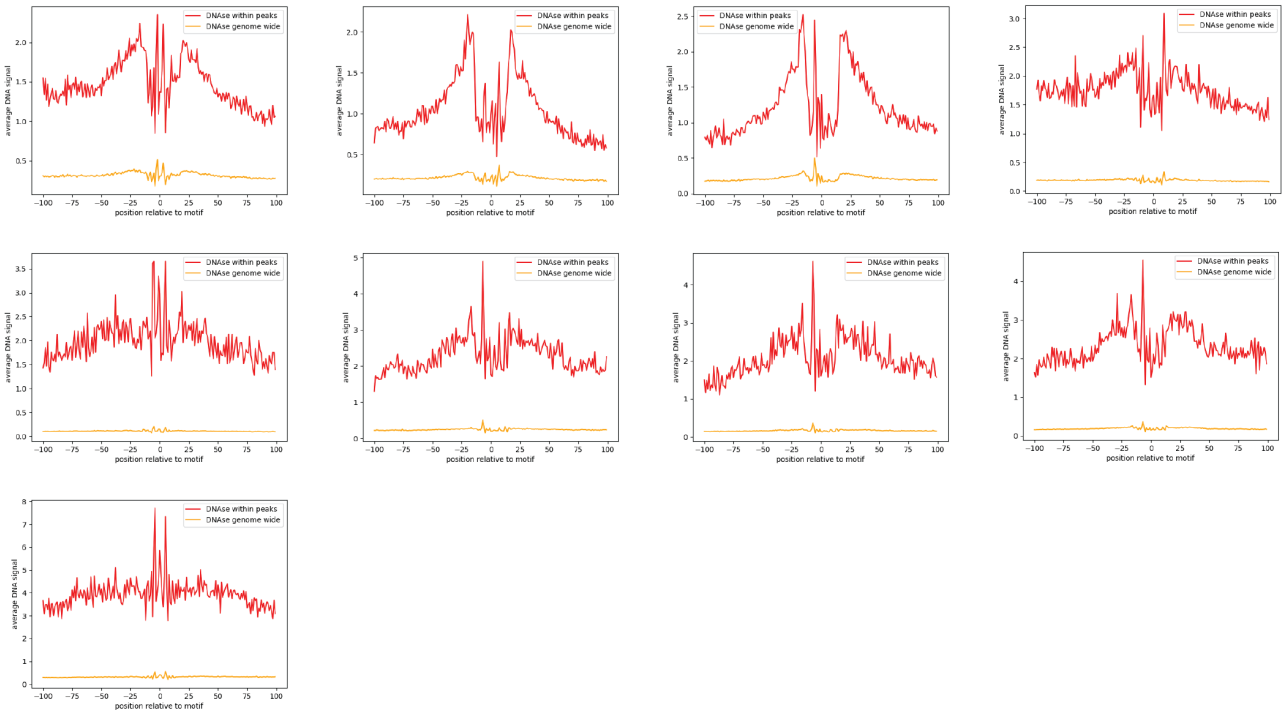
DNAse within peaks
DNAse genome wide
average DNA signal
position relative to motif

H

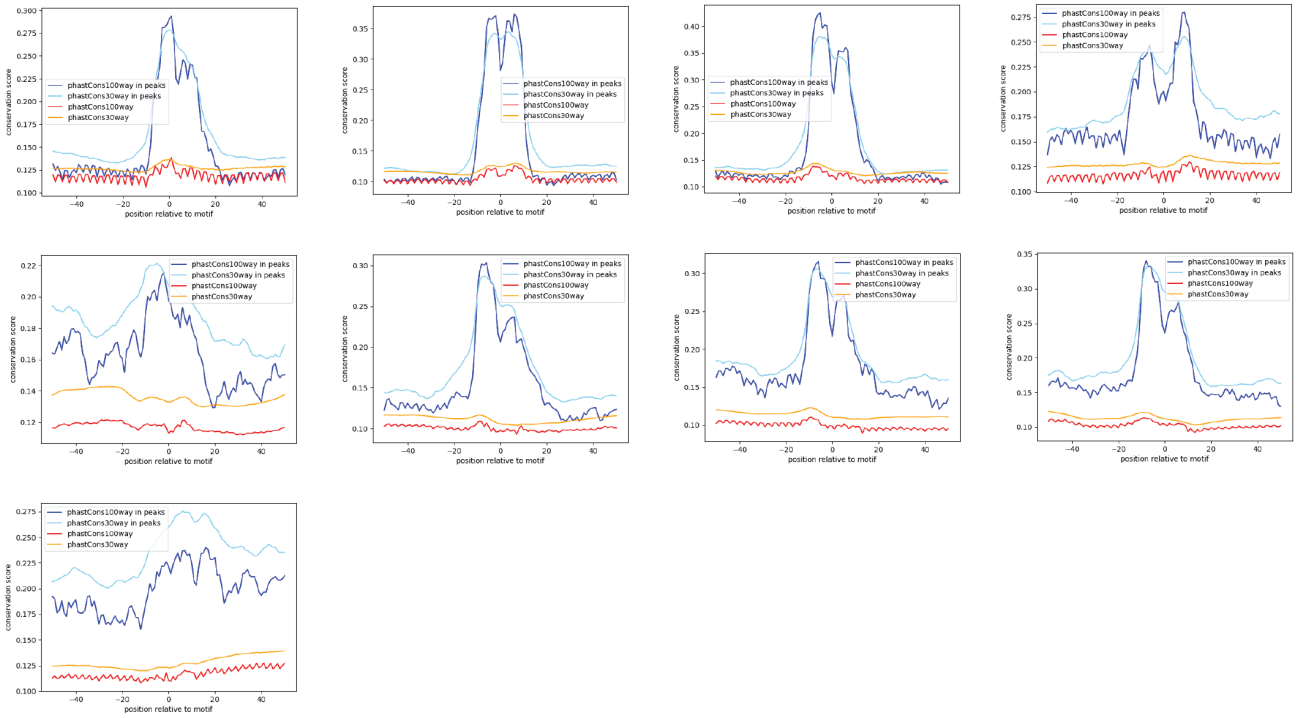
phastCons100way in peaks
phastCons30way in peaks
phastCons100way
phastCons30way
conservation score
position relative to motif

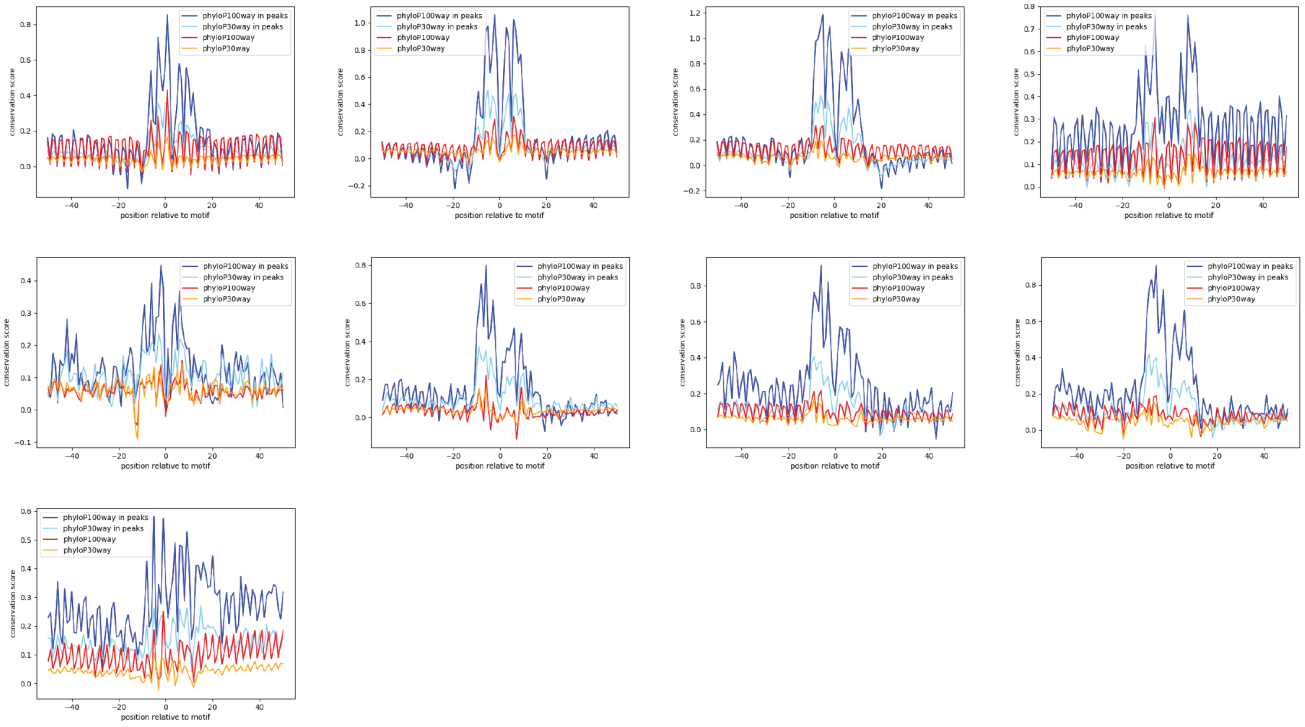

Supplementary Figure 244: Properties and genomic distribution of motifs identified for the REST transcription factor in K562 (accession ENCSR000BMW).

TF-MoDisCO pattern_10 n=205, CWM

pattern_10, n=205; subpattern_0, ns=53

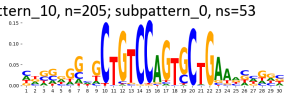

pattern_10, n=205; subpattern_1, ns=46

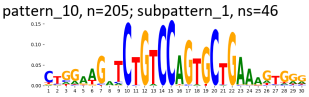

pattern_10, n=205; subpattern_2, ns=43

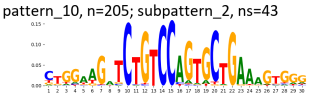

pattern_10, n=205; subpattern_3, ns=32

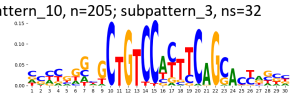

pattern_10, n=205; subpattern_4, ns=26

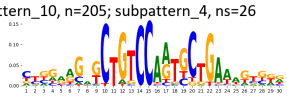

pattern_10, n=205; subpattern_5, ns=5

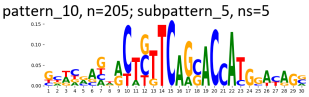

TF-MoDisCO pattern_10 n=205, PWM

pattern_10, n=205; subpattern_0, ns=53

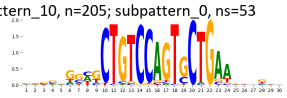

pattern_10, n=205; subpattern_1, ns=46

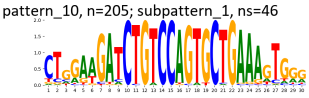

pattern_10, n=205; subpattern_2, ns=43

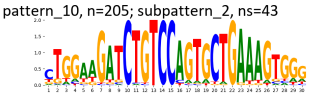

pattern_10, n=205; subpattern_3, ns=32

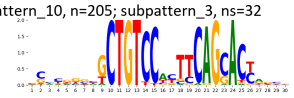

pattern_10, n=205; subpattern_4, ns=26

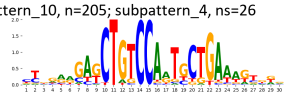

pattern_10, n=205; subpattern_5, ns=5

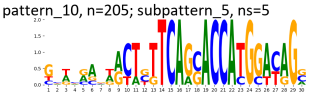

TF-MoDisCO pattern_13 n=97, CWM

pattern_13, n=97; subpattern_0, ns=37

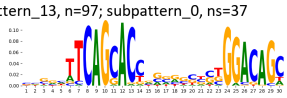

pattern_13, n=97; subpattern_1, ns=35

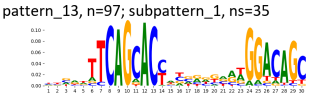

pattern_13, n=97; subpattern_2, ns=25

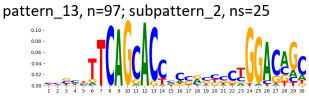

TF-MoDisCO pattern_13 n=97, PWM

pattern_13, n=97; subpattern_0, ns=37

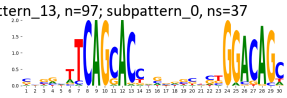

pattern_13, n=97; subpattern_1, ns=35

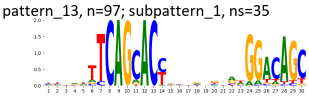

pattern_13, n=97; subpattern_2, ns=25

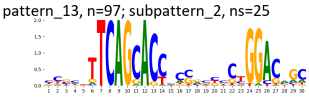

TF-MoDisCO pattern_15 n=81, CWM

pattern_15, n=81; subpattern_0, ns=30

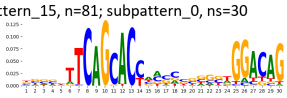

pattern_15, n=81; subpattern_1, ns=29

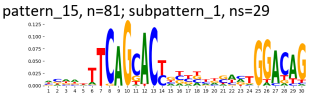

pattern_15, n=81; subpattern_2, ns=15

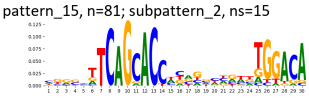

pattern_15, n=81; subpattern_3, ns=7

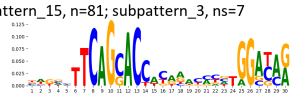

TF-MoDisCO pattern_15 n=81, PWM

pattern_15, n=81; subpattern_0, ns=30

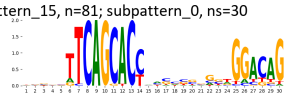

pattern_15, n=81; subpattern_1, ns=29

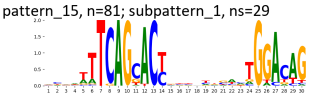

pattern_15, n=81; subpattern_2, ns=15

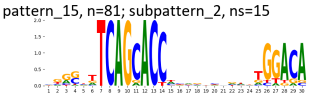

pattern_15, n=81; subpattern_3, ns=7

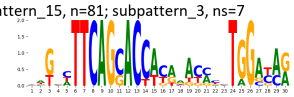

TF-MoDisCO pattern_16 n=63, CWM

pattern_16, n=63; subpattern_0, ns=24

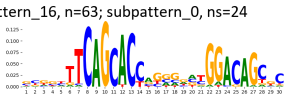

pattern_16, n=63; subpattern_1, ns=23

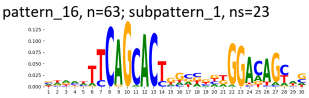

pattern_16, n=63; subpattern_2, ns=16

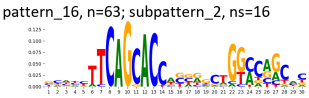

TF-MoDisCO pattern_16 n=63, PWM

pattern_16, n=63; subpattern_0, ns=24

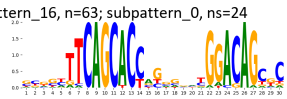

pattern_16, n=63; subpattern_1, ns=23

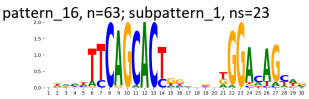

pattern_16, n=63; subpattern_2, ns=16

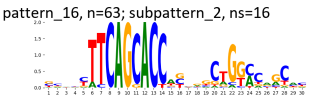

TF-MoDisCO pattern_18 n=28, CWM

pattern_18, n=28; subpattern_0, ns=28

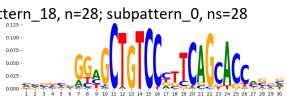

TF-MoDisCO pattern_18 n=28, PWM

pattern_18, n=28; subpattern_0, ns=28

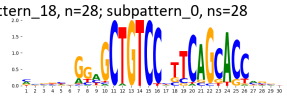

TF-MoDisCO pattern_2 n=4398, CWM

pattern_2, n=4398; subpattern_0, ns=955

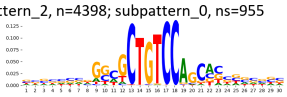

pattern_2, n=4398; subpattern_1, ns=781

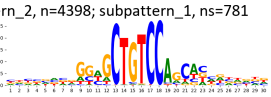

pattern_2, n=4398; subpattern_2, ns=704

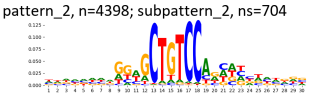

pattern_2, n=4398; subpattern_3, ns=601

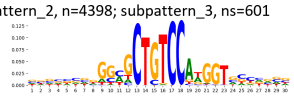

pattern_2, n=4398; subpattern_4, ns=556

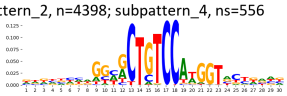

pattern_2, n=4398; subpattern_5, ns=449

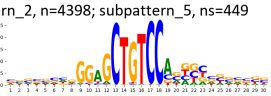

pattern_2, n=4398; subpattern_6, ns=218

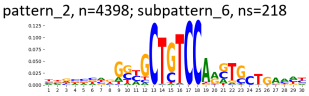

pattern_2, n=4398; subpattern_7, ns=88

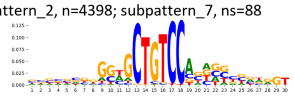

pattern_2, n=4398; subpattern_8, ns=46

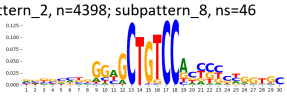

TF-MoDisCO pattern_2 n=4398, PWM

pattern_2, n=4398; subpattern_0, ns=955

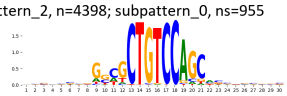

pattern_2, n=4398; subpattern_1, ns=781

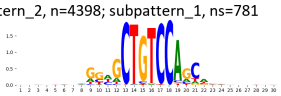

pattern_2, n=4398; subpattern_2, ns=704

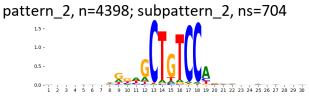

pattern_2, n=4398; subpattern_3, ns=601

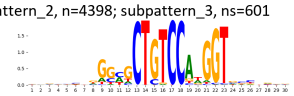

pattern_2, n=4398; subpattern_4, ns=556

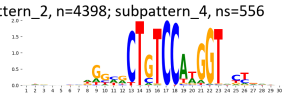

pattern_2, n=4398; subpattern_5, ns=449

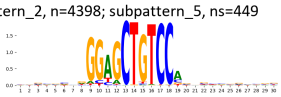

pattern_2, n=4398; subpattern_6, ns=218

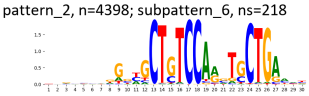

pattern_2, n=4398; subpattern_7, ns=88

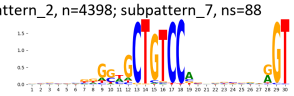

pattern_2, n=4398; subpattern_8, ns=46

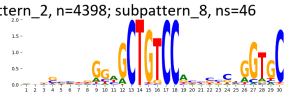

TF-MoDisCO pattern_3 n=2181, CWM

pattern_3, n=2181; subpattern_0, ns=570

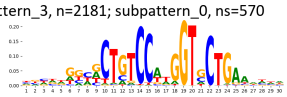

pattern_3, n=2181; subpattern_1, ns=427

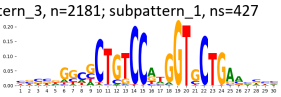

pattern_3, n=2181; subpattern_2, ns=413

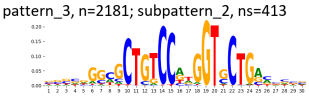

pattern_3, n=2181; subpattern_3, ns=411

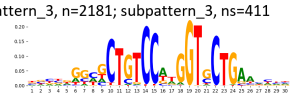

pattern_3, n=2181; subpattern_4, ns=360

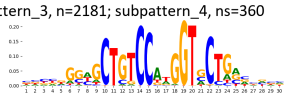

TF-MoDisCO pattern_3 n=2181, PWM

pattern_3, n=2181; subpattern_0, ns=570

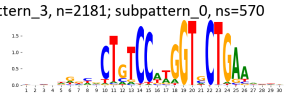

pattern_3, n=2181; subpattern_1, ns=427

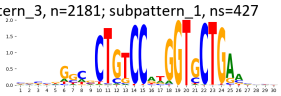

pattern_3, n=2181; subpattern_2, ns=413

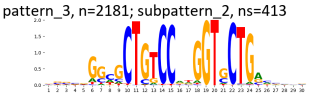

pattern_3, n=2181; subpattern_3, ns=411

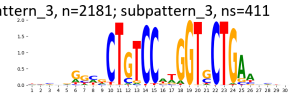

pattern_3, n=2181; subpattern_4, ns=360

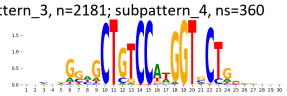

TF-MoDisCO pattern_4 n=713, CWM

pattern_4, n=713; subpattern_0, ns=206

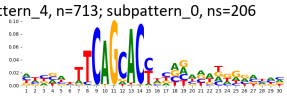

pattern_4, n=713; subpattern_1, ns=192

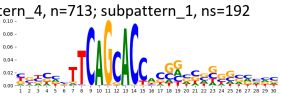

pattern_4, n=713; subpattern_2, ns=177

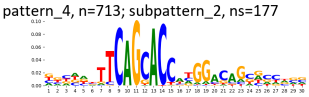

pattern_4, n=713; subpattern_3, ns=122

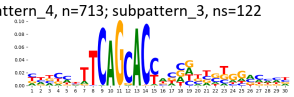

pattern_4, n=713; subpattern_4, ns=12

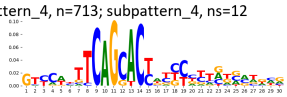

pattern_4, n=713; subpattern_5, ns=4

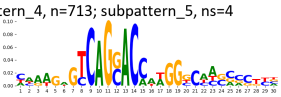

TF-MoDisCO pattern_4 n=713, PWM

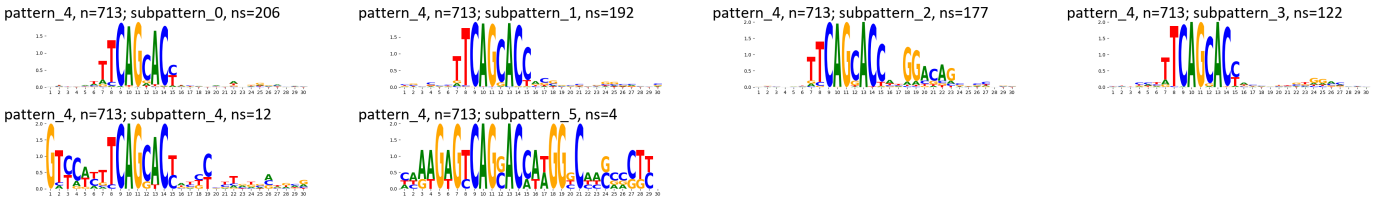

TF-MoDisCO pattern_7 n=334, CWM

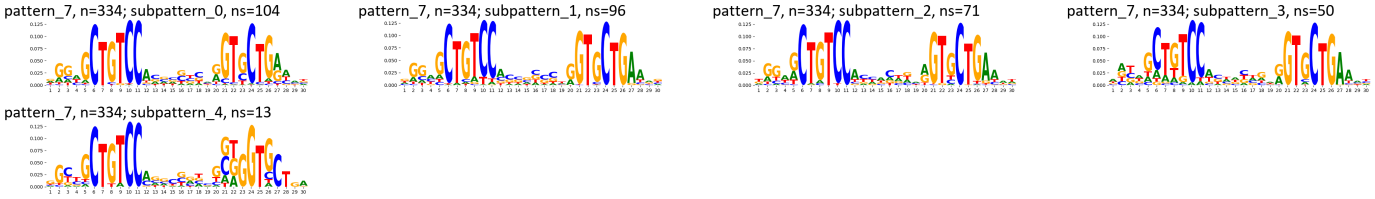

TF-MoDisCO pattern_7 n=334, PWM

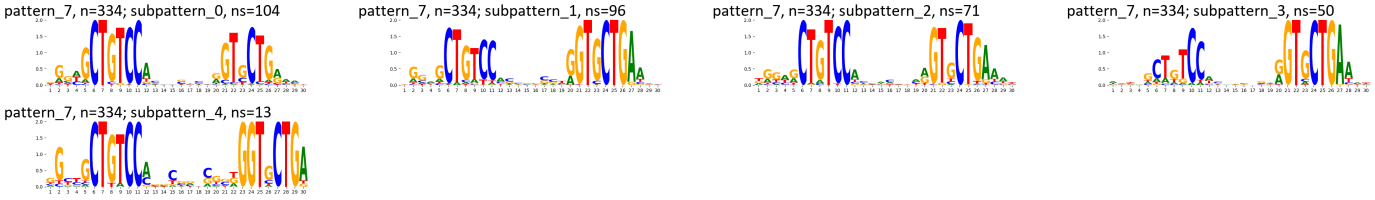

Supplementary Figure 245: TF-MoDisCO subpatterns for the REST transcription factor in K562 (accession ENCSR000BMW).

A

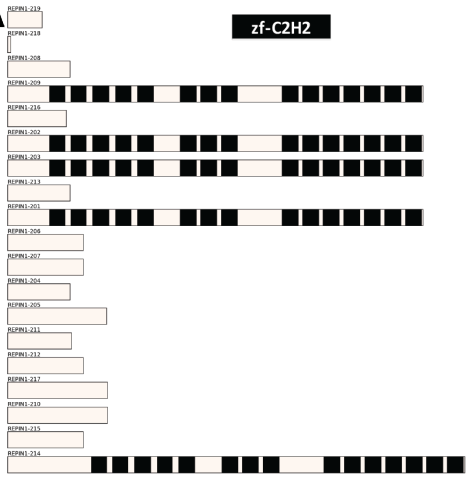

B

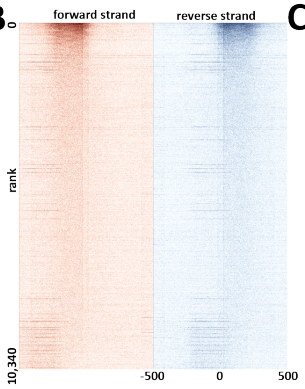

C

peaks	
state	fraction
TssA	0.36
TssFlnkU	0.29
TssFlnkD	0.11
EnhWk	0.11
EnhA1	0.10
TssFlnk	0.10
ReprPCWk	0.07
Quies	0.06
TxWk	0.03
ReprPC	0.03
EnhA2	0.03
EnhBiv	0.02
EnhG1	0.01
EnhG2	0.01
Tx	0.01
TssBiv	0.01
Het	0.00
ZNF/Rpts	0.00

D

peaks		peaks	
repeat	fraction	repeat	fraction
Simple_repeat	0.19	MIRb	0.03
SINE/MIR	0.08	G-rich	0.03
SINE/Alu	0.07	L2a	0.02
LINE/L2	0.05	MIR3	0.02
LTR/ERV1	0.04	MIR	0.02
Low_complexity	0.04	MIRc	0.02
LINE/L1	0.02	L2c	0.01
DNA/hAT-Charlie	0.02	L2b	0.01
LTR/ERVL-MaLR	0.02	MER41B	0.01
LTR/ERVL	0.02	(GGC)n	0.01
LINE/CR1	0.01	GA-rich	0.01
DNA/hAT-Tip100	0.00	AluSx	0.01
DNA/TcMar-Tigger	0.00	AluJb	0.01
tRNA	0.00	(GCG)n	0.01
LTR/ERVK	0.00	AluSx1	0.01
snRNA	0.00	(GCC)n	0.01
DNA/hAT-Blackjack	0.00	AluSz	0.01
Unknown	0.00	AluJr	0.01

E

Ontology	Term	FDR Q-val
GO Biological Process	cellular response to topologically incorrect protein	14.40
GO Biological Process	endoplasmic reticulum unfolded protein response	13.20
GO Biological Process	viral gene expression	10.34
GO Biological Process	regulation of mitochondrial membrane permeability	9.94
GO Biological Process	'de novo' protein folding	8.95
GO Biological Process	transcription from RNA polymerase III promoter	7.49
GO Biological Process	posttranscriptional gene silencing by RNA	7.06
GO Biological Process	mitochondrial DNA metabolic process	6.92
GO Biological Process	RNA methylation	6.05
GO Biological Process	positive regulation of nuclease activity	5.47
GO Biological Process	mitochondrial genome maintenance	5.25
GO Biological Process	termination of RNA polymerase II transcription	5.01
GO Biological Process	platelet formation	4.95
GO Biological Process	translesion synthesis	4.57
GO Biological Process	platelet morphogenesis	4.16
GO Biological Process	positive regulation of mitochondrial membrane permeability	3.68
GO Biological Process	positive regulation of membrane permeability	3.14
GO Biological Process	mitochondrial outer membrane permeabilization involved in programmed cell death	3.11
GO Biological Process	regulation of establishment of protein localization to chromosome	2.96
GO Biological Process	activation of signaling protein activity involved in unfolded protein response	2.75

F

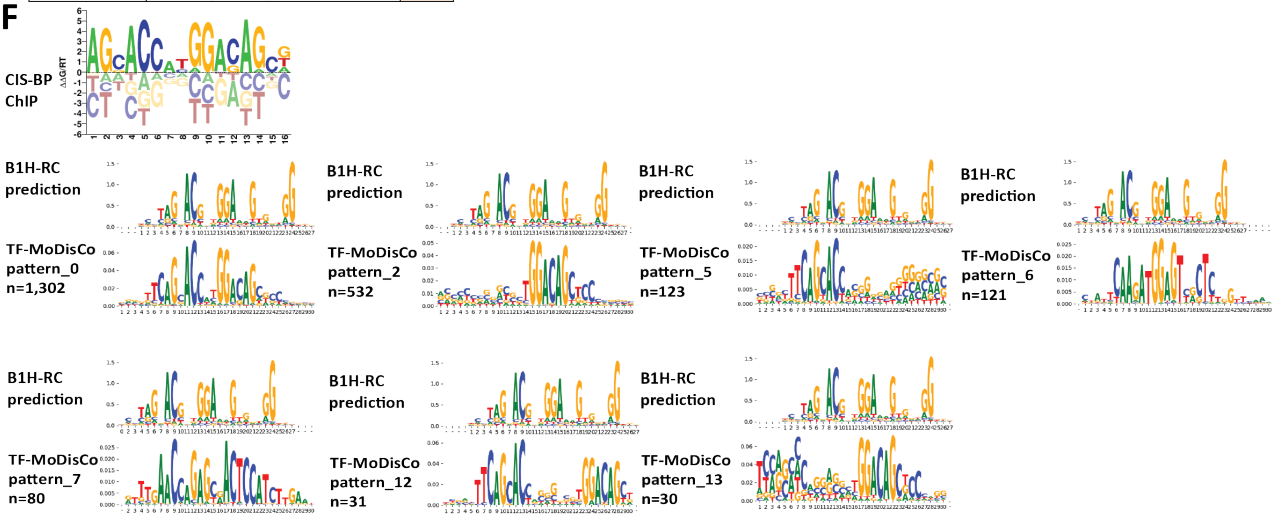

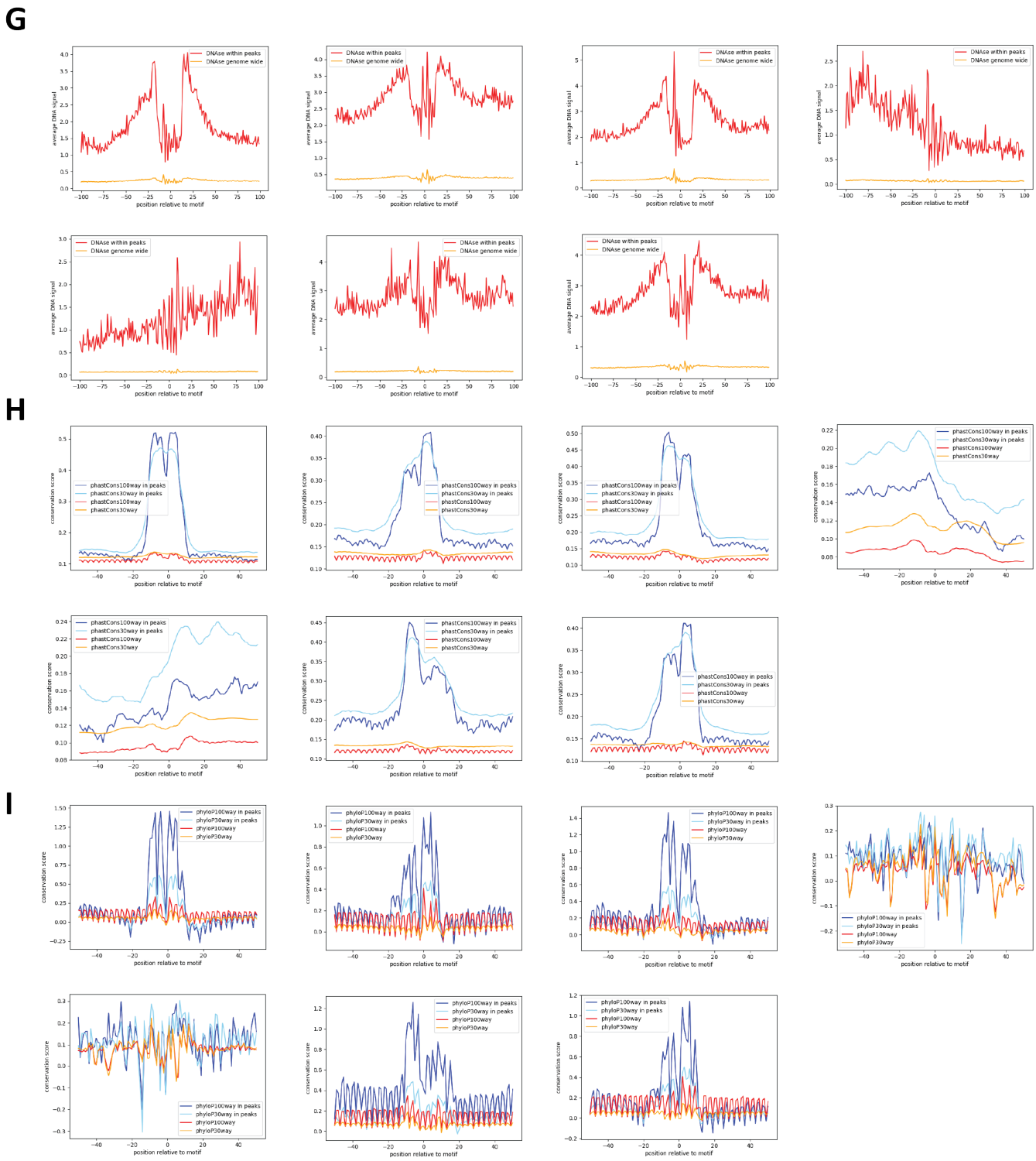

Supplementary Figure 246: Properties and genomic distribution of motifs identified for the REST transcription factor in K562 (accession ENCSR054JMQ).

TF-MoDisCO pattern_0 n=1302, CWM

pattern_0, n=1302; subpattern_0, ns=395

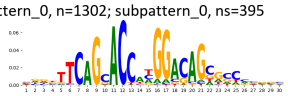

pattern_0, n=1302; subpattern_1, ns=361

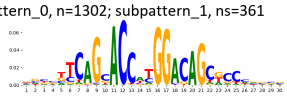

pattern_0, n=1302; subpattern_2, ns=292

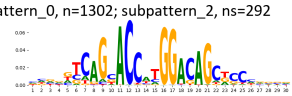

pattern_0, n=1302; subpattern_3, ns=252

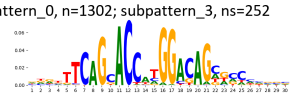

pattern_0, n=1302; subpattern_4, ns=2

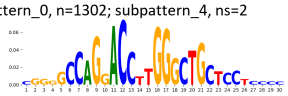

TF-MoDisCO pattern_0 n=1302, PWM

pattern_0, n=1302; subpattern_0, ns=395

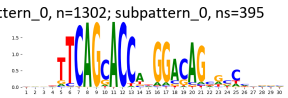

pattern_0, n=1302; subpattern_1, ns=361

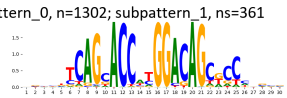

pattern_0, n=1302; subpattern_2, ns=292

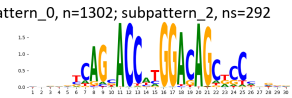

pattern_0, n=1302; subpattern_3, ns=252

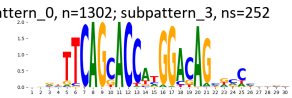

pattern_0, n=1302; subpattern_4, ns=2

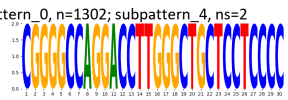

TF-MoDisCO pattern_12 n=31, CWM

pattern_12, n=31; subpattern_0, ns=31

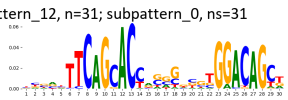

TF-MoDisCO pattern_12 n=31, PWM

pattern_12, n=31; subpattern_0, ns=31

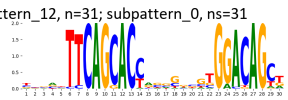

TF-MoDisCO pattern_13 n=30, CWM

pattern_13, n=30; subpattern_0, ns=30

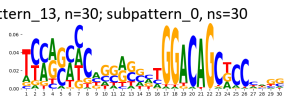

TF-MoDisCO pattern_13 n=30, PWM

pattern_13, n=30; subpattern_0, ns=30

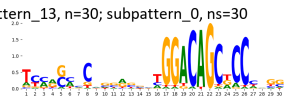

TF-MoDisCO pattern_2 n=532, CWM

pattern_2, n=532; subpattern_0, ns=184

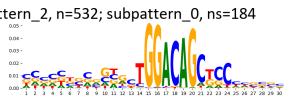

pattern_2, n=532; subpattern_1, ns=118

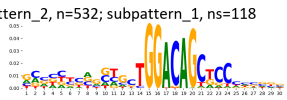

pattern_2, n=532; subpattern_2, ns=70

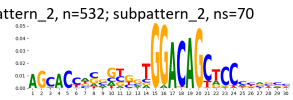

pattern_2, n=532; subpattern_3, ns=68

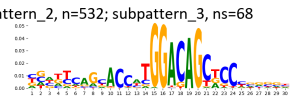

pattern_2, n=532; subpattern_4, ns=56

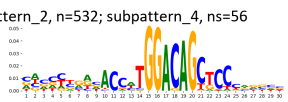

pattern_2, n=532; subpattern_5, ns=20

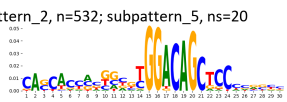

pattern_2, n=532; subpattern_6, ns=16

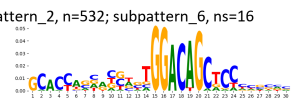

TF-MoDisCO pattern_2 n=532, PWM

pattern_2, n=532; subpattern_0, ns=184

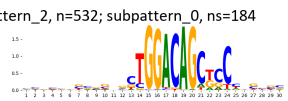

pattern_2, n=532; subpattern_1, ns=118

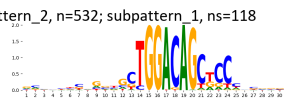

pattern_2, n=532; subpattern_2, ns=70

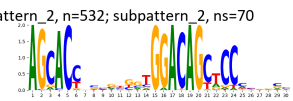

pattern_2, n=532; subpattern_3, ns=68

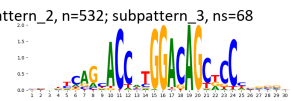

pattern_2, n=532; subpattern_4, ns=56

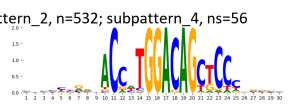

pattern_2, n=532; subpattern_5, ns=20

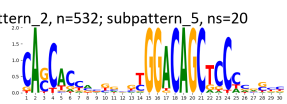

pattern_2, n=532; subpattern_6, ns=16

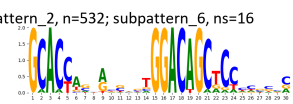

TF-MoDisCO pattern_5 n=123, CWM

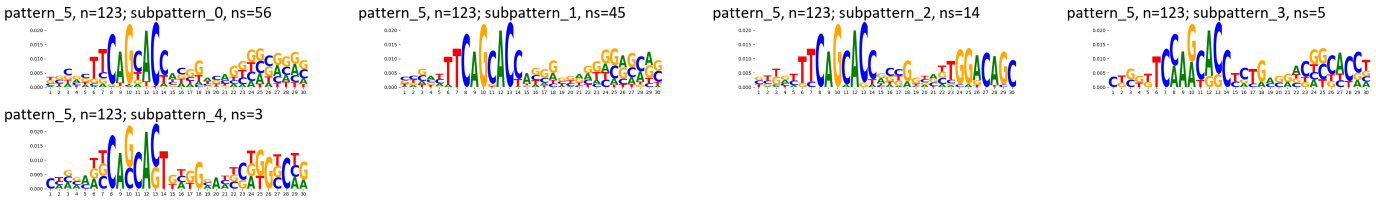

TF-MoDisCO pattern_5 n=123, PWM

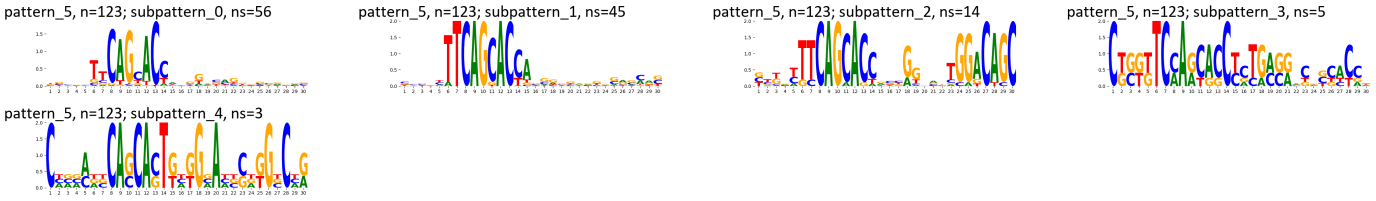

TF-MoDisCO pattern_6 n=121, CWM

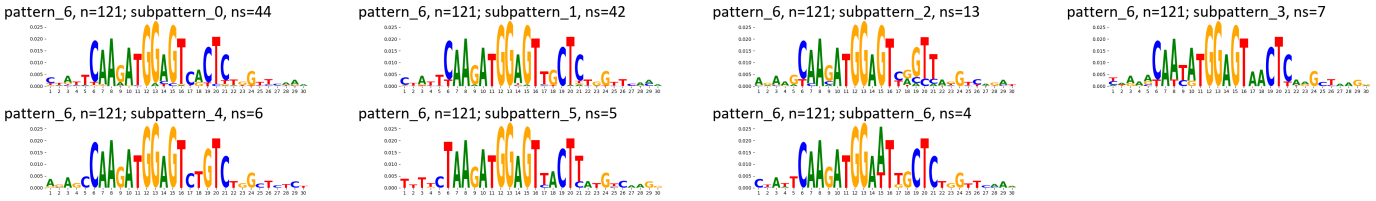

TF-MoDisCO pattern_6 n=121, PWM

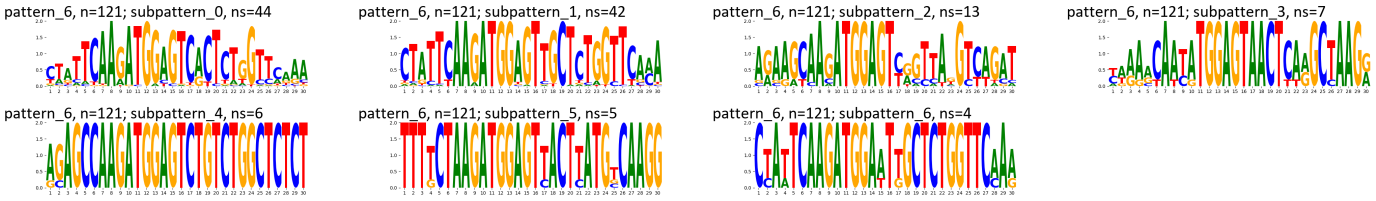

TF-MoDisCO pattern_7 n=80, CWM

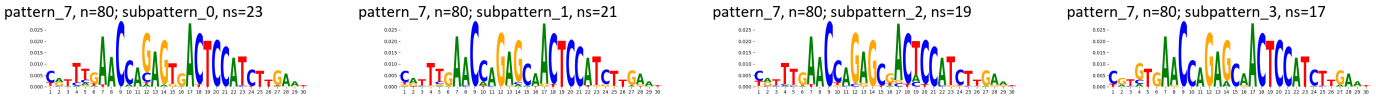

TF-MoDisCO pattern_7 n=80, PWM

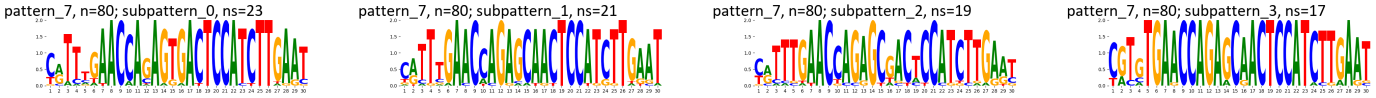

Supplementary Figure 247: TF-MoDisCO subpatterns for the REST transcription factor in K562 (accession ENCSR054JMQ).

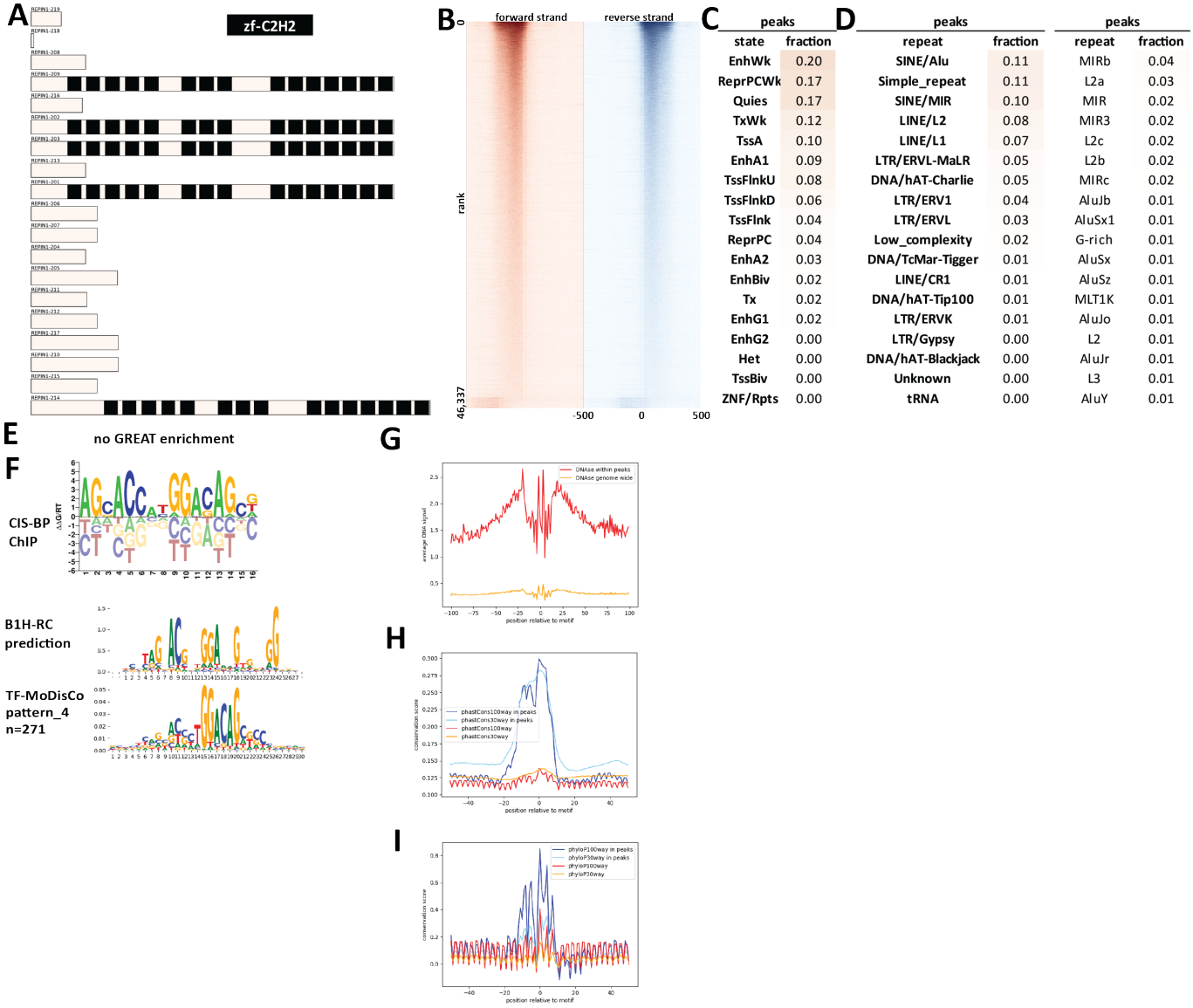

peaks

state	fraction
EnhWk	0.20
ReprPCWk	0.17
Quies	0.17
TxWk	0.12
TssA	0.10
EnhA1	0.09
TssFlnkU	0.08
TssFlnkD	0.06
TssFlnk	0.04
ReprPC	0.04
EnhA2	0.03
EnhBiv	0.02
Tx	0.02
EnhG1	0.02
EnhG2	0.00
Het	0.00
TssBiv	0.00
ZNF/Rpts	0.00

peaks

repeat	fraction
SINE/Alu	0.11
Simple_repeat	0.11
SINE/MIR	0.10
LINE/L2	0.08
LINE/L1	0.07
LTR/ERVL-MaLR	0.05
DNA/hAT-Charlie	0.05
LTR/ERV1	0.04
LTR/ERVL	0.03
Low_complexity	0.02
DNA/TcMar-Tigger	0.01
LINE/CR1	0.01
DNA/hAT-Tip100	0.01
LTR/ERVK	0.01
LTR/Gypsy	0.00
DNA/hAT-Blackjack	0.00
Unknown	0.00
tRNA	0.00

peaks

repeat	fraction
MIRb	0.04
L2a	0.03
MIR	0.02
MIR3	0.02
L2c	0.02
L2b	0.02
MIRc	0.02
AluJb	0.01
AluSx1	0.01
G-rich	0.01
AluSx	0.01
AluSz	0.01
MLT1K	0.01
AluJo	0.01
L2	0.01
AluJr	0.01
L3	0.01
AluY	0.01

Supplementary Figure 248: Properties and genomic distribution of motifs identified for the REST transcription factor in K562 (accession ENCSR137ZMQ).

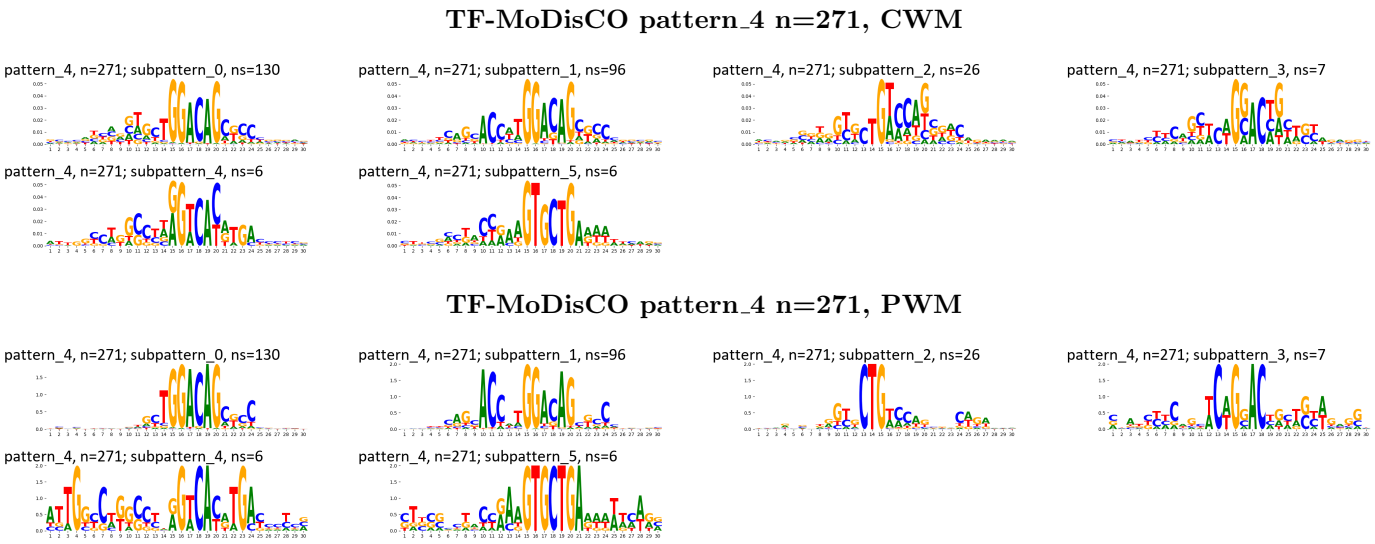

Supplementary Figure 249: TF-MoDisCO subpatterns for the REST transcription factor in K562 (accession ENCSR137ZMQ).

A

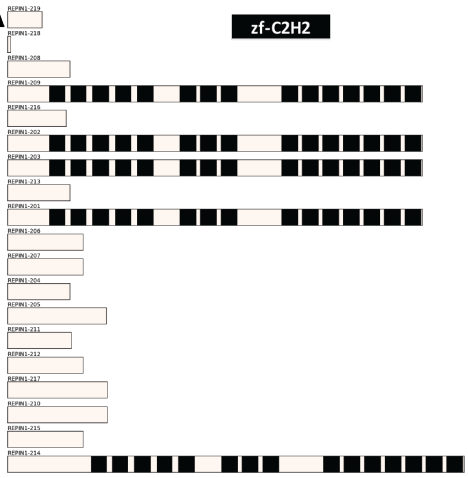

B

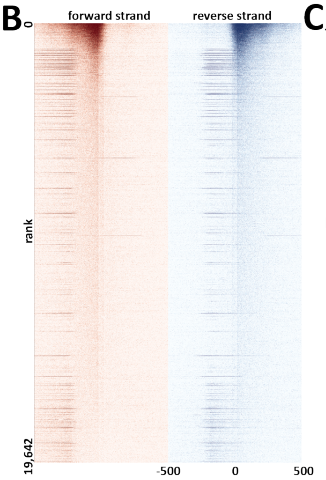

C

peaks	
state	fraction
TssA	0.27
EnhA2	0.21
Quies	0.20
TxWk	0.12
TssFlnk	0.08
EnhWk	0.07
EnhA1	0.05
ReprPCWk	0.03
TssFlnkU	0.02
TssFlnkD	0.01
Het	0.01
ReprPC	0.00
TssBiv	0.00
Tx	0.00
EnhBiv	0.00
ZNF/Rpts	0.00
EnhG1	0.00
EnhG2	0.00

D

peaks		peaks	
repeat	fraction	repeat	fraction
Simple_repeat	0.13	MIRb	0.05
SINE/MIR	0.13	MIR	0.03
SINE/Alu	0.12	L2a	0.03
LINE/L2	0.09	L2c	0.03
LINE/L1	0.08	MIR3	0.02
DNA/hAT-Charlie	0.05	MIRc	0.02
LTR/ERVL-MaLR	0.03	L2b	0.02
LTR/ERV1	0.03	AluJb	0.01
Low_complexity	0.03	AluSx	0.01
LTR/ERVL	0.02	AluSx1	0.01
LINE/CR1	0.01	AluSz	0.01
DNA/TcMar-Tigger	0.01	G-rich	0.01
DNA/hAT-Tip100	0.01	(T)n	0.01
DNA/hAT-Blackjack	0.00	AluJr	0.01
LINE/RTE-X	0.00	L3	0.01
LINE/RTE-BovB	0.00	L2	0.01
DNA/hAT	0.00	AluY	0.01
Unknown	0.00	AluJo	0.01

E

Ontology	Term	FDR Q-val
GO Biological Process	lipid homeostasis	44.59
GO Biological Process	triglyceride homeostasis	33.56
GO Biological Process	cellular response to xenobiotic stimulus	27.53
GO Biological Process	xenobiotic metabolic process	27.44
GO Biological Process	response to xenobiotic stimulus	24.73
GO Biological Process	regulation of cholesterol metabolic process	23.08
GO Biological Process	cholesterol homeostasis	21.20
GO Biological Process	regulation of lipid catabolic process	18.34
GO Biological Process	acute-phase response	17.11
GO Biological Process	positive regulation of lipid catabolic process	16.61
GO Biological Process	cotranslational protein targeting to membrane	16.48
GO Biological Process	reverse cholesterol transport	16.29
GO Biological Process	sterol transport	16.27
GO Biological Process	plasma lipoprotein particle clearance	15.75
GO Biological Process	SRP-dependent cotranslational protein targeting to membrane	15.33
GO Biological Process	regulation of cholesterol biosynthetic process	15.12
GO Biological Process	bile acid metabolic process	14.44
GO Biological Process	regulation of endoplasmic reticulum unfolded protein response	13.74
GO Biological Process	ethanol oxidation	9.52
GO Biological Process	cytoplasmic translation	9.49
Human Phenotype	Lipid accumulation in hepatocytes	14.71
Human Phenotype	Hepatic steatosis	14.47

F

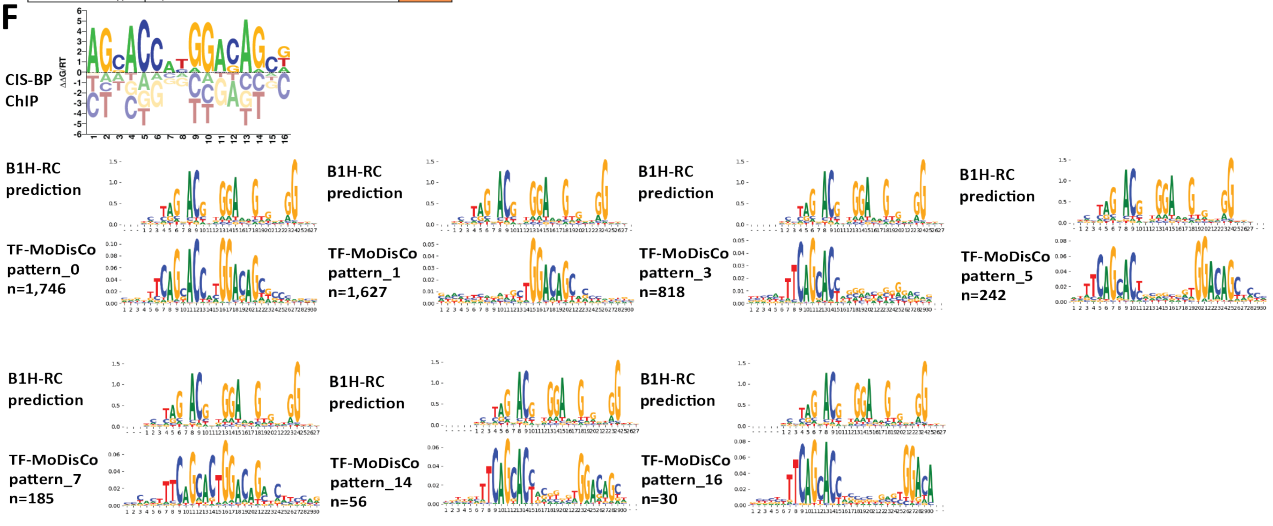

G n/a

H

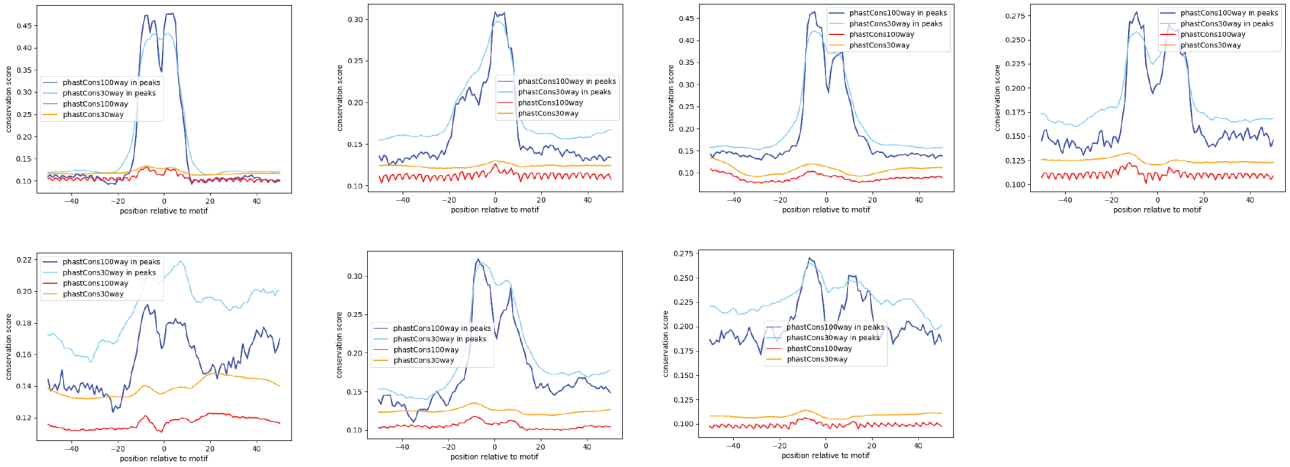

I

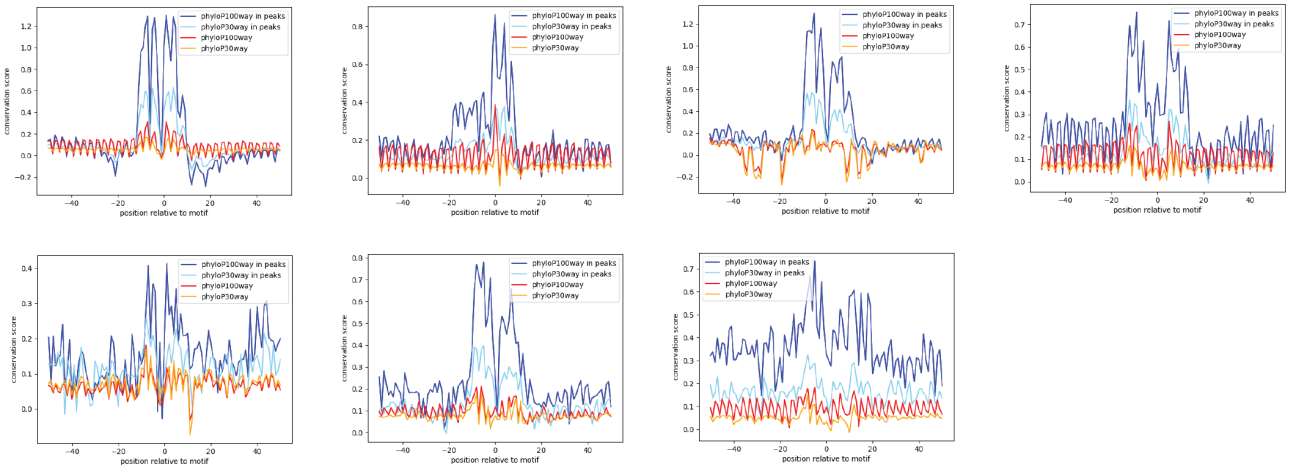

Supplementary Figure 250: Properties and genomic distribution of motifs identified for the REST transcription factor in liver (accession ENCSR893QWP).

TF-MoDisCO pattern_0 n=1746, CWM

pattern_0, n=1746; subpattern_0, ns=520

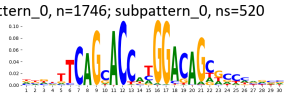

pattern_0, n=1746; subpattern_1, ns=425

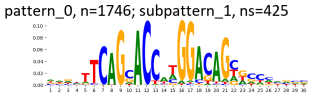

pattern_0, n=1746; subpattern_2, ns=325

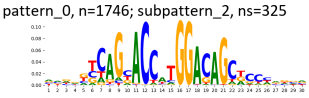

pattern_0, n=1746; subpattern_3, ns=321

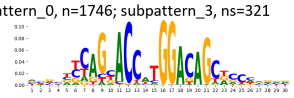

pattern_0, n=1746; subpattern_4, ns=153

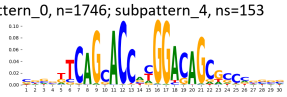

pattern_0, n=1746; subpattern_5, ns=2

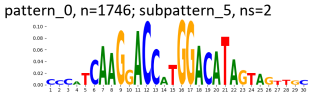

TF-MoDisCO pattern_0 n=1746, PWM

pattern_0, n=1746; subpattern_0, ns=520

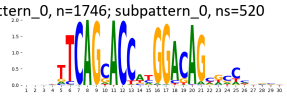

pattern_0, n=1746; subpattern_1, ns=425

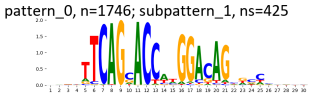

pattern_0, n=1746; subpattern_2, ns=325

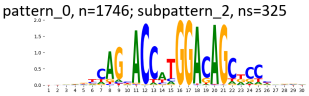

pattern_0, n=1746; subpattern_3, ns=321

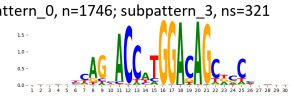

pattern_0, n=1746; subpattern_4, ns=153

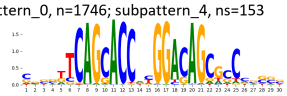

pattern_0, n=1746; subpattern_5, ns=2

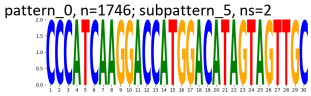

TF-MoDisCO pattern_1 n=1627, CWM

pattern_1, n=1627; subpattern_0, ns=501

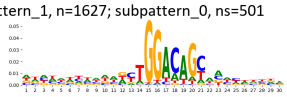

pattern_1, n=1627; subpattern_1, ns=338

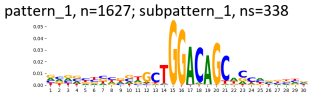

pattern_1, n=1627; subpattern_10, ns=2

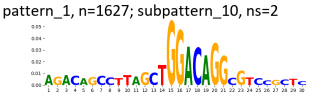

pattern_1, n=1627; subpattern_11, ns=2

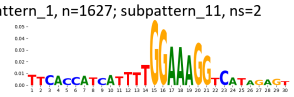

pattern_1, n=1627; subpattern_12, ns=2

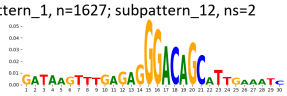

pattern_1, n=1627; subpattern_13, ns=2

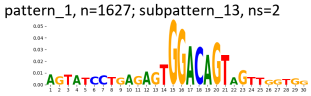

pattern_1, n=1627; subpattern_14, ns=2

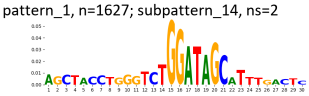

pattern_1, n=1627; subpattern_2, ns=277

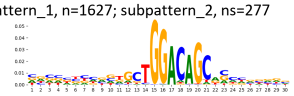

pattern_1, n=1627; subpattern_3, ns=261

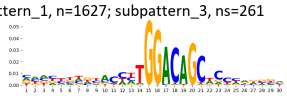

pattern_1, n=1627; subpattern_4, ns=90

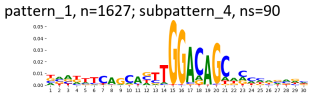

pattern_1, n=1627; subpattern_5, ns=68

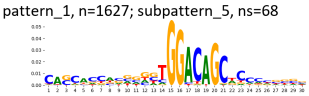

pattern_1, n=1627; subpattern_6, ns=63

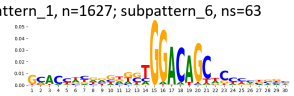

pattern_1, n=1627; subpattern_7, ns=11

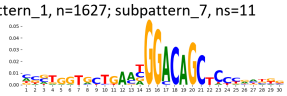

pattern_1, n=1627; subpattern_8, ns=4

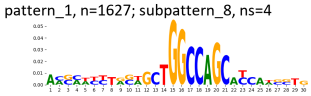

pattern_1, n=1627; subpattern_9, ns=4

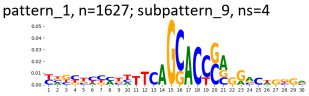

TF-MoDisCO pattern_1 n=1627, PWM

pattern_1, n=1627; subpattern_0, ns=501

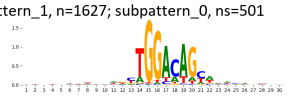

pattern_1, n=1627; subpattern_1, ns=338

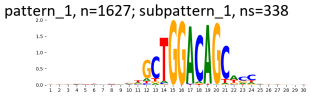

pattern_1, n=1627; subpattern_10, ns=2

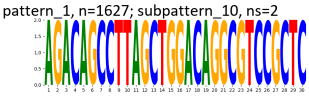

pattern_1, n=1627; subpattern_11, ns=2

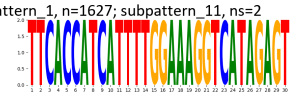

pattern_1, n=1627; subpattern_12, ns=2

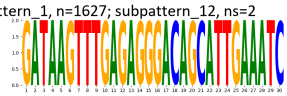

pattern_1, n=1627; subpattern_13, ns=2

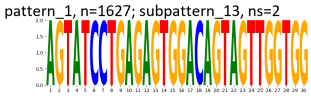

pattern_1, n=1627; subpattern_14, ns=2

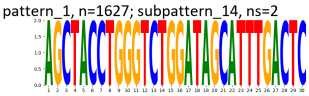

pattern_1, n=1627; subpattern_2, ns=277

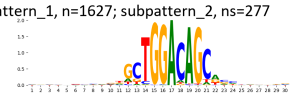

pattern_1, n=1627; subpattern_3, ns=261

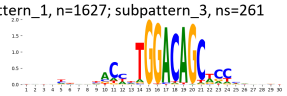

pattern_1, n=1627; subpattern_4, ns=90

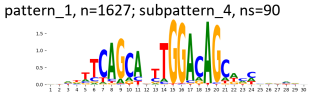

pattern_1, n=1627; subpattern_5, ns=68

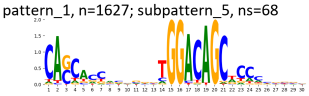

pattern_1, n=1627; subpattern_6, ns=63

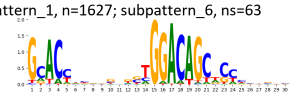

pattern_1, n=1627; subpattern_7, ns=11

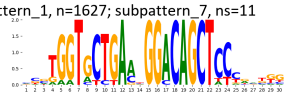

pattern_1, n=1627; subpattern_8, ns=4

pattern_1, n=1627; subpattern_9, ns=4

TF-MoDisCO pattern_14 n=56, CWM

pattern_14, n=56; subpattern_0, ns=22

pattern_14, n=56; subpattern_1, ns=21

pattern_14, n=56; subpattern_2, ns=9

pattern_14, n=56; subpattern_3, ns=4

TF-MoDisCO pattern_14 n=56, PWM

pattern_14, n=56; subpattern_0, ns=22

pattern_14, n=56; subpattern_1, ns=21

pattern_14, n=56; subpattern_2, ns=9

pattern_14, n=56; subpattern_3, ns=4

TF-MoDisCO pattern_16 n=30, CWM

pattern_16, n=30; subpattern_0, ns=30

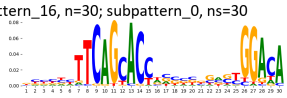

TF-MoDisCO pattern_16 n=30, PWM

pattern_16, n=30; subpattern_0, ns=30

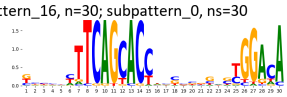

TF-MoDisCO pattern_3 n=818, CWM

pattern_3, n=818; subpattern_0, ns=218

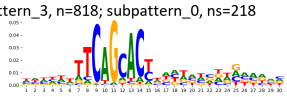

pattern_3, n=818; subpattern_1, ns=208

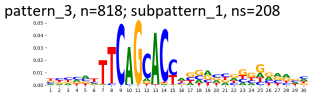

pattern_3, n=818; subpattern_2, ns=143

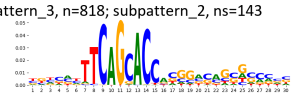

pattern_3, n=818; subpattern_3, ns=138

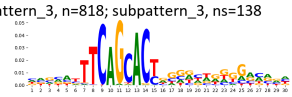

pattern_3, n=818; subpattern_4, ns=106

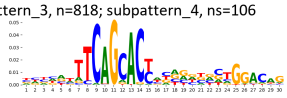

pattern_3, n=818; subpattern_5, ns=5

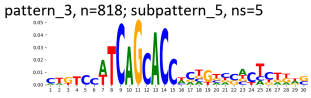

TF-MoDisCO pattern_3 n=818, PWM

pattern_3, n=818; subpattern_0, ns=218

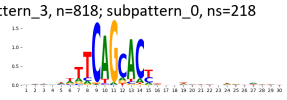

pattern_3, n=818; subpattern_1, ns=208

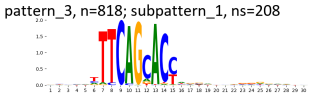

pattern_3, n=818; subpattern_2, ns=143

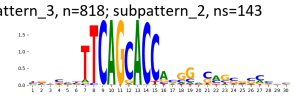

pattern_3, n=818; subpattern_3, ns=138

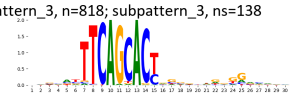

pattern_3, n=818; subpattern_4, ns=106

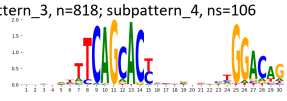

pattern_3, n=818; subpattern_5, ns=5

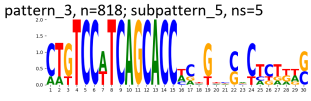

TF-MoDisCO pattern_5 n=242, CWM

pattern_5, n=242; subpattern_0, ns=76

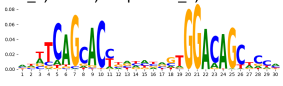

pattern_5, n=242; subpattern_1, ns=66

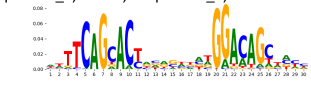

pattern_5, n=242; subpattern_2, ns=52

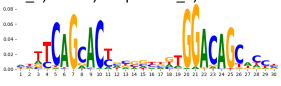

pattern_5, n=242; subpattern_3, ns=36

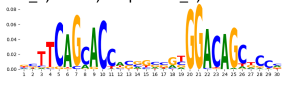

pattern_5, n=242; subpattern_4, ns=10

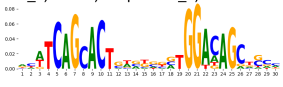

pattern_5, n=242; subpattern_5, ns=2

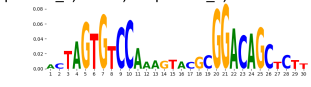

TF-MoDisCO pattern_5 n=242, PWM

pattern_5, n=242; subpattern_0, ns=76

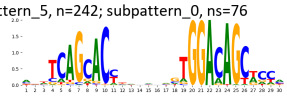

pattern_5, n=242; subpattern_1, ns=66

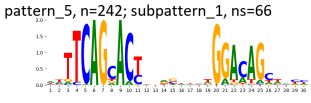

pattern_5, n=242; subpattern_2, ns=52

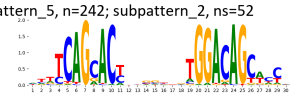

pattern_5, n=242; subpattern_3, ns=36

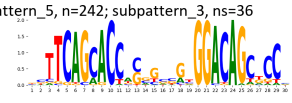

pattern_5, n=242; subpattern_4, ns=10

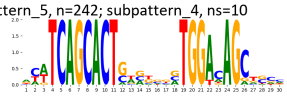

pattern_5, n=242; subpattern_5, ns=2

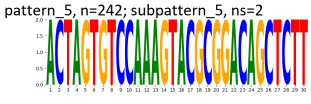

TF-MoDisCO pattern_7 n=185, CWM

pattern_7, n=185; subpattern_0, ns=65

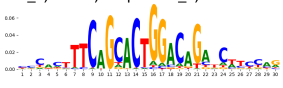

pattern_7, n=185; subpattern_1, ns=53

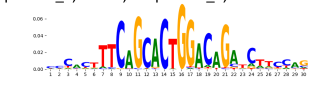

pattern_7, n=185; subpattern_2, ns=38

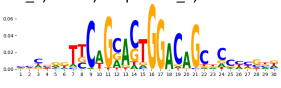

pattern_7, n=185; subpattern_3, ns=11

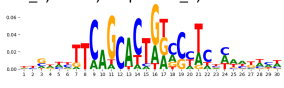

pattern_7, n=185; subpattern_4, ns=9

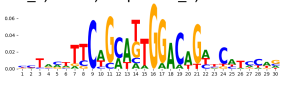

pattern_7, n=185; subpattern_5, ns=7

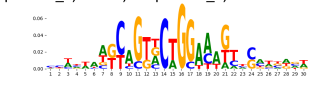

pattern_7, n=185; subpattern_6, ns=2

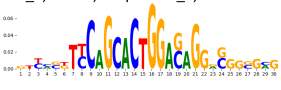

TF-MoDisCO pattern_7 n=185, PWM

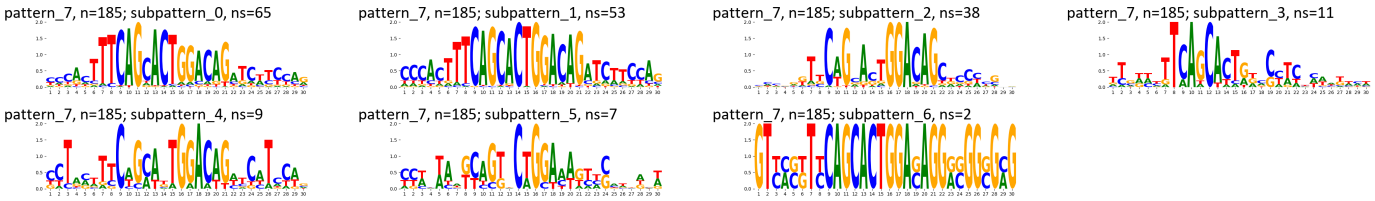

Supplementary Figure 251: TF-MoDisCO subpatterns for the REST transcription factor in liver (accession ENCSR893QWP).

A

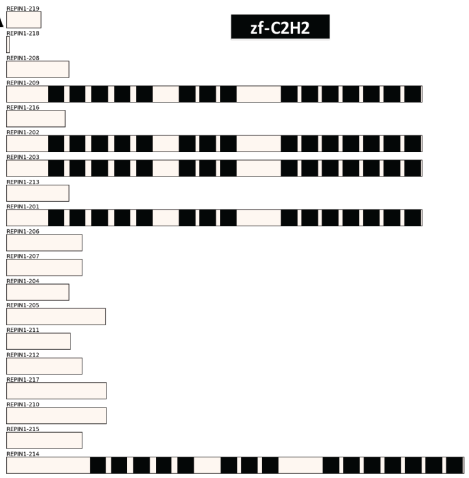

B

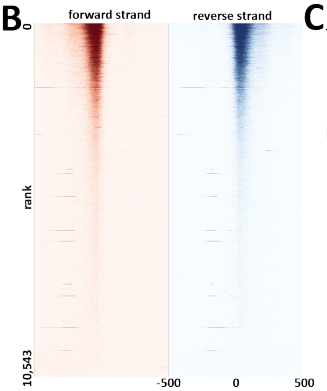

C

peaks	
state	fraction
Quies	0.33
TssA	0.15
EnhA1	0.12
ReprPCWk	0.09
EnhWk	0.09
TssFlnk	0.07
TxWk	0.06
TssFlnkU	0.05
EnhA2	0.04
TssFlnkD	0.02
ReprPC	0.01
Tx	0.01
Het	0.01
EnhG1	0.00
EnhBiv	0.00
EnhG2	0.00
TssBiv	0.00
ZNF/Rpts	0.00

D

peaks		peaks	
repeat	fraction	repeat	fraction
Simple_repeat	0.10	L2a	0.04
SINE/MIR	0.10	MIRb	0.04
LINE/L2	0.10	L2c	0.03
SINE/Alu	0.07	MIR	0.02
LINE/L1	0.07	L2b	0.02
LTR/ERVL-MaLR	0.04	MIR3	0.02
DNA/hAT-Charlie	0.04	MIRc	0.02
LTR/ERVL	0.03	G-rich	0.01
LTR/ERV1	0.02	L3	0.01
Low_complexity	0.02	AluJb	0.01
LINE/CR1	0.01	AluSx1	0.01
DNA/TcMar-Tigger	0.01	L2	0.01
DNA/hAT-Tip100	0.01	AluJr	0.01
Unknown	0.00	AluSz	0.01
LTR/Gypsy	0.00	GA-rich	0.01
LTR/Gypsy?	0.00	AluJo	0.01
LINE/RTE-BovB	0.00	L1M1	0.01
LINE/RTE-X	0.00	AluSx	0.01

E

Ontology	Term	FDR Q-val
GO Biological Process	negative regulation of fibroblast growth factor receptor signaling pathway	13.00
GO Biological Process	regulation of alpha-amino-3-hydroxy-5-methyl-4-isoxazole propionate selective glutamate receptor activity	4.56
GO Biological Process	response to corticosterone	3.92
GO Biological Process	vesicle transport along actin filament	2.65
GO Biological Process	signal complex assembly	1.73

F

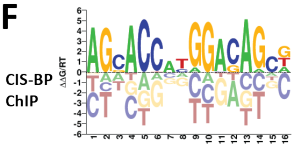

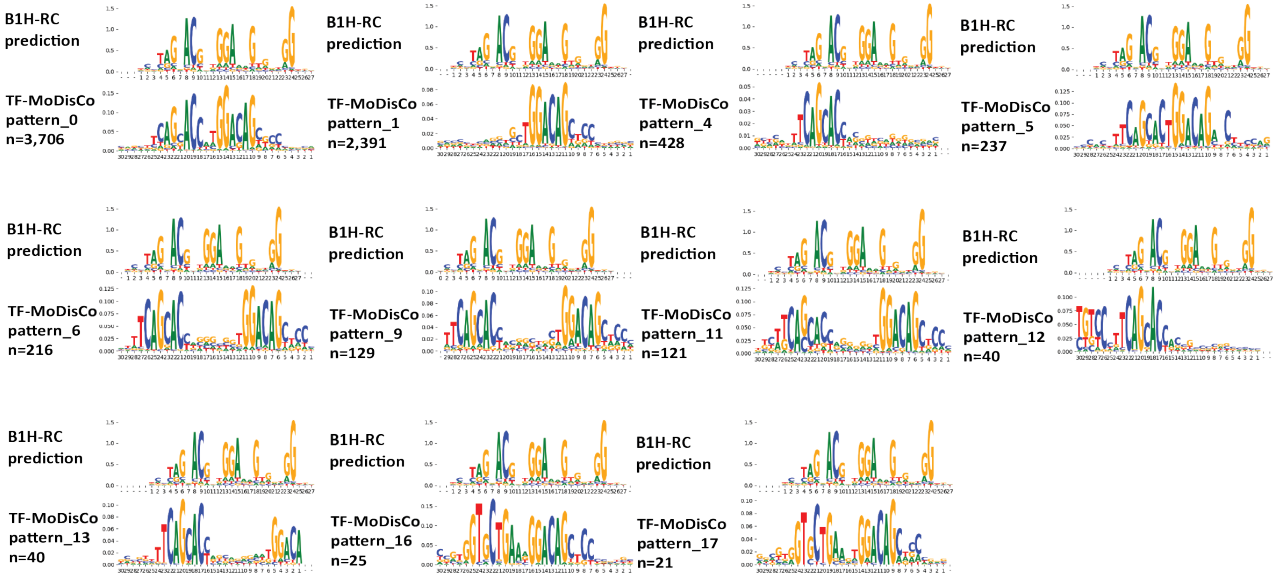

G n/a

H

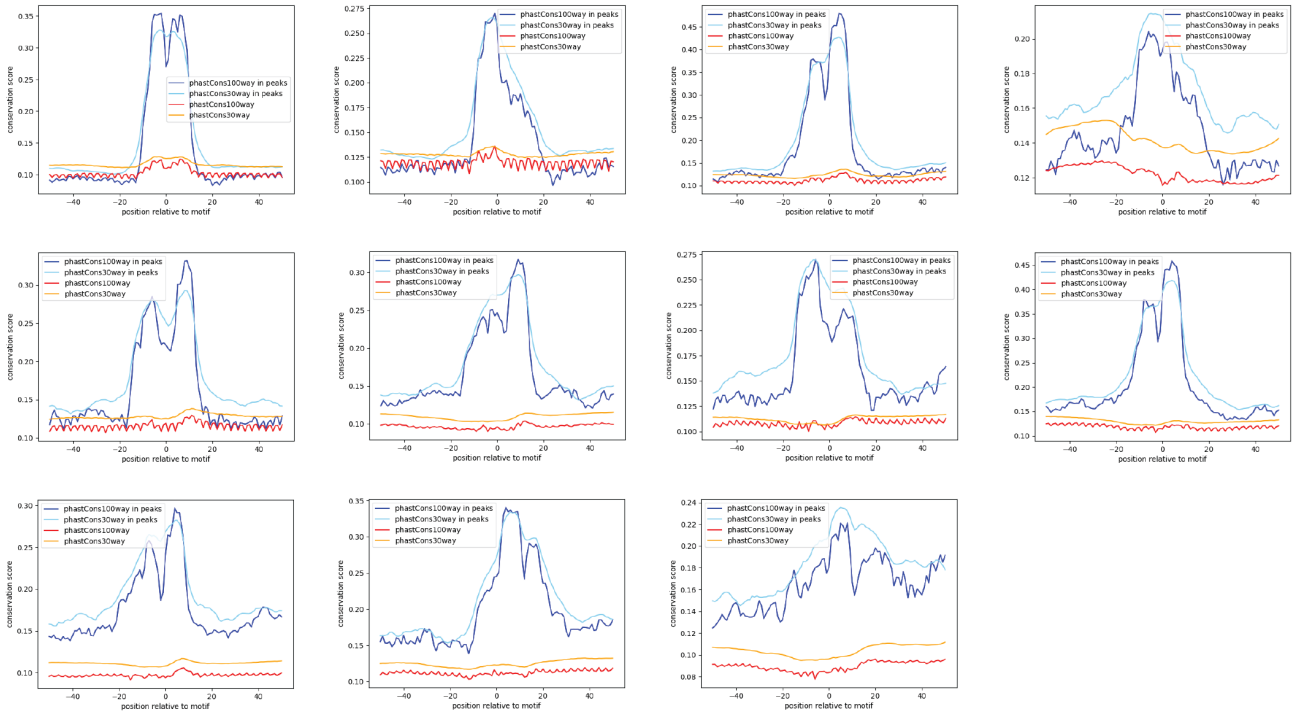

I

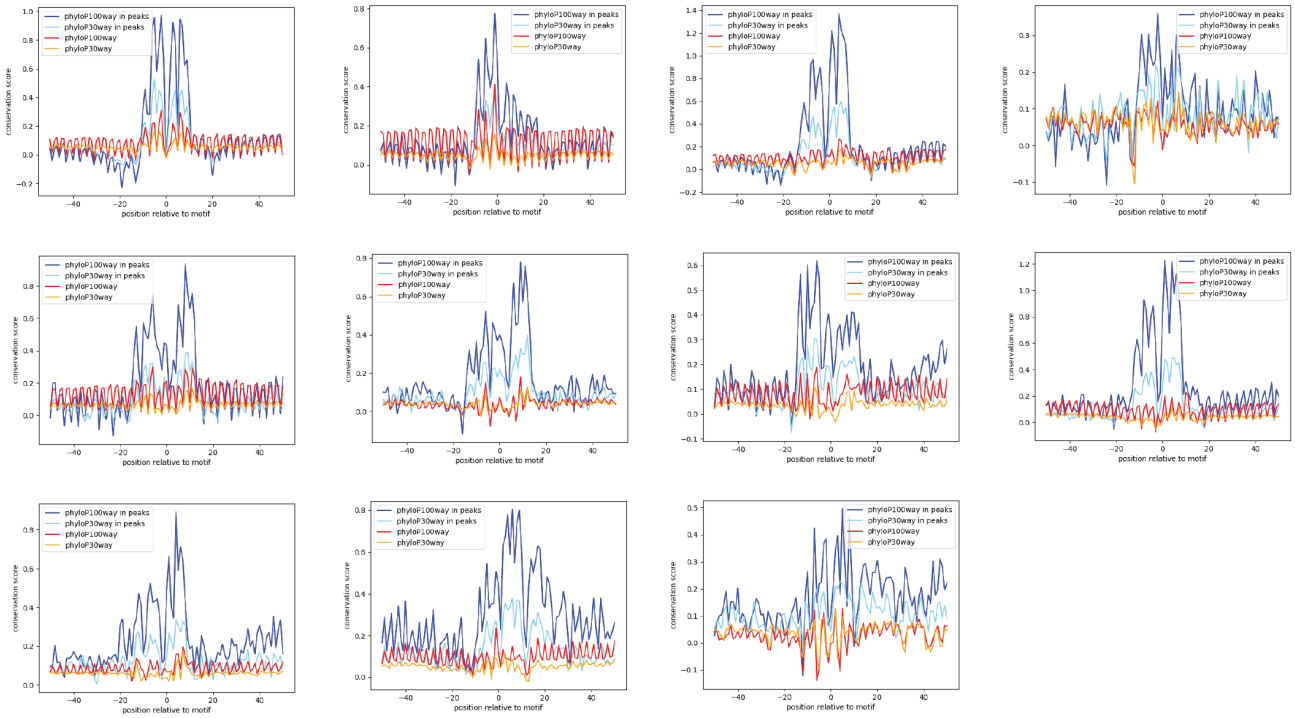

Supplementary Figure 252: Properties and genomic distribution of motifs identified for the REST transcription factor in MCF-7 (accession ENCSR000BSP).

TF-MoDisCO pattern_0 n=3706, CWM

pattern_0, n=3706; subpattern_0, ns=801

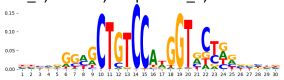

pattern_0, n=3706; subpattern_1, ns=777

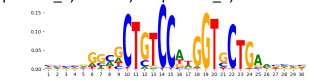

pattern_0, n=3706; subpattern_2, ns=745

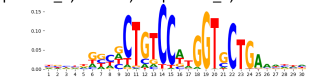

pattern_0, n=3706; subpattern_3, ns=609

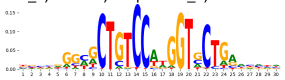

pattern_0, n=3706; subpattern_4, ns=411

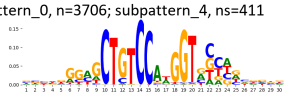

pattern_0, n=3706; subpattern_5, ns=323

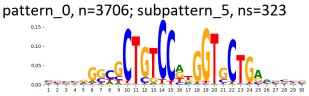

pattern_0, n=3706; subpattern_6, ns=40

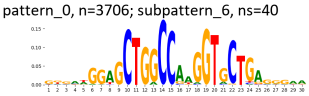

TF-MoDisCO pattern_0 n=3706, PWM

pattern_0, n=3706; subpattern_0, ns=801

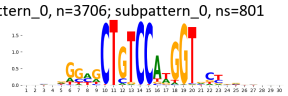

pattern_0, n=3706; subpattern_1, ns=777

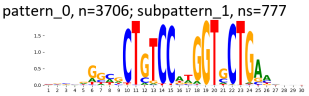

pattern_0, n=3706; subpattern_2, ns=745

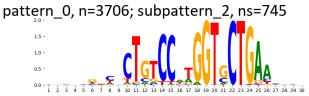

pattern_0, n=3706; subpattern_3, ns=609

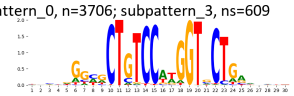

pattern_0, n=3706; subpattern_4, ns=411

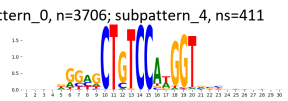

pattern_0, n=3706; subpattern_5, ns=323

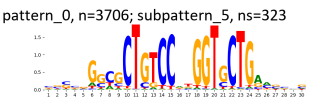

pattern_0, n=3706; subpattern_6, ns=40

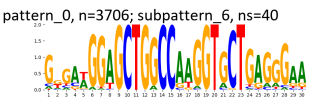

TF-MoDisCO pattern_1 n=2391, CWM

pattern_1, n=2391; subpattern_0, ns=482

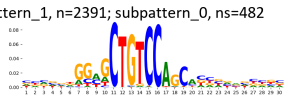

pattern_1, n=2391; subpattern_1, ns=450

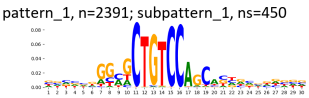

pattern_1, n=2391; subpattern_2, ns=448

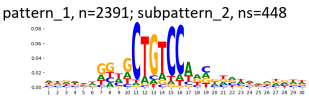

pattern_1, n=2391; subpattern_3, ns=398

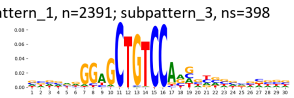

pattern_1, n=2391; subpattern_4, ns=298

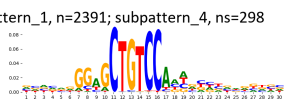

pattern_1, n=2391; subpattern_5, ns=154

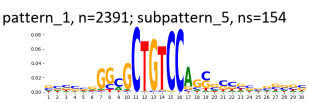

pattern_1, n=2391; subpattern_6, ns=145

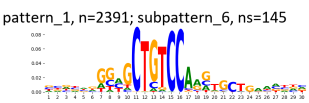

pattern_1, n=2391; subpattern_7, ns=13

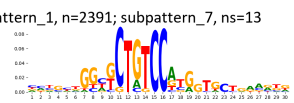

pattern_1, n=2391; subpattern_8, ns=3

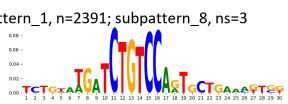

TF-MoDisCO pattern_1 n=2391, PWM

pattern_1, n=2391; subpattern_0, ns=482

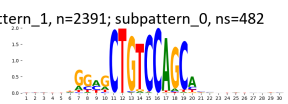

pattern_1, n=2391; subpattern_1, ns=450

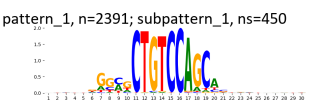

pattern_1, n=2391; subpattern_2, ns=448

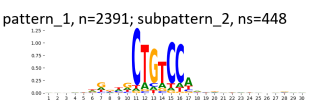

pattern_1, n=2391; subpattern_3, ns=398

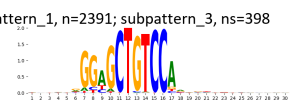

pattern_1, n=2391; subpattern_4, ns=298

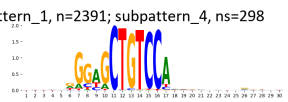

pattern_1, n=2391; subpattern_5, ns=154

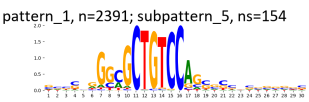

pattern_1, n=2391; subpattern_6, ns=145

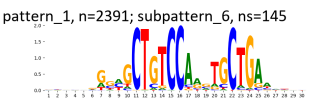

pattern_1, n=2391; subpattern_7, ns=13

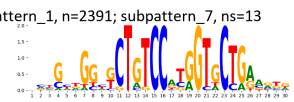

pattern_1, n=2391; subpattern_8, ns=3

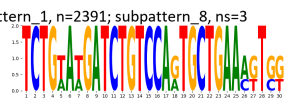

TF-MoDisCO pattern_11 n=121, CWM

pattern_11, n=121; subpattern_0, ns=47

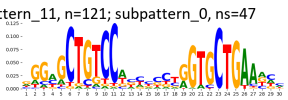

pattern_11, n=121; subpattern_1, ns=41

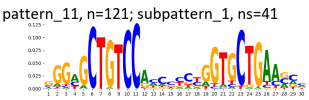

pattern_11, n=121; subpattern_2, ns=33

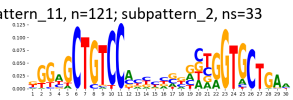

TF-MoDisCO pattern_11 n=121, PWM

pattern_11, n=121; subpattern_0, ns=47

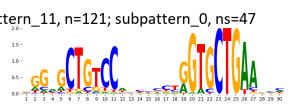

pattern_11, n=121; subpattern_1, ns=41

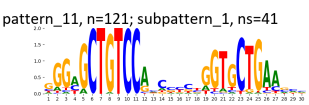

pattern_11, n=121; subpattern_2, ns=33

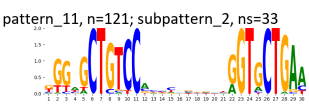

TF-MoDisCO pattern_12 n=40, CWM

pattern_12, n=40; subpattern_0, ns=40

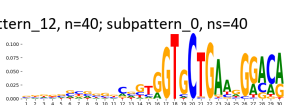

TF-MoDisCO pattern_12 n=40, PWM

pattern_12, n=40; subpattern_0, ns=40

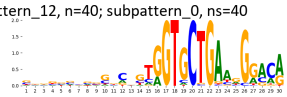

TF-MoDisCO pattern_13 n=40, CWM

pattern_13, n=40; subpattern_0, ns=40

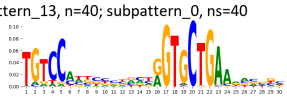

TF-MoDisCO pattern_13 n=40, PWM

pattern_13, n=40; subpattern_0, ns=40

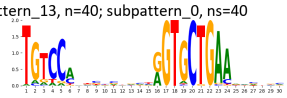

TF-MoDisCO pattern_16 n=25, CWM

pattern_16, n=25; subpattern_0, ns=25

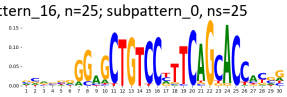

TF-MoDisCO pattern_16 n=25, PWM

pattern_16, n=25; subpattern_0, ns=25

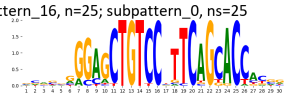

TF-MoDisCO pattern_17 n=21, CWM

pattern_17, n=21; subpattern_0, ns=21

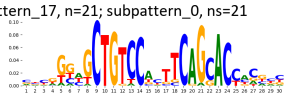

TF-MoDisCO pattern_17 n=21, PWM

pattern_17, n=21; subpattern_0, ns=21

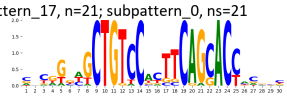

TF-MoDisCO pattern_4 n=428, CWM

pattern_4, n=428; subpattern_0, ns=129

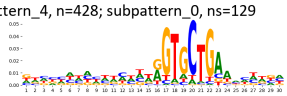

pattern_4, n=428; subpattern_1, ns=120

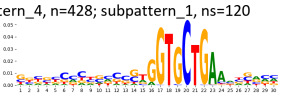

pattern_4, n=428; subpattern_2, ns=111

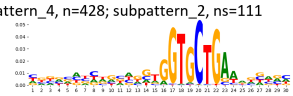

pattern_4, n=428; subpattern_3, ns=47

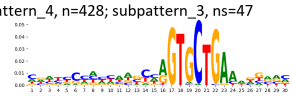

pattern_4, n=428; subpattern_4, ns=11

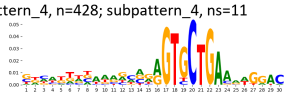

pattern_4, n=428; subpattern_5, ns=8

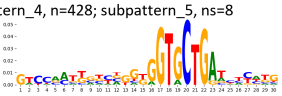

pattern_4, n=428; subpattern_6, ns=2

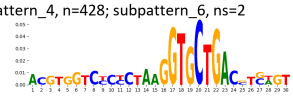

TF-MoDisCO pattern_4 n=428, PWM

pattern_4, n=428; subpattern_0, ns=129

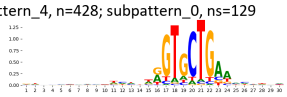

pattern_4, n=428; subpattern_1, ns=120

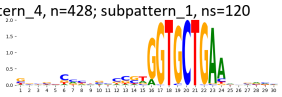

pattern_4, n=428; subpattern_2, ns=111

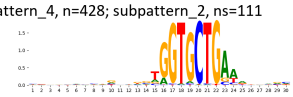

pattern_4, n=428; subpattern_3, ns=47

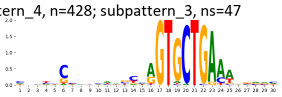

pattern_4, n=428; subpattern_4, ns=11

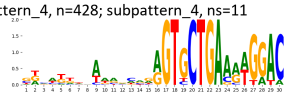

pattern_4, n=428; subpattern_5, ns=8

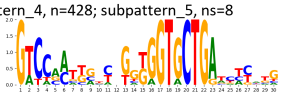

pattern_4, n=428; subpattern_6, ns=2

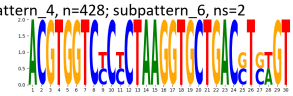

TF-MoDisCO pattern_5 n=237, CWM

pattern_5, n=237; subpattern_0, ns=71

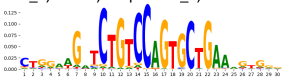

pattern_5, n=237; subpattern_1, ns=70

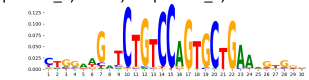

pattern_5, n=237; subpattern_2, ns=62

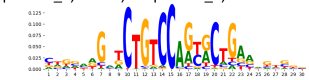

pattern_5, n=237; subpattern_3, ns=29

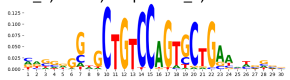

pattern_5, n=237; subpattern_4, ns=5

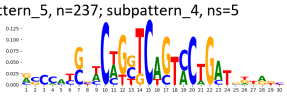

TF-MoDisCO pattern_5 n=237, PWM

pattern_5, n=237; subpattern_0, ns=71

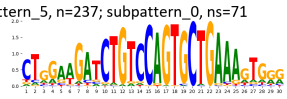

pattern_5, n=237; subpattern_1, ns=70

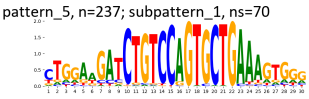

pattern_5, n=237; subpattern_2, ns=62

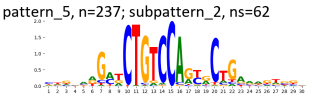

pattern_5, n=237; subpattern_3, ns=29

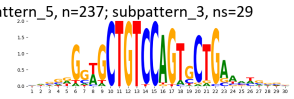

pattern_5, n=237; subpattern_4, ns=5

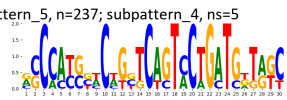

TF-MoDisCO pattern_6 n=216, CWM

pattern_6, n=216; subpattern_0, ns=87

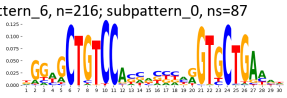

pattern_6, n=216; subpattern_1, ns=78

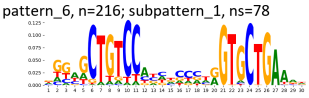

pattern_6, n=216; subpattern_2, ns=34

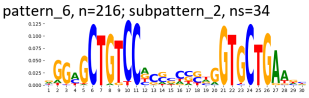

pattern_6, n=216; subpattern_3, ns=7

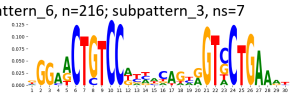

pattern_6, n=216; subpattern_4, ns=5

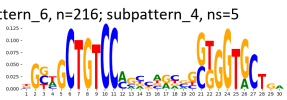

pattern_6, n=216; subpattern_5, ns=5

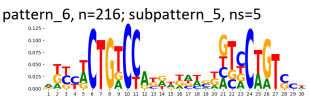

TF-MoDisCO pattern_6 n=216, PWM

pattern_6, n=216; subpattern_0, ns=87

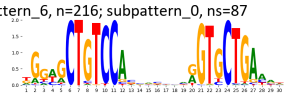

pattern_6, n=216; subpattern_1, ns=78

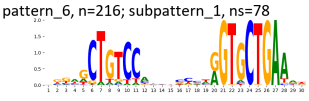

pattern_6, n=216; subpattern_2, ns=34

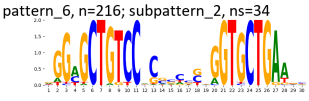

pattern_6, n=216; subpattern_3, ns=7

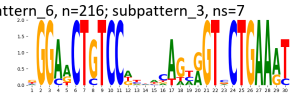

pattern_6, n=216; subpattern_4, ns=5

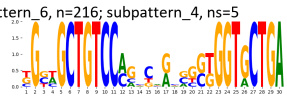

pattern_6, n=216; subpattern_5, ns=5

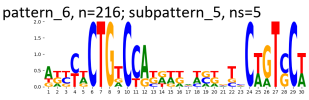

TF-MoDisCO pattern_9 n=129, CWM

pattern_9, n=129; subpattern_0, ns=40

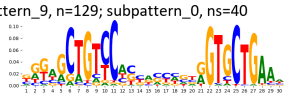

pattern_9, n=129; subpattern_1, ns=40

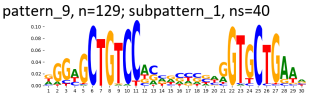

pattern_9, n=129; subpattern_2, ns=30

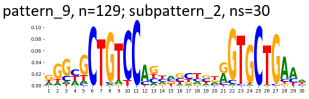

pattern_9, n=129; subpattern_3, ns=8

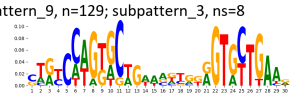

pattern_9, n=129; subpattern_4, ns=7

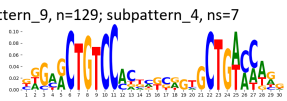

pattern_9, n=129; subpattern_5, ns=2

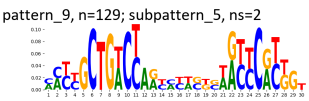

pattern_9, n=129; subpattern_6, ns=2

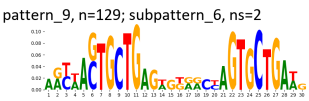

TF-MoDisCO pattern_9 n=129, PWM

pattern_9, n=129; subpattern_0, ns=40

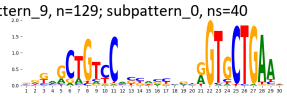

pattern_9, n=129; subpattern_1, ns=40

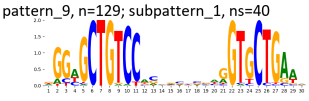

pattern_9, n=129; subpattern_2, ns=30

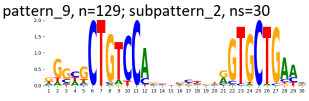

pattern_9, n=129; subpattern_3, ns=8

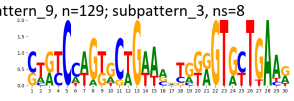

pattern_9, n=129; subpattern_4, ns=7

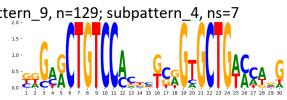

pattern_9, n=129; subpattern_5, ns=2

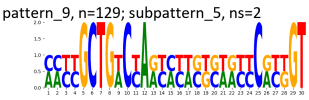

pattern_9, n=129; subpattern_6, ns=2

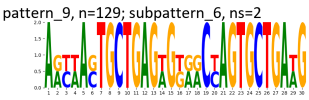

Supplementary Figure 253: TF-MoDisCO subpatterns for the REST transcription factor in MCF-7 (accession ENCSR000BSP).

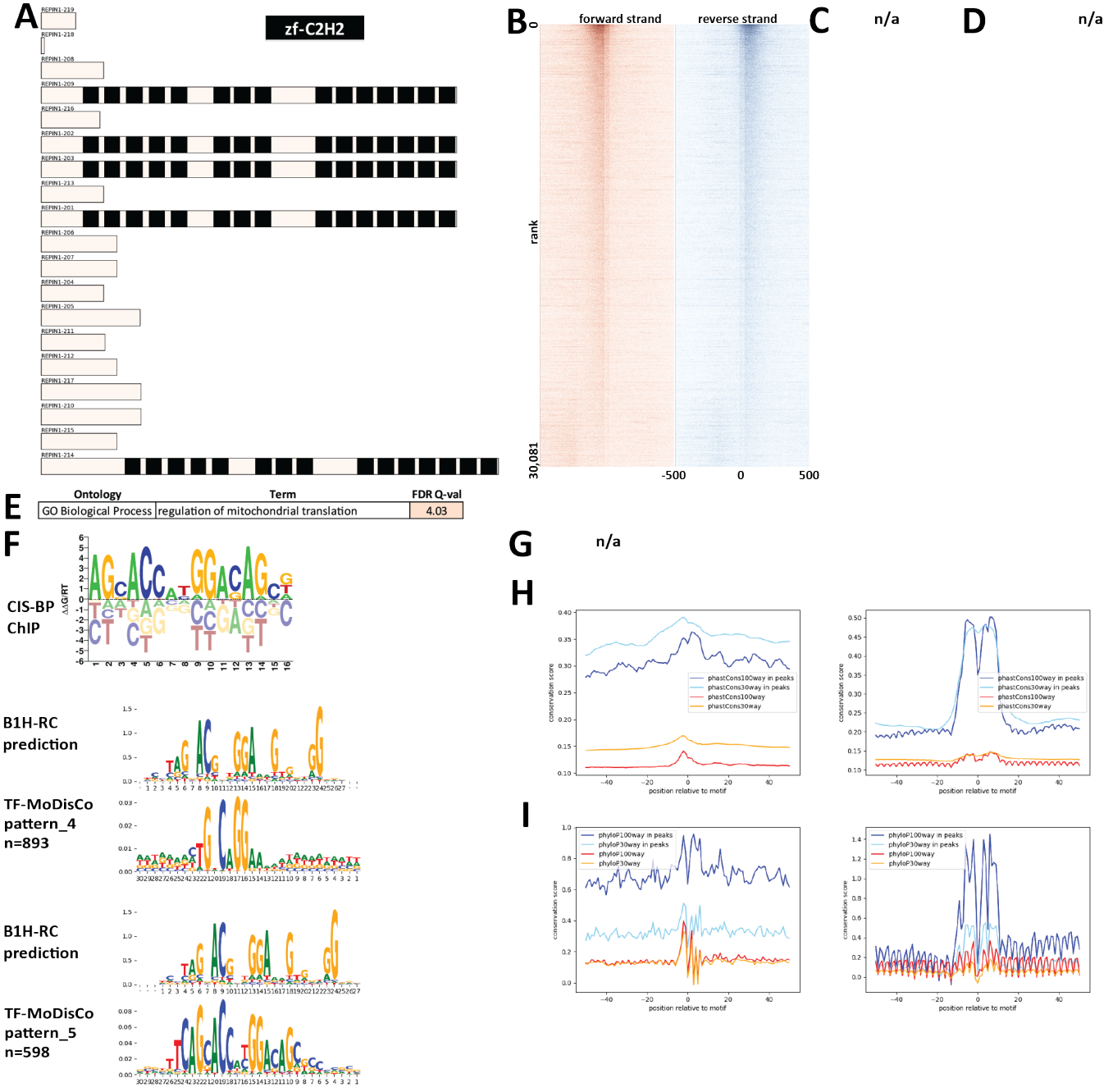

Supplementary Figure 254: Properties and genomic distribution of motifs identified for the REST transcription factor in neural cell (accession ENCSR000BTV).

TF-MoDisCO pattern_4 n=893, CWM

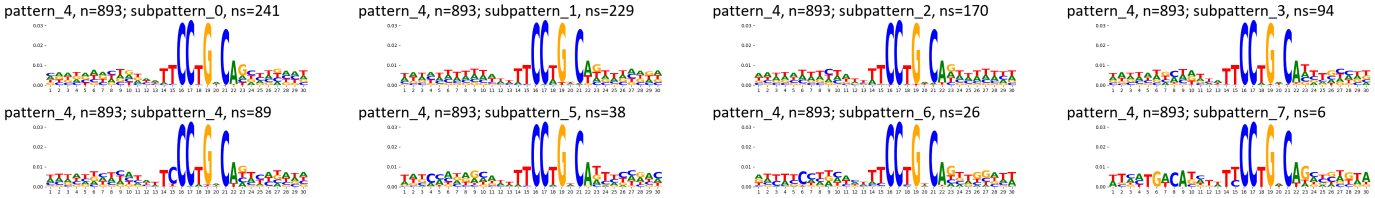

TF-MoDisCO pattern_4 n=893, PWM

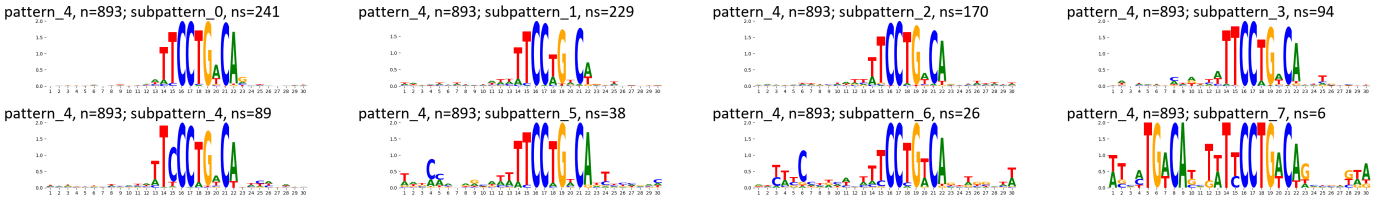

TF-MoDisCO pattern_5 n=598, CWM

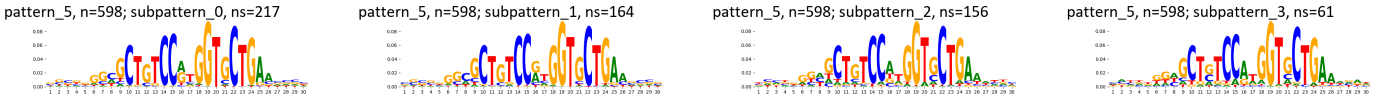

TF-MoDisCO pattern_5 n=598, PWM

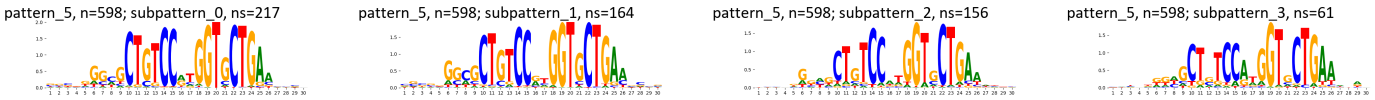

Supplementary Figure 255: TF-MoDisCO subpatterns for the REST transcription factor in neural cell (accession ENCSR000BTV).

A

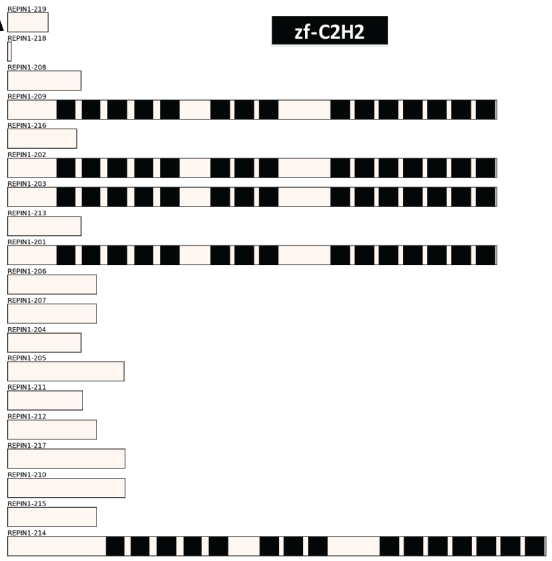

B

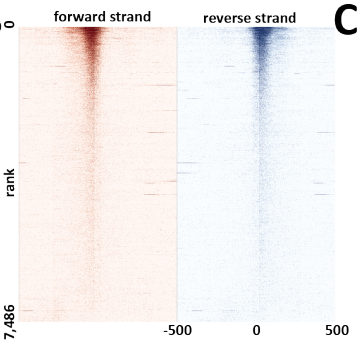

C n/a

D n/a

F

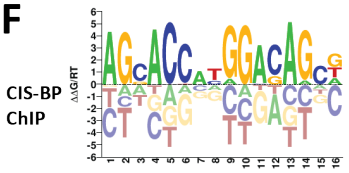

E

Ontology	Term	FDR Q-val
GO Biological Process	viral gene expression	10.43
GO Biological Process	translational elongation	8.89
GO Biological Process	mitochondrial translation	8.08
GO Biological Process	mitochondrial translational elongation	7.72
GO Biological Process	mitochondrial translational termination	7.48
GO Biological Process	translational termination	6.61
GO Biological Process	viral transcription	6.60
GO Biological Process	protein targeting to ER	6.56
GO Biological Process	cotranslational protein targeting to membrane	5.89
GO Biological Process	SRP-dependent cotranslational protein targeting to membrane	5.34
GO Biological Process	regulation of alternative mRNA splicing, via spliceosome	5.22
GO Biological Process	response to L-glutamate	4.35
GO Biological Process	positive regulation of transcription from RNA polymerase II promoter in response to stress	4.27
GO Biological Process	ribosome assembly	4.17
GO Biological Process	negative regulation of Notch signaling pathway	3.85
GO Biological Process	response to corticosterone	3.81
GO Biological Process	response to salt	3.24
GO Biological Process	regulation of alpha-amino-3-hydroxy-5-methyl-4-isoxazole propionate selective glutamate receptor activity	3.07
GO Biological Process	ribosomal large subunit assembly	2.26
GO Biological Process	positive regulation of mitochondrial membrane permeability	1.78

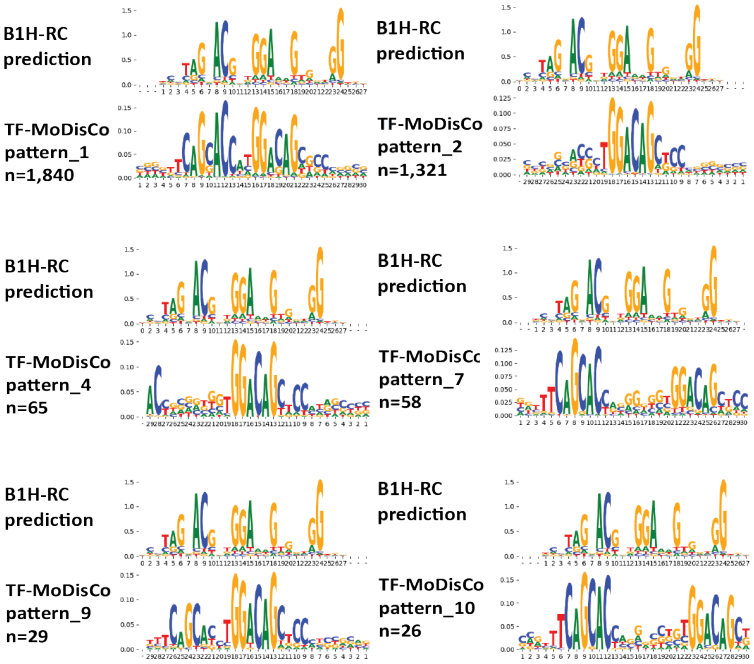

G n/a

H

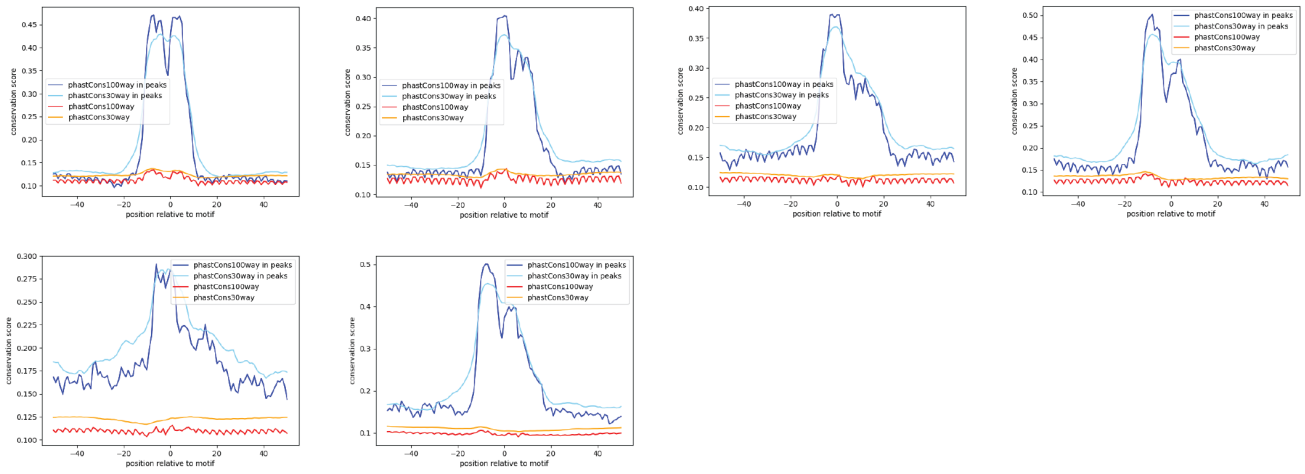

I

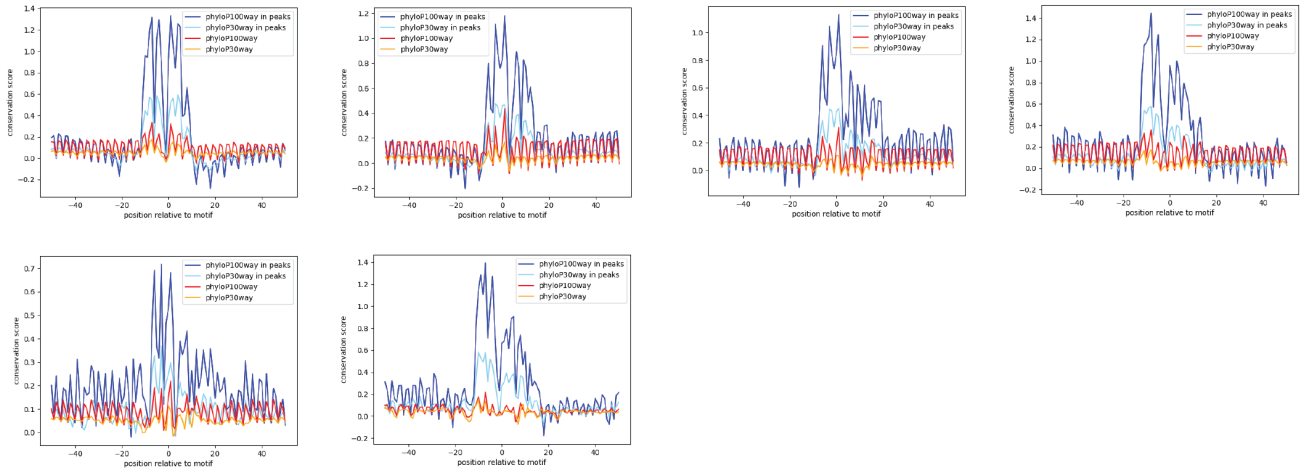

Supplementary Figure 256: Properties and genomic distribution of motifs identified for the REST transcription factor in Panc1 (accession ENCSR000BJO).

TF-MoDisCO pattern_1 n=1840, CWM

pattern_1, n=1840; subpattern_0, ns=418

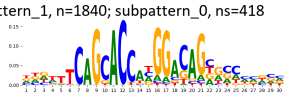

pattern_1, n=1840; subpattern_1, ns=355

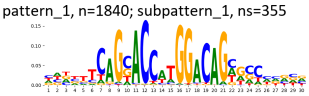

pattern_1, n=1840; subpattern_2, ns=341

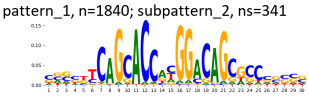

pattern_1, n=1840; subpattern_3, ns=322

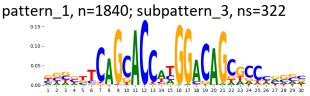

pattern_1, n=1840; subpattern_4, ns=268

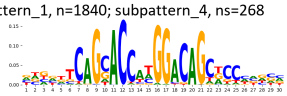

pattern_1, n=1840; subpattern_5, ns=136

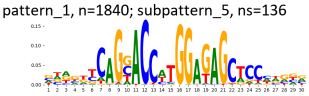

TF-MoDisCO pattern_1 n=1840, PWM

pattern_1, n=1840; subpattern_0, ns=418

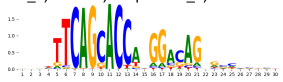

pattern_1, n=1840; subpattern_1, ns=355

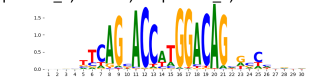

pattern_1, n=1840; subpattern_2, ns=341

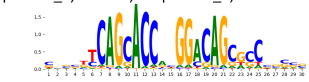

pattern_1, n=1840; subpattern_3, ns=322

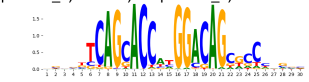

pattern_1, n=1840; subpattern_4, ns=268

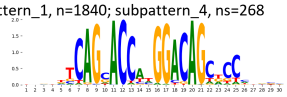

pattern_1, n=1840; subpattern_5, ns=136

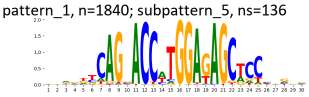

TF-MoDisCO pattern_10 n=26, CWM

pattern_10, n=26; subpattern_0, ns=26

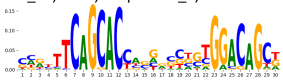

TF-MoDisCO pattern_10 n=26, PWM

pattern_10, n=26; subpattern_0, ns=26

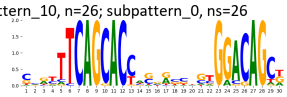

TF-MoDisCO pattern_2 n=1321, CWM

pattern_2, n=1321; subpattern_0, ns=316

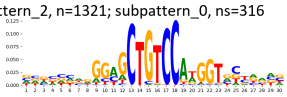

pattern_2, n=1321; subpattern_1, ns=313

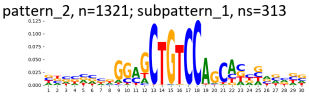

pattern_2, n=1321; subpattern_2, ns=269

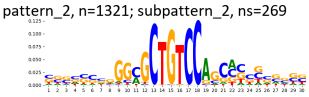

pattern_2, n=1321; subpattern_3, ns=187

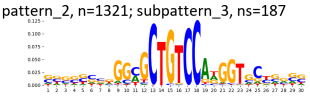

pattern_2, n=1321; subpattern_4, ns=134

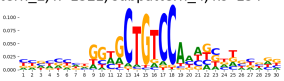

pattern_2, n=1321; subpattern_5, ns=55

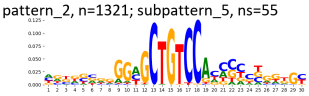

pattern_2, n=1321; subpattern_6, ns=37

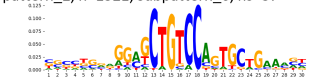

pattern_2, n=1321; subpattern_7, ns=10

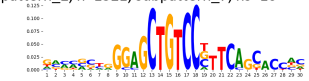

TF-MoDisCO pattern_2 n=1321, PWM

pattern_2, n=1321; subpattern_0, ns=316

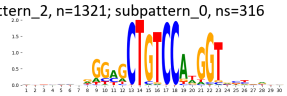

pattern_2, n=1321; subpattern_1, ns=313

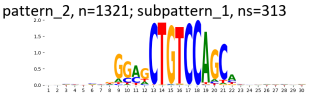

pattern_2, n=1321; subpattern_2, ns=269

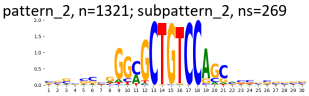

pattern_2, n=1321; subpattern_3, ns=187

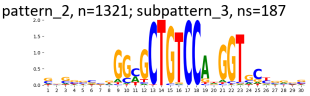

pattern_2, n=1321; subpattern_4, ns=134

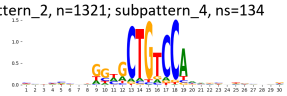

pattern_2, n=1321; subpattern_5, ns=55

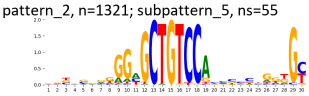

pattern_2, n=1321; subpattern_6, ns=37

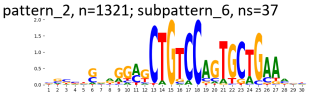

pattern_2, n=1321; subpattern_7, ns=10

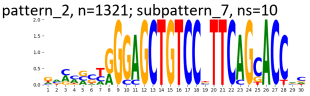

TF-MoDisCO pattern_4 n=65, CWM

pattern_4, n=65; subpattern_0, ns=21

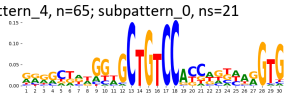

pattern_4, n=65; subpattern_1, ns=21

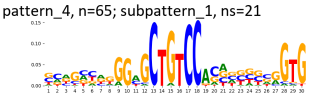

pattern_4, n=65; subpattern_2, ns=16

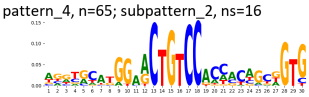

pattern_4, n=65; subpattern_3, ns=7

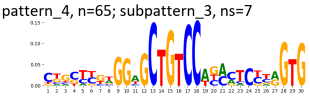

TF-MoDisCO pattern_4 n=65, PWM

pattern_4, n=65; subpattern_0, ns=21

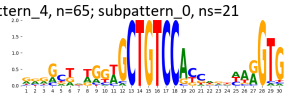

pattern_4, n=65; subpattern_1, ns=21

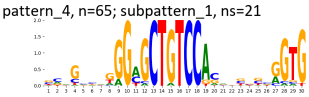

pattern_4, n=65; subpattern_2, ns=16

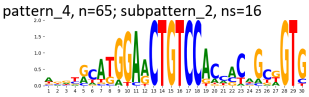

pattern_4, n=65; subpattern_3, ns=7

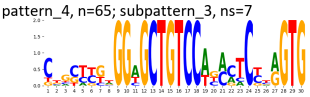

TF-MoDisCO pattern_7 n=58, CWM

pattern_7, n=58; subpattern_0, ns=20

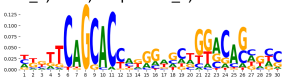

pattern_7, n=58; subpattern_1, ns=20

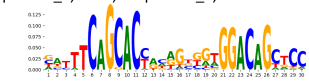

pattern_7, n=58; subpattern_2, ns=18

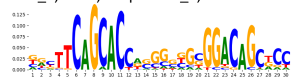

TF-MoDisCO pattern_7 n=58, PWM

pattern_7, n=58; subpattern_0, ns=20

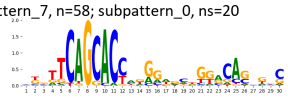

pattern_7, n=58; subpattern_1, ns=20

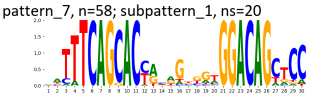

pattern_7, n=58; subpattern_2, ns=18

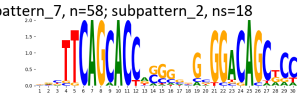

TF-MoDisCO pattern_9 n=29, CWM

pattern_9, n=29; subpattern_0, ns=29

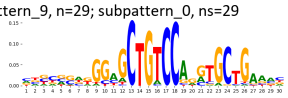

TF-MoDisCO pattern_9 n=29, PWM

pattern_9, n=29; subpattern_0, ns=29

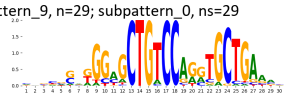

Supplementary Figure 257: TF-MoDisCO subpatterns for the REST transcription factor in Panc1 (accession ENCSR000BJO).

A

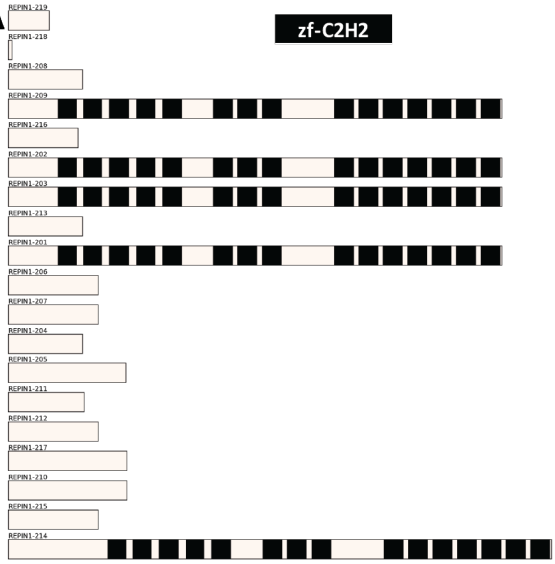

B

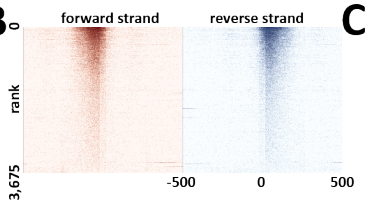

C n/a

D n/a

F

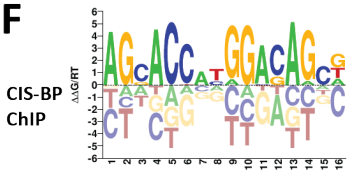

E

Ontology	Term	FDR Q-val
GO Biological Process	viral gene expression	9.75
GO Biological Process	viral transcription	8.43
GO Biological Process	SRP-dependent cotranslational protein targeting to membrane	7.52
GO Biological Process	cotranslational protein targeting to membrane	7.29
GO Biological Process	translational initiation	7.11
GO Biological Process	protein targeting to ER	7.11
GO Biological Process	multi-organism metabolic process	7.12
GO Biological Process	nuclear-transcribed mRNA catabolic process, nonsense-mediated decay	7.08
GO Biological Process	establishment of protein localization to endoplasmic reticulum	6.00
GO Biological Process	regulation of neuronal synaptic plasticity	4.17
GO Biological Process	cellular response to monosaccharide stimulus	4.12
GO Biological Process	cellular response to hexose stimulus	4.01
GO Biological Process	cellular response to glucose stimulus	3.85
GO Biological Process	cellular response to drug	3.77
GO Biological Process	regulation of posttranscriptional gene silencing	3.16
GO Biological Process	regulation of gene silencing by RNA	3.16
GO Biological Process	regulation of alpha-amino-3-hydroxy-5-methyl-4-isoxazole propionate selective glutamate receptor activity	2.81
GO Biological Process	regulation of short-term neuronal synaptic plasticity	2.45
GO Biological Process	positive regulation of TOR signaling	2.19
GO Biological Process	regulation of systemic arterial blood pressure by endothelin	1.81

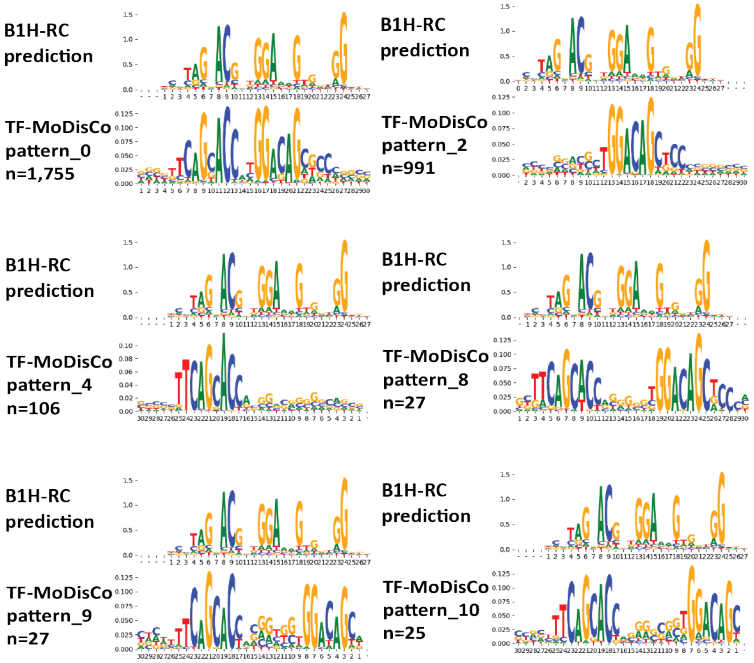

G n/a

H

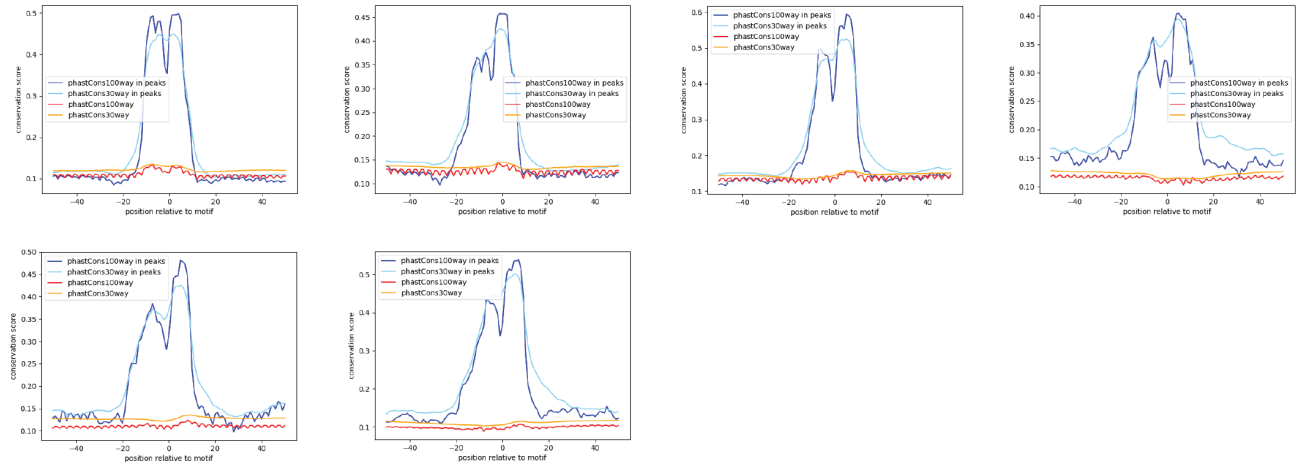

I

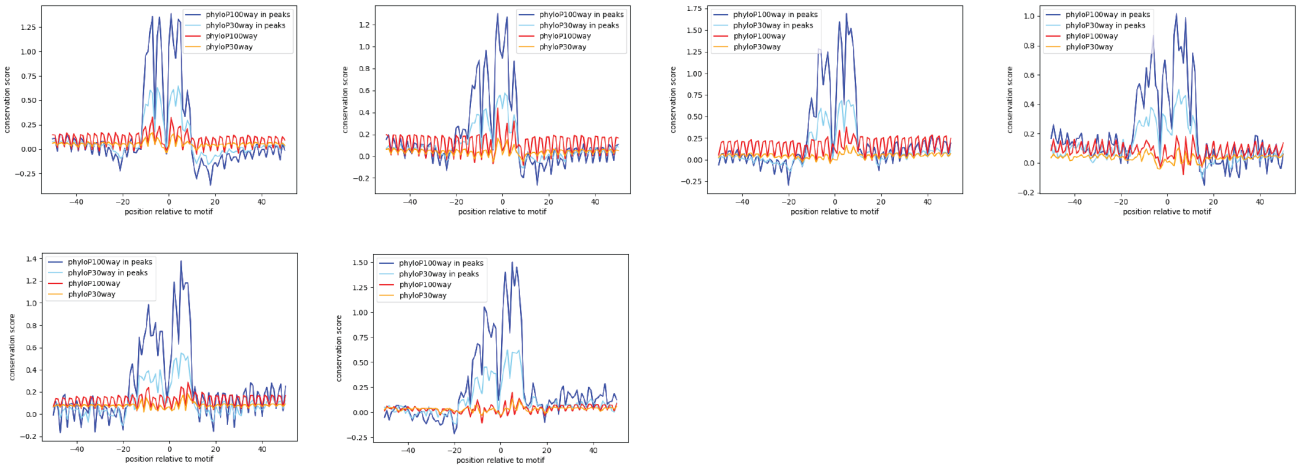

Supplementary Figure 258: Properties and genomic distribution of motifs identified for the REST transcription factor in Panc1 (accession ENCSR000BPK).

TF-MoDisCO pattern_0 n=1755, CWM

pattern_0, n=1755; subpattern_0, ns=465

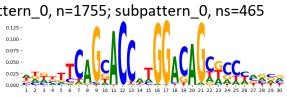

pattern_0, n=1755; subpattern_1, ns=374

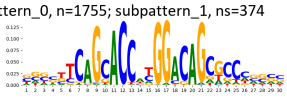

pattern_0, n=1755; subpattern_2, ns=344

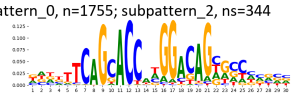

pattern_0, n=1755; subpattern_3, ns=335

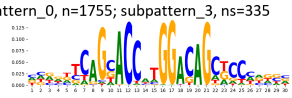

pattern_0, n=1755; subpattern_4, ns=237

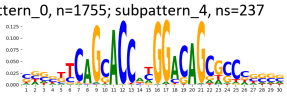

TF-MoDisCO pattern_0 n=1755, PWM

pattern_0, n=1755; subpattern_0, ns=465

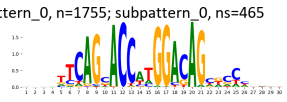

pattern_0, n=1755; subpattern_1, ns=374

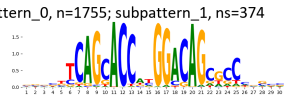

pattern_0, n=1755; subpattern_2, ns=344

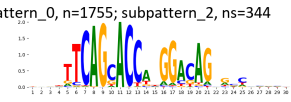

pattern_0, n=1755; subpattern_3, ns=335

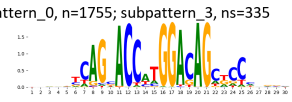

pattern_0, n=1755; subpattern_4, ns=237

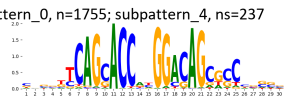

TF-MoDisCO pattern_10 n=25, CWM

pattern_10, n=25; subpattern_0, ns=25

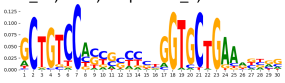

TF-MoDisCO pattern_10 n=25, PWM

pattern_10, n=25; subpattern_0, ns=25

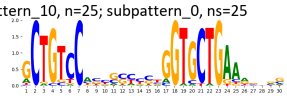

TF-MoDisCO pattern_2 n=991, CWM

pattern_2, n=991; subpattern_0, ns=207

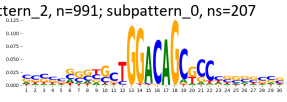

pattern_2, n=991; subpattern_1, ns=193

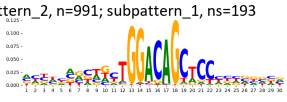

pattern_2, n=991; subpattern_2, ns=158

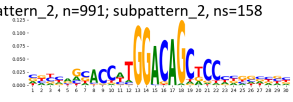

pattern_2, n=991; subpattern_3, ns=136

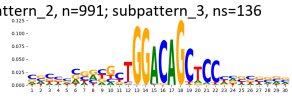

pattern_2, n=991; subpattern_4, ns=131

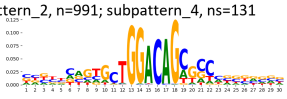

pattern_2, n=991; subpattern_5, ns=110

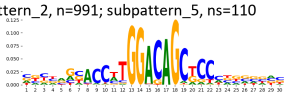

pattern_2, n=991; subpattern_6, ns=53

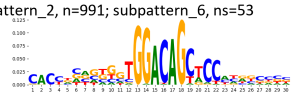

pattern_2, n=991; subpattern_7, ns=3

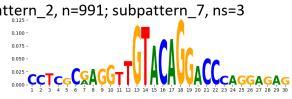

TF-MoDisCO pattern_2 n=991, PWM

pattern_2, n=991; subpattern_0, ns=207

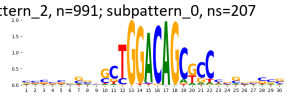

pattern_2, n=991; subpattern_1, ns=193

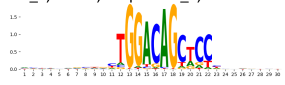

pattern_2, n=991; subpattern_2, ns=158

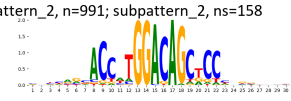

pattern_2, n=991; subpattern_3, ns=136

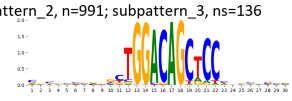

pattern_2, n=991; subpattern_4, ns=131

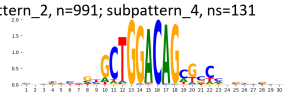

pattern_2, n=991; subpattern_5, ns=110

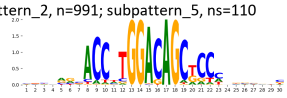

pattern_2, n=991; subpattern_6, ns=53

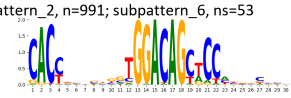

pattern_2, n=991; subpattern_7, ns=3

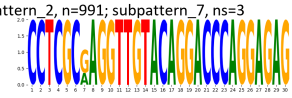

TF-MoDisCO pattern_4 n=106, CWM

pattern_4, n=106; subpattern_0, ns=29

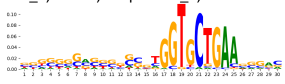

pattern_4, n=106; subpattern_1, ns=24

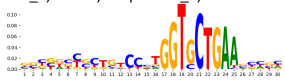

pattern_4, n=106; subpattern_2, ns=22

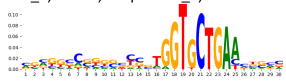

pattern_4, n=106; subpattern_3, ns=18

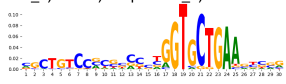

pattern_4, n=106; subpattern_4, ns=6

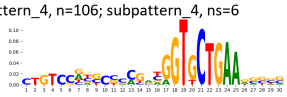

pattern_4, n=106; subpattern_5, ns=5

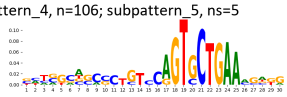

pattern_4, n=106; subpattern_6, ns=2

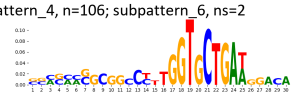

TF-MoDisCO pattern_4 n=106, PWM

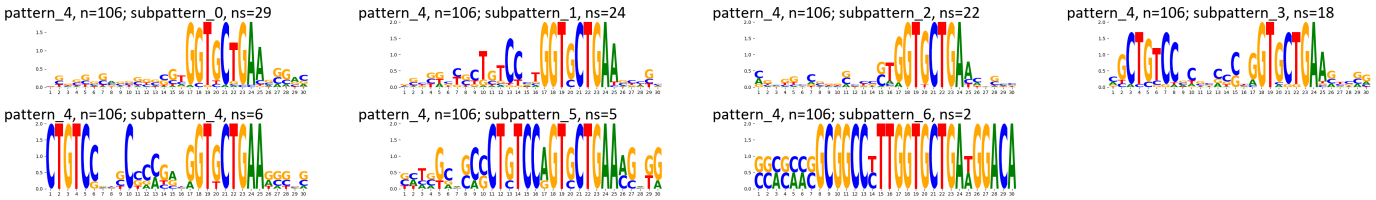

TF-MoDisCO pattern_8 n=27, CWM

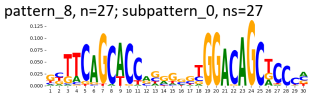

TF-MoDisCO pattern_8 n=27, PWM

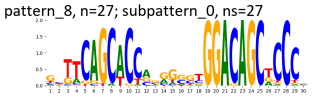

TF-MoDisCO pattern_9 n=27, CWM

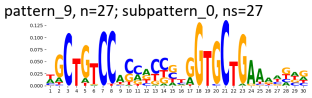

TF-MoDisCO pattern_9 n=27, PWM

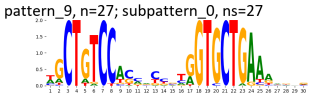

Supplementary Figure 259: TF-MoDisCO subpatterns for the REST transcription factor in Panc1 (accession ENCSR000BPK).

A

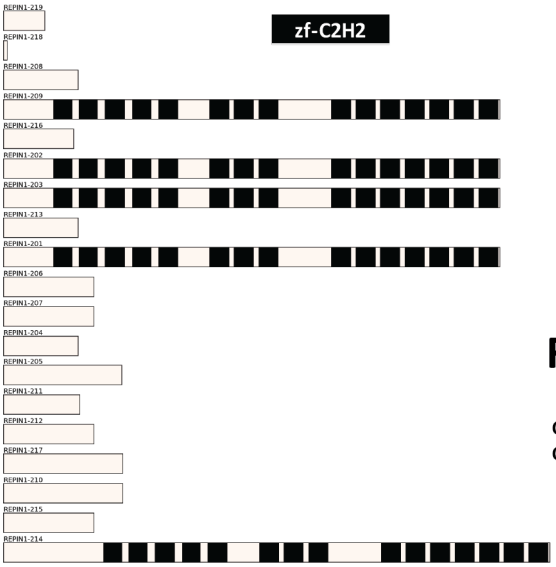

B

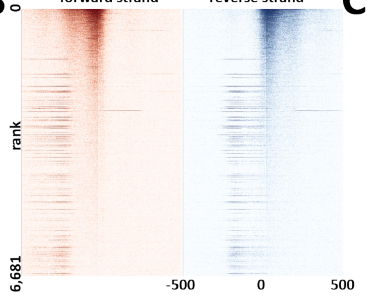

C n/a

D n/a

E

Ontology	Term	FDR Q-val
GO Biological Process	membrane depolarization	7.59
GO Biological Process	peptide hormone secretion	7.26
GO Biological Process	peptide secretion	7.21
GO Biological Process	synaptic vesicle exocytosis	6.77
GO Biological Process	regulation of neuronal synaptic plasticity	6.33
GO Biological Process	regulation of type B pancreatic cell apoptotic process	6.25
GO Biological Process	regulation of short-term neuronal synaptic plasticity	5.12
GO Biological Process	regulation of alpha-amino-3-hydroxy-5-methyl-4-isoxazole propionate selective glutamate receptor activity	4.10
GO Biological Process	positive regulation of intrinsic apoptotic signaling pathway	3.34
GO Biological Process	glutamine family amino acid catabolic process	2.75
GO Biological Process	regulation of systemic arterial blood pressure by endothelin	2.13
GO Biological Process	stress fiber assembly	1.50

F

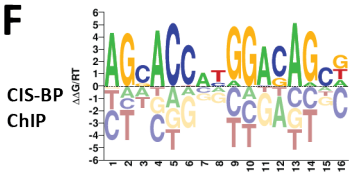

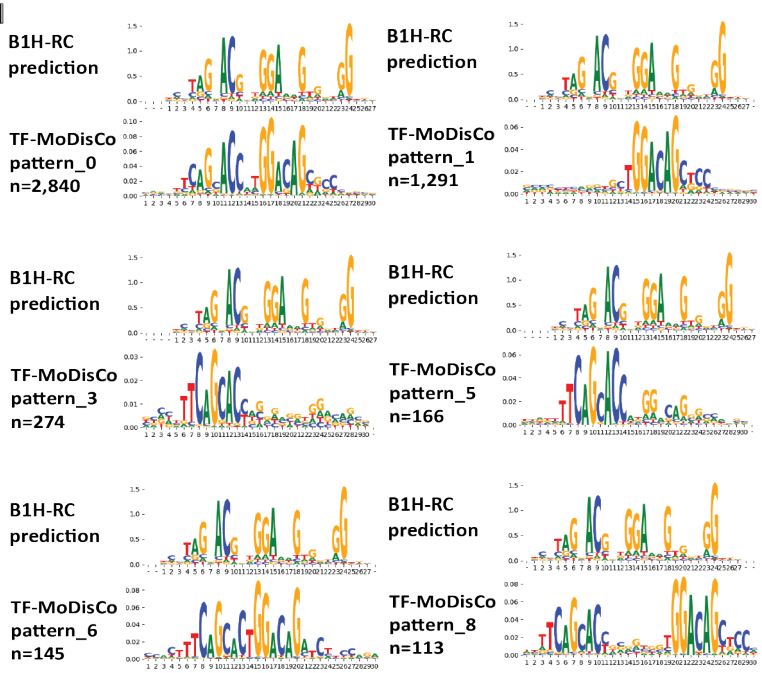

G n/a

H

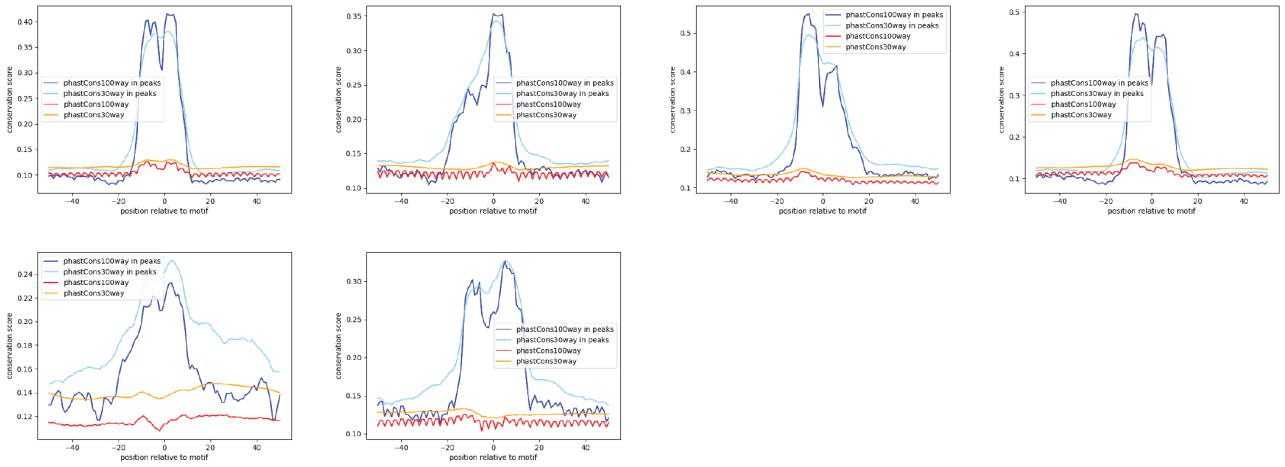

I

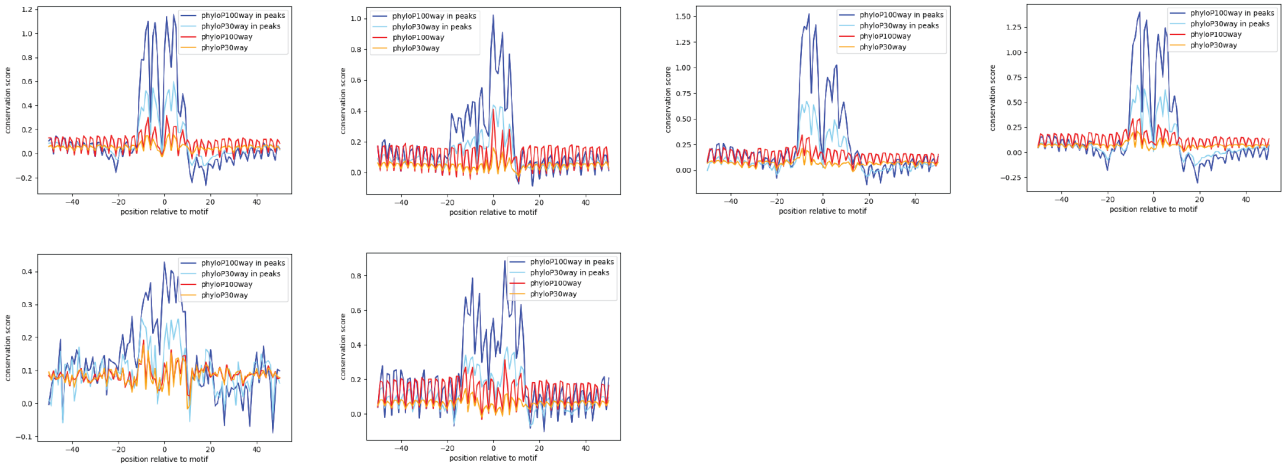

Supplementary Figure 260: Properties and genomic distribution of motifs identified for the REST transcription factor in Panc1 (accession ENCSR000BUP).

TF-MoDisCO pattern_0 n=2840, CWM

pattern_0, n=2840; subpattern_0, ns=757

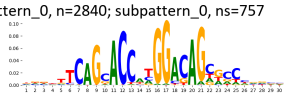

pattern_0, n=2840; subpattern_1, ns=650

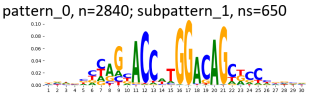

pattern_0, n=2840; subpattern_2, ns=603

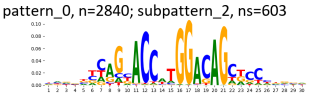

pattern_0, n=2840; subpattern_3, ns=388

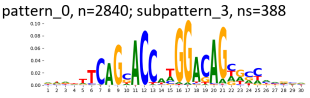

pattern_0, n=2840; subpattern_4, ns=365

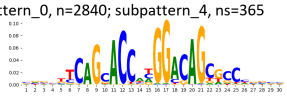

pattern_0, n=2840; subpattern_5, ns=30

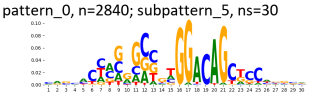

pattern_0, n=2840; subpattern_6, ns=26

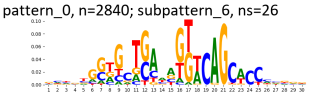

pattern_0, n=2840; subpattern_7, ns=21

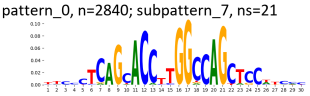

TF-MoDisCO pattern_0 n=2840, PWM

pattern_0, n=2840; subpattern_0, ns=757

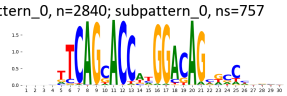

pattern_0, n=2840; subpattern_1, ns=650

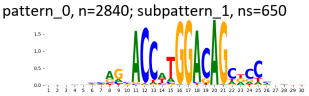

pattern_0, n=2840; subpattern_2, ns=603

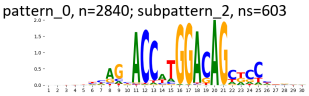

pattern_0, n=2840; subpattern_3, ns=388

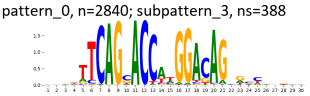

pattern_0, n=2840; subpattern_4, ns=365

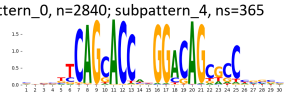

pattern_0, n=2840; subpattern_5, ns=30

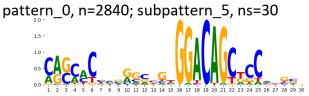

pattern_0, n=2840; subpattern_6, ns=26

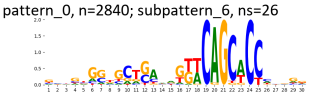

pattern_0, n=2840; subpattern_7, ns=21

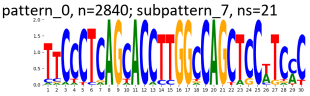

TF-MoDisCO pattern_1 n=1291, CWM

pattern_1, n=1291; subpattern_0, ns=254

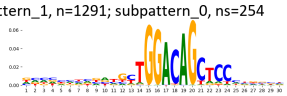

pattern_1, n=1291; subpattern_1, ns=248

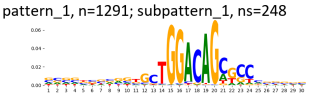

pattern_1, n=1291; subpattern_2, ns=236

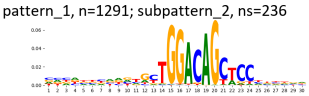

pattern_1, n=1291; subpattern_3, ns=189

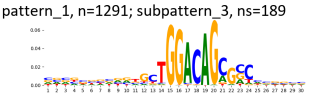

pattern_1, n=1291; subpattern_4, ns=156

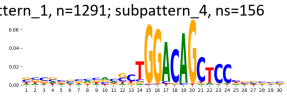

pattern_1, n=1291; subpattern_5, ns=85

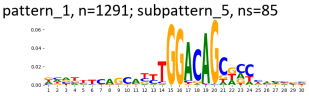

pattern_1, n=1291; subpattern_6, ns=58

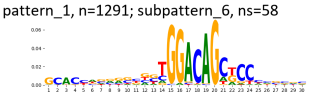

pattern_1, n=1291; subpattern_7, ns=47

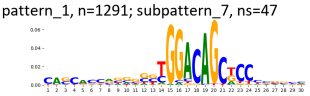

pattern_1, n=1291; subpattern_8, ns=15

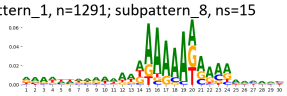

pattern_1, n=1291; subpattern_9, ns=3

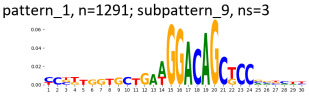

TF-MoDisCO pattern_1 n=1291, PWM

pattern_1, n=1291; subpattern_0, ns=254

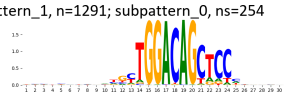

pattern_1, n=1291; subpattern_1, ns=248

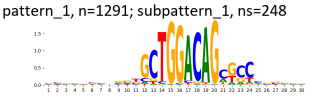

pattern_1, n=1291; subpattern_2, ns=236

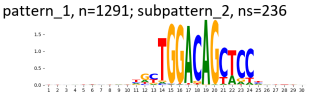

pattern_1, n=1291; subpattern_3, ns=189

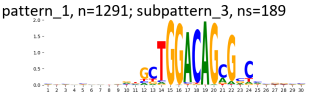

pattern_1, n=1291; subpattern_4, ns=156

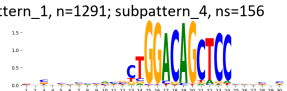

pattern_1, n=1291; subpattern_5, ns=85

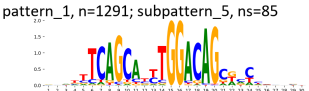

pattern_1, n=1291; subpattern_6, ns=58

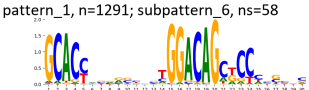

pattern_1, n=1291; subpattern_7, ns=47

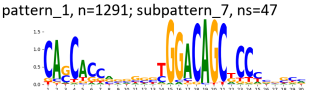

pattern_1, n=1291; subpattern_8, ns=15

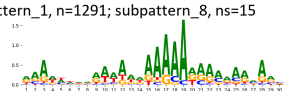

pattern_1, n=1291; subpattern_9, ns=3



TF-MoDisCO pattern_3 n=274, CWM

pattern_3, n=274; subpattern_0, ns=76

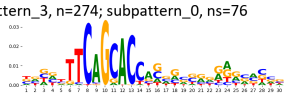

pattern_3, n=274; subpattern_1, ns=48

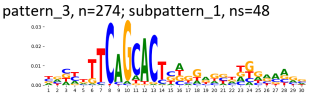

pattern_3, n=274; subpattern_2, ns=42

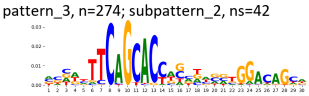

pattern_3, n=274; subpattern_3, ns=41

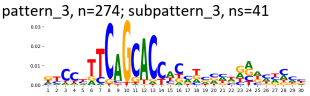

pattern_3, n=274; subpattern_4, ns=31

pattern_3, n=274; subpattern_5, ns=20

pattern_3, n=274; subpattern_6, ns=16

TF-MoDisCO pattern_3 n=274, PWM

pattern_3, n=274; subpattern_0, ns=76

pattern_3, n=274; subpattern_1, ns=48

pattern_3, n=274; subpattern_2, ns=42

pattern_3, n=274; subpattern_3, ns=41

pattern_3, n=274; subpattern_4, ns=31

pattern_3, n=274; subpattern_5, ns=20

pattern_3, n=274; subpattern_6, ns=16

TF-MoDisCO pattern_5 n=166, CWM

pattern_5, n=166; subpattern_0, ns=42

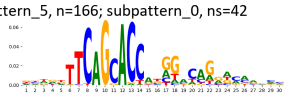

pattern_5, n=166; subpattern_1, ns=41

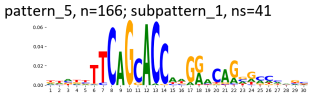

pattern_5, n=166; subpattern_2, ns=35

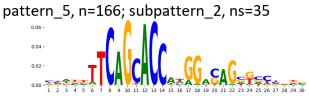

pattern_5, n=166; subpattern_3, ns=31

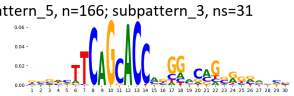

pattern_5, n=166; subpattern_4, ns=12

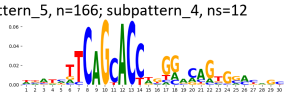

pattern_5, n=166; subpattern_5, ns=3

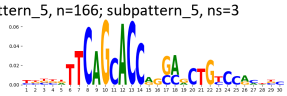

pattern_5, n=166; subpattern_6, ns=2

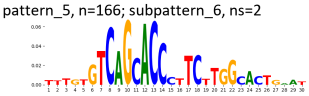

TF-MoDisCO pattern_5 n=166, PWM

pattern_5, n=166; subpattern_0, ns=42

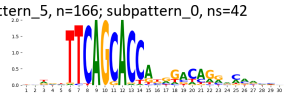

pattern_5, n=166; subpattern_1, ns=41

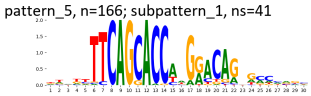

pattern_5, n=166; subpattern_2, ns=35

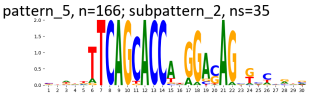

pattern_5, n=166; subpattern_3, ns=31

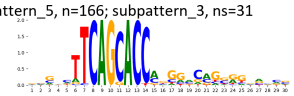

pattern_5, n=166; subpattern_4, ns=12

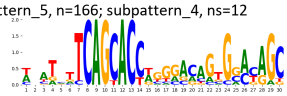

pattern_5, n=166; subpattern_5, ns=3

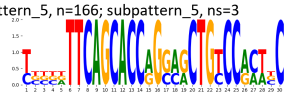

pattern_5, n=166; subpattern_6, ns=2

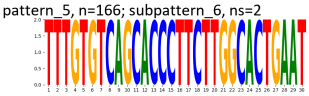

TF-MoDisCO pattern_6 n=145, CWM

pattern_6, n=145; subpattern_0, ns=54

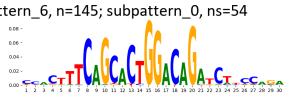

pattern_6, n=145; subpattern_1, ns=51

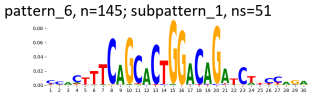

pattern_6, n=145; subpattern_2, ns=30

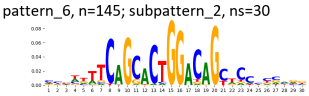

pattern_6, n=145; subpattern_3, ns=4

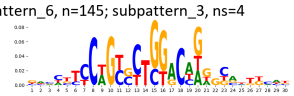

pattern_6, n=145; subpattern_4, ns=3

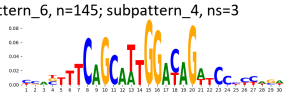

pattern_6, n=145; subpattern_5, ns=3

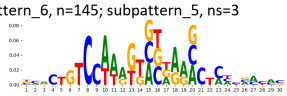

TF-MoDisCO pattern_6 n=145, PWM

pattern_6, n=145; subpattern_0, ns=54

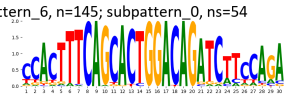

pattern_6, n=145; subpattern_1, ns=51

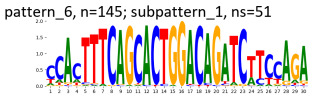

pattern_6, n=145; subpattern_2, ns=30

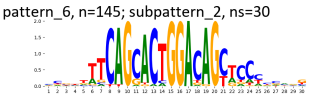

pattern_6, n=145; subpattern_3, ns=4

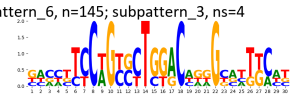

pattern_6, n=145; subpattern_4, ns=3

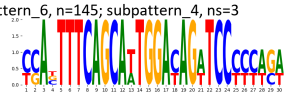

pattern_6, n=145; subpattern_5, ns=3

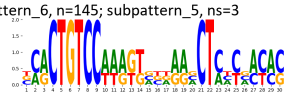

TF-MoDisCO pattern_8 n=113, CWM

pattern_8, n=113; subpattern_0, ns=33

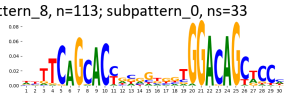

pattern_8, n=113; subpattern_1, ns=27

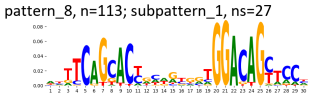

pattern_8, n=113; subpattern_2, ns=26

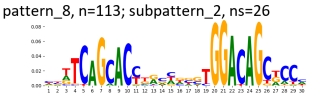

pattern_8, n=113; subpattern_3, ns=18

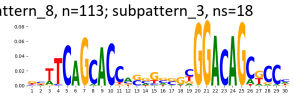

pattern_8, n=113; subpattern_4, ns=9

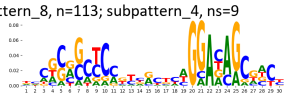

TF-MoDisCO pattern_8 n=113, PWM

pattern_8, n=113; subpattern_0, ns=33

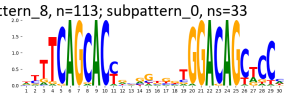

pattern_8, n=113; subpattern_1, ns=27

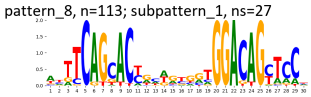

pattern_8, n=113; subpattern_2, ns=26

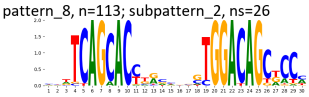

pattern_8, n=113; subpattern_3, ns=18

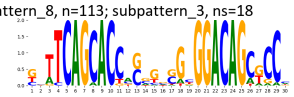

pattern_8, n=113; subpattern_4, ns=9

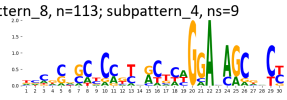

Supplementary Figure 261: TF-MoDisCO subpatterns for the REST transcription factor in Panc1 (accession ENCSR000BUP).

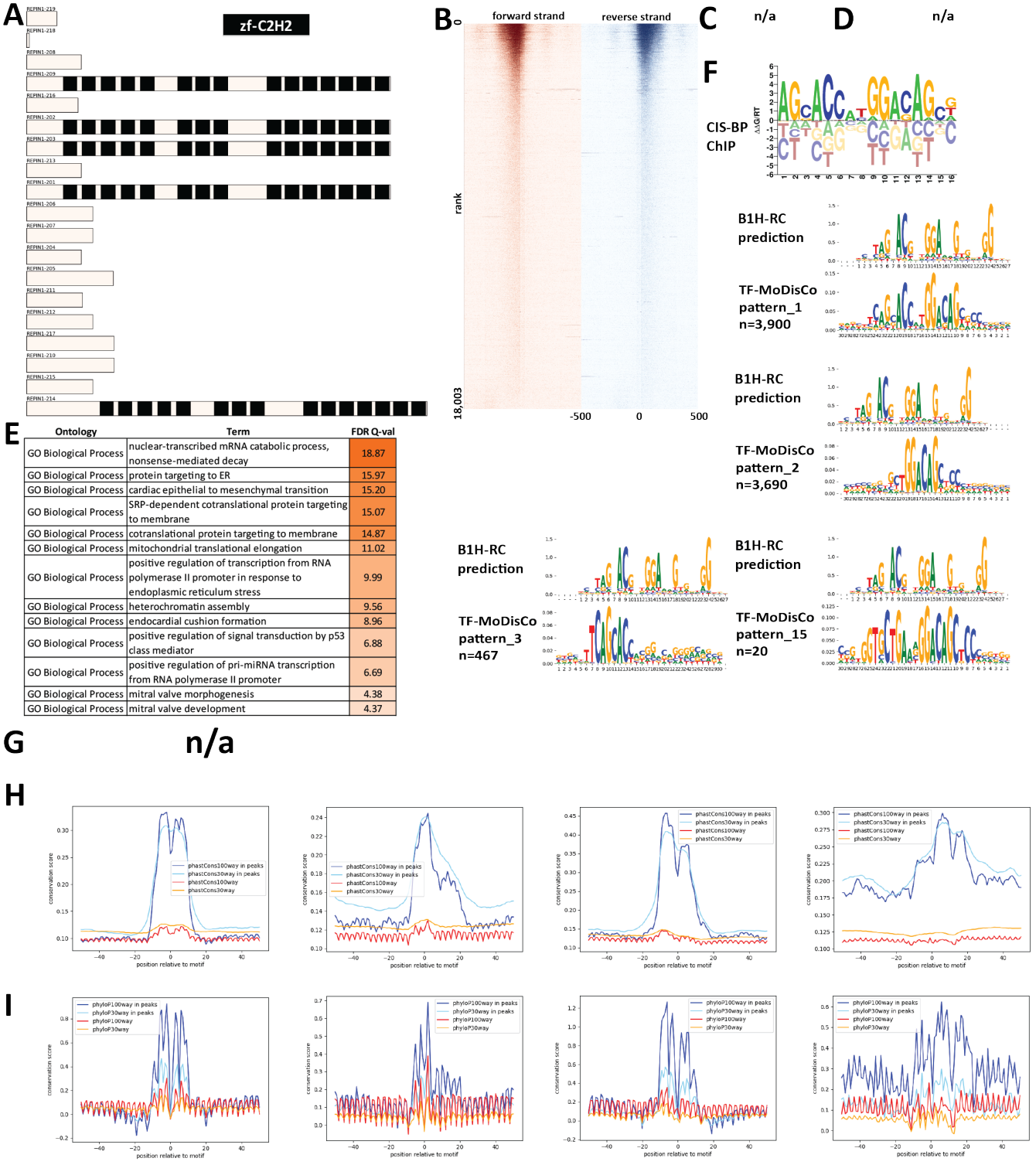

Ontology	Term	FDR Q-val
GO Biological Process	nuclear-transcribed mRNA catabolic process, nonsense-mediated decay	18.87
GO Biological Process	protein targeting to ER	15.97
GO Biological Process	cardiac epithelial to mesenchymal transition	15.20
GO Biological Process	SRP-dependent cotranslational protein targeting to membrane	15.07
GO Biological Process	cotranslational protein targeting to membrane	14.87
GO Biological Process	mitochondrial translational elongation	11.02
GO Biological Process	positive regulation of transcription from RNA polymerase II promoter in response to endoplasmic reticulum stress	9.99
GO Biological Process	heterochromatin assembly	9.56
GO Biological Process	endocardial cushion formation	8.96
GO Biological Process	positive regulation of signal transduction by p53 class mediator	6.88
GO Biological Process	positive regulation of pri-miRNA transcription from RNA polymerase II promoter	6.69
GO Biological Process	mitral valve morphogenesis	4.38
GO Biological Process	mitral valve development	4.37

Supplementary Figure 262: Properties and genomic distribution of motifs identified for the REST transcription factor in PFSK-1 (accession ENCSR000BOX).

TF-MoDisCO pattern_1 n=3900, CWM

pattern_1, n=3900; subpattern_0, ns=845

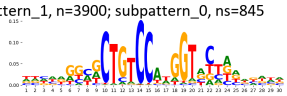

pattern_1, n=3900; subpattern_1, ns=793

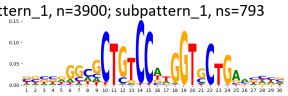

pattern_1, n=3900; subpattern_2, ns=675

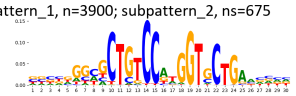

pattern_1, n=3900; subpattern_3, ns=623

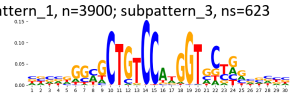

pattern_1, n=3900; subpattern_4, ns=551

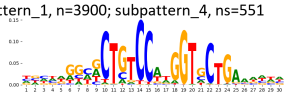

pattern_1, n=3900; subpattern_5, ns=413

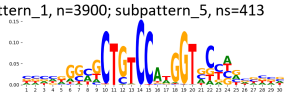

TF-MoDisCO pattern_1 n=3900, PWM

pattern_1, n=3900; subpattern_0, ns=845

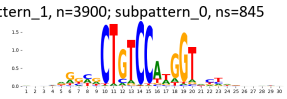

pattern_1, n=3900; subpattern_1, ns=793

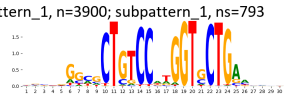

pattern_1, n=3900; subpattern_2, ns=675

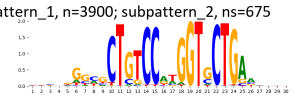

pattern_1, n=3900; subpattern_3, ns=623

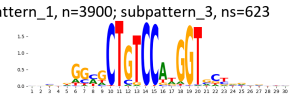

pattern_1, n=3900; subpattern_4, ns=551

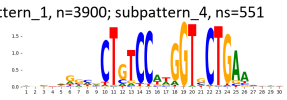

pattern_1, n=3900; subpattern_5, ns=413

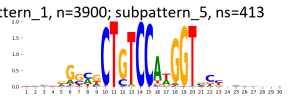

TF-MoDisCO pattern_15 n=20, CWM

pattern_15, n=20; subpattern_0, ns=20

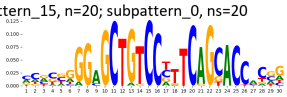

TF-MoDisCO pattern_15 n=20, PWM

pattern_15, n=20; subpattern_0, ns=20

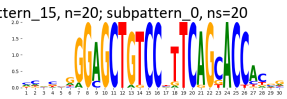

TF-MoDisCO pattern_2 n=3690, CWM

pattern_2, n=3690; subpattern_0, ns=926

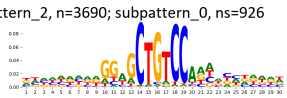

pattern_2, n=3690; subpattern_1, ns=718

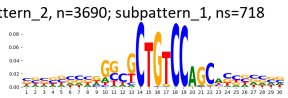

pattern_2, n=3690; subpattern_2, ns=644

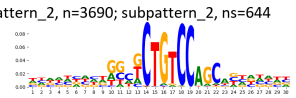

pattern_2, n=3690; subpattern_3, ns=613

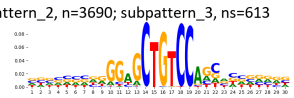

pattern_2, n=3690; subpattern_4, ns=593

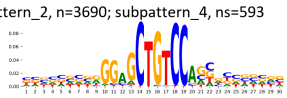

pattern_2, n=3690; subpattern_5, ns=88

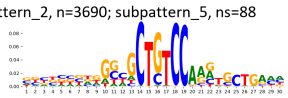

pattern_2, n=3690; subpattern_6, ns=78

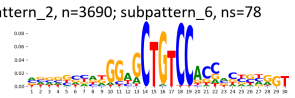

pattern_2, n=3690; subpattern_7, ns=19

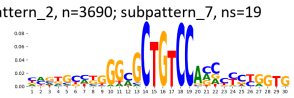

pattern_2, n=3690; subpattern_8, ns=9

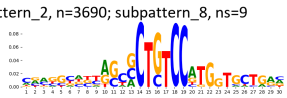

pattern_2, n=3690; subpattern_9, ns=2

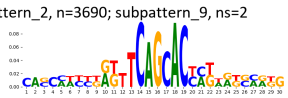

TF-MoDisCO pattern_2 n=3690, PWM

pattern_2, n=3690; subpattern_0, ns=926

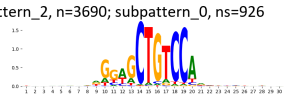

pattern_2, n=3690; subpattern_1, ns=718

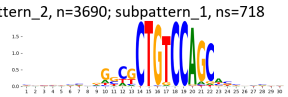

pattern_2, n=3690; subpattern_2, ns=644

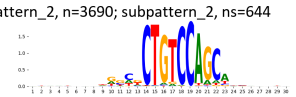

pattern_2, n=3690; subpattern_3, ns=613

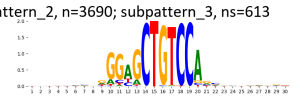

pattern_2, n=3690; subpattern_4, ns=593

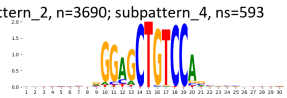

pattern_2, n=3690; subpattern_5, ns=88

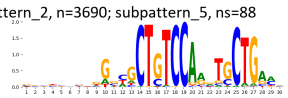

pattern_2, n=3690; subpattern_6, ns=78

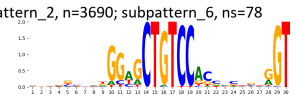

pattern_2, n=3690; subpattern_7, ns=19

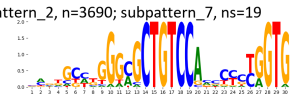

pattern_2, n=3690; subpattern_8, ns=9

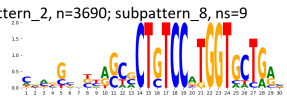

pattern_2, n=3690; subpattern_9, ns=2

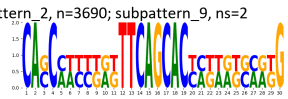

TF-MoDisCO pattern_3 n=467, CWM

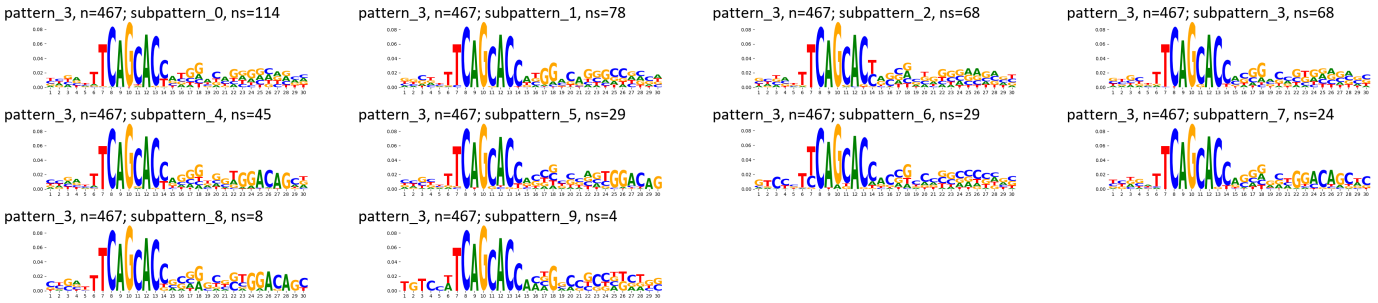

TF-MoDisCO pattern_3 n=467, PWM

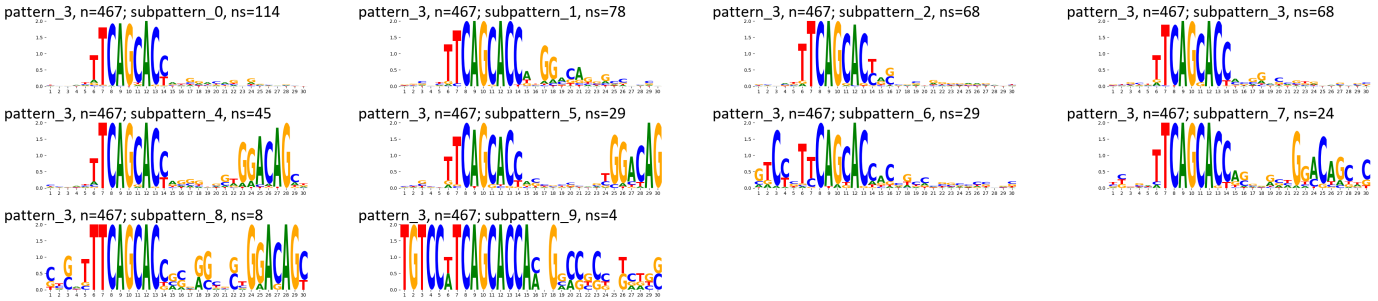

Supplementary Figure 263: TF-MoDisCO subpatterns for the REST transcription factor in PFSK-1 (accession ENCSR000BOX).

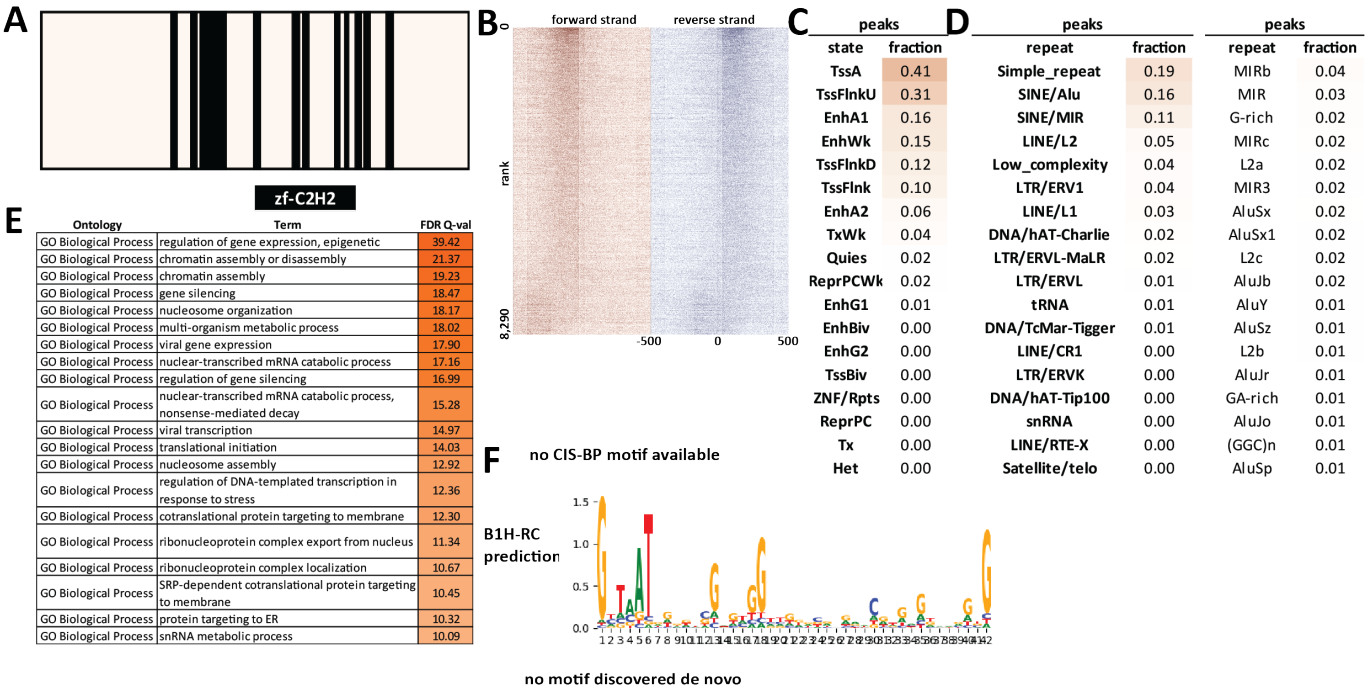

Supplementary Figure 264: Properties and genomic distribution of motifs identified for the RLF transcription factor in K562 (accession ENCSR718SDE).

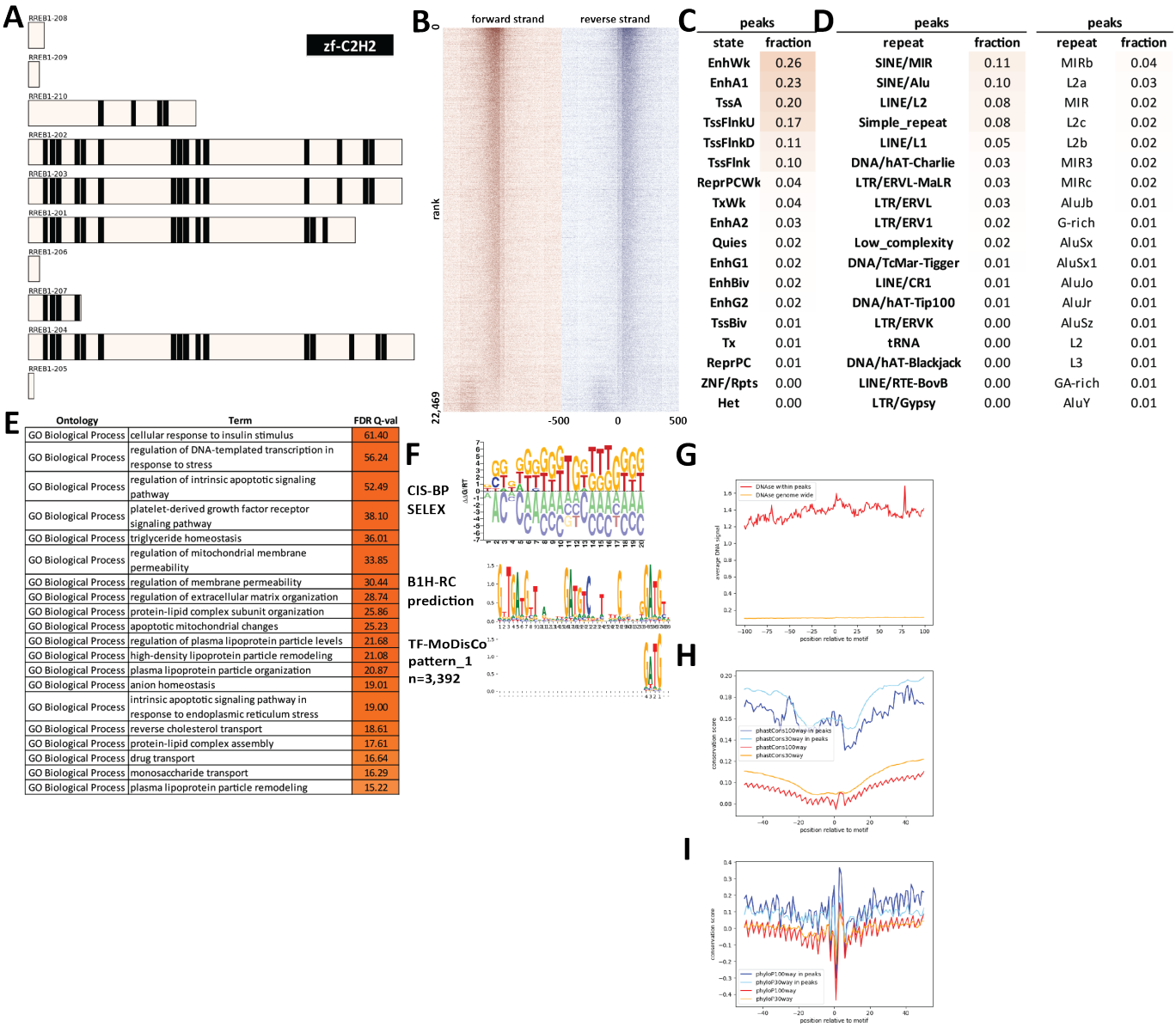

Supplementary Figure 265: Properties and genomic distribution of motifs identified for the RREB1 transcription factor in HepG2 (accession ENCSR180MUU).

TF-MoDisCO pattern_1 n=3392, CWM

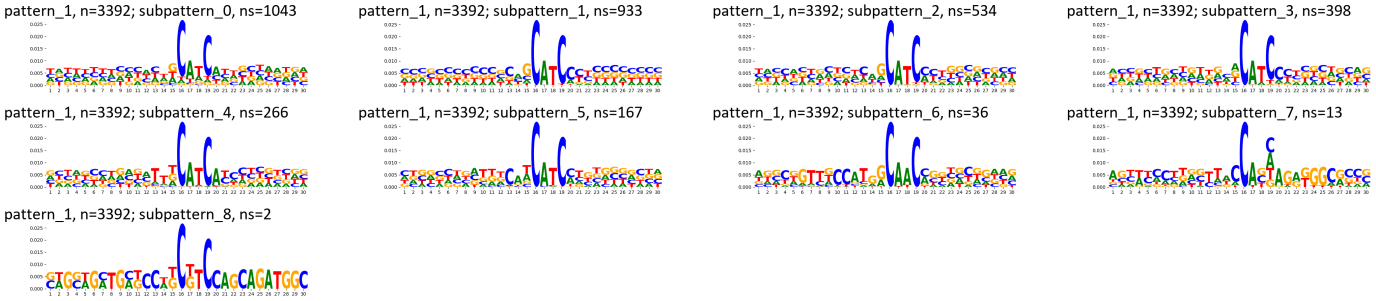

TF-MoDisCO pattern_1 n=3392, PWM

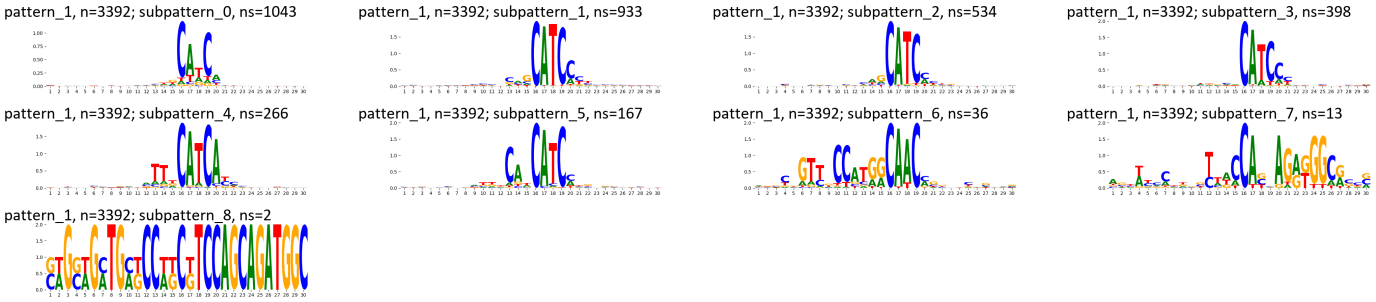

Supplementary Figure 266: TF-MoDisCO subpatterns for the RREB1 transcription factor in HepG2 (accession ENCSR180MUU).

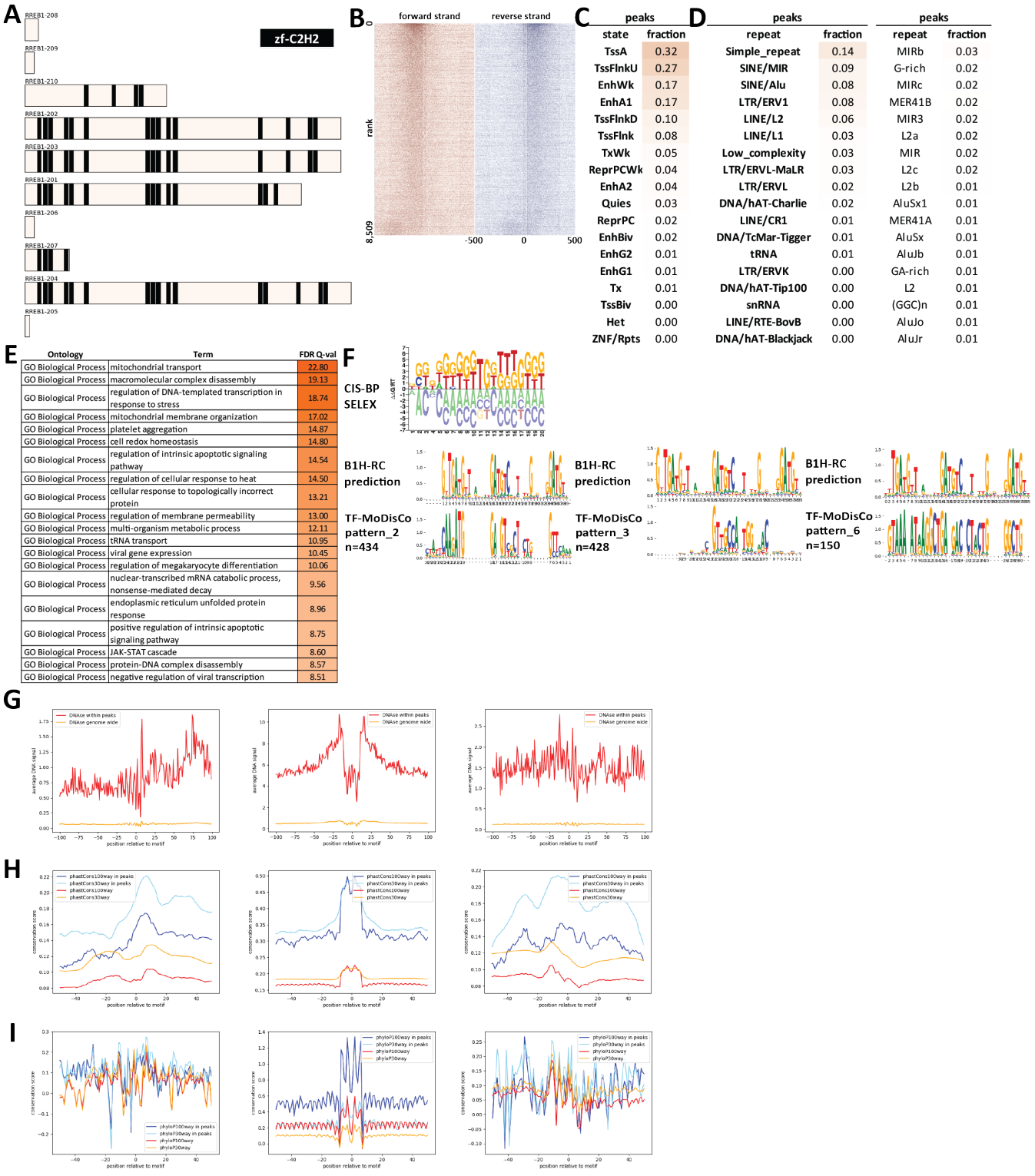

Supplementary Figure 267: Properties and genomic distribution of motifs identified for the RREB1 transcription factor in K562 (accession ENCSR250WFW).

TF-MoDisCO pattern_2 n=434, CWM

pattern_2, n=434; subpattern_0, ns=138

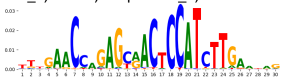

pattern_2, n=434; subpattern_1, ns=119

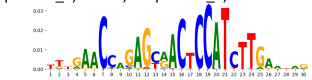

pattern_2, n=434; subpattern_2, ns=51

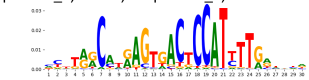

pattern_2, n=434; subpattern_3, ns=43

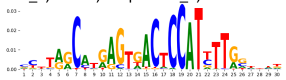

pattern_2, n=434; subpattern_4, ns=36

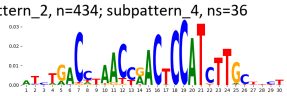

pattern_2, n=434; subpattern_5, ns=21

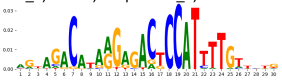

pattern_2, n=434; subpattern_6, ns=21

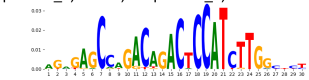

pattern_2, n=434; subpattern_7, ns=3

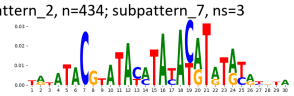

pattern_2, n=434; subpattern_8, ns=2

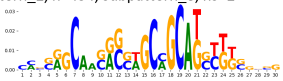

TF-MoDisCO pattern_2 n=434, PWM

pattern_2, n=434; subpattern_0, ns=138

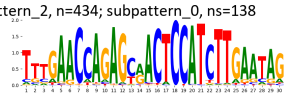

pattern_2, n=434; subpattern_1, ns=119

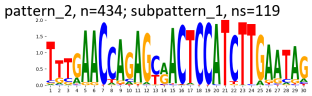

pattern_2, n=434; subpattern_2, ns=51

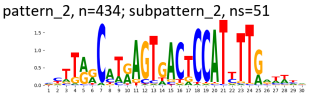

pattern_2, n=434; subpattern_3, ns=43

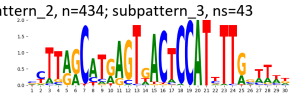

pattern_2, n=434; subpattern_4, ns=36

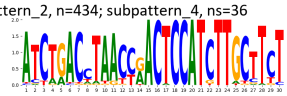

pattern_2, n=434; subpattern_5, ns=21

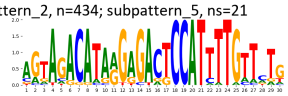

pattern_2, n=434; subpattern_6, ns=21

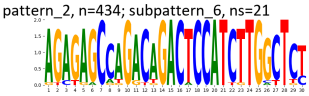

pattern_2, n=434; subpattern_7, ns=3

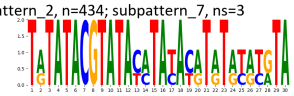

pattern_2, n=434; subpattern_8, ns=2

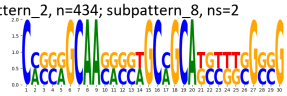

TF-MoDisCO pattern_3 n=428, CWM

pattern_3, n=428; subpattern_0, ns=135

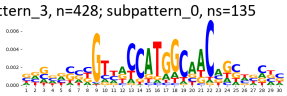

pattern_3, n=428; subpattern_1, ns=122

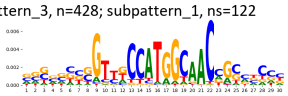

pattern_3, n=428; subpattern_2, ns=90

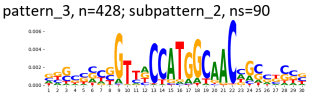

pattern_3, n=428; subpattern_3, ns=51

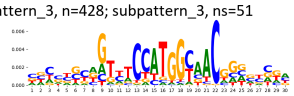

pattern_3, n=428; subpattern_4, ns=28

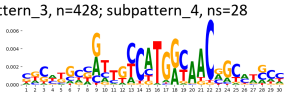

pattern_3, n=428; subpattern_5, ns=2

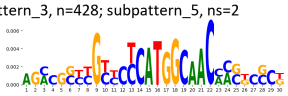

TF-MoDisCO pattern_3 n=428, PWM

pattern_3, n=428; subpattern_0, ns=135

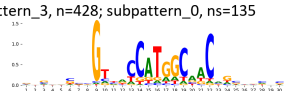

pattern_3, n=428; subpattern_1, ns=122

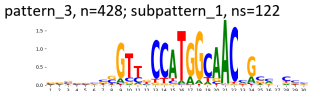

pattern_3, n=428; subpattern_2, ns=90



pattern_3, n=428; subpattern_3, ns=51

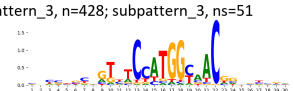

pattern_3, n=428; subpattern_4, ns=28

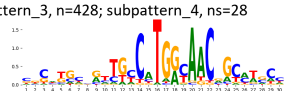

pattern_3, n=428; subpattern_5, ns=2

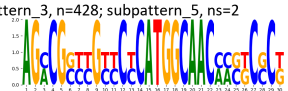

TF-MoDisCO pattern_6 n=150, CWM

pattern_6, n=150; subpattern_0, ns=65

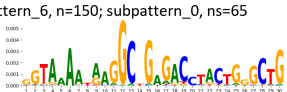

pattern_6, n=150; subpattern_1, ns=64

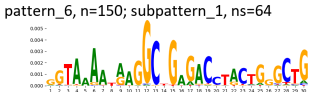

pattern_6, n=150; subpattern_2, ns=21

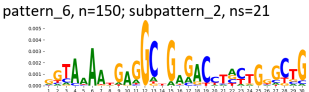

TF-MoDisCO pattern_6 n=150, PWM

pattern_6, n=150; subpattern_0, ns=65

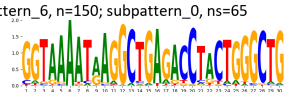

pattern_6, n=150; subpattern_1, ns=64

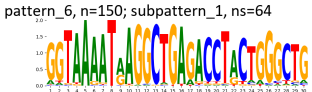

pattern_6, n=150; subpattern_2, ns=21

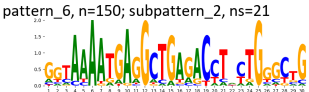

Supplementary Figure 268: TF-MoDisCO subpatterns for the RREB1 transcription factor in K562 (accession ENCSR250WFW).

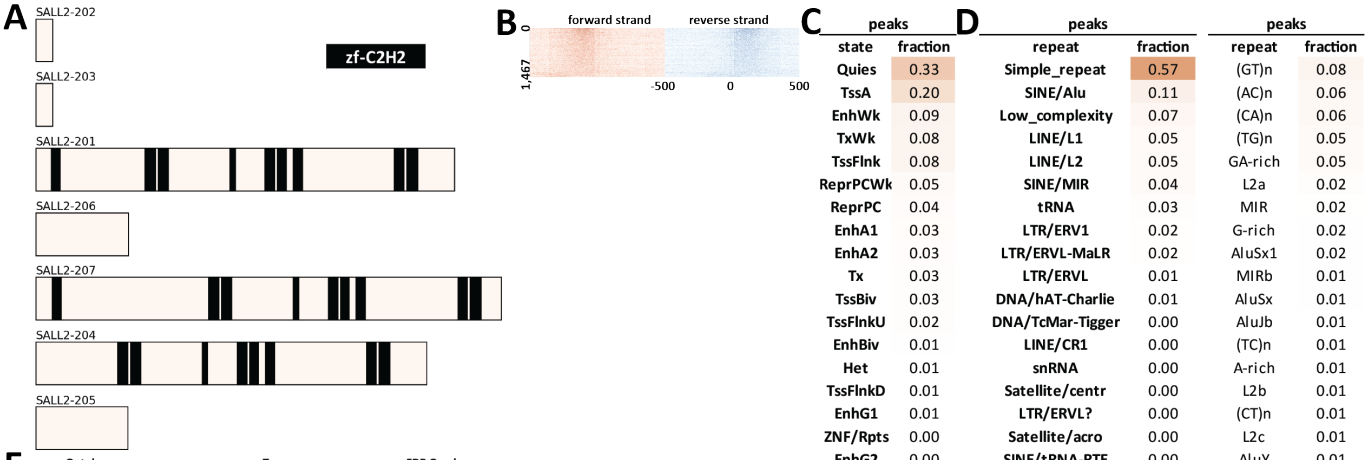

C

peaks	
state	fraction
Quies	0.33
TssA	0.20
EnhWk	0.09
TxWk	0.08
TssFlnk	0.08
ReprPCWk	0.05
ReprPC	0.04
EnhA1	0.03
EnhA2	0.03
Tx	0.03
TssBiv	0.03
TssFlnkU	0.02
EnhBiv	0.01
Het	0.01
TssFlnkD	0.01
EnhG1	0.01
ZNF/Rpts	0.00
EnhG2	0.00

D

peaks		peaks	
repeat	fraction	repeat	fraction
Simple_repeat	0.57	(GT)n	0.08
SINE/Alu	0.11	(AC)n	0.06
Low_complexity	0.07	(CA)n	0.06
LINE/L1	0.05	(TG)n	0.05
LINE/L2	0.05	GA-rich	0.05
SINE/MIR	0.04	L2a	0.02
tRNA	0.03	MIR	0.02
LTR/ERV1	0.02	G-rich	0.02
LTR/ERVL-MaLR	0.02	AluSx1	0.02
LTR/ERVL	0.01	MIRb	0.01
DNA/hAT-Charlie	0.01	AluSx	0.01
DNA/TcMar-Tigger	0.00	AluJb	0.01
LINE/CR1	0.00	(TC)n	0.01
snRNA	0.00	A-rich	0.01
Satellite/centr	0.00	L2b	0.01
LTR/ERVL?	0.00	(CT)n	0.01
Satellite/acro	0.00	L2c	0.01
SINE/tRNA-RTE	0.00	AluY	0.01

E

Ontology	Term	FDR Q-val
GO Biological Process	regulation of transforming growth factor beta receptor signaling pathway	9.04
GO Biological Process	regulation of cellular response to transforming growth factor beta stimulus	9.03
GO Biological Process	regulation of epithelial to mesenchymal transition	6.65
GO Biological Process	regulation of transcription from RNA polymerase II promoter in response to stress	3.94
GO Biological Process	regulation of DNA-templated transcription in response to stress	3.50
GO Biological Process	lung epithelium development	2.87
GO Biological Process	wound healing, spreading of epidermal cells	2.79
GO Biological Process	trachea cartilage development	2.22
GO Biological Process	animal organ regeneration	2.05
GO Biological Process	nephron tubule formation	1.62
GO Biological Process	trachea development	1.56
GO Biological Process	TOR signaling	1.37
GO Biological Process	metanephric tubule development	1.32
Human Phenotype	Abnormality of the hip joint	4.09
Human Phenotype	Abnormality of the synovia	3.85
Human Phenotype	Hypotelorism	3.77
Human Phenotype	Aplasia/Hypoplasia involving the vertebral column	3.23

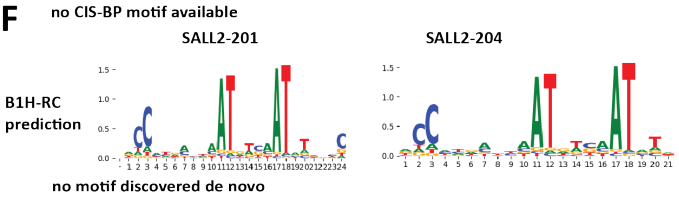

Supplementary Figure 269: Properties and genomic distribution of motifs identified for the SALL2 transcription factor in HEK293 (accession ENCSR044FMM).

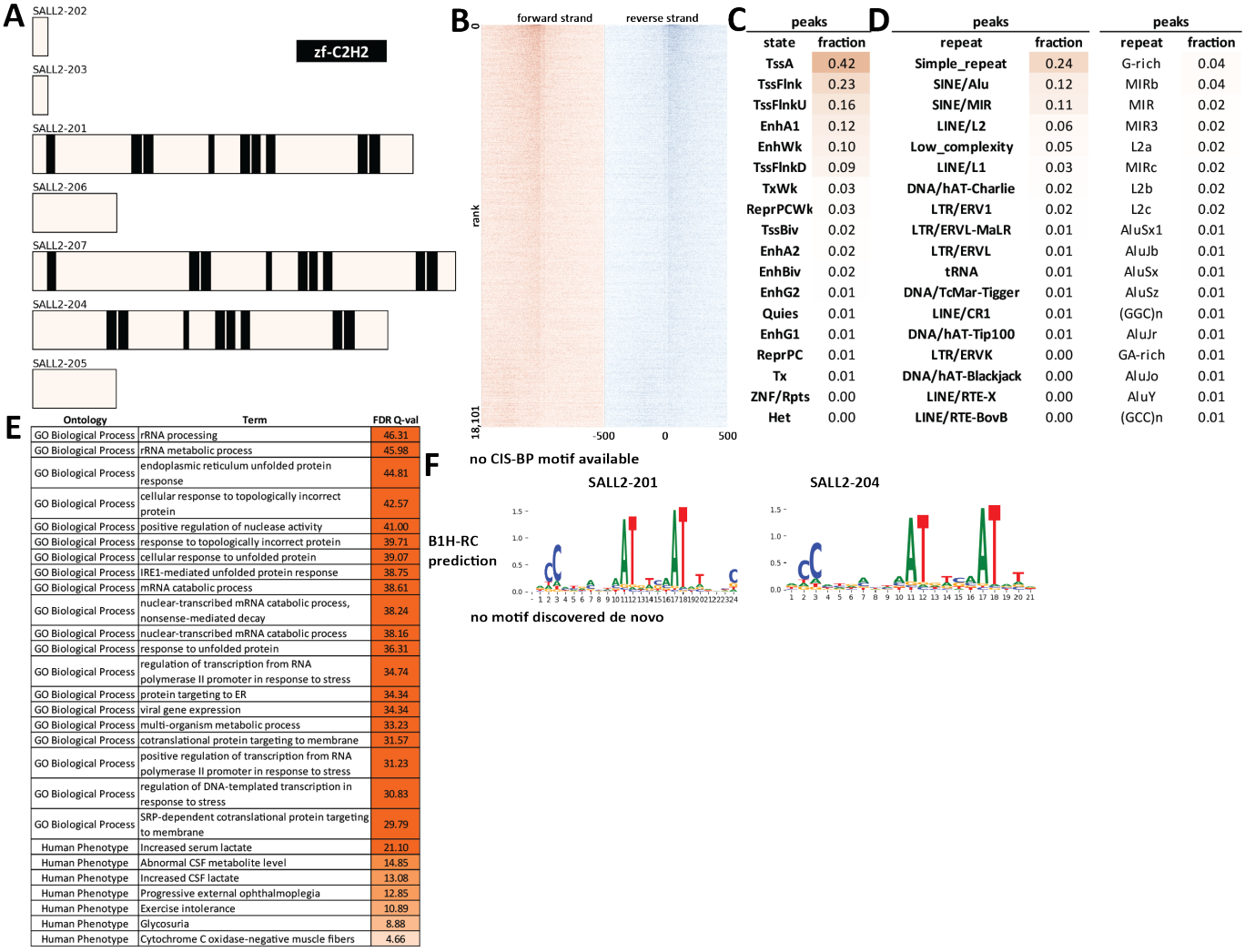

Supplementary Figure 270: Properties and genomic distribution of motifs identified for the SALL2 transcription factor in HepG2 (accession ENCSR062TDX).

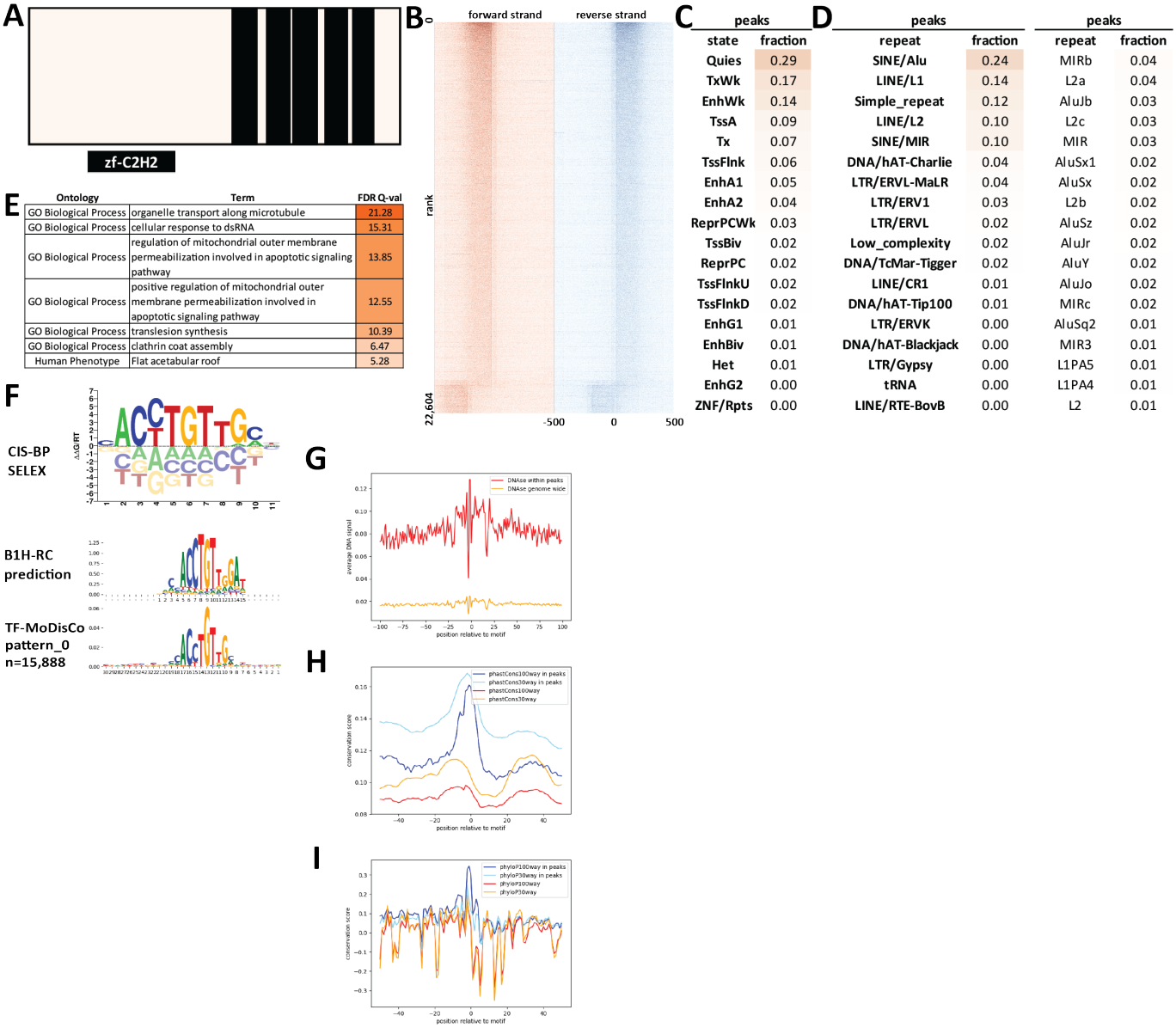

Supplementary Figure 271: Properties and genomic distribution of motifs identified for the SCRT1 transcription factor in HEK293 (accession ENCSR605MGM).

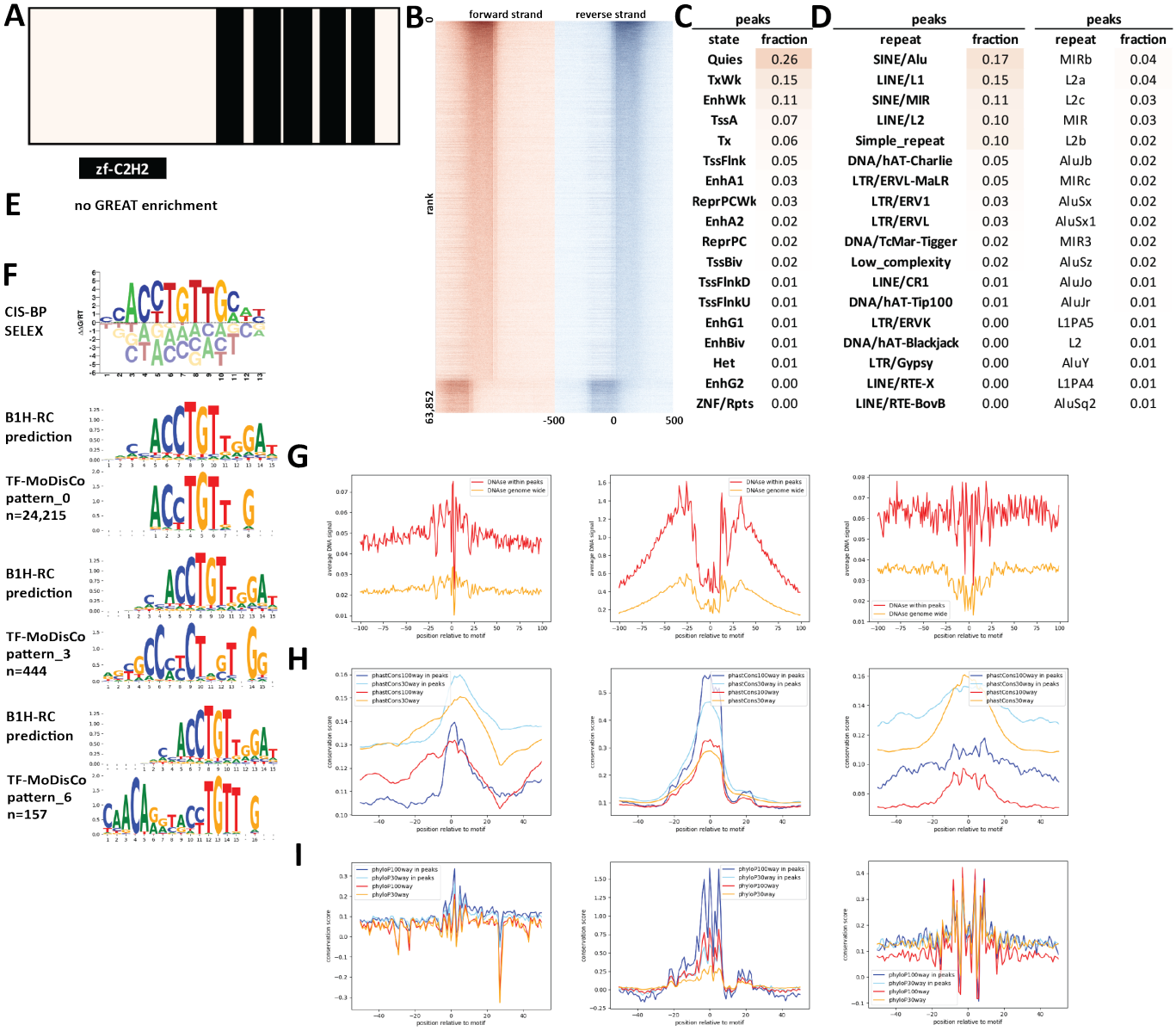

peaks	
state	fraction
Quies	0.26
TxWk	0.15
EnhWk	0.11
TssA	0.07
Tx	0.06
TssFlnk	0.05
EnhA1	0.03
ReprPCWk	0.03
EnhA2	0.02
ReprPC	0.02
TssBiv	0.02
TssFlnkD	0.01
TssFlnkU	0.01
EnhG1	0.01
EnhBiv	0.01
Het	0.01
EnhG2	0.00
ZNF/Rpts	0.00

peaks	
repeat	fraction
SINE/Alu	0.17
LINE/L1	0.15
SINE/MIR	0.11
LINE/L2	0.10
Simple_repeat	0.10
DNA/hAT-Charlie	0.05
LTR/ERVL-MaLR	0.05
LTR/ERV1	0.03
LTR/ERVL	0.03
DNA/TcMar-Tigger	0.02
Low_complexity	0.02
LINE/CR1	0.01
DNA/hAT-Tip100	0.01
LTR/ERVK	0.00
DNA/hAT-Blackjack	0.00
LTR/Gypsy	0.00
LINE/RTE-X	0.00
LINE/RTE-BovB	0.00

peaks	
repeat	fraction
MIRb	0.04
L2a	0.04
L2c	0.03
MIR	0.03
L2b	0.02
AluJb	0.02
MIRc	0.02
AluSx	0.02
AluSx1	0.02
MIR3	0.02
AluSz	0.02
AluJo	0.01
AluJr	0.01
L1PA5	0.01
L2	0.01
AluY	0.01
L1PA4	0.01
AluSq2	0.01

Supplementary Figure 272: Properties and genomic distribution of motifs identified for the SCRT2 transcription factor in HEK293 (accession ENCSR338DGO).

TF-MoDisCO pattern_0 n=24215, CWM

pattern_0, n=24215; subpattern_0, ns=4200

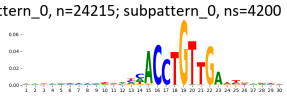

pattern_0, n=24215; subpattern_1, ns=3287

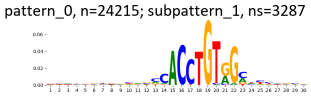

pattern_0, n=24215; subpattern_10, ns=975

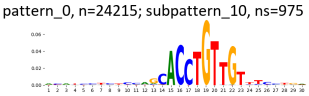

pattern_0, n=24215; subpattern_11, ns=284

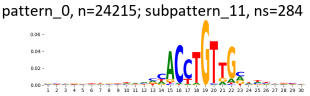

pattern_0, n=24215; subpattern_12, ns=38

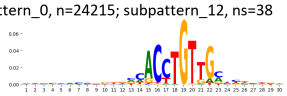

pattern_0, n=24215; subpattern_2, ns=2595

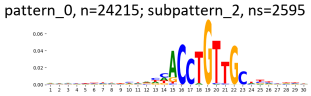

pattern_0, n=24215; subpattern_3, ns=2542

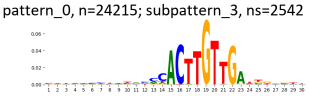

pattern_0, n=24215; subpattern_4, ns=2474

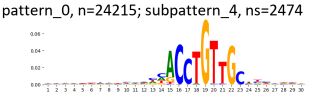

pattern_0, n=24215; subpattern_5, ns=2102

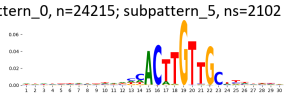

pattern_0, n=24215; subpattern_6, ns=2095

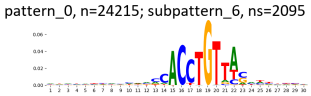

pattern_0, n=24215; subpattern_7, ns=1491

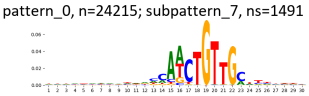

pattern_0, n=24215; subpattern_8, ns=1092

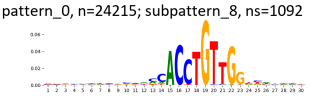

pattern_0, n=24215; subpattern_9, ns=1040

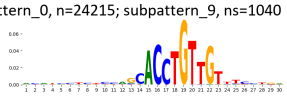

TF-MoDisCO pattern_0 n=24215, PWM

pattern_0, n=24215; subpattern_0, ns=4200

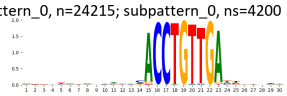

pattern_0, n=24215; subpattern_1, ns=3287

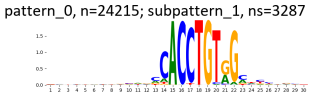

pattern_0, n=24215; subpattern_10, ns=975

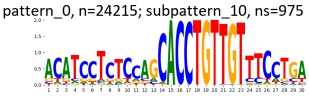

pattern_0, n=24215; subpattern_11, ns=284

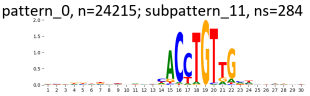

pattern_0, n=24215; subpattern_12, ns=38

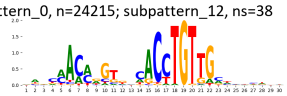

pattern_0, n=24215; subpattern_2, ns=2595

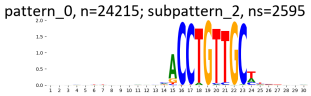

pattern_0, n=24215; subpattern_3, ns=2542

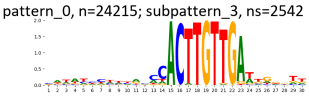

pattern_0, n=24215; subpattern_4, ns=2474

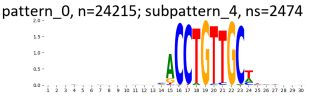

pattern_0, n=24215; subpattern_5, ns=2102

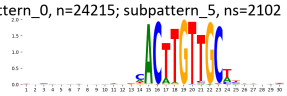

pattern_0, n=24215; subpattern_6, ns=2095

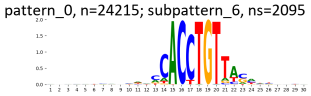

pattern_0, n=24215; subpattern_7, ns=1491

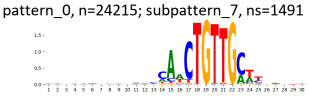

pattern_0, n=24215; subpattern_8, ns=1092

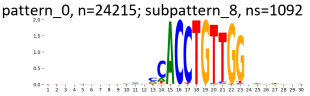

pattern_0, n=24215; subpattern_9, ns=1040

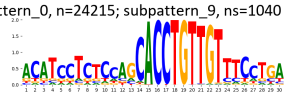

TF-MoDisCO pattern_3 n=444, CWM

pattern_3, n=444; subpattern_0, ns=117

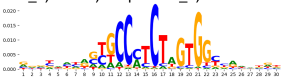

pattern_3, n=444; subpattern_1, ns=115

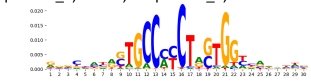

pattern_3, n=444; subpattern_2, ns=111

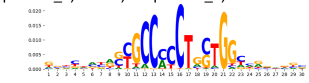

pattern_3, n=444; subpattern_3, ns=99

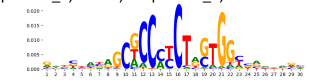

pattern_3, n=444; subpattern_4, ns=2

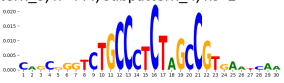

TF-MoDisCO pattern_3 n=444, PWM

pattern_3, n=444; subpattern_0, ns=117

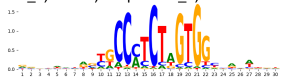

pattern_3, n=444; subpattern_1, ns=115

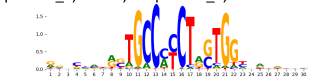

pattern_3, n=444; subpattern_2, ns=111

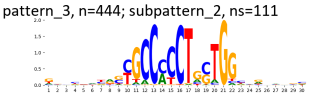

pattern_3, n=444; subpattern_3, ns=99

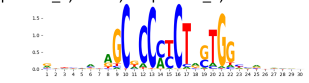

pattern_3, n=444; subpattern_4, ns=2

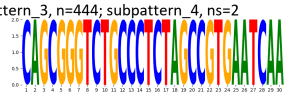

TF-MoDisCO pattern_6 n=157, CWM

pattern_6, n=157; subpattern_0, ns=45

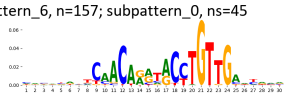

pattern_6, n=157; subpattern_1, ns=37

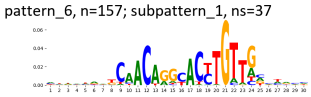

pattern_6, n=157; subpattern_2, ns=32

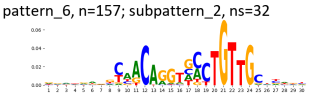

pattern_6, n=157; subpattern_3, ns=24

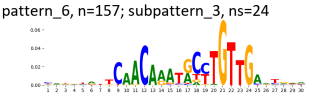

pattern_6, n=157; subpattern_4, ns=19

TF-MoDisCO pattern_6 n=157, PWM

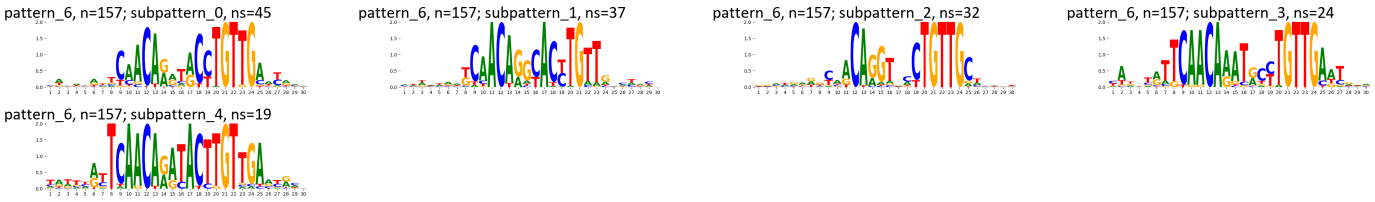

Supplementary Figure 273: TF-MoDisCO subpatterns for the SCRT2 transcription factor in HEK293 (accession ENCSR338DGO).

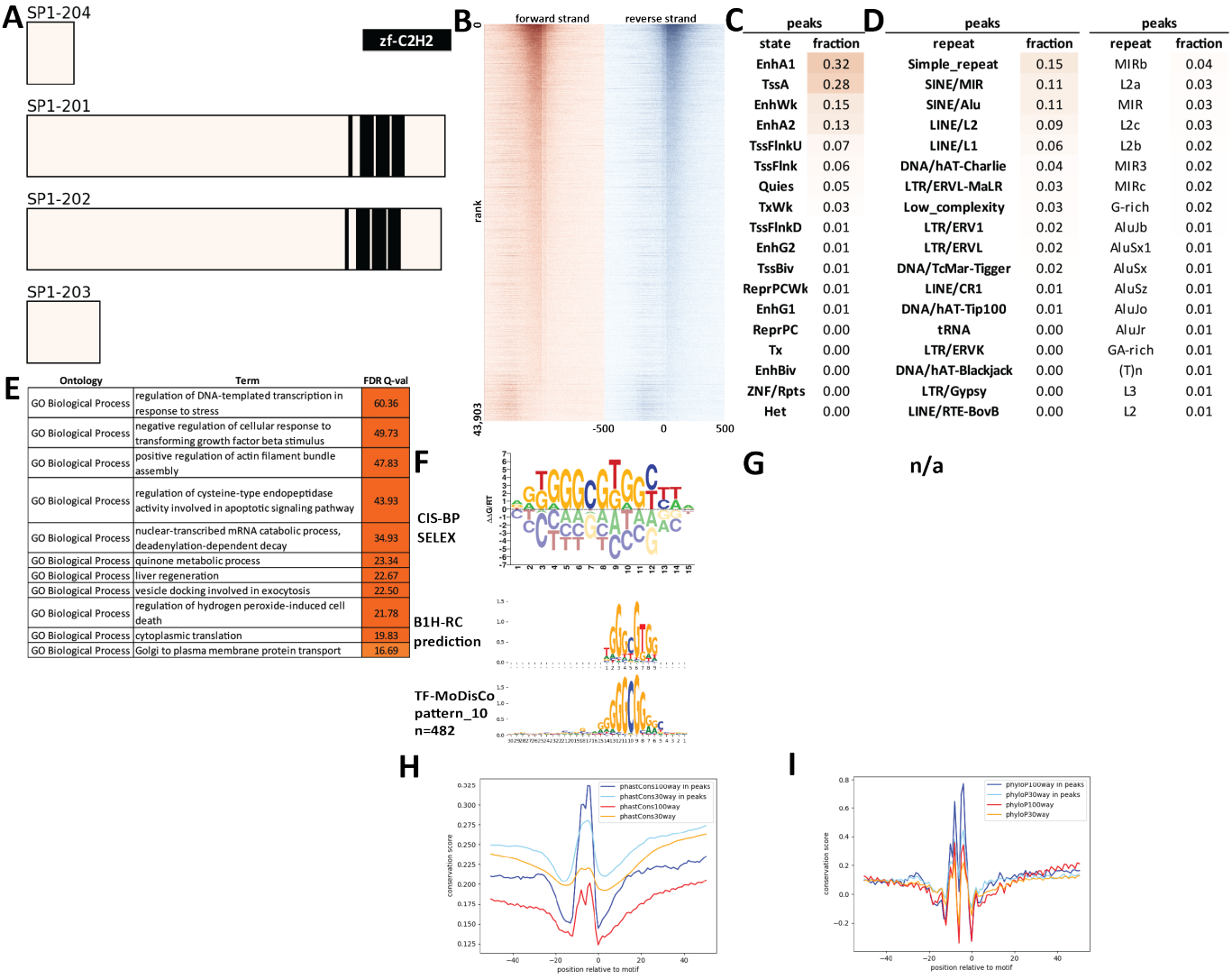

Supplementary Figure 274: Properties and genomic distribution of motifs identified for the SP1 transcription factor in A549 (accession ENCSR000BPE).

TF-MoDisCO pattern_10 n=482, CWM

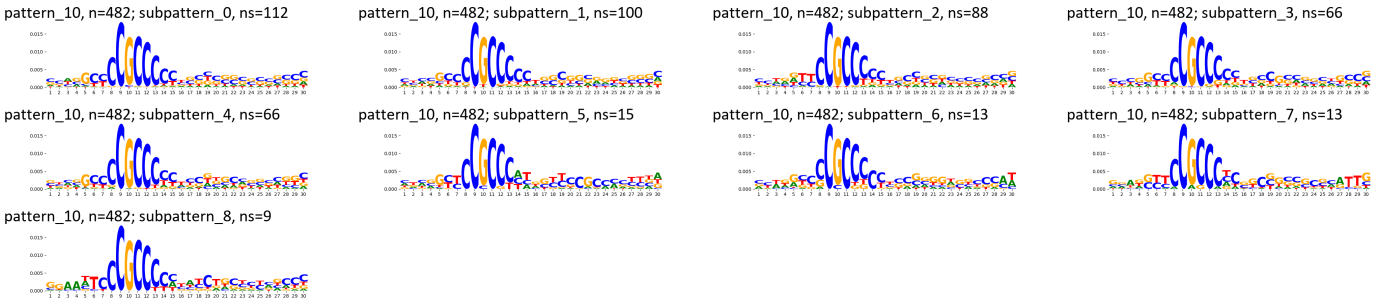

TF-MoDisCO pattern_10 n=482, PWM

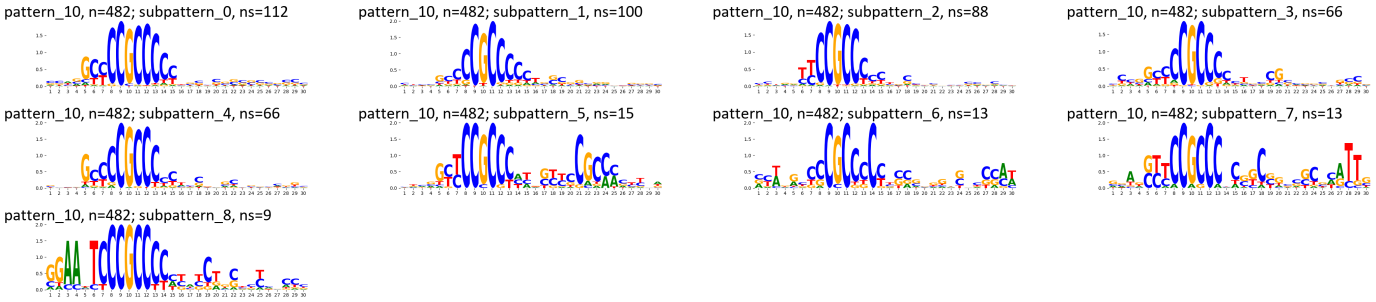

Supplementary Figure 275: TF-MoDisCO subpatterns for the SP1 transcription factor in A549 (accession ENCSR000BPE).

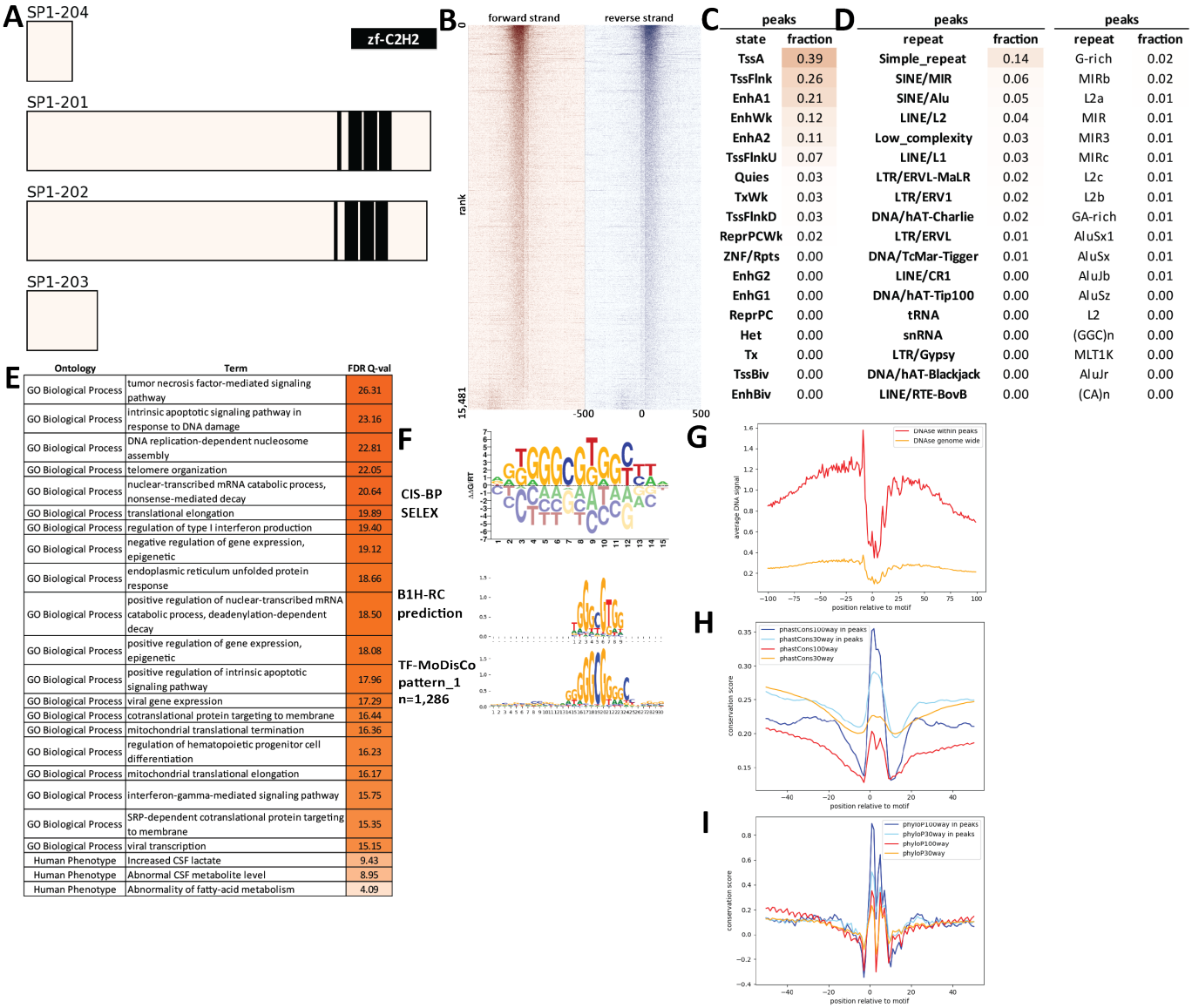

Supplementary Figure 276: Properties and genomic distribution of motifs identified for the SP1 transcription factor in GM12878 (accession ENCSR000BHK).

TF-MoDisCO pattern_1 n=1206, CWM

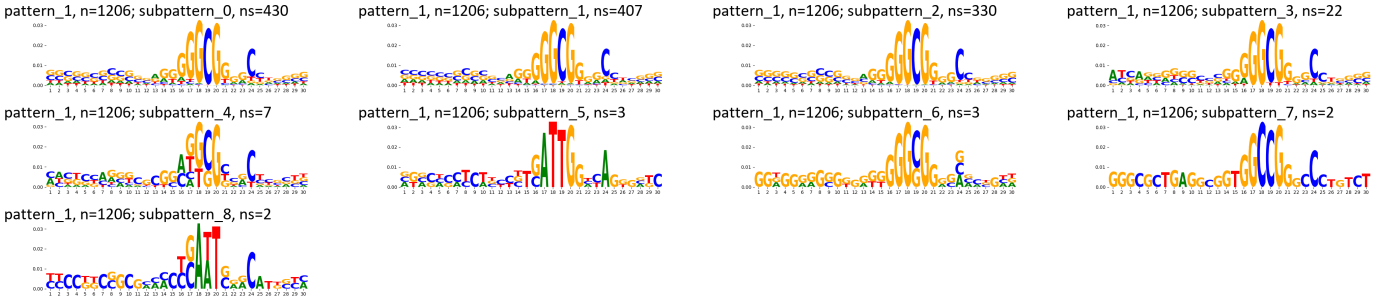

TF-MoDisCO pattern_1 n=1206, PWM

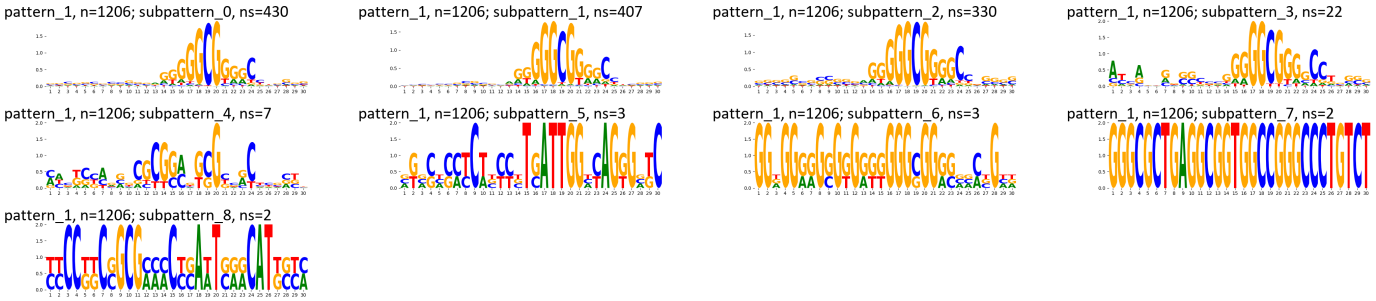

Supplementary Figure 277: TF-MoDisCO subpatterns for the SP1 transcription factor in GM12878 (accession ENCSR000BHK).

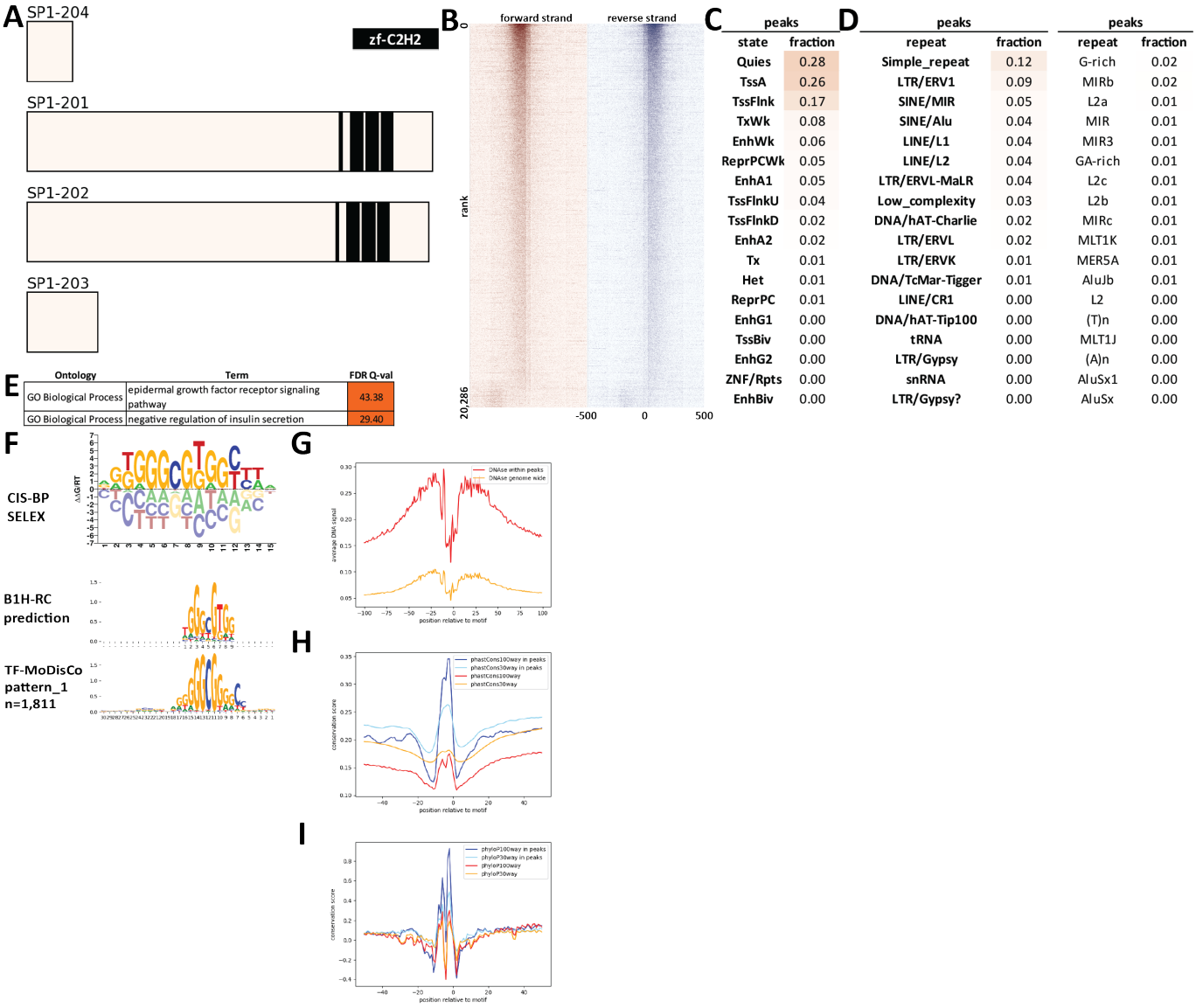

peaks	
state	fraction
Quies	0.28
TssA	0.26
TssFlnk	0.17
TxWk	0.08
EnhWk	0.06
ReprPCWk	0.05
EnhA1	0.05
TssFlnkU	0.04
TssFlnkD	0.02
EnhA2	0.02
Tx	0.01
Het	0.01
ReprPC	0.01
EnhG1	0.00
TssBiv	0.00
EnhG2	0.00
ZNF/Rpts	0.00
EnhBiv	0.00

peaks	
repeat	fraction
Simple_repeat	0.12
LTR/ERV1	0.09
SINE/MIR	0.05
SINE/Alu	0.04
LINE/L1	0.04
LINE/L2	0.04
LTR/ERVL-MaLR	0.04
Low_complexity	0.03
DNA/hAT-Charlie	0.02
LTR/ERVL	0.02
LTR/ERVK	0.01
DNA/TcMar-Tigger	0.01
LINE/CR1	0.00
DNA/hAT-Tip100	0.00
tRNA	0.00
LTR/Gypsy	0.00
snRNA	0.00
LTR/Gypsy?	0.00

peaks	
repeat	fraction
G-rich	0.02
MIRb	0.02
L2a	0.01
MIR	0.01
MIR3	0.01
GA-rich	0.01
L2c	0.01
L2b	0.01
MIRc	0.01
MLT1K	0.01
MER5A	0.01
AluJb	0.01
L2	0.00
(T)n	0.00
MLT1J	0.00
(A)n	0.00
AluSx1	0.00
AluSx	0.00

Supplementary Figure 278: Properties and genomic distribution of motifs identified for the SP1 transcription factor in H1 (accession ENCSR000BIR).

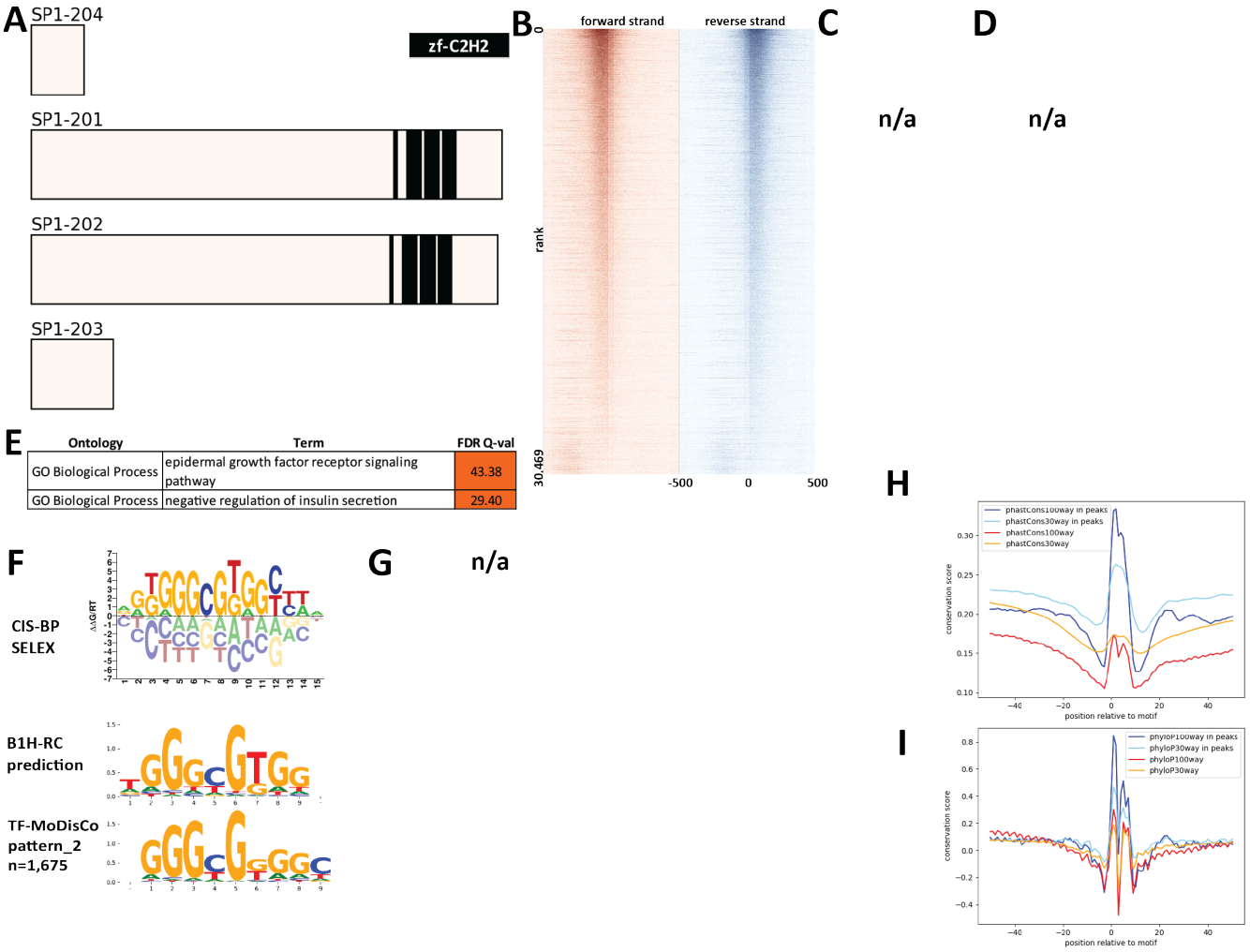

Supplementary Figure 279: Properties and genomic distribution of motifs identified for the SP1 transcription factor in HCT116 (accession ENCSR000BSF).

TF-MoDisCO pattern_2 n=1675, CWM

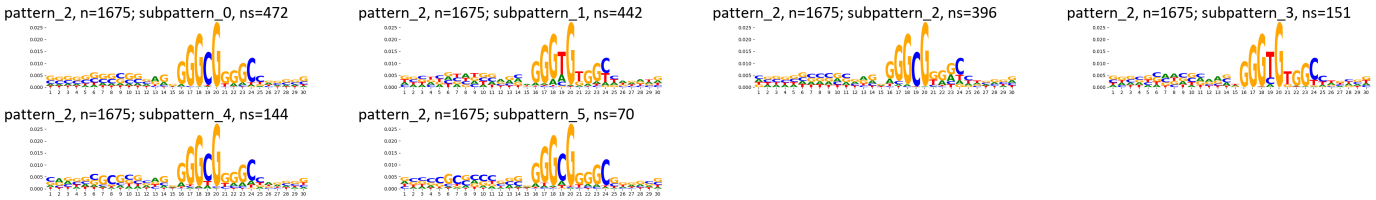

TF-MoDisCO pattern_2 n=1675, PWM

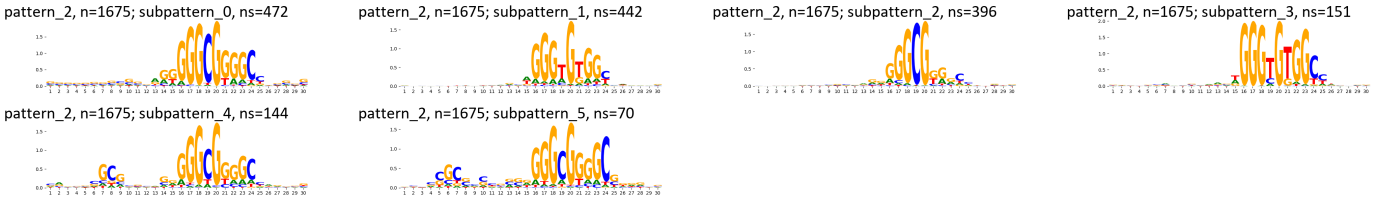

Supplementary Figure 280: TF-MoDisCO subpatterns for the SP1 transcription factor in HCT116 (accession ENCSR000BSF).

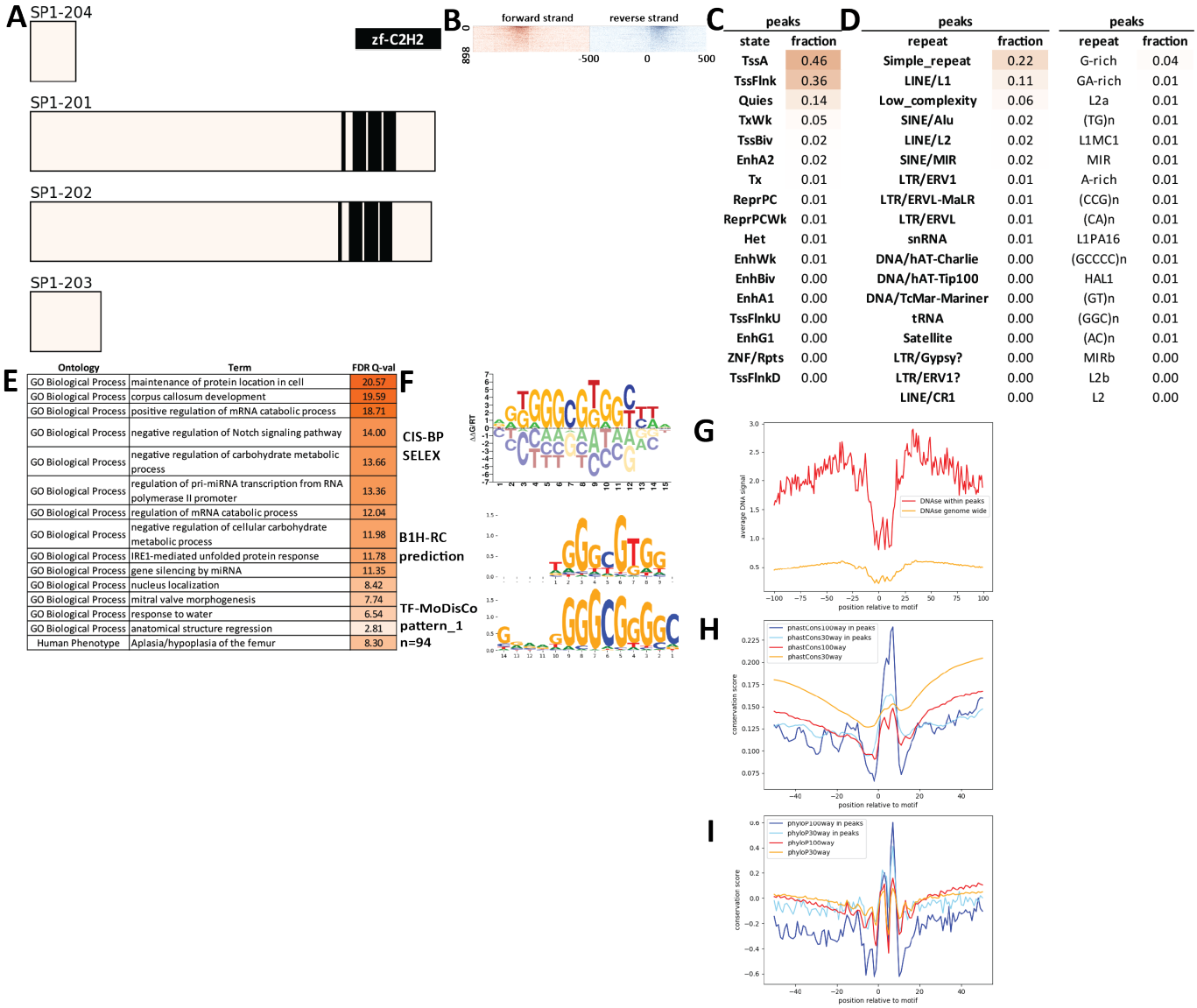

Supplementary Figure 281: Properties and genomic distribution of motifs identified for the SP1 transcription factor in HEK293T (accession ENCSR906PEI).

TF-MoDisCO pattern_1 n=94, CWM

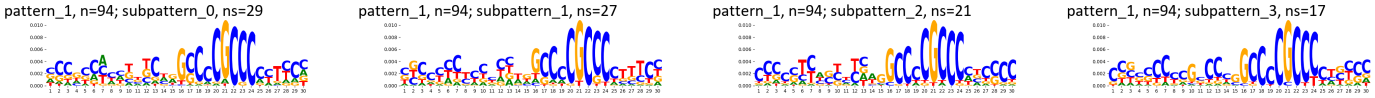

TF-MoDisCO pattern_1 n=94, PWM

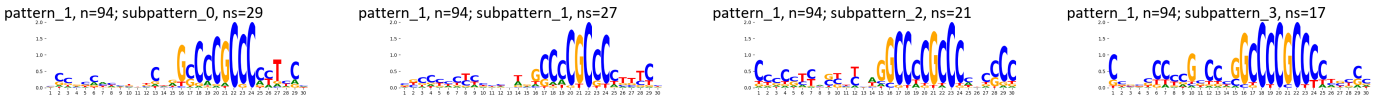

Supplementary Figure 282: TF-MoDisCO subpatterns for the SP1 transcription factor in HEK293T (accession ENCSR906PEI).

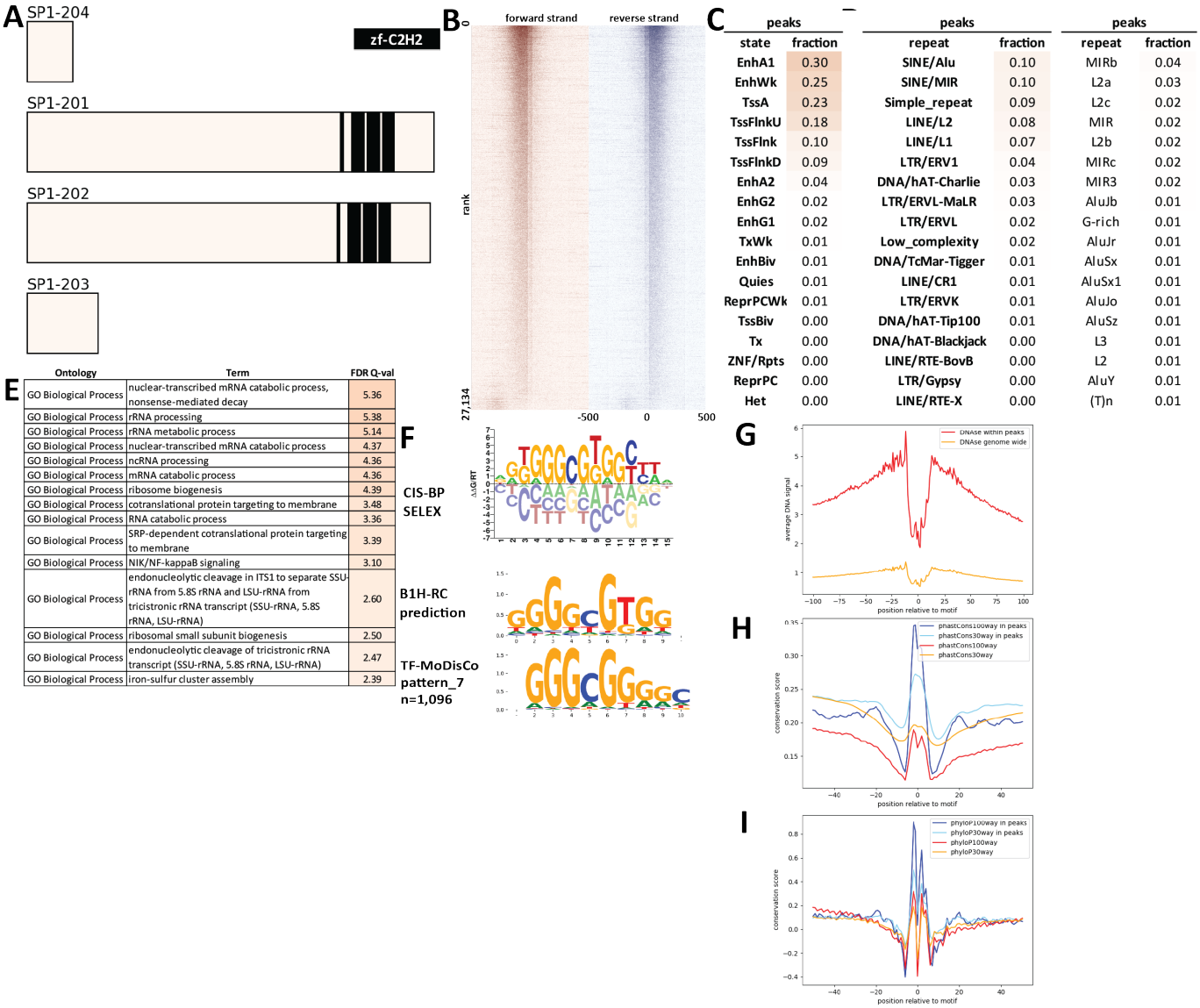

Supplementary Figure 283: Properties and genomic distribution of motifs identified for the SP1 transcription factor in HepG2 (accession ENCSR000BJX).

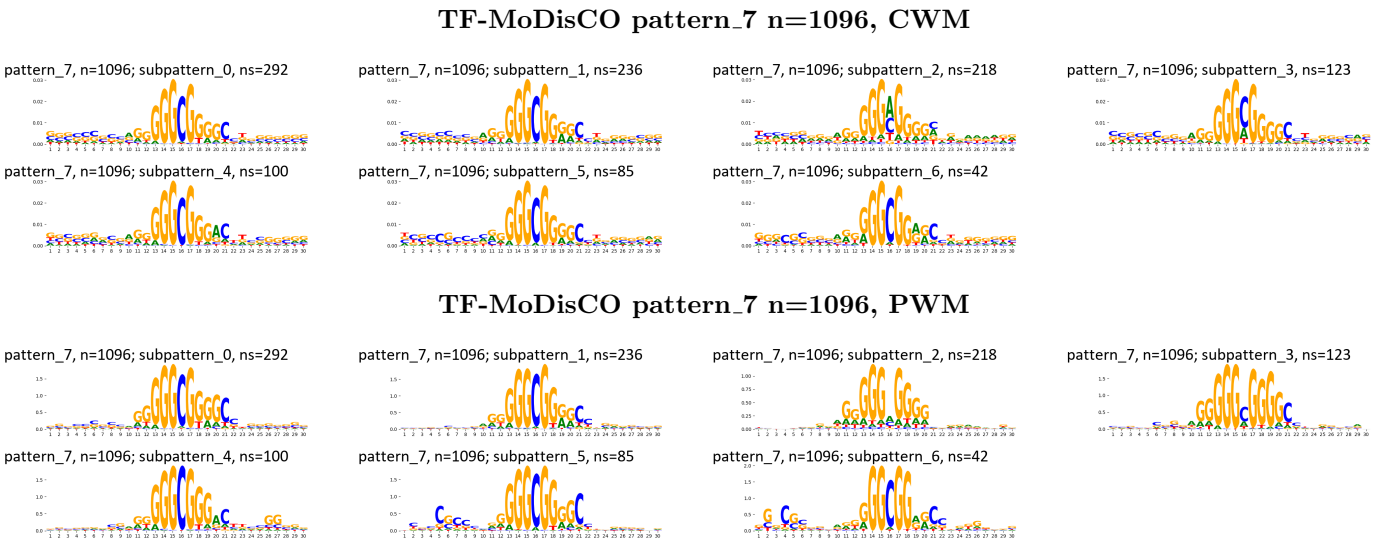

Supplementary Figure 284: TF-MoDisCO subpatterns for the SP1 transcription factor in HepG2 (accession ENCSR000BJX).

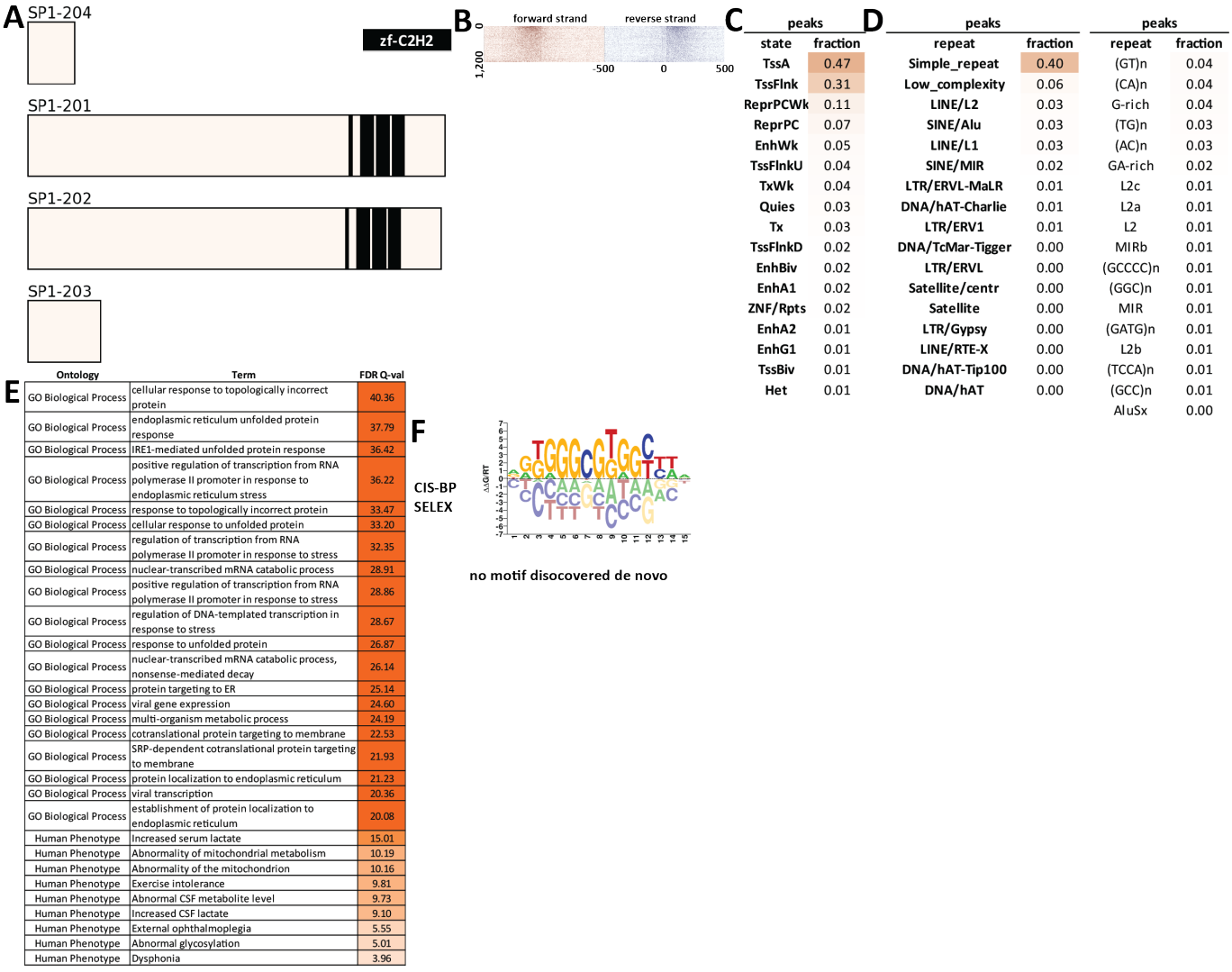

C

peaks	
state	fraction
TssA	0.47
TssFlnk	0.31
ReprPCWk	0.11
ReprPC	0.07
EnhWk	0.05
TssFlnkU	0.04
TxWk	0.04
Quies	0.03
Tx	0.03
TssFlnkD	0.02
EnhBiv	0.02
EnhA1	0.02
ZNF/Rpts	0.02
EnhA2	0.01
EnhG1	0.01
TssBiv	0.01
Het	0.01

D

peaks		peaks	
repeat	fraction	repeat	fraction
Simple_repeat	0.40	(GT)n	0.04
Low_complexity	0.06	(CA)n	0.04
LINE/L2	0.03	G-rich	0.04
SINE/Alu	0.03	(TG)n	0.03
LINE/L1	0.03	(AC)n	0.03
SINE/MIR	0.02	GA-rich	0.02
LTR/ERVL-MaLR	0.01	L2c	0.01
DNA/hAT-Charlie	0.01	L2a	0.01
LTR/ERV1	0.01	L2	0.01
DNA/TcMar-Tigger	0.00	MIRb	0.01
LTR/ERVL	0.00	(GCCCC)n	0.01
Satellite/centr	0.00	(GGC)n	0.01
Satellite	0.00	MIR	0.01
LTR/Gypsy	0.00	(GATG)n	0.01
LINE/RTE-X	0.00	L2b	0.01
DNA/hAT-Tip100	0.00	(TCCA)n	0.01
DNA/hAT	0.00	(GCC)n	0.01
		AluSx	0.00

E

Ontology	Term	FDR Q-val
GO Biological Process	cellular response to topologically incorrect protein	40.36
GO Biological Process	endoplasmic reticulum unfolded protein response	37.79
GO Biological Process	IRE1-mediated unfolded protein response	36.42
GO Biological Process	positive regulation of transcription from RNA polymerase II promoter in response to endoplasmic reticulum stress	36.22
GO Biological Process	response to topologically incorrect protein	33.47
GO Biological Process	cellular response to unfolded protein	33.20
GO Biological Process	regulation of transcription from RNA polymerase II promoter in response to stress	32.35
GO Biological Process	nuclear-transcribed mRNA catabolic process	28.91
GO Biological Process	positive regulation of transcription from RNA polymerase II promoter in response to stress	28.86
GO Biological Process	regulation of DNA-templated transcription in response to stress	28.67
GO Biological Process	response to unfolded protein	26.87
GO Biological Process	nuclear-transcribed mRNA catabolic process, nonsense-mediated decay	26.14
GO Biological Process	protein targeting to ER	25.14
GO Biological Process	viral gene expression	24.60
GO Biological Process	multi-organism metabolic process	24.19
GO Biological Process	cotranslational protein targeting to membrane	22.53
GO Biological Process	SRP-dependent cotranslational protein targeting to membrane	21.93
GO Biological Process	protein localization to endoplasmic reticulum	21.23
GO Biological Process	viral transcription	20.36
GO Biological Process	establishment of protein localization to endoplasmic reticulum	20.08
Human Phenotype	Increased serum lactate	15.01
Human Phenotype	Abnormality of mitochondrial metabolism	10.19
Human Phenotype	Abnormality of the mitochondrion	10.16
Human Phenotype	Exercise intolerance	9.81
Human Phenotype	Abnormal CSF metabolite level	9.73
Human Phenotype	Increased CSF lactate	9.10
Human Phenotype	External ophthalmoplegia	5.55
Human Phenotype	Abnormal glycosylation	5.01
Human Phenotype	Dysphonia	3.96

Supplementary Figure 285: Properties and genomic distribution of motifs identified for the SP1 transcription factor in HepG2 (accession ENCSR334KIQ).

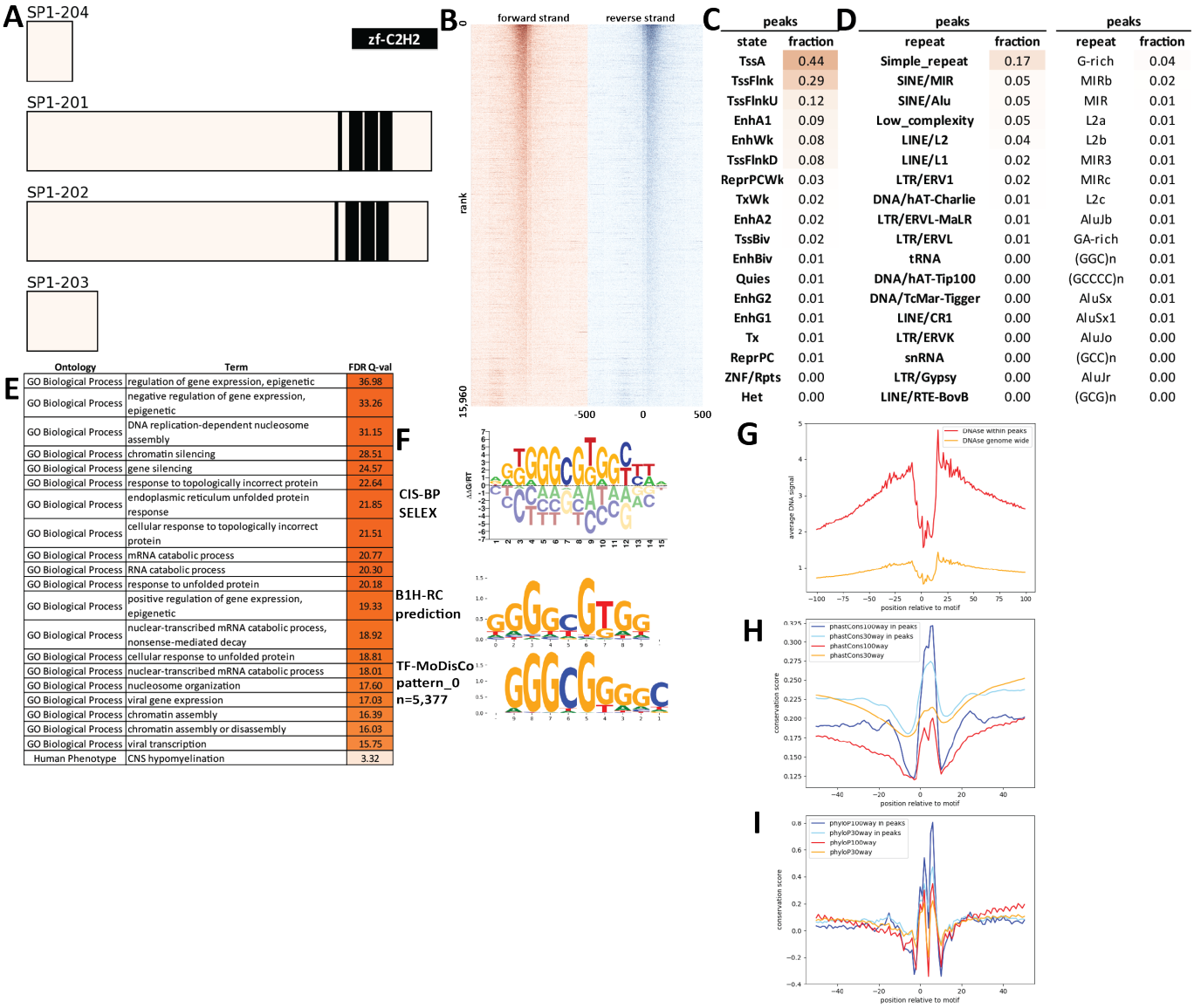

peaks	
state	fraction
TssA	0.44
TssFlnk	0.29
TssFlnkU	0.12
EnhA1	0.09
EnhWk	0.08
TssFlnkD	0.08
ReprPCWk	0.03
TxWk	0.02
EnhA2	0.02
TssBiv	0.02
EnhBiv	0.01
Quies	0.01
EnhG2	0.01
EnhG1	0.01
Tx	0.01
ReprPC	0.01
ZNF/Rpts	0.00
Het	0.00

peaks	
repeat	fraction
Simple_repeat	0.17
SINE/MIR	0.05
SINE/Alu	0.05
Low_complexity	0.05
LINE/L2	0.04
LINE/L1	0.02
LTR/ERV1	0.02
DNA/hAT-Charlie	0.01
LTR/ERVL-MaLR	0.01
LTR/ERVL	0.01
tRNA	0.00
DNA/hAT-Tip100	0.00
DNA/TcMar-Tigger	0.00
LINE/CR1	0.00
LTR/ERVK	0.00
snRNA	0.00
LTR/Gypsy	0.00
LINE/RTE-BovB	0.00

peaks	
repeat	fraction
G-rich	0.04
MIRb	0.02
MIR	0.01
L2a	0.01
L2b	0.01
MIR3	0.01
MIRc	0.01
L2c	0.01
AluJb	0.01
GA-rich	0.01
(GGC)n	0.01
(GCCCC)n	0.01
AluSx	0.01
AluSx1	0.01
AluJo	0.00
(GCC)n	0.00
AluJr	0.00
(GCG)n	0.00

Ontology	Term	FDR Q-val
GO Biological Process	regulation of gene expression, epigenetic	36.98
GO Biological Process	negative regulation of gene expression, epigenetic	33.26
GO Biological Process	DNA replication-dependent nucleosome assembly	31.15
GO Biological Process	chromatin silencing	28.51
GO Biological Process	gene silencing	24.57
GO Biological Process	response to topologically incorrect protein	22.64
GO Biological Process	endoplasmic reticulum unfolded protein response	21.85
GO Biological Process	cellular response to topologically incorrect protein	21.51
GO Biological Process	mRNA catabolic process	20.77
GO Biological Process	RNA catabolic process	20.30
GO Biological Process	response to unfolded protein	20.18
GO Biological Process	positive regulation of gene expression, epigenetic	19.33
GO Biological Process	nuclear-transcribed mRNA catabolic process, nonsense-mediated decay	18.92
GO Biological Process	cellular response to unfolded protein	18.81
GO Biological Process	nuclear-transcribed mRNA catabolic process	18.01
GO Biological Process	nucleosome organization	17.60
GO Biological Process	viral gene expression	17.03
GO Biological Process	chromatin assembly	16.39
GO Biological Process	chromatin assembly or disassembly	16.03
GO Biological Process	viral transcription	15.75
Human Phenotype	CNS hypomyelination	3.32

Supplementary Figure 286: Properties and genomic distribution of motifs identified for the SP1 transcription factor in HepG2 (accession ENCSR460YAM).

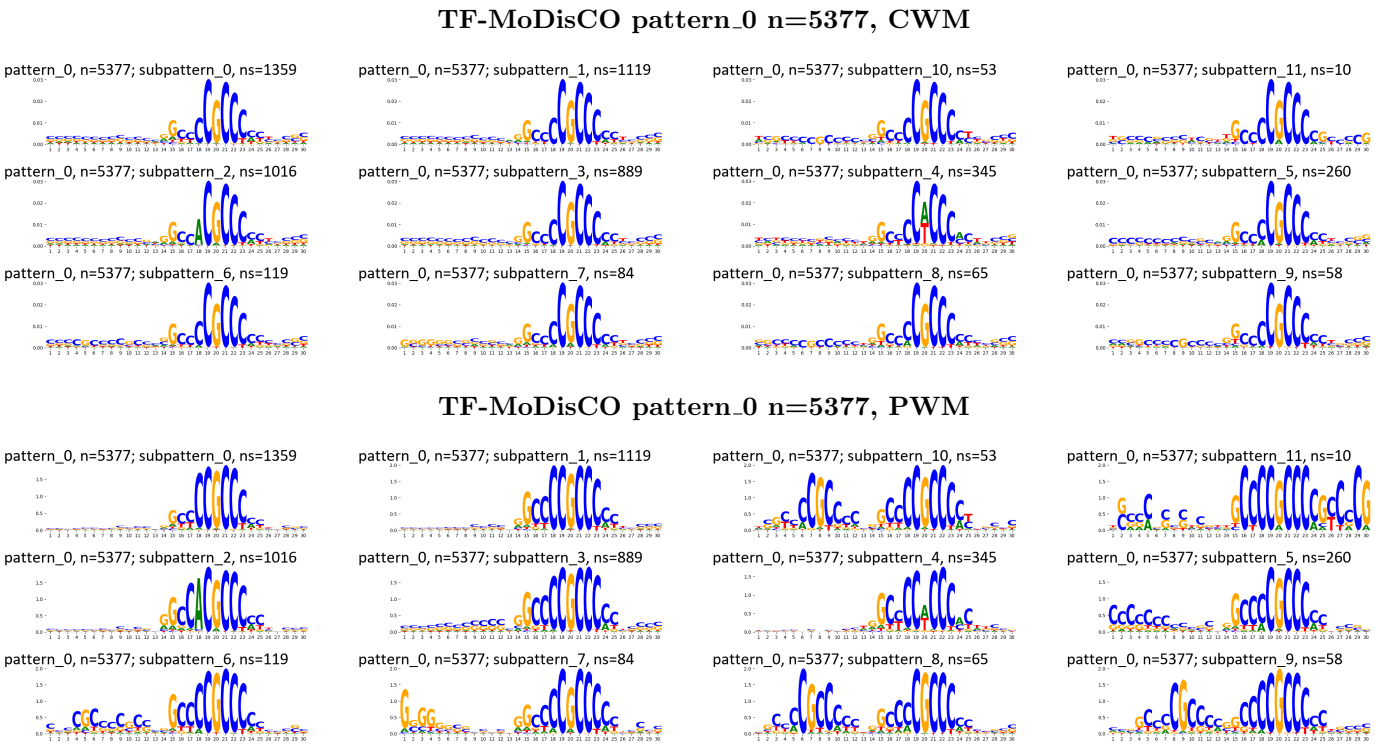

Supplementary Figure 287: TF-MoDisCO subpatterns for the SP1 transcription factor in HepG2 (accession ENCSR460YAM).

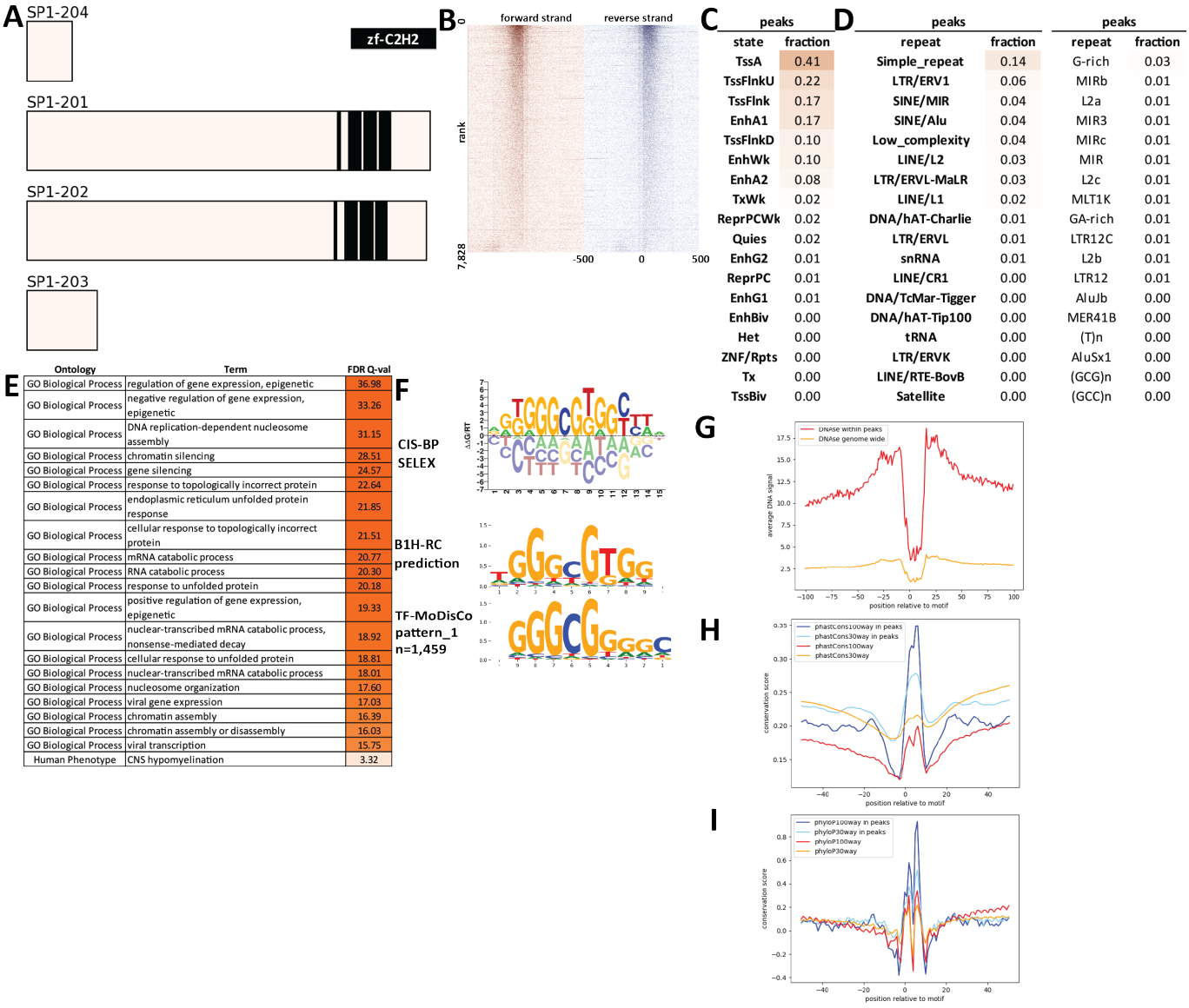

peaks	
state	fraction
TssA	0.41
TssFlnkU	0.22
TssFlnk	0.17
EnhA1	0.17
TssFlnkD	0.10
EnhWk	0.10
EnhA2	0.08
TxWk	0.02
ReprPCWk	0.02
Quies	0.02
EnhG2	0.01
ReprPC	0.01
EnhG1	0.01
EnhBiv	0.00
Het	0.00
ZNF/Rpts	0.00
Tx	0.00
TssBiv	0.00

peaks		peaks	
repeat	fraction	repeat	fraction
Simple_repeat	0.14	G-rich	0.03
LTR/ERV1	0.06	MIRb	0.01
SINE/MIR	0.04	L2a	0.01
SINE/Alu	0.04	MIR3	0.01
Low_complexity	0.04	MIRc	0.01
LINE/L2	0.03	MIR	0.01
LTR/ERVL-MaLR	0.03	L2c	0.01
LINE/L1	0.02	MLT1K	0.01
DNA/hAT-Charlie	0.01	GA-rich	0.01
LTR/ERVL	0.01	LTR12C	0.01
snRNA	0.01	L2b	0.01
LINE/CR1	0.00	LTR12	0.01
DNA/TcMar-Tigger	0.00	AluJb	0.00
DNA/hAT-Tip100	0.00	MER41B	0.00
tRNA	0.00	(T)n	0.00
LTR/ERVK	0.00	AluSx1	0.00
LINE/RTE-BovB	0.00	(GCG)n	0.00
Satellite	0.00	(GCC)n	0.00

Ontology	Term	FDR Q-val
GO Biological Process	regulation of gene expression, epigenetic	36.98
GO Biological Process	negative regulation of gene expression, epigenetic	33.26
GO Biological Process	DNA replication-dependent nucleosome assembly	31.15
GO Biological Process	chromatin silencing	28.51
GO Biological Process	gene silencing	24.57
GO Biological Process	response to topologically incorrect protein	22.64
GO Biological Process	endoplasmic reticulum unfolded protein response	21.85
GO Biological Process	cellular response to topologically incorrect protein	21.51
GO Biological Process	mRNA catabolic process	20.77
GO Biological Process	RNA catabolic process	20.30
GO Biological Process	response to unfolded protein	20.18
GO Biological Process	positive regulation of gene expression, epigenetic	19.33
GO Biological Process	nuclear-transcribed mRNA catabolic process, nonsense-mediated decay	18.92
GO Biological Process	cellular response to unfolded protein	18.81
GO Biological Process	nuclear-transcribed mRNA catabolic process	18.01
GO Biological Process	nucleosome organization	17.60
GO Biological Process	viral gene expression	17.03
GO Biological Process	chromatin assembly	16.39
GO Biological Process	chromatin assembly or disassembly	16.03
GO Biological Process	viral transcription	15.75
Human Phenotype	CNS hypomyelination	3.32

Supplementary Figure 288: Properties and genomic distribution of motifs identified for the SP1 transcription factor in K562 (accession ENCSR000BKO).

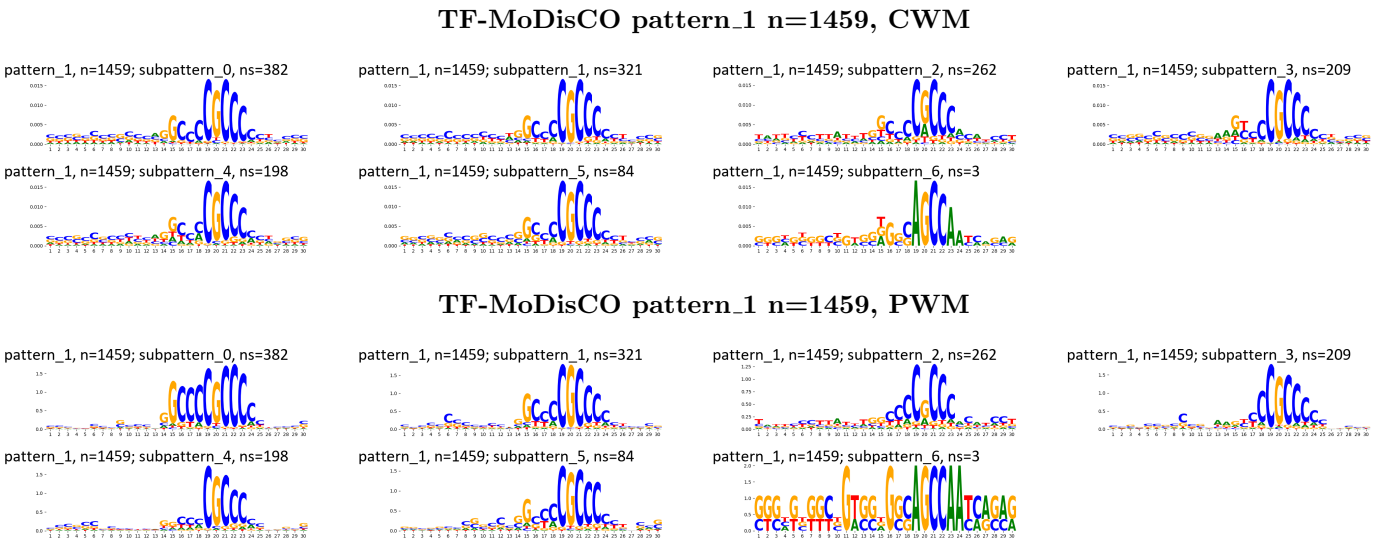

Supplementary Figure 289: TF-MoDisCO subpatterns for the SP1 transcription factor in K562 (accession ENCSR000BKO).

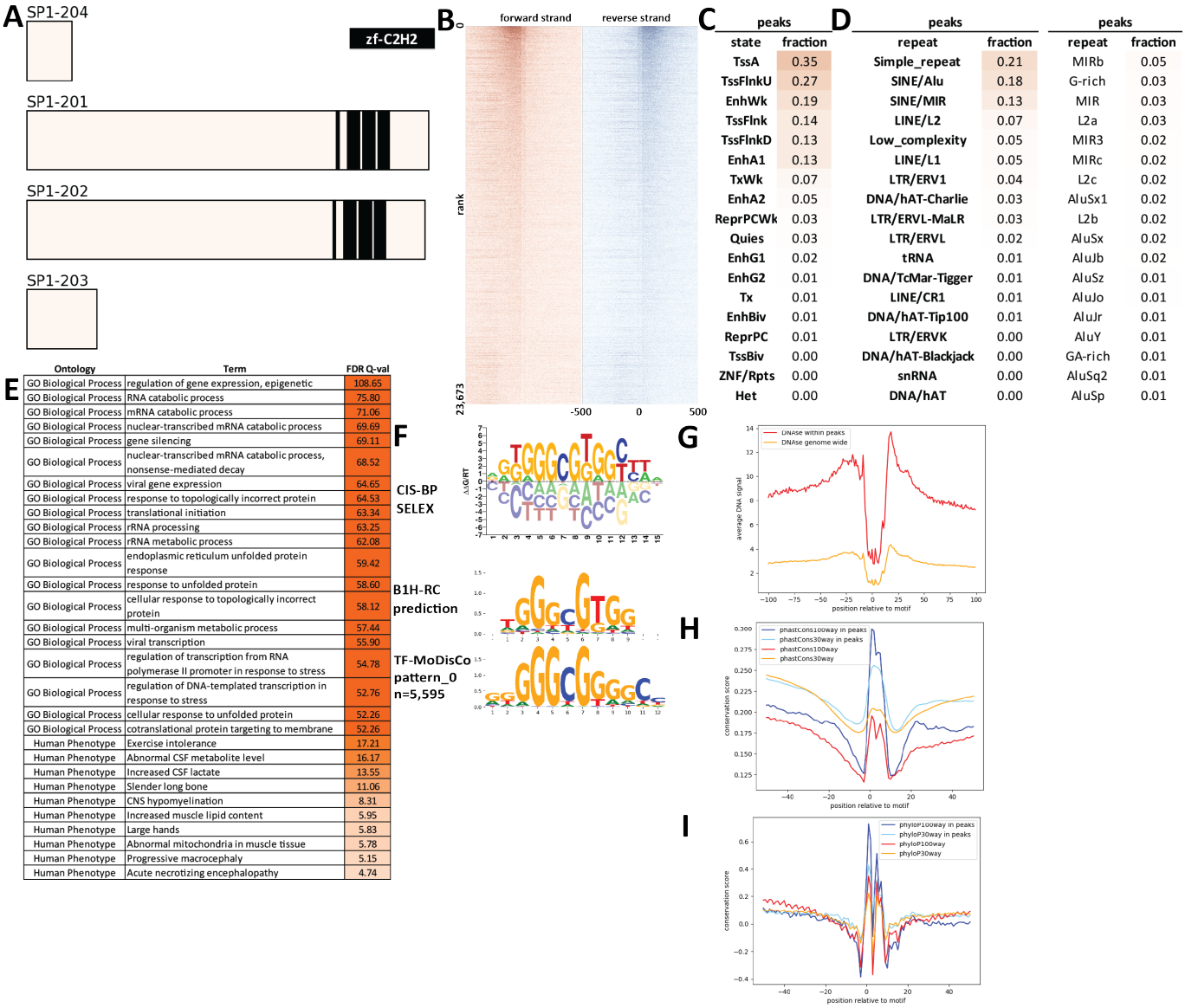

Supplementary Figure 290: Properties and genomic distribution of motifs identified for the SP1 transcription factor in K562 (accession ENCSR372IML).

TF-MoDisCO pattern_0 n=5595, CWM

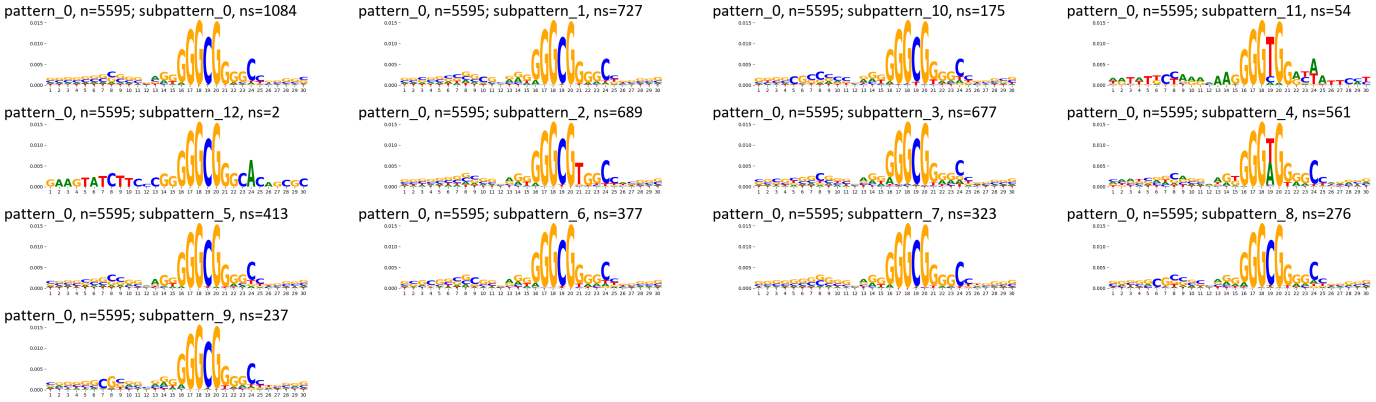

TF-MoDisCO pattern_0 n=5595, PWM

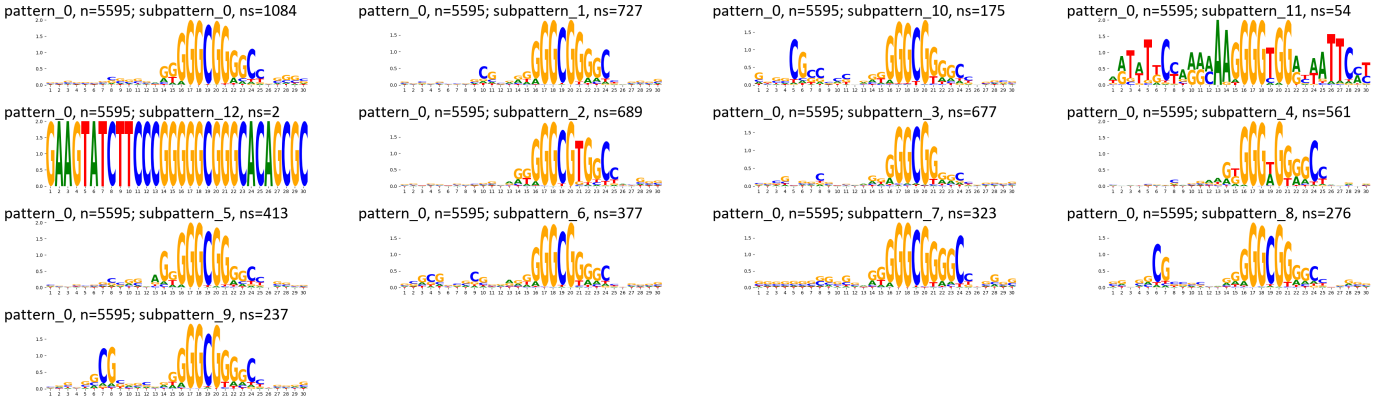

Supplementary Figure 291: TF-MoDisCO subpatterns for the SP1 transcription factor in K562 (accession ENCSR372IML).

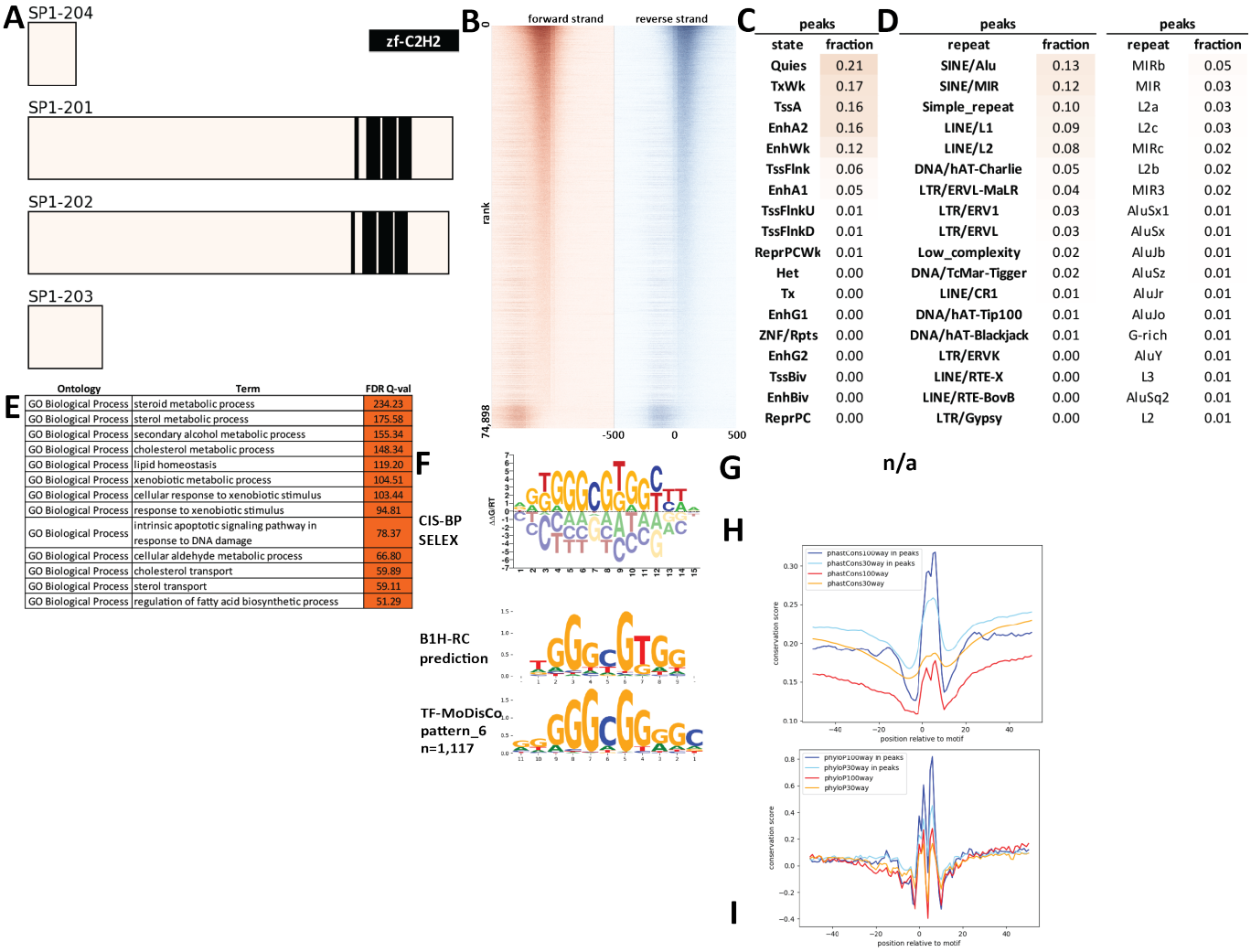

C

peaks	
state	fraction
Quies	0.21
TxWk	0.17
TssA	0.16
EnhA2	0.16
EnhWk	0.12
TssFlnk	0.06
EnhA1	0.05
TssFlnkU	0.01
TssFlnkD	0.01
ReprPCWk	0.01
Het	0.00
Tx	0.00
EnhG1	0.00
ZNF/Rpts	0.00
EnhG2	0.00
TssBiv	0.00
EnhBiv	0.00
ReprPC	0.00

D

peaks		peaks	
repeat	fraction	repeat	fraction
SINE/Alu	0.13	MIRb	0.05
SINE/MIR	0.12	MIR	0.03
Simple_repeat	0.10	L2a	0.03
LINE/L1	0.09	L2c	0.03
LINE/L2	0.08	MIRc	0.02
DNA/hAT-Charlie	0.05	L2b	0.02
LTR/ERVL-MaLR	0.04	MIR3	0.02
LTR/ERV1	0.03	AluSx1	0.01
LTR/ERVL	0.03	AluSx	0.01
Low_complexity	0.02	AluJb	0.01
DNA/TcMar-Tigger	0.02	AluSz	0.01
LINE/CR1	0.01	AluJr	0.01
DNA/hAT-Tip100	0.01	AluJo	0.01
DNA/hAT-Blackjack	0.01	G-rich	0.01
LTR/ERVK	0.00	AluY	0.01
LINE/RTE-X	0.00	L3	0.01
LINE/RTE-BovB	0.00	AluSq2	0.01
LTR/Gypsy	0.00	L2	0.01

E

Ontology	Term	FDR Q-val
GO Biological Process	steroid metabolic process	234.23
GO Biological Process	sterol metabolic process	175.58
GO Biological Process	secondary alcohol metabolic process	155.34
GO Biological Process	cholesterol metabolic process	148.34
GO Biological Process	lipid homeostasis	119.20
GO Biological Process	xenobiotic metabolic process	104.51
GO Biological Process	cellular response to xenobiotic stimulus	103.44
GO Biological Process	response to xenobiotic stimulus	94.81
GO Biological Process	intrinsic apoptotic signaling pathway in response to DNA damage	78.37
GO Biological Process	cellular aldehyde metabolic process	66.80
GO Biological Process	cholesterol transport	59.89
GO Biological Process	sterol transport	59.11
GO Biological Process	regulation of fatty acid biosynthetic process	51.29

Supplementary Figure 292: Properties and genomic distribution of motifs identified for the SP1 transcription factor in liver (accession ENCSR085IXF).

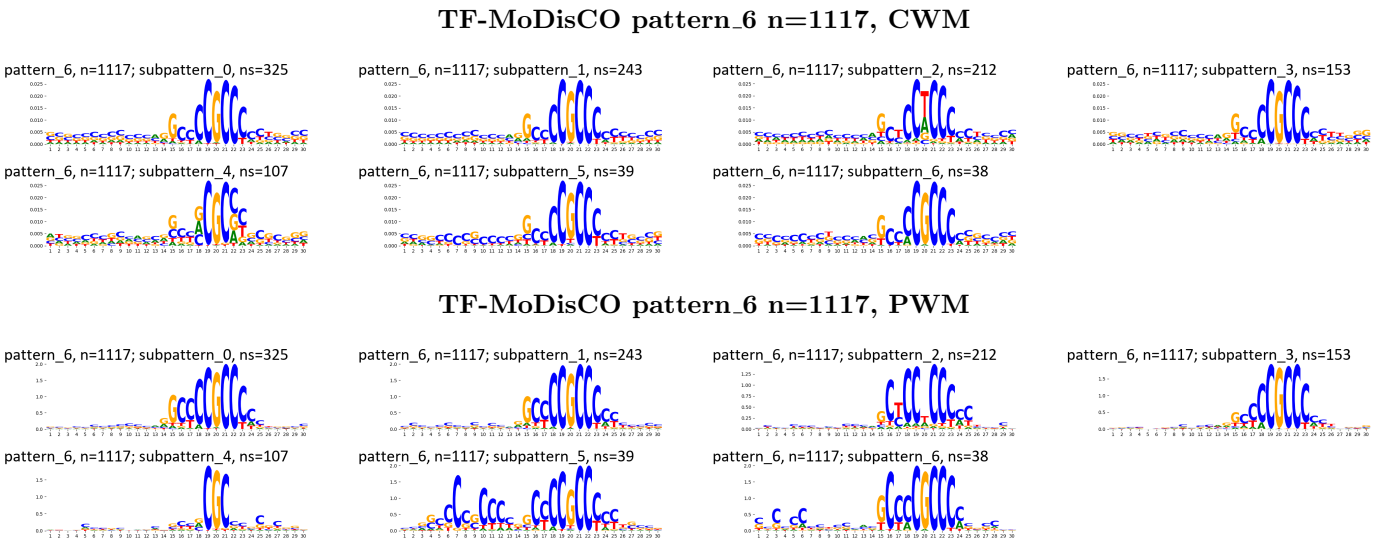

Supplementary Figure 293: TF-MoDisCO subpatterns for the SP1 transcription factor in liver (accession ENCSR085IXF).

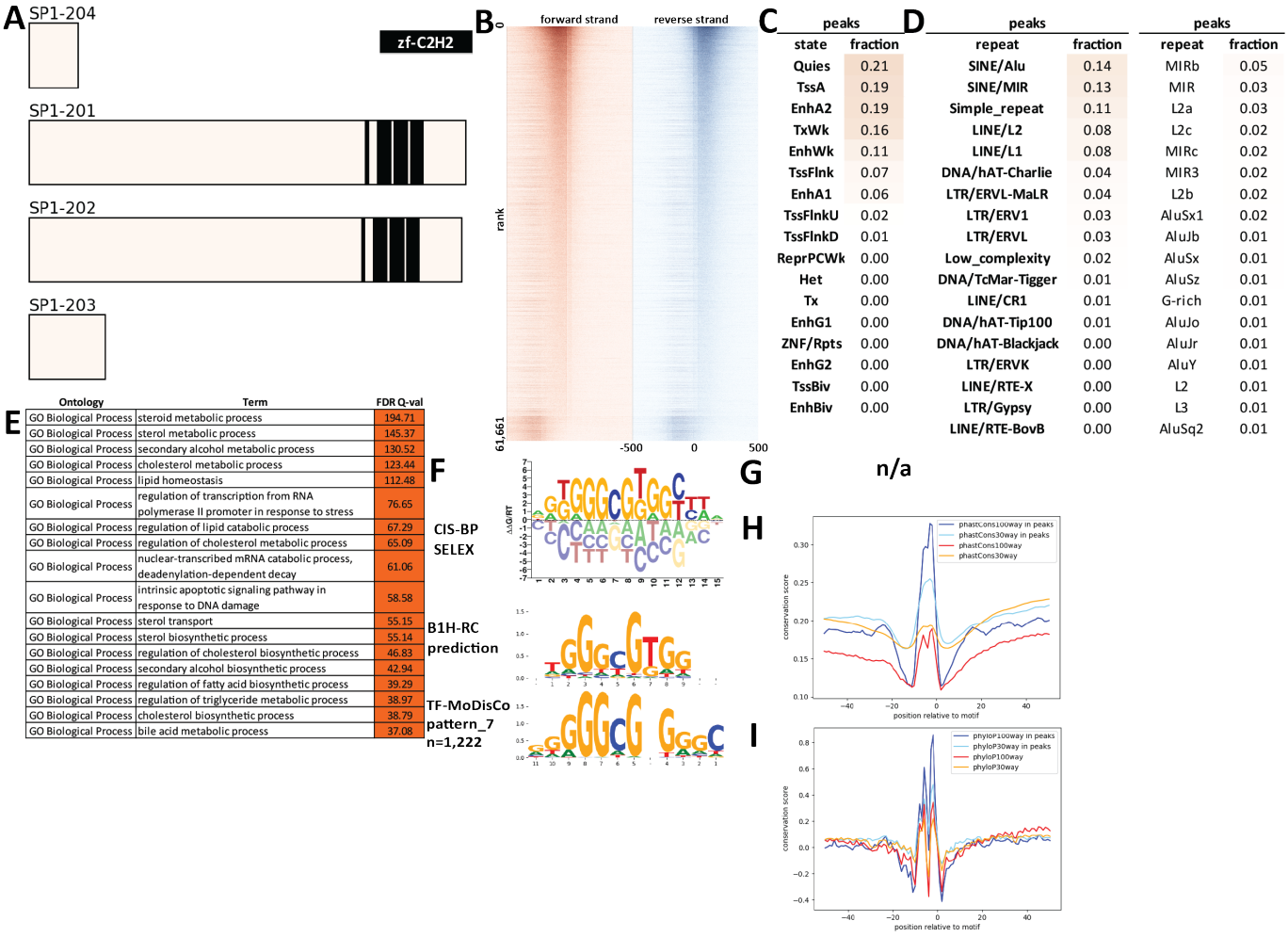

C

peaks	
state	fraction
Quies	0.21
TssA	0.19
EnhA2	0.19
TxWk	0.16
EnhWk	0.11
TssFlnk	0.07
EnhA1	0.06
TssFlnkU	0.02
TssFlnkD	0.01
ReprPCWk	0.00
Het	0.00
Tx	0.00
EnhG1	0.00
ZNF/Rpts	0.00
EnhG2	0.00
TssBiv	0.00
EnhBiv	0.00

D

peaks		peaks	
repeat	fraction	repeat	fraction
SINE/Alu	0.14	MIRb	0.05
SINE/MIR	0.13	MIR	0.03
Simple_repeat	0.11	L2a	0.03
LINE/L2	0.08	L2c	0.02
LINE/L1	0.08	MIRc	0.02
DNA/hAT-Charlie	0.04	MIR3	0.02
LTR/ERVL-MaLR	0.04	L2b	0.02
LTR/ERV1	0.03	AluSx1	0.02
LTR/ERVL	0.03	AluJb	0.01
Low_complexity	0.02	AluSx	0.01
DNA/TcMar-Tigger	0.01	AluSz	0.01
LINE/CR1	0.01	G-rich	0.01
DNA/hAT-Tip100	0.01	AluJo	0.01
DNA/hAT-Blackjack	0.00	AluJr	0.01
LTR/ERVK	0.00	AluY	0.01
LINE/RTE-X	0.00	L2	0.01
LTR/Gypsy	0.00	L3	0.01
LINE/RTE-BovB	0.00	AluSq2	0.01

E

Ontology	Term	FDR Q-val
GO Biological Process	steroid metabolic process	194.71
GO Biological Process	sterol metabolic process	145.37
GO Biological Process	secondary alcohol metabolic process	130.52
GO Biological Process	cholesterol metabolic process	123.44
GO Biological Process	lipid homeostasis	112.48
GO Biological Process	regulation of transcription from RNA polymerase II promoter in response to stress	76.65
GO Biological Process	regulation of lipid catabolic process	67.29
GO Biological Process	regulation of cholesterol metabolic process	65.09
GO Biological Process	nuclear-transcribed mRNA catabolic process, deadenylation-dependent decay	61.06
GO Biological Process	intrinsic apoptotic signaling pathway in response to DNA damage	58.58
GO Biological Process	sterol transport	55.15
GO Biological Process	sterol biosynthetic process	55.14
GO Biological Process	regulation of cholesterol biosynthetic process	46.83
GO Biological Process	secondary alcohol biosynthetic process	42.94
GO Biological Process	regulation of fatty acid biosynthetic process	39.29
GO Biological Process	regulation of triglyceride metabolic process	38.97
GO Biological Process	cholesterol biosynthetic process	38.79
GO Biological Process	bile acid metabolic process	37.08

Supplementary Figure 294: Properties and genomic distribution of motifs identified for the SP1 transcription factor in liver (accession ENCSR386YIH).

TF-MoDisCO pattern_7 n=1222, CWM

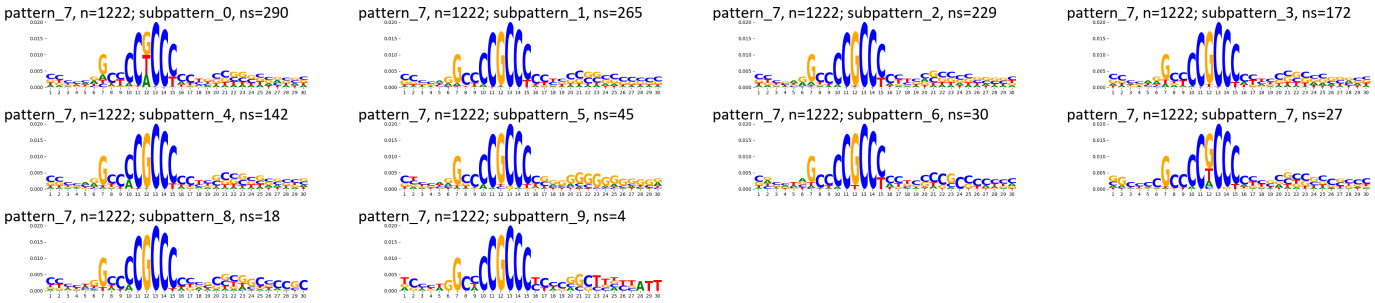

TF-MoDisCO pattern_7 n=1222, PWM

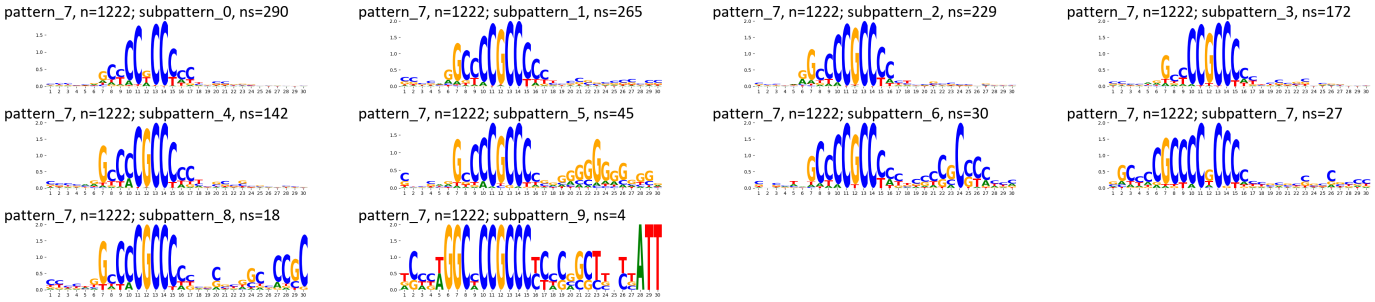

Supplementary Figure 295: TF-MoDisCO subpatterns for the SP1 transcription factor in liver (accession ENCSR386YIH).

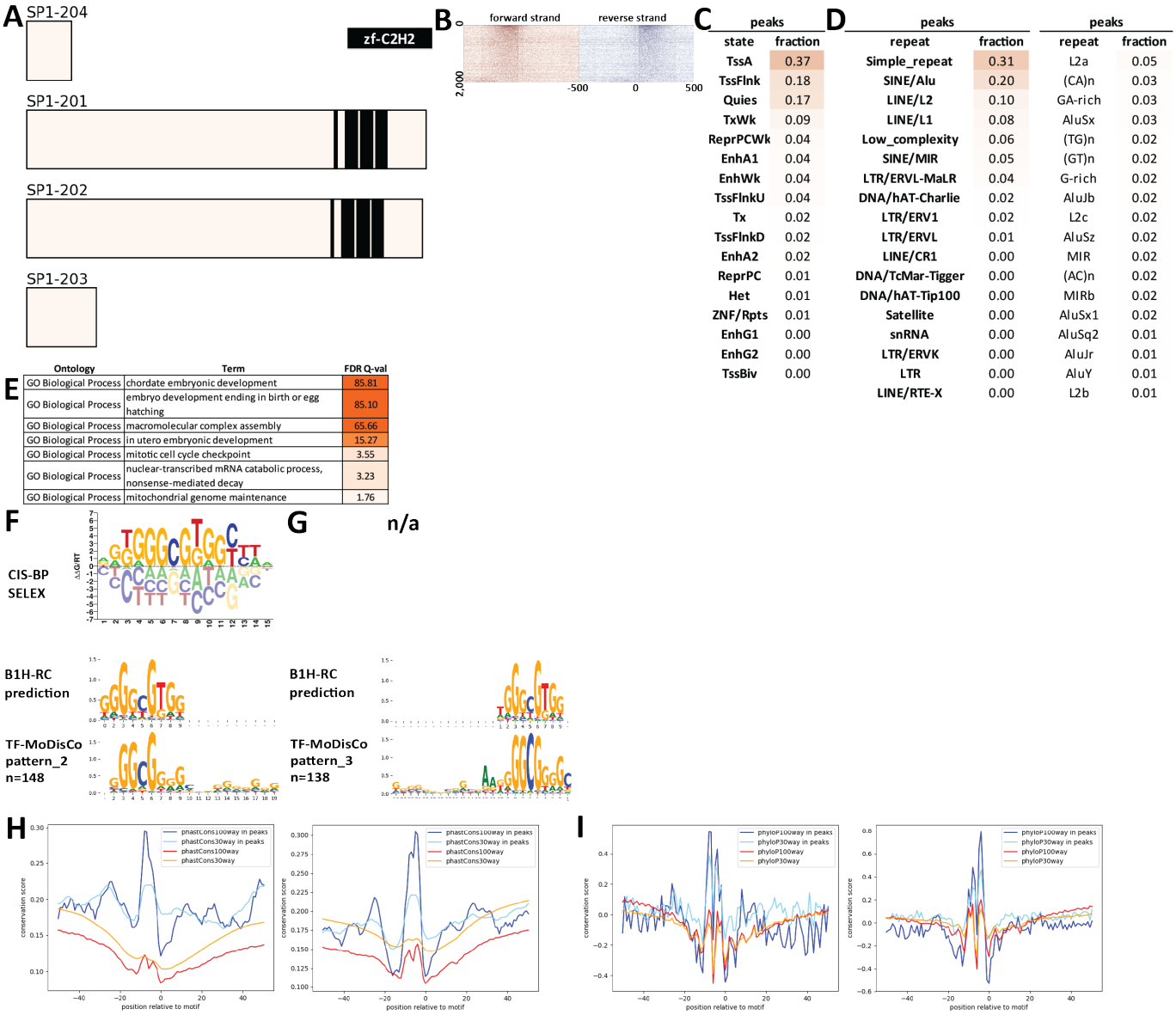

peaks	
state	fraction
TssA	0.37
TssFlnk	0.18
Quies	0.17
TxWk	0.09
ReprPCWk	0.04
EnhA1	0.04
EnhWk	0.04
TssFlnkU	0.04
Tx	0.02
TssFlnkD	0.02
EnhA2	0.02
ReprPC	0.01
Het	0.01
ZNF/Rpts	0.01
EnhG1	0.00
EnhG2	0.00
TssBiv	0.00

peaks		peaks	
repeat	fraction	repeat	fraction
Simple_repeat	0.31	L2a	0.05
SINE/Alu	0.20	(CA)n	0.03
LINE/L2	0.10	GA-rich	0.03
LINE/L1	0.08	AluSx	0.03
Low_complexity	0.06	(TG)n	0.02
SINE/MIR	0.05	(GT)n	0.02
LTR/ERVL-MaLR	0.04	G-rich	0.02
DNA/hAT-Charlie	0.02	AluJb	0.02
LTR/ERV1	0.02	L2c	0.02
LTR/ERVL	0.01	AluSz	0.02
LINE/CR1	0.00	MIR	0.02
DNA/TcMar-Tigger	0.00	(AC)n	0.02
DNA/hAT-Tip100	0.00	MIRb	0.02
Satellite	0.00	AluSx1	0.02
snRNA	0.00	AluSq2	0.01
LTR/ERVK	0.00	AluJr	0.01
LTR	0.00	AluY	0.01
LINE/RTE-X	0.00	L2b	0.01

Ontology	Term	FDR Q-val
GO Biological Process	chordate embryonic development	85.81
GO Biological Process	embryo development ending in birth or egg hatching	85.10
GO Biological Process	macromolecular complex assembly	65.66
GO Biological Process	in utero embryonic development	15.27
GO Biological Process	mitotic cell cycle checkpoint	3.55
GO Biological Process	nuclear-transcribed mRNA catabolic process, nonsense-mediated decay	3.23
GO Biological Process	mitochondrial genome maintenance	1.76

Supplementary Figure 296: Properties and genomic distribution of motifs identified for the SP1 transcription factor in MCF-7 (accession ENCSR729LGA).

TF-MoDisCO pattern_2 n=148, CWM

pattern_2, n=148; subpattern_0, ns=31

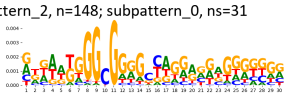

pattern_2, n=148; subpattern_1, ns=30

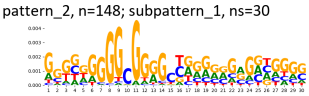

pattern_2, n=148; subpattern_2, ns=28

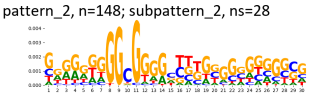

pattern_2, n=148; subpattern_3, ns=27

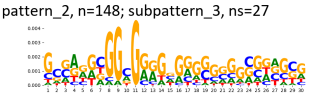

pattern_2, n=148; subpattern_4, ns=25

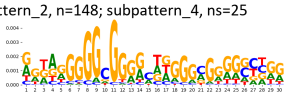

pattern_2, n=148; subpattern_5, ns=7

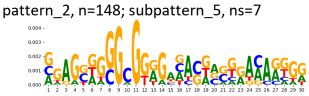

TF-MoDisCO pattern_2 n=148, PWM

pattern_2, n=148; subpattern_0, ns=31

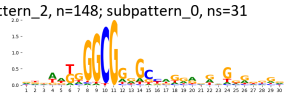

pattern_2, n=148; subpattern_1, ns=30

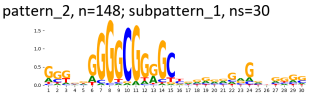

pattern_2, n=148; subpattern_2, ns=28

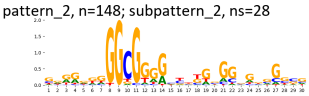

pattern_2, n=148; subpattern_3, ns=27

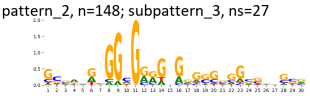

pattern_2, n=148; subpattern_4, ns=25

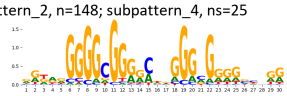

pattern_2, n=148; subpattern_5, ns=7

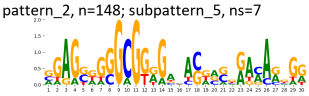

TF-MoDisCO pattern_3 n=138, CWM

pattern_3, n=138; subpattern_0, ns=42

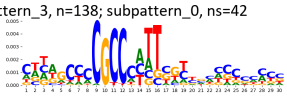

pattern_3, n=138; subpattern_1, ns=38

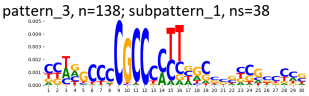

pattern_3, n=138; subpattern_2, ns=25

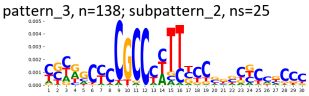

pattern_3, n=138; subpattern_3, ns=17

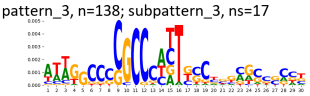

pattern_3, n=138; subpattern_4, ns=16

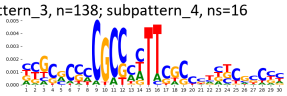

TF-MoDisCO pattern_3 n=138, PWM

pattern_3, n=138; subpattern_0, ns=42

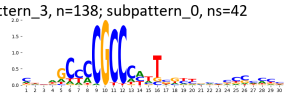

pattern_3, n=138; subpattern_1, ns=38

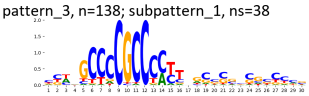

pattern_3, n=138; subpattern_2, ns=25

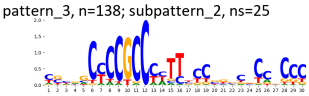

pattern_3, n=138; subpattern_3, ns=17

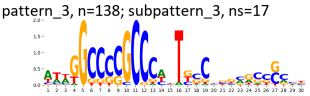

pattern_3, n=138; subpattern_4, ns=16

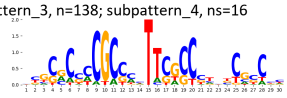

Supplementary Figure 297: TF-MoDisCO subpatterns for the SP1 transcription factor in MCF-7 (accession ENCSR729LGA).

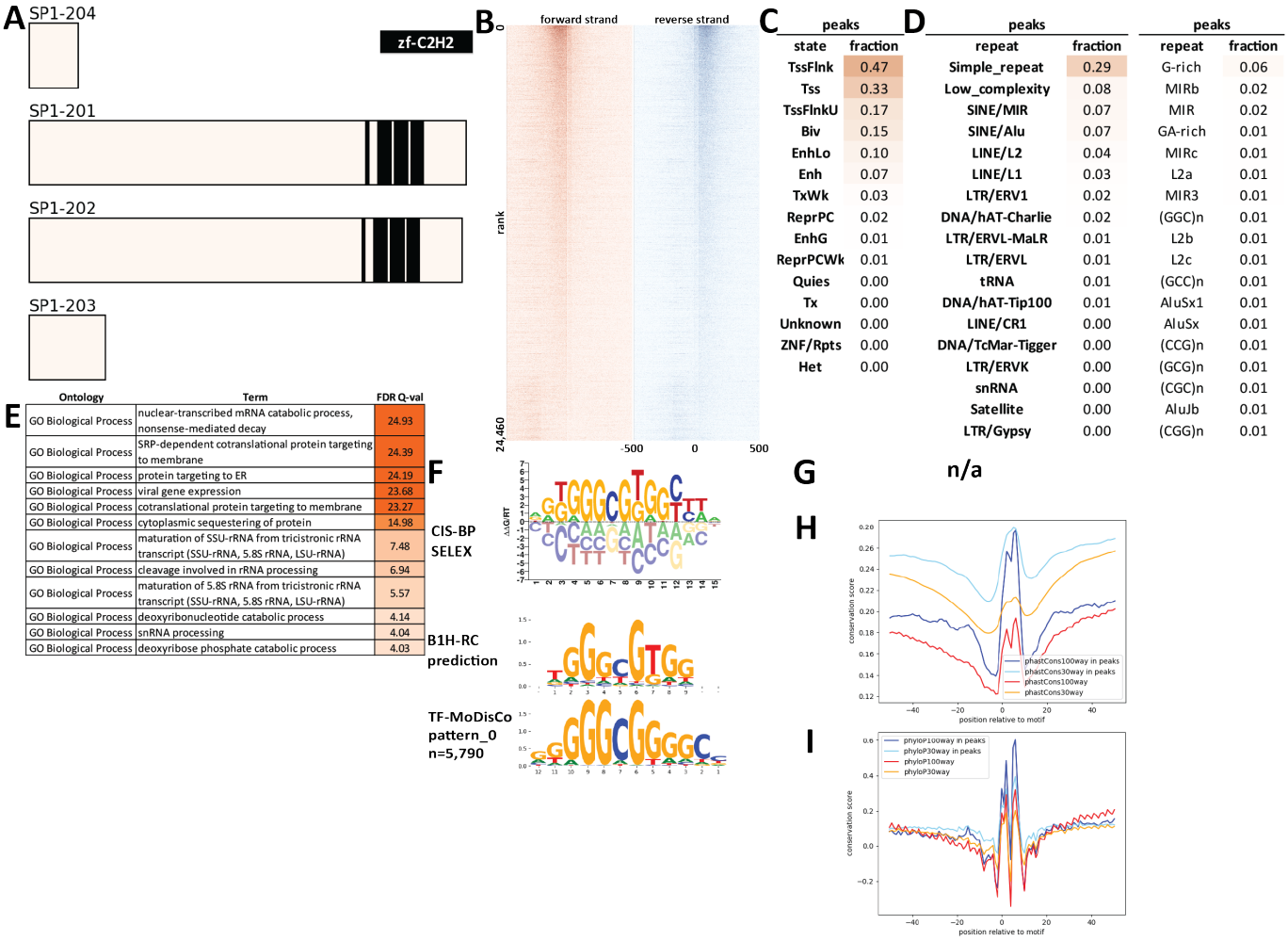

Supplementary Figure 298: Properties and genomic distribution of motifs identified for the SP1 transcription factor in WTC11 (accession ENCSR583CGO).

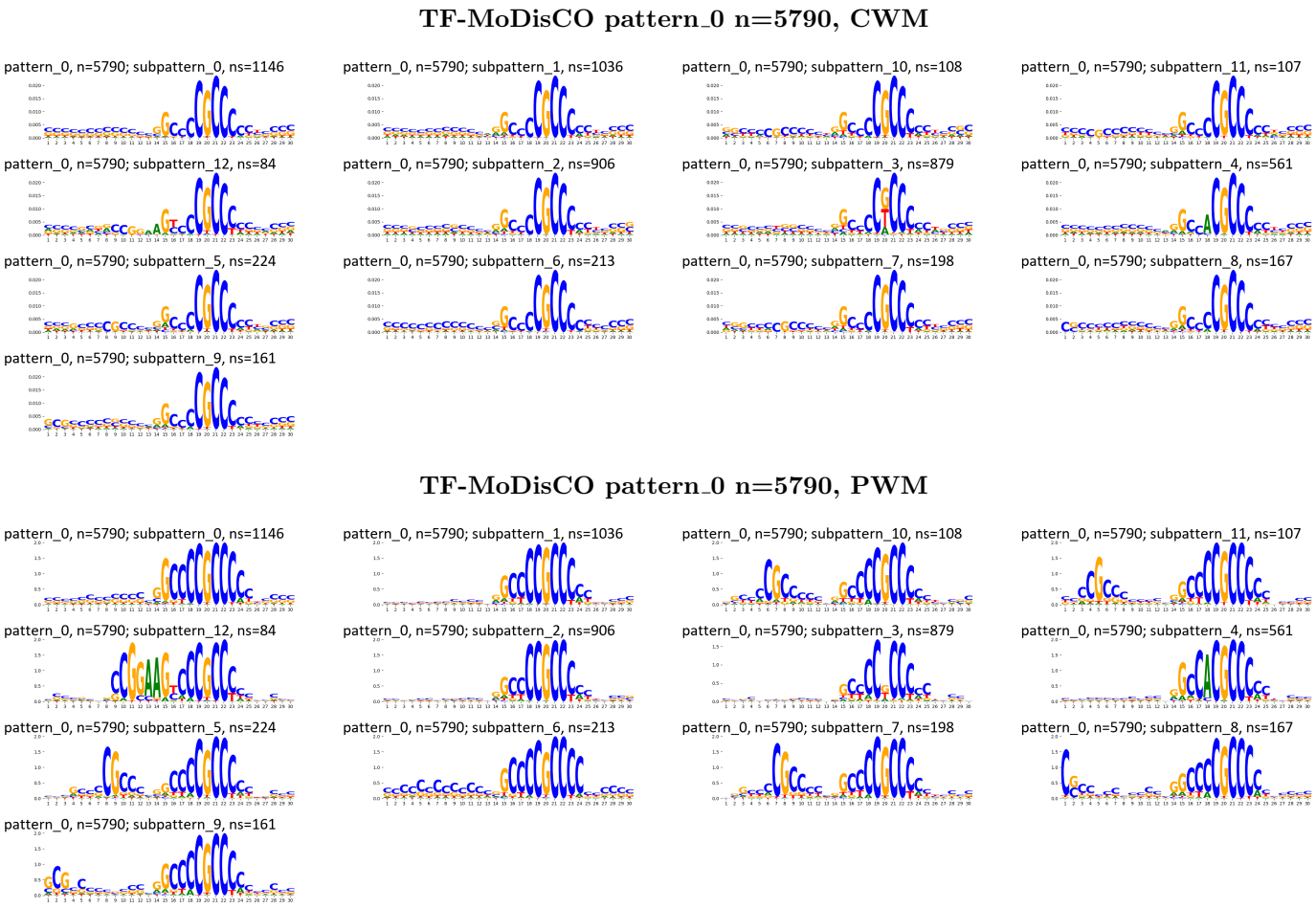

Supplementary Figure 299: TF-MoDisCO subpatterns for the SP1 transcription factor in WTC11 (accession ENCSR583CGO).

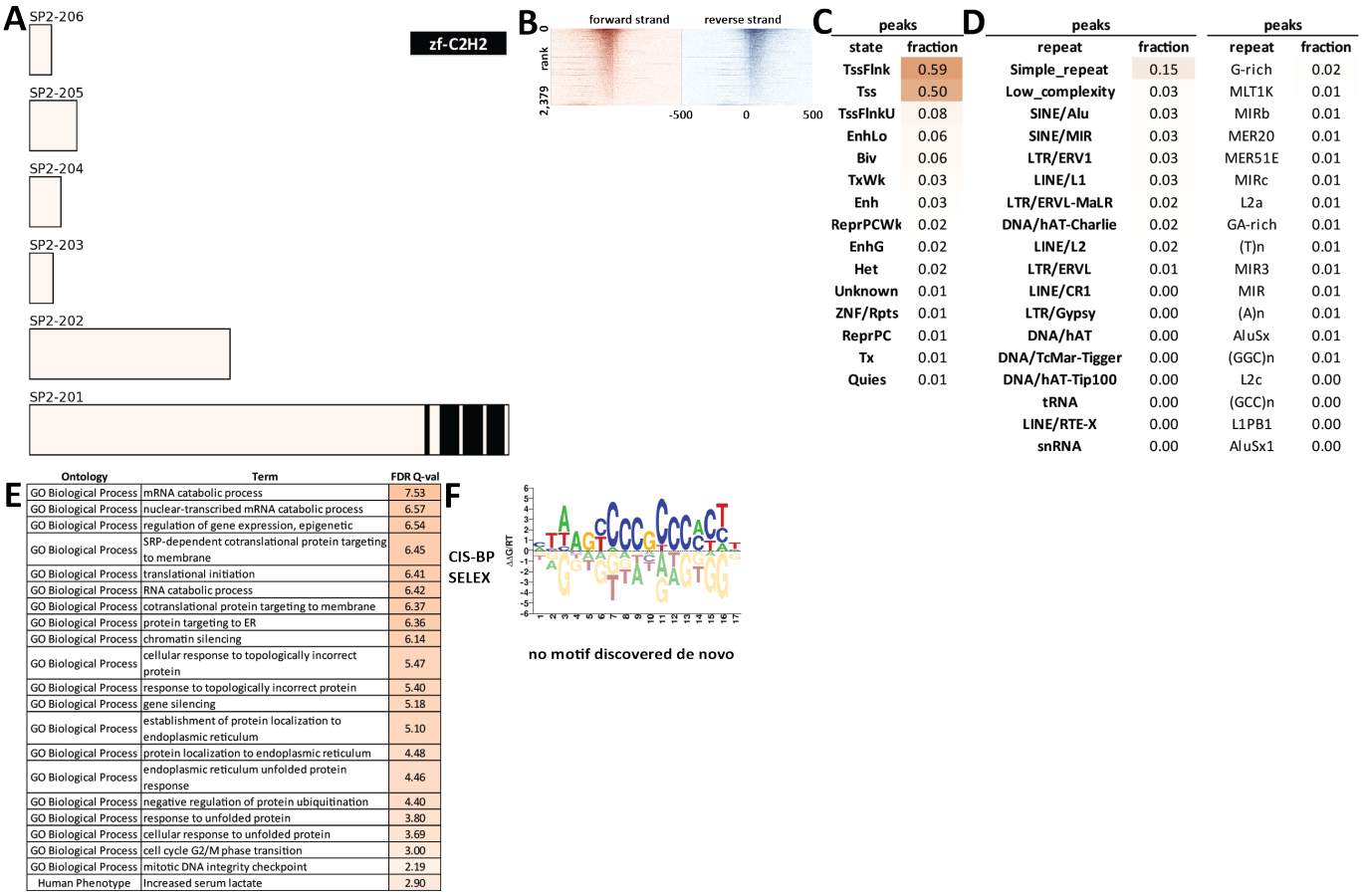

C

peaks	
state	fraction
TssFlnk	0.59
Tss	0.50
TssFlnkU	0.08
EnhLo	0.06
Biv	0.06
TxWk	0.03
Enh	0.03
ReprPCWk	0.02
EnhG	0.02
Het	0.02
Unknown	0.01
ZNF/Rpts	0.01
ReprPC	0.01
Tx	0.01
Quies	0.01

D

peaks		peaks	
repeat	fraction	repeat	fraction
Simple_repeat	0.15	G-rich	0.02
Low_complexity	0.03	MLT1K	0.01
SINE/Alu	0.03	MIRb	0.01
SINE/MIR	0.03	MER20	0.01
LTR/ERV1	0.03	MER51E	0.01
LINE/L1	0.03	MIRc	0.01
LTR/ERVL-MaLR	0.02	L2a	0.01
DNA/hAT-Charlie	0.02	GA-rich	0.01
LINE/L2	0.02	(T)n	0.01
LTR/ERVL	0.01	MIR3	0.01
LINE/CR1	0.00	MIR	0.01
LTR/Gypsy	0.00	(A)n	0.01
DNA/hAT	0.00	AluSx	0.01
DNA/TcMar-Tigger	0.00	(GGC)n	0.01
DNA/hAT-Tip100	0.00	L2c	0.00
tRNA	0.00	(GCC)n	0.00
LINE/RTE-X	0.00	L1PB1	0.00
snRNA	0.00	AluSx1	0.00

E

Ontology	Term	FDR Q-val
GO Biological Process	mRNA catabolic process	7.53
GO Biological Process	nuclear-transcribed mRNA catabolic process	6.57
GO Biological Process	regulation of gene expression, epigenetic	6.54
GO Biological Process	SRP-dependent cotranslational protein targeting to membrane	6.45
GO Biological Process	translational initiation	6.41
GO Biological Process	RNA catabolic process	6.42
GO Biological Process	cotranslational protein targeting to membrane	6.37
GO Biological Process	protein targeting to ER	6.36
GO Biological Process	chromatin silencing	6.14
GO Biological Process	cellular response to topologically incorrect protein	5.47
GO Biological Process	response to topologically incorrect protein	5.40
GO Biological Process	gene silencing	5.18
GO Biological Process	establishment of protein localization to endoplasmic reticulum	5.10
GO Biological Process	protein localization to endoplasmic reticulum	4.48
GO Biological Process	endoplasmic reticulum unfolded protein response	4.46
GO Biological Process	negative regulation of protein ubiquitination	4.40
GO Biological Process	response to unfolded protein	3.80
GO Biological Process	cellular response to unfolded protein	3.69
GO Biological Process	cell cycle G2/M phase transition	3.00
GO Biological Process	mitotic DNA integrity checkpoint	2.19
Human Phenotype	Increased serum lactate	2.90

Supplementary Figure 300: Properties and genomic distribution of motifs identified for the SP2 transcription factor in H1 (accession ENCSR000BQG).

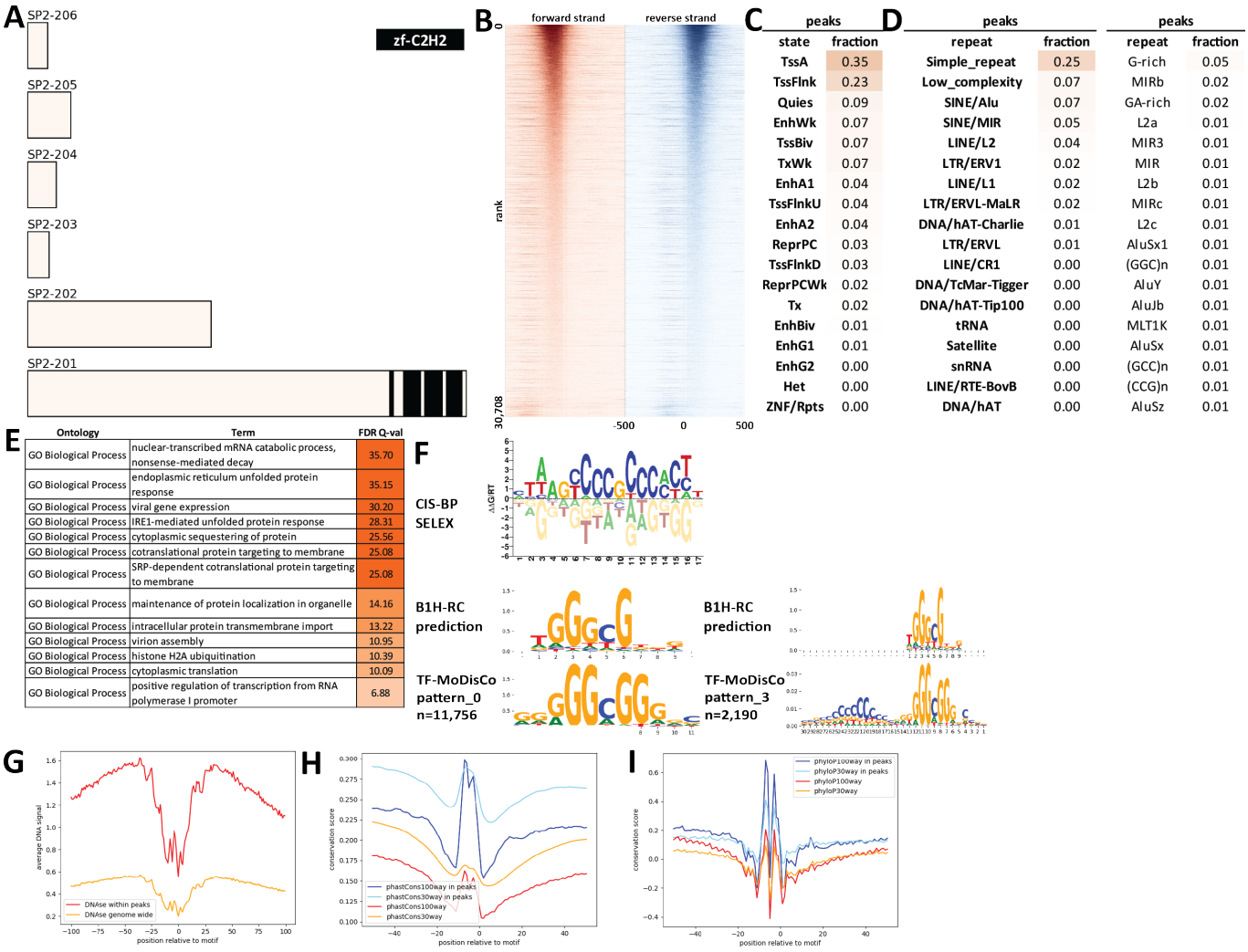

Supplementary Figure 301: Properties and genomic distribution of motifs identified for the SP2 transcription factor in HEK293 (accession ENCSR807LQP).

TF-MoDisCO pattern_0 n=11756, CWM

pattern_0, n=11756; subpattern_0, ns=2850

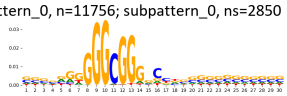

pattern_0, n=11756; subpattern_1, ns=2005

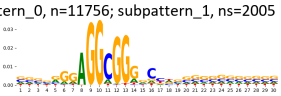

pattern_0, n=11756; subpattern_10, ns=399

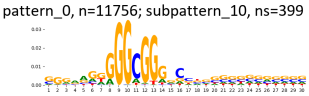

pattern_0, n=11756; subpattern_11, ns=278

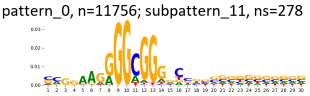

pattern_0, n=11756; subpattern_12, ns=253

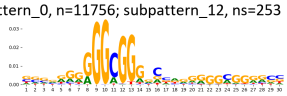

pattern_0, n=11756; subpattern_13, ns=203

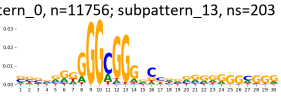

pattern_0, n=11756; subpattern_14, ns=164

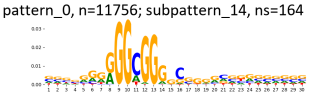

pattern_0, n=11756; subpattern_15, ns=62

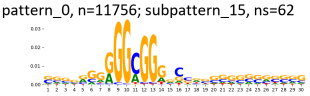

pattern_0, n=11756; subpattern_16, ns=53

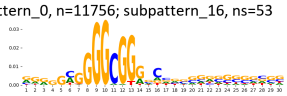

pattern_0, n=11756; subpattern_2, ns=1625

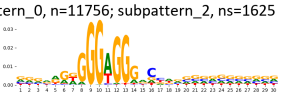

pattern_0, n=11756; subpattern_3, ns=862

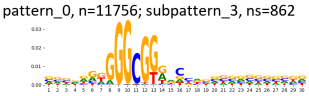

pattern_0, n=11756; subpattern_4, ns=659

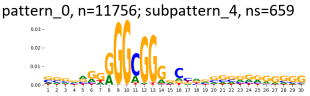

pattern_0, n=11756; subpattern_5, ns=561

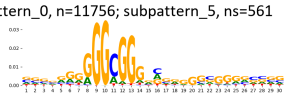

pattern_0, n=11756; subpattern_6, ns=484

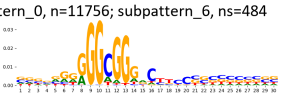

pattern_0, n=11756; subpattern_7, ns=471

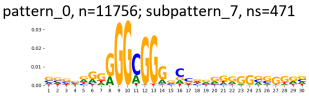

pattern_0, n=11756; subpattern_8, ns=424

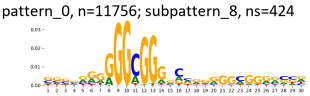

pattern_0, n=11756; subpattern_9, ns=403

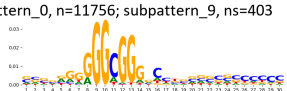

TF-MoDisCO pattern_0 n=11756, PWM

pattern_0, n=11756; subpattern_0, ns=2850

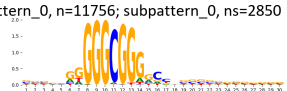

pattern_0, n=11756; subpattern_1, ns=2005

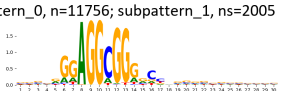

pattern_0, n=11756; subpattern_10, ns=399

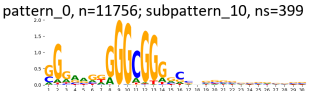

pattern_0, n=11756; subpattern_11, ns=278

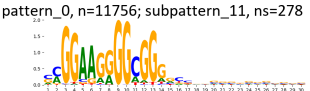

pattern_0, n=11756; subpattern_12, ns=253

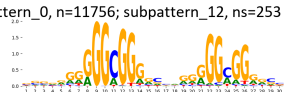

pattern_0, n=11756; subpattern_13, ns=203

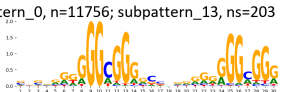

pattern_0, n=11756; subpattern_14, ns=164



pattern_0, n=11756; subpattern_15, ns=62

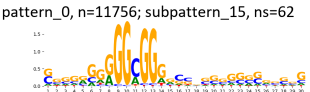

pattern_0, n=11756; subpattern_16, ns=53

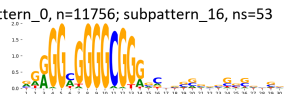

pattern_0, n=11756; subpattern_2, ns=1625

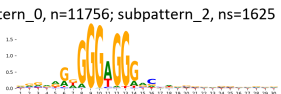

pattern_0, n=11756; subpattern_3, ns=862

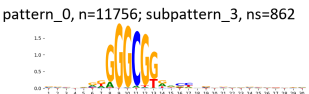

pattern_0, n=11756; subpattern_4, ns=659



pattern_0, n=11756; subpattern_5, ns=561

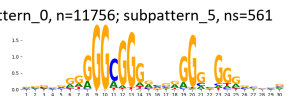

pattern_0, n=11756; subpattern_6, ns=484

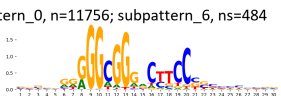

pattern_0, n=11756; subpattern_7, ns=471

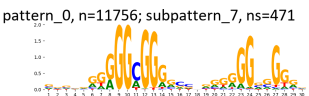

pattern_0, n=11756; subpattern_8, ns=424

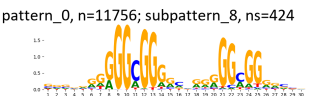

pattern_0, n=11756; subpattern_9, ns=403

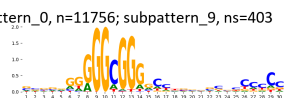

TF-MoDisCO pattern_3 n=2190, CWM

pattern_3, n=2190; subpattern_0, ns=469

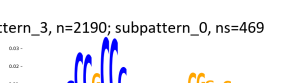

pattern_3, n=2190; subpattern_1, ns=364

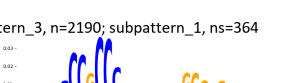

pattern_3, n=2190; subpattern_2, ns=349

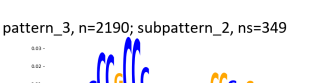

pattern_3, n=2190; subpattern_3, ns=233

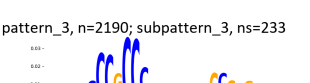

pattern_3, n=2190; subpattern_4, ns=206

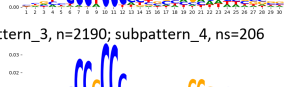

pattern_3, n=2190; subpattern_5, ns=175

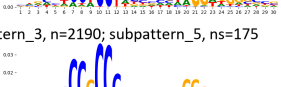

pattern_3, n=2190; subpattern_6, ns=170

pattern_3, n=2190; subpattern_7, ns=123

pattern_3, n=2190; subpattern_8, ns=101

TF-MoDisCO pattern_3 n=2190, PWM

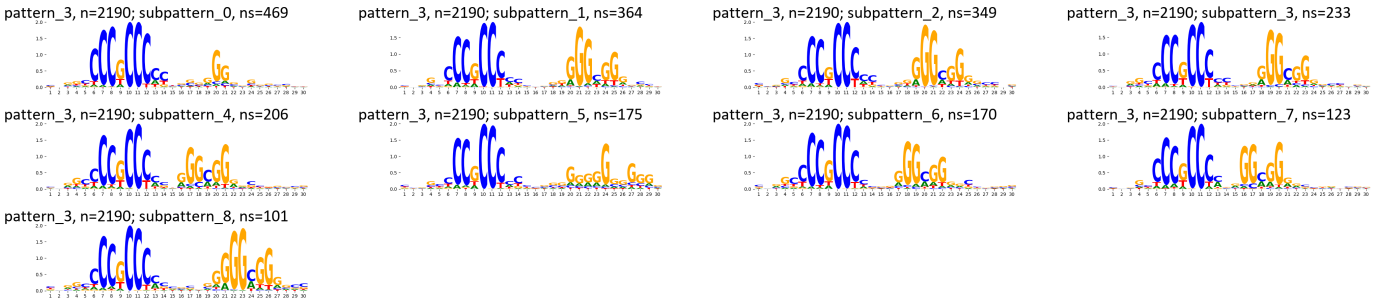

Supplementary Figure 302: TF-MoDisCO subpatterns for the SP2 transcription factor in HEK293 (accession ENCSR807LQP).

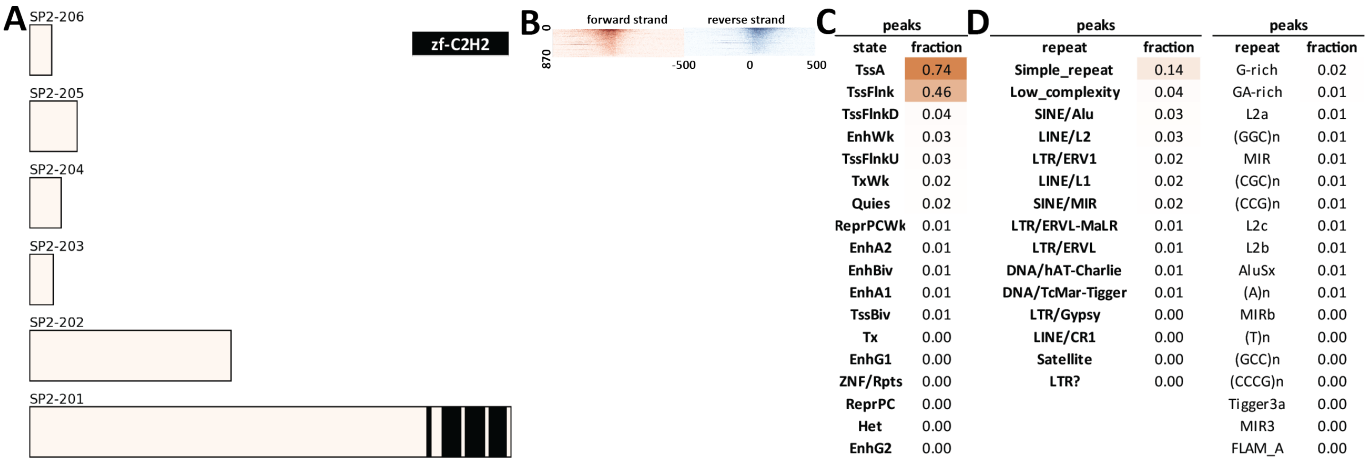

C

peaks	
state	fraction
TssA	0.74
TssFlnk	0.46
TssFlnkD	0.04
EnhWk	0.03
TssFlnkU	0.03
TxWk	0.02
Quies	0.02
ReprPCWk	0.01
EnhA2	0.01
EnhBiv	0.01
EnhA1	0.01
TssBiv	0.01
Tx	0.00
EnhG1	0.00
ZNF/Rpts	0.00
ReprPC	0.00
Het	0.00
EnhG2	0.00

D

peaks		peaks	
repeat	fraction	repeat	fraction
Simple_repeat	0.14	G-rich	0.02
Low_complexity	0.04	GA-rich	0.01
SINE/Alu	0.03	L2a	0.01
LINE/L2	0.03	(GGC)n	0.01
LTR/ERV1	0.02	MIR	0.01
LINE/L1	0.02	(CGC)n	0.01
SINE/MIR	0.02	(CCG)n	0.01
LTR/ERVL-MaLR	0.01	L2c	0.01
LTR/ERVL	0.01	L2b	0.01
DNA/hAT-Charlie	0.01	AluSx	0.01
DNA/TcMar-Tigger	0.01	(A)n	0.01
LTR/Gypsy	0.00	MIRb	0.00
LINE/CR1	0.00	(T)n	0.00
Satellite	0.00	(GCC)n	0.00
LTR?	0.00	(CCCG)n	0.00
		Tigger3a	0.00
		MIR3	0.00
		FLAM_A	0.00

E

Ontology	Term	FDR Q-val
GO Biological Process	mRNA metabolic process	5.34
GO Biological Process	RNA splicing, via transesterification reactions	3.89
GO Biological Process	ncRNA metabolic process	3.79
GO Biological Process	RNA splicing	3.25
GO Biological Process	mRNA splicing, via spliceosome	3.24
GO Biological Process	ribonucleoprotein complex biogenesis	3.16
GO Biological Process	mRNA catabolic process	3.15
GO Biological Process	RNA catabolic process	2.77
GO Biological Process	negative regulation of protein ubiquitination	2.77
GO Biological Process	negative regulation of protein modification by small protein conjugation or removal	2.02
GO Biological Process	regulation of telomerase RNA localization to Cajal body	1.65
GO Biological Process	ribonucleoprotein complex assembly	1.49
GO Biological Process	ribonucleoprotein complex subunit organization	1.31

F

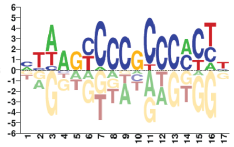

no motif discovered de novo

Supplementary Figure 303: Properties and genomic distribution of motifs identified for the SP2 transcription factor in HepG2 (accession ENCSR000BOU).

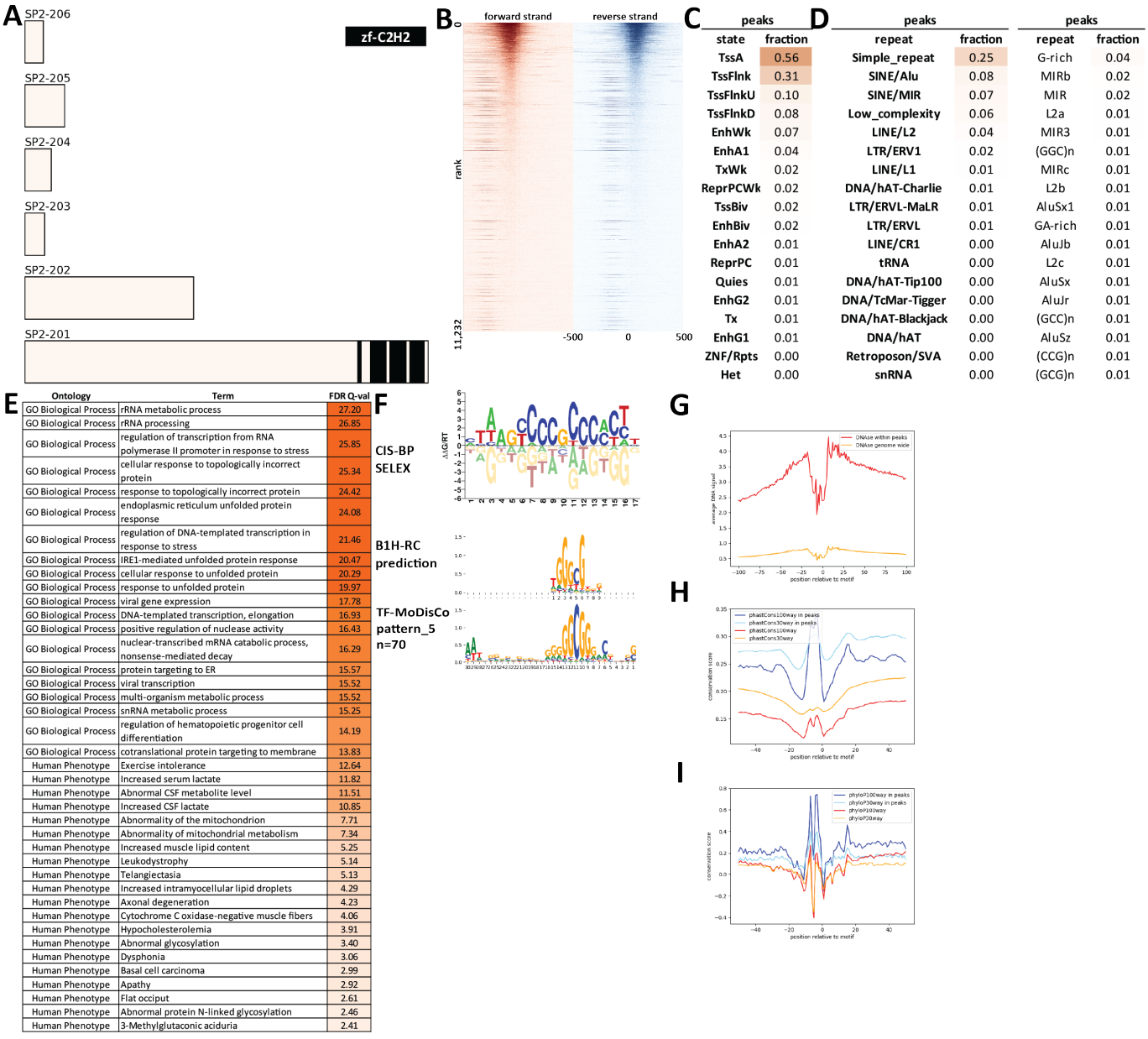

C	peaks	
	state	fraction
	TssA	0.56
	TssFlnk	0.31
	TssFlnkU	0.10
	TssFlnkD	0.08
	EnhWk	0.07
	EnhA1	0.04
	TxWk	0.02
	ReprPCWk	0.02
	TssBiv	0.02
	EnhBiv	0.02
	EnhA2	0.01
	ReprPC	0.01
	Quies	0.01
	EnhG2	0.01
	Tx	0.01
	EnhG1	0.01
	ZNF/Rpts	0.00
	Het	0.00

D	peaks		peaks	
	repeat	fraction	repeat	fraction
	Simple_repeat	0.25	G-rich	0.04
	SINE/Alu	0.08	MIRb	0.02
	SINE/MIR	0.07	MIR	0.02
	Low_complexity	0.06	L2a	0.01
	LINE/L2	0.04	MIR3	0.01
	LTR/ERV1	0.02	(GGC)n	0.01
	LINE/L1	0.01	MIRc	0.01
	DNA/hAT-Charlie	0.01	L2b	0.01
	LTR/ERVL-MaLR	0.01	AluSx1	0.01
	LTR/ERVL	0.01	GA-rich	0.01
	LINE/CR1	0.00	AluJb	0.01
	tRNA	0.00	L2c	0.01
	DNA/hAT-Tip100	0.00	AluSx	0.01
	DNA/TcMar-Tigger	0.00	AluJr	0.01
	DNA/hAT-Blackjack	0.00	(GCC)n	0.01
	DNA/hAT	0.00	AluSz	0.01
	Retroposon/SVA	0.00	(CCG)n	0.01
	snRNA	0.00	(GCG)n	0.01

E	Ontology	Term	FDR Q-val
	GO Biological Process	rRNA metabolic process	27.20
	GO Biological Process	rRNA processing	26.85
	GO Biological Process	regulation of transcription from RNA polymerase II promoter in response to stress	25.85
	GO Biological Process	cellular response to topologically incorrect protein	25.34
	GO Biological Process	response to topologically incorrect protein	24.42
	GO Biological Process	endoplasmic reticulum unfolded protein response	24.08
	GO Biological Process	regulation of DNA-templated transcription in response to stress	21.46
	GO Biological Process	IRE1-mediated unfolded protein response	20.47
	GO Biological Process	cellular response to unfolded protein	20.29
	GO Biological Process	response to unfolded protein	19.97
	GO Biological Process	viral gene expression	17.78
	GO Biological Process	DNA-templated transcription, elongation	16.93
	GO Biological Process	positive regulation of nuclease activity	16.43
	GO Biological Process	nuclear-transcribed mRNA catabolic process, nonsense-mediated decay	16.29
	GO Biological Process	protein targeting to ER	15.57
	GO Biological Process	viral transcription	15.52
	GO Biological Process	multi-organism metabolic process	15.52
	GO Biological Process	snRNA metabolic process	15.25
	GO Biological Process	regulation of hematopoietic progenitor cell differentiation	14.19
	GO Biological Process	cotranslational protein targeting to membrane	13.83
	Human Phenotype	Exercise intolerance	12.64
	Human Phenotype	Increased serum lactate	11.82
	Human Phenotype	Abnormal CSF metabolite level	11.51
	Human Phenotype	Increased CSF lactate	10.85
	Human Phenotype	Abnormality of the mitochondrion	7.71
	Human Phenotype	Abnormality of mitochondrial metabolism	7.34
	Human Phenotype	Increased muscle lipid content	5.25
	Human Phenotype	Leukodystrophy	5.14
	Human Phenotype	Telangiectasia	5.13
	Human Phenotype	Increased intramyocellular lipid droplets	4.29
	Human Phenotype	Axonal degeneration	4.23
	Human Phenotype	Cytochrome C oxidase-negative muscle fibers	4.06
	Human Phenotype	Hypocholesterolemia	3.91
	Human Phenotype	Abnormal glycosylation	3.40
	Human Phenotype	Dysphonia	3.06
	Human Phenotype	Basal cell carcinoma	2.99
	Human Phenotype	Apathy	2.92
	Human Phenotype	Flat occiput	2.61
	Human Phenotype	Abnormal protein N-linked glycosylation	2.46
	Human Phenotype	3-Methylglutaconic aciduria	2.41

Supplementary Figure 304: Properties and genomic distribution of motifs identified for the SP2 transcription factor in HepG2 (accession ENCSR946RZN).

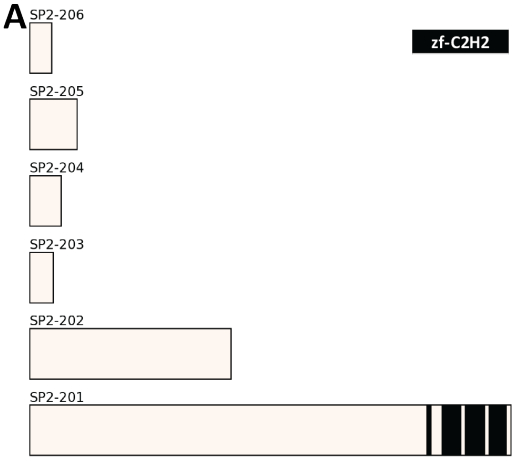

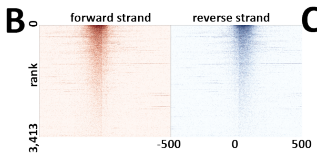

C

peaks	
state	fraction
TssA	0.52
TssFlnk	0.27
TssFlnkU	0.15
TssFlnkD	0.11
EnhWk	0.08
ReprPCWk	0.03
TxWk	0.03
Quies	0.02
EnhA1	0.02
EnhA2	0.02
ReprPC	0.02
EnhG1	0.01
Tx	0.01
EnhBiv	0.01
EnhG2	0.01
TssBiv	0.01
Het	0.00
ZNF/Rpts	0.00

D

peaks		peaks	
repeat	fraction	repeat	fraction
Simple_repeat	0.13	G-rich	0.03
Low_complexity	0.03	MLT1K	0.01
SINE/Alu	0.02	(GGC)n	0.01
LTR/ERV1	0.02	MER51E	0.01
LTR/ERVL-MaLR	0.02	AluJb	0.01
SINE/MIR	0.02	MIRc	0.00
LINE/L2	0.01	MIRb	0.00
LINE/L1	0.01	L2a	0.00
DNA/hAT-Charlie	0.01	(GCC)n	0.00
LTR/ERVL	0.01	(GCG)n	0.00
LINE/CR1	0.00	(CGC)n	0.00
DNA/hAT-Tip100	0.00	MIR3	0.00
snRNA	0.00	MIR	0.00
DNA/TcMar-Tigger	0.00	L2b	0.00
LTR/Gypsy	0.00	L2c	0.00
LTR/ERVK	0.00	GA-rich	0.00
LINE/RTE-BovB	0.00	(GGCGG)n	0.00
DNA/hAT-Blackjack	0.00	(CCG)n	0.00

E

Ontology	Term	FDR Q-val
GO Biological Process	protein folding	14.65
GO Biological Process	cellular response to topologically incorrect protein	10.67
GO Biological Process	response to topologically incorrect protein	10.14
GO Biological Process	ribosome biogenesis	9.28
GO Biological Process	rRNA metabolic process	8.78
GO Biological Process	protein transmembrane transport	8.22
GO Biological Process	rRNA processing	8.20
GO Biological Process	mitochondrial transport	8.17
GO Biological Process	viral gene expression	8.08
GO Biological Process	endoplasmic reticulum unfolded protein response	7.98
GO Biological Process	multi-organism metabolic process	7.82
GO Biological Process	translational initiation	7.53
GO Biological Process	viral transcription	7.13
GO Biological Process	cotranslational protein targeting to membrane	6.79
GO Biological Process	cellular response to unfolded protein	6.68
GO Biological Process	SRP-dependent cotranslational protein targeting to membrane	6.69
GO Biological Process	response to unfolded protein	6.64
GO Biological Process	mRNA catabolic process	6.29
GO Biological Process	protein targeting to ER	6.20
GO Biological Process	nuclear-transcribed mRNA catabolic process	5.60
Human Phenotype	Increased serum lactate	7.15
Human Phenotype	Lactic acidosis	4.08

F

CIS-BP
SELEX

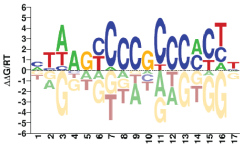

no motif discovered de novo

Supplementary Figure 305: Properties and genomic distribution of motifs identified for the SP2 transcription factor in K562 (accession ENCSR000BNL).

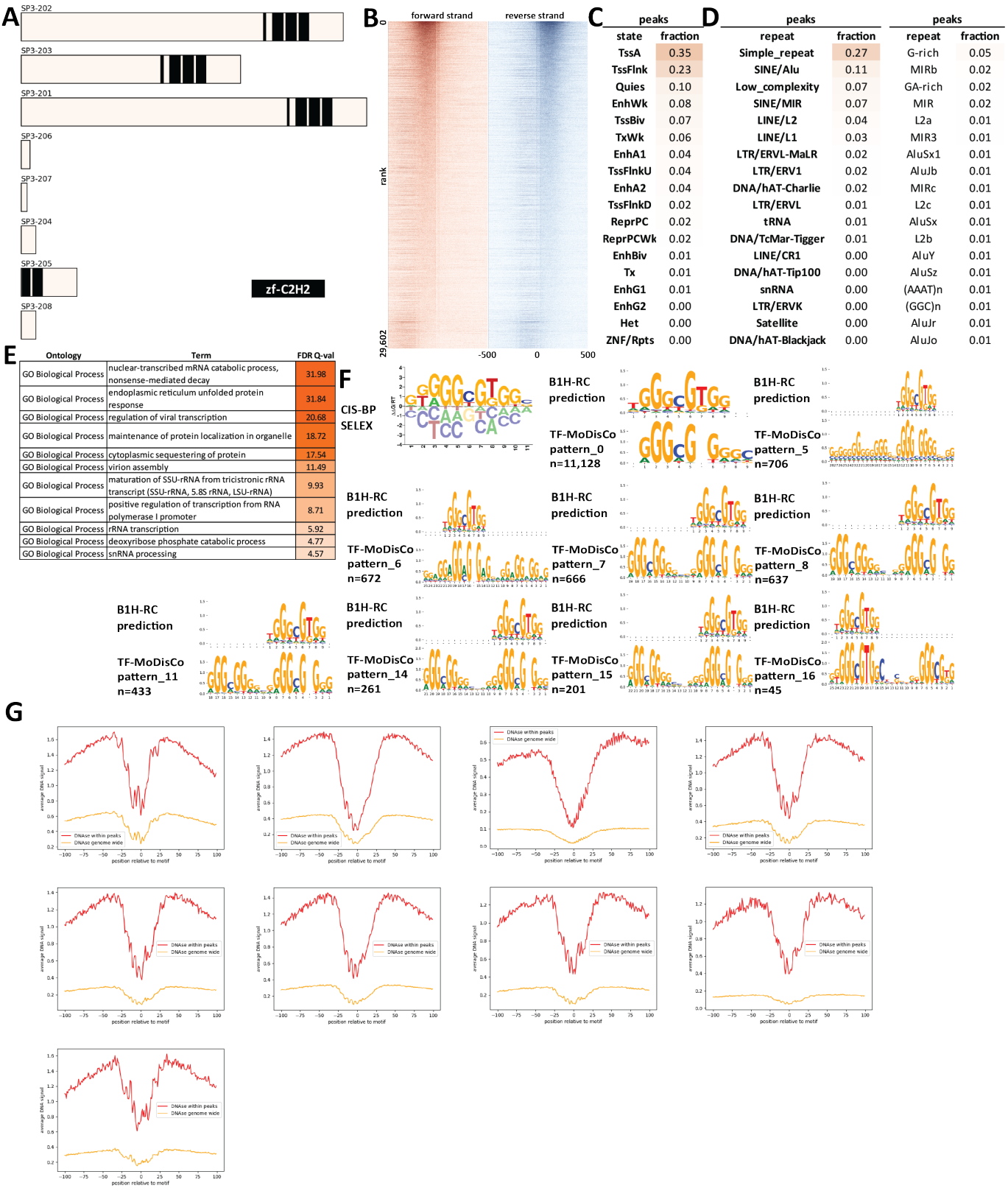
A
SP3-202
SP3-203
SP3-201
SP3-206
SP3-207
SP3-204
SP3-205
SP3-208
zf-C2H2
B
forward strand
reverse strand
rank
29,602
-500
0
500
C
peaks
state
fraction
TssA 0.35
TssFlnk 0.23
Quies 0.10
EnhWk 0.08
TssBiv 0.07
TxWk 0.06
EnhA1 0.04
TssFlnkU 0.04
EnhA2 0.04
TssFlnkD 0.02
ReprPC 0.02
ReprPCWk 0.02
EnhBiv 0.01
Tx 0.01
EnhG1 0.01
EnhG2 0.00
Het 0.00
ZNF/Rpts 0.00
D
peaks
repeat
fraction
Simple_repeat 0.27
SINE/Alu 0.11
Low_complexity 0.07
SINE/MIR 0.07
LINE/L2 0.04
LINE/L1 0.03
LTR/ERVL-MaLR 0.02
LTR/ERV1 0.02
DNA/hAT-Charlie 0.02
LTR/ERVL 0.01
tRNA 0.01
DNA/TcMar-Tigger 0.01
LINE/CR1 0.00
DNA/hAT-Tip100 0.00
snRNA 0.00
LTR/ERVK 0.00
Satellite 0.00
DNA/hAT-Blackjack 0.00
peaks
repeat
fraction
G-rich 0.05
MIRb 0.02
GA-rich 0.02
MIR 0.02
L2a 0.01
MIR3 0.01
AluSx1 0.01
AluJb 0.01
MIRc 0.01
L2c 0.01
AluSx 0.01
L2b 0.01
AluY 0.01
AluSz 0.01
(AAAT)n 0.01
(GGC)n 0.01
AluJr 0.01
AluJo 0.01
E
Ontology
Term
FDR Q-val
GO Biological Process nuclear-transcribed mRNA catabolic process, nonsense-mediated decay 31.98
GO Biological Process endoplasmic reticulum unfolded protein response 31.84
GO Biological Process regulation of viral transcription 20.68
GO Biological Process maintenance of protein localization in organelle 18.72
GO Biological Process cytoplasmic sequestering of protein 17.54
GO Biological Process virion assembly 11.49
GO Biological Process maturation of SSU-rRNA from tricistronic rRNA transcript (SSU-rRNA, 5.8S rRNA, LSU-rRNA) 9.93
GO Biological Process positive regulation of transcription from RNA polymerase I promoter 8.71
GO Biological Process rRNA transcription 5.92
GO Biological Process deoxyribose phosphate catabolic process 4.77
GO Biological Process snRNA processing 4.57
F
CIS-BP SELEX
B1H-RC prediction
TF-MoDisCo pattern_0 n=11,128
B1H-RC prediction
TF-MoDisCo pattern_5 n=706
B1H-RC prediction
TF-MoDisCo pattern_6 n=672
B1H-RC prediction
TF-MoDisCo pattern_7 n=666
B1H-RC prediction
TF-MoDisCo pattern_8 n=637
B1H-RC prediction
TF-MoDisCo pattern_11 n=433
B1H-RC prediction
TF-MoDisCo pattern_14 n=261
B1H-RC prediction
TF-MoDisCo pattern_15 n=201
B1H-RC prediction
TF-MoDisCo pattern_16 n=45
G
average DNA signal
DNAse within peaks
DNAse genome wide
position relative to motif

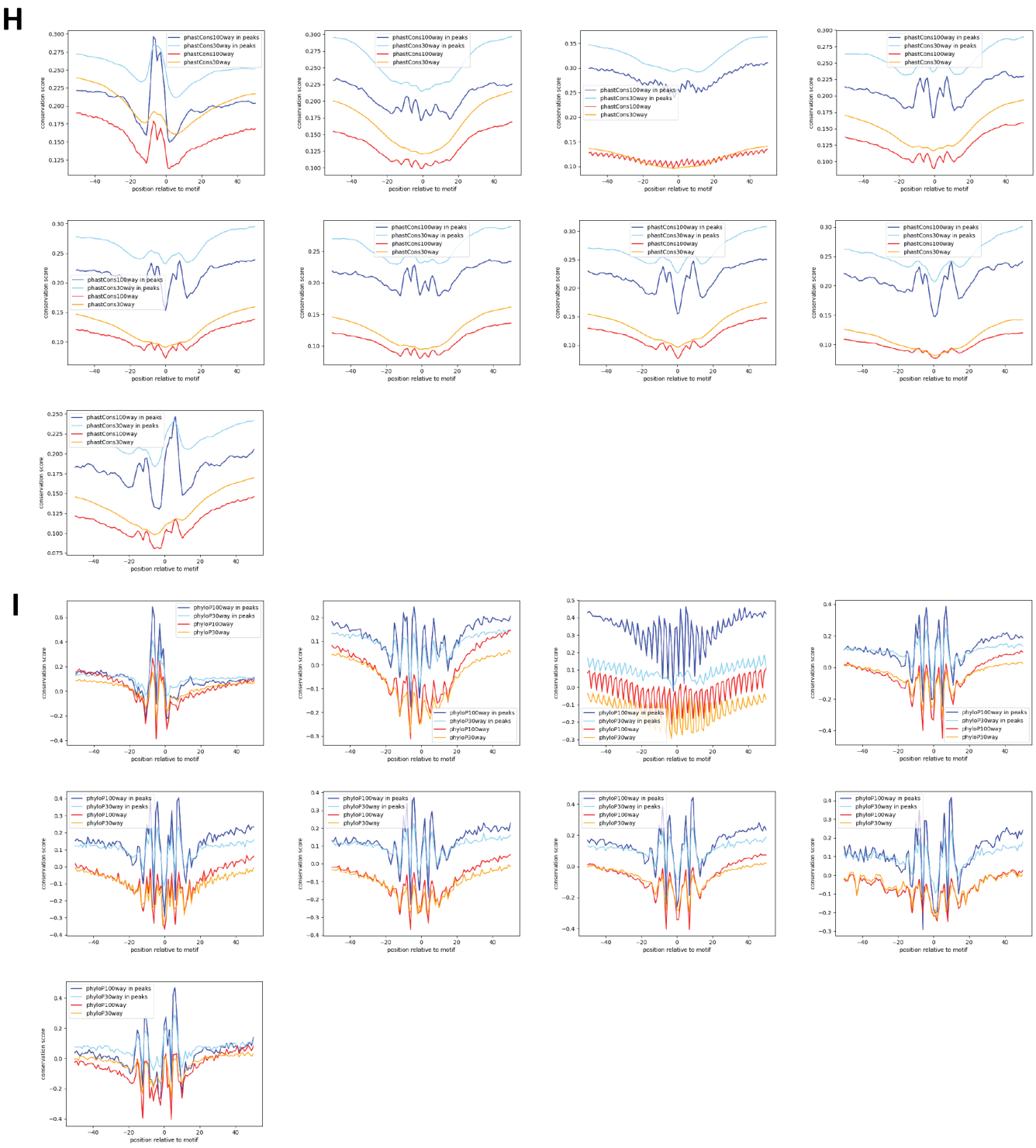

Supplementary Figure 306: Properties and genomic distribution of motifs identified for the SP3 transcription factor in HEK293 (accession ENCSR141PZA).

TF-MoDisCO pattern_0 n=11128, CWM

pattern_0, n=11128; subpattern_0, ns=2280

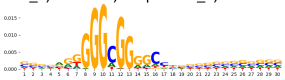

pattern_0, n=11128; subpattern_1, ns=2202

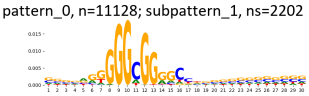

pattern_0, n=11128; subpattern_10, ns=353

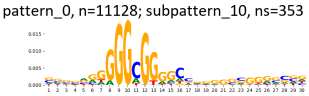

pattern_0, n=11128; subpattern_11, ns=245

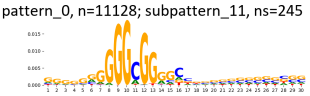

pattern_0, n=11128; subpattern_12, ns=242

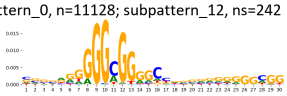

pattern_0, n=11128; subpattern_13, ns=207

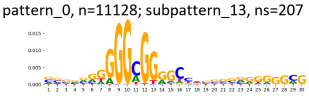

pattern_0, n=11128; subpattern_14, ns=47

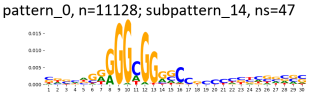

pattern_0, n=11128; subpattern_15, ns=2

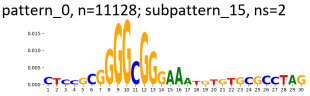

pattern_0, n=11128; subpattern_16, ns=2

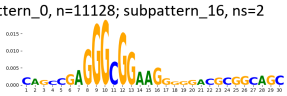

pattern_0, n=11128; subpattern_2, ns=1248

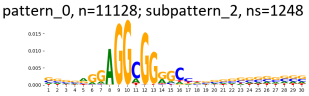

pattern_0, n=11128; subpattern_3, ns=969

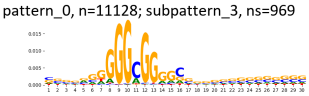

pattern_0, n=11128; subpattern_4, ns=835

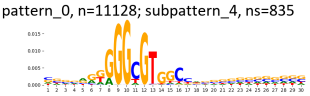

pattern_0, n=11128; subpattern_5, ns=567

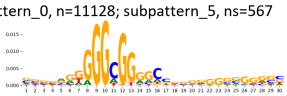

pattern_0, n=11128; subpattern_6, ns=532

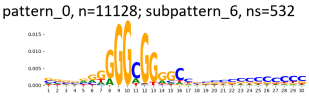

pattern_0, n=11128; subpattern_7, ns=514

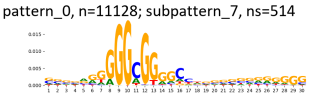

pattern_0, n=11128; subpattern_8, ns=460

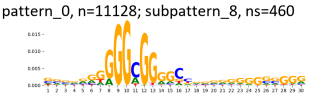

pattern_0, n=11128; subpattern_9, ns=423

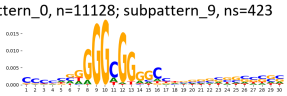

TF-MoDisCO pattern_0 n=11128, PWM

pattern_0, n=11128; subpattern_0, ns=2280

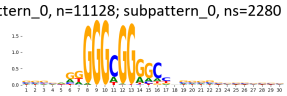

pattern_0, n=11128; subpattern_1, ns=2202

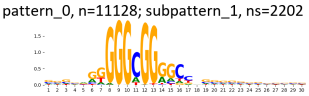

pattern_0, n=11128; subpattern_10, ns=353

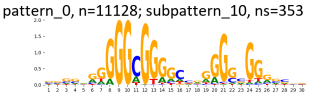

pattern_0, n=11128; subpattern_11, ns=245

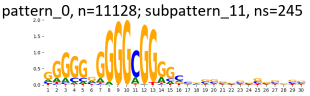

pattern_0, n=11128; subpattern_12, ns=242

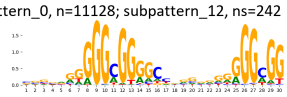

pattern_0, n=11128; subpattern_13, ns=207

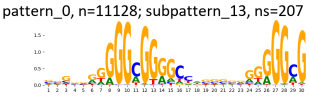

pattern_0, n=11128; subpattern_14, ns=47

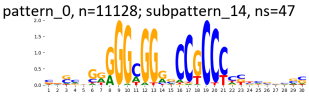

pattern_0, n=11128; subpattern_15, ns=2

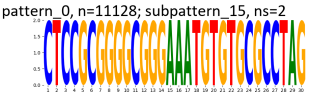

pattern_0, n=11128; subpattern_16, ns=2

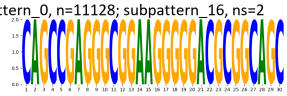

pattern_0, n=11128; subpattern_2, ns=1248

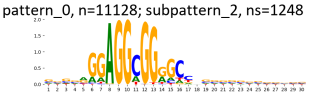

pattern_0, n=11128; subpattern_3, ns=969

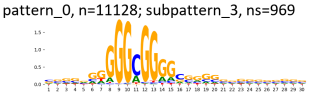

pattern_0, n=11128; subpattern_4, ns=835

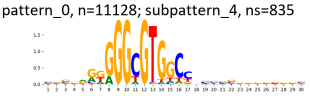

pattern_0, n=11128; subpattern_5, ns=567

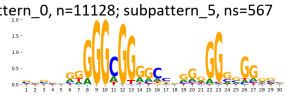

pattern_0, n=11128; subpattern_6, ns=532

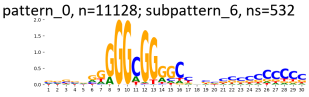

pattern_0, n=11128; subpattern_7, ns=514

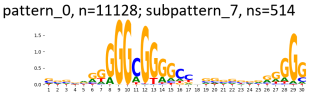

pattern_0, n=11128; subpattern_8, ns=460

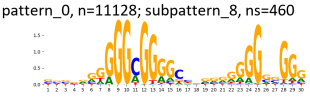

pattern_0, n=11128; subpattern_9, ns=423

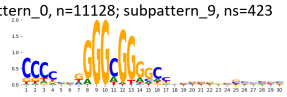

TF-MoDisCO pattern_11 n=433, CWM

pattern_11, n=433; subpattern_0, ns=130

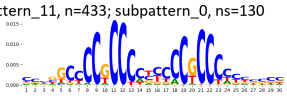

pattern_11, n=433; subpattern_1, ns=92

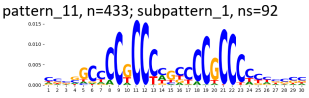

pattern_11, n=433; subpattern_2, ns=74

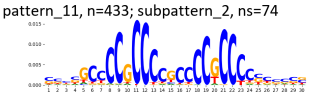

pattern_11, n=433; subpattern_3, ns=62

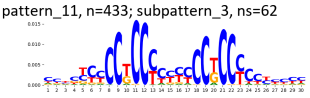

pattern_11, n=433; subpattern_4, ns=31

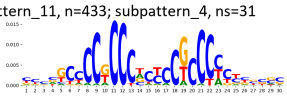

pattern_11, n=433; subpattern_5, ns=19

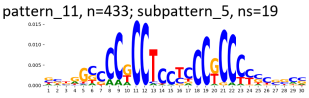

pattern_11, n=433; subpattern_6, ns=16

pattern_11, n=433; subpattern_7, ns=5

pattern_11, n=433; subpattern_8, ns=2

pattern_11, n=433; subpattern_9, ns=2

TF-MoDisCO pattern_11 n=433, PWM

pattern_11, n=433; subpattern_0, ns=130

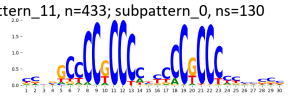

pattern_11, n=433; subpattern_1, ns=92

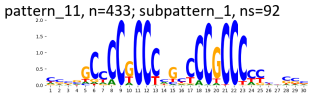

pattern_11, n=433; subpattern_2, ns=74

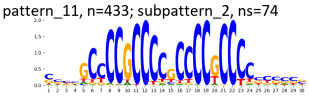

pattern_11, n=433; subpattern_3, ns=62

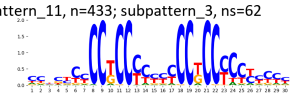

pattern_11, n=433; subpattern_4, ns=31

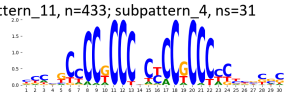

pattern_11, n=433; subpattern_5, ns=19

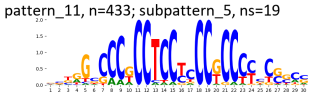

pattern_11, n=433; subpattern_6, ns=16

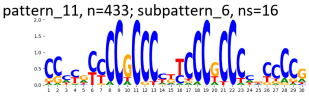

pattern_11, n=433; subpattern_7, ns=5

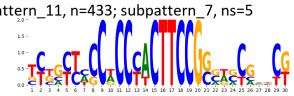

pattern_11, n=433; subpattern_8, ns=2

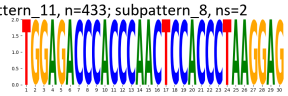

pattern_11, n=433; subpattern_9, ns=2

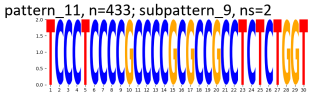

TF-MoDisCO pattern_14 n=261, CWM

pattern_14, n=261; subpattern_0, ns=72

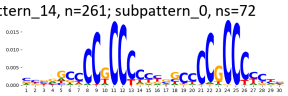

pattern_14, n=261; subpattern_1, ns=69

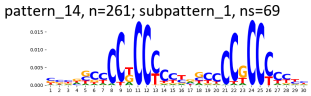

pattern_14, n=261; subpattern_2, ns=62

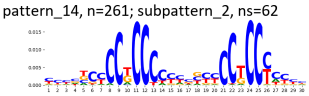

pattern_14, n=261; subpattern_3, ns=50

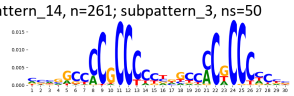

pattern_14, n=261; subpattern_4, ns=4

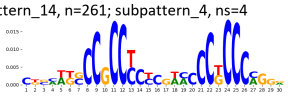

pattern_14, n=261; subpattern_5, ns=2

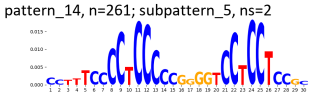

pattern_14, n=261; subpattern_6, ns=2

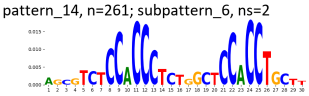

TF-MoDisCO pattern_14 n=261, PWM

pattern_14, n=261; subpattern_0, ns=72

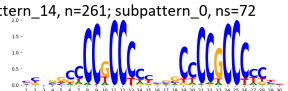

pattern_14, n=261; subpattern_1, ns=69

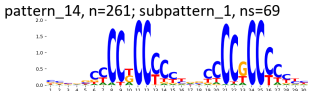

pattern_14, n=261; subpattern_2, ns=62

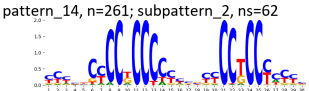

pattern_14, n=261; subpattern_3, ns=50

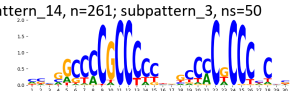

pattern_14, n=261; subpattern_4, ns=4

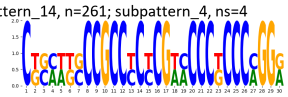

pattern_14, n=261; subpattern_5, ns=2

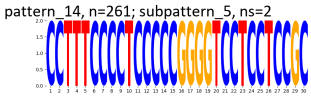

pattern_14, n=261; subpattern_6, ns=2

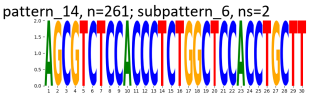

TF-MoDisCO pattern_15 n=201, CWM

pattern_15, n=201; subpattern_0, ns=47

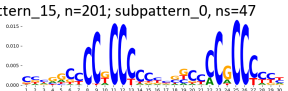

pattern_15, n=201; subpattern_1, ns=37

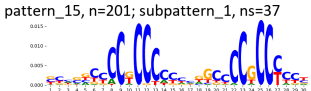

pattern_15, n=201; subpattern_2, ns=37

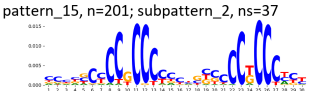

pattern_15, n=201; subpattern_3, ns=33

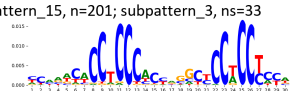

pattern_15, n=201; subpattern_4, ns=24

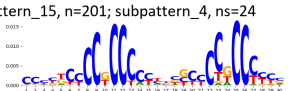

pattern_15, n=201; subpattern_5, ns=11

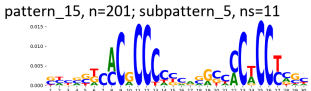

pattern_15, n=201; subpattern_6, ns=6

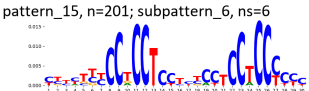

pattern_15, n=201; subpattern_7, ns=2

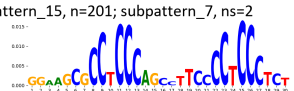

pattern_15, n=201; subpattern_8, ns=2

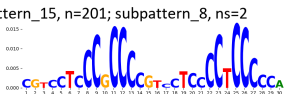

pattern_15, n=201; subpattern_9, ns=2

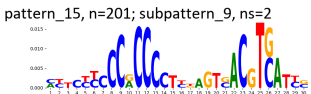

TF-MoDisCO pattern_15 n=201, PWM

pattern_15, n=201; subpattern_0, ns=47

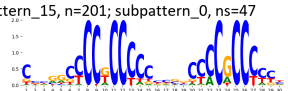

pattern_15, n=201; subpattern_1, ns=37

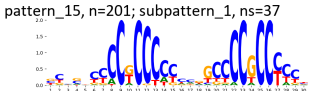

pattern_15, n=201; subpattern_2, ns=37

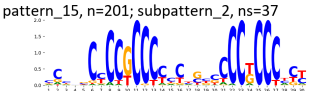

pattern_15, n=201; subpattern_3, ns=33

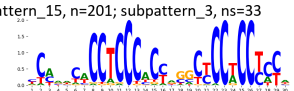

pattern_15, n=201; subpattern_4, ns=24

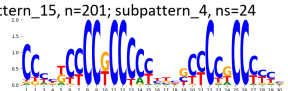

pattern_15, n=201; subpattern_5, ns=11

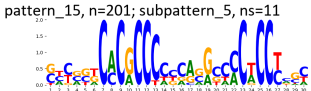

pattern_15, n=201; subpattern_6, ns=6

pattern_15, n=201; subpattern_7, ns=2

pattern_15, n=201; subpattern_8, ns=2

pattern_15, n=201; subpattern_9, ns=2

TF-MoDisCO pattern_16 n=45, CWM

pattern_16, n=45; subpattern_0, ns=45

TF-MoDisCO pattern_16 n=45, PWM

pattern_16, n=45; subpattern_0, ns=45

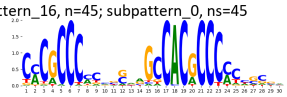

TF-MoDisCO pattern_5 n=706, CWM

pattern_5, n=706; subpattern_0, ns=252

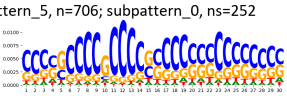

pattern_5, n=706; subpattern_1, ns=158

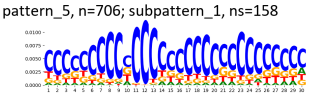

pattern_5, n=706; subpattern_2, ns=125

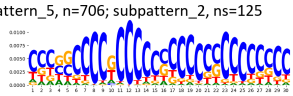

pattern_5, n=706; subpattern_3, ns=114

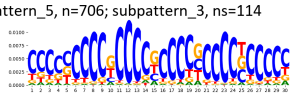

pattern_5, n=706; subpattern_4, ns=27

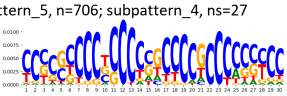

pattern_5, n=706; subpattern_5, ns=25

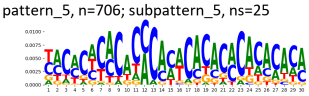

pattern_5, n=706; subpattern_6, ns=5

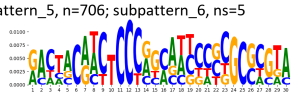

TF-MoDisCO pattern_5 n=706, PWM

pattern_5, n=706; subpattern_0, ns=252

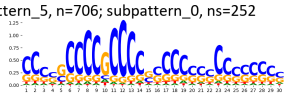

pattern_5, n=706; subpattern_1, ns=158

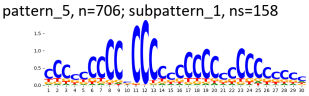

pattern_5, n=706; subpattern_2, ns=125

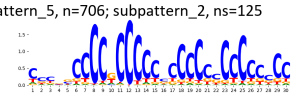

pattern_5, n=706; subpattern_3, ns=114

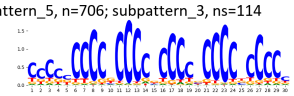

pattern_5, n=706; subpattern_4, ns=27

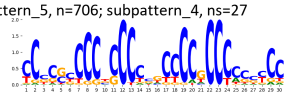

pattern_5, n=706; subpattern_5, ns=25

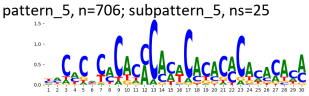

pattern_5, n=706; subpattern_6, ns=5

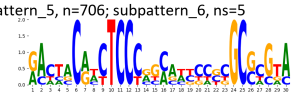

TF-MoDisCO pattern_6 n=672, CWM

pattern_6, n=672; subpattern_0, ns=194

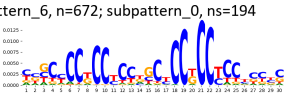

pattern_6, n=672; subpattern_1, ns=134

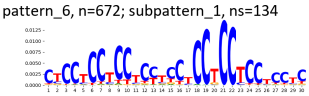

pattern_6, n=672; subpattern_2, ns=105

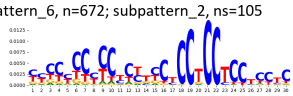

pattern_6, n=672; subpattern_3, ns=99

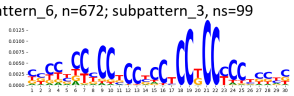

pattern_6, n=672; subpattern_4, ns=80

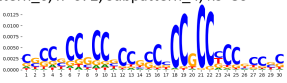

pattern_6, n=672; subpattern_5, ns=58

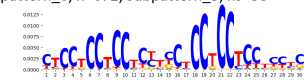

pattern_6, n=672; subpattern_6, ns=2

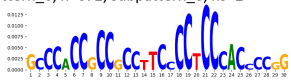

TF-MoDisCO pattern_6 n=672, PWM

pattern_6, n=672; subpattern_0, ns=194

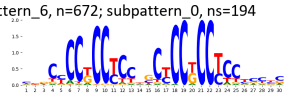

pattern_6, n=672; subpattern_1, ns=134

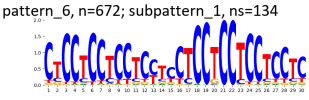

pattern_6, n=672; subpattern_2, ns=105

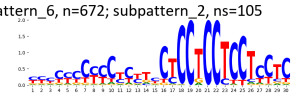

pattern_6, n=672; subpattern_3, ns=99

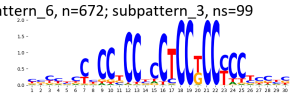

pattern_6, n=672; subpattern_4, ns=80

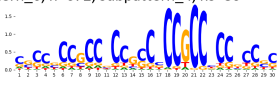

pattern_6, n=672; subpattern_5, ns=58

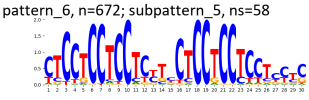

pattern_6, n=672; subpattern_6, ns=2

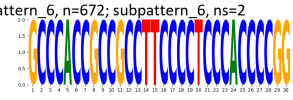

TF-MoDisCO pattern_7 n=666, CWM

pattern_7, n=666; subpattern_0, ns=156

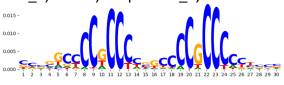

pattern_7, n=666; subpattern_1, ns=121

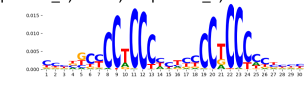

pattern_7, n=666; subpattern_2, ns=114

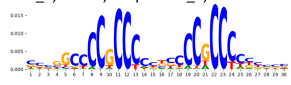

pattern_7, n=666; subpattern_3, ns=96

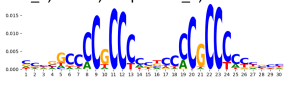

pattern_7, n=666; subpattern_4, ns=83

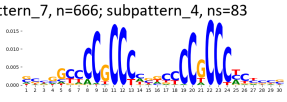

pattern_7, n=666; subpattern_5, ns=58

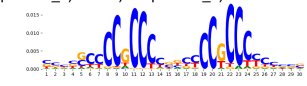

pattern_7, n=666; subpattern_6, ns=25

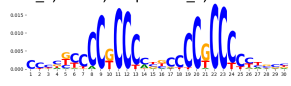

pattern_7, n=666; subpattern_7, ns=8

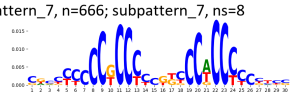

pattern_7, n=666; subpattern_8, ns=3

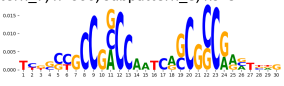

pattern_7, n=666; subpattern_9, ns=2

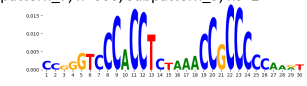

TF-MoDisCO pattern_7 n=666, PWM

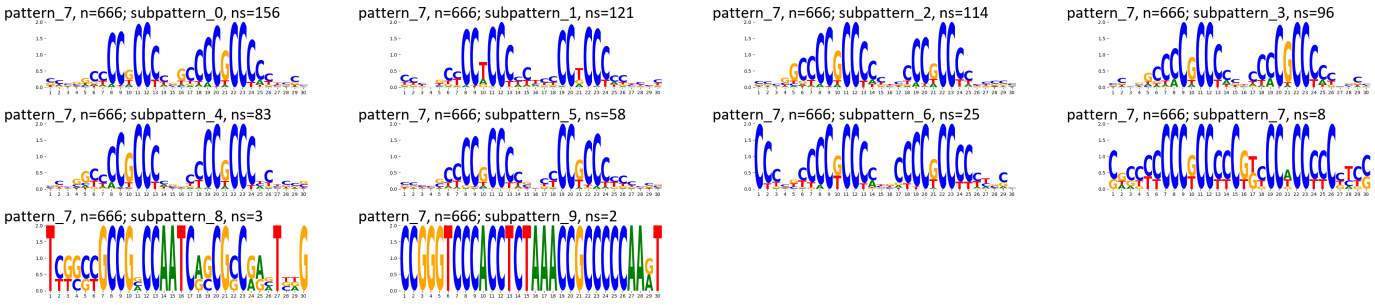

TF-MoDisCO pattern_8 n=637, CWM

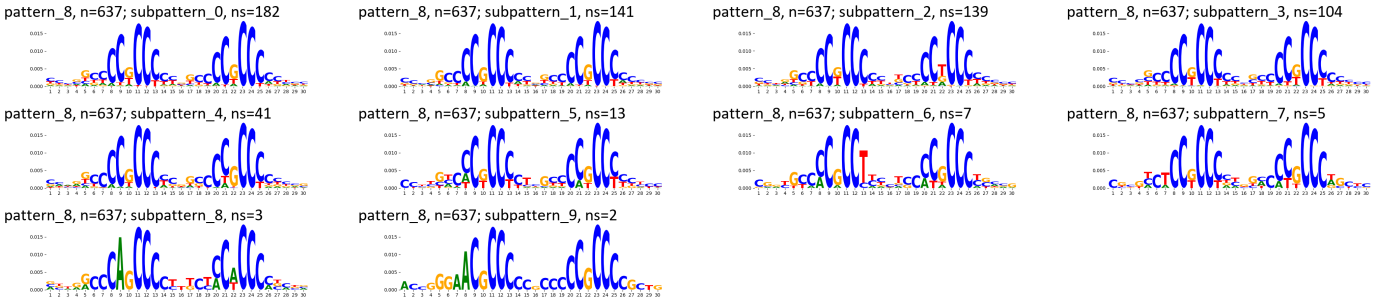

TF-MoDisCO pattern_8 n=637, PWM

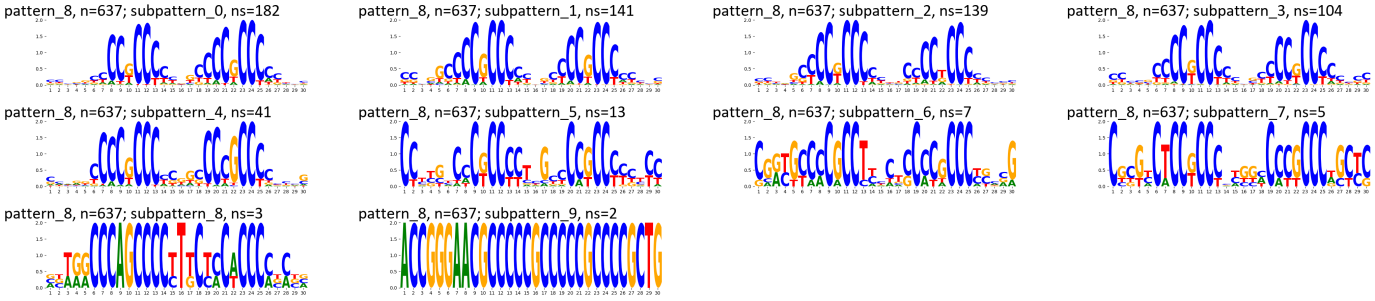

Supplementary Figure 307: TF-MoDisCO subpatterns for the SP3 transcription factor in HEK293 (accession ENCSR141PZA).

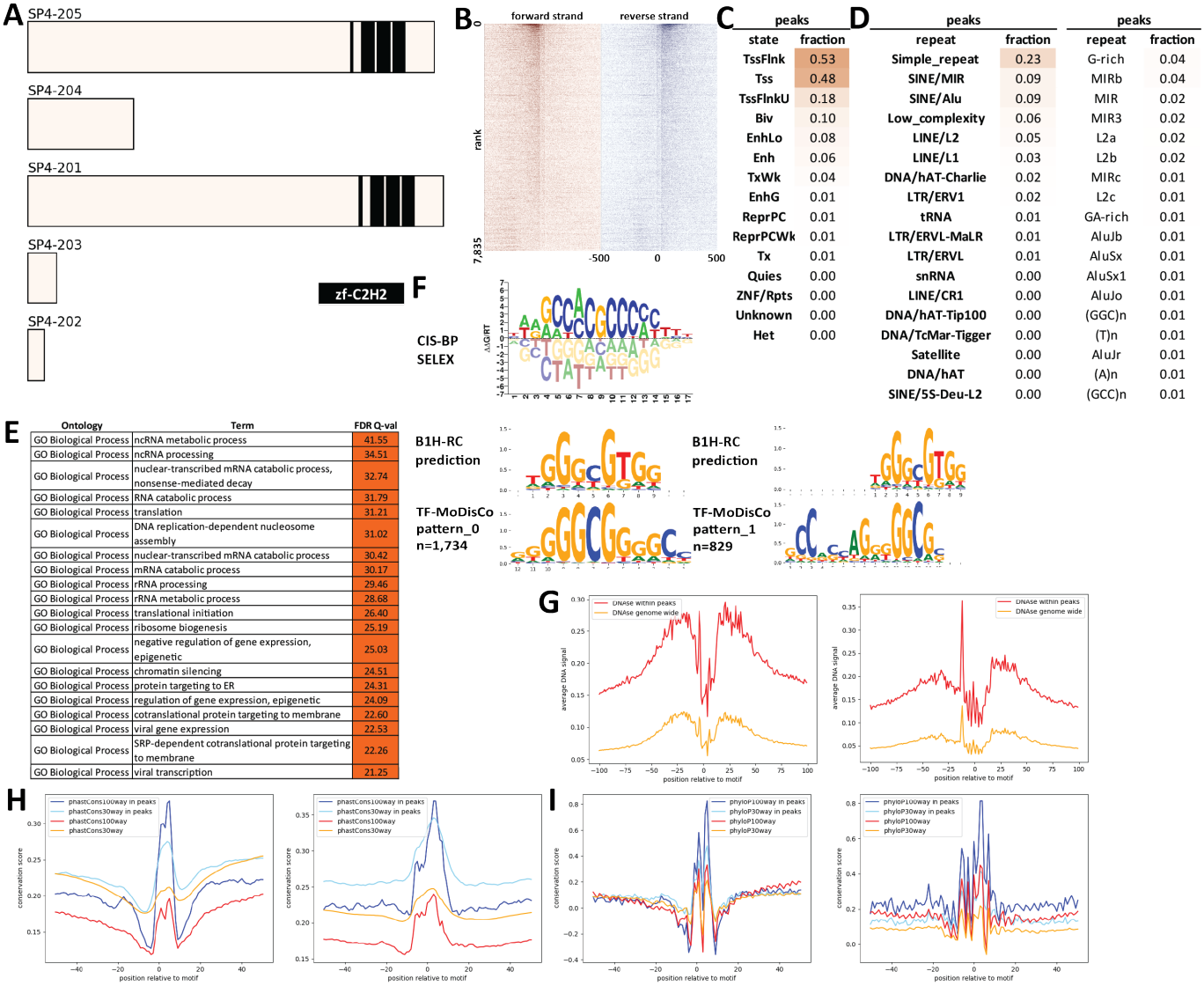

Supplementary Figure 308: Properties and genomic distribution of motifs identified for the SP4 transcription factor in H1 (accession ENCSR000BQV).

TF-MoDisCO pattern_0 n=1734, CWM

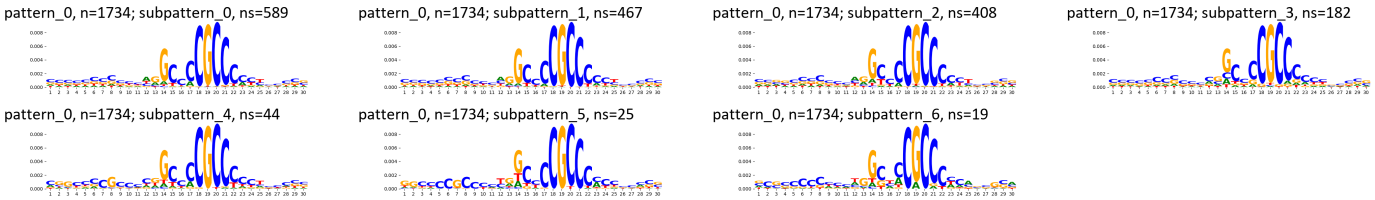

TF-MoDisCO pattern_0 n=1734, PWM

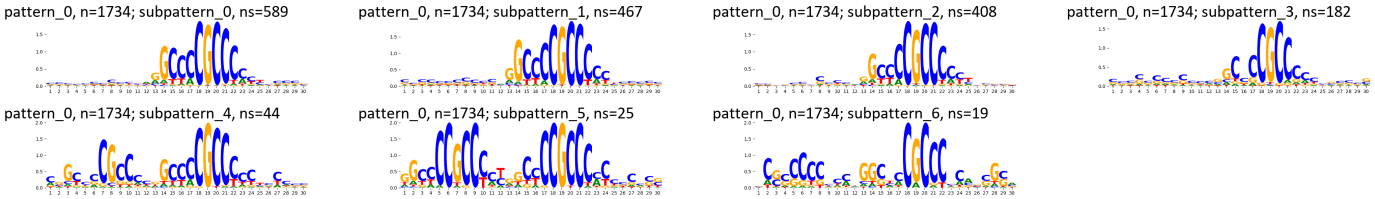

TF-MoDisCO pattern_1 n=829, CWM

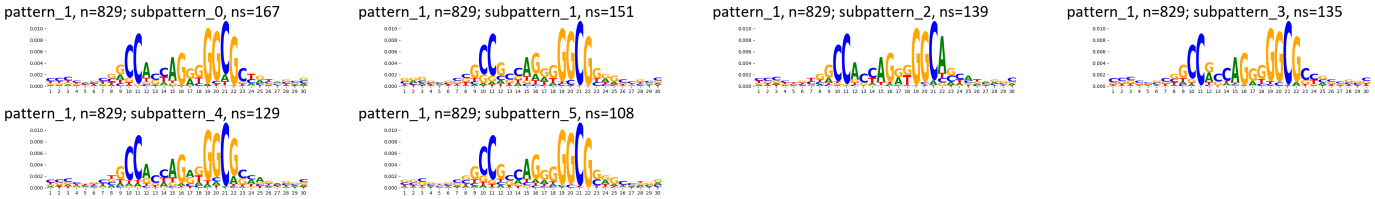

TF-MoDisCO pattern_1 n=829, PWM

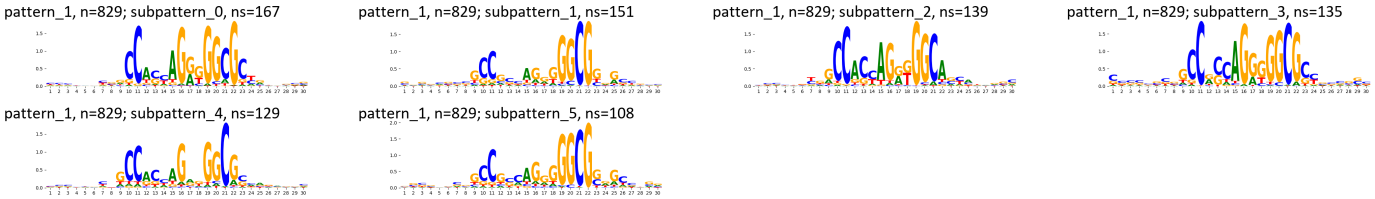

Supplementary Figure 309: TF-MoDisCO subpatterns for the SP4 transcription factor in H1 (accession ENCSR000BQV).

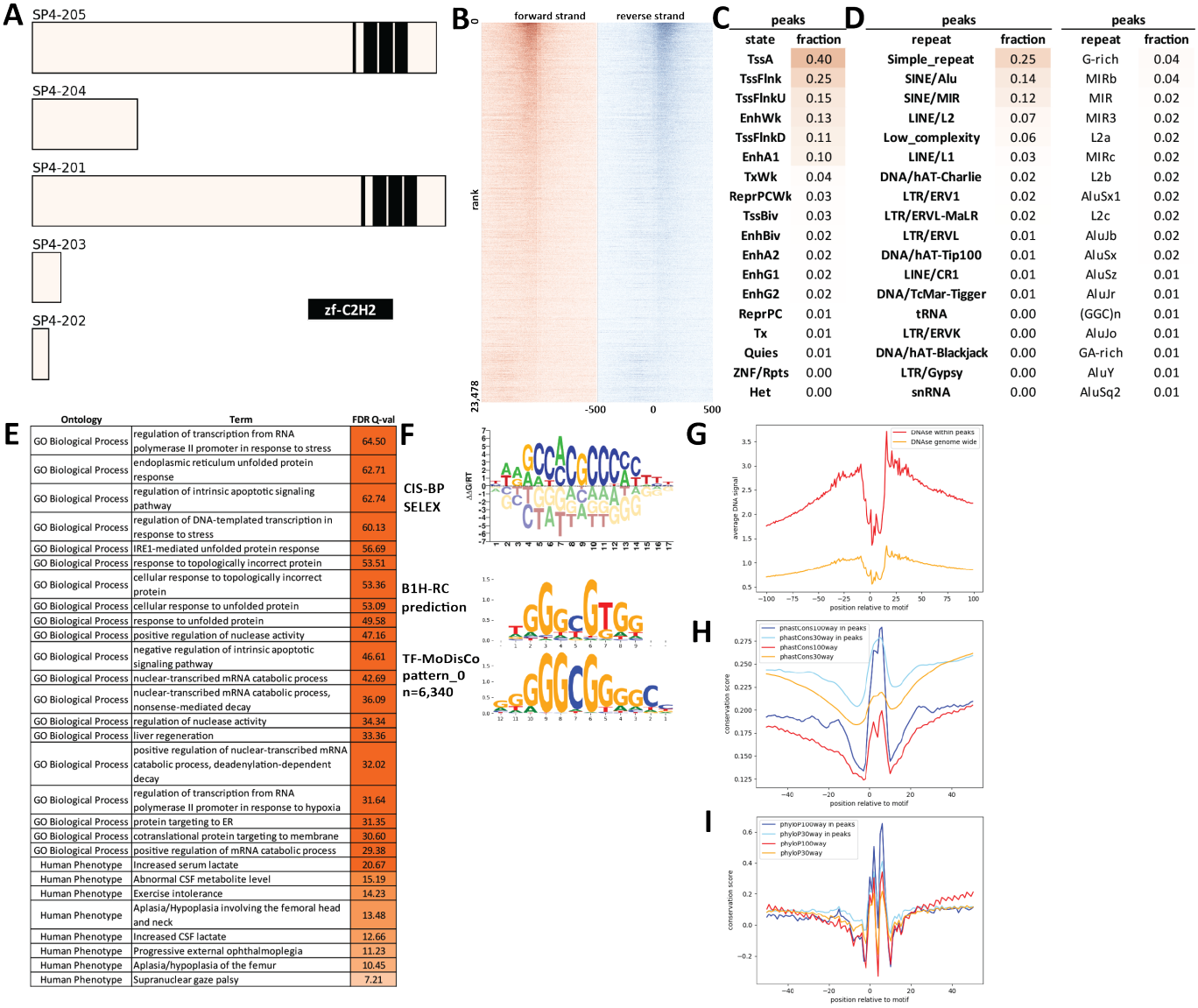

Supplementary Figure 310: Properties and genomic distribution of motifs identified for the SP4 transcription factor in HepG2 (accession ENCSR642PQK).

TF-MoDisCO pattern_0 n=6340, CWM

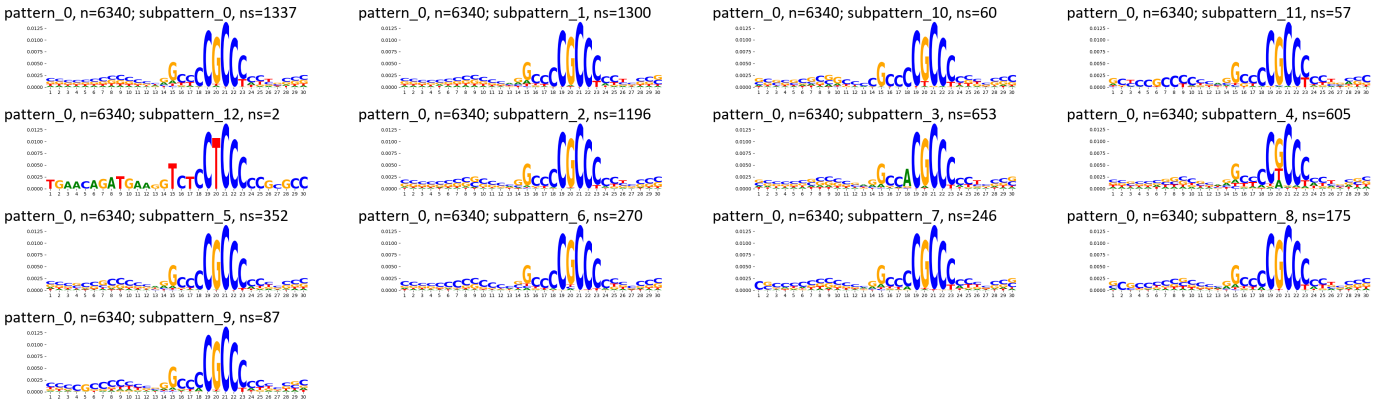

TF-MoDisCO pattern_0 n=6340, PWM

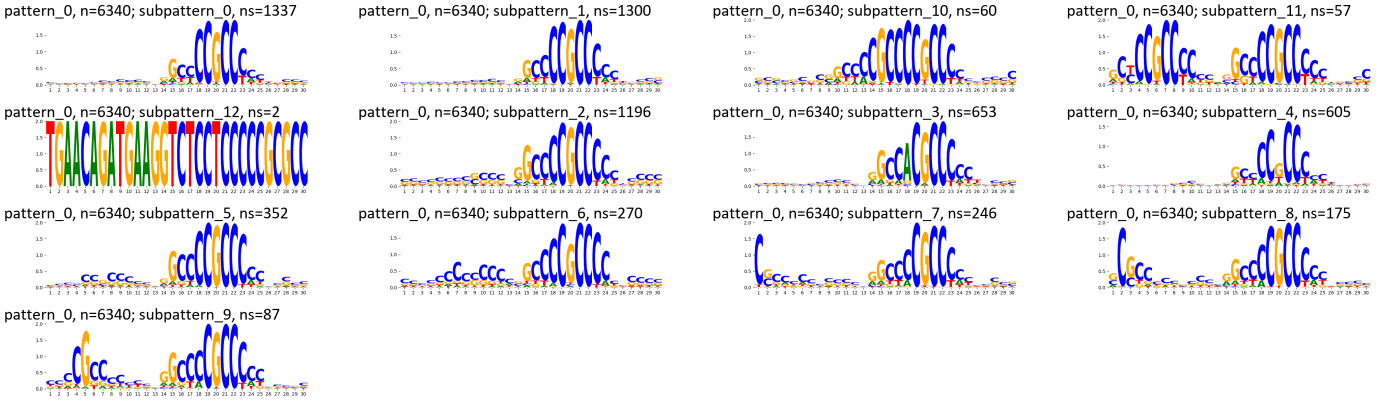

Supplementary Figure 311: TF-MoDisCO subpatterns for the SP4 transcription factor in HepG2 (accession ENCSR642PQK).

A



zf-C2H2

B

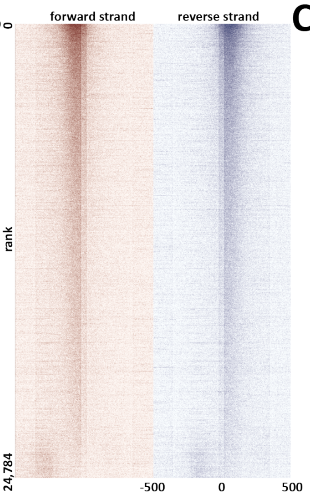

C

peaks	
state	fraction
TssA	0.30
EnhA1	0.19
TssFlnk	0.18
EnhWk	0.17
TssFlnkU	0.16
TssFlnkD	0.10
EnhA2	0.03
TxWk	0.02
ReprPCWk	0.02
EnhBiv	0.02
Quies	0.01
TssBiv	0.01
EnhG2	0.01
EnhG1	0.01
ReprPC	0.00
Tx	0.00
Het	0.00
ZNF/Rpts	0.00

D

peaks		peaks	
repeat	fraction	repeat	fraction
Simple_repeat	0.13	MIRb	0.03
SINE/Alu	0.10	G-rich	0.03
SINE/MIR	0.07	L2a	0.02
LINE/L2	0.06	MIR	0.02
LINE/L1	0.06	L2c	0.02
Low_complexity	0.04	L2b	0.02
DNA/hAT-Charlie	0.02	AluJb	0.01
LTR/ERV1	0.02	MIRc	0.01
LTR/ERVL-MaLR	0.02	MIR3	0.01
LTR/ERVL	0.02	AluJr	0.01
DNA/TcMar-Tigger	0.01	AluSx1	0.01
LINE/CR1	0.01	AluSx	0.01
LTR/ERVK	0.00	AluSz	0.01
DNA/hAT-Tip100	0.00	AluJo	0.01
tRNA	0.00	GA-rich	0.01
Retroposon/SVA	0.00	AluY	0.01
LINE/RTE-BovB	0.00	L2	0.01
DNA/hAT-Blackjack	0.00	(GGC)n	0.00

E

Ontology	Term	FDR Q-val
GO Biological Process	mitochondrial transport	66.94
GO Biological Process	nuclear-transcribed mRNA catabolic process	45.55
GO Biological Process	mitochondrial membrane organization	39.82
GO Biological Process	regulation of transcription from RNA polymerase II promoter in response to stress	38.94
GO Biological Process	endoplasmic reticulum unfolded protein response	36.97
GO Biological Process	liver regeneration	36.35
GO Biological Process	regulation of membrane permeability	36.13
GO Biological Process	regulation of mitochondrial membrane permeability	36.06
GO Biological Process	regulation of DNA-templated transcription in response to stress	35.99
GO Biological Process	negative regulation of intrinsic apoptotic signaling pathway	35.94
GO Biological Process	cellular response to epidermal growth factor stimulus	31.14
GO Biological Process	nuclear-transcribed mRNA catabolic process, nonsense-mediated decay	30.96
GO Biological Process	positive regulation of nuclease activity	30.32
GO Biological Process	mitochondrial transmembrane transport	28.78
GO Biological Process	nuclear-transcribed mRNA catabolic process, deadenylation-dependent decay	27.72
GO Biological Process	cotranslational protein targeting to membrane	25.11
GO Biological Process	regulation of release of cytochrome c from mitochondria	22.94
GO Biological Process	intrinsic apoptotic signaling pathway in response to DNA damage	22.78
GO Biological Process	regulation of endoplasmic reticulum unfolded protein response	21.51
GO Biological Process	snRNA metabolic process	21.45
Human Phenotype	Abnormal CSF metabolite level	17.55
Human Phenotype	Aplasia/hypoplasia of the femur	16.11
Human Phenotype	Increased CSF lactate	14.15
Human Phenotype	Increased mean platelet volume	11.75
Human Phenotype	Glycosuria	9.59
Human Phenotype	Hyperphosphaturia	8.82
Human Phenotype	Abnormality of transition element cation homeostasis	8.45
Human Phenotype	Increased serum ferritin	8.20
Human Phenotype	Abnormality of iron homeostasis	7.64

F

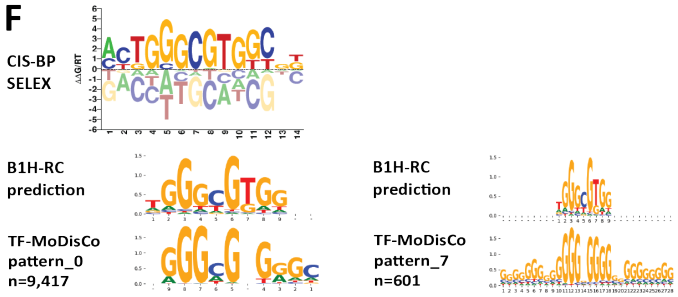

G

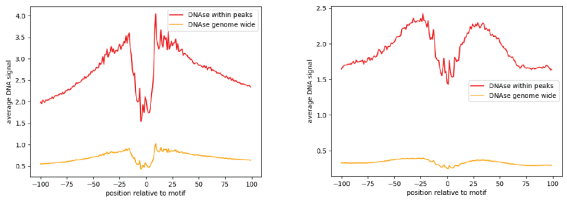

H

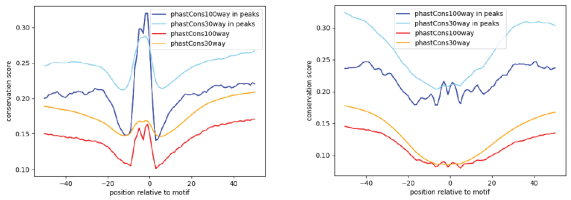

I

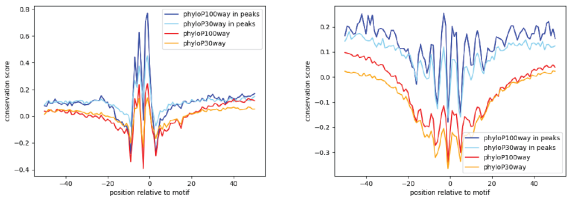

Supplementary Figure 312: Properties and genomic distribution of motifs identified for the SP5 transcription factor in HepG2 (accession ENCSR019NPF).

TF-MoDisCO pattern_0 n=9417, CWM

pattern_0, n=9417; subpattern_0, ns=1315

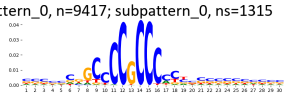

pattern_0, n=9417; subpattern_1, ns=1179

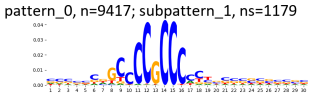

pattern_0, n=9417; subpattern_10, ns=358

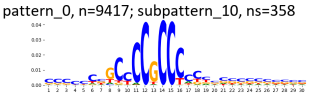

pattern_0, n=9417; subpattern_11, ns=335

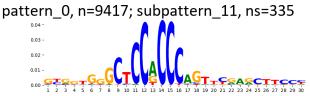

pattern_0, n=9417; subpattern_12, ns=122

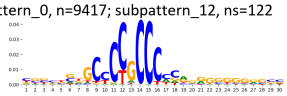

pattern_0, n=9417; subpattern_13, ns=51

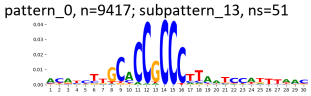

pattern_0, n=9417; subpattern_14, ns=29

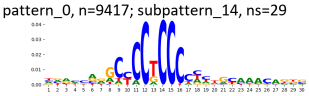

pattern_0, n=9417; subpattern_2, ns=1166

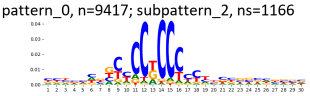

pattern_0, n=9417; subpattern_3, ns=1001

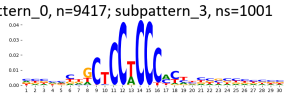

pattern_0, n=9417; subpattern_4, ns=955

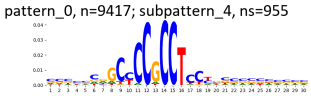

pattern_0, n=9417; subpattern_5, ns=774

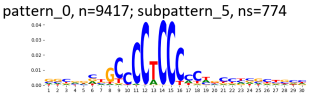

pattern_0, n=9417; subpattern_6, ns=684

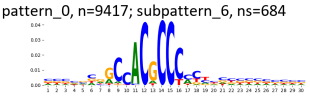

pattern_0, n=9417; subpattern_7, ns=528

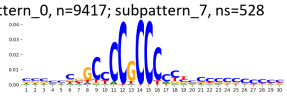

pattern_0, n=9417; subpattern_8, ns=524

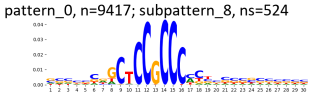

pattern_0, n=9417; subpattern_9, ns=396

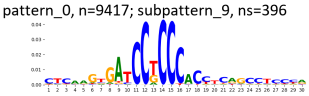

TF-MoDisCO pattern_0 n=9417, PWM

pattern_0, n=9417; subpattern_0, ns=1315

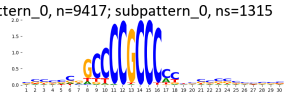

pattern_0, n=9417; subpattern_1, ns=1179

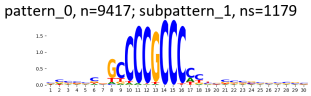

pattern_0, n=9417; subpattern_10, ns=358

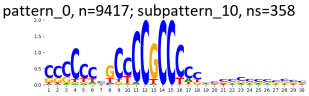

pattern_0, n=9417; subpattern_11, ns=335

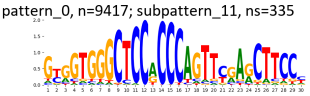

pattern_0, n=9417; subpattern_12, ns=122

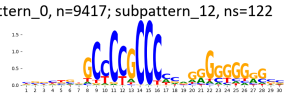

pattern_0, n=9417; subpattern_13, ns=51

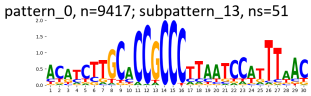

pattern_0, n=9417; subpattern_14, ns=29

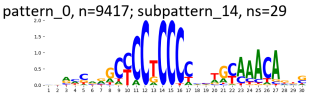

pattern_0, n=9417; subpattern_2, ns=1166

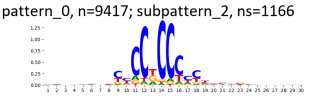

pattern_0, n=9417; subpattern_3, ns=1001

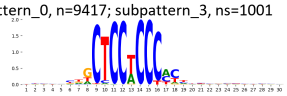

pattern_0, n=9417; subpattern_4, ns=955

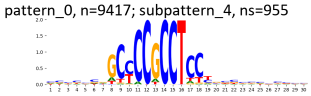

pattern_0, n=9417; subpattern_5, ns=774

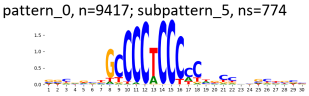

pattern_0, n=9417; subpattern_6, ns=684

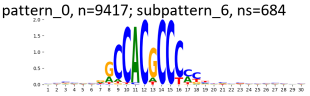

pattern_0, n=9417; subpattern_7, ns=528

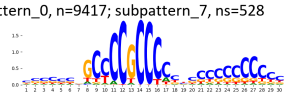

pattern_0, n=9417; subpattern_8, ns=524

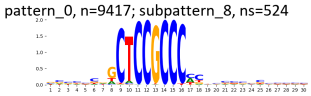

pattern_0, n=9417; subpattern_9, ns=396

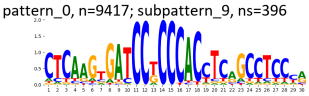

TF-MoDisCO pattern_7 n=601, CWM

pattern_7, n=601; subpattern_0, ns=97

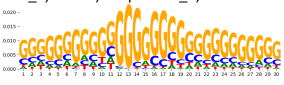

pattern_7, n=601; subpattern_1, ns=95

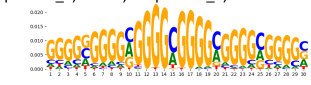

pattern_7, n=601; subpattern_2, ns=91

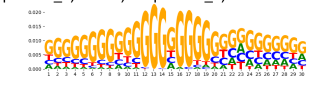

pattern_7, n=601; subpattern_3, ns=77

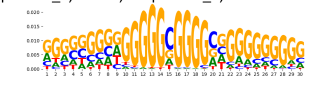

pattern_7, n=601; subpattern_4, ns=76

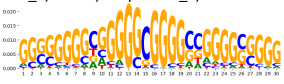

pattern_7, n=601; subpattern_5, ns=65

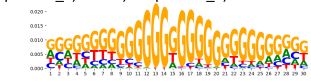

pattern_7, n=601; subpattern_6, ns=57

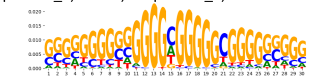

pattern_7, n=601; subpattern_7, ns=39

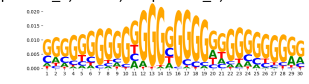

pattern_7, n=601; subpattern_8, ns=4

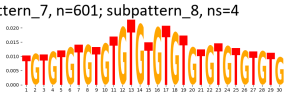

TF-MoDisCO pattern_7 n=601, PWM

pattern_7, n=601; subpattern_0, ns=97

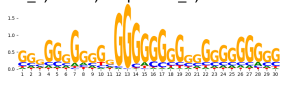

pattern_7, n=601; subpattern_1, ns=95

pattern_7, n=601; subpattern_2, ns=91

pattern_7, n=601; subpattern_3, ns=77

pattern_7, n=601; subpattern_4, ns=76

pattern_7, n=601; subpattern_5, ns=65

pattern_7, n=601; subpattern_6, ns=57

pattern_7, n=601; subpattern_7, ns=39

pattern_7, n=601; subpattern_8, ns=4

Supplementary Figure 313: TF-MoDisCO subpatterns for the SP5 transcription factor in HepG2 (accession ENCSR019NPF).

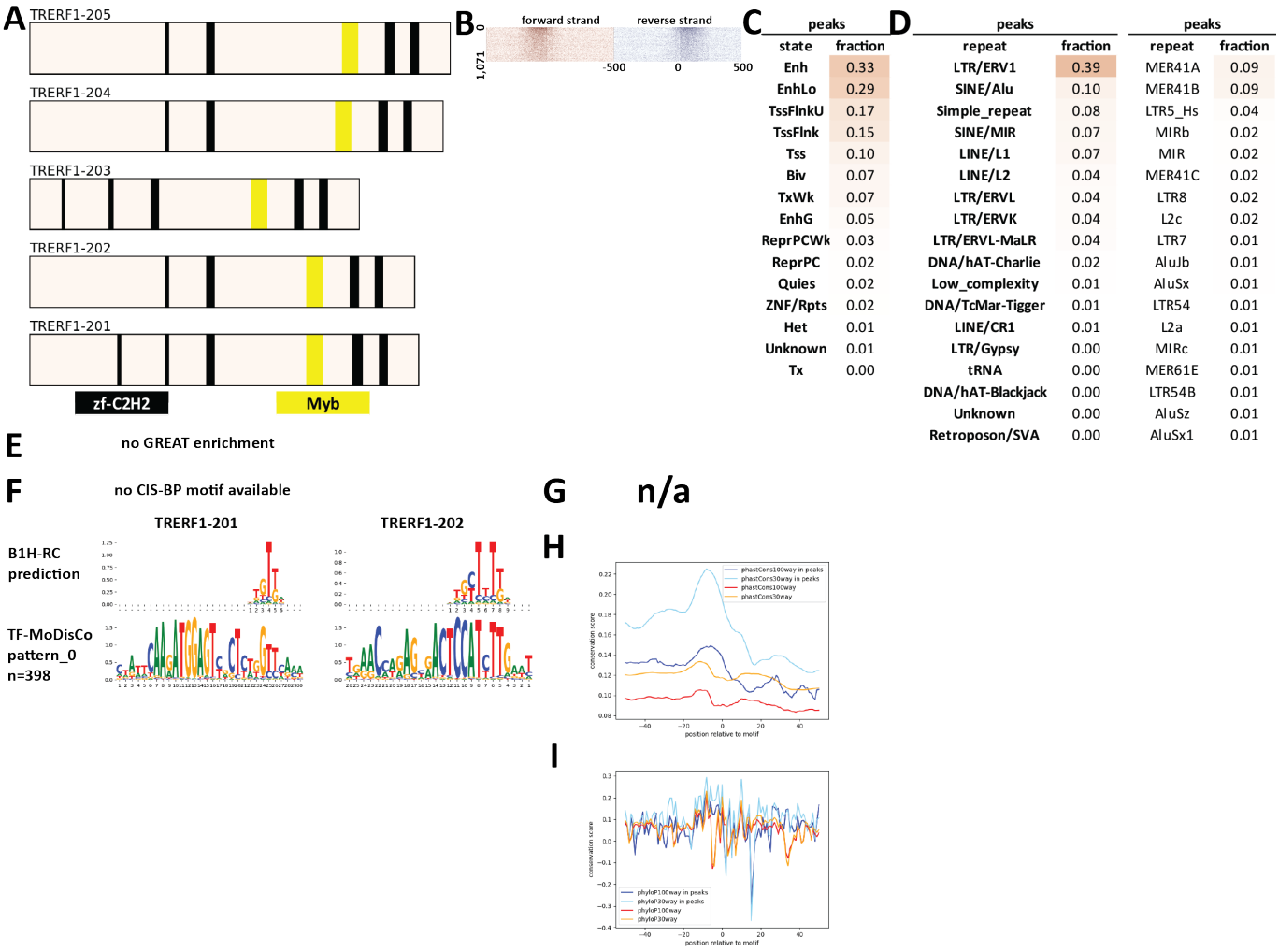

peaks	
state	fraction
Enh	0.33
EnhLo	0.29
TssFlnkU	0.17
TssFlnk	0.15
Tss	0.10
Biv	0.07
TxWk	0.07
EnhG	0.05
ReprPCWk	0.03
ReprPC	0.02
Quies	0.02
ZNF/Rpts	0.02
Het	0.01
Unknown	0.01
Tx	0.00

peaks		peaks	
repeat	fraction	repeat	fraction
LTR/ERV1	0.39	MER41A	0.09
SINE/Alu	0.10	MER41B	0.09
Simple_repeat	0.08	LTR5_Hs	0.04
SINE/MIR	0.07	MIRb	0.02
LINE/L1	0.07	MIR	0.02
LINE/L2	0.04	MER41C	0.02
LTR/ERVL	0.04	LTR8	0.02
LTR/ERVK	0.04	L2c	0.02
LTR/ERVL-MaLR	0.04	LTR7	0.01
DNA/hAT-Charlie	0.02	AluJb	0.01
Low_complexity	0.01	AluSx	0.01
DNA/TcMar-Tigger	0.01	LTR54	0.01
LINE/CR1	0.01	L2a	0.01
LTR/Gypsy	0.00	MIRc	0.01
tRNA	0.00	MER61E	0.01
DNA/hAT-Blackjack	0.00	LTR54B	0.01
Unknown	0.00	AluSz	0.01
Retroposon/SVA	0.00	AluSx1	0.01

Supplementary Figure 314: Properties and genomic distribution of motifs identified for the TRERF1 transcription factor in WTC11 (accession ENCSR547WSB).

TF-MoDisCO pattern_0 n=398, CWM

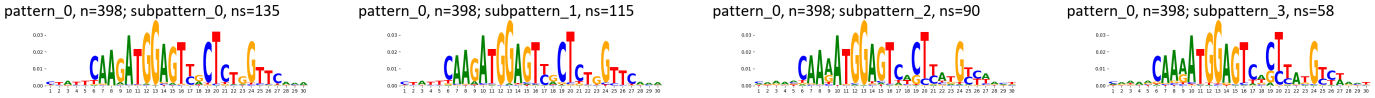

TF-MoDisCO pattern_0 n=398, PWM

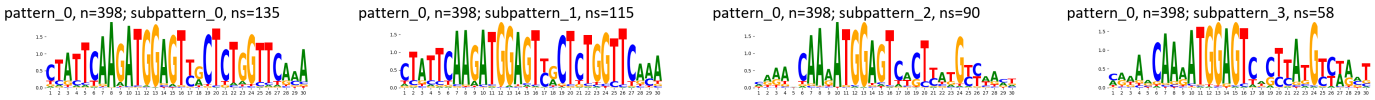

Supplementary Figure 315: TF-MoDisCO subpatterns for the TRERF1 transcription factor in WTC11 (accession ENCSR547WSB).

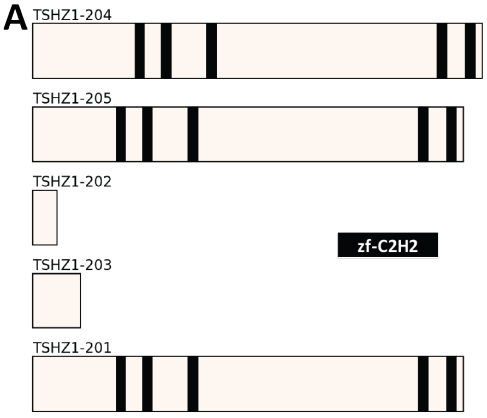

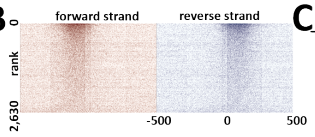

C

peaks	
state	fraction
Quies	0.41
TssA	0.15
TxWk	0.13
EnhWk	0.06
TssFlnk	0.05
EnhA2	0.04
EnhA1	0.03
Tx	0.03
TssFlnkU	0.03
ReprPCWk	0.03
ReprPC	0.01
TssFlnkD	0.01
TssBiv	0.00
EnhG1	0.00
Het	0.00
ZNF/Rpts	0.00
EnhG2	0.00
EnhBiv	0.00

D

peaks		peaks	
repeat	fraction	repeat	fraction
LTR/ERV1	0.33	MER41B	0.08
SINE/Alu	0.14	MER41A	0.05
SINE/MIR	0.09	MIRb	0.03
LINE/L2	0.07	LTR8	0.03
LINE/L1	0.07	L2a	0.02
Simple_repeat	0.06	L2c	0.02
LTR/ERVL	0.05	MIR	0.02
LTR/ERVL-MaLR	0.05	MIRc	0.02
DNA/hAT-Charlie	0.03	AluJb	0.02
LTR/ERVK	0.02	LTR54	0.02
DNA/TcMar-Tigger	0.02	AluSz	0.02
Low_complexity	0.01	L2b	0.02
LINE/CR1	0.01	MIR3	0.01
snRNA	0.01	AluSx1	0.01
DNA/hAT-Tip100	0.01	AluJr	0.01
tRNA	0.00	AluJo	0.01
Retroposon/SVA	0.00	L2	0.01
LTR/Gypsy	0.00	AluSx	0.01

E

Ontology	Term	FDR Q-val
GO Biological Process	positive regulation of interleukin-8 production	11.02
GO Biological Process	positive regulation of T cell activation	8.91
GO Biological Process	regulation of CD4-positive, alpha-beta T cell activation	8.67
GO Biological Process	negative regulation of extrinsic apoptotic signaling pathway in absence of ligand	6.32
GO Biological Process	negative regulation of tissue remodeling	5.02
GO Biological Process	cytokine production involved in immune response	4.69
GO Biological Process	negative regulation of transcription from RNA polymerase II promoter in response to stress	4.45
GO Biological Process	regulation of bone remodeling	4.34
GO Biological Process	regulation of ATPase activity	4.07
GO Biological Process	JAK-STAT cascade	3.85
GO Biological Process	4-hydroxyproline metabolic process	3.85
GO Biological Process	placenta blood vessel development	3.50
GO Biological Process	cellular response to growth hormone stimulus	1.32
GO Biological Process	positive regulation of growth hormone secretion	1.31

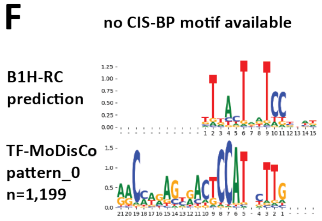

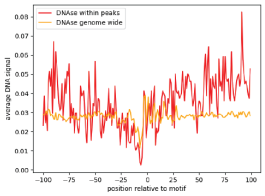

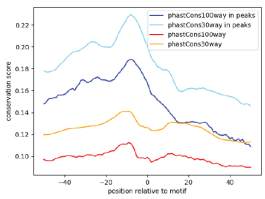

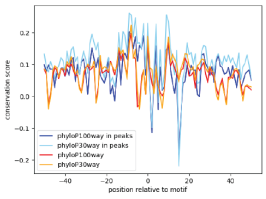

Supplementary Figure 316: Properties and genomic distribution of motifs identified for the TSHZ1 transcription factor in HEK293 (accession ENCSR958JPH).

TF-MoDisCO pattern_0 n=1199, CWM

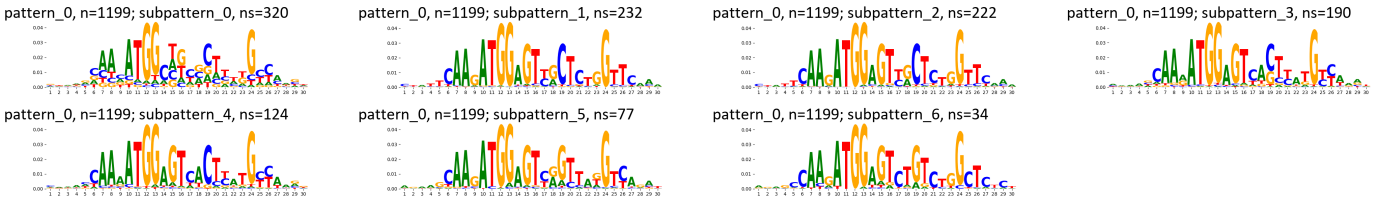

TF-MoDisCO pattern_0 n=1199, PWM

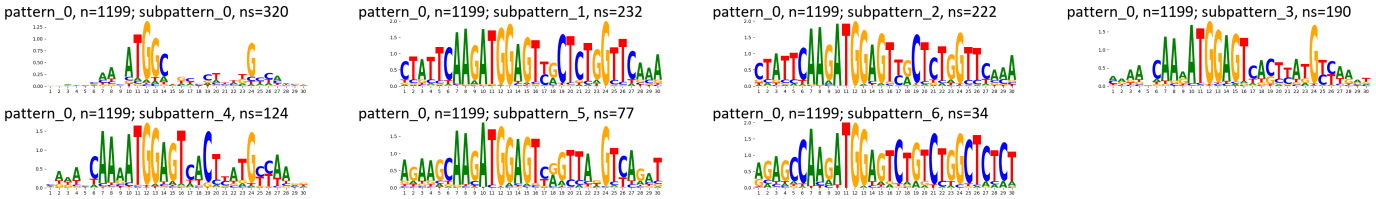

Supplementary Figure 317: TF-MoDisCO subpatterns for the TSHZ1 transcription factor in HEK293 (accession ENCSR958JPH).

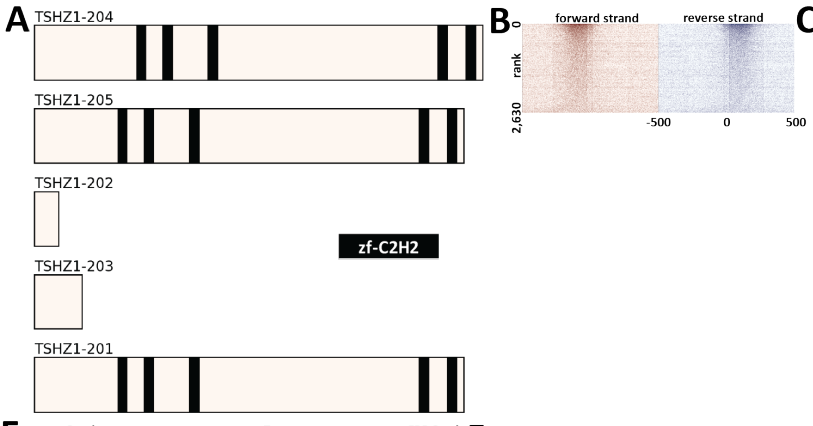

C

peaks	
state	fraction
EnhA1	0.30
EnhWk	0.20
TssFlnkU	0.14
TssA	0.14
TxWk	0.11
EnhA2	0.10
Quies	0.09
ReprPCWk	0.05
TssFlnkD	0.02
EnhG2	0.02
TssFlnk	0.02
EnhG1	0.01
Tx	0.01
ReprPC	0.01
EnhBiv	0.01
Het	0.00
ZNF/Rpts	0.00
TssBiv	0.00

D

peaks		peaks	
repeat	fraction	repeat	fraction
LTR/ERV1	0.33	MER41B	0.08
SINE/Alu	0.14	MER41A	0.05
SINE/MIR	0.09	MIRb	0.03
LINE/L2	0.07	LTR8	0.03
LINE/L1	0.07	L2a	0.02
Simple_repeat	0.06	L2c	0.02
LTR/ERVL	0.05	MIR	0.02
LTR/ERVL-MaLR	0.05	MIRc	0.02
DNA/hAT-Charlie	0.03	AluJb	0.02
LTR/ERVK	0.02	LTR54	0.02
DNA/TcMar-Tigger	0.02	AluSz	0.02
Low_complexity	0.01	L2b	0.02
LINE/CR1	0.01	MIR3	0.01
snRNA	0.01	AluSx1	0.01
DNA/hAT-Tip100	0.01	AluJr	0.01
tRNA	0.00	AluJo	0.01
Retroposon/SVA	0.00	L2	0.01
LTR/Gypsy	0.00	AluSx	0.01

E

Ontology	Term	FDR Q-val
GO Biological Process	positive regulation of interleukin-8 production	11.02
GO Biological Process	positive regulation of T cell activation	8.91
GO Biological Process	regulation of CD4-positive, alpha-beta T cell activation	8.67
GO Biological Process	negative regulation of extrinsic apoptotic signaling pathway in absence of ligand	6.32
GO Biological Process	negative regulation of tissue remodeling	5.02
GO Biological Process	cytokine production involved in immune response	4.69
GO Biological Process	negative regulation of transcription from RNA polymerase II promoter in response to stress	4.45
GO Biological Process	regulation of bone remodeling	4.34
GO Biological Process	regulation of ATPase activity	4.07
GO Biological Process	JAK-STAT cascade	3.85
GO Biological Process	4-hydroxyproline metabolic process	3.85
GO Biological Process	placenta blood vessel development	3.50
GO Biological Process	cellular response to growth hormone stimulus	1.32
GO Biological Process	positive regulation of growth hormone secretion	1.31

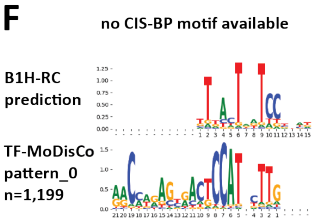

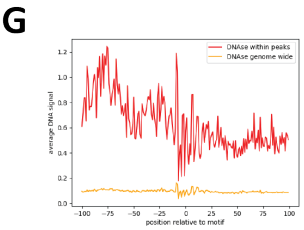

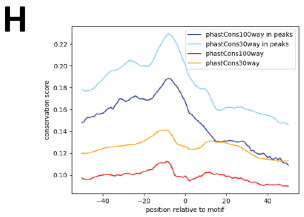

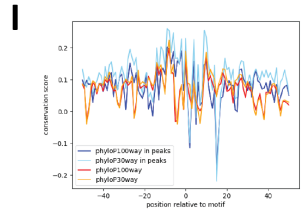

Supplementary Figure 318: Properties and genomic distribution of motifs identified for the TSHZ1 transcription factor in K562 (accession ENCSR958JPH).

TF-MoDisCO pattern_0 n=1199, CWM

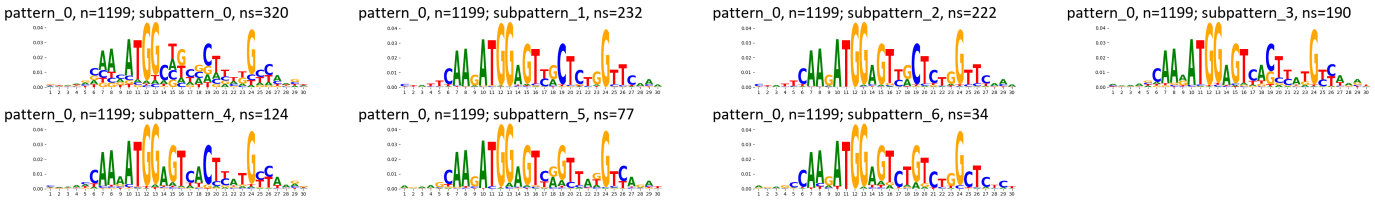

TF-MoDisCO pattern_0 n=1199, PWM

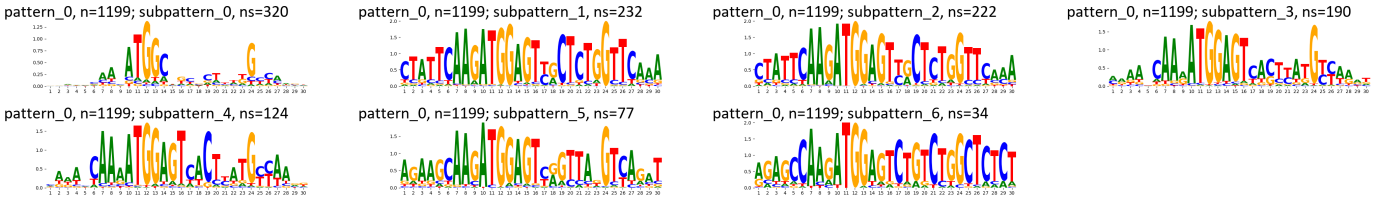

Supplementary Figure 319: TF-MoDisCO subpatterns for the TSHZ1 transcription factor in K562 (accession ENCSR958JPH).

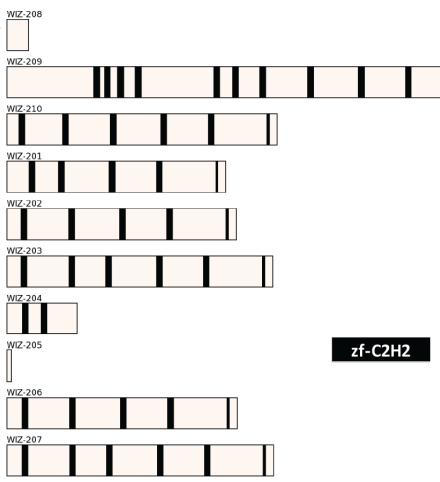

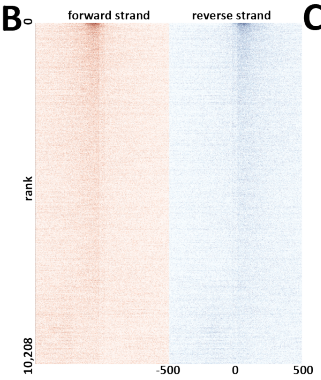

C

peaks	
state	fraction
TssA	0.39
TssFlnk	0.19
TssFlnkU	0.18
EnhA1	0.15
EnhWk	0.14
TssFlnkD	0.10
ReprPCWk	0.04
Quies	0.03
TxWk	0.02
TssBiv	0.02
EnhA2	0.02
EnhBiv	0.02
ReprPC	0.01
EnhG2	0.01
EnhG1	0.01
Tx	0.00
ZNF/Rpts	0.00
Het	0.00

D

peaks		peaks	
repeat	fraction	repeat	fraction
Simple_repeat	0.20	MIRb	0.05
SINE/Alu	0.14	MIR	0.03
SINE/MIR	0.13	L2a	0.03
LINE/L2	0.08	G-rich	0.03
LINE/L1	0.05	L2c	0.02
Low_complexity	0.04	MIR3	0.02
DNA/hAT-Charlie	0.03	MIRc	0.02
LTR/ERVL-MaLR	0.03	L2b	0.02
LTR/ERV1	0.03	AluJb	0.02
LTR/ERVL	0.02	AluSx1	0.02
DNA/hAT-Tip100	0.01	AluSx	0.01
LINE/CR1	0.01	AluSz	0.01
DNA/TcMar-Tigger	0.01	AluJo	0.01
tRNA	0.00	AluJr	0.01
DNA/hAT-Blackjack	0.00	GA-rich	0.01
LTR/ERVK	0.00	AluY	0.01
DNA/hAT	0.00	AluSq2	0.01
DNA/TcMar-Mariner	0.00	L2	0.01

E

Ontology	Term	FDR Q-val
GO Biological Process	regulation of transcription from RNA polymerase II promoter in response to stress	21.99
GO Biological Process	regulation of DNA-templated transcription in response to stress	19.51
GO Biological Process	activation of signaling protein activity involved in unfolded protein response	17.69
GO Biological Process	translational elongation	15.85
GO Biological Process	regulation of cellular amino acid metabolic process	15.54
GO Biological Process	regulation of transcription from RNA polymerase II promoter in response to hypoxia	14.20
GO Biological Process	regulation of mitochondrial membrane permeability	12.93
GO Biological Process	RNA phosphodiester bond hydrolysis	12.74
GO Biological Process	positive regulation of mRNA catabolic process	12.56
GO Biological Process	regulation of translational fidelity	12.04
GO Biological Process	regulation of membrane permeability	11.22
GO Biological Process	negative regulation of ubiquitin protein ligase activity	11.08
GO Biological Process	RNA phosphodiester bond hydrolysis, endonucleolytic	11.02
GO Biological Process	negative regulation of ubiquitin-protein ligase activity involved in mitotic cell cycle	9.96
GO Biological Process	negative regulation of ubiquitin-protein transferase activity	9.91
GO Biological Process	regulation of ubiquitin-protein ligase activity involved in mitotic cell cycle	9.85
GO Biological Process	regulation of endoplasmic reticulum unfolded protein response	8.67
GO Biological Process	anaphase-promoting complex-dependent catabolic process	8.48
GO Biological Process	positive regulation of endoplasmic reticulum unfolded protein response	7.14
GO Biological Process	regulation of translational elongation	6.57

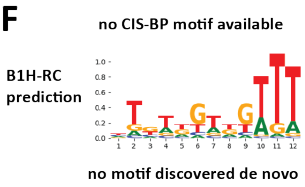

Supplementary Figure 320: Properties and genomic distribution of motifs identified for the WIZ transcription factor in HepG2 (accession ENCSR434ZNS).

A

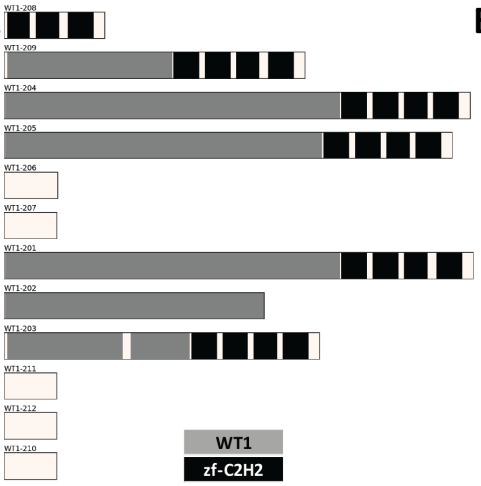

B

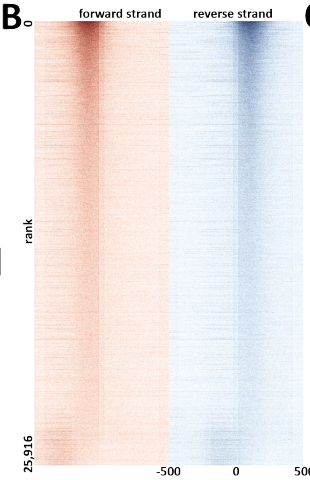

C

peaks	
state	fraction
EnhWk	0.25
TssA	0.19
Quies	0.15
TxWk	0.11
EnhA1	0.10
TssFlnk	0.09
EnhA2	0.07
TssBiv	0.03
TssFlnkU	0.03
Tx	0.02
TssFlnkD	0.02
ReprPCWk	0.02
ReprPC	0.02
EnhBiv	0.01
EnhG1	0.01
EnhG2	0.00
Het	0.00
ZNF/Rpts	0.00

D

peaks		peaks	
repeat	fraction	repeat	fraction
Simple_repeat	0.15	MIRb	0.03
SINE/Alu	0.14	L2a	0.02
SINE/MIR	0.08	AluJb	0.02
LINE/L2	0.07	L2c	0.02
LINE/L1	0.06	MIR	0.02
Low_complexity	0.04	G-rich	0.02
LTR/ERVL-MaLR	0.03	GA-rich	0.02
DNA/hAT-Charlie	0.02	MIRc	0.02
LTR/ERV1	0.02	L2b	0.02
LTR/ERVL	0.01	MIR3	0.01
DNA/TcMar-Tigger	0.01	AluSx	0.01
LINE/CR1	0.01	AluSx1	0.01
LTR/ERVK	0.01	AluJr	0.01
tRNA	0.00	AluSz	0.01
DNA/hAT-Tip100	0.00	AluJo	0.01
LINE/RTE-X	0.00	L2	0.01
Unknown	0.00	AluY	0.01
Retroposon/SVA	0.00	(GT)n	0.01

E

Ontology	Term	FDR Q-val
GO Biological Process	mRNA transcription	29.06
GO Biological Process	regulation of viral transcription	28.17
GO Biological Process	cellular response to epidermal growth factor stimulus	27.16
GO Biological Process	response to epidermal growth factor	25.64
GO Biological Process	nuclear-transcribed mRNA catabolic process, nonsense-mediated decay	23.75
GO Biological Process	negative regulation of cardiac muscle hypertrophy	21.82
GO Biological Process	negative regulation of muscle hypertrophy	20.80
GO Biological Process	intrinsic apoptotic signaling pathway in response to DNA damage	20.54
GO Biological Process	posttranscriptional gene silencing by RNA	18.96
GO Biological Process	regulation of pri-miRNA transcription from RNA polymerase II promoter	18.95
GO Biological Process	posttranscriptional gene silencing	18.38
GO Biological Process	gene silencing by miRNA	18.18
GO Biological Process	thyroid gland development	17.98
GO Biological Process	positive regulation of mRNA catabolic process	17.41
GO Biological Process	histone ubiquitination	16.88
GO Biological Process	positive regulation of pri-miRNA transcription from RNA polymerase II promoter	15.08
GO Biological Process	paraxial mesoderm development	11.83
GO Biological Process	production of miRNAs involved in gene silencing by miRNA	11.37
GO Biological Process	coenzyme A metabolic process	9.78
GO Biological Process	negative regulation of cyclin-dependent protein serine/threonine kinase activity	9.46
Human Phenotype	Hamartoma	13.77
Human Phenotype	Missing ribs	13.44
Human Phenotype	Neonatal death	10.37

F

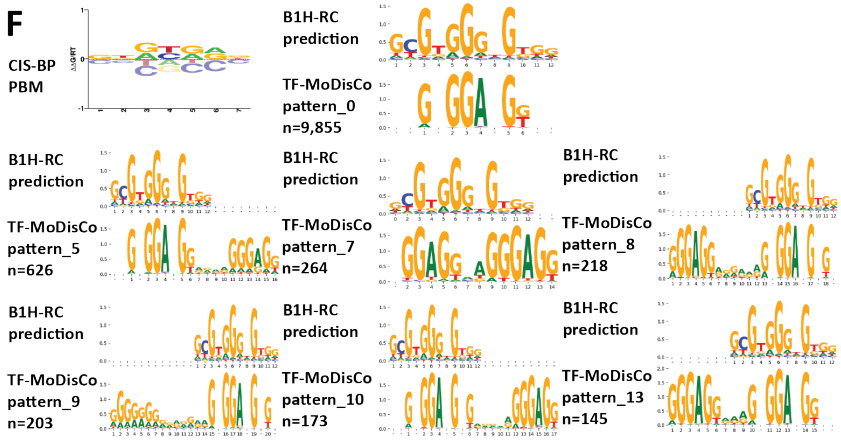

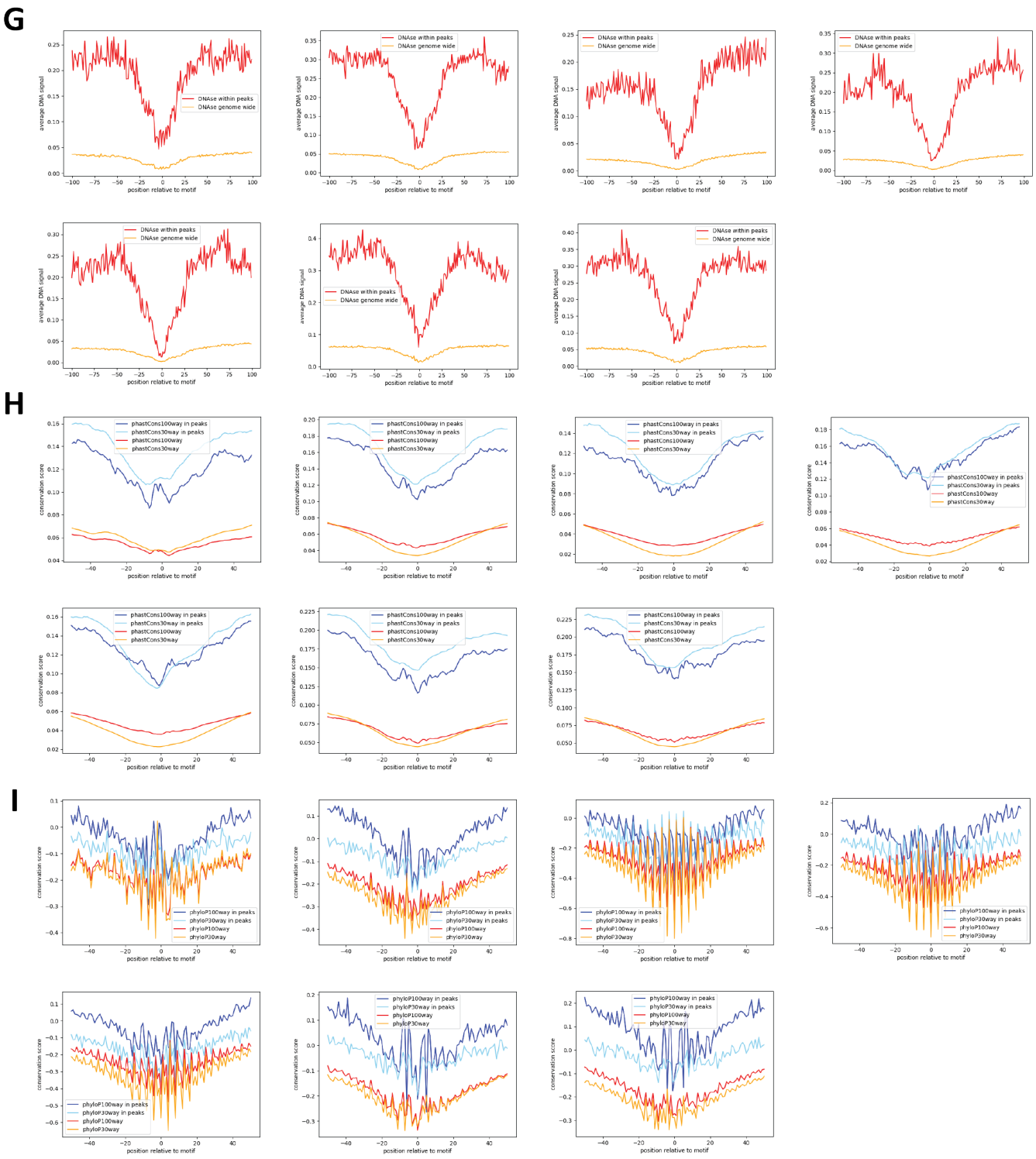

Supplementary Figure 321: Properties and genomic distribution of motifs identified for the WT1 transcription factor in HEK293 (accession ENCSR966PJJ).

TF-MoDisCO pattern_0 n=9855, CWM

pattern_0, n=9855; subpattern_0, ns=1913

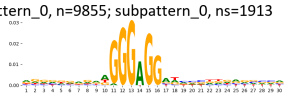

pattern_0, n=9855; subpattern_1, ns=1812

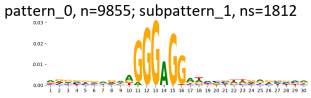

pattern_0, n=9855; subpattern_2, ns=1679

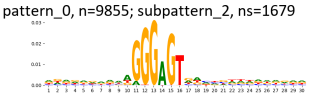

pattern_0, n=9855; subpattern_3, ns=1673

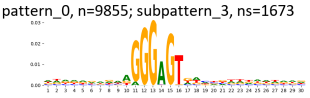

pattern_0, n=9855; subpattern_4, ns=1351

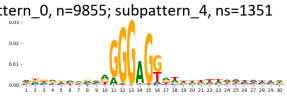

pattern_0, n=9855; subpattern_5, ns=697

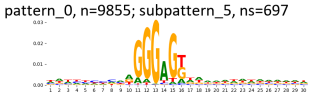

pattern_0, n=9855; subpattern_6, ns=424

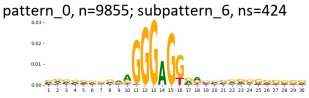

pattern_0, n=9855; subpattern_7, ns=181

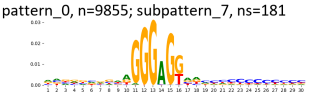

pattern_0, n=9855; subpattern_8, ns=125

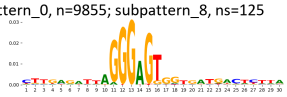

TF-MoDisCO pattern_0 n=9855, PWM

pattern_0, n=9855; subpattern_0, ns=1913

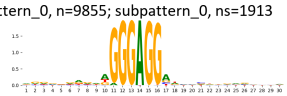

pattern_0, n=9855; subpattern_1, ns=1812

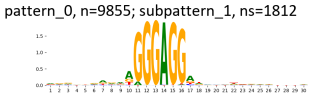

pattern_0, n=9855; subpattern_2, ns=1679

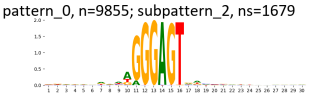

pattern_0, n=9855; subpattern_3, ns=1673

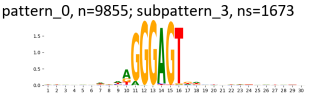

pattern_0, n=9855; subpattern_4, ns=1351

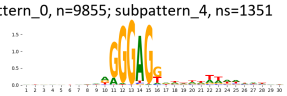

pattern_0, n=9855; subpattern_5, ns=697

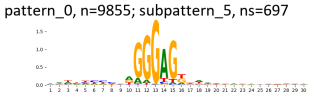

pattern_0, n=9855; subpattern_6, ns=424

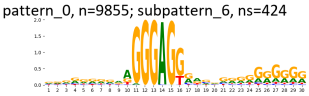

pattern_0, n=9855; subpattern_7, ns=181

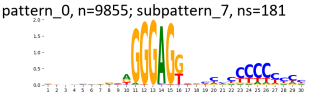

pattern_0, n=9855; subpattern_8, ns=125

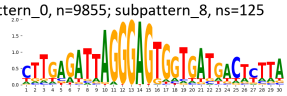

TF-MoDisCO pattern_10 n=173, CWM

pattern_10, n=173; subpattern_0, ns=62

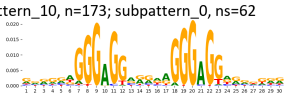

pattern_10, n=173; subpattern_1, ns=53

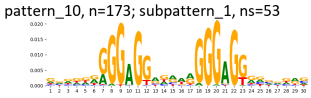

pattern_10, n=173; subpattern_2, ns=33

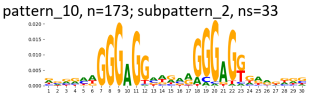

pattern_10, n=173; subpattern_3, ns=25

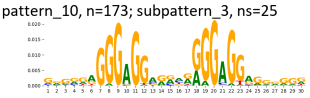

TF-MoDisCO pattern_10 n=173, PWM

pattern_10, n=173; subpattern_0, ns=62

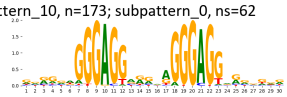

pattern_10, n=173; subpattern_1, ns=53

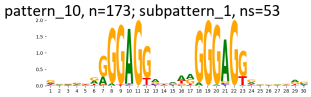

pattern_10, n=173; subpattern_2, ns=33

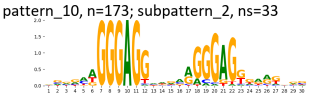

pattern_10, n=173; subpattern_3, ns=25

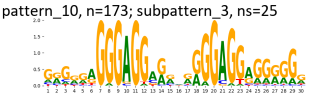

TF-MoDisCO pattern_13 n=145, CWM

pattern_13, n=145; subpattern_0, ns=61

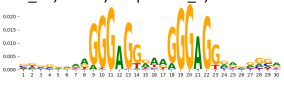

pattern_13, n=145; subpattern_1, ns=58

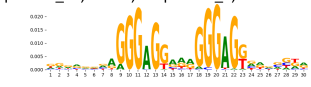

pattern_13, n=145; subpattern_2, ns=10

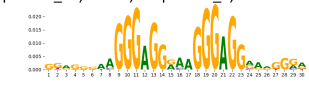

pattern_13, n=145; subpattern_3, ns=9

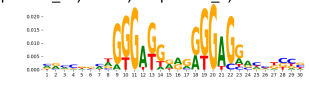

pattern_13, n=145; subpattern_4, ns=7

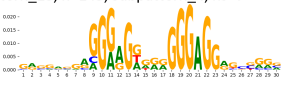

TF-MoDisCO pattern_13 n=145, PWM

pattern_13, n=145; subpattern_0, ns=61

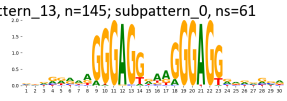

pattern_13, n=145; subpattern_1, ns=58

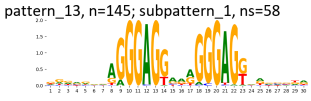

pattern_13, n=145; subpattern_2, ns=10

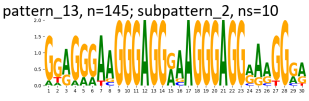

pattern_13, n=145; subpattern_3, ns=9

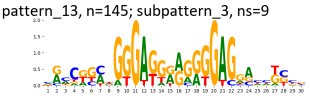

pattern_13, n=145; subpattern_4, ns=7

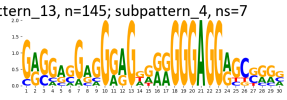

TF-MoDisCO pattern_5 n=626, CWM

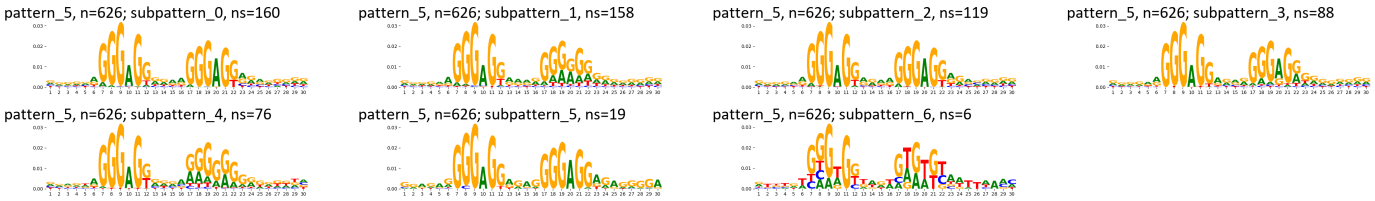

TF-MoDisCO pattern_5 n=626, PWM

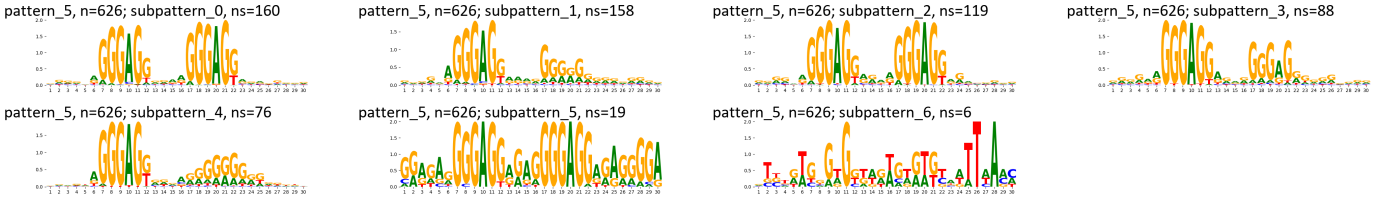

TF-MoDisCO pattern_7 n=264, CWM

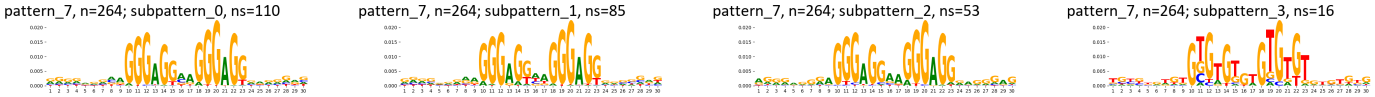

TF-MoDisCO pattern_7 n=264, PWM



TF-MoDisCO pattern_8 n=218, CWM

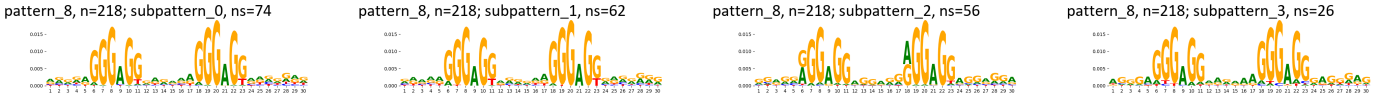

TF-MoDisCO pattern_8 n=218, PWM

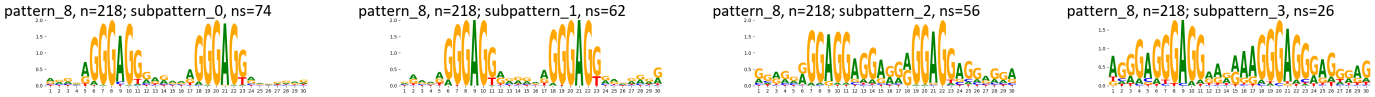

TF-MoDisCO pattern_9 n=203, CWM



TF-MoDisCO pattern_9 n=203, PWM

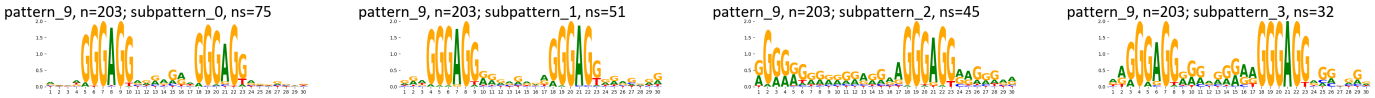

Supplementary Figure 322: TF-MoDisCO subpatterns for the WT1 transcription factor in HEK293 (accession ENCSR966PJJ).

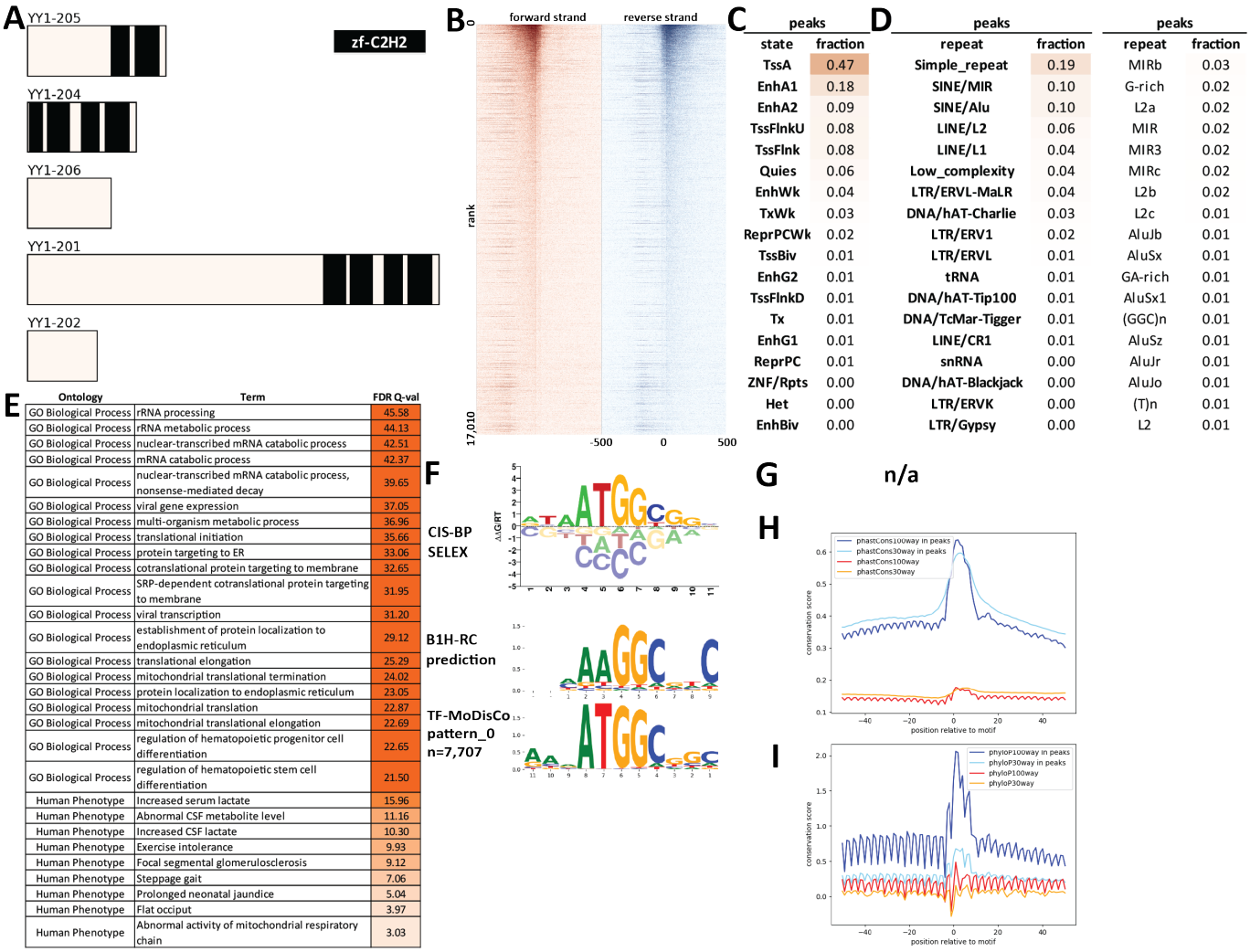

peaks	
state	fraction
TssA	0.47
EnhA1	0.18
EnhA2	0.09
TssFlnkU	0.08
TssFlnk	0.08
Quies	0.06
EnhWk	0.04
TxWk	0.03
ReprPCWk	0.02
TssBiv	0.01
EnhG2	0.01
TssFlnkD	0.01
Tx	0.01
EnhG1	0.01
ReprPC	0.01
ZNF/Rpts	0.00
Het	0.00
EnhBiv	0.00

peaks		peaks	
repeat	fraction	repeat	fraction
Simple_repeat	0.19	MIRb	0.03
SINE/MIR	0.10	G-rich	0.02
SINE/Alu	0.10	L2a	0.02
LINE/L2	0.06	MIR	0.02
LINE/L1	0.04	MIR3	0.02
Low_complexity	0.04	MIRc	0.02
LTR/ERVL-MaLR	0.04	L2b	0.02
DNA/hAT-Charlie	0.03	L2c	0.01
LTR/ERV1	0.02	AluJb	0.01
LTR/ERVL	0.01	AluSx	0.01
tRNA	0.01	GA-rich	0.01
DNA/hAT-Tip100	0.01	AluSx1	0.01
DNA/TcMar-Tigger	0.01	(GGC)n	0.01
LINE/CR1	0.01	AluSz	0.01
snRNA	0.00	AluJr	0.01
DNA/hAT-Blackjack	0.00	AluJo	0.01
LTR/ERVK	0.00	(T)n	0.01
LTR/Gypsy	0.00	L2	0.01

Ontology	Term	FDR Q-val
GO Biological Process	rRNA processing	45.58
GO Biological Process	rRNA metabolic process	44.13
GO Biological Process	nuclear-transcribed mRNA catabolic process	42.51
GO Biological Process	mRNA catabolic process	42.37
GO Biological Process	nuclear-transcribed mRNA catabolic process, nonsense-mediated decay	39.65
GO Biological Process	viral gene expression	37.05
GO Biological Process	multi-organism metabolic process	36.96
GO Biological Process	translational initiation	35.66
GO Biological Process	protein targeting to ER	33.06
GO Biological Process	cotranslational protein targeting to membrane	32.65
GO Biological Process	SRP-dependent cotranslational protein targeting to membrane	31.95
GO Biological Process	viral transcription	31.20
GO Biological Process	establishment of protein localization to endoplasmic reticulum	29.12
GO Biological Process	translational elongation	25.29
GO Biological Process	mitochondrial translational termination	24.02
GO Biological Process	protein localization to endoplasmic reticulum	23.05
GO Biological Process	mitochondrial translation	22.87
GO Biological Process	mitochondrial translational elongation	22.69
GO Biological Process	regulation of hematopoietic progenitor cell differentiation	22.65
GO Biological Process	regulation of hematopoietic stem cell differentiation	21.50
Human Phenotype	Increased serum lactate	15.96
Human Phenotype	Abnormal CSF metabolite level	11.16
Human Phenotype	Increased CSF lactate	10.30
Human Phenotype	Exercise intolerance	9.93
Human Phenotype	Focal segmental glomerulosclerosis	9.12
Human Phenotype	Steppage gait	7.06
Human Phenotype	Prolonged neonatal jaundice	5.04
Human Phenotype	Flat occiput	3.97
Human Phenotype	Abnormal activity of mitochondrial respiratory chain	3.03

Supplementary Figure 323: Properties and genomic distribution of motifs identified for the YY1 transcription factor in A549 (accession ENCSR000BPM).

TF-MoDisCO pattern_0 n=7707, CWM

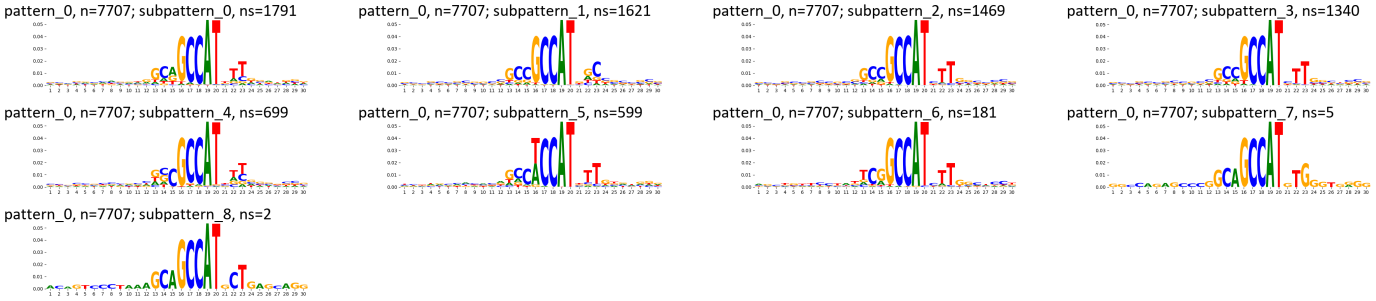

TF-MoDisCO pattern_0 n=7707, PWM

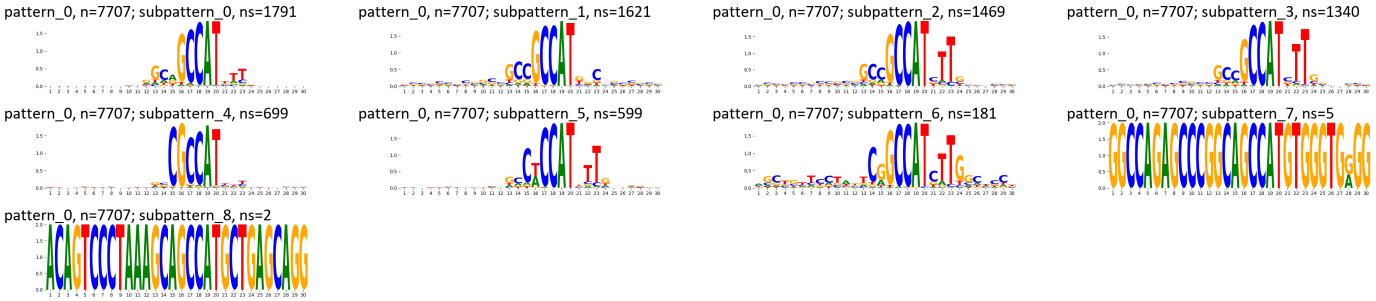

Supplementary Figure 324: TF-MoDisCO subpatterns for the YY1 transcription factor in A549 (accession ENCSR000BPM).

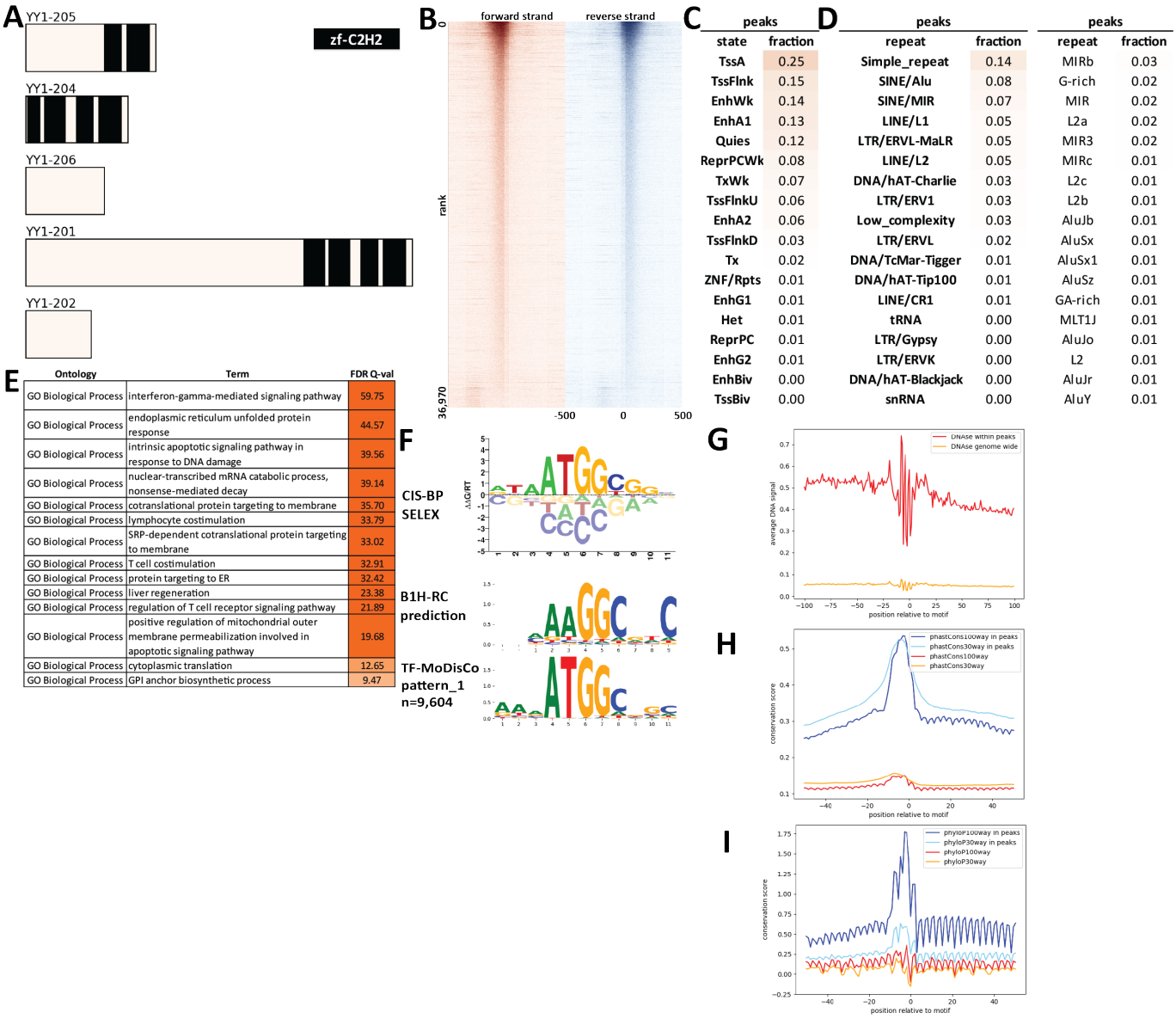

Supplementary Figure 325: Properties and genomic distribution of motifs identified for the YY1 transcription factor in GM12878 (accession ENCSR000BNP).

TF-MoDisCO pattern_1 n=9604, CWM

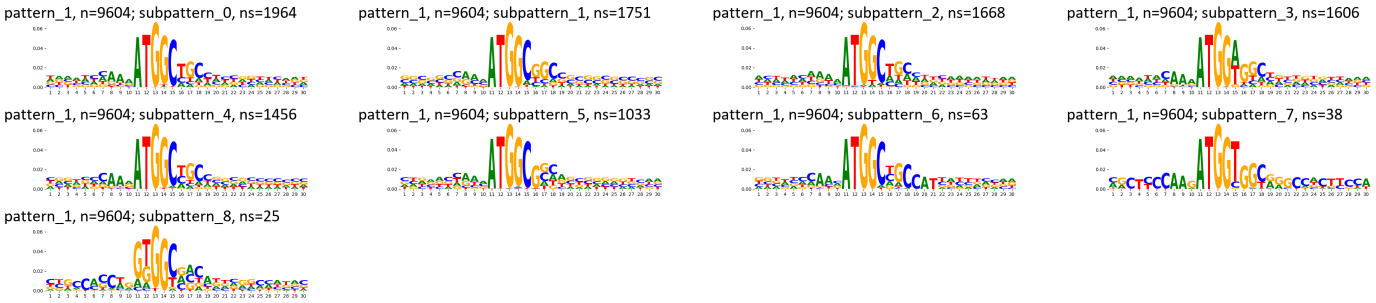

TF-MoDisCO pattern_1 n=9604, PWM

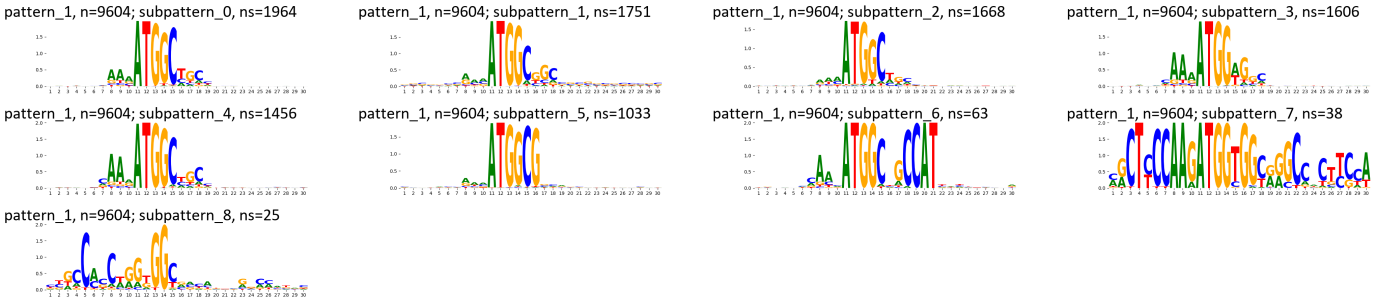

Supplementary Figure 326: TF-MoDisCO subpatterns for the YY1 transcription factor in GM12878 (accession ENCSR000BNP).

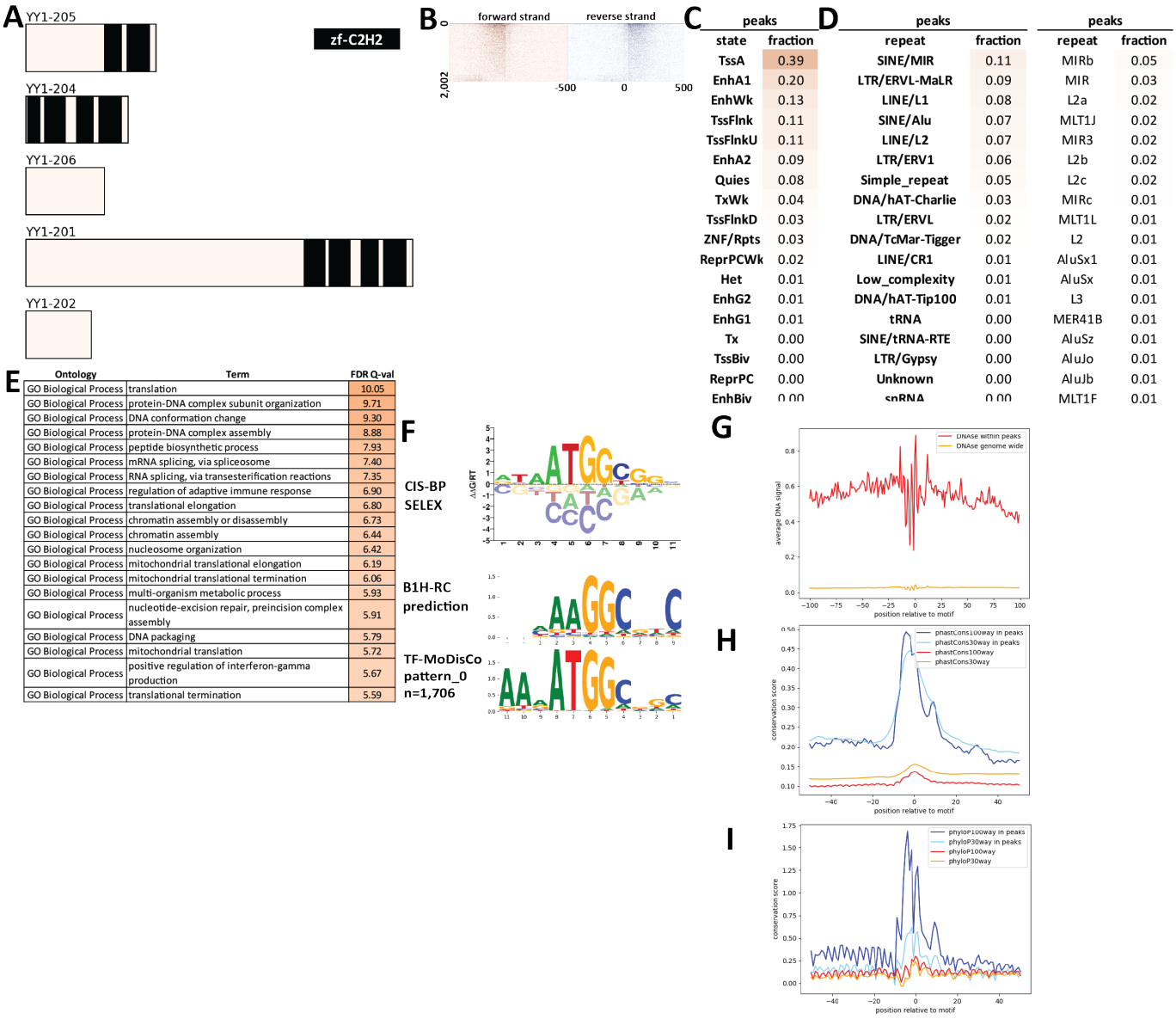

C

peaks	
state	fraction
TssA	0.39
EnhA1	0.20
EnhWk	0.13
TssFlnk	0.11
TssFlnkU	0.11
EnhA2	0.09
Quies	0.08
TxWk	0.04
TssFlnkD	0.03
ZNF/Rpts	0.03
ReprPCWk	0.02
Het	0.01
EnhG2	0.01
EnhG1	0.01
Tx	0.00
TssBiv	0.00
ReprPC	0.00
EnhBiv	0.00

D

peaks		peaks	
repeat	fraction	repeat	fraction
SINE/MIR	0.11	MIRb	0.05
LTR/ERVL-MaLR	0.09	MIR	0.03
LINE/L1	0.08	L2a	0.02
SINE/Alu	0.07	MLT1J	0.02
LINE/L2	0.07	MIR3	0.02
LTR/ERV1	0.06	L2b	0.02
Simple_repeat	0.05	L2c	0.02
DNA/hAT-Charlie	0.03	MIRc	0.01
LTR/ERVL	0.02	MLT1L	0.01
DNA/TcMar-Tigger	0.02	L2	0.01
LINE/CR1	0.01	AluSx1	0.01
Low_complexity	0.01	AluSx	0.01
DNA/hAT-Tip100	0.01	L3	0.01
tRNA	0.00	MER41B	0.01
SINE/tRNA-RTE	0.00	AluSz	0.01
LTR/Gypsy	0.00	AluJo	0.01
Unknown	0.00	AluJb	0.01
snRNA	0.00	MLT1F	0.01

E

Ontology	Term	FDR Q-val
GO Biological Process	translation	10.05
GO Biological Process	protein-DNA complex subunit organization	9.71
GO Biological Process	DNA conformation change	9.30
GO Biological Process	protein-DNA complex assembly	8.88
GO Biological Process	peptide biosynthetic process	7.93
GO Biological Process	mRNA splicing, via spliceosome	7.40
GO Biological Process	RNA splicing, via transesterification reactions	7.35
GO Biological Process	regulation of adaptive immune response	6.90
GO Biological Process	translational elongation	6.80
GO Biological Process	chromatin assembly or disassembly	6.73
GO Biological Process	chromatin assembly	6.44
GO Biological Process	nucleosome organization	6.42
GO Biological Process	mitochondrial translational elongation	6.19
GO Biological Process	mitochondrial translational termination	6.06
GO Biological Process	multi-organism metabolic process	5.93
GO Biological Process	nucleotide-excision repair, preincision complex assembly	5.91
GO Biological Process	DNA packaging	5.79
GO Biological Process	mitochondrial translation	5.72
GO Biological Process	positive regulation of interferon-gamma production	5.67
GO Biological Process	translational termination	5.59

Supplementary Figure 327: Properties and genomic distribution of motifs identified for the YY1 transcription factor in GM12878 (accession ENCSR000EUM).

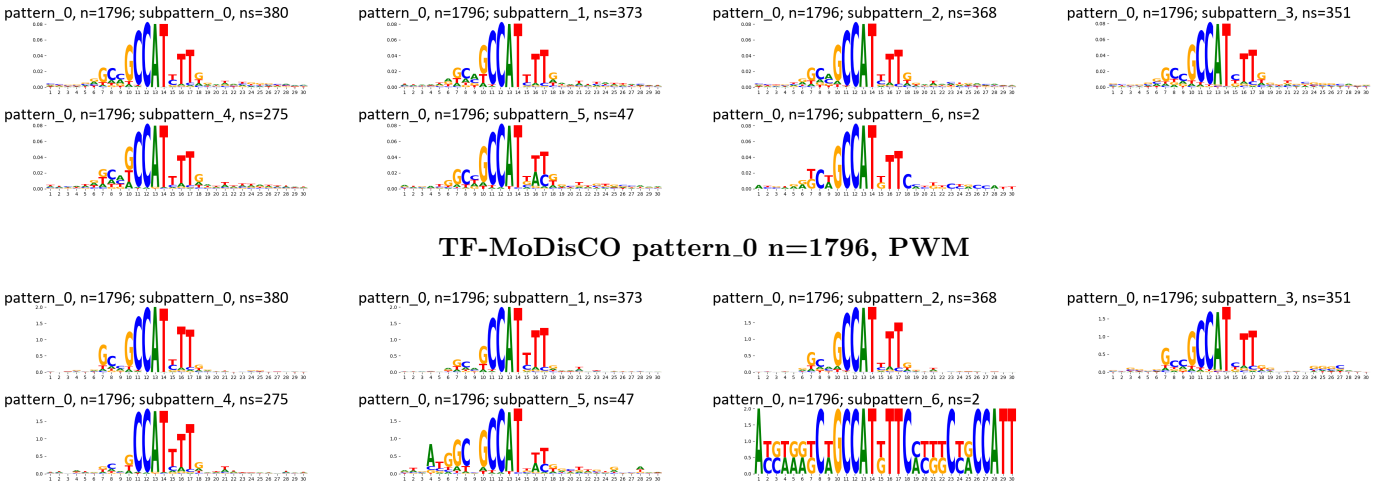

Supplementary Figure 328: TF-MoDisCO subpatterns for the YY1 transcription factor in GM12878 (accession ENCSR000EUM).

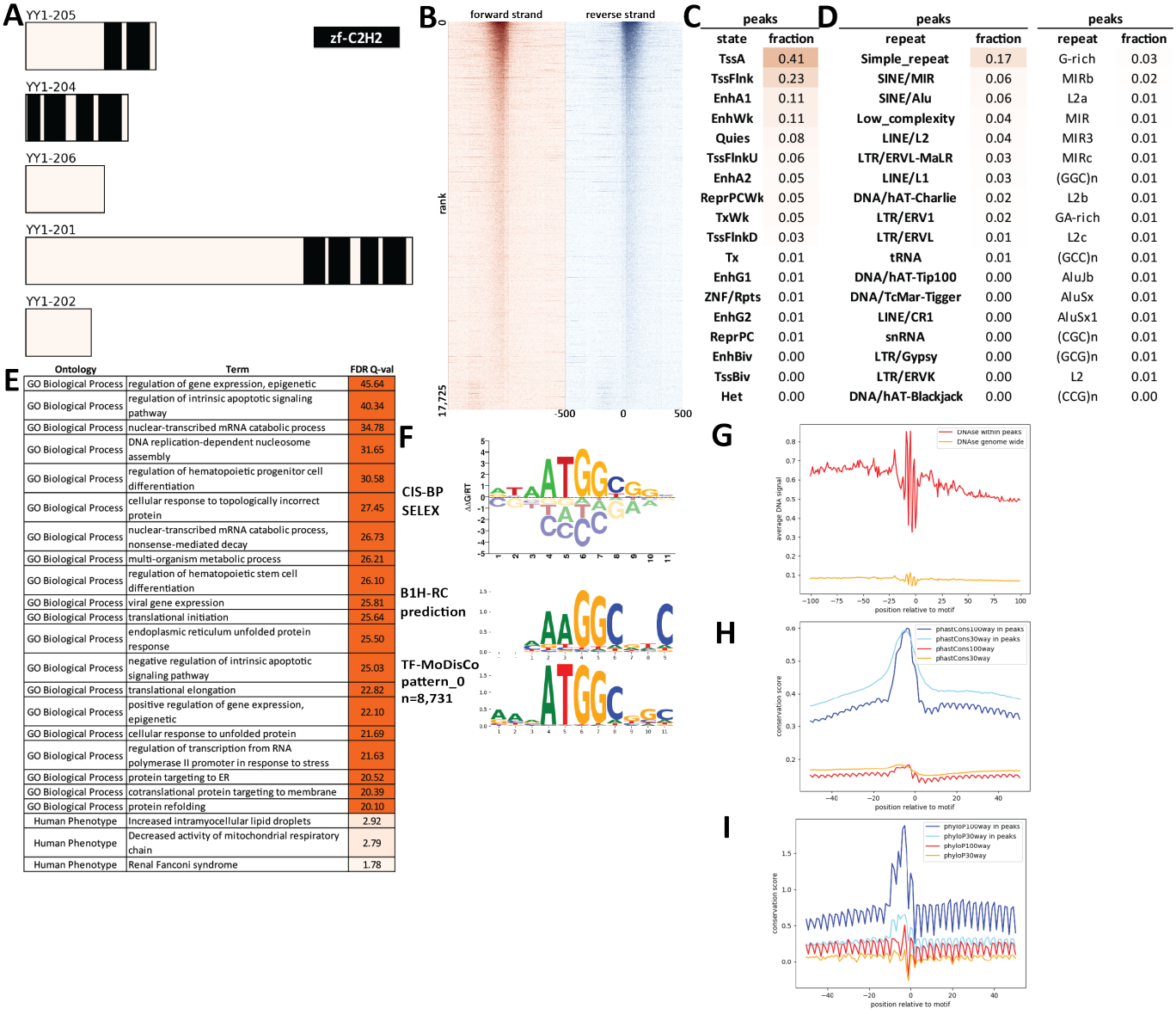

C

peaks	
state	fraction
TssA	0.41
TssFlnk	0.23
EnhA1	0.11
EnhWk	0.11
Quies	0.08
TssFlnkU	0.06
EnhA2	0.05
ReprPCWk	0.05
TxWk	0.05
TssFlnkD	0.03
Tx	0.01
EnhG1	0.01
ZNF/Rpts	0.01
EnhG2	0.01
ReprPC	0.01
EnhBiv	0.00
TssBiv	0.00
Het	0.00

D

peaks		peaks	
repeat	fraction	repeat	fraction
Simple_repeat	0.17	G-rich	0.03
SINE/MIR	0.06	MIRb	0.02
SINE/Alu	0.06	L2a	0.01
Low_complexity	0.04	MIR	0.01
LINE/L2	0.04	MIR3	0.01
LTR/ERVL-MaLR	0.03	MIRc	0.01
LINE/L1	0.03	(GGC)n	0.01
DNA/hAT-Charlie	0.02	L2b	0.01
LTR/ERV1	0.02	GA-rich	0.01
LTR/ERVL	0.01	L2c	0.01
tRNA	0.01	(GCC)n	0.01
DNA/hAT-Tip100	0.00	AluJb	0.01
DNA/TcMar-Tigger	0.00	AluSx	0.01
LINE/CR1	0.00	AluSx1	0.01
snRNA	0.00	(CGC)n	0.01
LTR/Gypsy	0.00	(GCG)n	0.01
LTR/ERVK	0.00	L2	0.01
DNA/hAT-Blackjack	0.00	(CCG)n	0.00

E

Ontology	Term	FDR Q-val
GO Biological Process	regulation of gene expression, epigenetic	45.64
GO Biological Process	regulation of intrinsic apoptotic signaling pathway	40.34
GO Biological Process	nuclear-transcribed mRNA catabolic process	34.78
GO Biological Process	DNA replication-dependent nucleosome assembly	31.65
GO Biological Process	regulation of hematopoietic progenitor cell differentiation	30.58
GO Biological Process	cellular response to topologically incorrect protein	27.45
GO Biological Process	nuclear-transcribed mRNA catabolic process, nonsense-mediated decay	26.73
GO Biological Process	multi-organism metabolic process	26.21
GO Biological Process	regulation of hematopoietic stem cell differentiation	26.10
GO Biological Process	viral gene expression	25.81
GO Biological Process	translational initiation	25.64
GO Biological Process	endoplasmic reticulum unfolded protein response	25.50
GO Biological Process	negative regulation of intrinsic apoptotic signaling pathway	25.03
GO Biological Process	translational elongation	22.82
GO Biological Process	positive regulation of gene expression, epigenetic	22.10
GO Biological Process	cellular response to unfolded protein	21.69
GO Biological Process	regulation of transcription from RNA polymerase II promoter in response to stress	21.63
GO Biological Process	protein targeting to ER	20.52
GO Biological Process	cotranslational protein targeting to membrane	20.39
GO Biological Process	protein refolding	20.10
Human Phenotype	Increased intramyocellular lipid droplets	2.92
Human Phenotype	Decreased activity of mitochondrial respiratory chain	2.79
Human Phenotype	Renal Fanconi syndrome	1.78

Supplementary Figure 329: Properties and genomic distribution of motifs identified for the YY1 transcription factor in GM12891 (accession ENCSR000BKJ).

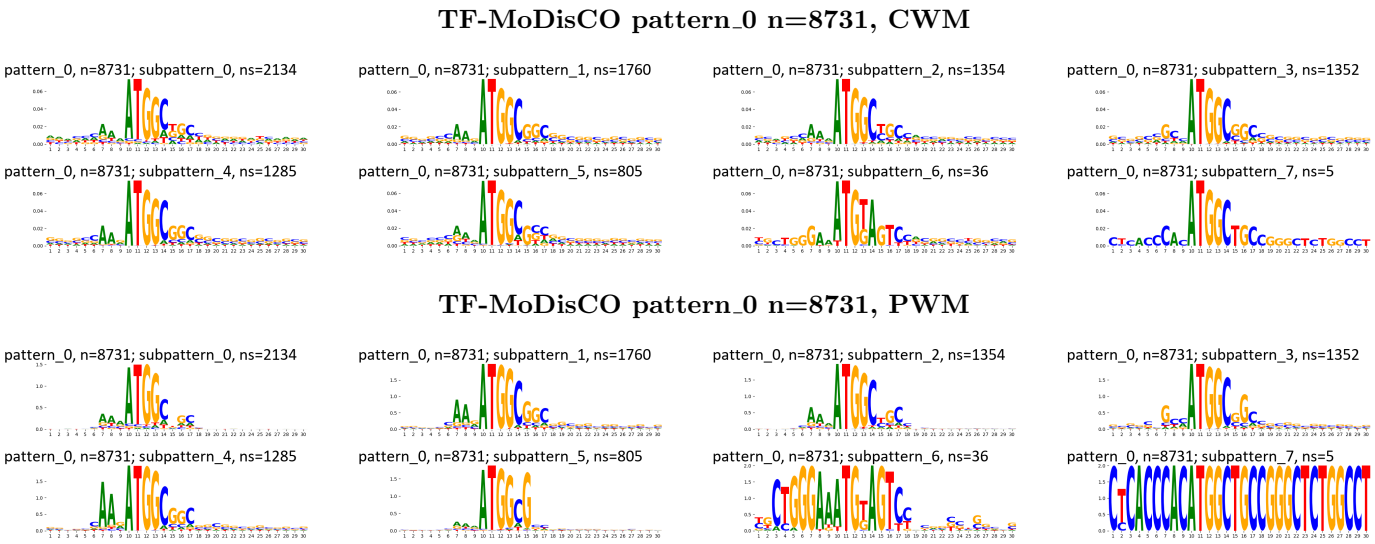

Supplementary Figure 330: TF-MoDisCO subpatterns for the YY1 transcription factor in GM12891 (accession ENCSR000BKJ).

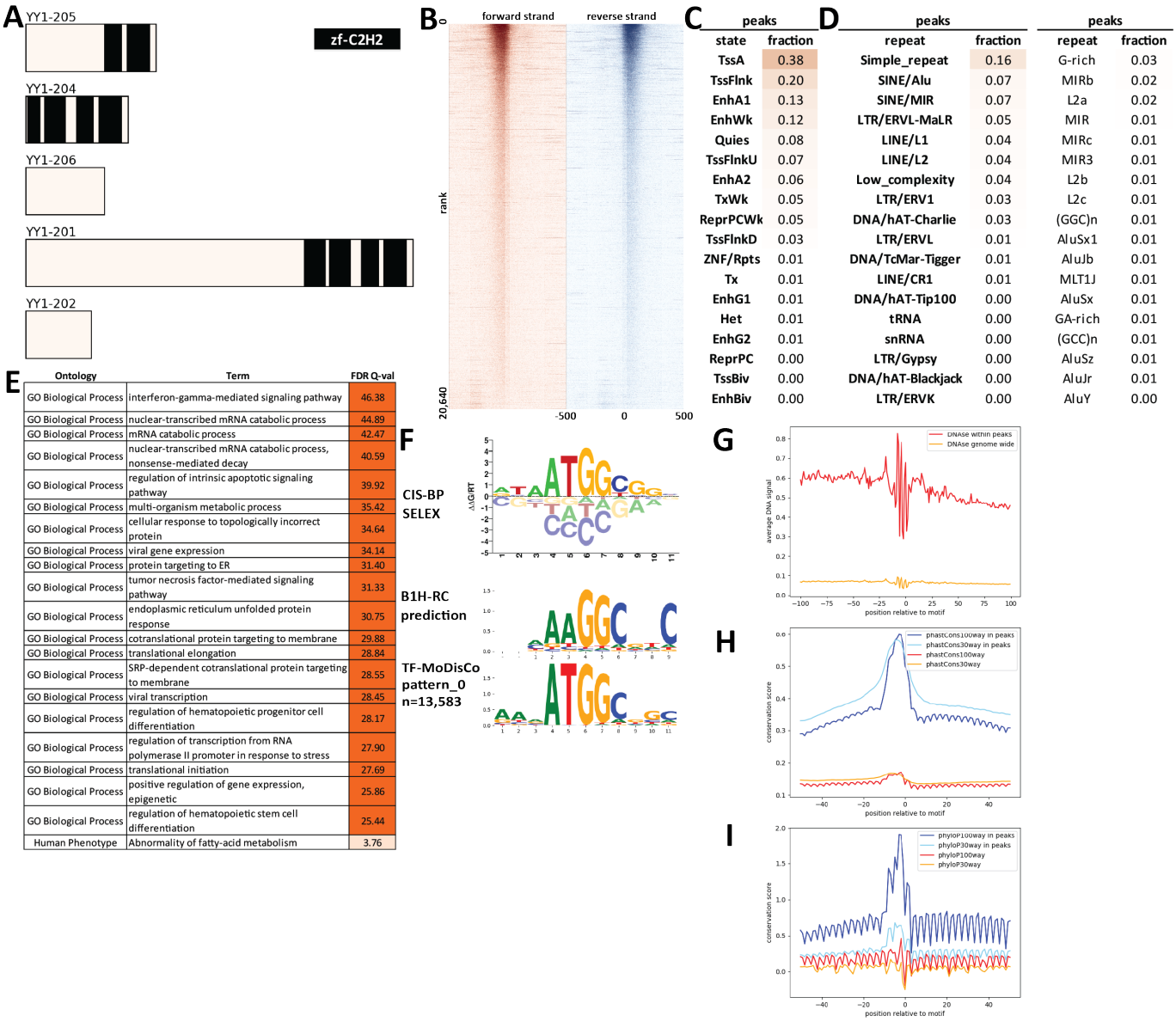

Supplementary Figure 331: Properties and genomic distribution of motifs identified for the YY1 transcription factor in GM12892 (accession ENCSR000BLT).

TF-MoDisCO pattern_0 n=13583, CWM

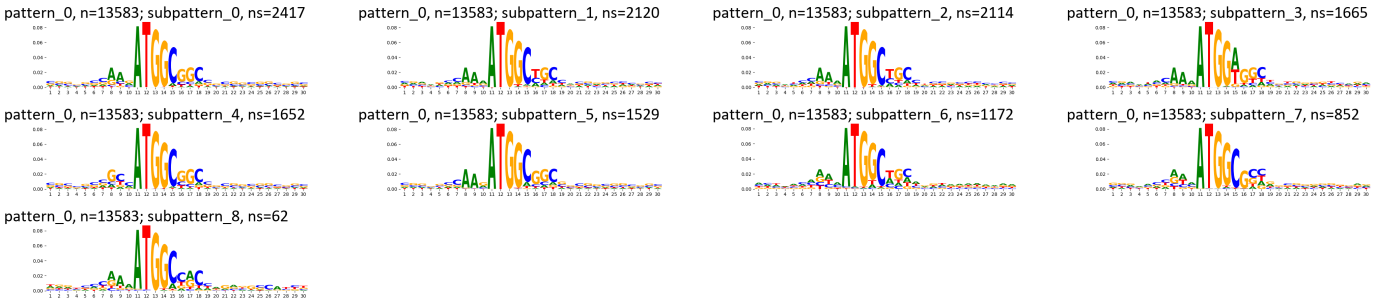

TF-MoDisCO pattern_0 n=13583, PWM

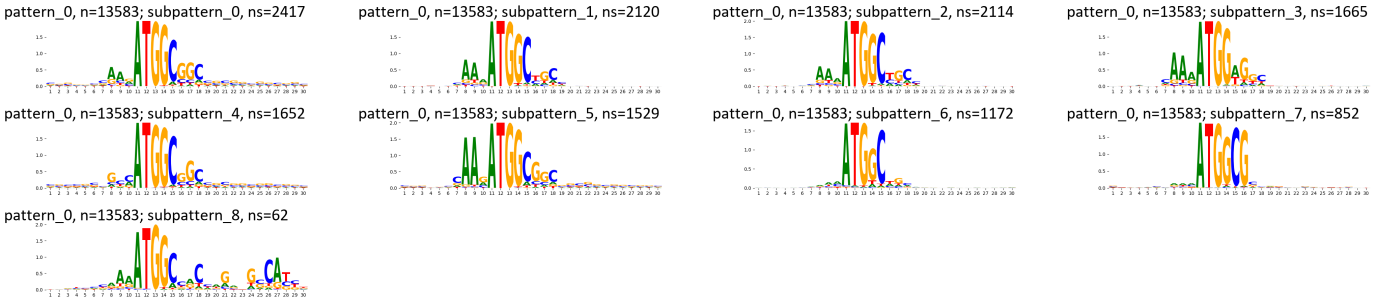

Supplementary Figure 332: TF-MoDisCO subpatterns for the YY1 transcription factor in GM12892 (accession ENCSR000BLT).

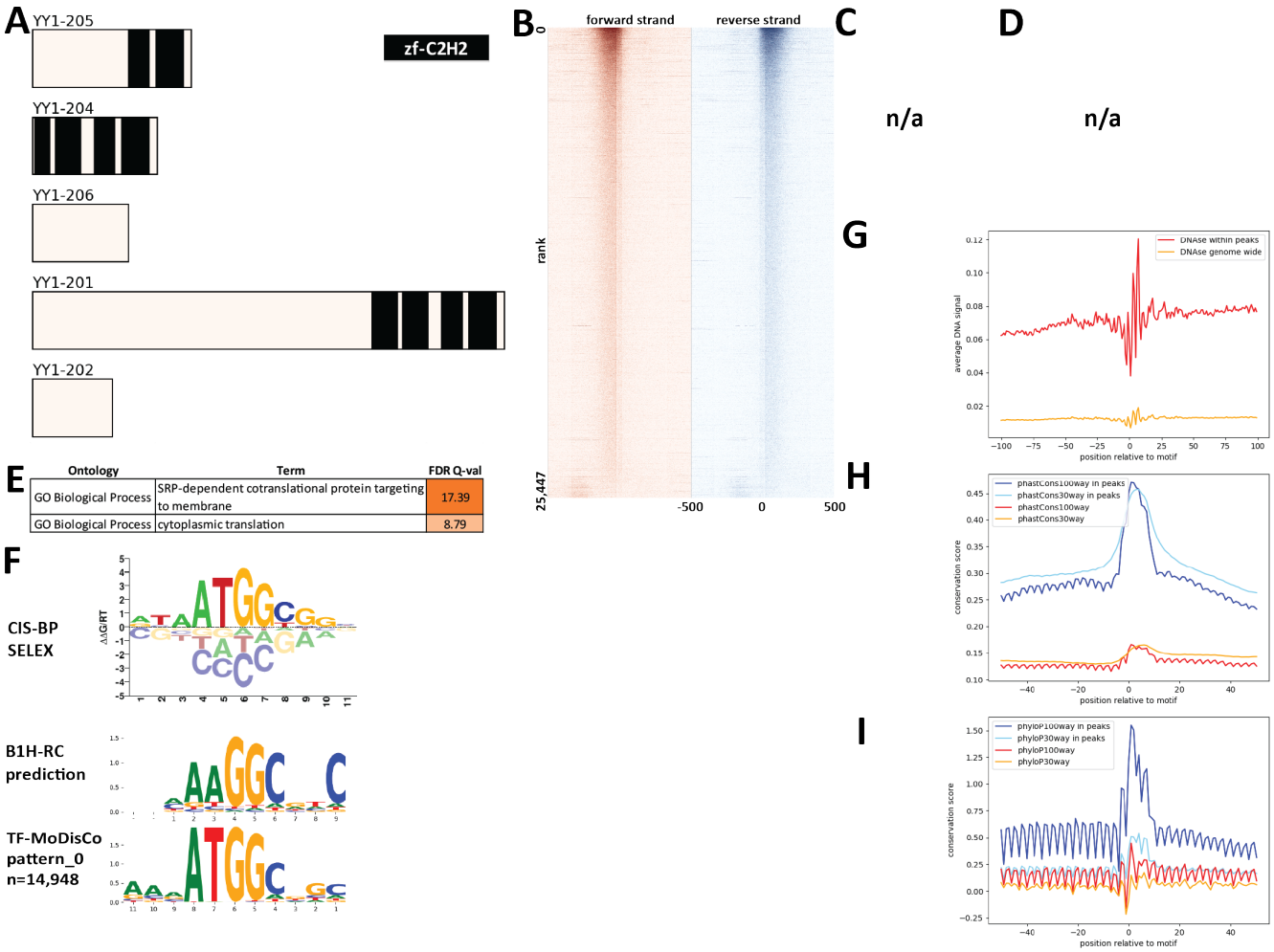

Supplementary Figure 333: Properties and genomic distribution of motifs identified for the YY1 transcription factor in H1 (accession ENCSR000BKD).

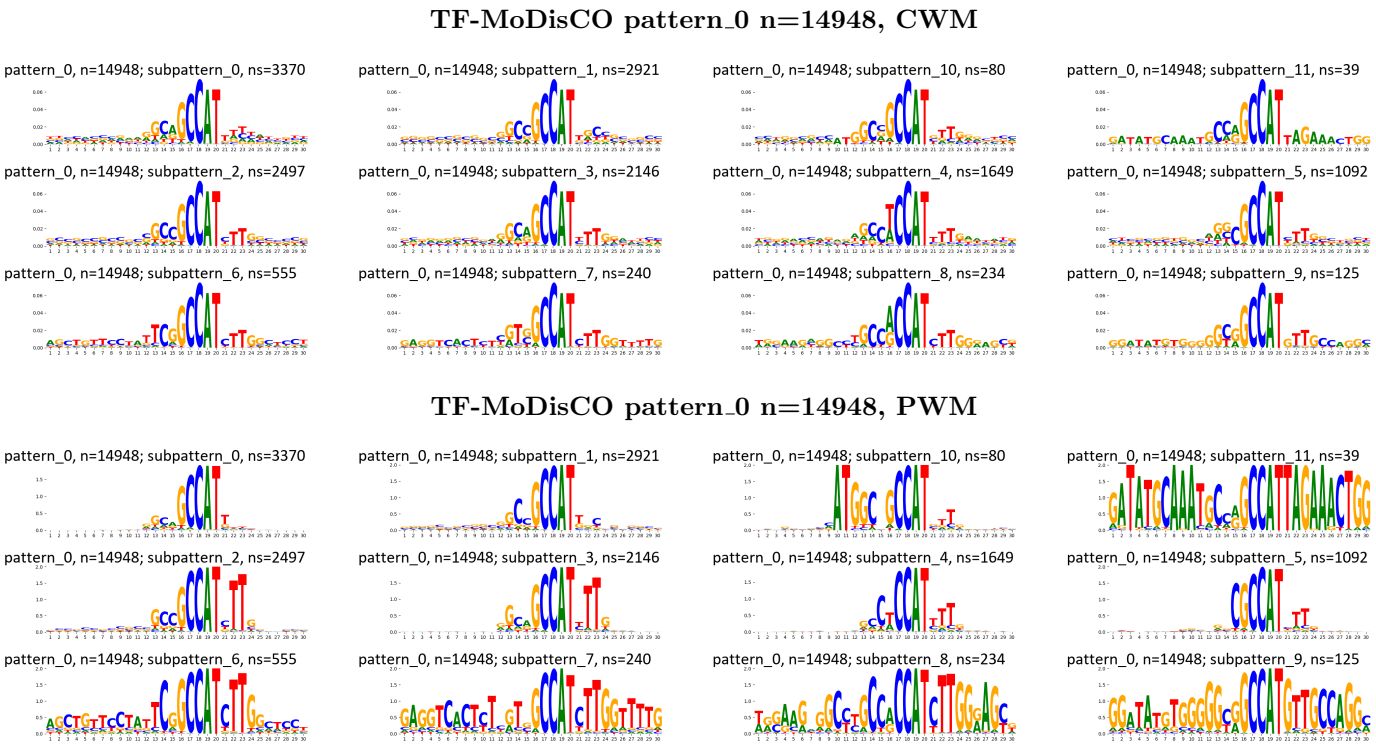

Supplementary Figure 334: TF-MoDisCO subpatterns for the YY1 transcription factor in H1 (accession ENCSR000BKD).

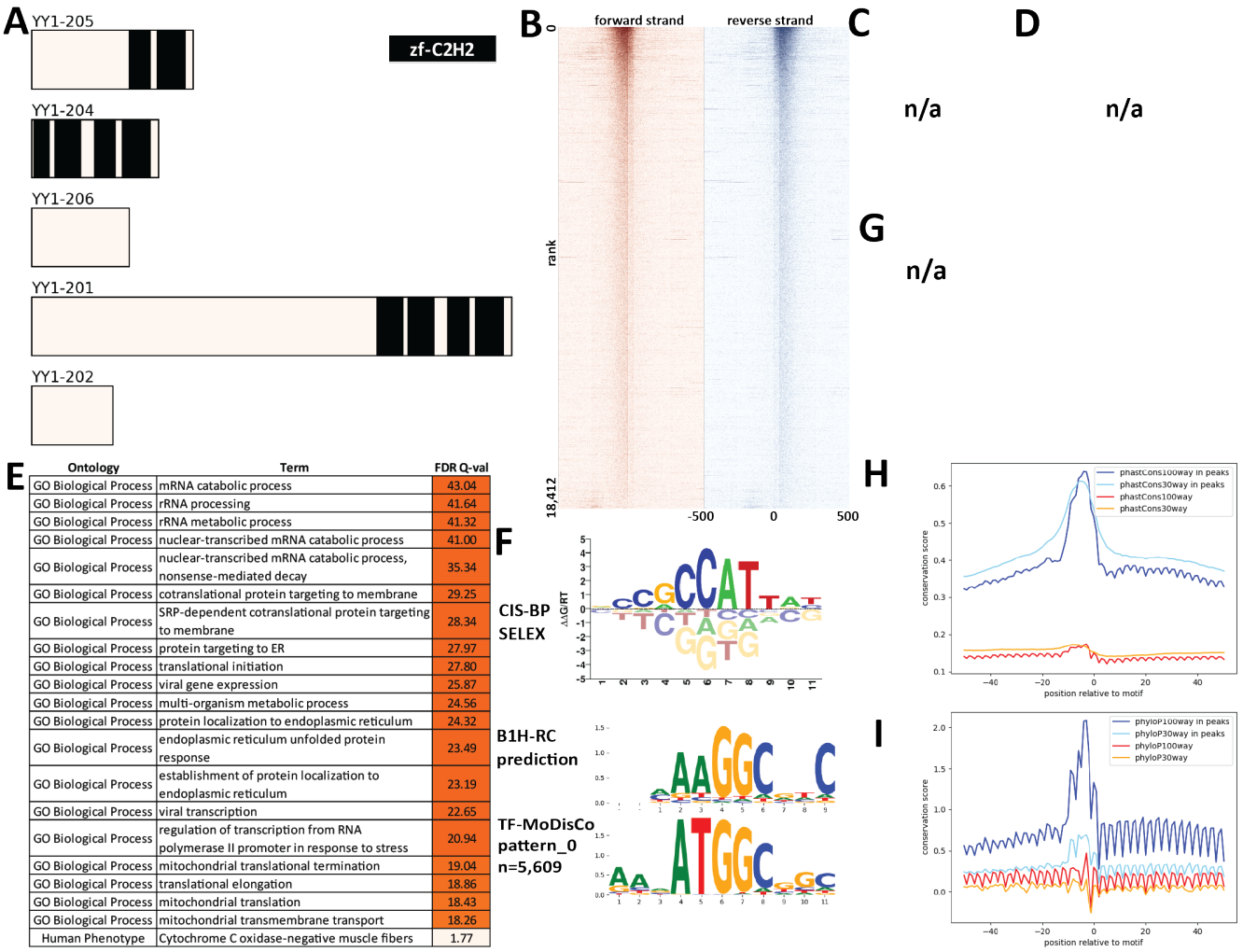

Ontology	Term	FDR Q-val
GO Biological Process	mRNA catabolic process	43.04
GO Biological Process	rRNA processing	41.64
GO Biological Process	rRNA metabolic process	41.32
GO Biological Process	nuclear-transcribed mRNA catabolic process	41.00
GO Biological Process	nuclear-transcribed mRNA catabolic process, nonsense-mediated decay	35.34
GO Biological Process	cotranslational protein targeting to membrane	29.25
GO Biological Process	SRP-dependent cotranslational protein targeting to membrane	28.34
GO Biological Process	protein targeting to ER	27.97
GO Biological Process	translational initiation	27.80
GO Biological Process	viral gene expression	25.87
GO Biological Process	multi-organism metabolic process	24.56
GO Biological Process	protein localization to endoplasmic reticulum	24.32
GO Biological Process	endoplasmic reticulum unfolded protein response	23.49
GO Biological Process	establishment of protein localization to endoplasmic reticulum	23.19
GO Biological Process	viral transcription	22.65
GO Biological Process	regulation of transcription from RNA polymerase II promoter in response to stress	20.94
GO Biological Process	mitochondrial translational termination	19.04
GO Biological Process	translational elongation	18.86
GO Biological Process	mitochondrial translation	18.43
GO Biological Process	mitochondrial transmembrane transport	18.26
Human Phenotype	Cytochrome C oxidase-negative muscle fibers	1.77

Supplementary Figure 335: Properties and genomic distribution of motifs identified for the YY1 transcription factor in HCT116 (accession ENCSR000BNX).

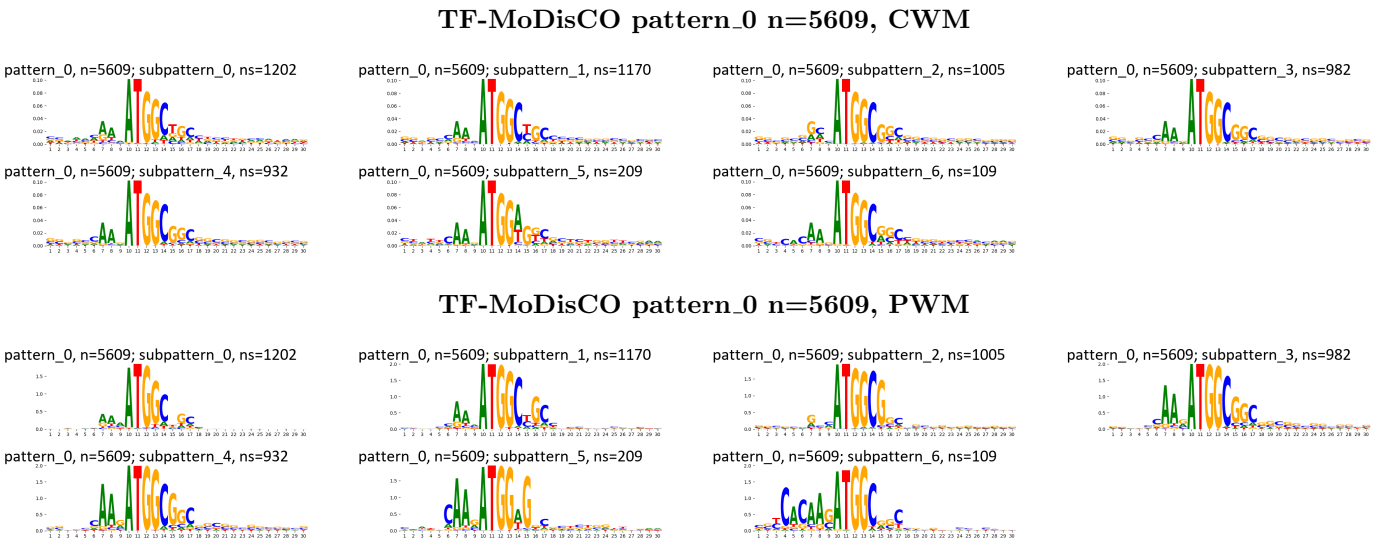

Supplementary Figure 336: TF-MoDisCO subpatterns for the YY1 transcription factor in HCT116 (accession ENCSR000BNX).

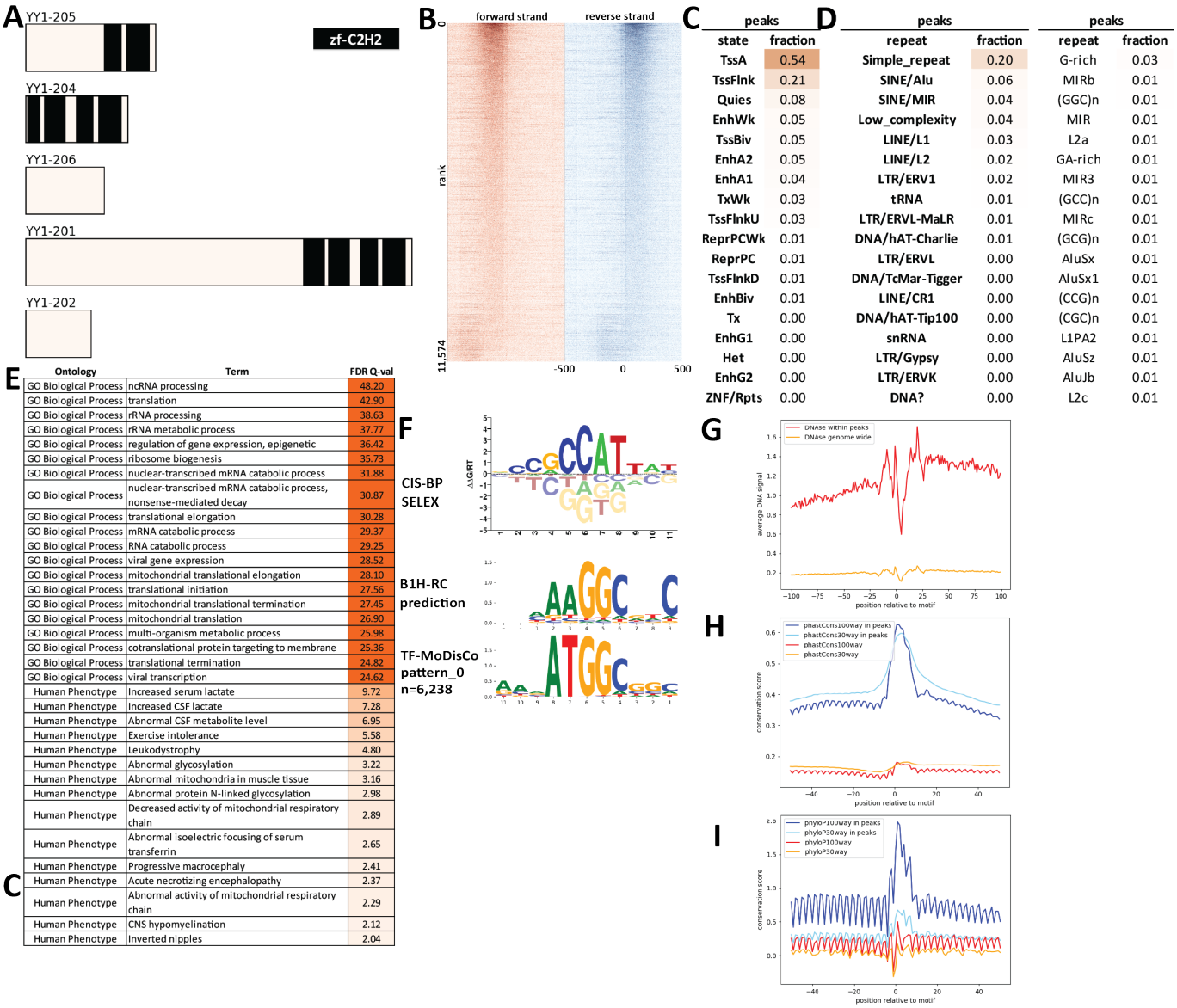

Supplementary Figure 337: Properties and genomic distribution of motifs identified for the YY1 transcription factor in HEK293 (accession ENCSR859RAO).

TF-MoDisCO pattern_0 n=6283, CWM

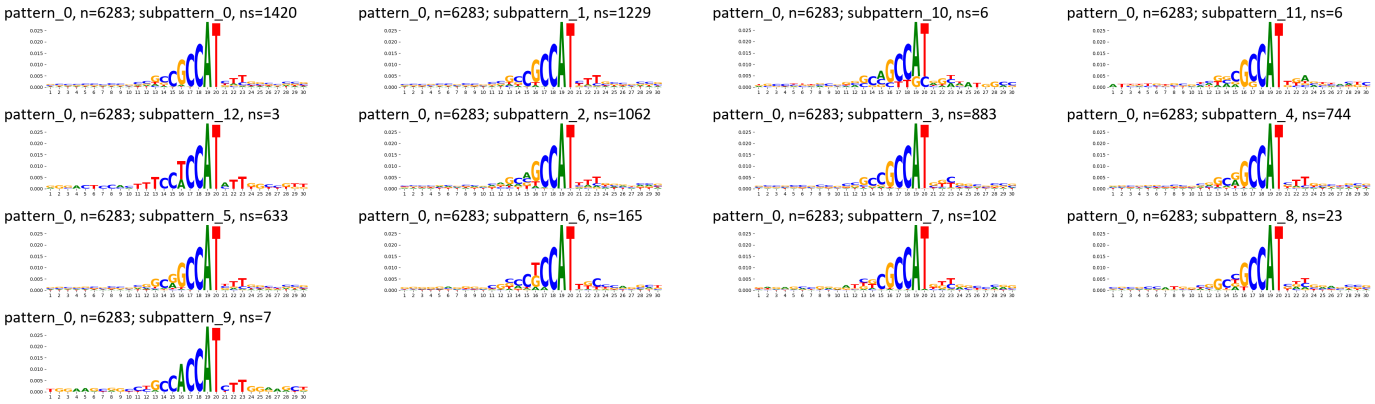

TF-MoDisCO pattern_0 n=6283, PWM

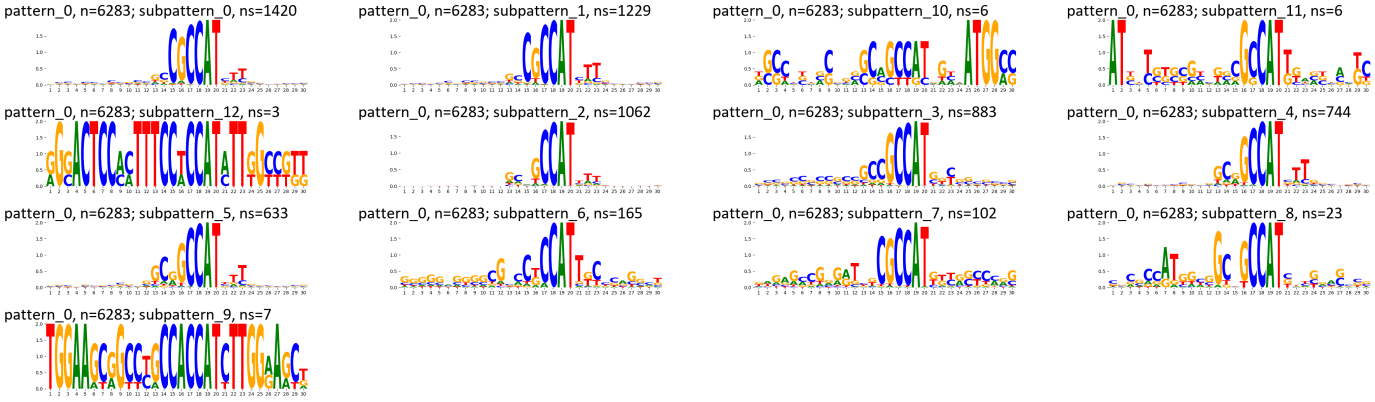

Supplementary Figure 338: TF-MoDisCO subpatterns for the YY1 transcription factor in HEK293 (accession ENCSR859RAO).

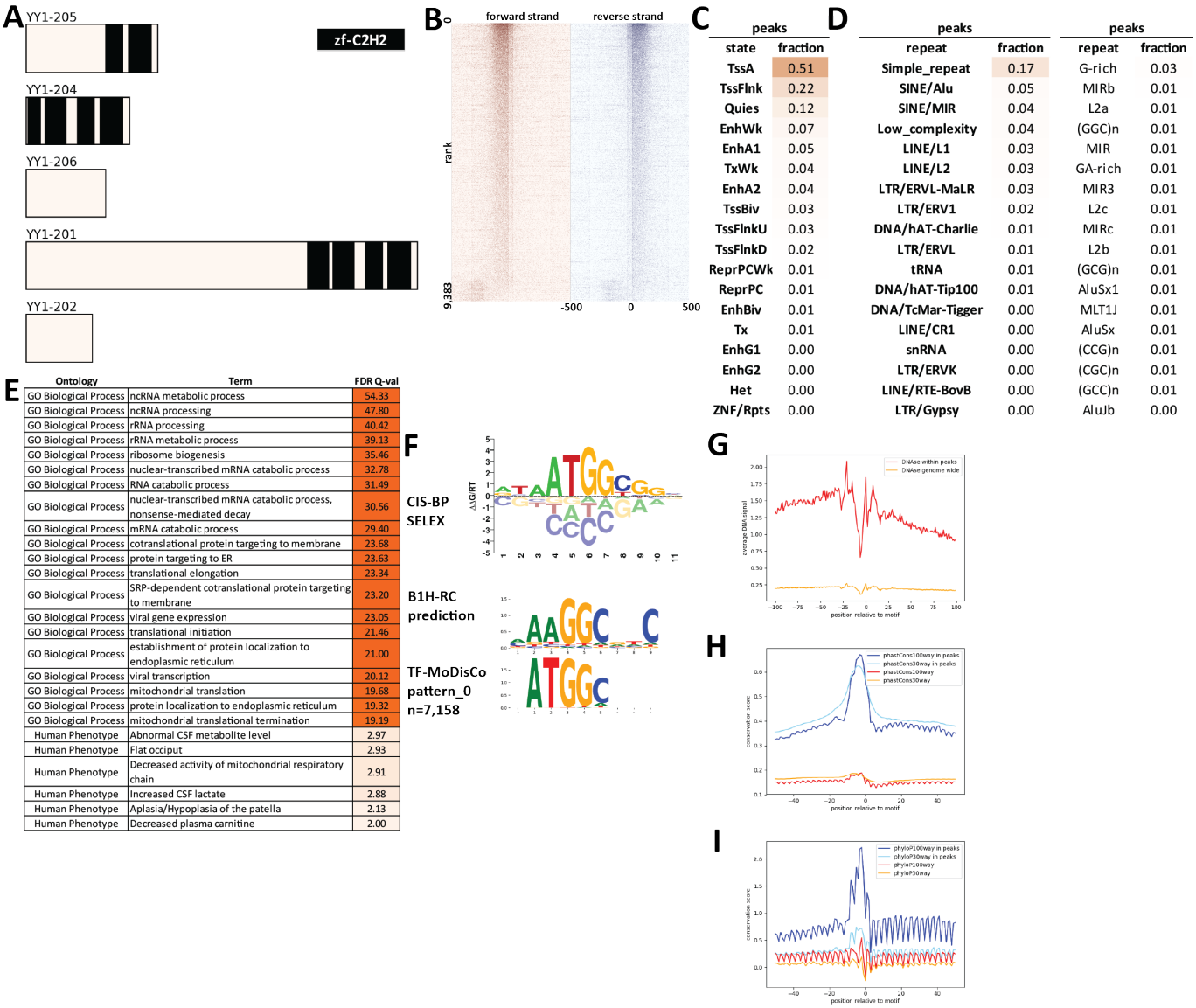

C

peaks	
state	fraction
TssA	0.51
TssFlnk	0.22
Quies	0.12
EnhWk	0.07
EnhA1	0.05
TxWk	0.04
EnhA2	0.04
TssBiv	0.03
TssFlnkU	0.03
TssFlnkD	0.02
ReprPCWk	0.01
ReprPC	0.01
EnhBiv	0.01
Tx	0.01
EnhG1	0.00
EnhG2	0.00
Het	0.00
ZNF/Rpts	0.00

D

peaks		peaks	
repeat	fraction	repeat	fraction
Simple_repeat	0.17	G-rich	0.03
SINE/Alu	0.05	MIRb	0.01
SINE/MIR	0.04	L2a	0.01
Low_complexity	0.04	(GGC)n	0.01
LINE/L1	0.03	MIR	0.01
LINE/L2	0.03	GA-rich	0.01
LTR/ERVL-MaLR	0.03	MIR3	0.01
LTR/ERV1	0.02	L2c	0.01
DNA/hAT-Charlie	0.01	MIRc	0.01
LTR/ERVL	0.01	L2b	0.01
tRNA	0.01	(GCG)n	0.01
DNA/hAT-Tip100	0.01	AluSx1	0.01
DNA/TcMar-Tigger	0.00	MLT1J	0.01
LINE/CR1	0.00	AluSx	0.01
snRNA	0.00	(CCG)n	0.01
LTR/ERVK	0.00	(CGC)n	0.01
LINE/RTE-BovB	0.00	(GCC)n	0.01
LTR/Gypsy	0.00	AluJb	0.00

E

Ontology	Term	FDR Q-val
GO Biological Process	ncRNA metabolic process	54.33
GO Biological Process	ncRNA processing	47.80
GO Biological Process	rRNA processing	40.42
GO Biological Process	rRNA metabolic process	39.13
GO Biological Process	ribosome biogenesis	35.46
GO Biological Process	nuclear-transcribed mRNA catabolic process	32.78
GO Biological Process	RNA catabolic process	31.49
GO Biological Process	nuclear-transcribed mRNA catabolic process, nonsense-mediated decay	30.56
GO Biological Process	mRNA catabolic process	29.40
GO Biological Process	cotranslational protein targeting to membrane	23.68
GO Biological Process	protein targeting to ER	23.63
GO Biological Process	translational elongation	23.34
GO Biological Process	SRP-dependent cotranslational protein targeting to membrane	23.20
GO Biological Process	viral gene expression	23.05
GO Biological Process	translational initiation	21.46
GO Biological Process	establishment of protein localization to endoplasmic reticulum	21.00
GO Biological Process	viral transcription	20.12
GO Biological Process	mitochondrial translation	19.68
GO Biological Process	protein localization to endoplasmic reticulum	19.32
GO Biological Process	mitochondrial translational termination	19.19
Human Phenotype	Abnormal CSF metabolite level	2.97
Human Phenotype	Flat occiput	2.93
Human Phenotype	Decreased activity of mitochondrial respiratory chain	2.91
Human Phenotype	Increased CSF lactate	2.88
Human Phenotype	Aplasia/Hypoplasia of the patella	2.13
Human Phenotype	Decreased plasma carnitine	2.00

Supplementary Figure 339: Properties and genomic distribution of motifs identified for the YY1 transcription factor in HEK293 (accession Hughes NB models).

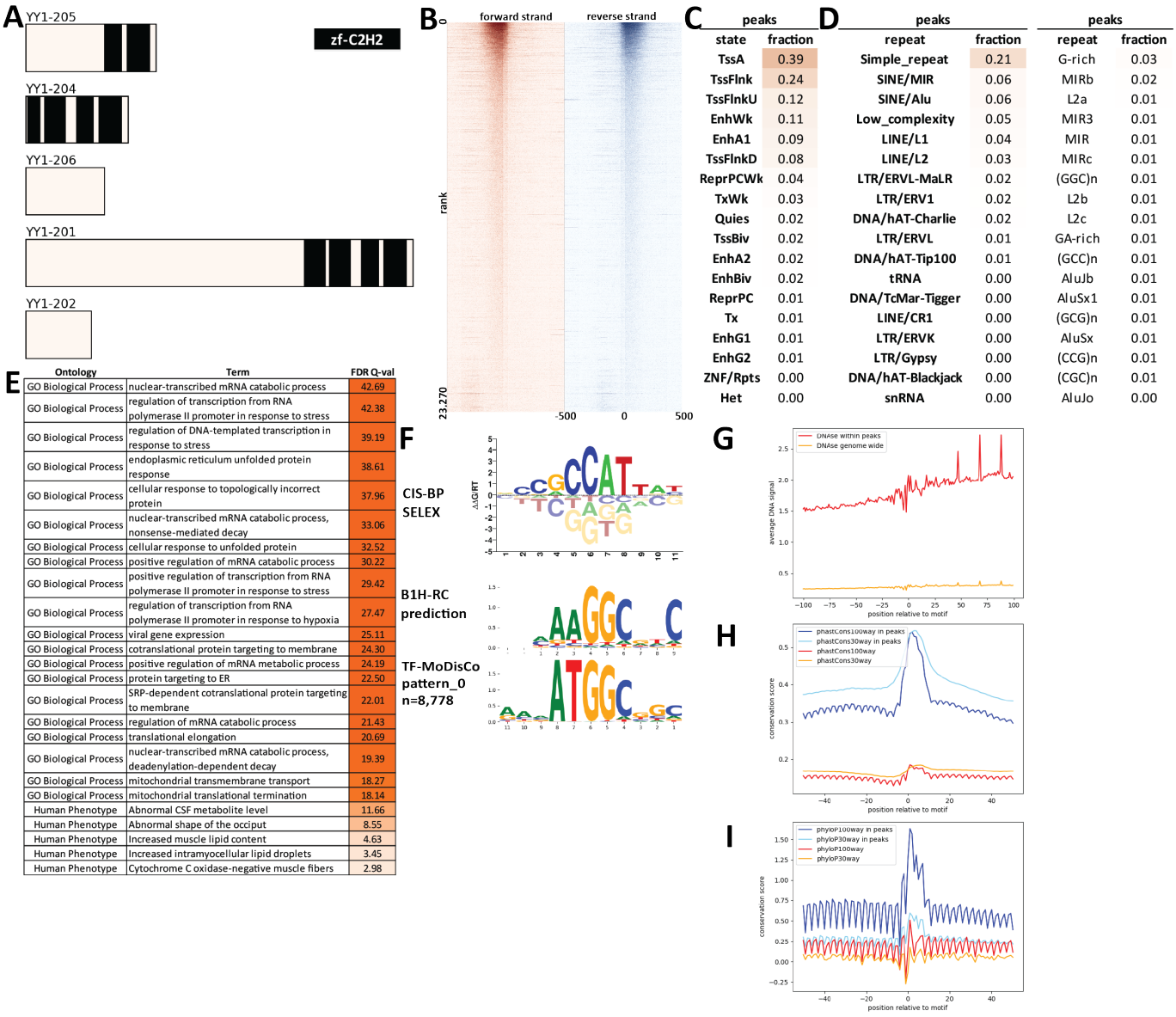

Supplementary Figure 340: Properties and genomic distribution of motifs identified for the YY1 transcription factor in HepG2 (accession ENCSR000BNT).

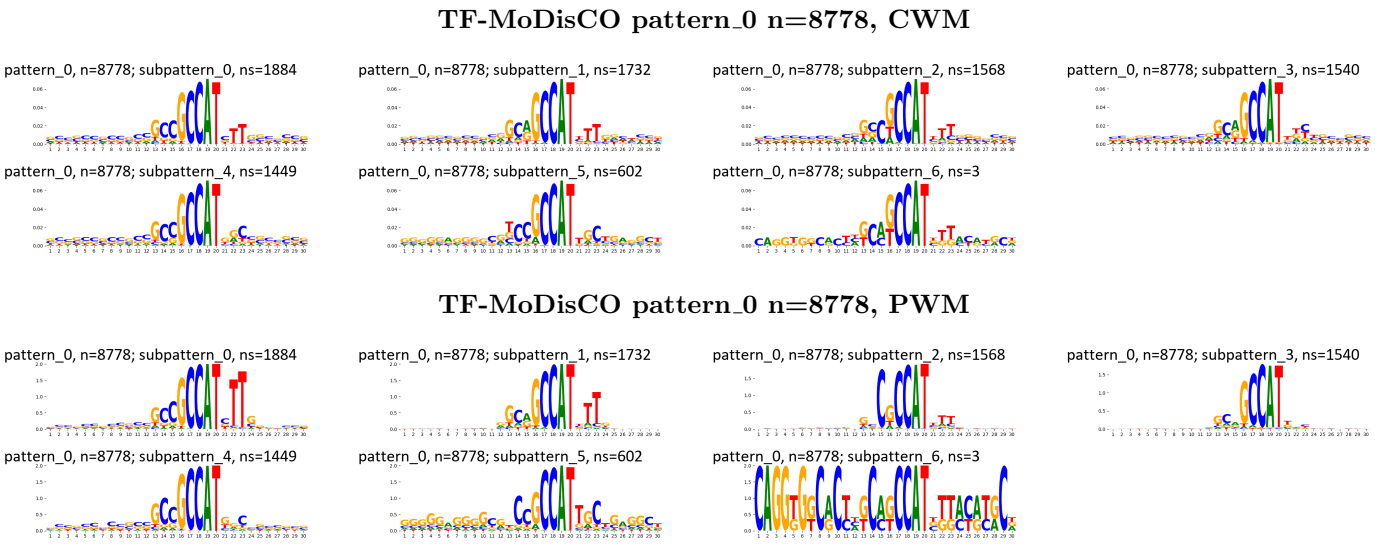

Supplementary Figure 341: TF-MoDisCO subpatterns for the YY1 transcription factor in HepG2 (accession ENCSR000BNT).

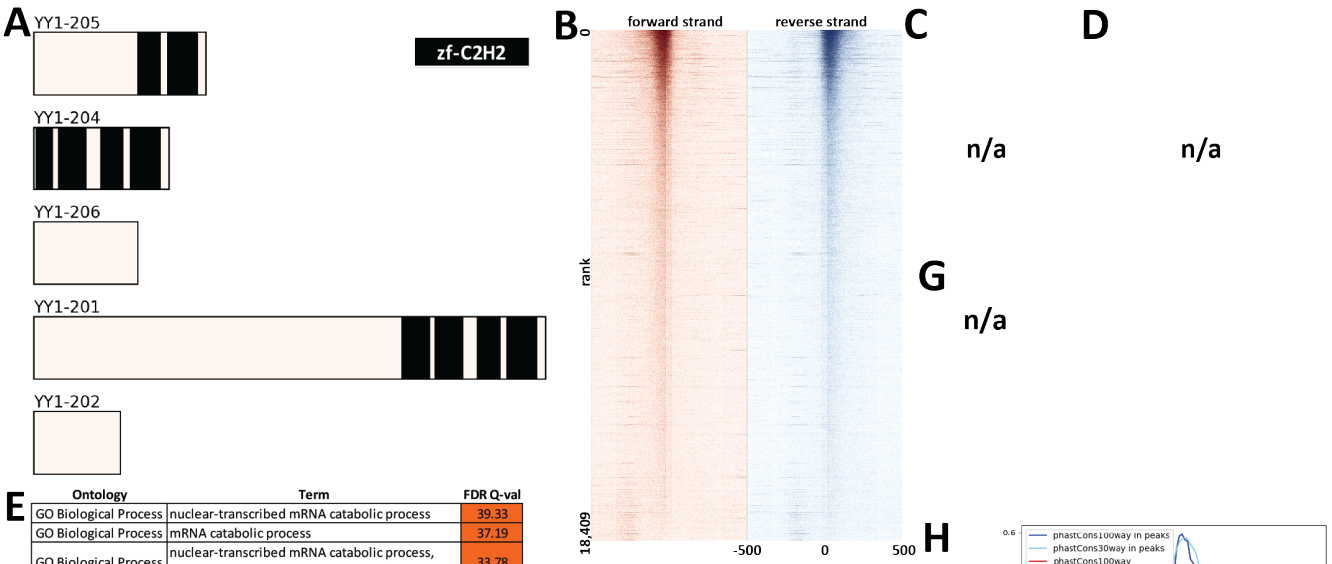

E

Ontology	Term	FDR Q-val
GO Biological Process	nuclear-transcribed mRNA catabolic process	39.33
GO Biological Process	mRNA catabolic process	37.19
GO Biological Process	nuclear-transcribed mRNA catabolic process, nonsense-mediated decay	33.78
GO Biological Process	viral gene expression	29.72
GO Biological Process	endoplasmic reticulum unfolded protein response	29.09
GO Biological Process	cotranslational protein targeting to membrane	28.07
GO Biological Process	protein targeting to ER	27.59
GO Biological Process	multi-organism metabolic process	26.97
GO Biological Process	cellular response to topologically incorrect protein	26.88
GO Biological Process	SRP-dependent cotranslational protein targeting to membrane	26.77
GO Biological Process	viral transcription	26.75
GO Biological Process	translational initiation	25.92
GO Biological Process	protein localization to endoplasmic reticulum	24.27
GO Biological Process	protein targeting to membrane	23.63
GO Biological Process	cellular response to unfolded protein	23.22
GO Biological Process	establishment of protein localization to endoplasmic reticulum	22.45
GO Biological Process	regulation of mitochondrial membrane permeability	18.03
GO Biological Process	intrinsic apoptotic signaling pathway in response to DNA damage	17.83
GO Biological Process	regulation of viral transcription	16.33
GO Biological Process	regulation of release of cytochrome c from mitochondria	15.60
Human Phenotype	Abnormal CSF metabolite level	10.30
Human Phenotype	Increased CSF lactate	7.90
Human Phenotype	Abnormal activity of mitochondrial respiratory chain	3.81
Human Phenotype	Decreased activity of mitochondrial respiratory chain	3.78

Supplementary Figure 342: Properties and genomic distribution of motifs identified for the YY1 transcription factor in Ishikawa (accession ENCSR000BSY).

TF-MoDisCO pattern_0 n=9922, CWM

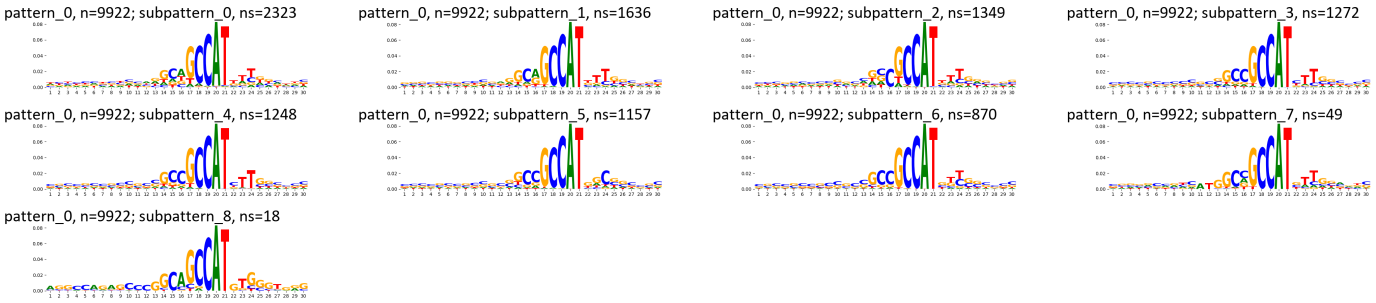

TF-MoDisCO pattern_0 n=9922, PWM

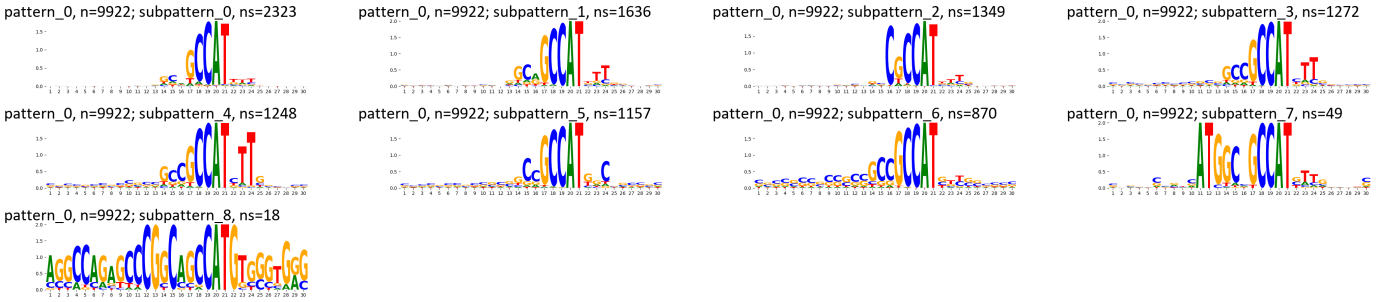

Supplementary Figure 343: TF-MoDisCO subpatterns for the YY1 transcription factor in Ishikawa (accession ENCSR000BSY).

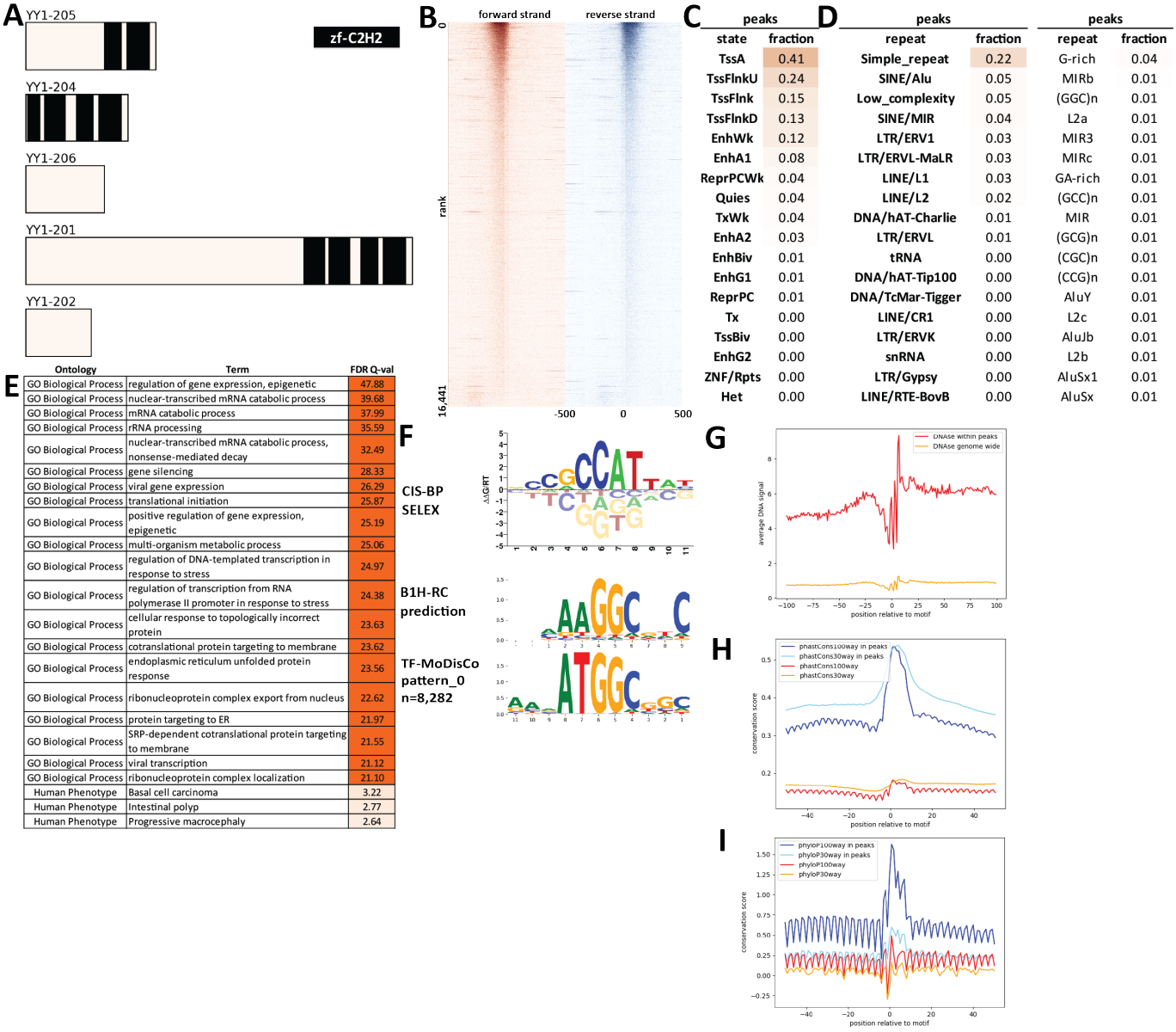

Supplementary Figure 344: Properties and genomic distribution of motifs identified for the YY1 transcription factor in K562 (accession ENCSR000BKU).

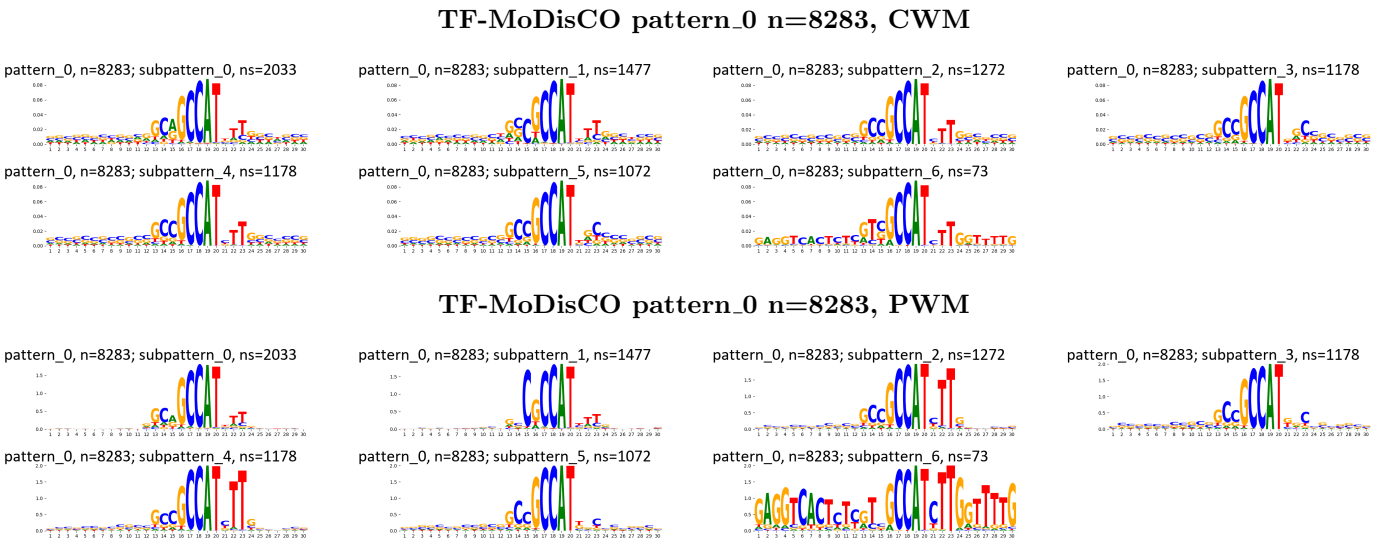

Supplementary Figure 345: TF-MoDisCO subpatterns for the YY1 transcription factor in K562 (accession ENCSR000BKU).

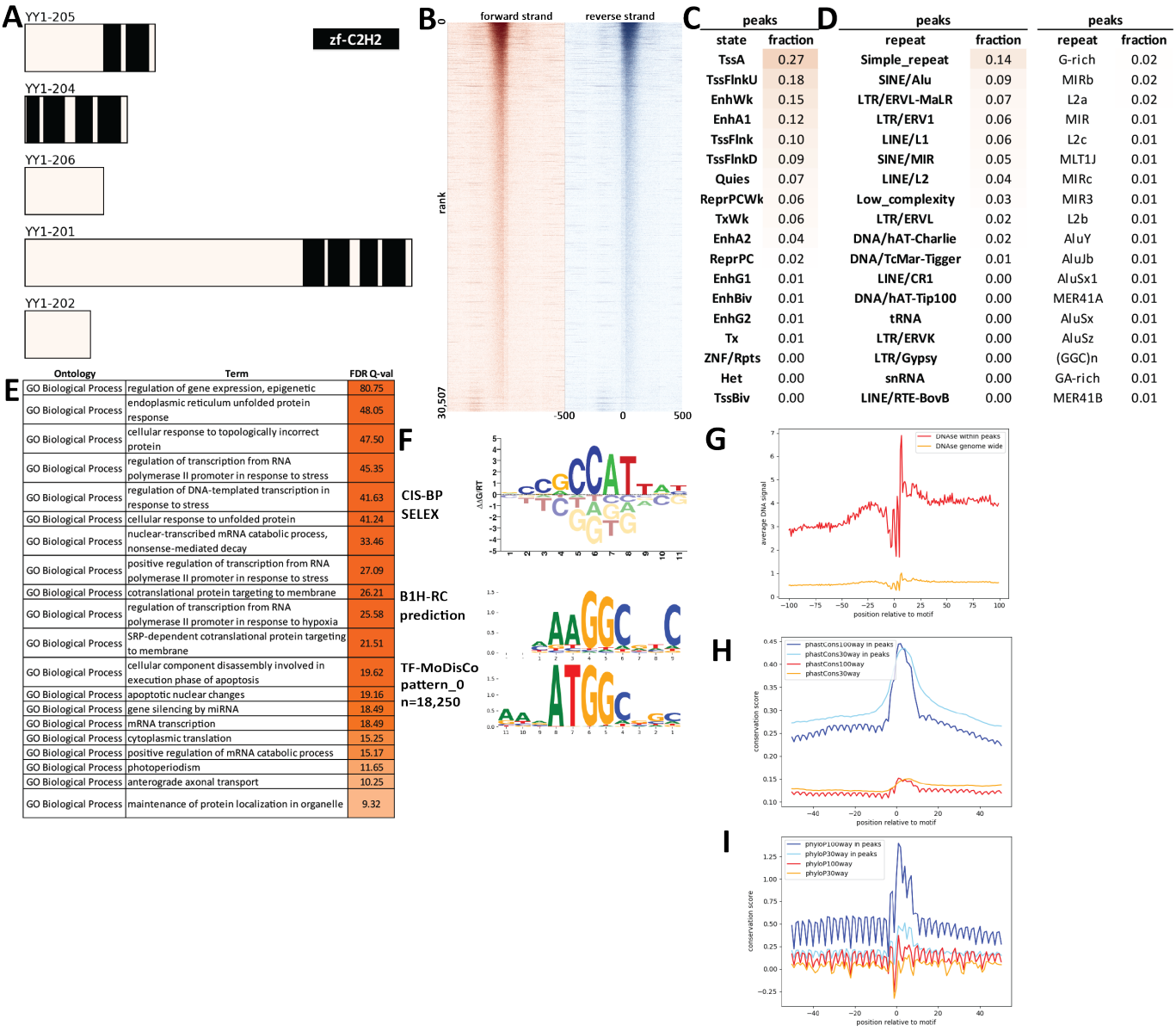

Supplementary Figure 346: Properties and genomic distribution of motifs identified for the YY1 transcription factor in K562 (accession ENCSR000BMH).

TF-MoDisCO pattern_0 n=18250, CWM

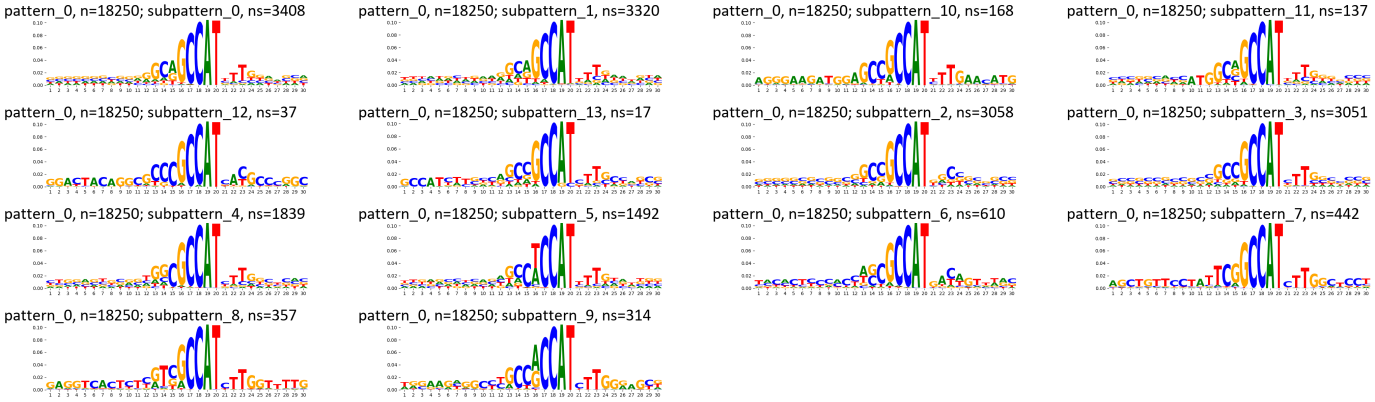

TF-MoDisCO pattern_0 n=18250, PWM

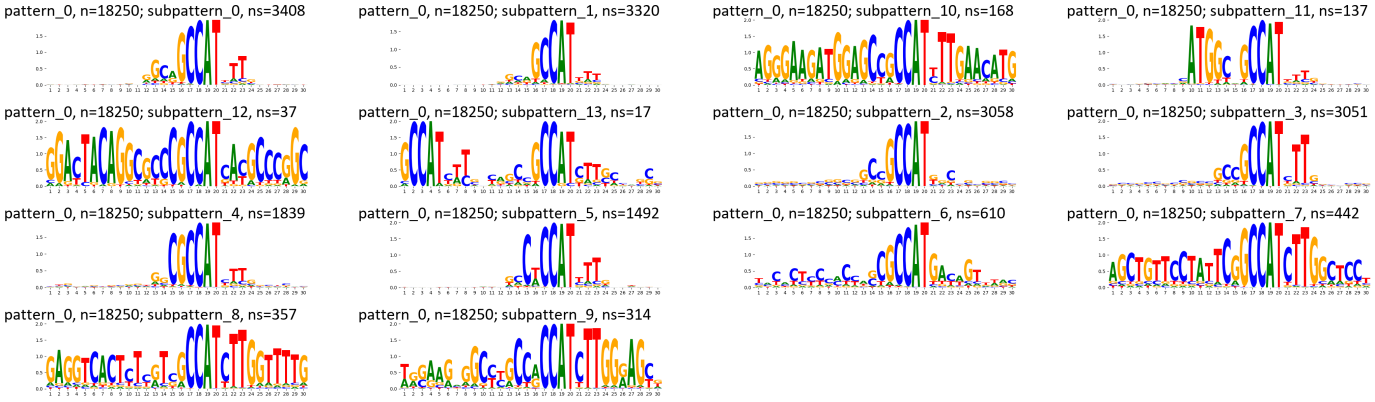

Supplementary Figure 347: TF-MoDisCO subpatterns for the YY1 transcription factor in K562 (accession ENCSR000BMH).

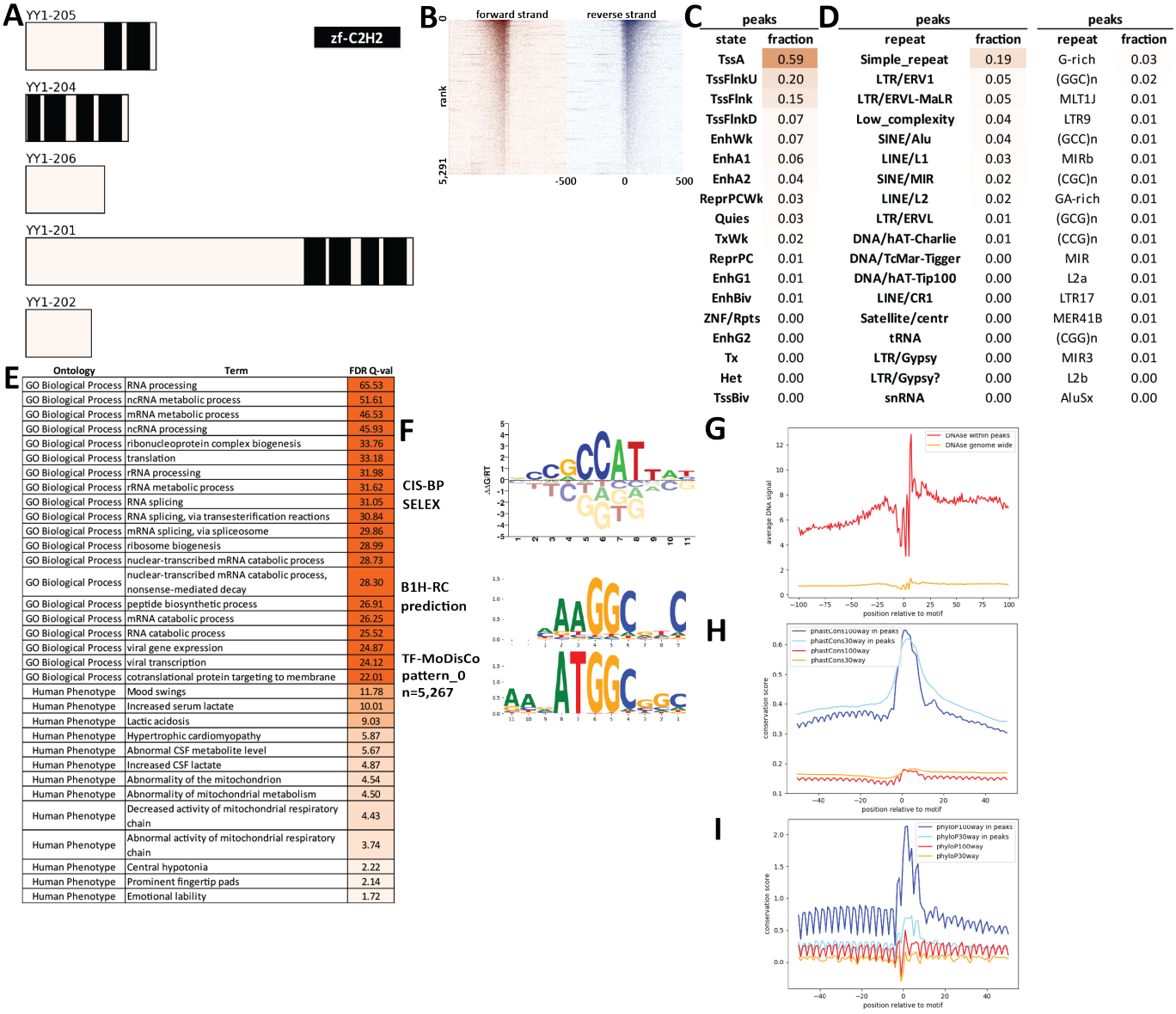

peaks	
state	fraction
TssA	0.59
TssFlnkU	0.20
TssFlnk	0.15
TssFlnkD	0.07
EnhWk	0.07
EnhA1	0.06
EnhA2	0.04
ReprPCWk	0.03
Quies	0.03
TxWk	0.02
ReprPC	0.01
EnhG1	0.01
EnhBiv	0.01
ZNF/Rpts	0.00
EnhG2	0.00
Tx	0.00
Het	0.00
TssBiv	0.00

peaks		peaks	
repeat	fraction	repeat	fraction
Simple_repeat	0.19	G-rich	0.03
LTR/ERV1	0.05	(GGC)n	0.02
LTR/ERVL-MaLR	0.05	MLT1J	0.01
Low_complexity	0.04	LTR9	0.01
SINE/Alu	0.04	(GCC)n	0.01
LINE/L1	0.03	MIRb	0.01
SINE/MIR	0.02	(CGC)n	0.01
LINE/L2	0.02	GA-rich	0.01
LTR/ERVL	0.01	(GCG)n	0.01
DNA/hAT-Charlie	0.01	(CCG)n	0.01
DNA/TcMar-Tigger	0.00	MIR	0.01
DNA/hAT-Tip100	0.00	L2a	0.01
LINE/CR1	0.00	LTR17	0.01
Satellite/centr	0.00	MER41B	0.01
tRNA	0.00	(CGG)n	0.01
LTR/Gypsy	0.00	MIR3	0.01
LTR/Gypsy?	0.00	L2b	0.00
snRNA	0.00	AluSx	0.00

Ontology	Term	FDR Q-val
GO Biological Process	RNA processing	65.53
GO Biological Process	ncRNA metabolic process	51.61
GO Biological Process	mRNA metabolic process	46.53
GO Biological Process	ncRNA processing	45.93
GO Biological Process	ribonucleoprotein complex biogenesis	33.76
GO Biological Process	translation	33.18
GO Biological Process	rRNA processing	31.98
GO Biological Process	rRNA metabolic process	31.62
GO Biological Process	RNA splicing	31.05
GO Biological Process	RNA splicing, via transesterification reactions	30.84
GO Biological Process	mRNA splicing, via spliceosome	29.86
GO Biological Process	ribosome biogenesis	28.99
GO Biological Process	nuclear-transcribed mRNA catabolic process	28.73
GO Biological Process	nuclear-transcribed mRNA catabolic process, nonsense-mediated decay	28.30
GO Biological Process	peptide biosynthetic process	26.91
GO Biological Process	mRNA catabolic process	26.25
GO Biological Process	RNA catabolic process	25.52
GO Biological Process	viral gene expression	24.87
GO Biological Process	viral transcription	24.12
GO Biological Process	cotranslational protein targeting to membrane	22.01
Human Phenotype	Mood swings	11.78
Human Phenotype	Increased serum lactate	10.01
Human Phenotype	Lactic acidosis	9.03
Human Phenotype	Hypertrophic cardiomyopathy	5.87
Human Phenotype	Abnormal CSF metabolite level	5.67
Human Phenotype	Increased CSF lactate	4.87
Human Phenotype	Abnormality of the mitochondrion	4.54
Human Phenotype	Abnormality of mitochondrial metabolism	4.50
Human Phenotype	Decreased activity of mitochondrial respiratory chain	4.43
Human Phenotype	Abnormal activity of mitochondrial respiratory chain	3.74
Human Phenotype	Central hypotonia	2.22
Human Phenotype	Prominent fingertip pads	2.14
Human Phenotype	Emotional lability	1.72

Supplementary Figure 348: Properties and genomic distribution of motifs identified for the YY1 transcription factor in K562 (accession ENCSR000EWF).

TF-MoDisCO pattern_0 n=5267, CWM

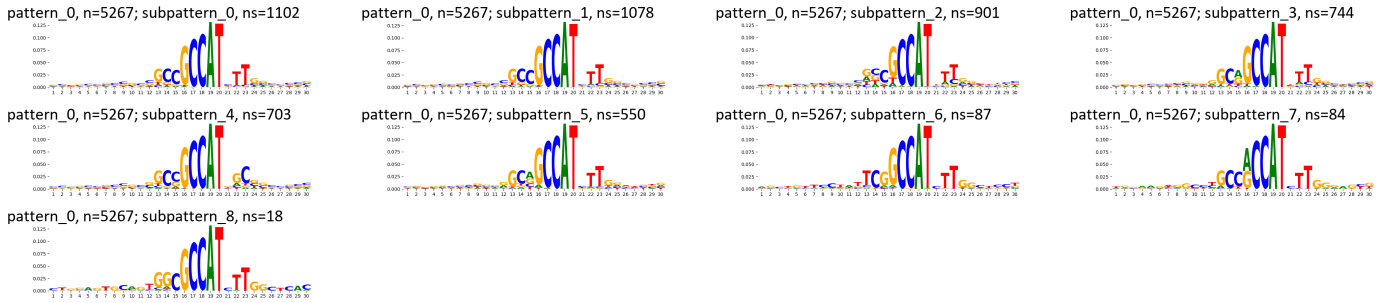

TF-MoDisCO pattern_0 n=5267, PWM

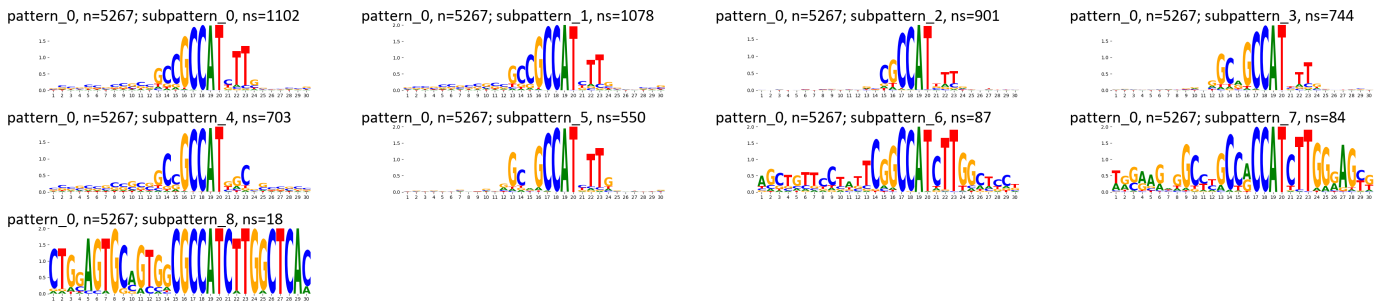

Supplementary Figure 349: TF-MoDisCO subpatterns for the YY1 transcription factor in K562 (accession ENCSR000EWF).

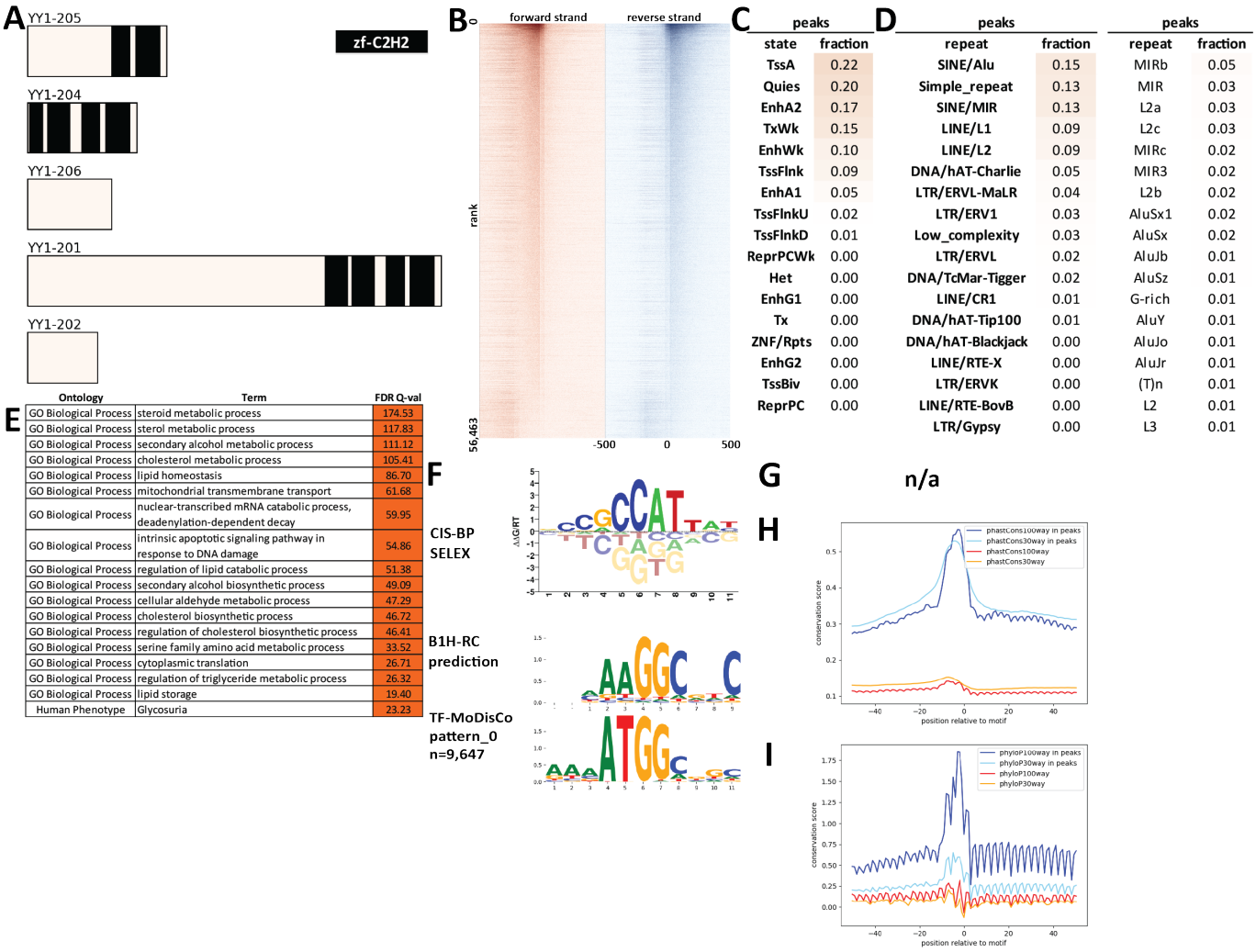

Supplementary Figure 350: Properties and genomic distribution of motifs identified for the YY1 transcription factor in liver (accession ENCSR382MOM).

TF-MoDisCO pattern_0 n=9647, CWM

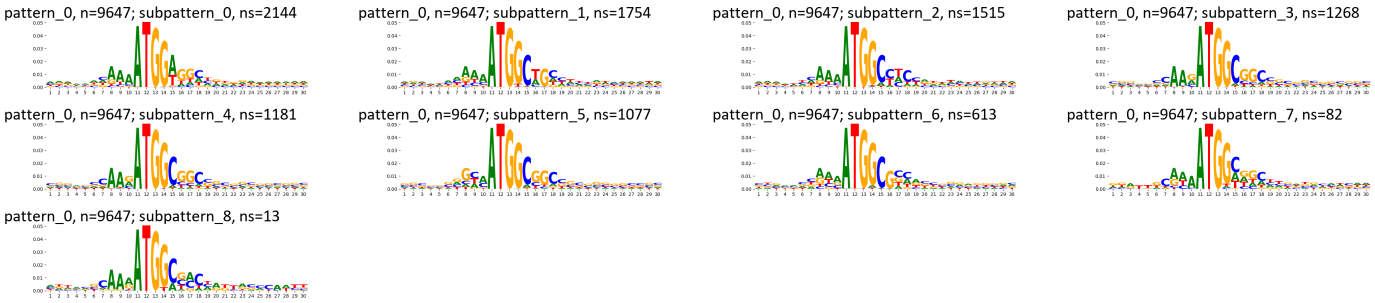

TF-MoDisCO pattern_0 n=9647, PWM

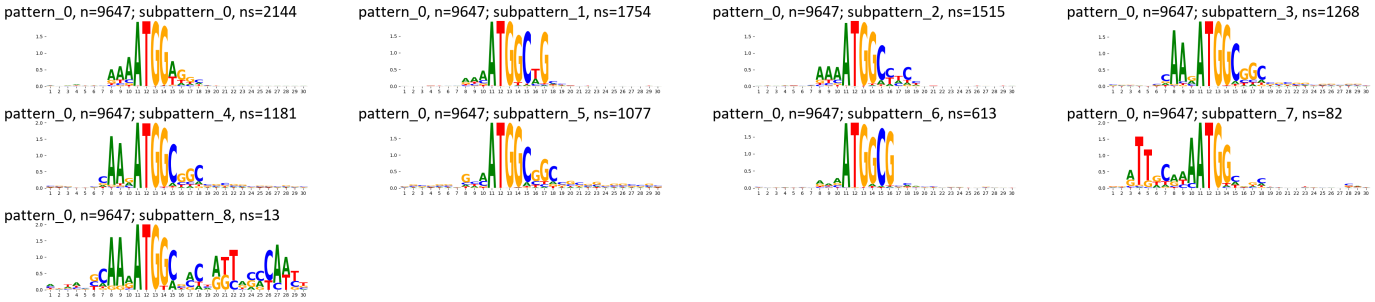

Supplementary Figure 351: TF-MoDisCO subpatterns for the YY1 transcription factor in liver (accession ENCSR382MOM).

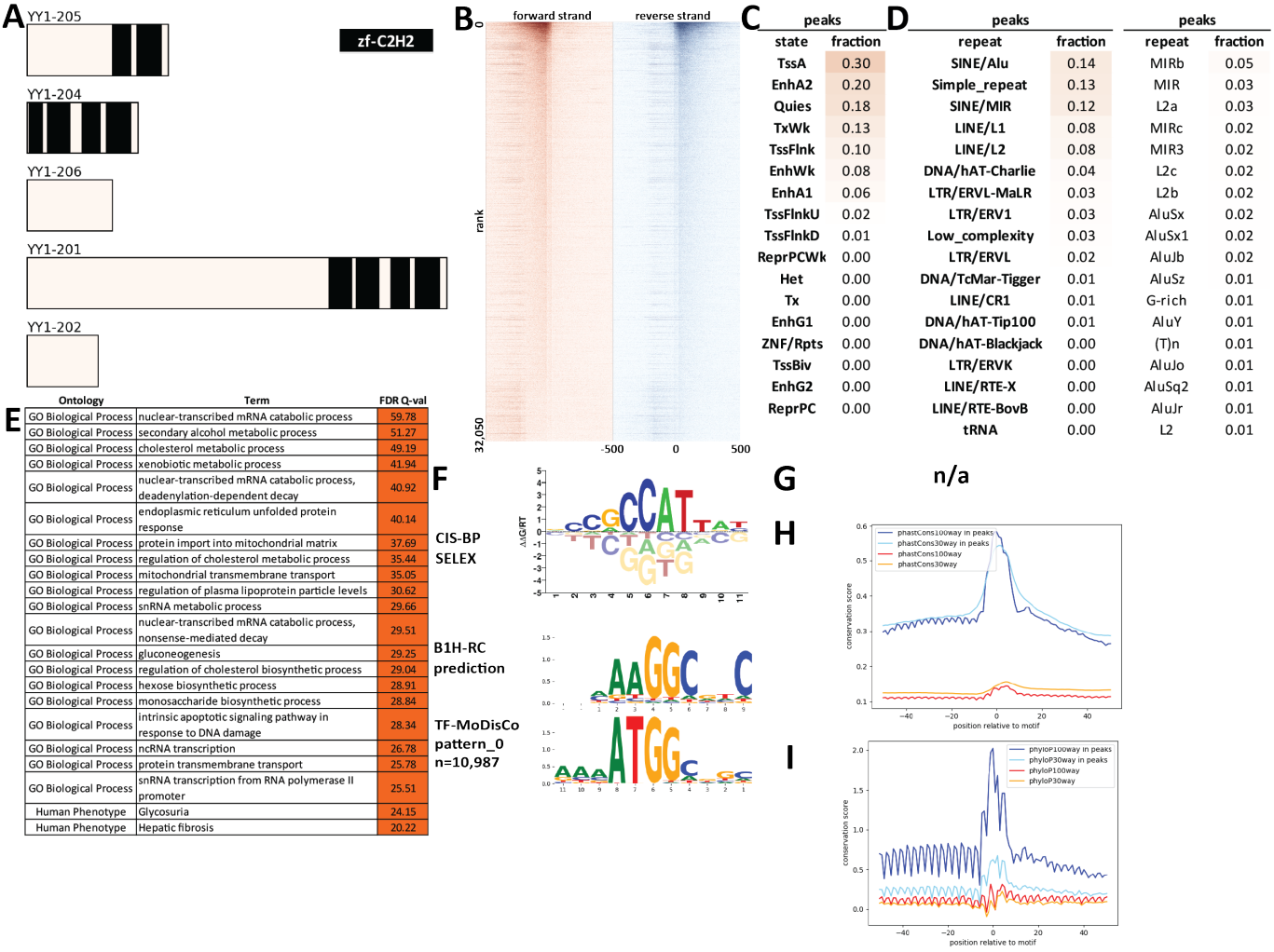

Supplementary Figure 352: Properties and genomic distribution of motifs identified for the YY1 transcription factor in liver (accession ENCSR994YLZ).

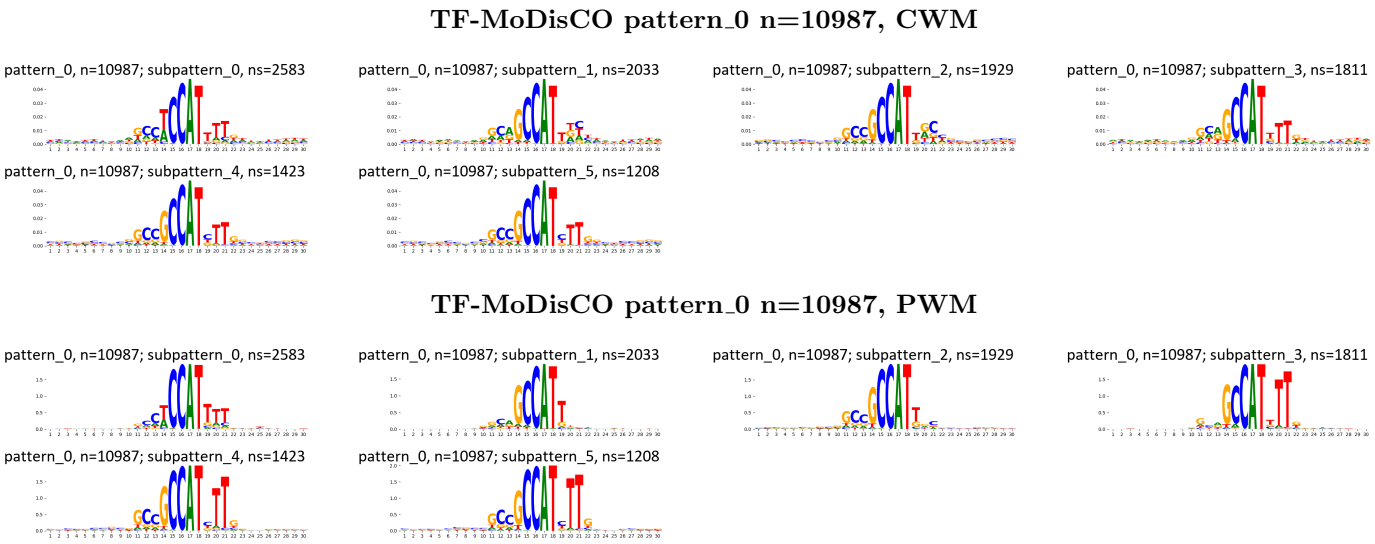

Supplementary Figure 353: TF-MoDisCO subpatterns for the YY1 transcription factor in liver (accession ENCSR994YLZ).

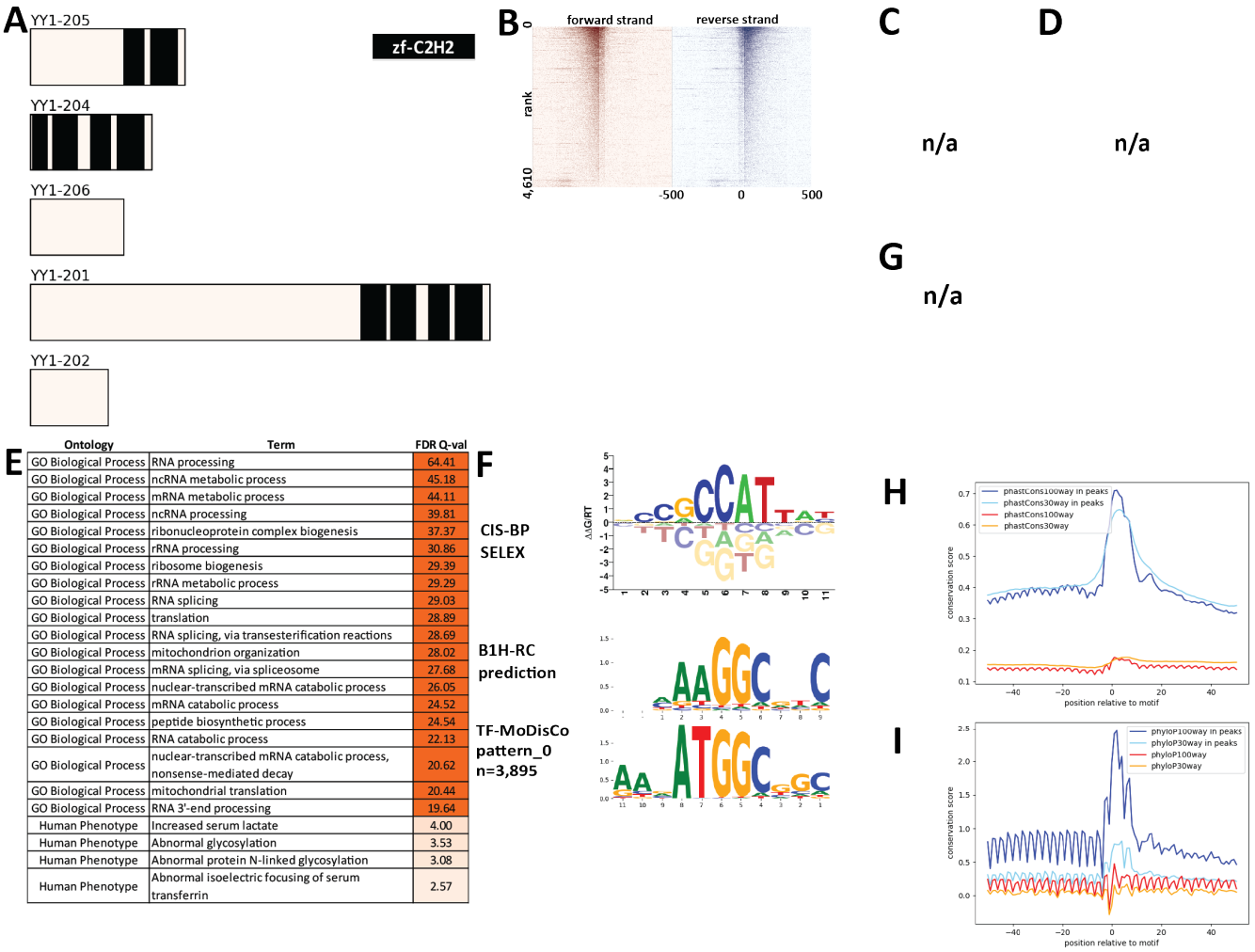

Ontology	Term	FDR Q-val
GO Biological Process	RNA processing	64.41
GO Biological Process	ncRNA metabolic process	45.18
GO Biological Process	mRNA metabolic process	44.11
GO Biological Process	ncRNA processing	39.81
GO Biological Process	ribonucleoprotein complex biogenesis	37.37
GO Biological Process	rRNA processing	30.86
GO Biological Process	ribosome biogenesis	29.39
GO Biological Process	rRNA metabolic process	29.29
GO Biological Process	RNA splicing	29.03
GO Biological Process	translation	28.89
GO Biological Process	RNA splicing, via transesterification reactions	28.69
GO Biological Process	mitochondrion organization	28.02
GO Biological Process	mRNA splicing, via spliceosome	27.68
GO Biological Process	nuclear-transcribed mRNA catabolic process	26.05
GO Biological Process	mRNA catabolic process	24.52
GO Biological Process	peptide biosynthetic process	24.54
GO Biological Process	RNA catabolic process	22.13
GO Biological Process	nuclear-transcribed mRNA catabolic process, nonsense-mediated decay	20.62
GO Biological Process	mitochondrial translation	20.44
GO Biological Process	RNA 3'-end processing	19.64
Human Phenotype	Increased serum lactate	4.00
Human Phenotype	Abnormal glycosylation	3.53
Human Phenotype	Abnormal protein N-linked glycosylation	3.08
Human Phenotype	Abnormal isoelectric focusing of serum transferrin	2.57

Supplementary Figure 354: Properties and genomic distribution of motifs identified for the YY1 transcription factor in NT2D1 (accession ENCSR000EXG).

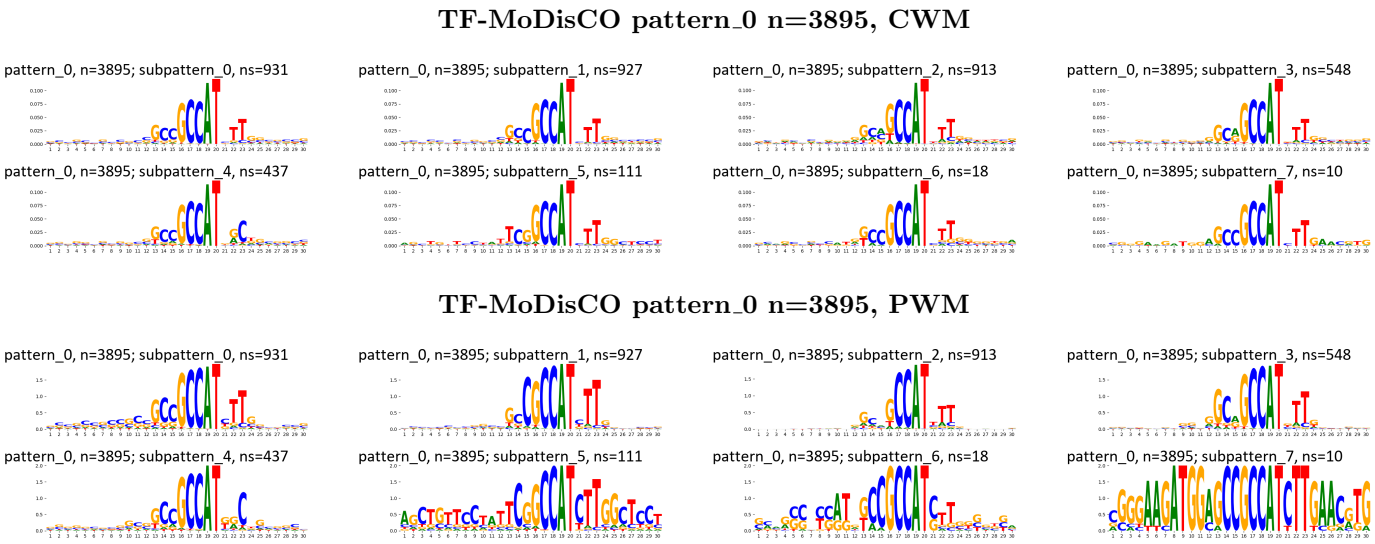

Supplementary Figure 355: TF-MoDisCO subpatterns for the YY1 transcription factor in NT2D1 (accession ENCSR000EXG).

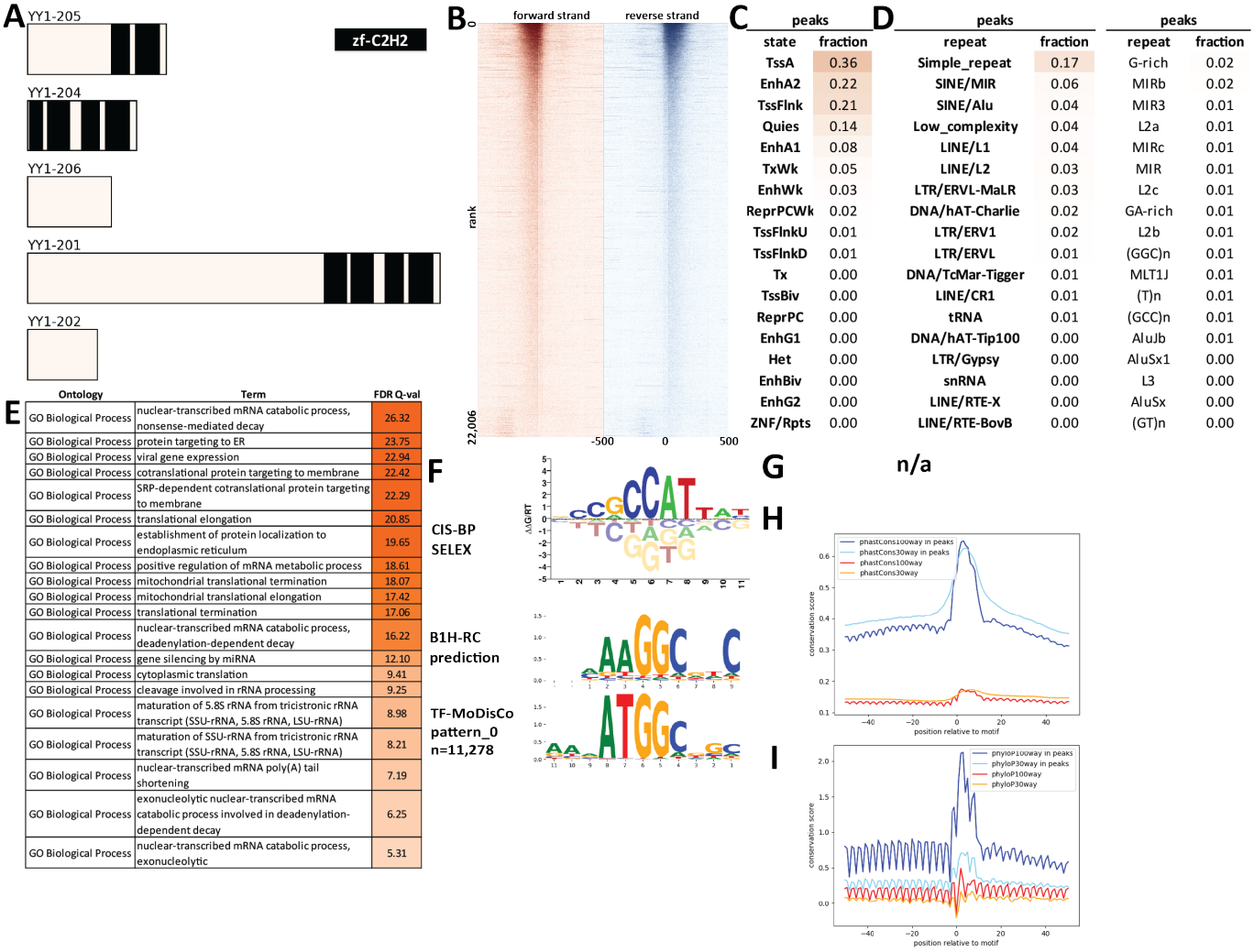

Supplementary Figure 356: Properties and genomic distribution of motifs identified for the YY1 transcription factor in SK-N-SH (accession ENCSR000BLZ).

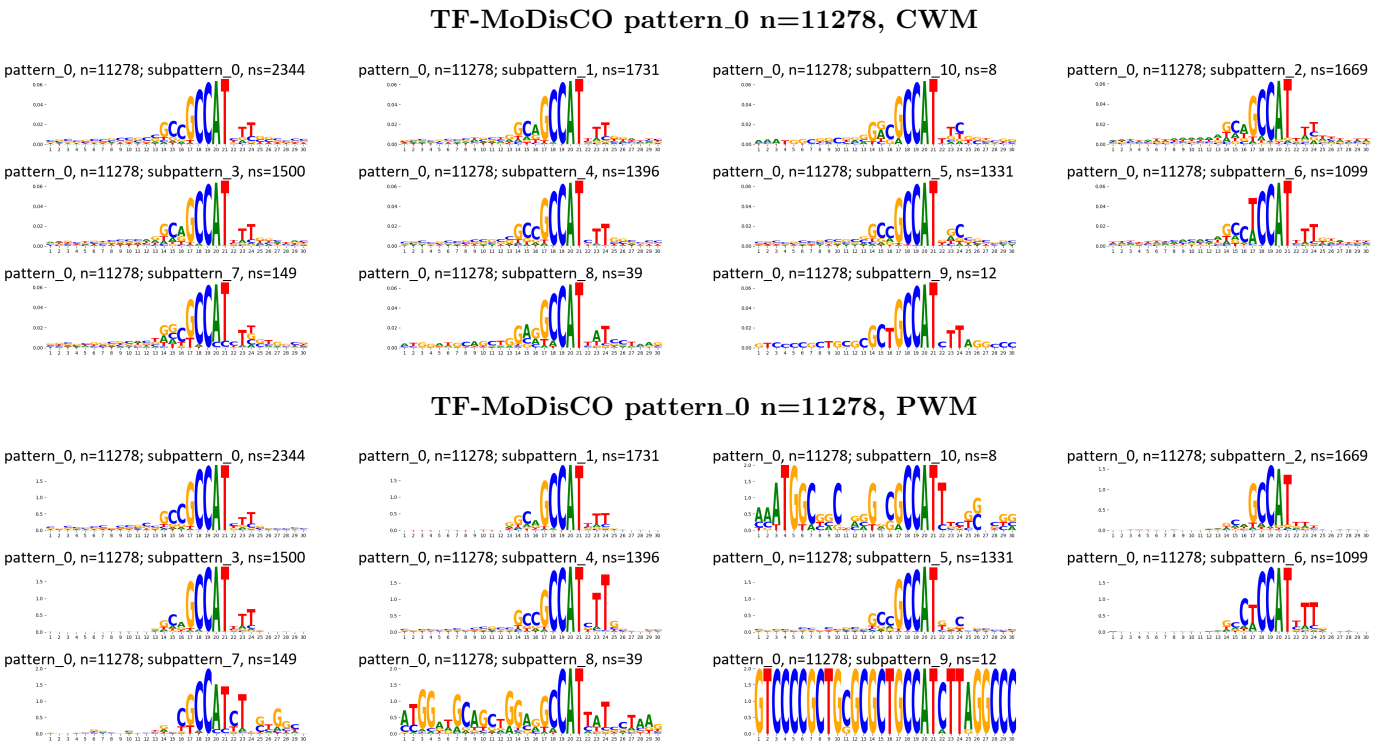

Supplementary Figure 357: TF-MoDisCO subpatterns for the YY1 transcription factor in SK-N-SH (accession ENCSR000BLZ).

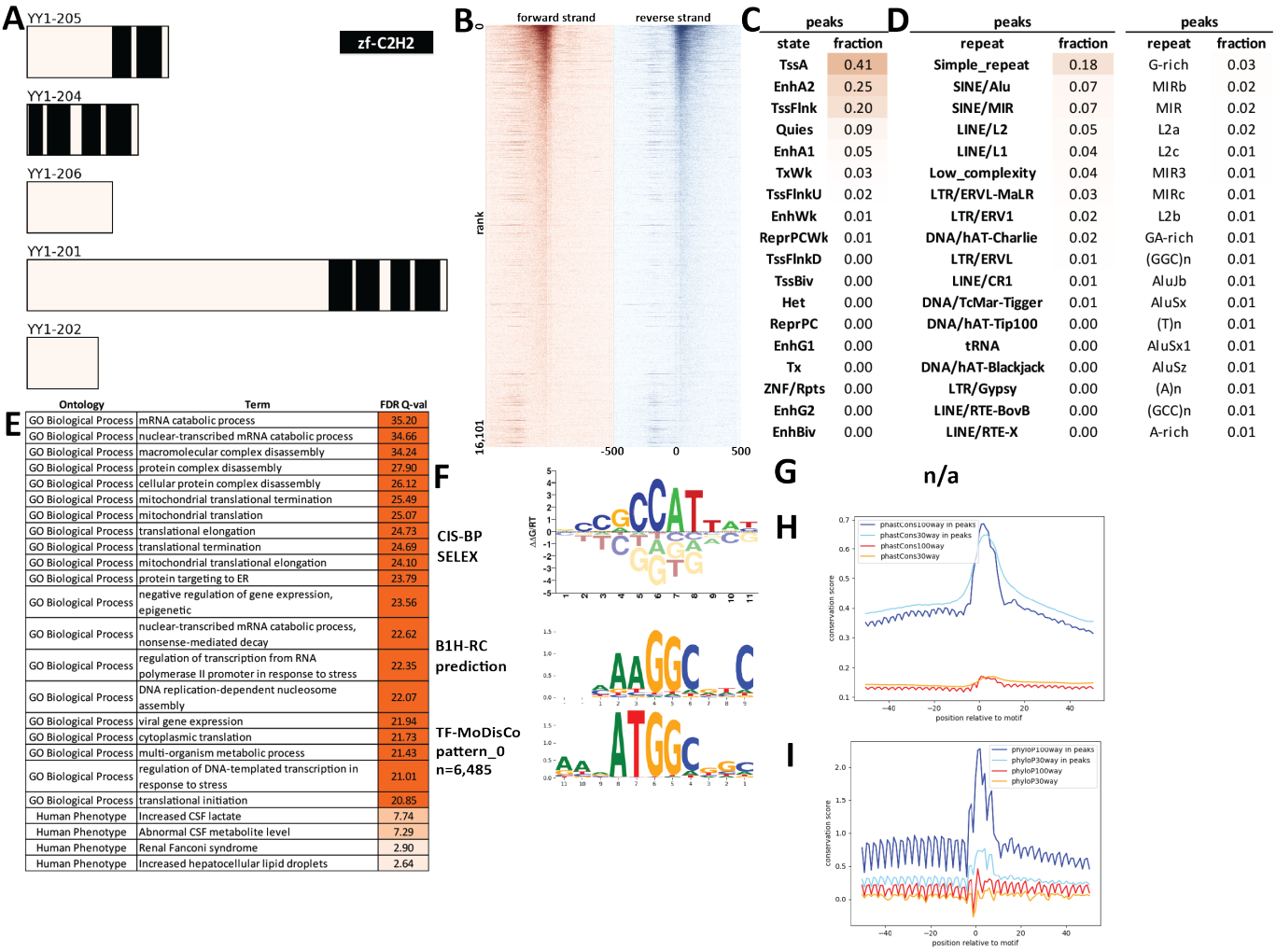

Supplementary Figure 358: Properties and genomic distribution of motifs identified for the YY1 transcription factor in SK-N-SH (accession ENCSR000BSM).

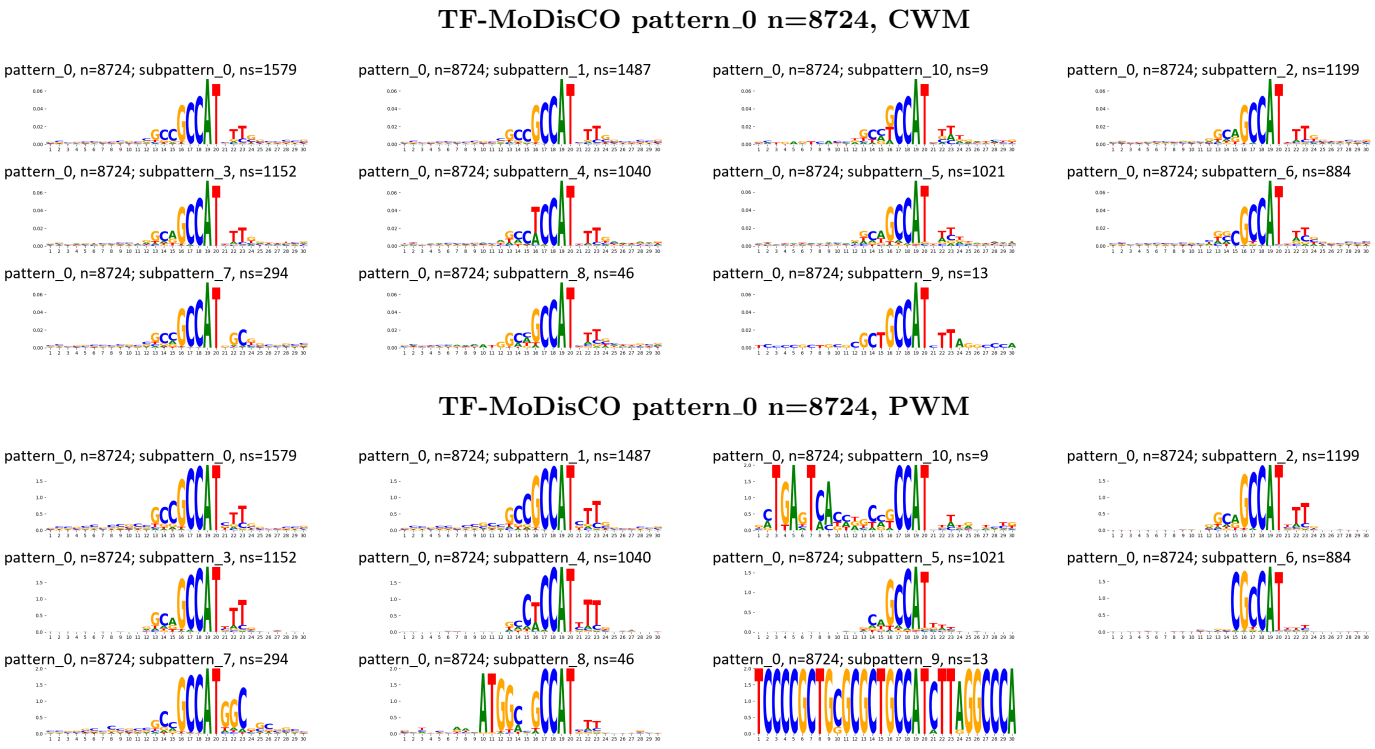

Supplementary Figure 359: TF-MoDisCO subpatterns for the YY1 transcription factor in SK-N-SH (accession ENCSR000BSM).

A



B

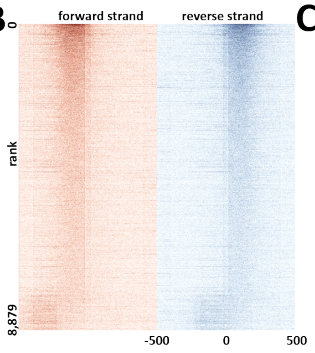

C

peaks	
state	fraction
TssA	0.49
TssFlnk	0.19
Quies	0.13
EnhWk	0.08
TxWk	0.06
EnhA1	0.04
TssBiv	0.04
EnhA2	0.03
TssFlnkU	0.03
ReprPCWk	0.02
ReprPC	0.01
TssFlnkD	0.01
Tx	0.01
EnhBiv	0.01
EnhG1	0.01
EnhG2	0.00
Het	0.00
ZNF/Rpts	0.00

D

peaks		peaks	
repeat	fraction	repeat	fraction
Simple_repeat	0.26	G-rich	0.02
SINE/Alu	0.10	(GT)n	0.02
SINE/MIR	0.04	MIRb	0.02
LINE/L2	0.04	(AC)n	0.02
Low_complexity	0.04	(TG)n	0.01
LINE/L1	0.03	L2a	0.01
LTR/ERVL-MaLR	0.03	GA-rich	0.01
LTR/ERV1	0.01	(CA)n	0.01
DNA/hAT-Charlie	0.01	AluSx	0.01
tRNA	0.01	AluSx1	0.01
LTR/ERVL	0.01	L2c	0.01
DNA/TcMar-Tigger	0.01	AluSz	0.01
LINE/CR1	0.00	(GGC)n	0.01
DNA/hAT-Tip100	0.00	MIR	0.01
snRNA	0.00	L2b	0.01
LTR/Gypsy	0.00	MIRc	0.01
LINE/RTE-BovB	0.00	AluJb	0.01
LINE/RTE-X	0.00	AluY	0.01

E

Ontology	Term	FDR Q-val
GO Biological Process	ncRNA metabolic process	69.52
GO Biological Process	ncRNA processing	62.56
GO Biological Process	ribonucleoprotein complex biogenesis	58.74
GO Biological Process	rRNA processing	54.64
GO Biological Process	rRNA metabolic process	53.59
GO Biological Process	ribosome biogenesis	52.17
GO Biological Process	translation	51.14
GO Biological Process	peptide biosynthetic process	43.70
GO Biological Process	nuclear-transcribed mRNA catabolic process, nonsense-mediated decay	43.04
GO Biological Process	viral gene expression	39.73
GO Biological Process	cotranslational protein targeting to membrane	38.31
GO Biological Process	protein targeting to ER	38.07
GO Biological Process	nuclear-transcribed mRNA catabolic process	37.88
GO Biological Process	SRP-dependent cotranslational protein targeting to membrane	37.37
GO Biological Process	mRNA catabolic process	37.10
GO Biological Process	viral transcription	35.83
GO Biological Process	multi-organism metabolic process	35.83
GO Biological Process	establishment of protein localization to endoplasmic reticulum	35.45
GO Biological Process	translational initiation	34.53
GO Biological Process	protein localization to endoplasmic reticulum	33.74
Human Phenotype	Increased serum lactate	6.22
Human Phenotype	Abnormality of the mitochondrion	5.64
Human Phenotype	Abnormality of mitochondrial metabolism	5.34
Human Phenotype	Abnormal CSF metabolite level	5.05
Human Phenotype	Increased intramyocellular lipid droplets	4.65
Human Phenotype	Increased CSF lactate	4.66
Human Phenotype	Decreased activity of mitochondrial respiratory chain	4.10
Human Phenotype	Abnormal activity of mitochondrial respiratory chain	3.44
Human Phenotype	3-Methylglutaconic aciduria	1.80

F

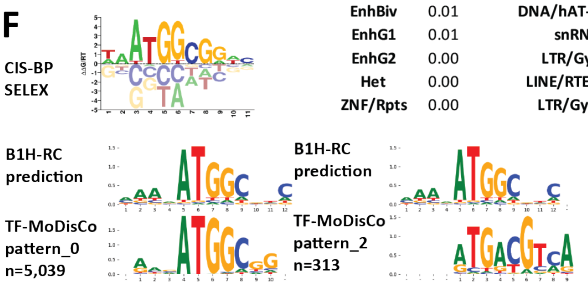

G

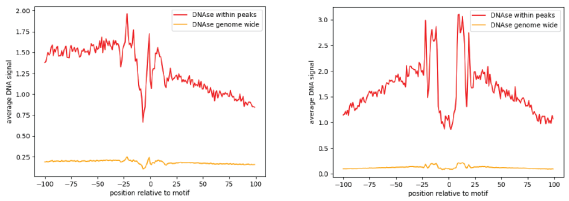

H

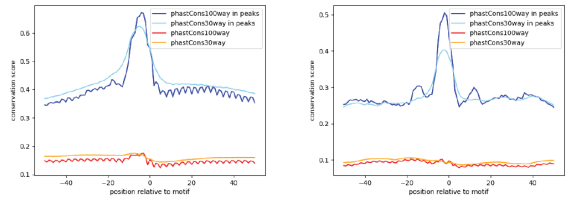

I

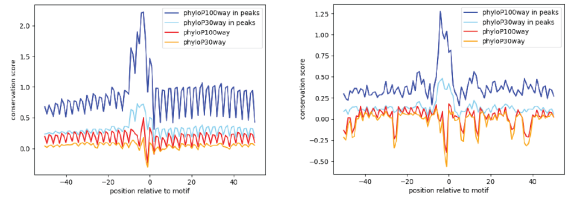

Supplementary Figure 360: Properties and genomic distribution of motifs identified for the YY2 transcription factor in HEK293 (accession ENCSR692HSE).

TF-MoDisCO pattern_0 n=5039, CWM

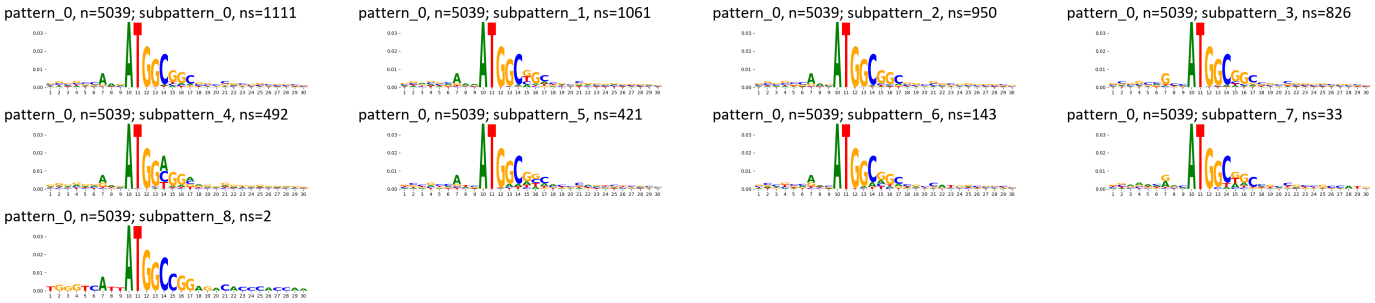

TF-MoDisCO pattern_0 n=5039, PWM

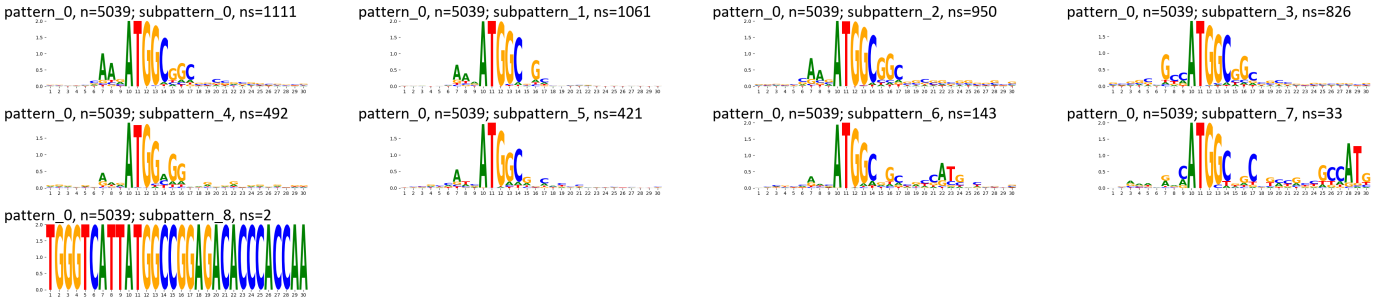

TF-MoDisCO pattern_2 n=313, CWM

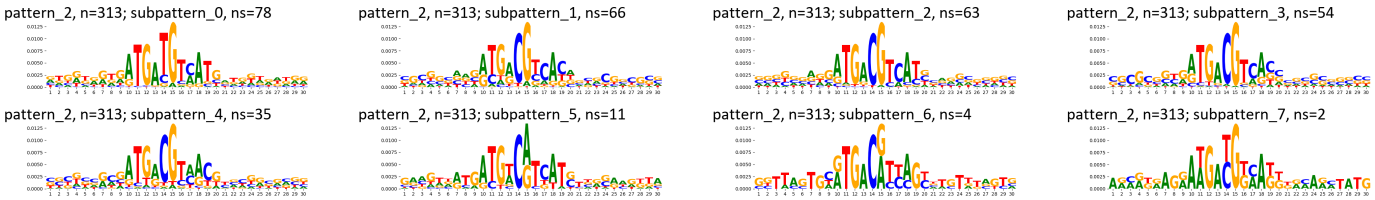

TF-MoDisCO pattern_2 n=313, PWM

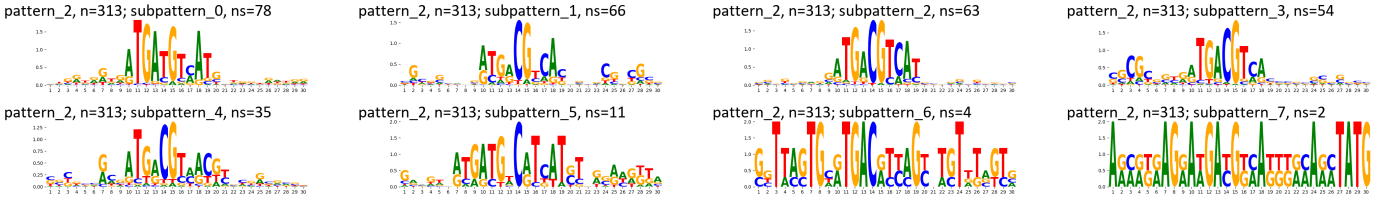

Supplementary Figure 361: TF-MoDisCO subpatterns for the YY2 transcription factor in HEK293 (accession ENCSR692HSE).

A

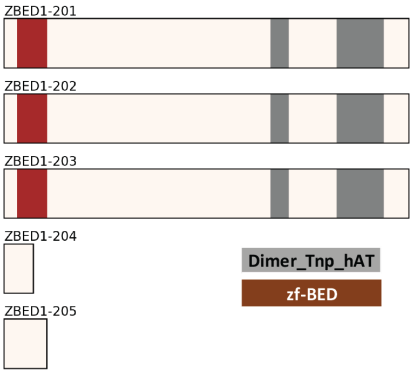

B

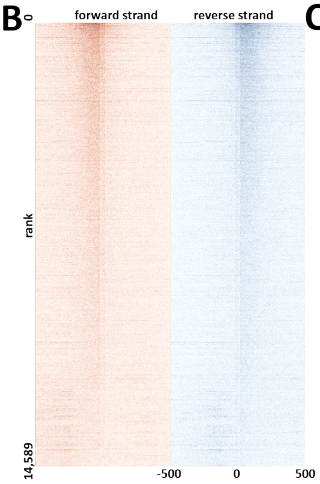

C

peaks	
state	fraction
Quies	0.25
TssA	0.15
TxWk	0.13
EnhWk	0.09
TssFlnk	0.07
Tx	0.05
EnhA1	0.03
EnhA2	0.02
TssFlnkU	0.02
ReprPCWk	0.01
TssFlnkD	0.01
EnhG1	0.01
ReprPC	0.01
TssBiv	0.01
EnhG2	0.00
Het	0.00
EnhBiv	0.00
ZNF/Rpts	0.00

D

peaks		peaks	
repeat	fraction	repeat	fraction
SINE/Alu	0.16	MIRb	0.05
SINE/MIR	0.14	MIR	0.03
Simple_repeat	0.13	L2a	0.03
LINE/L1	0.09	MIR3	0.03
LINE/L2	0.08	MIRc	0.02
LTR/ERVL-MaLR	0.05	L2c	0.02
DNA/hAT-Charlie	0.05	L2b	0.02
LTR/ERV1	0.03	AluSx	0.02
Low_complexity	0.02	AluJb	0.02
LTR/ERVL	0.02	AluSx1	0.02
DNA/TcMar-Tigger	0.02	AluSz	0.01
LINE/CR1	0.01	AluJo	0.01
DNA/hAT-Tip100	0.01	L2	0.01
tRNA	0.01	AluJr	0.01
DNA/hAT-Blackjack	0.00	L3	0.01
LTR/Gypsy	0.00	MER5A	0.01
LINE/RTE-X	0.00	AluY	0.01
LTR/ERVK	0.00	(AC)n	0.01

E

Ontology	Term	FDR Q-val
GO Biological Process	regulation of immune response	199.68
GO Biological Process	positive regulation of immune response	132.87
GO Biological Process	lymphocyte activation	123.45
GO Biological Process	regulation of lymphocyte activation	115.57
GO Biological Process	innate immune response	113.56
GO Biological Process	adaptive immune response	110.53
GO Biological Process	regulation of immune effector process	104.47
GO Biological Process	positive regulation of cytokine production	101.72
GO Biological Process	cytokine-mediated signaling pathway	101.13
GO Biological Process	leukocyte differentiation	98.32
GO Biological Process	immune response-activating signal transduction	98.05
GO Biological Process	activation of immune response	94.72
GO Biological Process	immune response-regulating signaling pathway	93.96
GO Biological Process	leukocyte cell-cell adhesion	87.90
GO Biological Process	regulation of innate immune response	86.89
GO Biological Process	positive regulation of cell activation	86.88
GO Biological Process	regulation of leukocyte cell-cell adhesion	85.55
GO Biological Process	leukocyte aggregation	83.41
GO Biological Process	regulation of T cell activation	83.33
GO Biological Process	lymphocyte differentiation	83.29
Human Phenotype	Abnormality of leukocytes	51.68
Human Phenotype	Abnormality of lymphocytes	42.23
Human Phenotype	Decreased antibody level in blood	36.56
Human Phenotype	Recurrent bacterial infections	35.39
Human Phenotype	Abnormality of B cell physiology	34.92
Human Phenotype	Abnormal immunoglobulin level	34.64
Human Phenotype	Abnormality of bone marrow cell morphology	26.81
Human Phenotype	Abnormality of cells of the lymphoid lineage	17.19
Human Phenotype	Abnormality of the lymph nodes	16.80
Human Phenotype	Lymphadenopathy	15.72

F

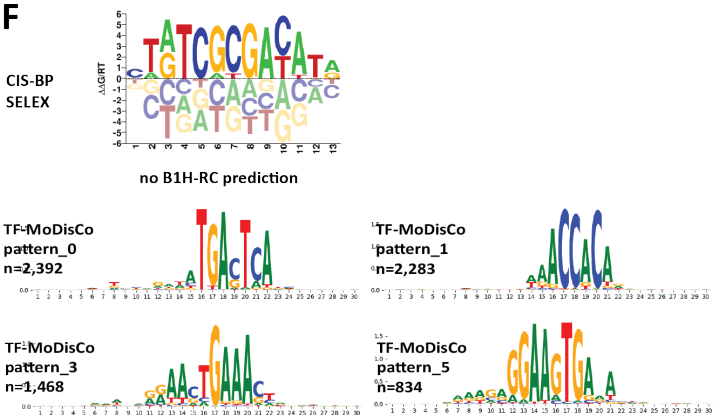

G

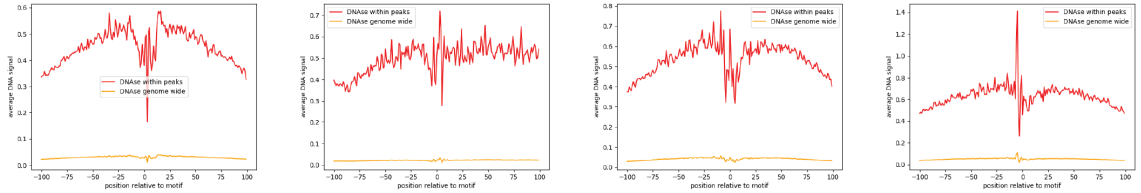

H

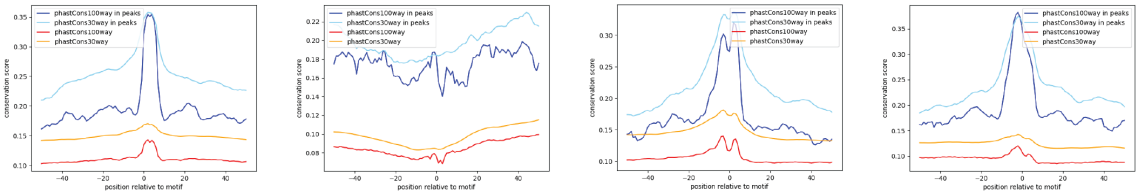

I

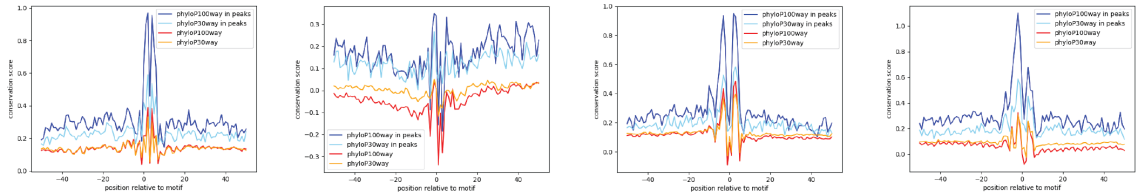

Supplementary Figure 362: Properties and genomic distribution of motifs identified for the ZBED1 transcription factor in GM12878 (accession ENCSR207PFI).

TF-MoDisCO pattern_0 n=2392, CWM

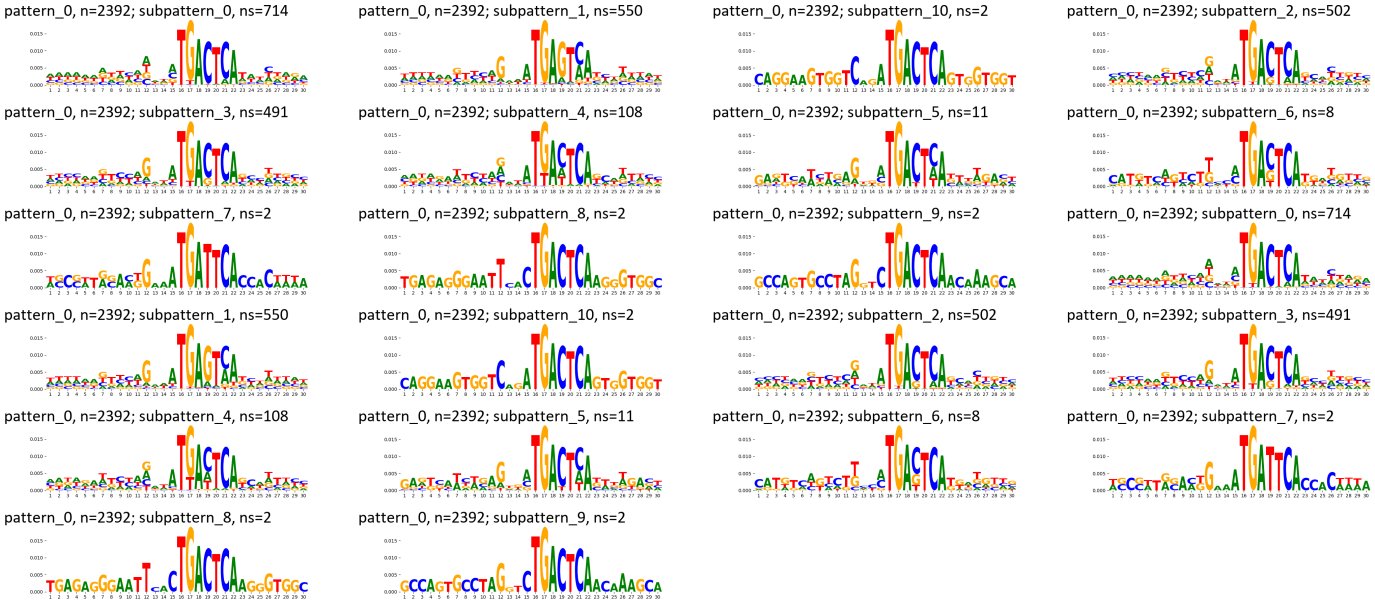

TF-MoDisCO pattern_0 n=2392, PWM

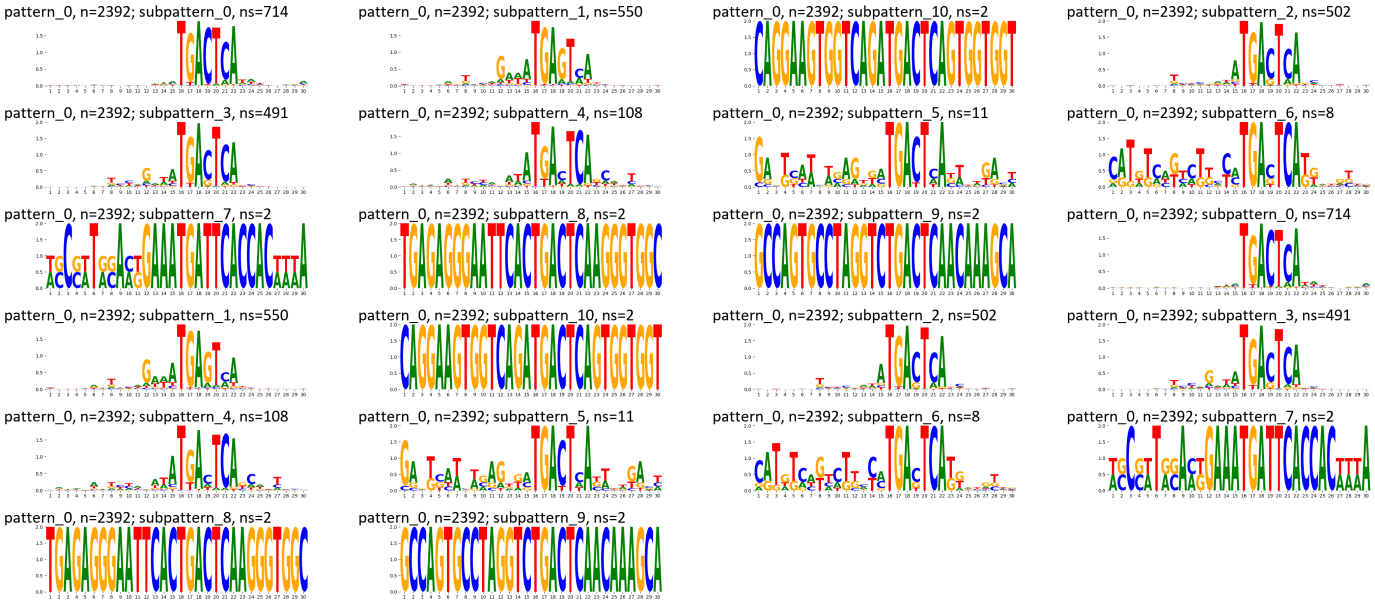

TF-MoDisCO pattern_1 n=2283, CWM

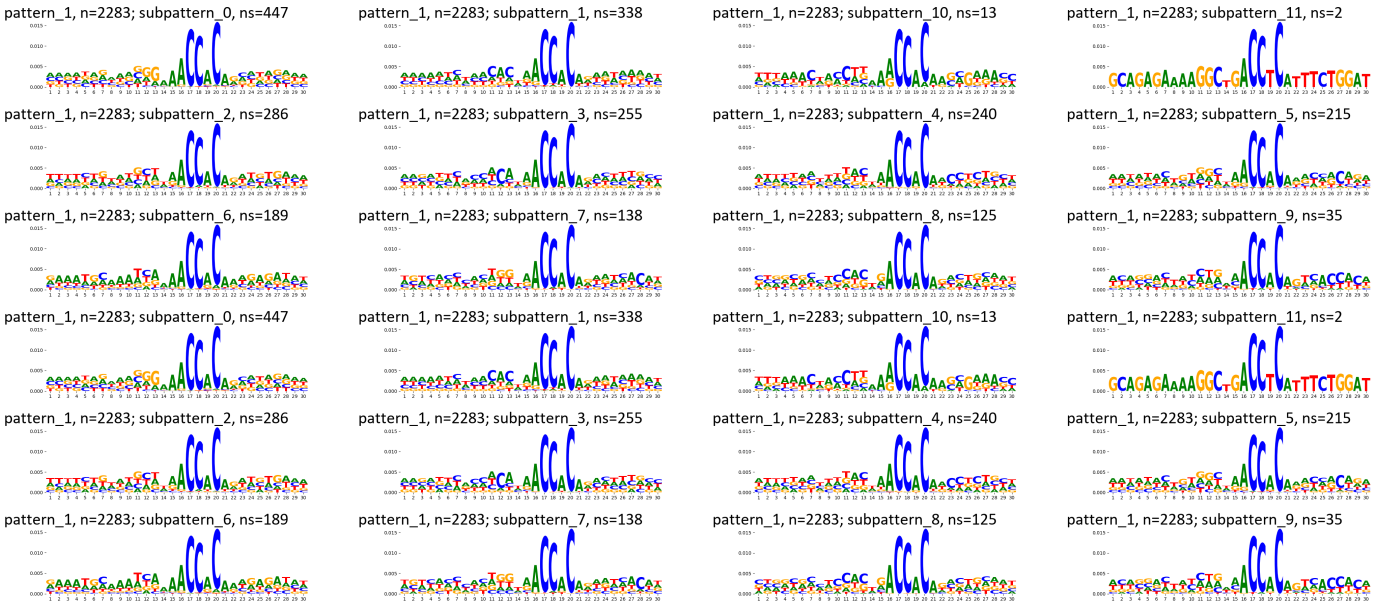

TF-MoDisCO pattern_1 n=2283, PWM

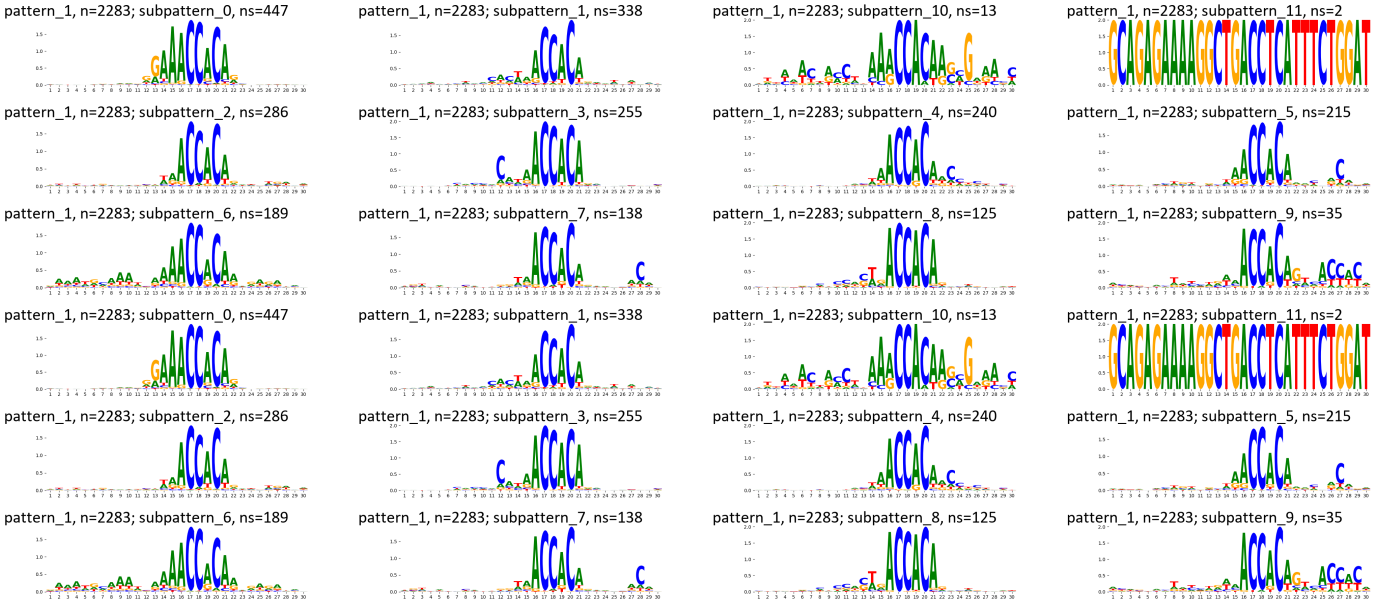

TF-MoDisCO pattern_3 n=1468, CWM

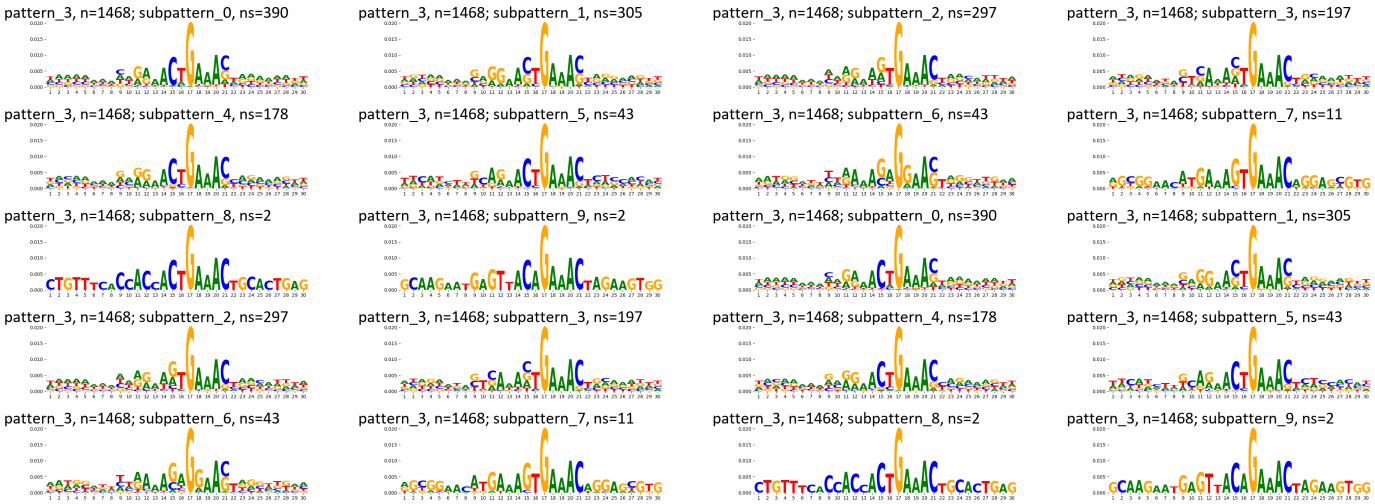

TF-MoDisCO pattern_3 n=1468, PWM

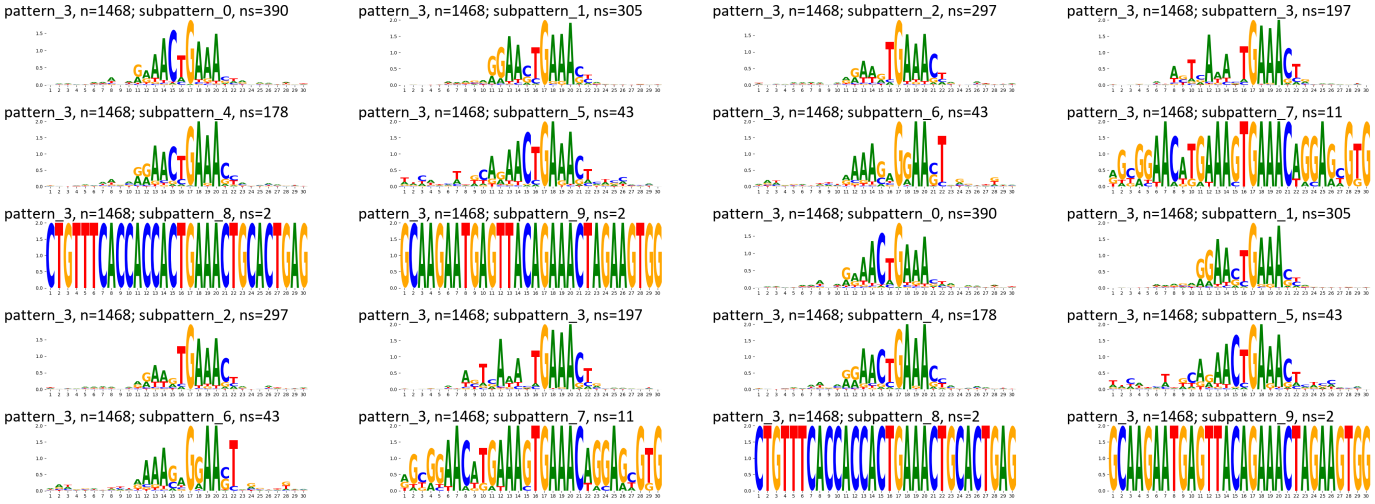

TF-MoDisCO pattern_5 n=834, CWM

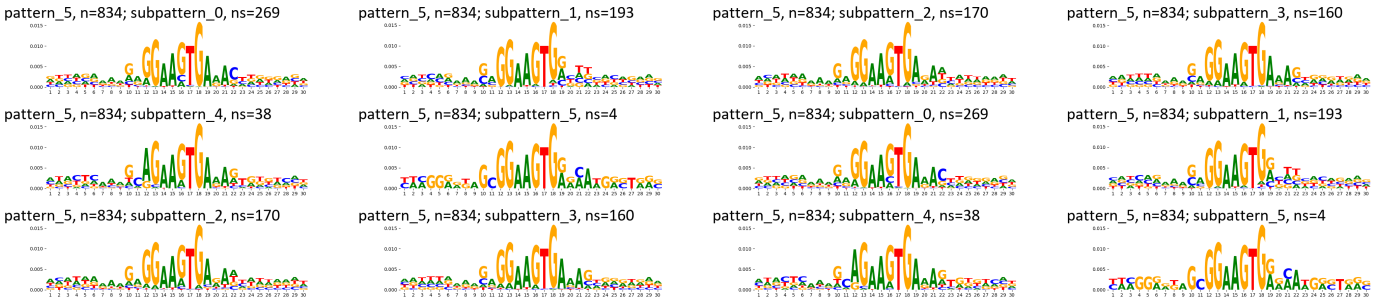

TF-MoDisCO pattern_5 n=834, PWM

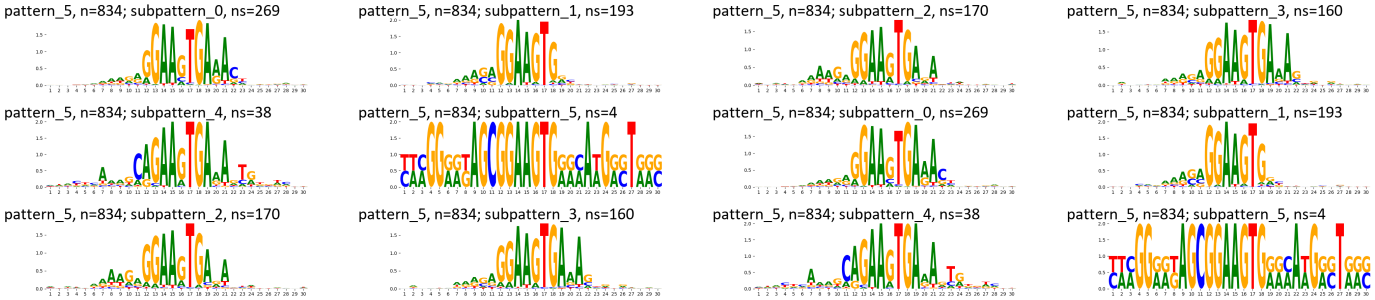

Supplementary Figure 363: TF-MoDisCO subpatterns for the ZBED1 transcription factor in GM12878 (accession ENCSR207PFI).

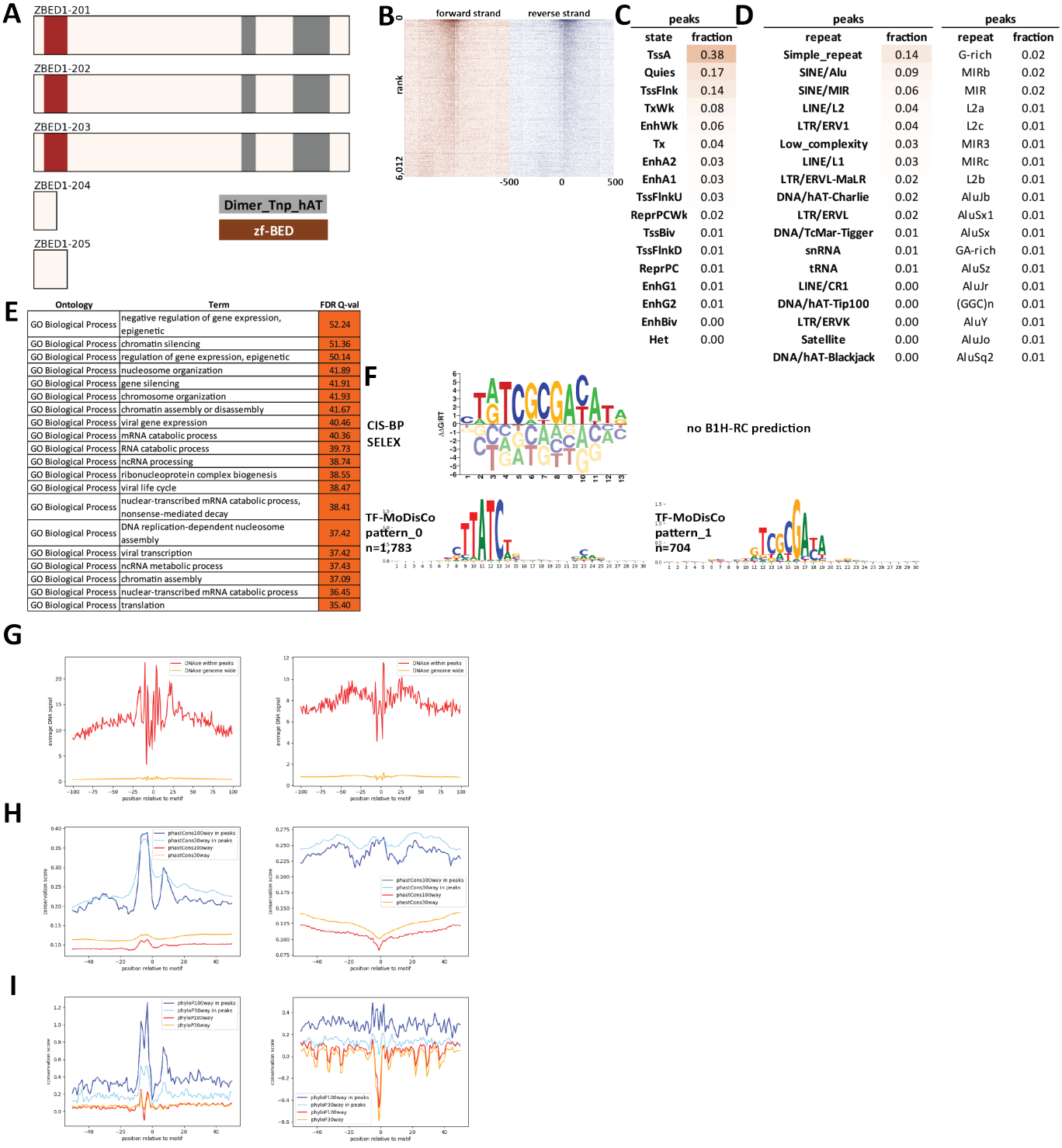

Supplementary Figure 364: Properties and genomic distribution of motifs identified for the ZBED1 transcription factor in K562 (accession ENCSR286PCG).

TF-MoDisCO pattern_0 n=1783, CWM

pattern_0, n=1783; subpattern_0, ns=442

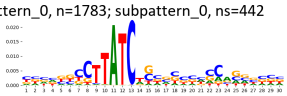

pattern_0, n=1783; subpattern_1, ns=359

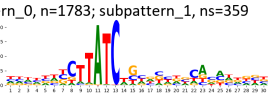

pattern_0, n=1783; subpattern_2, ns=357

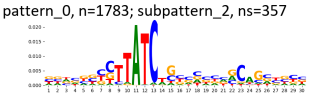

pattern_0, n=1783; subpattern_3, ns=326

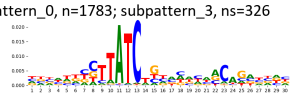

pattern_0, n=1783; subpattern_4, ns=297

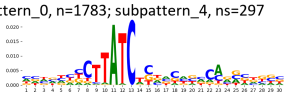

pattern_0, n=1783; subpattern_5, ns=2

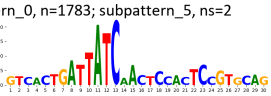

pattern_0, n=1783; subpattern_0, ns=442

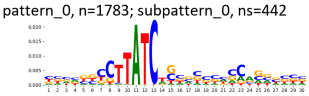

pattern_0, n=1783; subpattern_1, ns=359

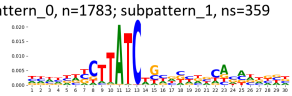

pattern_0, n=1783; subpattern_2, ns=357

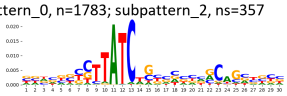

pattern_0, n=1783; subpattern_3, ns=326

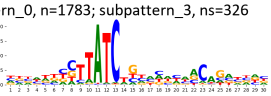

pattern_0, n=1783; subpattern_4, ns=297

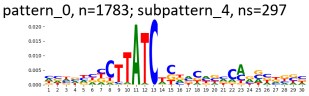

pattern_0, n=1783; subpattern_5, ns=2

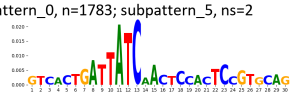

TF-MoDisCO pattern_0 n=1783, PWM

pattern_0, n=1783; subpattern_0, ns=442

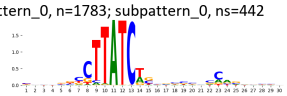

pattern_0, n=1783; subpattern_1, ns=359

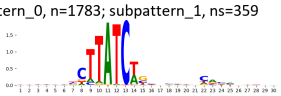

pattern_0, n=1783; subpattern_2, ns=357

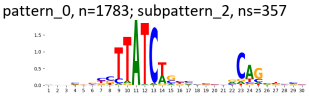

pattern_0, n=1783; subpattern_3, ns=326

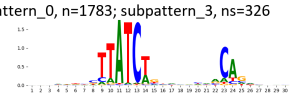

pattern_0, n=1783; subpattern_4, ns=297

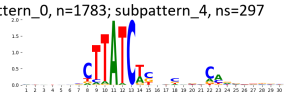

pattern_0, n=1783; subpattern_5, ns=2

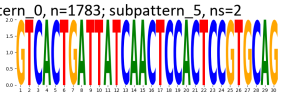

pattern_0, n=1783; subpattern_0, ns=442

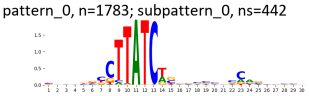

pattern_0, n=1783; subpattern_1, ns=359

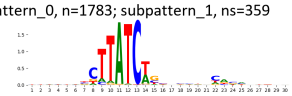

pattern_0, n=1783; subpattern_2, ns=357

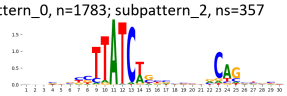

pattern_0, n=1783; subpattern_3, ns=326

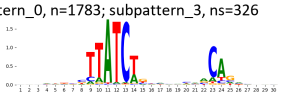

pattern_0, n=1783; subpattern_4, ns=297

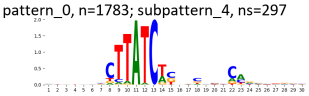

pattern_0, n=1783; subpattern_5, ns=2

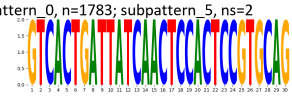

TF-MoDisCO pattern_1 n=704, CWM

pattern_1, n=704; subpattern_0, ns=140

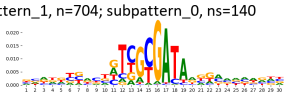

pattern_1, n=704; subpattern_1, ns=136

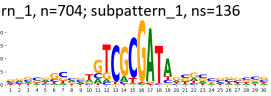

pattern_1, n=704; subpattern_2, ns=136

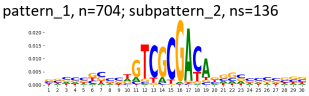

pattern_1, n=704; subpattern_3, ns=116

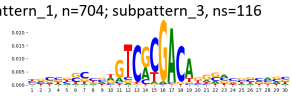

pattern_1, n=704; subpattern_4, ns=90

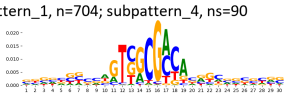

pattern_1, n=704; subpattern_5, ns=76

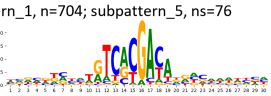

pattern_1, n=704; subpattern_6, ns=7

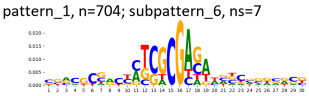

pattern_1, n=704; subpattern_7, ns=3

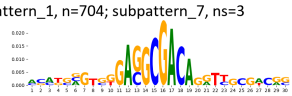

pattern_1, n=704; subpattern_0, ns=140

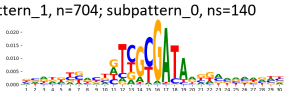

pattern_1, n=704; subpattern_1, ns=136

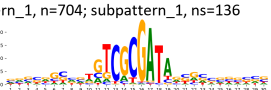

pattern_1, n=704; subpattern_2, ns=136

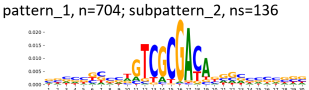

pattern_1, n=704; subpattern_3, ns=116

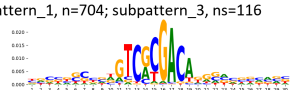

pattern_1, n=704; subpattern_4, ns=90

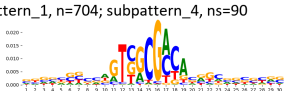

pattern_1, n=704; subpattern_5, ns=76

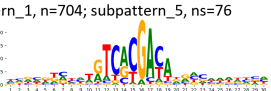

pattern_1, n=704; subpattern_6, ns=7

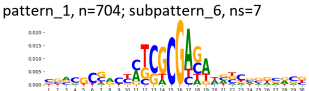

pattern_1, n=704; subpattern_7, ns=3

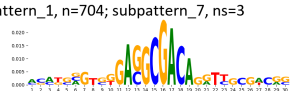

TF-MoDisCO pattern_1 n=704, PWM

pattern_1, n=704; subpattern_0, ns=140

pattern_1, n=704; subpattern_1, ns=136

pattern_1, n=704; subpattern_2, ns=136

pattern_1, n=704; subpattern_3, ns=116

pattern_1, n=704; subpattern_4, ns=90

pattern_1, n=704; subpattern_5, ns=76

pattern_1, n=704; subpattern_6, ns=7

pattern_1, n=704; subpattern_7, ns=3

pattern_1, n=704; subpattern_0, ns=140

pattern_1, n=704; subpattern_1, ns=136

pattern_1, n=704; subpattern_2, ns=136

pattern_1, n=704; subpattern_3, ns=116

pattern_1, n=704; subpattern_4, ns=90

pattern_1, n=704; subpattern_5, ns=76

pattern_1, n=704; subpattern_6, ns=7

pattern_1, n=704; subpattern_7, ns=3

Supplementary Figure 365: TF-MoDisCO subpatterns for the ZBED1 transcription factor in K562 (accession ENCSR286PCG).

A

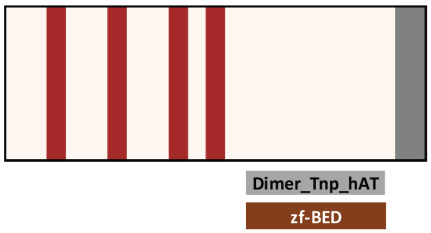

B

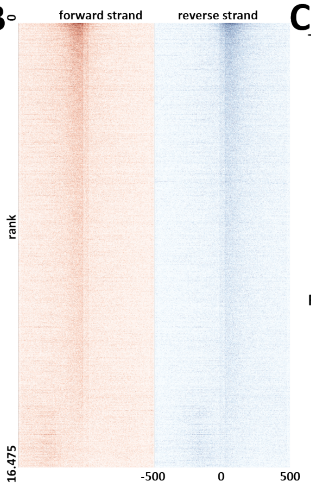

C

peaks	
state	fraction
TssA	0.31
Quies	0.20
TssFlnk	0.16
TxWk	0.10
EnhWk	0.07
TssFlnkU	0.03
Tx	0.03
EnhA1	0.03
TssBiv	0.03
EnhA2	0.03
ReprPCWk	0.02
ReprPC	0.02
TssFlnkD	0.02
EnhG1	0.01
EnhBiv	0.01
Het	0.00
EnhG2	0.00
ZNF/Rpts	0.00

D

peaks		peaks	
repeat	fraction	repeat	fraction
Simple_repeat	0.16	MIRb	0.04
SINE/MIR	0.11	G-rich	0.03
SINE/Alu	0.10	MIR	0.02
LINE/L2	0.06	MIR3	0.02
LINE/L1	0.04	MIRc	0.02
Low_complexity	0.04	L2a	0.02
DNA/hAT-Charlie	0.03	L2b	0.02
LTR/ERV1	0.02	L2c	0.02
LTR/ERVL-MaLR	0.02	AluJb	0.01
LTR/ERVL	0.02	AluSx1	0.01
LINE/CR1	0.01	AluSx	0.01
DNA/TcMar-Tigger	0.01	AluSz	0.01
tRNA	0.01	AluJr	0.01
DNA/hAT-Tip100	0.01	AluJo	0.01
LTR/ERVK	0.00	AluY	0.01
DNA/hAT-Blackjack	0.00	GA-rich	0.01
DNA/hAT	0.00	(GGC)n	0.01
LTR/Gypsy	0.00	L3	0.01

E

Ontology	Term	FDR Q-val
GO Biological Process	endoplasmic reticulum unfolded protein response	41.70
GO Biological Process	cellular response to topologically incorrect protein	38.68
GO Biological Process	cellular response to unfolded protein	36.68
GO Biological Process	regulation of DNA-templated transcription in response to stress	36.10
GO Biological Process	IRE1-mediated unfolded protein response	35.54
GO Biological Process	response to topologically incorrect protein	35.50
GO Biological Process	response to unfolded protein	32.99
GO Biological Process	liver regeneration	29.63
GO Biological Process	nuclear-transcribed mRNA catabolic process	29.63
GO Biological Process	nuclear-transcribed mRNA catabolic process, nonsense-mediated decay	26.81
GO Biological Process	negative regulation of intrinsic apoptotic signaling pathway	22.96
GO Biological Process	regulation of mitochondrial membrane permeability	19.92
GO Biological Process	response to epidermal growth factor	18.58
GO Biological Process	cellular response to epidermal growth factor stimulus	17.80
GO Biological Process	translational elongation	17.44
GO Biological Process	cotranslational protein targeting to membrane	16.39
GO Biological Process	platelet-derived growth factor receptor signaling pathway	16.09
GO Biological Process	viral gene expression	16.09
GO Biological Process	mitochondrial genome maintenance	14.78
GO Biological Process	mitochondrial transmembrane transport	14.54
Human Phenotype	Abnormal CSF metabolite level	9.18
Human Phenotype	Increased CSF lactate	7.39

F

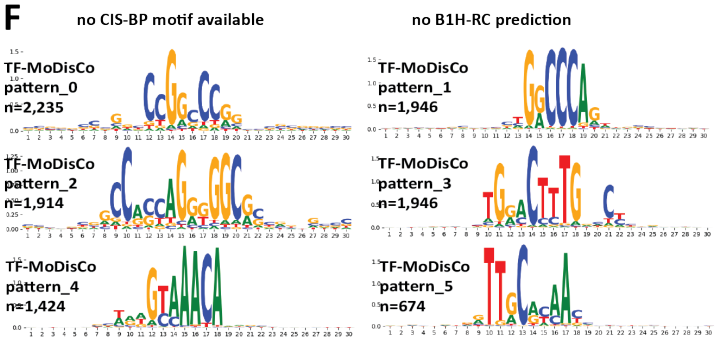

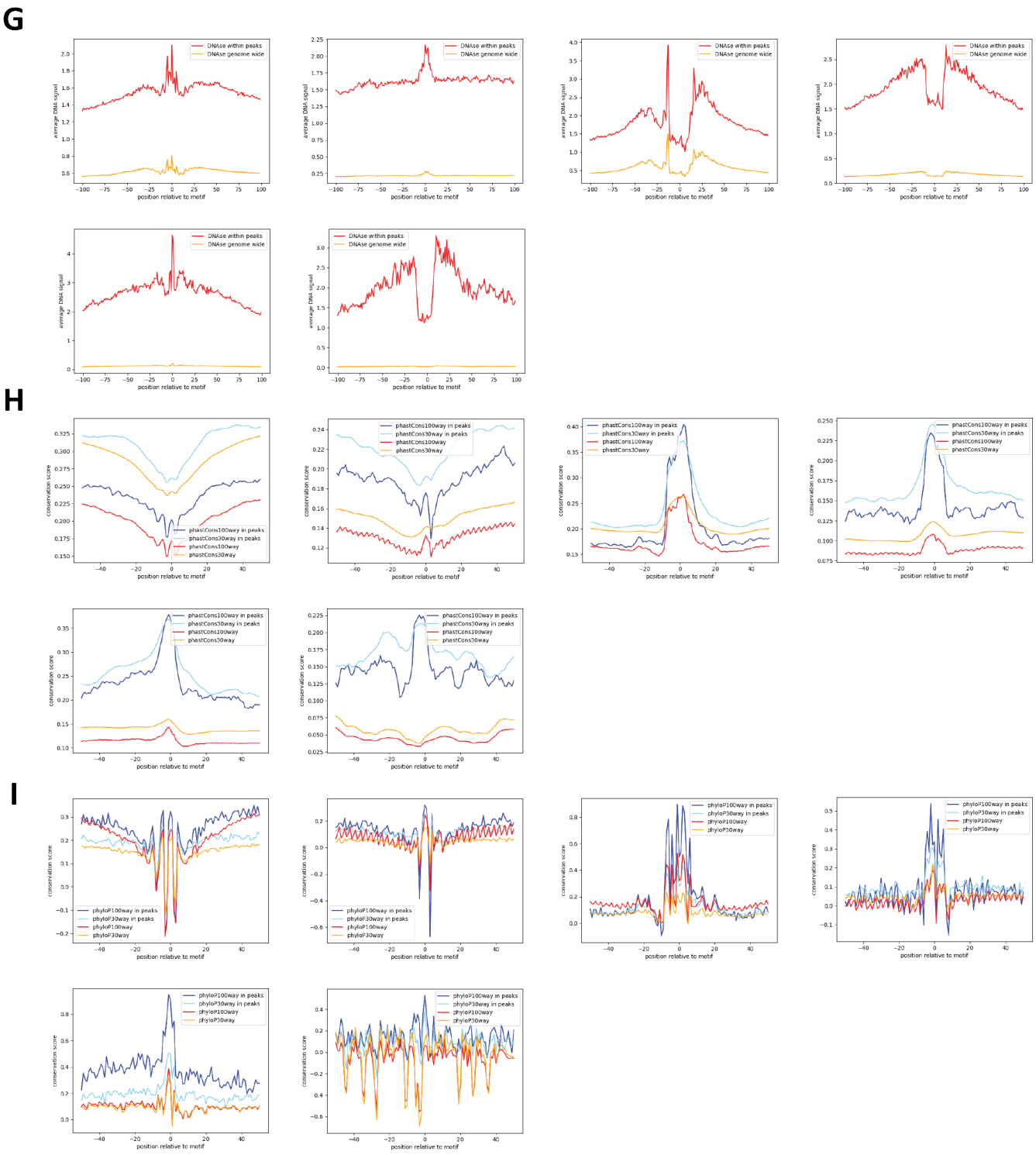

Supplementary Figure 366: Properties and genomic distribution of motifs identified for the ZBED4 transcription factor in HepG2 (accession ENCSR409PMR).

TF-MoDisCO pattern_0 n=2235, CWM

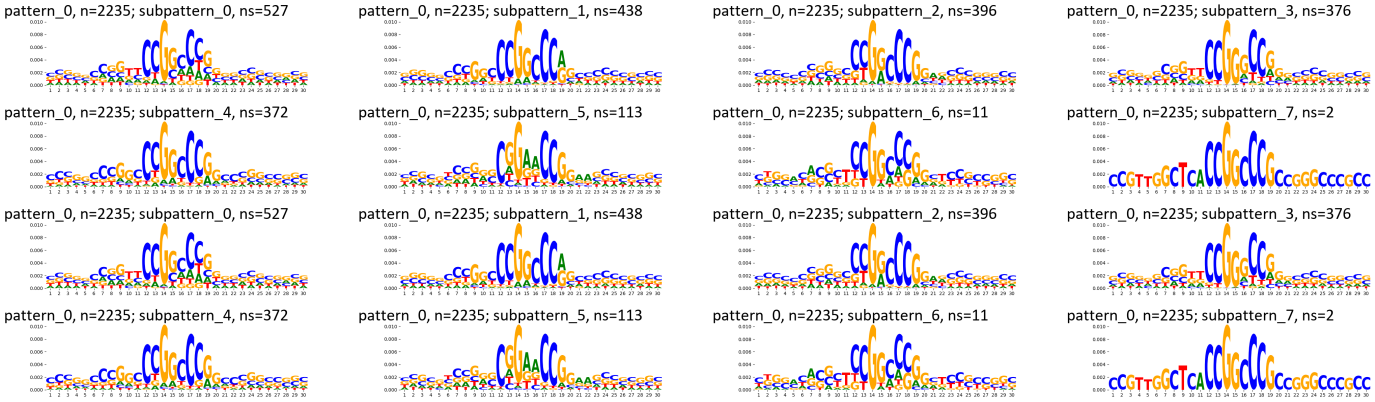

TF-MoDisCO pattern_0 n=2235, PWM

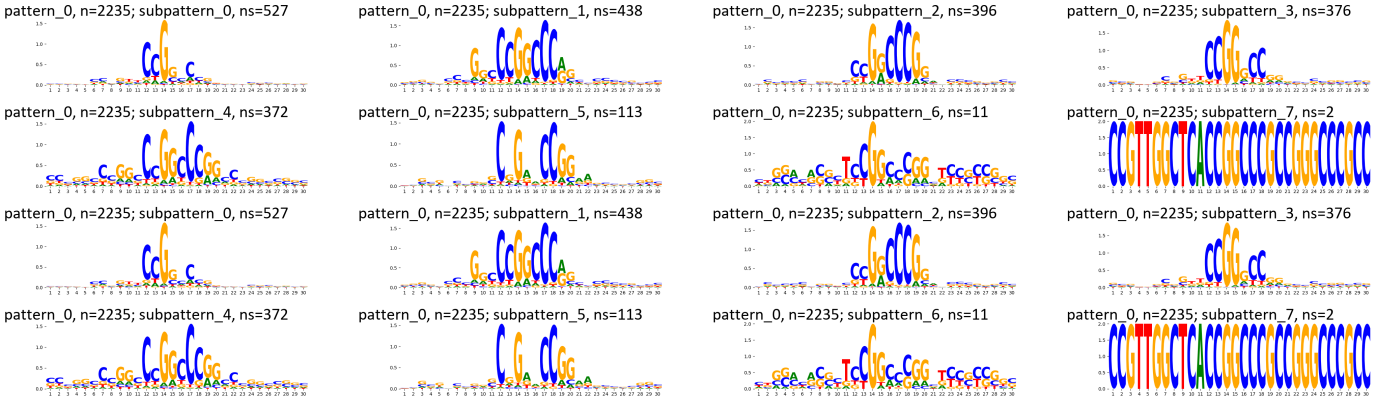

TF-MoDisCO pattern_1 n=1946, CWM

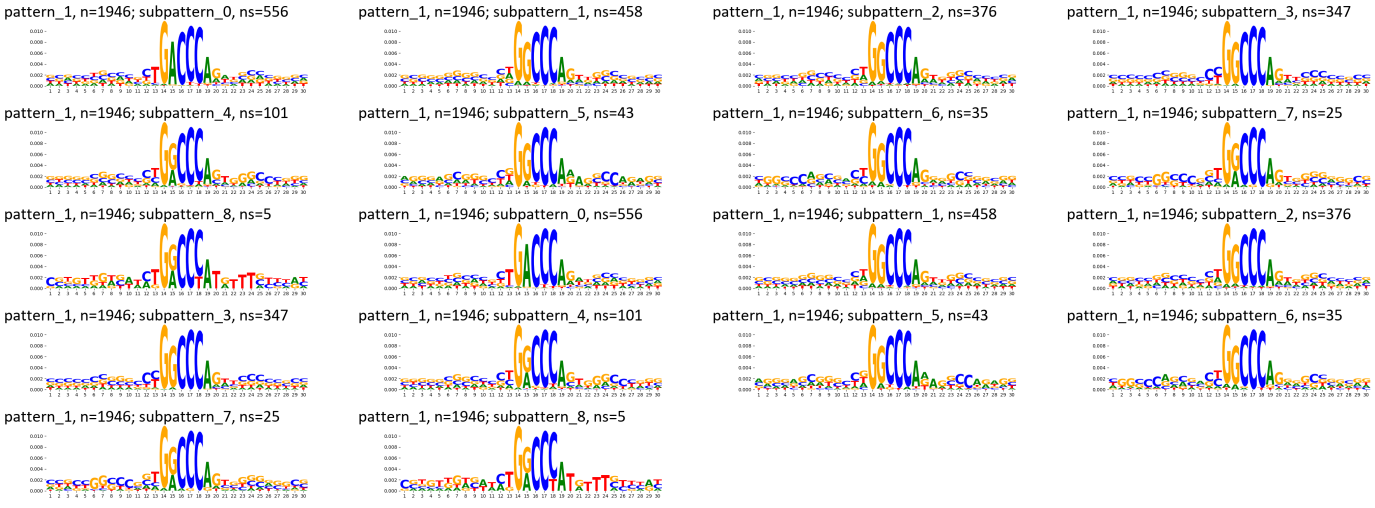

TF-MoDisCO pattern_1 n=1946, PWM

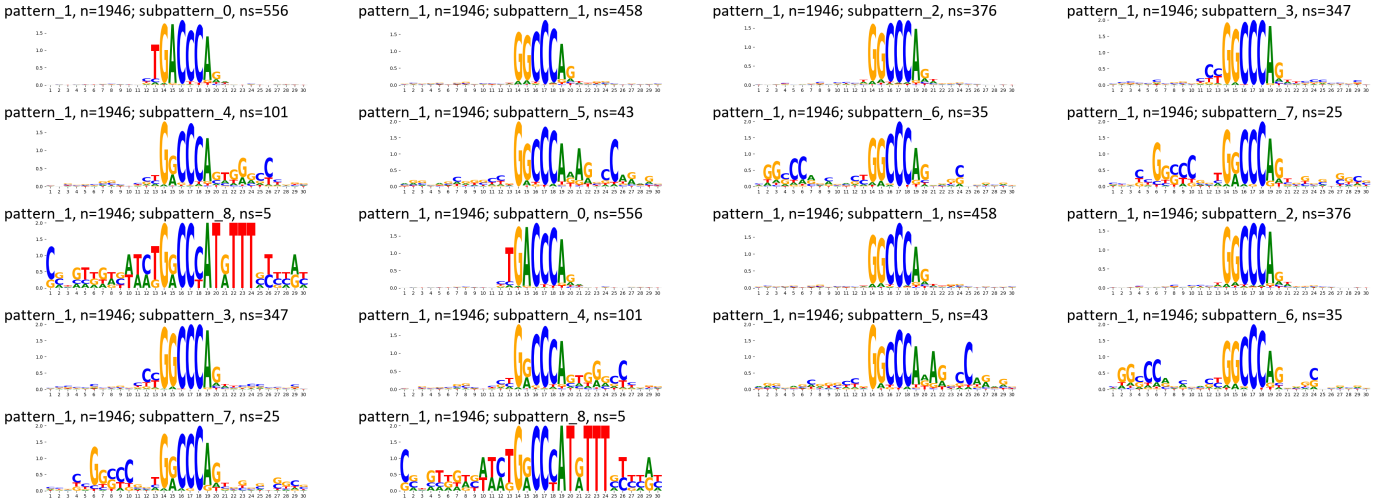

TF-MoDisCO pattern_2 n=1914, CWM

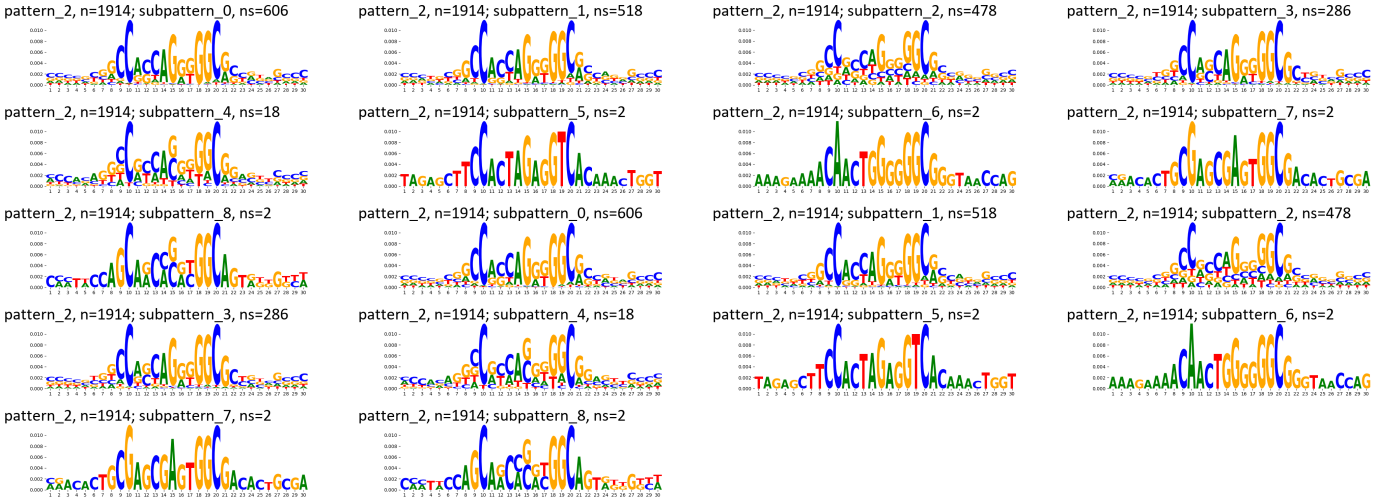

TF-MoDisCO pattern_2 n=1914, PWM

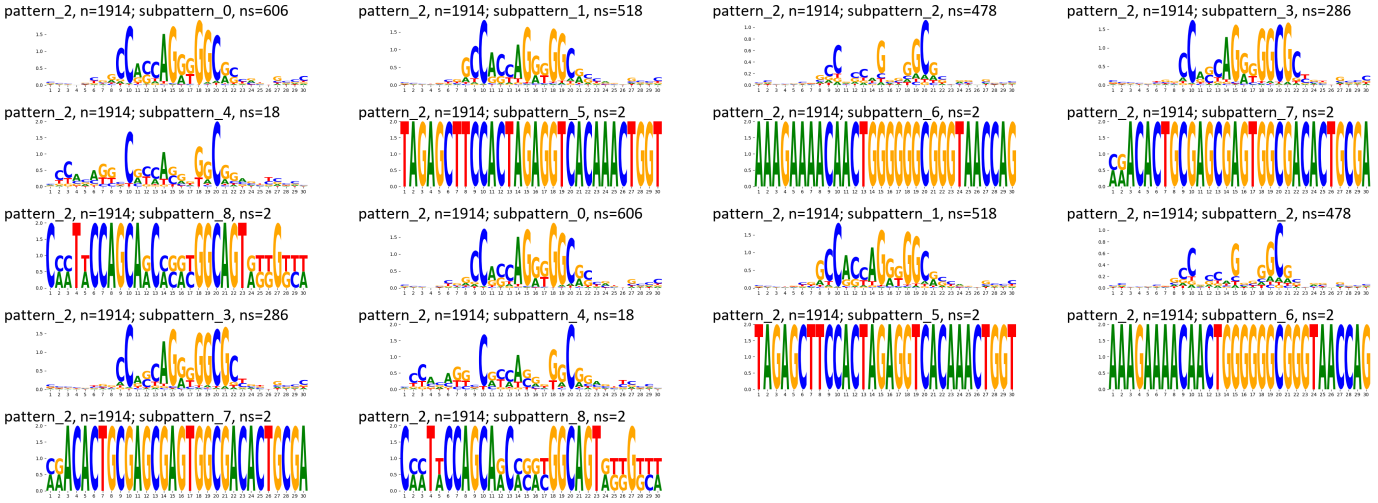

TF-MoDisCO pattern_3 n=1885, CWM

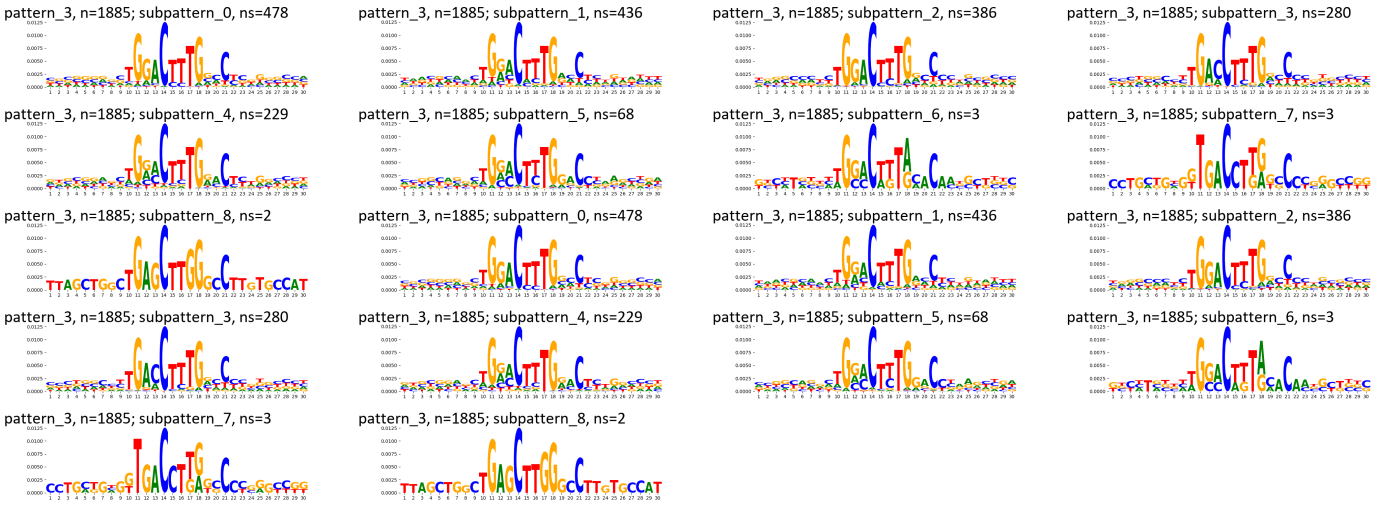

TF-MoDisCO pattern_3 n=1885, PWM

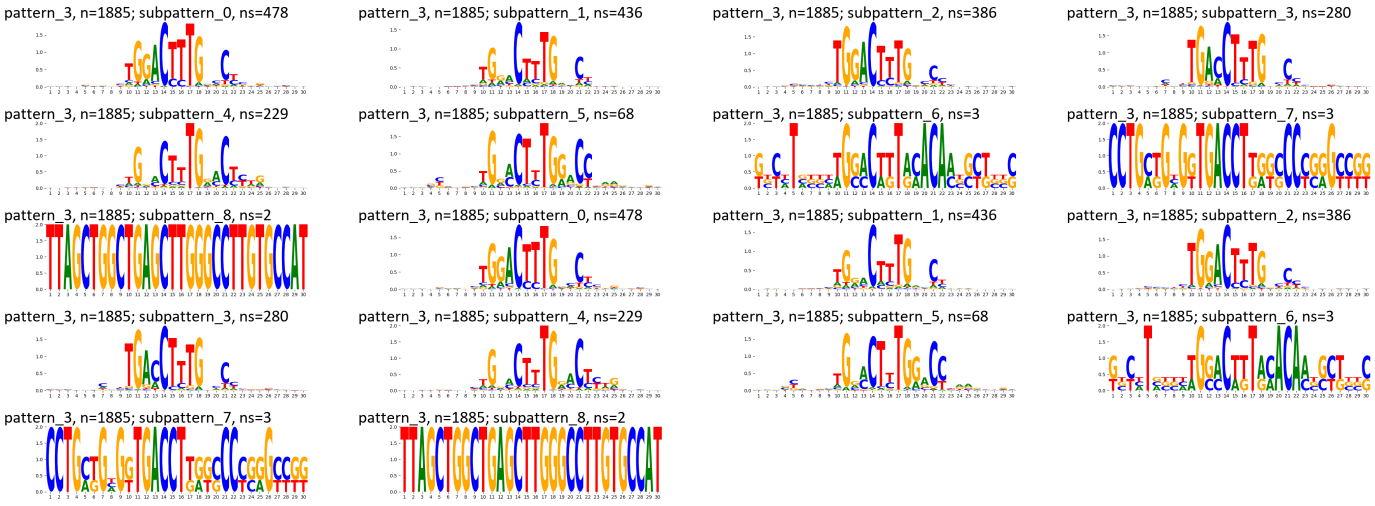

TF-MoDisCO pattern_4 n=1424, CWM

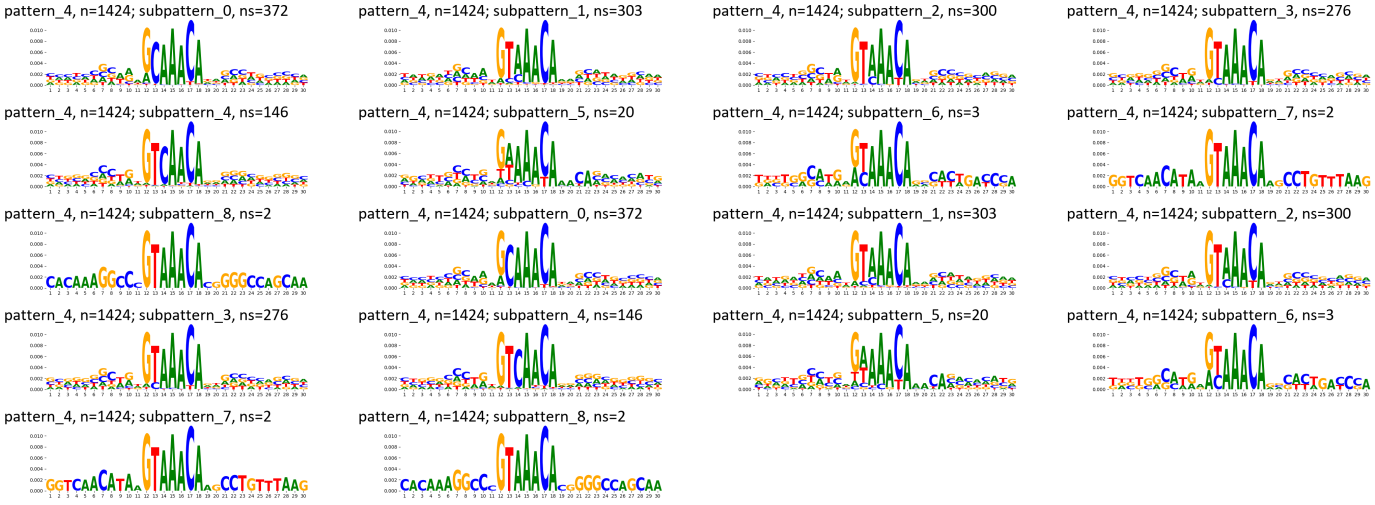

TF-MoDisCO pattern_4 n=1424, PWM

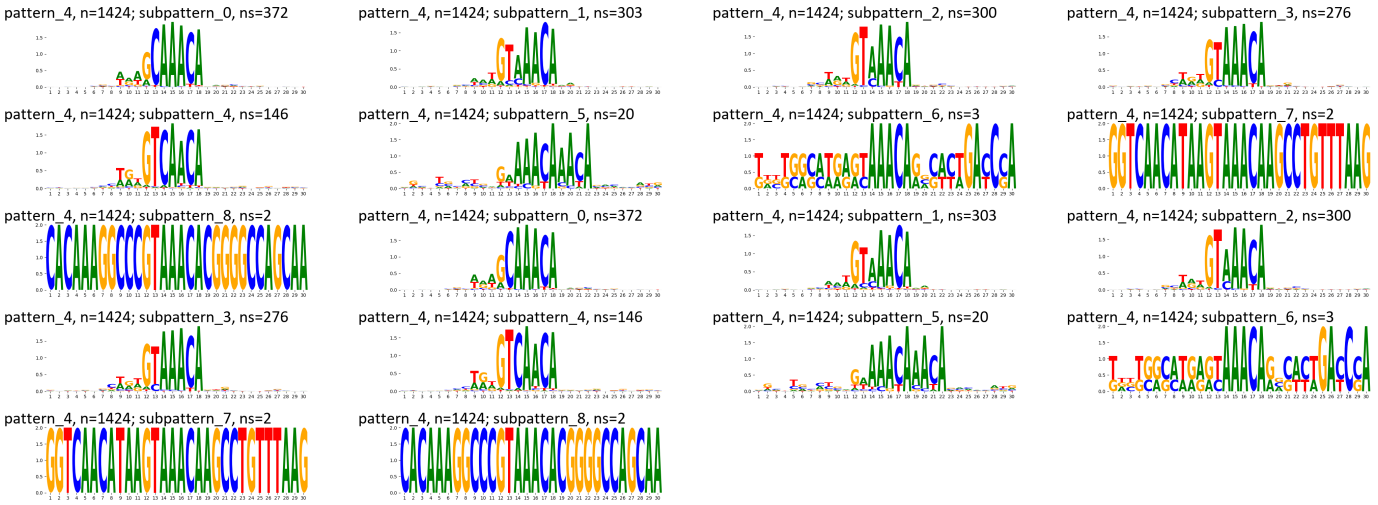

TF-MoDisCO pattern_5 n=674, CWM

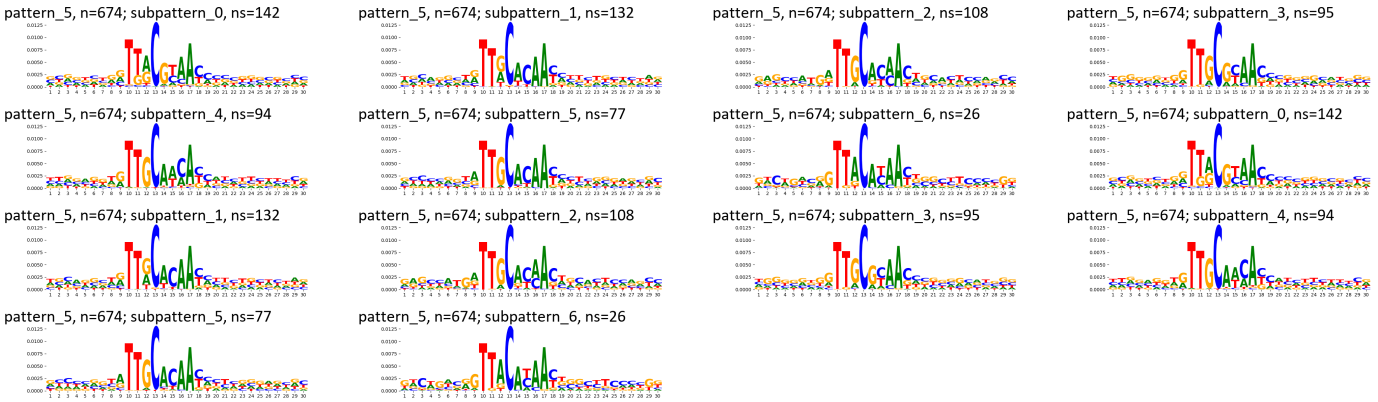

TF-MoDisCO pattern_5 n=674, PWM

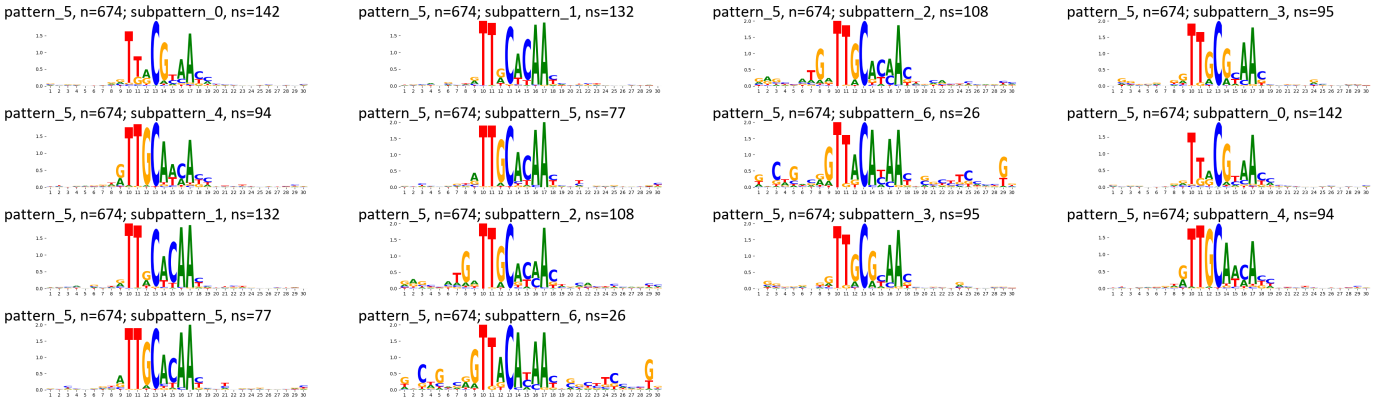

Supplementary Figure 367: TF-MoDisCO subpatterns for the ZBED4 transcription factor in HepG2 (accession ENCSR409PMR).

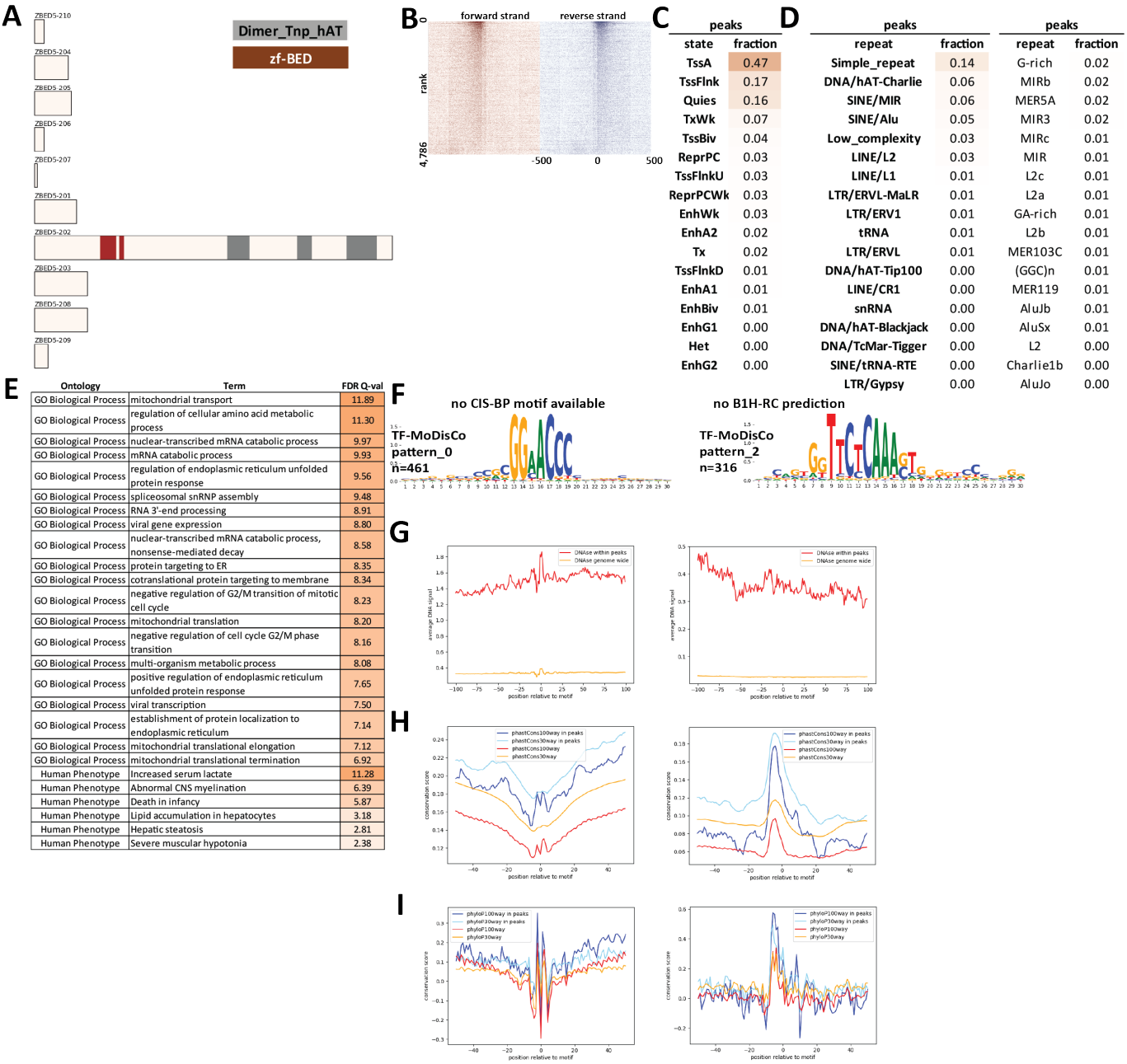

peaks	
state	fraction
TssA	0.47
TssFlnk	0.17
Quies	0.16
TxWk	0.07
TssBiv	0.04
ReprPC	0.03
TssFlnkU	0.03
ReprPCWk	0.03
EnhWk	0.03
EnhA2	0.02
Tx	0.02
TssFlnkD	0.01
EnhA1	0.01
EnhBiv	0.01
EnhG1	0.00
Het	0.00
EnhG2	0.00

peaks		peaks	
repeat	fraction	repeat	fraction
Simple_repeat	0.14	G-rich	0.02
DNA/hAT-Charlie	0.06	MIRb	0.02
SINE/MIR	0.06	MER5A	0.02
SINE/Alu	0.05	MIR3	0.02
Low_complexity	0.03	MIRc	0.01
LINE/L2	0.03	MIR	0.01
LINE/L1	0.01	L2c	0.01
LTR/ERVL-MaLR	0.01	L2a	0.01
LTR/ERV1	0.01	GA-rich	0.01
tRNA	0.01	L2b	0.01
LTR/ERVL	0.01	MER103C	0.01
DNA/hAT-Tip100	0.00	(GGC)n	0.01
LINE/CR1	0.00	MER119	0.01
snRNA	0.00	AluJb	0.01
DNA/hAT-Blackjack	0.00	AluSx	0.01
DNA/TcMar-Tigger	0.00	L2	0.00
SINE/tRNA-RTE	0.00	Charlie1b	0.00
LTR/Gypsy	0.00	AluJo	0.00

Ontology	Term	FDR Q-val
GO Biological Process	mitochondrial transport	11.89
GO Biological Process	regulation of cellular amino acid metabolic process	11.30
GO Biological Process	nuclear-transcribed mRNA catabolic process	9.97
GO Biological Process	mRNA catabolic process	9.93
GO Biological Process	regulation of endoplasmic reticulum unfolded protein response	9.56
GO Biological Process	spliceosomal snRNP assembly	9.48
GO Biological Process	RNA 3'-end processing	8.91
GO Biological Process	viral gene expression	8.80
GO Biological Process	nuclear-transcribed mRNA catabolic process, nonsense-mediated decay	8.58
GO Biological Process	protein targeting to ER	8.35
GO Biological Process	cotranslational protein targeting to membrane	8.34
GO Biological Process	negative regulation of G2/M transition of mitotic cell cycle	8.23
GO Biological Process	mitochondrial translation	8.20
GO Biological Process	negative regulation of cell cycle G2/M phase transition	8.16
GO Biological Process	multi-organism metabolic process	8.08
GO Biological Process	positive regulation of endoplasmic reticulum unfolded protein response	7.65
GO Biological Process	viral transcription	7.50
GO Biological Process	establishment of protein localization to endoplasmic reticulum	7.14
GO Biological Process	mitochondrial translational elongation	7.12
GO Biological Process	mitochondrial translational termination	6.92
Human Phenotype	Increased serum lactate	11.28
Human Phenotype	Abnormal CNS myelination	6.39
Human Phenotype	Death in infancy	5.87
Human Phenotype	Lipid accumulation in hepatocytes	3.18
Human Phenotype	Hepatic steatosis	2.81
Human Phenotype	Severe muscular hypotonia	2.38

Supplementary Figure 368: Properties and genomic distribution of motifs identified for the ZBED5 transcription factor in HepG2 (accession ENCSR656SIB).

TF-MoDisCO pattern_0 n=461, CWM

pattern_0, n=461; subpattern_0, ns=157

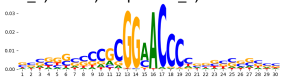

pattern_0, n=461; subpattern_1, ns=127

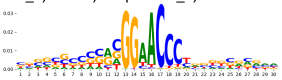

pattern_0, n=461; subpattern_2, ns=96

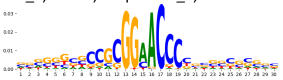

pattern_0, n=461; subpattern_3, ns=72

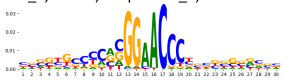

pattern_0, n=461; subpattern_4, ns=7

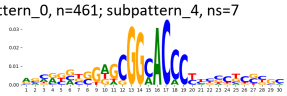

pattern_0, n=461; subpattern_5, ns=2

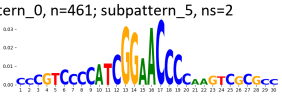

TF-MoDisCO pattern_0 n=461, PWM

pattern_0, n=461; subpattern_0, ns=157

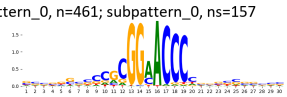

pattern_0, n=461; subpattern_1, ns=127

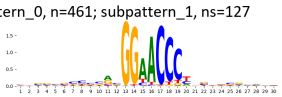

pattern_0, n=461; subpattern_2, ns=96

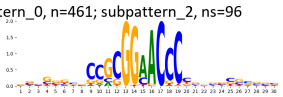

pattern_0, n=461; subpattern_3, ns=72

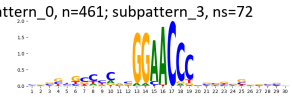

pattern_0, n=461; subpattern_4, ns=7

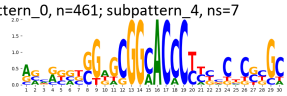

pattern_0, n=461; subpattern_5, ns=2

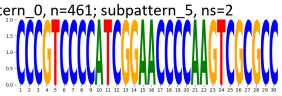

TF-MoDisCO pattern_2 n=316, CWM

pattern_2, n=316; subpattern_0, ns=87

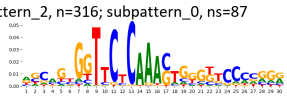

pattern_2, n=316; subpattern_1, ns=83

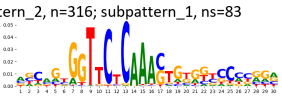

pattern_2, n=316; subpattern_2, ns=78

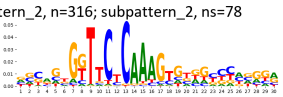

pattern_2, n=316; subpattern_3, ns=42

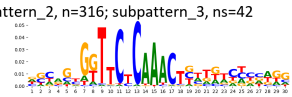

pattern_2, n=316; subpattern_4, ns=26

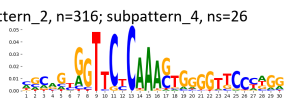

TF-MoDisCO pattern_2 n=316, PWM

pattern_2, n=316; subpattern_0, ns=87

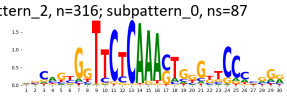

pattern_2, n=316; subpattern_1, ns=83

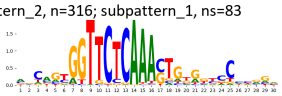

pattern_2, n=316; subpattern_2, ns=78

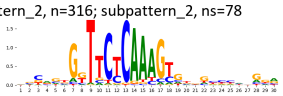

pattern_2, n=316; subpattern_3, ns=42

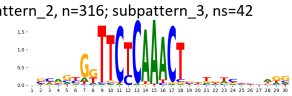

pattern_2, n=316; subpattern_4, ns=26

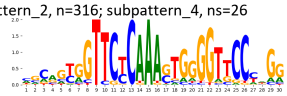

Supplementary Figure 369: TF-MoDisCO subpatterns for the ZBED5 transcription factor in HepG2 (accession ENCSR656SIB).

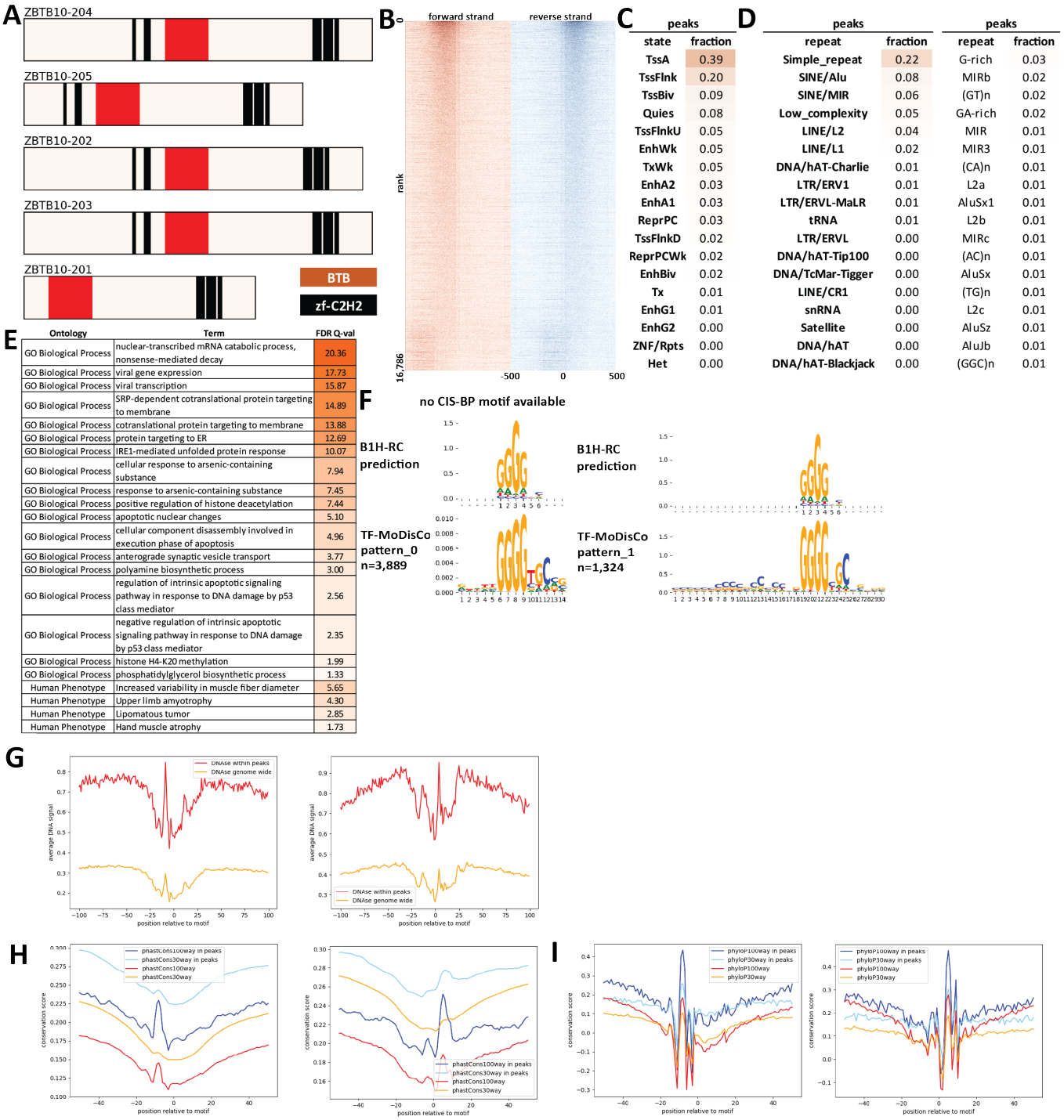

Supplementary Figure 370: Properties and genomic distribution of motifs identified for the ZBTB10 transcription factor in HEK293 (accession ENCSR004PLU).

TF-MoDisCO pattern_0 n=3889, CWM

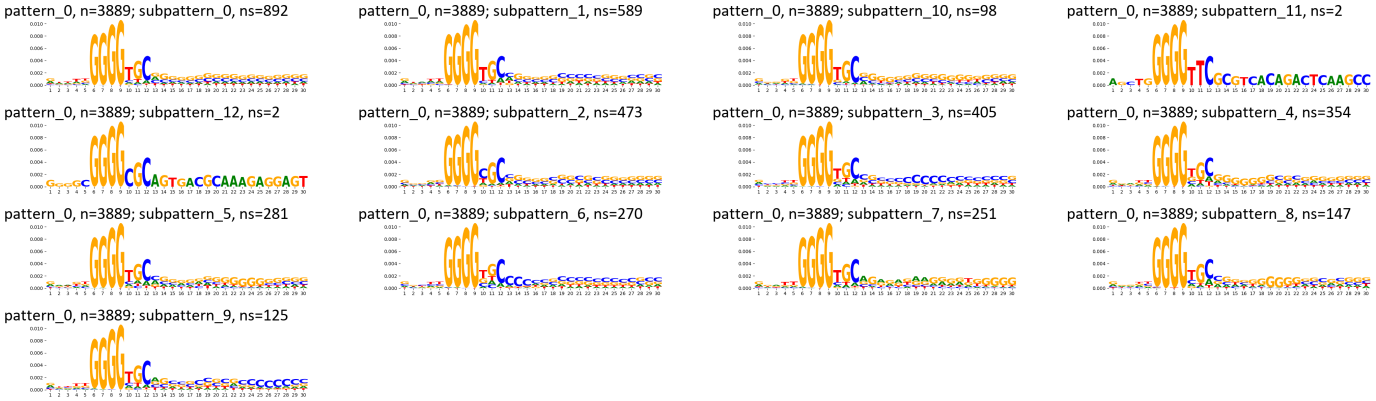

TF-MoDisCO pattern_0 n=3889, PWM

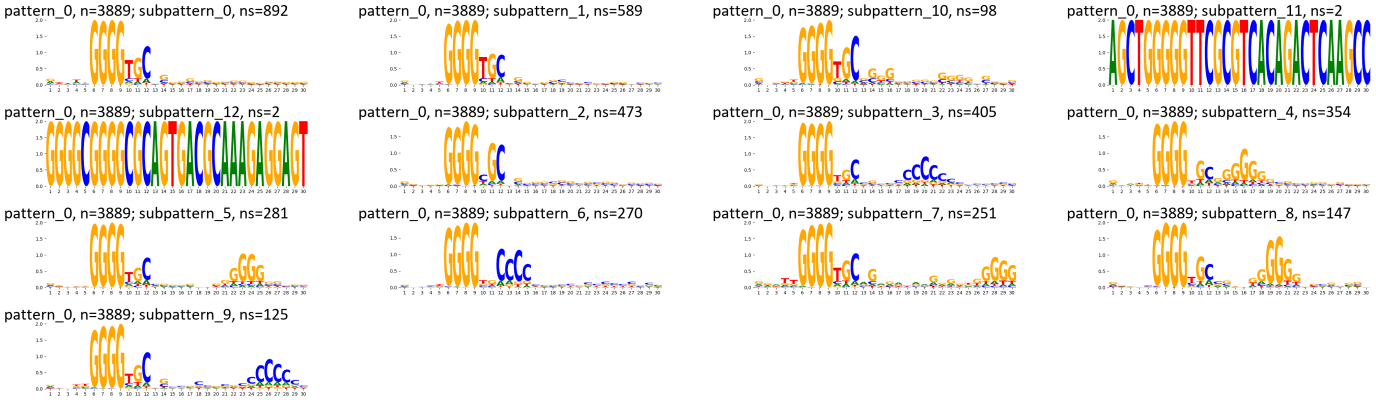

TF-MoDisCO pattern_1 n=1324, CWM

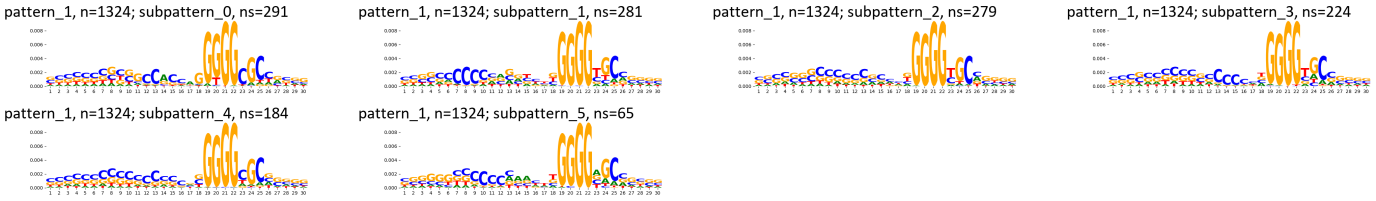

TF-MoDisCO pattern_1 n=1324, PWM

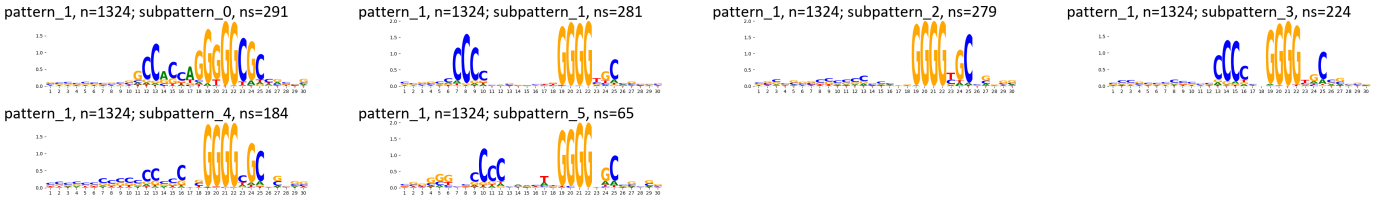

Supplementary Figure 371: TF-MoDisCO subpatterns for the ZBTB10 transcription factor in HEK293 (accession ENCSR004PLU).

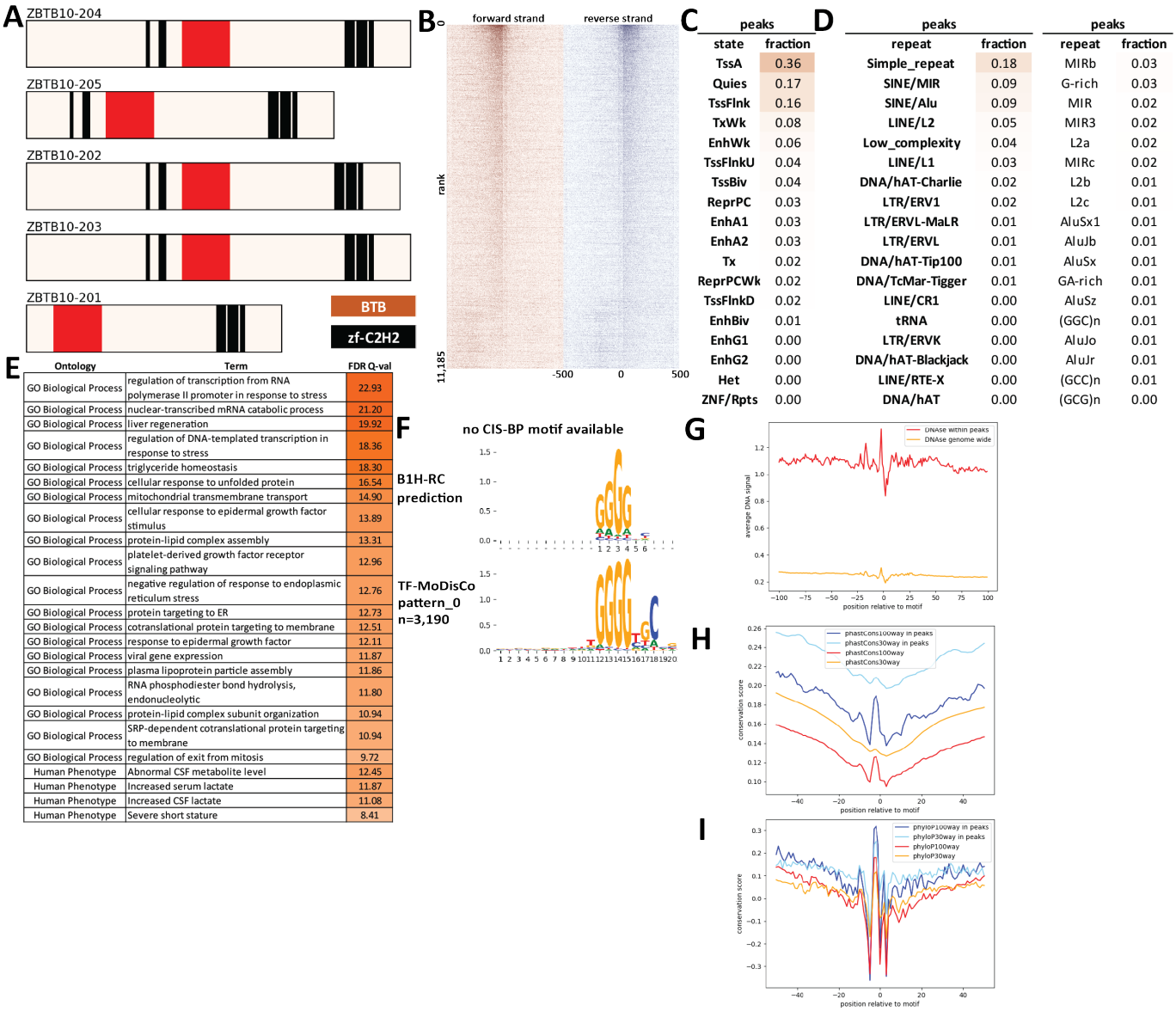

Supplementary Figure 372: Properties and genomic distribution of motifs identified for the ZBTB10 transcription factor in HepG2 (accession ENCSR959COF).

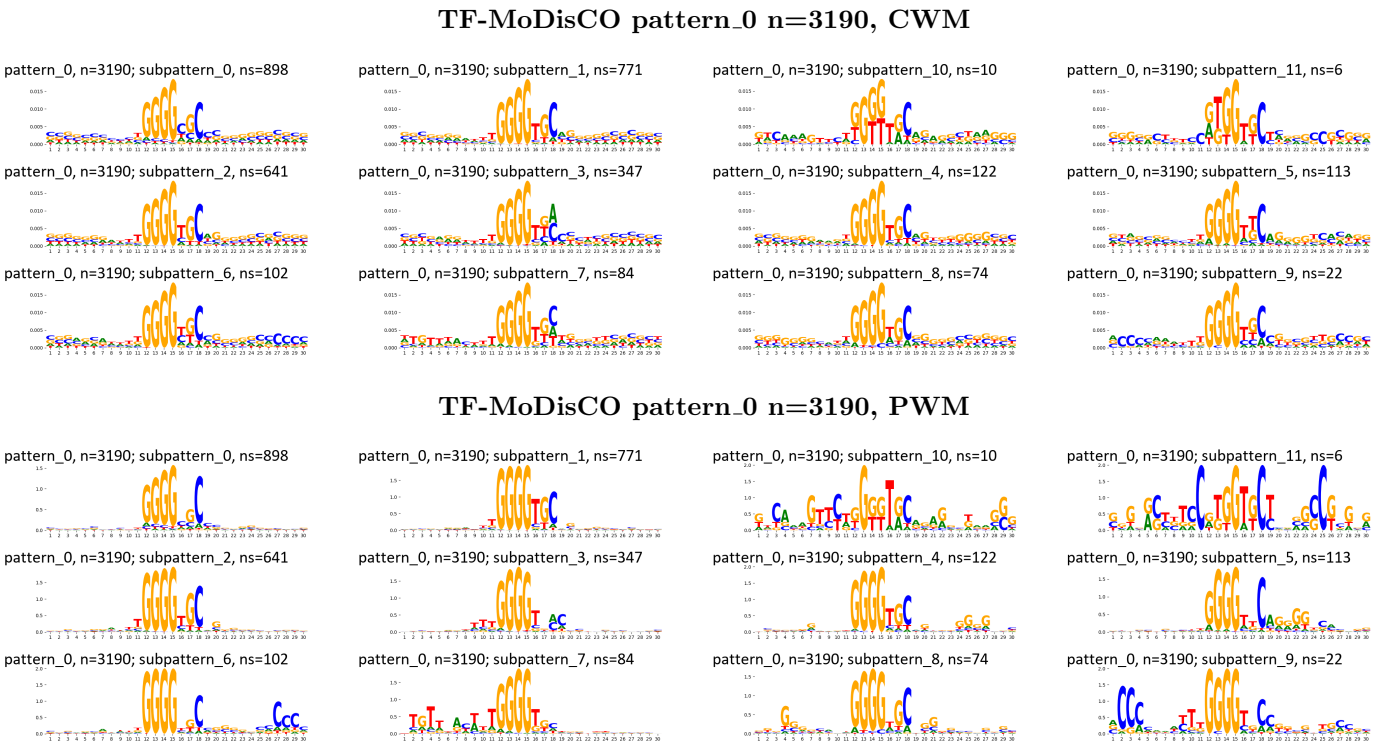

Supplementary Figure 373: TF-MoDisCO subpatterns for the ZBTB10 transcription factor in HepG2 (accession ENCSR959COF).

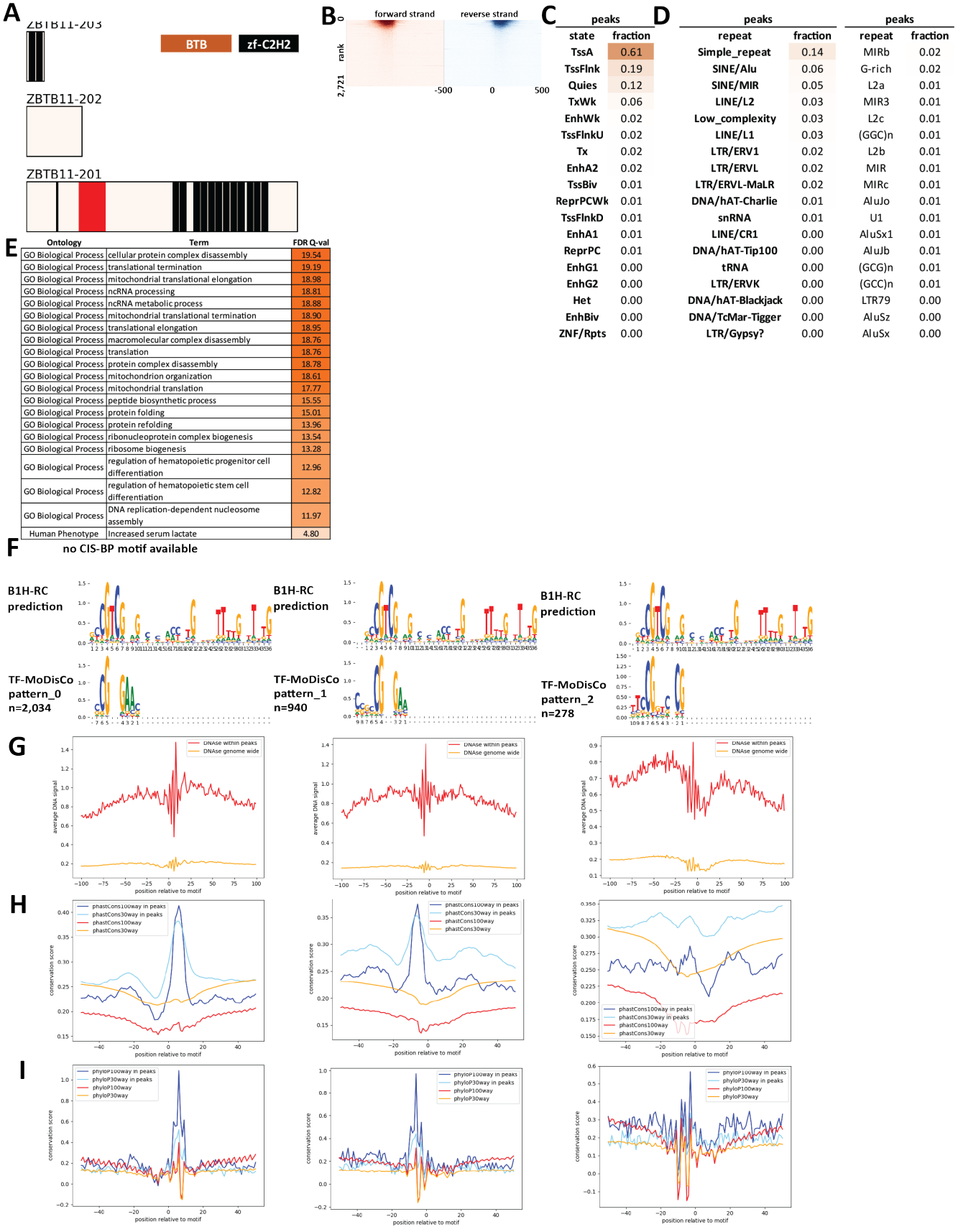

Supplementary Figure 374: Properties and genomic distribution of motifs identified for the ZBTB11 transcription factor in GM12878 (accession ENCSR057DTZ).

TF-MoDisCO pattern_0 n=2034, CWM

pattern_0, n=2034; subpattern_0, ns=410

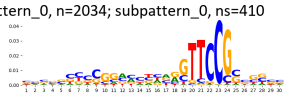

pattern_0, n=2034; subpattern_1, ns=323

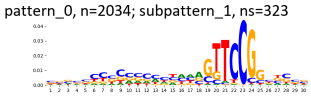

pattern_0, n=2034; subpattern_2, ns=318

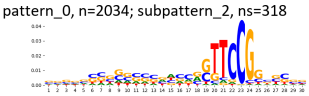

pattern_0, n=2034; subpattern_3, ns=305

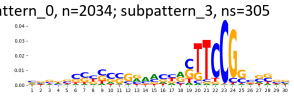

pattern_0, n=2034; subpattern_4, ns=276

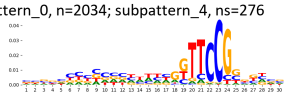

pattern_0, n=2034; subpattern_5, ns=167

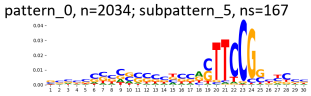

pattern_0, n=2034; subpattern_6, ns=136

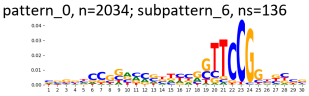

pattern_0, n=2034; subpattern_7, ns=99

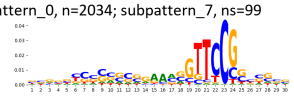

TF-MoDisCO pattern_0 n=2034, PWM

pattern_0, n=2034; subpattern_0, ns=410

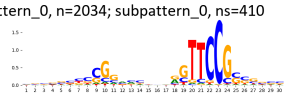

pattern_0, n=2034; subpattern_1, ns=323

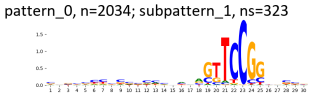

pattern_0, n=2034; subpattern_2, ns=318

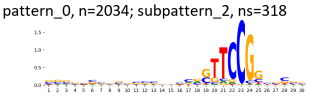

pattern_0, n=2034; subpattern_3, ns=305

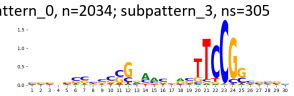

pattern_0, n=2034; subpattern_4, ns=276

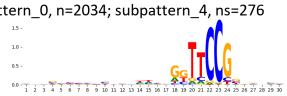

pattern_0, n=2034; subpattern_5, ns=167

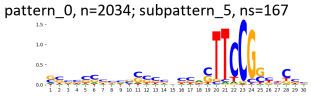

pattern_0, n=2034; subpattern_6, ns=136

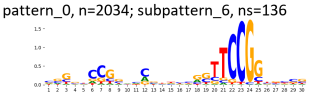

pattern_0, n=2034; subpattern_7, ns=99

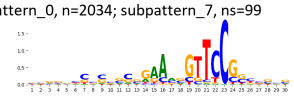

TF-MoDisCO pattern_1 n=940, CWM

pattern_1, n=940; subpattern_0, ns=234

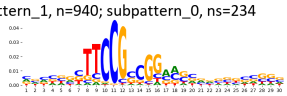

pattern_1, n=940; subpattern_1, ns=229

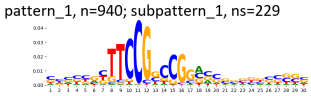

pattern_1, n=940; subpattern_2, ns=166

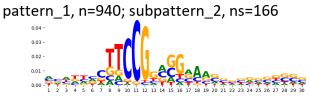

pattern_1, n=940; subpattern_3, ns=152

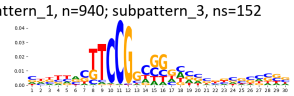

pattern_1, n=940; subpattern_4, ns=136

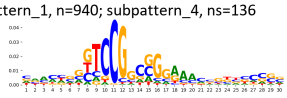

pattern_1, n=940; subpattern_5, ns=21

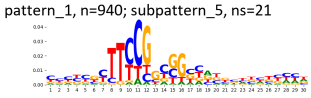

pattern_1, n=940; subpattern_6, ns=2

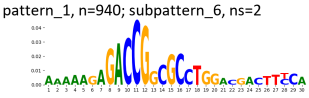

TF-MoDisCO pattern_1 n=940, PWM

pattern_1, n=940; subpattern_0, ns=234

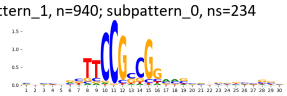

pattern_1, n=940; subpattern_1, ns=229

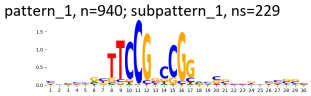

pattern_1, n=940; subpattern_2, ns=166

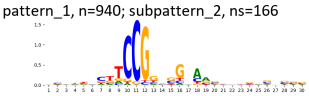

pattern_1, n=940; subpattern_3, ns=152

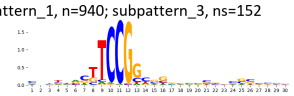

pattern_1, n=940; subpattern_4, ns=136

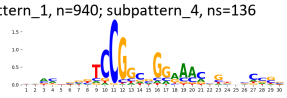

pattern_1, n=940; subpattern_5, ns=21

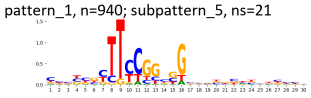

pattern_1, n=940; subpattern_6, ns=2

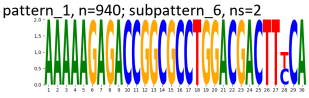

TF-MoDisCO pattern_2 n=278, CWM

pattern_2, n=278; subpattern_0, ns=62

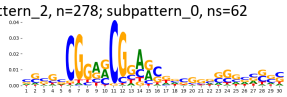

pattern_2, n=278; subpattern_1, ns=50

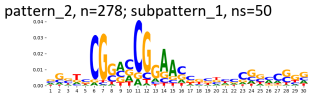

pattern_2, n=278; subpattern_2, ns=49

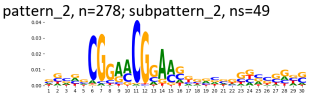

pattern_2, n=278; subpattern_3, ns=48

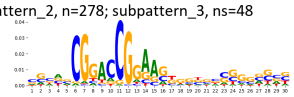

pattern_2, n=278; subpattern_4, ns=38

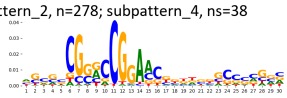

pattern_2, n=278; subpattern_5, ns=31

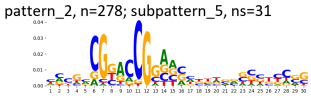

TF-MoDisCO pattern_2 n=278, PWM

pattern_2, n=278; subpattern_0, ns=62

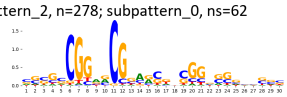

pattern_2, n=278; subpattern_1, ns=50

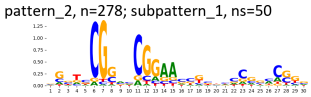

pattern_2, n=278; subpattern_2, ns=49

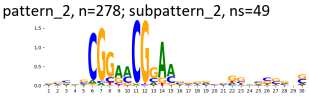

pattern_2, n=278; subpattern_3, ns=48

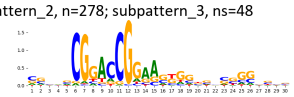

pattern_2, n=278; subpattern_4, ns=38

pattern_2, n=278; subpattern_5, ns=31

Supplementary Figure 375: TF-MoDisCO subpatterns for the ZBTB11 transcription factor in GM12878 (accession ENCSR057DTZ).

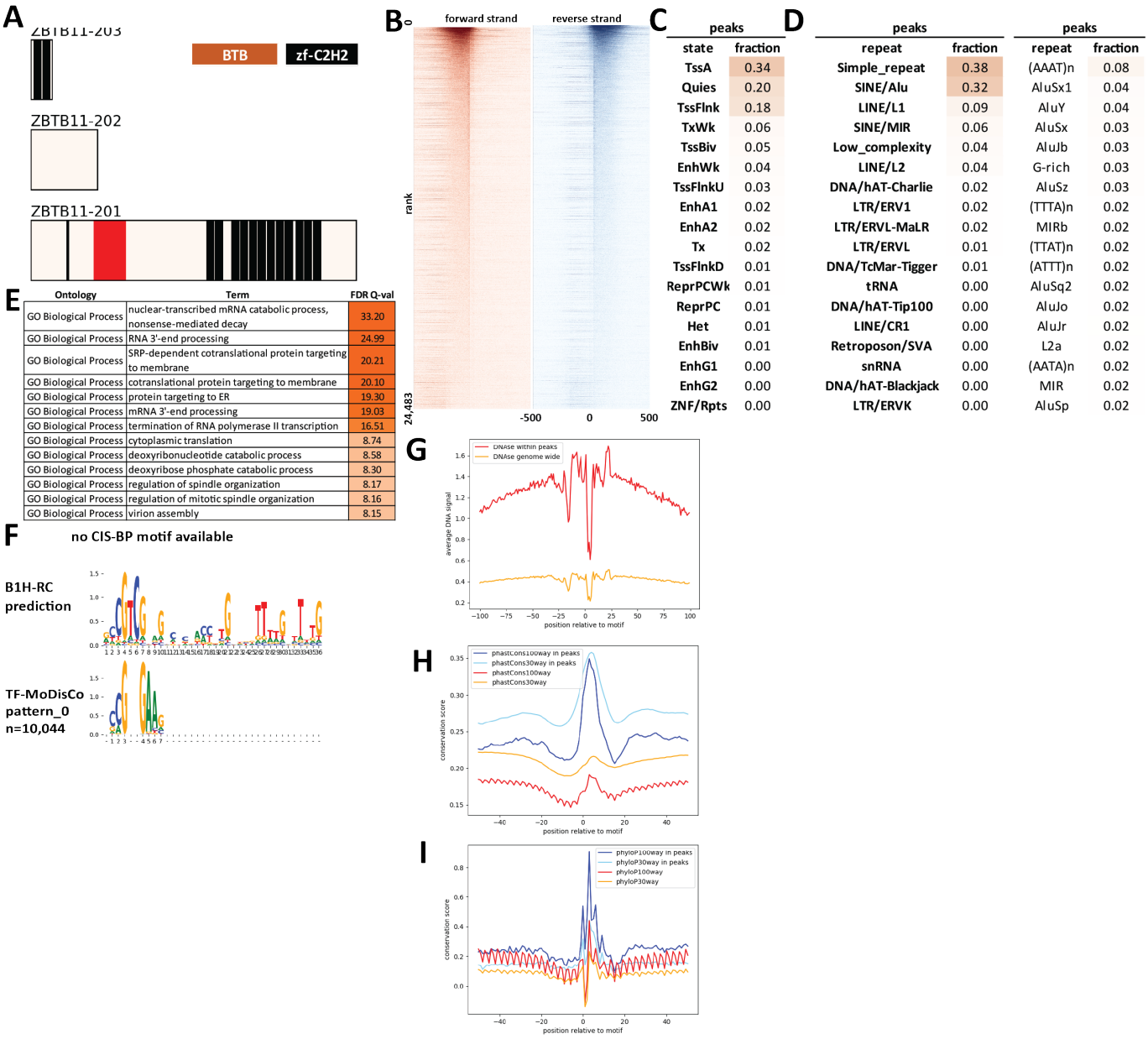

C

peaks	
state	fraction
TssA	0.34
Quies	0.20
TssFlnk	0.18
TxWk	0.06
TssBiv	0.05
EnhWk	0.04
TssFlnkU	0.03
EnhA1	0.02
EnhA2	0.02
Tx	0.02
TssFlnkD	0.01
ReprPCWk	0.01
ReprPC	0.01
Het	0.01
EnhBiv	0.01
EnhG1	0.00
EnhG2	0.00
ZNF/Rpts	0.00

D

peaks		peaks	
repeat	fraction	repeat	fraction
Simple_repeat	0.38	(AAAT)n	0.08
SINE/Alu	0.32	AluSx1	0.04
LINE/L1	0.09	AluY	0.04
SINE/MIR	0.06	AluSx	0.03
Low_complexity	0.04	AluJb	0.03
LINE/L2	0.04	G-rich	0.03
DNA/hAT-Charlie	0.02	AluSz	0.03
LTR/ERV1	0.02	(TTTA)n	0.02
LTR/ERVL-MaLR	0.02	MIRb	0.02
LTR/ERVL	0.01	(TTAT)n	0.02
DNA/TcMar-Tigger	0.01	(ATTT)n	0.02
tRNA	0.00	AluSq2	0.02
DNA/hAT-Tip100	0.00	AluJo	0.02
LINE/CR1	0.00	AluJr	0.02
Retroposon/SVA	0.00	L2a	0.02
snRNA	0.00	(AATA)n	0.02
DNA/hAT-Blackjack	0.00	MIR	0.02
LTR/ERVK	0.00	AluSp	0.02

E

Ontology	Term	FDR Q-val
GO Biological Process	nuclear-transcribed mRNA catabolic process, nonsense-mediated decay	33.20
GO Biological Process	RNA 3'-end processing	24.99
GO Biological Process	SRP-dependent cotranslational protein targeting to membrane	20.21
GO Biological Process	cotranslational protein targeting to membrane	20.10
GO Biological Process	protein targeting to ER	19.30
GO Biological Process	mRNA 3'-end processing	19.03
GO Biological Process	termination of RNA polymerase II transcription	16.51
GO Biological Process	cytoplasmic translation	8.74
GO Biological Process	deoxyribonucleotide catabolic process	8.58
GO Biological Process	deoxyribose phosphate catabolic process	8.30
GO Biological Process	regulation of spindle organization	8.17
GO Biological Process	regulation of mitotic spindle organization	8.16
GO Biological Process	virion assembly	8.15

Supplementary Figure 376: Properties and genomic distribution of motifs identified for the ZBTB11 transcription factor in HEK293 (accession ENCSR882ZTS).

TF-MoDisCO pattern_0 n=10044, CWM

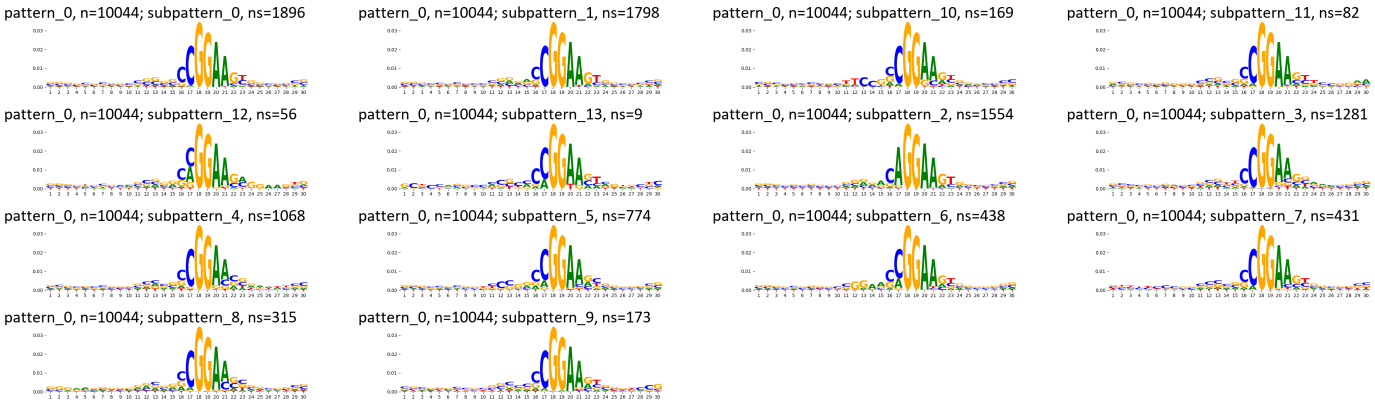

TF-MoDisCO pattern_0 n=10044, PWM

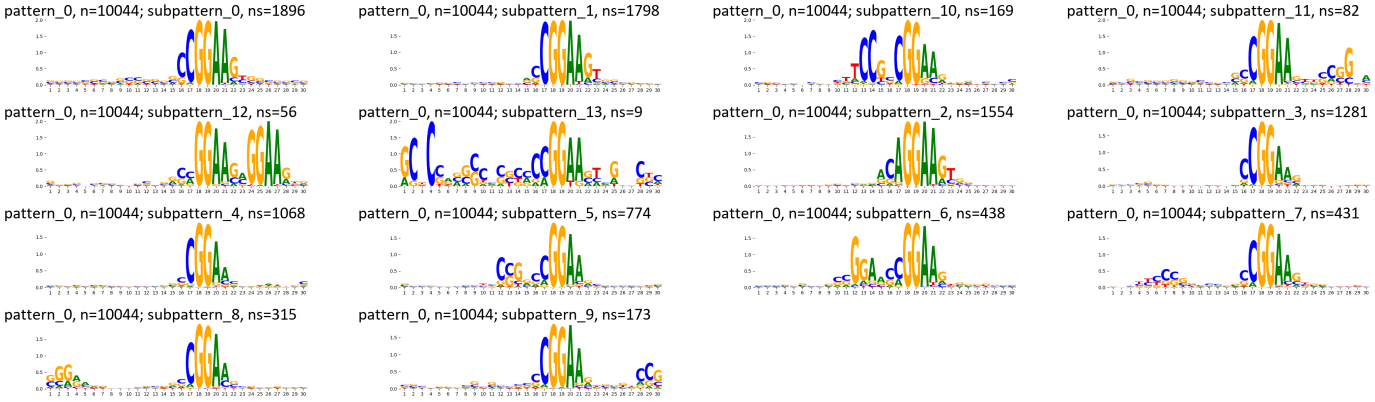

Supplementary Figure 377: TF-MoDisCO subpatterns for the ZBTB11 transcription factor in HEK293 (accession ENCSR882ZTS).

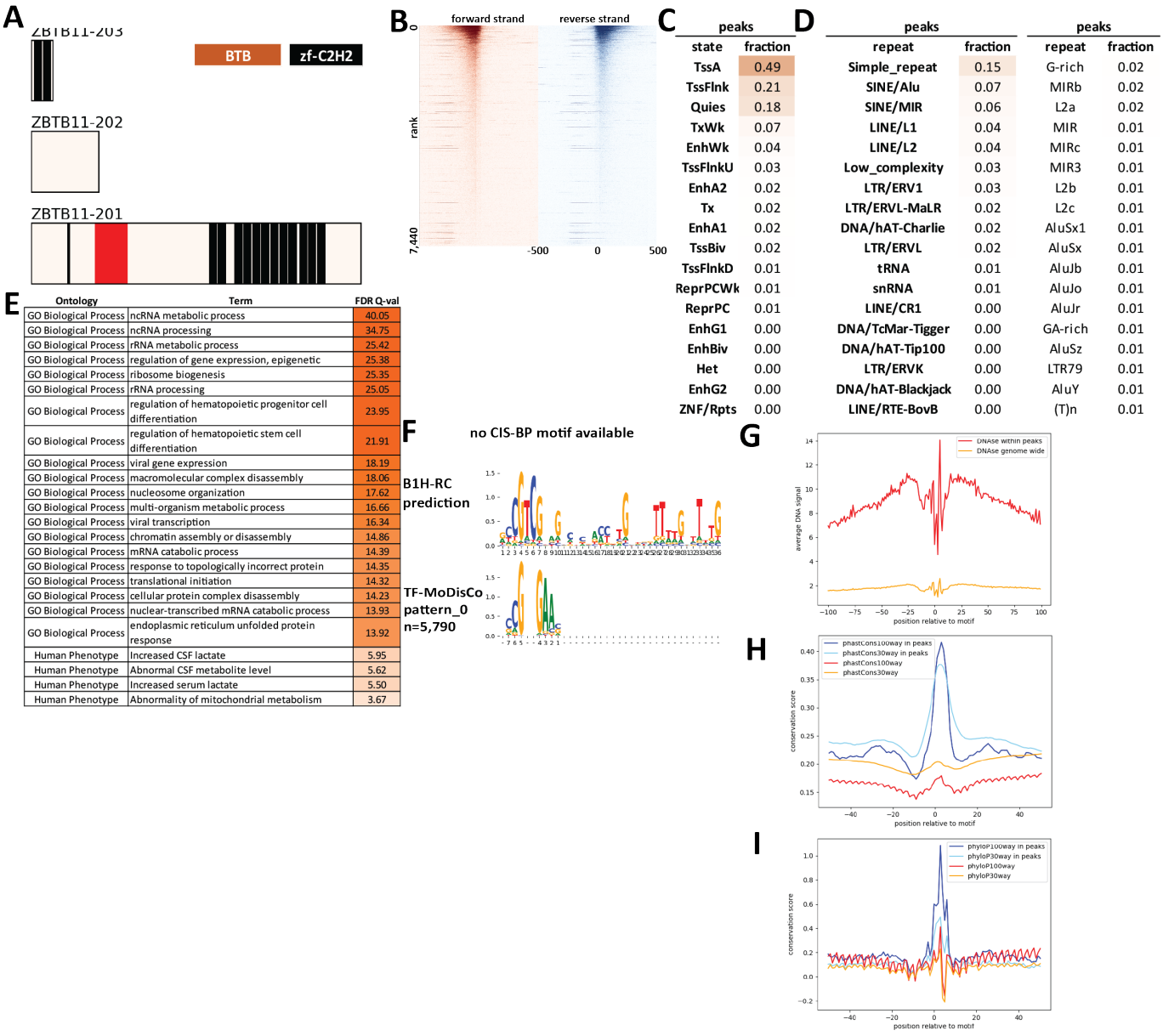

C

peaks	
state	fraction
TssA	0.49
TssFlnk	0.21
Quies	0.18
TxWk	0.07
EnhWk	0.04
TssFlnkU	0.03
EnhA2	0.02
Tx	0.02
EnhA1	0.02
TssBiv	0.02
TssFlnkD	0.01
ReprPCWk	0.01
ReprPC	0.01
EnhG1	0.00
EnhBiv	0.00
Het	0.00
EnhG2	0.00
ZNF/Rpts	0.00

D

peaks		peaks	
repeat	fraction	repeat	fraction
Simple_repeat	0.15	G-rich	0.02
SINE/Alu	0.07	MIRb	0.02
SINE/MIR	0.06	L2a	0.02
LINE/L1	0.04	MIR	0.01
LINE/L2	0.04	MIRc	0.01
Low_complexity	0.03	MIR3	0.01
LTR/ERV1	0.03	L2b	0.01
LTR/ERVL-MaLR	0.02	L2c	0.01
DNA/hAT-Charlie	0.02	AluSx1	0.01
LTR/ERVL	0.02	AluSx	0.01
tRNA	0.01	AluJb	0.01
snRNA	0.01	AluJo	0.01
LINE/CR1	0.00	AluJr	0.01
DNA/TcMar-Tigger	0.00	GA-rich	0.01
DNA/hAT-Tip100	0.00	AluSz	0.01
LTR/ERVK	0.00	LTR79	0.01
DNA/hAT-Blackjack	0.00	AluY	0.01
LINE/RTE-BovB	0.00	(T)n	0.01

E

Ontology	Term	FDR Q-val
GO Biological Process	ncRNA metabolic process	40.05
GO Biological Process	ncRNA processing	34.75
GO Biological Process	rRNA metabolic process	25.42
GO Biological Process	regulation of gene expression, epigenetic	25.38
GO Biological Process	ribosome biogenesis	25.35
GO Biological Process	rRNA processing	25.05
GO Biological Process	regulation of hematopoietic progenitor cell differentiation	23.95
GO Biological Process	regulation of hematopoietic stem cell differentiation	21.91
GO Biological Process	viral gene expression	18.19
GO Biological Process	macromolecular complex disassembly	18.06
GO Biological Process	nucleosome organization	17.62
GO Biological Process	multi-organism metabolic process	16.66
GO Biological Process	viral transcription	16.34
GO Biological Process	chromatin assembly or disassembly	14.86
GO Biological Process	mRNA catabolic process	14.39
GO Biological Process	response to topologically incorrect protein	14.35
GO Biological Process	translational initiation	14.32
GO Biological Process	cellular protein complex disassembly	14.23
GO Biological Process	nuclear-transcribed mRNA catabolic process	13.93
GO Biological Process	endoplasmic reticulum unfolded protein response	13.92
Human Phenotype	Increased CSF lactate	5.95
Human Phenotype	Abnormal CSF metabolite level	5.62
Human Phenotype	Increased serum lactate	5.50
Human Phenotype	Abnormality of mitochondrial metabolism	3.67

Supplementary Figure 378: Properties and genomic distribution of motifs identified for the ZBTB11 transcription factor in K562 (accession ENCSR331GDC).

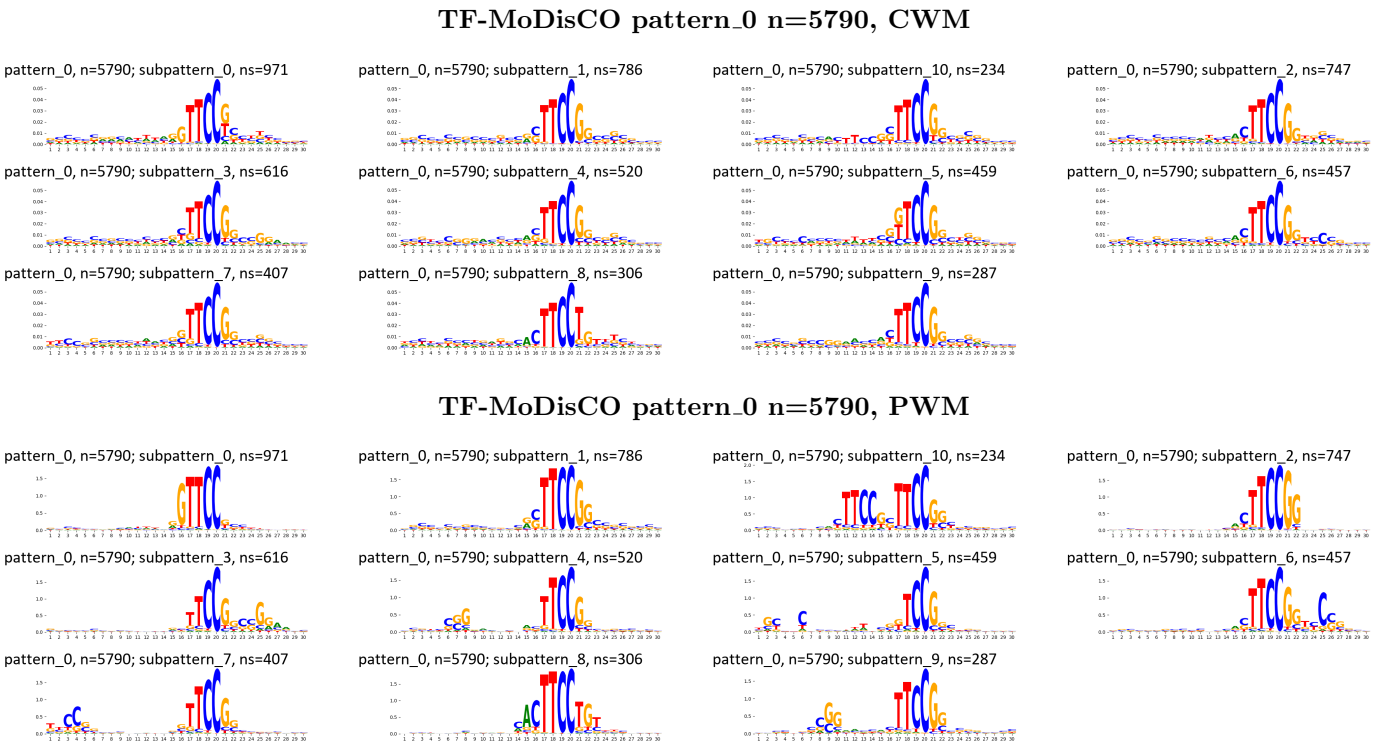

Supplementary Figure 379: TF-MoDisCO subpatterns for the ZBTB11 transcription factor in K562 (accession ENCSR331GDC).

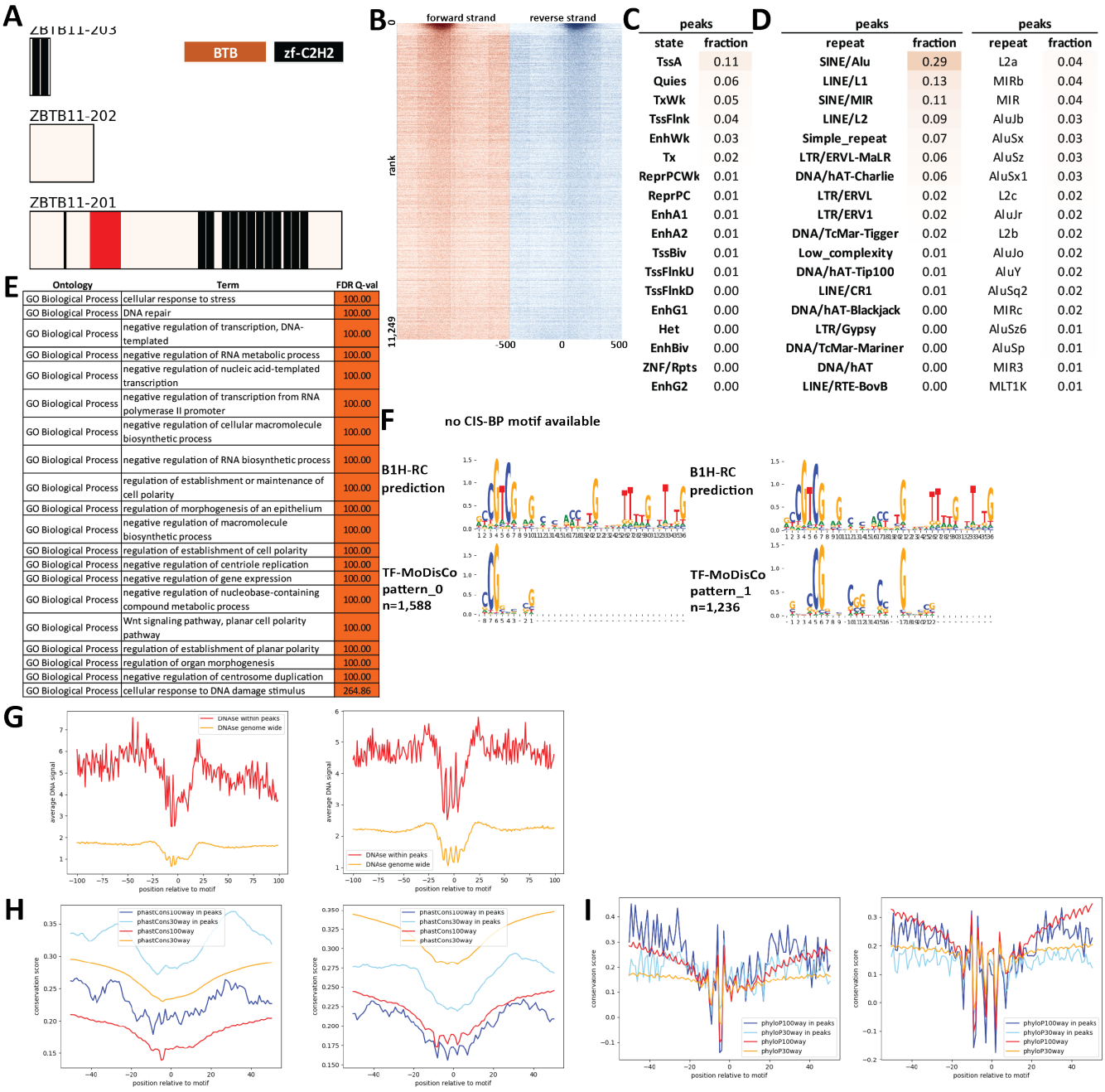

Supplementary Figure 380: Properties and genomic distribution of motifs identified for the ZBTB11 transcription factor in K562 (accession ENCSR468DVP).

TF-MoDisCO pattern_0 n=1588, CWM

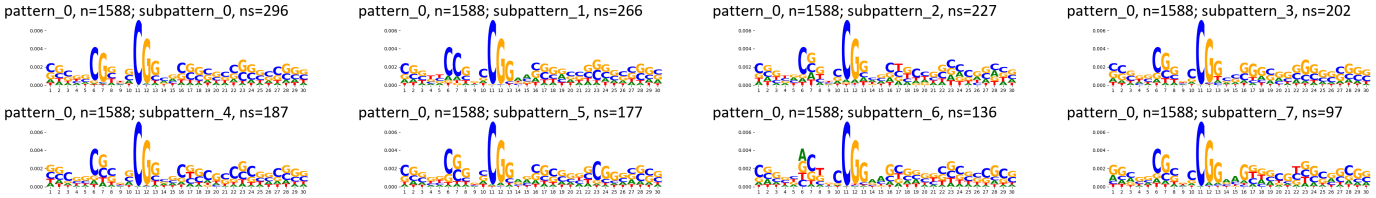

TF-MoDisCO pattern_0 n=1588, PWM

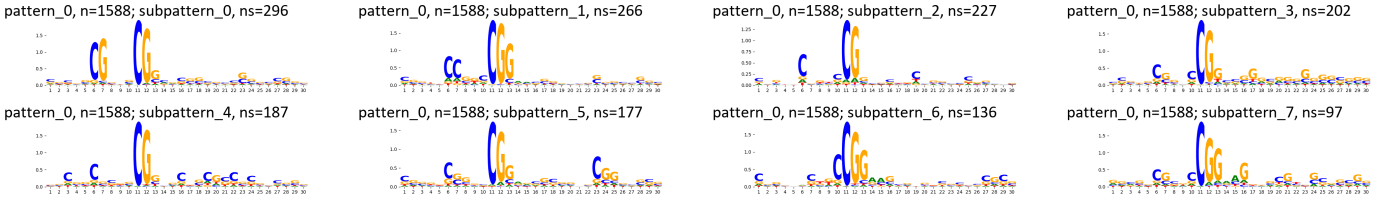

TF-MoDisCO pattern_1 n=1236, CWM

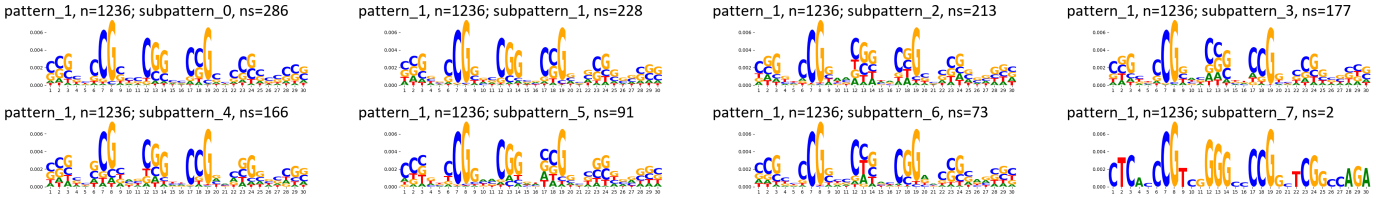

TF-MoDisCO pattern_1 n=1236, PWM

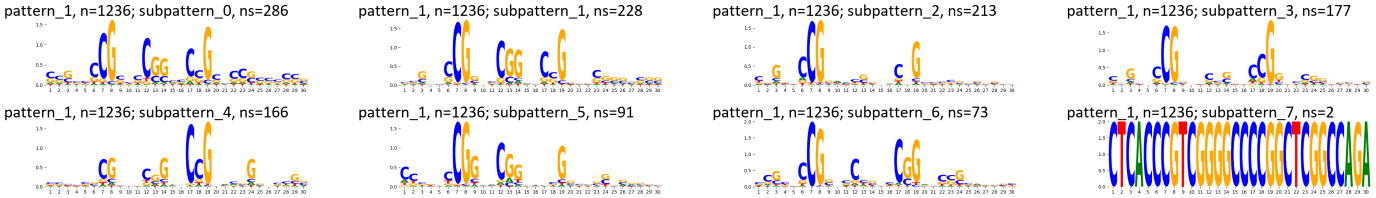

Supplementary Figure 381: TF-MoDisCO subpatterns for the ZBTB11 transcription factor in K562 (accession ENCSR468DVP).

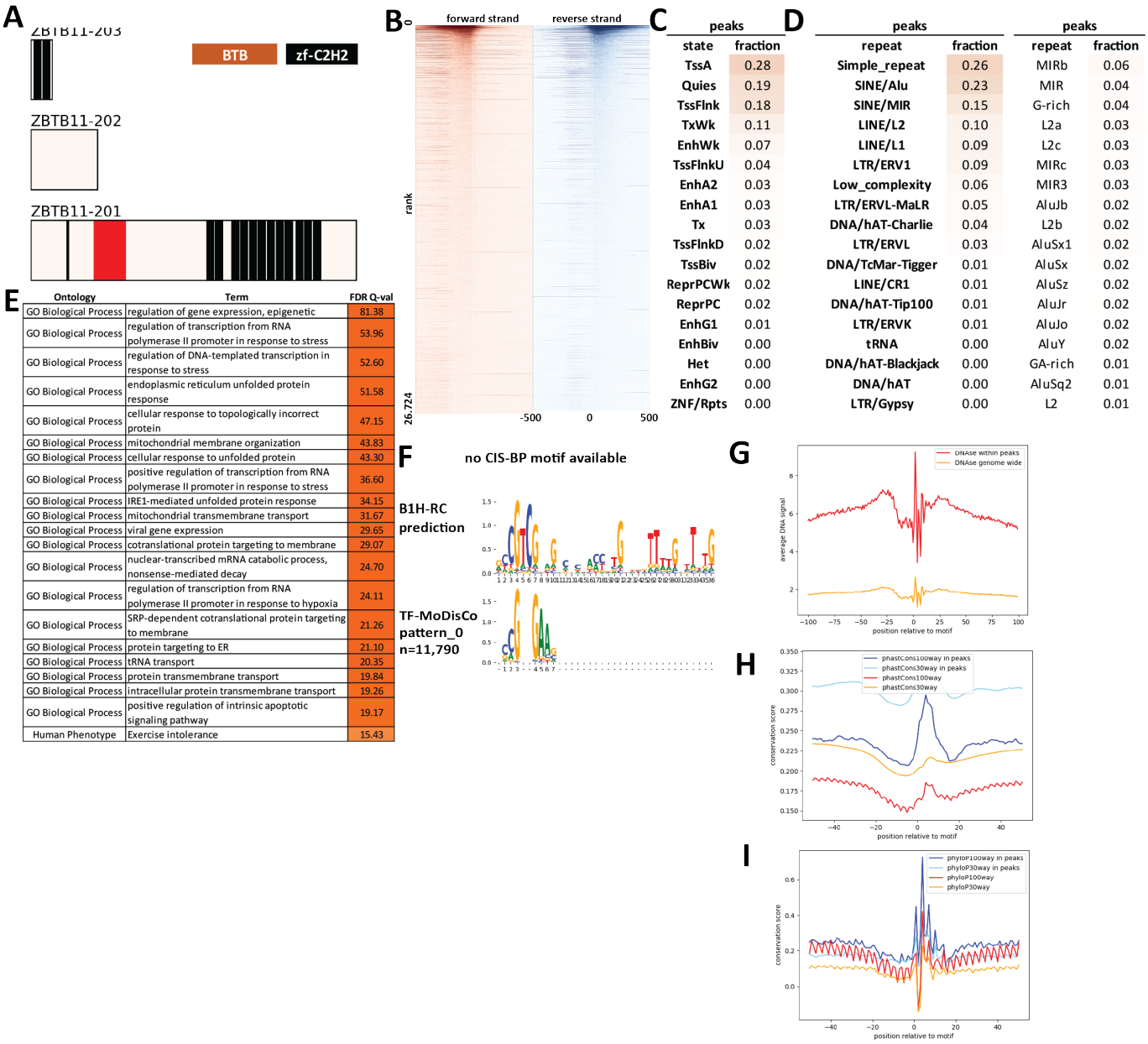

peaks	
state	fraction
TssA	0.28
Quies	0.19
TssFlnk	0.18
TxWk	0.11
EnhWk	0.07
TssFlnkU	0.04
EnhA2	0.03
EnhA1	0.03
Tx	0.03
TssFlnkD	0.02
TssBiv	0.02
ReprPCWk	0.02
ReprPC	0.02
EnhG1	0.01
EnhBiv	0.00
Het	0.00
EnhG2	0.00
ZNF/Rpts	0.00

peaks	
repeat	fraction
Simple_repeat	0.26
SINE/Alu	0.23
SINE/MIR	0.15
LINE/L2	0.10
LINE/L1	0.09
LTR/ERV1	0.09
Low_complexity	0.06
LTR/ERVL-MaLR	0.05
DNA/hAT-Charlie	0.04
LTR/ERVL	0.03
DNA/TcMar-Tigger	0.01
LINE/CR1	0.01
DNA/hAT-Tip100	0.01
LTR/ERVK	0.01
tRNA	0.00
DNA/hAT-Blackjack	0.00
DNA/hAT	0.00
LTR/Gypsy	0.00

peaks	
repeat	fraction
MIRb	0.06
MIR	0.04
G-rich	0.04
L2a	0.03
L2c	0.03
MIRc	0.03
MIR3	0.03
AluJb	0.02
L2b	0.02
AluSx1	0.02
AluSx	0.02
AluSz	0.02
AluJr	0.02
AluJo	0.02
AluY	0.02
GA-rich	0.01
AluSq2	0.01
L2	0.01

Ontology	Term	FDR Q-val
GO Biological Process	regulation of gene expression, epigenetic	81.38
GO Biological Process	regulation of transcription from RNA polymerase II promoter in response to stress	53.96
GO Biological Process	regulation of DNA-templated transcription in response to stress	52.60
GO Biological Process	endoplasmic reticulum unfolded protein response	51.58
GO Biological Process	cellular response to topologically incorrect protein	47.15
GO Biological Process	mitochondrial membrane organization	43.83
GO Biological Process	cellular response to unfolded protein	43.30
GO Biological Process	positive regulation of transcription from RNA polymerase II promoter in response to stress	36.60
GO Biological Process	IRE1-mediated unfolded protein response	34.15
GO Biological Process	mitochondrial transmembrane transport	31.67
GO Biological Process	viral gene expression	29.65
GO Biological Process	cotranslational protein targeting to membrane	29.07
GO Biological Process	nuclear-transcribed mRNA catabolic process, nonsense-mediated decay	24.70
GO Biological Process	regulation of transcription from RNA polymerase II promoter in response to hypoxia	24.11
GO Biological Process	SRP-dependent cotranslational protein targeting to membrane	21.26
GO Biological Process	protein targeting to ER	21.10
GO Biological Process	tRNA transport	20.35
GO Biological Process	protein transmembrane transport	19.84
GO Biological Process	intracellular protein transmembrane transport	19.26
GO Biological Process	positive regulation of intrinsic apoptotic signaling pathway	19.17
Human Phenotype	Exercise intolerance	15.43

Supplementary Figure 382: Properties and genomic distribution of motifs identified for the ZBTB11 transcription factor in K562 (accession ENCSR706BJO).

TF-MoDisCO pattern_0 n=11790, CWM

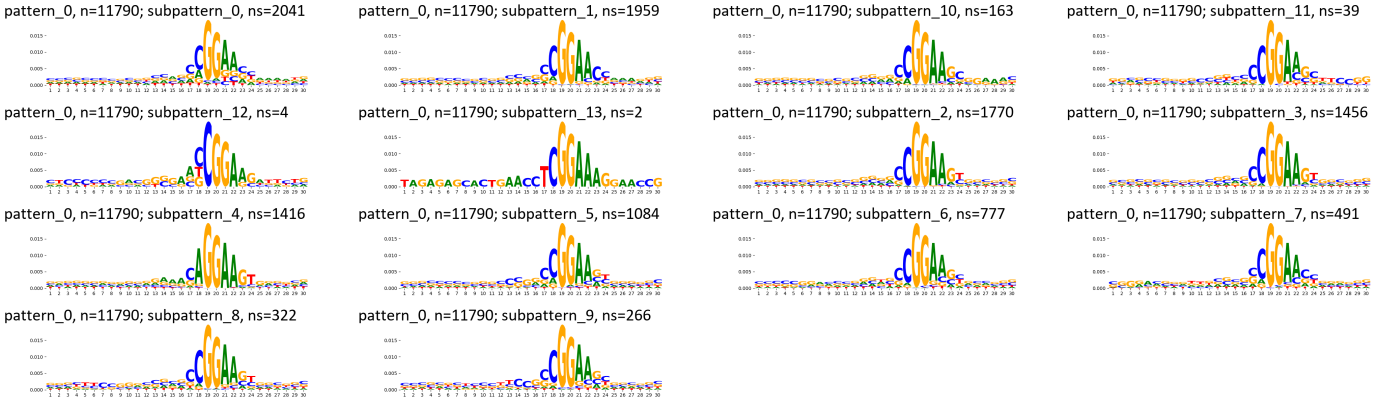

TF-MoDisCO pattern_0 n=11790, PWM

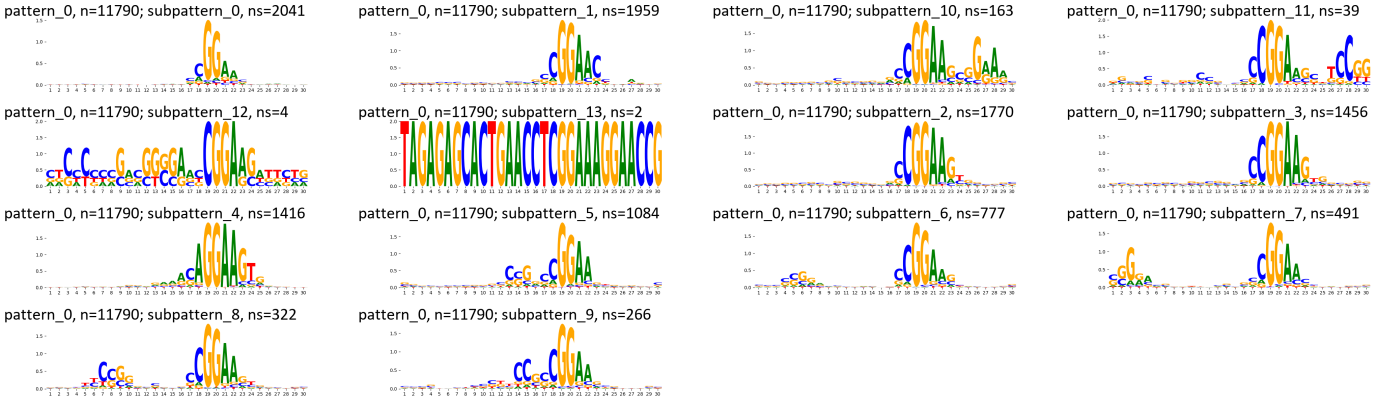

Supplementary Figure 383: TF-MoDisCO subpatterns for the ZBTB11 transcription factor in K562 (accession ENCSR706BJO).



Supplementary Figure 384: Properties and genomic distribution of motifs identified for the ZBTB11 transcription factor in K562 (accession ENCSR985OYK).

TF-MoDisCO pattern_0 n=2671, CWM

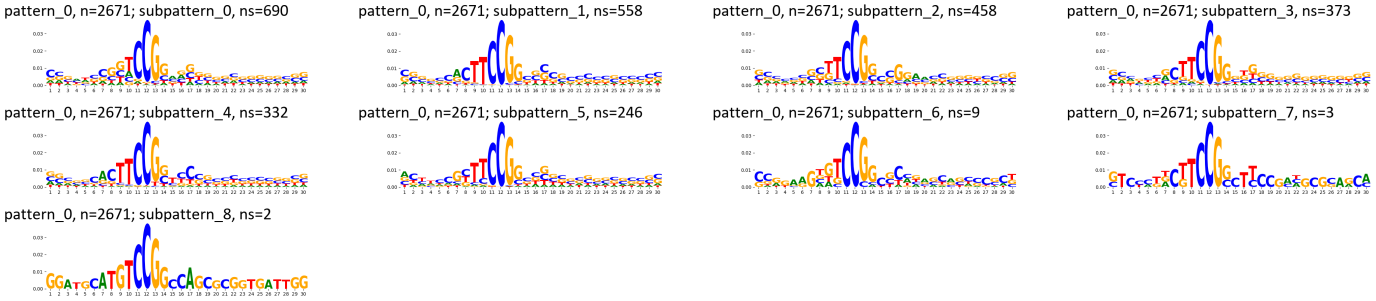

TF-MoDisCO pattern_0 n=2671, PWM

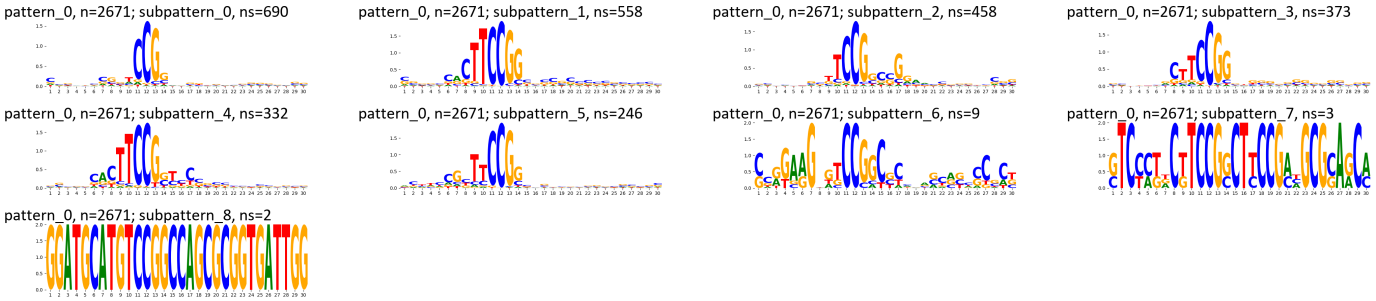

TF-MoDisCO pattern_1 n=1335, CWM

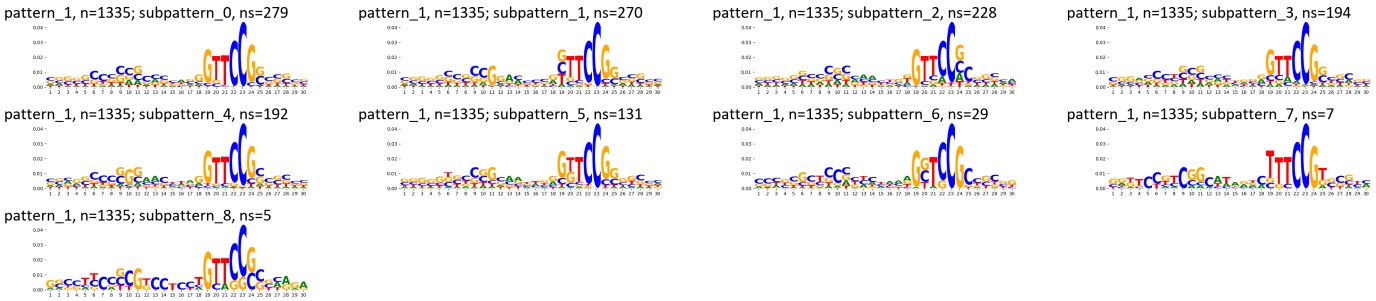

TF-MoDisCO pattern_1 n=1335, PWM

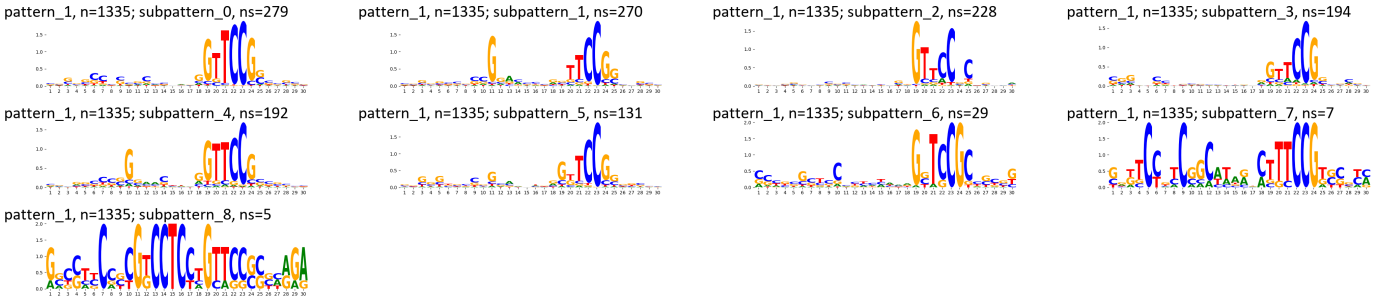

Supplementary Figure 385: TF-MoDisCO subpatterns for the ZBTB11 transcription factor in K562 (accession ENCSR985OYK).

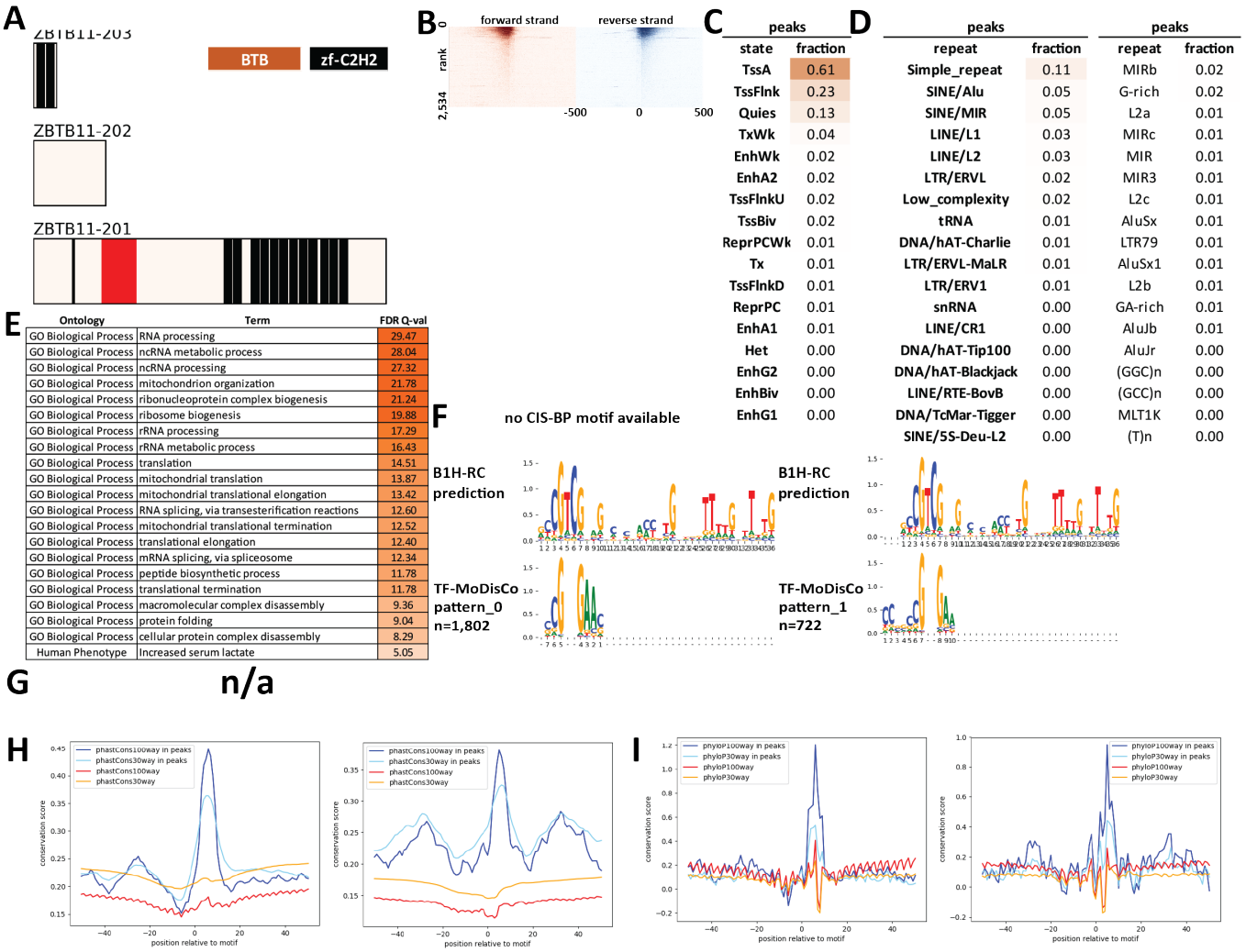

Supplementary Figure 386: Properties and genomic distribution of motifs identified for the ZBTB11 transcription factor in MCF-7 (accession ENCSR155VDK).

TF-MoDisCO pattern_0 n=1802, CWM

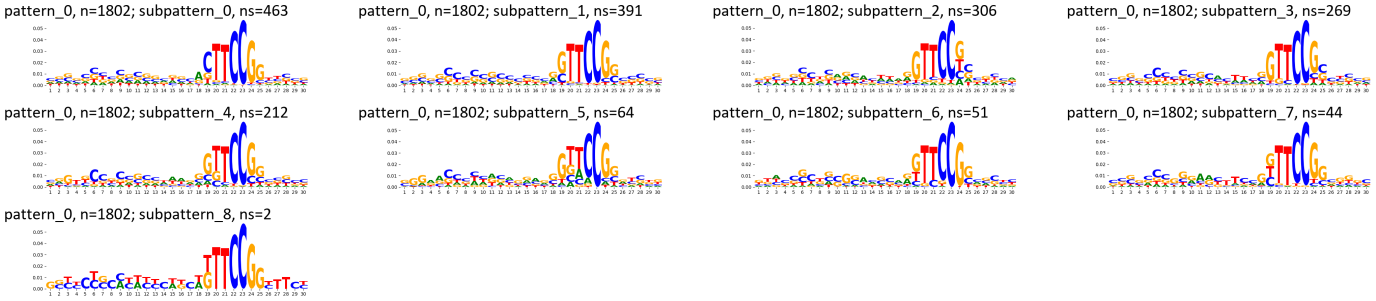

TF-MoDisCO pattern_0 n=1802, PWM

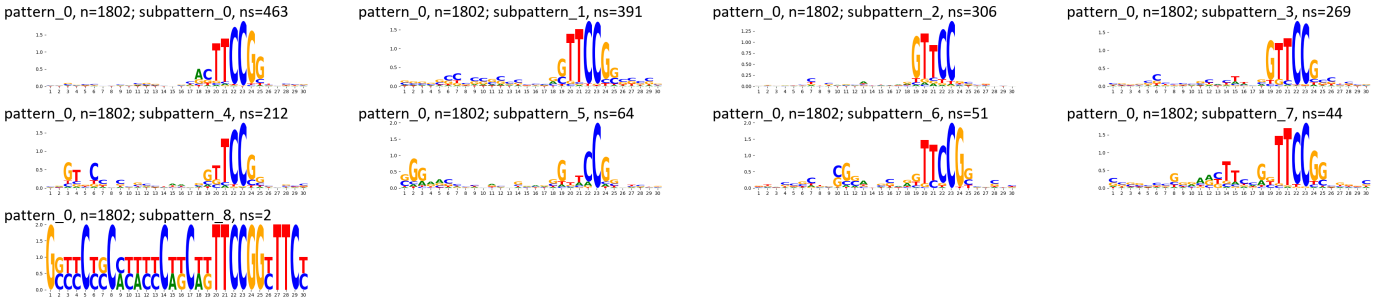

TF-MoDisCO pattern_1 n=722, CWM

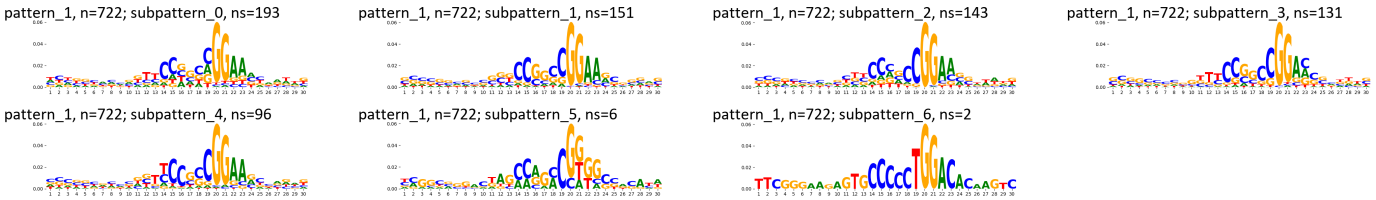

TF-MoDisCO pattern_1 n=722, PWM

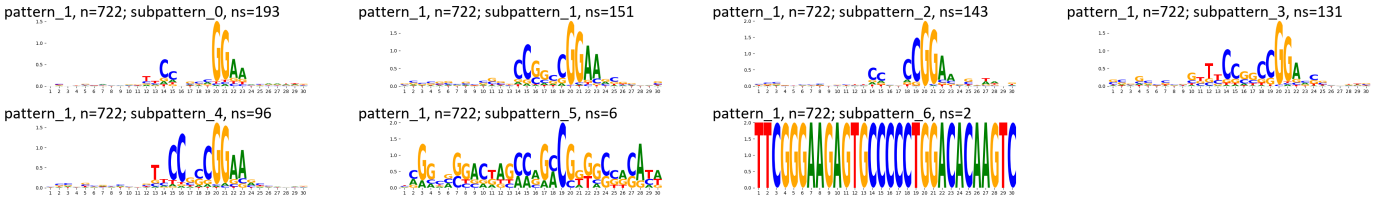

Supplementary Figure 387: TF-MoDisCO subpatterns for the ZBTB11 transcription factor in MCF-7 (accession ENCSR155VDK).

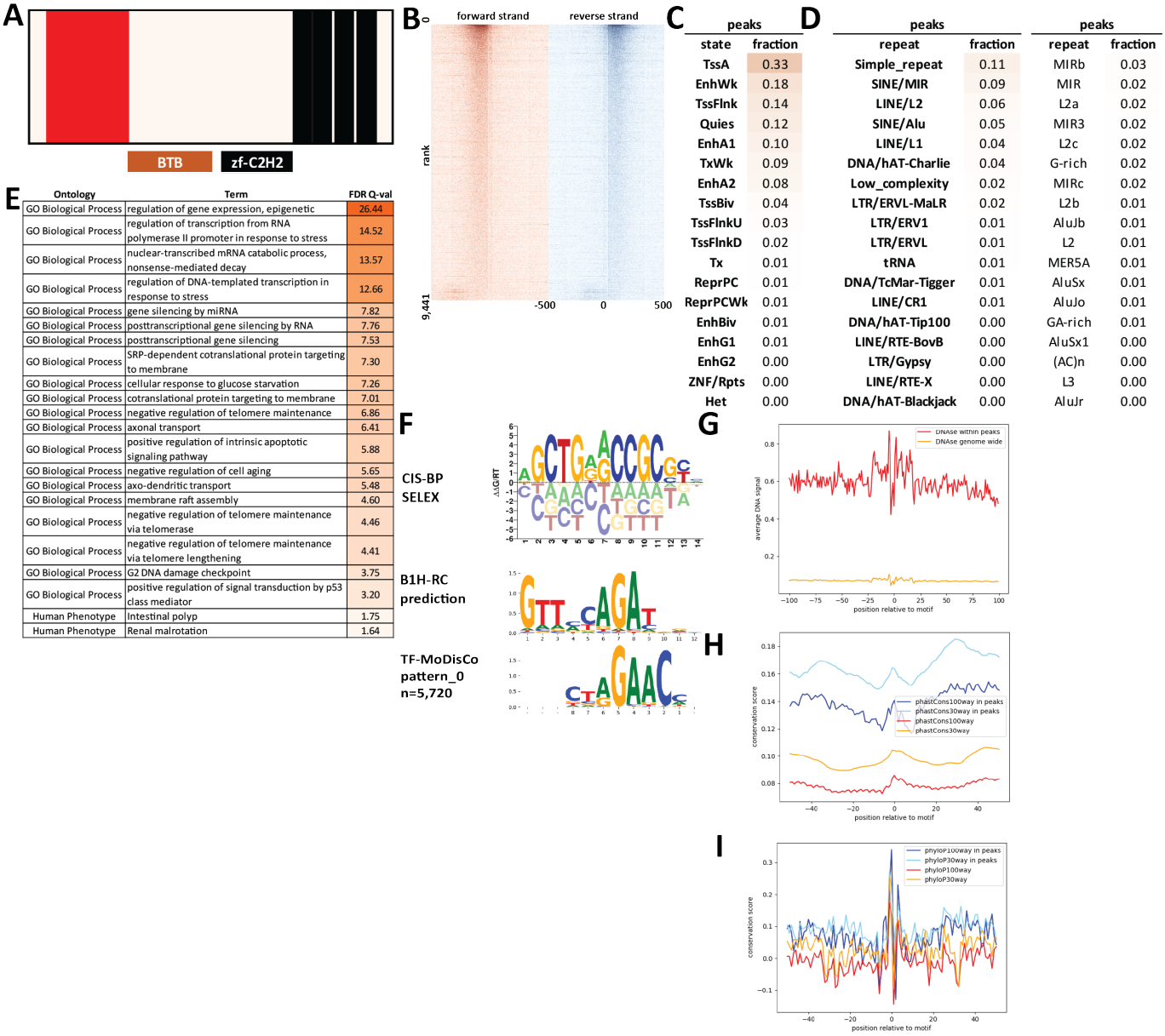

Supplementary Figure 388: Properties and genomic distribution of motifs identified for the ZBTB12 transcription factor in HEK293 (accession ENCSR543KOA).

TF-MoDisCO pattern_0 n=5720, CWM

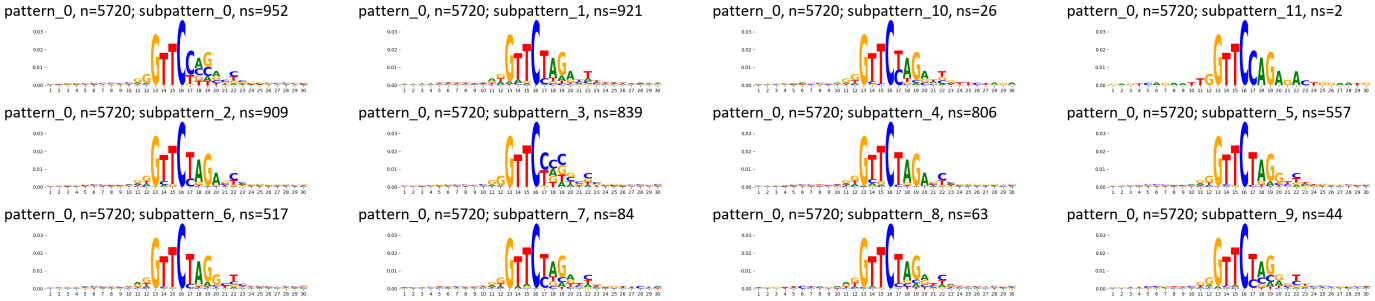

TF-MoDisCO pattern_0 n=5720, PWM

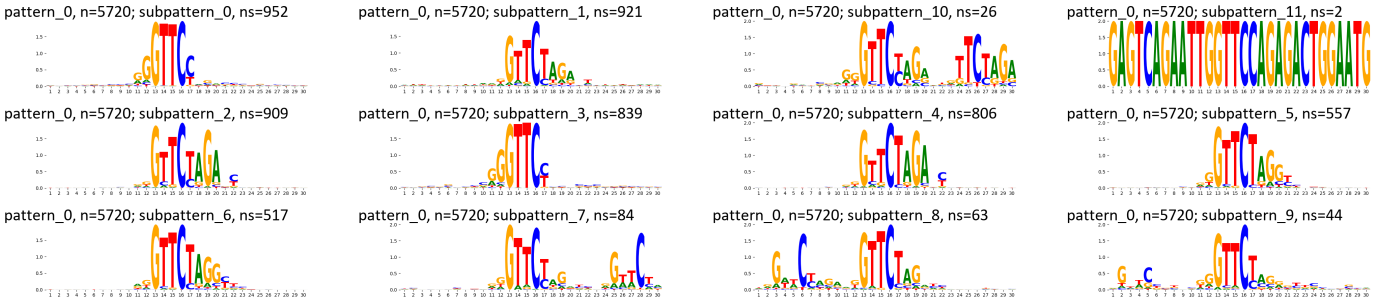

Supplementary Figure 389: TF-MoDisCO subpatterns for the ZBTB12 transcription factor in HEK293 (accession ENCSR543KOA).

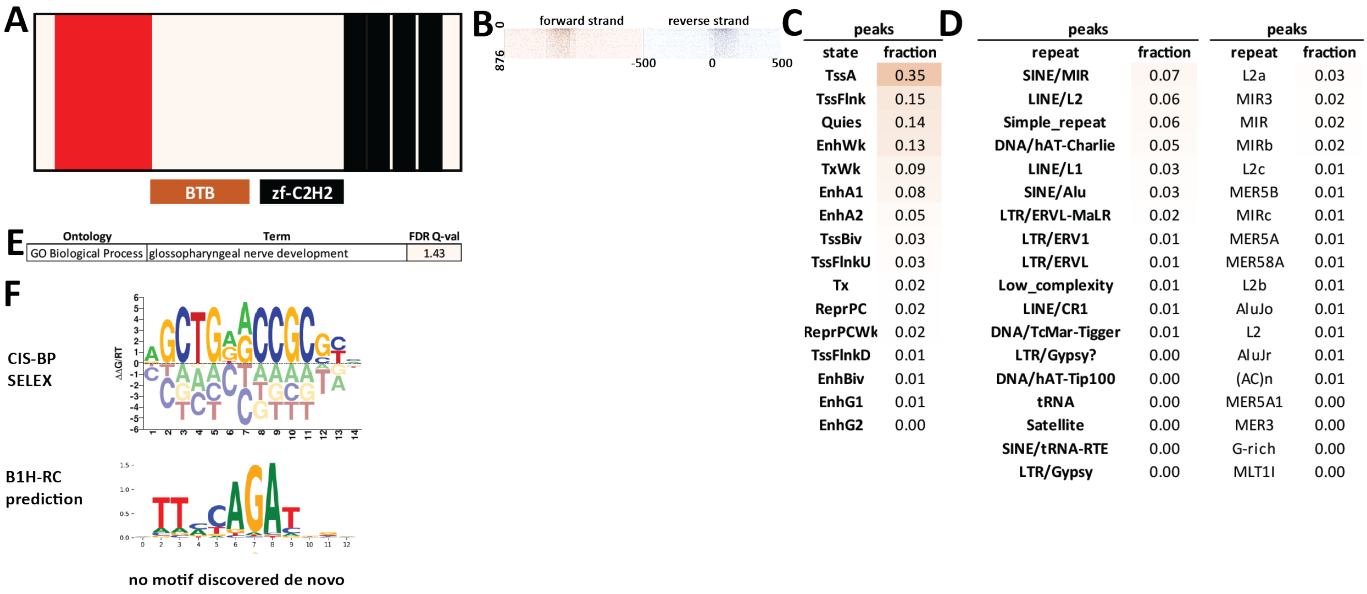

Supplementary Figure 390: Properties and genomic distribution of motifs identified for the ZBTB12 transcription factor in HEK293 (accession Hughes NB models).

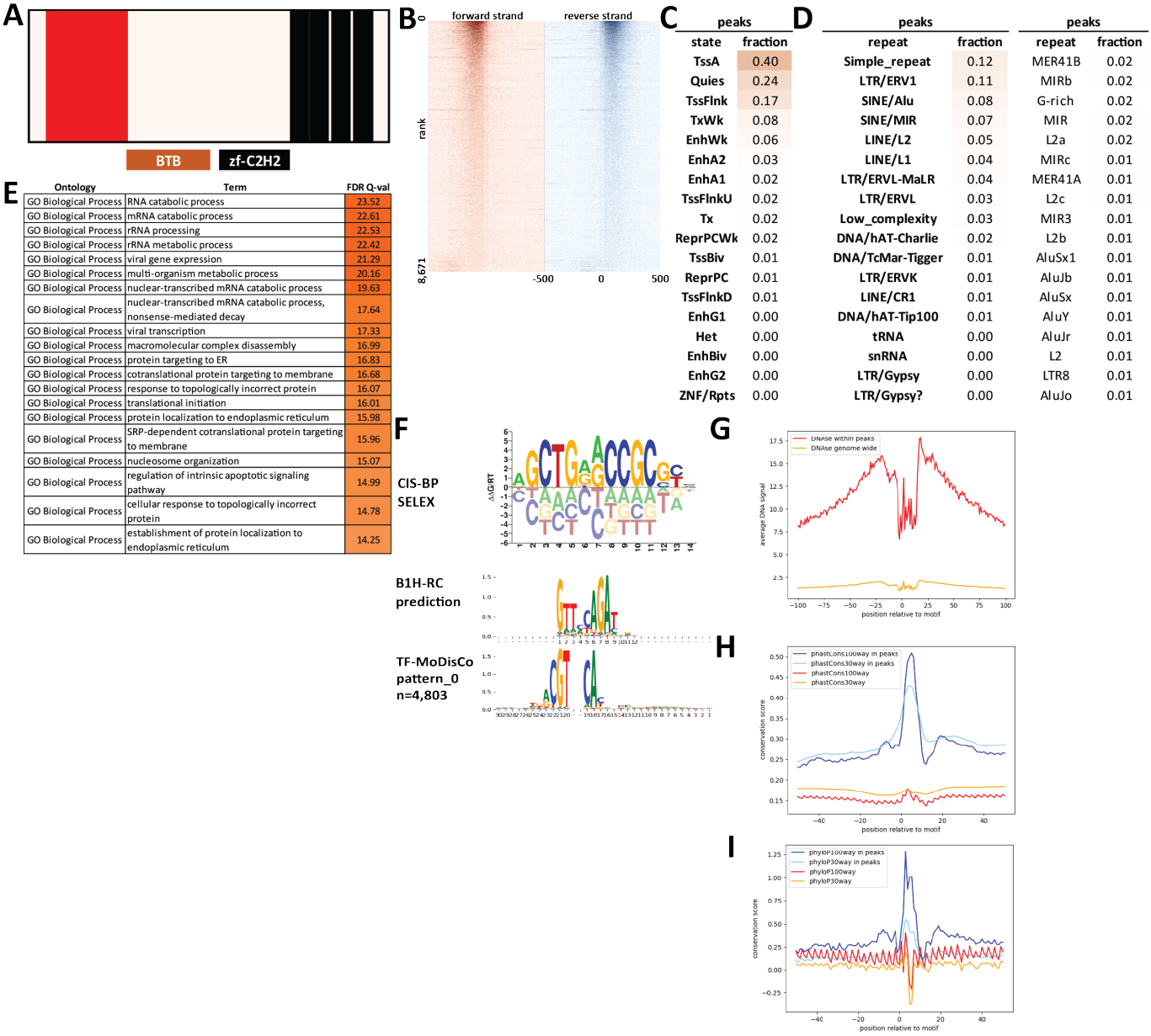

Supplementary Figure 391: Properties and genomic distribution of motifs identified for the ZBTB12 transcription factor in K562 (accession ENCSR172OSX).

TF-MoDisCO pattern_0 n=4803, CWM

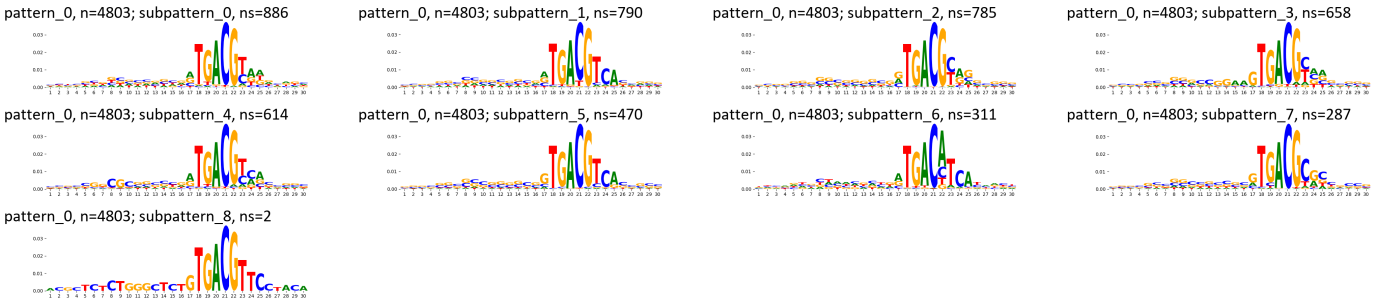

TF-MoDisCO pattern_0 n=4803, PWM

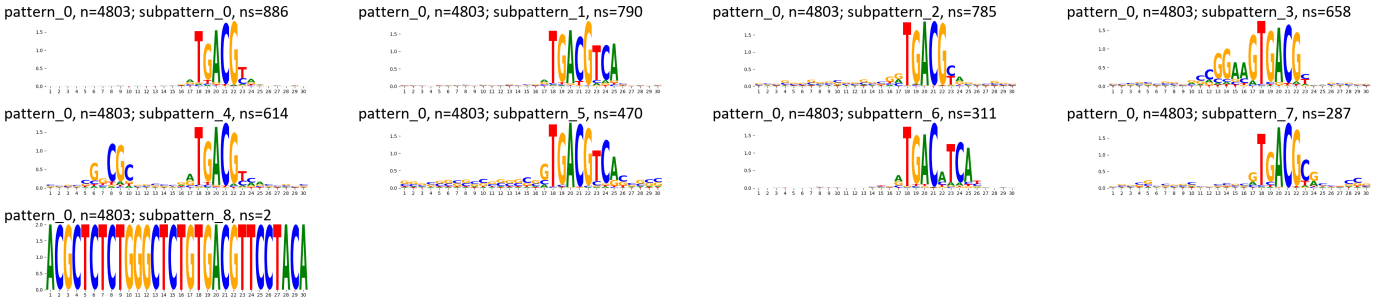

Supplementary Figure 392: TF-MoDisCO subpatterns for the ZBTB12 transcription factor in K562 (accession ENCSR172OSX).

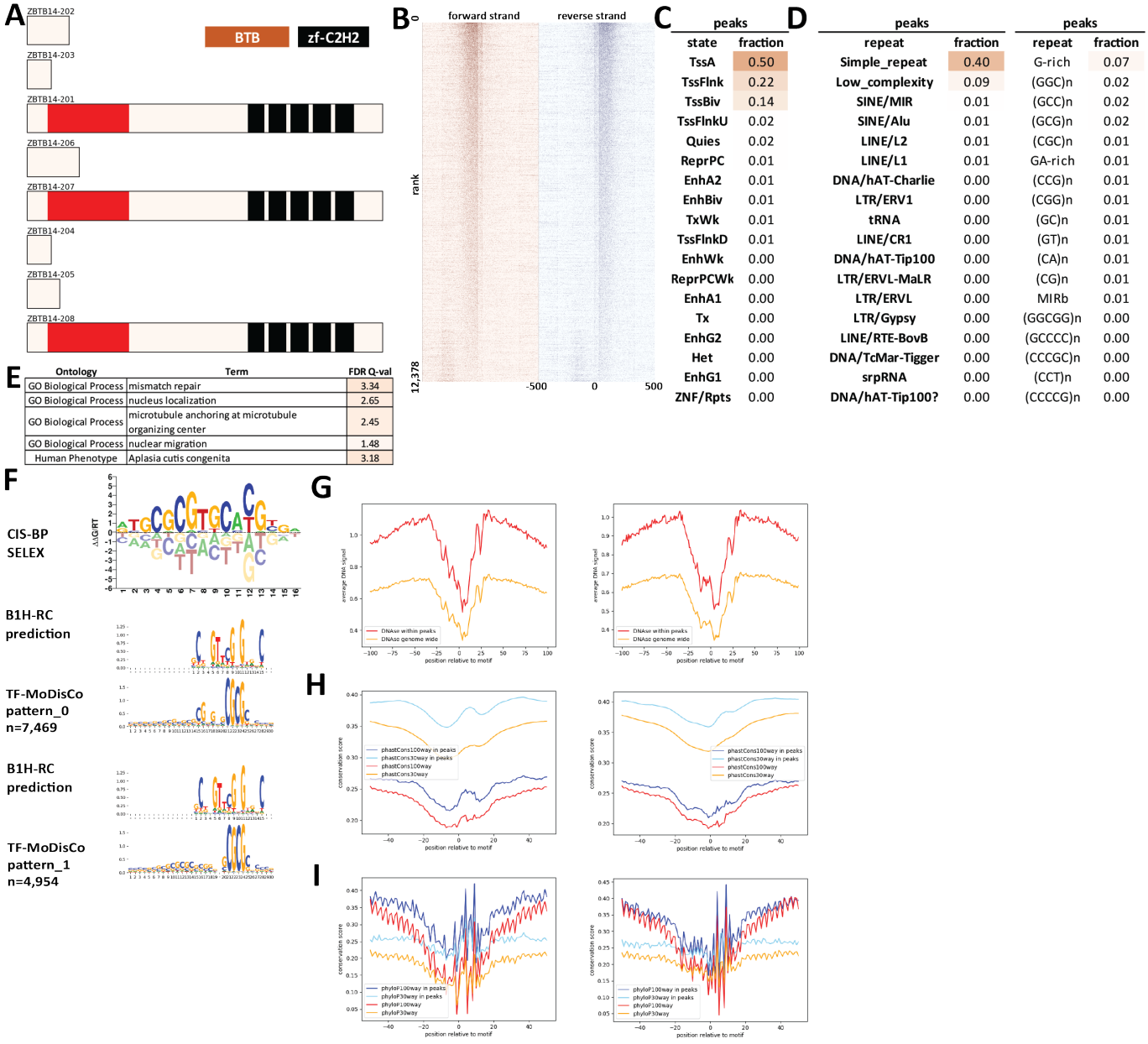

C

peaks	
state	fraction
TssA	0.50
TssFlnk	0.22
TssBiv	0.14
TssFlnkU	0.02
Quies	0.02
ReprPC	0.01
EnhA2	0.01
EnhBiv	0.01
TxWk	0.01
TssFlnkD	0.01
EnhWk	0.00
ReprPCWk	0.00
EnhA1	0.00
Tx	0.00
EnhG2	0.00
Het	0.00
EnhG1	0.00
ZNF/Rpts	0.00

D

peaks		peaks	
repeat	fraction	repeat	fraction
Simple_repeat	0.40	G-rich	0.07
Low_complexity	0.09	(GGC)n	0.02
SINE/MIR	0.01	(GCC)n	0.02
SINE/Alu	0.01	(GCG)n	0.02
LINE/L2	0.01	(CGC)n	0.01
LINE/L1	0.01	GA-rich	0.01
DNA/hAT-Charlie	0.00	(CCG)n	0.01
LTR/ERV1	0.00	(CGG)n	0.01
tRNA	0.00	(GC)n	0.01
LINE/CR1	0.00	(GT)n	0.01
DNA/hAT-Tip100	0.00	(CA)n	0.01
LTR/ERVL-MaLR	0.00	(CG)n	0.01
LTR/ERVL	0.00	MIRb	0.01
LTR/Gypsy	0.00	(GGCGG)n	0.00
LINE/RTE-BovB	0.00	(GCCCC)n	0.00
DNA/TcMar-Tigger	0.00	(CCCGC)n	0.00
srpRNA	0.00	(CCT)n	0.00
DNA/hAT-Tip100?	0.00	(CCCCG)n	0.00

E

Ontology	Term	FDR Q-val
GO Biological Process	mismatch repair	3.34
GO Biological Process	nucleus localization	2.65
GO Biological Process	microtubule anchoring at microtubule organizing center	2.45
GO Biological Process	nuclear migration	1.48
Human Phenotype	Aplasia cutis congenita	3.18

Supplementary Figure 393: Properties and genomic distribution of motifs identified for the ZBTB14 transcription factor in HEK293 (accession Hughes GR models).

TF-MoDisCO pattern_0 n=7469, CWM

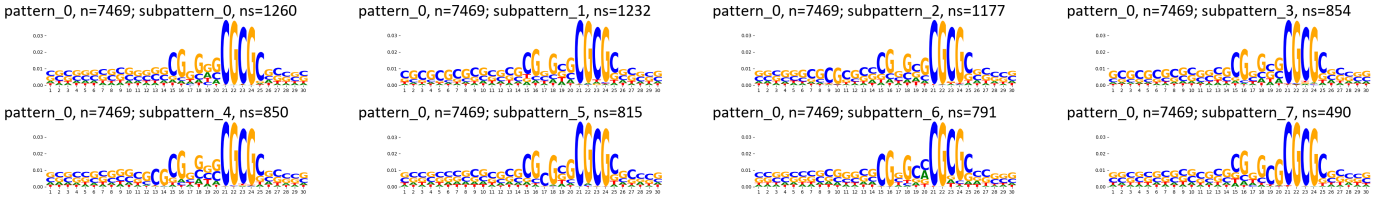

TF-MoDisCO pattern_0 n=7469, PWM

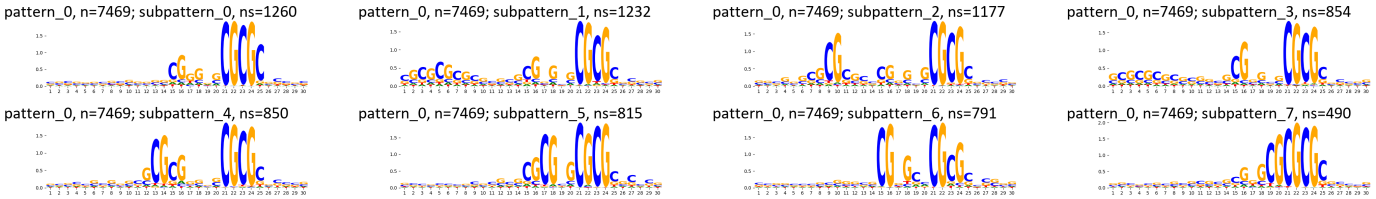

TF-MoDisCO pattern_1 n=4954, CWM

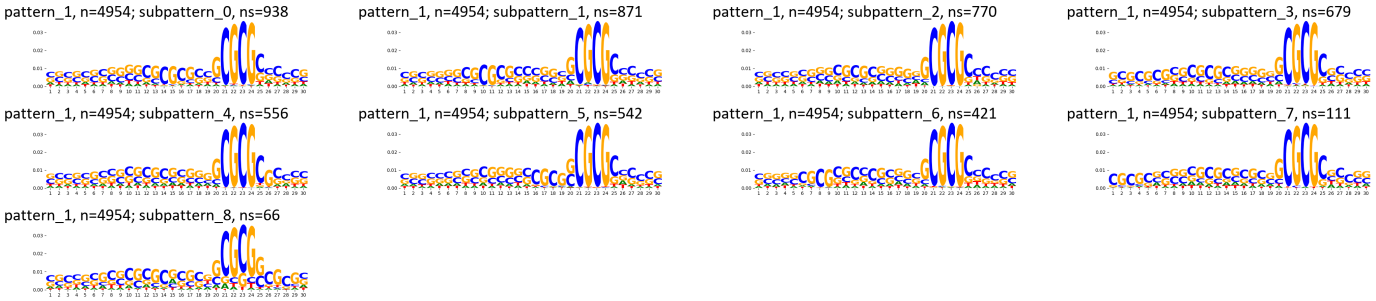

TF-MoDisCO pattern_1 n=4954, PWM

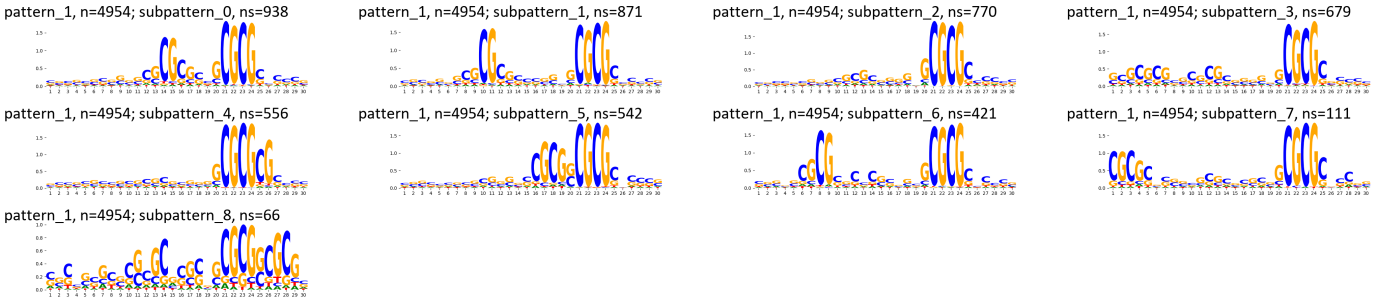

Supplementary Figure 394: TF-MoDisCO subpatterns for the ZBTB14 transcription factor in HEK293 (accession Hughes GR models).

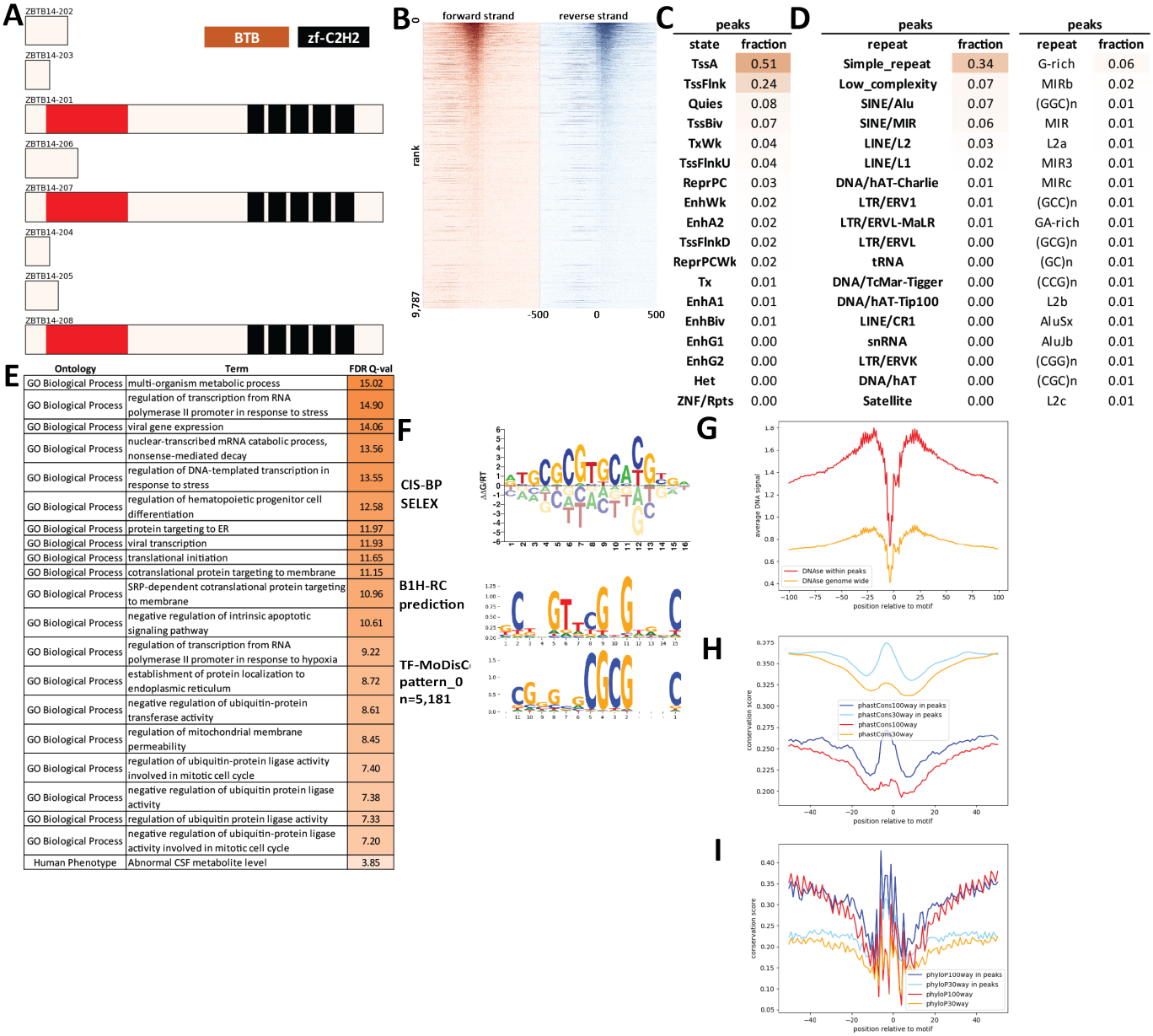

Supplementary Figure 395: Properties and genomic distribution of motifs identified for the ZBTB14 transcription factor in HepG2 (accession ENCSR532WFC).

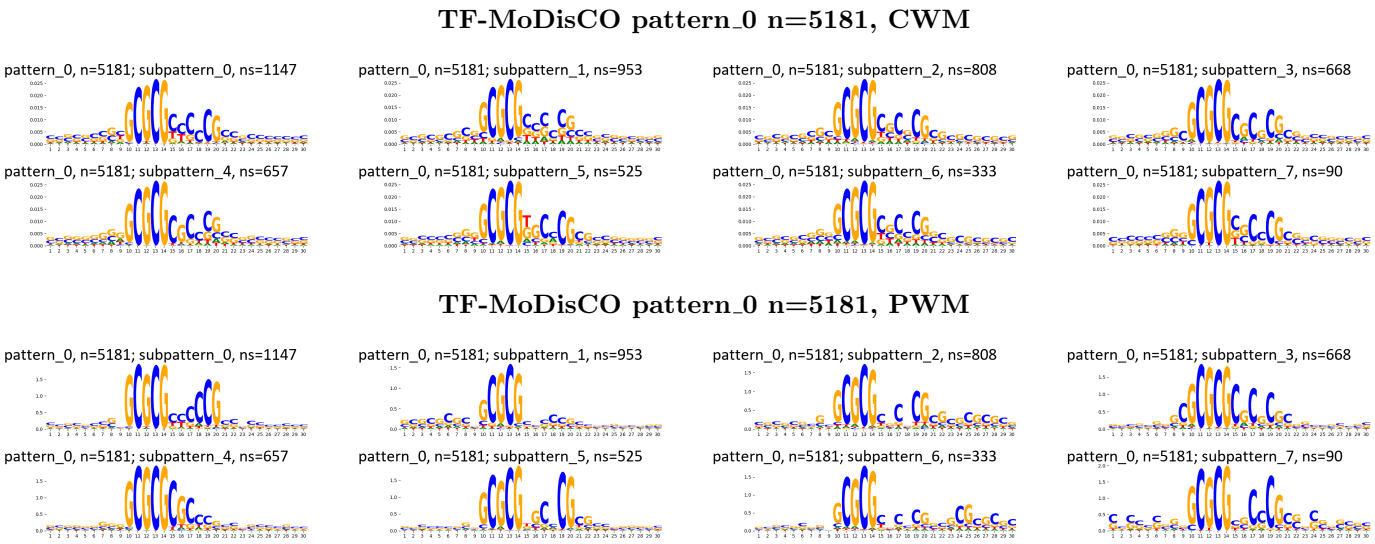

Supplementary Figure 396: TF-MoDisCO subpatterns for the ZBTB14 transcription factor in HepG2 (accession ENCSR532WFC).

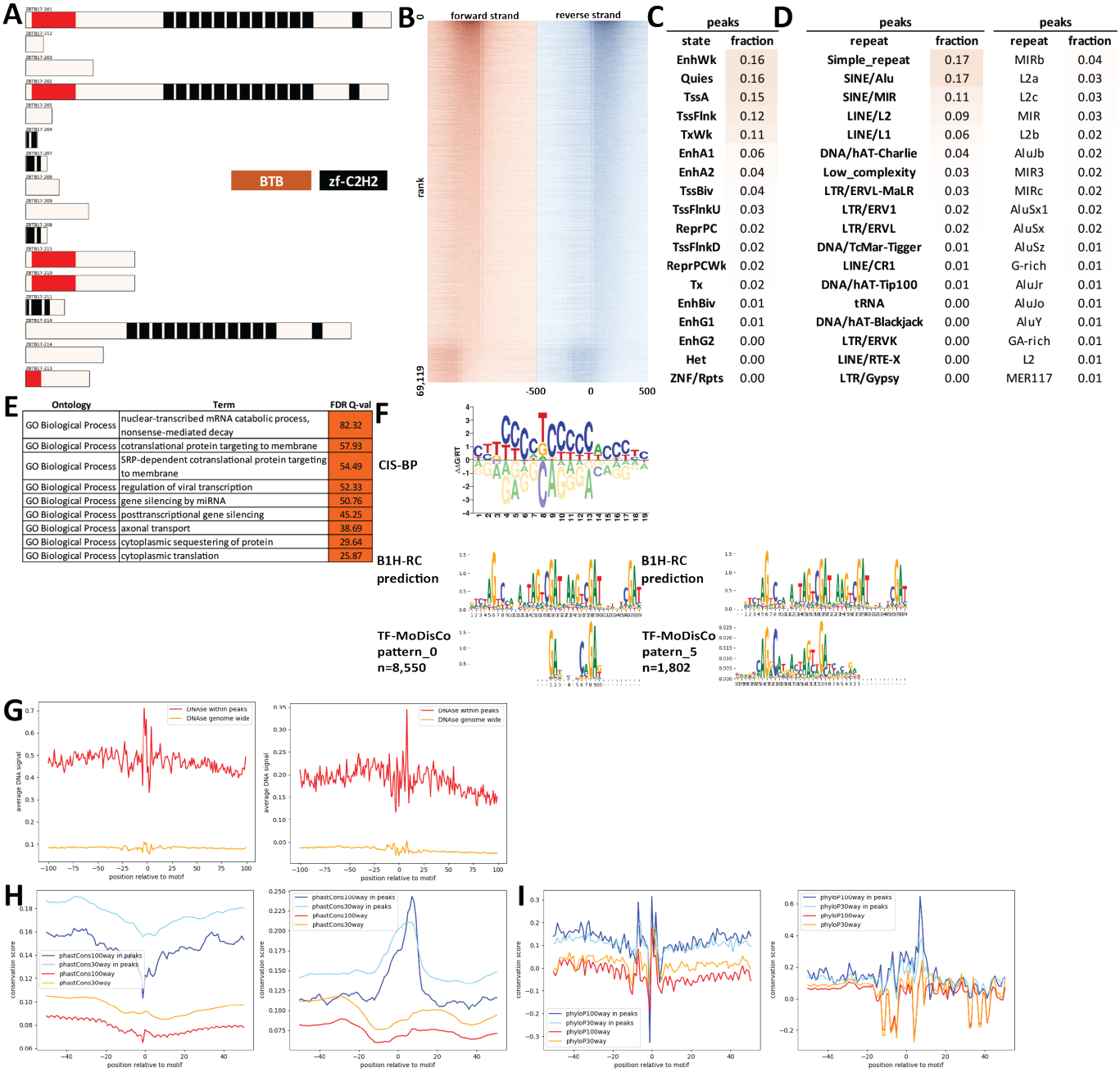

Supplementary Figure 397: Properties and genomic distribution of motifs identified for the ZBTB17 transcription factor in HEK293 (accession ENCSR631WAA).

TF-MoDisCO pattern_0 n=8550, CWM

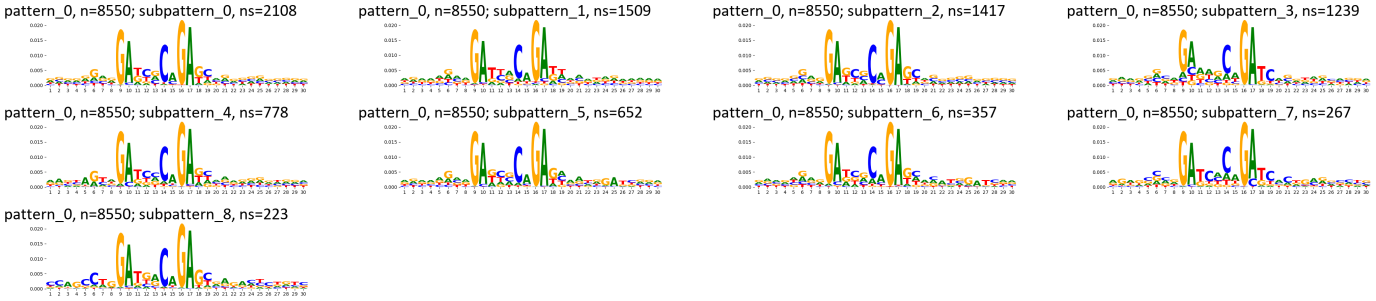

TF-MoDisCO pattern_0 n=8550, PWM

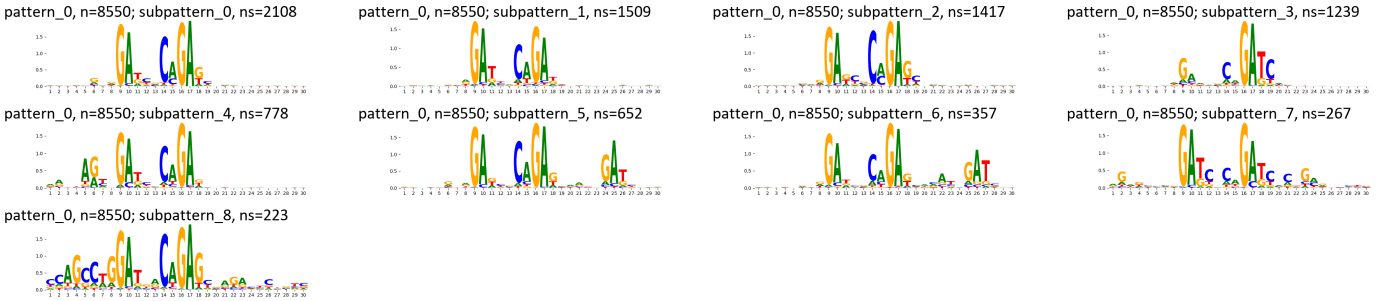

TF-MoDisCO pattern_5 n=1802, CWM

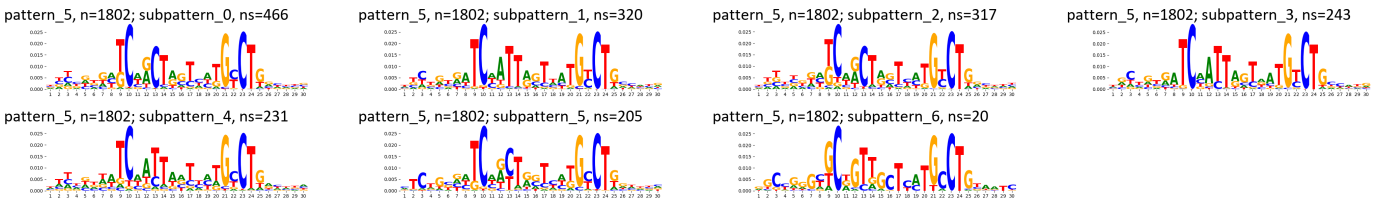

TF-MoDisCO pattern_5 n=1802, PWM

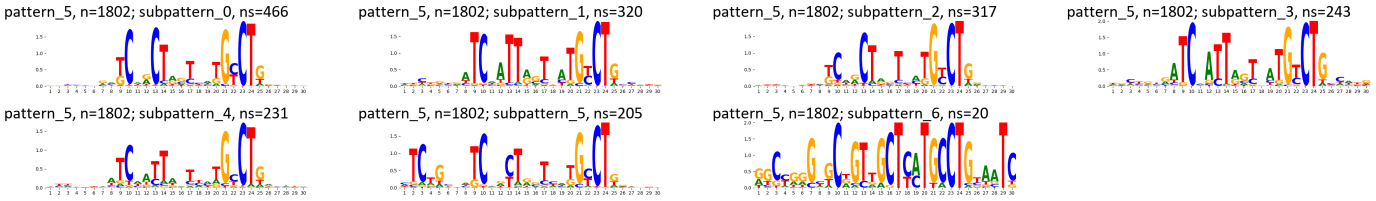

Supplementary Figure 398: TF-MoDisCO subpatterns for the ZBTB17 transcription factor in HEK293 (accession ENCSR631WAA).

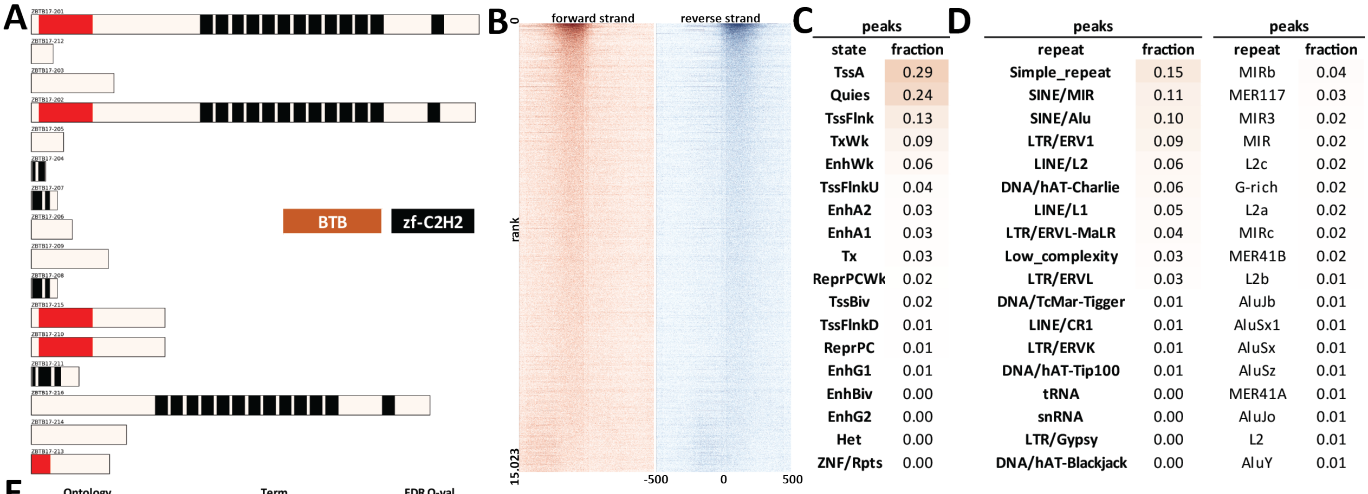

C

peaks	
state	fraction
TssA	0.29
Quies	0.24
TssFlnk	0.13
TxWk	0.09
EnhWk	0.06
TssFlnkU	0.04
EnhA2	0.03
EnhA1	0.03
Tx	0.03
ReprPCWk	0.02
TssBiv	0.02
TssFlnkD	0.01
ReprPC	0.01
EnhG1	0.01
EnhBiv	0.00
EnhG2	0.00
Het	0.00
ZNF/Rpts	0.00

D

peaks		peaks	
repeat	fraction	repeat	fraction
Simple_repeat	0.15	MIRb	0.04
SINE/MIR	0.11	MER117	0.03
SINE/Alu	0.10	MIR3	0.02
LTR/ERV1	0.09	MIR	0.02
LINE/L2	0.06	L2c	0.02
DNA/hAT-Charlie	0.06	G-rich	0.02
LINE/L1	0.05	L2a	0.02
LTR/ERVL-MaLR	0.04	MIRc	0.02
Low_complexity	0.03	MER41B	0.02
LTR/ERVL	0.03	L2b	0.01
DNA/TcMar-Tigger	0.01	AluJb	0.01
LINE/CR1	0.01	AluSx1	0.01
LTR/ERVK	0.01	AluSx	0.01
DNA/hAT-Tip100	0.01	AluSz	0.01
tRNA	0.00	MER41A	0.01
snRNA	0.00	AluJo	0.01
LTR/Gypsy	0.00	L2	0.01
DNA/hAT-Blackjack	0.00	AluY	0.01

E

Ontology	Term	FDR Q-val
GO Biological Process	regulation of DNA-templated transcription in response to stress	48.32
GO Biological Process	regulation of gene expression, epigenetic	43.37
GO Biological Process	regulation of intrinsic apoptotic signaling pathway	32.31
GO Biological Process	gene silencing	31.57
GO Biological Process	mitochondrial membrane organization	30.06
GO Biological Process	regulation of megakaryocyte differentiation	26.12
GO Biological Process	cellular response to topologically incorrect protein	22.55
GO Biological Process	endoplasmic reticulum unfolded protein response	22.42
GO Biological Process	regulation of mitochondrial membrane permeability	19.77
GO Biological Process	erythrocyte homeostasis	19.26
GO Biological Process	coronary artery morphogenesis	19.08
GO Biological Process	regulation of receptor catabolic process	19.00
GO Biological Process	cellular response to unfolded protein	18.64
GO Biological Process	regulation of membrane permeability	18.46
GO Biological Process	viral gene expression	18.01
GO Biological Process	regulation of posttranscriptional gene silencing	16.76
GO Biological Process	regulation of gene silencing by RNA	16.76
GO Biological Process	regulation of gene silencing by miRNA	16.33
GO Biological Process	erythrocyte differentiation	16.25
GO Biological Process	translational elongation	16.22
Human Phenotype	Abnormal concentration of calcium in blood	7.39

F

CIS-BP

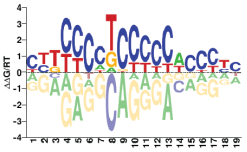

no motif discovered de novo

Supplementary Figure 399: Properties and genomic distribution of motifs identified for the ZBTB17 transcription factor in K562 (accession ENCSR026KKZ).

A

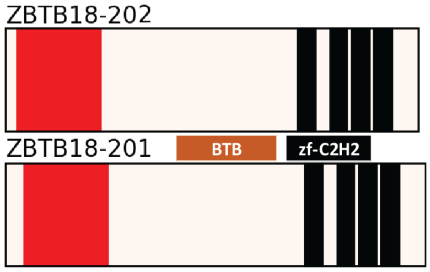

B

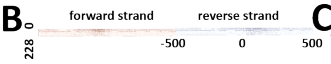

C

peaks	
state	fraction
TssA	0.49
TssFlnk	0.21
Quies	0.14
TssBiv	0.06
TxWk	0.05
EnhWk	0.05
EnhA1	0.04
EnhA2	0.03
TssFlnkU	0.02
Tx	0.01
EnhBiv	0.01
ReprPCWk	0.01
ReprPC	0.01
Het	0.01
ZNF/Rpts	0.00

D

peaks		peaks	
repeat	fraction	repeat	fraction
Simple_repeat	0.15	G-rich	0.02
Low_complexity	0.04	MIR3	0.01
SINE/MIR	0.02	MER20	0.01
DNA/hAT-Charlie	0.02	MER5A	0.01
LTR/ERVL-MaLR	0.02	GA-rich	0.01
tRNA	0.01	A-rich	0.01
SINE/Alu	0.01	(TG)n	0.01
LTR/ERV1	0.01	(GGC)n	0.01
LINE/L1	0.01	tRNA-Thr-AC/	0.00
LINE/L2	0.01	tRNA-Leu-TTA(I	0.00
snRNA	0.00	tRNA-Gly-GG'	0.00
rRNA	0.00	U1	0.00
LTR/ERVL	0.00	OldhAT1	0.00
DNA?	0.00	MamRep187!	0.00
DNA/hAT-Tip100?	0.00	MSTA-int	0.00
DNA/hAT-Ac	0.00	MLT1O	0.00
		MLT1I	0.00
		MLT1B	0.00

E

Ontology	Term	FDR Q-val
GO Biological Process	mitochondrial electron transport, NADH to ubiquinone	9.49
GO Biological Process	mitochondrial respiratory chain complex I assembly	7.54
GO Biological Process	mitochondrial respiratory chain complex assembly	6.66
GO Biological Process	mitochondrial ATP synthesis coupled electron transport	5.42
GO Biological Process	ATP synthesis coupled electron transport	5.28
GO Biological Process	oxidative phosphorylation	5.13
GO Biological Process	respiratory electron transport chain	4.59
GO Biological Process	ATP metabolic process	3.68
GO Biological Process	purine ribonucleoside monophosphate metabolic process	3.50
GO Biological Process	purine nucleoside monophosphate metabolic process	3.52
GO Biological Process	cellular respiration	3.20
GO Biological Process	electron transport chain	3.07
GO Biological Process	ribonucleoside monophosphate metabolic process	3.06
GO Biological Process	purine ribonucleoside triphosphate metabolic process	2.89
GO Biological Process	nucleoside monophosphate metabolic process	2.90
GO Biological Process	ribonucleoside triphosphate metabolic process	2.75
GO Biological Process	purine nucleoside triphosphate metabolic process	2.74
GO Biological Process	energy derivation by oxidation of organic compounds	2.48
GO Biological Process	nucleoside triphosphate metabolic process	2.34
GO Biological Process	generation of precursor metabolites and energy	1.71
Human Phenotype	Leber optic atrophy	35.68
Human Phenotype	Central retinal vessel vascular tortuosity	35.68
Human Phenotype	Hemianopia	35.68
Human Phenotype	Stroke-like episode	20.51
Human Phenotype	Centrocecal scotoma	19.35
Human Phenotype	Optic neuropathy	18.62
Human Phenotype	Wolff-Parkinson-White syndrome	17.37
Human Phenotype	Episodic vomiting	16.57
Human Phenotype	Mitochondrial myopathy	15.96
Human Phenotype	Retinal vascular tortuosity	13.89
Human Phenotype	Ragged-red muscle fibers	13.91
Human Phenotype	Hemiparesis	12.66
Human Phenotype	Abnormal retinal artery morphology	12.63
Human Phenotype	Bilateral sensorineural hearing impairment	12.55
Human Phenotype	Arterial tortuosity	12.58
Human Phenotype	Vascular tortuosity	12.39
Human Phenotype	Migraine	12.07
Human Phenotype	Abnormality of head blood vessel	11.75
Human Phenotype	Muscle abnormality related to mitochondrial dysfunction	11.73
Human Phenotype	Hemiplegia/hemiparesis	11.29

F

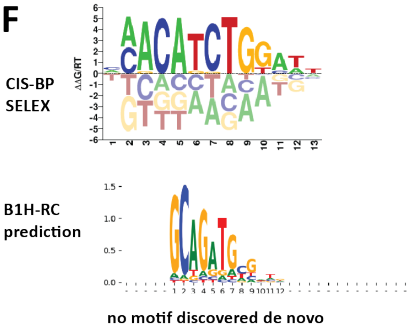

Supplementary Figure 400: Properties and genomic distribution of motifs identified for the ZBTB18 transcription factor in HEK293 (accession Hughes NB models).

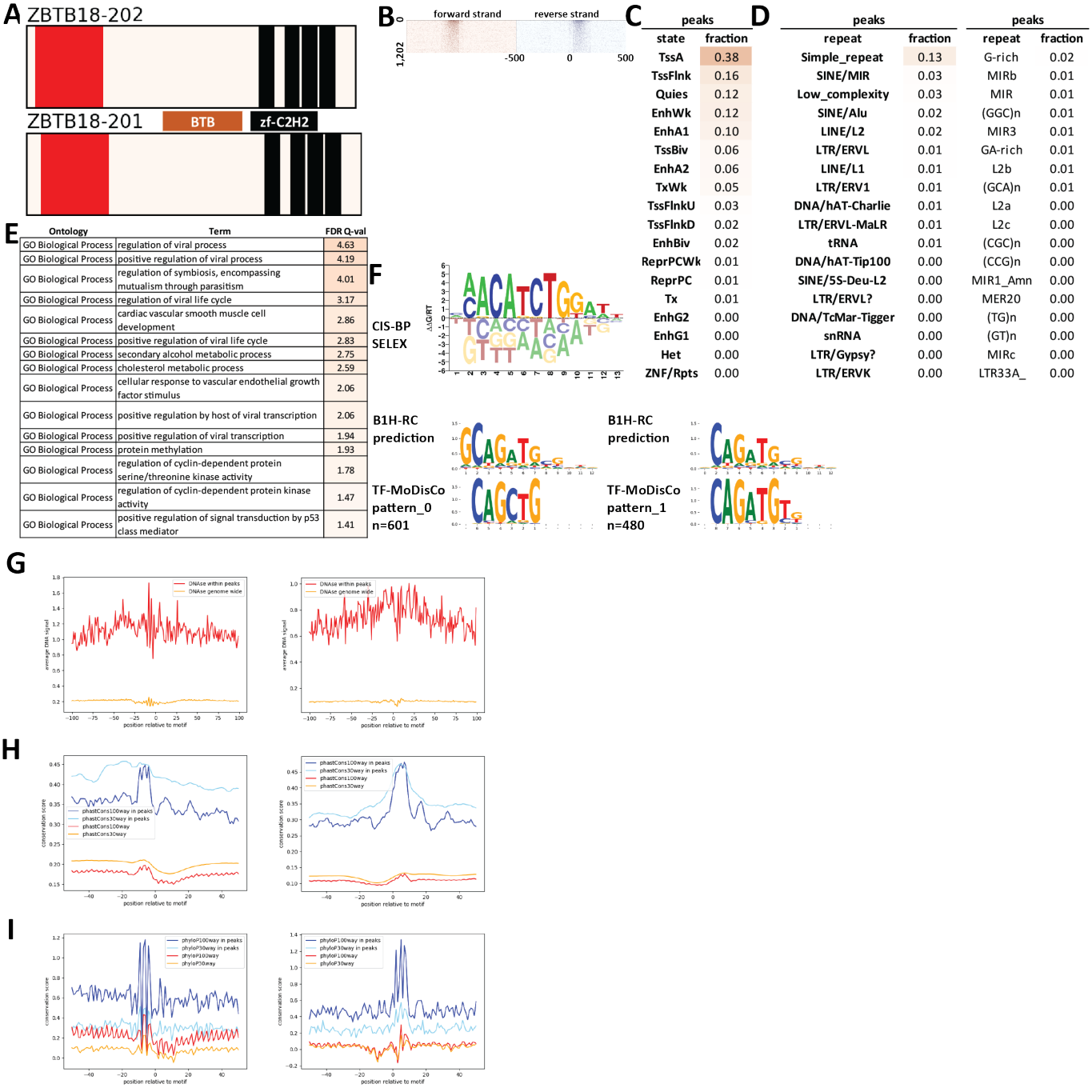

Supplementary Figure 401: Properties and genomic distribution of motifs identified for the ZBTB18 transcription factor in HEK293 (accession Hughes GR models).

TF-MoDisCO pattern_0 n=601, CWM

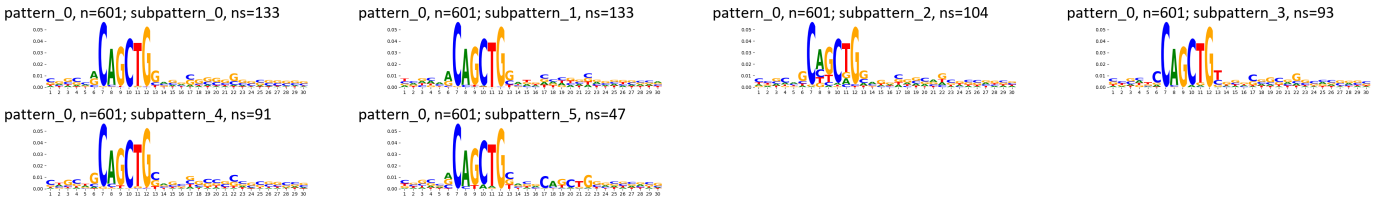

TF-MoDisCO pattern_0 n=601, PWM

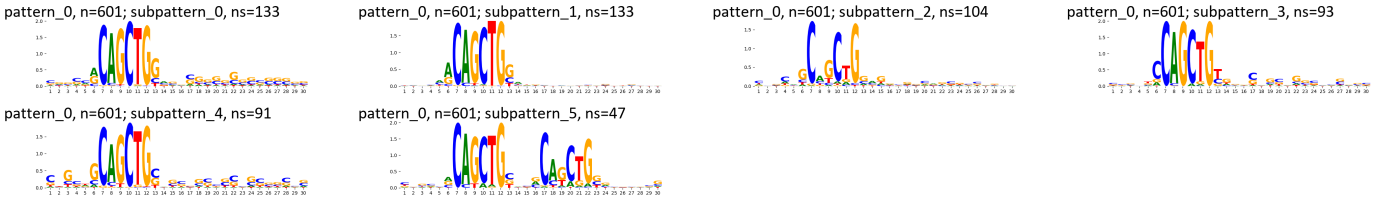

TF-MoDisCO pattern_1 n=480, CWM

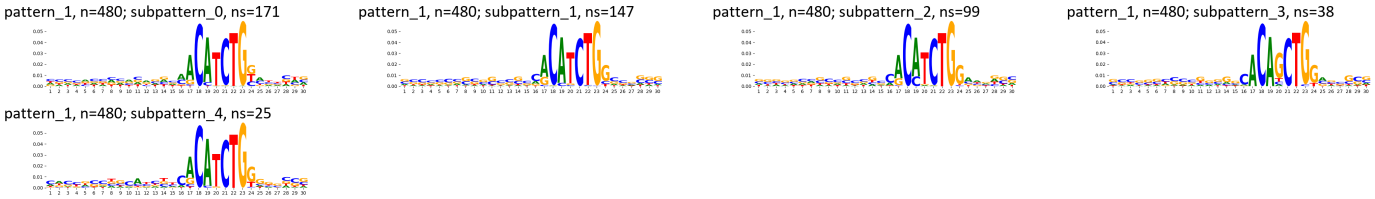

TF-MoDisCO pattern_1 n=480, PWM

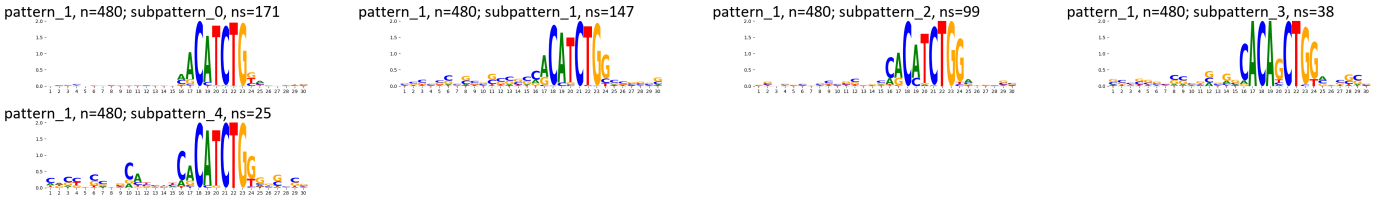

Supplementary Figure 402: TF-MoDisCO subpatterns for the ZBTB18 transcription factor in HEK293 (accession Hughes GR models).

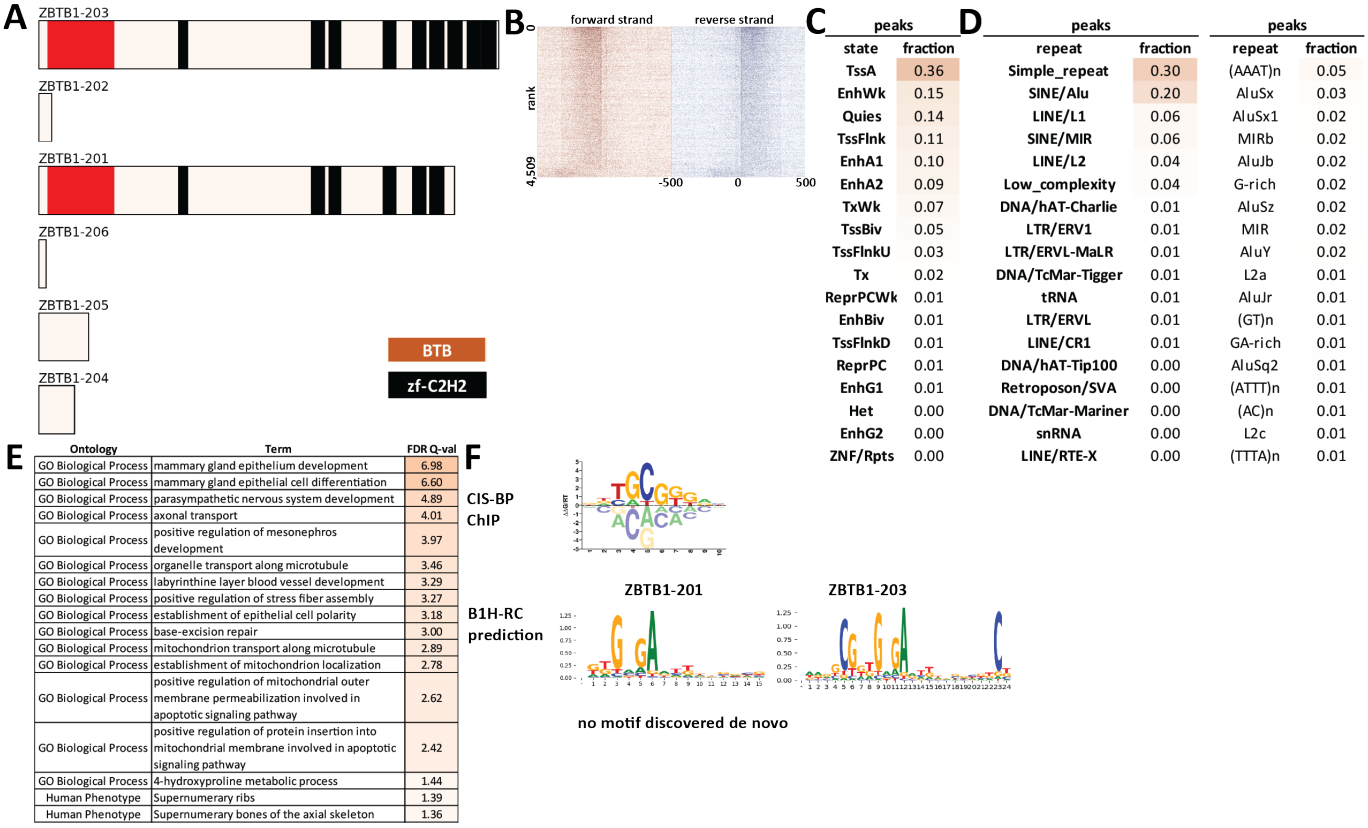

C

peaks	
state	fraction
TssA	0.36
EnhWk	0.15
Quies	0.14
TssFlnk	0.11
EnhA1	0.10
EnhA2	0.09
TxWk	0.07
TssBiv	0.05
TssFlnkU	0.03
Tx	0.02
ReprPCWk	0.01
EnhBiv	0.01
TssFlnkD	0.01
ReprPC	0.01
EnhG1	0.01
Het	0.00
EnhG2	0.00
ZNF/Rpts	0.00

D

peaks		peaks	
repeat	fraction	repeat	fraction
Simple_repeat	0.30	(AAAT)n	0.05
SINE/Alu	0.20	AluSx	0.03
LINE/L1	0.06	AluSx1	0.02
SINE/MIR	0.06	MIRb	0.02
LINE/L2	0.04	AluJb	0.02
Low_complexity	0.04	G-rich	0.02
DNA/hAT-Charlie	0.01	AluSz	0.02
LTR/ERV1	0.01	MIR	0.02
LTR/ERVL-MaLR	0.01	AluY	0.02
DNA/TcMar-Tigger	0.01	L2a	0.01
tRNA	0.01	AluJr	0.01
LTR/ERVL	0.01	(GT)n	0.01
LINE/CR1	0.01	GA-rich	0.01
DNA/hAT-Tip100	0.00	AluSq2	0.01
Retroposon/SVA	0.00	(ATTT)n	0.01
DNA/TcMar-Mariner	0.00	(AC)n	0.01
snRNA	0.00	L2c	0.01
LINE/RTE-X	0.00	(TTTA)n	0.01

E

Ontology	Term	FDR Q-val
GO Biological Process	mammary gland epithelium development	6.98
GO Biological Process	mammary gland epithelial cell differentiation	6.60
GO Biological Process	parasympathetic nervous system development	4.89
GO Biological Process	axonal transport	4.01
GO Biological Process	positive regulation of mesonephros development	3.97
GO Biological Process	organelle transport along microtubule	3.46
GO Biological Process	labyrinthine layer blood vessel development	3.29
GO Biological Process	positive regulation of stress fiber assembly	3.27
GO Biological Process	establishment of epithelial cell polarity	3.18
GO Biological Process	base-excision repair	3.00
GO Biological Process	mitochondrion transport along microtubule	2.89
GO Biological Process	establishment of mitochondrion localization	2.78
GO Biological Process	positive regulation of mitochondrial outer membrane permeabilization involved in apoptotic signaling pathway	2.62
GO Biological Process	positive regulation of protein insertion into mitochondrial membrane involved in apoptotic signaling pathway	2.42
GO Biological Process	4-hydroxyproline metabolic process	1.44
Human Phenotype	Supernumerary ribs	1.39
Human Phenotype	Supernumerary bones of the axial skeleton	1.36

Supplementary Figure 403: Properties and genomic distribution of motifs identified for the ZBTB1 transcription factor in HEK293 (accession ENCSR927UJQ).

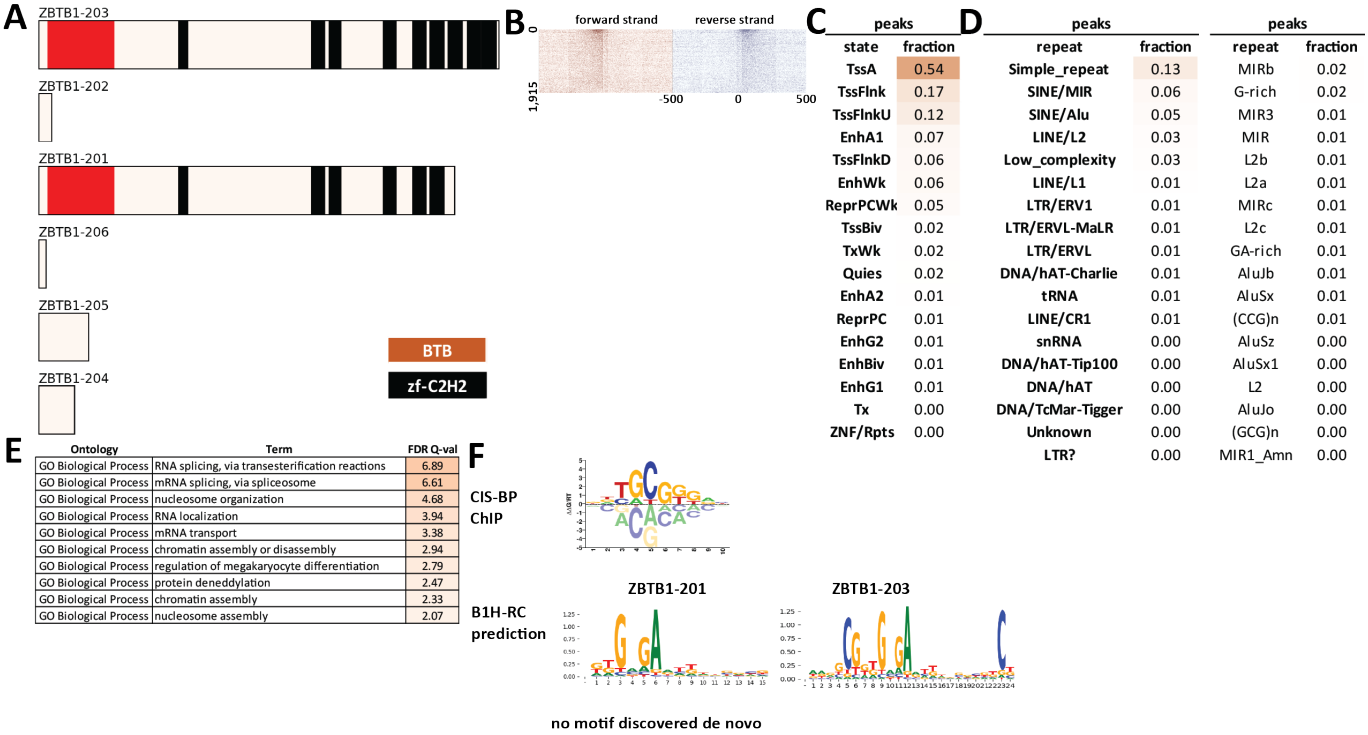

C

peaks	
state	fraction
TssA	0.54
TssFlnk	0.17
TssFlnkU	0.12
EnhA1	0.07
TssFlnkD	0.06
EnhWk	0.06
ReprPCWk	0.05
TssBiv	0.02
TxWk	0.02
Quies	0.02
EnhA2	0.01
ReprPC	0.01
EnhG2	0.01
EnhBiv	0.01
EnhG1	0.01
Tx	0.00
ZNF/Rpts	0.00

D

peaks		peaks	
repeat	fraction	repeat	fraction
Simple_repeat	0.13	MIRb	0.02
SINE/MIR	0.06	G-rich	0.02
SINE/Alu	0.05	MIR3	0.01
LINE/L2	0.03	MIR	0.01
Low_complexity	0.03	L2b	0.01
LINE/L1	0.01	L2a	0.01
LTR/ERV1	0.01	MIRc	0.01
LTR/ERVL-MaLR	0.01	L2c	0.01
LTR/ERVL	0.01	GA-rich	0.01
DNA/hAT-Charlie	0.01	AluJb	0.01
tRNA	0.01	AluSx	0.01
LINE/CR1	0.01	(CCG)n	0.01
snRNA	0.00	AluSz	0.00
DNA/hAT-Tip100	0.00	AluSx1	0.00
DNA/hAT	0.00	L2	0.00
DNA/TcMar-Tigger	0.00	AluJo	0.00
Unknown	0.00	(GCG)n	0.00
LTR?	0.00	MIR1_Amn	0.00

E

Ontology	Term	FDR Q-val
GO Biological Process	RNA splicing, via transesterification reactions	6.89
GO Biological Process	mRNA splicing, via spliceosome	6.61
GO Biological Process	nucleosome organization	4.68
GO Biological Process	RNA localization	3.94
GO Biological Process	mRNA transport	3.38
GO Biological Process	chromatin assembly or disassembly	2.94
GO Biological Process	regulation of megakaryocyte differentiation	2.79
GO Biological Process	protein deneddylation	2.47
GO Biological Process	chromatin assembly	2.33
GO Biological Process	nucleosome assembly	2.07

Supplementary Figure 404: Properties and genomic distribution of motifs identified for the ZBTB1 transcription factor in HepG2 (accession ENCSR331HWO).

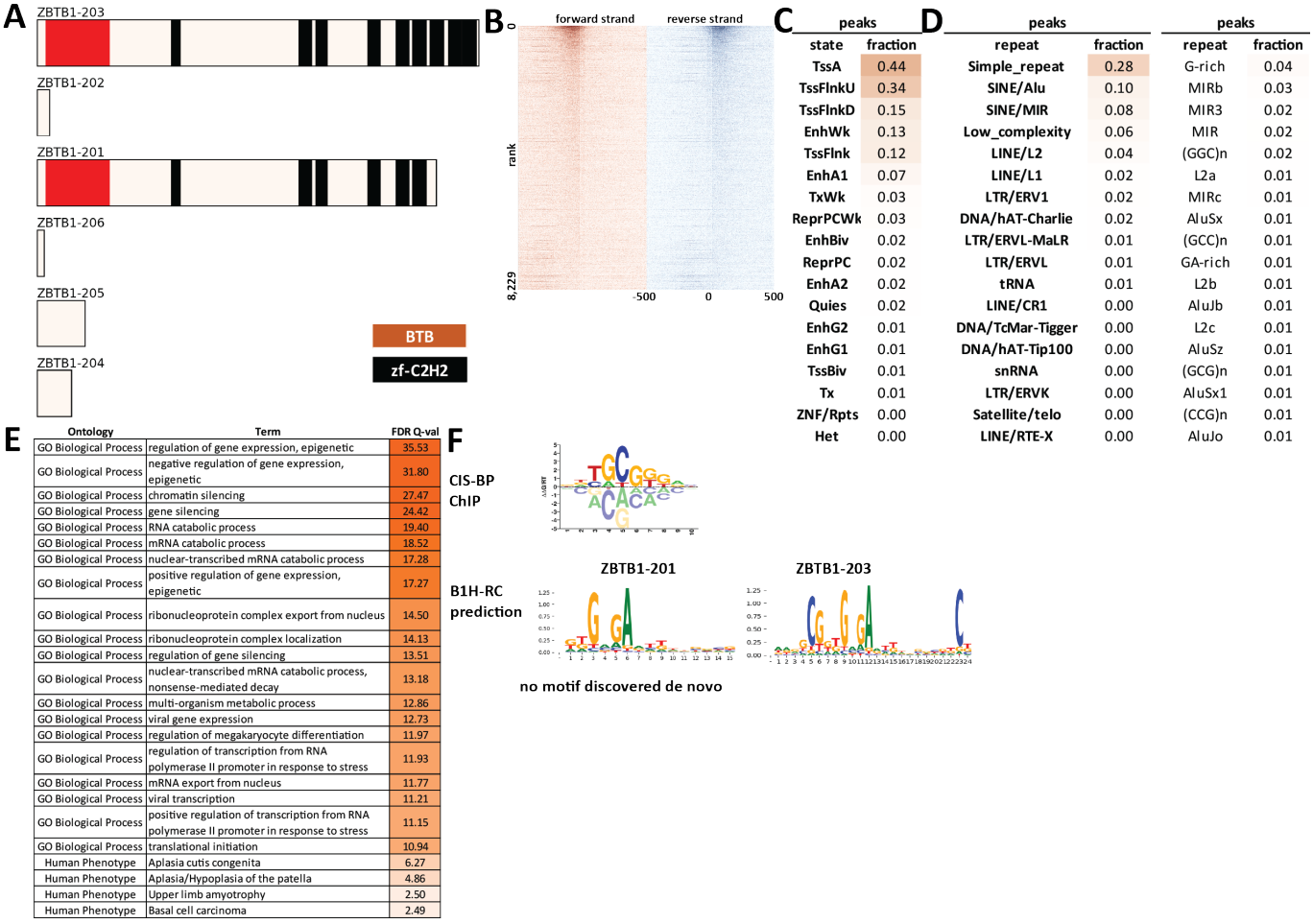

C

peaks	
state	fraction
TssA	0.44
TssFlnkU	0.34
TssFlnkD	0.15
EnhWk	0.13
TssFlnk	0.12
EnhA1	0.07
TxWk	0.03
ReprPCWk	0.03
EnhBiv	0.02
ReprPC	0.02
EnhA2	0.02
Quies	0.02
EnhG2	0.01
EnhG1	0.01
TssBiv	0.01
Tx	0.01
ZNF/Rpts	0.00
Het	0.00

D

peaks		peaks	
repeat	fraction	repeat	fraction
Simple_repeat	0.28	G-rich	0.04
SINE/Alu	0.10	MIRb	0.03
SINE/MIR	0.08	MIR3	0.02
Low_complexity	0.06	MIR	0.02
LINE/L2	0.04	(GGC)n	0.02
LINE/L1	0.02	L2a	0.01
LTR/ERV1	0.02	MIRc	0.01
DNA/hAT-Charlie	0.02	AluSx	0.01
LTR/ERVL-MaLR	0.01	(GCC)n	0.01
LTR/ERVL	0.01	GA-rich	0.01
tRNA	0.01	L2b	0.01
LINE/CR1	0.00	AluJb	0.01
DNA/TcMar-Tigger	0.00	L2c	0.01
DNA/hAT-Tip100	0.00	AluSz	0.01
snRNA	0.00	(GCG)n	0.01
LTR/ERVK	0.00	AluSx1	0.01
Satellite/telo	0.00	(CCG)n	0.01
LINE/RTE-X	0.00	AluJo	0.01

E

Ontology	Term	FDR Q-val
GO Biological Process	regulation of gene expression, epigenetic	35.53
GO Biological Process	negative regulation of gene expression, epigenetic	31.80
GO Biological Process	chromatin silencing	27.47
GO Biological Process	gene silencing	24.42
GO Biological Process	RNA catabolic process	19.40
GO Biological Process	mRNA catabolic process	18.52
GO Biological Process	nuclear-transcribed mRNA catabolic process	17.28
GO Biological Process	positive regulation of gene expression, epigenetic	17.27
GO Biological Process	ribonucleoprotein complex export from nucleus	14.50
GO Biological Process	ribonucleoprotein complex localization	14.13
GO Biological Process	regulation of gene silencing	13.51
GO Biological Process	nuclear-transcribed mRNA catabolic process, nonsense-mediated decay	13.18
GO Biological Process	multi-organism metabolic process	12.86
GO Biological Process	viral gene expression	12.73
GO Biological Process	regulation of megakaryocyte differentiation	11.97
GO Biological Process	regulation of transcription from RNA polymerase II promoter in response to stress	11.93
GO Biological Process	mRNA export from nucleus	11.77
GO Biological Process	viral transcription	11.21
GO Biological Process	positive regulation of transcription from RNA polymerase II promoter in response to stress	11.15
GO Biological Process	translational initiation	10.94
Human Phenotype	Aplasia cutis congenita	6.27
Human Phenotype	Aplasia/Hypoplasia of the patella	4.86
Human Phenotype	Upper limb amyotrophy	2.50
Human Phenotype	Basal cell carcinoma	2.49

Supplementary Figure 405: Properties and genomic distribution of motifs identified for the ZBTB1 transcription factor in K562 (accession ENCSR166BAY).

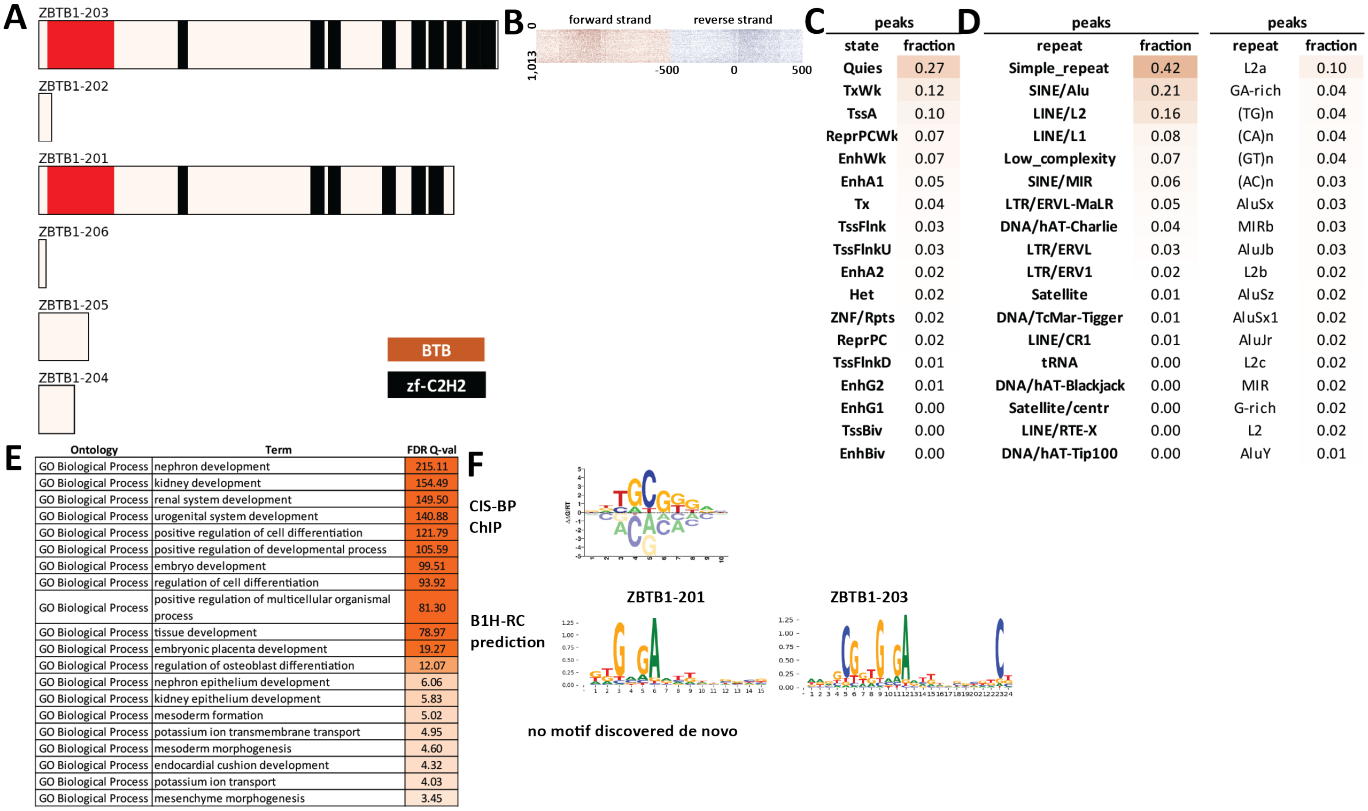

Supplementary Figure 406: Properties and genomic distribution of motifs identified for the ZBTB1 transcription factor in MCF-7 (accession ENCSR309ELI).

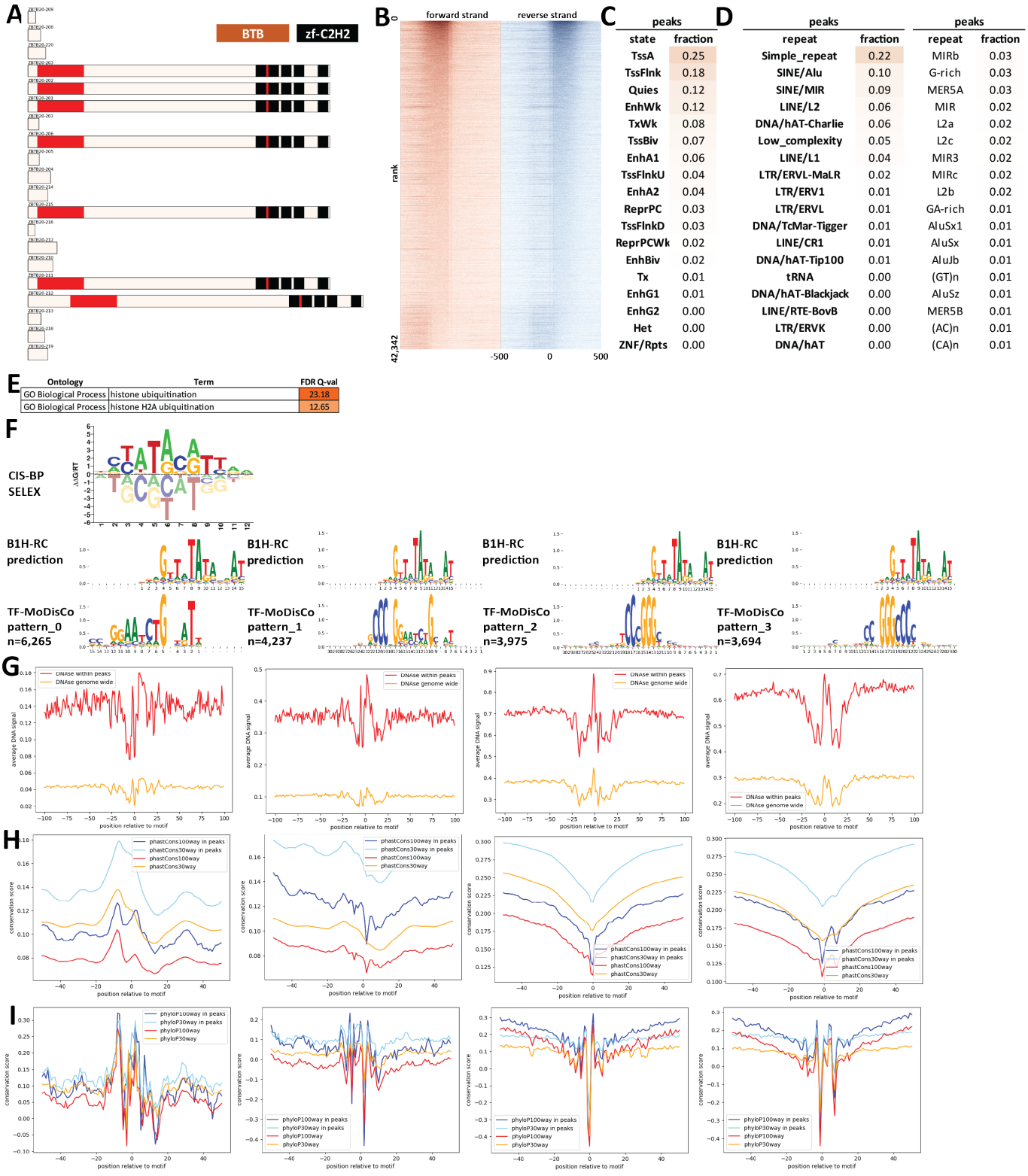

Supplementary Figure 407: Properties and genomic distribution of motifs identified for the ZBTB20 transcription factor in HEK293 (accession ENCSR460MBI).

TF-MoDisCO pattern_0 n=6265, CWM

pattern_0, n=6265; subpattern_0, ns=1213

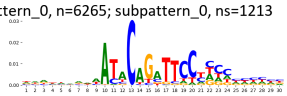

pattern_0, n=6265; subpattern_1, ns=1121

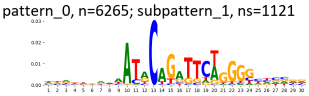

pattern_0, n=6265; subpattern_2, ns=1004

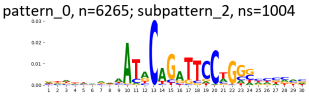

pattern_0, n=6265; subpattern_3, ns=928

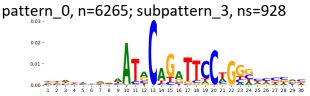

pattern_0, n=6265; subpattern_4, ns=844

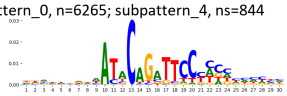

pattern_0, n=6265; subpattern_5, ns=802

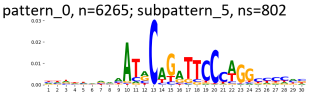

pattern_0, n=6265; subpattern_6, ns=329

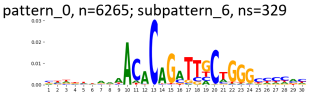

pattern_0, n=6265; subpattern_7, ns=24

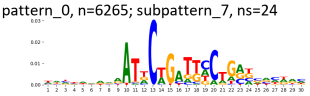

TF-MoDisCO pattern_0 n=6265, PWM

pattern_0, n=6265; subpattern_0, ns=1213

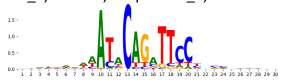

pattern_0, n=6265; subpattern_1, ns=1121

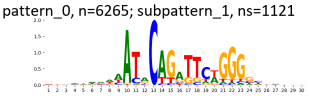

pattern_0, n=6265; subpattern_2, ns=1004

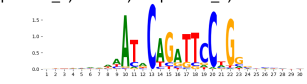

pattern_0, n=6265; subpattern_3, ns=928

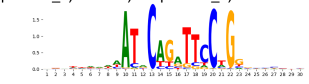

pattern_0, n=6265; subpattern_4, ns=844

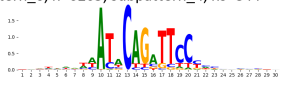

pattern_0, n=6265; subpattern_5, ns=802

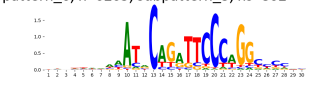

pattern_0, n=6265; subpattern_6, ns=329

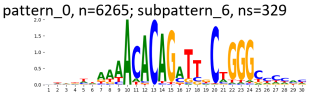

pattern_0, n=6265; subpattern_7, ns=24

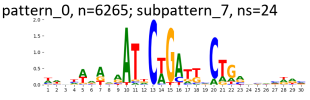

TF-MoDisCO pattern_1 n=4237, CWM

pattern_1, n=4237; subpattern_0, ns=1061

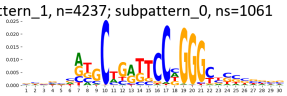

pattern_1, n=4237; subpattern_1, ns=852

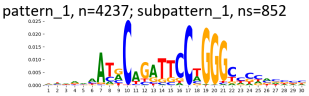

pattern_1, n=4237; subpattern_10, ns=2

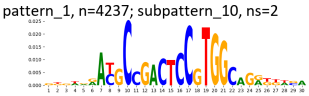

pattern_1, n=4237; subpattern_11, ns=2

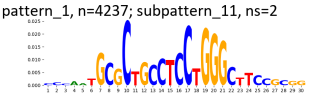

pattern_1, n=4237; subpattern_2, ns=794

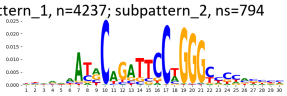

pattern_1, n=4237; subpattern_3, ns=666

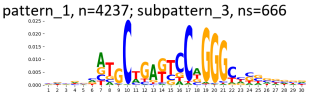

pattern_1, n=4237; subpattern_4, ns=635

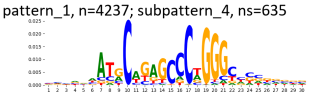

pattern_1, n=4237; subpattern_5, ns=188

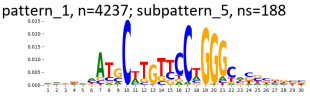

pattern_1, n=4237; subpattern_6, ns=25

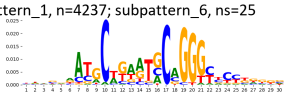

pattern_1, n=4237; subpattern_7, ns=7

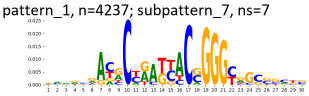

pattern_1, n=4237; subpattern_8, ns=3

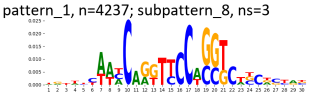

pattern_1, n=4237; subpattern_9, ns=2

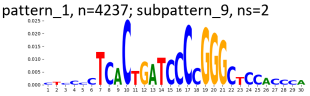

TF-MoDisCO pattern_1 n=4237, PWM

pattern_1, n=4237; subpattern_0, ns=1061

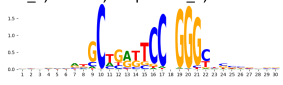

pattern_1, n=4237; subpattern_1, ns=852

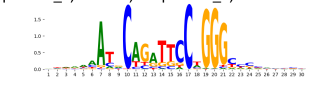

pattern_1, n=4237; subpattern_10, ns=2

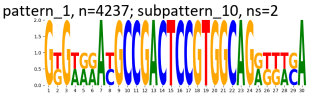

pattern_1, n=4237; subpattern_11, ns=2

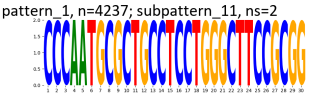

pattern_1, n=4237; subpattern_2, ns=794

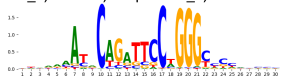

pattern_1, n=4237; subpattern_3, ns=666

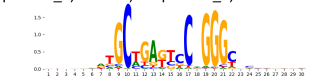

pattern_1, n=4237; subpattern_4, ns=635

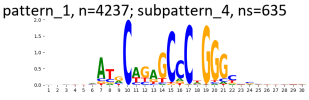

pattern_1, n=4237; subpattern_5, ns=188

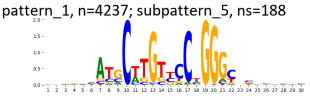

pattern_1, n=4237; subpattern_6, ns=25

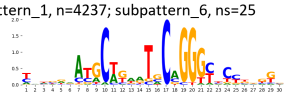

pattern_1, n=4237; subpattern_7, ns=7

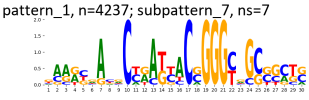

pattern_1, n=4237; subpattern_8, ns=3

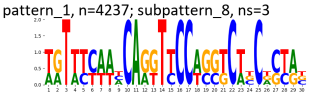

pattern_1, n=4237; subpattern_9, ns=2

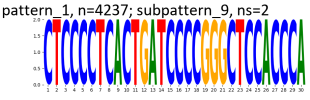

TF-MoDisCO pattern_2 n=3975, CWM

pattern_2, n=3975; subpattern_0, ns=842

pattern_2, n=3975; subpattern_1, ns=778

pattern_2, n=3975; subpattern_2, ns=755

pattern_2, n=3975; subpattern_3, ns=627

pattern_2, n=3975; subpattern_4, ns=550

pattern_2, n=3975; subpattern_5, ns=212

pattern_2, n=3975; subpattern_6, ns=83

pattern_2, n=3975; subpattern_7, ns=72

pattern_2, n=3975; subpattern_8, ns=56

TF-MoDisCO pattern_2 n=3975, PWM

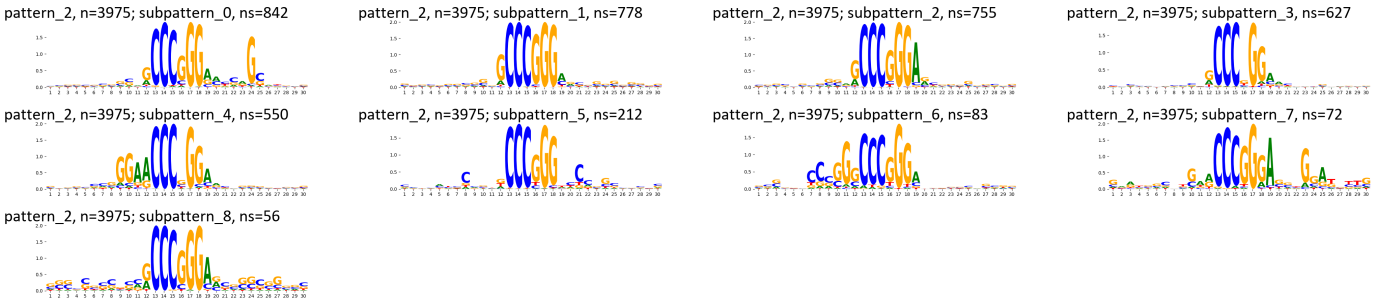

TF-MoDisCO pattern_3 n=3694, CWM

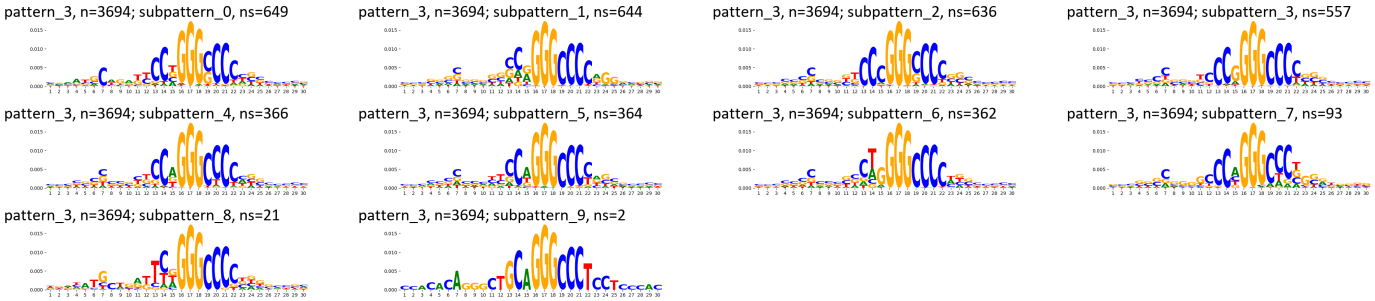

TF-MoDisCO pattern_3 n=3694, PWM

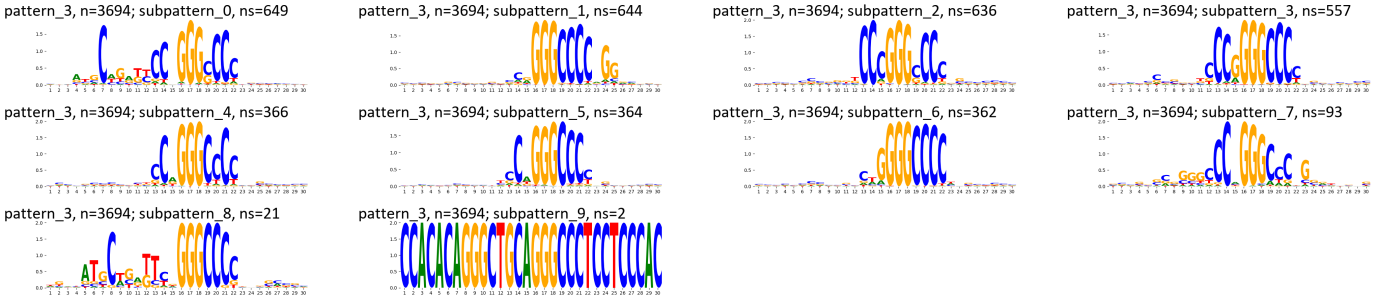

Supplementary Figure 408: TF-MoDisCO subpatterns for the ZBTB20 transcription factor in HEK293 (accession ENCSR460MBI).

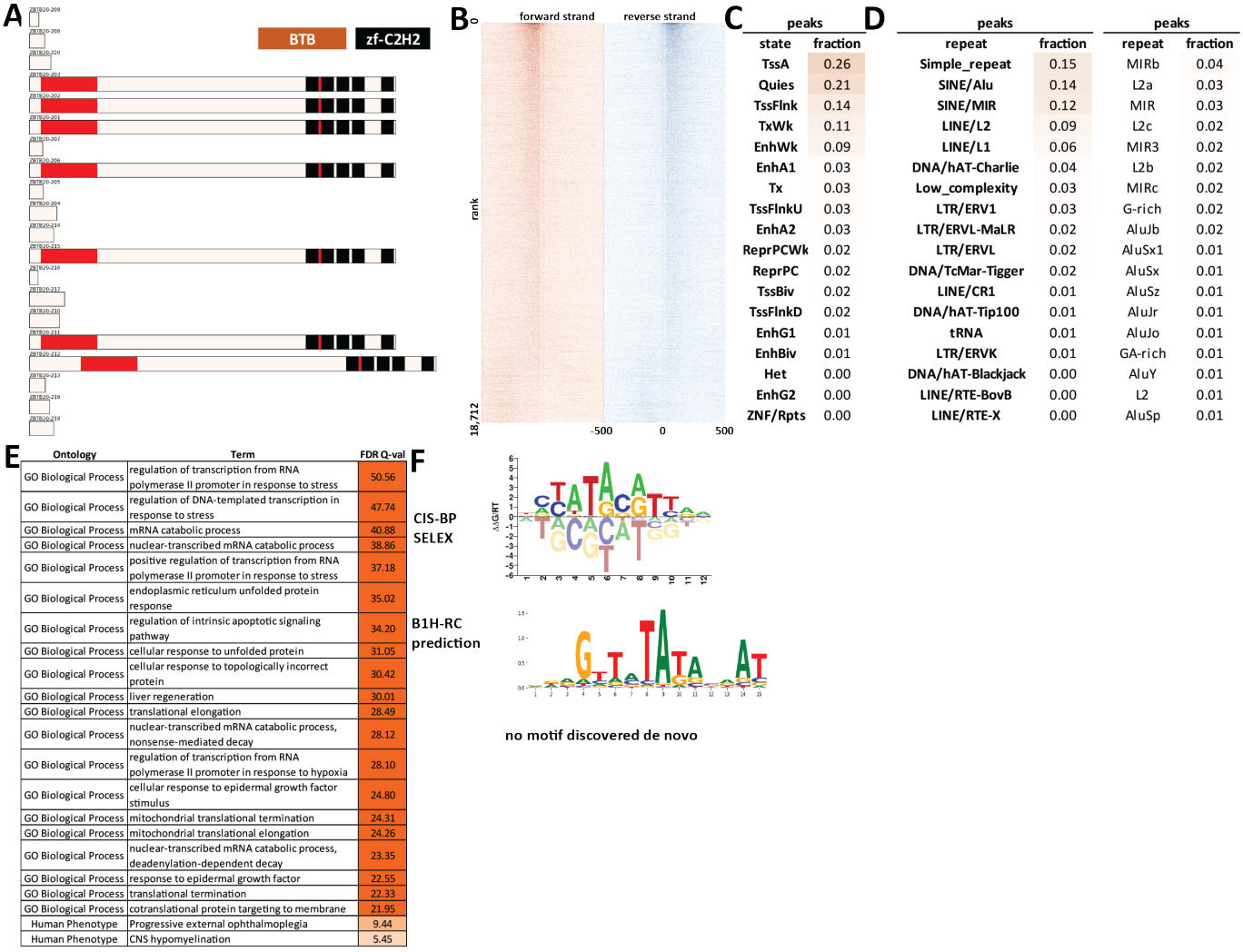

Supplementary Figure 409: Properties and genomic distribution of motifs identified for the ZBTB20 transcription factor in HepG2 (accession ENCSR392TWV).

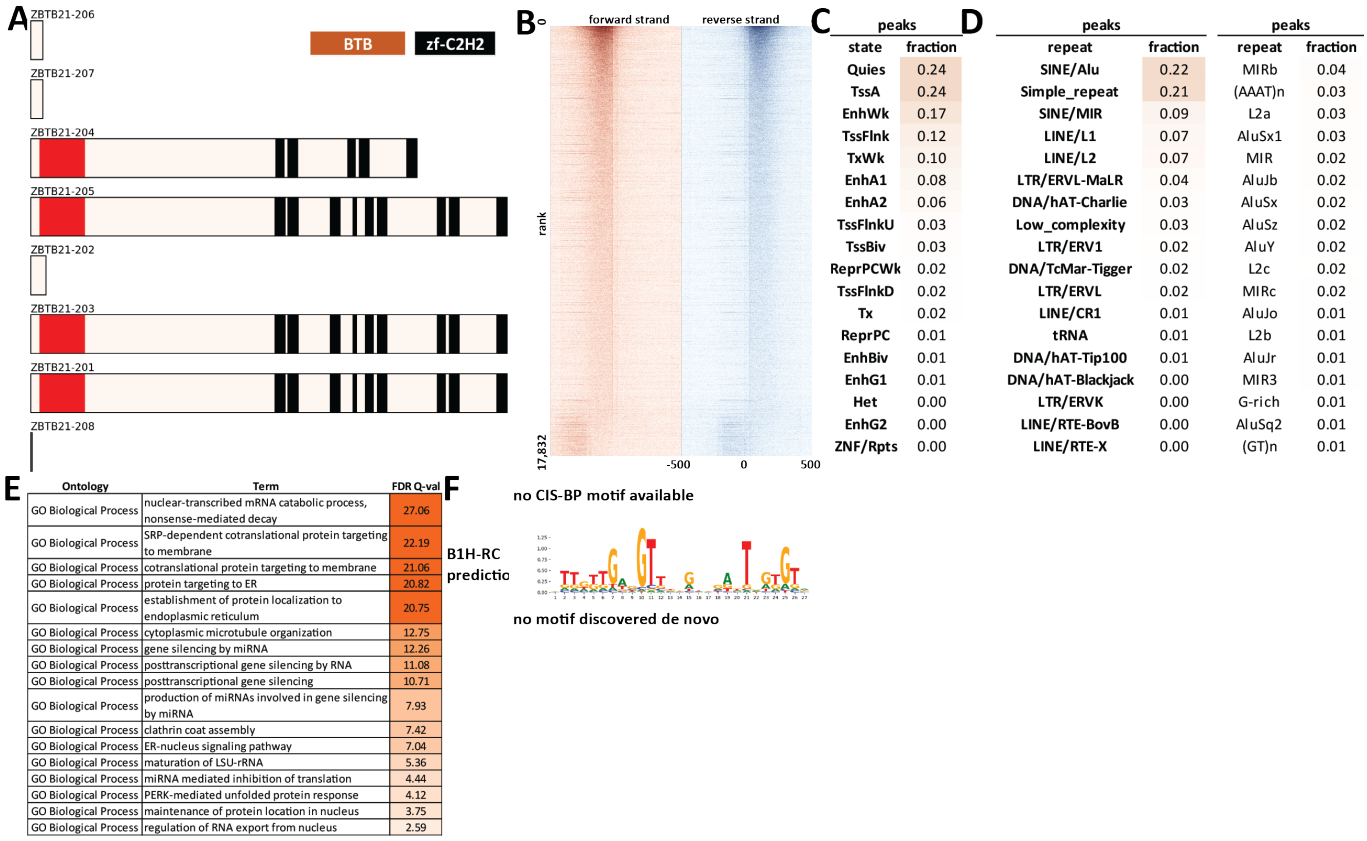

peaks

state	fraction
Quies	0.24
TssA	0.24
EnhWk	0.17
TssFlnk	0.12
TxWk	0.10
EnhA1	0.08
EnhA2	0.06
TssFlnkU	0.03
TssBiv	0.03
ReprPCWk	0.02
TssFlnkD	0.02
Tx	0.02
ReprPC	0.01
EnhBiv	0.01
EnhG1	0.01
Het	0.00
EnhG2	0.00
ZNF/Rpts	0.00

peaks

repeat	fraction	repeat	fraction
SINE/Alu	0.22	MIRb	0.04
Simple_repeat	0.21	(AAAT)n	0.03
SINE/MIR	0.09	L2a	0.03
LINE/L1	0.07	AluSx1	0.03
LINE/L2	0.07	MIR	0.02
LTR/ERVL-MaLR	0.04	AluJb	0.02
DNA/hAT-Charlie	0.03	AluSx	0.02
Low_complexity	0.03	AluSz	0.02
LTR/ERV1	0.02	AluY	0.02
DNA/TcMar-Tigger	0.02	L2c	0.02
LTR/ERVL	0.02	MIRc	0.02
LINE/CR1	0.01	AluJo	0.01
tRNA	0.01	L2b	0.01
DNA/hAT-Tip100	0.01	AluJr	0.01
DNA/hAT-Blackjack	0.00	MIR3	0.01
LTR/ERVK	0.00	G-rich	0.01
LINE/RTE-BovB	0.00	AluSq2	0.01
LINE/RTE-X	0.00	(GT)n	0.01

Supplementary Figure 410: Properties and genomic distribution of motifs identified for the ZBTB21 transcription factor in HEK293 (accession ENCSR321MSF).

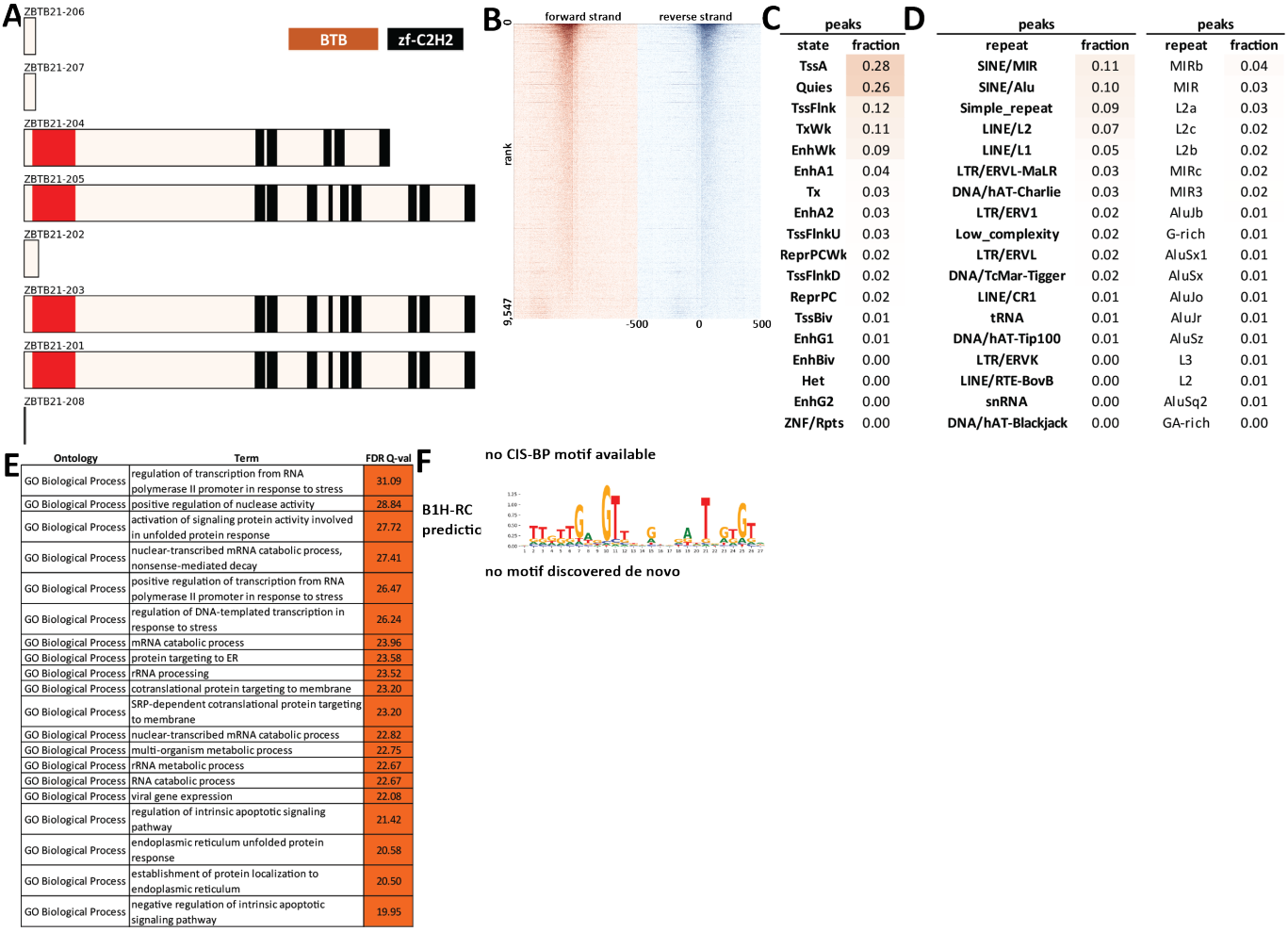

C

peaks	
state	fraction
TssA	0.28
Quies	0.26
TssFlnk	0.12
TxWk	0.11
EnhWk	0.09
EnhA1	0.04
Tx	0.03
EnhA2	0.03
TssFlnkU	0.03
ReprPCWk	0.02
TssFlnkD	0.02
ReprPC	0.02
TssBiv	0.01
EnhG1	0.01
EnhBiv	0.00
Het	0.00
EnhG2	0.00
ZNF/Rpts	0.00

D

peaks		peaks	
repeat	fraction	repeat	fraction
SINE/MIR	0.11	MIRb	0.04
SINE/Alu	0.10	MIR	0.03
Simple_repeat	0.09	L2a	0.03
LINE/L2	0.07	L2c	0.02
LINE/L1	0.05	L2b	0.02
LTR/ERVL-MaLR	0.03	MIRc	0.02
DNA/hAT-Charlie	0.03	MIR3	0.02
LTR/ERV1	0.02	AluJb	0.01
Low_complexity	0.02	G-rich	0.01
LTR/ERVL	0.02	AluSx1	0.01
DNA/TcMar-Tigger	0.02	AluSx	0.01
LINE/CR1	0.01	AluJo	0.01
tRNA	0.01	AluJr	0.01
DNA/hAT-Tip100	0.01	AluSz	0.01
LTR/ERVK	0.00	L3	0.01
LINE/RTE-BovB	0.00	L2	0.01
snRNA	0.00	AluSq2	0.01
DNA/hAT-Blackjack	0.00	GA-rich	0.00

E

Ontology	Term	FDR Q-val
GO Biological Process	regulation of transcription from RNA polymerase II promoter in response to stress	31.09
GO Biological Process	positive regulation of nuclease activity	28.84
GO Biological Process	activation of signaling protein activity involved in unfolded protein response	27.72
GO Biological Process	nuclear-transcribed mRNA catabolic process, nonsense-mediated decay	27.41
GO Biological Process	positive regulation of transcription from RNA polymerase II promoter in response to stress	26.47
GO Biological Process	regulation of DNA-templated transcription in response to stress	26.24
GO Biological Process	mRNA catabolic process	23.96
GO Biological Process	protein targeting to ER	23.58
GO Biological Process	rRNA processing	23.52
GO Biological Process	cotranslational protein targeting to membrane	23.20
GO Biological Process	SRP-dependent cotranslational protein targeting to membrane	23.20
GO Biological Process	nuclear-transcribed mRNA catabolic process	22.82
GO Biological Process	multi-organism metabolic process	22.75
GO Biological Process	rRNA metabolic process	22.67
GO Biological Process	RNA catabolic process	22.67
GO Biological Process	viral gene expression	22.08
GO Biological Process	regulation of intrinsic apoptotic signaling pathway	21.42
GO Biological Process	endoplasmic reticulum unfolded protein response	20.58
GO Biological Process	establishment of protein localization to endoplasmic reticulum	20.50
GO Biological Process	negative regulation of intrinsic apoptotic signaling pathway	19.95

Supplementary Figure 411: Properties and genomic distribution of motifs identified for the ZBTB21 transcription factor in HepG2 (accession ENCSR549PAU).

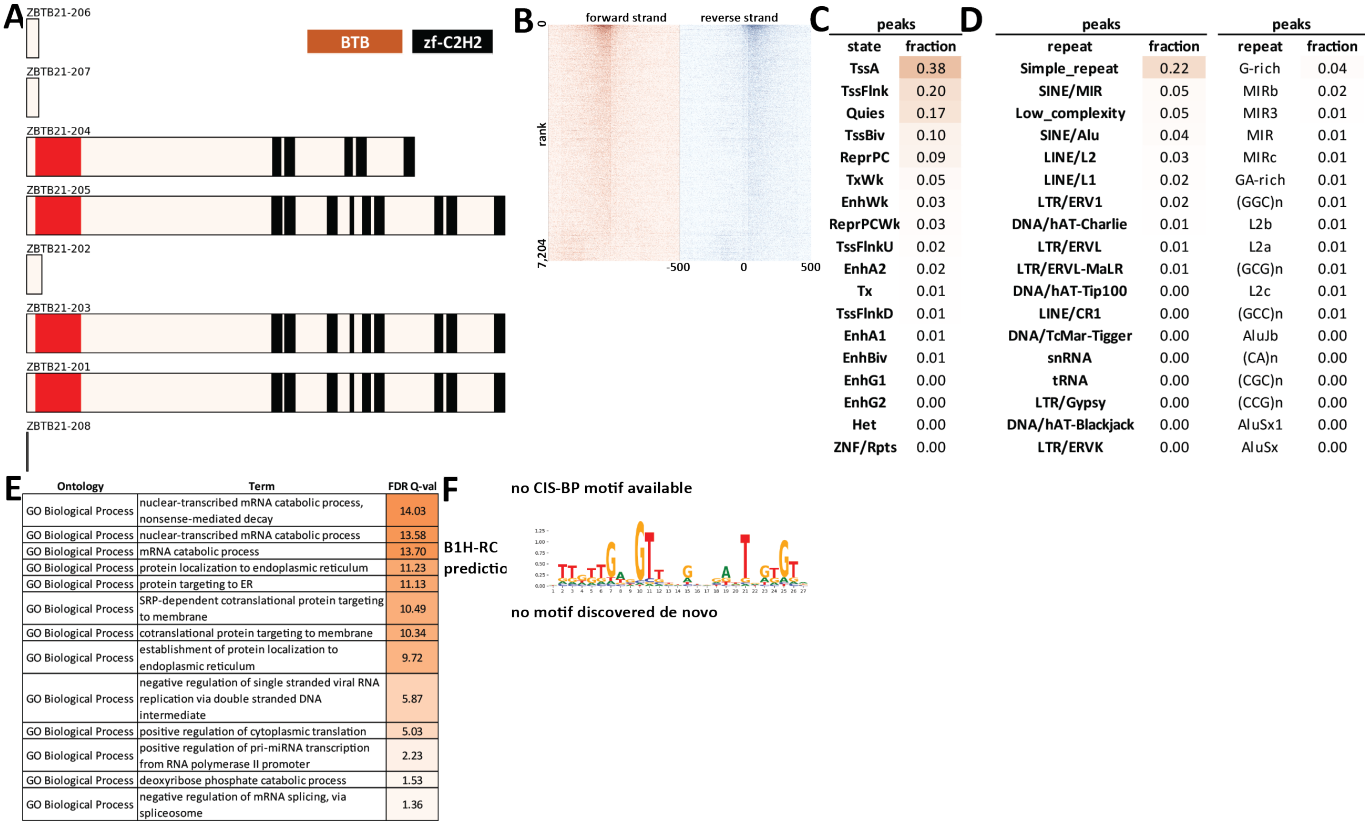

peaks	
state	fraction
TssA	0.38
TssFlnk	0.20
Quies	0.17
TssBiv	0.10
ReprPC	0.09
TxWk	0.05
EnhWk	0.03
ReprPCWk	0.03
TssFlnkU	0.02
EnhA2	0.02
Tx	0.01
TssFlnkD	0.01
EnhA1	0.01
EnhBiv	0.01
EnhG1	0.00
EnhG2	0.00
Het	0.00
ZNF/Rpts	0.00

peaks		peaks	
repeat	fraction	repeat	fraction
Simple_repeat	0.22	G-rich	0.04
SINE/MIR	0.05	MIRb	0.02
Low_complexity	0.05	MIR3	0.01
SINE/Alu	0.04	MIR	0.01
LINE/L2	0.03	MIRc	0.01
LINE/L1	0.02	GA-rich	0.01
LTR/ERV1	0.02	(GGC)n	0.01
DNA/hAT-Charlie	0.01	L2b	0.01
LTR/ERVL	0.01	L2a	0.01
LTR/ERVL-MaLR	0.01	(GCG)n	0.01
DNA/hAT-Tip100	0.00	L2c	0.01
LINE/CR1	0.00	(GCC)n	0.01
DNA/TcMar-Tigger	0.00	AluJb	0.00
snRNA	0.00	(CA)n	0.00
tRNA	0.00	(CGC)n	0.00
LTR/Gypsy	0.00	(CCG)n	0.00
DNA/hAT-Blackjack	0.00	AluSx1	0.00
LTR/ERVK	0.00	AluSx	0.00

Ontology	Term	FDR Q-val
GO Biological Process	nuclear-transcribed mRNA catabolic process, nonsense-mediated decay	14.03
GO Biological Process	nuclear-transcribed mRNA catabolic process	13.58
GO Biological Process	mRNA catabolic process	13.70
GO Biological Process	protein localization to endoplasmic reticulum	11.23
GO Biological Process	protein targeting to ER	11.13
GO Biological Process	SRP-dependent cotranslational protein targeting to membrane	10.49
GO Biological Process	cotranslational protein targeting to membrane	10.34
GO Biological Process	establishment of protein localization to endoplasmic reticulum	9.72
GO Biological Process	negative regulation of single stranded viral RNA replication via double stranded DNA intermediate	5.87
GO Biological Process	positive regulation of cytoplasmic translation	5.03
GO Biological Process	positive regulation of pri-miRNA transcription from RNA polymerase II promoter	2.23
GO Biological Process	deoxyribose phosphate catabolic process	1.53
GO Biological Process	negative regulation of mRNA splicing, via spliceosome	1.36

Supplementary Figure 412: Properties and genomic distribution of motifs identified for the ZBTB21 transcription factor in WTC11 (accession ENCSR962BEI).

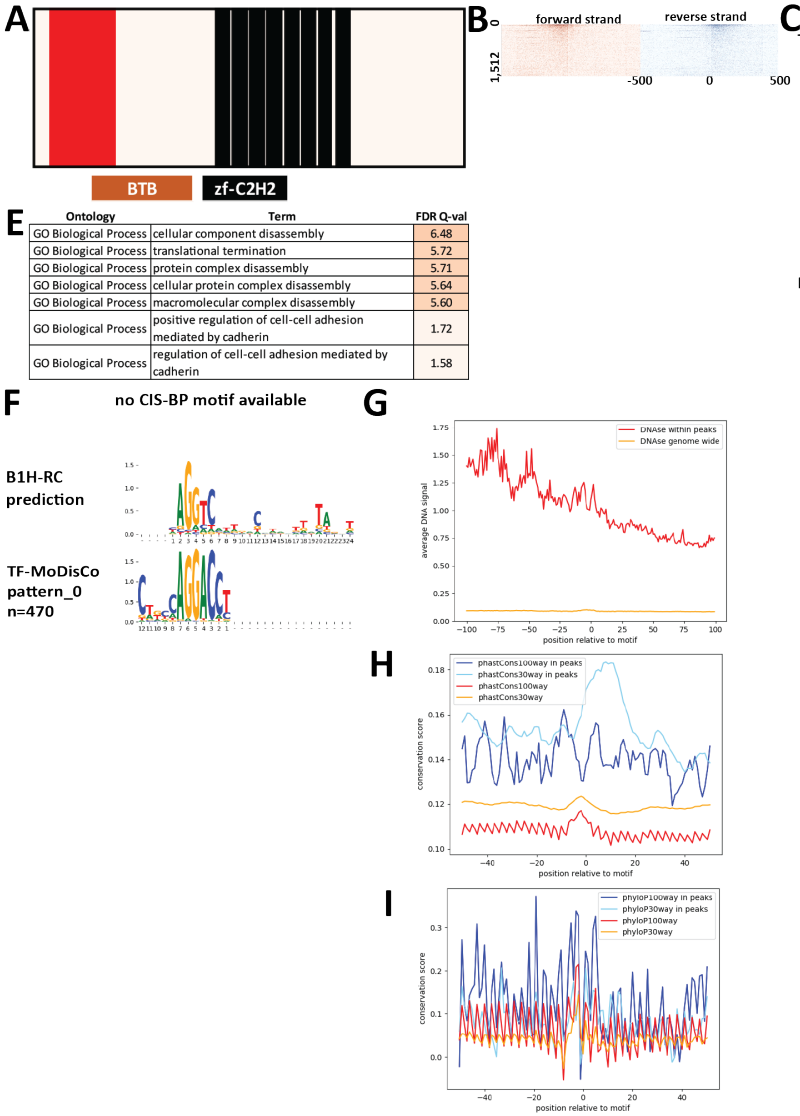

E

Ontology	Term	FDR Q-val
GO Biological Process	cellular component disassembly	6.48
GO Biological Process	translational termination	5.72
GO Biological Process	protein complex disassembly	5.71
GO Biological Process	cellular protein complex disassembly	5.64
GO Biological Process	macromolecular complex disassembly	5.60
GO Biological Process	positive regulation of cell-cell adhesion mediated by cadherin	1.72
GO Biological Process	regulation of cell-cell adhesion mediated by cadherin	1.58

C

peaks	
state	fraction
TssA	0.39
Quies	0.21
TssFlnk	0.16
TxWk	0.10
EnhWk	0.05
TssFlnkU	0.05
TssBiv	0.04
ReprPC	0.03
TssFlnkD	0.03
ReprPCWk	0.03
EnhA1	0.02
Tx	0.02
EnhA2	0.02
EnhBiv	0.01
EnhG1	0.00
Het	0.00
EnhG2	0.00

D

peaks		peaks	
repeat	fraction	repeat	fraction
Simple_repeat	0.16	L2a	0.03
SINE/MIR	0.09	MIRb	0.03
SINE/Alu	0.08	MIR3	0.02
LINE/L2	0.07	L2b	0.02
Low_complexity	0.03	G-rich	0.02
LINE/L1	0.02	MIRc	0.02
LTR/ERV1	0.02	MIR	0.02
LTR/ERVL-MaLR	0.02	L2c	0.01
LTR/ERVL	0.02	AluJb	0.01
DNA/hAT-Charlie	0.01	(TG)n	0.01
LINE/CR1	0.01	AluSq2	0.01
DNA/hAT-Tip100	0.01	AluJo	0.01
DNA/TcMar-Tigger	0.00	L2	0.01
DNA/hAT-Blackjack	0.00	GA-rich	0.01
LTR/Gypsy	0.00	AluJr	0.01
LTR/ERVK	0.00	(T)n	0.01
tRNA	0.00	(GT)n	0.01
LTR?	0.00	AluSx	0.01

Supplementary Figure 413: Properties and genomic distribution of motifs identified for the ZBTB24 transcription factor in HepG2 (accession ENCSR396XDF).

TF-MoDisCO pattern_0 n=470, CWM

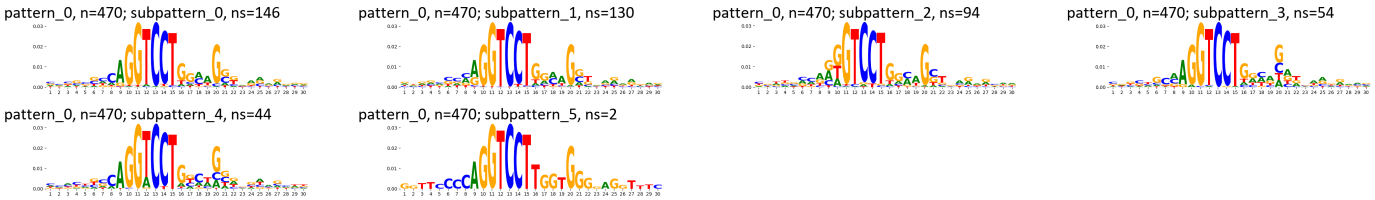

TF-MoDisCO pattern_0 n=470, PWM

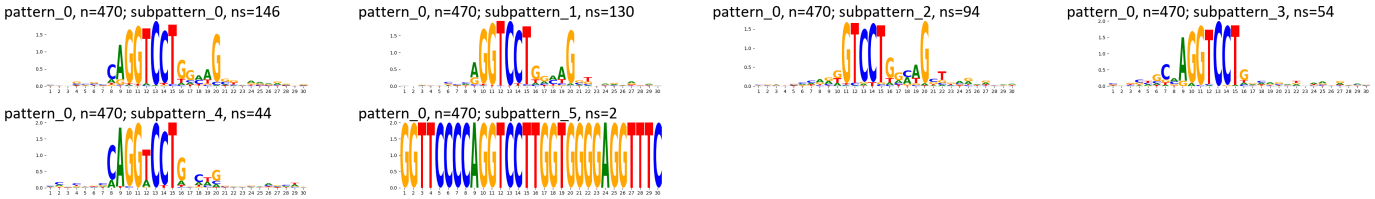

Supplementary Figure 414: TF-MoDisCO subpatterns for the ZBTB24 transcription factor in HepG2 (accession ENCSR396XDF).

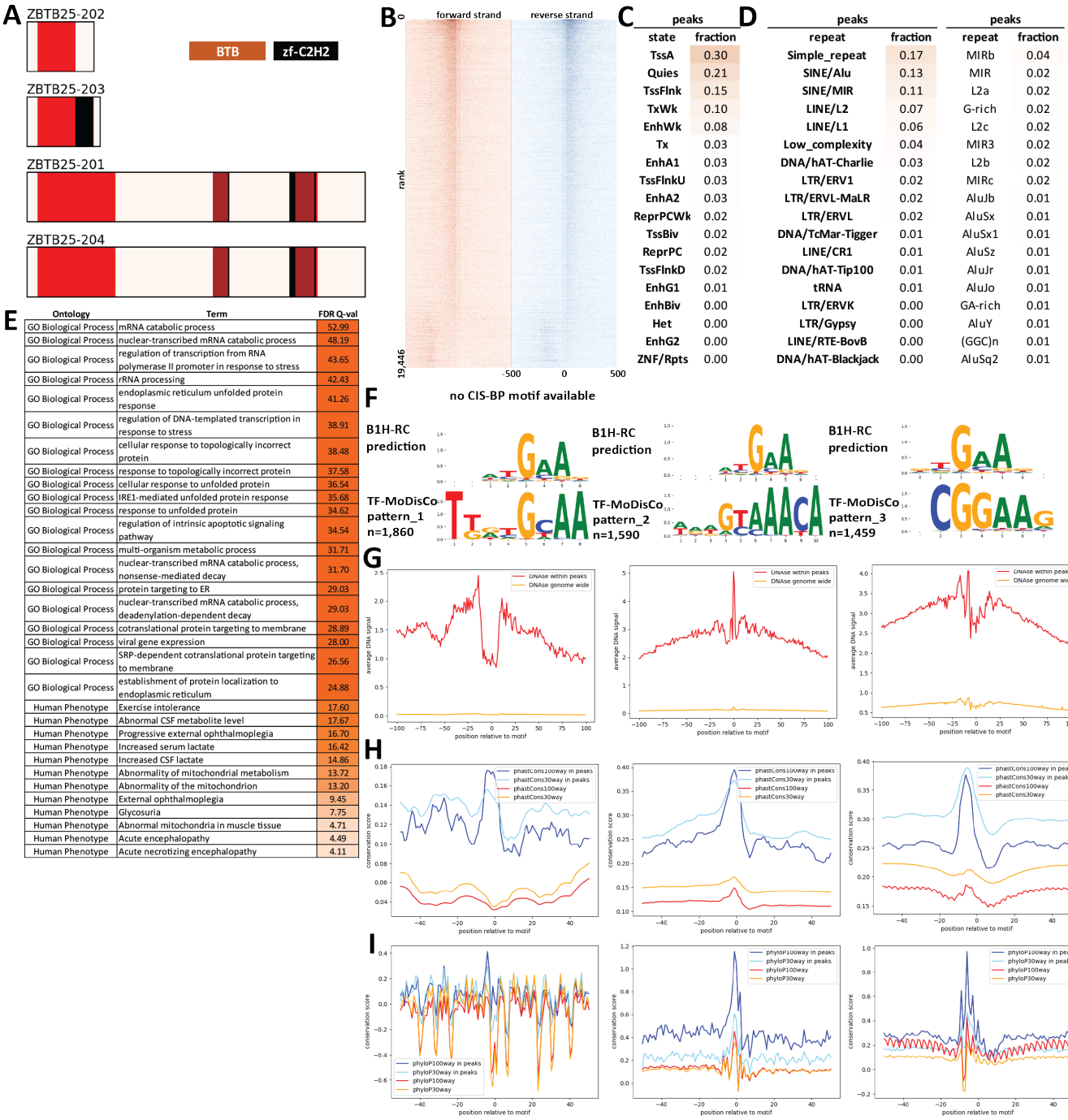

C

peaks	
state	fraction
TssA	0.30
Quies	0.21
TssFlnk	0.15
TxWk	0.10
EnhWk	0.08
Tx	0.03
EnhA1	0.03
TssFlnkU	0.03
EnhA2	0.03
ReprPCWk	0.02
TssBiv	0.02
ReprPC	0.02
TssFlnkD	0.02
EnhG1	0.01
EnhBiv	0.00
Het	0.00
EnhG2	0.00
ZNF/Rpts	0.00

D

peaks		peaks	
repeat	fraction	repeat	fraction
Simple_repeat	0.17	MIRb	0.04
SINE/Alu	0.13	MIR	0.02
SINE/MIR	0.11	L2a	0.02
LINE/L2	0.07	G-rich	0.02
LINE/L1	0.06	L2c	0.02
Low_complexity	0.04	MIR3	0.02
DNA/hAT-Charlie	0.03	L2b	0.02
LTR/ERV1	0.02	MIRc	0.02
LTR/ERVL-MaLR	0.02	AluJb	0.01
LTR/ERVL	0.02	AluSx	0.01
DNA/TcMar-Tigger	0.01	AluSx1	0.01
LINE/CR1	0.01	AluSz	0.01
DNA/hAT-Tip100	0.01	AluJr	0.01
tRNA	0.01	AluJo	0.01
LTR/ERVK	0.00	GA-rich	0.01
LTR/Gypsy	0.00	AluY	0.01
LINE/RTE-BovB	0.00	(GGC)n	0.01
DNA/hAT-Blackjack	0.00	AluSq2	0.01

E

Ontology	Term	FDR Q-val
GO Biological Process	mRNA catabolic process	52.99
GO Biological Process	nuclear-transcribed mRNA catabolic process	48.19
GO Biological Process	regulation of transcription from RNA polymerase II promoter in response to stress	43.65
GO Biological Process	rRNA processing	42.43
GO Biological Process	endoplasmic reticulum unfolded protein response	41.26
GO Biological Process	regulation of DNA-templated transcription in response to stress	38.91
GO Biological Process	cellular response to topologically incorrect protein	38.48
GO Biological Process	response to topologically incorrect protein	37.58
GO Biological Process	cellular response to unfolded protein	36.54
GO Biological Process	IRE1-mediated unfolded protein response	35.68
GO Biological Process	response to unfolded protein	34.62
GO Biological Process	regulation of intrinsic apoptotic signaling pathway	34.54
GO Biological Process	multi-organism metabolic process	31.71
GO Biological Process	nuclear-transcribed mRNA catabolic process, nonsense-mediated decay	31.70
GO Biological Process	protein targeting to ER	29.03
GO Biological Process	nuclear-transcribed mRNA catabolic process, deadenylation-dependent decay	29.03
GO Biological Process	cotranslational protein targeting to membrane	28.89
GO Biological Process	viral gene expression	28.00
GO Biological Process	SRP-dependent cotranslational protein targeting to membrane	26.56
GO Biological Process	establishment of protein localization to endoplasmic reticulum	24.88
Human Phenotype	Exercise intolerance	17.60
Human Phenotype	Abnormal CSF metabolite level	17.67
Human Phenotype	Progressive external ophthalmoplegia	16.70
Human Phenotype	Increased serum lactate	16.42
Human Phenotype	Increased CSF lactate	14.86
Human Phenotype	Abnormality of mitochondrial metabolism	13.72
Human Phenotype	Abnormality of the mitochondrion	13.20
Human Phenotype	External ophthalmoplegia	9.45
Human Phenotype	Glycosuria	7.75
Human Phenotype	Abnormal mitochondria in muscle tissue	4.71
Human Phenotype	Acute encephalopathy	4.49
Human Phenotype	Acute necrotizing encephalopathy	4.11

Supplementary Figure 415: Properties and genomic distribution of motifs identified for the ZBTB25 transcription factor in HepG2 (accession ENCSR485OYR).

TF-MoDiSCO pattern_1 n=1860, CWM

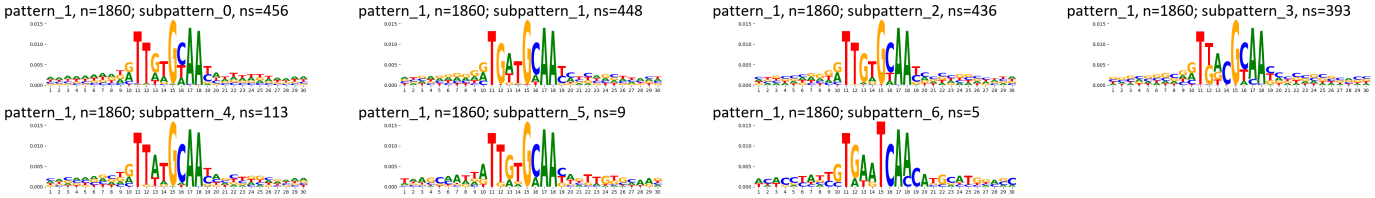

TF-MoDiSCO pattern_1 n=1860, PWM

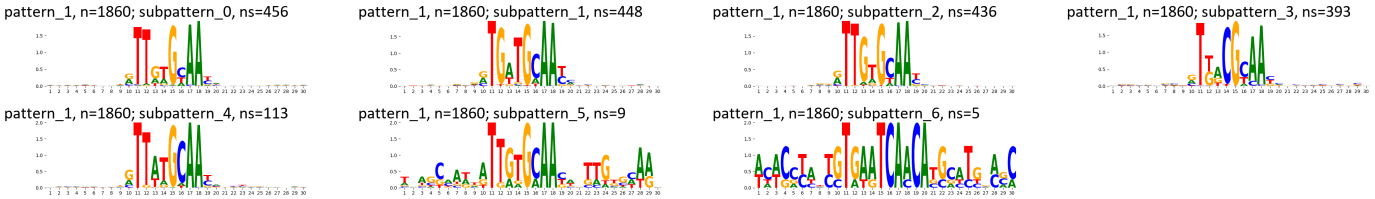

TF-MoDiSCO pattern_2 n=1590, CWM

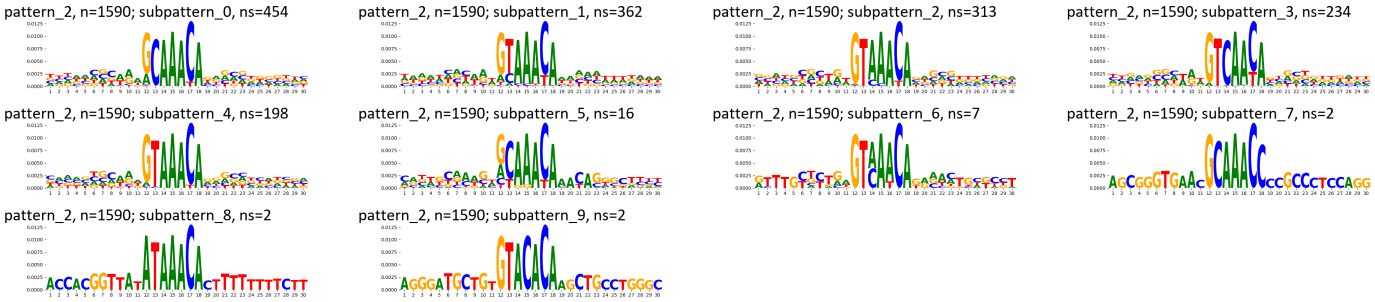

TF-MoDiSCO pattern_2 n=1590, PWM

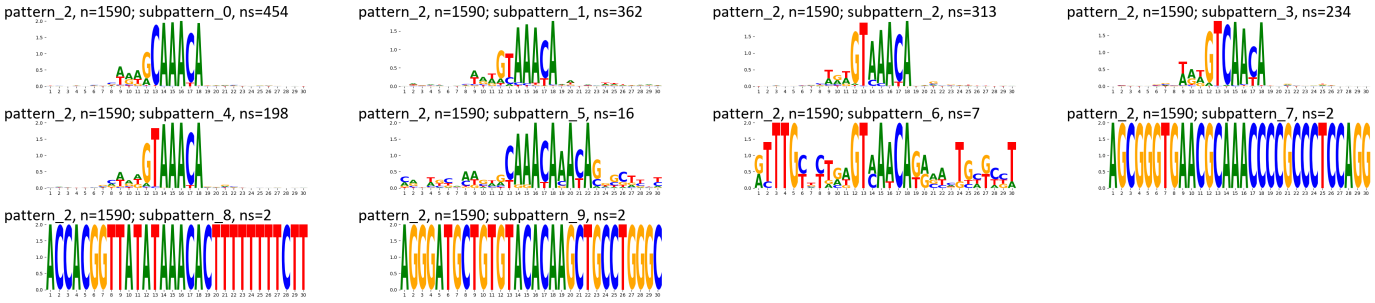

TF-MoDiSCO pattern_3 n=1459, CWM

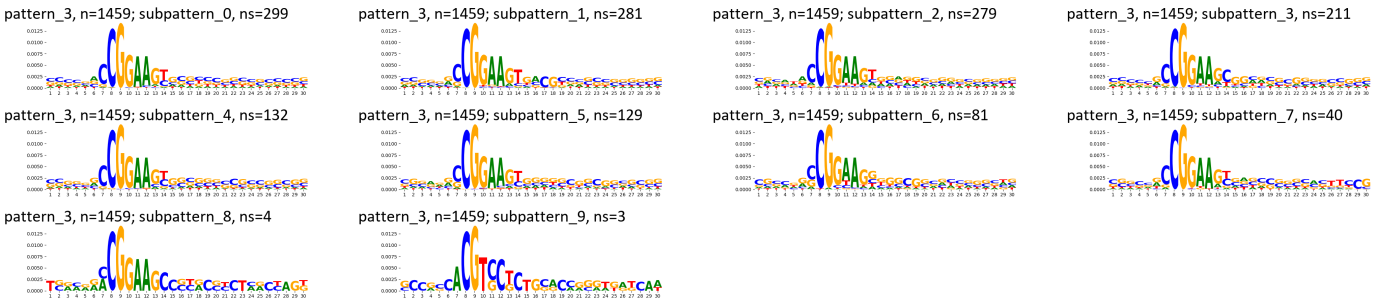

TF-MoDiSCO pattern_3 n=1459, PWM

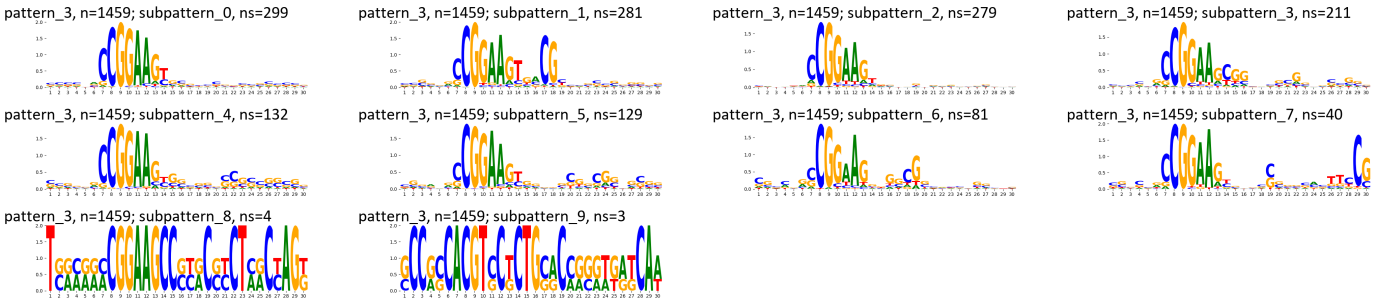

Supplementary Figure 416: TF-MoDisCO subpatterns for the ZBTB25 transcription factor in HepG2 (accession ENCSR485OYR).

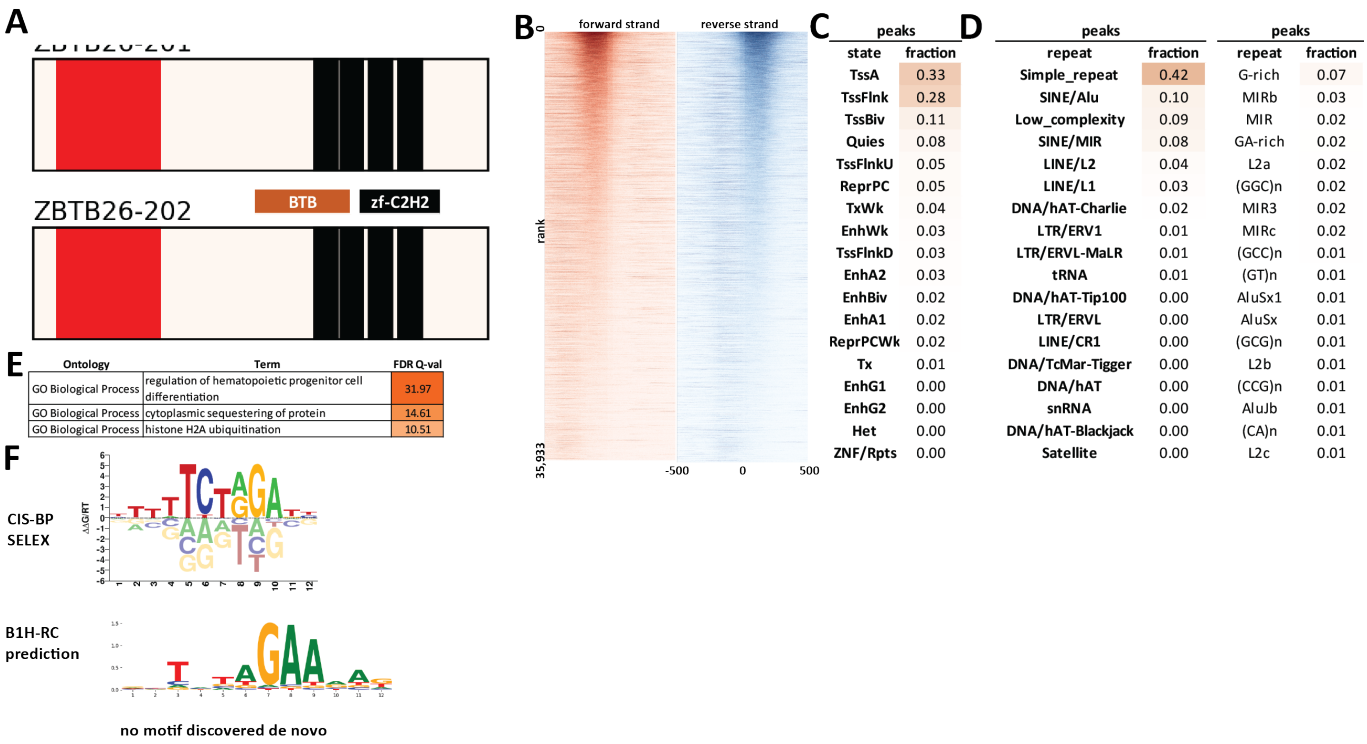

Supplementary Figure 417: Properties and genomic distribution of motifs identified for the ZBTB26 transcription factor in HEK293 (accession ENCSR229DYF).

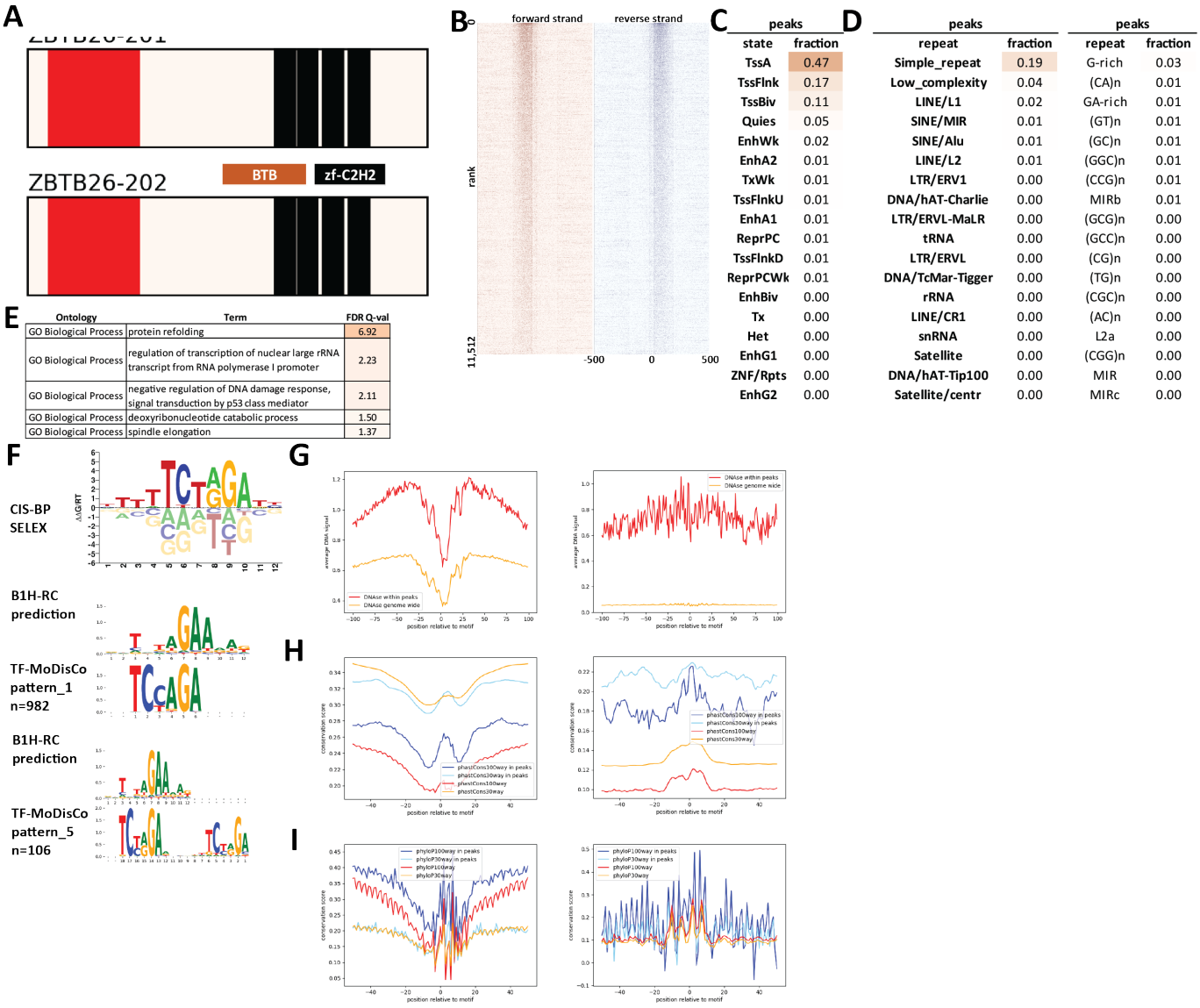

Supplementary Figure 418: Properties and genomic distribution of motifs identified for the ZBTB26 transcription factor in HEK293 (accession Hughes GR models).

TF-MoDisCO pattern_1 n=982, CWM

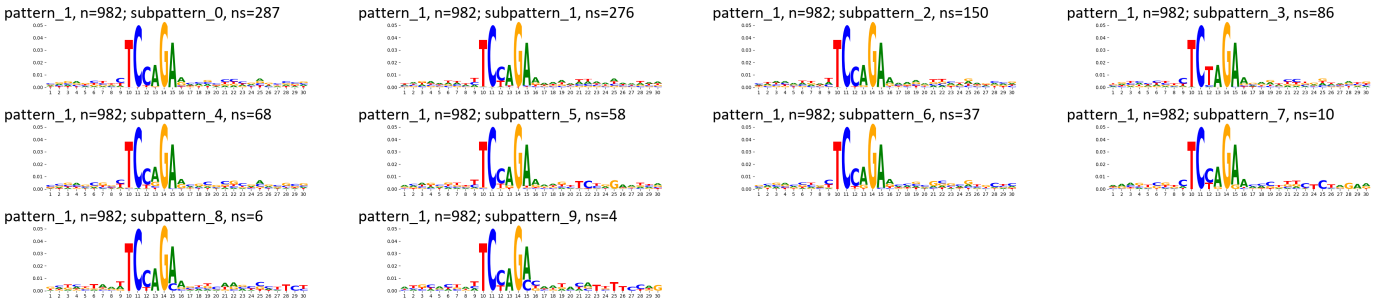

TF-MoDisCO pattern_1 n=982, PWM

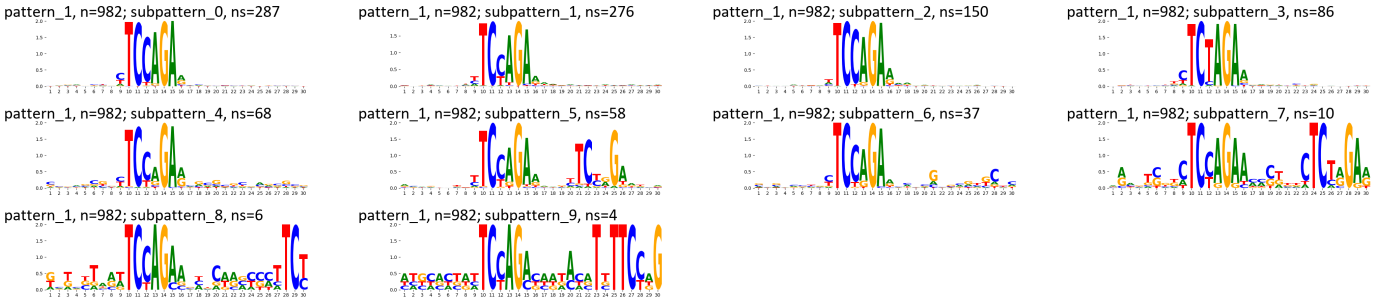

TF-MoDisCO pattern_5 n=106, CWM

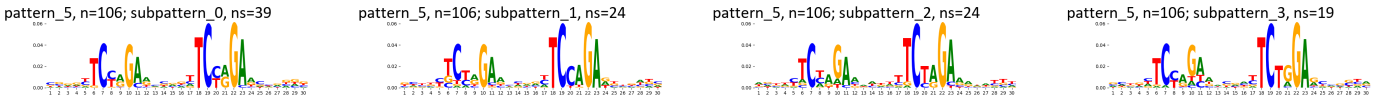

TF-MoDisCO pattern_5 n=106, PWM

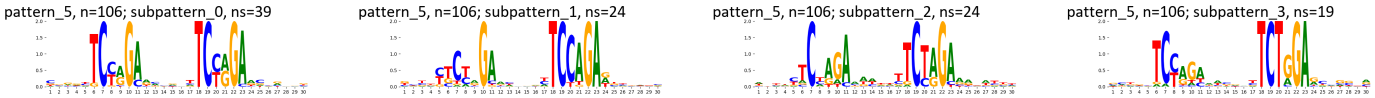

Supplementary Figure 419: TF-MoDisCO subpatterns for the ZBTB26 transcription factor in HEK293 (accession Hughes GR models).

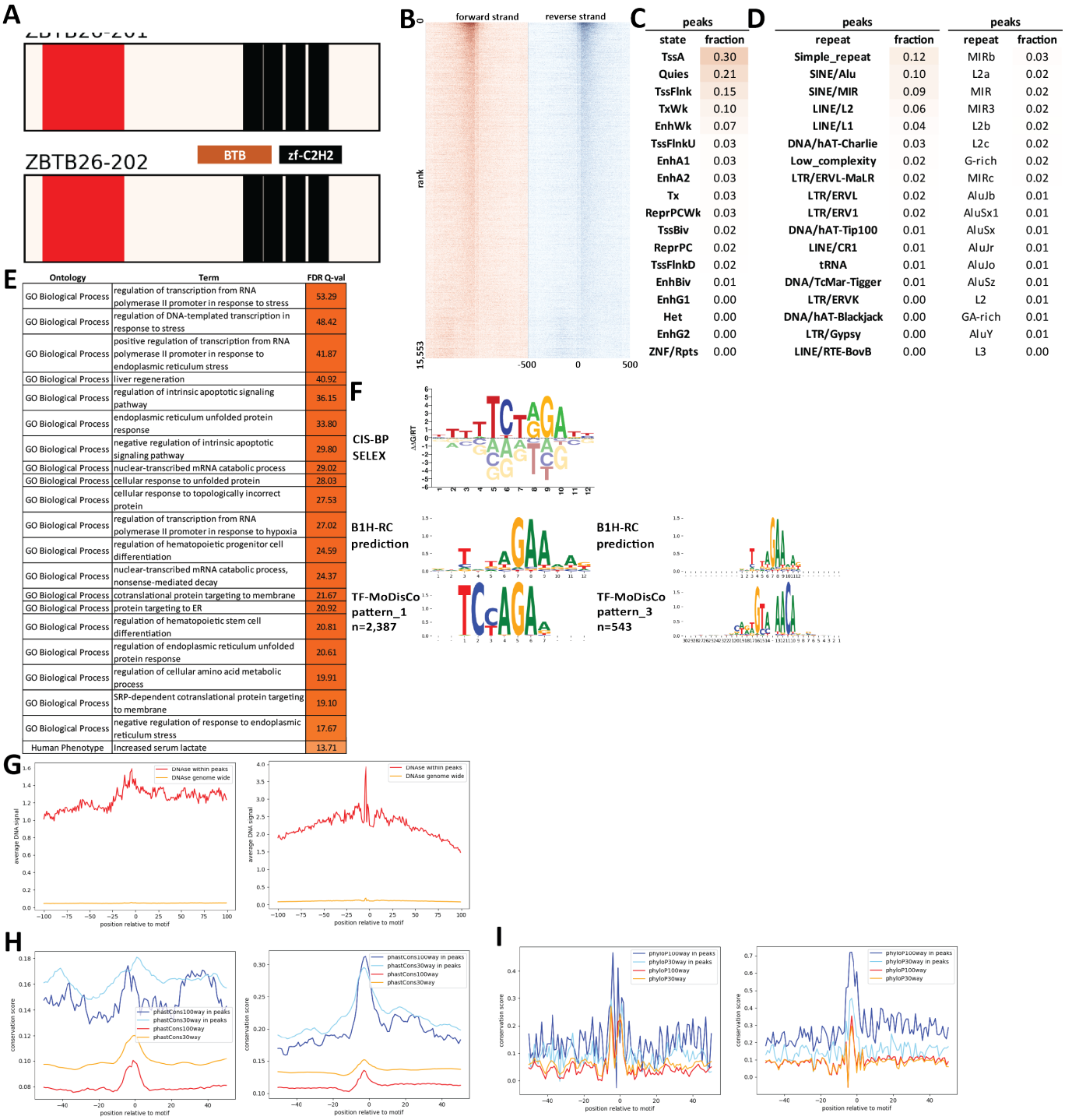

Supplementary Figure 420: Properties and genomic distribution of motifs identified for the ZBTB26 transcription factor in HepG2 (accession ENCSR184SVO).

TF-MoDisCO pattern_1 n=2387, CWM

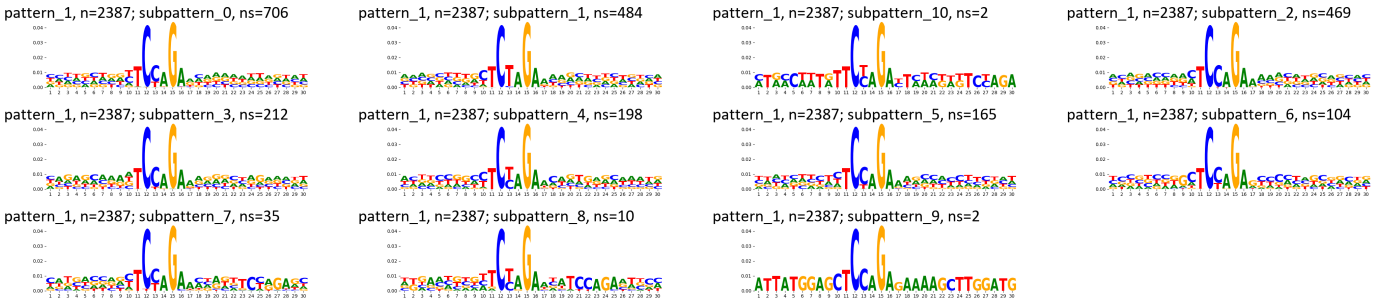

TF-MoDisCO pattern_1 n=2387, PWM

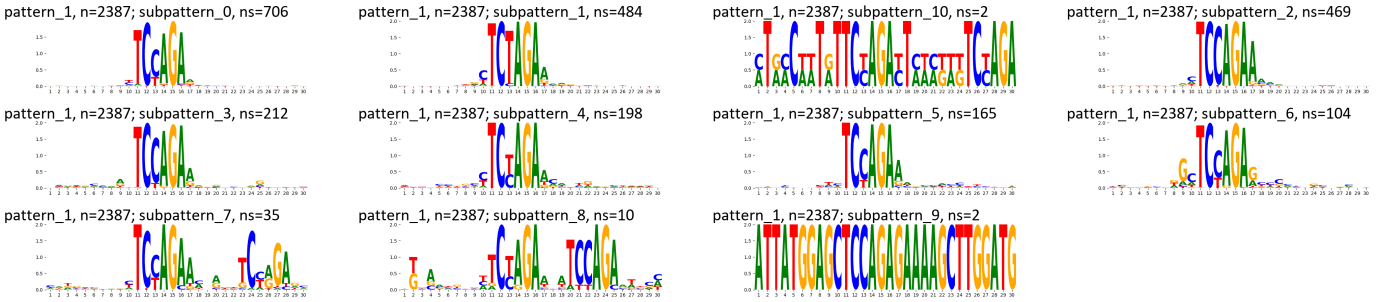

TF-MoDisCO pattern_3 n=543, CWM

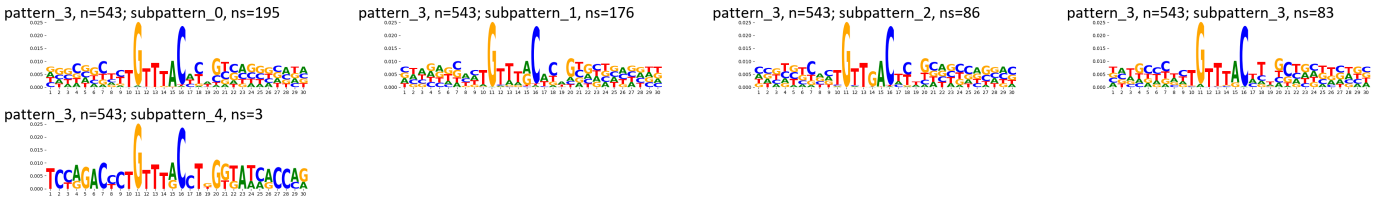

TF-MoDisCO pattern_3 n=543, PWM

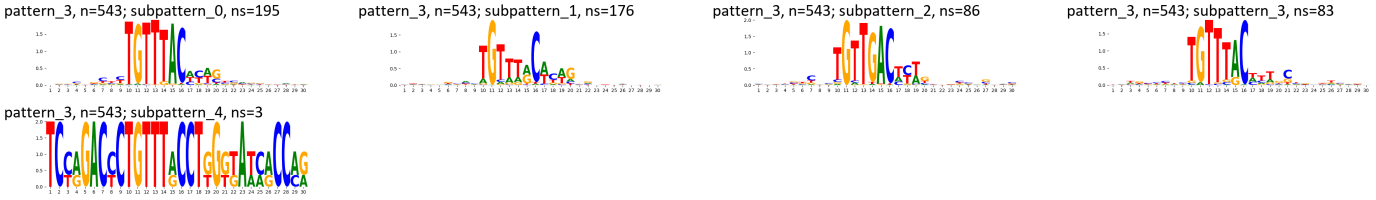

Supplementary Figure 421: TF-MoDisCO subpatterns for the ZBTB26 transcription factor in HepG2 (accession ENCSR184SVO).

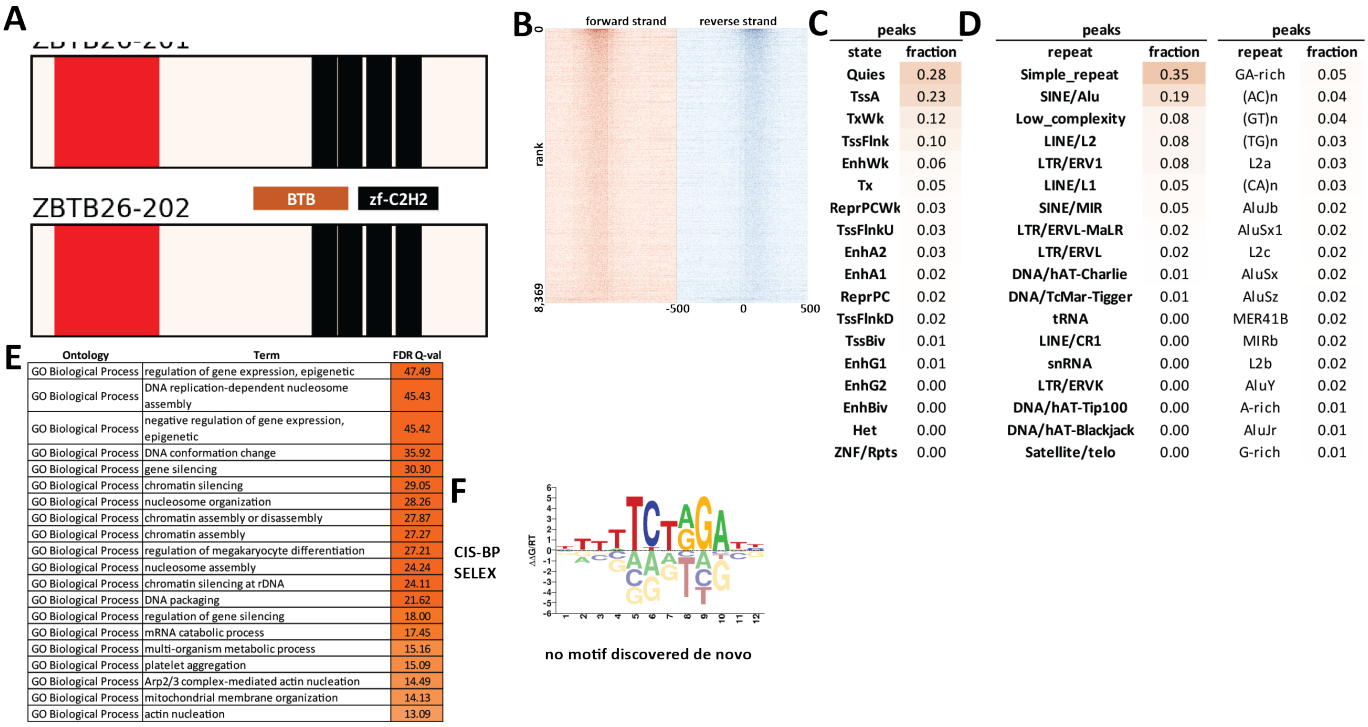

C

peaks	
state	fraction
Quies	0.28
TssA	0.23
TxWk	0.12
TssFlnk	0.10
EnhWk	0.06
Tx	0.05
ReprPCWk	0.03
TssFlnkU	0.03
EnhA2	0.03
EnhA1	0.02
ReprPC	0.02
TssFlnkD	0.02
TssBiv	0.01
EnhG1	0.01
EnhG2	0.00
EnhBiv	0.00
Het	0.00
ZNF/Rpts	0.00

D

peaks		peaks	
repeat	fraction	repeat	fraction
Simple_repeat	0.35	GA-rich	0.05
SINE/Alu	0.19	(AC)n	0.04
Low_complexity	0.08	(GT)n	0.04
LINE/L2	0.08	(TG)n	0.03
LTR/ERV1	0.08	L2a	0.03
LINE/L1	0.05	(CA)n	0.03
SINE/MIR	0.05	AluJb	0.02
LTR/ERVL-MaLR	0.02	AluSx1	0.02
LTR/ERVL	0.02	L2c	0.02
DNA/hAT-Charlie	0.01	AluSx	0.02
DNA/TcMar-Tigger	0.01	AluSz	0.02
tRNA	0.00	MER41B	0.02
LINE/CR1	0.00	MIRb	0.02
snRNA	0.00	L2b	0.02
LTR/ERVK	0.00	AluY	0.02
DNA/hAT-Tip100	0.00	A-rich	0.01
DNA/hAT-Blackjack	0.00	AluJr	0.01
Satellite/telo	0.00	G-rich	0.01

E

Ontology	Term	FDR Q-val
GO Biological Process	regulation of gene expression, epigenetic	47.49
GO Biological Process	DNA replication-dependent nucleosome assembly	45.43
GO Biological Process	negative regulation of gene expression, epigenetic	45.42
GO Biological Process	DNA conformation change	35.92
GO Biological Process	gene silencing	30.30
GO Biological Process	chromatin silencing	29.05
GO Biological Process	nucleosome organization	28.26
GO Biological Process	chromatin assembly or disassembly	27.87
GO Biological Process	chromatin assembly	27.27
GO Biological Process	regulation of megakaryocyte differentiation	27.21
GO Biological Process	nucleosome assembly	24.24
GO Biological Process	chromatin silencing at rDNA	24.11
GO Biological Process	DNA packaging	21.62
GO Biological Process	regulation of gene silencing	18.00
GO Biological Process	mRNA catabolic process	17.45
GO Biological Process	multi-organism metabolic process	15.16
GO Biological Process	platelet aggregation	15.09
GO Biological Process	Arp2/3 complex-mediated actin nucleation	14.49
GO Biological Process	mitochondrial membrane organization	14.13
GO Biological Process	actin nucleation	13.09

Supplementary Figure 422: Properties and genomic distribution of motifs identified for the ZBTB26 transcription factor in K562 (accession ENCSR115HLM).

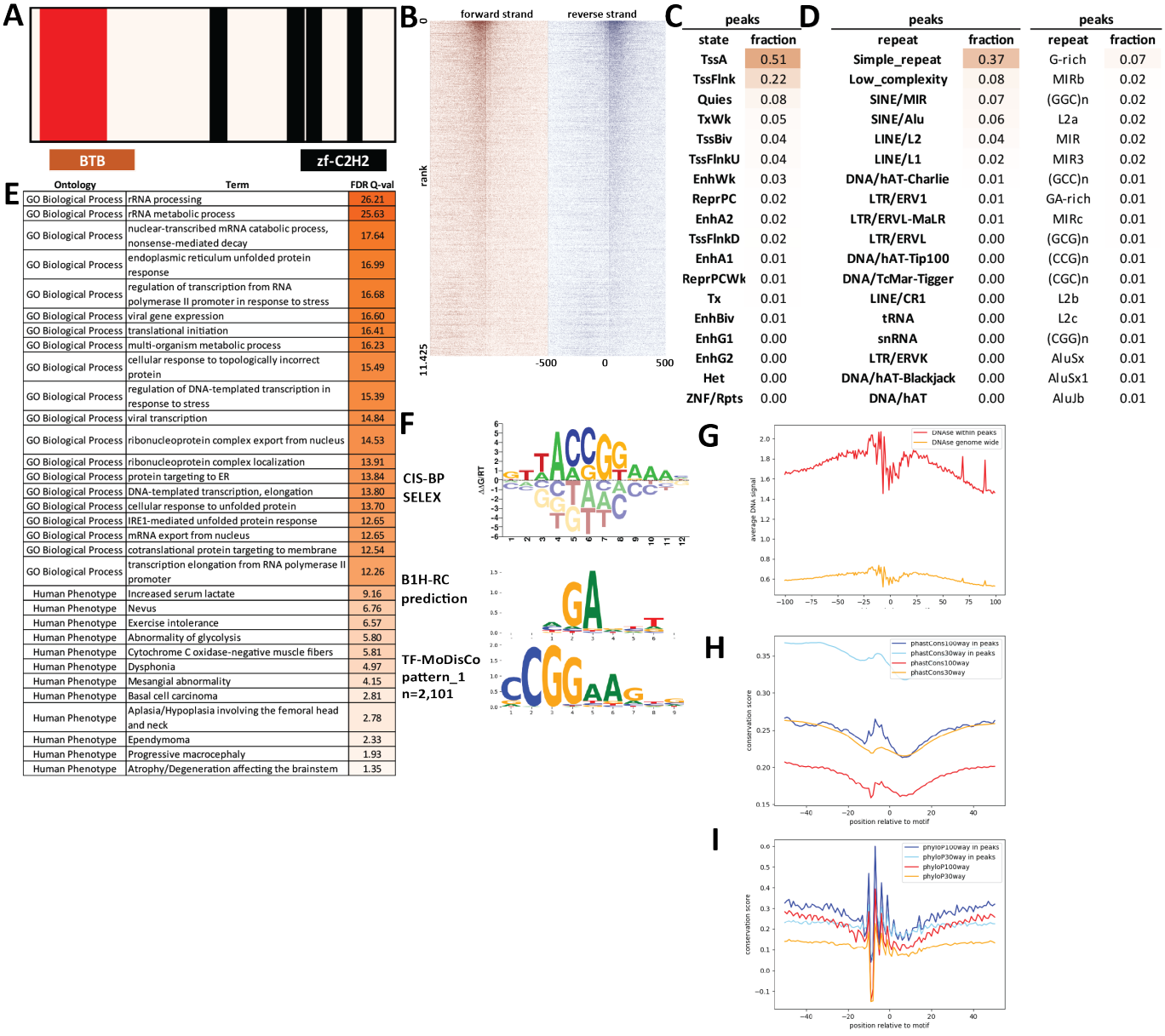

Supplementary Figure 423: Properties and genomic distribution of motifs identified for the ZBTB2 transcription factor in HepG2 (accession ENCSR175MIA).

TF-MoDisCO pattern_1 n=2101, CWM

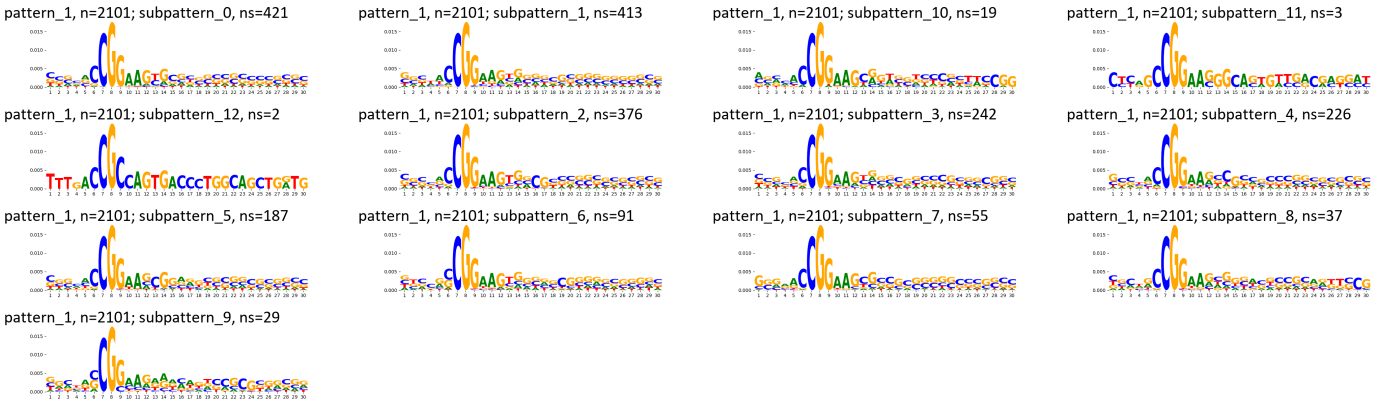

TF-MoDisCO pattern_1 n=2101, PWM

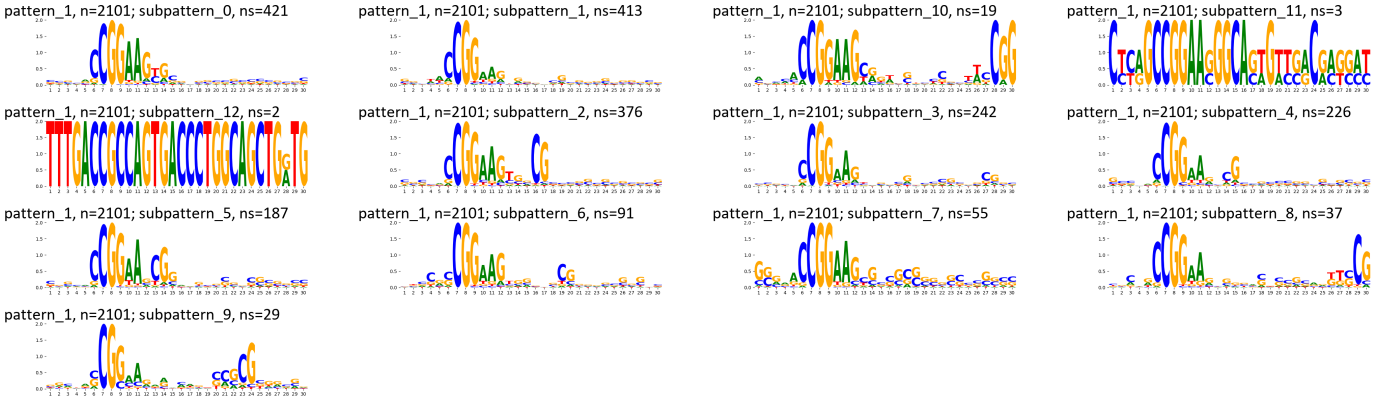

Supplementary Figure 424: TF-MoDisCO subpatterns for the ZBTB2 transcription factor in HepG2 (accession ENCSR175MIA).

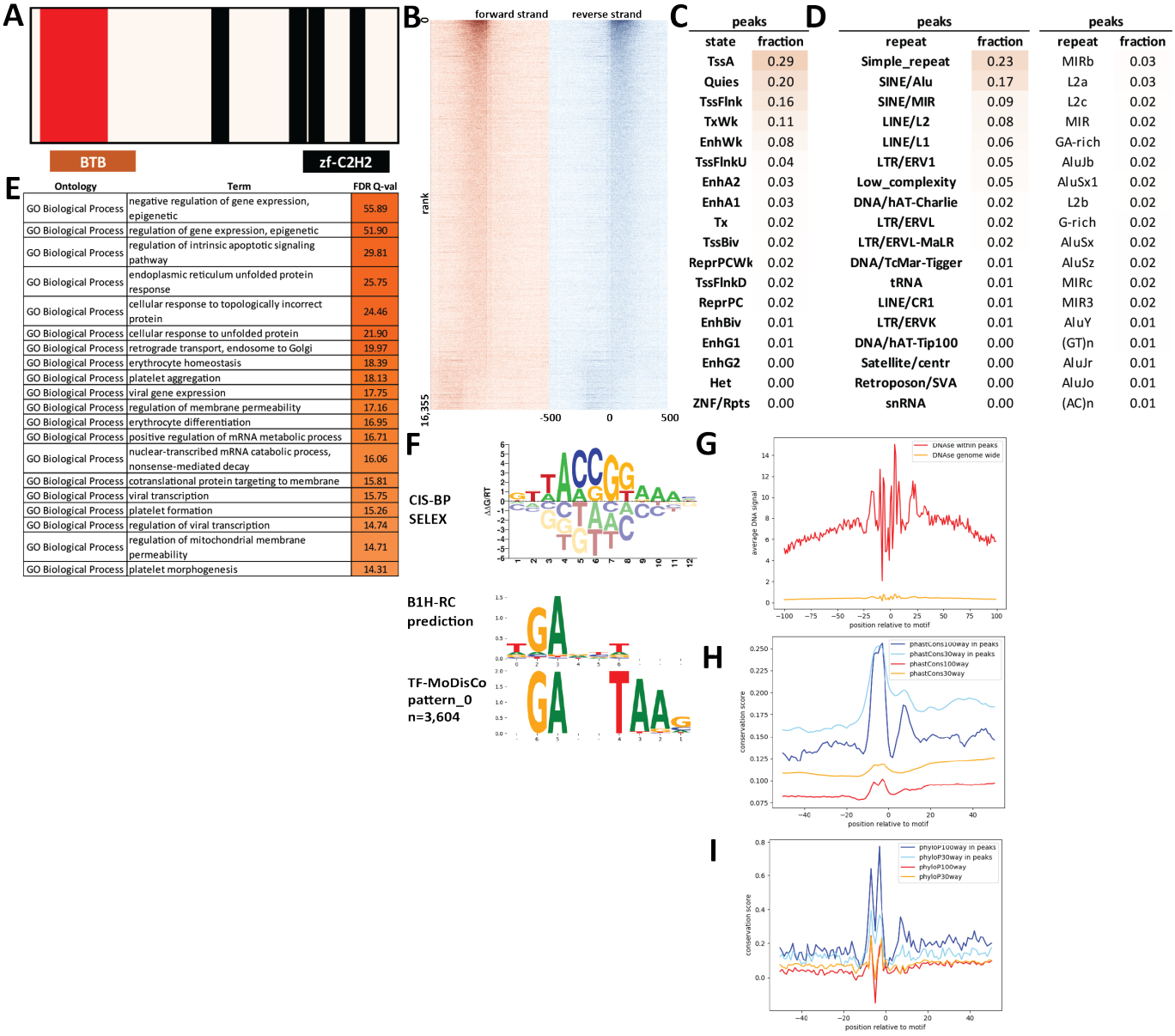

Supplementary Figure 425: Properties and genomic distribution of motifs identified for the ZBTB2 transcription factor in K562 (accession ENCSR230PTV).

TF-MoDisCO pattern_0 n=3604, CWM

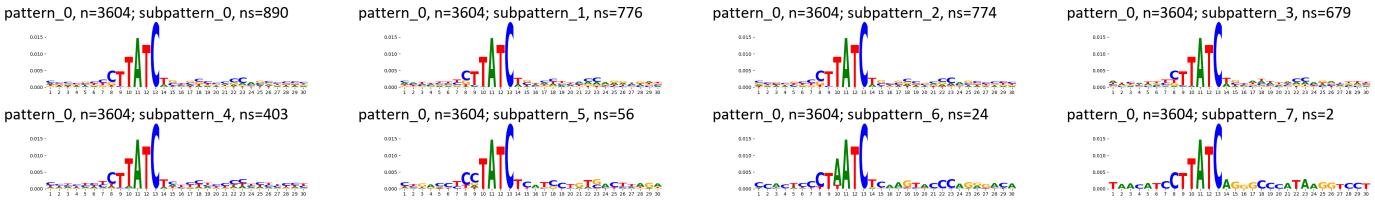

TF-MoDisCO pattern_0 n=3604, PWM

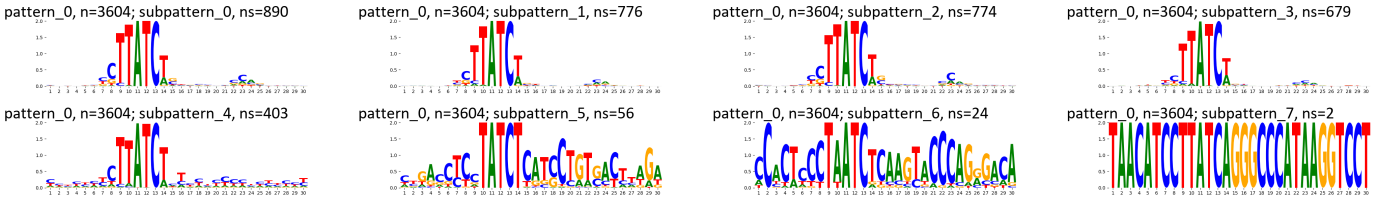

Supplementary Figure 426: TF-MoDisCO subpatterns for the ZBTB2 transcription factor in K562 (accession ENCSR230PTV).

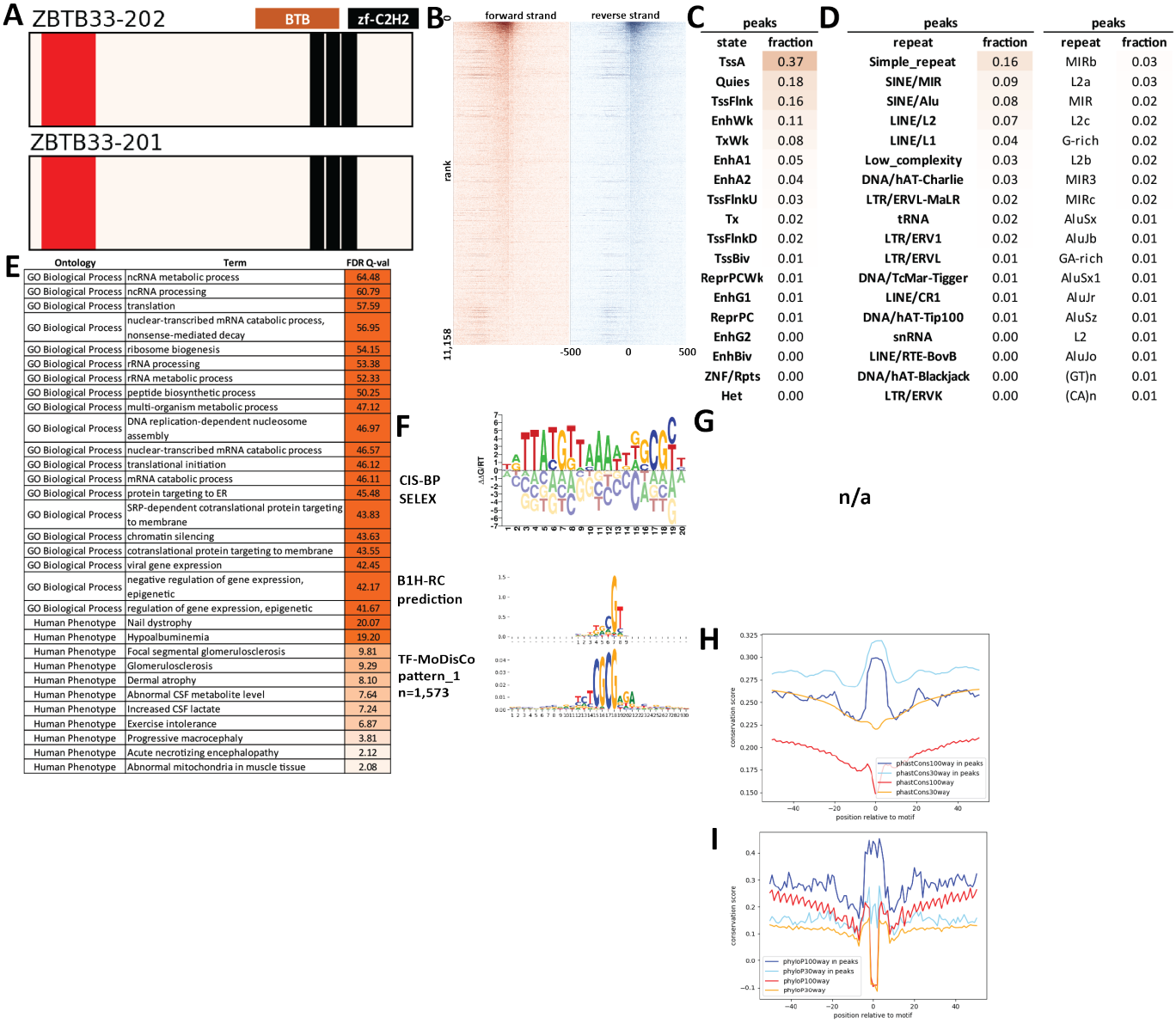

Supplementary Figure 427: Properties and genomic distribution of motifs identified for the ZBTB33 transcription factor in A549 (accession ENCSR000BPZ).

TF-MoDisCO pattern_1 n=1573, CWM

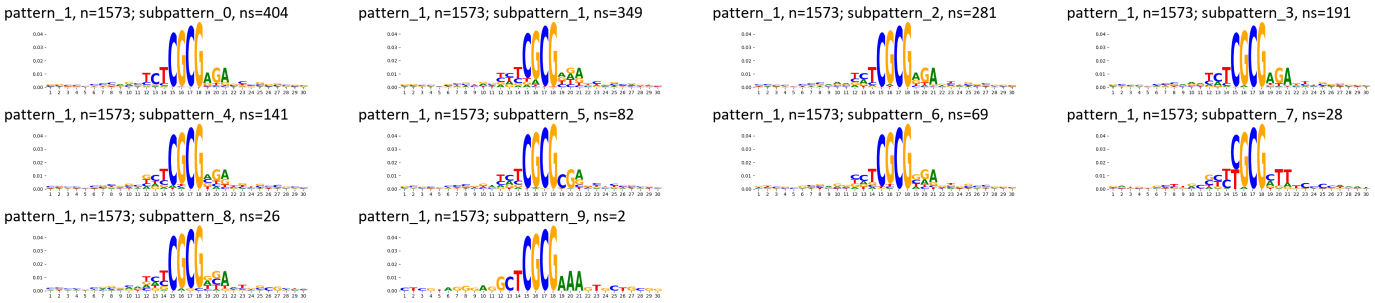

TF-MoDisCO pattern_1 n=1573, PWM

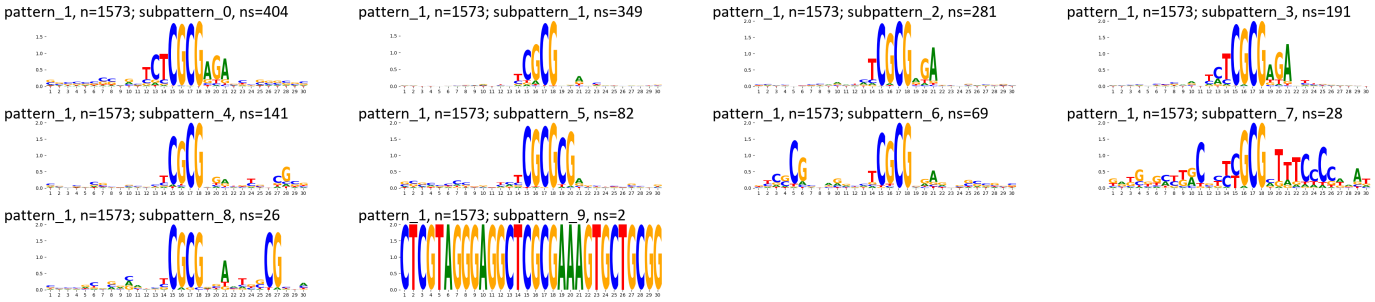

Supplementary Figure 428: TF-MoDisCO subpatterns for the ZBTB33 transcription factor in A549 (accession ENCSR000BPZ).

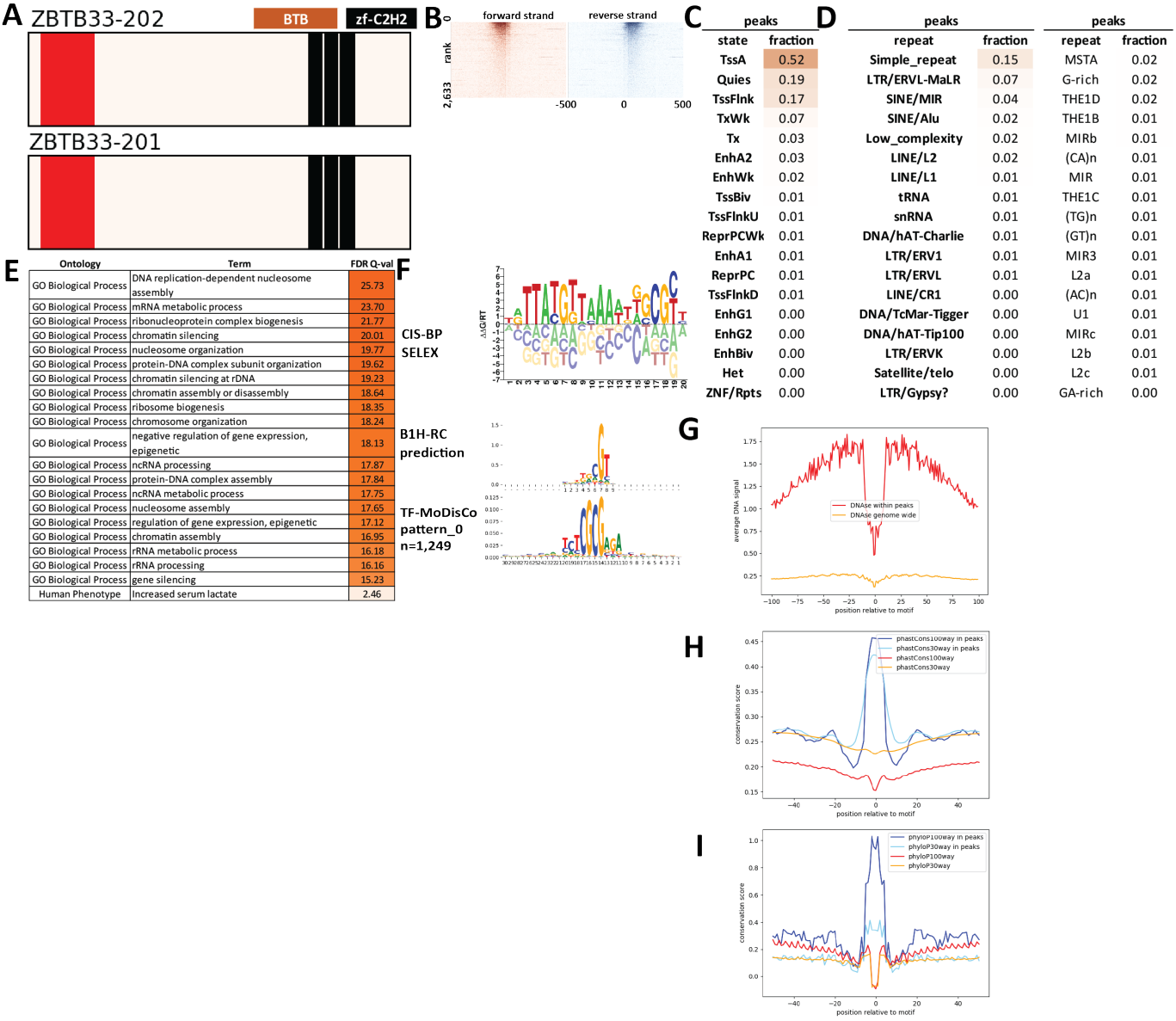

Supplementary Figure 429: Properties and genomic distribution of motifs identified for the ZBTB33 transcription factor in GM12878 (accession ENCSR000BHC).

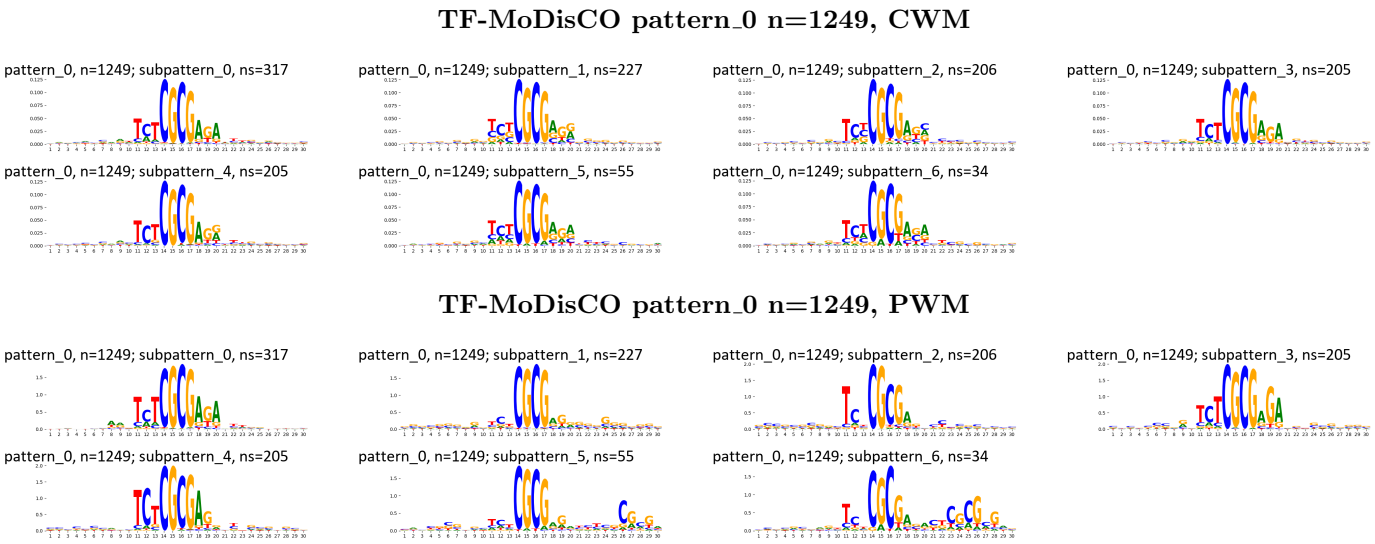

Supplementary Figure 430: TF-MoDisCO subpatterns for the ZBTB33 transcription factor in GM12878 (accession ENCSR000BHC).

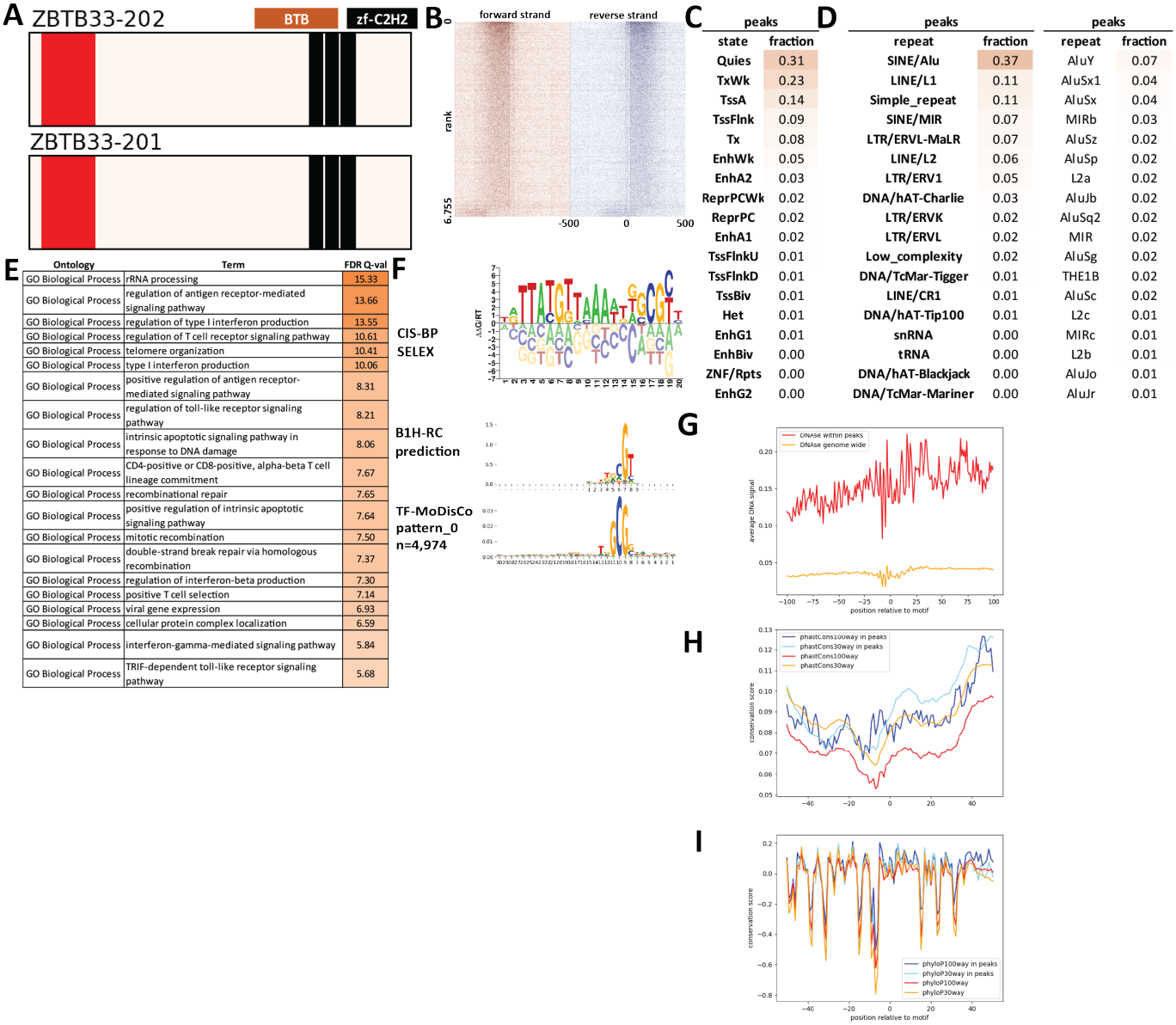

Supplementary Figure 431: Properties and genomic distribution of motifs identified for the ZBTB33 transcription factor in GM12878 (accession ENCSR542FLV).

TF-MoDisCO pattern_0 n=4974, CWM

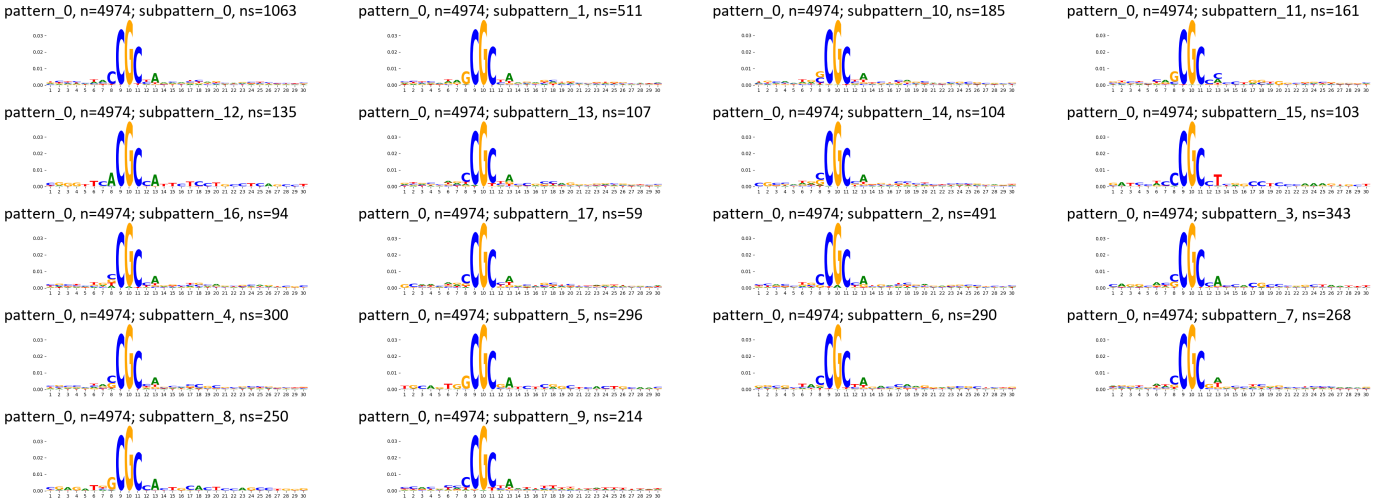

TF-MoDisCO pattern_0 n=4974, PWM

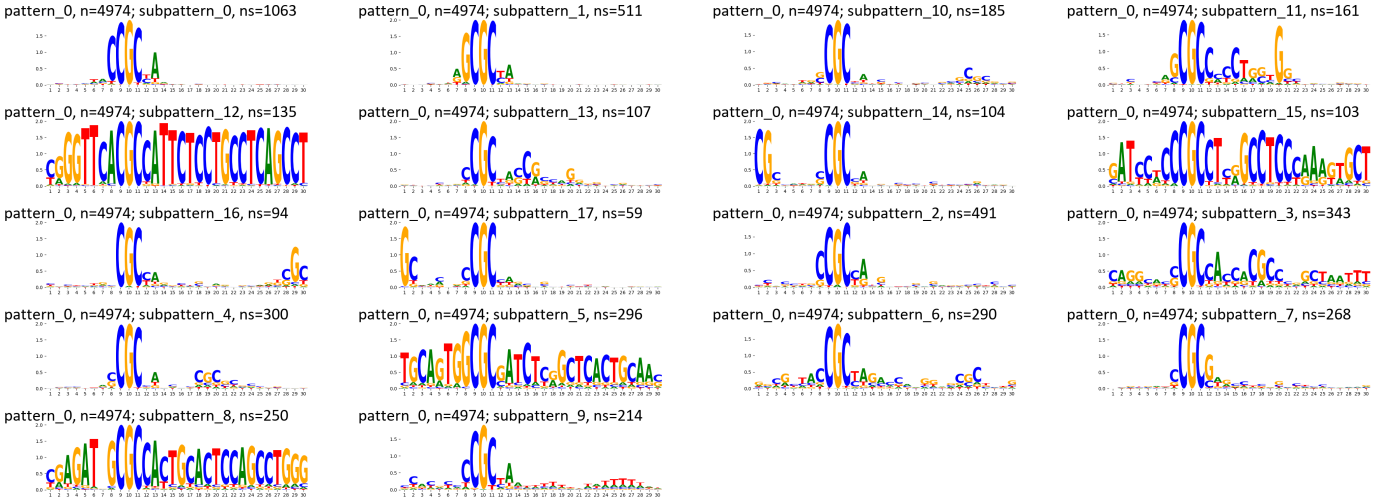

Supplementary Figure 432: TF-MoDisCO subpatterns for the ZBTB33 transcription factor in GM12878 (accession ENCSR542FLV).

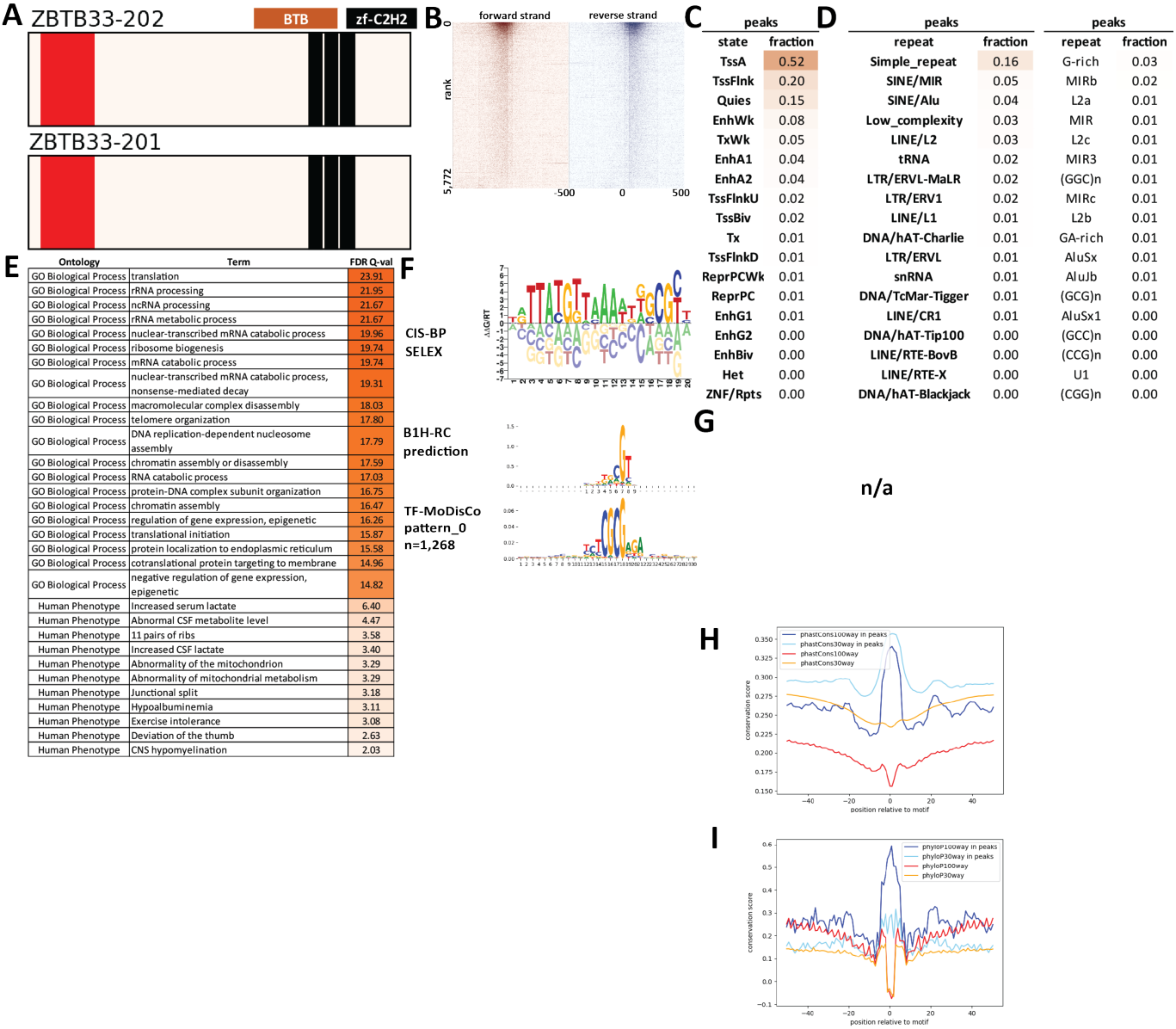

Supplementary Figure 433: Properties and genomic distribution of motifs identified for the ZBTB33 transcription factor in HCT116 (accession ENCSR000BNY).

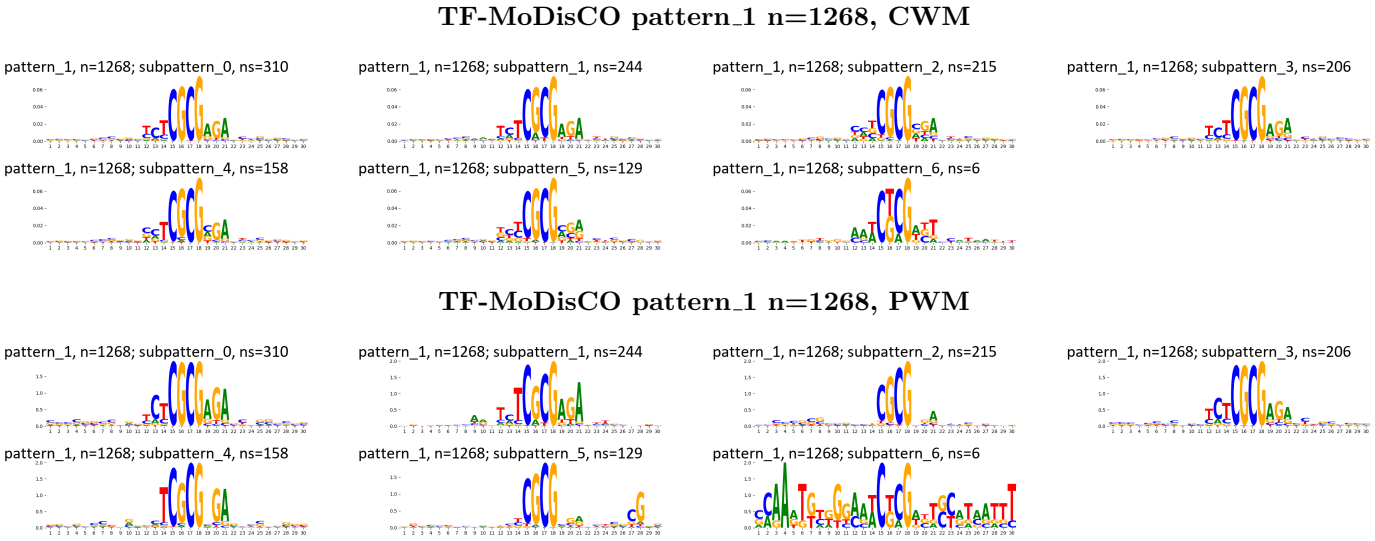

Supplementary Figure 434: TF-MoDisCO subpatterns for the ZBTB33 transcription factor in HCT116 (accession ENCSR000BNY).

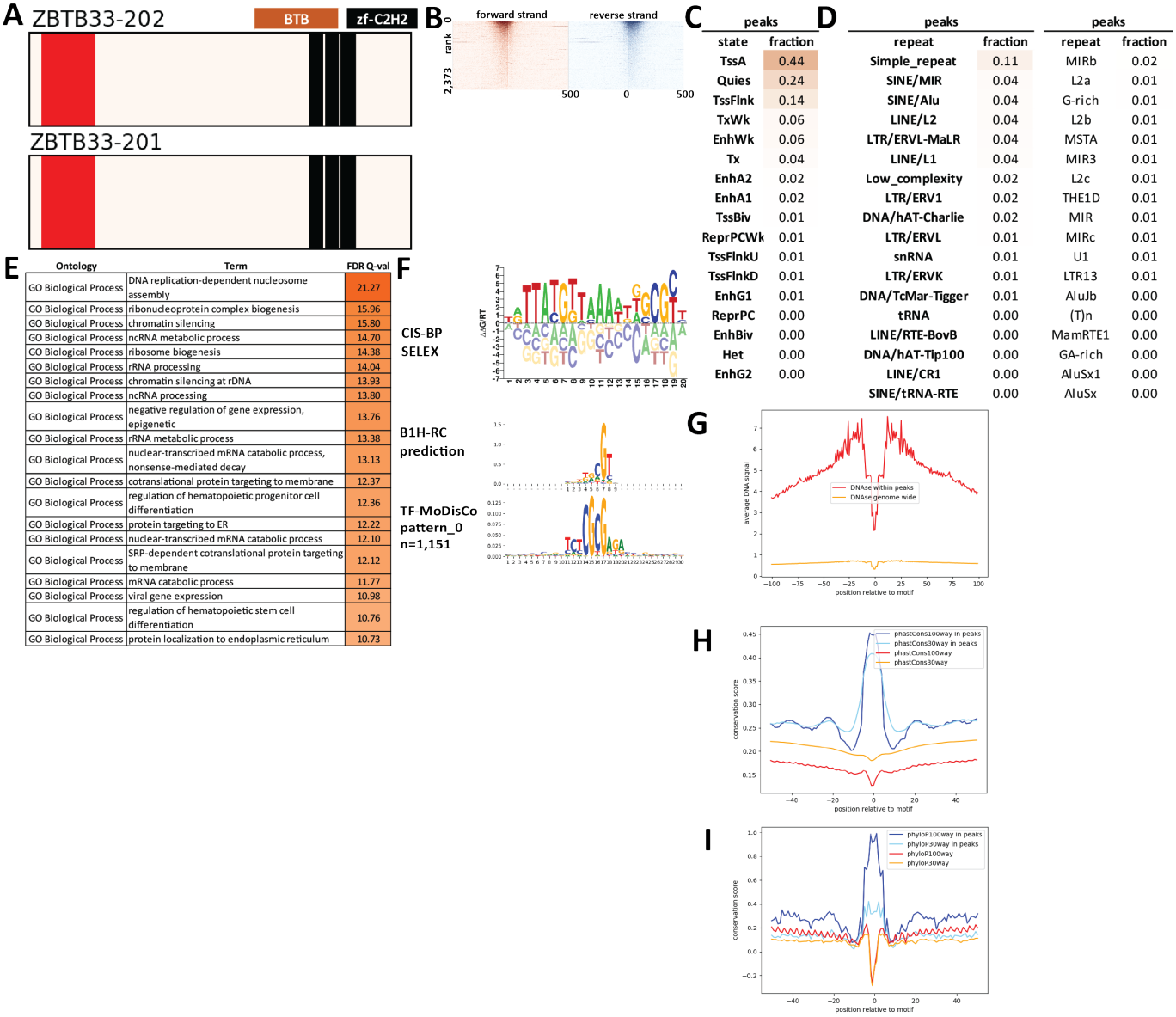

Supplementary Figure 435: Properties and genomic distribution of motifs identified for the ZBTB33 transcription factor in HepG2 (accession ENCSR000BHR).

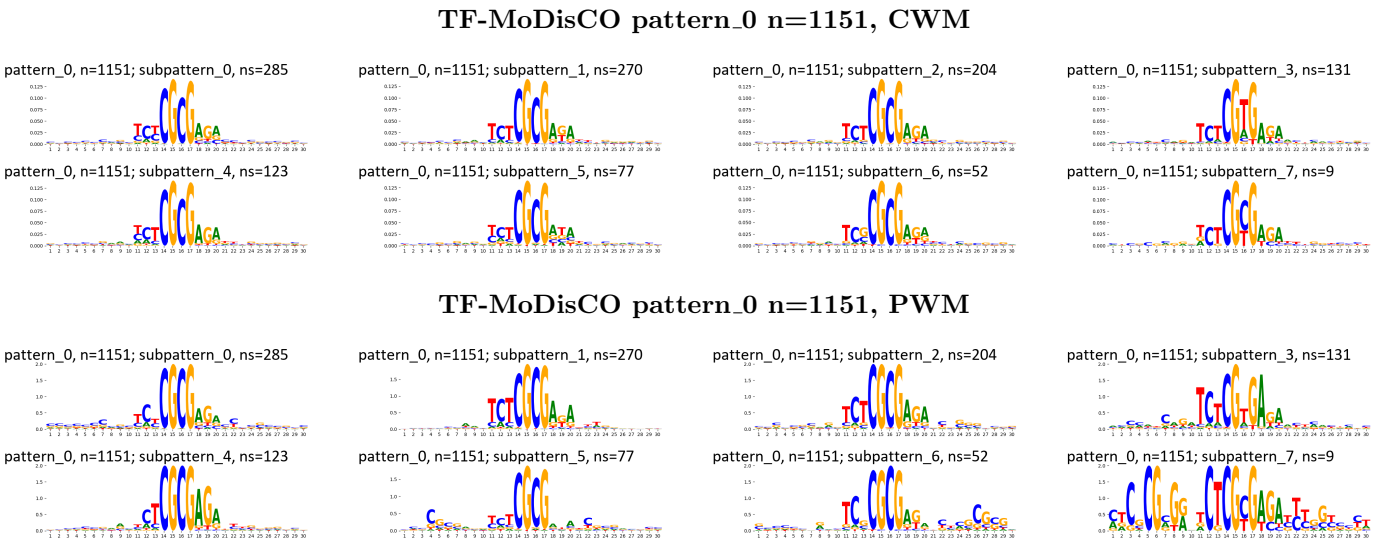

Supplementary Figure 436: TF-MoDisCO subpatterns for the ZBTB33 transcription factor in HepG2 (accession ENCSR000BHR).

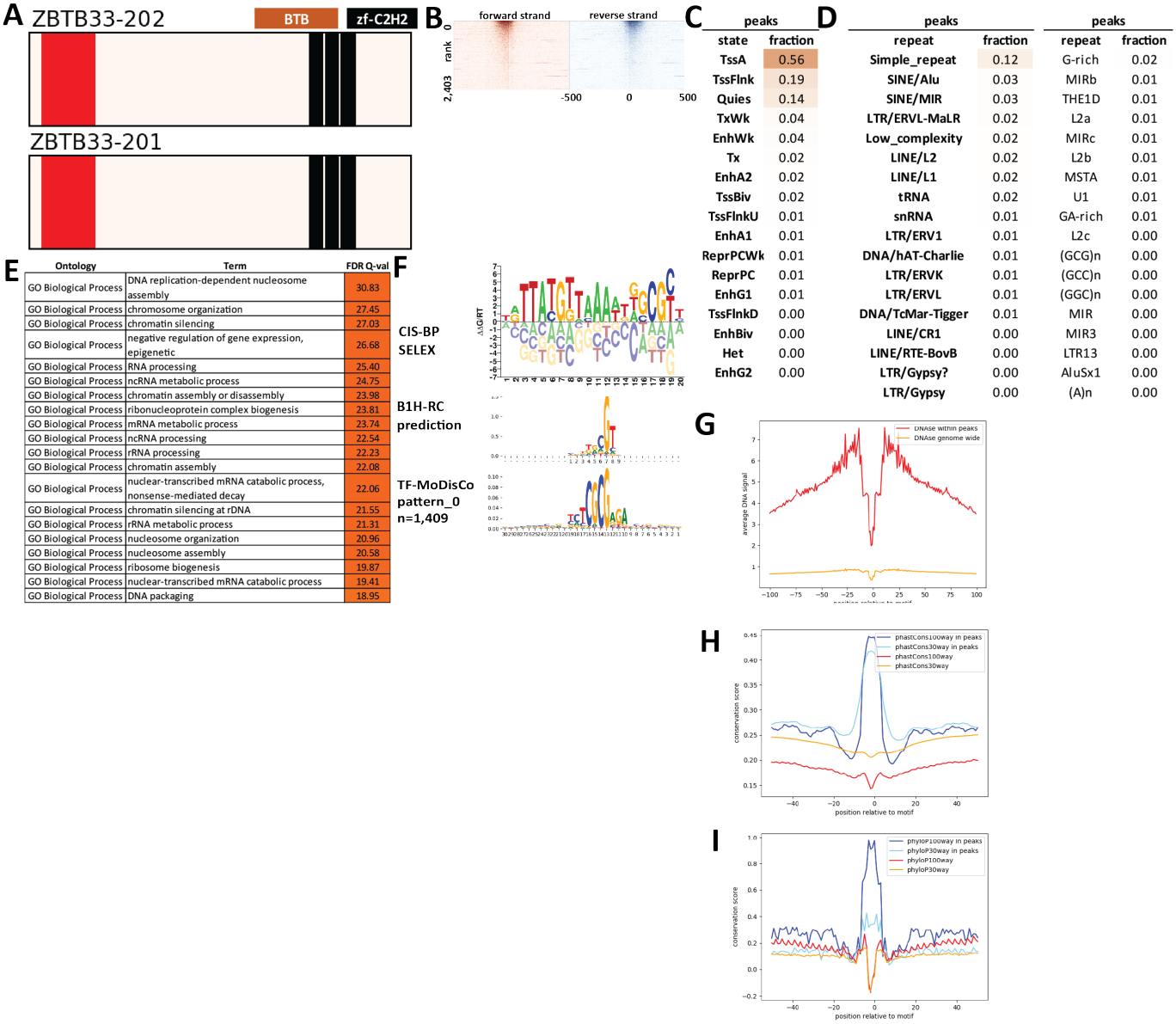

Supplementary Figure 437: Properties and genomic distribution of motifs identified for the ZBTB33 transcription factor in HepG2 (accession ENCSR000BNA).

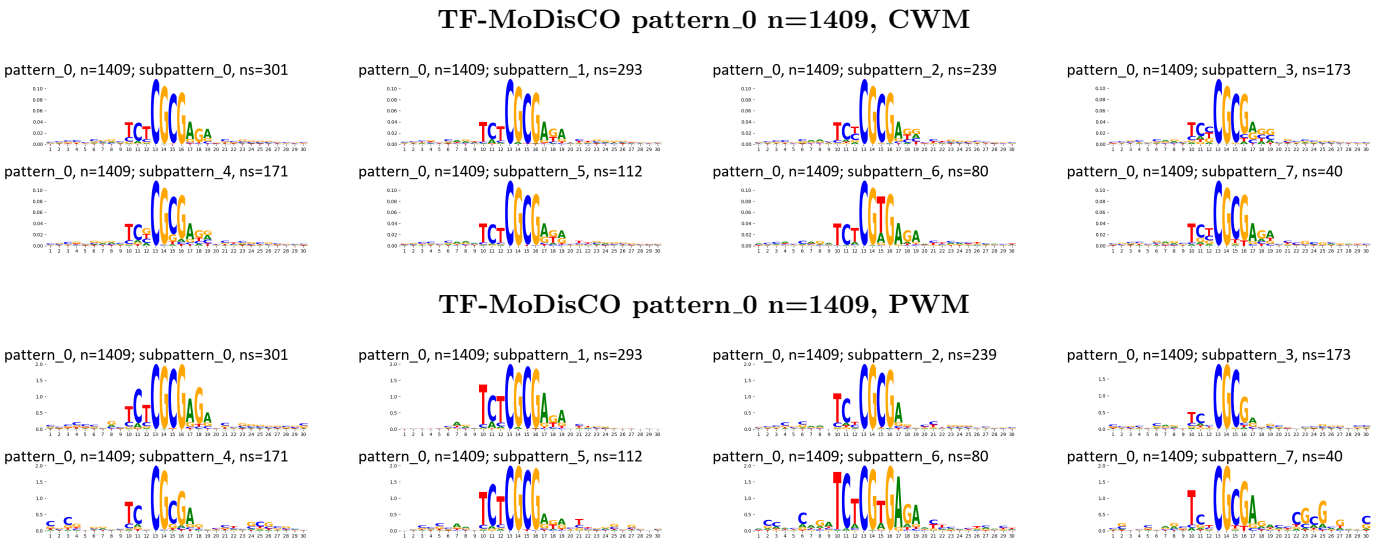

Supplementary Figure 438: TF-MoDisCO subpatterns for the ZBTB33 transcription factor in HepG2 (accession ENCSR000BNA).

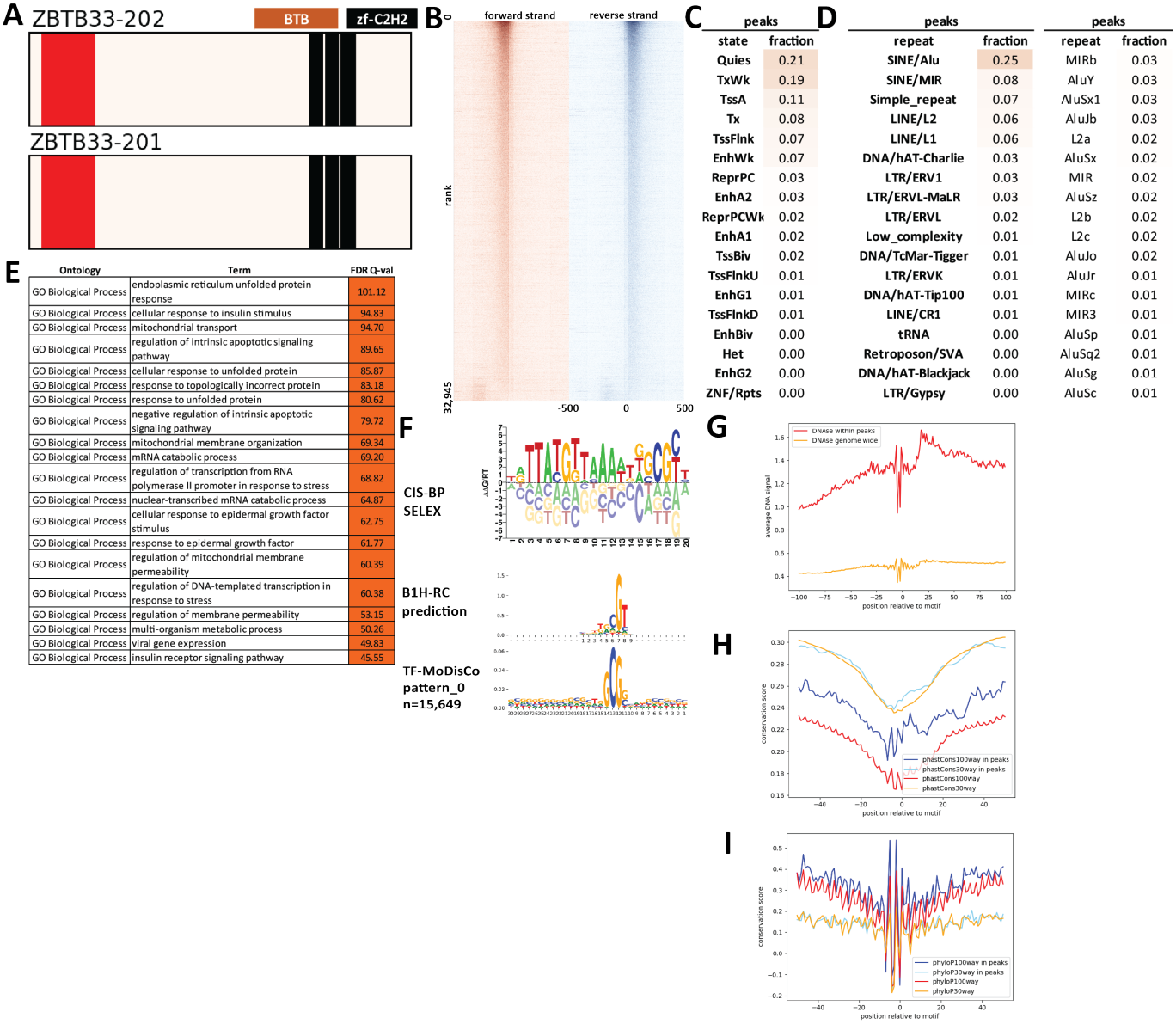

Supplementary Figure 439: Properties and genomic distribution of motifs identified for the ZBTB33 transcription factor in HepG2 (accession ENCSR421DAO).

TF-MoDisCO pattern_0 n=15649, CWM

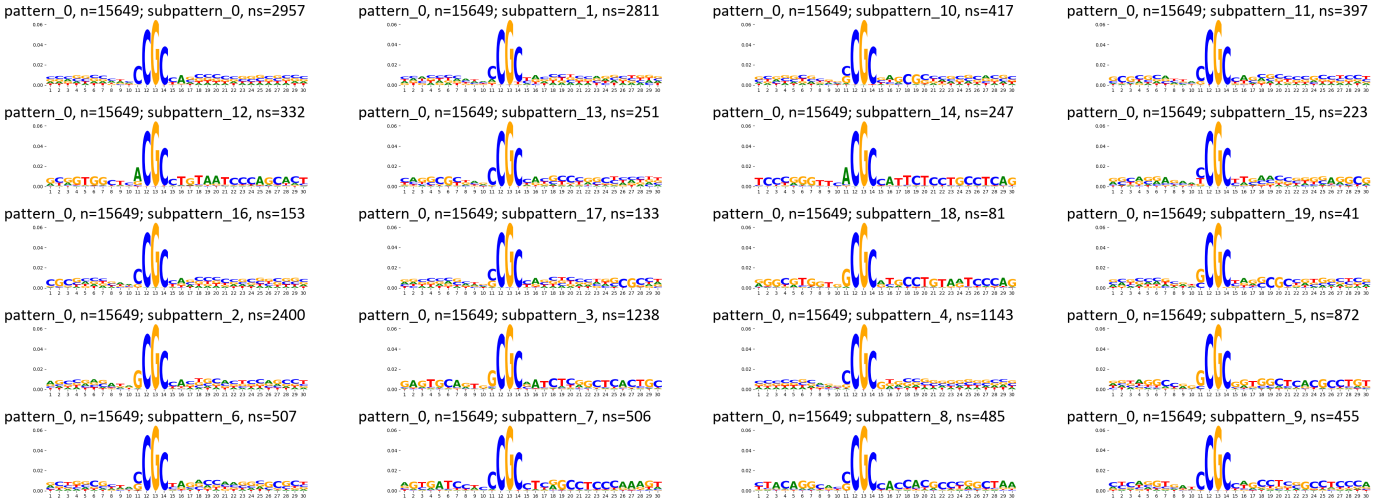

TF-MoDisCO pattern_0 n=15649, PWM

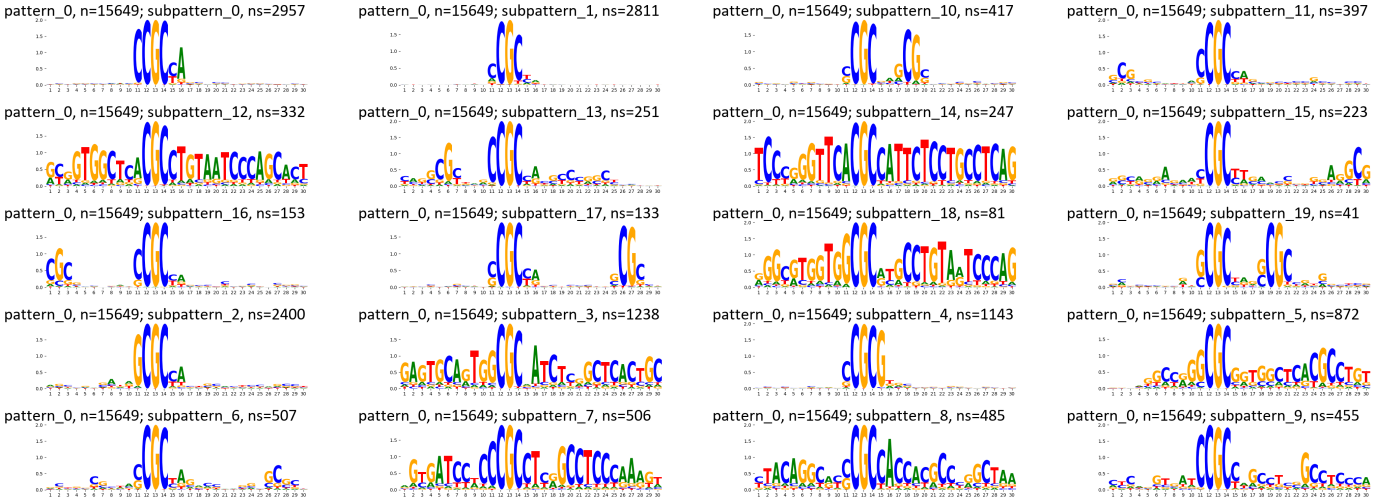

Supplementary Figure 440: TF-MoDisCO subpatterns for the ZBTB33 transcription factor in HepG2 (accession ENCSR421DAO).

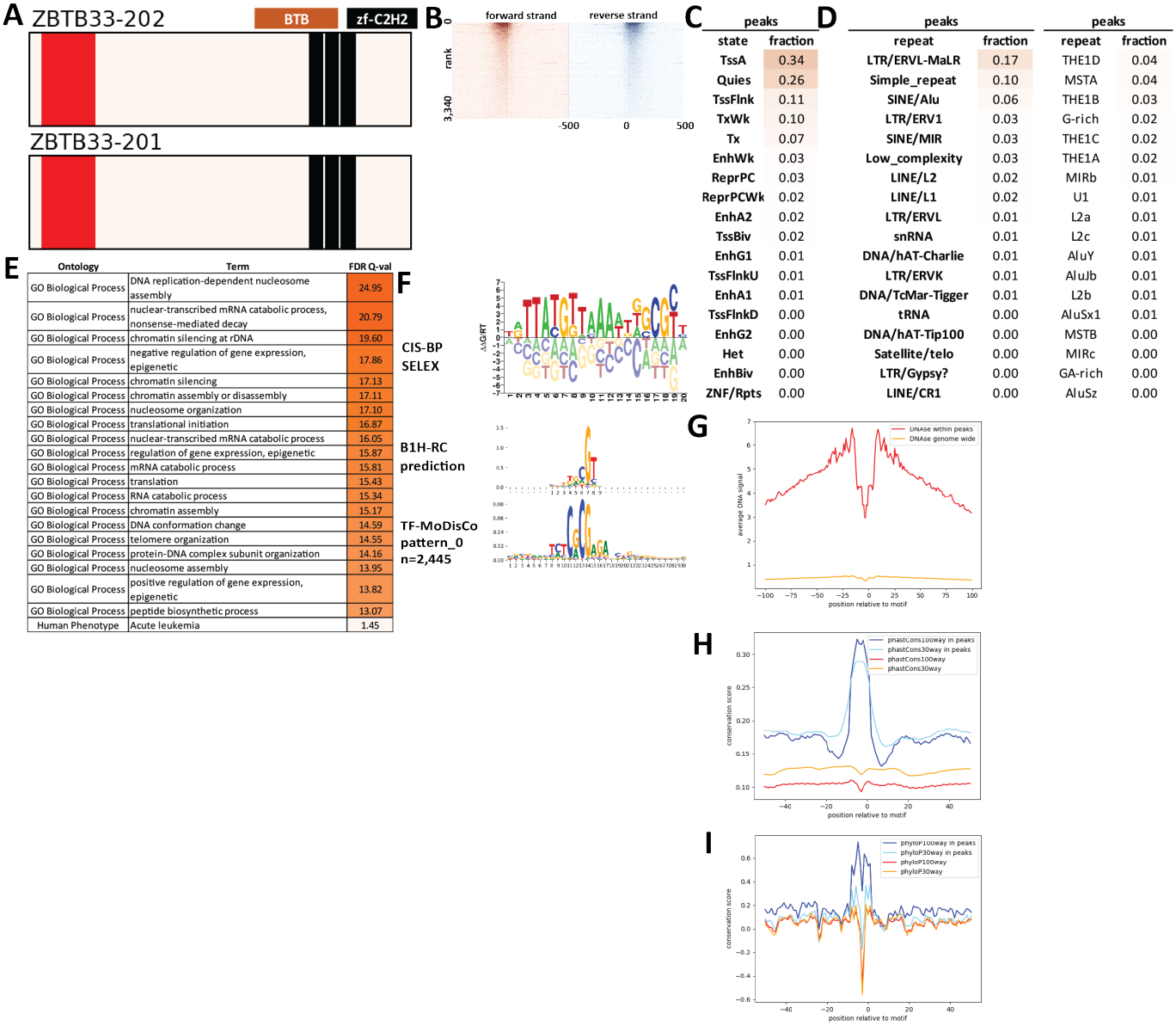

Supplementary Figure 441: Properties and genomic distribution of motifs identified for the ZBTB33 transcription factor in K562 (accession ENCSR000BKF).

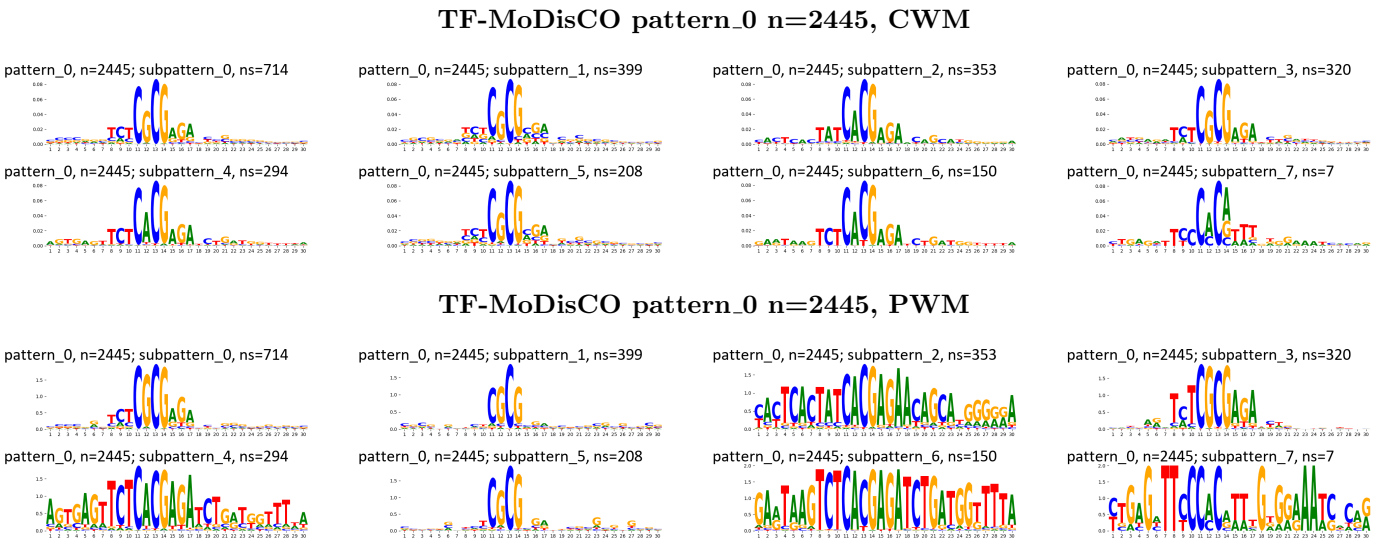

Supplementary Figure 442: TF-MoDisCO subpatterns for the ZBTB33 transcription factor in K562 (accession ENCSR000BKF).

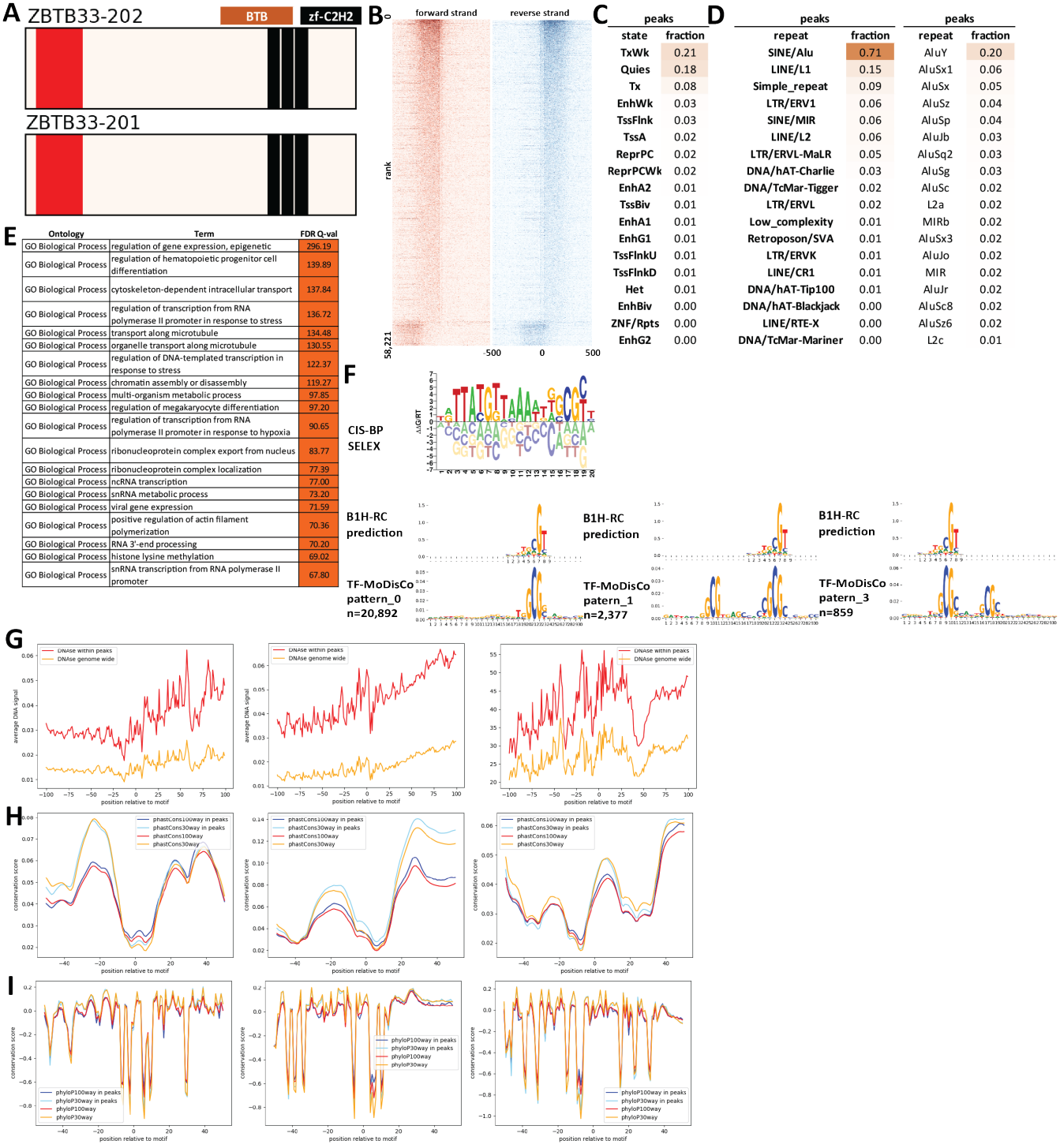

Supplementary Figure 443: Properties and genomic distribution of motifs identified for the ZBTB33 transcription factor in K562 (accession ENCSR876GXA).

TF-MoDisCO pattern_0 n=20892, CWM

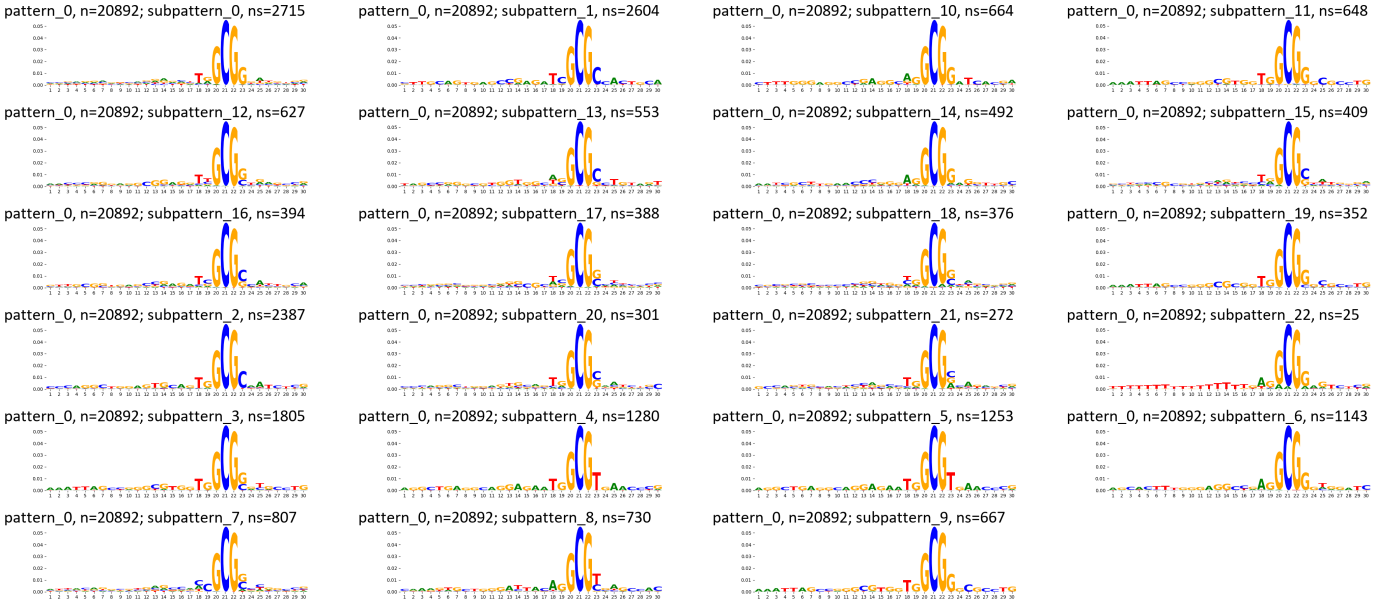

TF-MoDisCO pattern_0 n=20892, PWM

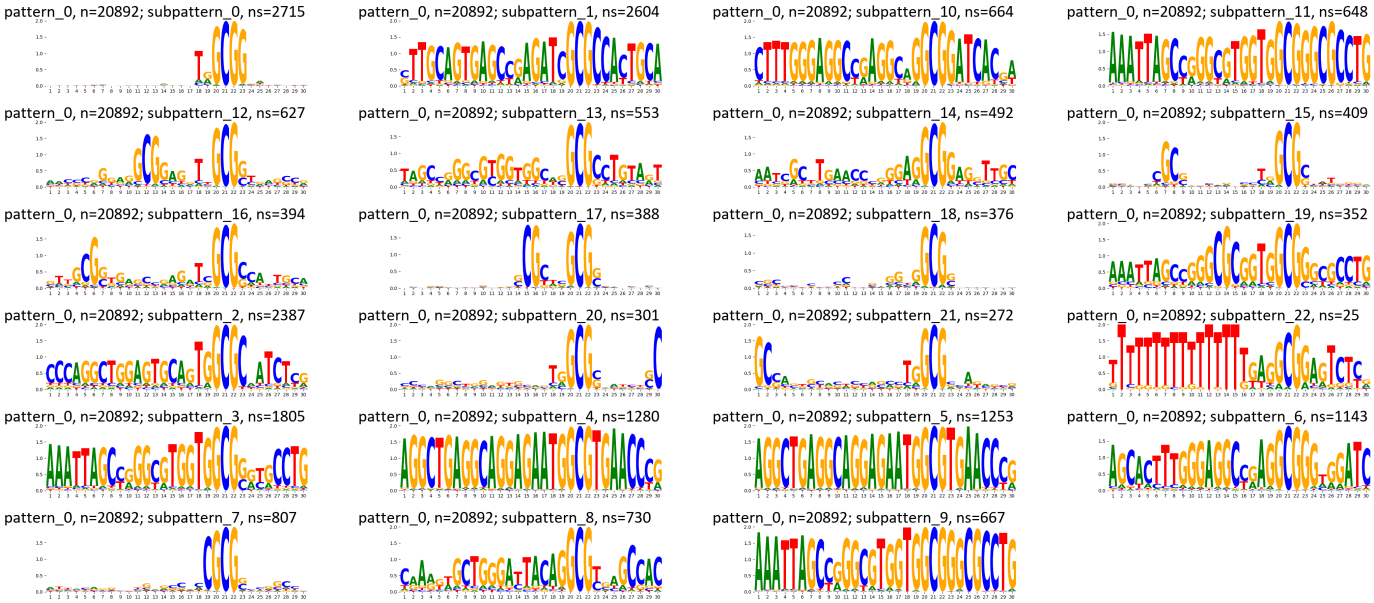

TF-MoDisCO pattern_1 n=2377, CWM

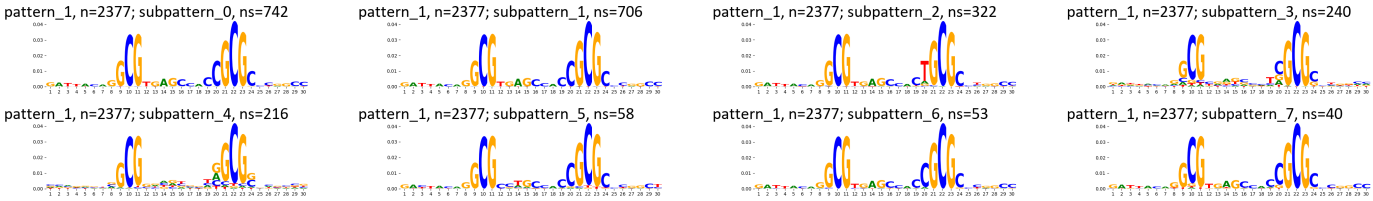

TF-MoDisCO pattern_1 n=2377, PWM

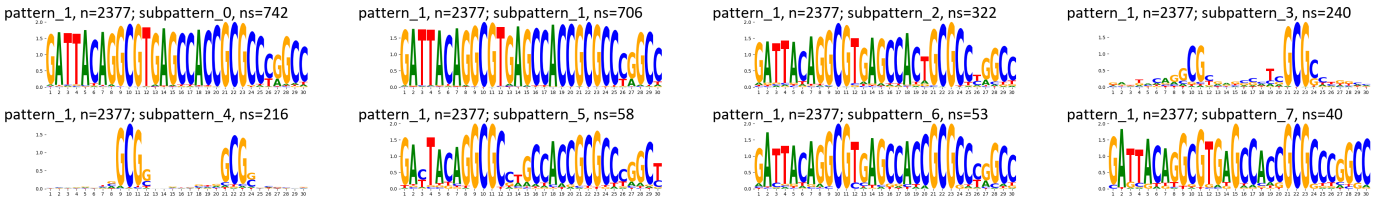

TF-MoDisCO pattern_3 n=859, CWM

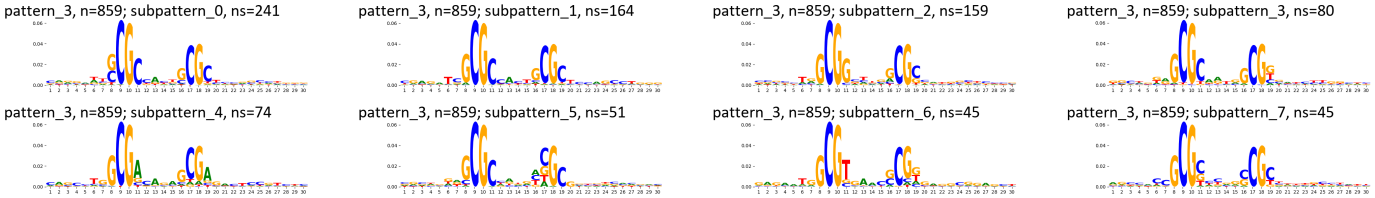

TF-MoDisCO pattern_3 n=859, PWM

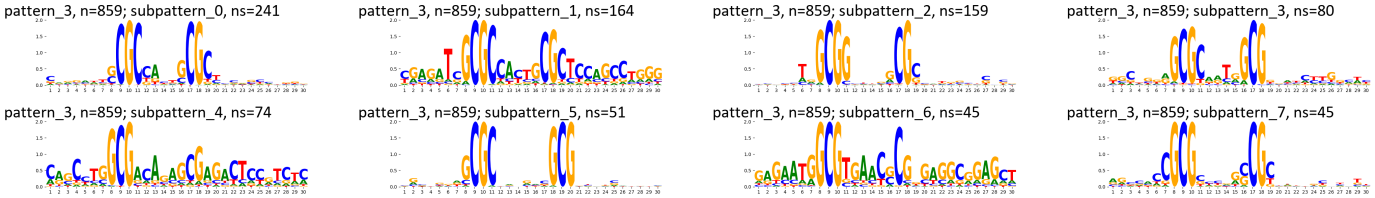

Supplementary Figure 444: TF-MoDisCO subpatterns for the ZBTB33 transcription factor in K562 (accession ENCSR876GXA).

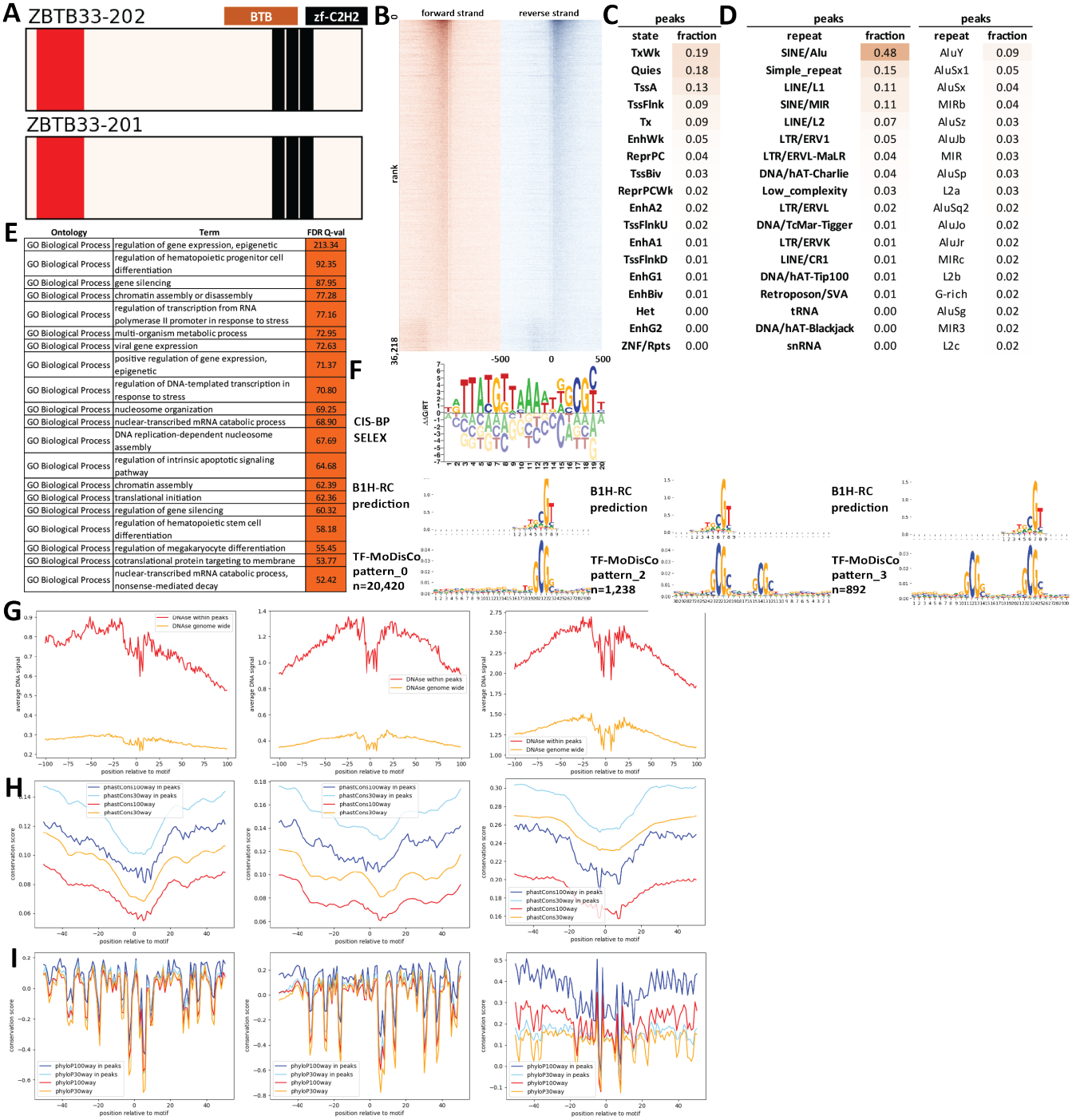

Supplementary Figure 445: Properties and genomic distribution of motifs identified for the ZBTB33 transcription factor in K562 (accession ENCSR955LXM).

TF-MoDisCO pattern_0 n=20420, CWM

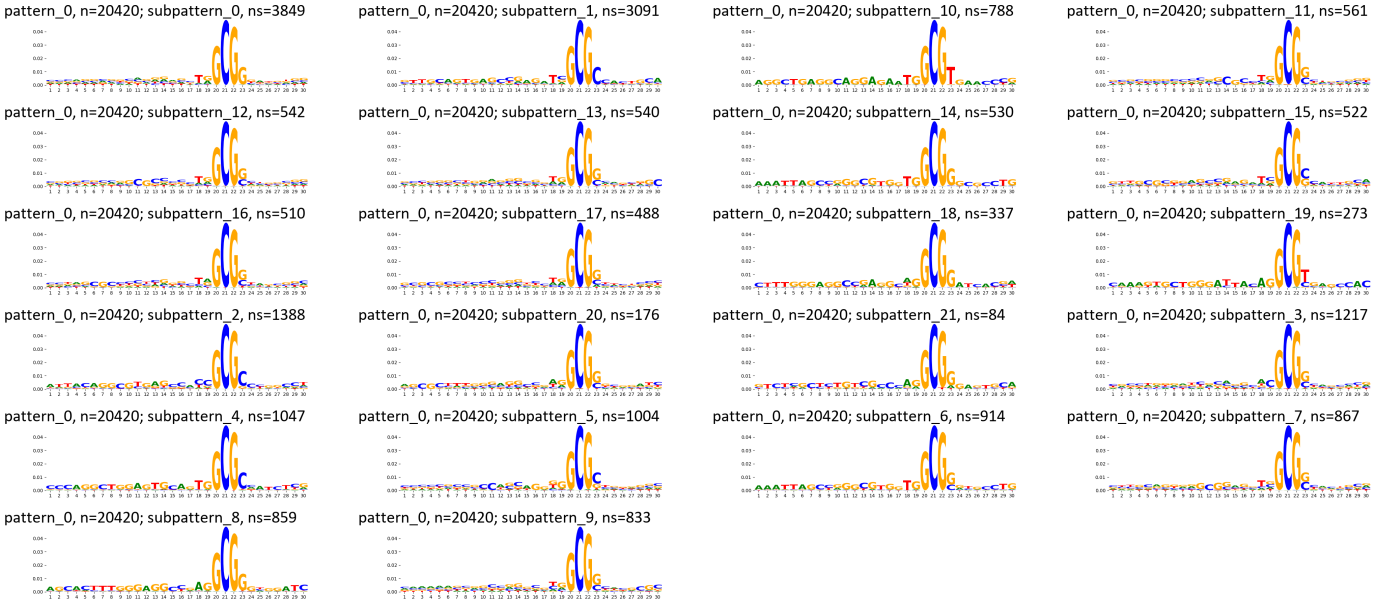

TF-MoDisCO pattern_0 n=20420, PWM

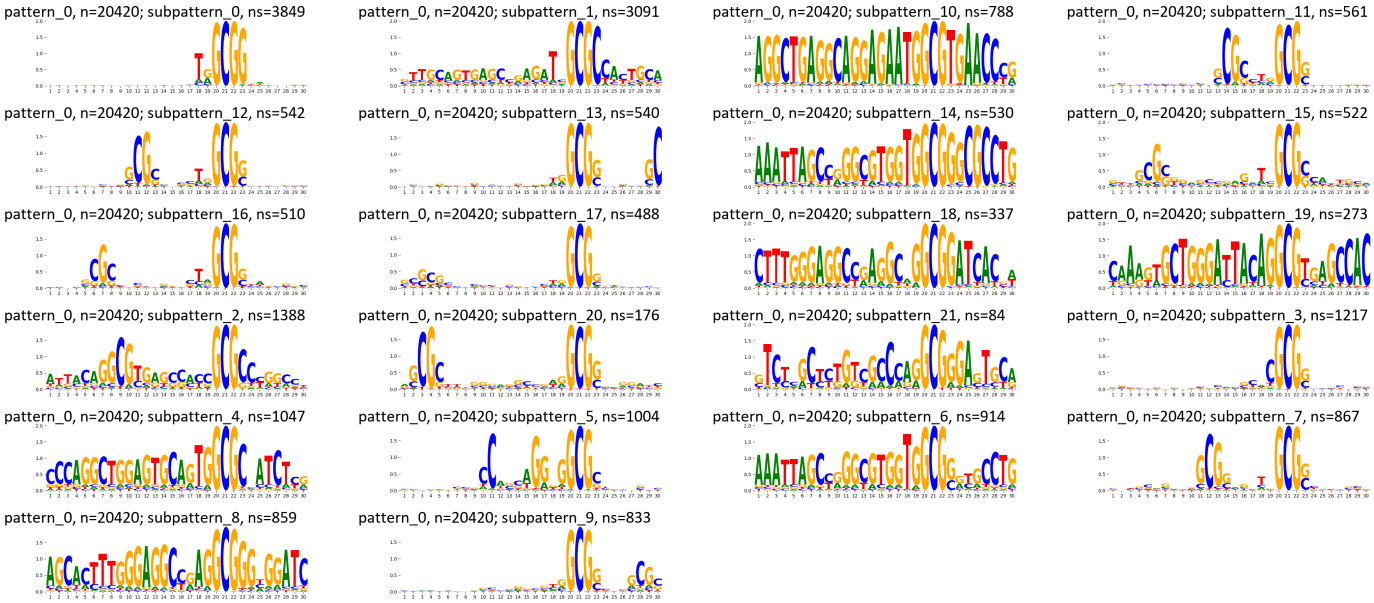

TF-MoDisCO pattern_2 n=1238, CWM

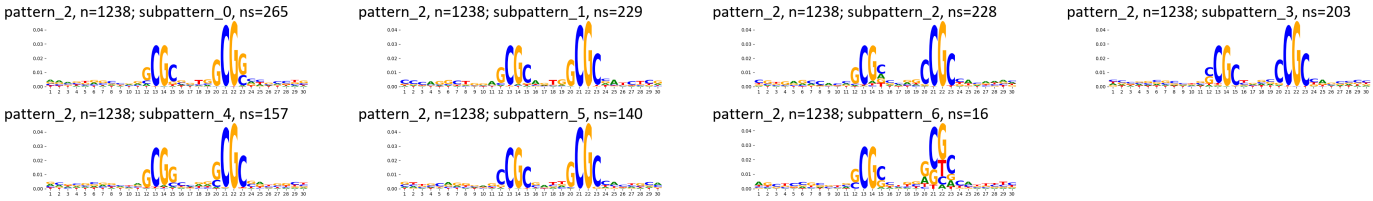

TF-MoDisCO pattern_2 n=1238, PWM

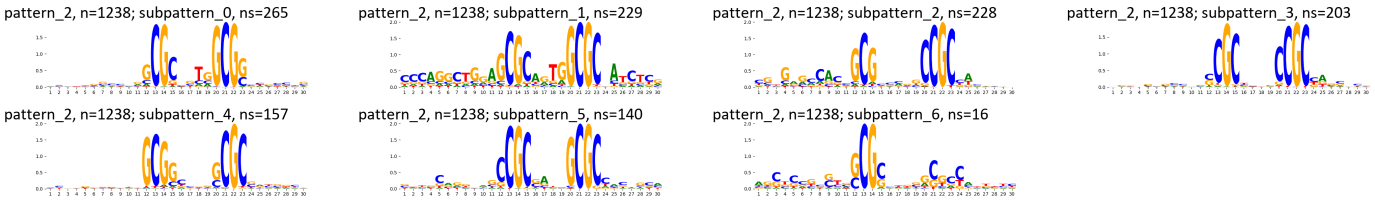

TF-MoDisCO pattern_3 n=892, CWM

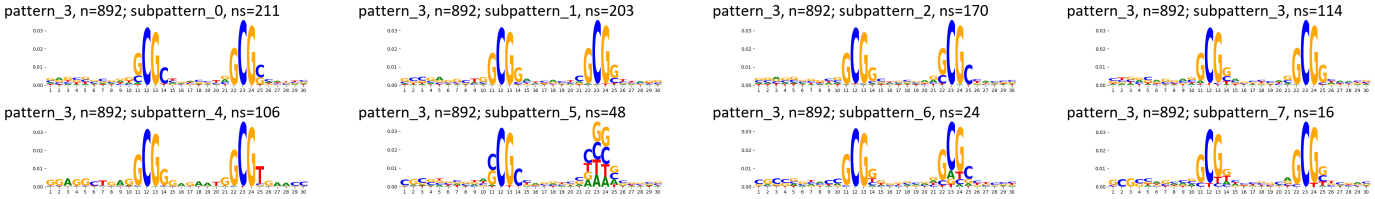

TF-MoDisCO pattern_3 n=892, PWM

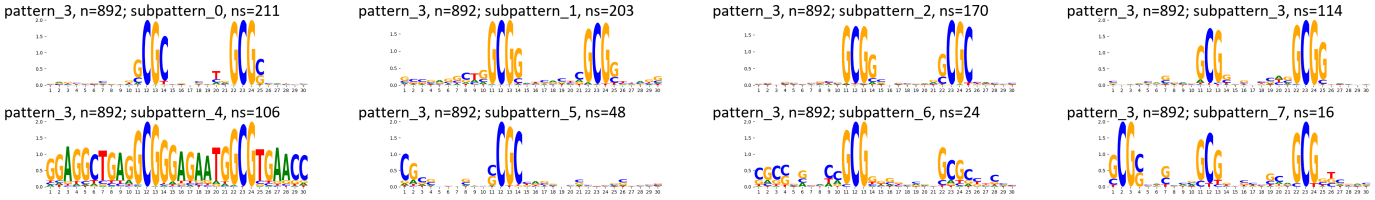

Supplementary Figure 446: TF-MoDisCO subpatterns for the ZBTB33 transcription factor in K562 (accession ENCSR955LXM).

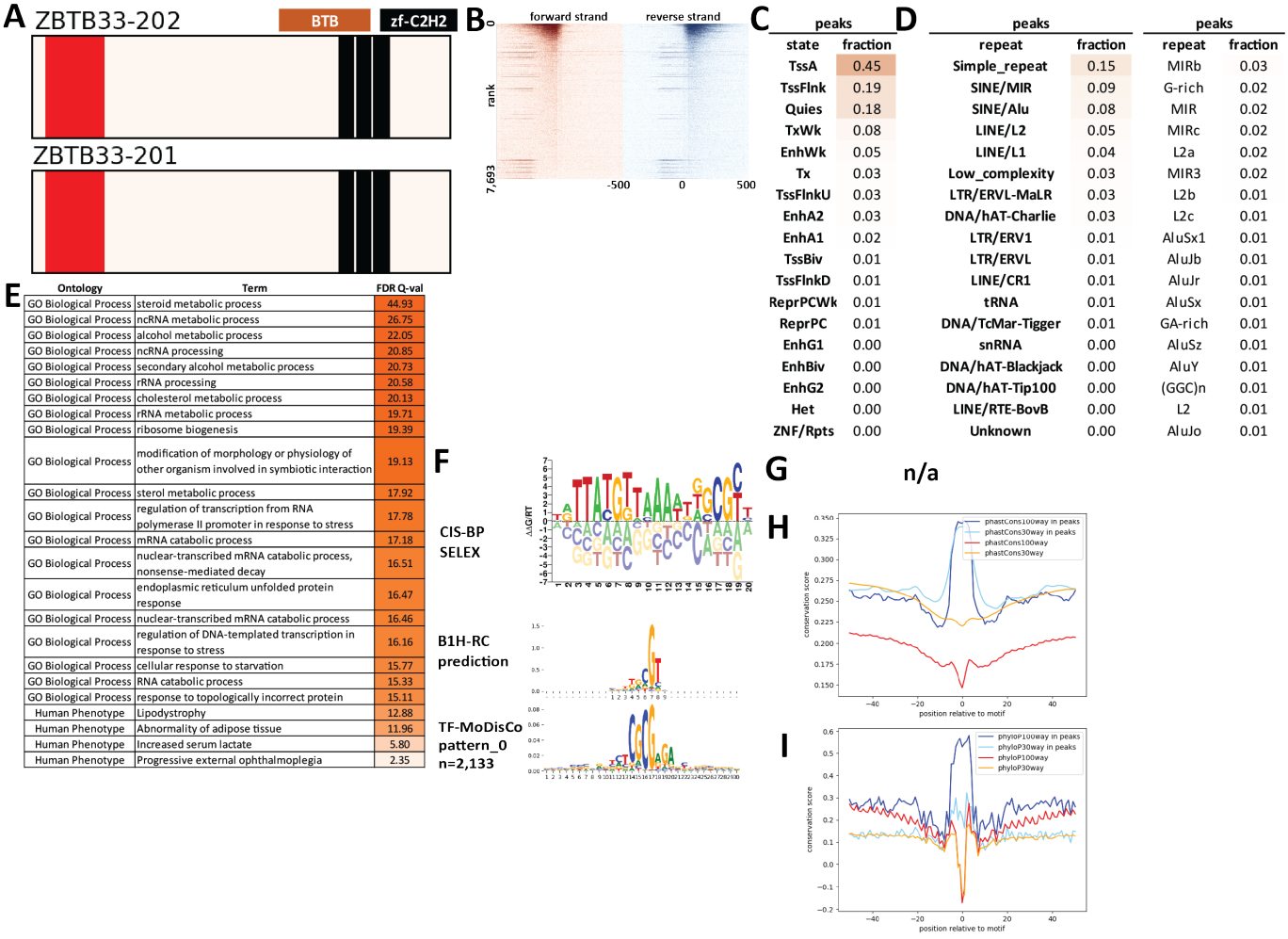

Supplementary Figure 447: Properties and genomic distribution of motifs identified for the ZBTB33 transcription factor in liver (accession ENCSR345YWJ).

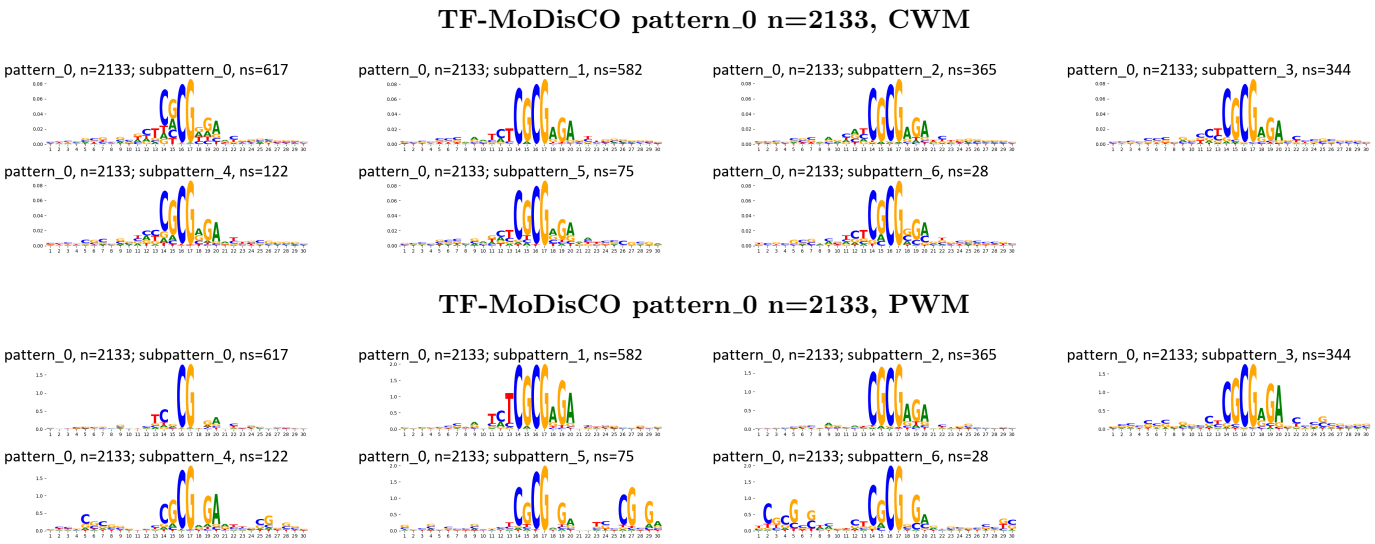

Supplementary Figure 448: TF-MoDisCO subpatterns for the ZBTB33 transcription factor in liver (accession ENCSR345YWJ).

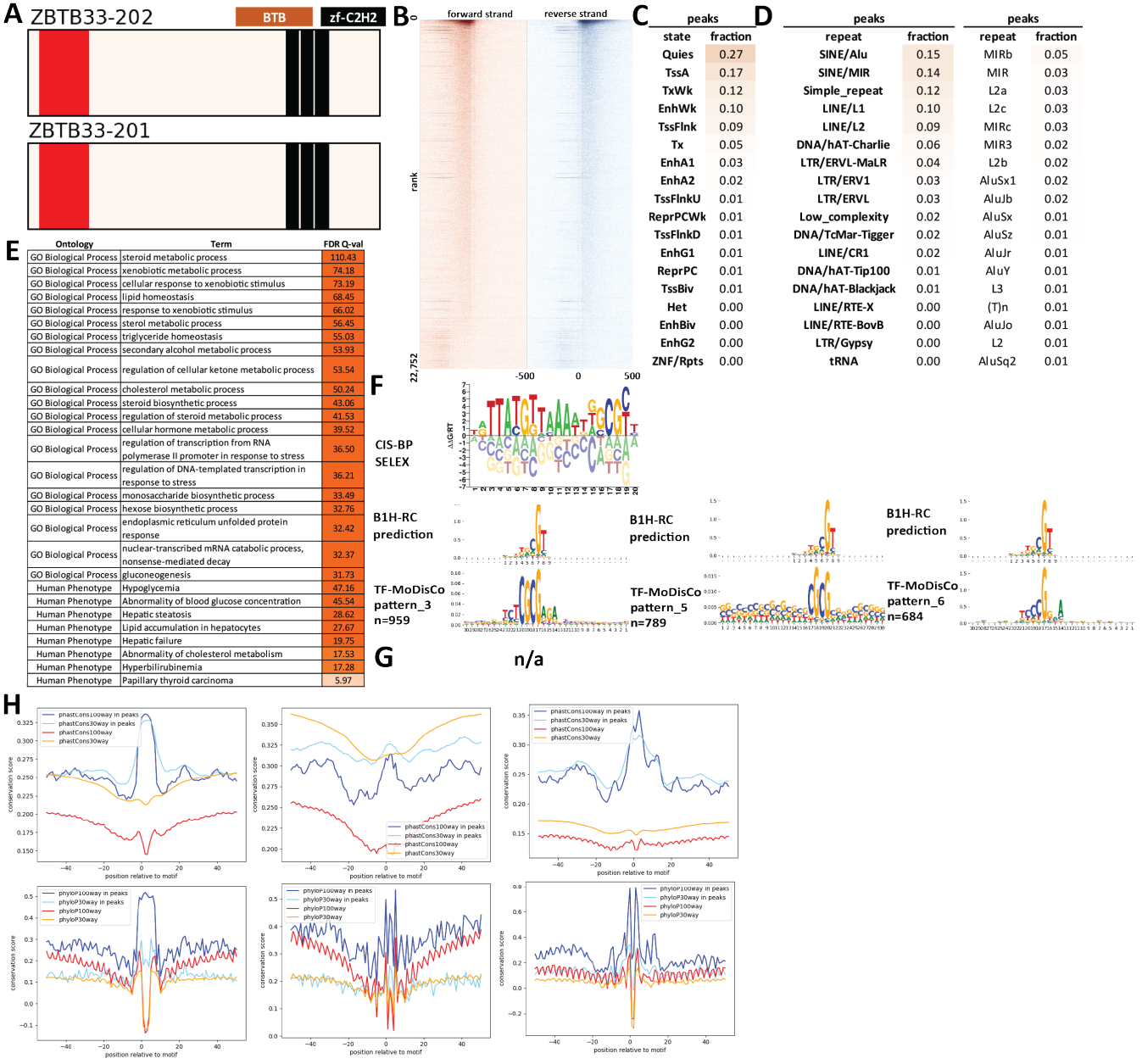

Supplementary Figure 449: Properties and genomic distribution of motifs identified for the ZBTB33 transcription factor in liver (accession ENCSR516HUP).

TF-MoDisCO pattern_3 n=959, CWM

pattern_3, n=959; subpattern_0, ns=218

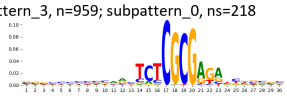

pattern_3, n=959; subpattern_1, ns=192

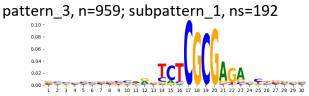

pattern_3, n=959; subpattern_2, ns=171

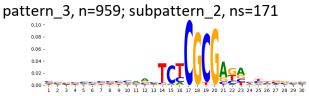

pattern_3, n=959; subpattern_3, ns=166

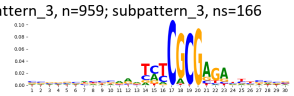

pattern_3, n=959; subpattern_4, ns=129

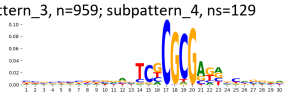

pattern_3, n=959; subpattern_5, ns=70

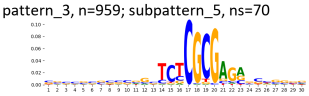

pattern_3, n=959; subpattern_6, ns=11

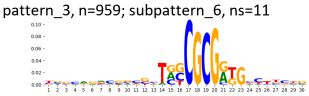

pattern_3, n=959; subpattern_7, ns=2

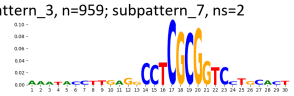

TF-MoDisCO pattern_3 n=959, PWM

pattern_3, n=959; subpattern_0, ns=218

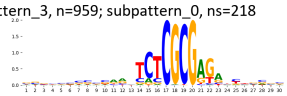

pattern_3, n=959; subpattern_1, ns=192

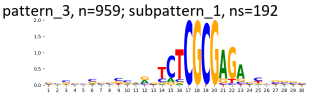

pattern_3, n=959; subpattern_2, ns=171

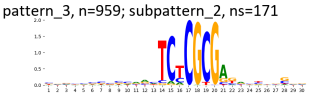

pattern_3, n=959; subpattern_3, ns=166

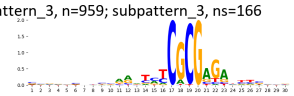

pattern_3, n=959; subpattern_4, ns=129

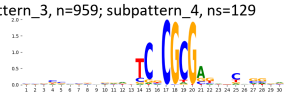

pattern_3, n=959; subpattern_5, ns=70

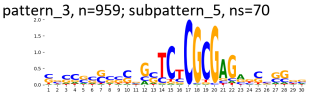

pattern_3, n=959; subpattern_6, ns=11

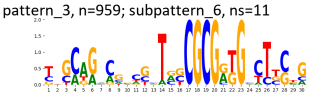

pattern_3, n=959; subpattern_7, ns=2

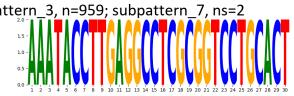

TF-MoDisCO pattern_5 n=789, CWM

pattern_5, n=789; subpattern_0, ns=141

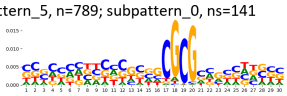

pattern_5, n=789; subpattern_1, ns=140

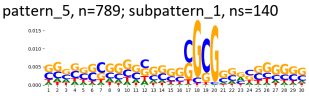

pattern_5, n=789; subpattern_2, ns=131

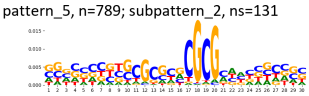

pattern_5, n=789; subpattern_3, ns=102

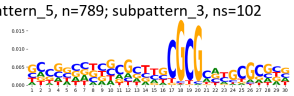

pattern_5, n=789; subpattern_4, ns=77

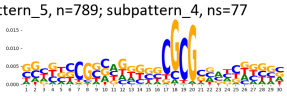

pattern_5, n=789; subpattern_5, ns=74

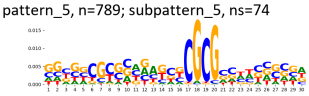

pattern_5, n=789; subpattern_6, ns=61

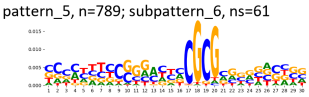

pattern_5, n=789; subpattern_7, ns=32

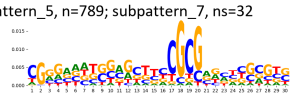

pattern_5, n=789; subpattern_8, ns=31

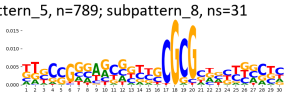

TF-MoDisCO pattern_5 n=789, PWM

pattern_5, n=789; subpattern_0, ns=141

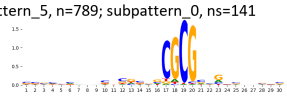

pattern_5, n=789; subpattern_1, ns=140

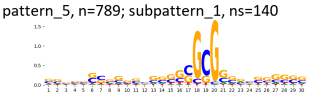

pattern_5, n=789; subpattern_2, ns=131

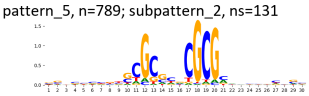

pattern_5, n=789; subpattern_3, ns=102

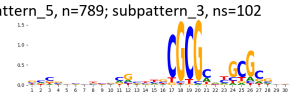

pattern_5, n=789; subpattern_4, ns=77

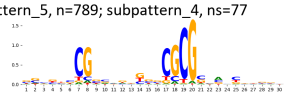

pattern_5, n=789; subpattern_5, ns=74

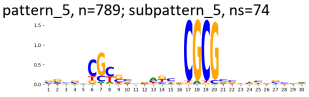

pattern_5, n=789; subpattern_6, ns=61

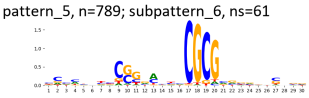

pattern_5, n=789; subpattern_7, ns=32

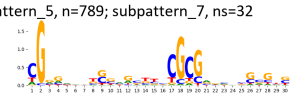

pattern_5, n=789; subpattern_8, ns=31

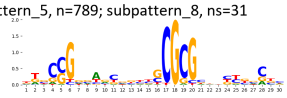

TF-MoDisCO pattern_6 n=684, CWM

pattern_6, n=684; subpattern_0, ns=228

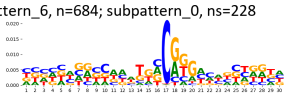

pattern_6, n=684; subpattern_1, ns=103

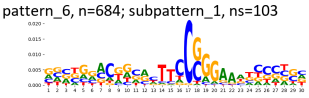

pattern_6, n=684; subpattern_2, ns=97

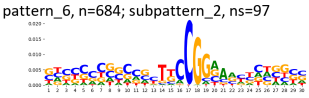

pattern_6, n=684; subpattern_3, ns=85

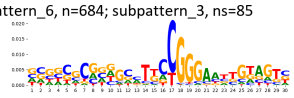

pattern_6, n=684; subpattern_4, ns=74

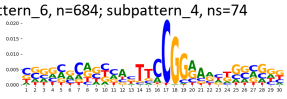

pattern_6, n=684; subpattern_5, ns=65

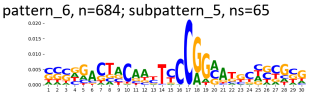

pattern_6, n=684; subpattern_6, ns=19

pattern_6, n=684; subpattern_7, ns=13

TF-MoDisCO pattern_6 n=684, PWM

pattern_6, n=684; subpattern_0, ns=228

pattern_6, n=684; subpattern_1, ns=103

pattern_6, n=684; subpattern_2, ns=97

pattern_6, n=684; subpattern_3, ns=85

pattern_6, n=684; subpattern_4, ns=74

pattern_6, n=684; subpattern_5, ns=65

pattern_6, n=684; subpattern_6, ns=19

pattern_6, n=684; subpattern_7, ns=13

Supplementary Figure 450: TF-MoDisCO subpatterns for the ZBTB33 transcription factor in liver (accession ENCSR516HUP).

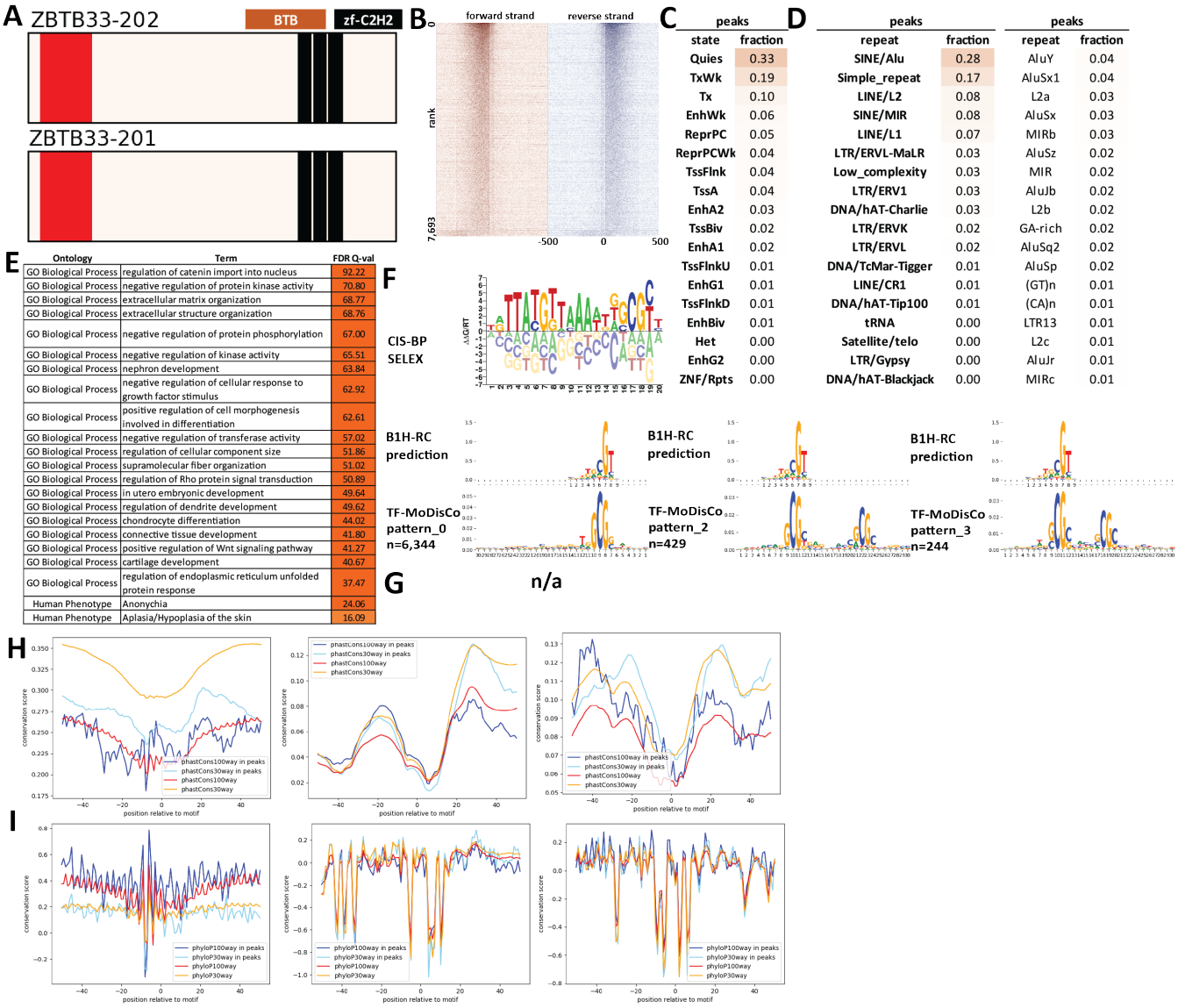

Supplementary Figure 451: Properties and genomic distribution of motifs identified for the ZBTB33 transcription factor in MCF-7 (accession ENCSR231YFE).

TF-MoDisCO pattern_0 n=6344, CWM

pattern_0, n=6344; subpattern_0, ns=1840

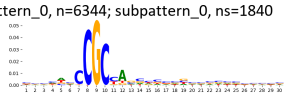

pattern_0, n=6344; subpattern_1, ns=1366

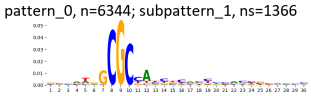

pattern_0, n=6344; subpattern_10, ns=169

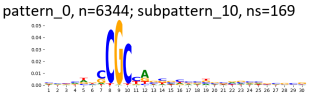

pattern_0, n=6344; subpattern_11, ns=125

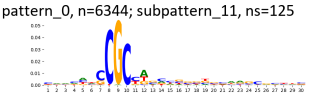

pattern_0, n=6344; subpattern_12, ns=106

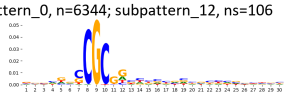

pattern_0, n=6344; subpattern_13, ns=105

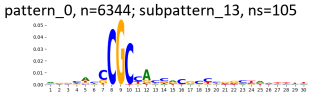

pattern_0, n=6344; subpattern_14, ns=70

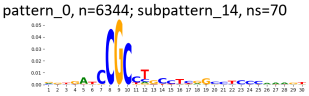

pattern_0, n=6344; subpattern_15, ns=2

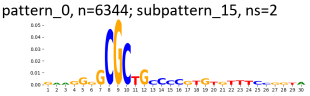

pattern_0, n=6344; subpattern_2, ns=427

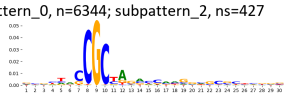

pattern_0, n=6344; subpattern_3, ns=408

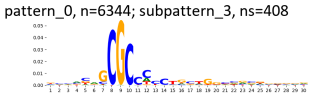

pattern_0, n=6344; subpattern_4, ns=378

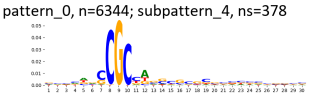

pattern_0, n=6344; subpattern_5, ns=378

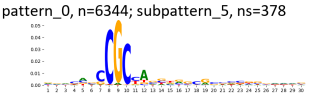

pattern_0, n=6344; subpattern_6, ns=331

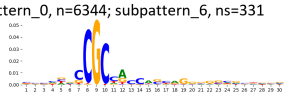

pattern_0, n=6344; subpattern_7, ns=241

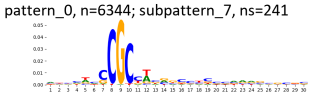

pattern_0, n=6344; subpattern_8, ns=223

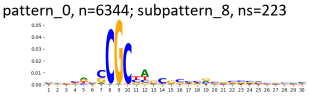

pattern_0, n=6344; subpattern_9, ns=175

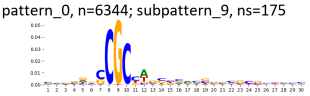

TF-MoDisCO pattern_0 n=6344, PWM

pattern_0, n=6344; subpattern_0, ns=1840

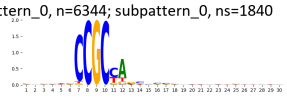

pattern_0, n=6344; subpattern_1, ns=1366

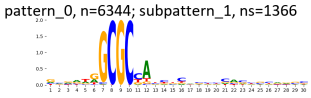

pattern_0, n=6344; subpattern_10, ns=169

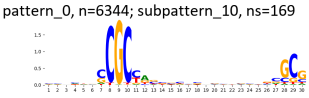

pattern_0, n=6344; subpattern_11, ns=125

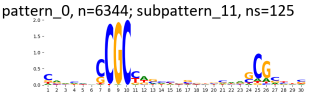

pattern_0, n=6344; subpattern_12, ns=106

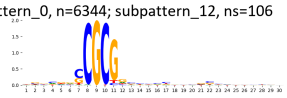

pattern_0, n=6344; subpattern_13, ns=105

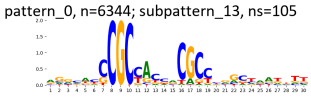

pattern_0, n=6344; subpattern_14, ns=70

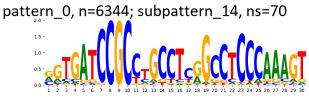

pattern_0, n=6344; subpattern_15, ns=2

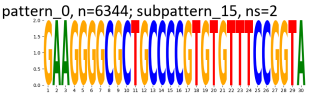

pattern_0, n=6344; subpattern_2, ns=427

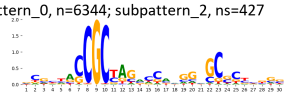

pattern_0, n=6344; subpattern_3, ns=408

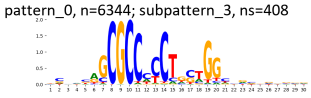

pattern_0, n=6344; subpattern_4, ns=378

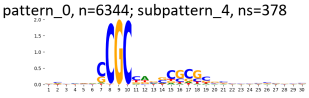

pattern_0, n=6344; subpattern_5, ns=378

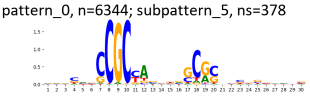

pattern_0, n=6344; subpattern_6, ns=331

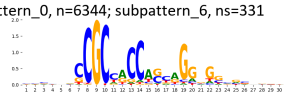

pattern_0, n=6344; subpattern_7, ns=241

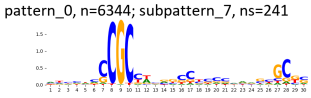

pattern_0, n=6344; subpattern_8, ns=223

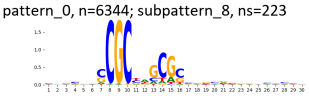

pattern_0, n=6344; subpattern_9, ns=175

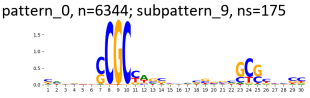

TF-MoDisCO pattern_2 n=429, CWM

pattern_2, n=429; subpattern_0, ns=123

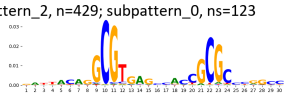

pattern_2, n=429; subpattern_1, ns=101

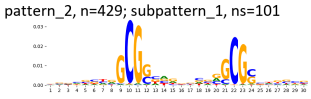

pattern_2, n=429; subpattern_2, ns=67

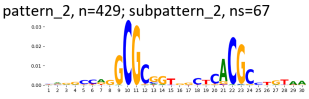

pattern_2, n=429; subpattern_3, ns=48

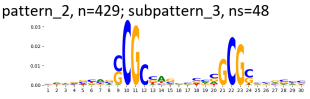

pattern_2, n=429; subpattern_4, ns=47

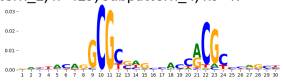

pattern_2, n=429; subpattern_5, ns=36

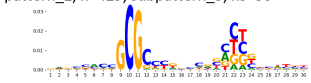

pattern_2, n=429; subpattern_6, ns=7

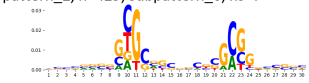

TF-MoDisCO pattern_2 n=429, PWM

pattern_2, n=429; subpattern_0, ns=123

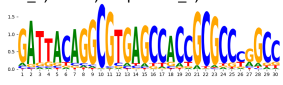

pattern_2, n=429; subpattern_1, ns=101

pattern_2, n=429; subpattern_2, ns=67

pattern_2, n=429; subpattern_3, ns=48

pattern_2, n=429; subpattern_4, ns=47

pattern_2, n=429; subpattern_5, ns=36

pattern_2, n=429; subpattern_6, ns=7

TF-MoDisCO pattern_3 n=244, CWM

pattern_3, n=244; subpattern_0, ns=78

pattern_3, n=244; subpattern_1, ns=52

pattern_3, n=244; subpattern_2, ns=52

pattern_3, n=244; subpattern_3, ns=32

pattern_3, n=244; subpattern_4, ns=18

pattern_3, n=244; subpattern_5, ns=8

pattern_3, n=244; subpattern_6, ns=4

TF-MoDisCO pattern_3 n=244, PWM

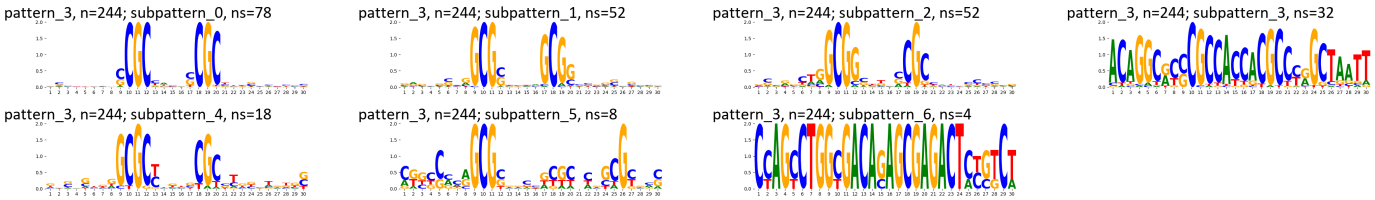

Supplementary Figure 452: TF-MoDisCO subpatterns for the ZBTB33 transcription factor in MCF-7 (accession ENCSR231YFE).

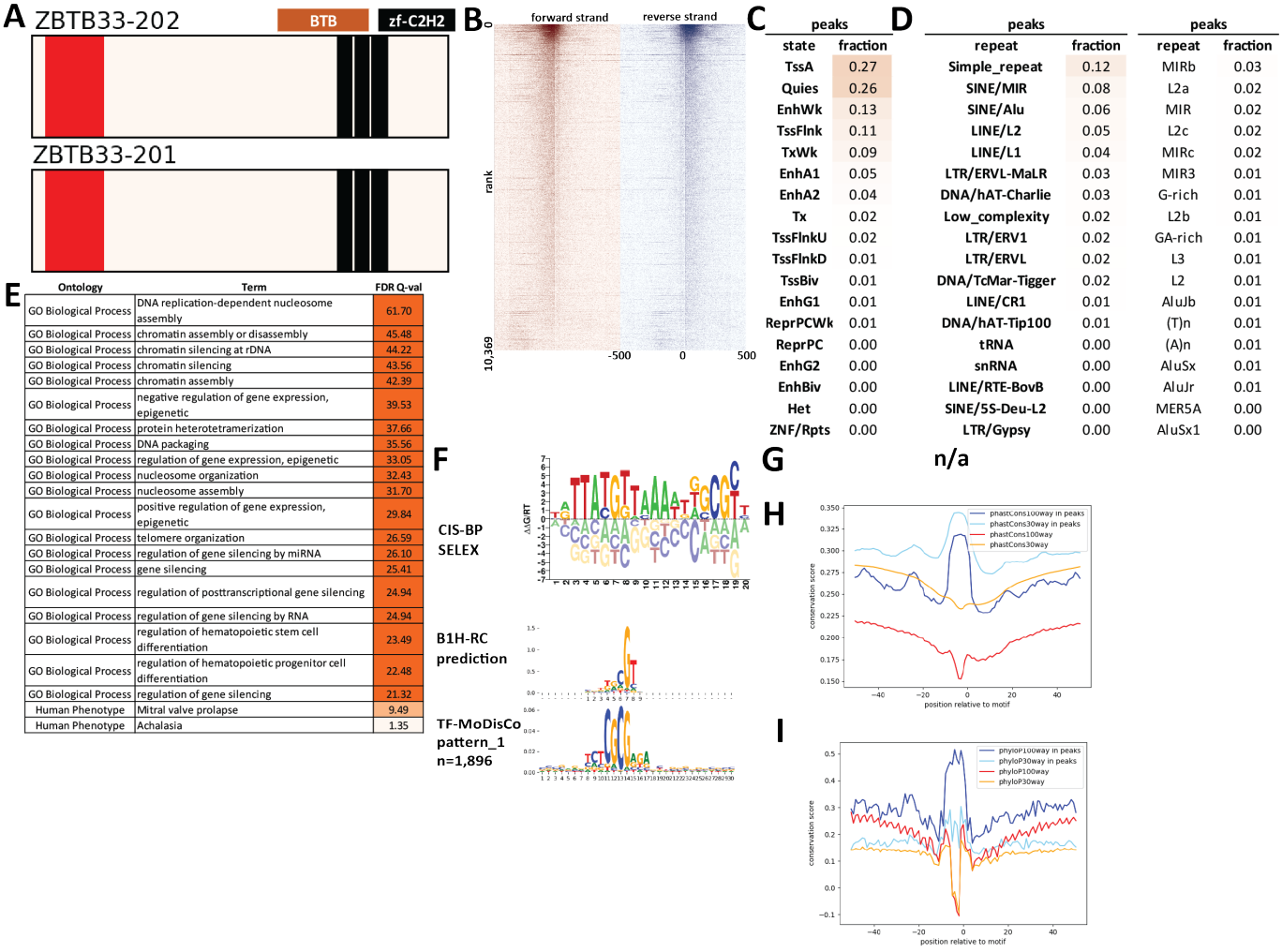

Supplementary Figure 453: Properties and genomic distribution of motifs identified for the ZBTB33 transcription factor in SK-N-SH (accession ENCSR000BTS).

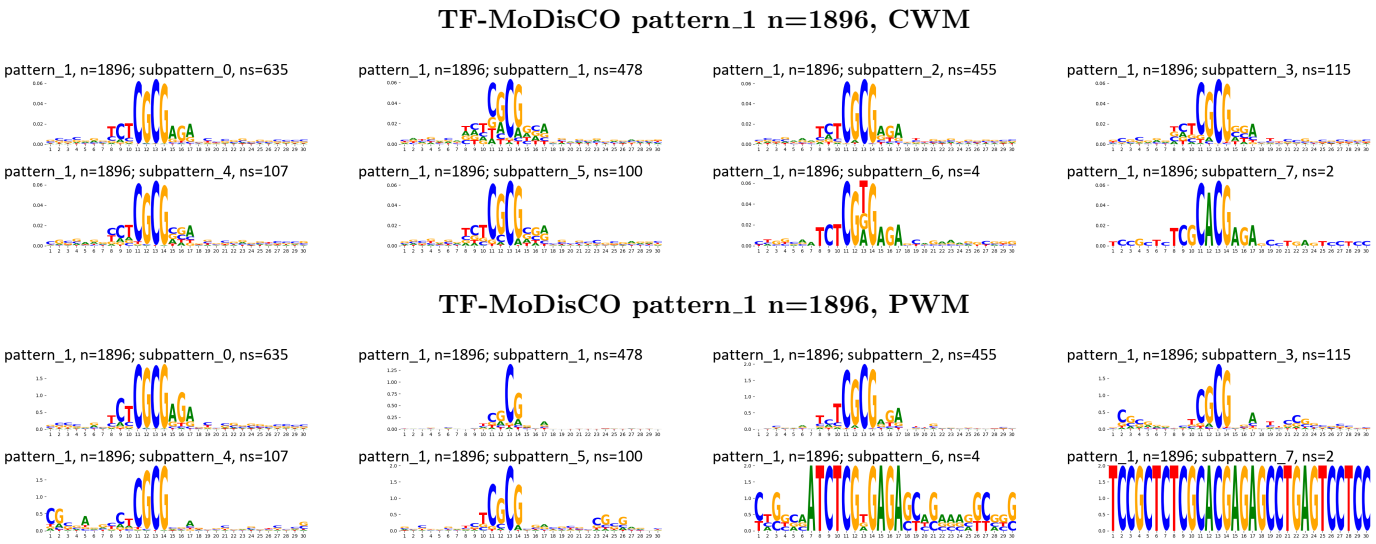

Supplementary Figure 454: TF-MoDisCO subpatterns for the ZBTB33 transcription factor in SK-N-SH (accession ENCSR000BTS).

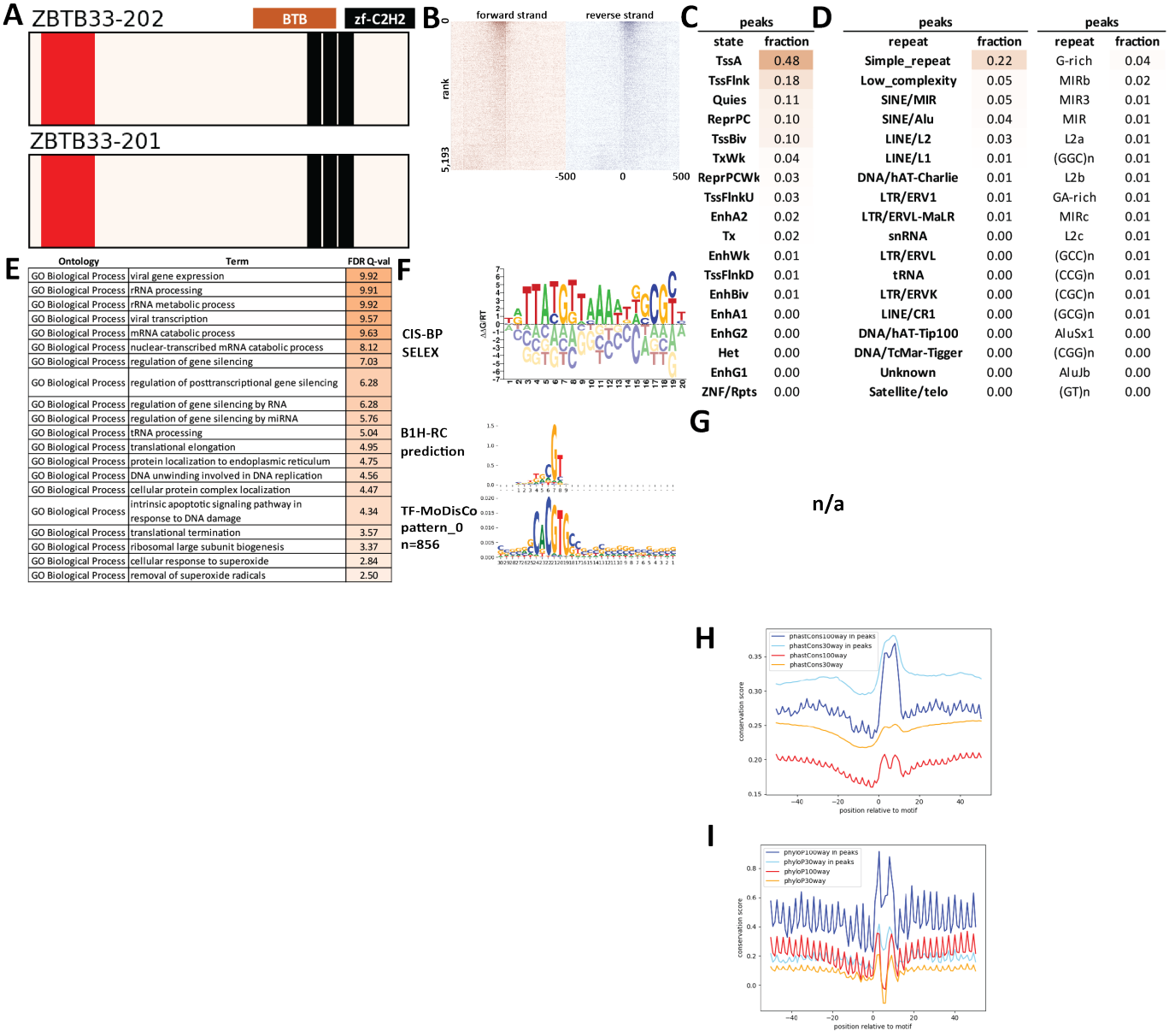

Supplementary Figure 455: Properties and genomic distribution of motifs identified for the ZBTB33 transcription factor in WTC11 (accession ENCSR943MQH).

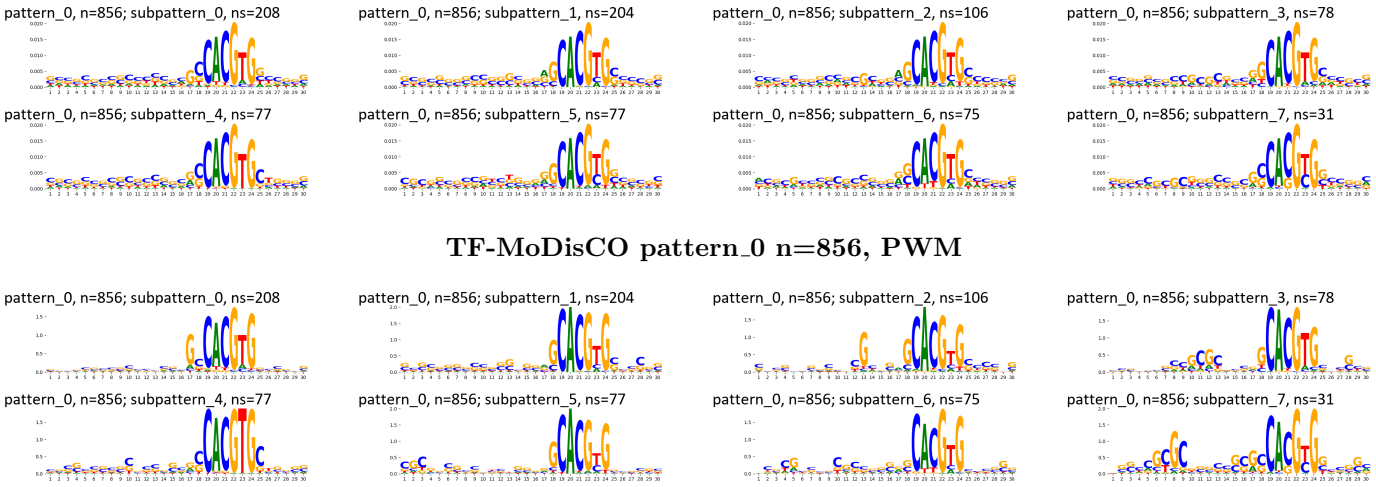

Supplementary Figure 456: TF-MoDisCO subpatterns for the ZBTB33 transcription factor in WTC11 (accession ENCSR943MQH).

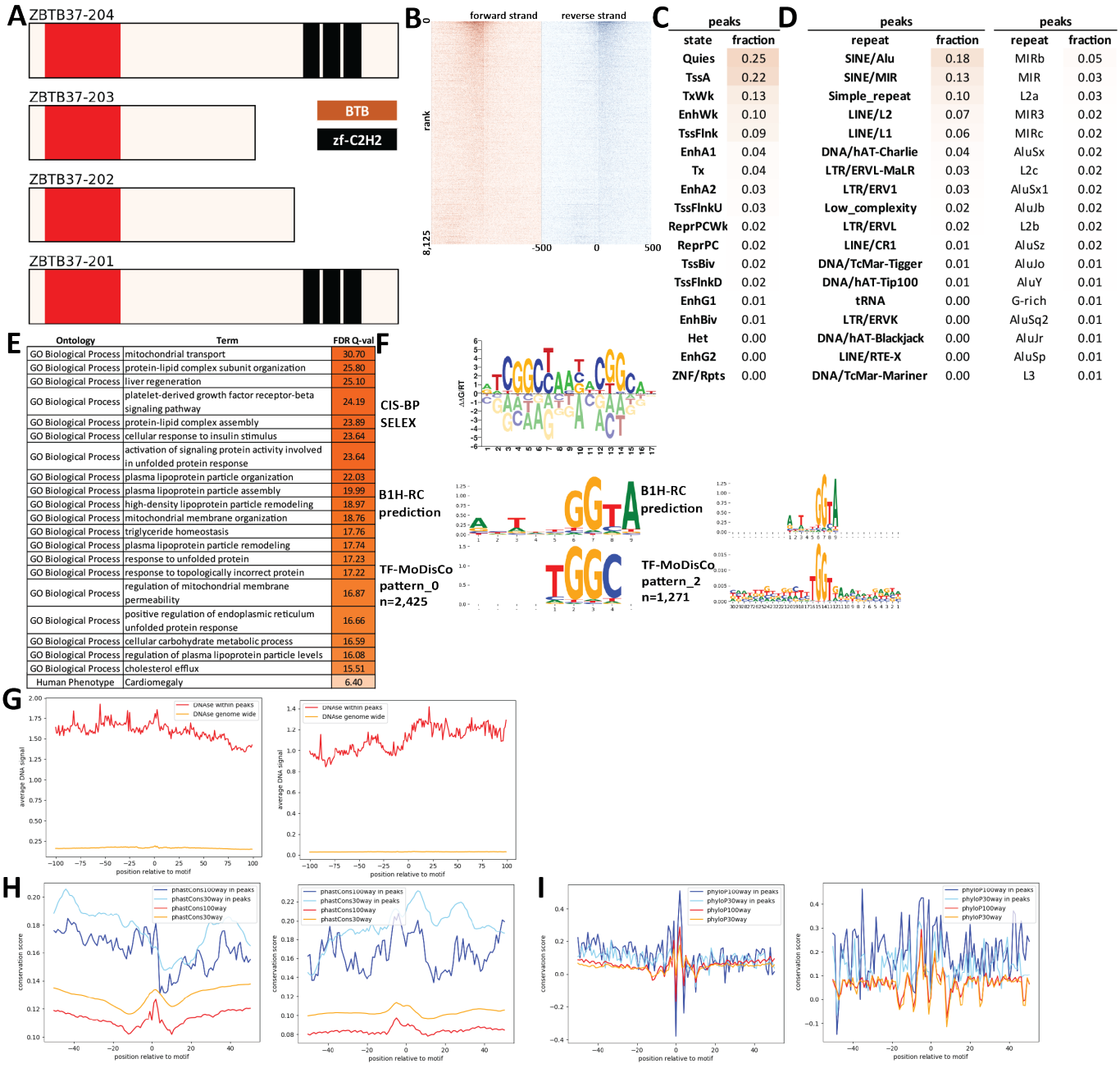

peaks	
state	fraction
Quies	0.25
TssA	0.22
TxWk	0.13
EnhWk	0.10
TssFlnk	0.09
EnhA1	0.04
Tx	0.04
EnhA2	0.03
TssFlnkU	0.03
ReprPCWk	0.02
ReprPC	0.02
TssBiv	0.02
TssFlnkD	0.02
EnhG1	0.01
EnhBiv	0.01
Het	0.00
EnhG2	0.00
ZNF/Rpts	0.00

peaks		peaks	
repeat	fraction	repeat	fraction
SINE/Alu	0.18	MIRb	0.05
SINE/MIR	0.13	MIR	0.03
Simple_repeat	0.10	L2a	0.03
LINE/L2	0.07	MIR3	0.02
LINE/L1	0.06	MIRc	0.02
DNA/hAT-Charlie	0.04	AluSx	0.02
LTR/ERVL-MaLR	0.03	L2c	0.02
LTR/ERV1	0.03	AluSx1	0.02
Low_complexity	0.02	AluJb	0.02
LTR/ERVL	0.02	L2b	0.02
LINE/CR1	0.01	AluSz	0.02
DNA/TcMar-Tigger	0.01	AluJo	0.01
DNA/hAT-Tip100	0.01	AluY	0.01
tRNA	0.00	G-rich	0.01
LTR/ERVK	0.00	AluSq2	0.01
DNA/hAT-Blackjack	0.00	AluJr	0.01
LINE/RTE-X	0.00	AluSp	0.01
DNA/TcMar-Mariner	0.00	L3	0.01

Ontology	Term	FDR Q-val
GO Biological Process	mitochondrial transport	30.70
GO Biological Process	protein-lipid complex subunit organization	25.80
GO Biological Process	liver regeneration	25.10
GO Biological Process	platelet-derived growth factor receptor-beta signaling pathway	24.19
GO Biological Process	protein-lipid complex assembly	23.89
GO Biological Process	cellular response to insulin stimulus	23.64
GO Biological Process	activation of signaling protein activity involved in unfolded protein response	23.64
GO Biological Process	plasma lipoprotein particle organization	22.03
GO Biological Process	plasma lipoprotein particle assembly	19.99
GO Biological Process	high-density lipoprotein particle remodeling	18.97
GO Biological Process	mitochondrial membrane organization	18.76
GO Biological Process	triglyceride homeostasis	17.76
GO Biological Process	plasma lipoprotein particle remodeling	17.74
GO Biological Process	response to unfolded protein	17.23
GO Biological Process	response to topologically incorrect protein	17.22
GO Biological Process	regulation of mitochondrial membrane permeability	16.87
GO Biological Process	positive regulation of endoplasmic reticulum unfolded protein response	16.66
GO Biological Process	cellular carbohydrate metabolic process	16.59
GO Biological Process	regulation of plasma lipoprotein particle levels	16.08
GO Biological Process	cholesterol efflux	15.51
Human Phenotype	Cardiomegaly	6.40

Supplementary Figure 457: Properties and genomic distribution of motifs identified for the ZBTB37 transcription factor in HepG2 (accession ENCSR775YXE).

TF-MoDiSCO pattern_0 n=2425, CWM

pattern_0, n=2425; subpattern_0, ns=565

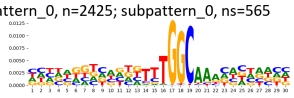

pattern_0, n=2425; subpattern_1, ns=529

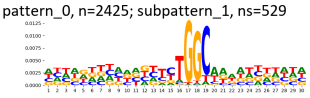

pattern_0, n=2425; subpattern_10, ns=2

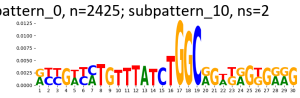

pattern_0, n=2425; subpattern_11, ns=2

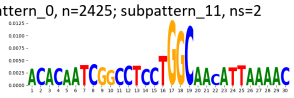

pattern_0, n=2425; subpattern_2, ns=463

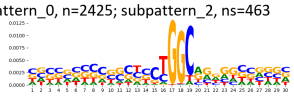

pattern_0, n=2425; subpattern_3, ns=332

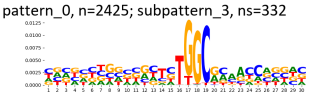

pattern_0, n=2425; subpattern_4, ns=318

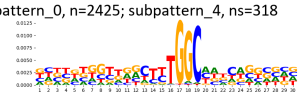

pattern_0, n=2425; subpattern_5, ns=142

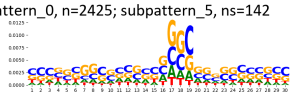

pattern_0, n=2425; subpattern_6, ns=35

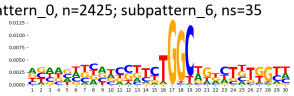

pattern_0, n=2425; subpattern_7, ns=31

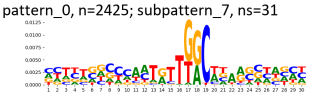

pattern_0, n=2425; subpattern_8, ns=4

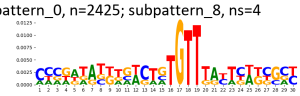

pattern_0, n=2425; subpattern_9, ns=2

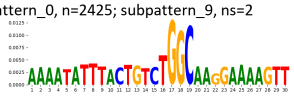

TF-MoDiSCO pattern_0 n=2425, PWM

pattern_0, n=2425; subpattern_0, ns=565

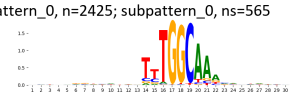

pattern_0, n=2425; subpattern_1, ns=529

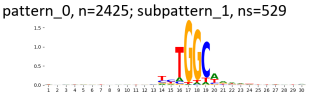

pattern_0, n=2425; subpattern_10, ns=2

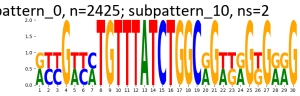

pattern_0, n=2425; subpattern_11, ns=2

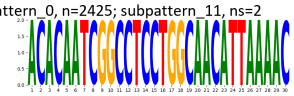

pattern_0, n=2425; subpattern_2, ns=463

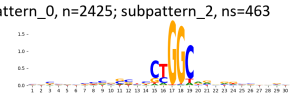

pattern_0, n=2425; subpattern_3, ns=332

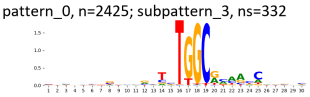

pattern_0, n=2425; subpattern_4, ns=318

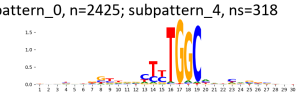

pattern_0, n=2425; subpattern_5, ns=142

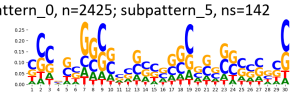

pattern_0, n=2425; subpattern_6, ns=35

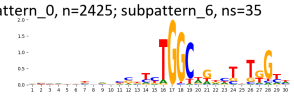

pattern_0, n=2425; subpattern_7, ns=31

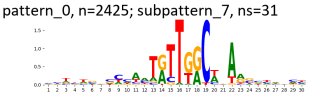

pattern_0, n=2425; subpattern_8, ns=4

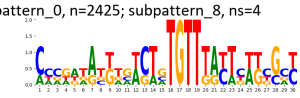

pattern_0, n=2425; subpattern_9, ns=2

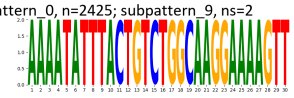

TF-MoDiSCO pattern_2 n=1271, CWM

pattern_2, n=1271; subpattern_0, ns=320

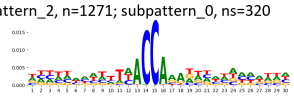

pattern_2, n=1271; subpattern_1, ns=253

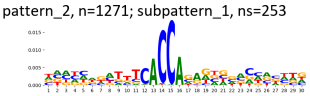

pattern_2, n=1271; subpattern_2, ns=179

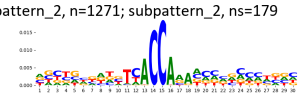

pattern_2, n=1271; subpattern_3, ns=155

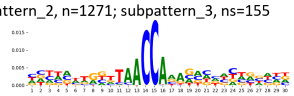

pattern_2, n=1271; subpattern_4, ns=119

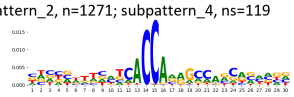

pattern_2, n=1271; subpattern_5, ns=92

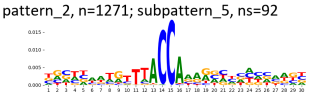

pattern_2, n=1271; subpattern_6, ns=71

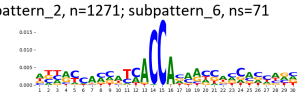

pattern_2, n=1271; subpattern_7, ns=48

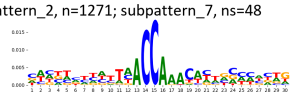

pattern_2, n=1271; subpattern_8, ns=26

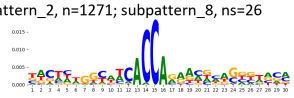

pattern_2, n=1271; subpattern_9, ns=8

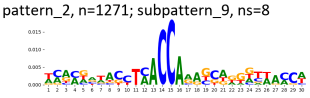

TF-MoDiSCO pattern_2 n=1271, CWM

pattern_2, n=1271; subpattern_0, ns=320

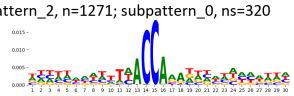

pattern_2, n=1271; subpattern_1, ns=253

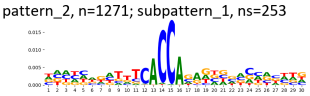

pattern_2, n=1271; subpattern_2, ns=179

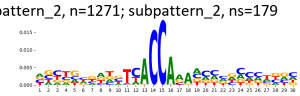

pattern_2, n=1271; subpattern_3, ns=155

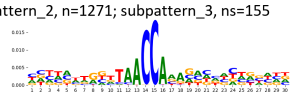

pattern_2, n=1271; subpattern_4, ns=119

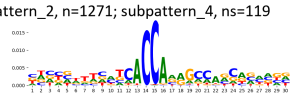

pattern_2, n=1271; subpattern_5, ns=92

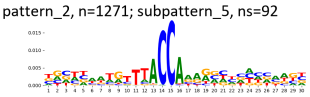

pattern_2, n=1271; subpattern_6, ns=71

pattern_2, n=1271; subpattern_7, ns=48

pattern_2, n=1271; subpattern_8, ns=26

pattern_2, n=1271; subpattern_9, ns=8

TF-MoDiSCO pattern_2 n=1271, PWM

pattern_2, n=1271; subpattern_0, ns=320

pattern_2, n=1271; subpattern_1, ns=253

pattern_2, n=1271; subpattern_2, ns=179

pattern_2, n=1271; subpattern_3, ns=155

pattern_2, n=1271; subpattern_4, ns=119

pattern_2, n=1271; subpattern_5, ns=92

pattern_2, n=1271; subpattern_6, ns=71

pattern_2, n=1271; subpattern_7, ns=48

pattern_2, n=1271; subpattern_8, ns=26

pattern_2, n=1271; subpattern_9, ns=8

TF-MoDisCO pattern_2 n=1271, PWM

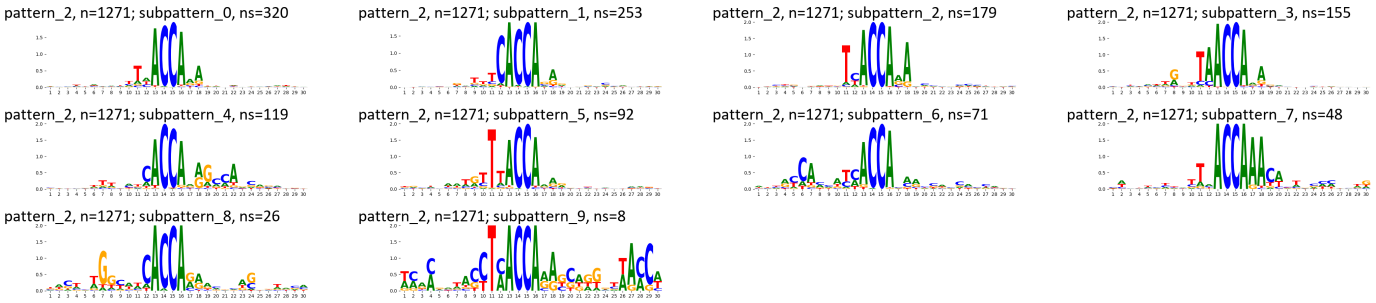

Supplementary Figure 458: TF-MoDisCO subpatterns for the ZBTB37 transcription factor in HepG2 (accession ENCSR775YXE).

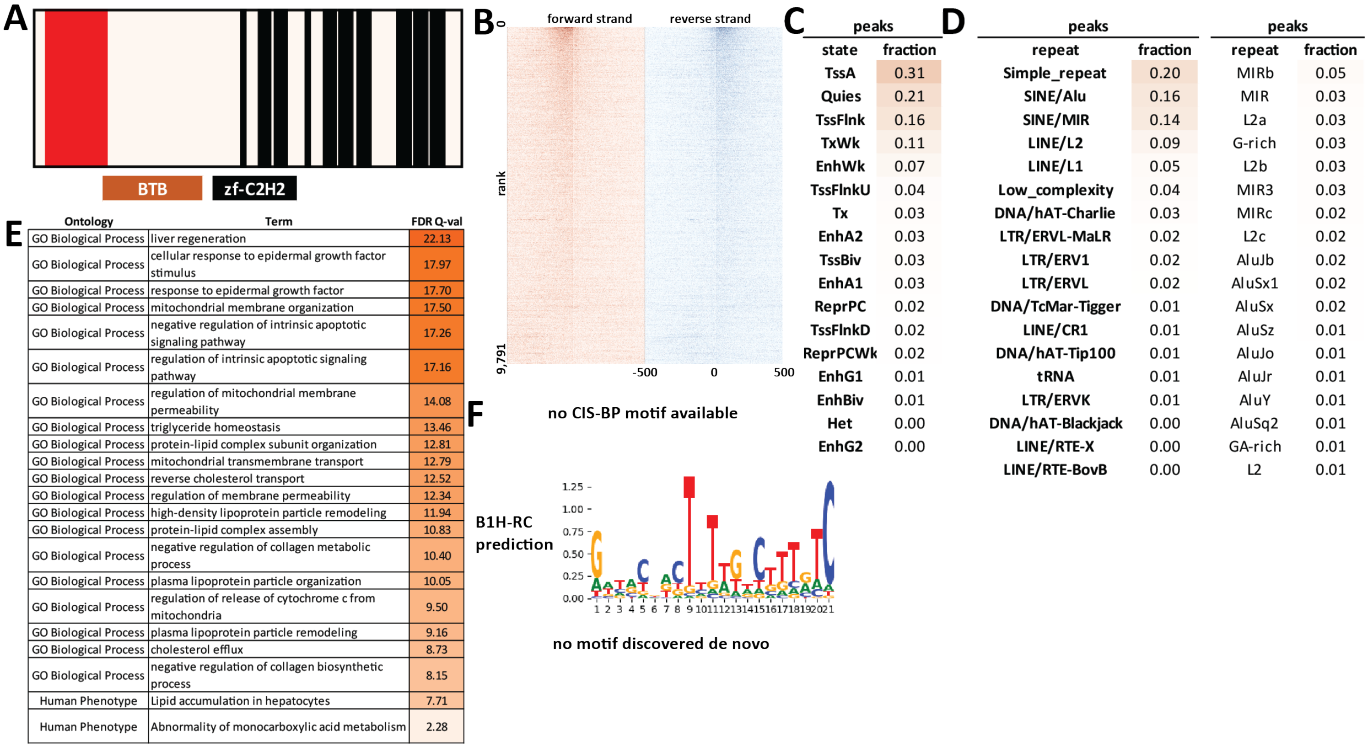

Supplementary Figure 459: Properties and genomic distribution of motifs identified for the ZBTB39 transcription factor in HepG2 (accession ENCSR087NSZ).

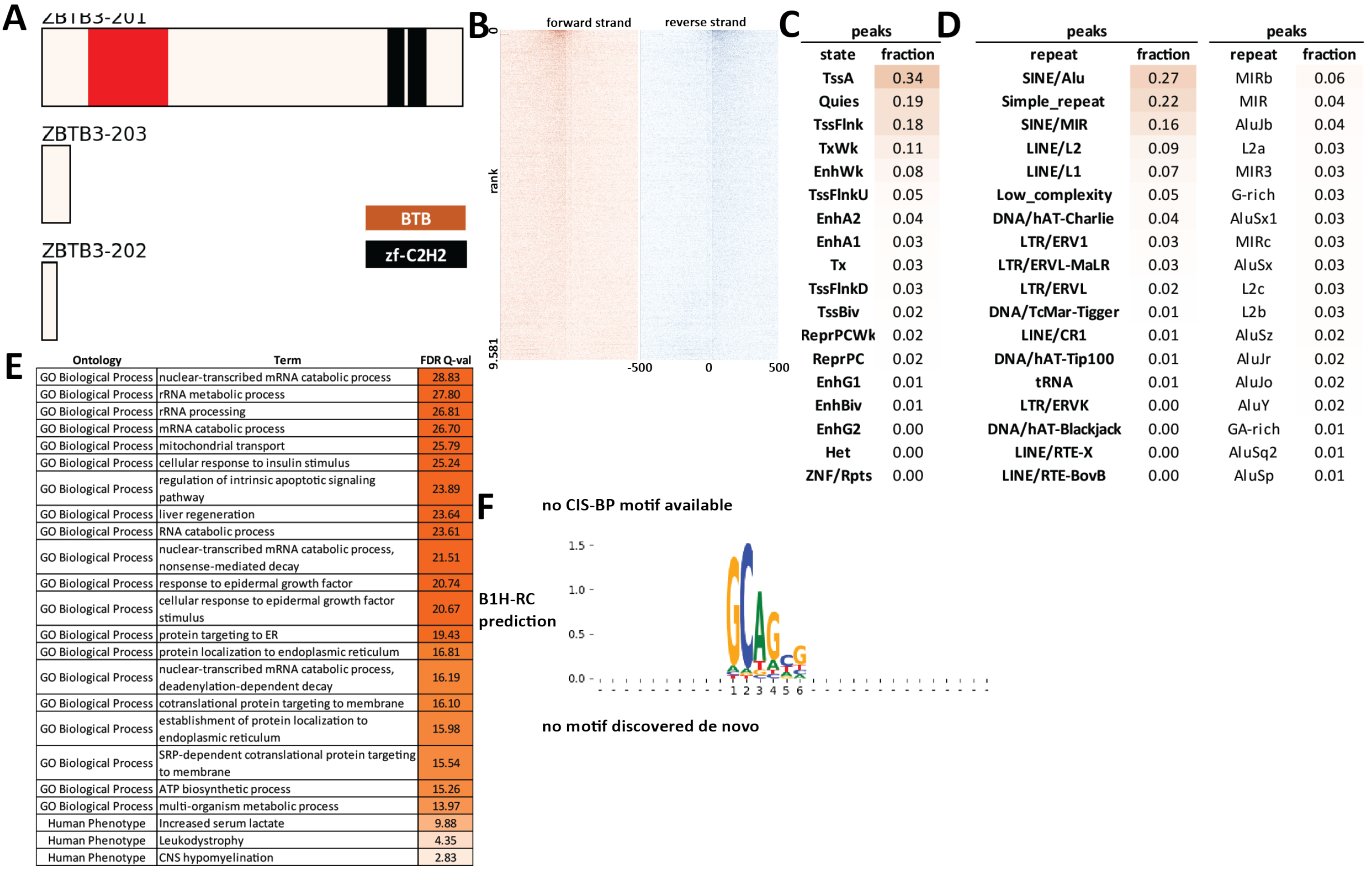

C

peaks	
state	fraction
TssA	0.34
Quies	0.19
TssFlnk	0.18
TxWk	0.11
EnhWk	0.08
TssFlnkU	0.05
EnhA2	0.04
EnhA1	0.03
Tx	0.03
TssFlnkD	0.03
TssBiv	0.02
ReprPCWk	0.02
ReprPC	0.02
EnhG1	0.01
EnhBiv	0.01
EnhG2	0.00
Het	0.00
ZNF/Rpts	0.00

D

peaks		peaks	
repeat	fraction	repeat	fraction
SINE/Alu	0.27	MIRb	0.06
Simple_repeat	0.22	MIR	0.04
SINE/MIR	0.16	AluJb	0.04
LINE/L2	0.09	L2a	0.03
LINE/L1	0.07	MIR3	0.03
Low_complexity	0.05	G-rich	0.03
DNA/hAT-Charlie	0.04	AluSx1	0.03
LTR/ERV1	0.03	MIRc	0.03
LTR/ERVL-MaLR	0.03	AluSx	0.03
LTR/ERVL	0.02	L2c	0.03
DNA/TcMar-Tigger	0.01	L2b	0.03
LINE/CR1	0.01	AluSz	0.02
DNA/hAT-Tip100	0.01	AluJr	0.02
tRNA	0.01	AluJo	0.02
LTR/ERVK	0.00	AluY	0.02
DNA/hAT-Blackjack	0.00	GA-rich	0.01
LINE/RTE-X	0.00	AluSq2	0.01
LINE/RTE-BovB	0.00	AluSp	0.01

E

Ontology	Term	FDR Q-val
GO Biological Process	nuclear-transcribed mRNA catabolic process	28.83
GO Biological Process	rRNA metabolic process	27.80
GO Biological Process	rRNA processing	26.81
GO Biological Process	mRNA catabolic process	26.70
GO Biological Process	mitochondrial transport	25.79
GO Biological Process	cellular response to insulin stimulus	25.24
GO Biological Process	regulation of intrinsic apoptotic signaling pathway	23.89
GO Biological Process	liver regeneration	23.64
GO Biological Process	RNA catabolic process	23.61
GO Biological Process	nuclear-transcribed mRNA catabolic process, nonsense-mediated decay	21.51
GO Biological Process	response to epidermal growth factor	20.74
GO Biological Process	cellular response to epidermal growth factor stimulus	20.67
GO Biological Process	protein targeting to ER	19.43
GO Biological Process	protein localization to endoplasmic reticulum	16.81
GO Biological Process	nuclear-transcribed mRNA catabolic process, deadenylation-dependent decay	16.19
GO Biological Process	cotranslational protein targeting to membrane	16.10
GO Biological Process	establishment of protein localization to endoplasmic reticulum	15.98
GO Biological Process	SRP-dependent cotranslational protein targeting to membrane	15.54
GO Biological Process	ATP biosynthetic process	15.26
GO Biological Process	multi-organism metabolic process	13.97
Human Phenotype	Increased serum lactate	9.88
Human Phenotype	Leukodystrophy	4.35
Human Phenotype	CNS hypomyelination	2.83

Supplementary Figure 460: Properties and genomic distribution of motifs identified for the ZBTB3 transcription factor in HepG2 (accession ENCSR481AIK).

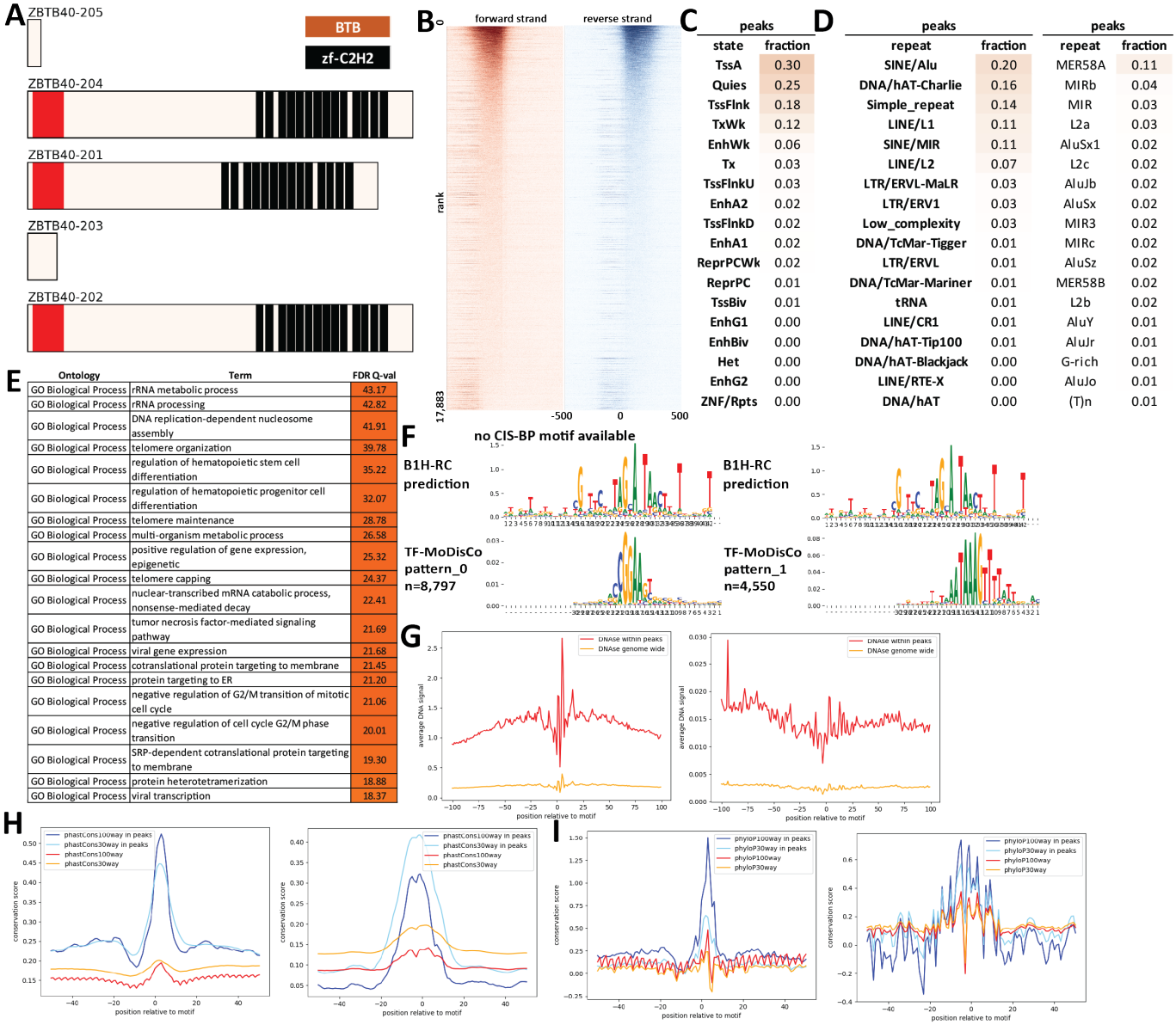

Supplementary Figure 461: Properties and genomic distribution of motifs identified for the ZBTB40 transcription factor in GM12878 (accession ENCSR189YYK).

TF-MoDisCO pattern_0 n=8797, CWM

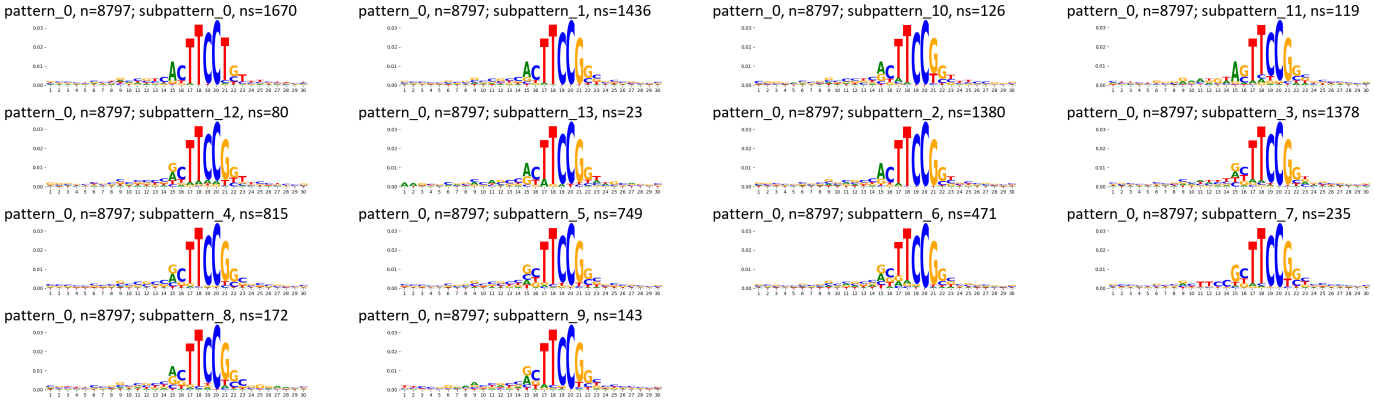

TF-MoDisCO pattern_0 n=8797, PWM

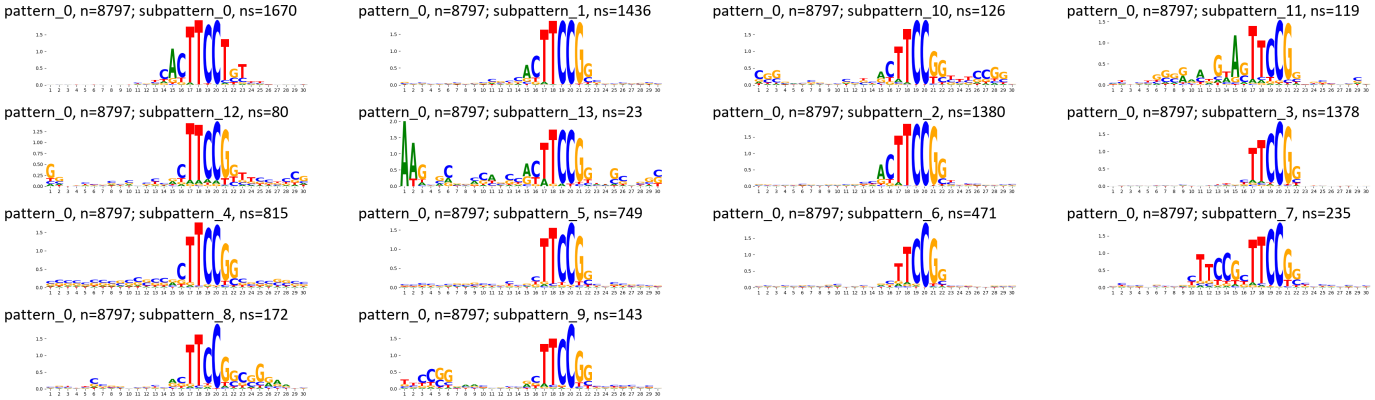

TF-MoDisCO pattern_1 n=4550, CWM

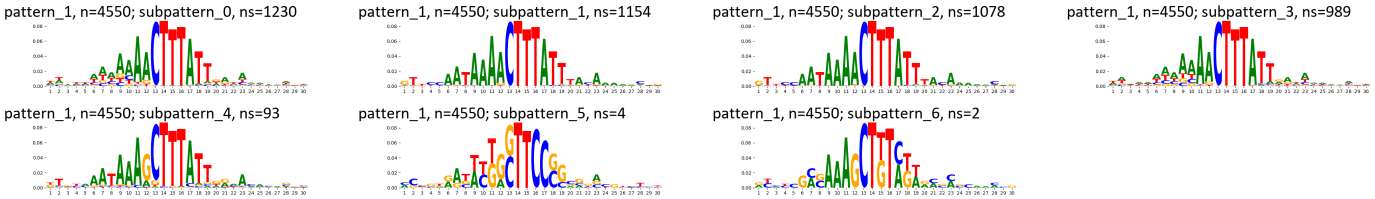

TF-MoDisCO pattern_1 n=4550, PWM

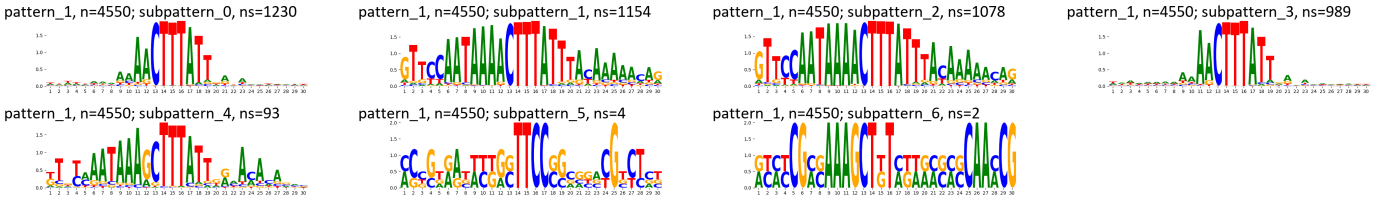

Supplementary Figure 462: TF-MoDisCO subpatterns for the ZBTB40 transcription factor in GM12878 (accession ENCSR189YYK).

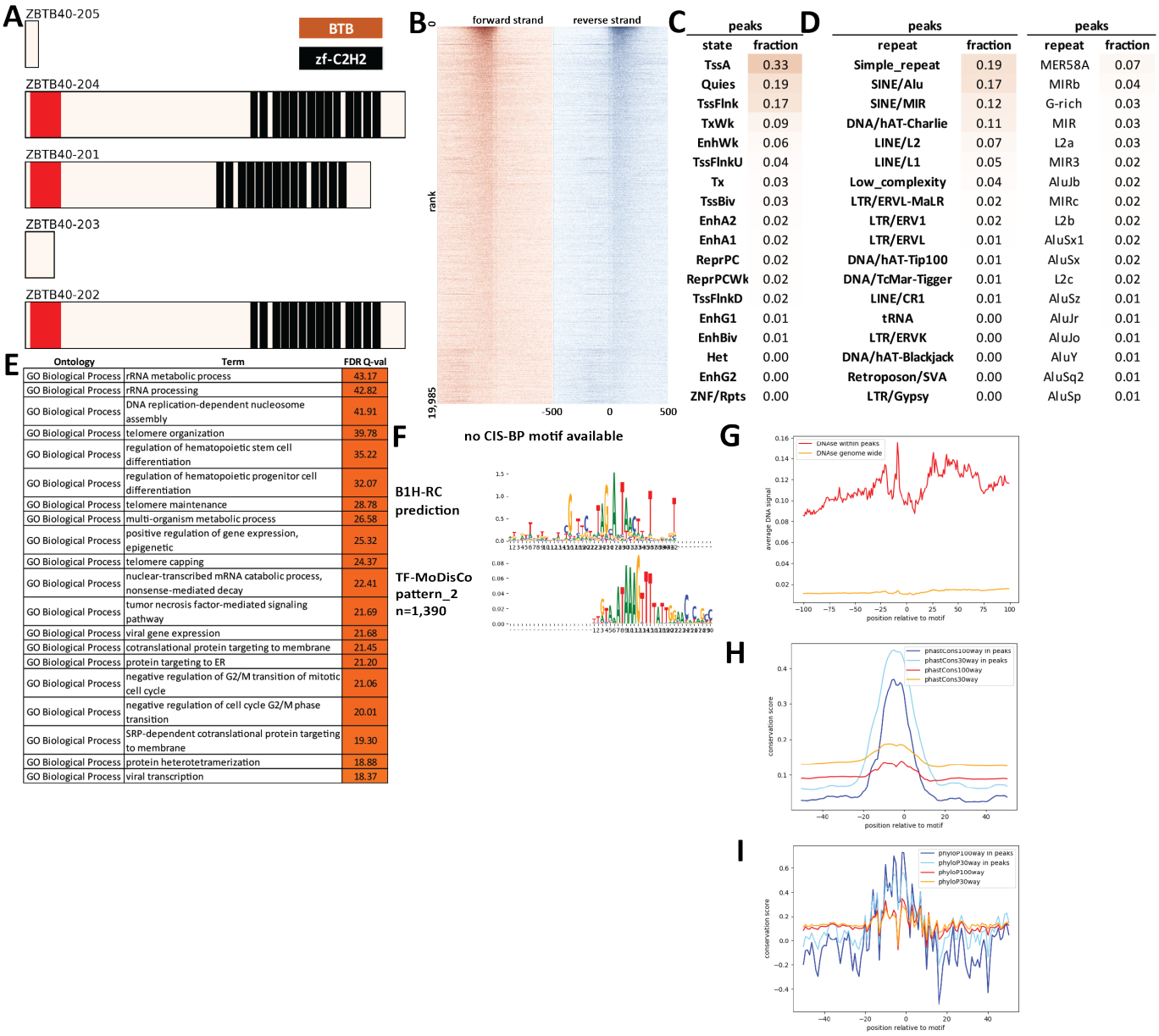

Supplementary Figure 463: Properties and genomic distribution of motifs identified for the ZBTB40 transcription factor in HepG2 (accession ENCSR200AWS).

TF-MoDisCO pattern_2 n=1390, CWM

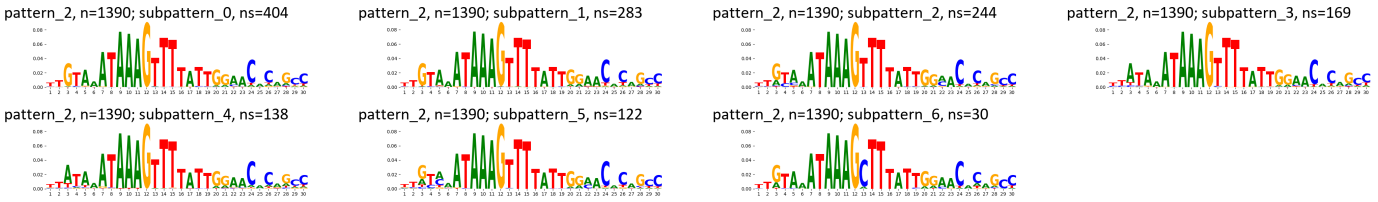

TF-MoDisCO pattern_2 n=1390, CWM

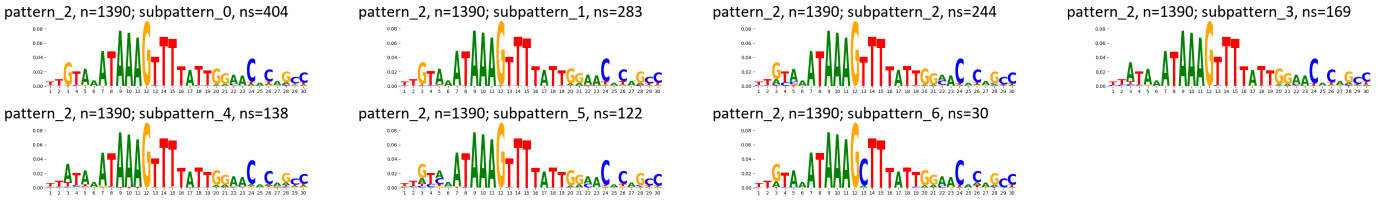

TF-MoDisCO pattern_2 n=1390, PWM

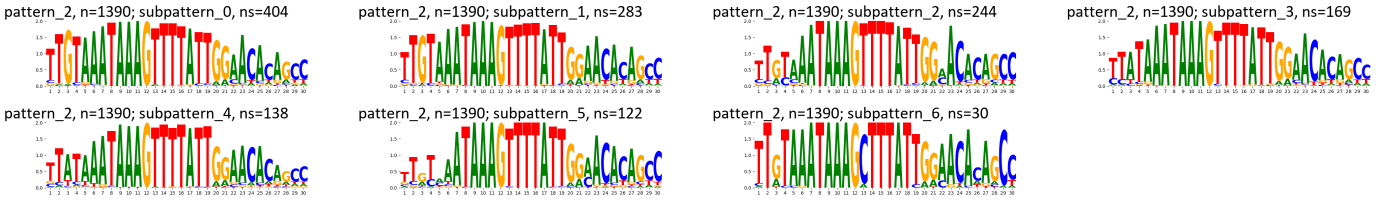

TF-MoDisCO pattern_2 n=1390, PWM

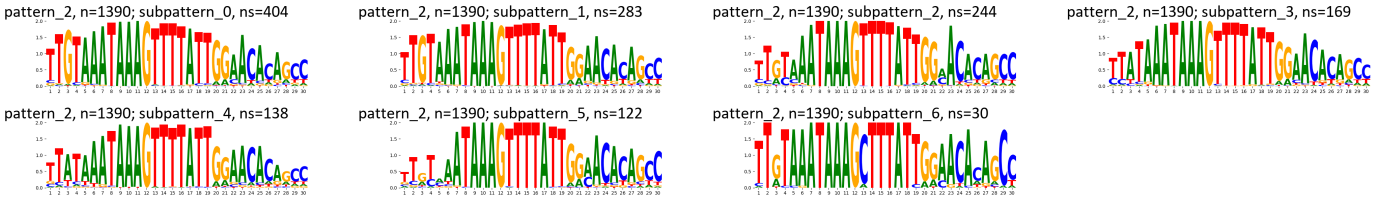

Supplementary Figure 464: TF-MoDisCO subpatterns for the ZBTB40 transcription factor in HepG2 (accession ENCSR200AWS).

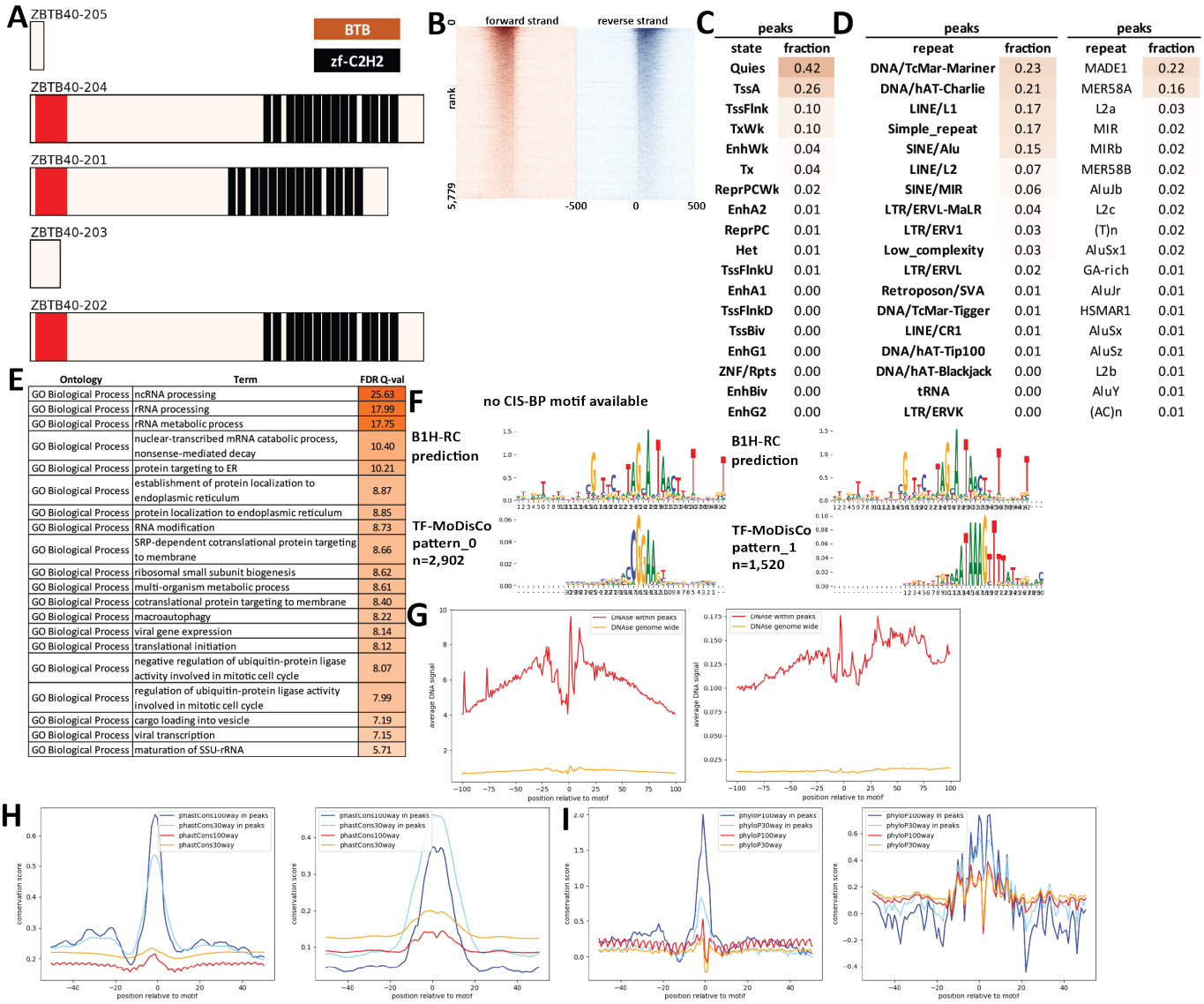

peaks	
state	fraction
Quies	0.42
TssA	0.26
TssFlnk	0.10
TxWk	0.10
EnhWk	0.04
Tx	0.04
ReprPCWk	0.02
EnhA2	0.01
ReprPC	0.01
Het	0.01
TssFlnkU	0.01
EnhA1	0.00
TssFlnkD	0.00
TssBiv	0.00
EnhG1	0.00
ZNF/Rpts	0.00
EnhBiv	0.00
EnhG2	0.00

peaks	
repeat	fraction
DNA/TcMar-Mariner	0.23
DNA/hAT-Charlie	0.21
LINE/L1	0.17
Simple_repeat	0.17
SINE/Alu	0.15
LINE/L2	0.07
SINE/MIR	0.06
LTR/ERVL-MaLR	0.04
LTR/ERV1	0.03
Low_complexity	0.03
LTR/ERVL	0.02
Retroposon/SVA	0.01
DNA/TcMar-Tigger	0.01
LINE/CR1	0.01
DNA/hAT-Tip100	0.01
DNA/hAT-Blackjack	0.00
tRNA	0.00
LTR/ERVK	0.00

peaks	
repeat	fraction
MADE1	0.22
MER58A	0.16
L2a	0.03
MIR	0.02
MIRb	0.02
MER58B	0.02
AluJb	0.02
L2c	0.02
(T)n	0.02
AluSx1	0.02
GA-rich	0.01
AluJr	0.01
HSMAR1	0.01
AluSx	0.01
AluSz	0.01
L2b	0.01
AluY	0.01
(AC)n	0.01

Ontology	Term	FDR Q-val
GO Biological Process	ncRNA processing	25.63
GO Biological Process	rRNA processing	17.99
GO Biological Process	rRNA metabolic process	17.75
GO Biological Process	nuclear-transcribed mRNA catabolic process, nonsense-mediated decay	10.40
GO Biological Process	protein targeting to ER	10.21
GO Biological Process	establishment of protein localization to endoplasmic reticulum	8.87
GO Biological Process	protein localization to endoplasmic reticulum	8.85
GO Biological Process	RNA modification	8.73
GO Biological Process	SRP-dependent cotranslational protein targeting to membrane	8.66
GO Biological Process	ribosomal small subunit biogenesis	8.62
GO Biological Process	multi-organism metabolic process	8.61
GO Biological Process	cotranslational protein targeting to membrane	8.40
GO Biological Process	macroautophagy	8.22
GO Biological Process	viral gene expression	8.14
GO Biological Process	translational initiation	8.12
GO Biological Process	negative regulation of ubiquitin-protein ligase activity involved in mitotic cell cycle	8.07
GO Biological Process	regulation of ubiquitin-protein ligase activity involved in mitotic cell cycle	7.99
GO Biological Process	cargo loading into vesicle	7.19
GO Biological Process	viral transcription	7.15
GO Biological Process	maturation of SSU-rRNA	5.71

Supplementary Figure 465: Properties and genomic distribution of motifs identified for the ZBTB40 transcription factor in HepG2 (accession ENCSR525YFS).

TF-MoDisCO pattern_0 n=2902, CWM

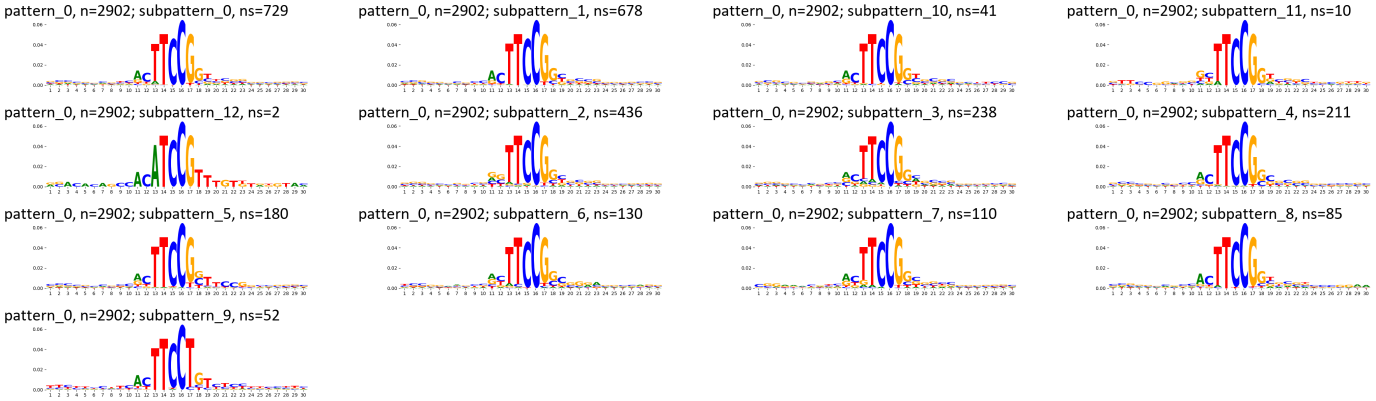

TF-MoDisCO pattern_0 n=2902, PWM

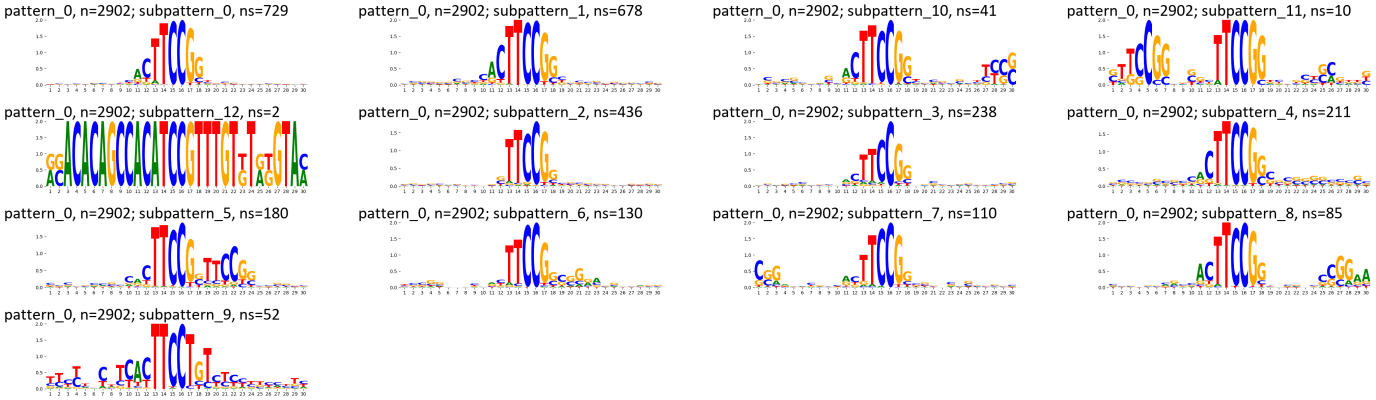

TF-MoDisCO pattern_1 n=1520, CWM

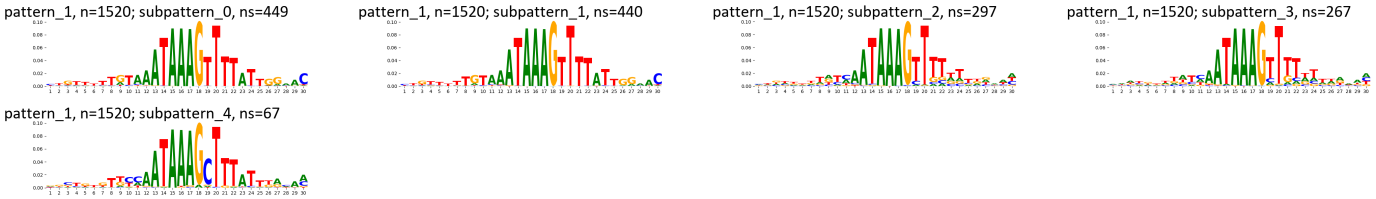

TF-MoDisCO pattern_1 n=1520, PWM

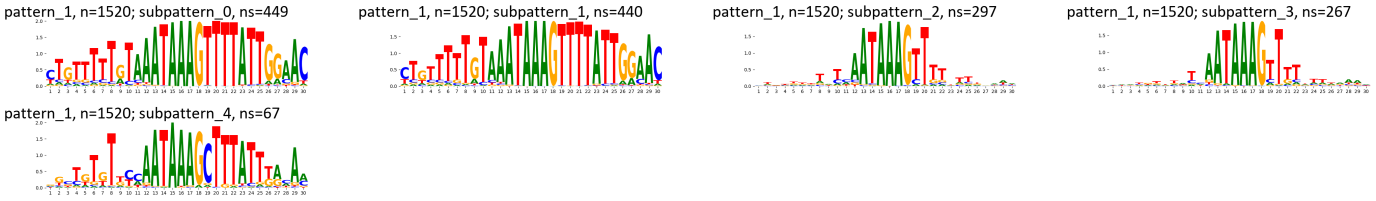

Supplementary Figure 466: TF-MoDisCO subpatterns for the ZBTB40 transcription factor in HepG2 (accession ENCSR525YFS).

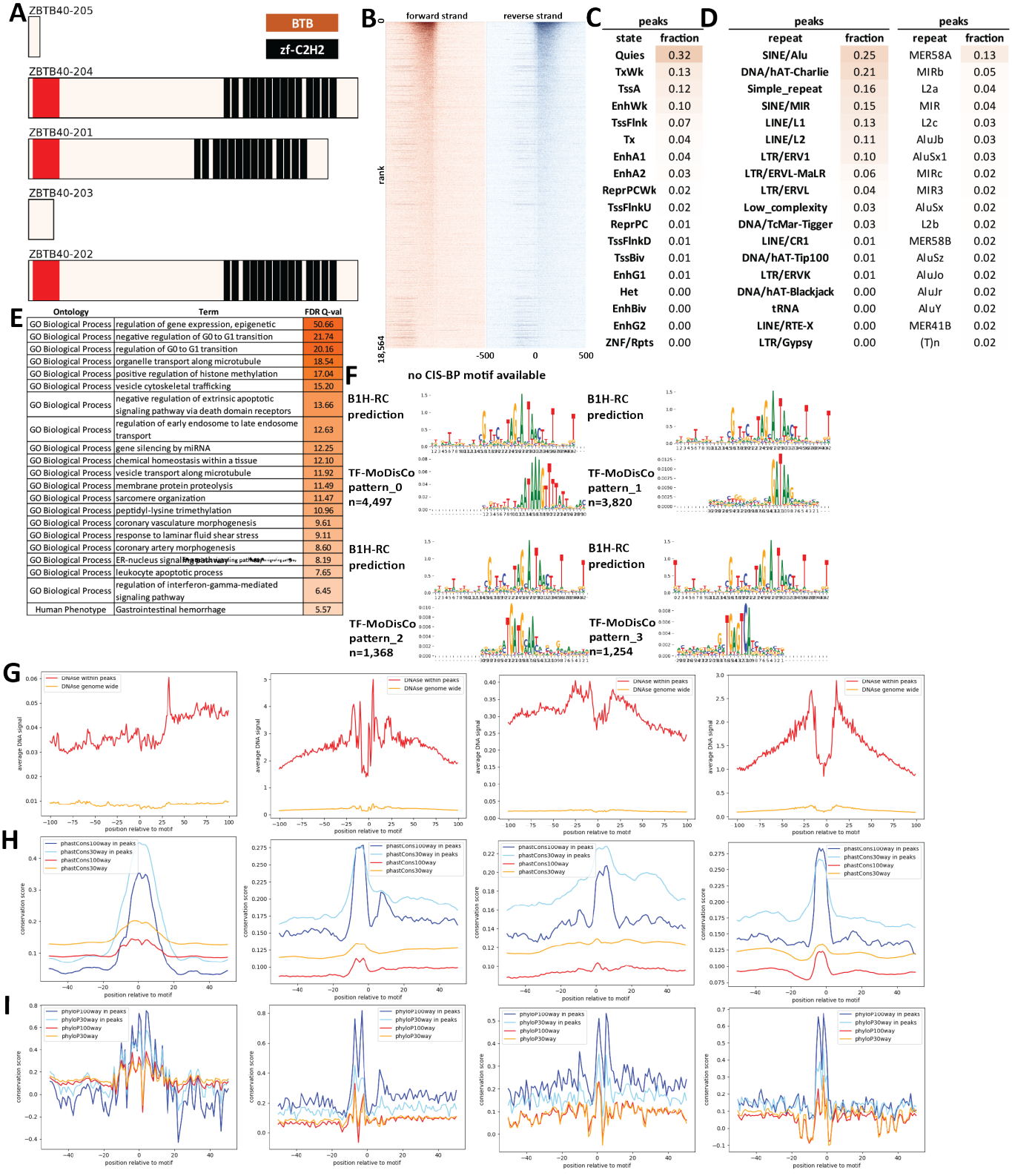

Supplementary Figure 467: Properties and genomic distribution of motifs identified for the ZBTB40 transcription factor in K562 (accession ENCSR158RYZ).

TF-MoDisCO pattern_0 n=4497, CWM

pattern_0, n=4497; subpattern_0, ns=1149

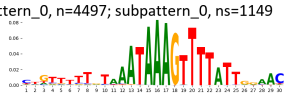

pattern_0, n=4497; subpattern_1, ns=1108

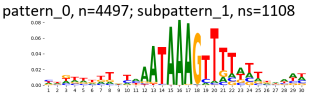

pattern_0, n=4497; subpattern_2, ns=1070

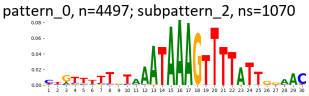

pattern_0, n=4497; subpattern_3, ns=888

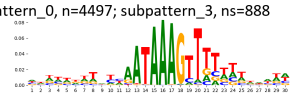

pattern_0, n=4497; subpattern_4, ns=143

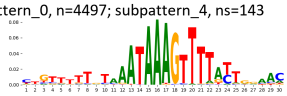

pattern_0, n=4497; subpattern_5, ns=133

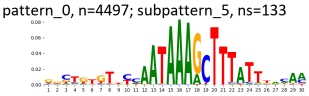

pattern_0, n=4497; subpattern_6, ns=4

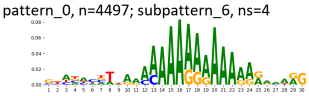

pattern_0, n=4497; subpattern_7, ns=2

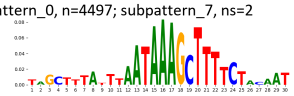

TF-MoDisCO pattern_0 n=4497, PWM

pattern_0, n=4497; subpattern_0, ns=1149

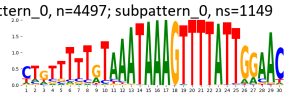

pattern_0, n=4497; subpattern_1, ns=1108

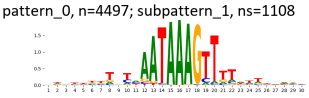

pattern_0, n=4497; subpattern_2, ns=1070

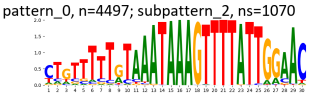

pattern_0, n=4497; subpattern_3, ns=888

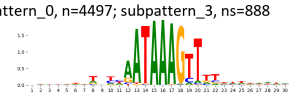

pattern_0, n=4497; subpattern_4, ns=143

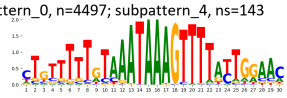

pattern_0, n=4497; subpattern_5, ns=133

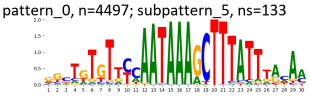

pattern_0, n=4497; subpattern_6, ns=4

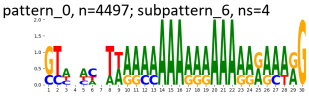

pattern_0, n=4497; subpattern_7, ns=2

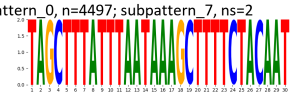

TF-MoDisCO pattern_1 n=3820, CWM

pattern_1, n=3820; subpattern_0, ns=1118

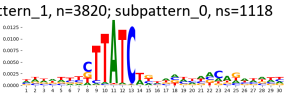

pattern_1, n=3820; subpattern_1, ns=993

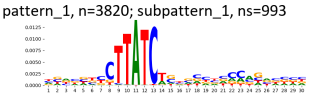

pattern_1, n=3820; subpattern_2, ns=830

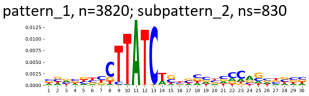

pattern_1, n=3820; subpattern_3, ns=414

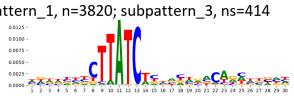

pattern_1, n=3820; subpattern_4, ns=145

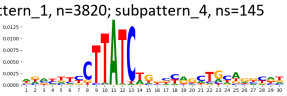

pattern_1, n=3820; subpattern_5, ns=107

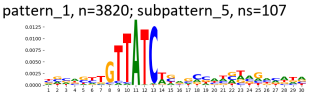

pattern_1, n=3820; subpattern_6, ns=105

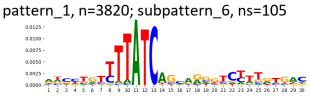

pattern_1, n=3820; subpattern_7, ns=78

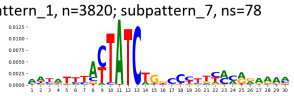

pattern_1, n=3820; subpattern_8, ns=27

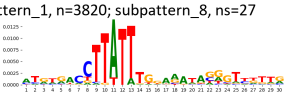

pattern_1, n=3820; subpattern_9, ns=3

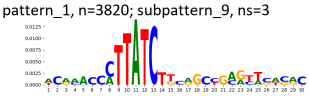

TF-MoDisCO pattern_1 n=3820, PWM

pattern_1, n=3820; subpattern_0, ns=1118

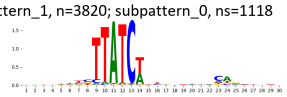

pattern_1, n=3820; subpattern_1, ns=993

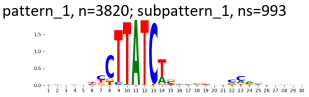

pattern_1, n=3820; subpattern_2, ns=830

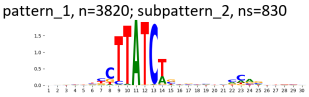

pattern_1, n=3820; subpattern_3, ns=414

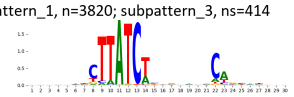

pattern_1, n=3820; subpattern_4, ns=145

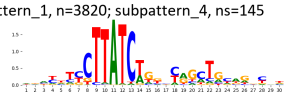

pattern_1, n=3820; subpattern_5, ns=107

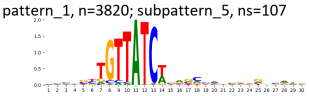

pattern_1, n=3820; subpattern_6, ns=105

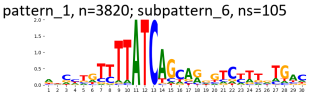

pattern_1, n=3820; subpattern_7, ns=78

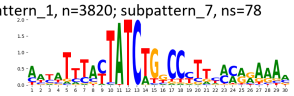

pattern_1, n=3820; subpattern_8, ns=27

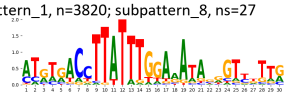

pattern_1, n=3820; subpattern_9, ns=3

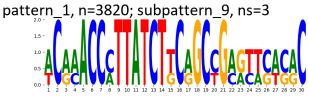

TF-MoDisCO pattern_2 n=1368, CWM

pattern_2, n=1368; subpattern_0, ns=349

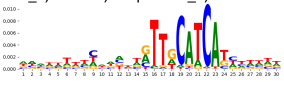

pattern_2, n=1368; subpattern_1, ns=326

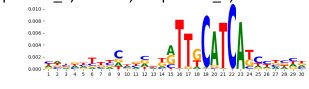

pattern_2, n=1368; subpattern_2, ns=283

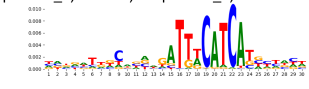

pattern_2, n=1368; subpattern_3, ns=270

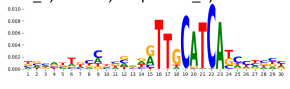

pattern_2, n=1368; subpattern_4, ns=124

pattern_2, n=1368; subpattern_5, ns=6

pattern_2, n=1368; subpattern_6, ns=4

pattern_2, n=1368; subpattern_7, ns=4

pattern_2, n=1368; subpattern_8, ns=2

TF-MoDisCO pattern_2 n=1368, PWM

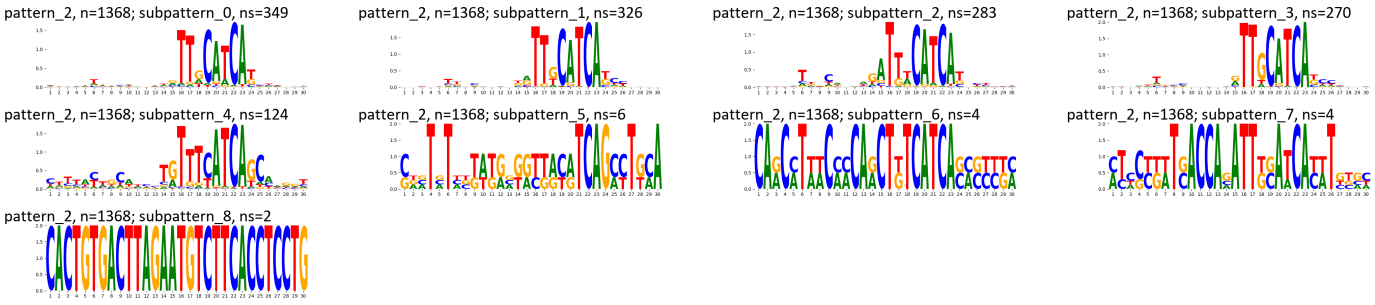

TF-MoDisCO pattern_3 n=1254, CWM

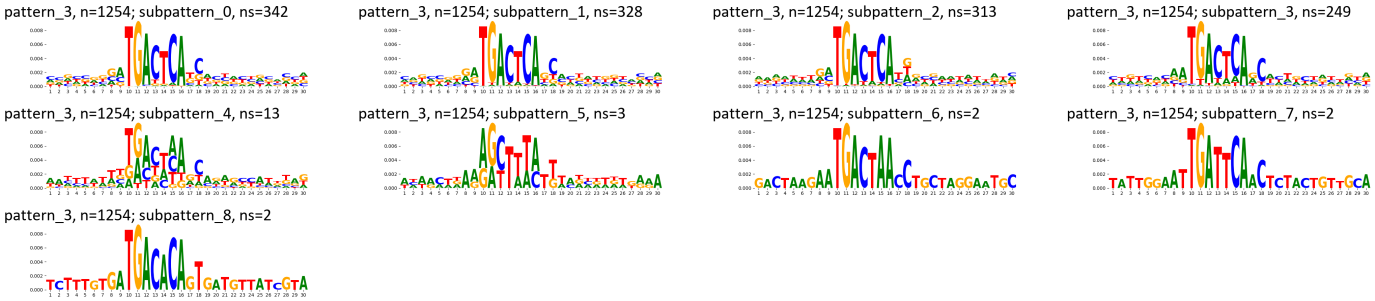

TF-MoDisCO pattern_3 n=1254, PWM

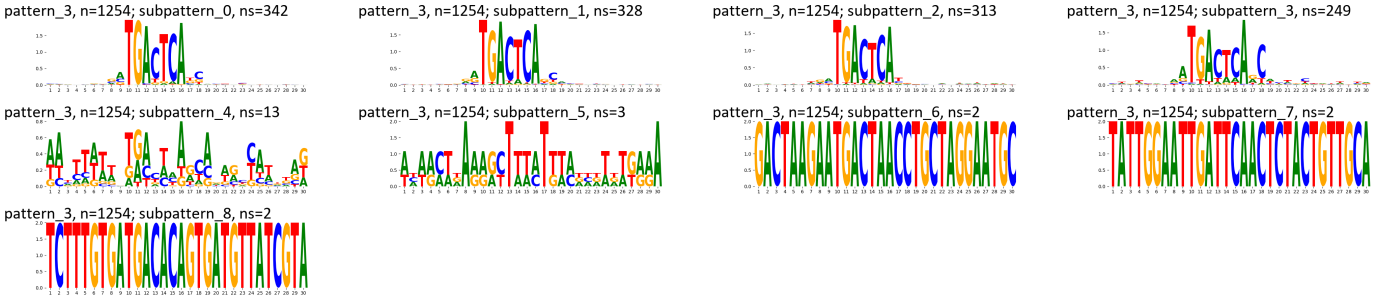

Supplementary Figure 468: TF-MoDisCO subpatterns for the ZBTB40 transcription factor in K562 (accession ENCSR158RYZ).

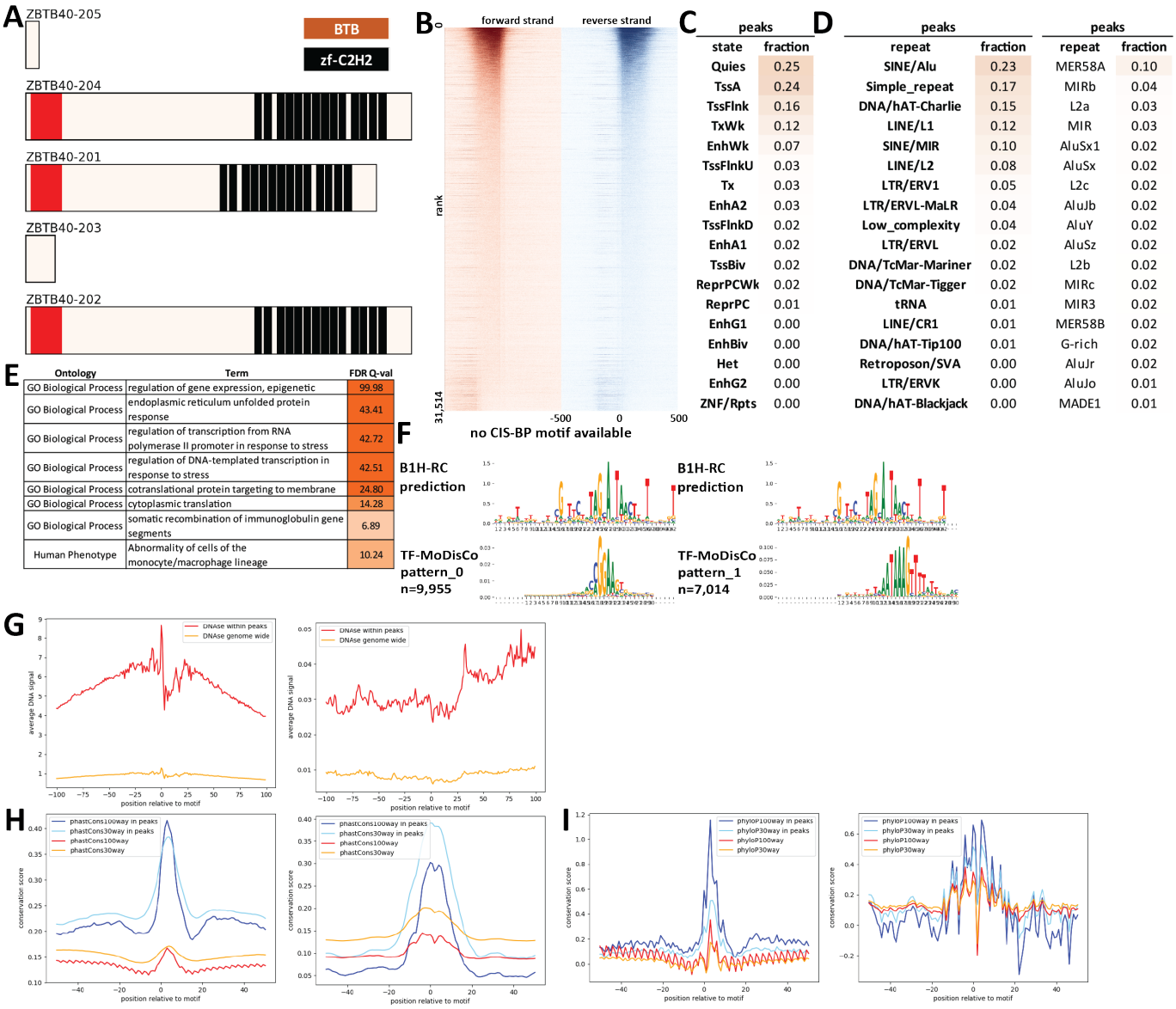

peaks	
state	fraction
Quies	0.25
TssA	0.24
TssFlnk	0.16
TxWk	0.12
EnhWk	0.07
TssFlnkU	0.03
Tx	0.03
EnhA2	0.03
TssFlnkD	0.02
EnhA1	0.02
TssBiv	0.02
ReprPCWk	0.02
ReprPC	0.01
EnhG1	0.00
EnhBiv	0.00
Het	0.00
EnhG2	0.00
ZNF/Rpts	0.00

peaks	
repeat	fraction
SINE/Alu	0.23
Simple_repeat	0.17
DNA/hAT-Charlie	0.15
LINE/L1	0.12
SINE/MIR	0.10
LINE/L2	0.08
LTR/ERV1	0.05
LTR/ERVL-MaLR	0.04
Low_complexity	0.04
LTR/ERVL	0.02
DNA/TcMar-Mariner	0.02
DNA/TcMar-Tigger	0.02
tRNA	0.01
LINE/CR1	0.01
DNA/hAT-Tip100	0.01
Retroposon/SVA	0.00
LTR/ERVK	0.00
DNA/hAT-Blackjack	0.00

peaks	
repeat	fraction
MER58A	0.10
MIRb	0.04
L2a	0.03
MIR	0.03
AluSx1	0.02
AluSx	0.02
L2c	0.02
AluJb	0.02
AluY	0.02
AluSz	0.02
L2b	0.02
MIRc	0.02
MIR3	0.02
MER58B	0.02
G-rich	0.02
AluJr	0.02
AluJo	0.01
MADE1	0.01

Ontology	Term	FDR Q-val
GO Biological Process	regulation of gene expression, epigenetic	99.98
GO Biological Process	endoplasmic reticulum unfolded protein response	43.41
GO Biological Process	regulation of transcription from RNA polymerase II promoter in response to stress	42.72
GO Biological Process	regulation of DNA-templated transcription in response to stress	42.51
GO Biological Process	cotranslational protein targeting to membrane	24.80
GO Biological Process	cytoplasmic translation	14.28
GO Biological Process	somatic recombination of immunoglobulin gene segments	6.89
Human Phenotype	Abnormality of cells of the monocyte/macrophage lineage	10.24

Supplementary Figure 469: Properties and genomic distribution of motifs identified for the ZBTB40 transcription factor in K562 (accession ENCSR237VLT).

TF-MoDisCO pattern_0 n=9955, CWM

pattern_0, n=9955; subpattern_0, ns=2592

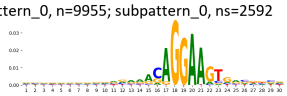

pattern_0, n=9955; subpattern_1, ns=1864

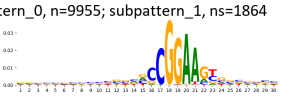

pattern_0, n=9955; subpattern_10, ns=74

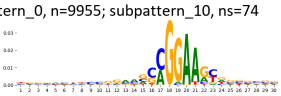

pattern_0, n=9955; subpattern_11, ns=64

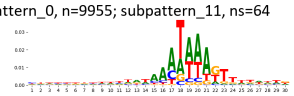

pattern_0, n=9955; subpattern_12, ns=44

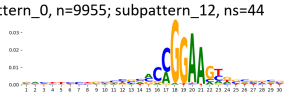

pattern_0, n=9955; subpattern_13, ns=42

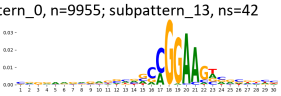

pattern_0, n=9955; subpattern_14, ns=11

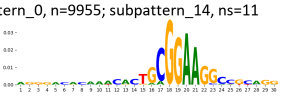

pattern_0, n=9955; subpattern_15, ns=2

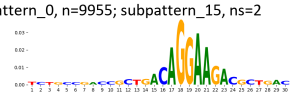

pattern_0, n=9955; subpattern_2, ns=1384

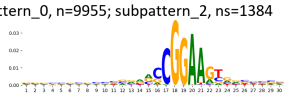

pattern_0, n=9955; subpattern_3, ns=1353

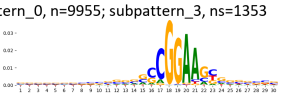

pattern_0, n=9955; subpattern_4, ns=978

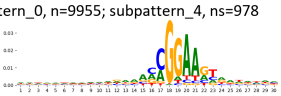

pattern_0, n=9955; subpattern_5, ns=680

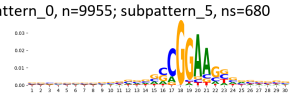

pattern_0, n=9955; subpattern_6, ns=508

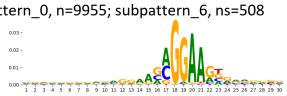

pattern_0, n=9955; subpattern_7, ns=156

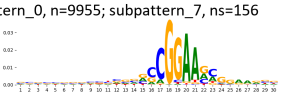

pattern_0, n=9955; subpattern_8, ns=116

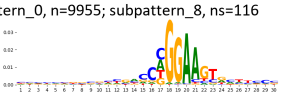

pattern_0, n=9955; subpattern_9, ns=87

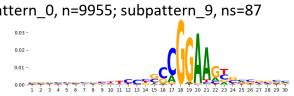

TF-MoDisCO pattern_0 n=9955, PWM

pattern_0, n=9955; subpattern_0, ns=2592

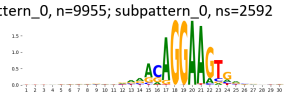

pattern_0, n=9955; subpattern_1, ns=1864

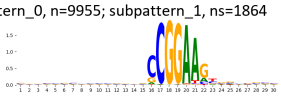

pattern_0, n=9955; subpattern_10, ns=74

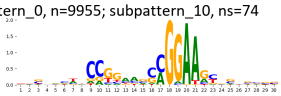

pattern_0, n=9955; subpattern_11, ns=64

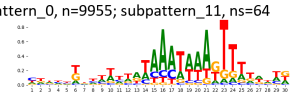

pattern_0, n=9955; subpattern_12, ns=44

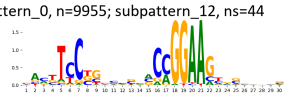

pattern_0, n=9955; subpattern_13, ns=42

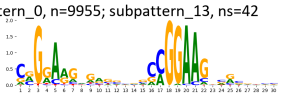

pattern_0, n=9955; subpattern_14, ns=11

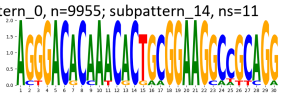

pattern_0, n=9955; subpattern_15, ns=2

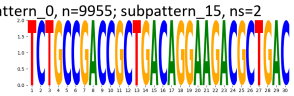

pattern_0, n=9955; subpattern_2, ns=1384

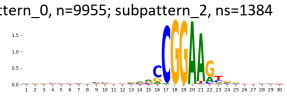

pattern_0, n=9955; subpattern_3, ns=1353

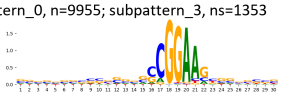

pattern_0, n=9955; subpattern_4, ns=978

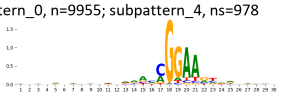

pattern_0, n=9955; subpattern_5, ns=680

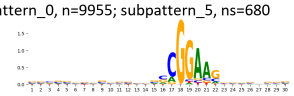

pattern_0, n=9955; subpattern_6, ns=508

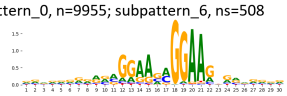

pattern_0, n=9955; subpattern_7, ns=156

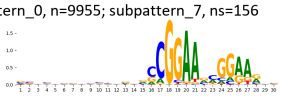

pattern_0, n=9955; subpattern_8, ns=116

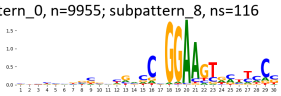

pattern_0, n=9955; subpattern_9, ns=87

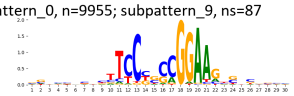

TF-MoDisCO pattern_1 n=7014, CWM

pattern_1, n=7014; subpattern_0, ns=2050

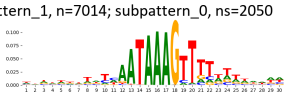

pattern_1, n=7014; subpattern_1, ns=2044

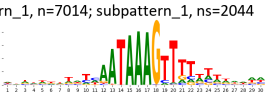

pattern_1, n=7014; subpattern_2, ns=1308

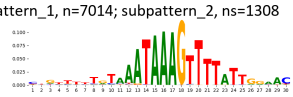

pattern_1, n=7014; subpattern_3, ns=1294

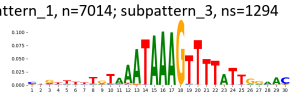

pattern_1, n=7014; subpattern_4, ns=151

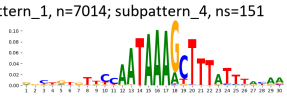

pattern_1, n=7014; subpattern_5, ns=117

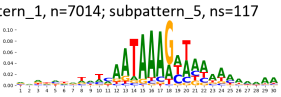

pattern_1, n=7014; subpattern_6, ns=25

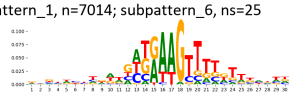

pattern_1, n=7014; subpattern_7, ns=18

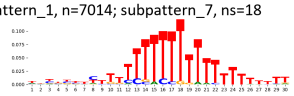

pattern_1, n=7014; subpattern_8, ns=7

TF-MoDisCO pattern_1 n=7014, PWM

pattern_1, n=7014; subpattern_0, ns=2050

pattern_1, n=7014; subpattern_1, ns=2044

pattern_1, n=7014; subpattern_2, ns=1308

pattern_1, n=7014; subpattern_3, ns=1294

pattern_1, n=7014; subpattern_4, ns=151

pattern_1, n=7014; subpattern_5, ns=117

pattern_1, n=7014; subpattern_6, ns=25

pattern_1, n=7014; subpattern_7, ns=18

pattern_1, n=7014; subpattern_8, ns=7

Supplementary Figure 470: TF-MoDisCO subpatterns for the ZBTB40 transcription factor in K562 (accession ENCSR237VLT).

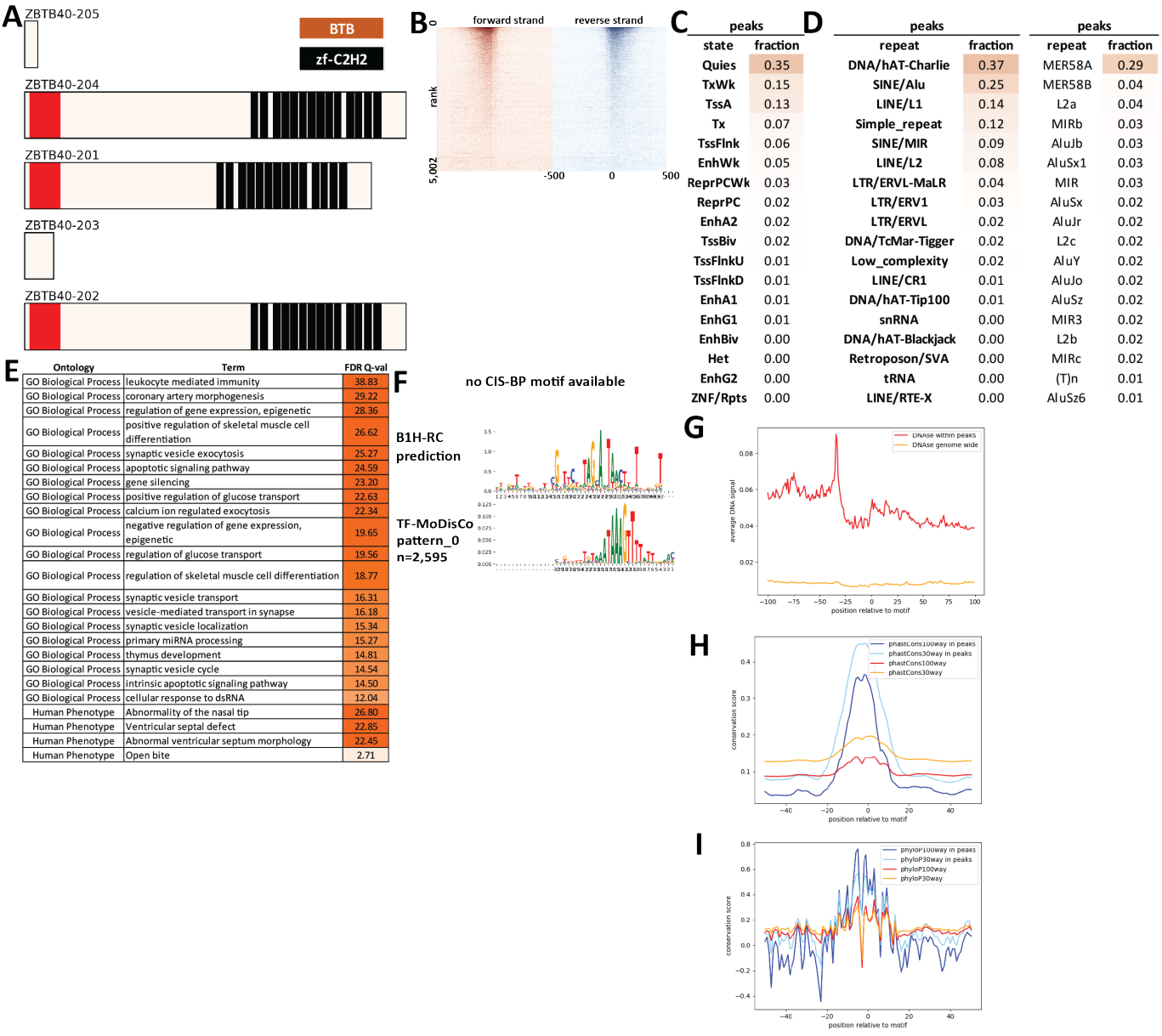

C

peaks	
state	fraction
Quies	0.35
TxWk	0.15
TssA	0.13
Tx	0.07
TssFlnk	0.06
EnhWk	0.05
ReprPCWk	0.03
ReprPC	0.02
EnhA2	0.02
TssBiv	0.02
TssFlnkU	0.01
TssFlnkD	0.01
EnhA1	0.01
EnhG1	0.01
EnhBiv	0.00
Het	0.00
EnhG2	0.00
ZNF/Rpts	0.00

D

peaks		peaks	
repeat	fraction	repeat	fraction
DNA/hAT-Charlie	0.37	MER58A	0.29
SINE/Alu	0.25	MER58B	0.04
LINE/L1	0.14	L2a	0.04
Simple_repeat	0.12	MIRb	0.03
SINE/MIR	0.09	AluJb	0.03
LINE/L2	0.08	AluSx1	0.03
LTR/ERVL-MaLR	0.04	MIR	0.03
LTR/ERV1	0.03	AluSx	0.02
LTR/ERVL	0.02	AluJr	0.02
DNA/TcMar-Tigger	0.02	L2c	0.02
Low_complexity	0.02	AluY	0.02
LINE/CR1	0.01	AluJo	0.02
DNA/hAT-Tip100	0.01	AluSz	0.02
snRNA	0.00	MIR3	0.02
DNA/hAT-Blackjack	0.00	L2b	0.02
Retroposon/SVA	0.00	MIRc	0.02
tRNA	0.00	(T)n	0.01
LINE/RTE-X	0.00	AluSz6	0.01

E

Ontology	Term	FDR Q-val
GO Biological Process	leukocyte mediated immunity	38.83
GO Biological Process	coronary artery morphogenesis	29.22
GO Biological Process	regulation of gene expression, epigenetic	28.36
GO Biological Process	positive regulation of skeletal muscle cell differentiation	26.62
GO Biological Process	synaptic vesicle exocytosis	25.27
GO Biological Process	apoptotic signaling pathway	24.59
GO Biological Process	gene silencing	23.20
GO Biological Process	positive regulation of glucose transport	22.63
GO Biological Process	calcium ion regulated exocytosis	22.34
GO Biological Process	negative regulation of gene expression, epigenetic	19.65
GO Biological Process	regulation of glucose transport	19.56
GO Biological Process	regulation of skeletal muscle cell differentiation	18.77
GO Biological Process	synaptic vesicle transport	16.31
GO Biological Process	vesicle-mediated transport in synapse	16.18
GO Biological Process	synaptic vesicle localization	15.34
GO Biological Process	primary miRNA processing	15.27
GO Biological Process	thymus development	14.81
GO Biological Process	synaptic vesicle cycle	14.54
GO Biological Process	intrinsic apoptotic signaling pathway	14.50
GO Biological Process	cellular response to dsRNA	12.04
Human Phenotype	Abnormality of the nasal tip	26.80
Human Phenotype	Ventricular septal defect	22.85
Human Phenotype	Abnormal ventricular septum morphology	22.45
Human Phenotype	Open bite	2.71

Supplementary Figure 471: Properties and genomic distribution of motifs identified for the ZBTB40 transcription factor in K562 (accession ENCSR579YNY).

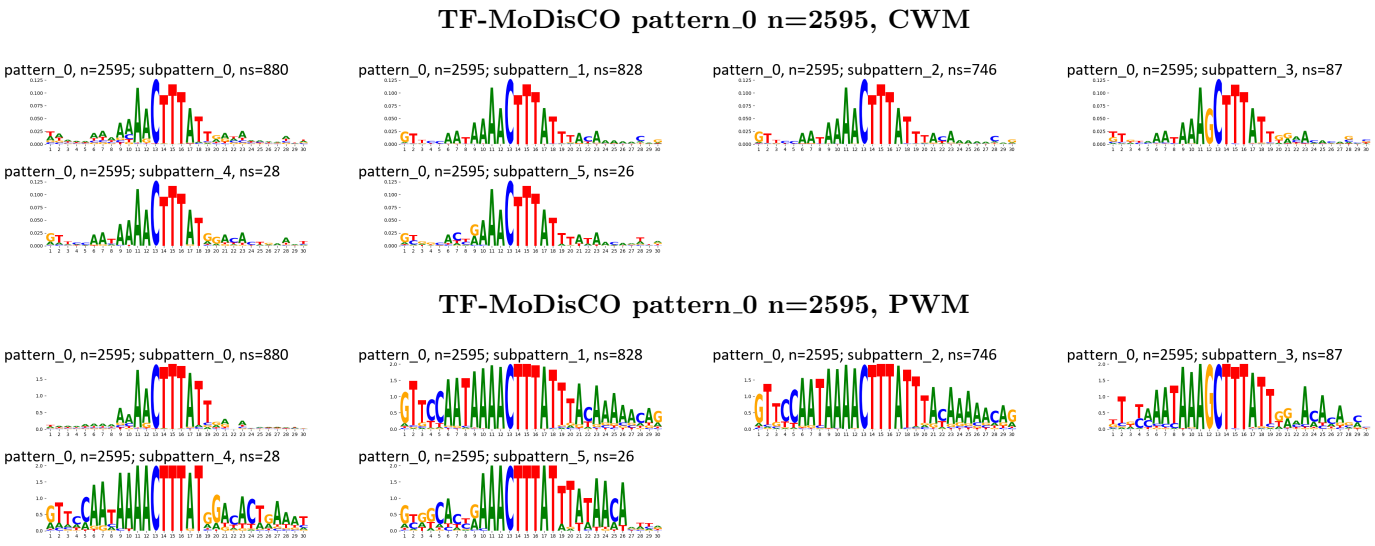

Supplementary Figure 472: TF-MoDisCO subpatterns for the ZBTB40 transcription factor in K562 (accession ENCSR579YNY).

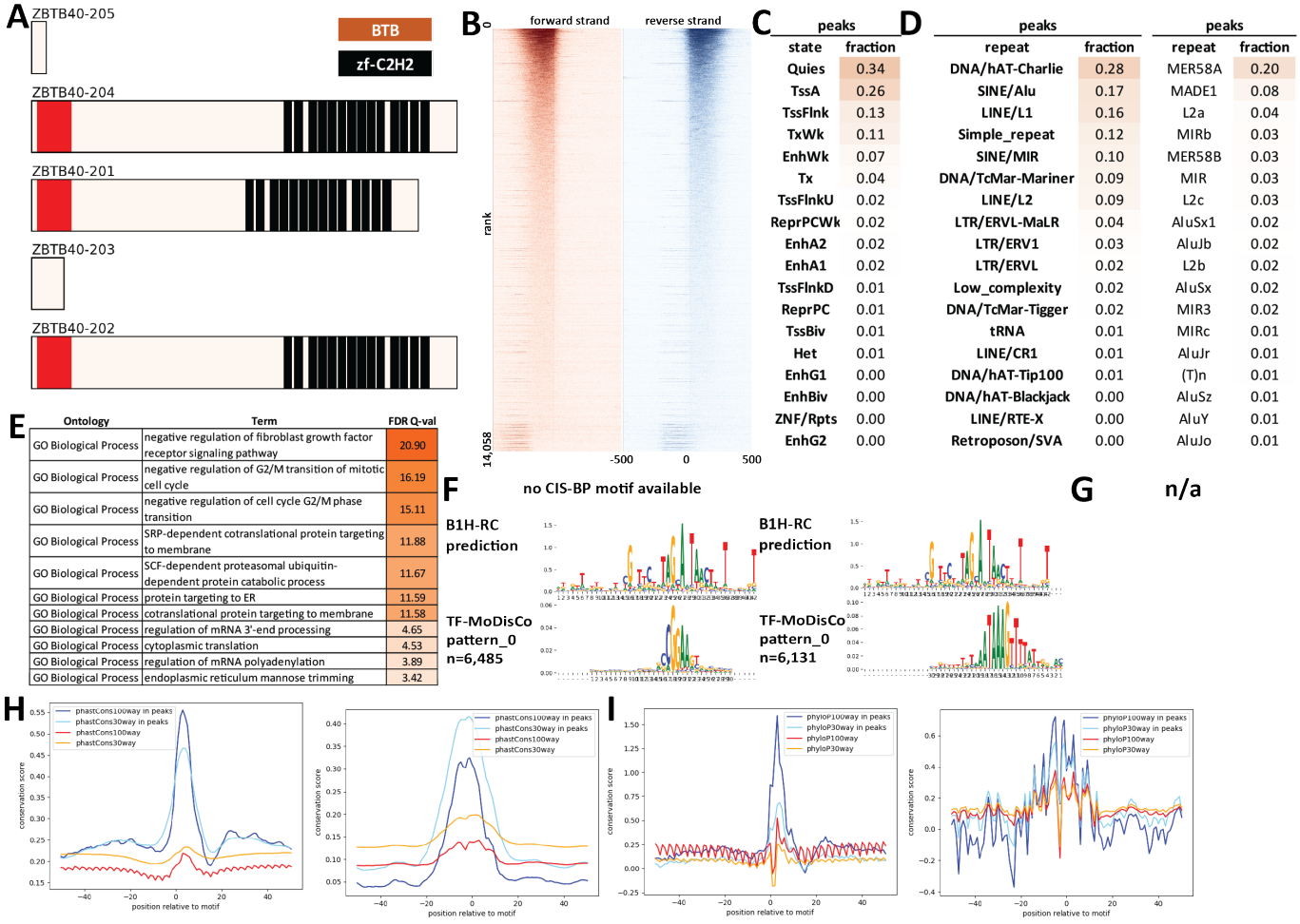

Supplementary Figure 473: Properties and genomic distribution of motifs identified for the ZBTB40 transcription factor in MCF-7 (accession ENCSR318LVG).

TF-MoDisCO pattern_0 n=6485, CWM

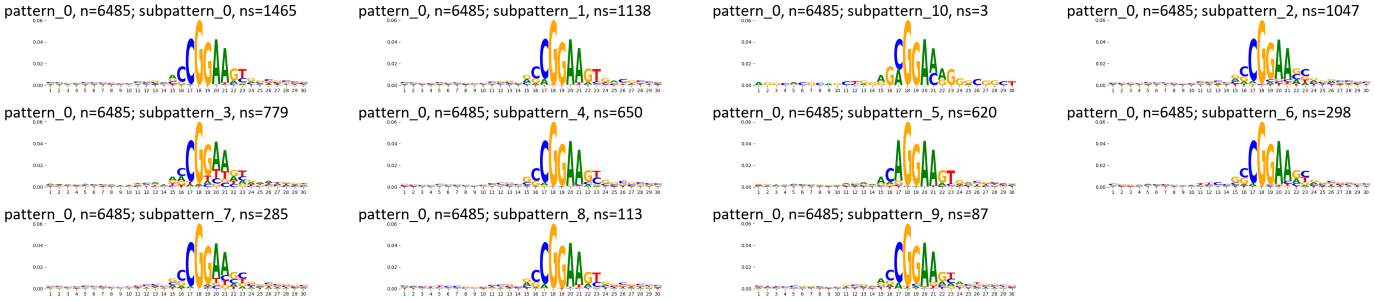

TF-MoDisCO pattern_0 n=6485, PWM

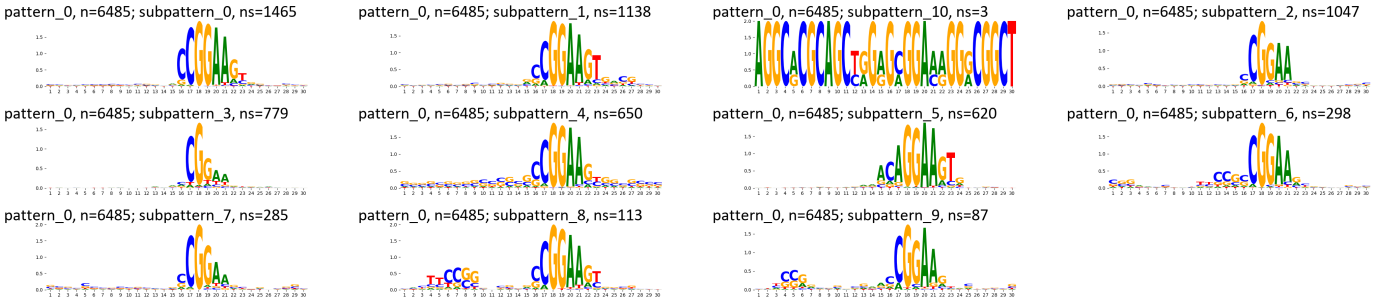

TF-MoDisCO pattern_1 n=6131, CWM

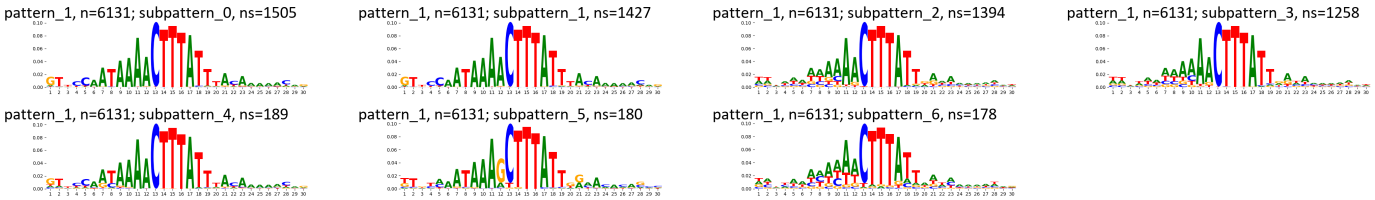

TF-MoDisCO pattern_1 n=6131, PWM

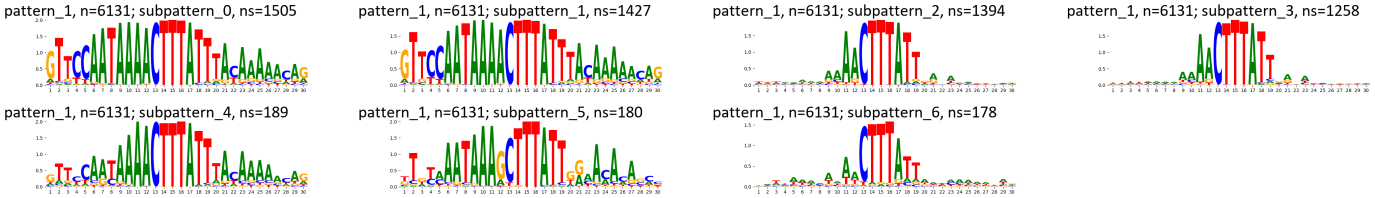

Supplementary Figure 474: TF-MoDisCO subpatterns for the ZBTB40 transcription factor in MCF-7 (accession ENCSR318LVG).

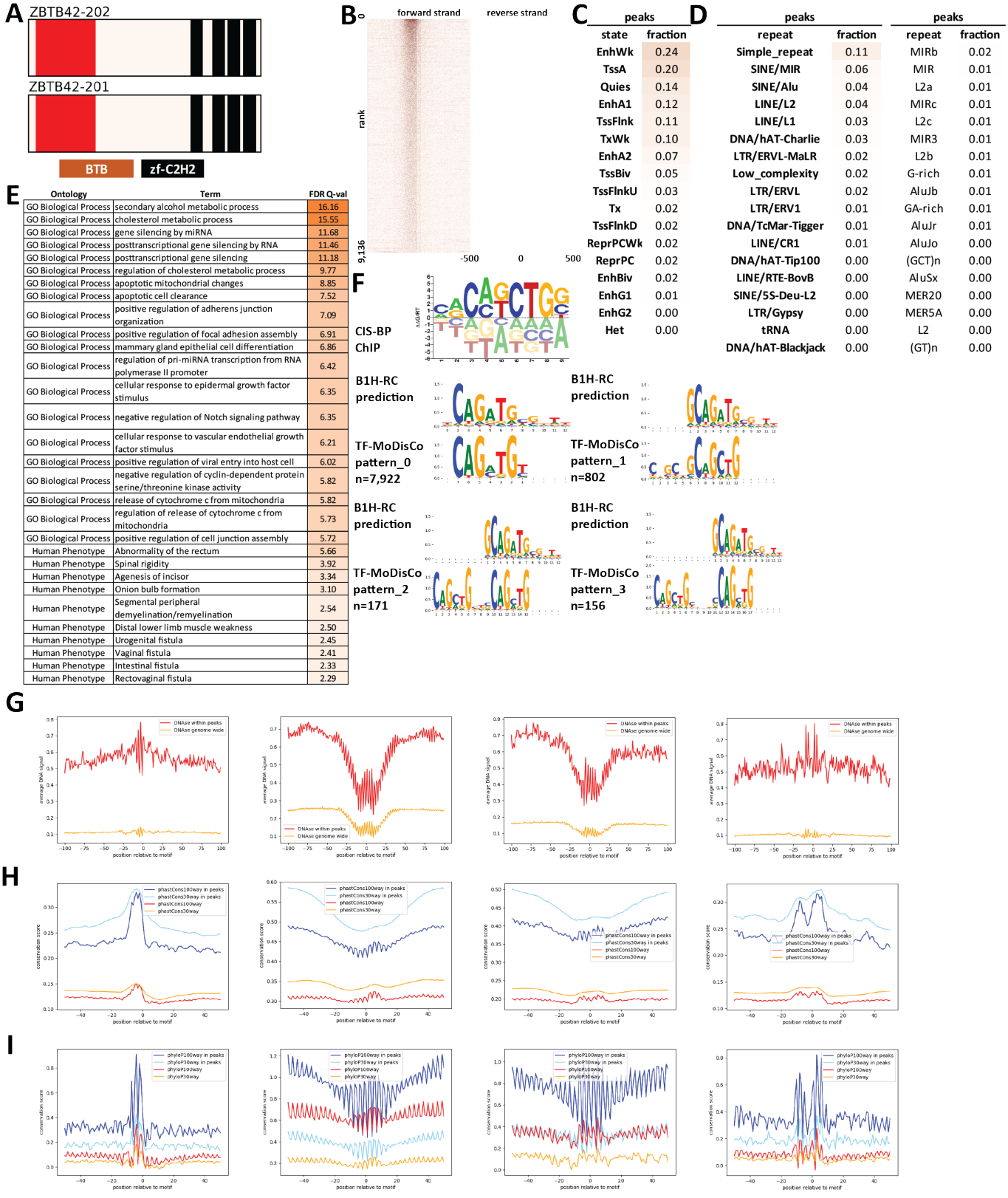

Supplementary Figure 475: Properties and genomic distribution of motifs identified for the ZBTB42 transcription factor in HEK293 (accession Hughes GR models).

TF-MoDisCO pattern_0 n=7922, CWM

pattern_0, n=7922; subpattern_0, ns=1926

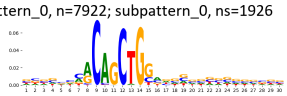

pattern_0, n=7922; subpattern_1, ns=1822

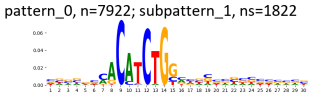

pattern_0, n=7922; subpattern_10, ns=149

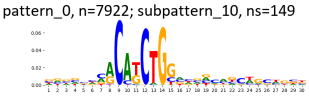

pattern_0, n=7922; subpattern_11, ns=68

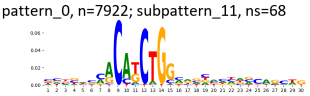

pattern_0, n=7922; subpattern_12, ns=38

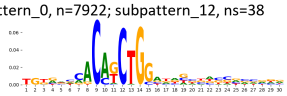

pattern_0, n=7922; subpattern_2, ns=1184

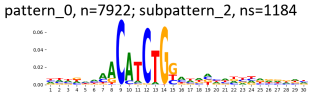

pattern_0, n=7922; subpattern_3, ns=776

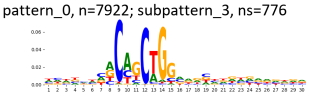

pattern_0, n=7922; subpattern_4, ns=513

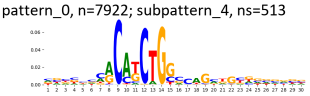

pattern_0, n=7922; subpattern_5, ns=483

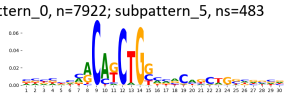

pattern_0, n=7922; subpattern_6, ns=395

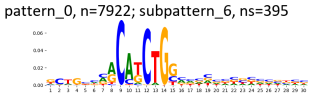

pattern_0, n=7922; subpattern_7, ns=214

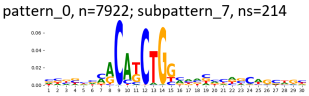

pattern_0, n=7922; subpattern_8, ns=188

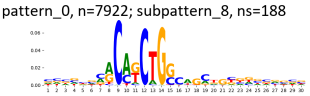

pattern_0, n=7922; subpattern_9, ns=166

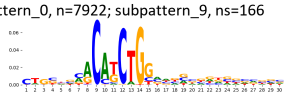

TF-MoDisCO pattern_0 n=7922, PWM

pattern_0, n=7922; subpattern_0, ns=1926

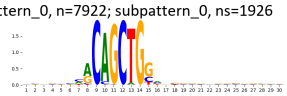

pattern_0, n=7922; subpattern_1, ns=1822

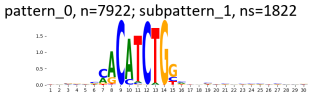

pattern_0, n=7922; subpattern_10, ns=149

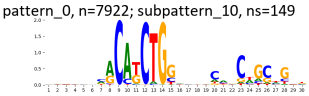

pattern_0, n=7922; subpattern_11, ns=68

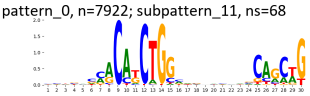

pattern_0, n=7922; subpattern_12, ns=38

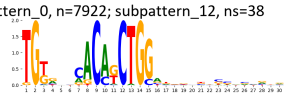

pattern_0, n=7922; subpattern_2, ns=1184

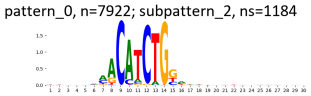

pattern_0, n=7922; subpattern_3, ns=776

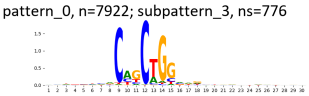

pattern_0, n=7922; subpattern_4, ns=513

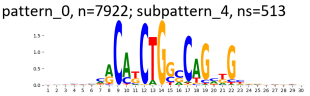

pattern_0, n=7922; subpattern_5, ns=483

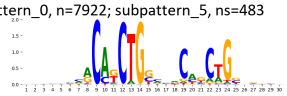

pattern_0, n=7922; subpattern_6, ns=395

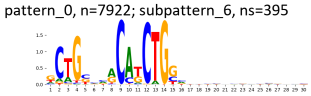

pattern_0, n=7922; subpattern_7, ns=214

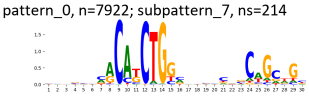

pattern_0, n=7922; subpattern_8, ns=188

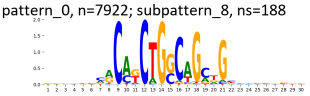

pattern_0, n=7922; subpattern_9, ns=166

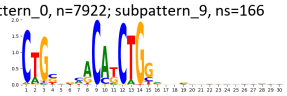

TF-MoDisCO pattern_1 n=802, CWM

pattern_1, n=802; subpattern_0, ns=200

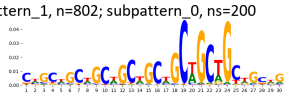

pattern_1, n=802; subpattern_1, ns=146

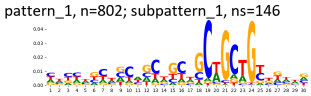

pattern_1, n=802; subpattern_2, ns=144

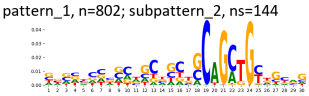

pattern_1, n=802; subpattern_3, ns=132

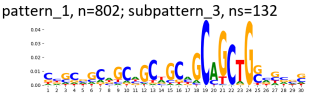

pattern_1, n=802; subpattern_4, ns=119

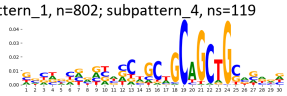

pattern_1, n=802; subpattern_5, ns=61

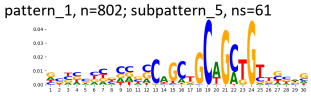

TF-MoDisCO pattern_1 n=802, PWM

pattern_1, n=802; subpattern_0, ns=200

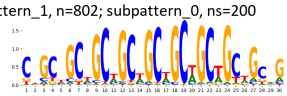

pattern_1, n=802; subpattern_1, ns=146

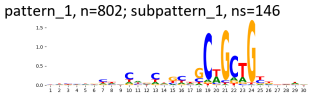

pattern_1, n=802; subpattern_2, ns=144

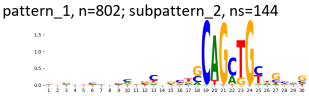

pattern_1, n=802; subpattern_3, ns=132

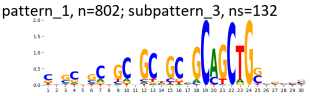

pattern_1, n=802; subpattern_4, ns=119

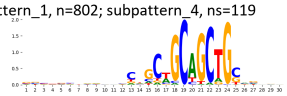

pattern_1, n=802; subpattern_5, ns=61

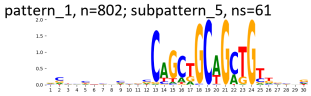

TF-MoDisCO pattern_2 n=171, CWM

pattern_2, n=171; subpattern_0, ns=39

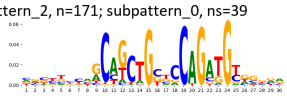

pattern_2, n=171; subpattern_1, ns=38

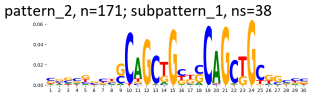

pattern_2, n=171; subpattern_2, ns=36

pattern_2, n=171; subpattern_3, ns=32

pattern_2, n=171; subpattern_4, ns=19

pattern_2, n=171; subpattern_5, ns=7

TF-MoDisCO pattern_2 n=171, PWM

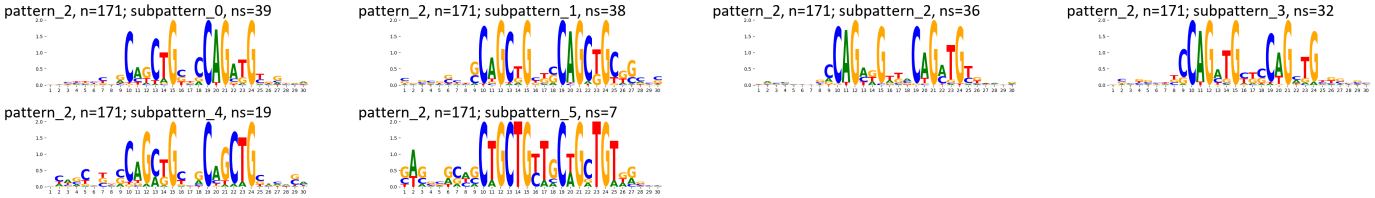

TF-MoDisCO pattern_3 n=156, CWM

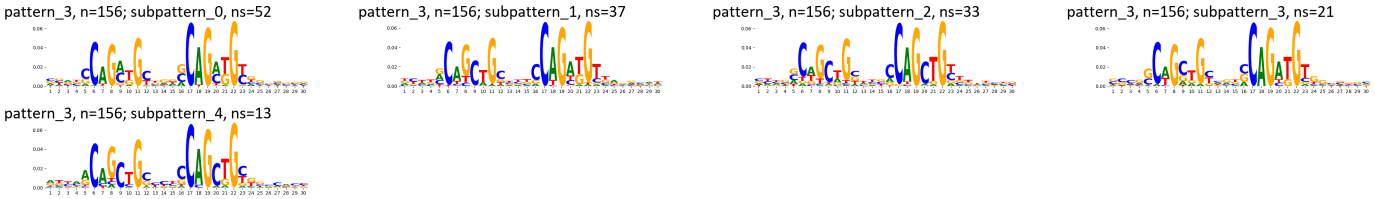

TF-MoDisCO pattern_3 n=156, PWM

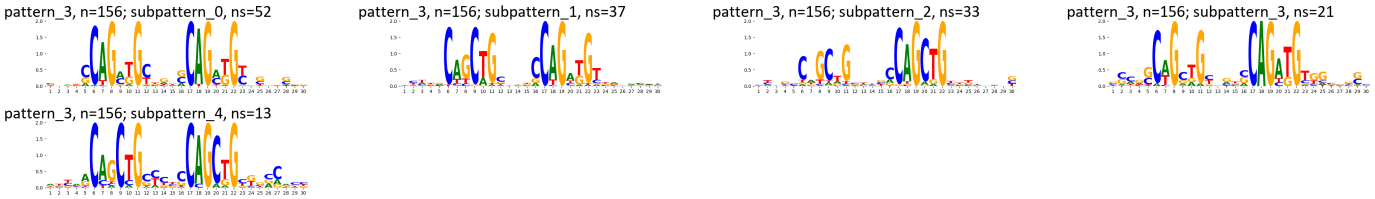

Supplementary Figure 476: TF-MoDisCO subpatterns for the ZBTB42 transcription factor in HEK293 (accession Hughes GR models).

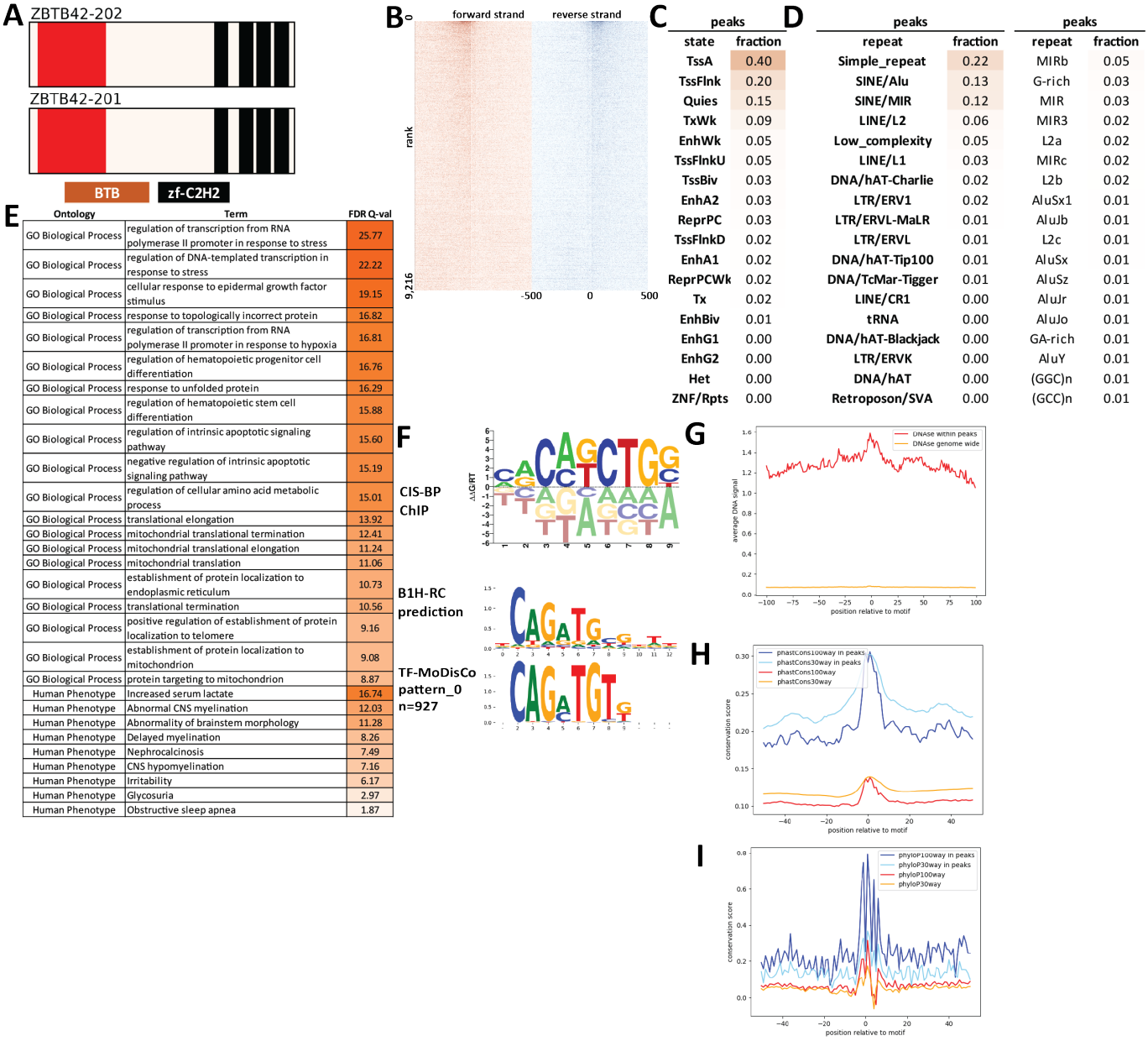

Supplementary Figure 477: Properties and genomic distribution of motifs identified for the ZBTB42 transcription factor in HepG2 (accession ENCSR232AAR).

TF-MoDisCO pattern_0 n=927, CWM

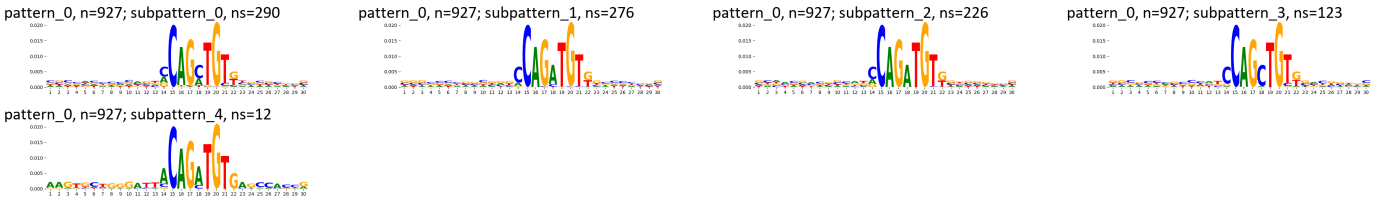

TF-MoDisCO pattern_0 n=927, PWM

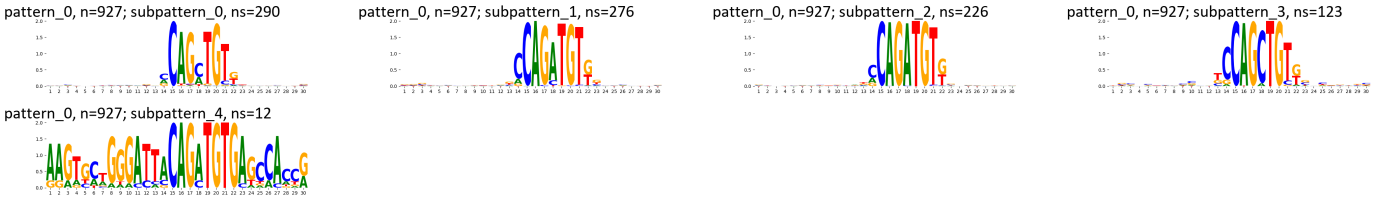

Supplementary Figure 478: TF-MoDisCO subpatterns for the ZBTB42 transcription factor in HepG2 (accession ENCSR232AAR).

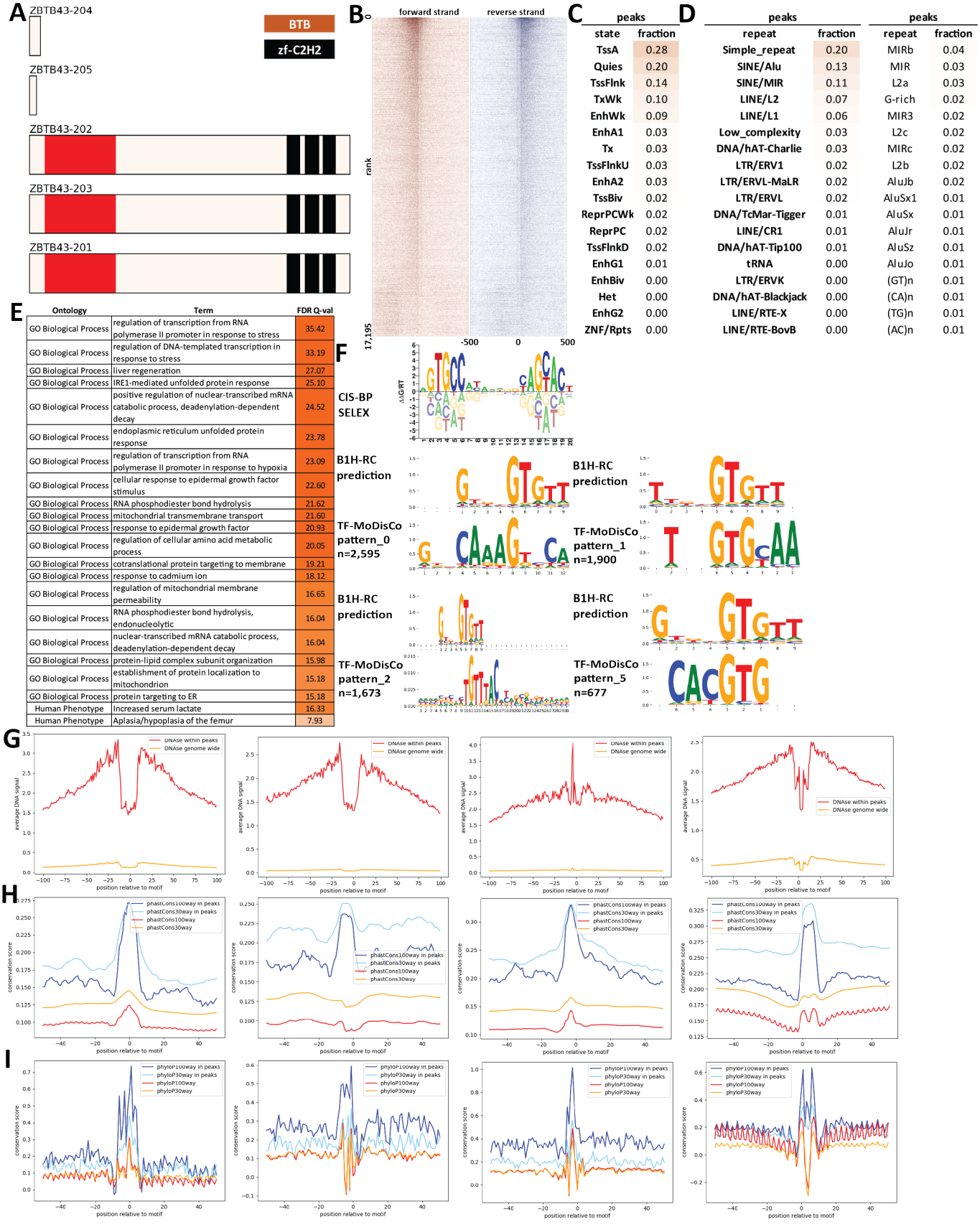

Supplementary Figure 479: Properties and genomic distribution of motifs identified for the ZBTB43 transcription factor in HepG2 (accession ENCSR173USN).

TF-MoDisCO pattern_0 n=2595, CWM

pattern_0, n=2595; subpattern_0, ns=626

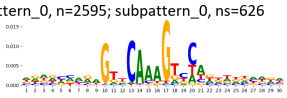

pattern_0, n=2595; subpattern_1, ns=409

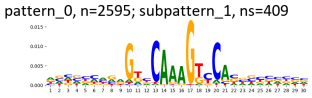

pattern_0, n=2595; subpattern_2, ns=394

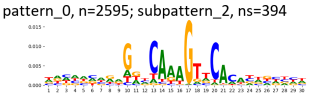

pattern_0, n=2595; subpattern_3, ns=389

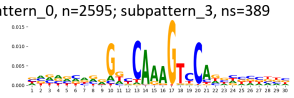

pattern_0, n=2595; subpattern_4, ns=303

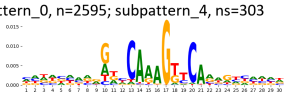

pattern_0, n=2595; subpattern_5, ns=195

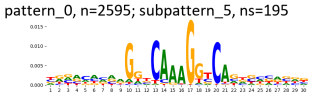

pattern_0, n=2595; subpattern_6, ns=125

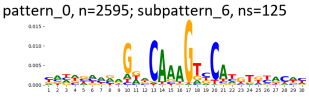

pattern_0, n=2595; subpattern_7, ns=105

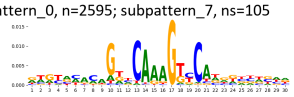

pattern_0, n=2595; subpattern_8, ns=49

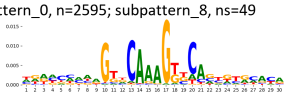

TF-MoDisCO pattern_0 n=2595, PWM

pattern_0, n=2595; subpattern_0, ns=626

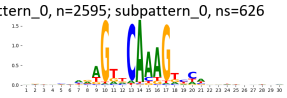

pattern_0, n=2595; subpattern_1, ns=409

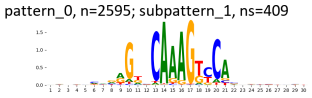

pattern_0, n=2595; subpattern_2, ns=394

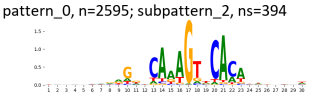

pattern_0, n=2595; subpattern_3, ns=389

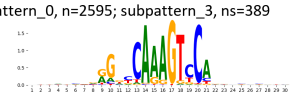

pattern_0, n=2595; subpattern_4, ns=303

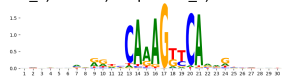

pattern_0, n=2595; subpattern_5, ns=195

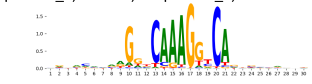

pattern_0, n=2595; subpattern_6, ns=125

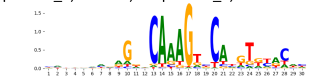

pattern_0, n=2595; subpattern_7, ns=105

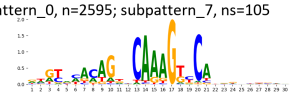

pattern_0, n=2595; subpattern_8, ns=49

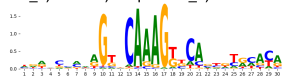

TF-MoDisCO pattern_1 n=1900, CWM

pattern_1, n=1900; subpattern_0, ns=410

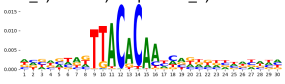

pattern_1, n=1900; subpattern_1, ns=357

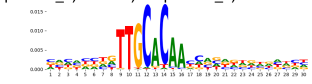

pattern_1, n=1900; subpattern_2, ns=286

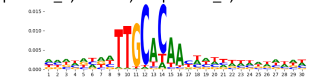

pattern_1, n=1900; subpattern_3, ns=253

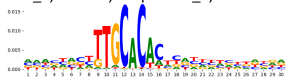

pattern_1, n=1900; subpattern_4, ns=226

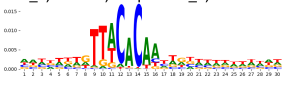

pattern_1, n=1900; subpattern_5, ns=155

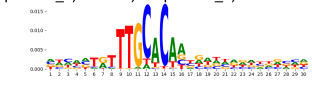

pattern_1, n=1900; subpattern_6, ns=148

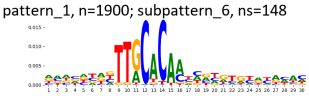

pattern_1, n=1900; subpattern_7, ns=36

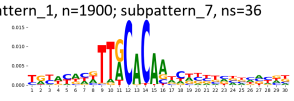

pattern_1, n=1900; subpattern_8, ns=29

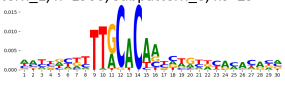

TF-MoDisCO pattern_1 n=1900, PWM

pattern_1, n=1900; subpattern_0, ns=410

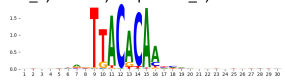

pattern_1, n=1900; subpattern_1, ns=357

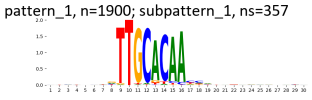

pattern_1, n=1900; subpattern_2, ns=286

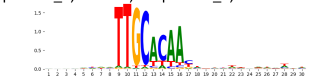

pattern_1, n=1900; subpattern_3, ns=253

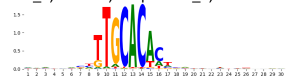

pattern_1, n=1900; subpattern_4, ns=226

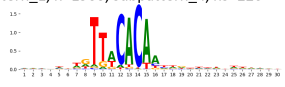

pattern_1, n=1900; subpattern_5, ns=155

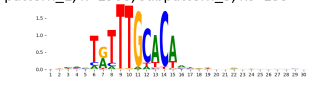

pattern_1, n=1900; subpattern_6, ns=148

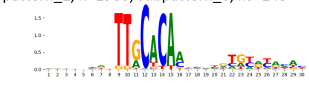

pattern_1, n=1900; subpattern_7, ns=36

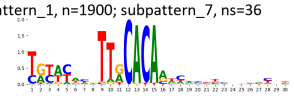

pattern_1, n=1900; subpattern_8, ns=29

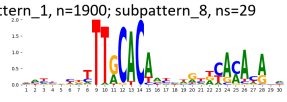

TF-MoDisCO pattern_2 n=1673, CWM

pattern_2, n=1673; subpattern_0, ns=456

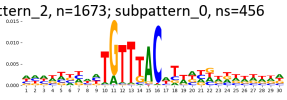

pattern_2, n=1673; subpattern_1, ns=318

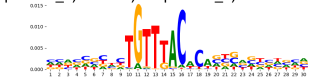

pattern_2, n=1673; subpattern_2, ns=291

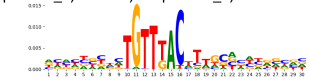

pattern_2, n=1673; subpattern_3, ns=153

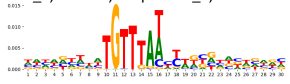

pattern_2, n=1673; subpattern_4, ns=129

pattern_2, n=1673; subpattern_5, ns=119

pattern_2, n=1673; subpattern_6, ns=96

pattern_2, n=1673; subpattern_7, ns=68

pattern_2, n=1673; subpattern_8, ns=43

TF-MoDisCO pattern_2 n=1673, PWM

pattern_2, n=1673; subpattern_0, ns=456

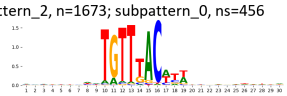

pattern_2, n=1673; subpattern_1, ns=318

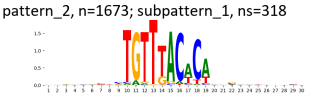

pattern_2, n=1673; subpattern_2, ns=291

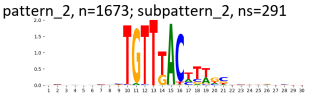

pattern_2, n=1673; subpattern_3, ns=153

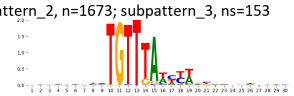

pattern_2, n=1673; subpattern_4, ns=129

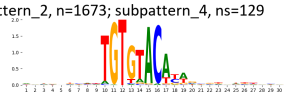

pattern_2, n=1673; subpattern_5, ns=119

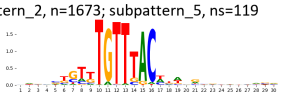

pattern_2, n=1673; subpattern_6, ns=96

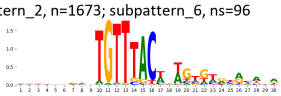

pattern_2, n=1673; subpattern_7, ns=68

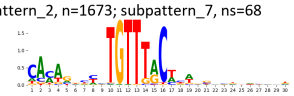

pattern_2, n=1673; subpattern_8, ns=43

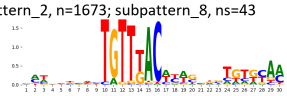

TF-MoDisCO pattern_5 n=677, CWM

pattern_5, n=677; subpattern_0, ns=148

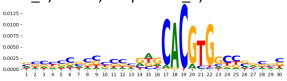

pattern_5, n=677; subpattern_1, ns=120

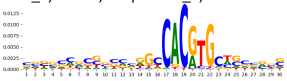

pattern_5, n=677; subpattern_2, ns=112

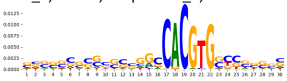

pattern_5, n=677; subpattern_3, ns=71

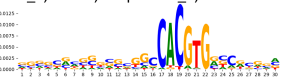

pattern_5, n=677; subpattern_4, ns=69

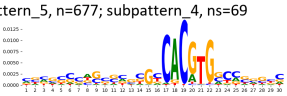

pattern_5, n=677; subpattern_5, ns=66

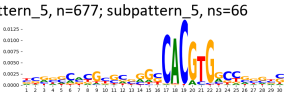

pattern_5, n=677; subpattern_6, ns=59

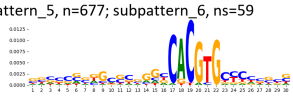

pattern_5, n=677; subpattern_7, ns=30

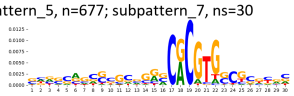

pattern_5, n=677; subpattern_8, ns=2

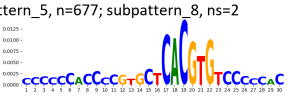

TF-MoDisCO pattern_5 n=677, PWM

pattern_5, n=677; subpattern_0, ns=148

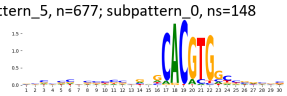

pattern_5, n=677; subpattern_1, ns=120

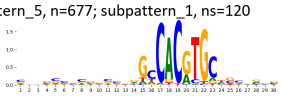

pattern_5, n=677; subpattern_2, ns=112

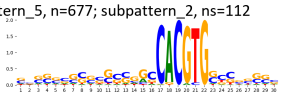

pattern_5, n=677; subpattern_3, ns=71

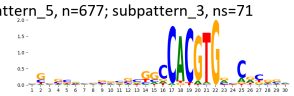

pattern_5, n=677; subpattern_4, ns=69

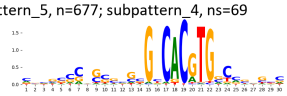

pattern_5, n=677; subpattern_5, ns=66

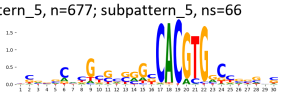

pattern_5, n=677; subpattern_6, ns=59

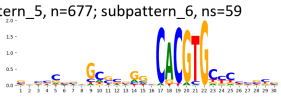

pattern_5, n=677; subpattern_7, ns=30

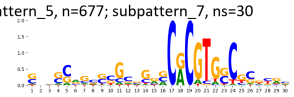

pattern_5, n=677; subpattern_8, ns=2

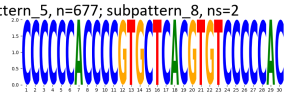

Supplementary Figure 480: TF-MoDisCO subpatterns for the ZBTB43 transcription factor in HepG2 (accession ENCSR173USN).

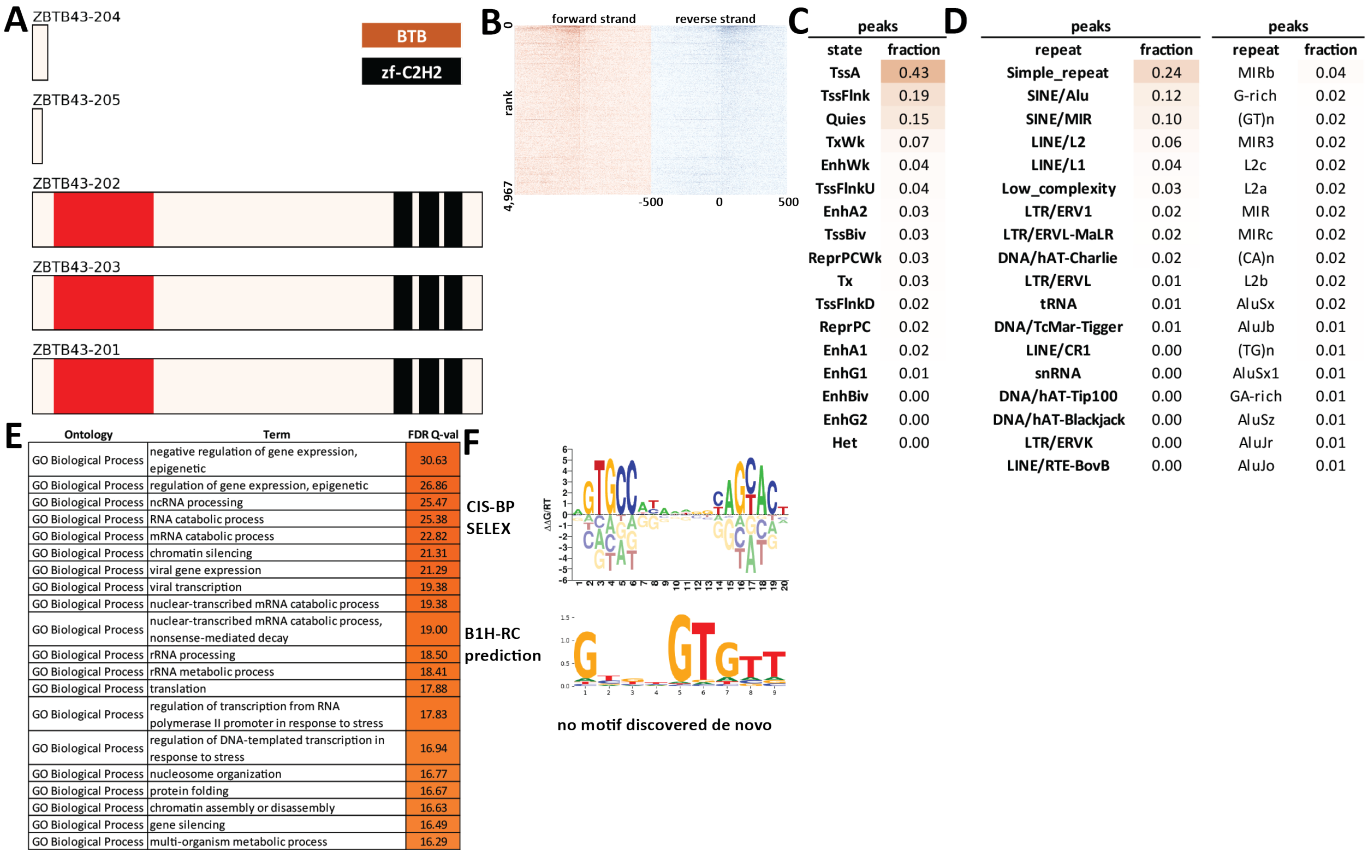

Supplementary Figure 481: Properties and genomic distribution of motifs identified for the ZBTB43 transcription factor in K562 (accession ENCSR800KMQ).

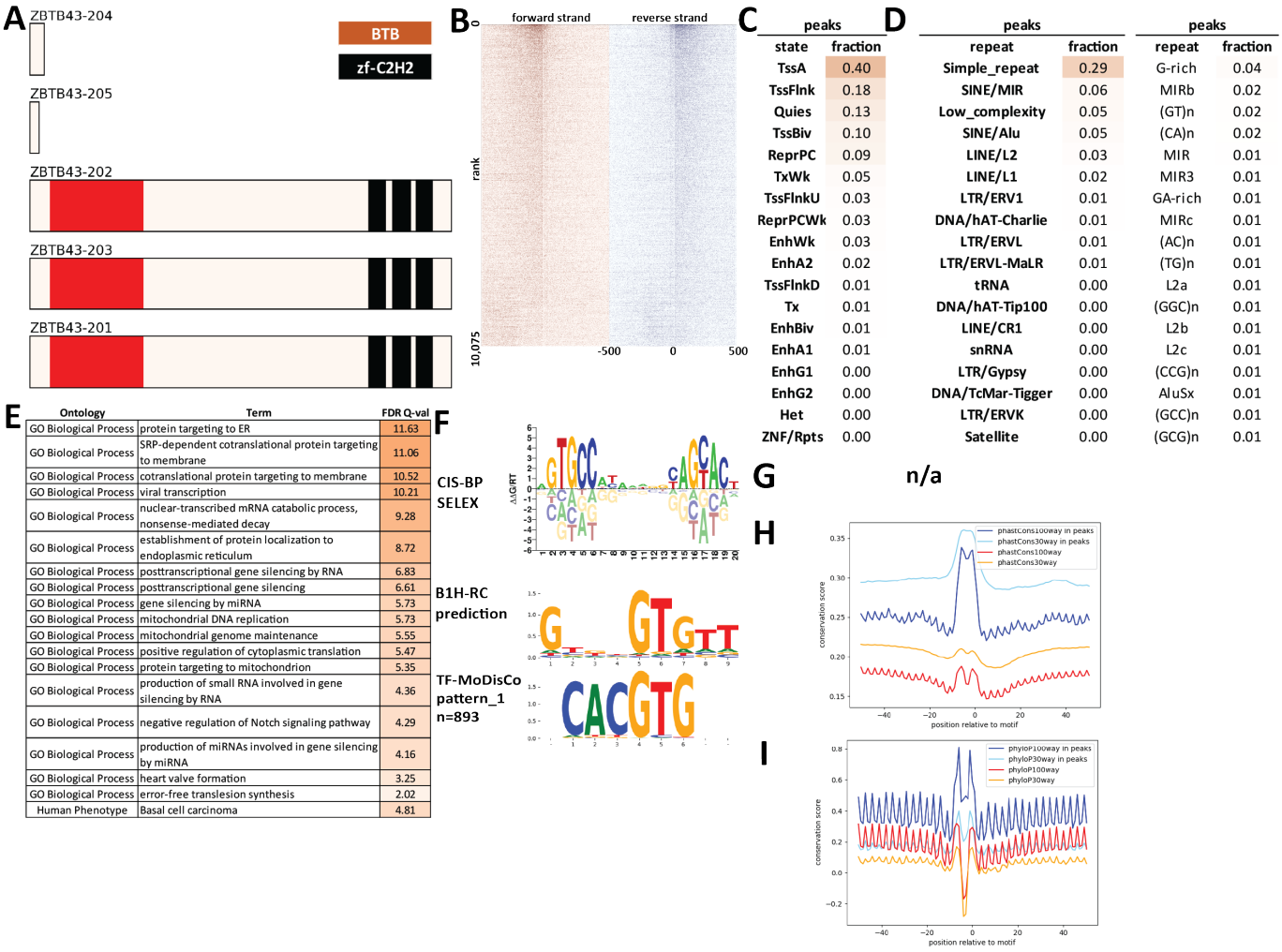

Supplementary Figure 482: Properties and genomic distribution of motifs identified for the ZBTB43 transcription factor in WTC11 (accession ENCSR199PXS).

TF-MoDisCO pattern_1 n=893, CWM

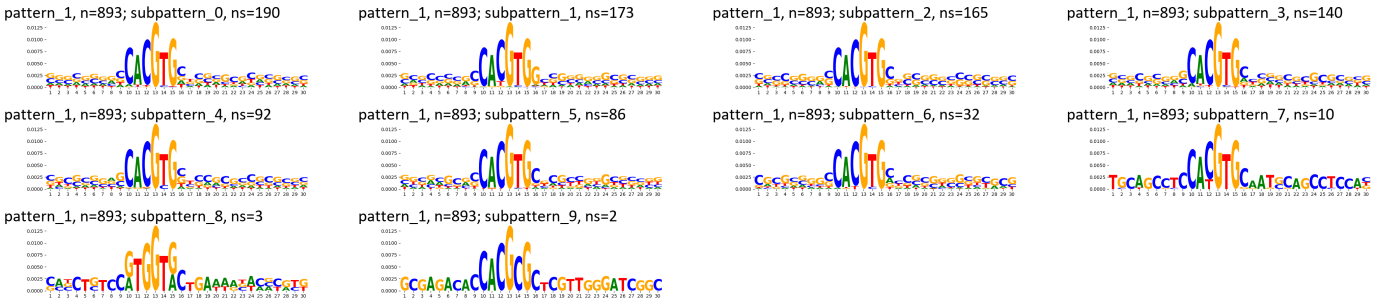

TF-MoDisCO pattern_1 n=893, PWM

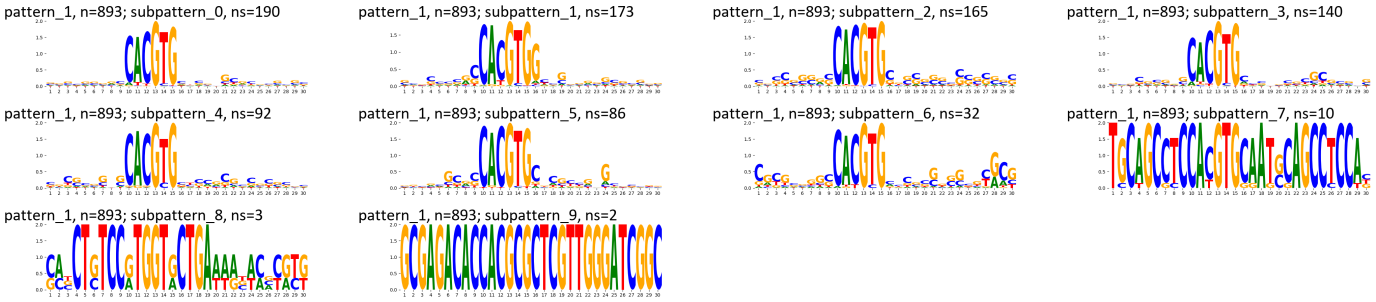

Supplementary Figure 483: TF-MoDisCO subpatterns for the ZBTB43 transcription factor in WTC11 (accession ENCSR199PXS).

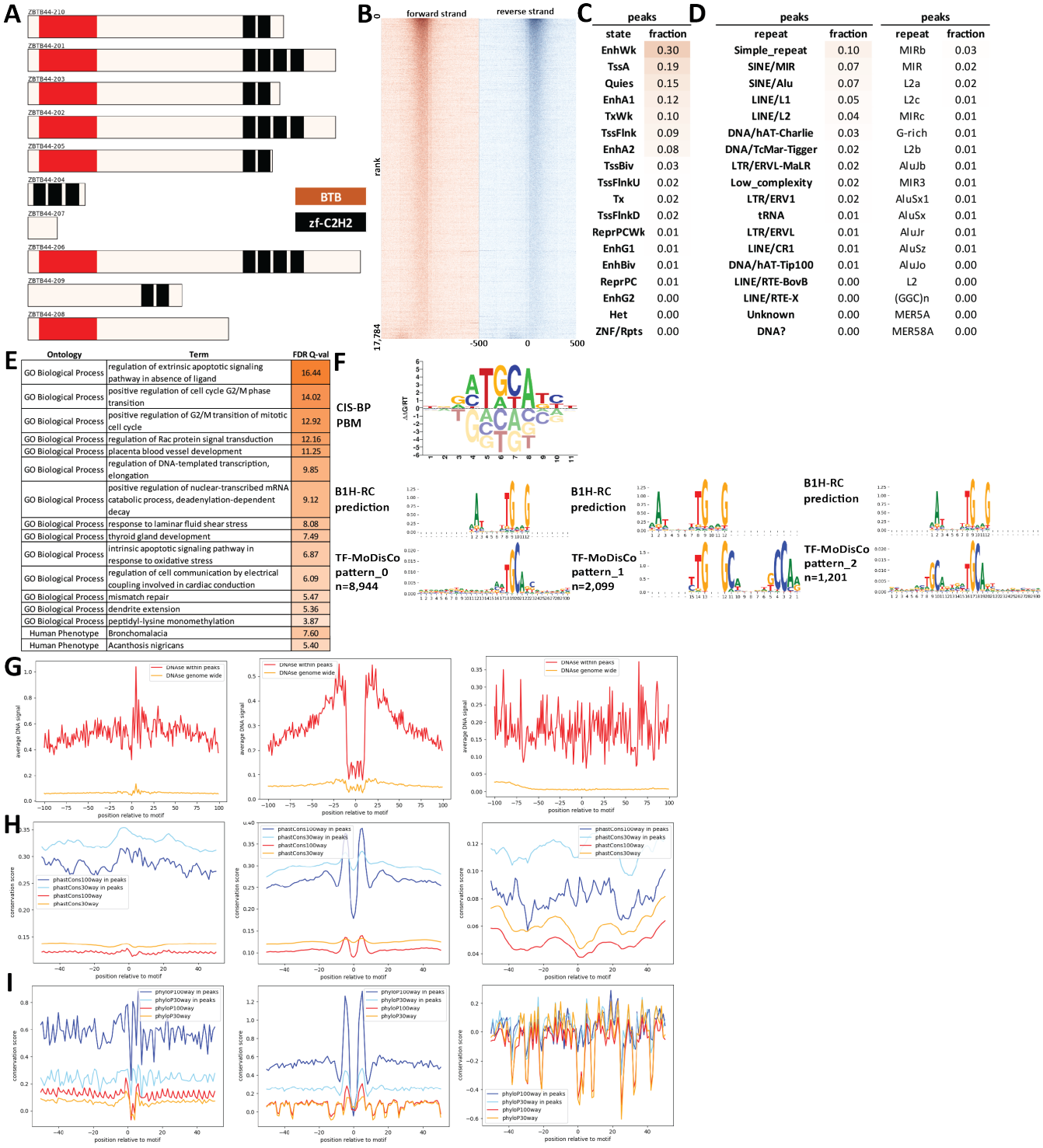

Supplementary Figure 484: Properties and genomic distribution of motifs identified for the ZBTB44 transcription factor in HEK293 (accession ENCSR076STQ).

TF-MoDisCO pattern_0 n=8944, CWM

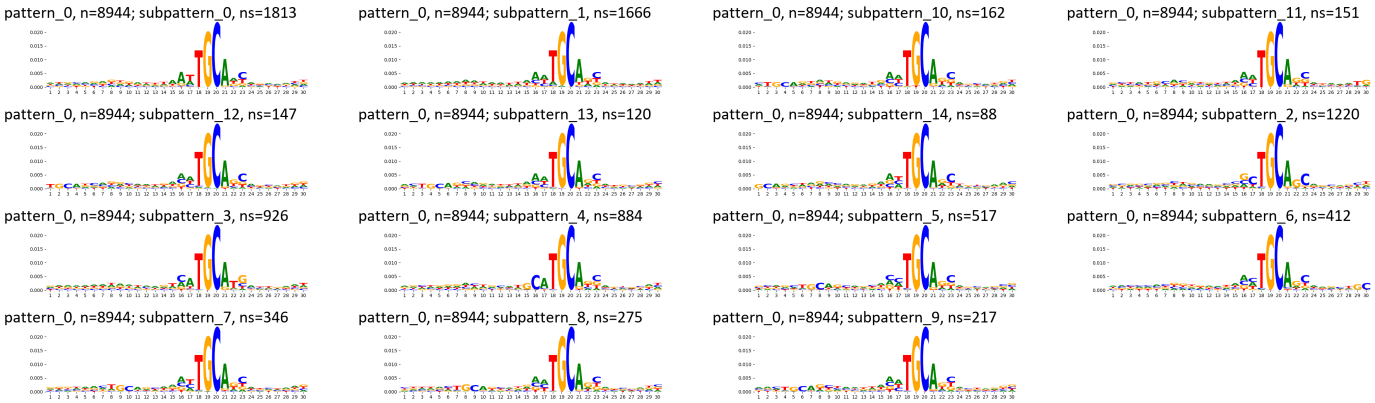

TF-MoDisCO pattern_0 n=8944, PWM

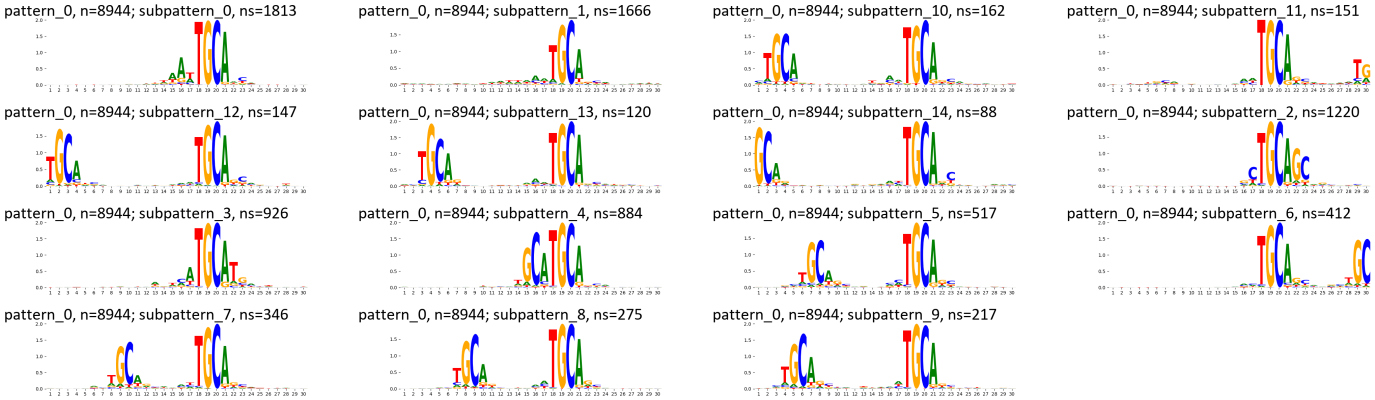

TF-MoDisCO pattern_1 n=2099, CWM

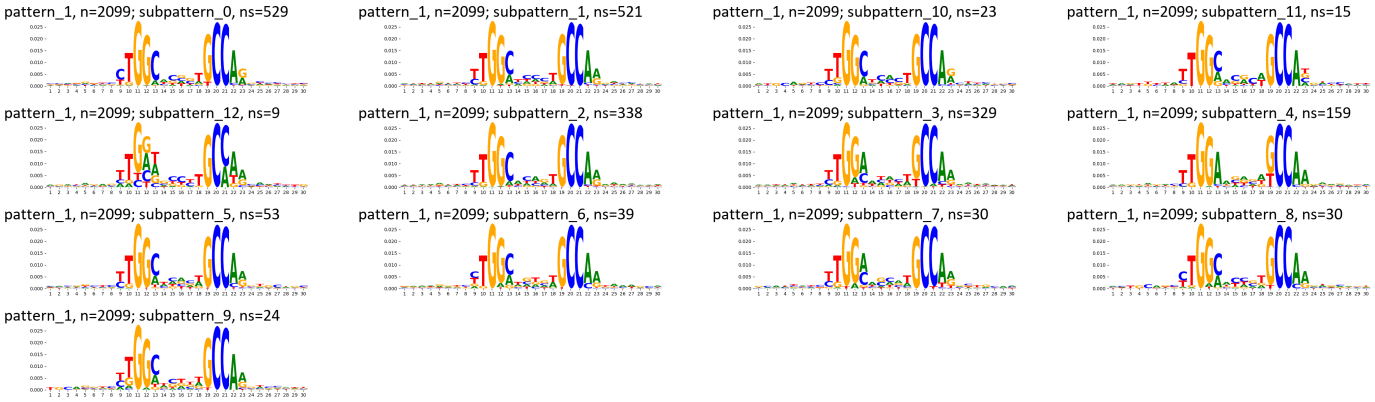

TF-MoDisCO pattern_1 n=2099, PWM

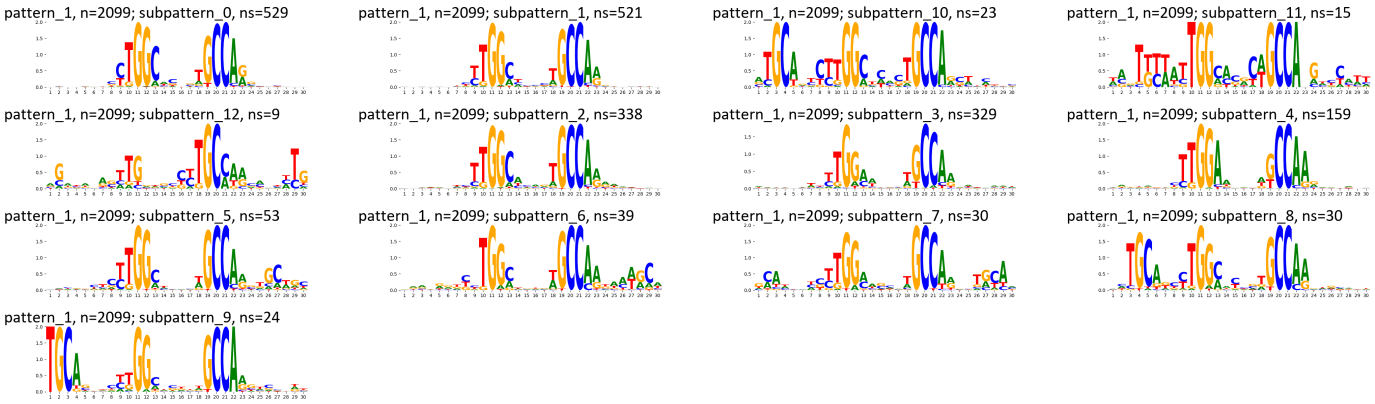

TF-MoDisCO pattern_2 n=1201, CWM

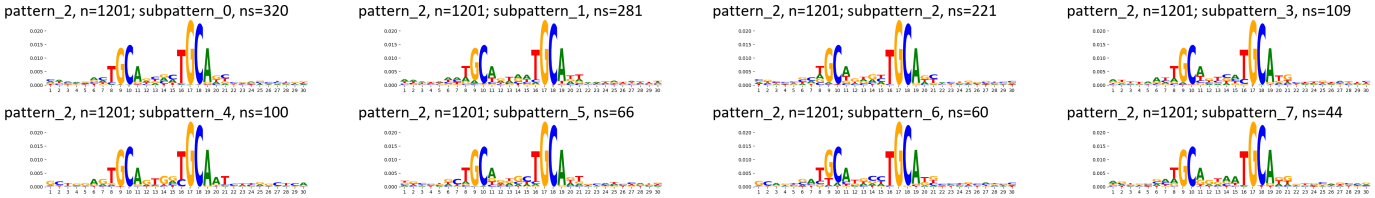

TF-MoDisCO pattern_2 n=1201, PWM

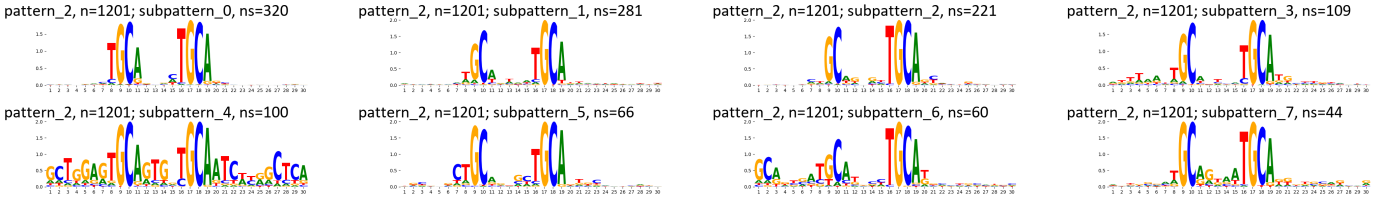

Supplementary Figure 485: TF-MoDisCO subpatterns for the ZBTB44 transcription factor in HEK293 (accession ENCSR076STQ).

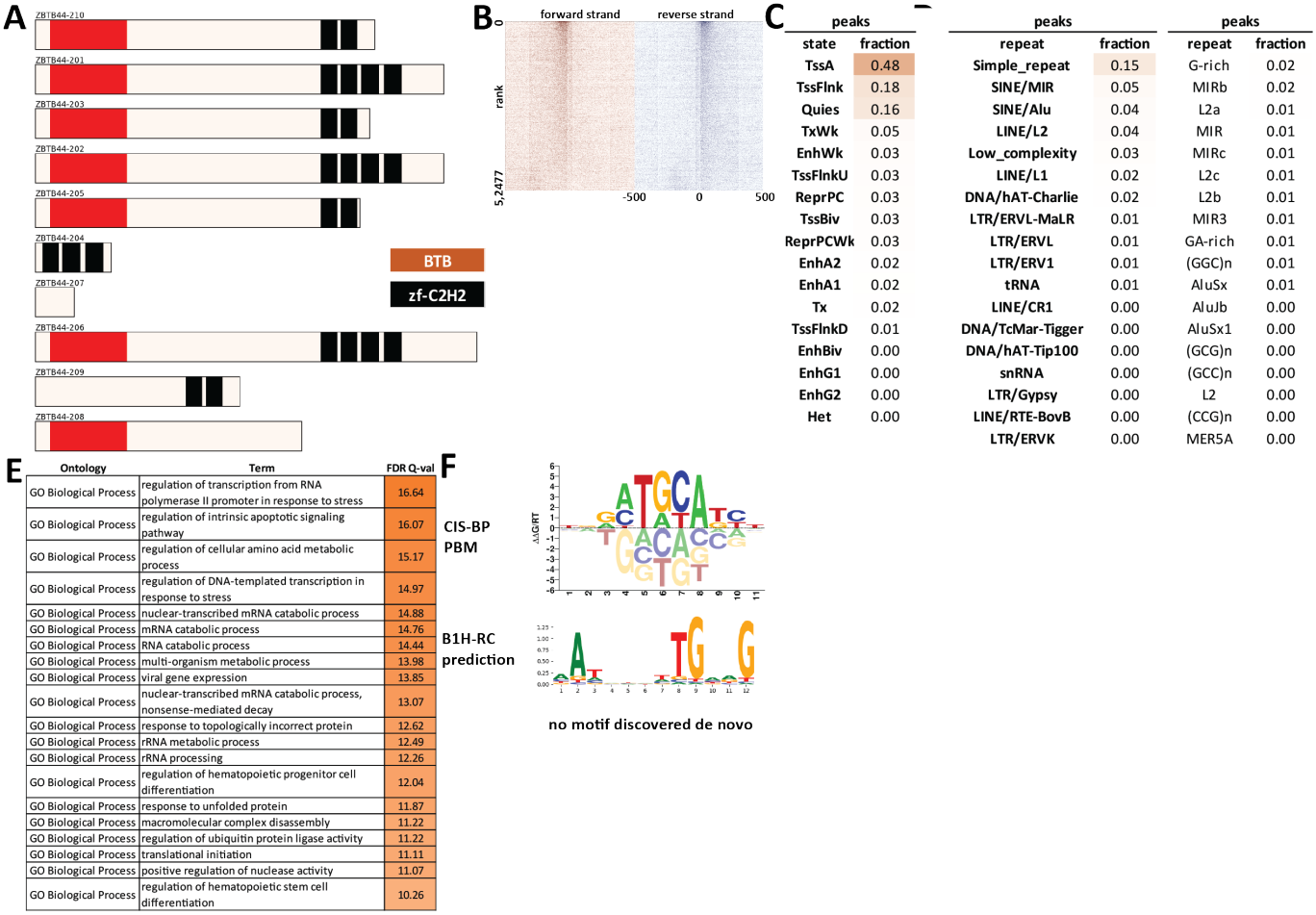

Supplementary Figure 486: Properties and genomic distribution of motifs identified for the ZBTB44 transcription factor in HepG2 (accession ENCSR269MEF).

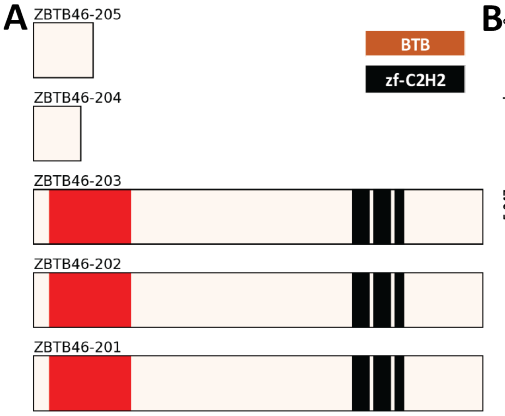

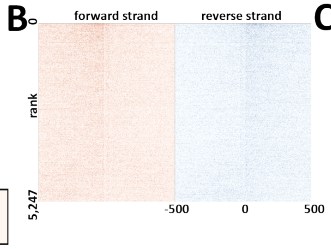

C

peaks	
state	fraction
TssA	0.35
TssFlnk	0.18
Quies	0.17
TxWk	0.10
EnhWk	0.06
TssFlnkU	0.05
TssBiv	0.04
TssFlnkD	0.03
ReprPC	0.03
EnhA1	0.03
Tx	0.03
EnhA2	0.03
ReprPCWk	0.02
EnhBiv	0.01
EnhG1	0.01
EnhG2	0.00
Het	0.00

peaks	
repeat	fraction
Simple_repeat	0.20
SINE/MIR	0.14
SINE/Alu	0.13
LINE/L2	0.08
Low_complexity	0.04
LINE/L1	0.03
DNA/hAT-Charlie	0.02
LTR/ERVL-MaLR	0.02
LTR/ERV1	0.02
LTR/ERVL	0.01
LINE/CR1	0.01
DNA/TcMar-Tigger	0.01
DNA/hAT-Tip100	0.01
tRNA	0.00
DNA/hAT-Blackjack	0.00
LTR/ERVK	0.00
LTR/Gypsy	0.00
LINE/RTE-X	0.00

peaks	
repeat	fraction
MIRb	0.05
MIR	0.03
G-rich	0.03
MIR3	0.03
L2a	0.03
L2b	0.03
MIRc	0.02
L2c	0.02
AluSx1	0.02
AluJb	0.02
AluSz	0.01
AluSx	0.01
GA-rich	0.01
AluJo	0.01
AluJr	0.01
AluY	0.01
L3	0.01
(GGC)n	0.01

E

Ontology	Term	FDR Q-val
GO Biological Process	regulation of transcription from RNA polymerase II promoter in response to stress	29.84
GO Biological Process	regulation of DNA-templated transcription in response to stress	28.38
GO Biological Process	liver regeneration	26.02
GO Biological Process	endoplasmic reticulum unfolded protein response	22.82
GO Biological Process	cellular response to epidermal growth factor stimulus	20.72
GO Biological Process	cellular response to topologically incorrect protein	19.51
GO Biological Process	cellular response to unfolded protein	19.20
GO Biological Process	response to topologically incorrect protein	17.61
GO Biological Process	response to unfolded protein	17.27
GO Biological Process	regulation of transcription from RNA polymerase II promoter in response to hypoxia	15.97
GO Biological Process	response to endoplasmic reticulum stress	15.90
GO Biological Process	protein-lipid complex assembly	10.67
GO Biological Process	regulation of pri-miRNA transcription from RNA polymerase II promoter	10.40
GO Biological Process	embryonic placenta development	10.02
GO Biological Process	negative regulation of pri-miRNA transcription from RNA polymerase II promoter	9.31
GO Biological Process	protein-lipid complex subunit organization	8.54
GO Biological Process	insulin receptor signaling pathway	8.51
GO Biological Process	negative regulation of protein localization to plasma membrane	8.15
GO Biological Process	cortical cytoskeleton organization	7.84
GO Biological Process	regulation of mitochondrial membrane permeability	7.68
Human Phenotype	Abnormal CNS myelination	9.87
Human Phenotype	Increased serum lactate	7.28
Human Phenotype	Leukodystrophy	5.86

F

no CIS-BP motif available

B1H-RC prediction

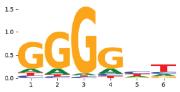

no motif discovered de novo

Supplementary Figure 487: Properties and genomic distribution of motifs identified for the ZBTB46 transcription factor in HepG2 (accession ENCSR931SYA).

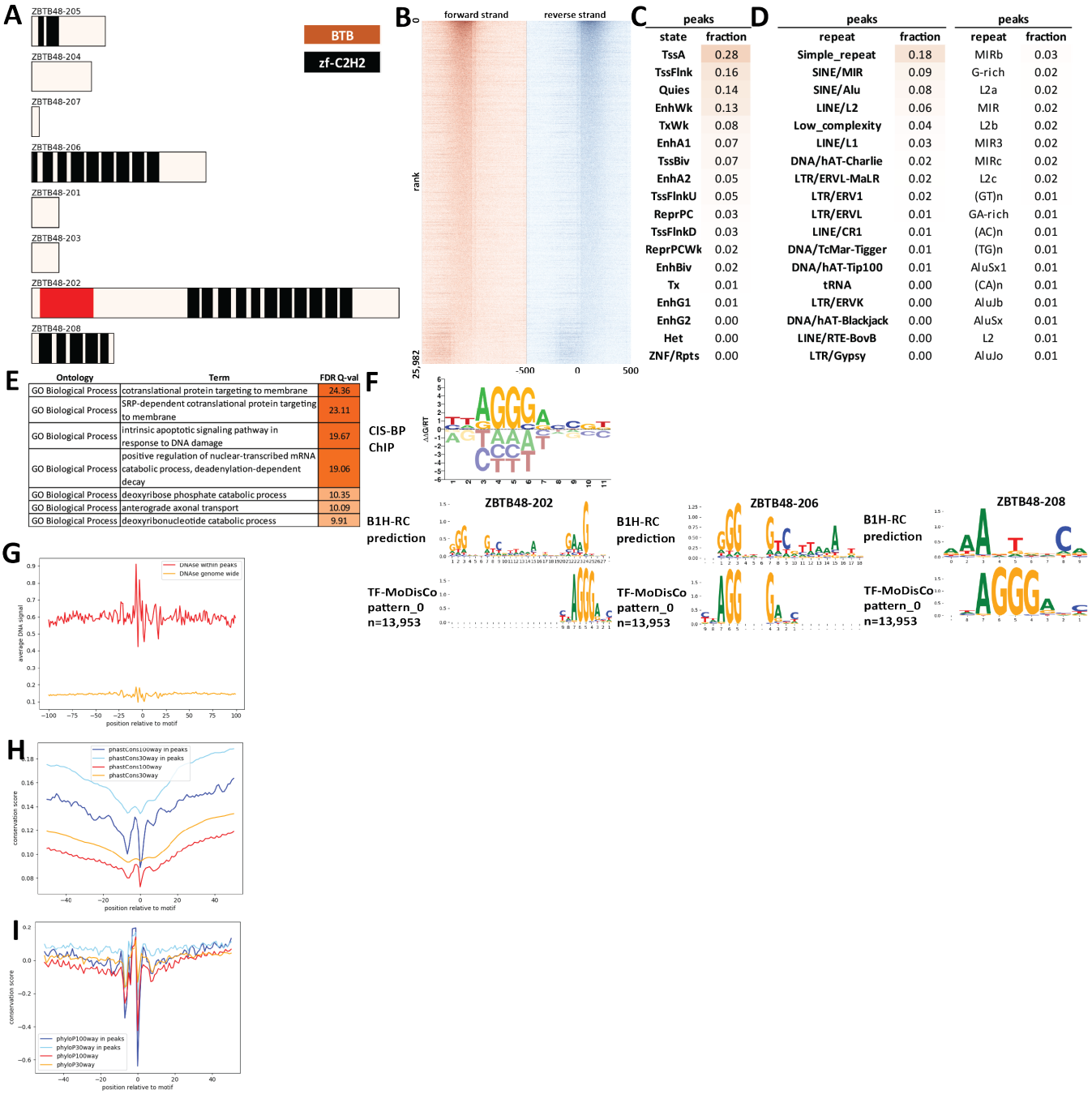

Supplementary Figure 488: Properties and genomic distribution of motifs identified for the ZBTB48 transcription factor in HEK293 (accession ENCSR781EQJ).

TF-MoDisCO pattern_0 n=13953, CWM

pattern_0, n=13953; subpattern_0, ns=3086

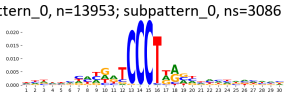

pattern_0, n=13953; subpattern_1, ns=2897

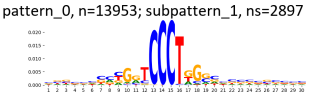

pattern_0, n=13953; subpattern_10, ns=167

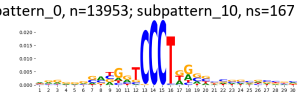

pattern_0, n=13953; subpattern_11, ns=123

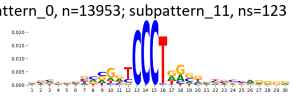

pattern_0, n=13953; subpattern_12, ns=80

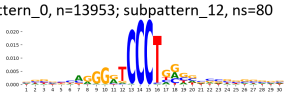

pattern_0, n=13953; subpattern_13, ns=41

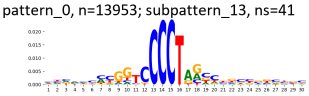

pattern_0, n=13953; subpattern_14, ns=2

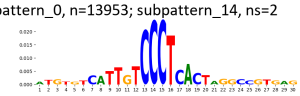

pattern_0, n=13953; subpattern_15, ns=2

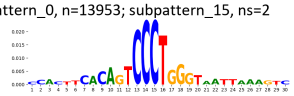

pattern_0, n=13953; subpattern_16, ns=2

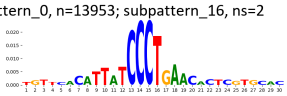

pattern_0, n=13953; subpattern_17, ns=2

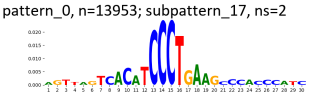

pattern_0, n=13953; subpattern_18, ns=2

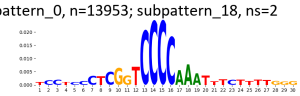

pattern_0, n=13953; subpattern_2, ns=2622

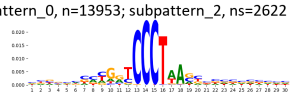

pattern_0, n=13953; subpattern_3, ns=2419

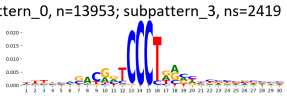

pattern_0, n=13953; subpattern_4, ns=650

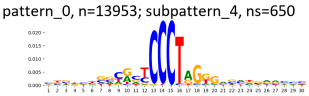

pattern_0, n=13953; subpattern_5, ns=558

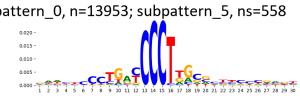

pattern_0, n=13953; subpattern_6, ns=405

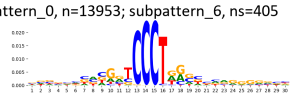

pattern_0, n=13953; subpattern_7, ns=329

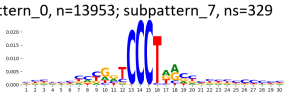

pattern_0, n=13953; subpattern_8, ns=291

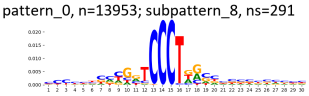

pattern_0, n=13953; subpattern_9, ns=275

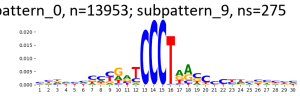

TF-MoDisCO pattern_0 n=13953, CWM

pattern_0, n=13953; subpattern_0, ns=3086

pattern_0, n=13953; subpattern_1, ns=2897

pattern_0, n=13953; subpattern_10, ns=167

pattern_0, n=13953; subpattern_11, ns=123

pattern_0, n=13953; subpattern_12, ns=80

pattern_0, n=13953; subpattern_13, ns=41

pattern_0, n=13953; subpattern_14, ns=2

pattern_0, n=13953; subpattern_15, ns=2

pattern_0, n=13953; subpattern_16, ns=2

pattern_0, n=13953; subpattern_17, ns=2

pattern_0, n=13953; subpattern_18, ns=2

pattern_0, n=13953; subpattern_2, ns=2622

pattern_0, n=13953; subpattern_3, ns=2419

pattern_0, n=13953; subpattern_4, ns=650

pattern_0, n=13953; subpattern_5, ns=558

pattern_0, n=13953; subpattern_6, ns=405

pattern_0, n=13953; subpattern_7, ns=329

pattern_0, n=13953; subpattern_8, ns=291

pattern_0, n=13953; subpattern_9, ns=275

TF-MoDisCO pattern_0 n=13953, CWM

pattern_0, n=13953; subpattern_0, ns=3086

pattern_0, n=13953; subpattern_1, ns=2897

pattern_0, n=13953; subpattern_10, ns=167

pattern_0, n=13953; subpattern_11, ns=123

pattern_0, n=13953; subpattern_12, ns=80

pattern_0, n=13953; subpattern_13, ns=41

pattern_0, n=13953; subpattern_14, ns=2

pattern_0, n=13953; subpattern_15, ns=2

pattern_0, n=13953; subpattern_16, ns=2

pattern_0, n=13953; subpattern_17, ns=2

pattern_0, n=13953; subpattern_18, ns=2

pattern_0, n=13953; subpattern_2, ns=2622

pattern_0, n=13953; subpattern_3, ns=2419

pattern_0, n=13953; subpattern_4, ns=650

pattern_0, n=13953; subpattern_5, ns=558

pattern_0, n=13953; subpattern_6, ns=405

pattern_0, n=13953; subpattern_7, ns=329

pattern_0, n=13953; subpattern_8, ns=291

pattern_0, n=13953; subpattern_9, ns=275

TF-MoDisCO pattern_0 n=13953, PWM

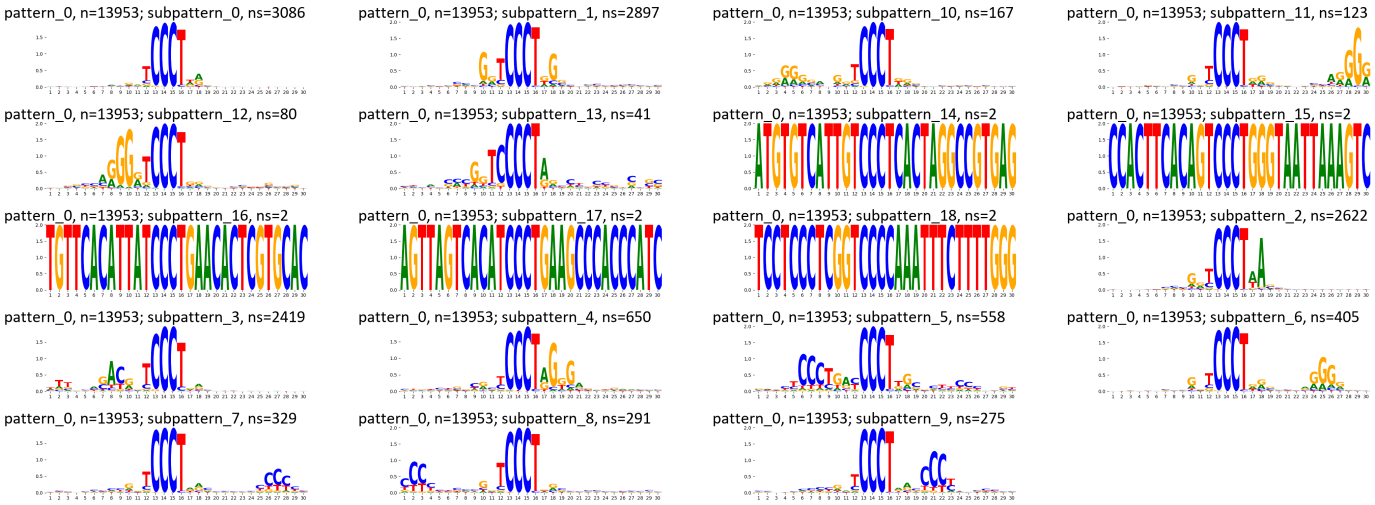

TF-MoDisCO pattern_0 n=13953, PWM

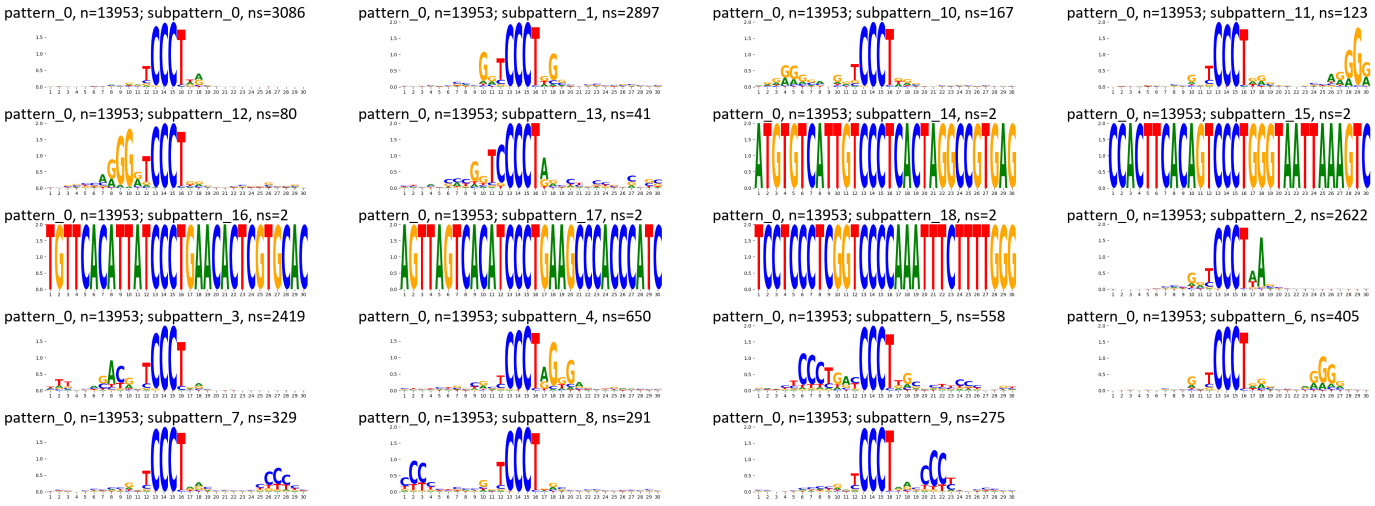
pattern_0, n=13953; subpattern_0, ns=3086
pattern_0, n=13953; subpattern_1, ns=2897
pattern_0, n=13953; subpattern_10, ns=167
pattern_0, n=13953; subpattern_11, ns=123
pattern_0, n=13953; subpattern_12, ns=80
pattern_0, n=13953; subpattern_13, ns=41
pattern_0, n=13953; subpattern_14, ns=2
pattern_0, n=13953; subpattern_15, ns=2
pattern_0, n=13953; subpattern_16, ns=2
pattern_0, n=13953; subpattern_17, ns=2
pattern_0, n=13953; subpattern_18, ns=2
pattern_0, n=13953; subpattern_2, ns=2622
pattern_0, n=13953; subpattern_3, ns=2419
pattern_0, n=13953; subpattern_4, ns=650
pattern_0, n=13953; subpattern_5, ns=558
pattern_0, n=13953; subpattern_6, ns=405
pattern_0, n=13953; subpattern_7, ns=329
pattern_0, n=13953; subpattern_8, ns=291
pattern_0, n=13953; subpattern_9, ns=275

TF-MoDisCO pattern_0 n=13953, PWM

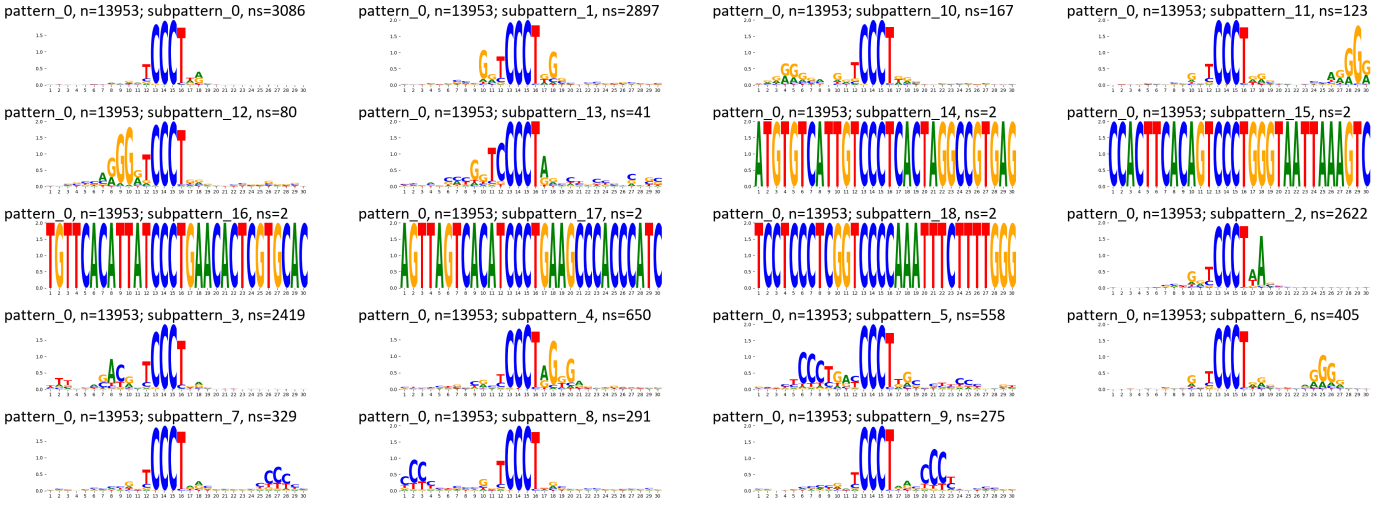
pattern_0, n=13953; subpattern_0, ns=3086
pattern_0, n=13953; subpattern_1, ns=2897
pattern_0, n=13953; subpattern_10, ns=167
pattern_0, n=13953; subpattern_11, ns=123
pattern_0, n=13953; subpattern_12, ns=80
pattern_0, n=13953; subpattern_13, ns=41
pattern_0, n=13953; subpattern_14, ns=2
pattern_0, n=13953; subpattern_15, ns=2
pattern_0, n=13953; subpattern_16, ns=2
pattern_0, n=13953; subpattern_17, ns=2
pattern_0, n=13953; subpattern_18, ns=2
pattern_0, n=13953; subpattern_2, ns=2622
pattern_0, n=13953; subpattern_3, ns=2419
pattern_0, n=13953; subpattern_4, ns=650
pattern_0, n=13953; subpattern_5, ns=558
pattern_0, n=13953; subpattern_6, ns=405
pattern_0, n=13953; subpattern_7, ns=329
pattern_0, n=13953; subpattern_8, ns=291
pattern_0, n=13953; subpattern_9, ns=275

Supplementary Figure 489: TF-MoDisCO subpatterns for the ZBTB48 transcription factor in HEK293 (accession ENCSR781EQJ).

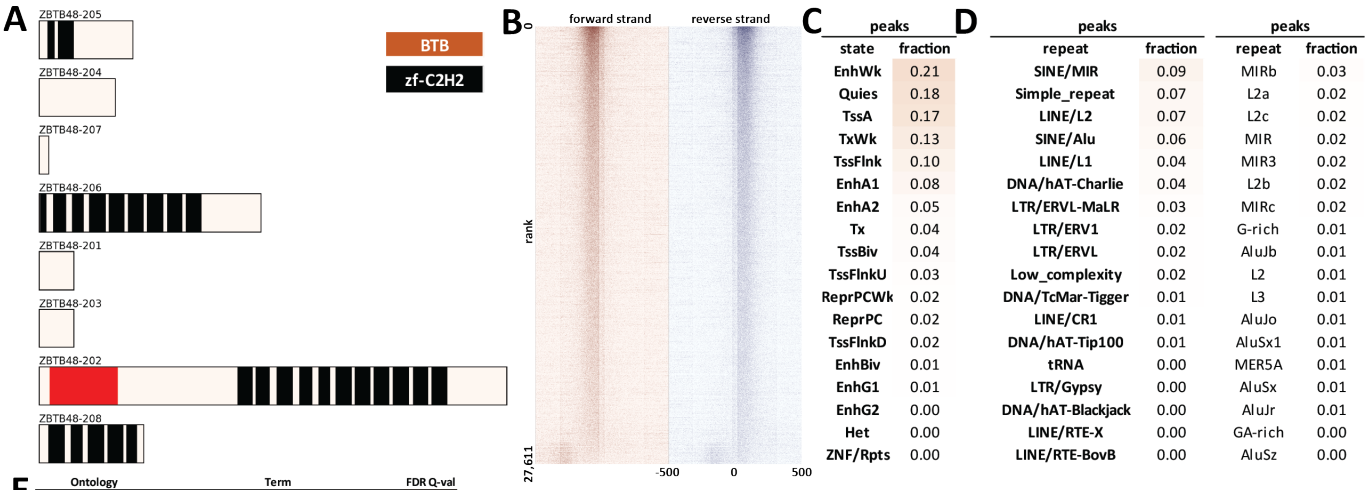

C

peaks	
state	fraction
EnhWk	0.21
Quies	0.18
TssA	0.17
TxWk	0.13
TssFlnk	0.10
EnhA1	0.08
EnhA2	0.05
Tx	0.04
TssBiv	0.04
TssFlnkU	0.03
ReprPCWk	0.02
ReprPC	0.02
TssFlnkD	0.02
EnhBiv	0.01
EnhG1	0.01
EnhG2	0.00
Het	0.00
ZNF/Rpts	0.00

D

peaks		peaks	
repeat	fraction	repeat	fraction
SINE/MIR	0.09	MIRb	0.03
Simple_repeat	0.07	L2a	0.02
LINE/L2	0.07	L2c	0.02
SINE/Alu	0.06	MIR	0.02
LINE/L1	0.04	MIR3	0.02
DNA/hAT-Charlie	0.04	L2b	0.02
LTR/ERVL-MaLR	0.03	MIRc	0.02
LTR/ERV1	0.02	G-rich	0.01
LTR/ERVL	0.02	AluJb	0.01
Low_complexity	0.02	L2	0.01
DNA/TcMar-Tigger	0.01	L3	0.01
LINE/CR1	0.01	AluJo	0.01
DNA/hAT-Tip100	0.01	AluSx1	0.01
tRNA	0.00	MER5A	0.01
LTR/Gypsy	0.00	AluSx	0.01
DNA/hAT-Blackjack	0.00	AluJr	0.01
LINE/RTE-X	0.00	GA-rich	0.00
LINE/RTE-BovB	0.00	AluSz	0.00

E

Ontology	Term	FDR Q-val
GO Biological Process	posttranscriptional gene silencing	33.58
GO Biological Process	gene silencing by miRNA	32.96
GO Biological Process	posttranscriptional gene silencing by RNA	32.86
GO Biological Process	adherens junction assembly	24.05
GO Biological Process	cellular response to dsRNA	20.34
GO Biological Process	production of miRNAs involved in gene silencing by miRNA	20.28
GO Biological Process	positive regulation of nuclear-transcribed mRNA catabolic process, deadenylation-dependent decay	19.41
GO Biological Process	positive regulation of intrinsic apoptotic signaling pathway	19.11
GO Biological Process	positive regulation of mRNA catabolic process	17.26
GO Biological Process	production of small RNA involved in gene silencing by RNA	16.78
GO Biological Process	negative regulation of homotypic cell-cell adhesion	15.67
GO Biological Process	nucleotide-binding domain, leucine rich repeat containing receptor signaling pathway	15.35
GO Biological Process	paraxial mesoderm development	14.44
GO Biological Process	nucleus localization	9.02
GO Biological Process	regulation of nucleobase-containing compound transport	8.20
Human Phenotype	Coxa vara	16.28
Human Phenotype	Ectopic kidney	14.85

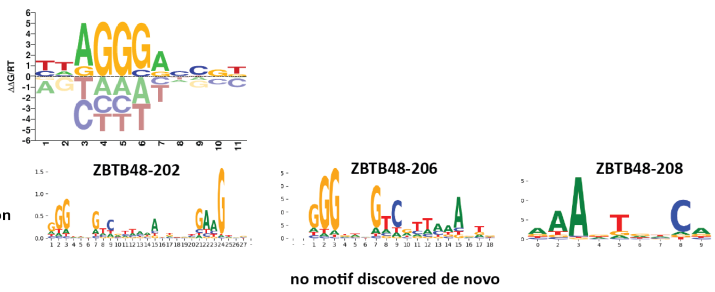

Supplementary Figure 490: Properties and genomic distribution of motifs identified for the ZBTB48 transcription factor in HEK293 (accession Hughes GR models).

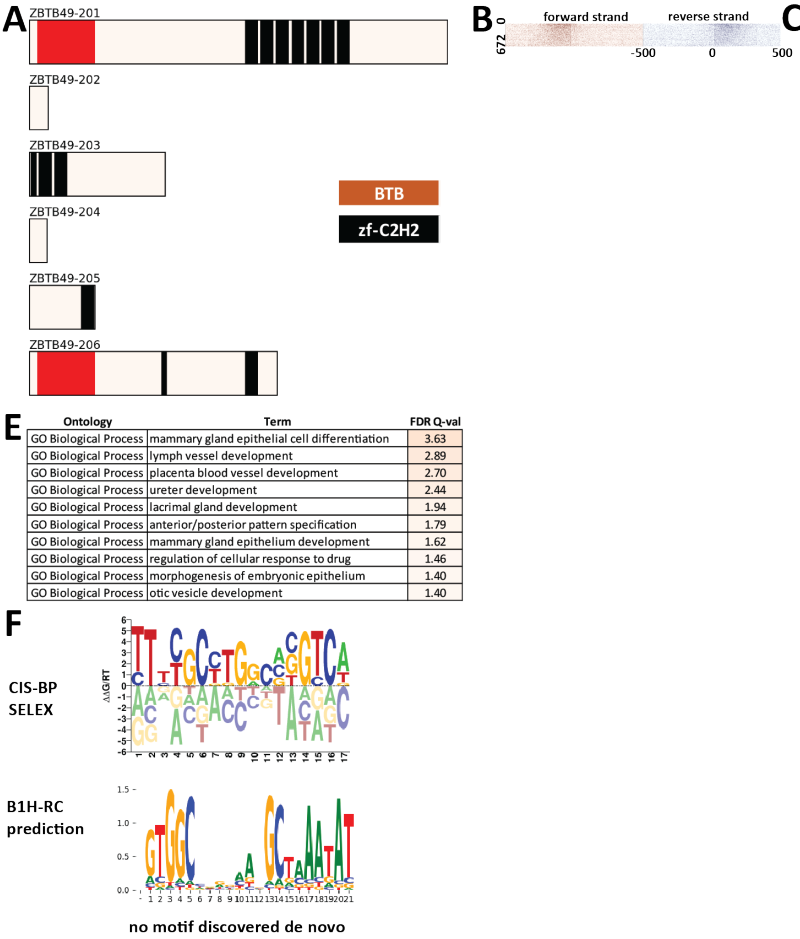

C

peaks	
state	fraction
Quies	0.21
EnhWk	0.21
EnhA2	0.17
TssA	0.17
TxWk	0.14
EnhA1	0.12
TssFlnk	0.05
Tx	0.02
ReprPCWk	0.02
TssFlnkU	0.02
EnhBiv	0.02
TssFlnkD	0.01
TssBiv	0.01
ReprPC	0.01
EnhG1	0.01
ZNF/Rpts	0.00
EnhG2	0.00
Het	0.00

D

peaks		peaks	
repeat	fraction	repeat	fraction
SINE/Alu	0.27	AluSz	0.06
Simple_repeat	0.11	AluSx1	0.05
LINE/L1	0.09	AluSx	0.04
SINE/MIR	0.08	MIR	0.03
LINE/L2	0.06	MIRb	0.03
LTR/ERVL-MaLR	0.03	L2a	0.03
Low_complexity	0.02	AluJb	0.03
LTR/ERV1	0.02	AluSz6	0.02
DNA/hAT-Charlie	0.02	MIRc	0.01
LTR/ERVL	0.02	L2c	0.01
LINE/CR1	0.01	(T)n	0.01
DNA/TcMar-Tigger	0.01	GA-rich	0.01
LINE/RTE-BovB	0.00	AluSq2	0.01
DNA/hAT-Tip100	0.00	(GT)n	0.01
Unknown	0.00	L3	0.01
DNA?	0.00	L2b	0.01
DNA/hAT-Blackjack	0.00	AluJo	0.01
tRNA	0.00	(TG)n	0.01

E

Ontology	Term	FDR Q-val
GO Biological Process	mammary gland epithelial cell differentiation	3.63
GO Biological Process	lymph vessel development	2.89
GO Biological Process	placenta blood vessel development	2.70
GO Biological Process	ureter development	2.44
GO Biological Process	lacrimal gland development	1.94
GO Biological Process	anterior/posterior pattern specification	1.79
GO Biological Process	mammary gland epithelium development	1.62
GO Biological Process	regulation of cellular response to drug	1.46
GO Biological Process	morphogenesis of embryonic epithelium	1.40
GO Biological Process	otic vesicle development	1.40

Supplementary Figure 491: Properties and genomic distribution of motifs identified for the ZBTB49 transcription factor in HEK293 (accession ENCSR924GRG).

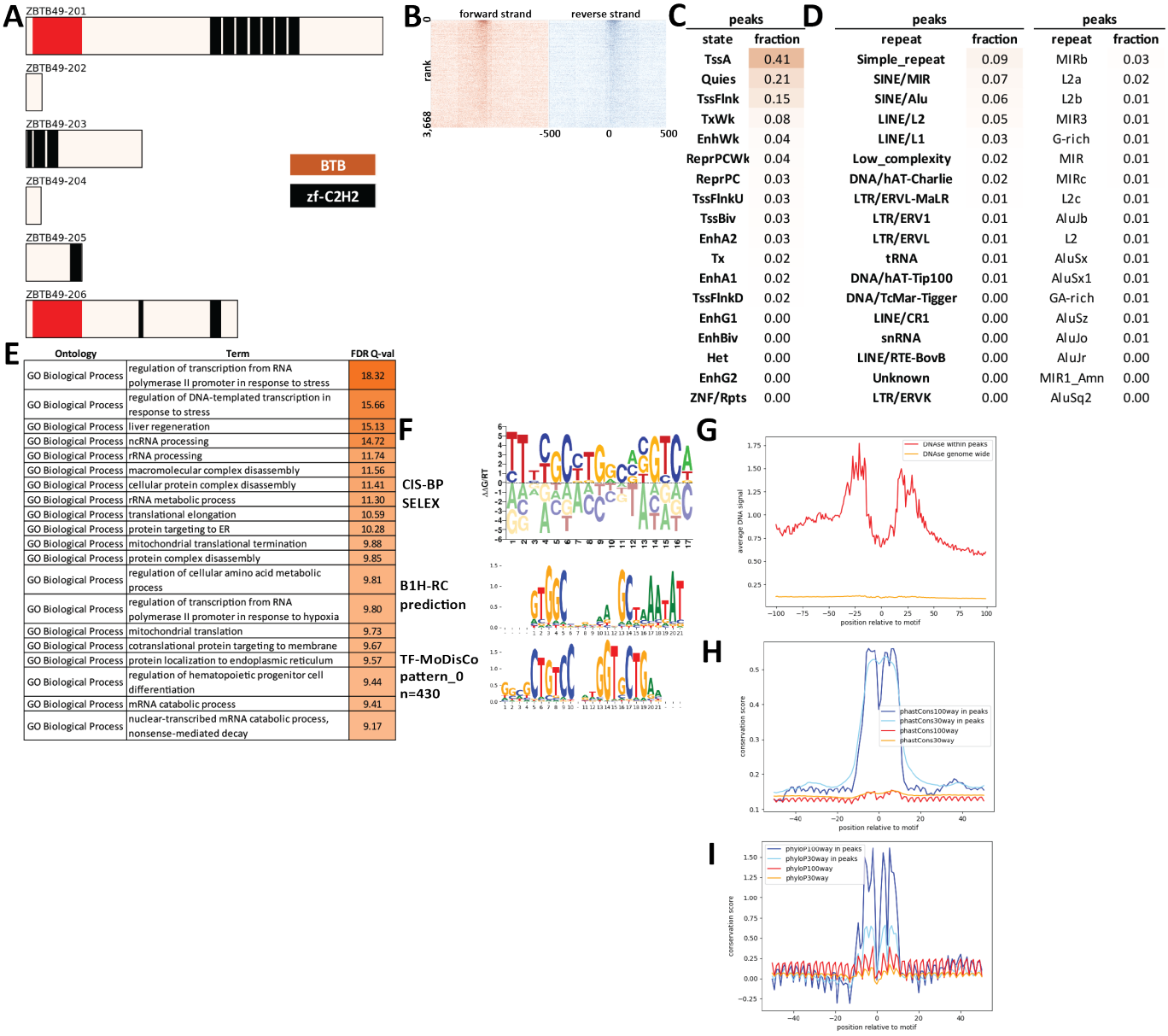

C

peaks	
state	fraction
TssA	0.41
Quies	0.21
TssFlnk	0.15
TxWk	0.08
EnhWk	0.04
ReprPCWk	0.04
ReprPC	0.03
TssFlnkU	0.03
TssBiv	0.03
EnhA2	0.03
Tx	0.02
EnhA1	0.02
TssFlnkD	0.02
EnhG1	0.00
EnhBiv	0.00
Het	0.00
EnhG2	0.00
ZNF/Rpts	0.00

D

peaks		peaks	
repeat	fraction	repeat	fraction
Simple_repeat	0.09	MIRb	0.03
SINE/MIR	0.07	L2a	0.02
SINE/Alu	0.06	L2b	0.01
LINE/L2	0.05	MIR3	0.01
LINE/L1	0.03	G-rich	0.01
Low_complexity	0.02	MIR	0.01
DNA/hAT-Charlie	0.02	MIRc	0.01
LTR/ERVL-MaLR	0.01	L2c	0.01
LTR/ERV1	0.01	AluJb	0.01
LTR/ERVL	0.01	L2	0.01
tRNA	0.01	AluSx	0.01
DNA/hAT-Tip100	0.01	AluSx1	0.01
DNA/TcMar-Tigger	0.00	GA-rich	0.01
LINE/CR1	0.00	AluSz	0.01
snRNA	0.00	AluJo	0.01
LINE/RTE-BovB	0.00	AluJr	0.00
Unknown	0.00	MIR1_Amn	0.00
LTR/ERVK	0.00	AluSq2	0.00

E

Ontology	Term	FDR Q-val
GO Biological Process	regulation of transcription from RNA polymerase II promoter in response to stress	18.32
GO Biological Process	regulation of DNA-templated transcription in response to stress	15.66
GO Biological Process	liver regeneration	15.13
GO Biological Process	ncRNA processing	14.72
GO Biological Process	rRNA processing	11.74
GO Biological Process	macromolecular complex disassembly	11.56
GO Biological Process	cellular protein complex disassembly	11.41
GO Biological Process	rRNA metabolic process	11.30
GO Biological Process	translational elongation	10.59
GO Biological Process	protein targeting to ER	10.28
GO Biological Process	mitochondrial translational termination	9.88
GO Biological Process	protein complex disassembly	9.85
GO Biological Process	regulation of cellular amino acid metabolic process	9.81
GO Biological Process	regulation of transcription from RNA polymerase II promoter in response to hypoxia	9.80
GO Biological Process	mitochondrial translation	9.73
GO Biological Process	cotranslational protein targeting to membrane	9.67
GO Biological Process	protein localization to endoplasmic reticulum	9.57
GO Biological Process	regulation of hematopoietic progenitor cell differentiation	9.44
GO Biological Process	mRNA catabolic process	9.41
GO Biological Process	nuclear-transcribed mRNA catabolic process, nonsense-mediated decay	9.17

Supplementary Figure 492: Properties and genomic distribution of motifs identified for the ZBTB49 transcription factor in HepG2 (accession ENCSR803IYP).

TF-MoDisCO pattern_0 n=430, CWM

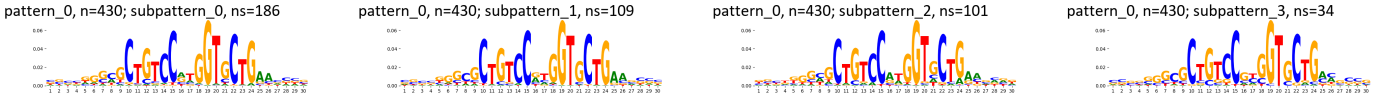

TF-MoDisCO pattern_0 n=430, PWM

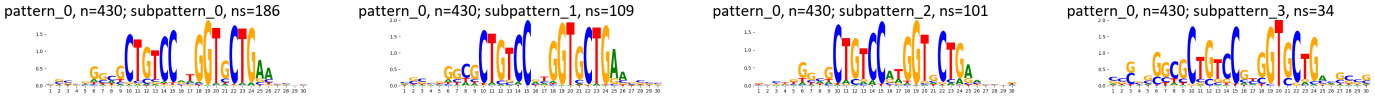

Supplementary Figure 493: TF-MoDisCO subpatterns for the ZBTB49 transcription factor in HepG2 (accession ENCSR803IYP).

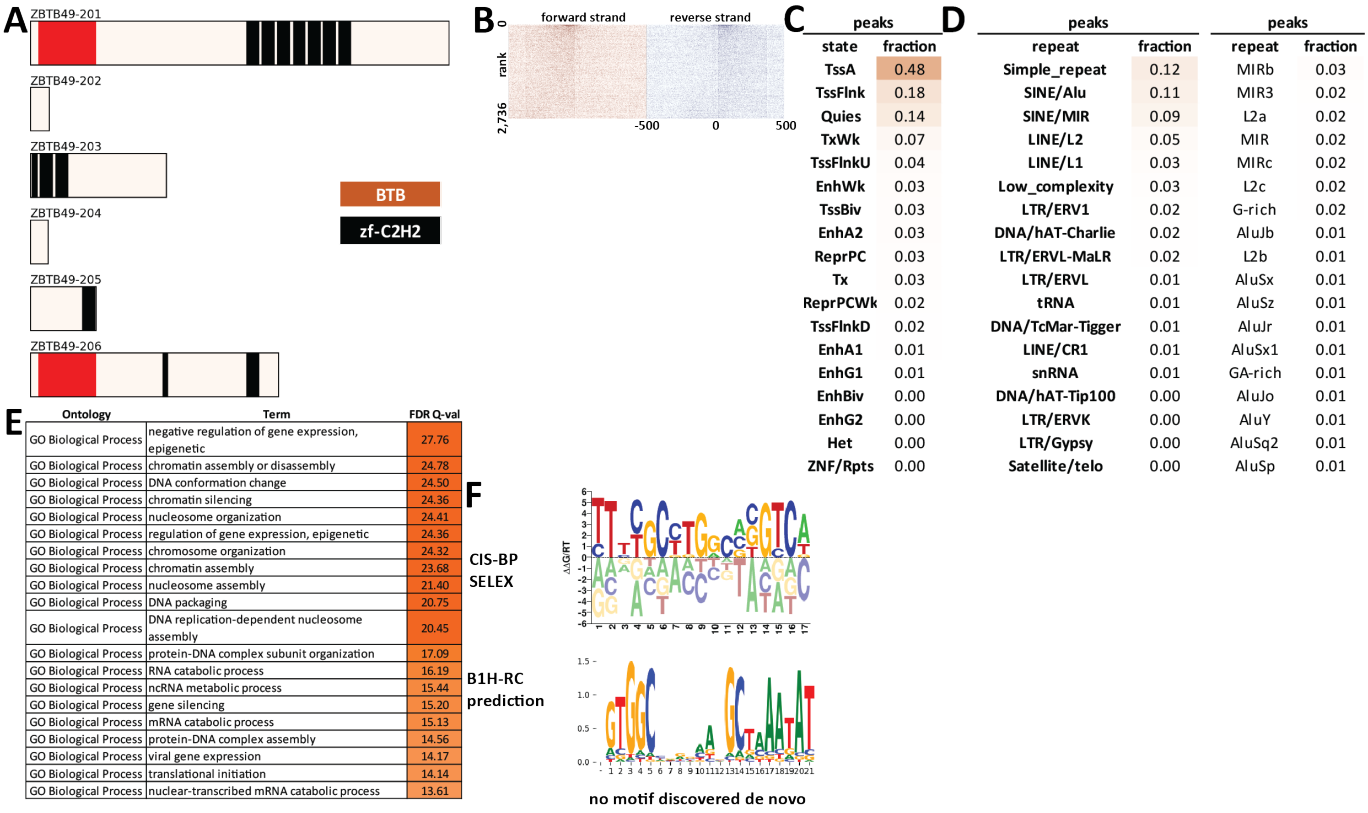

Supplementary Figure 494: Properties and genomic distribution of motifs identified for the ZBTB49 transcription factor in K562 (accession ENCSR249VFB).

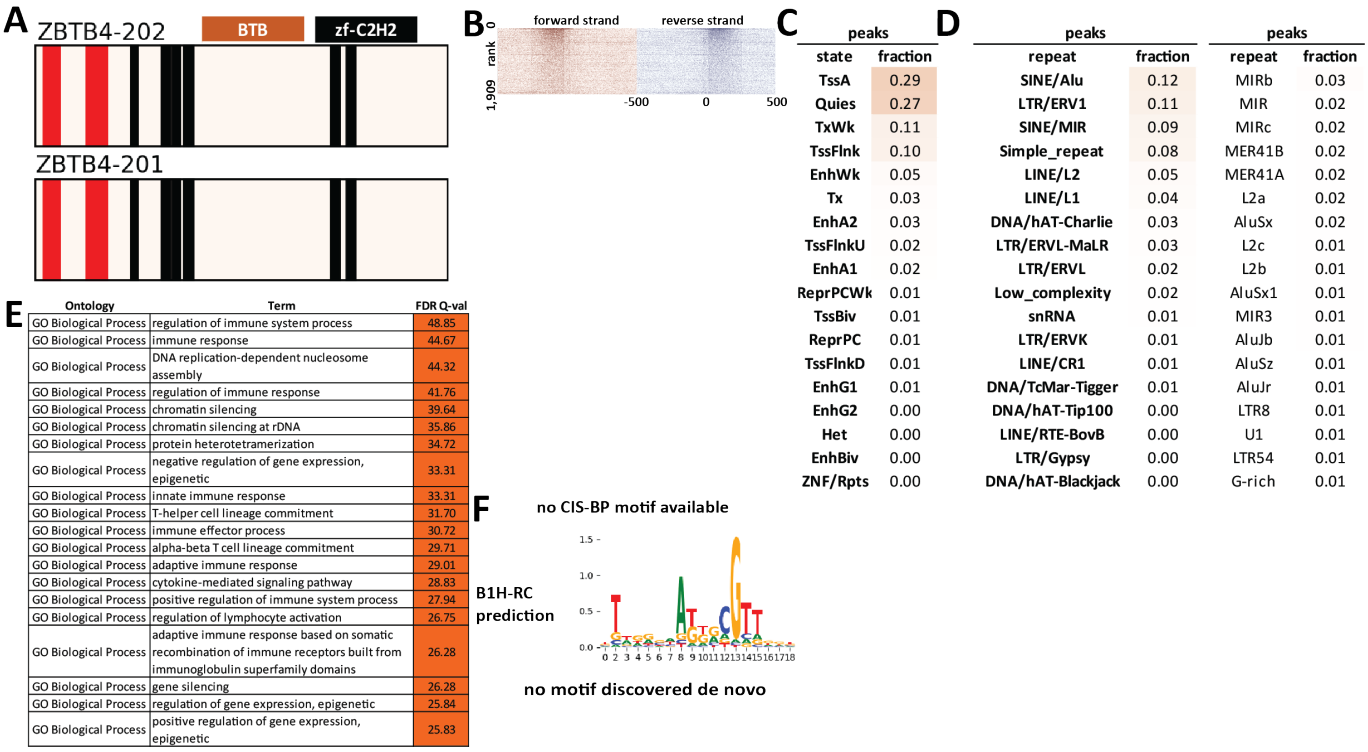

C

peaks	
state	fraction
TssA	0.29
Quies	0.27
TxWk	0.11
TssFlnk	0.10
EnhWk	0.05
Tx	0.03
EnhA2	0.03
TssFlnkU	0.02
EnhA1	0.02
ReprPCWk	0.01
TssBiv	0.01
ReprPC	0.01
TssFlnkD	0.01
EnhG1	0.01
EnhG2	0.00
Het	0.00
EnhBiv	0.00
ZNF/Rpts	0.00

D

peaks		peaks	
repeat	fraction	repeat	fraction
SINE/Alu	0.12	MIRb	0.03
LTR/ERV1	0.11	MIR	0.02
SINE/MIR	0.09	MIRc	0.02
Simple_repeat	0.08	MER41B	0.02
LINE/L2	0.05	MER41A	0.02
LINE/L1	0.04	L2a	0.02
DNA/hAT-Charlie	0.03	AluSx	0.02
LTR/ERVL-MaLR	0.03	L2c	0.01
LTR/ERVL	0.02	L2b	0.01
Low_complexity	0.02	AluSx1	0.01
snRNA	0.01	MIR3	0.01
LTR/ERVK	0.01	AluJb	0.01
LINE/CR1	0.01	AluSz	0.01
DNA/TcMar-Tigger	0.01	AluJr	0.01
DNA/hAT-Tip100	0.00	LTR8	0.01
LINE/RTE-BovB	0.00	U1	0.01
LTR/Gypsy	0.00	LTR54	0.01
DNA/hAT-Blackjack	0.00	G-rich	0.01

E

Ontology	Term	FDR Q-val
GO Biological Process	regulation of immune system process	48.85
GO Biological Process	immune response	44.67
GO Biological Process	DNA replication-dependent nucleosome assembly	44.32
GO Biological Process	regulation of immune response	41.76
GO Biological Process	chromatin silencing	39.64
GO Biological Process	chromatin silencing at rDNA	35.86
GO Biological Process	protein heterotetramerization	34.72
GO Biological Process	negative regulation of gene expression, epigenetic	33.31
GO Biological Process	innate immune response	33.31
GO Biological Process	T-helper cell lineage commitment	31.70
GO Biological Process	immune effector process	30.72
GO Biological Process	alpha-beta T cell lineage commitment	29.71
GO Biological Process	adaptive immune response	29.01
GO Biological Process	cytokine-mediated signaling pathway	28.83
GO Biological Process	positive regulation of immune system process	27.94
GO Biological Process	regulation of lymphocyte activation	26.75
GO Biological Process	adaptive immune response based on somatic recombination of immune receptors built from immunoglobulin superfamily domains	26.28
GO Biological Process	gene silencing	26.28
GO Biological Process	regulation of gene expression, epigenetic	25.84
GO Biological Process	positive regulation of gene expression, epigenetic	25.83

Supplementary Figure 495: Properties and genomic distribution of motifs identified for the ZBTB4 transcription factor in GM12878 (accession ENCSR691IQB).

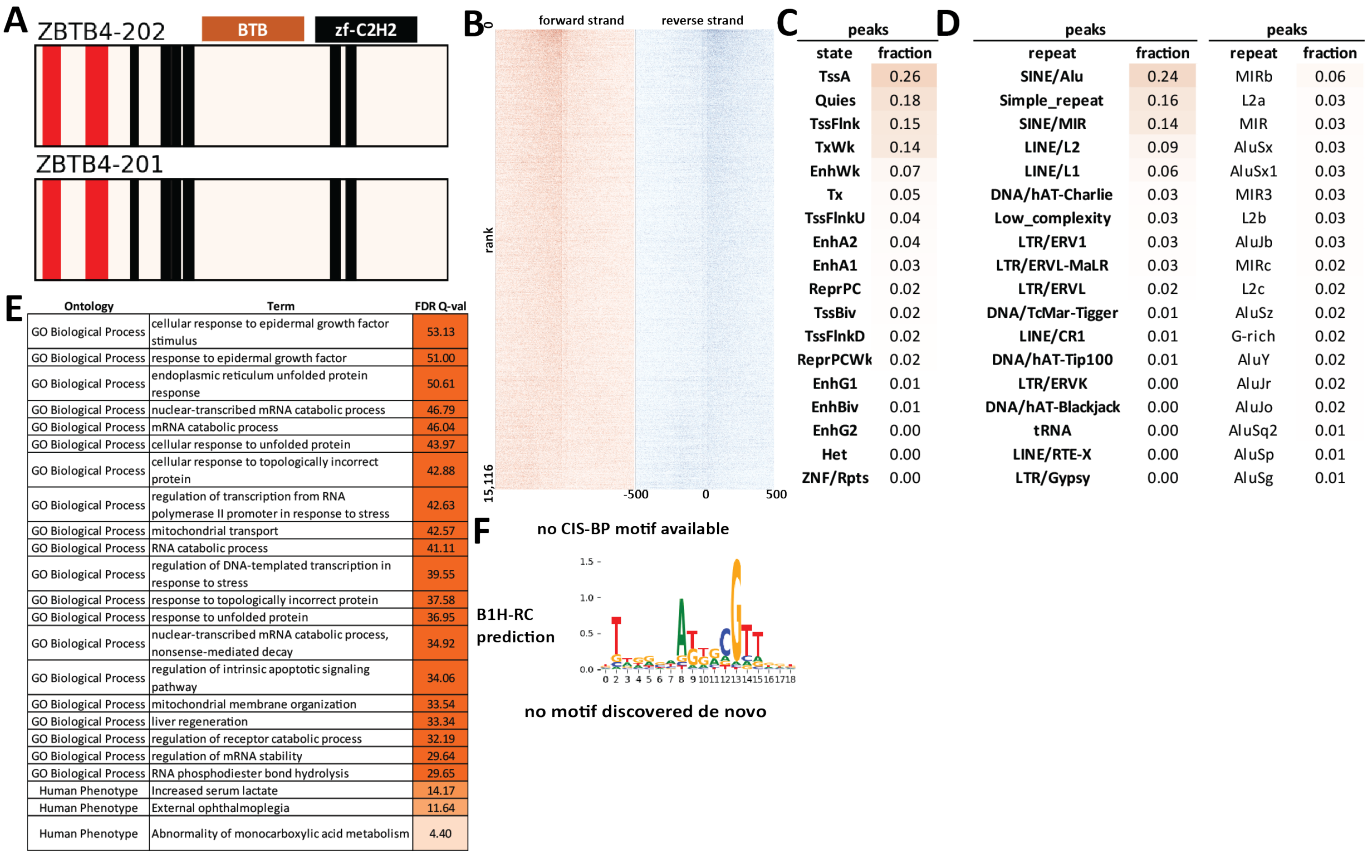

peaks	
state	fraction
TssA	0.26
Quies	0.18
TssFlnk	0.15
TxWk	0.14
EnhWk	0.07
Tx	0.05
TssFlnkU	0.04
EnhA2	0.04
EnhA1	0.03
ReprPC	0.02
TssBiv	0.02
TssFlnkD	0.02
ReprPCWk	0.02
EnhG1	0.01
EnhBiv	0.01
EnhG2	0.00
Het	0.00
ZNF/Rpts	0.00

peaks		peaks	
repeat	fraction	repeat	fraction
SINE/Alu	0.24	MIRb	0.06
Simple_repeat	0.16	L2a	0.03
SINE/MIR	0.14	MIR	0.03
LINE/L2	0.09	AluSx	0.03
LINE/L1	0.06	AluSx1	0.03
DNA/hAT-Charlie	0.03	MIR3	0.03
Low_complexity	0.03	L2b	0.03
LTR/ERV1	0.03	AluJb	0.03
LTR/ERVL-MaLR	0.03	MIRc	0.02
LTR/ERVL	0.02	L2c	0.02
DNA/TcMar-Tigger	0.01	AluSz	0.02
LINE/CR1	0.01	G-rich	0.02
DNA/hAT-Tip100	0.01	AluY	0.02
LTR/ERVK	0.00	AluJr	0.02
DNA/hAT-Blackjack	0.00	AluJo	0.02
tRNA	0.00	AluSq2	0.01
LINE/RTE-X	0.00	AluSp	0.01
LTR/Gypsy	0.00	AluSg	0.01

Ontology	Term	FDR Q-val
GO Biological Process	cellular response to epidermal growth factor stimulus	53.13
GO Biological Process	response to epidermal growth factor	51.00
GO Biological Process	endoplasmic reticulum unfolded protein response	50.61
GO Biological Process	nuclear-transcribed mRNA catabolic process	46.79
GO Biological Process	mRNA catabolic process	46.04
GO Biological Process	cellular response to unfolded protein	43.97
GO Biological Process	cellular response to topologically incorrect protein	42.88
GO Biological Process	regulation of transcription from RNA polymerase II promoter in response to stress	42.63
GO Biological Process	mitochondrial transport	42.57
GO Biological Process	RNA catabolic process	41.11
GO Biological Process	regulation of DNA-templated transcription in response to stress	39.55
GO Biological Process	response to topologically incorrect protein	37.58
GO Biological Process	response to unfolded protein	36.95
GO Biological Process	nuclear-transcribed mRNA catabolic process, nonsense-mediated decay	34.92
GO Biological Process	regulation of intrinsic apoptotic signaling pathway	34.06
GO Biological Process	mitochondrial membrane organization	33.54
GO Biological Process	liver regeneration	33.34
GO Biological Process	regulation of receptor catabolic process	32.19
GO Biological Process	regulation of mRNA stability	29.64
GO Biological Process	RNA phosphodiester bond hydrolysis	29.65
Human Phenotype	Increased serum lactate	14.17
Human Phenotype	External ophthalmoplegia	11.64
Human Phenotype	Abnormality of monocarboxylic acid metabolism	4.40

Supplementary Figure 496: Properties and genomic distribution of motifs identified for the ZBTB4 transcription factor in HepG2 (accession ENCSR479PRL).

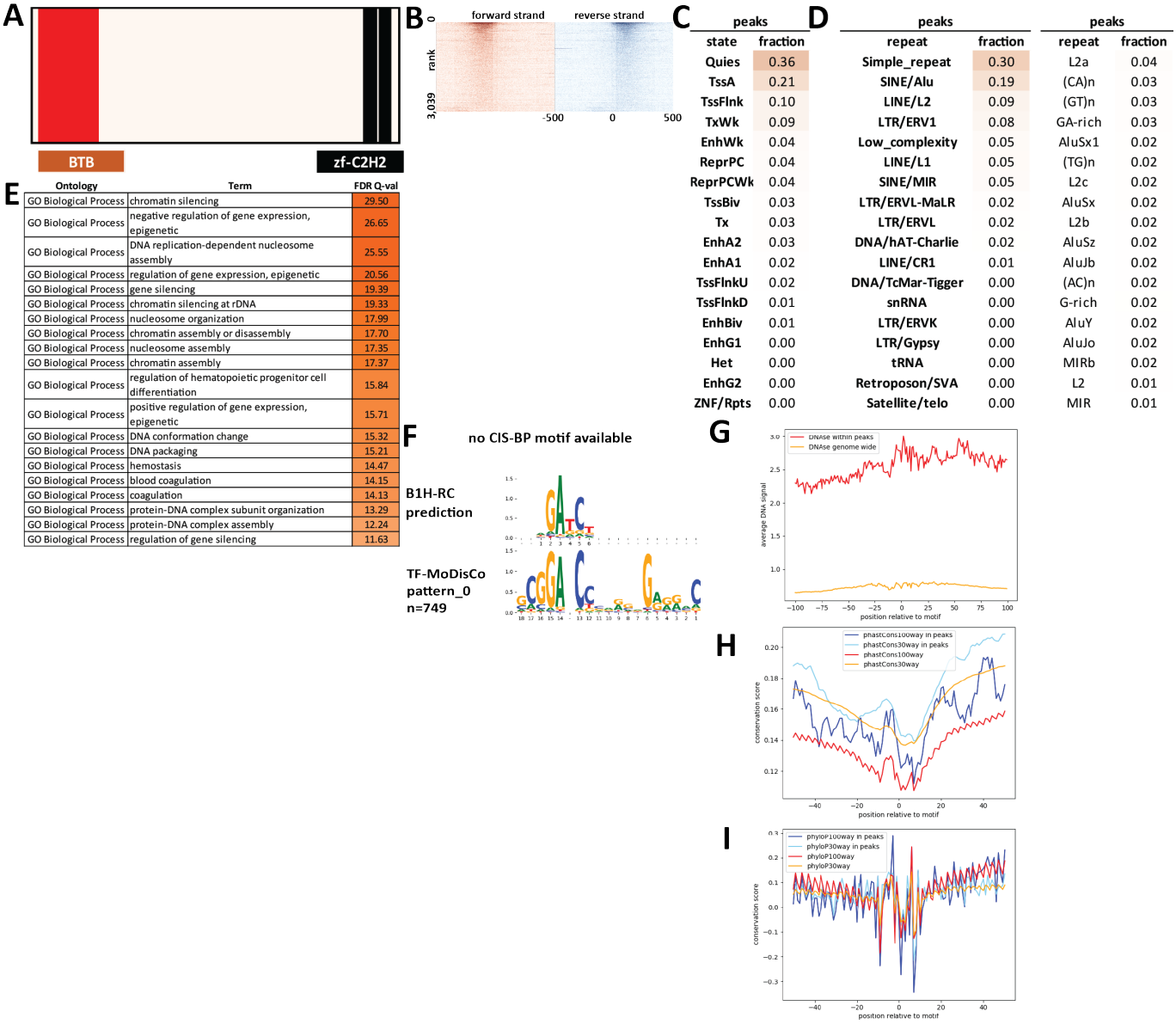

Supplementary Figure 497: Properties and genomic distribution of motifs identified for the ZBTB5 transcription factor in K562 (accession ENCSR389PWB).

TF-MoDisCO pattern_0 n=749, CWM

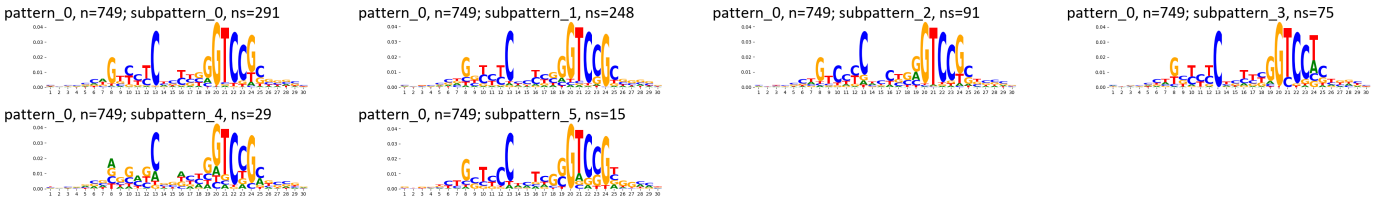

TF-MoDisCO pattern_0 n=749, PWM

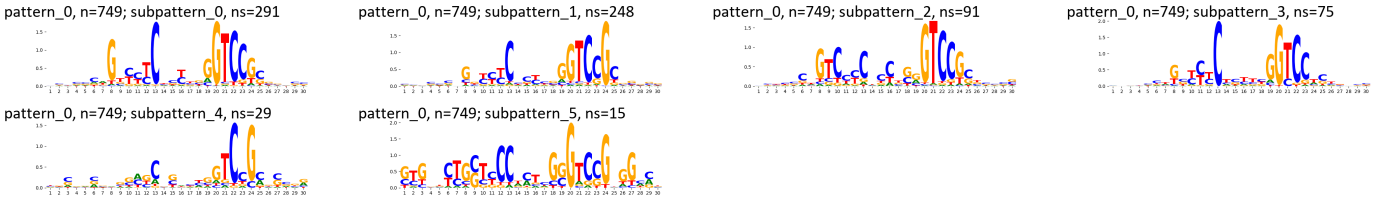

Supplementary Figure 498: TF-MoDisCO subpatterns for the ZBTB5 transcription factor in K562 (accession ENCSR389PWB).

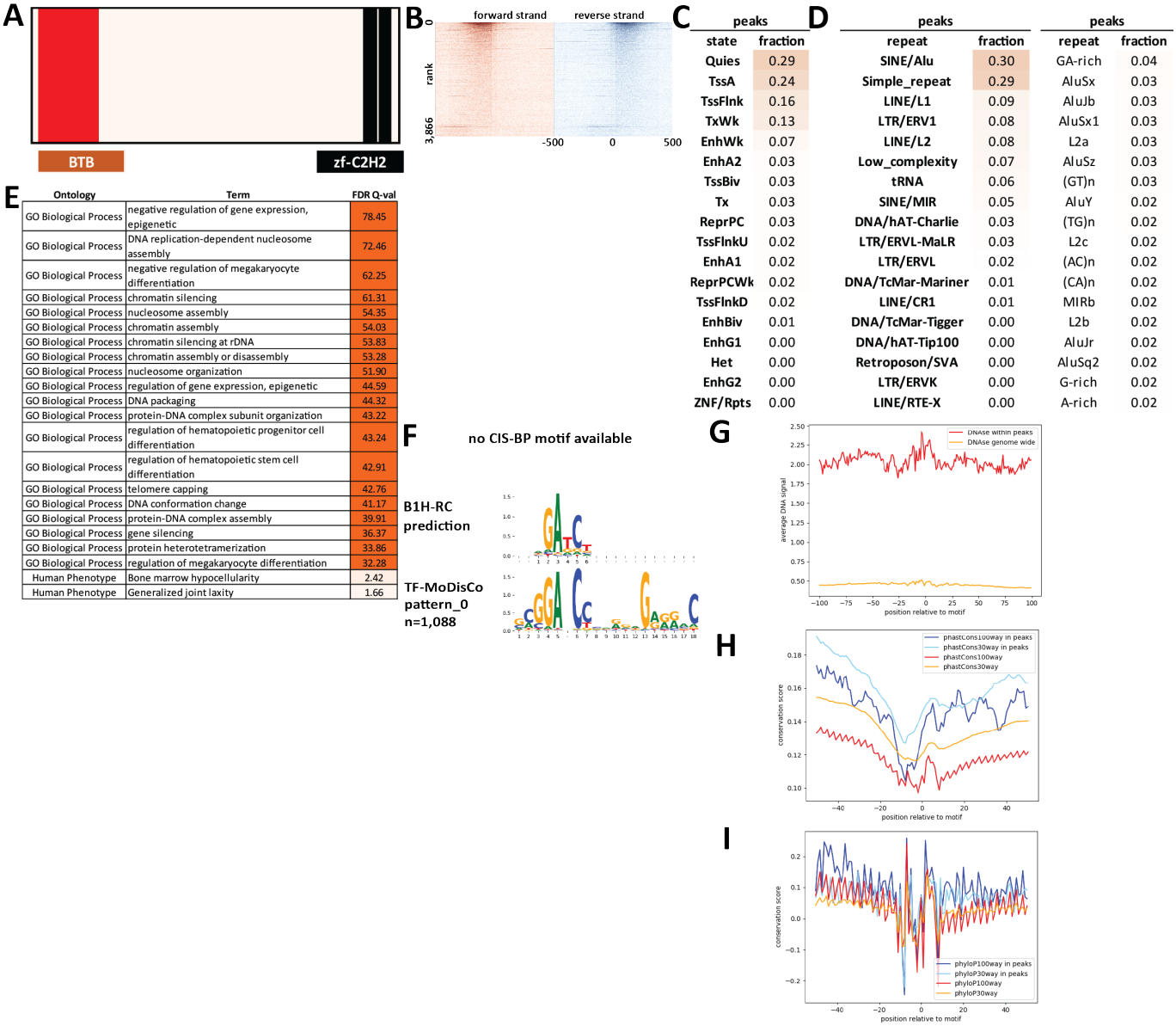

Supplementary Figure 499: Properties and genomic distribution of motifs identified for the ZBTB5 transcription factor in K562 (accession ENCSR786OQY).

TF-MoDisCO pattern_0 n=1088, CWM

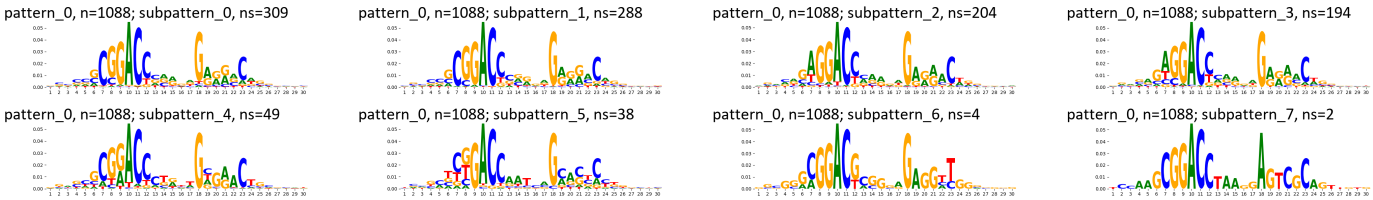

TF-MoDisCO pattern_0 n=1088, PWM

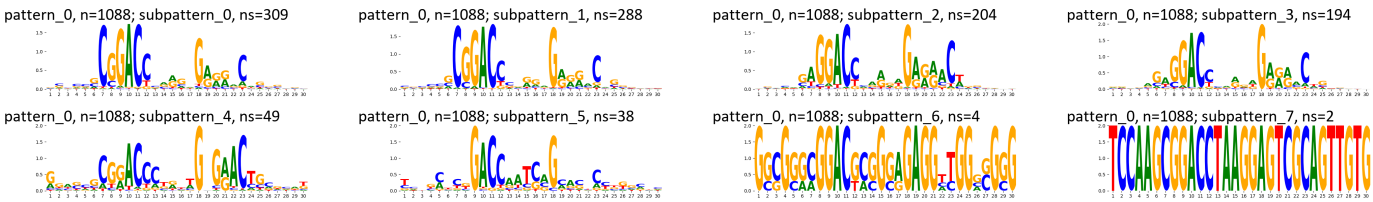

Supplementary Figure 500: TF-MoDisCO subpatterns for the ZBTB5 transcription factor in K562 (accession ENCSR786OQY).

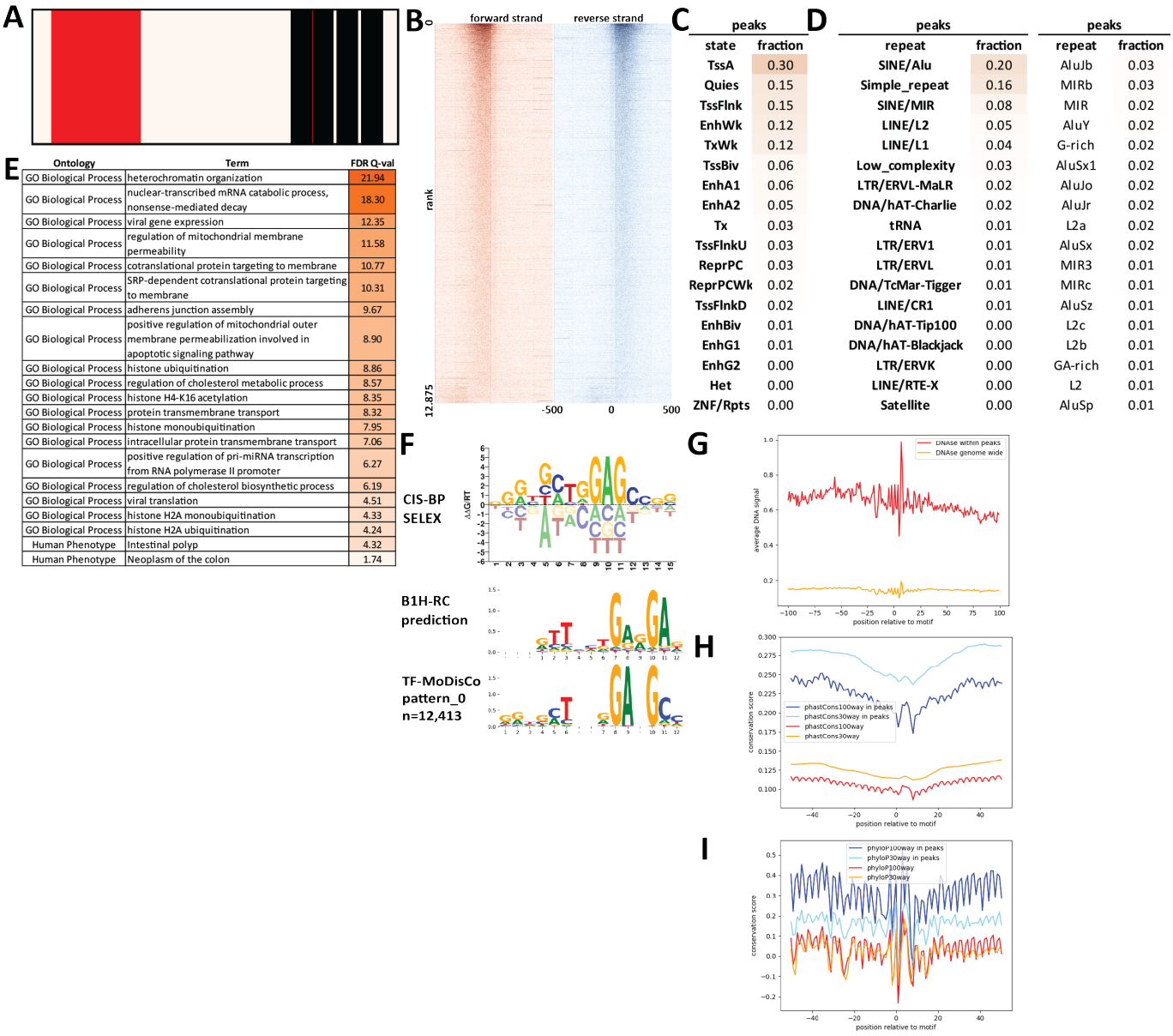

Ontology	Term	FDR Q-val
GO Biological Process	heterochromatin organization	21.94
GO Biological Process	nuclear-transcribed mRNA catabolic process, nonsense-mediated decay	18.30
GO Biological Process	viral gene expression	12.35
GO Biological Process	regulation of mitochondrial membrane permeability	11.58
GO Biological Process	cotranslational protein targeting to membrane	10.77
GO Biological Process	SRP-dependent cotranslational protein targeting to membrane	10.31
GO Biological Process	adherens junction assembly	9.67
GO Biological Process	positive regulation of mitochondrial outer membrane permeabilization involved in apoptotic signaling pathway	8.90
GO Biological Process	histone ubiquitination	8.86
GO Biological Process	regulation of cholesterol metabolic process	8.57
GO Biological Process	histone H4-K16 acetylation	8.35
GO Biological Process	protein transmembrane transport	8.32
GO Biological Process	histone monoubiquitination	7.95
GO Biological Process	intracellular protein transmembrane transport	7.06
GO Biological Process	positive regulation of pri-miRNA transcription from RNA polymerase II promoter	6.27
GO Biological Process	regulation of cholesterol biosynthetic process	6.19
GO Biological Process	viral translation	4.51
GO Biological Process	histone H2A monoubiquitination	4.33
GO Biological Process	histone H2A ubiquitination	4.24
Human Phenotype	Intestinal polyp	4.32
Human Phenotype	Neoplasm of the colon	1.74

peaks	
state	fraction
TssA	0.30
Quies	0.15
TssFlnk	0.15
EnhWk	0.12
TxWk	0.12
TssBiv	0.06
EnhA1	0.06
EnhA2	0.05
Tx	0.03
TssFlnkU	0.03
ReprPC	0.03
ReprPCWk	0.02
TssFlnkD	0.02
EnhBiv	0.01
EnhG1	0.01
EnhG2	0.00
Het	0.00
ZNF/Rpts	0.00

peaks		peaks	
repeat	fraction	repeat	fraction
SINE/Alu	0.20	AluJb	0.03
Simple_repeat	0.16	MIRb	0.03
SINE/MIR	0.08	MIR	0.02
LINE/L2	0.05	AluY	0.02
LINE/L1	0.04	G-rich	0.02
Low_complexity	0.03	AluSx1	0.02
LTR/ERVL-MaLR	0.02	AluJo	0.02
DNA/hAT-Charlie	0.02	AluJr	0.02
tRNA	0.01	L2a	0.02
LTR/ERV1	0.01	AluSx	0.02
LTR/ERVL	0.01	MIR3	0.01
DNA/TcMar-Tigger	0.01	MIRc	0.01
LINE/CR1	0.01	AluSz	0.01
DNA/hAT-Tip100	0.00	L2c	0.01
DNA/hAT-Blackjack	0.00	L2b	0.01
LTR/ERVK	0.00	GA-rich	0.01
LINE/RTE-X	0.00	L2	0.01
Satellite	0.00	AluSp	0.01

Supplementary Figure 501: Properties and genomic distribution of motifs identified for the ZBTB6 transcription factor in HEK293 (accession ENCSR619OUC).

TF-MoDisCO pattern_0 n=12413, CWM

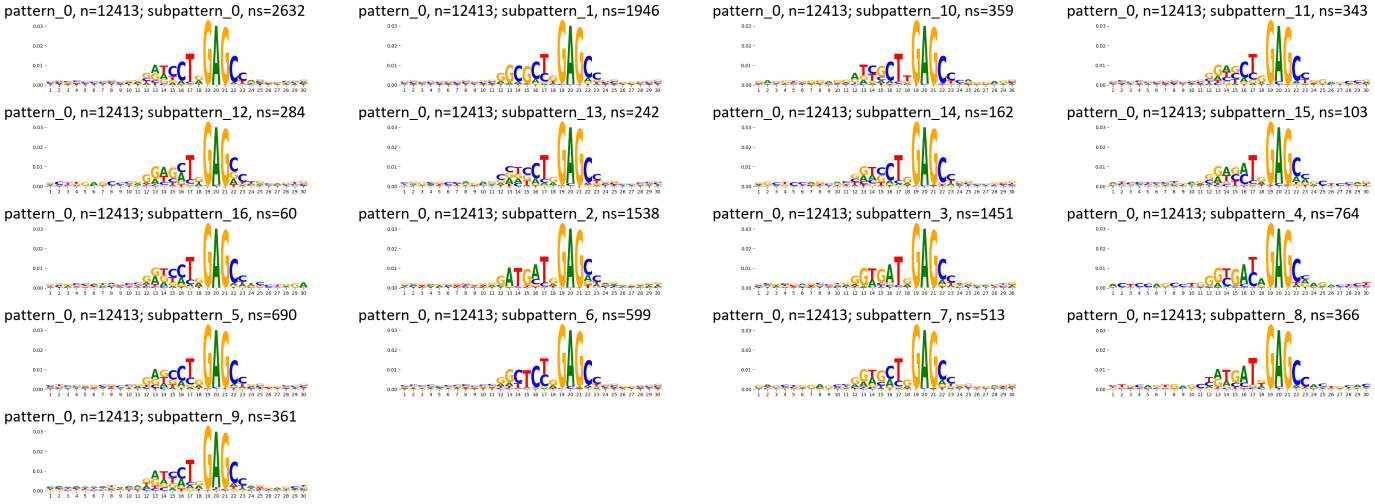

TF-MoDisCO pattern_0 n=12413, PWM

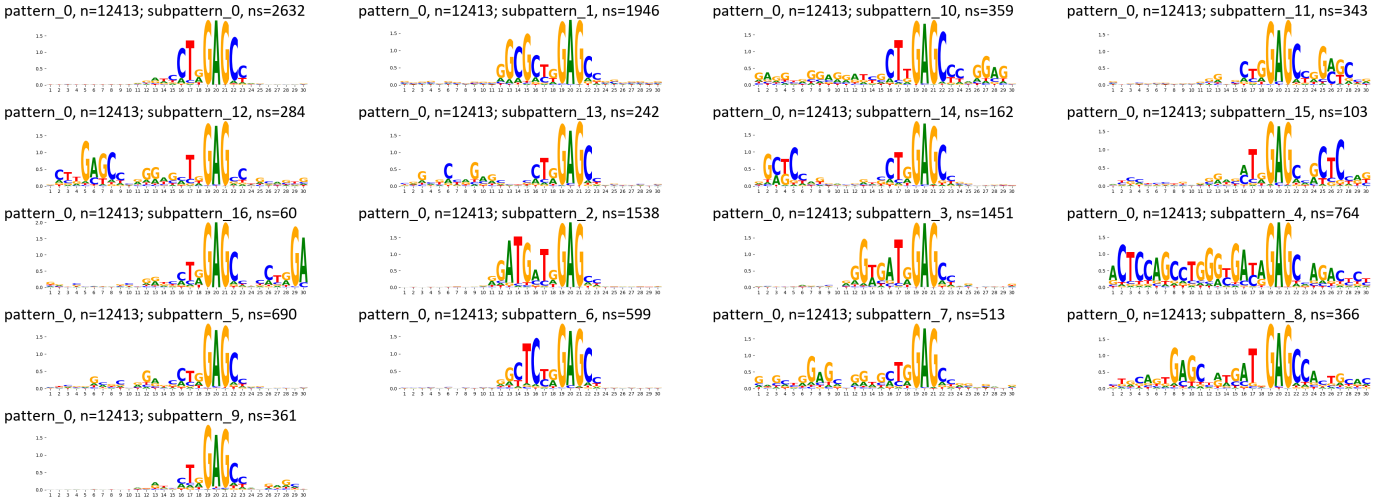

Supplementary Figure 502: TF-MoDisCO subpatterns for the ZBTB6 transcription factor in HEK293 (accession ENCSR619OUC).

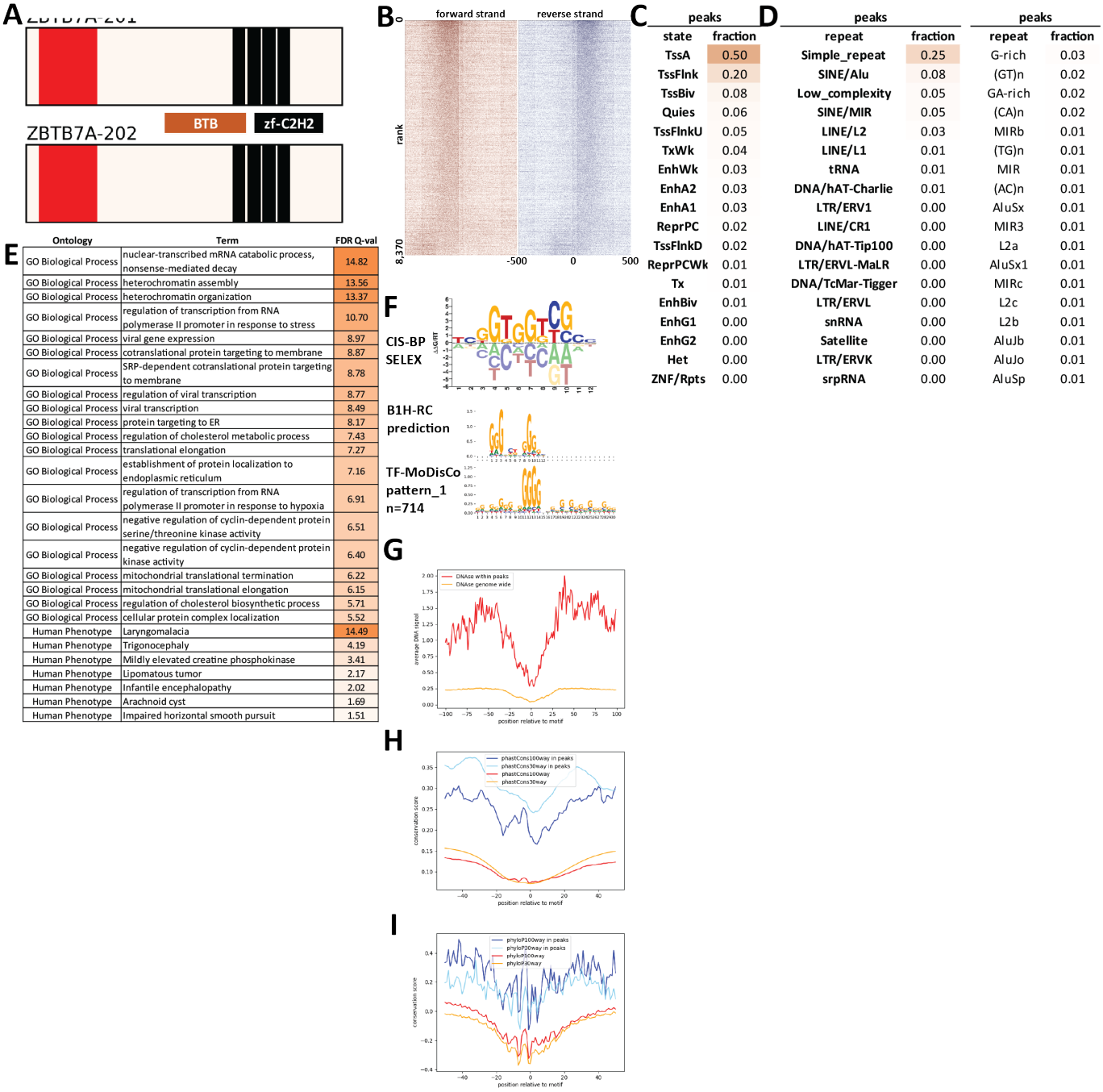

Supplementary Figure 503: Properties and genomic distribution of motifs identified for the ZBTB7A transcription factor in HEK293 (accession ENCSR773REP).

TF-MoDisCO pattern_1 n=714, CWM

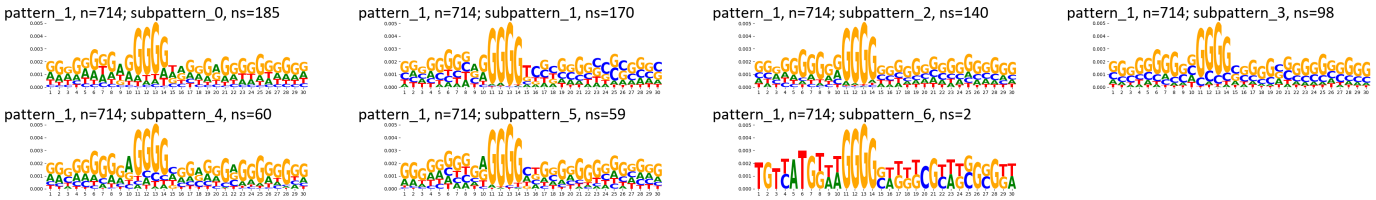

TF-MoDisCO pattern_1 n=714, PWM

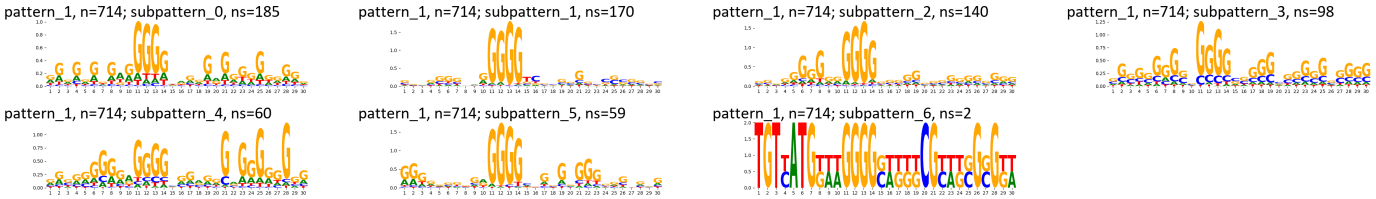

Supplementary Figure 504: TF-MoDisCO subpatterns for the ZBTB7A transcription factor in HEK293 (accession ENCSR773REP).

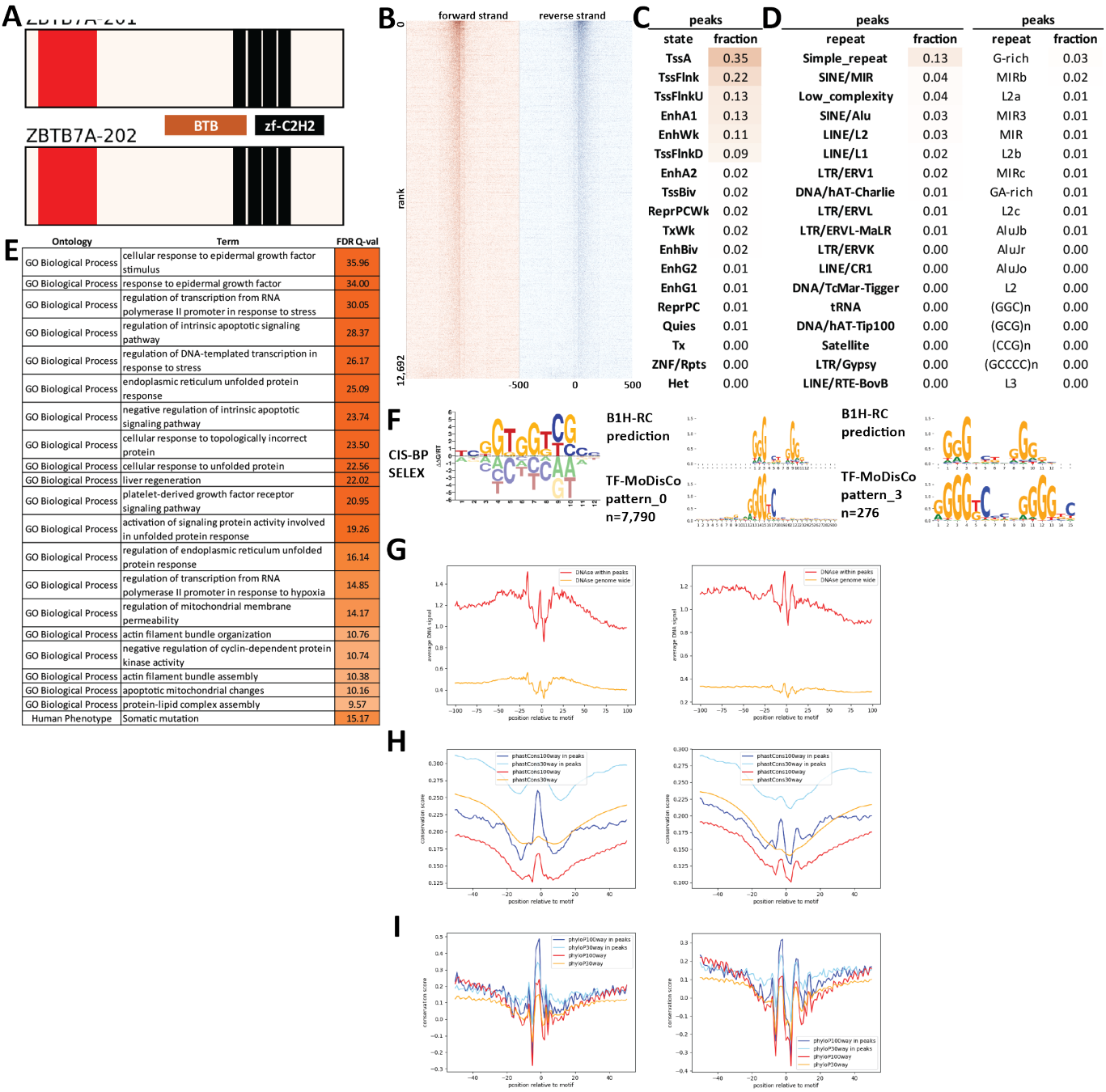

peaks	
state	fraction
TssA	0.35
TssFlnk	0.22
TssFlnkU	0.13
EnhA1	0.13
EnhWk	0.11
TssFlnkD	0.09
EnhA2	0.02
TssBiv	0.02
ReprPCWk	0.02
TxWk	0.02
EnhBiv	0.02
EnhG2	0.01
EnhG1	0.01
ReprPC	0.01
Quies	0.01
Tx	0.00
ZNF/Rpts	0.00
Het	0.00

peaks		peaks	
repeat	fraction	repeat	fraction
Simple_repeat	0.13	G-rich	0.03
SINE/MIR	0.04	MIRb	0.02
Low_complexity	0.04	L2a	0.01
SINE/Alu	0.03	MIR3	0.01
LINE/L2	0.03	MIR	0.01
LINE/L1	0.02	L2b	0.01
LTR/ERV1	0.02	MIRc	0.01
DNA/hAT-Charlie	0.01	GA-rich	0.01
LTR/ERVL	0.01	L2c	0.01
LTR/ERVL-MaLR	0.01	AluJb	0.01
LTR/ERVK	0.00	AluJr	0.00
LINE/CR1	0.00	AluJo	0.00
DNA/TcMar-Tigger	0.00	L2	0.00
tRNA	0.00	(GGC)n	0.00
DNA/hAT-Tip100	0.00	(GCG)n	0.00
Satellite	0.00	(CCG)n	0.00
LTR/Gypsy	0.00	(GCCCC)n	0.00
LINE/RTE-BovB	0.00	L3	0.00

Ontology	Term	FDR Q-val
GO Biological Process	cellular response to epidermal growth factor stimulus	35.96
GO Biological Process	response to epidermal growth factor	34.00
GO Biological Process	regulation of transcription from RNA polymerase II promoter in response to stress	30.05
GO Biological Process	regulation of intrinsic apoptotic signaling pathway	28.37
GO Biological Process	regulation of DNA-templated transcription in response to stress	26.17
GO Biological Process	endoplasmic reticulum unfolded protein response	25.09
GO Biological Process	negative regulation of intrinsic apoptotic signaling pathway	23.74
GO Biological Process	cellular response to topologically incorrect protein	23.50
GO Biological Process	cellular response to unfolded protein	22.56
GO Biological Process	liver regeneration	22.02
GO Biological Process	platelet-derived growth factor receptor signaling pathway	20.95
GO Biological Process	activation of signaling protein activity involved in unfolded protein response	19.26
GO Biological Process	regulation of endoplasmic reticulum unfolded protein response	16.14
GO Biological Process	regulation of transcription from RNA polymerase II promoter in response to hypoxia	14.85
GO Biological Process	regulation of mitochondrial membrane permeability	14.17
GO Biological Process	actin filament bundle organization	10.76
GO Biological Process	negative regulation of cyclin-dependent protein kinase activity	10.74
GO Biological Process	actin filament bundle assembly	10.38
GO Biological Process	apoptotic mitochondrial changes	10.16
GO Biological Process	protein-lipid complex assembly	9.57
Human Phenotype	Somatic mutation	15.17

Supplementary Figure 505: Properties and genomic distribution of motifs identified for the ZBTB7A transcription factor in HepG2 (accession ENCSR000BQA).

TF-MoDisCO pattern_0 n=7790, CWM

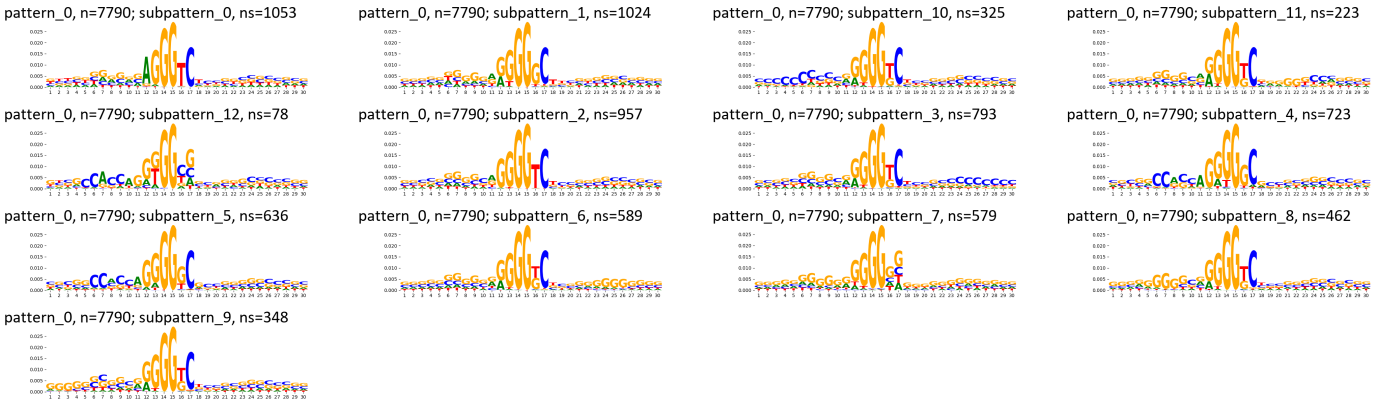

TF-MoDisCO pattern_0 n=7790, PWM

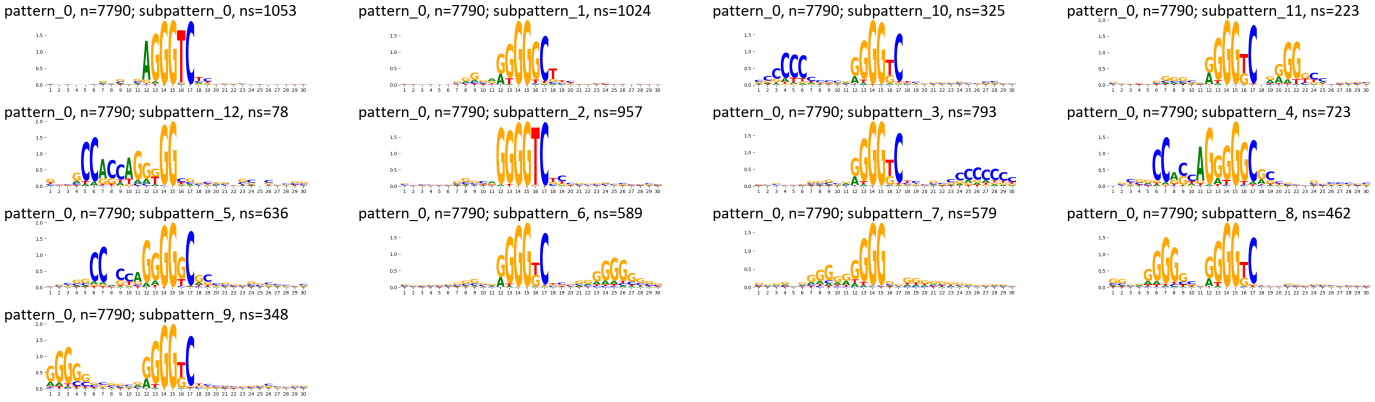

TF-MoDisCO pattern_3 n=276, CWM

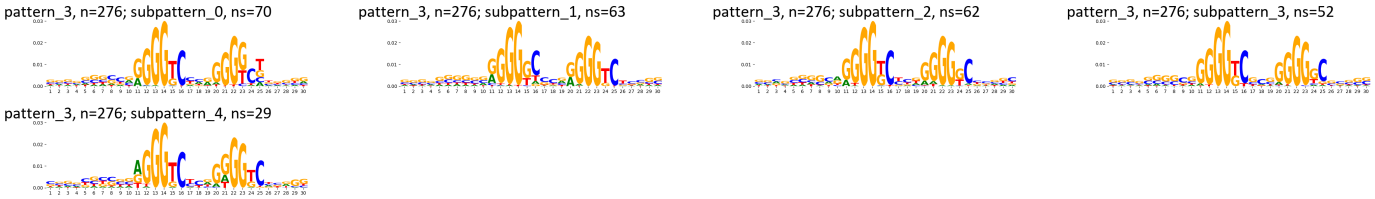

TF-MoDisCO pattern_3 n=276, PWM

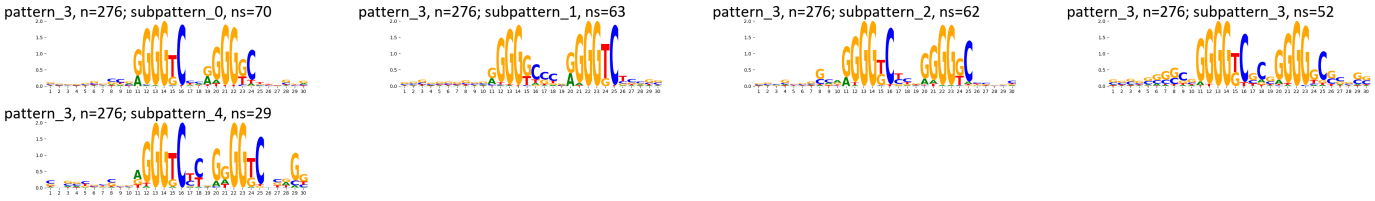

Supplementary Figure 506: TF-MoDisCO subpatterns for the ZBTB7A transcription factor in HepG2 (accession ENCSR000BQA).

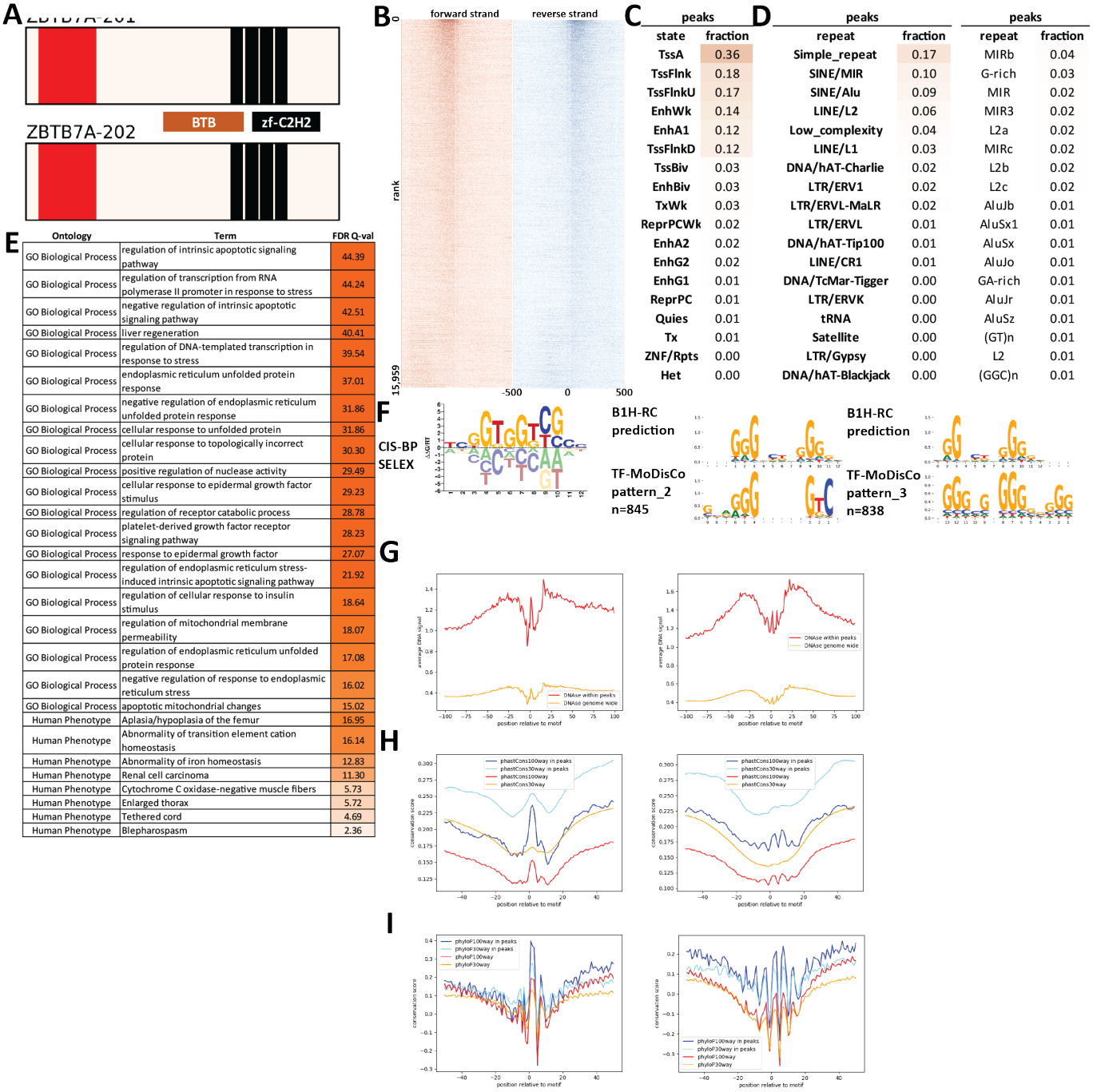

Supplementary Figure 507: Properties and genomic distribution of motifs identified for the ZBTB7A transcription factor in HepG2 (accession ENCSR850YDX).

TF-MoDisCO pattern_2 n=845, CWM

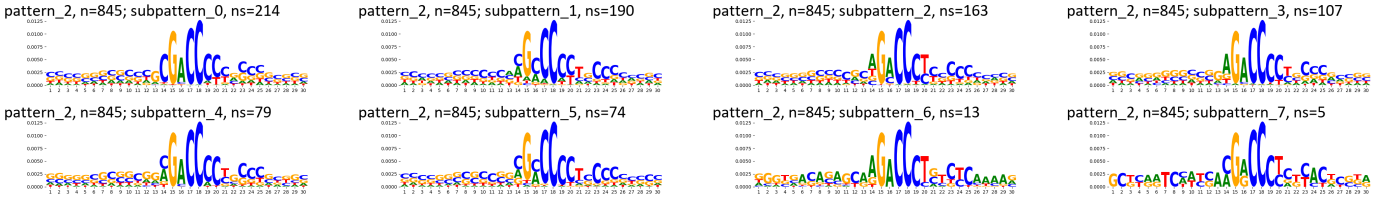

TF-MoDisCO pattern_2 n=845, PWM

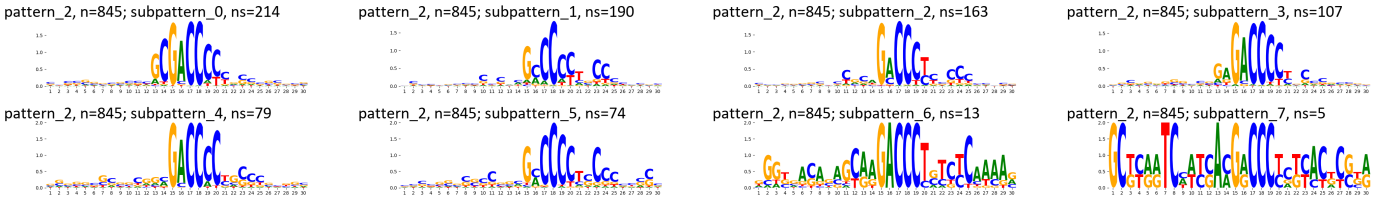

TF-MoDisCO pattern_3 n=838, CWM

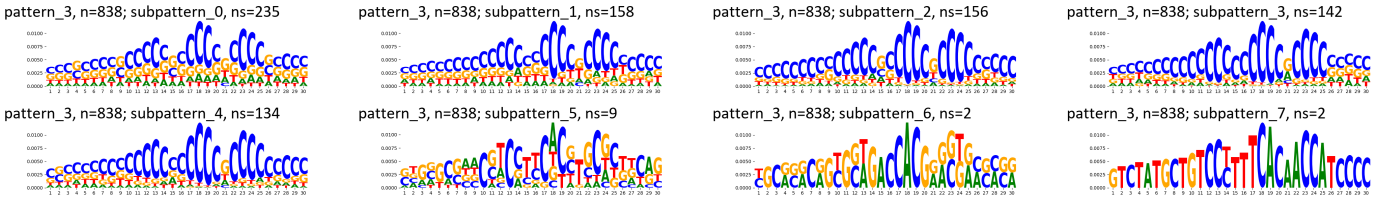

TF-MoDisCO pattern_3 n=838, PWM

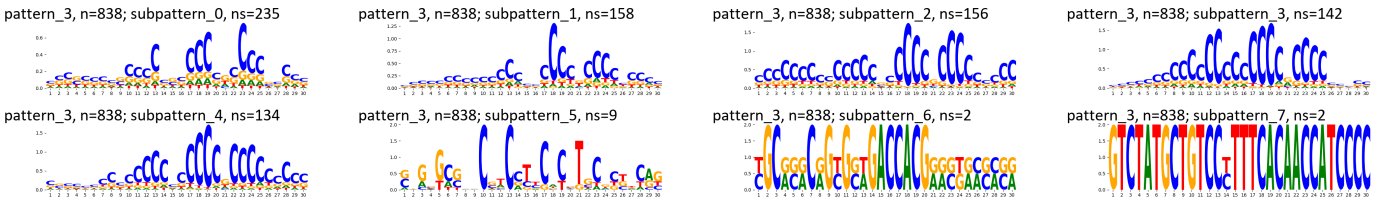

Supplementary Figure 508: TF-MoDisCO subpatterns for the ZBTB7A transcription factor in HepG2 (accession ENCSR850YDX).

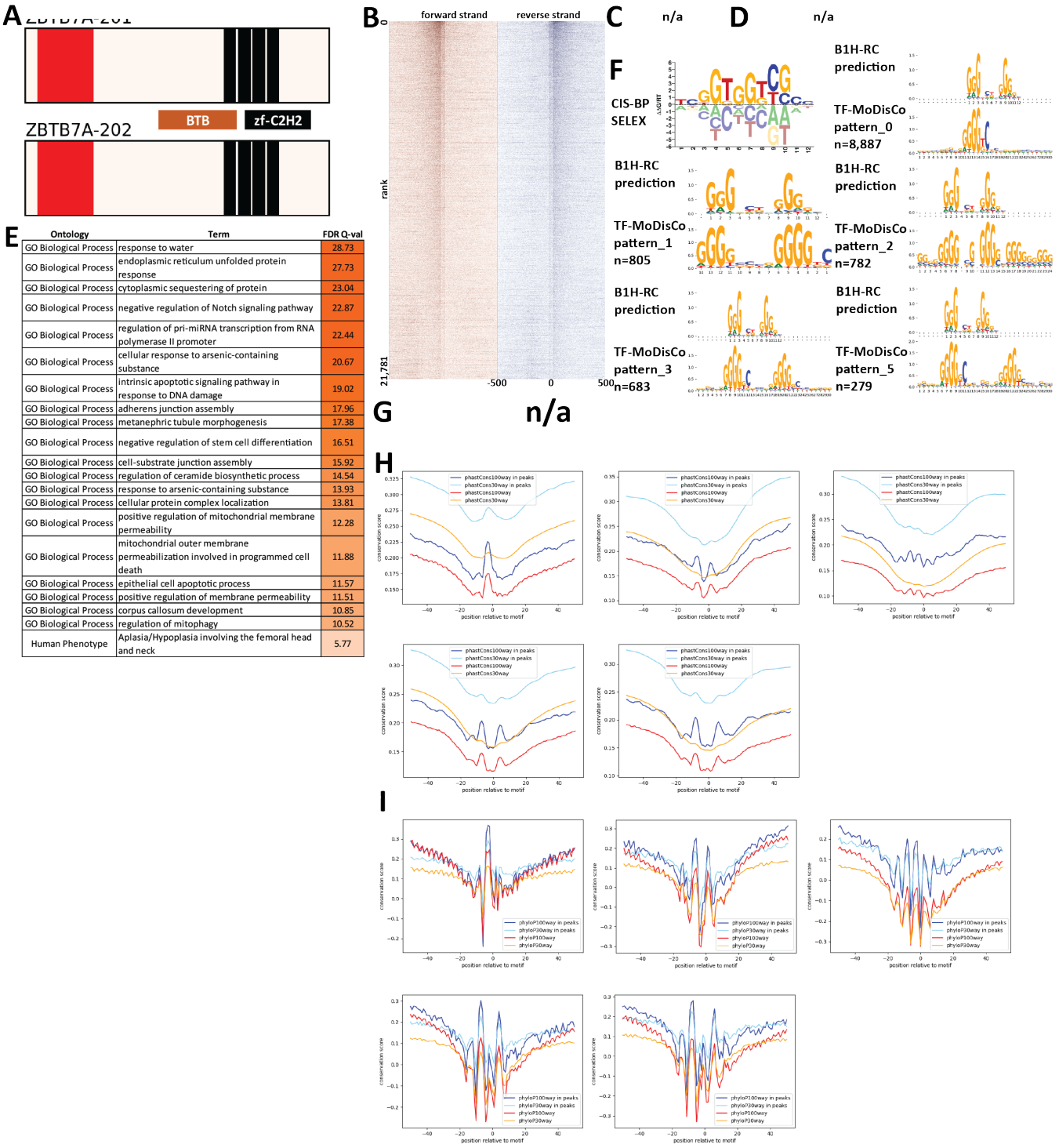

E

Ontology	Term	FDR Q-val
GO Biological Process	response to water	28.73
GO Biological Process	endoplasmic reticulum unfolded protein response	27.73
GO Biological Process	cytoplasmic sequestering of protein	23.04
GO Biological Process	negative regulation of Notch signaling pathway	22.87
GO Biological Process	regulation of pri-miRNA transcription from RNA polymerase II promoter	22.44
GO Biological Process	cellular response to arsenic-containing substance	20.67
GO Biological Process	intrinsic apoptotic signaling pathway in response to DNA damage	19.02
GO Biological Process	adherens junction assembly	17.96
GO Biological Process	metanephric tubule morphogenesis	17.38
GO Biological Process	negative regulation of stem cell differentiation	16.51
GO Biological Process	cell-substrate junction assembly	15.92
GO Biological Process	regulation of ceramide biosynthetic process	14.54
GO Biological Process	response to arsenic-containing substance	13.93
GO Biological Process	cellular protein complex localization	13.81
GO Biological Process	positive regulation of mitochondrial membrane permeability	12.28
GO Biological Process	mitochondrial outer membrane permeabilization involved in programmed cell death	11.88
GO Biological Process	epithelial cell apoptotic process	11.57
GO Biological Process	positive regulation of membrane permeability	11.51
GO Biological Process	corpus callosum development	10.85
GO Biological Process	regulation of mitophagy	10.52
Human Phenotype	Aplasia/Hypoplasia involving the femoral head and neck	5.77

Supplementary Figure 509: Properties and genomic distribution of motifs identified for the ZBTB7A transcription factor in Ishikawa (accession ENCSR000BSZ).

TF-MoDisCO pattern_0 n=8887, CWM

pattern_0, n=8887; subpattern_0, ns=2306

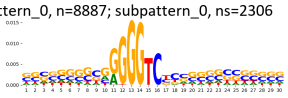

pattern_0, n=8887; subpattern_1, ns=1404

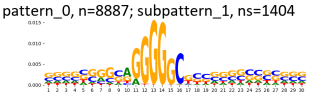

pattern_0, n=8887; subpattern_10, ns=179

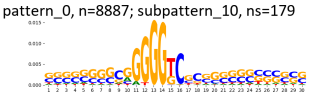

pattern_0, n=8887; subpattern_2, ns=1053

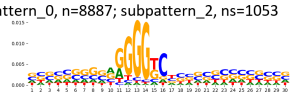

pattern_0, n=8887; subpattern_3, ns=721

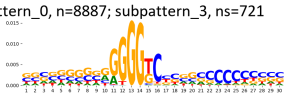

pattern_0, n=8887; subpattern_4, ns=710

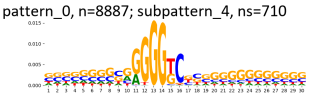

pattern_0, n=8887; subpattern_5, ns=662

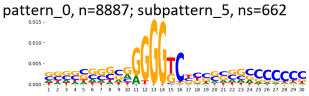

pattern_0, n=8887; subpattern_6, ns=653

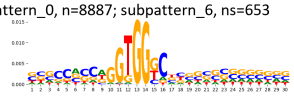

pattern_0, n=8887; subpattern_7, ns=477

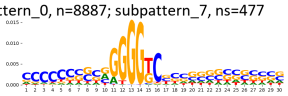

pattern_0, n=8887; subpattern_8, ns=373

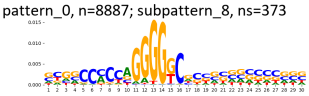

pattern_0, n=8887; subpattern_9, ns=349

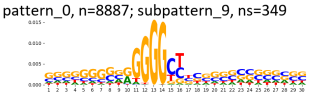

TF-MoDisCO pattern_0 n=8887, PWM

pattern_0, n=8887; subpattern_0, ns=2306

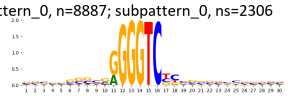

pattern_0, n=8887; subpattern_1, ns=1404

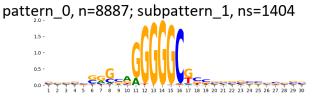

pattern_0, n=8887; subpattern_10, ns=179

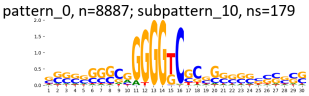

pattern_0, n=8887; subpattern_2, ns=1053

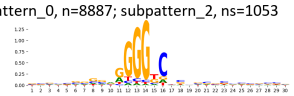

pattern_0, n=8887; subpattern_3, ns=721

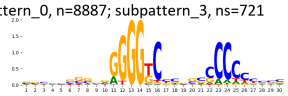

pattern_0, n=8887; subpattern_4, ns=710

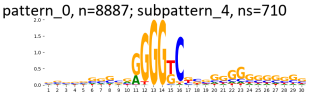

pattern_0, n=8887; subpattern_5, ns=662

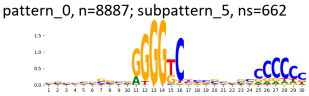

pattern_0, n=8887; subpattern_6, ns=653

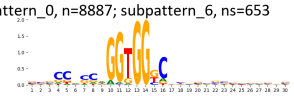

pattern_0, n=8887; subpattern_7, ns=477

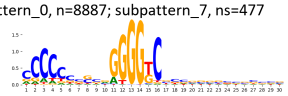

pattern_0, n=8887; subpattern_8, ns=373

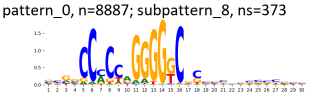

pattern_0, n=8887; subpattern_9, ns=349

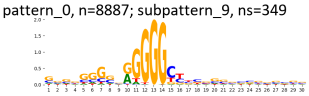

TF-MoDisCO pattern_1 n=805, CWM

pattern_1, n=805; subpattern_0, ns=171

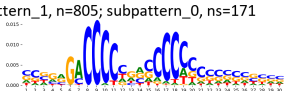

pattern_1, n=805; subpattern_1, ns=155

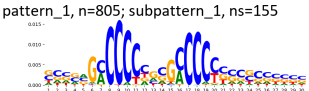

pattern_1, n=805; subpattern_2, ns=140

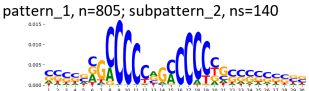

pattern_1, n=805; subpattern_3, ns=124

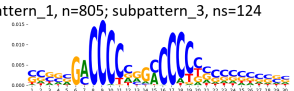

pattern_1, n=805; subpattern_4, ns=103

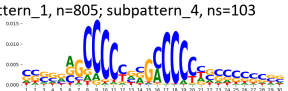

pattern_1, n=805; subpattern_5, ns=103

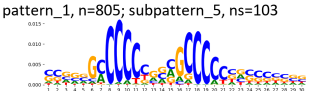

pattern_1, n=805; subpattern_6, ns=9

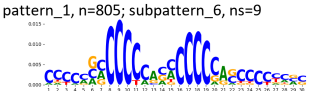

TF-MoDisCO pattern_1 n=805, PWM

pattern_1, n=805; subpattern_0, ns=171

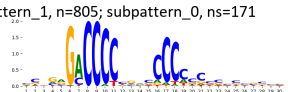

pattern_1, n=805; subpattern_1, ns=155

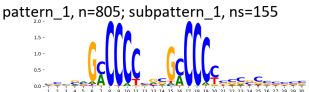

pattern_1, n=805; subpattern_2, ns=140

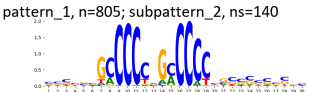

pattern_1, n=805; subpattern_3, ns=124

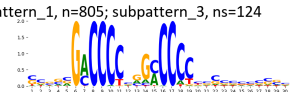

pattern_1, n=805; subpattern_4, ns=103

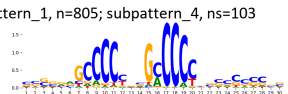

pattern_1, n=805; subpattern_5, ns=103

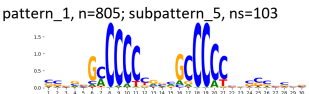

pattern_1, n=805; subpattern_6, ns=9

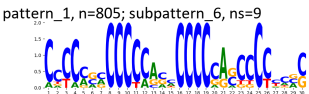

TF-MoDisCO pattern_2 n=782, CWM

pattern_2, n=782; subpattern_0, ns=205

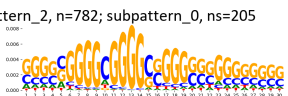

pattern_2, n=782; subpattern_1, ns=137

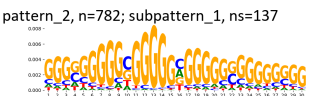

pattern_2, n=782; subpattern_2, ns=120

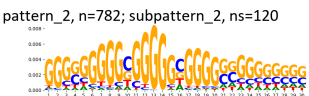

pattern_2, n=782; subpattern_3, ns=96

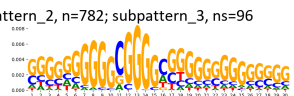

pattern_2, n=782; subpattern_4, ns=93

pattern_2, n=782; subpattern_5, ns=73

pattern_2, n=782; subpattern_6, ns=58

TF-MoDisCO pattern_2 n=782, PWM

pattern_2, n=782; subpattern_0, ns=205

pattern_2, n=782; subpattern_1, ns=137

pattern_2, n=782; subpattern_2, ns=120

pattern_2, n=782; subpattern_3, ns=96

pattern_2, n=782; subpattern_4, ns=93

pattern_2, n=782; subpattern_5, ns=73

pattern_2, n=782; subpattern_6, ns=58

TF-MoDisCO pattern_3 n=683, CWM

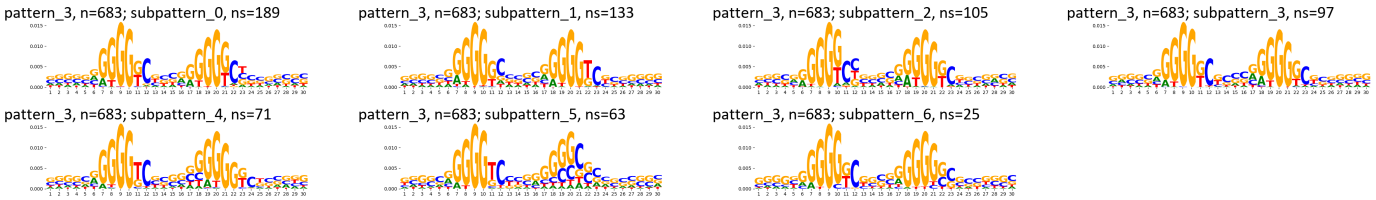

TF-MoDisCO pattern_3 n=683, PWM

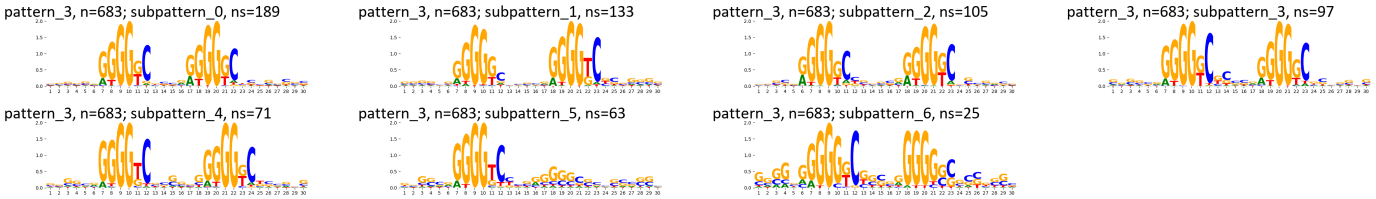

TF-MoDisCO pattern_5 n=279, CWM

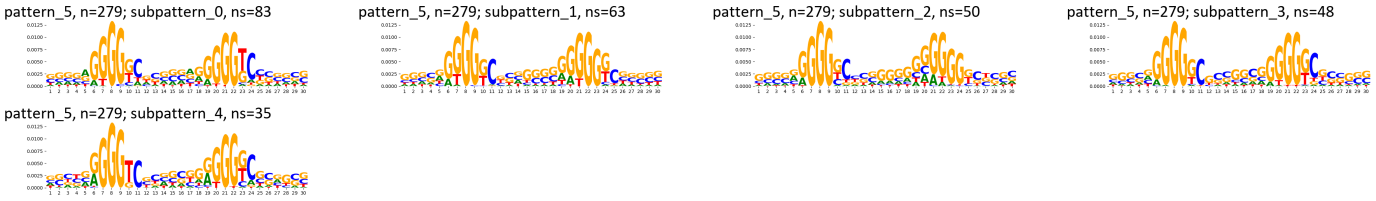

TF-MoDisCO pattern_5 n=279, PWM

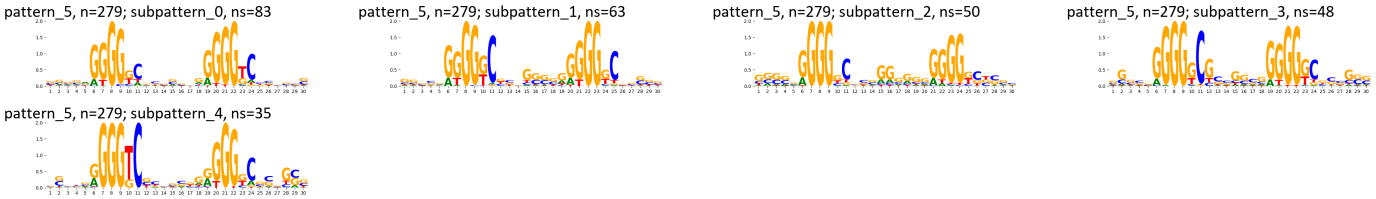

Supplementary Figure 510: TF-MoDisCO subpatterns for the ZBTB7A transcription factor in Ishikawa (accession ENCSR000BSZ).

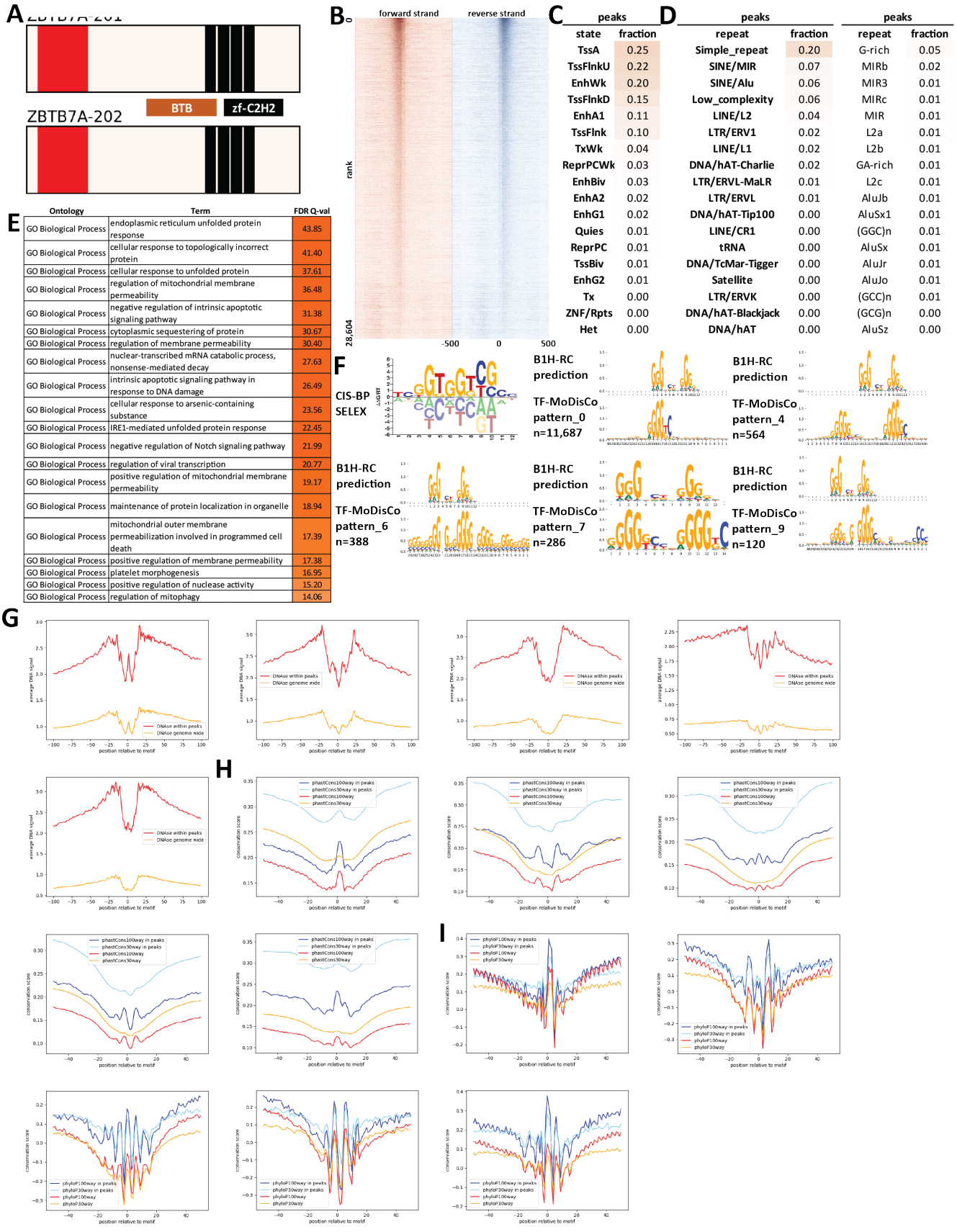

Supplementary Figure 511: Properties and genomic distribution of motifs identified for the ZBTB7A transcription factor in K562 (accession ENCSR000BME).

TF-MoDisCO pattern_0 n=11687, CWM

pattern_0, n=11687; subpattern_0, ns=2326

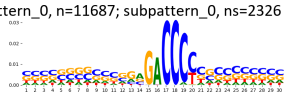

pattern_0, n=11687; subpattern_1, ns=2092

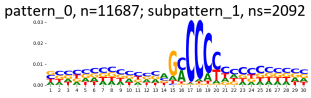

pattern_0, n=11687; subpattern_2, ns=1713

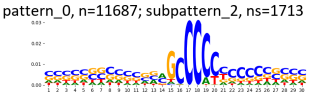

pattern_0, n=11687; subpattern_3, ns=1361

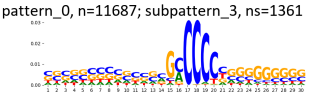

pattern_0, n=11687; subpattern_4, ns=1138

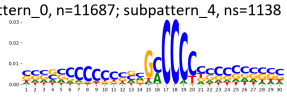

pattern_0, n=11687; subpattern_5, ns=1056

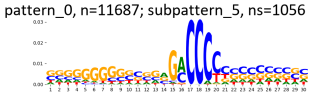

pattern_0, n=11687; subpattern_6, ns=1023

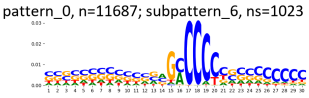

pattern_0, n=11687; subpattern_7, ns=504

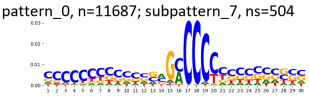

pattern_0, n=11687; subpattern_8, ns=474

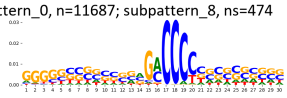

TF-MoDisCO pattern_0 n=11687, PWM

pattern_0, n=11687; subpattern_0, ns=2326

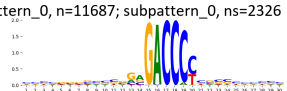

pattern_0, n=11687; subpattern_1, ns=2092

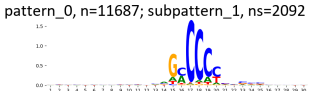

pattern_0, n=11687; subpattern_2, ns=1713

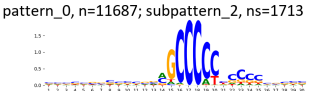

pattern_0, n=11687; subpattern_3, ns=1361

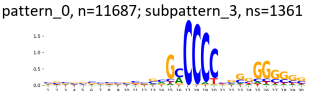

pattern_0, n=11687; subpattern_4, ns=1138

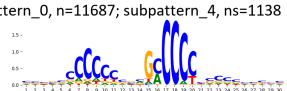

pattern_0, n=11687; subpattern_5, ns=1056

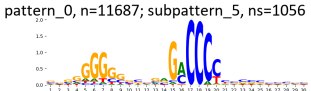

pattern_0, n=11687; subpattern_6, ns=1023

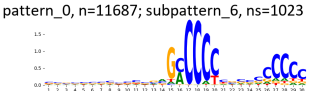

pattern_0, n=11687; subpattern_7, ns=504

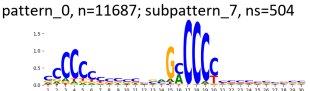

pattern_0, n=11687; subpattern_8, ns=474

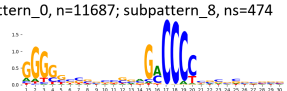

TF-MoDisCO pattern_4 n=564, CWM

pattern_4, n=564; subpattern_0, ns=156

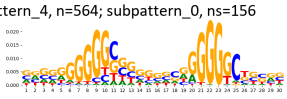

pattern_4, n=564; subpattern_1, ns=147

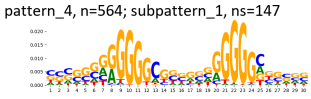

pattern_4, n=564; subpattern_2, ns=124

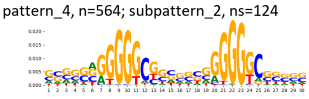

pattern_4, n=564; subpattern_3, ns=118

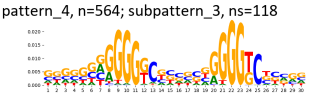

pattern_4, n=564; subpattern_4, ns=19

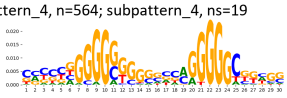

TF-MoDisCO pattern_4 n=564, PWM

pattern_4, n=564; subpattern_0, ns=156

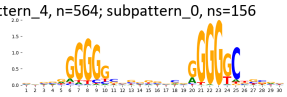

pattern_4, n=564; subpattern_1, ns=147

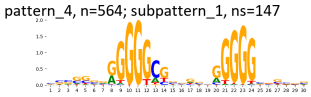

pattern_4, n=564; subpattern_2, ns=124

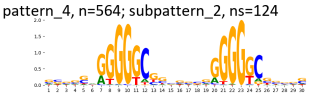

pattern_4, n=564; subpattern_3, ns=118

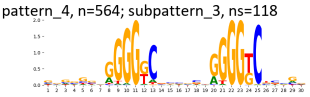

pattern_4, n=564; subpattern_4, ns=19

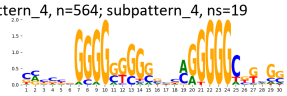

TF-MoDisCO pattern_6 n=388, CWM

pattern_6, n=388; subpattern_0, ns=110

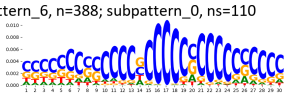

pattern_6, n=388; subpattern_1, ns=74

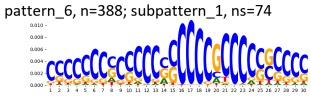

pattern_6, n=388; subpattern_2, ns=52

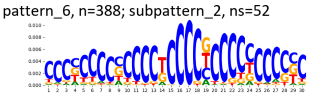

pattern_6, n=388; subpattern_3, ns=52

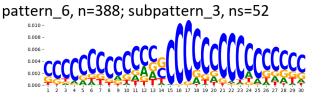

pattern_6, n=388; subpattern_4, ns=50

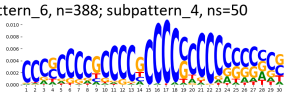

pattern_6, n=388; subpattern_5, ns=41

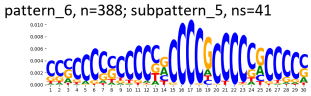

pattern_6, n=388; subpattern_6, ns=7

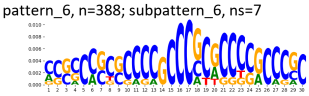

pattern_6, n=388; subpattern_7, ns=2

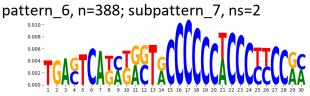

TF-MoDisCO pattern_6 n=388, PWM

pattern_6, n=388; subpattern_0, ns=110

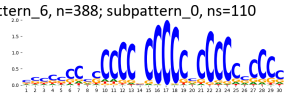

pattern_6, n=388; subpattern_1, ns=74

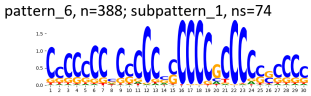

pattern_6, n=388; subpattern_2, ns=52

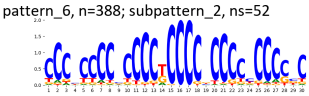

pattern_6, n=388; subpattern_3, ns=52

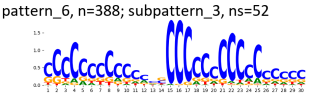

pattern_6, n=388; subpattern_4, ns=50

pattern_6, n=388; subpattern_5, ns=41

pattern_6, n=388; subpattern_6, ns=7

pattern_6, n=388; subpattern_7, ns=2

TF-MoDisCO pattern_7 n=286, CWM

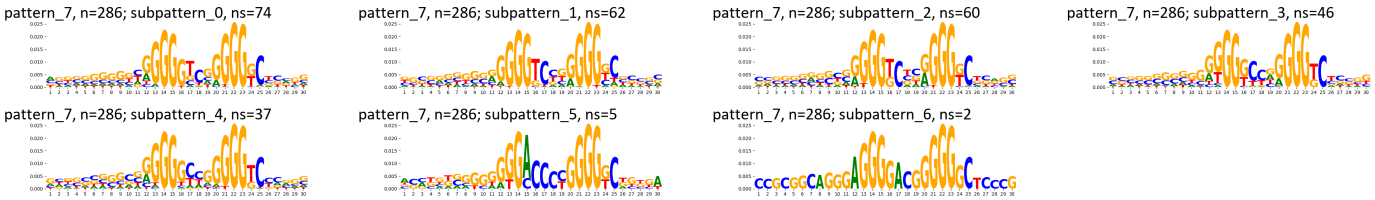

TF-MoDisCO pattern_7 n=286, PWM

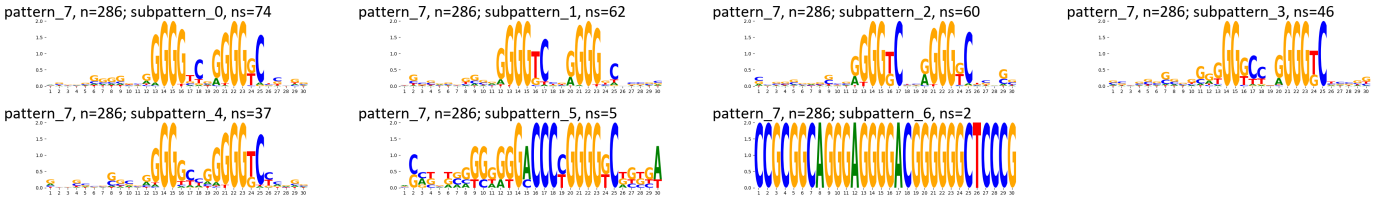

TF-MoDisCO pattern_9 n=120, CWM

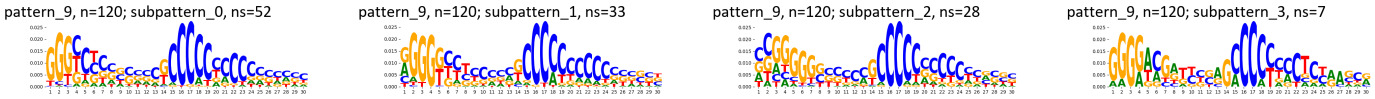

TF-MoDisCO pattern_9 n=120, PWM

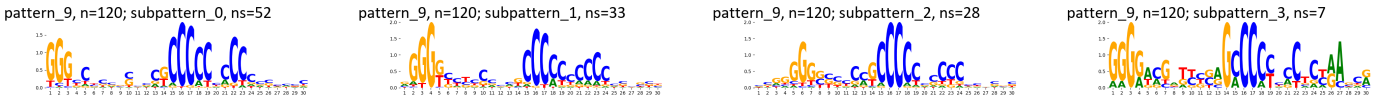

Supplementary Figure 512: TF-MoDisCO subpatterns for the ZBTB7A transcription factor in K562 (accession ENCSR000BME).

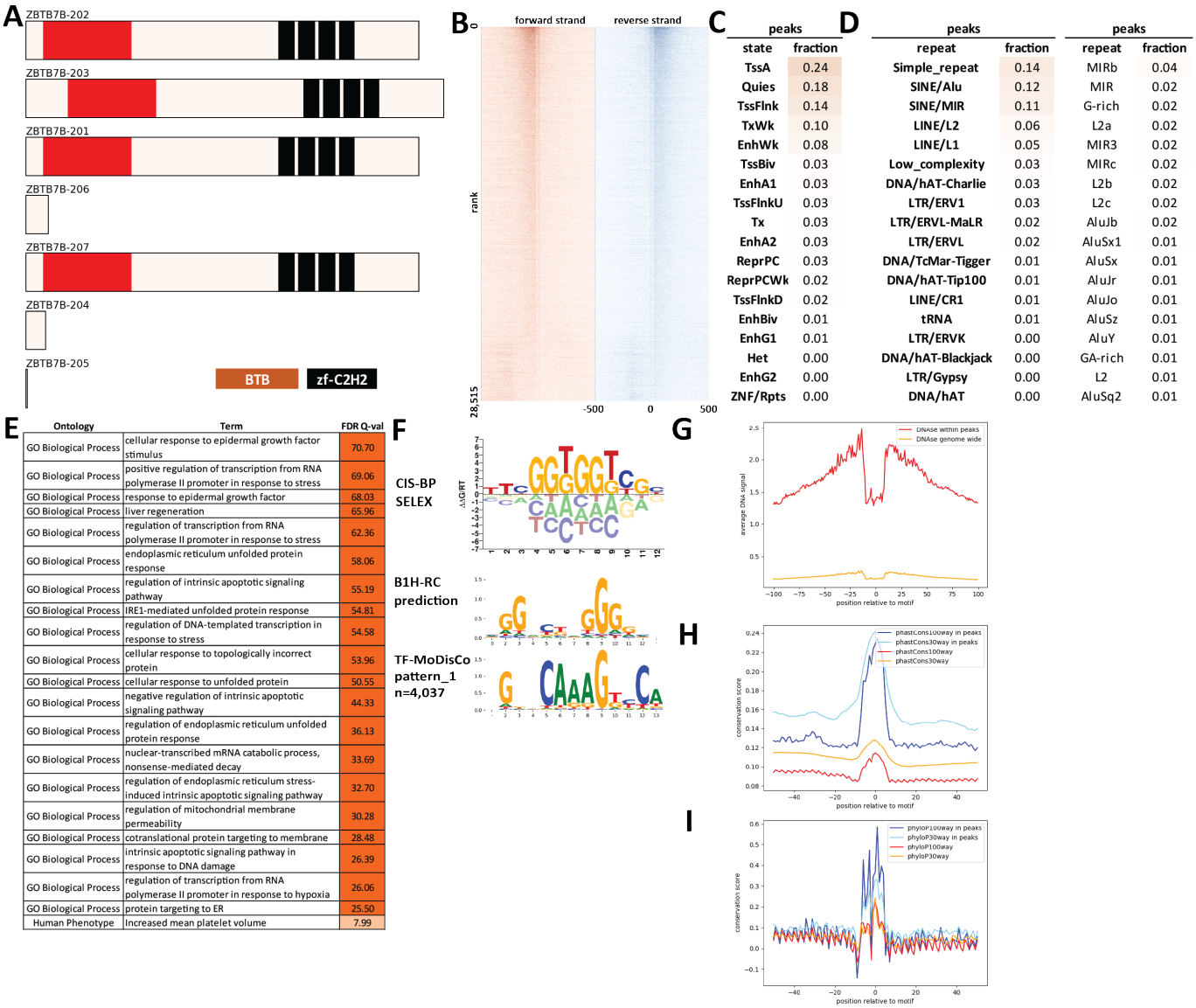

peaks	
state	fraction
TssA	0.24
Quies	0.18
TssFlnk	0.14
TxWk	0.10
EnhWk	0.08
TssBiv	0.03
EnhA1	0.03
TssFlnkU	0.03
Tx	0.03
EnhA2	0.03
ReprPC	0.03
ReprPCWk	0.02
TssFlnkD	0.02
EnhBiv	0.01
EnhG1	0.01
Het	0.00
EnhG2	0.00
ZNF/Rpts	0.00

peaks		peaks	
repeat	fraction	repeat	fraction
Simple_repeat	0.14	MIRb	0.04
SINE/Alu	0.12	MIR	0.02
SINE/MIR	0.11	G-rich	0.02
LINE/L2	0.06	L2a	0.02
LINE/L1	0.05	MIR3	0.02
Low_complexity	0.03	MIRc	0.02
DNA/hAT-Charlie	0.03	L2b	0.02
LTR/ERV1	0.03	L2c	0.02
LTR/ERVL-MaLR	0.02	AluJb	0.02
LTR/ERVL	0.02	AluSx1	0.01
DNA/TcMar-Tigger	0.01	AluSx	0.01
DNA/hAT-Tip100	0.01	AluJr	0.01
LINE/CR1	0.01	AluJo	0.01
tRNA	0.01	AluSz	0.01
LTR/ERVK	0.00	AluY	0.01
DNA/hAT-Blackjack	0.00	GA-rich	0.01
LTR/Gypsy	0.00	L2	0.01
DNA/hAT	0.00	AluSq2	0.01

Ontology	Term	FDR Q-val
GO Biological Process	cellular response to epidermal growth factor stimulus	70.70
GO Biological Process	positive regulation of transcription from RNA polymerase II promoter in response to stress	69.06
GO Biological Process	response to epidermal growth factor	68.03
GO Biological Process	liver regeneration	65.96
GO Biological Process	regulation of transcription from RNA polymerase II promoter in response to stress	62.36
GO Biological Process	endoplasmic reticulum unfolded protein response	58.06
GO Biological Process	regulation of intrinsic apoptotic signaling pathway	55.19
GO Biological Process	IRE1-mediated unfolded protein response	54.81
GO Biological Process	regulation of DNA-templated transcription in response to stress	54.58
GO Biological Process	cellular response to topologically incorrect protein	53.96
GO Biological Process	cellular response to unfolded protein	50.55
GO Biological Process	negative regulation of intrinsic apoptotic signaling pathway	44.33
GO Biological Process	regulation of endoplasmic reticulum unfolded protein response	36.13
GO Biological Process	nuclear-transcribed mRNA catabolic process, nonsense-mediated decay	33.69
GO Biological Process	regulation of endoplasmic reticulum stress-induced intrinsic apoptotic signaling pathway	32.70
GO Biological Process	regulation of mitochondrial membrane permeability	30.28
GO Biological Process	cotranslational protein targeting to membrane	28.48
GO Biological Process	intrinsic apoptotic signaling pathway in response to DNA damage	26.39
GO Biological Process	regulation of transcription from RNA polymerase II promoter in response to hypoxia	26.06
GO Biological Process	protein targeting to ER	25.50
Human Phenotype	Increased mean platelet volume	7.99

Supplementary Figure 513: Properties and genomic distribution of motifs identified for the ZBTB7B transcription factor in HepG2 (accession ENCSR322ULL).

TF-MoDisCO pattern_1 n=4037, CWM

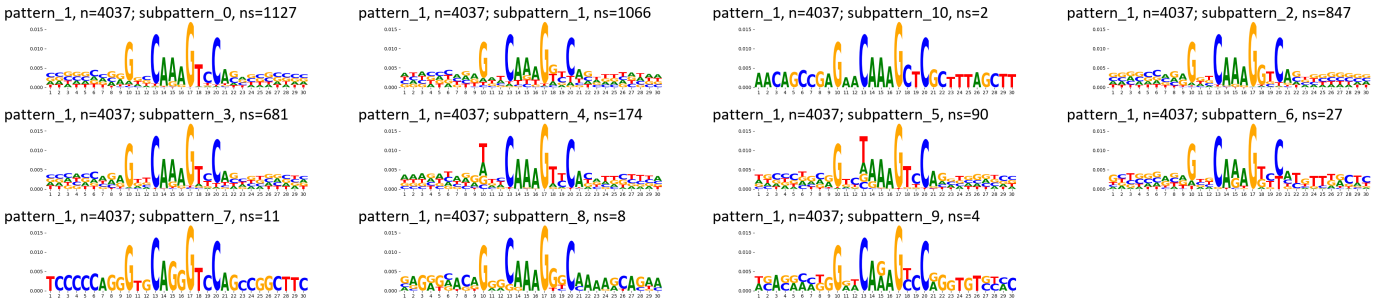

TF-MoDisCO pattern_1 n=4037, PWM

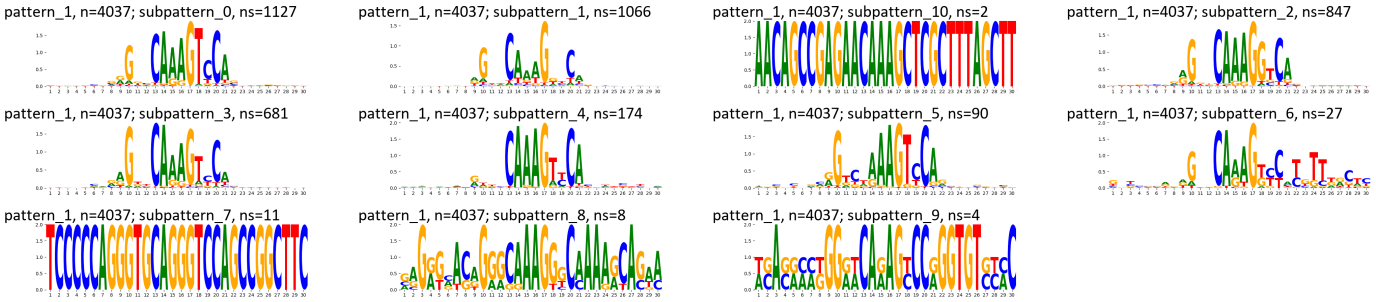

Supplementary Figure 514: TF-MoDisCO subpatterns for the ZBTB7B transcription factor in HepG2 (accession ENCSR322ULL).

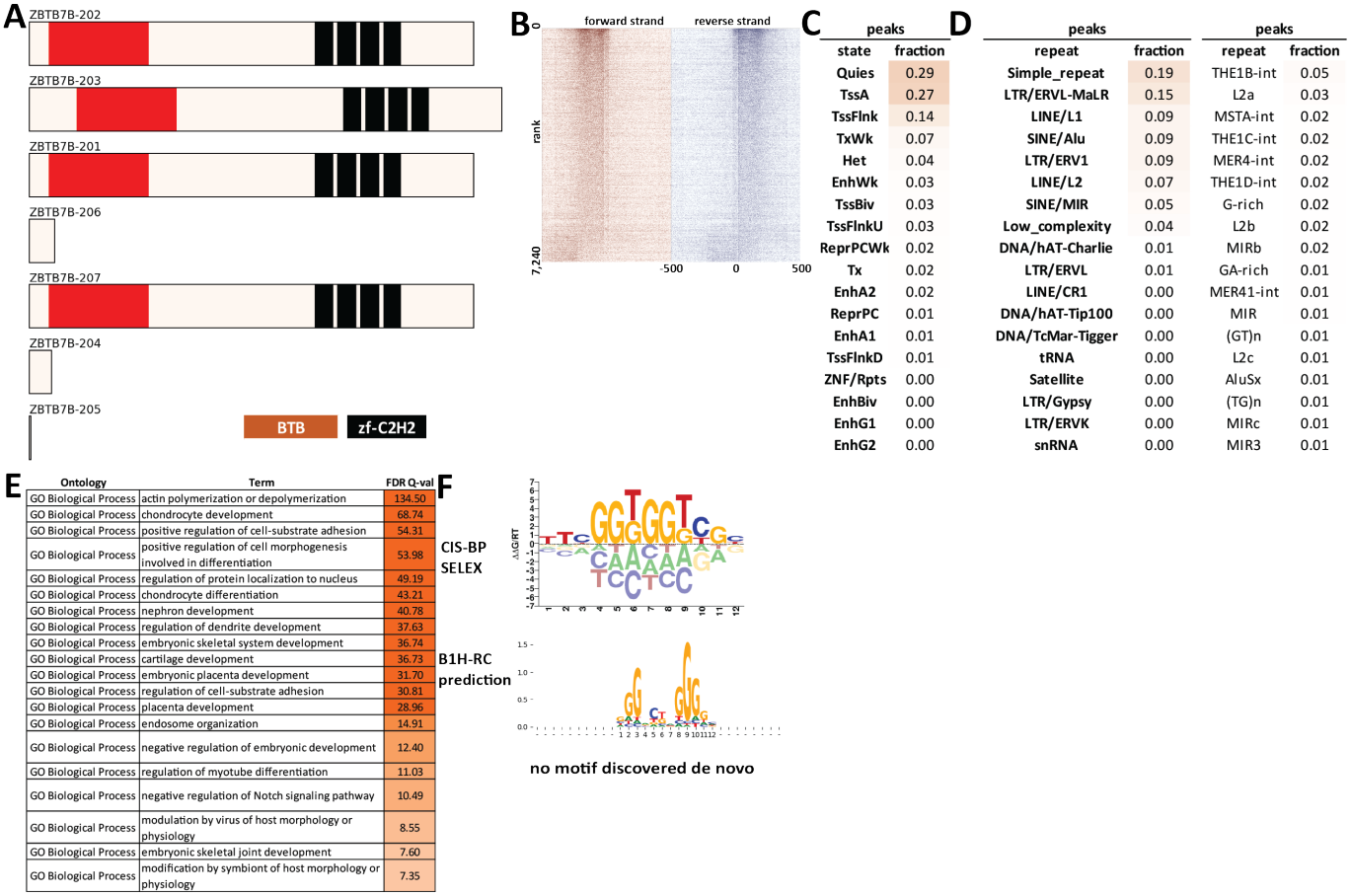

peaks	
state	fraction
Quies	0.29
TssA	0.27
TssFlnk	0.14
TxWk	0.07
Het	0.04
EnhWk	0.03
TssBiv	0.03
TssFlnkU	0.03
ReprPCWk	0.02
Tx	0.02
EnhA2	0.02
ReprPC	0.01
EnhA1	0.01
TssFlnkD	0.01
ZNF/Rpts	0.00
EnhBiv	0.00
EnhG1	0.00
EnhG2	0.00

peaks		peaks	
repeat	fraction	repeat	fraction
Simple_repeat	0.19	THE1B-int	0.05
LTR/ERVL-MaLR	0.15	L2a	0.03
LINE/L1	0.09	MSTA-int	0.02
SINE/Alu	0.09	THE1C-int	0.02
LTR/ERV1	0.09	MER4-int	0.02
LINE/L2	0.07	THE1D-int	0.02
SINE/MIR	0.05	G-rich	0.02
Low_complexity	0.04	L2b	0.02
DNA/hAT-Charlie	0.01	MIRb	0.02
LTR/ERVL	0.01	GA-rich	0.01
LINE/CR1	0.00	MER41-int	0.01
DNA/hAT-Tip100	0.00	MIR	0.01
DNA/TcMar-Tigger	0.00	(GT)n	0.01
tRNA	0.00	L2c	0.01
Satellite	0.00	AluSx	0.01
LTR/Gypsy	0.00	(TG)n	0.01
LTR/ERVK	0.00	MIRc	0.01
snRNA	0.00	MIR3	0.01

Ontology	Term	FDR Q-val
GO Biological Process	actin polymerization or depolymerization	134.50
GO Biological Process	chondrocyte development	68.74
GO Biological Process	positive regulation of cell-substrate adhesion	54.31
GO Biological Process	positive regulation of cell morphogenesis involved in differentiation	53.98
GO Biological Process	regulation of protein localization to nucleus	49.19
GO Biological Process	chondrocyte differentiation	43.21
GO Biological Process	nephron development	40.78
GO Biological Process	regulation of dendrite development	37.63
GO Biological Process	embryonic skeletal system development	36.74
GO Biological Process	cartilage development	36.73
GO Biological Process	embryonic placenta development	31.70
GO Biological Process	regulation of cell-substrate adhesion	30.81
GO Biological Process	placenta development	28.96
GO Biological Process	endosome organization	14.91
GO Biological Process	negative regulation of embryonic development	12.40
GO Biological Process	regulation of myotube differentiation	11.03
GO Biological Process	negative regulation of Notch signaling pathway	10.49
GO Biological Process	modulation by virus of host morphology or physiology	8.55
GO Biological Process	embryonic skeletal joint development	7.60
GO Biological Process	modification by symbiont of host morphology or physiology	7.35

Supplementary Figure 515: Properties and genomic distribution of motifs identified for the ZBTB7B transcription factor in MCF-7 (accession ENCSR277BXW).

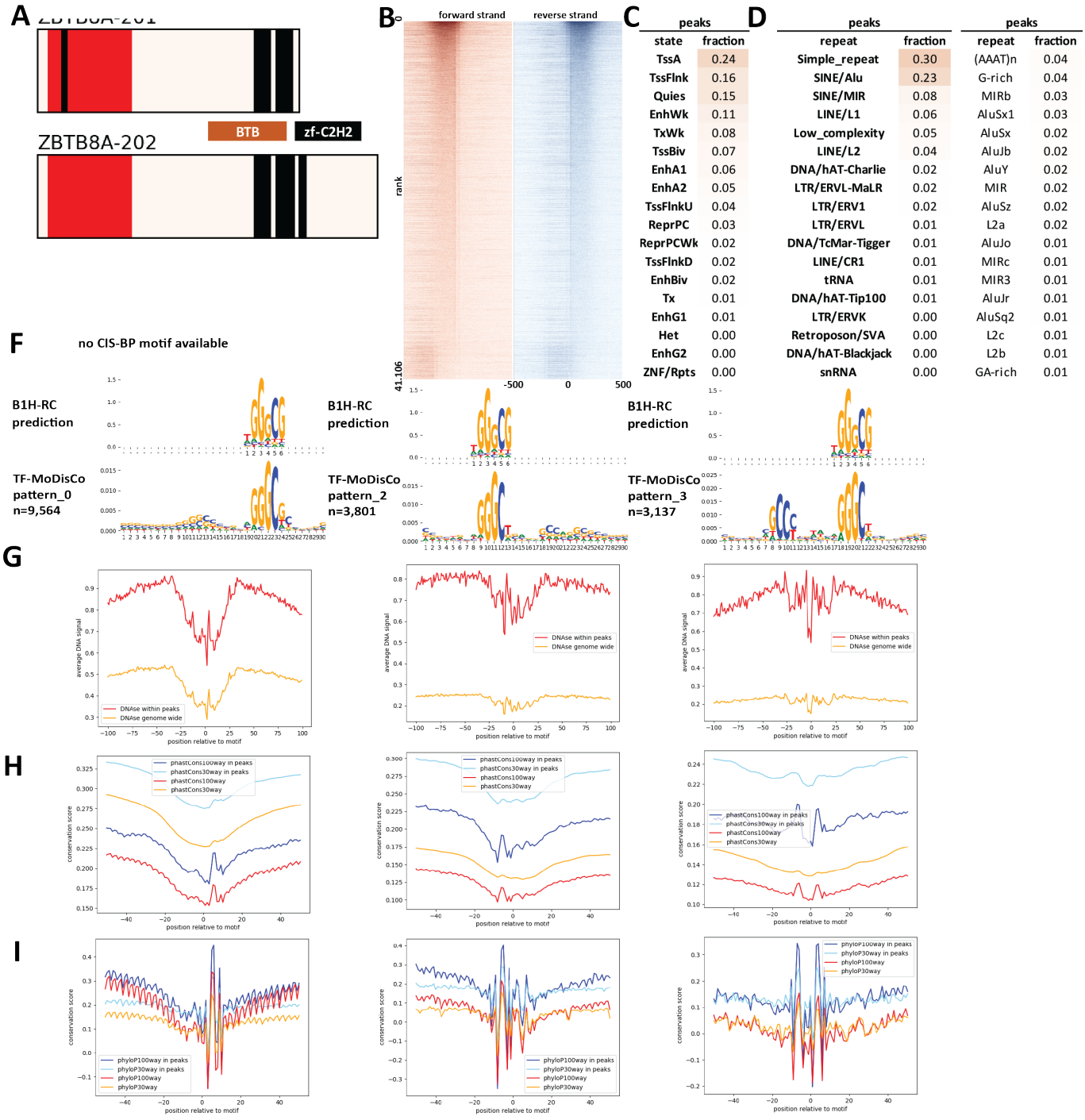

Supplementary Figure 516: Properties and genomic distribution of motifs identified for the ZBTB8A transcription factor in HEK293 (accession ENCSR481FEC).

TF-MoDisCO pattern_0 n=9564, CWM

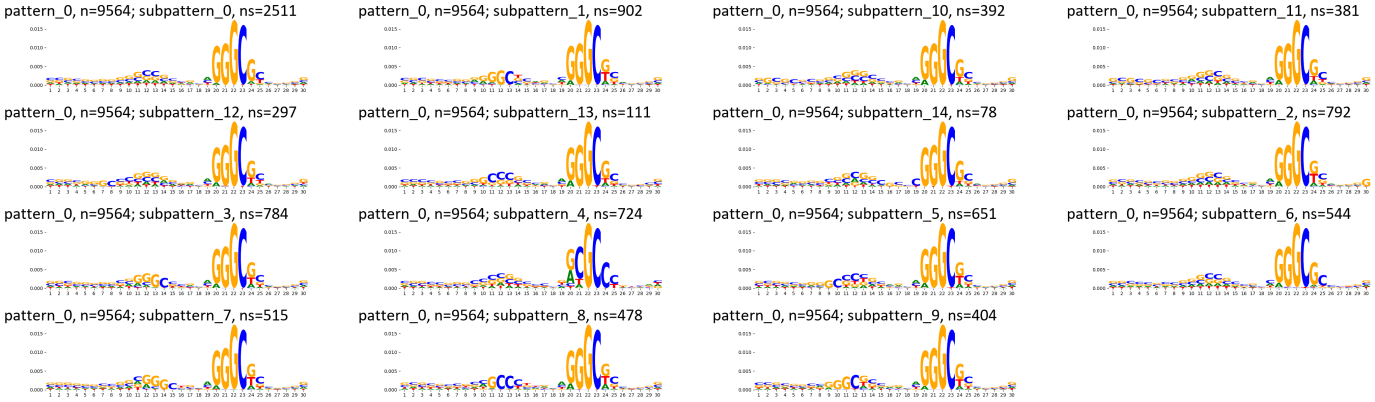

TF-MoDisCO pattern_0 n=9564, PWM

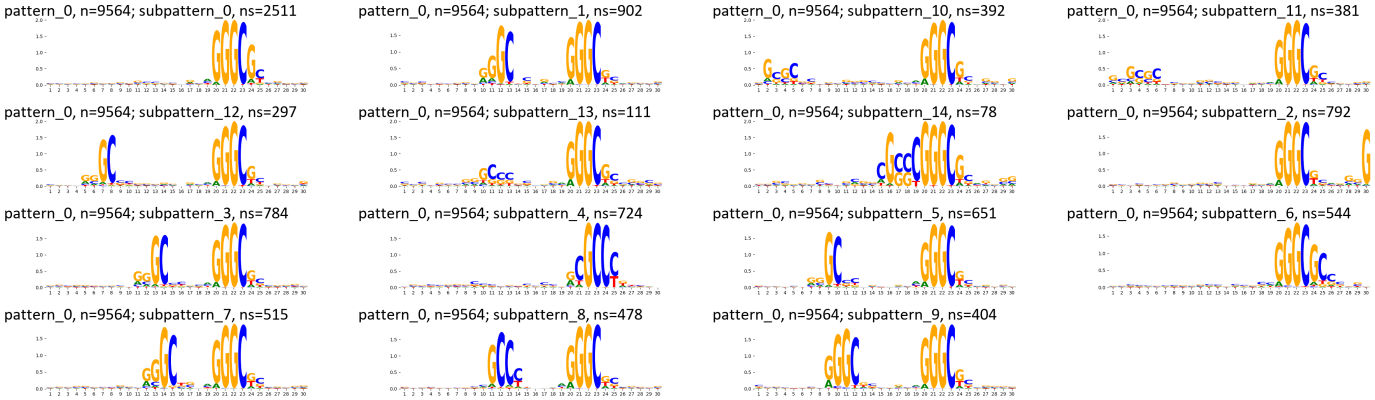

TF-MoDisCO pattern_2 n=3801, CWM

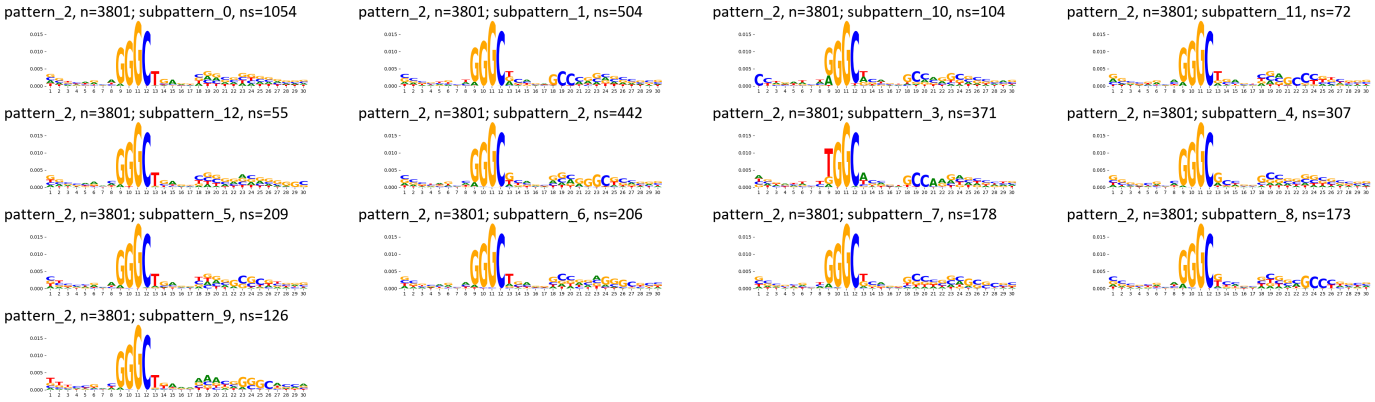

TF-MoDisCO pattern_2 n=3801, PWM

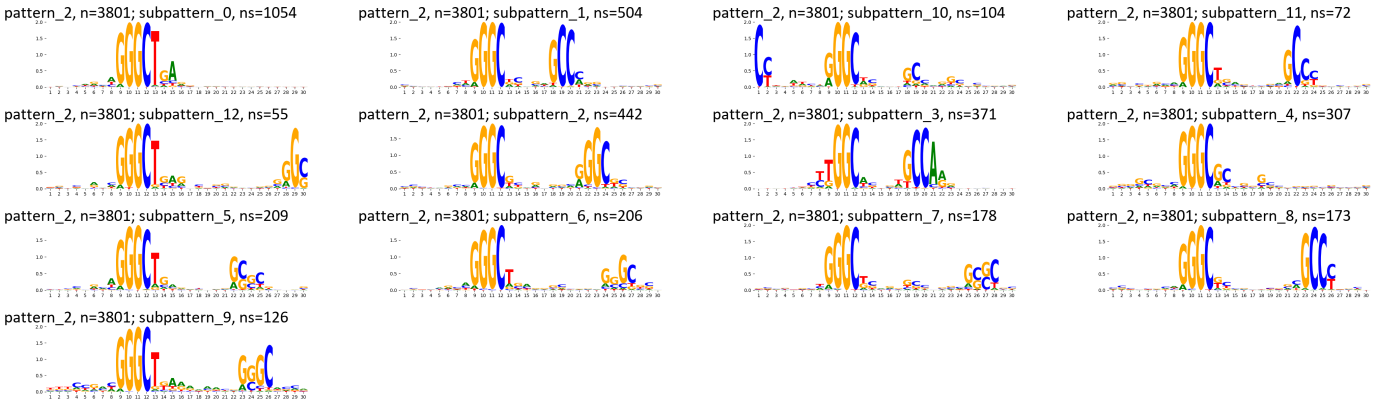

TF-MoDisCO pattern_3 n=3137, CWM

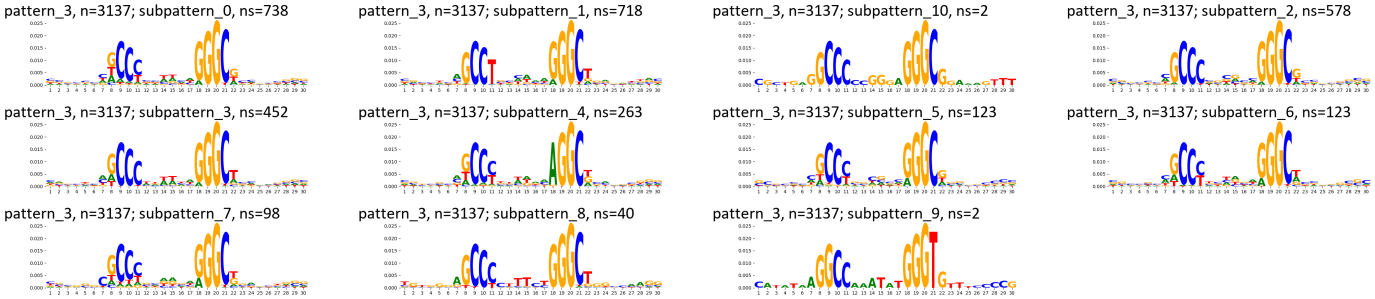

TF-MoDisCO pattern_3 n=3137, PWM

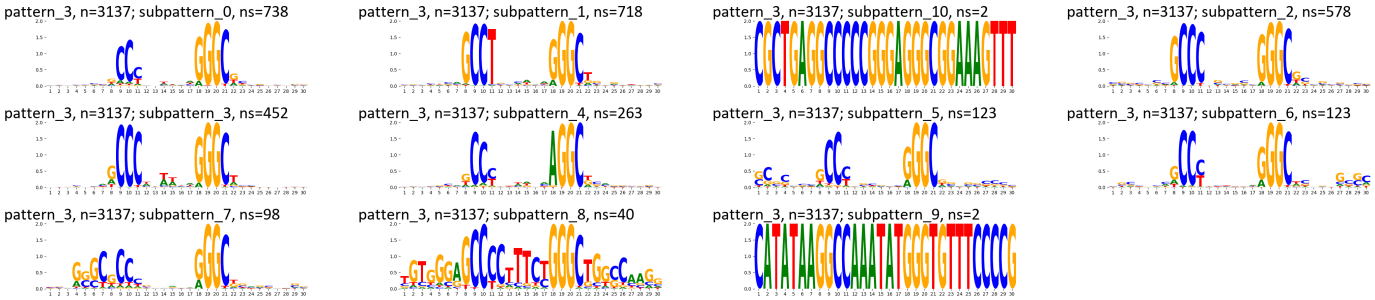

Supplementary Figure 517: TF-MoDisCO subpatterns for the ZBTB8A transcription factor in HEK293 (accession ENCSR481FEC).

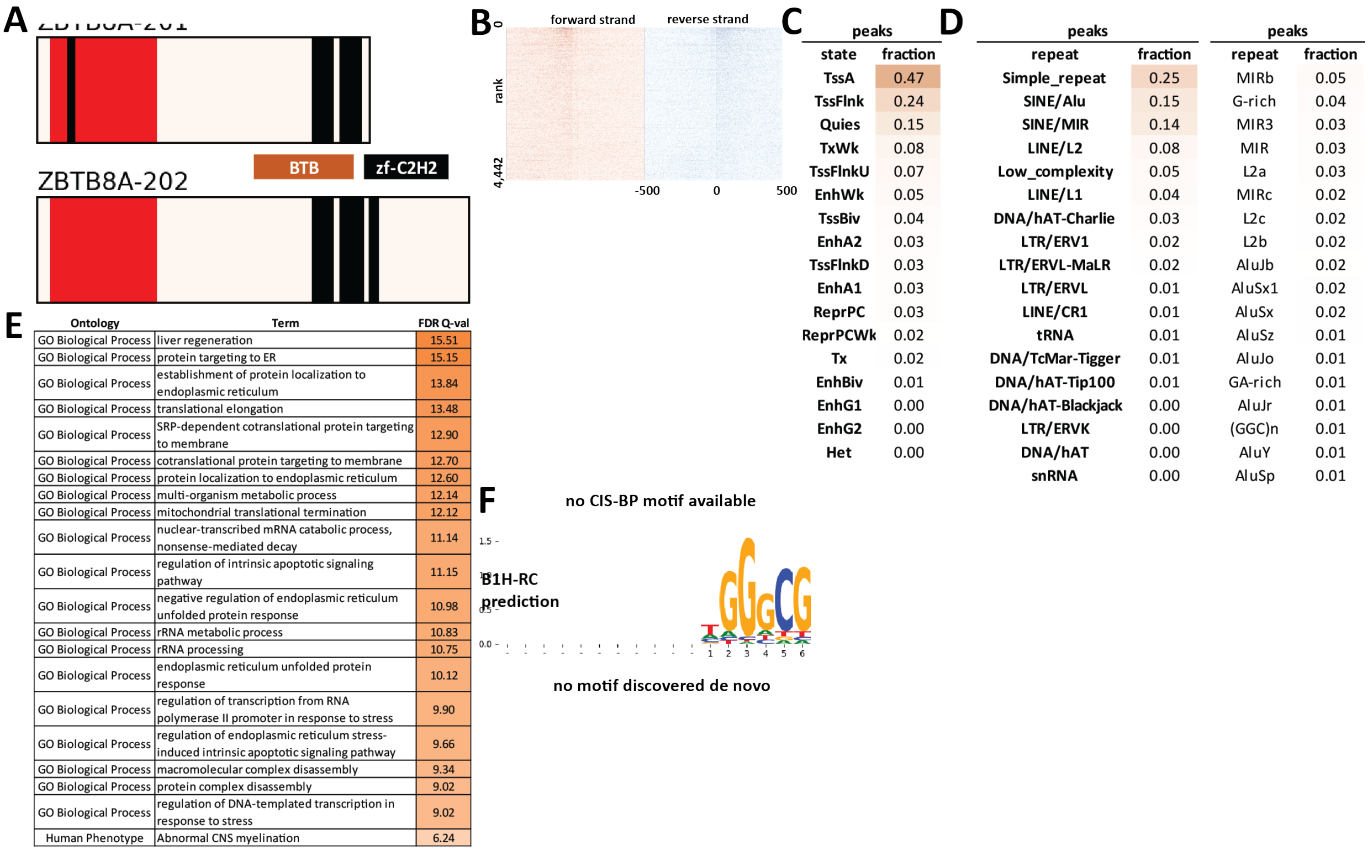

C

peaks	
state	fraction
TssA	0.47
TssFlnk	0.24
Quies	0.15
TxWk	0.08
TssFlnkU	0.07
EnhWk	0.05
TssBiv	0.04
EnhA2	0.03
TssFlnkD	0.03
EnhA1	0.03
ReprPC	0.03
ReprPCWk	0.02
Tx	0.02
EnhBiv	0.01
EnhG1	0.00
EnhG2	0.00
Het	0.00

D

peaks		peaks	
repeat	fraction	repeat	fraction
Simple_repeat	0.25	MIRb	0.05
SINE/Alu	0.15	G-rich	0.04
SINE/MIR	0.14	MIR3	0.03
LINE/L2	0.08	MIR	0.03
Low_complexity	0.05	L2a	0.03
LINE/L1	0.04	MIRc	0.02
DNA/hAT-Charlie	0.03	L2c	0.02
LTR/ERV1	0.02	L2b	0.02
LTR/ERVL-MaLR	0.02	AluJb	0.02
LTR/ERVL	0.01	AluSx1	0.02
LINE/CR1	0.01	AluSx	0.02
tRNA	0.01	AluSz	0.01
DNA/TcMar-Tigger	0.01	AluJo	0.01
DNA/hAT-Tip100	0.01	GA-rich	0.01
DNA/hAT-Blackjack	0.00	AluJr	0.01
LTR/ERVK	0.00	(GGC)n	0.01
DNA/hAT	0.00	AluY	0.01
snRNA	0.00	AluSp	0.01

E

Ontology	Term	FDR Q-val
GO Biological Process	liver regeneration	15.51
GO Biological Process	protein targeting to ER	15.15
GO Biological Process	establishment of protein localization to endoplasmic reticulum	13.84
GO Biological Process	translational elongation	13.48
GO Biological Process	SRP-dependent cotranslational protein targeting to membrane	12.90
GO Biological Process	cotranslational protein targeting to membrane	12.70
GO Biological Process	protein localization to endoplasmic reticulum	12.60
GO Biological Process	multi-organism metabolic process	12.14
GO Biological Process	mitochondrial translational termination	12.12
GO Biological Process	nuclear-transcribed mRNA catabolic process, nonsense-mediated decay	11.14
GO Biological Process	regulation of intrinsic apoptotic signaling pathway	11.15
GO Biological Process	negative regulation of endoplasmic reticulum unfolded protein response	10.98
GO Biological Process	rRNA metabolic process	10.83
GO Biological Process	rRNA processing	10.75
GO Biological Process	endoplasmic reticulum unfolded protein response	10.12
GO Biological Process	regulation of transcription from RNA polymerase II promoter in response to stress	9.90
GO Biological Process	regulation of endoplasmic reticulum stress-induced intrinsic apoptotic signaling pathway	9.66
GO Biological Process	macromolecular complex disassembly	9.34
GO Biological Process	protein complex disassembly	9.02
GO Biological Process	regulation of DNA-templated transcription in response to stress	9.02
Human Phenotype	Abnormal CNS myelination	6.24

Supplementary Figure 518: Properties and genomic distribution of motifs identified for the ZBTB8A transcription factor in HepG2 (accession ENCSR625XAV).

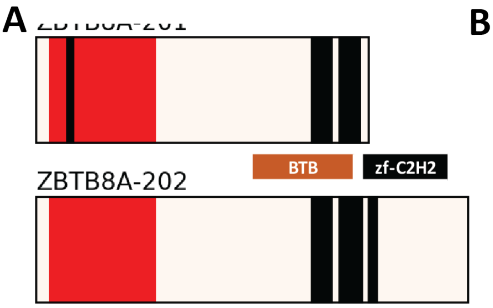

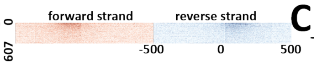

C

peaks	
state	fraction
TssA	0.33
Quies	0.27
TssFlnk	0.26
TxWk	0.11
EnhWk	0.06
EnhA2	0.04
Tx	0.02
TssBiv	0.02
ReprPCWk	0.02
ReprPC	0.02
TssFlnkD	0.01
TssFlnkU	0.01
EnhA1	0.01
Het	0.00
EnhG2	0.00
EnhG1	0.00

D

peaks		peaks	
repeat	fraction	repeat	fraction
tRNA	0.28	U1	0.03
LINE/L1	0.16	L2a	0.02
Simple_repeat	0.08	L2c	0.02
SINE/Alu	0.07	MIR	0.02
LINE/L2	0.06	A-rich	0.02
SINE/MIR	0.05	tRNA-Lys-AA/	0.01
snRNA	0.05	MIRb	0.01
LTR/ERV1	0.04	tRNA-Ile-ATT	0.01
DNA/hAT-Charlie	0.03	tRNA-Asp-GA'	0.01
Low_complexity	0.03	L2	0.01
DNA/TcMar-Tigger	0.03	L1M5	0.01
LTR/ERVL-MaLR	0.02	tRNA-Val-GTC	0.01
LTR/ERVL	0.01	tRNA-Ser-TCY	0.01
DNA/hAT-Tip100	0.00	tRNA-Arg-CGY	0.01
Unknown	0.00	tRNA-Ala-GCY	0.01
Satellite/telo	0.00	U5	0.01
SINE/tRNA	0.00	GA-rich	0.01
Retroposon/SVA	0.00	tRNA-Tyr-TAC	0.01

E

Ontology	Term	FDR Q-val
GO Biological Process	nucleosome assembly	30.46
GO Biological Process	chromatin assembly	28.33
GO Biological Process	nucleosome organization	28.11
GO Biological Process	chromatin assembly or disassembly	26.00
GO Biological Process	DNA packaging	24.46
GO Biological Process	DNA conformation change	21.73
GO Biological Process	chromosome organization	21.03
GO Biological Process	chromatin organization	19.09
GO Biological Process	regulation of cellular amide metabolic process	8.43
GO Biological Process	protein folding	7.69
GO Biological Process	protein peptidyl-prolyl isomerization	5.61
GO Biological Process	cellular hyperosmotic response	2.67
GO Biological Process	positive regulation of TOR signaling	1.75
GO Biological Process	cellular response to glucocorticoid stimulus	1.43

F

no CIS-BP motif available



no motif discovered de novo

Supplementary Figure 519: Properties and genomic distribution of motifs identified for the ZBTB8A transcription factor in K562 (accession ENCSR283ZNI).

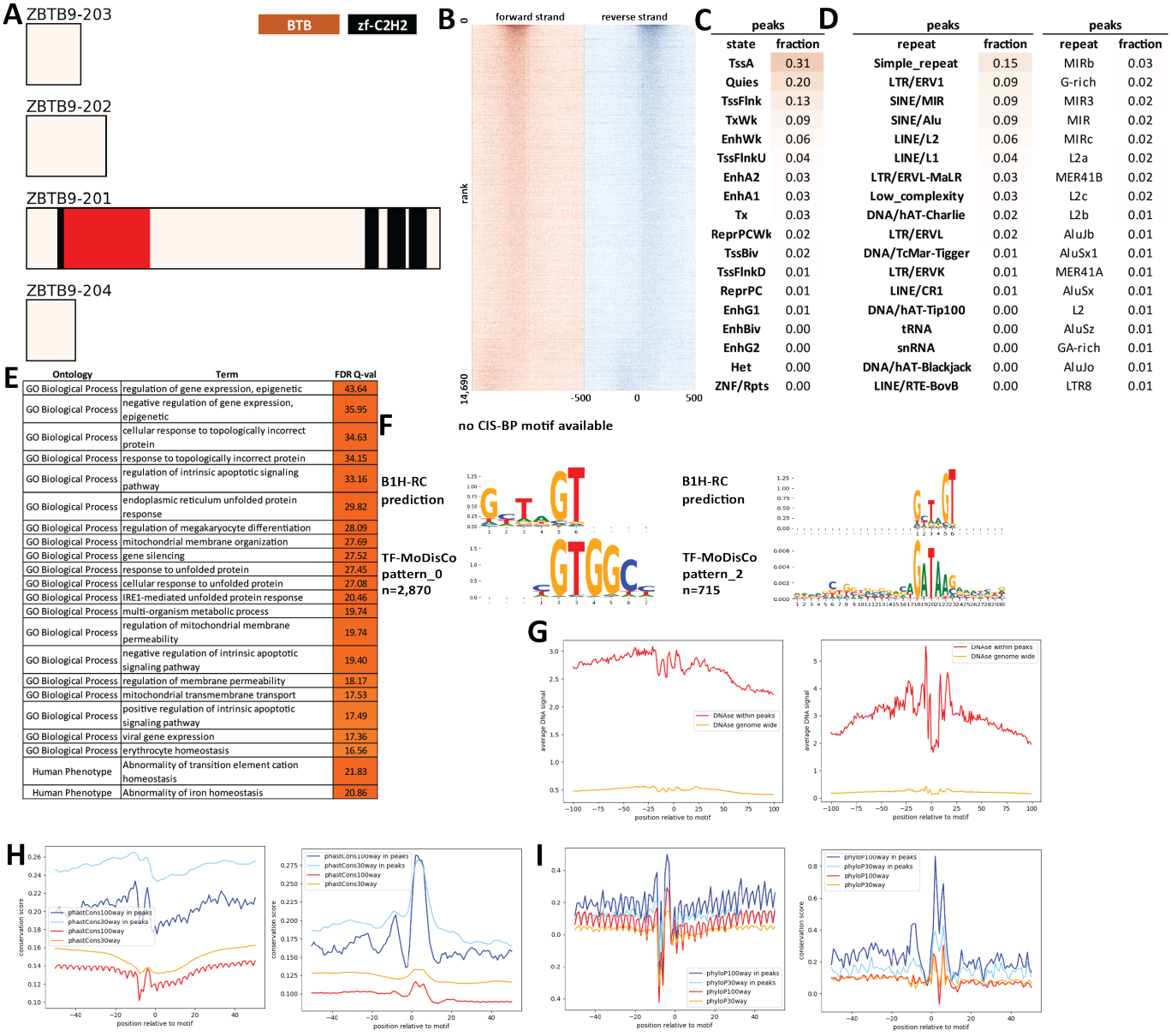

peaks	
state	fraction
TssA	0.31
Quies	0.20
TssFlnk	0.13
TxWk	0.09
EnhWk	0.06
TssFlnkU	0.04
EnhA2	0.03
EnhA1	0.03
Tx	0.03
ReprPCWk	0.02
TssBiv	0.02
TssFlnkD	0.01
ReprPC	0.01
EnhG1	0.01
EnhBiv	0.00
EnhG2	0.00
Het	0.00
ZNF/Rpts	0.00

peaks	
repeat	fraction
Simple_repeat	0.15
LTR/ERV1	0.09
SINE/MIR	0.09
SINE/Alu	0.09
LINE/L2	0.06
LINE/L1	0.04
LTR/ERVL-MaLR	0.03
Low_complexity	0.03
DNA/hAT-Charlie	0.02
LTR/ERVL	0.02
DNA/TcMar-Tigger	0.01
LTR/ERVK	0.01
LINE/CR1	0.01
DNA/hAT-Tip100	0.00
tRNA	0.00
snRNA	0.00
DNA/hAT-Blackjack	0.00
LINE/RTE-BovB	0.00

peaks	
repeat	fraction
MIRb	0.03
G-rich	0.02
MIR3	0.02
MIR	0.02
MIRc	0.02
L2a	0.02
MER41B	0.02
L2c	0.02
L2b	0.01
AluJb	0.01
AluSx1	0.01
MER41A	0.01
AluSx	0.01
L2	0.01
AluSz	0.01
GA-rich	0.01
AluJo	0.01
LTR8	0.01

Ontology	Term	FDR Q-val
GO Biological Process	regulation of gene expression, epigenetic	43.64
GO Biological Process	negative regulation of gene expression, epigenetic	35.95
GO Biological Process	cellular response to topologically incorrect protein	34.63
GO Biological Process	response to topologically incorrect protein	34.15
GO Biological Process	regulation of intrinsic apoptotic signaling pathway	33.16
GO Biological Process	endoplasmic reticulum unfolded protein response	29.82
GO Biological Process	regulation of megakaryocyte differentiation	28.09
GO Biological Process	mitochondrial membrane organization	27.69
GO Biological Process	gene silencing	27.52
GO Biological Process	response to unfolded protein	27.45
GO Biological Process	cellular response to unfolded protein	27.08
GO Biological Process	IRE1-mediated unfolded protein response	20.46
GO Biological Process	multi-organism metabolic process	19.74
GO Biological Process	regulation of mitochondrial membrane permeability	19.74
GO Biological Process	negative regulation of intrinsic apoptotic signaling pathway	19.40
GO Biological Process	regulation of membrane permeability	18.17
GO Biological Process	mitochondrial transmembrane transport	17.53
GO Biological Process	positive regulation of intrinsic apoptotic signaling pathway	17.49
GO Biological Process	viral gene expression	17.36
GO Biological Process	erythrocyte homeostasis	16.56
Human Phenotype	Abnormality of transition element cation homeostasis	21.83
Human Phenotype	Abnormality of iron homeostasis	20.86

Supplementary Figure 520: Properties and genomic distribution of motifs identified for the ZBTB9 transcription factor in K562 (accession ENCSR536CBU).

TF-MoDisCO pattern_0 n=2870, CWM

pattern_0, n=2870; subpattern_0, ns=658

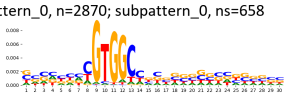

pattern_0, n=2870; subpattern_1, ns=654

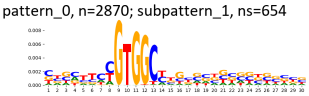

pattern_0, n=2870; subpattern_10, ns=31

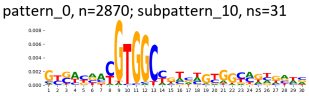

pattern_0, n=2870; subpattern_11, ns=13

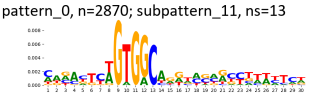

pattern_0, n=2870; subpattern_12, ns=3

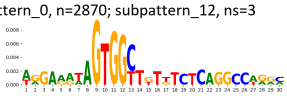

pattern_0, n=2870; subpattern_13, ns=3

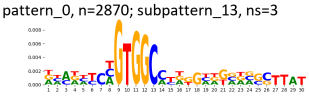

pattern_0, n=2870; subpattern_14, ns=3

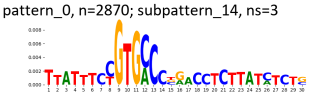

pattern_0, n=2870; subpattern_15, ns=2

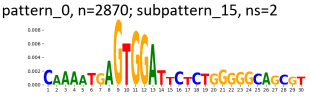

pattern_0, n=2870; subpattern_2, ns=282

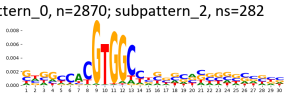

pattern_0, n=2870; subpattern_3, ns=260

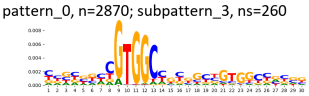

pattern_0, n=2870; subpattern_4, ns=224

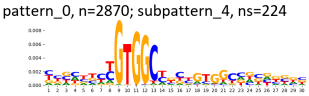

pattern_0, n=2870; subpattern_5, ns=222

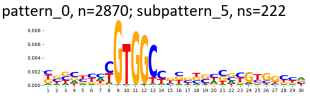

pattern_0, n=2870; subpattern_6, ns=194

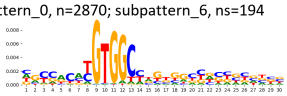

pattern_0, n=2870; subpattern_7, ns=189

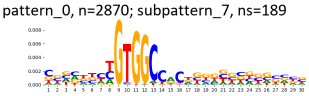

pattern_0, n=2870; subpattern_8, ns=80

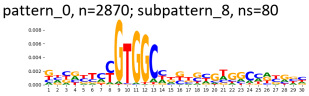

pattern_0, n=2870; subpattern_9, ns=52

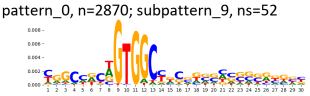

TF-MoDisCO pattern_0 n=2870, PWM

pattern_0, n=2870; subpattern_0, ns=658

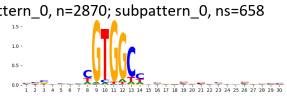

pattern_0, n=2870; subpattern_1, ns=654

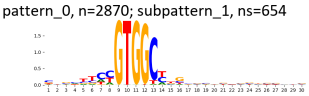

pattern_0, n=2870; subpattern_10, ns=31

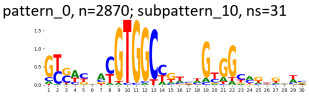

pattern_0, n=2870; subpattern_11, ns=13

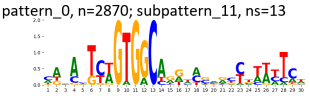

pattern_0, n=2870; subpattern_12, ns=3

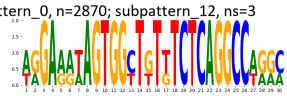

pattern_0, n=2870; subpattern_13, ns=3

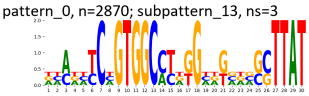

pattern_0, n=2870; subpattern_14, ns=3

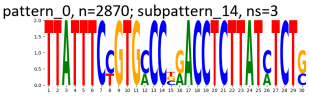

pattern_0, n=2870; subpattern_15, ns=2

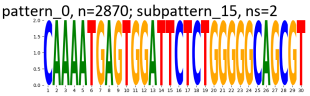

pattern_0, n=2870; subpattern_2, ns=282

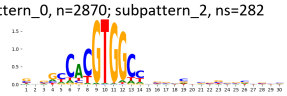

pattern_0, n=2870; subpattern_3, ns=260

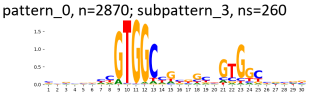

pattern_0, n=2870; subpattern_4, ns=224

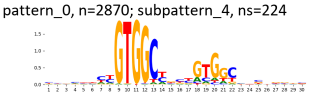

pattern_0, n=2870; subpattern_5, ns=222

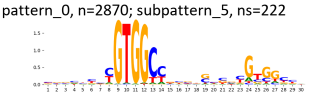

pattern_0, n=2870; subpattern_6, ns=194

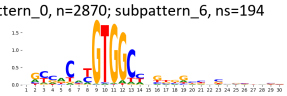

pattern_0, n=2870; subpattern_7, ns=189

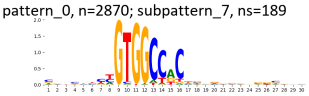

pattern_0, n=2870; subpattern_8, ns=80

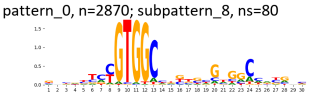

pattern_0, n=2870; subpattern_9, ns=52

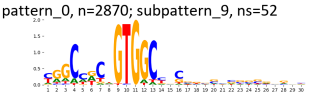

TF-MoDisCO pattern_2 n=715, CWM

pattern_2, n=715; subpattern_0, ns=141

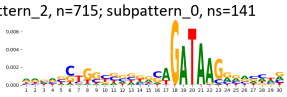

pattern_2, n=715; subpattern_1, ns=141

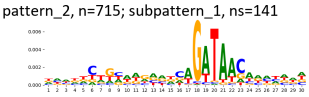

pattern_2, n=715; subpattern_2, ns=105

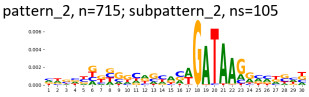

pattern_2, n=715; subpattern_3, ns=94

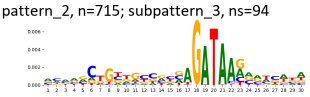

pattern_2, n=715; subpattern_4, ns=65

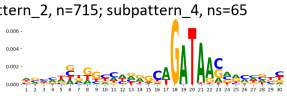

pattern_2, n=715; subpattern_5, ns=59

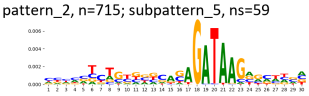

pattern_2, n=715; subpattern_6, ns=57

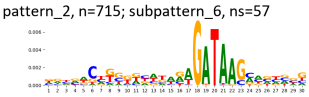

pattern_2, n=715; subpattern_7, ns=51

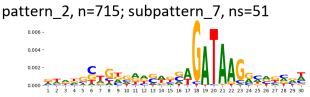

pattern_2, n=715; subpattern_8, ns=2

TF-MoDisCO pattern_2 n=715, PWM

pattern_2, n=715; subpattern_0, ns=141

pattern_2, n=715; subpattern_1, ns=141

pattern_2, n=715; subpattern_2, ns=105

pattern_2, n=715; subpattern_3, ns=94

pattern_2, n=715; subpattern_4, ns=65

pattern_2, n=715; subpattern_5, ns=59

pattern_2, n=715; subpattern_6, ns=57

pattern_2, n=715; subpattern_7, ns=51

pattern_2, n=715; subpattern_8, ns=2

Supplementary Figure 521: TF-MoDisCO subpatterns for the ZBTB9 transcription factor in K562 (accession ENCSR536CBU).

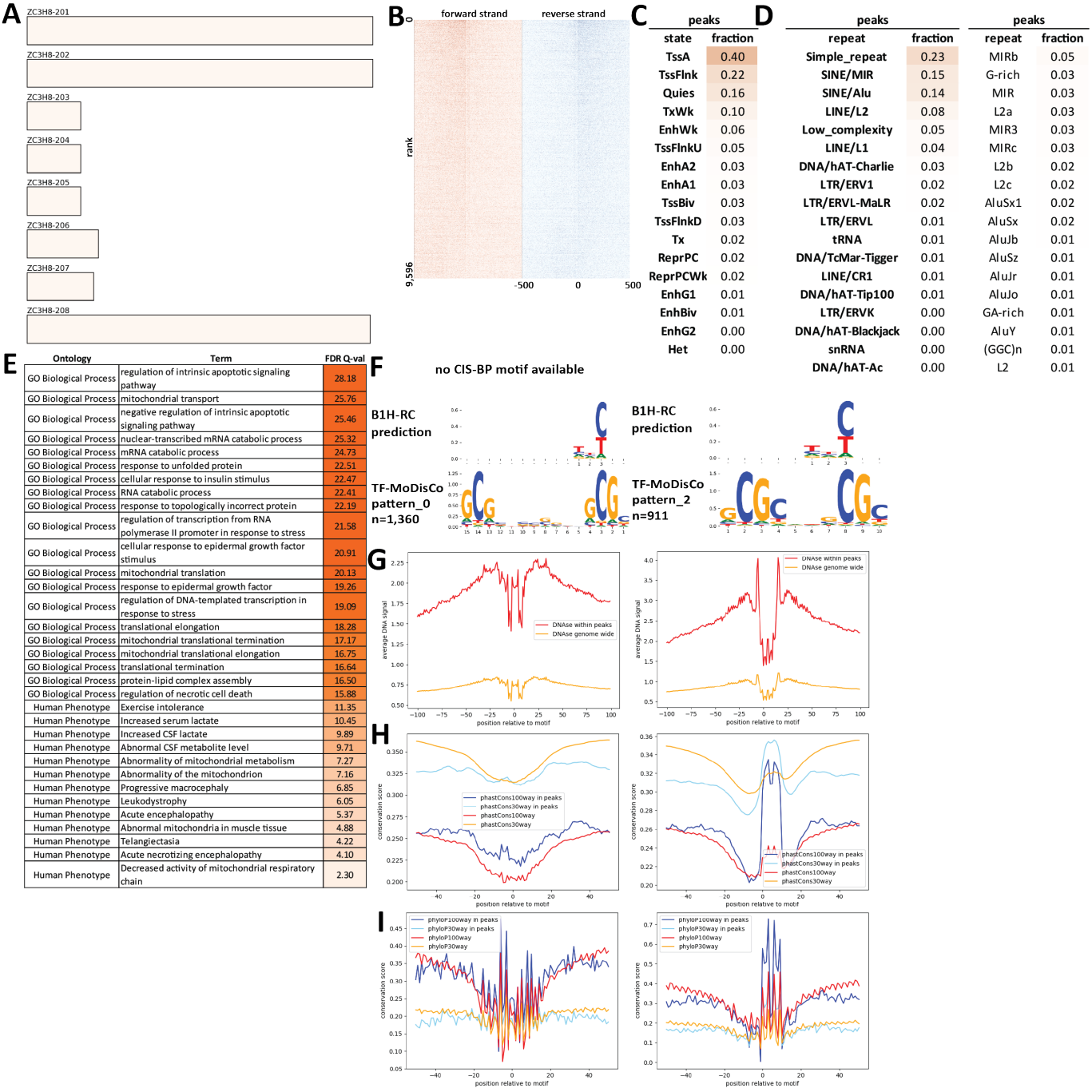

peaks	
state	fraction
TssA	0.40
TssFlnk	0.22
Quies	0.16
TxWk	0.10
EnhWk	0.06
TssFlnkU	0.05
EnhA2	0.03
EnhA1	0.03
TssBiv	0.03
TssFlnkD	0.03
Tx	0.02
ReprPC	0.02
ReprPCWk	0.02
EnhG1	0.01
EnhBiv	0.01
EnhG2	0.00
Het	0.00

peaks	
repeat	fraction
Simple_repeat	0.23
SINE/MIR	0.15
SINE/Alu	0.14
LINE/L2	0.08
Low_complexity	0.05
LINE/L1	0.04
DNA/hAT-Charlie	0.03
LTR/ERV1	0.02
LTR/ERVL-MaLR	0.02
LTR/ERVL	0.01
tRNA	0.01
DNA/TcMar-Tigger	0.01
LINE/CR1	0.01
DNA/hAT-Tip100	0.01
LTR/ERVK	0.00
DNA/hAT-Blackjack	0.00
snRNA	0.00
DNA/hAT-Ac	0.00

peaks	
repeat	fraction
MIRb	0.05
G-rich	0.03
MIR	0.03
L2a	0.03
MIR3	0.03
MIRc	0.03
L2b	0.02
L2c	0.02
AluSx1	0.02
AluSx	0.02
AluJb	0.01
AluSz	0.01
AluJr	0.01
AluJo	0.01
GA-rich	0.01
AluY	0.01
(GGC)n	0.01
L2	0.01

Ontology	Term	FDR Q-val
GO Biological Process	regulation of intrinsic apoptotic signaling pathway	28.18
GO Biological Process	mitochondrial transport	25.76
GO Biological Process	negative regulation of intrinsic apoptotic signaling pathway	25.46
GO Biological Process	nuclear-transcribed mRNA catabolic process	25.32
GO Biological Process	mRNA catabolic process	24.73
GO Biological Process	response to unfolded protein	22.51
GO Biological Process	cellular response to insulin stimulus	22.47
GO Biological Process	RNA catabolic process	22.41
GO Biological Process	response to topologically incorrect protein	22.19
GO Biological Process	regulation of transcription from RNA polymerase II promoter in response to stress	21.58
GO Biological Process	cellular response to epidermal growth factor stimulus	20.91
GO Biological Process	mitochondrial translation	20.13
GO Biological Process	response to epidermal growth factor	19.26
GO Biological Process	regulation of DNA-templated transcription in response to stress	19.09
GO Biological Process	translational elongation	18.28
GO Biological Process	mitochondrial translational termination	17.17
GO Biological Process	mitochondrial translational elongation	16.75
GO Biological Process	translational termination	16.64
GO Biological Process	protein-lipid complex assembly	16.50
GO Biological Process	regulation of necrotic cell death	15.88
Human Phenotype	Exercise intolerance	11.35
Human Phenotype	Increased serum lactate	10.45
Human Phenotype	Increased CSF lactate	9.89
Human Phenotype	Abnormal CSF metabolite level	9.71
Human Phenotype	Abnormality of mitochondrial metabolism	7.27
Human Phenotype	Abnormality of the mitochondrion	7.16
Human Phenotype	Progressive macrocephaly	6.85
Human Phenotype	Leukodystrophy	6.05
Human Phenotype	Acute encephalopathy	5.37
Human Phenotype	Abnormal mitochondria in muscle tissue	4.88
Human Phenotype	Telangiectasia	4.22
Human Phenotype	Acute necrotizing encephalopathy	4.10
Human Phenotype	Decreased activity of mitochondrial respiratory chain	2.30

Supplementary Figure 522: Properties and genomic distribution of motifs identified for the ZC3H8 transcription factor in HepG2 (accession ENCSR734CRN).

TF-MoDisCO pattern_0 n=1360, CWM

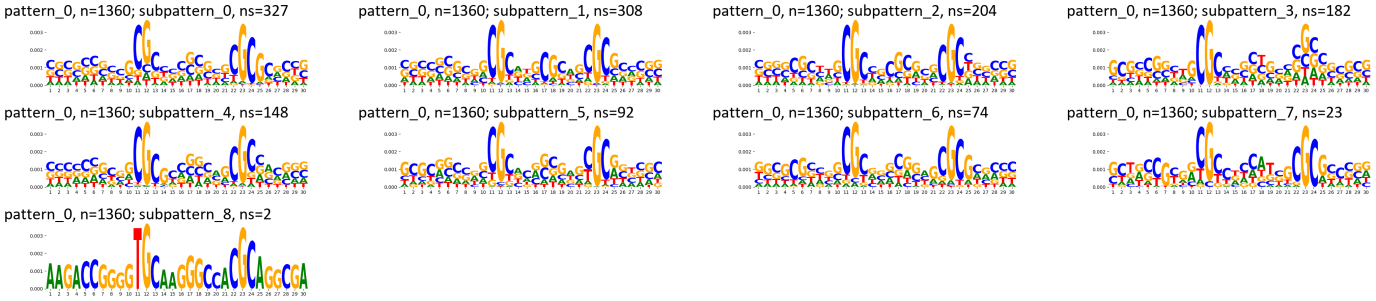

TF-MoDisCO pattern_0 n=1360, PWM

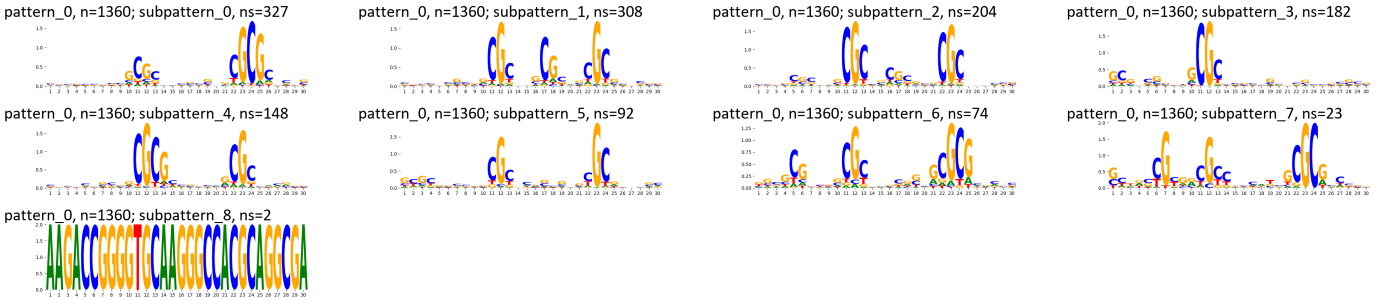

TF-MoDisCO pattern_2 n=911, CWM

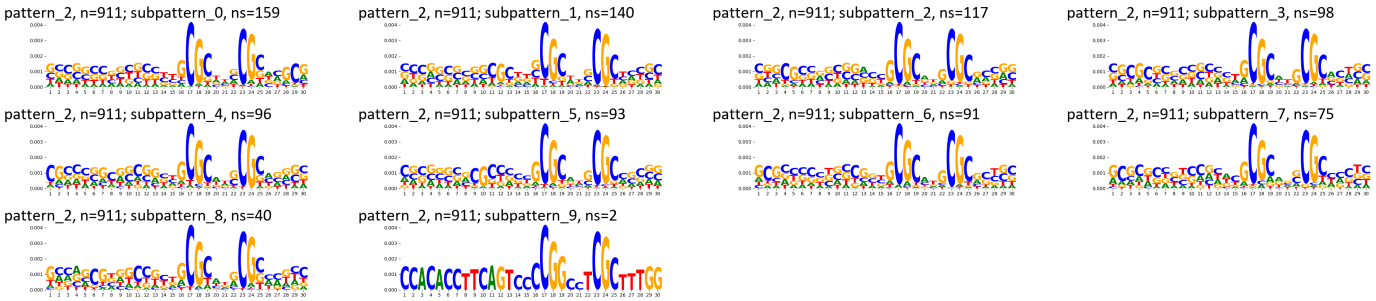

TF-MoDisCO pattern_2 n=911, PWM

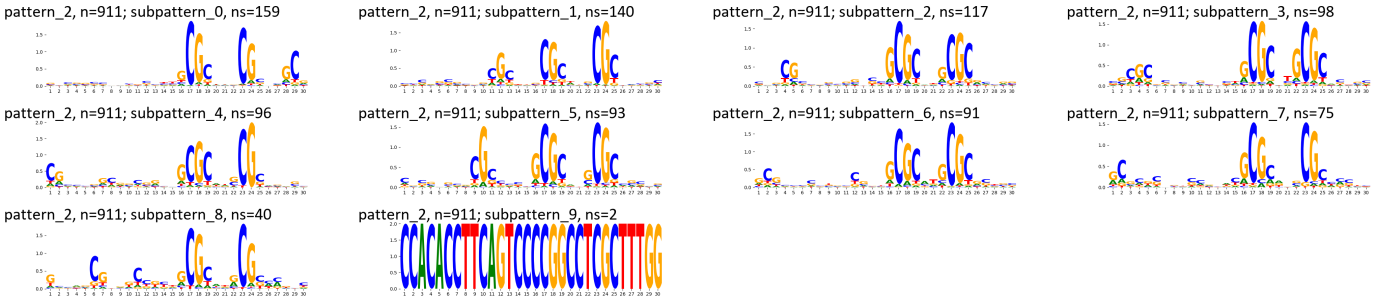

Supplementary Figure 523: TF-MoDisCO subpatterns for the ZC3H8 transcription factor in HepG2 (accession ENCSR734CRN).

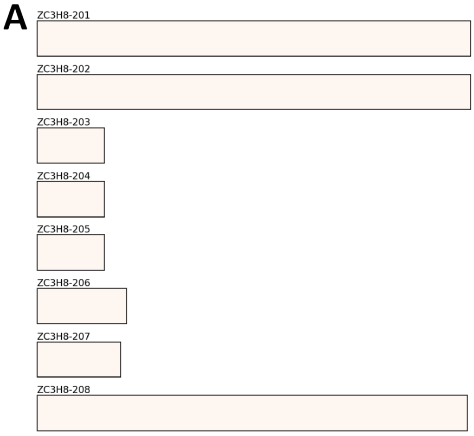

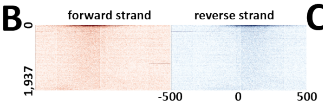

C

peaks	
state	fraction
TssA	0.33
Quies	0.28
TssFlnk	0.13
TxWk	0.13
EnhWk	0.08
TssFlnkU	0.04
EnhA2	0.03
EnhA1	0.03
Tx	0.03
ReprPCWk	0.02
ReprPC	0.02
TssBiv	0.02
TssFlnkD	0.02
EnhG1	0.00
EnhBiv	0.00
EnhG2	0.00
Het	0.00

D

peaks		peaks	
repeat	fraction	repeat	fraction
Simple_repeat	0.27	GA-rich	0.04
SINE/Alu	0.25	AluSx	0.03
Low_complexity	0.08	L2a	0.03
LINE/L2	0.08	(GT)n	0.03
LINE/L1	0.08	AluSx1	0.03
SINE/MIR	0.06	AluJb	0.03
LTR/ERV1	0.05	(AC)n	0.03
snRNA	0.02	(TG)n	0.03
LTR/ERVL-MaLR	0.02	AluSz	0.02
DNA/hAT-Charlie	0.02	AluY	0.02
LTR/ERVL	0.01	A-rich	0.02
tRNA	0.01	(CA)n	0.02
DNA/TcMar-Tigger	0.01	MIRc	0.02
LINE/CR1	0.01	MIRb	0.02
DNA/hAT-Tip100	0.00	L2	0.02
LTR/Gypsy?	0.00	L2c	0.02
LTR/ERVK	0.00	MIR	0.01
DNA/hAT-Blackjack	0.00	U1	0.01

E

Ontology	Term	FDR Q-val
GO Biological Process	negative regulation of gene expression, epigenetic	30.24
GO Biological Process	regulation of gene expression, epigenetic	20.77
GO Biological Process	nucleosome organization	18.98
GO Biological Process	nucleosome assembly	17.73
GO Biological Process	chromatin assembly	16.50
GO Biological Process	chromatin assembly or disassembly	16.49
GO Biological Process	protein-DNA complex subunit organization	16.26
GO Biological Process	protein-DNA complex assembly	15.03
GO Biological Process	DNA packaging	13.77
GO Biological Process	DNA conformation change	13.08
GO Biological Process	DNA replication-independent nucleosome assembly	10.25
GO Biological Process	DNA replication-independent nucleosome organization	10.07
GO Biological Process	chromatin remodeling at centromere	9.25
GO Biological Process	histone exchange	8.27
GO Biological Process	regulation of gene silencing	7.93
GO Biological Process	viral transcription	7.81
GO Biological Process	centromere complex assembly	7.76
GO Biological Process	viral gene expression	7.49
GO Biological Process	protein peptidyl-prolyl isomerization	7.46
GO Biological Process	regulation of posttranscriptional gene silencing	7.41

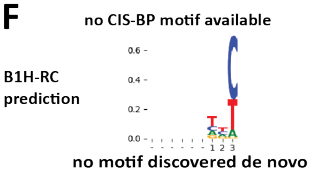

Supplementary Figure 524: Properties and genomic distribution of motifs identified for the ZC3H8 transcription factor in K562 (accession ENCSR143CEO).

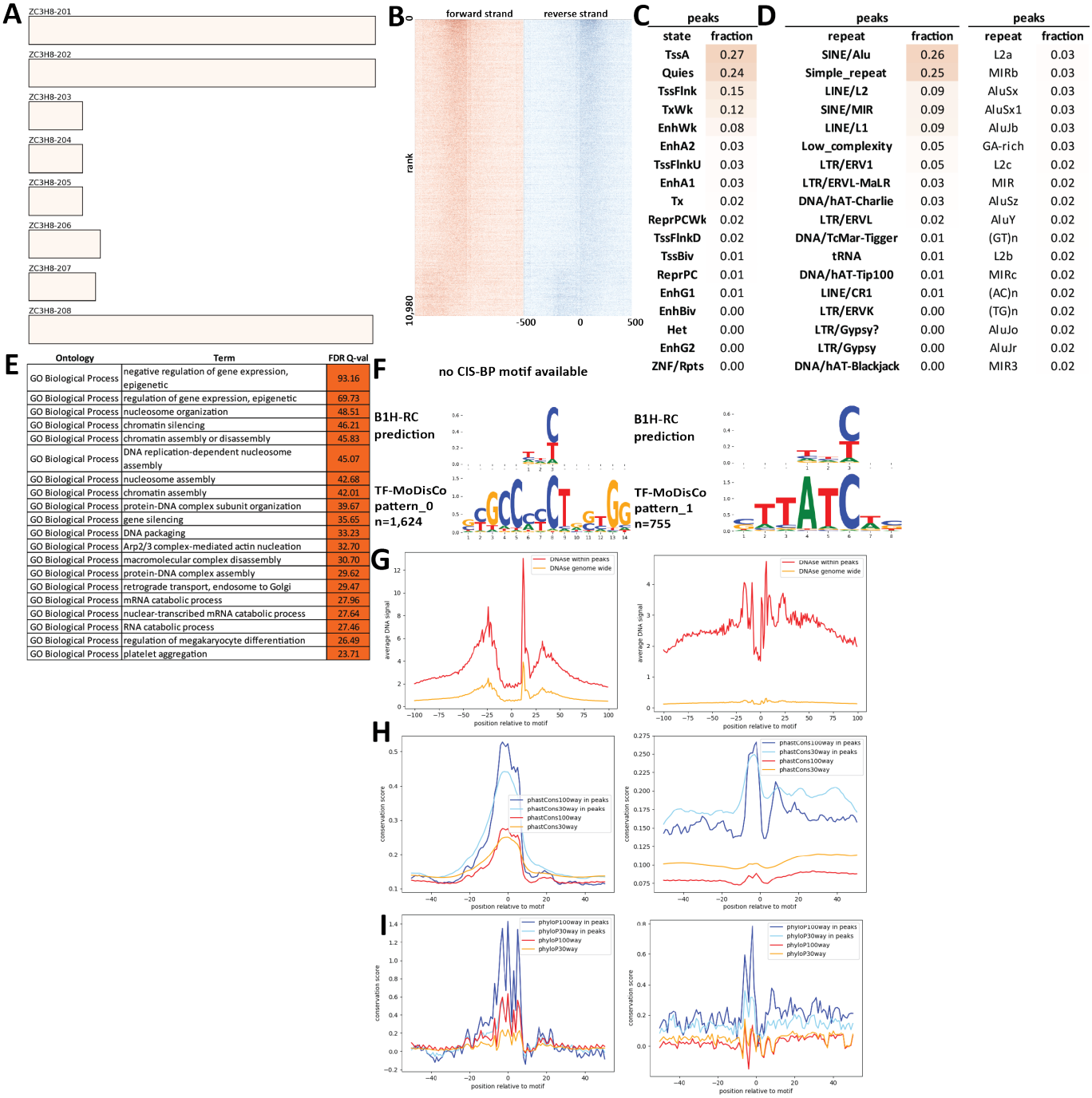

peaks	
state	fraction
TssA	0.27
Quies	0.24
TssFlnk	0.15
TxWk	0.12
EnhWk	0.08
EnhA2	0.03
TssFlnkU	0.03
EnhA1	0.03
Tx	0.02
ReprPCWk	0.02
TssFlnkD	0.02
TssBiv	0.01
ReprPC	0.01
EnhG1	0.01
EnhBiv	0.00
Het	0.00
EnhG2	0.00
ZNF/Rpts	0.00

peaks		peaks	
repeat	fraction	repeat	fraction
SINE/Alu	0.26	L2a	0.03
Simple_repeat	0.25	MIRb	0.03
LINE/L2	0.09	AluSx	0.03
SINE/MIR	0.09	AluSx1	0.03
LINE/L1	0.09	AluJb	0.03
Low_complexity	0.05	GA-rich	0.03
LTR/ERV1	0.05	L2c	0.02
LTR/ERVL-MaLR	0.03	MIR	0.02
DNA/hAT-Charlie	0.03	AluSz	0.02
LTR/ERVL	0.02	AluY	0.02
DNA/TcMar-Tigger	0.01	(GT)n	0.02
tRNA	0.01	L2b	0.02
DNA/hAT-Tip100	0.01	MIRc	0.02
LINE/CR1	0.01	(AC)n	0.02
LTR/ERVK	0.00	(TG)n	0.02
LTR/Gypsy?	0.00	AluJo	0.02
LTR/Gypsy	0.00	AluJr	0.02
DNA/hAT-Blackjack	0.00	MIR3	0.02

Ontology	Term	FDR Q-val
GO Biological Process	negative regulation of gene expression, epigenetic	93.16
GO Biological Process	regulation of gene expression, epigenetic	69.73
GO Biological Process	nucleosome organization	48.51
GO Biological Process	chromatin silencing	46.21
GO Biological Process	chromatin assembly or disassembly	45.83
GO Biological Process	DNA replication-dependent nucleosome assembly	45.07
GO Biological Process	nucleosome assembly	42.68
GO Biological Process	chromatin assembly	42.01
GO Biological Process	protein-DNA complex subunit organization	39.67
GO Biological Process	gene silencing	35.65
GO Biological Process	DNA packaging	33.23
GO Biological Process	Arp2/3 complex-mediated actin nucleation	32.70
GO Biological Process	macromolecular complex disassembly	30.70
GO Biological Process	protein-DNA complex assembly	29.62
GO Biological Process	retrograde transport, endosome to Golgi	29.47
GO Biological Process	mRNA catabolic process	27.96
GO Biological Process	nuclear-transcribed mRNA catabolic process	27.64
GO Biological Process	RNA catabolic process	27.46
GO Biological Process	regulation of megakaryocyte differentiation	26.49
GO Biological Process	platelet aggregation	23.71

Supplementary Figure 525: Properties and genomic distribution of motifs identified for the ZC3H8 transcription factor in K562 (accession ENCSR494PWZ).

TF-MoDisCO pattern_0 n=1624, CWM

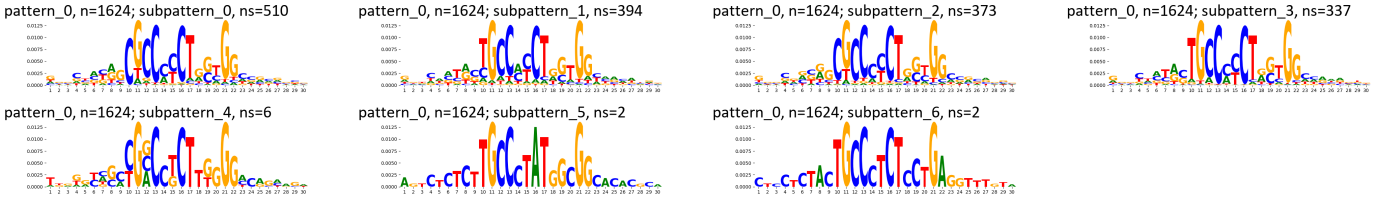

TF-MoDisCO pattern_0 n=1624, PWM

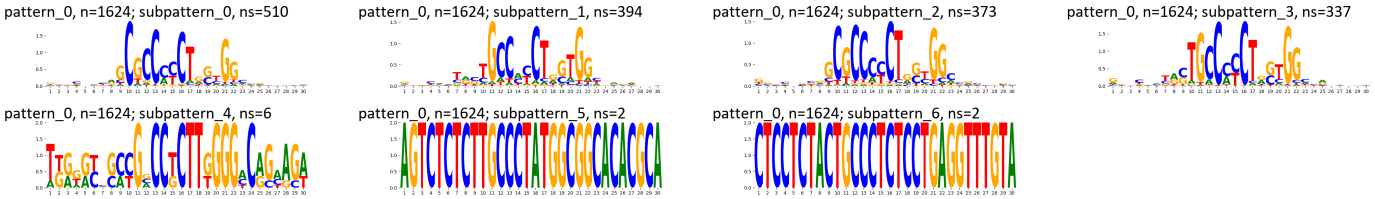

TF-MoDisCO pattern_1 n=755, CWM

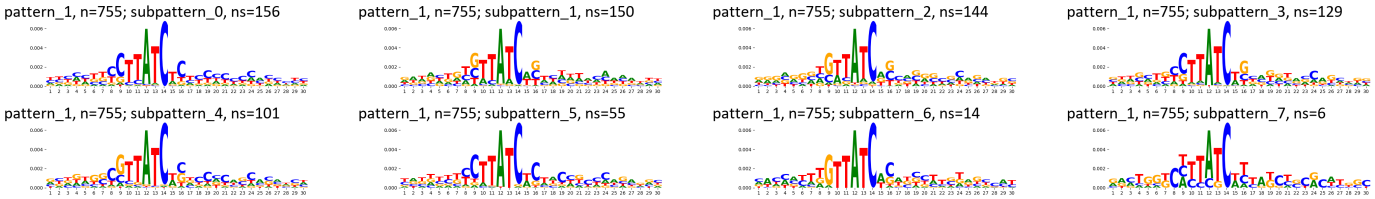

TF-MoDisCO pattern_1 n=755, PWM

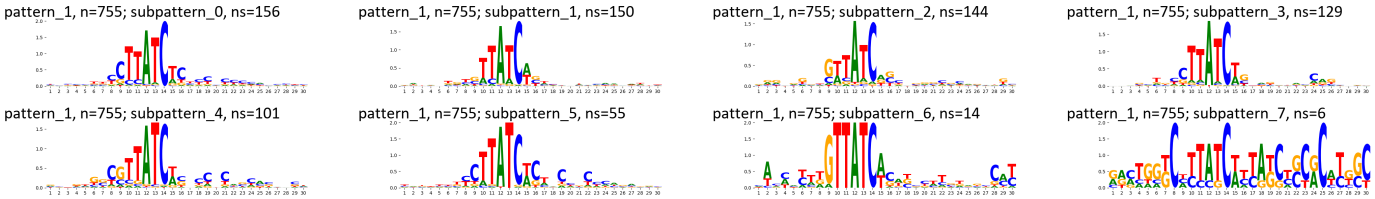

Supplementary Figure 526: TF-MoDisCO subpatterns for the ZC3H8 transcription factor in K562 (accession ENCSR494PWZ).

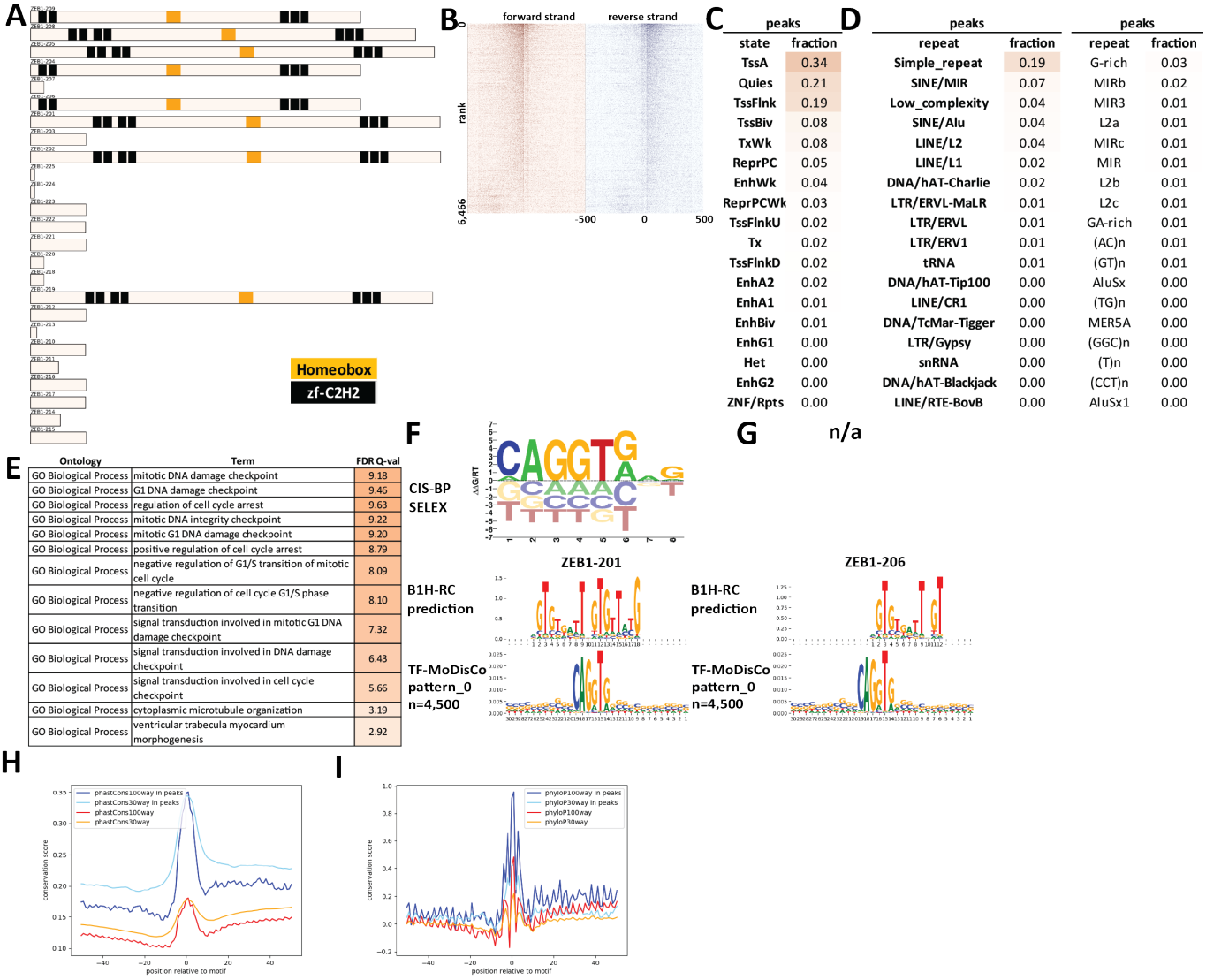

Supplementary Figure 527: Properties and genomic distribution of motifs identified for the ZEB1 transcription factor in bipolar neuron (accession ENCSR418KUS).

TF-MoDisCO pattern_0 n=4500, CWM

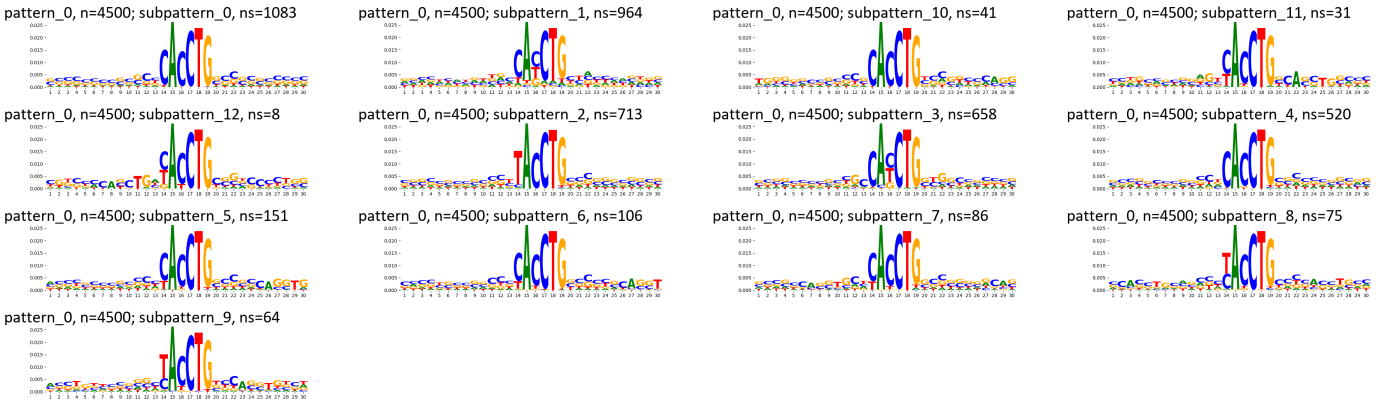

TF-MoDisCO pattern_0 n=4500, PWM

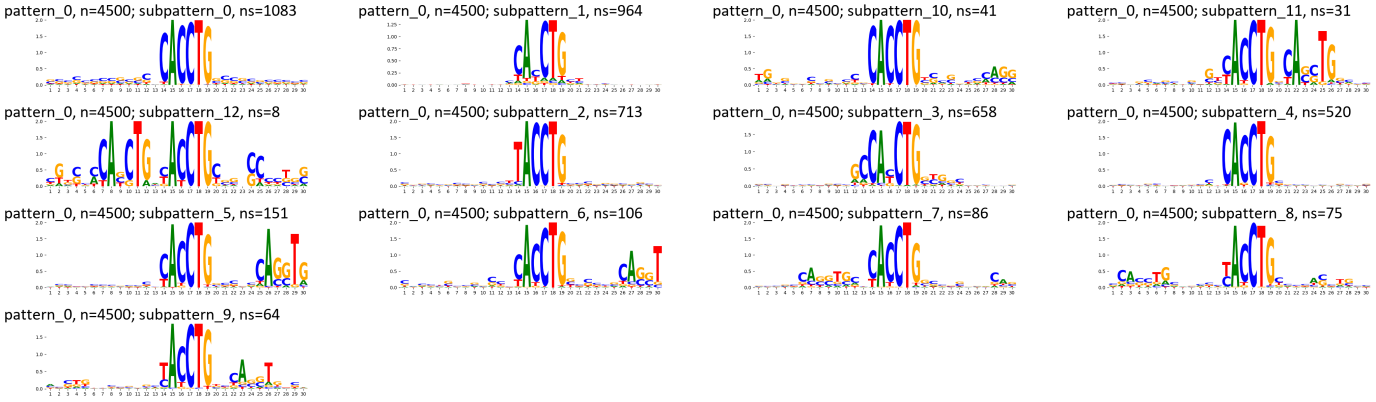

Supplementary Figure 528: TF-MoDisCO subpatterns for the ZEB1 transcription factor in bipolar neuron (accession ENCSR418KUS).

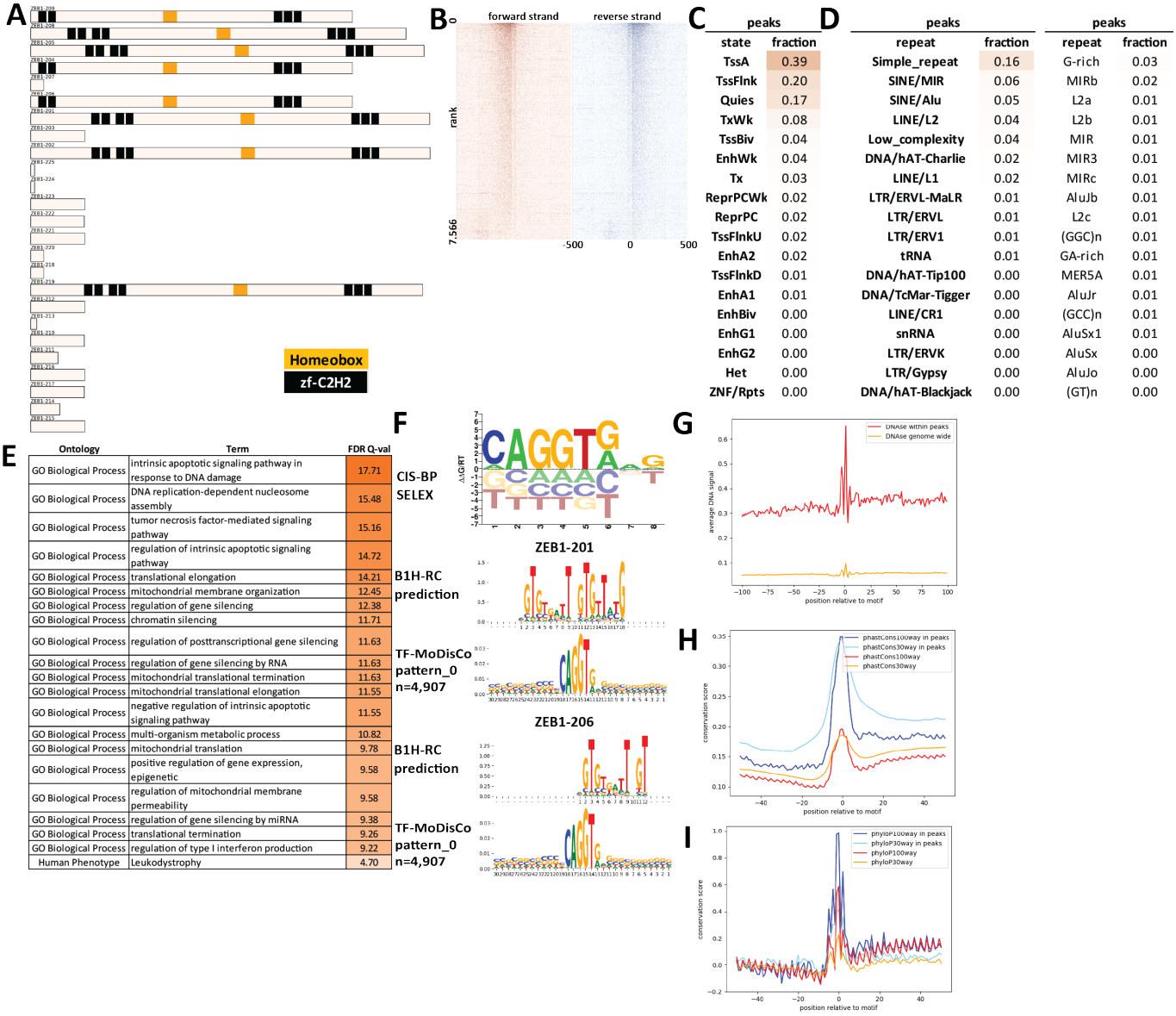

peaks	
state	fraction
TssA	0.39
TssFlnk	0.20
Quies	0.17
TxWk	0.08
TssBiv	0.04
EnhWk	0.04
Tx	0.03
ReprPCWk	0.02
ReprPC	0.02
TssFlnkU	0.02
EnhA2	0.02
TssFlnkD	0.01
EnhA1	0.01
EnhBiv	0.00
EnhG1	0.00
EnhG2	0.00
Het	0.00
ZNF/Rpts	0.00

peaks		peaks	
repeat	fraction	repeat	fraction
Simple_repeat	0.16	G-rich	0.03
SINE/MIR	0.06	MIRb	0.02
SINE/Alu	0.05	L2a	0.01
LINE/L2	0.04	L2b	0.01
Low_complexity	0.04	MIR	0.01
DNA/hAT-Charlie	0.02	MIR3	0.01
LINE/L1	0.02	MIRc	0.01
LTR/ERVL-MaLR	0.01	AluJb	0.01
LTR/ERVL	0.01	L2c	0.01
LTR/ERV1	0.01	(GGC)n	0.01
tRNA	0.01	GA-rich	0.01
DNA/hAT-Tip100	0.00	MER5A	0.01
DNA/TcMar-Tigger	0.00	AluJr	0.01
LINE/CR1	0.00	(GCC)n	0.01
snRNA	0.00	AluSx1	0.01
LTR/ERVK	0.00	AluSx	0.00
LTR/Gypsy	0.00	AluJo	0.00
DNA/hAT-Blackjack	0.00	(GT)n	0.00

Ontology	Term	FDR Q-val
GO Biological Process	intrinsic apoptotic signaling pathway in response to DNA damage	17.71
GO Biological Process	DNA replication-dependent nucleosome assembly	15.48
GO Biological Process	tumor necrosis factor-mediated signaling pathway	15.16
GO Biological Process	regulation of intrinsic apoptotic signaling pathway	14.72
GO Biological Process	translational elongation	14.21
GO Biological Process	mitochondrial membrane organization	12.45
GO Biological Process	regulation of gene silencing	12.38
GO Biological Process	chromatin silencing	11.71
GO Biological Process	regulation of posttranscriptional gene silencing	11.63
GO Biological Process	regulation of gene silencing by RNA	11.63
GO Biological Process	mitochondrial translational termination	11.63
GO Biological Process	mitochondrial translational elongation	11.55
GO Biological Process	negative regulation of intrinsic apoptotic signaling pathway	11.55
GO Biological Process	multi-organism metabolic process	10.82
GO Biological Process	mitochondrial translation	9.78
GO Biological Process	positive regulation of gene expression, epigenetic	9.58
GO Biological Process	regulation of mitochondrial membrane permeability	9.58
GO Biological Process	regulation of gene silencing by miRNA	9.38
GO Biological Process	translational termination	9.26
GO Biological Process	regulation of type I interferon production	9.22
Human Phenotype	Leukodystrophy	4.70

Supplementary Figure 529: Properties and genomic distribution of motifs identified for the ZEB1 transcription factor in GM12878 (accession ENCSR000BND).

TF-MoDisCO pattern_0 n=4907, CWM

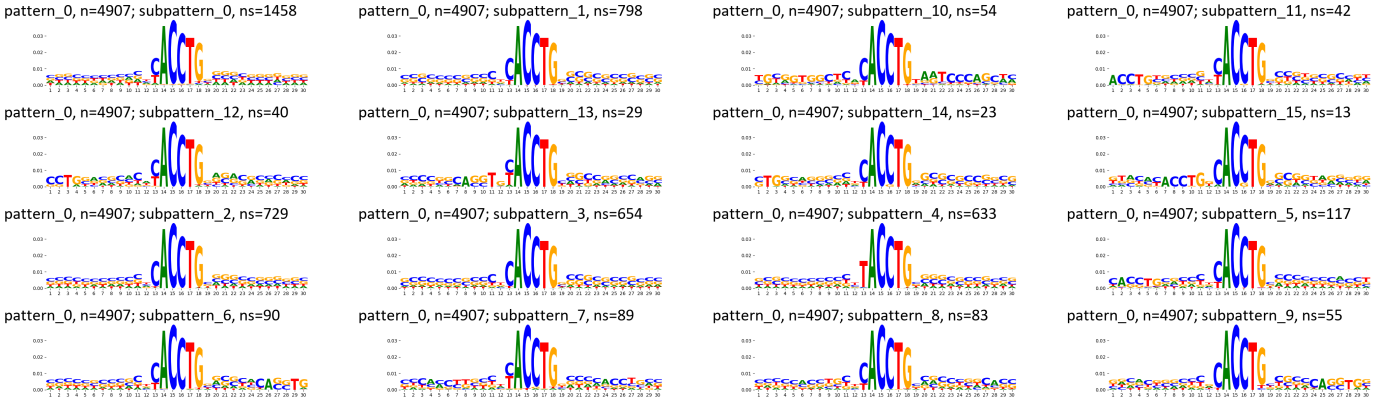

TF-MoDisCO pattern_0 n=4907, PWM

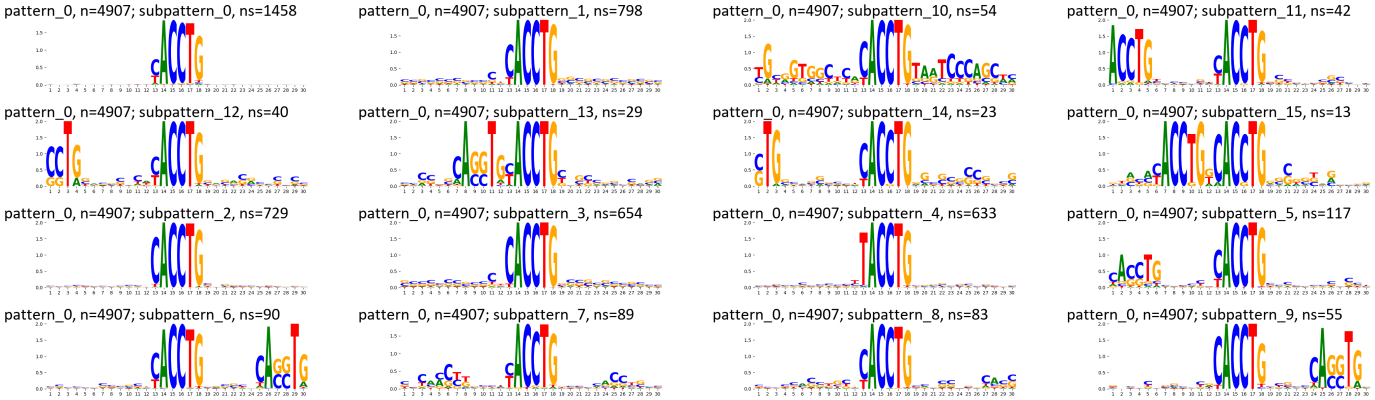

Supplementary Figure 530: TF-MoDisCO subpatterns for the ZEB1 transcription factor in GM12878 (accession ENCSR000BND).

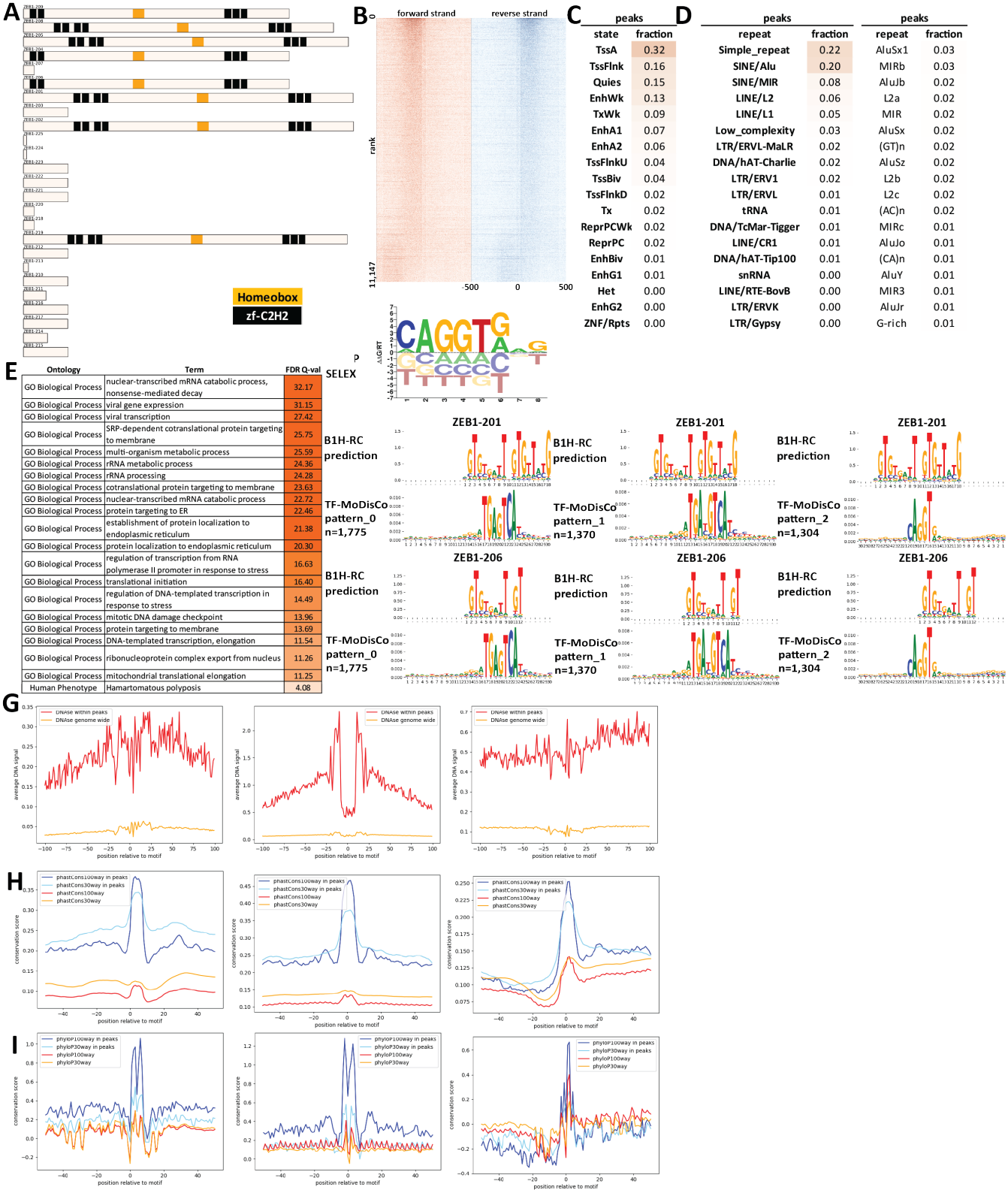

C

peaks	
state	fraction
TssA	0.32
TssFlnk	0.16
Quies	0.15
EnhWk	0.13
TxWk	0.09
EnhA1	0.07
EnhA2	0.06
TssFlnkU	0.04
TssBiv	0.04
TssFlnkD	0.02
Tx	0.02
ReprPCWk	0.02
ReprPC	0.02
EnhBiv	0.01
EnhG1	0.01
Het	0.00
EnhG2	0.00
ZNF/Rpts	0.00

D

peaks		peaks	
repeat	fraction	repeat	fraction
Simple_repeat	0.22	AluSx1	0.03
SINE/Alu	0.20	MIRb	0.03
SINE/MIR	0.08	AluJb	0.02
LINE/L2	0.06	L2a	0.02
LINE/L1	0.05	MIR	0.02
Low_complexity	0.03	AluSx	0.02
LTR/ERVL-MaLR	0.02	(GT)n	0.02
DNA/hAT-Charlie	0.02	AluSz	0.02
LTR/ERV1	0.02	L2b	0.02
LTR/ERVL	0.01	L2c	0.02
tRNA	0.01	(AC)n	0.02
DNA/TcMar-Tigger	0.01	MIRc	0.01
LINE/CR1	0.01	AluJo	0.01
DNA/hAT-Tip100	0.01	(CA)n	0.01
snRNA	0.00	AluY	0.01
LINE/RTE-BovB	0.00	MIR3	0.01
LTR/ERVK	0.00	AluJr	0.01
LTR/Gypsy	0.00	G-rich	0.01

E

Ontology	Term	FDR Q-val
GO Biological Process	nuclear-transcribed mRNA catabolic process, nonsense-mediated decay	32.17
GO Biological Process	viral gene expression	31.15
GO Biological Process	viral transcription	27.42
GO Biological Process	SRP-dependent cotranslational protein targeting to membrane	25.75
GO Biological Process	multi-organism metabolic process	25.59
GO Biological Process	rRNA metabolic process	24.36
GO Biological Process	rRNA processing	24.28
GO Biological Process	cotranslational protein targeting to membrane	23.63
GO Biological Process	nuclear-transcribed mRNA catabolic process	22.72
GO Biological Process	protein targeting to ER	22.46
GO Biological Process	establishment of protein localization to endoplasmic reticulum	21.38
GO Biological Process	protein localization to endoplasmic reticulum	20.30
GO Biological Process	regulation of transcription from RNA polymerase II promoter in response to stress	16.63
GO Biological Process	translational initiation	16.40
GO Biological Process	regulation of DNA-templated transcription in response to stress	14.49
GO Biological Process	mitotic DNA damage checkpoint	13.96
GO Biological Process	protein targeting to membrane	13.69
GO Biological Process	DNA-templated transcription, elongation	11.54
GO Biological Process	ribonucleoprotein complex export from nucleus	11.26
GO Biological Process	mitochondrial translational elongation	11.25
Human Phenotype	Hamartomatous polyposis	4.08

Supplementary Figure 531: Properties and genomic distribution of motifs identified for the ZEB1 transcription factor in HEK293 (accession ENCSR909HMT).

TF-MoDisCO pattern_0 n=1775, CWM

pattern_0, n=1775; subpattern_0, ns=533

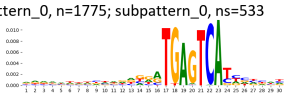

pattern_0, n=1775; subpattern_1, ns=426

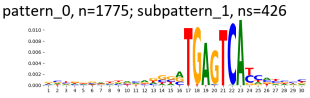

pattern_0, n=1775; subpattern_2, ns=368

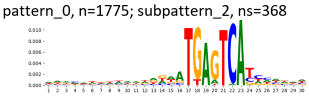

pattern_0, n=1775; subpattern_3, ns=268

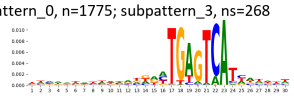

pattern_0, n=1775; subpattern_4, ns=82

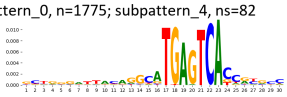

pattern_0, n=1775; subpattern_5, ns=43

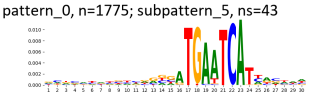

pattern_0, n=1775; subpattern_6, ns=29

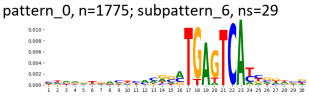

pattern_0, n=1775; subpattern_7, ns=14

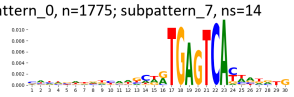

pattern_0, n=1775; subpattern_8, ns=12

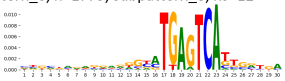

TF-MoDisCO pattern_0 n=1775, PWM

pattern_0, n=1775; subpattern_0, ns=533

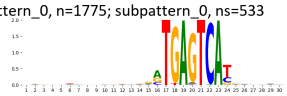

pattern_0, n=1775; subpattern_1, ns=426

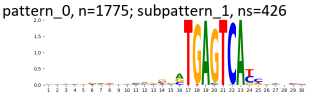

pattern_0, n=1775; subpattern_2, ns=368

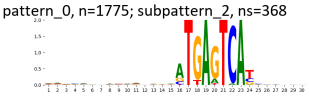

pattern_0, n=1775; subpattern_3, ns=268

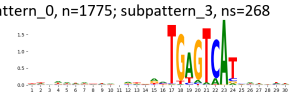

pattern_0, n=1775; subpattern_4, ns=82

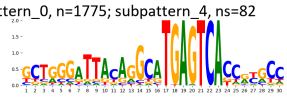

pattern_0, n=1775; subpattern_5, ns=43

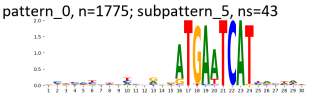

pattern_0, n=1775; subpattern_6, ns=29

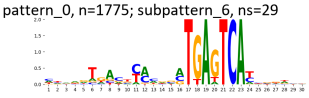

pattern_0, n=1775; subpattern_7, ns=14

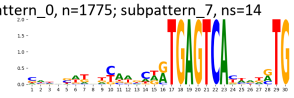

pattern_0, n=1775; subpattern_8, ns=12

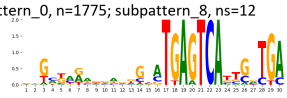

TF-MoDisCO pattern_1 n=1370, CWM

pattern_1, n=1370; subpattern_0, ns=328

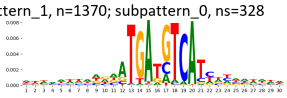

pattern_1, n=1370; subpattern_1, ns=328

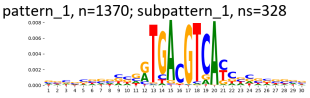

pattern_1, n=1370; subpattern_2, ns=304

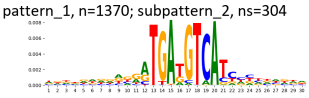

pattern_1, n=1370; subpattern_3, ns=226

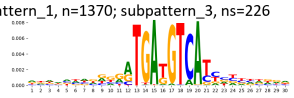

pattern_1, n=1370; subpattern_4, ns=137

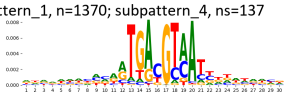

pattern_1, n=1370; subpattern_5, ns=18

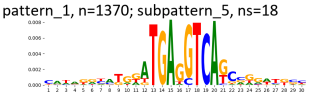

pattern_1, n=1370; subpattern_6, ns=16

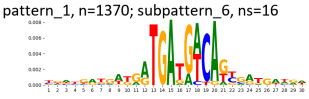

pattern_1, n=1370; subpattern_7, ns=7

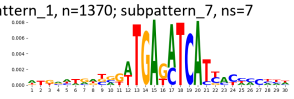

pattern_1, n=1370; subpattern_8, ns=4

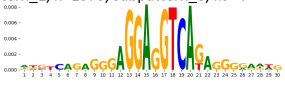

pattern_1, n=1370; subpattern_9, ns=2

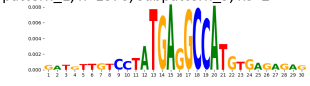

TF-MoDisCO pattern_1 n=1370, PWM

pattern_1, n=1370; subpattern_0, ns=328

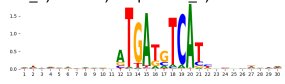

pattern_1, n=1370; subpattern_1, ns=328

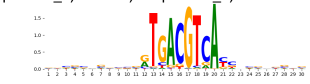

pattern_1, n=1370; subpattern_2, ns=304

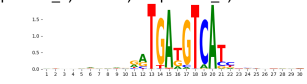

pattern_1, n=1370; subpattern_3, ns=226

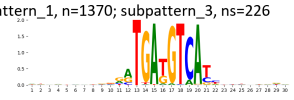

pattern_1, n=1370; subpattern_4, ns=137

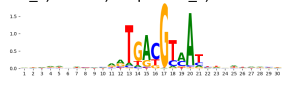

pattern_1, n=1370; subpattern_5, ns=18

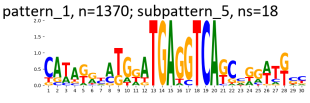

pattern_1, n=1370; subpattern_6, ns=16

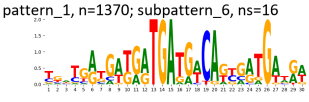

pattern_1, n=1370; subpattern_7, ns=7

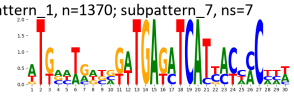

pattern_1, n=1370; subpattern_8, ns=4

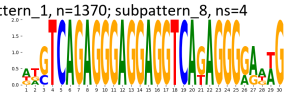

pattern_1, n=1370; subpattern_9, ns=2

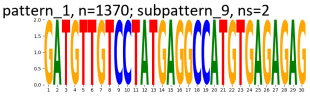

TF-MoDisCO pattern_2 n=1304, CWM

pattern_2, n=1304; subpattern_0, ns=269

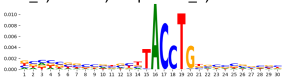

pattern_2, n=1304; subpattern_1, ns=252

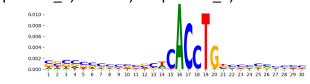

pattern_2, n=1304; subpattern_10, ns=9

pattern_2, n=1304; subpattern_11, ns=4

pattern_2, n=1304; subpattern_2, ns=216

pattern_2, n=1304; subpattern_3, ns=208

pattern_2, n=1304; subpattern_4, ns=81

pattern_2, n=1304; subpattern_5, ns=80

pattern_2, n=1304; subpattern_6, ns=61

pattern_2, n=1304; subpattern_7, ns=47

pattern_2, n=1304; subpattern_8, ns=43

pattern_2, n=1304; subpattern_9, ns=34

TF-MoDisCO pattern_2 n=1304, PWM

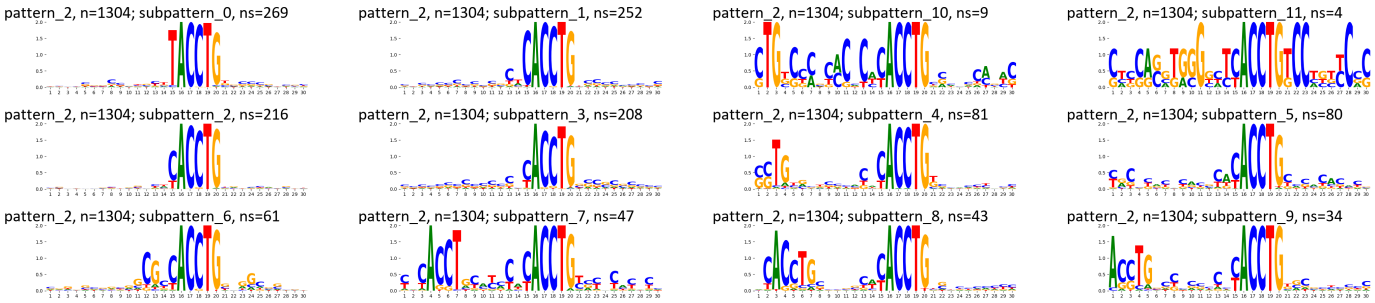

Supplementary Figure 532: TF-MoDisCO subpatterns for the ZEB1 transcription factor in HEK293 (accession ENCSR909HMT).

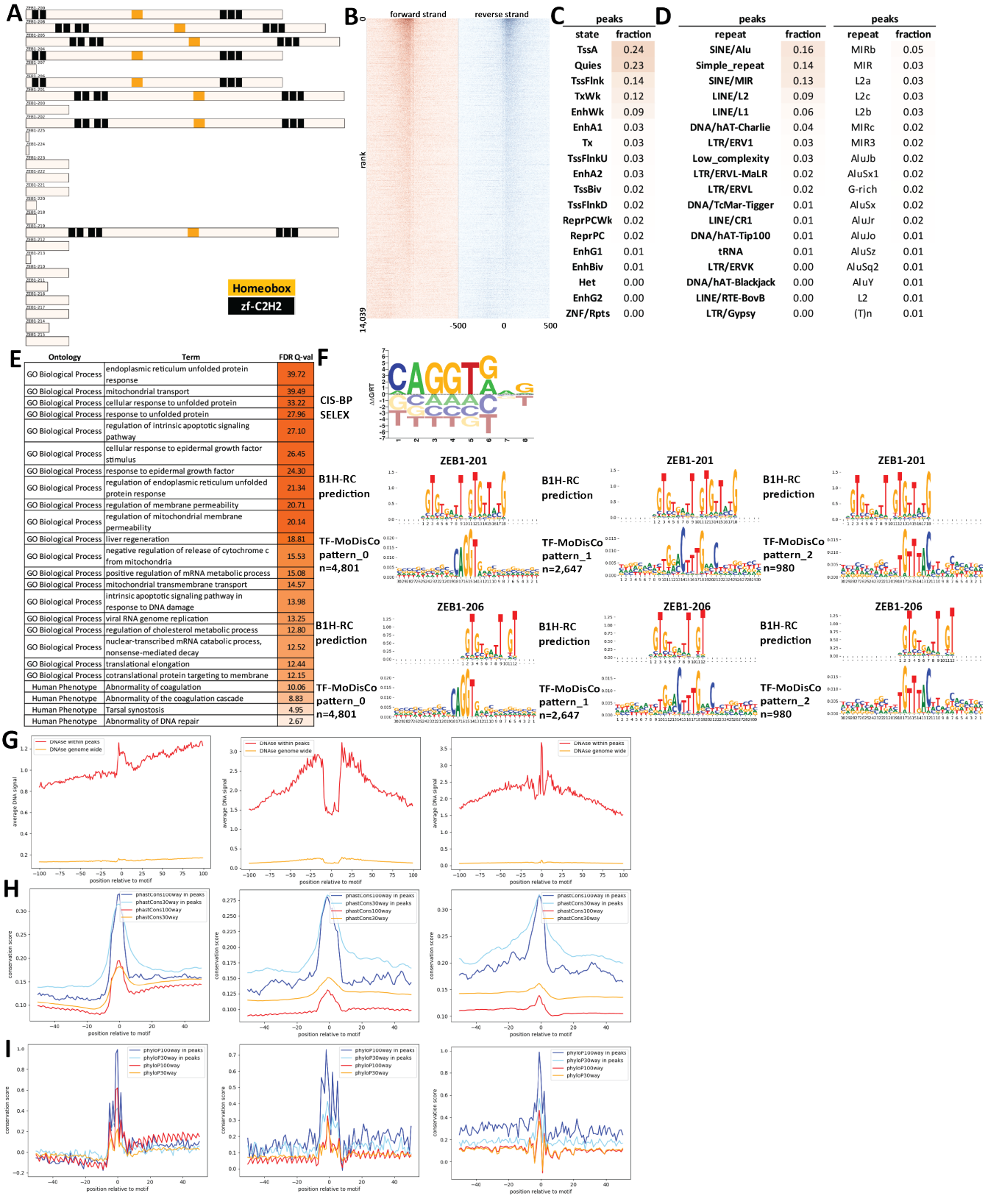

Supplementary Figure 533: Properties and genomic distribution of motifs identified for the ZEB1 transcription factor in HepG2 (accession ENCSR000BVN).

TF-MoDisCO pattern_0 n=4801, CWM

pattern_0, n=4801; subpattern_0, ns=1362

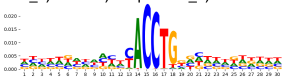

pattern_0, n=4801; subpattern_1, ns=991

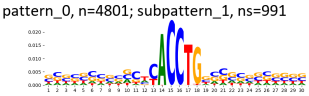

pattern_0, n=4801; subpattern_10, ns=62

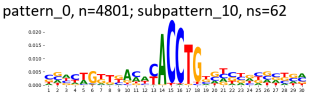

pattern_0, n=4801; subpattern_11, ns=60

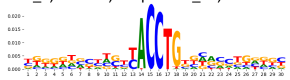

pattern_0, n=4801; subpattern_12, ns=43

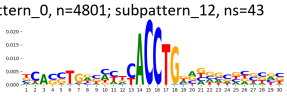

pattern_0, n=4801; subpattern_13, ns=38

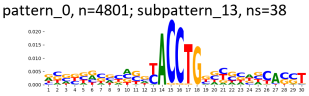

pattern_0, n=4801; subpattern_14, ns=22

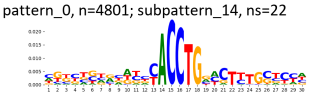

pattern_0, n=4801; subpattern_15, ns=2

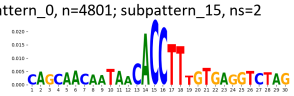

pattern_0, n=4801; subpattern_2, ns=921

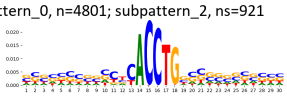

pattern_0, n=4801; subpattern_3, ns=395

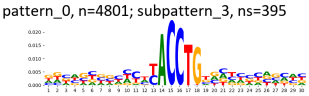

pattern_0, n=4801; subpattern_4, ns=369

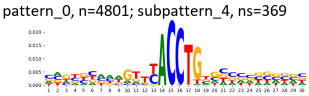

pattern_0, n=4801; subpattern_5, ns=205

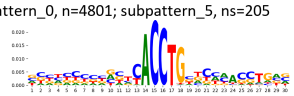

pattern_0, n=4801; subpattern_6, ns=110

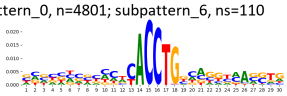

pattern_0, n=4801; subpattern_7, ns=79

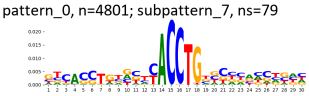

pattern_0, n=4801; subpattern_8, ns=71

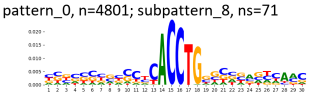

pattern_0, n=4801; subpattern_9, ns=71

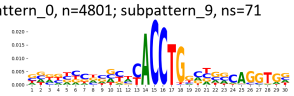

TF-MoDisCO pattern_0 n=4801, PWM

pattern_0, n=4801; subpattern_0, ns=1362

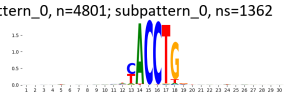

pattern_0, n=4801; subpattern_1, ns=991

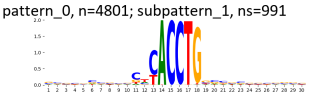

pattern_0, n=4801; subpattern_10, ns=62

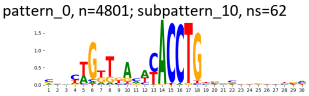

pattern_0, n=4801; subpattern_11, ns=60

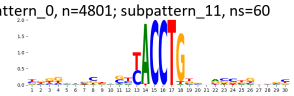

pattern_0, n=4801; subpattern_12, ns=43

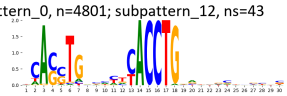

pattern_0, n=4801; subpattern_13, ns=38

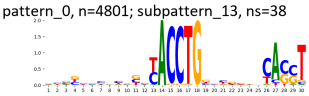

pattern_0, n=4801; subpattern_14, ns=22

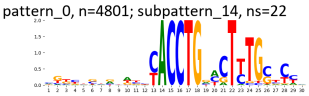

pattern_0, n=4801; subpattern_15, ns=2

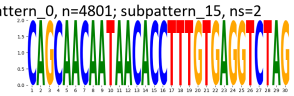

pattern_0, n=4801; subpattern_2, ns=921

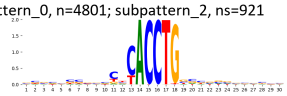

pattern_0, n=4801; subpattern_3, ns=395

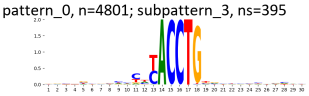

pattern_0, n=4801; subpattern_4, ns=369

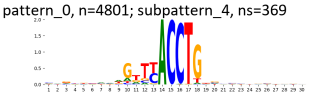

pattern_0, n=4801; subpattern_5, ns=205

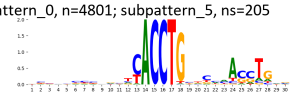

pattern_0, n=4801; subpattern_6, ns=110

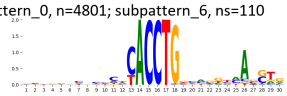

pattern_0, n=4801; subpattern_7, ns=79

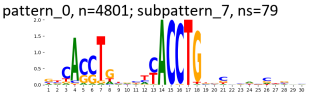

pattern_0, n=4801; subpattern_8, ns=71

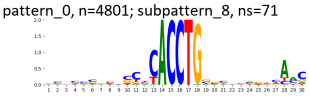

pattern_0, n=4801; subpattern_9, ns=71

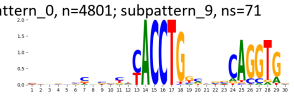

TF-MoDisCO pattern_1 n=2647, CWM

pattern_1, n=2647; subpattern_0, ns=546

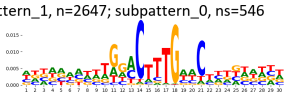

pattern_1, n=2647; subpattern_1, ns=493

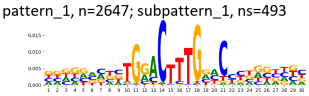

pattern_1, n=2647; subpattern_10, ns=2

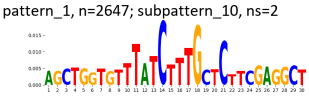

pattern_1, n=2647; subpattern_2, ns=462

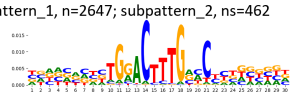

pattern_1, n=2647; subpattern_3, ns=403

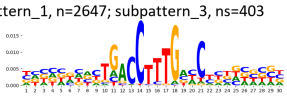

pattern_1, n=2647; subpattern_4, ns=363

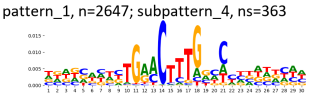

pattern_1, n=2647; subpattern_5, ns=283

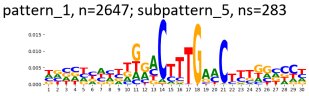

pattern_1, n=2647; subpattern_6, ns=80

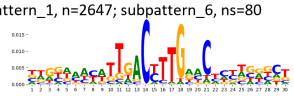

pattern_1, n=2647; subpattern_7, ns=9

pattern_1, n=2647; subpattern_8, ns=4

pattern_1, n=2647; subpattern_9, ns=2

TF-MoDisCO pattern_1 n=2647, PWM

pattern_1, n=2647; subpattern_0, ns=546

pattern_1, n=2647; subpattern_1, ns=493

pattern_1, n=2647; subpattern_10, ns=2

pattern_1, n=2647; subpattern_2, ns=462

pattern_1, n=2647; subpattern_3, ns=403

pattern_1, n=2647; subpattern_4, ns=363

pattern_1, n=2647; subpattern_5, ns=283

pattern_1, n=2647; subpattern_6, ns=80

pattern_1, n=2647; subpattern_7, ns=9

pattern_1, n=2647; subpattern_8, ns=4

pattern_1, n=2647; subpattern_9, ns=2

TF-MoDisCO pattern_2 n=980, CWM

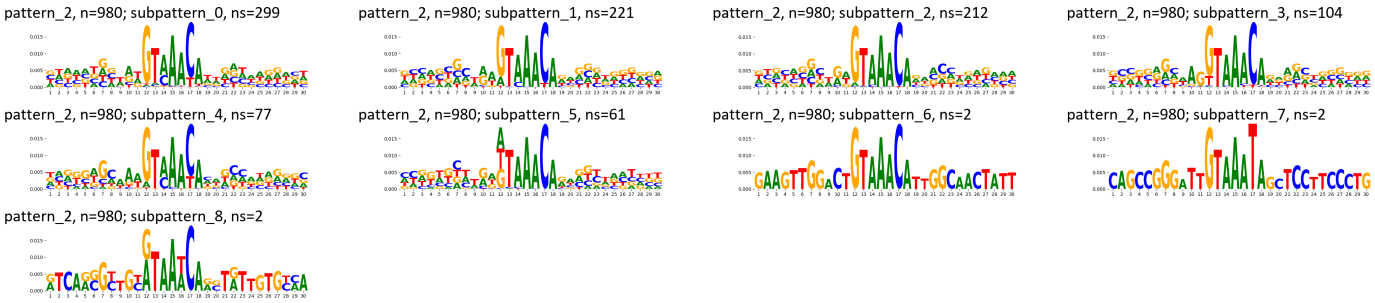

TF-MoDisCO pattern_2 n=980, PWM

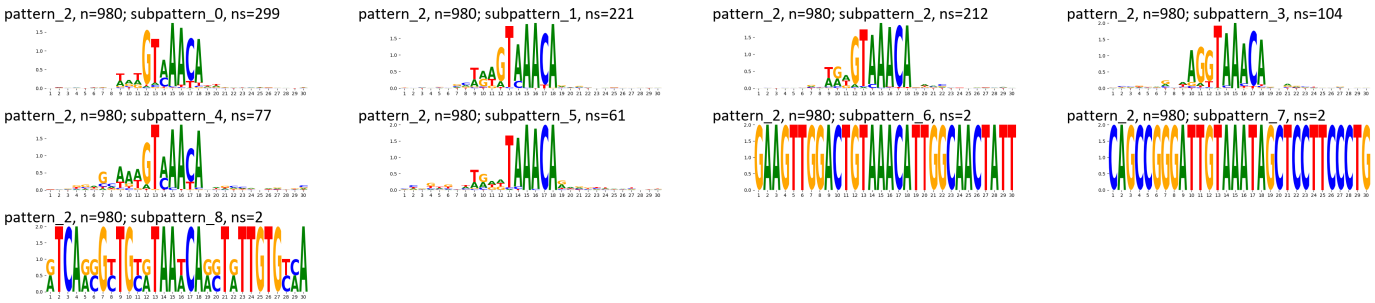

Supplementary Figure 534: TF-MoDisCO subpatterns for the ZEB1 transcription factor in HepG2 (accession ENCSR000BVN).

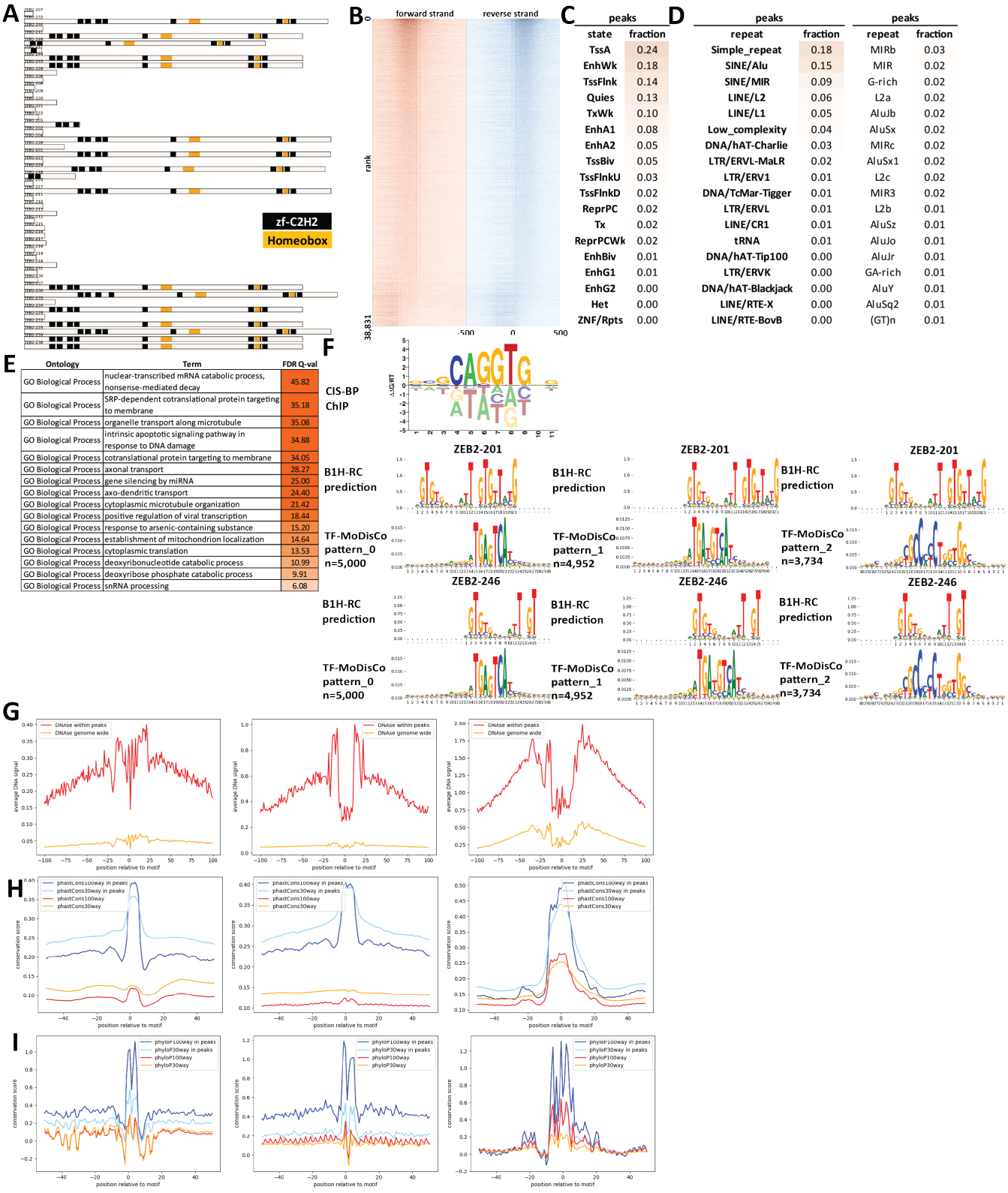

Supplementary Figure 535: Properties and genomic distribution of motifs identified for the ZEB2 transcription factor in HEK293 (accession ENCSR417VWF).

TF-MoDisCO pattern_0 n=5000, CWM

pattern_0, n=5000; subpattern_0, ns=1143

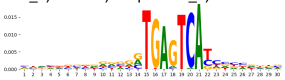

pattern_0, n=5000; subpattern_1, ns=1008

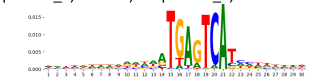

pattern_0, n=5000; subpattern_10, ns=47

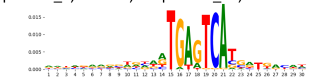

pattern_0, n=5000; subpattern_11, ns=37

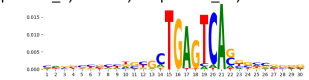

pattern_0, n=5000; subpattern_2, ns=840

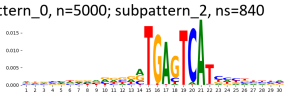

pattern_0, n=5000; subpattern_3, ns=767

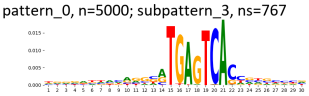

pattern_0, n=5000; subpattern_4, ns=274

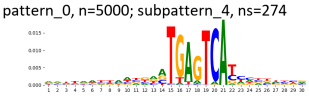

pattern_0, n=5000; subpattern_5, ns=249

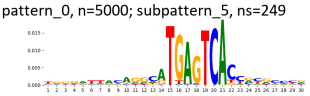

pattern_0, n=5000; subpattern_6, ns=227

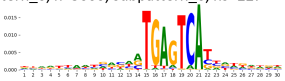

pattern_0, n=5000; subpattern_7, ns=181

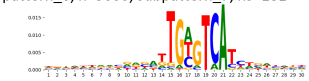

pattern_0, n=5000; subpattern_8, ns=123

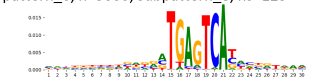

pattern_0, n=5000; subpattern_9, ns=104

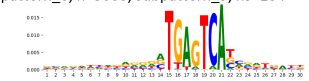

TF-MoDisCO pattern_0 n=5000, PWM

pattern_0, n=5000; subpattern_0, ns=1143

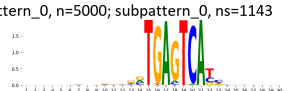

pattern_0, n=5000; subpattern_1, ns=1008

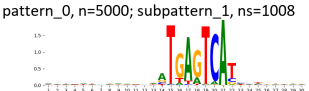

pattern_0, n=5000; subpattern_10, ns=47

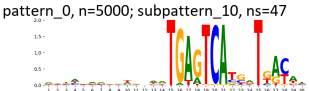

pattern_0, n=5000; subpattern_11, ns=37

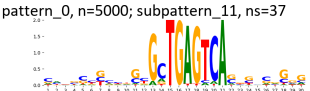

pattern_0, n=5000; subpattern_2, ns=840

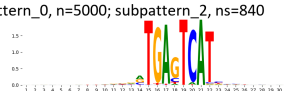

pattern_0, n=5000; subpattern_3, ns=767

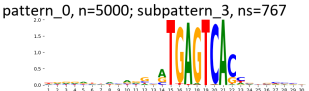

pattern_0, n=5000; subpattern_4, ns=274

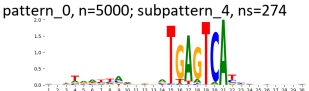

pattern_0, n=5000; subpattern_5, ns=249

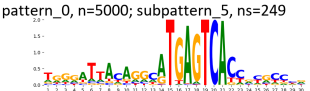

pattern_0, n=5000; subpattern_6, ns=227

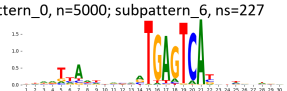

pattern_0, n=5000; subpattern_7, ns=181

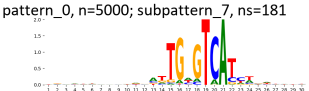

pattern_0, n=5000; subpattern_8, ns=123

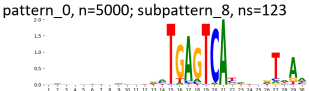

pattern_0, n=5000; subpattern_9, ns=104

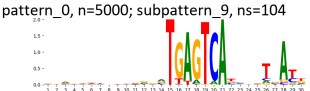

TF-MoDisCO pattern_1 n=4952, CWM

pattern_1, n=4952; subpattern_0, ns=1226

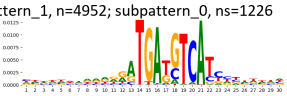

pattern_1, n=4952; subpattern_1, ns=1067

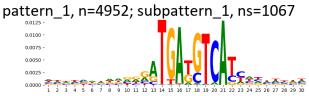

pattern_1, n=4952; subpattern_2, ns=964

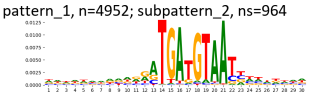

pattern_1, n=4952; subpattern_3, ns=831

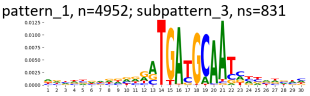

pattern_1, n=4952; subpattern_4, ns=770

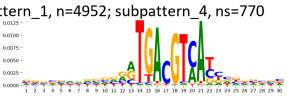

pattern_1, n=4952; subpattern_5, ns=57

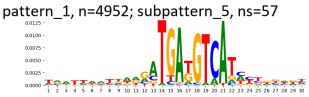

pattern_1, n=4952; subpattern_6, ns=17

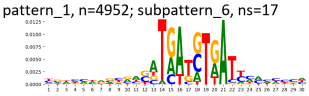

pattern_1, n=4952; subpattern_7, ns=17

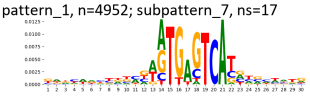

pattern_1, n=4952; subpattern_8, ns=3

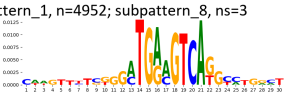

TF-MoDisCO pattern_1 n=4952, PWM

pattern_1, n=4952; subpattern_0, ns=1226

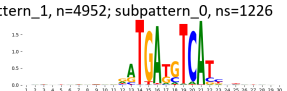

pattern_1, n=4952; subpattern_1, ns=1067

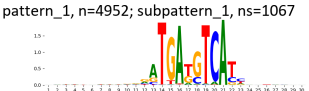

pattern_1, n=4952; subpattern_2, ns=964

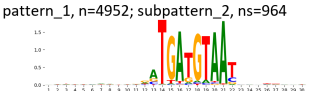

pattern_1, n=4952; subpattern_3, ns=831

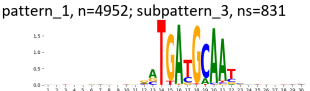

pattern_1, n=4952; subpattern_4, ns=770

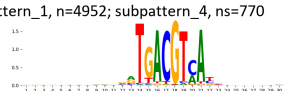

pattern_1, n=4952; subpattern_5, ns=57

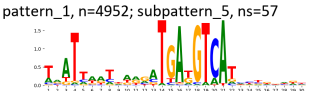

pattern_1, n=4952; subpattern_6, ns=17

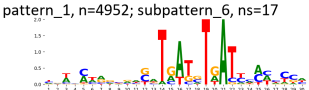

pattern_1, n=4952; subpattern_7, ns=17

pattern_1, n=4952; subpattern_8, ns=3

TF-MoDisCO pattern_2 n=3734, CWM

pattern_2, n=3734; subpattern_0, ns=778

pattern_2, n=3734; subpattern_1, ns=755

pattern_2, n=3734; subpattern_2, ns=745

pattern_2, n=3734; subpattern_3, ns=666

pattern_2, n=3734; subpattern_4, ns=411

pattern_2, n=3734; subpattern_5, ns=379

TF-MoDisCO pattern_2 n=3734, PWM

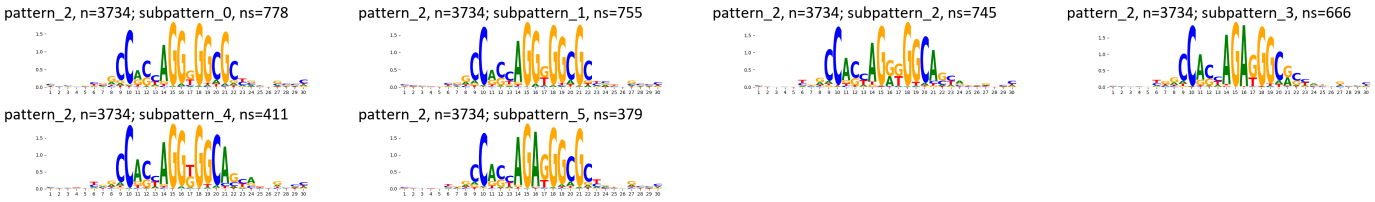

Supplementary Figure 536: TF-MoDisCO subpatterns for the ZEB2 transcription factor in HEK293 (accession ENCSR417VWF).

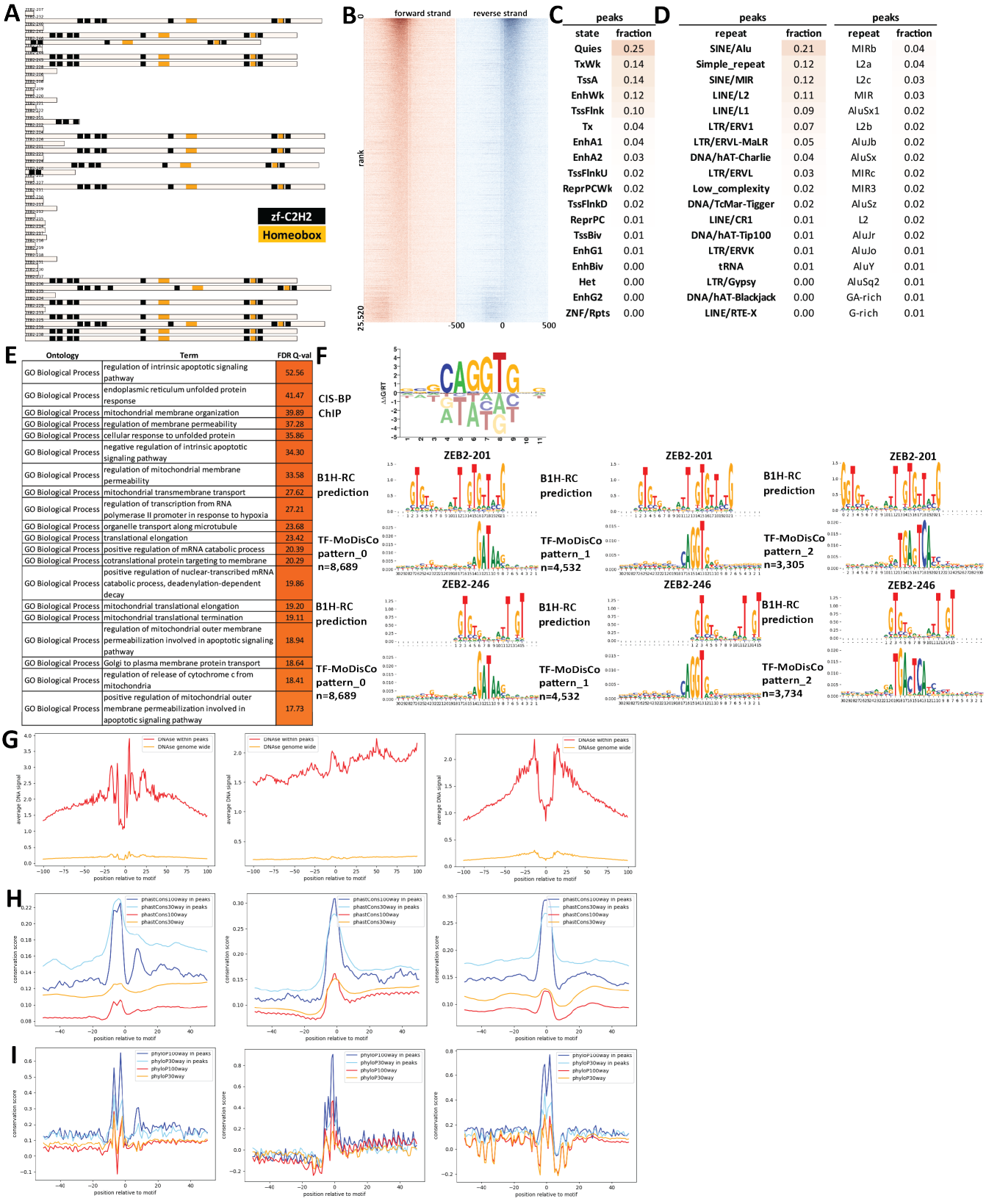

Supplementary Figure 537: Properties and genomic distribution of motifs identified for the ZEB2 transcription factor in K562 (accession ENCSR004GKA).

TF-MoDisCO pattern_1 n=6662, CWM

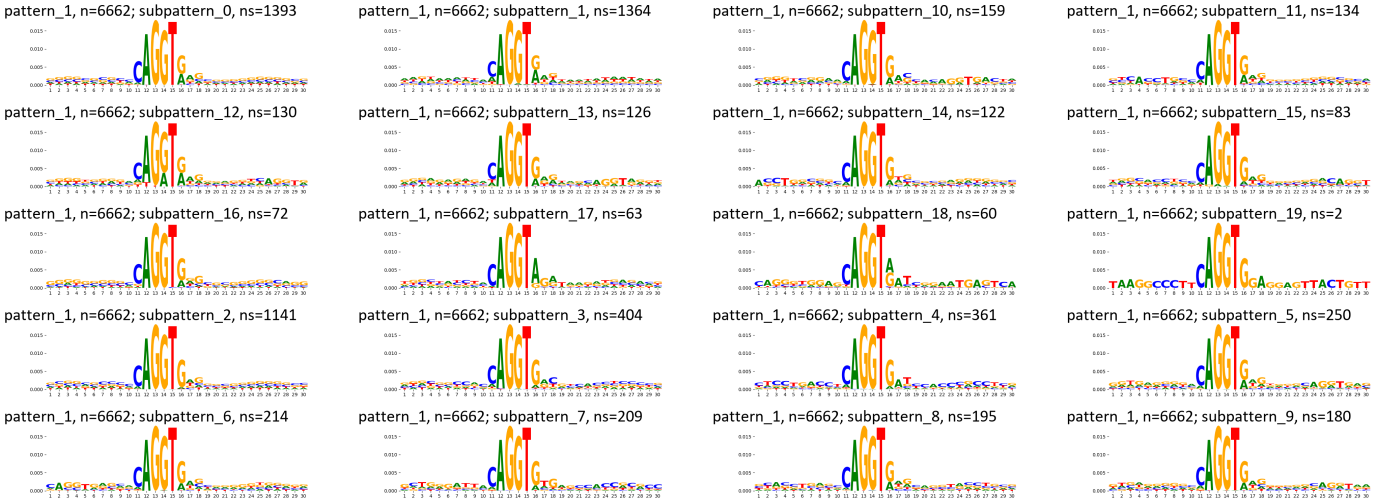

TF-MoDisCO pattern_1 n=6662, PWM

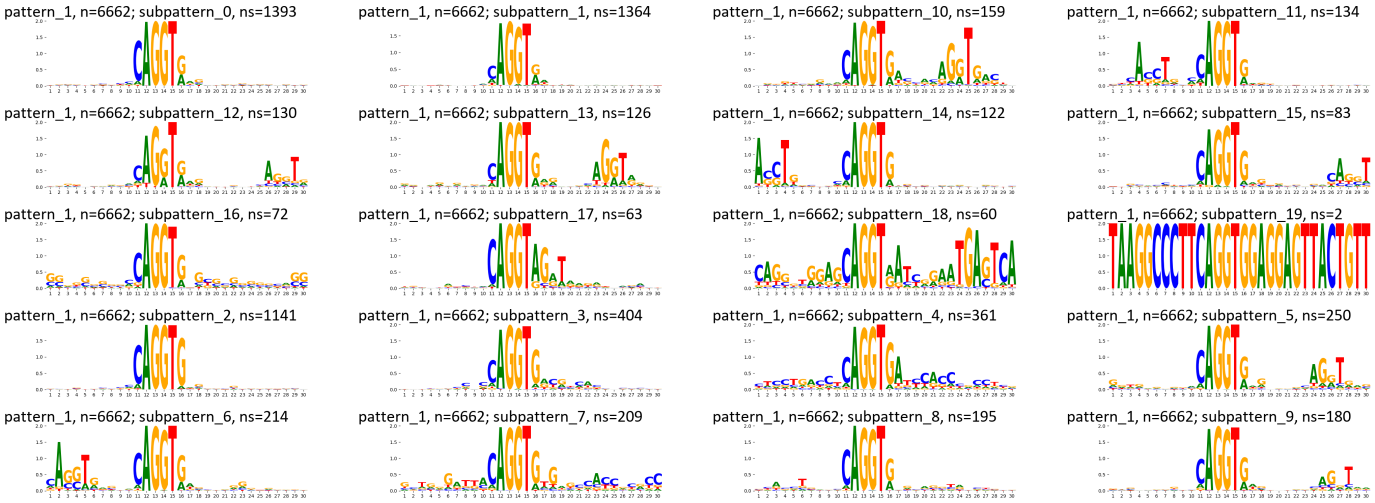

TF-MoDisCO pattern_3 n=1610, CWM

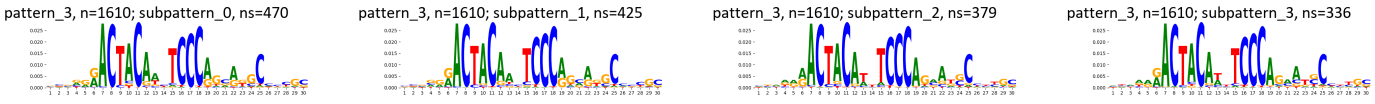

TF-MoDisCO pattern_3 n=1610, PWM

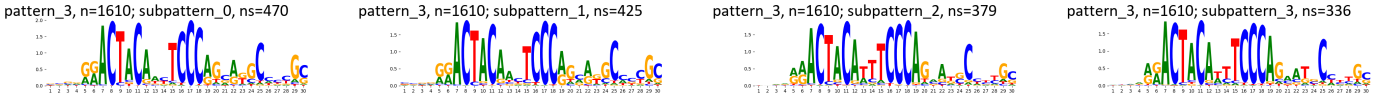

Supplementary Figure 538: TF-MoDisCO subpatterns for the ZEB2 transcription factor in K562 (accession ENCSR004GKA).

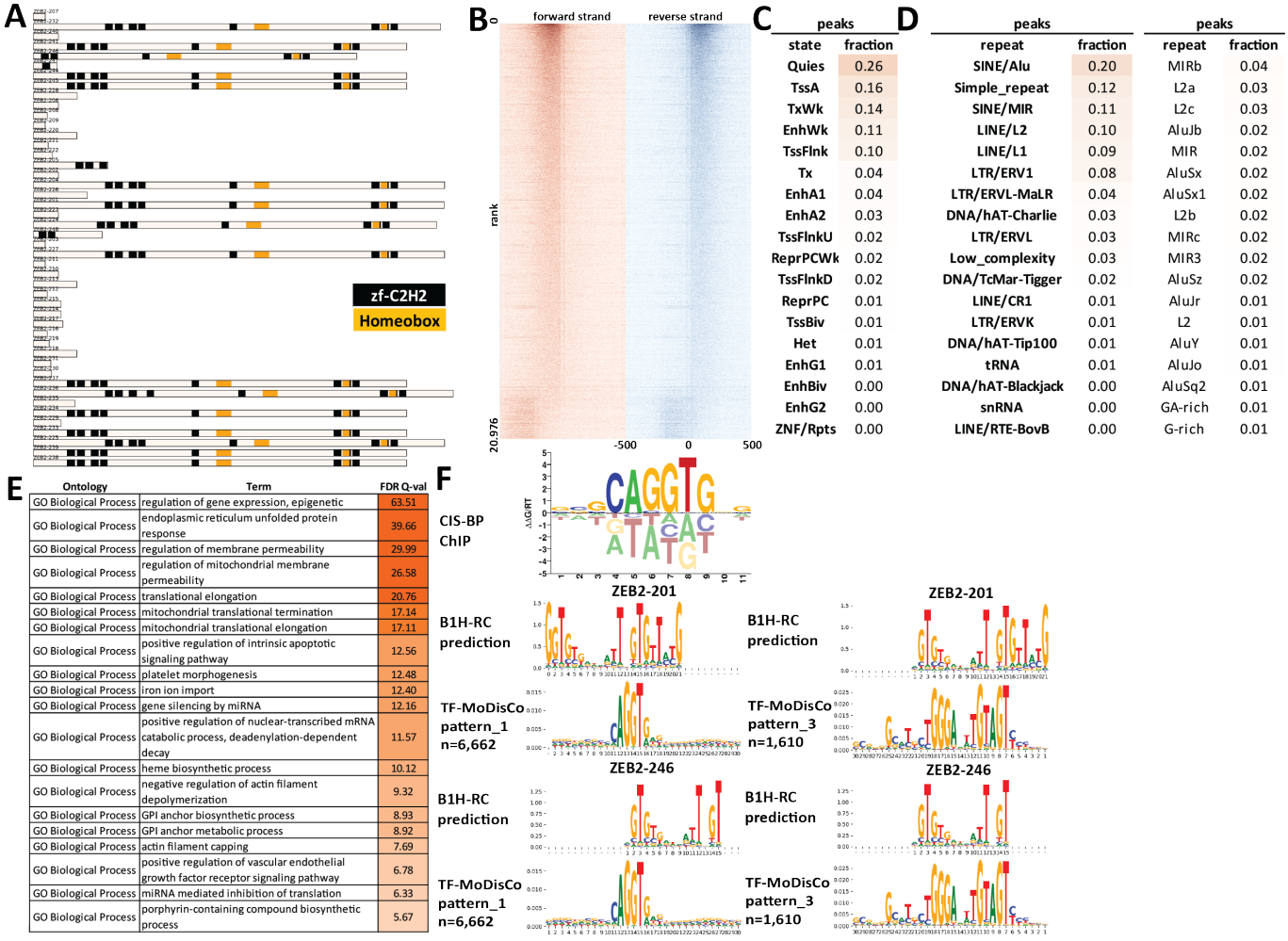

Supplementary Figure 539: Properties and genomic distribution of motifs identified for the ZEB2 transcription factor in K562 (accession ENCSR322CFO).

TF-MoDisCO pattern_0 n=8689, CWM

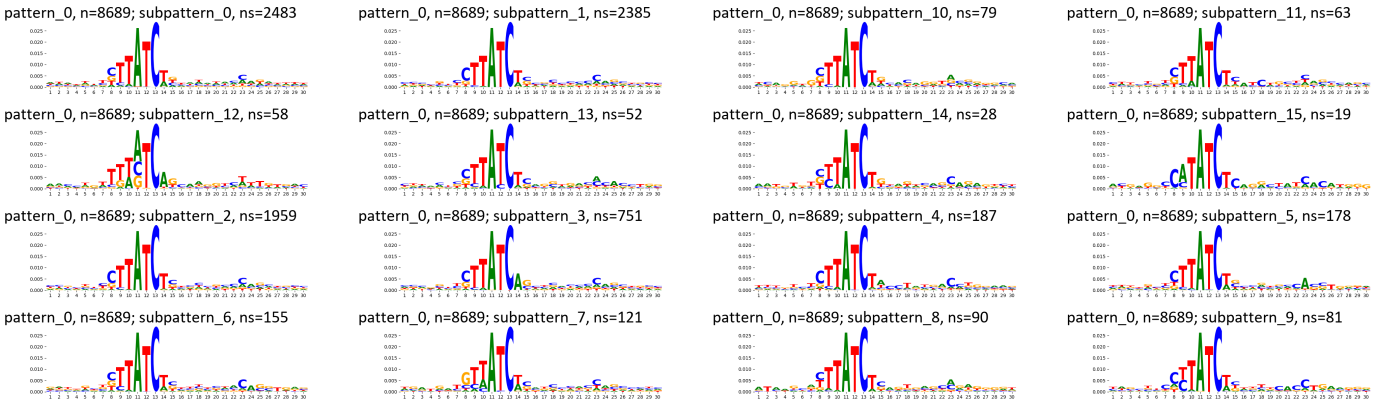

TF-MoDisCO pattern_0 n=8689, PWM

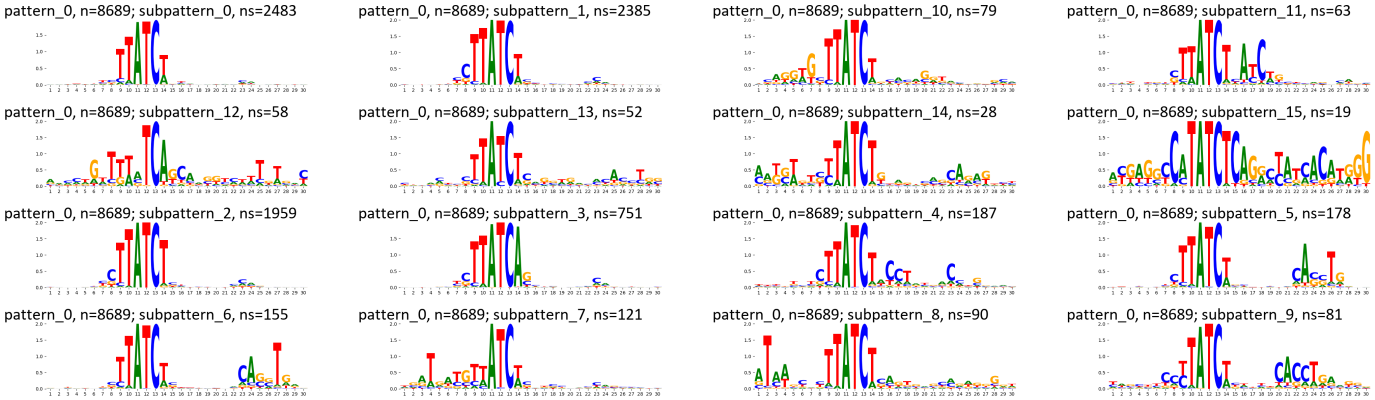

TF-MoDisCO pattern_1 n=4532, CWM

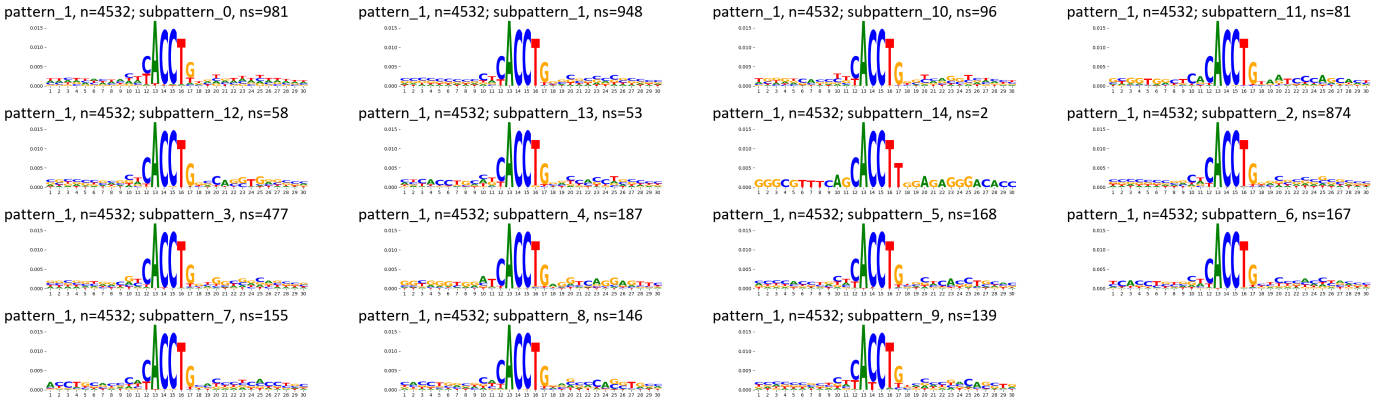

TF-MoDisCO pattern_1 n=4532, PWM

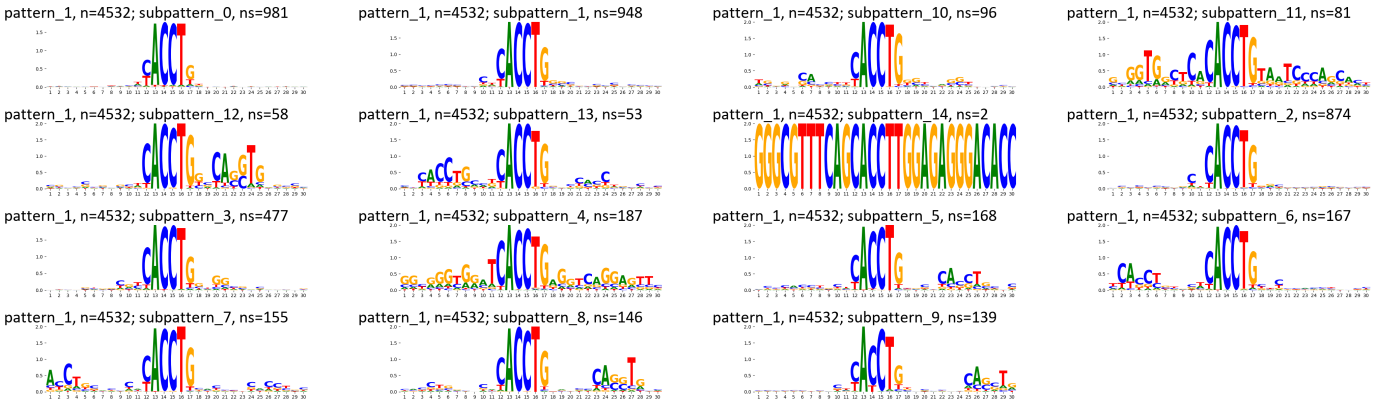

TF-MoDisCO pattern_2 n=3305, CWM

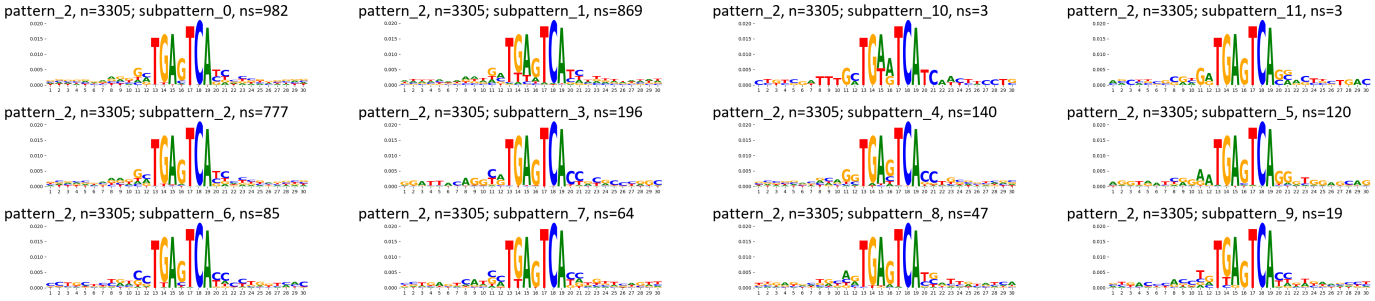

TF-MoDisCO pattern_2 n=3305, PWM

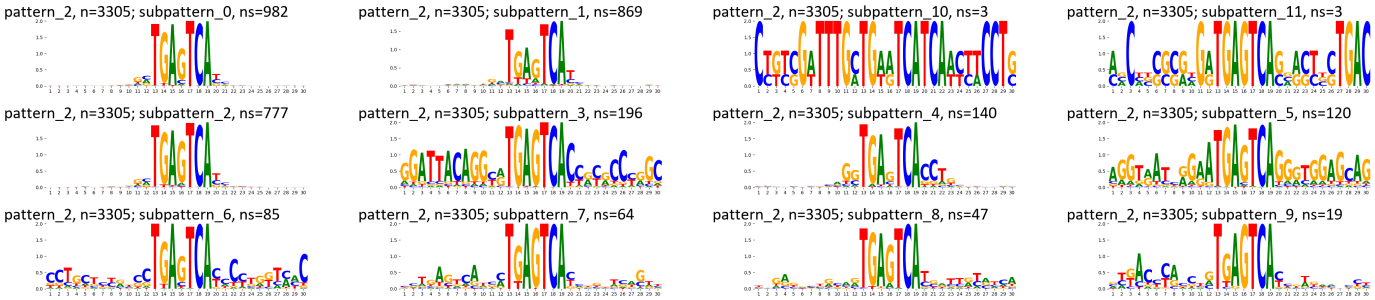

Supplementary Figure 540: TF-MoDisCO subpatterns for the ZEB2 transcription factor in K562 (accession ENCSR322CFO).

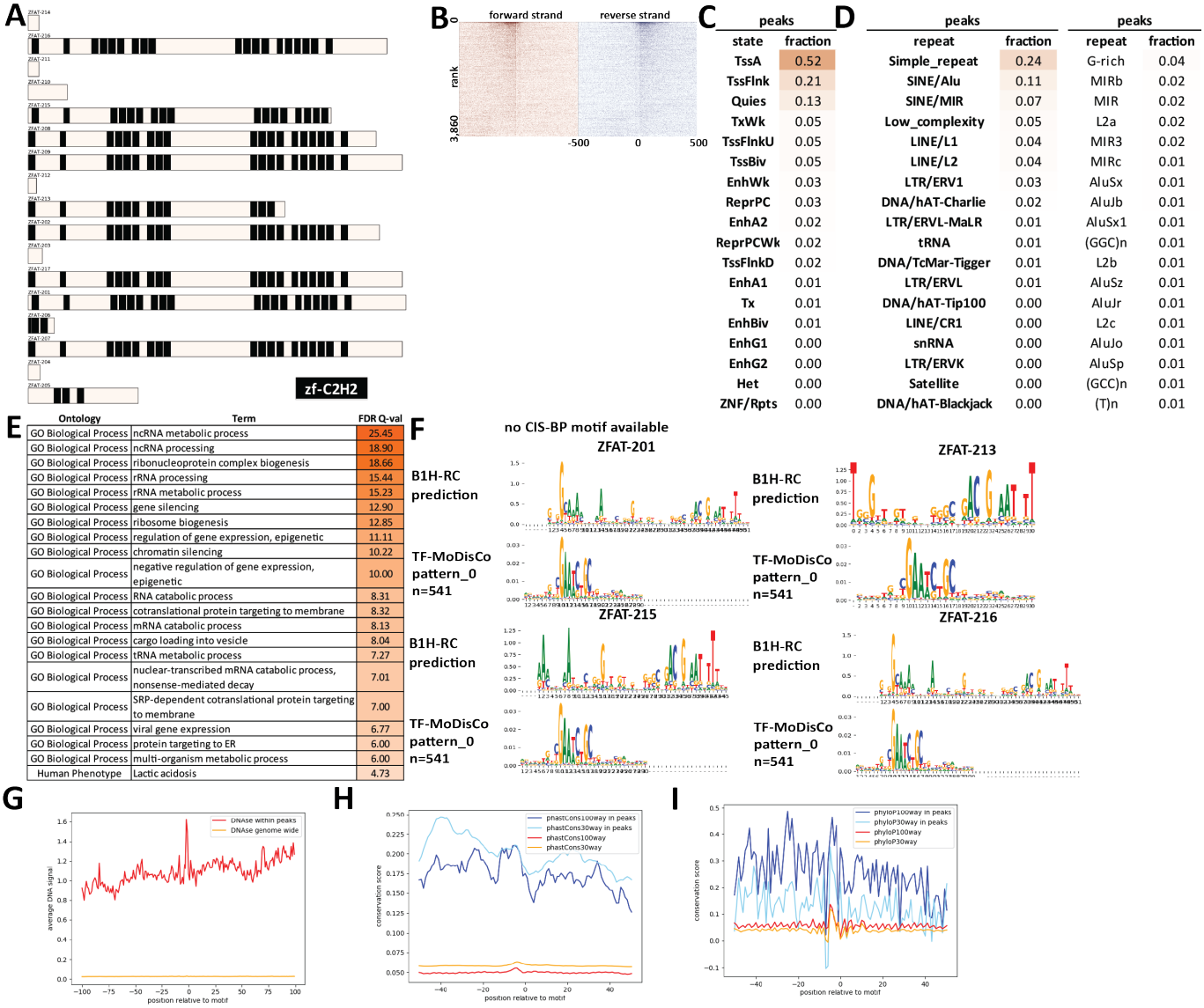

Supplementary Figure 541: Properties and genomic distribution of motifs identified for the ZFAT transcription factor in HepG2 (accession ENCSR409DYM).

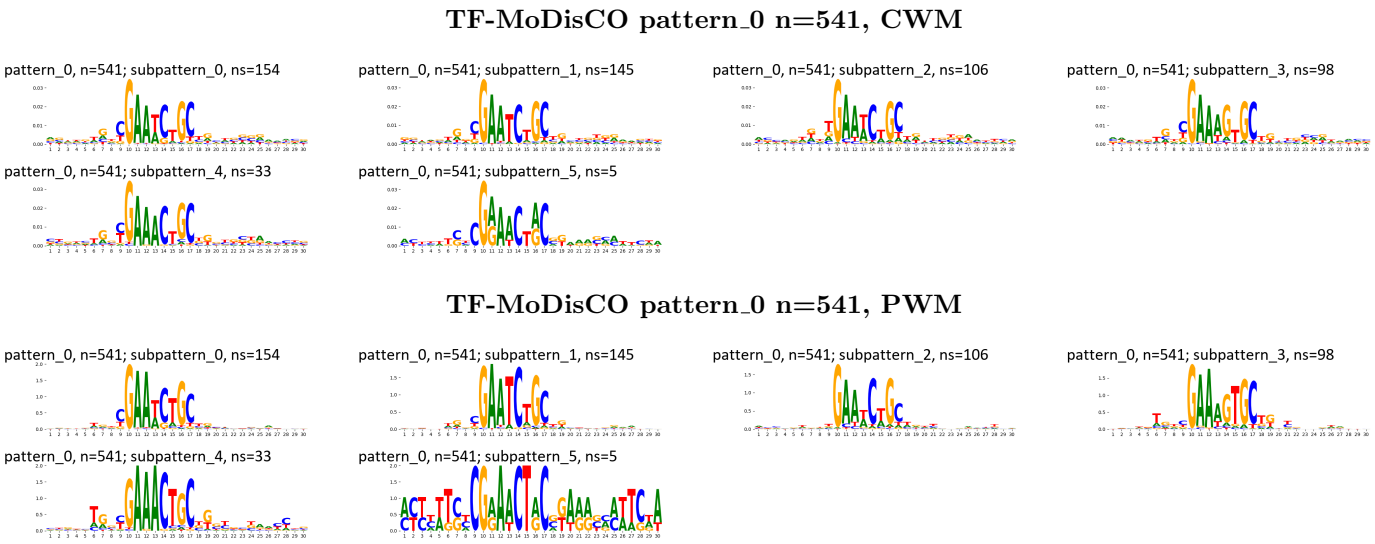

Supplementary Figure 542: TF-MoDisCO subpatterns for the ZFAT transcription factor in HepG2 (accession ENCSR409DYM).

A

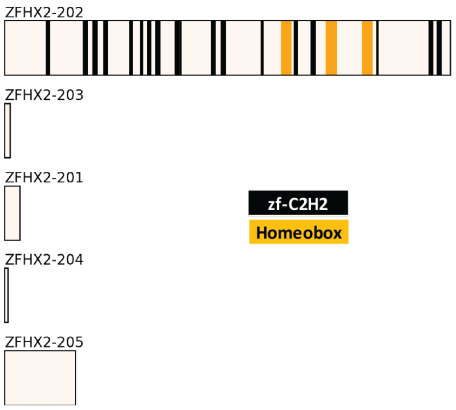

B

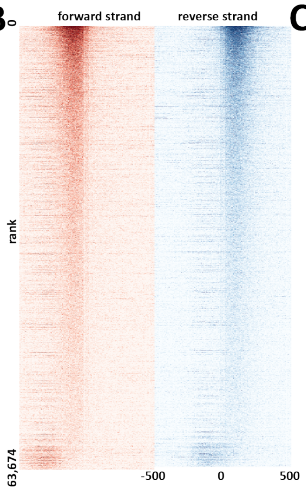

C

peaks	
state	fraction
Quies	0.19
TssA	0.14
TxWk	0.11
EnhWk	0.09
TssFlnk	0.09
TssBiv	0.04
Tx	0.04
ReprPC	0.03
ReprPCWk	0.03
EnhA1	0.03
EnhA2	0.02
TssFlnkU	0.02
TssFlnkD	0.01
EnhBiv	0.01
EnhG1	0.01
EnhG2	0.00
Het	0.00
ZNF/Rpts	0.00

D

peaks		peaks	
repeat	fraction	repeat	fraction
Simple_repeat	0.23	L2a	0.03
SINE/Alu	0.15	MIRb	0.03
LINE/L2	0.09	G-rich	0.03
SINE/MIR	0.08	L2c	0.02
LINE/L1	0.05	L2b	0.02
Low_complexity	0.04	AluJb	0.02
LTR/ERVL-MaLR	0.04	AluSx1	0.02
DNA/hAT-Charlie	0.02	MIR	0.02
LTR/ERVL	0.02	AluSx	0.02
LTR/ERV1	0.01	(GT)n	0.02
DNA/TcMar-Tigger	0.01	GA-rich	0.01
LINE/CR1	0.01	MIRc	0.01
DNA/hAT-Tip100	0.01	MIR3	0.01
DNA/hAT-Blackjack	0.00	AluSz	0.01
tRNA	0.00	(CA)n	0.01
LTR/ERVK	0.00	(AC)n	0.01
LTR/Gypsy?	0.00	(TG)n	0.01
LINE/RTE-BovB	0.00	L2	0.01

E

Ontology	Term	FDR Q-val
GO Biological Process	regulation of mitochondrial membrane permeability	59.37
GO Biological Process	gene silencing by miRNA	50.37
GO Biological Process	posttranscriptional gene silencing by RNA	43.02
GO Biological Process	posttranscriptional gene silencing	41.96

F

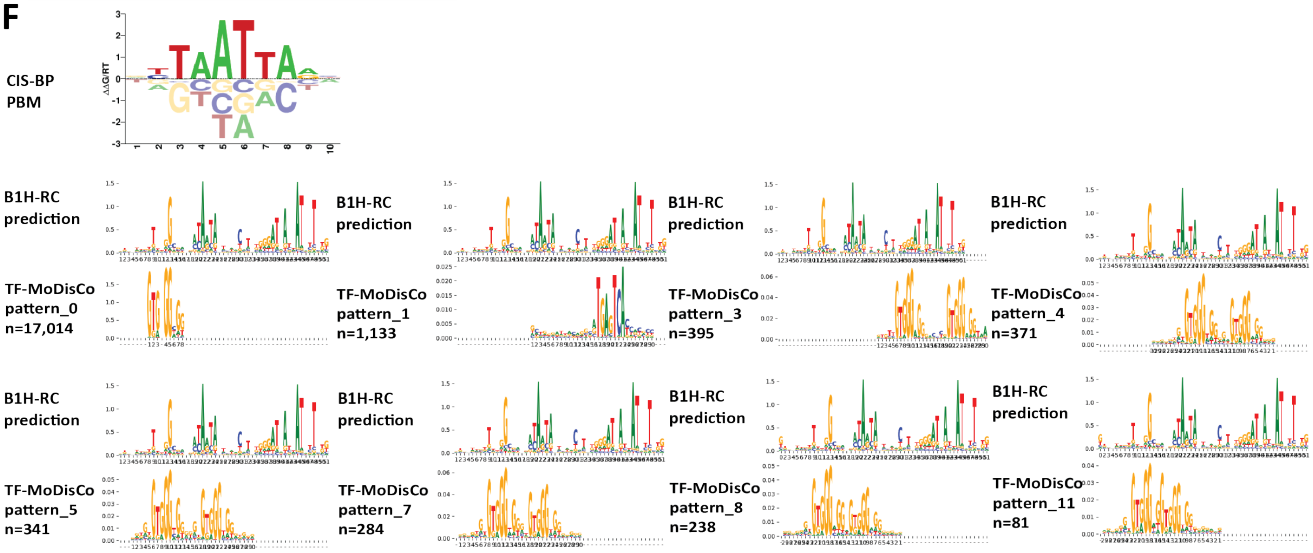

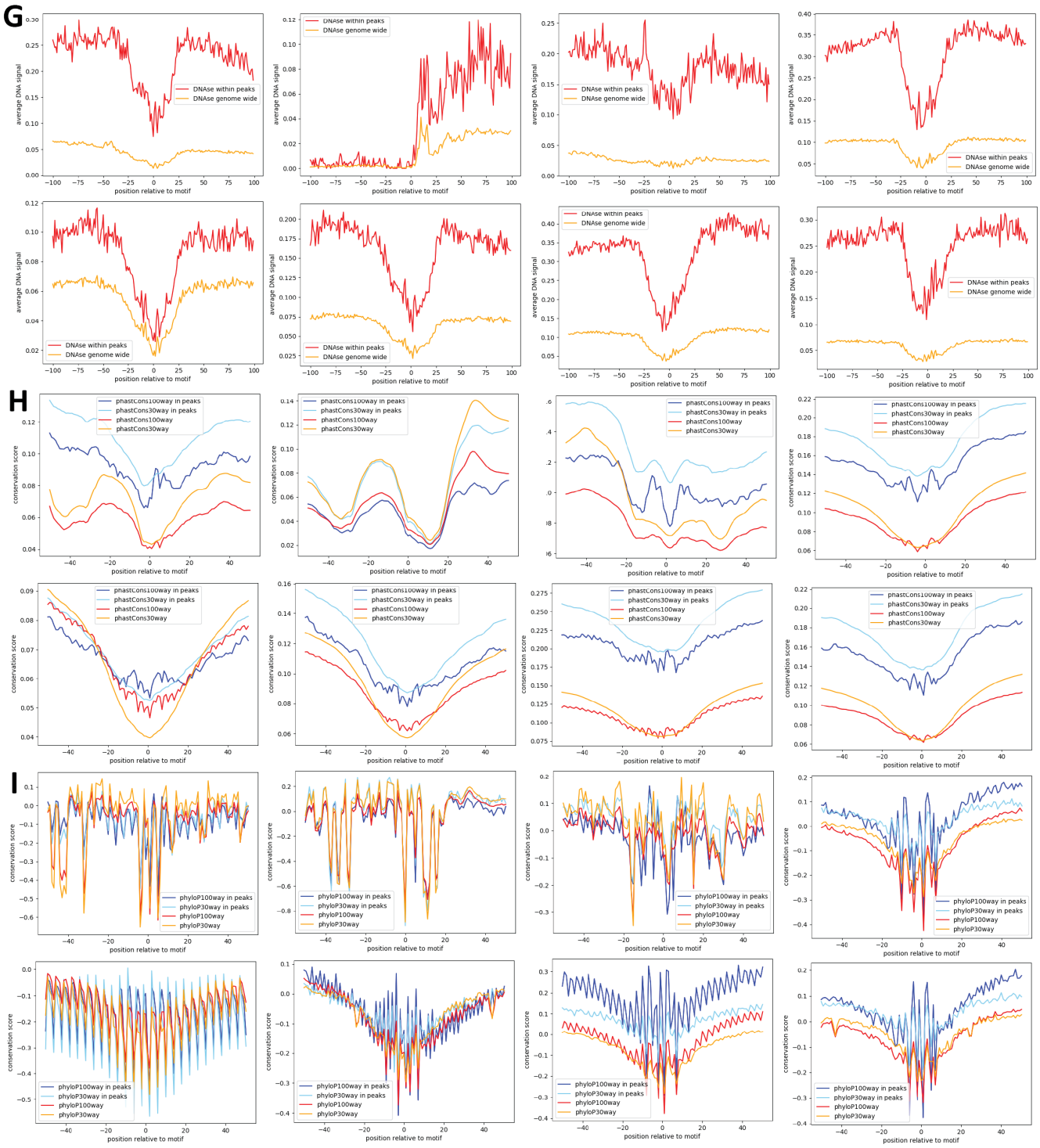

Supplementary Figure 543: Properties and genomic distribution of motifs identified for the ZFHX2 transcription factor in HEK293 (accession ENCSR632SIM).

TF-MoDisCO pattern_0 n=17014, CWM

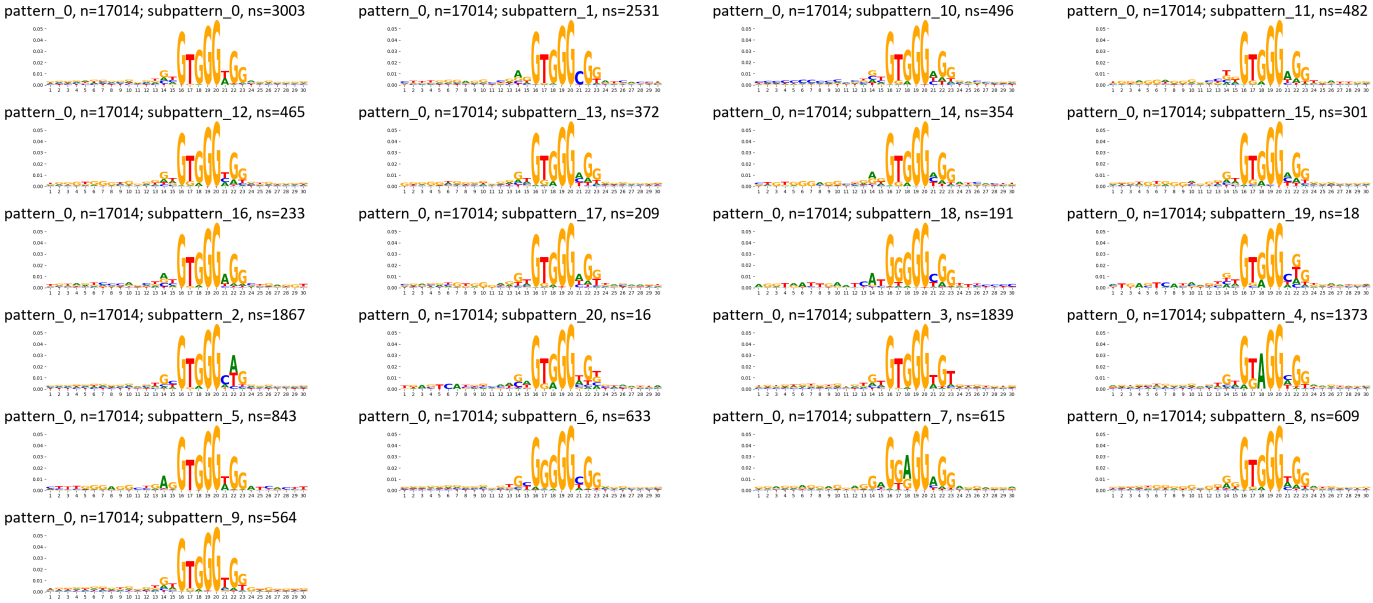

TF-MoDisCO pattern_0 n=17014, PWM

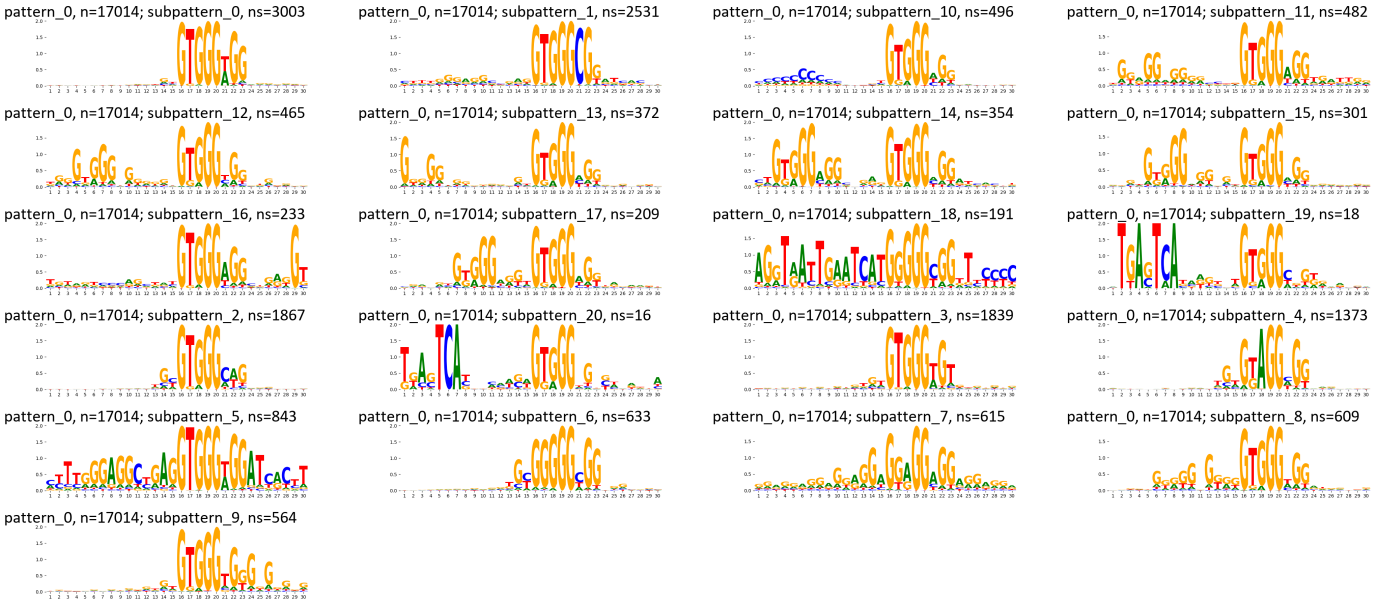

TF-MoDisCO pattern_1 n=1133, CWM

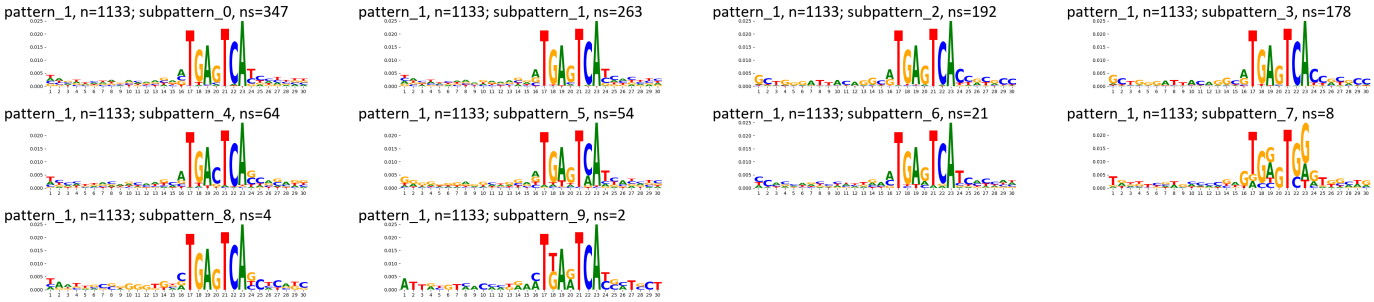

TF-MoDisCO pattern_1 n=1133, PWM

pattern_1, n=1133; subpattern_0, ns=347

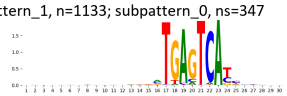

pattern_1, n=1133; subpattern_1, ns=263

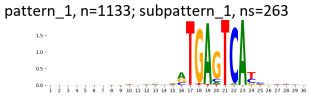

pattern_1, n=1133; subpattern_2, ns=192

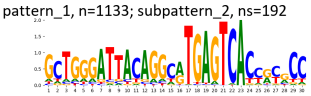

pattern_1, n=1133; subpattern_3, ns=178

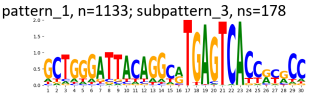

pattern_1, n=1133; subpattern_4, ns=64

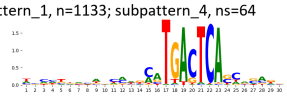

pattern_1, n=1133; subpattern_5, ns=54

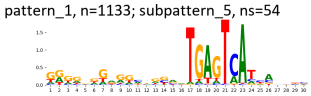

pattern_1, n=1133; subpattern_6, ns=21

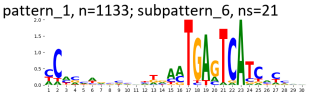

pattern_1, n=1133; subpattern_7, ns=8

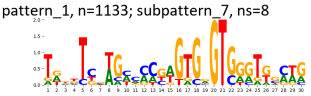

pattern_1, n=1133; subpattern_8, ns=4

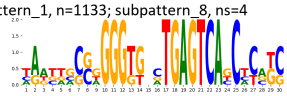

pattern_1, n=1133; subpattern_9, ns=2

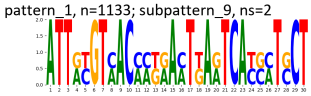

TF-MoDisCO pattern_11 n=80, CWM

pattern_11, n=80; subpattern_0, ns=23

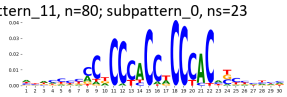

pattern_11, n=80; subpattern_1, ns=19

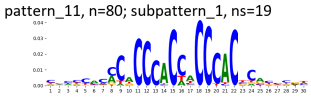

pattern_11, n=80; subpattern_2, ns=17

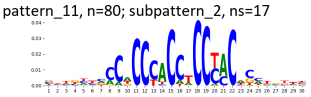

pattern_11, n=80; subpattern_3, ns=14

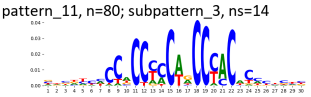

pattern_11, n=80; subpattern_4, ns=7

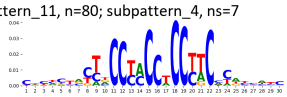

TF-MoDisCO pattern_11 n=80, PWM

pattern_11, n=80; subpattern_0, ns=23

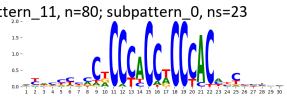

pattern_11, n=80; subpattern_1, ns=19

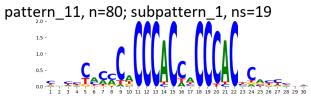

pattern_11, n=80; subpattern_2, ns=17

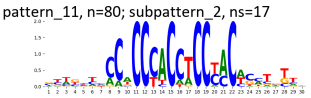

pattern_11, n=80; subpattern_3, ns=14

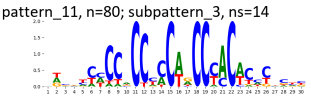

pattern_11, n=80; subpattern_4, ns=7

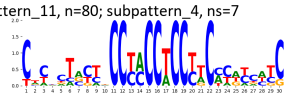

TF-MoDisCO pattern_3 n=395, CWM

pattern_3, n=395; subpattern_0, ns=113

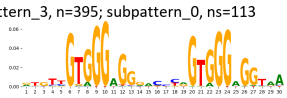

pattern_3, n=395; subpattern_1, ns=91

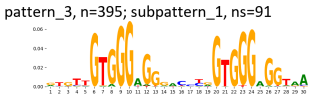

pattern_3, n=395; subpattern_2, ns=76

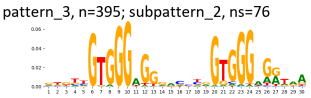

pattern_3, n=395; subpattern_3, ns=70

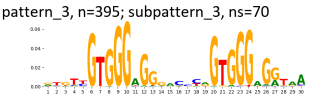

pattern_3, n=395; subpattern_4, ns=41

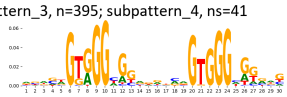

pattern_3, n=395; subpattern_5, ns=4

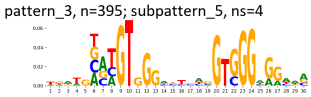

TF-MoDisCO pattern_3 n=395, PWM

pattern_3, n=395; subpattern_0, ns=113

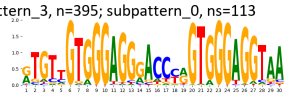

pattern_3, n=395; subpattern_1, ns=91

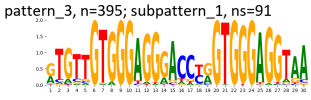

pattern_3, n=395; subpattern_2, ns=76

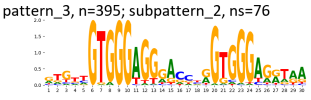

pattern_3, n=395; subpattern_3, ns=70

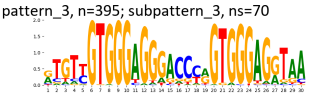

pattern_3, n=395; subpattern_4, ns=41

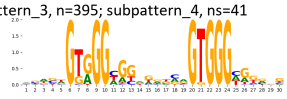

pattern_3, n=395; subpattern_5, ns=4

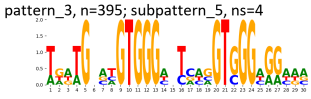

TF-MoDisCO pattern_4 n=371, CWM

pattern_4, n=371; subpattern_0, ns=124

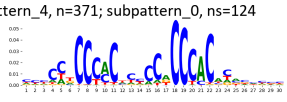

pattern_4, n=371; subpattern_1, ns=118

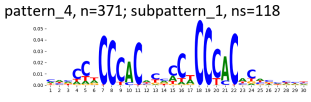

pattern_4, n=371; subpattern_2, ns=69

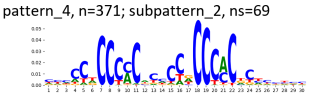

pattern_4, n=371; subpattern_3, ns=25

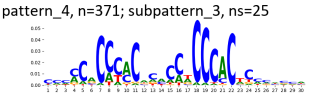

pattern_4, n=371; subpattern_4, ns=18

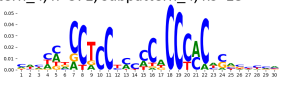

pattern_4, n=371; subpattern_5, ns=15

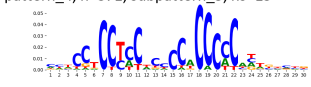

pattern_4, n=371; subpattern_6, ns=2



TF-MoDisCO pattern_4 n=371, PWM

pattern_4, n=371; subpattern_0, ns=124

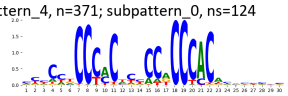

pattern_4, n=371; subpattern_1, ns=118

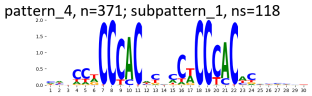

pattern_4, n=371; subpattern_2, ns=69

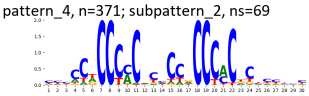

pattern_4, n=371; subpattern_3, ns=25

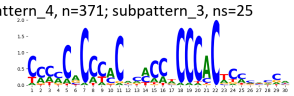

pattern_4, n=371; subpattern_4, ns=18

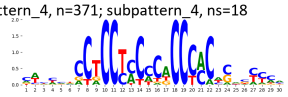

pattern_4, n=371; subpattern_5, ns=15

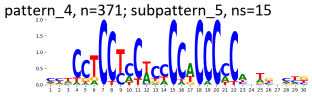

pattern_4, n=371; subpattern_6, ns=2

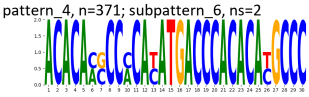

TF-MoDisCO pattern_5 n=341, CWM

pattern_5, n=341; subpattern_0, ns=106

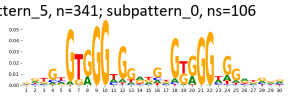

pattern_5, n=341; subpattern_1, ns=88

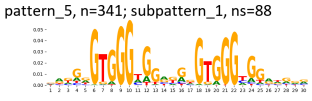

pattern_5, n=341; subpattern_2, ns=68

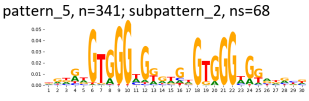

pattern_5, n=341; subpattern_3, ns=38

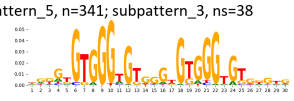

pattern_5, n=341; subpattern_4, ns=26

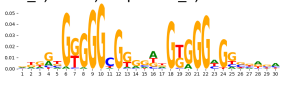

pattern_5, n=341; subpattern_5, ns=9

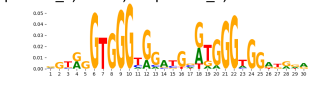

pattern_5, n=341; subpattern_6, ns=6

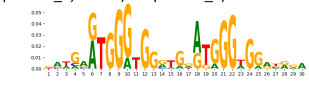

TF-MoDisCO pattern_5 n=341, PWM

pattern_5, n=341; subpattern_0, ns=106

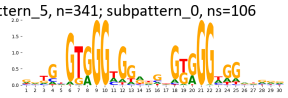

pattern_5, n=341; subpattern_1, ns=88

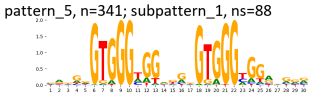

pattern_5, n=341; subpattern_2, ns=68

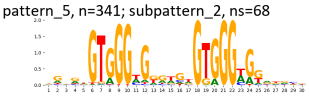

pattern_5, n=341; subpattern_3, ns=38

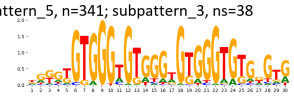

pattern_5, n=341; subpattern_4, ns=26

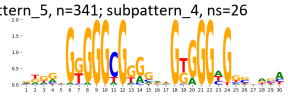

pattern_5, n=341; subpattern_5, ns=9

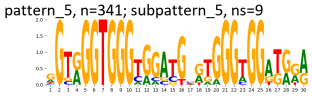

pattern_5, n=341; subpattern_6, ns=6

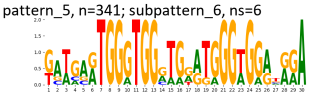

TF-MoDisCO pattern_7 n=284, CWM

pattern_7, n=284; subpattern_0, ns=90

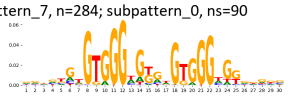

pattern_7, n=284; subpattern_1, ns=81

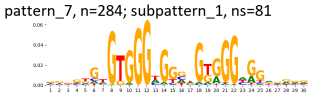

pattern_7, n=284; subpattern_2, ns=40

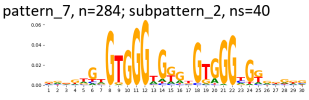

pattern_7, n=284; subpattern_3, ns=38

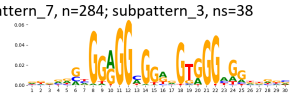

pattern_7, n=284; subpattern_4, ns=31

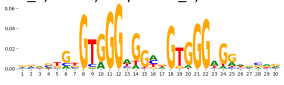

pattern_7, n=284; subpattern_5, ns=2



pattern_7, n=284; subpattern_6, ns=2

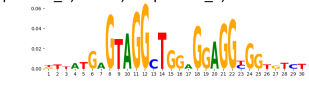

TF-MoDisCO pattern_7 n=284, PWM

pattern_7, n=284; subpattern_0, ns=90

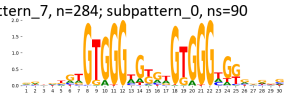

pattern_7, n=284; subpattern_1, ns=81

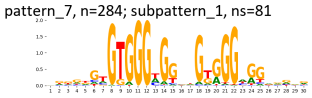

pattern_7, n=284; subpattern_2, ns=40

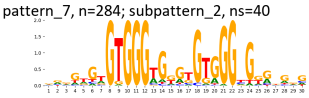

pattern_7, n=284; subpattern_3, ns=38

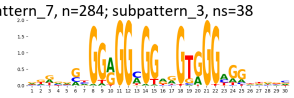

pattern_7, n=284; subpattern_4, ns=31

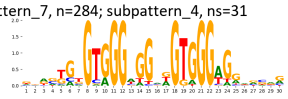

pattern_7, n=284; subpattern_5, ns=2

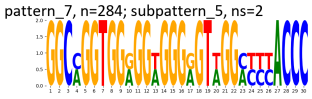

pattern_7, n=284; subpattern_6, ns=2

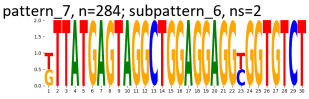

TF-MoDisCO pattern_8 n=238, CWM

pattern_8, n=238; subpattern_0, ns=72

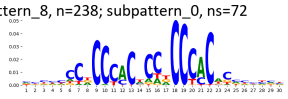

pattern_8, n=238; subpattern_1, ns=67

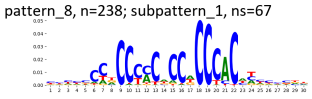

pattern_8, n=238; subpattern_2, ns=38

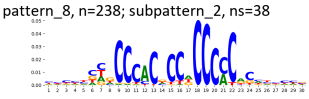

pattern_8, n=238; subpattern_3, ns=25

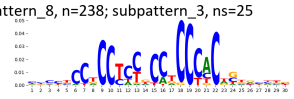

pattern_8, n=238; subpattern_4, ns=15

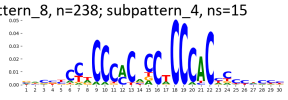

pattern_8, n=238; subpattern_5, ns=8

pattern_8, n=238; subpattern_6, ns=8

pattern_8, n=238; subpattern_7, ns=5

TF-MoDisCO pattern_8 n=238, PWM

pattern_8, n=238; subpattern_0, ns=72

pattern_8, n=238; subpattern_1, ns=67

pattern_8, n=238; subpattern_2, ns=38

pattern_8, n=238; subpattern_3, ns=25

pattern_8, n=238; subpattern_4, ns=15

pattern_8, n=238; subpattern_5, ns=8

pattern_8, n=238; subpattern_6, ns=8

pattern_8, n=238; subpattern_7, ns=5

Supplementary Figure 544: TF-MoDisCO subpatterns for the ZFHX2 transcription factor in HEK293 (accession ENCSR632SIM).

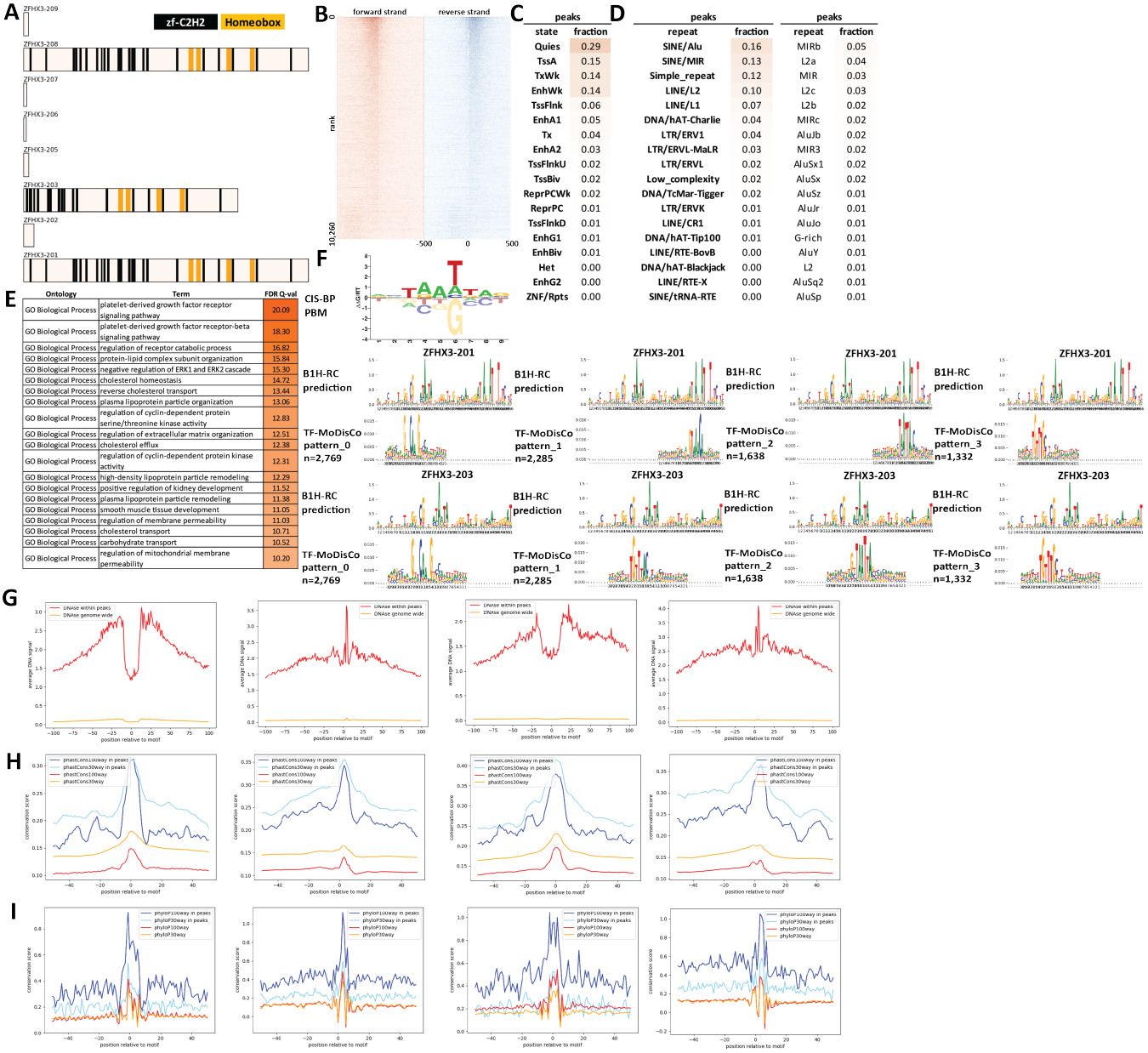

Supplementary Figure 545: Properties and genomic distribution of motifs identified for the ZFHX3 transcription factor in HepG2 (accession ENCSR879RGN).

TF-MoDisCO pattern_0 n=2769, CWM

pattern_0, n=2769; subpattern_0, ns=619

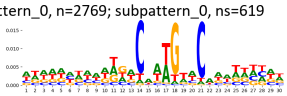

pattern_0, n=2769; subpattern_1, ns=616

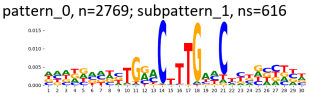

pattern_0, n=2769; subpattern_2, ns=475

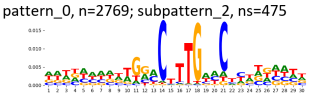

pattern_0, n=2769; subpattern_3, ns=423

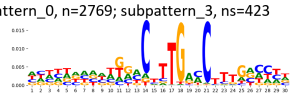

pattern_0, n=2769; subpattern_4, ns=377

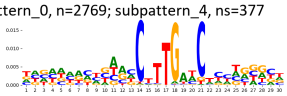

pattern_0, n=2769; subpattern_5, ns=99

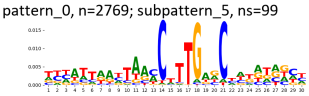

pattern_0, n=2769; subpattern_6, ns=75

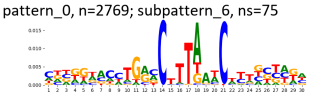

pattern_0, n=2769; subpattern_7, ns=57

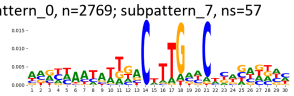

pattern_0, n=2769; subpattern_8, ns=24

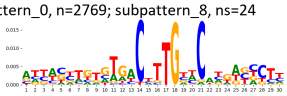

pattern_0, n=2769; subpattern_9, ns=4

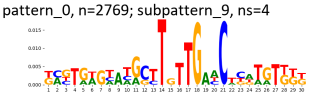

TF-MoDisCO pattern_0 n=2769, PWM

pattern_0, n=2769; subpattern_0, ns=619

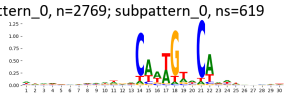

pattern_0, n=2769; subpattern_1, ns=616

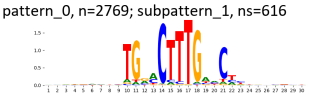

pattern_0, n=2769; subpattern_2, ns=475

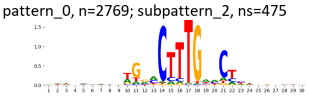

pattern_0, n=2769; subpattern_3, ns=423

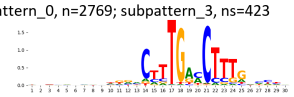

pattern_0, n=2769; subpattern_4, ns=377

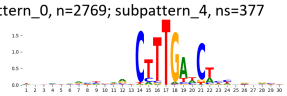

pattern_0, n=2769; subpattern_5, ns=99

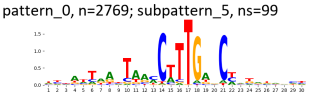

pattern_0, n=2769; subpattern_6, ns=75

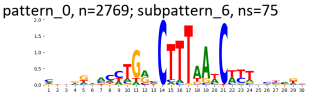

pattern_0, n=2769; subpattern_7, ns=57

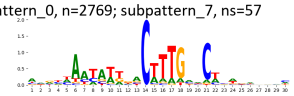

pattern_0, n=2769; subpattern_8, ns=24

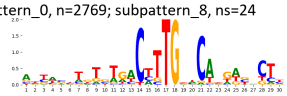

pattern_0, n=2769; subpattern_9, ns=4

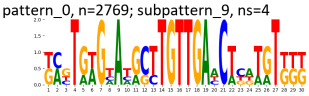

TF-MoDisCO pattern_1 n=2285, CWM

pattern_1, n=2285; subpattern_0, ns=571

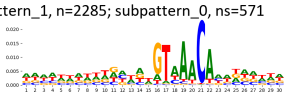

pattern_1, n=2285; subpattern_1, ns=450

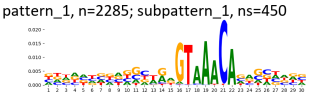

pattern_1, n=2285; subpattern_2, ns=363

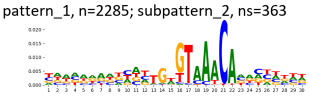

pattern_1, n=2285; subpattern_3, ns=326

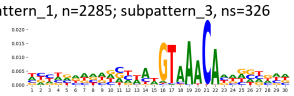

pattern_1, n=2285; subpattern_4, ns=279

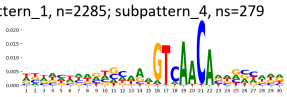

pattern_1, n=2285; subpattern_5, ns=276

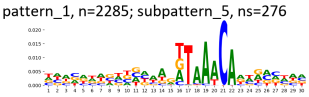

pattern_1, n=2285; subpattern_6, ns=7

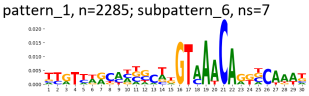

pattern_1, n=2285; subpattern_7, ns=7

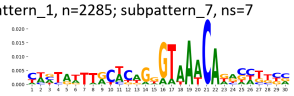

pattern_1, n=2285; subpattern_8, ns=4

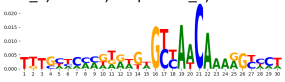

pattern_1, n=2285; subpattern_9, ns=2

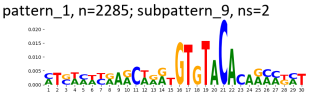

TF-MoDisCO pattern_1 n=2285, PWM

pattern_1, n=2285; subpattern_0, ns=571

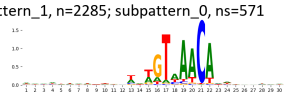

pattern_1, n=2285; subpattern_1, ns=450

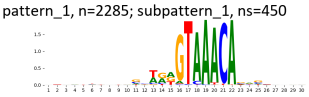

pattern_1, n=2285; subpattern_2, ns=363

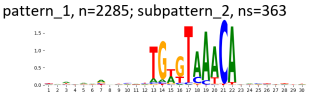

pattern_1, n=2285; subpattern_3, ns=326

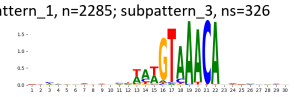

pattern_1, n=2285; subpattern_4, ns=279

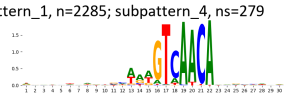

pattern_1, n=2285; subpattern_5, ns=276

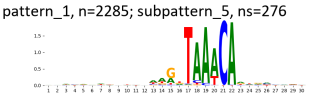

pattern_1, n=2285; subpattern_6, ns=7

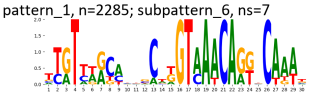

pattern_1, n=2285; subpattern_7, ns=7

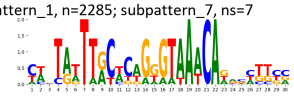

pattern_1, n=2285; subpattern_8, ns=4

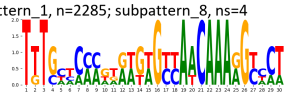

pattern_1, n=2285; subpattern_9, ns=2

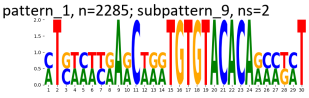

TF-MoDisCO pattern_2 n=1638, CWM

pattern_2, n=1638; subpattern_0, ns=437

pattern_2, n=1638; subpattern_1, ns=371

pattern_2, n=1638; subpattern_2, ns=266

pattern_2, n=1638; subpattern_3, ns=161

pattern_2, n=1638; subpattern_4, ns=154

pattern_2, n=1638; subpattern_5, ns=129

pattern_2, n=1638; subpattern_6, ns=78

pattern_2, n=1638; subpattern_7, ns=42

TF-MoDisCO pattern_2 n=1638, PWM

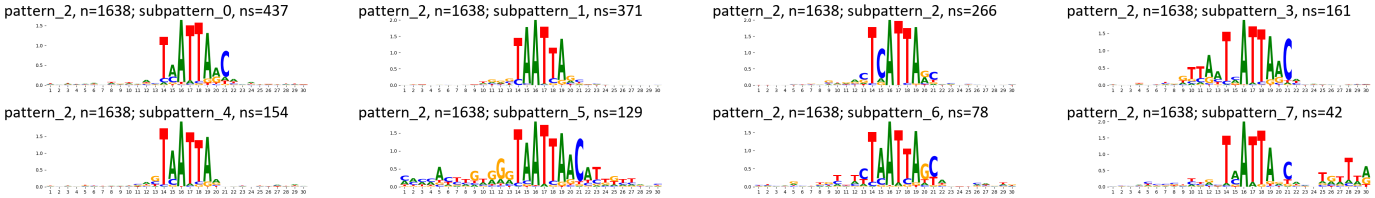

TF-MoDisCO pattern_3 n=1332, CWM

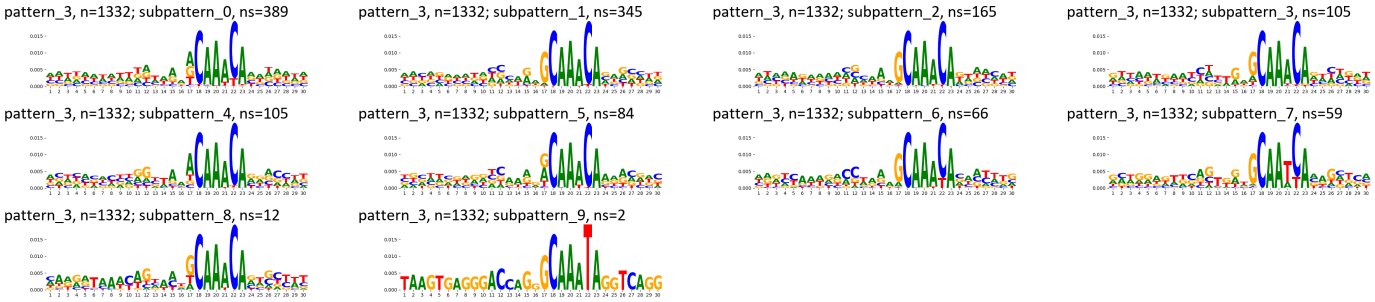

TF-MoDisCO pattern_3 n=1332, PWM

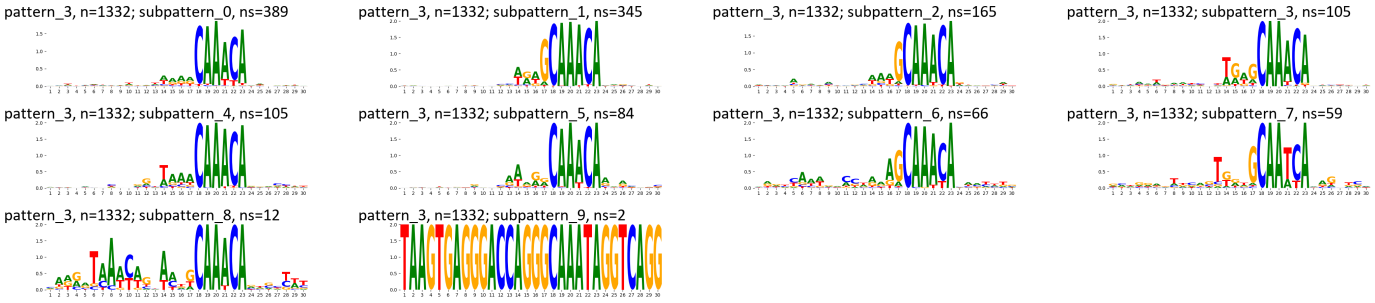

Supplementary Figure 546: TF-MoDisCO subpatterns for the ZFHX3 transcription factor in HepG2 (accession ENCSR879RGN).

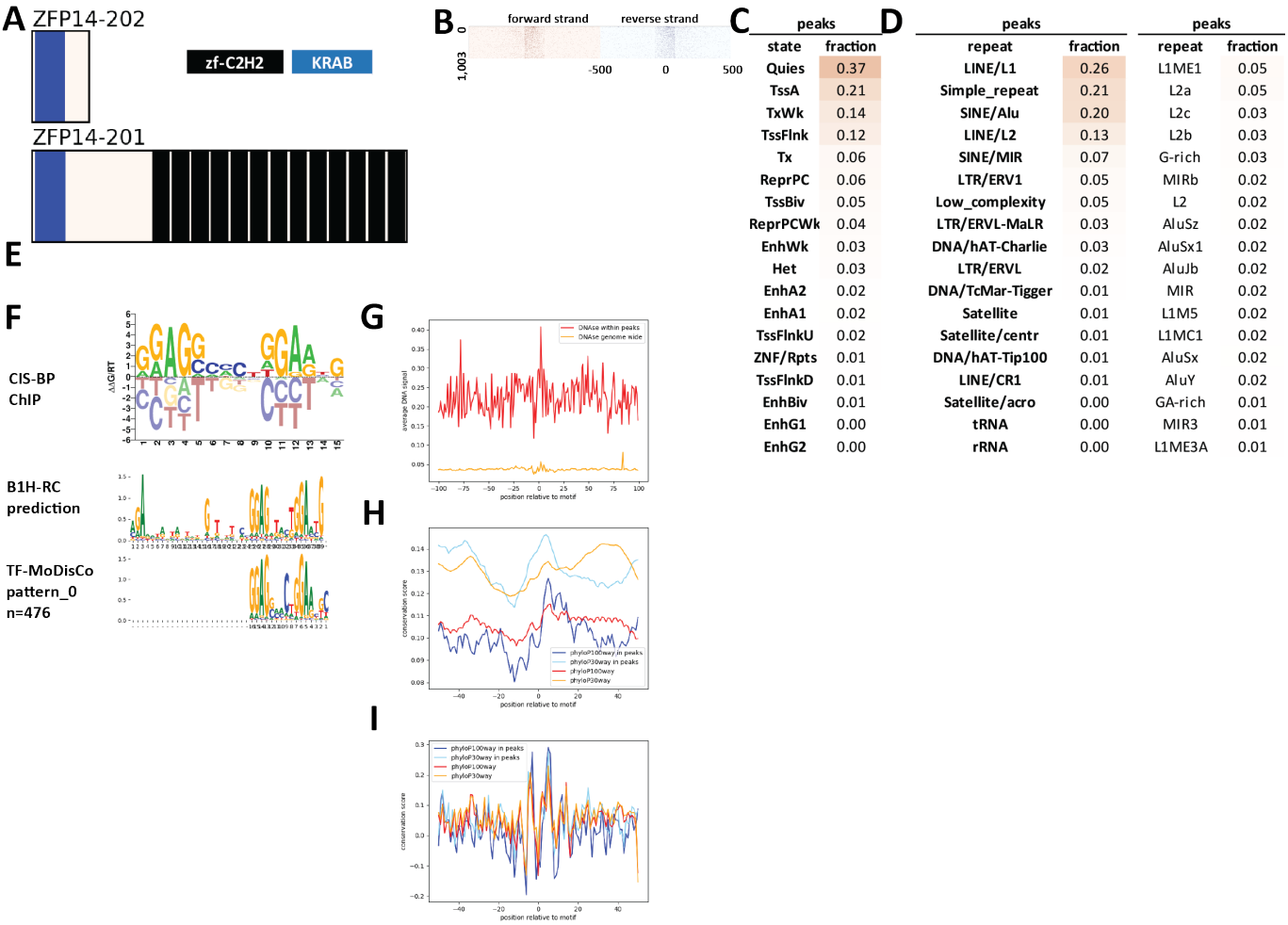

peaks	
state	fraction
Quies	0.37
TssA	0.21
TxWk	0.14
TssFlnk	0.12
Tx	0.06
ReprPC	0.06
TssBiv	0.05
ReprPCWk	0.04
EnhWk	0.03
Het	0.03
EnhA2	0.02
EnhA1	0.02
TssFlnkU	0.02
ZNF/Rpts	0.01
TssFlnkD	0.01
EnhBiv	0.01
EnhG1	0.00
EnhG2	0.00

peaks	
repeat	fraction
LINE/L1	0.26
Simple_repeat	0.21
SINE/Alu	0.20
LINE/L2	0.13
SINE/MIR	0.07
LTR/ERV1	0.05
Low_complexity	0.05
LTR/ERVL-MaLR	0.03
DNA/hAT-Charlie	0.03
LTR/ERVL	0.02
DNA/TcMar-Tigger	0.01
Satellite	0.01
Satellite/centr	0.01
DNA/hAT-Tip100	0.01
LINE/CR1	0.01
Satellite/acro	0.00
tRNA	0.00
rRNA	0.00

peaks	
repeat	fraction
L1ME1	0.05
L2a	0.05
L2c	0.03
L2b	0.03
G-rich	0.03
MIRb	0.02
L2	0.02
AluSz	0.02
AluSx1	0.02
AluJb	0.02
MIR	0.02
L1M5	0.02
L1MC1	0.02
AluSx	0.02
AluY	0.02
GA-rich	0.01
MIR3	0.01
L1ME3A	0.01

Supplementary Figure 547: Properties and genomic distribution of motifs identified for the ZFP14 transcription factor in HEK293 (accession ChipExo models).

TF-MoDisCO pattern_0 n=476, CWM

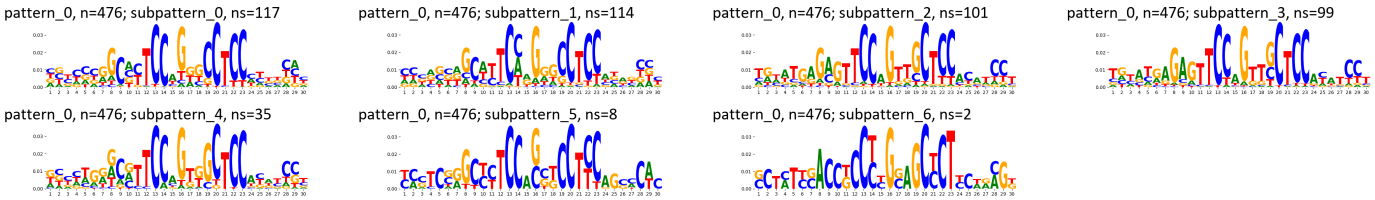

TF-MoDisCO pattern_0 n=476, PWM

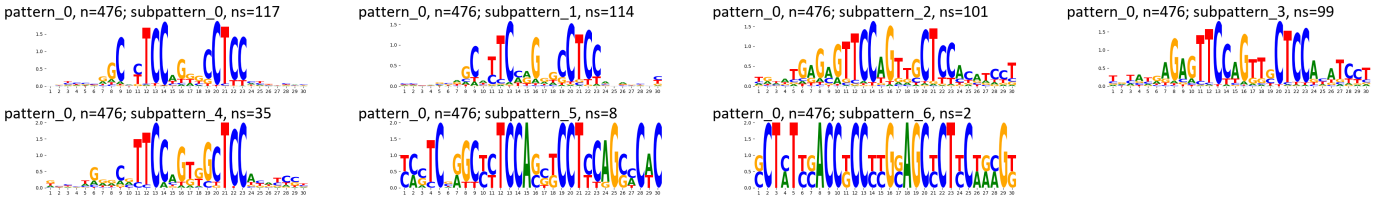

Supplementary Figure 548: TF-MoDisCO subpatterns for the ZFP14 transcription factor in HEK293 (accession ChipExo models).

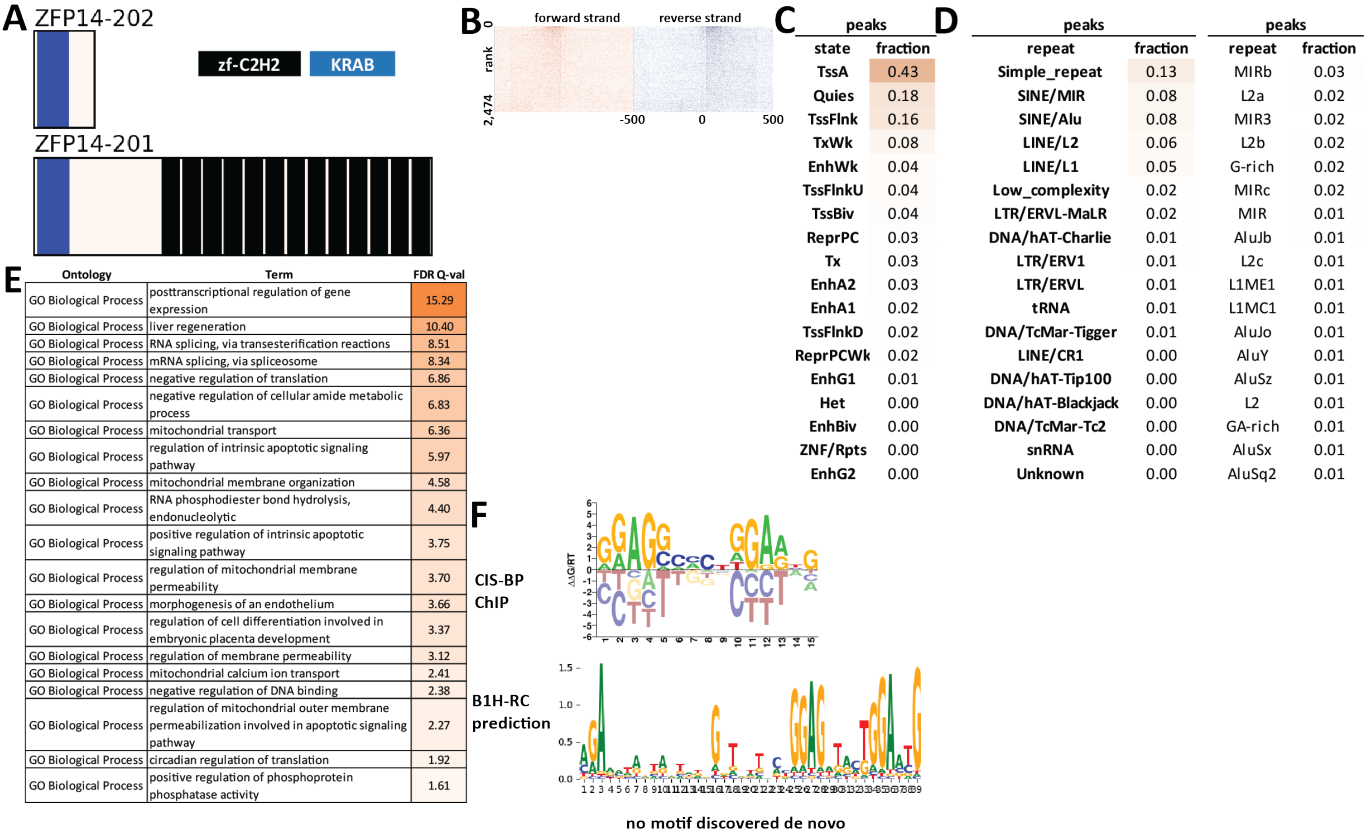

Supplementary Figure 549: Properties and genomic distribution of motifs identified for the ZFP14 transcription factor in HepG2 (accession ENCSR620DBD).

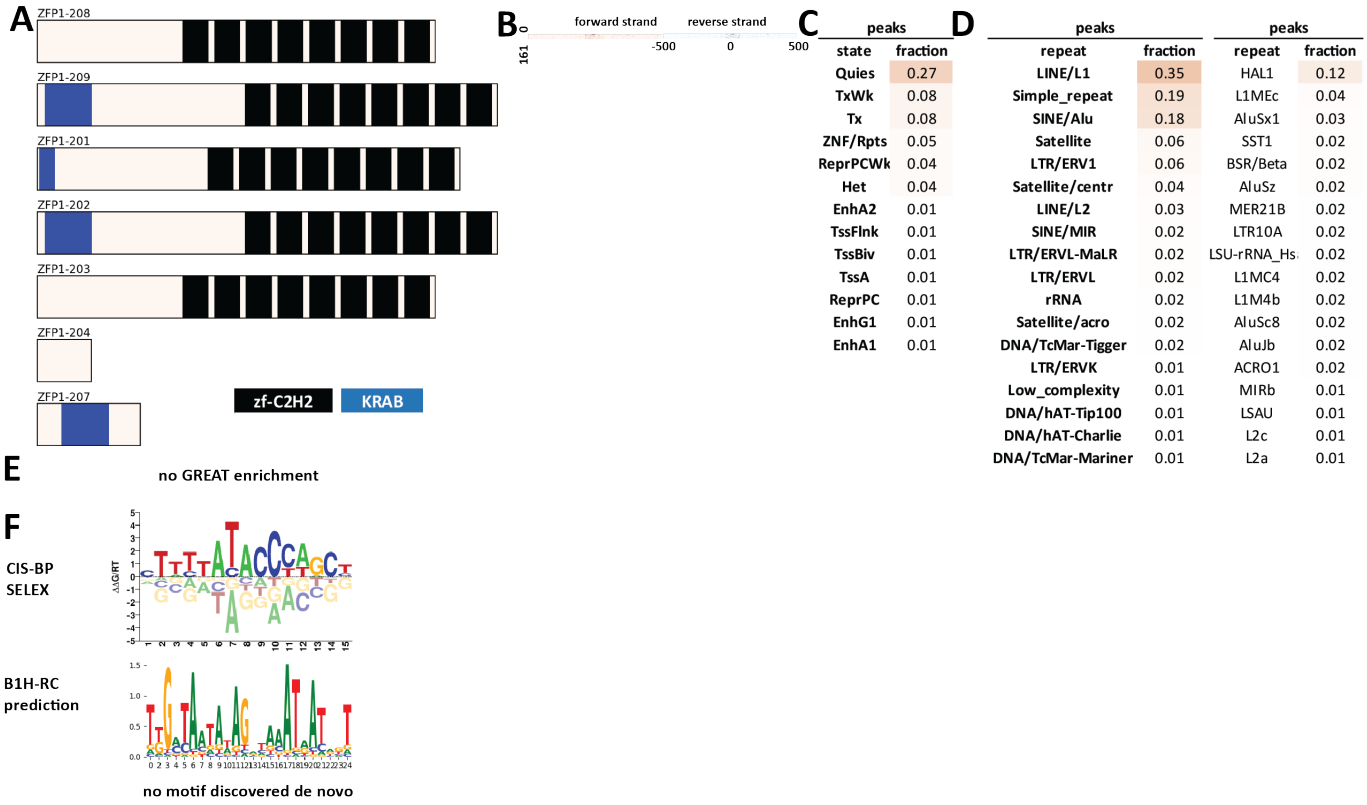

Supplementary Figure 550: Properties and genomic distribution of motifs identified for the ZFP1 transcription factor in HEK293 (accession ChipExo models).

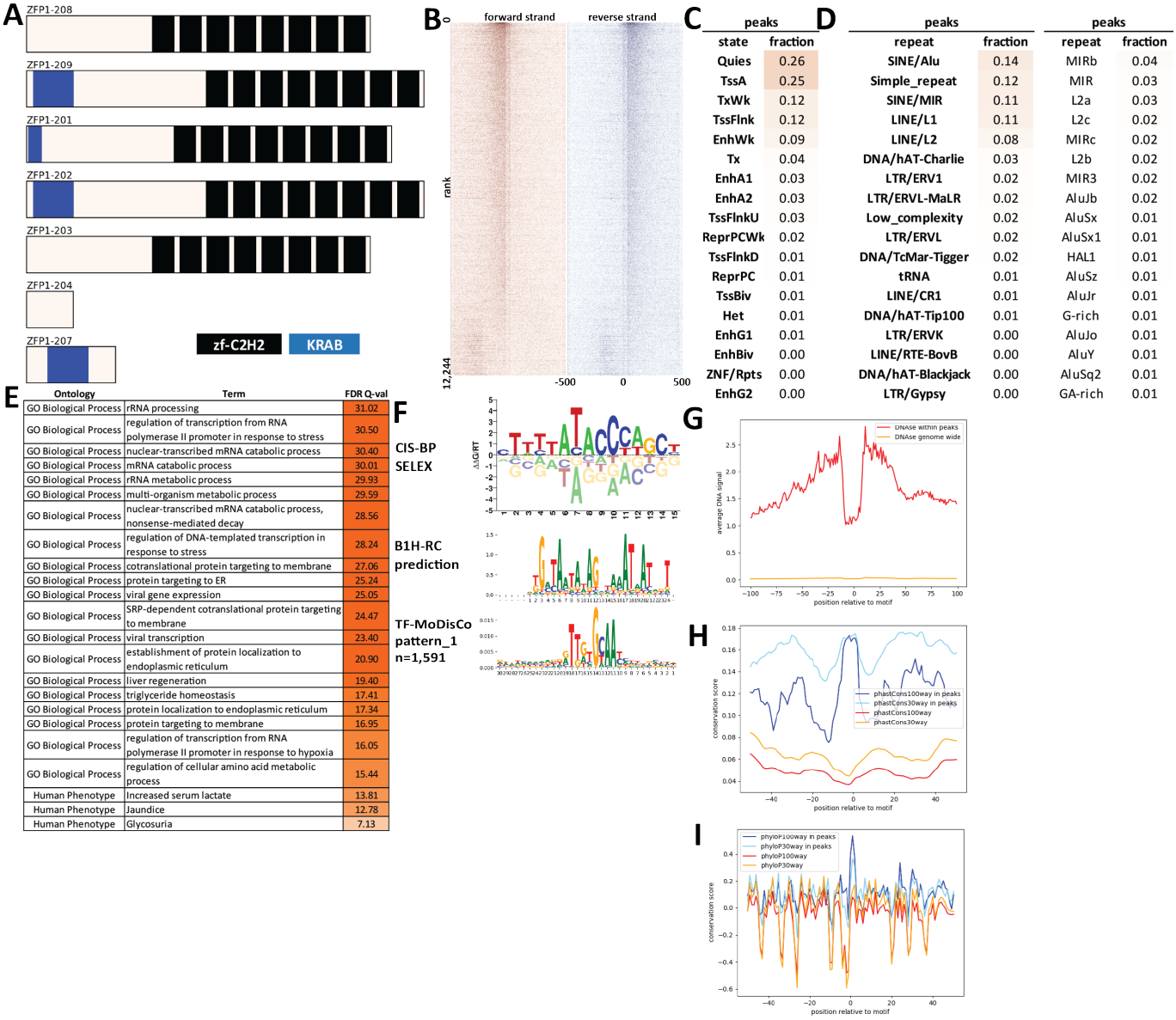

Supplementary Figure 551: Properties and genomic distribution of motifs identified for the ZFP1 transcription factor in HepG2 (accession ENCSR586DEH).

TF-MoDisCO pattern_1 n=1591, CWM

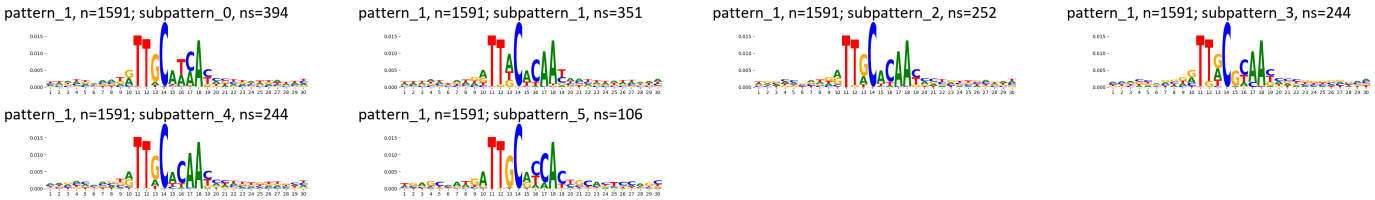

TF-MoDisCO pattern_1 n=1591, PWM

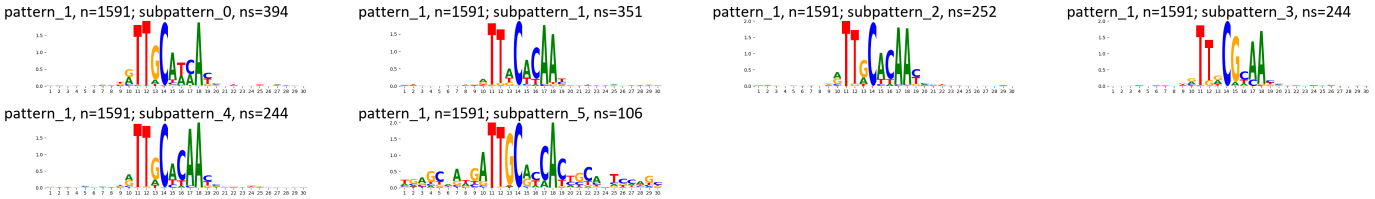

Supplementary Figure 552: TF-MoDisCO subpatterns for the ZFP1 transcription factor in HepG2 (accession ENCSR586DEH).

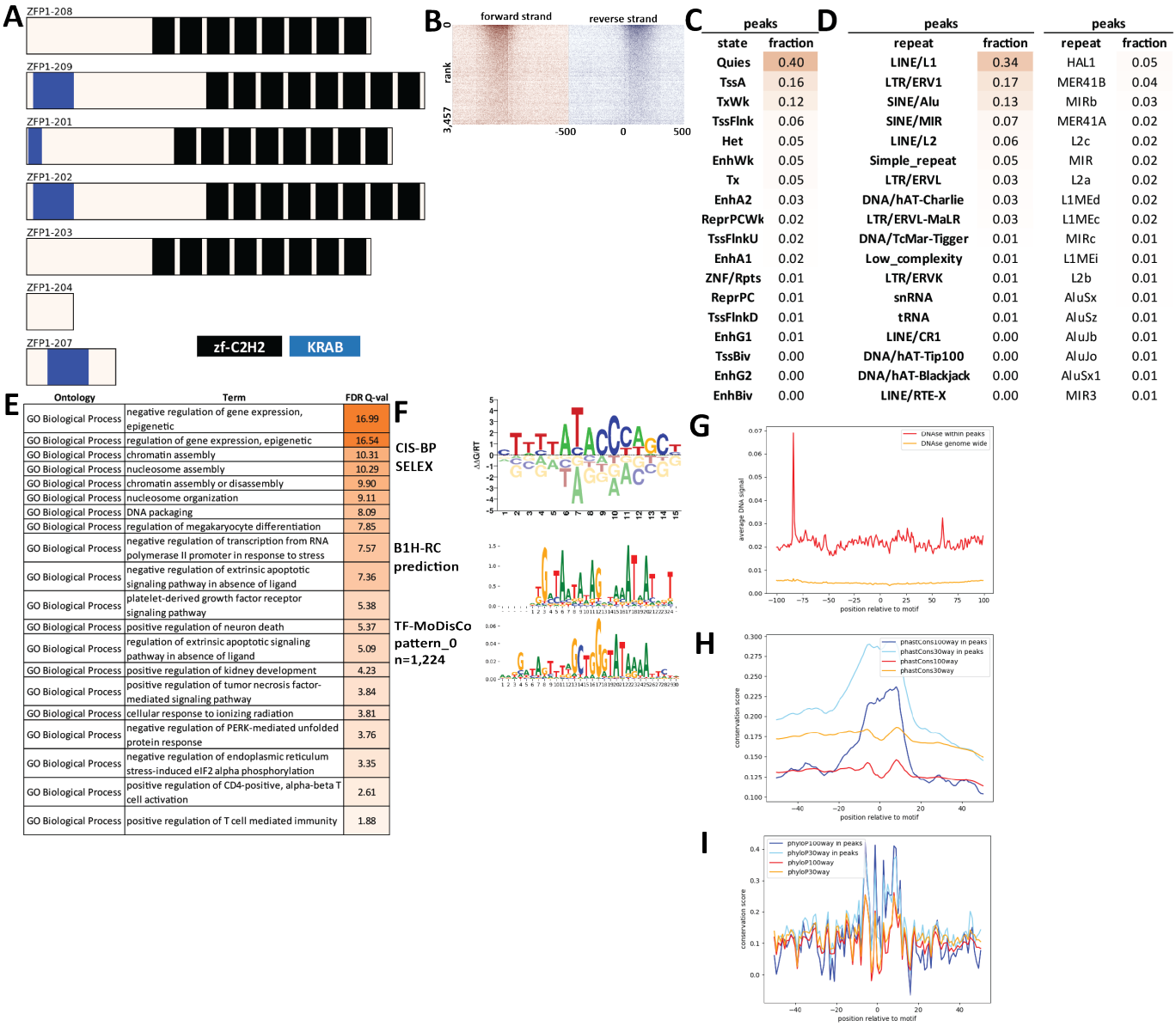

C

peaks	
state	fraction
Quies	0.40
TssA	0.16
TxWk	0.12
TssFlnk	0.06
Het	0.05
EnhWk	0.05
Tx	0.05
EnhA2	0.03
ReprPCWk	0.02
TssFlnkU	0.02
EnhA1	0.02
ZNF/Rpts	0.01
ReprPC	0.01
TssFlnkD	0.01
EnhG1	0.01
TssBiv	0.00
EnhG2	0.00
EnhBiv	0.00

D

peaks		peaks	
repeat	fraction	repeat	fraction
LINE/L1	0.34	HAL1	0.05
LTR/ERV1	0.17	MER41B	0.04
SINE/Alu	0.13	MIRb	0.03
SINE/MIR	0.07	MER41A	0.02
LINE/L2	0.06	L2c	0.02
Simple_repeat	0.05	MIR	0.02
LTR/ERVL	0.03	L2a	0.02
DNA/hAT-Charlie	0.03	L1MEd	0.02
LTR/ERVL-MaLR	0.03	L1MEc	0.02
DNA/TcMar-Tigger	0.01	MIRc	0.01
Low_complexity	0.01	L1MEi	0.01
LTR/ERVK	0.01	L2b	0.01
snRNA	0.01	AluSx	0.01
tRNA	0.01	AluSz	0.01
LINE/CR1	0.00	AluJb	0.01
DNA/hAT-Tip100	0.00	AluJo	0.01
DNA/hAT-Blackjack	0.00	AluSx1	0.01
LINE/RTE-X	0.00	MIR3	0.01

E

Ontology	Term	FDR Q-val
GO Biological Process	negative regulation of gene expression, epigenetic	16.99
GO Biological Process	regulation of gene expression, epigenetic	16.54
GO Biological Process	chromatin assembly	10.31
GO Biological Process	nucleosome assembly	10.29
GO Biological Process	chromatin assembly or disassembly	9.90
GO Biological Process	nucleosome organization	9.11
GO Biological Process	DNA packaging	8.09
GO Biological Process	regulation of megakaryocyte differentiation	7.85
GO Biological Process	negative regulation of transcription from RNA polymerase II promoter in response to stress	7.57
GO Biological Process	negative regulation of extrinsic apoptotic signaling pathway in absence of ligand	7.36
GO Biological Process	platelet-derived growth factor receptor signaling pathway	5.38
GO Biological Process	positive regulation of neuron death	5.37
GO Biological Process	regulation of extrinsic apoptotic signaling pathway in absence of ligand	5.09
GO Biological Process	positive regulation of kidney development	4.23
GO Biological Process	positive regulation of tumor necrosis factor-mediated signaling pathway	3.84
GO Biological Process	cellular response to ionizing radiation	3.81
GO Biological Process	negative regulation of PERK-mediated unfolded protein response	3.76
GO Biological Process	negative regulation of endoplasmic reticulum stress-induced eIF2 alpha phosphorylation	3.35
GO Biological Process	positive regulation of CD4-positive, alpha-beta T cell activation	2.61
GO Biological Process	positive regulation of T cell mediated immunity	1.88

Supplementary Figure 553: Properties and genomic distribution of motifs identified for the ZFP1 transcription factor in K562 (accession ENCSR617POJ).

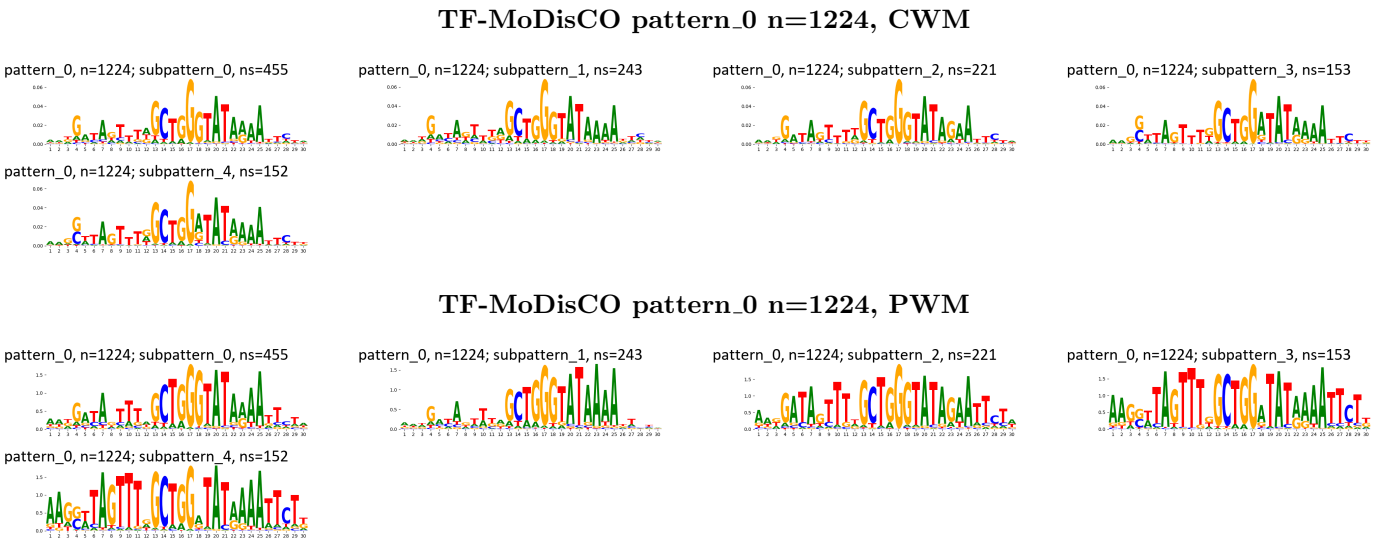

Supplementary Figure 554: TF-MoDisCO subpatterns for the ZFP1 transcription factor in K562 (accession ENCSR617POJ).

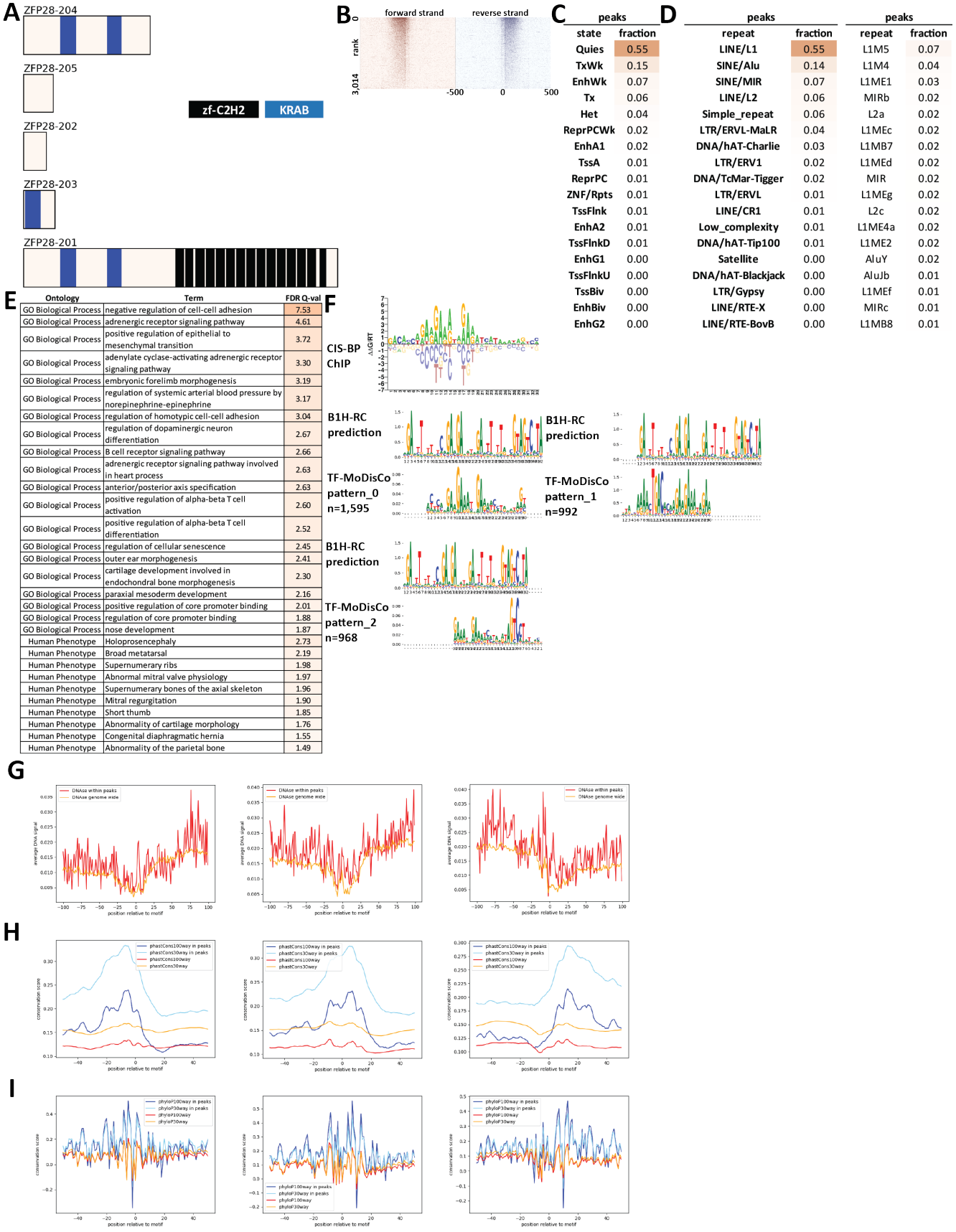

Supplementary Figure 555: Properties and genomic distribution of motifs identified for the ZFP28 transcription factor in HEK293 (accession Hughes GR models).

TF-MoDisCO pattern_0 n=1595, CWM

pattern_0, n=1595; subpattern_0, ns=408

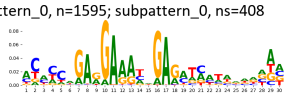

pattern_0, n=1595; subpattern_1, ns=336

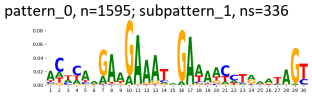

pattern_0, n=1595; subpattern_2, ns=218

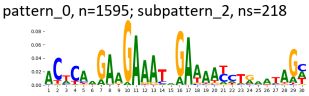

pattern_0, n=1595; subpattern_3, ns=187

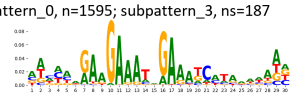

pattern_0, n=1595; subpattern_4, ns=159

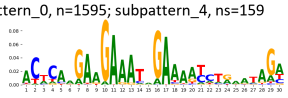

pattern_0, n=1595; subpattern_5, ns=146

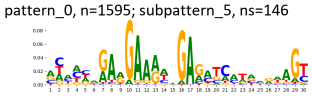

pattern_0, n=1595; subpattern_6, ns=141

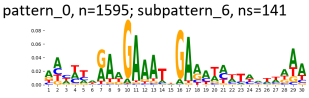

TF-MoDisCO pattern_0 n=1595, PWM

pattern_0, n=1595; subpattern_0, ns=408

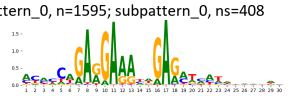

pattern_0, n=1595; subpattern_1, ns=336

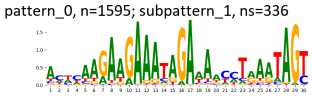

pattern_0, n=1595; subpattern_2, ns=218

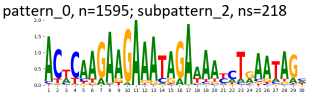

pattern_0, n=1595; subpattern_3, ns=187

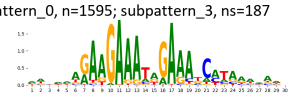

pattern_0, n=1595; subpattern_4, ns=159

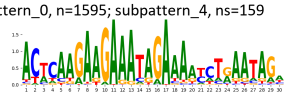

pattern_0, n=1595; subpattern_5, ns=146

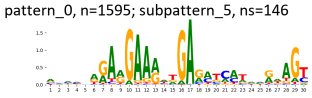

pattern_0, n=1595; subpattern_6, ns=141

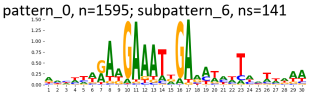

TF-MoDisCO pattern_1 n=992, CWM

pattern_1, n=992; subpattern_0, ns=286

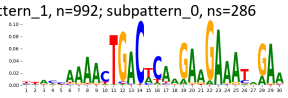

pattern_1, n=992; subpattern_1, ns=274

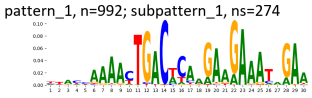

pattern_1, n=992; subpattern_2, ns=246

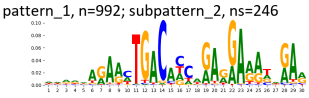

pattern_1, n=992; subpattern_3, ns=179

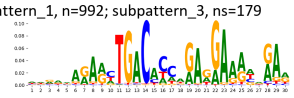

pattern_1, n=992; subpattern_4, ns=5

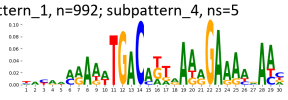

pattern_1, n=992; subpattern_5, ns=2

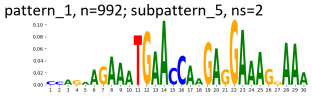

TF-MoDisCO pattern_1 n=992, PWM

pattern_1, n=992; subpattern_0, ns=286

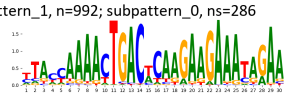

pattern_1, n=992; subpattern_1, ns=274

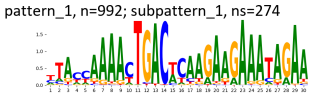

pattern_1, n=992; subpattern_2, ns=246

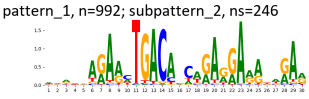

pattern_1, n=992; subpattern_3, ns=179

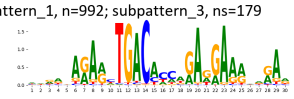

pattern_1, n=992; subpattern_4, ns=5

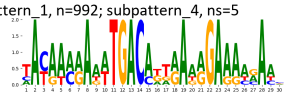

pattern_1, n=992; subpattern_5, ns=2

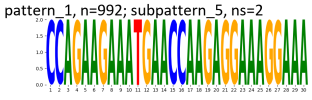

TF-MoDisCO pattern_2 n=968, CWM

pattern_2, n=968; subpattern_0, ns=250

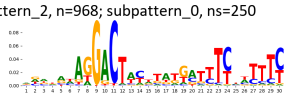

pattern_2, n=968; subpattern_1, ns=243

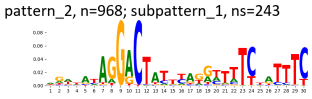

pattern_2, n=968; subpattern_2, ns=201

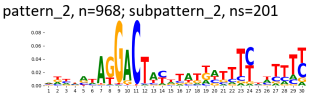

pattern_2, n=968; subpattern_3, ns=145

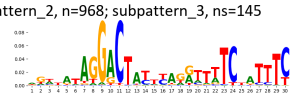

pattern_2, n=968; subpattern_4, ns=112

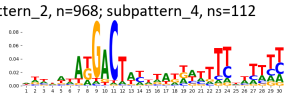

pattern_2, n=968; subpattern_5, ns=15

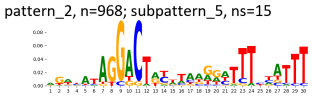

pattern_2, n=968; subpattern_6, ns=2

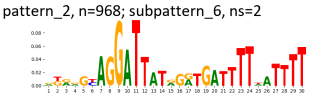

TF-MoDisCO pattern_2 n=968, PWM

pattern_2, n=968; subpattern_0, ns=250

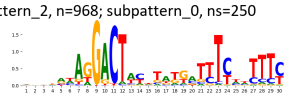

pattern_2, n=968; subpattern_1, ns=243

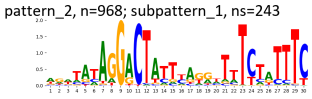

pattern_2, n=968; subpattern_2, ns=201

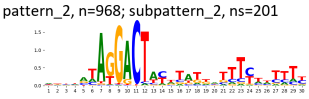

pattern_2, n=968; subpattern_3, ns=145

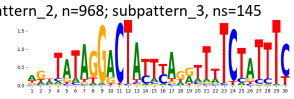

pattern_2, n=968; subpattern_4, ns=112

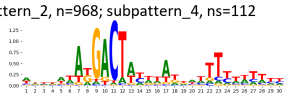

pattern_2, n=968; subpattern_5, ns=15

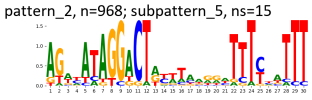

pattern_2, n=968; subpattern_6, ns=2

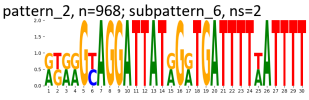

Supplementary Figure 556: TF-MoDisCO subpatterns for the ZFP28 transcription factor in HEK293 (accession Hughes GR models).

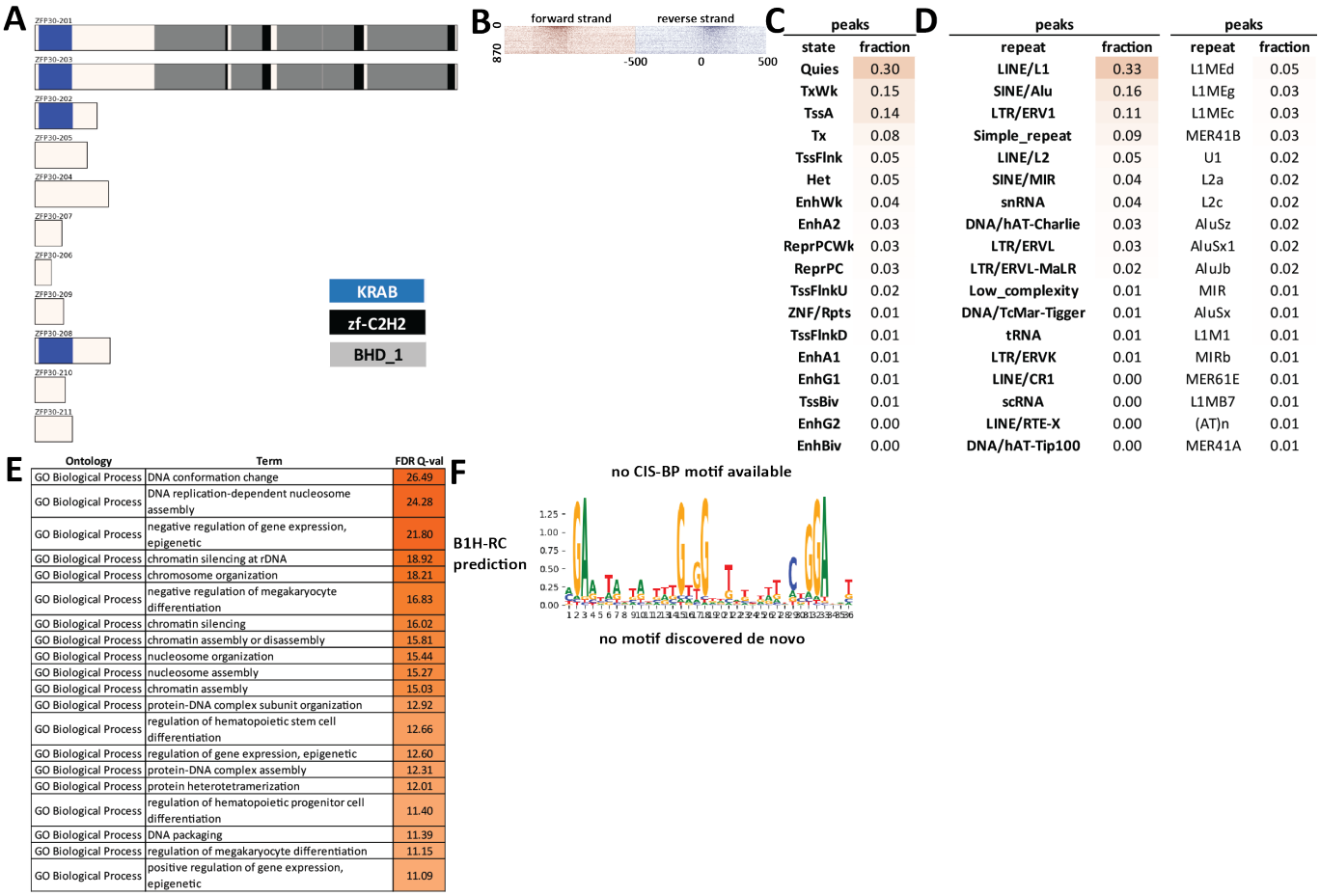

C

peaks	
state	fraction
Quies	0.30
TxWk	0.15
TssA	0.14
Tx	0.08
TssFlnk	0.05
Het	0.05
EnhWk	0.04
EnhA2	0.03
ReprPCWk	0.03
ReprPC	0.03
TssFlnkU	0.02
ZNF/Rpts	0.01
TssFlnkD	0.01
EnhA1	0.01
EnhG1	0.01
TssBiv	0.01
EnhG2	0.00
EnhBiv	0.00

D

peaks		peaks	
repeat	fraction	repeat	fraction
LINE/L1	0.33	L1MEd	0.05
SINE/Alu	0.16	L1MEg	0.03
LTR/ERV1	0.11	L1MEc	0.03
Simple_repeat	0.09	MER41B	0.03
LINE/L2	0.05	U1	0.02
SINE/MIR	0.04	L2a	0.02
snRNA	0.04	L2c	0.02
DNA/hAT-Charlie	0.03	AluSz	0.02
LTR/ERVL	0.03	AluSx1	0.02
LTR/ERVL-MaLR	0.02	AluJb	0.02
Low_complexity	0.01	MIR	0.01
DNA/TcMar-Tigger	0.01	AluSx	0.01
tRNA	0.01	L1M1	0.01
LTR/ERVK	0.01	MIRb	0.01
LINE/CR1	0.00	MER61E	0.01
scRNA	0.00	L1MB7	0.01
LINE/RTE-X	0.00	(AT)n	0.01
DNA/hAT-Tip100	0.00	MER41A	0.01

E

Ontology	Term	FDR Q-val
GO Biological Process	DNA conformation change	26.49
GO Biological Process	DNA replication-dependent nucleosome assembly	24.28
GO Biological Process	negative regulation of gene expression, epigenetic	21.80
GO Biological Process	chromatin silencing at rDNA	18.92
GO Biological Process	chromosome organization	18.21
GO Biological Process	negative regulation of megakaryocyte differentiation	16.83
GO Biological Process	chromatin silencing	16.02
GO Biological Process	chromatin assembly or disassembly	15.81
GO Biological Process	nucleosome organization	15.44
GO Biological Process	nucleosome assembly	15.27
GO Biological Process	chromatin assembly	15.03
GO Biological Process	protein-DNA complex subunit organization	12.92
GO Biological Process	regulation of hematopoietic stem cell differentiation	12.66
GO Biological Process	regulation of gene expression, epigenetic	12.60
GO Biological Process	protein-DNA complex assembly	12.31
GO Biological Process	protein heterotetramerization	12.01
GO Biological Process	regulation of hematopoietic progenitor cell differentiation	11.40
GO Biological Process	DNA packaging	11.39
GO Biological Process	regulation of megakaryocyte differentiation	11.15
GO Biological Process	positive regulation of gene expression, epigenetic	11.09

Supplementary Figure 557: Properties and genomic distribution of motifs identified for the ZFP30 transcription factor in K562 (accession ENCSR279OXE).

A

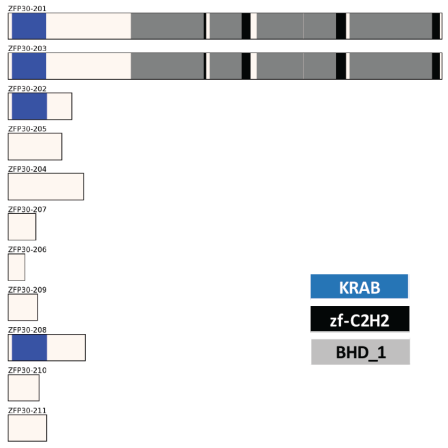

B

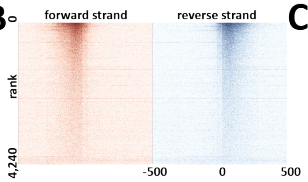

C

peaks	
state	fraction
Quies	0.47
TxWk	0.11
TssA	0.11
Het	0.07
EnhWk	0.06
Tx	0.04
TssFlnk	0.04
EnhA2	0.02
EnhA1	0.02
TssFlnkU	0.01
ReprPCWk	0.01
ZNF/Rpts	0.01
ReprPC	0.01
TssBiv	0.01
TssFlnkD	0.01
EnhG1	0.00
EnhG2	0.00
EnhBiv	0.00

D

peaks		peaks	
repeat	fraction	repeat	fraction
LINE/L1	0.48	L1MEd	0.09
Simple_repeat	0.08	L1MEg	0.06
SINE/Alu	0.07	L1MEc	0.05
SINE/MIR	0.04	MIRb	0.02
LINE/L2	0.04	L1M1	0.02
LTR/ERV1	0.03	L1ME1	0.02
LTR/ERVL-MaLR	0.02	L2a	0.02
LTR/ERVL	0.02	L2c	0.01
DNA/hAT-Charlie	0.02	MIR	0.01
Low_complexity	0.01	L1MEf	0.01
DNA/TcMar-Tigger	0.01	AluJb	0.01
LINE/CR1	0.01	L1MEi	0.01
snRNA	0.01	L1MA4A	0.01
DNA/hAT-Tip100	0.00	L1MA3	0.01
LTR/ERVK	0.00	L1ME3B	0.01
DNA/TcMar-Mariner	0.00	L1M2	0.01
DNA/hAT-Blackjack	0.00	AluSz	0.01
LINE/RTE-X	0.00	MIR3	0.01

E

Ontology	Term	FDR Q-val
GO Biological Process	positive regulation of nuclear-transcribed mRNA catabolic process, deadenylation-dependent decay	9.07
GO Biological Process	response to epidermal growth factor	7.41
GO Biological Process	regulation of heart morphogenesis	7.27
GO Biological Process	cellular response to epidermal growth factor stimulus	7.24
GO Biological Process	positive regulation of mRNA catabolic process	7.15
GO Biological Process	noradrenergic neuron differentiation	6.21
GO Biological Process	regulation of mRNA catabolic process	5.57
GO Biological Process	positive regulation of nuclear-transcribed mRNA poly(A) tail shortening	5.18
GO Biological Process	positive regulation of cardiac muscle hypertrophy	5.04
GO Biological Process	regulation of cardiac muscle hypertrophy	4.36
GO Biological Process	regulation of pri-miRNA transcription from RNA polymerase II promoter	4.29
GO Biological Process	gene silencing by miRNA	4.13
GO Biological Process	cardiac right ventricle morphogenesis	3.71
GO Biological Process	regulation of cell adhesion mediated by integrin	3.63
GO Biological Process	negative regulation of mesenchymal cell proliferation	3.41
GO Biological Process	regulation of glucose import in response to insulin stimulus	3.00
GO Biological Process	catecholamine biosynthetic process	2.79
GO Biological Process	positive regulation of glucose import in response to insulin stimulus	2.65
GO Biological Process	positive regulation of transcription regulatory region DNA binding	2.53
GO Biological Process	limb bud formation	2.50

F

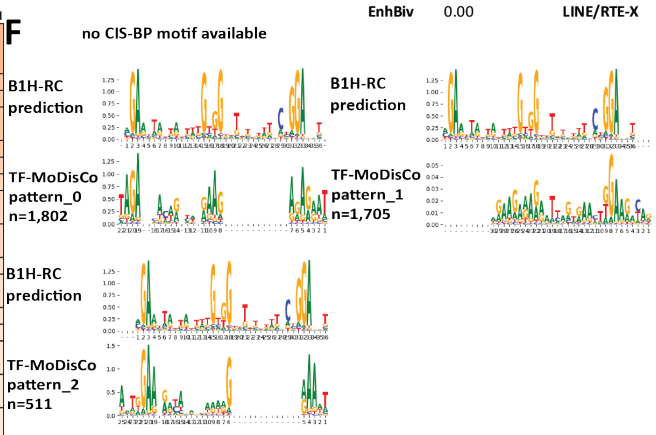

G

n/a

H

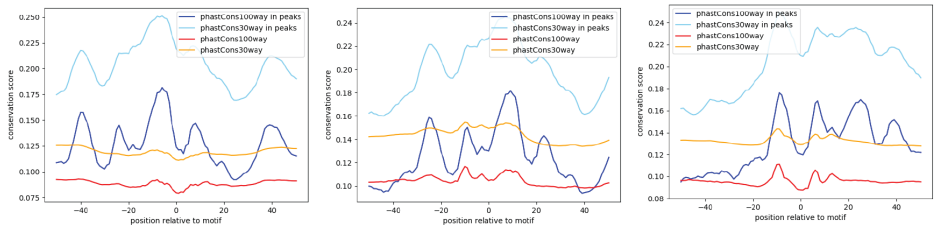

I

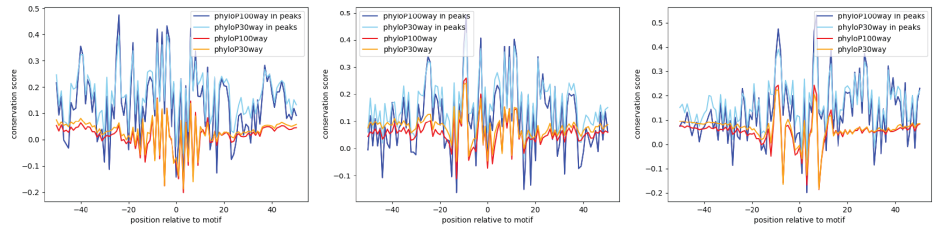

Supplementary Figure 558: Properties and genomic distribution of motifs identified for the ZFP30 transcription factor in SK-N-SH (accession ENCSR376QPI).

TF-MoDisCO pattern_0 n=1802, CWM

pattern_0, n=1802; subpattern_0, ns=438

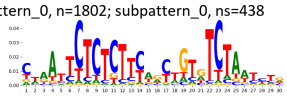

pattern_0, n=1802; subpattern_1, ns=363

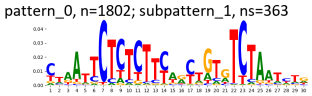

pattern_0, n=1802; subpattern_2, ns=281

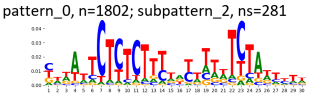

pattern_0, n=1802; subpattern_3, ns=242

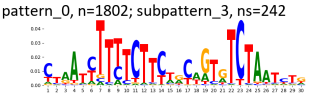

pattern_0, n=1802; subpattern_4, ns=173

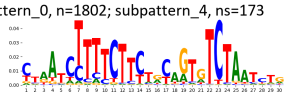

pattern_0, n=1802; subpattern_5, ns=91

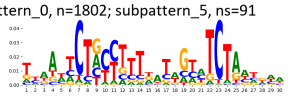

pattern_0, n=1802; subpattern_6, ns=85

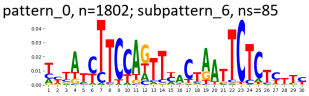

pattern_0, n=1802; subpattern_7, ns=82

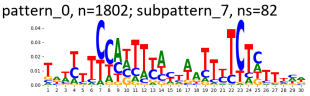

pattern_0, n=1802; subpattern_8, ns=47

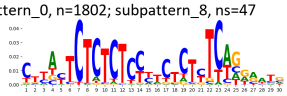

TF-MoDisCO pattern_0 n=1802, PWM

pattern_0, n=1802; subpattern_0, ns=438

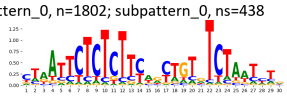

pattern_0, n=1802; subpattern_1, ns=363

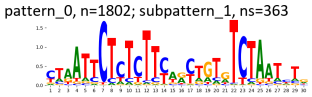

pattern_0, n=1802; subpattern_2, ns=281

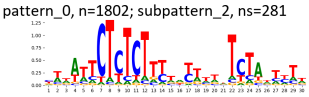

pattern_0, n=1802; subpattern_3, ns=242

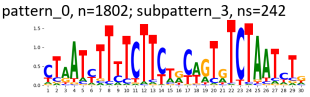

pattern_0, n=1802; subpattern_4, ns=173

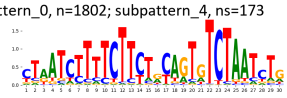

pattern_0, n=1802; subpattern_5, ns=91

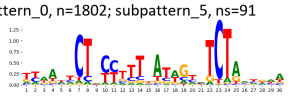

pattern_0, n=1802; subpattern_6, ns=85

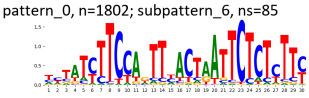

pattern_0, n=1802; subpattern_7, ns=82

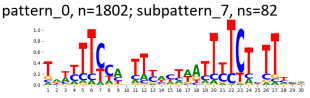

pattern_0, n=1802; subpattern_8, ns=47

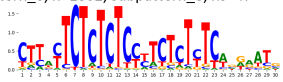

TF-MoDisCO pattern_1 n=1705, CWM

pattern_1, n=1705; subpattern_0, ns=341

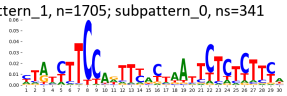

pattern_1, n=1705; subpattern_1, ns=305

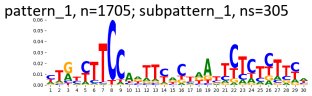

pattern_1, n=1705; subpattern_2, ns=218

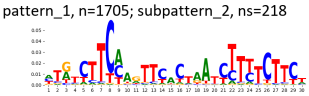

pattern_1, n=1705; subpattern_3, ns=195

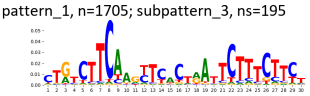

pattern_1, n=1705; subpattern_4, ns=174

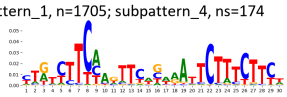

pattern_1, n=1705; subpattern_5, ns=150

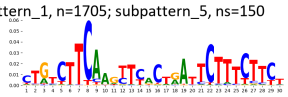

pattern_1, n=1705; subpattern_6, ns=144

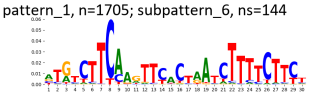

pattern_1, n=1705; subpattern_7, ns=143

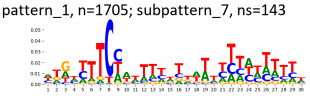

pattern_1, n=1705; subpattern_8, ns=35

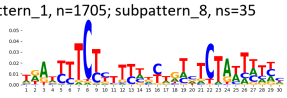

TF-MoDisCO pattern_1 n=1705, PWM

pattern_1, n=1705; subpattern_0, ns=341

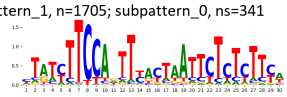

pattern_1, n=1705; subpattern_1, ns=305

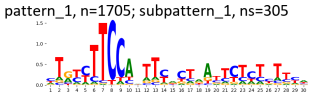

pattern_1, n=1705; subpattern_2, ns=218

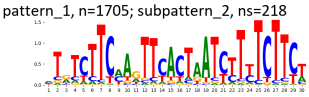

pattern_1, n=1705; subpattern_3, ns=195

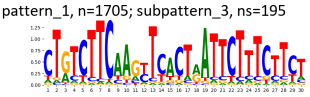

pattern_1, n=1705; subpattern_4, ns=174

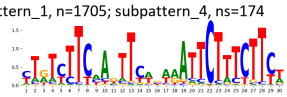

pattern_1, n=1705; subpattern_5, ns=150

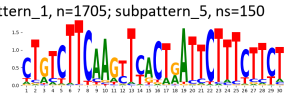

pattern_1, n=1705; subpattern_6, ns=144

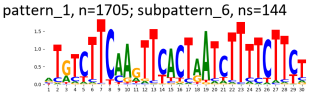

pattern_1, n=1705; subpattern_7, ns=143

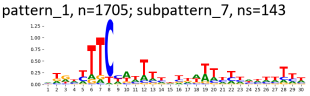

pattern_1, n=1705; subpattern_8, ns=35

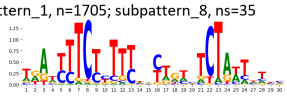

TF-MoDisCO pattern_2 n=511, CWM

pattern_2, n=511; subpattern_0, ns=98

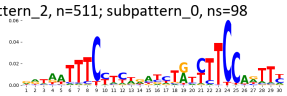

pattern_2, n=511; subpattern_1, ns=90

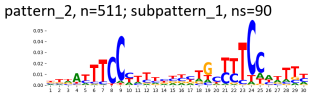

pattern_2, n=511; subpattern_2, ns=90

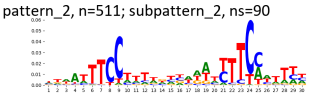

pattern_2, n=511; subpattern_3, ns=85

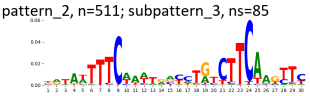

pattern_2, n=511; subpattern_4, ns=73

pattern_2, n=511; subpattern_5, ns=70

pattern_2, n=511; subpattern_6, ns=5

TF-MoDisCO pattern_2 n=511, PWM

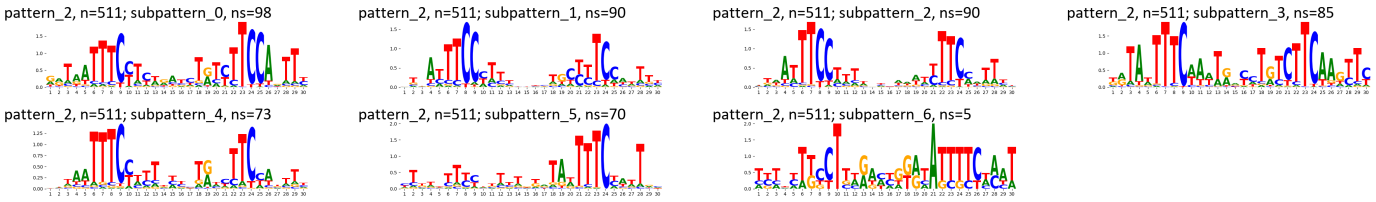

Supplementary Figure 559: TF-MoDisCO subpatterns for the ZFP30 transcription factor in SK-N-SH (accession ENCSR376QPI).

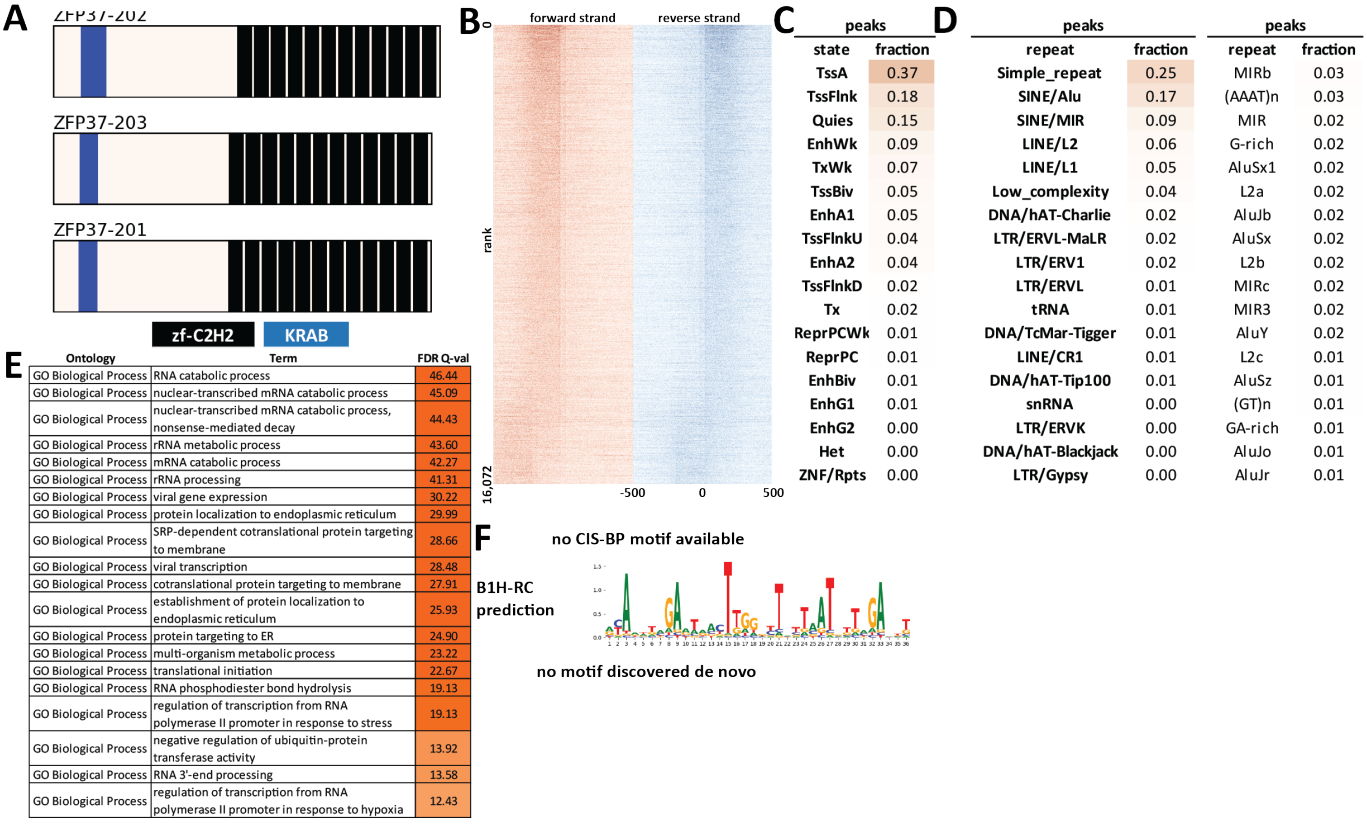

Supplementary Figure 560: Properties and genomic distribution of motifs identified for the ZFP37 transcription factor in HEK293 (accession ENCSR365GRX).

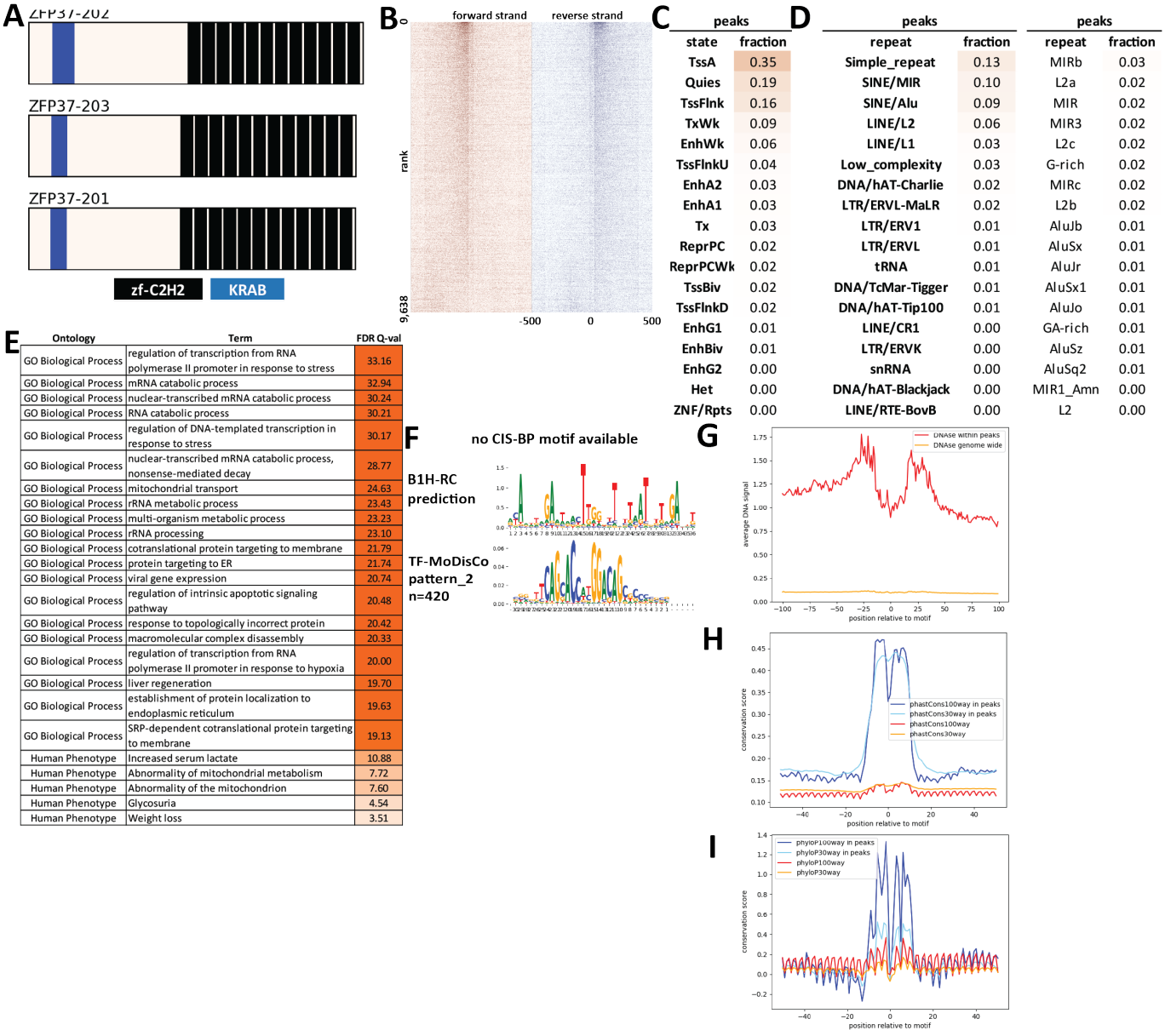

Supplementary Figure 561: Properties and genomic distribution of motifs identified for the ZFP37 transcription factor in HepG2 (accession ENCSR505LJT).

TF-MoDisCO pattern_2 n=420, CWM

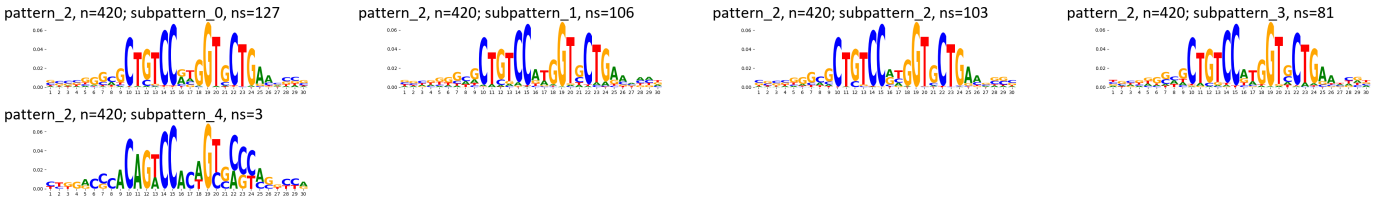

TF-MoDisCO pattern_2 n=420, PWM

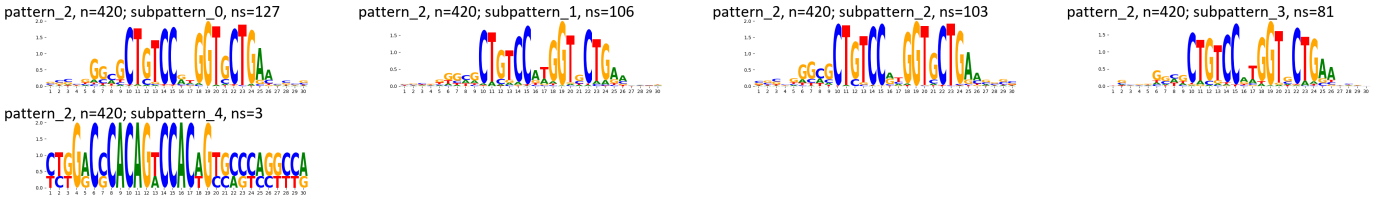

Supplementary Figure 562: TF-MoDisCO subpatterns for the ZFP37 transcription factor in HepG2 (accession ENCSR505LJT).

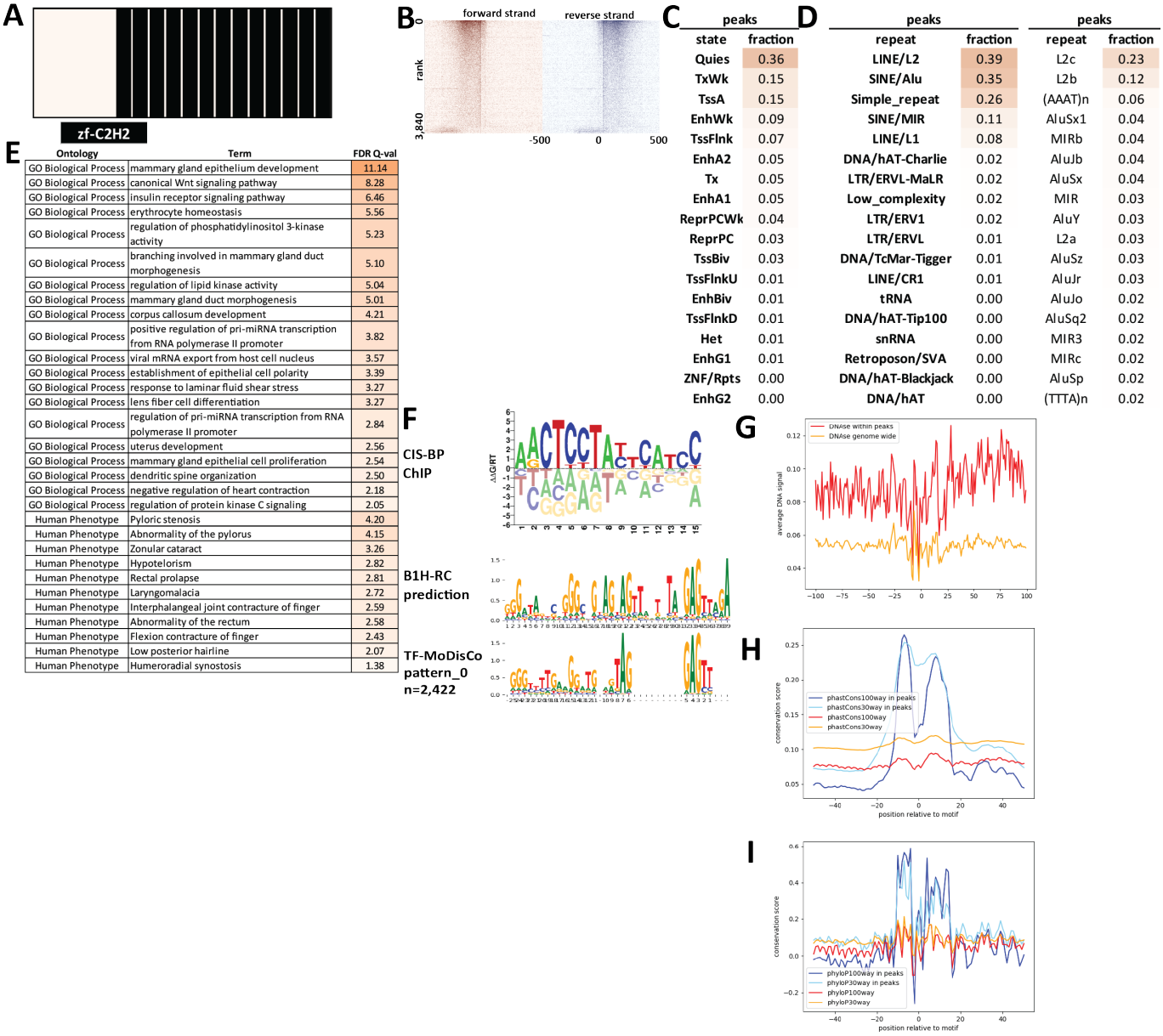

Supplementary Figure 563: Properties and genomic distribution of motifs identified for the ZFP3 transcription factor in HEK293 (accession ENCSR134QIE).

TF-MoDisCO pattern_0 n=2422, CWM

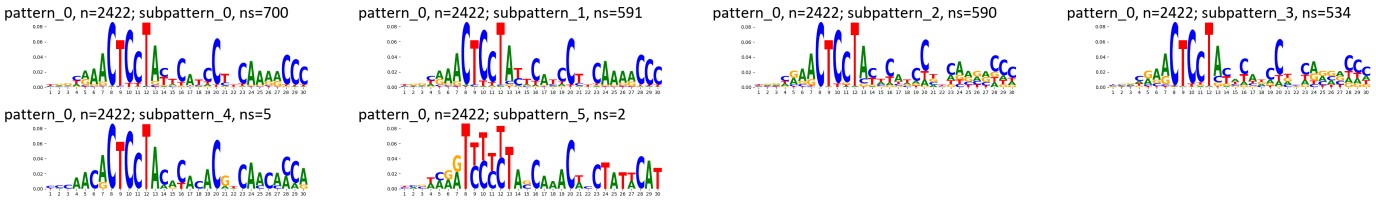

TF-MoDisCO pattern_0 n=2422, PWM

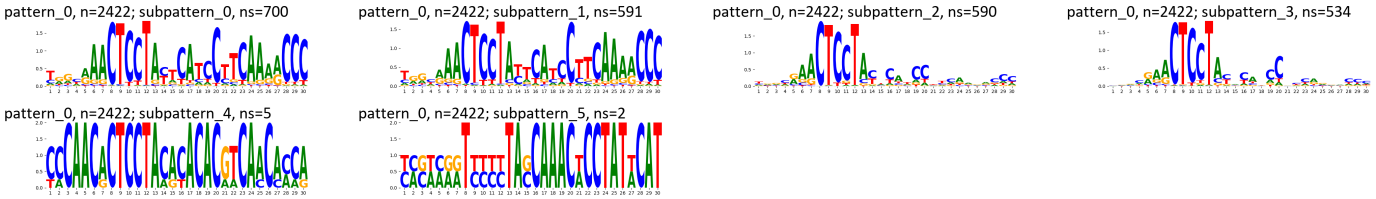

Supplementary Figure 564: TF-MoDisCO subpatterns for the ZFP3 transcription factor in HEK293 (accession ENCSR134QIE).

A



B

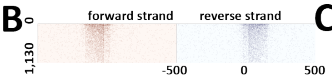

C

peaks	
state	fraction
Quies	0.42
TxWk	0.15
TssA	0.07
EnhWk	0.06
Tx	0.06
ReprPCWk	0.06
ReprPC	0.04
TssFlnk	0.03
EnhA1	0.03
TssBiv	0.02
EnhA2	0.02
EnhBiv	0.01
Het	0.01
TssFlnkU	0.01
TssFlnkD	0.01
EnhG1	0.00
EnhG2	0.00
ZNF/Rpts	0.00

D

peaks		peaks	
repeat	fraction	repeat	fraction
LINE/L2	0.64	L2c	0.39
SINE/MIR	0.06	L2b	0.22
SINE/Alu	0.05	L2a	0.03
LINE/L1	0.04	MIRb	0.02
Simple_repeat	0.02	MIR	0.02
DNA/hAT-Charlie	0.01	MIRc	0.01
LTR/ERVL-MaLR	0.01	MIR3	0.01
Low_complexity	0.01	AluSx	0.01
LTR/ERV1	0.01	AluJb	0.01
LTR/ERVL	0.00	AluSz	0.01
LINE/CR1	0.00	G-rich	0.01
DNA/hAT-Tip100	0.00	FLAM_C	0.01
DNA/TcMar-Tigger	0.00	AluJr	0.00
srpRNA	0.00	L2	0.00
snRNA	0.00	AluSx1	0.00
rRNA	0.00	AluJo	0.00
SINE/tRNA-Deu	0.00	(AC)n	0.00
LTR/Gypsy	0.00	MLT1K	0.00

E

Ontology	Term	FDR Q-val
GO Biological Process	Fc-gamma receptor signaling pathway involved in phagocytosis	6.54
GO Biological Process	Fc-gamma receptor signaling pathway	6.47
GO Biological Process	Fc receptor mediated stimulatory signaling pathway	6.26
GO Biological Process	mammary gland epithelium development	6.11
GO Biological Process	amelogenesis	5.58
GO Biological Process	dendritic spine organization	5.57
GO Biological Process	response to light stimulus	5.47
GO Biological Process	regulation of ATP metabolic process	5.41
GO Biological Process	vascular endothelial growth factor receptor signaling pathway	5.35
GO Biological Process	positive regulation of T cell activation	5.22
GO Biological Process	regulation of cellular response to insulin stimulus	4.89
GO Biological Process	positive regulation of leukocyte cell-cell adhesion	4.60
GO Biological Process	regulation of phosphatidylinositol 3-kinase activity	4.34
GO Biological Process	regulation of lipid kinase activity	4.31
GO Biological Process	lens fiber cell differentiation	4.27
GO Biological Process	regulation of lymphocyte differentiation	4.15
GO Biological Process	platelet-derived growth factor receptor signaling pathway	3.80
GO Biological Process	intracellular receptor signaling pathway	3.64
GO Biological Process	establishment of endothelial barrier	3.55
GO Biological Process	dendritic spine morphogenesis	3.52

F

CIS-BP ChIP

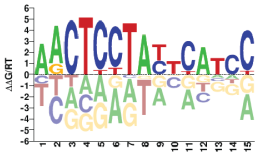

B1H-RC prediction

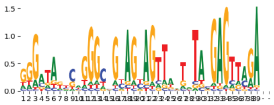

TF-MoDisCo pattern_0 n=1,077

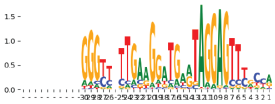

G

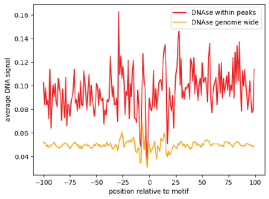

H

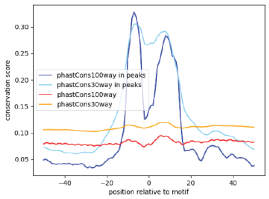

I

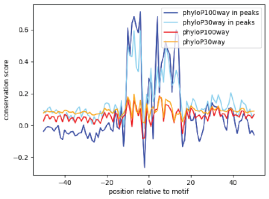

Supplementary Figure 565: Properties and genomic distribution of motifs identified for the ZFP3 transcription factor in HEK293 (accession Hughes NB models).

TF-MoDisCO pattern_0 n=1077, CWM

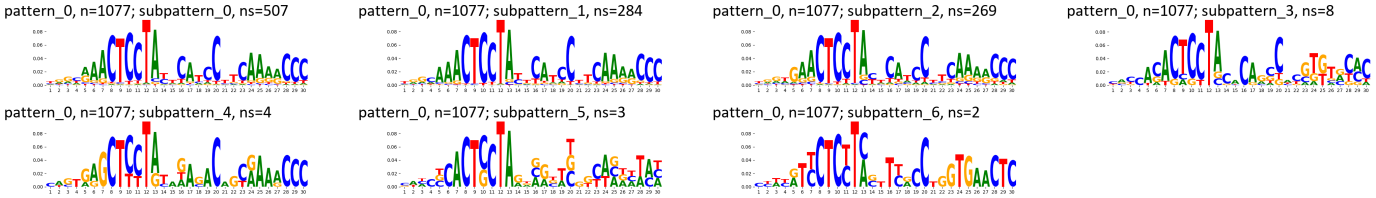

TF-MoDisCO pattern_0 n=1077, PWM

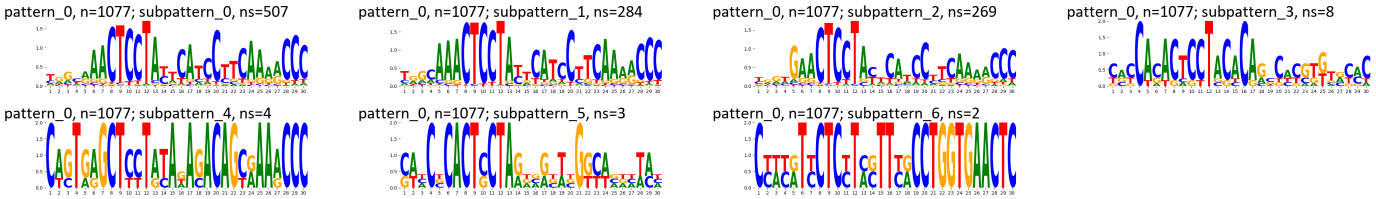

Supplementary Figure 566: TF-MoDisCO subpatterns for the ZFP3 transcription factor in HEK293 (accession Hughes NB models).

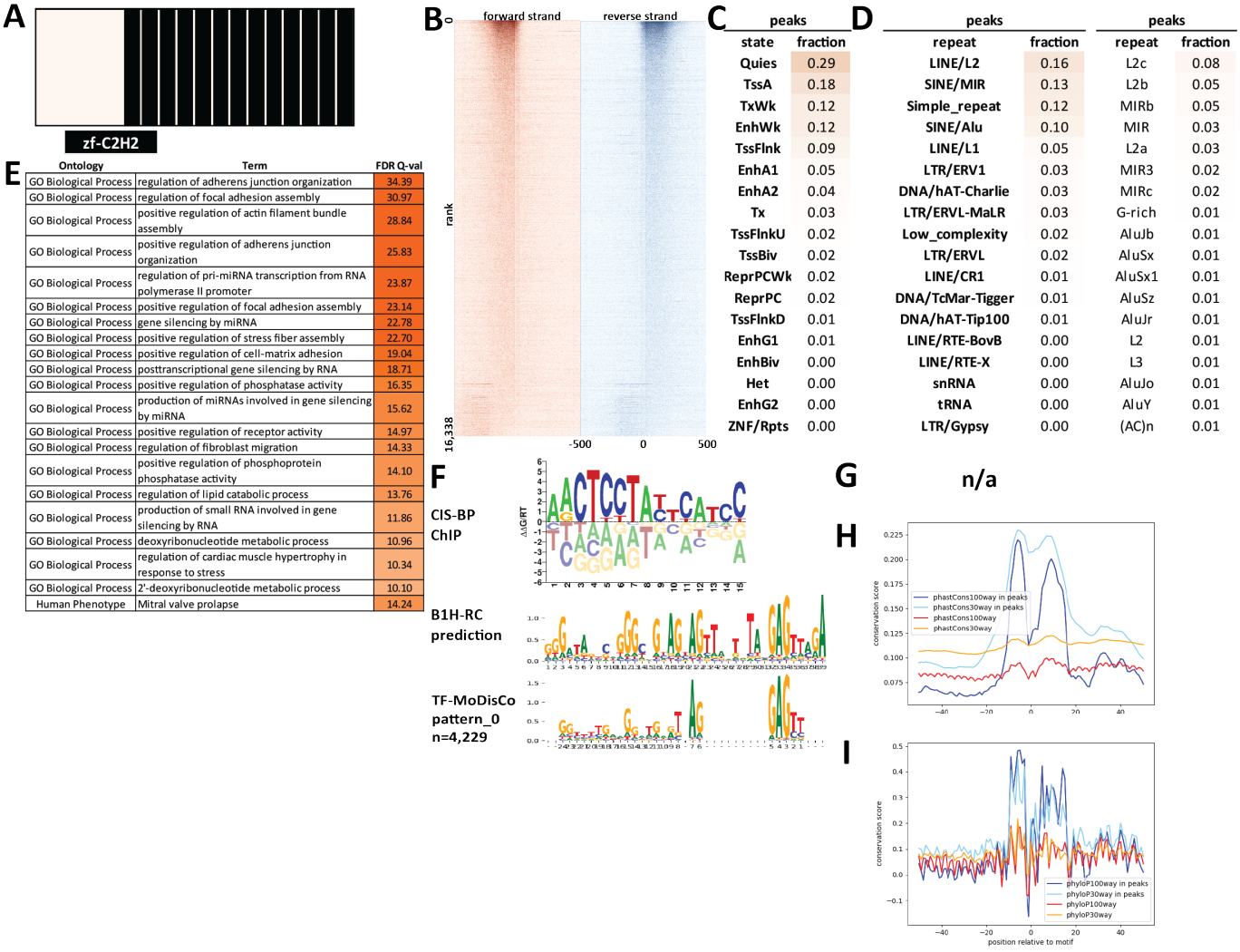

Supplementary Figure 567: Properties and genomic distribution of motifs identified for the ZFP3 transcription factor in SK-N-SH (accession ENCSR581GUY).

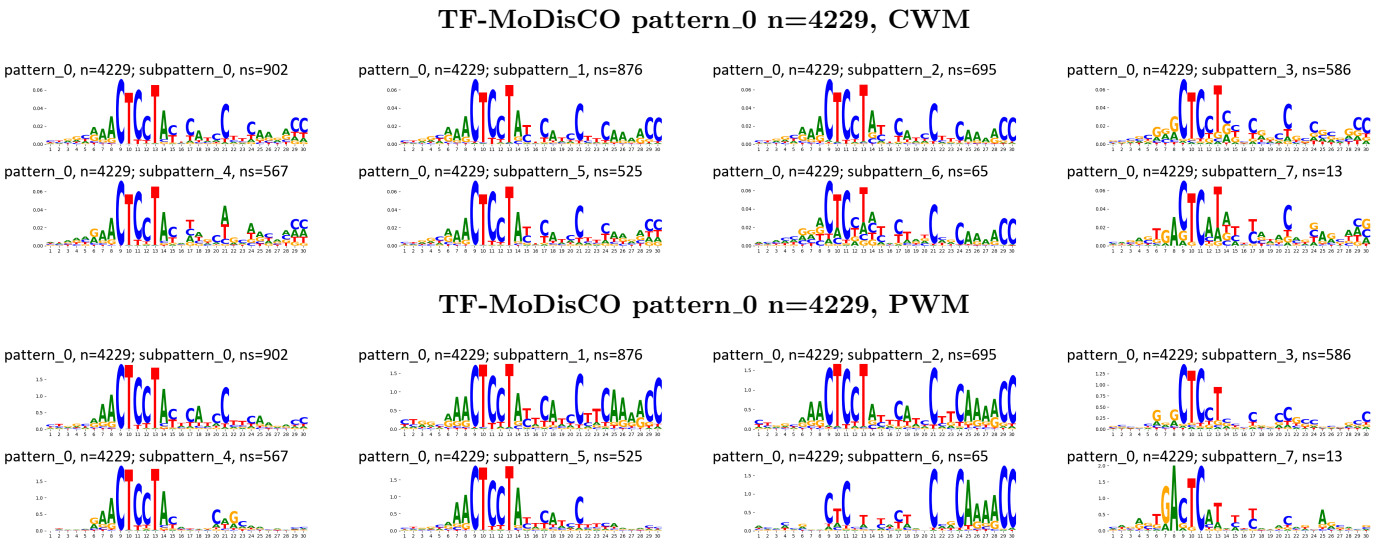

Supplementary Figure 568: TF-MoDisCO subpatterns for the ZFP3 transcription factor in SK-N-SH (accession ENCSR581GUY).

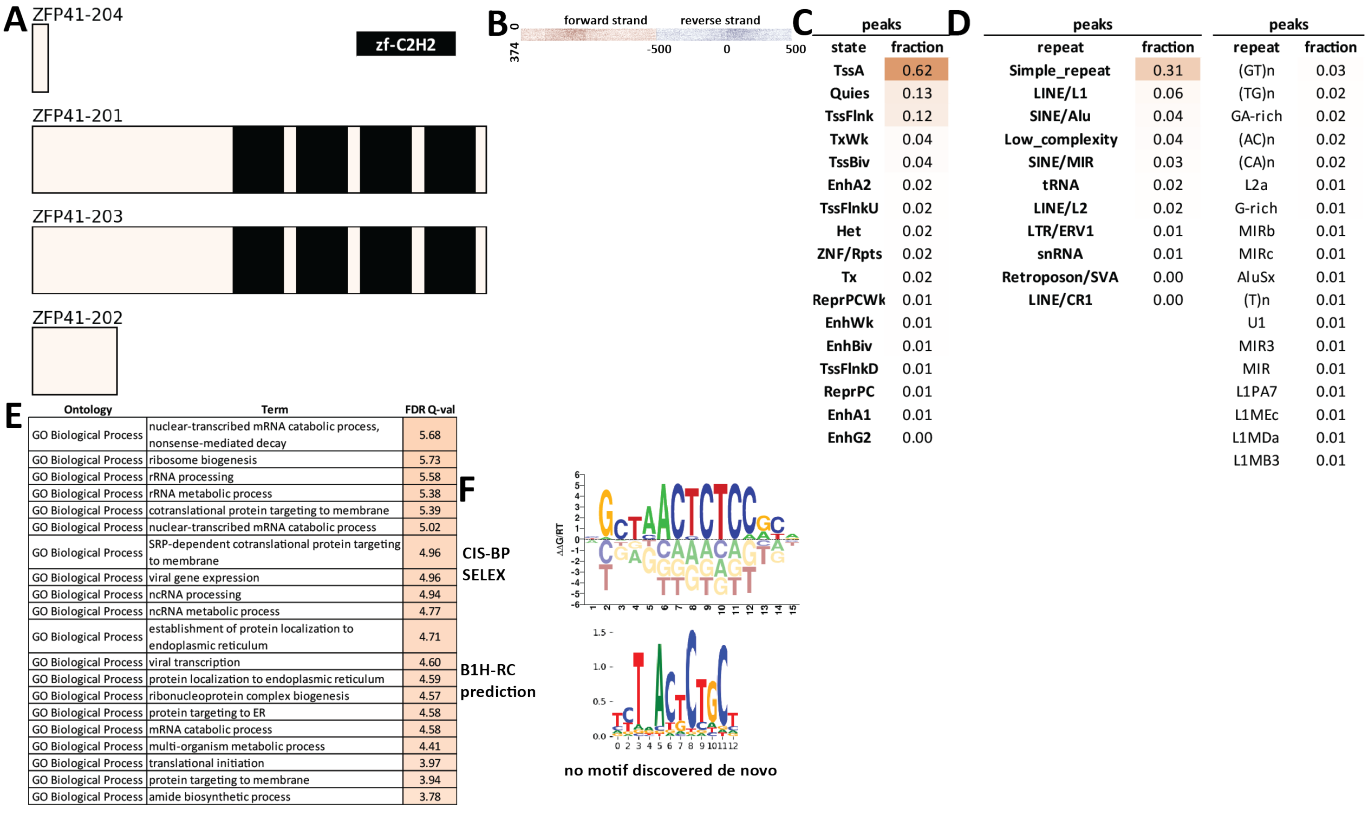

C

peaks	
state	fraction
TssA	0.62
Quies	0.13
TssFlnk	0.12
TxWk	0.04
TssBiv	0.04
EnhA2	0.02
TssFlnkU	0.02
Het	0.02
ZNF/Rpts	0.02
Tx	0.02
ReprPCWk	0.01
EnhWk	0.01
EnhBiv	0.01
TssFlnkD	0.01
ReprPC	0.01
EnhA1	0.01
EnhG2	0.00

D

peaks		peaks	
repeat	fraction	repeat	fraction
Simple_repeat	0.31	(GT)n	0.03
LINE/L1	0.06	(TG)n	0.02
SINE/Alu	0.04	GA-rich	0.02
Low_complexity	0.04	(AC)n	0.02
SINE/MIR	0.03	(CA)n	0.02
tRNA	0.02	L2a	0.01
LINE/L2	0.02	G-rich	0.01
LTR/ERV1	0.01	MIRb	0.01
snRNA	0.01	MIRc	0.01
Retroposon/SVA	0.00	AluSx	0.01
LINE/CR1	0.00	(T)n	0.01
		U1	0.01
		MIR3	0.01
		MIR	0.01
		L1PA7	0.01
		L1MEc	0.01
		L1MDa	0.01
		L1MB3	0.01

E

Ontology	Term	FDR Q-val
GO Biological Process	nuclear-transcribed mRNA catabolic process, nonsense-mediated decay	5.68
GO Biological Process	ribosome biogenesis	5.73
GO Biological Process	rRNA processing	5.58
GO Biological Process	rRNA metabolic process	5.38
GO Biological Process	cotranslational protein targeting to membrane	5.39
GO Biological Process	nuclear-transcribed mRNA catabolic process	5.02
GO Biological Process	SRP-dependent cotranslational protein targeting to membrane	4.96
GO Biological Process	viral gene expression	4.96
GO Biological Process	ncRNA processing	4.94
GO Biological Process	ncRNA metabolic process	4.77
GO Biological Process	establishment of protein localization to endoplasmic reticulum	4.71
GO Biological Process	viral transcription	4.60
GO Biological Process	protein localization to endoplasmic reticulum	4.59
GO Biological Process	ribonucleoprotein complex biogenesis	4.57
GO Biological Process	protein targeting to ER	4.58
GO Biological Process	mRNA catabolic process	4.58
GO Biological Process	multi-organism metabolic process	4.41
GO Biological Process	translational initiation	3.97
GO Biological Process	protein targeting to membrane	3.94
GO Biological Process	amide biosynthetic process	3.78

Supplementary Figure 569: Properties and genomic distribution of motifs identified for the ZFP41 transcription factor in HEK293 (accession ENCSR348ONY).

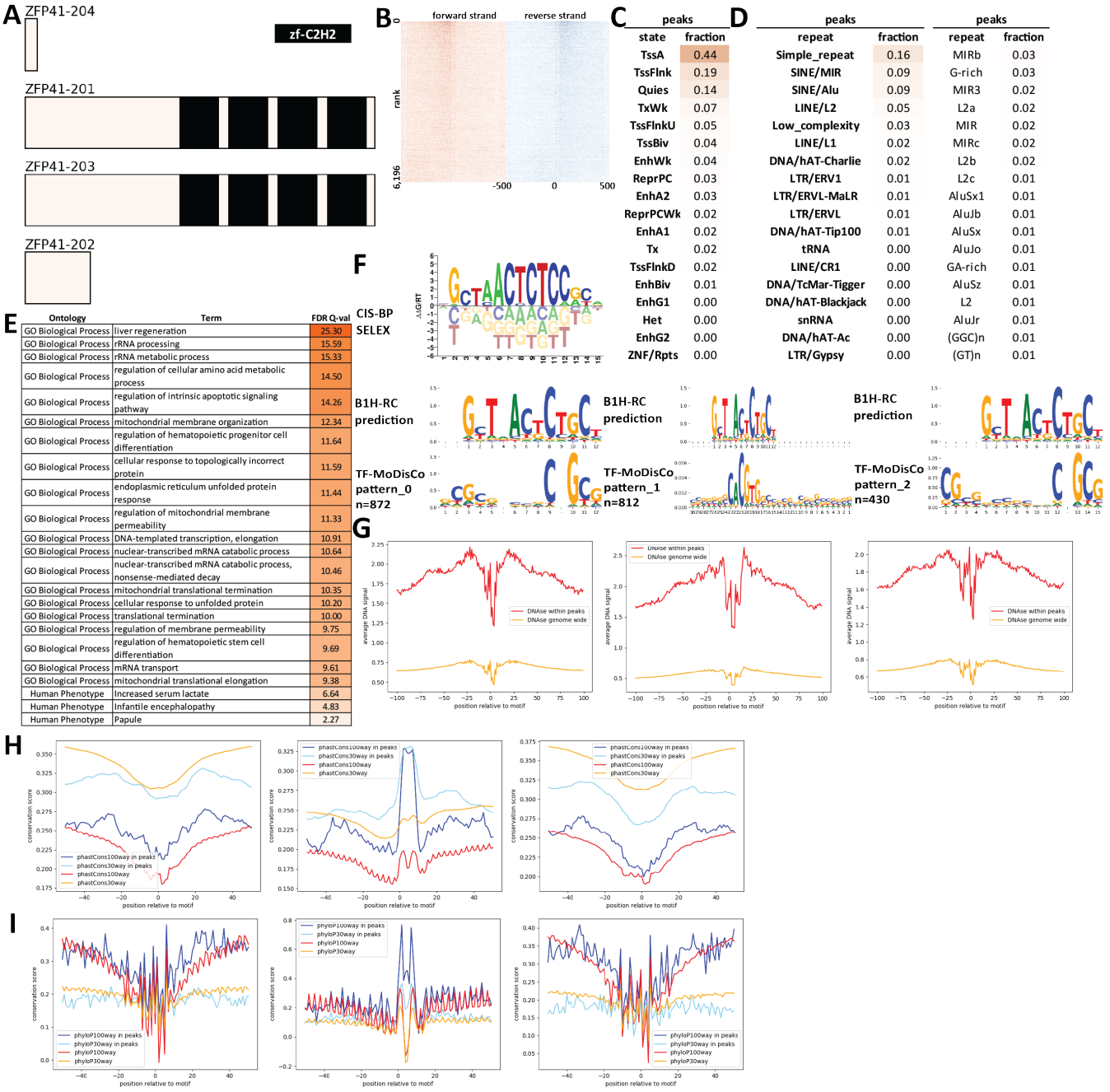

Supplementary Figure 570: Properties and genomic distribution of motifs identified for the ZFP41 transcription factor in HepG2 (accession ENCSR731UPJ).

TF-MoDisCO pattern_0 n=872, CWM

pattern_0, n=872; subpattern_0, ns=172

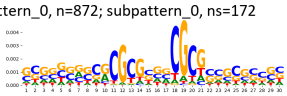

pattern_0, n=872; subpattern_1, ns=153

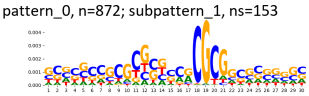

pattern_0, n=872; subpattern_2, ns=141

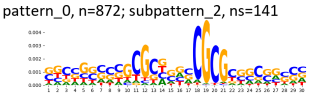

pattern_0, n=872; subpattern_3, ns=137

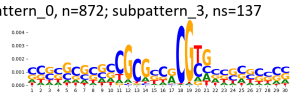

pattern_0, n=872; subpattern_4, ns=121

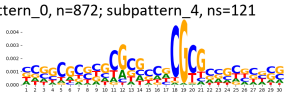

pattern_0, n=872; subpattern_5, ns=102

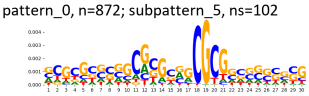

pattern_0, n=872; subpattern_6, ns=44

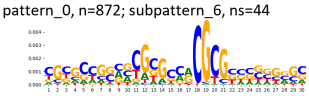

pattern_0, n=872; subpattern_7, ns=2

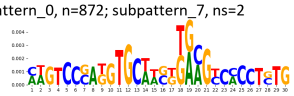

TF-MoDisCO pattern_0 n=872, PWM

pattern_0, n=872; subpattern_0, ns=172

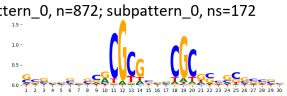

pattern_0, n=872; subpattern_1, ns=153

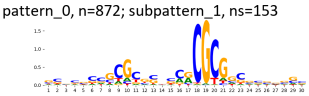

pattern_0, n=872; subpattern_2, ns=141

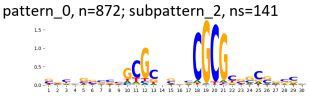

pattern_0, n=872; subpattern_3, ns=137

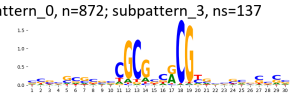

pattern_0, n=872; subpattern_4, ns=121

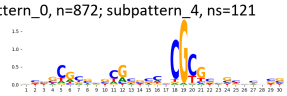

pattern_0, n=872; subpattern_5, ns=102

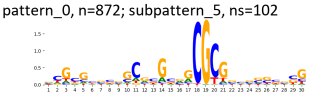

pattern_0, n=872; subpattern_6, ns=44

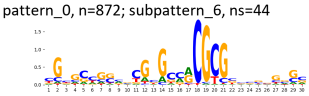

pattern_0, n=872; subpattern_7, ns=2

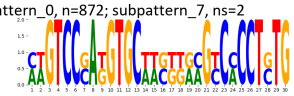

TF-MoDisCO pattern_1 n=812, CWM

pattern_1, n=812; subpattern_0, ns=148

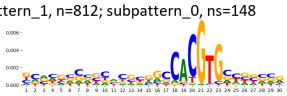

pattern_1, n=812; subpattern_1, ns=141

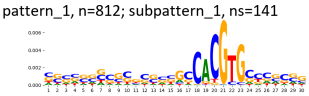

pattern_1, n=812; subpattern_2, ns=134

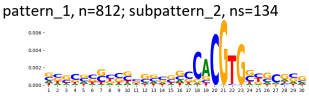

pattern_1, n=812; subpattern_3, ns=120

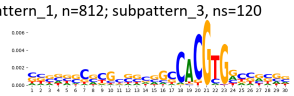

pattern_1, n=812; subpattern_4, ns=84

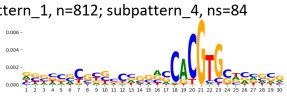

pattern_1, n=812; subpattern_5, ns=83

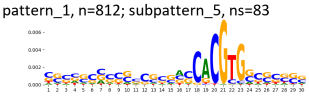

pattern_1, n=812; subpattern_6, ns=77

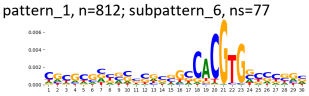

pattern_1, n=812; subpattern_7, ns=25

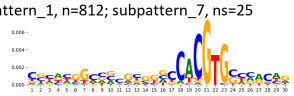

TF-MoDisCO pattern_1 n=812, PWM

pattern_1, n=812; subpattern_0, ns=148

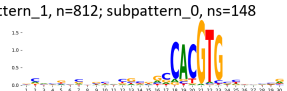

pattern_1, n=812; subpattern_1, ns=141

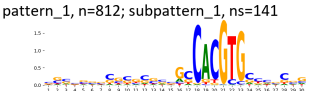

pattern_1, n=812; subpattern_2, ns=134

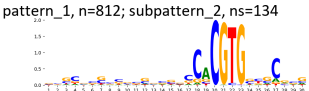

pattern_1, n=812; subpattern_3, ns=120

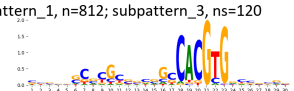

pattern_1, n=812; subpattern_4, ns=84

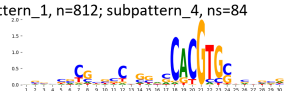

pattern_1, n=812; subpattern_5, ns=83

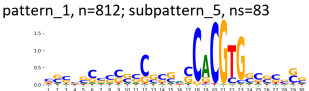

pattern_1, n=812; subpattern_6, ns=77

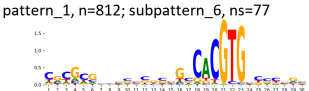

pattern_1, n=812; subpattern_7, ns=25

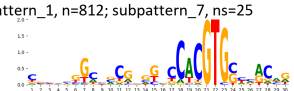

TF-MoDisCO pattern_2 n=430, CWM

pattern_2, n=430; subpattern_0, ns=101

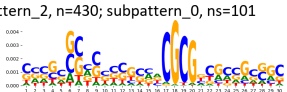

pattern_2, n=430; subpattern_1, ns=101

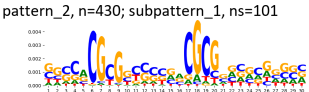

pattern_2, n=430; subpattern_2, ns=72

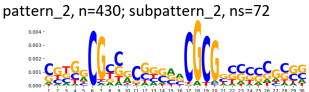

pattern_2, n=430; subpattern_3, ns=58

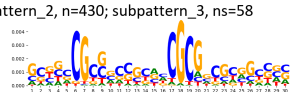

pattern_2, n=430; subpattern_4, ns=45

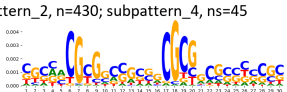

pattern_2, n=430; subpattern_5, ns=38

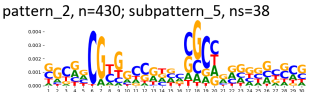

pattern_2, n=430; subpattern_6, ns=13

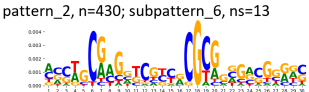

pattern_2, n=430; subpattern_7, ns=2

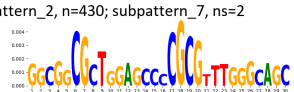

TF-MoDisCO pattern_2 n=430, PWM

pattern_2, n=430; subpattern_0, ns=101

pattern_2, n=430; subpattern_1, ns=101

pattern_2, n=430; subpattern_2, ns=72

pattern_2, n=430; subpattern_3, ns=58

pattern_2, n=430; subpattern_4, ns=45

pattern_2, n=430; subpattern_5, ns=38

pattern_2, n=430; subpattern_6, ns=13

pattern_2, n=430; subpattern_7, ns=2

Supplementary Figure 571: TF-MoDisCO subpatterns for the ZFP41 transcription factor in HepG2 (accession ENCSR731UPJ).

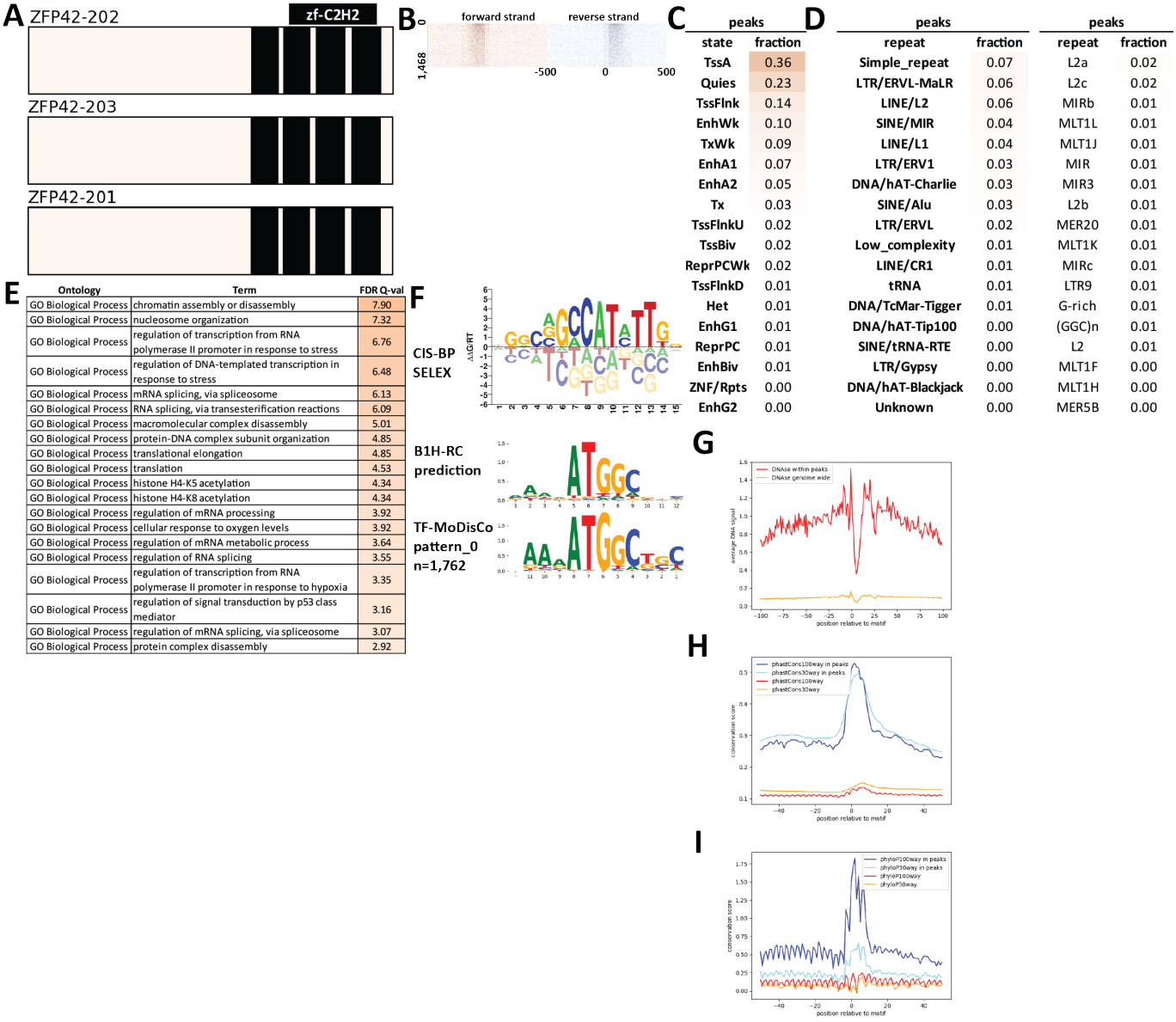

Supplementary Figure 572: Properties and genomic distribution of motifs identified for the ZFP42 transcription factor in HEK293 (accession Hughes GR models).

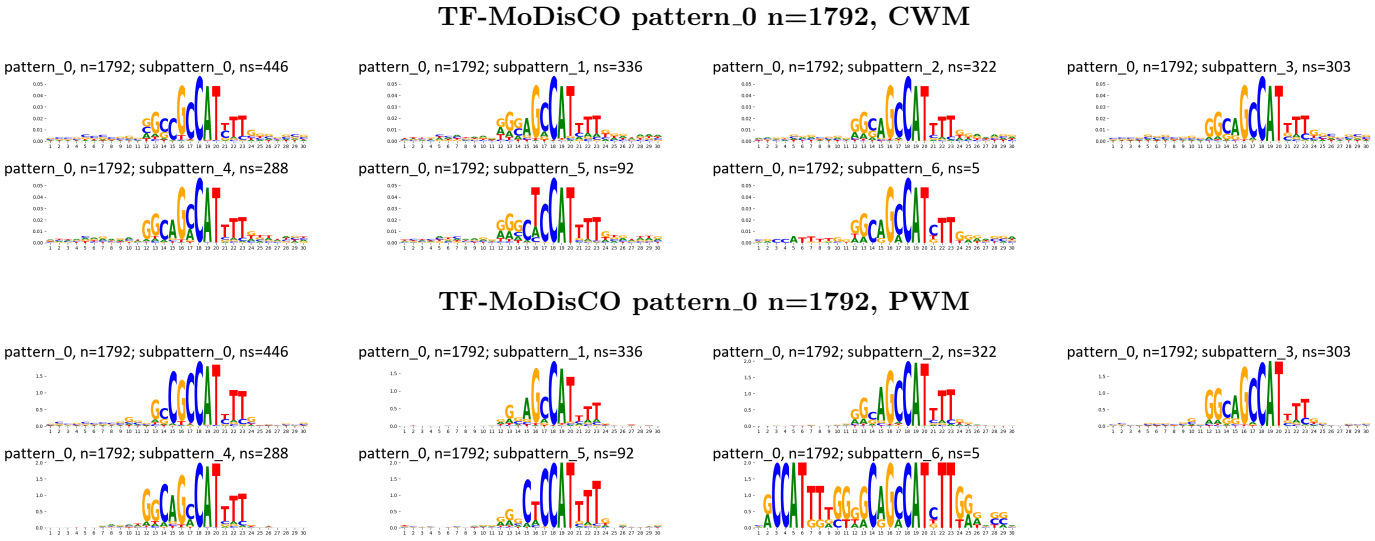

Supplementary Figure 573: TF-MoDisCO subpatterns for the ZFP42 transcription factor in HEK293 (accession Hughes GR models).

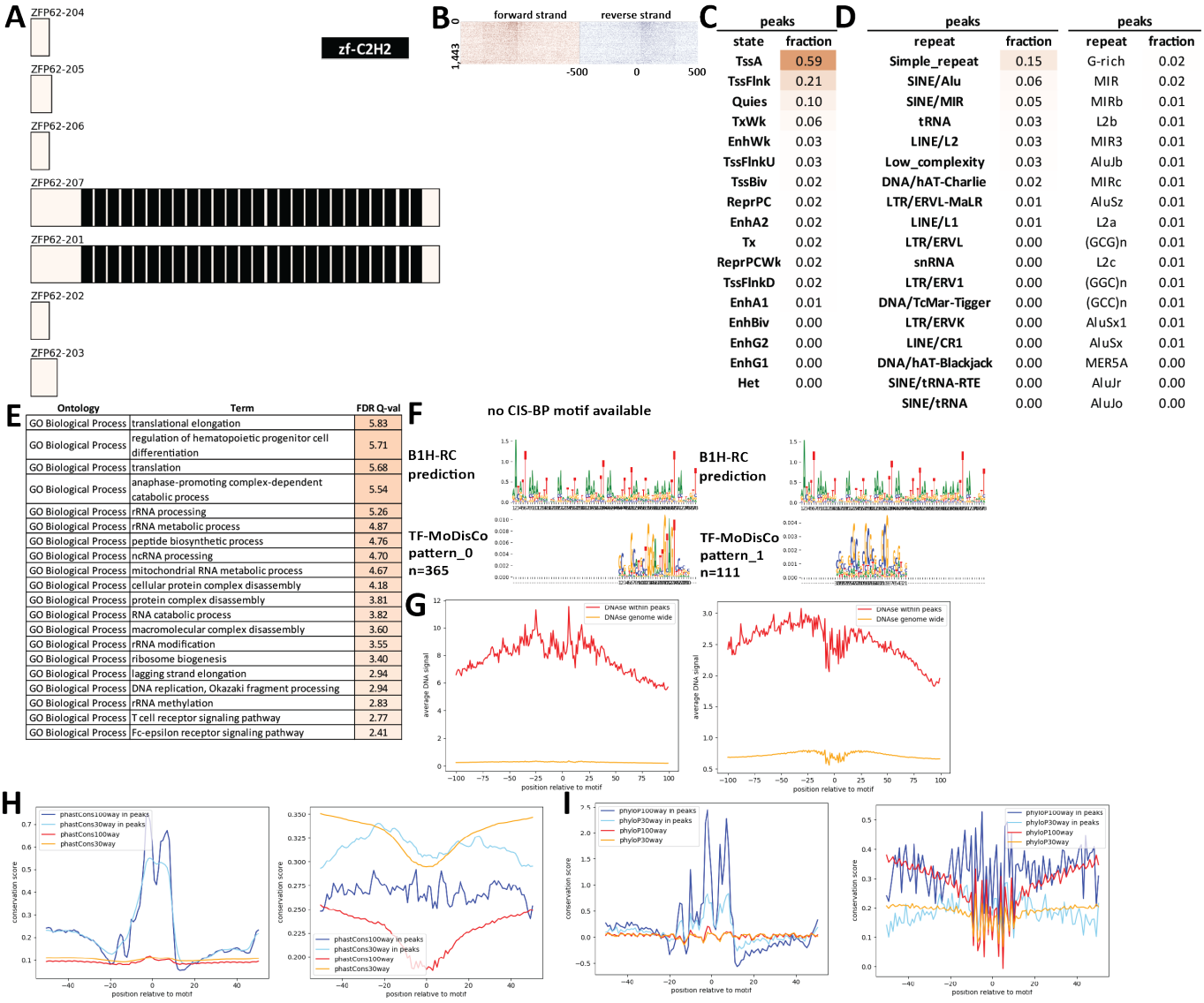

Supplementary Figure 574: Properties and genomic distribution of motifs identified for the ZFP62 transcription factor in HepG2 (accession ENCSR495RMN).

TF-MoDisCO pattern_0 n=365, CWM

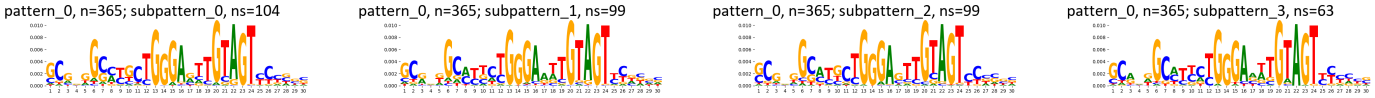

TF-MoDisCO pattern_0 n=365, PWM

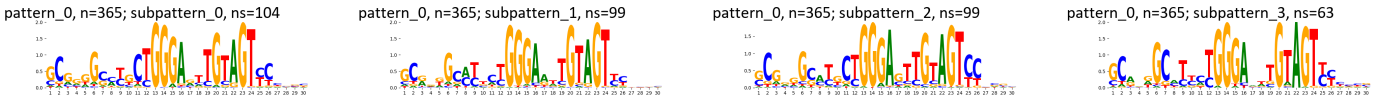

TF-MoDisCO pattern_1 n=111, CWM

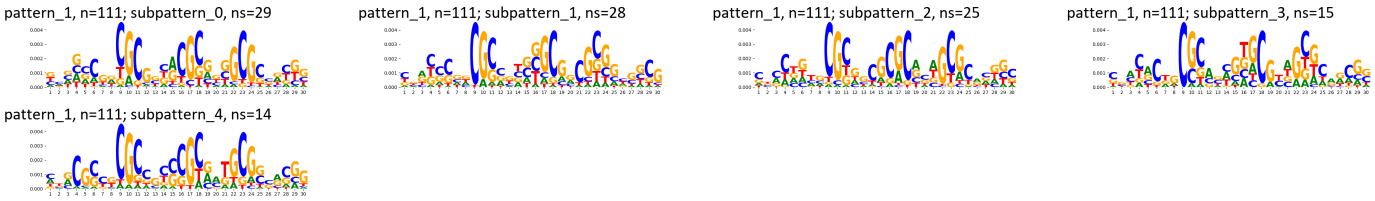

TF-MoDisCO pattern_1 n=111, PWM

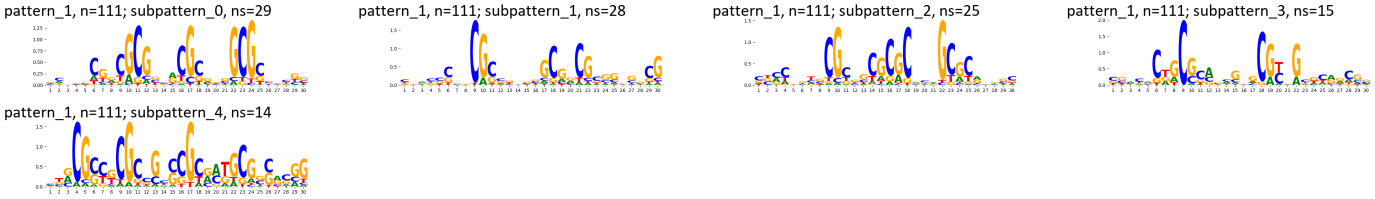

Supplementary Figure 575: TF-MoDisCO subpatterns for the ZFP62 transcription factor in HepG2 (accession ENCSR495RMN).

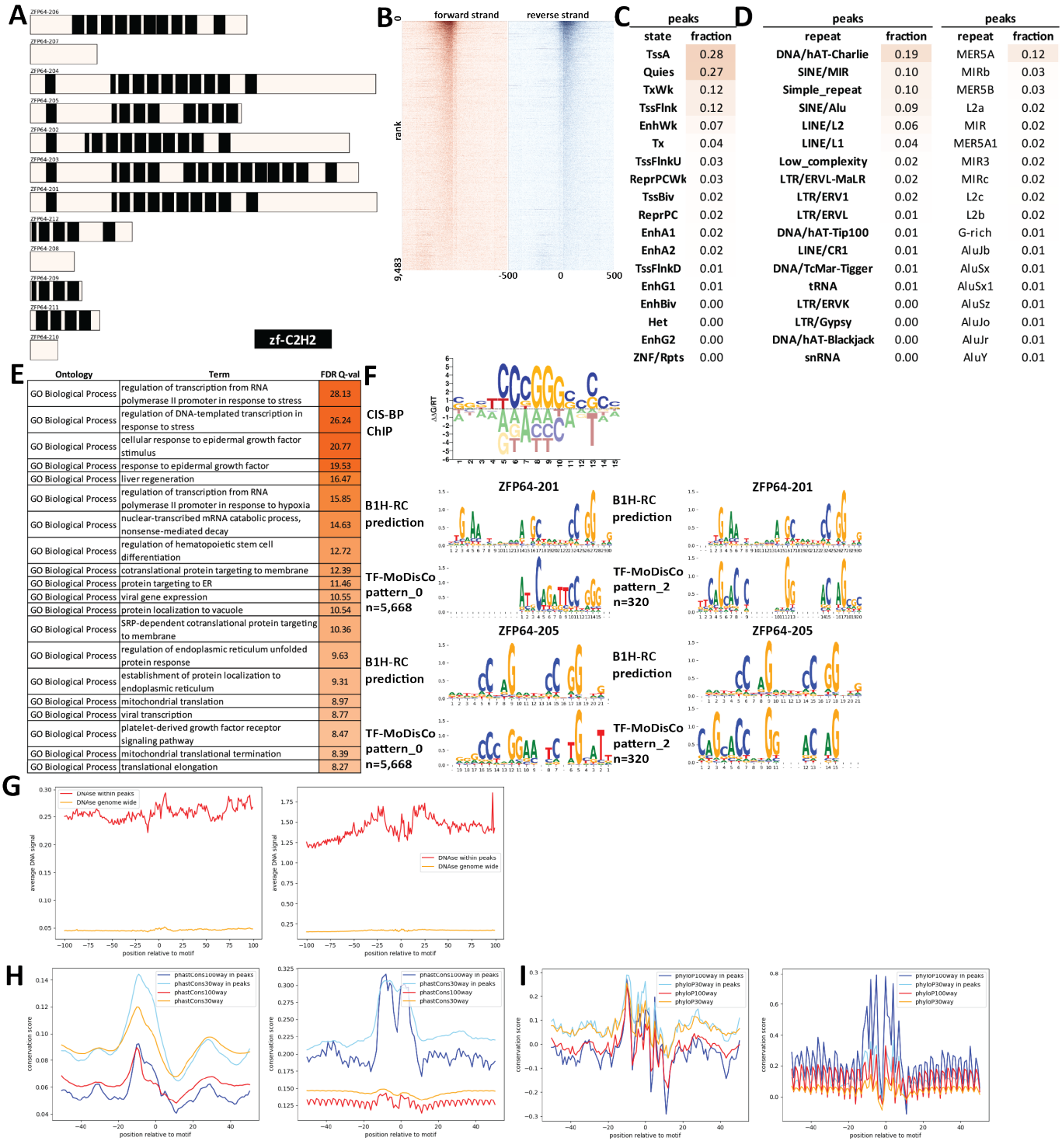

Supplementary Figure 576: Properties and genomic distribution of motifs identified for the ZFP64 transcription factor in HepG2 (accession ENCSR487CPI).

TF-MoDisCO pattern_0 n=5668, CWM

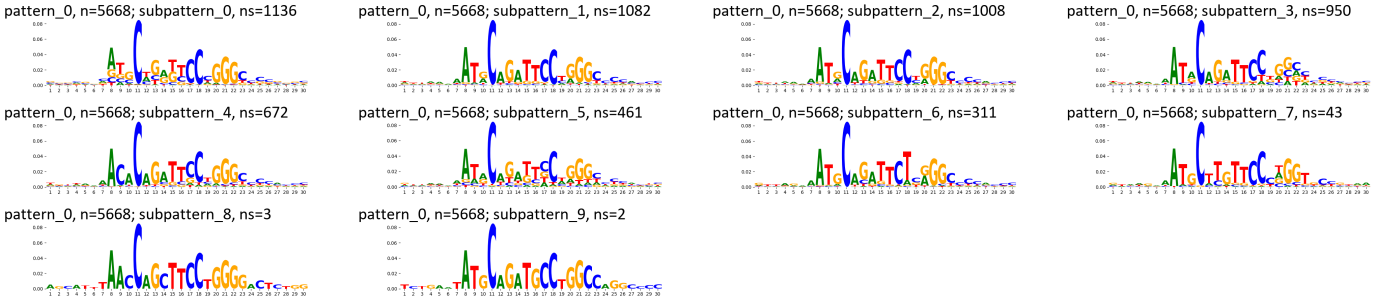

TF-MoDisCO pattern_0 n=5668, PWM

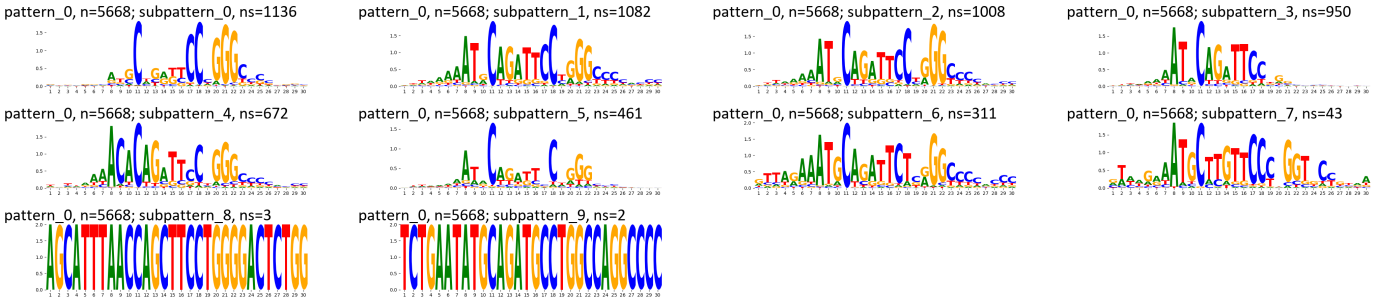

TF-MoDisCO pattern_2 n=320, CWM

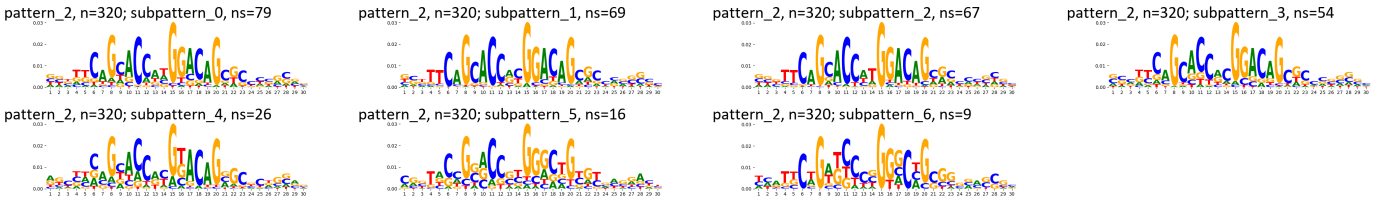

TF-MoDisCO pattern_2 n=320, PWM

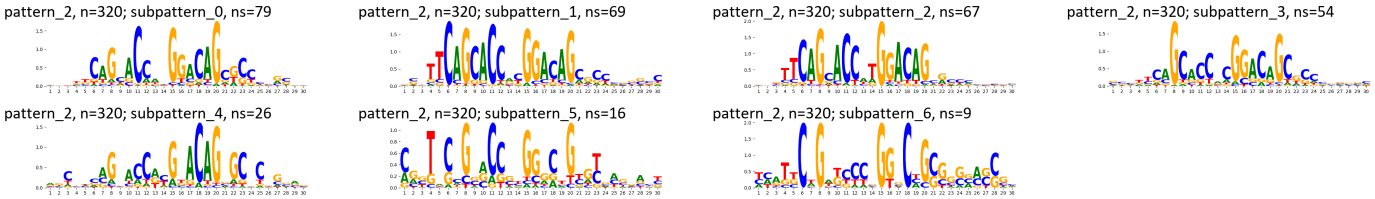

Supplementary Figure 577: TF-MoDisCO subpatterns for the ZFP64 transcription factor in HepG2 (accession ENCSR487CPI).

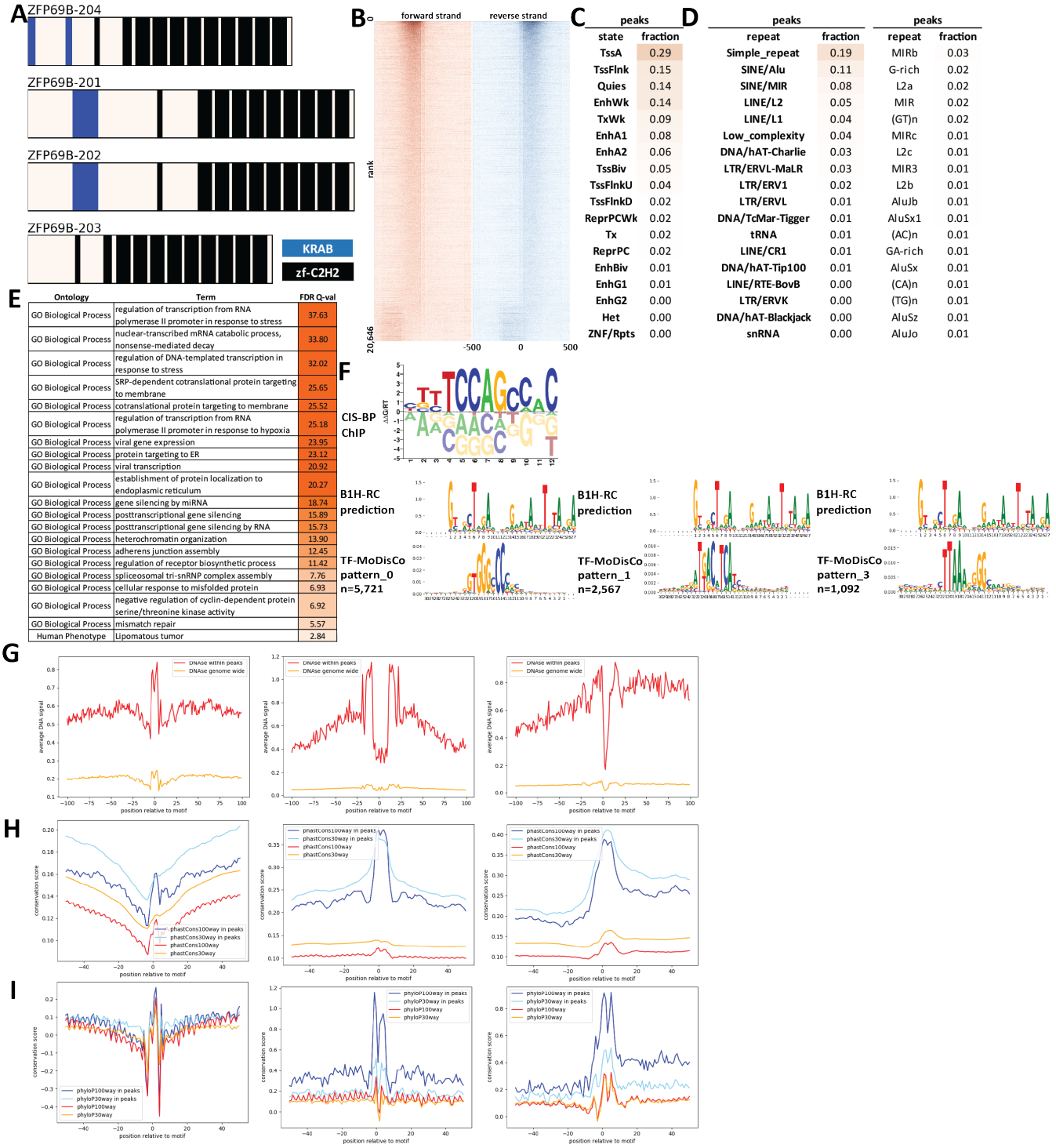

Supplementary Figure 578: Properties and genomic distribution of motifs identified for the ZFP69B transcription factor in HEK293 (accession ENCSR381VYR).

TF-MoDisCO pattern_0 n=5721, CWM

pattern_0, n=5721; subpattern_0, ns=1245

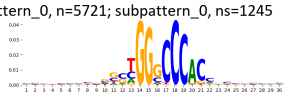

pattern_0, n=5721; subpattern_1, ns=1227

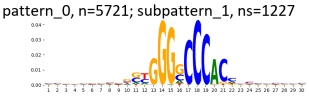

pattern_0, n=5721; subpattern_2, ns=1053

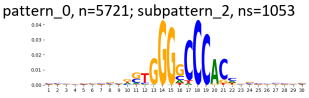

pattern_0, n=5721; subpattern_3, ns=1031

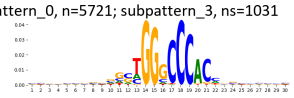

pattern_0, n=5721; subpattern_4, ns=804

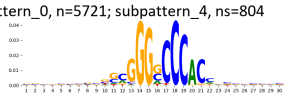

pattern_0, n=5721; subpattern_5, ns=258

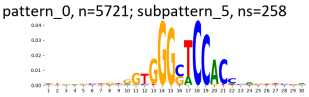

pattern_0, n=5721; subpattern_6, ns=67

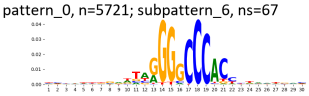

pattern_0, n=5721; subpattern_7, ns=26

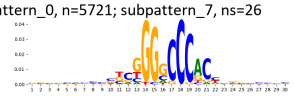

pattern_0, n=5721; subpattern_8, ns=10

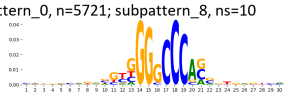

TF-MoDisCO pattern_0 n=5721, PWM

pattern_0, n=5721; subpattern_0, ns=1245

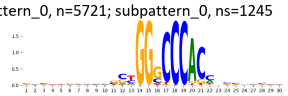

pattern_0, n=5721; subpattern_1, ns=1227

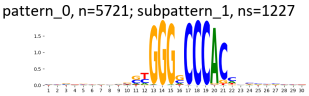

pattern_0, n=5721; subpattern_2, ns=1053

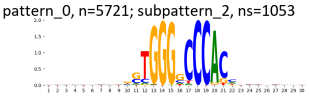

pattern_0, n=5721; subpattern_3, ns=1031

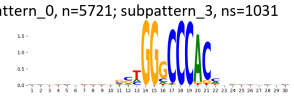

pattern_0, n=5721; subpattern_4, ns=804

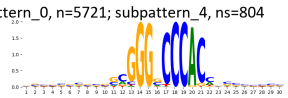

pattern_0, n=5721; subpattern_5, ns=258

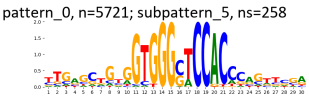

pattern_0, n=5721; subpattern_6, ns=67

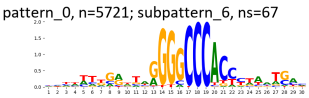

pattern_0, n=5721; subpattern_7, ns=26

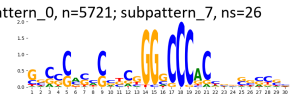

pattern_0, n=5721; subpattern_8, ns=10

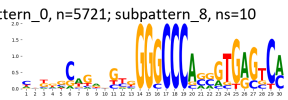

TF-MoDisCO pattern_1 n=2567, CWM

pattern_1, n=2567; subpattern_0, ns=618

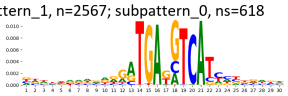

pattern_1, n=2567; subpattern_1, ns=547

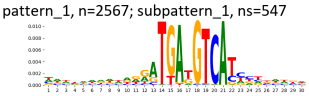

pattern_1, n=2567; subpattern_2, ns=513

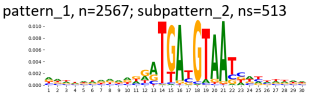

pattern_1, n=2567; subpattern_3, ns=474

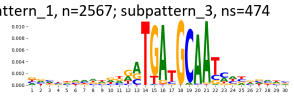

pattern_1, n=2567; subpattern_4, ns=339

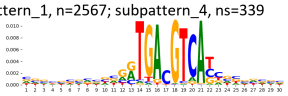

pattern_1, n=2567; subpattern_5, ns=65

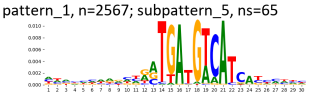

pattern_1, n=2567; subpattern_6, ns=9

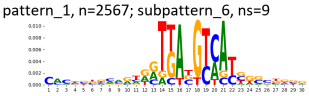

pattern_1, n=2567; subpattern_7, ns=2

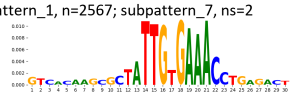

TF-MoDisCO pattern_1 n=2567, PWM

pattern_1, n=2567; subpattern_0, ns=618

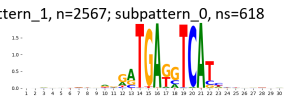

pattern_1, n=2567; subpattern_1, ns=547

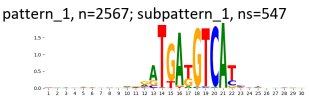

pattern_1, n=2567; subpattern_2, ns=513

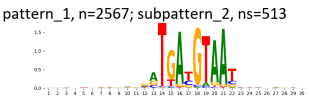

pattern_1, n=2567; subpattern_3, ns=474

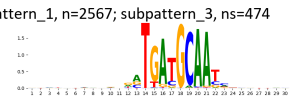

pattern_1, n=2567; subpattern_4, ns=339

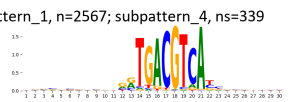

pattern_1, n=2567; subpattern_5, ns=65

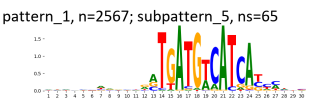

pattern_1, n=2567; subpattern_6, ns=9

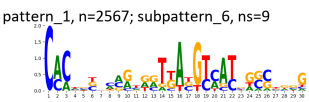

pattern_1, n=2567; subpattern_7, ns=2

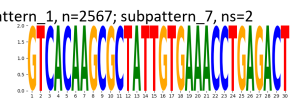

TF-MoDisCO pattern_2 n=1600, CWM

pattern_2, n=1600; subpattern_0, ns=590

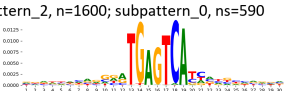

pattern_2, n=1600; subpattern_1, ns=537

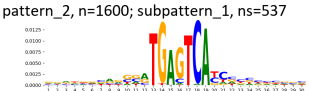

pattern_2, n=1600; subpattern_2, ns=432

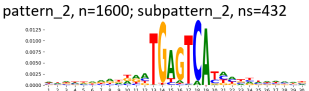

pattern_2, n=1600; subpattern_3, ns=16

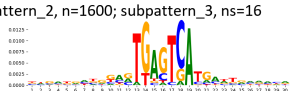

pattern_2, n=1600; subpattern_4, ns=11

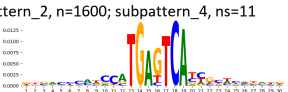

pattern_2, n=1600; subpattern_5, ns=10

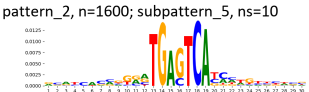

pattern_2, n=1600; subpattern_6, ns=4

TF-MoDisCO pattern_2 n=1600, PWM

pattern_2, n=1600; subpattern_0, ns=590

pattern_2, n=1600; subpattern_1, ns=537

pattern_2, n=1600; subpattern_2, ns=432

pattern_2, n=1600; subpattern_3, ns=16

pattern_2, n=1600; subpattern_4, ns=11

pattern_2, n=1600; subpattern_5, ns=10

pattern_2, n=1600; subpattern_6, ns=4

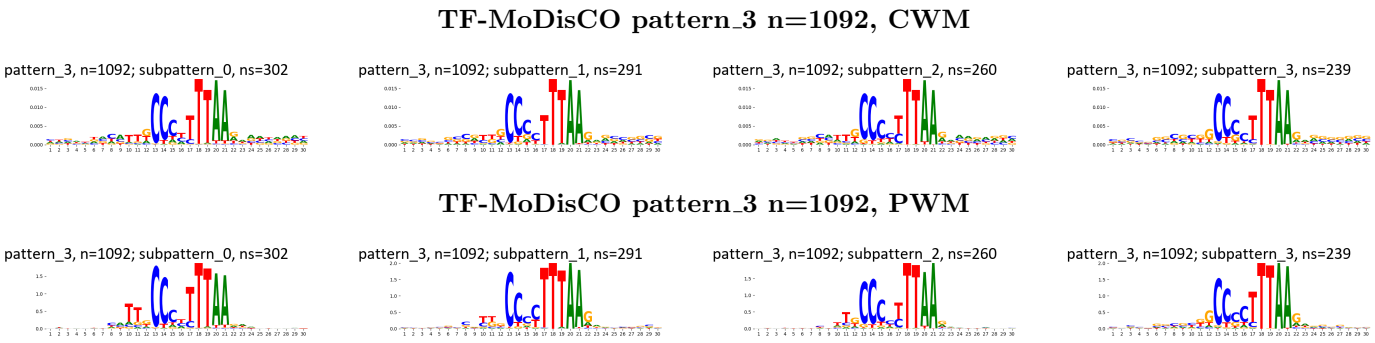

Supplementary Figure 579: TF-MoDisCO subpatterns for the ZFP69B transcription factor in HEK293 (accession ENCSR381VYR).

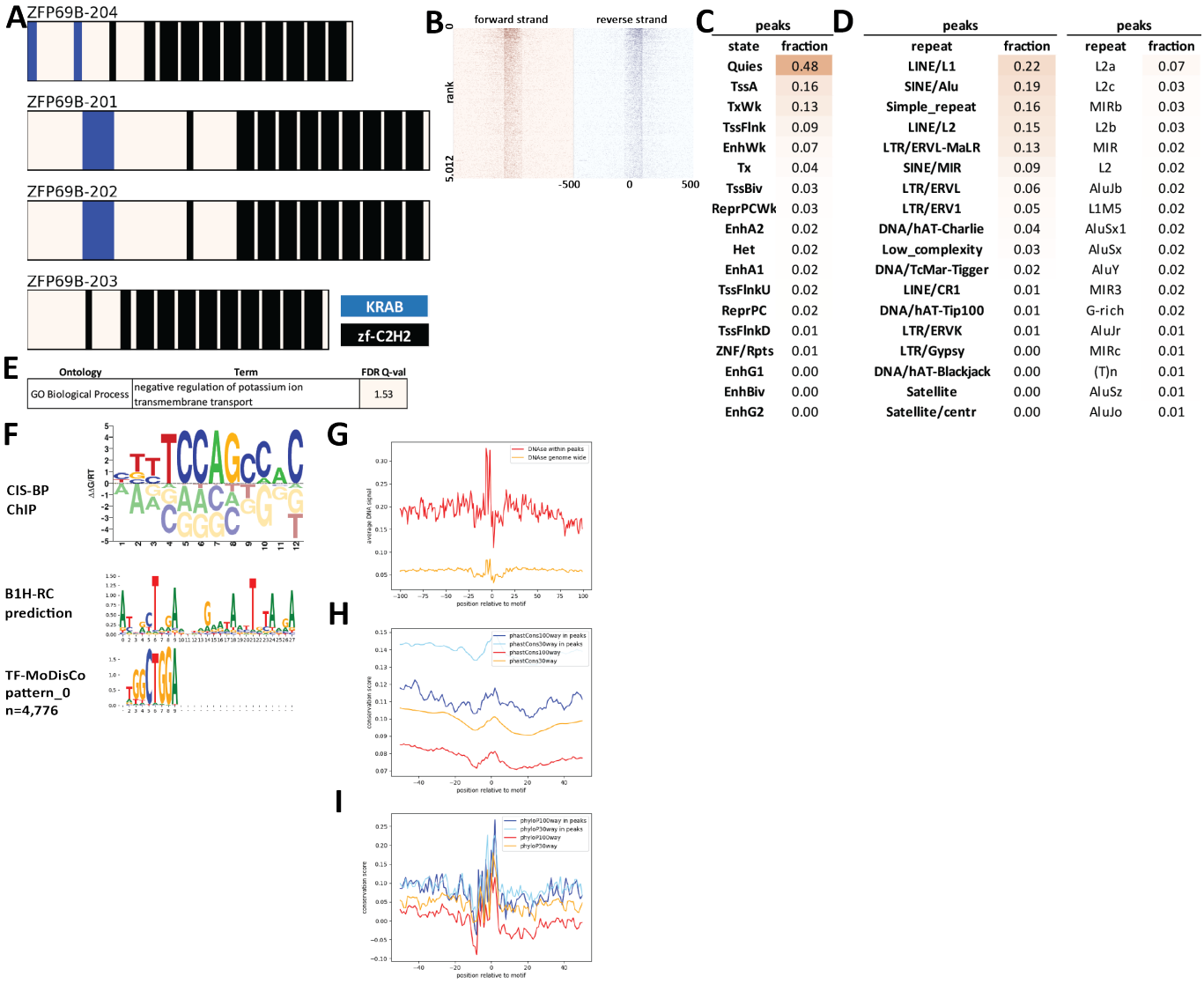

peaks

state	fraction
Quies	0.48
TssA	0.16
TxWk	0.13
TssFlnk	0.09
EnhWk	0.07
Tx	0.04
TssBiv	0.03
ReprPCWk	0.03
EnhA2	0.02
Het	0.02
EnhA1	0.02
TssFlnkU	0.02
ReprPC	0.02
TssFlnkD	0.01
ZNF/Rpts	0.01
EnhG1	0.00
EnhBiv	0.00
EnhG2	0.00

peaks

repeat	fraction
LINE/L1	0.22
SINE/Alu	0.19
Simple_repeat	0.16
LINE/L2	0.15
LTR/ERVL-MaLR	0.13
SINE/MIR	0.09
LTR/ERVL	0.06
LTR/ERV1	0.05
DNA/hAT-Charlie	0.04
Low_complexity	0.03
DNA/TcMar-Tigger	0.02
LINE/CR1	0.01
DNA/hAT-Tip100	0.01
LTR/ERVK	0.01
LTR/Gypsy	0.00
DNA/hAT-Blackjack	0.00
Satellite	0.00
Satellite/centr	0.00

peaks

repeat	fraction
L2a	0.07
L2c	0.03
MIRb	0.03
L2b	0.03
MIR	0.02
L2	0.02
AluJb	0.02
L1M5	0.02
AluSx1	0.02
AluSx	0.02
AluY	0.02
MIR3	0.02
G-rich	0.02
AluJr	0.01
MIRc	0.01
(T)n	0.01
AluSz	0.01
AluJo	0.01

Supplementary Figure 580: Properties and genomic distribution of motifs identified for the ZFP69B transcription factor in HEK293 (accession ChipExo models).

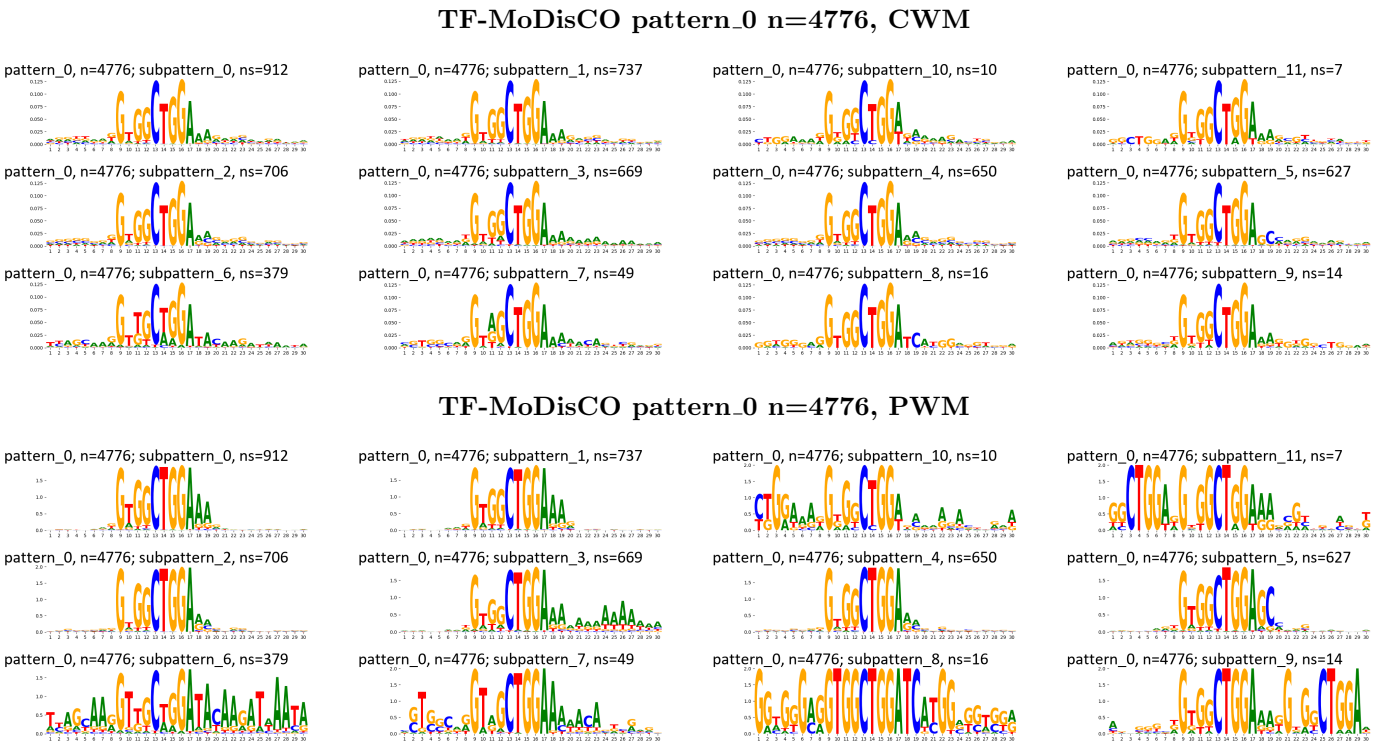

Supplementary Figure 581: TF-MoDisCO subpatterns for the ZFP69B transcription factor in HEK293 (accession ChipExo models).

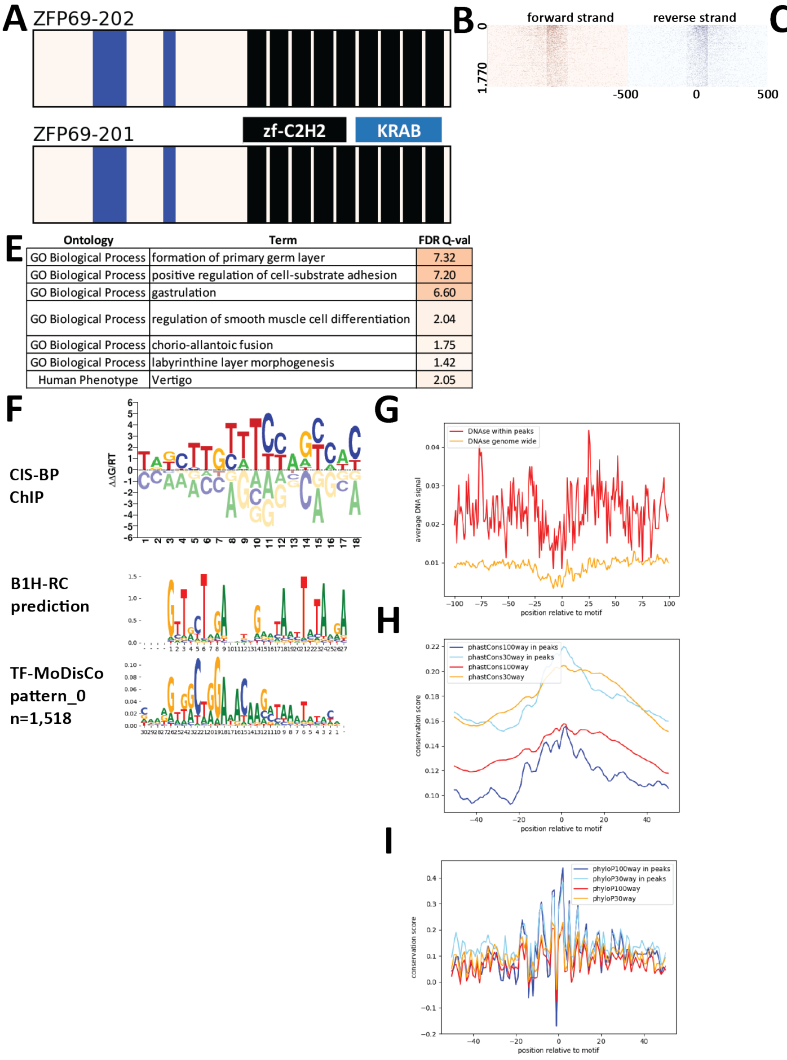

Ontology	Term	FDR Q-val
GO Biological Process	formation of primary germ layer	7.32
GO Biological Process	positive regulation of cell-substrate adhesion	7.20
GO Biological Process	gastrulation	6.60
GO Biological Process	regulation of smooth muscle cell differentiation	2.04
GO Biological Process	chorio-allantoic fusion	1.75
GO Biological Process	labyrinthine layer morphogenesis	1.42
Human Phenotype	Vertigo	2.05

peaks	
state	fraction
Quies	0.57
TxWk	0.15
Tx	0.08
EnhWk	0.04
ReprPCWk	0.03
TssA	0.03
Het	0.02
TssFlnk	0.02
ReprPC	0.01
EnhA1	0.01
EnhA2	0.01
TssBiv	0.01
EnhG1	0.01
ZNF/Rpts	0.00
TssFlnkU	0.00
TssFlnkD	0.00
EnhBiv	0.00
EnhG2	0.00

peaks		peaks	
repeat	fraction	repeat	fraction
LINE/L1	0.65	L1M5	0.06
SINE/Alu	0.25	L1ME4b	0.06
Simple_repeat	0.09	L1MC1	0.04
LTR/ERVL-MaLR	0.08	L1M4	0.04
LINE/L2	0.07	L1ME1	0.04
SINE/MIR	0.06	L1MB7	0.03
LTR/ERV1	0.05	L2a	0.03
DNA/hAT-Charlie	0.04	AluJb	0.03
LTR/ERVL	0.04	AluSz	0.02
DNA/TcMar-Tigger	0.03	MIRb	0.02
Low_complexity	0.01	AluSx	0.02
LINE/CR1	0.01	L1MC	0.02
DNA/hAT-Tip100	0.01	L1ME4a	0.02
Satellite/centr	0.01	AluSx1	0.02
Satellite	0.01	AluY	0.02
LTR/ERVK	0.01	L1MB8	0.02
LINE/RTE-X	0.00	L2c	0.02
Satellite/acro	0.00	L1MD	0.02

Supplementary Figure 582: Properties and genomic distribution of motifs identified for the ZFP69 transcription factor in HEK293 (accession ChipExo models).

TF-MoDisCO pattern_0 n=1518, CWM

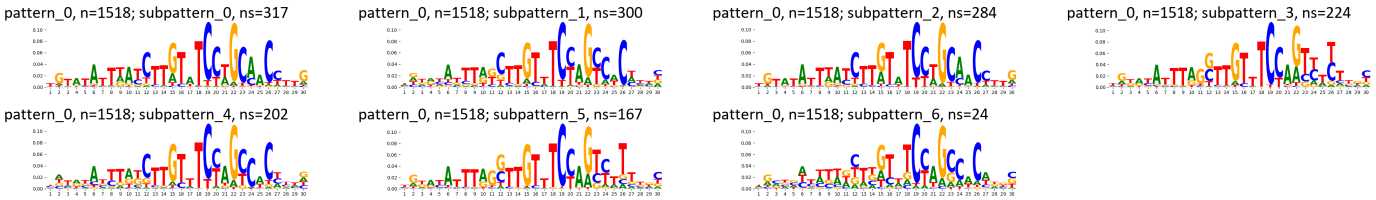

TF-MoDisCO pattern_0 n=1518, PWM

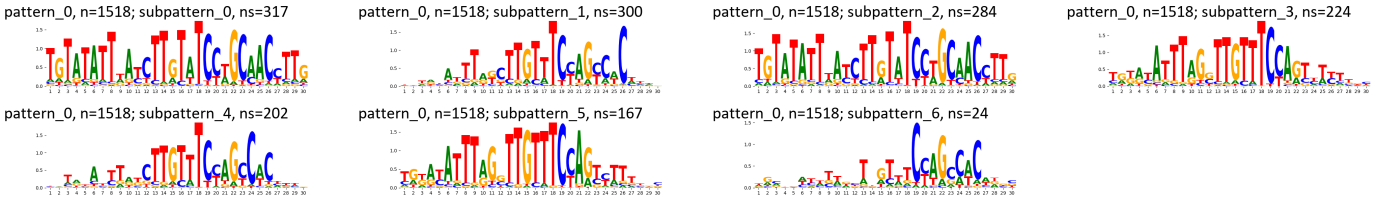

Supplementary Figure 583: TF-MoDisCO subpatterns for the ZFP69 transcription factor in HEK293 (accession ChipExo models).

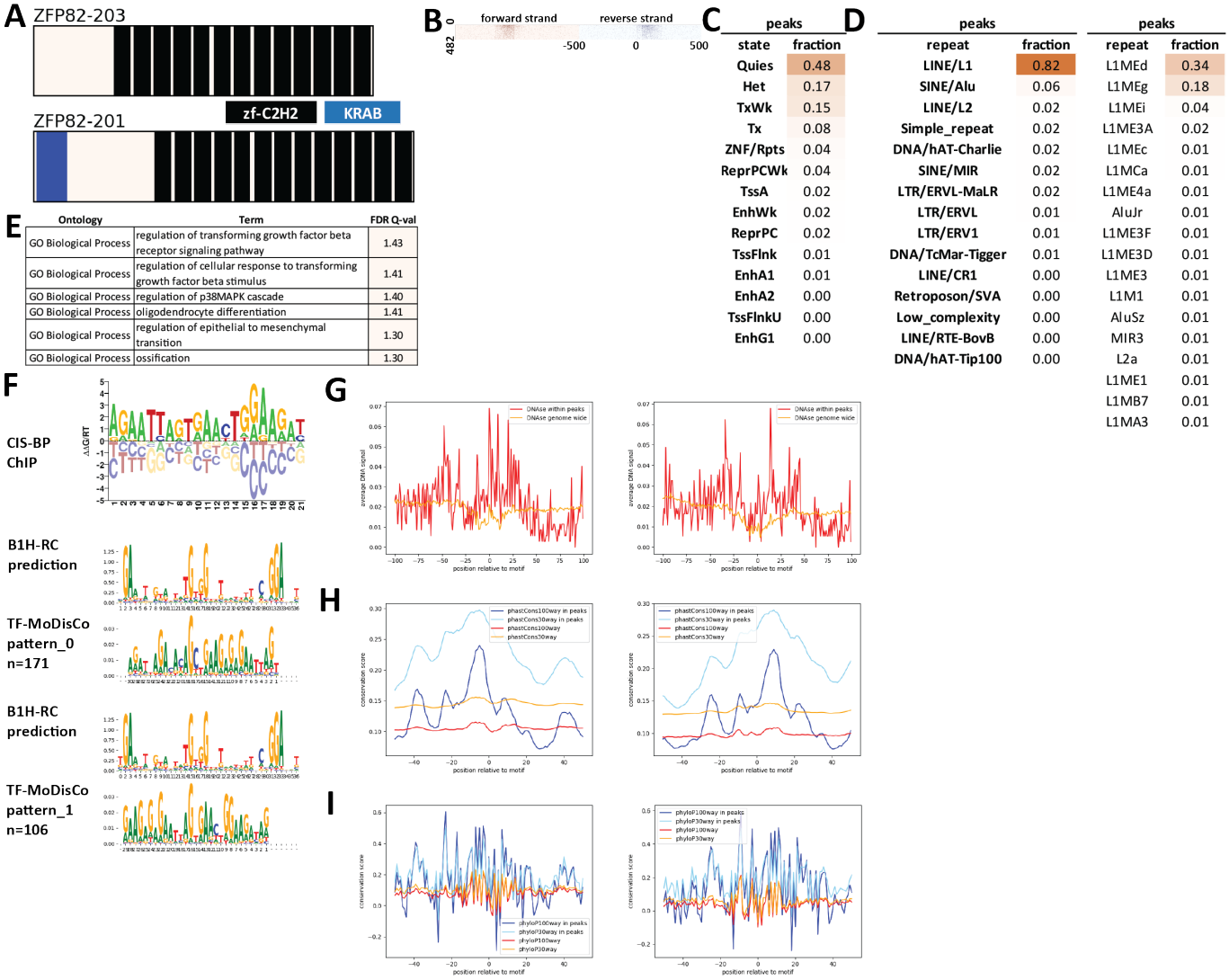

Supplementary Figure 584: Properties and genomic distribution of motifs identified for the ZFP82 transcription factor in HEK293 (accession Hughes GR models).

TF-MoDisCO pattern_0 n=171, CWM

pattern_0, n=171; subpattern_0, ns=52

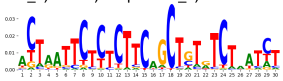

pattern_0, n=171; subpattern_1, ns=43

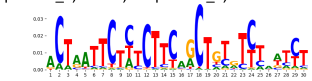

pattern_0, n=171; subpattern_2, ns=42

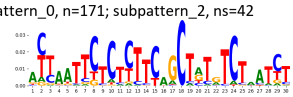

pattern_0, n=171; subpattern_3, ns=34

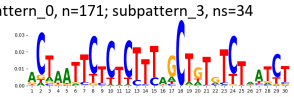

TF-MoDisCO pattern_0 n=171, PWM

pattern_0, n=171; subpattern_0, ns=52

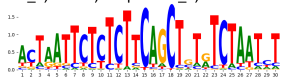

pattern_0, n=171; subpattern_1, ns=43

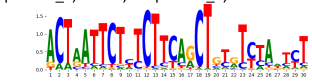

pattern_0, n=171; subpattern_2, ns=42

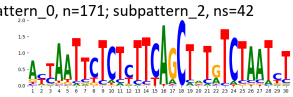

pattern_0, n=171; subpattern_3, ns=34

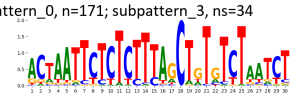

TF-MoDisCO pattern_1 n=106, CWM

pattern_1, n=106; subpattern_0, ns=34

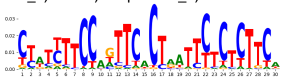

pattern_1, n=106; subpattern_1, ns=23

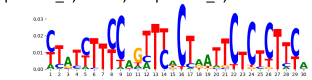

pattern_1, n=106; subpattern_2, ns=19

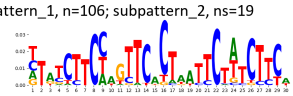

pattern_1, n=106; subpattern_3, ns=15

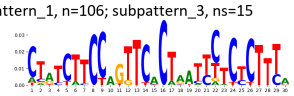

pattern_1, n=106; subpattern_4, ns=15

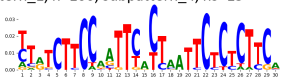

TF-MoDisCO pattern_1 n=106, PWM

pattern_1, n=106; subpattern_0, ns=34

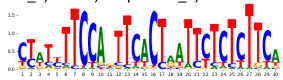

pattern_1, n=106; subpattern_1, ns=23

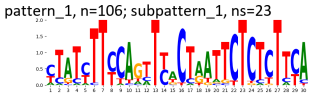

pattern_1, n=106; subpattern_2, ns=19

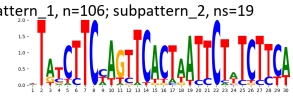

pattern_1, n=106; subpattern_3, ns=15

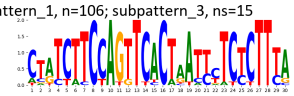

pattern_1, n=106; subpattern_4, ns=15

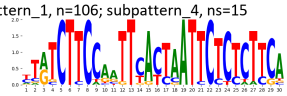

Supplementary Figure 585: TF-MoDisCO subpatterns for the ZFP82 transcription factor in HEK293 (accession Hughes GR models).

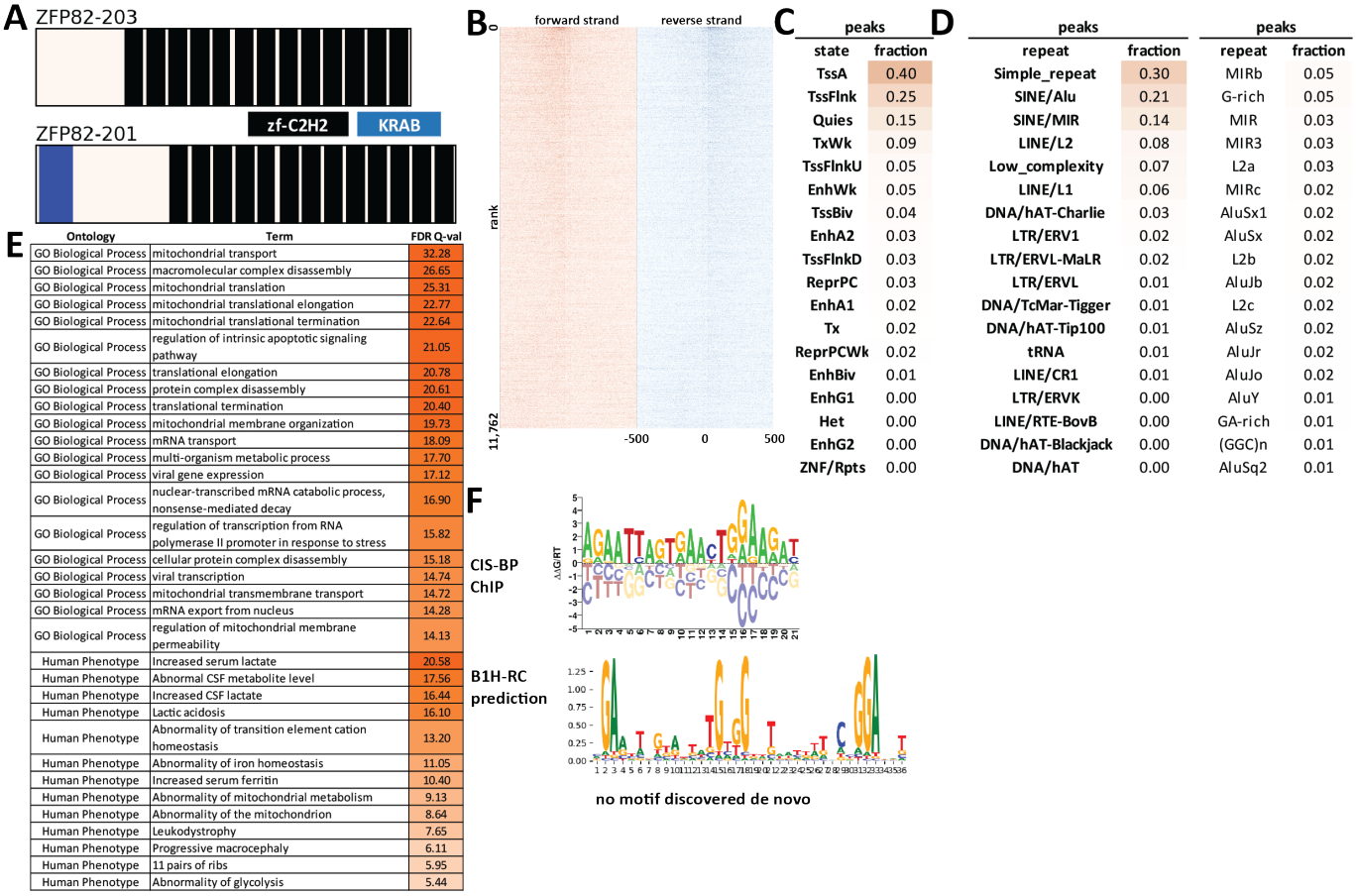

E

Ontology	Term	FDR Q-val
GO Biological Process	mitochondrial transport	32.28
GO Biological Process	macromolecular complex disassembly	26.65
GO Biological Process	mitochondrial translation	25.31
GO Biological Process	mitochondrial translational elongation	22.77
GO Biological Process	mitochondrial translational termination	22.64
GO Biological Process	regulation of intrinsic apoptotic signaling pathway	21.05
GO Biological Process	translational elongation	20.78
GO Biological Process	protein complex disassembly	20.61
GO Biological Process	translational termination	20.40
GO Biological Process	mitochondrial membrane organization	19.73
GO Biological Process	mRNA transport	18.09
GO Biological Process	multi-organism metabolic process	17.70
GO Biological Process	viral gene expression	17.12
GO Biological Process	nuclear-transcribed mRNA catabolic process, nonsense-mediated decay	16.90
GO Biological Process	regulation of transcription from RNA polymerase II promoter in response to stress	15.82
GO Biological Process	cellular protein complex disassembly	15.18
GO Biological Process	viral transcription	14.74
GO Biological Process	mitochondrial transmembrane transport	14.72
GO Biological Process	mRNA export from nucleus	14.28
GO Biological Process	regulation of mitochondrial membrane permeability	14.13
Human Phenotype	Increased serum lactate	20.58
Human Phenotype	Abnormal CSF metabolite level	17.56
Human Phenotype	Increased CSF lactate	16.44
Human Phenotype	Lactic acidosis	16.10
Human Phenotype	Abnormality of transition element cation homeostasis	13.20
Human Phenotype	Abnormality of iron homeostasis	11.05
Human Phenotype	Increased serum ferritin	10.40
Human Phenotype	Abnormality of mitochondrial metabolism	9.13
Human Phenotype	Abnormality of the mitochondrion	8.64
Human Phenotype	Leukodystrophy	7.65
Human Phenotype	Progressive macrocephaly	6.11
Human Phenotype	11 pairs of ribs	5.95
Human Phenotype	Abnormality of glycolysis	5.44

C

peaks	
state	fraction
TssA	0.40
TssFlnk	0.25
Quies	0.15
TxWk	0.09
TssFlnkU	0.05
EnhWk	0.05
TssBiv	0.04
EnhA2	0.03
TssFlnkD	0.03
ReprPC	0.03
EnhA1	0.02
Tx	0.02
ReprPCWk	0.02
EnhBiv	0.01
EnhG1	0.00
Het	0.00
EnhG2	0.00
ZNF/Rpts	0.00

D

peaks		peaks	
repeat	fraction	repeat	fraction
Simple_repeat	0.30	MIRb	0.05
SINE/Alu	0.21	G-rich	0.05
SINE/MIR	0.14	MIR	0.03
LINE/L2	0.08	MIR3	0.03
Low_complexity	0.07	L2a	0.03
LINE/L1	0.06	MIRc	0.02
DNA/hAT-Charlie	0.03	AluSx1	0.02
LTR/ERV1	0.02	AluSx	0.02
LTR/ERVL-MaLR	0.02	L2b	0.02
LTR/ERVL	0.01	AluJb	0.02
DNA/TcMar-Tigger	0.01	L2c	0.02
DNA/hAT-Tip100	0.01	AluSz	0.02
tRNA	0.01	AluJr	0.02
LINE/CR1	0.01	AluJo	0.02
LTR/ERVK	0.00	AluY	0.01
LINE/RTE-BovB	0.00	GA-rich	0.01
DNA/hAT-Blackjack	0.00	(GGC)n	0.01
DNA/hAT	0.00	AluSq2	0.01

Supplementary Figure 586: Properties and genomic distribution of motifs identified for the ZFP82 transcription factor in HepG2 (accession ENCSR196FSX).

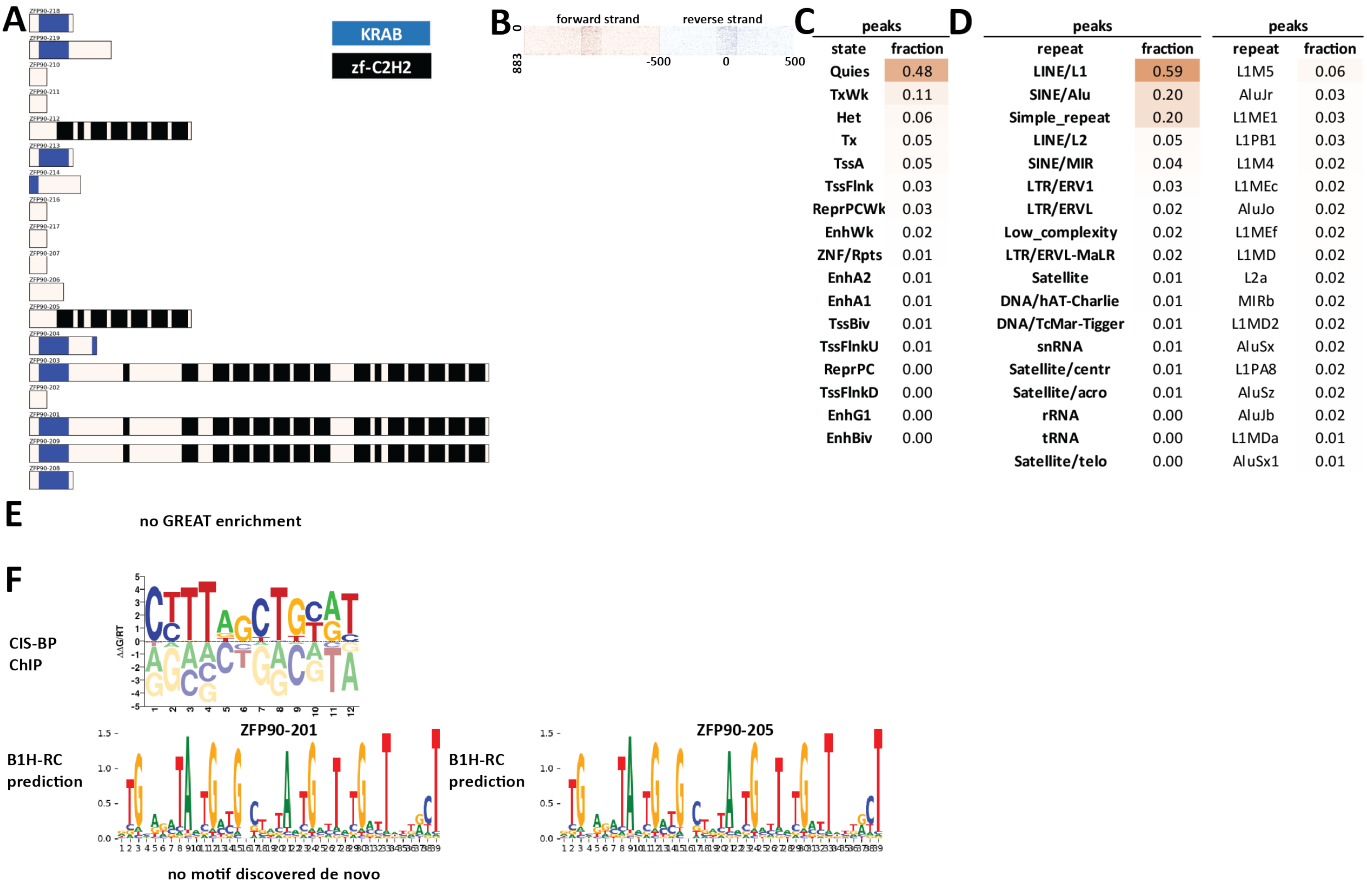

Supplementary Figure 587: Properties and genomic distribution of motifs identified for the ZFP90 transcription factor in HEK293 (accession ChipExo models).

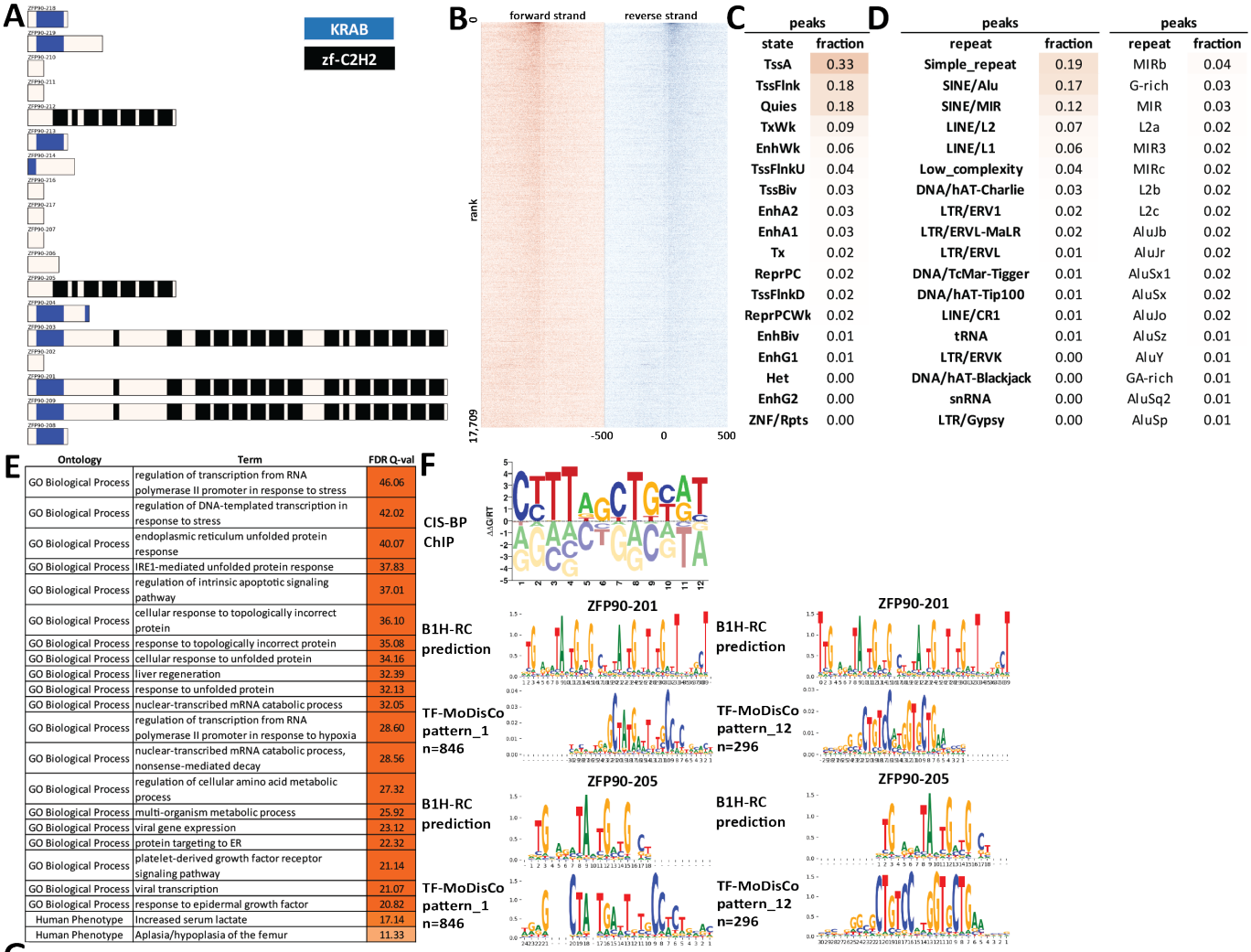

Supplementary Figure 588: Properties and genomic distribution of motifs identified for the ZFP90 transcription factor in HepG2 (accession ENCSR377GZS).

TF-MoDisCO pattern_1 n=846, CWM

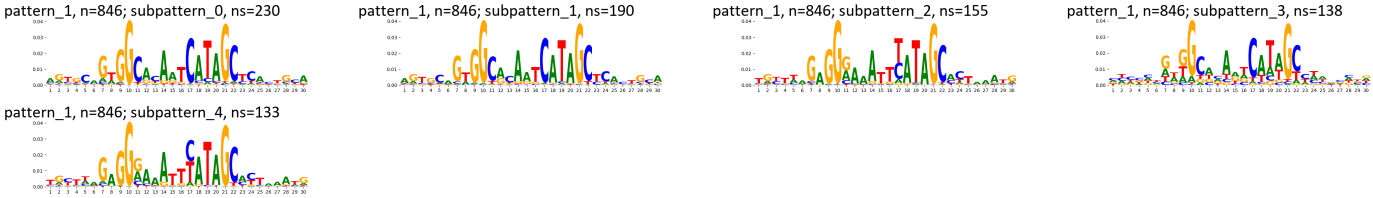

TF-MoDisCO pattern_1 n=846, PWM

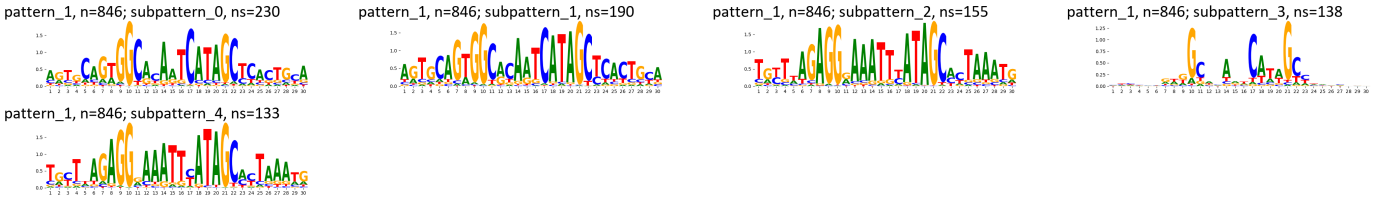

TF-MoDisCO pattern_12 n=296, CWM

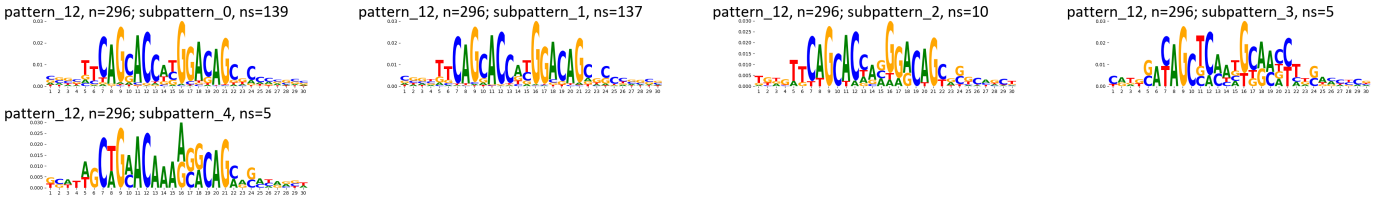

TF-MoDisCO pattern_12 n=296, PWM

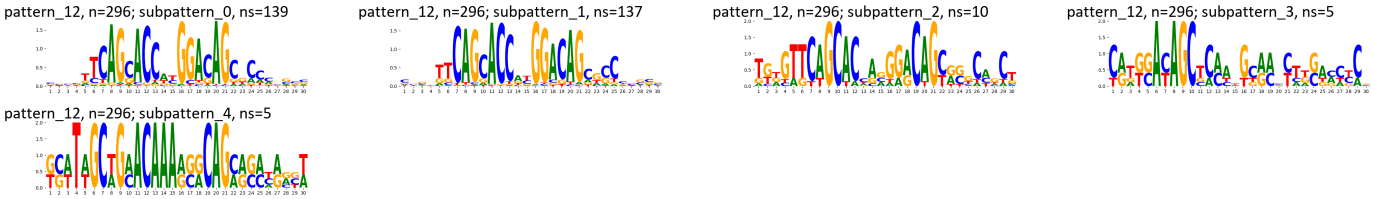

Supplementary Figure 589: TF-MoDisCO subpatterns for the ZFP90 transcription factor in HepG2 (accession ENCSR377GZS).

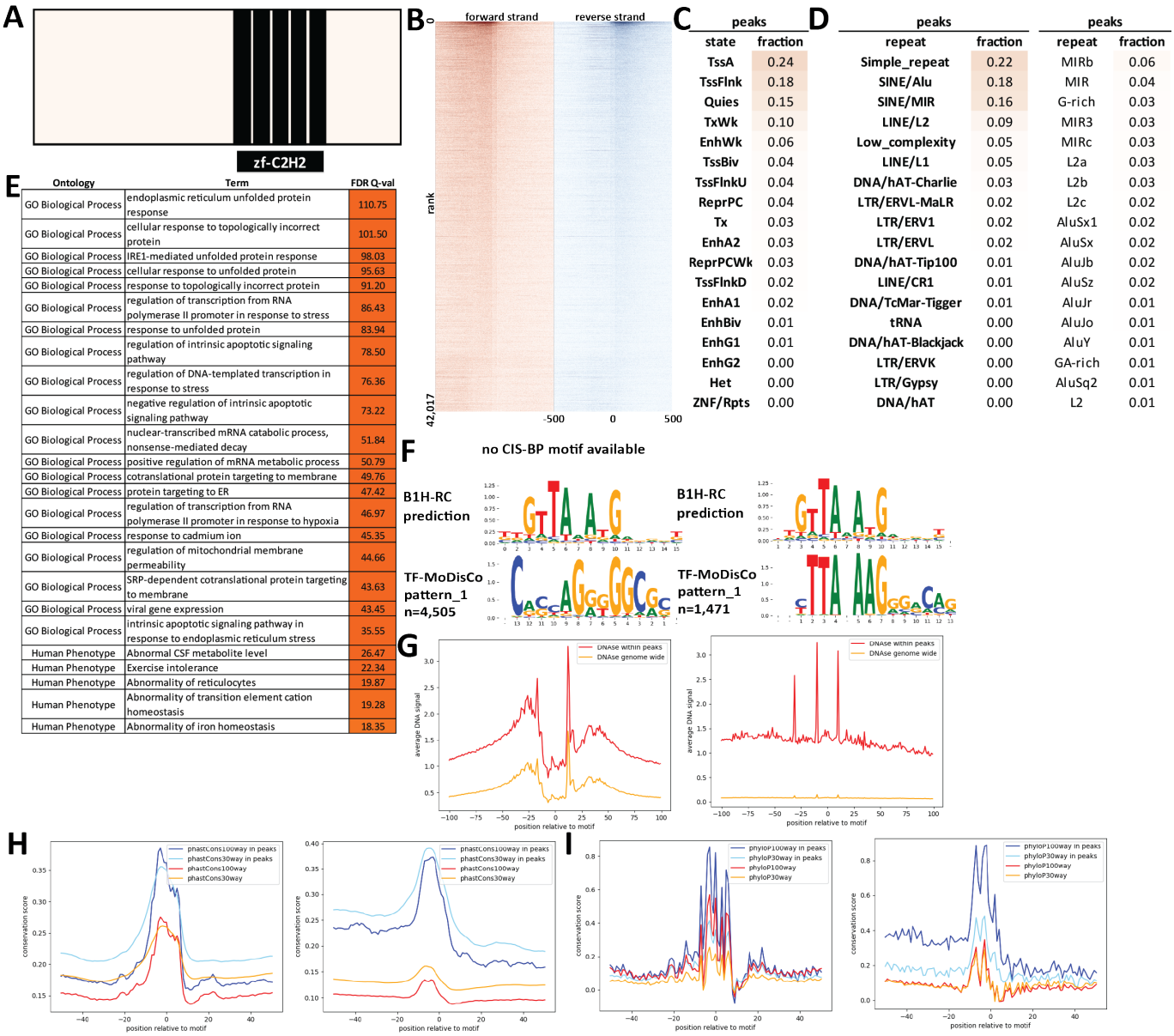

Supplementary Figure 590: Properties and genomic distribution of motifs identified for the ZFP91 transcription factor in HepG2 (accession ENCSR678KUJ).

TF-MoDisCO pattern_1 n=4505, CWM

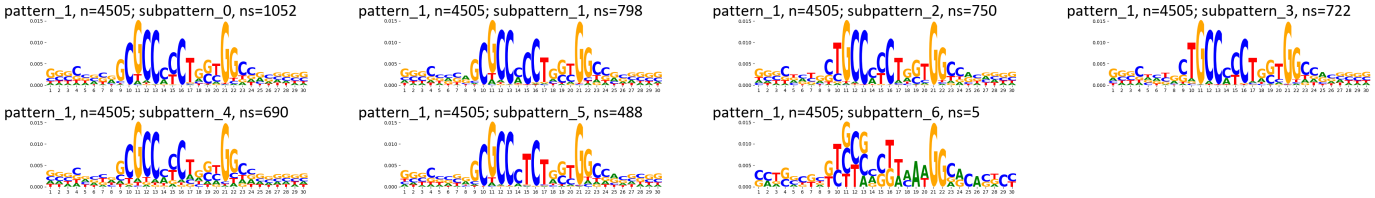

TF-MoDisCO pattern_1 n=4505, PWM

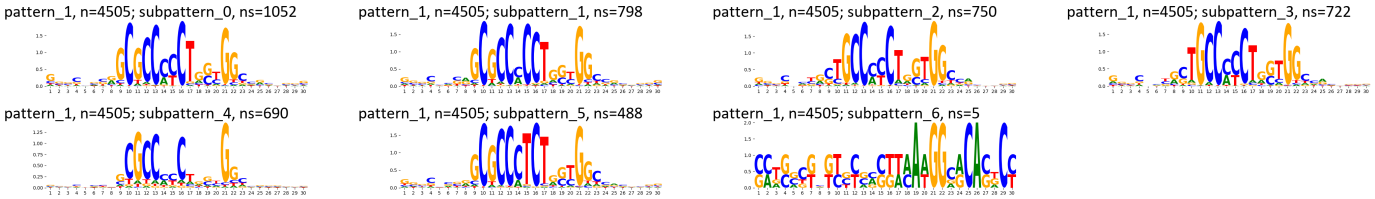

TF-MoDisCO pattern_4 n=1471, CWM

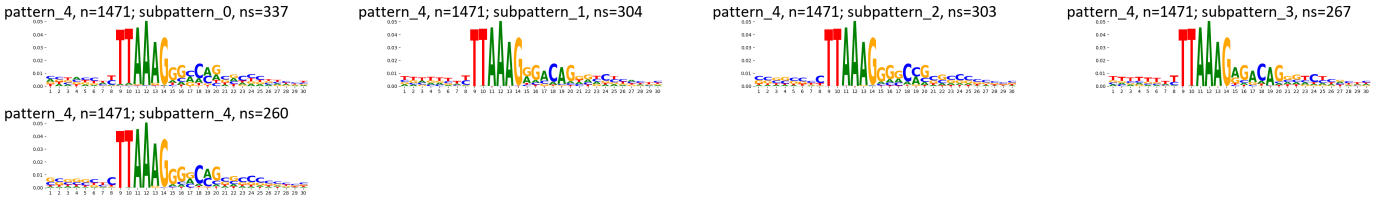

TF-MoDisCO pattern_4 n=1471, PWM

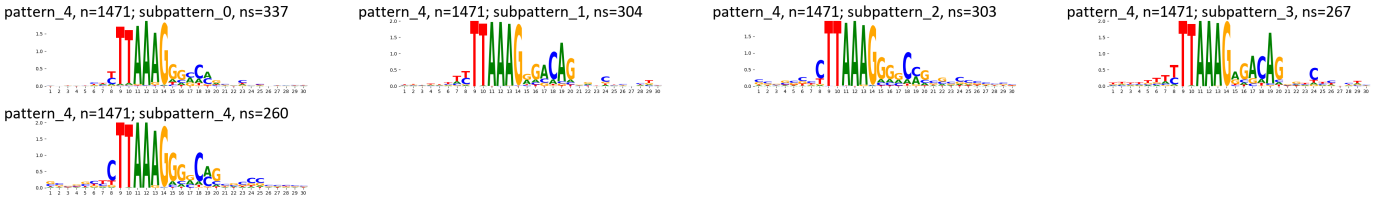

Supplementary Figure 591: TF-MoDisCO subpatterns for the ZFP91 transcription factor in HepG2 (accession ENCSR678KUJ).

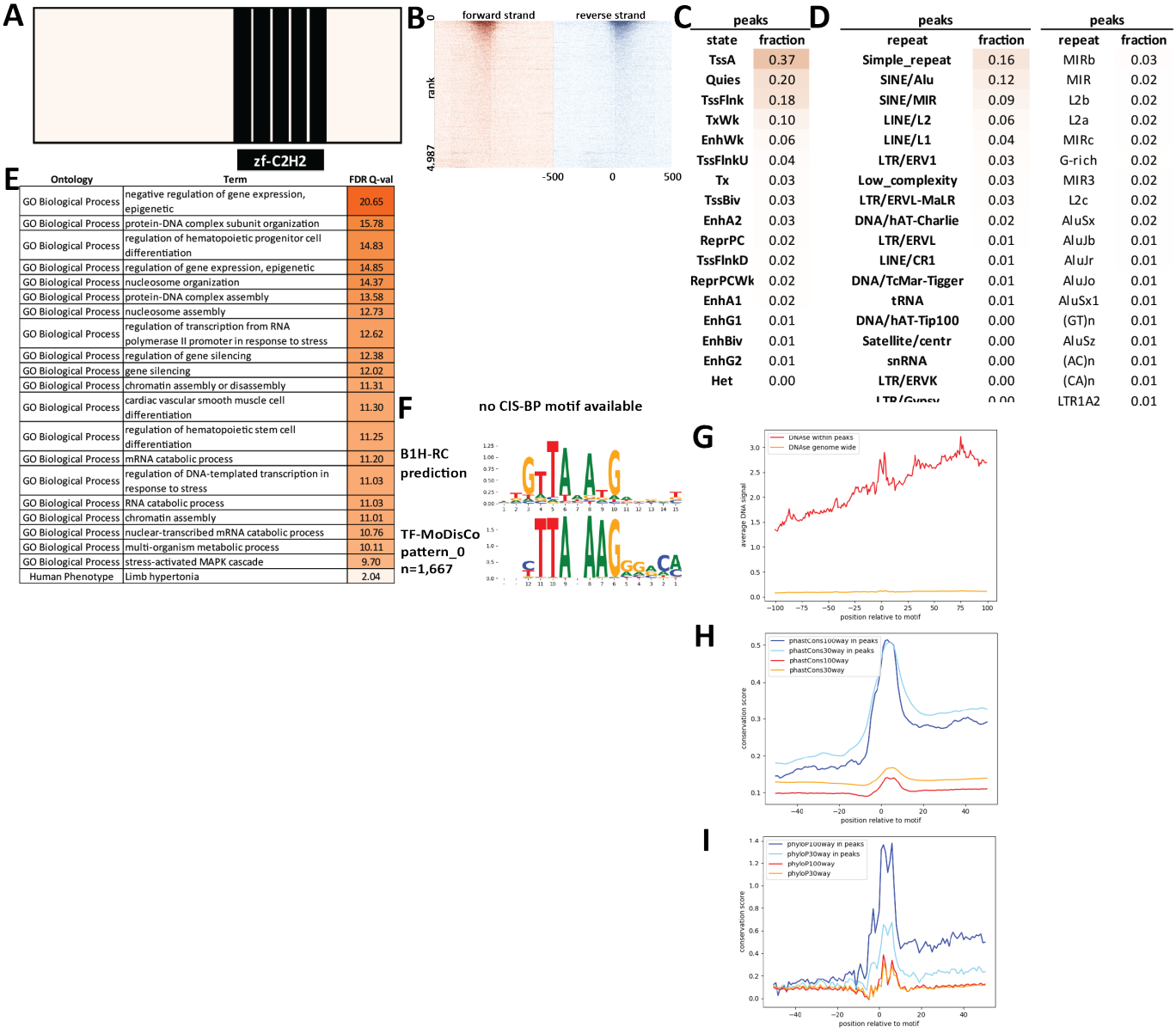

Supplementary Figure 592: Properties and genomic distribution of motifs identified for the ZFP91 transcription factor in K562 (accession ENCSR201DCF).

TF-MoDisCO pattern_0 n=1667, CWM

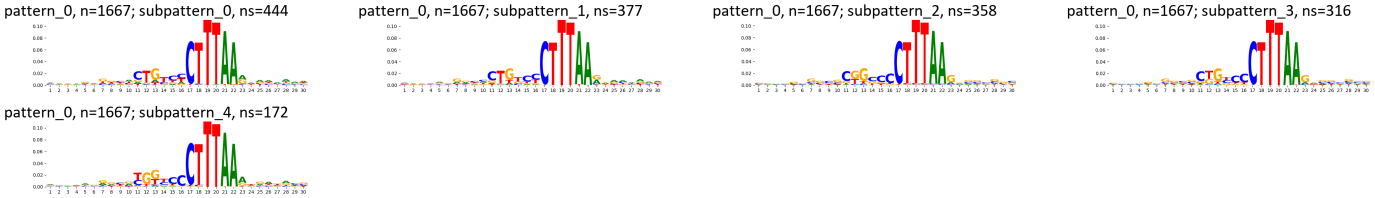

TF-MoDisCO pattern_0 n=1667, PWM

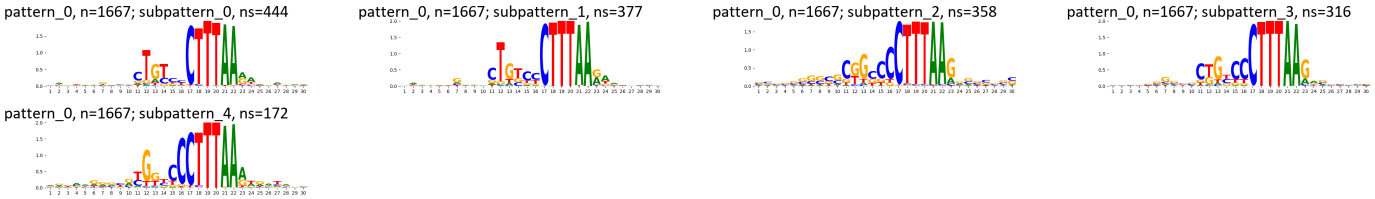

Supplementary Figure 593: TF-MoDisCO subpatterns for the ZFP91 transcription factor in K562 (accession ENCSR201DCF).

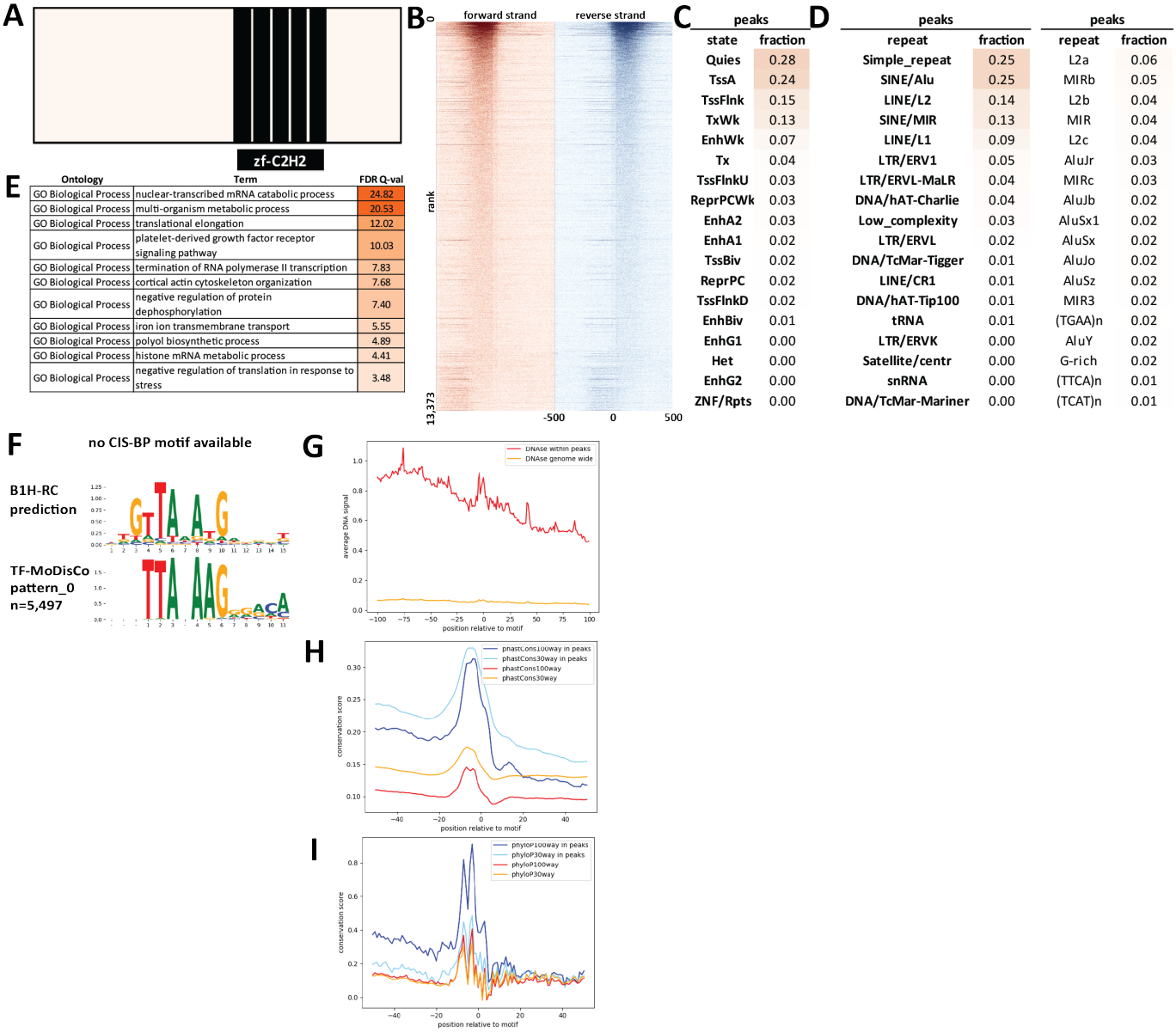

Supplementary Figure 594: Properties and genomic distribution of motifs identified for the ZFP91 transcription factor in K562 (accession ENCSR898XMH).

TF-MoDisCO pattern_0 n=5497, CWM

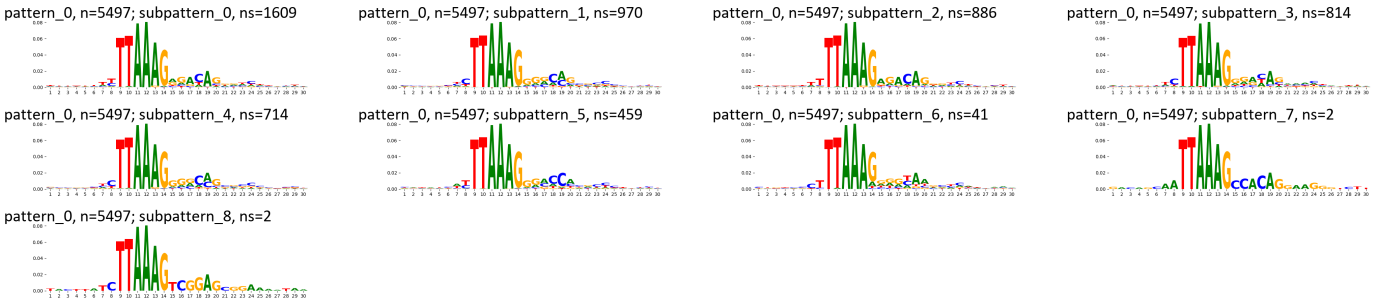

TF-MoDisCO pattern_0 n=5497, PWM

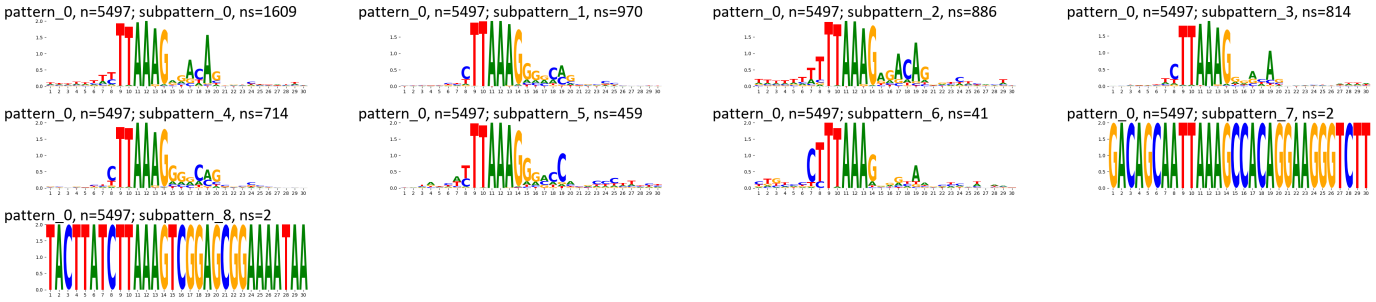

Supplementary Figure 595: TF-MoDisCO subpatterns for the ZFP91 transcription factor in K562 (accession ENCSR898XMH).

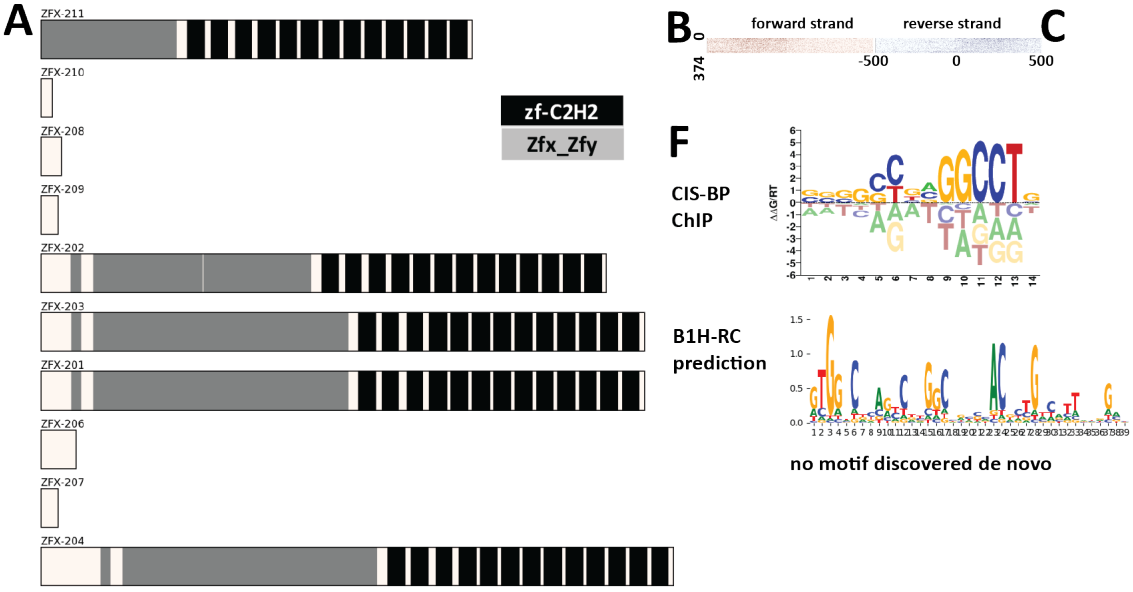

E

Ontology	Term	FDR Q-val
GO Biological Process	RNA processing	10.02
GO Biological Process	mRNA metabolic process	9.40
GO Biological Process	ribonucleoprotein complex biogenesis	8.26
GO Biological Process	ribonucleoprotein complex assembly	4.69
GO Biological Process	ribonucleoprotein complex subunit organization	4.46
GO Biological Process	translational initiation	4.06
GO Biological Process	ncRNA processing	3.95
GO Biological Process	viral gene expression	3.79
GO Biological Process	RNA splicing	3.73
GO Biological Process	mRNA processing	3.63
GO Biological Process	cellular macromolecule catabolic process	3.53
GO Biological Process	nuclear-transcribed mRNA catabolic process	3.55
GO Biological Process	cellular macromolecular complex assembly	3.48
GO Biological Process	ribosome biogenesis	3.26
GO Biological Process	mRNA catabolic process	3.06
GO Biological Process	ncRNA metabolic process	2.78
GO Biological Process	RNA catabolic process	2.77
GO Biological Process	multi-organism metabolic process	2.78
GO Biological Process	translation	2.57
GO Biological Process	mRNA splicing, via spliceosome	2.41

Supplementary Figure 596: Properties and genomic distribution of motifs identified for the ZFX transcription factor in 22Rv1 (accession ENCSR246MLJ).

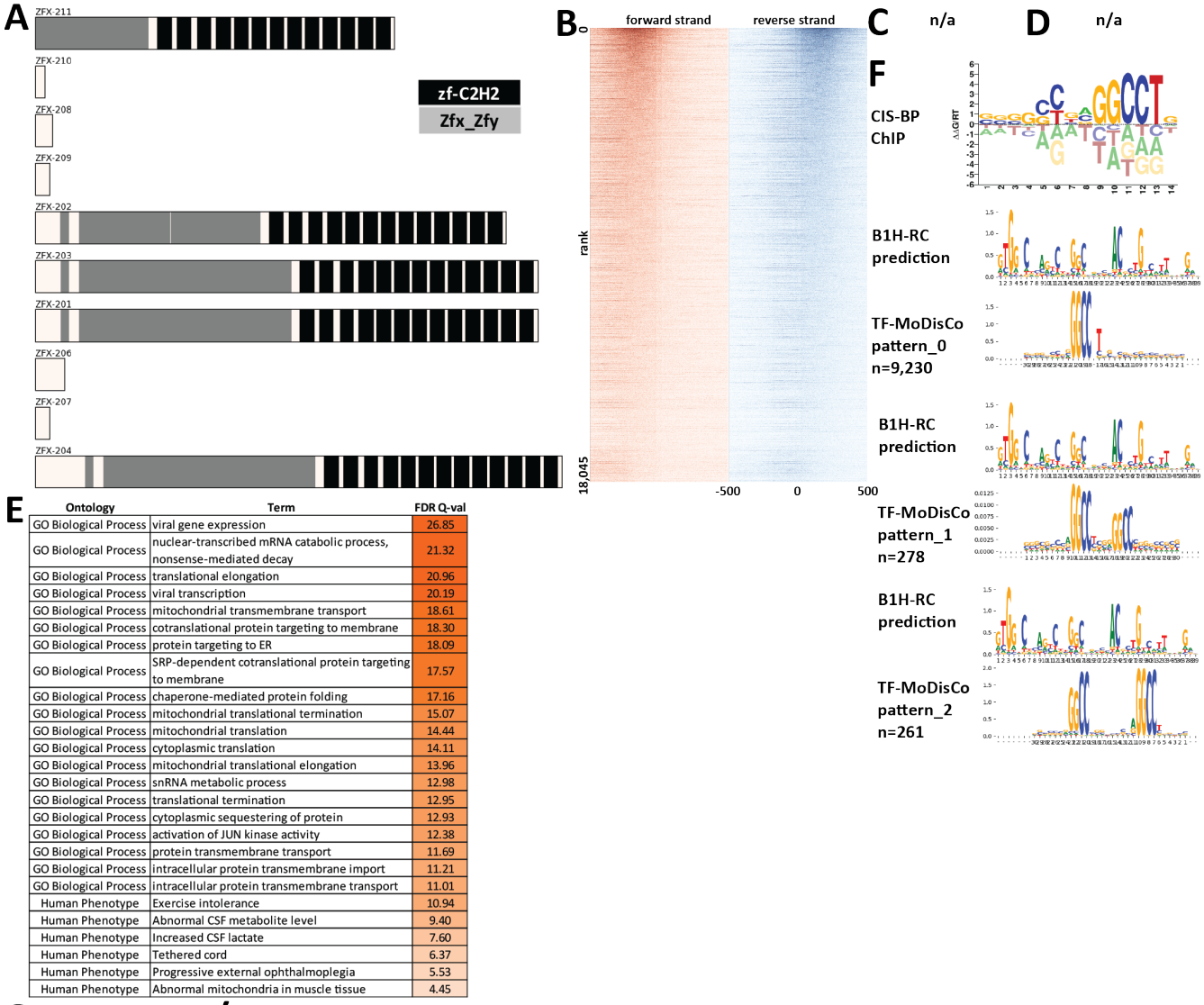

E

Ontology	Term	FDR Q-val
GO Biological Process	viral gene expression	26.85
GO Biological Process	nuclear-transcribed mRNA catabolic process, nonsense-mediated decay	21.32
GO Biological Process	translational elongation	20.96
GO Biological Process	viral transcription	20.19
GO Biological Process	mitochondrial transmembrane transport	18.61
GO Biological Process	cotranslational protein targeting to membrane	18.30
GO Biological Process	protein targeting to ER	18.09
GO Biological Process	SRP-dependent cotranslational protein targeting to membrane	17.57
GO Biological Process	chaperone-mediated protein folding	17.16
GO Biological Process	mitochondrial translational termination	15.07
GO Biological Process	mitochondrial translation	14.44
GO Biological Process	cytoplasmic translation	14.11
GO Biological Process	mitochondrial translational elongation	13.96
GO Biological Process	snRNA metabolic process	12.98
GO Biological Process	translational termination	12.95
GO Biological Process	cytoplasmic sequestering of protein	12.93
GO Biological Process	activation of JUN kinase activity	12.38
GO Biological Process	protein transmembrane transport	11.69
GO Biological Process	intracellular protein transmembrane import	11.21
GO Biological Process	intracellular protein transmembrane transport	11.01
Human Phenotype	Exercise intolerance	10.94
Human Phenotype	Abnormal CSF metabolite level	9.40
Human Phenotype	Increased CSF lactate	7.60
Human Phenotype	Tethered cord	6.37
Human Phenotype	Progressive external ophthalmoplegia	5.53
Human Phenotype	Abnormal mitochondria in muscle tissue	4.45

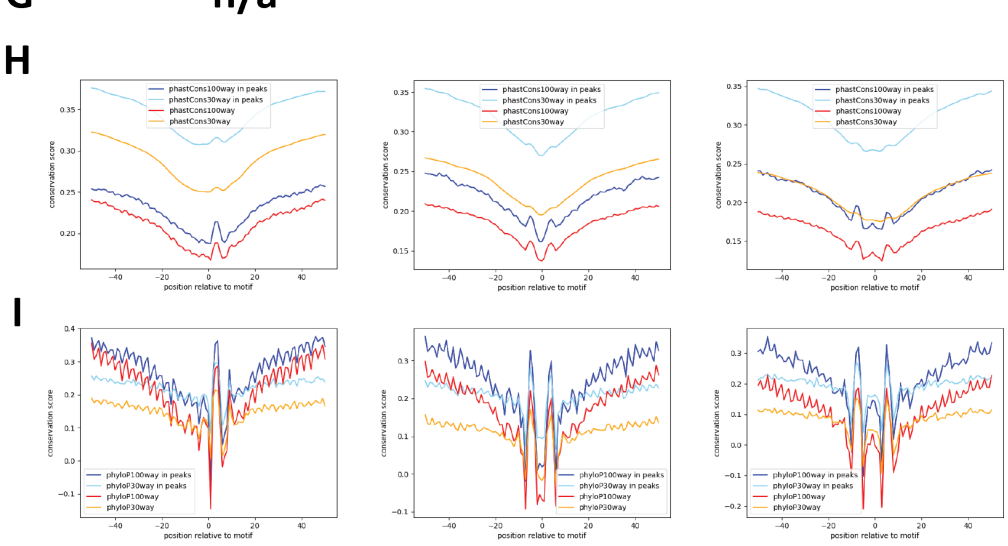

Supplementary Figure 597: Properties and genomic distribution of motifs identified for the ZFX transcription factor in C4-2B (accession ENCSR027UFT).

TF-MoDisCO pattern_0 n=9230, CWM

pattern_0, n=9230; subpattern_0, ns=2608

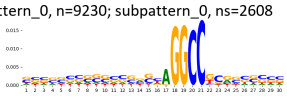

pattern_0, n=9230; subpattern_1, ns=1768

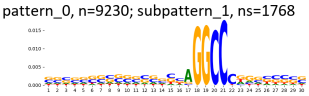

pattern_0, n=9230; subpattern_10, ns=232

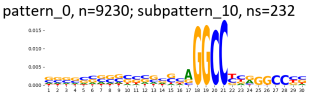

pattern_0, n=9230; subpattern_11, ns=209

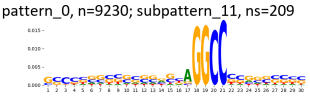

pattern_0, n=9230; subpattern_12, ns=125

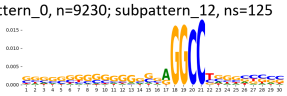

pattern_0, n=9230; subpattern_13, ns=79

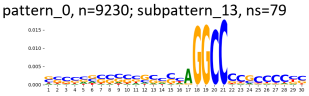

pattern_0, n=9230; subpattern_14, ns=2

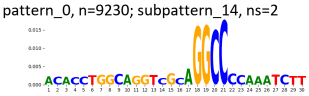

pattern_0, n=9230; subpattern_2, ns=1616

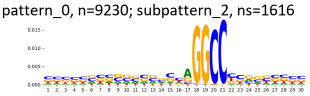

pattern_0, n=9230; subpattern_3, ns=564

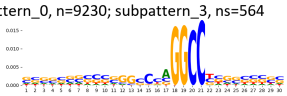

pattern_0, n=9230; subpattern_4, ns=412

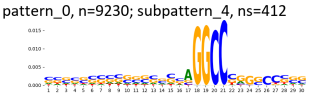

pattern_0, n=9230; subpattern_5, ns=381

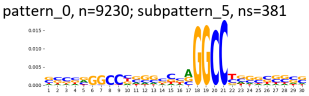

pattern_0, n=9230; subpattern_6, ns=379

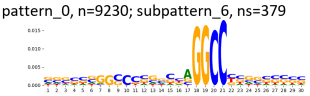

pattern_0, n=9230; subpattern_7, ns=312

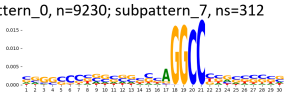

pattern_0, n=9230; subpattern_8, ns=277

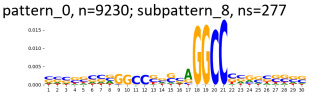

pattern_0, n=9230; subpattern_9, ns=266

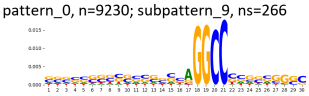

TF-MoDisCO pattern_0 n=9230, PWM

pattern_0, n=9230; subpattern_0, ns=2608

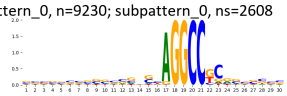

pattern_0, n=9230; subpattern_1, ns=1768

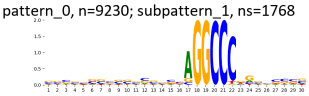

pattern_0, n=9230; subpattern_10, ns=232

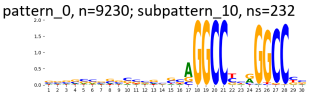

pattern_0, n=9230; subpattern_11, ns=209

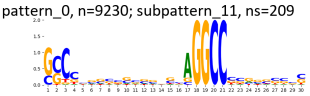

pattern_0, n=9230; subpattern_12, ns=125

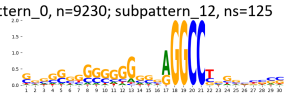

pattern_0, n=9230; subpattern_13, ns=79

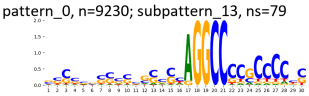

pattern_0, n=9230; subpattern_14, ns=2

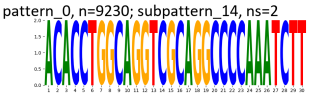

pattern_0, n=9230; subpattern_2, ns=1616

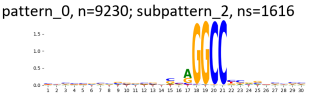

pattern_0, n=9230; subpattern_3, ns=564

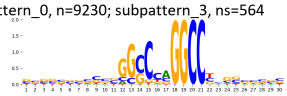

pattern_0, n=9230; subpattern_4, ns=412

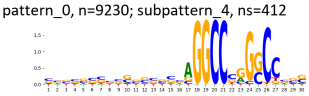

pattern_0, n=9230; subpattern_5, ns=381

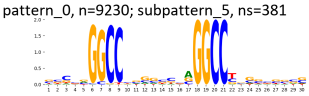

pattern_0, n=9230; subpattern_6, ns=379

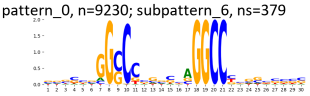

pattern_0, n=9230; subpattern_7, ns=312

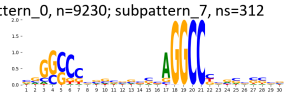

pattern_0, n=9230; subpattern_8, ns=277

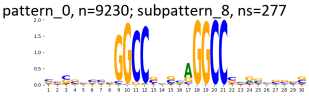

pattern_0, n=9230; subpattern_9, ns=266

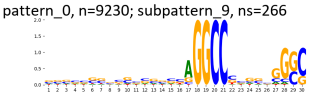

TF-MoDisCO pattern_1 n=278, CWM

pattern_1, n=278; subpattern_0, ns=66

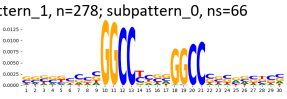

pattern_1, n=278; subpattern_1, ns=58

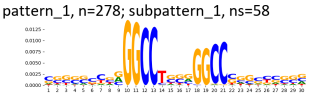

pattern_1, n=278; subpattern_2, ns=47

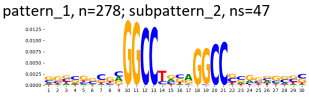

pattern_1, n=278; subpattern_3, ns=40

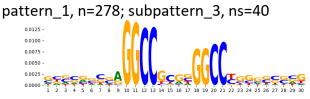

pattern_1, n=278; subpattern_4, ns=32

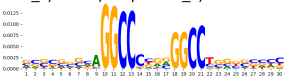

pattern_1, n=278; subpattern_5, ns=31

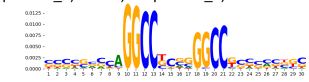

pattern_1, n=278; subpattern_6, ns=4

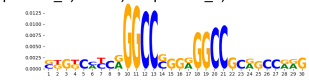

TF-MoDisCO pattern_1 n=278, PWM

pattern_1, n=278; subpattern_0, ns=66

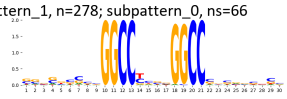

pattern_1, n=278; subpattern_1, ns=58

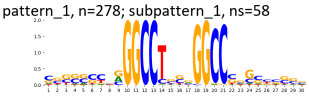

pattern_1, n=278; subpattern_2, ns=47

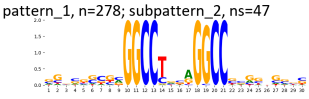

pattern_1, n=278; subpattern_3, ns=40

pattern_1, n=278; subpattern_4, ns=32

pattern_1, n=278; subpattern_5, ns=31

pattern_1, n=278; subpattern_6, ns=4

TF-MoDisCO pattern_2 n=261, CWM

pattern_2, n=261; subpattern_0, ns=67

pattern_2, n=261; subpattern_1, ns=52

pattern_2, n=261; subpattern_2, ns=48

pattern_2, n=261; subpattern_3, ns=45

pattern_2, n=261; subpattern_4, ns=38

pattern_2, n=261; subpattern_5, ns=7

pattern_2, n=261; subpattern_6, ns=4

TF-MoDisCO pattern_2 n=261, PWM

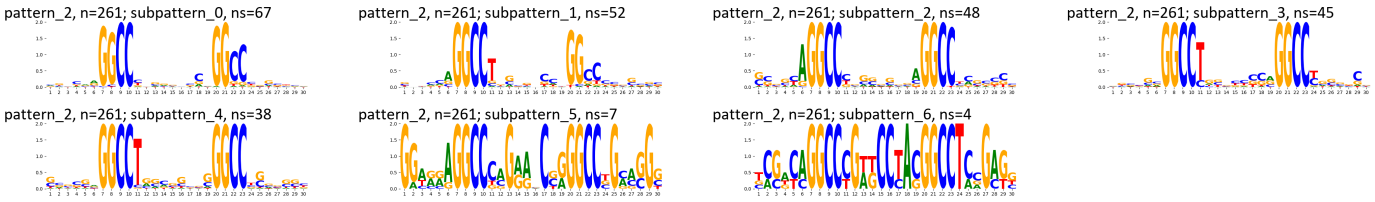

Supplementary Figure 598: TF-MoDisCO subpatterns for the ZFX transcription factor in C4-2B (accession ENCSR027UFT).

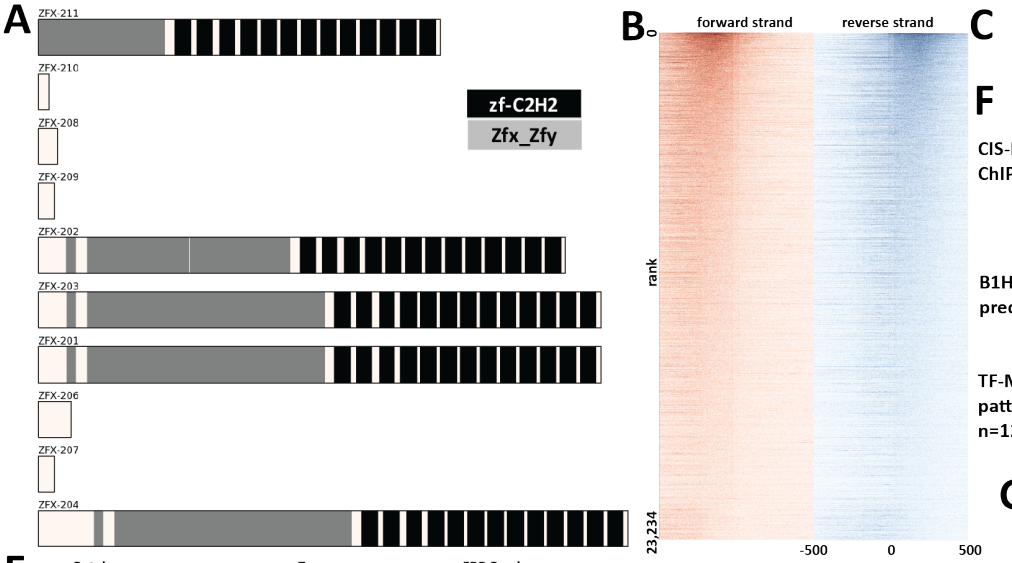

E

Ontology	Term	FDR Q-val
GO Biological Process	nuclear-transcribed mRNA catabolic process	41.94
GO Biological Process	nuclear-transcribed mRNA catabolic process, nonsense-mediated decay	40.80
GO Biological Process	viral gene expression	36.56
GO Biological Process	viral transcription	31.00
GO Biological Process	multi-organism metabolic process	30.65
GO Biological Process	translational initiation	29.21
GO Biological Process	cotranslational protein targeting to membrane	28.81
GO Biological Process	SRP-dependent cotranslational protein targeting to membrane	28.28
GO Biological Process	protein targeting to ER	27.45
GO Biological Process	establishment of protein localization to endoplasmic reticulum	21.75
GO Biological Process	mitochondrial translational termination	18.74
GO Biological Process	mitochondrial translational elongation	16.83
GO Biological Process	regulation of pri-miRNA transcription from RNA polymerase II promoter	16.03
GO Biological Process	regulation of cellular amino acid metabolic process	14.51
GO Biological Process	cytoplasmic sequestering of protein	14.12
GO Biological Process	IRE1-mediated unfolded protein response	13.96
GO Biological Process	positive regulation of pri-miRNA transcription from RNA polymerase II promoter	13.43
GO Biological Process	termination of RNA polymerase II transcription	11.89
GO Biological Process	DNA replication checkpoint	10.04
GO Biological Process	intra-S DNA damage checkpoint	8.79
Human Phenotype	Abnormal CSF metabolite level	11.86
Human Phenotype	Increased CSF lactate	10.07
Human Phenotype	Cytochrome C oxidase-negative muscle fibers	4.86
Human Phenotype	Abnormal mitochondria in muscle tissue	4.66
Human Phenotype	Progressive macrocephaly	4.07
Human Phenotype	Progressive external ophthalmoplegia	3.95
Human Phenotype	Increased muscle lipid content	3.75
Human Phenotype	Acute necrotizing encephalopathy	3.68

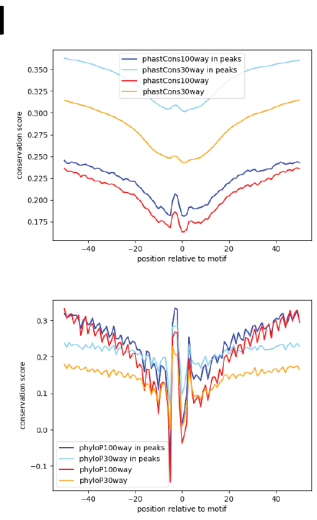

Supplementary Figure 599: Properties and genomic distribution of motifs identified for the ZFX transcription factor in HCT116 (accession ENCSR503GVO).

TF-MoDisCO pattern_0 n=12729, CWM

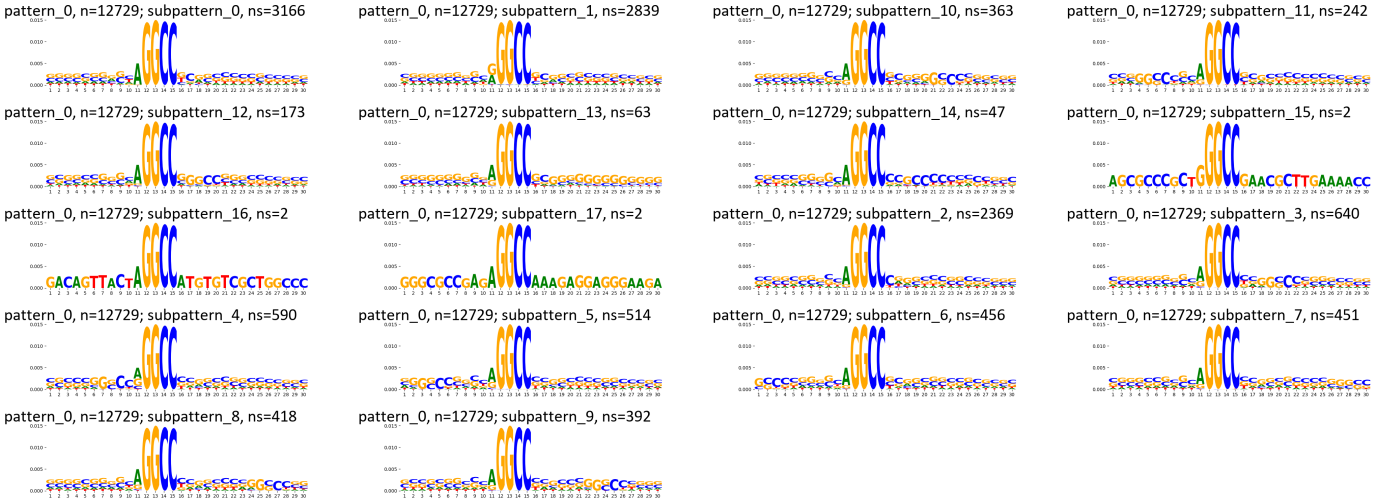

TF-MoDisCO pattern_0 n=12729, PWM

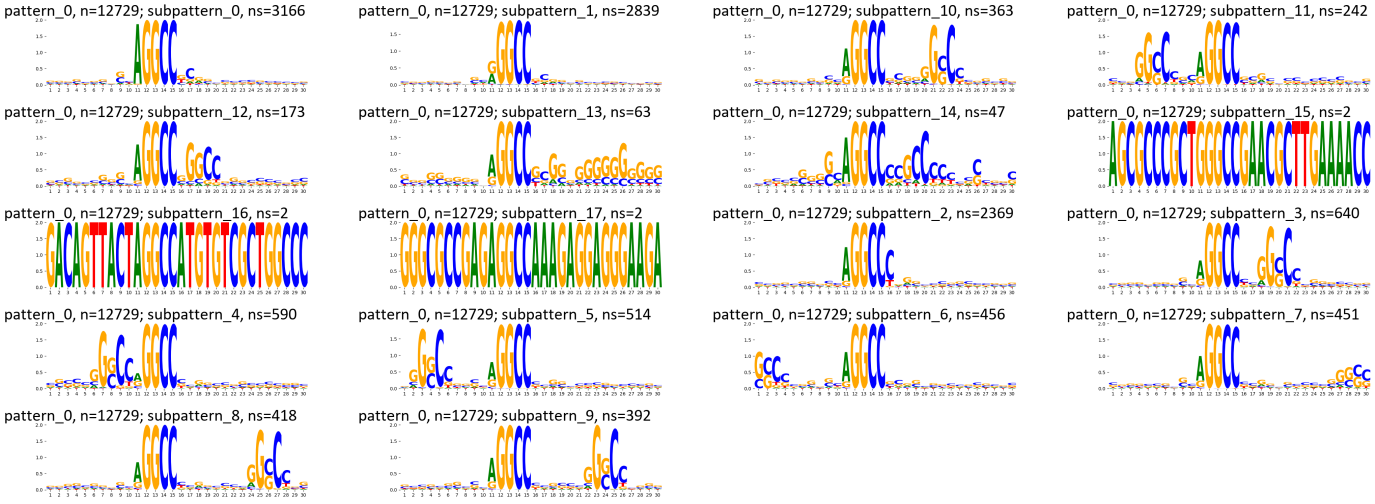

Supplementary Figure 600: TF-MoDisCO subpatterns for the ZFX transcription factor in HCT116 (accession ENCSR503GVO).

A

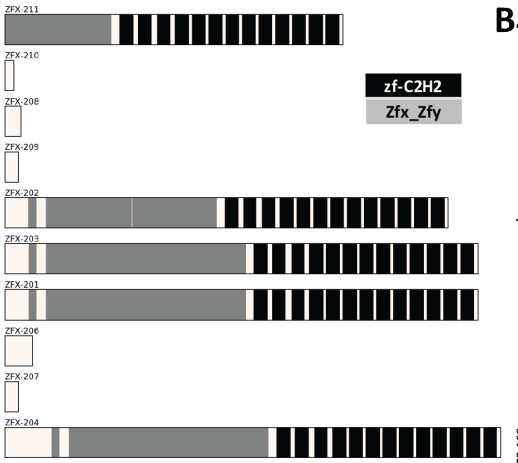

B

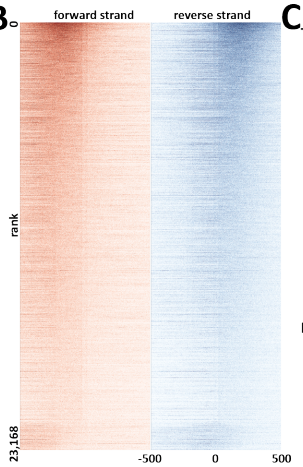

C

peaks	
state	fraction
TssA	0.38
TssFlnk	0.21
Quies	0.10
TssBiv	0.05
TssFlnkU	0.04
TxWk	0.04
EnhA2	0.03
EnhWk	0.02
EnhA1	0.02
Tx	0.01
ReprPC	0.01
TssFlnkD	0.01
ReprPCWk	0.01
EnhBiv	0.01
Het	0.00
EnhG1	0.00
EnhG2	0.00
ZNF/Rpts	0.00

D

peaks		peaks	
repeat	fraction	repeat	fraction
Simple_repeat	0.29	G-rich	0.05
SINE/Alu	0.11	MIRb	0.03
SINE/MIR	0.08	L2a	0.02
Low_complexity	0.07	MIR3	0.02
LINE/L2	0.05	MIR	0.02
LINE/L1	0.03	AluJb	0.02
LTR/ERVL-MaLR	0.02	MIRc	0.01
DNA/hAT-Charlie	0.02	L2b	0.01
LTR/ERV1	0.02	(GGC)n	0.01
LTR/ERVL	0.01	L2c	0.01
DNA/hAT-Tip100	0.01	(GCC)n	0.01
DNA/TcMar-Tigger	0.01	GA-rich	0.01
LINE/CR1	0.00	AluSx	0.01
LTR/Gypsy	0.00	AluJo	0.01
tRNA	0.00	AluSz	0.01
LTR/ERVK	0.00	AluJr	0.01
DNA/hAT	0.00	AluSx1	0.01
DNA/hAT-Blackjack	0.00	(CCG)n	0.01

E

Ontology	Term	FDR Q-val
GO Biological Process	viral gene expression	40.23
GO Biological Process	multi-organism metabolic process	33.97
GO Biological Process	viral transcription	33.98
GO Biological Process	cotranslational protein targeting to membrane	33.00
GO Biological Process	mitochondrial transmembrane transport	32.60
GO Biological Process	SRP-dependent cotranslational protein targeting to membrane	31.42
GO Biological Process	protein targeting to ER	30.10
GO Biological Process	nuclear-transcribed mRNA catabolic process, nonsense-mediated decay	29.32
GO Biological Process	protein localization to endoplasmic reticulum	26.46
GO Biological Process	establishment of protein localization to endoplasmic reticulum	25.73
GO Biological Process	tRNA transport	23.85
GO Biological Process	translational elongation	23.21
GO Biological Process	purine ribonucleoside monophosphate biosynthetic process	22.51
GO Biological Process	heterochromatin organization	21.19
GO Biological Process	protein targeting to mitochondrion	19.65
GO Biological Process	mitochondrial translational termination	18.52
GO Biological Process	mitochondrial genome maintenance	18.37
GO Biological Process	intracellular protein transmembrane transport	17.77
GO Biological Process	protein transmembrane transport	17.70
GO Biological Process	mitochondrial translational elongation	17.26
Human Phenotype	Exercise intolerance	20.15
Human Phenotype	Increased serum lactate	20.23
Human Phenotype	Increased CSF lactate	16.10
Human Phenotype	Abnormal CSF metabolite level	16.17
Human Phenotype	Increased muscle lipid content	13.16
Human Phenotype	Cytochrome C oxidase-negative muscle fibers	12.90
Human Phenotype	Increased intramyocellular lipid droplets	11.84
Human Phenotype	Renal Fanconi syndrome	7.66
Human Phenotype	Increased hepatocellular lipid droplets	6.98
Human Phenotype	Abnormality of renal resorption	6.26
Human Phenotype	CNS hypomyelination	5.35
Human Phenotype	Abnormal mitochondria in muscle tissue	4.39
Human Phenotype	Progressive macrocephaly	4.37
Human Phenotype	Acute necrotizing encephalopathy	3.95
Human Phenotype	Vertebral compression fractures	3.84

F

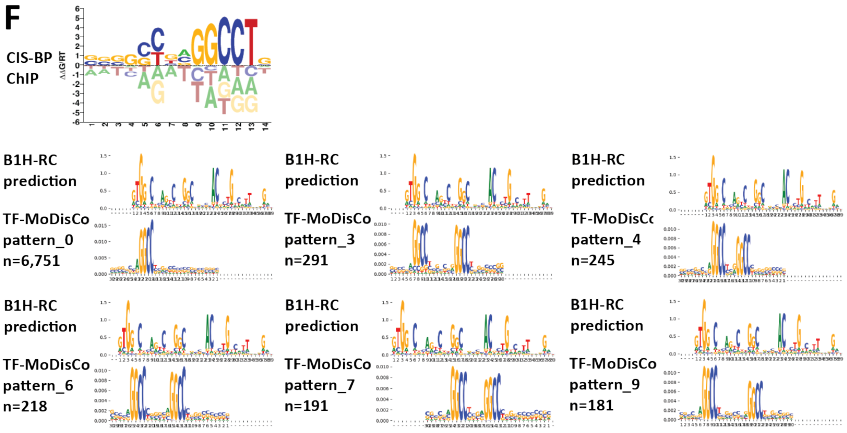

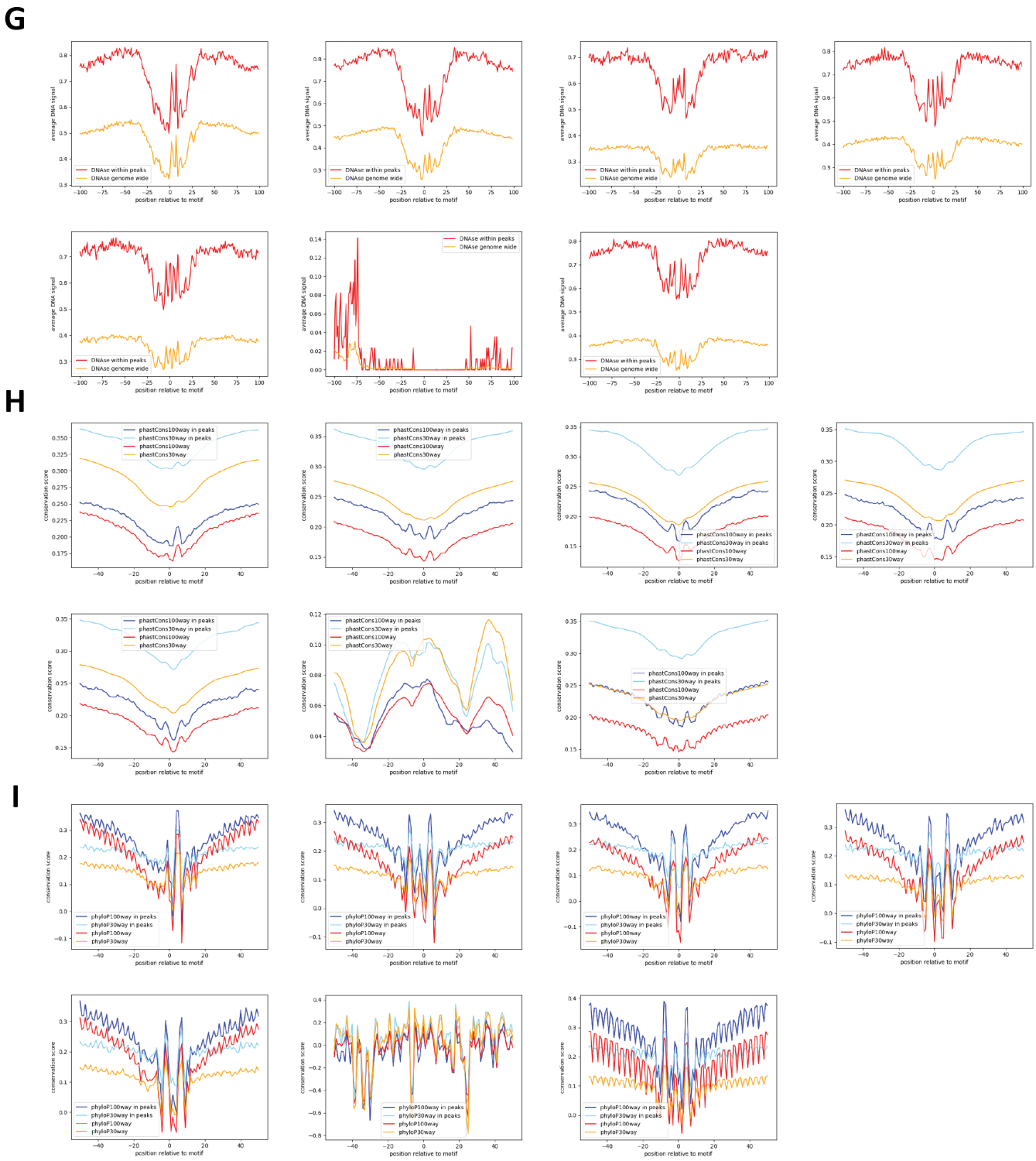

Supplementary Figure 601: Properties and genomic distribution of motifs identified for the ZFX transcription factor in HEK293T (accession ENCSR218GSN).

TF-MoDisCO pattern_0 n=6751, CWM

pattern_0, n=6751; subpattern_0, ns=1541

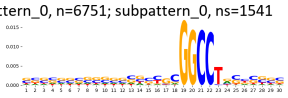

pattern_0, n=6751; subpattern_1, ns=1407

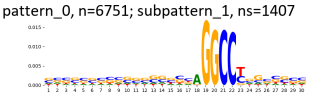

pattern_0, n=6751; subpattern_10, ns=139

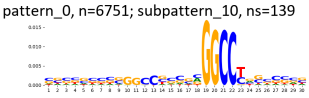

pattern_0, n=6751; subpattern_11, ns=128

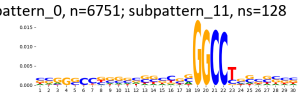

pattern_0, n=6751; subpattern_12, ns=23

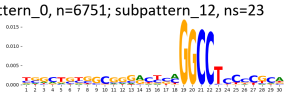

pattern_0, n=6751; subpattern_13, ns=2

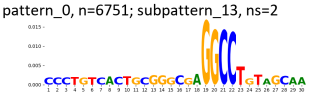

pattern_0, n=6751; subpattern_14, ns=2

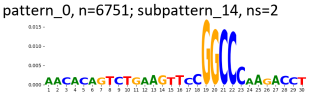

pattern_0, n=6751; subpattern_15, ns=2

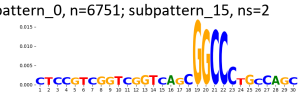

pattern_0, n=6751; subpattern_2, ns=1263

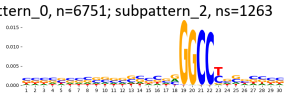

pattern_0, n=6751; subpattern_3, ns=828

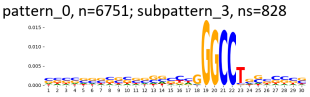

pattern_0, n=6751; subpattern_4, ns=355

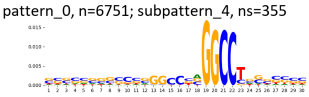

pattern_0, n=6751; subpattern_5, ns=305

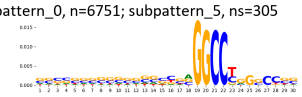

pattern_0, n=6751; subpattern_6, ns=224

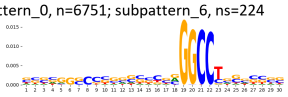

pattern_0, n=6751; subpattern_7, ns=193

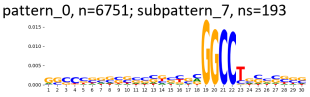

pattern_0, n=6751; subpattern_8, ns=177

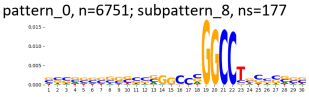

pattern_0, n=6751; subpattern_9, ns=162

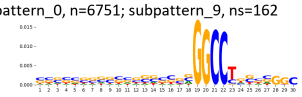

TF-MoDisCO pattern_0 n=6751, PWM

pattern_0, n=6751; subpattern_0, ns=1541

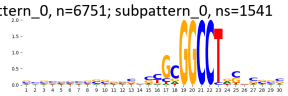

pattern_0, n=6751; subpattern_1, ns=1407

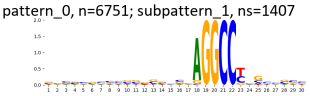

pattern_0, n=6751; subpattern_10, ns=139

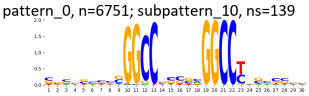

pattern_0, n=6751; subpattern_11, ns=128

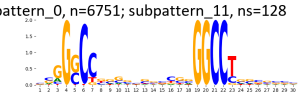

pattern_0, n=6751; subpattern_12, ns=23

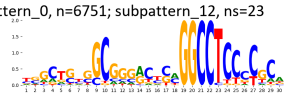

pattern_0, n=6751; subpattern_13, ns=2

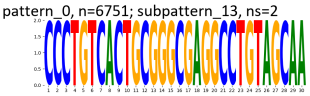

pattern_0, n=6751; subpattern_14, ns=2

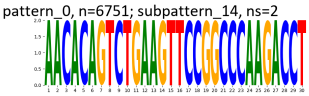

pattern_0, n=6751; subpattern_15, ns=2

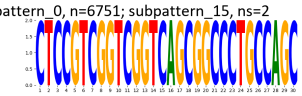

pattern_0, n=6751; subpattern_2, ns=1263

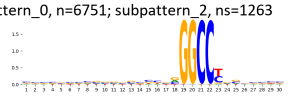

pattern_0, n=6751; subpattern_3, ns=828

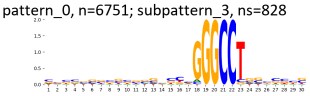

pattern_0, n=6751; subpattern_4, ns=355

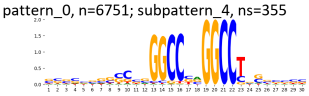

pattern_0, n=6751; subpattern_5, ns=305

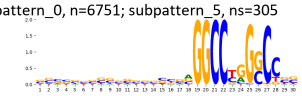

pattern_0, n=6751; subpattern_6, ns=224

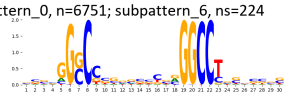

pattern_0, n=6751; subpattern_7, ns=193

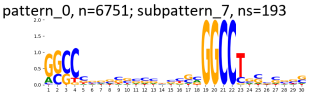

pattern_0, n=6751; subpattern_8, ns=177

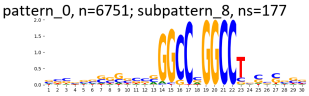

pattern_0, n=6751; subpattern_9, ns=162

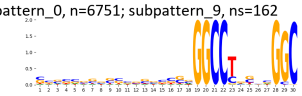

TF-MoDisCO pattern_3 n=291, CWM

pattern_3, n=291; subpattern_0, ns=114

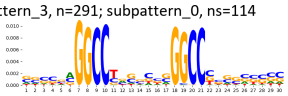

pattern_3, n=291; subpattern_1, ns=73

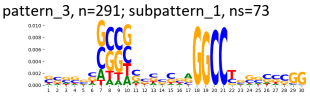

pattern_3, n=291; subpattern_2, ns=58

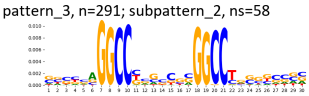

pattern_3, n=291; subpattern_3, ns=39

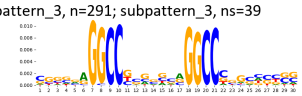

pattern_3, n=291; subpattern_4, ns=5

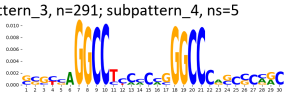

pattern_3, n=291; subpattern_5, ns=2

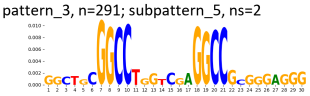

TF-MoDisCO pattern_3 n=291, PWM

pattern_3, n=291; subpattern_0, ns=114

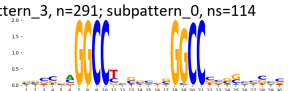

pattern_3, n=291; subpattern_1, ns=73

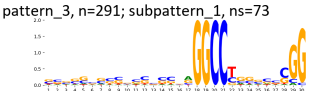

pattern_3, n=291; subpattern_2, ns=58

pattern_3, n=291; subpattern_3, ns=39

pattern_3, n=291; subpattern_4, ns=5

pattern_3, n=291; subpattern_5, ns=2

TF-MoDisCO pattern_4 n=245, CWM

pattern_4, n=245; subpattern_0, ns=49

pattern_4, n=245; subpattern_1, ns=48

pattern_4, n=245; subpattern_2, ns=44

pattern_4, n=245; subpattern_3, ns=34

pattern_4, n=245; subpattern_4, ns=26

pattern_4, n=245; subpattern_5, ns=16

pattern_4, n=245; subpattern_6, ns=15

pattern_4, n=245; subpattern_7, ns=11

pattern_4, n=245; subpattern_8, ns=2

TF-MoDisCO pattern_4 n=245, PWM

pattern_4, n=245; subpattern_0, ns=49

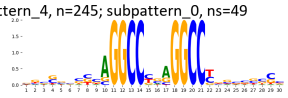

pattern_4, n=245; subpattern_1, ns=48

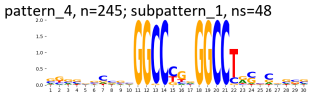

pattern_4, n=245; subpattern_2, ns=44

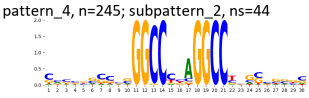

pattern_4, n=245; subpattern_3, ns=34

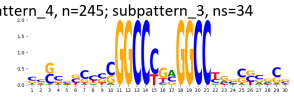

pattern_4, n=245; subpattern_4, ns=26

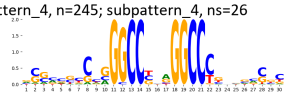

pattern_4, n=245; subpattern_5, ns=16

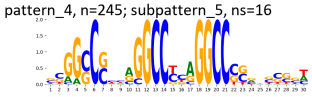

pattern_4, n=245; subpattern_6, ns=15

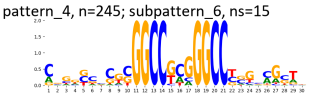

pattern_4, n=245; subpattern_7, ns=11

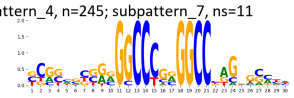

pattern_4, n=245; subpattern_8, ns=2

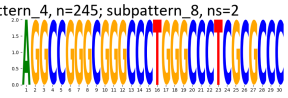

TF-MoDisCO pattern_6 n=218, CWM

pattern_6, n=218; subpattern_0, ns=78

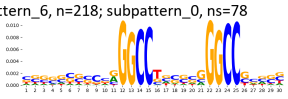

pattern_6, n=218; subpattern_1, ns=71

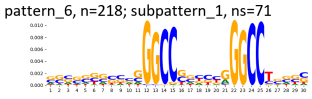

pattern_6, n=218; subpattern_2, ns=25

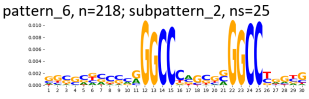

pattern_6, n=218; subpattern_3, ns=25

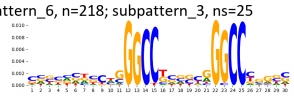

pattern_6, n=218; subpattern_4, ns=15

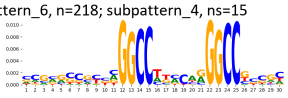

pattern_6, n=218; subpattern_5, ns=2

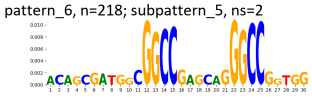

pattern_6, n=218; subpattern_6, ns=2

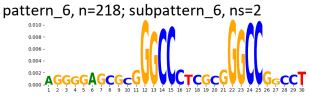

TF-MoDisCO pattern_6 n=218, PWM

pattern_6, n=218; subpattern_0, ns=78

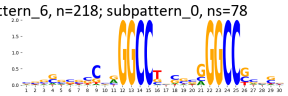

pattern_6, n=218; subpattern_1, ns=71

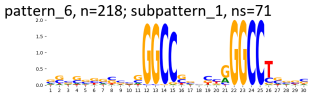

pattern_6, n=218; subpattern_2, ns=25

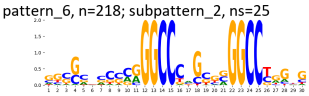

pattern_6, n=218; subpattern_3, ns=25

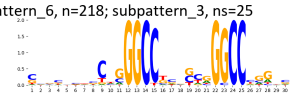

pattern_6, n=218; subpattern_4, ns=15

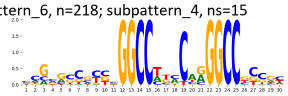

pattern_6, n=218; subpattern_5, ns=2

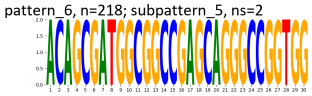

pattern_6, n=218; subpattern_6, ns=2

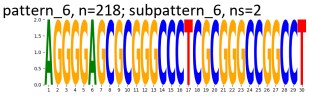

TF-MoDisCO pattern_7 n=191, CWM

pattern_7, n=191; subpattern_0, ns=47

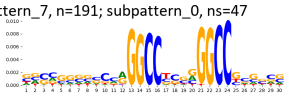

pattern_7, n=191; subpattern_1, ns=47

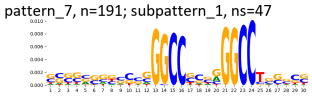

pattern_7, n=191; subpattern_2, ns=37

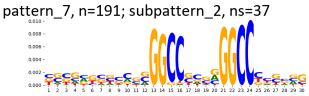

pattern_7, n=191; subpattern_3, ns=35

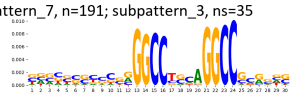

pattern_7, n=191; subpattern_4, ns=18

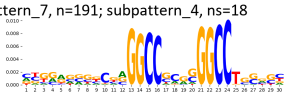

pattern_7, n=191; subpattern_5, ns=7

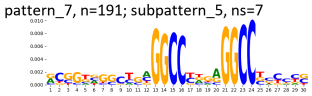

TF-MoDisCO pattern_7 n=191, PWM

pattern_7, n=191; subpattern_0, ns=47

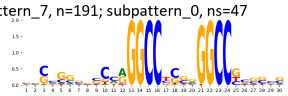

pattern_7, n=191; subpattern_1, ns=47

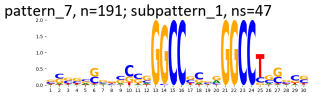

pattern_7, n=191; subpattern_2, ns=37

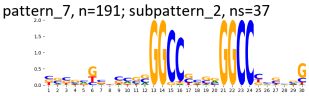

pattern_7, n=191; subpattern_3, ns=35

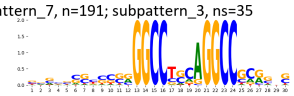

pattern_7, n=191; subpattern_4, ns=18

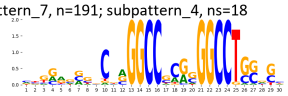

pattern_7, n=191; subpattern_5, ns=7

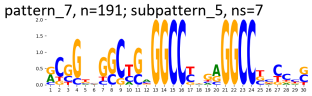

TF-MoDisCO pattern_9 n=181, CWM

pattern_9, n=181; subpattern_0, ns=38

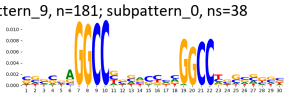

pattern_9, n=181; subpattern_1, ns=37

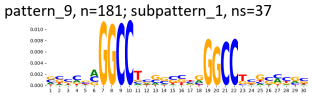

pattern_9, n=181; subpattern_2, ns=28

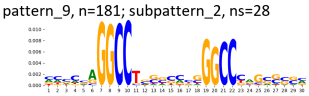

pattern_9, n=181; subpattern_3, ns=28

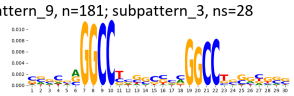

pattern_9, n=181; subpattern_4, ns=26

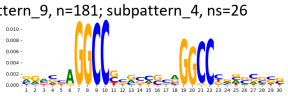

pattern_9, n=181; subpattern_5, ns=11

pattern_9, n=181; subpattern_6, ns=7

pattern_9, n=181; subpattern_7, ns=4

pattern_9, n=181; subpattern_8, ns=2

TF-MoDisCO pattern_9 n=181, PWM

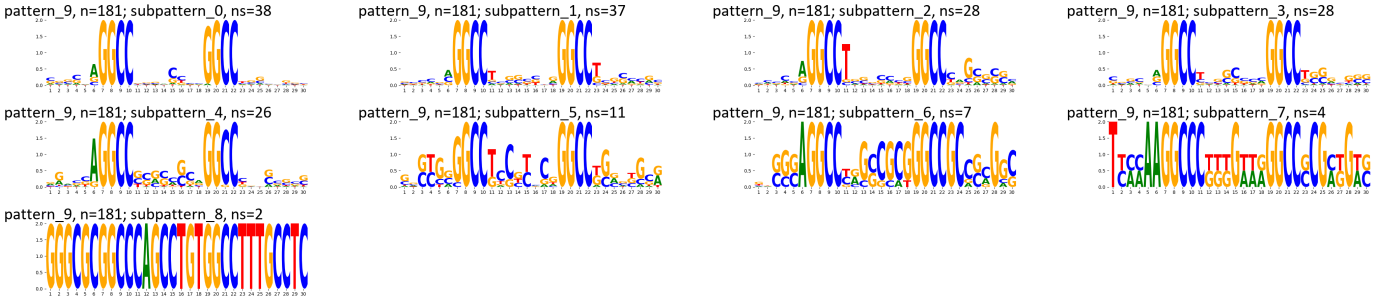

Supplementary Figure 602: TF-MoDisCO subpatterns for the ZFX transcription factor in HEK293T (accession ENCSR218GSN).

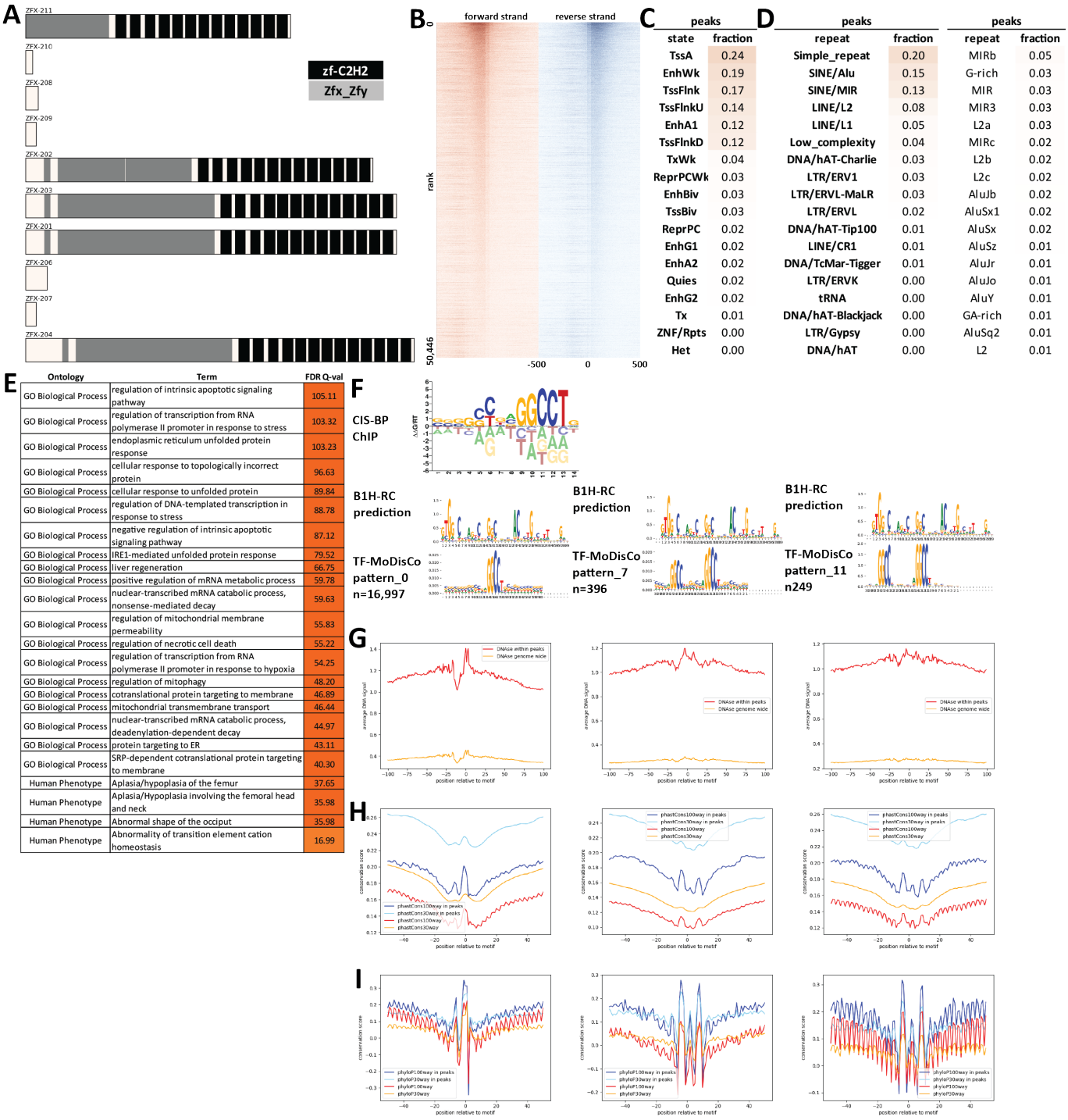

Supplementary Figure 603: Properties and genomic distribution of motifs identified for the ZFX transcription factor in HepG2 (accession ENCSR266HHO).

TF-MoDisCO pattern_0 n=16997, CWM

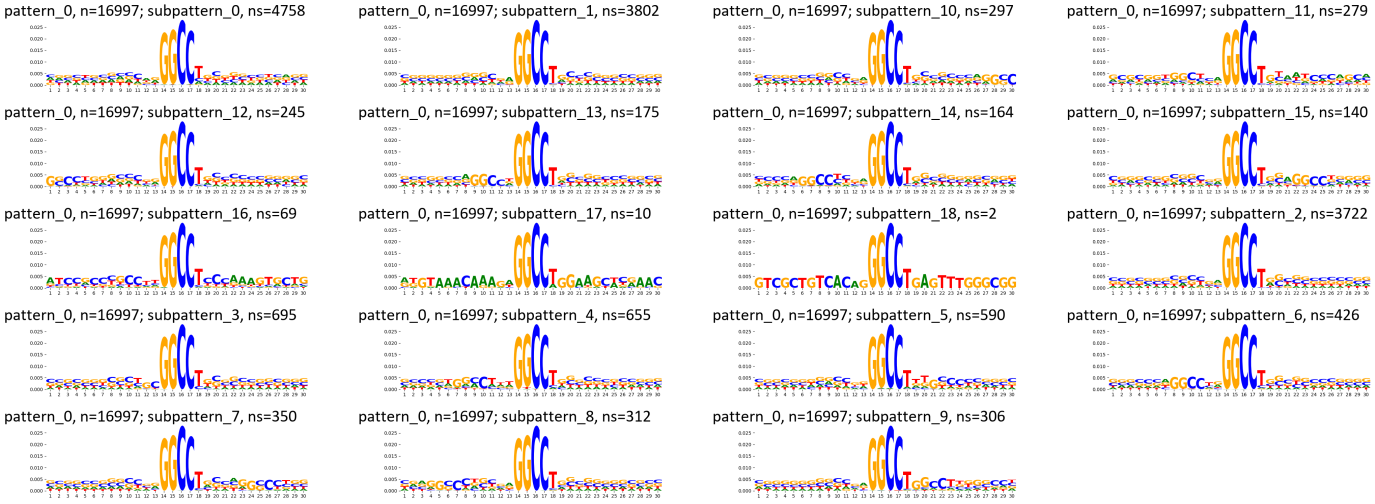

TF-MoDisCO pattern_0 n=16997, PWM

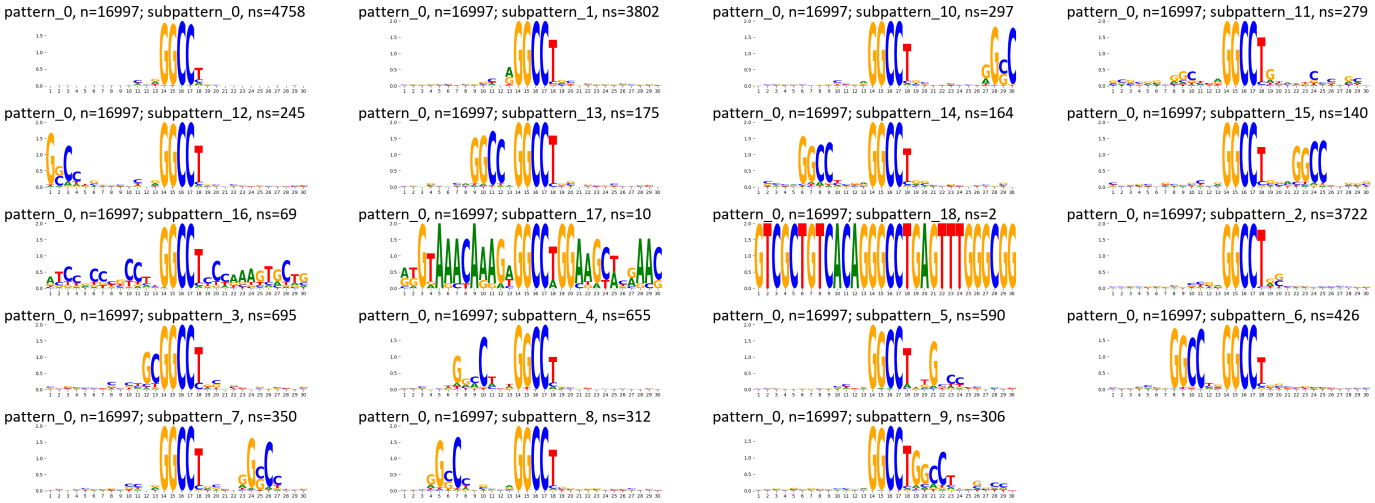

TF-MoDisCO pattern_11 n=249, CWM

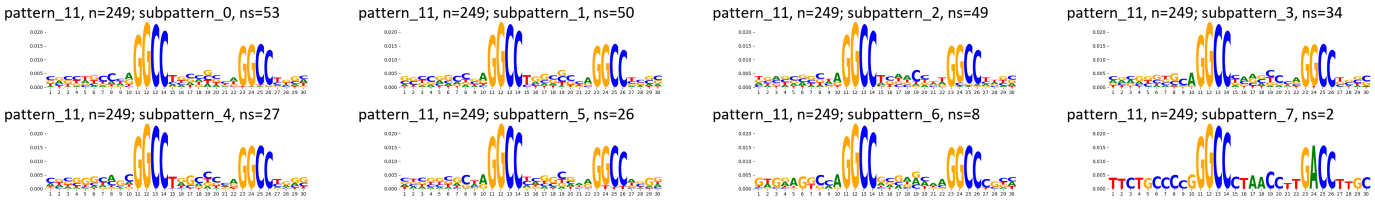

TF-MoDisCO pattern_11 n=249, PWM

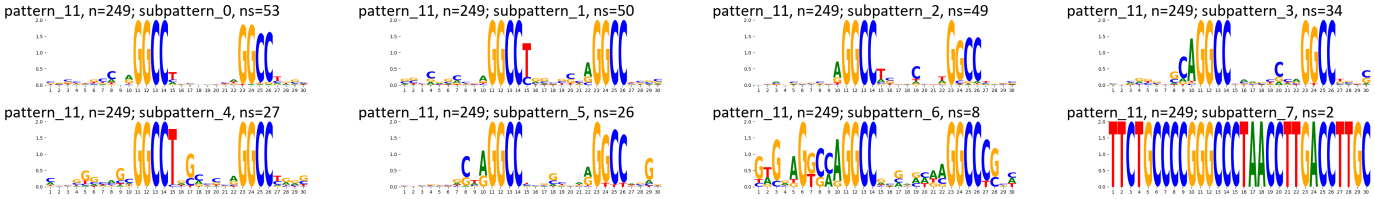

TF-MoDisCO pattern_7 n=396, CWM

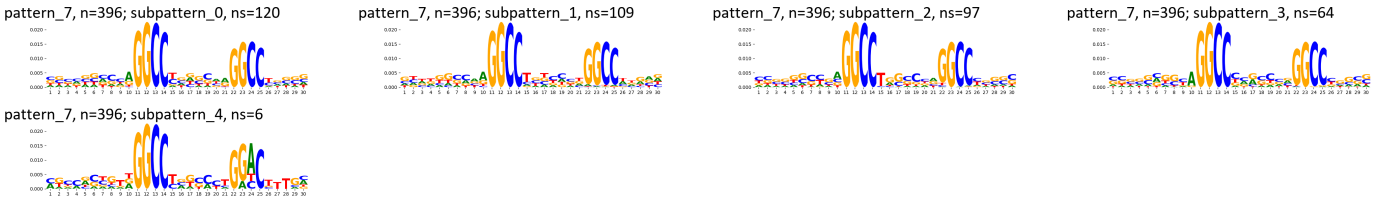

TF-MoDisCO pattern_7 n=396, PWM

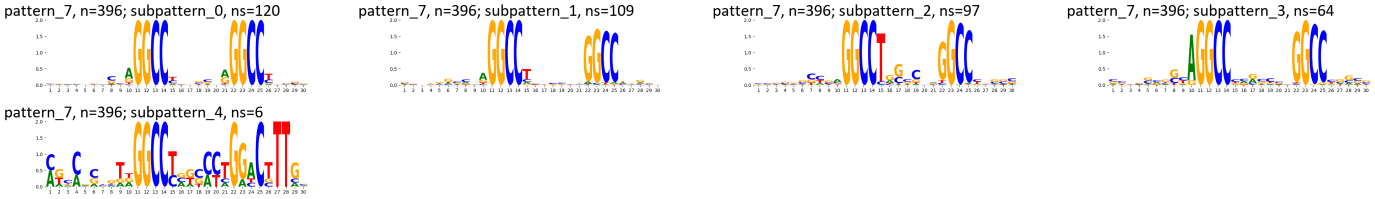

Supplementary Figure 604: TF-MoDisCO subpatterns for the ZFX transcription factor in HepG2 (accession ENCSR266HHO).

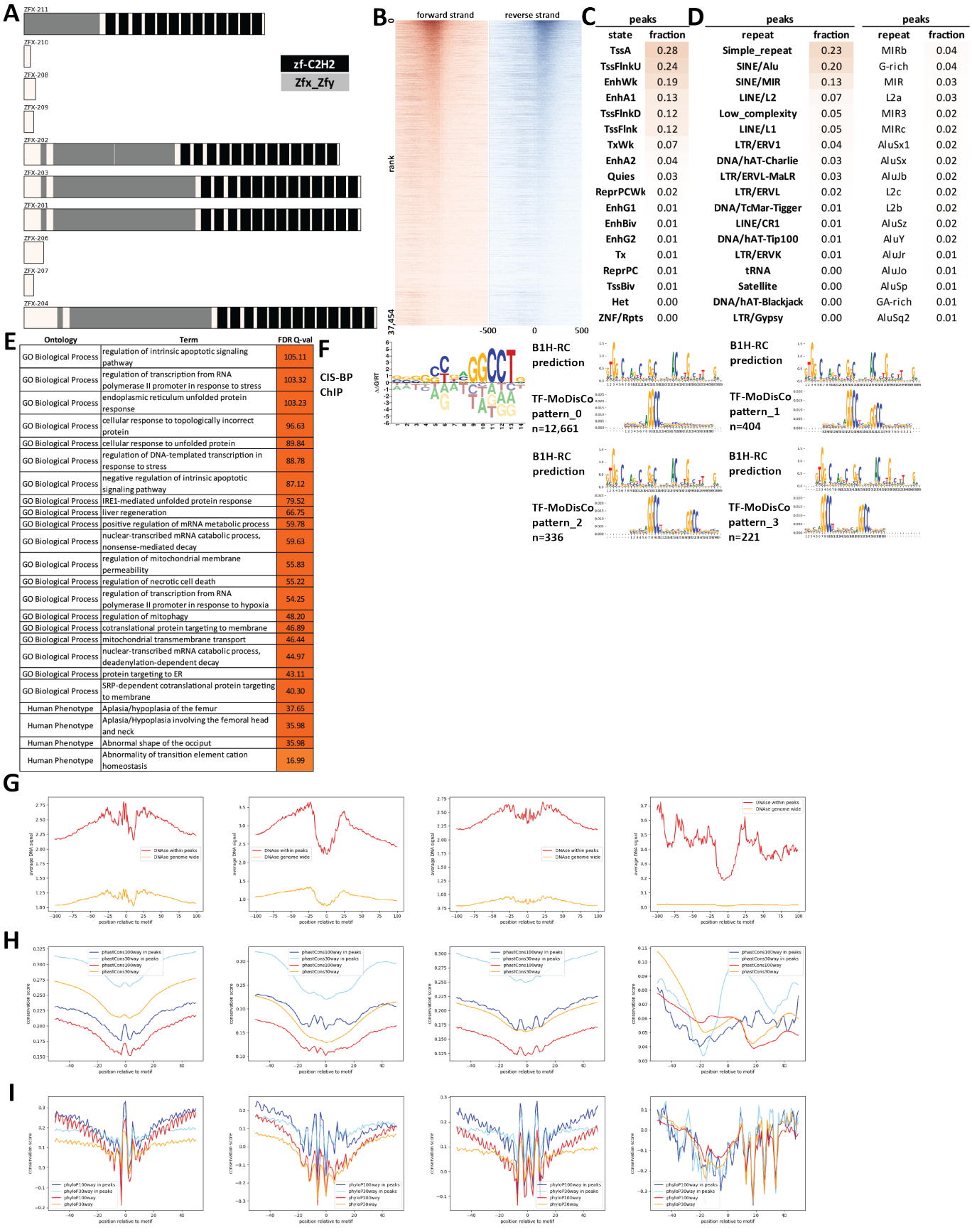

Supplementary Figure 605: Properties and genomic distribution of motifs identified for the ZFX transcription factor in K562 (accession ENCSR628DJK).

TF-MoDisCO pattern_0 n=15446, CWM

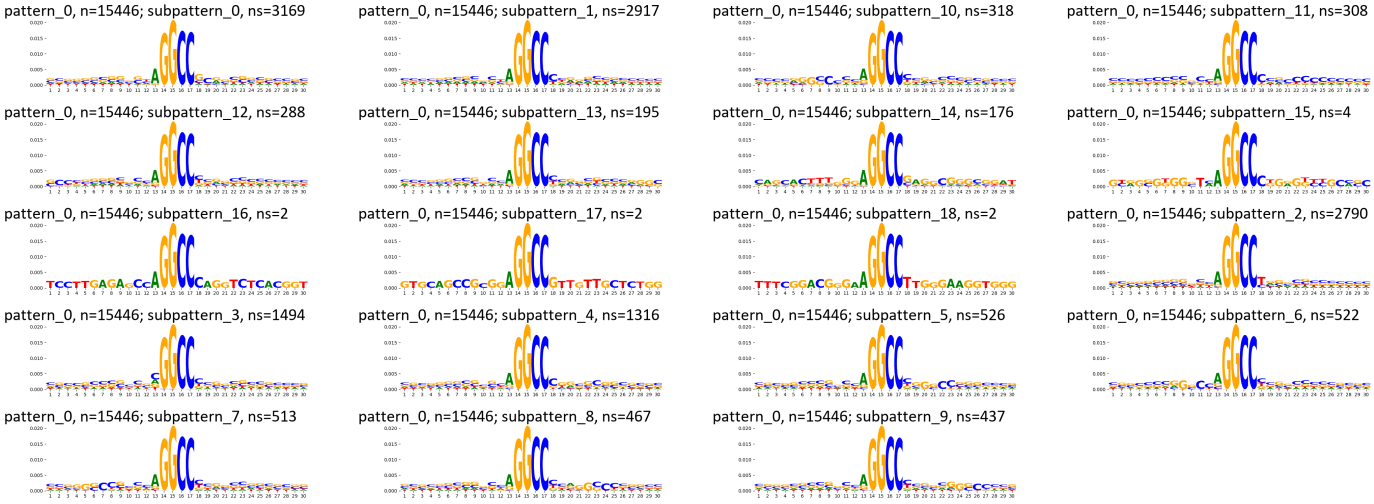

TF-MoDisCO pattern_0 n=15446, PWM

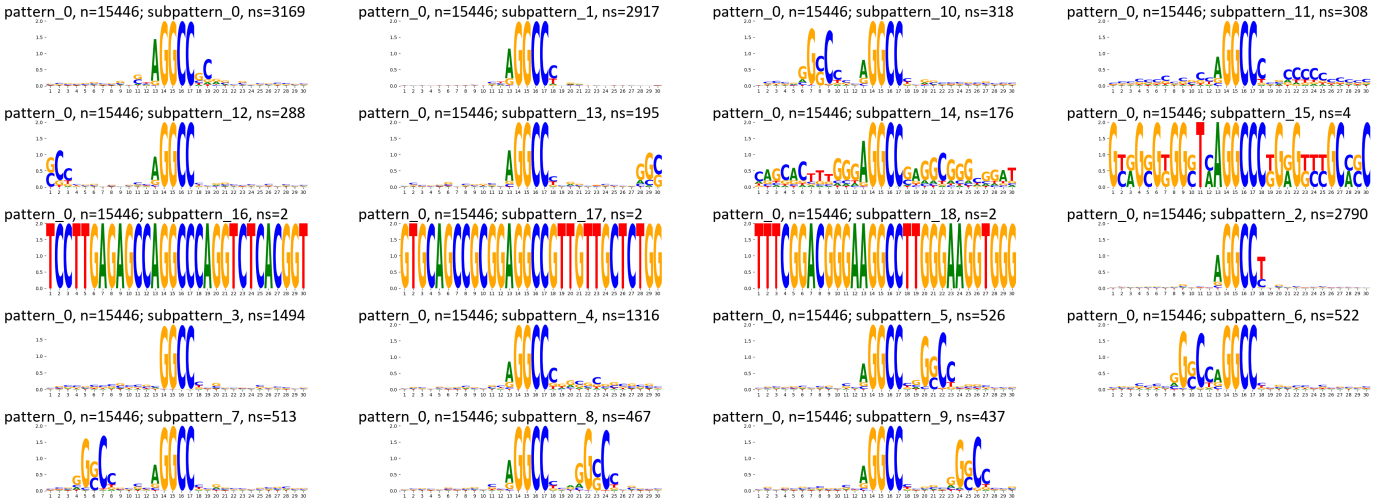

TF-MoDisCO pattern_2 n=501, CWM

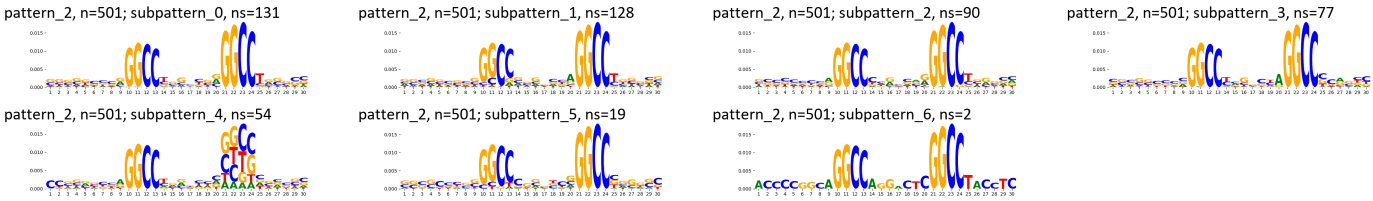

TF-MoDisCO pattern_2 n=501, PWM

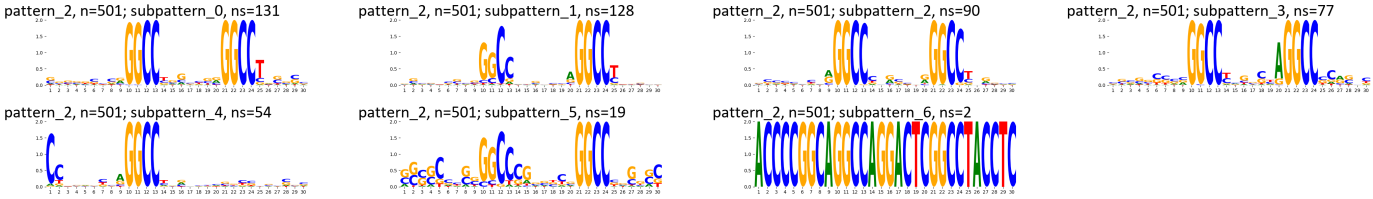

TF-MoDisCO pattern_4 n=297, CWM

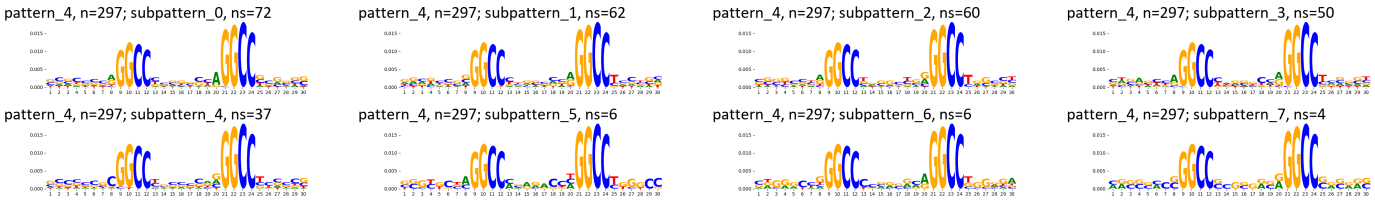

TF-MoDisCO pattern_4 n=297, PWM

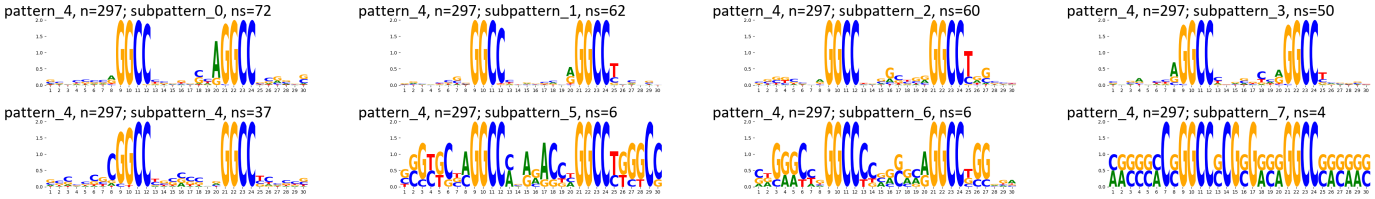

TF-MoDisCO pattern_7 n=275, CWM

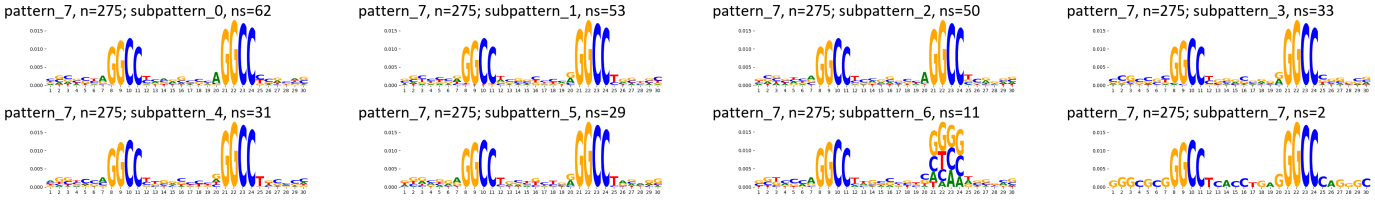

TF-MoDisCO pattern_7 n=275, PWM

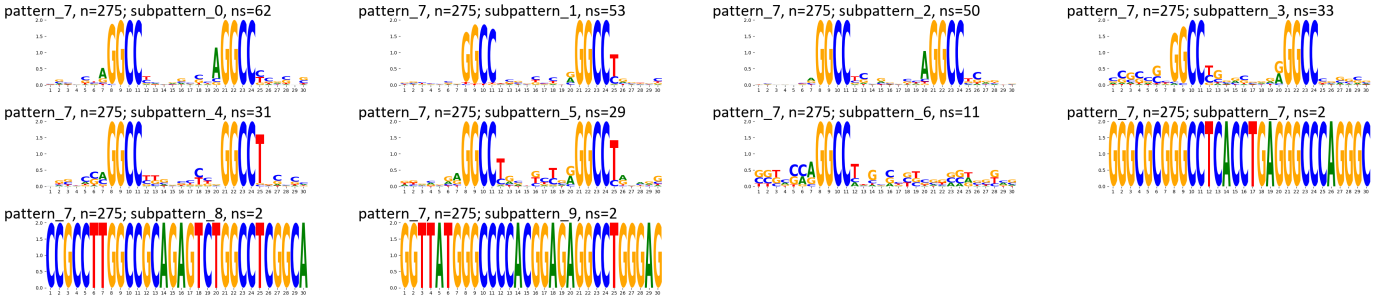

TF-MoDisCO pattern_8 n=235, CWM

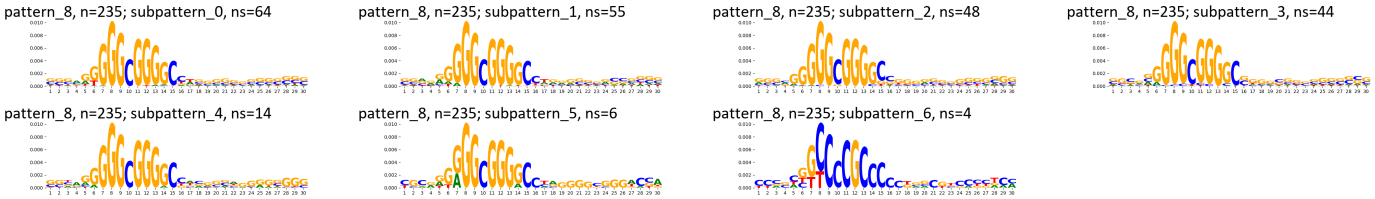

TF-MoDisCO pattern_8 n=235, PWM

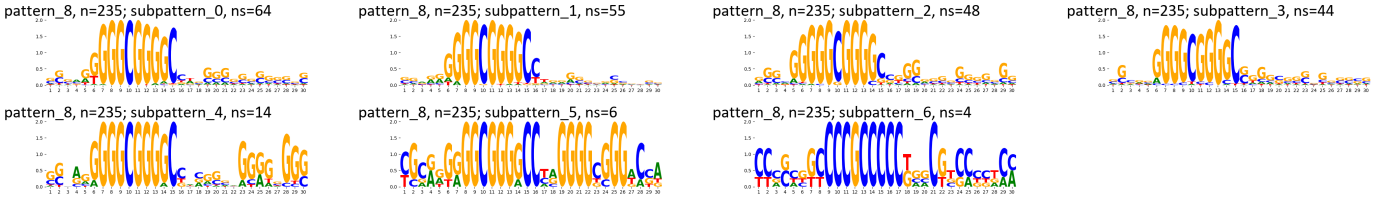

Supplementary Figure 606: TF-MoDisCO subpatterns for the ZFX transcription factor in K562 (accession ENCSR628DJK).

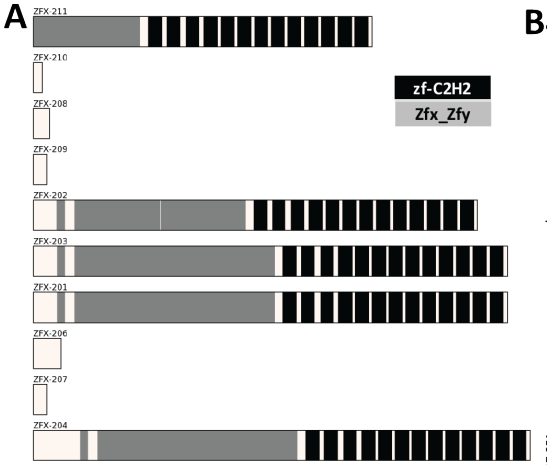

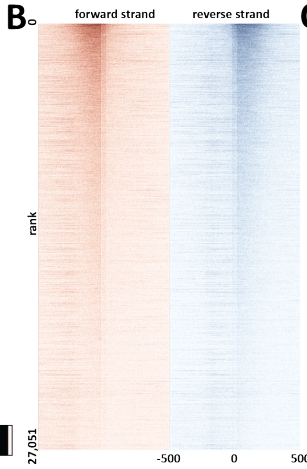

C

peaks	
state	fraction
TssA	0.34
TssFlnkU	0.27
EnhWk	0.15
TssFlnk	0.13
TssFlnkD	0.13
EnhA1	0.12
TxWk	0.04
EnhA2	0.04
Quies	0.03
ReprPCWk	0.02
EnhBiv	0.01
EnhG2	0.01
ReprPC	0.01
EnhG1	0.01
TssBiv	0.01
Tx	0.00
Het	0.00
ZNF/Rpts	0.00

D

peaks		peaks	
repeat	fraction	repeat	fraction
Simple_repeat	0.27	G-rich	0.05
SINE/Alu	0.11	MIRb	0.04
SINE/MIR	0.10	MIR	0.02
Low_complexity	0.07	MIR3	0.02
LINE/L2	0.06	L2a	0.02
LTR/ERV1	0.04	MIRc	0.02
LINE/L1	0.03	L2b	0.02
LTR/ERVL-MaLR	0.03	L2c	0.02
DNA/hAT-Charlie	0.02	AluSx1	0.01
LTR/ERVL	0.01	AluSx	0.01
DNA/hAT-Tip100	0.01	GA-rich	0.01
LINE/CR1	0.01	AluJb	0.01
DNA/TcMar-Tigger	0.01	(GGC)n	0.01
LTR/ERVK	0.00	AluSz	0.01
tRNA	0.00	(GCC)n	0.01
DNA/hAT-Blackjack	0.00	AluY	0.01
LTR/Gypsy	0.00	AluJr	0.01
Satellite	0.00	AluJo	0.01

E

Ontology	Term	FDR Q-val
GO Biological Process	regulation of gene expression, epigenetic	108.09
GO Biological Process	mRNA catabolic process	79.10
GO Biological Process	nuclear-transcribed mRNA catabolic process	78.45
GO Biological Process	regulation of hematopoietic progenitor cell differentiation	75.28
GO Biological Process	gene silencing	68.54
GO Biological Process	nuclear-transcribed mRNA catabolic process, nonsense-mediated decay	65.05
GO Biological Process	regulation of transcription from RNA polymerase II promoter in response to stress	62.50
GO Biological Process	cotranslational protein targeting to membrane	60.71
GO Biological Process	positive regulation of transcription from RNA polymerase II promoter in response to stress	59.84
GO Biological Process	regulation of DNA-templated transcription in response to stress	59.81
GO Biological Process	viral gene expression	54.36
GO Biological Process	multi-organism metabolic process	53.49
GO Biological Process	SRP-dependent cotranslational protein targeting to membrane	52.22
GO Biological Process	protein targeting to ER	50.46
GO Biological Process	translational initiation	48.95
GO Biological Process	endoplasmic reticulum unfolded protein response	48.30
GO Biological Process	protein localization to endoplasmic reticulum	43.96
GO Biological Process	viral transcription	43.86
GO Biological Process	regulation of megakaryocyte differentiation	41.28
GO Biological Process	establishment of protein localization to endoplasmic reticulum	41.01
Human Phenotype	Abnormal CSF metabolite level	20.67
Human Phenotype	Increased CSF lactate	19.53
Human Phenotype	Progressive macrocephaly	8.94
Human Phenotype	Cytochrome C oxidase-negative muscle fibers	6.00
Human Phenotype	Increased muscle lipid content	5.59

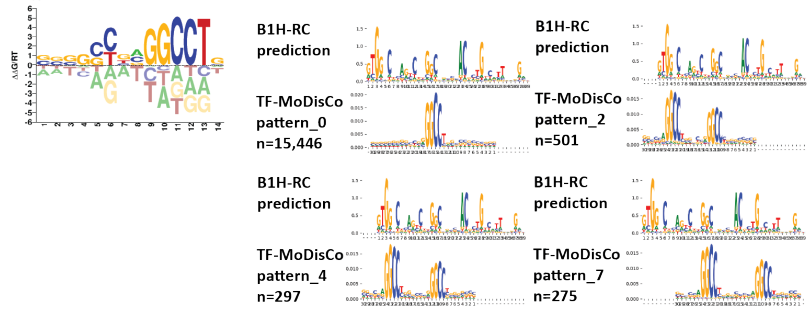

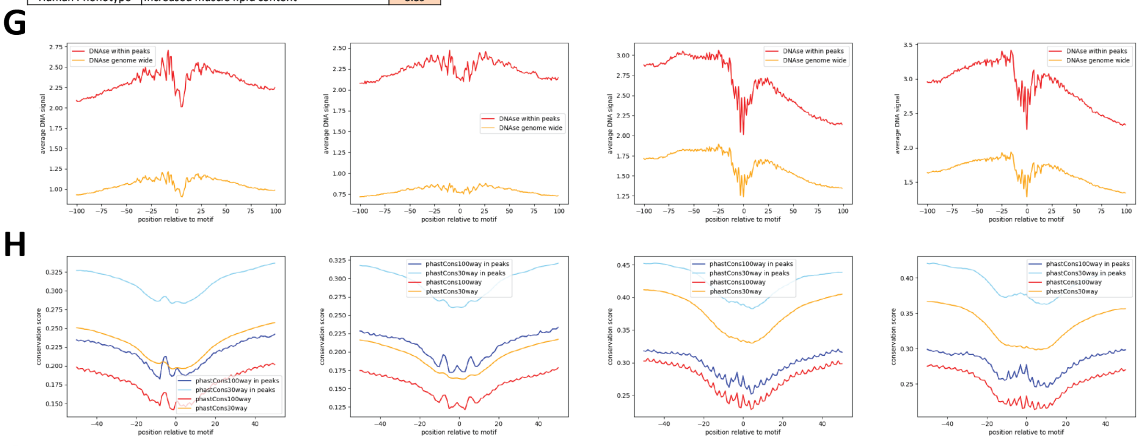

Supplementary Figure 607: Properties and genomic distribution of motifs identified for the ZFX transcription factor in K562 (accession ENCSR920ASP).

TF-MoDisCO pattern_0 n=12661, CWM

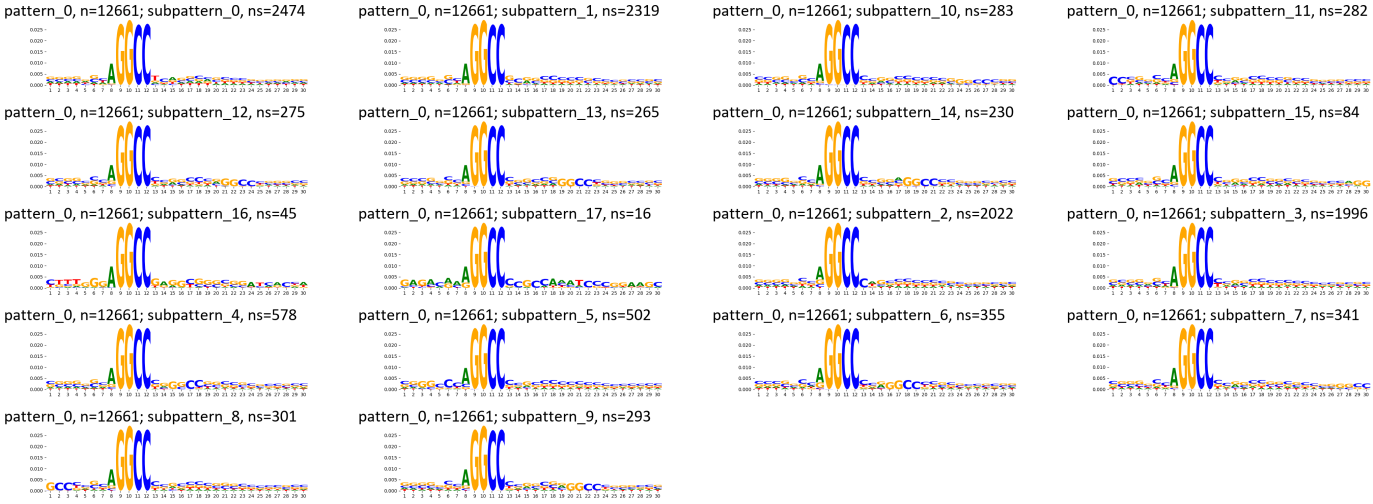

TF-MoDisCO pattern_0 n=12661, PWM

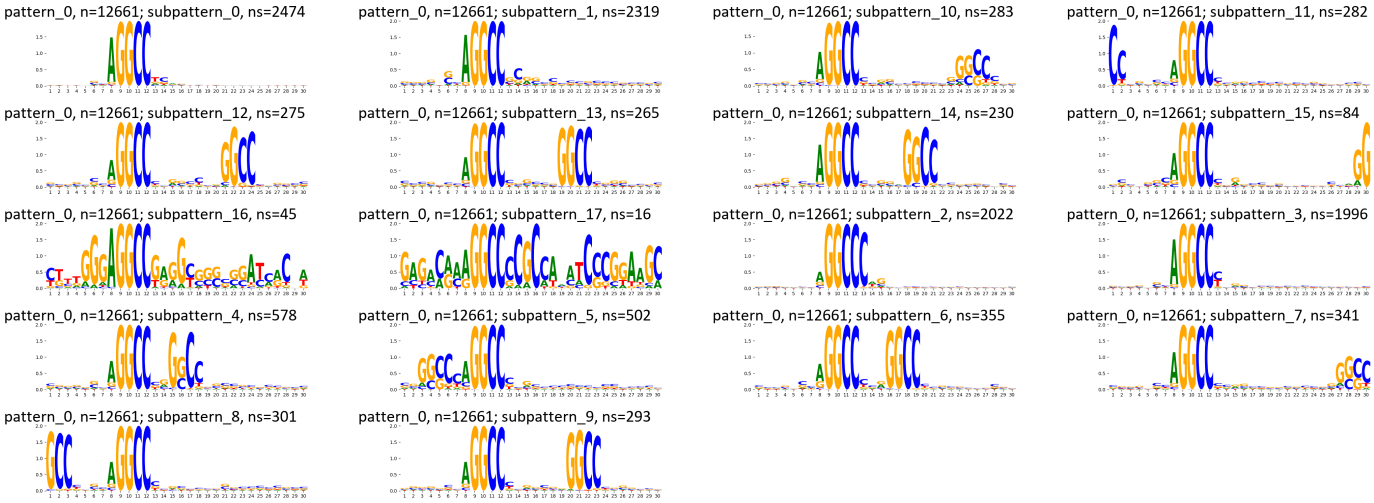

TF-MoDisCO pattern_1 n=404, CWM

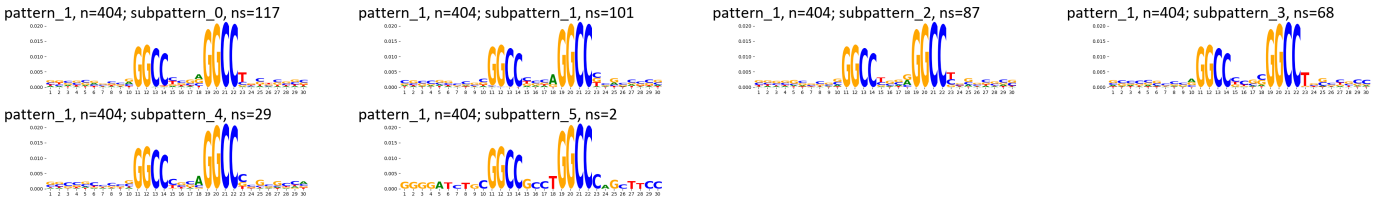

TF-MoDisCO pattern_1 n=404, PWM

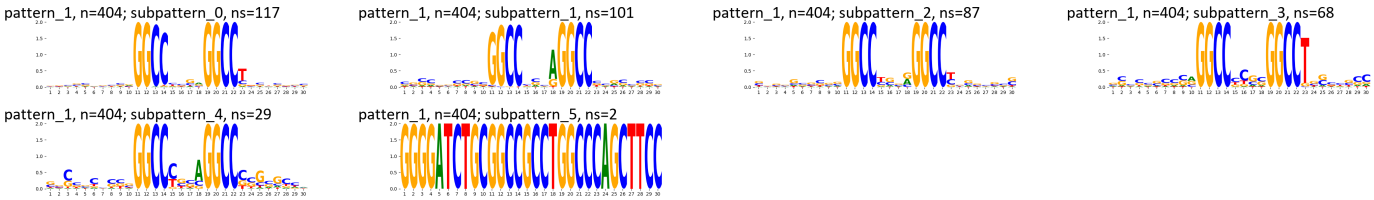

TF-MoDisCO pattern_2 n=336, CWM

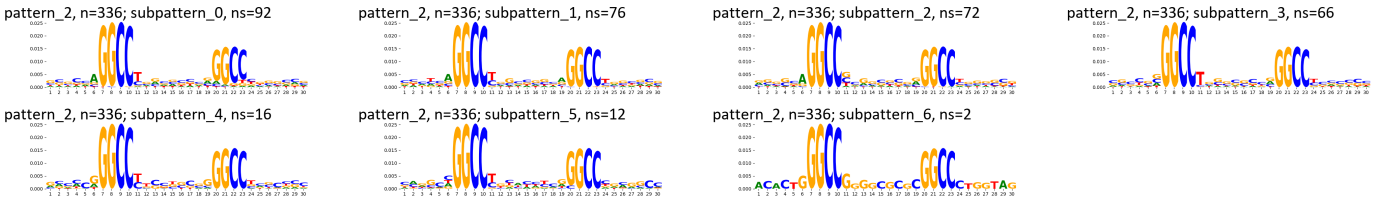

TF-MoDisCO pattern_2 n=336, PWM

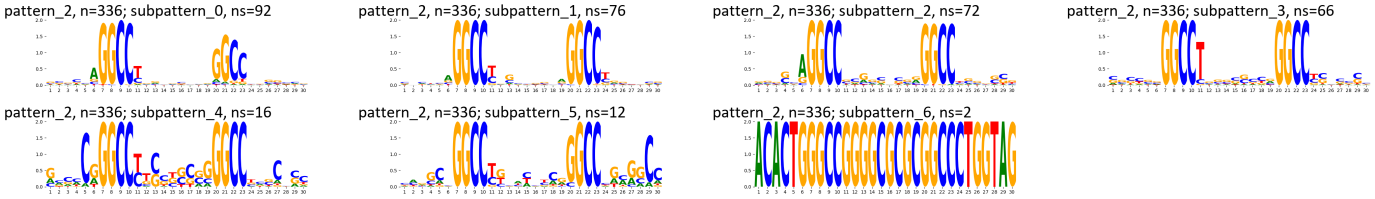

TF-MoDisCO pattern_3 n=221, CWM

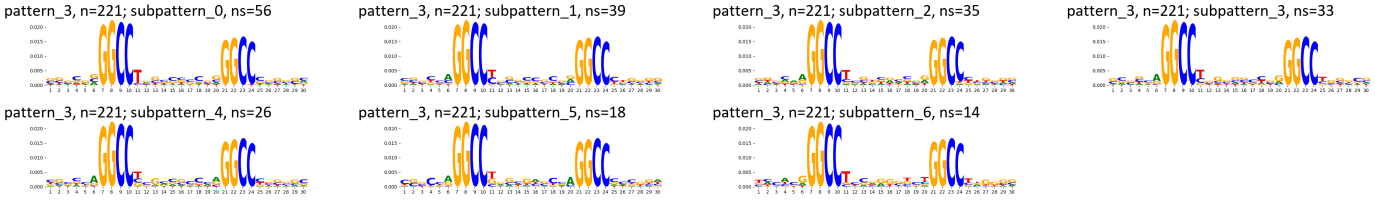

TF-MoDisCO pattern_3 n=221, PWM

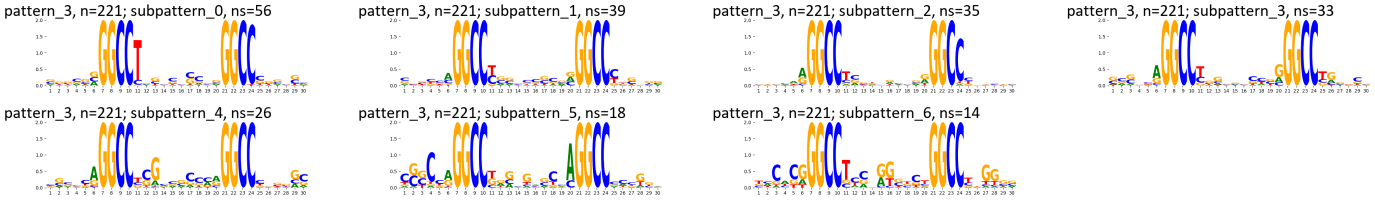

Supplementary Figure 608: TF-MoDisCO subpatterns for the ZFX transcription factor in K562 (accession ENCSR920ASP).

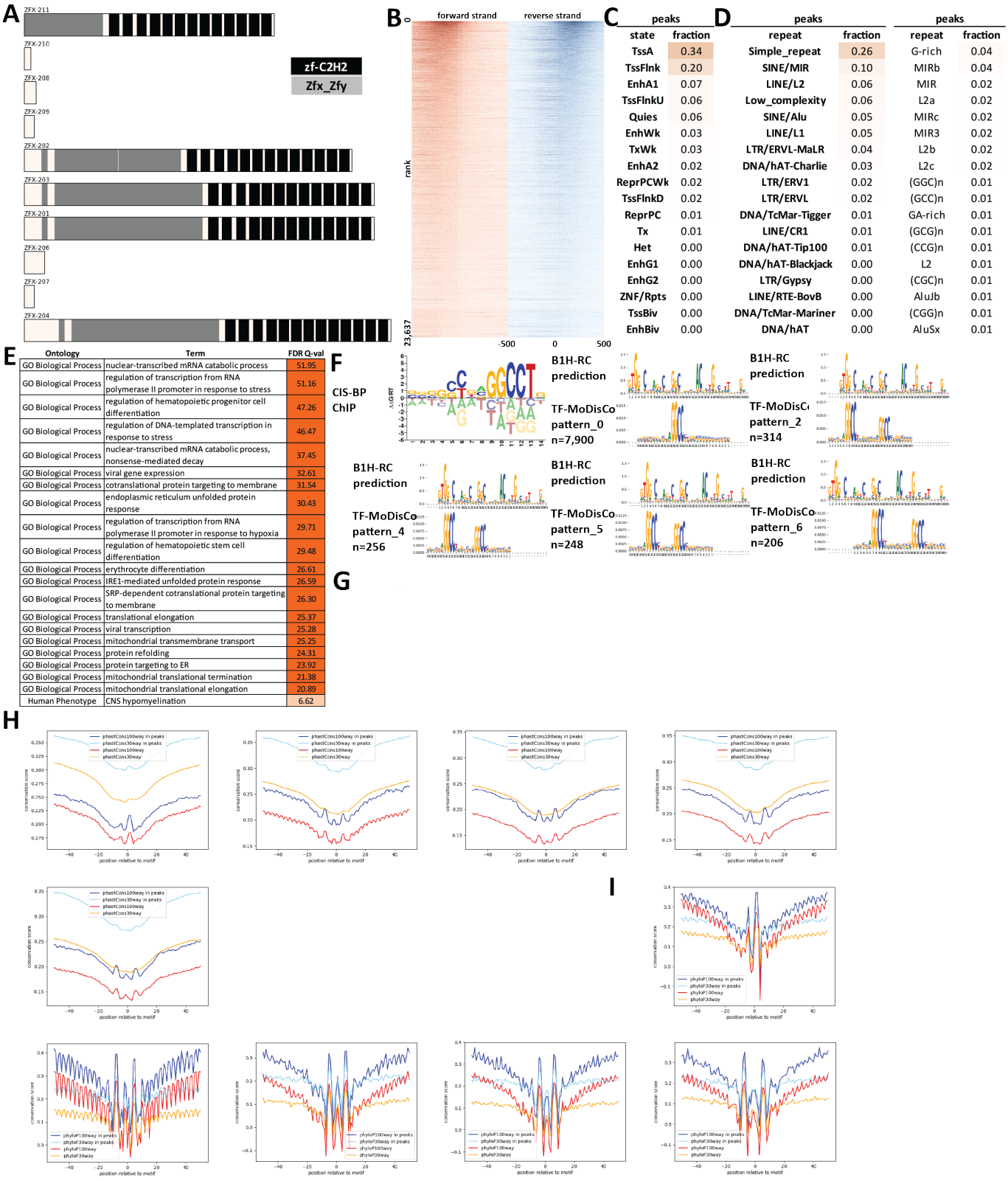

peaks	
state	fraction
TssA	0.34
TssFlnk	0.20
EnhA1	0.07
TssFlnkU	0.06
Quies	0.06
EnhWk	0.03
TxWk	0.03
EnhA2	0.02
ReprPCWk	0.02
TssFlnkD	0.02
ReprPC	0.01
Tx	0.01
Het	0.00
EnhG1	0.00
EnhG2	0.00
ZNF/Rpts	0.00
TssBiv	0.00
EnhBiv	0.00

peaks		peaks	
repeat	fraction	repeat	fraction
Simple_repeat	0.26	G-rich	0.04
SINE/MIR	0.10	MIRb	0.04
LINE/L2	0.06	MIR	0.02
Low_complexity	0.06	L2a	0.02
SINE/Alu	0.05	MIRc	0.02
LINE/L1	0.05	MIR3	0.02
LTR/ERVL-MaLR	0.04	L2b	0.02
DNA/hAT-Charlie	0.03	L2c	0.02
LTR/ERV1	0.02	(GGC)n	0.01
LTR/ERVL	0.02	(GCC)n	0.01
DNA/TcMar-Tigger	0.01	GA-rich	0.01
LINE/CR1	0.01	(GCG)n	0.01
DNA/hAT-Tip100	0.01	(CCG)n	0.01
DNA/hAT-Blackjack	0.00	L2	0.01
LTR/Gypsy	0.00	(CGC)n	0.01
LINE/RTE-BovB	0.00	AluJb	0.01
DNA/TcMar-Mariner	0.00	(CGG)n	0.01
DNA/hAT	0.00	AluSx	0.01

Ontology	Term	FDR Q-val
GO Biological Process	nuclear-transcribed mRNA catabolic process	51.95
GO Biological Process	regulation of transcription from RNA polymerase II promoter in response to stress	51.16
GO Biological Process	regulation of hematopoietic progenitor cell differentiation	47.26
GO Biological Process	regulation of DNA-templated transcription in response to stress	46.47
GO Biological Process	nuclear-transcribed mRNA catabolic process, nonsense-mediated decay	37.45
GO Biological Process	viral gene expression	32.61
GO Biological Process	cotranslational protein targeting to membrane	31.54
GO Biological Process	endoplasmic reticulum unfolded protein response	30.43
GO Biological Process	regulation of transcription from RNA polymerase II promoter in response to hypoxia	29.71
GO Biological Process	regulation of hematopoietic stem cell differentiation	29.48
GO Biological Process	erythrocyte differentiation	26.61
GO Biological Process	IRE1-mediated unfolded protein response	26.59
GO Biological Process	SRP-dependent cotranslational protein targeting to membrane	26.30
GO Biological Process	translational elongation	25.37
GO Biological Process	viral transcription	25.28
GO Biological Process	mitochondrial transmembrane transport	25.25
GO Biological Process	protein refolding	24.31
GO Biological Process	protein targeting to ER	23.92
GO Biological Process	mitochondrial translational termination	21.38
GO Biological Process	mitochondrial translational elongation	20.89
Human Phenotype	CNS hypomyelination	6.62

Supplementary Figure 609: Properties and genomic distribution of motifs identified for the ZFX transcription factor in MCF-7 (accession ENCSR435OQD).

TF-MoDisCO pattern_0 n=7900, CWM

pattern_0, n=7900; subpattern_0, ns=1827

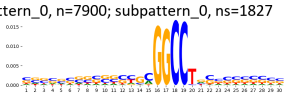

pattern_0, n=7900; subpattern_1, ns=1671

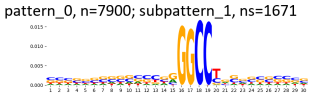

pattern_0, n=7900; subpattern_10, ns=77

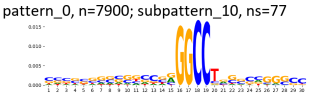

pattern_0, n=7900; subpattern_11, ns=47

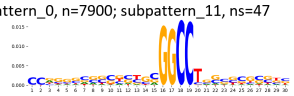

pattern_0, n=7900; subpattern_12, ns=18

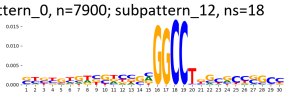

pattern_0, n=7900; subpattern_13, ns=3

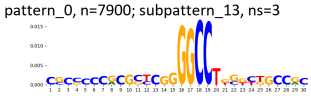

pattern_0, n=7900; subpattern_14, ns=2

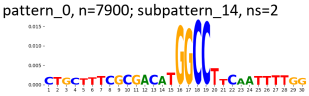

pattern_0, n=7900; subpattern_2, ns=1483

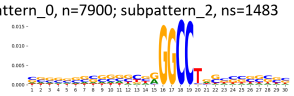

pattern_0, n=7900; subpattern_3, ns=1071

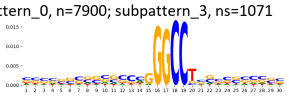

pattern_0, n=7900; subpattern_4, ns=548

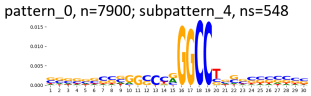

pattern_0, n=7900; subpattern_5, ns=337

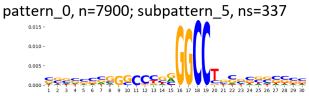

pattern_0, n=7900; subpattern_6, ns=253

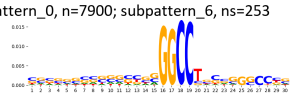

pattern_0, n=7900; subpattern_7, ns=238

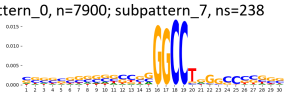

pattern_0, n=7900; subpattern_8, ns=211

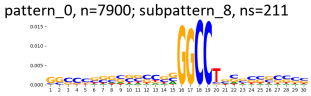

pattern_0, n=7900; subpattern_9, ns=114

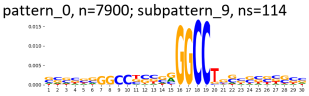

TF-MoDisCO pattern_0 n=7900, PWM

pattern_0, n=7900; subpattern_0, ns=1827

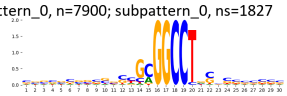

pattern_0, n=7900; subpattern_1, ns=1671

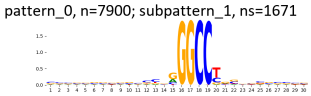

pattern_0, n=7900; subpattern_10, ns=77

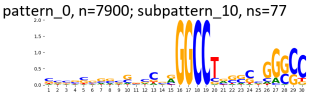

pattern_0, n=7900; subpattern_11, ns=47

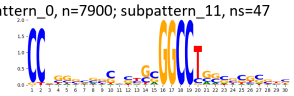

pattern_0, n=7900; subpattern_12, ns=18

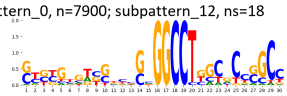

pattern_0, n=7900; subpattern_13, ns=3

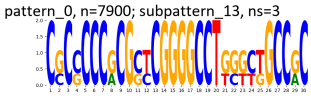

pattern_0, n=7900; subpattern_14, ns=2

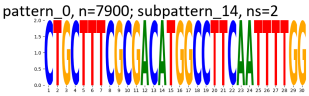

pattern_0, n=7900; subpattern_2, ns=1483

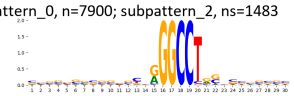

pattern_0, n=7900; subpattern_3, ns=1071

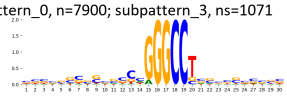

pattern_0, n=7900; subpattern_4, ns=548

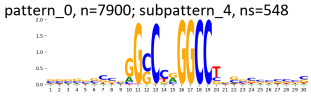

pattern_0, n=7900; subpattern_5, ns=337

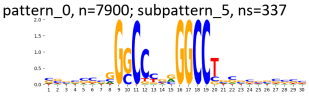

pattern_0, n=7900; subpattern_6, ns=253

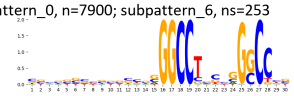

pattern_0, n=7900; subpattern_7, ns=238

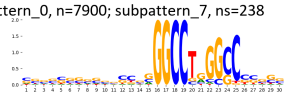

pattern_0, n=7900; subpattern_8, ns=211

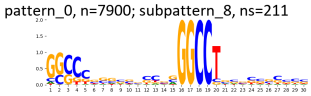

pattern_0, n=7900; subpattern_9, ns=114

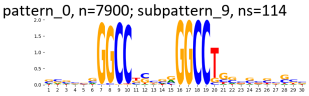

TF-MoDisCO pattern_2 n=314, CWM

pattern_2, n=314; subpattern_0, ns=102

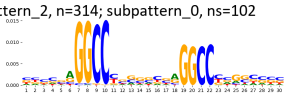

pattern_2, n=314; subpattern_1, ns=90

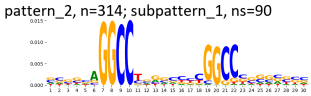

pattern_2, n=314; subpattern_2, ns=50

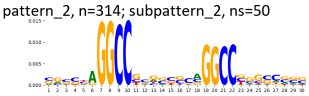

pattern_2, n=314; subpattern_3, ns=31

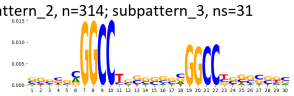

pattern_2, n=314; subpattern_4, ns=22

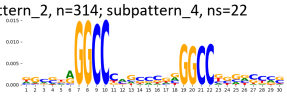

pattern_2, n=314; subpattern_5, ns=17

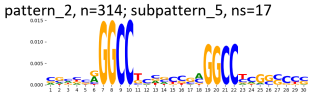

pattern_2, n=314; subpattern_6, ns=2

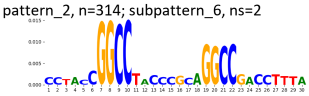

TF-MoDisCO pattern_2 n=314, PWM

pattern_2, n=314; subpattern_0, ns=102

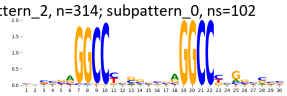

pattern_2, n=314; subpattern_1, ns=90

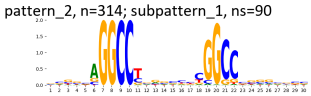

pattern_2, n=314; subpattern_2, ns=50

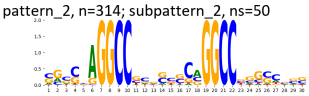

pattern_2, n=314; subpattern_3, ns=31

pattern_2, n=314; subpattern_4, ns=22

pattern_2, n=314; subpattern_5, ns=17

pattern_2, n=314; subpattern_6, ns=2

TF-MoDisCO pattern_4 n=256, CWM

pattern_4, n=256; subpattern_0, ns=67

pattern_4, n=256; subpattern_1, ns=60

pattern_4, n=256; subpattern_2, ns=46

pattern_4, n=256; subpattern_3, ns=36

pattern_4, n=256; subpattern_4, ns=27

pattern_4, n=256; subpattern_5, ns=12

pattern_4, n=256; subpattern_6, ns=8

TF-MoDisCO pattern_4 n=256, PWM

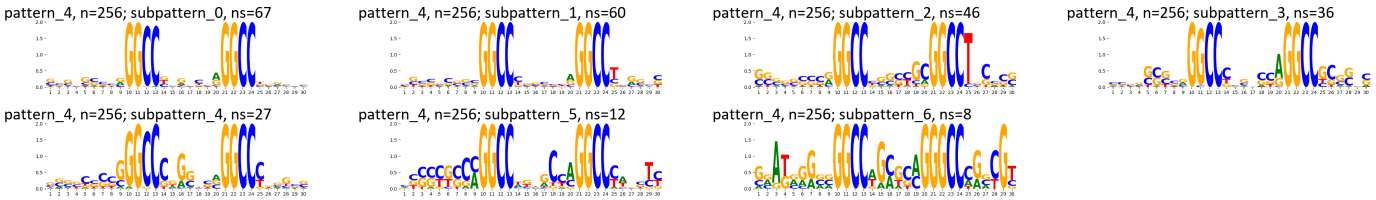

TF-MoDisCO pattern_5 n=248, CWM

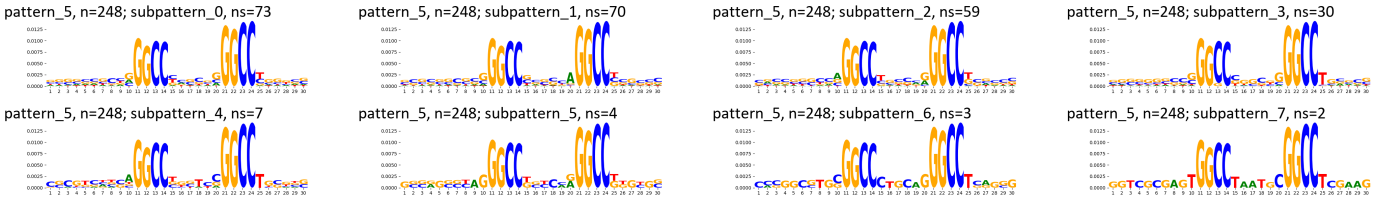

TF-MoDisCO pattern_5 n=248, PWM

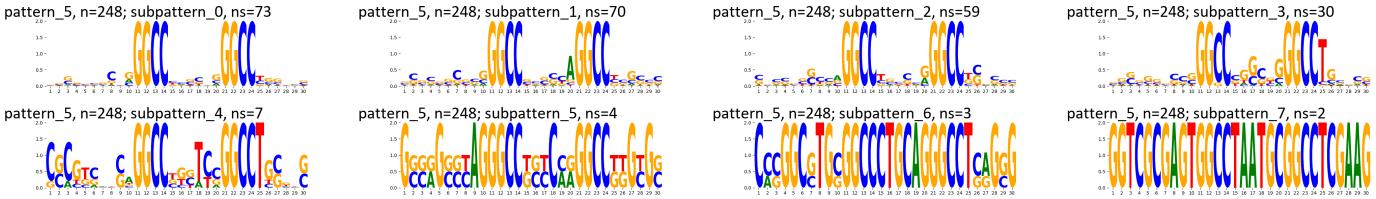

TF-MoDisCO pattern_6 n=206, CWM

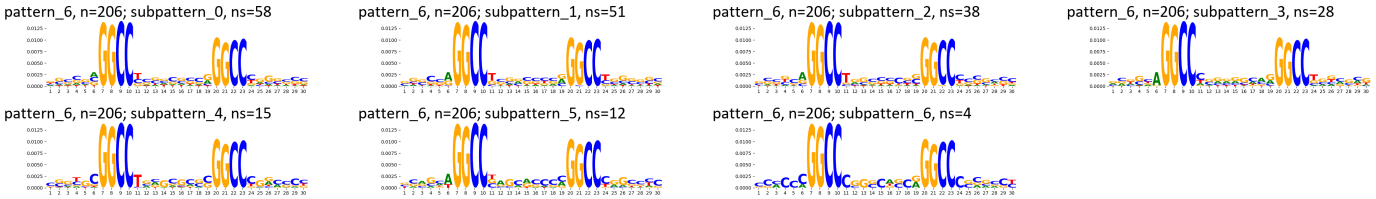

TF-MoDisCO pattern_6 n=206, PWM

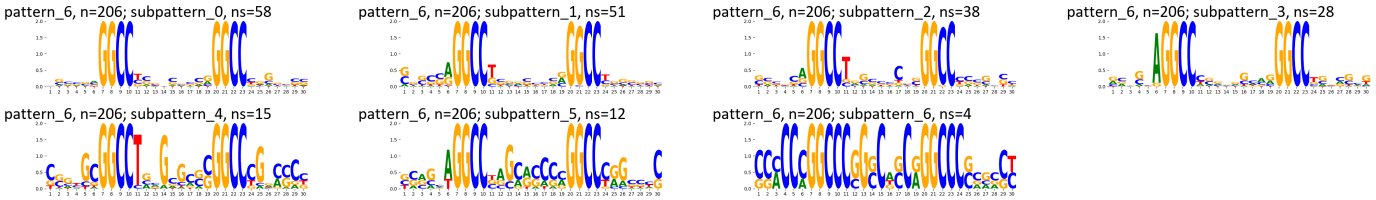

Supplementary Figure 610: TF-MoDisCO subpatterns for the ZFX transcription factor in MCF-7 (accession ENCSR435OQD).

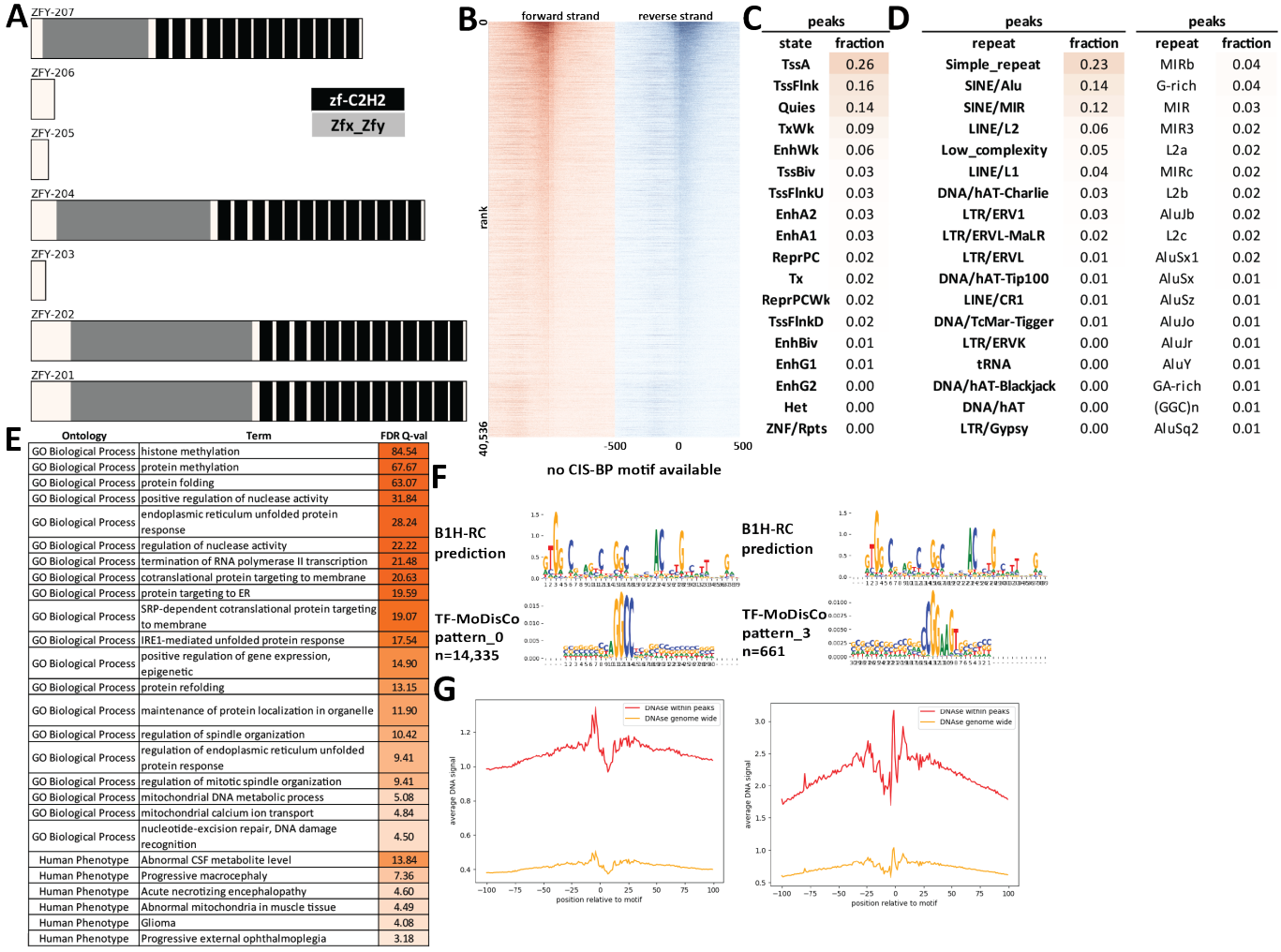

Supplementary Figure 611: Properties and genomic distribution of motifs identified for the ZFY transcription factor in HepG2 (accession ENCSR949OEV).

TF-MoDisCO pattern_0 n=14335, CWM

pattern_0, n=14335; subpattern_0, ns=3654

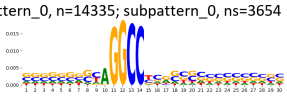

pattern_0, n=14335; subpattern_1, ns=2691

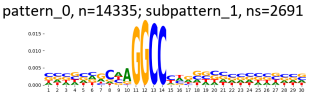

pattern_0, n=14335; subpattern_10, ns=291

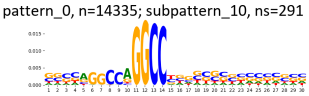

pattern_0, n=14335; subpattern_11, ns=285

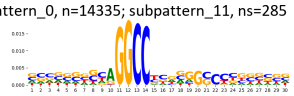

pattern_0, n=14335; subpattern_12, ns=252

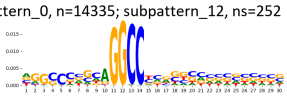

pattern_0, n=14335; subpattern_13, ns=222

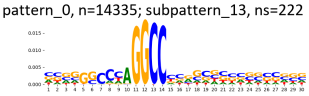

pattern_0, n=14335; subpattern_14, ns=216

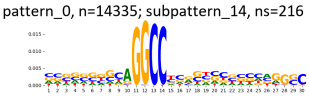

pattern_0, n=14335; subpattern_15, ns=35

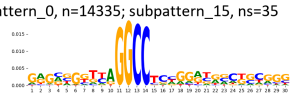

pattern_0, n=14335; subpattern_16, ns=5

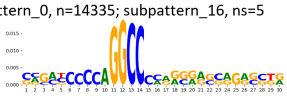

pattern_0, n=14335; subpattern_17, ns=4

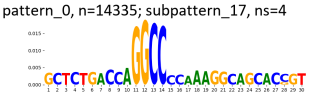

pattern_0, n=14335; subpattern_18, ns=3

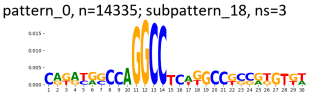

pattern_0, n=14335; subpattern_19, ns=3

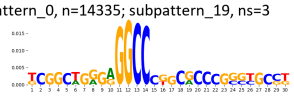

pattern_0, n=14335; subpattern_2, ns=2452

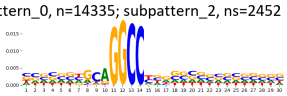

pattern_0, n=14335; subpattern_20, ns=2

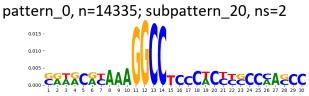

pattern_0, n=14335; subpattern_21, ns=2

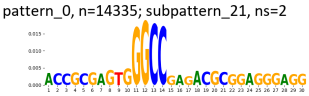

pattern_0, n=14335; subpattern_22, ns=2

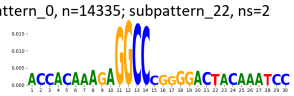

pattern_0, n=14335; subpattern_3, ns=1375

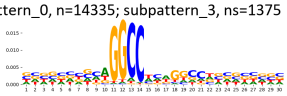

pattern_0, n=14335; subpattern_4, ns=1218

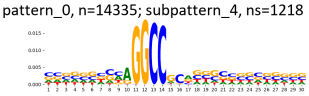

pattern_0, n=14335; subpattern_5, ns=393

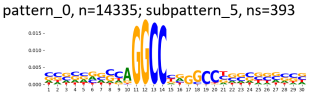

pattern_0, n=14335; subpattern_6, ns=347

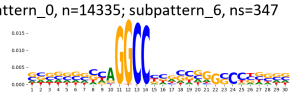

pattern_0, n=14335; subpattern_7, ns=301

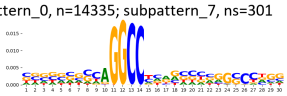

pattern_0, n=14335; subpattern_8, ns=291

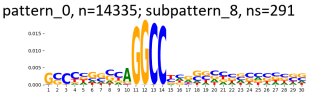

pattern_0, n=14335; subpattern_9, ns=291

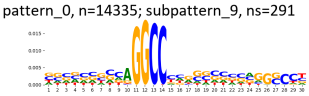

TF-MoDisCO pattern_0 n=14335, PWM

pattern_0, n=14335; subpattern_0, ns=3654

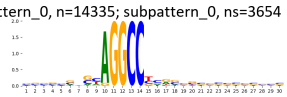

pattern_0, n=14335; subpattern_1, ns=2691

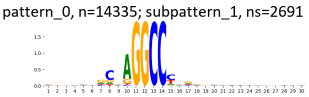

pattern_0, n=14335; subpattern_10, ns=291

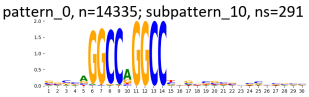

pattern_0, n=14335; subpattern_11, ns=285

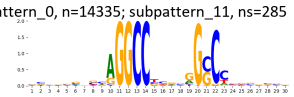

pattern_0, n=14335; subpattern_12, ns=252

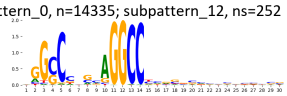

pattern_0, n=14335; subpattern_13, ns=222

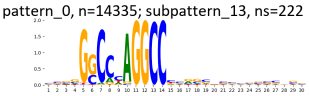

pattern_0, n=14335; subpattern_14, ns=216

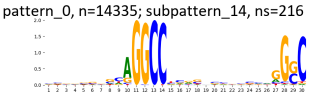

pattern_0, n=14335; subpattern_15, ns=35

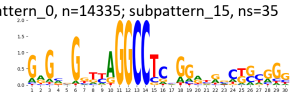

pattern_0, n=14335; subpattern_16, ns=5



pattern_0, n=14335; subpattern_17, ns=4

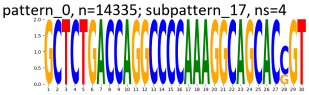

pattern_0, n=14335; subpattern_18, ns=3



pattern_0, n=14335; subpattern_19, ns=3

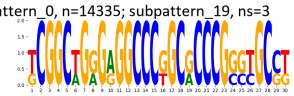

pattern_0, n=14335; subpattern_2, ns=2452

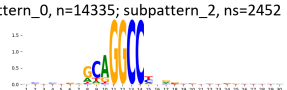

pattern_0, n=14335; subpattern_20, ns=2

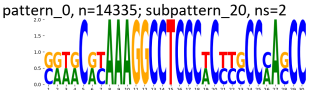

pattern_0, n=14335; subpattern_21, ns=2



pattern_0, n=14335; subpattern_22, ns=2

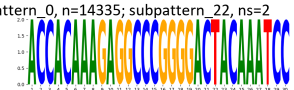

pattern_0, n=14335; subpattern_3, ns=1375

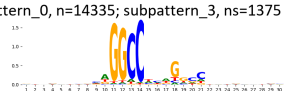

pattern_0, n=14335; subpattern_4, ns=1218

pattern_0, n=14335; subpattern_5, ns=393

pattern_0, n=14335; subpattern_6, ns=347

pattern_0, n=14335; subpattern_7, ns=301

pattern_0, n=14335; subpattern_8, ns=291

pattern_0, n=14335; subpattern_9, ns=291

TF-MoDisCO pattern_3 n=661, CWM

pattern_3, n=661; subpattern_0, ns=191

pattern_3, n=661; subpattern_1, ns=155

pattern_3, n=661; subpattern_2, ns=105

pattern_3, n=661; subpattern_3, ns=61

pattern_3, n=661; subpattern_4, ns=57

pattern_3, n=661; subpattern_5, ns=56

pattern_3, n=661; subpattern_6, ns=31

pattern_3, n=661; subpattern_7, ns=5

TF-MoDisCO pattern_3 n=661, PWM

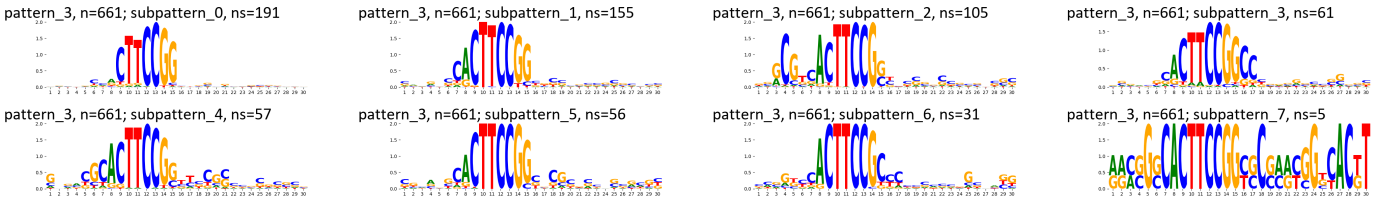

Supplementary Figure 612: TF-MoDisCO subpatterns for the ZFY transcription factor in HepG2 (accession ENCSR949OEV).

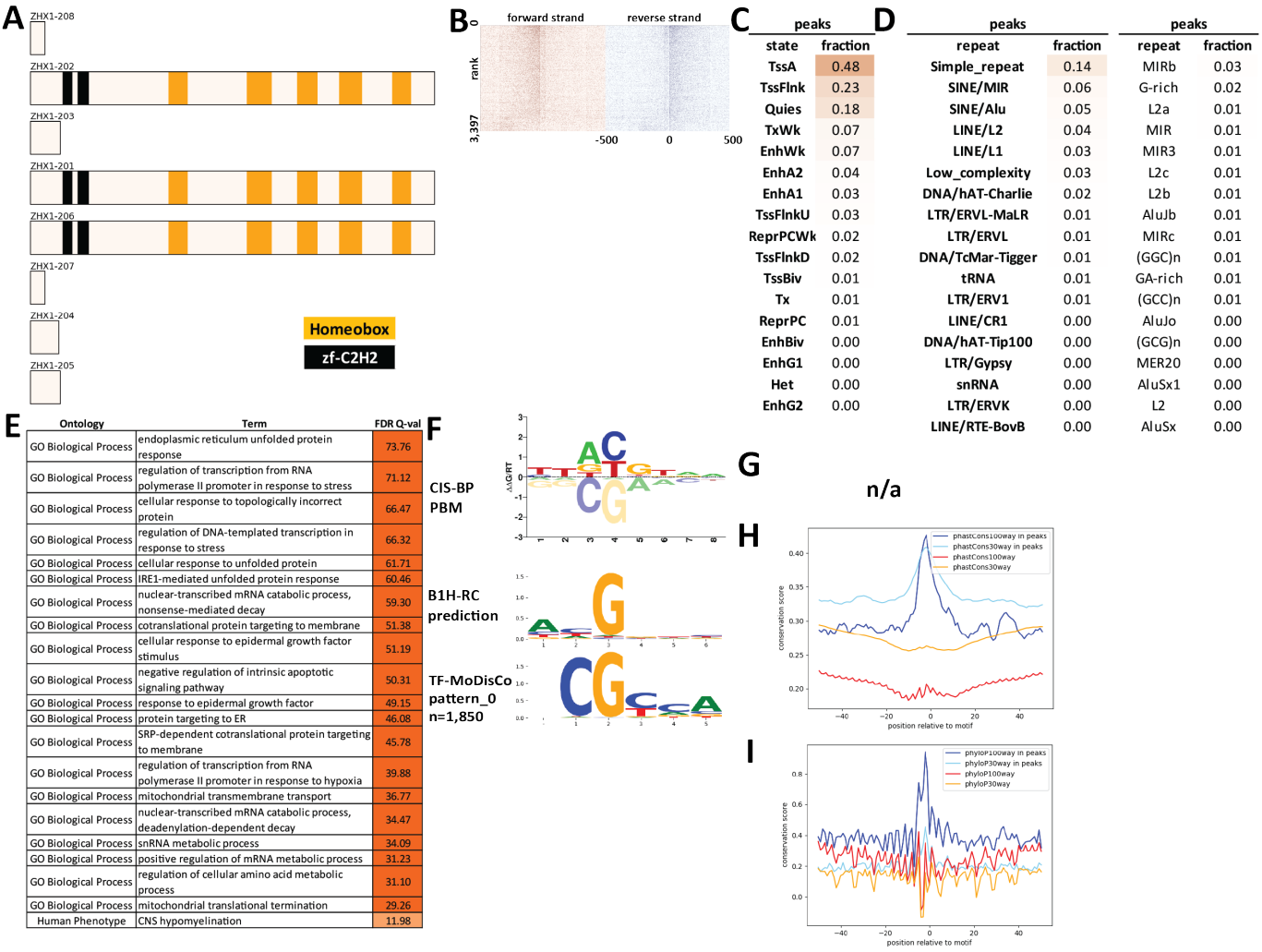

peaks	
state	fraction
TssA	0.48
TssFlnk	0.23
Quies	0.18
TxWk	0.07
EnhWk	0.07
EnhA2	0.04
EnhA1	0.03
TssFlnkU	0.03
ReprPCWk	0.02
TssFlnkD	0.02
TssBiv	0.01
Tx	0.01
ReprPC	0.01
EnhBiv	0.00
EnhG1	0.00
Het	0.00
EnhG2	0.00

peaks		peaks	
repeat	fraction	repeat	fraction
Simple_repeat	0.14	MIRb	0.03
SINE/MIR	0.06	G-rich	0.02
SINE/Alu	0.05	L2a	0.01
LINE/L2	0.04	MIR	0.01
LINE/L1	0.03	MIR3	0.01
Low_complexity	0.03	L2c	0.01
DNA/hAT-Charlie	0.02	L2b	0.01
LTR/ERVL-MaLR	0.01	AluJb	0.01
LTR/ERVL	0.01	MIRc	0.01
DNA/TcMar-Tigger	0.01	(GGC)n	0.01
tRNA	0.01	GA-rich	0.01
LTR/ERV1	0.01	(GCC)n	0.01
LINE/CR1	0.00	AluJo	0.00
DNA/hAT-Tip100	0.00	(GCG)n	0.00
LTR/Gypsy	0.00	MER20	0.00
snRNA	0.00	AluSx1	0.00
LTR/ERVK	0.00	L2	0.00
LINE/RTE-BovB	0.00	AluSx	0.00

Ontology	Term	FDR Q-val
GO Biological Process	endoplasmic reticulum unfolded protein response	73.76
GO Biological Process	regulation of transcription from RNA polymerase II promoter in response to stress	71.12
GO Biological Process	cellular response to topologically incorrect protein	66.47
GO Biological Process	regulation of DNA-templated transcription in response to stress	66.32
GO Biological Process	cellular response to unfolded protein	61.71
GO Biological Process	IRE1-mediated unfolded protein response	60.46
GO Biological Process	nuclear-transcribed mRNA catabolic process, nonsense-mediated decay	59.30
GO Biological Process	cotranslational protein targeting to membrane	51.38
GO Biological Process	cellular response to epidermal growth factor stimulus	51.19
GO Biological Process	negative regulation of intrinsic apoptotic signaling pathway	50.31
GO Biological Process	response to epidermal growth factor	49.15
GO Biological Process	protein targeting to ER	46.08
GO Biological Process	SRP-dependent cotranslational protein targeting to membrane	45.78
GO Biological Process	regulation of transcription from RNA polymerase II promoter in response to hypoxia	39.88
GO Biological Process	mitochondrial transmembrane transport	36.77
GO Biological Process	nuclear-transcribed mRNA catabolic process, deadenylation-dependent decay	34.47
GO Biological Process	snRNA metabolic process	34.09
GO Biological Process	positive regulation of mRNA metabolic process	31.23
GO Biological Process	regulation of cellular amino acid metabolic process	31.10
GO Biological Process	mitochondrial translational termination	29.26
Human Phenotype	CNS hypomyelination	11.98

Supplementary Figure 613: Properties and genomic distribution of motifs identified for the ZHX1 transcription factor in HeLa-S3 (accession ENCSR887MXT).

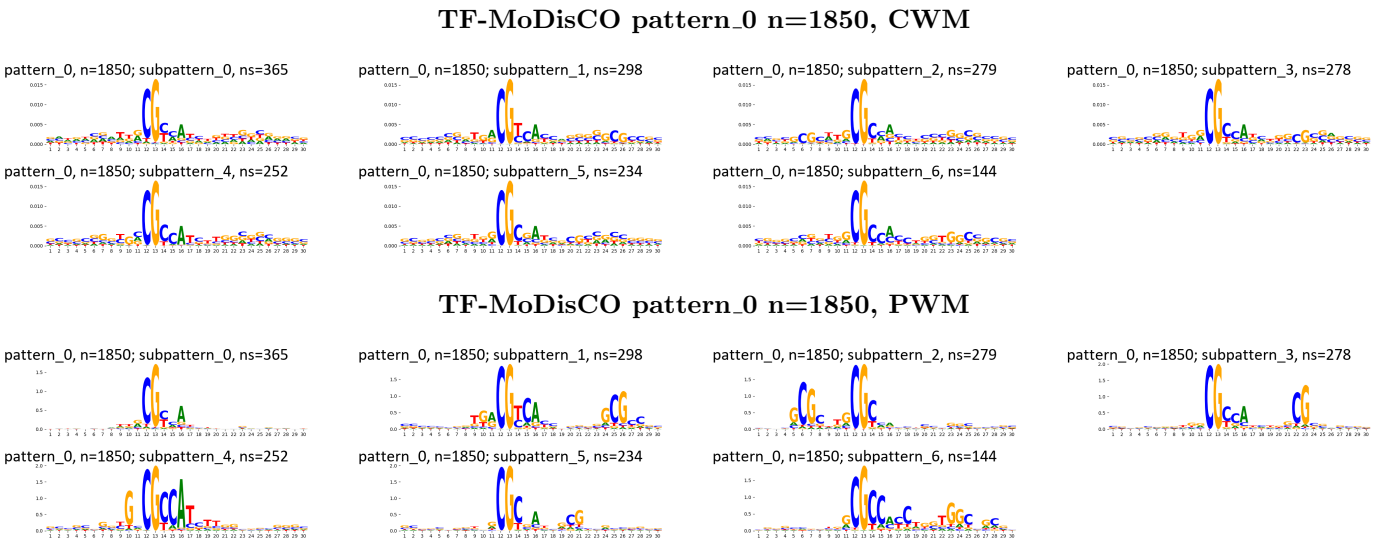

Supplementary Figure 614: TF-MoDisCO subpatterns for the ZHX1 transcription factor in HeLa-S3 (accession ENCSR887MXT).

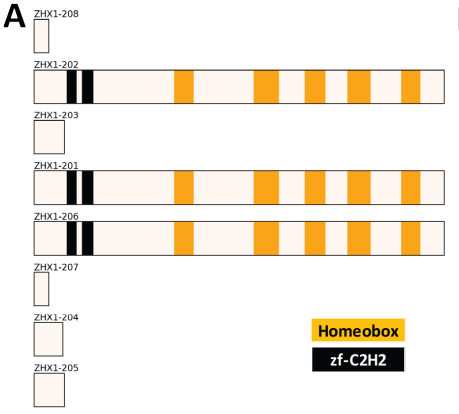



C

peaks	
state	fraction
TssA	0.36
Quies	0.17
TssFlnk	0.17
TxWk	0.10
EnhWk	0.06
Tx	0.04
TssFlnkU	0.03
TssBiv	0.03
EnhA2	0.03
ReprPC	0.02
EnhA1	0.02
TssFlnkD	0.02
ReprPCWk	0.02
EnhG1	0.01
EnhBiv	0.01
EnhG2	0.00
Het	0.00
ZNF/Rpts	0.00

D

peaks		peaks	
repeat	fraction	repeat	fraction
Simple_repeat	0.19	MIRb	0.04
SINE/Alu	0.12	G-rich	0.03
SINE/MIR	0.10	MIR	0.02
LINE/L2	0.06	L2a	0.02
Low_complexity	0.04	MIRc	0.02
LINE/L1	0.04	MIR3	0.02
DNA/hAT-Charlie	0.02	L2b	0.02
LTR/ERV1	0.02	L2c	0.02
LTR/ERVL-MaLR	0.02	AluJb	0.01
LTR/ERVL	0.01	AluSx1	0.01
DNA/TcMar-Tigger	0.01	AluSx	0.01
tRNA	0.01	AluSz	0.01
LINE/CR1	0.01	AluJr	0.01
DNA/hAT-Tip100	0.01	AluJo	0.01
DNA/hAT-Blackjack	0.00	AluY	0.01
LTR/ERVK	0.00	(GGC)n	0.01
LINE/RTE-BovB	0.00	GA-rich	0.01
snRNA	0.00	AluSq2	0.01

E

Ontology	Term	FDR Q-val
GO Biological Process	viral gene expression	22.66
GO Biological Process	ncRNA metabolic process	21.50
GO Biological Process	multi-organism metabolic process	21.66
GO Biological Process	viral transcription	18.60
GO Biological Process	translation	17.72
GO Biological Process	ncRNA processing	17.19
GO Biological Process	viral life cycle	16.67
GO Biological Process	peptide biosynthetic process	16.45
GO Biological Process	ribonucleoprotein complex biogenesis	16.25
GO Biological Process	positive regulation of transcription from RNA polymerase II promoter in response to stress	15.30
GO Biological Process	translational initiation	15.22
GO Biological Process	response to topologically incorrect protein	13.72
GO Biological Process	cellular response to topologically incorrect protein	13.27
GO Biological Process	nuclear-transcribed mRNA catabolic process	13.26
GO Biological Process	protein targeting to ER	13.20
GO Biological Process	ribosome biogenesis	12.92
GO Biological Process	response to endoplasmic reticulum stress	12.86
GO Biological Process	cotranslational protein targeting to membrane	12.54
GO Biological Process	rRNA processing	12.12
GO Biological Process	rRNA metabolic process	12.04

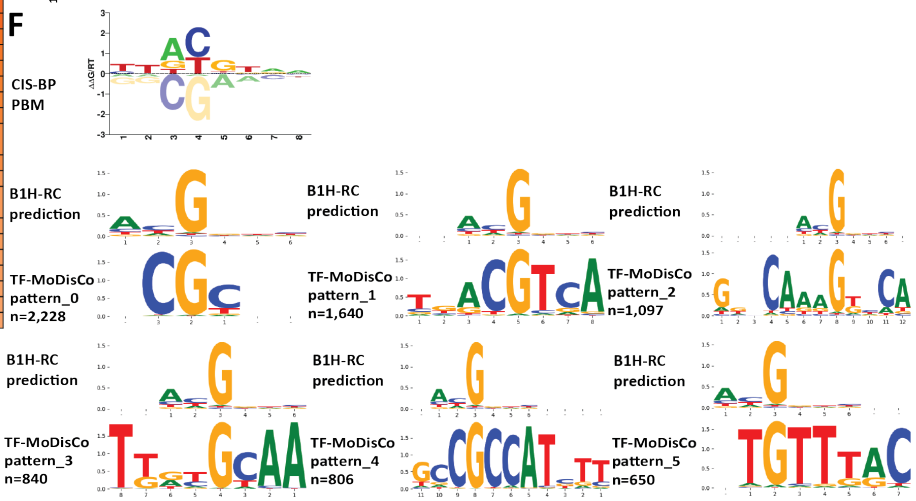

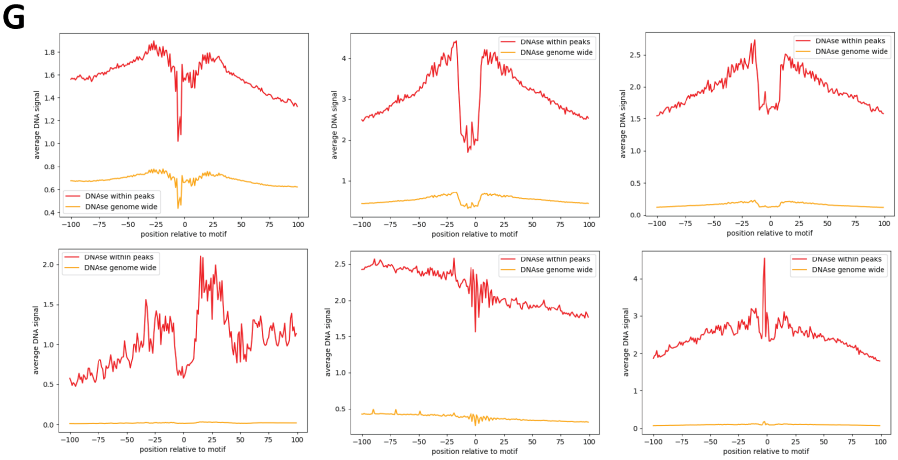

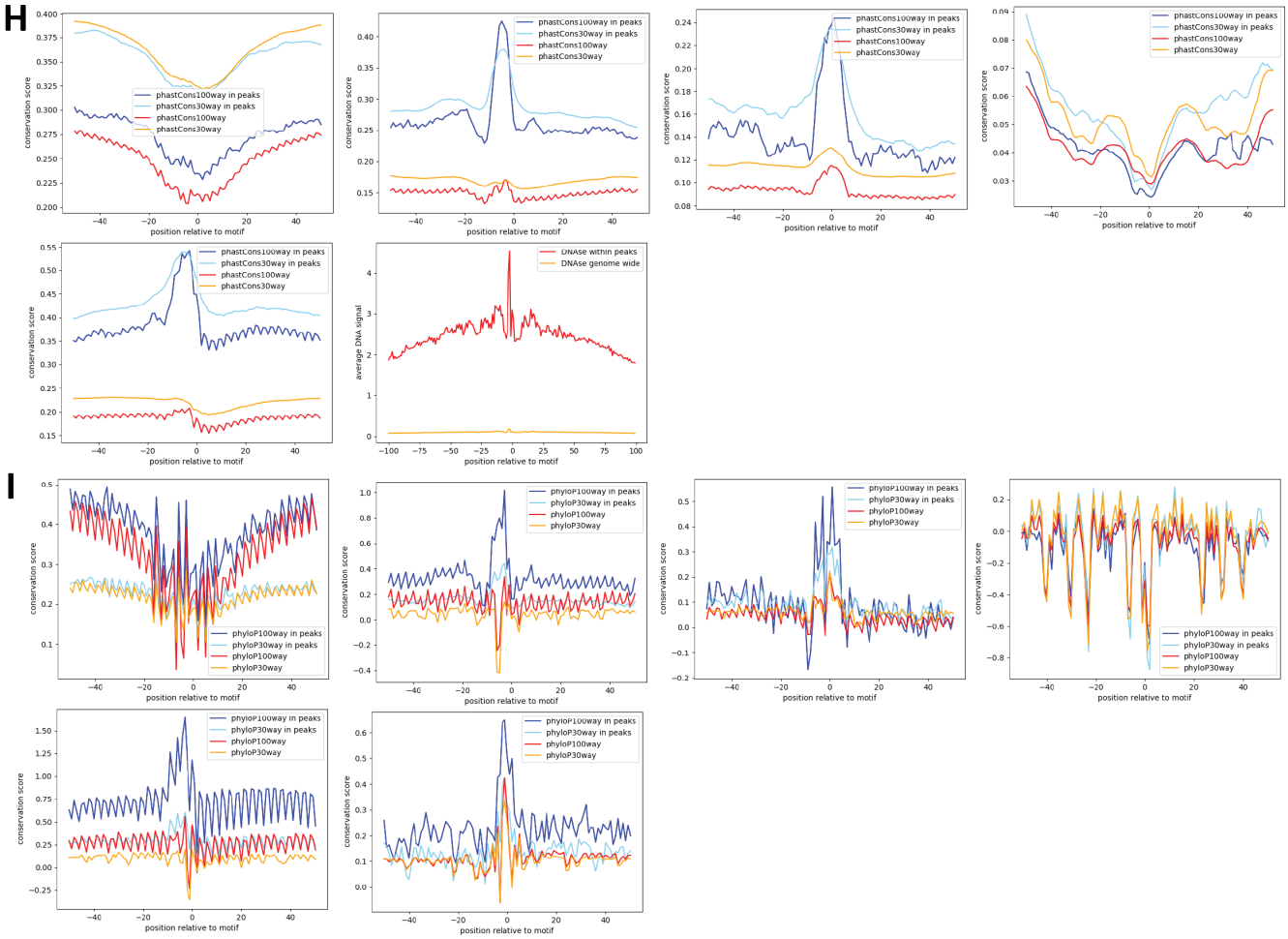

Supplementary Figure 615: Properties and genomic distribution of motifs identified for the ZHX1 transcription factor in HepG2 (accession ENCSR978DQT).

TF-MoDisCO pattern_0 n=2228, CWM

pattern_0, n=2228; subpattern_0, ns=392

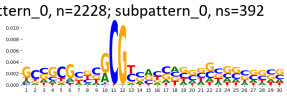

pattern_0, n=2228; subpattern_1, ns=367

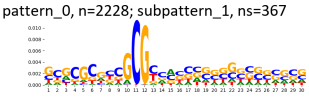

pattern_0, n=2228; subpattern_2, ns=326

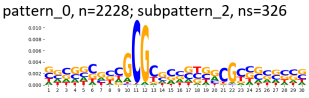

pattern_0, n=2228; subpattern_3, ns=302

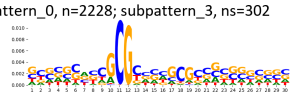

pattern_0, n=2228; subpattern_4, ns=204

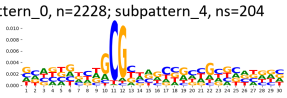

pattern_0, n=2228; subpattern_5, ns=190

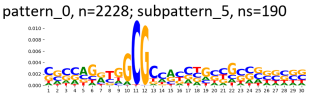

pattern_0, n=2228; subpattern_6, ns=121

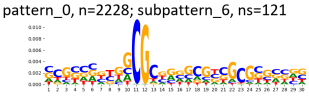

pattern_0, n=2228; subpattern_7, ns=119

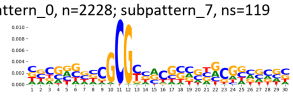

pattern_0, n=2228; subpattern_8, ns=112

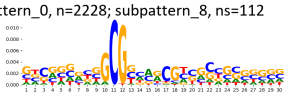

pattern_0, n=2228; subpattern_9, ns=95

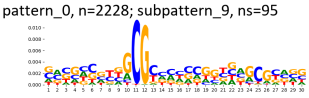

TF-MoDisCO pattern_0 n=2228, PWM

pattern_0, n=2228; subpattern_0, ns=392

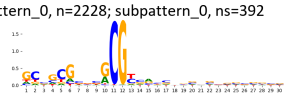

pattern_0, n=2228; subpattern_1, ns=367

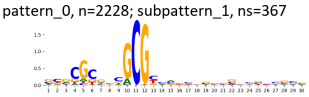

pattern_0, n=2228; subpattern_2, ns=326

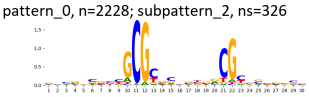

pattern_0, n=2228; subpattern_3, ns=302

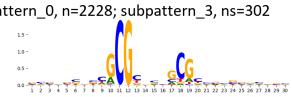

pattern_0, n=2228; subpattern_4, ns=204

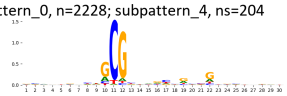

pattern_0, n=2228; subpattern_5, ns=190

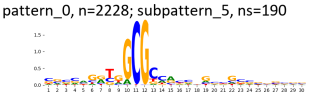

pattern_0, n=2228; subpattern_6, ns=121

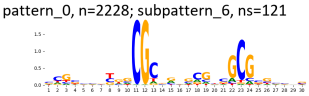

pattern_0, n=2228; subpattern_7, ns=119

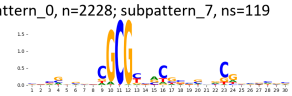

pattern_0, n=2228; subpattern_8, ns=112

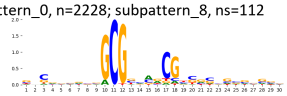

pattern_0, n=2228; subpattern_9, ns=95

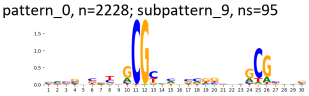

TF-MoDisCO pattern_1 n=1640, CWM

pattern_1, n=1640; subpattern_0, ns=356

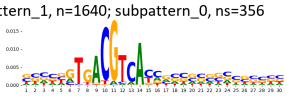

pattern_1, n=1640; subpattern_1, ns=320

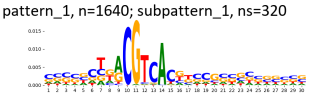

pattern_1, n=1640; subpattern_2, ns=288

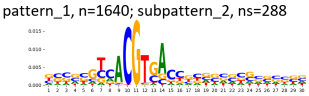

pattern_1, n=1640; subpattern_3, ns=263

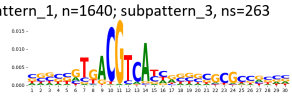

pattern_1, n=1640; subpattern_4, ns=210

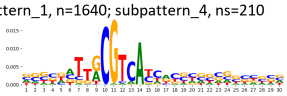

pattern_1, n=1640; subpattern_5, ns=113

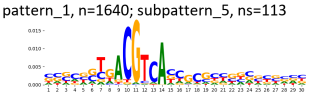

pattern_1, n=1640; subpattern_6, ns=90

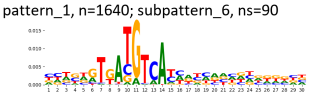

TF-MoDisCO pattern_1 n=1640, PWM

pattern_1, n=1640; subpattern_0, ns=356

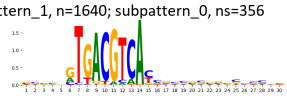

pattern_1, n=1640; subpattern_1, ns=320

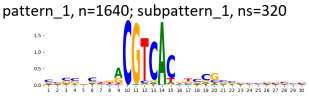

pattern_1, n=1640; subpattern_2, ns=288

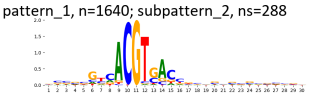

pattern_1, n=1640; subpattern_3, ns=263

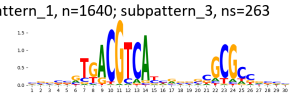

pattern_1, n=1640; subpattern_4, ns=210

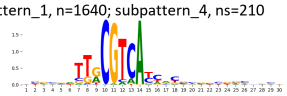

pattern_1, n=1640; subpattern_5, ns=113

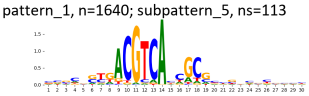

pattern_1, n=1640; subpattern_6, ns=90

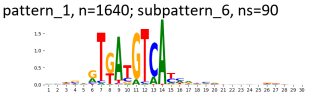

TF-MoDisCO pattern_2 n=1097, CWM

pattern_2, n=1097; subpattern_0, ns=253

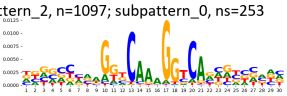

pattern_2, n=1097; subpattern_1, ns=235

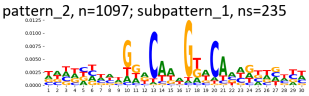

pattern_2, n=1097; subpattern_2, ns=194

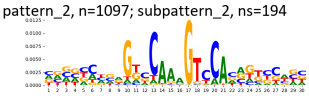

pattern_2, n=1097; subpattern_3, ns=165

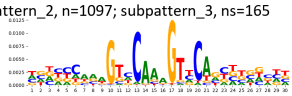

pattern_2, n=1097; subpattern_4, ns=139

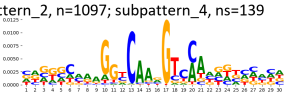

pattern_2, n=1097; subpattern_5, ns=102

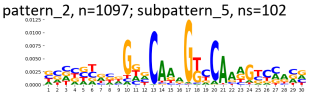

pattern_2, n=1097; subpattern_6, ns=6

pattern_2, n=1097; subpattern_7, ns=3

TF-MoDisCO pattern_2 n=1097, PWM

pattern_2, n=1097; subpattern_0, ns=253

pattern_2, n=1097; subpattern_1, ns=235

pattern_2, n=1097; subpattern_2, ns=194

pattern_2, n=1097; subpattern_3, ns=165

pattern_2, n=1097; subpattern_4, ns=139

pattern_2, n=1097; subpattern_5, ns=102

pattern_2, n=1097; subpattern_6, ns=6

pattern_2, n=1097; subpattern_7, ns=3

TF-MoDisCO pattern_3 n=840, CWM

pattern_3, n=840; subpattern_0, ns=200

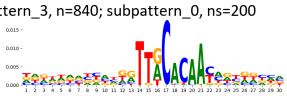

pattern_3, n=840; subpattern_1, ns=192

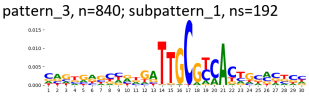

pattern_3, n=840; subpattern_2, ns=164

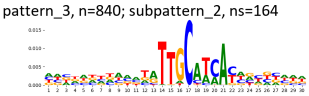

pattern_3, n=840; subpattern_3, ns=160

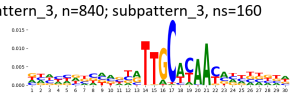

pattern_3, n=840; subpattern_4, ns=84

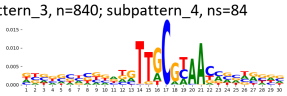

pattern_3, n=840; subpattern_5, ns=37

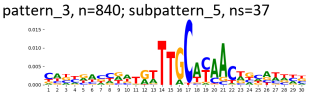

pattern_3, n=840; subpattern_6, ns=3

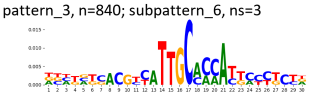

TF-MoDisCO pattern_3 n=840, PWM

pattern_3, n=840; subpattern_0, ns=200

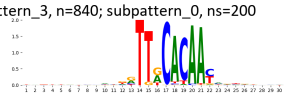

pattern_3, n=840; subpattern_1, ns=192

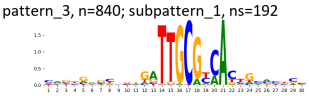

pattern_3, n=840; subpattern_2, ns=164

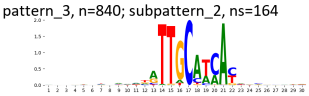

pattern_3, n=840; subpattern_3, ns=160

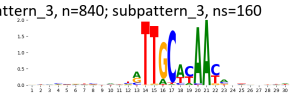

pattern_3, n=840; subpattern_4, ns=84

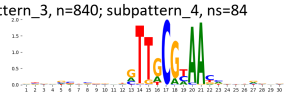

pattern_3, n=840; subpattern_5, ns=37

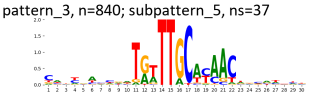

pattern_3, n=840; subpattern_6, ns=3

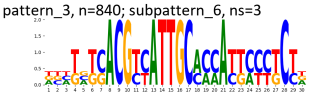

TF-MoDisCO pattern_4 n=806, CWM

pattern_4, n=806; subpattern_0, ns=169

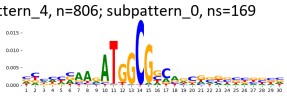

pattern_4, n=806; subpattern_1, ns=165

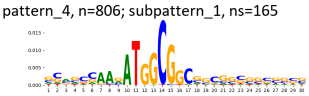

pattern_4, n=806; subpattern_2, ns=160

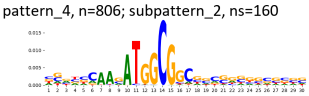

pattern_4, n=806; subpattern_3, ns=95

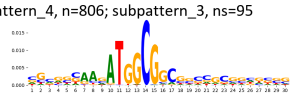

pattern_4, n=806; subpattern_4, ns=76

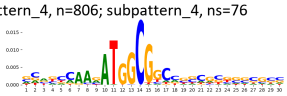

pattern_4, n=806; subpattern_5, ns=71

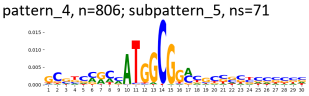

pattern_4, n=806; subpattern_6, ns=70

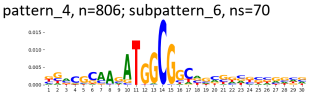

TF-MoDisCO pattern_4 n=806, PWM

pattern_4, n=806; subpattern_0, ns=169

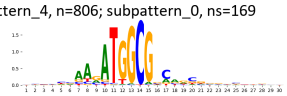

pattern_4, n=806; subpattern_1, ns=165

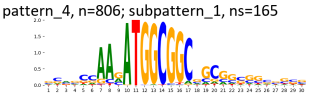

pattern_4, n=806; subpattern_2, ns=160

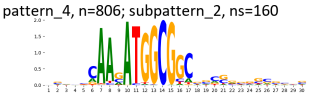

pattern_4, n=806; subpattern_3, ns=95

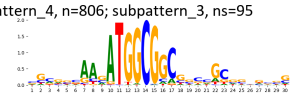

pattern_4, n=806; subpattern_4, ns=76

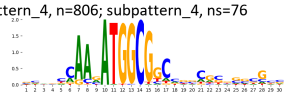

pattern_4, n=806; subpattern_5, ns=71

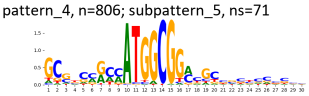

pattern_4, n=806; subpattern_6, ns=70

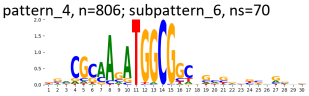

TF-MoDisCO pattern_5 n=650, CWM

pattern_5, n=650; subpattern_0, ns=155

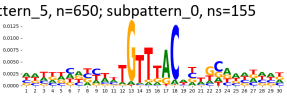

pattern_5, n=650; subpattern_1, ns=141

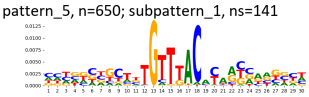

pattern_5, n=650; subpattern_2, ns=131

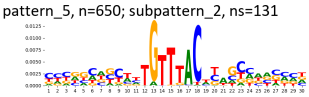

pattern_5, n=650; subpattern_3, ns=118

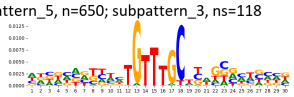

pattern_5, n=650; subpattern_4, ns=90

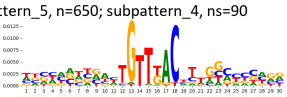

pattern_5, n=650; subpattern_5, ns=15

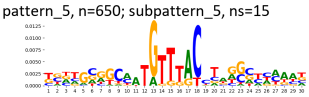

TF-MoDisCO pattern_5 n=650, PWM

pattern_5, n=650; subpattern_0, ns=155

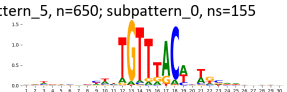

pattern_5, n=650; subpattern_1, ns=141

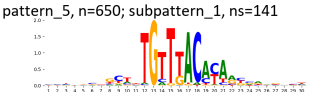

pattern_5, n=650; subpattern_2, ns=131

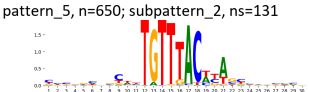

pattern_5, n=650; subpattern_3, ns=118

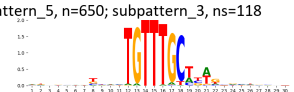

pattern_5, n=650; subpattern_4, ns=90

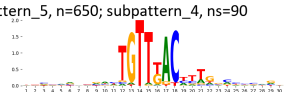

pattern_5, n=650; subpattern_5, ns=15

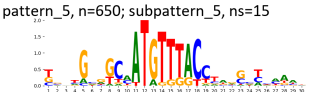

Supplementary Figure 616: TF-MoDisCO subpatterns for the ZHX1 transcription factor in HepG2 (accession ENCSR978DQT).

A

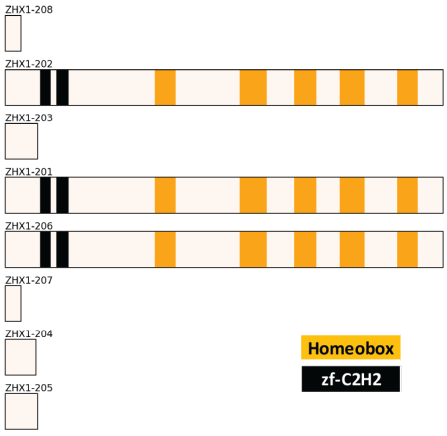

B

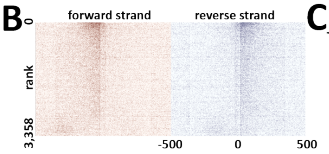

C

peaks	
state	fraction
TssA	0.51
TssFlnk	0.21
Quies	0.15
TxWk	0.07
EnhWk	0.04
EnhA2	0.03
TssFlnkU	0.02
Tx	0.02
EnhA1	0.02
ReprPCWk	0.02
TssBiv	0.02
ReprPC	0.01
TssFlnkD	0.01
EnhBiv	0.00
EnhG1	0.00
Het	0.00
EnhG2	0.00
ZNF/Rpts	0.00

D

peaks		peaks	
repeat	fraction	repeat	fraction
Simple_repeat	0.14	MIRb	0.02
SINE/MIR	0.06	G-rich	0.02
SINE/Alu	0.06	L2a	0.02
LINE/L2	0.04	MIR	0.01
Low_complexity	0.03	MIR3	0.01
LTR/ERV1	0.03	L2b	0.01
LINE/L1	0.03	MIRc	0.01
tRNA	0.02	GA-rich	0.01
LTR/ERVL-MaLR	0.02	L2c	0.01
DNA/hAT-Charlie	0.02	(GGC)n	0.01
LTR/ERVL	0.01	U1	0.01
snRNA	0.01	AluJb	0.01
DNA/hAT-Tip100	0.01	AluSz	0.01
DNA/TcMar-Tigger	0.00	AluY	0.01
LINE/CR1	0.00	L2	0.00
Satellite/telo	0.00	LTR17	0.00
LTR/Gypsy	0.00	AluSx1	0.00
LTR/ERVK	0.00	AluSx	0.00

E

Ontology	Term	FDR Q-val
GO Biological Process	mRNA catabolic process	45.72
GO Biological Process	nuclear-transcribed mRNA catabolic process	44.53
GO Biological Process	RNA catabolic process	43.69
GO Biological Process	regulation of transcription from RNA polymerase II promoter in response to stress	30.19
GO Biological Process	nuclear-transcribed mRNA catabolic process, deadenylation-dependent decay	29.63
GO Biological Process	nuclear-transcribed mRNA catabolic process, nonsense-mediated decay	29.07
GO Biological Process	multi-organism metabolic process	27.02
GO Biological Process	endoplasmic reticulum unfolded protein response	26.05
GO Biological Process	regulation of DNA-templated transcription in response to stress	25.84
GO Biological Process	viral gene expression	25.13
GO Biological Process	IRE1-mediated unfolded protein response	23.62
GO Biological Process	cellular response to topologically incorrect protein	22.42
GO Biological Process	cellular response to unfolded protein	22.33
GO Biological Process	mitochondrial translation	22.20
GO Biological Process	mitochondrial translational elongation	22.14
GO Biological Process	protein targeting to ER	21.85
GO Biological Process	response to epidermal growth factor	21.63
GO Biological Process	liver regeneration	21.41
GO Biological Process	cotranslational protein targeting to membrane	21.33
GO Biological Process	mitochondrial translational termination	21.12
Human Phenotype	Increased serum lactate	16.52
Human Phenotype	Abnormal CSF metabolite level	11.95
Human Phenotype	Increased CSF lactate	11.02
Human Phenotype	Exercise intolerance	10.22
Human Phenotype	Abnormal glycosylation	5.00
Human Phenotype	Abnormality of monocarboxylic acid metabolism	4.97
Human Phenotype	Abnormal protein N-linked glycosylation	4.68
Human Phenotype	Abnormal isoelectric focusing of serum transferrin	4.35

F

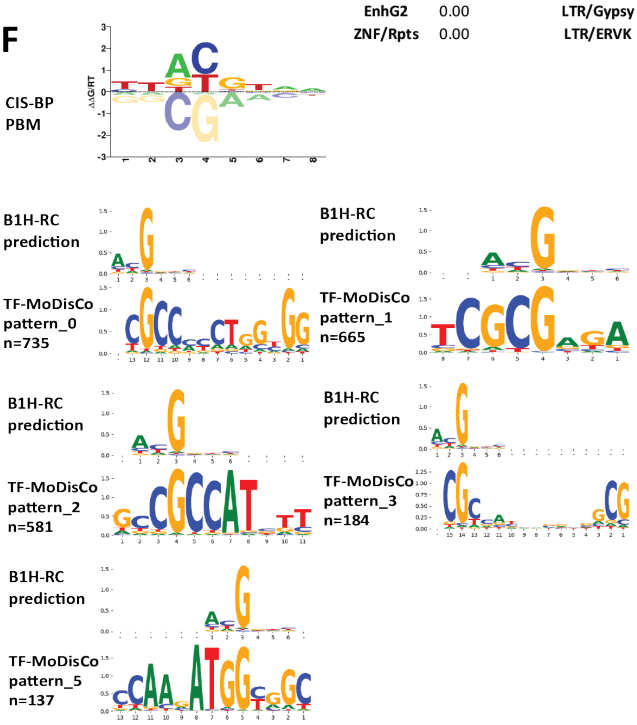

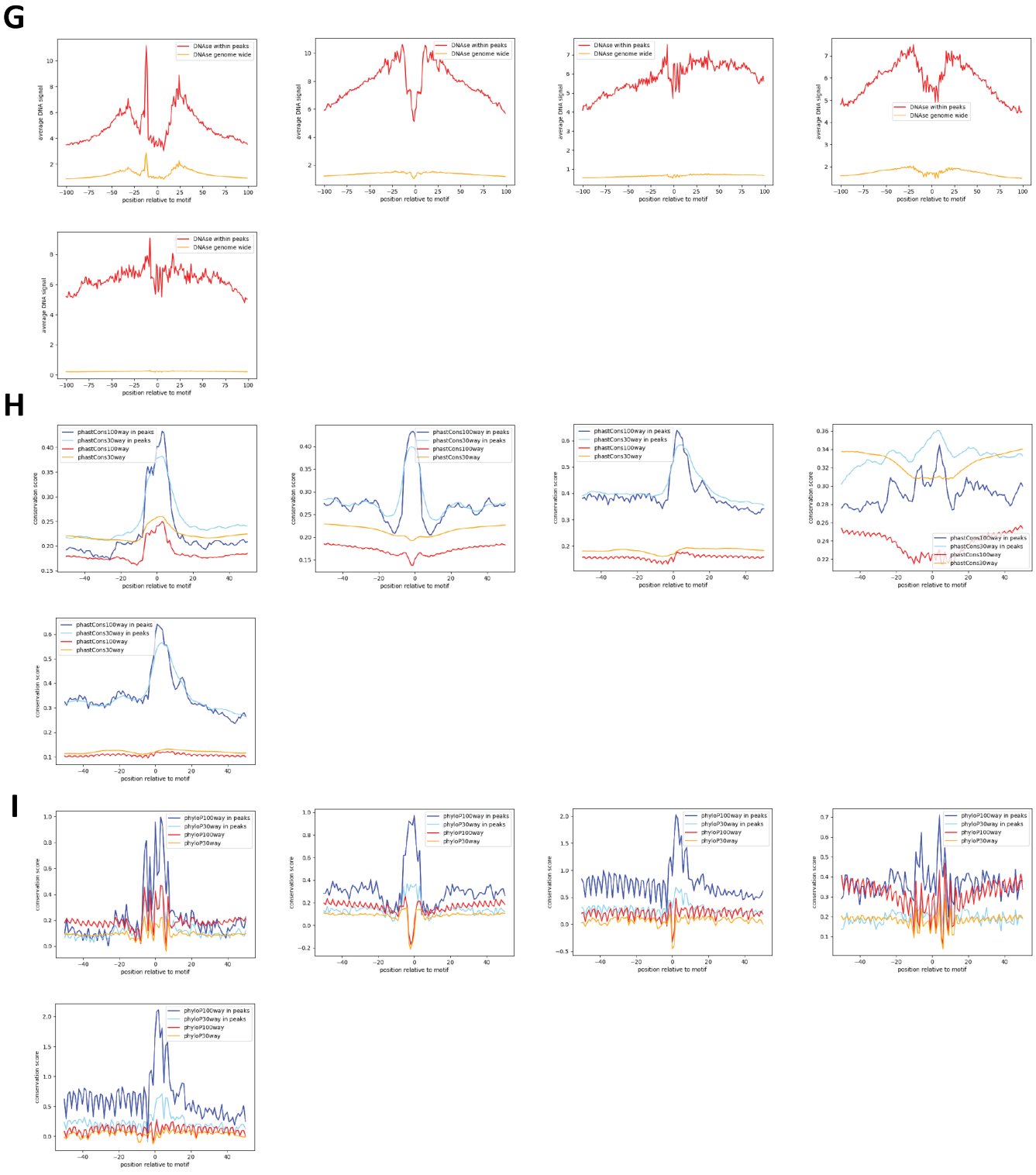

Supplementary Figure 617: Properties and genomic distribution of motifs identified for the ZHX1 transcription factor in K562 (accession ENCSR557RVF).

TF-MoDisCO pattern_0 n=735, CWM

pattern_0, n=735; subpattern_0, ns=214

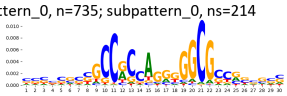

pattern_0, n=735; subpattern_1, ns=149

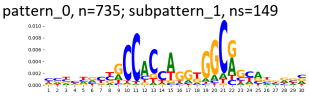

pattern_0, n=735; subpattern_2, ns=147

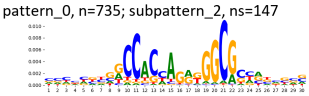

pattern_0, n=735; subpattern_3, ns=89

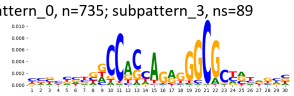

pattern_0, n=735; subpattern_4, ns=73

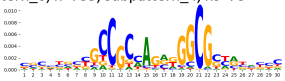

pattern_0, n=735; subpattern_5, ns=59

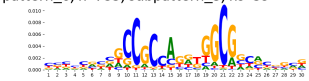

pattern_0, n=735; subpattern_6, ns=2



pattern_0, n=735; subpattern_7, ns=2



TF-MoDisCO pattern_0 n=735, PWM

pattern_0, n=735; subpattern_0, ns=214

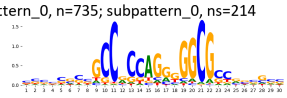

pattern_0, n=735; subpattern_1, ns=149

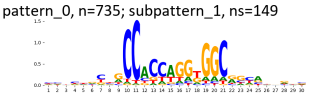

pattern_0, n=735; subpattern_2, ns=147

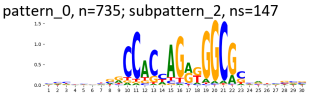

pattern_0, n=735; subpattern_3, ns=89

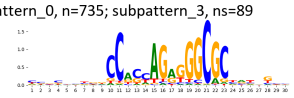

pattern_0, n=735; subpattern_4, ns=73

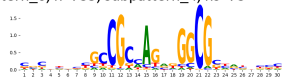

pattern_0, n=735; subpattern_5, ns=59

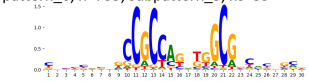

pattern_0, n=735; subpattern_6, ns=2

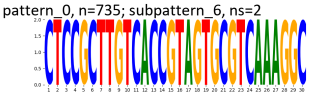

pattern_0, n=735; subpattern_7, ns=2

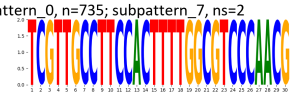

TF-MoDisCO pattern_1 n=665, CWM

pattern_1, n=665; subpattern_0, ns=205

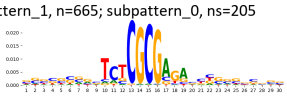

pattern_1, n=665; subpattern_1, ns=129

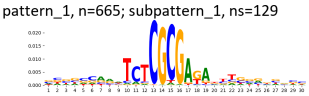

pattern_1, n=665; subpattern_2, ns=128

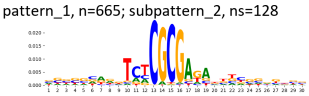

pattern_1, n=665; subpattern_3, ns=108

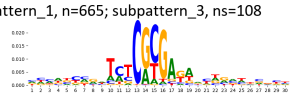

pattern_1, n=665; subpattern_4, ns=48

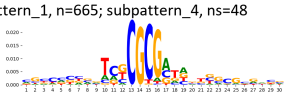

pattern_1, n=665; subpattern_5, ns=44

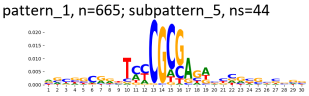

pattern_1, n=665; subpattern_6, ns=3

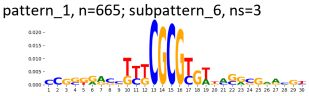

TF-MoDisCO pattern_1 n=665, PWM

pattern_1, n=665; subpattern_0, ns=205

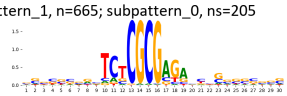

pattern_1, n=665; subpattern_1, ns=129

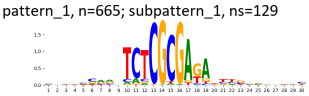

pattern_1, n=665; subpattern_2, ns=128

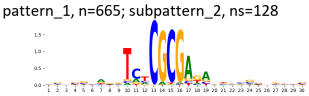

pattern_1, n=665; subpattern_3, ns=108

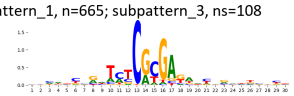

pattern_1, n=665; subpattern_4, ns=48

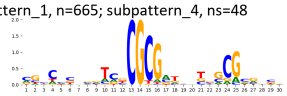

pattern_1, n=665; subpattern_5, ns=44

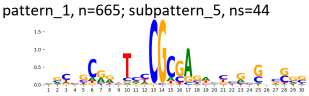

pattern_1, n=665; subpattern_6, ns=3

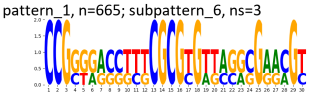

TF-MoDisCO pattern_2 n=581, CWM

pattern_2, n=581; subpattern_0, ns=170

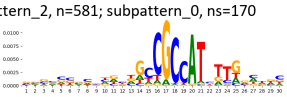

pattern_2, n=581; subpattern_1, ns=164

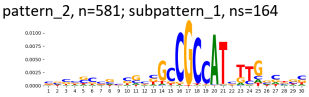

pattern_2, n=581; subpattern_2, ns=124

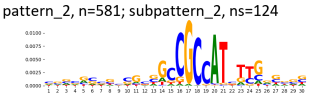

pattern_2, n=581; subpattern_3, ns=123

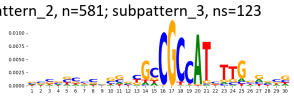

TF-MoDisCO pattern_2 n=581, PWM

pattern_2, n=581; subpattern_0, ns=170

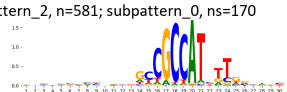

pattern_2, n=581; subpattern_1, ns=164

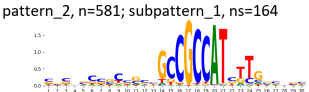

pattern_2, n=581; subpattern_2, ns=124

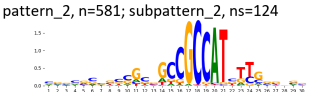

pattern_2, n=581; subpattern_3, ns=123

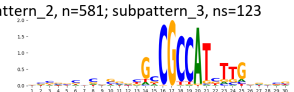

TF-MoDisCO pattern_3 n=184, CWM

pattern_3, n=184; subpattern_0, ns=41

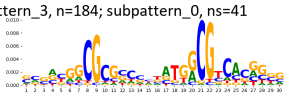

pattern_3, n=184; subpattern_1, ns=40

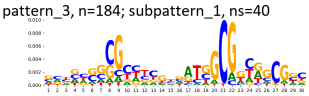

pattern_3, n=184; subpattern_2, ns=37

pattern_3, n=184; subpattern_3, ns=36

pattern_3, n=184; subpattern_4, ns=30

TF-MoDisCO pattern_3 n=184, PWM

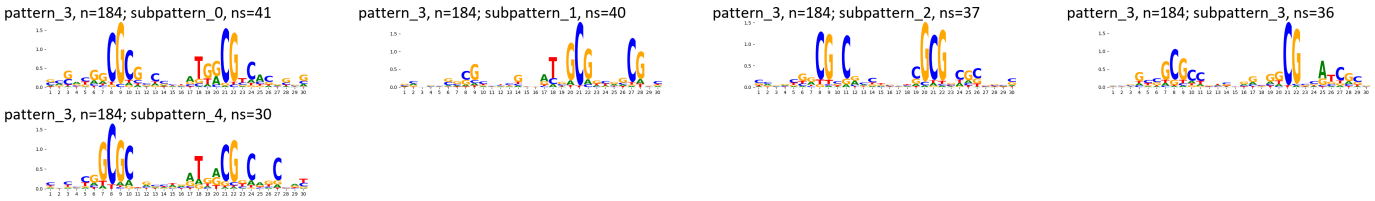

TF-MoDisCO pattern_5 n=137, CWM

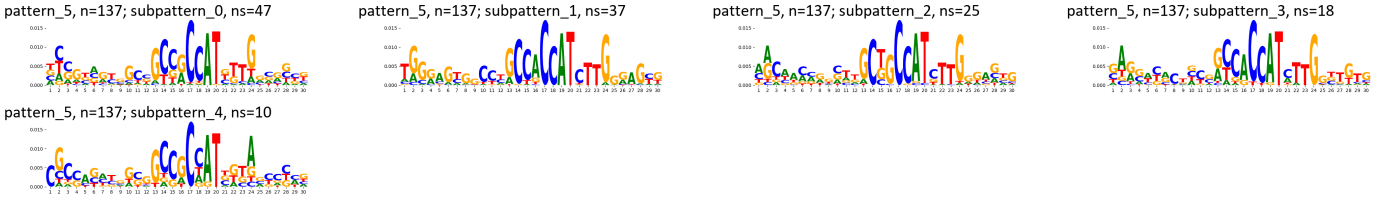

TF-MoDisCO pattern_5 n=137, PWM

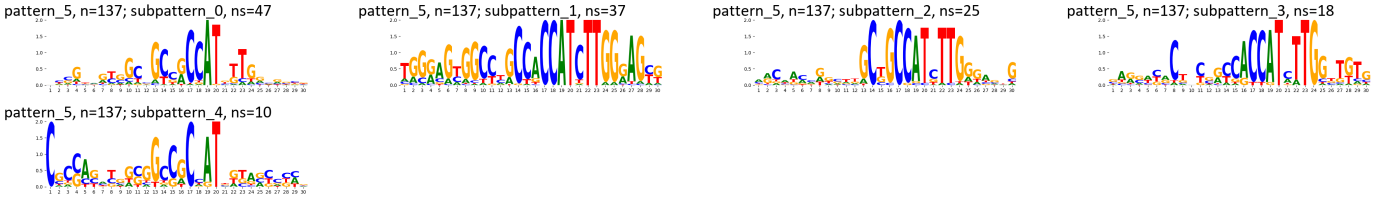

Supplementary Figure 618: TF-MoDisCO subpatterns for the ZHX1 transcription factor in K562 (accession ENCSR557RVF).

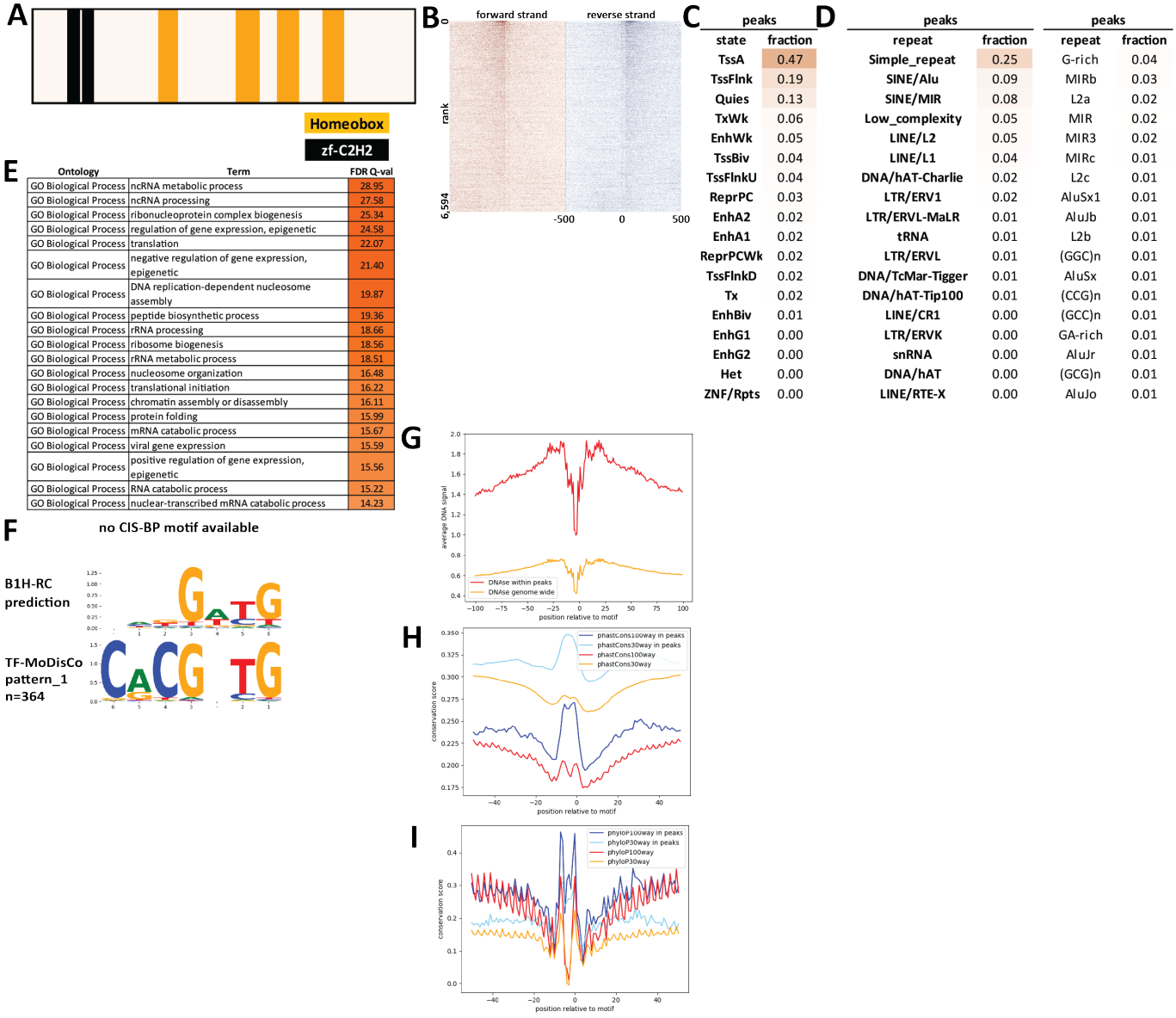

Supplementary Figure 619: Properties and genomic distribution of motifs identified for the ZHX2 transcription factor in HepG2 (accession ENCSR401VBM).

TF-MoDisCO pattern_1 n=364, CWM

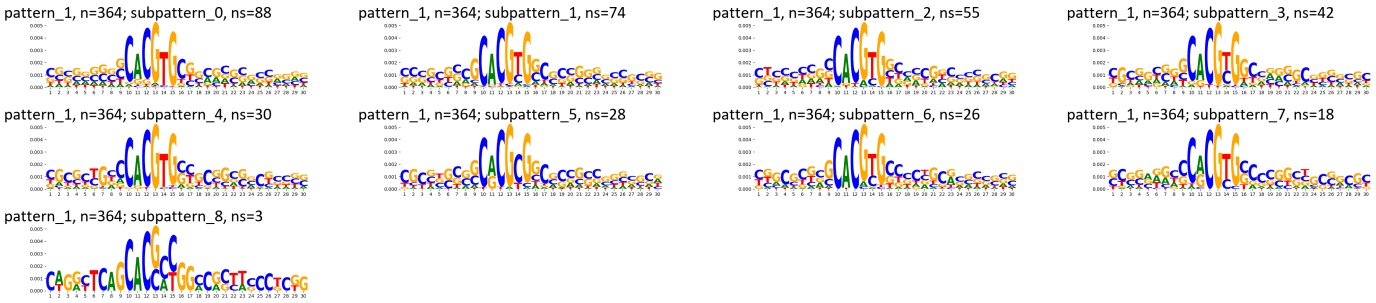

TF-MoDisCO pattern_1 n=364, PWM

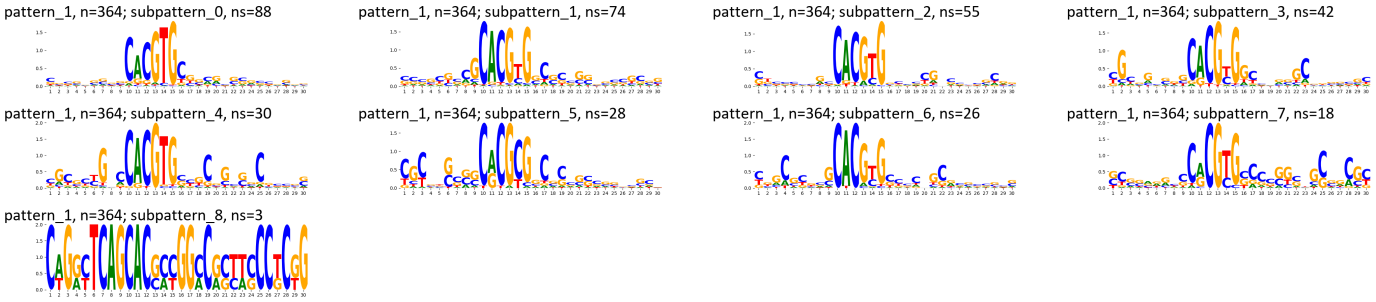

Supplementary Figure 620: TF-MoDisCO subpatterns for the ZHX2 transcription factor in HepG2 (accession ENCSR401VBM).

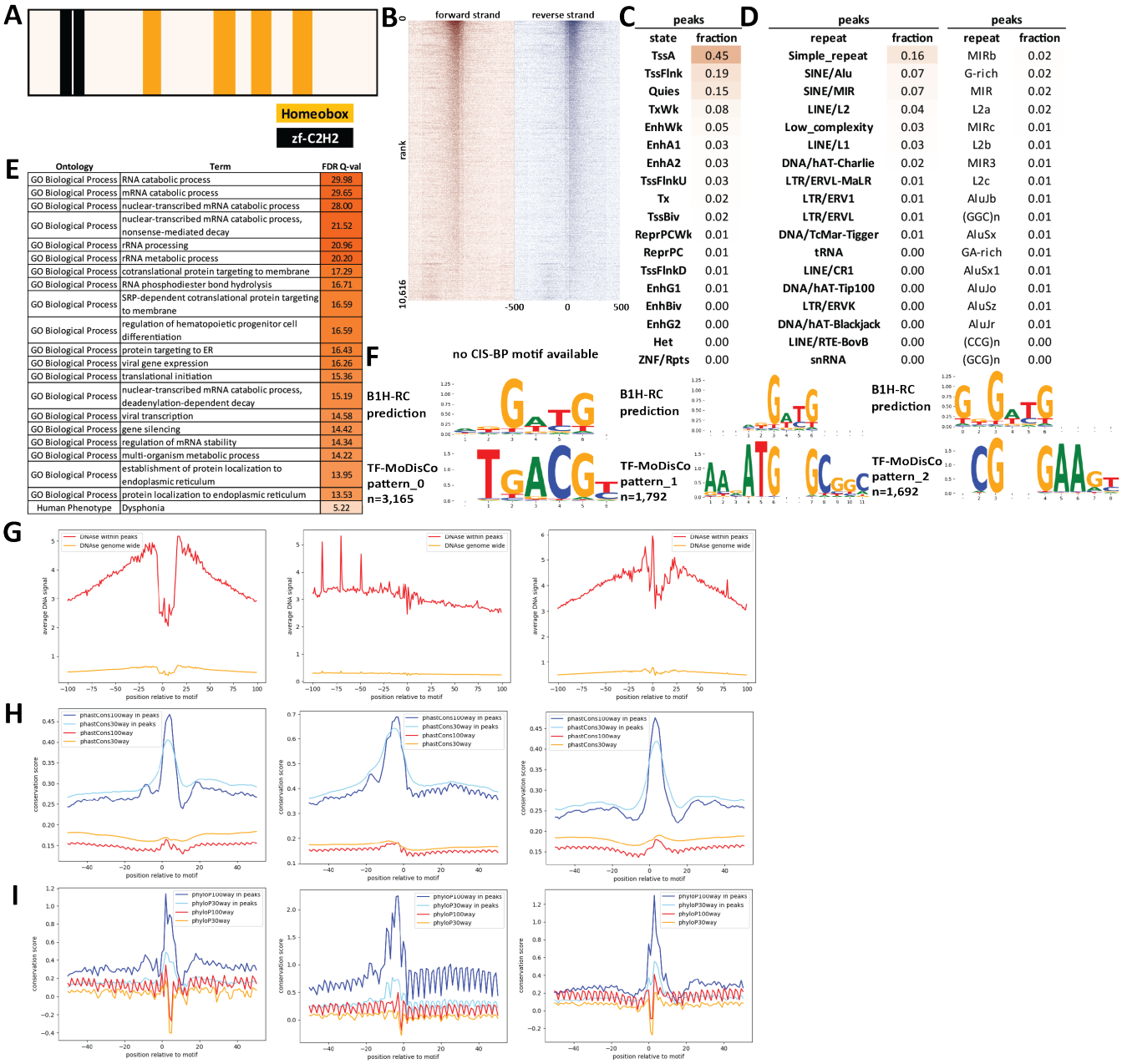

Supplementary Figure 621: Properties and genomic distribution of motifs identified for the ZHX2 transcription factor in HepG2 (accession ENCSR407BEZ).

TF-MoDisCO pattern_0 n=3165, CWM

pattern_0, n=3165; subpattern_0, ns=783

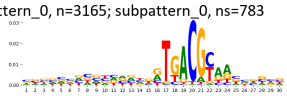

pattern_0, n=3165; subpattern_1, ns=466

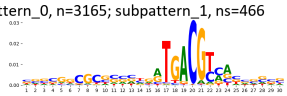

pattern_0, n=3165; subpattern_2, ns=457

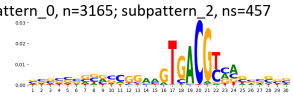

pattern_0, n=3165; subpattern_3, ns=434

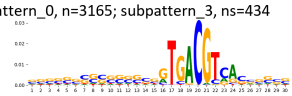

pattern_0, n=3165; subpattern_4, ns=373

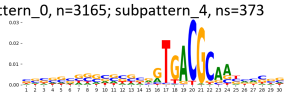

pattern_0, n=3165; subpattern_5, ns=336

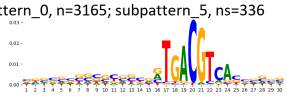

pattern_0, n=3165; subpattern_6, ns=313

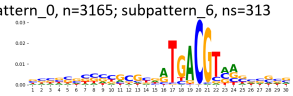

pattern_0, n=3165; subpattern_7, ns=3

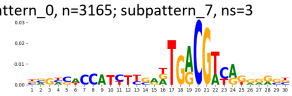

TF-MoDisCO pattern_0 n=3165, PWM

pattern_0, n=3165; subpattern_0, ns=783

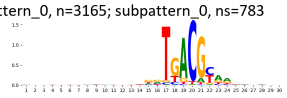

pattern_0, n=3165; subpattern_1, ns=466

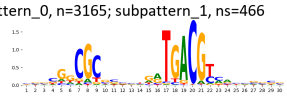

pattern_0, n=3165; subpattern_2, ns=457

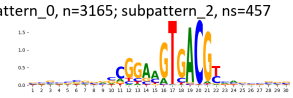

pattern_0, n=3165; subpattern_3, ns=434

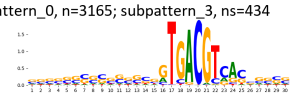

pattern_0, n=3165; subpattern_4, ns=373

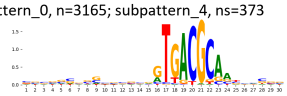

pattern_0, n=3165; subpattern_5, ns=336

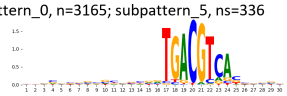

pattern_0, n=3165; subpattern_6, ns=313

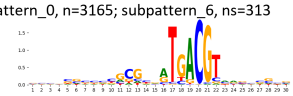

pattern_0, n=3165; subpattern_7, ns=3

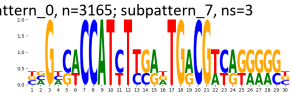

TF-MoDisCO pattern_1 n=1792, CWM

pattern_1, n=1792; subpattern_0, ns=466

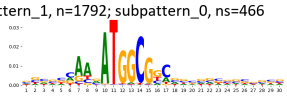

pattern_1, n=1792; subpattern_1, ns=432

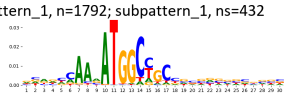

pattern_1, n=1792; subpattern_2, ns=380

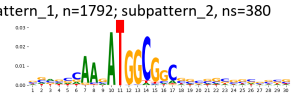

pattern_1, n=1792; subpattern_3, ns=290

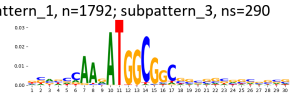

pattern_1, n=1792; subpattern_4, ns=224

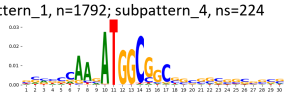

TF-MoDisCO pattern_1 n=1792, PWM

pattern_1, n=1792; subpattern_0, ns=466

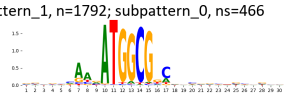

pattern_1, n=1792; subpattern_1, ns=432

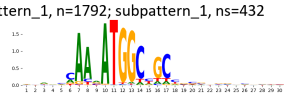

pattern_1, n=1792; subpattern_2, ns=380

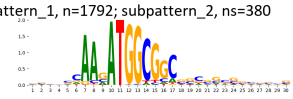

pattern_1, n=1792; subpattern_3, ns=290

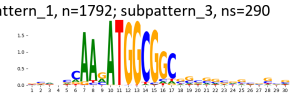

pattern_1, n=1792; subpattern_4, ns=224

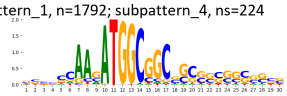

TF-MoDisCO pattern_2 n=1692, CWM

pattern_2, n=1692; subpattern_0, ns=541

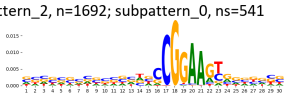

pattern_2, n=1692; subpattern_1, ns=351

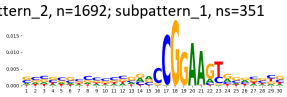

pattern_2, n=1692; subpattern_2, ns=272

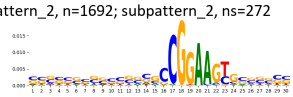

pattern_2, n=1692; subpattern_3, ns=238

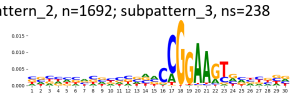

pattern_2, n=1692; subpattern_4, ns=158

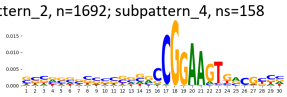

pattern_2, n=1692; subpattern_5, ns=86

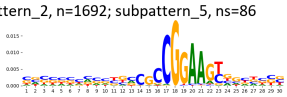

pattern_2, n=1692; subpattern_6, ns=43

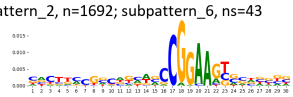

pattern_2, n=1692; subpattern_7, ns=3

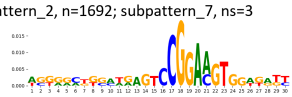

TF-MoDisCO pattern_2 n=1692, PWM

pattern_2, n=1692; subpattern_0, ns=541

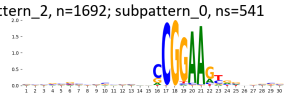

pattern_2, n=1692; subpattern_1, ns=351

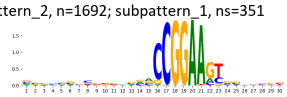

pattern_2, n=1692; subpattern_2, ns=272

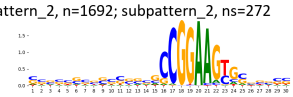

pattern_2, n=1692; subpattern_3, ns=238

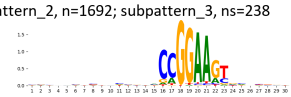

pattern_2, n=1692; subpattern_4, ns=158

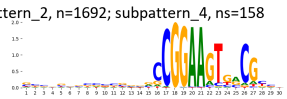

pattern_2, n=1692; subpattern_5, ns=86

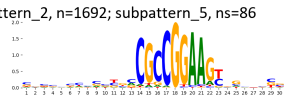

pattern_2, n=1692; subpattern_6, ns=43

pattern_2, n=1692; subpattern_7, ns=3

Supplementary Figure 622: TF-MoDisCO subpatterns for the ZHX2 transcription factor in HepG2 (accession ENCSR407BEZ).

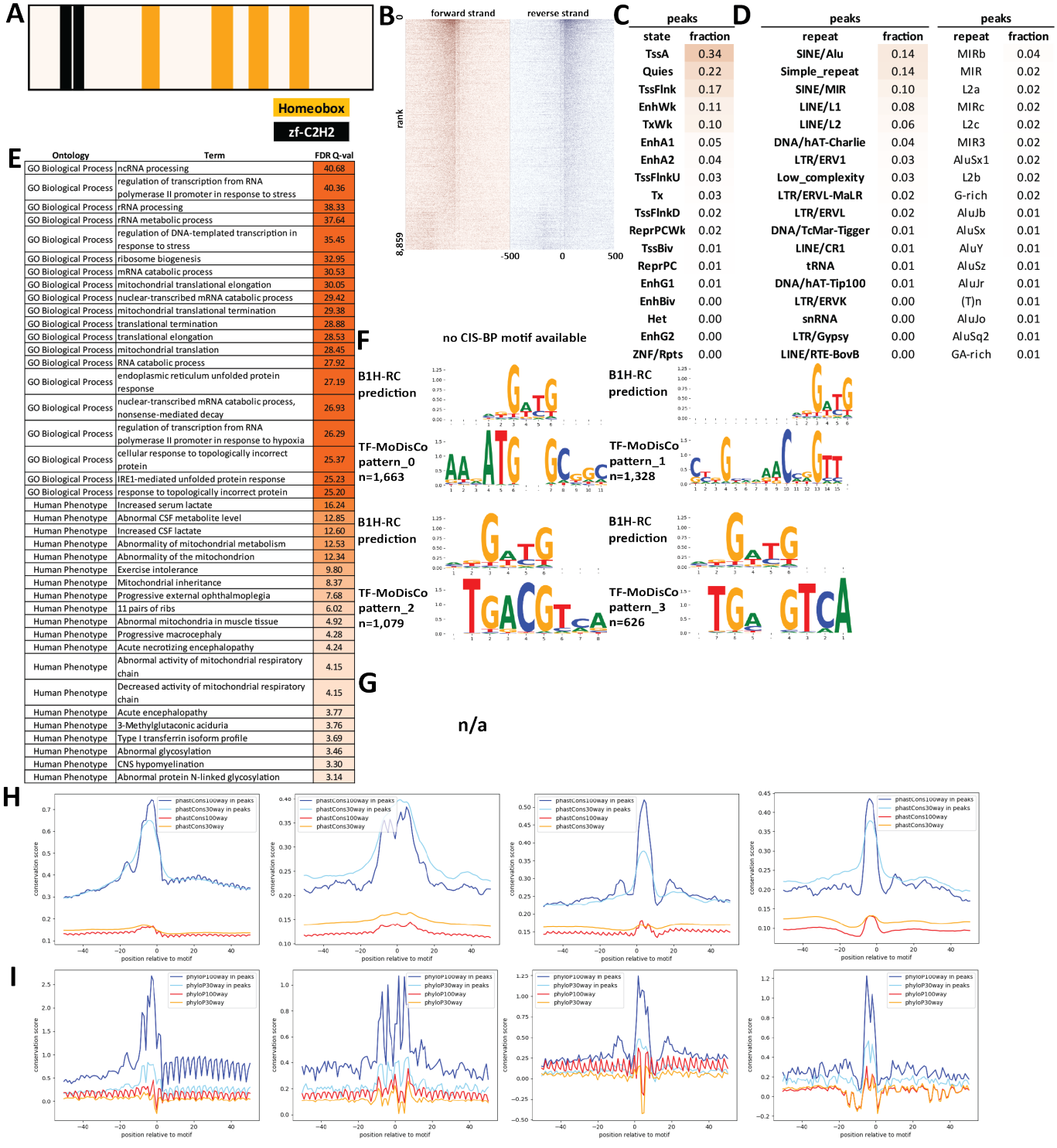

Supplementary Figure 623: Properties and genomic distribution of motifs identified for the ZHX2 transcription factor in MCF-7 (accession ENCSR876UYH).

TF-MoDisCO pattern_0 n=1663, CWM

pattern_0, n=1663; subpattern_0, ns=351

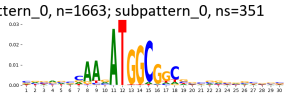

pattern_0, n=1663; subpattern_1, ns=337

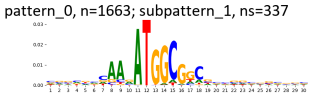

pattern_0, n=1663; subpattern_2, ns=323

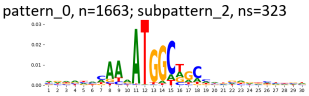

pattern_0, n=1663; subpattern_3, ns=286

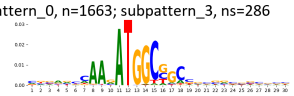

pattern_0, n=1663; subpattern_4, ns=184

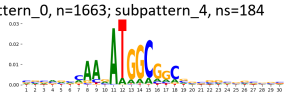

pattern_0, n=1663; subpattern_5, ns=179

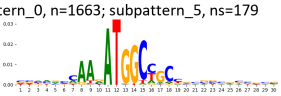

pattern_0, n=1663; subpattern_6, ns=3

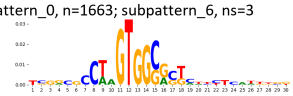

TF-MoDisCO pattern_0 n=1663, PWM

pattern_0, n=1663; subpattern_0, ns=351

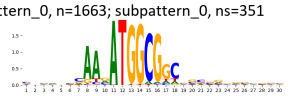

pattern_0, n=1663; subpattern_1, ns=337

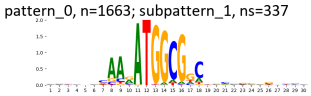

pattern_0, n=1663; subpattern_2, ns=323

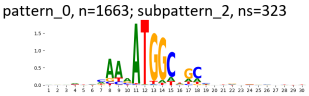

pattern_0, n=1663; subpattern_3, ns=286

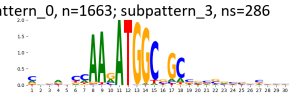

pattern_0, n=1663; subpattern_4, ns=184

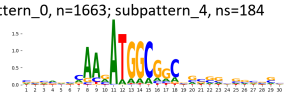

pattern_0, n=1663; subpattern_5, ns=179

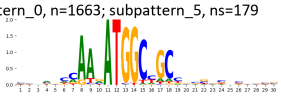

pattern_0, n=1663; subpattern_6, ns=3

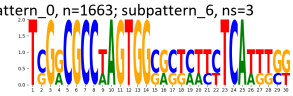

TF-MoDisCO pattern_1 n=1328, CWM

pattern_1, n=1328; subpattern_0, ns=327

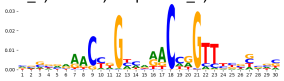

pattern_1, n=1328; subpattern_1, ns=305

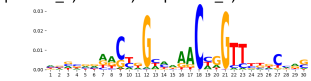

pattern_1, n=1328; subpattern_2, ns=262

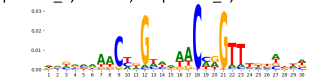

pattern_1, n=1328; subpattern_3, ns=176

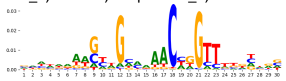

pattern_1, n=1328; subpattern_4, ns=115

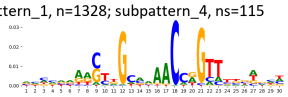

pattern_1, n=1328; subpattern_5, ns=79

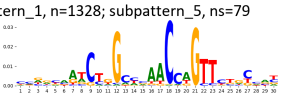

pattern_1, n=1328; subpattern_6, ns=62

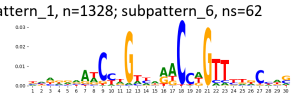

pattern_1, n=1328; subpattern_7, ns=2

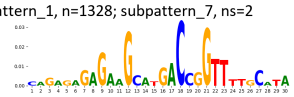

TF-MoDisCO pattern_1 n=1328, PWM

pattern_1, n=1328; subpattern_0, ns=327

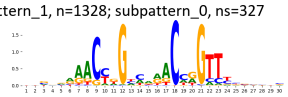

pattern_1, n=1328; subpattern_1, ns=305

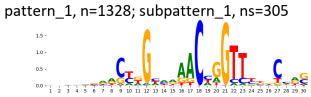

pattern_1, n=1328; subpattern_2, ns=262

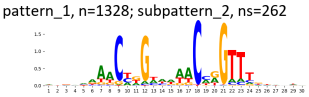

pattern_1, n=1328; subpattern_3, ns=176

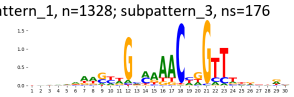

pattern_1, n=1328; subpattern_4, ns=115

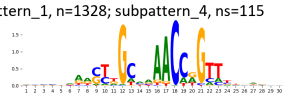

pattern_1, n=1328; subpattern_5, ns=79

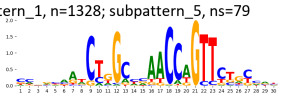

pattern_1, n=1328; subpattern_6, ns=62

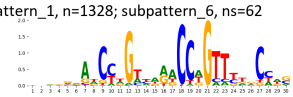

pattern_1, n=1328; subpattern_7, ns=2

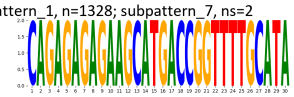

TF-MoDisCO pattern_2 n=1079, CWM

pattern_2, n=1079; subpattern_0, ns=267

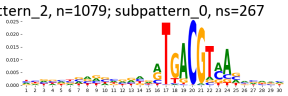

pattern_2, n=1079; subpattern_1, ns=254

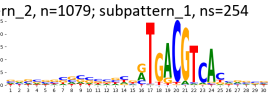

pattern_2, n=1079; subpattern_2, ns=212

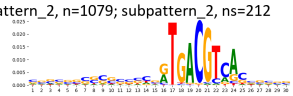

pattern_2, n=1079; subpattern_3, ns=118

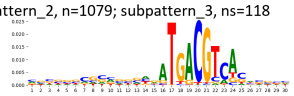

pattern_2, n=1079; subpattern_4, ns=114

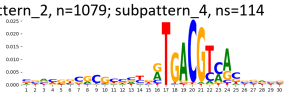

pattern_2, n=1079; subpattern_5, ns=103

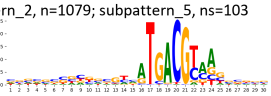

pattern_2, n=1079; subpattern_6, ns=9

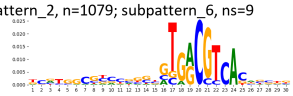

pattern_2, n=1079; subpattern_7, ns=2

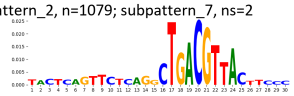

TF-MoDisCO pattern_2 n=1079, PWM

pattern_2, n=1079; subpattern_0, ns=267

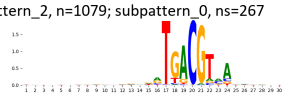

pattern_2, n=1079; subpattern_1, ns=254

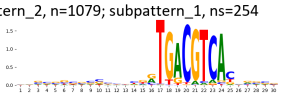

pattern_2, n=1079; subpattern_2, ns=212

pattern_2, n=1079; subpattern_3, ns=118

pattern_2, n=1079; subpattern_4, ns=114

pattern_2, n=1079; subpattern_5, ns=103

pattern_2, n=1079; subpattern_6, ns=9

pattern_2, n=1079; subpattern_7, ns=2

TF-MoDisCO pattern_4 n=626, CWM

pattern_4, n=626; subpattern_0, ns=164

pattern_4, n=626; subpattern_1, ns=159

pattern_4, n=626; subpattern_2, ns=157

pattern_4, n=626; subpattern_3, ns=146

TF-MoDisCO pattern_4 n=626, PWM



Supplementary Figure 624: TF-MoDisCO subpatterns for the ZHX2 transcription factor in MCF-7 (accession ENCSR876UYH).

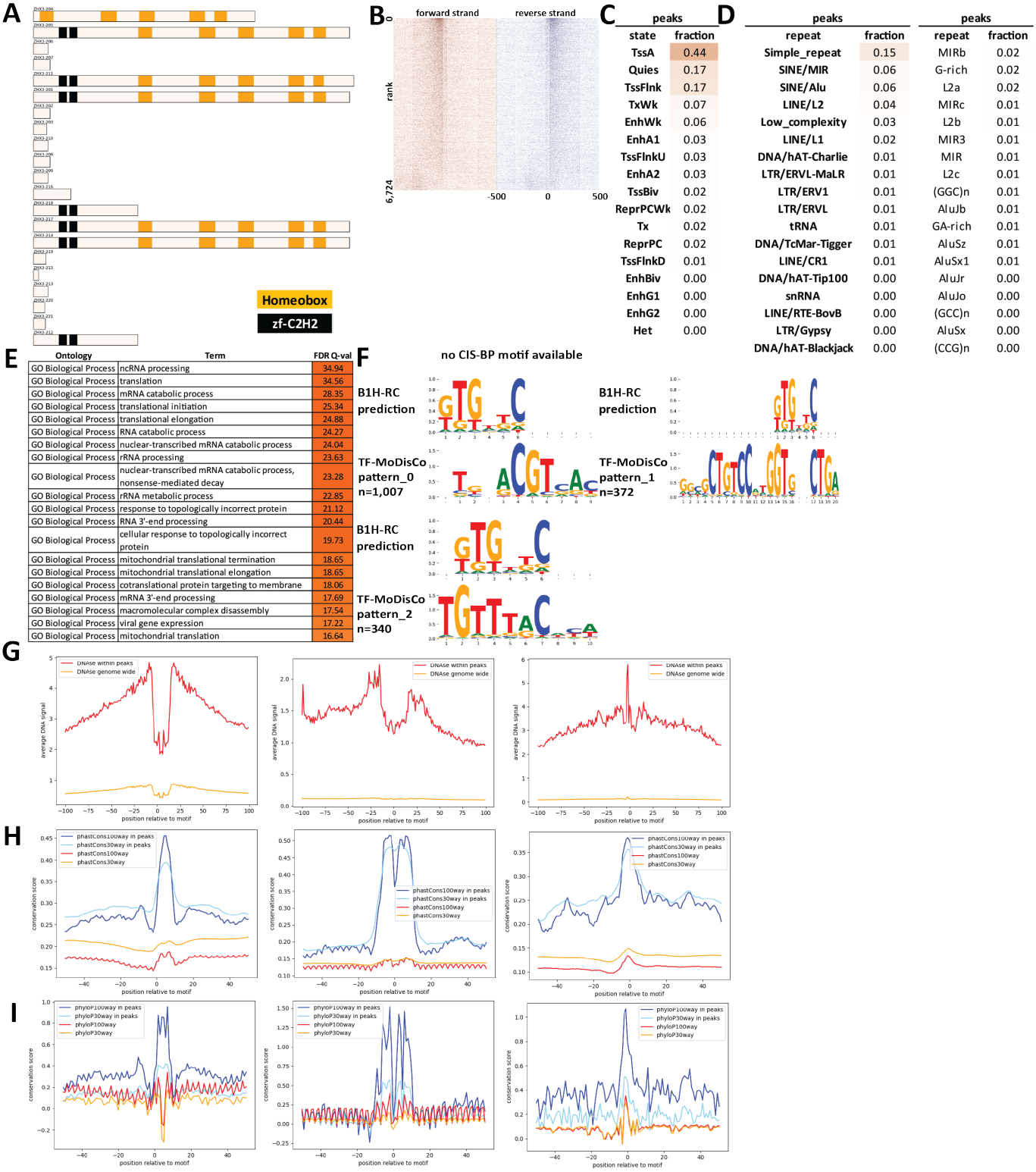

Supplementary Figure 625: Properties and genomic distribution of motifs identified for the ZHX3 transcription factor in HepG2 (accession ENCSR367KYL).

TF-MoDisCO pattern_0 n=1007, CWM

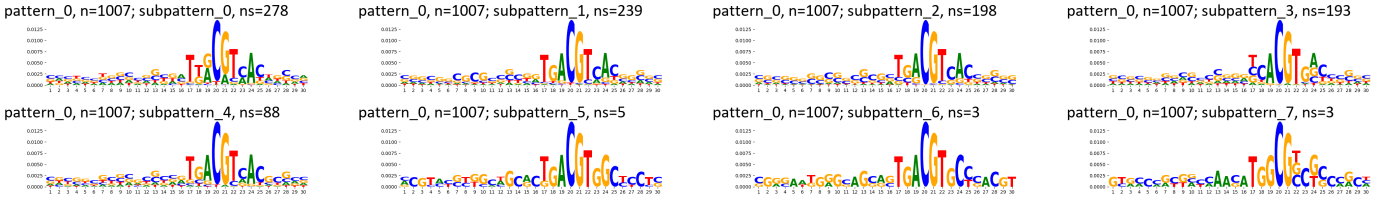

TF-MoDisCO pattern_0 n=1007, PWM

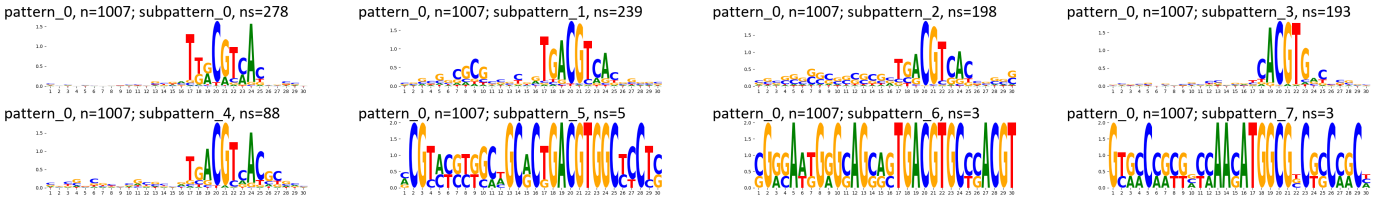

TF-MoDisCO pattern_1 n=372, CWM

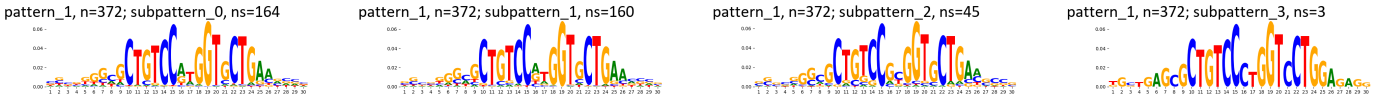

TF-MoDisCO pattern_1 n=372, PWM

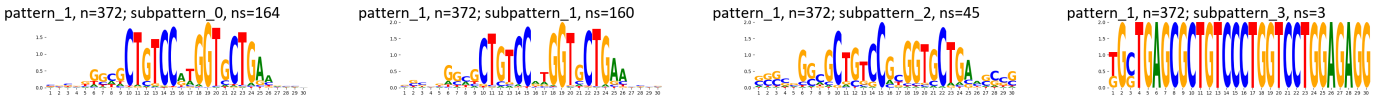

TF-MoDisCO pattern_2 n=340, CWM

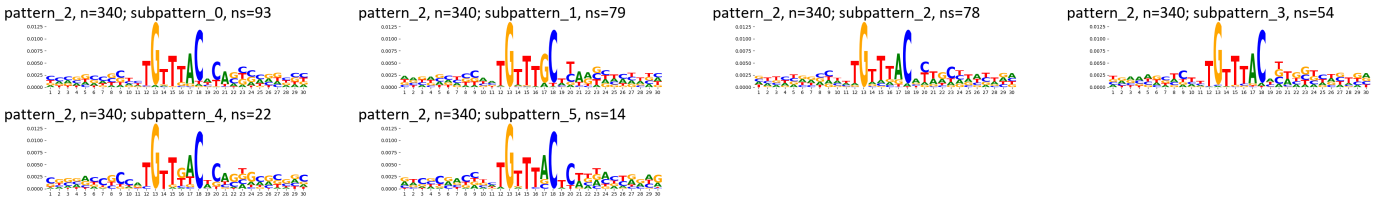

TF-MoDisCO pattern_2 n=340, PWM

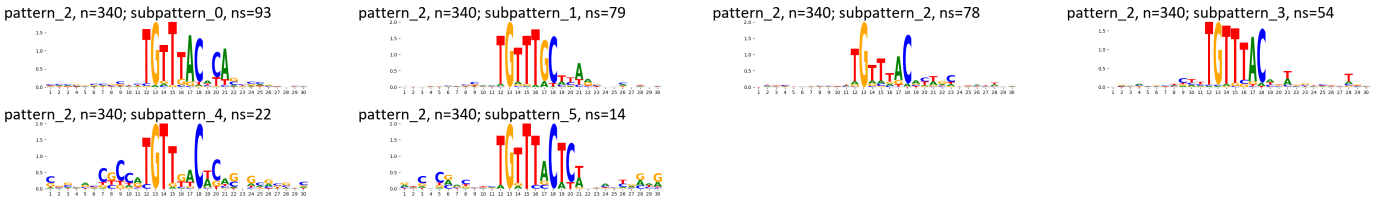

Supplementary Figure 626: TF-MoDisCO subpatterns for the ZHX3 transcription factor in HepG2 (accession ENCSR367KYL).

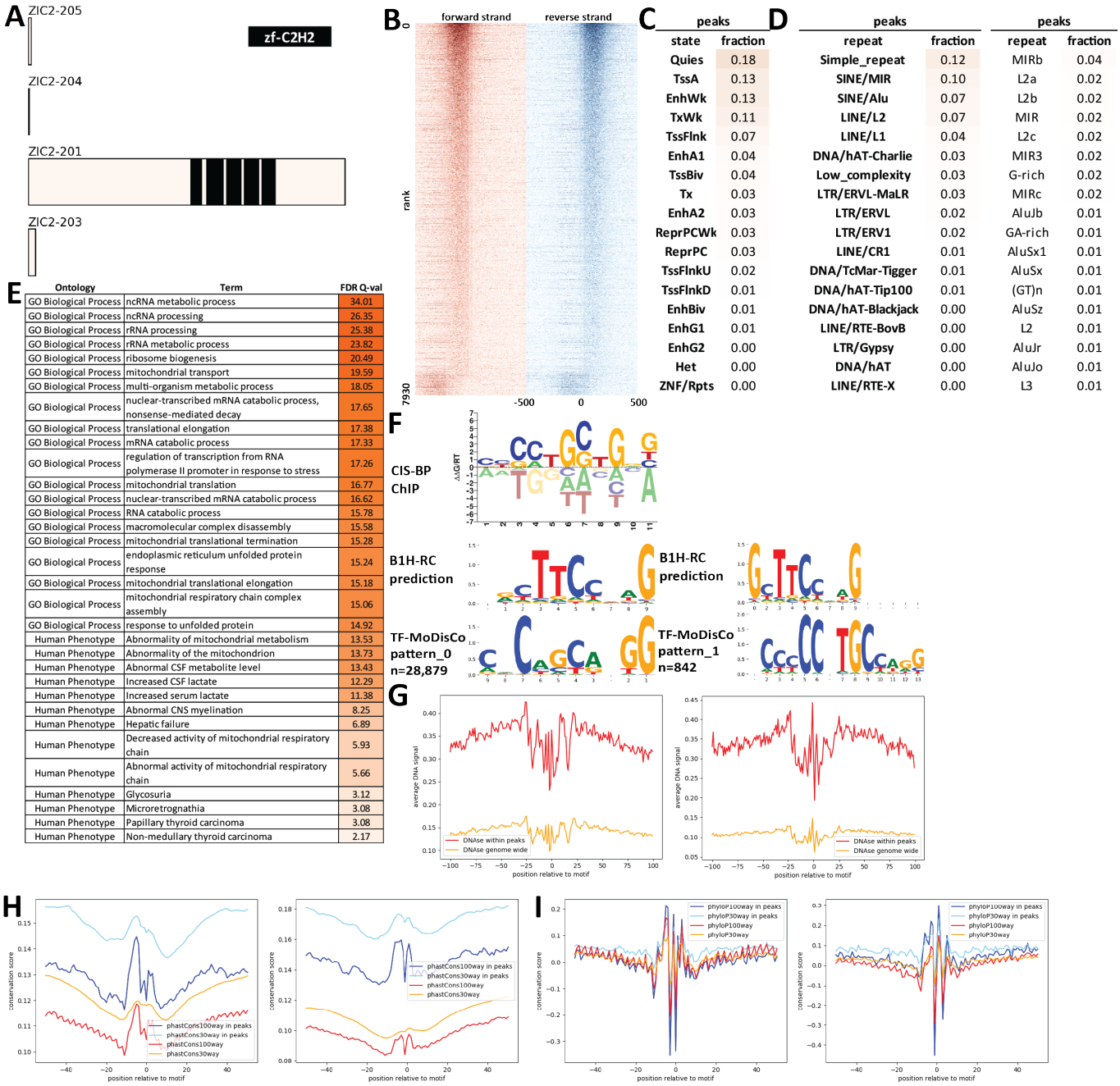

Supplementary Figure 627: Properties and genomic distribution of motifs identified for the ZIC2 transcription factor in HEK293 (accession ENCSR728MWW).

TF-MoDisCO pattern_0 n=28879, CWM

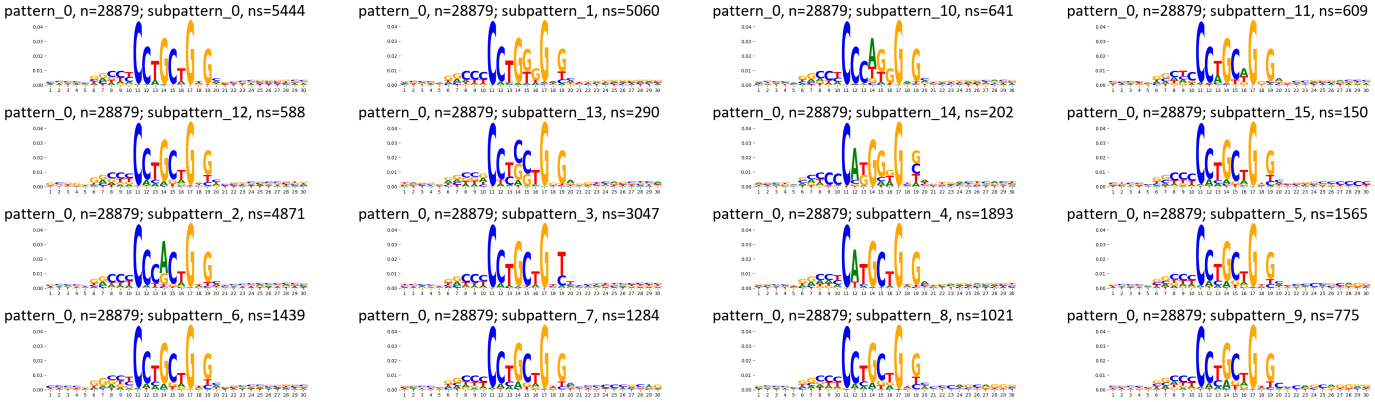

TF-MoDisCO pattern_0 n=28879, PWM

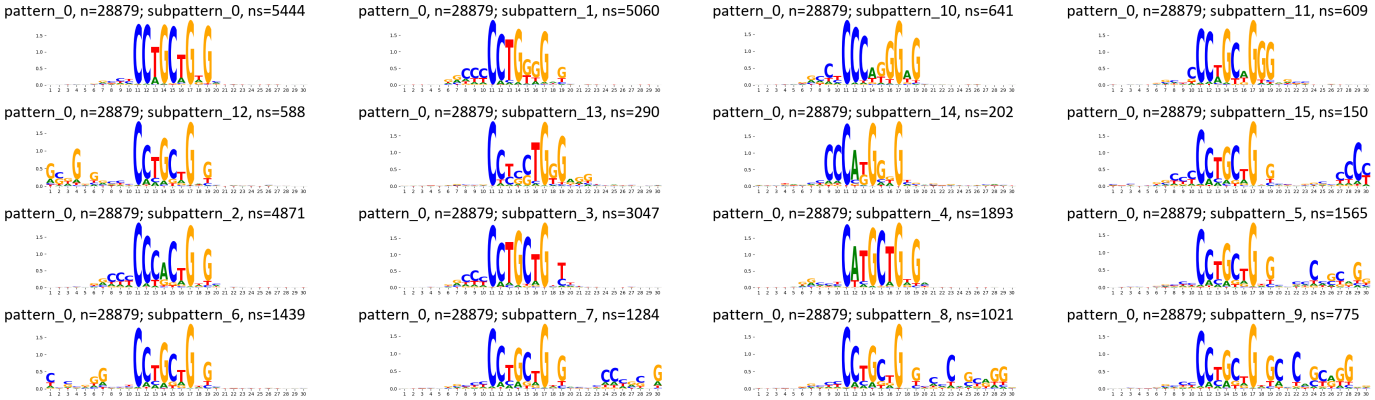

TF-MoDisCO pattern_1 n=842, CWM

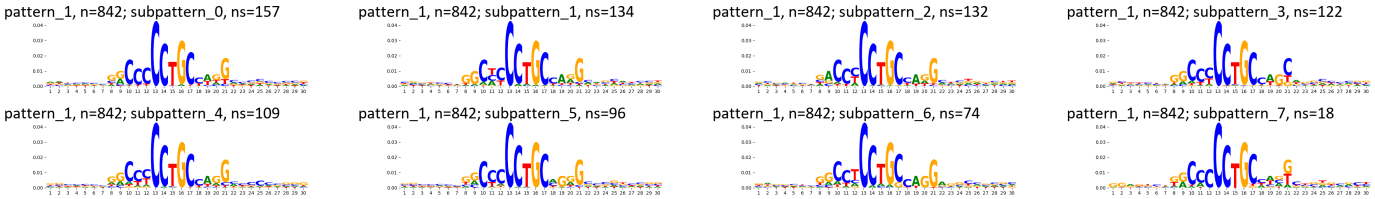

TF-MoDisCO pattern_1 n=842, PWM

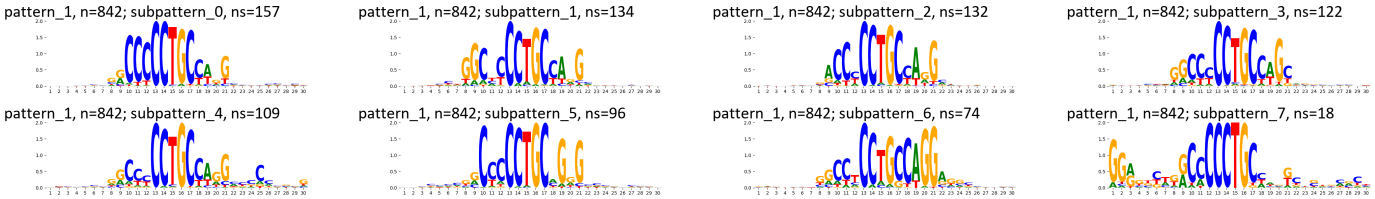

Supplementary Figure 628: TF-MoDisCO subpatterns for the ZIC2 transcription factor in HEK293 (accession ENCSR728MWW).

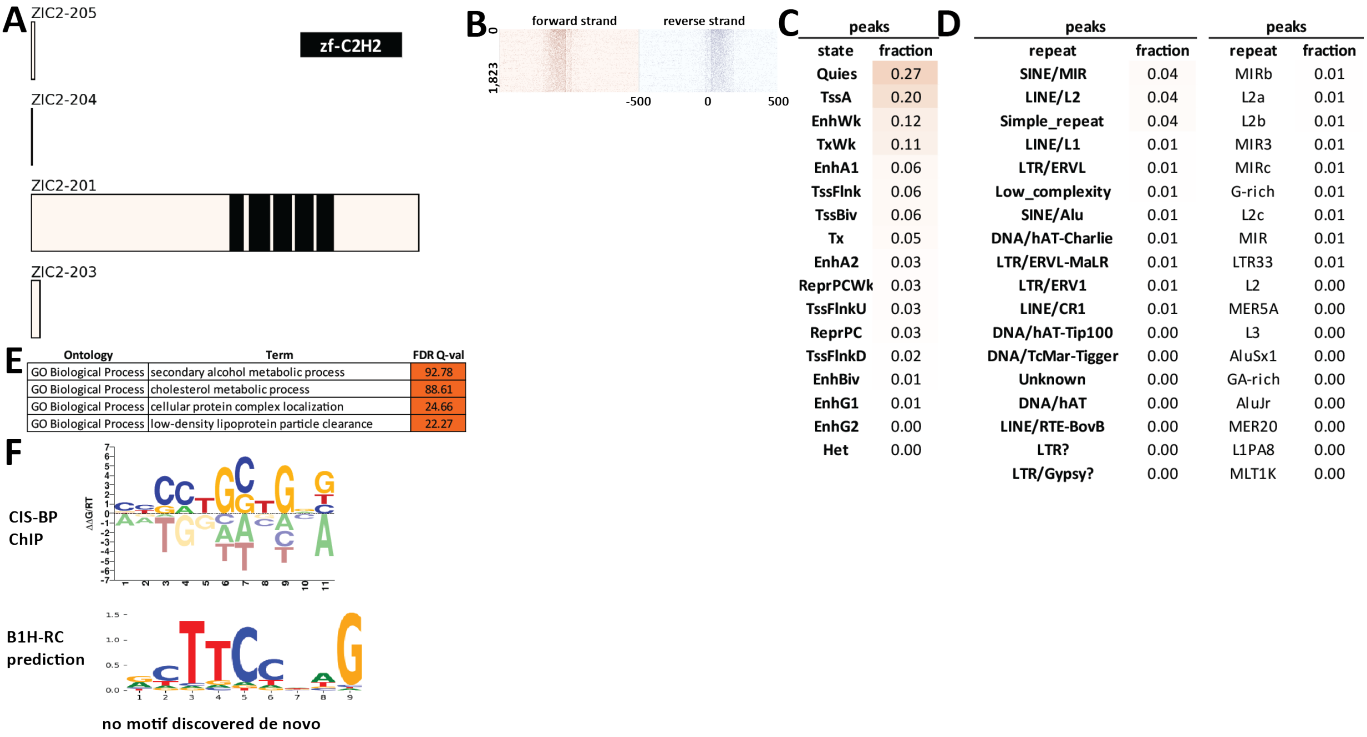

peaks	
state	fraction
Quies	0.27
TssA	0.20
EnhWk	0.12
TxWk	0.11
EnhA1	0.06
TssFlnk	0.06
TssBiv	0.06
Tx	0.05
EnhA2	0.03
ReprPCWk	0.03
TssFlnkU	0.03
ReprPC	0.03
TssFlnkD	0.02
EnhBiv	0.01
EnhG1	0.01
EnhG2	0.00
Het	0.00

peaks		peaks	
repeat	fraction	repeat	fraction
SINE/MIR	0.04	MIRb	0.01
LINE/L2	0.04	L2a	0.01
Simple_repeat	0.04	L2b	0.01
LINE/L1	0.01	MIR3	0.01
LTR/ERVL	0.01	MIRc	0.01
Low_complexity	0.01	G-rich	0.01
SINE/Alu	0.01	L2c	0.01
DNA/hAT-Charlie	0.01	MIR	0.01
LTR/ERVL-MaLR	0.01	LTR33	0.01
LTR/ERV1	0.01	L2	0.00
LINE/CR1	0.01	MER5A	0.00
DNA/hAT-Tip100	0.00	L3	0.00
DNA/TcMar-Tigger	0.00	AluSx1	0.00
Unknown	0.00	GA-rich	0.00
DNA/hAT	0.00	AluJr	0.00
LINE/RTE-BovB	0.00	MER20	0.00
LTR?	0.00	L1PA8	0.00
LTR/Gypsy?	0.00	MLT1K	0.00

Supplementary Figure 629: Properties and genomic distribution of motifs identified for the ZIC2 transcription factor in HEK293 (accession Hughes NB models).

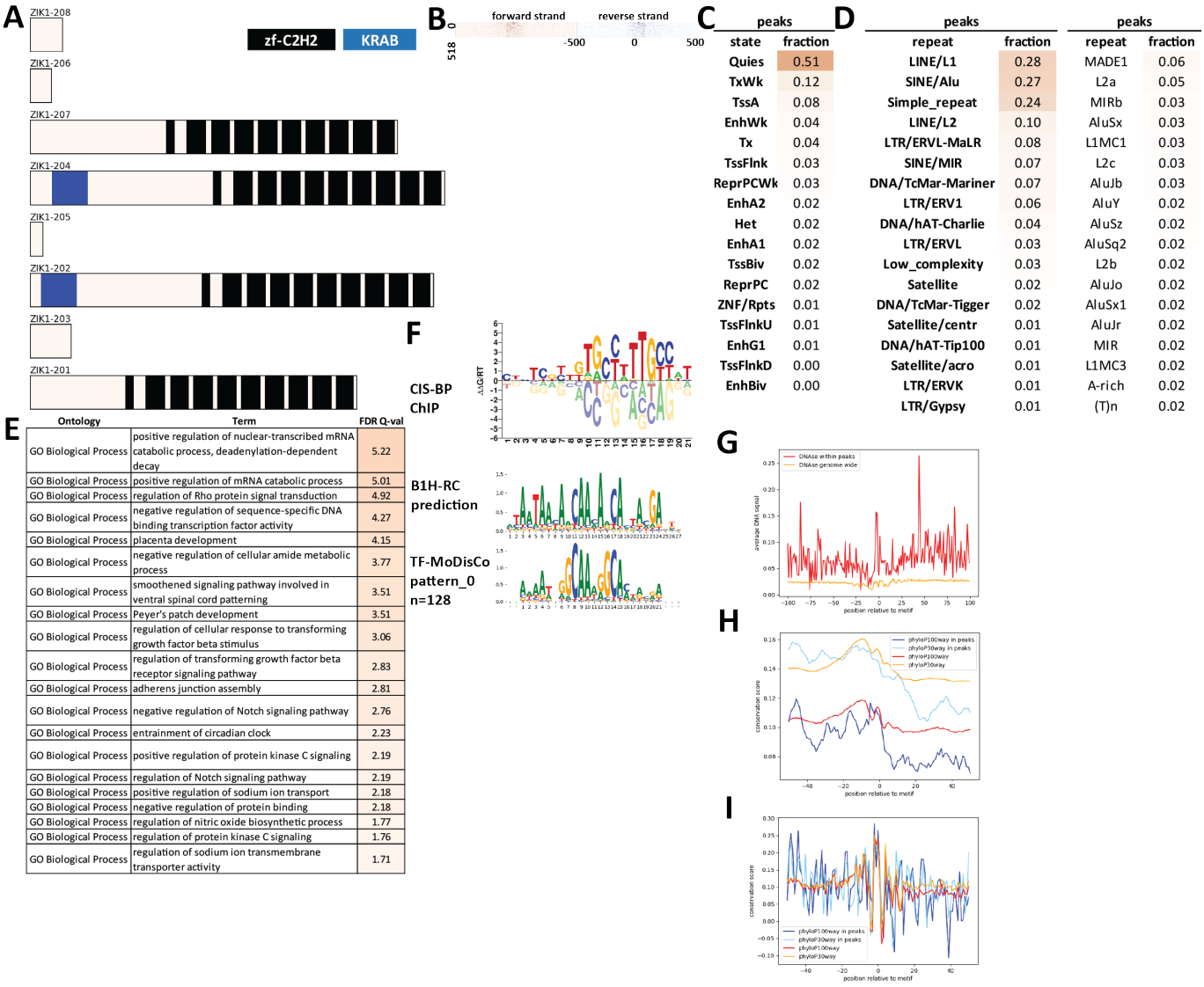

peaks	
state	fraction
Quies	0.51
TxWk	0.12
TssA	0.08
EnhWk	0.04
Tx	0.04
TssFlnk	0.03
ReprPCWk	0.03
EnhA2	0.02
Het	0.02
EnhA1	0.02
TssBiv	0.02
ReprPC	0.02
ZNF/Rpts	0.01
TssFlnkU	0.01
EnhG1	0.01
TssFlnkD	0.00
EnhBiv	0.00

peaks		peaks	
repeat	fraction	repeat	fraction
LINE/L1	0.28	MADE1	0.06
SINE/Alu	0.27	L2a	0.05
Simple_repeat	0.24	MIRb	0.03
LINE/L2	0.10	AluSx	0.03
LTR/ERVL-MaLR	0.08	L1MC1	0.03
SINE/MIR	0.07	L2c	0.03
DNA/TcMar-Mariner	0.07	AluJb	0.03
LTR/ERV1	0.06	AluY	0.02
DNA/hAT-Charlie	0.04	AluSz	0.02
LTR/ERVL	0.03	AluSq2	0.02
Low_complexity	0.03	L2b	0.02
Satellite	0.02	AluJo	0.02
DNA/TcMar-Tigger	0.02	AluSx1	0.02
Satellite/centr	0.01	AluJr	0.02
DNA/hAT-Tip100	0.01	MIR	0.02
Satellite/acro	0.01	L1MC3	0.02
LTR/ERVK	0.01	A-rich	0.02
LTR/Gypsy	0.01	(T)n	0.02

Ontology	Term	FDR Q-val
GO Biological Process	positive regulation of nuclear-transcribed mRNA catabolic process, deadenylation-dependent decay	5.22
GO Biological Process	positive regulation of mRNA catabolic process	5.01
GO Biological Process	regulation of Rho protein signal transduction	4.92
GO Biological Process	negative regulation of sequence-specific DNA binding transcription factor activity	4.27
GO Biological Process	placenta development	4.15
GO Biological Process	negative regulation of cellular amide metabolic process	3.77
GO Biological Process	smoothened signaling pathway involved in ventral spinal cord patterning	3.51
GO Biological Process	Peyer's patch development	3.51
GO Biological Process	regulation of cellular response to transforming growth factor beta stimulus	3.06
GO Biological Process	regulation of transforming growth factor beta receptor signaling pathway	2.83
GO Biological Process	adherens junction assembly	2.81
GO Biological Process	negative regulation of Notch signaling pathway	2.76
GO Biological Process	entrainment of circadian clock	2.23
GO Biological Process	positive regulation of protein kinase C signaling	2.19
GO Biological Process	regulation of Notch signaling pathway	2.19
GO Biological Process	positive regulation of sodium ion transport	2.18
GO Biological Process	negative regulation of protein binding	2.18
GO Biological Process	regulation of nitric oxide biosynthetic process	1.77
GO Biological Process	regulation of protein kinase C signaling	1.76
GO Biological Process	regulation of sodium ion transmembrane transporter activity	1.71

Supplementary Figure 630: Properties and genomic distribution of motifs identified for the ZIK1 transcription factor in HEK293 (accession ChipExo models).

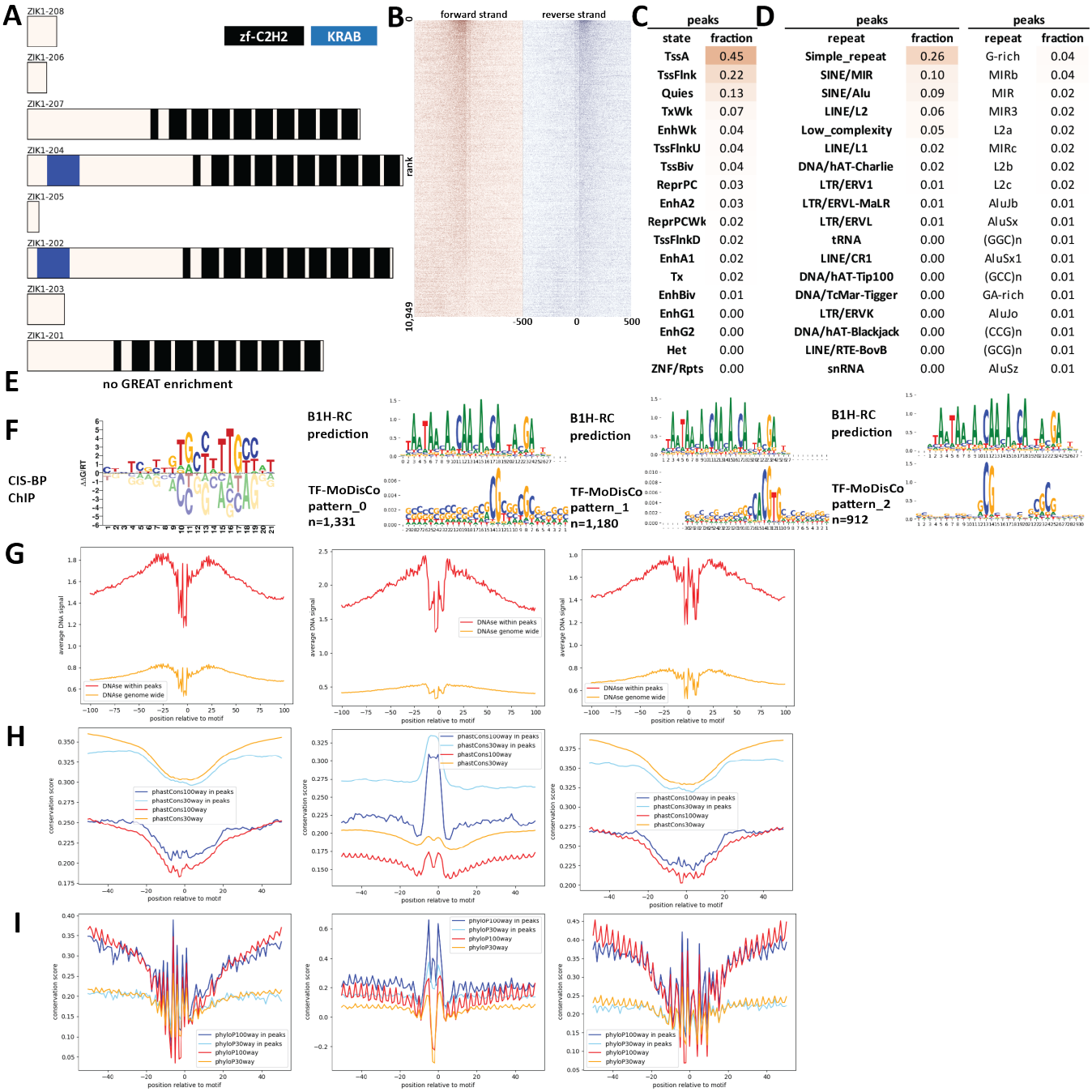

Supplementary Figure 631: Properties and genomic distribution of motifs identified for the ZIK1 transcription factor in HepG2 (accession ENCSR862VDD).

TF-MoDisCO pattern_0 n=1331, CWM

pattern_0, n=1331; subpattern_0, ns=227

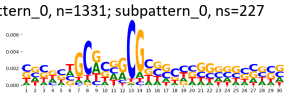

pattern_0, n=1331; subpattern_1, ns=223

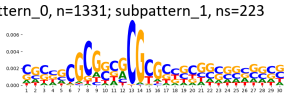

pattern_0, n=1331; subpattern_2, ns=173

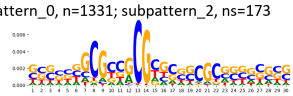

pattern_0, n=1331; subpattern_3, ns=170

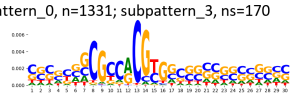

pattern_0, n=1331; subpattern_4, ns=164

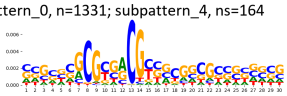

pattern_0, n=1331; subpattern_5, ns=117

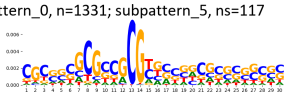

pattern_0, n=1331; subpattern_6, ns=112

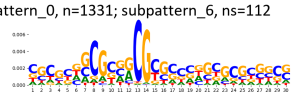

pattern_0, n=1331; subpattern_7, ns=96

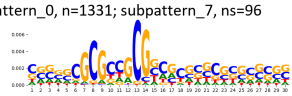

pattern_0, n=1331; subpattern_8, ns=42

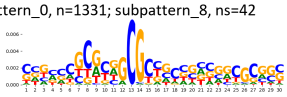

pattern_0, n=1331; subpattern_9, ns=7

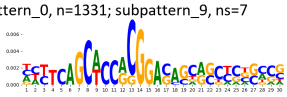

TF-MoDisCO pattern_0 n=1331, PWM

pattern_0, n=1331; subpattern_0, ns=227

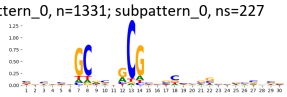

pattern_0, n=1331; subpattern_1, ns=223

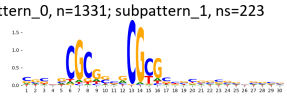

pattern_0, n=1331; subpattern_2, ns=173

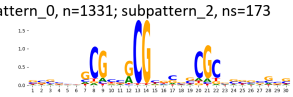

pattern_0, n=1331; subpattern_3, ns=170

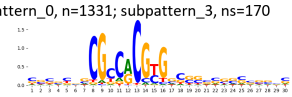

pattern_0, n=1331; subpattern_4, ns=164

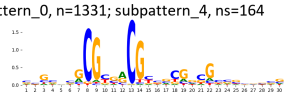

pattern_0, n=1331; subpattern_5, ns=117

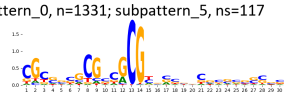

pattern_0, n=1331; subpattern_6, ns=112

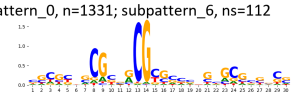

pattern_0, n=1331; subpattern_7, ns=96

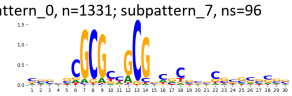

pattern_0, n=1331; subpattern_8, ns=42

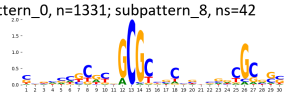

pattern_0, n=1331; subpattern_9, ns=7

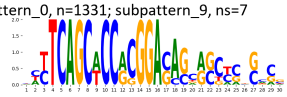

TF-MoDisCO pattern_1 n=1180, CWM

pattern_1, n=1180; subpattern_0, ns=236

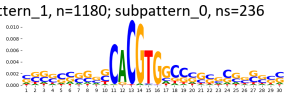

pattern_1, n=1180; subpattern_1, ns=228

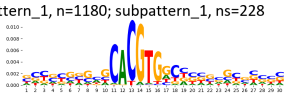

pattern_1, n=1180; subpattern_2, ns=186

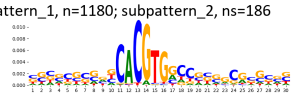

pattern_1, n=1180; subpattern_3, ns=173

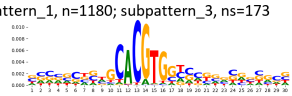

pattern_1, n=1180; subpattern_4, ns=170

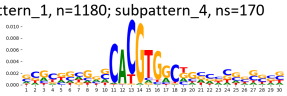

pattern_1, n=1180; subpattern_5, ns=108

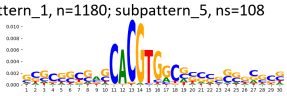

pattern_1, n=1180; subpattern_6, ns=68

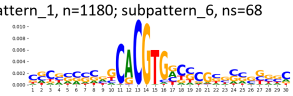

pattern_1, n=1180; subpattern_7, ns=11

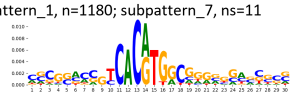

TF-MoDisCO pattern_1 n=1180, PWM

pattern_1, n=1180; subpattern_0, ns=236

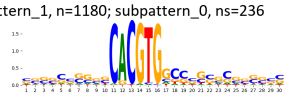

pattern_1, n=1180; subpattern_1, ns=228

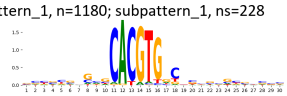

pattern_1, n=1180; subpattern_2, ns=186

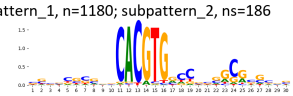

pattern_1, n=1180; subpattern_3, ns=173

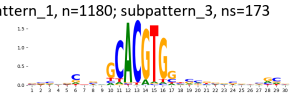

pattern_1, n=1180; subpattern_4, ns=170

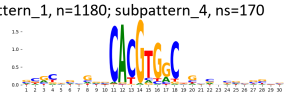

pattern_1, n=1180; subpattern_5, ns=108

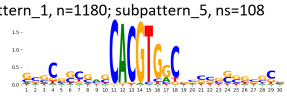

pattern_1, n=1180; subpattern_6, ns=68

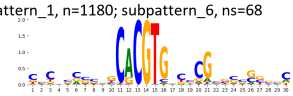

pattern_1, n=1180; subpattern_7, ns=11

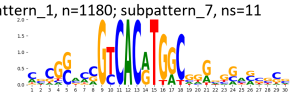

TF-MoDisCO pattern_2 n=912, CWM

pattern_2, n=912; subpattern_0, ns=162

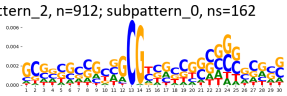

pattern_2, n=912; subpattern_1, ns=146

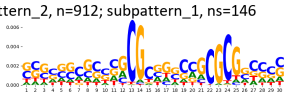

pattern_2, n=912; subpattern_2, ns=131

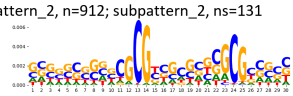

pattern_2, n=912; subpattern_3, ns=113

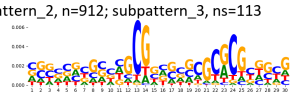

pattern_2, n=912; subpattern_4, ns=83

pattern_2, n=912; subpattern_5, ns=81

pattern_2, n=912; subpattern_6, ns=75

pattern_2, n=912; subpattern_7, ns=62

pattern_2, n=912; subpattern_8, ns=59

TF-MoDisCO pattern_2 n=912, PWM

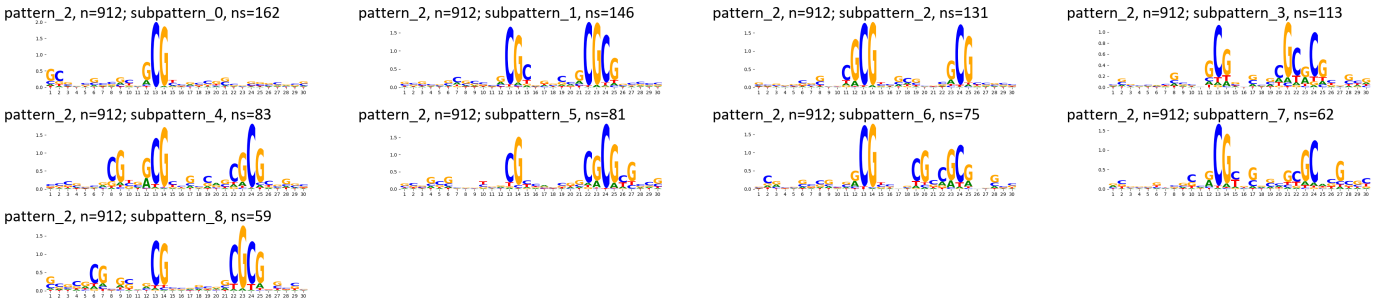

Supplementary Figure 632: TF-MoDisCO subpatterns for the ZIK1 transcription factor in HepG2 (accession ENCSR862VDD).

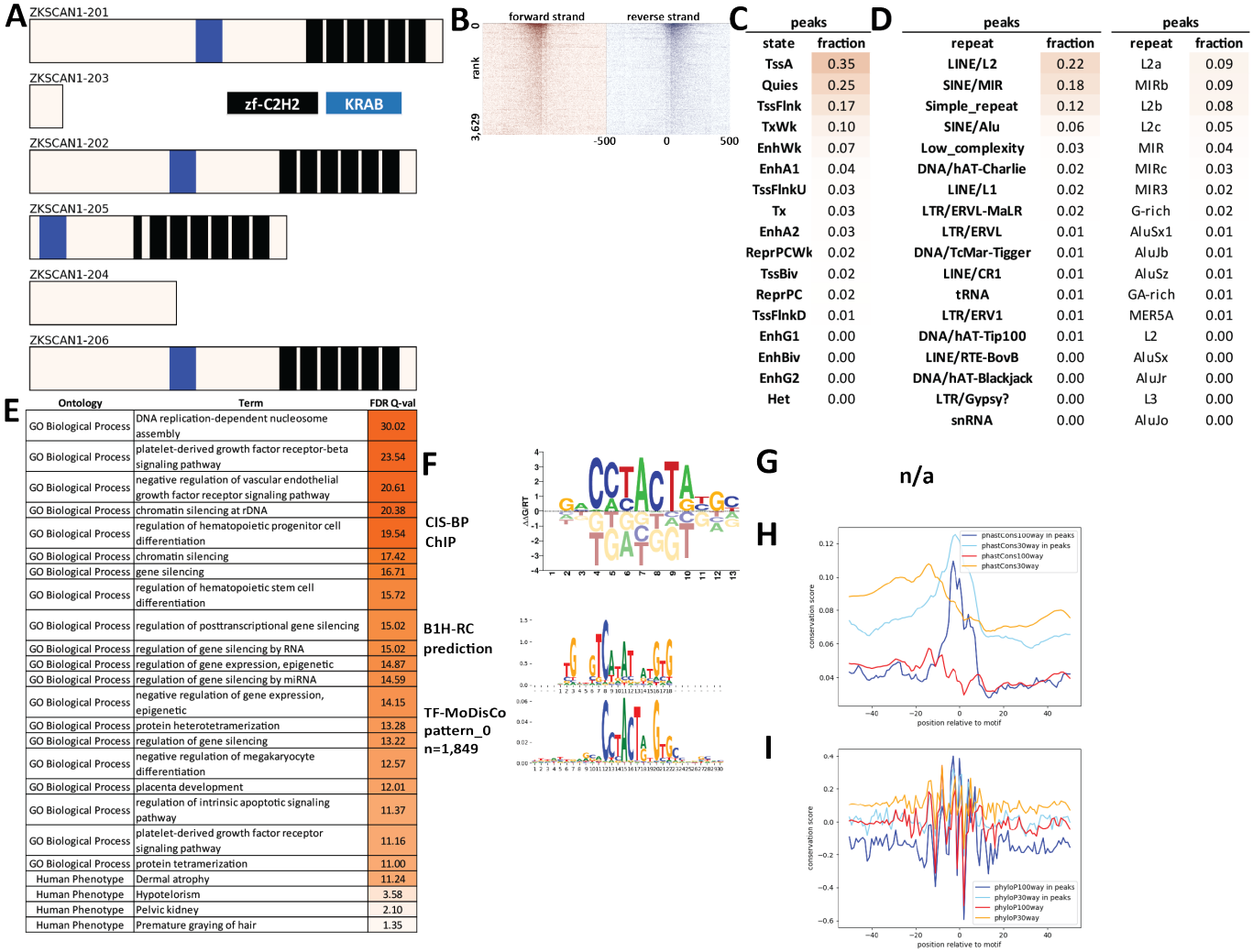

C

peaks	
state	fraction
TssA	0.35
Quies	0.25
TssFlnk	0.17
TxWk	0.10
EnhWk	0.07
EnhA1	0.04
TssFlnkU	0.03
Tx	0.03
EnhA2	0.03
ReprPCWk	0.02
TssBiv	0.02
ReprPC	0.02
TssFlnkD	0.01
EnhG1	0.00
EnhBiv	0.00
EnhG2	0.00
Het	0.00

D

peaks		peaks	
repeat	fraction	repeat	fraction
LINE/L2	0.22	L2a	0.09
SINE/MIR	0.18	MIRb	0.09
Simple_repeat	0.12	L2b	0.08
SINE/Alu	0.06	L2c	0.05
Low_complexity	0.03	MIR	0.04
DNA/hAT-Charlie	0.02	MIRc	0.03
LINE/L1	0.02	MIR3	0.02
LTR/ERVL-MaLR	0.02	G-rich	0.02
LTR/ERVL	0.01	AluSx1	0.01
DNA/TcMar-Tigger	0.01	AluJb	0.01
LINE/CR1	0.01	AluSz	0.01
tRNA	0.01	GA-rich	0.01
LTR/ERV1	0.01	MER5A	0.01
DNA/hAT-Tip100	0.01	L2	0.00
LINE/RTE-BovB	0.00	AluSx	0.00
DNA/hAT-Blackjack	0.00	AluJr	0.00
LTR/Gypsy?	0.00	L3	0.00
snRNA	0.00	AluJo	0.00

E

Ontology	Term	FDR Q-val
GO Biological Process	DNA replication-dependent nucleosome assembly	30.02
GO Biological Process	platelet-derived growth factor receptor-beta signaling pathway	23.54
GO Biological Process	negative regulation of vascular endothelial growth factor receptor signaling pathway	20.61
GO Biological Process	chromatin silencing at rDNA	20.38
GO Biological Process	regulation of hematopoietic progenitor cell differentiation	19.54
GO Biological Process	chromatin silencing	17.42
GO Biological Process	gene silencing	16.71
GO Biological Process	regulation of hematopoietic stem cell differentiation	15.72
GO Biological Process	regulation of posttranscriptional gene silencing	15.02
GO Biological Process	regulation of gene silencing by RNA	15.02
GO Biological Process	regulation of gene expression, epigenetic	14.87
GO Biological Process	regulation of gene silencing by miRNA	14.59
GO Biological Process	negative regulation of gene expression, epigenetic	14.15
GO Biological Process	protein heterotetramerization	13.28
GO Biological Process	regulation of gene silencing	13.22
GO Biological Process	negative regulation of megakaryocyte differentiation	12.57
GO Biological Process	placenta development	12.01
GO Biological Process	regulation of intrinsic apoptotic signaling pathway	11.37
GO Biological Process	platelet-derived growth factor receptor signaling pathway	11.16
GO Biological Process	protein tetramerization	11.00
Human Phenotype	Dermal atrophy	11.24
Human Phenotype	Hypotelorism	3.58
Human Phenotype	Pelvic kidney	2.10
Human Phenotype	Premature graying of hair	1.35

Supplementary Figure 633: Properties and genomic distribution of motifs identified for the ZKSCAN1 transcription factor in HeLa-S3 (accession ENCSR000ECJ).

TF-MoDisCO pattern_0 n=1849, CWM

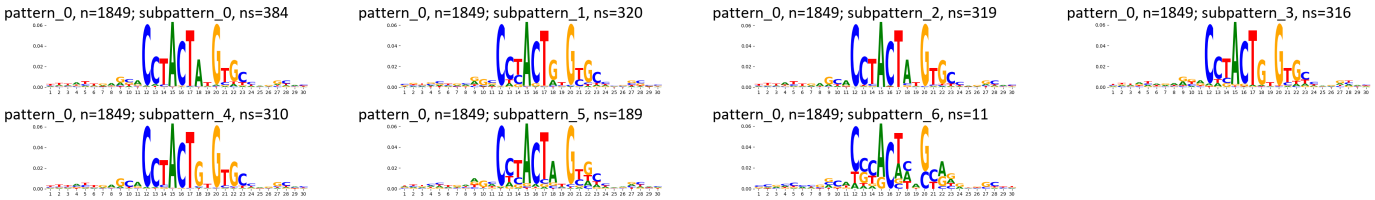

TF-MoDisCO pattern_0 n=1849, PWM

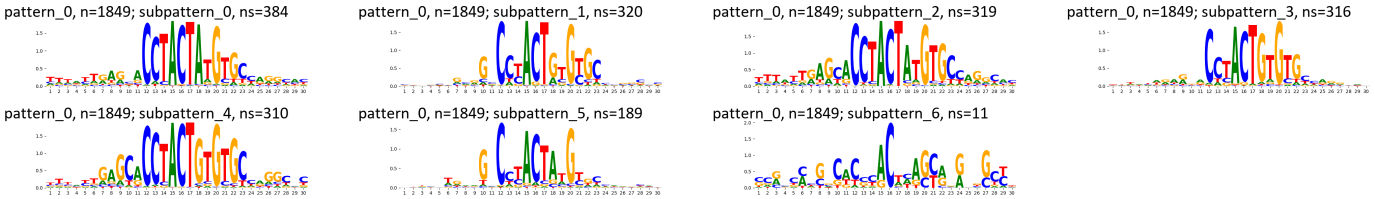

Supplementary Figure 634: TF-MoDisCO subpatterns for the ZKSCAN1 transcription factor in HeLa-S3 (accession ENCSR000ECJ).

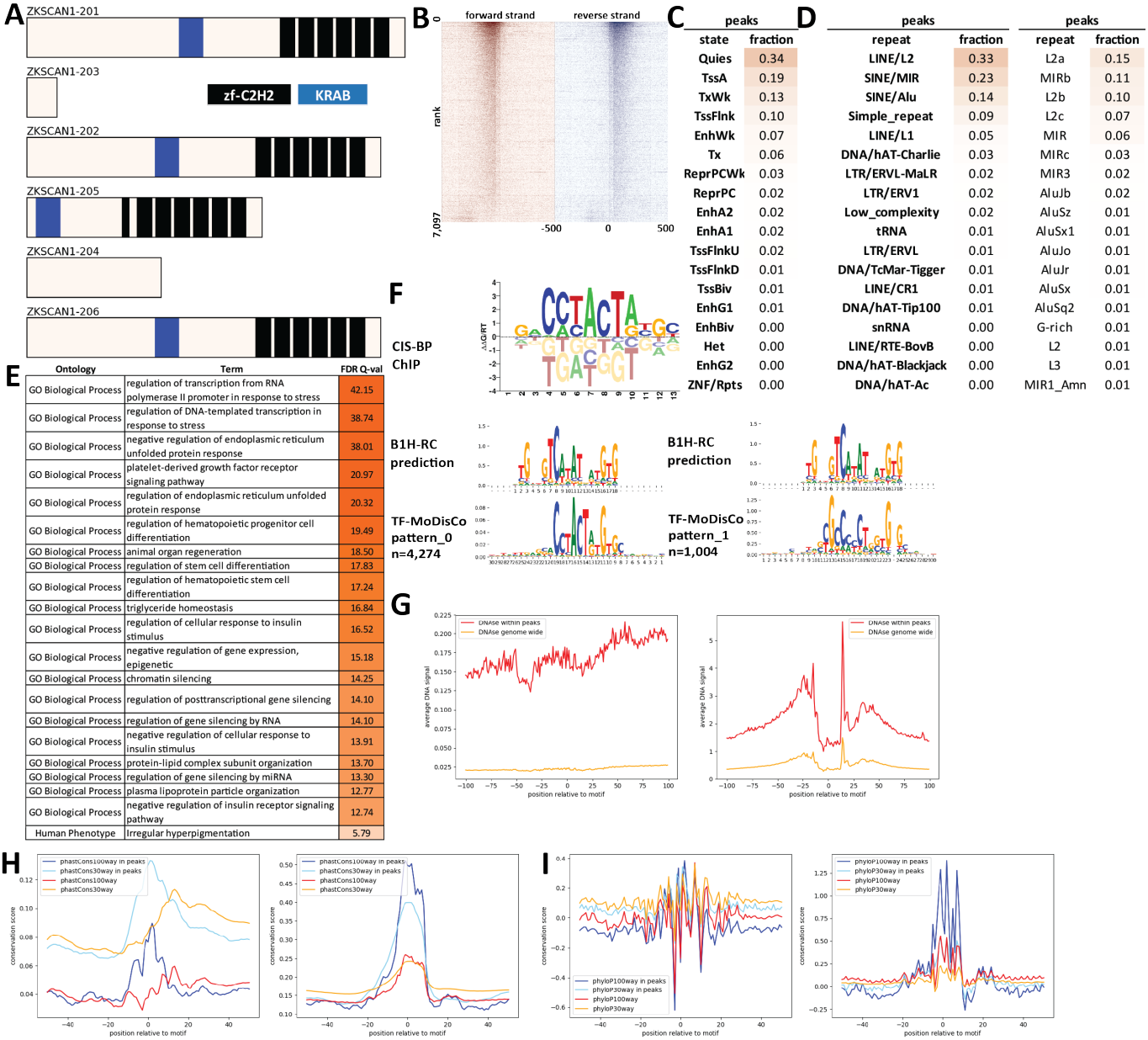

Supplementary Figure 635: Properties and genomic distribution of motifs identified for the ZKSCAN1 transcription factor in HepG2 (accession ENCSR157CAU).

TF-MoDisCO pattern_0 n=4274, CWM

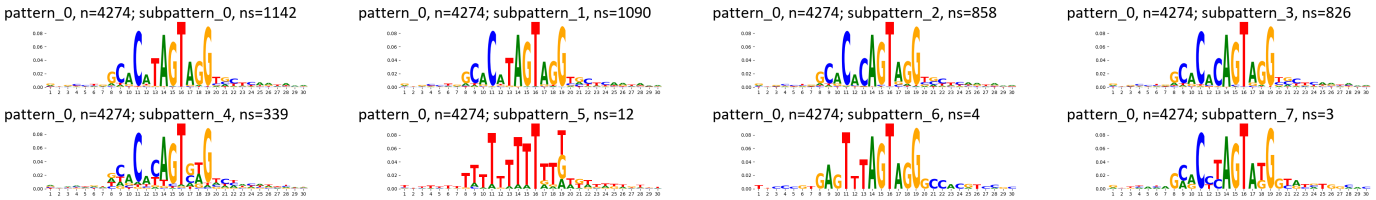

TF-MoDisCO pattern_0 n=4274, PWM

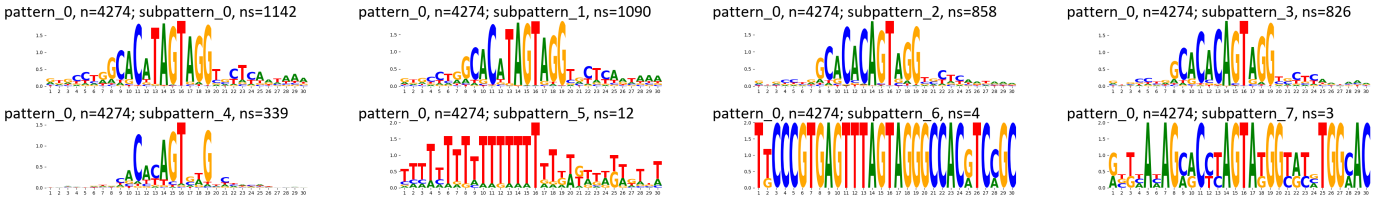

TF-MoDisCO pattern_1 n=1004, CWM

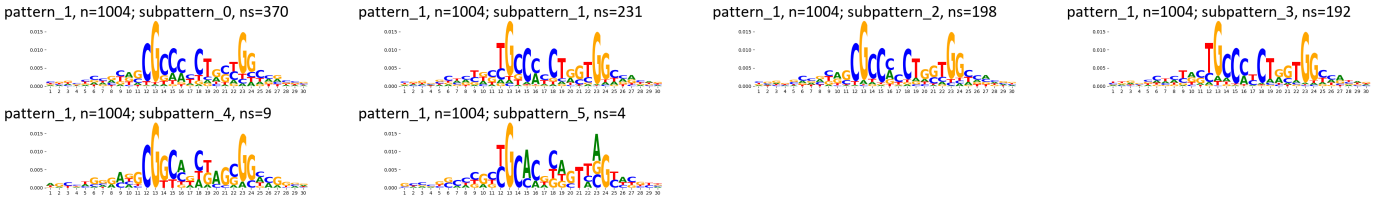

TF-MoDisCO pattern_1 n=1004, PWM

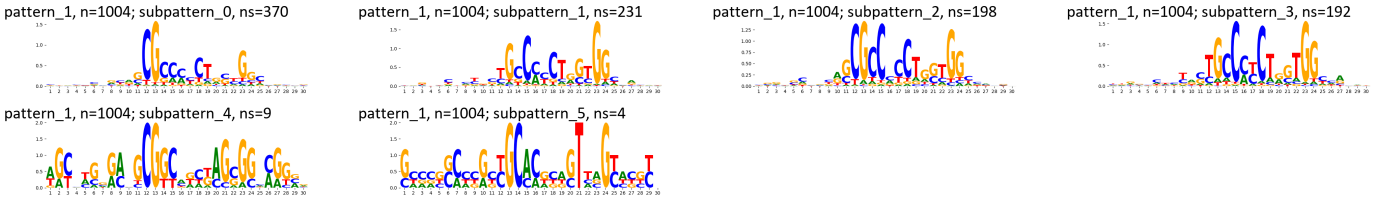

Supplementary Figure 636: TF-MoDisCO subpatterns for the ZKSCAN1 transcription factor in HepG2 (accession ENCSR157CAU).

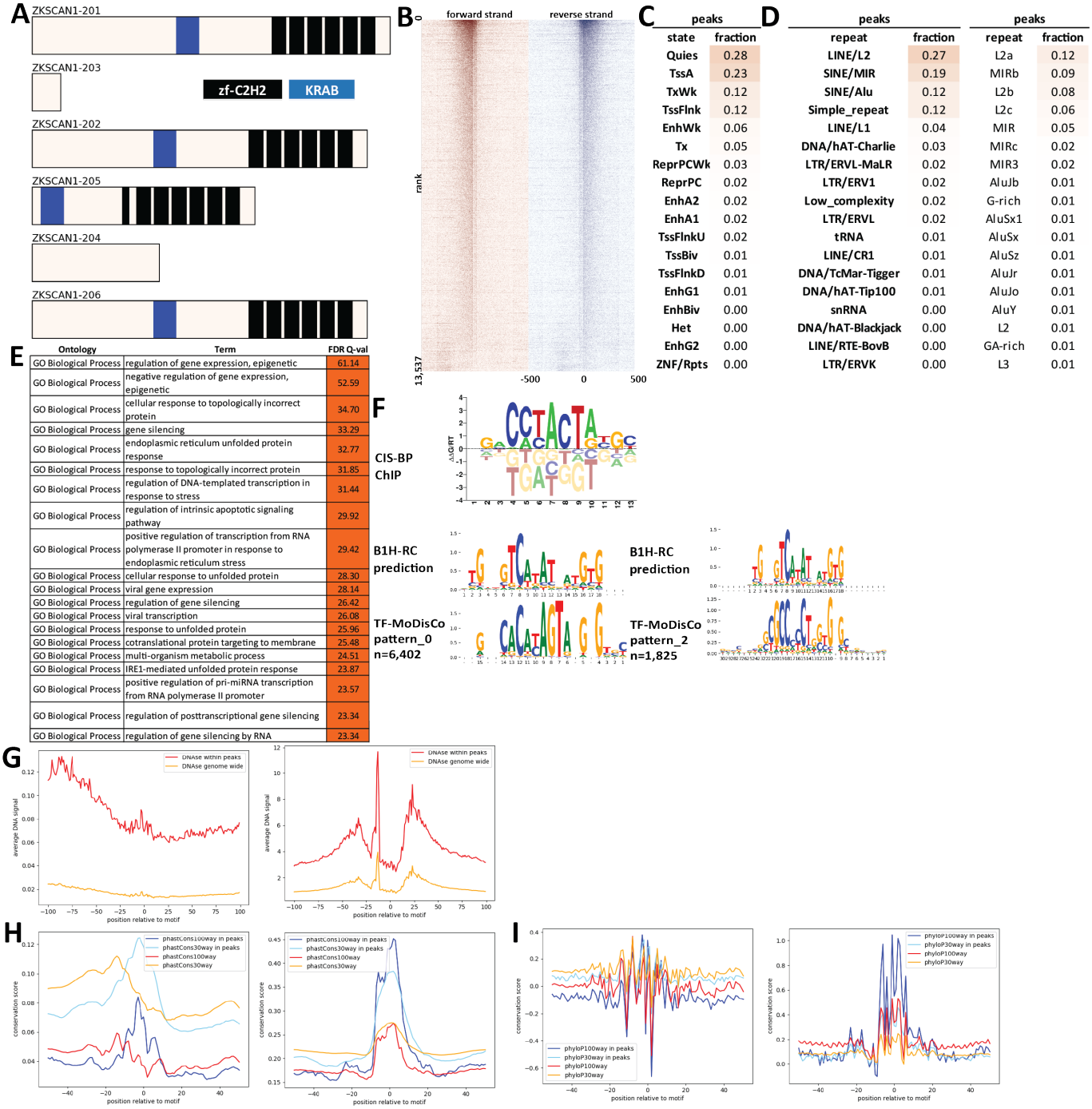

peaks	
state	fraction
Quies	0.28
TssA	0.23
TxWk	0.12
TssFlnk	0.12
EnhWk	0.06
Tx	0.05
ReprPCWk	0.03
ReprPC	0.02
EnhA2	0.02
EnhA1	0.02
TssFlnkU	0.02
TssBiv	0.01
TssFlnkD	0.01
EnhG1	0.01
EnhBiv	0.00
Het	0.00
EnhG2	0.00
ZNF/Rpts	0.00

peaks	
repeat	fraction
LINE/L2	0.27
SINE/MIR	0.19
SINE/Alu	0.12
Simple_repeat	0.12
LINE/L1	0.04
DNA/hAT-Charlie	0.03
LTR/ERVL-MaLR	0.02
LTR/ERV1	0.02
Low_complexity	0.02
LTR/ERVL	0.02
tRNA	0.01
LINE/CR1	0.01
DNA/TcMar-Tigger	0.01
DNA/hAT-Tip100	0.01
snRNA	0.00
DNA/hAT-Blackjack	0.00
LINE/RTE-BovB	0.00
LTR/ERVK	0.00

peaks	
repeat	fraction
L2a	0.12
MIRb	0.09
L2b	0.08
L2c	0.06
MIR	0.05
MIRc	0.02
MIR3	0.02
AluJb	0.01
G-rich	0.01
AluSx1	0.01
AluSx	0.01
AluSz	0.01
AluJr	0.01
AluJo	0.01
AluY	0.01
L2	0.01
GA-rich	0.01
L3	0.01

Ontology	Term	FDR Q-val
GO Biological Process	regulation of gene expression, epigenetic	61.14
GO Biological Process	negative regulation of gene expression, epigenetic	52.59
GO Biological Process	cellular response to topologically incorrect protein	34.70
GO Biological Process	gene silencing	33.29
GO Biological Process	endoplasmic reticulum unfolded protein response	32.77
GO Biological Process	response to topologically incorrect protein	31.85
GO Biological Process	regulation of DNA-templated transcription in response to stress	31.44
GO Biological Process	regulation of intrinsic apoptotic signaling pathway	29.92
GO Biological Process	positive regulation of transcription from RNA polymerase II promoter in response to endoplasmic reticulum stress	29.42
GO Biological Process	cellular response to unfolded protein	28.30
GO Biological Process	viral gene expression	28.14
GO Biological Process	regulation of gene silencing	26.42
GO Biological Process	viral transcription	26.08
GO Biological Process	response to unfolded protein	25.96
GO Biological Process	cotranslational protein targeting to membrane	25.48
GO Biological Process	multi-organism metabolic process	24.51
GO Biological Process	IRE1-mediated unfolded protein response	23.87
GO Biological Process	positive regulation of pri-miRNA transcription from RNA polymerase II promoter	23.57
GO Biological Process	regulation of posttranscriptional gene silencing	23.34
GO Biological Process	regulation of gene silencing by RNA	23.34

Supplementary Figure 637: Properties and genomic distribution of motifs identified for the ZKSCAN1 transcription factor in K562 (accession ENCSR882ERE).

TF-MoDisCO pattern_0 n=6402, CWM

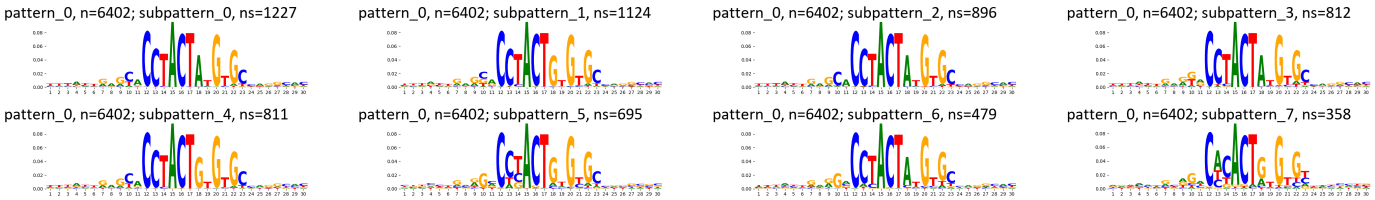

TF-MoDisCO pattern_0 n=6402, PWM

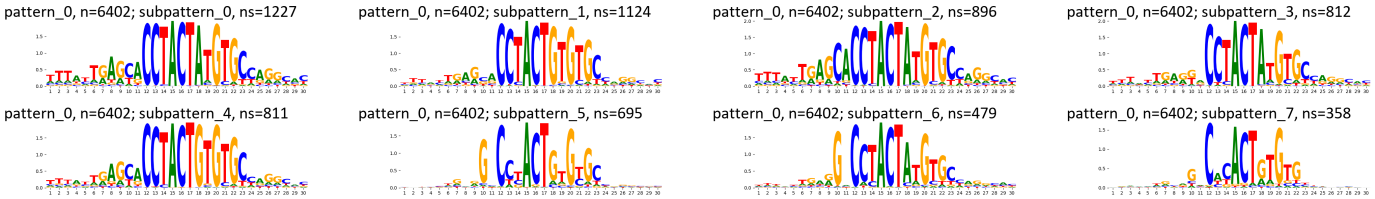

TF-MoDisCO pattern_2 n=1825, CWM

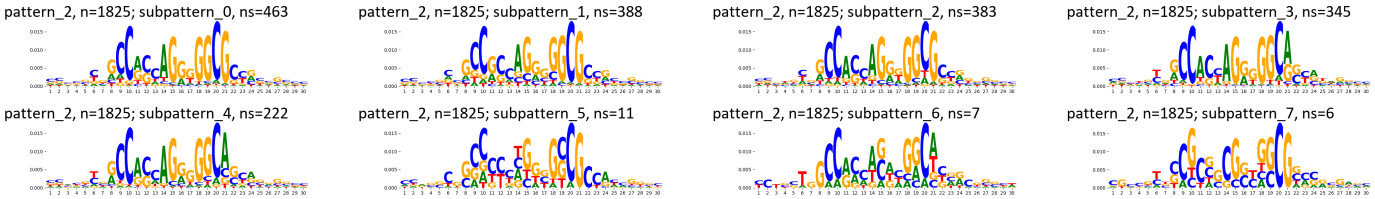

TF-MoDisCO pattern_2 n=1825, PWM

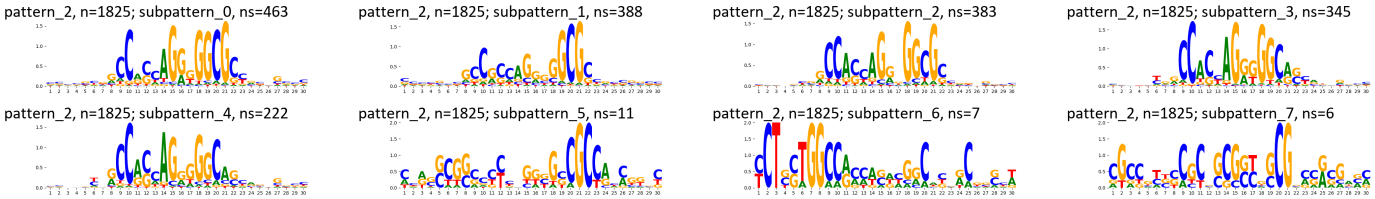

Supplementary Figure 638: TF-MoDisCO subpatterns for the ZKSCAN1 transcription factor in K562 (accession ENCSR882ERE).

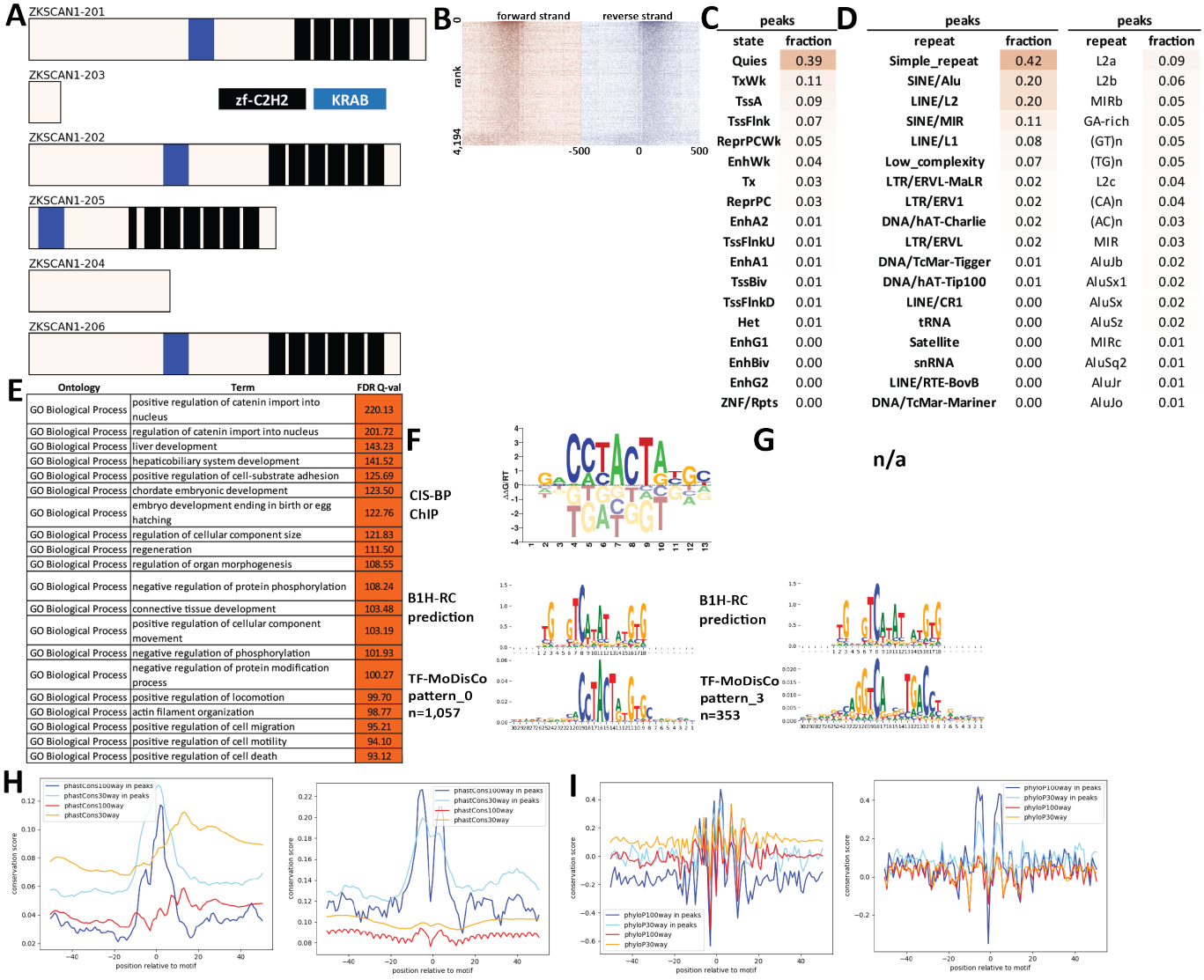

peaks	
state	fraction
Quies	0.39
TxWk	0.11
TssA	0.09
TssFlnk	0.07
ReprPCWk	0.05
EnhWk	0.04
Tx	0.03
ReprPC	0.03
EnhA2	0.01
TssFlnkU	0.01
EnhA1	0.01
TssBiv	0.01
TssFlnkD	0.01
Het	0.01
EnhG1	0.00
EnhBiv	0.00
EnhG2	0.00
ZNF/Rpts	0.00

peaks		peaks	
repeat	fraction	repeat	fraction
Simple_repeat	0.42	L2a	0.09
SINE/Alu	0.20	L2b	0.06
LINE/L2	0.20	MIRb	0.05
SINE/MIR	0.11	GA-rich	0.05
LINE/L1	0.08	(GT)n	0.05
Low_complexity	0.07	(TG)n	0.05
LTR/ERVL-MaLR	0.02	L2c	0.04
LTR/ERV1	0.02	(CA)n	0.04
DNA/hAT-Charlie	0.02	(AC)n	0.03
LTR/ERVL	0.02	MIR	0.03
DNA/TcMar-Tigger	0.01	AluJb	0.02
DNA/hAT-Tip100	0.01	AluSx1	0.02
LINE/CR1	0.00	AluSx	0.02
tRNA	0.00	AluSz	0.02
Satellite	0.00	MIRc	0.01
snRNA	0.00	AluSq2	0.01
LINE/RTE-BovB	0.00	AluJr	0.01
DNA/TcMar-Mariner	0.00	AluJo	0.01

Ontology	Term	FDR Q-val
GO Biological Process	positive regulation of catenin import into nucleus	220.13
GO Biological Process	regulation of catenin import into nucleus	201.72
GO Biological Process	liver development	143.23
GO Biological Process	hepaticobiliary system development	141.52
GO Biological Process	positive regulation of cell-substrate adhesion	125.69
GO Biological Process	chordate embryonic development	123.50
GO Biological Process	embryo development ending in birth or egg hatching	122.76
GO Biological Process	regulation of cellular component size	121.83
GO Biological Process	regeneration	111.50
GO Biological Process	regulation of organ morphogenesis	108.55
GO Biological Process	negative regulation of protein phosphorylation	108.24
GO Biological Process	connective tissue development	103.48
GO Biological Process	positive regulation of cellular component movement	103.19
GO Biological Process	negative regulation of phosphorylation	101.93
GO Biological Process	negative regulation of protein modification process	100.27
GO Biological Process	positive regulation of locomotion	99.70
GO Biological Process	actin filament organization	98.77
GO Biological Process	positive regulation of cell migration	95.21
GO Biological Process	positive regulation of cell motility	94.10
GO Biological Process	positive regulation of cell death	93.12

Supplementary Figure 639: Properties and genomic distribution of motifs identified for the ZKSCAN1 transcription factor in MCF-7 (accession ENCSR449UFF).

TF-MoDisCO pattern_0 n=1057, CWM

pattern_0, n=1057; subpattern_0, ns=294

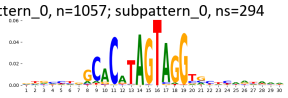

pattern_0, n=1057; subpattern_1, ns=283

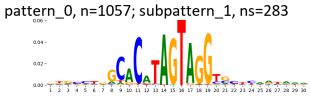

pattern_0, n=1057; subpattern_2, ns=240

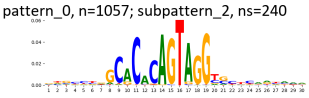

pattern_0, n=1057; subpattern_3, ns=235

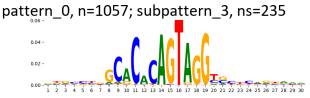

pattern_0, n=1057; subpattern_4, ns=5

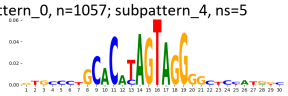

TF-MoDisCO pattern_0 n=1057, PWM

pattern_0, n=1057; subpattern_0, ns=294

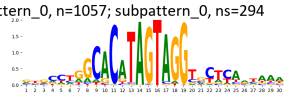

pattern_0, n=1057; subpattern_1, ns=283

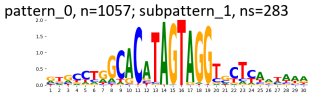

pattern_0, n=1057; subpattern_2, ns=240

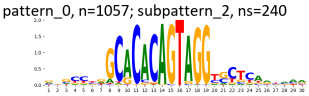

pattern_0, n=1057; subpattern_3, ns=235

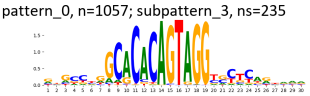

pattern_0, n=1057; subpattern_4, ns=5

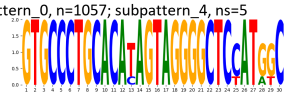

TF-MoDisCO pattern_3 n=353, CWM

pattern_3, n=353; subpattern_0, ns=86

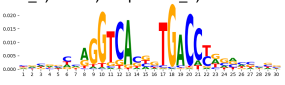

pattern_3, n=353; subpattern_1, ns=81

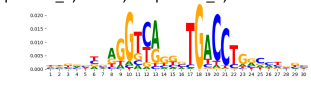

pattern_3, n=353; subpattern_2, ns=66

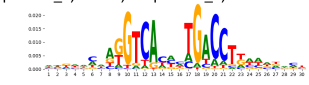

pattern_3, n=353; subpattern_3, ns=64

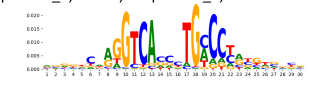

pattern_3, n=353; subpattern_4, ns=36

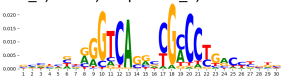

pattern_3, n=353; subpattern_5, ns=10

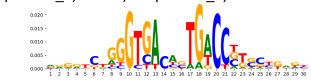

pattern_3, n=353; subpattern_6, ns=8

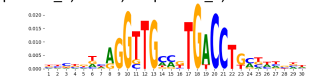

pattern_3, n=353; subpattern_7, ns=2

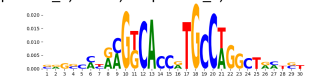

TF-MoDisCO pattern_3 n=353, PWM

pattern_3, n=353; subpattern_0, ns=86

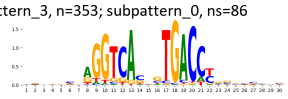

pattern_3, n=353; subpattern_1, ns=81

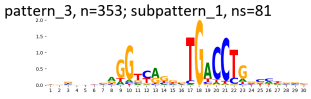

pattern_3, n=353; subpattern_2, ns=66

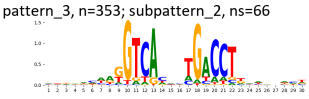

pattern_3, n=353; subpattern_3, ns=64

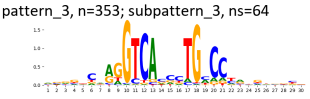

pattern_3, n=353; subpattern_4, ns=36

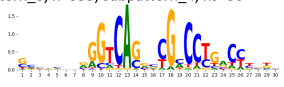

pattern_3, n=353; subpattern_5, ns=10

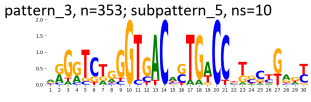

pattern_3, n=353; subpattern_6, ns=8

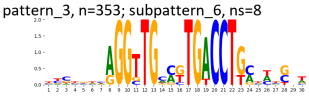

pattern_3, n=353; subpattern_7, ns=2

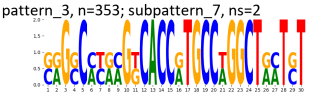

Supplementary Figure 640: TF-MoDisCO subpatterns for the ZKSCAN1 transcription factor in MCF-7 (accession ENCSR449UFF).

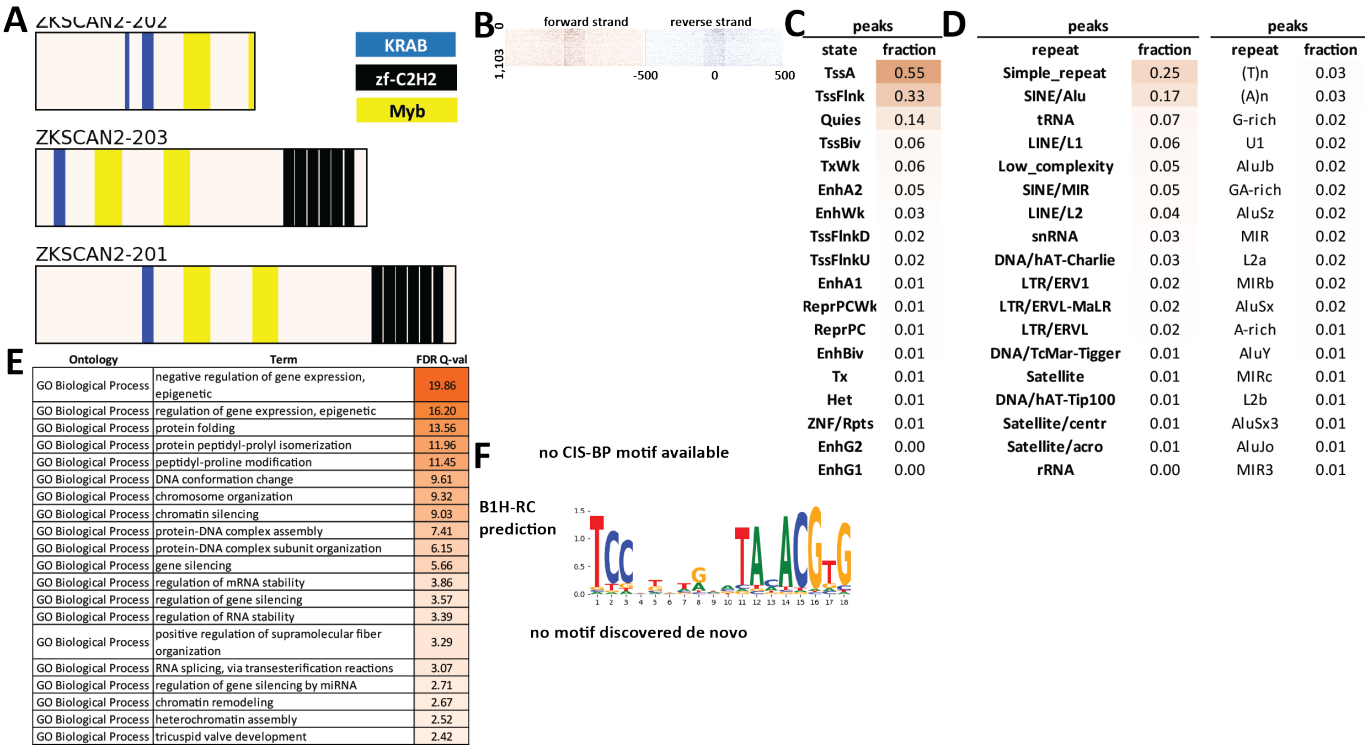

C

peaks	
state	fraction
TssA	0.55
TssFlnk	0.33
Quies	0.14
TssBiv	0.06
TxWk	0.06
EnhA2	0.05
EnhWk	0.03
TssFlnkD	0.02
TssFlnkU	0.02
EnhA1	0.01
ReprPCWk	0.01
ReprPC	0.01
EnhBiv	0.01
Tx	0.01
Het	0.01
ZNF/Rpts	0.01
EnhG2	0.00
EnhG1	0.00

D

peaks		peaks	
repeat	fraction	repeat	fraction
Simple_repeat	0.25	(T)n	0.03
SINE/Alu	0.17	(A)n	0.03
tRNA	0.07	G-rich	0.02
LINE/L1	0.06	U1	0.02
Low_complexity	0.05	AluJb	0.02
SINE/MIR	0.05	GA-rich	0.02
LINE/L2	0.04	AluSz	0.02
snRNA	0.03	MIR	0.02
DNA/hAT-Charlie	0.03	L2a	0.02
LTR/ERV1	0.02	MIRb	0.02
LTR/ERVL-MaLR	0.02	AluSx	0.02
LTR/ERVL	0.02	A-rich	0.01
DNA/TcMar-Tigger	0.01	AluY	0.01
Satellite	0.01	MIRc	0.01
DNA/hAT-Tip100	0.01	L2b	0.01
Satellite/centr	0.01	AluSx3	0.01
Satellite/acro	0.01	AluJo	0.01
rRNA	0.00	MIR3	0.01

E

Ontology	Term	FDR Q-val
GO Biological Process	negative regulation of gene expression, epigenetic	19.86
GO Biological Process	regulation of gene expression, epigenetic	16.20
GO Biological Process	protein folding	13.56
GO Biological Process	protein peptidyl-prolyl isomerization	11.96
GO Biological Process	peptidyl-proline modification	11.45
GO Biological Process	DNA conformation change	9.61
GO Biological Process	chromosome organization	9.32
GO Biological Process	chromatin silencing	9.03
GO Biological Process	protein-DNA complex assembly	7.41
GO Biological Process	protein-DNA complex subunit organization	6.15
GO Biological Process	gene silencing	5.66
GO Biological Process	regulation of mRNA stability	3.86
GO Biological Process	regulation of gene silencing	3.57
GO Biological Process	regulation of RNA stability	3.39
GO Biological Process	positive regulation of supramolecular fiber organization	3.29
GO Biological Process	RNA splicing, via transesterification reactions	3.07
GO Biological Process	regulation of gene silencing by miRNA	2.71
GO Biological Process	chromatin remodeling	2.67
GO Biological Process	heterochromatin assembly	2.52
GO Biological Process	tricuspid valve development	2.42

Supplementary Figure 641: Properties and genomic distribution of motifs identified for the ZKSCAN2 transcription factor in HEK293 (accession ChipExo models).

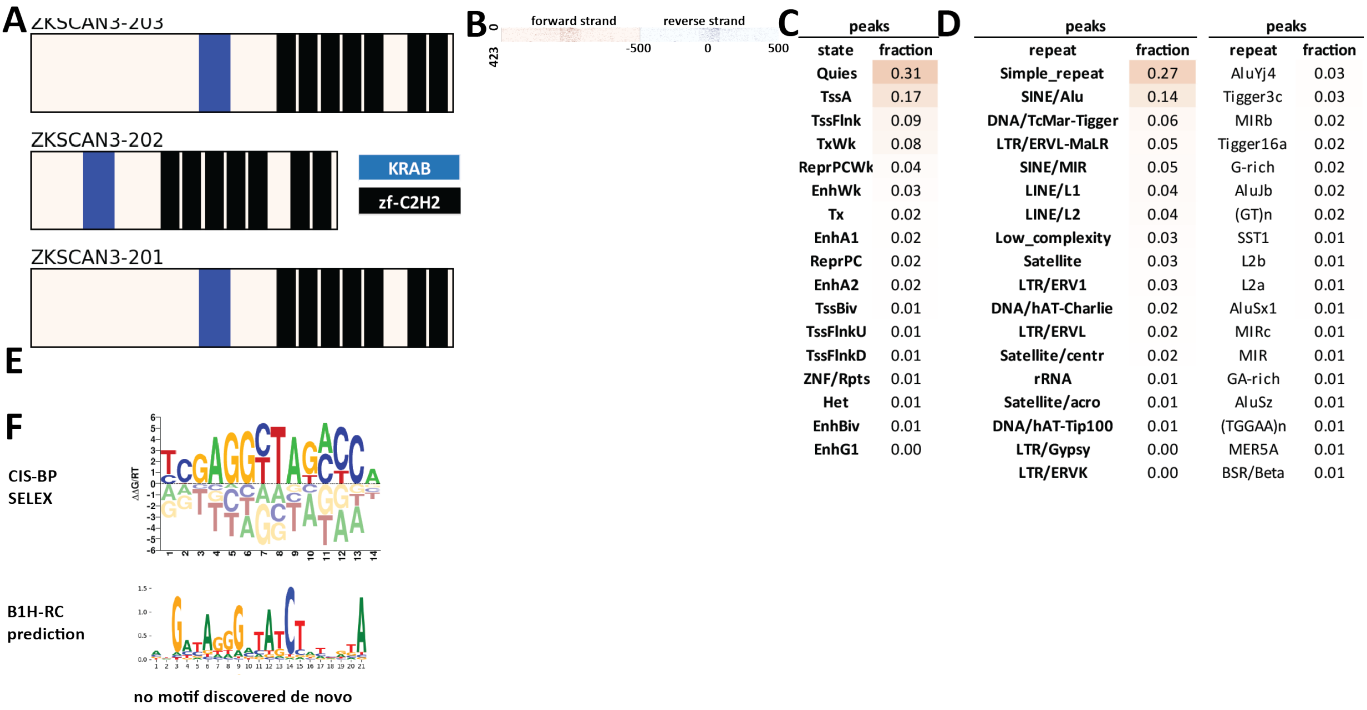

C

peaks	
state	fraction
Quies	0.31
TssA	0.17
TssFlnk	0.09
TxWk	0.08
ReprPCWk	0.04
EnhWk	0.03
Tx	0.02
EnhA1	0.02
ReprPC	0.02
EnhA2	0.02
TssBiv	0.01
TssFlnkU	0.01
TssFlnkD	0.01
ZNF/Rpts	0.01
Het	0.01
EnhBiv	0.01
EnhG1	0.00

D

peaks		peaks	
repeat	fraction	repeat	fraction
Simple_repeat	0.27	AluYj4	0.03
SINE/Alu	0.14	Tigger3c	0.03
DNA/TcMar-Tigger	0.06	MIRb	0.02
LTR/ERVL-MaLR	0.05	Tigger16a	0.02
SINE/MIR	0.05	G-rich	0.02
LINE/L1	0.04	AluJb	0.02
LINE/L2	0.04	(GT)n	0.02
Low_complexity	0.03	SST1	0.01
Satellite	0.03	L2b	0.01
LTR/ERV1	0.03	L2a	0.01
DNA/hAT-Charlie	0.02	AluSx1	0.01
LTR/ERVL	0.02	MIRc	0.01
Satellite/centr	0.02	MIR	0.01
rRNA	0.01	GA-rich	0.01
Satellite/acro	0.01	AluSz	0.01
DNA/hAT-Tip100	0.01	(TGGAA)n	0.01
LTR/Gypsy	0.00	MER5A	0.01
LTR/ERVK	0.00	BSR/Beta	0.01

Supplementary Figure 642: Properties and genomic distribution of motifs identified for the ZKSCAN3 transcription factor in HEK293 (accession ChipExo models).

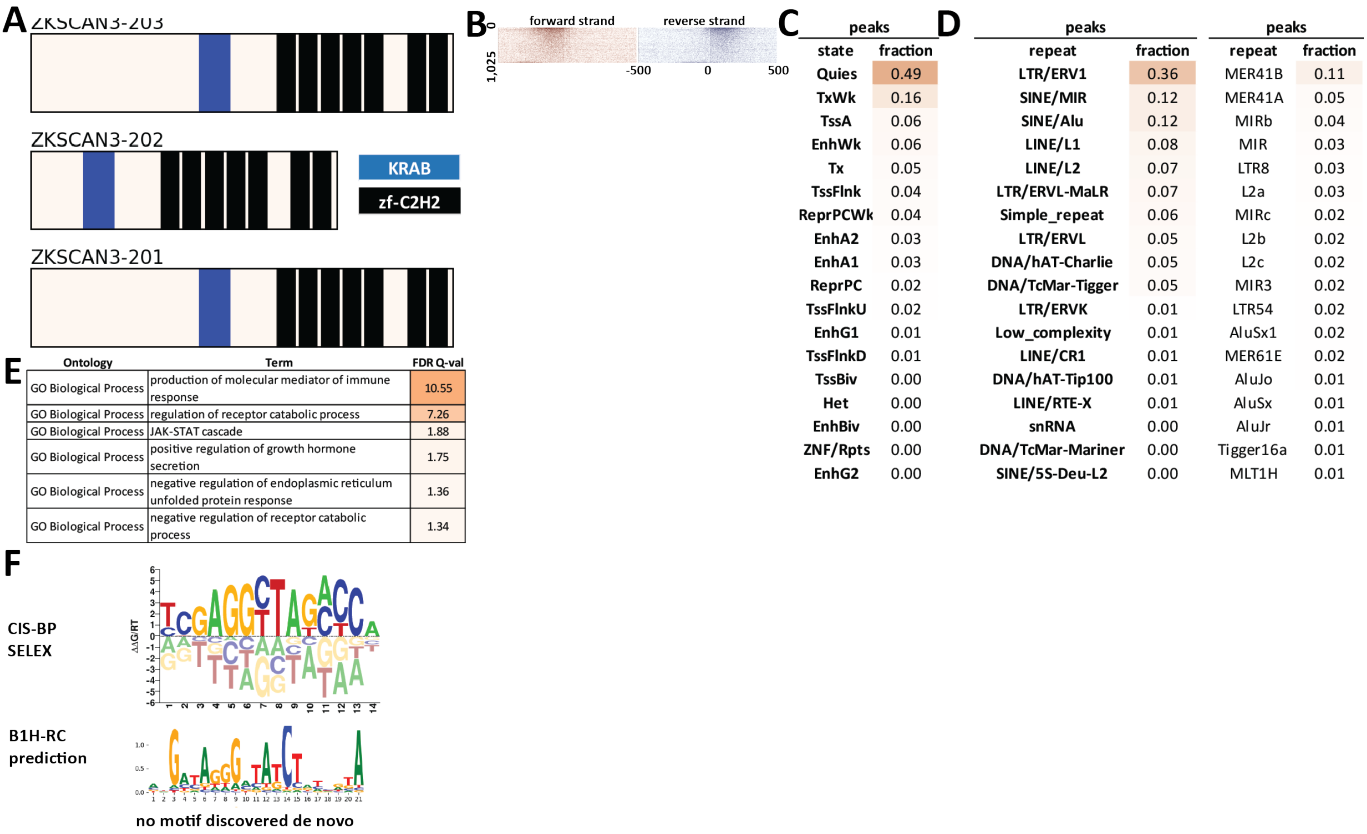

Supplementary Figure 643: Properties and genomic distribution of motifs identified for the ZKSCAN3 transcription factor in K562 (accession ENCSR199HGP).

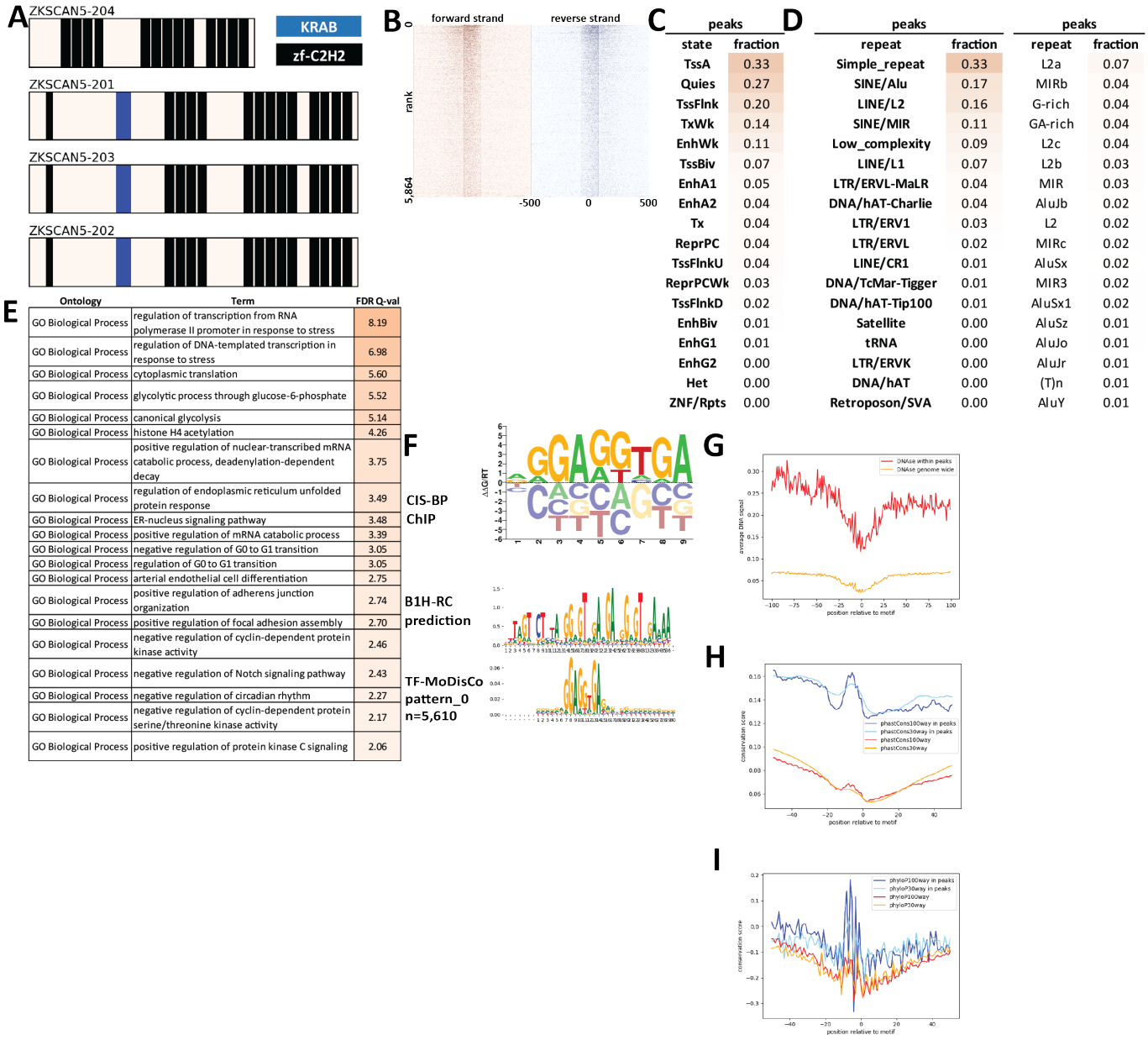

Supplementary Figure 644: Properties and genomic distribution of motifs identified for the ZKSCAN5 transcription factor in HEK293 (accession ChipExo models).

TF-MoDisCO pattern_0 n=5610, CWM

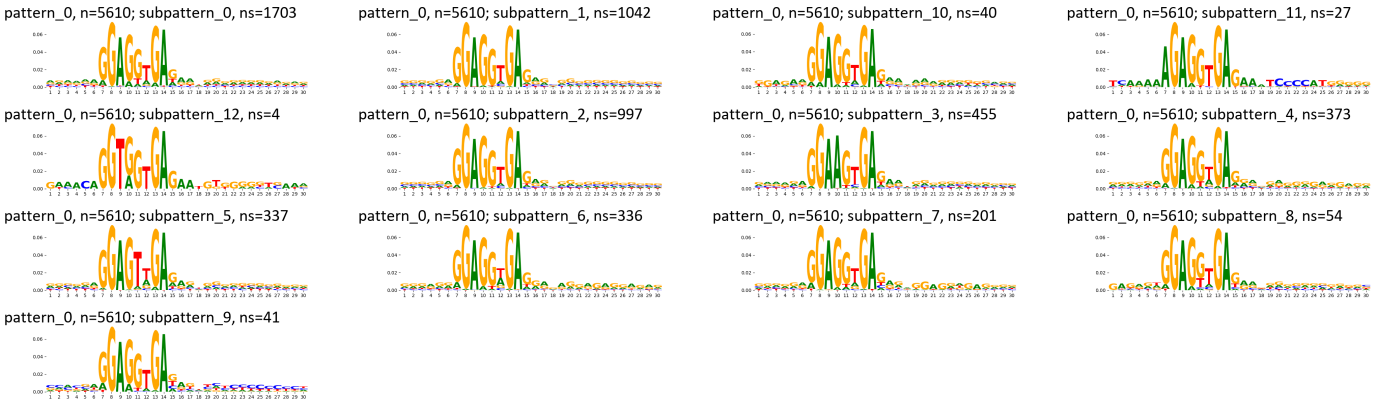

TF-MoDisCO pattern_0 n=5610, PWM

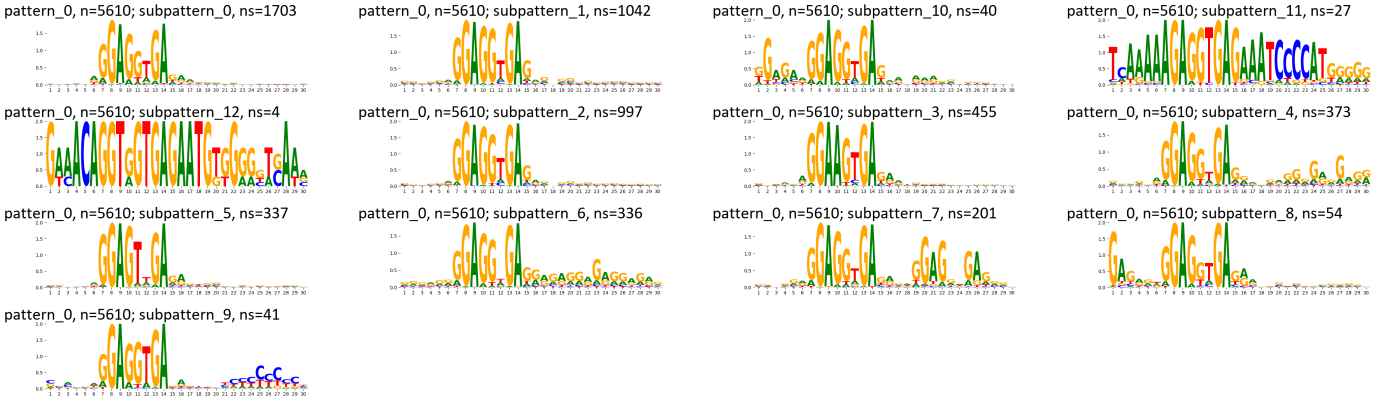

Supplementary Figure 645: TF-MoDisCO subpatterns for the ZKSCAN5 transcription factor in HEK293 (accession ChipExo models).

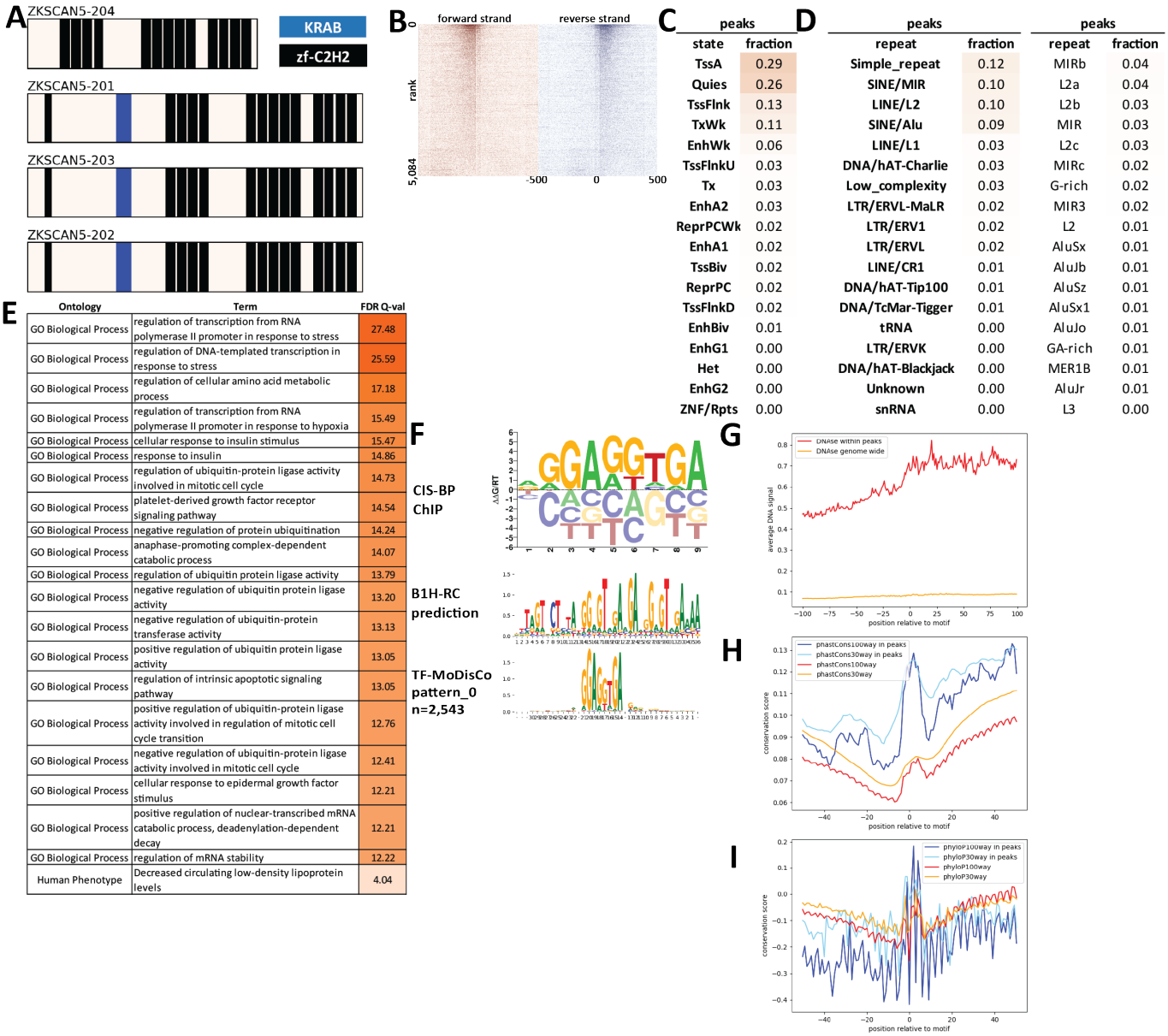

C

peaks	
state	fraction
TssA	0.29
Quies	0.26
TssFlnk	0.13
TxWk	0.11
EnhWk	0.06
TssFlnkU	0.03
Tx	0.03
EnhA2	0.03
ReprPCWk	0.02
EnhA1	0.02
TssBiv	0.02
ReprPC	0.02
TssFlnkD	0.02
EnhBiv	0.01
EnhG1	0.00
Het	0.00
EnhG2	0.00
ZNF/Rpts	0.00

D

peaks		peaks	
repeat	fraction	repeat	fraction
Simple_repeat	0.12	MIRb	0.04
SINE/MIR	0.10	L2a	0.04
LINE/L2	0.10	L2b	0.03
SINE/Alu	0.09	MIR	0.03
LINE/L1	0.03	L2c	0.03
DNA/hAT-Charlie	0.03	MIRc	0.02
Low_complexity	0.03	G-rich	0.02
LTR/ERVL-MaLR	0.02	MIR3	0.02
LTR/ERV1	0.02	L2	0.01
LTR/ERVL	0.02	AluSx	0.01
LINE/CR1	0.01	AluJb	0.01
DNA/hAT-Tip100	0.01	AluSz	0.01
DNA/TcMar-Tigger	0.01	AluSx1	0.01
tRNA	0.00	AluJo	0.01
LTR/ERVK	0.00	GA-rich	0.01
DNA/hAT-Blackjack	0.00	MER1B	0.01
Unknown	0.00	AluJr	0.01
snRNA	0.00	L3	0.00

E

Ontology	Term	FDR Q-val
GO Biological Process	regulation of transcription from RNA polymerase II promoter in response to stress	27.48
GO Biological Process	regulation of DNA-templated transcription in response to stress	25.59
GO Biological Process	regulation of cellular amino acid metabolic process	17.18
GO Biological Process	regulation of transcription from RNA polymerase II promoter in response to hypoxia	15.49
GO Biological Process	cellular response to insulin stimulus	15.47
GO Biological Process	response to insulin	14.86
GO Biological Process	regulation of ubiquitin-protein ligase activity involved in mitotic cell cycle	14.73
GO Biological Process	platelet-derived growth factor receptor signaling pathway	14.54
GO Biological Process	negative regulation of protein ubiquitination	14.24
GO Biological Process	anaphase-promoting complex-dependent catabolic process	14.07
GO Biological Process	regulation of ubiquitin protein ligase activity	13.79
GO Biological Process	negative regulation of ubiquitin protein ligase activity	13.20
GO Biological Process	negative regulation of ubiquitin-protein transferase activity	13.13
GO Biological Process	positive regulation of ubiquitin protein ligase activity	13.05
GO Biological Process	regulation of intrinsic apoptotic signaling pathway	13.05
GO Biological Process	positive regulation of ubiquitin-protein ligase activity involved in regulation of mitotic cell cycle transition	12.76
GO Biological Process	negative regulation of ubiquitin-protein ligase activity involved in mitotic cell cycle	12.41
GO Biological Process	cellular response to epidermal growth factor stimulus	12.21
GO Biological Process	positive regulation of nuclear-transcribed mRNA catabolic process, deadenylation-dependent decay	12.21
GO Biological Process	regulation of mRNA stability	12.22
Human Phenotype	Decreased circulating low-density lipoprotein levels	4.04

Supplementary Figure 646: Properties and genomic distribution of motifs identified for the ZKSCAN5 transcription factor in HepG2 (accession ENCSR159BTO).

TF-MoDisCO pattern_0 n=2543, CWM

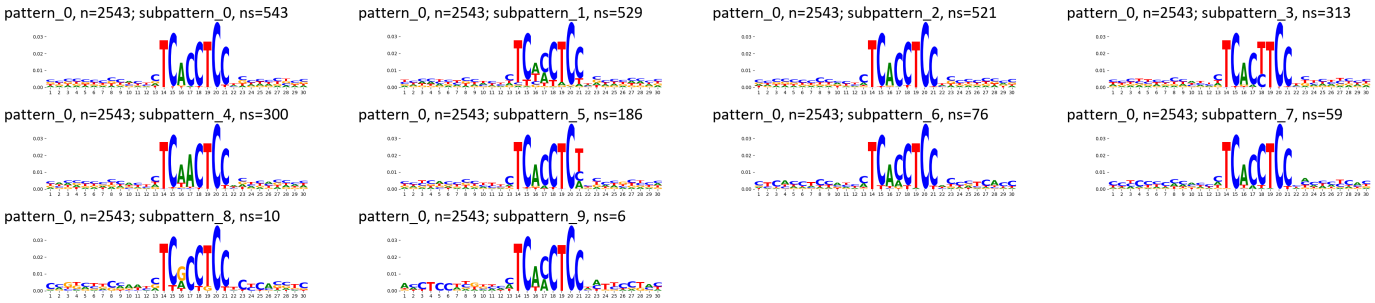

TF-MoDisCO pattern_0 n=2543, PWM

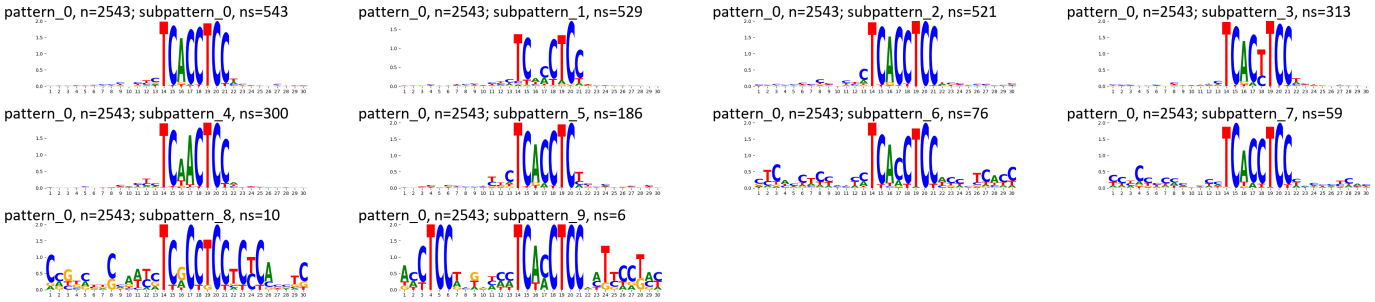

Supplementary Figure 647: TF-MoDisCO subpatterns for the ZKSCAN5 transcription factor in HepG2 (accession ENCSR159BTO).

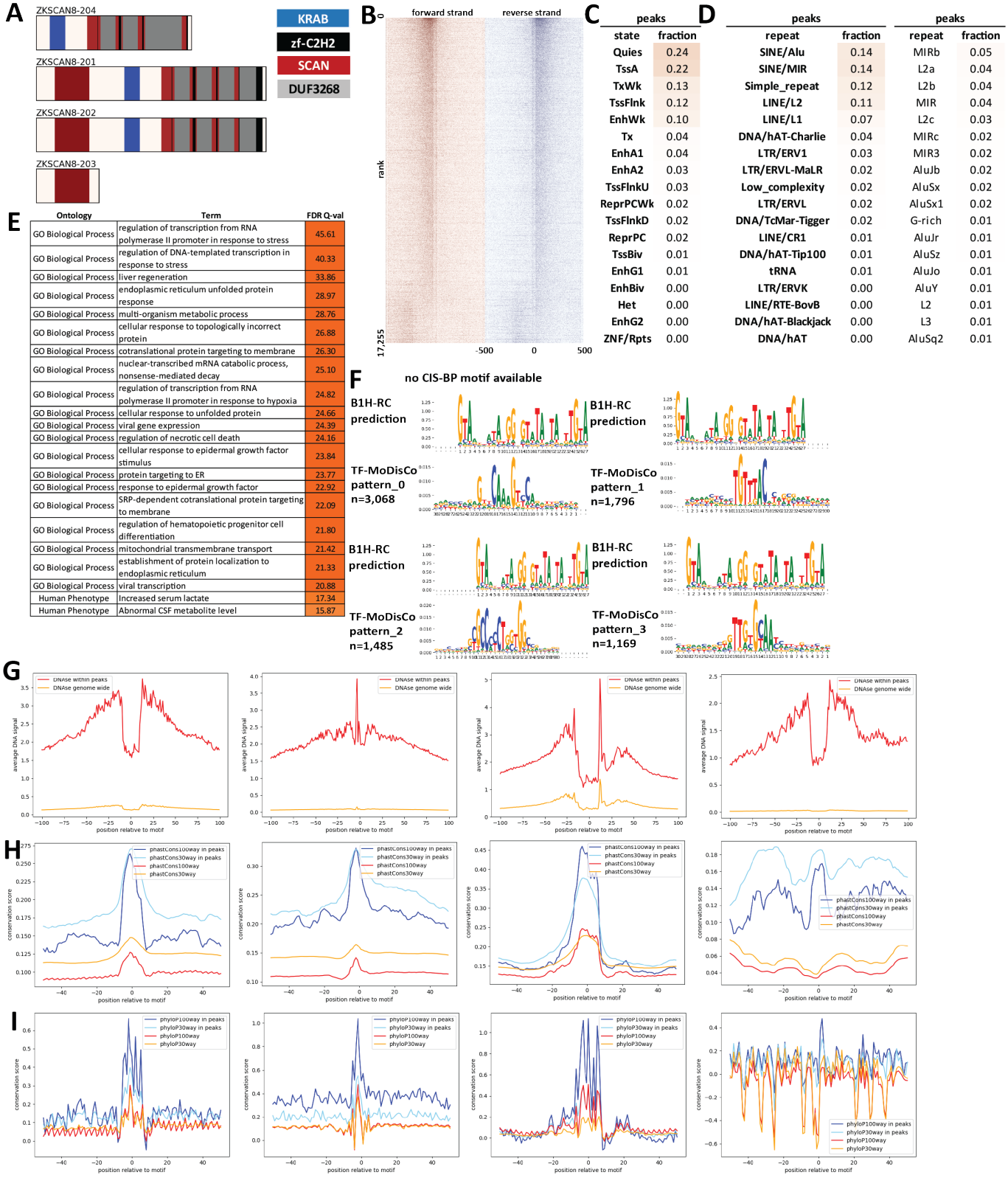

Supplementary Figure 648: Properties and genomic distribution of motifs identified for the ZKSCAN8 transcription factor in HepG2 (accession ENCSR808FFI).

TF-MoDisCO pattern_0 n=3068, CWM

pattern_0, n=3068; subpattern_0, ns=858

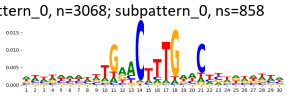

pattern_0, n=3068; subpattern_1, ns=622

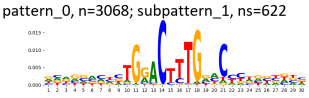

pattern_0, n=3068; subpattern_10, ns=2

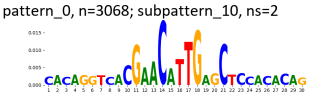

pattern_0, n=3068; subpattern_2, ns=566

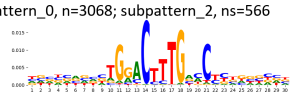

pattern_0, n=3068; subpattern_3, ns=506

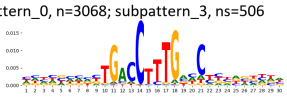

pattern_0, n=3068; subpattern_4, ns=239

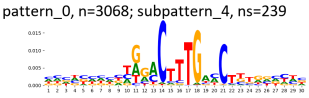

pattern_0, n=3068; subpattern_5, ns=237

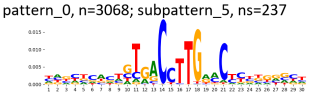

pattern_0, n=3068; subpattern_6, ns=23

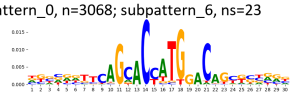

pattern_0, n=3068; subpattern_7, ns=8

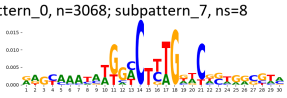

pattern_0, n=3068; subpattern_8, ns=5

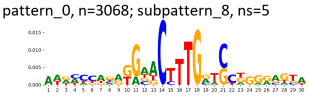

pattern_0, n=3068; subpattern_9, ns=2

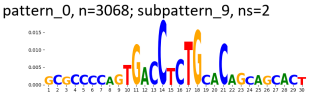

TF-MoDisCO pattern_0 n=3068, PWM

pattern_0, n=3068; subpattern_0, ns=858

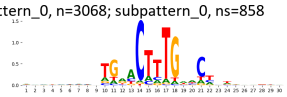

pattern_0, n=3068; subpattern_1, ns=622

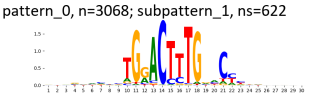

pattern_0, n=3068; subpattern_10, ns=2

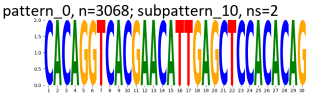

pattern_0, n=3068; subpattern_2, ns=566

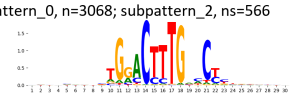

pattern_0, n=3068; subpattern_3, ns=506

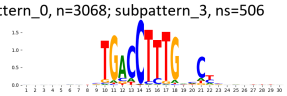

pattern_0, n=3068; subpattern_4, ns=239

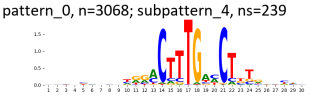

pattern_0, n=3068; subpattern_5, ns=237

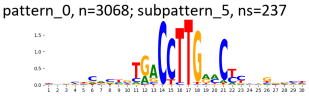

pattern_0, n=3068; subpattern_6, ns=23

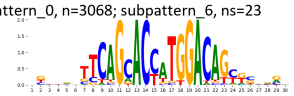

pattern_0, n=3068; subpattern_7, ns=8

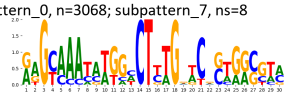

pattern_0, n=3068; subpattern_8, ns=5

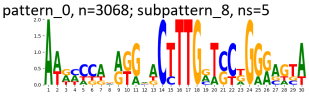

pattern_0, n=3068; subpattern_9, ns=2

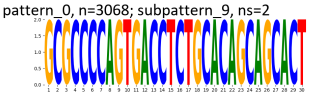

TF-MoDisCO pattern_1 n=1796, CWM

pattern_1, n=1796; subpattern_0, ns=489

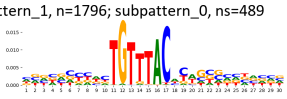

pattern_1, n=1796; subpattern_1, ns=472

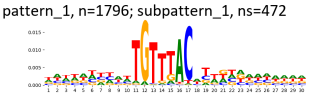

pattern_1, n=1796; subpattern_2, ns=282

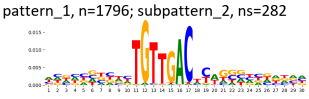

pattern_1, n=1796; subpattern_3, ns=258

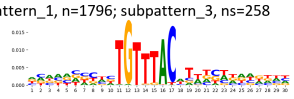

pattern_1, n=1796; subpattern_4, ns=160

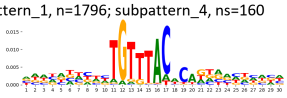

pattern_1, n=1796; subpattern_5, ns=125

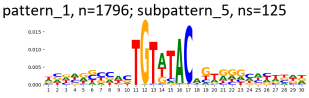

pattern_1, n=1796; subpattern_6, ns=7

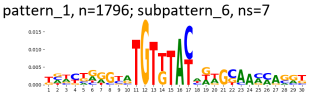

pattern_1, n=1796; subpattern_7, ns=3

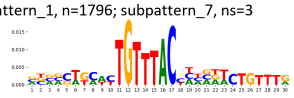

TF-MoDisCO pattern_1 n=1796, PWM

pattern_1, n=1796; subpattern_0, ns=489

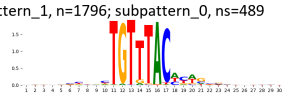

pattern_1, n=1796; subpattern_1, ns=472

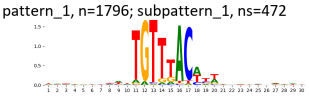

pattern_1, n=1796; subpattern_2, ns=282

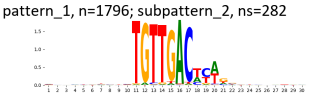

pattern_1, n=1796; subpattern_3, ns=258

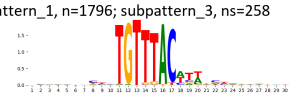

pattern_1, n=1796; subpattern_4, ns=160

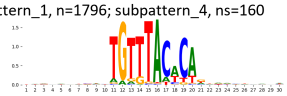

pattern_1, n=1796; subpattern_5, ns=125

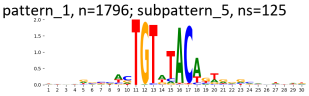

pattern_1, n=1796; subpattern_6, ns=7

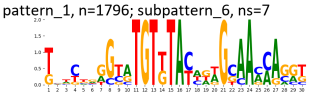

pattern_1, n=1796; subpattern_7, ns=3

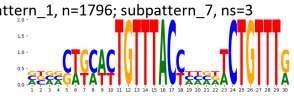

TF-MoDisCO pattern_2 n=1485, CWM

pattern_2, n=1485; subpattern_0, ns=389

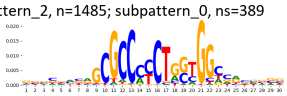

pattern_2, n=1485; subpattern_1, ns=316

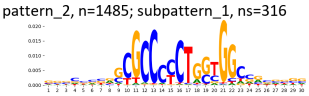

pattern_2, n=1485; subpattern_2, ns=312

pattern_2, n=1485; subpattern_3, ns=263

pattern_2, n=1485; subpattern_4, ns=203

pattern_2, n=1485; subpattern_5, ns=2

TF-MoDisCO pattern_2 n=1485, PWM

pattern_2, n=1485; subpattern_0, ns=389

pattern_2, n=1485; subpattern_1, ns=316

pattern_2, n=1485; subpattern_2, ns=312

pattern_2, n=1485; subpattern_3, ns=263

pattern_2, n=1485; subpattern_4, ns=203

pattern_2, n=1485; subpattern_5, ns=2

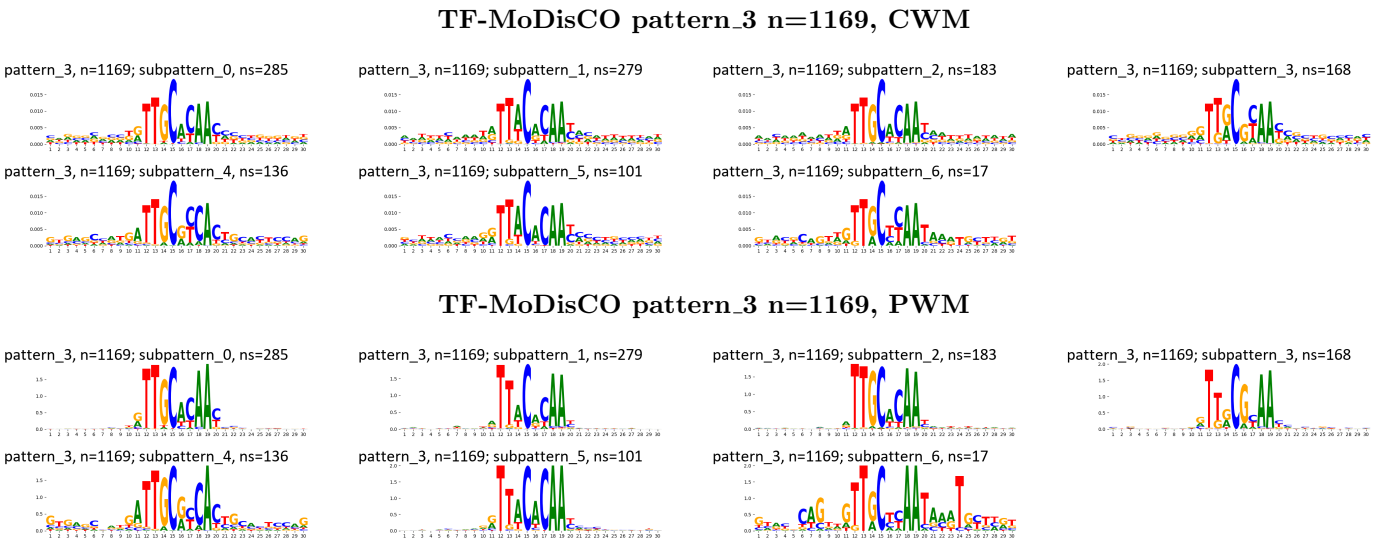

Supplementary Figure 649: TF-MoDisCO subpatterns for the ZKSCAN8 transcription factor in HepG2 (accession ENCSR808FFI).

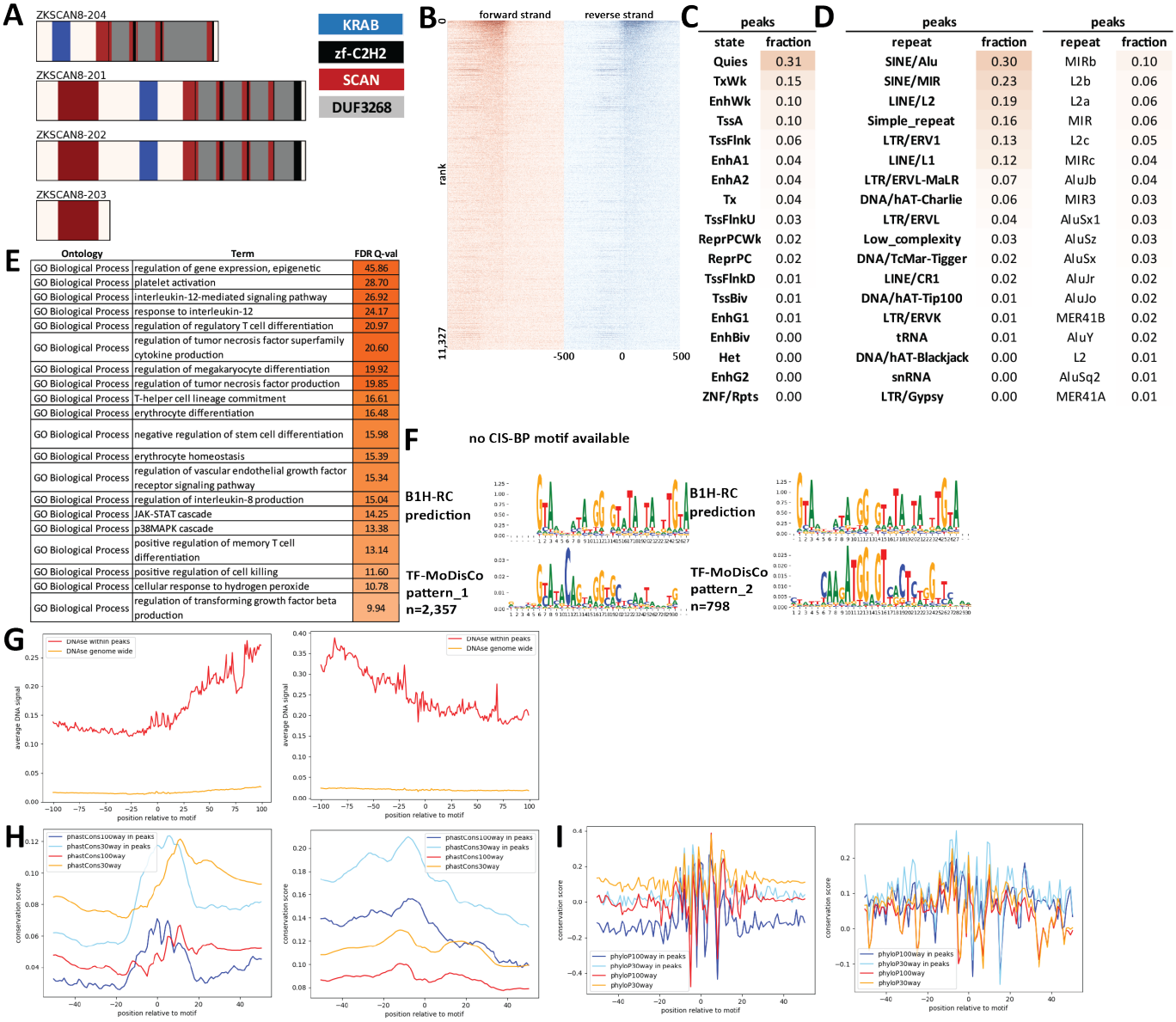

peaks	
state	fraction
Quies	0.31
TxWk	0.15
EnhWk	0.10
TssA	0.10
TssFlnk	0.06
EnhA1	0.04
EnhA2	0.04
Tx	0.04
TssFlnkU	0.03
ReprPCWk	0.02
ReprPC	0.02
TssFlnkD	0.01
TssBiv	0.01
EnhG1	0.01
EnhBiv	0.00
Het	0.00
EnhG2	0.00
ZNF/Rpts	0.00

peaks		peaks	
repeat	fraction	repeat	fraction
SINE/Alu	0.30	MIRb	0.10
SINE/MIR	0.23	L2b	0.06
LINE/L2	0.19	L2a	0.06
Simple_repeat	0.16	MIR	0.06
LTR/ERV1	0.13	L2c	0.05
LINE/L1	0.12	MIRc	0.04
LTR/ERVL-MaLR	0.07	AluJb	0.04
DNA/hAT-Charlie	0.06	MIR3	0.03
LTR/ERVL	0.04	AluSx1	0.03
Low_complexity	0.03	AluSz	0.03
DNA/TcMar-Tigger	0.02	AluSx	0.03
LINE/CR1	0.02	AluJr	0.02
DNA/hAT-Tip100	0.01	AluJo	0.02
LTR/ERVK	0.01	MER41B	0.02
tRNA	0.01	AluY	0.02
DNA/hAT-Blackjack	0.00	L2	0.01
snRNA	0.00	AluSq2	0.01
LTR/Gypsy	0.00	MER41A	0.01

Ontology	Term	FDR Q-val
GO Biological Process	regulation of gene expression, epigenetic	45.86
GO Biological Process	platelet activation	28.70
GO Biological Process	interleukin-12-mediated signaling pathway	26.92
GO Biological Process	response to interleukin-12	24.17
GO Biological Process	regulation of regulatory T cell differentiation	20.97
GO Biological Process	regulation of tumor necrosis factor superfamily cytokine production	20.60
GO Biological Process	regulation of megakaryocyte differentiation	19.92
GO Biological Process	regulation of tumor necrosis factor production	19.85
GO Biological Process	T-helper cell lineage commitment	16.61
GO Biological Process	erythrocyte differentiation	16.48
GO Biological Process	negative regulation of stem cell differentiation	15.98
GO Biological Process	erythrocyte homeostasis	15.39
GO Biological Process	regulation of vascular endothelial growth factor receptor signaling pathway	15.34
GO Biological Process	regulation of interleukin-8 production	15.04
GO Biological Process	JAK-STAT cascade	14.25
GO Biological Process	p38MAPK cascade	13.38
GO Biological Process	positive regulation of memory T cell differentiation	13.14
GO Biological Process	positive regulation of cell killing	11.60
GO Biological Process	cellular response to hydrogen peroxide	10.78
GO Biological Process	regulation of transforming growth factor beta production	9.94

Supplementary Figure 650: Properties and genomic distribution of motifs identified for the ZKSCAN8 transcription factor in K562 (accession ENCSR448UKK).

TF-MoDisCO pattern_1 n=2357, CWM

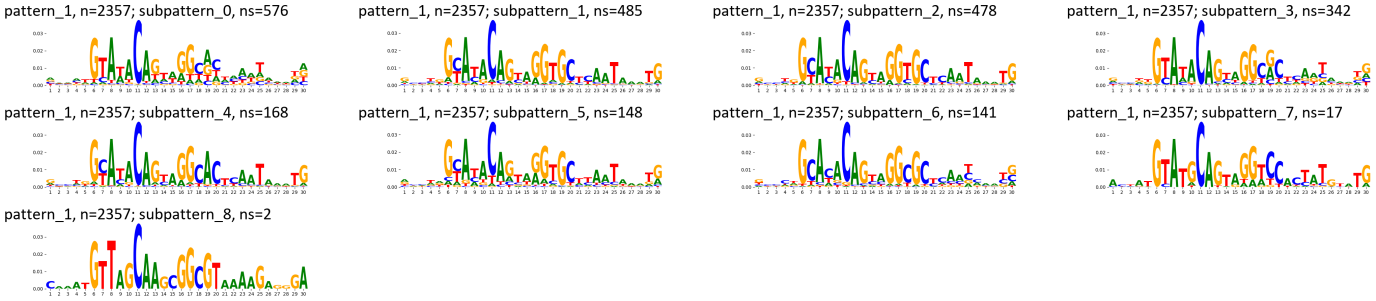

TF-MoDisCO pattern_1 n=2357, PWM

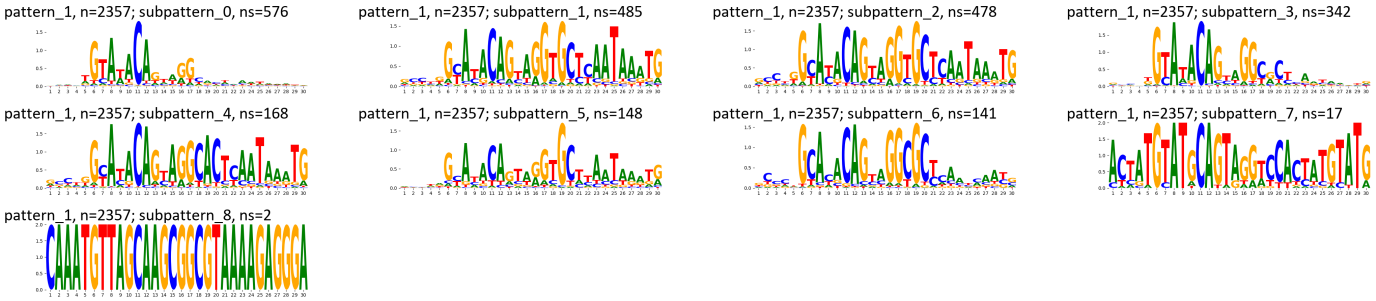

TF-MoDisCO pattern_2 n=798, CWM

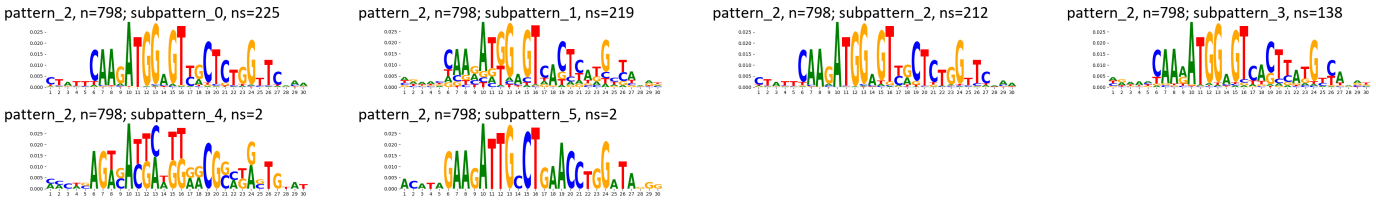

TF-MoDisCO pattern_2 n=798, PWM

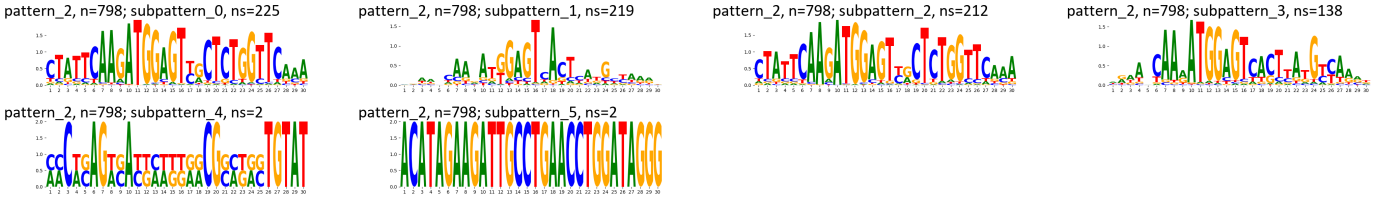

Supplementary Figure 651: TF-MoDisCO subpatterns for the ZKSCAN8 transcription factor in K562 (accession ENCSR448UKK).

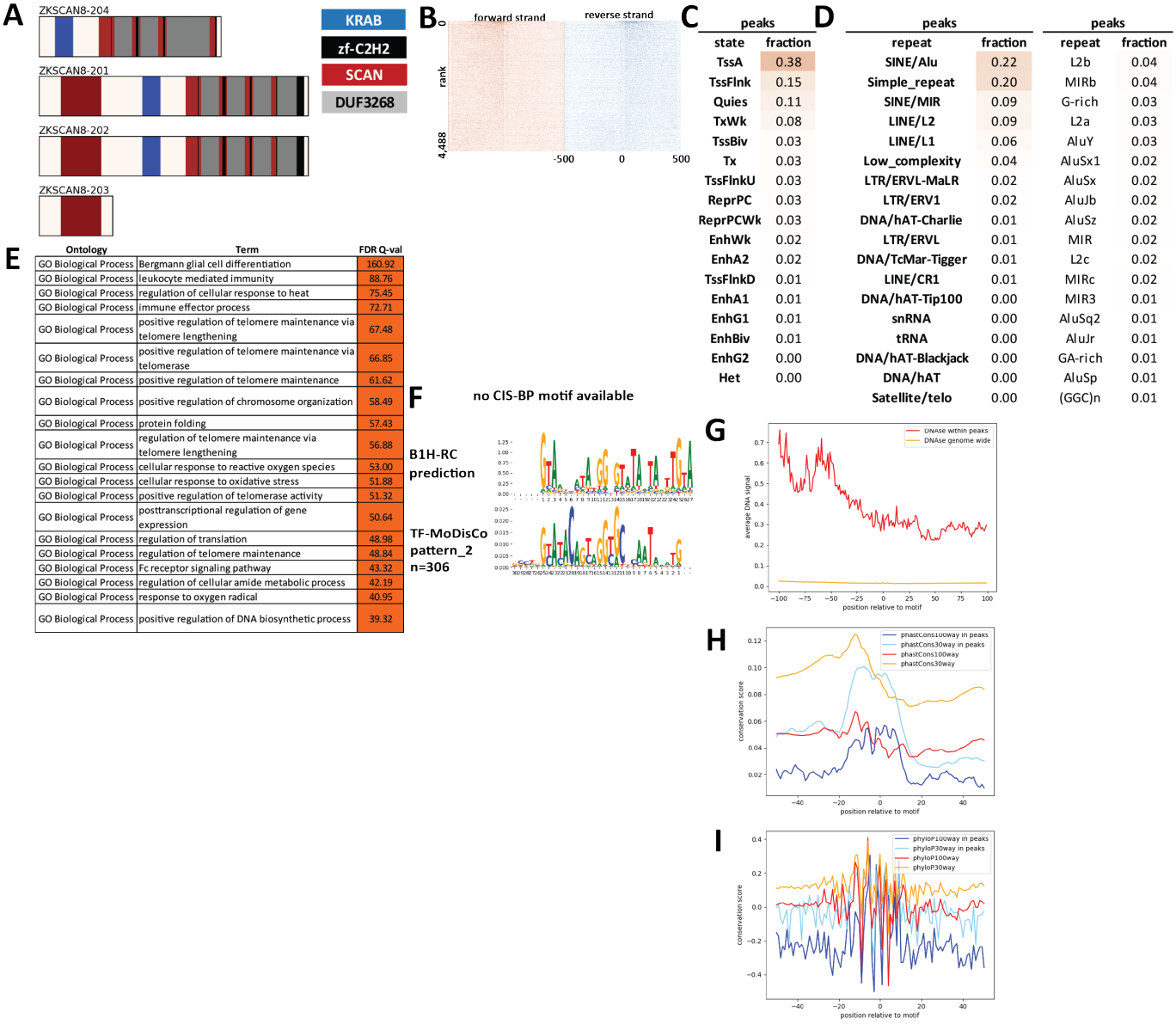

Supplementary Figure 652: Properties and genomic distribution of motifs identified for the ZKSCAN8 transcription factor in K562 (accession ENCSR755CRA).

TF-MoDisCO pattern_2 n=306, CWM

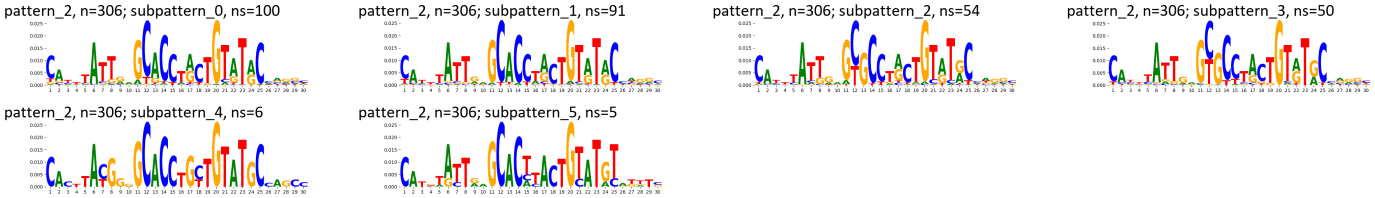

TF-MoDisCO pattern_2 n=306, PWM

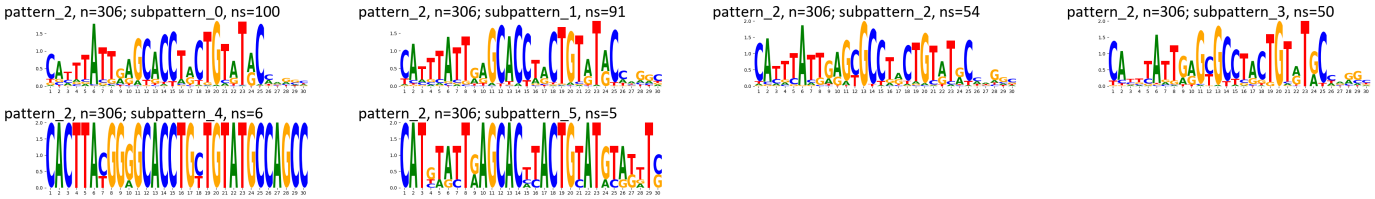

Supplementary Figure 653: TF-MoDisCO subpatterns for the ZKSCAN8 transcription factor in K562 (accession ENCSR755CRA).

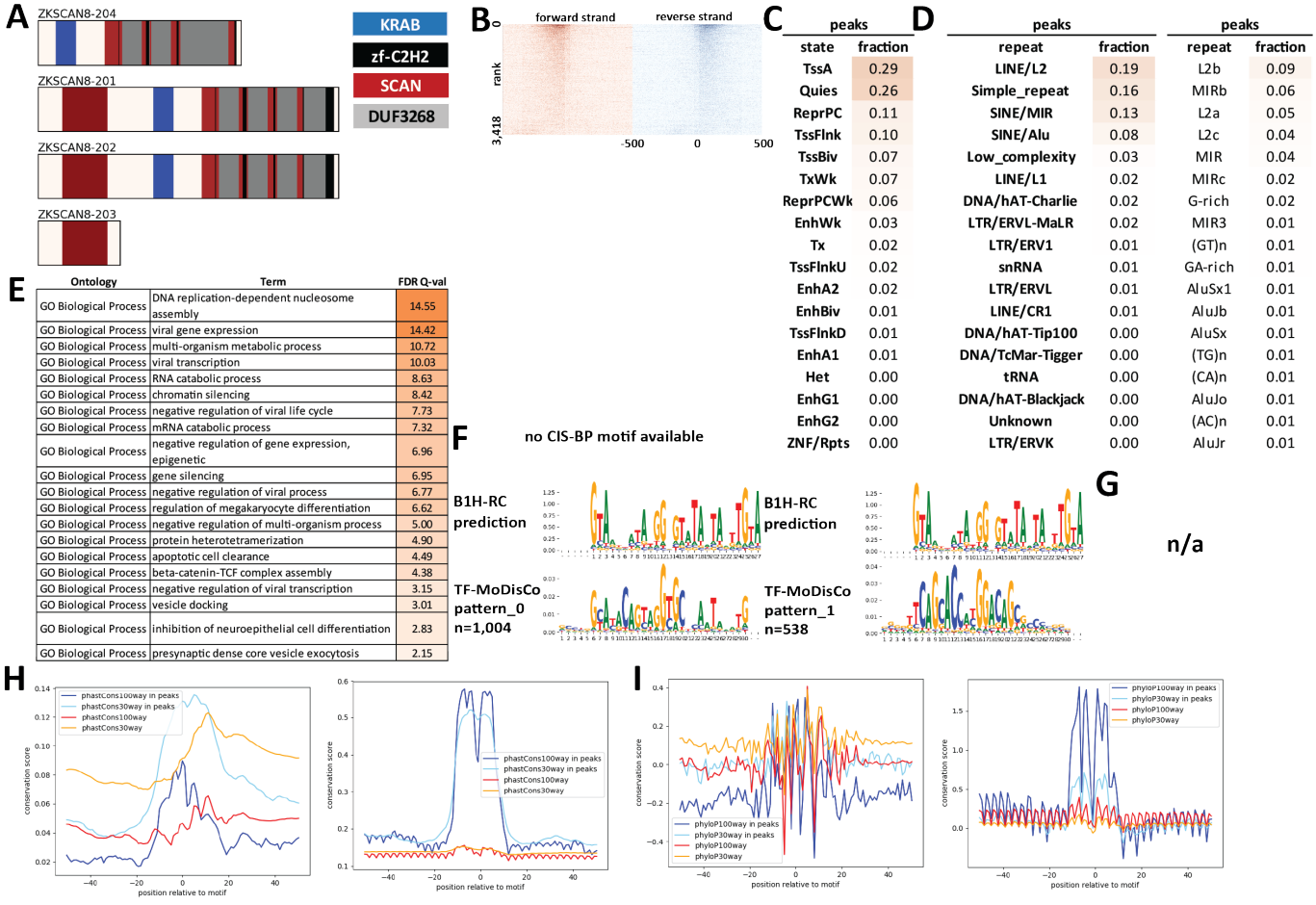

Supplementary Figure 654: Properties and genomic distribution of motifs identified for the ZKSCAN8 transcription factor in WTC11 (accession ENCSR115QIT).

TF-MoDisCO pattern_0 n=1004, CWM

pattern_0, n=1004; subpattern_0, ns=283

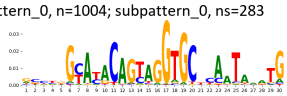

pattern_0, n=1004; subpattern_1, ns=218

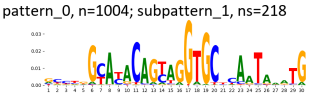

pattern_0, n=1004; subpattern_2, ns=201

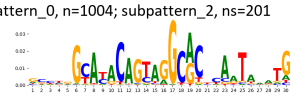

pattern_0, n=1004; subpattern_3, ns=139

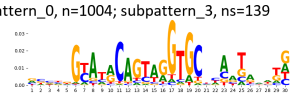

pattern_0, n=1004; subpattern_4, ns=102

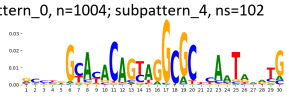

pattern_0, n=1004; subpattern_5, ns=61

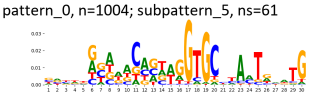

TF-MoDisCO pattern_0 n=1004, PWM

pattern_0, n=1004; subpattern_0, ns=283

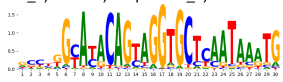

pattern_0, n=1004; subpattern_1, ns=218

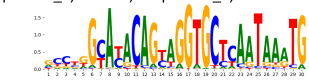

pattern_0, n=1004; subpattern_2, ns=201

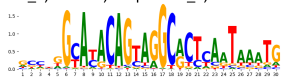

pattern_0, n=1004; subpattern_3, ns=139

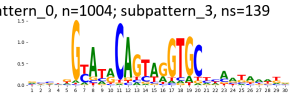

pattern_0, n=1004; subpattern_4, ns=102

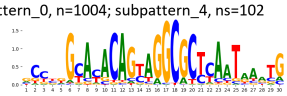

pattern_0, n=1004; subpattern_5, ns=61

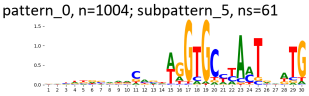

TF-MoDisCO pattern_1 n=538, CWM

pattern_1, n=538; subpattern_0, ns=202

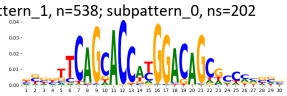

pattern_1, n=538; subpattern_1, ns=125

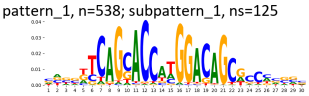

pattern_1, n=538; subpattern_2, ns=112

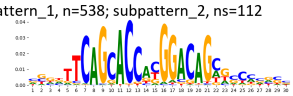

pattern_1, n=538; subpattern_3, ns=87

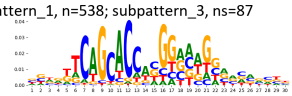

pattern_1, n=538; subpattern_4, ns=12

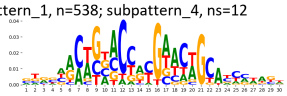

TF-MoDisCO pattern_1 n=538, PWM

pattern_1, n=538; subpattern_0, ns=202

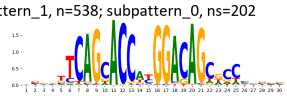

pattern_1, n=538; subpattern_1, ns=125

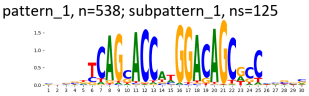

pattern_1, n=538; subpattern_2, ns=112

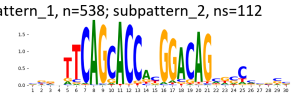

pattern_1, n=538; subpattern_3, ns=87

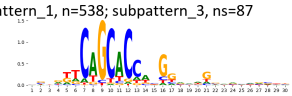

pattern_1, n=538; subpattern_4, ns=12

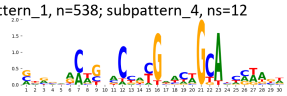

Supplementary Figure 655: TF-MoDisCO subpatterns for the ZKSCAN8 transcription factor in WTC11 (accession ENCSR115QIT).

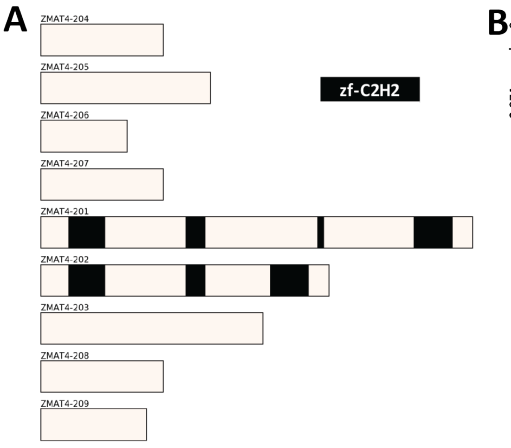

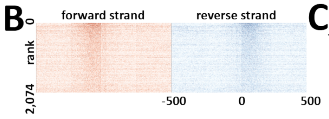

C

peaks	
state	fraction
TssA	0.30
Quies	0.21
TssFlnk	0.09
TxWk	0.08
Tx	0.05
EnhWk	0.04
ReprPC	0.03
ReprPCWk	0.02
EnhA2	0.02
EnhG1	0.02
TssBiv	0.01
TssFlnkU	0.01
EnhA1	0.01
EnhG2	0.01
Het	0.01
TssFlnkD	0.01
EnhBiv	0.01

D

peaks		peaks	
repeat	fraction	repeat	fraction
SINE/Alu	0.09	MIRb	0.02
LTR/ERV1	0.09	LTR7	0.02
Simple_repeat	0.08	MIR	0.02
SINE/MIR	0.05	L2a	0.01
LINE/L2	0.04	AluJb	0.01
LINE/L1	0.04	L2c	0.01
DNA/hAT-Charlie	0.02	L2b	0.01
LTR/ERVL-MaLR	0.02	AluSx1	0.01
Low_complexity	0.02	GA-rich	0.01
LTR/ERVL	0.02	AluY	0.01
snRNA	0.01	AluJr	0.01
LTR/ERVK	0.01	G-rich	0.01
DNA/TcMar-Tigger	0.01	AluSx	0.01
tRNA	0.01	MIRc	0.01
LTR/Gypsy	0.00	MER5A	0.01
LINE/CR1	0.00	AluSp	0.01
DNA/hAT-Tip100	0.00	AluJo	0.01
LINE/RTE-X	0.00	U1	0.01

E

Ontology	Term	FDR Q-val
GO Biological Process	nuclear-transcribed mRNA catabolic process, nonsense-mediated decay	26.68
GO Biological Process	translational initiation	25.38
GO Biological Process	protein targeting to ER	25.50
GO Biological Process	mRNA catabolic process	25.33
GO Biological Process	SRP-dependent cotranslational protein targeting to membrane	25.06
GO Biological Process	cotranslational protein targeting to membrane	24.52
GO Biological Process	protein localization to endoplasmic reticulum	24.41
GO Biological Process	nuclear-transcribed mRNA catabolic process	24.46
GO Biological Process	RNA catabolic process	23.56
GO Biological Process	establishment of protein localization to endoplasmic reticulum	22.99
GO Biological Process	translation	22.95
GO Biological Process	viral transcription	21.79
GO Biological Process	viral gene expression	21.59
GO Biological Process	mRNA metabolic process	21.25
GO Biological Process	peptide biosynthetic process	19.76
GO Biological Process	protein targeting to membrane	19.24
GO Biological Process	multi-organism metabolic process	18.26
GO Biological Process	nucleobase-containing compound catabolic process	17.59
GO Biological Process	posttranscriptional regulation of gene expression	17.49
GO Biological Process	ncRNA metabolic process	17.04
Human Phenotype	Somatic mosaicism	6.76
Human Phenotype	Cloverleaf skull	4.25

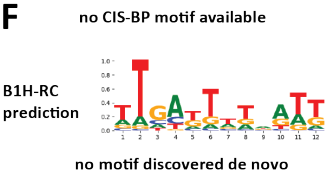

Supplementary Figure 656: Properties and genomic distribution of motifs identified for the ZMAT4 transcription factor in WTC11 (accession ENCSR807VQT).

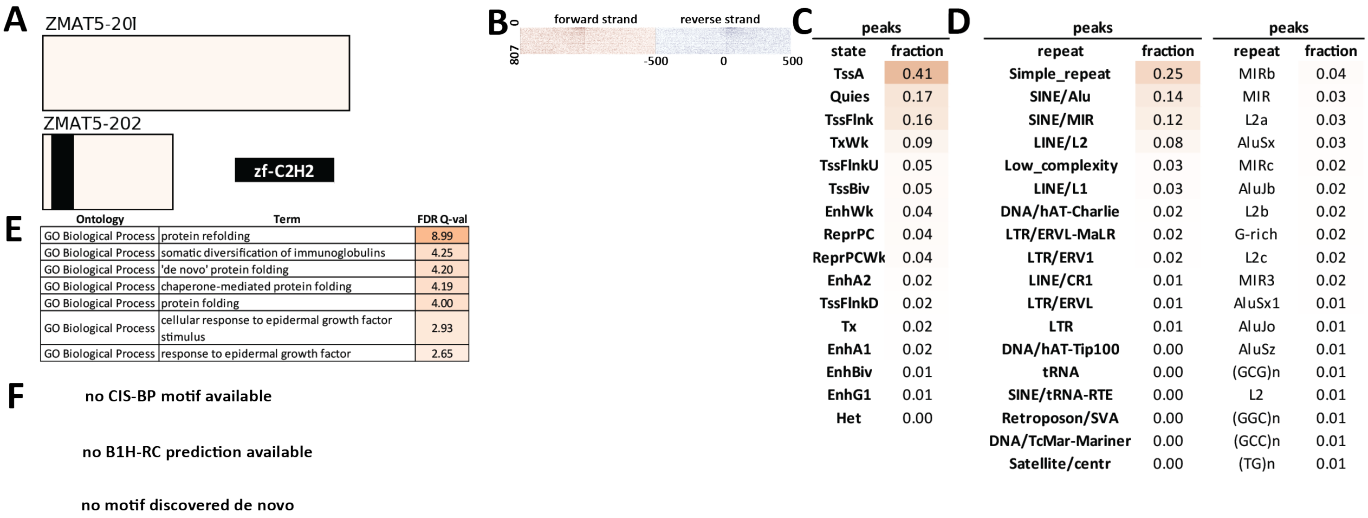

peaks	
state	fraction
TssA	0.41
Quies	0.17
TssFlnk	0.16
TxWk	0.09
TssFlnkU	0.05
TssBiv	0.05
EnhWk	0.04
ReprPC	0.04
ReprPCWk	0.04
EnhA2	0.02
TssFlnkD	0.02
Tx	0.02
EnhA1	0.02
EnhBiv	0.01
EnhG1	0.01
Het	0.00

peaks		peaks	
repeat	fraction	repeat	fraction
Simple_repeat	0.25	MIRb	0.04
SINE/Alu	0.14	MIR	0.03
SINE/MIR	0.12	L2a	0.03
LINE/L2	0.08	AluSx	0.03
Low_complexity	0.03	MIRc	0.02
LINE/L1	0.03	AluJb	0.02
DNA/hAT-Charlie	0.02	L2b	0.02
LTR/ERVL-MaLR	0.02	G-rich	0.02
LTR/ERV1	0.02	L2c	0.02
LINE/CR1	0.01	MIR3	0.02
LTR/ERVL	0.01	AluSx1	0.01
LTR	0.01	AluJo	0.01
DNA/hAT-Tip100	0.00	AluSz	0.01
tRNA	0.00	(GCG)n	0.01
SINE/tRNA-RTE	0.00	L2	0.01
Retroposon/SVA	0.00	(GGC)n	0.01
DNA/TcMar-Mariner	0.00	(GCC)n	0.01
Satellite/centr	0.00	(TG)n	0.01

Ontology	Term	FDR Q-val
GO Biological Process	protein refolding	8.99
GO Biological Process	somatic diversification of immunoglobulins	4.25
GO Biological Process	'de novo' protein folding	4.20
GO Biological Process	chaperone-mediated protein folding	4.19
GO Biological Process	protein folding	4.00
GO Biological Process	cellular response to epidermal growth factor stimulus	2.93
GO Biological Process	response to epidermal growth factor	2.65

Supplementary Figure 657: Properties and genomic distribution of motifs identified for the ZMAT5 transcription factor in HepG2 (accession ENCSR215XSZ).

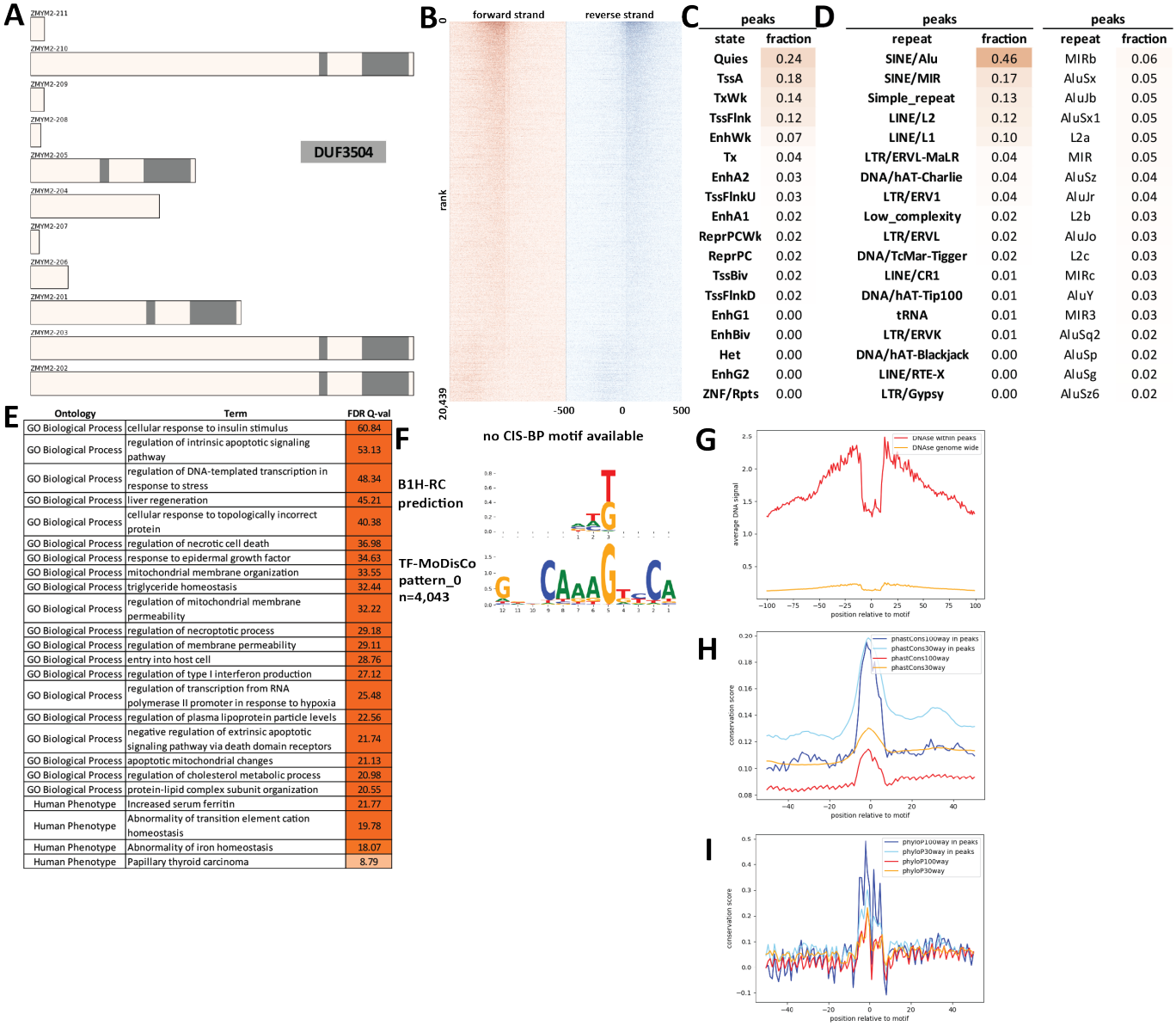

peaks	
state	fraction
Quies	0.24
TssA	0.18
TxWk	0.14
TssFlnk	0.12
EnhWk	0.07
Tx	0.04
EnhA2	0.03
TssFlnkU	0.03
EnhA1	0.02
ReprPCWk	0.02
ReprPC	0.02
TssBiv	0.02
TssFlnkD	0.02
EnhG1	0.00
EnhBiv	0.00
Het	0.00
EnhG2	0.00
ZNF/Rpts	0.00

peaks		peaks	
repeat	fraction	repeat	fraction
SINE/Alu	0.46	MIRb	0.06
SINE/MIR	0.17	AluSx	0.05
Simple_repeat	0.13	AluJb	0.05
LINE/L2	0.12	AluSx1	0.05
LINE/L1	0.10	L2a	0.05
LTR/ERVL-MaLR	0.04	MIR	0.05
DNA/hAT-Charlie	0.04	AluSz	0.04
LTR/ERV1	0.04	AluJr	0.04
Low_complexity	0.02	L2b	0.03
LTR/ERVL	0.02	AluJo	0.03
DNA/TcMar-Tigger	0.02	L2c	0.03
LINE/CR1	0.01	MIRc	0.03
DNA/hAT-Tip100	0.01	AluY	0.03
tRNA	0.01	MIR3	0.03
LTR/ERVK	0.01	AluSq2	0.02
DNA/hAT-Blackjack	0.00	AluSp	0.02
LINE/RTE-X	0.00	AluSg	0.02
LTR/Gypsy	0.00	AluSz6	0.02

Ontology	Term	FDR Q-val
GO Biological Process	cellular response to insulin stimulus	60.84
GO Biological Process	regulation of intrinsic apoptotic signaling pathway	53.13
GO Biological Process	regulation of DNA-templated transcription in response to stress	48.34
GO Biological Process	liver regeneration	45.21
GO Biological Process	cellular response to topologically incorrect protein	40.38
GO Biological Process	regulation of necrotic cell death	36.98
GO Biological Process	response to epidermal growth factor	34.63
GO Biological Process	mitochondrial membrane organization	33.55
GO Biological Process	triglyceride homeostasis	32.44
GO Biological Process	regulation of mitochondrial membrane permeability	32.22
GO Biological Process	regulation of necroptotic process	29.18
GO Biological Process	regulation of membrane permeability	29.11
GO Biological Process	entry into host cell	28.76
GO Biological Process	regulation of type I interferon production	27.12
GO Biological Process	regulation of transcription from RNA polymerase II promoter in response to hypoxia	25.48
GO Biological Process	regulation of plasma lipoprotein particle levels	22.56
GO Biological Process	negative regulation of extrinsic apoptotic signaling pathway via death domain receptors	21.74
GO Biological Process	apoptotic mitochondrial changes	21.13
GO Biological Process	regulation of cholesterol metabolic process	20.98
GO Biological Process	protein-lipid complex subunit organization	20.55
Human Phenotype	Increased serum ferritin	21.77
Human Phenotype	Abnormality of transition element cation homeostasis	19.78
Human Phenotype	Abnormality of iron homeostasis	18.07
Human Phenotype	Papillary thyroid carcinoma	8.79

Supplementary Figure 658: Properties and genomic distribution of motifs identified for the ZMYM2 transcription factor in HepG2 (accession ENCSR066EWR).

TF-MoDisCO pattern_0 n=4043, CWM

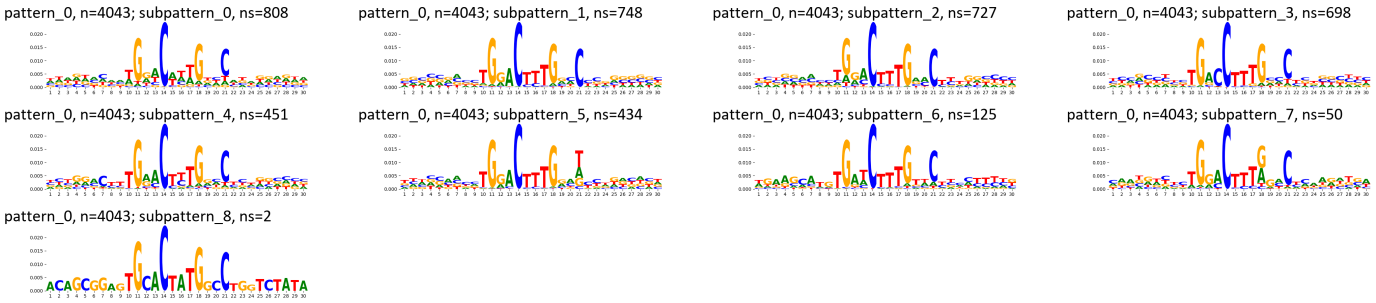

TF-MoDisCO pattern_0 n=4043, PWM

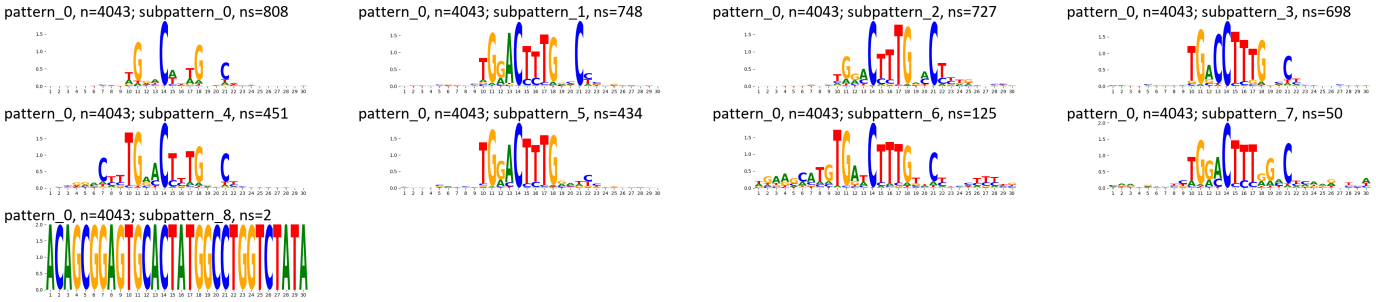

Supplementary Figure 659: TF-MoDisCO subpatterns for the ZMYM2 transcription factor in HepG2 (accession ENCSR066EWR).

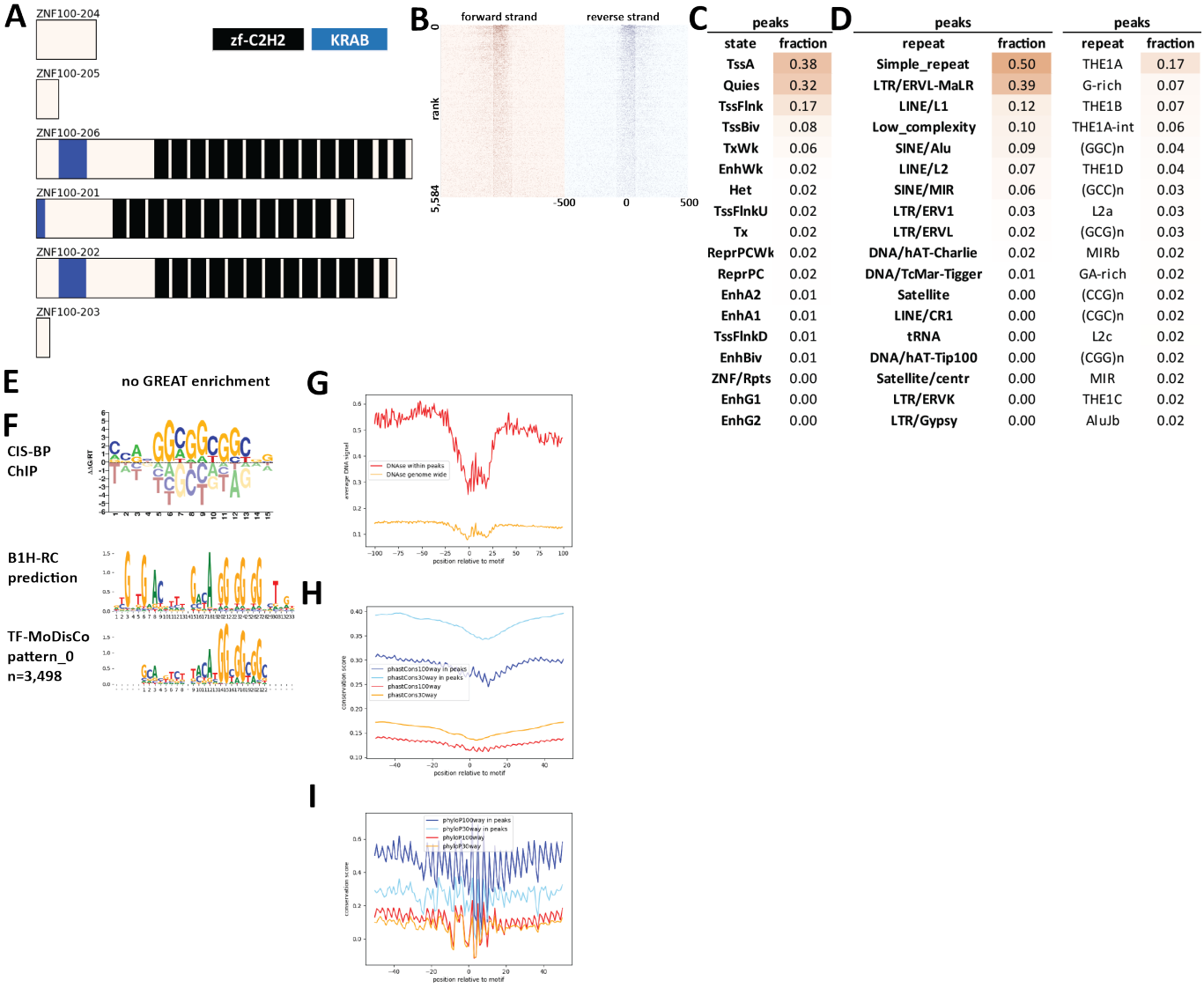

Supplementary Figure 660: Properties and genomic distribution of motifs identified for the ZNF100 transcription factor in HEK293 (accession ChipExo models).

TF-MoDisCO pattern_0 n=3498, CWM

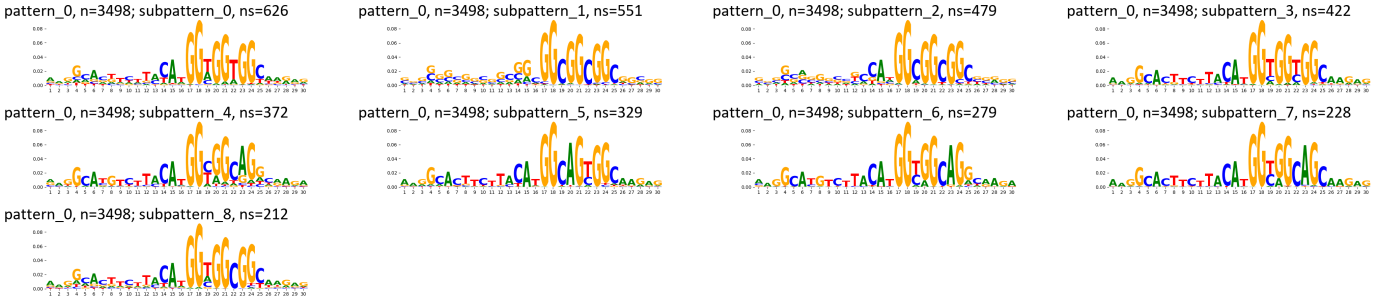

TF-MoDisCO pattern_0 n=3498, PWM

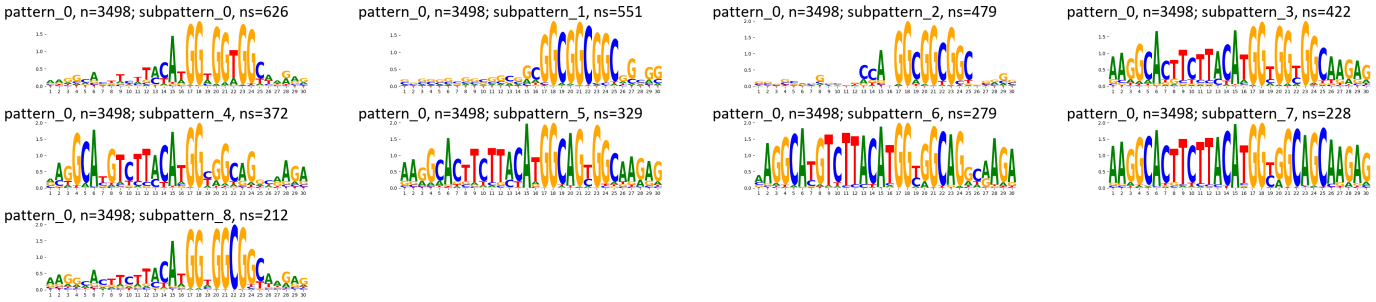

Supplementary Figure 661: TF-MoDisCO subpatterns for the ZNF100 transcription factor in HEK293 (accession ChipExo models).

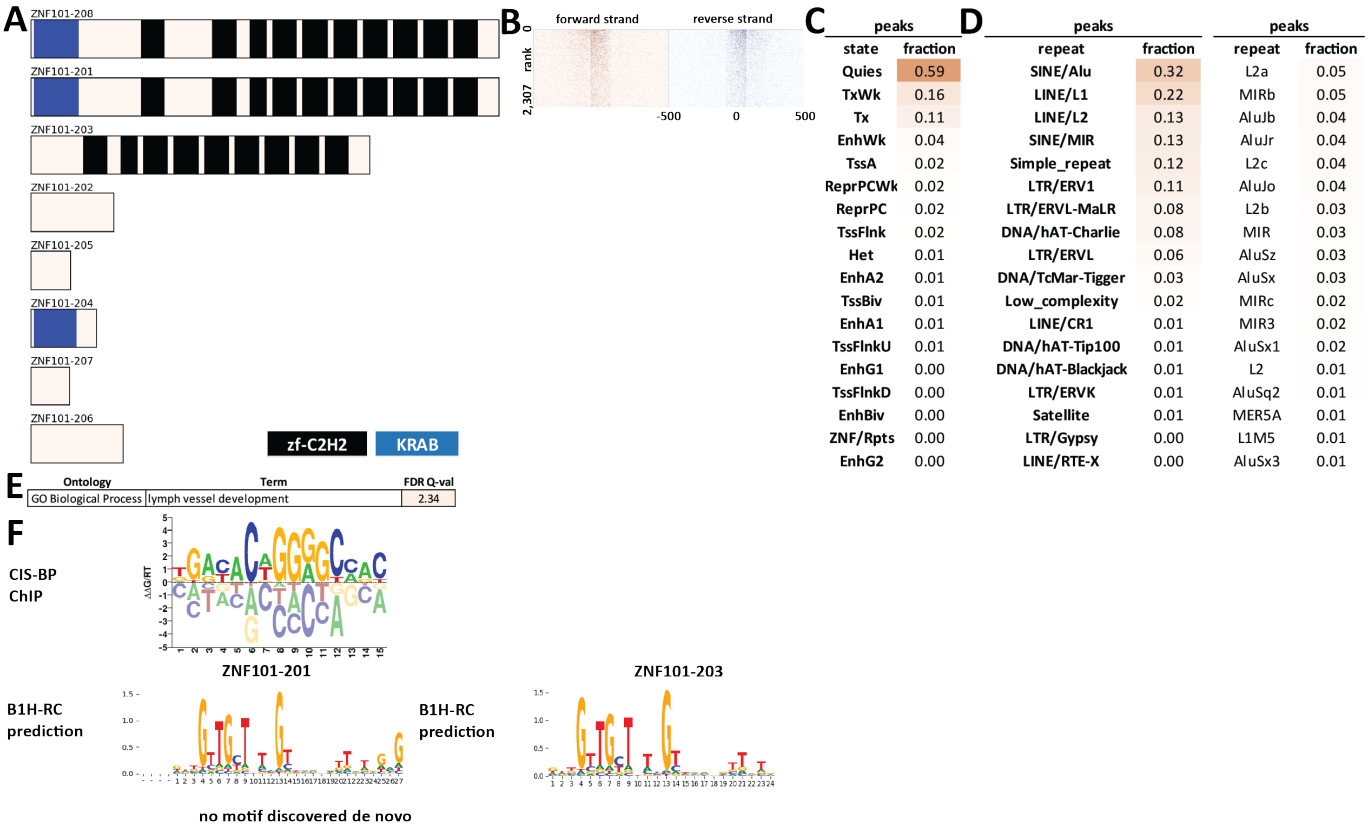

Supplementary Figure 662: Properties and genomic distribution of motifs identified for the ZNF101 transcription factor in HEK293 (accession ChipExo models).

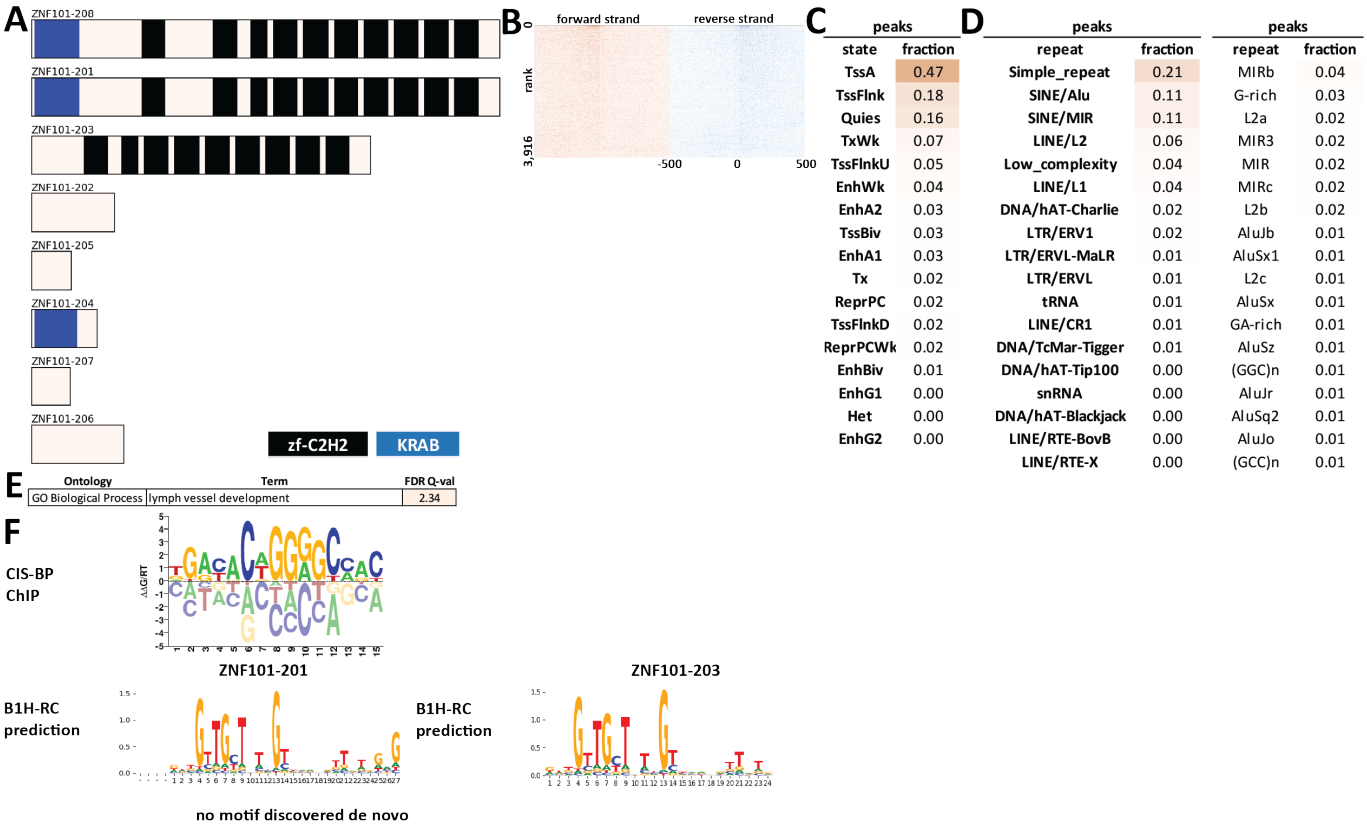

Supplementary Figure 663: Properties and genomic distribution of motifs identified for the ZNF101 transcription factor in HepG2 (accession ENCSR519QYU).

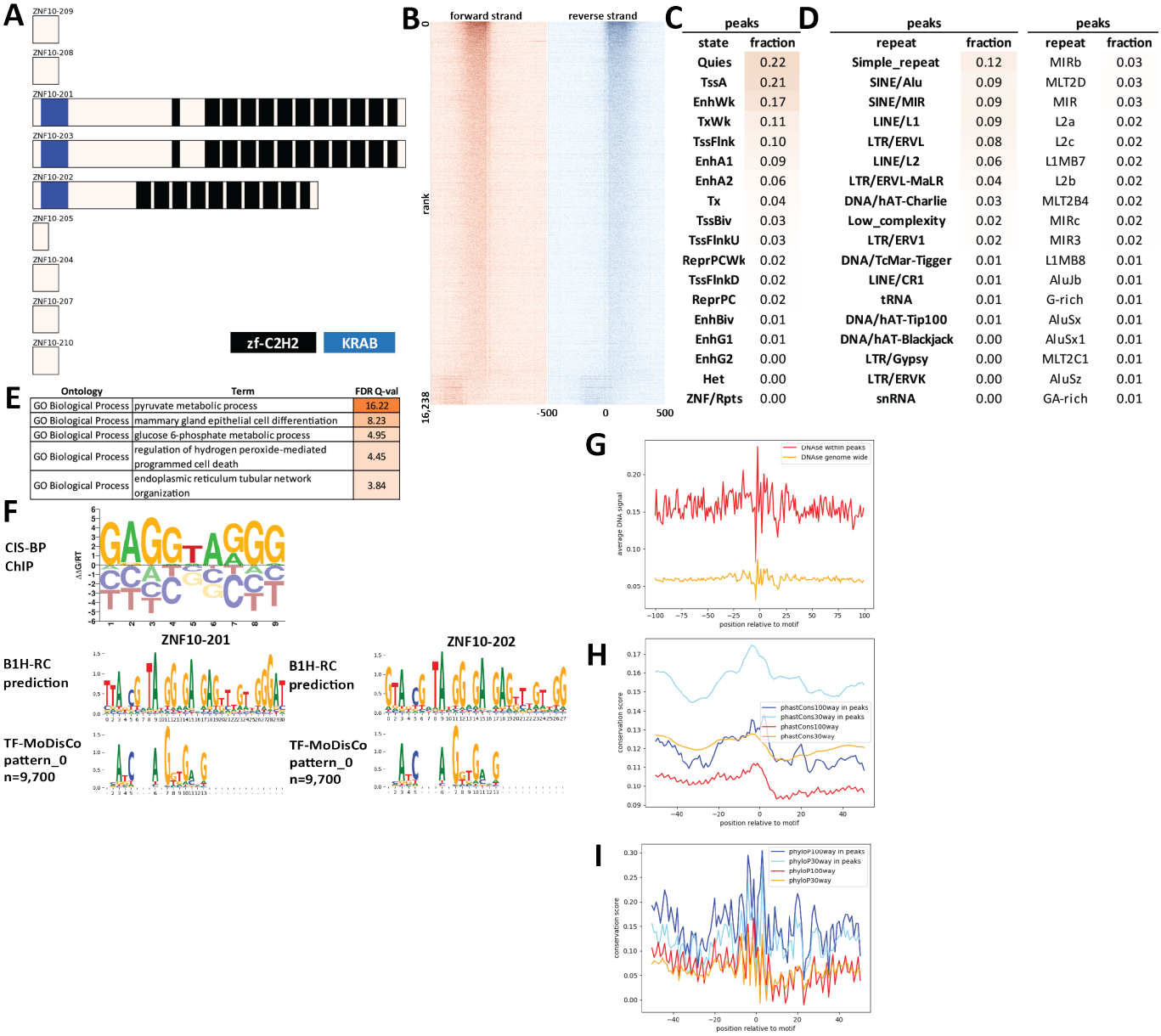

C

peaks	
state	fraction
Quies	0.22
TssA	0.21
EnhWk	0.17
TxWk	0.11
TssFlnk	0.10
EnhA1	0.09
EnhA2	0.06
Tx	0.04
TssBiv	0.03
TssFlnkU	0.03
ReprPCWk	0.02
TssFlnkD	0.02
ReprPC	0.02
EnhBiv	0.01
EnhG1	0.01
EnhG2	0.00
Het	0.00
ZNF/Rpts	0.00

D

peaks		peaks	
repeat	fraction	repeat	fraction
Simple_repeat	0.12	MIRb	0.03
SINE/Alu	0.09	MLT2D	0.03
SINE/MIR	0.09	MIR	0.03
LINE/L1	0.09	L2a	0.02
LTR/ERVL	0.08	L2c	0.02
LINE/L2	0.06	L1MB7	0.02
LTR/ERVL-MaLR	0.04	L2b	0.02
DNA/hAT-Charlie	0.03	MLT2B4	0.02
Low_complexity	0.02	MIRc	0.02
LTR/ERV1	0.02	MIR3	0.02
DNA/TcMar-Tigger	0.01	L1MB8	0.01
LINE/CR1	0.01	AluJb	0.01
tRNA	0.01	G-rich	0.01
DNA/hAT-Tip100	0.01	AluSx	0.01
DNA/hAT-Blackjack	0.00	AluSx1	0.01
LTR/Gypsy	0.00	MLT2C1	0.01
LTR/ERVK	0.00	AluSz	0.01
snRNA	0.00	GA-rich	0.01

E

Ontology	Term	FDR Q-val
GO Biological Process	pyruvate metabolic process	16.22
GO Biological Process	mammary gland epithelial cell differentiation	8.23
GO Biological Process	glucose 6-phosphate metabolic process	4.95
GO Biological Process	regulation of hydrogen peroxide-mediated programmed cell death	4.45
GO Biological Process	endoplasmic reticulum tubular network organization	3.84

Supplementary Figure 664: Properties and genomic distribution of motifs identified for the ZNF10 transcription factor in HEK293 (accession ENCSR019WUS).

TF-MoDisCO pattern_0 n=9700, CWM

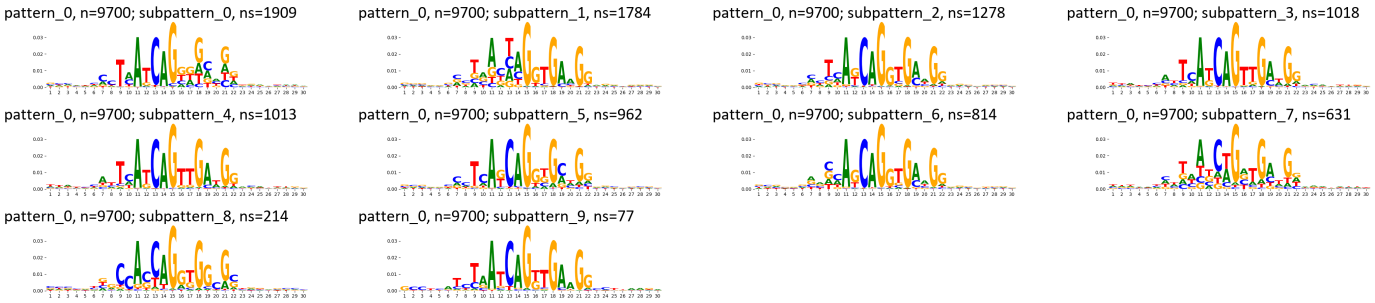

TF-MoDisCO pattern_0 n=9700, PWM

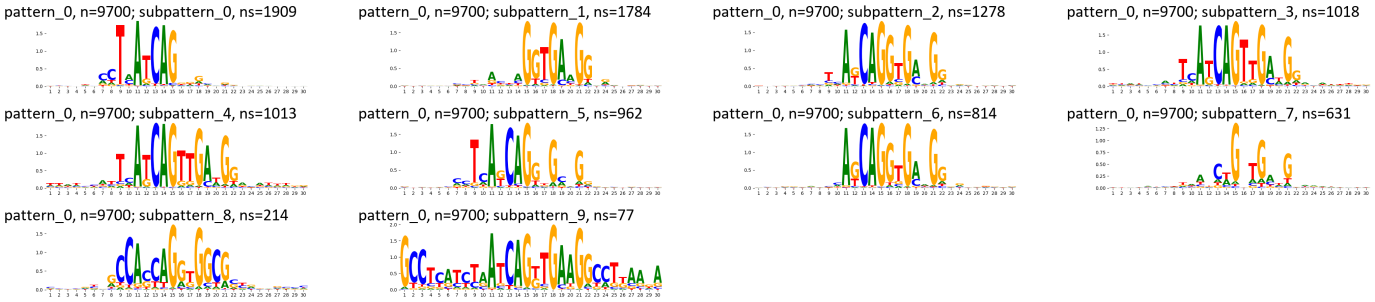

Supplementary Figure 665: TF-MoDisCO subpatterns for the ZNF10 transcription factor in HEK293 (accession ENCSR019WUS).

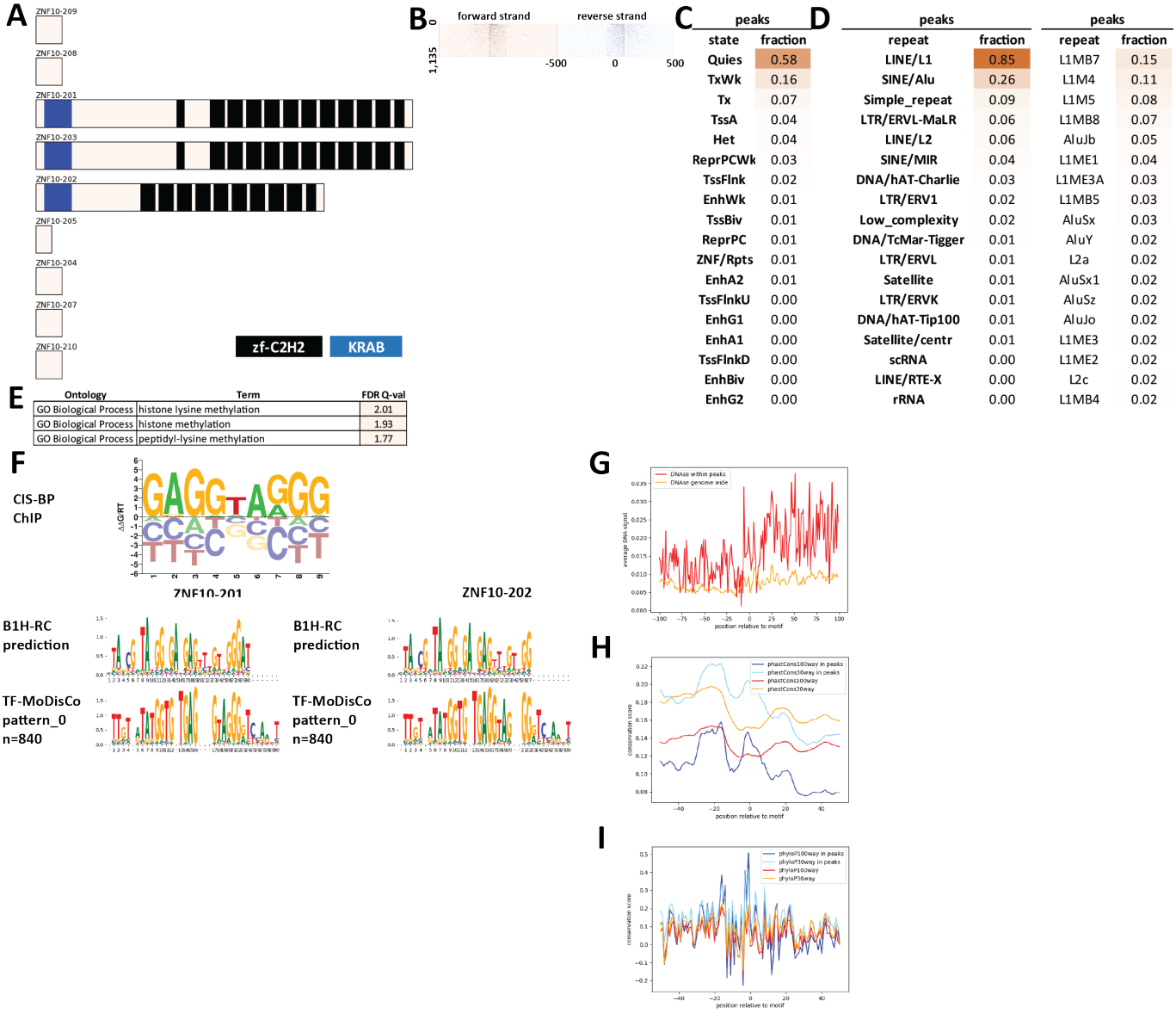

Supplementary Figure 666: Properties and genomic distribution of motifs identified for the ZNF10 transcription factor in HEK293 (accession ChipExo models).

TF-MoDisCO pattern_0 n=840, CWM

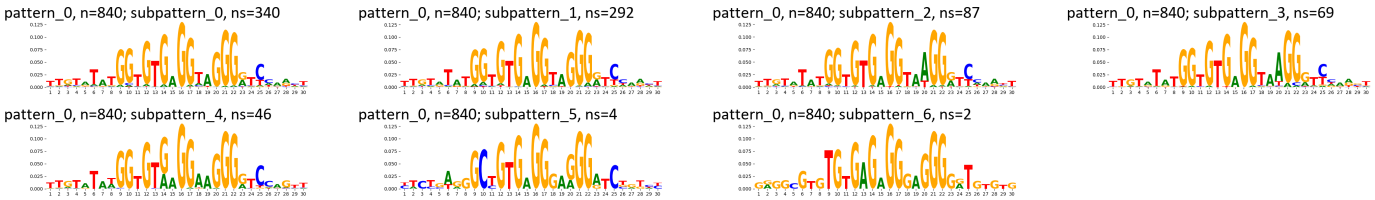

TF-MoDisCO pattern_0 n=840, PWM

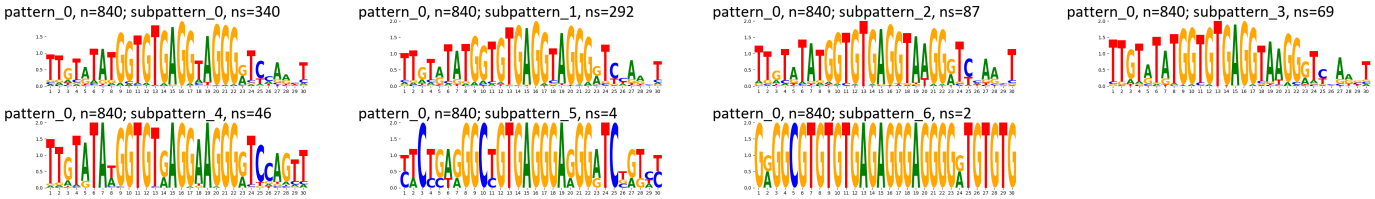

Supplementary Figure 667: TF-MoDisCO subpatterns for the ZNF10 transcription factor in HEK293 (accession ChipExo models).

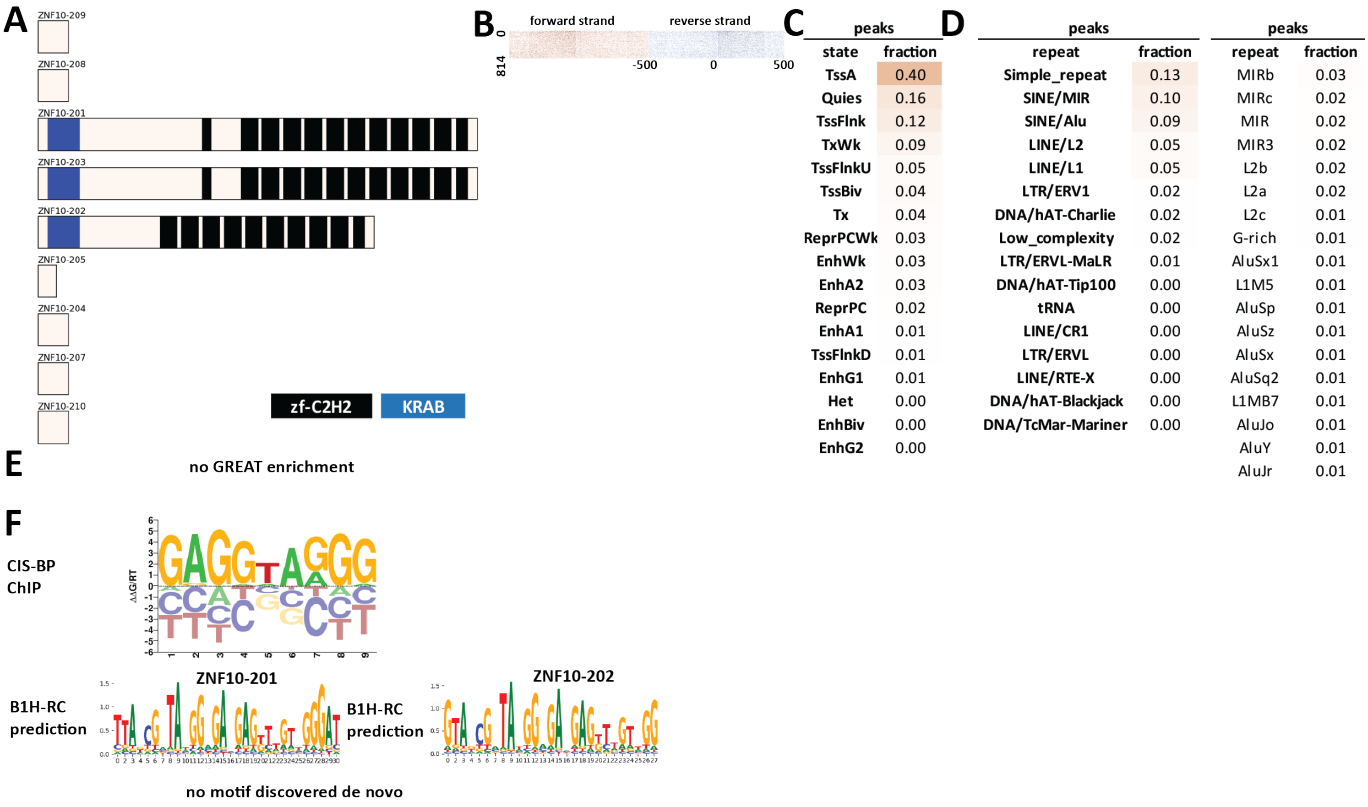

peaks	
state	fraction
TssA	0.40
Quies	0.16
TssFlnk	0.12
TxWk	0.09
TssFlnkU	0.05
TssBiv	0.04
Tx	0.04
ReprPCWk	0.03
EnhWk	0.03
EnhA2	0.03
ReprPC	0.02
EnhA1	0.01
TssFlnkD	0.01
EnhG1	0.01
Het	0.00
EnhBiv	0.00
EnhG2	0.00

peaks	
repeat	fraction
Simple_repeat	0.13
SINE/MIR	0.10
SINE/Alu	0.09
LINE/L2	0.05
LINE/L1	0.05
LTR/ERV1	0.02
DNA/hAT-Charlie	0.02
Low_complexity	0.02
LTR/ERVL-MaLR	0.01
DNA/hAT-Tip100	0.00
tRNA	0.00
LINE/CR1	0.00
LTR/ERVL	0.00
LINE/RTE-X	0.00
DNA/hAT-Blackjack	0.00
DNA/TcMar-Mariner	0.00

peaks	
repeat	fraction
MIRb	0.03
MIRc	0.02
MIR	0.02
MIR3	0.02
L2b	0.02
L2a	0.02
L2c	0.01
G-rich	0.01
AluSx1	0.01
L1M5	0.01
AluSp	0.01
AluSz	0.01
AluSx	0.01
AluSq2	0.01
L1MB7	0.01
AluJo	0.01
AluY	0.01
AluJr	0.01

Supplementary Figure 668: Properties and genomic distribution of motifs identified for the ZNF10 transcription factor in HepG2 (accession ENCSR009LIA).

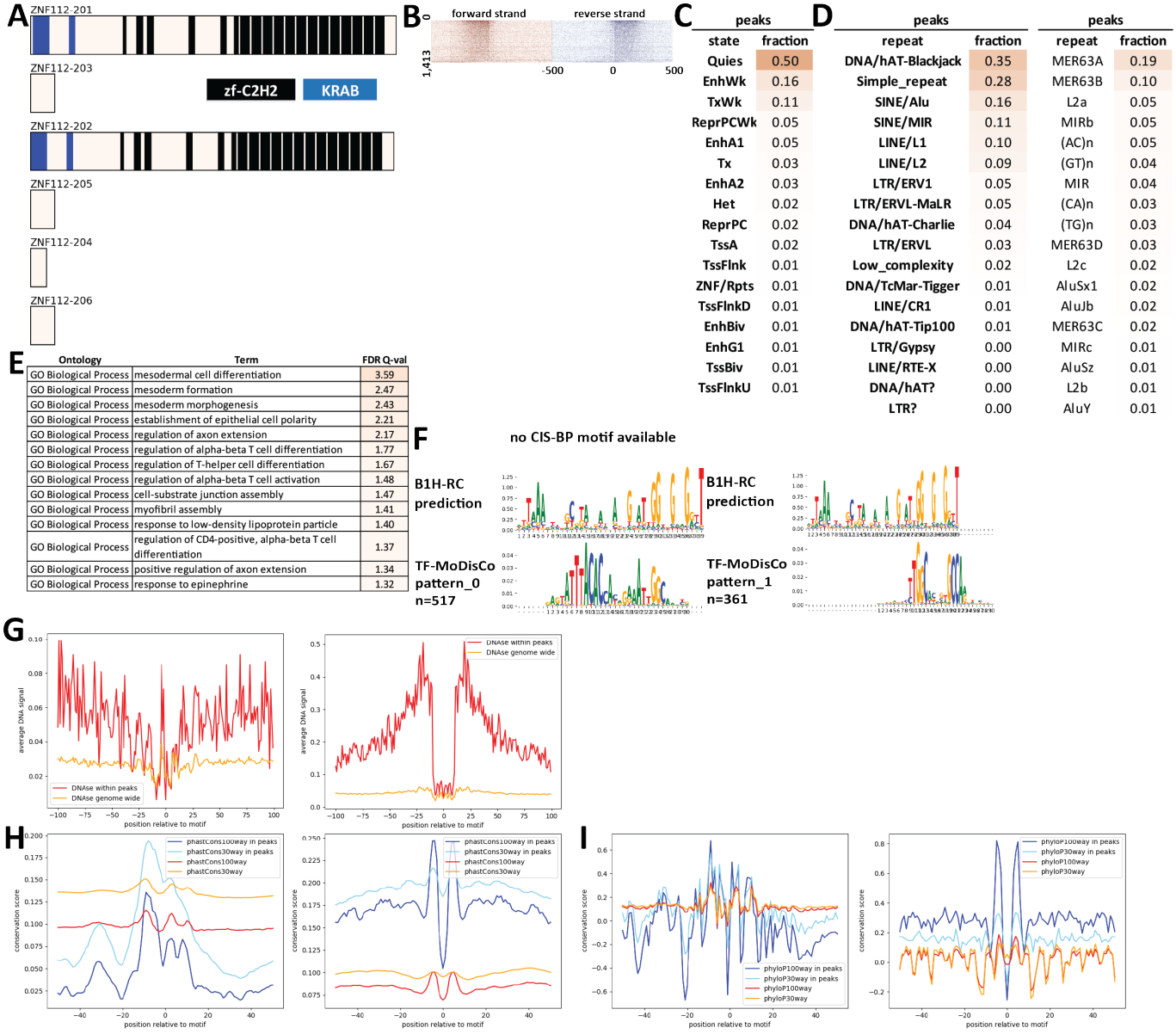

C

peaks	
state	fraction
Quies	0.50
EnhWk	0.16
TxWk	0.11
ReprPCWk	0.05
EnhA1	0.05
Tx	0.03
EnhA2	0.03
Het	0.02
ReprPC	0.02
TssA	0.02
TssFlnk	0.01
ZNF/Rpts	0.01
TssFlnkD	0.01
EnhBiv	0.01
EnhG1	0.01
TssBiv	0.01
TssFlnkU	0.01

D

peaks		peaks	
repeat	fraction	repeat	fraction
DNA/hAT-Blackjack	0.35	MER63A	0.19
Simple_repeat	0.28	MER63B	0.10
SINE/Alu	0.16	L2a	0.05
SINE/MIR	0.11	MIRb	0.05
LINE/L1	0.10	(AC)n	0.05
LINE/L2	0.09	(GT)n	0.04
LTR/ERV1	0.05	MIR	0.04
LTR/ERVL-MaLR	0.05	(CA)n	0.03
DNA/hAT-Charlie	0.04	(TG)n	0.03
LTR/ERVL	0.03	MER63D	0.03
Low_complexity	0.02	L2c	0.02
DNA/TcMar-Tigger	0.01	AluSx1	0.02
LINE/CR1	0.01	AluJb	0.02
DNA/hAT-Tip100	0.01	MER63C	0.02
LTR/Gypsy	0.00	MIRc	0.01
LINE/RTE-X	0.00	AluSz	0.01
DNA/hAT?	0.00	L2b	0.01
LTR?	0.00	AluY	0.01

E

Ontology	Term	FDR Q-val
GO Biological Process	mesodermal cell differentiation	3.59
GO Biological Process	mesoderm formation	2.47
GO Biological Process	mesoderm morphogenesis	2.43
GO Biological Process	establishment of epithelial cell polarity	2.21
GO Biological Process	regulation of axon extension	2.17
GO Biological Process	regulation of alpha-beta T cell differentiation	1.77
GO Biological Process	regulation of T-helper cell differentiation	1.67
GO Biological Process	regulation of alpha-beta T cell activation	1.48
GO Biological Process	cell-substrate junction assembly	1.47
GO Biological Process	myofibril assembly	1.41
GO Biological Process	response to low-density lipoprotein particle	1.40
GO Biological Process	regulation of CD4-positive, alpha-beta T cell differentiation	1.37
GO Biological Process	positive regulation of axon extension	1.34
GO Biological Process	response to epinephrine	1.32

Supplementary Figure 669: Properties and genomic distribution of motifs identified for the ZNF112 transcription factor in HEK293 (accession ENCSR751PNN).

TF-MoDisCO pattern_0 n=517, CWM

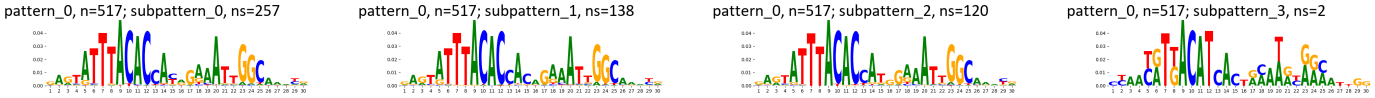

TF-MoDisCO pattern_0 n=517, PWM

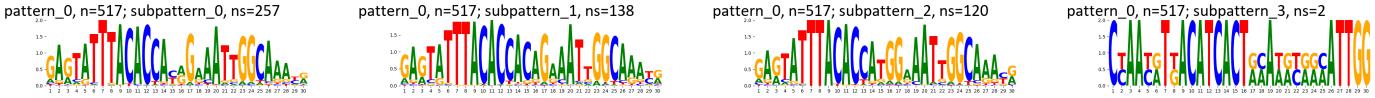

TF-MoDisCO pattern_1 n=361, CWM

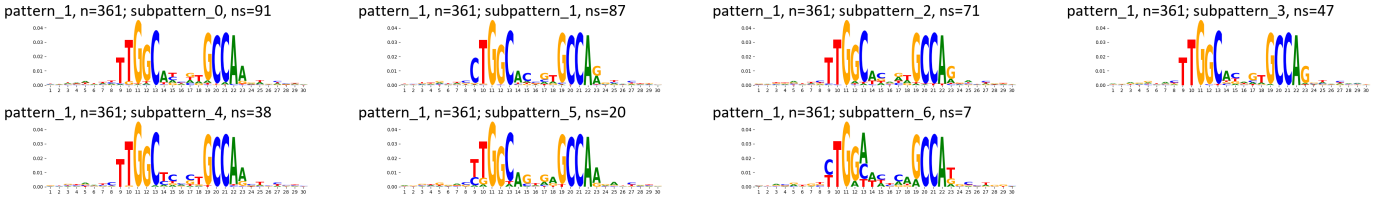

TF-MoDisCO pattern_1 n=361, PWM

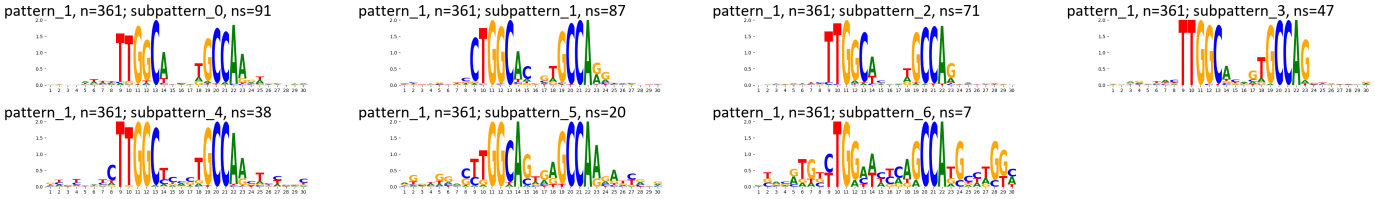

Supplementary Figure 670: TF-MoDisCO subpatterns for the ZNF112 transcription factor in HEK293 (accession ENCSR751PNN).

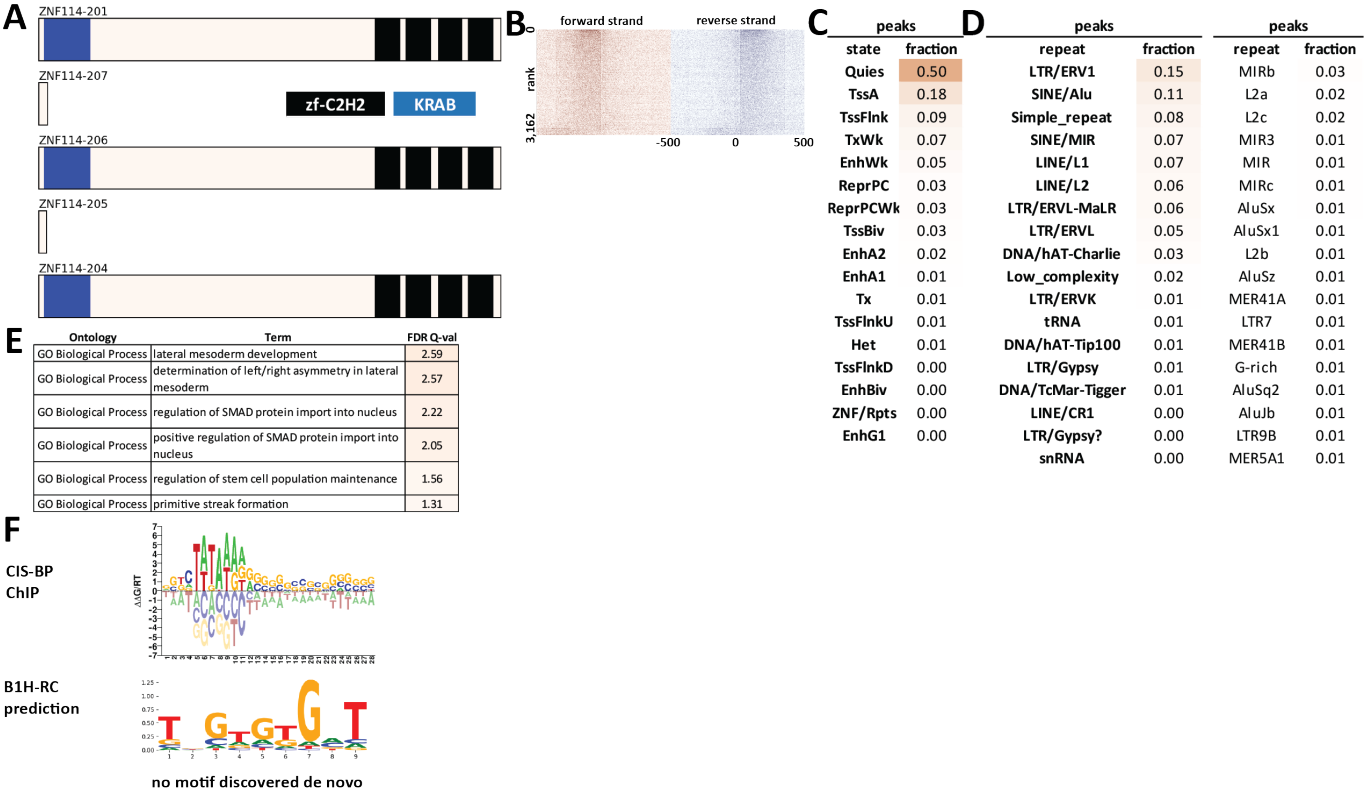

Supplementary Figure 671: Properties and genomic distribution of motifs identified for the ZNF114 transcription factor in GM23338 (accession ENCSR555KFE).

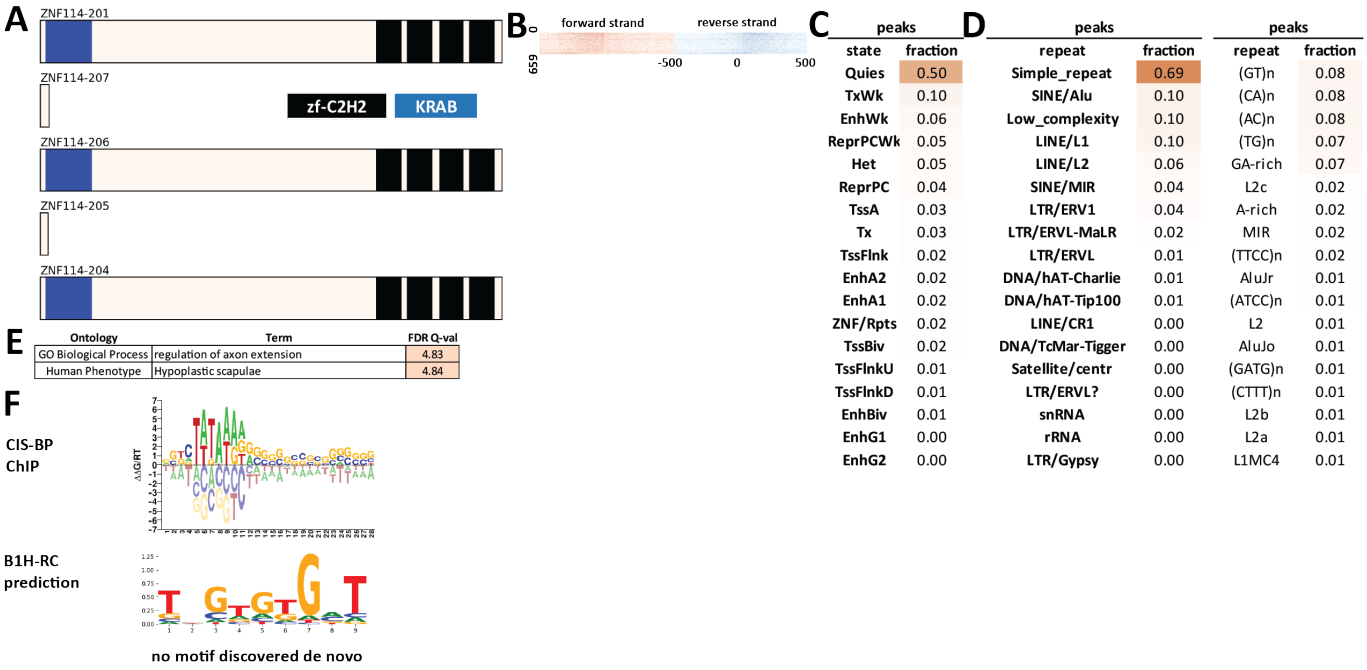

Supplementary Figure 672: Properties and genomic distribution of motifs identified for the ZNF114 transcription factor in HEK293 (accession ENCSR985MYI).

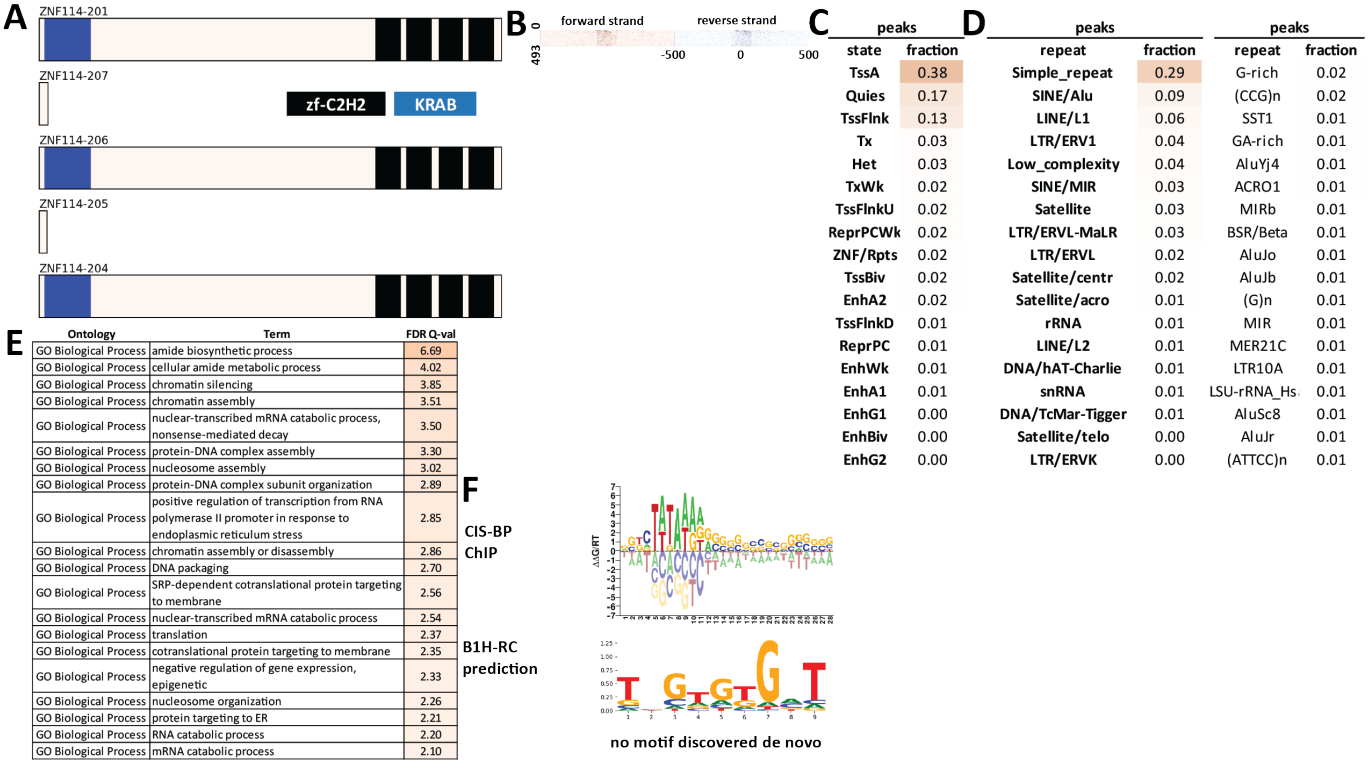

C

peaks	
state	fraction
TssA	0.38
Quies	0.17
TssFlnk	0.13
Tx	0.03
Het	0.03
TxWk	0.02
TssFlnkU	0.02
ReprPCWk	0.02
ZNF/Rpts	0.02
TssBiv	0.02
EnhA2	0.02
TssFlnkD	0.01
ReprPC	0.01
EnhWk	0.01
EnhA1	0.01
EnhG1	0.00
EnhBiv	0.00
EnhG2	0.00

D

peaks		peaks	
repeat	fraction	repeat	fraction
Simple_repeat	0.29	G-rich	0.02
SINE/Alu	0.09	(CCG)n	0.02
LINE/L1	0.06	SST1	0.01
LTR/ERV1	0.04	GA-rich	0.01
Low_complexity	0.04	AluYj4	0.01
SINE/MIR	0.03	ACRO1	0.01
Satellite	0.03	MIRb	0.01
LTR/ERVL-MaLR	0.03	BSR/Beta	0.01
LTR/ERVL	0.02	AluJo	0.01
Satellite/centr	0.02	AluJb	0.01
Satellite/acro	0.01	(G)n	0.01
rRNA	0.01	MIR	0.01
LINE/L2	0.01	MER21C	0.01
DNA/hAT-Charlie	0.01	LTR10A	0.01
snRNA	0.01	LSU-rRNA_Hs	0.01
DNA/TcMar-Tigger	0.01	AluSc8	0.01
Satellite/telo	0.00	AluJr	0.01
LTR/ERVK	0.00	(ATTCC)n	0.01

E

Ontology	Term	FDR Q-val
GO Biological Process	amide biosynthetic process	6.69
GO Biological Process	cellular amide metabolic process	4.02
GO Biological Process	chromatin silencing	3.85
GO Biological Process	chromatin assembly	3.51
GO Biological Process	nuclear-transcribed mRNA catabolic process, nonsense-mediated decay	3.50
GO Biological Process	protein-DNA complex assembly	3.30
GO Biological Process	nucleosome assembly	3.02
GO Biological Process	protein-DNA complex subunit organization	2.89
GO Biological Process	positive regulation of transcription from RNA polymerase II promoter in response to endoplasmic reticulum stress	2.85
GO Biological Process	chromatin assembly or disassembly	2.86
GO Biological Process	DNA packaging	2.70
GO Biological Process	SRP-dependent cotranslational protein targeting to membrane	2.56
GO Biological Process	nuclear-transcribed mRNA catabolic process	2.54
GO Biological Process	translation	2.37
GO Biological Process	cotranslational protein targeting to membrane	2.35
GO Biological Process	negative regulation of gene expression, epigenetic	2.33
GO Biological Process	nucleosome organization	2.26
GO Biological Process	protein targeting to ER	2.21
GO Biological Process	RNA catabolic process	2.20
GO Biological Process	mRNA catabolic process	2.10

Supplementary Figure 673: Properties and genomic distribution of motifs identified for the ZNF114 transcription factor in HEK293 (accession ChipExo models).

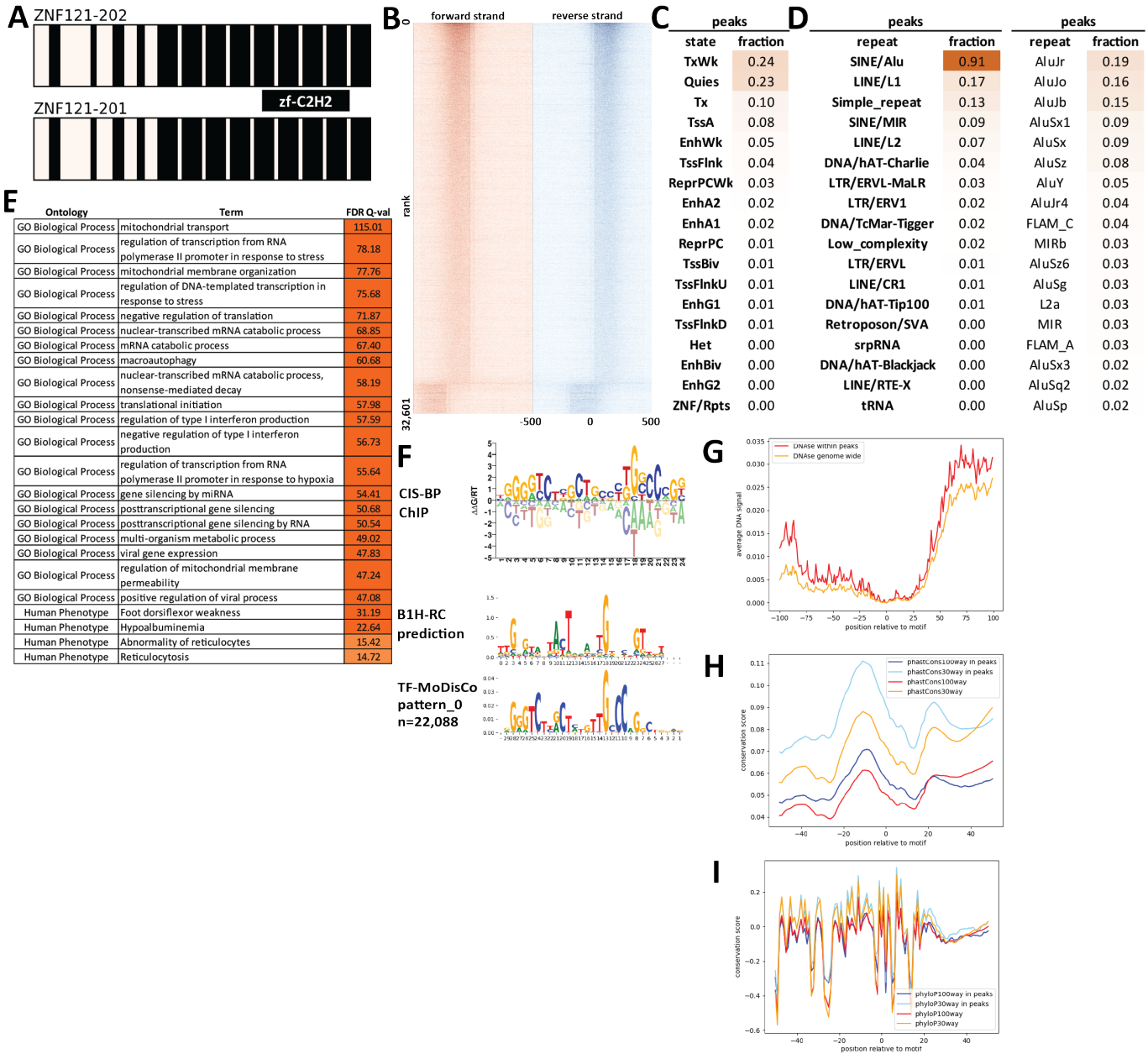

Supplementary Figure 674: Properties and genomic distribution of motifs identified for the ZNF121 transcription factor in HEK293 (accession ENCSR224QDY).

TF-MoDisCO pattern_0 n=22088, CWM

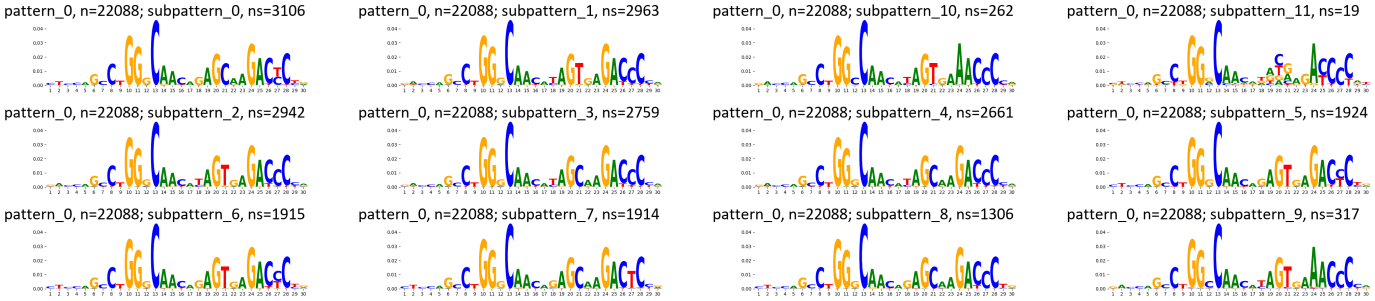

TF-MoDisCO pattern_0 n=22088, PWM

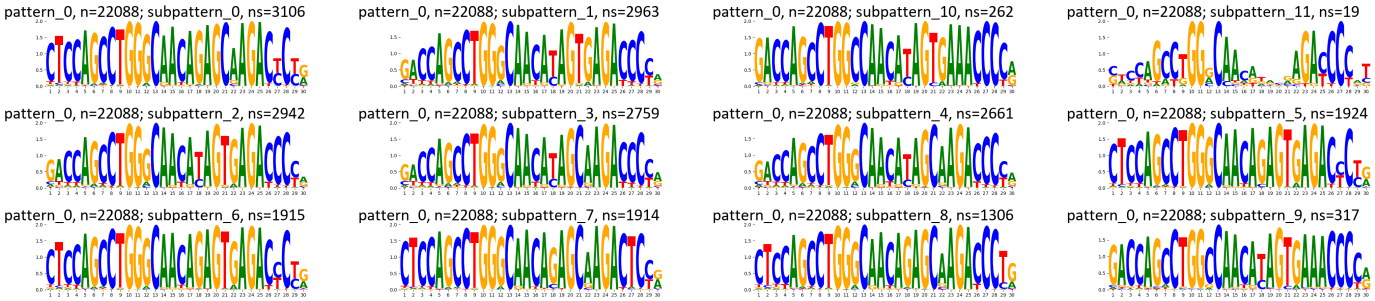

Supplementary Figure 675: TF-MoDisCO subpatterns for the ZNF121 transcription factor in HEK293 (accession ENCSR224QDY).

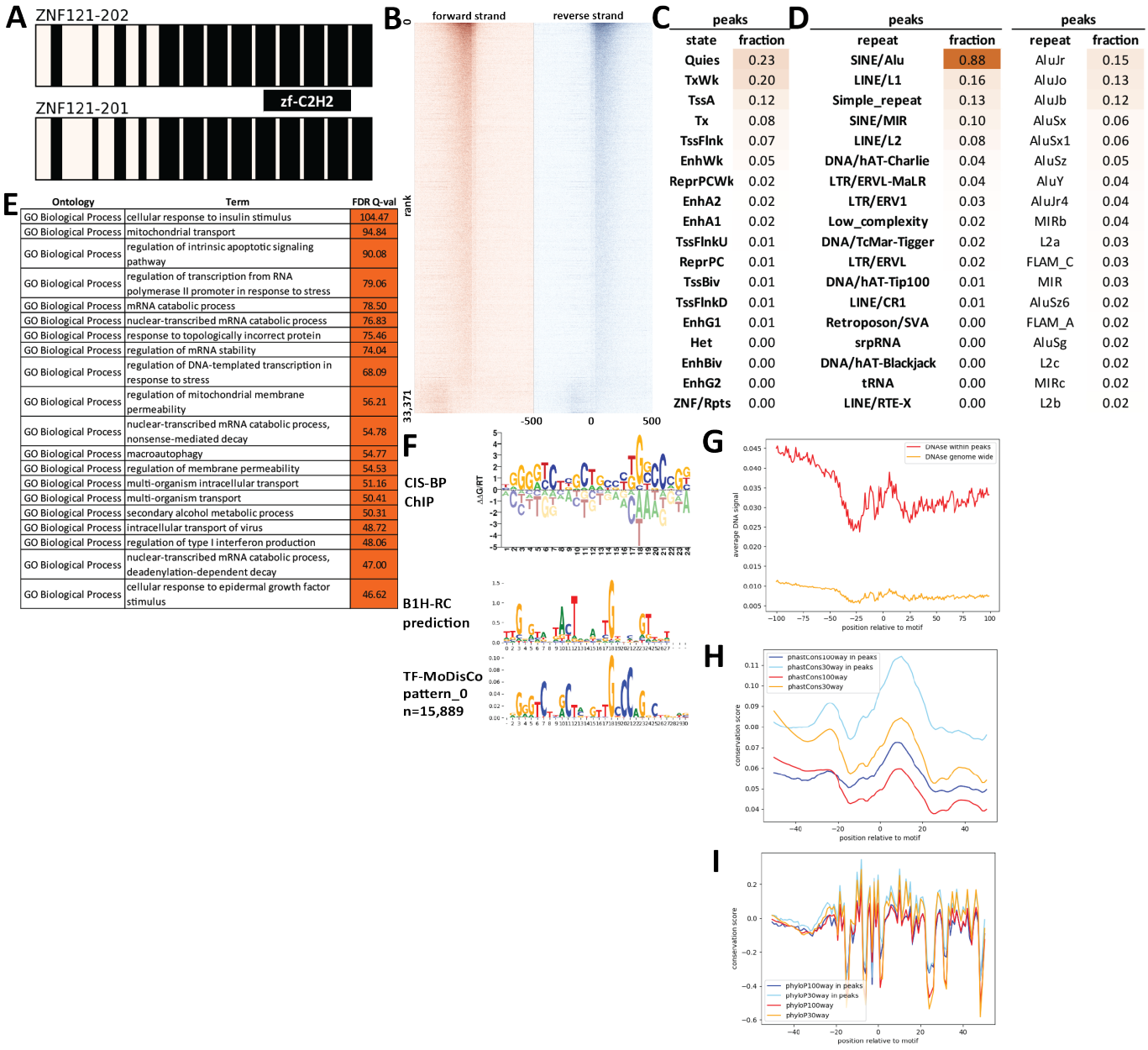

Supplementary Figure 676: Properties and genomic distribution of motifs identified for the ZNF121 transcription factor in HepG2 (accession ENCSR945QEW).

TF-MoDisCO pattern_0 n=15899, CWM

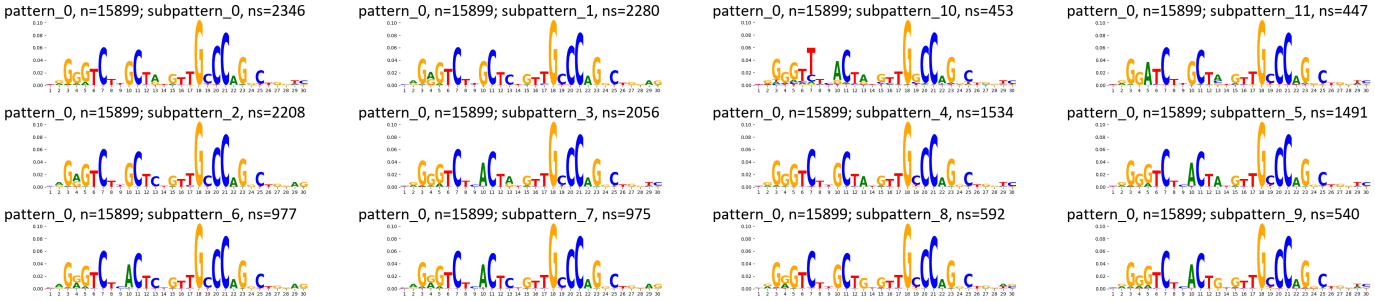

TF-MoDisCO pattern_0 n=15899, PWM

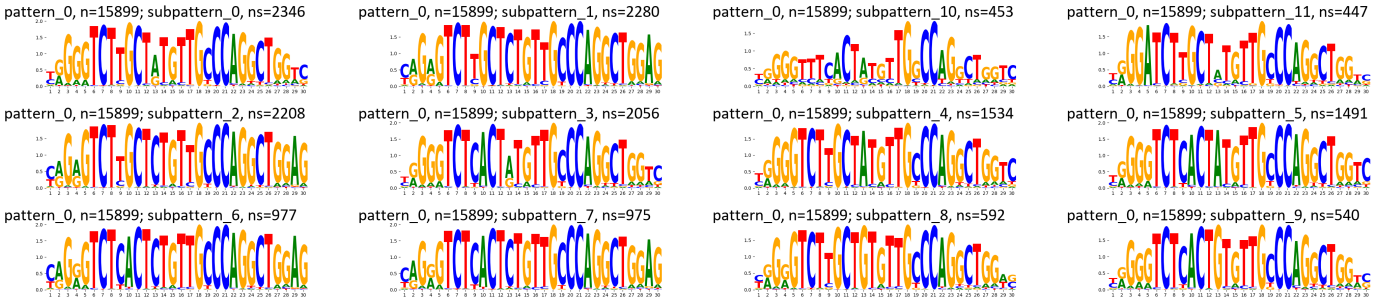

Supplementary Figure 677: TF-MoDisCO subpatterns for the ZNF121 transcription factor in HepG2 (accession ENCSR945QEW).

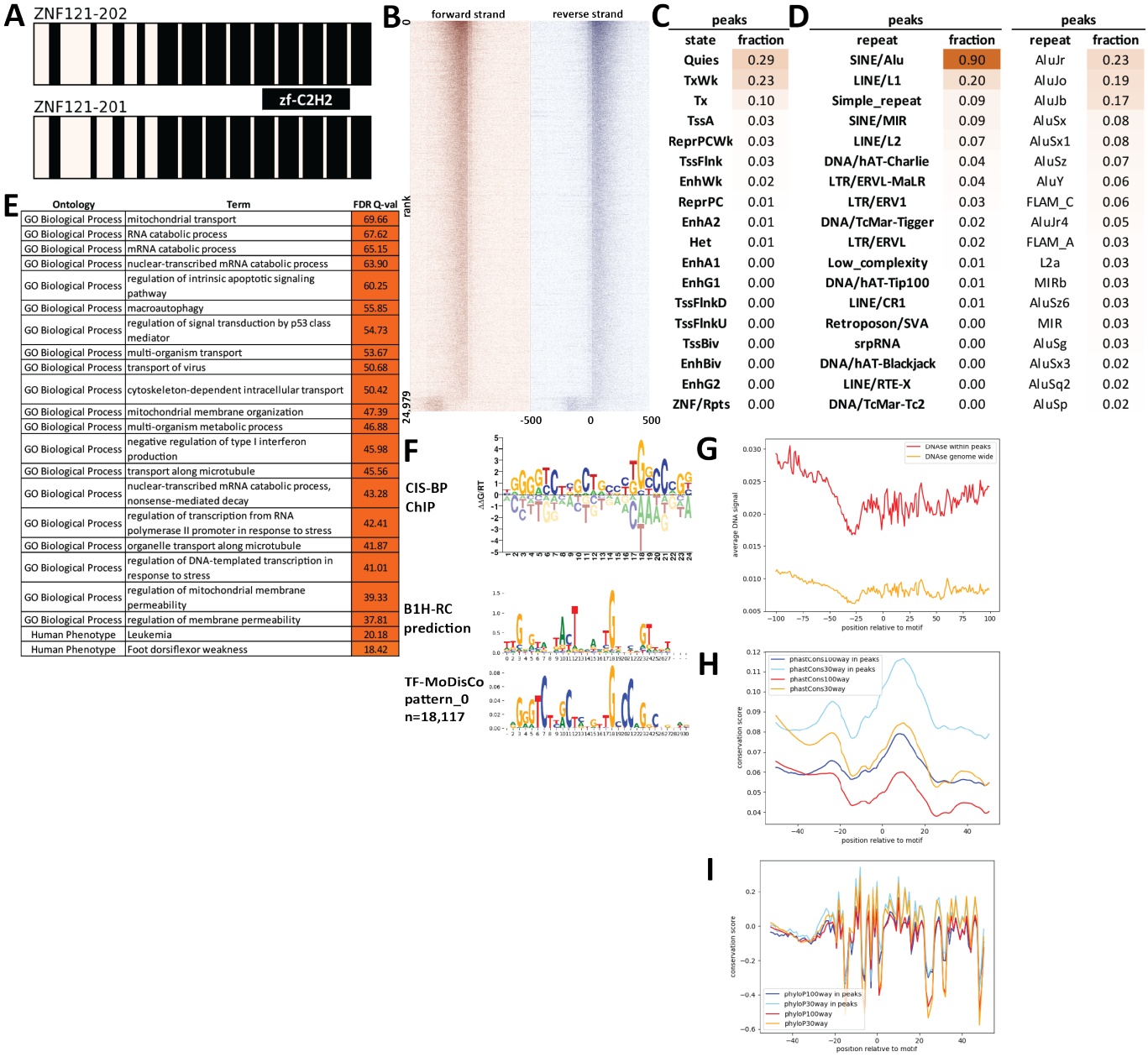

Supplementary Figure 678: Properties and genomic distribution of motifs identified for the ZNF121 transcription factor in K562 (accession ENCSR799URB).

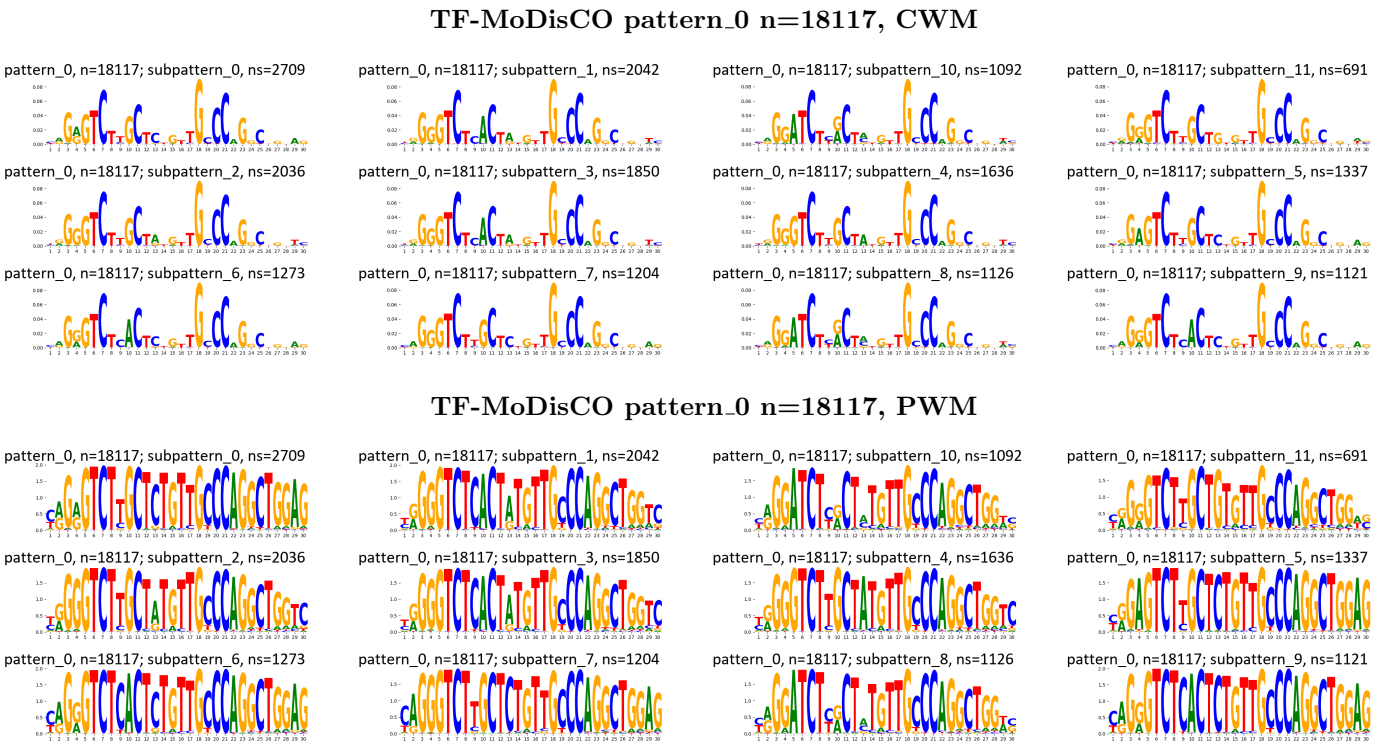

Supplementary Figure 679: TF-MoDisCO subpatterns for the ZNF121 transcription factor in K562 (accession ENCSR799URB).

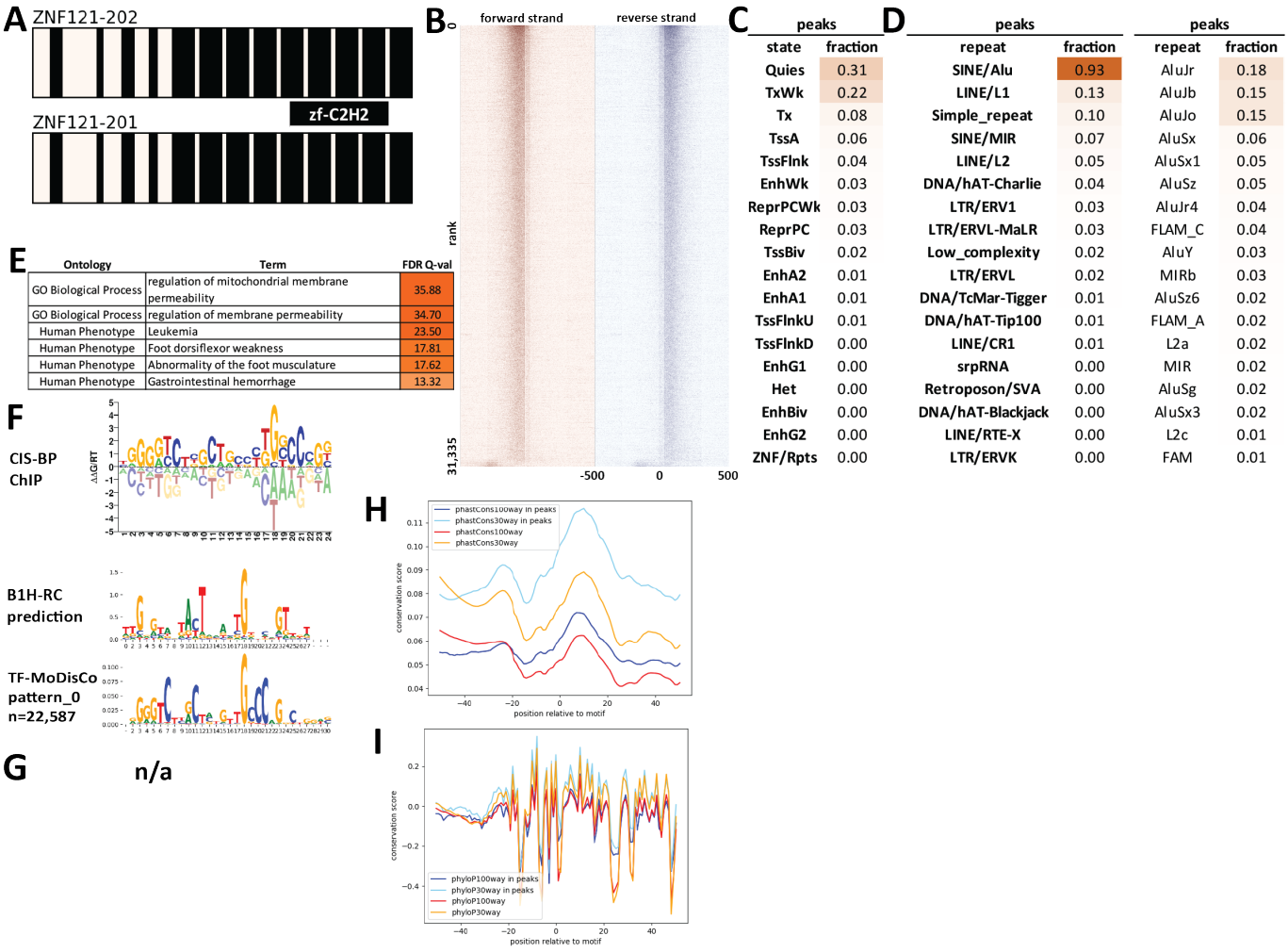

Supplementary Figure 680: Properties and genomic distribution of motifs identified for the ZNF121 transcription factor in WTC11 (accession ENCSR203PCF).

TF-MoDisCO pattern_0 n=22587, CWM

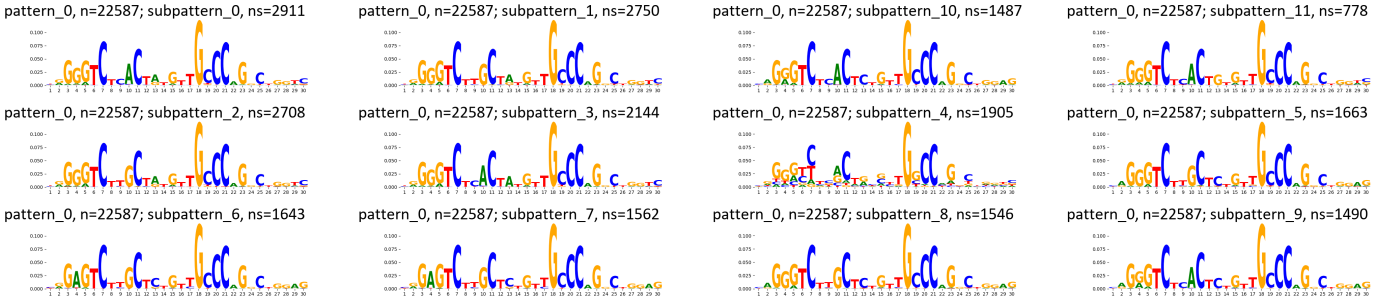

TF-MoDisCO pattern_0 n=22587, PWM

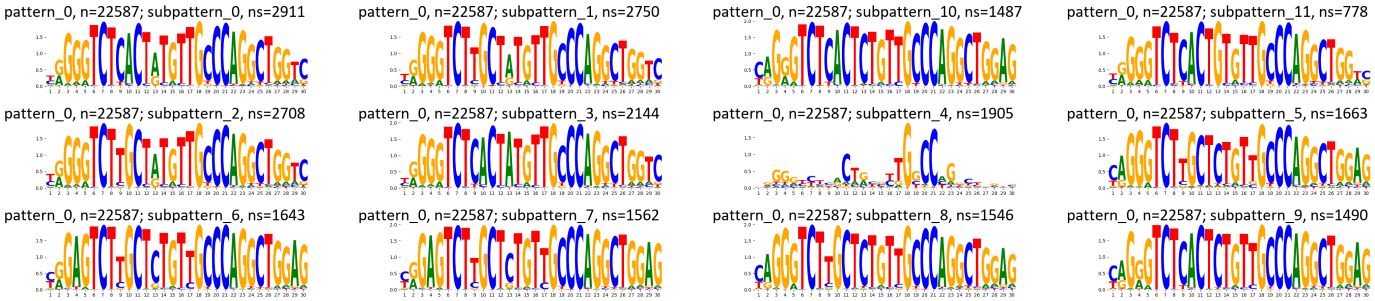

Supplementary Figure 681: TF-MoDisCO subpatterns for the ZNF121 transcription factor in WTC11 (accession ENCSR203PCF).

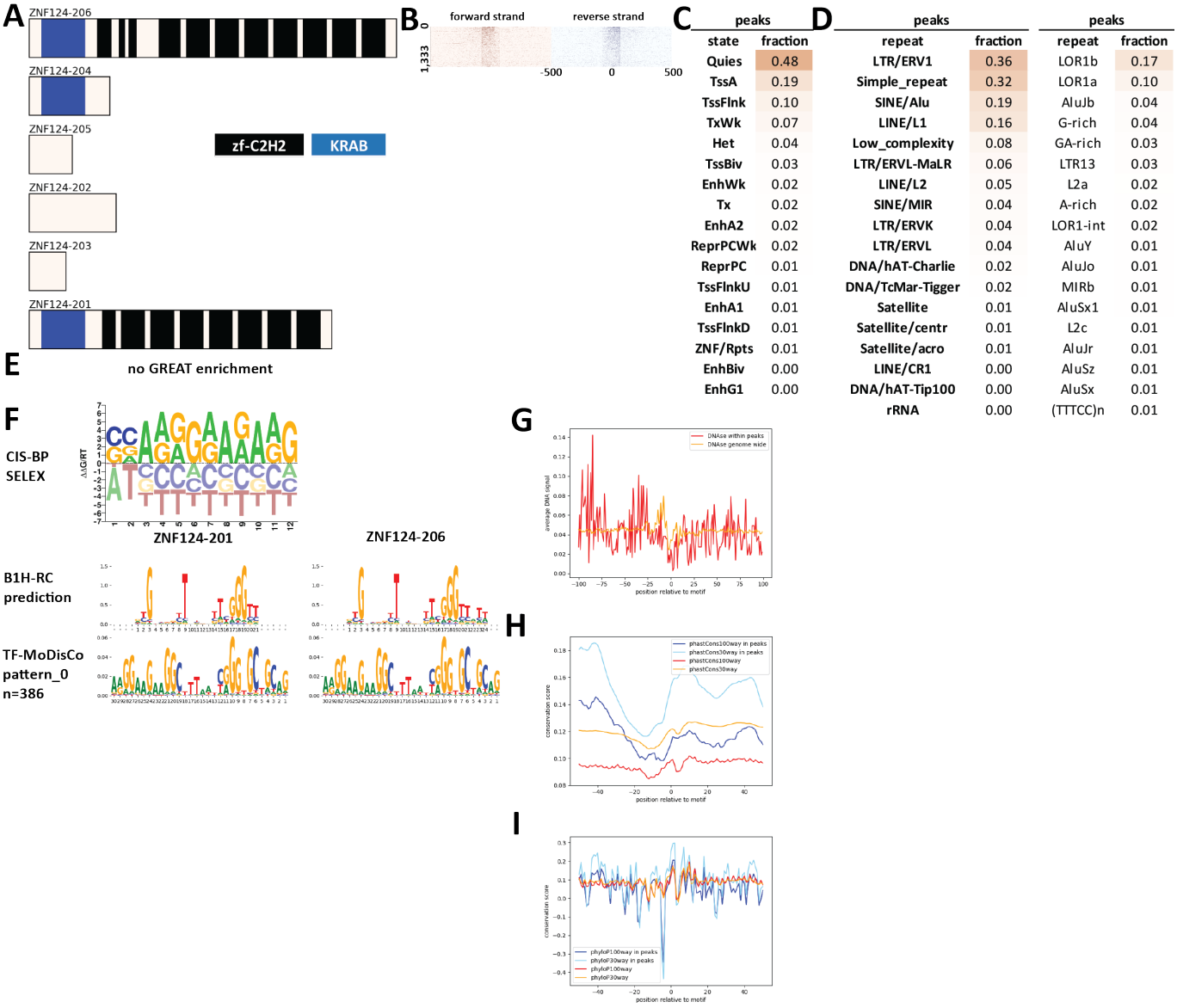

peaks	
state	fraction
Quies	0.48
TssA	0.19
TssFlnk	0.10
TxWk	0.07
Het	0.04
TssBiv	0.03
EnhWk	0.02
Tx	0.02
EnhA2	0.02
ReprPCWk	0.02
ReprPC	0.01
TssFlnkU	0.01
EnhA1	0.01
TssFlnkD	0.01
ZNF/Rpts	0.01
EnhBiv	0.00
EnhG1	0.00

peaks		peaks	
repeat	fraction	repeat	fraction
LTR/ERV1	0.36	LOR1b	0.17
Simple_repeat	0.32	LOR1a	0.10
SINE/Alu	0.19	AluJb	0.04
LINE/L1	0.16	G-rich	0.04
Low_complexity	0.08	GA-rich	0.03
LTR/ERVL-MaLR	0.06	LTR13	0.03
LINE/L2	0.05	L2a	0.02
SINE/MIR	0.04	A-rich	0.02
LTR/ERVK	0.04	LOR1-int	0.02
LTR/ERVL	0.04	AluY	0.01
DNA/hAT-Charlie	0.02	AluJo	0.01
DNA/TcMar-Tigger	0.02	MIRb	0.01
Satellite	0.01	AluSx1	0.01
Satellite/centr	0.01	L2c	0.01
Satellite/acro	0.01	AluJr	0.01
LINE/CR1	0.00	AluSz	0.01
DNA/hAT-Tip100	0.00	AluSx	0.01
rRNA	0.00	(TTTCC)n	0.01

Supplementary Figure 682: Properties and genomic distribution of motifs identified for the ZNF124 transcription factor in HEK293 (accession ChipExo models).

TF-MoDisCO pattern_0 n=386, CWM

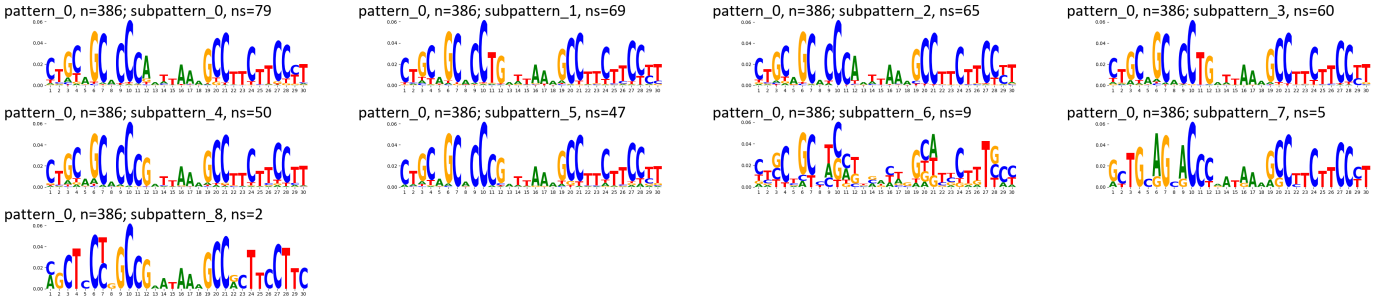

TF-MoDisCO pattern_0 n=386, PWM

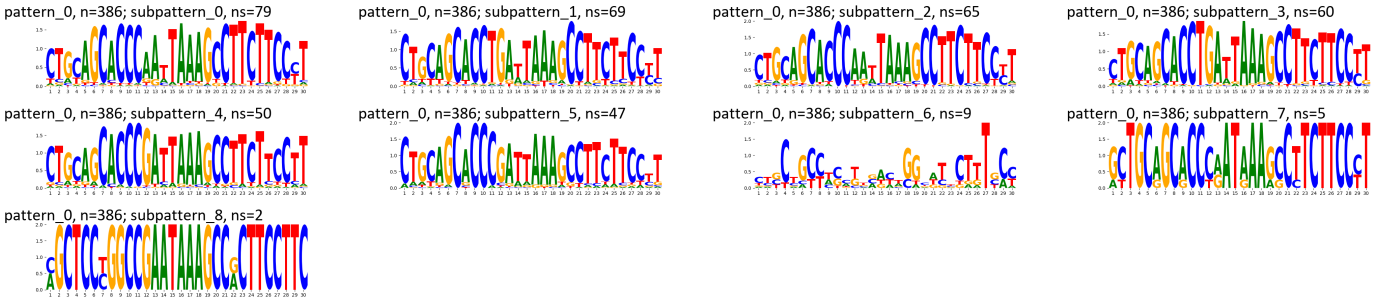

Supplementary Figure 683: TF-MoDisCO subpatterns for the ZNF124 transcription factor in HEK293 (accession ChipExo models).

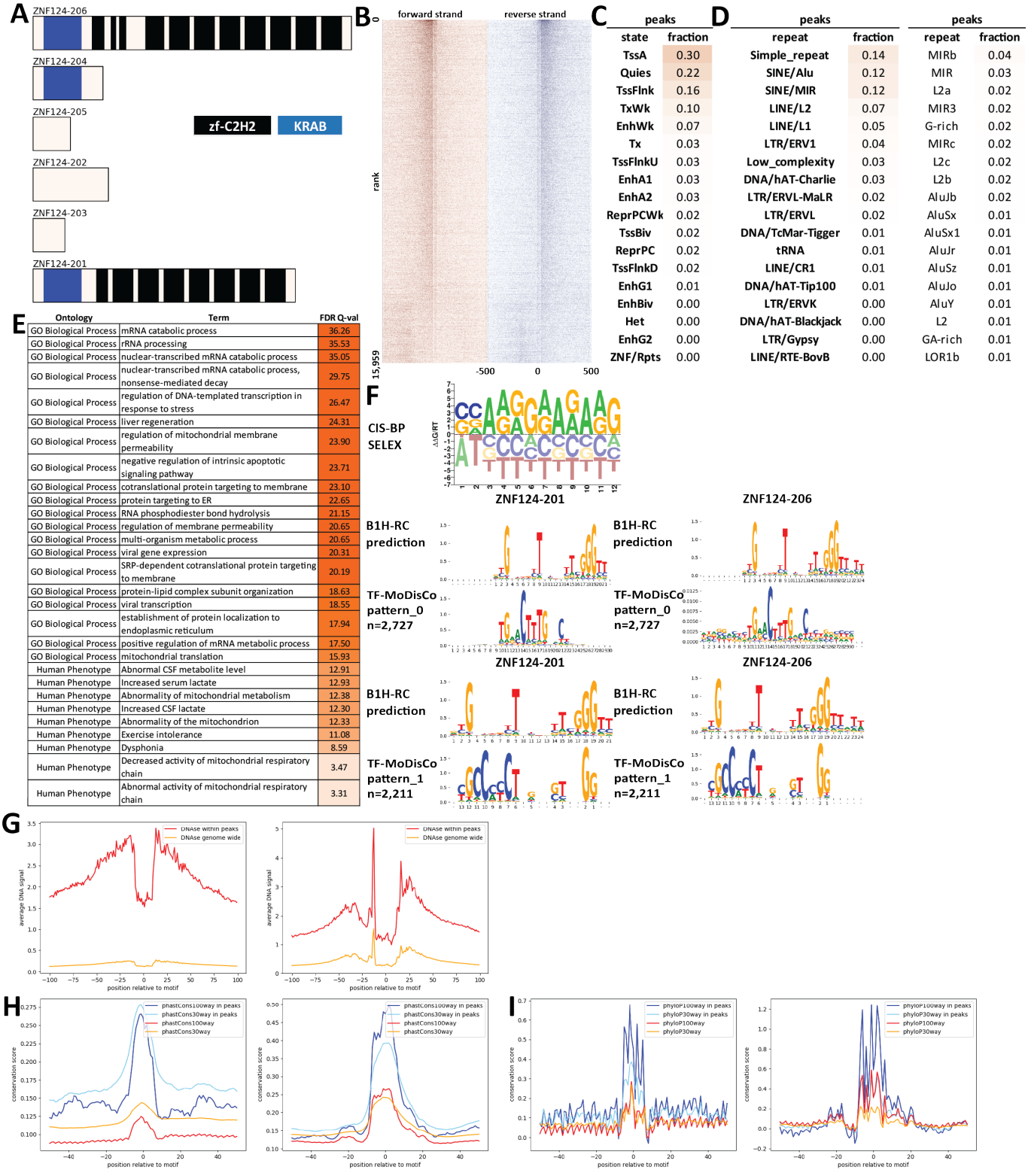

Supplementary Figure 684: Properties and genomic distribution of motifs identified for the ZNF124 transcription factor in HepG2 (accession ENCSR357YPP).

TF-MoDisCO pattern_0 n=2727, CWM

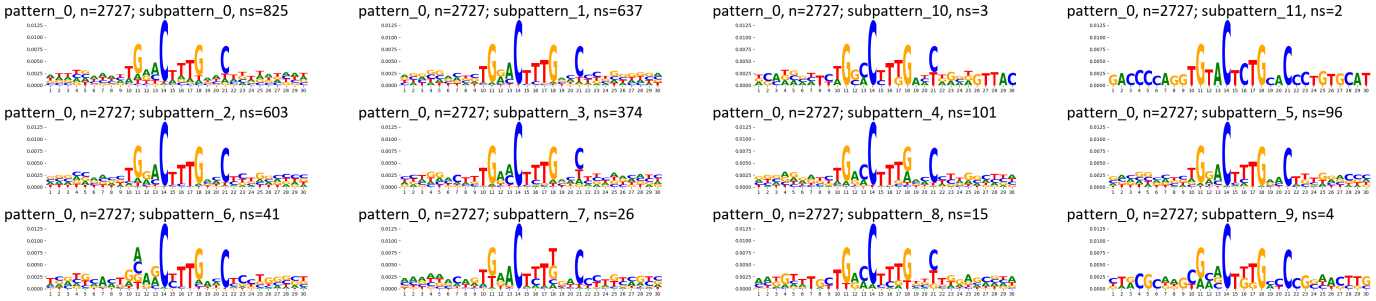

TF-MoDisCO pattern_0 n=2727, PWM

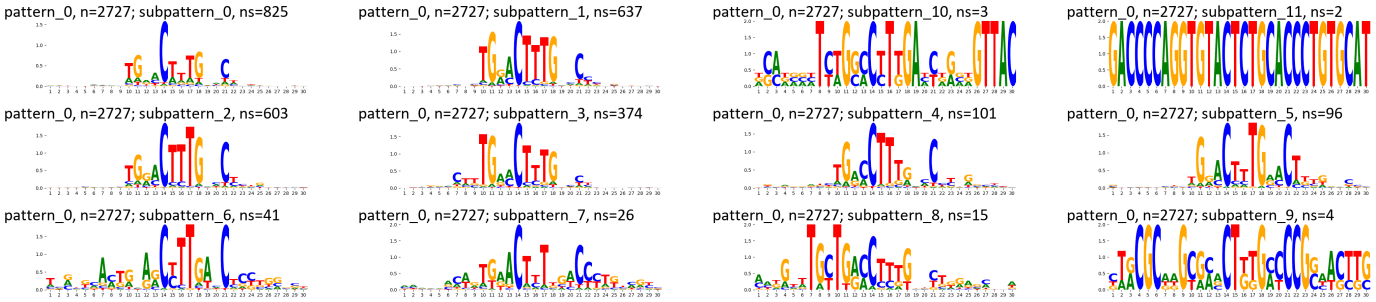

TF-MoDisCO pattern_1 n=2211, CWM

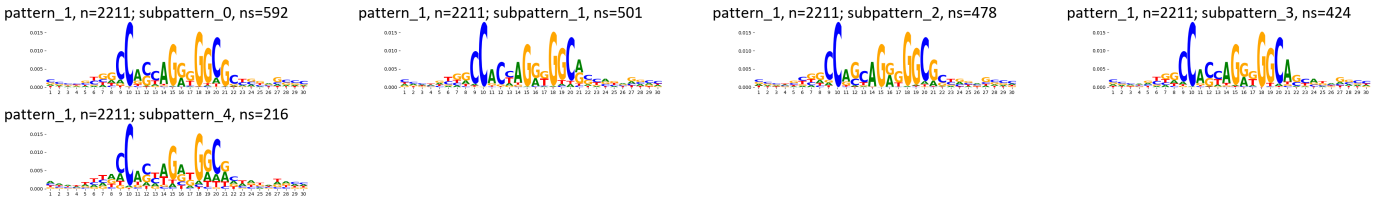

TF-MoDisCO pattern_1 n=2211, PWM

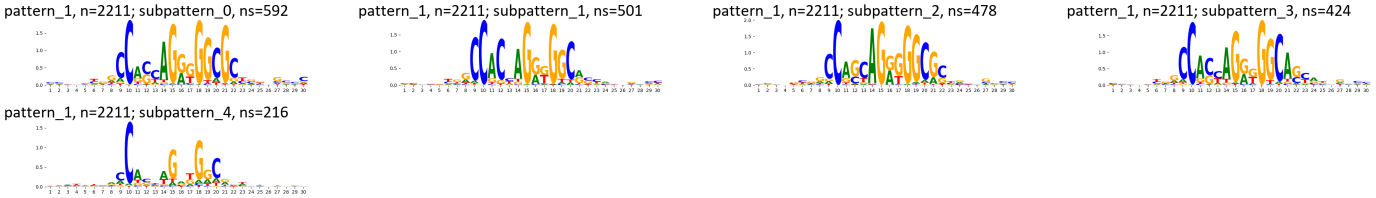

Supplementary Figure 685: TF-MoDisCO subpatterns for the ZNF124 transcription factor in HepG2 (accession ENCSR357YPP).

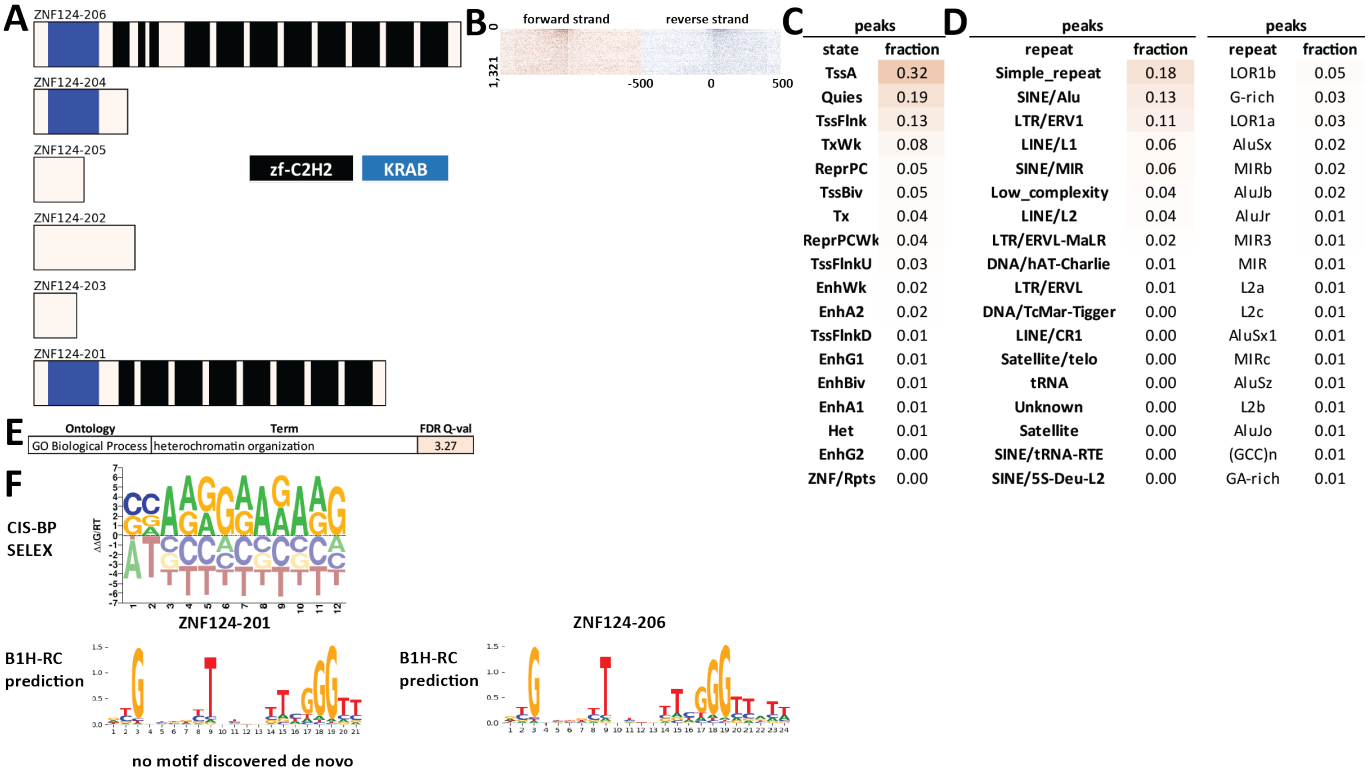

Supplementary Figure 686: Properties and genomic distribution of motifs identified for the ZNF124 transcription factor in K562 (accession ENCSR124YFA).

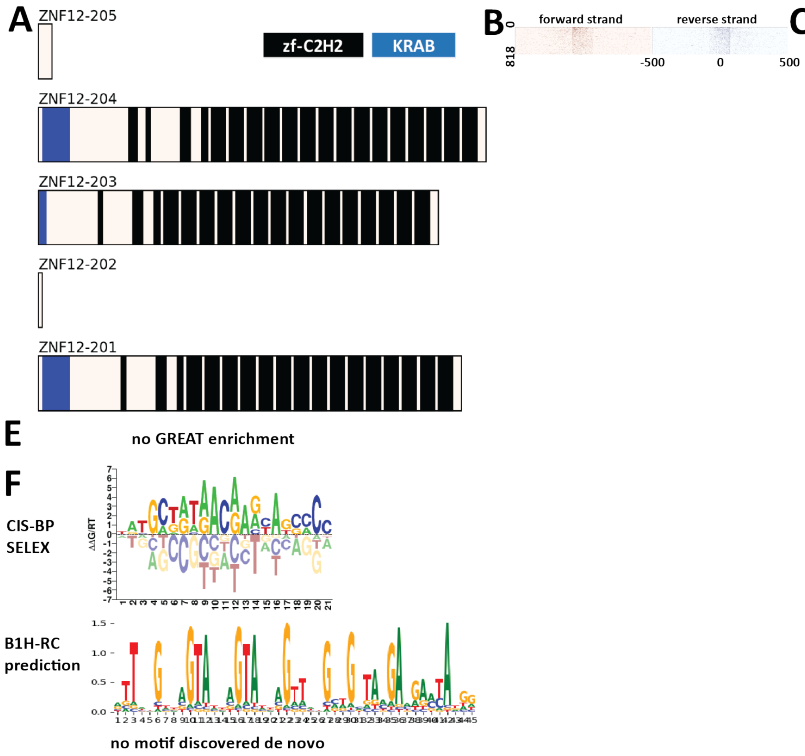

C

peaks	
state	fraction
Quies	0.40
TssA	0.24
TssFlnk	0.12
TxWk	0.08
TssBiv	0.04
ReprPCWk	0.04
EnhWk	0.04
Tx	0.03
EnhA2	0.03
ReprPC	0.02
EnhA1	0.02
TssFlnkU	0.02
Het	0.02
ZNF/Rpts	0.01
TssFlnkD	0.01
EnhBiv	0.00
EnhG1	0.00

D

peaks		peaks	
repeat	fraction	repeat	fraction
LTR/ERVL-MaLR	0.41	MLT1I	0.21
Simple_repeat	0.24	MIRb	0.05
SINE/Alu	0.17	MLT1J2	0.04
LINE/L2	0.10	L2a	0.04
SINE/MIR	0.10	L2c	0.03
LINE/L1	0.06	MLT1D	0.03
LTR/ERV1	0.04	MIR	0.03
Low_complexity	0.04	AluJr	0.02
DNA/hAT-Charlie	0.04	MLT1B	0.02
LTR/ERVL	0.03	G-rich	0.02
Satellite	0.01	AluSx1	0.02
Satellite/centr	0.01	MLT1A0	0.02
LINE/CR1	0.01	L2b	0.02
DNA/TcMar-Tigger	0.01	AluSx	0.02
rRNA	0.00	GA-rich	0.02
Satellite/telo	0.00	MIRc	0.01
Retroposon/SVA	0.00	AluY	0.01
LTR/ERVL?	0.00	AluSz	0.01

Supplementary Figure 687: Properties and genomic distribution of motifs identified for the ZNF12 transcription factor in HEK293 (accession ChipExo models).

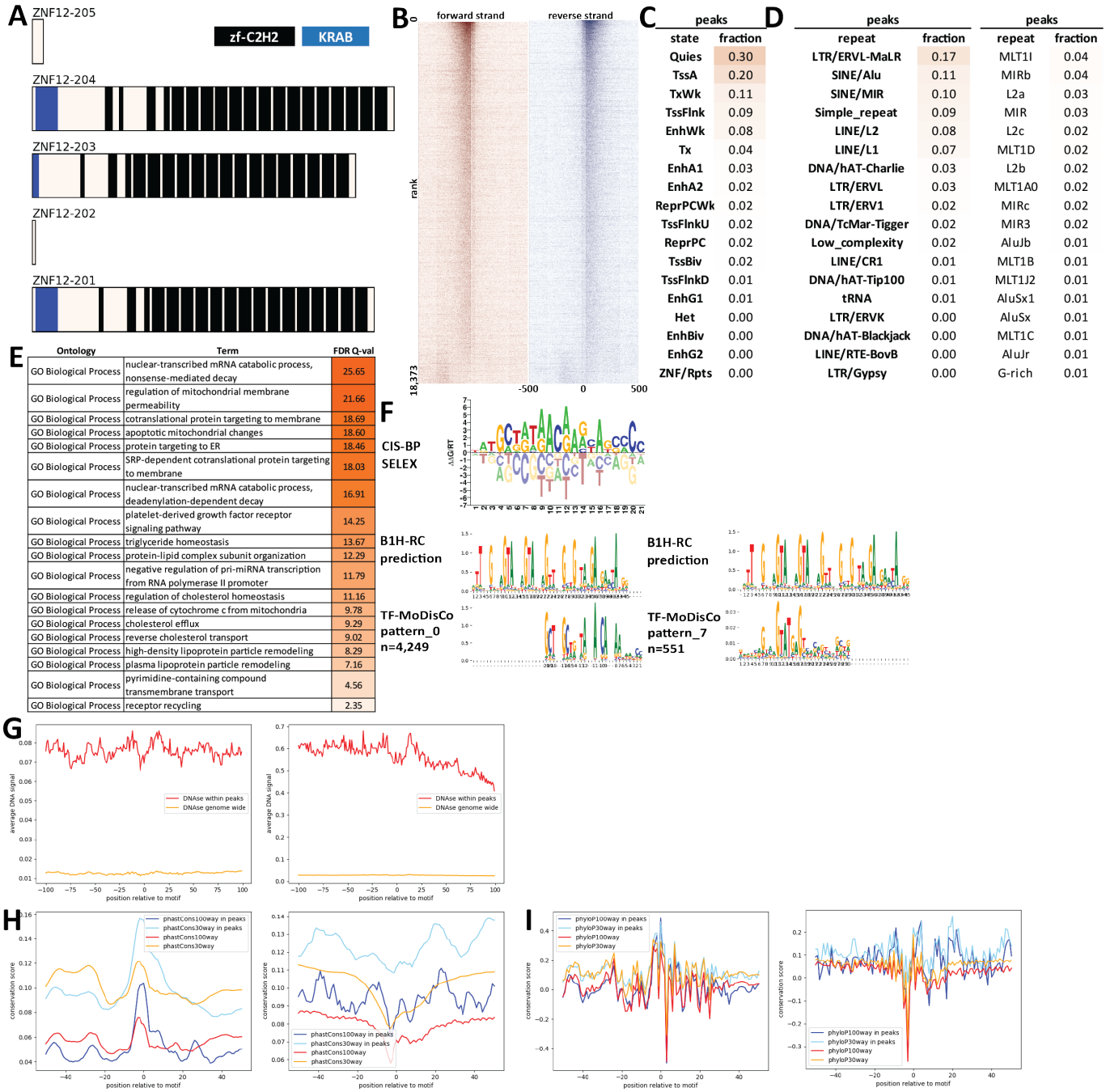

C

peaks	
state	fraction
Quies	0.30
TssA	0.20
TxWk	0.11
TssFlnk	0.09
EnhWk	0.08
Tx	0.04
EnhA1	0.03
EnhA2	0.02
ReprPCWk	0.02
TssFlnkU	0.02
ReprPC	0.02
TssBiv	0.02
TssFlnkD	0.01
EnhG1	0.01
Het	0.00
EnhBiv	0.00
EnhG2	0.00
ZNF/Rpts	0.00

D

peaks		peaks	
repeat	fraction	repeat	fraction
LTR/ERVL-MaLR	0.17	MLT1I	0.04
SINE/Alu	0.11	MIRb	0.04
SINE/MIR	0.10	L2a	0.03
Simple_repeat	0.09	MIR	0.03
LINE/L2	0.08	L2c	0.02
LINE/L1	0.07	MLT1D	0.02
DNA/hAT-Charlie	0.03	L2b	0.02
LTR/ERVL	0.03	MLT1A0	0.02
LTR/ERV1	0.02	MIRc	0.02
DNA/TcMar-Tigger	0.02	MIR3	0.02
Low_complexity	0.02	AluJb	0.01
LINE/CR1	0.01	MLT1B	0.01
DNA/hAT-Tip100	0.01	MLT1J2	0.01
tRNA	0.01	AluSx1	0.01
LTR/ERVK	0.00	AluSx	0.01
DNA/hAT-Blackjack	0.00	MLT1C	0.01
LINE/RTE-BovB	0.00	AluJr	0.01
LTR/Gypsy	0.00	G-rich	0.01

E

Ontology	Term	FDR Q-val
GO Biological Process	nuclear-transcribed mRNA catabolic process, nonsense-mediated decay	25.65
GO Biological Process	regulation of mitochondrial membrane permeability	21.66
GO Biological Process	cotranslational protein targeting to membrane	18.69
GO Biological Process	apoptotic mitochondrial changes	18.60
GO Biological Process	protein targeting to ER	18.46
GO Biological Process	SRP-dependent cotranslational protein targeting to membrane	18.03
GO Biological Process	nuclear-transcribed mRNA catabolic process, deadenylation-dependent decay	16.91
GO Biological Process	platelet-derived growth factor receptor signaling pathway	14.25
GO Biological Process	triglyceride homeostasis	13.67
GO Biological Process	protein-lipid complex subunit organization	12.29
GO Biological Process	negative regulation of pri-miRNA transcription from RNA polymerase II promoter	11.79
GO Biological Process	regulation of cholesterol homeostasis	11.16
GO Biological Process	release of cytochrome c from mitochondria	9.78
GO Biological Process	cholesterol efflux	9.29
GO Biological Process	reverse cholesterol transport	9.02
GO Biological Process	high-density lipoprotein particle remodeling	8.29
GO Biological Process	plasma lipoprotein particle remodeling	7.16
GO Biological Process	pyrimidine-containing compound transmembrane transport	4.56
GO Biological Process	receptor recycling	2.35

Supplementary Figure 688: Properties and genomic distribution of motifs identified for the ZNF12 transcription factor in HepG2 (accession ENCSR711KBM).

TF-MoDisCO pattern_0 n=4249, CWM

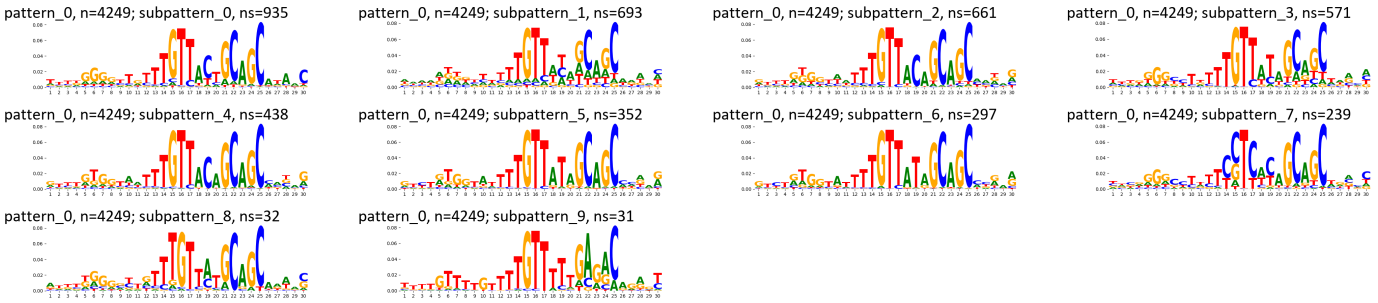

TF-MoDisCO pattern_0 n=4249, PWM

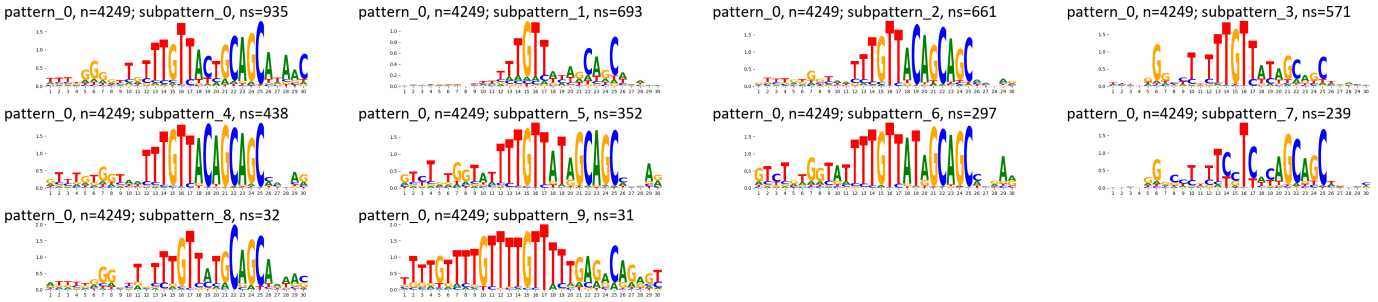

TF-MoDisCO pattern_7 n=551, CWM

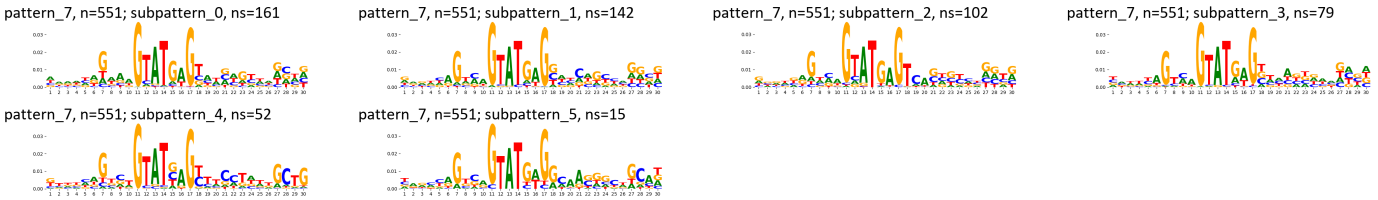

TF-MoDisCO pattern_7 n=551, PWM

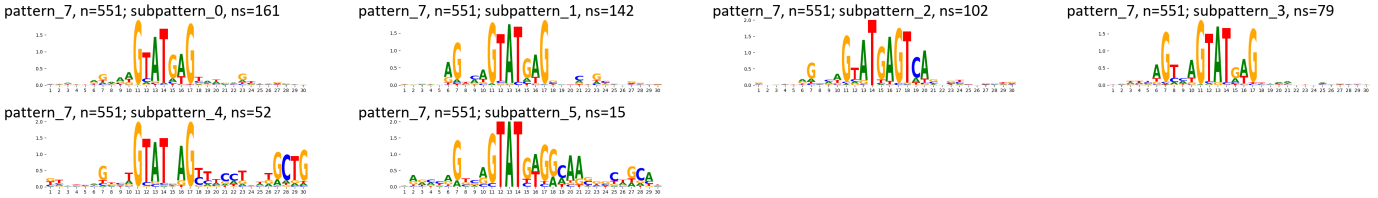

Supplementary Figure 689: TF-MoDisCO subpatterns for the ZNF12 transcription factor in HepG2 (accession ENCSR711KBM).

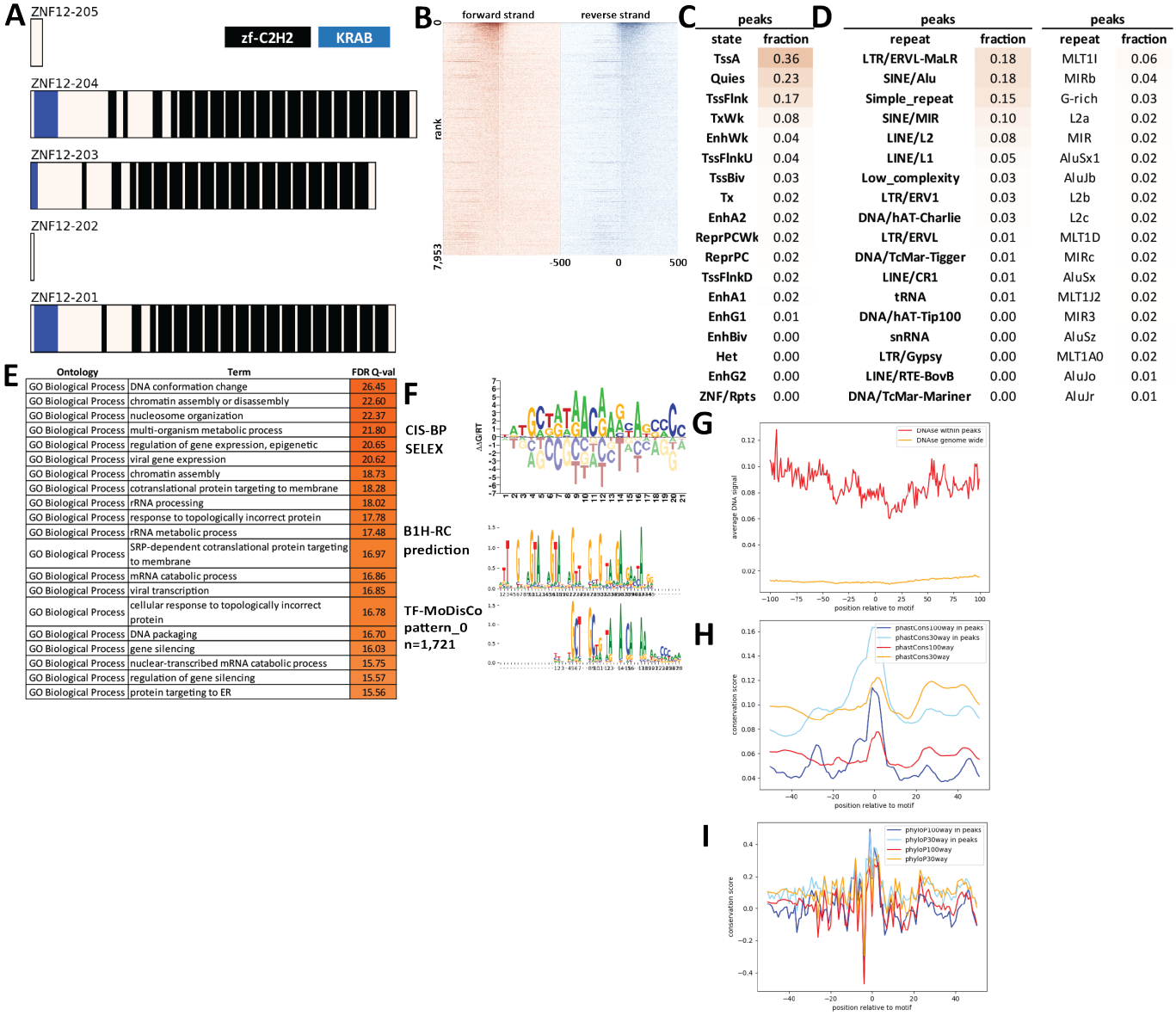

peaks	
state	fraction
TssA	0.36
Quies	0.23
TssFlnk	0.17
TxWk	0.08
EnhWk	0.04
TssFlnkU	0.04
TssBiv	0.03
Tx	0.02
EnhA2	0.02
ReprPCWk	0.02
ReprPC	0.02
TssFlnkD	0.02
EnhA1	0.02
EnhG1	0.01
EnhBiv	0.00
Het	0.00
EnhG2	0.00
ZNF/Rpts	0.00

peaks	
repeat	fraction
LTR/ERVL-MaLR	0.18
SINE/Alu	0.18
Simple_repeat	0.15
SINE/MIR	0.10
LINE/L2	0.08
LINE/L1	0.05
Low_complexity	0.03
LTR/ERV1	0.03
DNA/hAT-Charlie	0.03
LTR/ERVL	0.01
DNA/TcMar-Tigger	0.01
LINE/CR1	0.01
tRNA	0.01
DNA/hAT-Tip100	0.00
snRNA	0.00
LTR/Gypsy	0.00
LINE/RTE-BovB	0.00
DNA/TcMar-Mariner	0.00

peaks	
repeat	fraction
MLT1I	0.06
MIRb	0.04
G-rich	0.03
L2a	0.02
MIR	0.02
AluSx1	0.02
AluJb	0.02
L2b	0.02
L2c	0.02
MLT1D	0.02
MIRc	0.02
AluSx	0.02
MLT1J2	0.02
MIR3	0.02
AluSz	0.02
MLT1A0	0.02
AluJo	0.01
AluJr	0.01

Ontology	Term	FDR Q-val
GO Biological Process	DNA conformation change	26.45
GO Biological Process	chromatin assembly or disassembly	22.60
GO Biological Process	nucleosome organization	22.37
GO Biological Process	multi-organism metabolic process	21.80
GO Biological Process	regulation of gene expression, epigenetic	20.65
GO Biological Process	viral gene expression	20.62
GO Biological Process	chromatin assembly	18.73
GO Biological Process	cotranslational protein targeting to membrane	18.28
GO Biological Process	rRNA processing	18.02
GO Biological Process	response to topologically incorrect protein	17.78
GO Biological Process	rRNA metabolic process	17.48
GO Biological Process	SRP-dependent cotranslational protein targeting to membrane	16.97
GO Biological Process	mRNA catabolic process	16.86
GO Biological Process	viral transcription	16.85
GO Biological Process	cellular response to topologically incorrect protein	16.78
GO Biological Process	DNA packaging	16.70
GO Biological Process	gene silencing	16.03
GO Biological Process	nuclear-transcribed mRNA catabolic process	15.75
GO Biological Process	regulation of gene silencing	15.57
GO Biological Process	protein targeting to ER	15.56

Supplementary Figure 690: Properties and genomic distribution of motifs identified for the ZNF12 transcription factor in K562 (accession ENCSR041YBR).

TF-MoDisCO pattern_0 n=1721, CWM

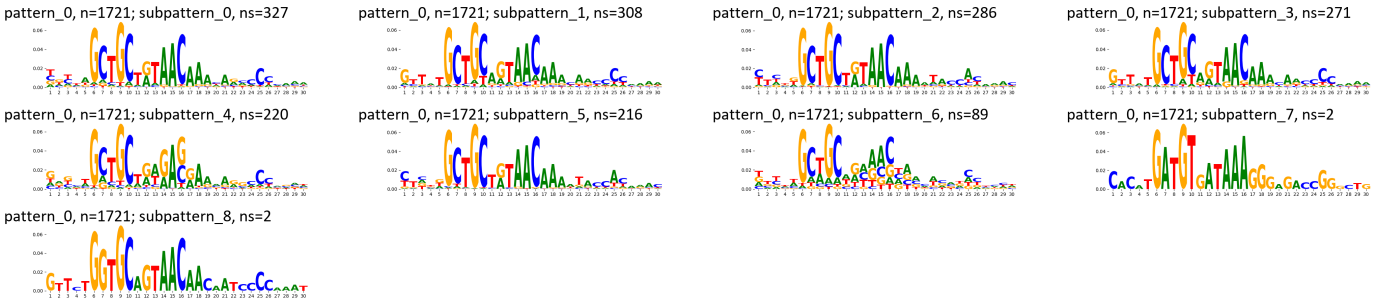

TF-MoDisCO pattern_0 n=1721, PWM

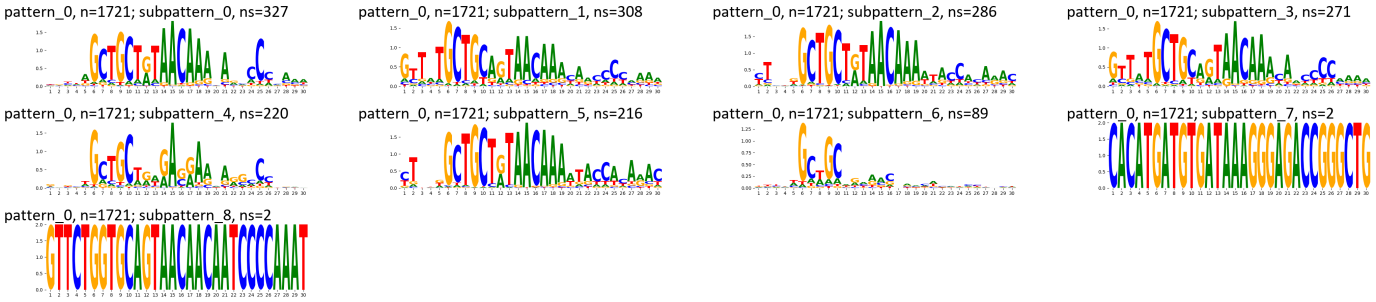

Supplementary Figure 691: TF-MoDisCO subpatterns for the ZNF12 transcription factor in K562 (accession ENCSR041YBR).

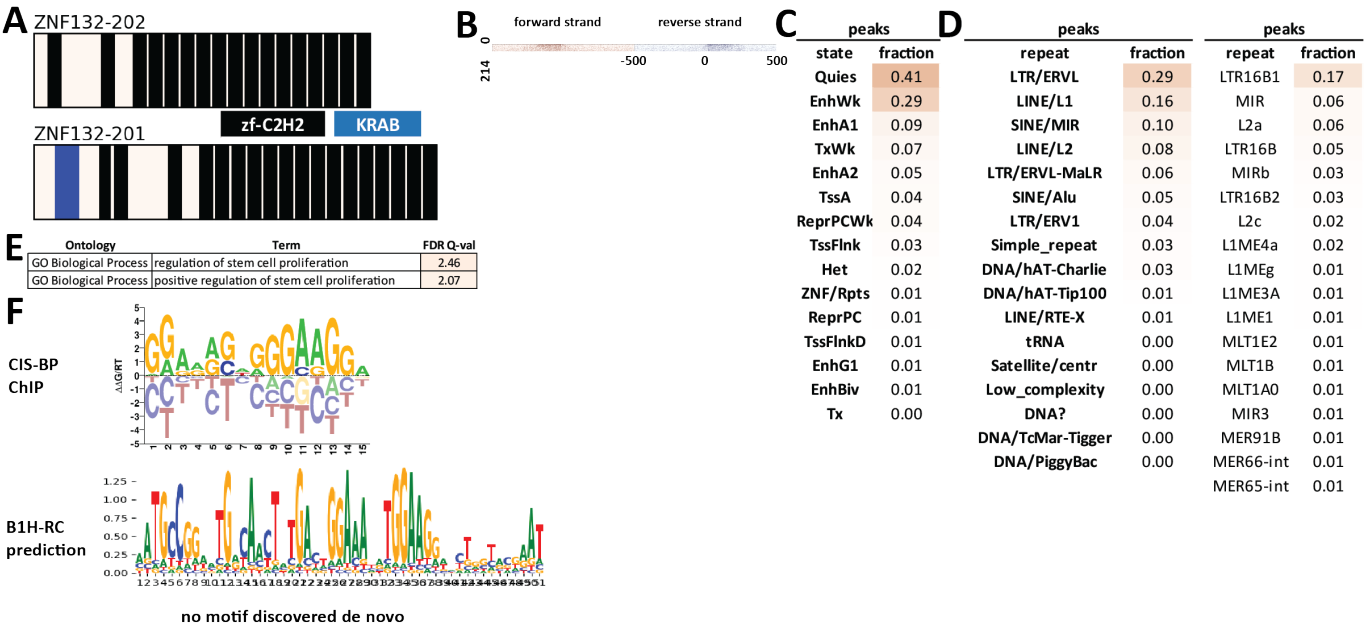

peaks	
state	fraction
Quies	0.41
EnhWk	0.29
EnhA1	0.09
TxWk	0.07
EnhA2	0.05
TssA	0.04
ReprPCWk	0.04
TssFlnk	0.03
Het	0.02
ZNF/Rpts	0.01
ReprPC	0.01
TssFlnkD	0.01
EnhG1	0.01
EnhBiv	0.01
Tx	0.00

peaks	
repeat	fraction
LTR/ERVL	0.29
LINE/L1	0.16
SINE/MIR	0.10
LINE/L2	0.08
LTR/ERVL-MaLR	0.06
SINE/Alu	0.05
LTR/ERV1	0.04
Simple_repeat	0.03
DNA/hAT-Charlie	0.03
DNA/hAT-Tip100	0.01
LINE/RTE-X	0.01
tRNA	0.00
Satellite/centr	0.00
Low_complexity	0.00
DNA?	0.00
DNA/TcMar-Tigger	0.00
DNA/PiggyBac	0.00

peaks	
repeat	fraction
LTR16B1	0.17
MIR	0.06
L2a	0.06
LTR16B	0.05
MIRb	0.03
LTR16B2	0.03
L2c	0.02
L1ME4a	0.02
L1MEg	0.01
L1ME3A	0.01
L1ME1	0.01
MLT1E2	0.01
MLT1B	0.01
MLT1A0	0.01
MIR3	0.01
MER91B	0.01
MER66-int	0.01
MER65-int	0.01

Supplementary Figure 692: Properties and genomic distribution of motifs identified for the ZNF132 transcription factor in HEK293 (accession ENCSR138RCE).

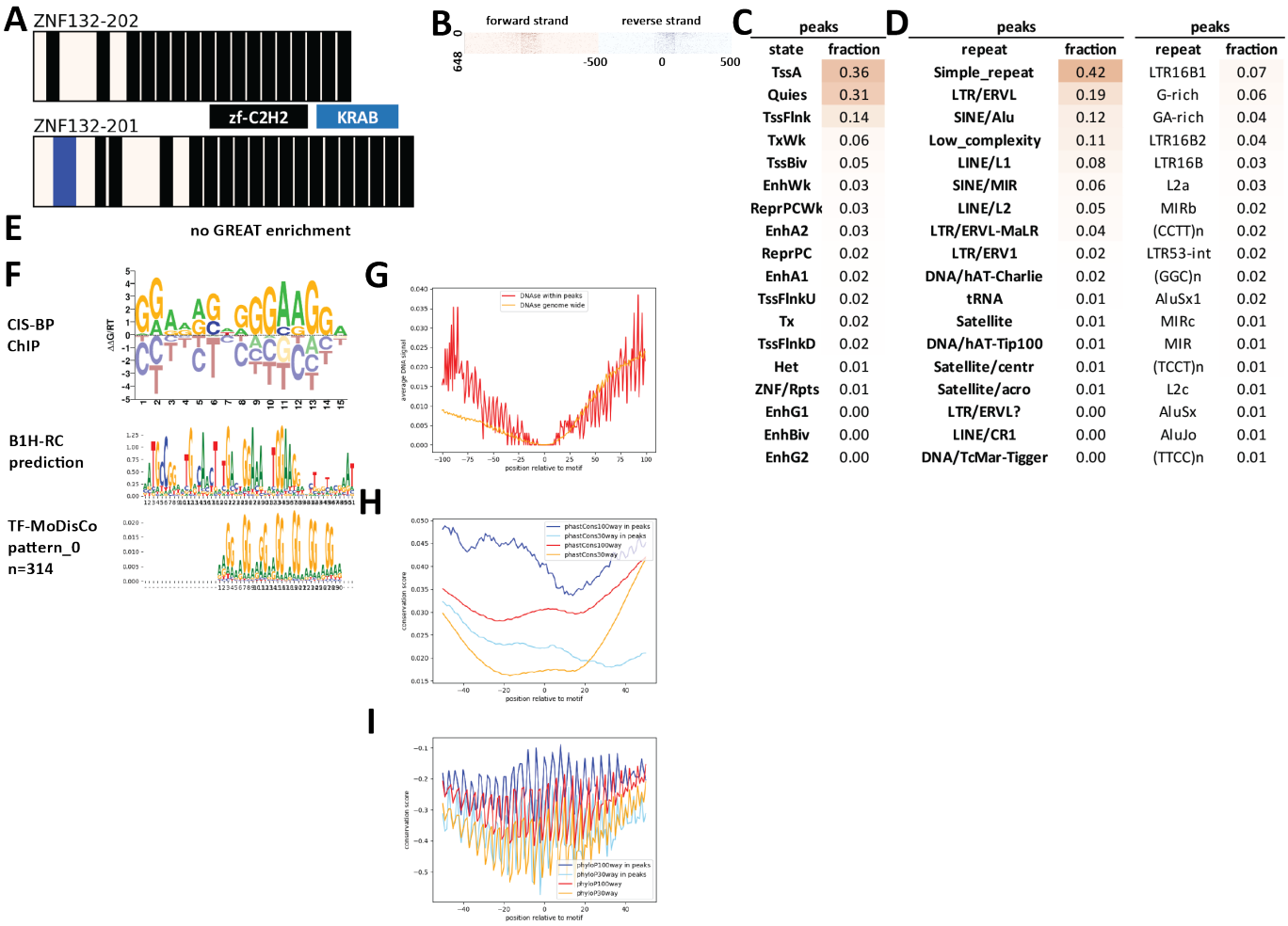

Supplementary Figure 693: Properties and genomic distribution of motifs identified for the ZNF132 transcription factor in HEK293 (accession ChipExo models).

TF-MoDisCO pattern_0 n=314, CWM

pattern_0, n=314; subpattern_0, ns=88

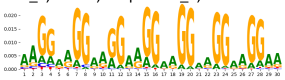

pattern_0, n=314; subpattern_1, ns=80

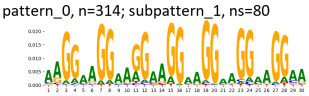

pattern_0, n=314; subpattern_2, ns=72

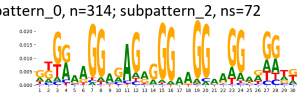

pattern_0, n=314; subpattern_3, ns=49

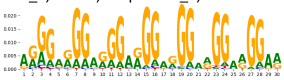

pattern_0, n=314; subpattern_4, ns=25

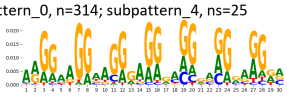

TF-MoDisCO pattern_0 n=314, PWM

pattern_0, n=314; subpattern_0, ns=88

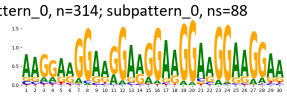

pattern_0, n=314; subpattern_1, ns=80

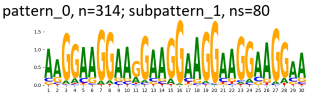

pattern_0, n=314; subpattern_2, ns=72

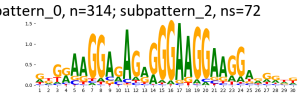

pattern_0, n=314; subpattern_3, ns=49

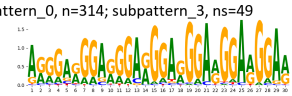

pattern_0, n=314; subpattern_4, ns=25

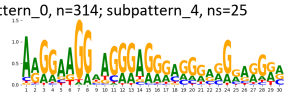

Supplementary Figure 694: TF-MoDisCO subpatterns for the ZNF132 transcription factor in HEK293 (accession ChipExo models).

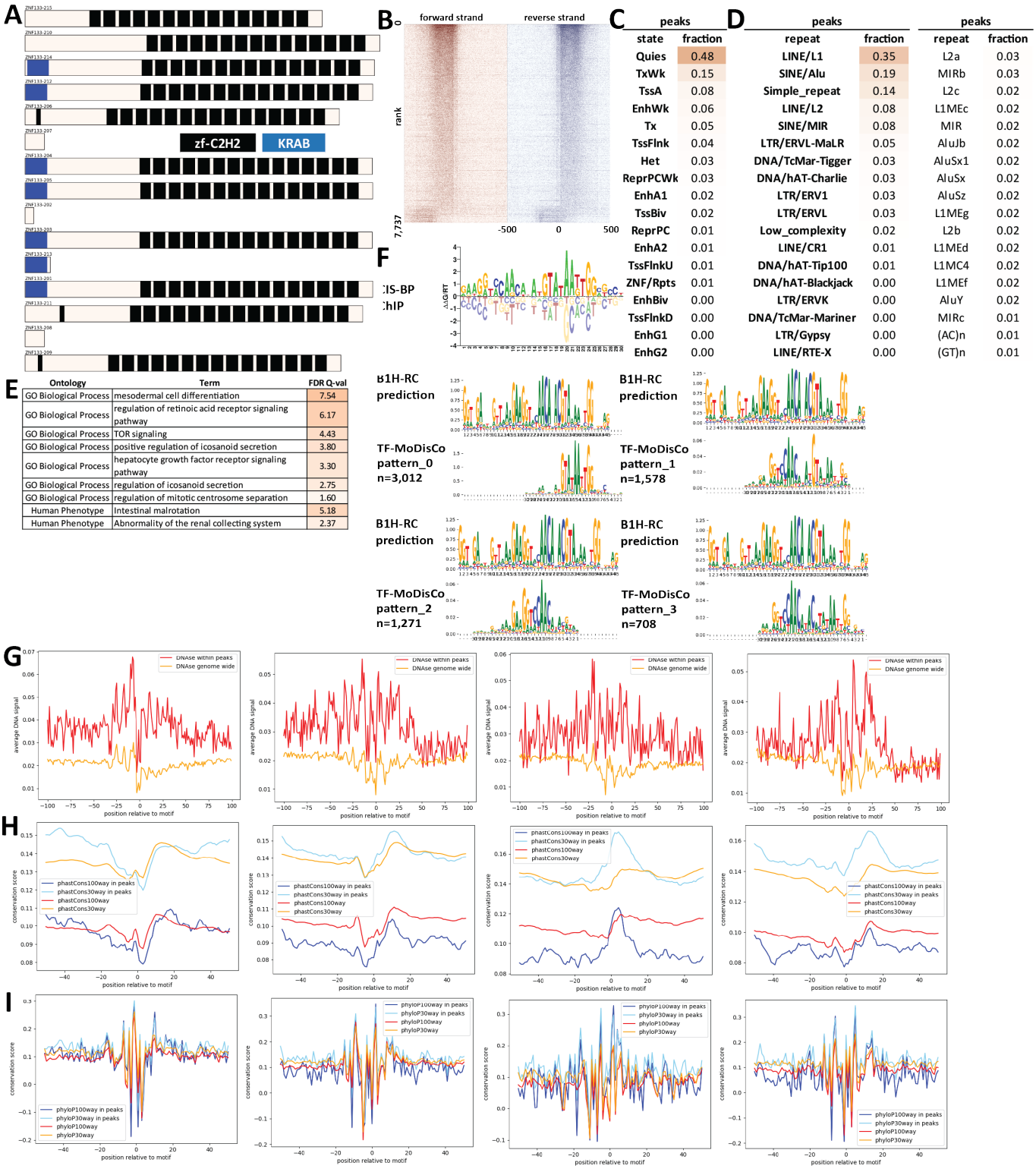

Supplementary Figure 695: Properties and genomic distribution of motifs identified for the ZNF133 transcription factor in HEK293 (accession ENCSR283MWQ).

TF-MoDisCO pattern_0 n=3012, CWM

pattern_0, n=3012; subpattern_0, ns=928

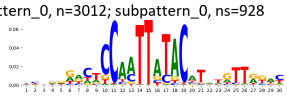

pattern_0, n=3012; subpattern_1, ns=726

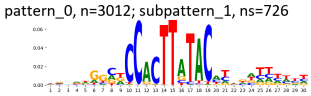

pattern_0, n=3012; subpattern_2, ns=529

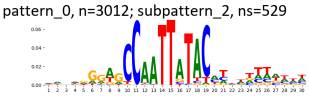

pattern_0, n=3012; subpattern_3, ns=310

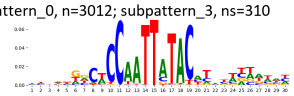

pattern_0, n=3012; subpattern_4, ns=291

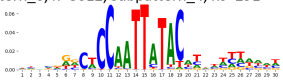

pattern_0, n=3012; subpattern_5, ns=140

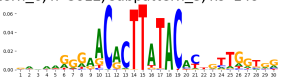

pattern_0, n=3012; subpattern_6, ns=86

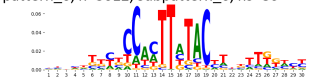

pattern_0, n=3012; subpattern_7, ns=2

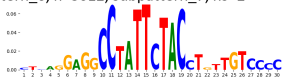

TF-MoDisCO pattern_0 n=3012, PWM

pattern_0, n=3012; subpattern_0, ns=928

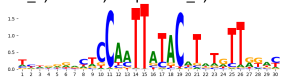

pattern_0, n=3012; subpattern_1, ns=726

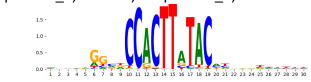

pattern_0, n=3012; subpattern_2, ns=529

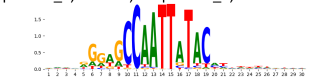

pattern_0, n=3012; subpattern_3, ns=310

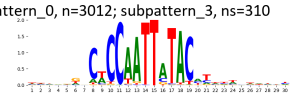

pattern_0, n=3012; subpattern_4, ns=291

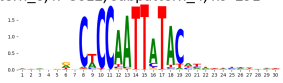

pattern_0, n=3012; subpattern_5, ns=140

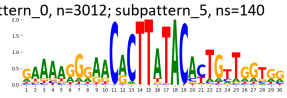

pattern_0, n=3012; subpattern_6, ns=86

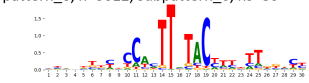

pattern_0, n=3012; subpattern_7, ns=2

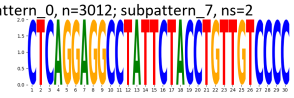

TF-MoDisCO pattern_1 n=1578, CWM

pattern_1, n=1578; subpattern_0, ns=264

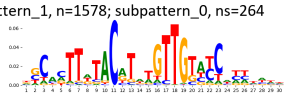

pattern_1, n=1578; subpattern_1, ns=259

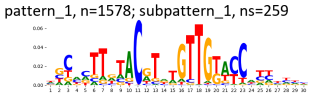

pattern_1, n=1578; subpattern_2, ns=246

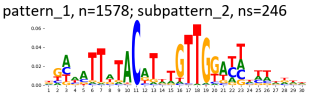

pattern_1, n=1578; subpattern_3, ns=236

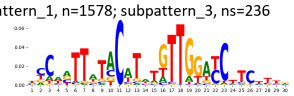

pattern_1, n=1578; subpattern_4, ns=216

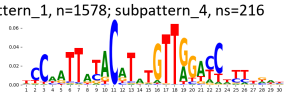

pattern_1, n=1578; subpattern_5, ns=215

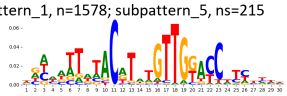

pattern_1, n=1578; subpattern_6, ns=140

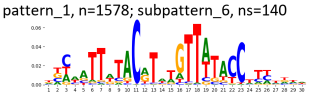

pattern_1, n=1578; subpattern_7, ns=2

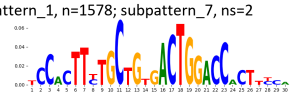

TF-MoDisCO pattern_1 n=1578, PWM

pattern_1, n=1578; subpattern_0, ns=264

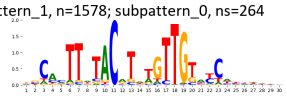

pattern_1, n=1578; subpattern_1, ns=259

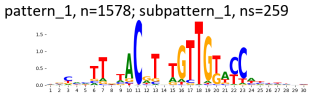

pattern_1, n=1578; subpattern_2, ns=246

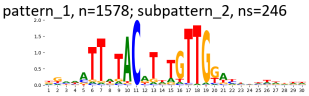

pattern_1, n=1578; subpattern_3, ns=236

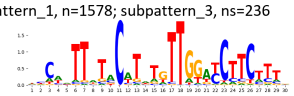

pattern_1, n=1578; subpattern_4, ns=216

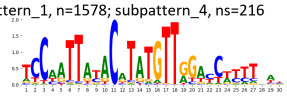

pattern_1, n=1578; subpattern_5, ns=215

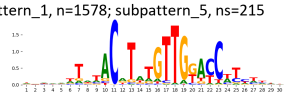

pattern_1, n=1578; subpattern_6, ns=140

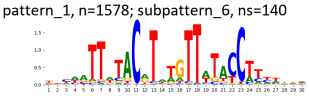

pattern_1, n=1578; subpattern_7, ns=2

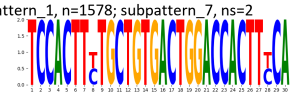

TF-MoDisCO pattern_2 n=1271, CWM

pattern_2, n=1271; subpattern_0, ns=284

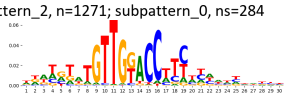

pattern_2, n=1271; subpattern_1, ns=277

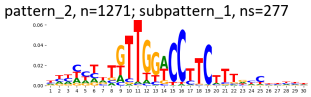

pattern_2, n=1271; subpattern_2, ns=266

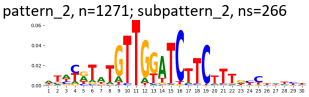

pattern_2, n=1271; subpattern_3, ns=154

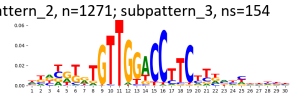

pattern_2, n=1271; subpattern_4, ns=124

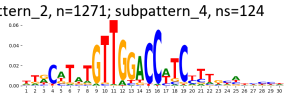

pattern_2, n=1271; subpattern_5, ns=88

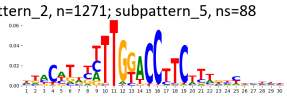

pattern_2, n=1271; subpattern_6, ns=78

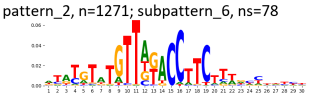

TF-MoDisCO pattern_2 n=1271, PWM

pattern_2, n=1271; subpattern_0, ns=284

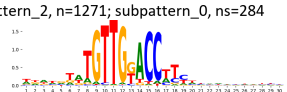

pattern_2, n=1271; subpattern_1, ns=277

pattern_2, n=1271; subpattern_2, ns=266

pattern_2, n=1271; subpattern_3, ns=154

pattern_2, n=1271; subpattern_4, ns=124

pattern_2, n=1271; subpattern_5, ns=88

pattern_2, n=1271; subpattern_6, ns=78

TF-MoDisCO pattern_3 n=708, CWM

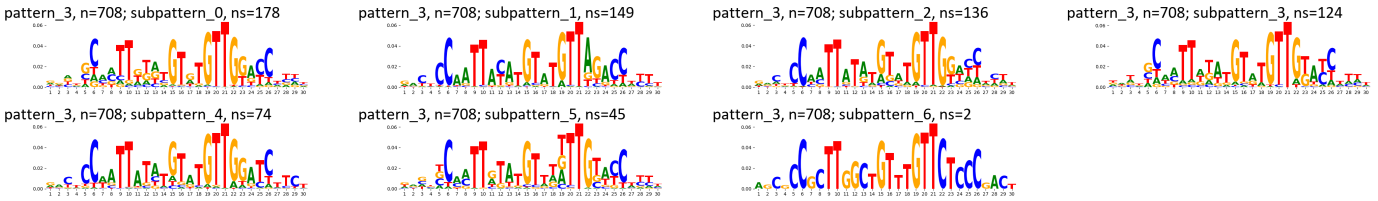

TF-MoDisCO pattern_3 n=708, PWM

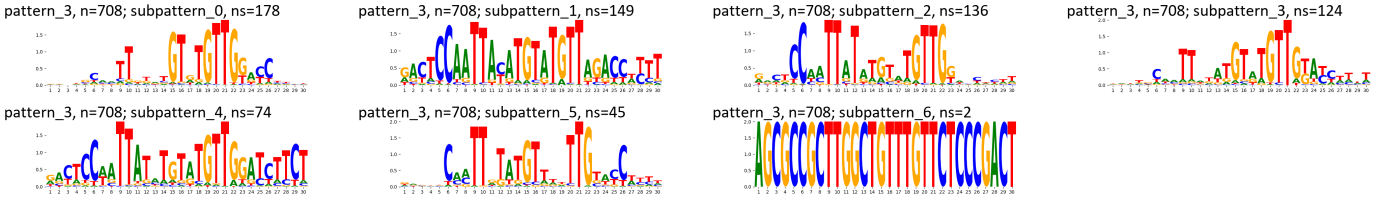

Supplementary Figure 696: TF-MoDisCO subpatterns for the ZNF133 transcription factor in HEK293 (accession ENCSR283MWQ).

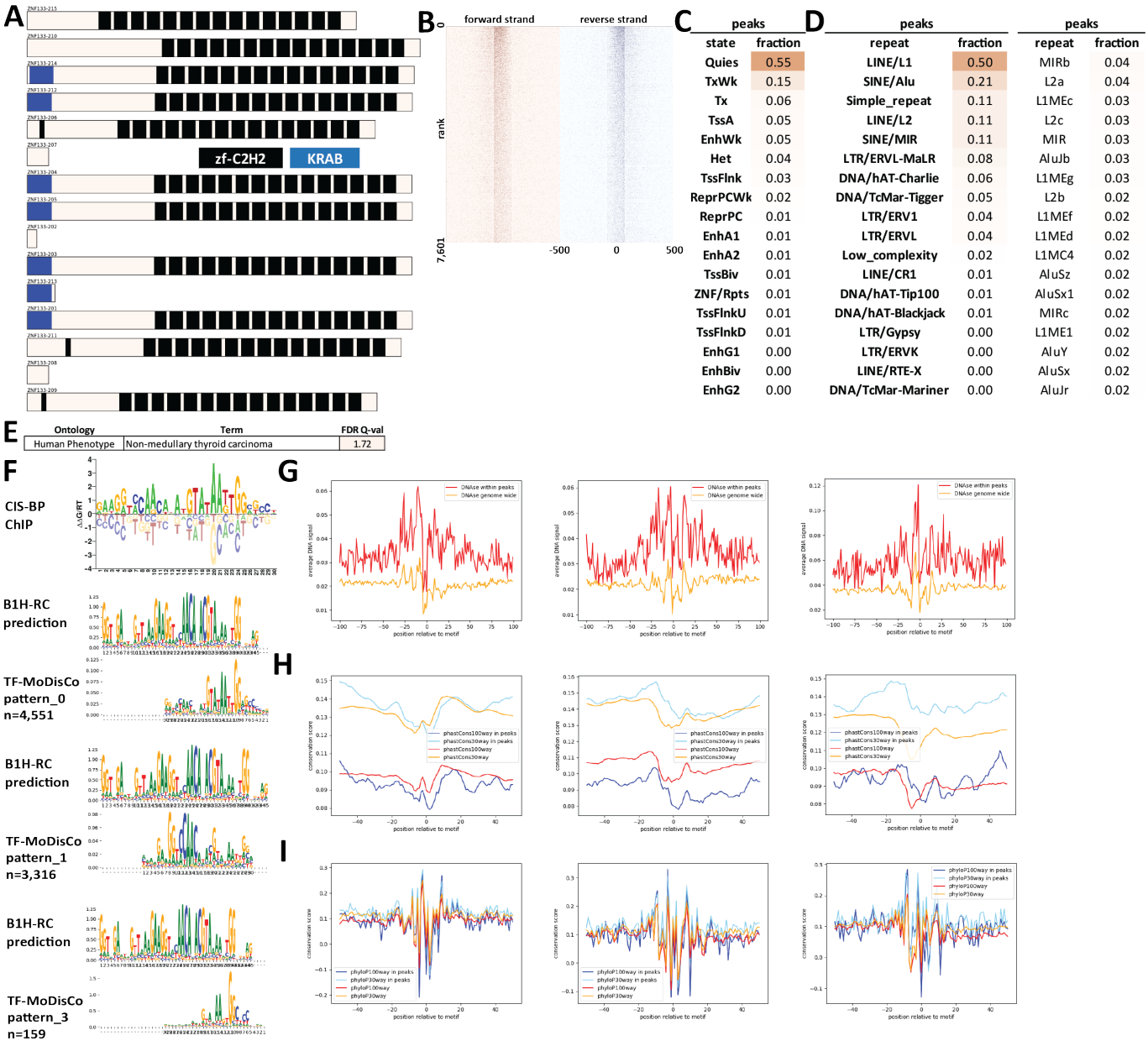

Supplementary Figure 697: Properties and genomic distribution of motifs identified for the ZNF133 transcription factor in HEK293 (accession ChipExo models).

TF-MoDisCO pattern_0 n=4551, CWM

pattern_0, n=4551; subpattern_0, ns=1118

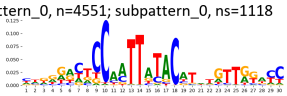

pattern_0, n=4551; subpattern_1, ns=1021

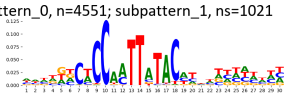

pattern_0, n=4551; subpattern_2, ns=1000

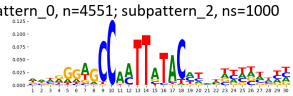

pattern_0, n=4551; subpattern_3, ns=593

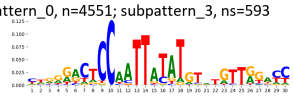

pattern_0, n=4551; subpattern_4, ns=362

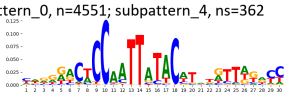

pattern_0, n=4551; subpattern_5, ns=267

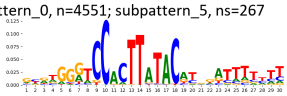

pattern_0, n=4551; subpattern_6, ns=96

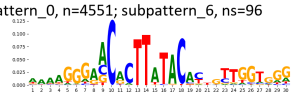

pattern_0, n=4551; subpattern_7, ns=91

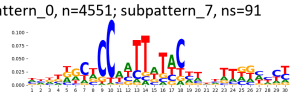

pattern_0, n=4551; subpattern_8, ns=3

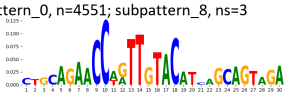

TF-MoDisCO pattern_0 n=4551, PWM

pattern_0, n=4551; subpattern_0, ns=1118

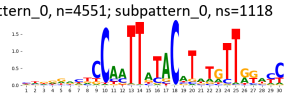

pattern_0, n=4551; subpattern_1, ns=1021

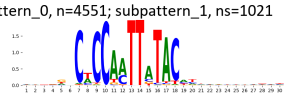

pattern_0, n=4551; subpattern_2, ns=1000

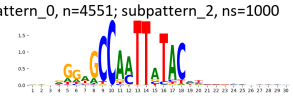

pattern_0, n=4551; subpattern_3, ns=593

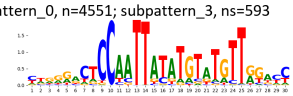

pattern_0, n=4551; subpattern_4, ns=362

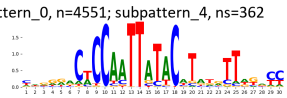

pattern_0, n=4551; subpattern_5, ns=267

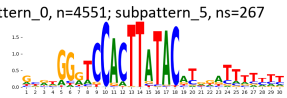

pattern_0, n=4551; subpattern_6, ns=96

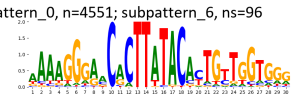

pattern_0, n=4551; subpattern_7, ns=91

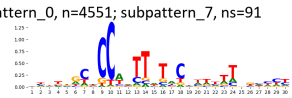

pattern_0, n=4551; subpattern_8, ns=3

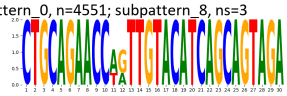

TF-MoDisCO pattern_1 n=3316, CWM

pattern_1, n=3316; subpattern_0, ns=746

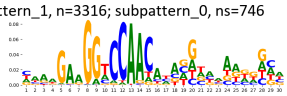

pattern_1, n=3316; subpattern_1, ns=672

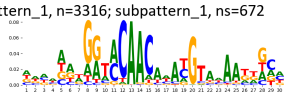

pattern_1, n=3316; subpattern_2, ns=547

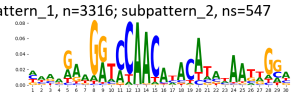

pattern_1, n=3316; subpattern_3, ns=544

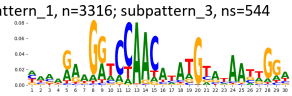

pattern_1, n=3316; subpattern_4, ns=448

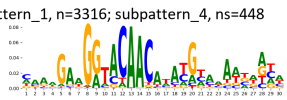

pattern_1, n=3316; subpattern_5, ns=332

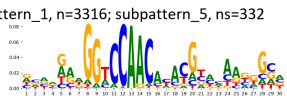

pattern_1, n=3316; subpattern_6, ns=15

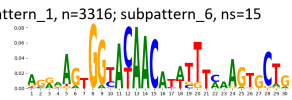

pattern_1, n=3316; subpattern_7, ns=9

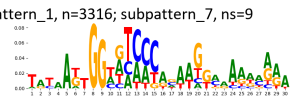

pattern_1, n=3316; subpattern_8, ns=3

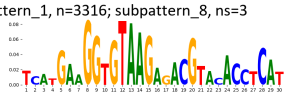

TF-MoDisCO pattern_1 n=3316, PWM

pattern_1, n=3316; subpattern_0, ns=746

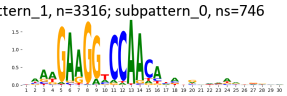

pattern_1, n=3316; subpattern_1, ns=672

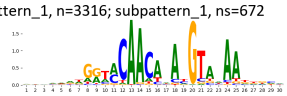

pattern_1, n=3316; subpattern_2, ns=547

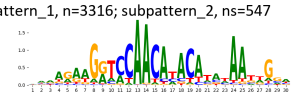

pattern_1, n=3316; subpattern_3, ns=544

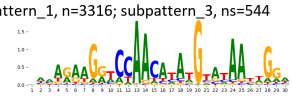

pattern_1, n=3316; subpattern_4, ns=448

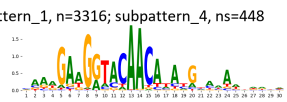

pattern_1, n=3316; subpattern_5, ns=332

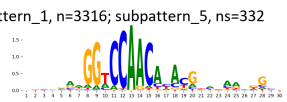

pattern_1, n=3316; subpattern_6, ns=15

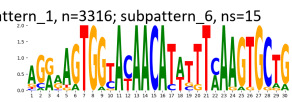

pattern_1, n=3316; subpattern_7, ns=9

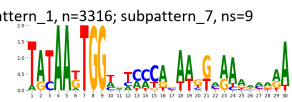

pattern_1, n=3316; subpattern_8, ns=3

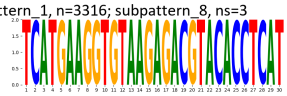

TF-MoDisCO pattern_3 n=159, CWM

pattern_3, n=159; subpattern_0, ns=56

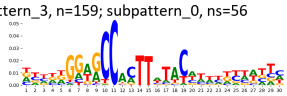

pattern_3, n=159; subpattern_1, ns=48

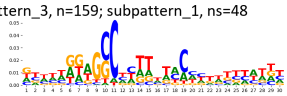

pattern_3, n=159; subpattern_2, ns=27

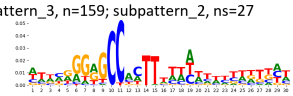

pattern_3, n=159; subpattern_3, ns=15

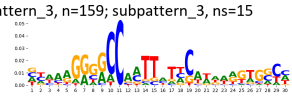

pattern_3, n=159; subpattern_4, ns=13

TF-MoDisCO pattern_3 n=159, PWM

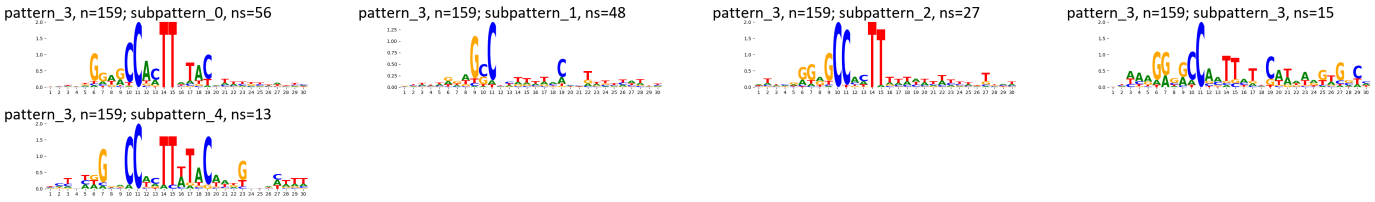

Supplementary Figure 698: TF-MoDisCO subpatterns for the ZNF133 transcription factor in HEK293 (accession ChipExo models).

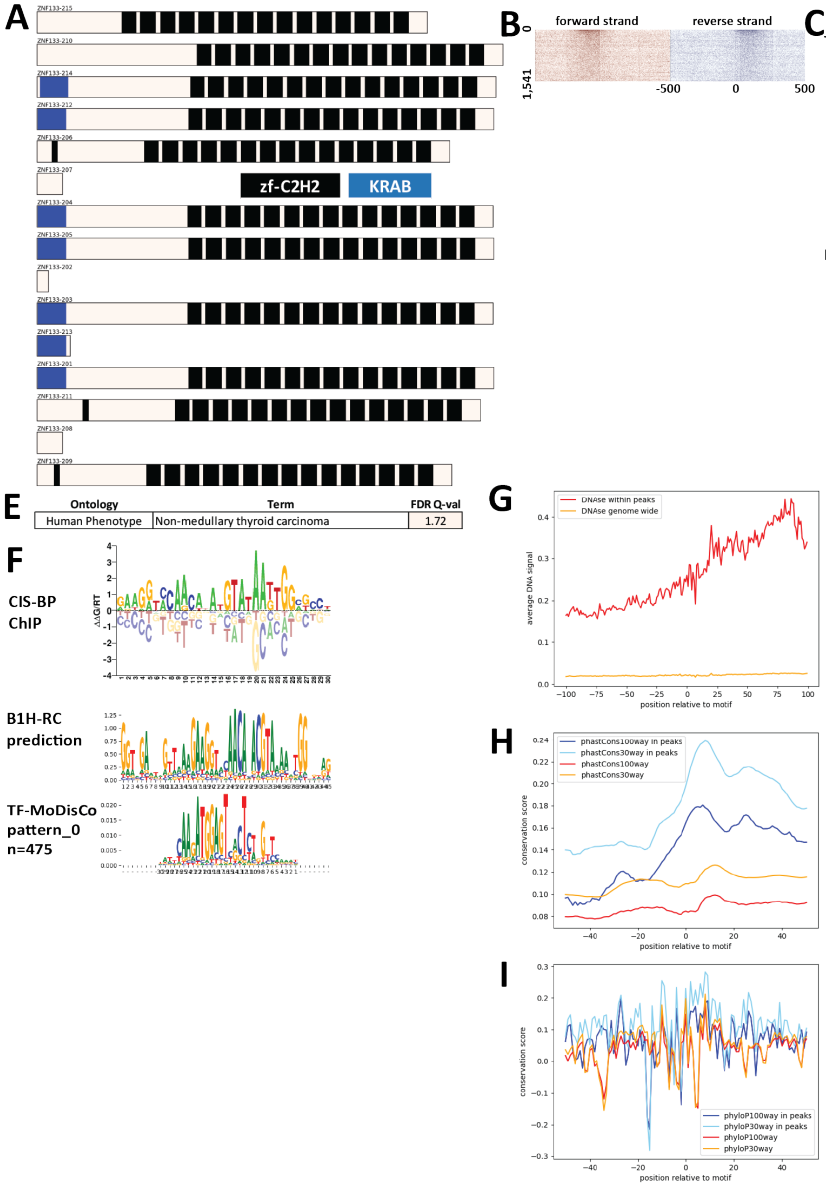

Supplementary Figure 699: Properties and genomic distribution of motifs identified for the ZNF133 transcription factor in K562 (accession ENCSR619UPN).

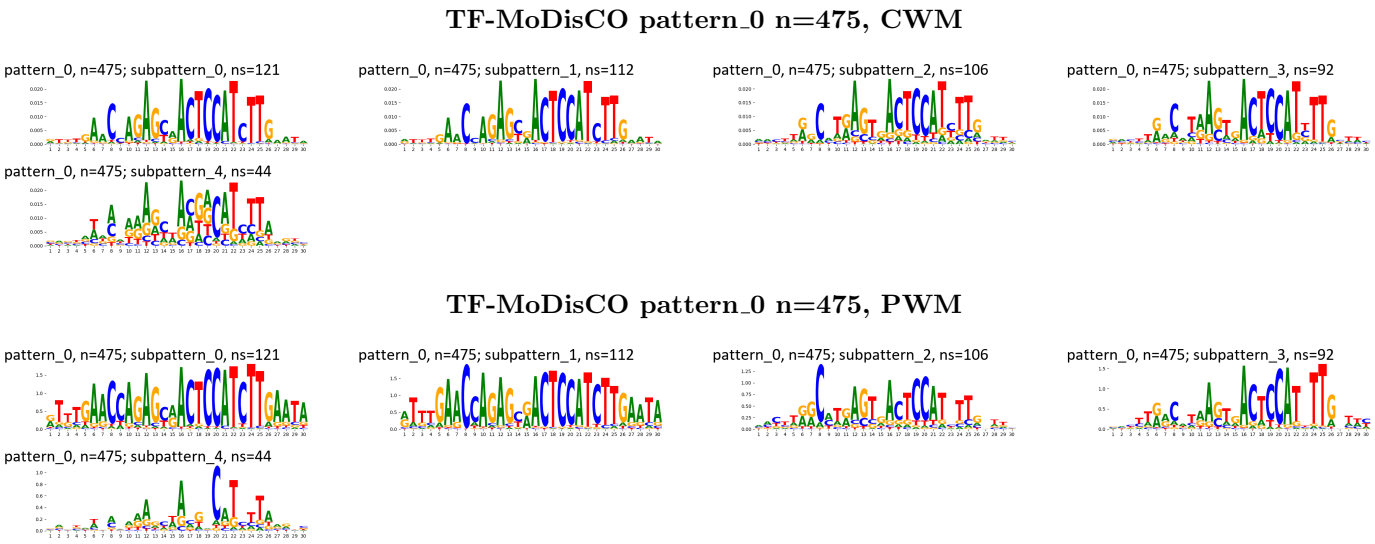

Supplementary Figure 700: TF-MoDisCO subpatterns for the ZNF133 transcription factor in K562 (accession ENCSR619UPN).

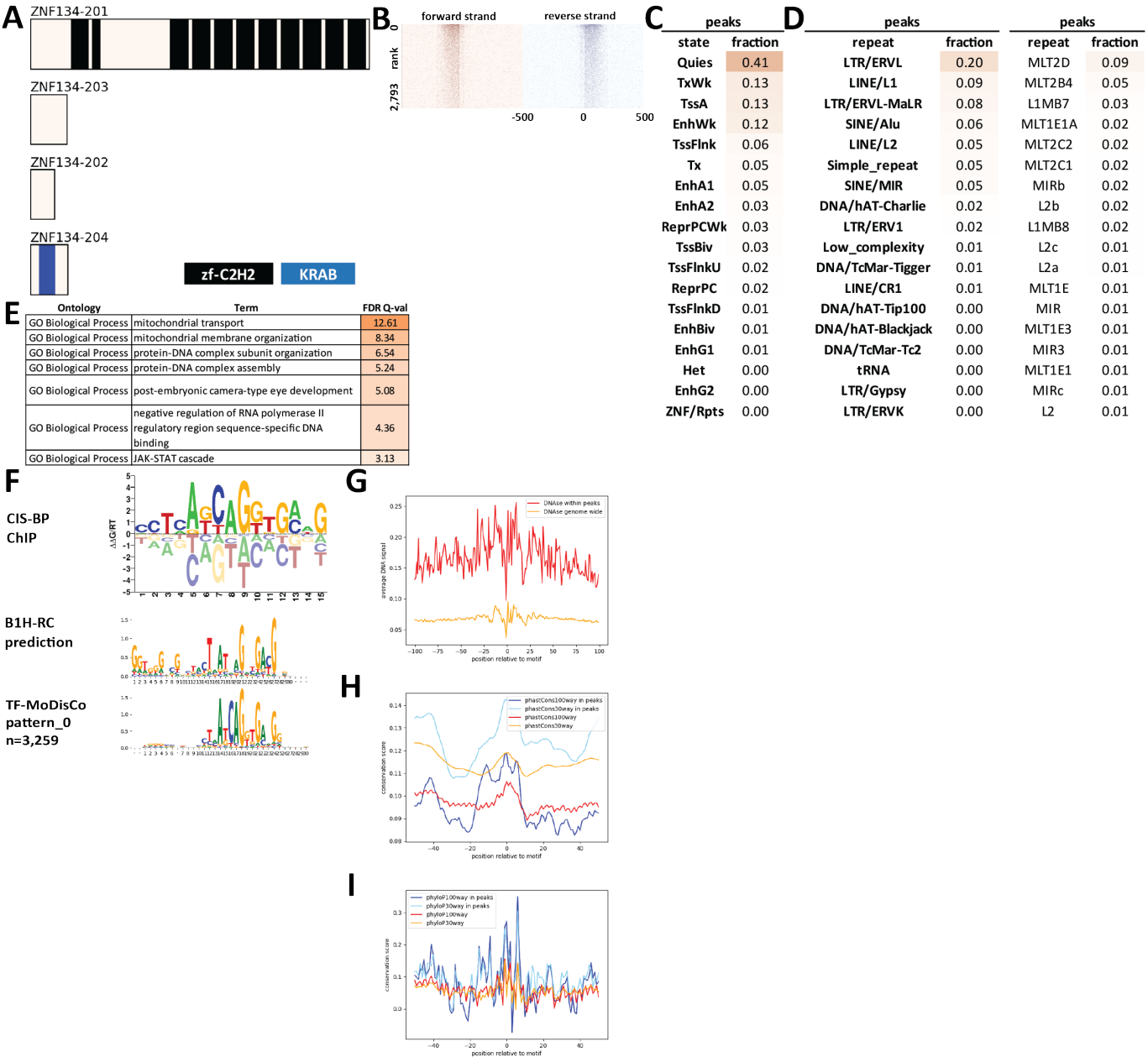

peaks	
state	fraction
Quies	0.41
TxWk	0.13
TssA	0.13
EnhWk	0.12
TssFlnk	0.06
Tx	0.05
EnhA1	0.05
EnhA2	0.03
ReprPCWk	0.03
TssBiv	0.03
TssFlnkU	0.02
ReprPC	0.02
TssFlnkD	0.01
EnhBiv	0.01
EnhG1	0.01
Het	0.00
EnhG2	0.00
ZNF/Rpts	0.00

peaks	
repeat	fraction
LTR/ERVL	0.20
LINE/L1	0.09
LTR/ERVL-MaLR	0.08
SINE/Alu	0.06
LINE/L2	0.05
Simple_repeat	0.05
SINE/MIR	0.05
DNA/hAT-Charlie	0.02
LTR/ERV1	0.02
Low_complexity	0.01
DNA/TcMar-Tigger	0.01
LINE/CR1	0.01
DNA/hAT-Tip100	0.00
DNA/hAT-Blackjack	0.00
DNA/TcMar-Tc2	0.00
tRNA	0.00
LTR/Gypsy	0.00
LTR/ERVK	0.00

peaks	
repeat	fraction
MLT2D	0.09
MLT2B4	0.05
L1MB7	0.03
MLT1E1A	0.02
MLT2C2	0.02
MLT2C1	0.02
MIRb	0.02
L2b	0.02
L1MB8	0.02
L2c	0.01
L2a	0.01
MLT1E	0.01
MIR	0.01
MLT1E3	0.01
MIR3	0.01
MLT1E1	0.01
MIRc	0.01
L2	0.01

Ontology	Term	FDR Q-val
GO Biological Process	mitochondrial transport	12.61
GO Biological Process	mitochondrial membrane organization	8.34
GO Biological Process	protein-DNA complex subunit organization	6.54
GO Biological Process	protein-DNA complex assembly	5.24
GO Biological Process	post-embryonic camera-type eye development	5.08
GO Biological Process	negative regulation of RNA polymerase II regulatory region sequence-specific DNA binding	4.36
GO Biological Process	JAK-STAT cascade	3.13

Supplementary Figure 701: Properties and genomic distribution of motifs identified for the ZNF134 transcription factor in HEK293 (accession Hughes GR models).

TF-MoDisCO pattern_0 n=3259, CWM

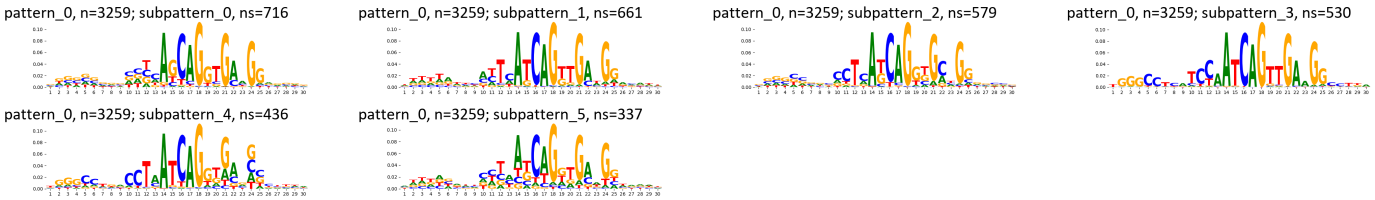

TF-MoDisCO pattern_0 n=3259, PWM

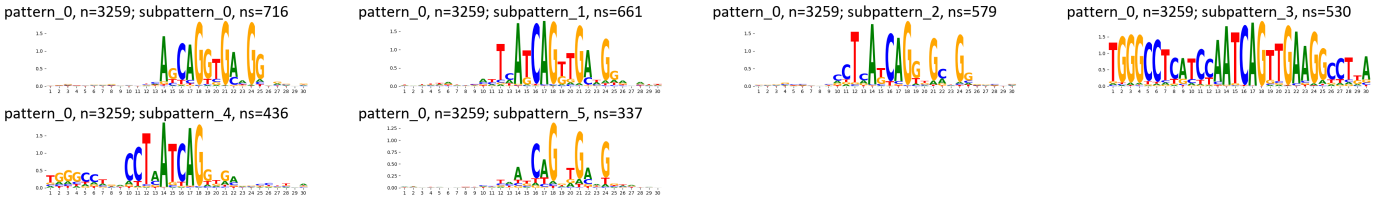

Supplementary Figure 702: TF-MoDisCO subpatterns for the ZNF134 transcription factor in HEK293 (accession Hughes GR models).

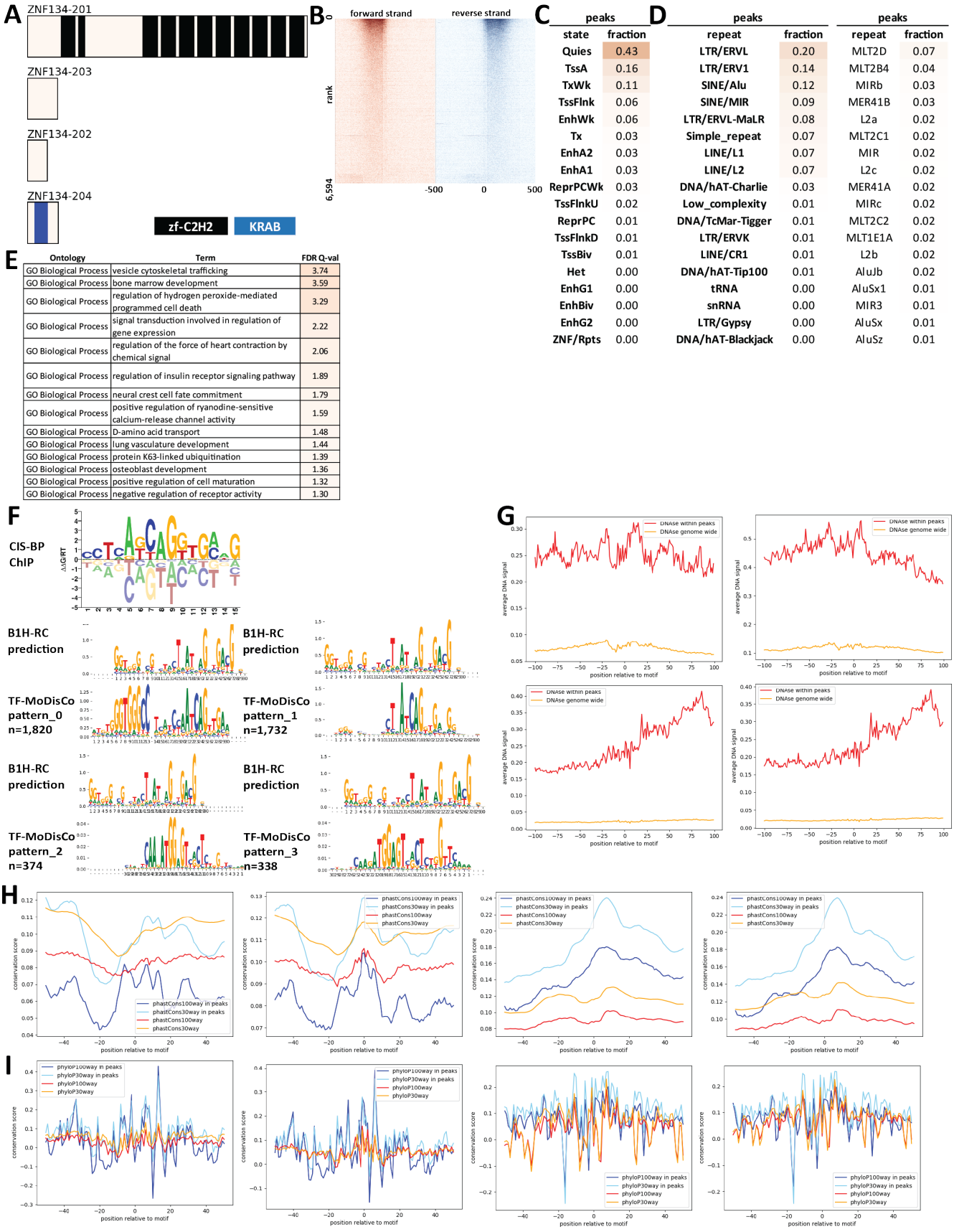

Supplementary Figure 703: Properties and genomic distribution of motifs identified for the ZNF134 transcription factor in K562 (accession ENCSR553NTC).

TF-MoDisCO pattern_0 n=1820, CWM

pattern_0, n=1820; subpattern_0, ns=466

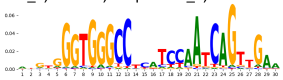

pattern_0, n=1820; subpattern_1, ns=383

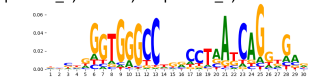

pattern_0, n=1820; subpattern_2, ns=379

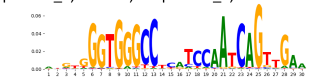

pattern_0, n=1820; subpattern_3, ns=377

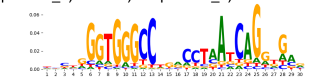

pattern_0, n=1820; subpattern_4, ns=101

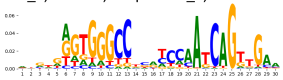

pattern_0, n=1820; subpattern_5, ns=98

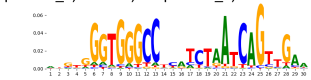

pattern_0, n=1820; subpattern_6, ns=9

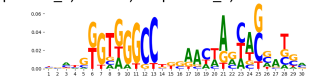

pattern_0, n=1820; subpattern_7, ns=7

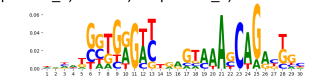

TF-MoDisCO pattern_0 n=1820, PWM

pattern_0, n=1820; subpattern_0, ns=466

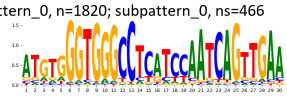

pattern_0, n=1820; subpattern_1, ns=383

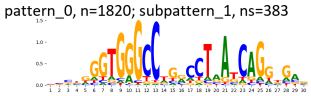

pattern_0, n=1820; subpattern_2, ns=379

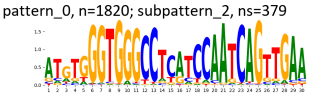

pattern_0, n=1820; subpattern_3, ns=377

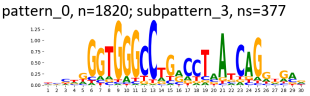

pattern_0, n=1820; subpattern_4, ns=101

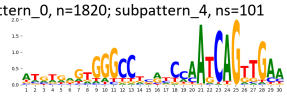

pattern_0, n=1820; subpattern_5, ns=98

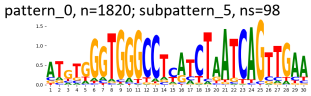

pattern_0, n=1820; subpattern_6, ns=9

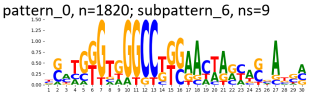

pattern_0, n=1820; subpattern_7, ns=7

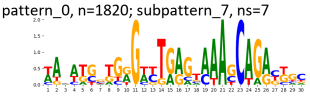

TF-MoDisCO pattern_1 n=1732, CWM

pattern_1, n=1732; subpattern_0, ns=430

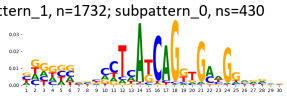

pattern_1, n=1732; subpattern_1, ns=303

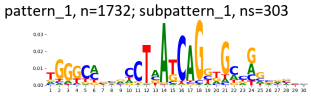

pattern_1, n=1732; subpattern_2, ns=293

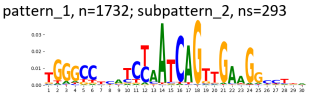

pattern_1, n=1732; subpattern_3, ns=263

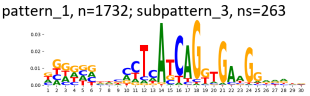

pattern_1, n=1732; subpattern_4, ns=247

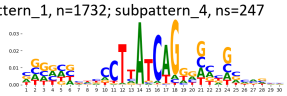

pattern_1, n=1732; subpattern_5, ns=192

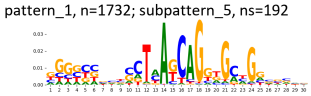

pattern_1, n=1732; subpattern_6, ns=2

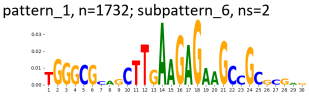

pattern_1, n=1732; subpattern_7, ns=2

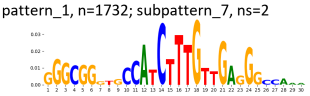

TF-MoDisCO pattern_1 n=1732, PWM

pattern_1, n=1732; subpattern_0, ns=430

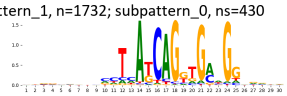

pattern_1, n=1732; subpattern_1, ns=303

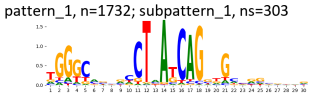

pattern_1, n=1732; subpattern_2, ns=293

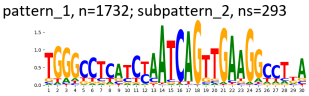

pattern_1, n=1732; subpattern_3, ns=263

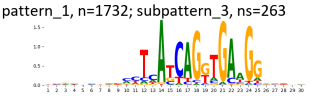

pattern_1, n=1732; subpattern_4, ns=247

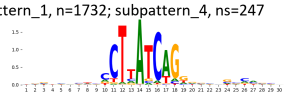

pattern_1, n=1732; subpattern_5, ns=192

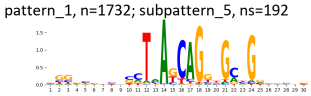

pattern_1, n=1732; subpattern_6, ns=2

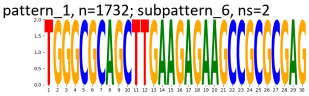

pattern_1, n=1732; subpattern_7, ns=2

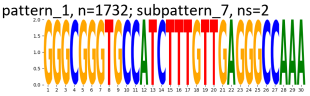

TF-MoDisCO pattern_2 n=374, CWM

pattern_2, n=374; subpattern_0, ns=110

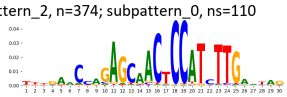

pattern_2, n=374; subpattern_1, ns=103

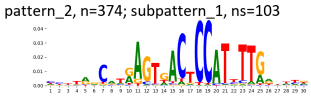

pattern_2, n=374; subpattern_2, ns=65

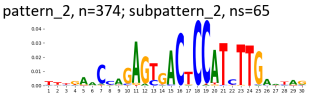

pattern_2, n=374; subpattern_3, ns=36

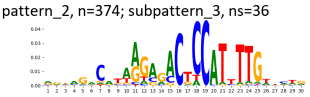

pattern_2, n=374; subpattern_4, ns=30

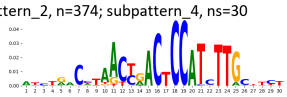

pattern_2, n=374; subpattern_5, ns=17

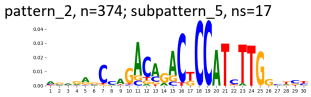

pattern_2, n=374; subpattern_6, ns=13

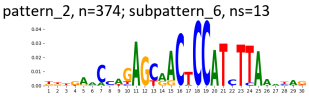

TF-MoDisCO pattern_2 n=374, PWM

pattern_2, n=374; subpattern_0, ns=110

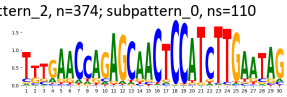

pattern_2, n=374; subpattern_1, ns=103

pattern_2, n=374; subpattern_2, ns=65

pattern_2, n=374; subpattern_3, ns=36

pattern_2, n=374; subpattern_4, ns=30

pattern_2, n=374; subpattern_5, ns=17

pattern_2, n=374; subpattern_6, ns=13

TF-MoDisCO pattern_3 n=338, CWM

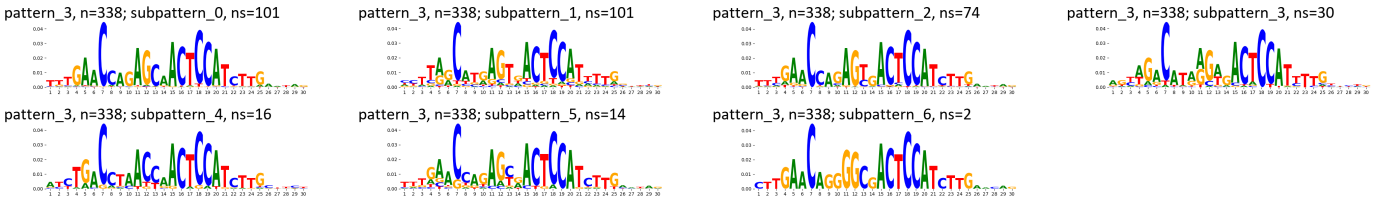

TF-MoDisCO pattern_3 n=338, PWM

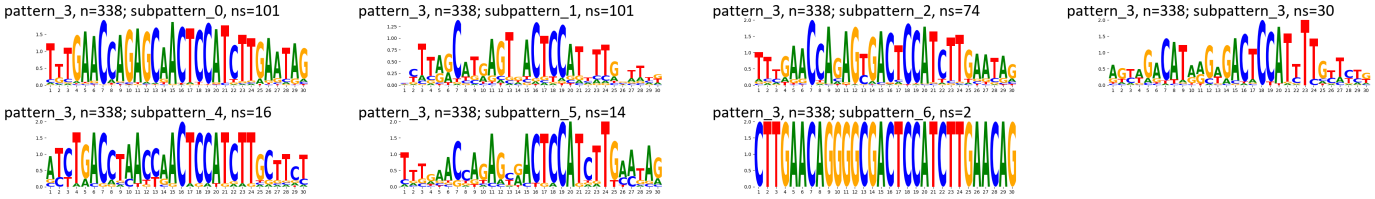

Supplementary Figure 704: TF-MoDisCO subpatterns for the ZNF134 transcription factor in K562 (accession ENCSR553NTC).

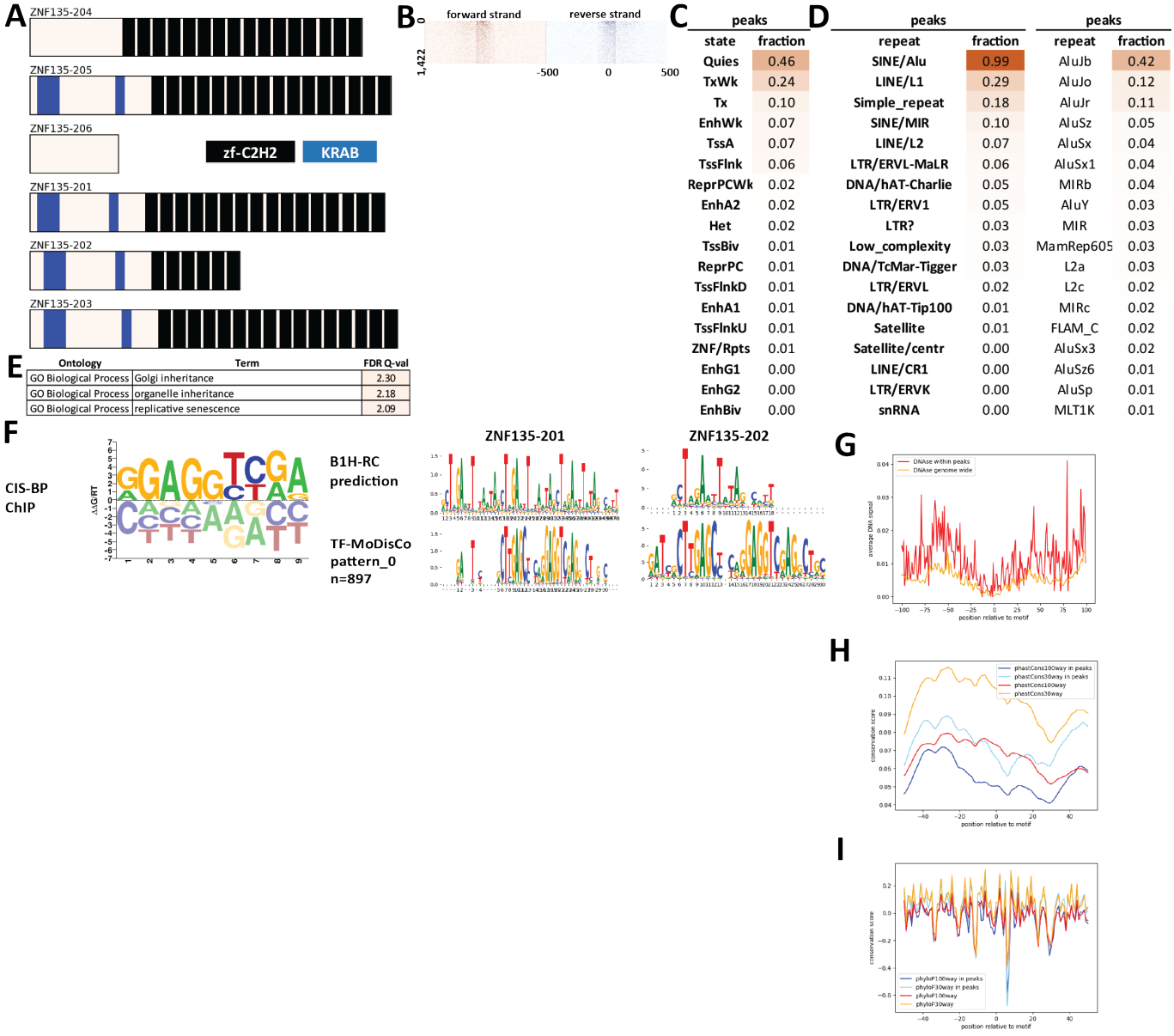

Supplementary Figure 705: Properties and genomic distribution of motifs identified for the ZNF135 transcription factor in HEK293 (accession ChipExo models).

TF-MoDisCO pattern_0 n=897, CWM

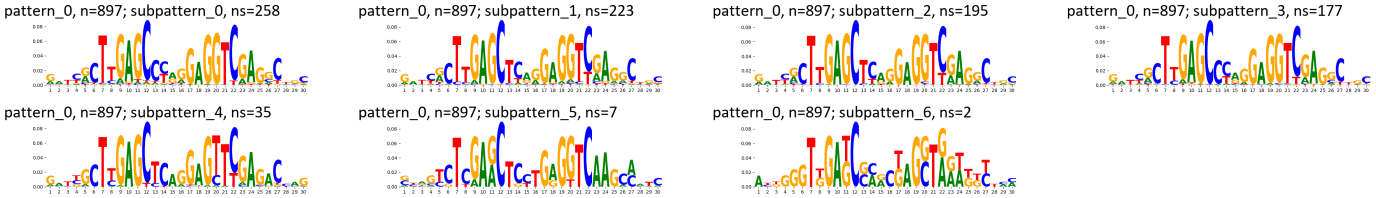

TF-MoDisCO pattern_0 n=897, PWM

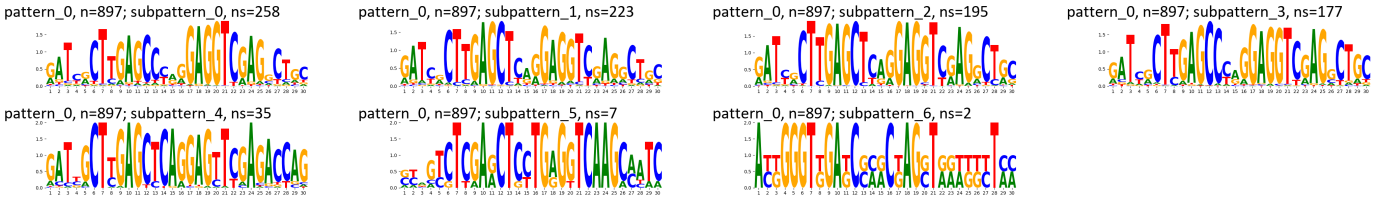

Supplementary Figure 706: TF-MoDisCO subpatterns for the ZNF135 transcription factor in HEK293 (accession ChipExo models).

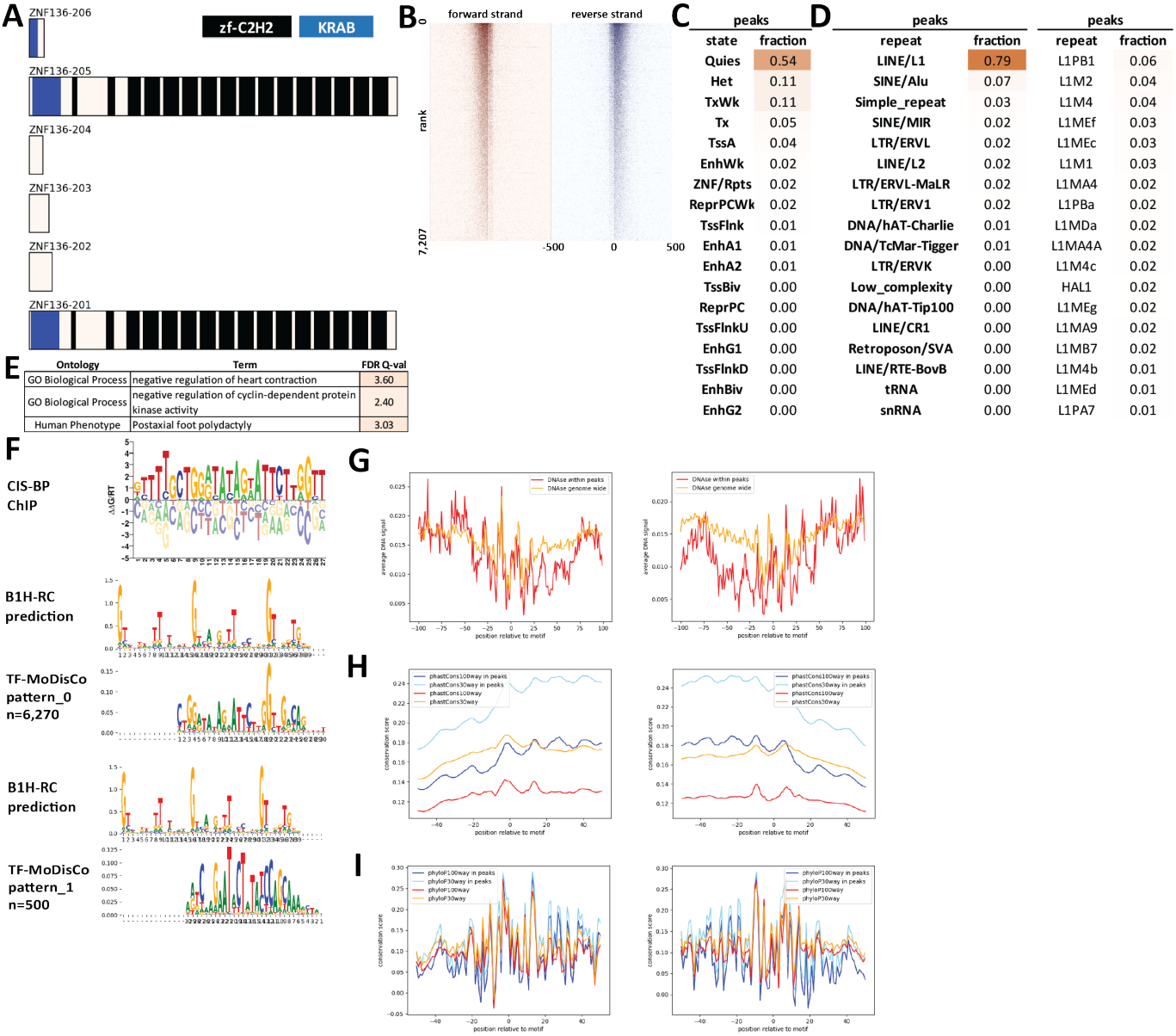

Supplementary Figure 707: Properties and genomic distribution of motifs identified for the ZNF136 transcription factor in HEK293 (accession Hughes NB models).

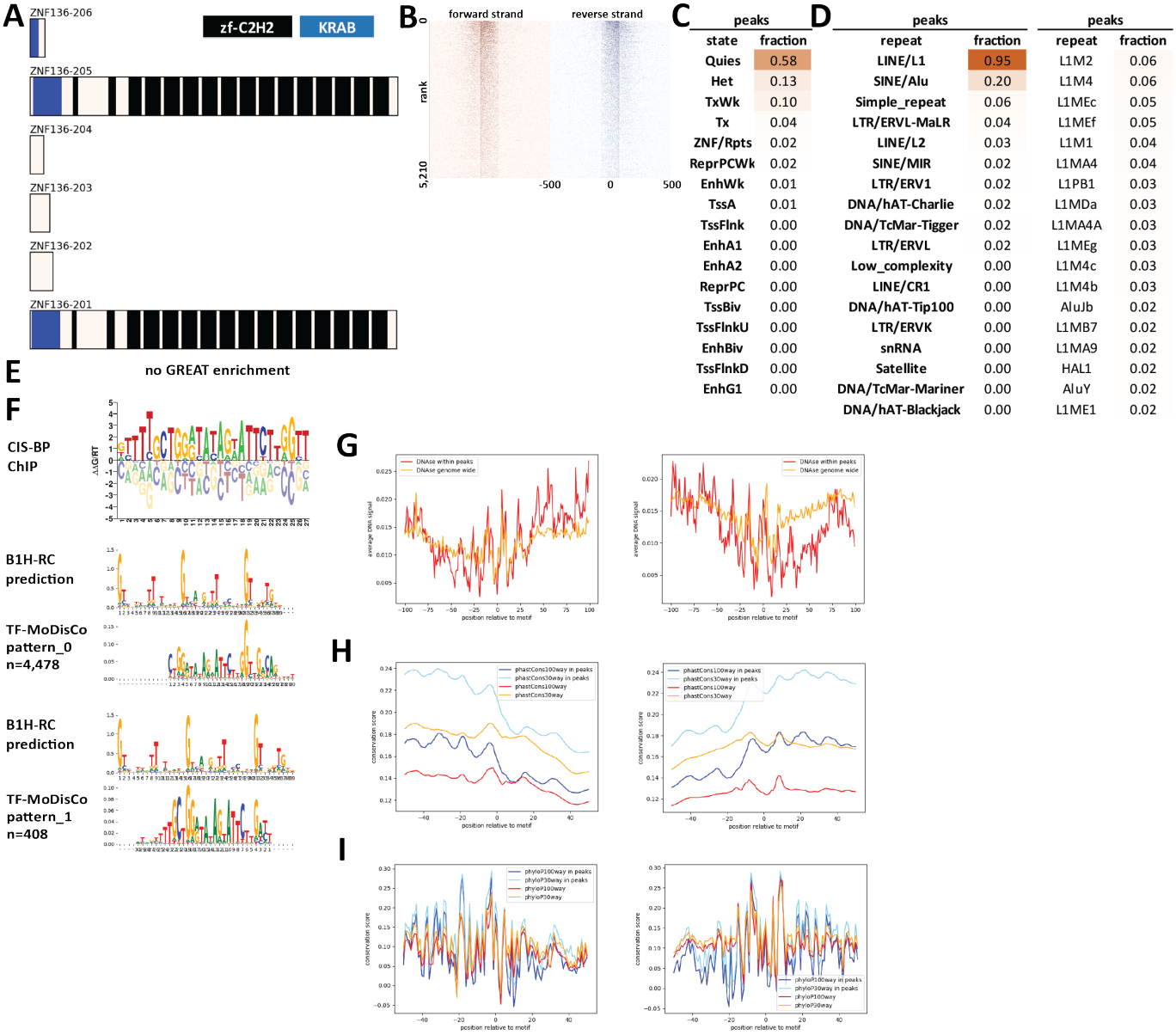

Supplementary Figure 708: Properties and genomic distribution of motifs identified for the ZNF136 transcription factor in HEK293 (accession ChipExo models).

TF-MoDisCO pattern_0 n=4478, CWM

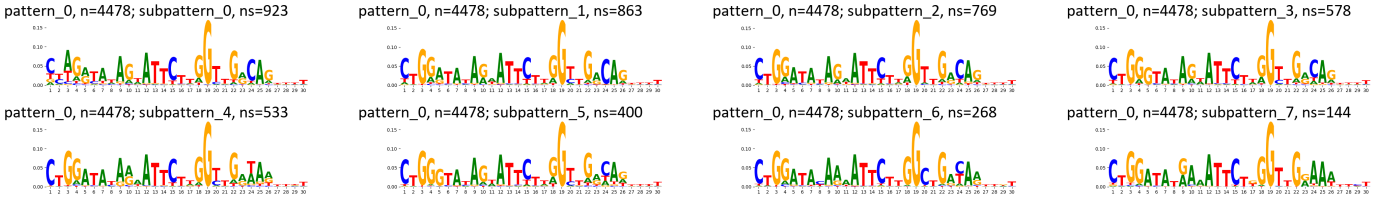

TF-MoDisCO pattern_0 n=4478, PWM

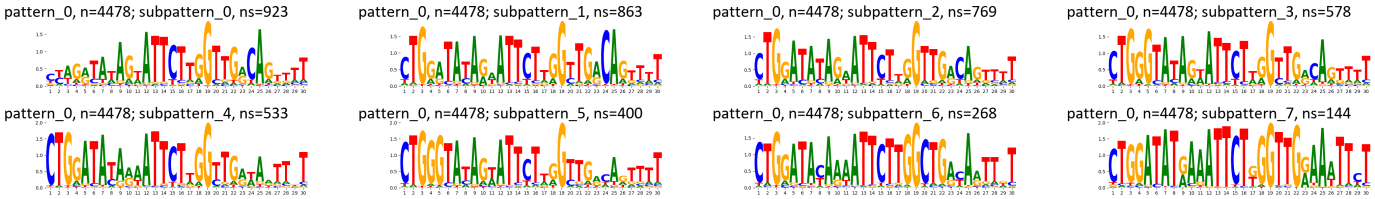

TF-MoDisCO pattern_1 n=408, CWM

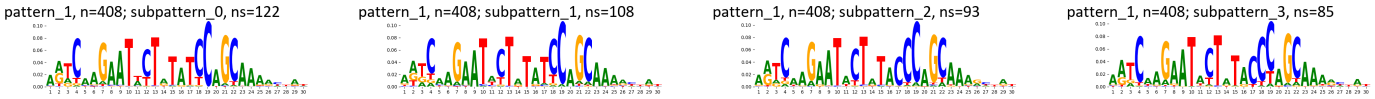

TF-MoDisCO pattern_1 n=408, PWM



Supplementary Figure 709: TF-MoDisCO subpatterns for the ZNF136 transcription factor in HEK293 (accession ChipExo models).

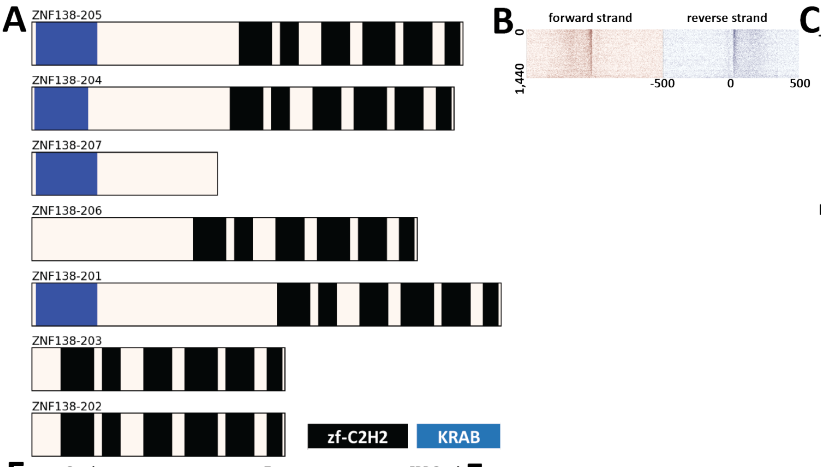

C

peaks	
state	fraction
Quies	0.50
TxWk	0.19
TssA	0.11
Tx	0.06
EnhWk	0.03
TssFlnk	0.03
ReprPCWk	0.03
Het	0.02
TssFlnkU	0.02
ReprPC	0.01
EnhA2	0.01
TssFlnkD	0.01
EnhA1	0.01
TssBiv	0.01
EnhG1	0.00
ZNF/Rpts	0.00
EnhG2	0.00
EnhBiv	0.00

D

peaks		peaks	
repeat	fraction	repeat	fraction
SINE/Alu	0.94	(AAAT)n	0.29
Simple_repeat	0.68	AluSx1	0.12
LINE/L1	0.20	AluSx	0.11
SINE/MIR	0.06	AluSz	0.09
LINE/L2	0.05	AluY	0.09
LTR/ERV1	0.03	AluJb	0.09
LTR/ERVL-MaLR	0.03	(ATTT)n	0.07
DNA/hAT-Charlie	0.02	(TTAT)n	0.07
LTR/ERVL	0.02	AluJo	0.06
DNA/TcMar-Tigger	0.01	AluSq2	0.06
Low_complexity	0.01	(TTTA)n	0.06
Retroposon/SVA	0.01	(AATA)n	0.05
LINE/CR1	0.00	AluSp	0.05
DNA/hAT-Tip100	0.00	AluJr	0.05
LTR/ERVK	0.00	AluSz6	0.04
DNA/TcMar-Mariner	0.00	(TATT)n	0.04
LINE/RTE-X	0.00	AluSc	0.03
tRNA	0.00	AluSg	0.03

E

Ontology	Term	FDR Q-val
GO Biological Process	glucose catabolic process	5.43
GO Biological Process	positive regulation of apoptotic signaling pathway	2.87
GO Biological Process	positive regulation of cellular senescence	2.23
GO Biological Process	positive regulation of cell aging	2.20
GO Biological Process	gap junction assembly	2.18
GO Biological Process	response to morphine	1.60
GO Biological Process	otic vesicle formation	1.47
Human Phenotype	Otitis media	1.95
Human Phenotype	Recurrent otitis media	1.37
Human Phenotype	Hirsutism	1.40

F

no CIS-BP motif available

B1H-RC prediction



no motif discovered de novo

Supplementary Figure 710: Properties and genomic distribution of motifs identified for the ZNF138 transcription factor in HEK293 (accession ENCSR551KAP).

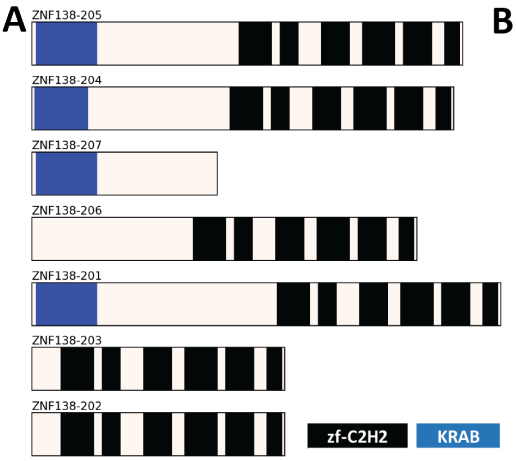

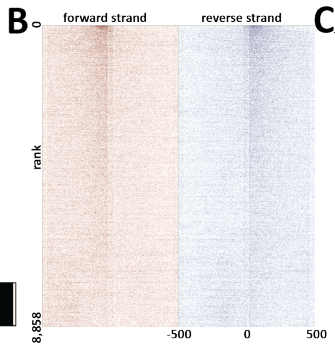

C

peaks

state	fraction
TssA	0.48
TssFlnk	0.20
Quies	0.11
TxWk	0.06
TssFlnkU	0.04
TssBiv	0.04
EnhWk	0.03
ReprPC	0.02
EnhA2	0.02
ReprPCWk	0.02
EnhA1	0.02
TssFlnkD	0.02
Tx	0.01
EnhBiv	0.00
EnhG1	0.00
Het	0.00
EnhG2	0.00
ZNF/Rpts	0.00

D

peaks

repeat	fraction
Simple_repeat	0.23
SINE/MIR	0.09
SINE/Alu	0.07
Low_complexity	0.05
LINE/L2	0.04
LINE/L1	0.02
DNA/hAT-Charlie	0.01
LTR/ERV1	0.01
LTR/ERVL-MaLR	0.01
LTR/ERVL	0.01
tRNA	0.00
DNA/hAT-Tip100	0.00
LINE/CR1	0.00
DNA/TcMar-Tigger	0.00
DNA/hAT-Blackjack	0.00
snRNA	0.00
LTR/ERVK	0.00
DNA/hAT	0.00

peaks

repeat	fraction
G-rich	0.04
MIRb	0.03
MIR3	0.02
MIR	0.02
MIRc	0.01
L2a	0.01
L2b	0.01
L2c	0.01
(GGC)n	0.01
GA-rich	0.01
AluSx	0.01
AluJb	0.01
(GCC)n	0.01
AluSx1	0.01
(GCG)n	0.01
(CCG)n	0.01
AluJo	0.01
(CGC)n	0.01

E

Ontology	Term	FDR Q-val
GO Biological Process	regulation of transcription from RNA polymerase II promoter in response to stress	33.66
GO Biological Process	regulation of DNA-templated transcription in response to stress	29.62
GO Biological Process	rRNA metabolic process	27.80
GO Biological Process	rRNA processing	27.70
GO Biological Process	ribosome biogenesis	27.60
GO Biological Process	regulation of intrinsic apoptotic signaling pathway	27.18
GO Biological Process	IRE1-mediated unfolded protein response	25.69
GO Biological Process	endoplasmic reticulum unfolded protein response	24.16
GO Biological Process	positive regulation of nuclease activity	23.79
GO Biological Process	activation of signaling protein activity involved in unfolded protein response	22.82
GO Biological Process	RNA catabolic process	21.76
GO Biological Process	nuclear-transcribed mRNA catabolic process	20.97
GO Biological Process	mRNA catabolic process	20.89
GO Biological Process	response to unfolded protein	20.88
GO Biological Process	response to topologically incorrect protein	20.51
GO Biological Process	negative regulation of intrinsic apoptotic signaling pathway	20.20
GO Biological Process	cellular response to unfolded protein	19.84
GO Biological Process	cellular response to topologically incorrect protein	19.46
GO Biological Process	protein targeting to ER	19.22
GO Biological Process	regulation of transcription from RNA polymerase II promoter in response to hypoxia	18.74
Human Phenotype	Exercise intolerance	11.14
Human Phenotype	Increased serum lactate	11.09
Human Phenotype	Increased CSF lactate	8.33
Human Phenotype	Abnormal CSF metabolite level	7.58
Human Phenotype	Progressive external ophthalmoplegia	5.05
Human Phenotype	Increased muscle lipid content	3.97
Human Phenotype	Increased intramyocellular lipid droplets	3.82
Human Phenotype	CNS hypomyelination	3.76
Human Phenotype	Dysphonia	3.51
Human Phenotype	Colon cancer	2.38
Human Phenotype	Weight loss	2.13
Human Phenotype	Abnormality of visual evoked potentials	1.86
Human Phenotype	Abnormal activity of mitochondrial respiratory chain	1.75
Human Phenotype	Decreased activity of mitochondrial respiratory chain	1.59

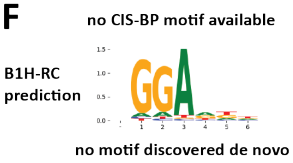

Supplementary Figure 711: Properties and genomic distribution of motifs identified for the ZNF138 transcription factor in HepG2 (accession ENCSR910MUD).

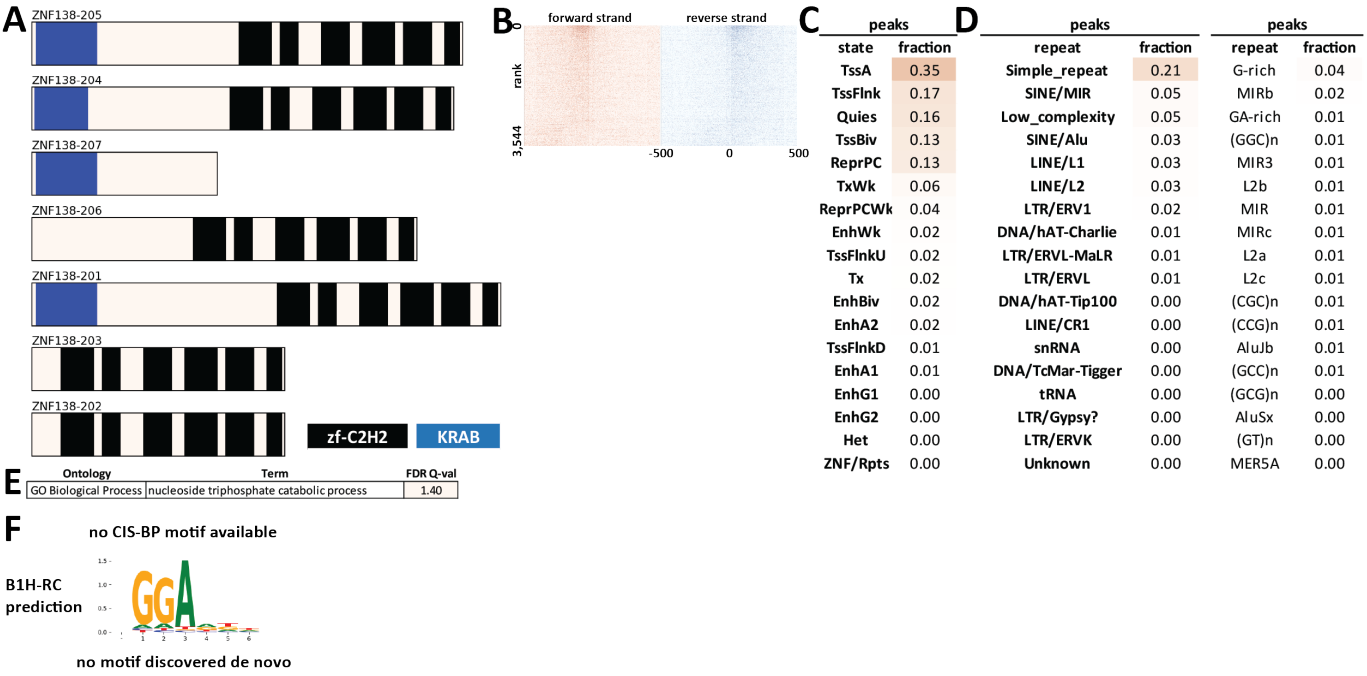

Supplementary Figure 712: Properties and genomic distribution of motifs identified for the ZNF138 transcription factor in WTC11 (accession ENCSR373KKV).

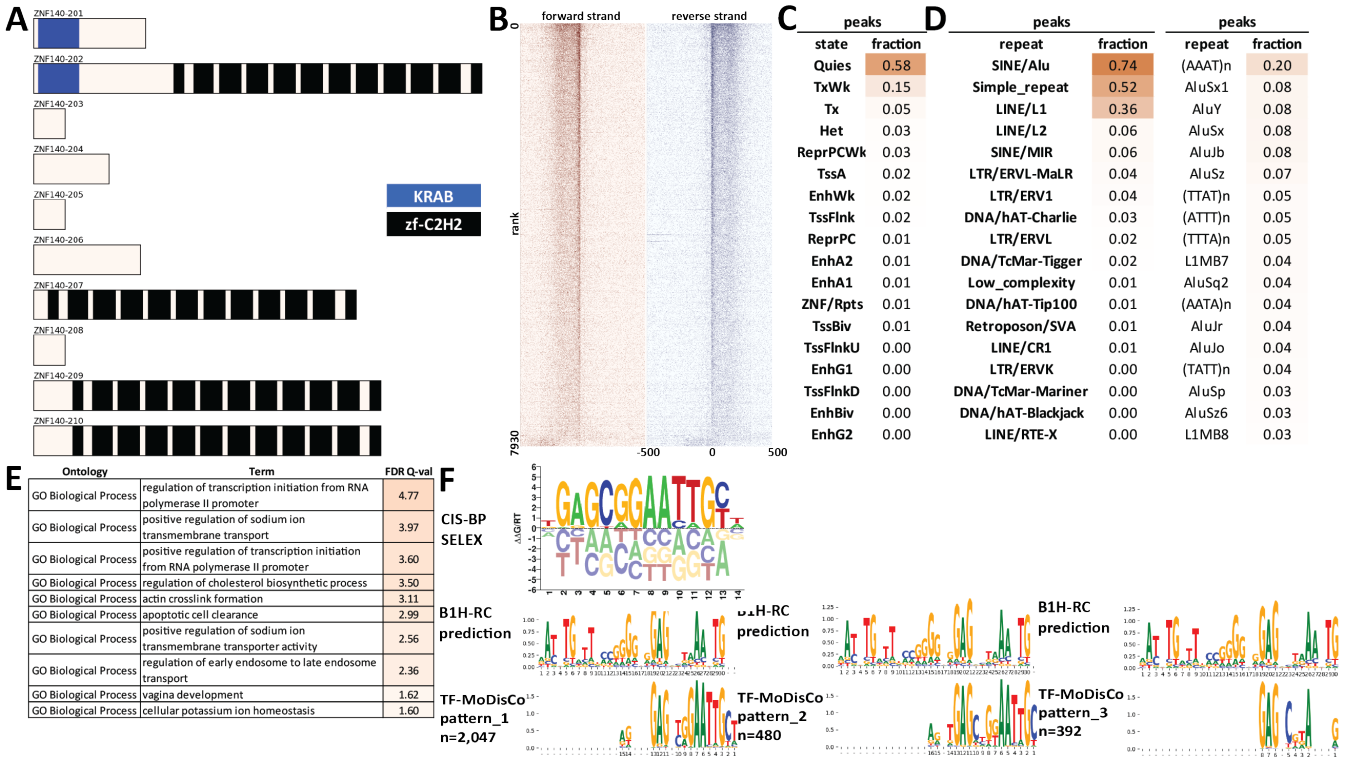

Supplementary Figure 713: Properties and genomic distribution of motifs identified for the ZNF140 transcription factor in HEK293 (accession ENCSR464KFG).

TF-MoDisCO pattern_1 n=2047, CWM

pattern_1, n=2047; subpattern_0, ns=591

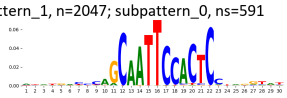

pattern_1, n=2047; subpattern_1, ns=572

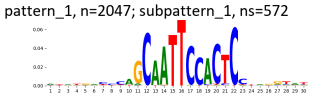

pattern_1, n=2047; subpattern_2, ns=449

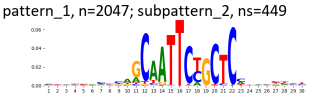

pattern_1, n=2047; subpattern_3, ns=435

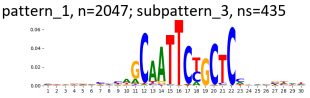

TF-MoDisCO pattern_1 n=2047, PWM

pattern_1, n=2047; subpattern_0, ns=591

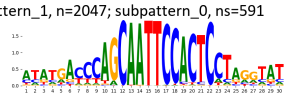

pattern_1, n=2047; subpattern_1, ns=572

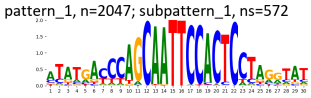

pattern_1, n=2047; subpattern_2, ns=449

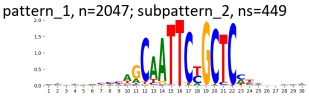

pattern_1, n=2047; subpattern_3, ns=435

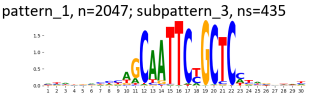

TF-MoDisCO pattern_2 n=480, CWM

pattern_2, n=480; subpattern_0, ns=120

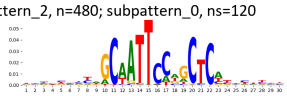

pattern_2, n=480; subpattern_1, ns=116

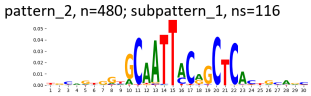

pattern_2, n=480; subpattern_2, ns=116

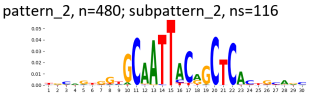

pattern_2, n=480; subpattern_3, ns=105

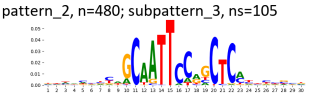

pattern_2, n=480; subpattern_4, ns=23

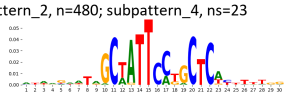

TF-MoDisCO pattern_2 n=480, PWM

pattern_2, n=480; subpattern_0, ns=120

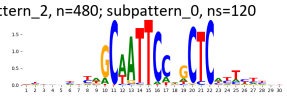

pattern_2, n=480; subpattern_1, ns=116

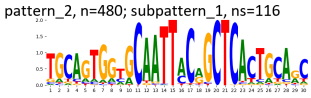

pattern_2, n=480; subpattern_2, ns=116

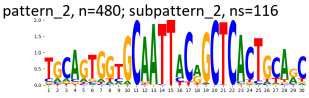

pattern_2, n=480; subpattern_3, ns=105

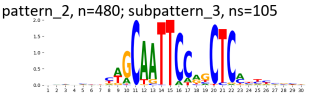

pattern_2, n=480; subpattern_4, ns=23

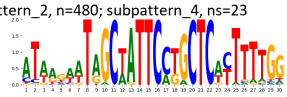

TF-MoDisCO pattern_3 n=392, CWM

pattern_3, n=392; subpattern_0, ns=119

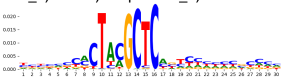

pattern_3, n=392; subpattern_1, ns=96

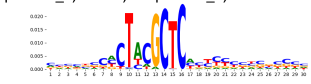

pattern_3, n=392; subpattern_2, ns=57

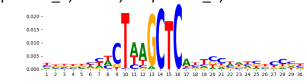

pattern_3, n=392; subpattern_3, ns=52

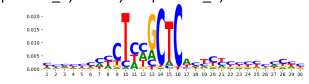

pattern_3, n=392; subpattern_4, ns=32

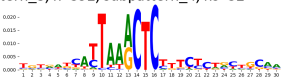

pattern_3, n=392; subpattern_5, ns=32

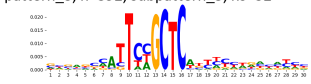

pattern_3, n=392; subpattern_6, ns=2

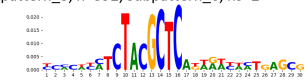

pattern_3, n=392; subpattern_7, ns=2

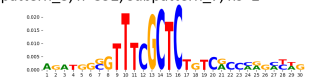

TF-MoDisCO pattern_3 n=392, PWM

pattern_3, n=392; subpattern_0, ns=119

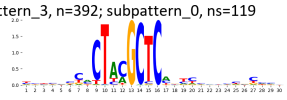

pattern_3, n=392; subpattern_1, ns=96

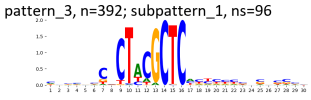

pattern_3, n=392; subpattern_2, ns=57

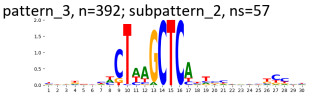

pattern_3, n=392; subpattern_3, ns=52

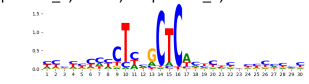

pattern_3, n=392; subpattern_4, ns=32

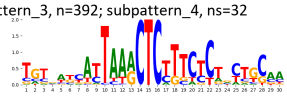

pattern_3, n=392; subpattern_5, ns=32

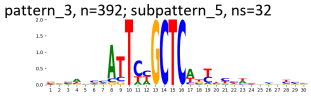

pattern_3, n=392; subpattern_6, ns=2

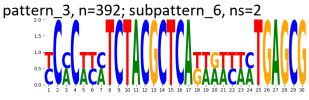

pattern_3, n=392; subpattern_7, ns=2

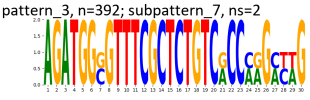

Supplementary Figure 714: TF-MoDisCO subpatterns for the ZNF140 transcription factor in HEK293 (accession ENCSR464KFG).

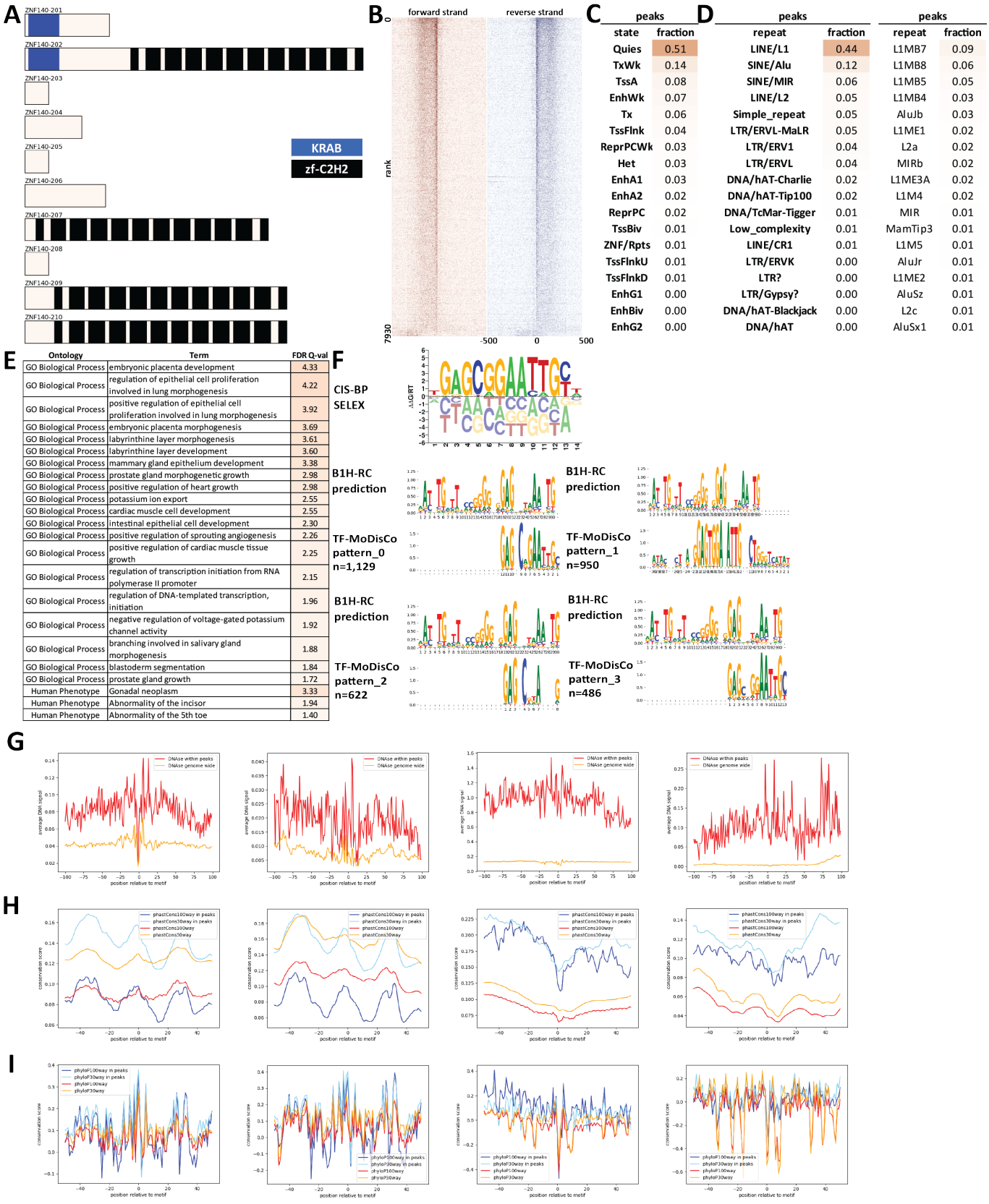

C

peaks	
state	fraction
Quies	0.51
TxWk	0.14
TssA	0.08
EnhWk	0.07
Tx	0.06
TssFlnk	0.04
ReprPCWk	0.03
Het	0.03
EnhA1	0.03
EnhA2	0.02
ReprPC	0.02
TssBiv	0.01
ZNF/Rpts	0.01
TssFlnkU	0.01
TssFlnkD	0.01
EnhG1	0.00
EnhBiv	0.00
EnhG2	0.00

D

peaks		peaks	
repeat	fraction	repeat	fraction
LINE/L1	0.44	L1MB7	0.09
SINE/Alu	0.12	L1MB8	0.06
SINE/MIR	0.06	L1MB5	0.05
LINE/L2	0.05	L1MB4	0.03
Simple_repeat	0.05	AluJb	0.03
LTR/ERVL-MaLR	0.05	L1ME1	0.02
LTR/ERV1	0.04	L2a	0.02
LTR/ERVL	0.04	MIRb	0.02
DNA/hAT-Charlie	0.02	L1ME3A	0.02
DNA/hAT-Tip100	0.02	L1M4	0.02
DNA/TcMar-Tigger	0.01	MIR	0.01
Low_complexity	0.01	MamTip3	0.01
LINE/CR1	0.01	L1M5	0.01
LTR/ERVK	0.00	AluJr	0.01
LTR?	0.00	L1ME2	0.01
LTR/Gypsy?	0.00	AluSz	0.01
DNA/hAT-Blackjack	0.00	L2c	0.01
DNA/hAT	0.00	AluSx1	0.01

E

Ontology	Term	FDR Q-val
GO Biological Process	embryonic placenta development	4.33
GO Biological Process	regulation of epithelial cell proliferation involved in lung morphogenesis	4.22
GO Biological Process	positive regulation of epithelial cell proliferation involved in lung morphogenesis	3.92
GO Biological Process	embryonic placenta morphogenesis	3.69
GO Biological Process	labyrinthine layer morphogenesis	3.61
GO Biological Process	labyrinthine layer development	3.60
GO Biological Process	mammary gland epithelium development	3.38
GO Biological Process	prostate gland morphogenetic growth	2.98
GO Biological Process	positive regulation of heart growth	2.98
GO Biological Process	potassium ion export	2.55
GO Biological Process	cardiac muscle cell development	2.55
GO Biological Process	intestinal epithelial cell development	2.30
GO Biological Process	positive regulation of sprouting angiogenesis	2.26
GO Biological Process	positive regulation of cardiac muscle tissue growth	2.25
GO Biological Process	regulation of transcription initiation from RNA polymerase II promoter	2.15
GO Biological Process	regulation of DNA-templated transcription, initiation	1.96
GO Biological Process	negative regulation of voltage-gated potassium channel activity	1.92
GO Biological Process	branching involved in salivary gland morphogenesis	1.88
GO Biological Process	blastoderm segmentation	1.84
GO Biological Process	prostate gland growth	1.72
Human Phenotype	Gonadal neoplasm	3.33
Human Phenotype	Abnormality of the incisor	1.94
Human Phenotype	Abnormality of the 5th toe	1.40

Supplementary Figure 715: Properties and genomic distribution of motifs identified for the ZNF140 transcription factor in HEK293 (accession Hughes GR models).

TF-MoDisCO pattern_0 n=1129, CWM

pattern_0, n=1129; subpattern_0, ns=305

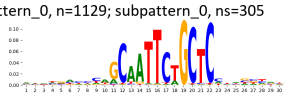

pattern_0, n=1129; subpattern_1, ns=267

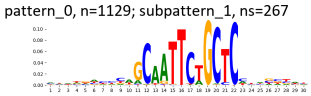

pattern_0, n=1129; subpattern_2, ns=184

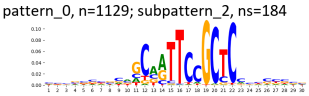

pattern_0, n=1129; subpattern_3, ns=133

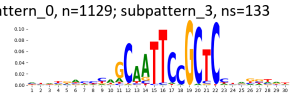

pattern_0, n=1129; subpattern_4, ns=122

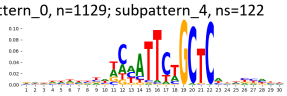

pattern_0, n=1129; subpattern_5, ns=118

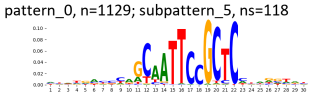

TF-MoDisCO pattern_0 n=1129, PWM

pattern_0, n=1129; subpattern_0, ns=305

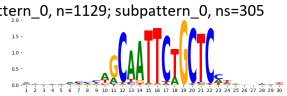

pattern_0, n=1129; subpattern_1, ns=267

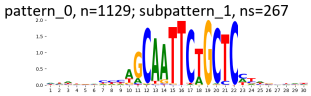

pattern_0, n=1129; subpattern_2, ns=184

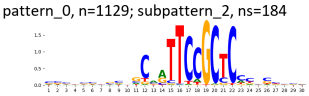

pattern_0, n=1129; subpattern_3, ns=133

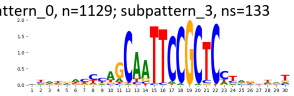

pattern_0, n=1129; subpattern_4, ns=122

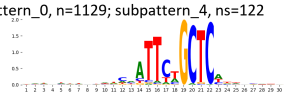

pattern_0, n=1129; subpattern_5, ns=118

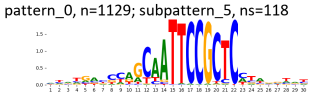

TF-MoDisCO pattern_1 n=950, CWM

pattern_1, n=950; subpattern_0, ns=271

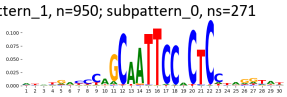

pattern_1, n=950; subpattern_1, ns=253

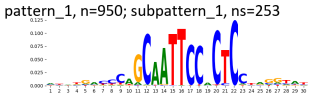

pattern_1, n=950; subpattern_2, ns=232

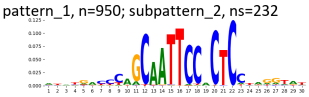

pattern_1, n=950; subpattern_3, ns=194

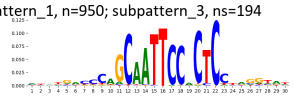

TF-MoDisCO pattern_1 n=950, PWM

pattern_1, n=950; subpattern_0, ns=271

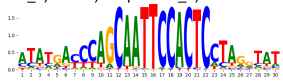

pattern_1, n=950; subpattern_1, ns=253

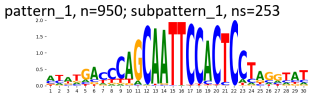

pattern_1, n=950; subpattern_2, ns=232

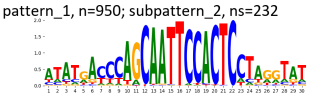

pattern_1, n=950; subpattern_3, ns=194

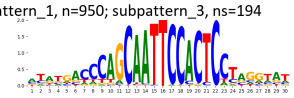

TF-MoDisCO pattern_2 n=622, CWM

pattern_2, n=622; subpattern_0, ns=189

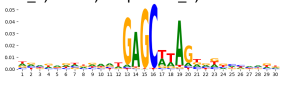

pattern_2, n=622; subpattern_1, ns=169

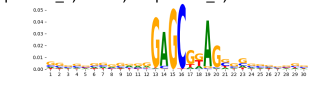

pattern_2, n=622; subpattern_2, ns=130

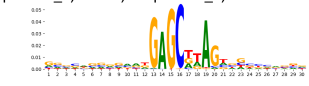

pattern_2, n=622; subpattern_3, ns=80

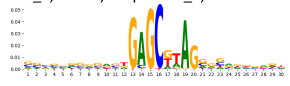

pattern_2, n=622; subpattern_4, ns=46

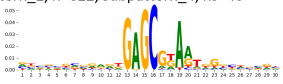

pattern_2, n=622; subpattern_5, ns=6

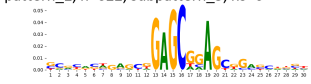

pattern_2, n=622; subpattern_6, ns=2

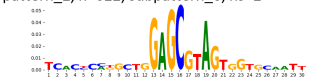

TF-MoDisCO pattern_2 n=622, PWM

pattern_2, n=622; subpattern_0, ns=189

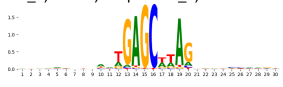

pattern_2, n=622; subpattern_1, ns=169

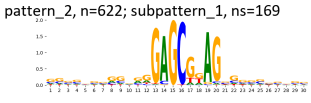

pattern_2, n=622; subpattern_2, ns=130

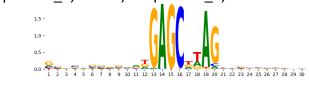

pattern_2, n=622; subpattern_3, ns=80

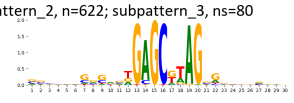

pattern_2, n=622; subpattern_4, ns=46

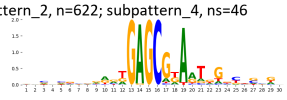

pattern_2, n=622; subpattern_5, ns=6

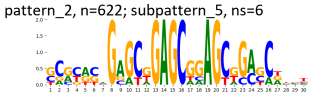

pattern_2, n=622; subpattern_6, ns=2

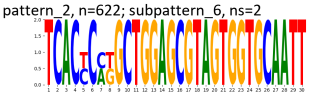

TF-MoDisCO pattern_3 n=486, CWM

pattern_3, n=486; subpattern_0, ns=126

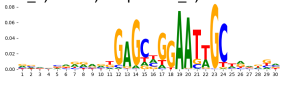

pattern_3, n=486; subpattern_1, ns=113

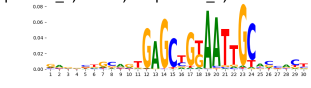

pattern_3, n=486; subpattern_2, ns=105

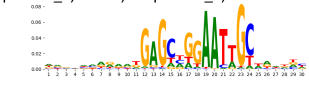

pattern_3, n=486; subpattern_3, ns=77

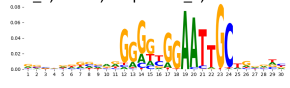

pattern_3, n=486; subpattern_4, ns=65

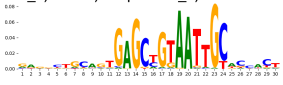

TF-MoDisCO pattern_3 n=486, PWM

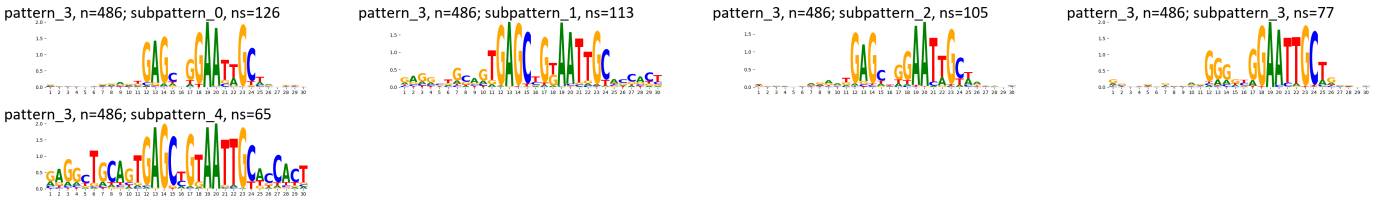

Supplementary Figure 716: TF-MoDisCO subpatterns for the ZNF140 transcription factor in HEK293 (accession Hughes GR models).

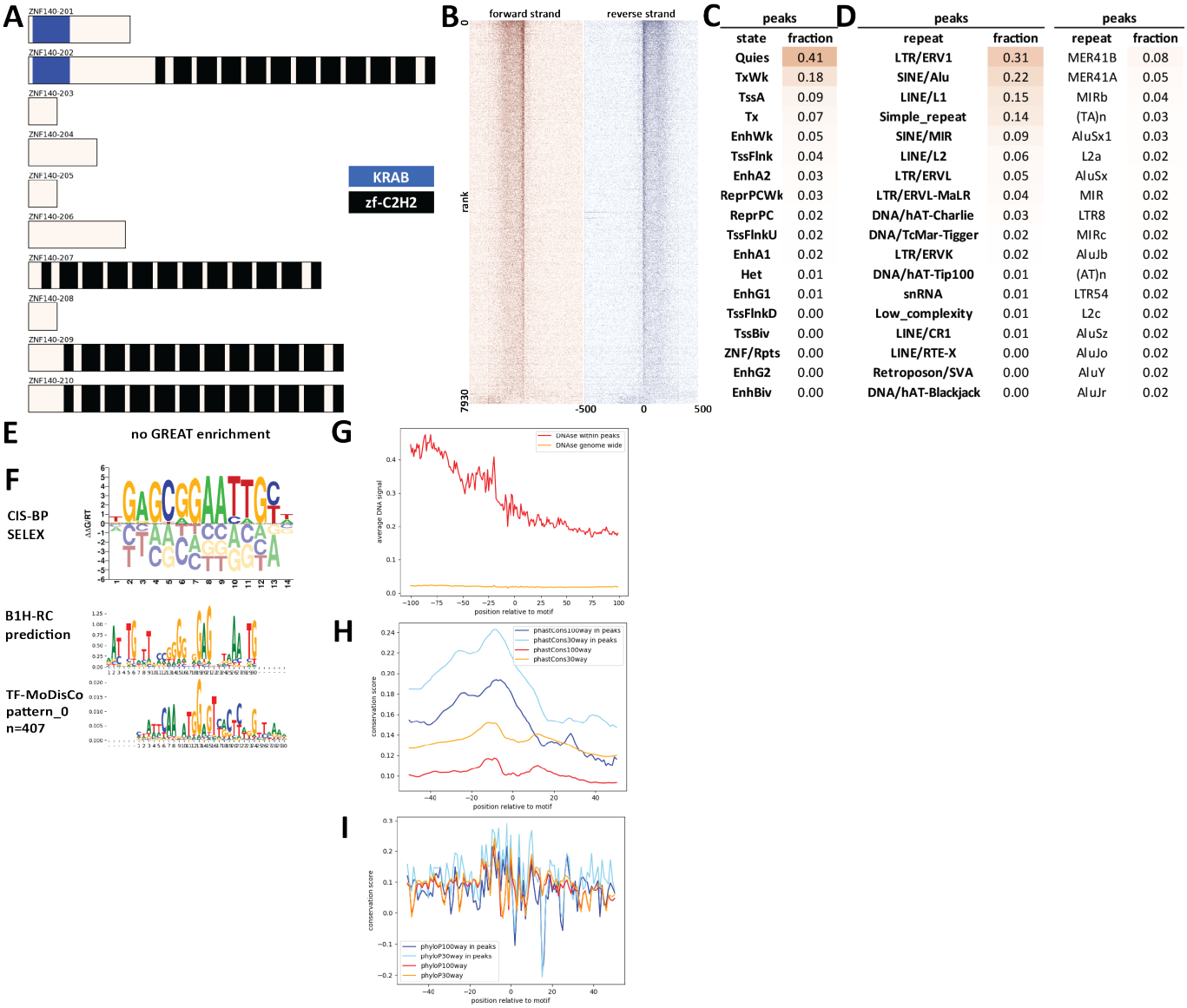

Supplementary Figure 717: Properties and genomic distribution of motifs identified for the ZNF140 transcription factor in K562 (accession ENCSR377HQG).

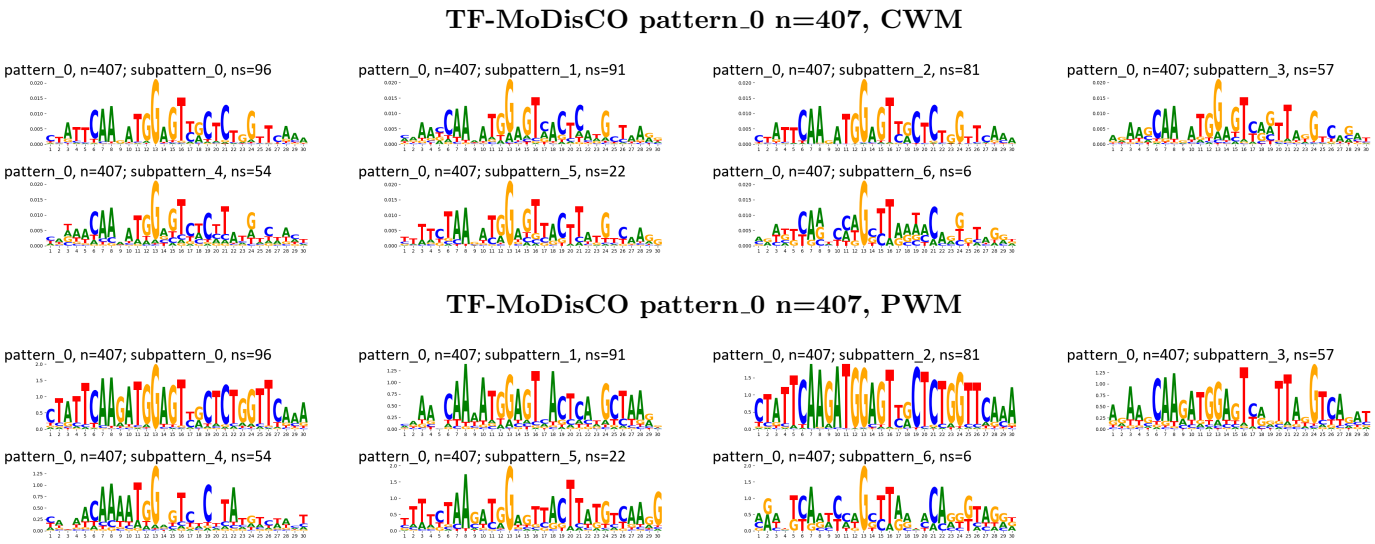

Supplementary Figure 718: TF-MoDisCO subpatterns for the ZNF140 transcription factor in K562 (accession ENCSR377HQG).

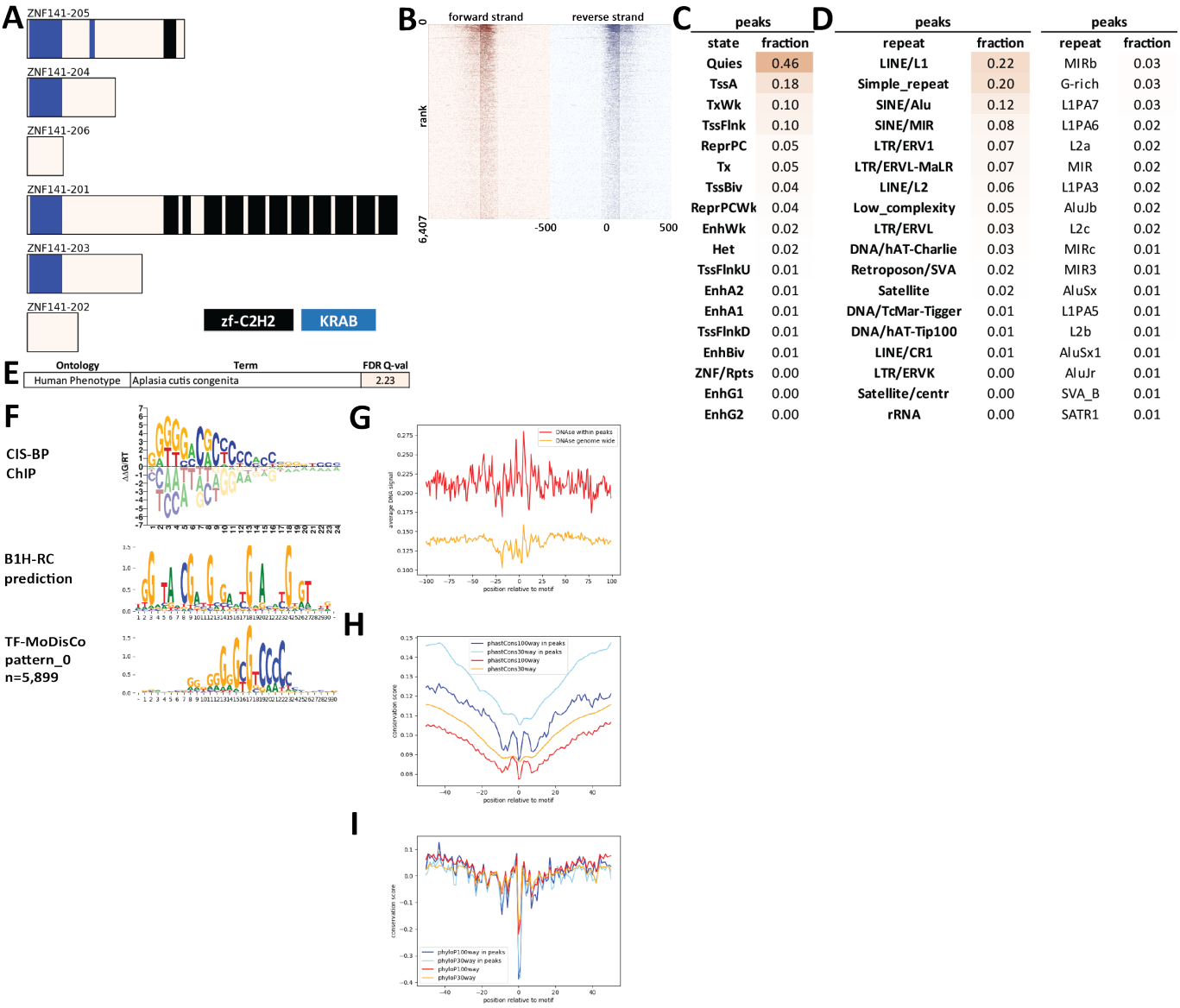

peaks	
state	fraction
Quies	0.46
TssA	0.18
TxWk	0.10
TssFlnk	0.10
ReprPC	0.05
Tx	0.05
TssBiv	0.04
ReprPCWk	0.04
EnhWk	0.02
Het	0.02
TssFlnkU	0.01
EnhA2	0.01
EnhA1	0.01
TssFlnkD	0.01
EnhBiv	0.01
ZNF/Rpts	0.00
EnhG1	0.00
EnhG2	0.00

peaks		peaks	
repeat	fraction	repeat	fraction
LINE/L1	0.22	MIRb	0.03
Simple_repeat	0.20	G-rich	0.03
SINE/Alu	0.12	L1PA7	0.03
SINE/MIR	0.08	L1PA6	0.02
LTR/ERV1	0.07	L2a	0.02
LTR/ERVL-MaLR	0.07	MIR	0.02
LINE/L2	0.06	L1PA3	0.02
Low_complexity	0.05	AluJb	0.02
LTR/ERVL	0.03	L2c	0.02
DNA/hAT-Charlie	0.03	MIRc	0.01
Retroposon/SVA	0.02	MIR3	0.01
Satellite	0.02	AluSx	0.01
DNA/TcMar-Tigger	0.01	L1PA5	0.01
DNA/hAT-Tip100	0.01	L2b	0.01
LINE/CR1	0.01	AluSx1	0.01
LTR/ERVK	0.00	AluJr	0.01
Satellite/centr	0.00	SVA_B	0.01
rRNA	0.00	SATR1	0.01

Supplementary Figure 719: Properties and genomic distribution of motifs identified for the ZNF141 transcription factor in HEK293 (accession ChipExo models).

TF-MoDisCO pattern_0 n=5899, CWM

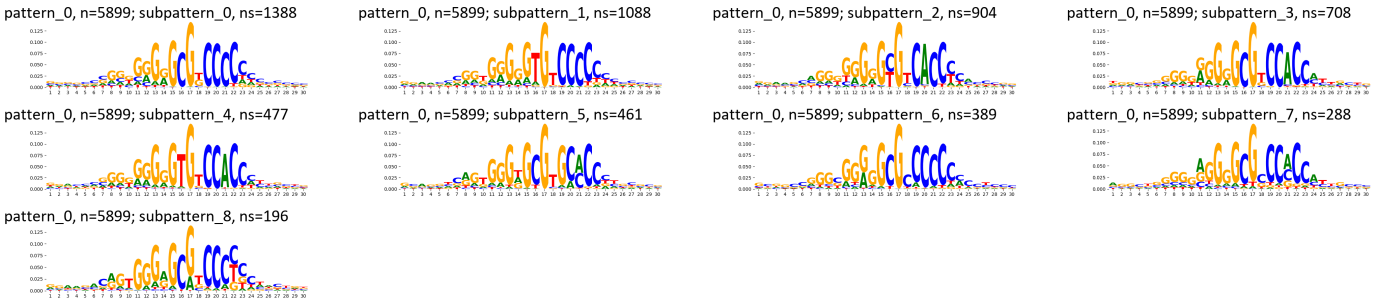

TF-MoDisCO pattern_0 n=5899, PWM

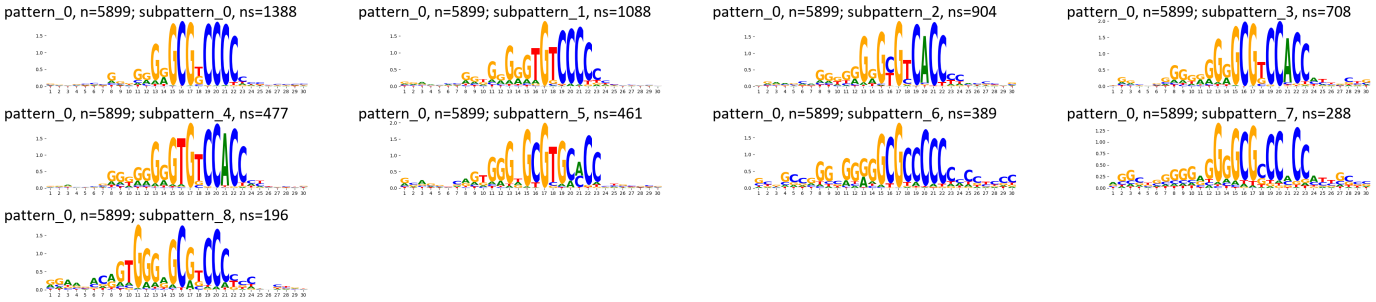

Supplementary Figure 720: TF-MoDisCO subpatterns for the ZNF141 transcription factor in HEK293 (accession ChipExo models).

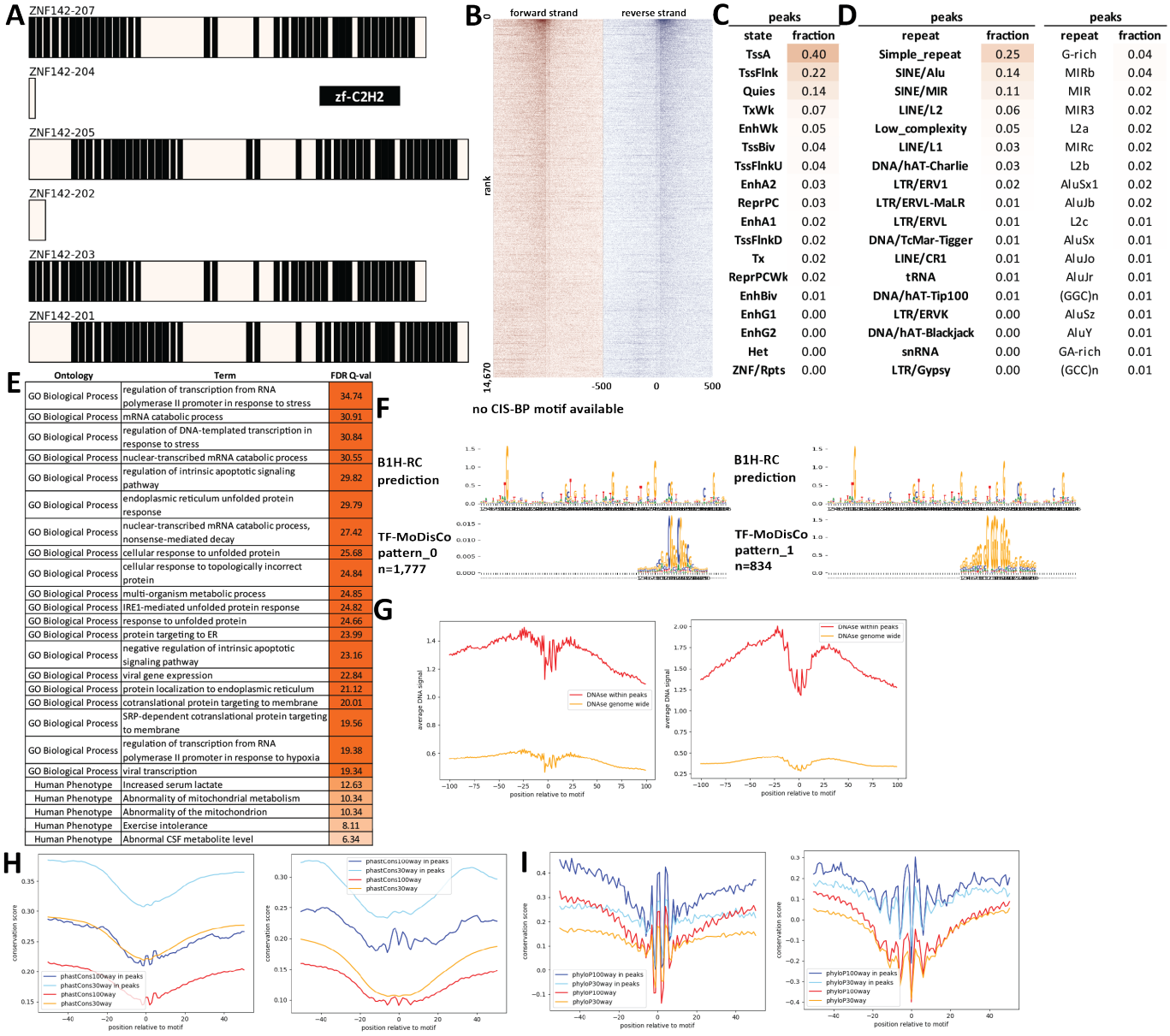

Supplementary Figure 721: Properties and genomic distribution of motifs identified for the ZNF142 transcription factor in HepG2 (accession ENCSR512ECF).

TF-MoDisCO pattern_0 n=1777, CWM

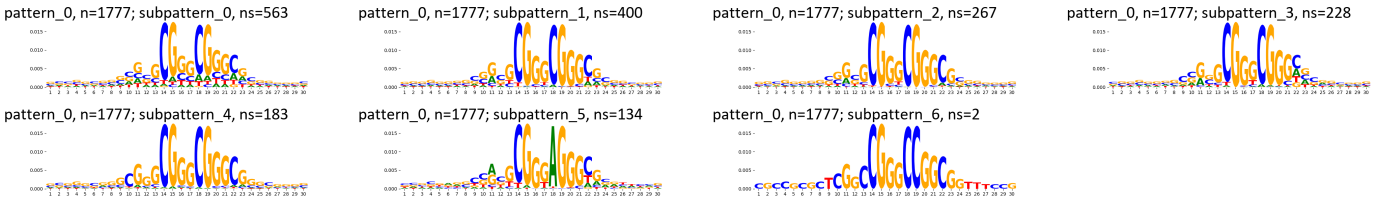

TF-MoDisCO pattern_0 n=1777, PWM

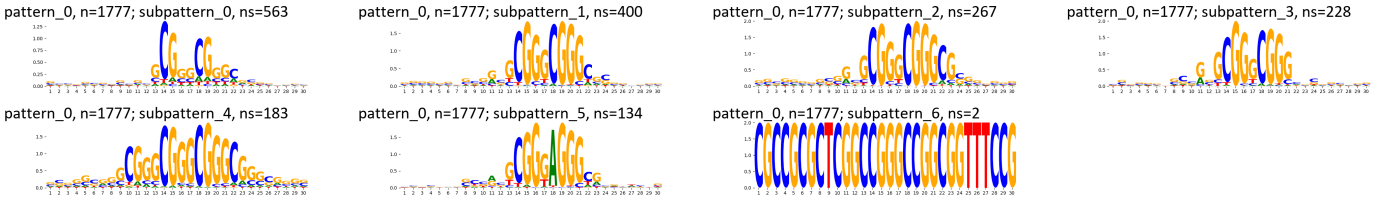

TF-MoDisCO pattern_1 n=834, CWM

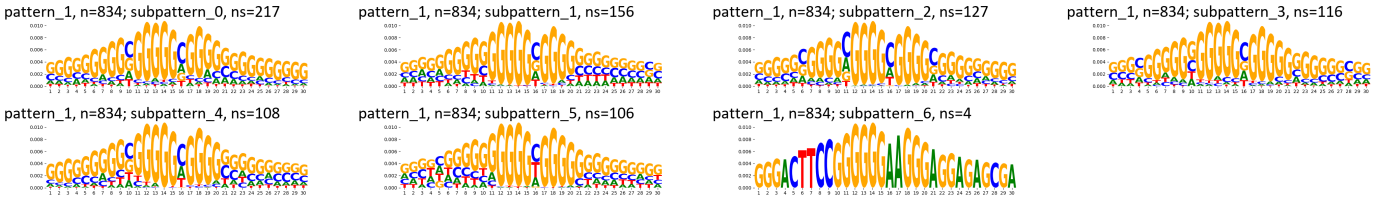

TF-MoDisCO pattern_1 n=834, PWM

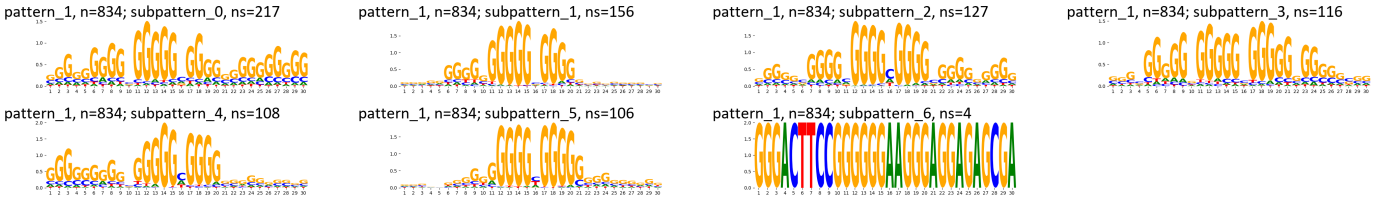

Supplementary Figure 722: TF-MoDisCO subpatterns for the ZNF142 transcription factor in HepG2 (accession ENCSR512ECF).

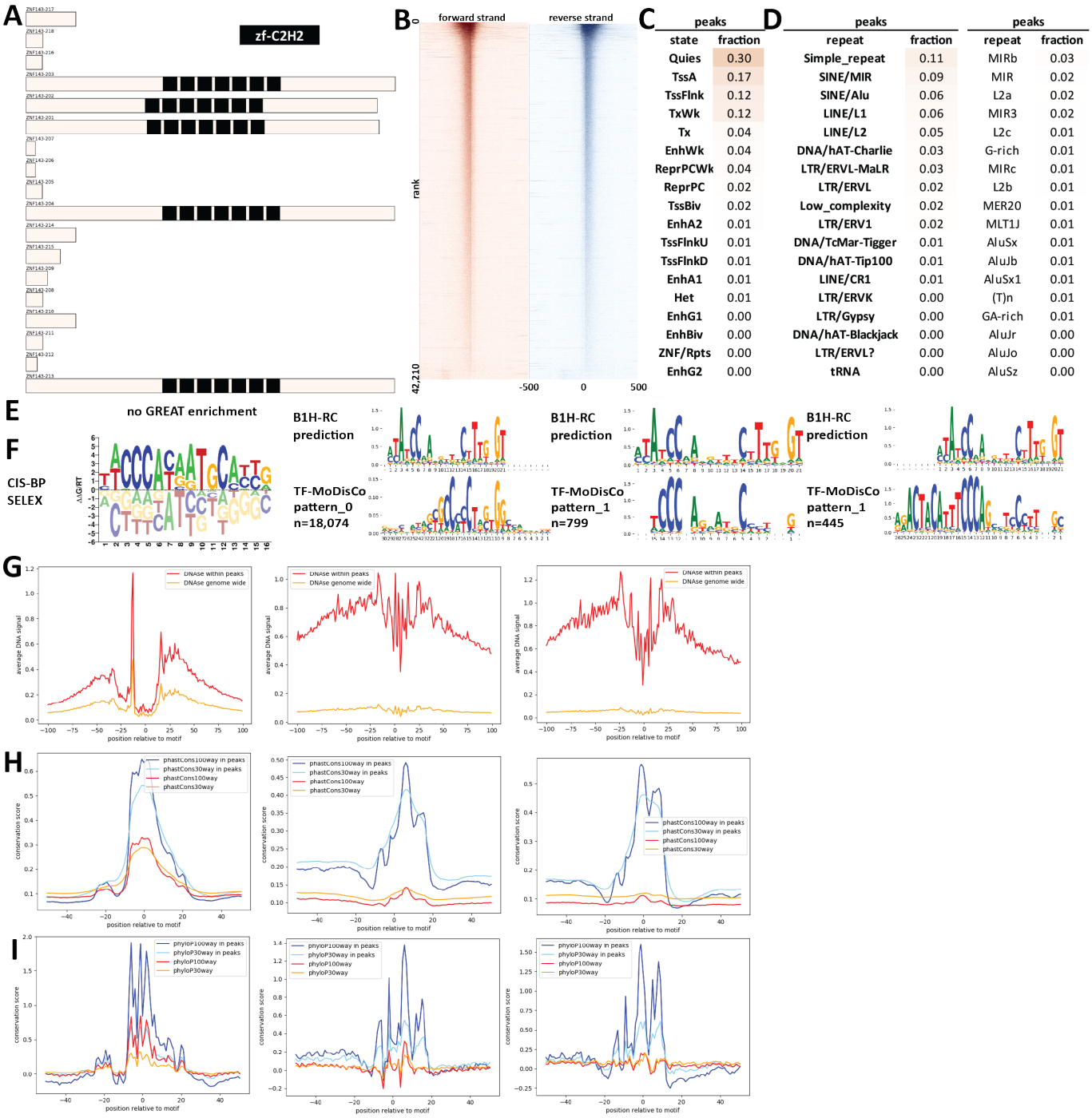

Supplementary Figure 723: Properties and genomic distribution of motifs identified for the ZNF143 transcription factor in GM12878 (accession ENCSR000DZL).

TF-MoDisCO pattern_0 n=18074, CWM

pattern_0, n=18074; subpattern_0, ns=3321

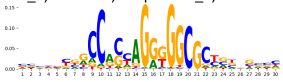

pattern_0, n=18074; subpattern_1, ns=2673

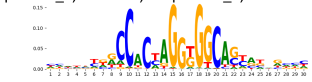

pattern_0, n=18074; subpattern_2, ns=2438

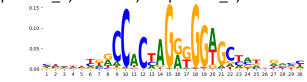

pattern_0, n=18074; subpattern_3, ns=2408

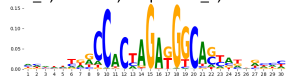

pattern_0, n=18074; subpattern_4, ns=2027

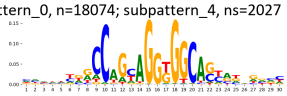

pattern_0, n=18074; subpattern_5, ns=2012

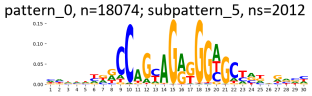

pattern_0, n=18074; subpattern_6, ns=1699

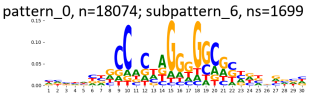

pattern_0, n=18074; subpattern_7, ns=1473

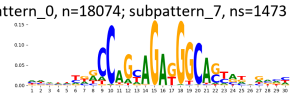

pattern_0, n=18074; subpattern_8, ns=17

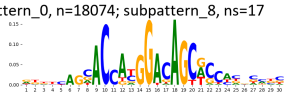

pattern_0, n=18074; subpattern_9, ns=6

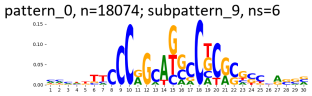

TF-MoDisCO pattern_0 n=18074, PWM

pattern_0, n=18074; subpattern_0, ns=3321

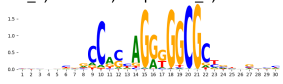

pattern_0, n=18074; subpattern_1, ns=2673

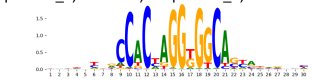

pattern_0, n=18074; subpattern_2, ns=2438

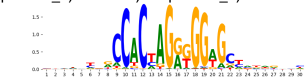

pattern_0, n=18074; subpattern_3, ns=2408

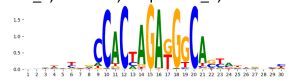

pattern_0, n=18074; subpattern_4, ns=2027

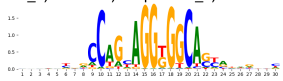

pattern_0, n=18074; subpattern_5, ns=2012

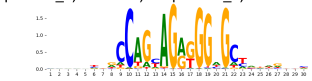

pattern_0, n=18074; subpattern_6, ns=1699

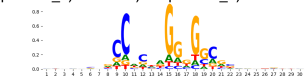

pattern_0, n=18074; subpattern_7, ns=1473

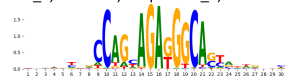

pattern_0, n=18074; subpattern_8, ns=17

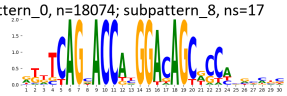

pattern_0, n=18074; subpattern_9, ns=6

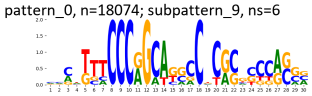

TF-MoDisCO pattern_1 n=799, CWM

pattern_1, n=799; subpattern_0, ns=173

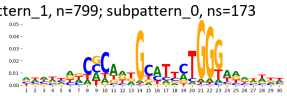

pattern_1, n=799; subpattern_1, ns=150

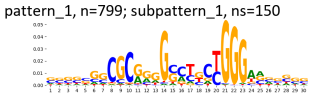

pattern_1, n=799; subpattern_2, ns=127

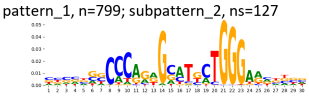

pattern_1, n=799; subpattern_3, ns=121

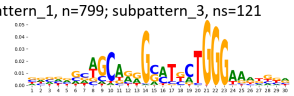

pattern_1, n=799; subpattern_4, ns=93

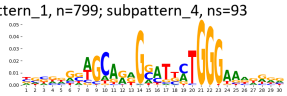

pattern_1, n=799; subpattern_5, ns=69

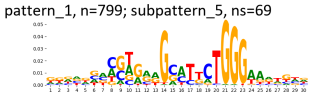

pattern_1, n=799; subpattern_6, ns=47

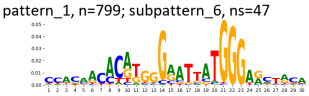

pattern_1, n=799; subpattern_7, ns=12

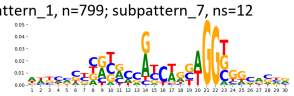

pattern_1, n=799; subpattern_8, ns=7

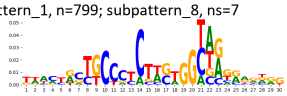

TF-MoDisCO pattern_1 n=799, PWM

pattern_1, n=799; subpattern_0, ns=173

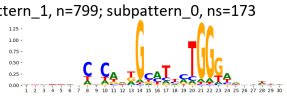

pattern_1, n=799; subpattern_1, ns=150

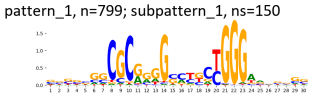

pattern_1, n=799; subpattern_2, ns=127

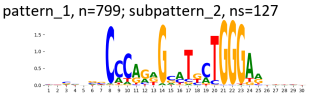

pattern_1, n=799; subpattern_3, ns=121

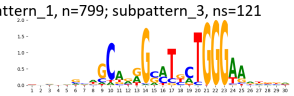

pattern_1, n=799; subpattern_4, ns=93

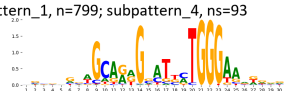

pattern_1, n=799; subpattern_5, ns=69

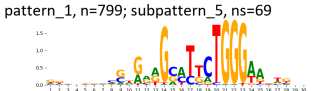

pattern_1, n=799; subpattern_6, ns=47

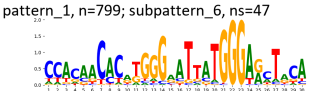

pattern_1, n=799; subpattern_7, ns=12

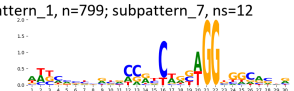

pattern_1, n=799; subpattern_8, ns=7

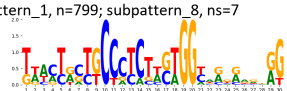

TF-MoDisCO pattern_3 n=445, CWM

pattern_3, n=445; subpattern_0, ns=194

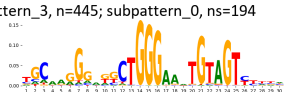

pattern_3, n=445; subpattern_1, ns=173

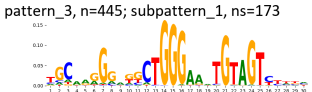

pattern_3, n=445; subpattern_2, ns=65

pattern_3, n=445; subpattern_3, ns=13

TF-MoDisCO pattern_3 n=445, PWM

pattern_3, n=445; subpattern_0, ns=194

pattern_3, n=445; subpattern_1, ns=173

pattern_3, n=445; subpattern_2, ns=65

pattern_3, n=445; subpattern_3, ns=13

Supplementary Figure 724: TF-MoDisCO subpatterns for the ZNF143 transcription factor in GM12878 (accession ENCSR000DZL).

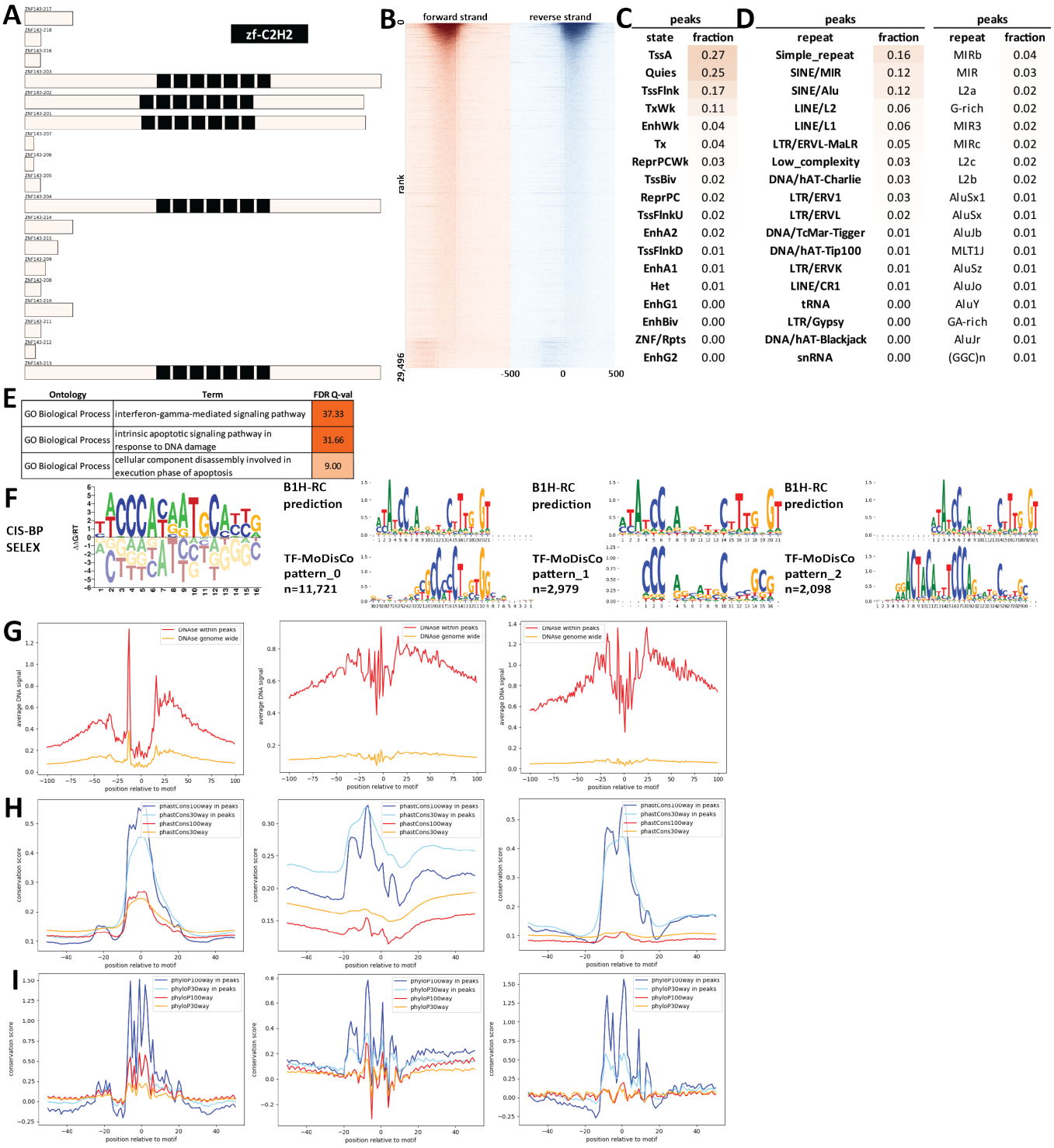

Supplementary Figure 725: Properties and genomic distribution of motifs identified for the ZNF143 transcription factor in GM12878 (accession ENCSR936XTK).

TF-MoDisCO pattern_0 n=11721, CWM

pattern_0, n=11721; subpattern_0, ns=2391

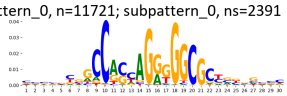

pattern_0, n=11721; subpattern_1, ns=2367

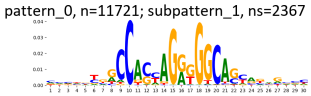

pattern_0, n=11721; subpattern_2, ns=2249

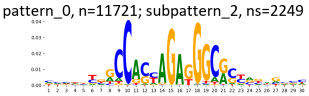

pattern_0, n=11721; subpattern_3, ns=2151

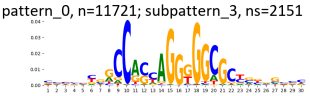

pattern_0, n=11721; subpattern_4, ns=1594

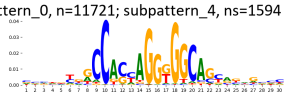

pattern_0, n=11721; subpattern_5, ns=912

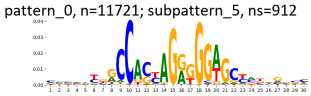

pattern_0, n=11721; subpattern_6, ns=50

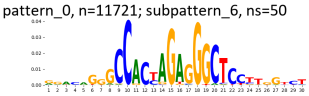

pattern_0, n=11721; subpattern_7, ns=4

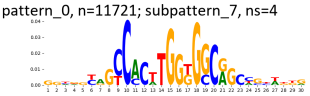

pattern_0, n=11721; subpattern_8, ns=3

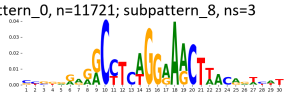

TF-MoDisCO pattern_0 n=11721, PWM

pattern_0, n=11721; subpattern_0, ns=2391

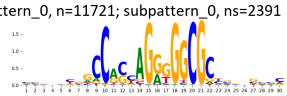

pattern_0, n=11721; subpattern_1, ns=2367

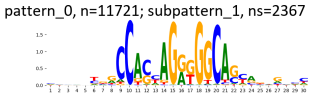

pattern_0, n=11721; subpattern_2, ns=2249

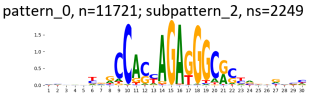

pattern_0, n=11721; subpattern_3, ns=2151

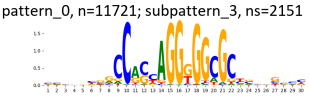

pattern_0, n=11721; subpattern_4, ns=1594

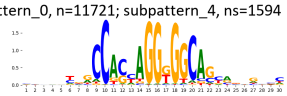

pattern_0, n=11721; subpattern_5, ns=912

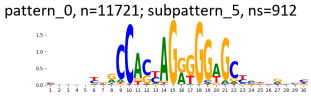

pattern_0, n=11721; subpattern_6, ns=50

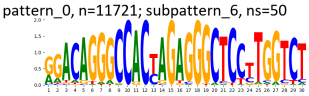

pattern_0, n=11721; subpattern_7, ns=4

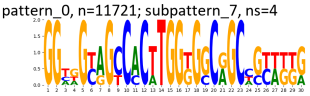

pattern_0, n=11721; subpattern_8, ns=3

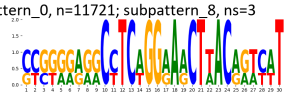

TF-MoDisCO pattern_1 n=2979, CWM

pattern_1, n=2979; subpattern_0, ns=605

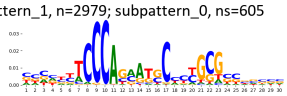

pattern_1, n=2979; subpattern_1, ns=598

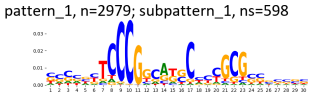

pattern_1, n=2979; subpattern_10, ns=2

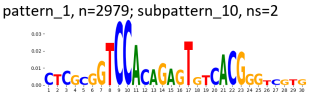

pattern_1, n=2979; subpattern_2, ns=547

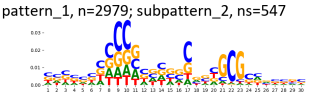

pattern_1, n=2979; subpattern_3, ns=537

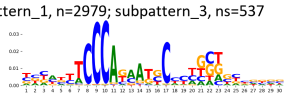

pattern_1, n=2979; subpattern_4, ns=382

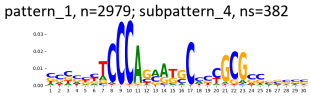

pattern_1, n=2979; subpattern_5, ns=259

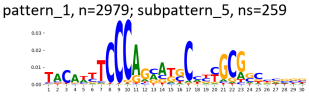

pattern_1, n=2979; subpattern_6, ns=28

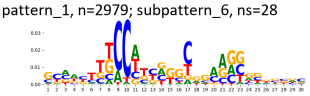

pattern_1, n=2979; subpattern_7, ns=14

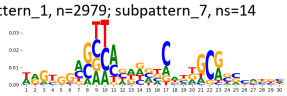

pattern_1, n=2979; subpattern_8, ns=5

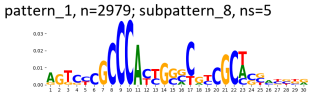

pattern_1, n=2979; subpattern_9, ns=2

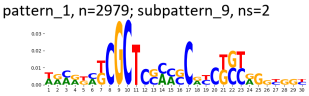

TF-MoDisCO pattern_1 n=2979, PWM

pattern_1, n=2979; subpattern_0, ns=605

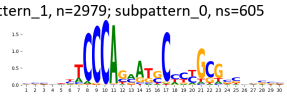

pattern_1, n=2979; subpattern_1, ns=598

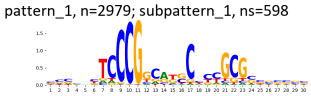

pattern_1, n=2979; subpattern_10, ns=2

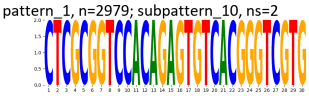

pattern_1, n=2979; subpattern_2, ns=547

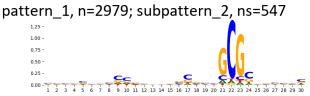

pattern_1, n=2979; subpattern_3, ns=537

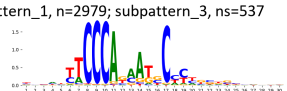

pattern_1, n=2979; subpattern_4, ns=382

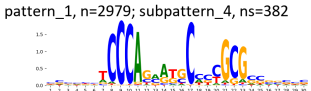

pattern_1, n=2979; subpattern_5, ns=259

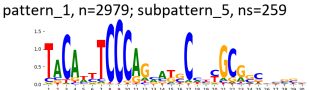

pattern_1, n=2979; subpattern_6, ns=28

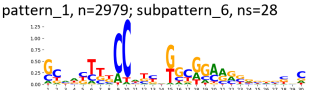

pattern_1, n=2979; subpattern_7, ns=14

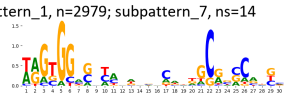

pattern_1, n=2979; subpattern_8, ns=5

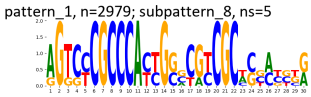

pattern_1, n=2979; subpattern_9, ns=2

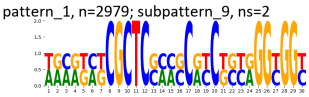

TF-MoDisCO pattern_2 n=2098, CWM

pattern_2, n=2098; subpattern_0, ns=530

pattern_2, n=2098; subpattern_1, ns=493

pattern_2, n=2098; subpattern_2, ns=487

pattern_2, n=2098; subpattern_3, ns=444

pattern_2, n=2098; subpattern_4, ns=144

TF-MoDisCO pattern_2 n=2098, PWM

pattern_2, n=2098; subpattern_0, ns=530

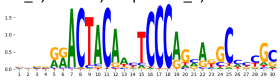

pattern_2, n=2098; subpattern_1, ns=493

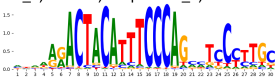

pattern_2, n=2098; subpattern_2, ns=487

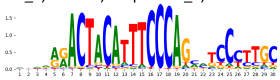

pattern_2, n=2098; subpattern_3, ns=444

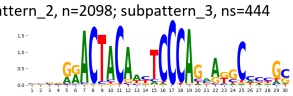

pattern_2, n=2098; subpattern_4, ns=144

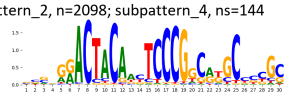

Supplementary Figure 726: TF-MoDisCO subpatterns for the ZNF143 transcription factor in GM12878 (accession ENCSR936XTK).

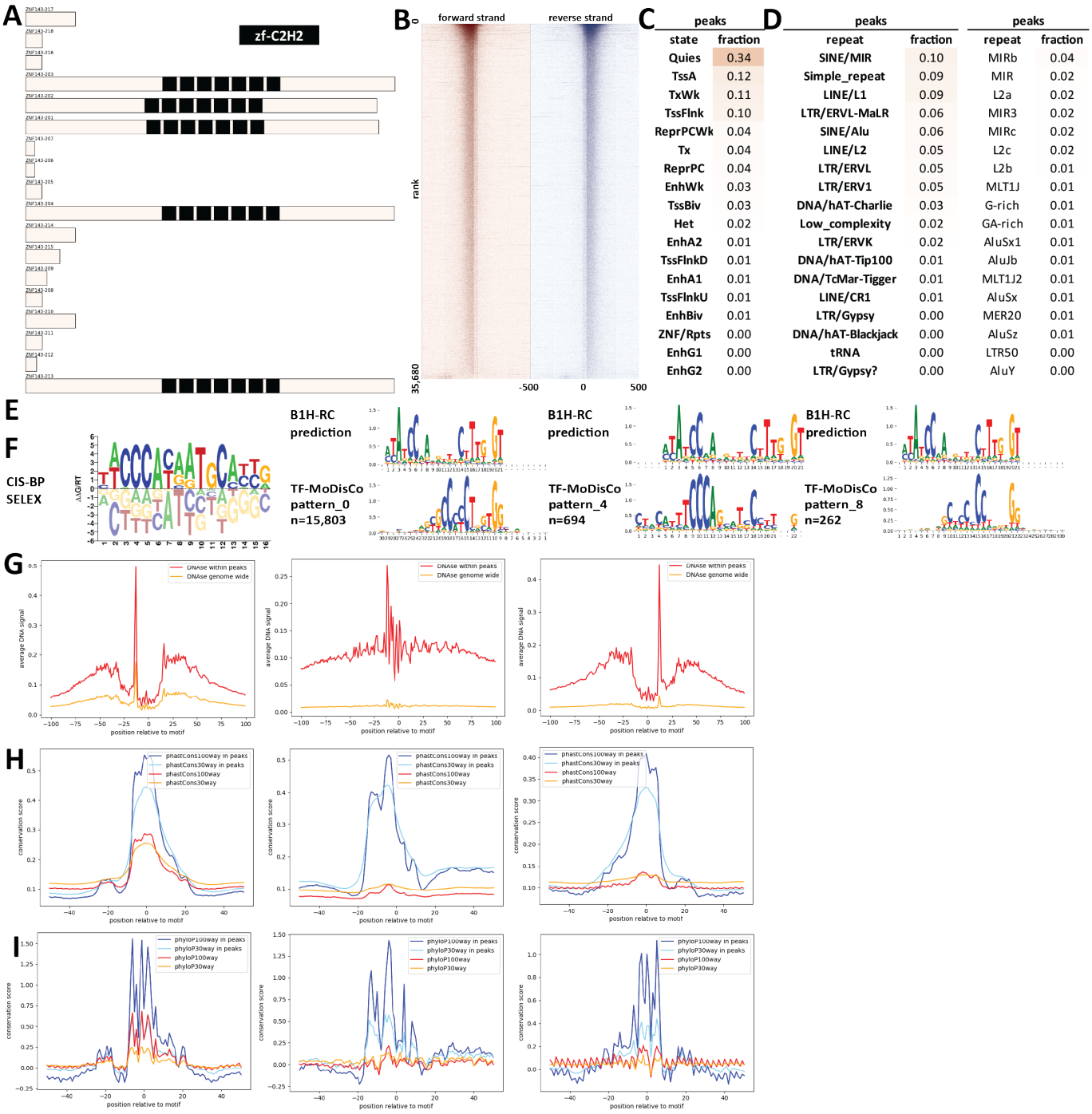

Supplementary Figure 727: Properties and genomic distribution of motifs identified for the ZNF143 transcription factor in H1 (accession ENCSR000EBW).

TF-MoDisCO pattern_0 n=15803, CWM

pattern_0, n=15803; subpattern_0, ns=2789

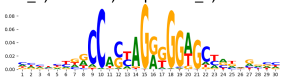

pattern_0, n=15803; subpattern_1, ns=2510

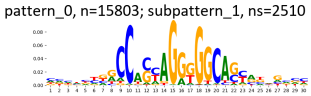

pattern_0, n=15803; subpattern_2, ns=2193

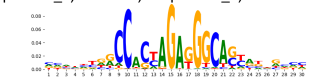

pattern_0, n=15803; subpattern_3, ns=2187

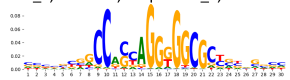

pattern_0, n=15803; subpattern_4, ns=2055

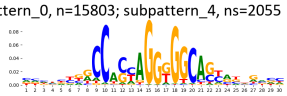

pattern_0, n=15803; subpattern_5, ns=1575

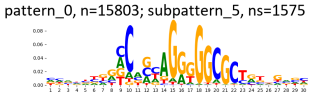

pattern_0, n=15803; subpattern_6, ns=1068

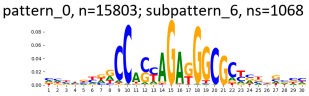

pattern_0, n=15803; subpattern_7, ns=766

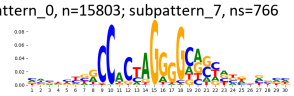

pattern_0, n=15803; subpattern_8, ns=660

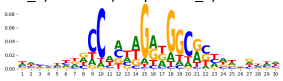

TF-MoDisCO pattern_0 n=15803, PWM

pattern_0, n=15803; subpattern_0, ns=2789

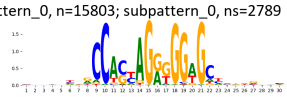

pattern_0, n=15803; subpattern_1, ns=2510

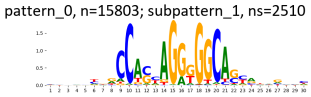

pattern_0, n=15803; subpattern_2, ns=2193

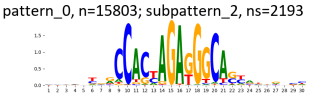

pattern_0, n=15803; subpattern_3, ns=2187

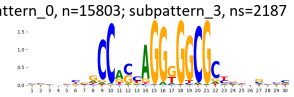

pattern_0, n=15803; subpattern_4, ns=2055

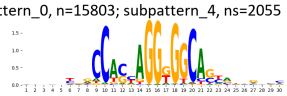

pattern_0, n=15803; subpattern_5, ns=1575

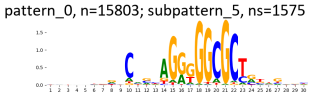

pattern_0, n=15803; subpattern_6, ns=1068

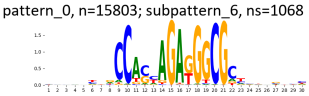

pattern_0, n=15803; subpattern_7, ns=766

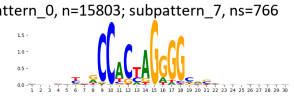

pattern_0, n=15803; subpattern_8, ns=660

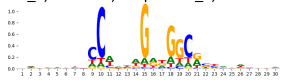

TF-MoDisCO pattern_4 n=694, CWM

pattern_4, n=694; subpattern_0, ns=187

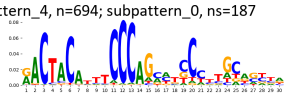

pattern_4, n=694; subpattern_1, ns=174

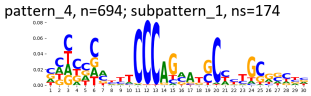

pattern_4, n=694; subpattern_2, ns=158

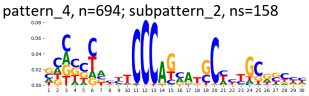

pattern_4, n=694; subpattern_3, ns=154

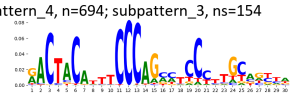

pattern_4, n=694; subpattern_4, ns=15

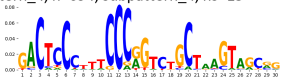

pattern_4, n=694; subpattern_5, ns=6

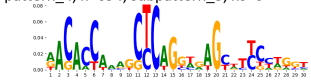

TF-MoDisCO pattern_4 n=694, PWM

pattern_4, n=694; subpattern_0, ns=187

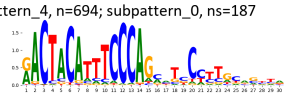

pattern_4, n=694; subpattern_1, ns=174

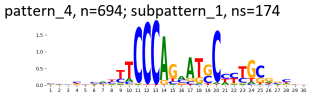

pattern_4, n=694; subpattern_2, ns=158

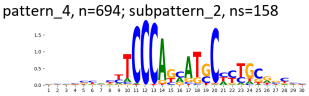

pattern_4, n=694; subpattern_3, ns=154

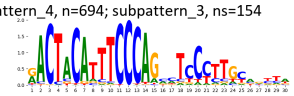

pattern_4, n=694; subpattern_4, ns=15

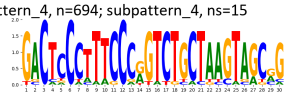

pattern_4, n=694; subpattern_5, ns=6

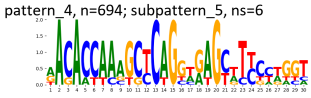

TF-MoDisCO pattern_8 n=262, CWM

pattern_8, n=262; subpattern_0, ns=70

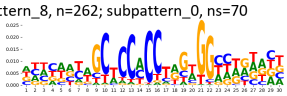

pattern_8, n=262; subpattern_1, ns=44

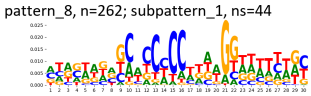

pattern_8, n=262; subpattern_2, ns=35

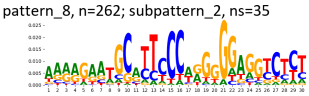

pattern_8, n=262; subpattern_3, ns=35

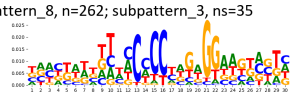

pattern_8, n=262; subpattern_4, ns=30

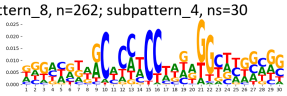

pattern_8, n=262; subpattern_5, ns=23

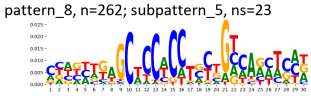

pattern_8, n=262; subpattern_6, ns=10

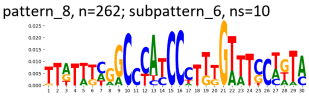

pattern_8, n=262; subpattern_7, ns=8

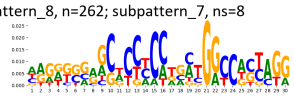

pattern_8, n=262; subpattern_8, ns=5

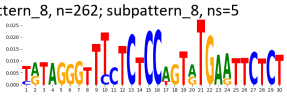

pattern_8, n=262; subpattern_9, ns=2

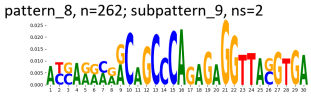

TF-MoDisCO pattern_8 n=262, PWM

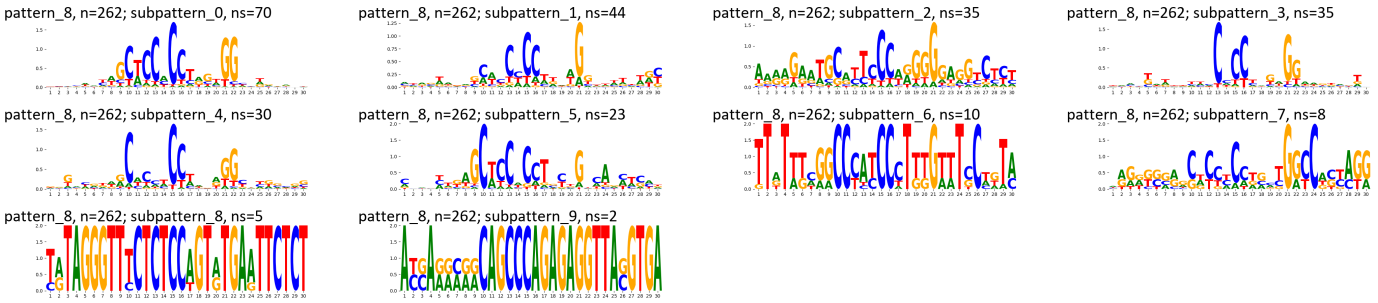

Supplementary Figure 728: TF-MoDisCO subpatterns for the ZNF143 transcription factor in H1 (accession ENCSR000EBW).

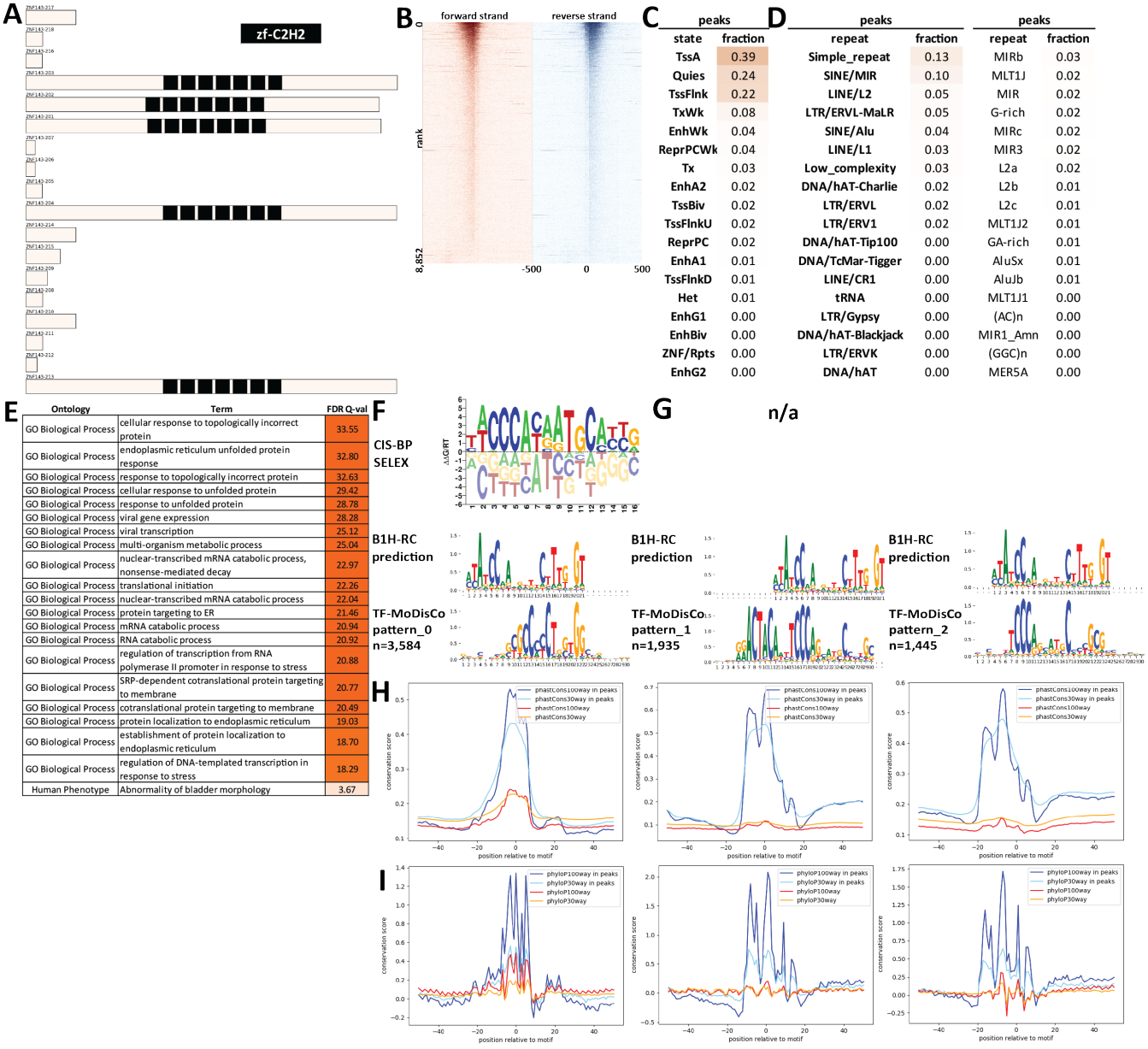

Supplementary Figure 729: Properties and genomic distribution of motifs identified for the ZNF143 transcription factor in HeLa-S3 (accession ENCSR000ECO).

TF-MoDisCO pattern_0 n=3584, CWM

pattern_0, n=3584; subpattern_0, ns=828

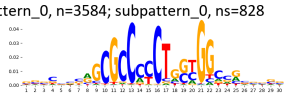

pattern_0, n=3584; subpattern_1, ns=695

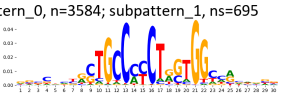

pattern_0, n=3584; subpattern_2, ns=641

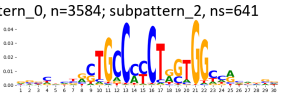

pattern_0, n=3584; subpattern_3, ns=545

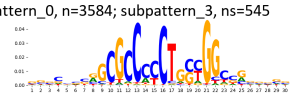

pattern_0, n=3584; subpattern_4, ns=539

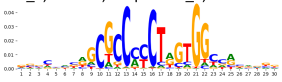

pattern_0, n=3584; subpattern_5, ns=312

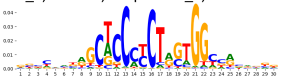

pattern_0, n=3584; subpattern_6, ns=24



TF-MoDisCO pattern_0 n=3584, PWM

pattern_0, n=3584; subpattern_0, ns=828

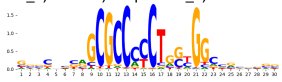

pattern_0, n=3584; subpattern_1, ns=695

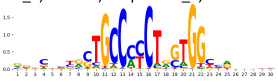

pattern_0, n=3584; subpattern_2, ns=641

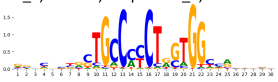

pattern_0, n=3584; subpattern_3, ns=545

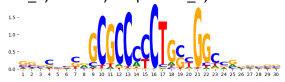

pattern_0, n=3584; subpattern_4, ns=539

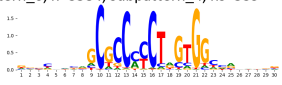

pattern_0, n=3584; subpattern_5, ns=312

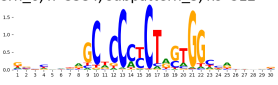

pattern_0, n=3584; subpattern_6, ns=24

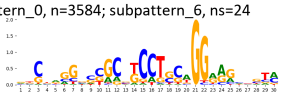

TF-MoDisCO pattern_1 n=1935, CWM

pattern_1, n=1935; subpattern_0, ns=440

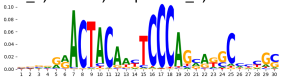

pattern_1, n=1935; subpattern_1, ns=434

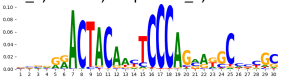

pattern_1, n=1935; subpattern_2, ns=387

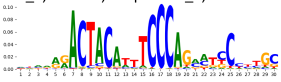

pattern_1, n=1935; subpattern_3, ns=373

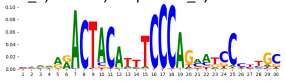

pattern_1, n=1935; subpattern_4, ns=299

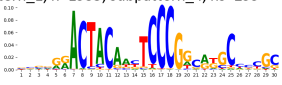

pattern_1, n=1935; subpattern_5, ns=2

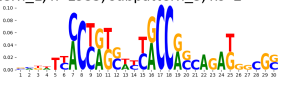

TF-MoDisCO pattern_1 n=1935, PWM

pattern_1, n=1935; subpattern_0, ns=440

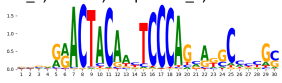

pattern_1, n=1935; subpattern_1, ns=434

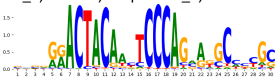

pattern_1, n=1935; subpattern_2, ns=387

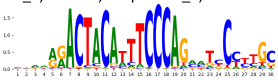

pattern_1, n=1935; subpattern_3, ns=373

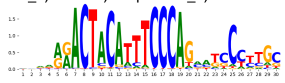

pattern_1, n=1935; subpattern_4, ns=299

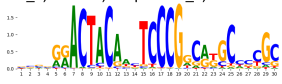

pattern_1, n=1935; subpattern_5, ns=2

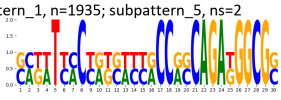

TF-MoDisCO pattern_2 n=1445, CWM

pattern_2, n=1445; subpattern_0, ns=343

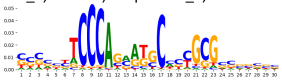

pattern_2, n=1445; subpattern_1, ns=321

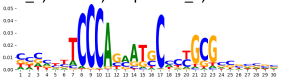

pattern_2, n=1445; subpattern_2, ns=313

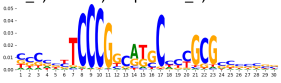

pattern_2, n=1445; subpattern_3, ns=256

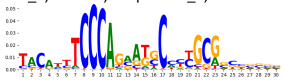

pattern_2, n=1445; subpattern_4, ns=204

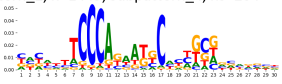

pattern_2, n=1445; subpattern_5, ns=5

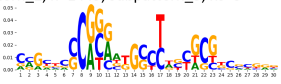

pattern_2, n=1445; subpattern_6, ns=3

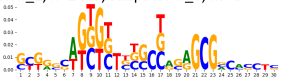

TF-MoDisCO pattern_2 n=1445, PWM

pattern_2, n=1445; subpattern_0, ns=343

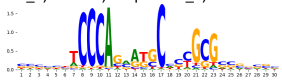

pattern_2, n=1445; subpattern_1, ns=321

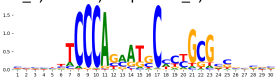

pattern_2, n=1445; subpattern_2, ns=313

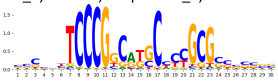

pattern_2, n=1445; subpattern_3, ns=256

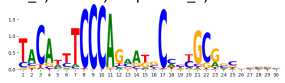

pattern_2, n=1445; subpattern_4, ns=204

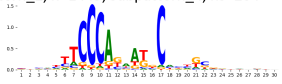

pattern_2, n=1445; subpattern_5, ns=5

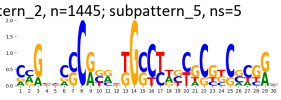

pattern_2, n=1445; subpattern_6, ns=3

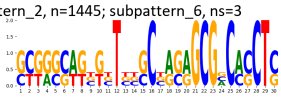

Supplementary Figure 730: TF-MoDisCO subpatterns for the ZNF143 transcription factor in HeLa-S3 (accession ENCSR000ECO).

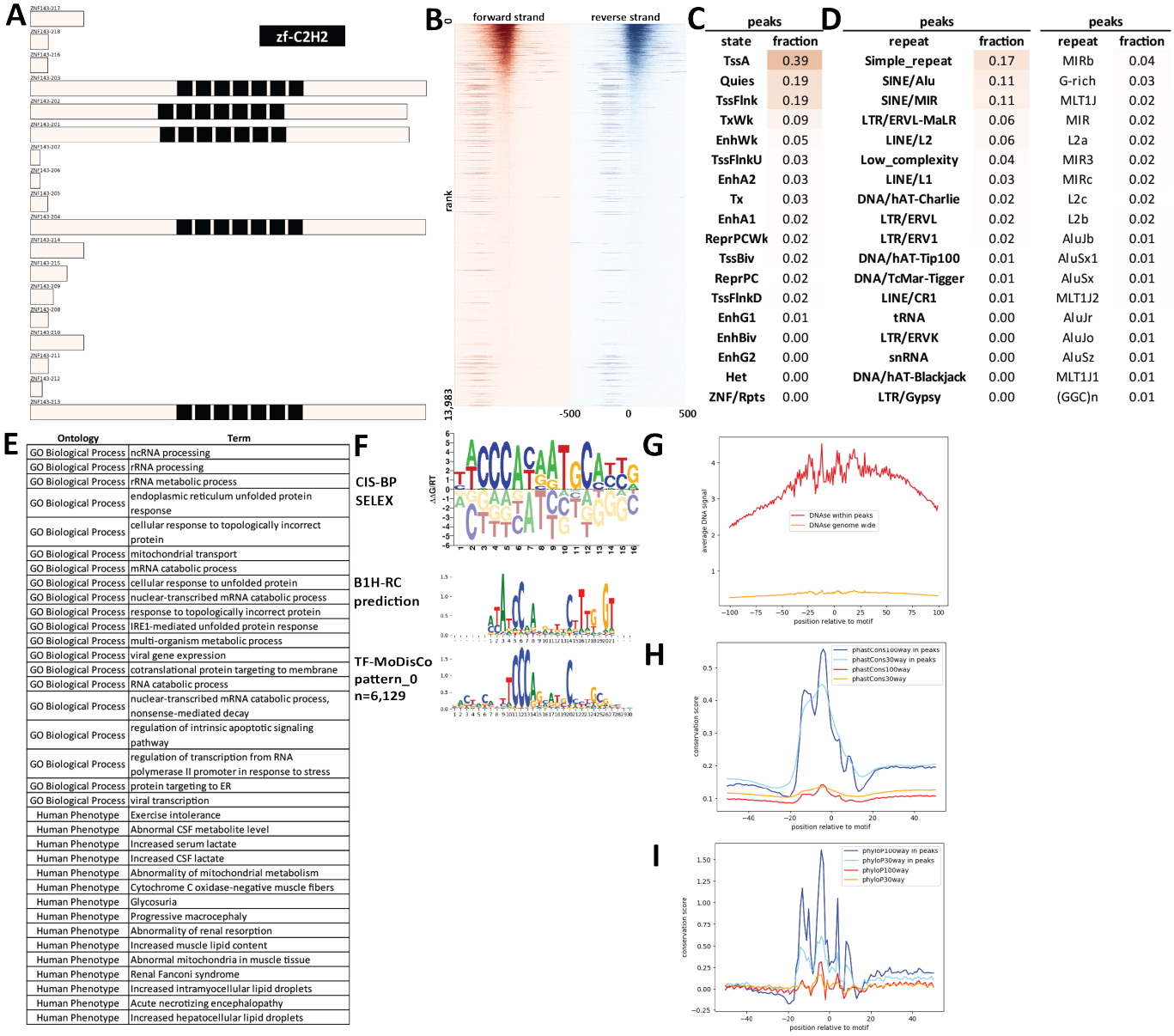

Supplementary Figure 731: Properties and genomic distribution of motifs identified for the ZNF143 transcription factor in HepG2 (accession ENCSR080UEM).

TF-MoDisCO pattern_0 n=6129, CWM

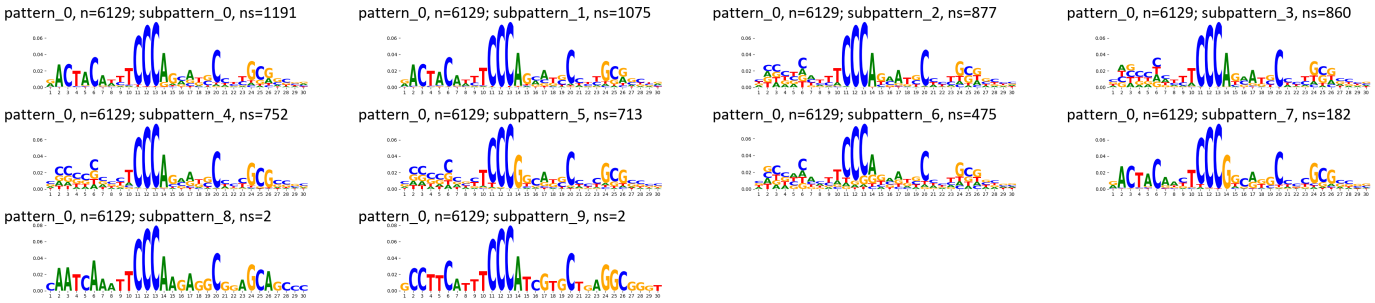

TF-MoDisCO pattern_0 n=6129, PWM

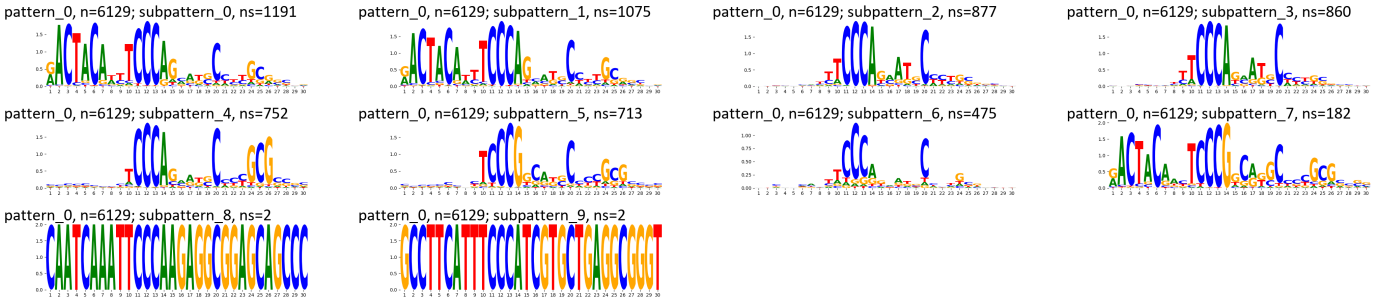

Supplementary Figure 732: TF-MoDisCO subpatterns for the ZNF143 transcription factor in HepG2 (accession ENCSR080UEM).

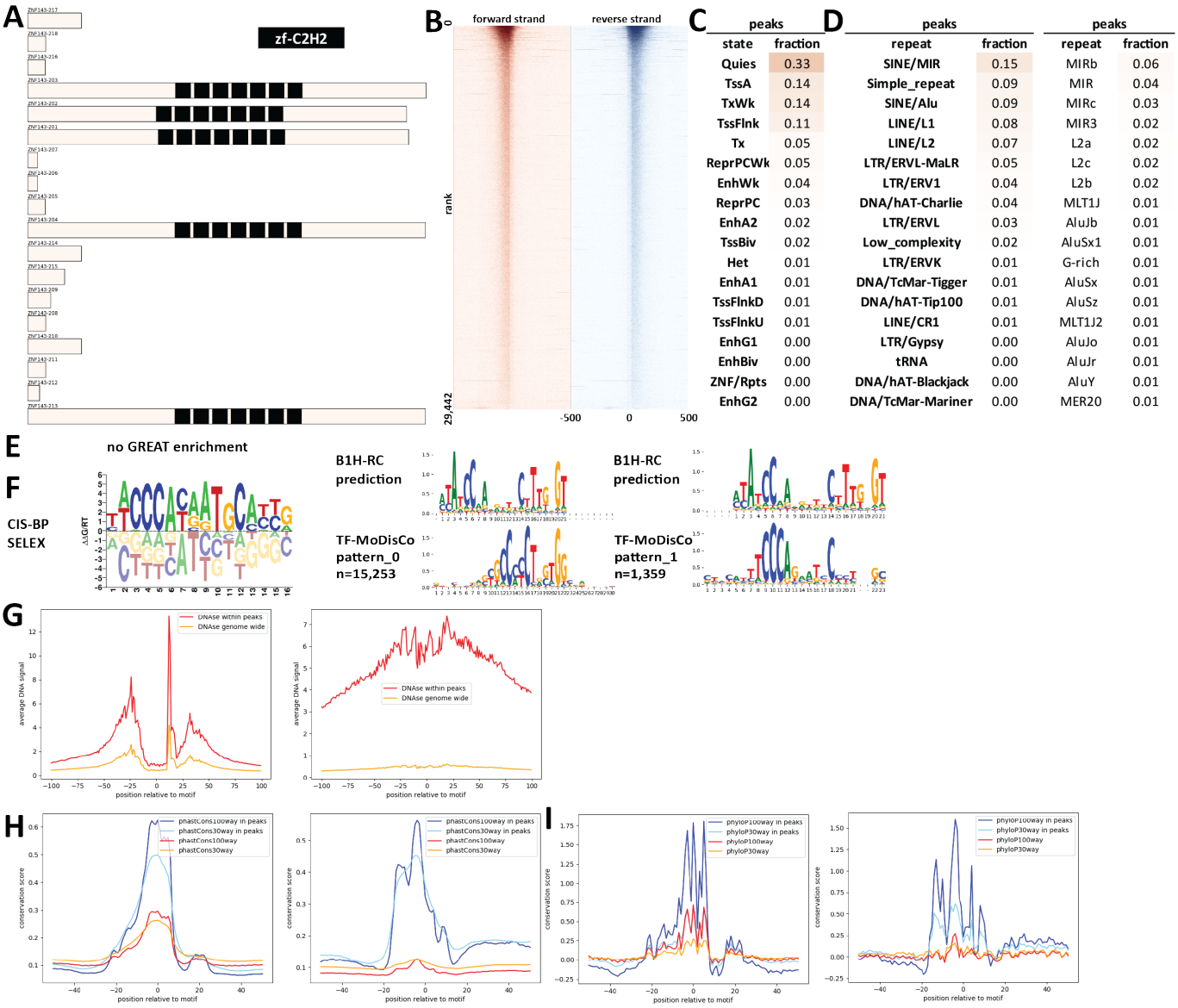

Supplementary Figure 733: Properties and genomic distribution of motifs identified for the ZNF143 transcription factor in K562 (accession ENCSR000EGP).

TF-MoDisCO pattern_0 n=15253, CWM

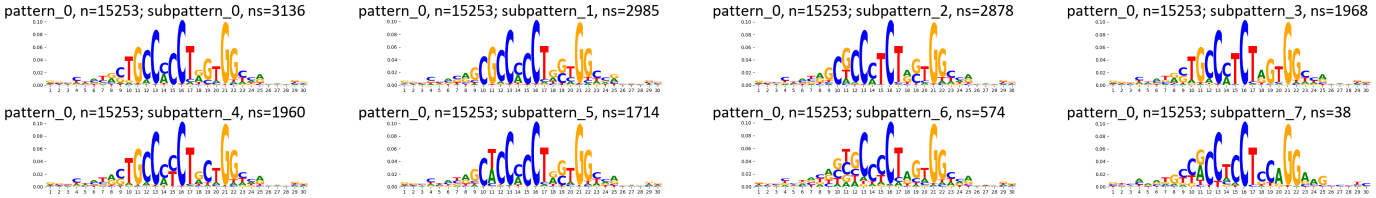

TF-MoDisCO pattern_0 n=15253, PWM

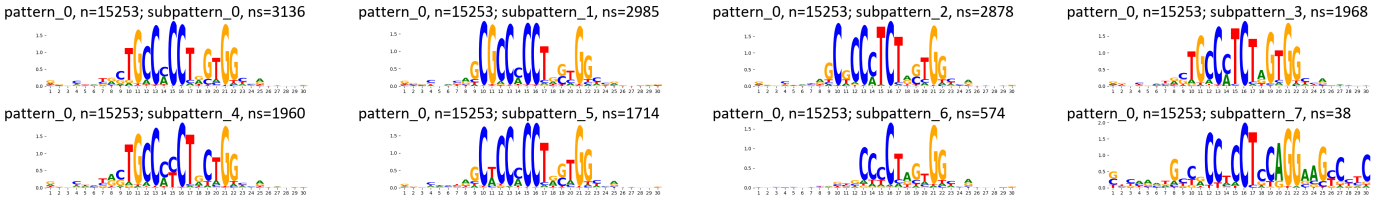

TF-MoDisCO pattern_1 n=1359, CWM

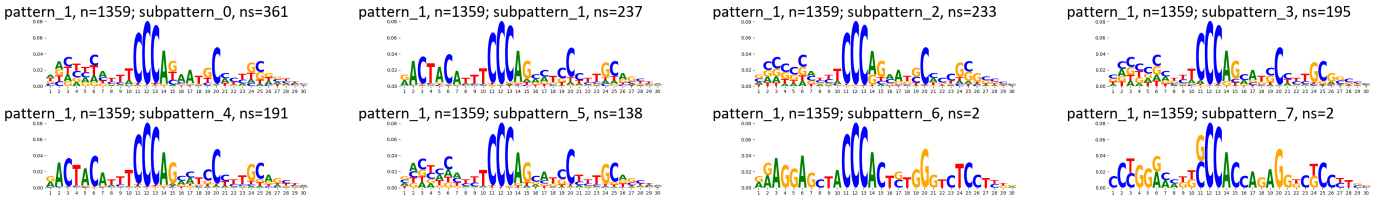

TF-MoDisCO pattern_1 n=1359, PWM

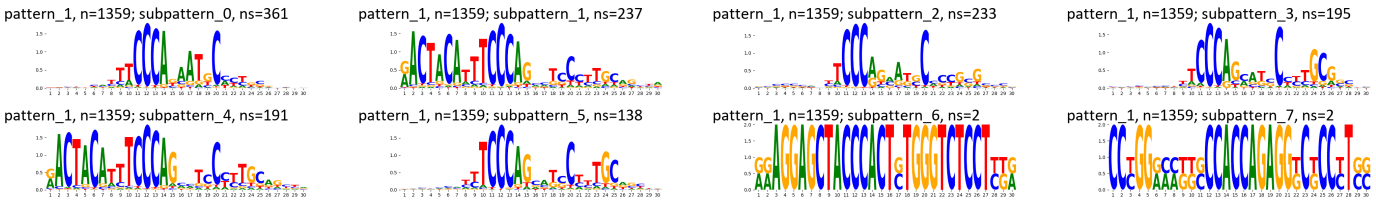

Supplementary Figure 734: TF-MoDisCO subpatterns for the ZNF143 transcription factor in K562 (accession ENCSR000EGP).

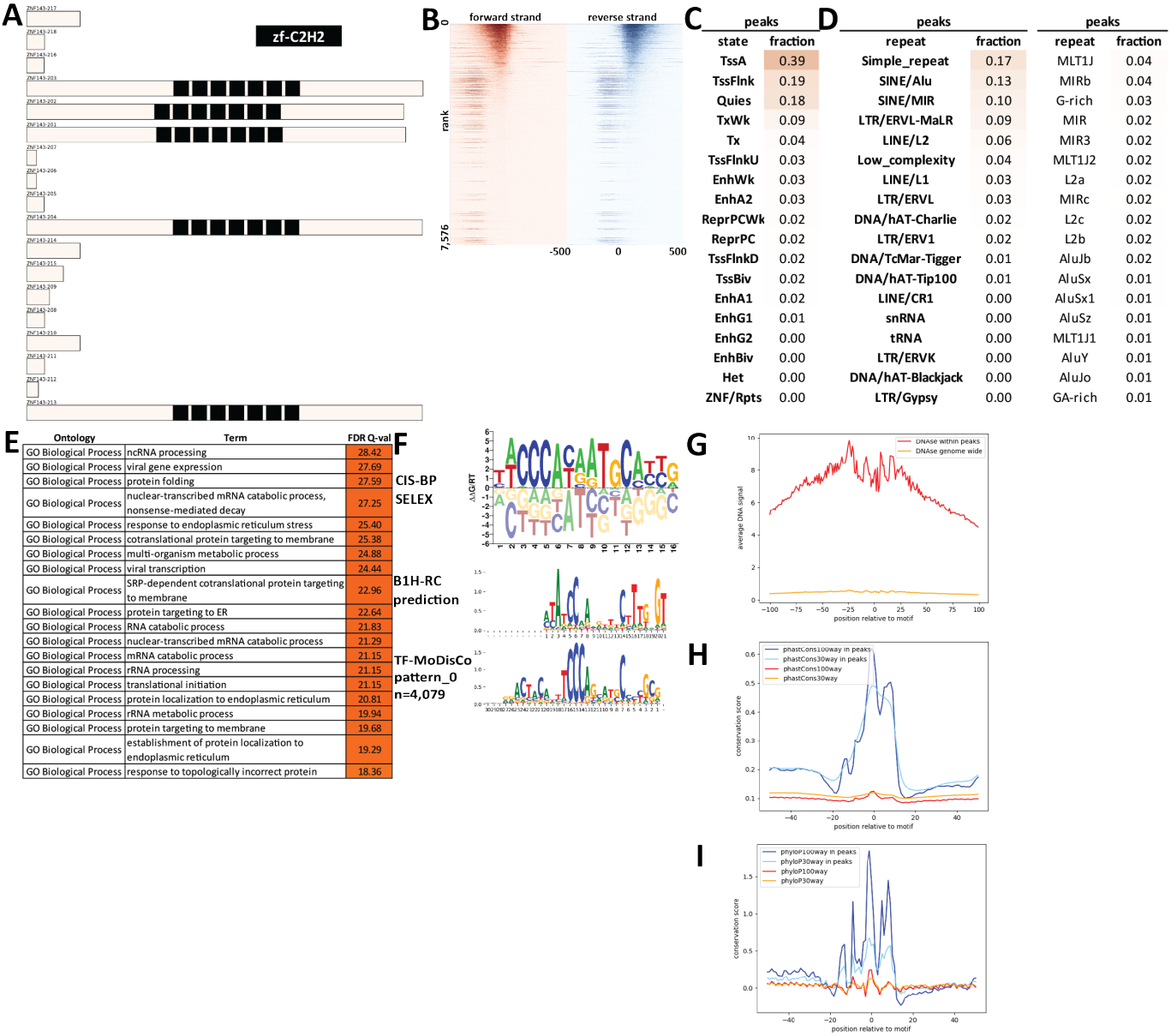

Supplementary Figure 735: Properties and genomic distribution of motifs identified for the ZNF143 transcription factor in K562 (accession ENCSR427WZJ).

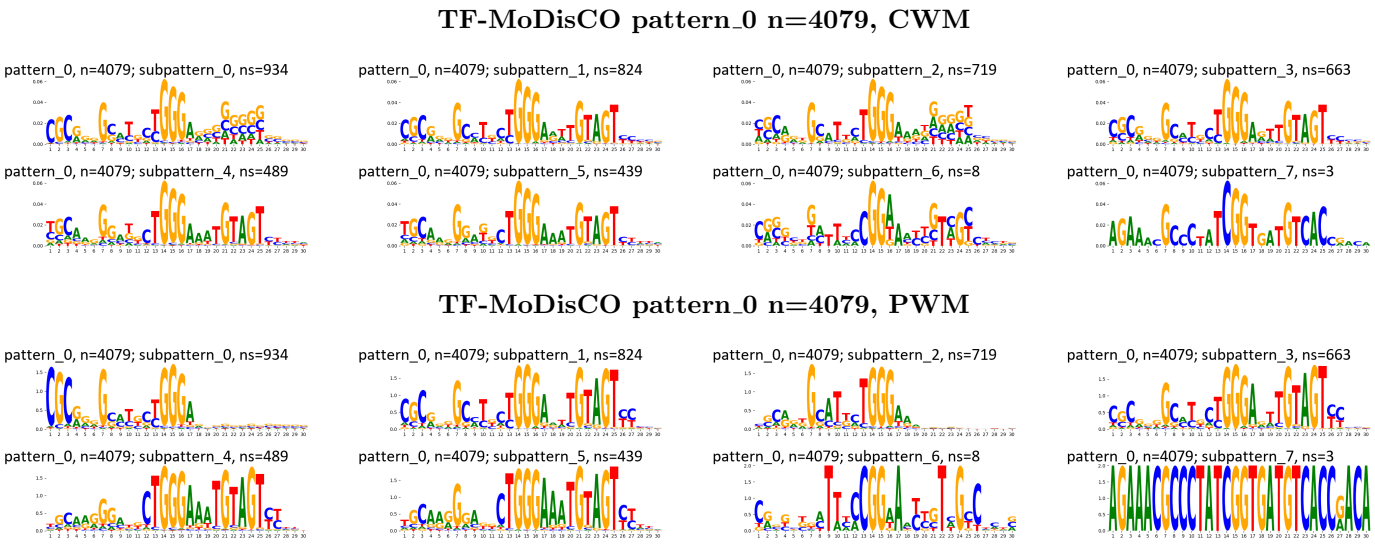

Supplementary Figure 736: TF-MoDisCO subpatterns for the ZNF143 transcription factor in K562 (accession ENCSR427WZJ).

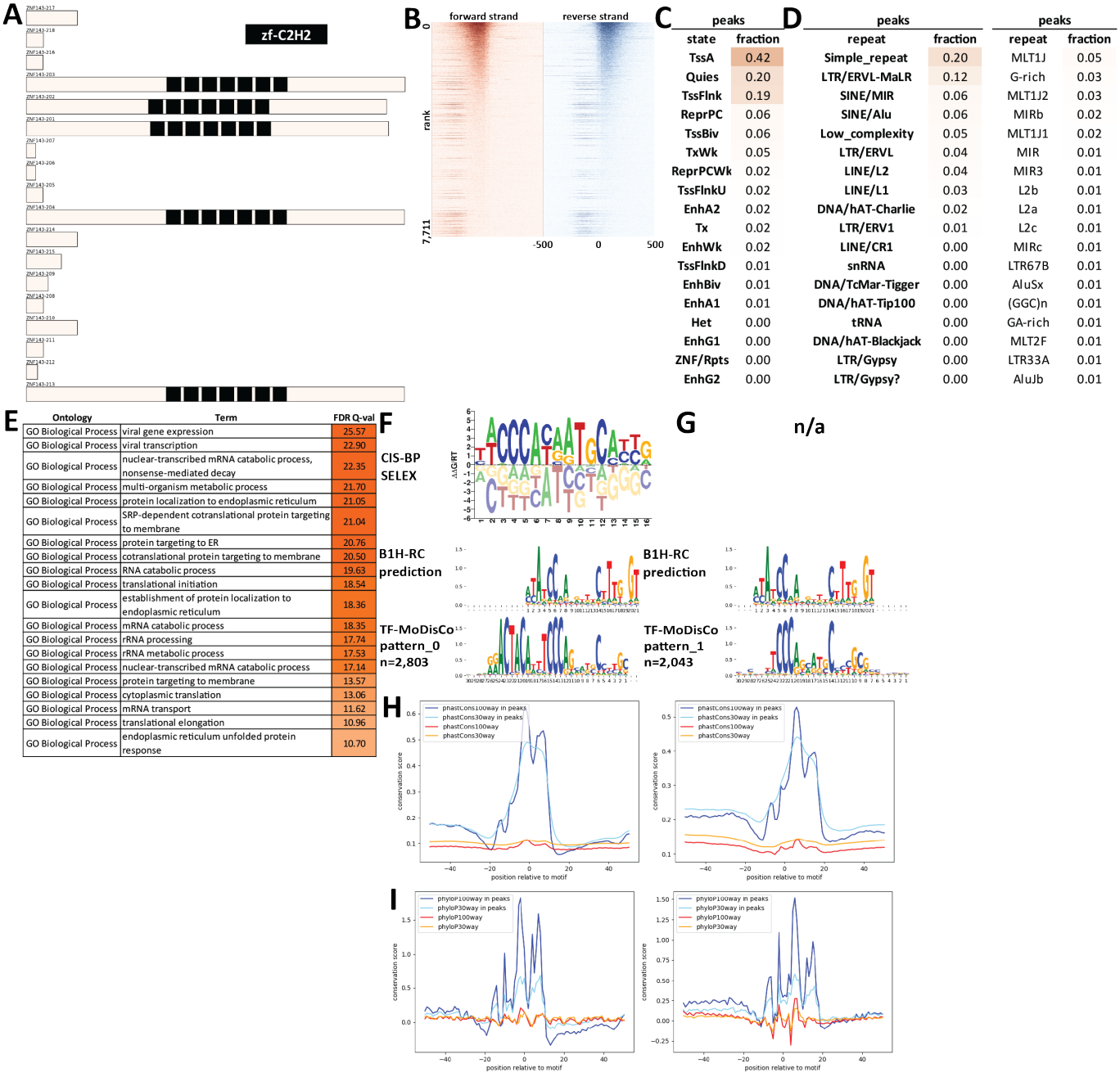

Supplementary Figure 737: Properties and genomic distribution of motifs identified for the ZNF143 transcription factor in WTC11 (accession ENCSR063FUV).

TF-MoDisCO pattern_0 n=2803, CWM

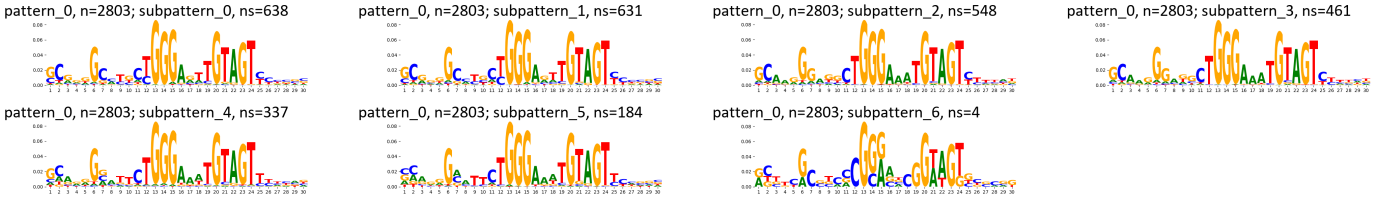

TF-MoDisCO pattern_0 n=2803, PWM

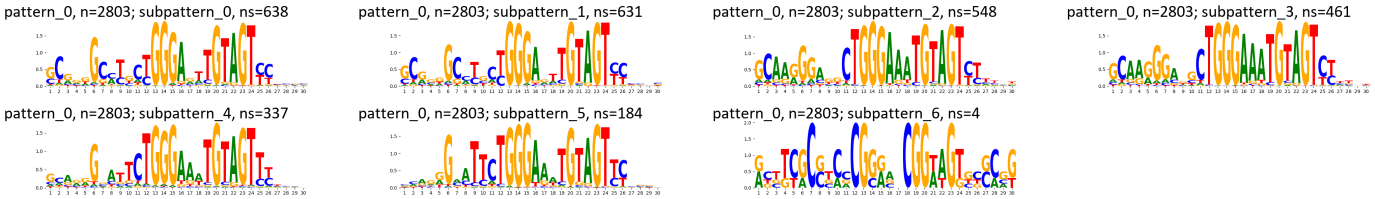

TF-MoDisCO pattern_1 n=2043, CWM

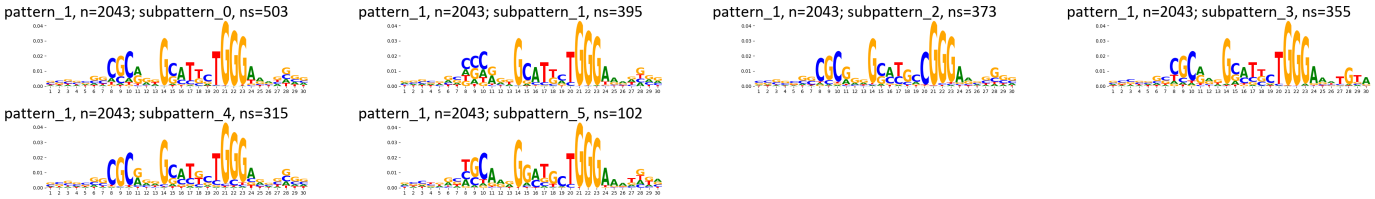

TF-MoDisCO pattern_1 n=2043, PWM

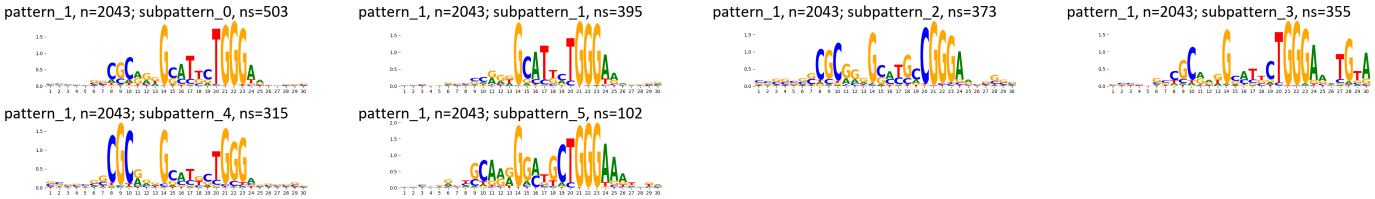

Supplementary Figure 738: TF-MoDisCO subpatterns for the ZNF143 transcription factor in WTC11 (accession ENCSR063FUV).

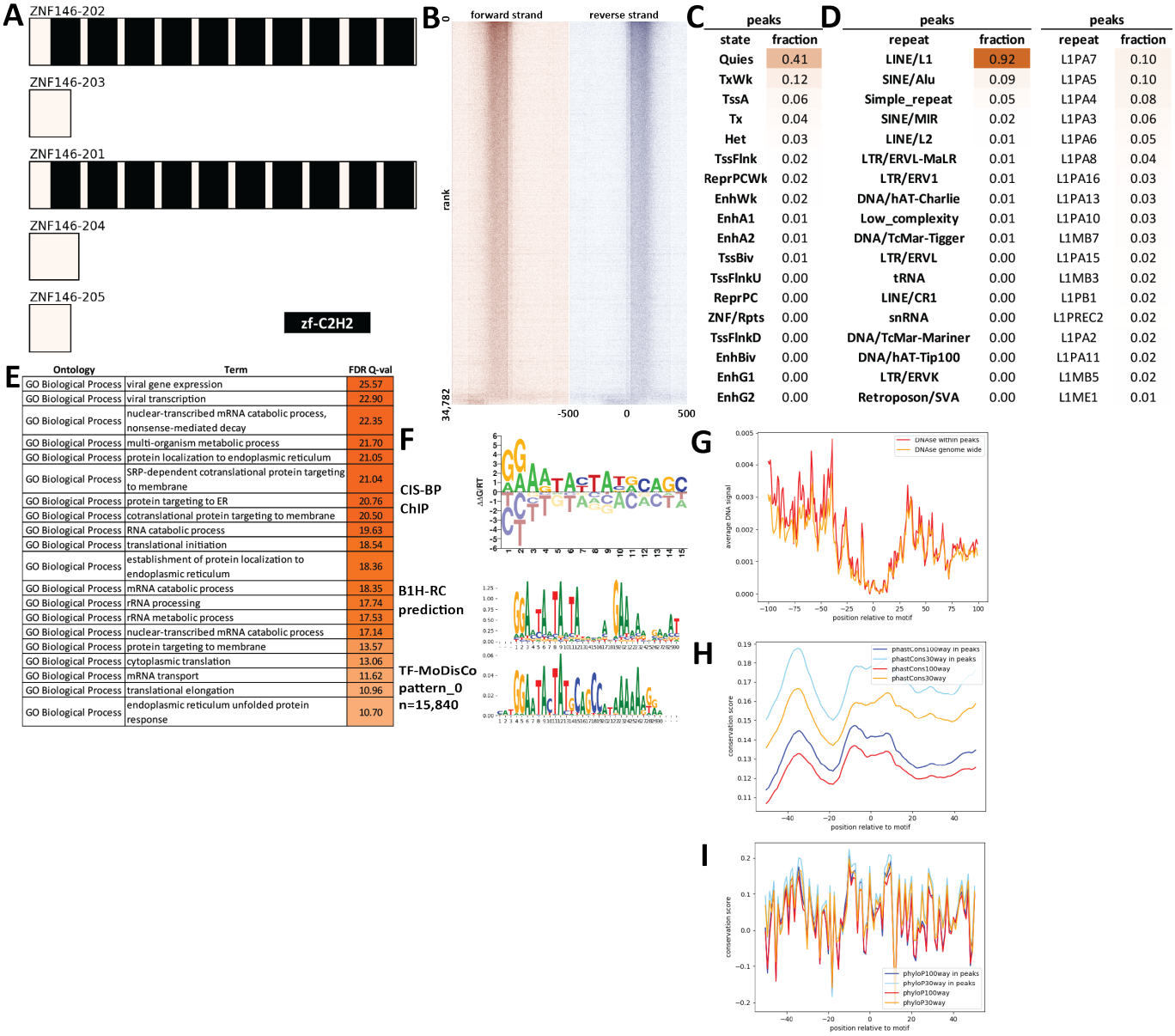

C

peaks	
state	fraction
Quies	0.41
TxWk	0.12
TssA	0.06
Tx	0.04
Het	0.03
TssFlnk	0.02
ReprPCWk	0.02
EnhWk	0.02
EnhA1	0.01
EnhA2	0.01
TssBiv	0.01
TssFlnkU	0.00
ReprPC	0.00
ZNF/Rpts	0.00
TssFlnkD	0.00
EnhBiv	0.00
EnhG1	0.00
EnhG2	0.00

D

peaks		peaks	
repeat	fraction	repeat	fraction
LINE/L1	0.92	L1PA7	0.10
SINE/Alu	0.09	L1PA5	0.10
Simple_repeat	0.05	L1PA4	0.08
SINE/MIR	0.02	L1PA3	0.06
LINE/L2	0.01	L1PA6	0.05
LTR/ERVL-MaLR	0.01	L1PA8	0.04
LTR/ERV1	0.01	L1PA16	0.03
DNA/hAT-Charlie	0.01	L1PA13	0.03
Low_complexity	0.01	L1PA10	0.03
DNA/TcMar-Tigger	0.01	L1MB7	0.03
LTR/ERVL	0.00	L1PA15	0.02
tRNA	0.00	L1MB3	0.02
LINE/CR1	0.00	L1PB1	0.02
snRNA	0.00	L1PREC2	0.02
DNA/TcMar-Mariner	0.00	L1PA2	0.02
DNA/hAT-Tip100	0.00	L1PA11	0.02
LTR/ERVK	0.00	L1MB5	0.02
Retroposon/SVA	0.00	L1ME1	0.01

E

Ontology	Term	FDR Q-val
GO Biological Process	viral gene expression	25.57
GO Biological Process	viral transcription	22.90
GO Biological Process	nuclear-transcribed mRNA catabolic process, nonsense-mediated decay	22.35
GO Biological Process	multi-organism metabolic process	21.70
GO Biological Process	protein localization to endoplasmic reticulum	21.05
GO Biological Process	SRP-dependent cotranslational protein targeting to membrane	21.04
GO Biological Process	protein targeting to ER	20.76
GO Biological Process	cotranslational protein targeting to membrane	20.50
GO Biological Process	RNA catabolic process	19.63
GO Biological Process	translational initiation	18.54
GO Biological Process	establishment of protein localization to endoplasmic reticulum	18.36
GO Biological Process	mRNA catabolic process	18.35
GO Biological Process	rRNA processing	17.74
GO Biological Process	rRNA metabolic process	17.53
GO Biological Process	nuclear-transcribed mRNA catabolic process	17.14
GO Biological Process	protein targeting to membrane	13.57
GO Biological Process	cytoplasmic translation	13.06
GO Biological Process	mRNA transport	11.62
GO Biological Process	translational elongation	10.96
GO Biological Process	endoplasmic reticulum unfolded protein response	10.70

Supplementary Figure 739: Properties and genomic distribution of motifs identified for the ZNF146 transcription factor in HEK293 (accession ENCSR689YFA).

TF-MoDisCO pattern_0 n=16840, CWM

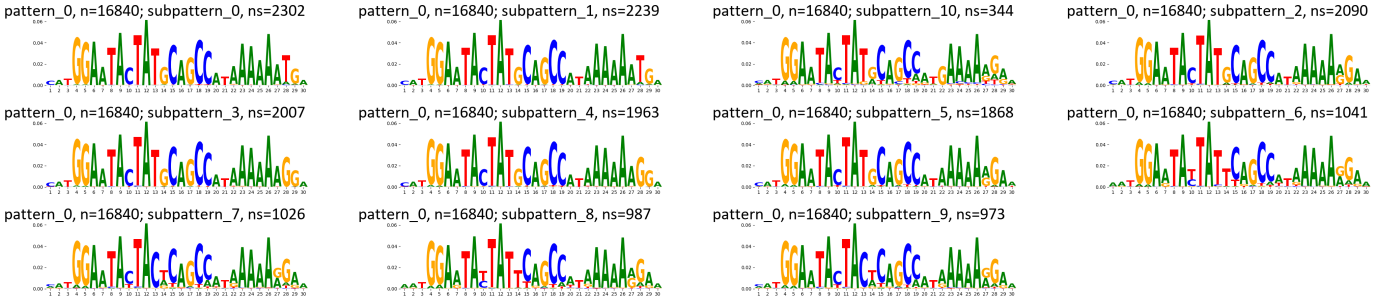

TF-MoDisCO pattern_0 n=16840, PWM

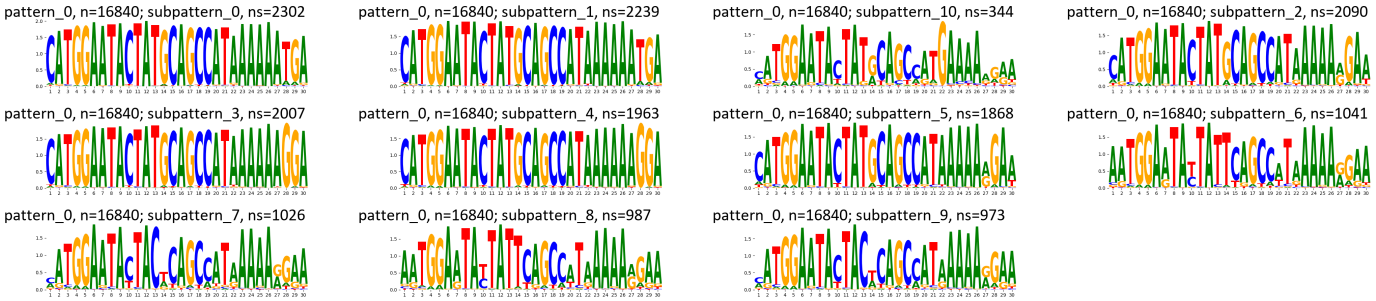

Supplementary Figure 740: TF-MoDisCO subpatterns for the ZNF146 transcription factor in HEK293 (accession ENCSR689YFA).

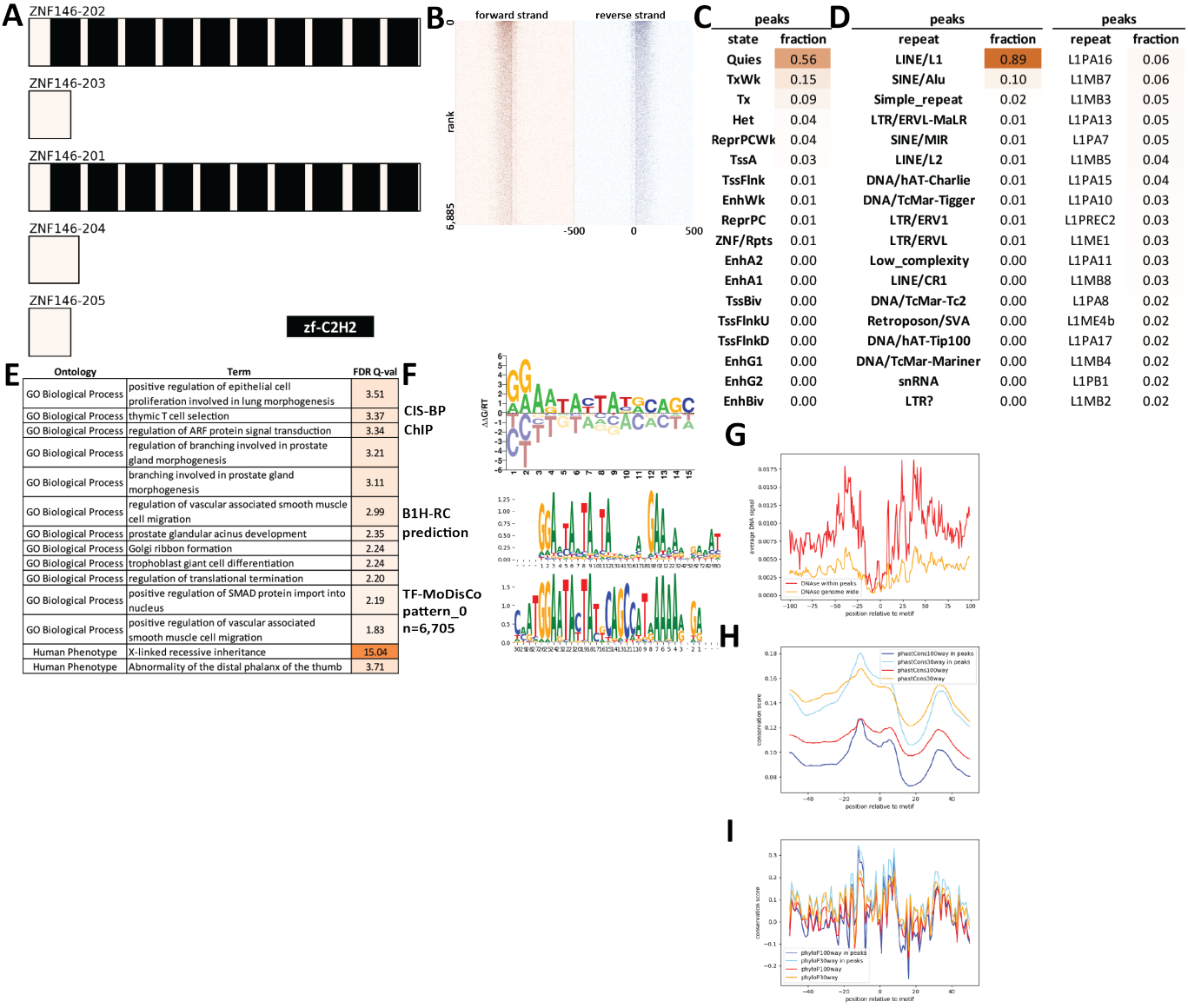

Supplementary Figure 741: Properties and genomic distribution of motifs identified for the ZNF146 transcription factor in HEK293 (accession Hughes GR models).

TF-MoDisCO pattern_0 n=6705, CWM

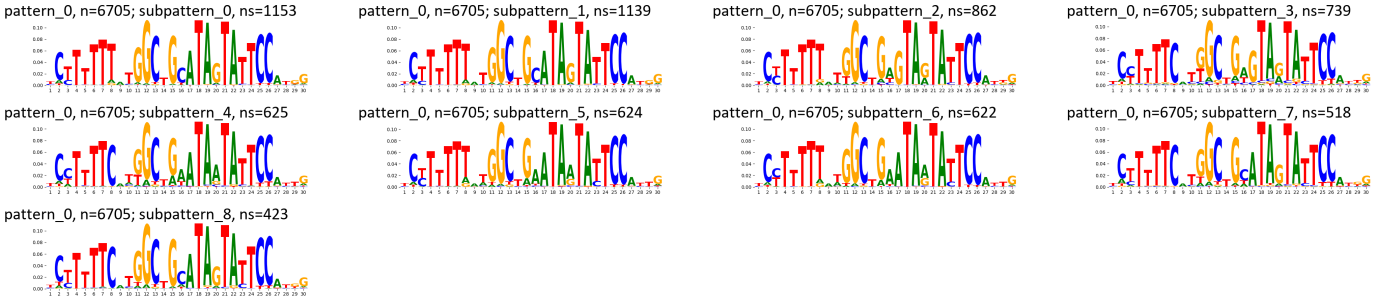

TF-MoDisCO pattern_0 n=6705, PWM

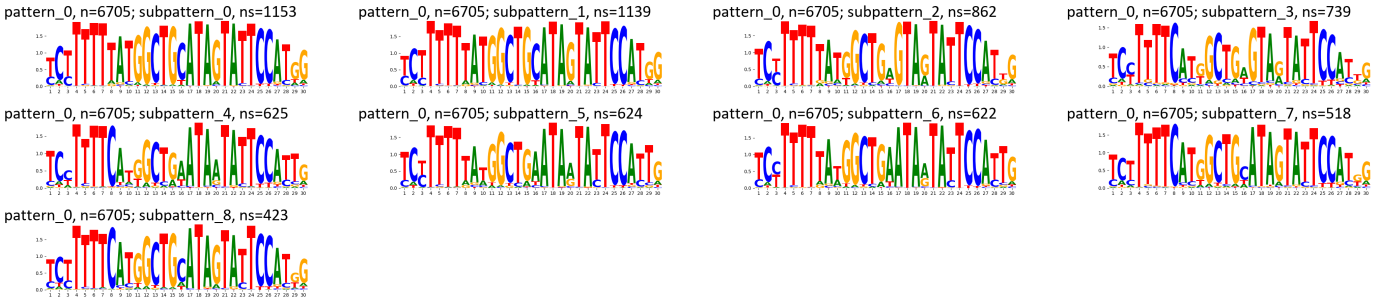

Supplementary Figure 742: TF-MoDisCO subpatterns for the ZNF146 transcription factor in HEK293 (accession Hughes GR models).

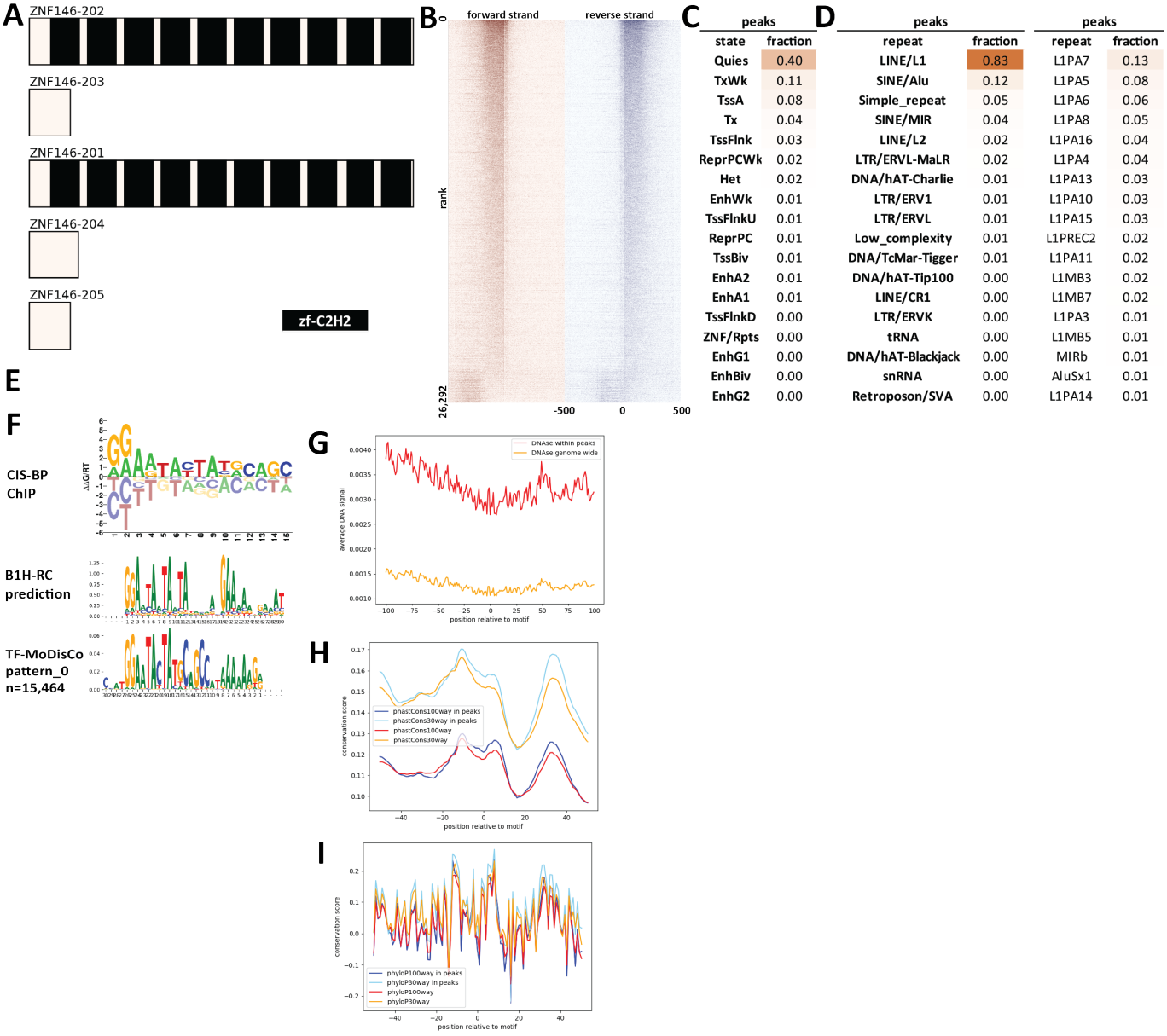

peaks	
state	fraction
Quies	0.40
TxWk	0.11
TssA	0.08
Tx	0.04
TssFlnk	0.03
ReprPCWk	0.02
Het	0.02
EnhWk	0.01
TssFlnkU	0.01
ReprPC	0.01
TssBiv	0.01
EnhA2	0.01
EnhA1	0.01
TssFlnkD	0.00
ZNF/Rpts	0.00
EnhG1	0.00
EnhBiv	0.00
EnhG2	0.00

peaks	
repeat	fraction
LINE/L1	0.83
SINE/Alu	0.12
Simple_repeat	0.05
SINE/MIR	0.04
LINE/L2	0.02
LTR/ERVL-MaLR	0.02
DNA/hAT-Charlie	0.01
LTR/ERV1	0.01
LTR/ERVL	0.01
Low_complexity	0.01
DNA/TcMar-Tigger	0.01
DNA/hAT-Tip100	0.00
LINE/CR1	0.00
LTR/ERVK	0.00
tRNA	0.00
DNA/hAT-Blackjack	0.00
snRNA	0.00
Retroposon/SVA	0.00

peaks	
repeat	fraction
L1PA7	0.13
L1PA5	0.08
L1PA6	0.06
L1PA8	0.05
L1PA16	0.04
L1PA4	0.04
L1PA13	0.03
L1PA10	0.03
L1PA15	0.03
L1PREC2	0.02
L1PA11	0.02
L1MB3	0.02
L1MB7	0.02
L1PA3	0.01
L1MB5	0.01
MIRb	0.01
AluSx1	0.01
L1PA14	0.01

Supplementary Figure 743: Properties and genomic distribution of motifs identified for the ZNF146 transcription factor in HepG2 (accession ENCSR957LTN).

TF-MoDisCO pattern_0 n=15464, CWM

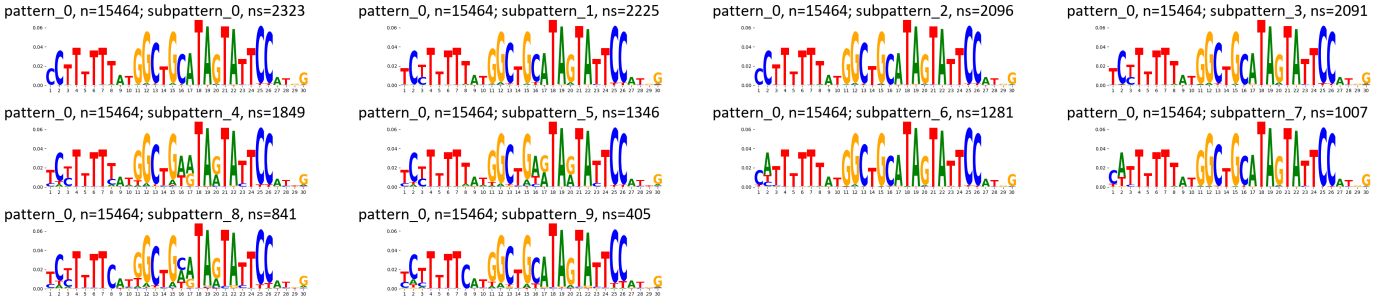

TF-MoDisCO pattern_0 n=15464, PWM

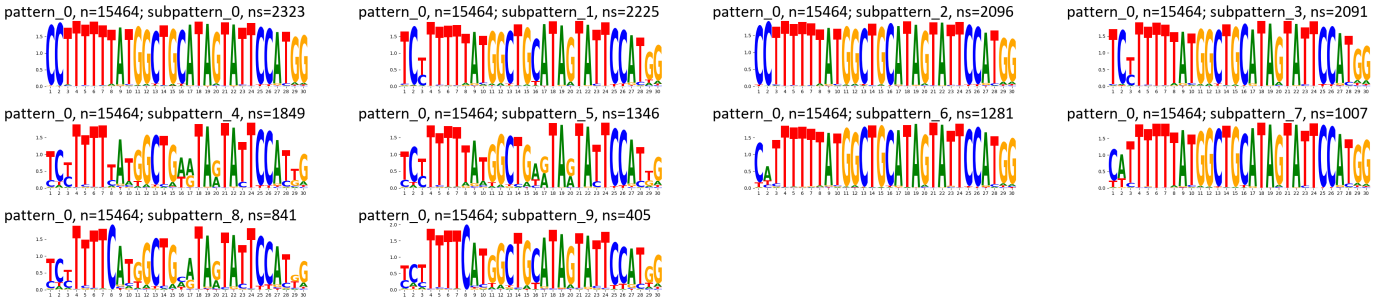

Supplementary Figure 744: TF-MoDisCO subpatterns for the ZNF146 transcription factor in HepG2 (accession ENCSR957LTN).

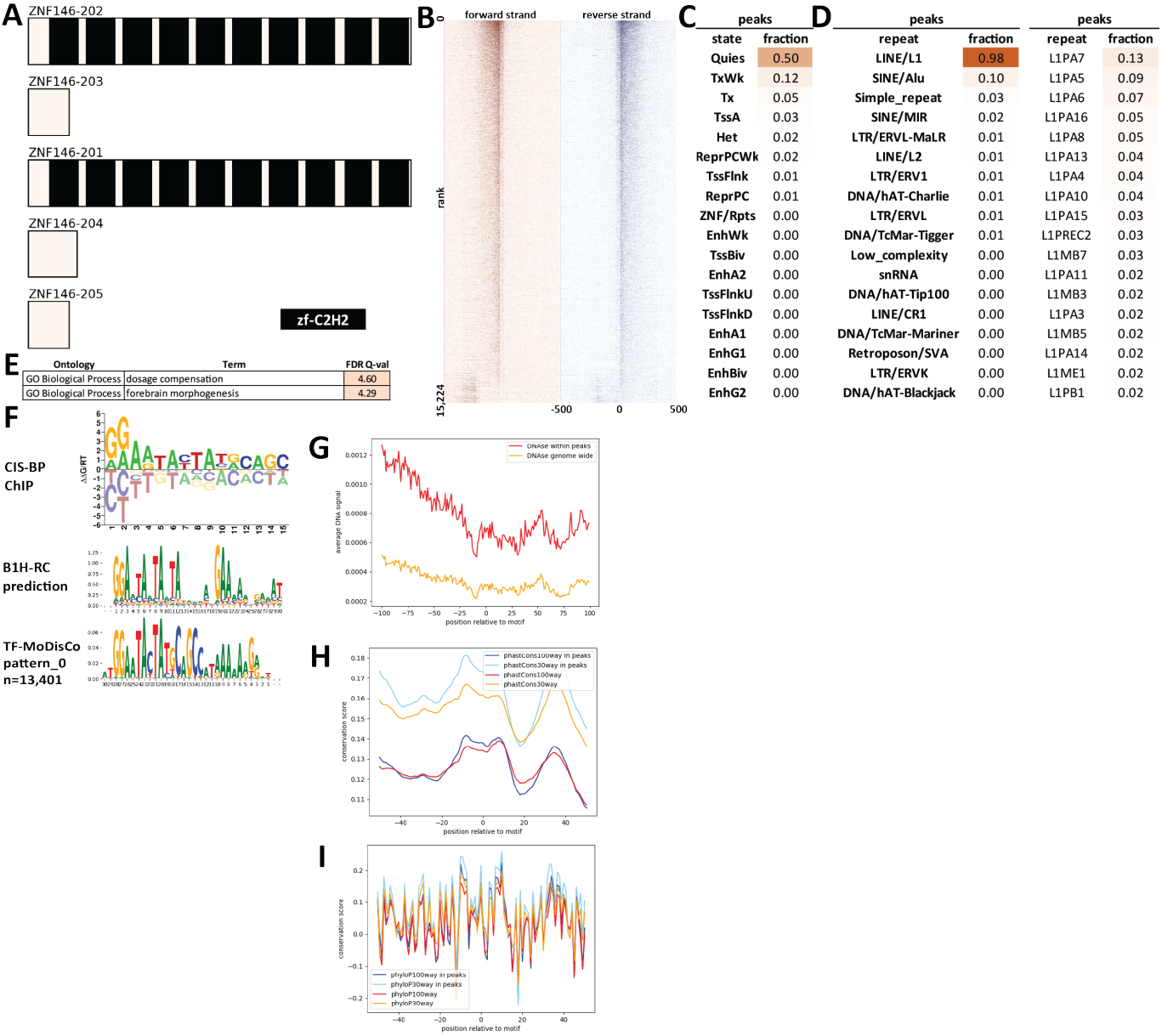

Supplementary Figure 745: Properties and genomic distribution of motifs identified for the ZNF146 transcription factor in K562 (accession ENCSR713IFY).

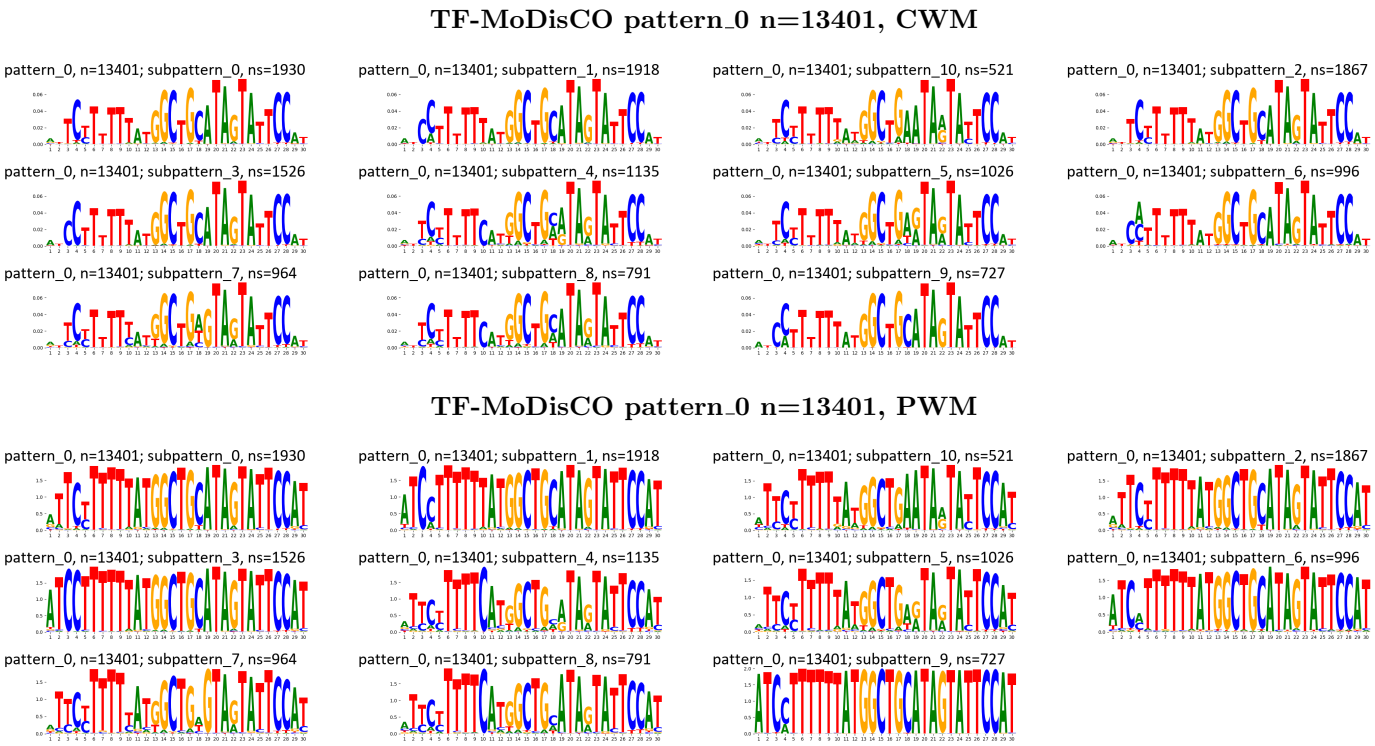

Supplementary Figure 746: TF-MoDisCO subpatterns for the ZNF146 transcription factor in K562 (accession ENCSR713IFY).

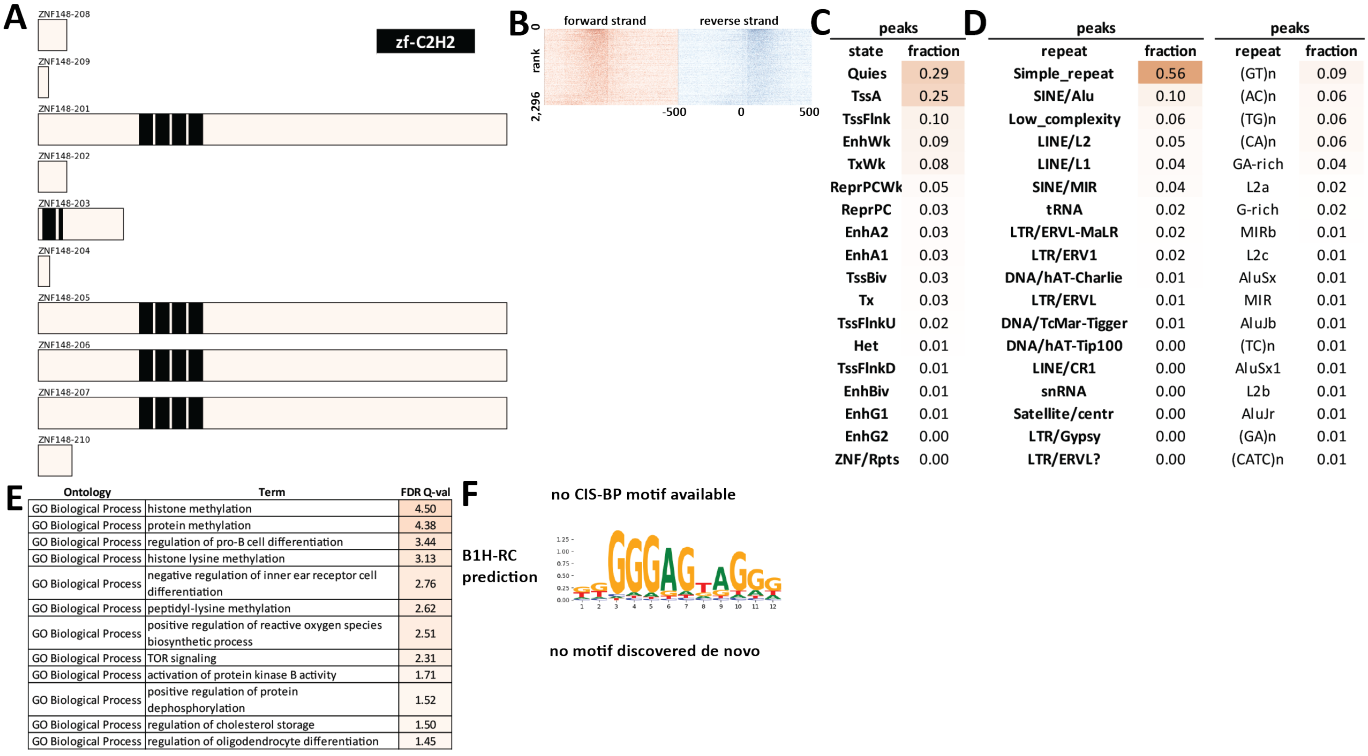

Supplementary Figure 747: Properties and genomic distribution of motifs identified for the ZNF148 transcription factor in HEK293 (accession ENCSR736ZKL).

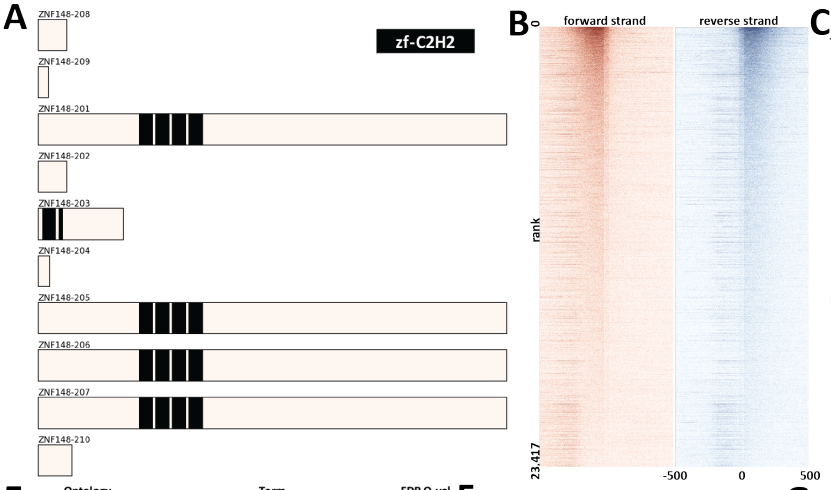

C

peaks	
state	fraction
TssA	0.22
Quies	0.22
TssFlnk	0.14
TxWk	0.10
EnhWk	0.09
EnhA1	0.04
TssFlnkU	0.03
EnhA2	0.03
TssBiv	0.03
Tx	0.02
ReprPCWk	0.02
TssFlnkD	0.02
ReprPC	0.02
EnhBiv	0.01
EnhG1	0.01
Het	0.00
EnhG2	0.00
ZNF/Rpts	0.00

D

peaks		peaks	
repeat	fraction	repeat	fraction
Simple_repeat	0.26	G-rich	0.05
SINE/Alu	0.13	MIRb	0.04
SINE/MIR	0.11	MIR	0.03
LINE/L1	0.09	L2a	0.03
LINE/L2	0.08	L2c	0.02
Low_complexity	0.07	MIR3	0.02
LTR/ERV1	0.06	MIRc	0.02
LTR/ERVL-MaLR	0.04	L2b	0.02
DNA/hAT-Charlie	0.04	GA-rich	0.02
LTR/ERVL	0.02	AluJb	0.01
DNA/TcMar-Tigger	0.01	AluSx1	0.01
LINE/CR1	0.01	AluSx	0.01
DNA/hAT-Tip100	0.01	AluSz	0.01
LTR/ERVK	0.01	AluJr	0.01
tRNA	0.00	AluJo	0.01
LTR/Gypsy	0.00	L2	0.01
DNA/hAT-Blackjack	0.00	AluY	0.01
LINE/RTE-X	0.00	(T)n	0.01

E

Ontology	Term	FDR Q-val
GO Biological Process	regulation of gene expression, epigenetic	83.83
GO Biological Process	regulation of transcription from RNA polymerase II promoter in response to stress	54.89
GO Biological Process	positive regulation of transcription from RNA polymerase II promoter in response to stress	50.75
GO Biological Process	regulation of DNA-templated transcription in response to stress	48.18
GO Biological Process	histone H2A ubiquitination	34.60
GO Biological Process	histone H2A monoubiquitination	34.43
GO Biological Process	endoplasmic reticulum unfolded protein response	34.05
GO Biological Process	histone monoubiquitination	33.46
GO Biological Process	histone ubiquitination	30.56
GO Biological Process	cellular response to unfolded protein	29.62
GO Biological Process	positive regulation of mRNA catabolic process	27.55
GO Biological Process	negative regulation of intrinsic apoptotic signaling pathway	27.50
GO Biological Process	erythrocyte homeostasis	26.06
GO Biological Process	positive regulation of mRNA metabolic process	25.99
GO Biological Process	gene silencing by miRNA	25.56
GO Biological Process	negative regulation of histone methylation	24.61
GO Biological Process	posttranscriptional gene silencing by RNA	23.69
GO Biological Process	posttranscriptional gene silencing	23.41
GO Biological Process	IRE1-mediated unfolded protein response	22.18
GO Biological Process	definitive hemopoiesis	18.68
Human Phenotype	Exotropia	16.33

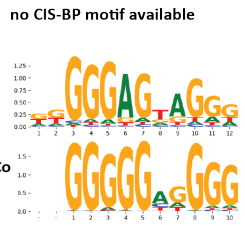

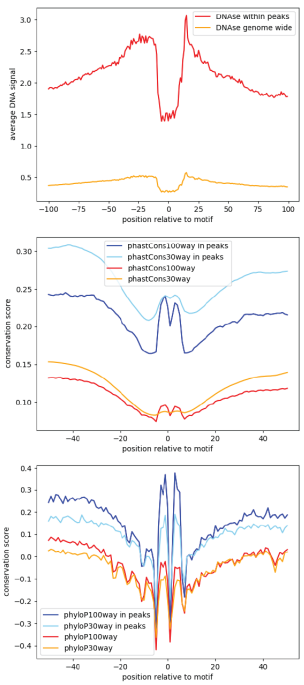

Supplementary Figure 748: Properties and genomic distribution of motifs identified for the ZNF148 transcription factor in K562 (accession ENCSR018MSO).

TF-MoDisCO pattern_0 n=11288, CWM

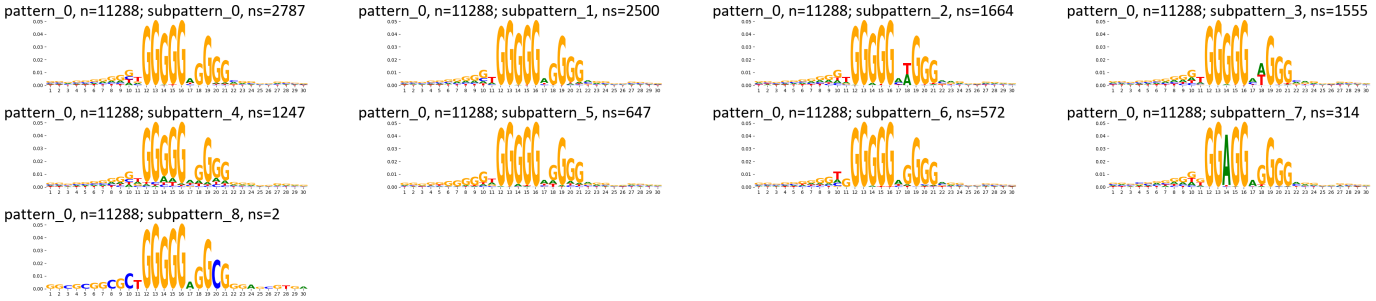

TF-MoDisCO pattern_0 n=11288, PWM

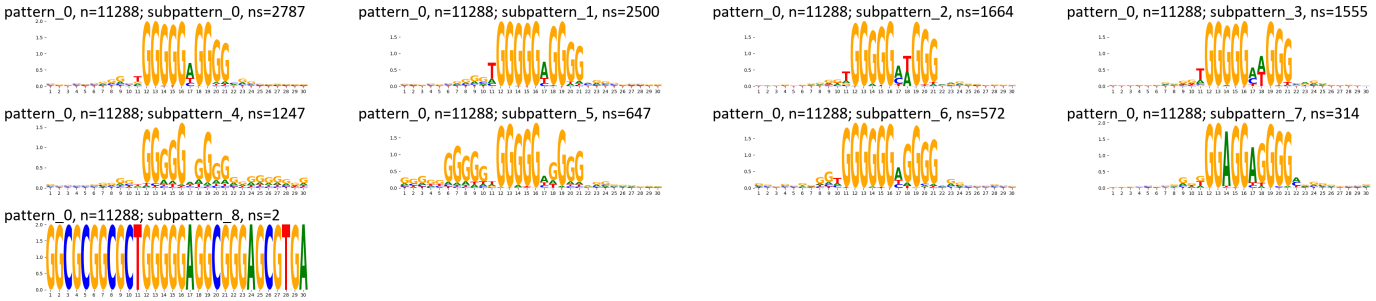

Supplementary Figure 749: TF-MoDisCO subpatterns for the ZNF148 transcription factor in K562 (accession ENCSR018MSO).

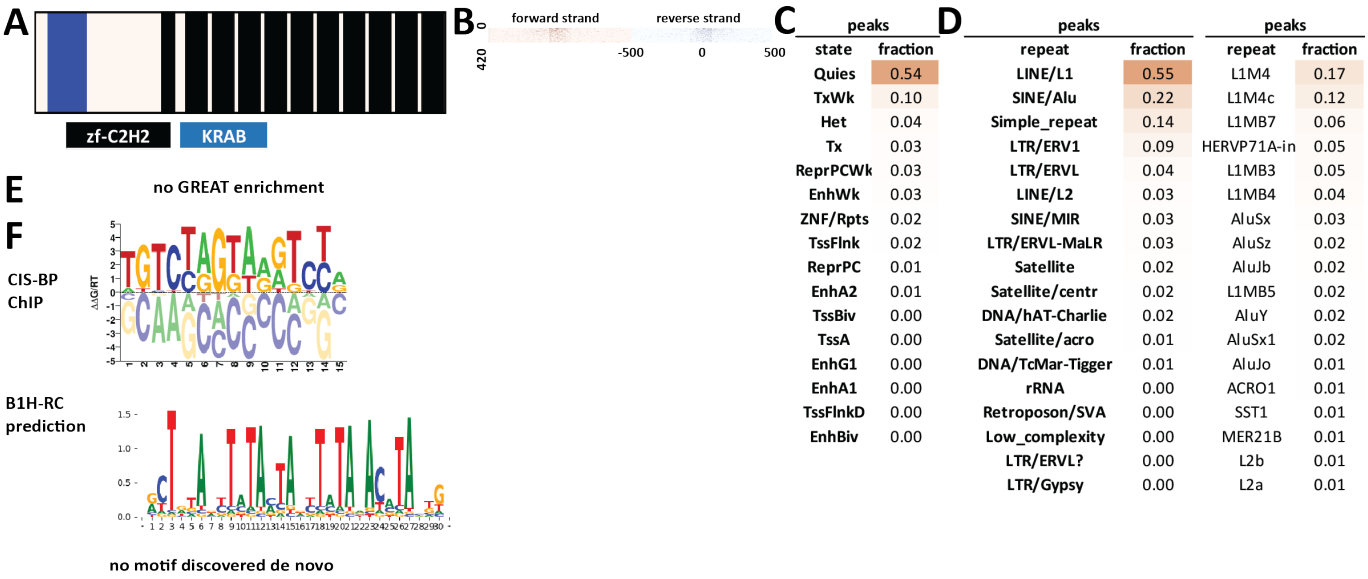

Supplementary Figure 750: Properties and genomic distribution of motifs identified for the ZNF154 transcription factor in HEK293 (accession ChipExo models).

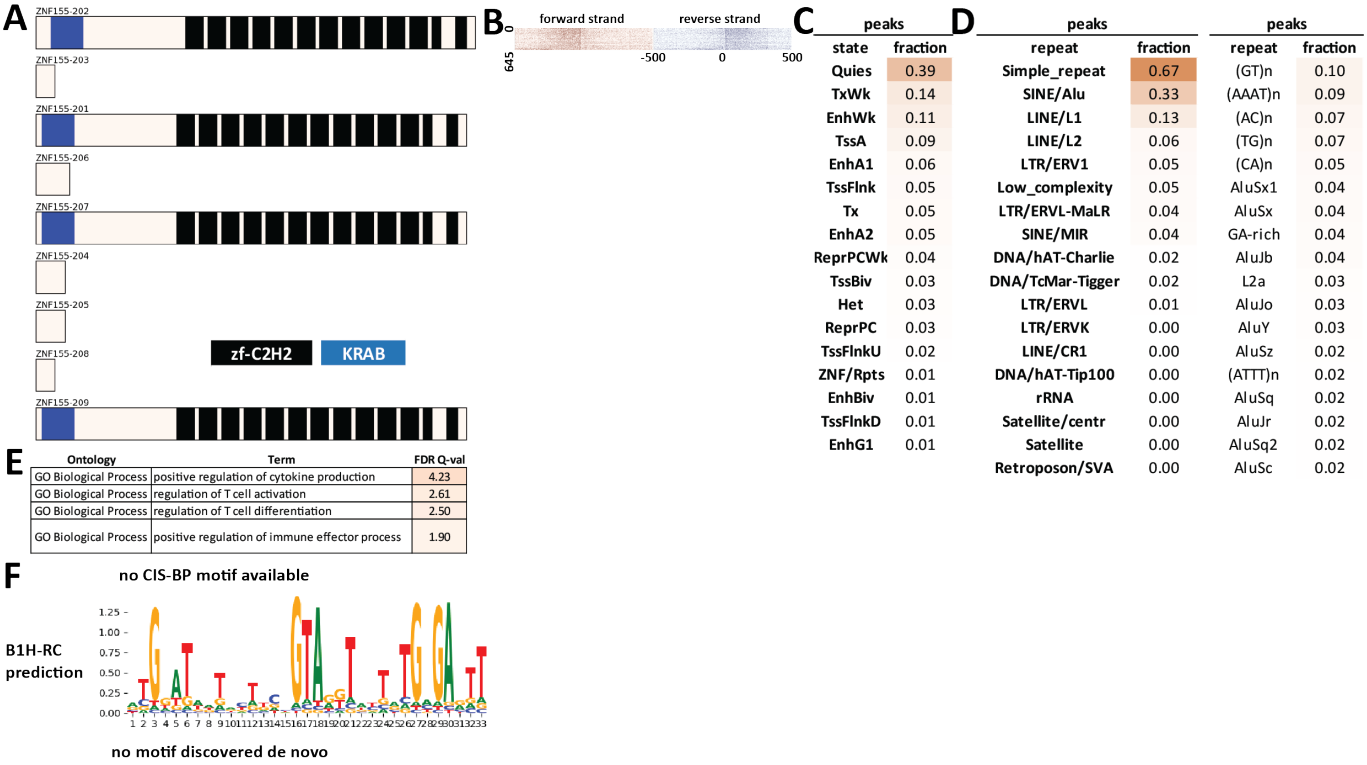

Supplementary Figure 751: Properties and genomic distribution of motifs identified for the ZNF155 transcription factor in HEK293 (accession ENCSR801BWR).

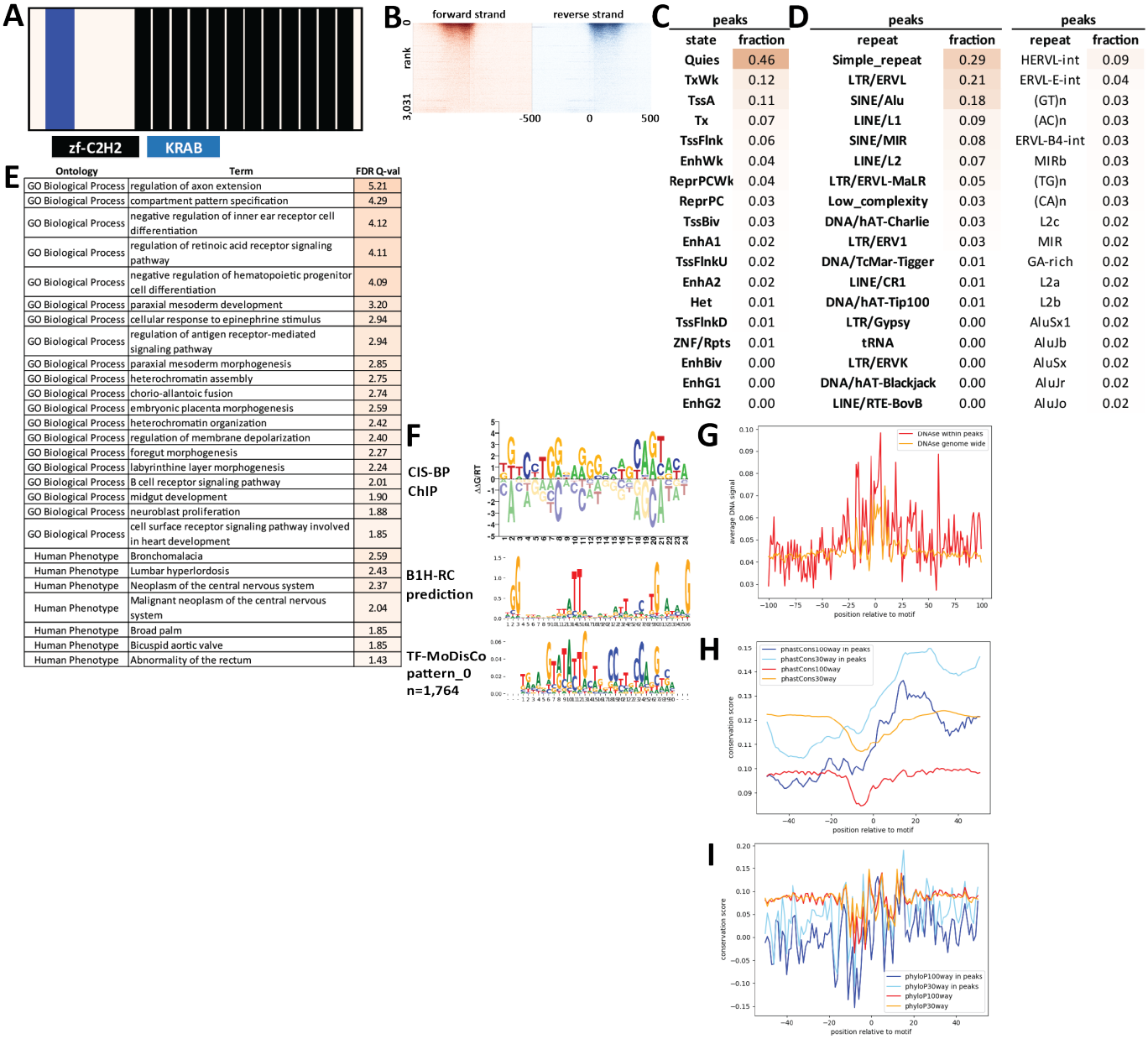

Supplementary Figure 752: Properties and genomic distribution of motifs identified for the ZNF157 transcription factor in HEK293 (accession ENCSR564YYW).

TF-MoDisCO pattern_0 n=1764, CWM

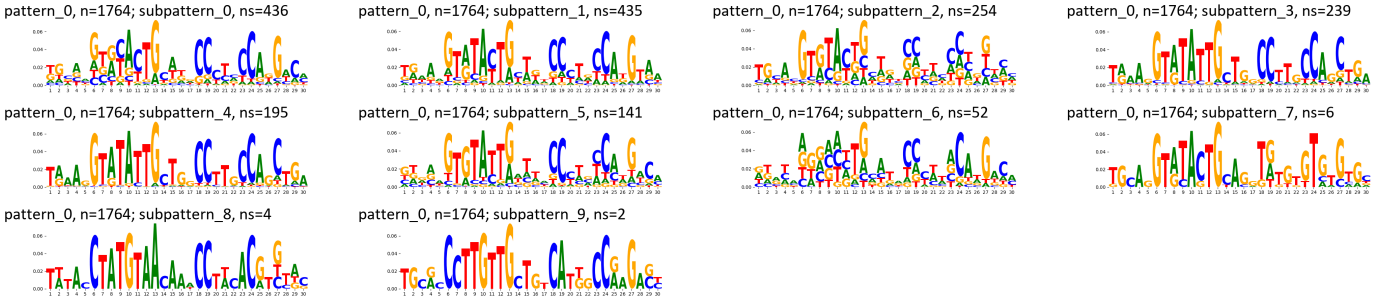

TF-MoDisCO pattern_0 n=1764, PWM

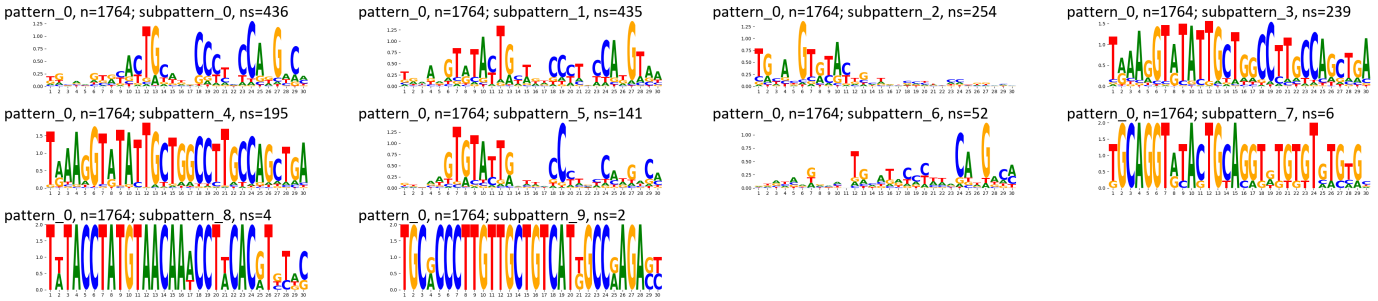

Supplementary Figure 753: TF-MoDisCO subpatterns for the ZNF157 transcription factor in HEK293 (accession ENCSR564YYW).

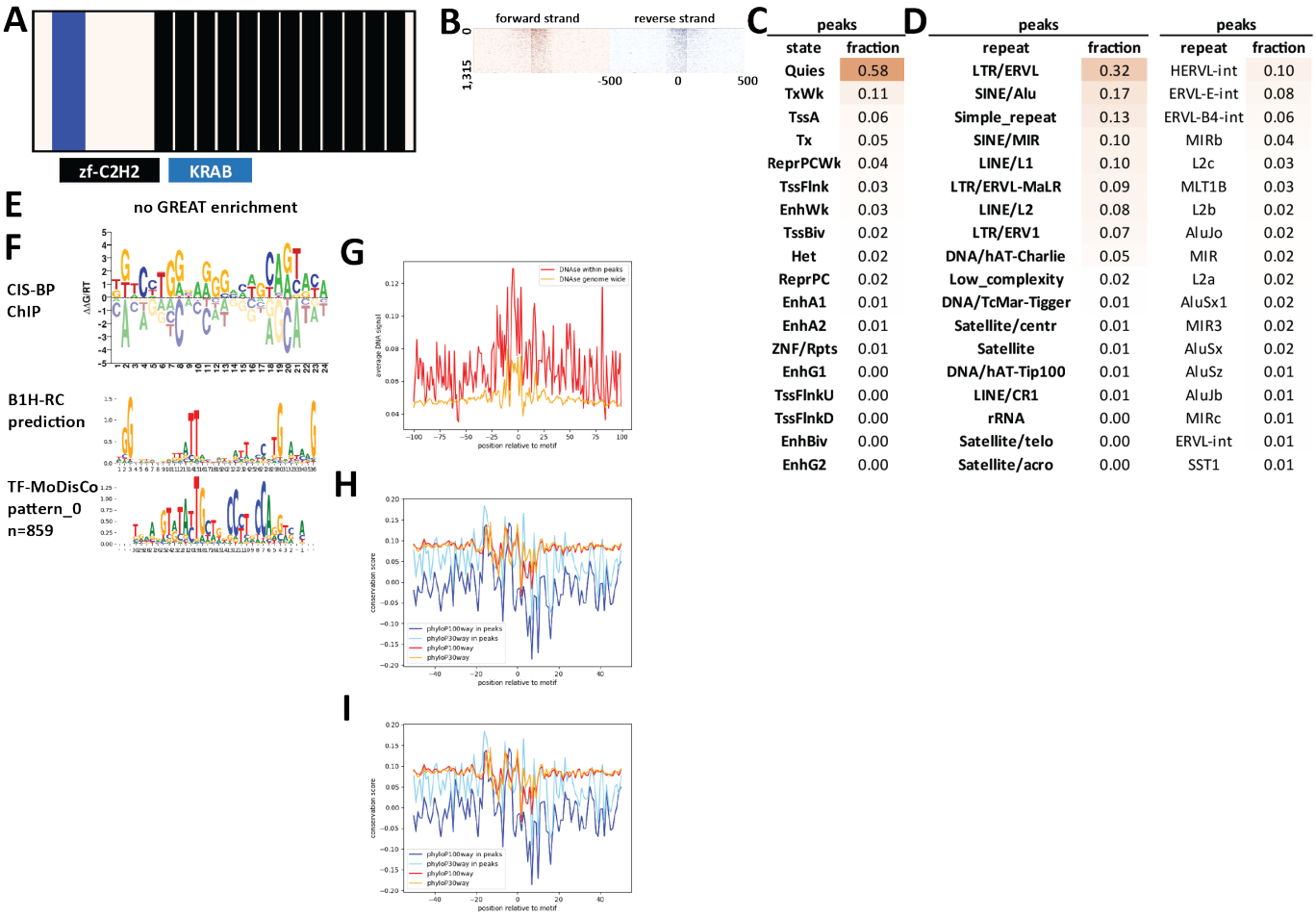

Supplementary Figure 754: Properties and genomic distribution of motifs identified for the ZNF157 transcription factor in HEK293 (accession ChipExo models).

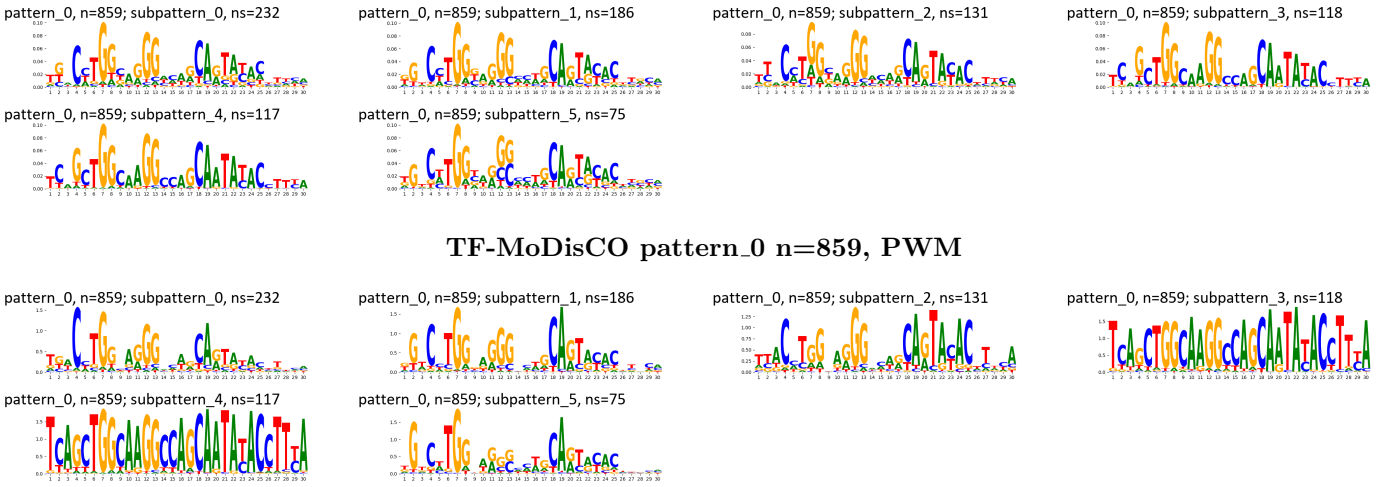

Supplementary Figure 755: TF-MoDisCO subpatterns for the ZNF157 transcription factor in HEK293 (accession ChipExo models).

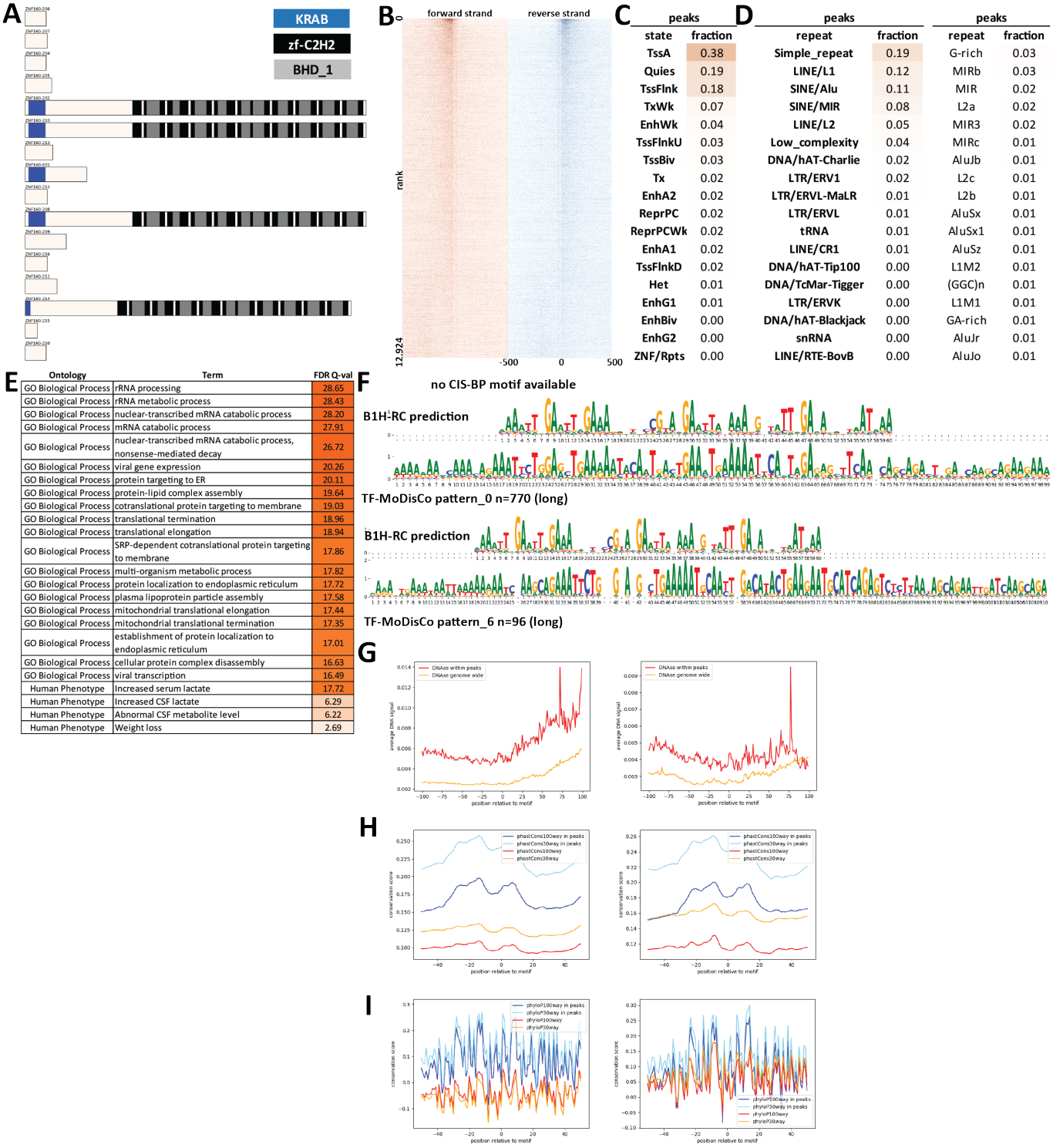

Supplementary Figure 756: Properties and genomic distribution of motifs identified for the ZNF160 transcription factor in HepG2 (accession ENCSR917SSX).

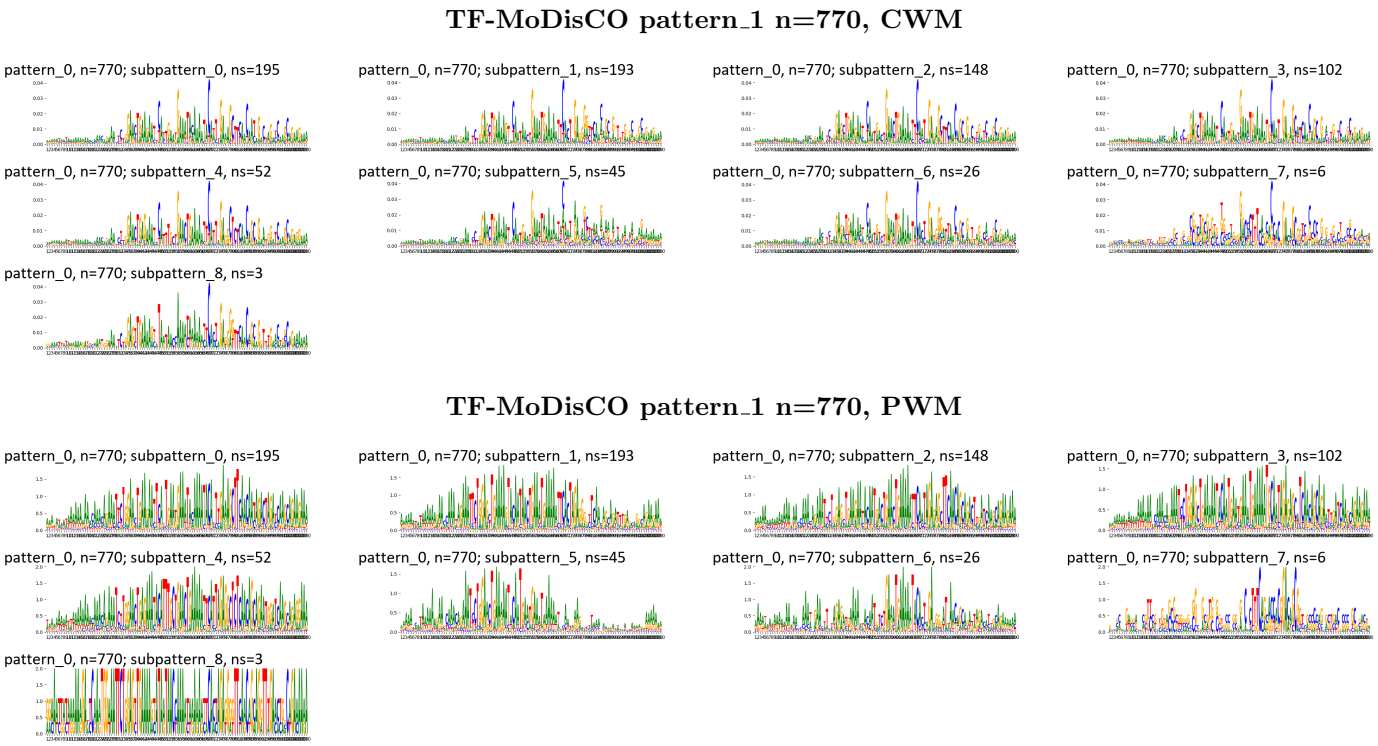

Supplementary Figure 757: TF-MoDisCO subpatterns for the ZNF160 transcription factor in HepG2 (accession ENCSR917SSX).

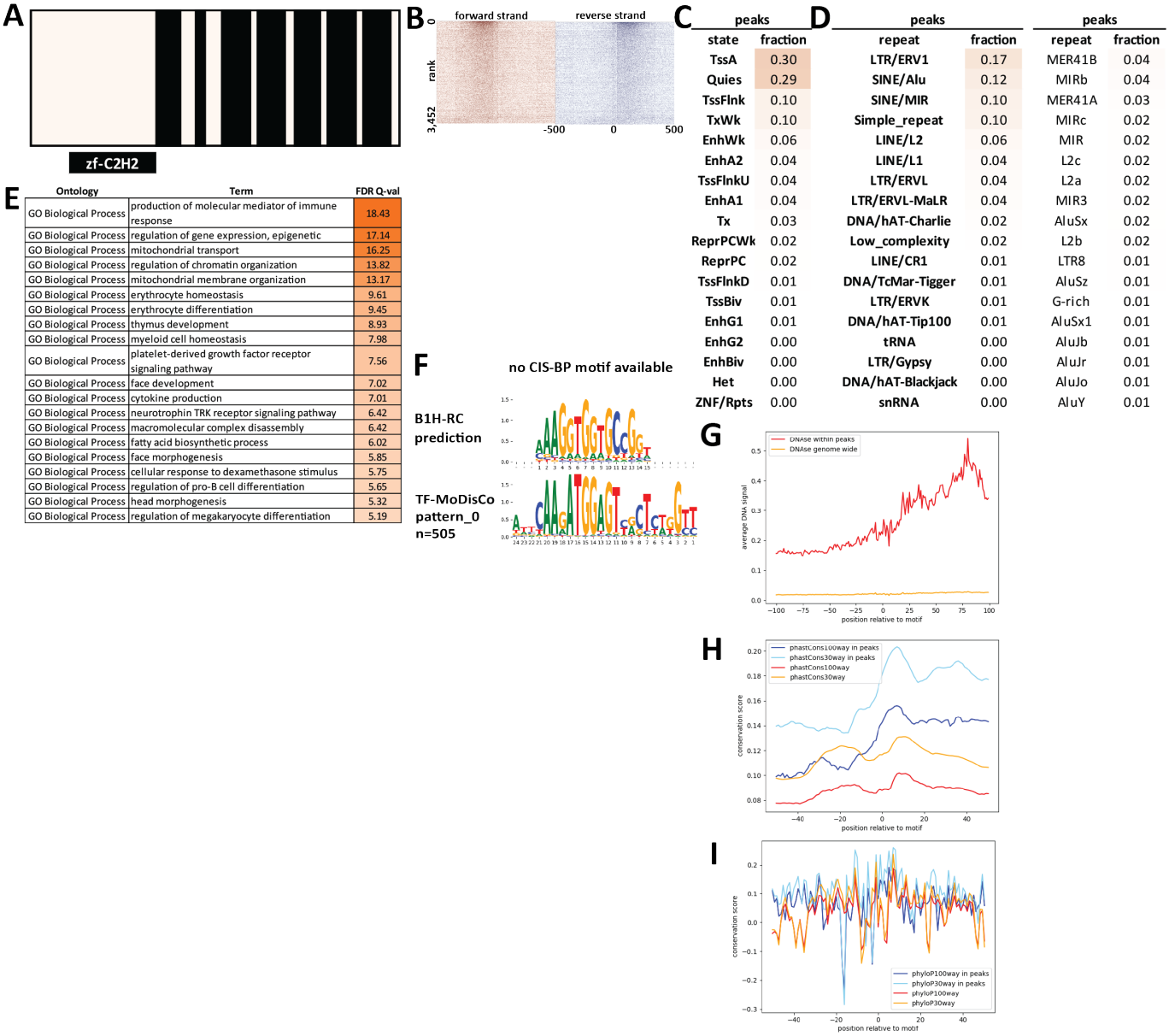

Supplementary Figure 758: Properties and genomic distribution of motifs identified for the ZNF165 transcription factor in K562 (accession ENCSR172XJS).

TF-MoDisCO pattern_0 n=505, CWM

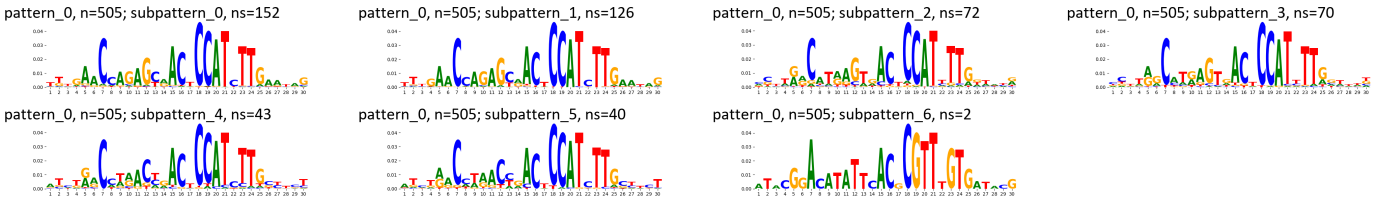

TF-MoDisCO pattern_0 n=505, PWM

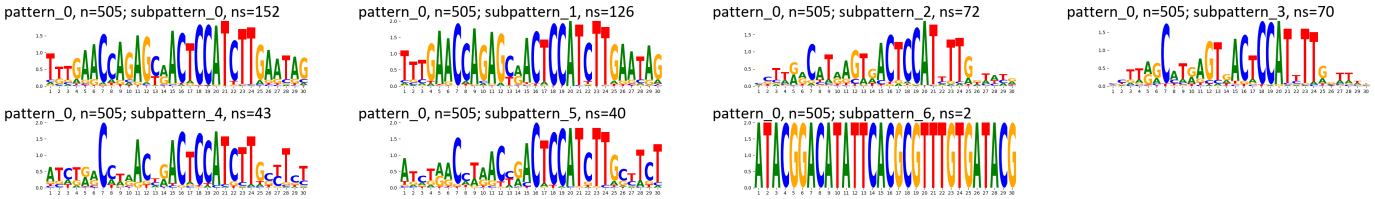

Supplementary Figure 759: TF-MoDisCO subpatterns for the ZNF165 transcription factor in K562 (accession ENCSR172XJS).

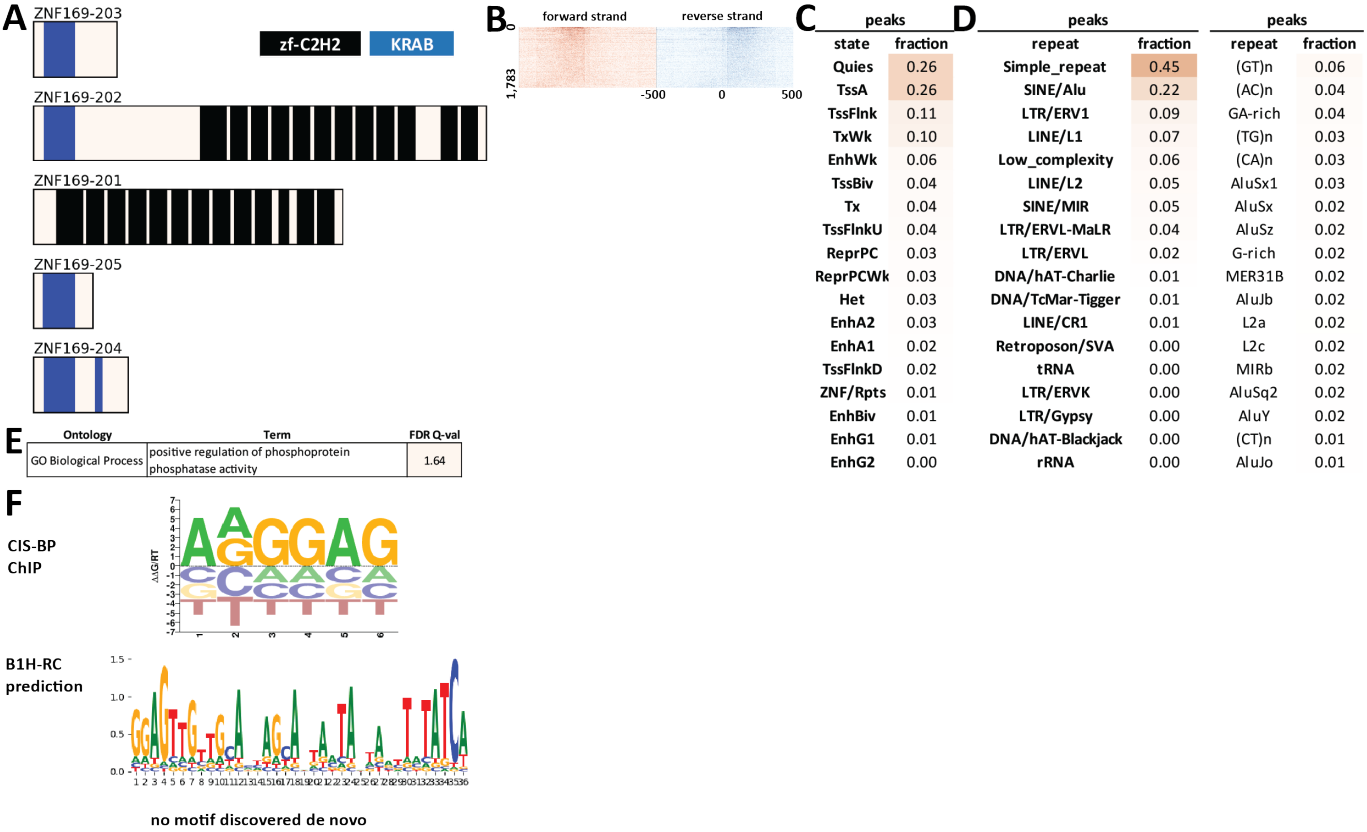

Supplementary Figure 760: Properties and genomic distribution of motifs identified for the ZNF169 transcription factor in HEK293 (accession ENCSR661AXW).

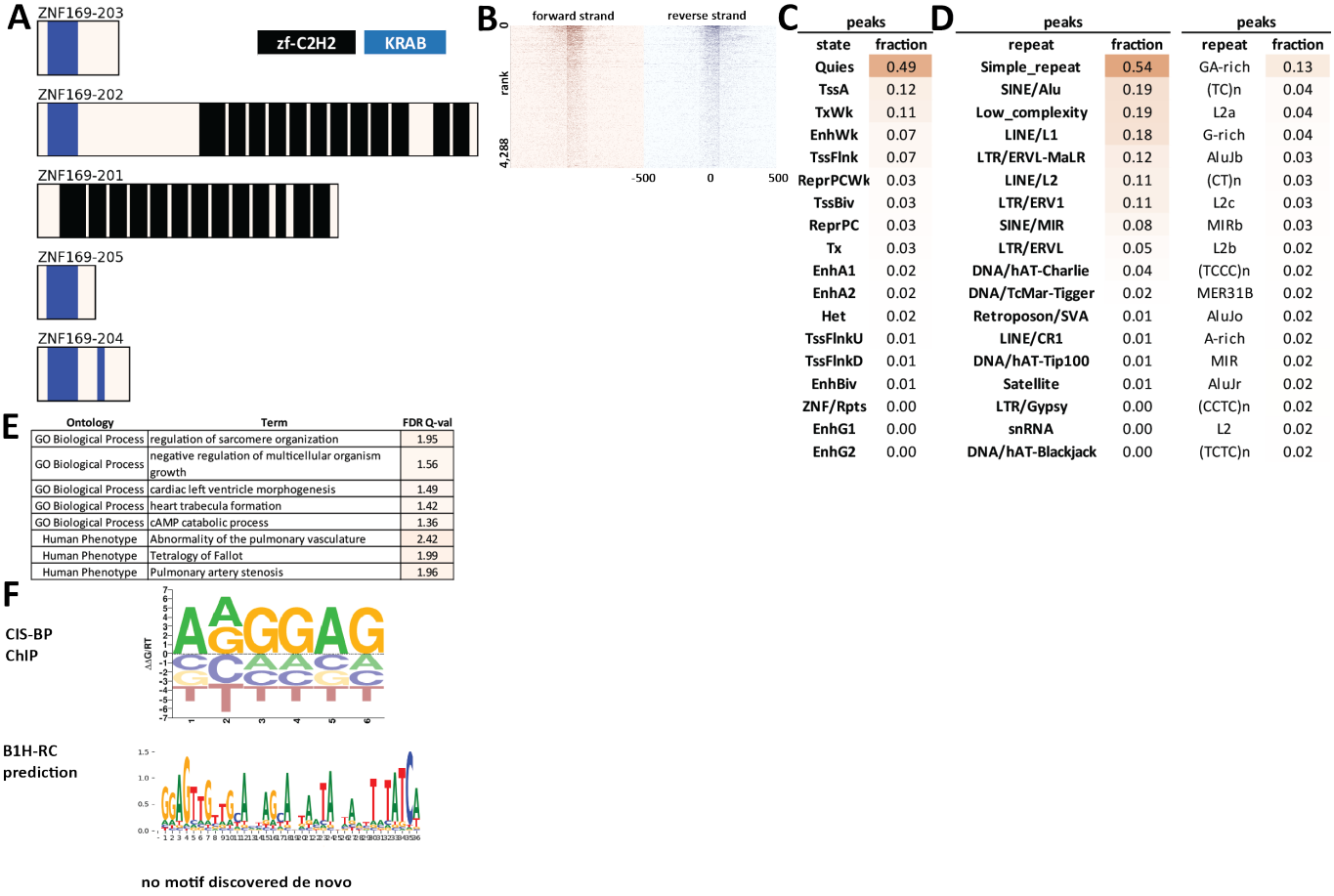

Supplementary Figure 761: Properties and genomic distribution of motifs identified for the ZNF169 transcription factor in HEK293 (accession ChipExo models).

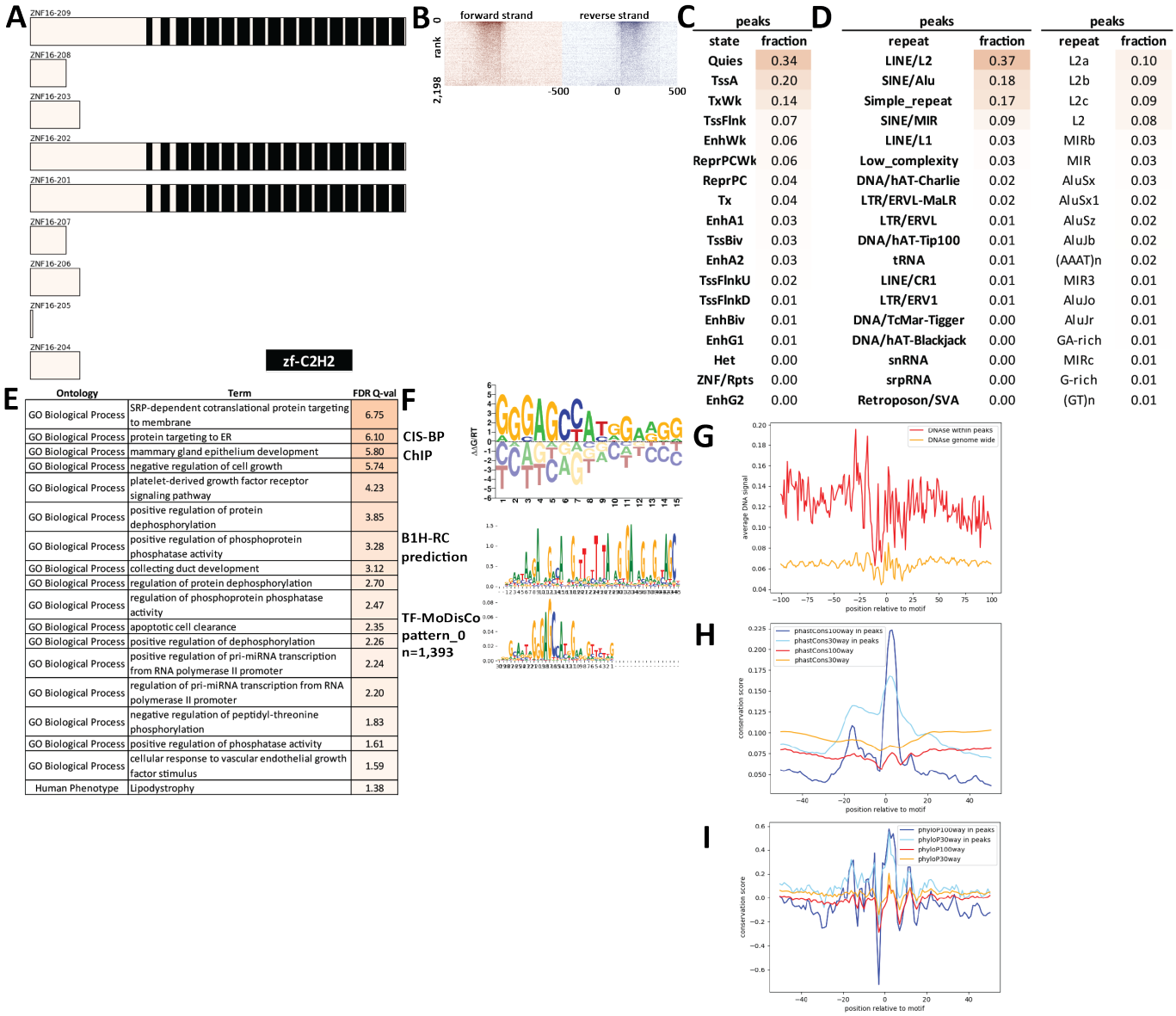

C

peaks	
state	fraction
Quies	0.34
TssA	0.20
TxWk	0.14
TssFlnk	0.07
EnhWk	0.06
ReprPCWk	0.06
ReprPC	0.04
Tx	0.04
EnhA1	0.03
TssBiv	0.03
EnhA2	0.03
TssFlnkU	0.02
TssFlnkD	0.01
EnhBiv	0.01
EnhG1	0.01
Het	0.00
ZNF/Rpts	0.00
EnhG2	0.00

D

peaks		peaks	
repeat	fraction	repeat	fraction
LINE/L2	0.37	L2a	0.10
SINE/Alu	0.18	L2b	0.09
Simple_repeat	0.17	L2c	0.09
SINE/MIR	0.09	L2	0.08
LINE/L1	0.03	MIRb	0.03
Low_complexity	0.03	MIR	0.03
DNA/hAT-Charlie	0.02	AluSx	0.03
LTR/ERVL-MaLR	0.02	AluSx1	0.02
LTR/ERVL	0.01	AluSz	0.02
DNA/hAT-Tip100	0.01	AluJb	0.02
tRNA	0.01	(AAAT)n	0.02
LINE/CR1	0.01	MIR3	0.01
LTR/ERV1	0.01	AluJo	0.01
DNA/TcMar-Tigger	0.00	AluJr	0.01
DNA/hAT-Blackjack	0.00	GA-rich	0.01
snRNA	0.00	MIRc	0.01
srpRNA	0.00	G-rich	0.01
Retroposon/SVA	0.00	(GT)n	0.01

E

Ontology	Term	FDR Q-val
GO Biological Process	SRP-dependent cotranslational protein targeting to membrane	6.75
GO Biological Process	protein targeting to ER	6.10
GO Biological Process	mammary gland epithelium development	5.80
GO Biological Process	negative regulation of cell growth	5.74
GO Biological Process	platelet-derived growth factor receptor signaling pathway	4.23
GO Biological Process	positive regulation of protein dephosphorylation	3.85
GO Biological Process	positive regulation of phosphoprotein phosphatase activity	3.28
GO Biological Process	collecting duct development	3.12
GO Biological Process	regulation of protein dephosphorylation	2.70
GO Biological Process	regulation of phosphoprotein phosphatase activity	2.47
GO Biological Process	apoptotic cell clearance	2.35
GO Biological Process	positive regulation of dephosphorylation	2.26
GO Biological Process	positive regulation of pri-miRNA transcription from RNA polymerase II promoter	2.24
GO Biological Process	regulation of pri-miRNA transcription from RNA polymerase II promoter	2.20
GO Biological Process	negative regulation of peptidyl-threonine phosphorylation	1.83
GO Biological Process	positive regulation of phosphatase activity	1.61
GO Biological Process	cellular response to vascular endothelial growth factor stimulus	1.59
Human Phenotype	Lipodystrophy	1.38

Supplementary Figure 762: Properties and genomic distribution of motifs identified for the ZNF16 transcription factor in HEK293 (accession ENCSR093HXE).

TF-MoDisCO pattern_0 n=1393, CWM

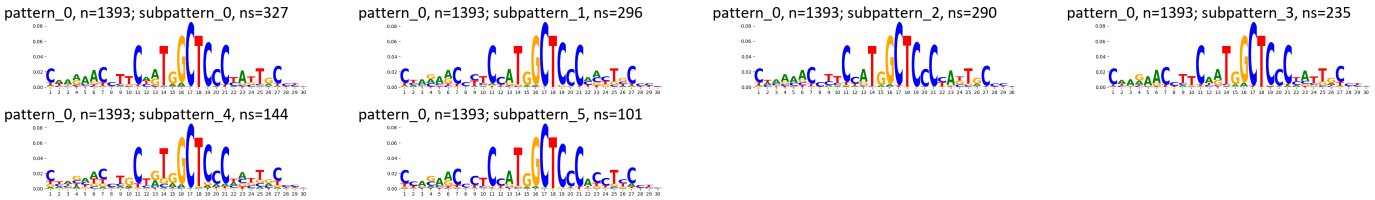

TF-MoDisCO pattern_0 n=1393, PWM

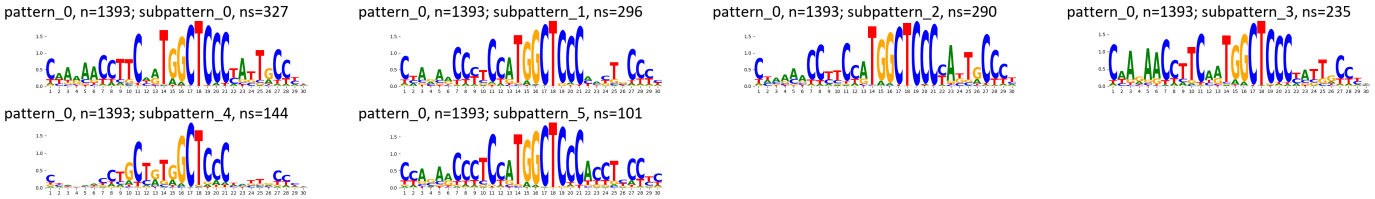

Supplementary Figure 763: TF-MoDisCO subpatterns for the ZNF16 transcription factor in HEK293 (accession ENCSR093HXE).

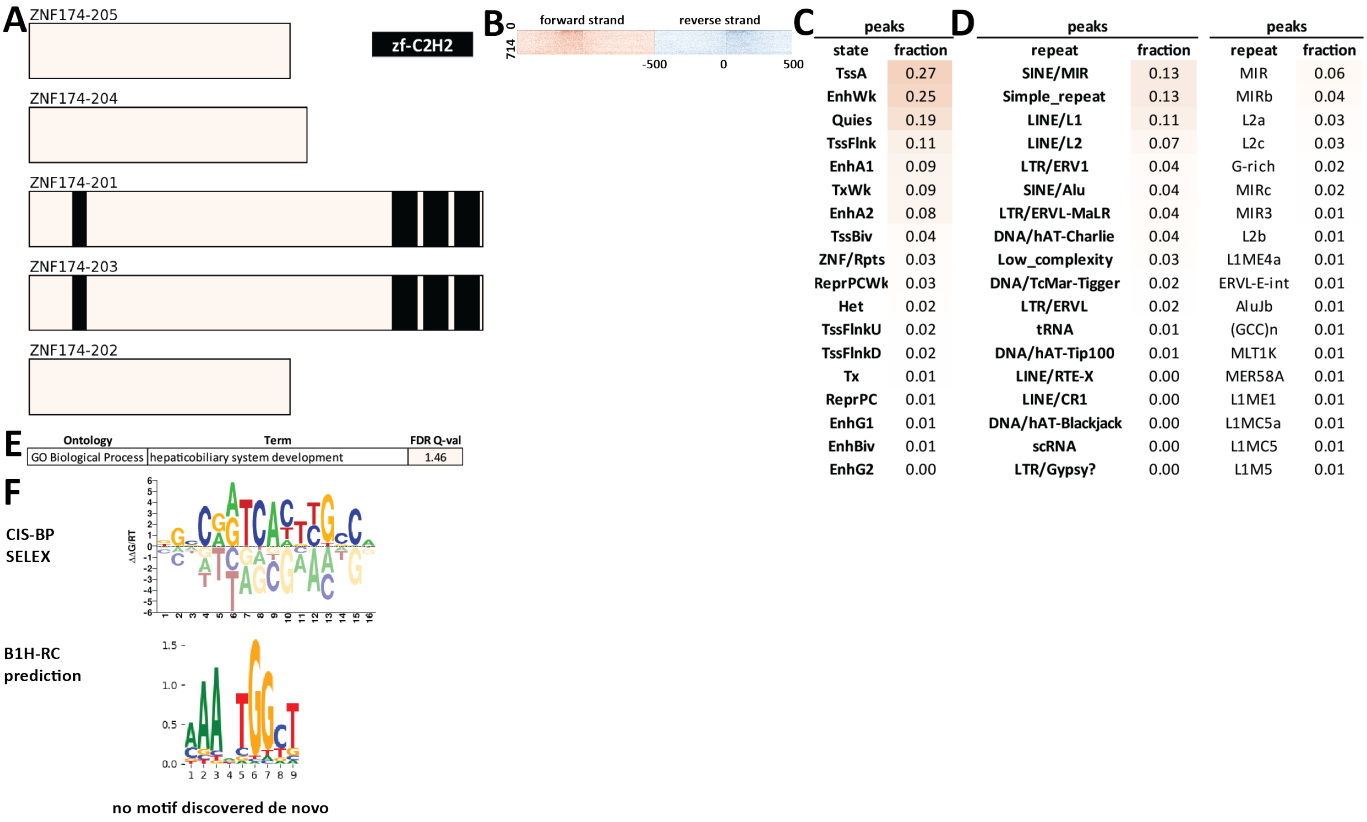

Supplementary Figure 764: Properties and genomic distribution of motifs identified for the ZNF174 transcription factor in HEK293 (accession ENCSR516VQK).

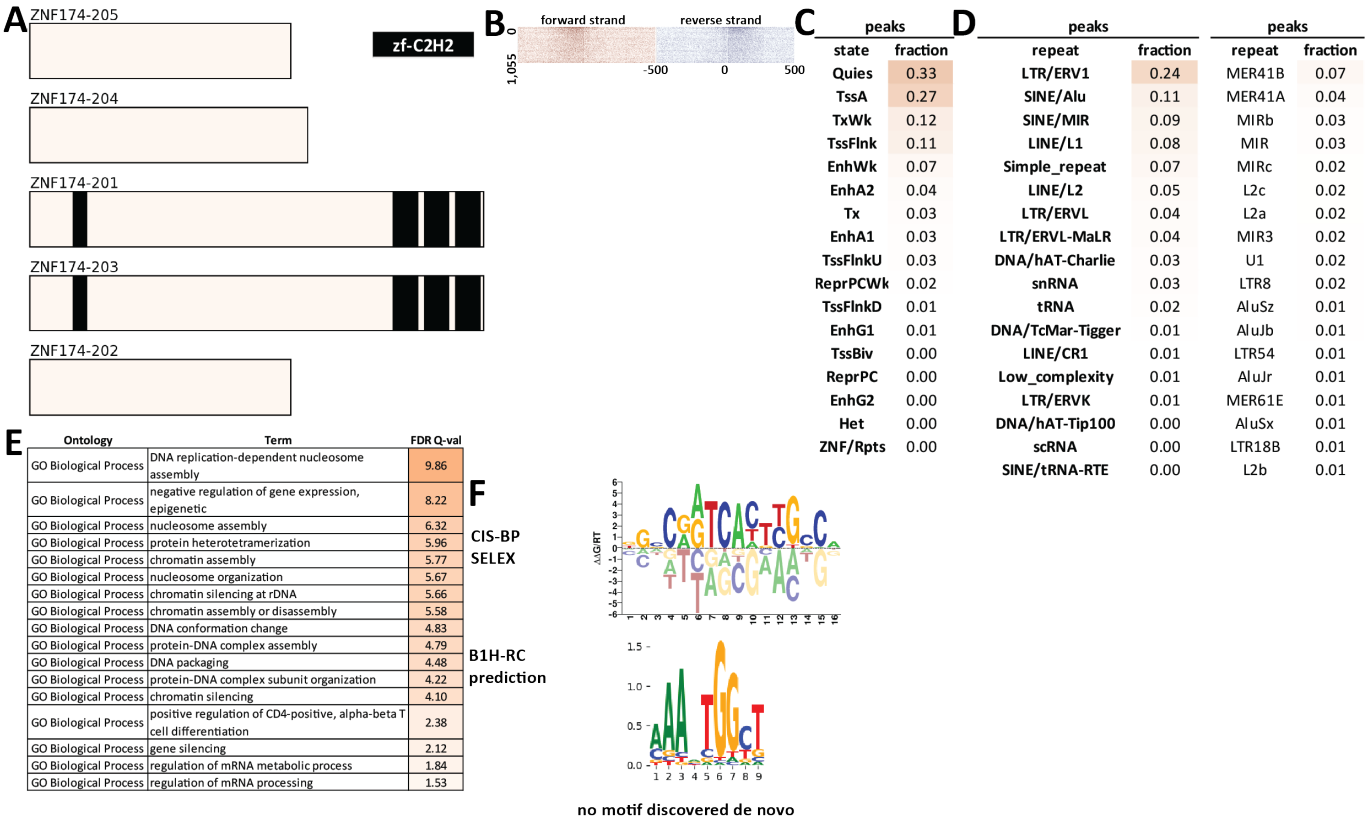

Supplementary Figure 765: Properties and genomic distribution of motifs identified for the ZNF174 transcription factor in K562 (accession ENCSR056VYW).

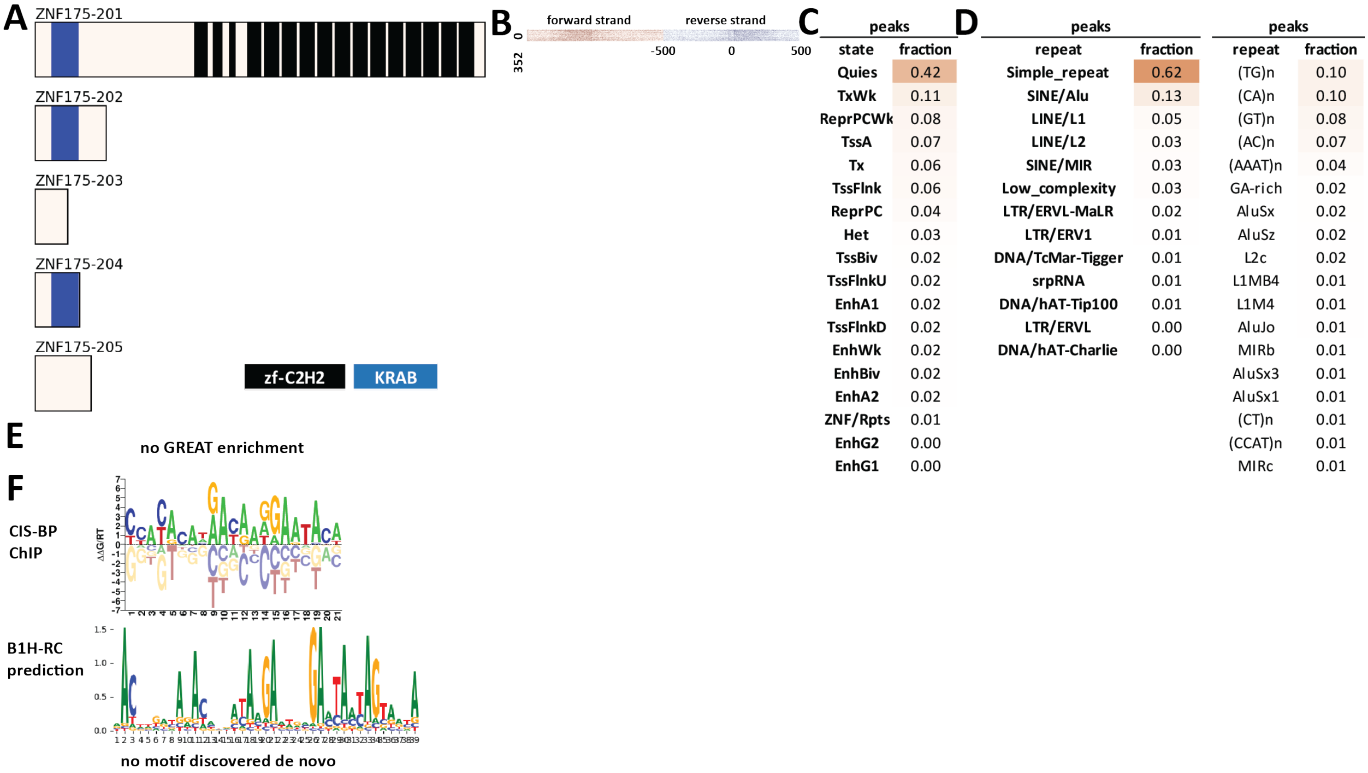

Supplementary Figure 766: Properties and genomic distribution of motifs identified for the ZNF175 transcription factor in HEK293 (accession ENCSR103GAK).

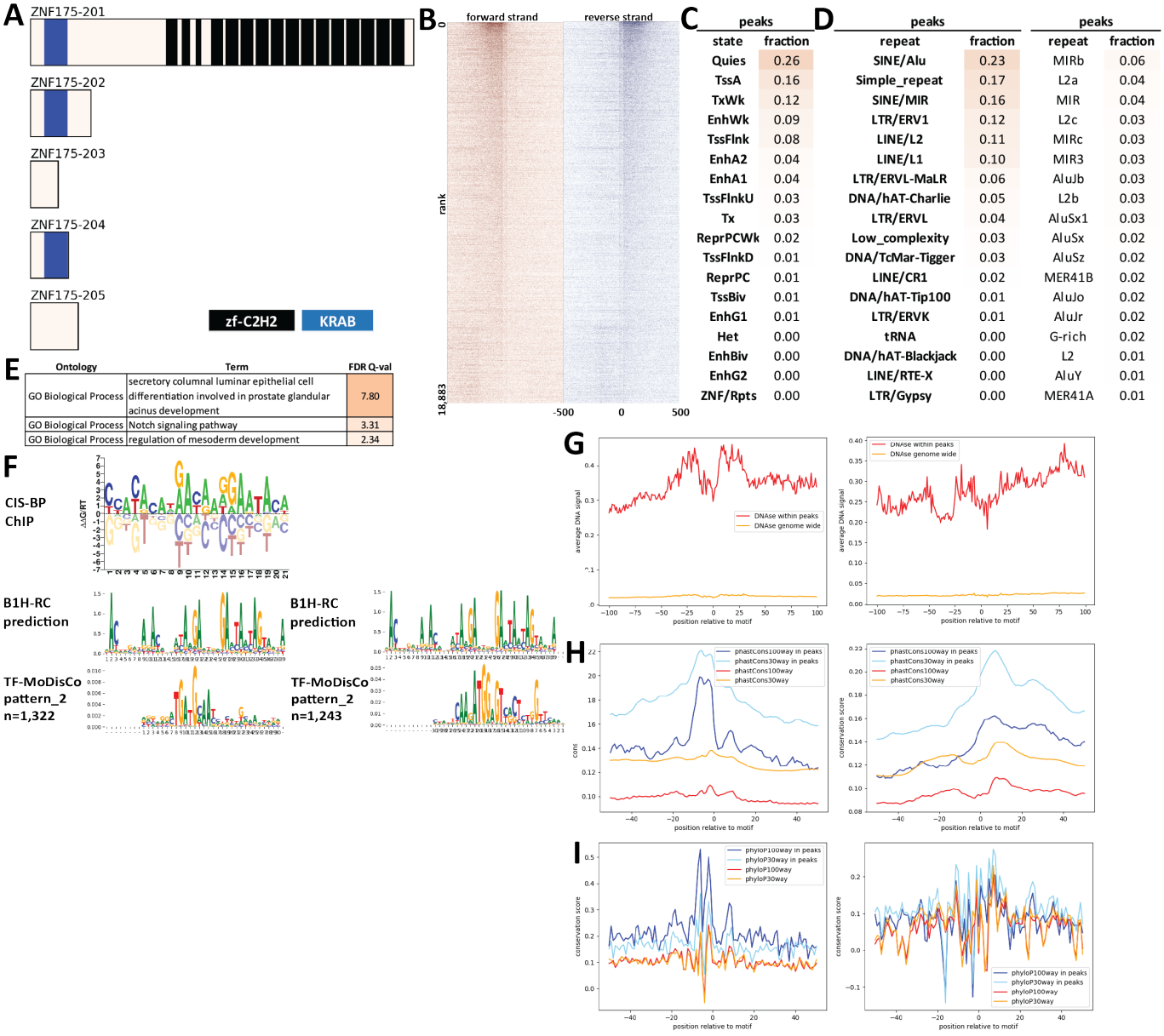

Supplementary Figure 767: Properties and genomic distribution of motifs identified for the ZNF175 transcription factor in K562 (accession ENCSR011PEI).

TF-MoDisCO pattern_2 n=1322, CWM

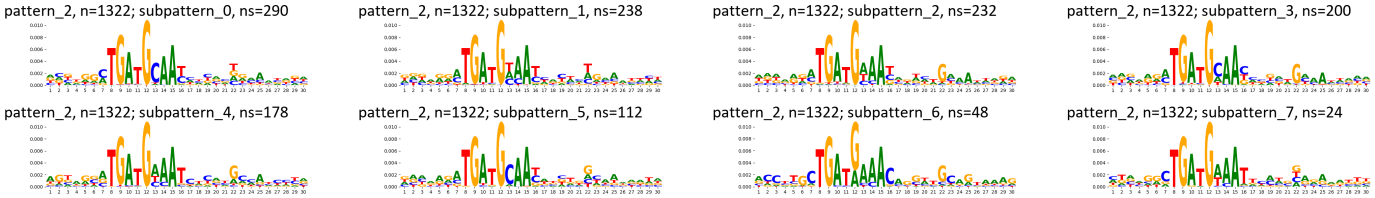

TF-MoDisCO pattern_2 n=1322, PWM

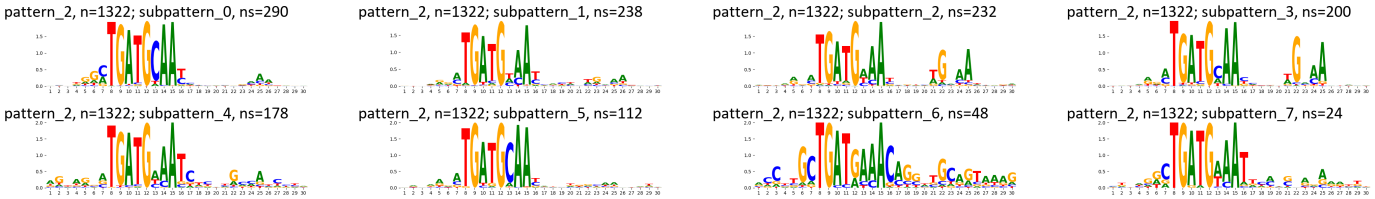

TF-MoDisCO pattern_3 n=1243, CWM

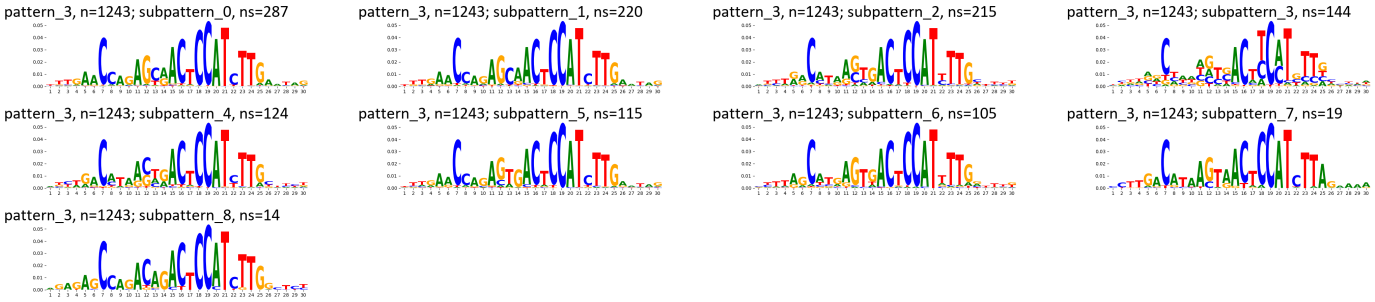

TF-MoDisCO pattern_3 n=1243, PWM

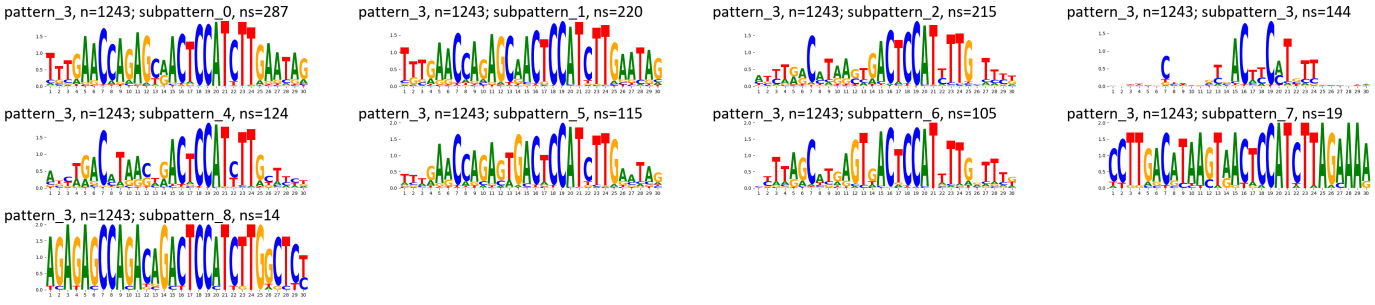

Supplementary Figure 768: TF-MoDisCO subpatterns for the ZNF175 transcription factor in K562 (accession ENCSR011PEI).

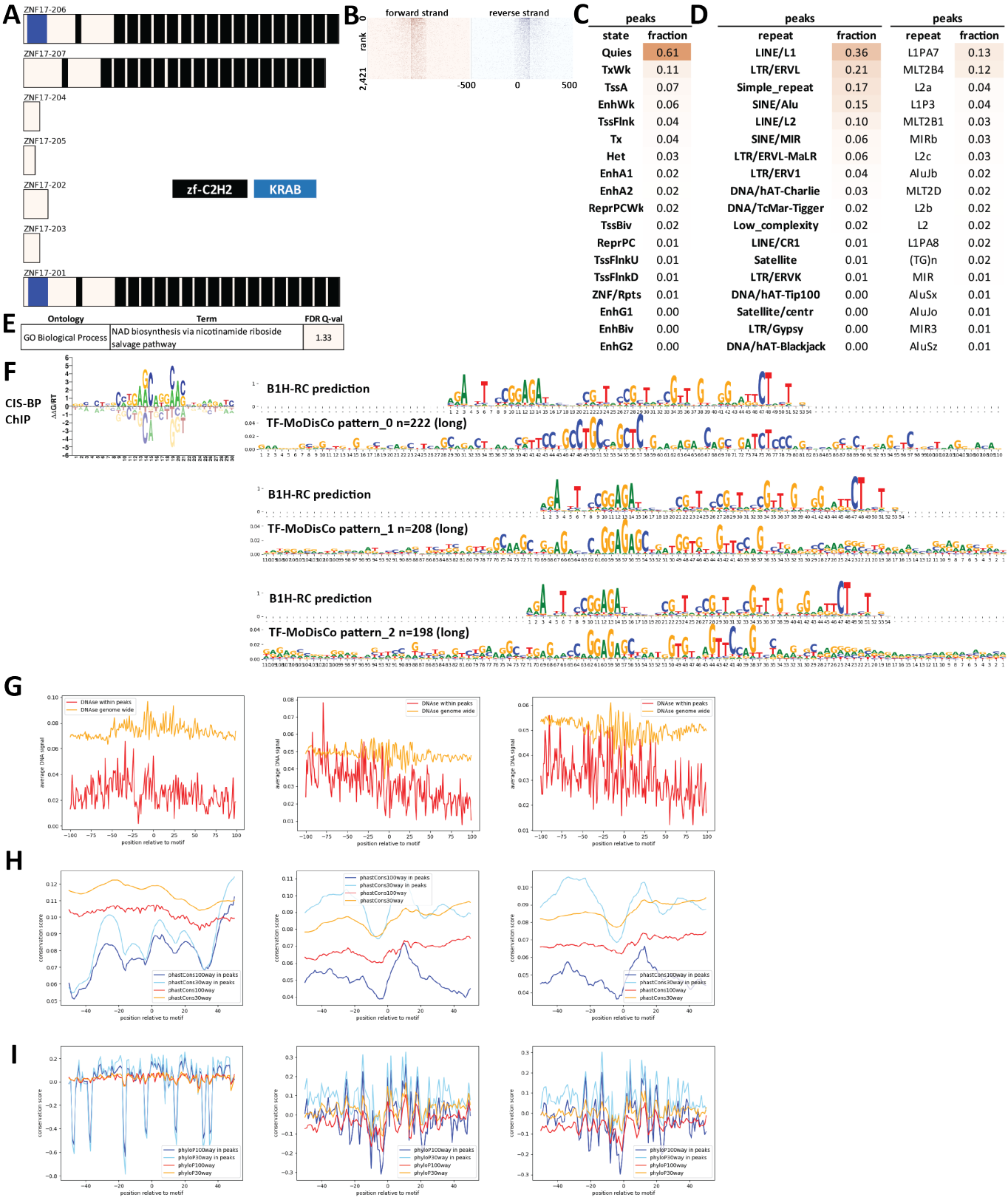

Supplementary Figure 769: Properties and genomic distribution of motifs identified for the ZNF17 transcription factor in HEK293 (accession ChipExo models).

TF-MoDisCO pattern_0 n=222, CWM

pattern_0, n=222; subpattern_0, ns=57

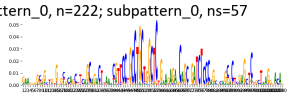

pattern_0, n=222; subpattern_1, ns=52

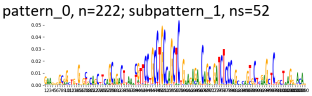

pattern_0, n=222; subpattern_2, ns=50

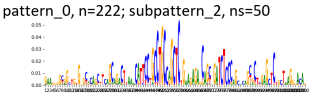

pattern_0, n=222; subpattern_3, ns=46

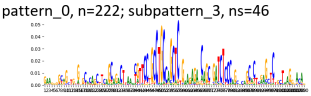

pattern_0, n=222; subpattern_4, ns=17

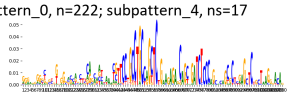

TF-MoDisCO pattern_0 n=222, PWM

pattern_0, n=222; subpattern_0, ns=57

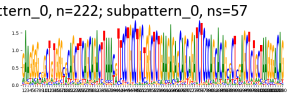

pattern_0, n=222; subpattern_1, ns=52

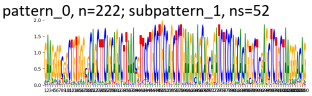

pattern_0, n=222; subpattern_2, ns=50

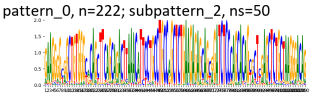

pattern_0, n=222; subpattern_3, ns=46

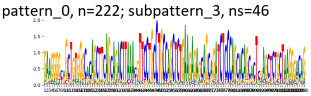

pattern_0, n=222; subpattern_4, ns=17

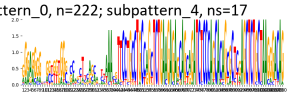

TF-MoDisCO pattern_1 n=208, CWM

pattern_1, n=208; subpattern_0, ns=54

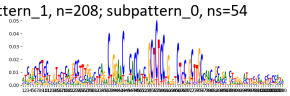

pattern_1, n=208; subpattern_1, ns=54

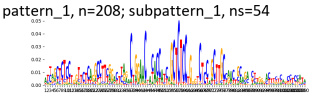

pattern_1, n=208; subpattern_2, ns=47

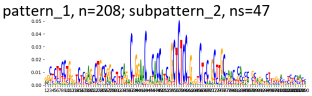

pattern_1, n=208; subpattern_3, ns=27

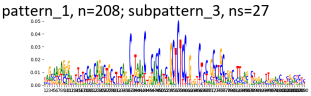

pattern_1, n=208; subpattern_4, ns=17

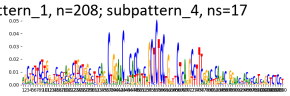

pattern_1, n=208; subpattern_5, ns=9

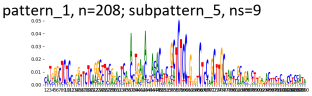

TF-MoDisCO pattern_1 n=208, PWM

pattern_1, n=208; subpattern_0, ns=54

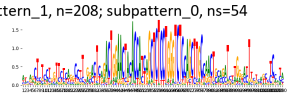

pattern_1, n=208; subpattern_1, ns=54

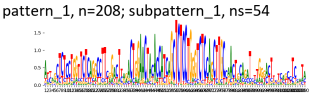

pattern_1, n=208; subpattern_2, ns=47

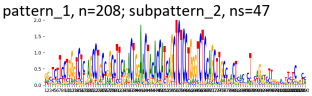

pattern_1, n=208; subpattern_3, ns=27

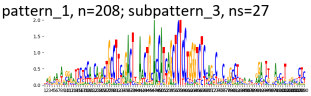

pattern_1, n=208; subpattern_4, ns=17

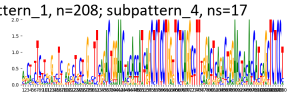

pattern_1, n=208; subpattern_5, ns=9

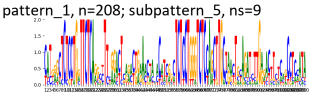

TF-MoDisCO pattern_2 n=198, CWM

pattern_2, n=198; subpattern_0, ns=53

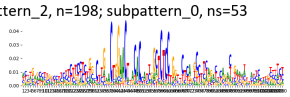

pattern_2, n=198; subpattern_1, ns=50

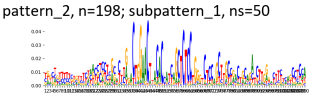

pattern_2, n=198; subpattern_2, ns=44

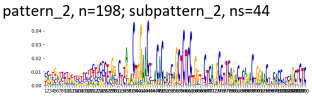

pattern_2, n=198; subpattern_3, ns=19

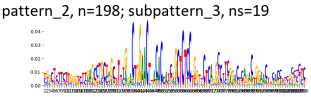

pattern_2, n=198; subpattern_4, ns=18

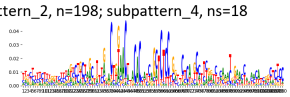

pattern_2, n=198; subpattern_5, ns=14

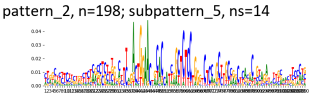

TF-MoDisCO pattern_2 n=198, PWM

pattern_2, n=198; subpattern_0, ns=53

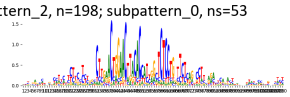

pattern_2, n=198; subpattern_1, ns=50

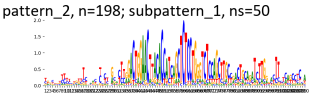

pattern_2, n=198; subpattern_2, ns=44

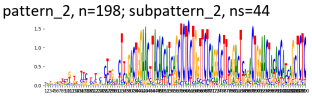

pattern_2, n=198; subpattern_3, ns=19

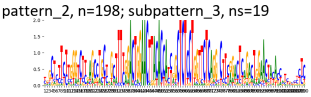

pattern_2, n=198; subpattern_4, ns=18

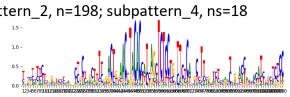

pattern_2, n=198; subpattern_5, ns=14

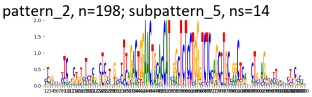

Supplementary Figure 770: TF-MoDisCO subpatterns for the ZNF17 transcription factor in HEK293 (accession ChipExo models).

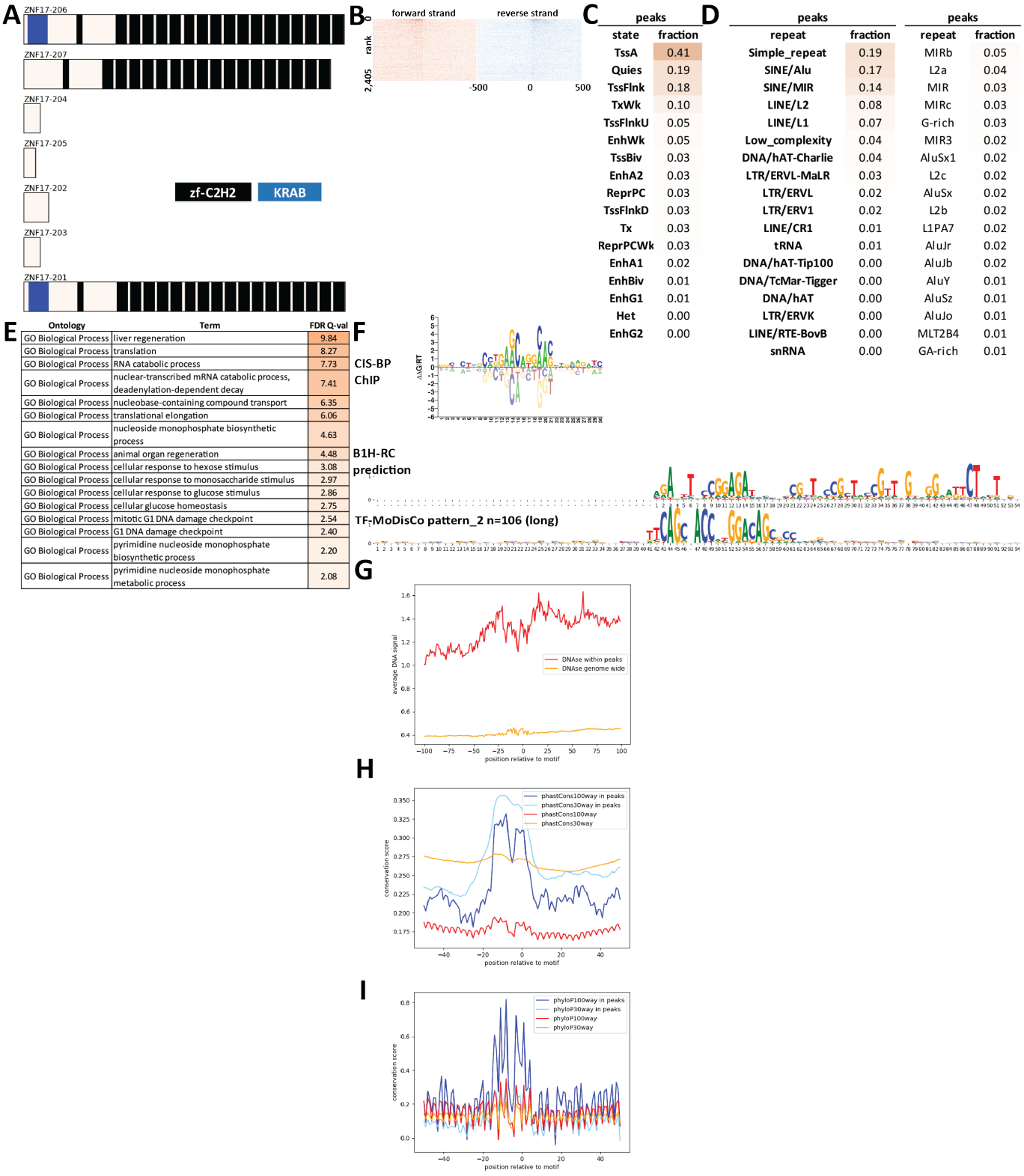

C

peaks	
state	fraction
TssA	0.41
Quies	0.19
TssFlnk	0.18
TxWk	0.10
TssFlnkU	0.05
EnhWk	0.05
TssBiv	0.03
EnhA2	0.03
ReprPC	0.03
TssFlnkD	0.03
Tx	0.03
ReprPCWk	0.03
EnhA1	0.02
EnhBiv	0.01
EnhG1	0.01
Het	0.00
EnhG2	0.00

D

peaks		peaks	
repeat	fraction	repeat	fraction
Simple_repeat	0.19	MIRb	0.05
SINE/Alu	0.17	L2a	0.04
SINE/MIR	0.14	MIR	0.03
LINE/L2	0.08	MIRc	0.03
LINE/L1	0.07	G-rich	0.03
Low_complexity	0.04	MIR3	0.02
DNA/hAT-Charlie	0.04	AluSx1	0.02
LTR/ERVL-MaLR	0.03	L2c	0.02
LTR/ERVL	0.02	AluSx	0.02
LTR/ERV1	0.02	L2b	0.02
LINE/CR1	0.01	L1PA7	0.02
tRNA	0.01	AluJr	0.02
DNA/hAT-Tip100	0.00	AluJb	0.02
DNA/TcMar-Tigger	0.00	AluY	0.01
DNA/hAT	0.00	AluSz	0.01
LTR/ERVK	0.00	AluJo	0.01
LINE/RTE-BovB	0.00	MLT2B4	0.01
snRNA	0.00	GA-rich	0.01

E

Ontology	Term	FDR Q-val
GO Biological Process	liver regeneration	9.84
GO Biological Process	translation	8.27
GO Biological Process	RNA catabolic process	7.73
GO Biological Process	nuclear-transcribed mRNA catabolic process, deadenylation-dependent decay	7.41
GO Biological Process	nucleobase-containing compound transport	6.35
GO Biological Process	translational elongation	6.06
GO Biological Process	nucleoside monophosphate biosynthetic process	4.63
GO Biological Process	animal organ regeneration	4.48
GO Biological Process	cellular response to hexose stimulus	3.08
GO Biological Process	cellular response to monosaccharide stimulus	2.97
GO Biological Process	cellular response to glucose stimulus	2.86
GO Biological Process	cellular glucose homeostasis	2.75
GO Biological Process	mitotic G1 DNA damage checkpoint	2.54
GO Biological Process	G1 DNA damage checkpoint	2.40
GO Biological Process	pyrimidine nucleoside monophosphate biosynthetic process	2.20
GO Biological Process	pyrimidine nucleoside monophosphate metabolic process	2.08

Supplementary Figure 771: Properties and genomic distribution of motifs identified for the ZNF17 transcription factor in HepG2 (accession ENCSR075BAS).

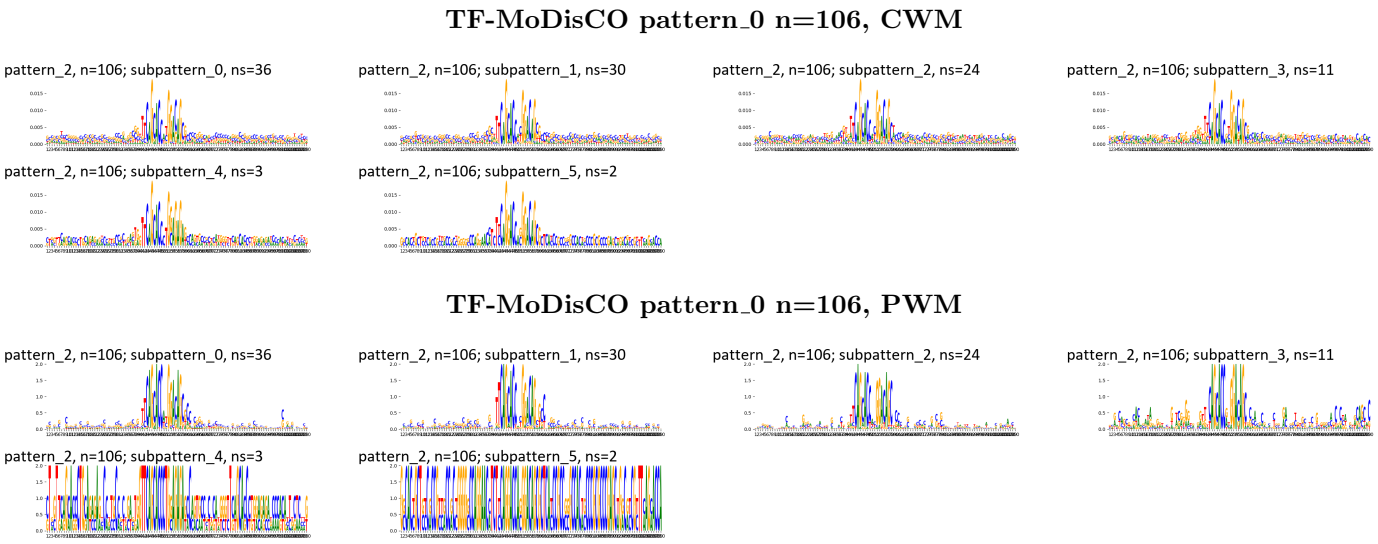

Supplementary Figure 772: TF-MoDisCO subpatterns for the ZNF17 transcription factor in HepG2 (accession ENCSR075BAS).

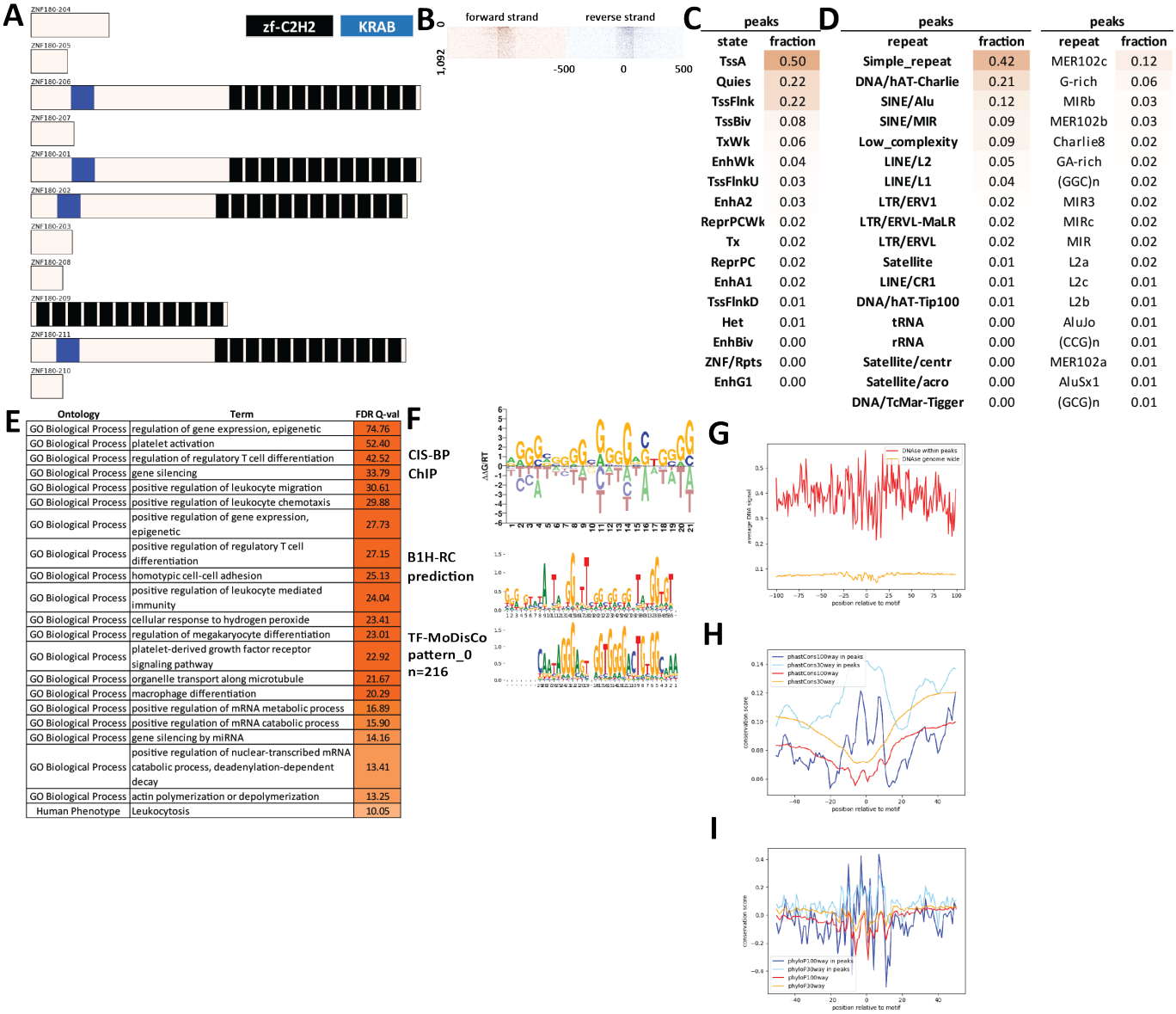

Supplementary Figure 773: Properties and genomic distribution of motifs identified for the ZNF180 transcription factor in HEK293 (accession ChipExo models).

TF-MoDisCO pattern_0 n=216, CWM

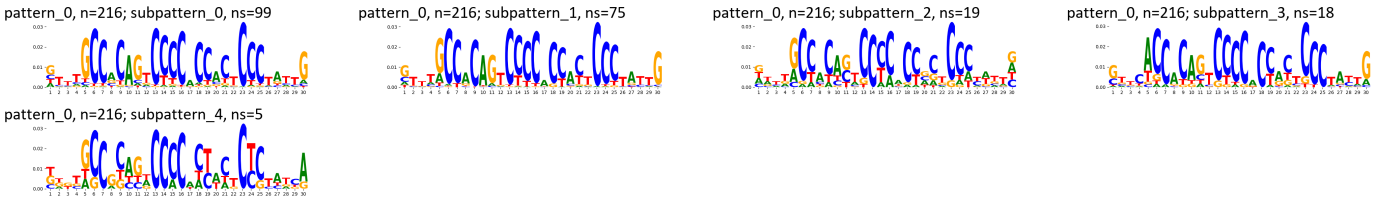

TF-MoDisCO pattern_0 n=216, PWM

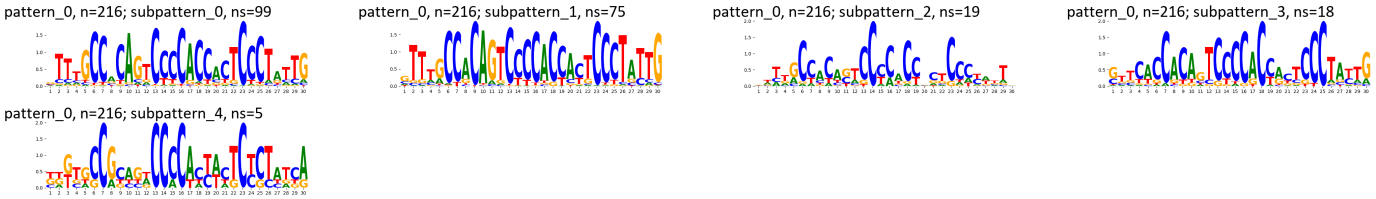

Supplementary Figure 774: TF-MoDisCO subpatterns for the ZNF180 transcription factor in HEK293 (accession ChipExo models).

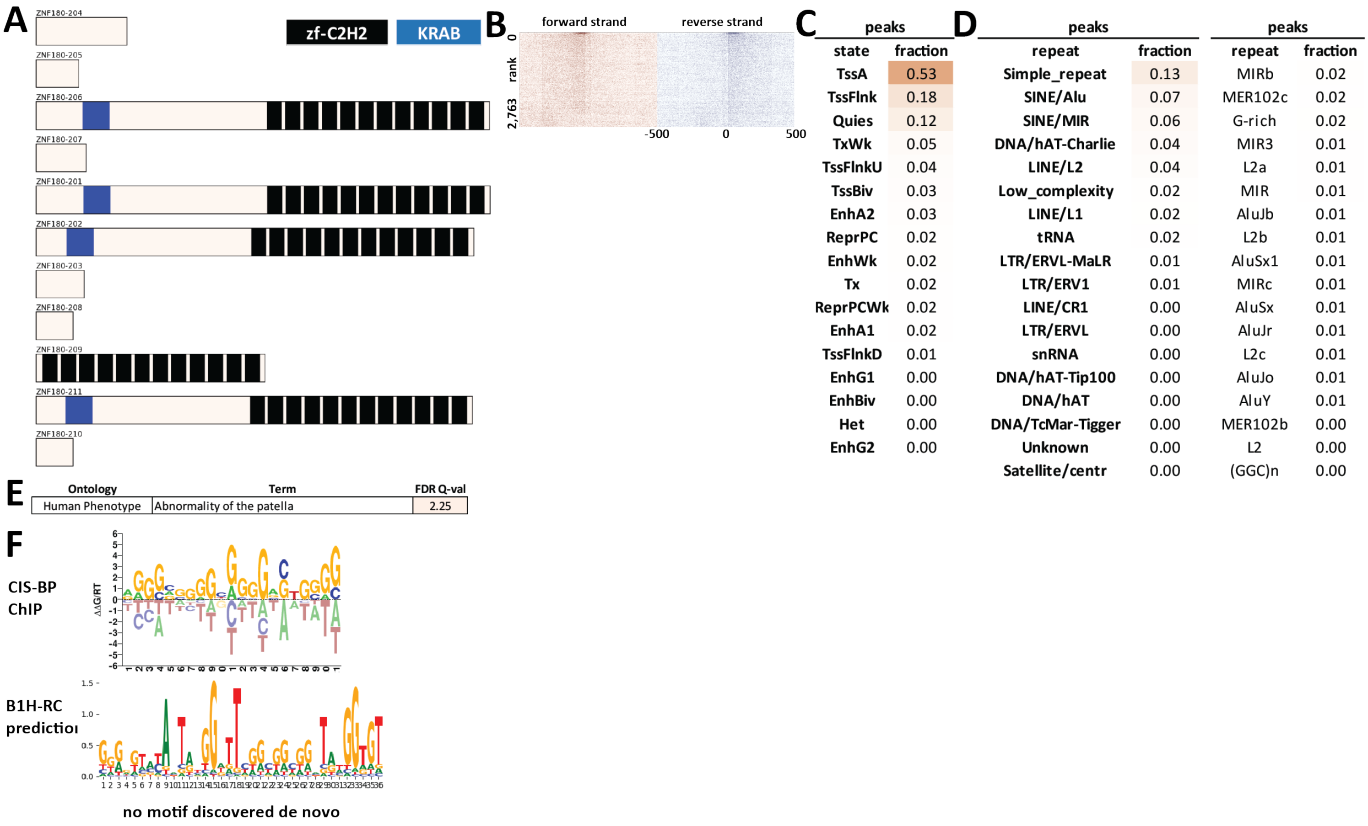

Supplementary Figure 775: Properties and genomic distribution of motifs identified for the ZNF180 transcription factor in HepG2 (accession ENCSR298DSB).

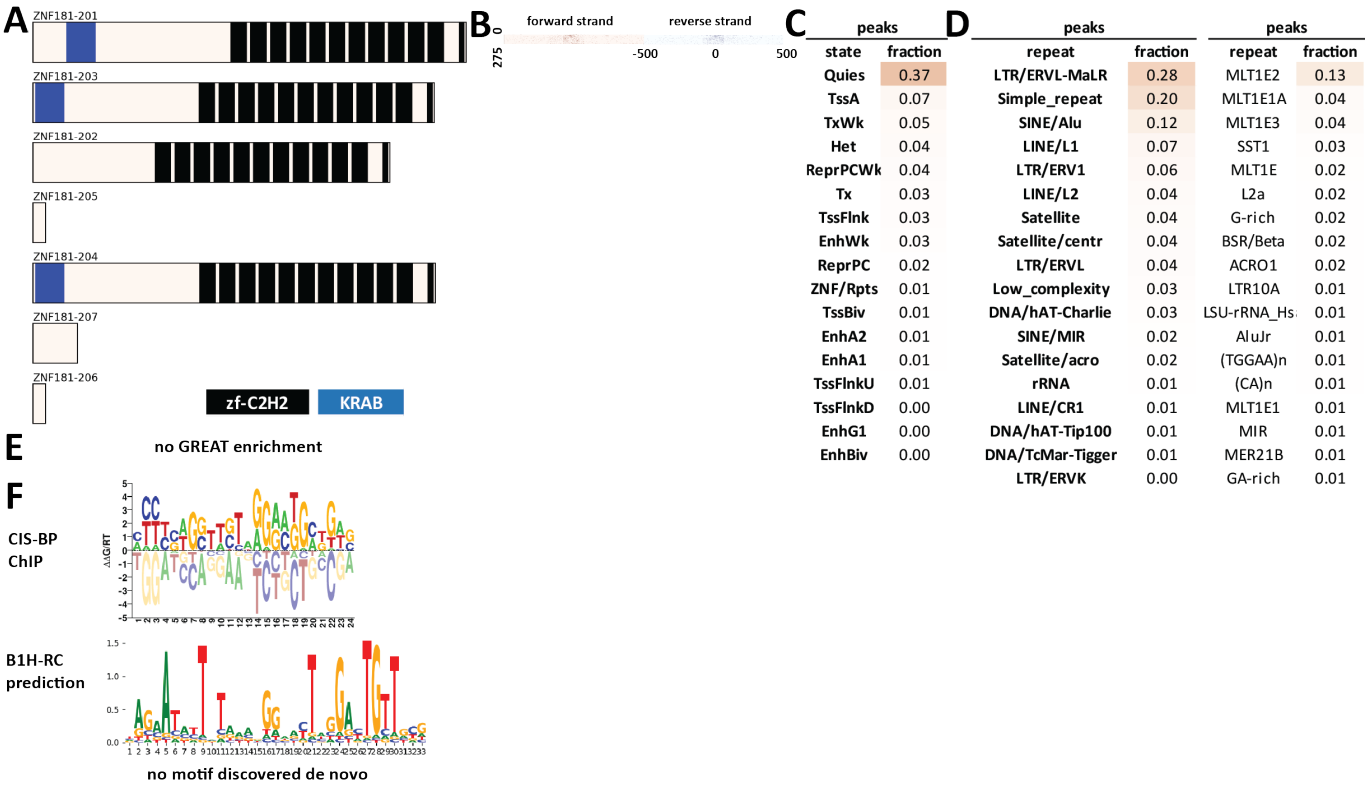

Supplementary Figure 776: Properties and genomic distribution of motifs identified for the ZNF181 transcription factor in HEK293 (accession ChipExo models).

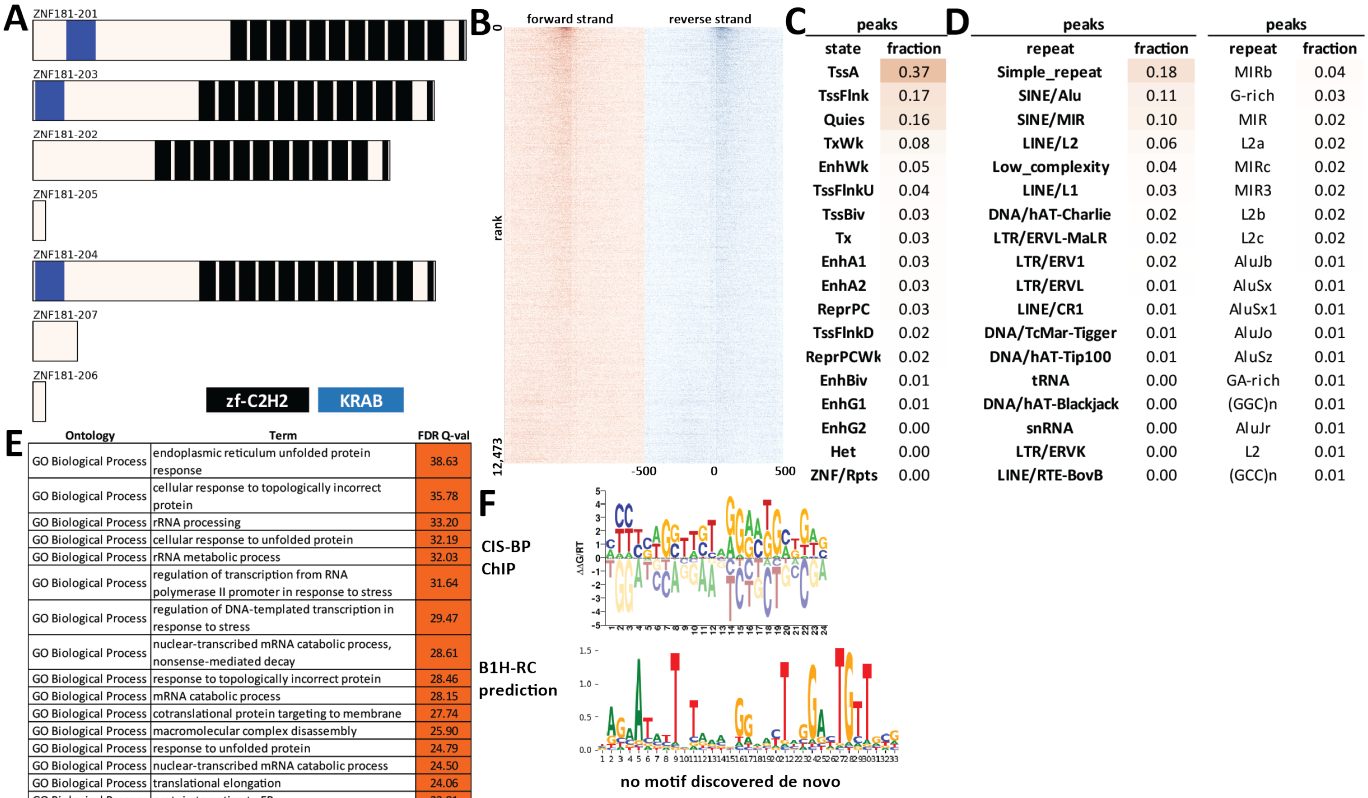

Supplementary Figure 777: Properties and genomic distribution of motifs identified for the ZNF181 transcription factor in HepG2 (accession ENCSR115LFG).

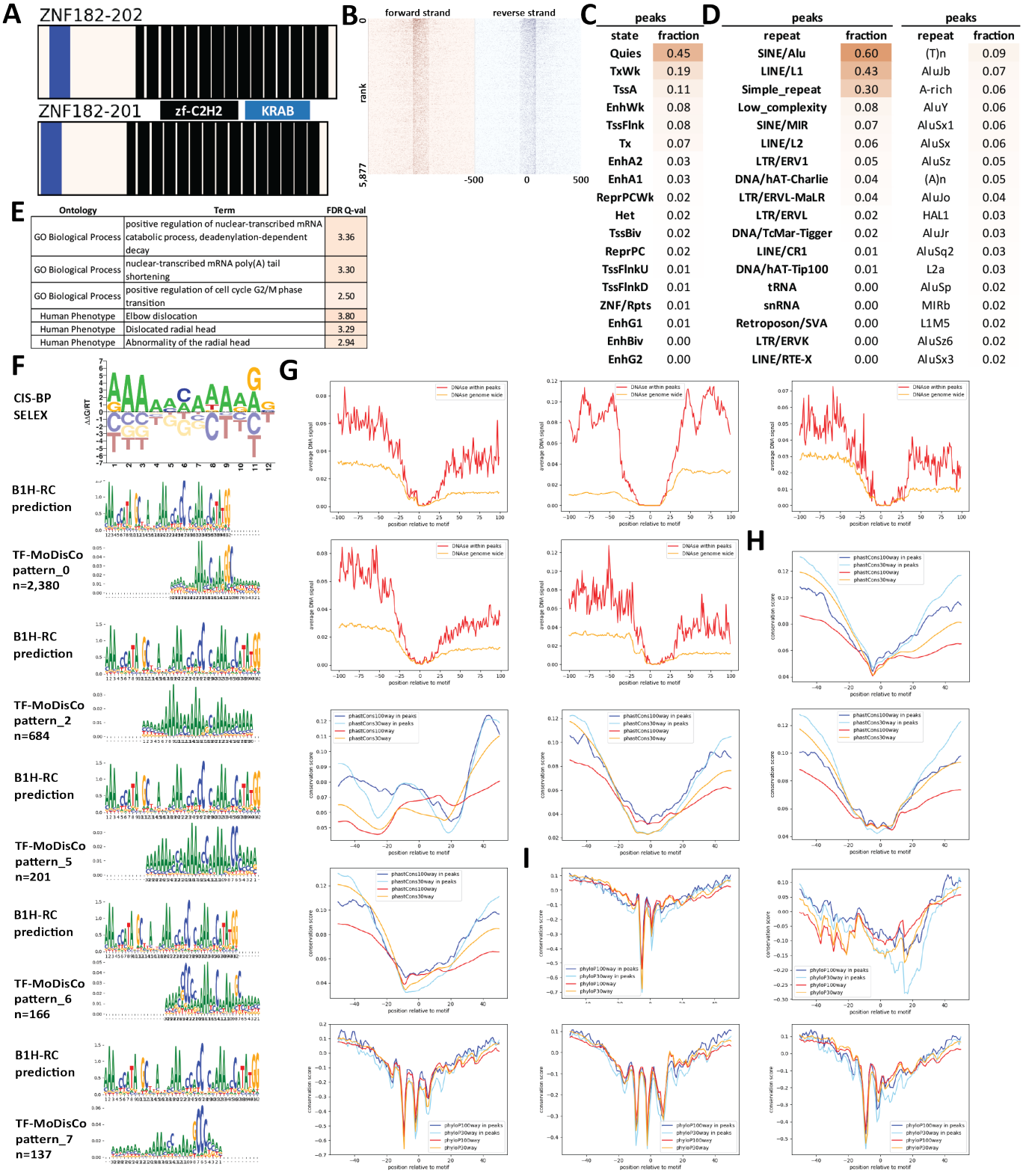

Supplementary Figure 778: Properties and genomic distribution of motifs identified for the ZNF182 transcription factor in HEK293 (accession ChipExo models).

TF-MoDisCO pattern_0 n=2380, CWM

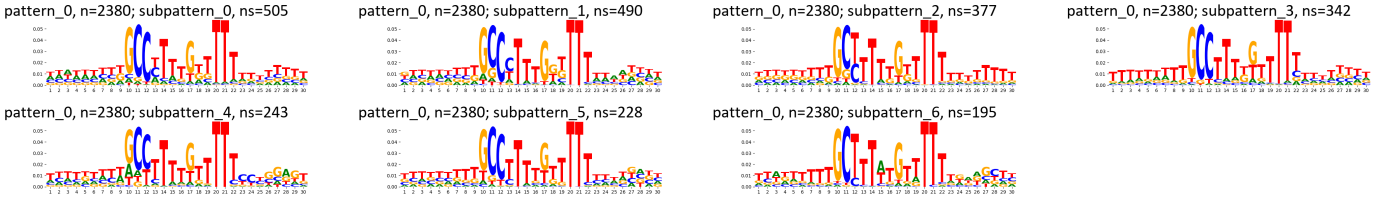

TF-MoDisCO pattern_0 n=2380, PWM

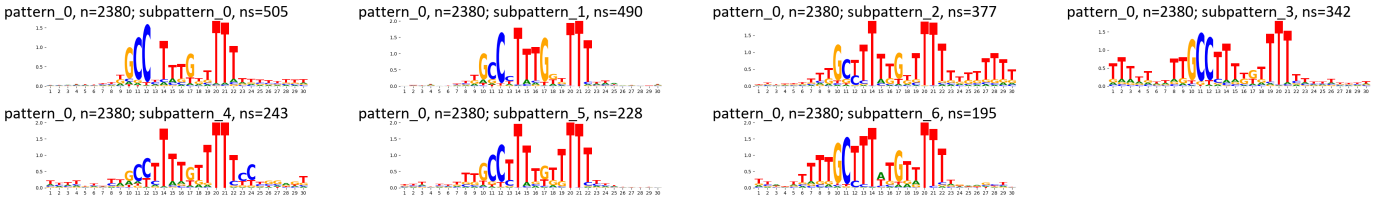

TF-MoDisCO pattern_2 n=684, CWM

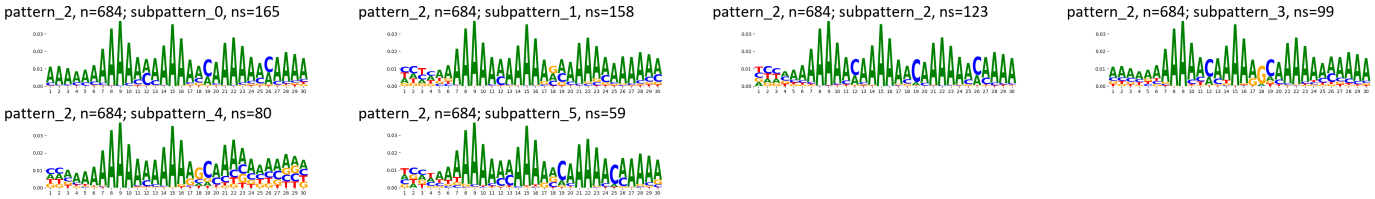

TF-MoDisCO pattern_2 n=684, PWM

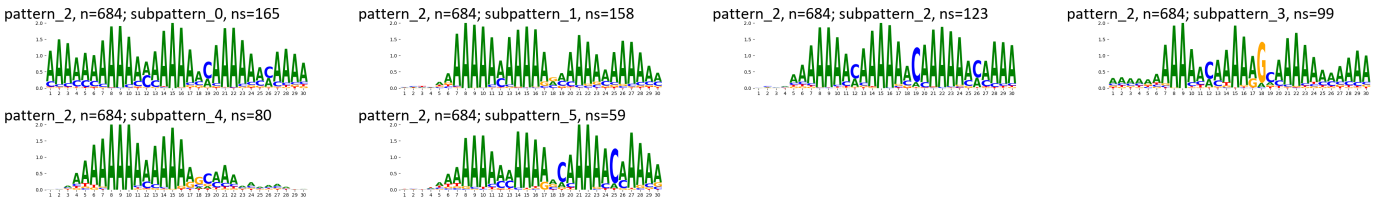

TF-MoDisCO pattern_5 n=201, CWM

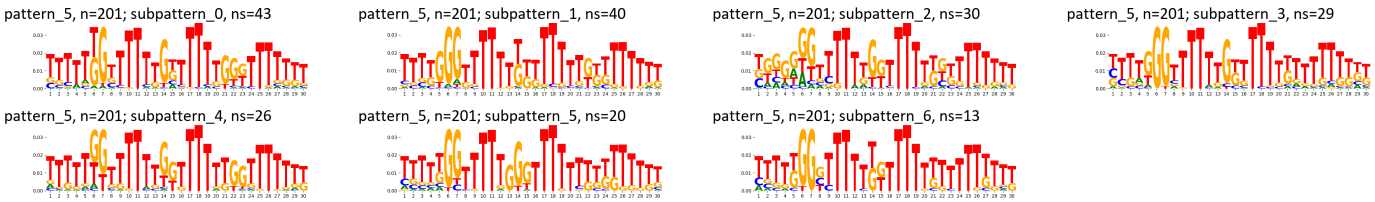

TF-MoDisCO pattern_5 n=201, PWM

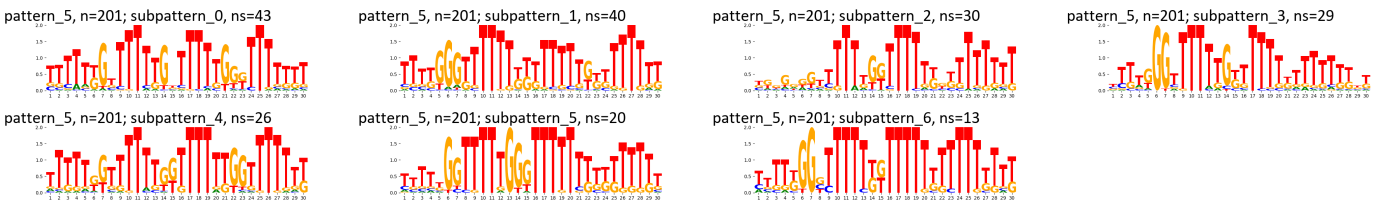

TF-MoDisCO pattern_6 n=166, CWM

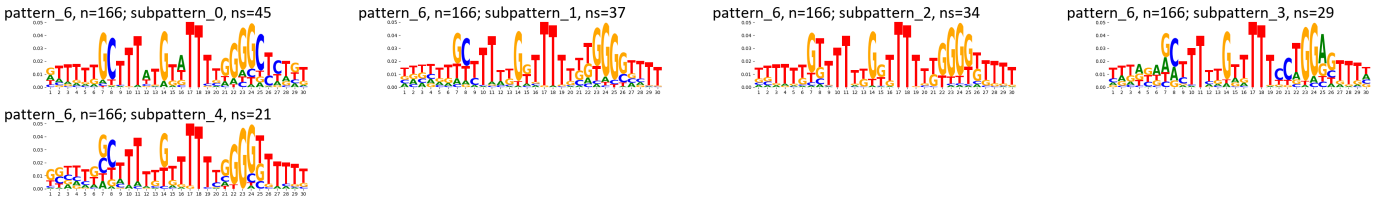

TF-MoDisCO pattern_6 n=166, PWM

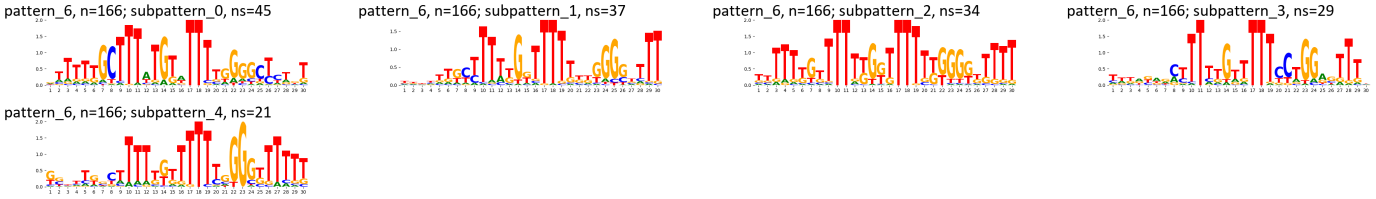

TF-MoDisCO pattern_7 n=137, CWM

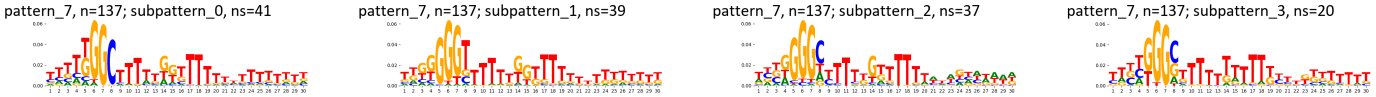

TF-MoDisCO pattern_7 n=137, PWM

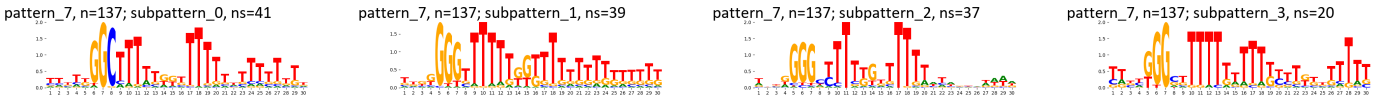

Supplementary Figure 779: TF-MoDisCO subpatterns for the ZNF182 transcription factor in HEK293 (accession ChipExo models).

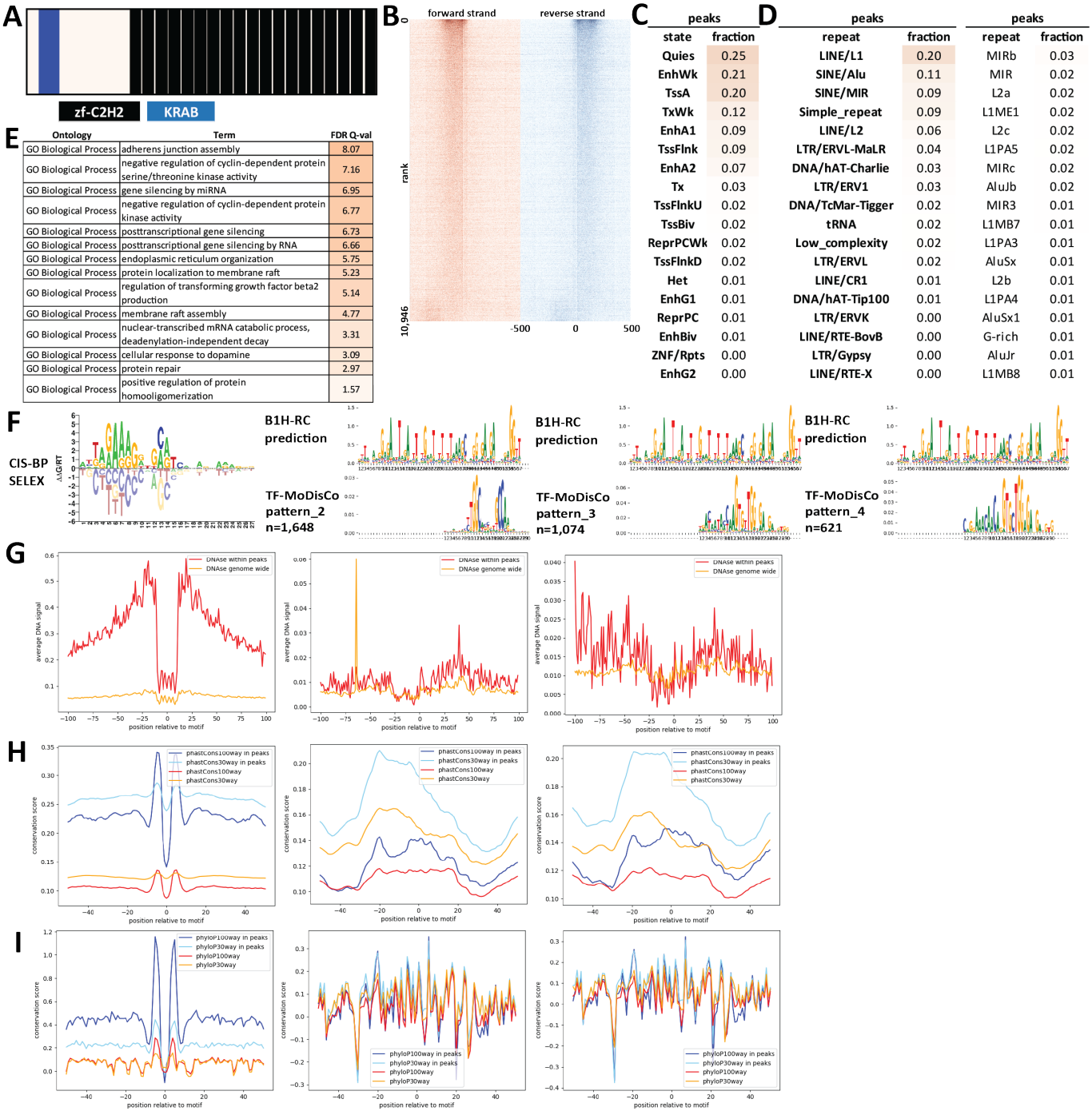

Supplementary Figure 780: Properties and genomic distribution of motifs identified for the ZNF184 transcription factor in HEK293 (accession ENCSR020UPN).

TF-MoDisCO pattern_2 n=1648, CWM

pattern_2, n=1648; subpattern_0, ns=473

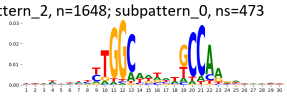

pattern_2, n=1648; subpattern_1, ns=326

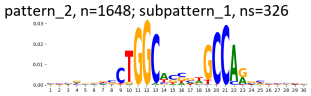

pattern_2, n=1648; subpattern_2, ns=306

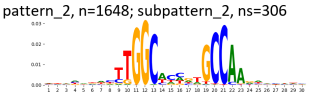

pattern_2, n=1648; subpattern_3, ns=258

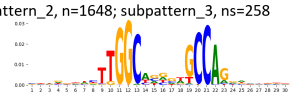

pattern_2, n=1648; subpattern_4, ns=251

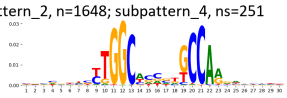

pattern_2, n=1648; subpattern_5, ns=22

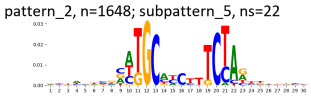

pattern_2, n=1648; subpattern_6, ns=6

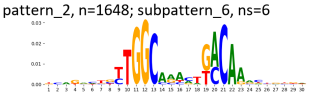

pattern_2, n=1648; subpattern_7, ns=4

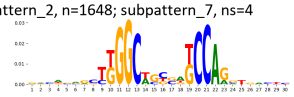

pattern_2, n=1648; subpattern_8, ns=2

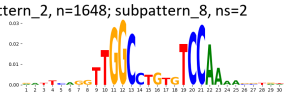

TF-MoDisCO pattern_2 n=1648, PWM

pattern_2, n=1648; subpattern_0, ns=473

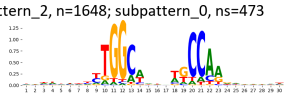

pattern_2, n=1648; subpattern_1, ns=326

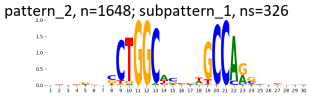

pattern_2, n=1648; subpattern_2, ns=306

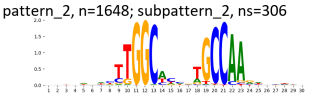

pattern_2, n=1648; subpattern_3, ns=258

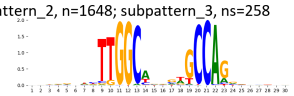

pattern_2, n=1648; subpattern_4, ns=251

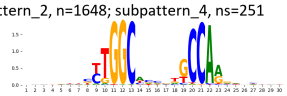

pattern_2, n=1648; subpattern_5, ns=22

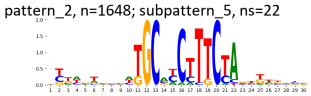

pattern_2, n=1648; subpattern_6, ns=6

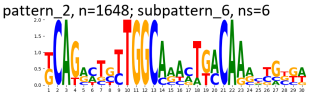

pattern_2, n=1648; subpattern_7, ns=4

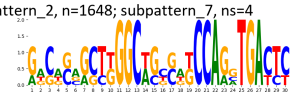

pattern_2, n=1648; subpattern_8, ns=2

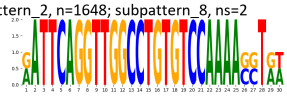

TF-MoDisCO pattern_3 n=1074, CWM

pattern_3, n=1074; subpattern_0, ns=239

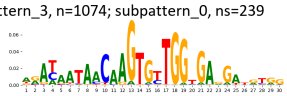

pattern_3, n=1074; subpattern_1, ns=218

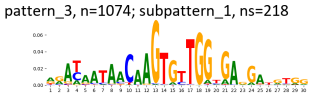

pattern_3, n=1074; subpattern_2, ns=209

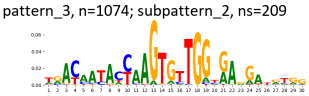

pattern_3, n=1074; subpattern_3, ns=206

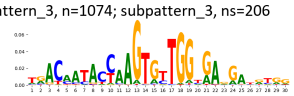

pattern_3, n=1074; subpattern_4, ns=101

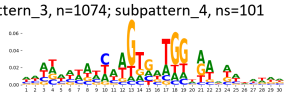

pattern_3, n=1074; subpattern_5, ns=93

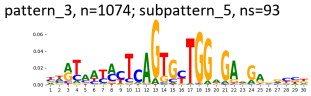

pattern_3, n=1074; subpattern_6, ns=8

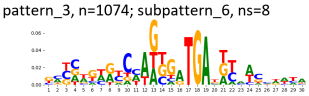

TF-MoDisCO pattern_3 n=1074, PWM

pattern_3, n=1074; subpattern_0, ns=239

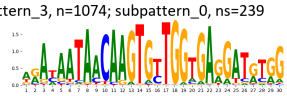

pattern_3, n=1074; subpattern_1, ns=218

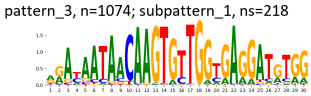

pattern_3, n=1074; subpattern_2, ns=209

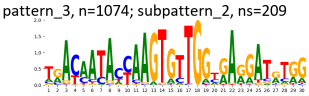

pattern_3, n=1074; subpattern_3, ns=206

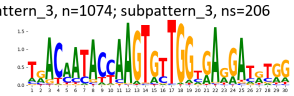

pattern_3, n=1074; subpattern_4, ns=101

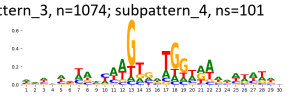

pattern_3, n=1074; subpattern_5, ns=93

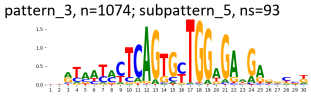

pattern_3, n=1074; subpattern_6, ns=8

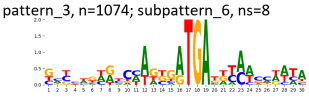

TF-MoDisCO pattern_4 n=621, CWM

pattern_4, n=621; subpattern_0, ns=309

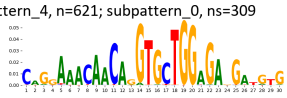

pattern_4, n=621; subpattern_1, ns=252

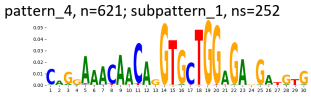

pattern_4, n=621; subpattern_2, ns=40

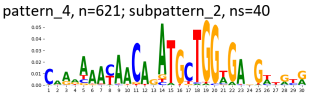

pattern_4, n=621; subpattern_3, ns=18

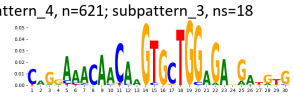

pattern_4, n=621; subpattern_4, ns=2

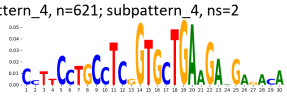

TF-MoDisCO pattern_4 n=621, PWM

pattern_4, n=621; subpattern_0, ns=309

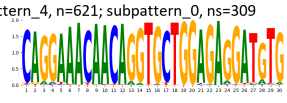

pattern_4, n=621; subpattern_1, ns=252

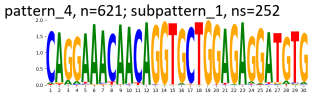

pattern_4, n=621; subpattern_2, ns=40

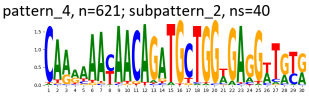

pattern_4, n=621; subpattern_3, ns=18

pattern_4, n=621; subpattern_4, ns=2

Supplementary Figure 781: TF-MoDisCO subpatterns for the ZNF184 transcription factor in HEK293 (accession ENCSR020UPN).

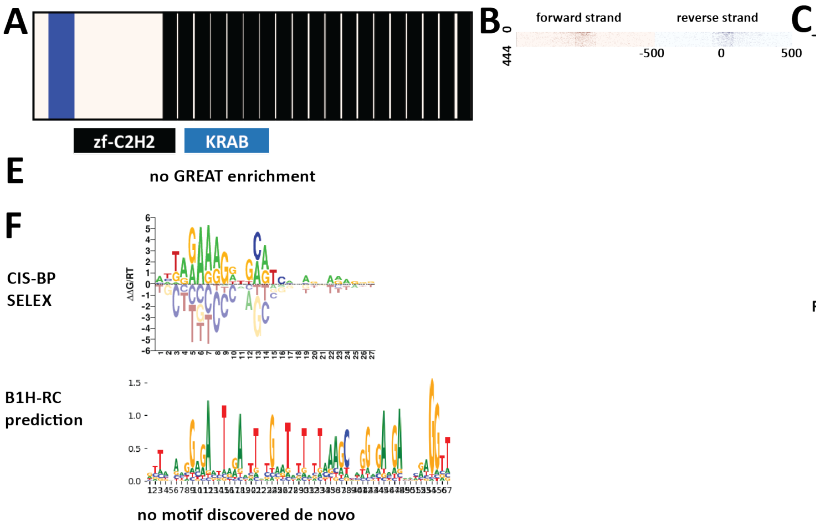

C

peaks	
state	fraction
Quies	0.34
TssA	0.19
TssFlnk	0.17
EnhWk	0.10
TxWk	0.10
EnhA2	0.05
EnhA1	0.04
Tx	0.04
TssBiv	0.03
TssFlnkD	0.03
ReprPCWk	0.03
TssFlnkU	0.02
Het	0.02
ZNF/Rpts	0.01
ReprPC	0.01
EnhG1	0.01
EnhBiv	0.01
EnhG2	0.00

D

peaks		peaks	
repeat	fraction	repeat	fraction
Simple_repeat	0.19	L2c	0.04
SINE/Alu	0.16	L2a	0.04
LINE/L1	0.13	MIRb	0.03
LINE/L2	0.11	AluJb	0.02
SINE/MIR	0.08	L2b	0.02
LTR/ERV1	0.05	L1ME1	0.02
Low_complexity	0.04	MIR3	0.02
LTR/ERVL-MaLR	0.03	L2	0.02
Satellite	0.02	AluJo	0.02
DNA/hAT-Charlie	0.02	GA-rich	0.02
LTR/ERVL	0.02	AluSz	0.02
Satellite/centr	0.01	AluSx	0.02
DNA/hAT-Tip100	0.01	A-rich	0.01
Satellite/acro	0.01	(GT)n	0.01
rRNA	0.01	MIRc	0.01
DNA/TcMar-Tigger	0.01	MIR	0.01
LTR/ERVK	0.00	MER5A	0.01
LINE/CR1	0.00	LTR10A	0.01

Supplementary Figure 782: Properties and genomic distribution of motifs identified for the ZNF184 transcription factor in HEK293 (accession ChipExo models).

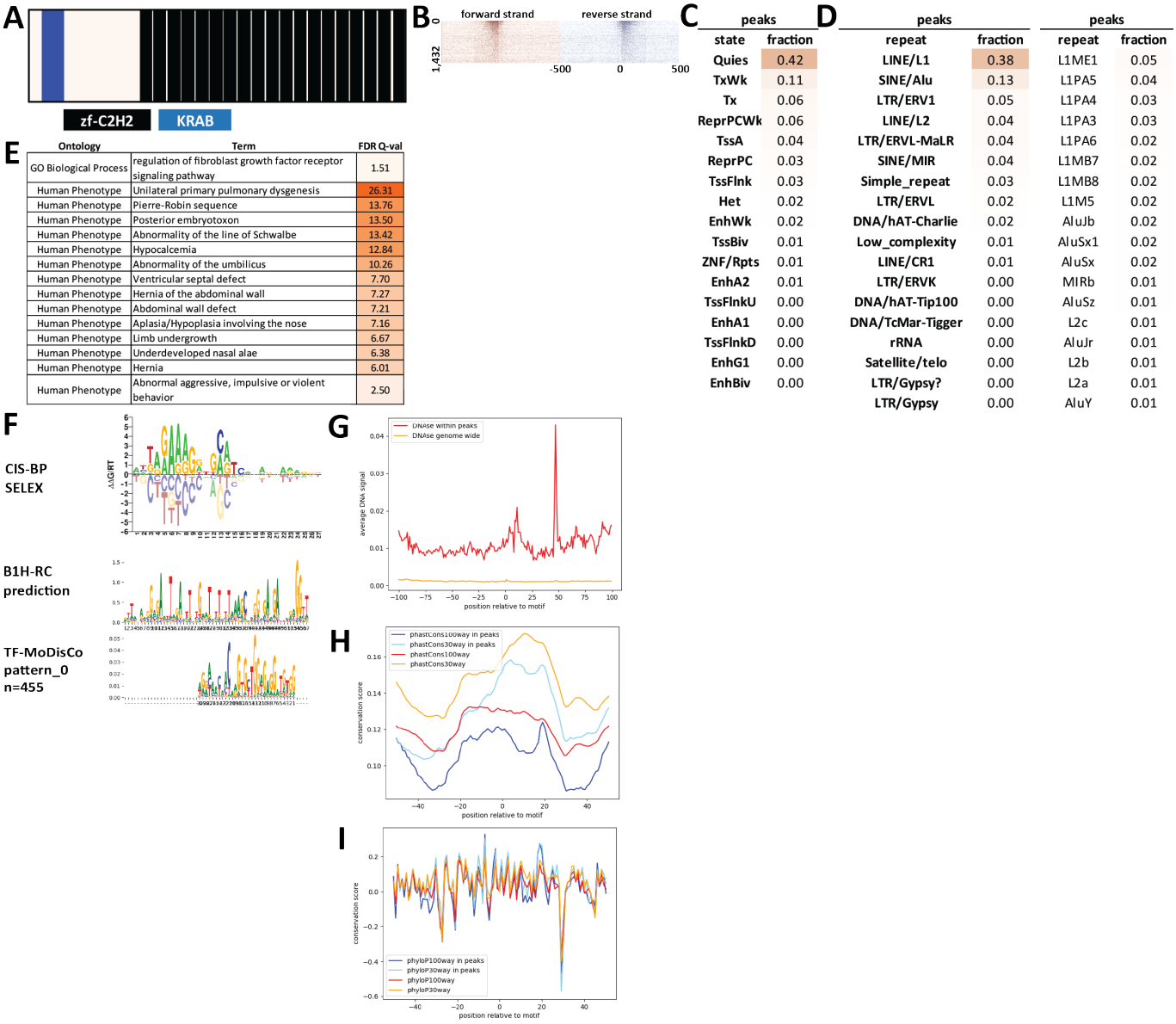

Supplementary Figure 783: Properties and genomic distribution of motifs identified for the ZNF184 transcription factor in K562 (accession ENCSR526HRN).

TF-MoDisCO pattern_0 n=455, CWM

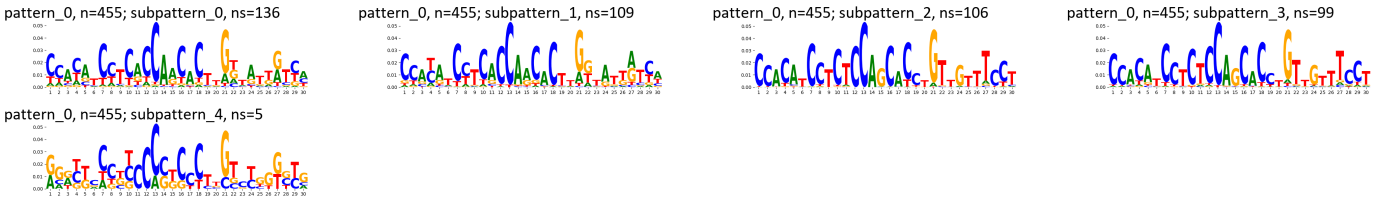

TF-MoDisCO pattern_0 n=455, PWM

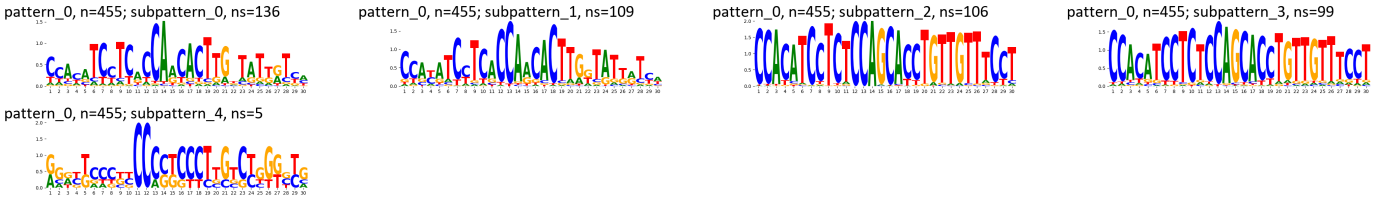

Supplementary Figure 784: TF-MoDisCO subpatterns for the ZNF184 transcription factor in K562 (accession ENCSR526HRN).



Supplementary Figure 785: Properties and genomic distribution of motifs identified for the ZNF184 transcription factor in K562 (accession ENCSR546IHU).

TF-MoDisCO pattern_0 n=1680, CWM

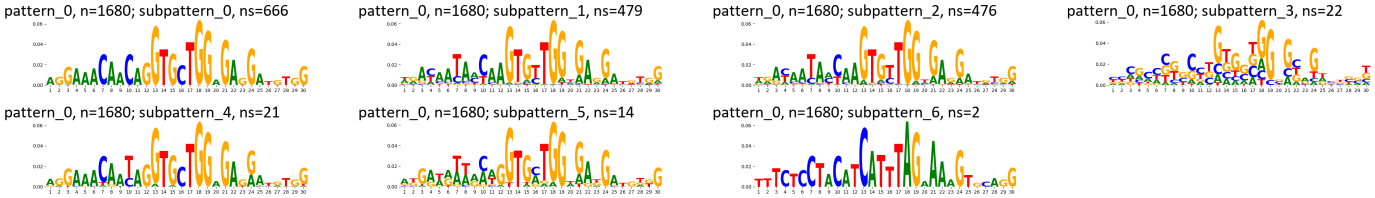

TF-MoDisCO pattern_0 n=1680, PWM

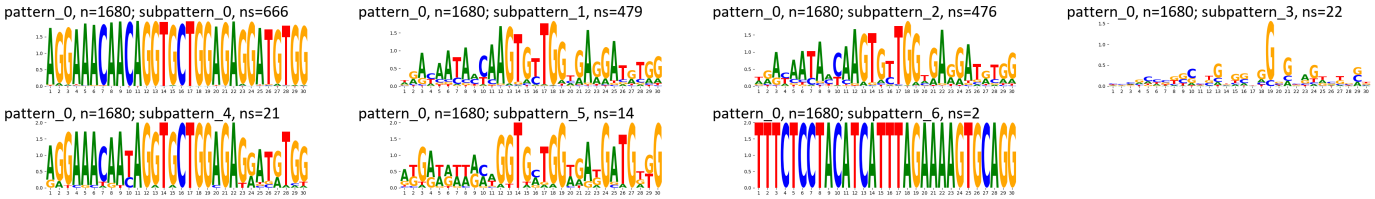

TF-MoDisCO pattern_2 n=935, CWM

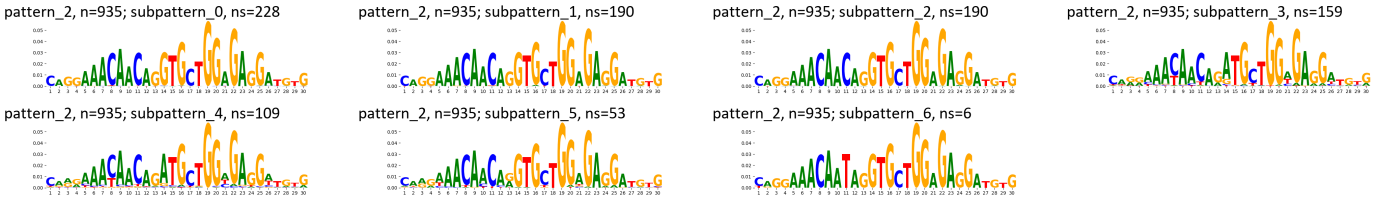

TF-MoDisCO pattern_2 n=935, PWM

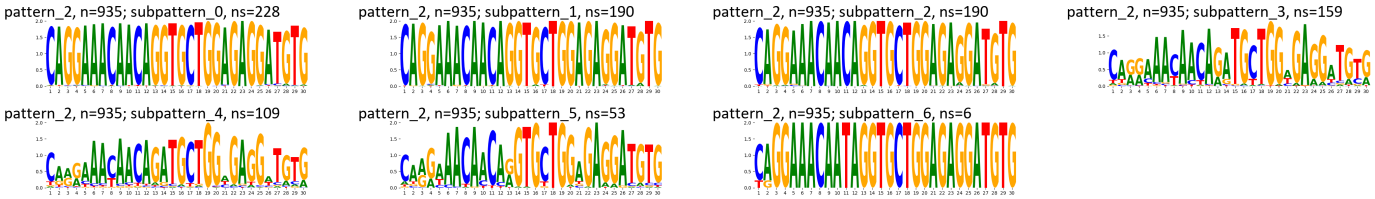

Supplementary Figure 786: TF-MoDisCO subpatterns for the ZNF184 transcription factor in K562 (accession ENCSR546IHU).

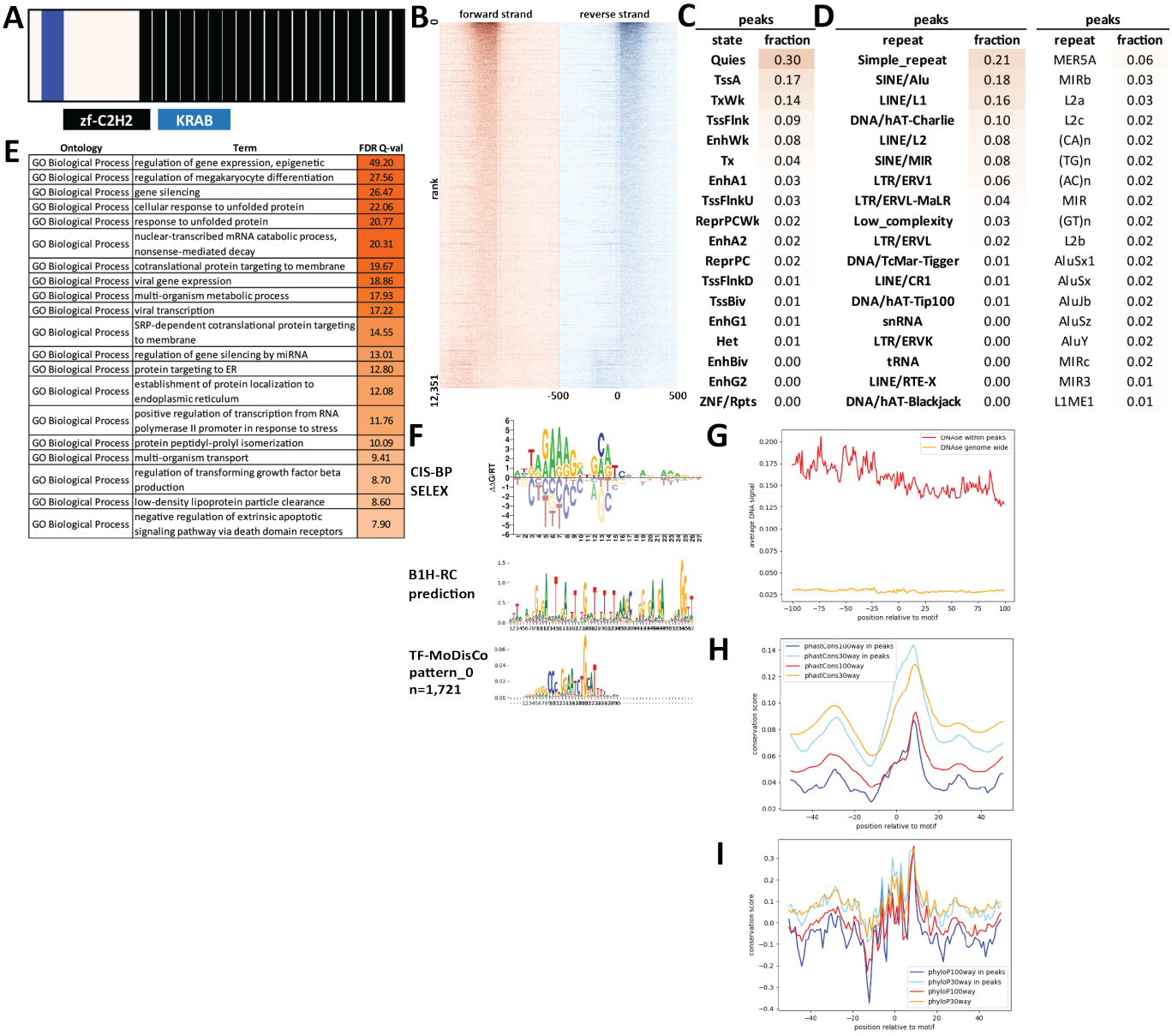

Supplementary Figure 787: Properties and genomic distribution of motifs identified for the ZNF184 transcription factor in K562 (accession ENCSR621ATC).

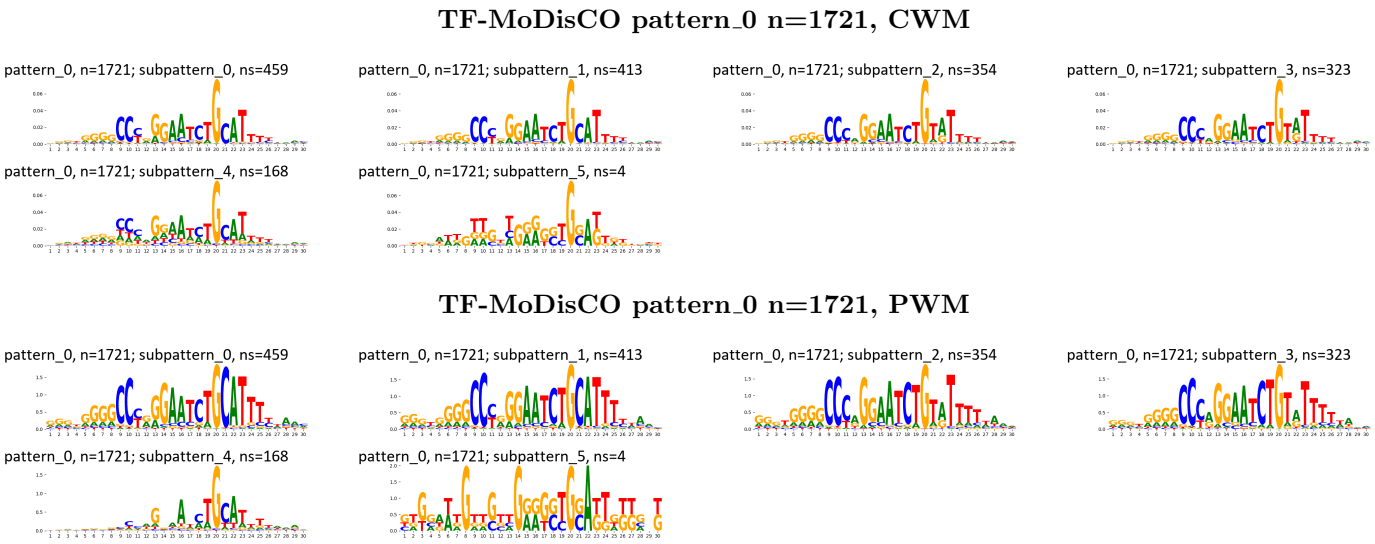

Supplementary Figure 788: TF-MoDisCO subpatterns for the ZNF184 transcription factor in K562 (accession ENCSR621ATC).

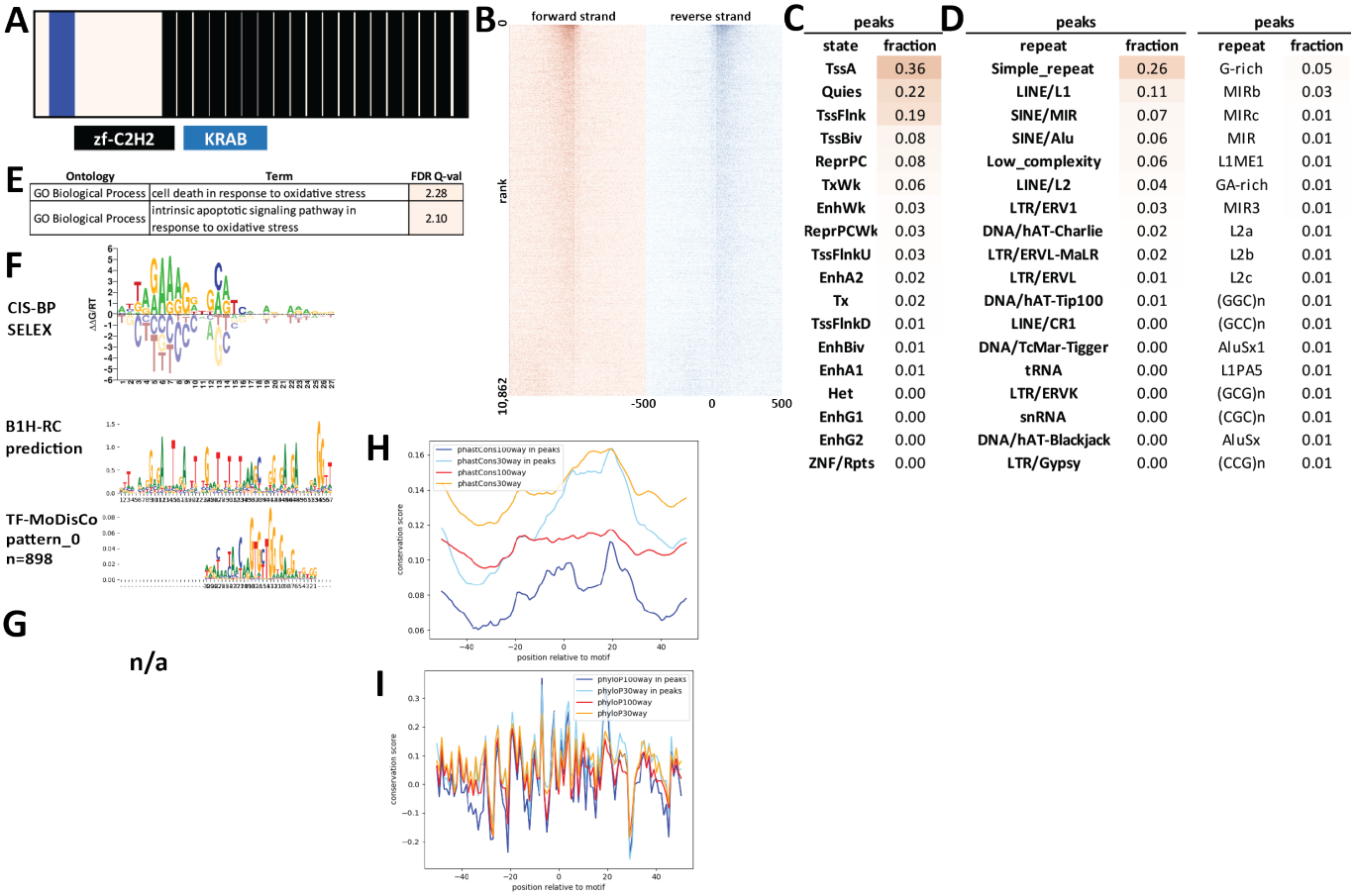

Supplementary Figure 789: Properties and genomic distribution of motifs identified for the ZNF184 transcription factor in WTC11 (accession ENCSR640STN).

TF-MoDisCO pattern_0 n=898, CWM

pattern_0, n=898; subpattern_0, ns=265

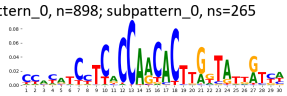

pattern_0, n=898; subpattern_1, ns=243

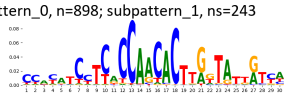

pattern_0, n=898; subpattern_2, ns=202

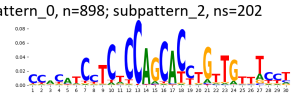

pattern_0, n=898; subpattern_3, ns=136

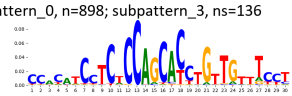

pattern_0, n=898; subpattern_4, ns=52

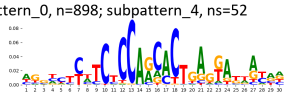

TF-MoDisCO pattern_0 n=898, PWM

pattern_0, n=898; subpattern_0, ns=265

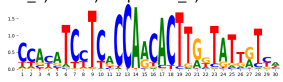

pattern_0, n=898; subpattern_1, ns=243

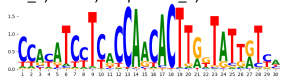

pattern_0, n=898; subpattern_2, ns=202

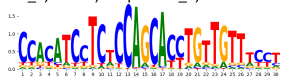

pattern_0, n=898; subpattern_3, ns=136

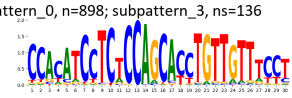

pattern_0, n=898; subpattern_4, ns=52

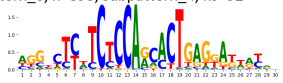

Supplementary Figure 790: TF-MoDisCO subpatterns for the ZNF184 transcription factor in WTC11 (accession ENCSR640STN).



Supplementary Figure 791: Properties and genomic distribution of motifs identified for the ZNF189 transcription factor in HEK293 (accession ENCSR163RYW).

TF-MoDisCO pattern_0 n=13283, CWM

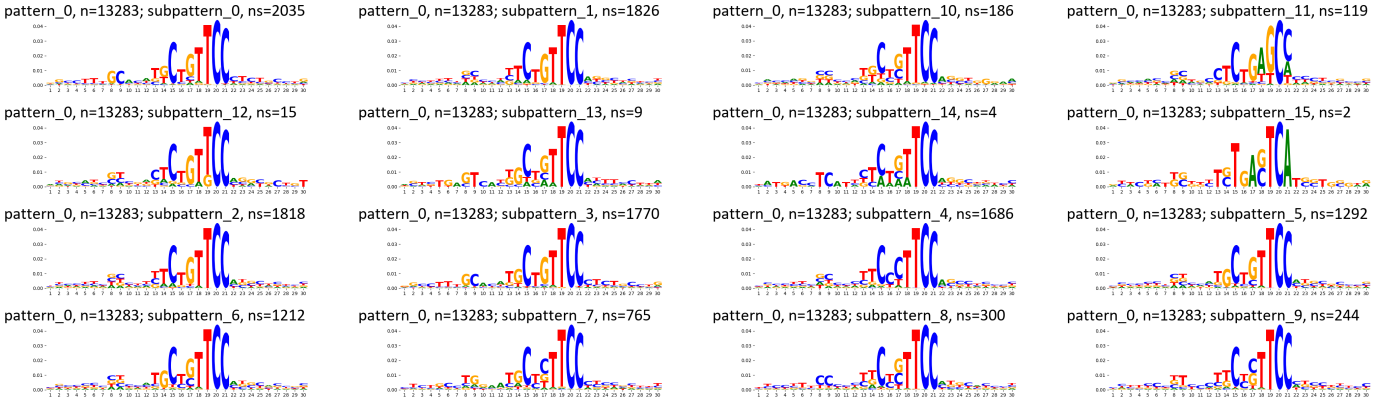

TF-MoDisCO pattern_0 n=13283, PWM

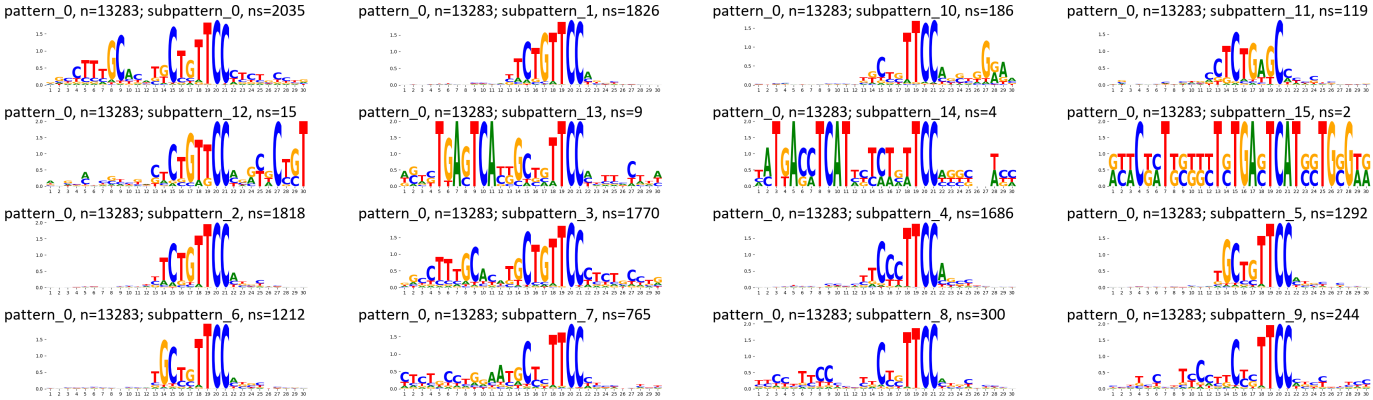

TF-MoDisCO pattern_1 n=3334, CWM

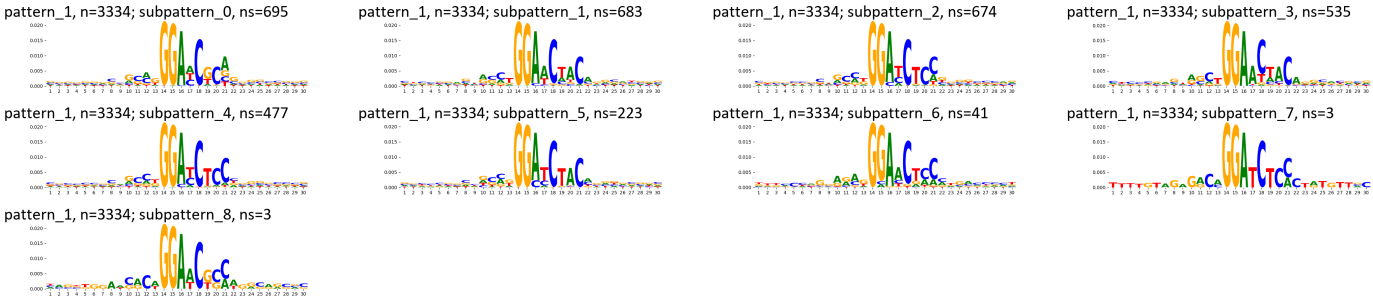

TF-MoDisCO pattern_1 n=3334, PWM

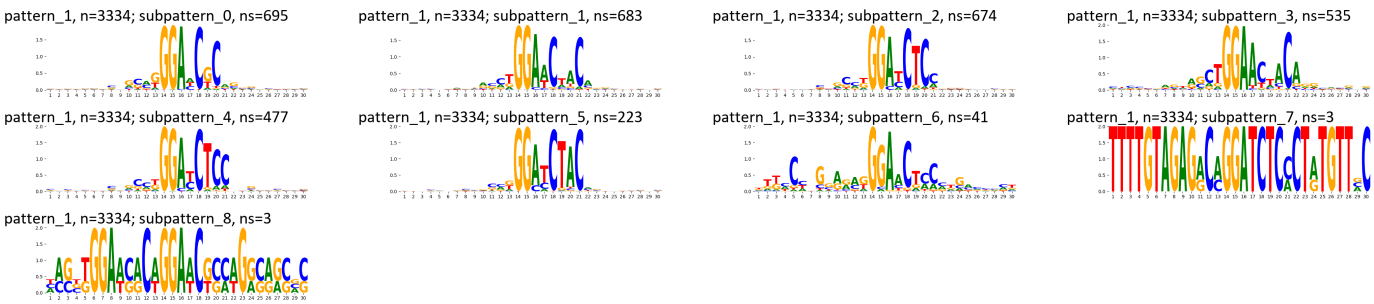

Supplementary Figure 792: TF-MoDisCO subpatterns for the ZNF189 transcription factor in HEK293 (accession ENCSR163RYW).

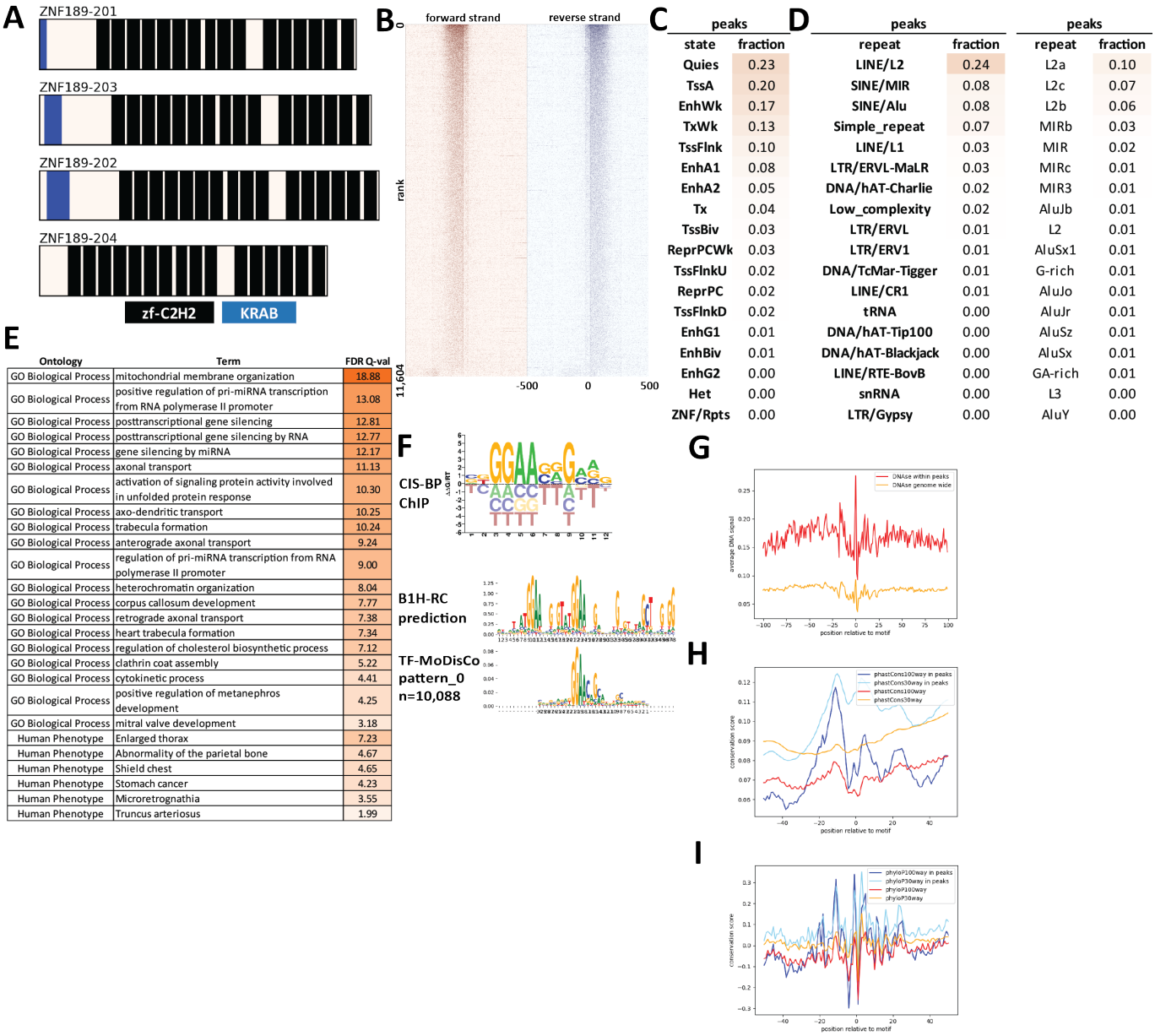

C

peaks	
state	fraction
Quies	0.23
TssA	0.20
EnhWk	0.17
TxWk	0.13
TssFlnk	0.10
EnhA1	0.08
EnhA2	0.05
Tx	0.04
TssBiv	0.03
ReprPCWk	0.03
TssFlnkU	0.02
ReprPC	0.02
TssFlnkD	0.02
EnhG1	0.01
EnhBiv	0.01
EnhG2	0.00
Het	0.00
ZNF/Rpts	0.00

D

peaks		peaks	
repeat	fraction	repeat	fraction
LINE/L2	0.24	L2a	0.10
SINE/MIR	0.08	L2c	0.07
SINE/Alu	0.08	L2b	0.06
Simple_repeat	0.07	MIRb	0.03
LINE/L1	0.03	MIR	0.02
LTR/ERVL-MaLR	0.03	MIRc	0.01
DNA/hAT-Charlie	0.02	MIR3	0.01
Low_complexity	0.02	AluJb	0.01
LTR/ERVL	0.01	L2	0.01
LTR/ERV1	0.01	AluSx1	0.01
DNA/TcMar-Tigger	0.01	G-rich	0.01
LINE/CR1	0.01	AluJo	0.01
tRNA	0.00	AluJr	0.01
DNA/hAT-Tip100	0.00	AluSz	0.01
DNA/hAT-Blackjack	0.00	AluSx	0.01
LINE/RTE-BovB	0.00	GA-rich	0.01
snRNA	0.00	L3	0.00
LTR/Gypsy	0.00	AluY	0.00

E

Ontology	Term	FDR Q-val
GO Biological Process	mitochondrial membrane organization	18.88
GO Biological Process	positive regulation of pri-miRNA transcription from RNA polymerase II promoter	13.08
GO Biological Process	posttranscriptional gene silencing	12.81
GO Biological Process	posttranscriptional gene silencing by RNA	12.77
GO Biological Process	gene silencing by miRNA	12.17
GO Biological Process	axonal transport	11.13
GO Biological Process	activation of signaling protein activity involved in unfolded protein response	10.30
GO Biological Process	axo-dendritic transport	10.25
GO Biological Process	trabecula formation	10.24
GO Biological Process	anterograde axonal transport	9.24
GO Biological Process	regulation of pri-miRNA transcription from RNA polymerase II promoter	9.00
GO Biological Process	heterochromatin organization	8.04
GO Biological Process	corpus callosum development	7.77
GO Biological Process	retrograde axonal transport	7.38
GO Biological Process	heart trabecula formation	7.34
GO Biological Process	regulation of cholesterol biosynthetic process	7.12
GO Biological Process	clathrin coat assembly	5.22
GO Biological Process	cytokinetic process	4.41
GO Biological Process	positive regulation of metanephros development	4.25
GO Biological Process	mitral valve development	3.18
Human Phenotype	Enlarged thorax	7.23
Human Phenotype	Abnormality of the parietal bone	4.67
Human Phenotype	Shield chest	4.65
Human Phenotype	Stomach cancer	4.23
Human Phenotype	Microretrognathia	3.55
Human Phenotype	Truncus arteriosus	1.99

Supplementary Figure 793: Properties and genomic distribution of motifs identified for the ZNF189 transcription factor in HEK293 (accession Hughes NB models).

TF-MoDisCO pattern_0 n=10088, CWM

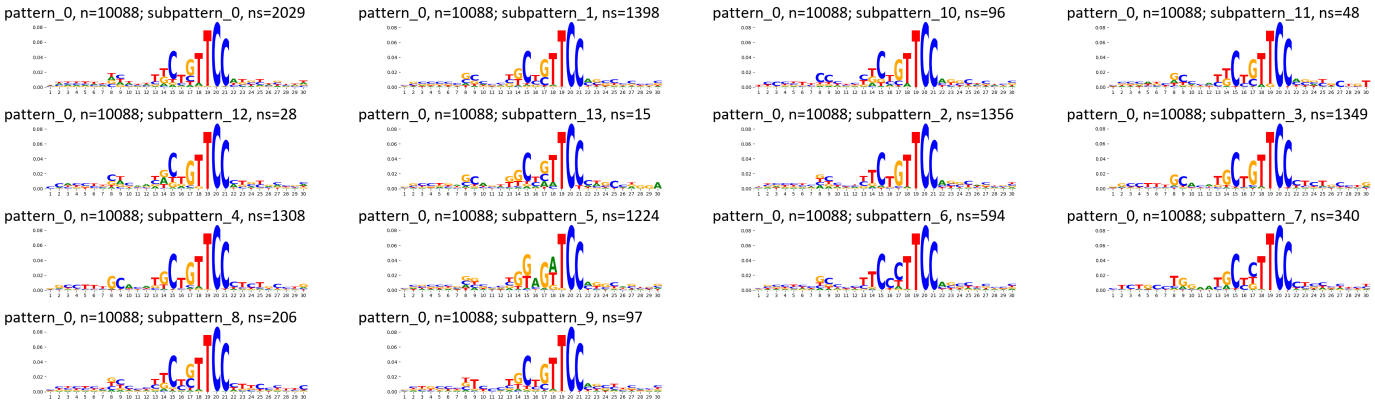

TF-MoDisCO pattern_0 n=10088, PWM

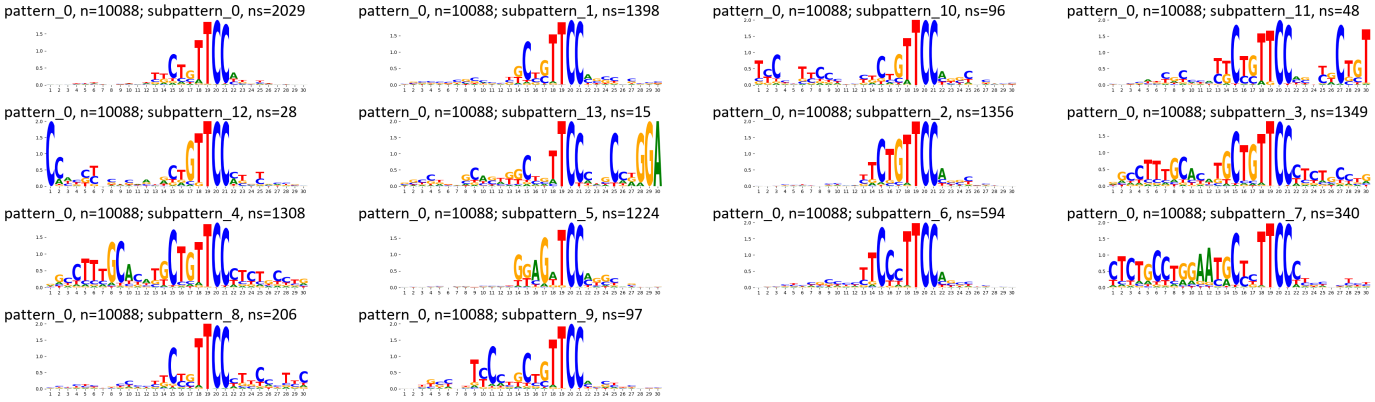

Supplementary Figure 794: TF-MoDisCO subpatterns for the ZNF189 transcription factor in HEK293 (accession Hughes NB models).

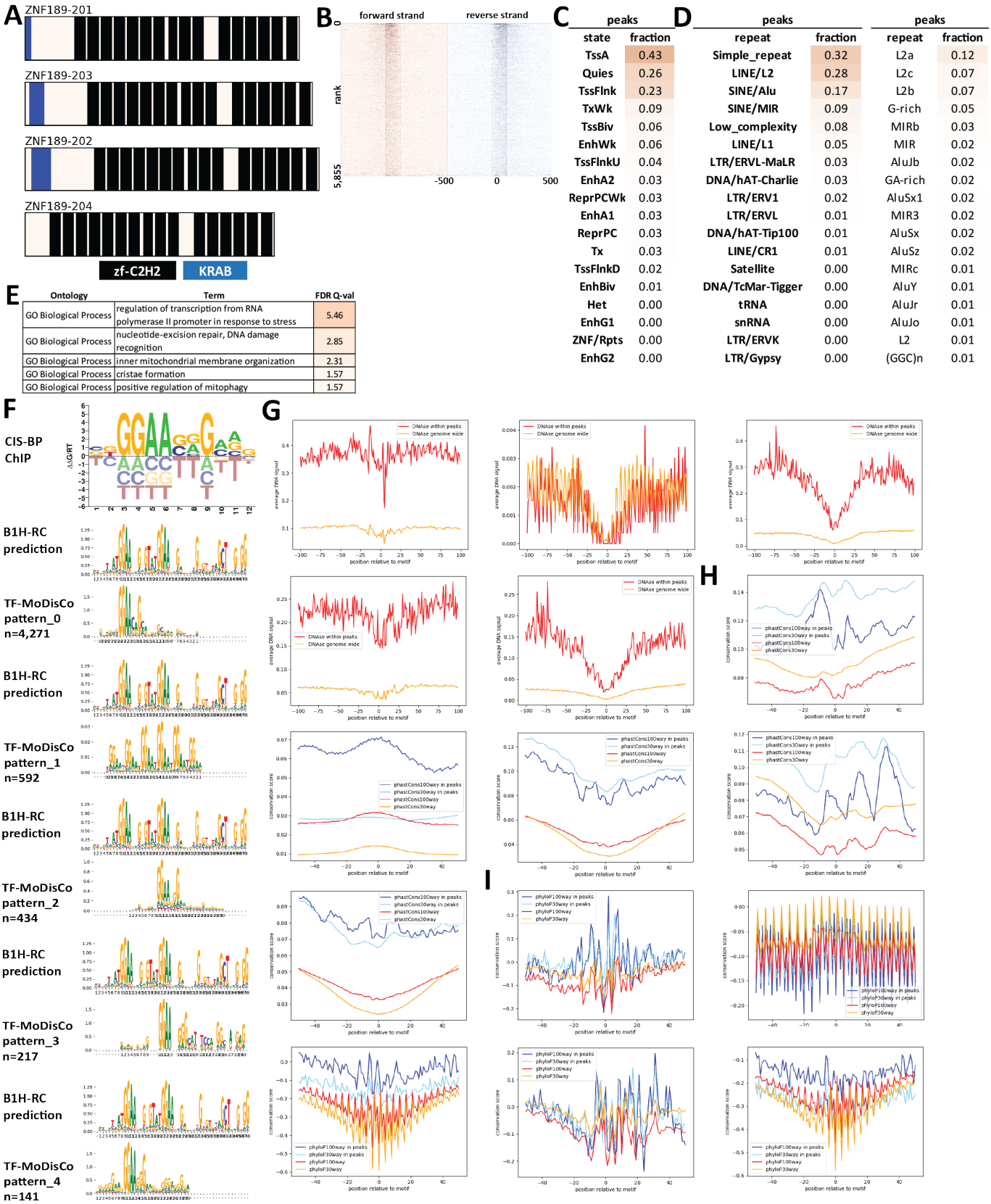

Supplementary Figure 795: Properties and genomic distribution of motifs identified for the ZNF189 transcription factor in HEK293 (accession ChipExo models).

TF-MoDisCO pattern_0 n=4271, CWM

pattern_0, n=4271; subpattern_0, ns=1158

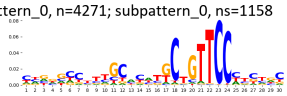

pattern_0, n=4271; subpattern_1, ns=884

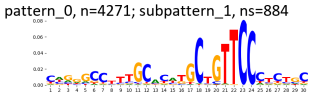

pattern_0, n=4271; subpattern_10, ns=5

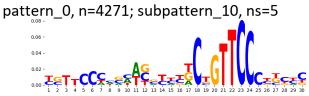

pattern_0, n=4271; subpattern_2, ns=849

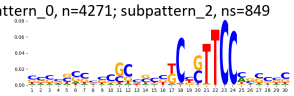

pattern_0, n=4271; subpattern_3, ns=593

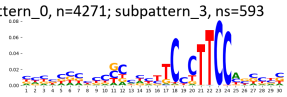

pattern_0, n=4271; subpattern_4, ns=567

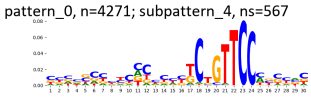

pattern_0, n=4271; subpattern_5, ns=117

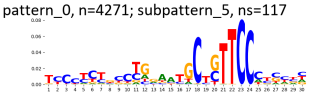

pattern_0, n=4271; subpattern_6, ns=56

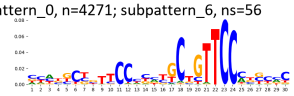

pattern_0, n=4271; subpattern_7, ns=18

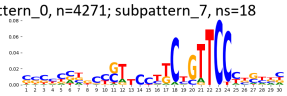

pattern_0, n=4271; subpattern_8, ns=17

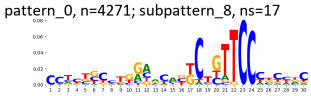

pattern_0, n=4271; subpattern_9, ns=7

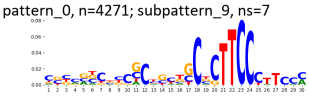

TF-MoDisCO pattern_0 n=4271, PWM

pattern_0, n=4271; subpattern_0, ns=1158

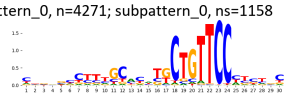

pattern_0, n=4271; subpattern_1, ns=884

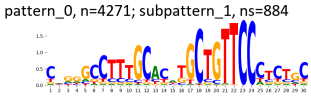

pattern_0, n=4271; subpattern_10, ns=5

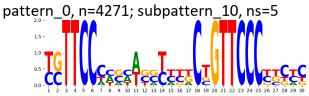

pattern_0, n=4271; subpattern_2, ns=849

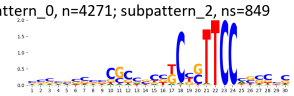

pattern_0, n=4271; subpattern_3, ns=593

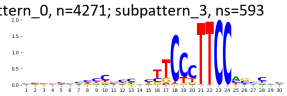

pattern_0, n=4271; subpattern_4, ns=567

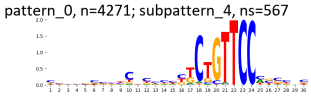

pattern_0, n=4271; subpattern_5, ns=117

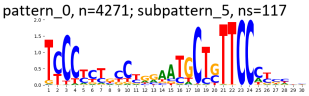

pattern_0, n=4271; subpattern_6, ns=56

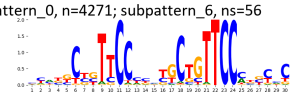

pattern_0, n=4271; subpattern_7, ns=18

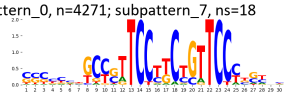

pattern_0, n=4271; subpattern_8, ns=17

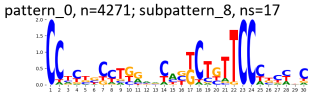

pattern_0, n=4271; subpattern_9, ns=7

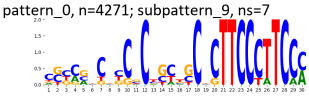

TF-MoDisCO pattern_1 n=592, CWM

pattern_1, n=592; subpattern_0, ns=168

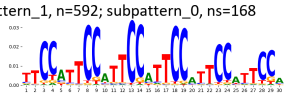

pattern_1, n=592; subpattern_1, ns=168

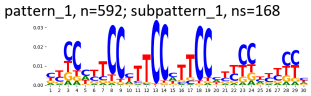

pattern_1, n=592; subpattern_2, ns=112

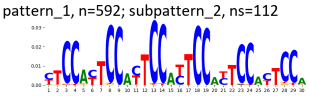

pattern_1, n=592; subpattern_3, ns=88

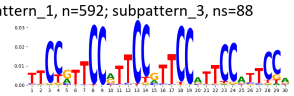

pattern_1, n=592; subpattern_4, ns=56

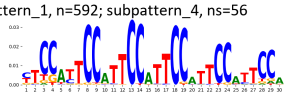

TF-MoDisCO pattern_1 n=592, PWM

pattern_1, n=592; subpattern_0, ns=168

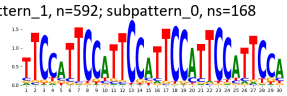

pattern_1, n=592; subpattern_1, ns=168

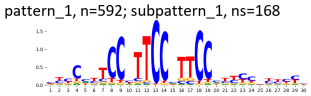

pattern_1, n=592; subpattern_2, ns=112

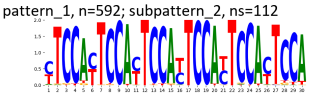

pattern_1, n=592; subpattern_3, ns=88

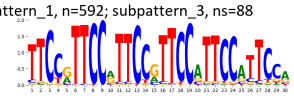

pattern_1, n=592; subpattern_4, ns=56

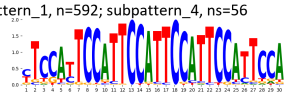

TF-MoDisCO pattern_2 n=434, CWM

pattern_2, n=434; subpattern_0, ns=137

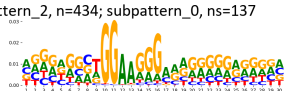

pattern_2, n=434; subpattern_1, ns=115

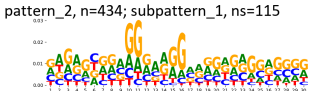

pattern_2, n=434; subpattern_2, ns=82

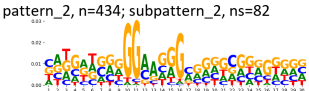

pattern_2, n=434; subpattern_3, ns=39

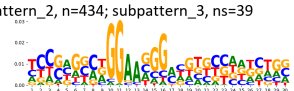

pattern_2, n=434; subpattern_4, ns=31

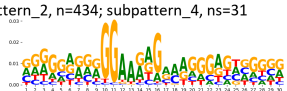

pattern_2, n=434; subpattern_5, ns=13

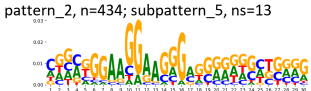

pattern_2, n=434; subpattern_6, ns=13

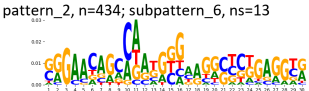

pattern_2, n=434; subpattern_7, ns=4

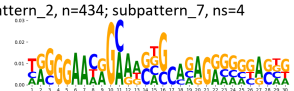

TF-MoDisCO pattern_2 n=434, PWM

pattern_2, n=434; subpattern_0, ns=137

pattern_2, n=434; subpattern_1, ns=115

pattern_2, n=434; subpattern_2, ns=82

pattern_2, n=434; subpattern_3, ns=39

pattern_2, n=434; subpattern_4, ns=31

pattern_2, n=434; subpattern_5, ns=13

pattern_2, n=434; subpattern_6, ns=13

pattern_2, n=434; subpattern_7, ns=4

TF-MoDisCO pattern_3 n=217, CWM

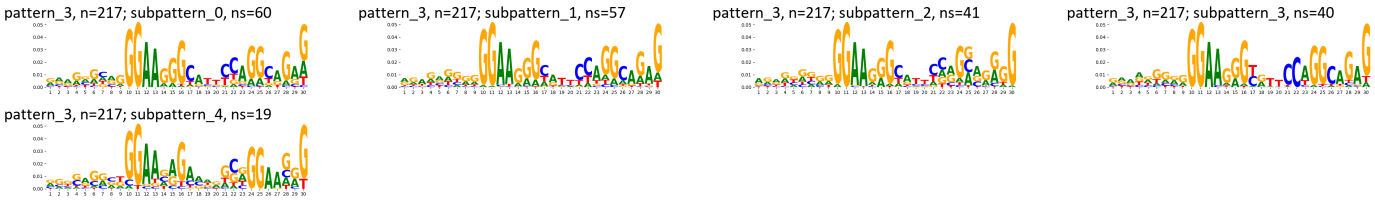

TF-MoDisCO pattern_3 n=217, PWM

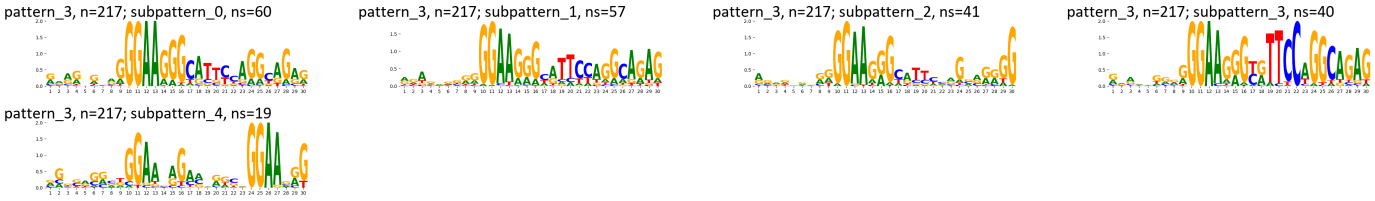

TF-MoDisCO pattern_4 n=141, CWM

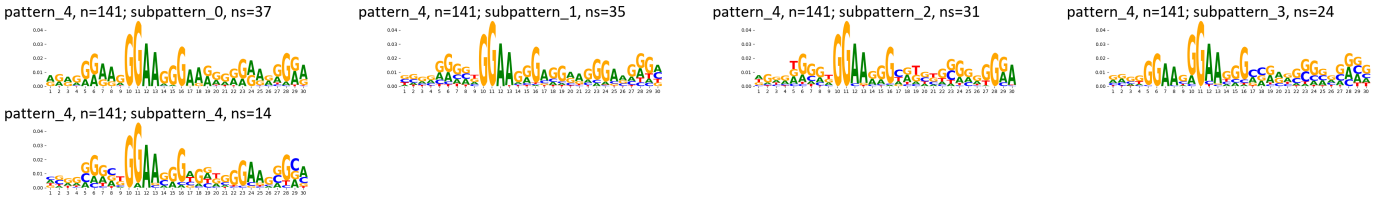

TF-MoDisCO pattern_4 n=141, PWM

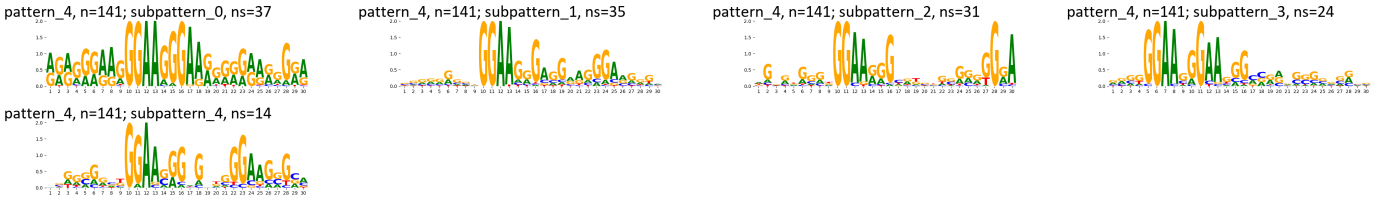

Supplementary Figure 796: TF-MoDisCO subpatterns for the ZNF189 transcription factor in HEK293 (accession ChipExo models).

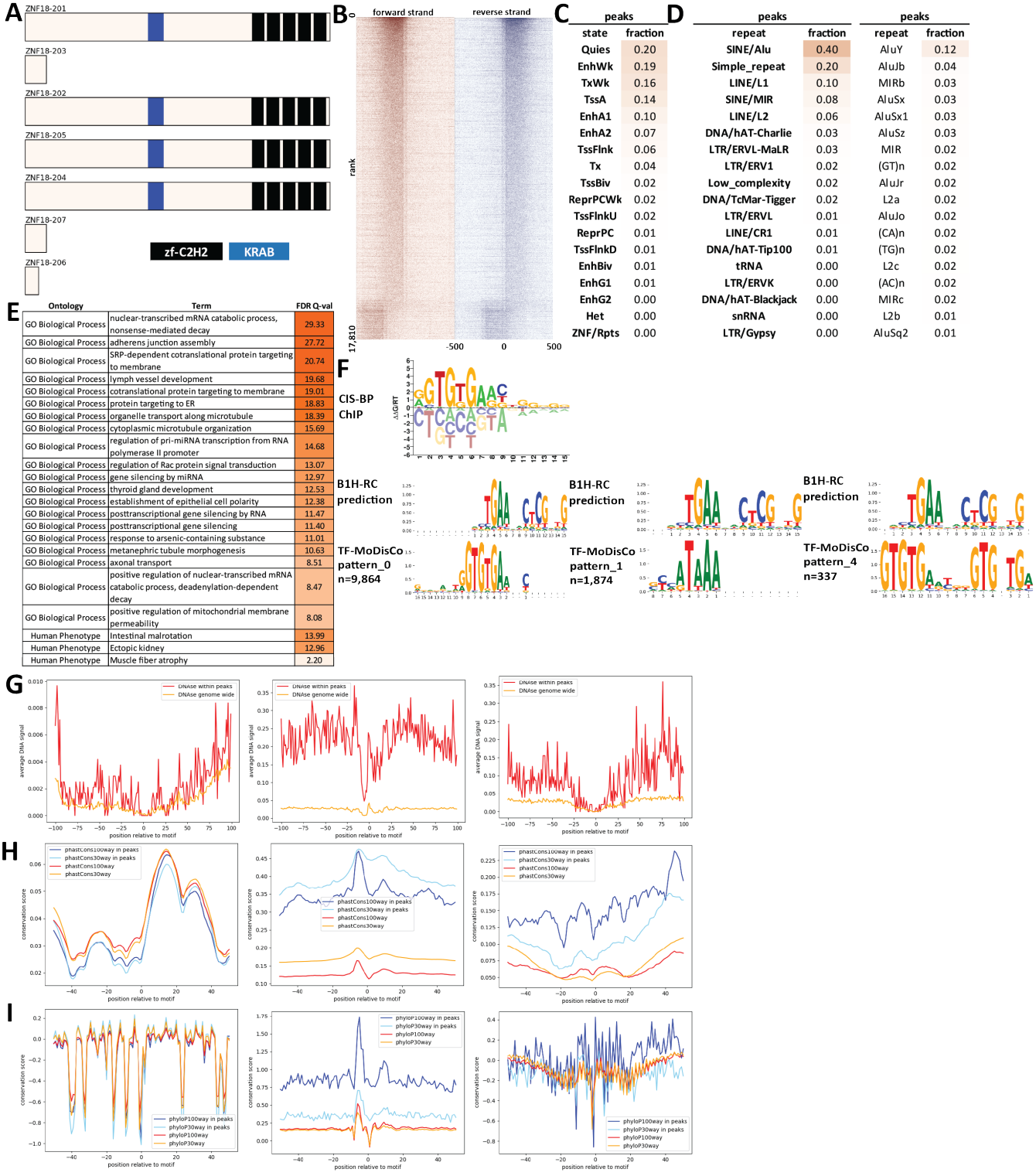

Supplementary Figure 797: Properties and genomic distribution of motifs identified for the ZNF18 transcription factor in HEK293 (accession ENCSR977HTH).

TF-MoDisCO pattern_0 n=9864, CWM

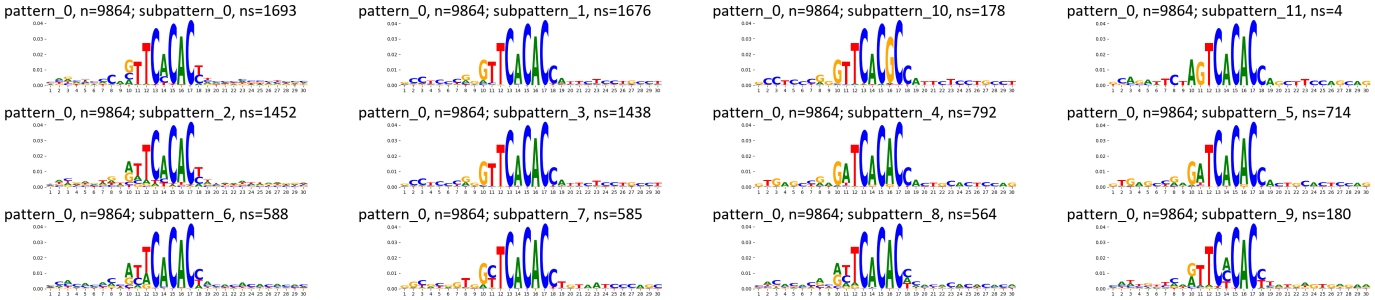

TF-MoDisCO pattern_0 n=9864, PWM

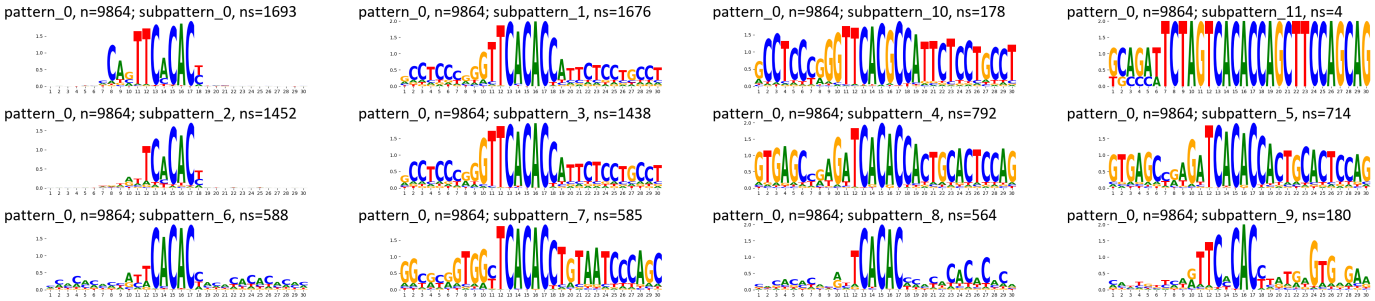

TF-MoDisCO pattern_1 n=1874, CWM

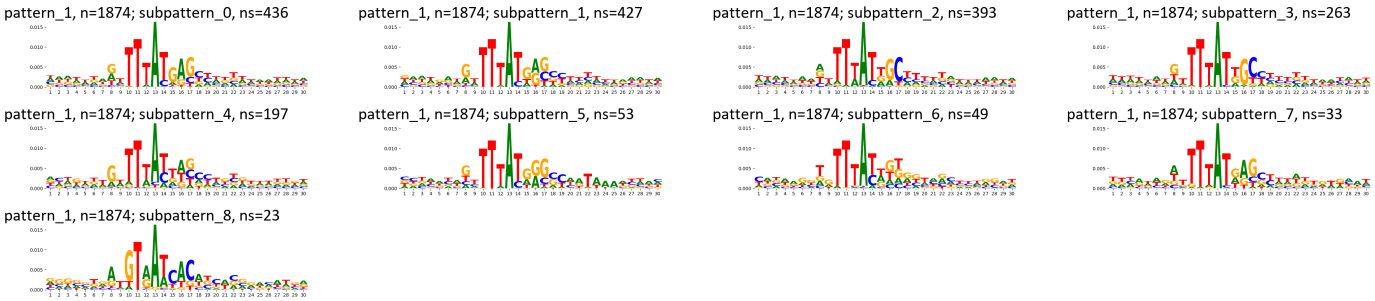

TF-MoDisCO pattern_1 n=1874, PWM

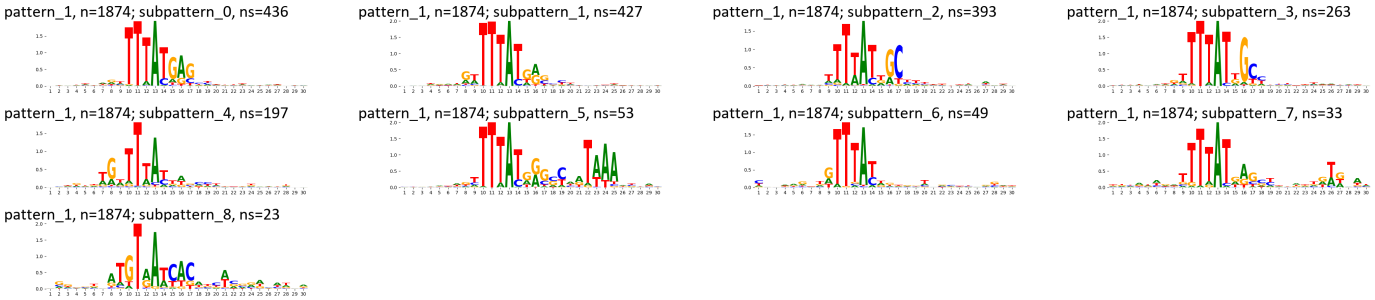

TF-MoDisCO pattern_4 n=337, CWM

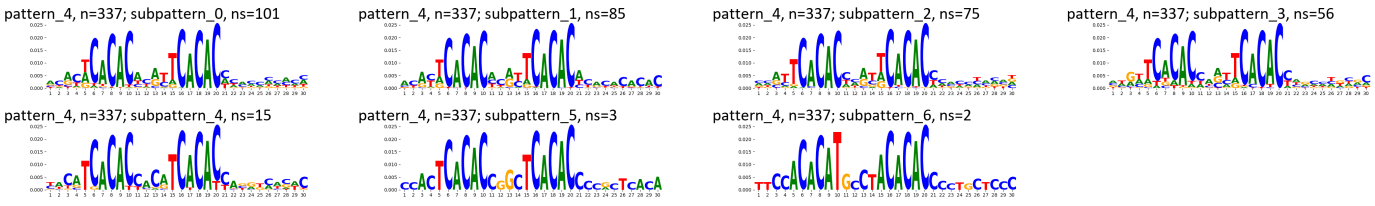

TF-MoDisCO pattern_4 n=337, PWM

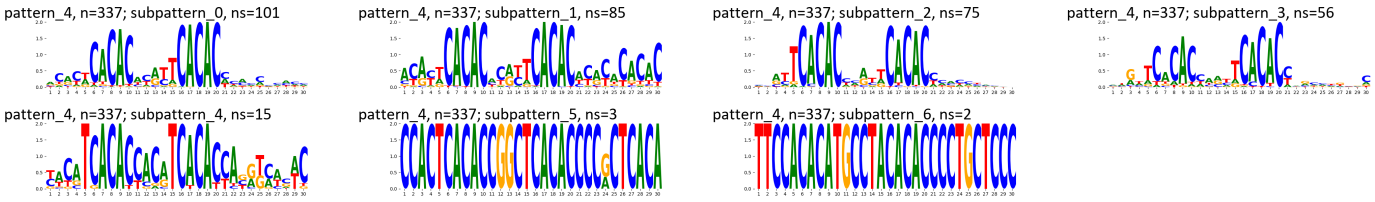

Supplementary Figure 798: TF-MoDisCO subpatterns for the ZNF18 transcription factor in HEK293 (accession ENCSR977HTH).

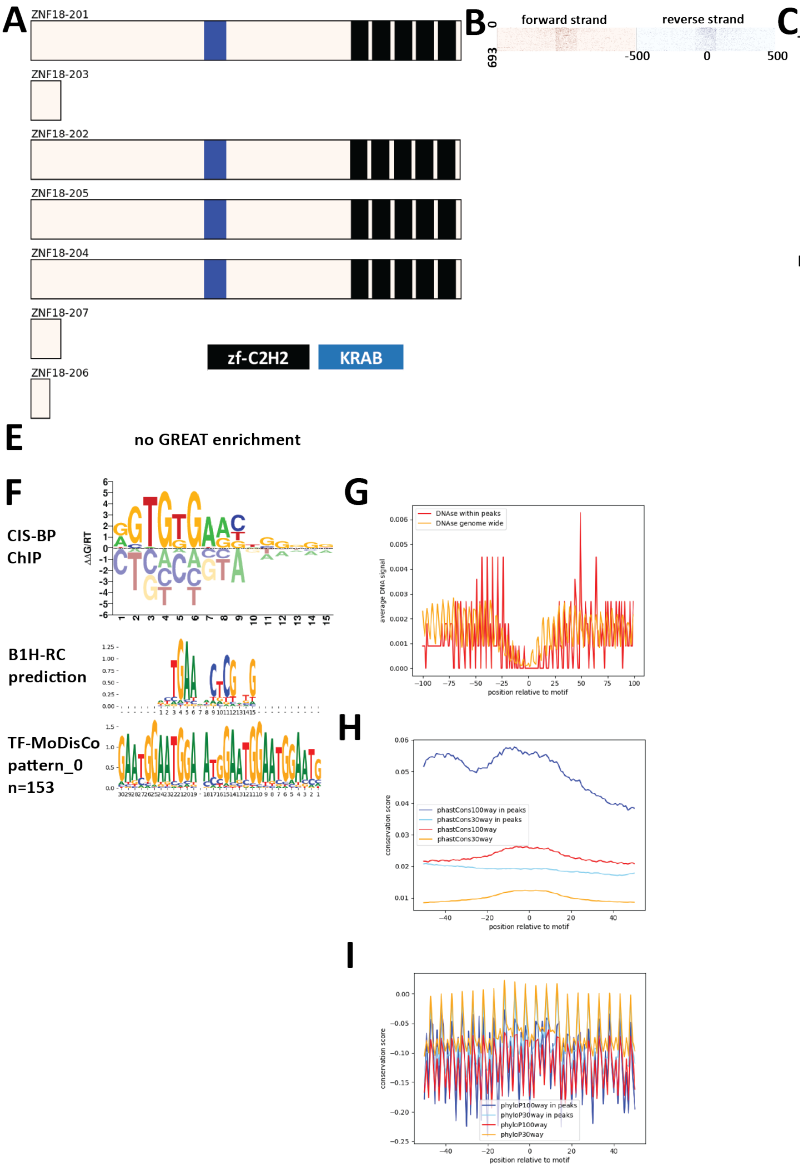

C

peaks	
state	fraction
Quies	0.27
TssA	0.23
TssFlnk	0.13
TxWk	0.10
EnhWk	0.08
EnhA2	0.05
EnhA1	0.05
TssBiv	0.04
ReprPCWk	0.04
TssFlnkU	0.03
ReprPC	0.03
Tx	0.03
TssFlnkD	0.01
EnhBiv	0.01
Het	0.01
ZNF/Rpts	0.01
EnhG1	0.01
EnhG2	0.00

D

peaks		peaks	
repeat	fraction	repeat	fraction
Simple_repeat	0.28	(GT)n	0.04
SINE/Alu	0.17	MIRb	0.03
SINE/MIR	0.09	AluJb	0.03
LINE/L2	0.05	MIR	0.02
LTR/ERV1	0.04	G-rich	0.02
LINE/L1	0.04	(CA)n	0.02
Low_complexity	0.03	L2a	0.02
LTR/ERVL-MaLR	0.03	AluSx	0.02
DNA/hAT-Charlie	0.03	L2c	0.01
LTR/ERVL	0.03	AluY	0.01
Satellite	0.02	AluJo	0.01
DNA/TcMar-Tigger	0.01	(AC)n	0.01
DNA/hAT-Tip100	0.01	AluSz	0.01
Satellite/centr	0.01	AluSx1	0.01
Satellite/acro	0.01	MIRc	0.01
tRNA	0.00	MIR3	0.01
Satellite/telo	0.00	AluJr	0.01
LTR/ERVK	0.00	L2b	0.01

Supplementary Figure 799: Properties and genomic distribution of motifs identified for the ZNF18 transcription factor in HEK293 (accession ChipExo models).

TF-MoDisCO pattern_0 n=153, CWM

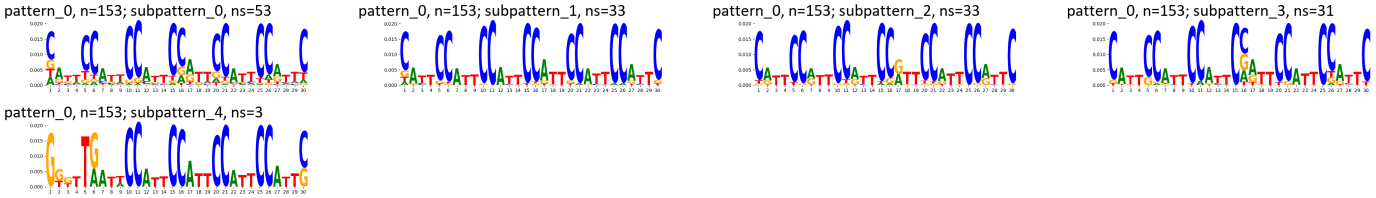

TF-MoDisCO pattern_0 n=153, PWM

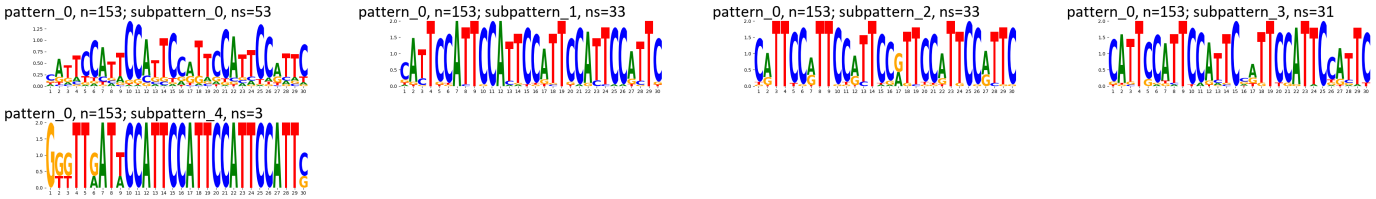

Supplementary Figure 800: TF-MoDisCO subpatterns for the ZNF18 transcription factor in HEK293 (accession ChipExo models).

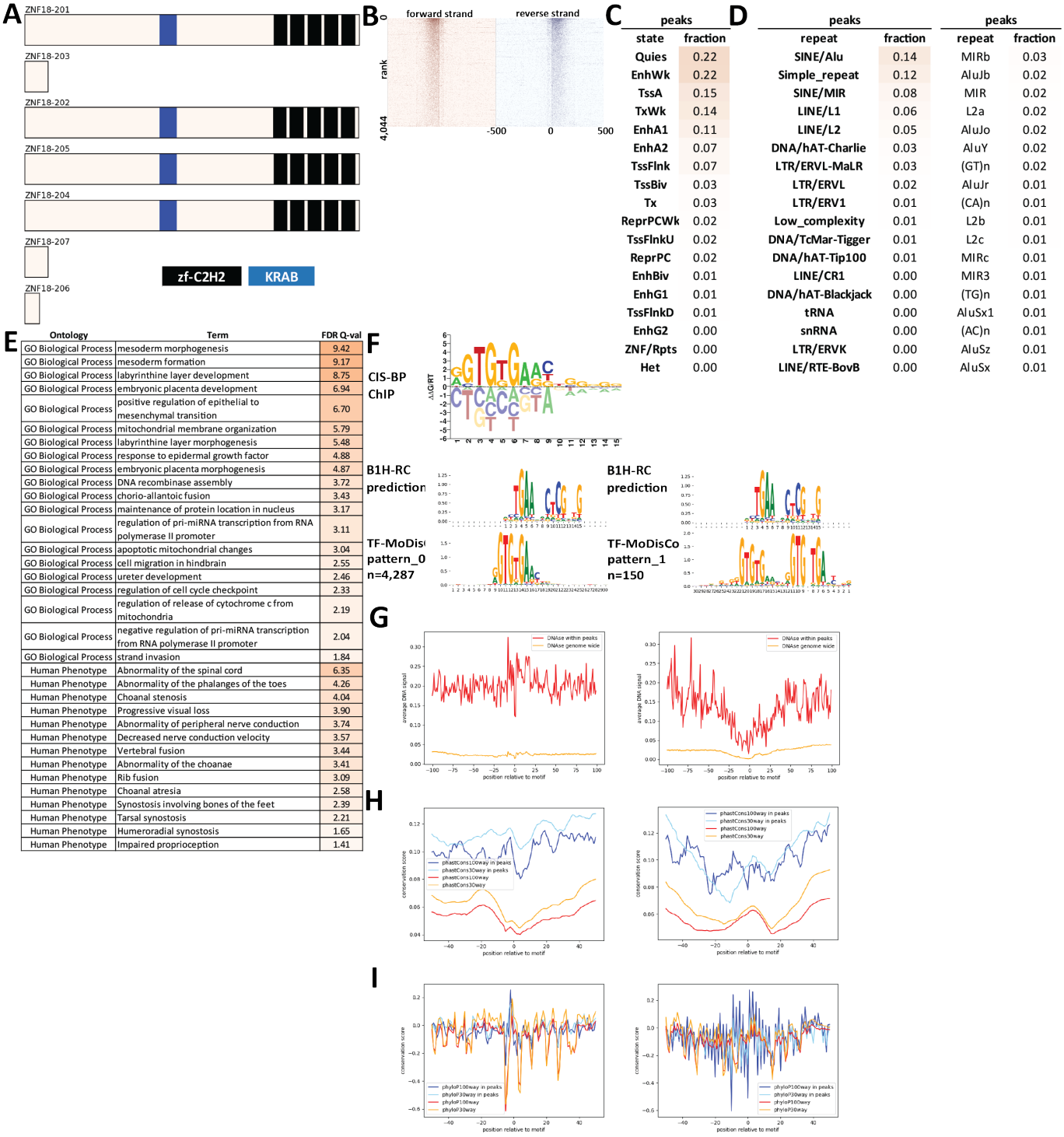

C

peaks	
state	fraction
Quies	0.22
EnhWk	0.22
TssA	0.15
TxWk	0.14
EnhA1	0.11
EnhA2	0.07
TssFlnk	0.07
TssBiv	0.03
Tx	0.03
ReprPCWk	0.02
TssFlnkU	0.02
ReprPC	0.02
EnhBiv	0.01
EnhG1	0.01
TssFlnkD	0.01
EnhG2	0.00
ZNF/Rpts	0.00
Het	0.00

D

peaks		peaks	
repeat	fraction	repeat	fraction
SINE/Alu	0.14	MIRb	0.03
Simple_repeat	0.12	AluJb	0.02
SINE/MIR	0.08	MIR	0.02
LINE/L1	0.06	L2a	0.02
LINE/L2	0.05	AluJo	0.02
DNA/hAT-Charlie	0.03	AluY	0.02
LTR/ERVL-MaLR	0.03	(GT)n	0.02
LTR/ERVL	0.02	AluJr	0.01
LTR/ERV1	0.01	(CA)n	0.01
Low_complexity	0.01	L2b	0.01
DNA/TcMar-Tigger	0.01	L2c	0.01
DNA/hAT-Tip100	0.01	MIRc	0.01
LINE/CR1	0.00	MIR3	0.01
DNA/hAT-Blackjack	0.00	(TG)n	0.01
tRNA	0.00	AluSx1	0.01
snRNA	0.00	(AC)n	0.01
LTR/ERVK	0.00	AluSz	0.01
LINE/RTE-BovB	0.00	AluSx	0.01

E

Ontology	Term	FDR Q-val
GO Biological Process	mesoderm morphogenesis	9.42
GO Biological Process	mesoderm formation	9.17
GO Biological Process	labyrinthine layer development	8.75
GO Biological Process	embryonic placenta development	6.94
GO Biological Process	positive regulation of epithelial to mesenchymal transition	6.70
GO Biological Process	mitochondrial membrane organization	5.79
GO Biological Process	labyrinthine layer morphogenesis	5.48
GO Biological Process	response to epidermal growth factor	4.88
GO Biological Process	embryonic placenta morphogenesis	4.87
GO Biological Process	DNA recombinase assembly	3.72
GO Biological Process	chorio-allantoic fusion	3.43
GO Biological Process	maintenance of protein location in nucleus	3.17
GO Biological Process	regulation of pri-miRNA transcription from RNA polymerase II promoter	3.11
GO Biological Process	apoptotic mitochondrial changes	3.04
GO Biological Process	cell migration in hindbrain	2.55
GO Biological Process	ureter development	2.46
GO Biological Process	regulation of cell cycle checkpoint	2.33
GO Biological Process	regulation of release of cytochrome c from mitochondria	2.19
GO Biological Process	negative regulation of pri-miRNA transcription from RNA polymerase II promoter	2.04
GO Biological Process	strand invasion	1.84
Human Phenotype	Abnormality of the spinal cord	6.35
Human Phenotype	Abnormality of the phalanges of the toes	4.26
Human Phenotype	Choanal stenosis	4.04
Human Phenotype	Progressive visual loss	3.90
Human Phenotype	Abnormality of peripheral nerve conduction	3.74
Human Phenotype	Decreased nerve conduction velocity	3.57
Human Phenotype	Vertebral fusion	3.44
Human Phenotype	Abnormality of the choanae	3.41
Human Phenotype	Rib fusion	3.09
Human Phenotype	Choanal atresia	2.58
Human Phenotype	Synostosis involving bones of the feet	2.39
Human Phenotype	Tarsal synostosis	2.21
Human Phenotype	Humeroradial synostosis	1.65
Human Phenotype	Impaired proprioception	1.41

Supplementary Figure 801: Properties and genomic distribution of motifs identified for the ZNF18 transcription factor in HEK293 (accession Hughes GR models).

TF-MoDisCO pattern_0 n=4287, CWM

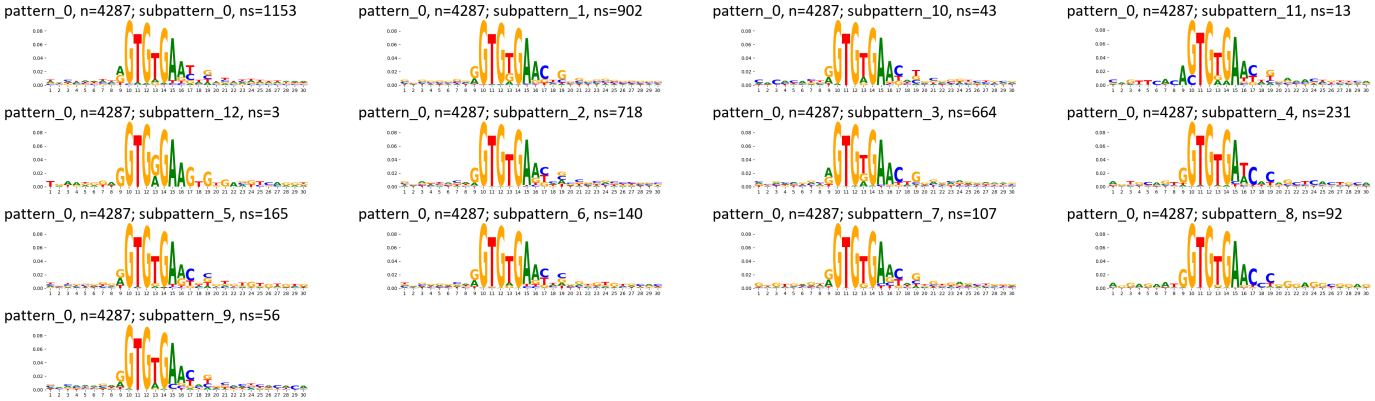

TF-MoDisCO pattern_0 n=4287, PWM

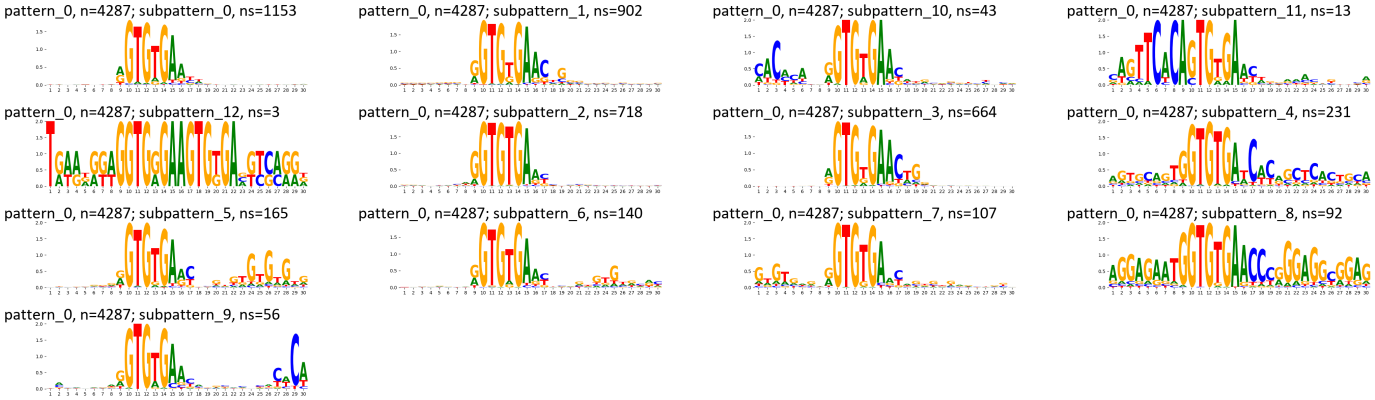

TF-MoDisCO pattern_1 n=150, CWM

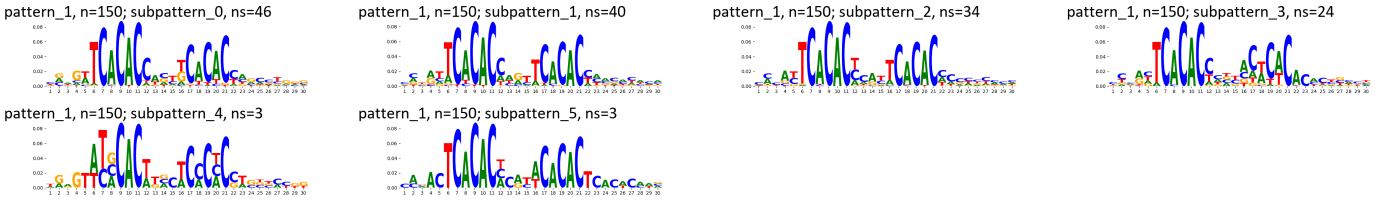

TF-MoDisCO pattern_1 n=150, PWM

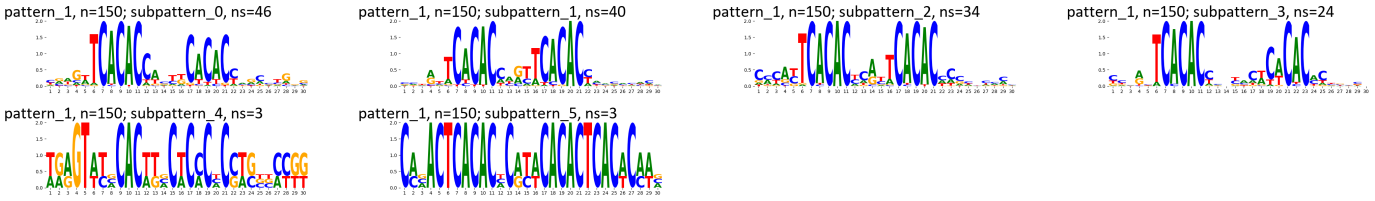

Supplementary Figure 802: TF-MoDisCO subpatterns for the ZNF18 transcription factor in HEK293 (accession Hughes GR models).

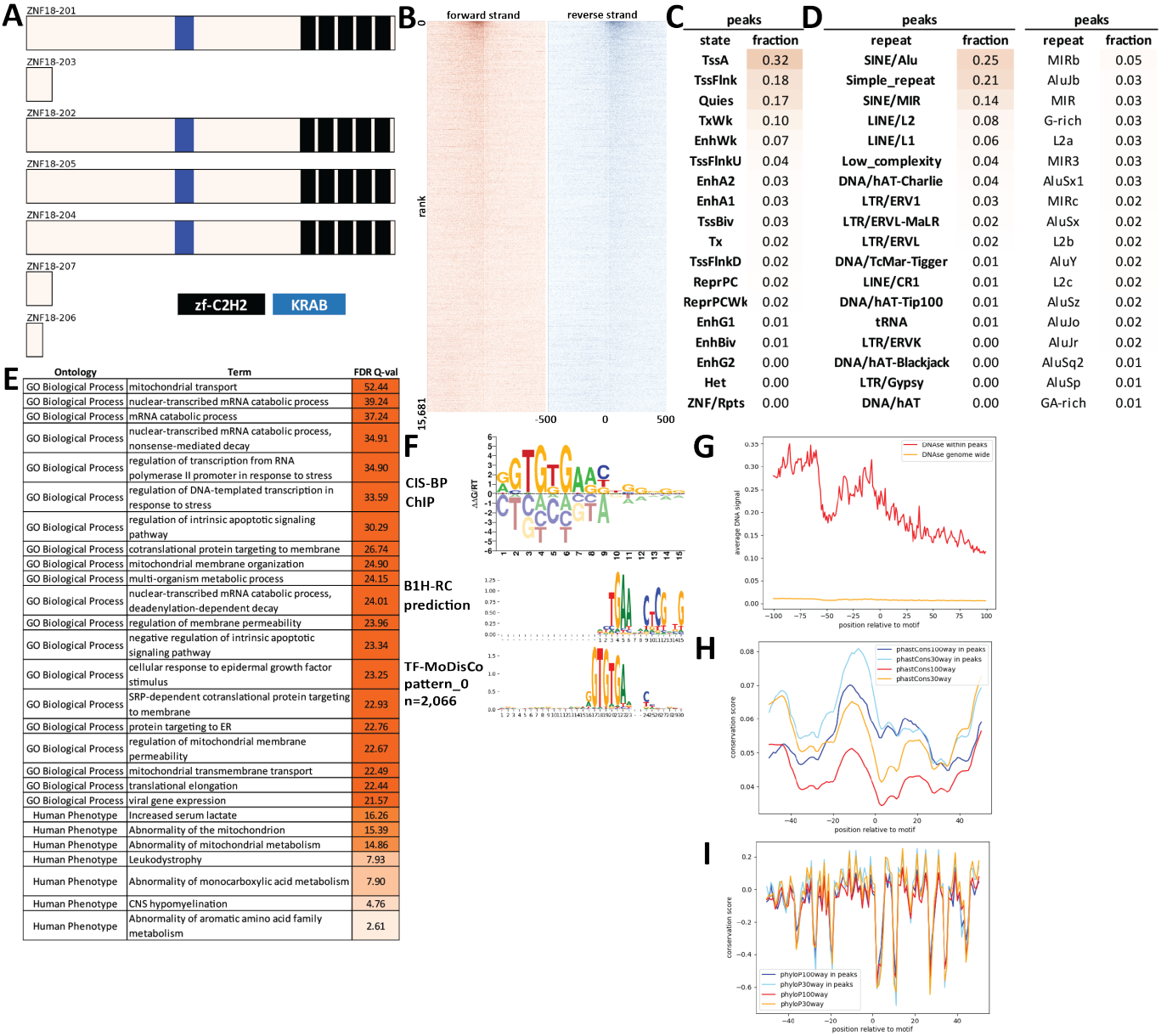

Supplementary Figure 803: Properties and genomic distribution of motifs identified for the ZNF18 transcription factor in HepG2 (accession ENCSR553ZJQ).

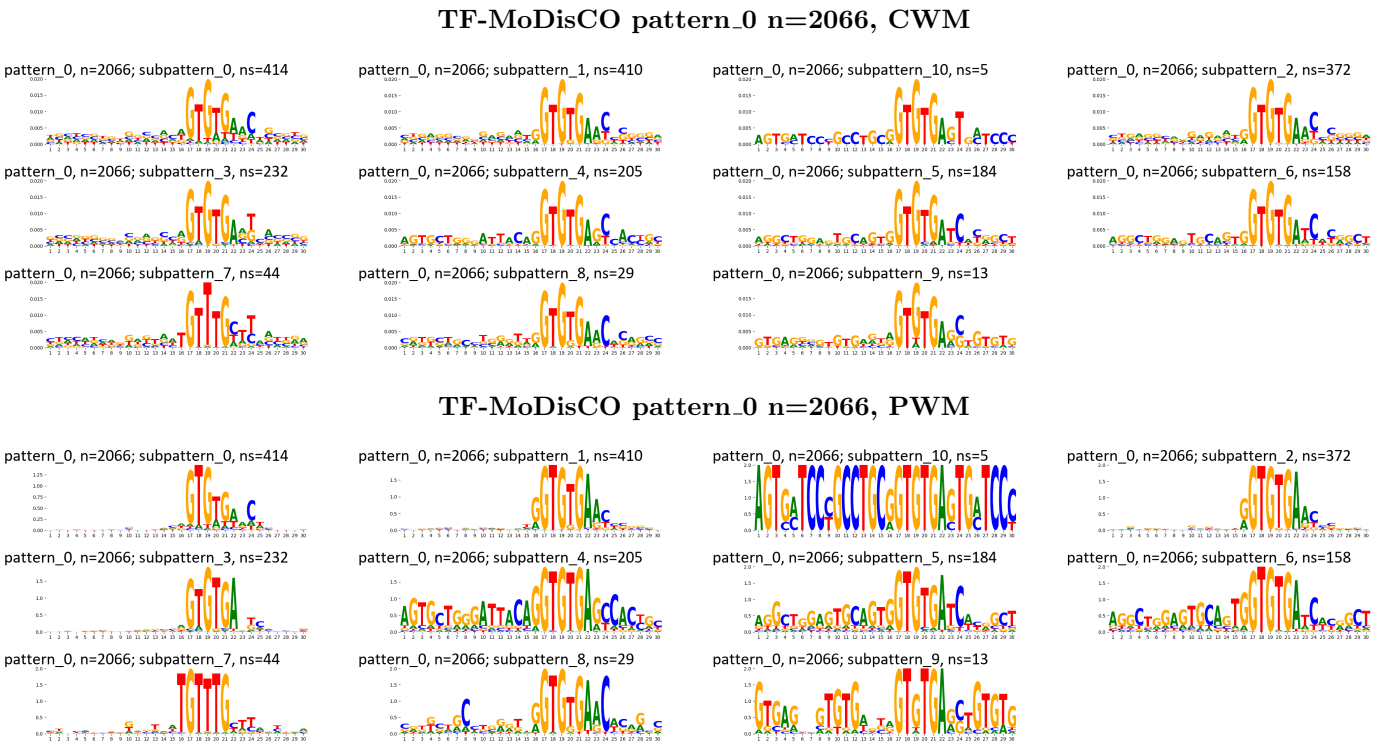

Supplementary Figure 804: TF-MoDisCO subpatterns for the ZNF18 transcription factor in HepG2 (accession ENCSR553ZJQ).

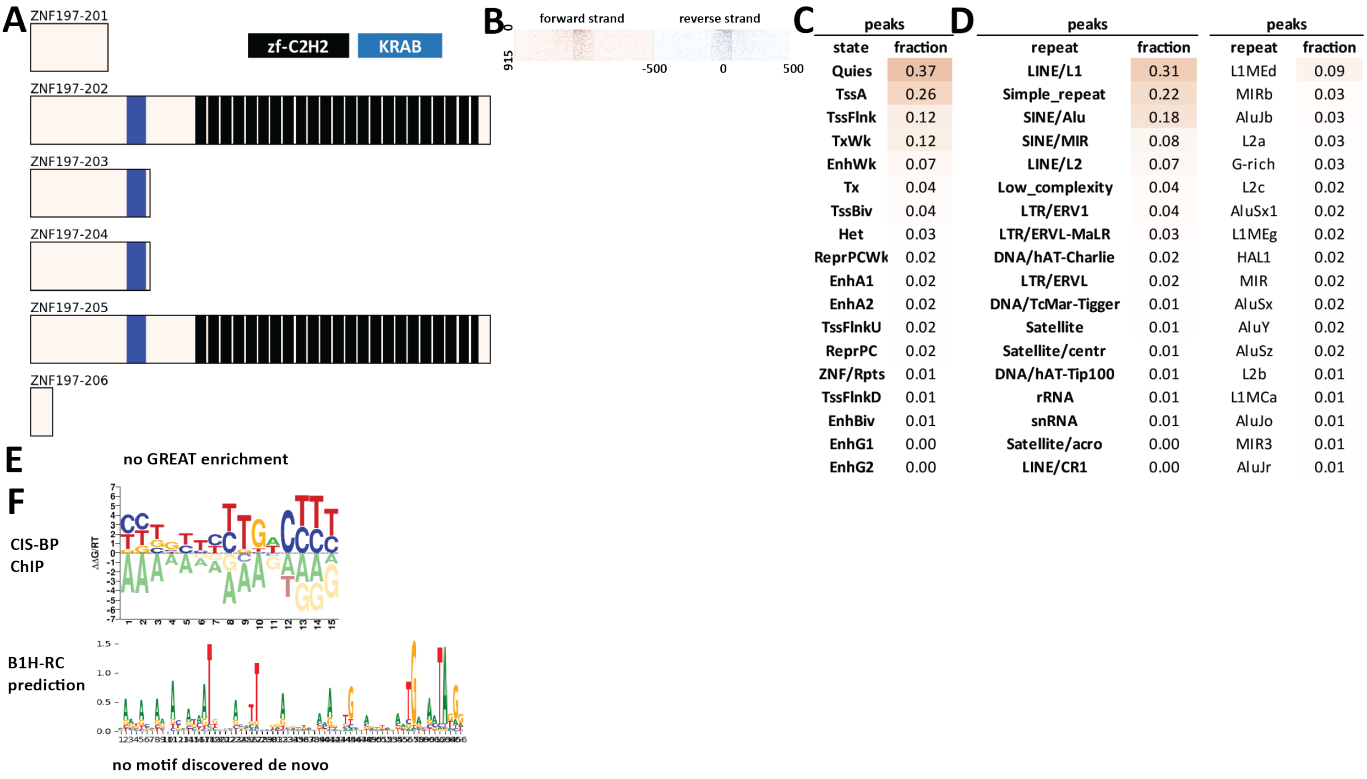

peaks	
state	fraction
Quies	0.37
TssA	0.26
TssFlnk	0.12
TxWk	0.12
EnhWk	0.07
Tx	0.04
TssBiv	0.04
Het	0.03
ReprPCWk	0.02
EnhA1	0.02
EnhA2	0.02
TssFlnkU	0.02
ReprPC	0.02
ZNF/Rpts	0.01
TssFlnkD	0.01
EnhBiv	0.01
EnhG1	0.00
EnhG2	0.00

peaks	
repeat	fraction
LINE/L1	0.31
Simple_repeat	0.22
SINE/Alu	0.18
SINE/MIR	0.08
LINE/L2	0.07
Low_complexity	0.04
LTR/ERV1	0.04
LTR/ERVL-MaLR	0.03
DNA/hAT-Charlie	0.02
LTR/ERVL	0.02
DNA/TcMar-Tigger	0.01
Satellite	0.01
Satellite/centr	0.01
DNA/hAT-Tip100	0.01
rRNA	0.01
snRNA	0.01
Satellite/acro	0.00
LINE/CR1	0.00

peaks	
repeat	fraction
L1MEd	0.09
MIRb	0.03
AluJb	0.03
L2a	0.03
G-rich	0.03
L2c	0.02
AluSx1	0.02
L1MEg	0.02
HAL1	0.02
MIR	0.02
AluSx	0.02
AluY	0.02
AluSz	0.02
L2b	0.01
L1MCa	0.01
AluJo	0.01
MIR3	0.01
AluJr	0.01

Supplementary Figure 805: Properties and genomic distribution of motifs identified for the ZNF197 transcription factor in HEK293 (accession ChipExo models).

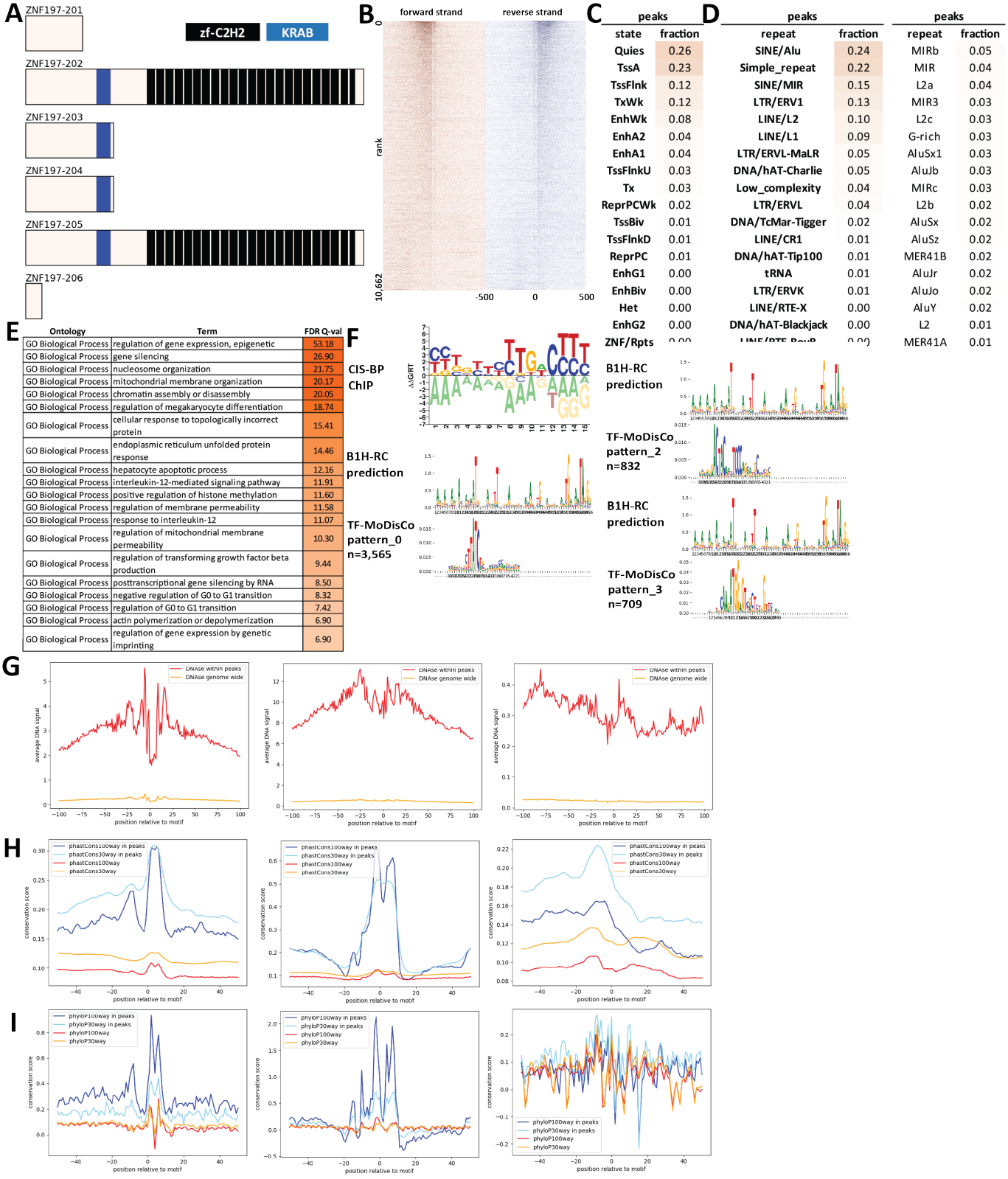

peaks	
state	fraction
Quies	0.26
TssA	0.23
TssFlnk	0.12
TxWk	0.12
EnhWk	0.08
EnhA2	0.04
EnhA1	0.04
TssFlnkU	0.03
Tx	0.03
ReprPCWk	0.02
TssBiv	0.01
TssFlnkD	0.01
ReprPC	0.01
EnhG1	0.00
EnhBiv	0.00
Het	0.00
EnhG2	0.00
ZNF/Rpts	0.00

peaks		peaks	
repeat	fraction	repeat	fraction
SINE/Alu	0.24	MIRb	0.05
Simple_repeat	0.22	MIR	0.04
SINE/MIR	0.15	L2a	0.04
LTR/ERV1	0.13	MIR3	0.03
LINE/L2	0.10	L2c	0.03
LINE/L1	0.09	G-rich	0.03
LTR/ERVL-MaLR	0.05	AluSx1	0.03
DNA/hAT-Charlie	0.05	AluJb	0.03
Low_complexity	0.04	MIRc	0.03
LTR/ERVL	0.04	L2b	0.02
DNA/TcMar-Tigger	0.02	AluSx	0.02
LINE/CR1	0.01	AluSz	0.02
DNA/hAT-Tip100	0.01	MER41B	0.02
tRNA	0.01	AluJr	0.02
LTR/ERVK	0.01	AluJo	0.02
LINE/RTE-X	0.00	AluY	0.02
DNA/hAT-Blackjack	0.00	L2	0.01
LINE/RTE-BovB	0.00	MER41A	0.01

Ontology	Term	FDR Q-val
GO Biological Process	regulation of gene expression, epigenetic	53.18
GO Biological Process	gene silencing	26.90
GO Biological Process	nucleosome organization	21.75
GO Biological Process	mitochondrial membrane organization	20.17
GO Biological Process	chromatin assembly or disassembly	20.05
GO Biological Process	regulation of megakaryocyte differentiation	18.74
GO Biological Process	cellular response to topologically incorrect protein	15.41
GO Biological Process	endoplasmic reticulum unfolded protein response	14.46
GO Biological Process	hepatocyte apoptotic process	12.16
GO Biological Process	interleukin-12-mediated signaling pathway	11.91
GO Biological Process	positive regulation of histone methylation	11.60
GO Biological Process	regulation of membrane permeability	11.58
GO Biological Process	response to interleukin-12	11.07
GO Biological Process	regulation of mitochondrial membrane permeability	10.30
GO Biological Process	regulation of transforming growth factor beta production	9.44
GO Biological Process	posttranscriptional gene silencing by RNA	8.50
GO Biological Process	negative regulation of G0 to G1 transition	8.32
GO Biological Process	regulation of G0 to G1 transition	7.42
GO Biological Process	actin polymerization or depolymerization	6.90
GO Biological Process	regulation of gene expression by genetic imprinting	6.90

Supplementary Figure 806: Properties and genomic distribution of motifs identified for the ZNF197 transcription factor in K562 (accession ENCSR580IAO).

TF-MoDisCO pattern_0 n=3565, CWM

pattern_0, n=3565; subpattern_0, ns=1029

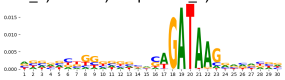

pattern_0, n=3565; subpattern_1, ns=863

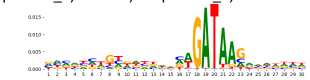

pattern_0, n=3565; subpattern_10, ns=6

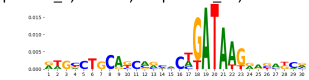

pattern_0, n=3565; subpattern_11, ns=2

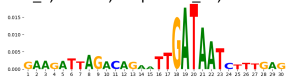

pattern_0, n=3565; subpattern_12, ns=2

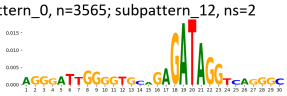

pattern_0, n=3565; subpattern_13, ns=2

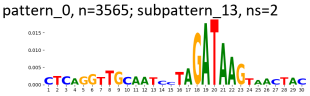

pattern_0, n=3565; subpattern_2, ns=780

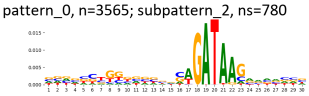

pattern_0, n=3565; subpattern_3, ns=569

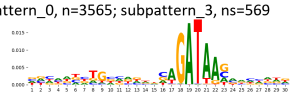

pattern_0, n=3565; subpattern_4, ns=156

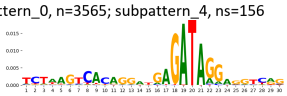

pattern_0, n=3565; subpattern_5, ns=62

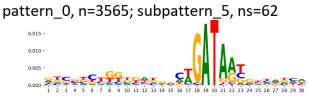

pattern_0, n=3565; subpattern_6, ns=34

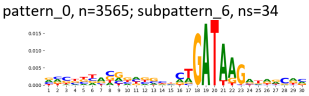

pattern_0, n=3565; subpattern_7, ns=30

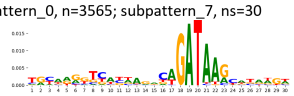

pattern_0, n=3565; subpattern_8, ns=15

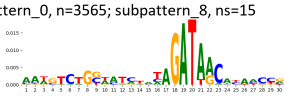

pattern_0, n=3565; subpattern_9, ns=15

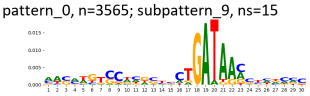

TF-MoDisCO pattern_0 n=3565, PWM

pattern_0, n=3565; subpattern_0, ns=1029

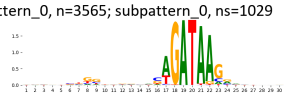

pattern_0, n=3565; subpattern_1, ns=863

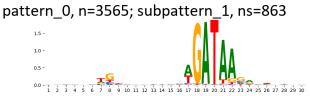

pattern_0, n=3565; subpattern_10, ns=6

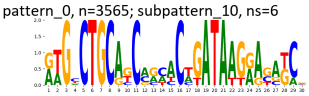

pattern_0, n=3565; subpattern_11, ns=2

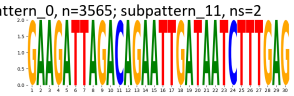

pattern_0, n=3565; subpattern_12, ns=2

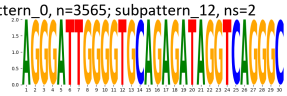

pattern_0, n=3565; subpattern_13, ns=2

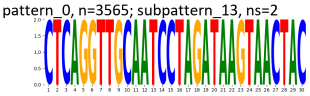

pattern_0, n=3565; subpattern_2, ns=780

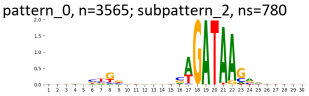

pattern_0, n=3565; subpattern_3, ns=569

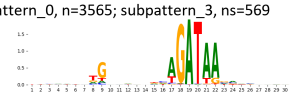

pattern_0, n=3565; subpattern_4, ns=156

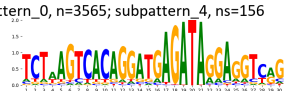

pattern_0, n=3565; subpattern_5, ns=62

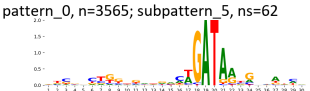

pattern_0, n=3565; subpattern_6, ns=34

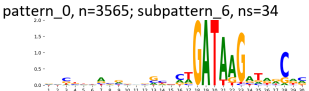

pattern_0, n=3565; subpattern_7, ns=30

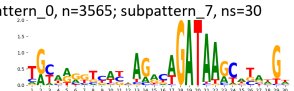

pattern_0, n=3565; subpattern_8, ns=15

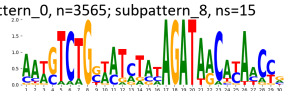

pattern_0, n=3565; subpattern_9, ns=15

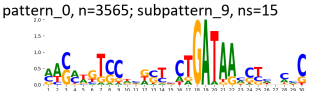

TF-MoDisCO pattern_2 n=832, CWM

pattern_2, n=832; subpattern_0, ns=376

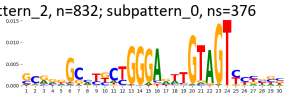

pattern_2, n=832; subpattern_1, ns=316

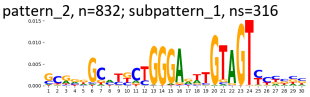

pattern_2, n=832; subpattern_2, ns=137

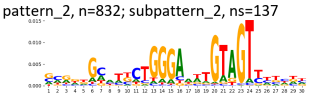

pattern_2, n=832; subpattern_3, ns=3

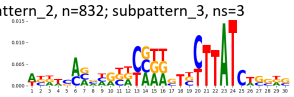

TF-MoDisCO pattern_2 n=832, PWM

pattern_2, n=832; subpattern_0, ns=376

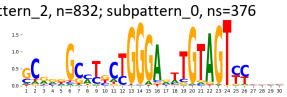

pattern_2, n=832; subpattern_1, ns=316

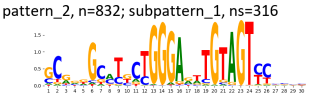

pattern_2, n=832; subpattern_2, ns=137

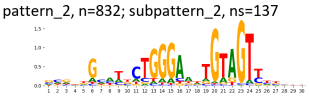

pattern_2, n=832; subpattern_3, ns=3

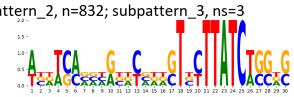

TF-MoDisCO pattern_3 n=709, CWM

pattern_3, n=709; subpattern_0, ns=187

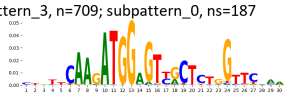

pattern_3, n=709; subpattern_1, ns=167

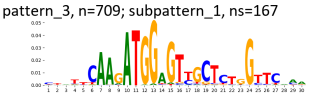

pattern_3, n=709; subpattern_2, ns=140

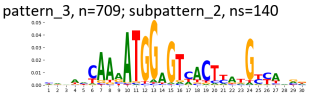

pattern_3, n=709; subpattern_3, ns=132

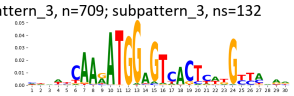

pattern_3, n=709; subpattern_4, ns=52

pattern_3, n=709; subpattern_5, ns=27

pattern_3, n=709; subpattern_6, ns=2

pattern_3, n=709; subpattern_7, ns=2

TF-MoDisCO pattern_3 n=709, PWM

pattern_3, n=709; subpattern_0, ns=187

pattern_3, n=709; subpattern_1, ns=167

pattern_3, n=709; subpattern_2, ns=140

pattern_3, n=709; subpattern_3, ns=132

pattern_3, n=709; subpattern_4, ns=52

pattern_3, n=709; subpattern_5, ns=27

pattern_3, n=709; subpattern_6, ns=2

pattern_3, n=709; subpattern_7, ns=2

Supplementary Figure 807: TF-MoDisCO subpatterns for the ZNF197 transcription factor in K562 (accession ENCSR580IAO).

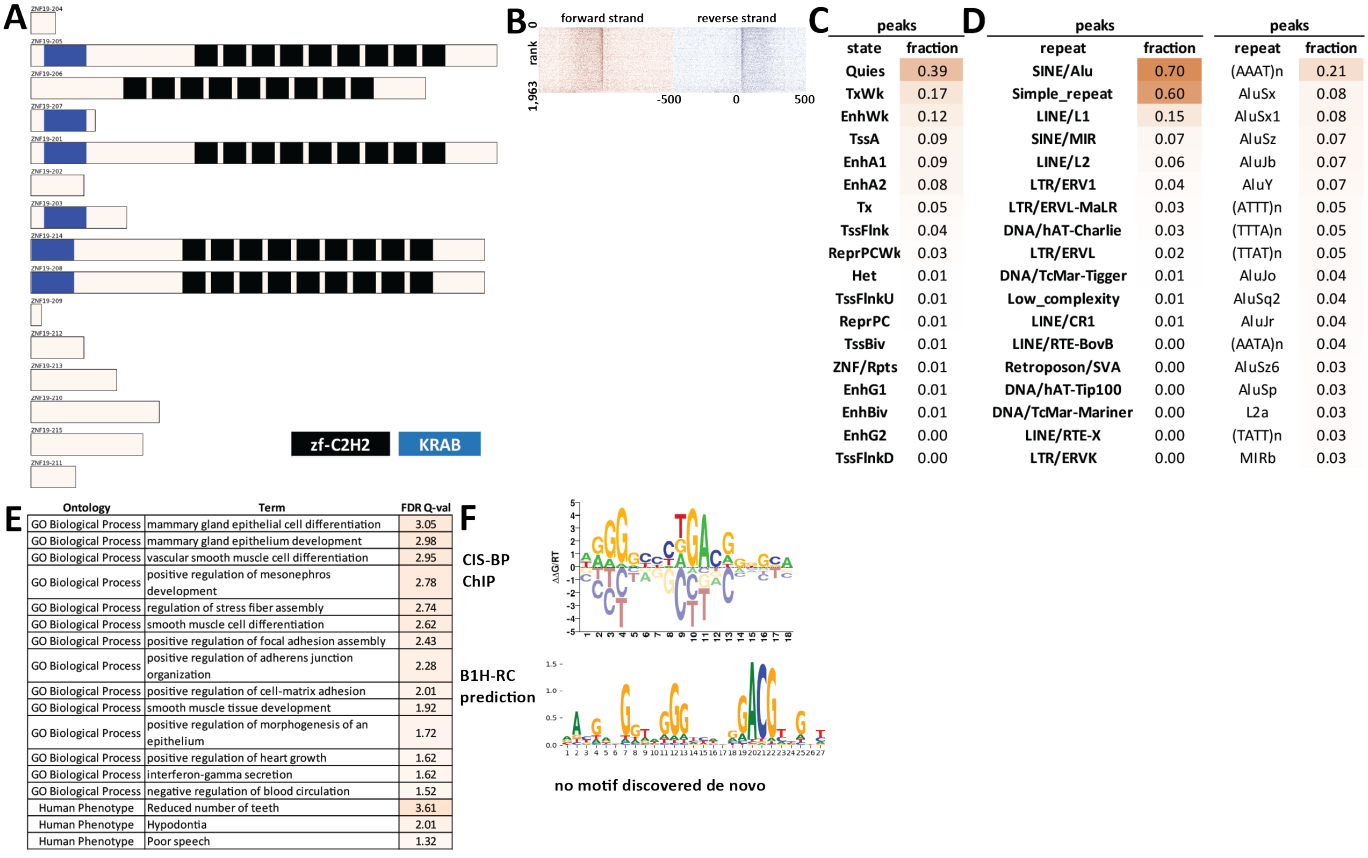

Supplementary Figure 808: Properties and genomic distribution of motifs identified for the ZNF19 transcription factor in HEK293 (accession ENCSR811JJM).

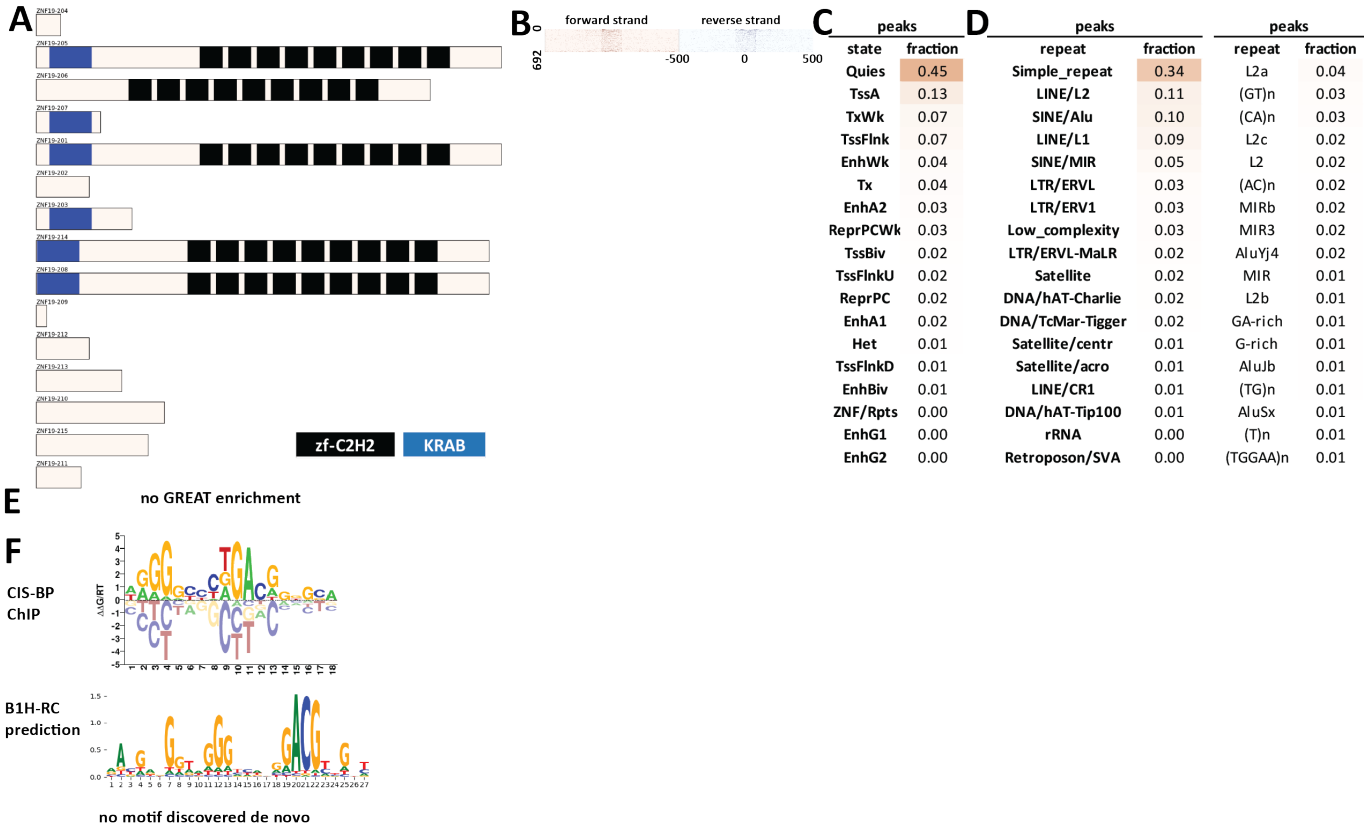

Supplementary Figure 809: Properties and genomic distribution of motifs identified for the ZNF19 transcription factor in HEK293 (accession ChipExo models).

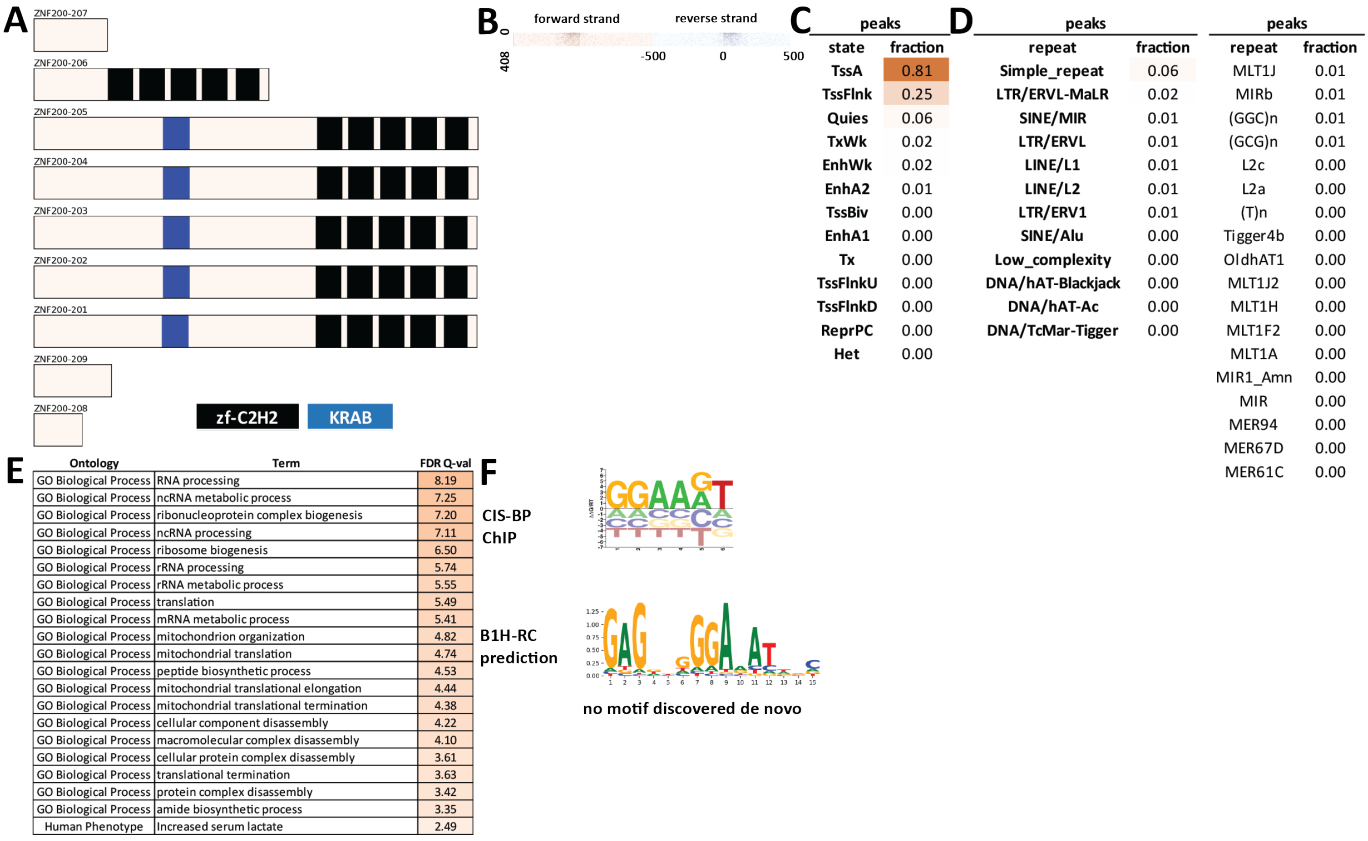

Supplementary Figure 810: Properties and genomic distribution of motifs identified for the ZNF200 transcription factor in HEK293 (accession Hughes NB models).

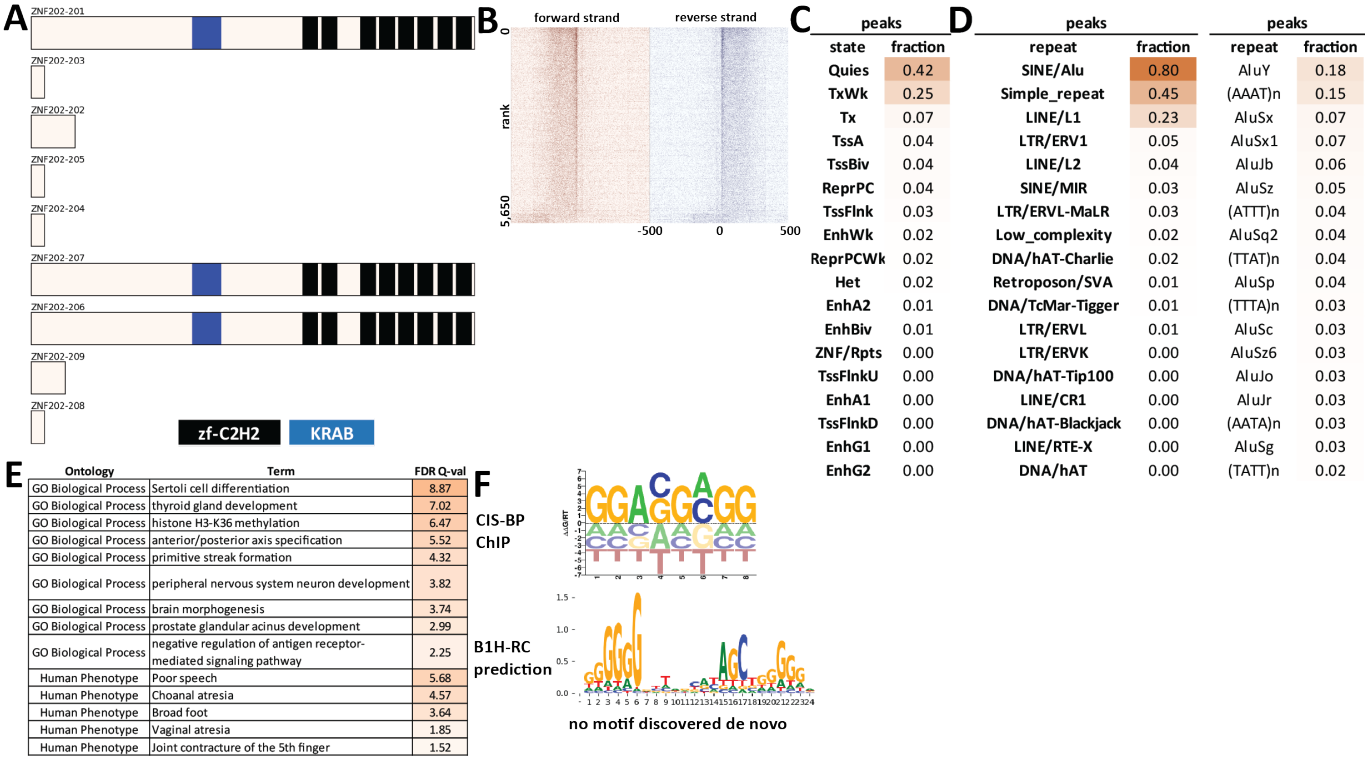

C

peaks	
state	fraction
Quies	0.42
TxWk	0.25
Tx	0.07
TssA	0.04
TssBiv	0.04
ReprPC	0.04
TssFlnk	0.03
EnhWk	0.02
ReprPCWk	0.02
Het	0.02
EnhA2	0.01
EnhBiv	0.01
ZNF/Rpts	0.00
TssFlnkU	0.00
EnhA1	0.00
TssFlnkD	0.00
EnhG1	0.00
EnhG2	0.00

D

peaks		peaks	
repeat	fraction	repeat	fraction
SINE/Alu	0.80	AluY	0.18
Simple_repeat	0.45	(AAAT)n	0.15
LINE/L1	0.23	AluSx	0.07
LTR/ERV1	0.05	AluSx1	0.07
LINE/L2	0.04	AluJb	0.06
SINE/MIR	0.03	AluSz	0.05
LTR/ERVL-MaLR	0.03	(ATTT)n	0.04
Low_complexity	0.02	AluSq2	0.04
DNA/hAT-Charlie	0.02	(TTAT)n	0.04
Retroposon/SVA	0.01	AluSp	0.04
DNA/TcMar-Tigger	0.01	(TTTA)n	0.03
LTR/ERVL	0.01	AluSc	0.03
LTR/ERVK	0.00	AluSz6	0.03
DNA/hAT-Tip100	0.00	AluJo	0.03
LINE/CR1	0.00	AluJr	0.03
DNA/hAT-Blackjack	0.00	(AATA)n	0.03
LINE/RTE-X	0.00	AluSg	0.03
DNA/hAT	0.00	(TATT)n	0.02

E

Ontology	Term	FDR Q-val
GO Biological Process	Sertoli cell differentiation	8.87
GO Biological Process	thyroid gland development	7.02
GO Biological Process	histone H3-K36 methylation	6.47
GO Biological Process	anterior/posterior axis specification	5.52
GO Biological Process	primitive streak formation	4.32
GO Biological Process	peripheral nervous system neuron development	3.82
GO Biological Process	brain morphogenesis	3.74
GO Biological Process	prostate glandular acinus development	2.99
GO Biological Process	negative regulation of antigen receptor-mediated signaling pathway	2.25
Human Phenotype	Poor speech	5.68
Human Phenotype	Choanal atresia	4.57
Human Phenotype	Broad foot	3.64
Human Phenotype	Vaginal atresia	1.85
Human Phenotype	Joint contracture of the 5th finger	1.52

Supplementary Figure 811: Properties and genomic distribution of motifs identified for the ZNF202 transcription factor in HEK293 (accession ENCSR996FYT).

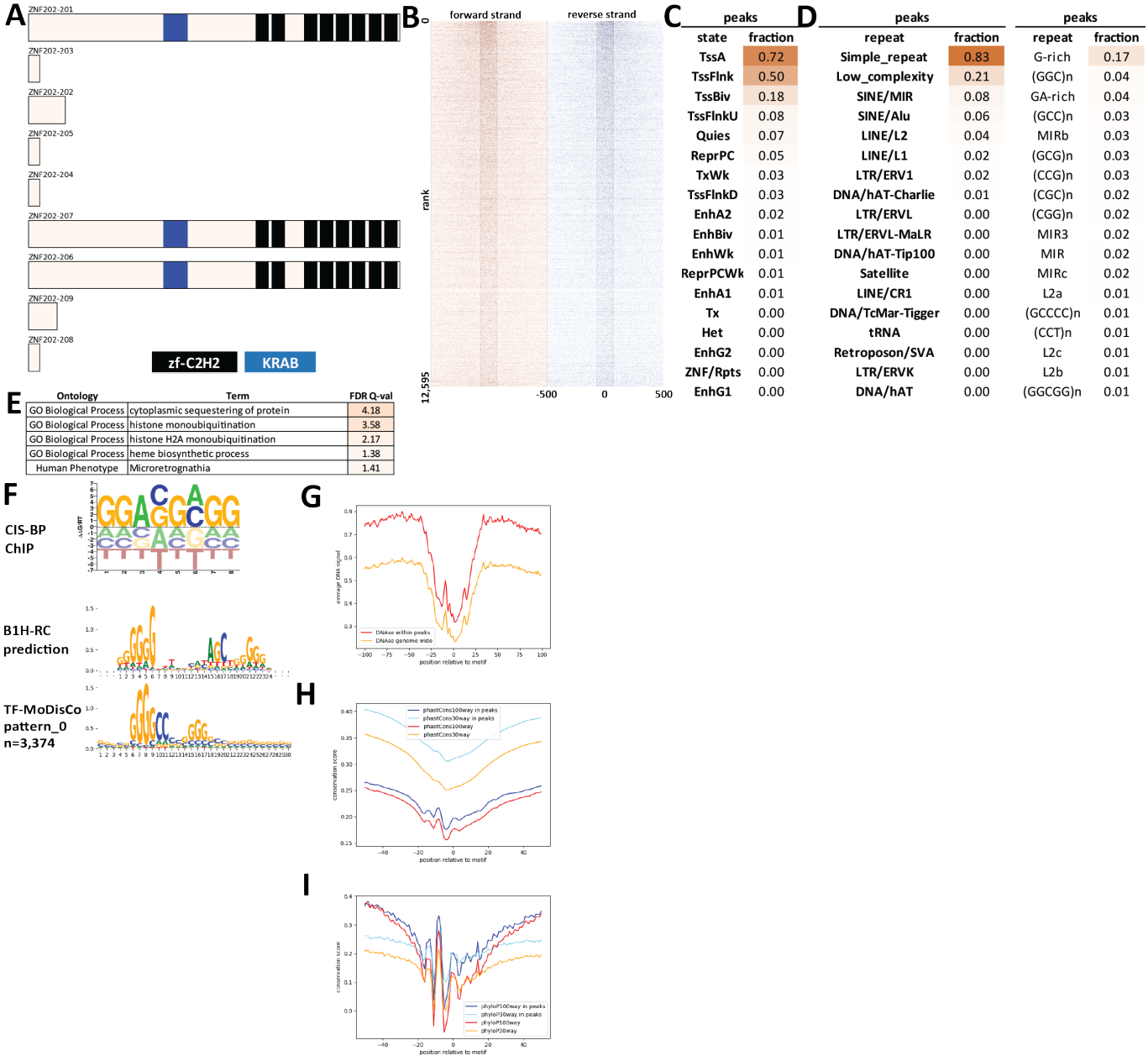

Supplementary Figure 812: Properties and genomic distribution of motifs identified for the ZNF202 transcription factor in HEK293 (accession ChipExo models).

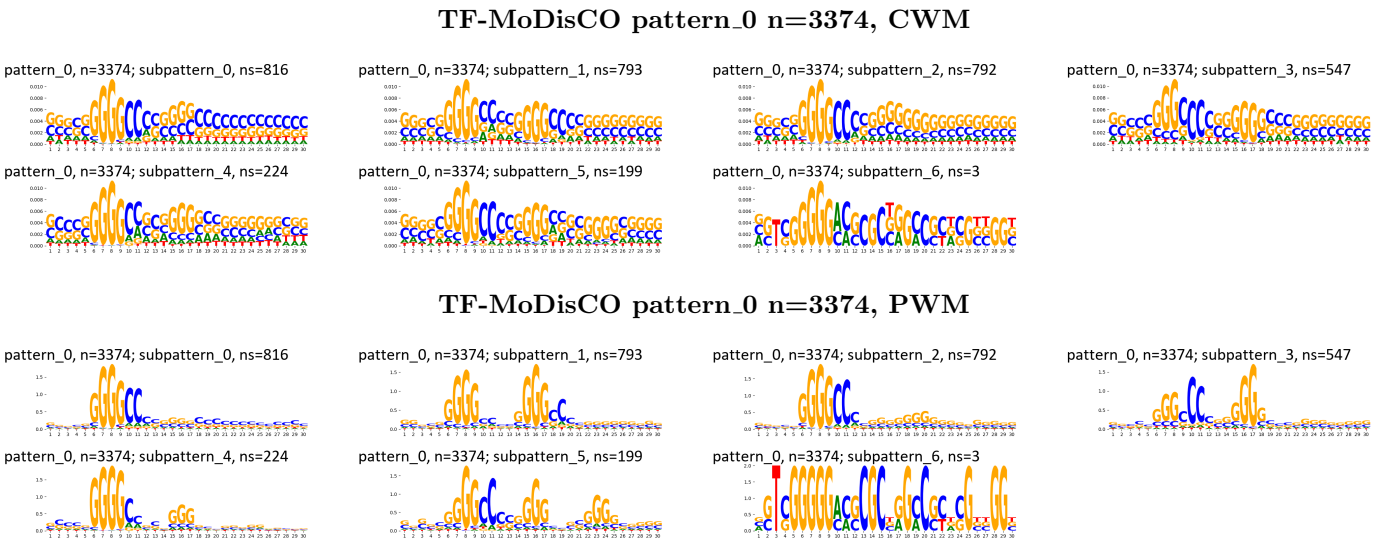

Supplementary Figure 813: TF-MoDisCO subpatterns for the ZNF202 transcription factor in HEK293 (accession ChipExo models).

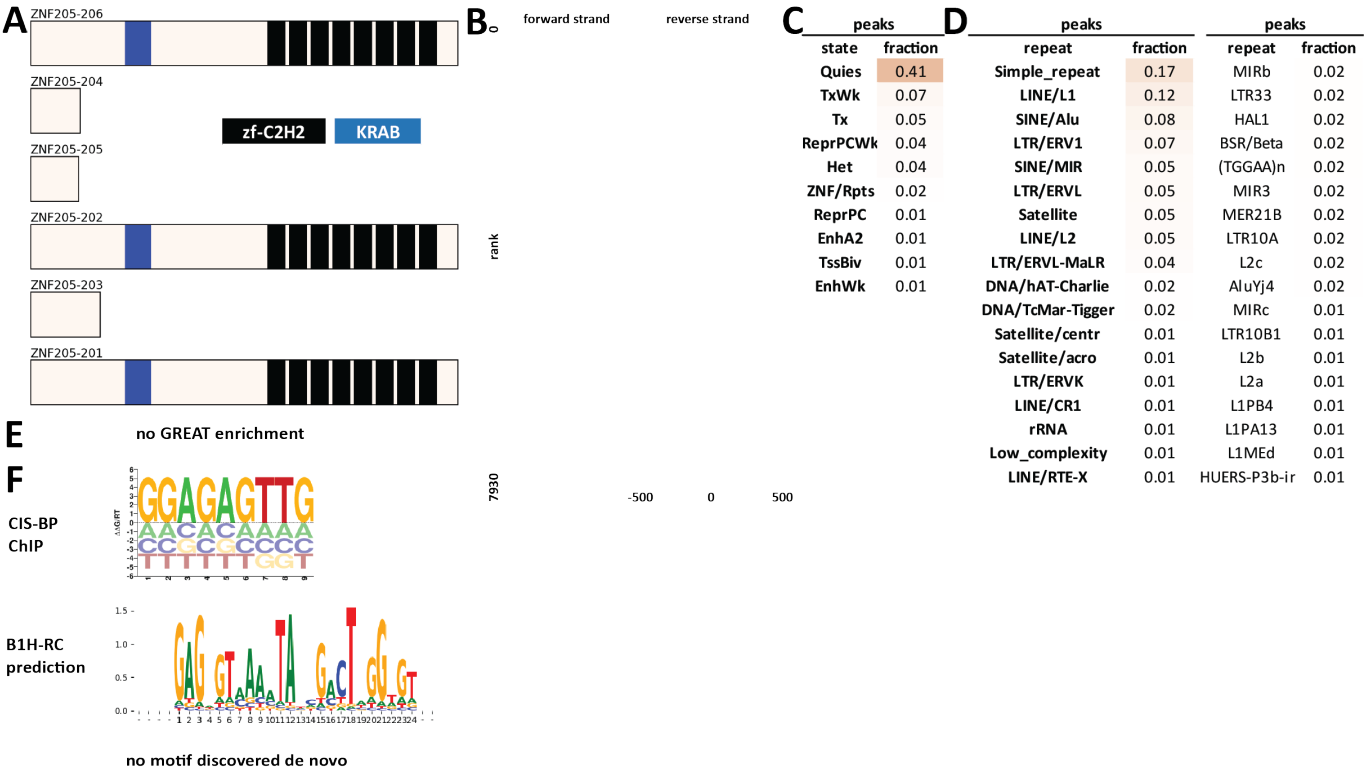

C

peaks	
state	fraction
Quies	0.41
TxWk	0.07
Tx	0.05
ReprPCWk	0.04
Het	0.04
ZNF/Rpts	0.02
ReprPC	0.01
EnhA2	0.01
TssBiv	0.01
EnhWk	0.01

D

peaks		peaks	
repeat	fraction	repeat	fraction
Simple_repeat	0.17	MIRb	0.02
LINE/L1	0.12	LTR33	0.02
SINE/Alu	0.08	HAL1	0.02
LTR/ERV1	0.07	BSR/Beta	0.02
SINE/MIR	0.05	(TGGAA)n	0.02
LTR/ERVL	0.05	MIR3	0.02
Satellite	0.05	MER21B	0.02
LINE/L2	0.05	LTR10A	0.02
LTR/ERVL-MaLR	0.04	L2c	0.02
DNA/hAT-Charlie	0.02	AluYj4	0.02
DNA/TcMar-Tigger	0.02	MIRc	0.01
Satellite/centr	0.01	LTR10B1	0.01
Satellite/acro	0.01	L2b	0.01
LTR/ERVK	0.01	L2a	0.01
LINE/CR1	0.01	L1PB4	0.01
rRNA	0.01	L1PA13	0.01
Low_complexity	0.01	L1MEd	0.01
LINE/RTE-X	0.01	HUERS-P3b-ir	0.01

Supplementary Figure 814: Properties and genomic distribution of motifs identified for the ZNF205 transcription factor in HEK293 (accession ChipExo models).

TF-MoDisCO pattern_0 n=128, CWM

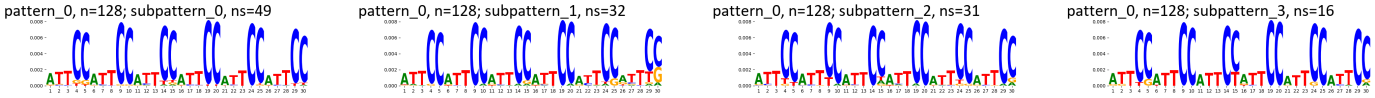

TF-MoDisCO pattern_0 n=128, PWM

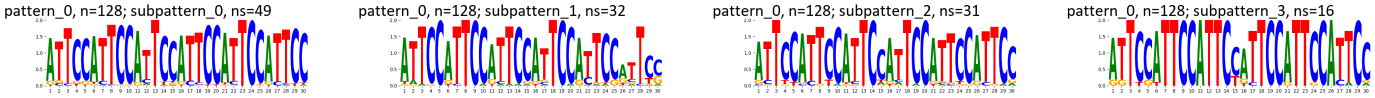

Supplementary Figure 815: TF-MoDisCO subpatterns for the ZNF205 transcription factor in HEK293 (accession ChipExo models).

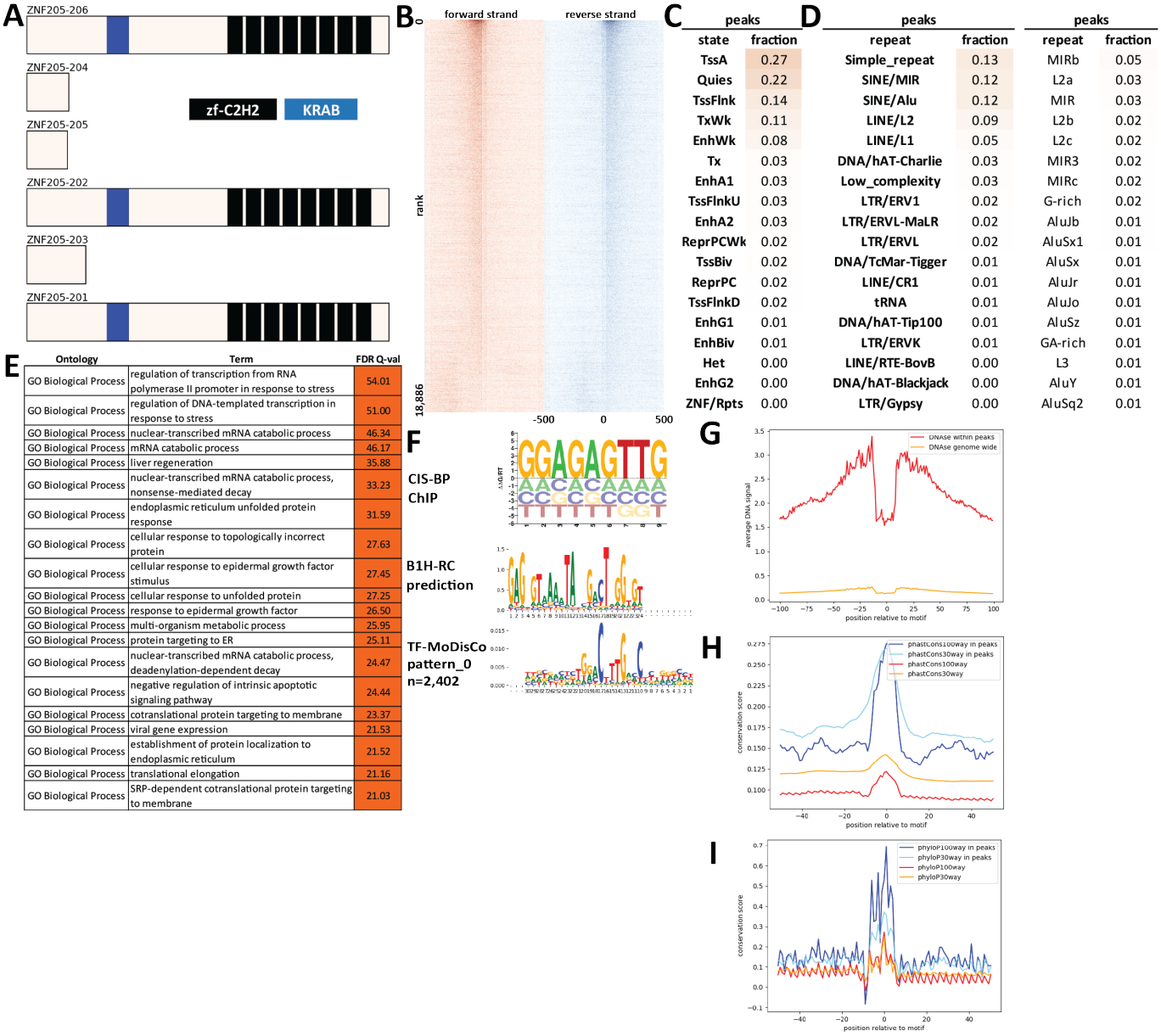

Supplementary Figure 816: Properties and genomic distribution of motifs identified for the ZNF205 transcription factor in HepG2 (accession ENCSR157CEN).

TF-MoDisCO pattern_0 n=2402, CWM

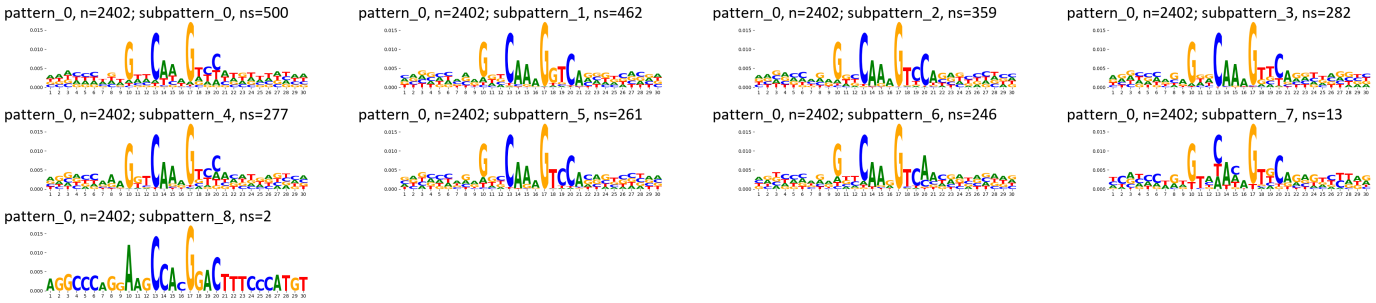

TF-MoDisCO pattern_0 n=2402, PWM

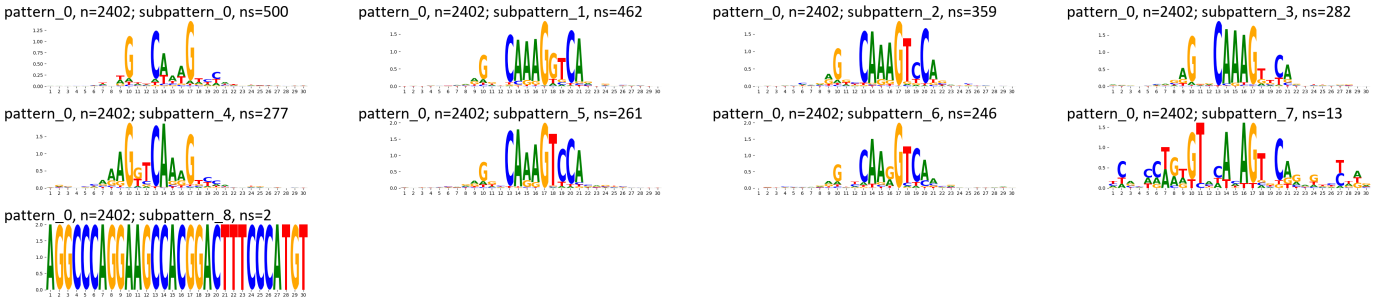

Supplementary Figure 817: TF-MoDisCO subpatterns for the ZNF205 transcription factor in HepG2 (accession ENCSR157CEN).

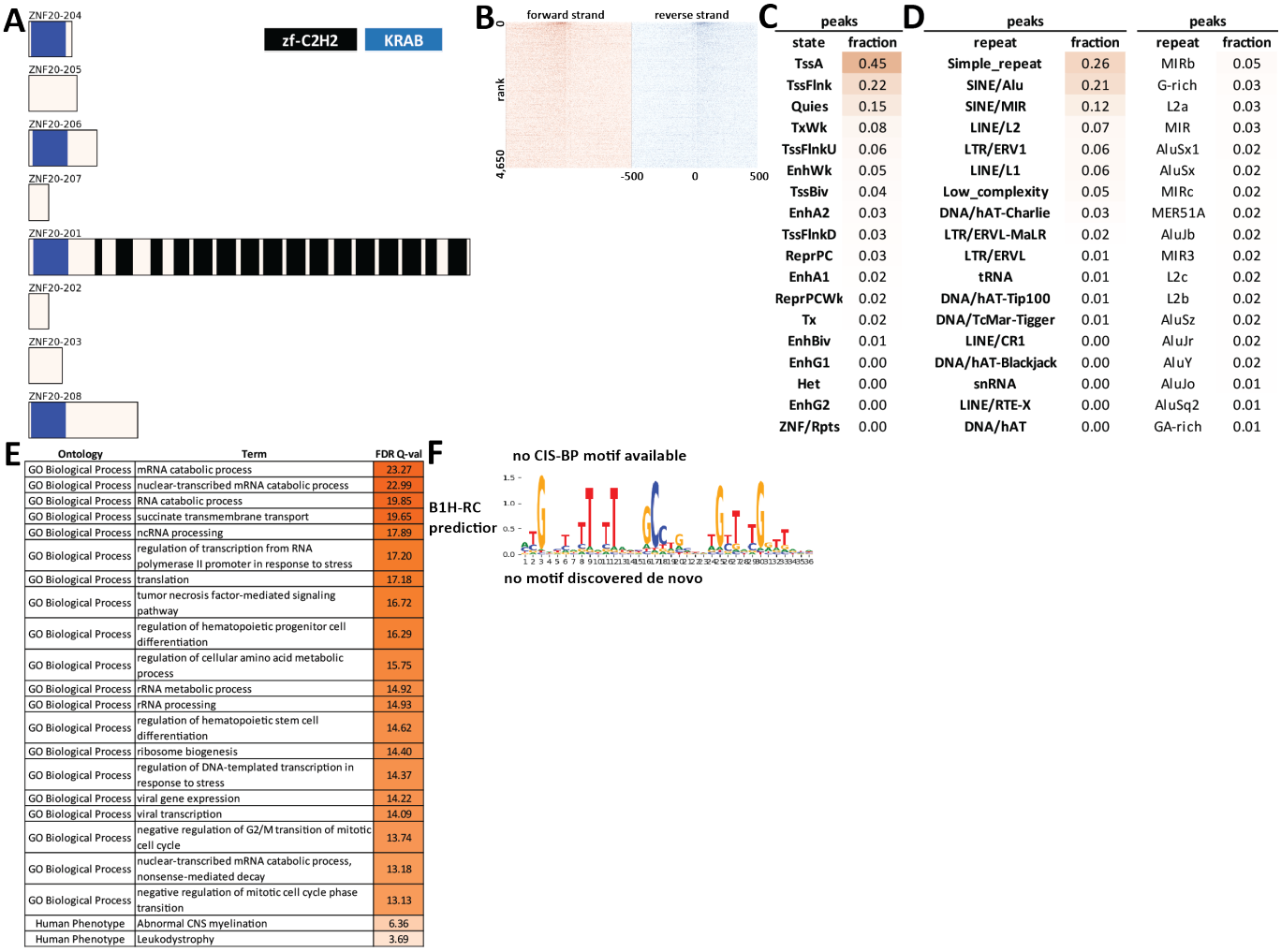

Supplementary Figure 818: Properties and genomic distribution of motifs identified for the ZNF20 transcription factor in HepG2 (accession ENCSR720PDY).

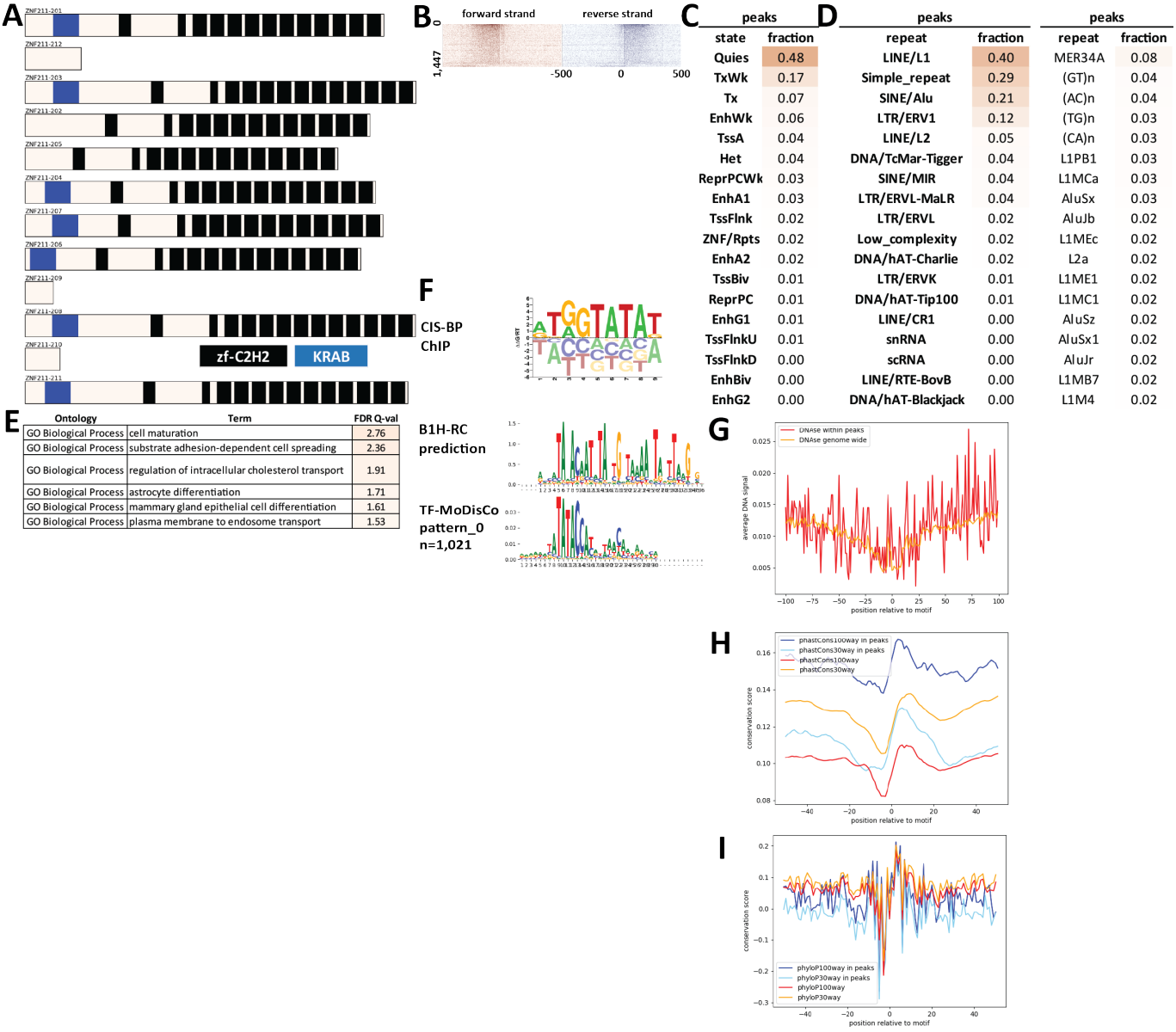

C

peaks	
state	fraction
Quies	0.48
TxWk	0.17
Tx	0.07
EnhWk	0.06
TssA	0.04
Het	0.04
ReprPCWk	0.03
EnhA1	0.03
TssFlnk	0.02
ZNF/Rpts	0.02
EnhA2	0.02
TssBiv	0.01
ReprPC	0.01
EnhG1	0.01
TssFlnkU	0.01
TssFlnkD	0.00
EnhBiv	0.00
EnhG2	0.00

D

peaks		peaks	
repeat	fraction	repeat	fraction
LINE/L1	0.40	MER34A	0.08
Simple_repeat	0.29	(GT)n	0.04
SINE/Alu	0.21	(AC)n	0.04
LTR/ERV1	0.12	(TG)n	0.03
LINE/L2	0.05	(CA)n	0.03
DNA/TcMar-Tigger	0.04	L1PB1	0.03
SINE/MIR	0.04	L1MCa	0.03
LTR/ERVL-MaLR	0.04	AluSx	0.03
LTR/ERVL	0.02	AluJb	0.02
Low_complexity	0.02	L1MEc	0.02
DNA/hAT-Charlie	0.02	L2a	0.02
LTR/ERVK	0.01	L1ME1	0.02
DNA/hAT-Tip100	0.01	L1MC1	0.02
LINE/CR1	0.00	AluSz	0.02
snRNA	0.00	AluSx1	0.02
scRNA	0.00	AluJr	0.02
LINE/RTE-BovB	0.00	L1MB7	0.02
DNA/hAT-Blackjack	0.00	L1M4	0.02

E

Ontology	Term	FDR Q-val
GO Biological Process	cell maturation	2.76
GO Biological Process	substrate adhesion-dependent cell spreading	2.36
GO Biological Process	regulation of intracellular cholesterol transport	1.91
GO Biological Process	astrocyte differentiation	1.71
GO Biological Process	mammary gland epithelial cell differentiation	1.61
GO Biological Process	plasma membrane to endosome transport	1.53

Supplementary Figure 819: Properties and genomic distribution of motifs identified for the ZNF211 transcription factor in HEK293 (accession ENCSR365DQH).

TF-MoDisCO pattern_0 n=1021, CWM

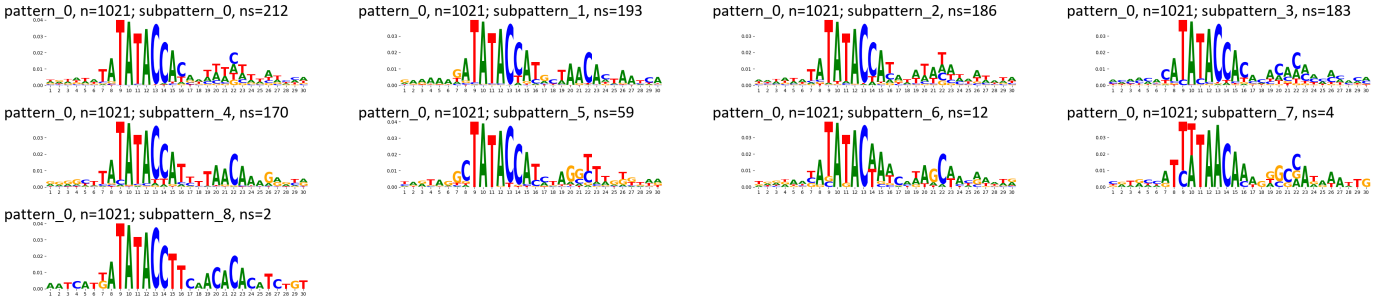

TF-MoDisCO pattern_0 n=1021, PWM

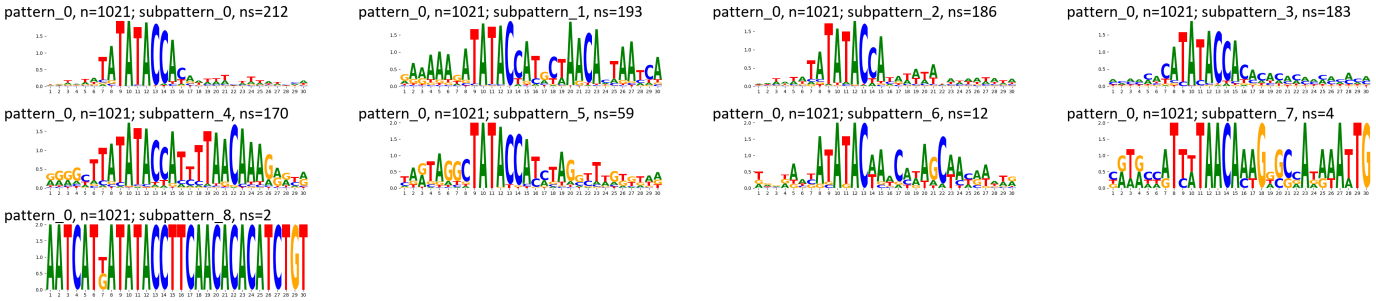

Supplementary Figure 820: TF-MoDisCO subpatterns for the ZNF211 transcription factor in HEK293 (accession ENCSR365DQH).

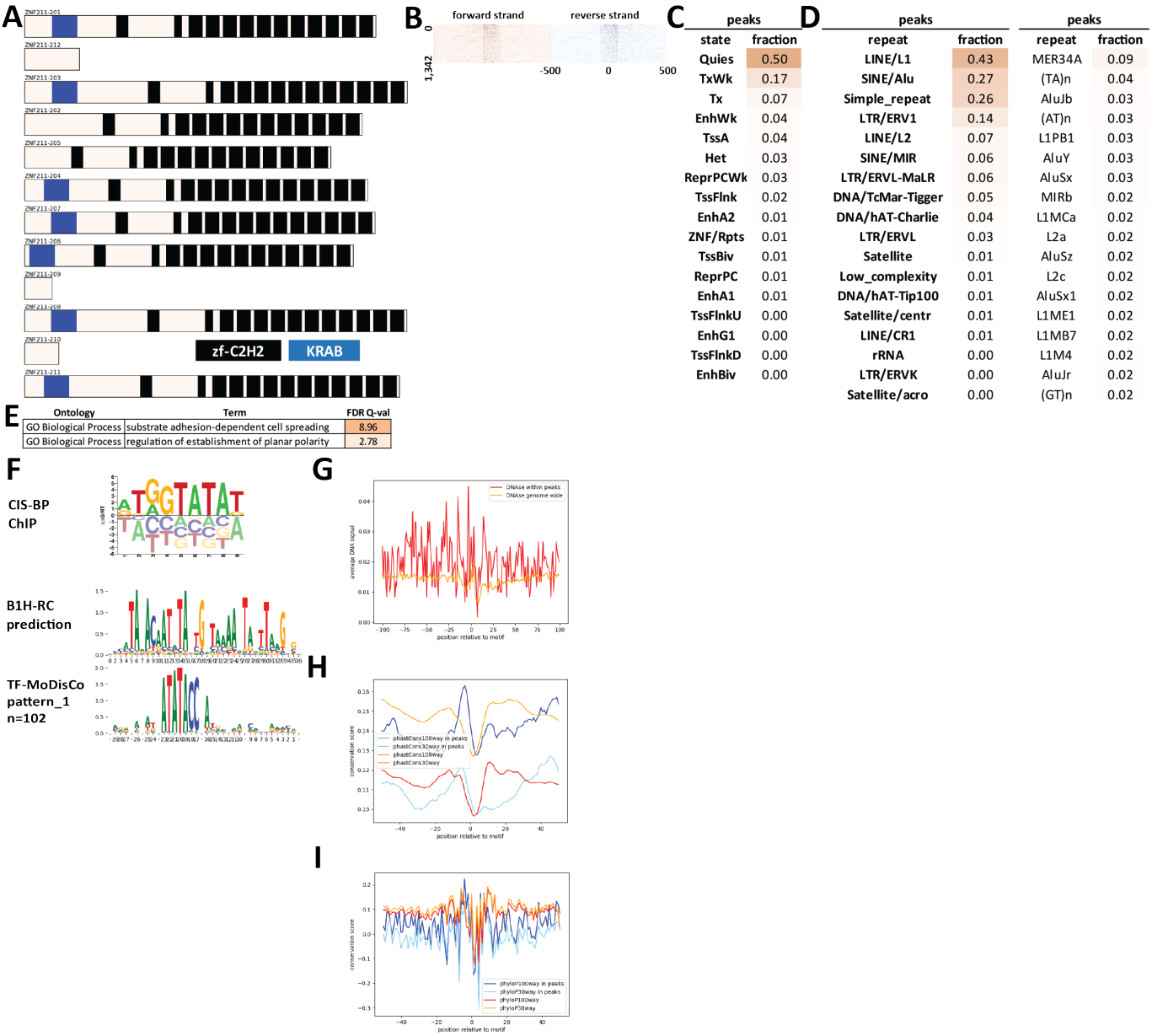

peaks	
state	fraction
Quies	0.50
TxWk	0.17
Tx	0.07
EnhWk	0.04
TssA	0.04
Het	0.03
ReprPCWk	0.03
TssFlnk	0.02
EnhA2	0.01
ZNF/Rpts	0.01
TssBiv	0.01
ReprPC	0.01
EnhA1	0.01
TssFlnkU	0.00
EnhG1	0.00
TssFlnkD	0.00
EnhBiv	0.00

peaks		peaks	
repeat	fraction	repeat	fraction
LINE/L1	0.43	MER34A	0.09
SINE/Alu	0.27	(TA)n	0.04
Simple_repeat	0.26	AluJb	0.03
LTR/ERV1	0.14	(AT)n	0.03
LINE/L2	0.07	L1PB1	0.03
SINE/MIR	0.06	AluY	0.03
LTR/ERVL-MaLR	0.06	AluSx	0.03
DNA/TcMar-Tigger	0.05	MIRb	0.02
DNA/hAT-Charlie	0.04	L1MCa	0.02
LTR/ERVL	0.03	L2a	0.02
Satellite	0.01	AluSz	0.02
Low_complexity	0.01	L2c	0.02
DNA/hAT-Tip100	0.01	AluSx1	0.02
Satellite/centr	0.01	L1ME1	0.02
LINE/CR1	0.01	L1MB7	0.02
rRNA	0.00	L1M4	0.02
LTR/ERVK	0.00	AluJr	0.02
Satellite/acro	0.00	(GT)n	0.02

Supplementary Figure 821: Properties and genomic distribution of motifs identified for the ZNF211 transcription factor in HEK293 (accession ChipExo models).

TF-MoDisCO pattern_1 n=102, CWM

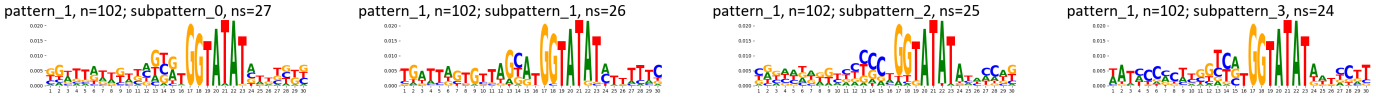

TF-MoDisCO pattern_1 n=102, PWM

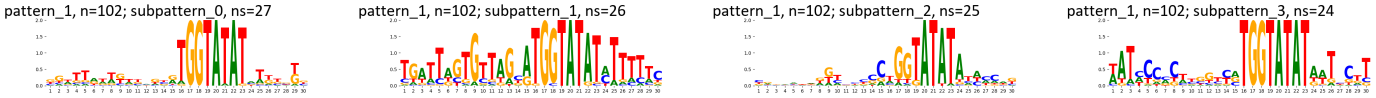

Supplementary Figure 822: TF-MoDisCO subpatterns for the ZNF211 transcription factor in HEK293 (accession ChipExo models).

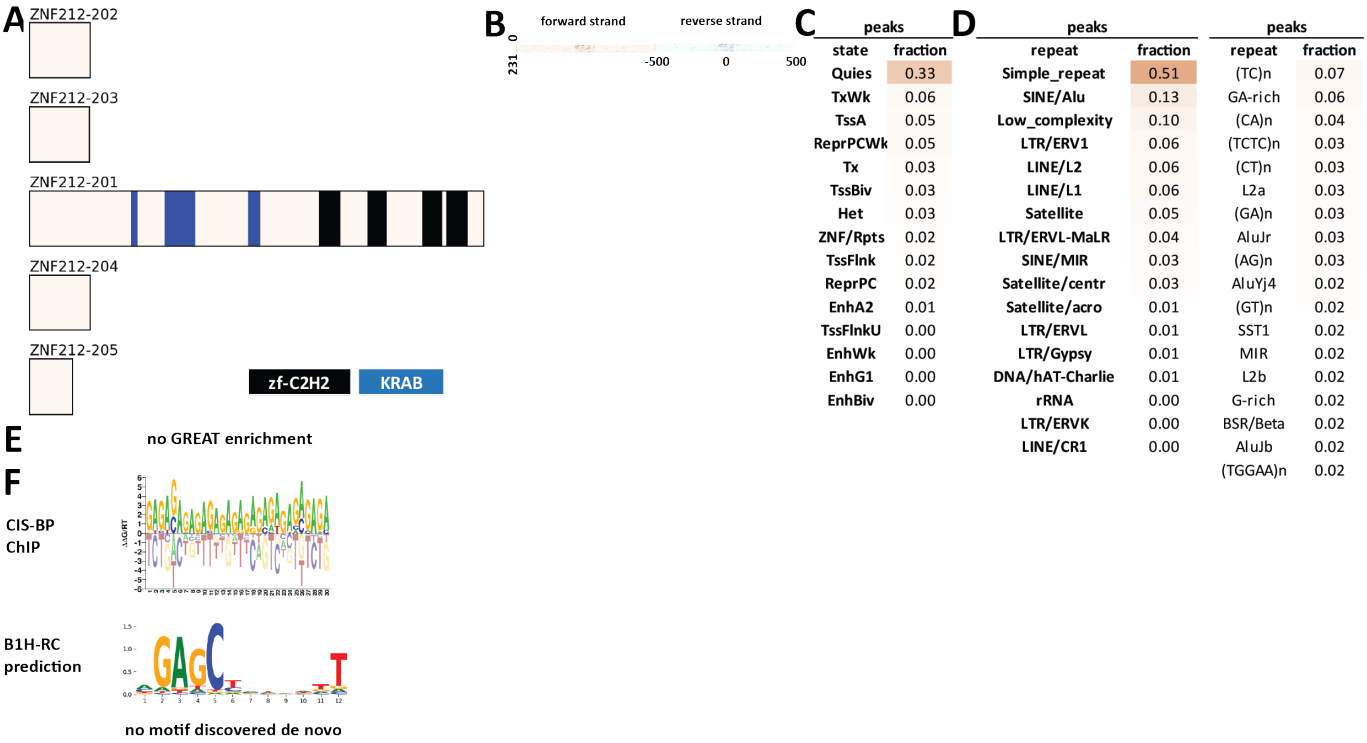

C

peaks	
state	fraction
Quies	0.33
TxWk	0.06
TssA	0.05
ReprPCWk	0.05
Tx	0.03
TssBiv	0.03
Het	0.03
ZNF/Rpts	0.02
TssFlnk	0.02
ReprPC	0.02
EnhA2	0.01
TssFlnkU	0.00
EnhWk	0.00
EnhG1	0.00
EnhBiv	0.00

D

peaks		peaks	
repeat	fraction	repeat	fraction
Simple_repeat	0.51	(TC)n	0.07
SINE/Alu	0.13	GA-rich	0.06
Low_complexity	0.10	(CA)n	0.04
LTR/ERV1	0.06	(TCTC)n	0.03
LINE/L2	0.06	(CT)n	0.03
LINE/L1	0.06	L2a	0.03
Satellite	0.05	(GA)n	0.03
LTR/ERVL-MaLR	0.04	AluJr	0.03
SINE/MIR	0.03	(AG)n	0.03
Satellite/centr	0.03	AluYj4	0.02
Satellite/acro	0.01	(GT)n	0.02
LTR/ERVL	0.01	SST1	0.02
LTR/Gypsy	0.01	MIR	0.02
DNA/hAT-Charlie	0.01	L2b	0.02
rRNA	0.00	G-rich	0.02
LTR/ERVK	0.00	BSR/Beta	0.02
LINE/CR1	0.00	AluJb	0.02
		(TGGAA)n	0.02

Supplementary Figure 823: Properties and genomic distribution of motifs identified for the ZNF212 transcription factor in HEK293 (accession ChipExo models).

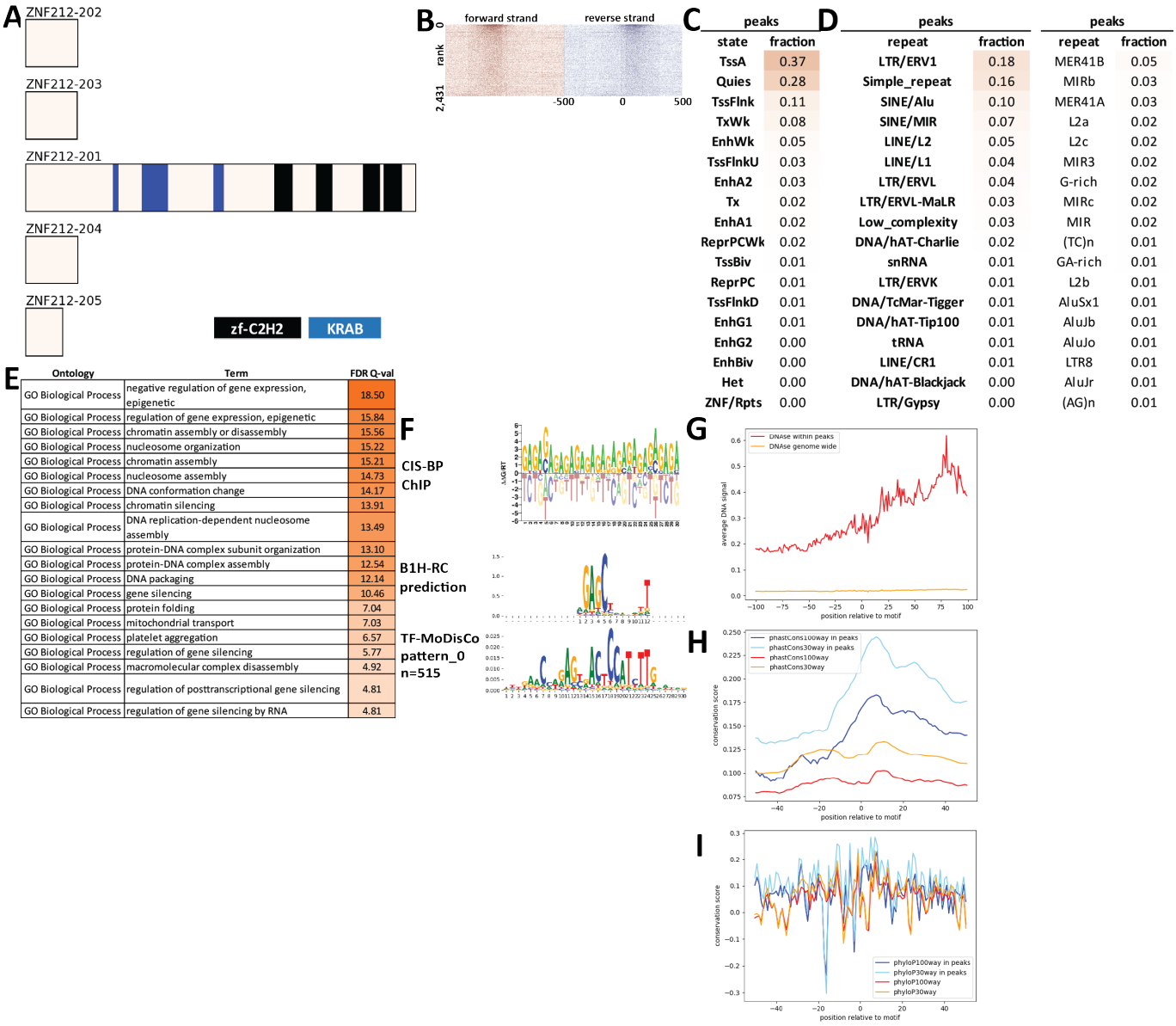

C

peaks	
state	fraction
TssA	0.37
Quies	0.28
TssFlnk	0.11
TxWk	0.08
EnhWk	0.05
TssFlnkU	0.03
EnhA2	0.03
Tx	0.02
EnhA1	0.02
ReprPCWk	0.02
TssBiv	0.01
ReprPC	0.01
TssFlnkD	0.01
EnhG1	0.01
EnhG2	0.00
EnhBiv	0.00
Het	0.00
ZNF/Rpts	0.00

D

peaks		peaks	
repeat	fraction	repeat	fraction
LTR/ERV1	0.18	MER41B	0.05
Simple_repeat	0.16	MIRb	0.03
SINE/Alu	0.10	MER41A	0.03
SINE/MIR	0.07	L2a	0.02
LINE/L2	0.05	L2c	0.02
LINE/L1	0.04	MIR3	0.02
LTR/ERVL	0.04	G-rich	0.02
LTR/ERVL-MaLR	0.03	MIRc	0.02
Low_complexity	0.03	MIR	0.02
DNA/hAT-Charlie	0.02	(TC)n	0.01
snRNA	0.01	GA-rich	0.01
LTR/ERVK	0.01	L2b	0.01
DNA/TcMar-Tigger	0.01	AluSx1	0.01
DNA/hAT-Tip100	0.01	AluJb	0.01
tRNA	0.01	AluJo	0.01
LINE/CR1	0.01	LTR8	0.01
DNA/hAT-Blackjack	0.00	AluJr	0.01
LTR/Gypsy	0.00	(AG)n	0.01

E

Ontology	Term	FDR Q-val
GO Biological Process	negative regulation of gene expression, epigenetic	18.50
GO Biological Process	regulation of gene expression, epigenetic	15.84
GO Biological Process	chromatin assembly or disassembly	15.56
GO Biological Process	nucleosome organization	15.22
GO Biological Process	chromatin assembly	15.21
GO Biological Process	nucleosome assembly	14.73
GO Biological Process	DNA conformation change	14.17
GO Biological Process	chromatin silencing	13.91
GO Biological Process	DNA replication-dependent nucleosome assembly	13.49
GO Biological Process	protein-DNA complex subunit organization	13.10
GO Biological Process	protein-DNA complex assembly	12.54
GO Biological Process	DNA packaging	12.14
GO Biological Process	gene silencing	10.46
GO Biological Process	protein folding	7.04
GO Biological Process	mitochondrial transport	7.03
GO Biological Process	platelet aggregation	6.57
GO Biological Process	regulation of gene silencing	5.77
GO Biological Process	macromolecular complex disassembly	4.92
GO Biological Process	regulation of posttranscriptional gene silencing	4.81
GO Biological Process	regulation of gene silencing by RNA	4.81

Supplementary Figure 824: Properties and genomic distribution of motifs identified for the ZNF212 transcription factor in K562 (accession ENCSR002ZGC).

TF-MoDisCO pattern_0 n=515, CWM

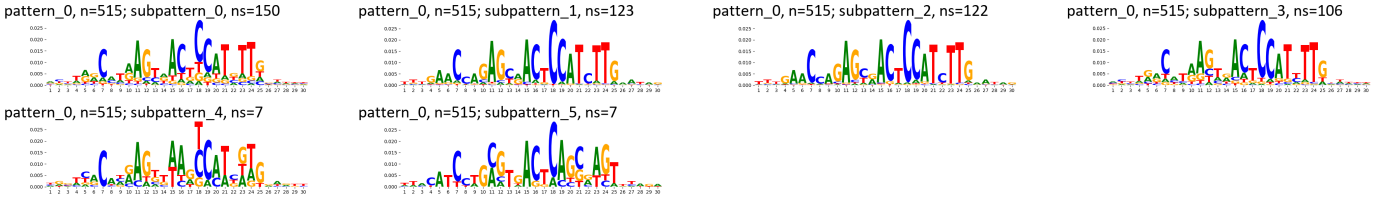

TF-MoDisCO pattern_0 n=515, PWM

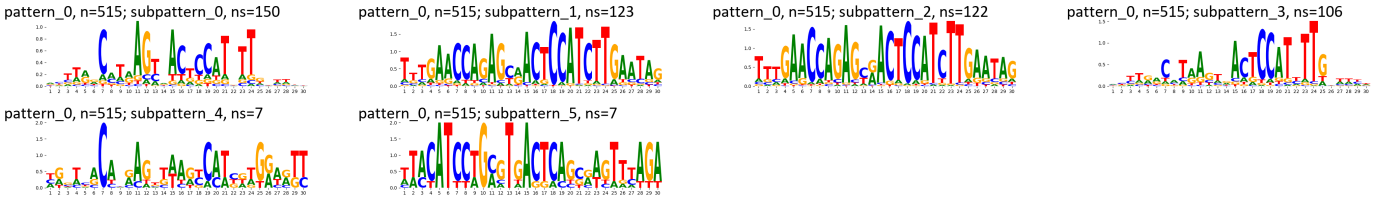

Supplementary Figure 825: TF-MoDisCO subpatterns for the ZNF212 transcription factor in K562 (accession ENCSR002ZGC).

A

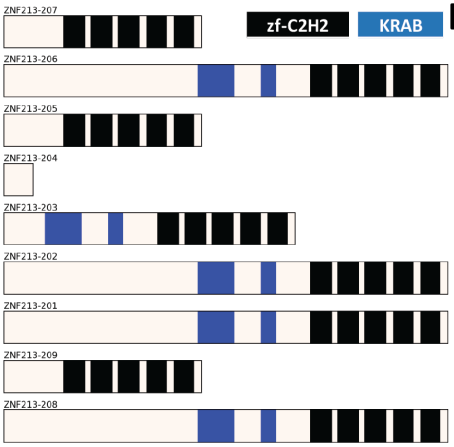

B

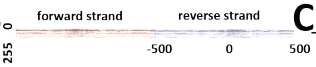

C

peaks	
state	fraction
TssA	0.52
TssFlnk	0.19
TssBiv	0.09
Quies	0.07
EnhA2	0.05
EnhWk	0.04
TxWk	0.03
EnhA1	0.03
ReprPCWk	0.02
ReprPC	0.02
TssFlnkU	0.01
EnhBiv	0.01
Tx	0.00
TssFlnkD	0.00
EnhG1	0.00

D

peaks		peaks	
repeat	fraction	repeat	fraction
Simple_repeat	0.13	G-rich	0.02
Low_complexity	0.03	(GGC)n	0.01
tRNA	0.02	MIRb	0.01
SINE/MIR	0.02	MIR3	0.01
LTR/ERVL-MaLR	0.02	GA-rich	0.01
SINE/Alu	0.01	(CGG)n	0.01
LINE/L2	0.01	tRNA-Val-GT(	0.00
DNA/hAT-Charlie	0.01	tRNA-Thr-AC\	0.00
snRNA	0.00	tRNA-Met-i	0.00
Unknown	0.00	tRNA-Leu-TT/	0.00
LTR/ERVL	0.00	tRNA-Asp-GA'	0.00
LINE/L1	0.00	UCON105	0.00
LINE/CR1	0.00	U1	0.00
DNA/hAT-Tip100	0.00	MamTip2	0.00
		MLT1J	0.00
		MLT1I	0.00
		MLT1H1	0.00
		MLT1C	0.00

E

Ontology	Term	FDR Q-val
GO Biological Process	mitochondrial electron transport, NADH to ubiquinone	19.70
GO Biological Process	mitochondrial ATP synthesis coupled electron transport	16.39
GO Biological Process	ATP synthesis coupled electron transport	16.10
GO Biological Process	oxidative phosphorylation	15.83
GO Biological Process	respiratory electron transport chain	13.15
GO Biological Process	ATP metabolic process	12.89
GO Biological Process	ribonucleoside triphosphate metabolic process	12.50
GO Biological Process	purine ribonucleoside triphosphate metabolic process	11.95
GO Biological Process	purine nucleoside triphosphate metabolic process	11.54
GO Biological Process	nucleoside triphosphate metabolic process	11.47
GO Biological Process	purine ribonucleoside monophosphate metabolic process	10.85
GO Biological Process	purine nucleoside monophosphate metabolic process	10.88
GO Biological Process	ribonucleoside monophosphate metabolic process	10.83
GO Biological Process	nucleoside monophosphate metabolic process	10.36
GO Biological Process	electron transport chain	9.91
GO Biological Process	purine ribonucleoside metabolic process	9.81
GO Biological Process	ribonucleoside metabolic process	9.75
GO Biological Process	purine nucleoside metabolic process	9.76
GO Biological Process	cellular respiration	9.34
GO Biological Process	glycosyl compound metabolic process	8.98
Human Phenotype	Leber optic atrophy	67.56
Human Phenotype	Central retinal vessel vascular tortuosity	67.56
Human Phenotype	Hemianopia	67.56
Human Phenotype	Stroke-like episode	40.91
Human Phenotype	Centrocecal scotoma	38.83
Human Phenotype	Optic neuropathy	37.51
Human Phenotype	Wolff-Parkinson-White syndrome	35.30
Human Phenotype	Episodic vomiting	33.87
Human Phenotype	Ragged-red muscle fibers	33.29
Human Phenotype	Mitochondrial myopathy	32.83
Human Phenotype	Retinal vascular tortuosity	29.20
Human Phenotype	Abnormal retinal artery morphology	26.85
Human Phenotype	Hemiparesis	25.98
Human Phenotype	Arterial tortuosity	25.71
Human Phenotype	Vascular tortuosity	25.37
Human Phenotype	Abnormality of head blood vessel	25.21
Human Phenotype	Muscle abnormality related to mitochondrial dysfunction	25.15
Human Phenotype	Hemiplegia/hemiparesis	25.14
Human Phenotype	Bilateral sensorineural hearing impairment	24.04
Human Phenotype	Mitochondrial inheritance	23.21

F

CIS-BP ChIP

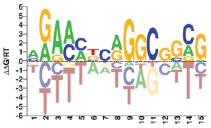

B1H-RC prediction

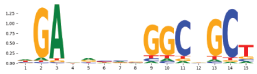

no motif discovered de novo

Supplementary Figure 826: Properties and genomic distribution of motifs identified for the ZNF213 transcription factor in HEK293 (accession Hughes GR models).

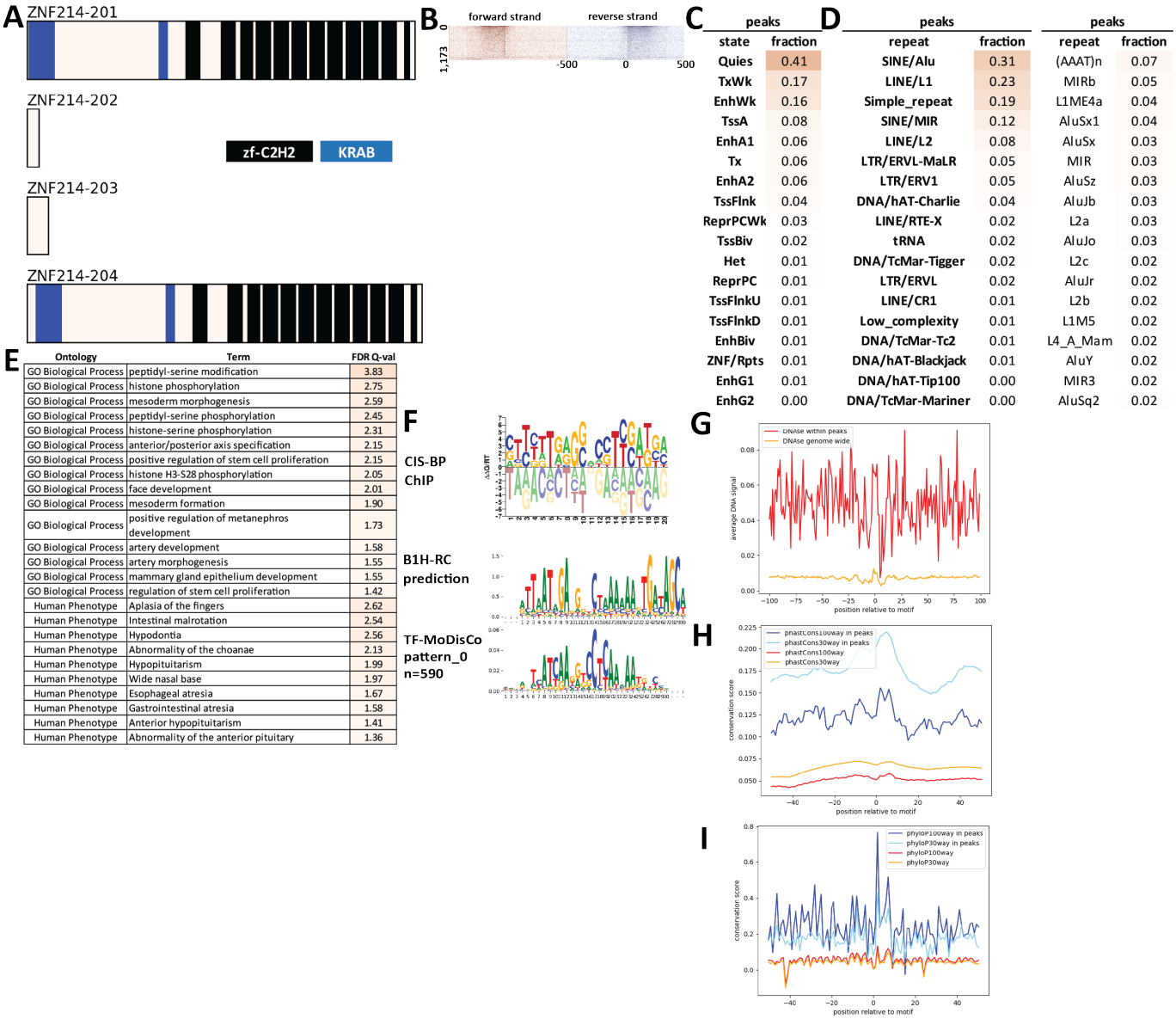

Supplementary Figure 827: Properties and genomic distribution of motifs identified for the ZNF214 transcription factor in HEK293 (accession ENCSR993DED).

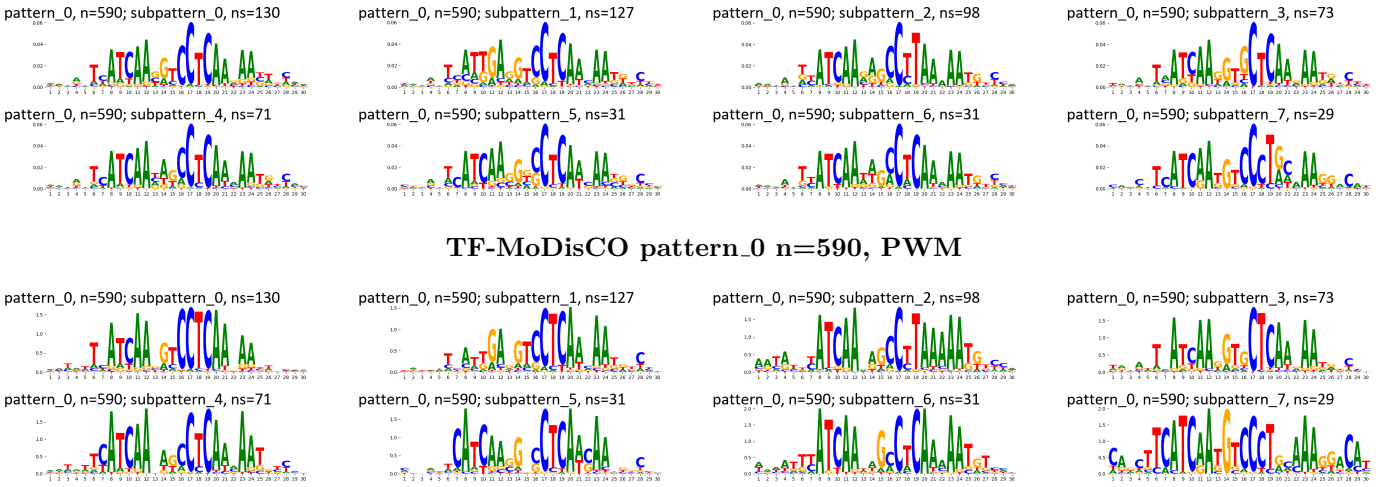

Supplementary Figure 828: TF-MoDisCO subpatterns for the ZNF214 transcription factor in HEK293 (accession ENCSR993DED).

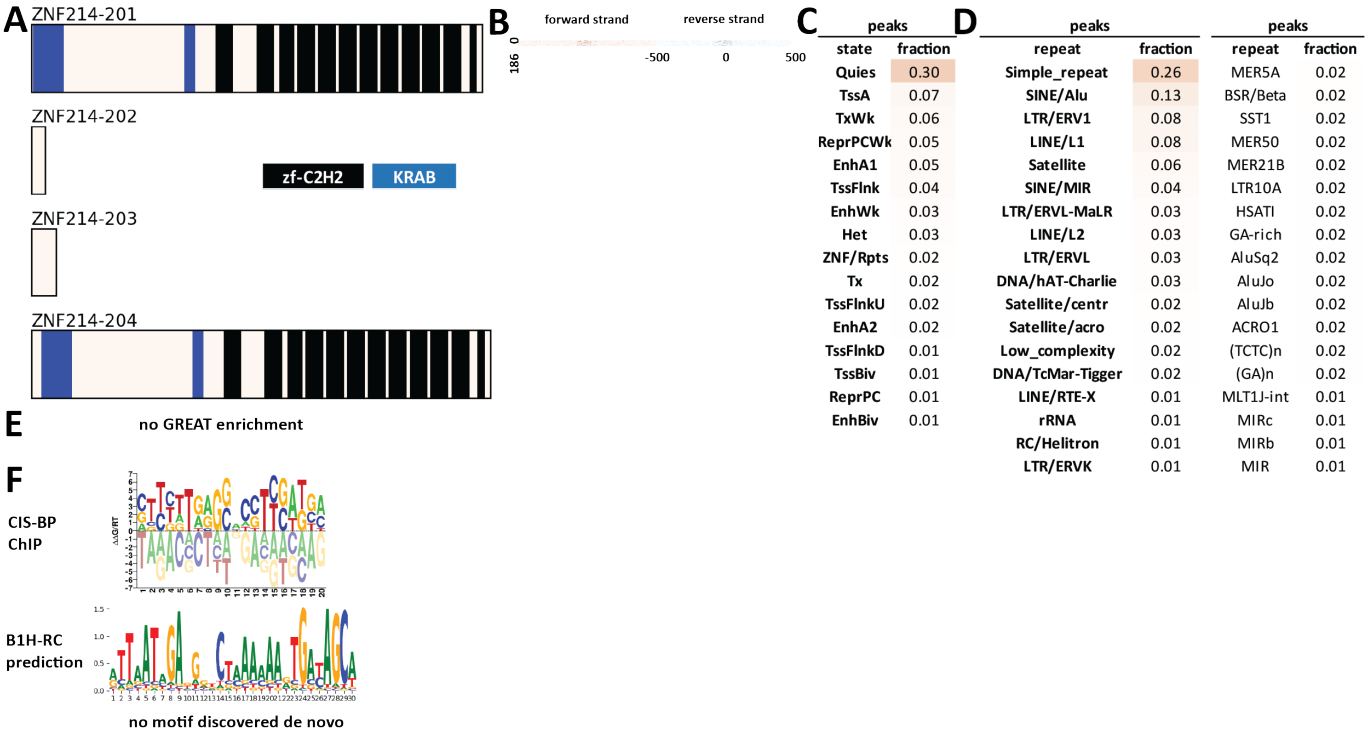

C

peaks	
state	fraction
Quies	0.30
TssA	0.07
TxWk	0.06
ReprPCWk	0.05
EnhA1	0.05
TssFlnk	0.04
EnhWk	0.03
Het	0.03
ZNF/Rpts	0.02
Tx	0.02
TssFlnkU	0.02
EnhA2	0.02
TssFlnkD	0.01
TssBiv	0.01
ReprPC	0.01
EnhBiv	0.01

D

peaks		peaks	
repeat	fraction	repeat	fraction
Simple_repeat	0.26	MER5A	0.02
SINE/Alu	0.13	BSR/Beta	0.02
LTR/ERV1	0.08	SST1	0.02
LINE/L1	0.08	MER50	0.02
Satellite	0.06	MER21B	0.02
SINE/MIR	0.04	LTR10A	0.02
LTR/ERVL-MaLR	0.03	HSATI	0.02
LINE/L2	0.03	GA-rich	0.02
LTR/ERVL	0.03	AluSq2	0.02
DNA/hAT-Charlie	0.03	AluJo	0.02
Satellite/centr	0.02	AluJb	0.02
Satellite/acro	0.02	ACRO1	0.02
Low_complexity	0.02	(TCTC)n	0.02
DNA/TcMar-Tigger	0.02	(GA)n	0.02
LINE/RTE-X	0.01	MLT1J-int	0.01
rRNA	0.01	MIRc	0.01
RC/Helitron	0.01	MIRb	0.01
LTR/ERVK	0.01	MIR	0.01

Supplementary Figure 829: Properties and genomic distribution of motifs identified for the ZNF214 transcription factor in HEK293 (accession ChipExo models).

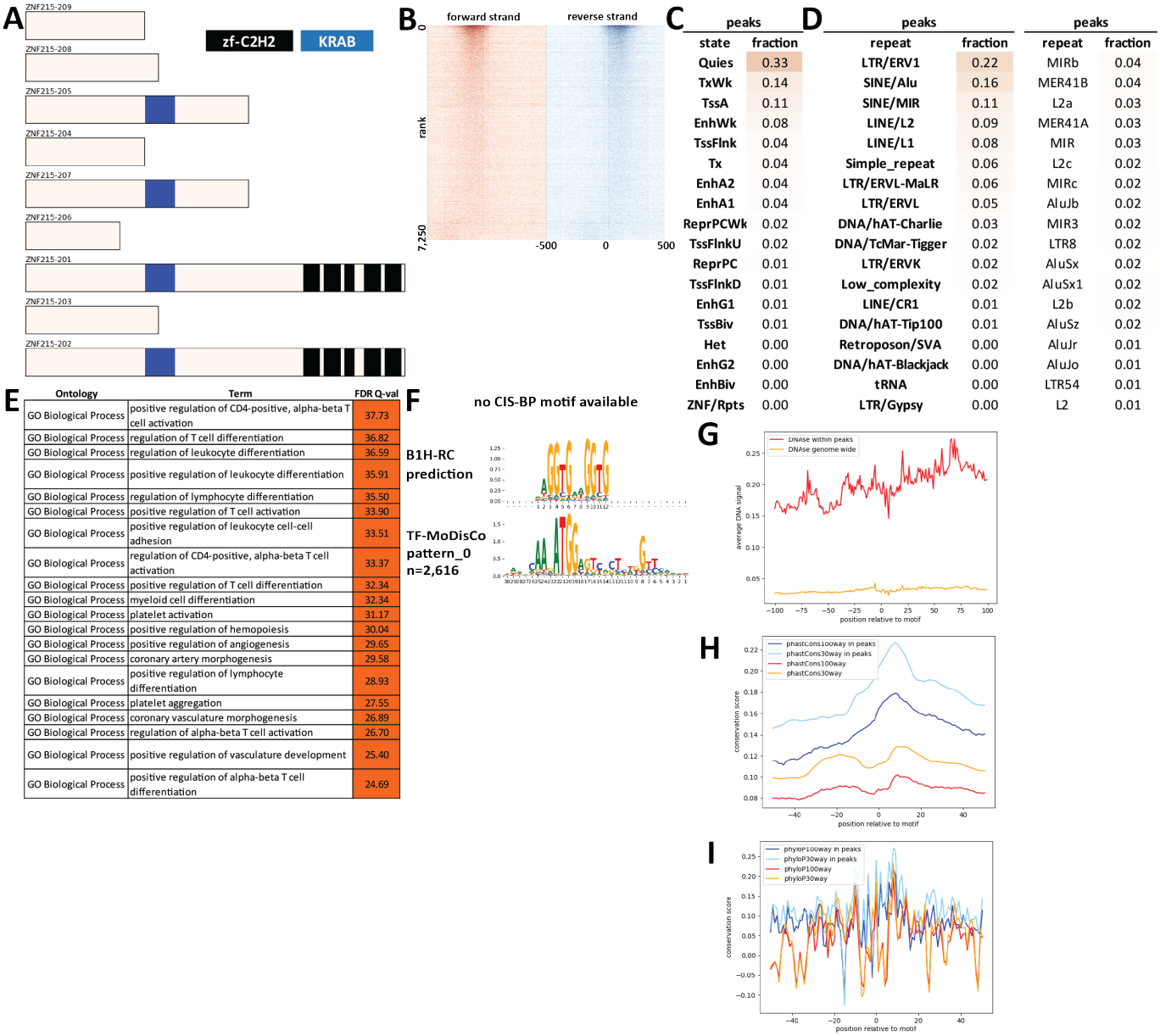

C

peaks	
state	fraction
Quies	0.33
TxWk	0.14
TssA	0.11
EnhWk	0.08
TssFlnk	0.04
Tx	0.04
EnhA2	0.04
EnhA1	0.04
ReprPCWk	0.02
TssFlnkU	0.02
ReprPC	0.01
TssFlnkD	0.01
EnhG1	0.01
TssBiv	0.01
Het	0.00
EnhG2	0.00
EnhBiv	0.00
ZNF/Rpts	0.00

D

peaks		peaks	
repeat	fraction	repeat	fraction
LTR/ERV1	0.22	MIRb	0.04
SINE/Alu	0.16	MER41B	0.04
SINE/MIR	0.11	L2a	0.03
LINE/L2	0.09	MER41A	0.03
LINE/L1	0.08	MIR	0.03
Simple_repeat	0.06	L2c	0.02
LTR/ERVL-MaLR	0.06	MIRc	0.02
LTR/ERVL	0.05	AluJb	0.02
DNA/hAT-Charlie	0.03	MIR3	0.02
DNA/TcMar-Tigger	0.02	LTR8	0.02
LTR/ERVK	0.02	AluSx	0.02
Low_complexity	0.02	AluSx1	0.02
LINE/CR1	0.01	L2b	0.02
DNA/hAT-Tip100	0.01	AluSz	0.02
Retroposon/SVA	0.00	AluJr	0.01
DNA/hAT-Blackjack	0.00	AluJo	0.01
tRNA	0.00	LTR54	0.01
LTR/Gypsy	0.00	L2	0.01

E

Ontology	Term	FDR Q-val
GO Biological Process	positive regulation of CD4-positive, alpha-beta T cell activation	37.73
GO Biological Process	regulation of T cell differentiation	36.82
GO Biological Process	regulation of leukocyte differentiation	36.59
GO Biological Process	positive regulation of leukocyte differentiation	35.91
GO Biological Process	regulation of lymphocyte differentiation	35.50
GO Biological Process	positive regulation of T cell activation	33.90
GO Biological Process	positive regulation of leukocyte cell-cell adhesion	33.51
GO Biological Process	regulation of CD4-positive, alpha-beta T cell activation	33.37
GO Biological Process	positive regulation of T cell differentiation	32.34
GO Biological Process	myeloid cell differentiation	32.34
GO Biological Process	platelet activation	31.17
GO Biological Process	positive regulation of hemopoiesis	30.04
GO Biological Process	positive regulation of angiogenesis	29.65
GO Biological Process	coronary artery morphogenesis	29.58
GO Biological Process	positive regulation of lymphocyte differentiation	28.93
GO Biological Process	platelet aggregation	27.55
GO Biological Process	coronary vasculature morphogenesis	26.89
GO Biological Process	regulation of alpha-beta T cell activation	26.70
GO Biological Process	positive regulation of vasculature development	25.40
GO Biological Process	positive regulation of alpha-beta T cell differentiation	24.69

Supplementary Figure 830: Properties and genomic distribution of motifs identified for the ZNF215 transcription factor in K562 (accession ENCSR699RWG).

TF-MoDisCO pattern_0 n=2616, CWM

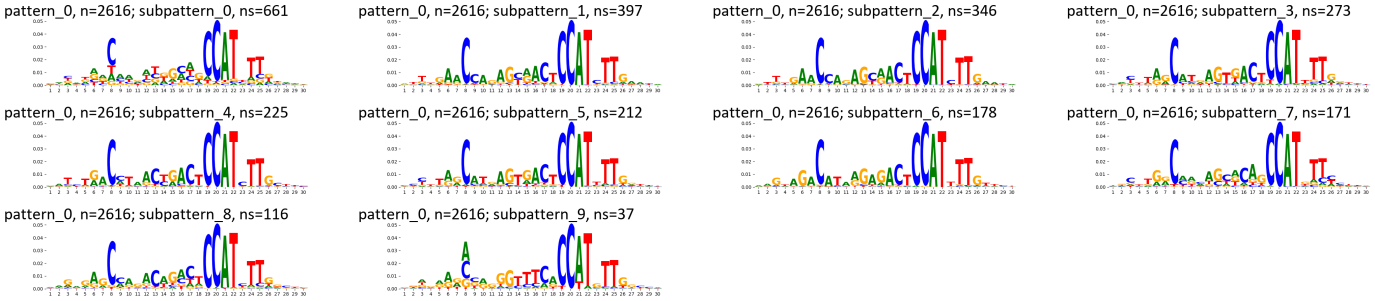

TF-MoDisCO pattern_0 n=2616, PWM

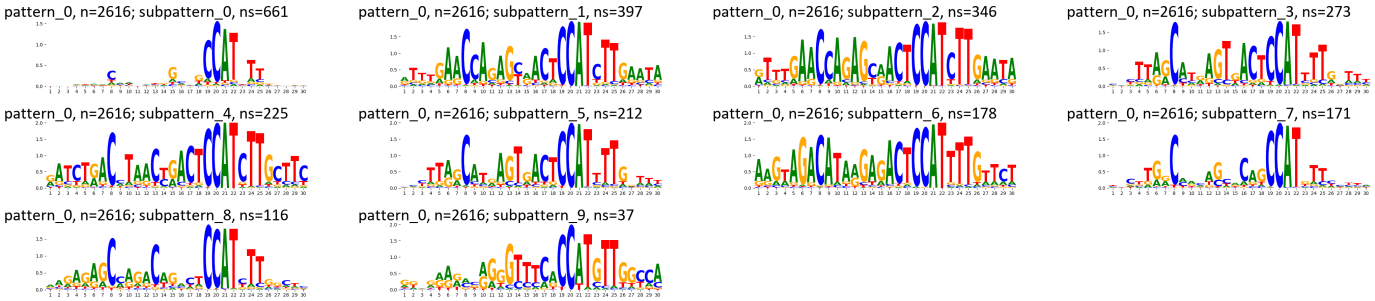

Supplementary Figure 831: TF-MoDisCO subpatterns for the ZNF215 transcription factor in K562 (accession ENCSR699RWG).

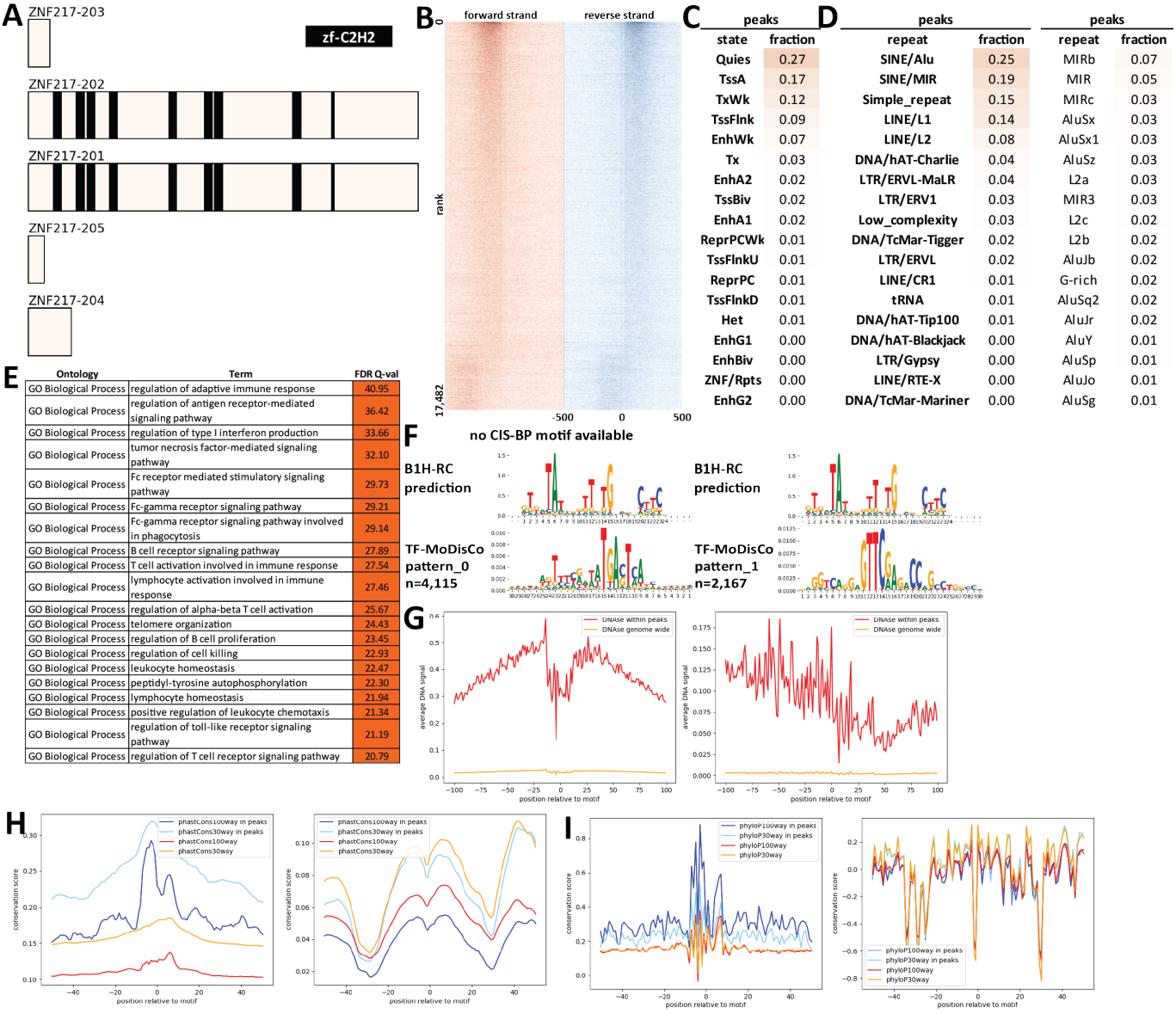

Supplementary Figure 832: Properties and genomic distribution of motifs identified for the ZNF217 transcription factor in GM12878 (accession ENCSR764CZW).

TF-MoDisCO pattern_0 n=4115, CWM

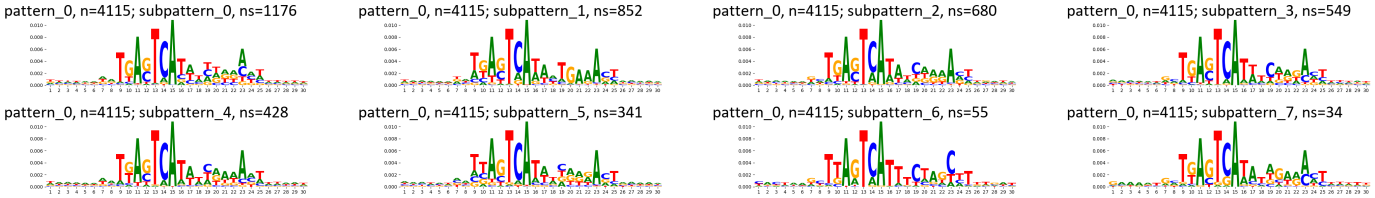

TF-MoDisCO pattern_0 n=4115, PWM

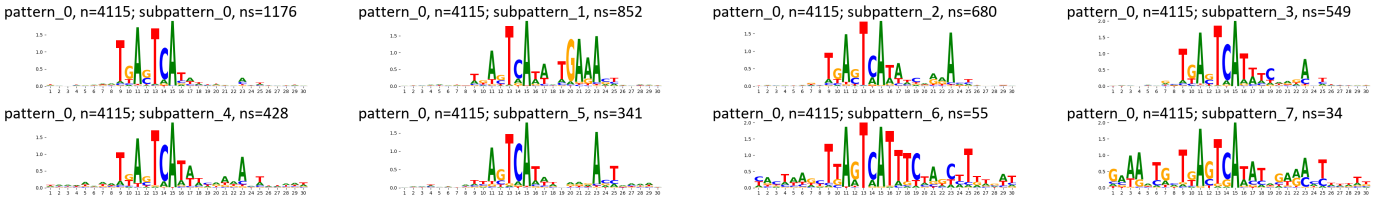

TF-MoDisCO pattern_1 n=2167, CWM

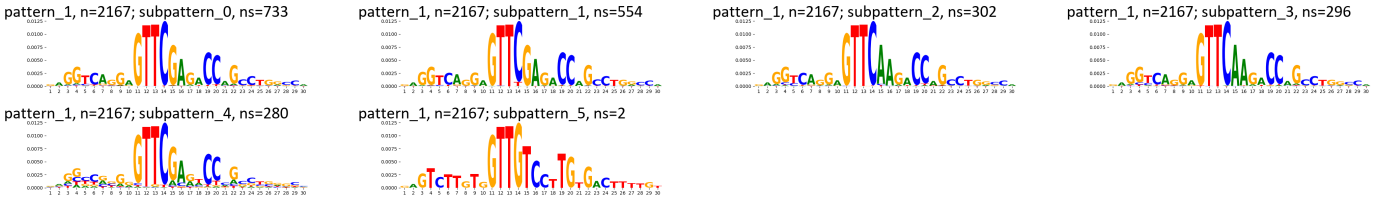

TF-MoDisCO pattern_1 n=2167, PWM

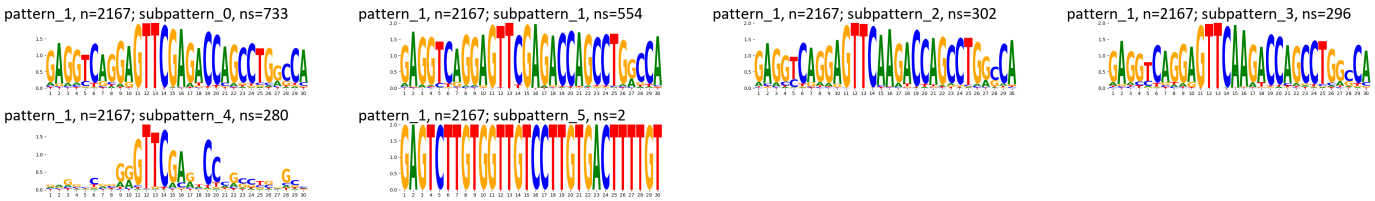

Supplementary Figure 833: TF-MoDisCO subpatterns for the ZNF217 transcription factor in GM12878 (accession ENCSR764CZW).

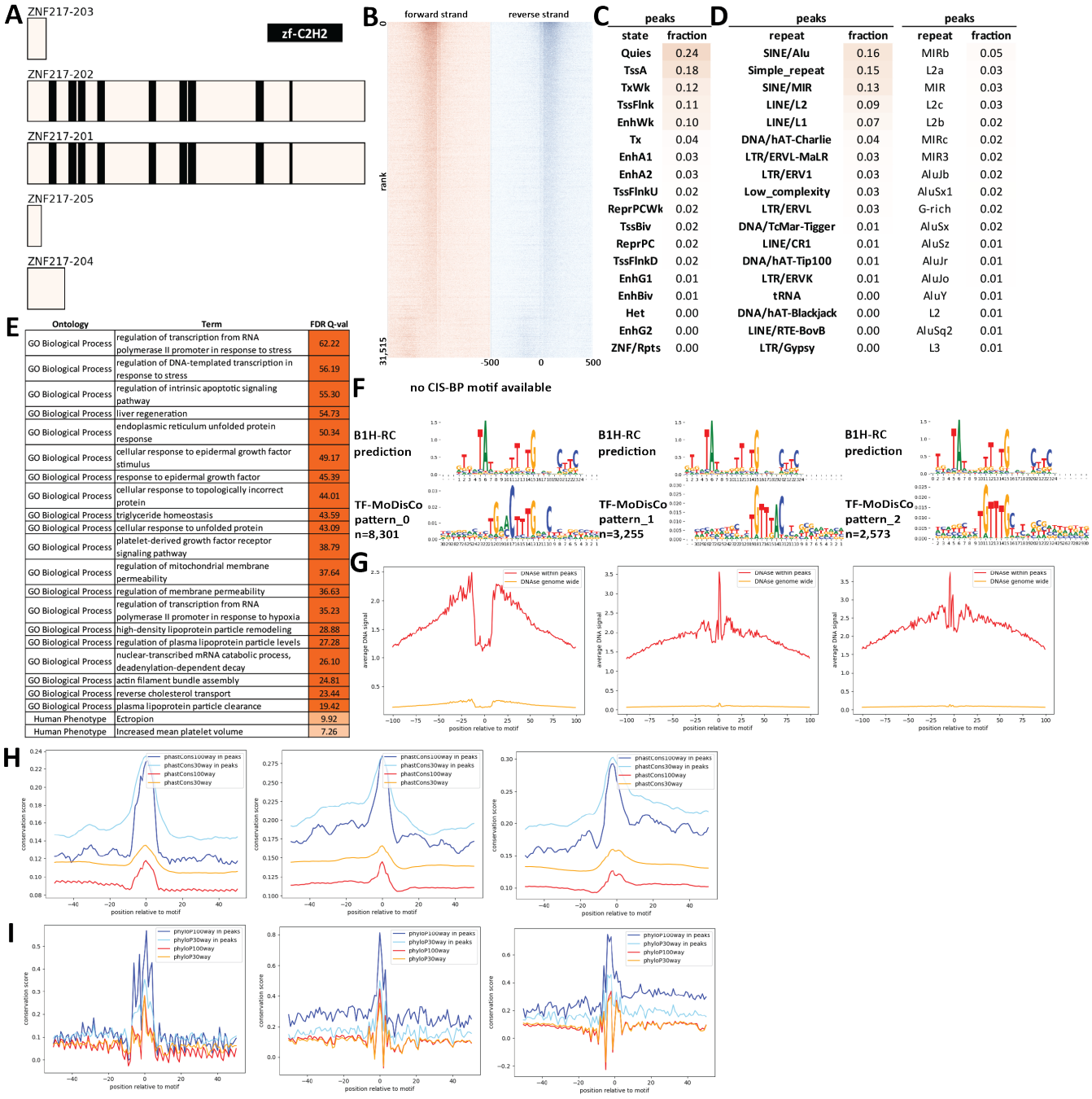

Supplementary Figure 834: Properties and genomic distribution of motifs identified for the ZNF217 transcription factor in HepG2 (accession ENCSR055FQB).

TF-MoDisCO pattern_0 n=8301, CWM

pattern_0, n=8301; subpattern_0, ns=2279

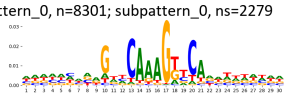

pattern_0, n=8301; subpattern_1, ns=1473

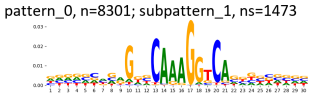

pattern_0, n=8301; subpattern_2, ns=1327

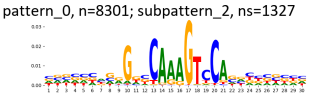

pattern_0, n=8301; subpattern_3, ns=1092

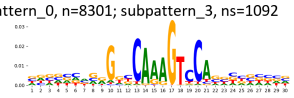

pattern_0, n=8301; subpattern_4, ns=997

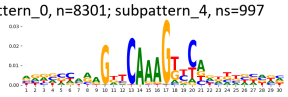

pattern_0, n=8301; subpattern_5, ns=740

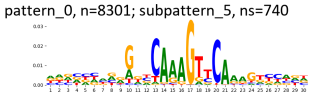

pattern_0, n=8301; subpattern_6, ns=365

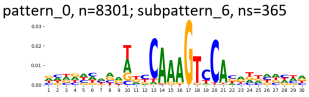

pattern_0, n=8301; subpattern_7, ns=25

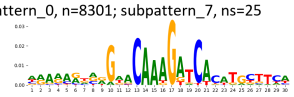

pattern_0, n=8301; subpattern_8, ns=3

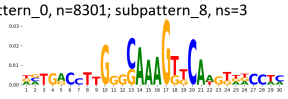

TF-MoDisCO pattern_0 n=8301, PWM

pattern_0, n=8301; subpattern_0, ns=2279

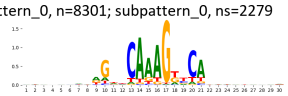

pattern_0, n=8301; subpattern_1, ns=1473

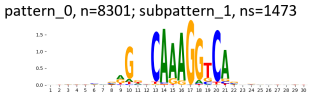

pattern_0, n=8301; subpattern_2, ns=1327

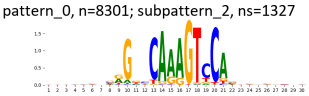

pattern_0, n=8301; subpattern_3, ns=1092

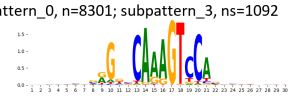

pattern_0, n=8301; subpattern_4, ns=997

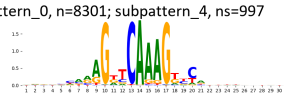

pattern_0, n=8301; subpattern_5, ns=740

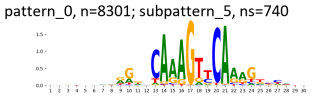

pattern_0, n=8301; subpattern_6, ns=365

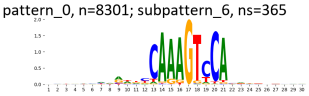

pattern_0, n=8301; subpattern_7, ns=25

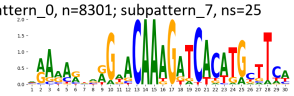

pattern_0, n=8301; subpattern_8, ns=3

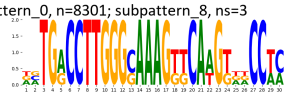

TF-MoDisCO pattern_1 n=3255, CWM

pattern_1, n=3255; subpattern_0, ns=892

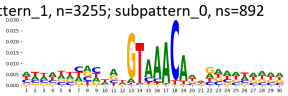

pattern_1, n=3255; subpattern_1, ns=669

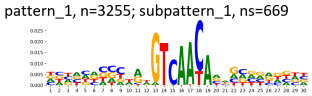

pattern_1, n=3255; subpattern_2, ns=648

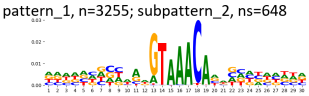

pattern_1, n=3255; subpattern_3, ns=495

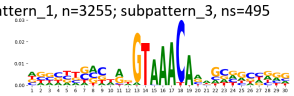

pattern_1, n=3255; subpattern_4, ns=481

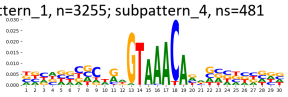

pattern_1, n=3255; subpattern_5, ns=41

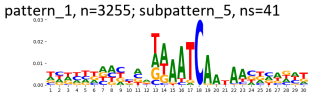

pattern_1, n=3255; subpattern_6, ns=21

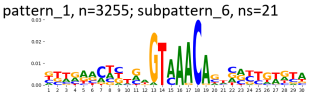

pattern_1, n=3255; subpattern_7, ns=6

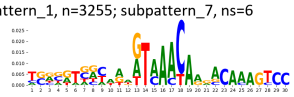

pattern_1, n=3255; subpattern_8, ns=2

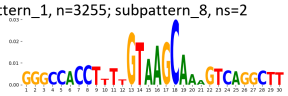

TF-MoDisCO pattern_1 n=3255, PWM

pattern_1, n=3255; subpattern_0, ns=892

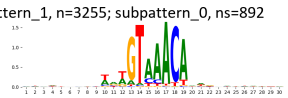

pattern_1, n=3255; subpattern_1, ns=669

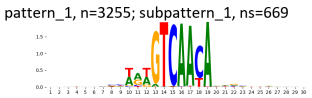

pattern_1, n=3255; subpattern_2, ns=648

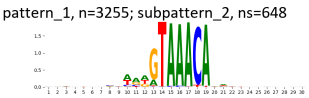

pattern_1, n=3255; subpattern_3, ns=495

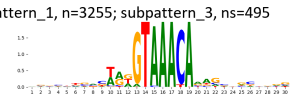

pattern_1, n=3255; subpattern_4, ns=481

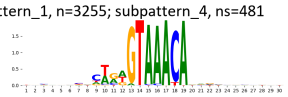

pattern_1, n=3255; subpattern_5, ns=41

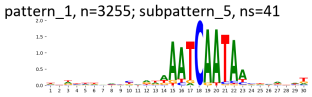

pattern_1, n=3255; subpattern_6, ns=21

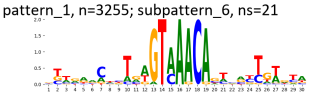

pattern_1, n=3255; subpattern_7, ns=6

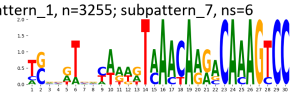

pattern_1, n=3255; subpattern_8, ns=2

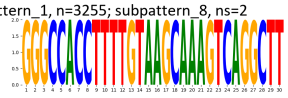

TF-MoDisCO pattern_2 n=2573, CWM

pattern_2, n=2573; subpattern_0, ns=782

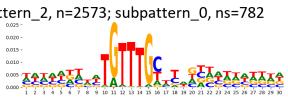

pattern_2, n=2573; subpattern_1, ns=746

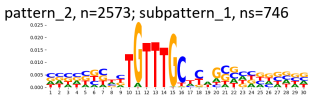

pattern_2, n=2573; subpattern_10, ns=2

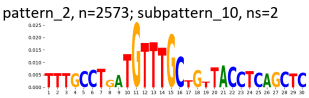

pattern_2, n=2573; subpattern_11, ns=2

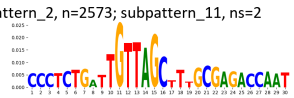

pattern_2, n=2573; subpattern_2, ns=498

pattern_2, n=2573; subpattern_3, ns=461

pattern_2, n=2573; subpattern_4, ns=34

pattern_2, n=2573; subpattern_5, ns=26

pattern_2, n=2573; subpattern_6, ns=10

pattern_2, n=2573; subpattern_7, ns=6

pattern_2, n=2573; subpattern_8, ns=3

pattern_2, n=2573; subpattern_9, ns=3

TF-MoDisCO pattern_2 n=2573, PWM

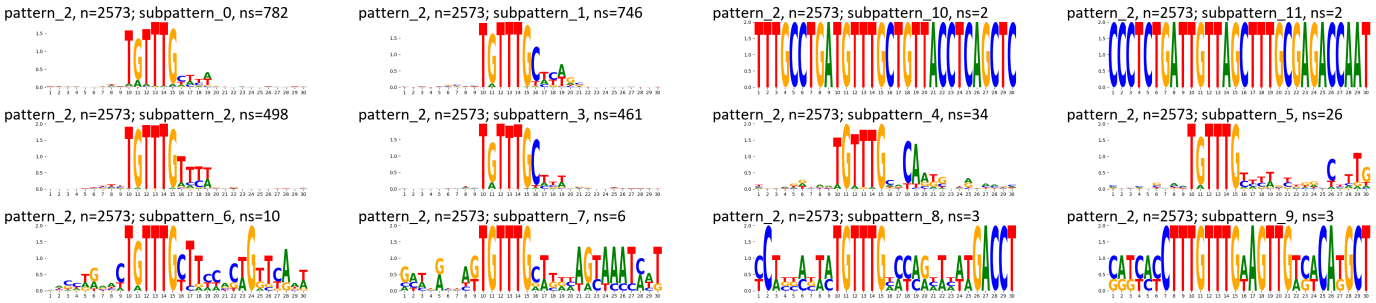

Supplementary Figure 835: TF-MoDisCO subpatterns for the ZNF217 transcription factor in HepG2 (accession ENCSR055FQB).

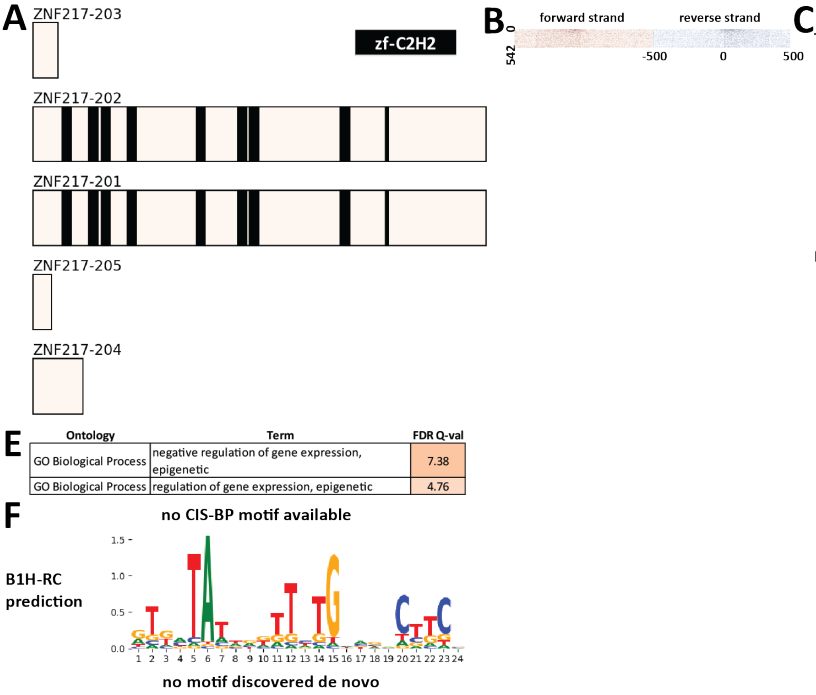

C

peaks	
state	fraction
TssA	0.32
Quies	0.19
TssFlnk	0.15
TxWk	0.10
ReprPC	0.06
TssBiv	0.05
Tx	0.05
TssFlnkU	0.04
ReprPCWk	0.04
EnhWk	0.03
EnhA2	0.02
EnhA1	0.02
TssFlnkD	0.01
EnhG1	0.01
EnhBiv	0.01
Het	0.00
EnhG2	0.00

D

peaks		peaks	
repeat	fraction	repeat	fraction
SINE/Alu	0.14	MIRc	0.03
Simple_repeat	0.13	MIR	0.02
SINE/MIR	0.09	AluJb	0.02
LINE/L2	0.07	L2a	0.02
LINE/L1	0.06	L2c	0.02
LTR/ERVL-MaLR	0.04	MIRb	0.02
Low_complexity	0.03	L2b	0.02
LTR/ERV1	0.03	AluY	0.02
LTR/ERVL	0.02	AluSx	0.02
DNA/TcMar-Tigger	0.02	MIR3	0.01
DNA/hAT-Charlie	0.01	G-rich	0.01
LINE/CR1	0.01	GA-rich	0.01
DNA/hAT-Tip100	0.01	AluSz	0.01
tRNA	0.00	AluSx1	0.01
srpRNA	0.00	AluSg	0.01
snRNA	0.00	AluJr	0.01
Satellite	0.00	L2	0.01
Satellite/centr	0.00	AluJo	0.01

E

Ontology	Term	FDR Q-val
GO Biological Process	negative regulation of gene expression, epigenetic	7.38
GO Biological Process	regulation of gene expression, epigenetic	4.76

F

Supplementary Figure 836: Properties and genomic distribution of motifs identified for the ZNF217 transcription factor in K562 (accession ENCSR841GLE).

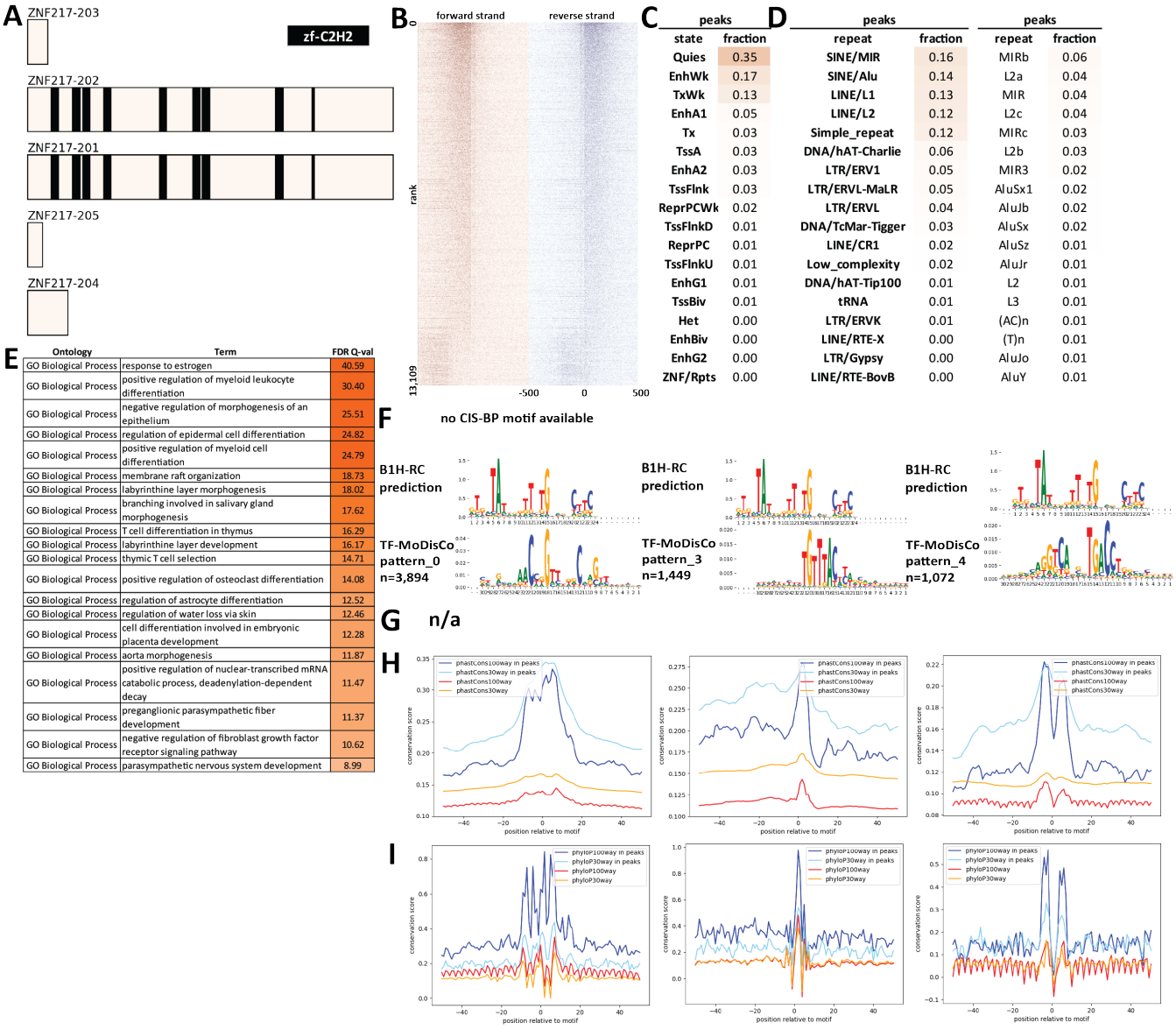

Supplementary Figure 837: Properties and genomic distribution of motifs identified for the ZNF217 transcription factor in MCF-7 (accession ENCSR000EWU).

TF-MoDisCO pattern_0 n=3894, CWM

pattern_0, n=3894; subpattern_0, ns=794

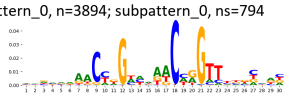

pattern_0, n=3894; subpattern_1, ns=737

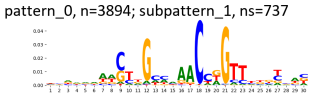

pattern_0, n=3894; subpattern_2, ns=648

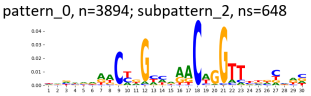

pattern_0, n=3894; subpattern_3, ns=610

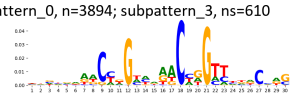

pattern_0, n=3894; subpattern_4, ns=580

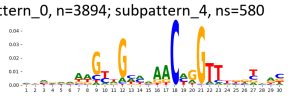

pattern_0, n=3894; subpattern_5, ns=493

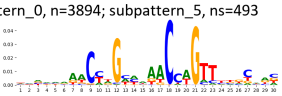

pattern_0, n=3894; subpattern_6, ns=26

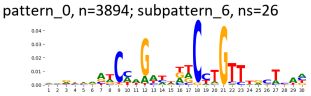

pattern_0, n=3894; subpattern_7, ns=2

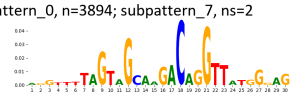

pattern_0, n=3894; subpattern_8, ns=2

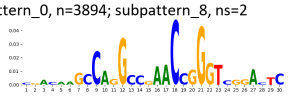

pattern_0, n=3894; subpattern_9, ns=2

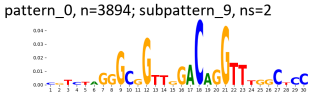

TF-MoDisCO pattern_0 n=3894, PWM

pattern_0, n=3894; subpattern_0, ns=794

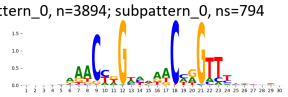

pattern_0, n=3894; subpattern_1, ns=737

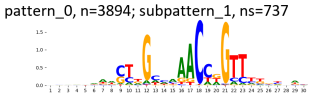

pattern_0, n=3894; subpattern_2, ns=648

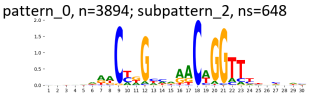

pattern_0, n=3894; subpattern_3, ns=610

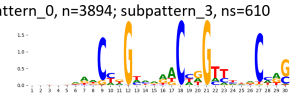

pattern_0, n=3894; subpattern_4, ns=580

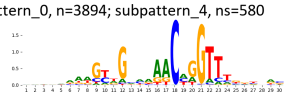

pattern_0, n=3894; subpattern_5, ns=493

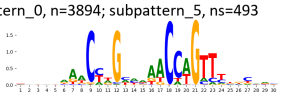

pattern_0, n=3894; subpattern_6, ns=26

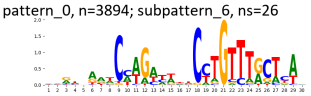

pattern_0, n=3894; subpattern_7, ns=2

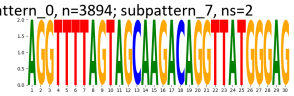

pattern_0, n=3894; subpattern_8, ns=2

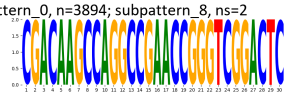

pattern_0, n=3894; subpattern_9, ns=2

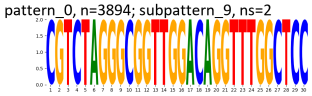

TF-MoDisCO pattern_3 n=1449, CWM

pattern_3, n=1449; subpattern_0, ns=319

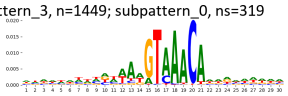

pattern_3, n=1449; subpattern_1, ns=310

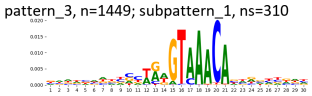

pattern_3, n=1449; subpattern_10, ns=2

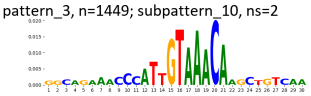

pattern_3, n=1449; subpattern_11, ns=2

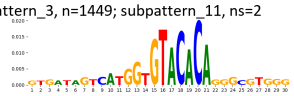

pattern_3, n=1449; subpattern_12, ns=2

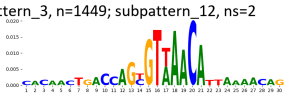

pattern_3, n=1449; subpattern_13, ns=2

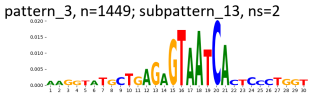

pattern_3, n=1449; subpattern_2, ns=267

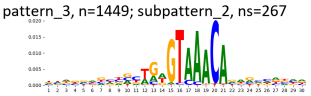

pattern_3, n=1449; subpattern_3, ns=195

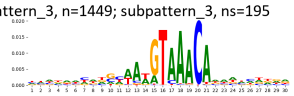

pattern_3, n=1449; subpattern_4, ns=183

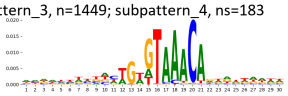

pattern_3, n=1449; subpattern_5, ns=145

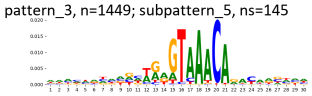

pattern_3, n=1449; subpattern_6, ns=7

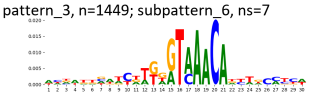

pattern_3, n=1449; subpattern_7, ns=6

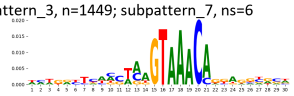

pattern_3, n=1449; subpattern_8, ns=5

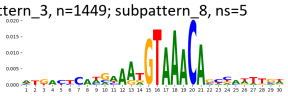

pattern_3, n=1449; subpattern_9, ns=4

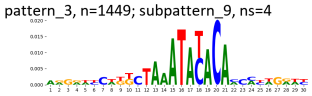

TF-MoDisCO pattern_3 n=1449, PWM

pattern_3, n=1449; subpattern_0, ns=319

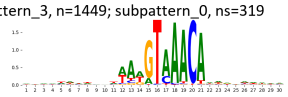

pattern_3, n=1449; subpattern_1, ns=310

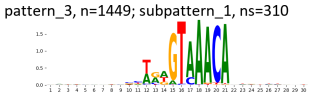

pattern_3, n=1449; subpattern_10, ns=2

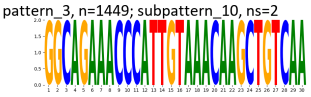

pattern_3, n=1449; subpattern_11, ns=2

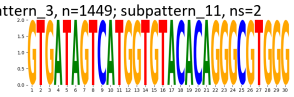

pattern_3, n=1449; subpattern_12, ns=2

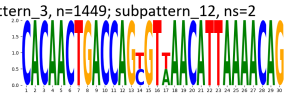

pattern_3, n=1449; subpattern_13, ns=2

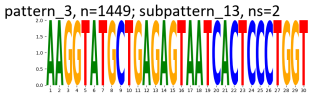

pattern_3, n=1449; subpattern_2, ns=267

pattern_3, n=1449; subpattern_3, ns=195

pattern_3, n=1449; subpattern_4, ns=183

pattern_3, n=1449; subpattern_5, ns=145

pattern_3, n=1449; subpattern_6, ns=7

pattern_3, n=1449; subpattern_7, ns=6

pattern_3, n=1449; subpattern_8, ns=5

pattern_3, n=1449; subpattern_9, ns=4

TF-MoDisCO pattern_4 n=1072, CWM

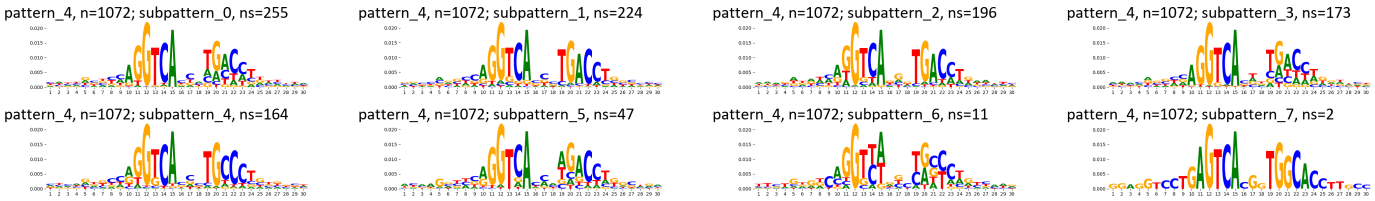

TF-MoDisCO pattern_4 n=1072, PWM

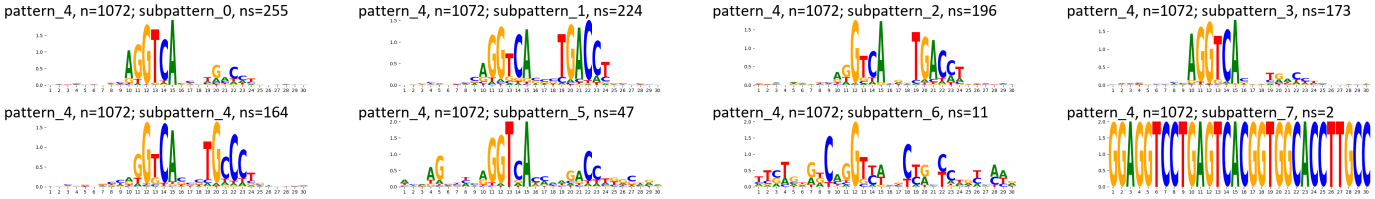

Supplementary Figure 838: TF-MoDisCO subpatterns for the ZNF217 transcription factor in MCF-7 (accession ENCSR000EWU).

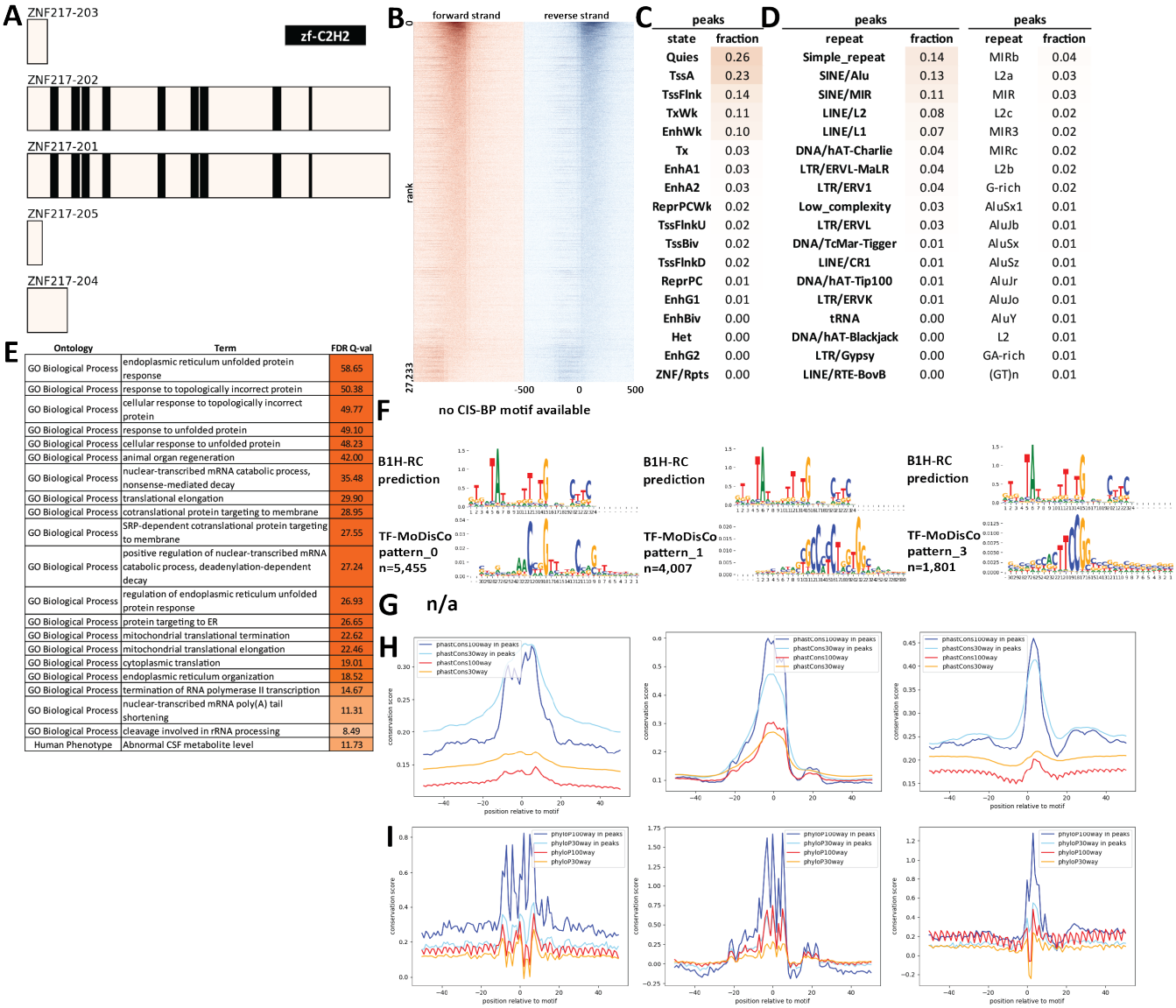

peaks	
state	fraction
Quies	0.26
TssA	0.23
TssFlnk	0.14
TxWk	0.11
EnhWk	0.10
Tx	0.03
EnhA1	0.03
EnhA2	0.03
ReprPCWk	0.02
TssFlnkU	0.02
TssBiv	0.02
TssFlnkD	0.02
ReprPC	0.01
EnhG1	0.01
EnhBiv	0.00
Het	0.00
EnhG2	0.00
ZNF/Rpts	0.00

peaks		peaks	
repeat	fraction	repeat	fraction
Simple_repeat	0.14	MIRb	0.04
SINE/Alu	0.13	L2a	0.03
SINE/MIR	0.11	MIR	0.03
LINE/L2	0.08	L2c	0.02
LINE/L1	0.07	MIR3	0.02
DNA/hAT-Charlie	0.04	MIRc	0.02
LTR/ERVL-MaLR	0.04	L2b	0.02
LTR/ERV1	0.04	G-rich	0.02
Low_complexity	0.03	AluSx1	0.01
LTR/ERVL	0.03	AluJb	0.01
DNA/TcMar-Tigger	0.01	AluSx	0.01
LINE/CR1	0.01	AluSz	0.01
DNA/hAT-Tip100	0.01	AluJr	0.01
LTR/ERVK	0.01	AluJo	0.01
tRNA	0.00	AluY	0.01
DNA/hAT-Blackjack	0.00	L2	0.01
LTR/Gypsy	0.00	GA-rich	0.01
LINE/RTE-BovB	0.00	(GT)n	0.01

Ontology	Term	FDR Q-val
GO Biological Process	endoplasmic reticulum unfolded protein response	58.65
GO Biological Process	response to topologically incorrect protein	50.38
GO Biological Process	cellular response to topologically incorrect protein	49.77
GO Biological Process	response to unfolded protein	49.10
GO Biological Process	cellular response to unfolded protein	48.23
GO Biological Process	animal organ regeneration	42.00
GO Biological Process	nuclear-transcribed mRNA catabolic process, nonsense-mediated decay	35.48
GO Biological Process	translational elongation	29.90
GO Biological Process	cotranslational protein targeting to membrane	28.95
GO Biological Process	SRP-dependent cotranslational protein targeting to membrane	27.55
GO Biological Process	positive regulation of nuclear-transcribed mRNA catabolic process, deadenylation-dependent decay	27.24
GO Biological Process	regulation of endoplasmic reticulum unfolded protein response	26.93
GO Biological Process	protein targeting to ER	26.65
GO Biological Process	mitochondrial translational termination	22.62
GO Biological Process	mitochondrial translational elongation	22.46
GO Biological Process	cytoplasmic translation	19.01
GO Biological Process	endoplasmic reticulum organization	18.52
GO Biological Process	termination of RNA polymerase II transcription	14.67
GO Biological Process	nuclear-transcribed mRNA poly(A) tail shortening	11.31
GO Biological Process	cleavage involved in rRNA processing	8.49
Human Phenotype	Abnormal CSF metabolite level	11.73

Supplementary Figure 839: Properties and genomic distribution of motifs identified for the ZNF217 transcription factor in MCF-7 (accession ENCSR465XQW).

TF-MoDisCO pattern_0 n=5455, CWM

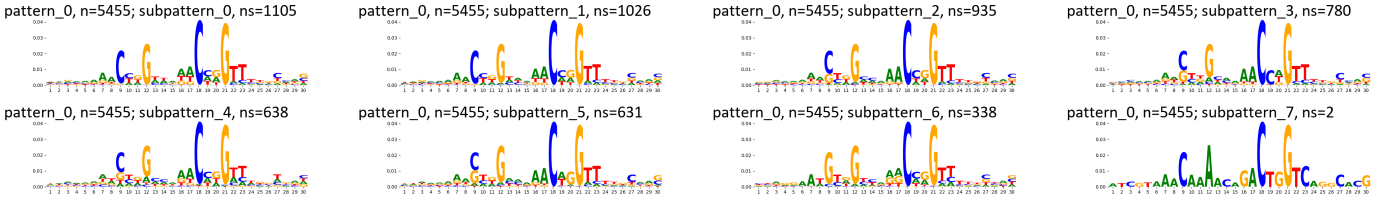

TF-MoDisCO pattern_0 n=5455, PWM

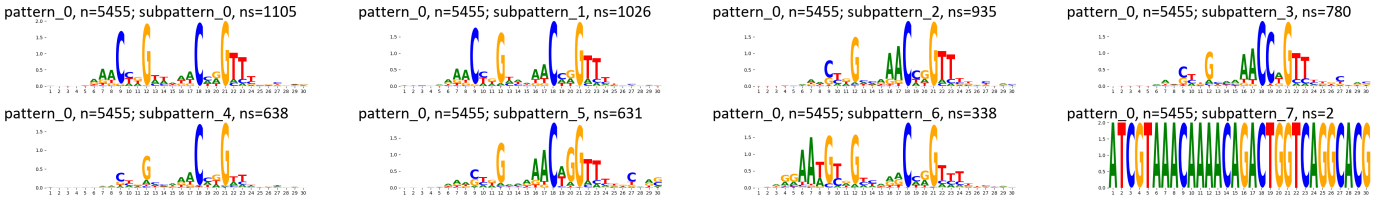

TF-MoDisCO pattern_1 n=4007, CWM

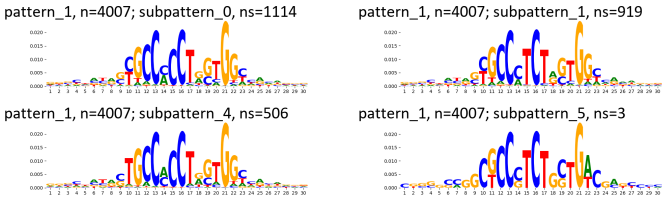

TF-MoDisCO pattern_1 n=4007, PWM

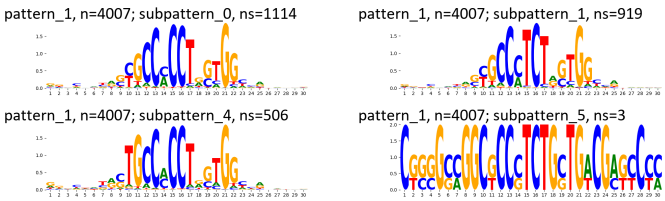

TF-MoDisCO pattern_3 n=1801, CWM

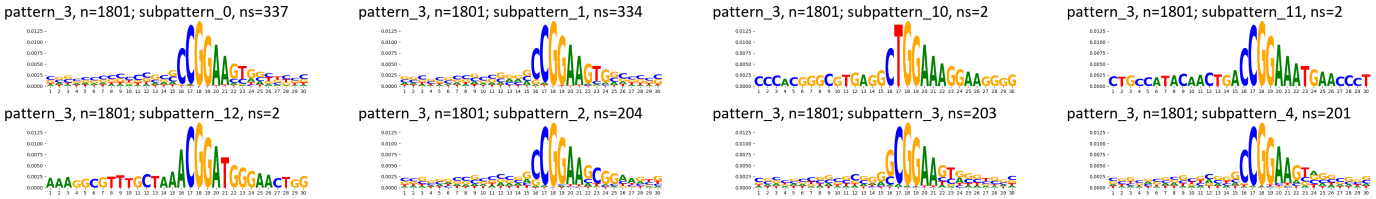

TF-MoDisCO pattern_3 n=1801, PWM

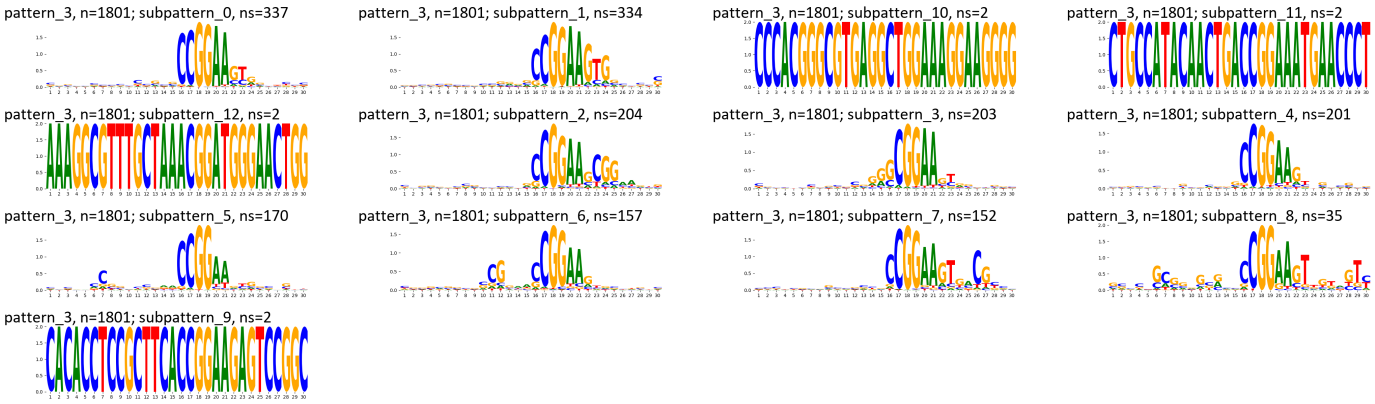

Supplementary Figure 840: TF-MoDisCO subpatterns for the ZNF217 transcription factor in MCF-7 (accession ENCSR465XQW).

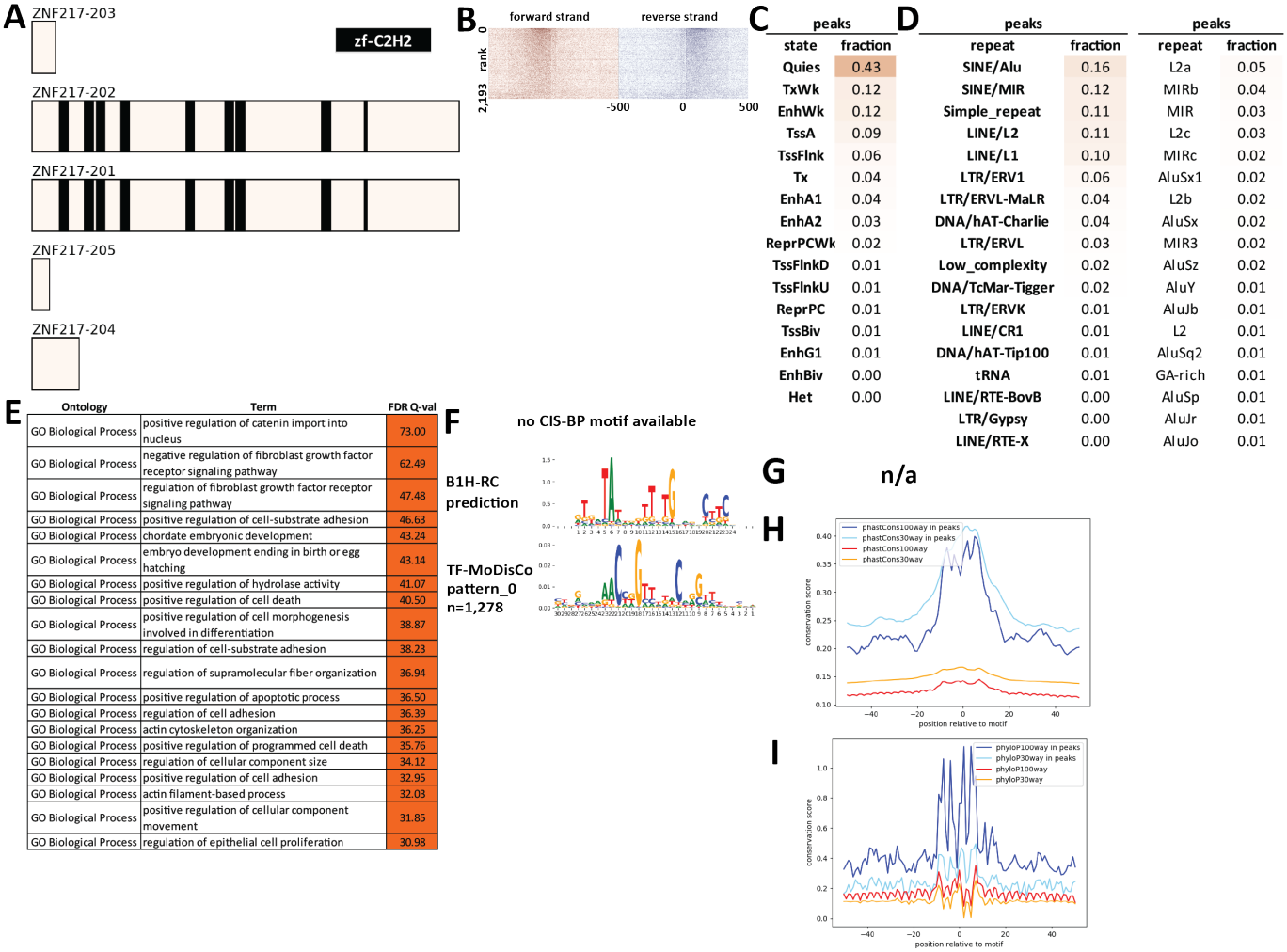

Supplementary Figure 841: Properties and genomic distribution of motifs identified for the ZNF217 transcription factor in MCF-7 (accession ENCSR912ATU).

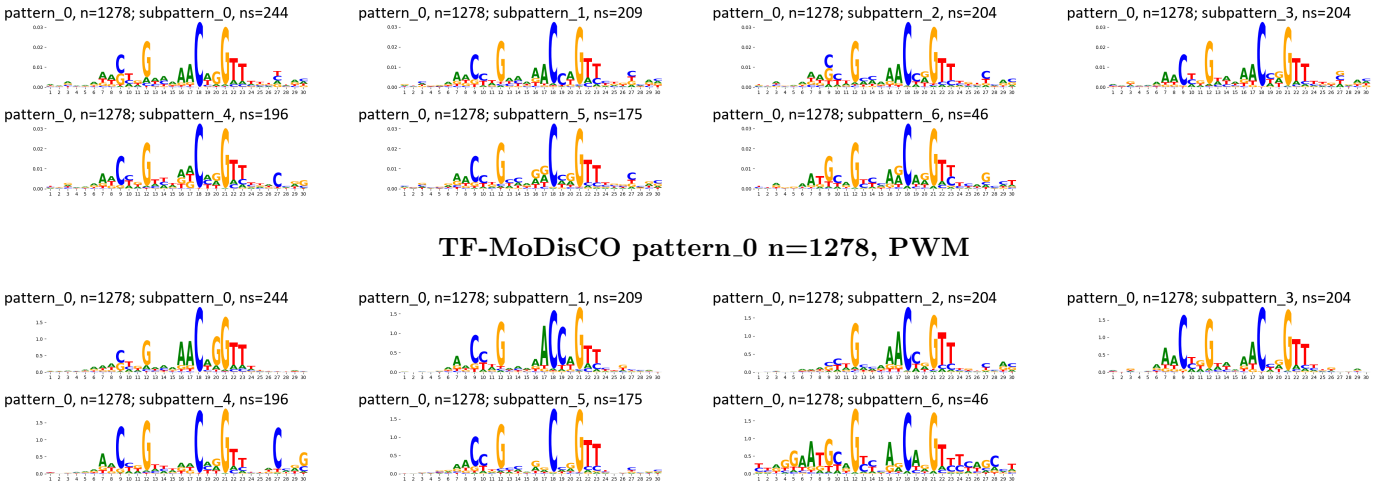

Supplementary Figure 842: TF-MoDisCO subpatterns for the ZNF217 transcription factor in MCF-7 (accession ENCSR912ATU).

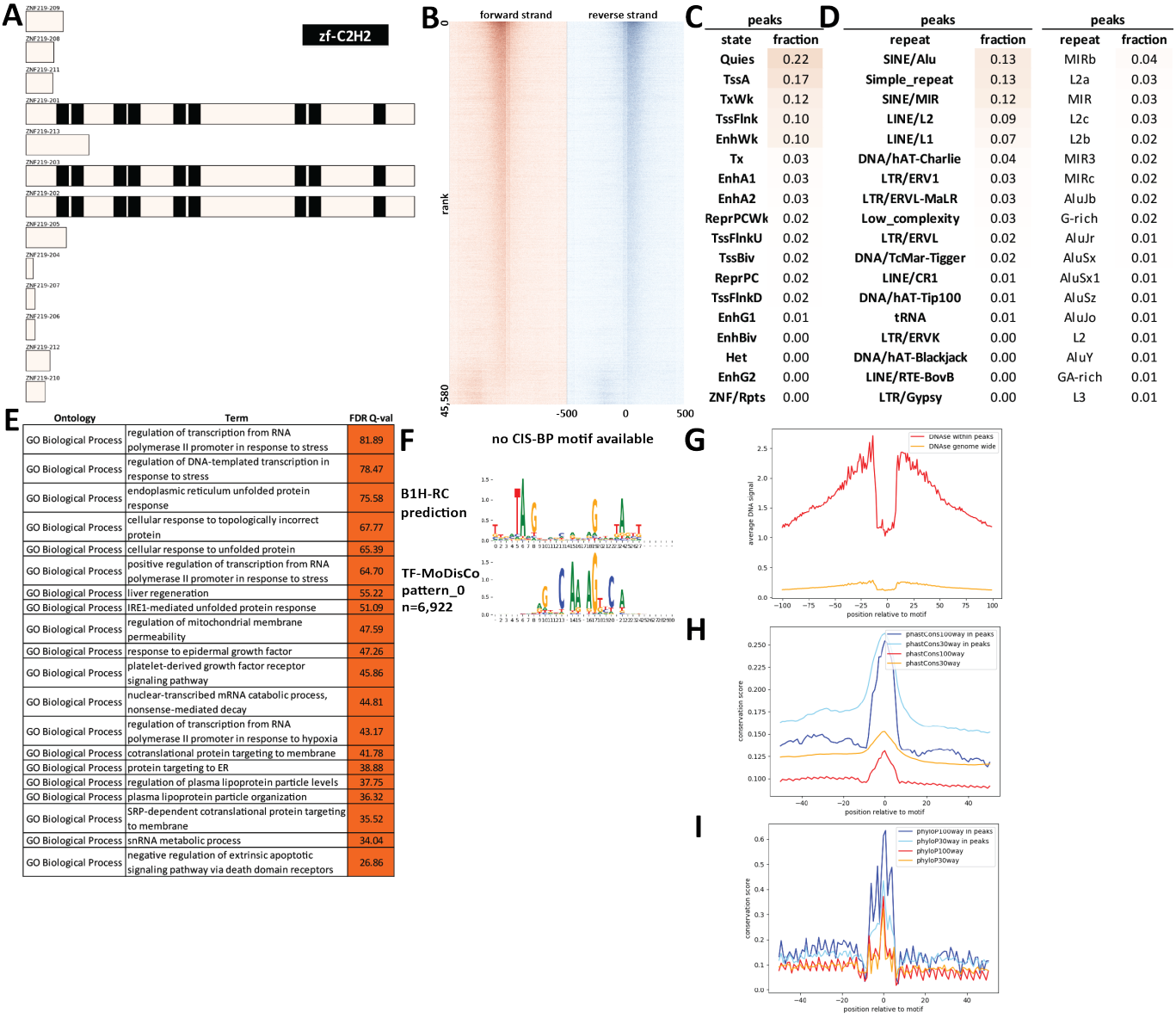

peaks	
state	fraction
Quies	0.22
TssA	0.17
TxWk	0.12
TssFlnk	0.10
EnhWk	0.10
Tx	0.03
EnhA1	0.03
EnhA2	0.03
ReprPCWk	0.02
TssFlnkU	0.02
TssBiv	0.02
ReprPC	0.02
TssFlnkD	0.02
EnhG1	0.01
EnhBiv	0.00
Het	0.00
EnhG2	0.00
ZNF/Rpts	0.00

peaks		peaks	
repeat	fraction	repeat	fraction
SINE/Alu	0.13	MIRb	0.04
Simple_repeat	0.13	L2a	0.03
SINE/MIR	0.12	MIR	0.03
LINE/L2	0.09	L2c	0.03
LINE/L1	0.07	L2b	0.02
DNA/hAT-Charlie	0.04	MIR3	0.02
LTR/ERV1	0.03	MIRc	0.02
LTR/ERVL-MaLR	0.03	AluJb	0.02
Low_complexity	0.03	G-rich	0.02
LTR/ERVL	0.02	AluJr	0.01
DNA/TcMar-Tigger	0.02	AluSx	0.01
LINE/CR1	0.01	AluSx1	0.01
DNA/hAT-Tip100	0.01	AluSz	0.01
tRNA	0.01	AluJo	0.01
LTR/ERVK	0.00	L2	0.01
DNA/hAT-Blackjack	0.00	AluY	0.01
LINE/RTE-BovB	0.00	GA-rich	0.01
LTR/Gypsy	0.00	L3	0.01

Ontology	Term	FDR Q-val
GO Biological Process	regulation of transcription from RNA polymerase II promoter in response to stress	81.89
GO Biological Process	regulation of DNA-templated transcription in response to stress	78.47
GO Biological Process	endoplasmic reticulum unfolded protein response	75.58
GO Biological Process	cellular response to topologically incorrect protein	67.77
GO Biological Process	cellular response to unfolded protein	65.39
GO Biological Process	positive regulation of transcription from RNA polymerase II promoter in response to stress	64.70
GO Biological Process	liver regeneration	55.22
GO Biological Process	IRE1-mediated unfolded protein response	51.09
GO Biological Process	regulation of mitochondrial membrane permeability	47.59
GO Biological Process	response to epidermal growth factor	47.26
GO Biological Process	platelet-derived growth factor receptor signaling pathway	45.86
GO Biological Process	nuclear-transcribed mRNA catabolic process, nonsense-mediated decay	44.81
GO Biological Process	regulation of transcription from RNA polymerase II promoter in response to hypoxia	43.17
GO Biological Process	cotranslational protein targeting to membrane	41.78
GO Biological Process	protein targeting to ER	38.88
GO Biological Process	regulation of plasma lipoprotein particle levels	37.75
GO Biological Process	plasma lipoprotein particle organization	36.32
GO Biological Process	SRP-dependent cotranslational protein targeting to membrane	35.52
GO Biological Process	snRNA metabolic process	34.04
GO Biological Process	negative regulation of extrinsic apoptotic signaling pathway via death domain receptors	26.86

Supplementary Figure 843: Properties and genomic distribution of motifs identified for the ZNF219 transcription factor in HepG2 (accession ENCSR243BPI).

TF-MoDisCO pattern_0 n=6922, CWM

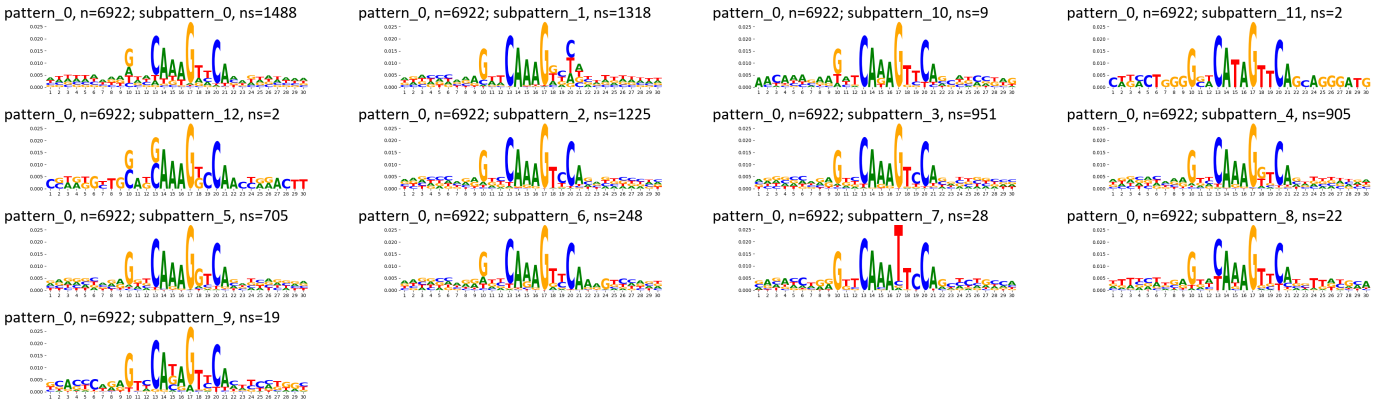

TF-MoDisCO pattern_0 n=6922, PWM

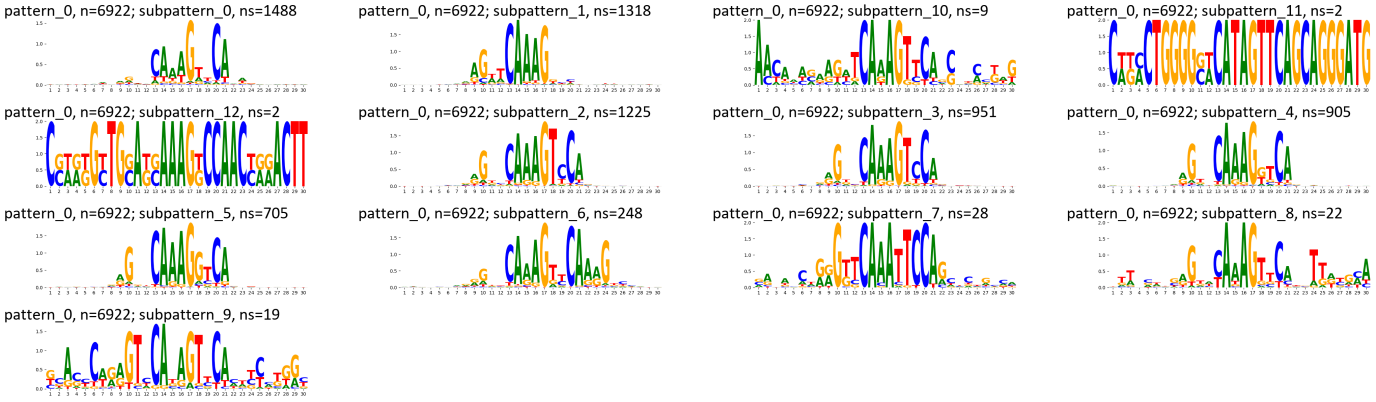

Supplementary Figure 844: TF-MoDisCO subpatterns for the ZNF219 transcription factor in HepG2 (accession ENCSR243BPI).

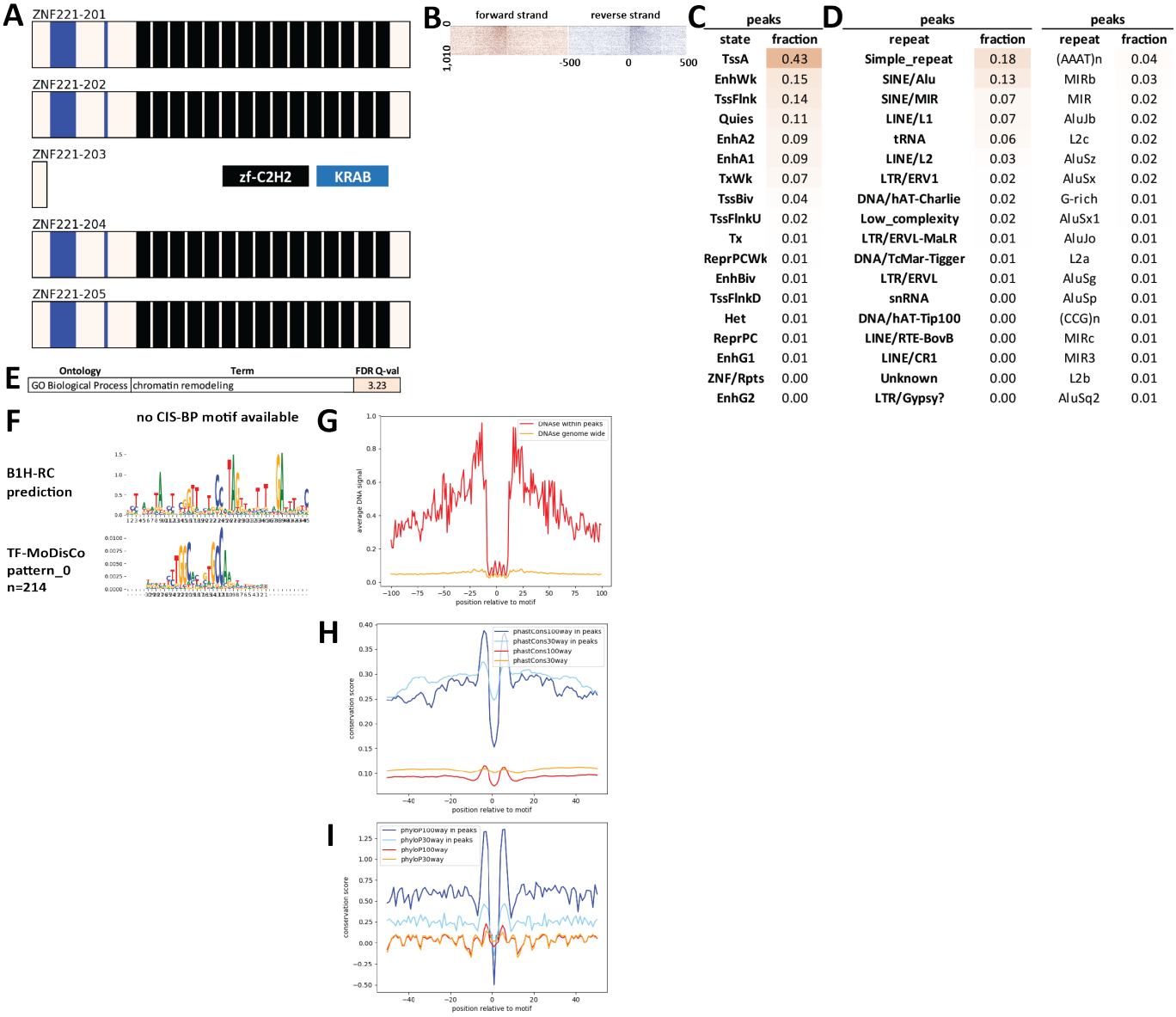

Supplementary Figure 845: Properties and genomic distribution of motifs identified for the ZNF221 transcription factor in HEK293 (accession ENCSR194BBY).

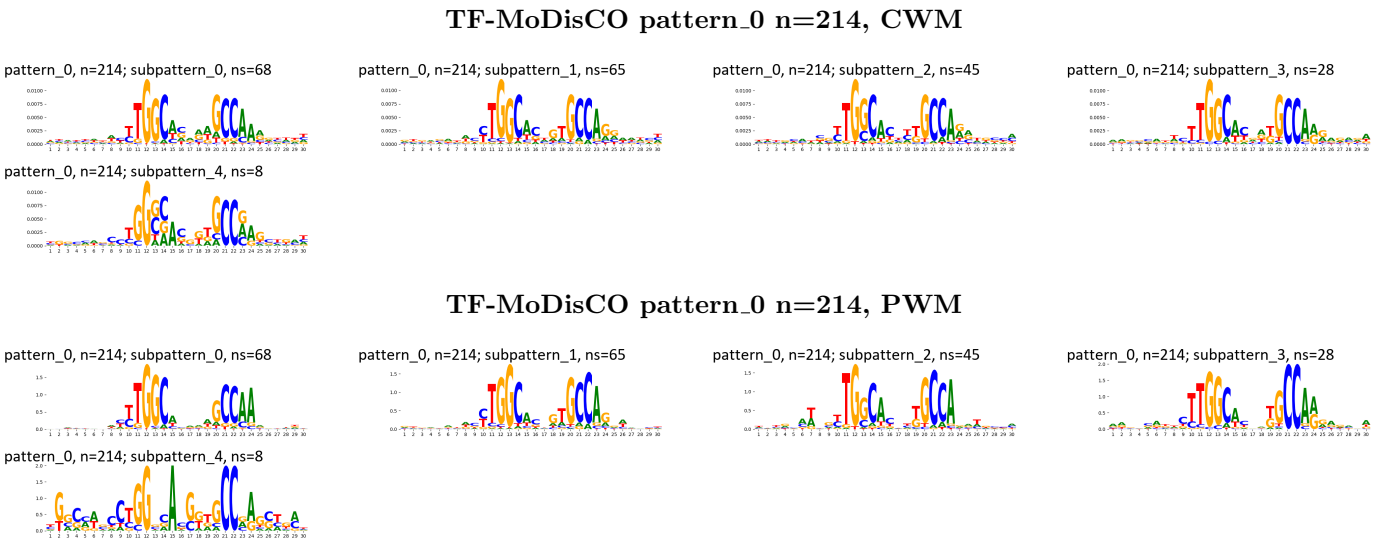

Supplementary Figure 846: TF-MoDisCO subpatterns for the ZNF221 transcription factor in HEK293 (accession ENCSR194BBY).

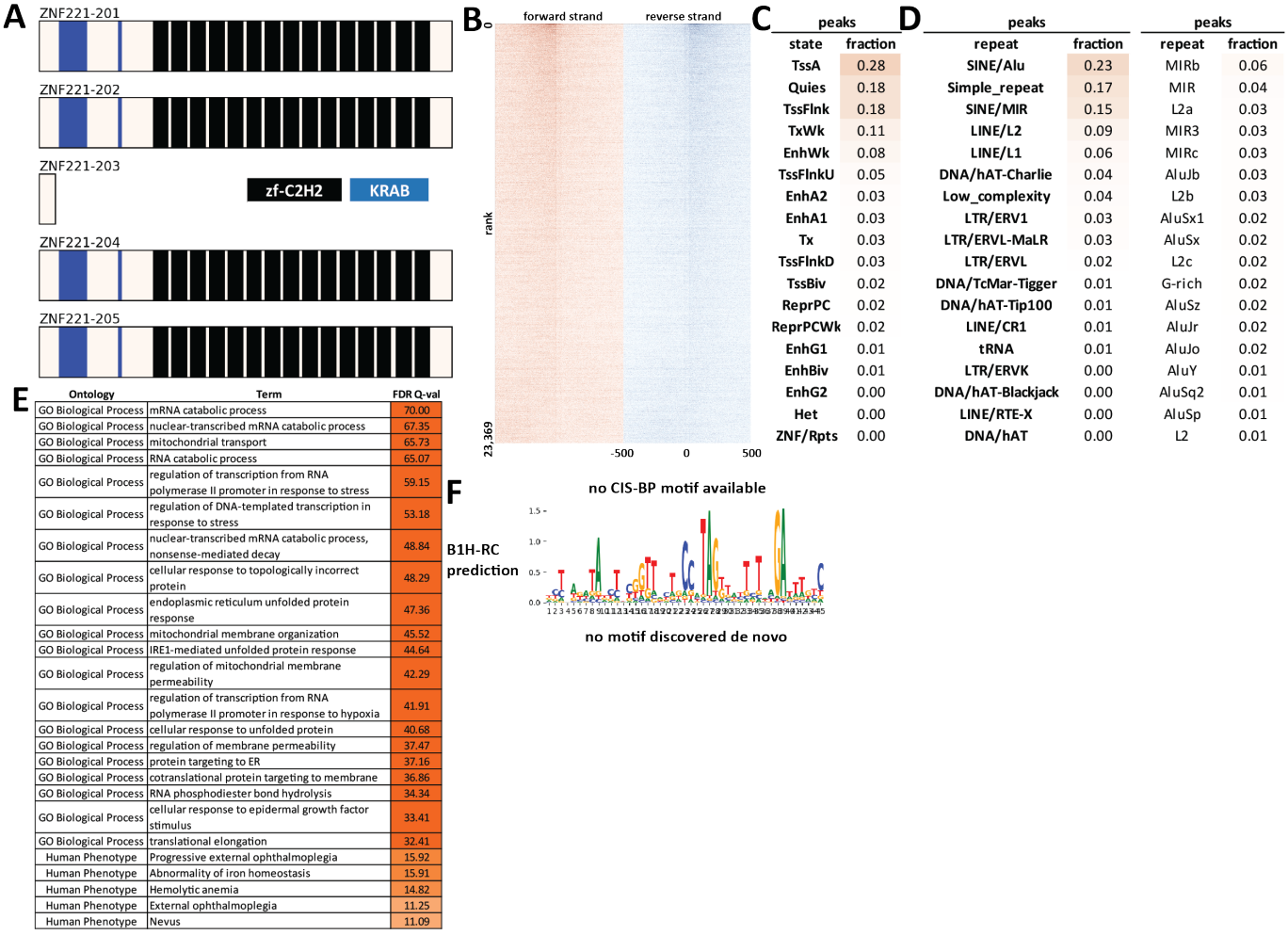

Supplementary Figure 847: Properties and genomic distribution of motifs identified for the ZNF221 transcription factor in HepG2 (accession ENCSR347HAM).

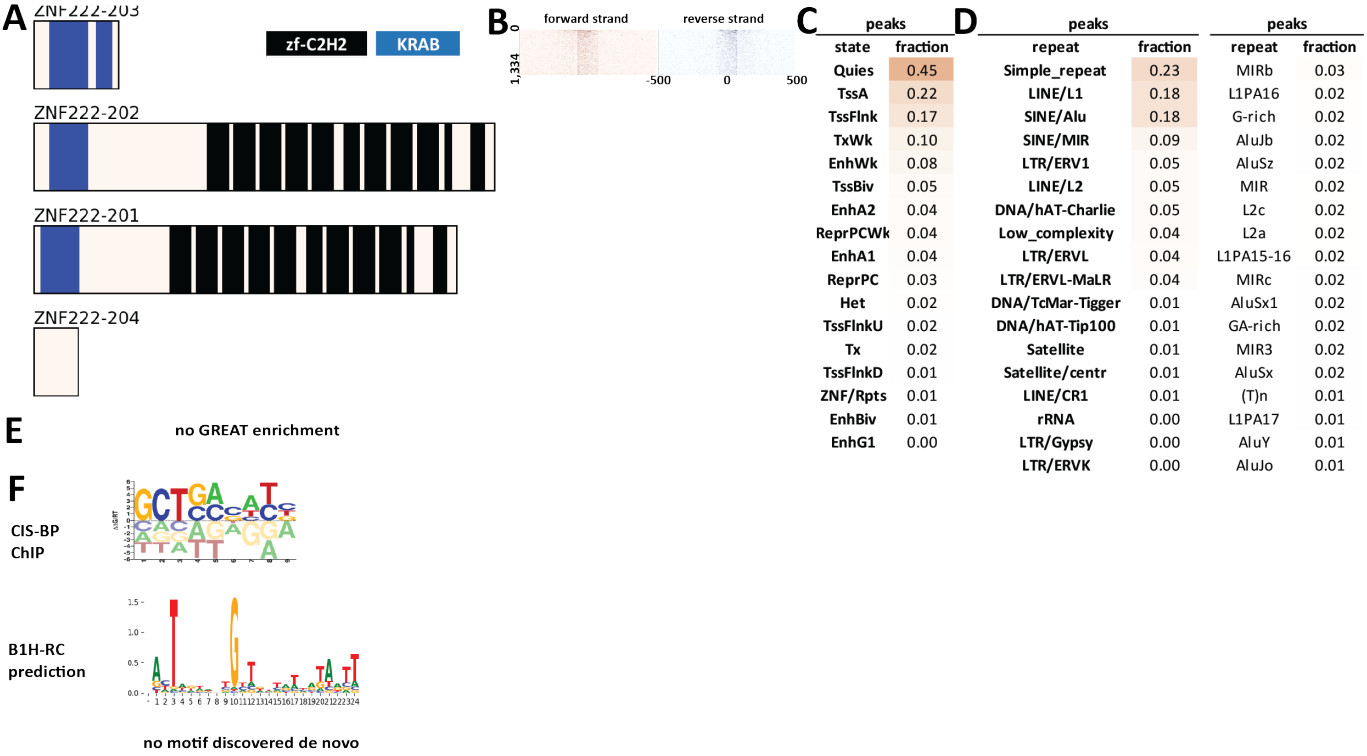

Supplementary Figure 848: Properties and genomic distribution of motifs identified for the ZNF222 transcription factor in HEK293 (accession ChipExo models).

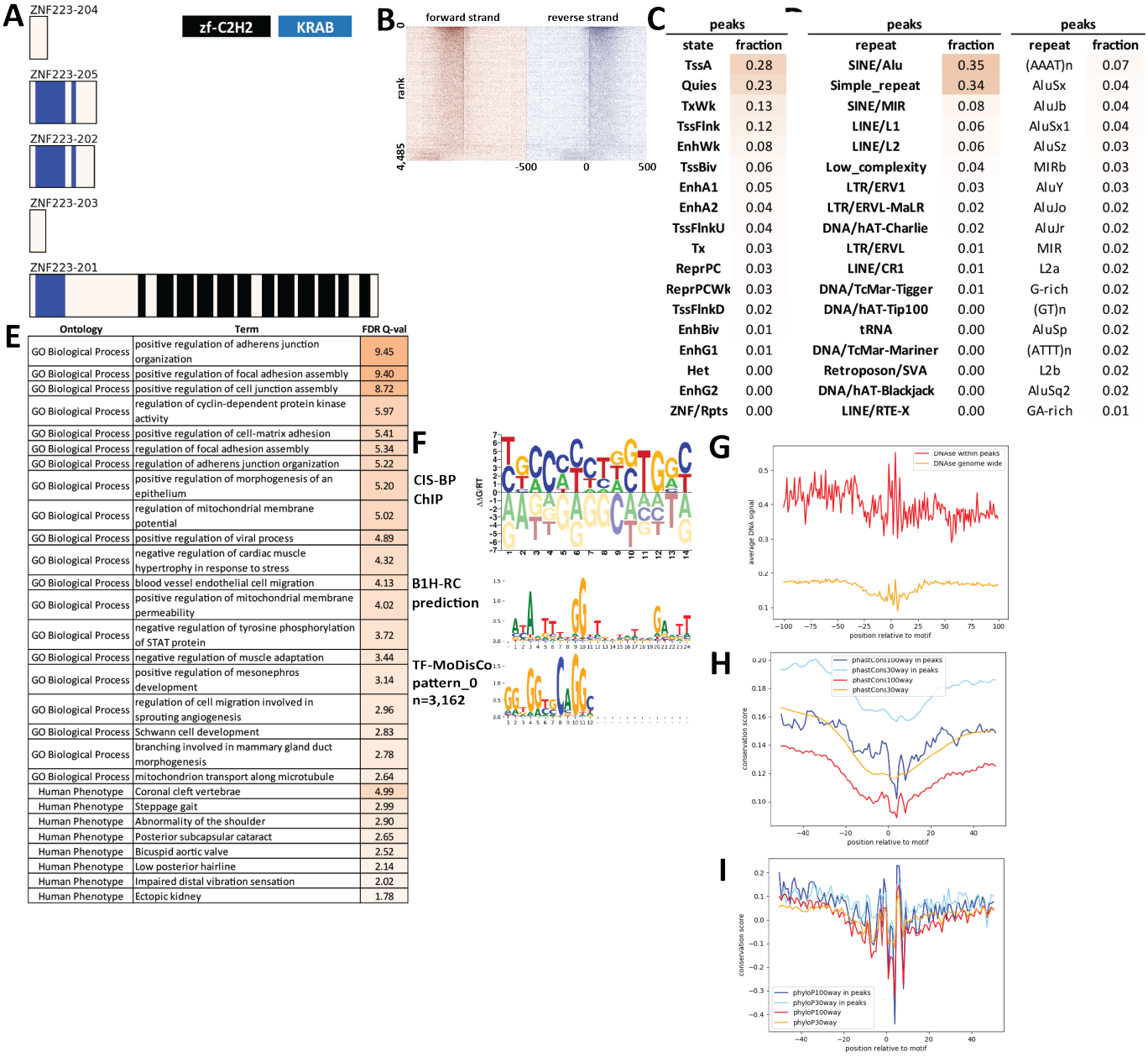

Supplementary Figure 849: Properties and genomic distribution of motifs identified for the ZNF223 transcription factor in HEK293 (accession ENCSR906PCS).

TF-MoDisCO pattern_0 n=3162, CWM

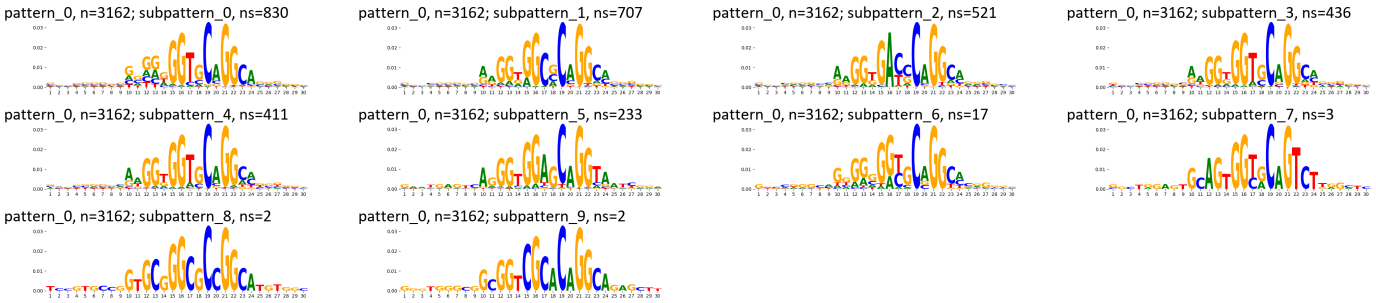

TF-MoDisCO pattern_0 n=3162, PWM

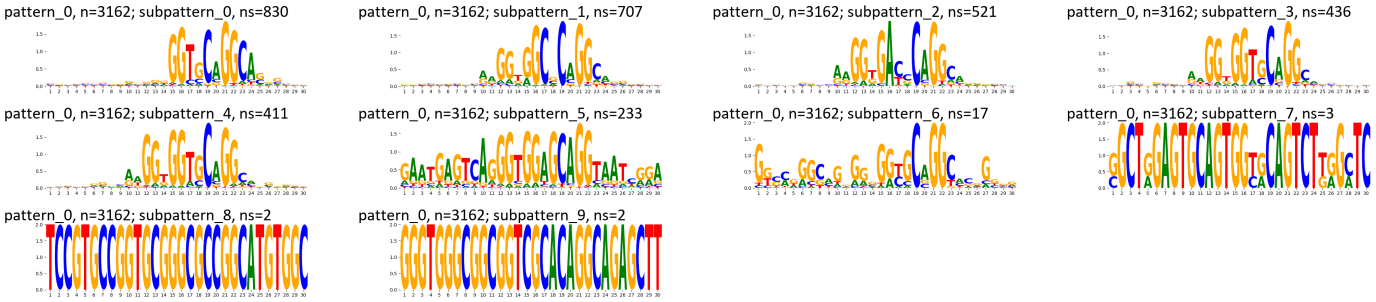

Supplementary Figure 850: TF-MoDisCO subpatterns for the ZNF223 transcription factor in HEK293 (accession ENCSR906PCS).

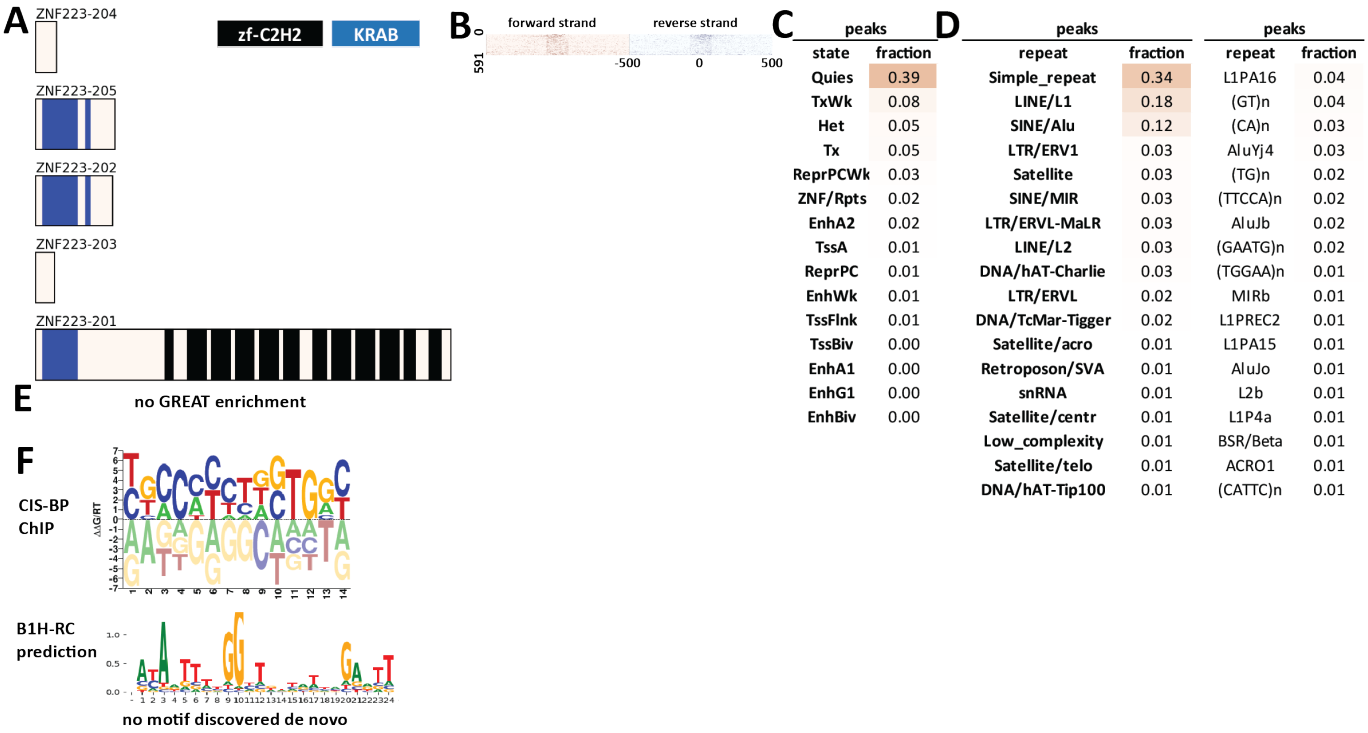

Supplementary Figure 851: Properties and genomic distribution of motifs identified for the ZNF223 transcription factor in HEK293 (accession ChipExo models).

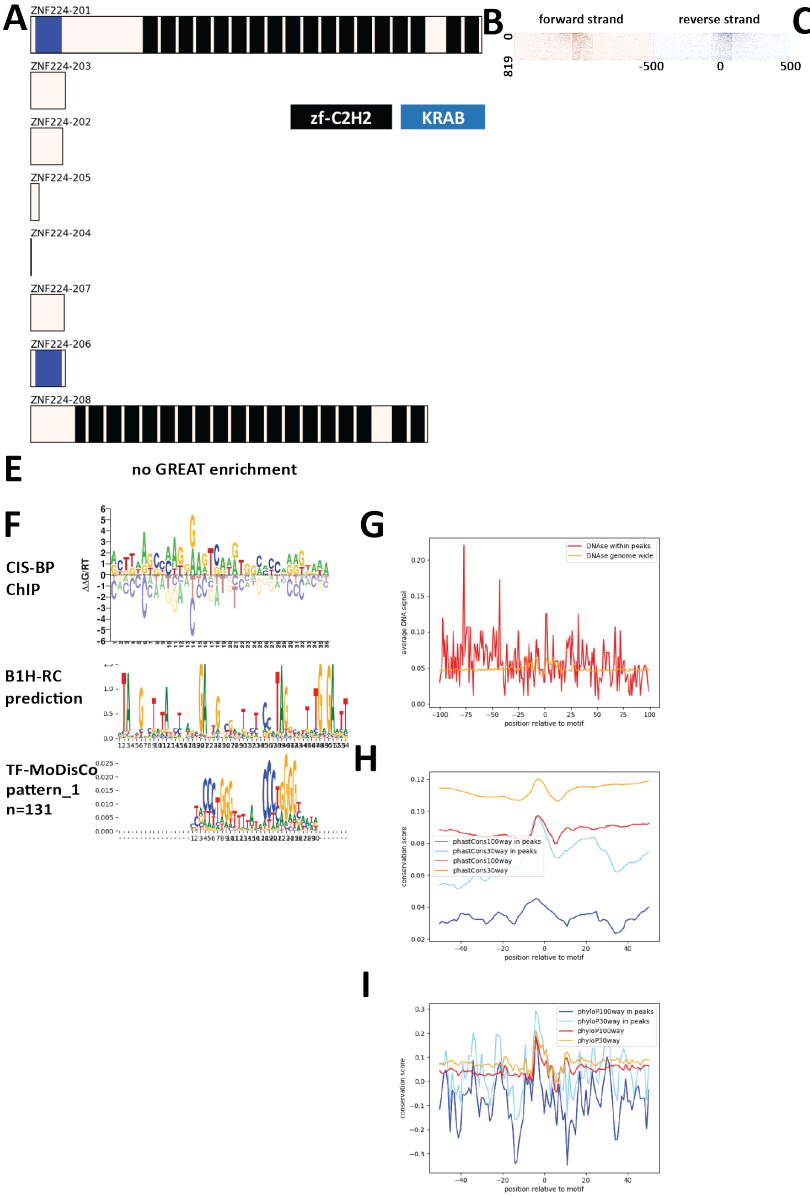

C

peaks	
state	fraction
Quies	0.51
TxWk	0.11
Tx	0.05
EnhWk	0.04
TssA	0.04
Het	0.04
TssFlnk	0.03
ReprPCWk	0.03
ReprPC	0.02
EnhA2	0.02
EnhA1	0.01
ZNF/Rpts	0.01
TssBiv	0.01
TssFlnkU	0.01
EnhG1	0.01
TssFlnkD	0.00
EnhBiv	0.00

D

peaks		peaks	
repeat	fraction	repeat	fraction
SINE/Alu	0.26	MER70A	0.09
LINE/L1	0.19	AluJb	0.06
Simple_repeat	0.18	MER70B	0.05
LTR/ERVL	0.17	AluJo	0.03
LTR/ERV1	0.10	MIRb	0.03
SINE/MIR	0.09	AluJr	0.03
LINE/L2	0.07	MER50	0.03
DNA/hAT-Charlie	0.06	L2a	0.03
LTR/ERVL-MaLR	0.05	MIR	0.02
Satellite	0.02	MIRc	0.02
Low_complexity	0.02	MIR3	0.02
DNA/TcMar-Tigger	0.02	L2c	0.02
DNA/hAT-Tip100	0.01	AluSx1	0.02
LTR/ERVK	0.01	MER50-int	0.02
LINE/CR1	0.01	AluY	0.02
Satellite/centr	0.01	L2	0.01
DNA/hAT-Blackjack	0.00	AluYj4	0.01
Retroposon/SVA	0.00	L2b	0.01

Supplementary Figure 852: Properties and genomic distribution of motifs identified for the ZNF224 transcription factor in HEK293 (accession ChipExo models).

TF-MoDisCO pattern_1 n=131, CWM

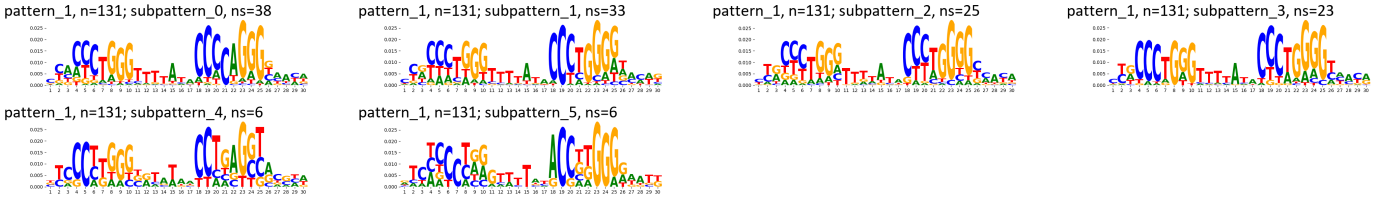

TF-MoDisCO pattern_1 n=131, PWM

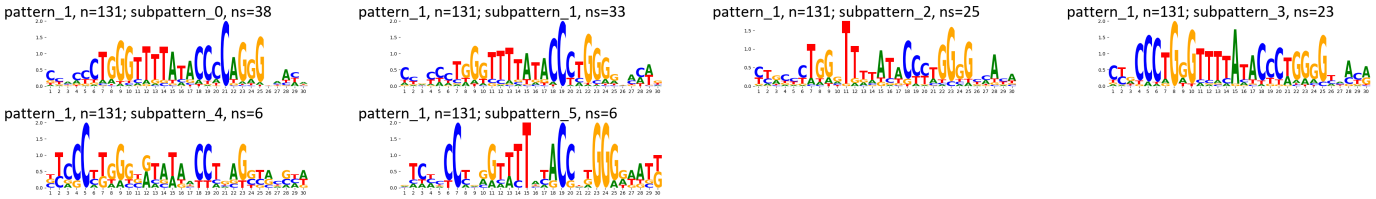

Supplementary Figure 853: TF-MoDisCO subpatterns for the ZNF224 transcription factor in HEK293 (accession ChipExo models).

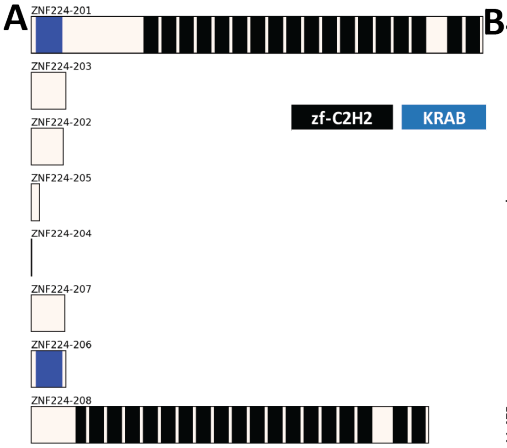

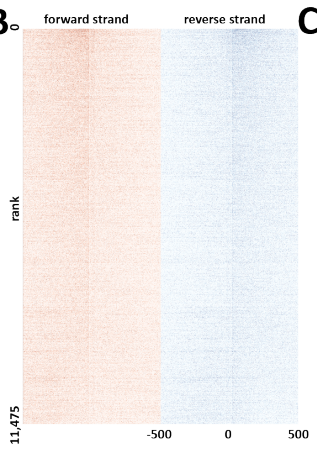

C

peaks	
state	fraction
TssA	0.39
TssFlnk	0.21
Quies	0.16
TxWk	0.09
EnhWk	0.05
TssFlnkU	0.05
EnhA2	0.03
TssBiv	0.03
EnhA1	0.03
Tx	0.02
TssFlnkD	0.02
ReprPC	0.02
ReprPCWk	0.02
EnhBiv	0.01
EnhG1	0.01
Het	0.00
EnhG2	0.00
ZNF/Rpts	0.00

D

peaks		peaks	
repeat	fraction	repeat	fraction
SINE/Alu	0.19	MIRb	0.05
Simple_repeat	0.19	MIR	0.03
SINE/MIR	0.14	L2a	0.03
LINE/L2	0.07	MIR3	0.03
LINE/L1	0.04	MIRc	0.03
Low_complexity	0.04	G-rich	0.02
DNA/hAT-Charlie	0.03	AluJb	0.02
LTR/ERV1	0.02	AluSx	0.02
LTR/ERVL-MaLR	0.02	AluSx1	0.02
LTR/ERVL	0.01	L2b	0.02
DNA/TcMar-Tigger	0.01	AluSz	0.02
LINE/CR1	0.01	L2c	0.02
tRNA	0.01	AluJr	0.01
DNA/hAT-Tip100	0.01	AluJo	0.01
DNA/hAT-Blackjack	0.00	AluY	0.01
LTR/ERVK	0.00	AluSq2	0.01
DNA/hAT	0.00	AluSp	0.01
LINE/RTE-X	0.00	GA-rich	0.01

E

Ontology	Term	FDR Q-val
GO Biological Process	rRNA metabolic process	39.28
GO Biological Process	rRNA processing	37.65
GO Biological Process	mRNA catabolic process	35.76
GO Biological Process	nuclear-transcribed mRNA catabolic process	34.55
GO Biological Process	protein targeting to ER	31.65
GO Biological Process	RNA catabolic process	31.39
GO Biological Process	regulation of transcription from RNA polymerase II promoter in response to stress	30.39
GO Biological Process	mitochondrial transport	29.13
GO Biological Process	translational elongation	28.85
GO Biological Process	cotranslational protein targeting to membrane	28.41
GO Biological Process	regulation of DNA-templated transcription in response to stress	28.38
GO Biological Process	nuclear-transcribed mRNA catabolic process, nonsense-mediated decay	28.14
GO Biological Process	protein localization to endoplasmic reticulum	27.97
GO Biological Process	cellular response to topologically incorrect protein	26.78
GO Biological Process	mitochondrial translational termination	26.76
GO Biological Process	establishment of protein localization to endoplasmic reticulum	26.44
GO Biological Process	macromolecular complex disassembly	26.44
GO Biological Process	mitochondrial translation	26.37
GO Biological Process	SRP-dependent cotranslational protein targeting to membrane	26.11
GO Biological Process	cellular response to unfolded protein	25.82
Human Phenotype	Elevated hepatic transaminases	12.31
Human Phenotype	Increased serum lactate	12.18
Human Phenotype	Exercise intolerance	9.72
Human Phenotype	Abnormal CSF metabolite level	8.58
Human Phenotype	Abnormality of the mitochondrion	7.25
Human Phenotype	Abnormality of mitochondrial metabolism	7.16
Human Phenotype	Abnormality of glycolysis	5.47
Human Phenotype	Generalized aminoaciduria	3.39
Human Phenotype	Glutaric aciduria	2.62

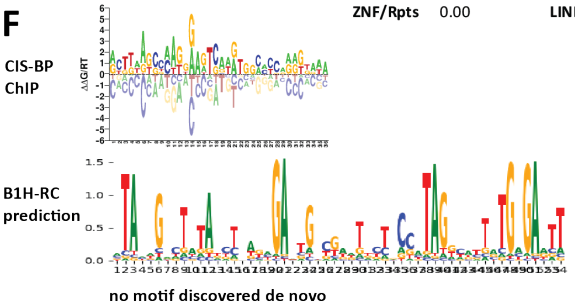

Supplementary Figure 854: Properties and genomic distribution of motifs identified for the ZNF224 transcription factor in HepG2 (accession ENCSR886VSY).

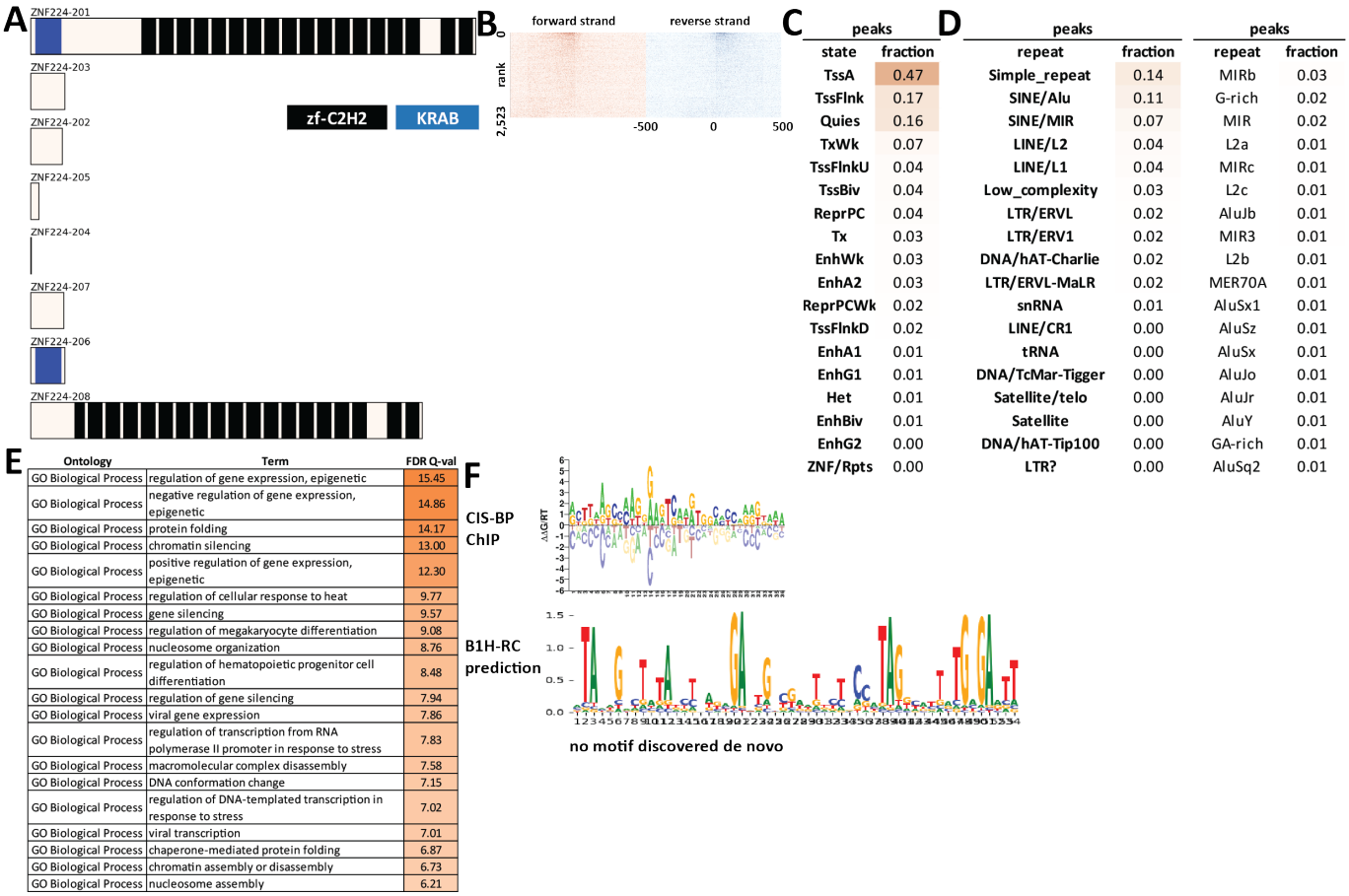

C

peaks	
state	fraction
TssA	0.47
TssFlnk	0.17
Quies	0.16
TxWk	0.07
TssFlnkU	0.04
TssBiv	0.04
ReprPC	0.04
Tx	0.03
EnhWk	0.03
EnhA2	0.03
ReprPCWk	0.02
TssFlnkD	0.02
EnhA1	0.01
EnhG1	0.01
Het	0.01
EnhBiv	0.01
EnhG2	0.00
ZNF/Rpts	0.00

D

peaks		peaks	
repeat	fraction	repeat	fraction
Simple_repeat	0.14	MIRb	0.03
SINE/Alu	0.11	G-rich	0.02
SINE/MIR	0.07	MIR	0.02
LINE/L2	0.04	L2a	0.01
LINE/L1	0.04	MIRc	0.01
Low_complexity	0.03	L2c	0.01
LTR/ERVL	0.02	AluJb	0.01
LTR/ERV1	0.02	MIR3	0.01
DNA/hAT-Charlie	0.02	L2b	0.01
LTR/ERVL-MaLR	0.02	MER70A	0.01
snRNA	0.01	AluSx1	0.01
LINE/CR1	0.00	AluSz	0.01
tRNA	0.00	AluSx	0.01
DNA/TcMar-Tigger	0.00	AluJo	0.01
Satellite/telo	0.00	AluJr	0.01
Satellite	0.00	AluY	0.01
DNA/hAT-Tip100	0.00	GA-rich	0.01
LTR?	0.00	AluSq2	0.01

E

Ontology	Term	FDR Q-val
GO Biological Process	regulation of gene expression, epigenetic	15.45
GO Biological Process	negative regulation of gene expression, epigenetic	14.86
GO Biological Process	protein folding	14.17
GO Biological Process	chromatin silencing	13.00
GO Biological Process	positive regulation of gene expression, epigenetic	12.30
GO Biological Process	regulation of cellular response to heat	9.77
GO Biological Process	gene silencing	9.57
GO Biological Process	regulation of megakaryocyte differentiation	9.08
GO Biological Process	nucleosome organization	8.76
GO Biological Process	regulation of hematopoietic progenitor cell differentiation	8.48
GO Biological Process	regulation of gene silencing	7.94
GO Biological Process	viral gene expression	7.86
GO Biological Process	regulation of transcription from RNA polymerase II promoter in response to stress	7.83
GO Biological Process	macromolecular complex disassembly	7.58
GO Biological Process	DNA conformation change	7.15
GO Biological Process	regulation of DNA-templated transcription in response to stress	7.02
GO Biological Process	viral transcription	7.01
GO Biological Process	chaperone-mediated protein folding	6.87
GO Biological Process	chromatin assembly or disassembly	6.73
GO Biological Process	nucleosome assembly	6.21

Supplementary Figure 855: Properties and genomic distribution of motifs identified for the ZNF224 transcription factor in K562 (accession ENCSR409PXW).

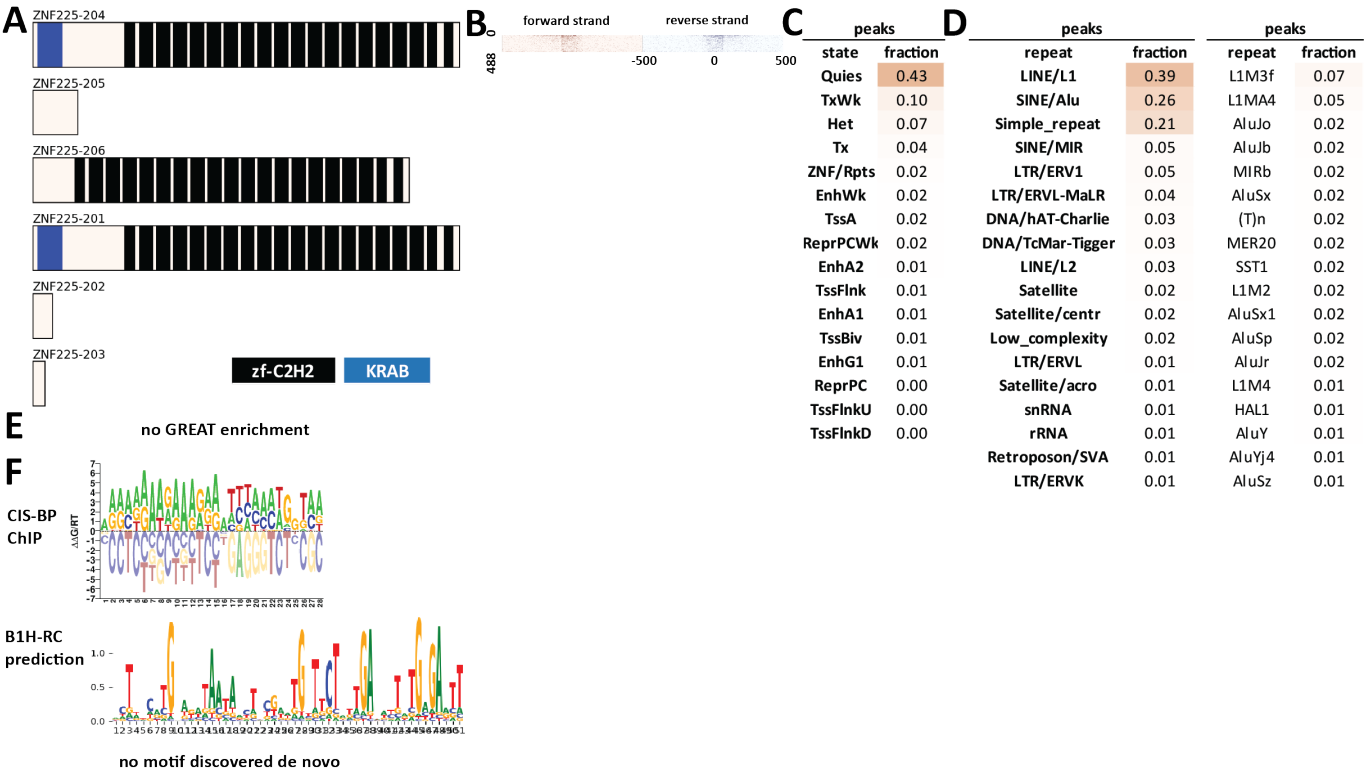

peaks	
state	fraction
Quies	0.43
TxWk	0.10
Het	0.07
Tx	0.04
ZNF/Rpts	0.02
EnhWk	0.02
TssA	0.02
ReprPCWk	0.02
EnhA2	0.01
TssFlnk	0.01
EnhA1	0.01
TssBiv	0.01
EnhG1	0.01
ReprPC	0.00
TssFlnkU	0.00
TssFlnkD	0.00

peaks	
repeat	fraction
LINE/L1	0.39
SINE/Alu	0.26
Simple_repeat	0.21
SINE/MIR	0.05
LTR/ERV1	0.05
LTR/ERVL-MaLR	0.04
DNA/hAT-Charlie	0.03
DNA/TcMar-Tigger	0.03
LINE/L2	0.03
Satellite	0.02
Satellite/centr	0.02
Low_complexity	0.02
LTR/ERVL	0.01
Satellite/acro	0.01
snRNA	0.01
rRNA	0.01
Retroposon/SVA	0.01
LTR/ERVK	0.01

peaks	
repeat	fraction
L1M3f	0.07
L1MA4	0.05
AluJo	0.02
AluJb	0.02
MIRb	0.02
AluSx	0.02
(T)n	0.02
MER20	0.02
SST1	0.02
L1M2	0.02
AluSx1	0.02
AluSp	0.02
AluJr	0.02
L1M4	0.01
HAL1	0.01
AluY	0.01
AluYj4	0.01
AluSz	0.01

Supplementary Figure 856: Properties and genomic distribution of motifs identified for the ZNF225 transcription factor in HEK293 (accession ChipExo models).

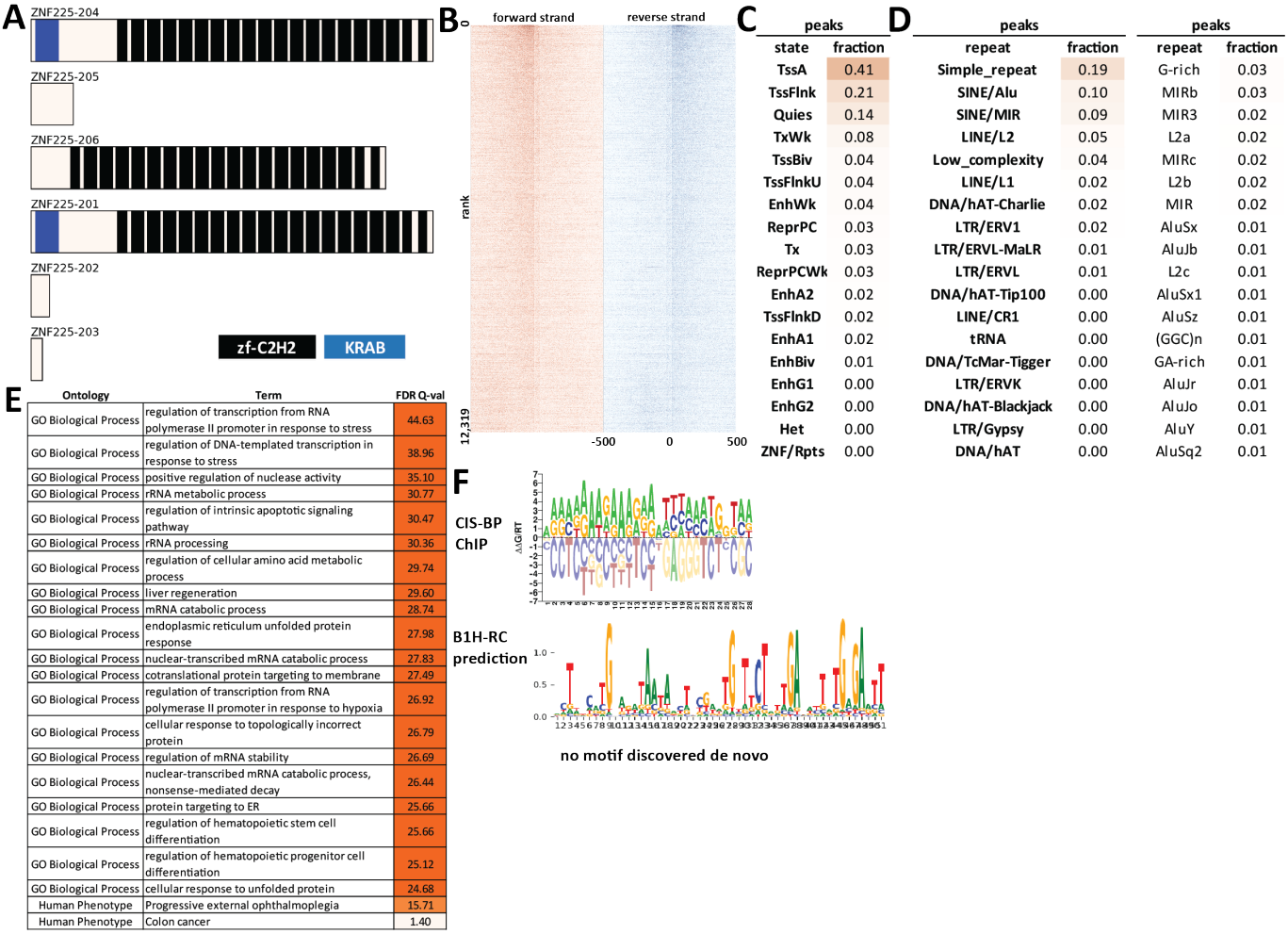

C

peaks	
state	fraction
TssA	0.41
TssFlnk	0.21
Quies	0.14
TxWk	0.08
TssBiv	0.04
TssFlnkU	0.04
EnhWk	0.04
ReprPC	0.03
Tx	0.03
ReprPCWk	0.03
EnhA2	0.02
TssFlnkD	0.02
EnhA1	0.02
EnhBiv	0.01
EnhG1	0.00
EnhG2	0.00
Het	0.00
ZNF/Rpts	0.00

D

peaks		peaks	
repeat	fraction	repeat	fraction
Simple_repeat	0.19	G-rich	0.03
SINE/Alu	0.10	MIRb	0.03
SINE/MIR	0.09	MIR3	0.02
LINE/L2	0.05	L2a	0.02
Low_complexity	0.04	MIRc	0.02
LINE/L1	0.02	L2b	0.02
DNA/hAT-Charlie	0.02	MIR	0.02
LTR/ERV1	0.02	AluSx	0.01
LTR/ERVL-MaLR	0.01	AluJb	0.01
LTR/ERVL	0.01	L2c	0.01
DNA/hAT-Tip100	0.00	AluSx1	0.01
LINE/CR1	0.00	AluSz	0.01
tRNA	0.00	(GGC)n	0.01
DNA/TcMar-Tigger	0.00	GA-rich	0.01
LTR/ERVK	0.00	AluJr	0.01
DNA/hAT-Blackjack	0.00	AluJo	0.01
LTR/Gypsy	0.00	AluY	0.01
DNA/hAT	0.00	AluSq2	0.01

E

Ontology	Term	FDR Q-val
GO Biological Process	regulation of transcription from RNA polymerase II promoter in response to stress	44.63
GO Biological Process	regulation of DNA-templated transcription in response to stress	38.96
GO Biological Process	positive regulation of nuclease activity	35.10
GO Biological Process	rRNA metabolic process	30.77
GO Biological Process	regulation of intrinsic apoptotic signaling pathway	30.47
GO Biological Process	rRNA processing	30.36
GO Biological Process	regulation of cellular amino acid metabolic process	29.74
GO Biological Process	liver regeneration	29.60
GO Biological Process	mRNA catabolic process	28.74
GO Biological Process	endoplasmic reticulum unfolded protein response	27.98
GO Biological Process	nuclear-transcribed mRNA catabolic process	27.83
GO Biological Process	cotranslational protein targeting to membrane	27.49
GO Biological Process	regulation of transcription from RNA polymerase II promoter in response to hypoxia	26.92
GO Biological Process	cellular response to topologically incorrect protein	26.79
GO Biological Process	regulation of mRNA stability	26.69
GO Biological Process	nuclear-transcribed mRNA catabolic process, nonsense-mediated decay	26.44
GO Biological Process	protein targeting to ER	25.66
GO Biological Process	regulation of hematopoietic stem cell differentiation	25.66
GO Biological Process	regulation of hematopoietic progenitor cell differentiation	25.12
GO Biological Process	cellular response to unfolded protein	24.68
Human Phenotype	Progressive external ophthalmoplegia	15.71
Human Phenotype	Colon cancer	1.40

Supplementary Figure 857: Properties and genomic distribution of motifs identified for the ZNF225 transcription factor in HepG2 (accession ENCSR075PWK).

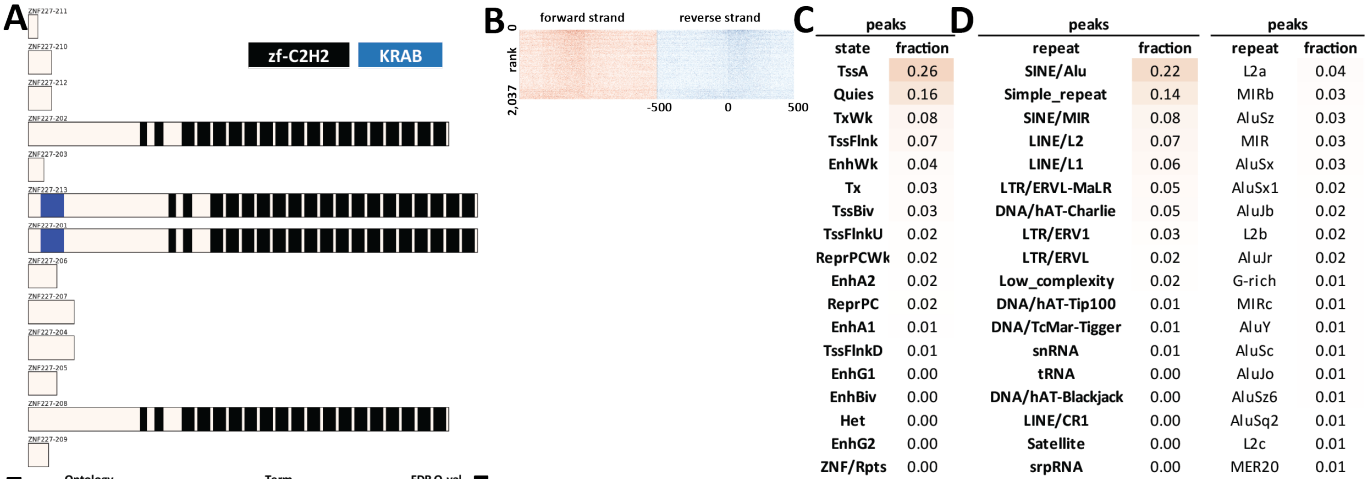

C

peaks

state	fraction
TssA	0.26
Quies	0.16
TxWk	0.08
TssFlnk	0.07
EnhWk	0.04
Tx	0.03
TssBiv	0.03
TssFlnkU	0.02
ReprPCWk	0.02
EnhA2	0.02
ReprPC	0.02
EnhA1	0.01
TssFlnkD	0.01
EnhG1	0.00
EnhBiv	0.00
Het	0.00
EnhG2	0.00
ZNF/Rpts	0.00

D

peaks

repeat	fraction
SINE/Alu	0.22
Simple_repeat	0.14
SINE/MIR	0.08
LINE/L2	0.07
LINE/L1	0.06
LTR/ERVL-MaLR	0.05
DNA/hAT-Charlie	0.05
LTR/ERV1	0.03
LTR/ERVL	0.02
Low_complexity	0.02
DNA/hAT-Tip100	0.01
DNA/TcMar-Tigger	0.01
snRNA	0.01
tRNA	0.00
DNA/hAT-Blackjack	0.00
LINE/CR1	0.00
Satellite	0.00
srpRNA	0.00

peaks

repeat	fraction
L2a	0.04
MIRb	0.03
AluSz	0.03
MIR	0.03
AluSx	0.03
AluSx1	0.02
AluJb	0.02
L2b	0.02
AluJr	0.02
G-rich	0.01
MIRc	0.01
AluY	0.01
AluSc	0.01
AluJo	0.01
AluSz6	0.01
AluSq2	0.01
L2c	0.01
MER20	0.01

E

Ontology	Term	FDR Q-val
GO Biological Process	gland development	119.03
GO Biological Process	chordate embryonic development	117.85
GO Biological Process	embryo development ending in birth or egg hatching	116.99
GO Biological Process	regulation of epithelial cell proliferation	111.61
GO Biological Process	macromolecular complex subunit organization	99.11
GO Biological Process	negative regulation of signal transduction	83.83
GO Biological Process	negative regulation of cell communication	73.23
GO Biological Process	negative regulation of signaling	72.99
GO Biological Process	embryo development	61.80
GO Biological Process	endoplasmic reticulum unfolded protein response	24.95
GO Biological Process	positive regulation of endoplasmic reticulum unfolded protein response	24.69
GO Biological Process	regulation of endoplasmic reticulum unfolded protein response	21.75
GO Biological Process	in utero embryonic development	15.71
GO Biological Process	response to endoplasmic reticulum stress	15.00
GO Biological Process	placenta development	14.20
GO Biological Process	embryonic placenta development	13.51
GO Biological Process	chromatin silencing	10.78
GO Biological Process	regulation of megakaryocyte differentiation	8.18
GO Biological Process	regulation of hematopoietic progenitor cell differentiation	8.17
GO Biological Process	negative regulation of megakaryocyte differentiation	7.91

F

no CIS-BP motif available

B1H-RC prediction

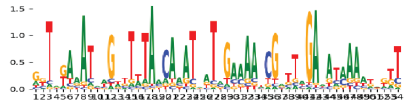

no motif discovered de novo

Supplementary Figure 858: Properties and genomic distribution of motifs identified for the ZNF227 transcription factor in MCF-7 (accession ENCSR877UJB).

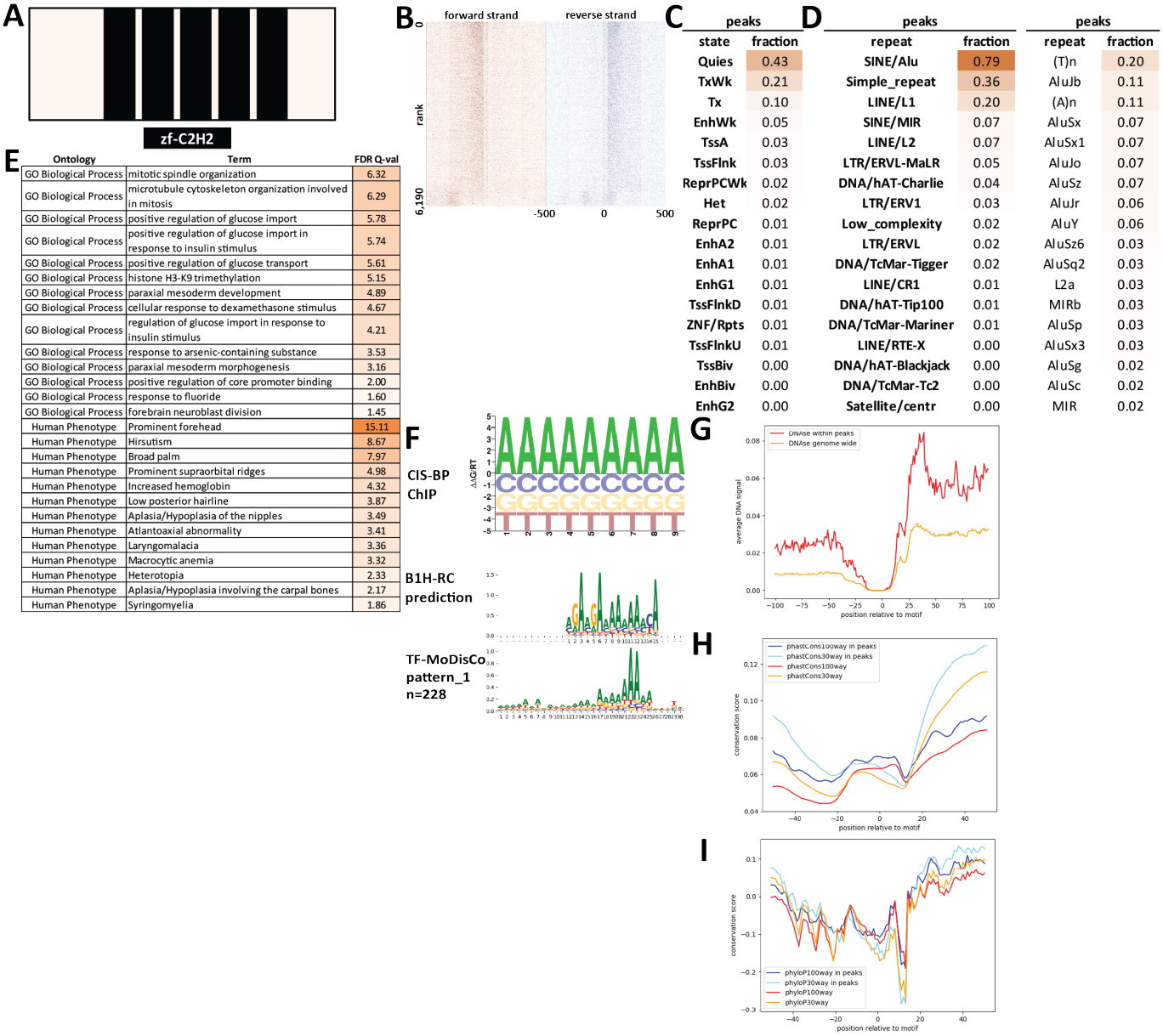

Supplementary Figure 859: Properties and genomic distribution of motifs identified for the ZNF22 transcription factor in HEK293 (accession Hughes GR models).

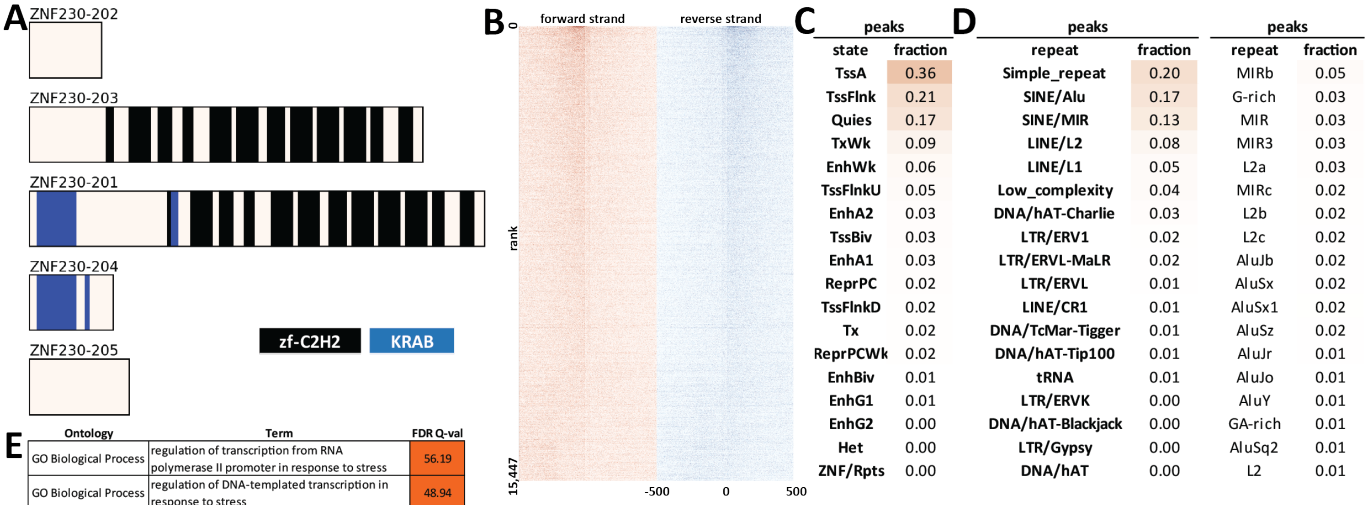

Supplementary Figure 860: Properties and genomic distribution of motifs identified for the ZNF230 transcription factor in HepG2 (accession ENCSR087HFN).

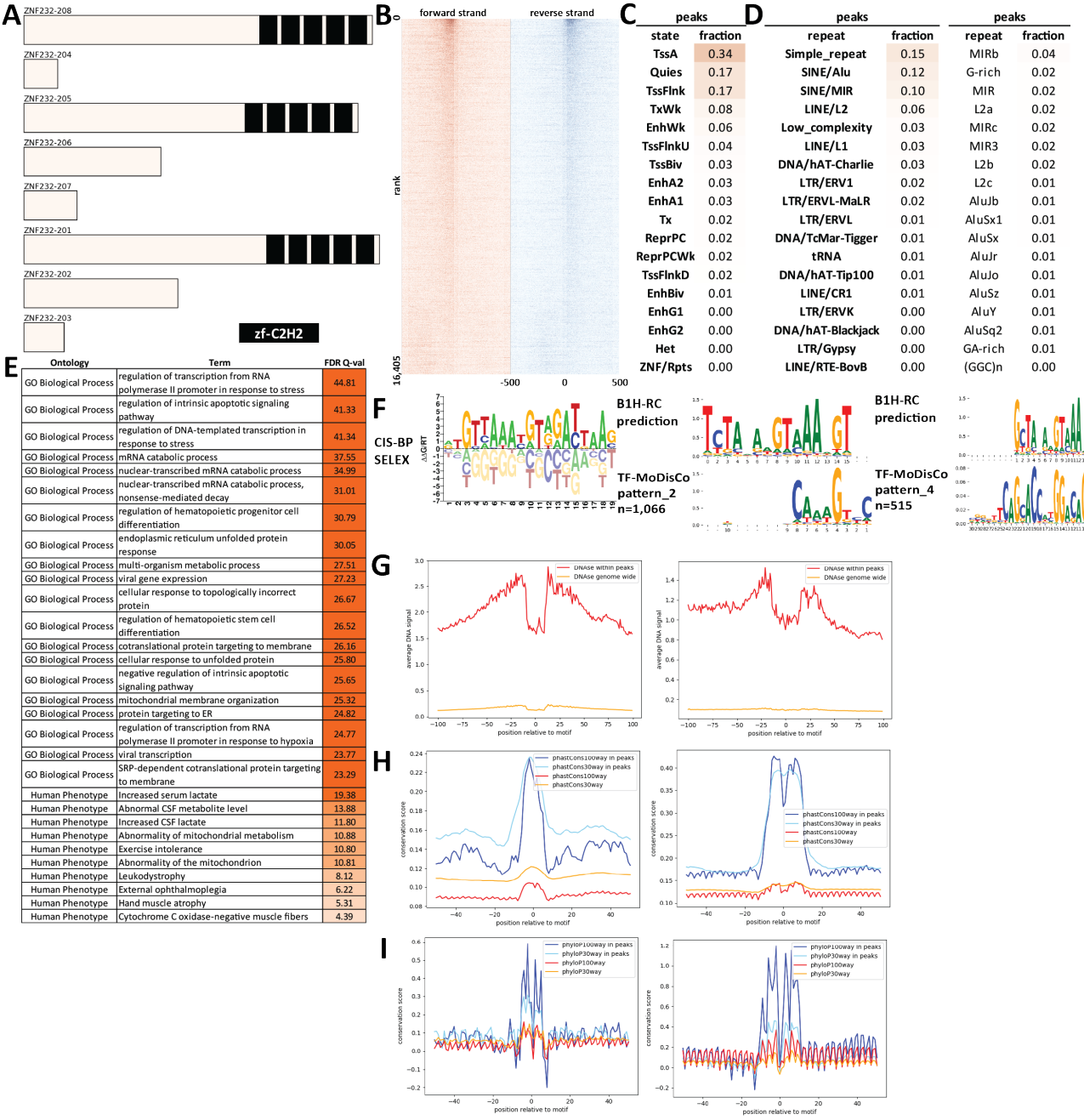

Supplementary Figure 861: Properties and genomic distribution of motifs identified for the ZNF232 transcription factor in HepG2 (accession ENCSR837GLU).

TF-MoDisCO pattern_2 n=1066, CWM

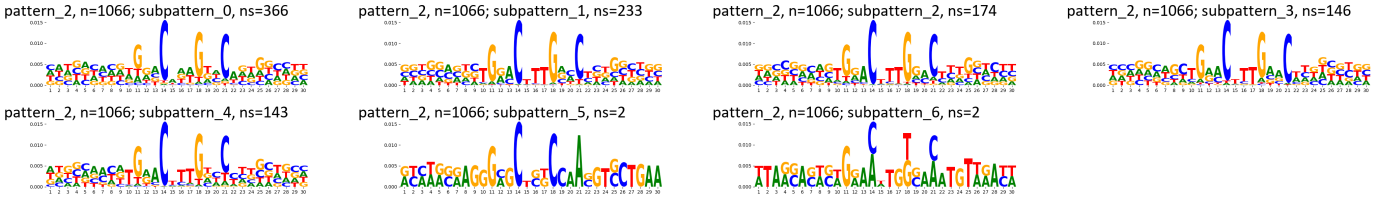

TF-MoDisCO pattern_2 n=1066, PWM

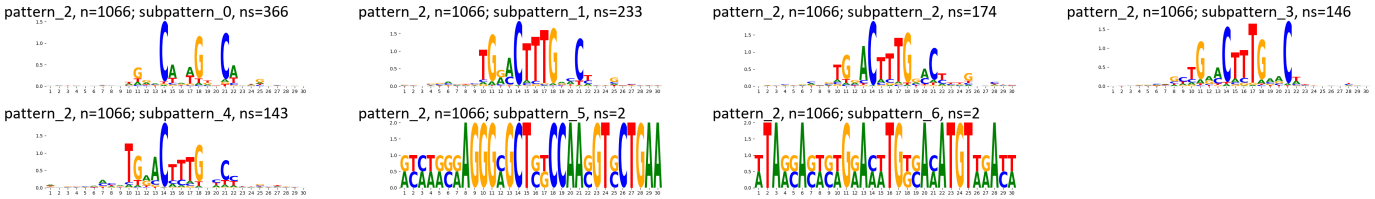

TF-MoDisCO pattern_4 n=515, CWM

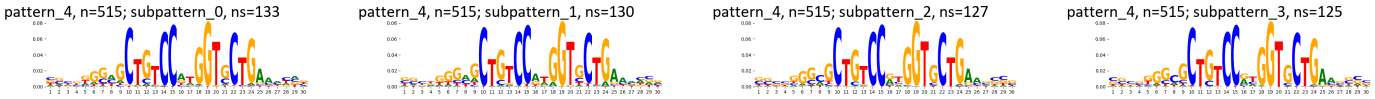

TF-MoDisCO pattern_4 n=515, PWM



Supplementary Figure 862: TF-MoDisCO subpatterns for the ZNF232 transcription factor in HepG2 (accession ENCSR837GLU).

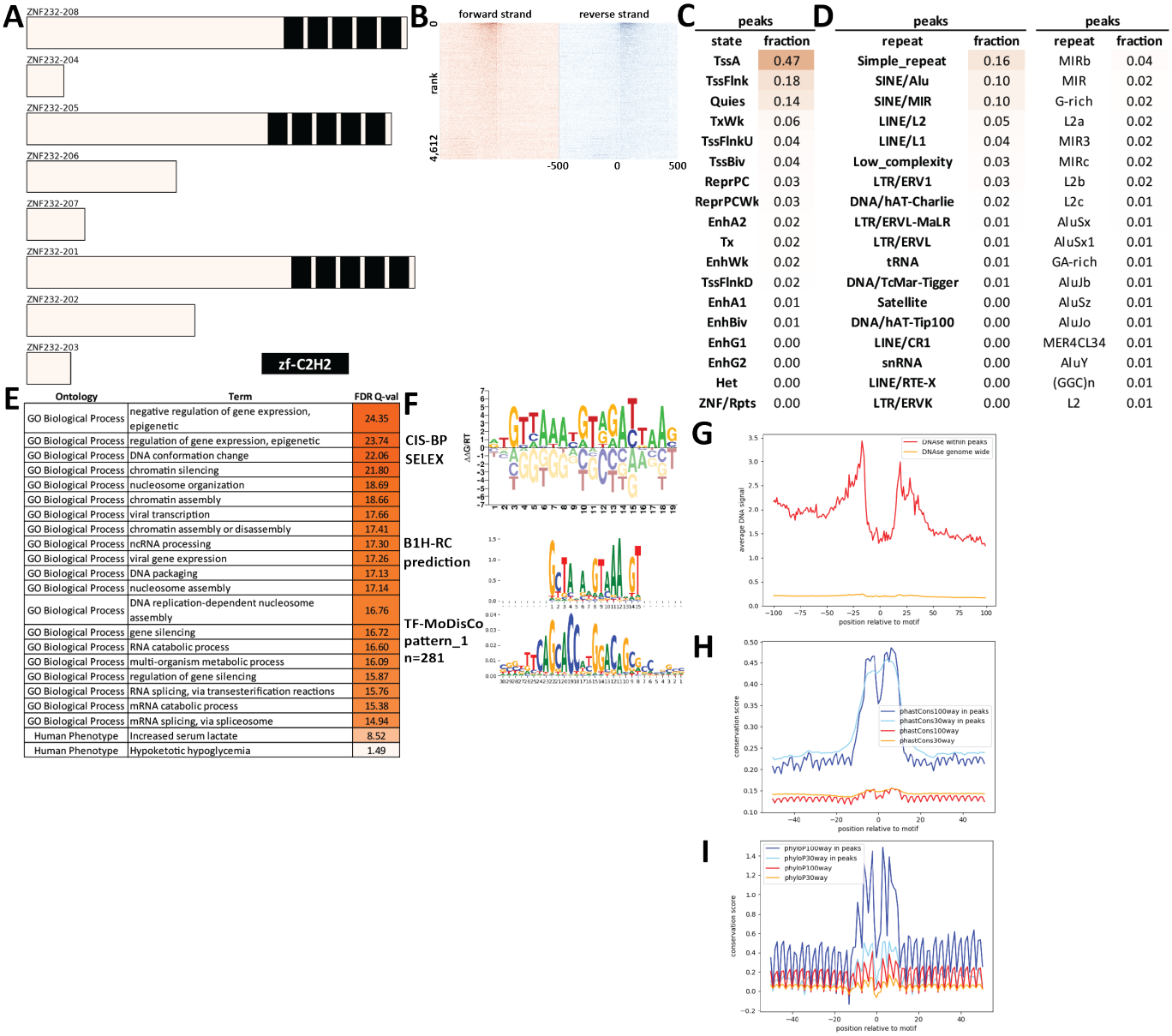

peaks	
state	fraction
TssA	0.47
TssFlnk	0.18
Quies	0.14
TxWk	0.06
TssFlnkU	0.04
TssBiv	0.04
ReprPC	0.03
ReprPCWk	0.03
EnhA2	0.02
Tx	0.02
EnhWk	0.02
TssFlnkD	0.02
EnhA1	0.01
EnhBiv	0.01
EnhG1	0.00
EnhG2	0.00
Het	0.00
ZNF/Rpts	0.00

peaks		peaks	
repeat	fraction	repeat	fraction
Simple_repeat	0.16	MIRb	0.04
SINE/Alu	0.10	MIR	0.02
SINE/MIR	0.10	G-rich	0.02
LINE/L2	0.05	L2a	0.02
LINE/L1	0.04	MIR3	0.02
Low_complexity	0.03	MIRc	0.02
LTR/ERV1	0.03	L2b	0.02
DNA/hAT-Charlie	0.02	L2c	0.01
LTR/ERVL-MaLR	0.01	AluSx	0.01
LTR/ERVL	0.01	AluSx1	0.01
tRNA	0.01	GA-rich	0.01
DNA/TcMar-Tigger	0.01	AluJb	0.01
Satellite	0.00	AluSz	0.01
DNA/hAT-Tip100	0.00	AluJo	0.01
LINE/CR1	0.00	MER4CL34	0.01
snRNA	0.00	AluY	0.01
LINE/RTE-X	0.00	(GGC)n	0.01
LTR/ERVK	0.00	L2	0.01

Ontology	Term	FDR Q-val
GO Biological Process	negative regulation of gene expression, epigenetic	24.35
GO Biological Process	regulation of gene expression, epigenetic	23.74
GO Biological Process	DNA conformation change	22.06
GO Biological Process	chromatin silencing	21.80
GO Biological Process	nucleosome organization	18.69
GO Biological Process	chromatin assembly	18.66
GO Biological Process	viral transcription	17.66
GO Biological Process	chromatin assembly or disassembly	17.41
GO Biological Process	ncRNA processing	17.30
GO Biological Process	viral gene expression	17.26
GO Biological Process	DNA packaging	17.13
GO Biological Process	nucleosome assembly	17.14
GO Biological Process	DNA replication-dependent nucleosome assembly	16.76
GO Biological Process	gene silencing	16.72
GO Biological Process	RNA catabolic process	16.60
GO Biological Process	multi-organism metabolic process	16.09
GO Biological Process	regulation of gene silencing	15.87
GO Biological Process	RNA splicing, via transesterification reactions	15.76
GO Biological Process	mRNA catabolic process	15.38
GO Biological Process	mRNA splicing, via spliceosome	14.94
Human Phenotype	Increased serum lactate	8.52
Human Phenotype	Hypoketotic hypoglycemia	1.49

Supplementary Figure 863: Properties and genomic distribution of motifs identified for the ZNF232 transcription factor in K562 (accession ENCSR360ECJ).

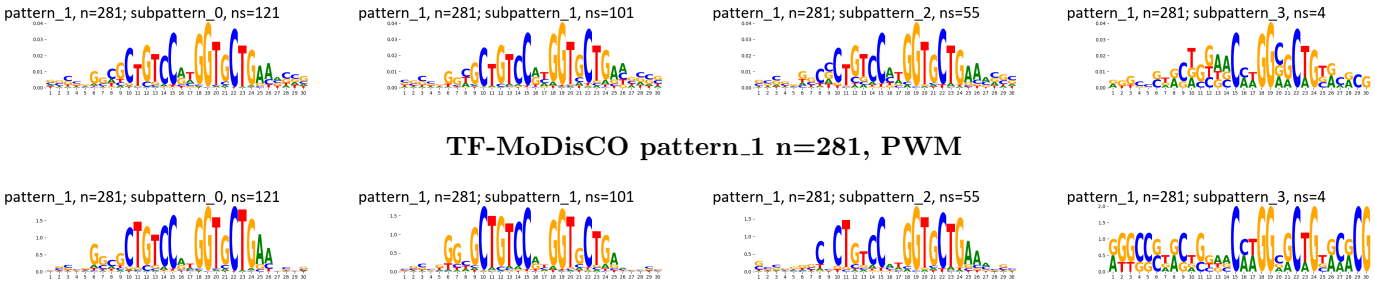

Supplementary Figure 864: TF-MoDisCO subpatterns for the ZNF232 transcription factor in K562 (accession ENCSR360ECJ).

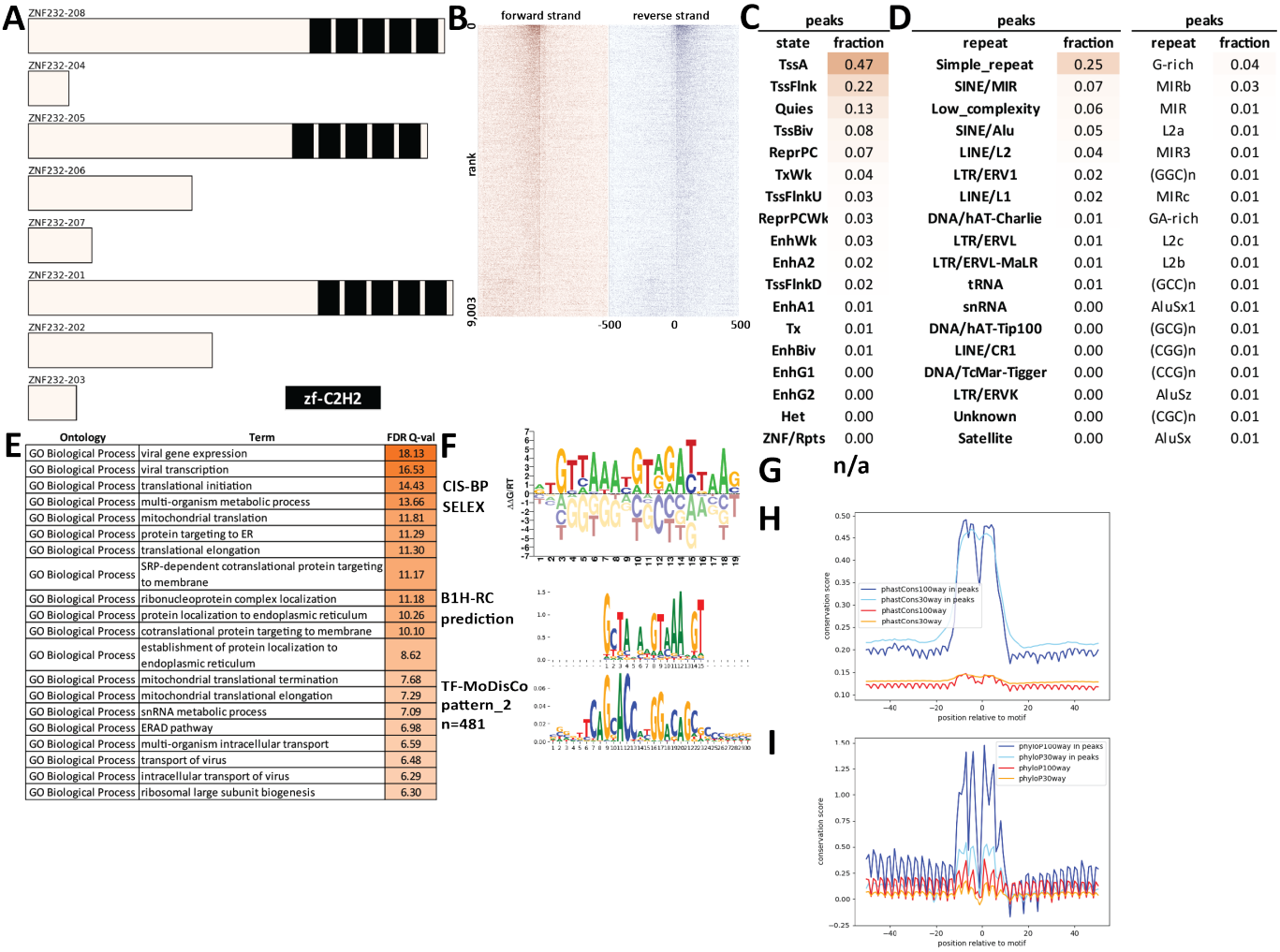

Supplementary Figure 865: Properties and genomic distribution of motifs identified for the ZNF232 transcription factor in WTC11 (accession ENCSR034IND).

TF-MoDisCO pattern_2 n=481, CWM

pattern_2, n=481; subpattern_0, ns=233

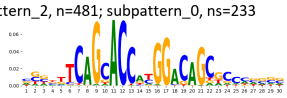

pattern_2, n=481; subpattern_1, ns=187

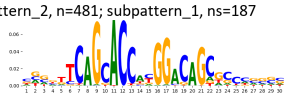

pattern_2, n=481; subpattern_2, ns=61

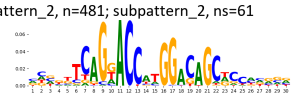

TF-MoDisCO pattern_2 n=481, PWM

pattern_2, n=481; subpattern_0, ns=233

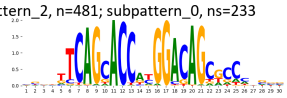

pattern_2, n=481; subpattern_1, ns=187

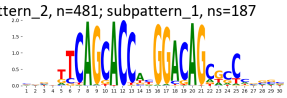

pattern_2, n=481; subpattern_2, ns=61

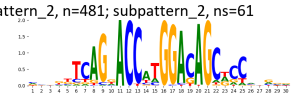

Supplementary Figure 866: TF-MoDisCO subpatterns for the ZNF232 transcription factor in WTC11 (accession ENCSR034IND).

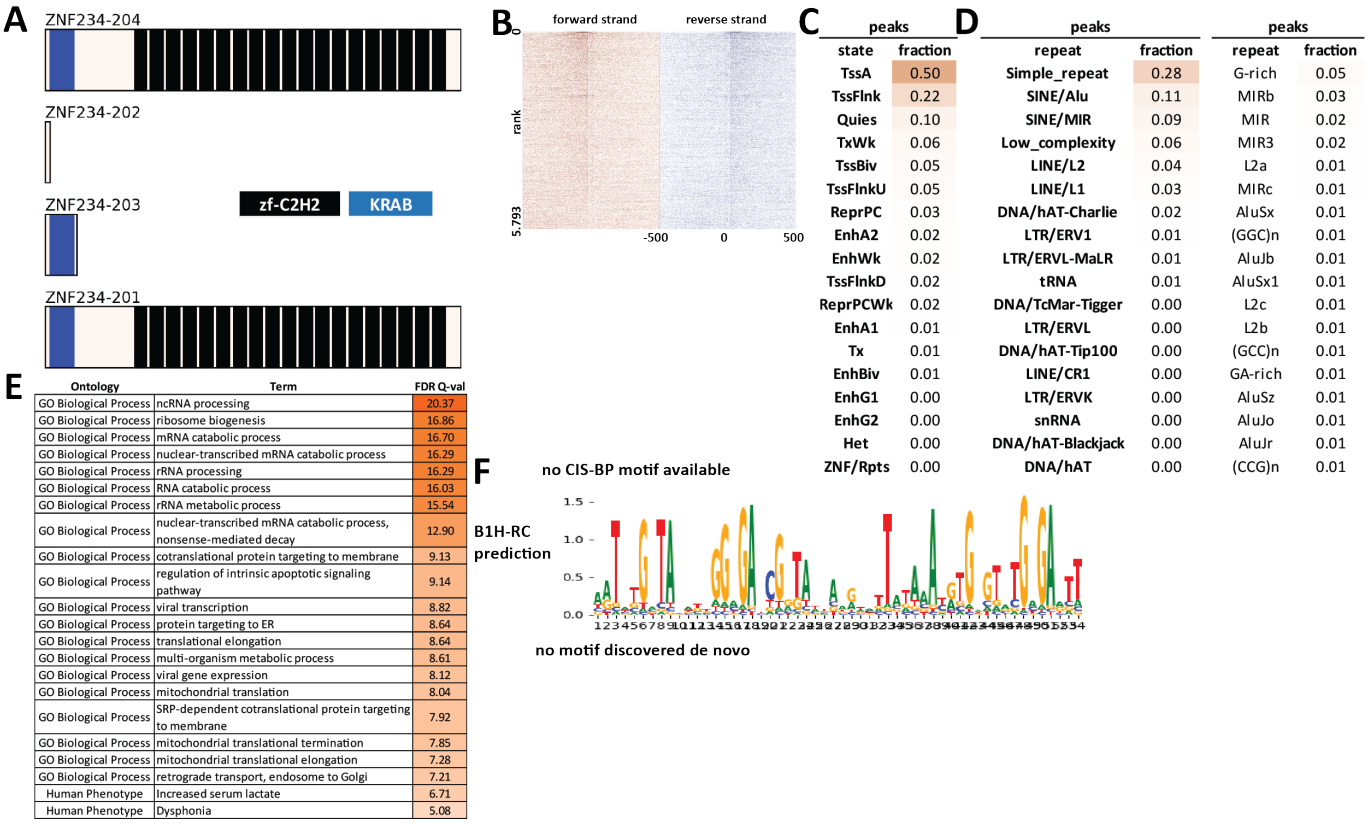

Supplementary Figure 867: Properties and genomic distribution of motifs identified for the ZNF234 transcription factor in HepG2 (accession ENCSR800ASH).

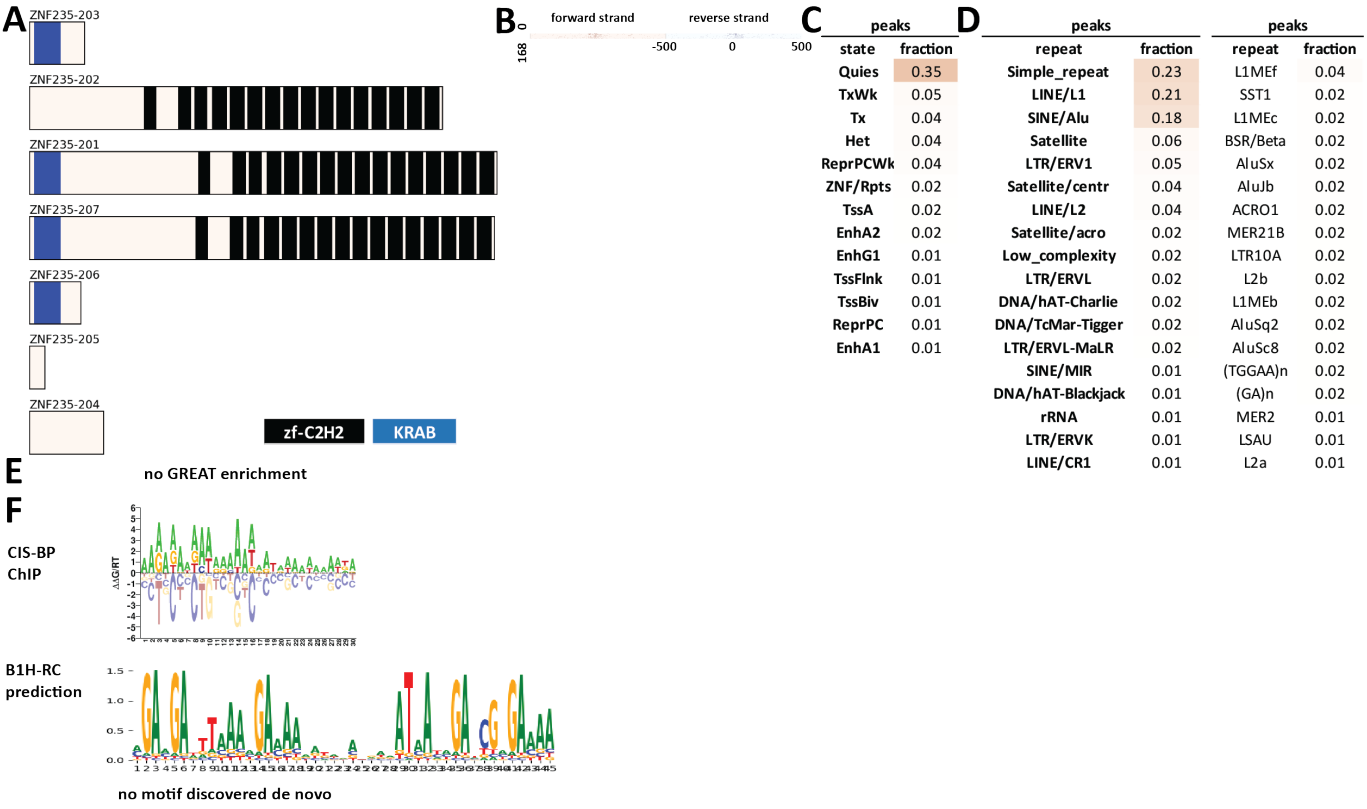

Supplementary Figure 868: Properties and genomic distribution of motifs identified for the ZNF235 transcription factor in HEK293 (accession ChipExo models).

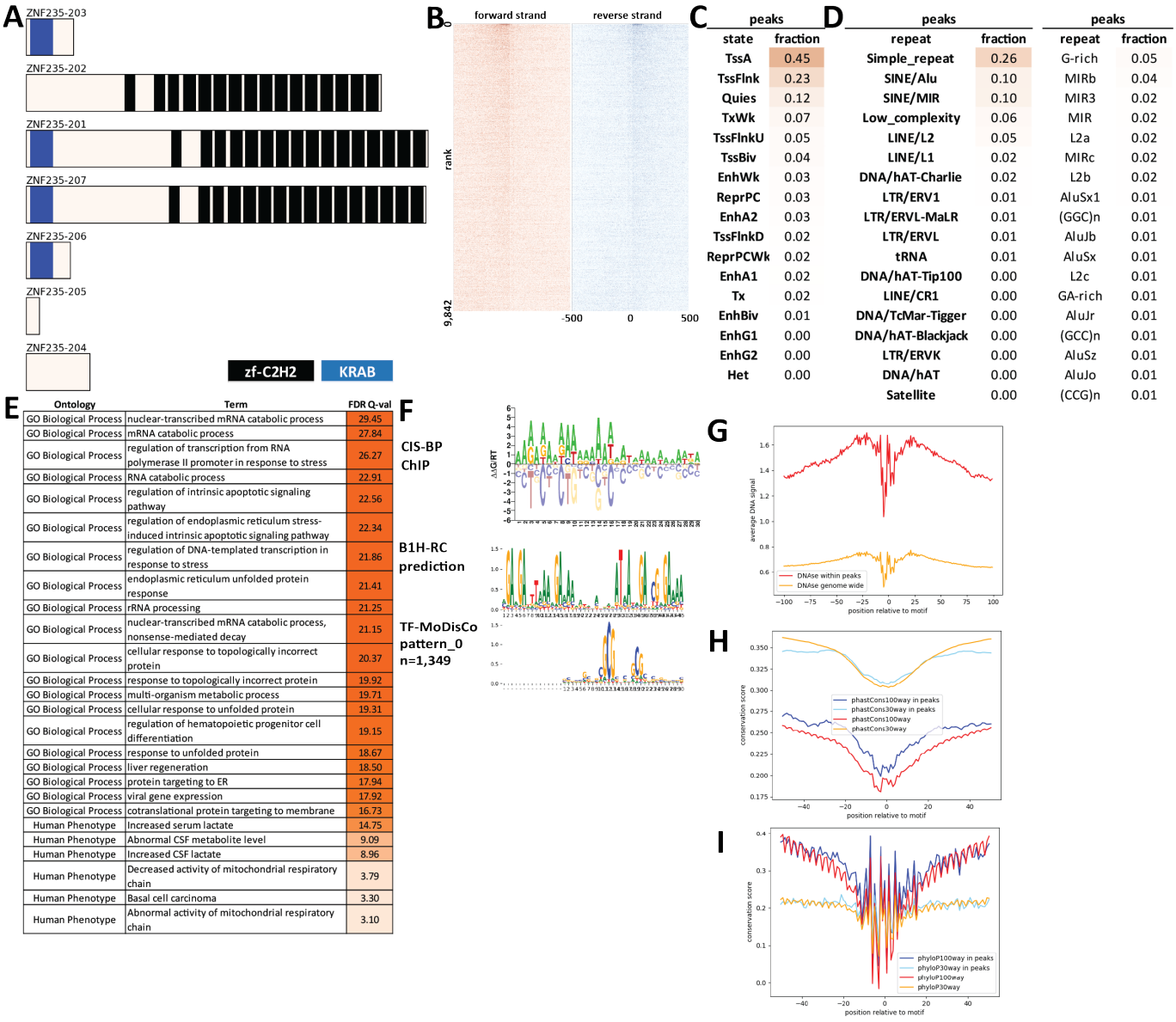

Supplementary Figure 869: Properties and genomic distribution of motifs identified for the ZNF235 transcription factor in HepG2 (accession ENCSR924KZA).

TF-MoDisCO pattern_0 n=1349, CWM

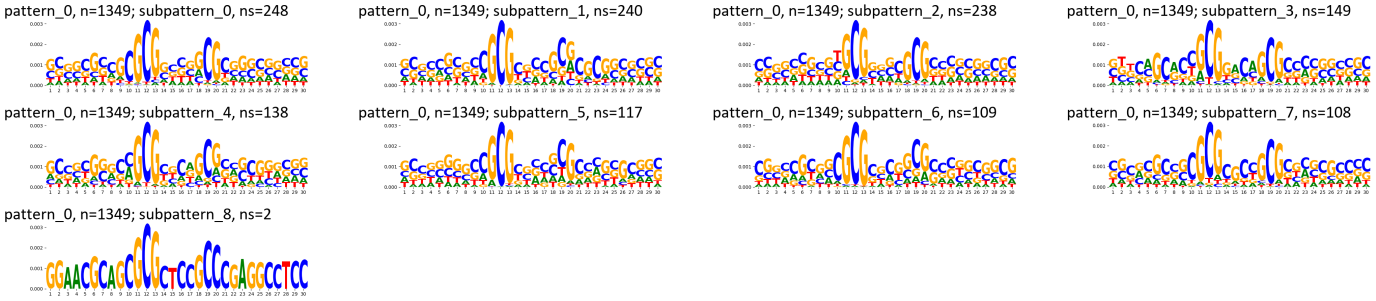

TF-MoDisCO pattern_0 n=1349, PWM

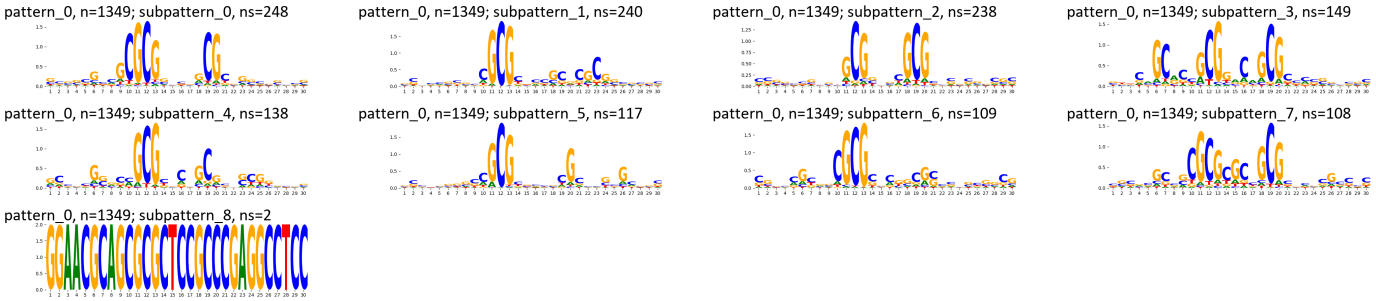

Supplementary Figure 870: TF-MoDisCO subpatterns for the ZNF235 transcription factor in HepG2 (accession ENCSR924KZA).

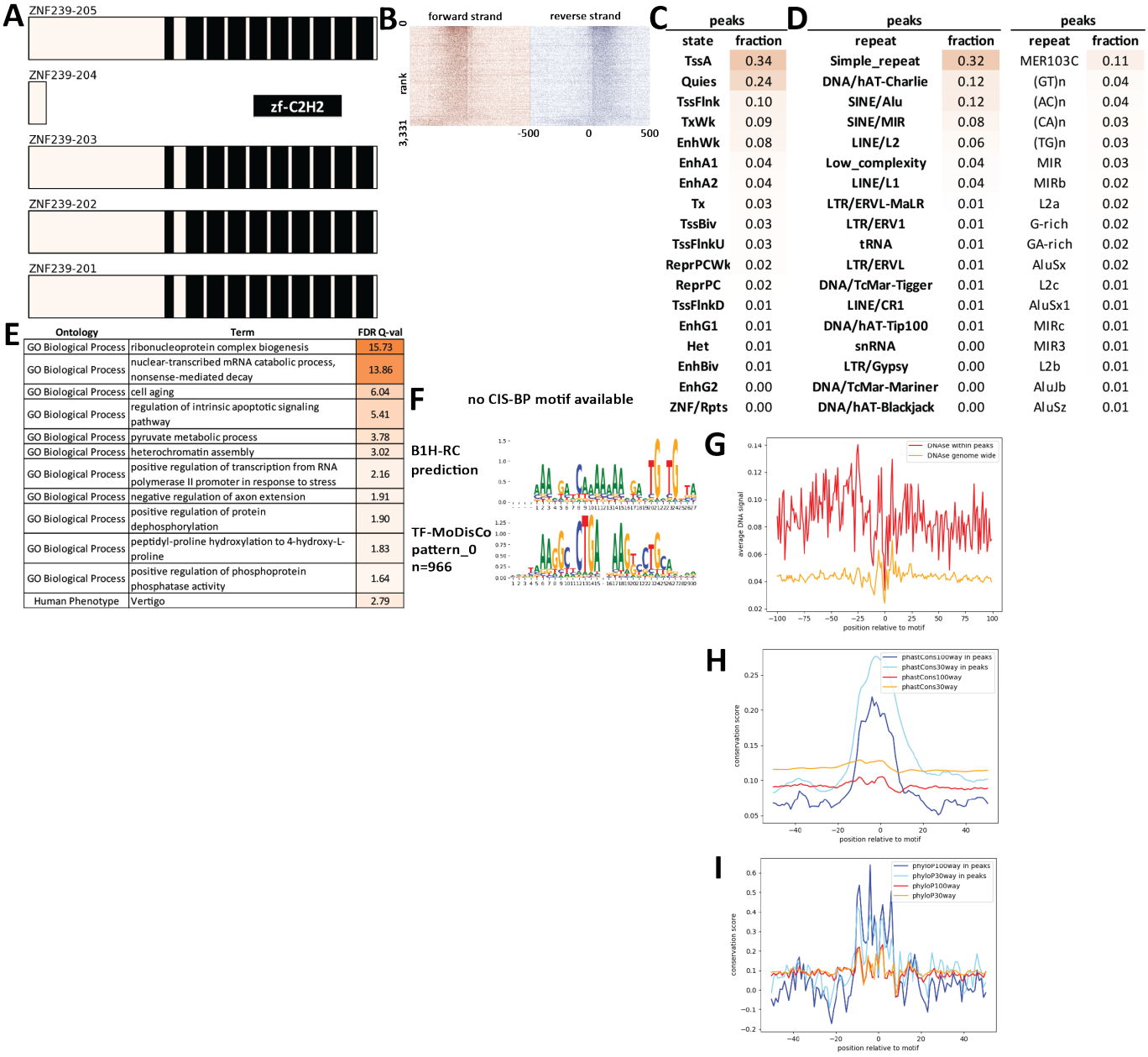

Supplementary Figure 871: Properties and genomic distribution of motifs identified for the ZNF239 transcription factor in HEK293 (accession ENCSR440COG).

TF-MoDisCO pattern_0 n=966, CWM

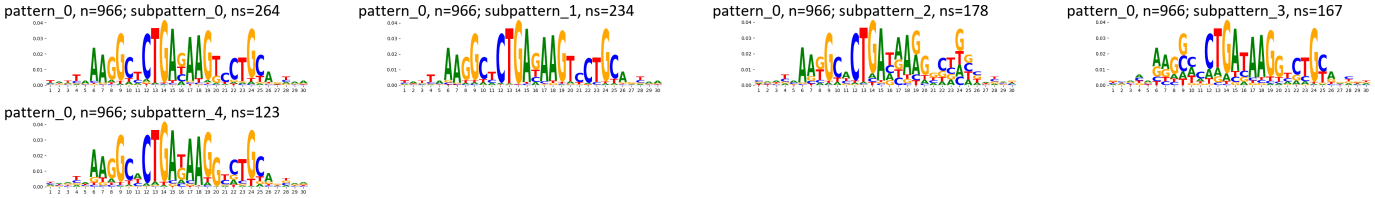

TF-MoDisCO pattern_0 n=966, PWM

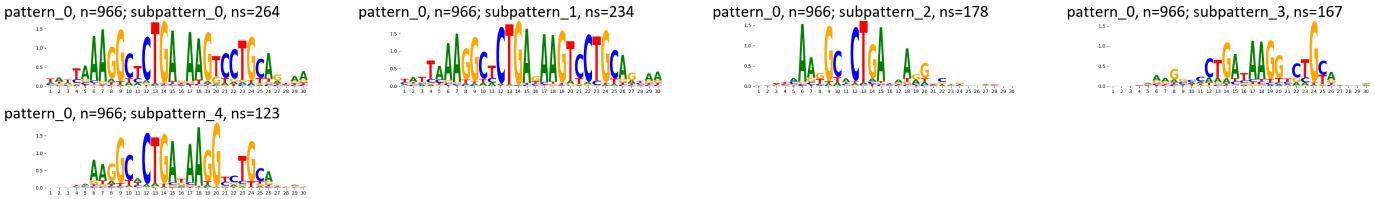

Supplementary Figure 872: TF-MoDisCO subpatterns for the ZNF239 transcription factor in HEK293 (accession ENCSR440COG).

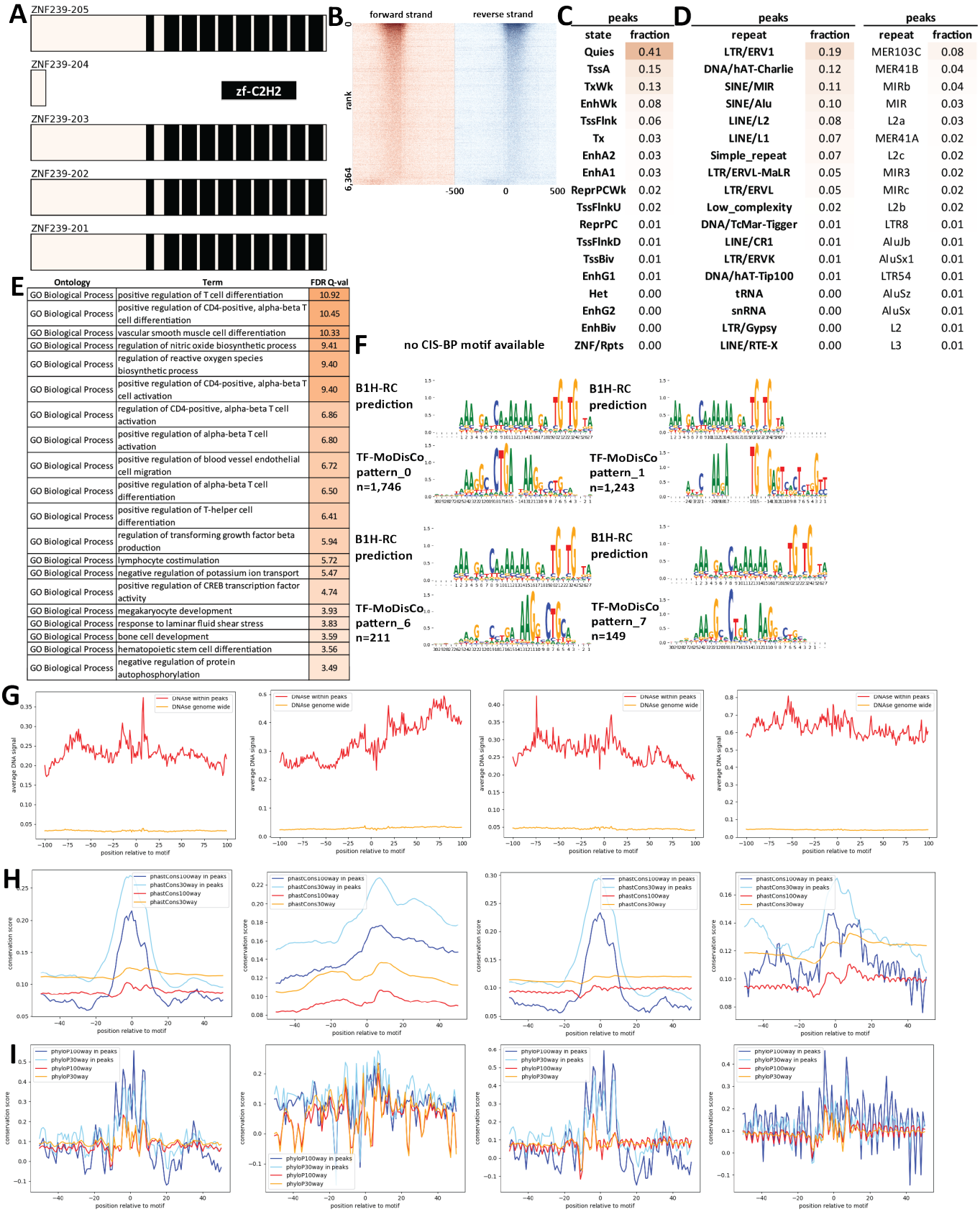

Supplementary Figure 873: Properties and genomic distribution of motifs identified for the ZNF239 transcription factor in K562 (accession ENCSR606KTL).

TF-MoDisCO pattern_0 n=1746, CWM

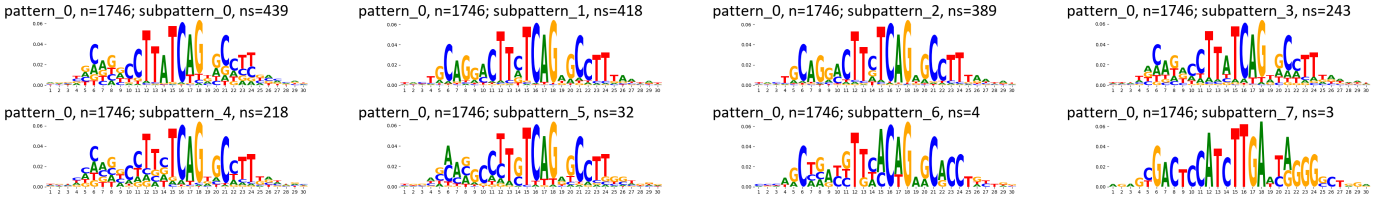

TF-MoDisCO pattern_0 n=1746, PWM

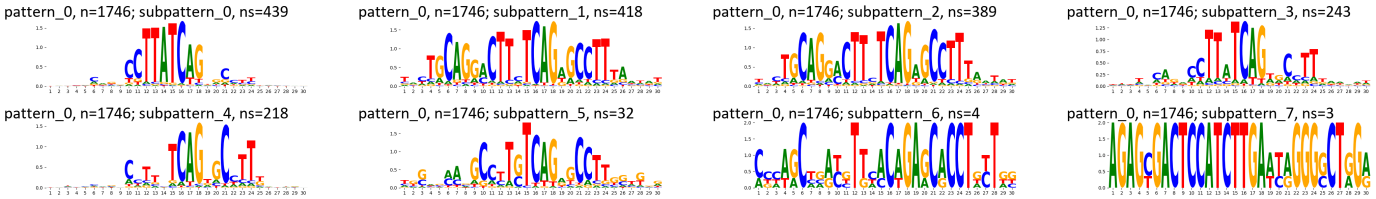

TF-MoDisCO pattern_1 n=1243, CWM

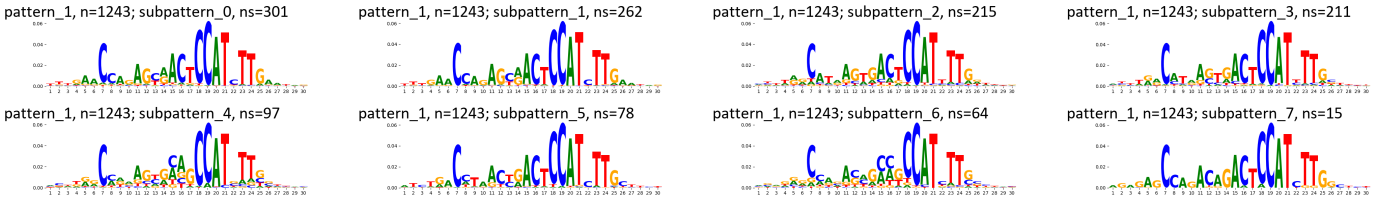

TF-MoDisCO pattern_1 n=1243, PWM

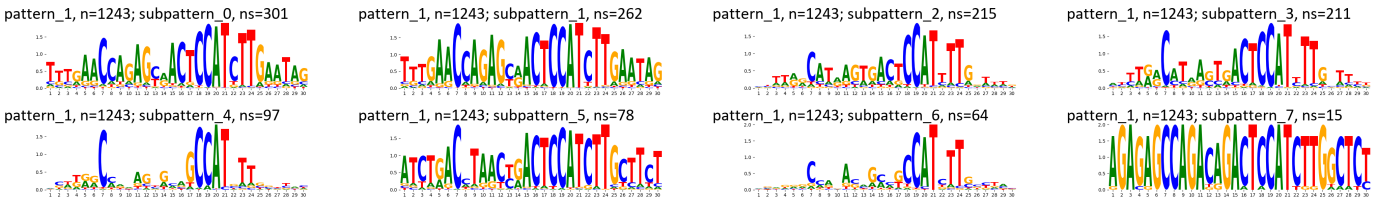

TF-MoDisCO pattern_6 n=211, CWM

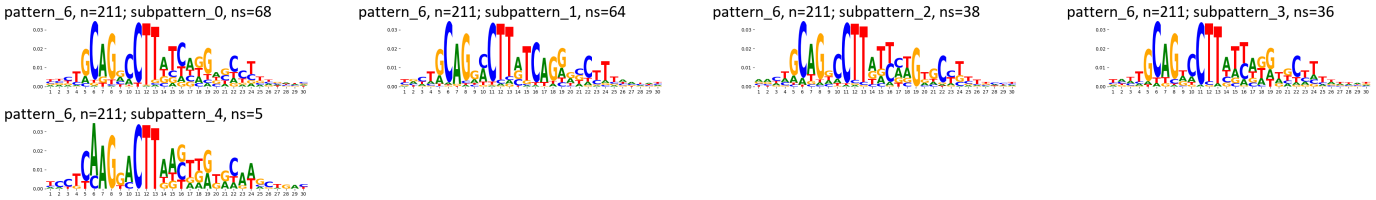

TF-MoDisCO pattern_6 n=211, PWM

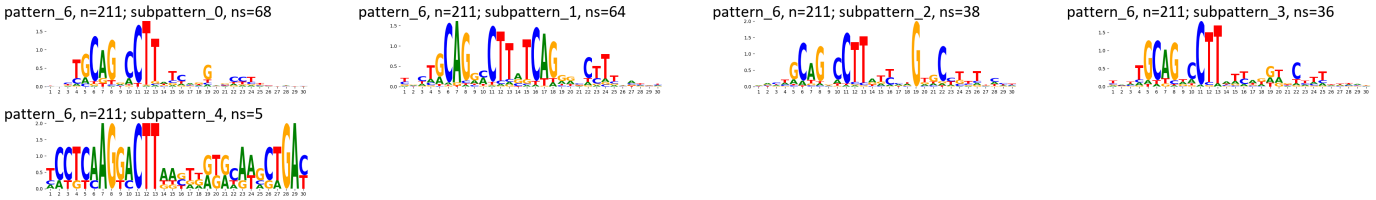

TF-MoDisCO pattern_7 n=149, CWM

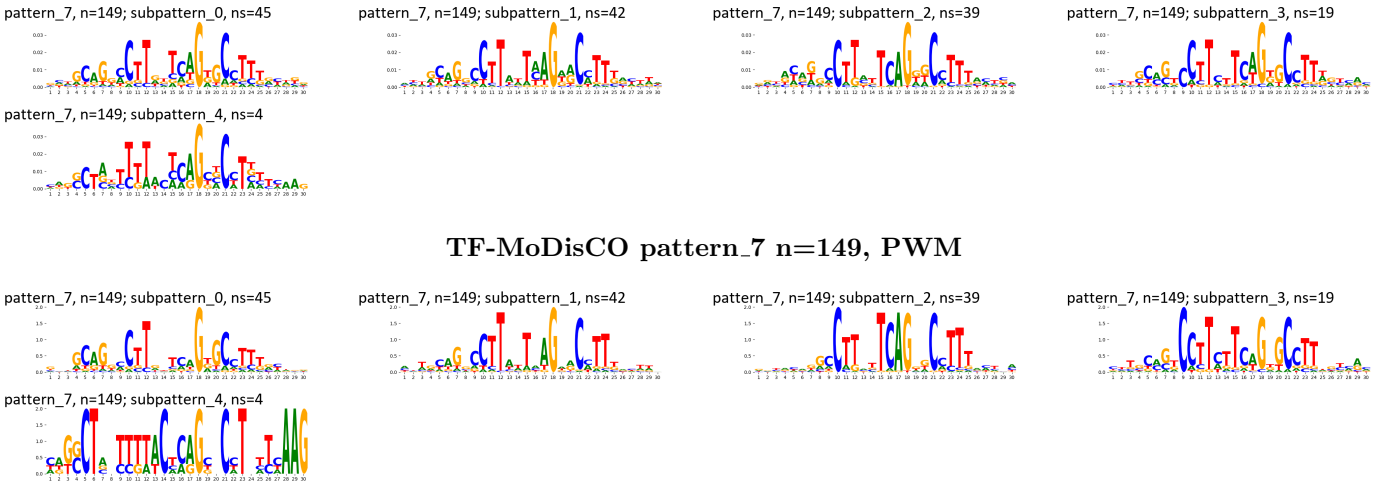

Supplementary Figure 874: TF-MoDisCO subpatterns for the ZNF239 transcription factor in K562 (accession ENCSR606KTL).

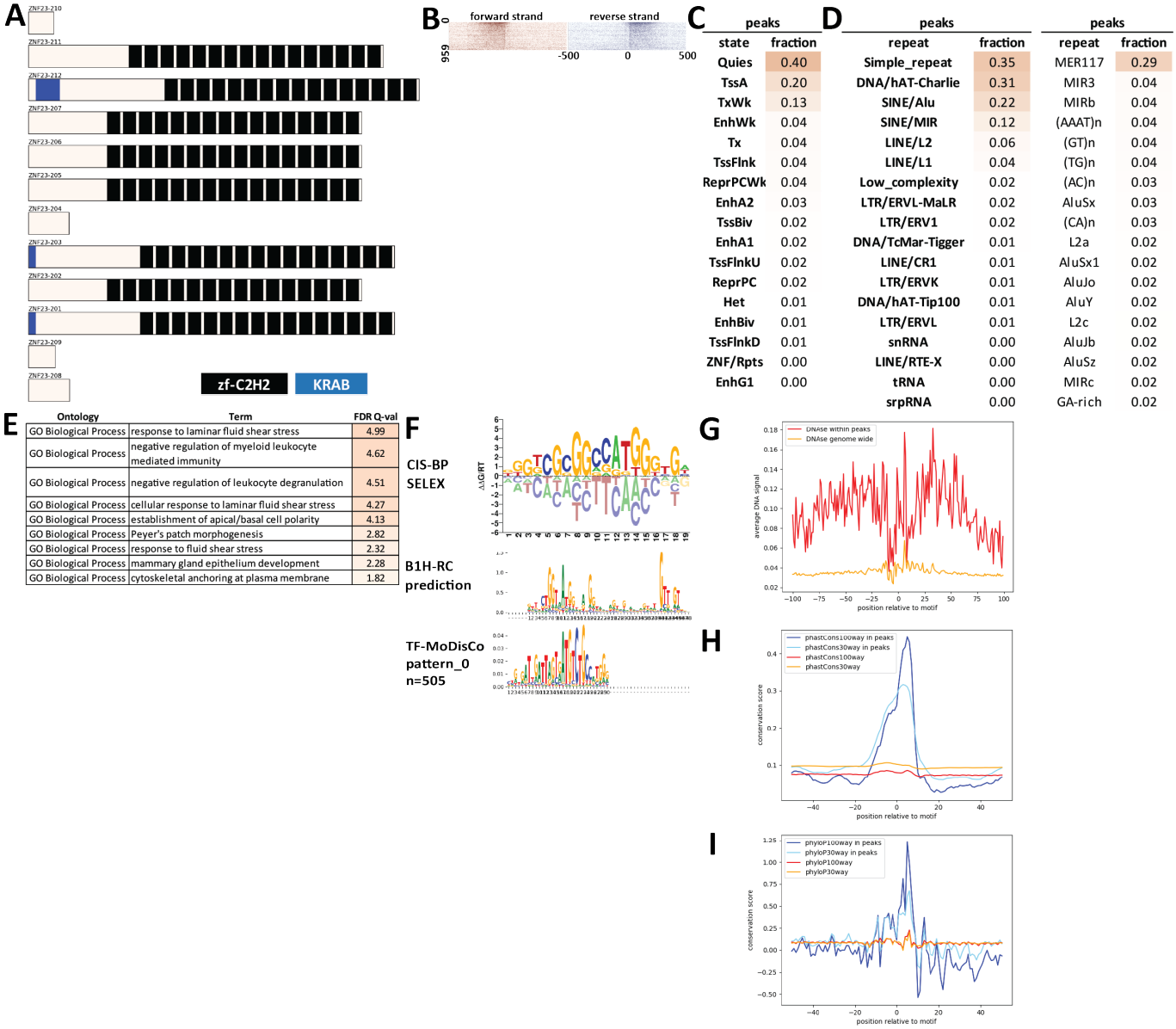

Supplementary Figure 875: Properties and genomic distribution of motifs identified for the ZNF23 transcription factor in HEK293 (accession ENCSR679KXF).

TF-MoDisCO pattern_0 n=505, CWM

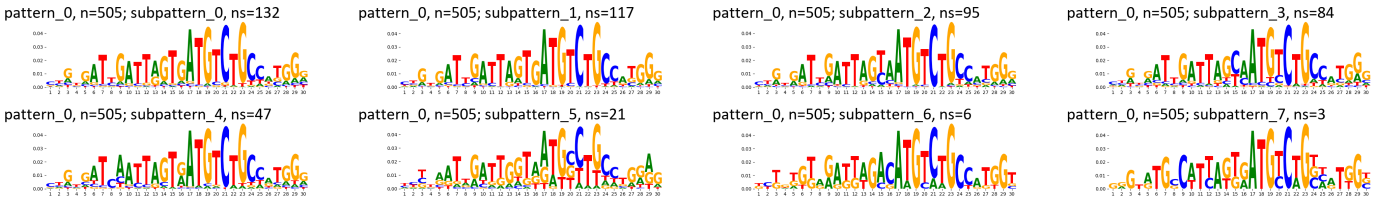

TF-MoDisCO pattern_0 n=505, PWM

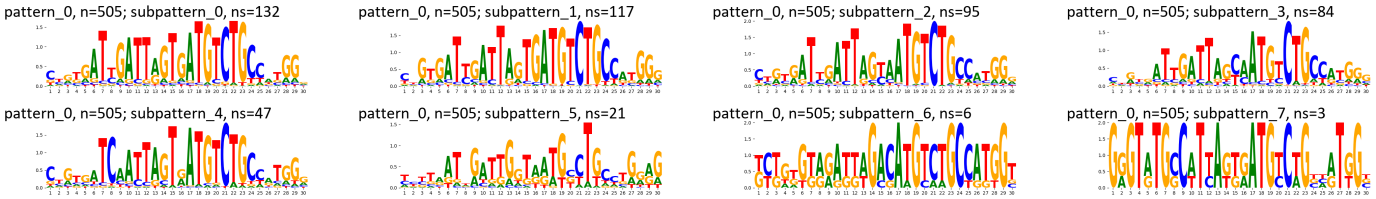

Supplementary Figure 876: TF-MoDisCO subpatterns for the ZNF23 transcription factor in HEK293 (accession ENCSR679KXF).

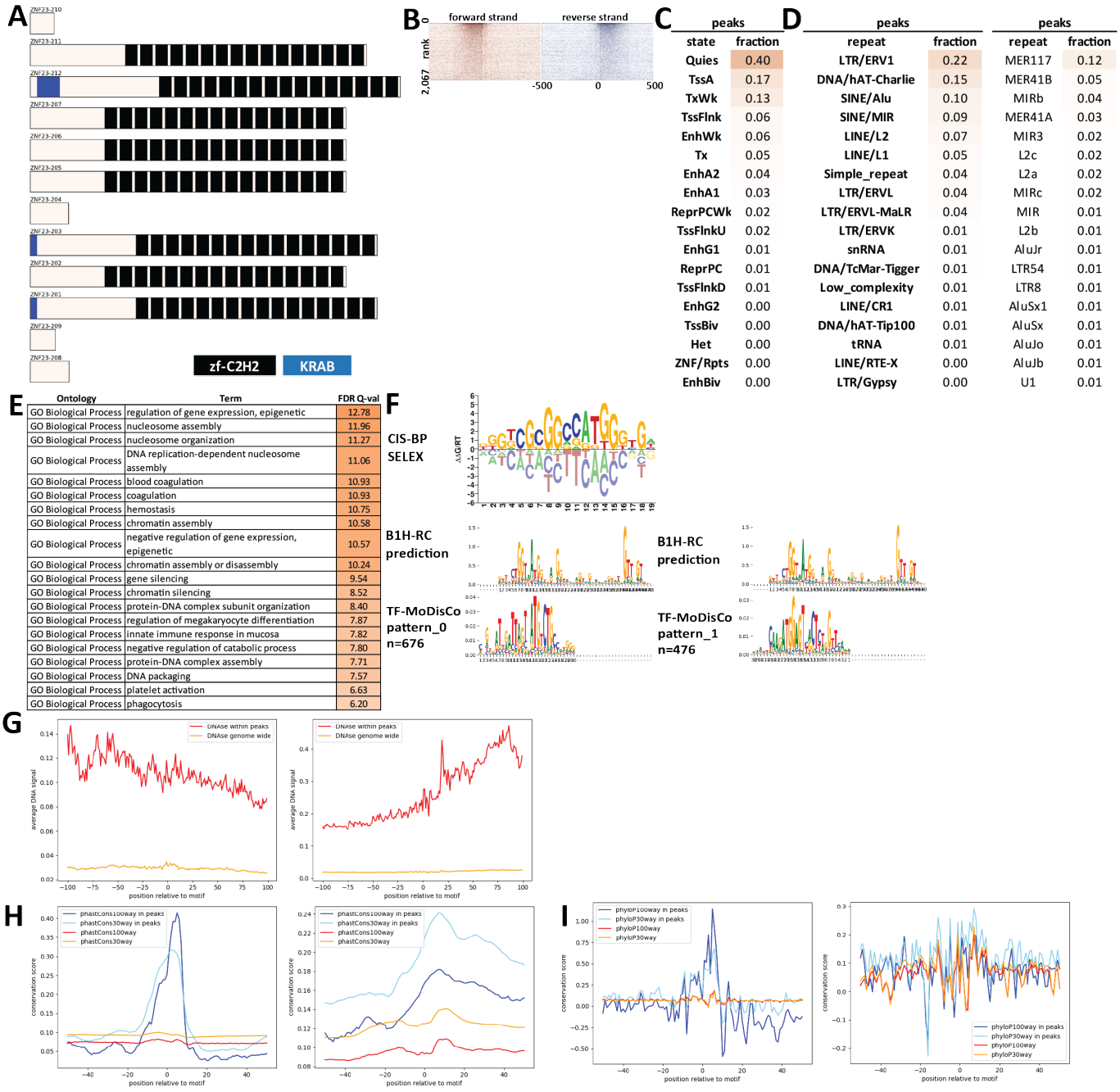

Supplementary Figure 877: Properties and genomic distribution of motifs identified for the ZNF23 transcription factor in K562 (accession ENCSR898IDK).

TF-MoDisCO pattern_0 n=676, CWM

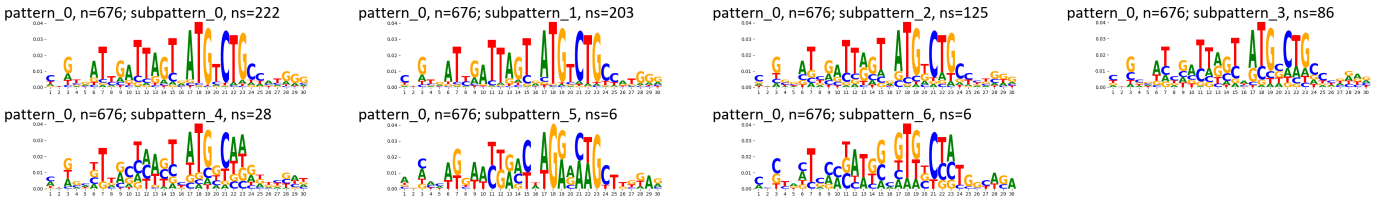

TF-MoDisCO pattern_0 n=676, PWM

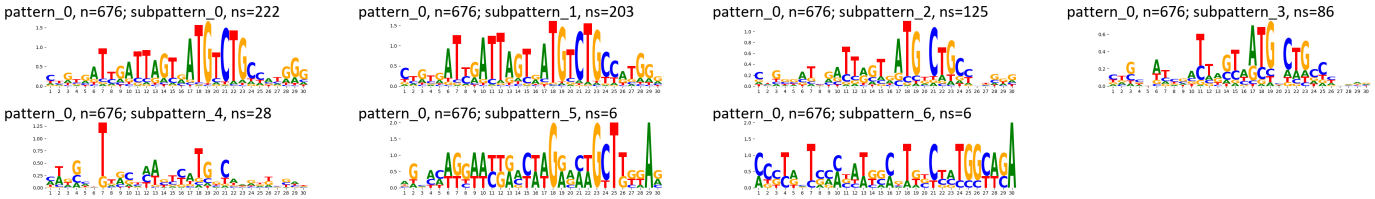

TF-MoDisCO pattern_1 n=485, CWM

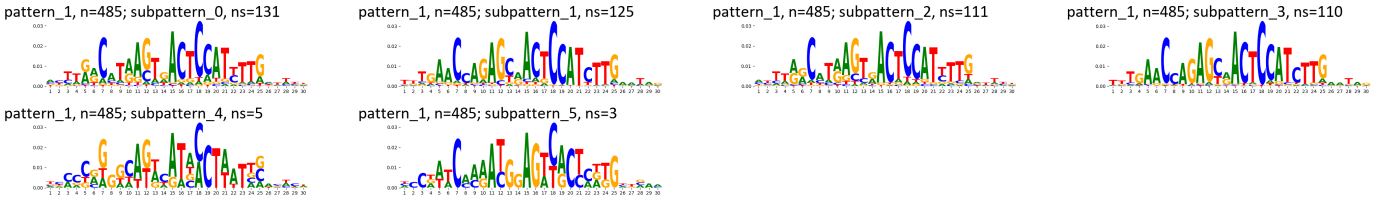

TF-MoDisCO pattern_1 n=485, PWM

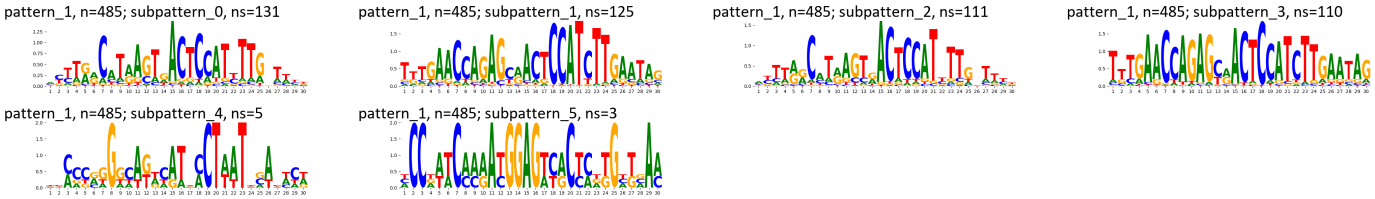

Supplementary Figure 878: TF-MoDisCO subpatterns for the ZNF23 transcription factor in K562 (accession ENCSR898IDK).

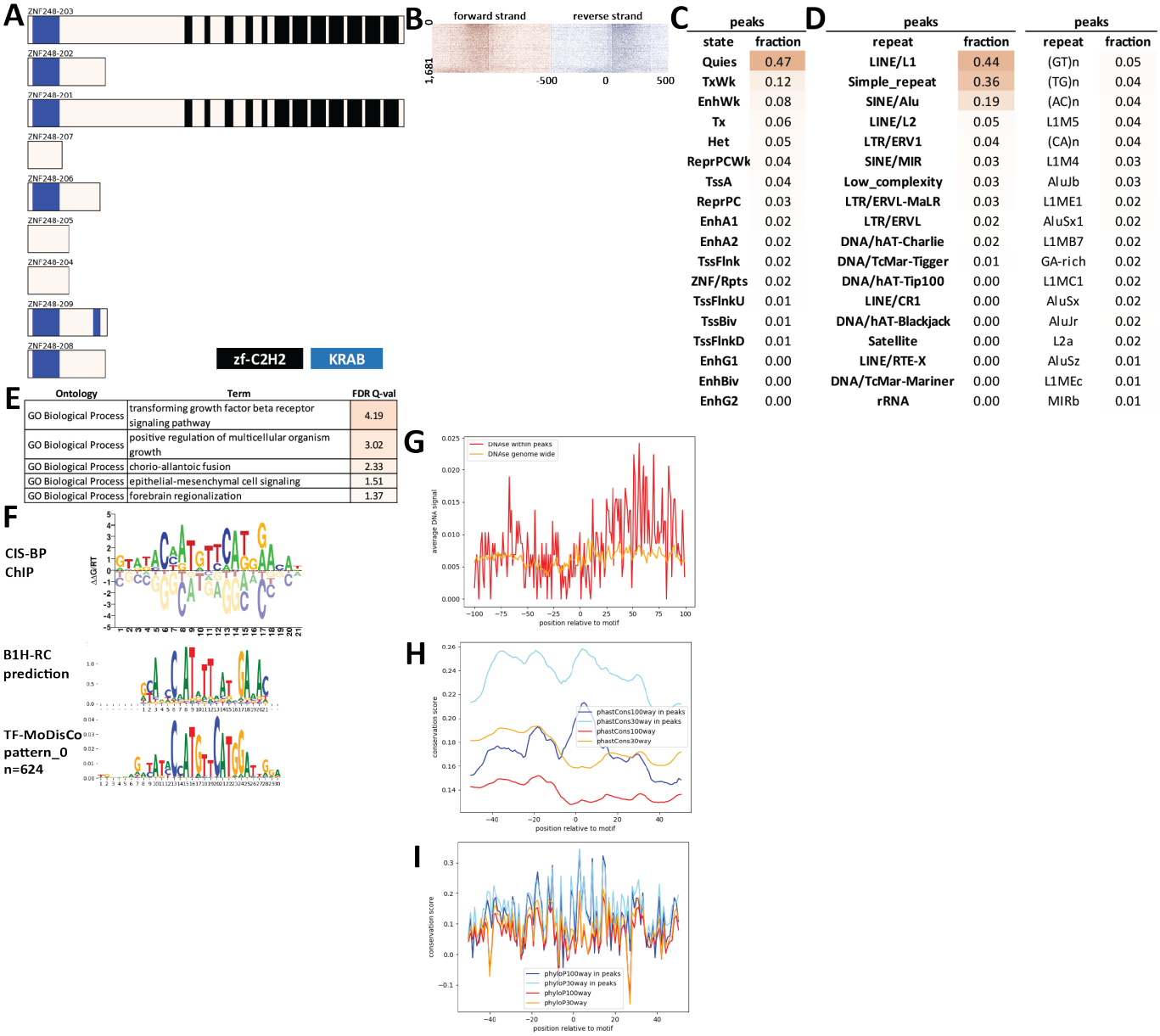

Supplementary Figure 879: Properties and genomic distribution of motifs identified for the ZNF248 transcription factor in HEK293 (accession ENCSR338SEM).

TF-MoDisCO pattern_0 n=624, CWM

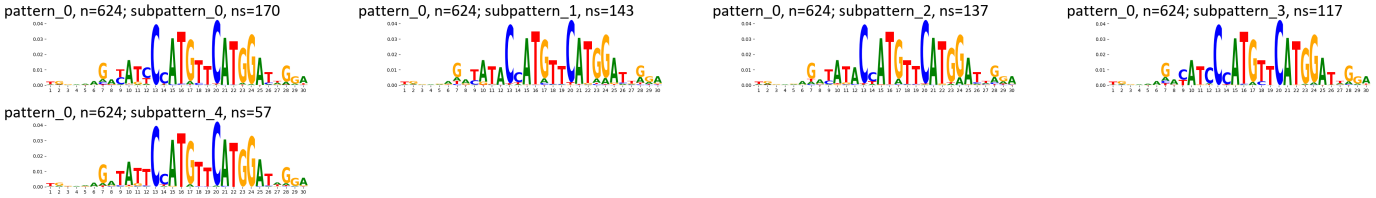

TF-MoDisCO pattern_0 n=624, PWM

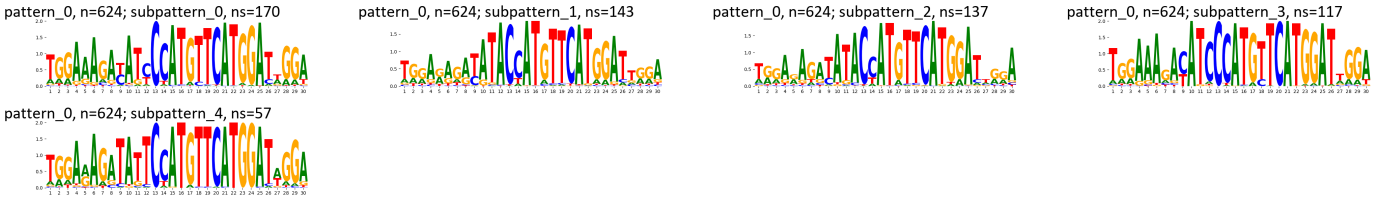

Supplementary Figure 880: TF-MoDisCO subpatterns for the ZNF248 transcription factor in HEK293 (accession ENCSR338SEM).

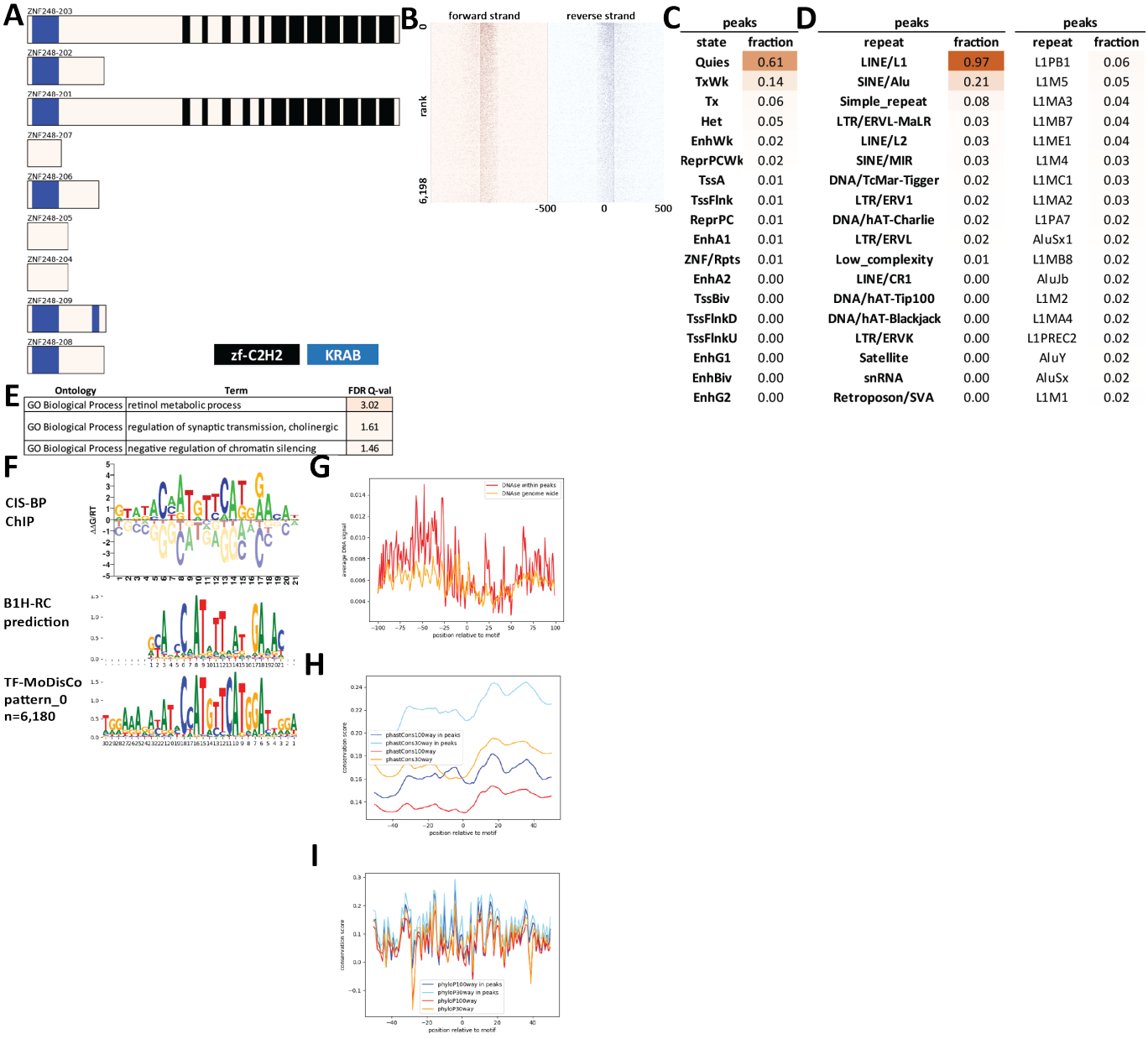

peaks

state	fraction
Quies	0.61
TxWk	0.14
Tx	0.06
Het	0.05
EnhWk	0.02
ReprPCWk	0.02
TssA	0.01
TssFlnk	0.01
ReprPC	0.01
EnhA1	0.01
ZNF/Rpts	0.01
EnhA2	0.00
TssBiv	0.00
TssFlnkD	0.00
TssFlnkU	0.00
EnhG1	0.00
EnhBiv	0.00
EnhG2	0.00

peaks

repeat	fraction
LINE/L1	0.97
SINE/Alu	0.21
Simple_repeat	0.08
LTR/ERVL-MaLR	0.03
LINE/L2	0.03
SINE/MIR	0.03
DNA/TcMar-Tigger	0.02
LTR/ERV1	0.02
DNA/hAT-Charlie	0.02
LTR/ERVL	0.02
Low_complexity	0.01
LINE/CR1	0.00
DNA/hAT-Tip100	0.00
DNA/hAT-Blackjack	0.00
LTR/ERVK	0.00
Satellite	0.00
snRNA	0.00
Retroposon/SVA	0.00

peaks

repeat	fraction
L1PB1	0.06
L1M5	0.05
L1MA3	0.04
L1MB7	0.04
L1ME1	0.04
L1M4	0.03
L1MC1	0.03
L1MA2	0.03
L1PA7	0.02
AluSx1	0.02
L1MB8	0.02
AluJb	0.02
L1M2	0.02
L1MA4	0.02
L1PREC2	0.02
AluY	0.02
AluSx	0.02
L1M1	0.02

Supplementary Figure 881: Properties and genomic distribution of motifs identified for the ZNF248 transcription factor in HEK293 (accession ChipExo models).

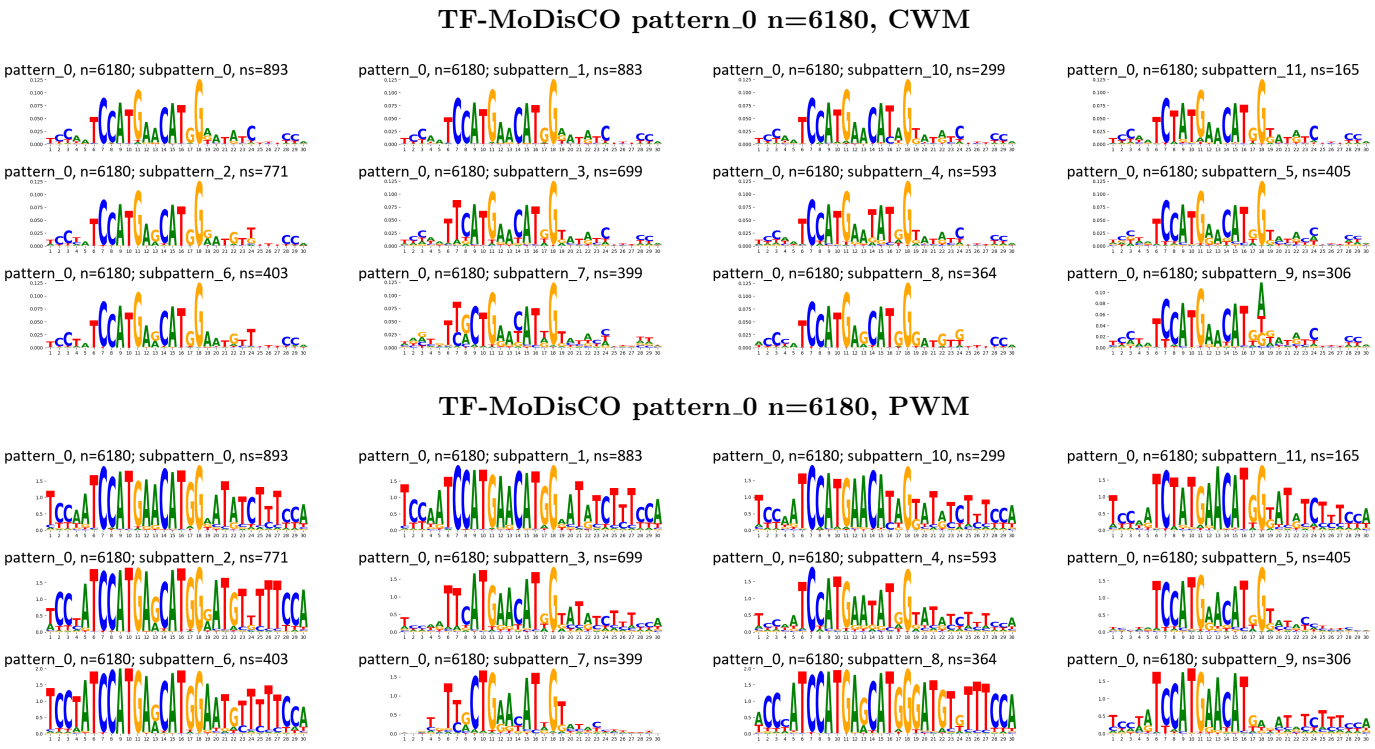

Supplementary Figure 882: TF-MoDisCO subpatterns for the ZNF248 transcription factor in HEK293 (accession ChipExo models).

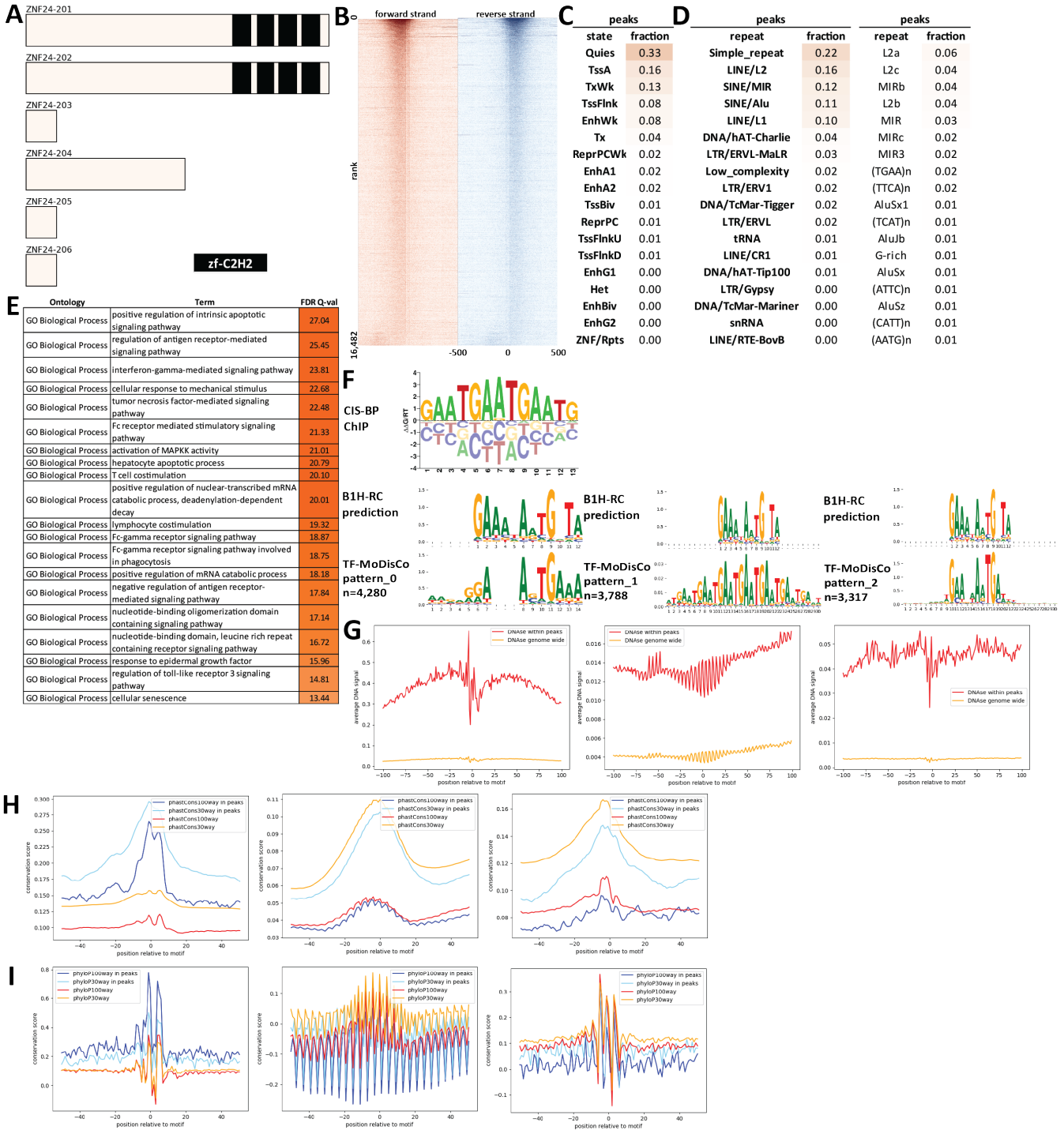

Supplementary Figure 883: Properties and genomic distribution of motifs identified for the ZNF24 transcription factor in GM12878 (accession ENCSR072PWP).

TF-MoDisCO pattern_0 n=4280, CWM

pattern_0, n=4280; subpattern_0, ns=1055

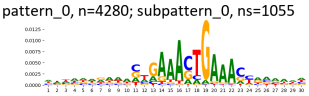

pattern_0, n=4280; subpattern_1, ns=789

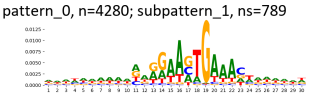

pattern_0, n=4280; subpattern_2, ns=753

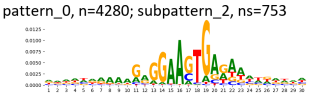

pattern_0, n=4280; subpattern_3, ns=694

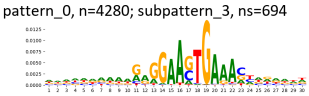

pattern_0, n=4280; subpattern_4, ns=519

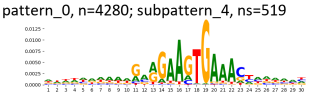

pattern_0, n=4280; subpattern_5, ns=459

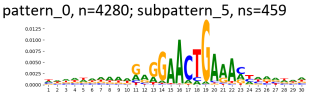

pattern_0, n=4280; subpattern_6, ns=9

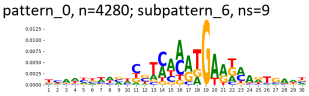

pattern_0, n=4280; subpattern_7, ns=2

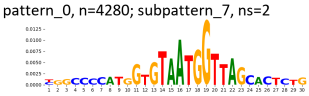

TF-MoDisCO pattern_0 n=4280, PWM

pattern_0, n=4280; subpattern_0, ns=1055

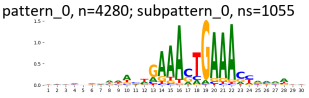

pattern_0, n=4280; subpattern_1, ns=789

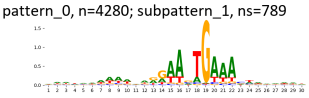

pattern_0, n=4280; subpattern_2, ns=753

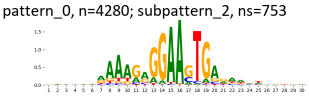

pattern_0, n=4280; subpattern_3, ns=694

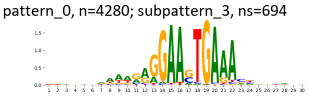

pattern_0, n=4280; subpattern_4, ns=519

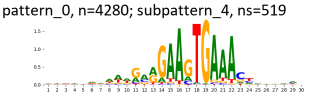

pattern_0, n=4280; subpattern_5, ns=459

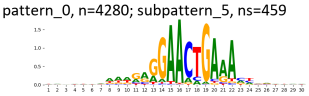

pattern_0, n=4280; subpattern_6, ns=9

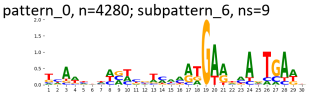

pattern_0, n=4280; subpattern_7, ns=2

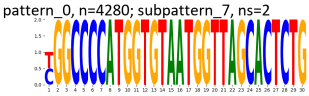

TF-MoDisCO pattern_1 n=3788, CWM

pattern_1, n=3788; subpattern_0, ns=646

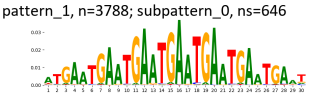

pattern_1, n=3788; subpattern_1, ns=597

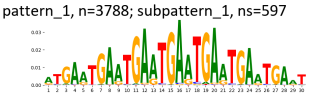

pattern_1, n=3788; subpattern_2, ns=540

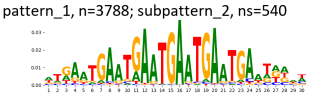

pattern_1, n=3788; subpattern_3, ns=532

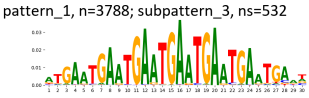

pattern_1, n=3788; subpattern_4, ns=525

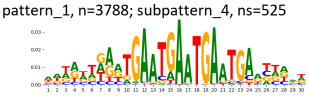

pattern_1, n=3788; subpattern_5, ns=524

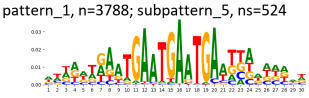

pattern_1, n=3788; subpattern_6, ns=407

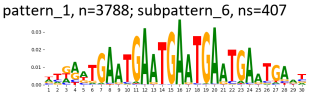

pattern_1, n=3788; subpattern_7, ns=17

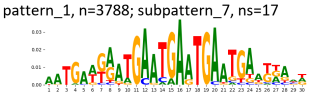

TF-MoDisCO pattern_1 n=3788, PWM

pattern_1, n=3788; subpattern_0, ns=646

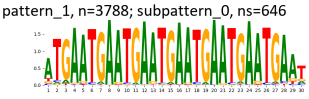

pattern_1, n=3788; subpattern_1, ns=597

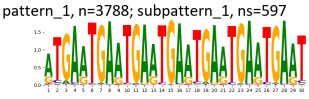

pattern_1, n=3788; subpattern_2, ns=540

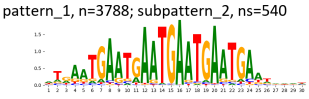

pattern_1, n=3788; subpattern_3, ns=532

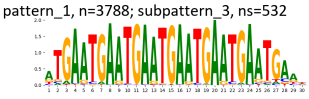

pattern_1, n=3788; subpattern_4, ns=525

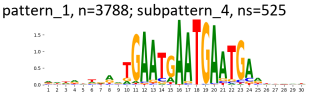

pattern_1, n=3788; subpattern_5, ns=524

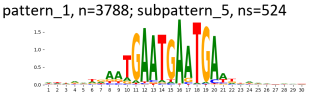

pattern_1, n=3788; subpattern_6, ns=407

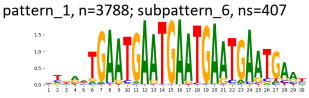

pattern_1, n=3788; subpattern_7, ns=17

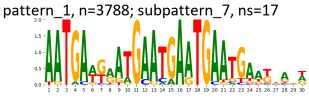

TF-MoDisCO pattern_2 n=3317, CWM

pattern_2, n=3317; subpattern_0, ns=723

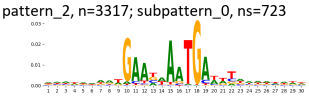

pattern_2, n=3317; subpattern_1, ns=622

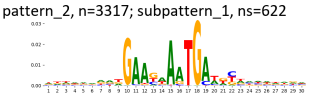

pattern_2, n=3317; subpattern_2, ns=608

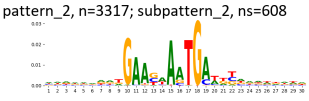

pattern_2, n=3317; subpattern_3, ns=584

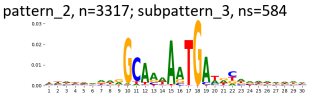

pattern_2, n=3317; subpattern_4, ns=409

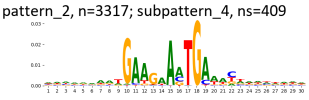

pattern_2, n=3317; subpattern_5, ns=166

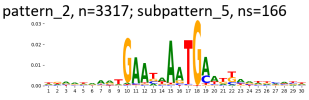

pattern_2, n=3317; subpattern_6, ns=116

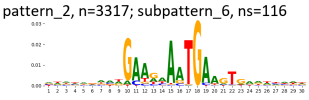

pattern_2, n=3317; subpattern_7, ns=89

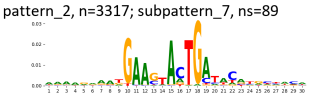

TF-MoDisCO pattern_2 n=3317, PWM

pattern_2, n=3317; subpattern_0, ns=723

pattern_2, n=3317; subpattern_1, ns=622

pattern_2, n=3317; subpattern_2, ns=608

pattern_2, n=3317; subpattern_3, ns=584

pattern_2, n=3317; subpattern_4, ns=409

pattern_2, n=3317; subpattern_5, ns=166

pattern_2, n=3317; subpattern_6, ns=116

pattern_2, n=3317; subpattern_7, ns=89

Supplementary Figure 884: TF-MoDisCO subpatterns for the ZNF24 transcription factor in GM12878 (accession ENCSR072PWP).

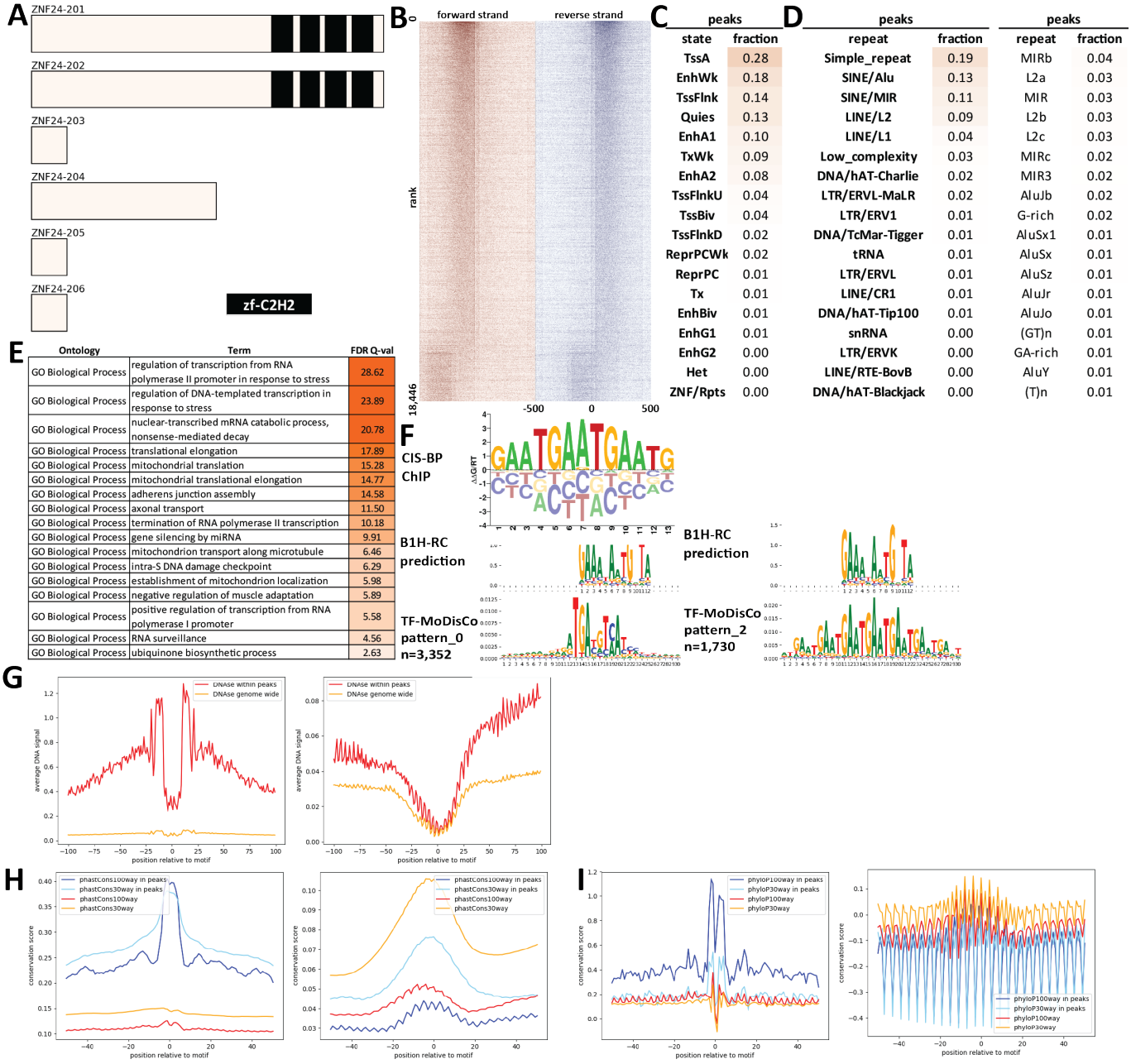

Supplementary Figure 885: Properties and genomic distribution of motifs identified for the ZNF24 transcription factor in HEK293 (accession ENCSR984MDV).

TF-MoDisCO pattern_0 n=3352, CWM

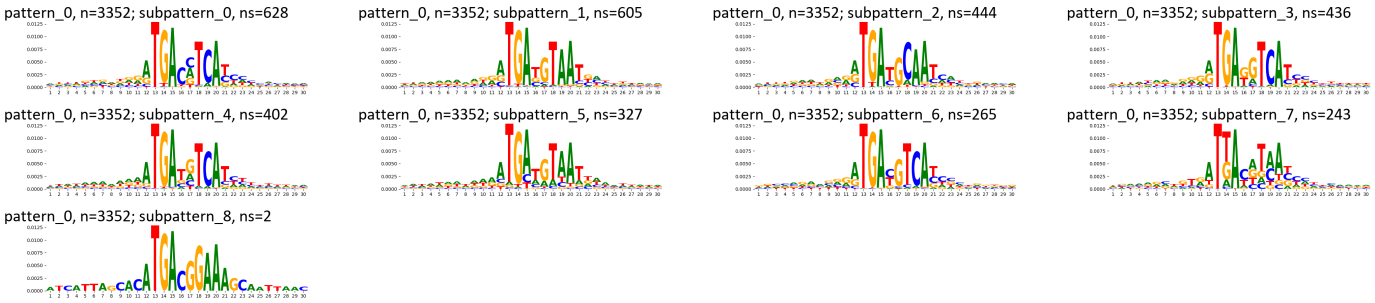

TF-MoDisCO pattern_0 n=3352, PWM

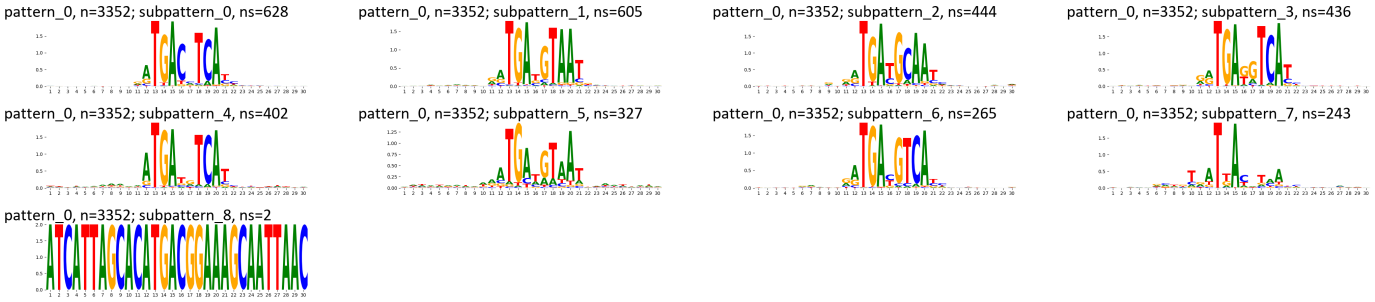

TF-MoDisCO pattern_2 n=1730, CWM

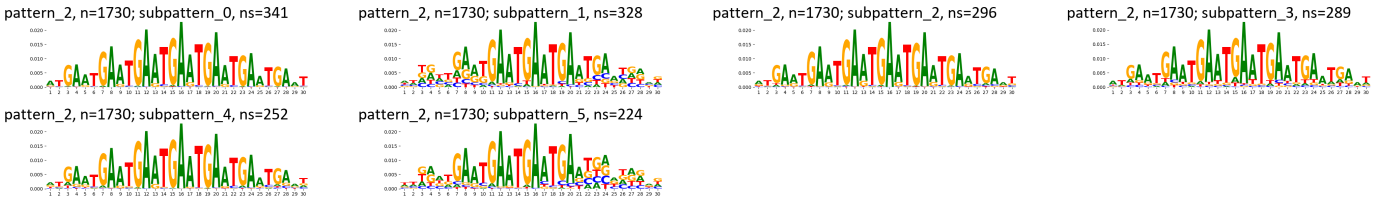

TF-MoDisCO pattern_2 n=1730, PWM

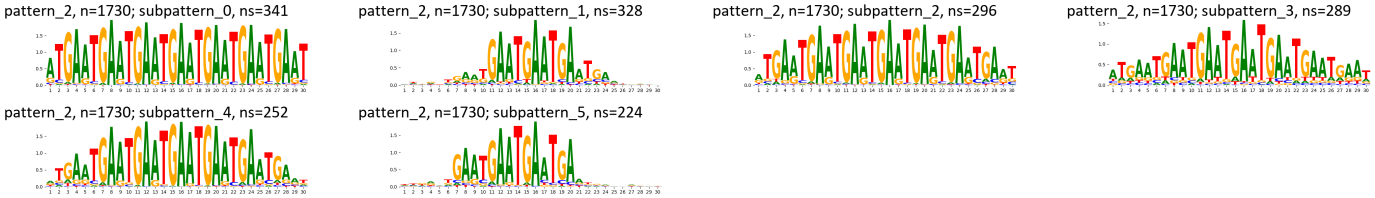

Supplementary Figure 886: TF-MoDisCO subpatterns for the ZNF24 transcription factor in HEK293 (accession ENCSR984MDV).

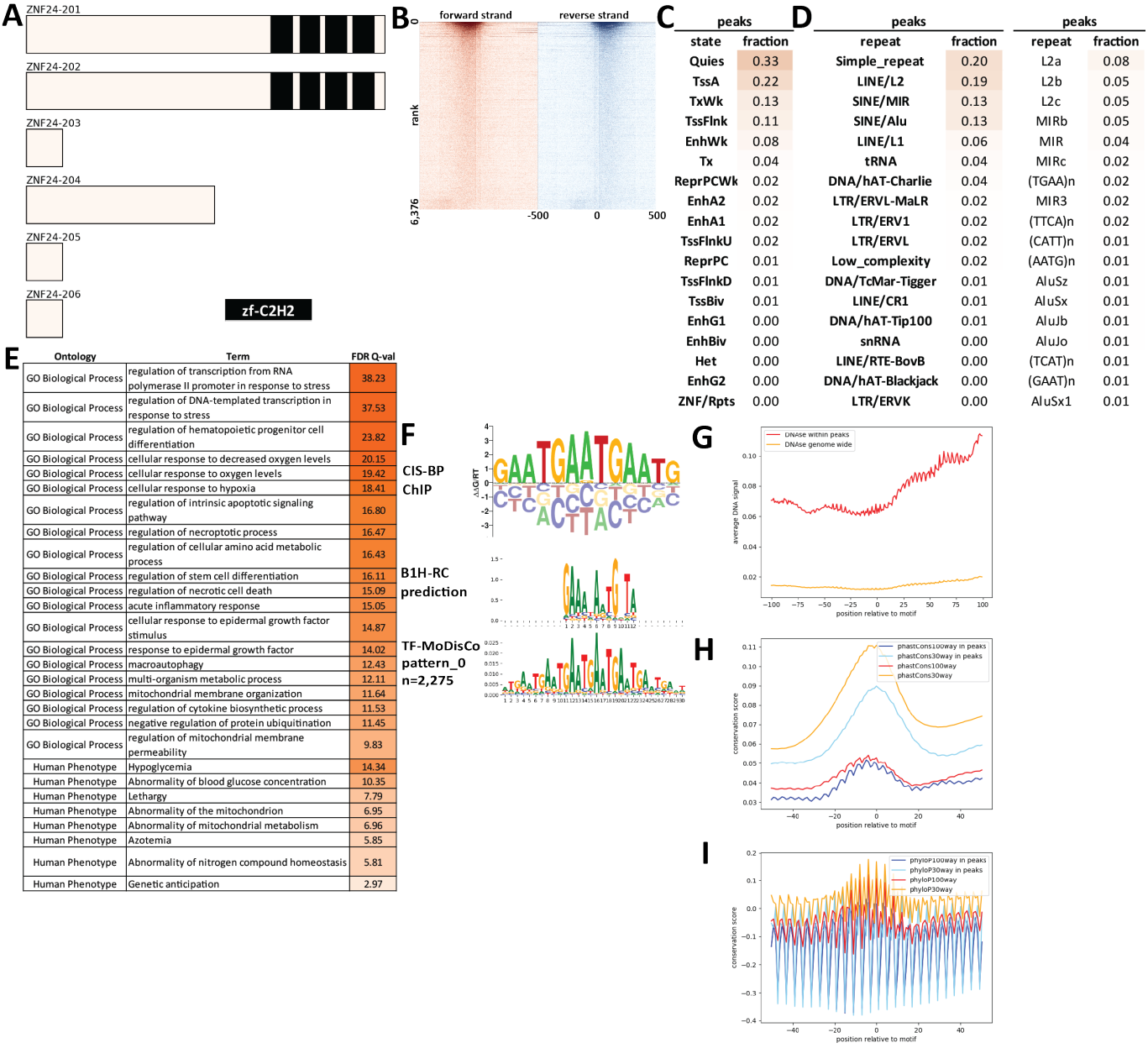

Supplementary Figure 887: Properties and genomic distribution of motifs identified for the ZNF24 transcription factor in HepG2 (accession ENCSR362NWP).

TF-MoDisCO pattern_0 n=2275, CWM

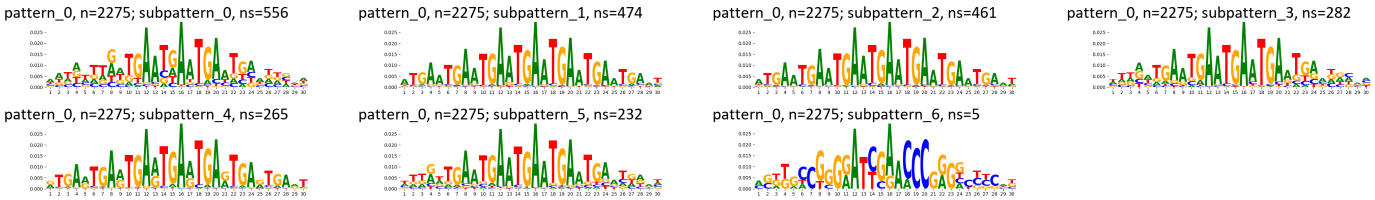

TF-MoDisCO pattern_0 n=2275, PWM

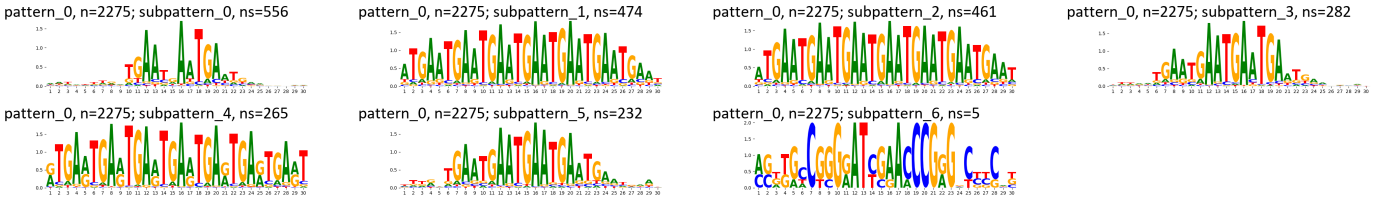

Supplementary Figure 888: TF-MoDisCO subpatterns for the ZNF24 transcription factor in HepG2 (accession ENCSR362NWP).

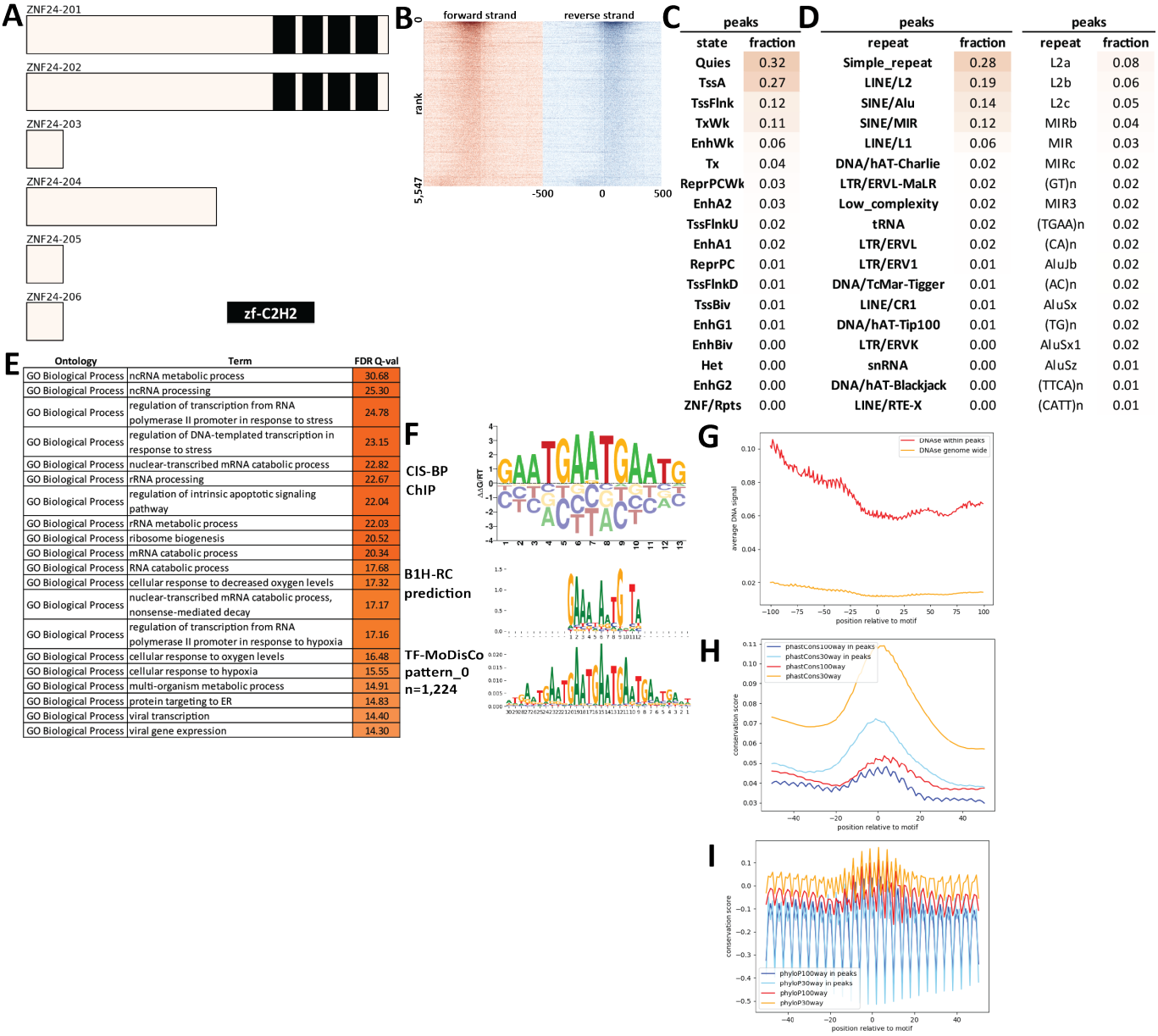

Supplementary Figure 889: Properties and genomic distribution of motifs identified for the ZNF24 transcription factor in HepG2 (accession ENCSR791AGT).

TF-MoDisCO pattern_0 n=1224, CWM

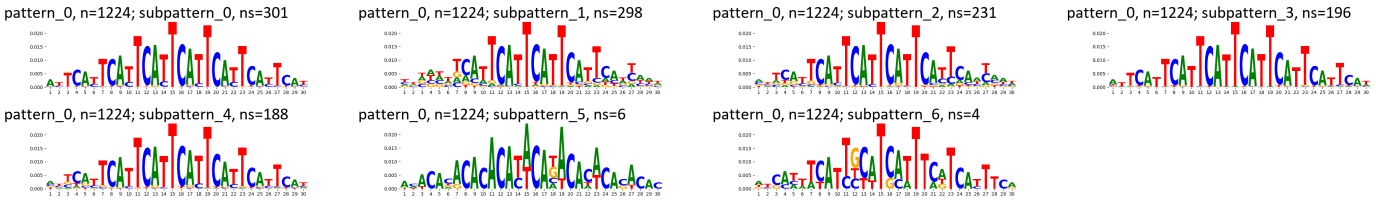

TF-MoDisCO pattern_0 n=1224, PWM

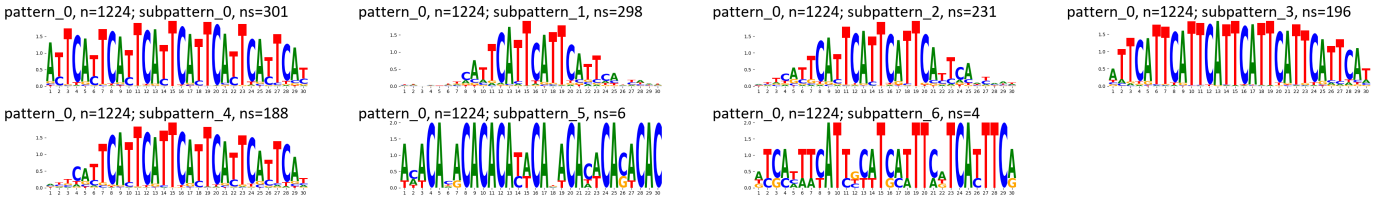

Supplementary Figure 890: TF-MoDisCO subpatterns for the ZNF24 transcription factor in HepG2 (accession ENCSR791AGT).

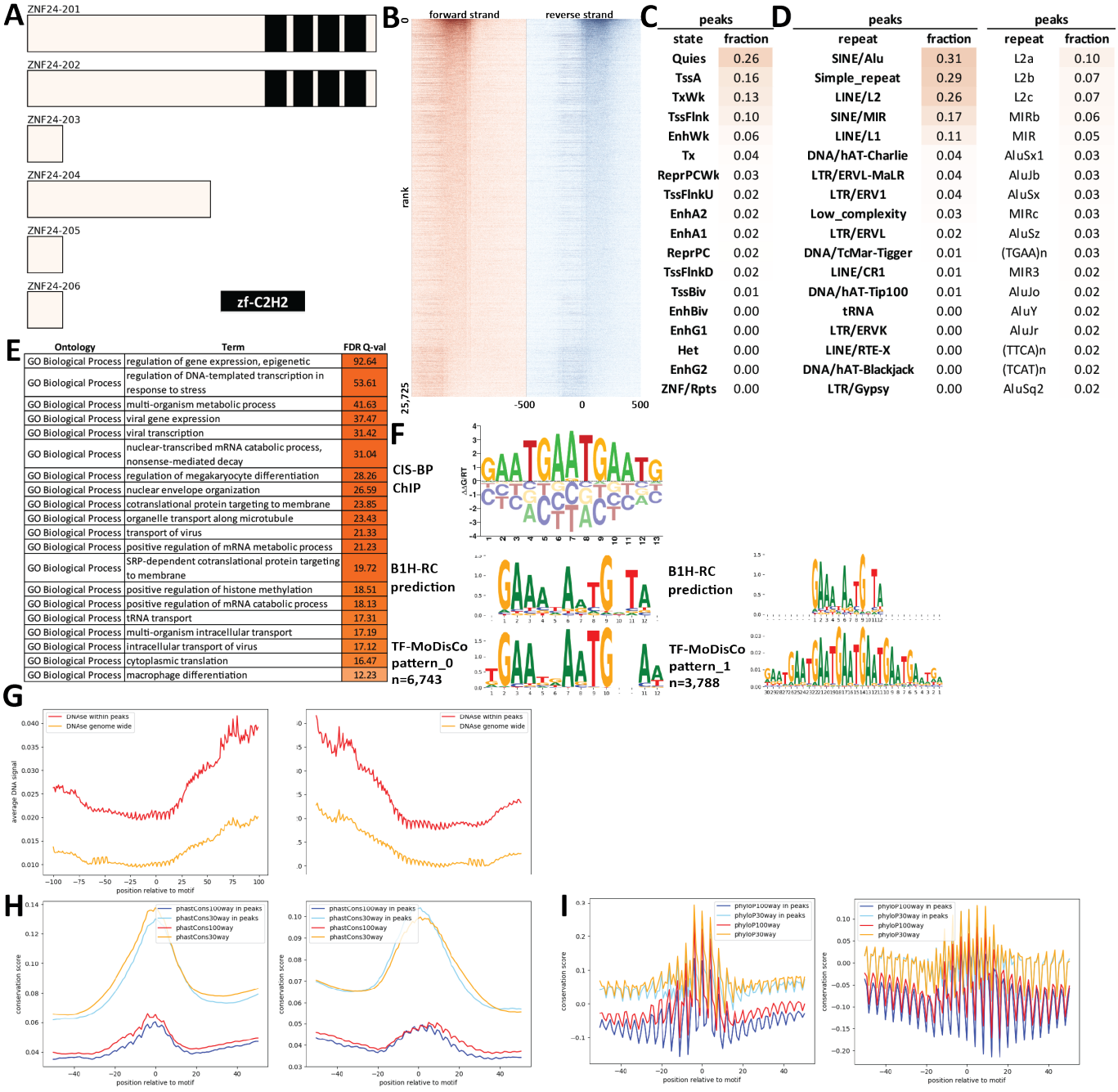

Supplementary Figure 891: Properties and genomic distribution of motifs identified for the ZNF24 transcription factor in K562 (accession ENCSR099NCH).

TF-MoDisCO pattern_0 n=6743, CWM

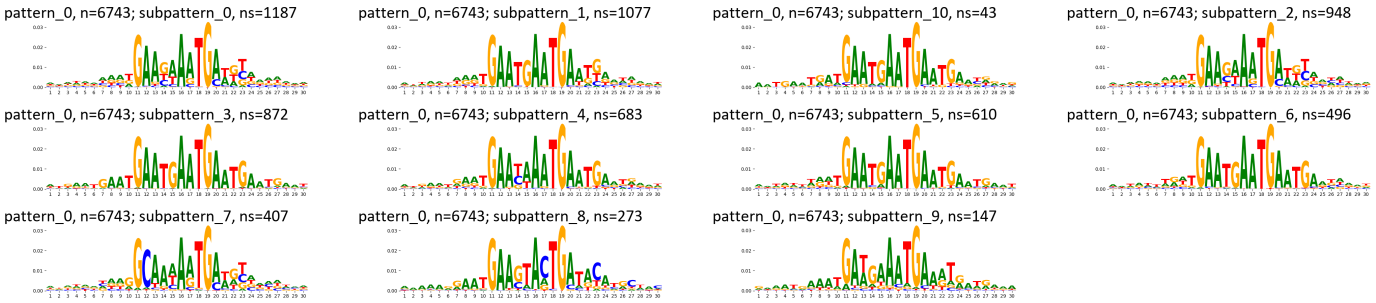

TF-MoDisCO pattern_0 n=6743, PWM

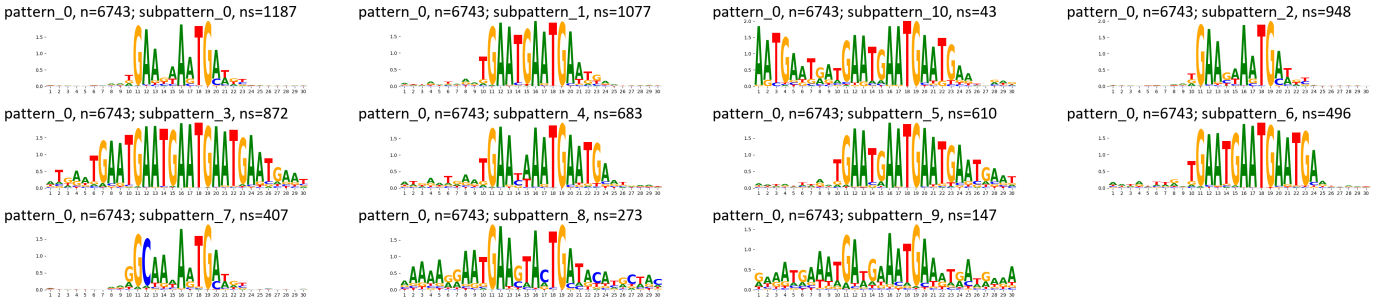

TF-MoDisCO pattern_1 n=3888, CWM

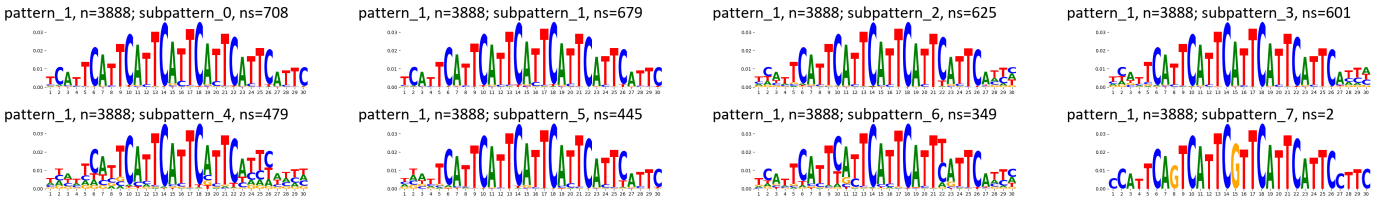

TF-MoDisCO pattern_1 n=3888, PWM

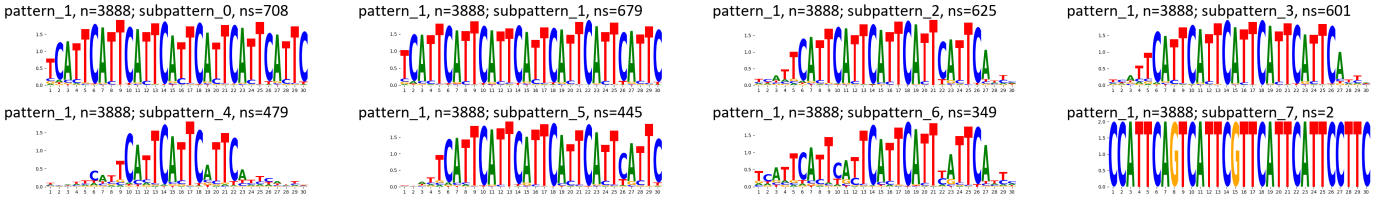

Supplementary Figure 892: TF-MoDisCO subpatterns for the ZNF24 transcription factor in K562 (accession ENCSR099NCH).

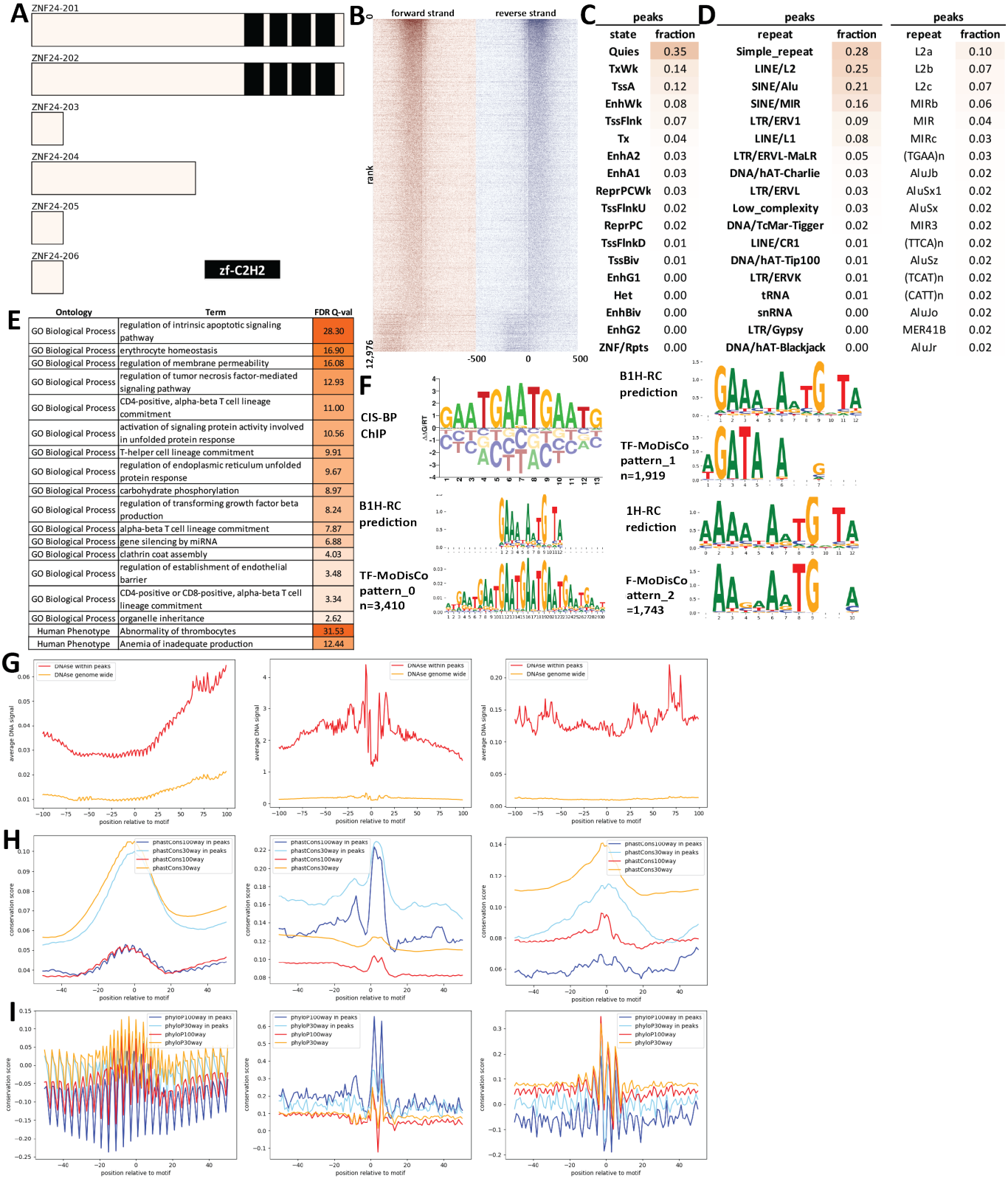

Supplementary Figure 893: Properties and genomic distribution of motifs identified for the ZNF24 transcription factor in K562 (accession ENCSR117WTM).

TF-MoDisCO pattern_0 n=3410, CWM

pattern_0, n=3410; subpattern_0, ns=735

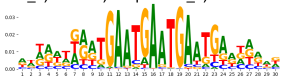

pattern_0, n=3410; subpattern_1, ns=507

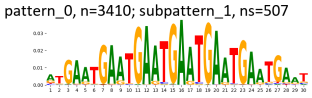

pattern_0, n=3410; subpattern_2, ns=501

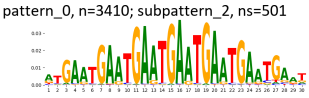

pattern_0, n=3410; subpattern_3, ns=448

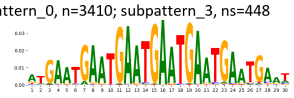

pattern_0, n=3410; subpattern_4, ns=440

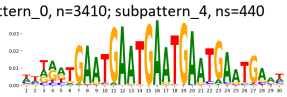

pattern_0, n=3410; subpattern_5, ns=405

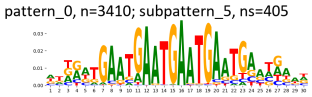

pattern_0, n=3410; subpattern_6, ns=355

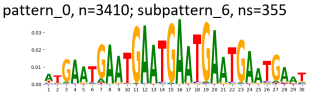

pattern_0, n=3410; subpattern_7, ns=17

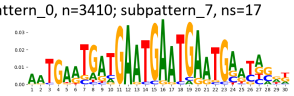

pattern_0, n=3410; subpattern_8, ns=2

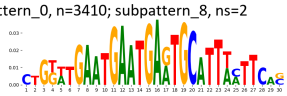

TF-MoDisCO pattern_0 n=3410, PWM

pattern_0, n=3410; subpattern_0, ns=735

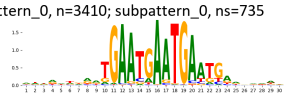

pattern_0, n=3410; subpattern_1, ns=507

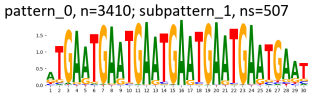

pattern_0, n=3410; subpattern_2, ns=501

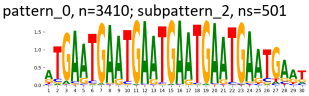

pattern_0, n=3410; subpattern_3, ns=448

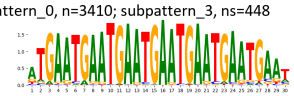

pattern_0, n=3410; subpattern_4, ns=440

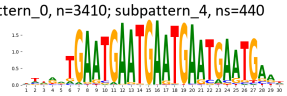

pattern_0, n=3410; subpattern_5, ns=405

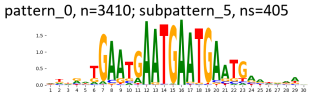

pattern_0, n=3410; subpattern_6, ns=355

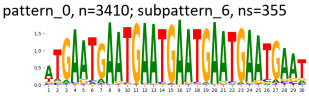

pattern_0, n=3410; subpattern_7, ns=17

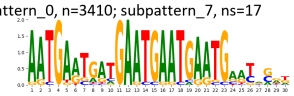

pattern_0, n=3410; subpattern_8, ns=2

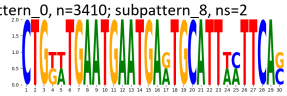

TF-MoDisCO pattern_1 n=1919, CWM

pattern_1, n=1919; subpattern_0, ns=523

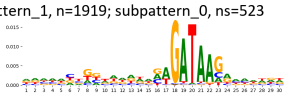

pattern_1, n=1919; subpattern_1, ns=472

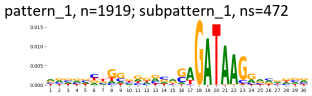

pattern_1, n=1919; subpattern_2, ns=390

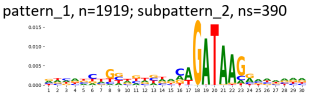

pattern_1, n=1919; subpattern_3, ns=353

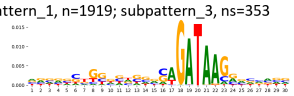

pattern_1, n=1919; subpattern_4, ns=94

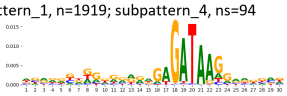

pattern_1, n=1919; subpattern_5, ns=65

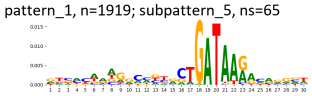

pattern_1, n=1919; subpattern_6, ns=13

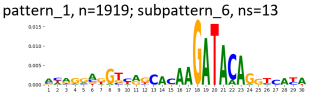

pattern_1, n=1919; subpattern_7, ns=9

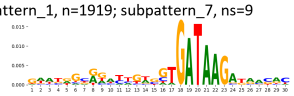

TF-MoDisCO pattern_1 n=1919, PWM

pattern_1, n=1919; subpattern_0, ns=523

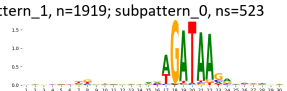

pattern_1, n=1919; subpattern_1, ns=472

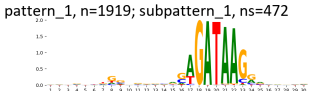

pattern_1, n=1919; subpattern_2, ns=390

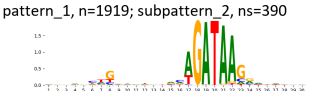

pattern_1, n=1919; subpattern_3, ns=353

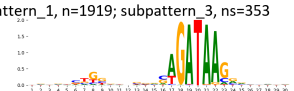

pattern_1, n=1919; subpattern_4, ns=94

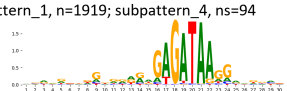

pattern_1, n=1919; subpattern_5, ns=65

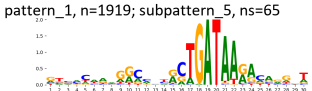

pattern_1, n=1919; subpattern_6, ns=13

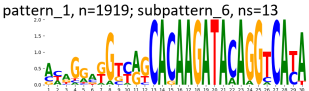

pattern_1, n=1919; subpattern_7, ns=9

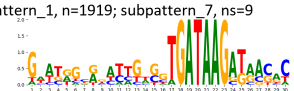

TF-MoDisCO pattern_2 n=1743, CWM

pattern_2, n=1743; subpattern_0, ns=391

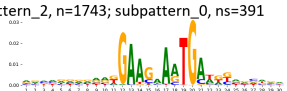

pattern_2, n=1743; subpattern_1, ns=381

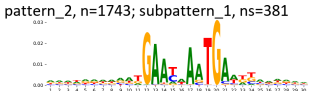

pattern_2, n=1743; subpattern_2, ns=322

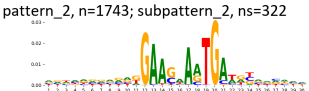

pattern_2, n=1743; subpattern_3, ns=306

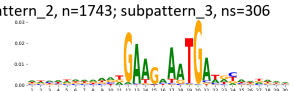

pattern_2, n=1743; subpattern_4, ns=175

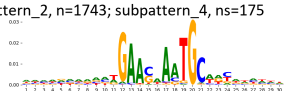

pattern_2, n=1743; subpattern_5, ns=158

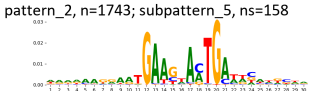

pattern_2, n=1743; subpattern_6, ns=8

pattern_2, n=1743; subpattern_7, ns=2

TF-MoDisCO pattern_2 n=1743, PWM

pattern_2, n=1743; subpattern_0, ns=391

pattern_2, n=1743; subpattern_1, ns=381

pattern_2, n=1743; subpattern_2, ns=322

pattern_2, n=1743; subpattern_3, ns=306

pattern_2, n=1743; subpattern_4, ns=175

pattern_2, n=1743; subpattern_5, ns=158

pattern_2, n=1743; subpattern_6, ns=8

pattern_2, n=1743; subpattern_7, ns=2

Supplementary Figure 894: TF-MoDisCO subpatterns for the ZNF24 transcription factor in K562 (accession ENCSR117WTM).

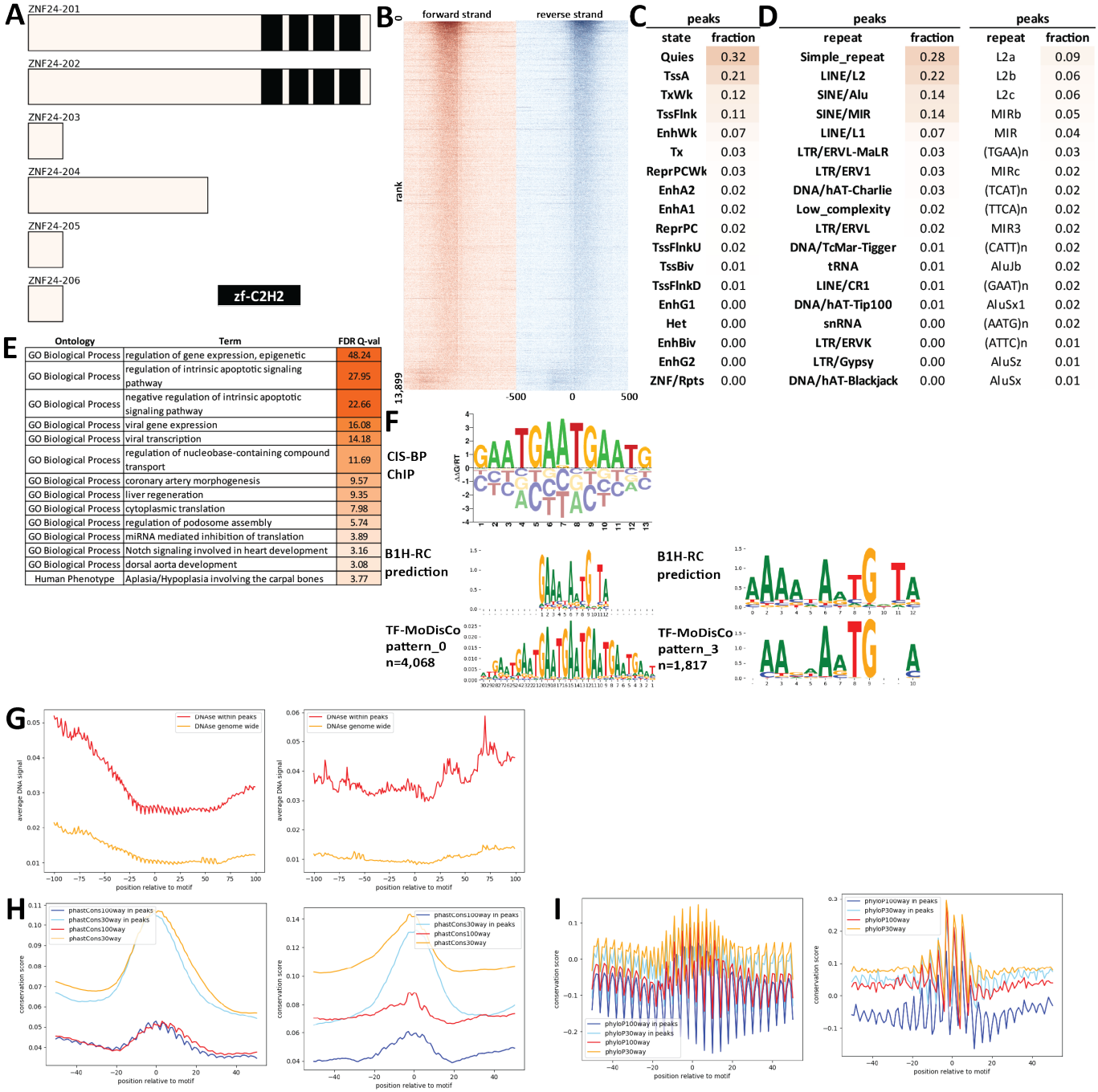

Supplementary Figure 895: Properties and genomic distribution of motifs identified for the ZNF24 transcription factor in K562 (accession ENCSR385AHH).

TF-MoDisCO pattern_0 n=4068, CWM

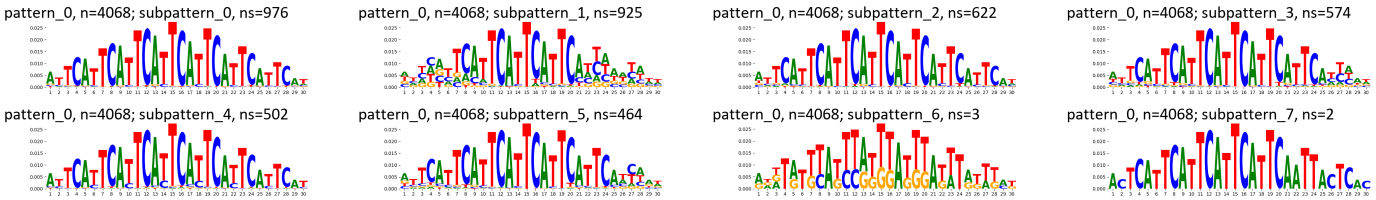

TF-MoDisCO pattern_0 n=4068, PWM

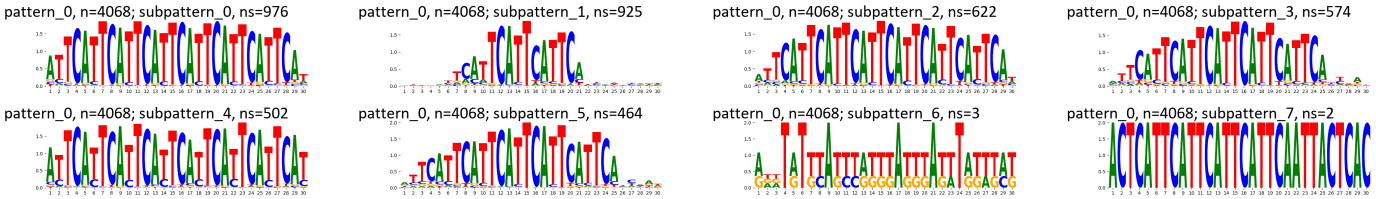

TF-MoDisCO pattern_3 n=1817, CWM

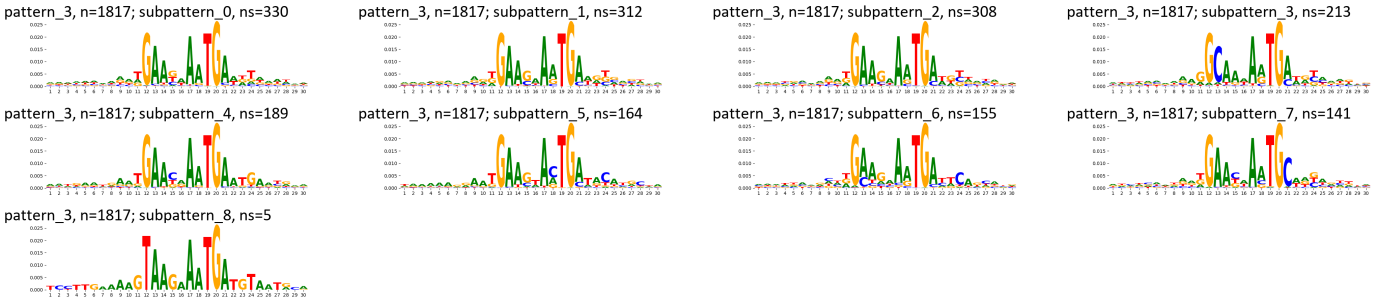

TF-MoDisCO pattern_3 n=1817, PWM

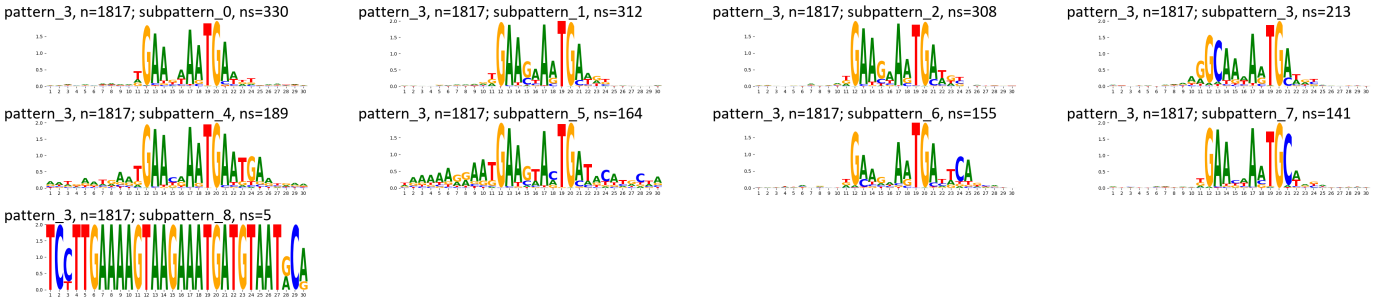

Supplementary Figure 896: TF-MoDisCO subpatterns for the ZNF24 transcription factor in K562 (accession ENCSR385AHH).

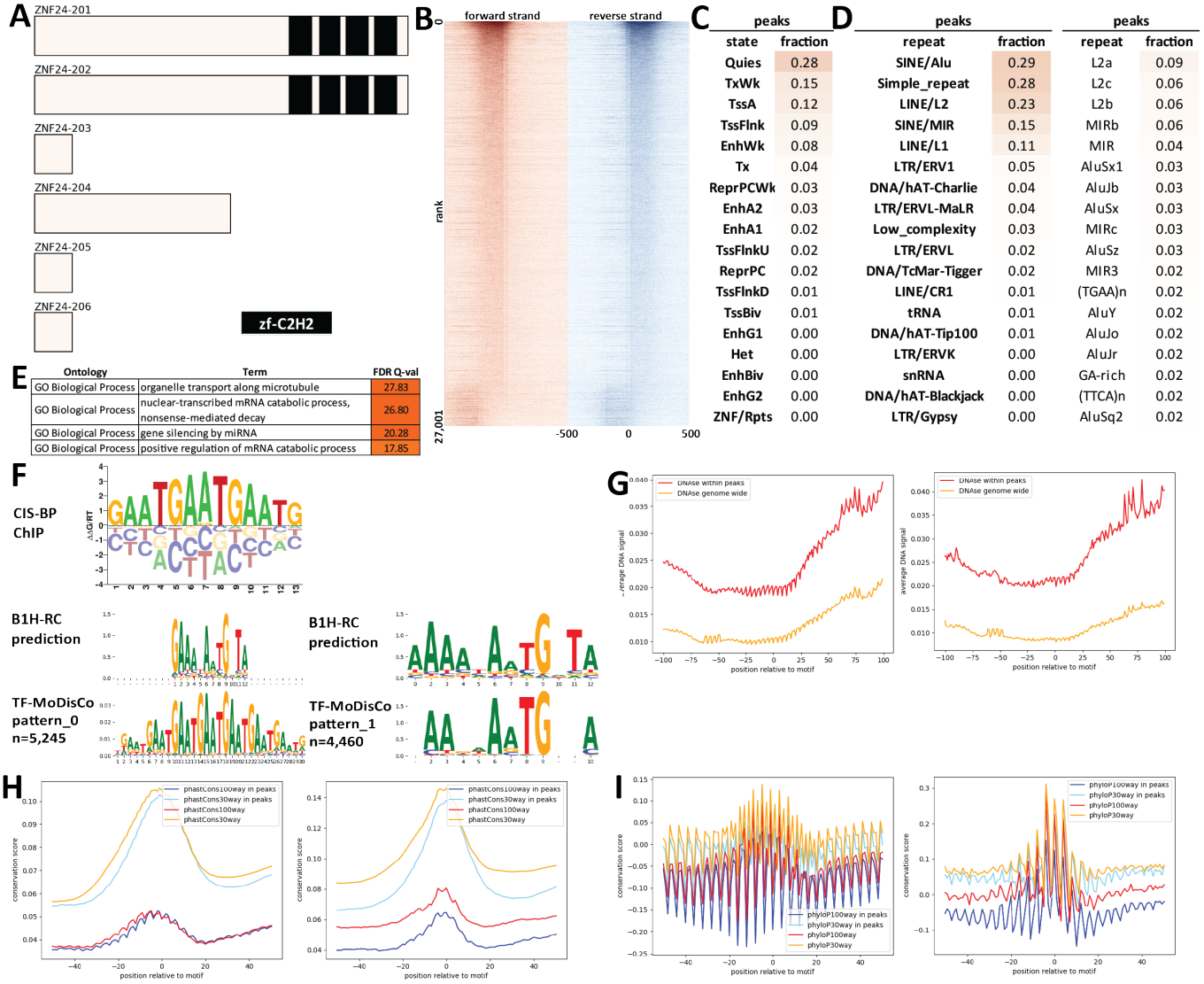

Supplementary Figure 897: Properties and genomic distribution of motifs identified for the ZNF24 transcription factor in K562 (accession ENCSR695EQB).

TF-MoDisCO pattern_0 n=5245, CWM

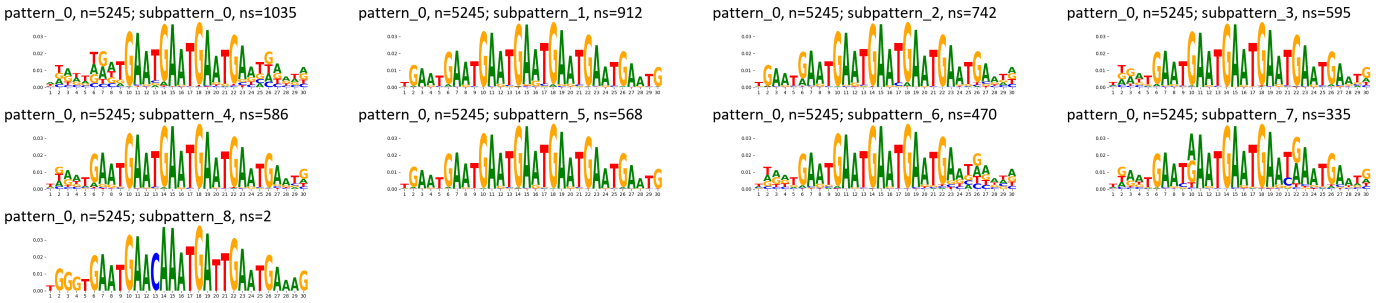

TF-MoDisCO pattern_0 n=5245, PWM

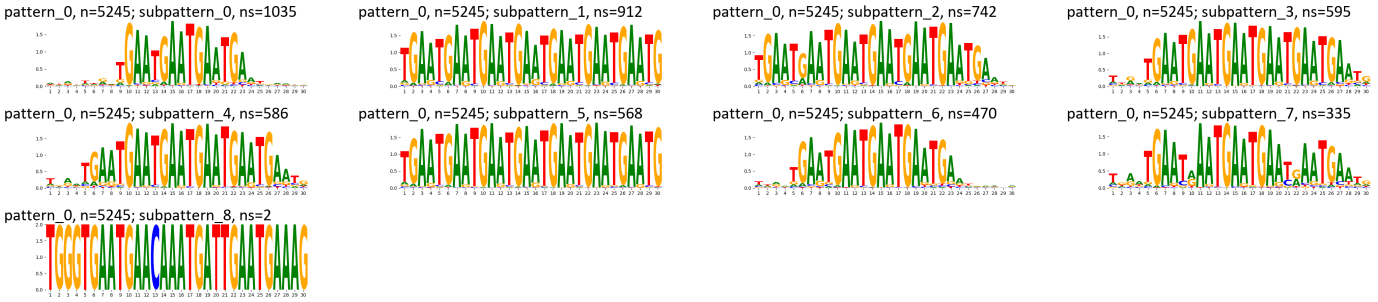

TF-MoDisCO pattern_1 n=4460, CWM

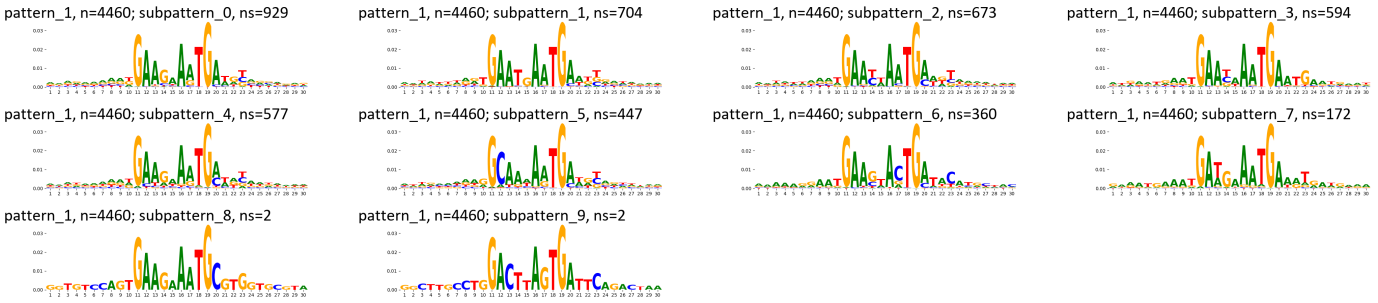

TF-MoDisCO pattern_1 n=4460, PWM

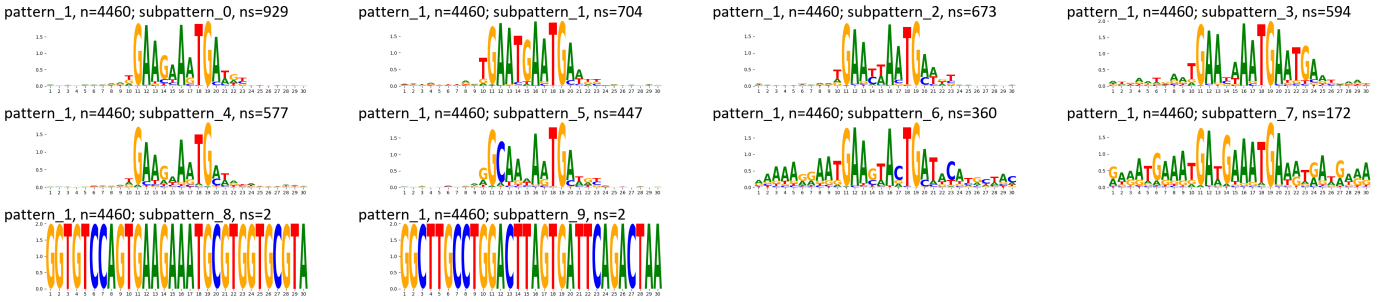

Supplementary Figure 898: TF-MoDisCO subpatterns for the ZNF24 transcription factor in K562 (accession ENCSR695EQB).

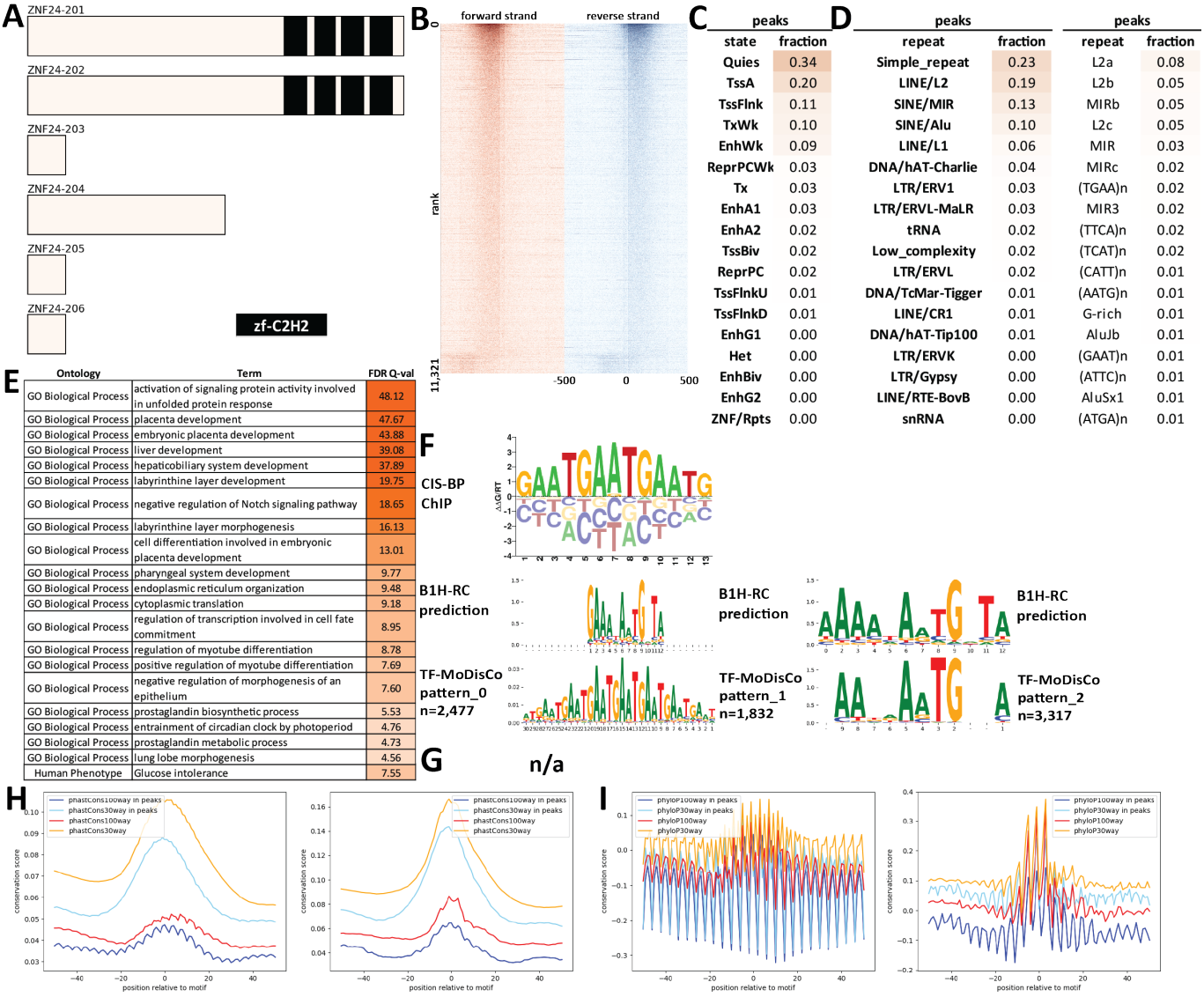

Supplementary Figure 899: Properties and genomic distribution of motifs identified for the ZNF24 transcription factor in MCF-7 (accession ENCSR503VTG).

TF-MoDisCO pattern_0 n=2477, CWM

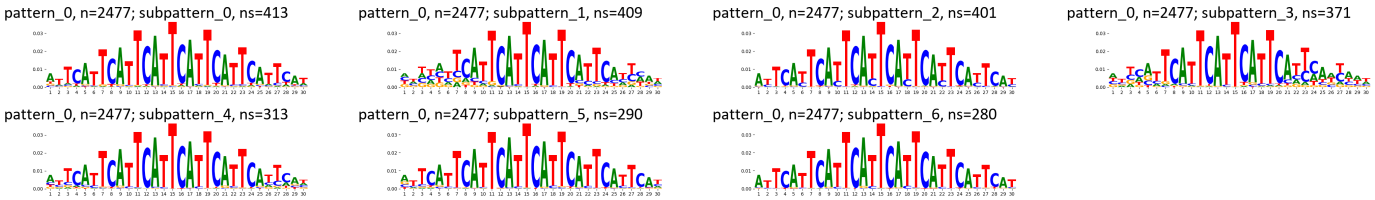

TF-MoDisCO pattern_0 n=2477, PWM

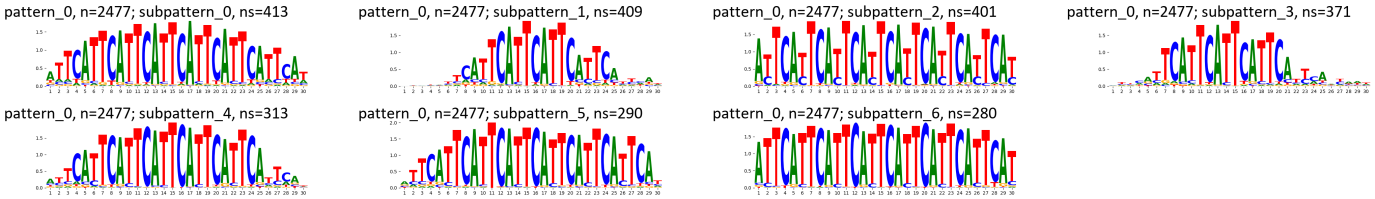

TF-MoDisCO pattern_2 n=1832, CWM

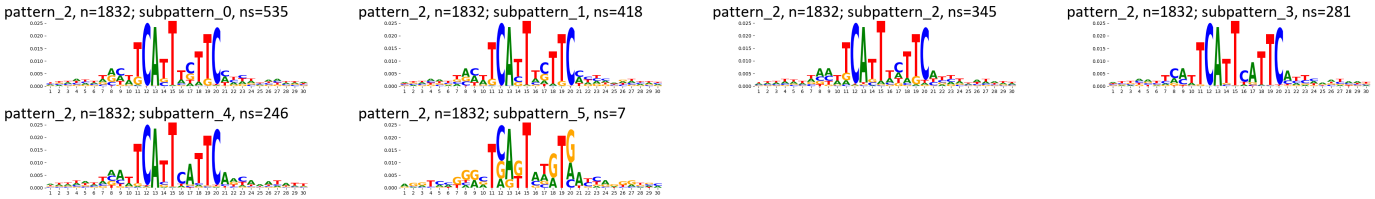

TF-MoDisCO pattern_2 n=1832, PWM

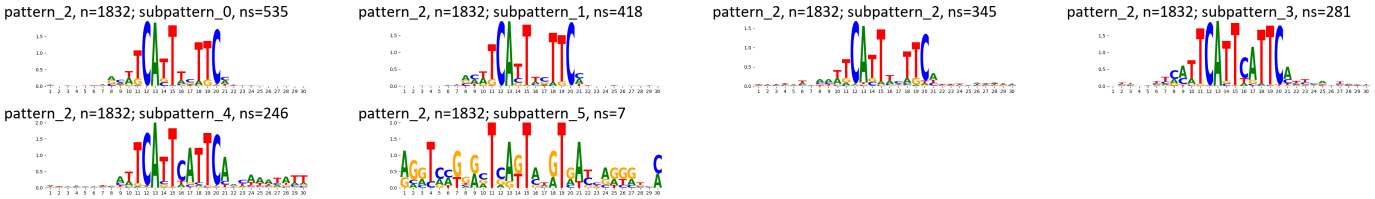

Supplementary Figure 900: TF-MoDisCO subpatterns for the ZNF24 transcription factor in MCF-7 (accession ENCSR503VTG).

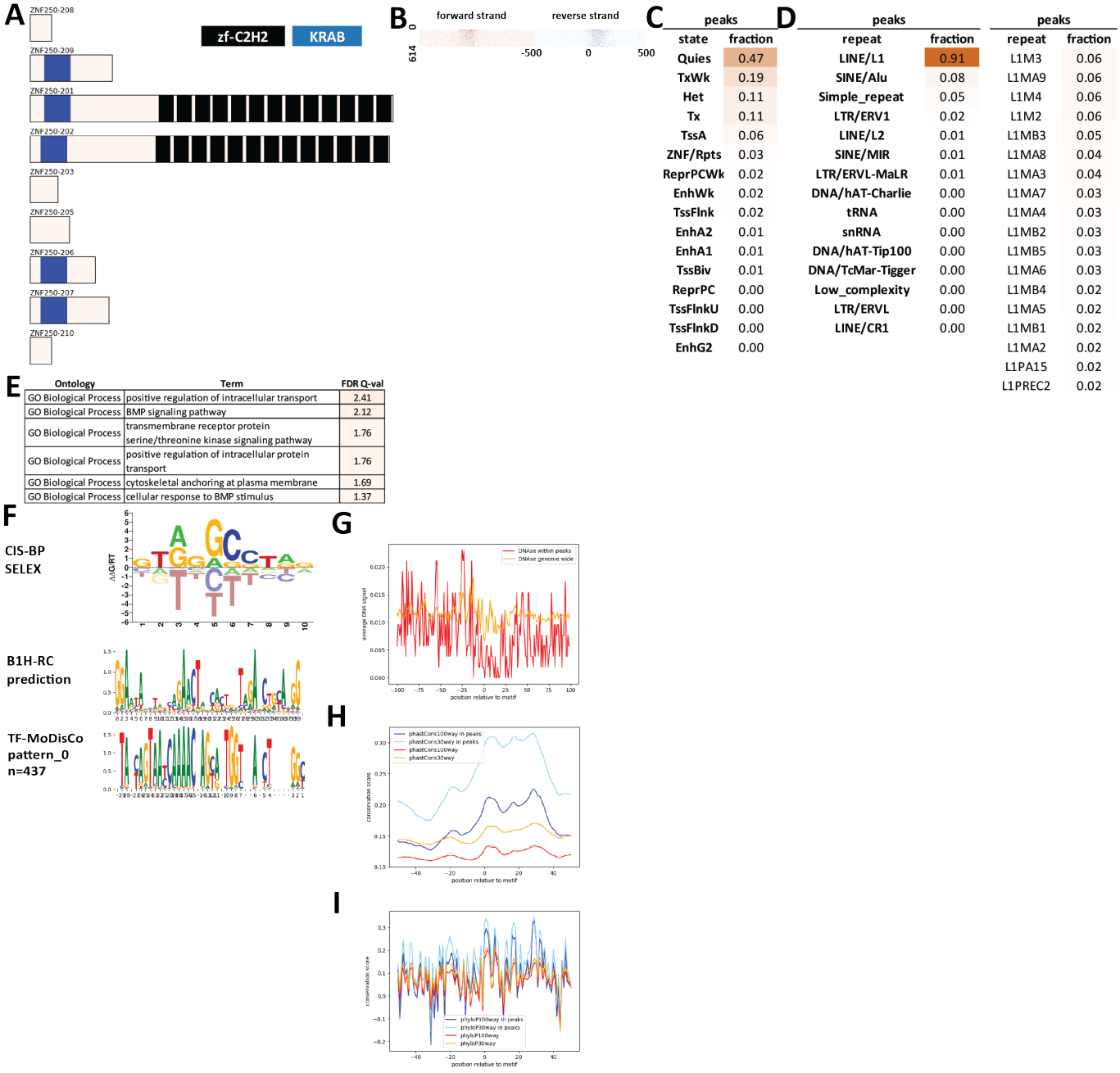

Supplementary Figure 901: Properties and genomic distribution of motifs identified for the ZNF250 transcription factor in HEK293 (accession Hughes GR models).

TF-MoDisCO pattern_0 n=437, CWM

pattern_0, n=437; subpattern_0, ns=147

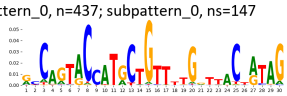

pattern_0, n=437; subpattern_1, ns=91

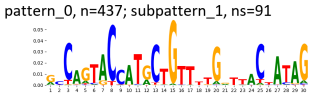

pattern_0, n=437; subpattern_2, ns=73

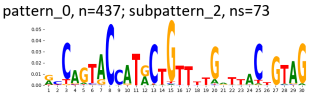

pattern_0, n=437; subpattern_3, ns=72

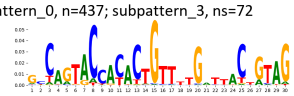

pattern_0, n=437; subpattern_4, ns=54

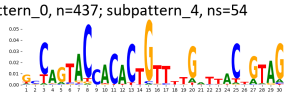

TF-MoDisCO pattern_0 n=437, PWM

pattern_0, n=437; subpattern_0, ns=147

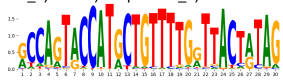

pattern_0, n=437; subpattern_1, ns=91

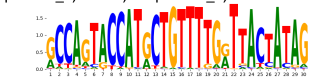

pattern_0, n=437; subpattern_2, ns=73

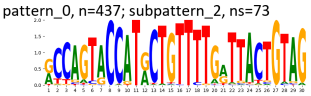

pattern_0, n=437; subpattern_3, ns=72

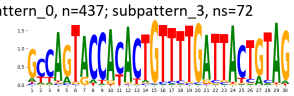

pattern_0, n=437; subpattern_4, ns=54

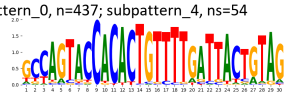

Supplementary Figure 902: TF-MoDisCO subpatterns for the ZNF250 transcription factor in HEK293 (accession Hughes GR models).

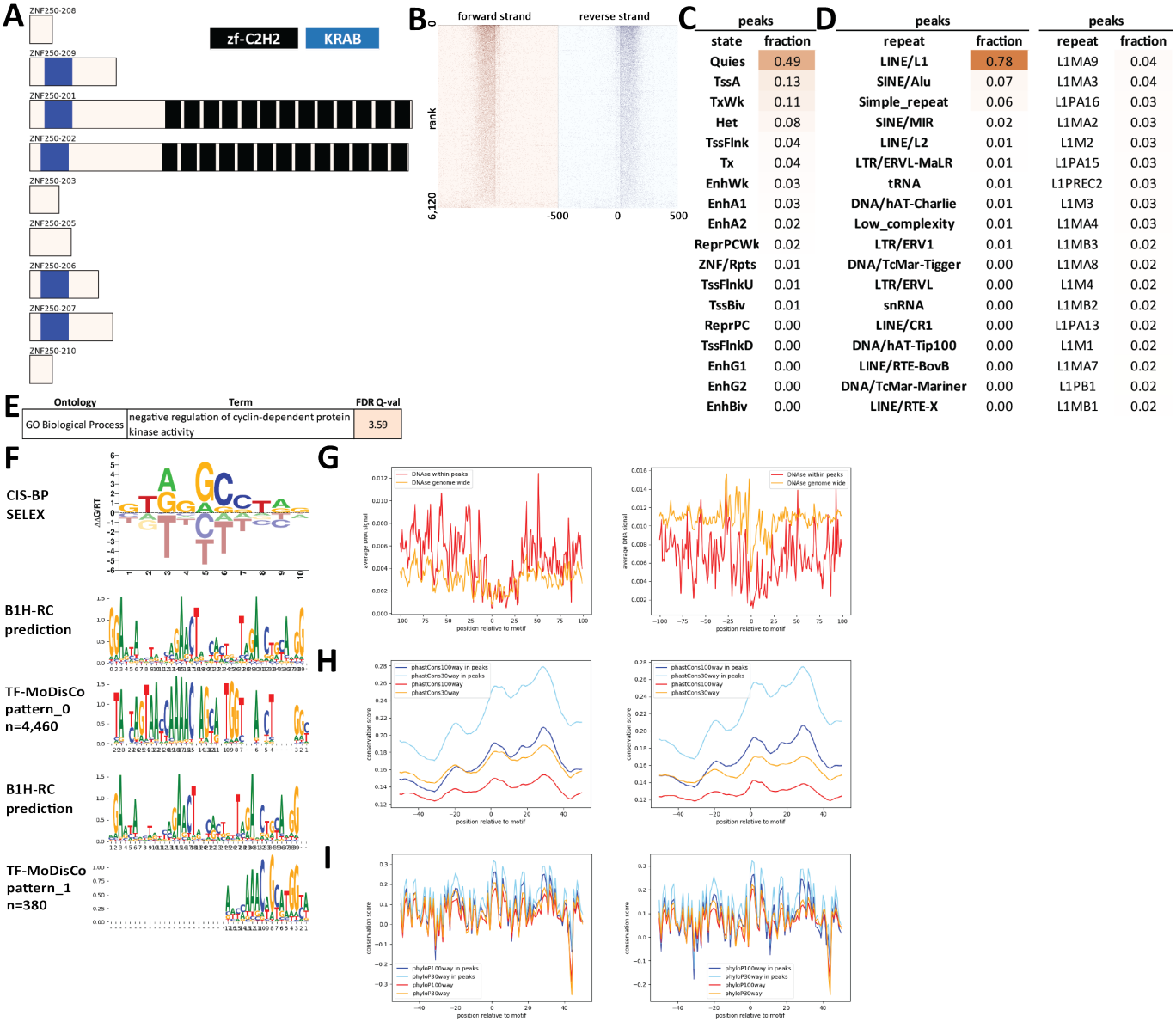

Supplementary Figure 903: Properties and genomic distribution of motifs identified for the ZNF250 transcription factor in HEK293 (accession Hughes NB models).

TF-MoDisCO pattern_0 n=4460, CWM

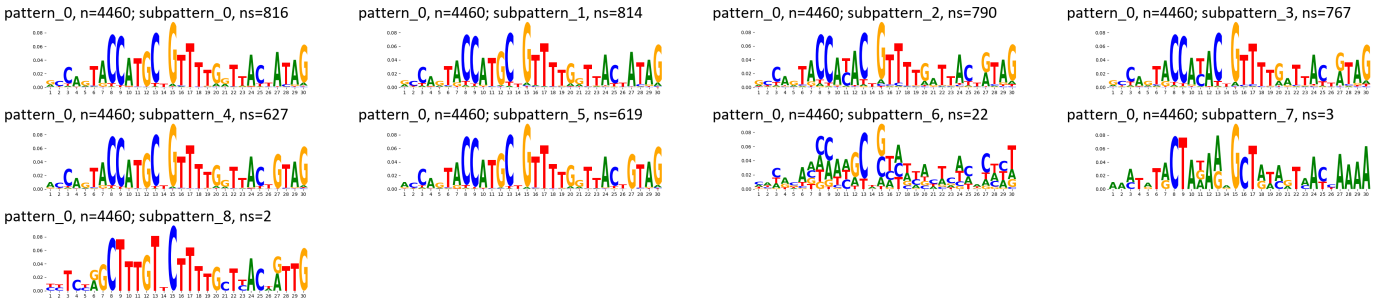

TF-MoDisCO pattern_0 n=4460, PWM

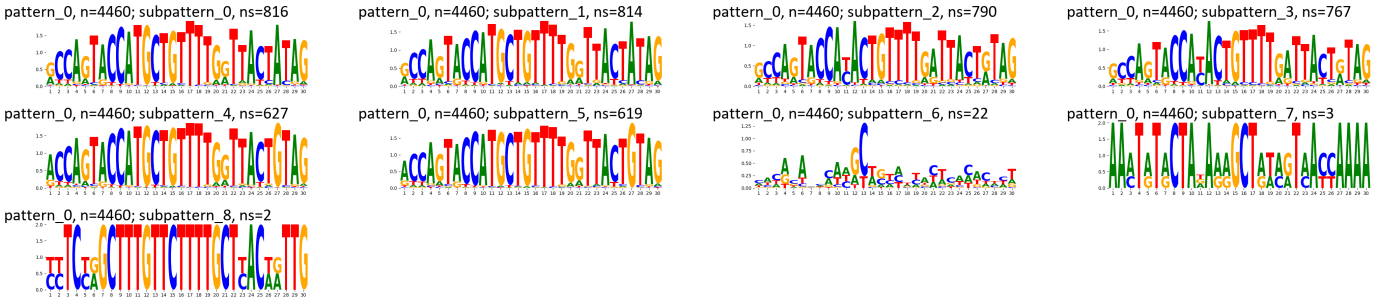

TF-MoDisCO pattern_1 n=380, CWM

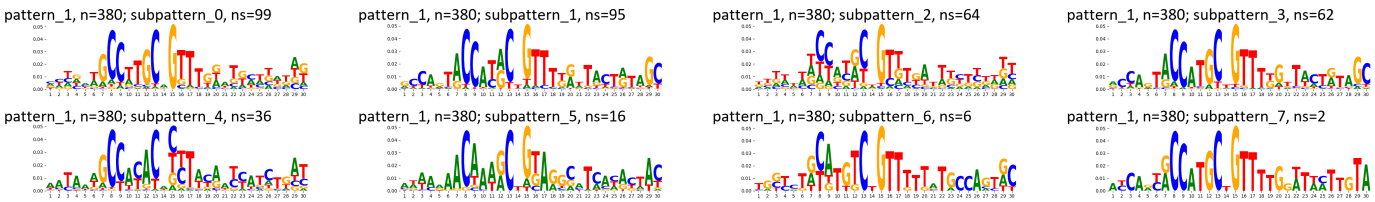

TF-MoDisCO pattern_1 n=380, PWM

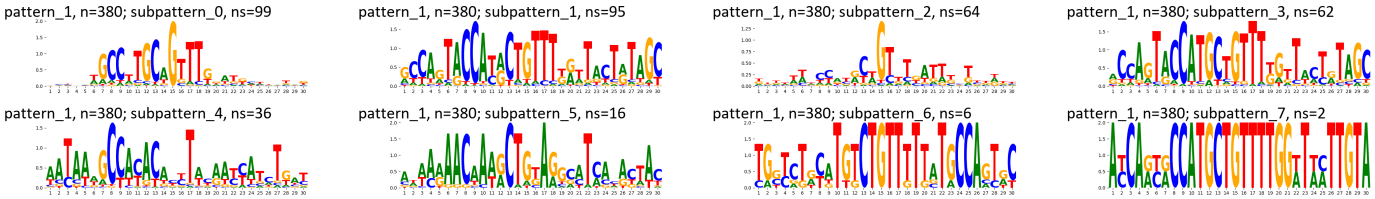

Supplementary Figure 904: TF-MoDisCO subpatterns for the ZNF250 transcription factor in HEK293 (accession Hughes NB models).

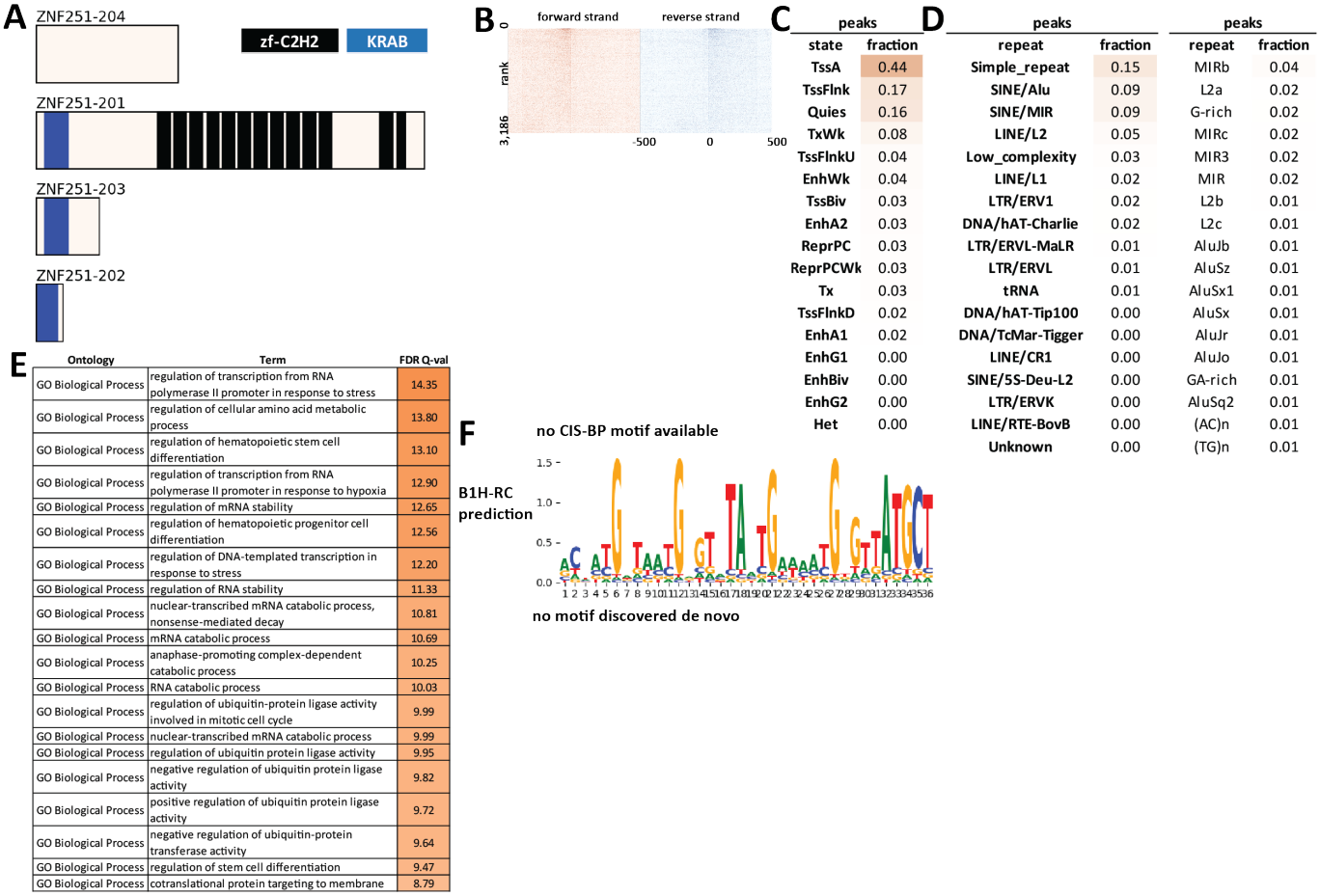

Supplementary Figure 905: Properties and genomic distribution of motifs identified for the ZNF251 transcription factor in HepG2 (accession ENCSR605KVV).

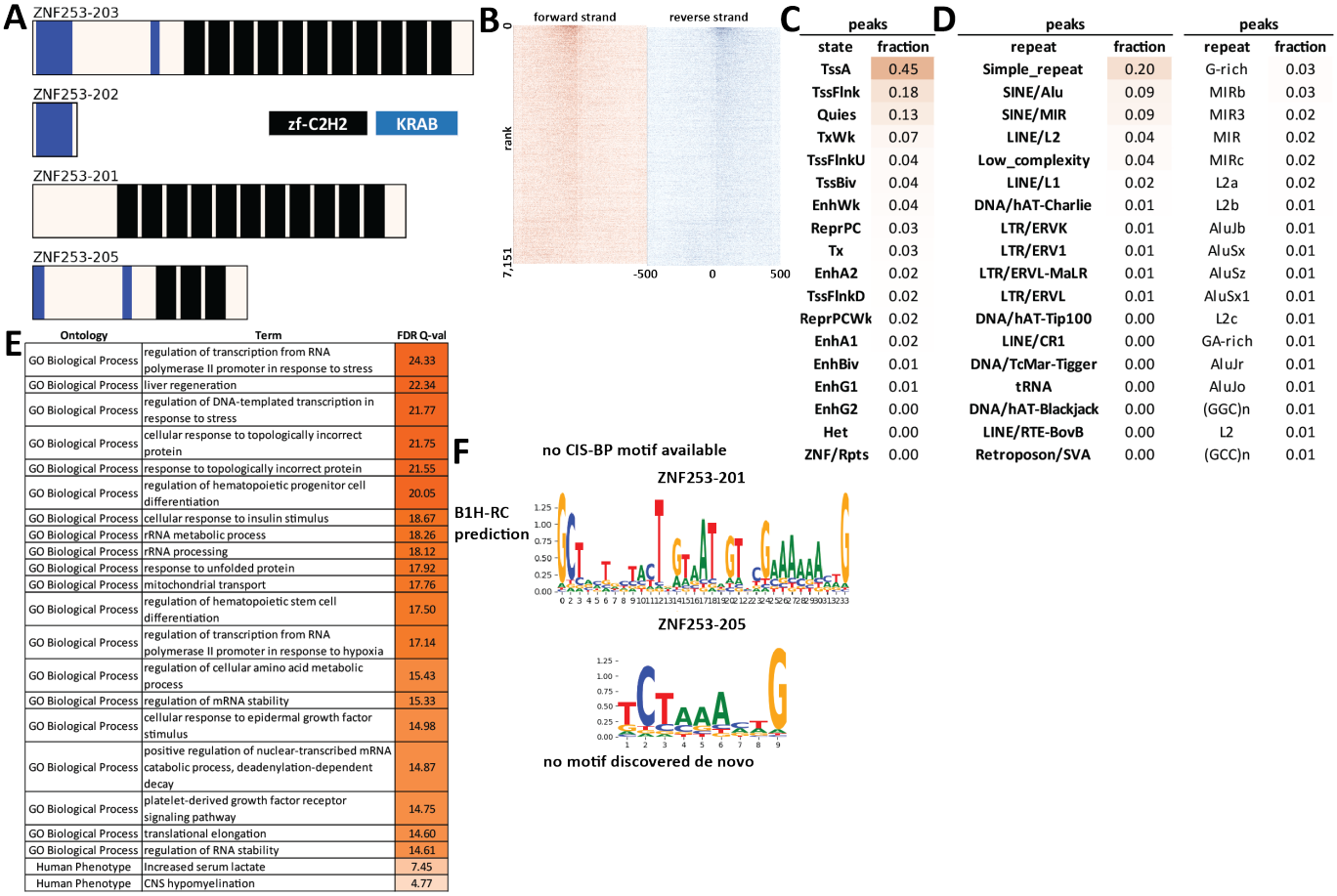

Supplementary Figure 906: Properties and genomic distribution of motifs identified for the ZNF253 transcription factor in HepG2 (accession ENCSR569GKR).

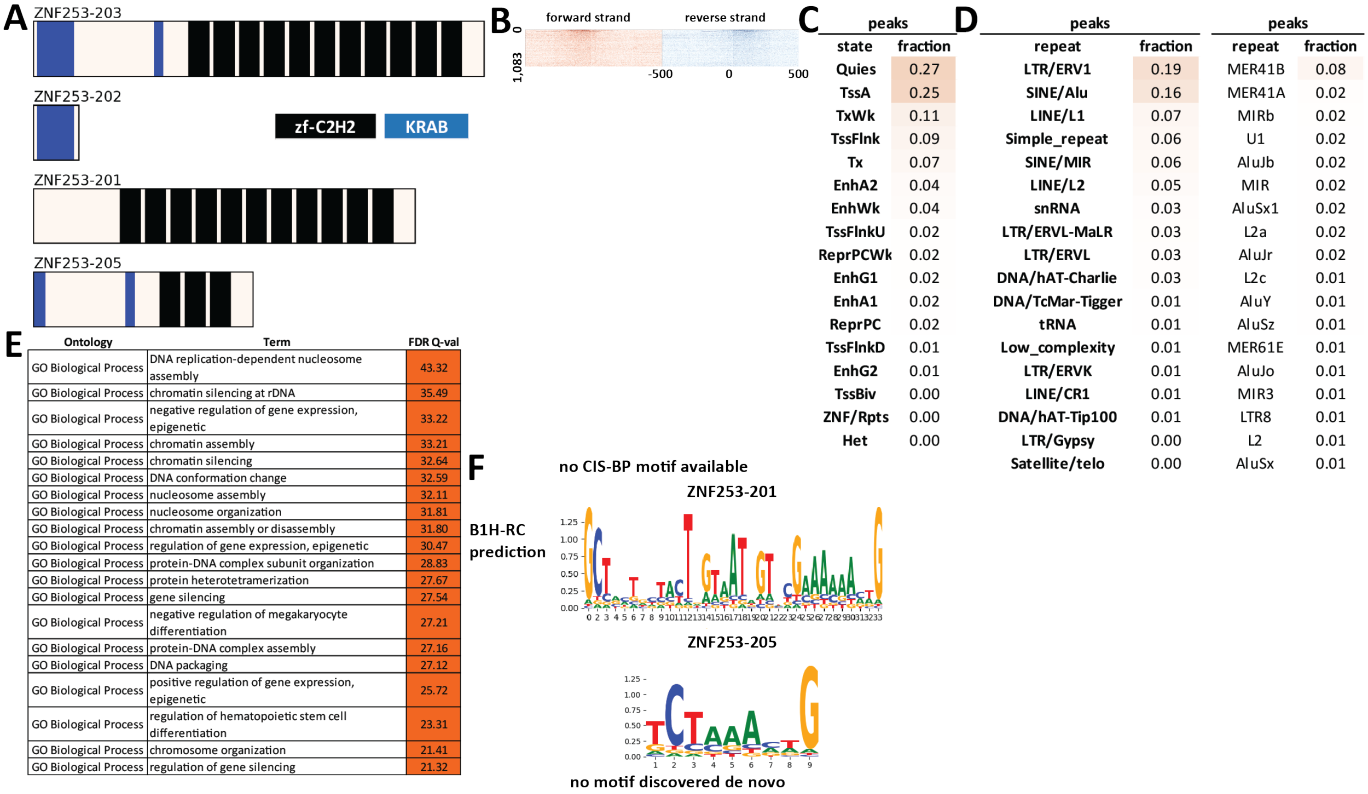

Supplementary Figure 907: Properties and genomic distribution of motifs identified for the ZNF253 transcription factor in K562 (accession ENCSR271RRH).

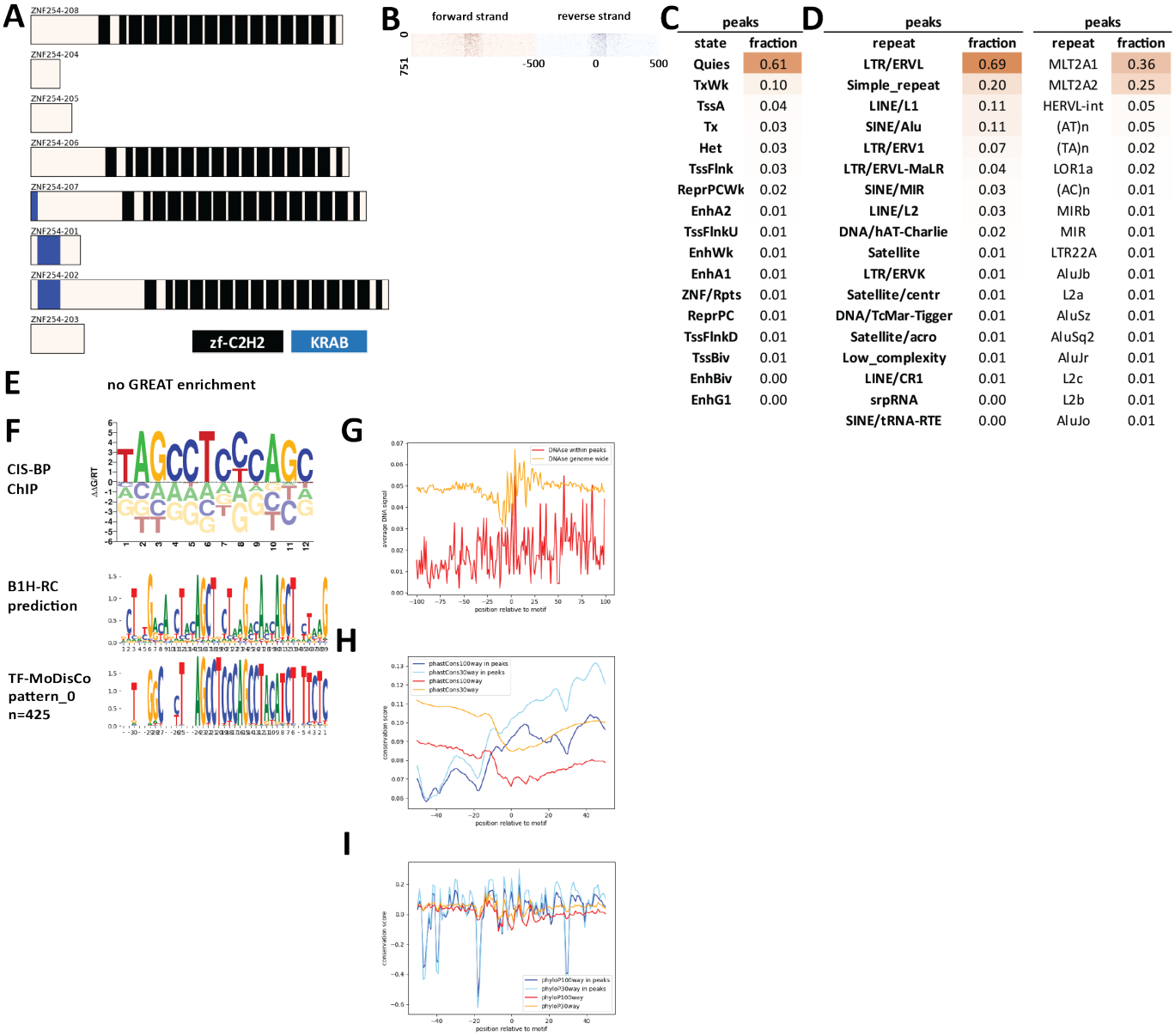

peaks	
state	fraction
Quies	0.61
TxWk	0.10
TssA	0.04
Tx	0.03
Het	0.03
TssFlnk	0.03
ReprPCWk	0.02
EnhA2	0.01
TssFlnkU	0.01
EnhWk	0.01
EnhA1	0.01
ZNF/Rpts	0.01
ReprPC	0.01
TssFlnkD	0.01
TssBiv	0.01
EnhBiv	0.00
EnhG1	0.00

peaks		peaks	
repeat	fraction	repeat	fraction
LTR/ERVL	0.69	MLT2A1	0.36
Simple_repeat	0.20	MLT2A2	0.25
LINE/L1	0.11	HERVL-int	0.05
SINE/Alu	0.11	(AT)n	0.05
LTR/ERV1	0.07	(TA)n	0.02
LTR/ERVL-MaLR	0.04	LOR1a	0.02
SINE/MIR	0.03	(AC)n	0.01
LINE/L2	0.03	MIRb	0.01
DNA/hAT-Charlie	0.02	MIR	0.01
Satellite	0.01	LTR22A	0.01
LTR/ERVK	0.01	AluJb	0.01
Satellite/centr	0.01	L2a	0.01
DNA/TcMar-Tigger	0.01	AluSz	0.01
Satellite/acro	0.01	AluSq2	0.01
Low_complexity	0.01	AluJr	0.01
LINE/CR1	0.01	L2c	0.01
srpRNA	0.00	L2b	0.01
SINE/tRNA-RTE	0.00	AluJo	0.01

Supplementary Figure 908: Properties and genomic distribution of motifs identified for the ZNF254 transcription factor in HEK293 (accession ChipExo models).

TF-MoDisCO pattern_0 n=425, CWM

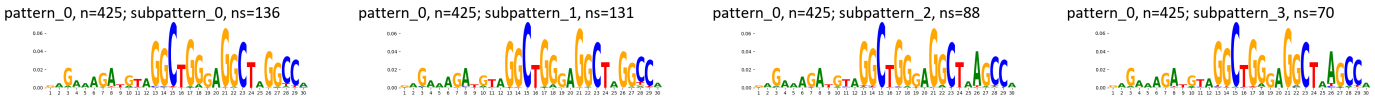

TF-MoDisCO pattern_0 n=425, PWM

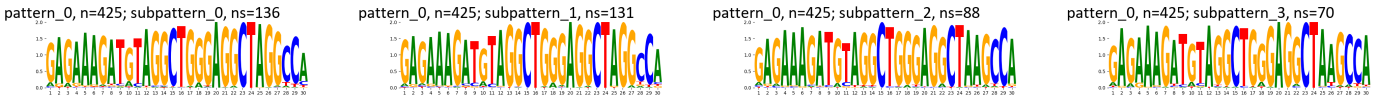

Supplementary Figure 909: TF-MoDisCO subpatterns for the ZNF254 transcription factor in HEK293 (accession ChipExo models).

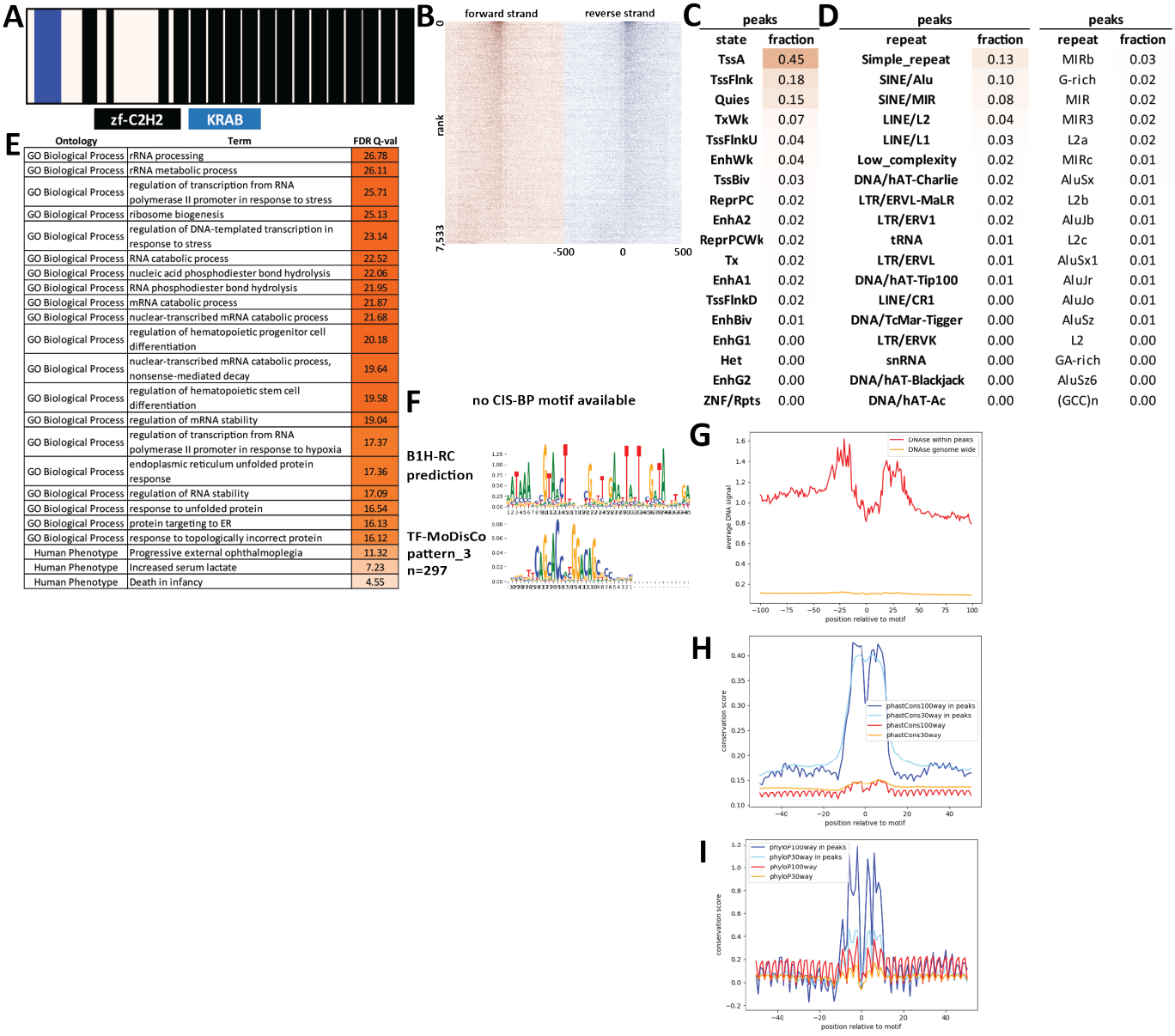

Supplementary Figure 910: Properties and genomic distribution of motifs identified for the ZNF256 transcription factor in HepG2 (accession ENCSR563JME).

TF-MoDisCO pattern_3 n=297, CWM

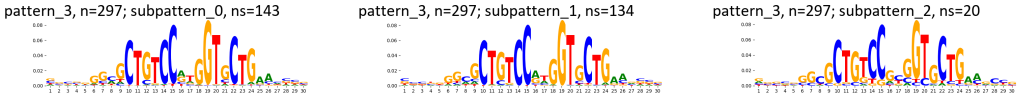

TF-MoDisCO pattern_3 n=297, PWM

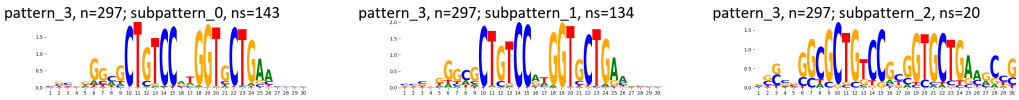

Supplementary Figure 911: TF-MoDisCO subpatterns for the ZNF256 transcription factor in HepG2 (accession ENCSR563JME).

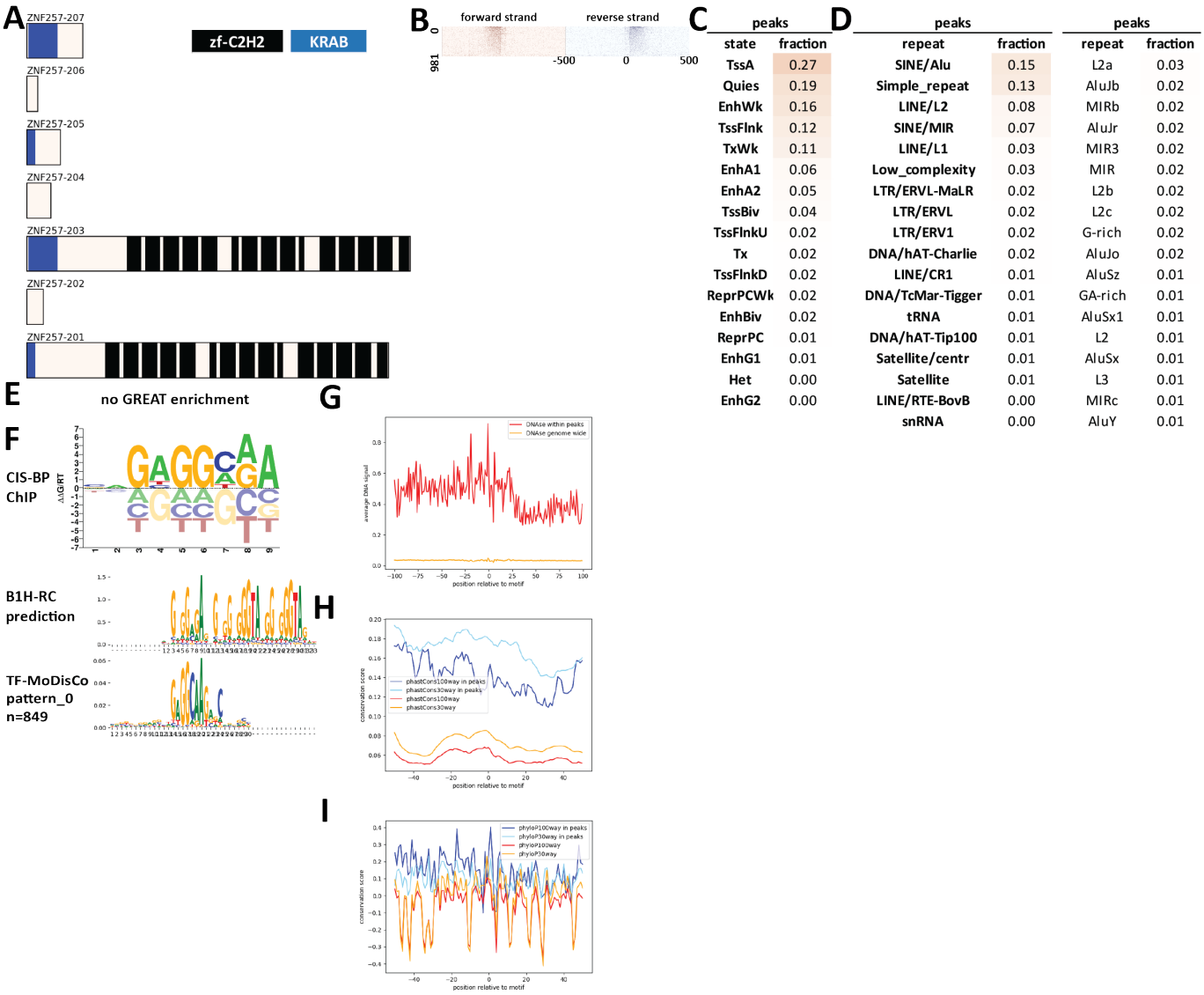

peaks	
state	fraction
TssA	0.27
Quies	0.19
EnhWk	0.16
TssFlnk	0.12
TxWk	0.11
EnhA1	0.06
EnhA2	0.05
TssBiv	0.04
TssFlnkU	0.02
Tx	0.02
TssFlnkD	0.02
ReprPCWk	0.02
EnhBiv	0.02
ReprPC	0.01
EnhG1	0.01
Het	0.00
EnhG2	0.00

peaks	
repeat	fraction
SINE/Alu	0.15
Simple_repeat	0.13
LINE/L2	0.08
SINE/MIR	0.07
LINE/L1	0.03
Low_complexity	0.03
LTR/ERVL-MaLR	0.02
LTR/ERVL	0.02
LTR/ERV1	0.02
DNA/hAT-Charlie	0.02
LINE/CR1	0.01
DNA/TcMar-Tigger	0.01
tRNA	0.01
DNA/hAT-Tip100	0.01
Satellite/centr	0.01
Satellite	0.01
LINE/RTE-BovB	0.00
snRNA	0.00

peaks	
repeat	fraction
L2a	0.03
AluJb	0.02
MIRb	0.02
AluJr	0.02
MIR3	0.02
MIR	0.02
L2b	0.02
L2c	0.02
G-rich	0.02
AluJo	0.02
AluSz	0.01
GA-rich	0.01
AluSx1	0.01
L2	0.01
AluSx	0.01
L3	0.01
MIRc	0.01
AluY	0.01

Supplementary Figure 912: Properties and genomic distribution of motifs identified for the ZNF257 transcription factor in HEK293 (accession Hughes GR models).

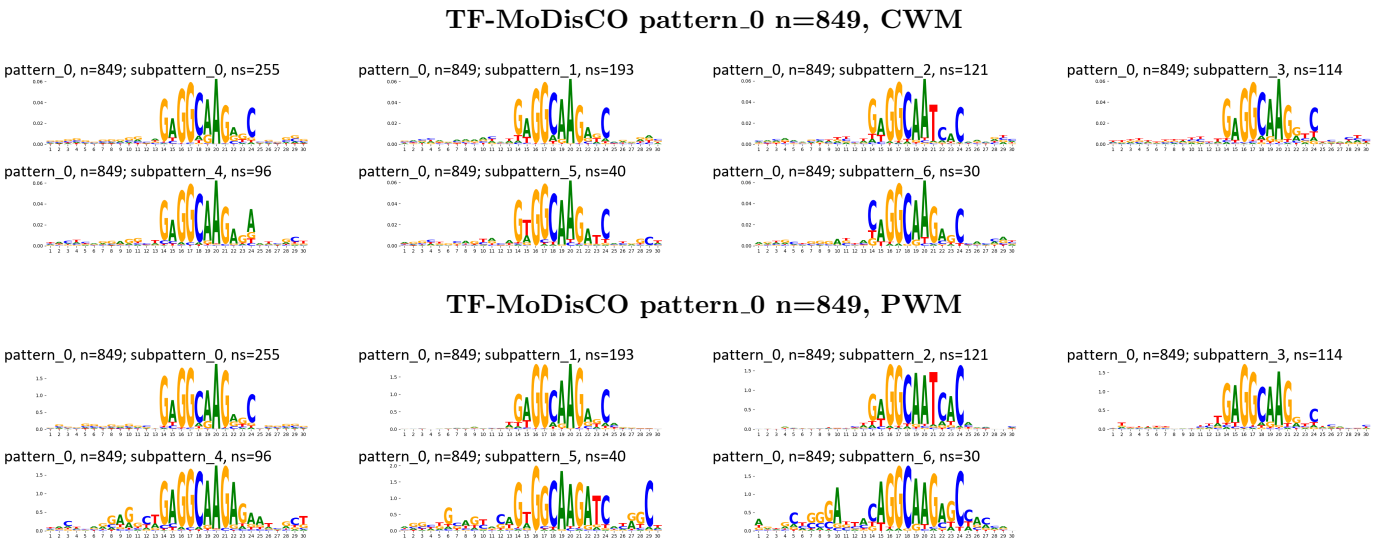

Supplementary Figure 913: TF-MoDisCO subpatterns for the ZNF257 transcription factor in HEK293 (accession Hughes GR models).

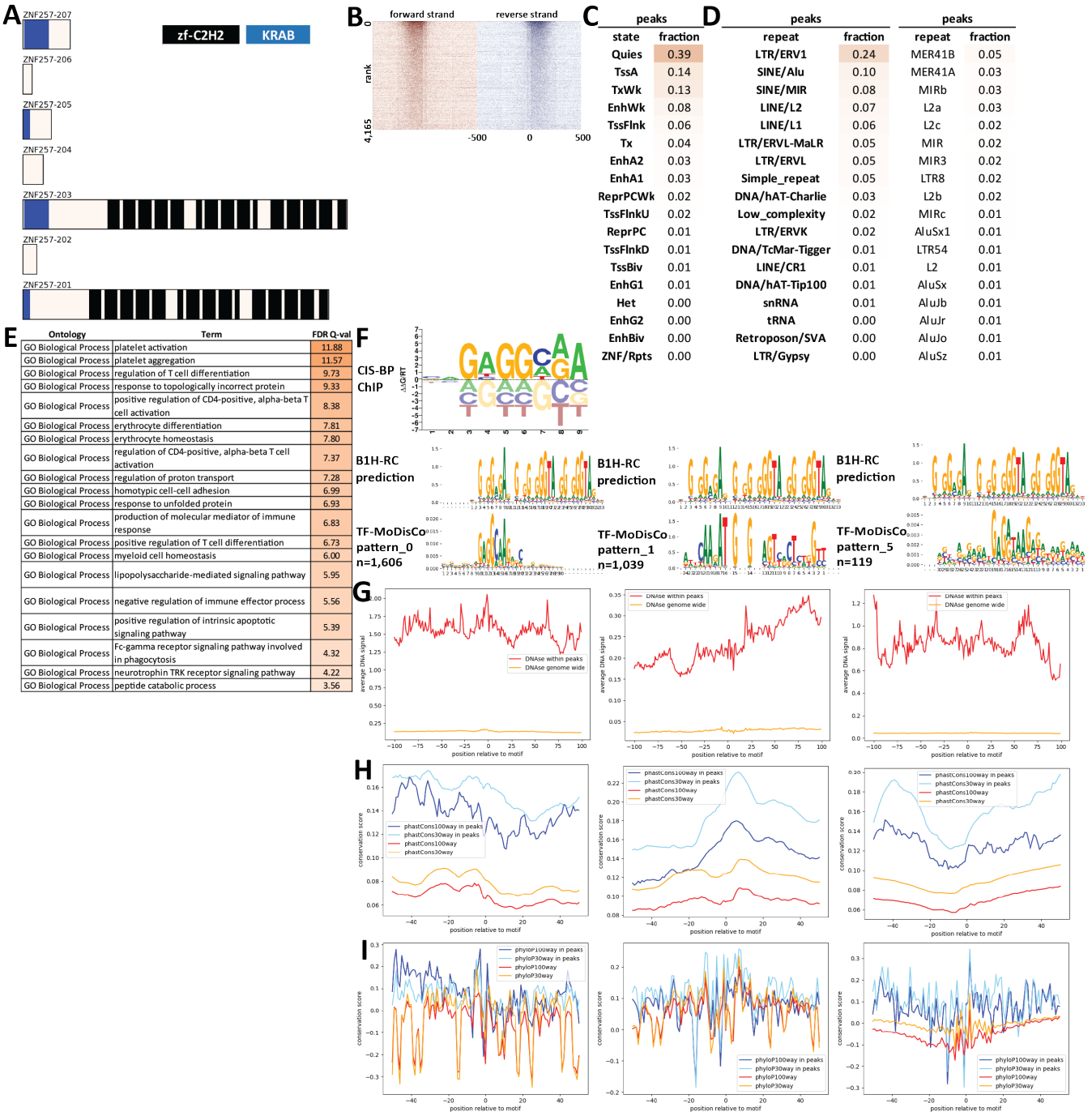

Supplementary Figure 914: Properties and genomic distribution of motifs identified for the ZNF257 transcription factor in K562 (accession ENCSR492FKD).

TF-MoDiSCO pattern_0 n=1606, CWM

pattern_0, n=1606; subpattern_0, ns=463

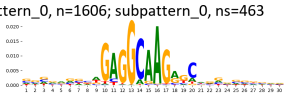

pattern_0, n=1606; subpattern_1, ns=395

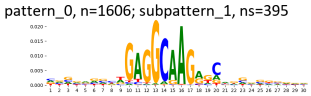

pattern_0, n=1606; subpattern_2, ns=269

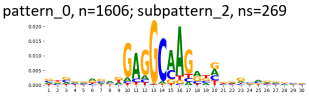

pattern_0, n=1606; subpattern_3, ns=196

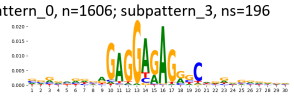

pattern_0, n=1606; subpattern_4, ns=138

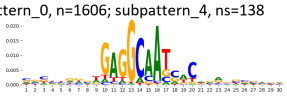

pattern_0, n=1606; subpattern_5, ns=114

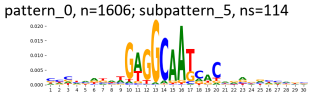

pattern_0, n=1606; subpattern_6, ns=31

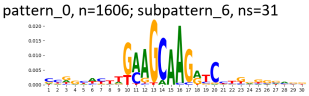

TF-MoDiSCO pattern_0 n=1606, PWM

pattern_0, n=1606; subpattern_0, ns=463

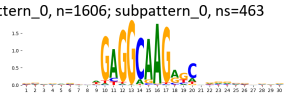

pattern_0, n=1606; subpattern_1, ns=395

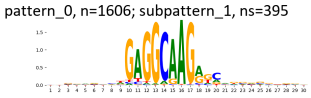

pattern_0, n=1606; subpattern_2, ns=269

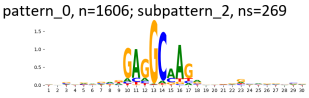

pattern_0, n=1606; subpattern_3, ns=196

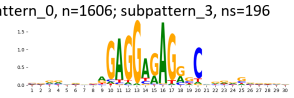

pattern_0, n=1606; subpattern_4, ns=138

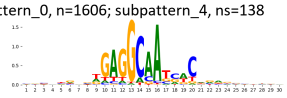

pattern_0, n=1606; subpattern_5, ns=114

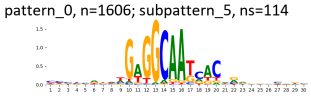

pattern_0, n=1606; subpattern_6, ns=31

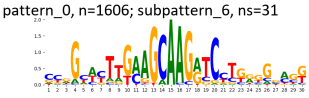

TF-MoDiSCO pattern_1 n=1039, CWM

pattern_1, n=1039; subpattern_0, ns=239

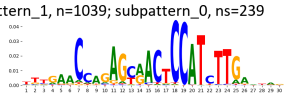

pattern_1, n=1039; subpattern_1, ns=218

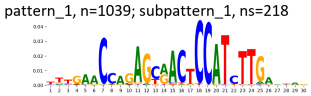

pattern_1, n=1039; subpattern_2, ns=195

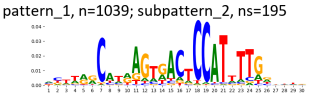

pattern_1, n=1039; subpattern_3, ns=121

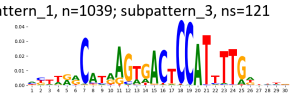

pattern_1, n=1039; subpattern_4, ns=94

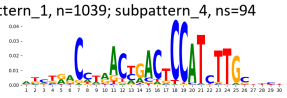

pattern_1, n=1039; subpattern_5, ns=69

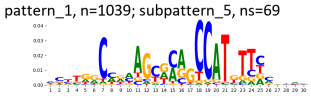

pattern_1, n=1039; subpattern_6, ns=60

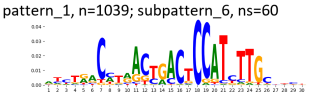

pattern_1, n=1039; subpattern_7, ns=29

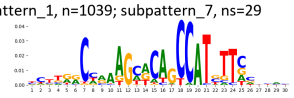

pattern_1, n=1039; subpattern_8, ns=14

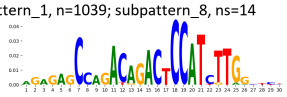

TF-MoDiSCO pattern_1 n=1039, CWM

pattern_1, n=1039; subpattern_0, ns=239

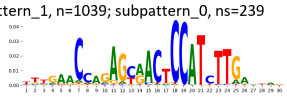

pattern_1, n=1039; subpattern_1, ns=218

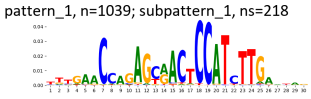

pattern_1, n=1039; subpattern_2, ns=195

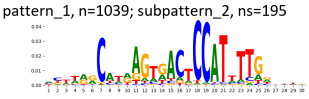

pattern_1, n=1039; subpattern_3, ns=121

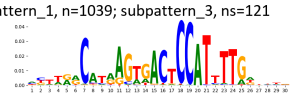

pattern_1, n=1039; subpattern_4, ns=94

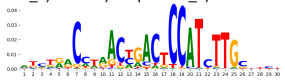

pattern_1, n=1039; subpattern_5, ns=69

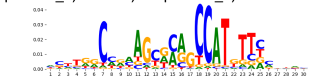

pattern_1, n=1039; subpattern_6, ns=60

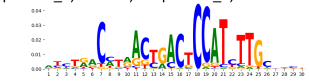

pattern_1, n=1039; subpattern_7, ns=29

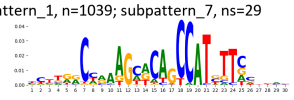

pattern_1, n=1039; subpattern_8, ns=14

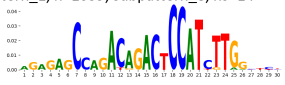

TF-MoDiSCO pattern_1 n=1039, PWM

pattern_1, n=1039; subpattern_0, ns=239

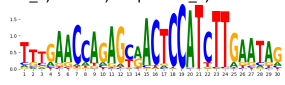

pattern_1, n=1039; subpattern_1, ns=218

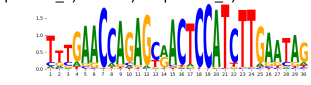

pattern_1, n=1039; subpattern_2, ns=195

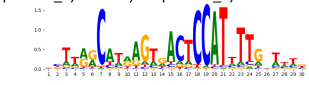

pattern_1, n=1039; subpattern_3, ns=121

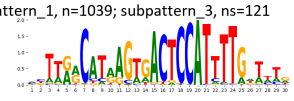

pattern_1, n=1039; subpattern_4, ns=94

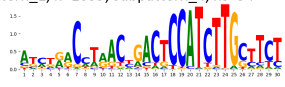

pattern_1, n=1039; subpattern_5, ns=69

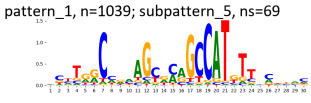

pattern_1, n=1039; subpattern_6, ns=60

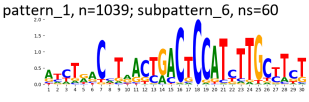

pattern_1, n=1039; subpattern_7, ns=29

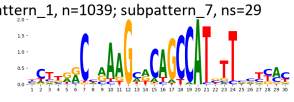

pattern_1, n=1039; subpattern_8, ns=14

TF-MoDiSCO pattern_1 n=1039, PWM

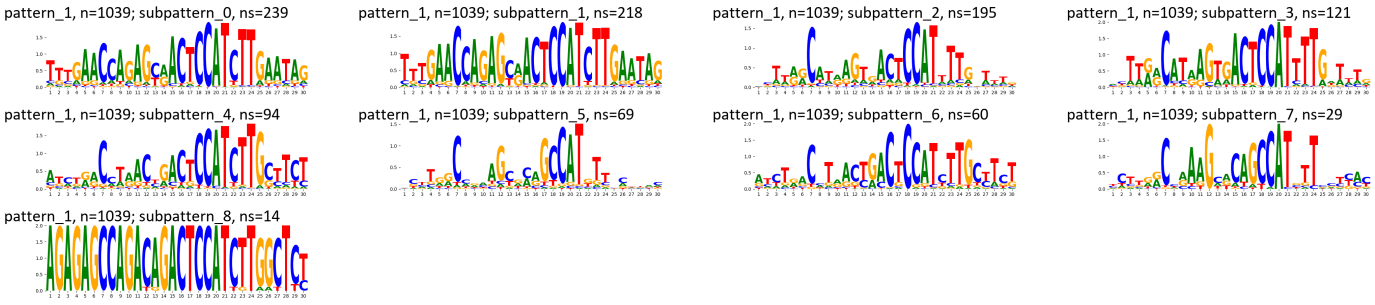

TF-MoDisCO pattern_5 n=119, CWM

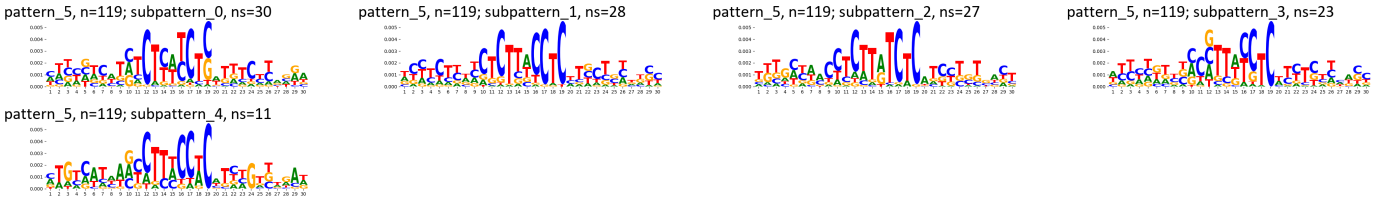

TF-MoDisCO pattern_5 n=119, PWM

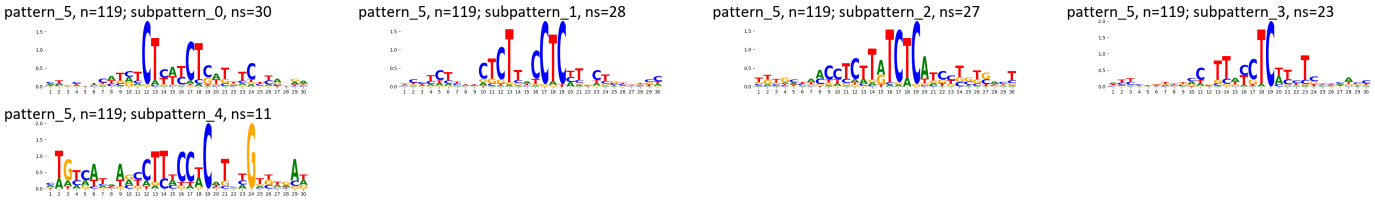

Supplementary Figure 915: TF-MoDisCO subpatterns for the ZNF257 transcription factor in K562 (accession ENCSR492FKD).

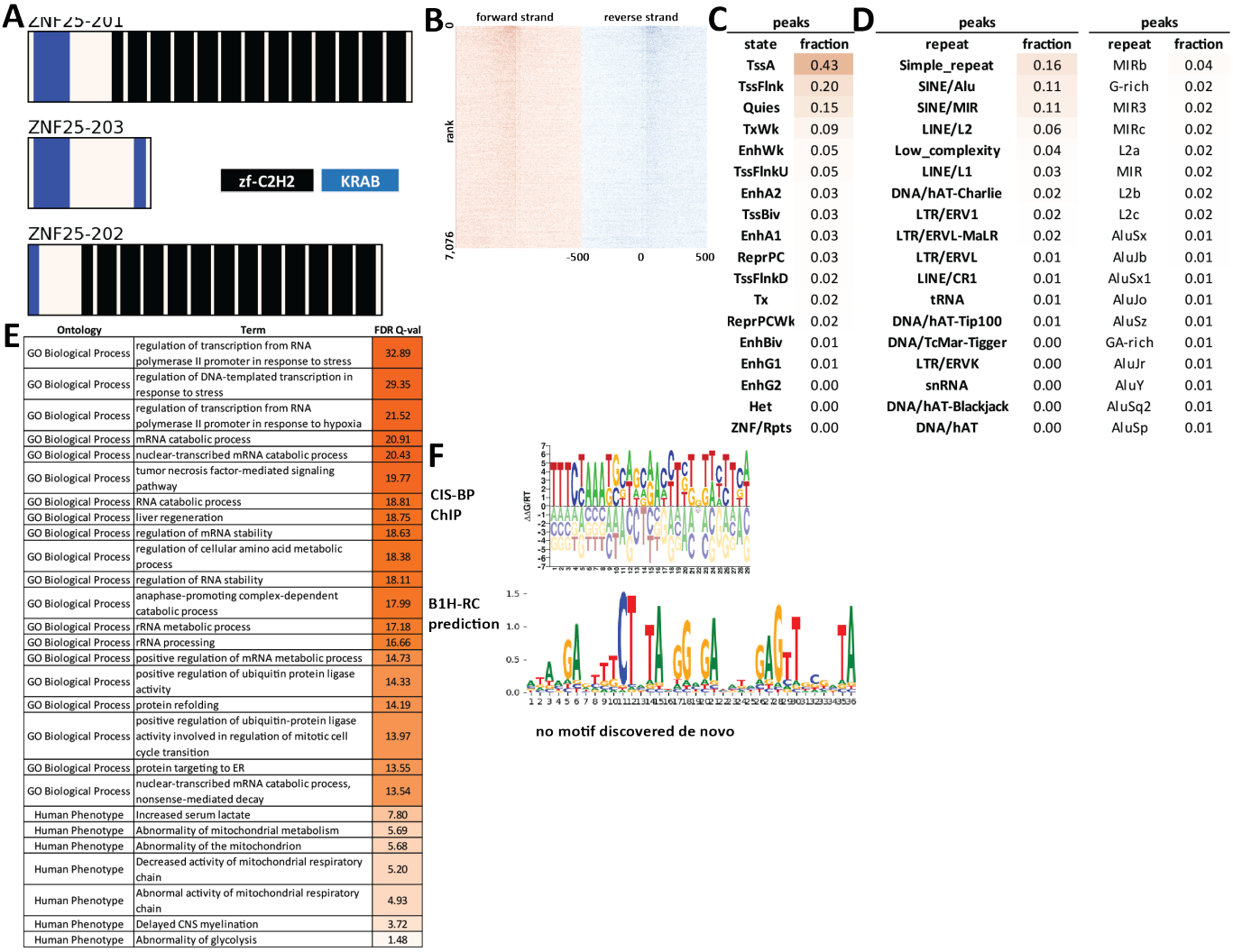

Supplementary Figure 916: Properties and genomic distribution of motifs identified for the ZNF25 transcription factor in HepG2 (accession ENCSR384SQB).

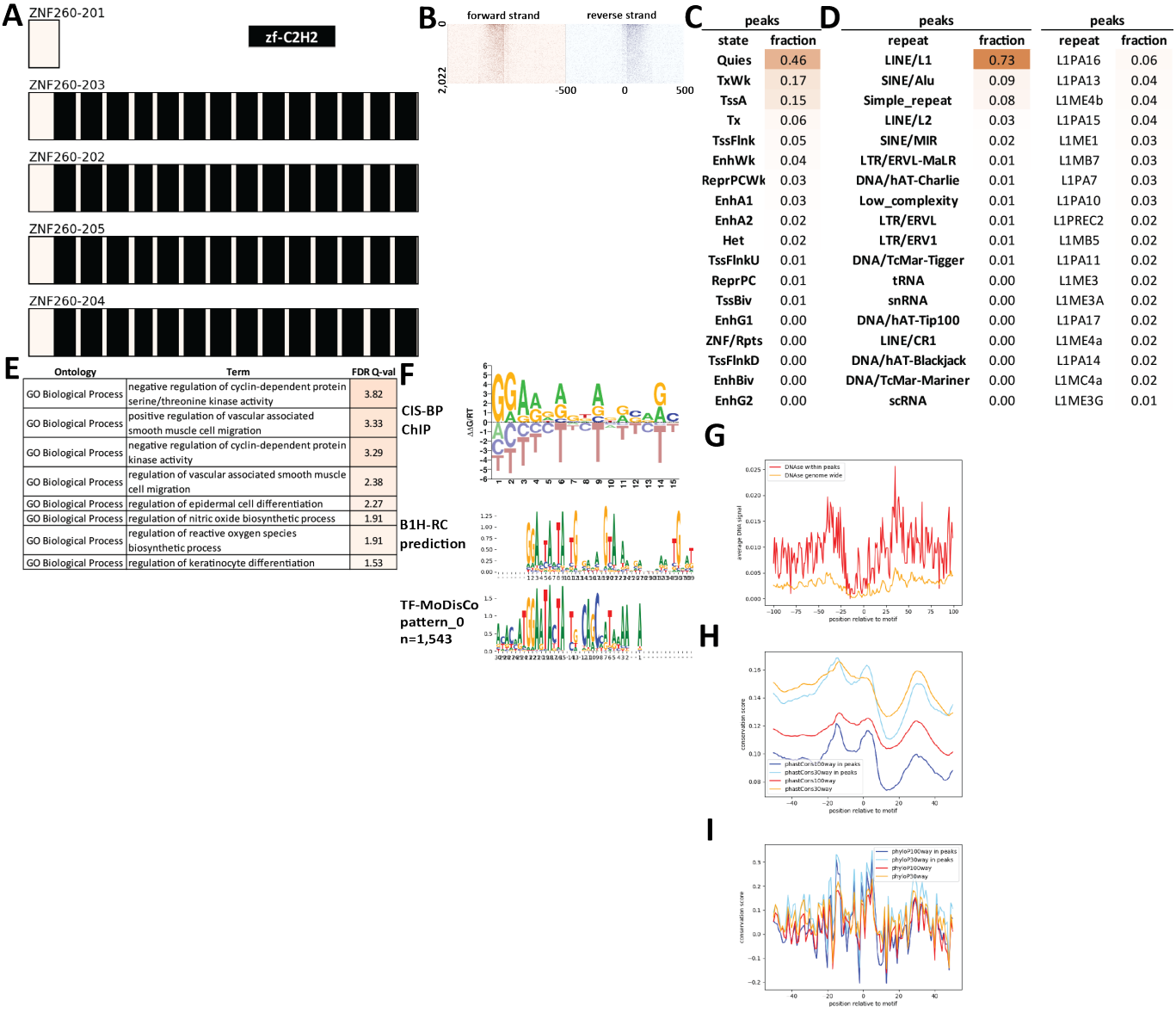

Supplementary Figure 917: Properties and genomic distribution of motifs identified for the ZNF260 transcription factor in HEK293 (accession Hughes GR models).

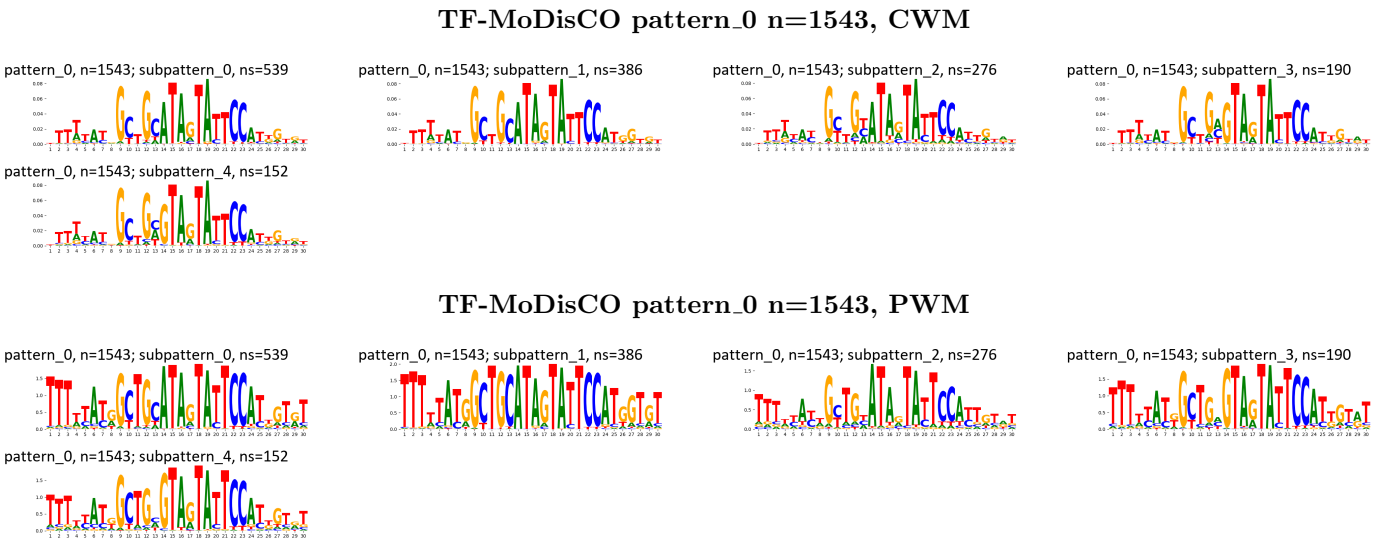

Supplementary Figure 918: TF-MoDisCO subpatterns for the ZNF260 transcription factor in HEK293 (accession Hughes GR models).

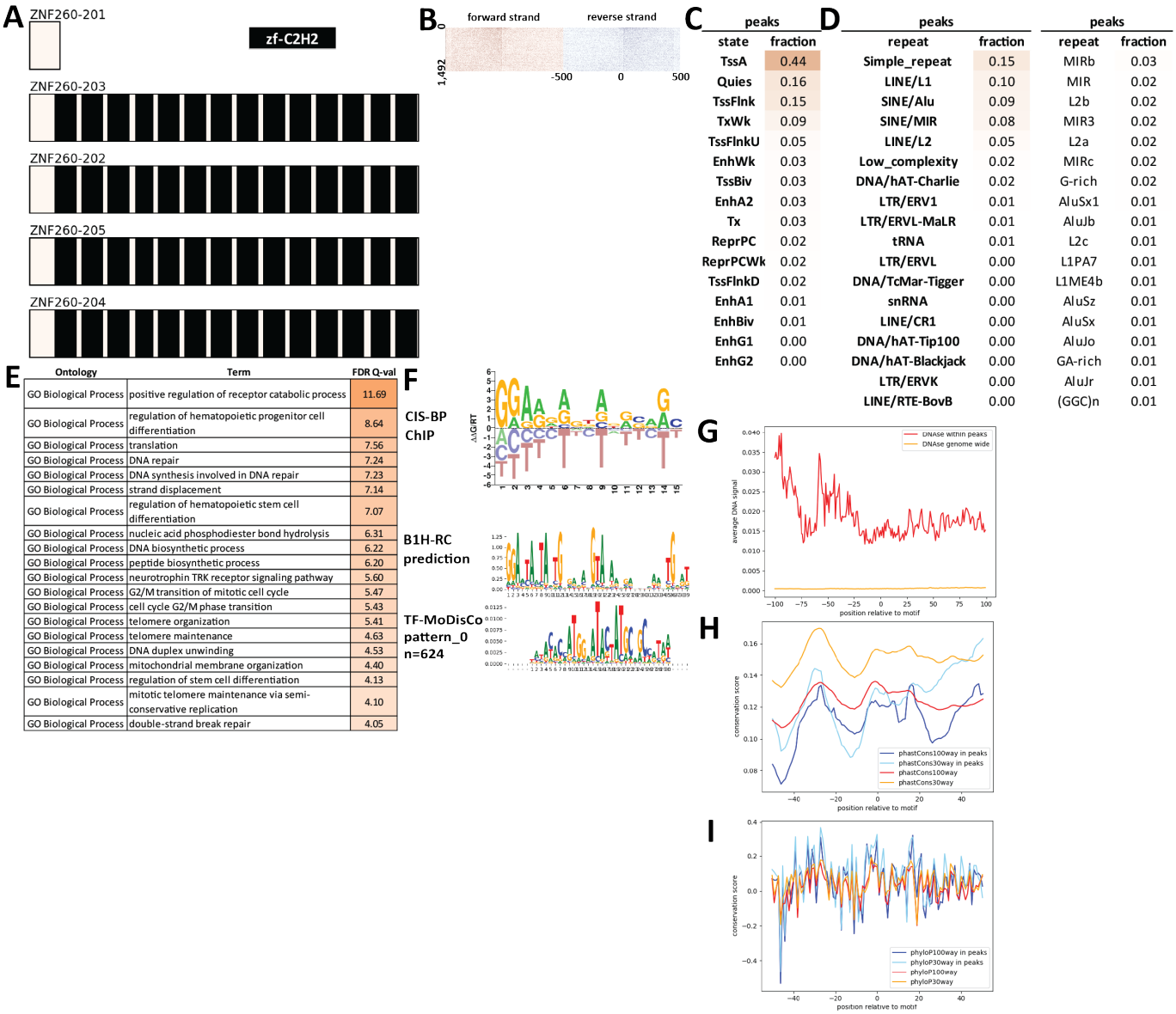

Supplementary Figure 919: Properties and genomic distribution of motifs identified for the ZNF260 transcription factor in HepG2 (accession ENCSR024ZIS).

TF-MoDisCO pattern_0 n=150, CWM

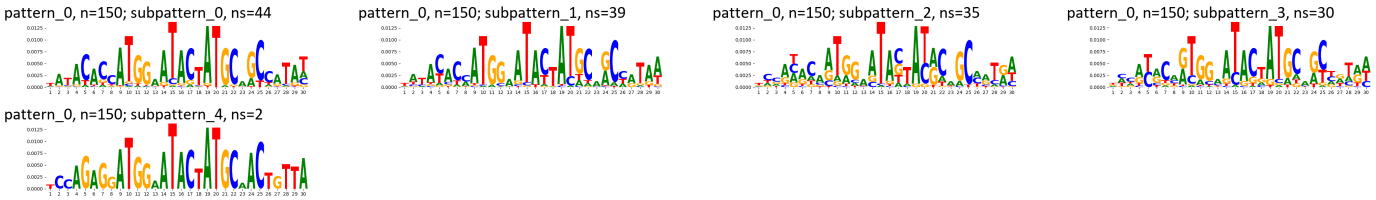

TF-MoDisCO pattern_0 n=150, PWM

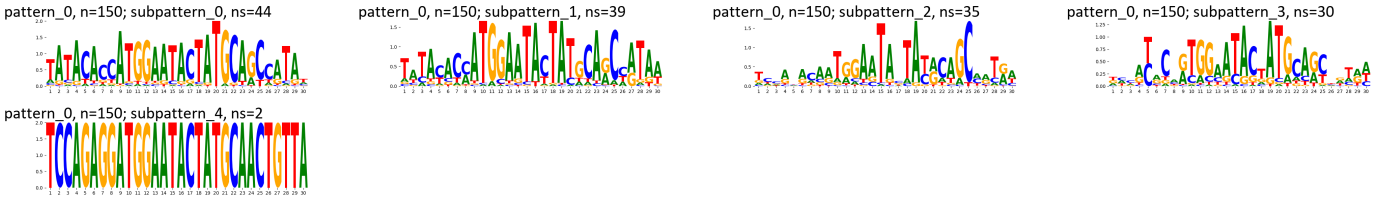

Supplementary Figure 920: TF-MoDisCO subpatterns for the ZNF260 transcription factor in HepG2 (accession ENCSR024ZIS).

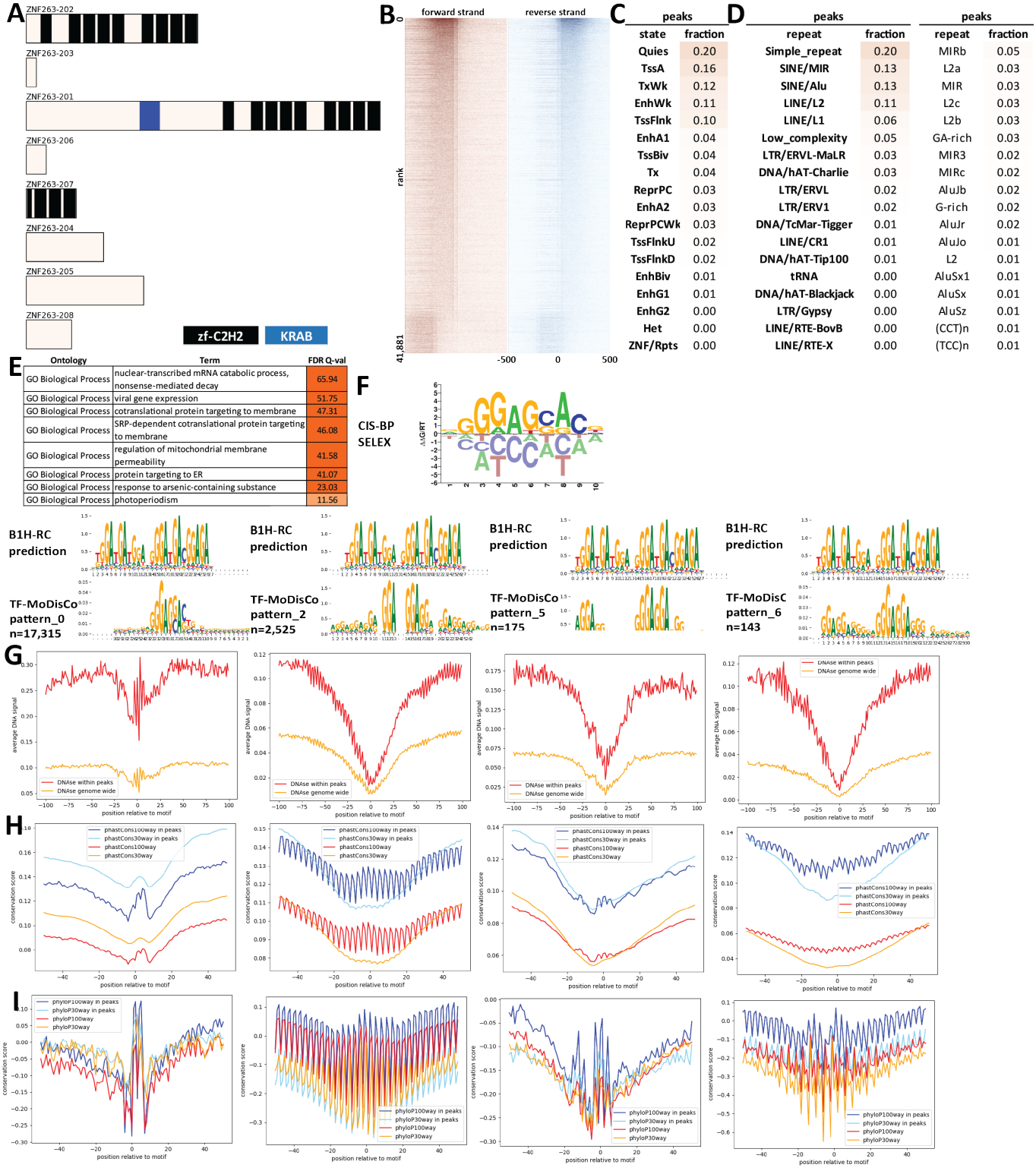

peaks	
state	fraction
Quies	0.20
TssA	0.16
TxWk	0.12
EnhWk	0.11
TssFlnk	0.10
EnhA1	0.04
TssBiv	0.04
Tx	0.04
ReprPC	0.03
EnhA2	0.03
ReprPCWk	0.03
TssFlnkU	0.02
TssFlnkD	0.02
EnhBiv	0.01
EnhG1	0.01
EnhG2	0.00
Het	0.00
ZNF/Rpts	0.00

peaks	
repeat	fraction
Simple_repeat	0.20
SINE/MIR	0.13
SINE/Alu	0.13
LINE/L2	0.11
LINE/L1	0.06
Low_complexity	0.05
LTR/ERVL-MaLR	0.03
DNA/hAT-Charlie	0.03
LTR/ERVL	0.02
LTR/ERV1	0.02
DNA/TcMar-Tigger	0.01
LINE/CR1	0.01
DNA/hAT-Tip100	0.01
tRNA	0.00
DNA/hAT-Blackjack	0.00
LTR/Gypsy	0.00
LINE/RTE-BovB	0.00
LINE/RTE-X	0.00

peaks	
repeat	fraction
MIRb	0.05
L2a	0.03
MIR	0.03
L2c	0.03
L2b	0.03
GA-rich	0.03
MIR3	0.02
MIRc	0.02
AluJb	0.02
G-rich	0.02
AluJr	0.02
AluJo	0.01
L2	0.01
AluSx1	0.01
AluSx	0.01
AluSz	0.01
(CCT)n	0.01
(TCC)n	0.01

Ontology	Term	FDR Q-val
GO Biological Process	nuclear-transcribed mRNA catabolic process, nonsense-mediated decay	65.94
GO Biological Process	viral gene expression	51.75
GO Biological Process	cotranslational protein targeting to membrane	47.31
GO Biological Process	SRP-dependent cotranslational protein targeting to membrane	46.08
GO Biological Process	regulation of mitochondrial membrane permeability	41.58
GO Biological Process	protein targeting to ER	41.07
GO Biological Process	response to arsenic-containing substance	23.03
GO Biological Process	photoperiodism	11.56

Supplementary Figure 921: Properties and genomic distribution of motifs identified for the ZNF263 transcription factor in HEK293 (accession ENCSR000EVD).

TF-MoDisCO pattern_0 n=17315, CWM

pattern_0, n=17315; subpattern_0, ns=4400

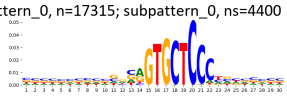

pattern_0, n=17315; subpattern_1, ns=3163

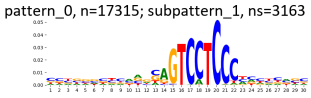

pattern_0, n=17315; subpattern_10, ns=45

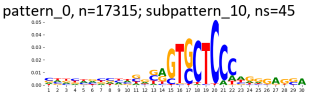

pattern_0, n=17315; subpattern_11, ns=43

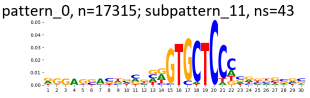

pattern_0, n=17315; subpattern_2, ns=3033

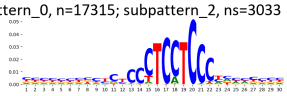

pattern_0, n=17315; subpattern_3, ns=2695

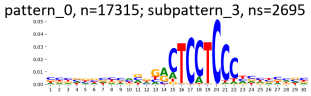

pattern_0, n=17315; subpattern_4, ns=1784

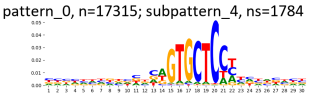

pattern_0, n=17315; subpattern_5, ns=1219

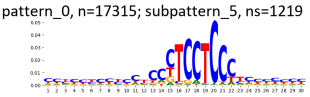

pattern_0, n=17315; subpattern_6, ns=339

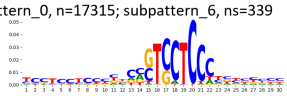

pattern_0, n=17315; subpattern_7, ns=324

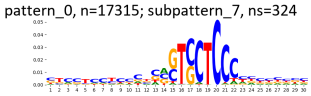

pattern_0, n=17315; subpattern_8, ns=212

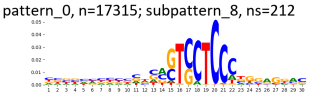

pattern_0, n=17315; subpattern_9, ns=58

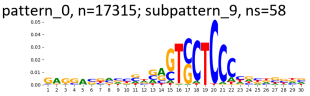

TF-MoDisCO pattern_0 n=17315, PWM

pattern_0, n=17315; subpattern_0, ns=4400

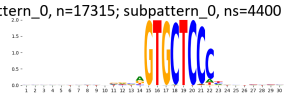

pattern_0, n=17315; subpattern_1, ns=3163

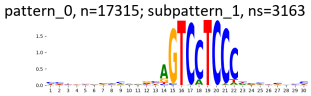

pattern_0, n=17315; subpattern_10, ns=45

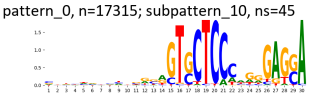

pattern_0, n=17315; subpattern_11, ns=43

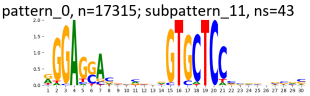

pattern_0, n=17315; subpattern_2, ns=3033

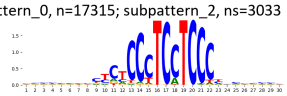

pattern_0, n=17315; subpattern_3, ns=2695

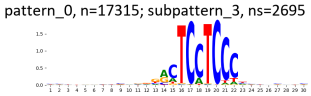

pattern_0, n=17315; subpattern_4, ns=1784

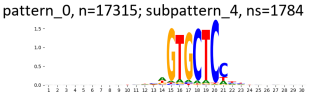

pattern_0, n=17315; subpattern_5, ns=1219

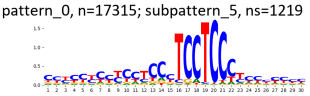

pattern_0, n=17315; subpattern_6, ns=339

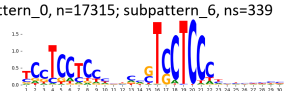

pattern_0, n=17315; subpattern_7, ns=324

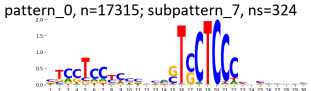

pattern_0, n=17315; subpattern_8, ns=212

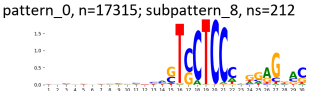

pattern_0, n=17315; subpattern_9, ns=58

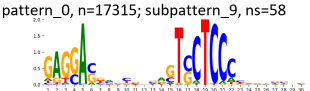

TF-MoDisCO pattern_2 n=2525, CWM

pattern_2, n=2525; subpattern_0, ns=412

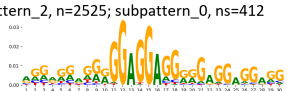

pattern_2, n=2525; subpattern_1, ns=388

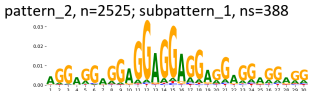

pattern_2, n=2525; subpattern_2, ns=387

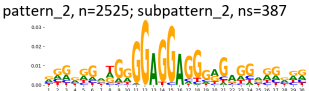

pattern_2, n=2525; subpattern_3, ns=385

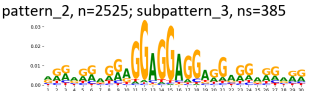

pattern_2, n=2525; subpattern_4, ns=249

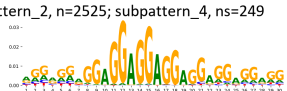

pattern_2, n=2525; subpattern_5, ns=229

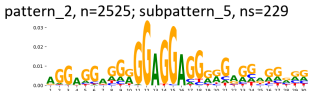

pattern_2, n=2525; subpattern_6, ns=213

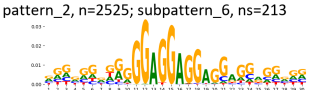

pattern_2, n=2525; subpattern_7, ns=180

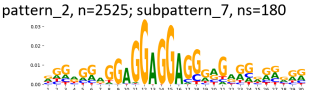

pattern_2, n=2525; subpattern_8, ns=80

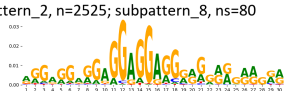

pattern_2, n=2525; subpattern_9, ns=2



TF-MoDisCO pattern_2 n=2525, PWM

pattern_2, n=2525; subpattern_0, ns=412

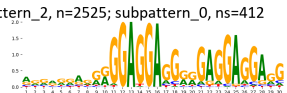

pattern_2, n=2525; subpattern_1, ns=388

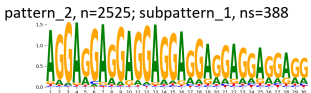

pattern_2, n=2525; subpattern_2, ns=387

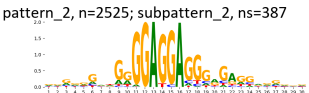

pattern_2, n=2525; subpattern_3, ns=385

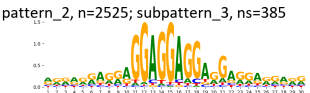

pattern_2, n=2525; subpattern_4, ns=249



pattern_2, n=2525; subpattern_5, ns=229

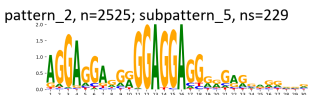

pattern_2, n=2525; subpattern_6, ns=213

pattern_2, n=2525; subpattern_7, ns=180

pattern_2, n=2525; subpattern_8, ns=80

pattern_2, n=2525; subpattern_9, ns=2

TF-MoDisCO pattern_5 n=175, CWM

pattern_5, n=175; subpattern_0, ns=65

pattern_5, n=175; subpattern_1, ns=62

pattern_5, n=175; subpattern_2, ns=48

TF-MoDisCO pattern_5 n=175, PWM

pattern_5, n=175; subpattern_0, ns=65

pattern_5, n=175; subpattern_1, ns=62

pattern_5, n=175; subpattern_2, ns=48

TF-MoDisCO pattern_6 n=143, CWM

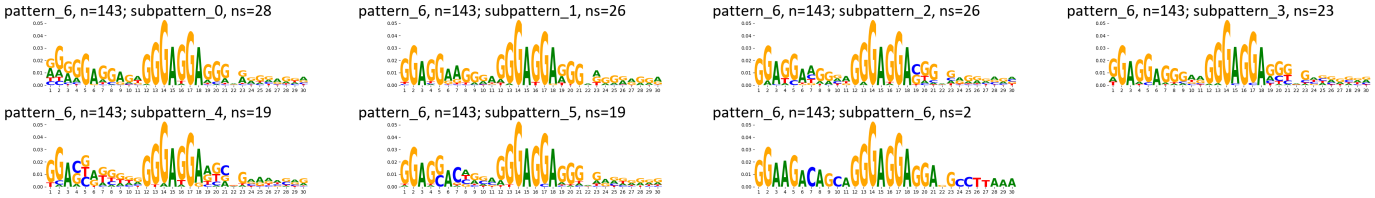

TF-MoDisCO pattern_6 n=143, PWM

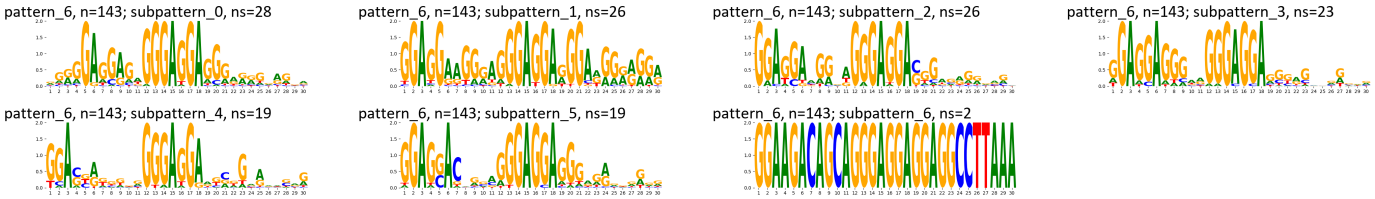

Supplementary Figure 922: TF-MoDisCO subpatterns for the ZNF263 transcription factor in HEK293 (accession ENCSR000EVD).

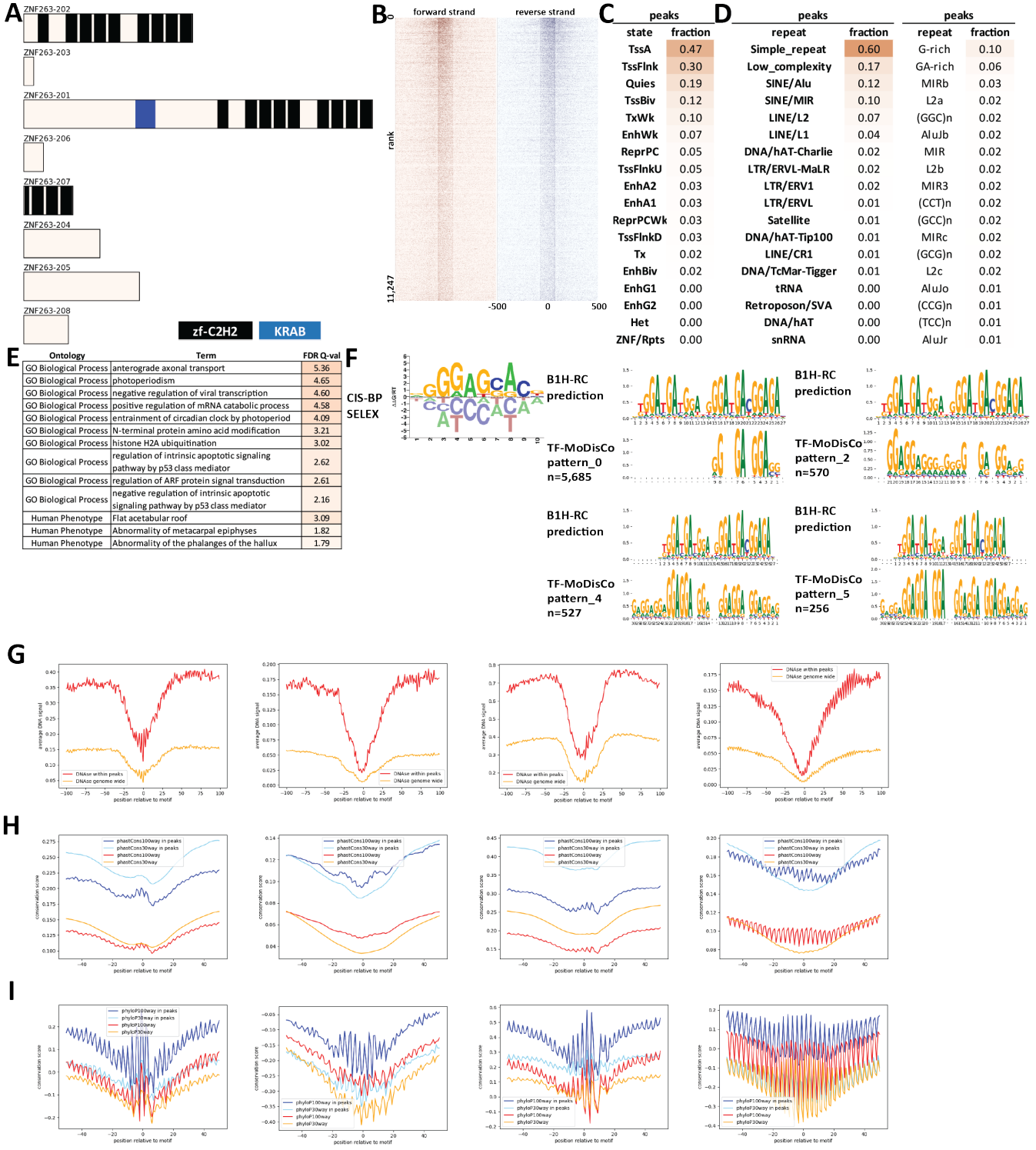

Supplementary Figure 923: Properties and genomic distribution of motifs identified for the ZNF263 transcription factor in HEK293 (accession ChipExo models).

TF-MoDisCO pattern_0 n=5685, CWM

pattern_0, n=5685; subpattern_0, ns=1054

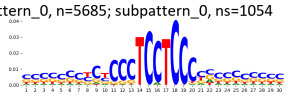

pattern_0, n=5685; subpattern_1, ns=982

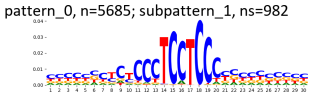

pattern_0, n=5685; subpattern_10, ns=109

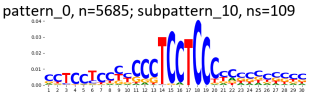

pattern_0, n=5685; subpattern_11, ns=24

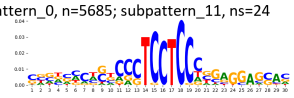

pattern_0, n=5685; subpattern_2, ns=819

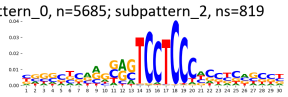

pattern_0, n=5685; subpattern_3, ns=803

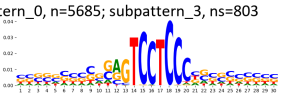

pattern_0, n=5685; subpattern_4, ns=665

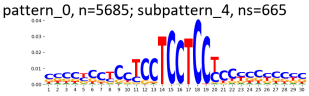

pattern_0, n=5685; subpattern_5, ns=422

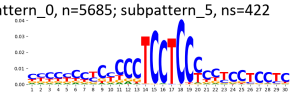

pattern_0, n=5685; subpattern_6, ns=284

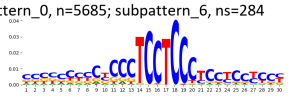

pattern_0, n=5685; subpattern_7, ns=282

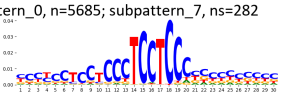

pattern_0, n=5685; subpattern_8, ns=131

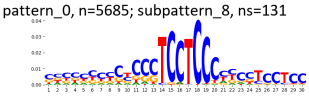

pattern_0, n=5685; subpattern_9, ns=110

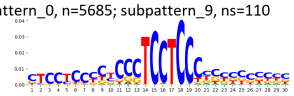

TF-MoDisCO pattern_0 n=5685, PWM

pattern_0, n=5685; subpattern_0, ns=1054

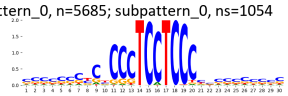

pattern_0, n=5685; subpattern_1, ns=982

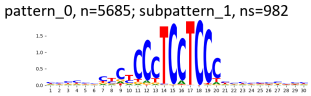

pattern_0, n=5685; subpattern_10, ns=109

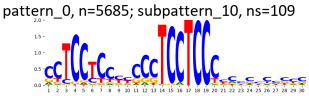

pattern_0, n=5685; subpattern_11, ns=24

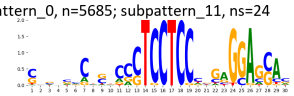

pattern_0, n=5685; subpattern_2, ns=819

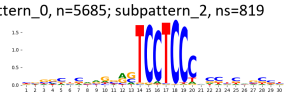

pattern_0, n=5685; subpattern_3, ns=803

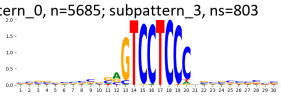

pattern_0, n=5685; subpattern_4, ns=665

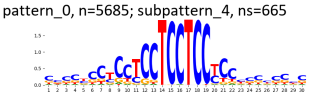

pattern_0, n=5685; subpattern_5, ns=422

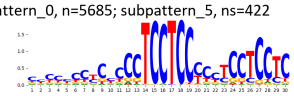

pattern_0, n=5685; subpattern_6, ns=284

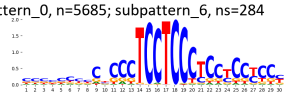

pattern_0, n=5685; subpattern_7, ns=282

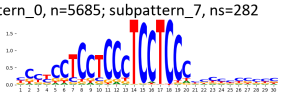

pattern_0, n=5685; subpattern_8, ns=131

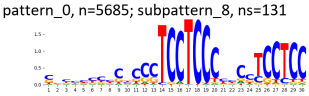

pattern_0, n=5685; subpattern_9, ns=110

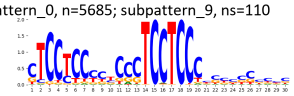

TF-MoDisCO pattern_2 n=570, CWM

pattern_2, n=570; subpattern_0, ns=167

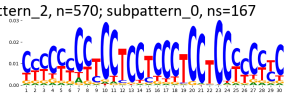

pattern_2, n=570; subpattern_1, ns=127

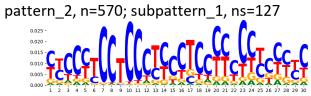

pattern_2, n=570; subpattern_2, ns=79

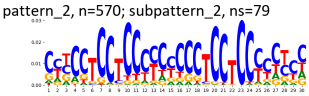

pattern_2, n=570; subpattern_3, ns=76

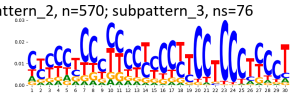

pattern_2, n=570; subpattern_4, ns=65

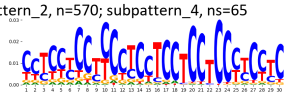

pattern_2, n=570; subpattern_5, ns=28

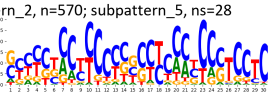

pattern_2, n=570; subpattern_6, ns=28

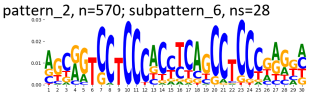

TF-MoDisCO pattern_2 n=570, PWM

pattern_2, n=570; subpattern_0, ns=167

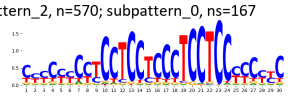

pattern_2, n=570; subpattern_1, ns=127

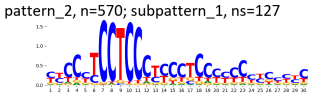

pattern_2, n=570; subpattern_2, ns=79

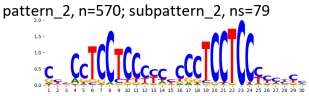

pattern_2, n=570; subpattern_3, ns=76

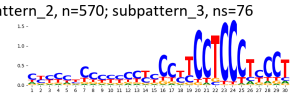

pattern_2, n=570; subpattern_4, ns=65

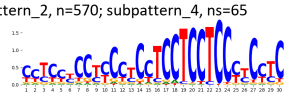

pattern_2, n=570; subpattern_5, ns=28

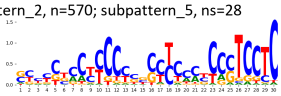

pattern_2, n=570; subpattern_6, ns=28

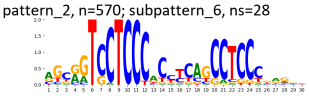

TF-MoDisCO pattern_4 n=527, CWM

pattern_4, n=527; subpattern_0, ns=104

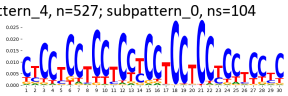

pattern_4, n=527; subpattern_1, ns=97

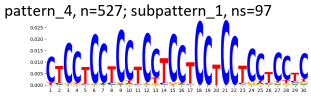

pattern_4, n=527; subpattern_2, ns=96

pattern_4, n=527; subpattern_3, ns=76

pattern_4, n=527; subpattern_4, ns=61

pattern_4, n=527; subpattern_5, ns=61

pattern_4, n=527; subpattern_6, ns=32

TF-MoDisCO pattern_4 n=527, PWM

pattern_4, n=527; subpattern_0, ns=104

pattern_4, n=527; subpattern_1, ns=97

pattern_4, n=527; subpattern_2, ns=96

pattern_4, n=527; subpattern_3, ns=76

pattern_4, n=527; subpattern_4, ns=61

pattern_4, n=527; subpattern_5, ns=61

pattern_4, n=527; subpattern_6, ns=32

TF-MoDisCO pattern_5 n=256, CWM

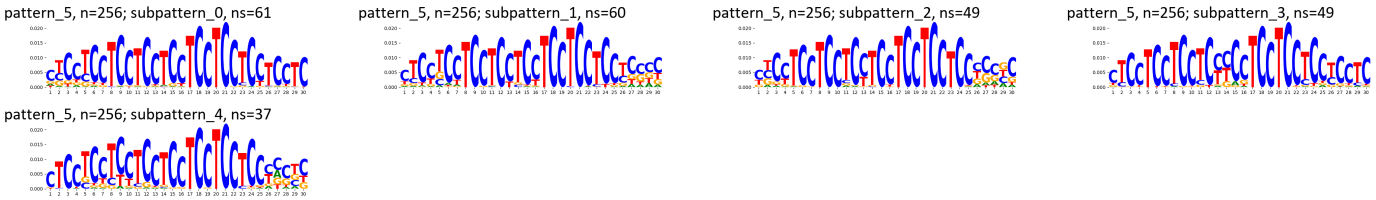

TF-MoDisCO pattern_5 n=256, PWM

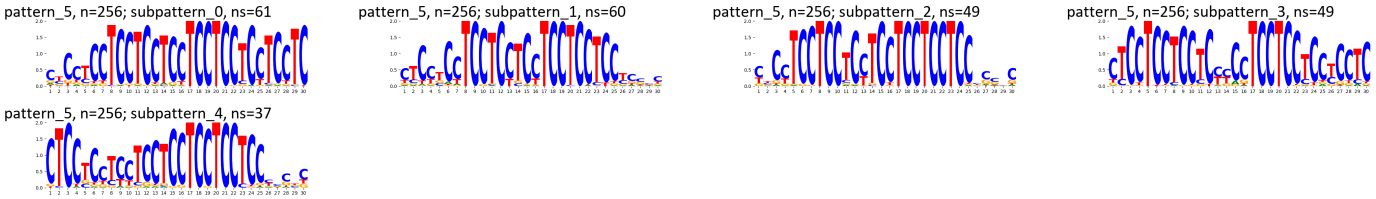

Supplementary Figure 924: TF-MoDisCO subpatterns for the ZNF263 transcription factor in HEK293 (accession ChipExo models).

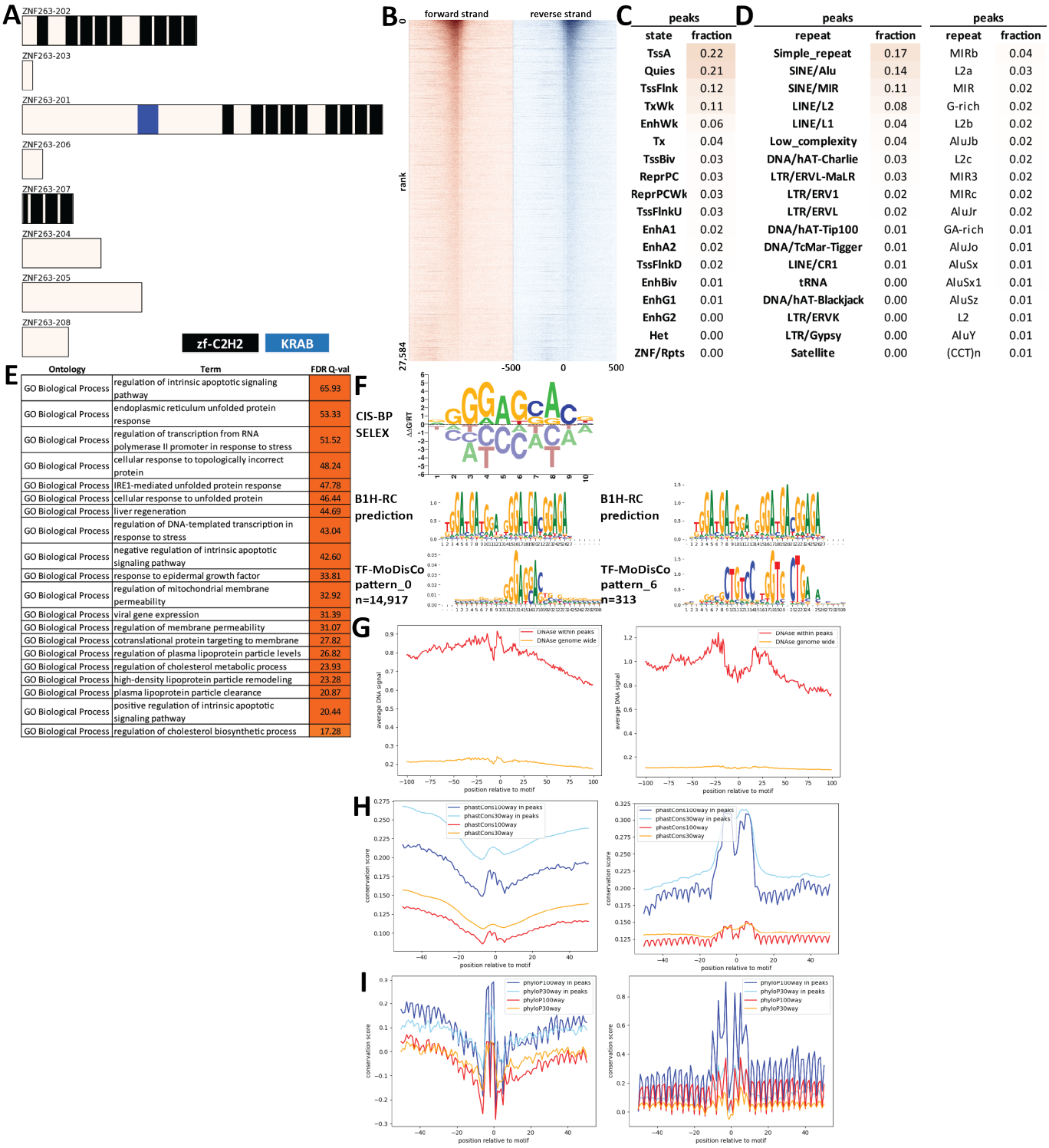

Supplementary Figure 925: Properties and genomic distribution of motifs identified for the ZNF263 transcription factor in HepG2 (accession ENCSR313MMD).

TF-MoDisCO pattern_0 n=14917, CWM

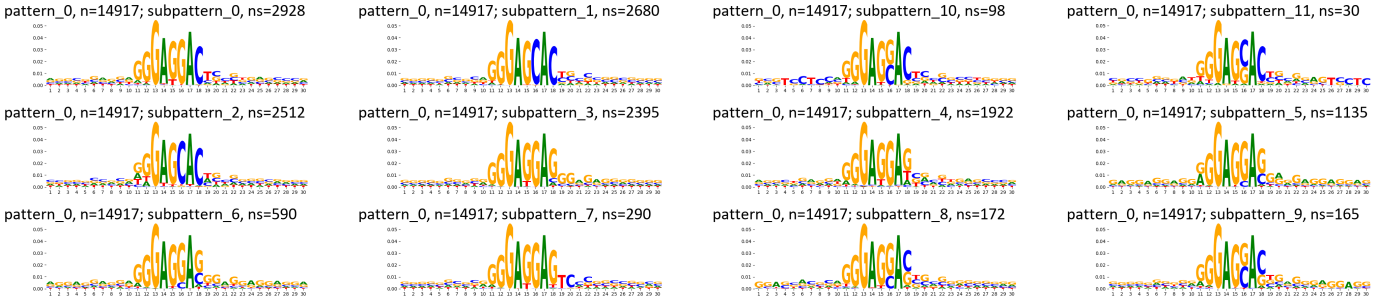

TF-MoDisCO pattern_0 n=14917, PWM

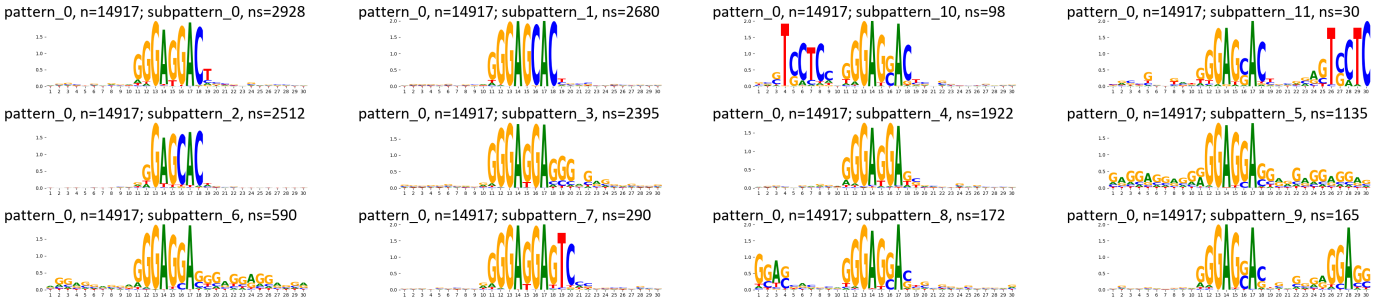

TF-MoDisCO pattern_7 n=313, CWM

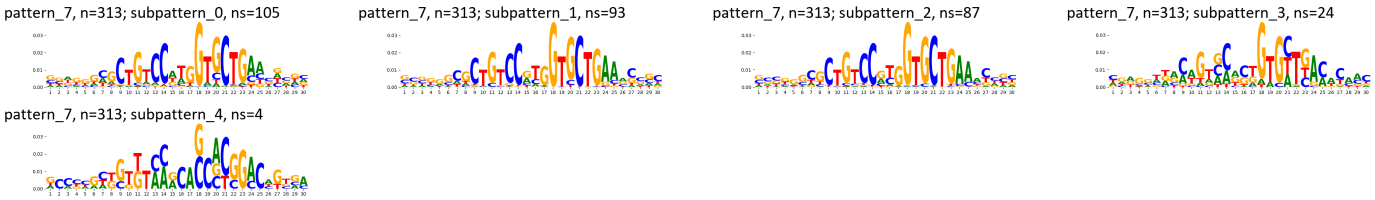

TF-MoDisCO pattern_7 n=313, PWM

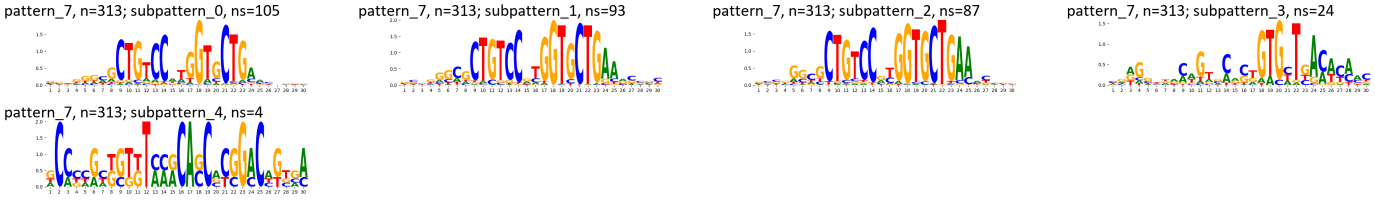

Supplementary Figure 926: TF-MoDisCO subpatterns for the ZNF263 transcription factor in HepG2 (accession ENCSR313MMD).

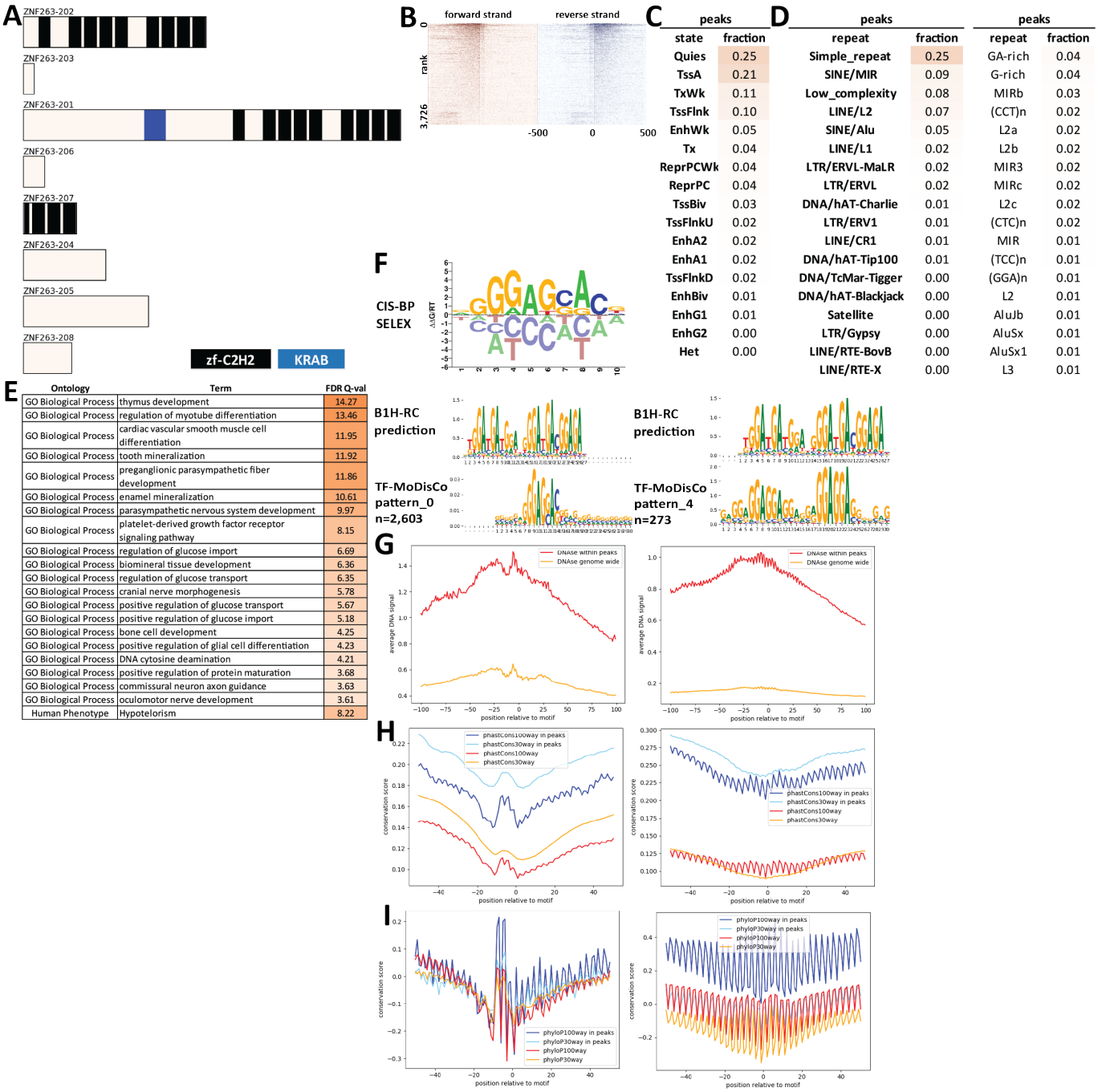

E

Ontology	Term	FDR Q-val
GO Biological Process	thymus development	14.27
GO Biological Process	regulation of myotube differentiation	13.46
GO Biological Process	cardiac vascular smooth muscle cell differentiation	11.95
GO Biological Process	tooth mineralization	11.92
GO Biological Process	preganglionic parasympathetic fiber development	11.86
GO Biological Process	enamel mineralization	10.61
GO Biological Process	parasympathetic nervous system development	9.97
GO Biological Process	platelet-derived growth factor receptor signaling pathway	8.15
GO Biological Process	regulation of glucose import	6.69
GO Biological Process	biomineral tissue development	6.36
GO Biological Process	regulation of glucose transport	6.35
GO Biological Process	cranial nerve morphogenesis	5.78
GO Biological Process	positive regulation of glucose transport	5.67
GO Biological Process	positive regulation of glucose import	5.18
GO Biological Process	bone cell development	4.25
GO Biological Process	positive regulation of glial cell differentiation	4.23
GO Biological Process	DNA cytosine deamination	4.21
GO Biological Process	positive regulation of protein maturation	3.68
GO Biological Process	commissural neuron axon guidance	3.63
GO Biological Process	oculomotor nerve development	3.61
Human Phenotype	Hypotelorism	8.22

C

peaks	
state	fraction
Quies	0.25
TssA	0.21
TxWk	0.11
TssFlnk	0.10
EnhWk	0.05
Tx	0.04
ReprPCWk	0.04
ReprPC	0.04
TssBiv	0.03
TssFlnkU	0.02
EnhA2	0.02
EnhA1	0.02
TssFlnkD	0.02
EnhBiv	0.01
EnhG1	0.01
EnhG2	0.00
Het	0.00

D

peaks		peaks	
repeat	fraction	repeat	fraction
Simple_repeat	0.25	GA-rich	0.04
SINE/MIR	0.09	G-rich	0.04
Low_complexity	0.08	MIRb	0.03
LINE/L2	0.07	(CCT)n	0.02
SINE/Alu	0.05	L2a	0.02
LINE/L1	0.02	L2b	0.02
LTR/ERVL-MaLR	0.02	MIR3	0.02
LTR/ERVL	0.02	MIRc	0.02
DNA/hAT-Charlie	0.01	L2c	0.02
LTR/ERV1	0.01	(CTC)n	0.02
LINE/CR1	0.01	MIR	0.01
DNA/hAT-Tip100	0.01	(TCC)n	0.01
DNA/TcMar-Tigger	0.00	(GGA)n	0.01
DNA/hAT-Blackjack	0.00	L2	0.01
Satellite	0.00	AluJb	0.01
LTR/Gypsy	0.00	AluSx	0.01
LINE/RTE-BovB	0.00	AluSx1	0.01
LINE/RTE-X	0.00	L3	0.01

Supplementary Figure 927: Properties and genomic distribution of motifs identified for the ZNF263 transcription factor in K562 (accession ENCSR000EWN).

TF-MoDisCO pattern_0 n=2603, CWM

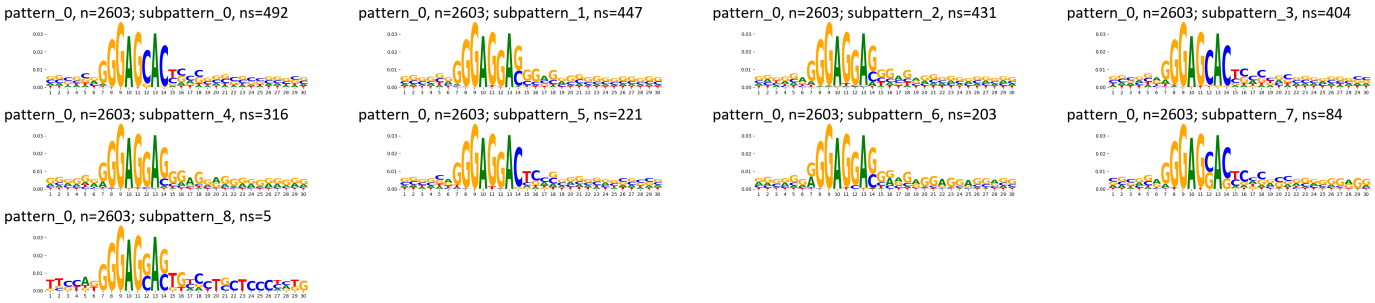

TF-MoDisCO pattern_0 n=2603, PWM

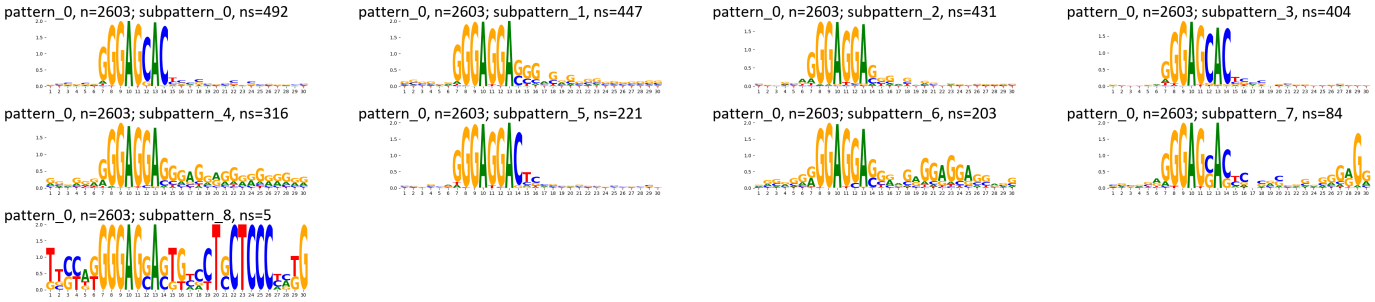

TF-MoDisCO pattern_4 n=273, CWM

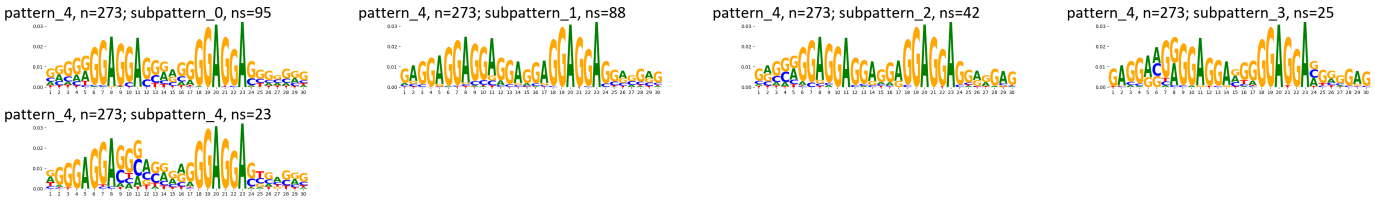

TF-MoDisCO pattern_4 n=273, PWM

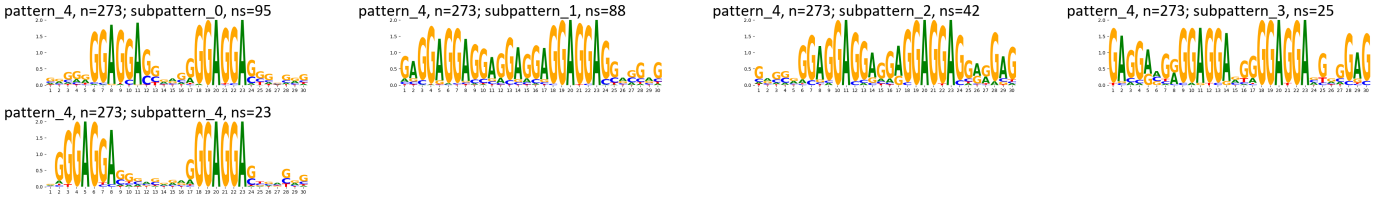

Supplementary Figure 928: TF-MoDisCO subpatterns for the ZNF263 transcription factor in K562 (accession ENCSR000EWN).

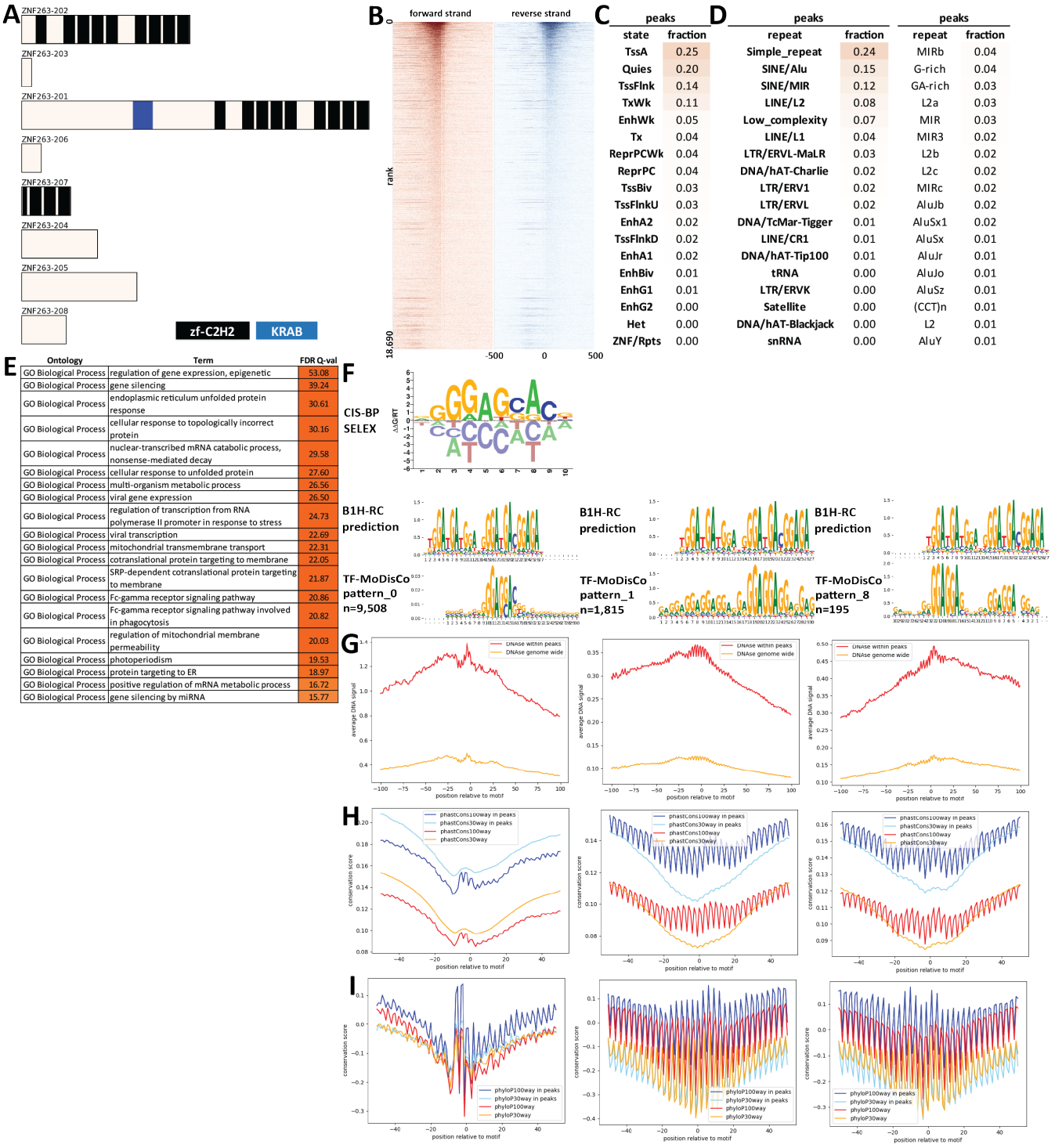

peaks	
state	fraction
TssA	0.25
Quies	0.20
TssFlnk	0.14
TxWk	0.11
EnhWk	0.05
Tx	0.04
ReprPCWk	0.04
ReprPC	0.04
TssBiv	0.03
TssFlnkU	0.03
EnhA2	0.02
TssFlnkD	0.02
EnhA1	0.02
EnhBiv	0.01
EnhG1	0.01
EnhG2	0.00
Het	0.00
ZNF/Rpts	0.00

peaks	
repeat	fraction
Simple_repeat	0.24
SINE/Alu	0.15
SINE/MIR	0.12
LINE/L2	0.08
Low_complexity	0.07
LINE/L1	0.04
LTR/ERVL-MaLR	0.03
DNA/hAT-Charlie	0.02
LTR/ERV1	0.02
LTR/ERVL	0.02
DNA/TcMar-Tigger	0.01
LINE/CR1	0.01
DNA/hAT-Tip100	0.01
tRNA	0.00
LTR/ERVK	0.00
Satellite	0.00
DNA/hAT-Blackjack	0.00
snRNA	0.00

peaks	
repeat	fraction
MIRb	0.04
G-rich	0.04
GA-rich	0.03
L2a	0.03
MIR	0.03
MIR3	0.02
L2b	0.02
L2c	0.02
MIRc	0.02
AluJb	0.02
AluSx1	0.02
AluSx	0.01
AluJr	0.01
AluJo	0.01
AluSz	0.01
(CCT)n	0.01
L2	0.01
AluY	0.01

Ontology	Term	FDR Q-val
GO Biological Process	regulation of gene expression, epigenetic	53.08
GO Biological Process	gene silencing	39.24
GO Biological Process	endoplasmic reticulum unfolded protein response	30.61
GO Biological Process	cellular response to topologically incorrect protein	30.16
GO Biological Process	nuclear-transcribed mRNA catabolic process, nonsense-mediated decay	29.58
GO Biological Process	cellular response to unfolded protein	27.60
GO Biological Process	multi-organism metabolic process	26.56
GO Biological Process	viral gene expression	26.50
GO Biological Process	regulation of transcription from RNA polymerase II promoter in response to stress	24.73
GO Biological Process	viral transcription	22.69
GO Biological Process	mitochondrial transmembrane transport	22.31
GO Biological Process	cotranslational protein targeting to membrane	22.05
GO Biological Process	SRP-dependent cotranslational protein targeting to membrane	21.87
GO Biological Process	Fc-gamma receptor signaling pathway	20.86
GO Biological Process	Fc-gamma receptor signaling pathway involved in phagocytosis	20.82
GO Biological Process	regulation of mitochondrial membrane permeability	20.03
GO Biological Process	photoperiodism	19.53
GO Biological Process	protein targeting to ER	18.97
GO Biological Process	positive regulation of mRNA metabolic process	16.72
GO Biological Process	gene silencing by miRNA	15.77

Supplementary Figure 929: Properties and genomic distribution of motifs identified for the ZNF263 transcription factor in K562 (accession ENCSR845GGY).

TF-MoDisCO pattern_0 n=9508, CWM

pattern_0, n=9508; subpattern_0, ns=2826

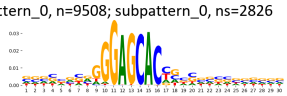

pattern_0, n=9508; subpattern_1, ns=1763

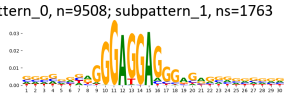

pattern_0, n=9508; subpattern_10, ns=32

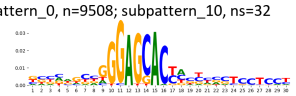

pattern_0, n=9508; subpattern_11, ns=29

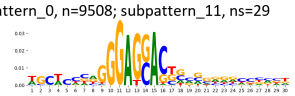

pattern_0, n=9508; subpattern_2, ns=1738

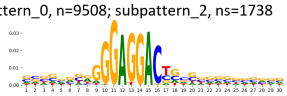

pattern_0, n=9508; subpattern_3, ns=1258

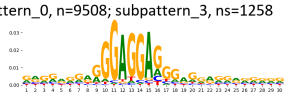

pattern_0, n=9508; subpattern_4, ns=745

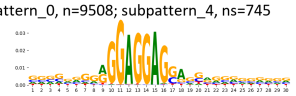

pattern_0, n=9508; subpattern_5, ns=334

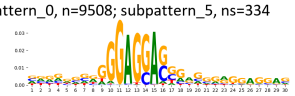

pattern_0, n=9508; subpattern_6, ns=276

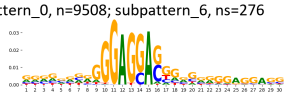

pattern_0, n=9508; subpattern_7, ns=232

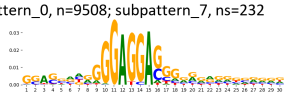

pattern_0, n=9508; subpattern_8, ns=192

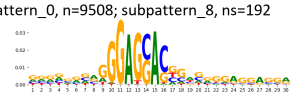

pattern_0, n=9508; subpattern_9, ns=83

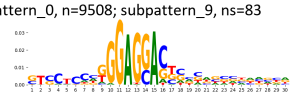

TF-MoDisCO pattern_0 n=9508, PWM

pattern_0, n=9508; subpattern_0, ns=2826

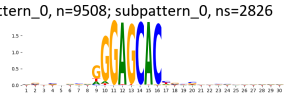

pattern_0, n=9508; subpattern_1, ns=1763

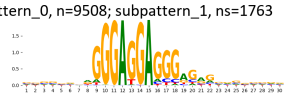

pattern_0, n=9508; subpattern_10, ns=32

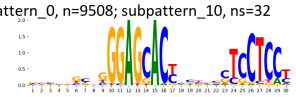

pattern_0, n=9508; subpattern_11, ns=29

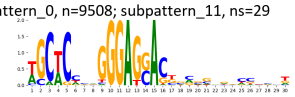

pattern_0, n=9508; subpattern_2, ns=1738

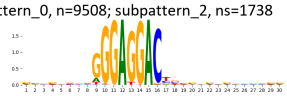

pattern_0, n=9508; subpattern_3, ns=1258

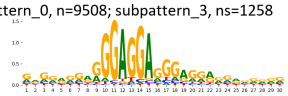

pattern_0, n=9508; subpattern_4, ns=745

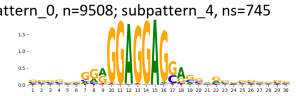

pattern_0, n=9508; subpattern_5, ns=334

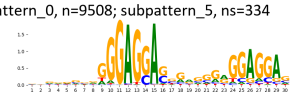

pattern_0, n=9508; subpattern_6, ns=276

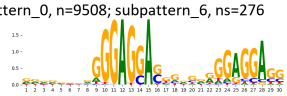

pattern_0, n=9508; subpattern_7, ns=232

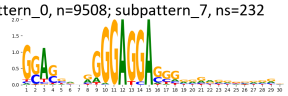

pattern_0, n=9508; subpattern_8, ns=192

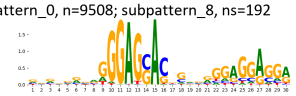

pattern_0, n=9508; subpattern_9, ns=83

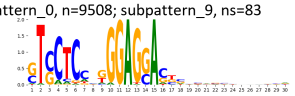

TF-MoDisCO pattern_1 n=1815, CWM

pattern_1, n=1815; subpattern_0, ns=444

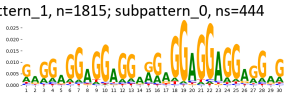

pattern_1, n=1815; subpattern_1, ns=352

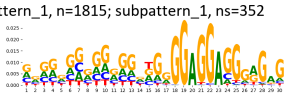

pattern_1, n=1815; subpattern_2, ns=344

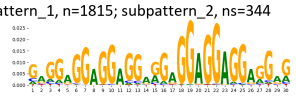

pattern_1, n=1815; subpattern_3, ns=266

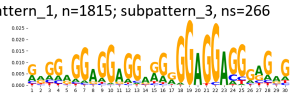

pattern_1, n=1815; subpattern_4, ns=179

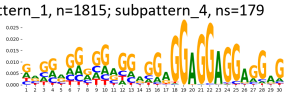

pattern_1, n=1815; subpattern_5, ns=129

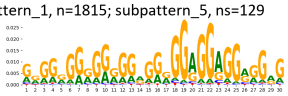

pattern_1, n=1815; subpattern_6, ns=101

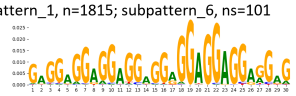

TF-MoDisCO pattern_1 n=1815, PWM

pattern_1, n=1815; subpattern_0, ns=444

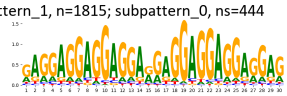

pattern_1, n=1815; subpattern_1, ns=352

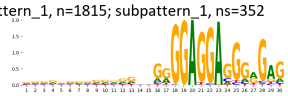

pattern_1, n=1815; subpattern_2, ns=344

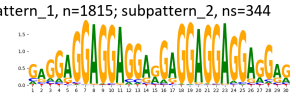

pattern_1, n=1815; subpattern_3, ns=266

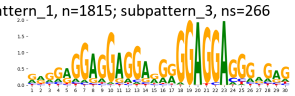

pattern_1, n=1815; subpattern_4, ns=179

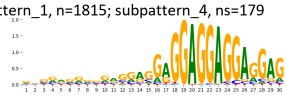

pattern_1, n=1815; subpattern_5, ns=129

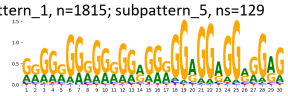

pattern_1, n=1815; subpattern_6, ns=101

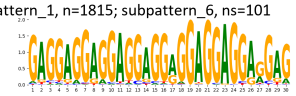

TF-MoDisCO pattern_8 n=195, CWM

pattern_8, n=195; subpattern_0, ns=72

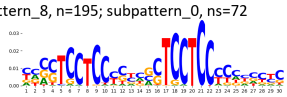

pattern_8, n=195; subpattern_1, ns=68

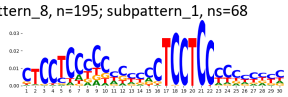

pattern_8, n=195; subpattern_2, ns=28

pattern_8, n=195; subpattern_3, ns=27

TF-MoDisCO pattern_8 n=195, PWM

pattern_8, n=195; subpattern_0, ns=72

pattern_8, n=195; subpattern_1, ns=68

pattern_8, n=195; subpattern_2, ns=28

pattern_8, n=195; subpattern_3, ns=27

Supplementary Figure 930: TF-MoDisCO subpatterns for the ZNF263 transcription factor in K562 (accession ENCSR845GGY).

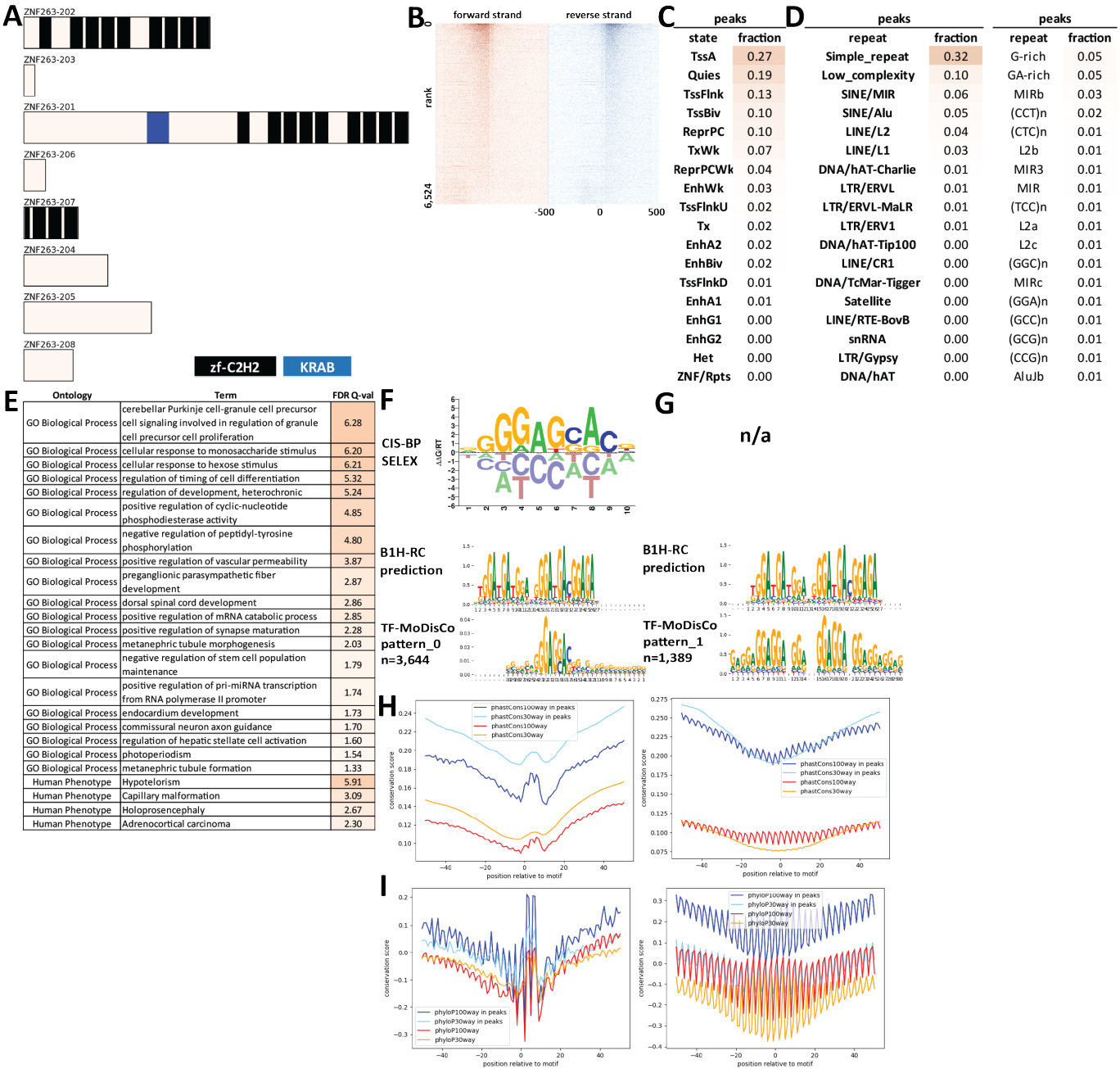

Supplementary Figure 931: Properties and genomic distribution of motifs identified for the ZNF263 transcription factor in WTC11 (accession ENCSR156JWW).

TF-MoDisCO pattern_0 n=3644, CWM

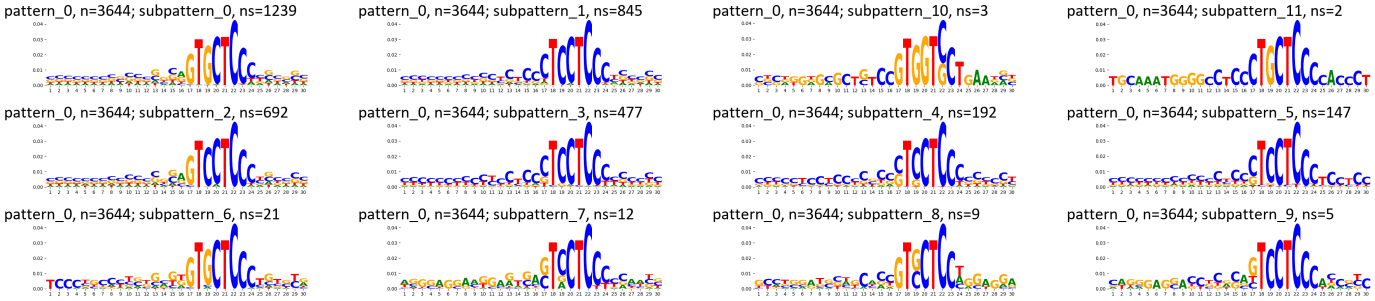

TF-MoDisCO pattern_0 n=3644, PWM

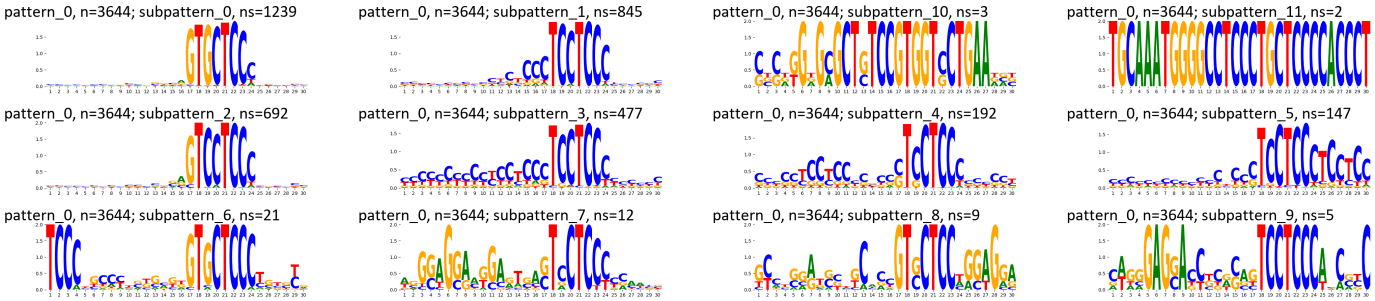

TF-MoDisCO pattern_1 n=1389, CWM

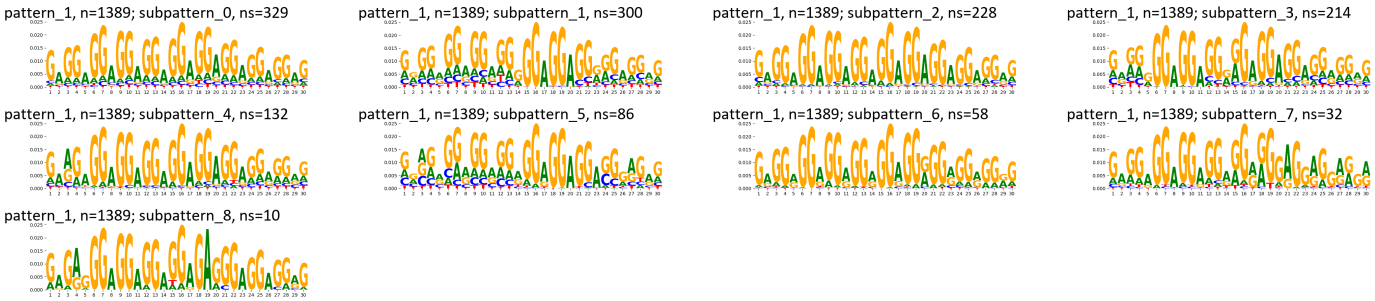

TF-MoDisCO pattern_1 n=1389, PWM

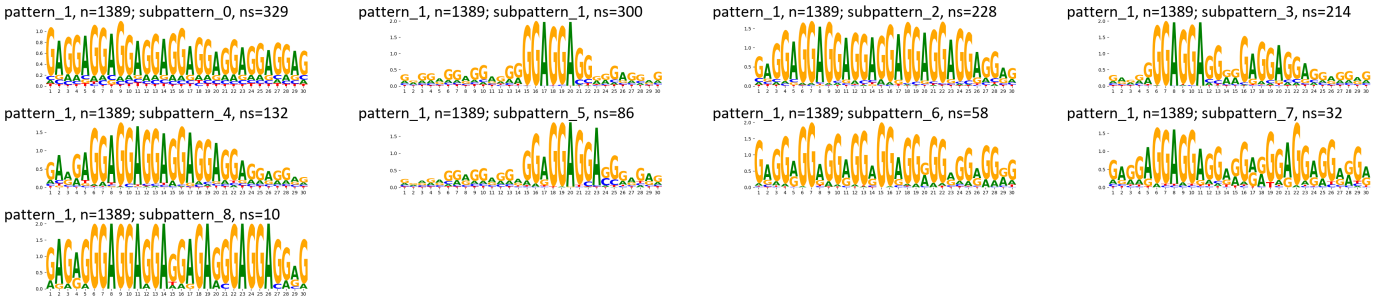

Supplementary Figure 932: TF-MoDisCO subpatterns for the ZNF263 transcription factor in WTC11 (accession ENCSR156JWW).

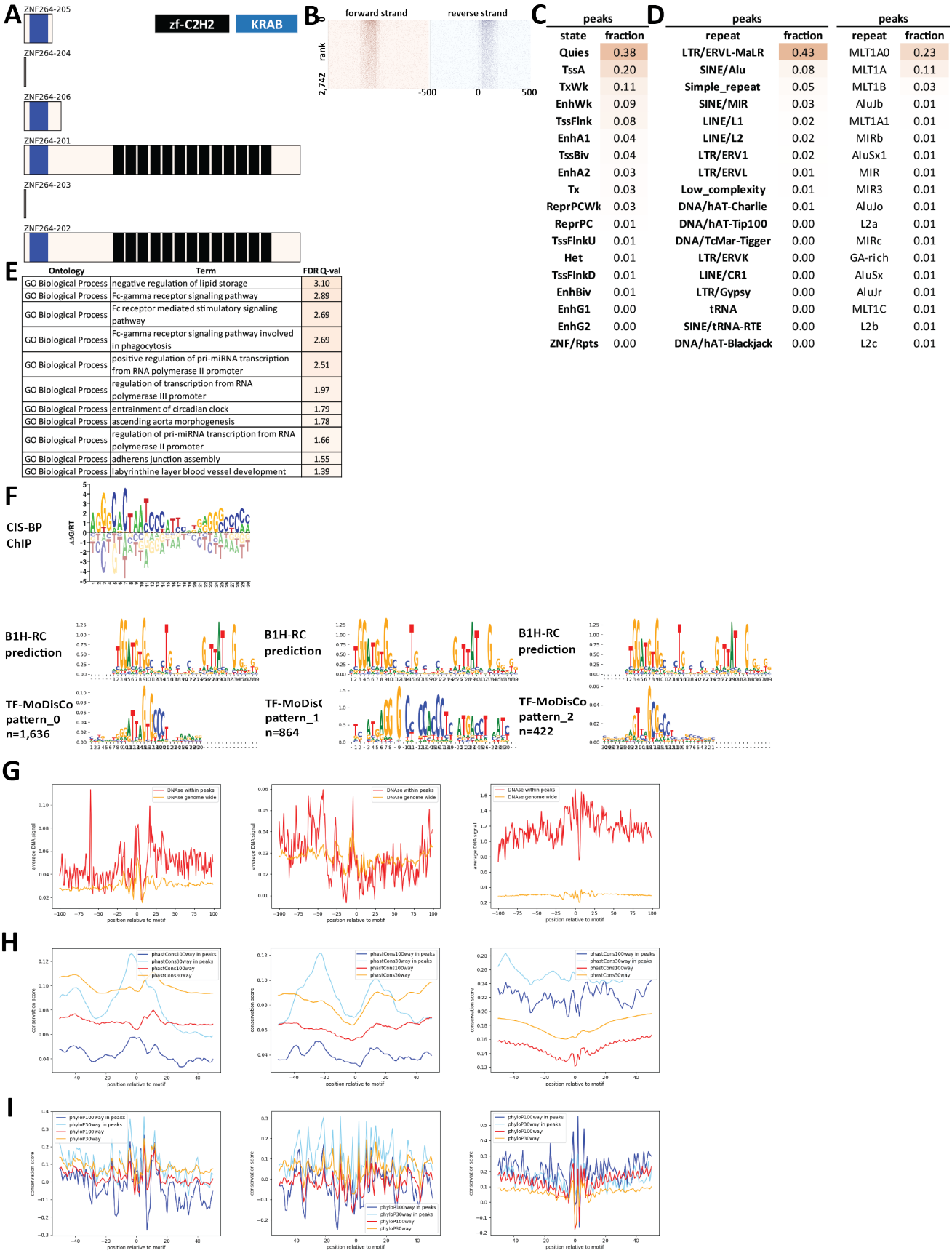

Supplementary Figure 933: Properties and genomic distribution of motifs identified for the ZNF264 transcription factor in HEK293 (accession Hughes NB models).

TF-MoDisCO pattern_0 n=1636, CWM

pattern_0, n=1636; subpattern_0, ns=385

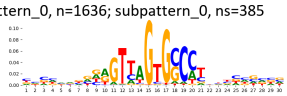

pattern_0, n=1636; subpattern_1, ns=361

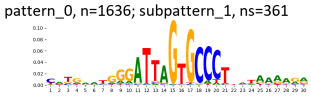

pattern_0, n=1636; subpattern_2, ns=360

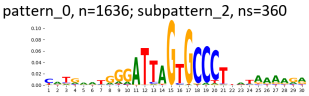

pattern_0, n=1636; subpattern_3, ns=224

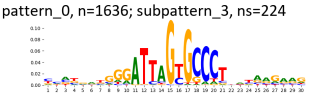

pattern_0, n=1636; subpattern_4, ns=166

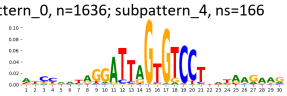

pattern_0, n=1636; subpattern_5, ns=119

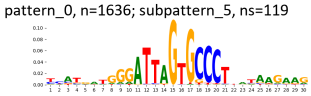

pattern_0, n=1636; subpattern_6, ns=18

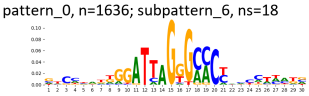

pattern_0, n=1636; subpattern_7, ns=3

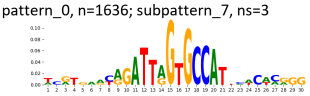

TF-MoDisCO pattern_0 n=1636, PWM

pattern_0, n=1636; subpattern_0, ns=385

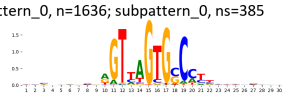

pattern_0, n=1636; subpattern_1, ns=361

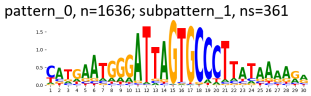

pattern_0, n=1636; subpattern_2, ns=360

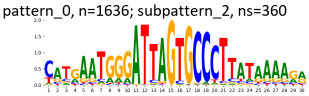

pattern_0, n=1636; subpattern_3, ns=224

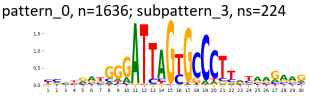

pattern_0, n=1636; subpattern_4, ns=166

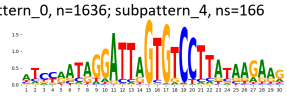

pattern_0, n=1636; subpattern_5, ns=119

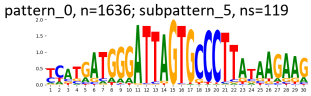

pattern_0, n=1636; subpattern_6, ns=18

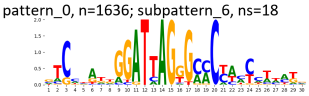

pattern_0, n=1636; subpattern_7, ns=3

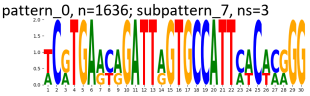

TF-MoDisCO pattern_1 n=864, CWM

pattern_1, n=864; subpattern_0, ns=223

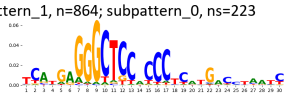

pattern_1, n=864; subpattern_1, ns=165

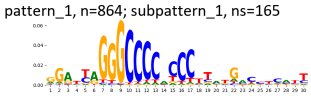

pattern_1, n=864; subpattern_2, ns=158

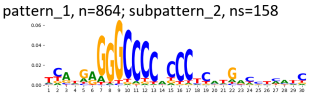

pattern_1, n=864; subpattern_3, ns=153

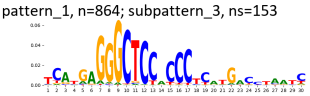

pattern_1, n=864; subpattern_4, ns=120

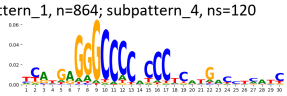

pattern_1, n=864; subpattern_5, ns=27

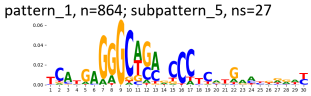

pattern_1, n=864; subpattern_6, ns=13

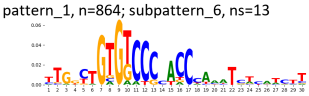

pattern_1, n=864; subpattern_7, ns=5

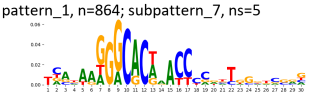

TF-MoDisCO pattern_1 n=864, PWM

pattern_1, n=864; subpattern_0, ns=223

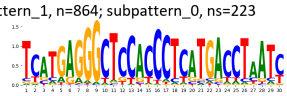

pattern_1, n=864; subpattern_1, ns=165

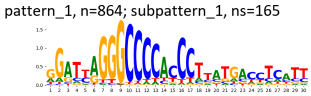

pattern_1, n=864; subpattern_2, ns=158

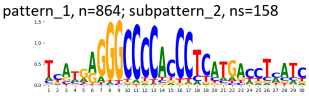

pattern_1, n=864; subpattern_3, ns=153

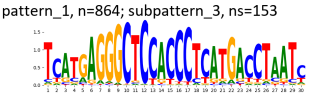

pattern_1, n=864; subpattern_4, ns=120

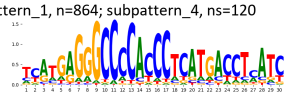

pattern_1, n=864; subpattern_5, ns=27

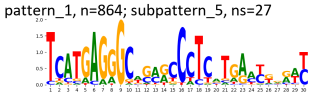

pattern_1, n=864; subpattern_6, ns=13

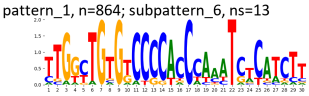

pattern_1, n=864; subpattern_7, ns=5

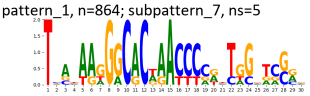

TF-MoDisCO pattern_2 n=422, CWM

pattern_2, n=422; subpattern_0, ns=142

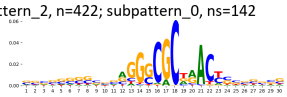

pattern_2, n=422; subpattern_1, ns=110

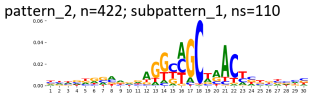

pattern_2, n=422; subpattern_2, ns=73

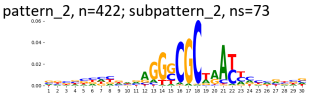

pattern_2, n=422; subpattern_3, ns=48

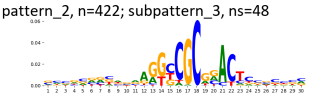

pattern_2, n=422; subpattern_4, ns=44

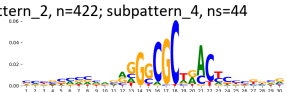

pattern_2, n=422; subpattern_5, ns=3

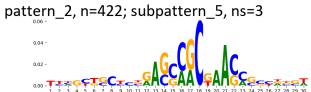

pattern_2, n=422; subpattern_6, ns=2

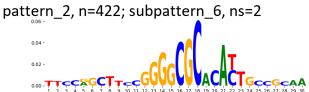

TF-MoDisCO pattern_2 n=422, CWM

pattern_2, n=422; subpattern_0, ns=142

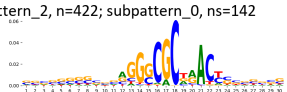

pattern_2, n=422; subpattern_1, ns=110

pattern_2, n=422; subpattern_2, ns=73

pattern_2, n=422; subpattern_3, ns=48

pattern_2, n=422; subpattern_4, ns=44

pattern_2, n=422; subpattern_5, ns=3

pattern_2, n=422; subpattern_6, ns=2

TF-MoDisCO pattern_2 n=422, PWM

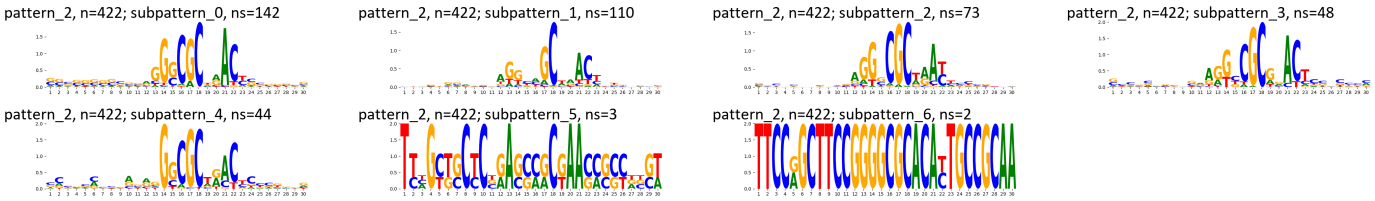

TF-MoDisCO pattern_2 n=422, PWM

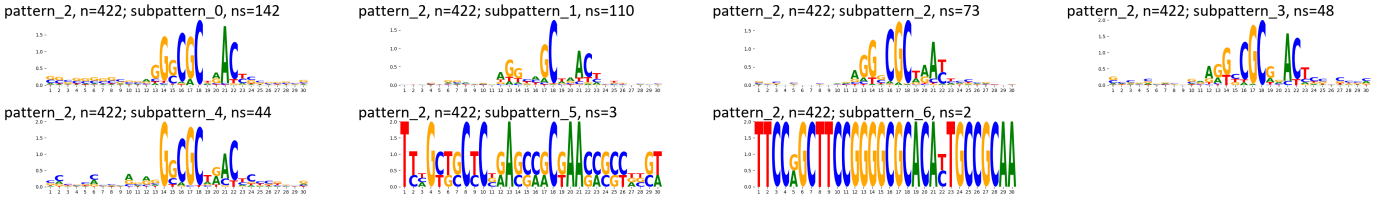

Supplementary Figure 934: TF-MoDisCO subpatterns for the ZNF264 transcription factor in HEK293 (accession Hughes NB models).

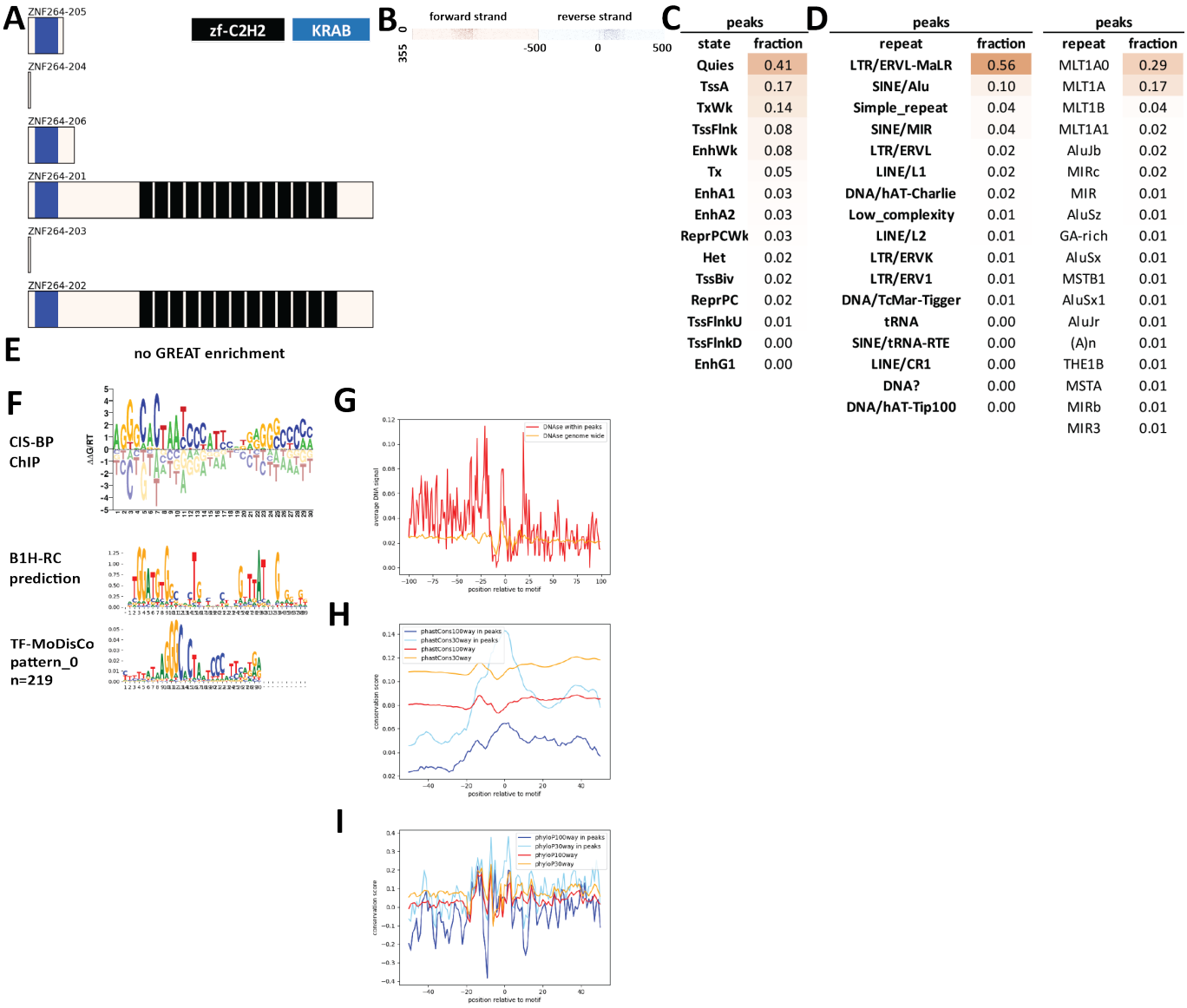

C

peaks	
state	fraction
Quies	0.41
TssA	0.17
TxWk	0.14
TssFlnk	0.08
EnhWk	0.08
Tx	0.05
EnhA1	0.03
EnhA2	0.03
ReprPCWk	0.03
Het	0.02
TssBiv	0.02
ReprPC	0.02
TssFlnkU	0.01
TssFlnkD	0.00
EnhG1	0.00

D

peaks		peaks	
repeat	fraction	repeat	fraction
LTR/ERVL-MaLR	0.56	MLT1A0	0.29
SINE/Alu	0.10	MLT1A	0.17
Simple_repeat	0.04	MLT1B	0.04
SINE/MIR	0.04	MLT1A1	0.02
LTR/ERVL	0.02	AluJb	0.02
LINE/L1	0.02	MIRc	0.02
DNA/hAT-Charlie	0.02	MIR	0.01
Low_complexity	0.01	AluSz	0.01
LINE/L2	0.01	GA-rich	0.01
LTR/ERVK	0.01	AluSx	0.01
LTR/ERV1	0.01	MSTB1	0.01
DNA/TcMar-Tigger	0.01	AluSx1	0.01
tRNA	0.00	AluJr	0.01
SINE/tRNA-RTE	0.00	(A)n	0.01
LINE/CR1	0.00	THE1B	0.01
DNA?	0.00	MSTA	0.01
DNA/hAT-Tip100	0.00	MIRb	0.01
		MIR3	0.01

Supplementary Figure 935: Properties and genomic distribution of motifs identified for the ZNF264 transcription factor in HEK293 (accession Hughes GR models).

TF-MoDisCO pattern_0 n=219, CWM

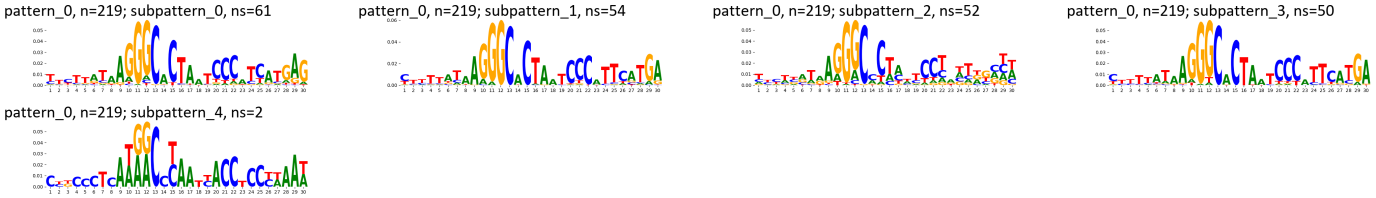

TF-MoDisCO pattern_0 n=219, PWM

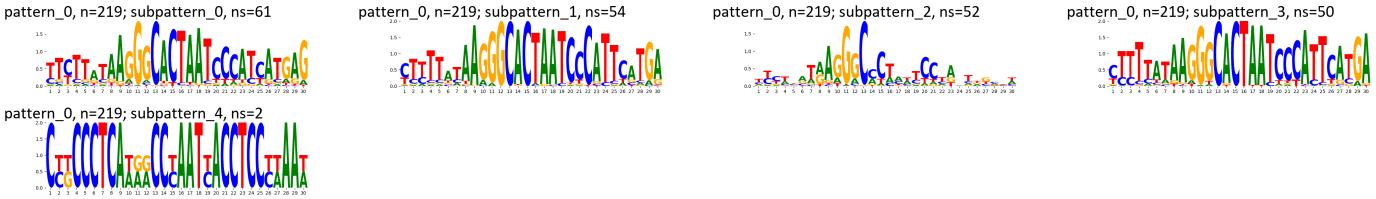

Supplementary Figure 936: TF-MoDisCO subpatterns for the ZNF264 transcription factor in HEK293 (accession Hughes GR models).

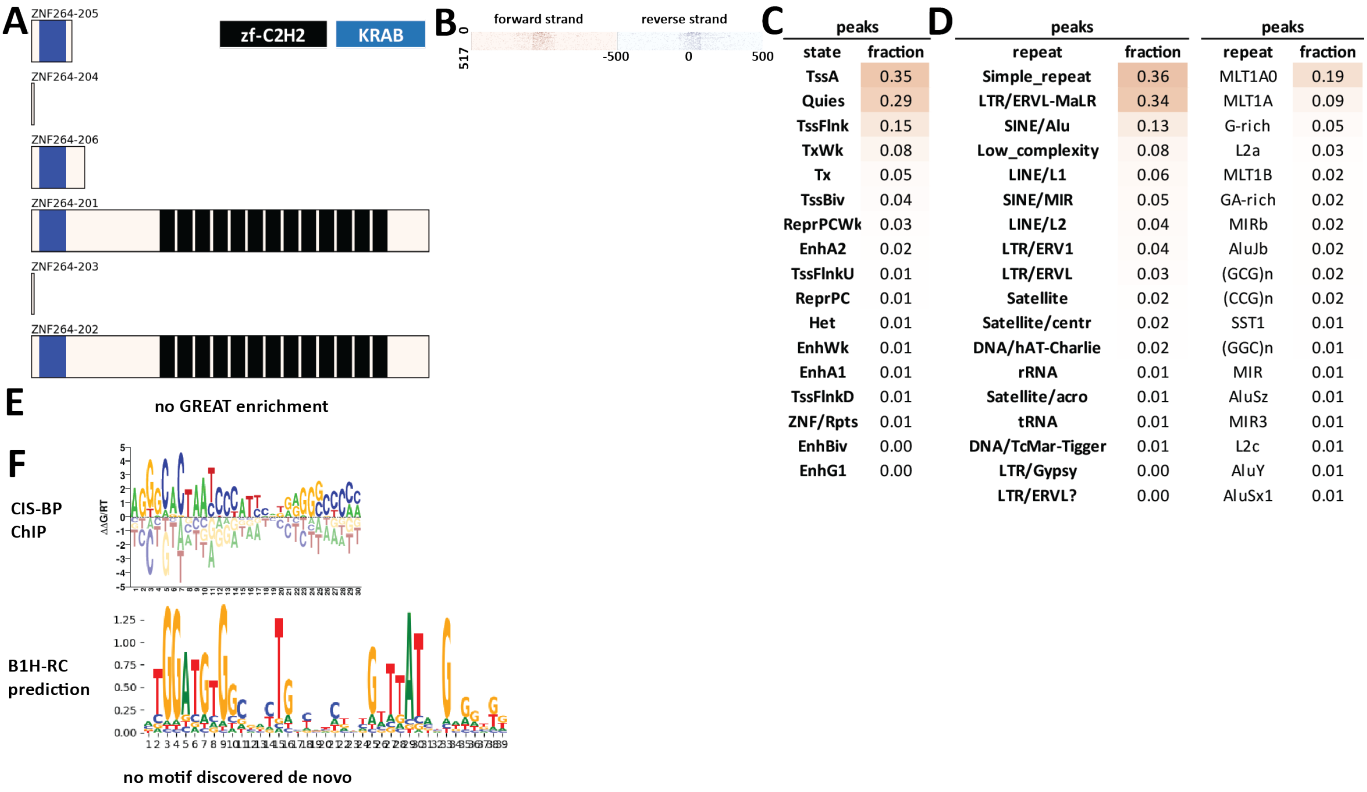

C

peaks	
state	fraction
TssA	0.35
Quies	0.29
TssFlnk	0.15
TxWk	0.08
Tx	0.05
TssBiv	0.04
ReprPCWk	0.03
EnhA2	0.02
TssFlnkU	0.01
ReprPC	0.01
Het	0.01
EnhWk	0.01
EnhA1	0.01
TssFlnkD	0.01
ZNF/Rpts	0.01
EnhBiv	0.00
EnhG1	0.00

D

peaks		peaks	
repeat	fraction	repeat	fraction
Simple_repeat	0.36	MLT1A0	0.19
LTR/ERVL-MaLR	0.34	MLT1A	0.09
SINE/Alu	0.13	G-rich	0.05
Low_complexity	0.08	L2a	0.03
LINE/L1	0.06	MLT1B	0.02
SINE/MIR	0.05	GA-rich	0.02
LINE/L2	0.04	MIRb	0.02
LTR/ERV1	0.04	AluJb	0.02
LTR/ERVL	0.03	(GCG)n	0.02
Satellite	0.02	(CCG)n	0.02
Satellite/centr	0.02	SST1	0.01
DNA/hAT-Charlie	0.02	(GGC)n	0.01
rRNA	0.01	MIR	0.01
Satellite/acro	0.01	AluSz	0.01
tRNA	0.01	MIR3	0.01
DNA/TcMar-Tigger	0.01	L2c	0.01
LTR/Gypsy	0.00	AluY	0.01
LTR/ERVL?	0.00	AluSx1	0.01

Supplementary Figure 937: Properties and genomic distribution of motifs identified for the ZNF264 transcription factor in HEK293 (accession ChipExo models).

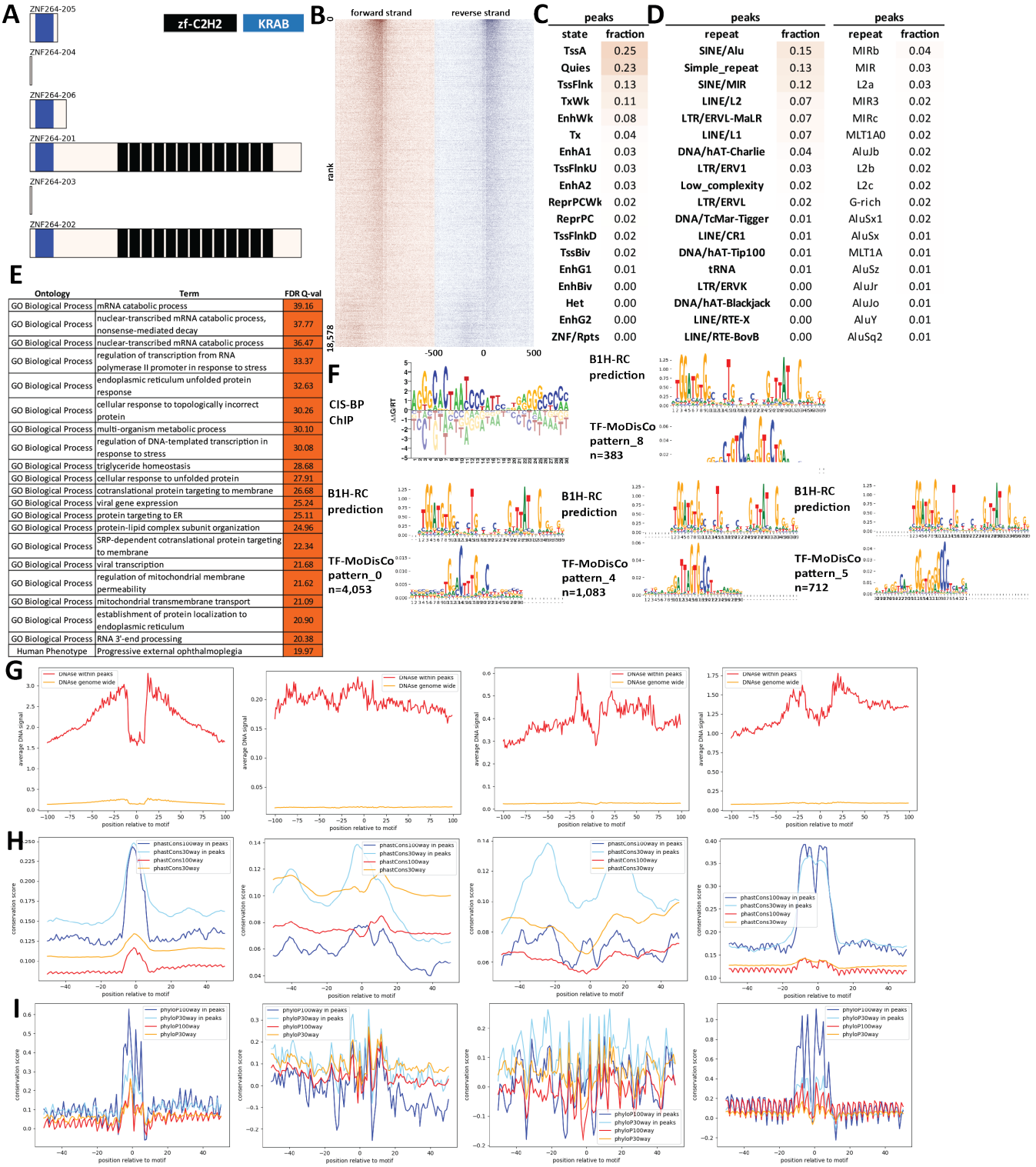

Supplementary Figure 938: Properties and genomic distribution of motifs identified for the ZNF264 transcription factor in HepG2 (accession ENCSR248BVU).

TF-MoDisCO pattern_0 n=4053, CWM

pattern_0, n=4053; subpattern_0, ns=897

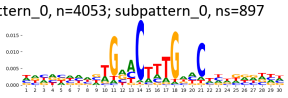

pattern_0, n=4053; subpattern_1, ns=826

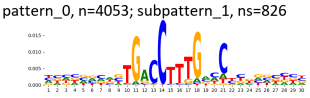

pattern_0, n=4053; subpattern_10, ns=4

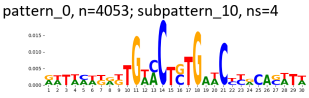

pattern_0, n=4053; subpattern_11, ns=2

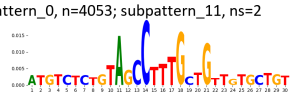

pattern_0, n=4053; subpattern_2, ns=651

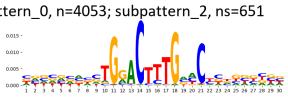

pattern_0, n=4053; subpattern_3, ns=591

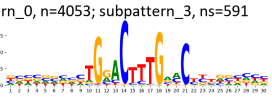

pattern_0, n=4053; subpattern_4, ns=383

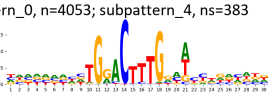

pattern_0, n=4053; subpattern_5, ns=347

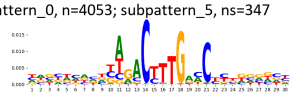

pattern_0, n=4053; subpattern_6, ns=182

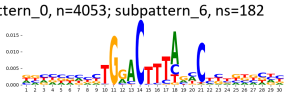

pattern_0, n=4053; subpattern_7, ns=130

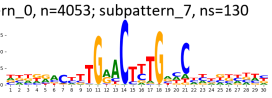

pattern_0, n=4053; subpattern_8, ns=30

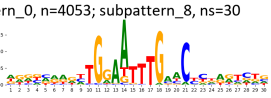

pattern_0, n=4053; subpattern_9, ns=10

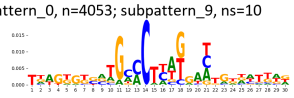

TF-MoDisCO pattern_0 n=4053, PWM

pattern_0, n=4053; subpattern_0, ns=897

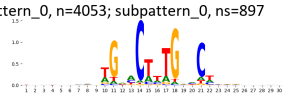

pattern_0, n=4053; subpattern_1, ns=826

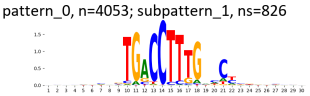

pattern_0, n=4053; subpattern_10, ns=4

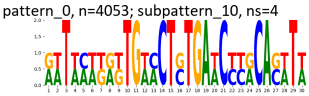

pattern_0, n=4053; subpattern_11, ns=2

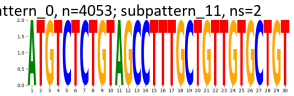

pattern_0, n=4053; subpattern_2, ns=651

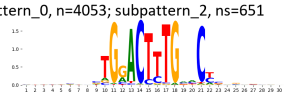

pattern_0, n=4053; subpattern_3, ns=591

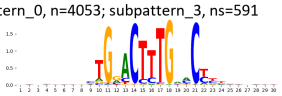

pattern_0, n=4053; subpattern_4, ns=383

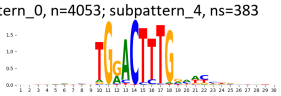

pattern_0, n=4053; subpattern_5, ns=347

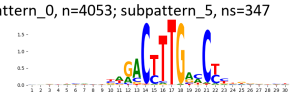

pattern_0, n=4053; subpattern_6, ns=182

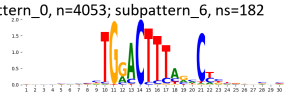

pattern_0, n=4053; subpattern_7, ns=130

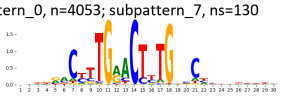

pattern_0, n=4053; subpattern_8, ns=30

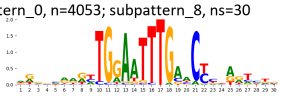

pattern_0, n=4053; subpattern_9, ns=10

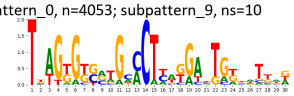

TF-MoDisCO pattern_4 n=1083, CWM

pattern_4, n=1083; subpattern_0, ns=367

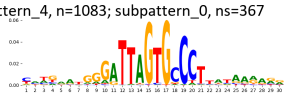

pattern_4, n=1083; subpattern_1, ns=345

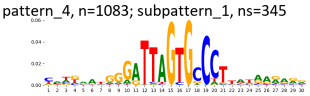

pattern_4, n=1083; subpattern_2, ns=249

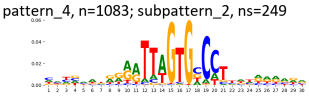

pattern_4, n=1083; subpattern_3, ns=68

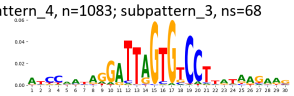

pattern_4, n=1083; subpattern_4, ns=35

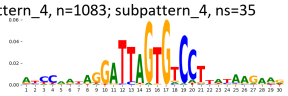

pattern_4, n=1083; subpattern_5, ns=19

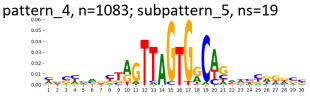

TF-MoDisCO pattern_4 n=1083, PWM

pattern_4, n=1083; subpattern_0, ns=367

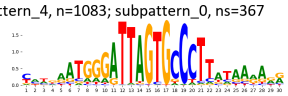

pattern_4, n=1083; subpattern_1, ns=345

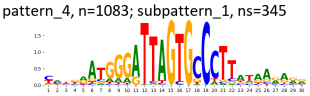

pattern_4, n=1083; subpattern_2, ns=249

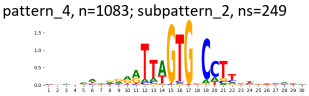

pattern_4, n=1083; subpattern_3, ns=68

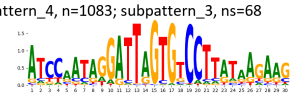

pattern_4, n=1083; subpattern_4, ns=35

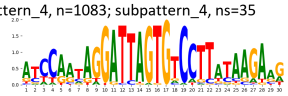

pattern_4, n=1083; subpattern_5, ns=19

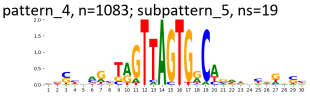

TF-MoDisCO pattern_5 n=712, CWM

pattern_5, n=712; subpattern_0, ns=148

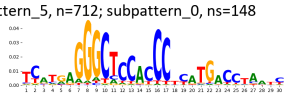

pattern_5, n=712; subpattern_1, ns=124

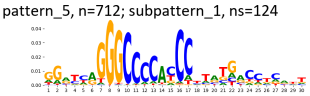

pattern_5, n=712; subpattern_2, ns=121

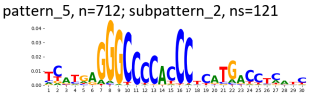

pattern_5, n=712; subpattern_3, ns=117

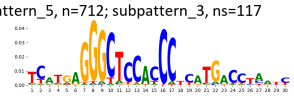

pattern_5, n=712; subpattern_4, ns=114

pattern_5, n=712; subpattern_5, ns=86

pattern_5, n=712; subpattern_6, ns=2

TF-MoDisCO pattern_5 n=712, PWM

pattern_5, n=712; subpattern_0, ns=148

pattern_5, n=712; subpattern_1, ns=124

pattern_5, n=712; subpattern_2, ns=121

pattern_5, n=712; subpattern_3, ns=117

pattern_5, n=712; subpattern_4, ns=114

pattern_5, n=712; subpattern_5, ns=86

pattern_5, n=712; subpattern_6, ns=2

TF-MoDisCO pattern_8 n=383, CWM

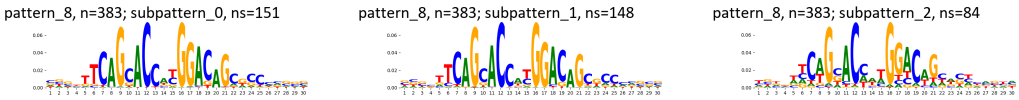

TF-MoDisCO pattern_8 n=383, PWM

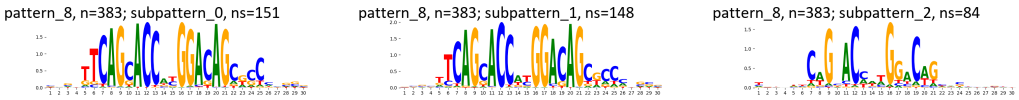

Supplementary Figure 939: TF-MoDisCO subpatterns for the ZNF264 transcription factor in HepG2 (accession ENCSR248BVU).

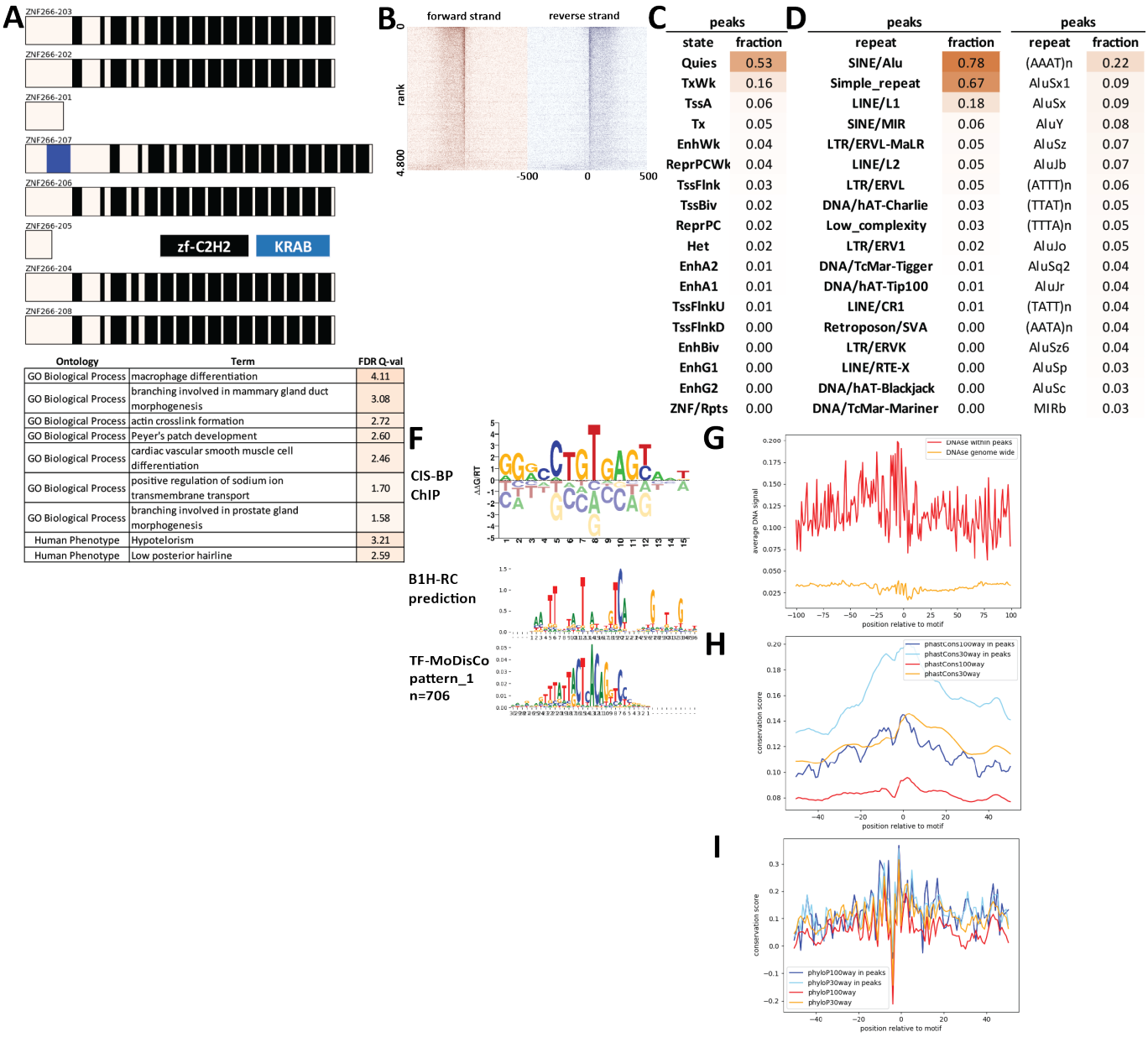

Ontology	Term	FDR Q-val
GO Biological Process	macrophage differentiation	4.11
GO Biological Process	branching involved in mammary gland duct morphogenesis	3.08
GO Biological Process	actin crosslink formation	2.72
GO Biological Process	Peyer's patch development	2.60
GO Biological Process	cardiac vascular smooth muscle cell differentiation	2.46
GO Biological Process	positive regulation of sodium ion transmembrane transport	1.70
GO Biological Process	branching involved in prostate gland morphogenesis	1.58
Human Phenotype	Hypotelorism	3.21
Human Phenotype	Low posterior hairline	2.59

C

peaks	
state	fraction
Quies	0.53
TxWk	0.16
TssA	0.06
Tx	0.05
EnhWk	0.04
ReprPCWk	0.04
TssFlnk	0.03
TssBiv	0.02
ReprPC	0.02
Het	0.02
EnhA2	0.01
EnhA1	0.01
TssFlnkU	0.01
TssFlnkD	0.00
EnhBiv	0.00
EnhG1	0.00
EnhG2	0.00
ZNF/Rpts	0.00

D

peaks		peaks	
repeat	fraction	repeat	fraction
SINE/Alu	0.78	(AAAT)n	0.22
Simple_repeat	0.67	AluSx1	0.09
LINE/L1	0.18	AluSx	0.09
SINE/MIR	0.06	AluY	0.08
LTR/ERVL-MaLR	0.05	AluSz	0.07
LINE/L2	0.05	AluJb	0.07
LTR/ERVL	0.05	(ATTT)n	0.06
DNA/hAT-Charlie	0.03	(TTAT)n	0.05
Low_complexity	0.03	(TTTA)n	0.05
LTR/ERV1	0.02	AluJo	0.05
DNA/TcMar-Tigger	0.01	AluSq2	0.04
DNA/hAT-Tip100	0.01	AluJr	0.04
LINE/CR1	0.01	(TATT)n	0.04
Retroposon/SVA	0.00	(AATA)n	0.04
LTR/ERVK	0.00	AluSz6	0.04
LINE/RTE-X	0.00	AluSp	0.03
DNA/hAT-Blackjack	0.00	AluSc	0.03
DNA/TcMar-Mariner	0.00	MIRb	0.03

Supplementary Figure 940: Properties and genomic distribution of motifs identified for the ZNF266 transcription factor in HEK293 (accession ENCSR466VYP).

TF-MoDisCO pattern_1 n=706, CWM

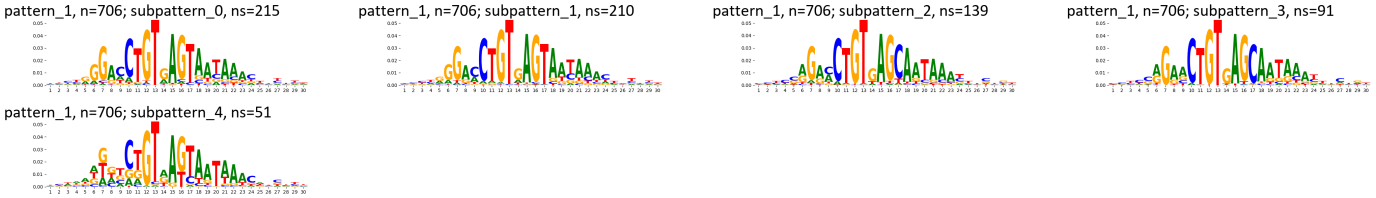

TF-MoDisCO pattern_1 n=706, PWM

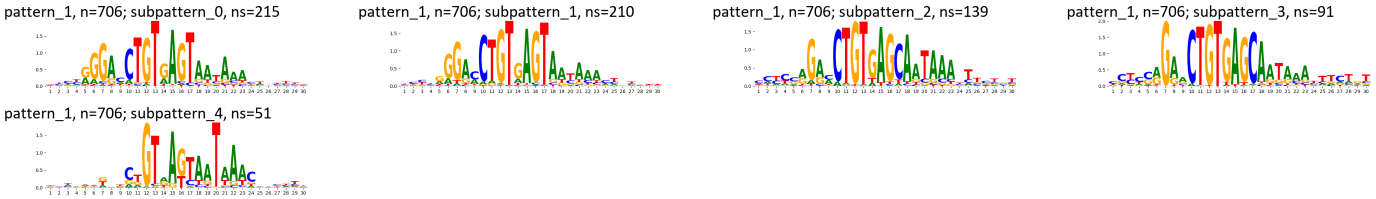

Supplementary Figure 941: TF-MoDisCO subpatterns for the ZNF266 transcription factor in HEK293 (accession ENCSR466VYP).

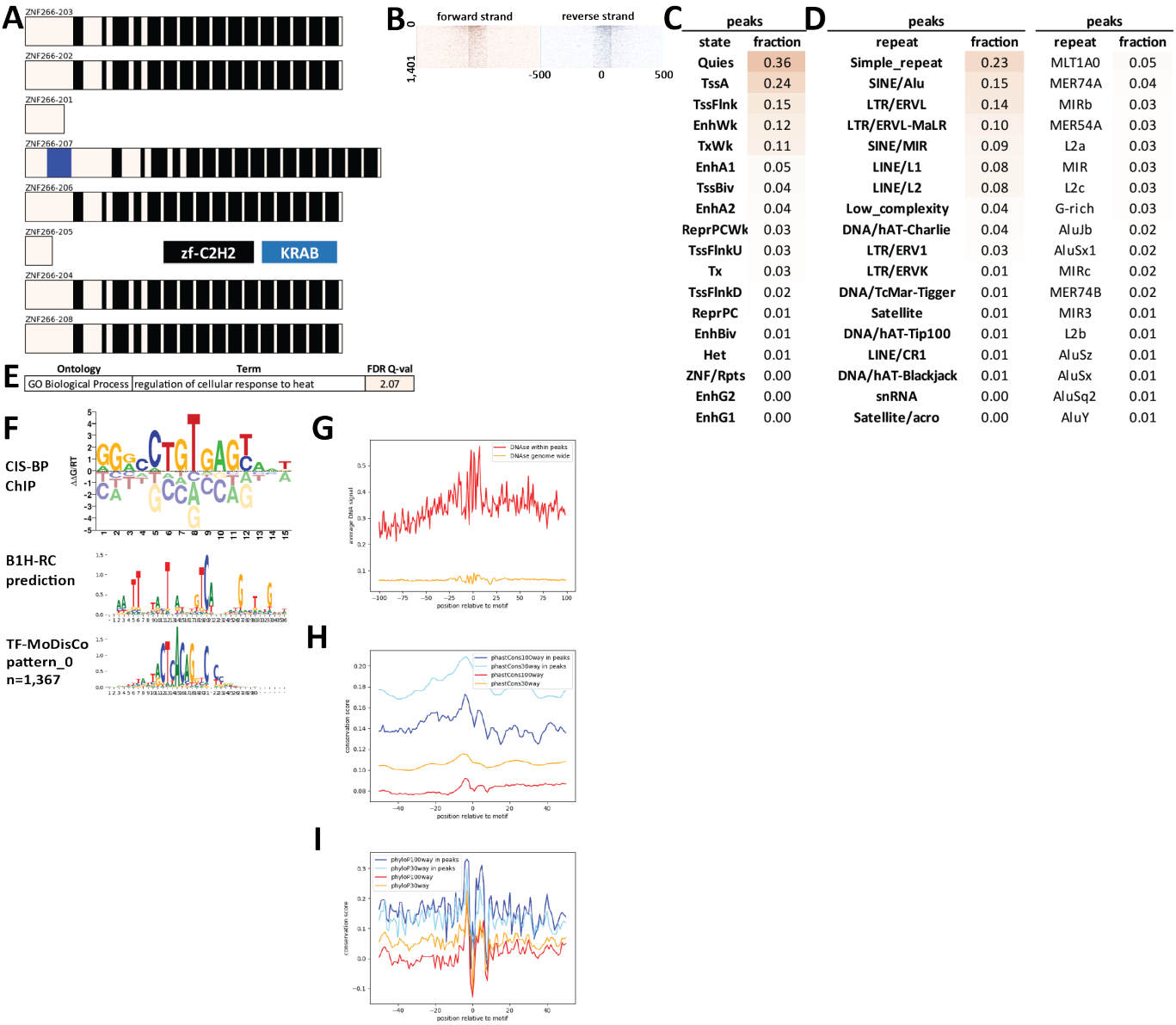

C

peaks	
state	fraction
Quies	0.36
TssA	0.24
TssFlnk	0.15
EnhWk	0.12
TxWk	0.11
EnhA1	0.05
TssBiv	0.04
EnhA2	0.04
ReprPCWk	0.03
TssFlnkU	0.03
Tx	0.03
TssFlnkD	0.02
ReprPC	0.01
EnhBiv	0.01
Het	0.01
ZNF/Rpts	0.00
EnhG2	0.00
EnhG1	0.00

D

peaks		peaks	
repeat	fraction	repeat	fraction
Simple_repeat	0.23	MLT1A0	0.05
SINE/Alu	0.15	MER74A	0.04
LTR/ERVL	0.14	MIRb	0.03
LTR/ERVL-MaLR	0.10	MER54A	0.03
SINE/MIR	0.09	L2a	0.03
LINE/L1	0.08	MIR	0.03
LINE/L2	0.08	L2c	0.03
Low_complexity	0.04	G-rich	0.03
DNA/hAT-Charlie	0.04	AluJb	0.02
LTR/ERV1	0.03	AluSx1	0.02
LTR/ERVK	0.01	MIRc	0.02
DNA/TcMar-Tigger	0.01	MER74B	0.02
Satellite	0.01	MIR3	0.01
DNA/hAT-Tip100	0.01	L2b	0.01
LINE/CR1	0.01	AluSz	0.01
DNA/hAT-Blackjack	0.01	AluSx	0.01
snRNA	0.00	AluSq2	0.01
Satellite/acro	0.00	AluY	0.01

Supplementary Figure 942: Properties and genomic distribution of motifs identified for the ZNF266 transcription factor in HEK293 (accession ChipExo models).

TF-MoDisCO pattern_0 n=1367, CWM

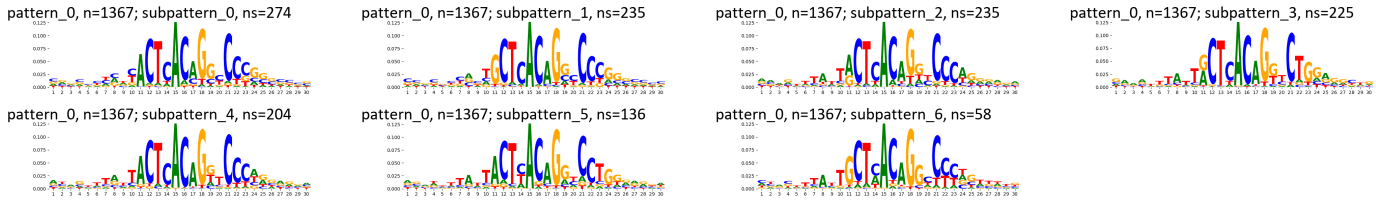

TF-MoDisCO pattern_0 n=1367, PWM

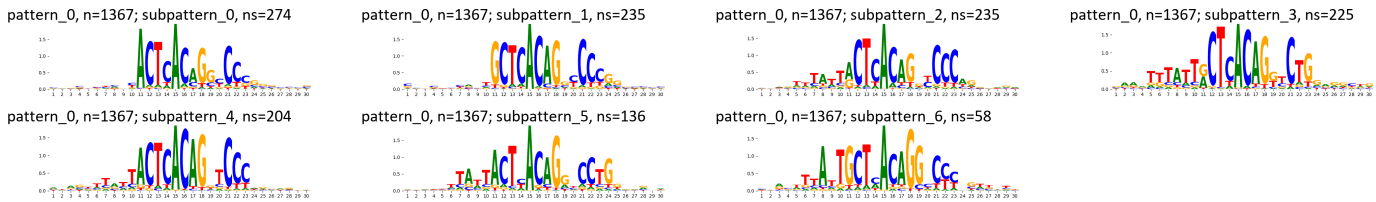

Supplementary Figure 943: TF-MoDisCO subpatterns for the ZNF266 transcription factor in HEK293 (accession ChipExo models).

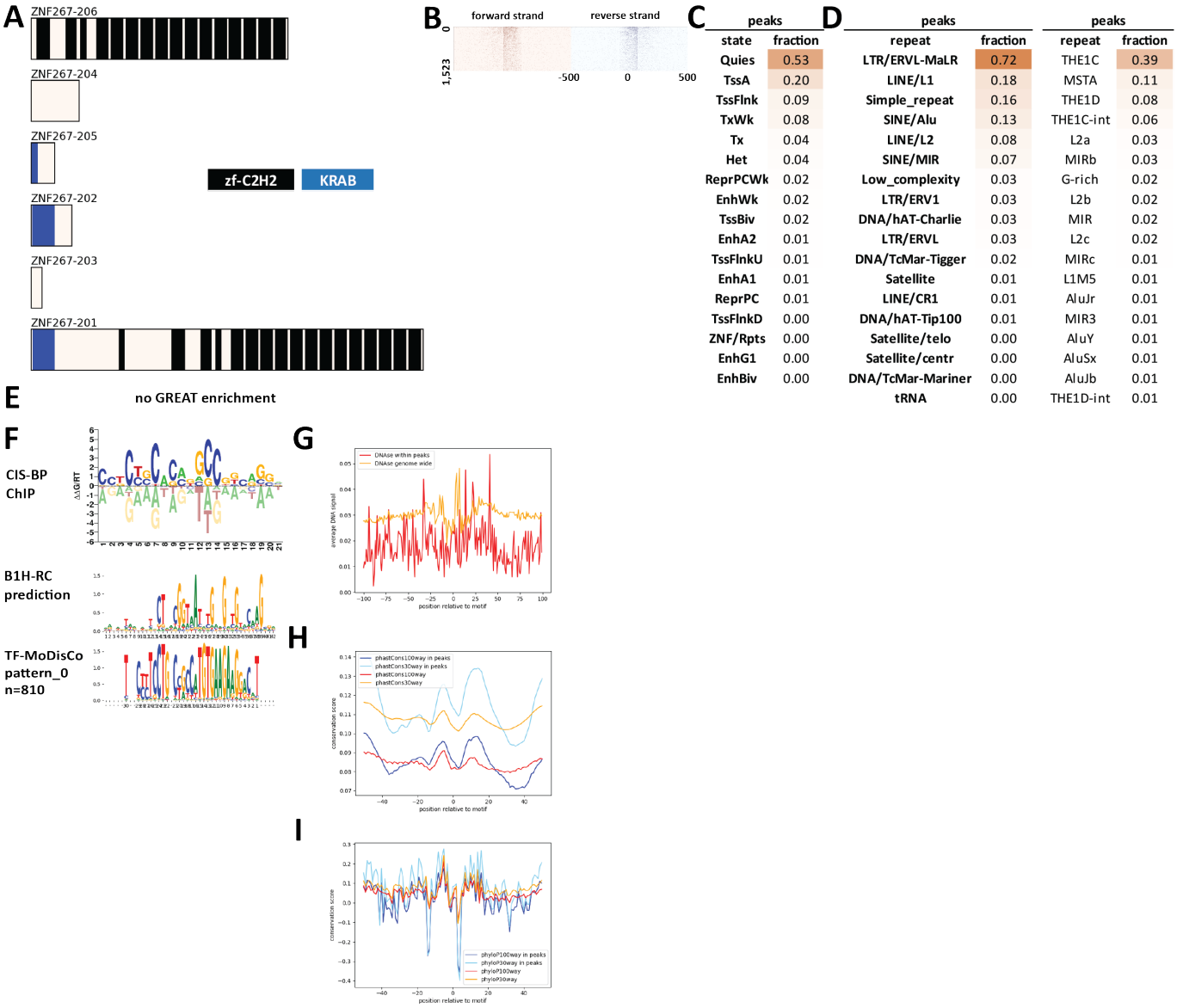

C

peaks	
state	fraction
Quies	0.53
TssA	0.20
TssFlnk	0.09
TxWk	0.08
Tx	0.04
Het	0.04
ReprPCWk	0.02
EnhWk	0.02
TssBiv	0.02
EnhA2	0.01
TssFlnkU	0.01
EnhA1	0.01
ReprPC	0.01
TssFlnkD	0.00
ZNF/Rpts	0.00
EnhG1	0.00
EnhBiv	0.00

D

peaks		peaks	
repeat	fraction	repeat	fraction
LTR/ERVL-MaLR	0.72	THE1C	0.39
LINE/L1	0.18	MSTA	0.11
Simple_repeat	0.16	THE1D	0.08
SINE/Alu	0.13	THE1C-int	0.06
LINE/L2	0.08	L2a	0.03
SINE/MIR	0.07	MIRb	0.03
Low_complexity	0.03	G-rich	0.02
LTR/ERV1	0.03	L2b	0.02
DNA/hAT-Charlie	0.03	MIR	0.02
LTR/ERVL	0.03	L2c	0.02
DNA/TcMar-Tigger	0.02	MIRc	0.01
Satellite	0.01	L1M5	0.01
LINE/CR1	0.01	AluJr	0.01
DNA/hAT-Tip100	0.01	MIR3	0.01
Satellite/telo	0.00	AluY	0.01
Satellite/centr	0.00	AluSx	0.01
DNA/TcMar-Mariner	0.00	AluJb	0.01
tRNA	0.00	THE1D-int	0.01

Supplementary Figure 944: Properties and genomic distribution of motifs identified for the ZNF267 transcription factor in HEK293 (accession ChipExo models).

TF-MoDisCO pattern_0 n=810, CWM

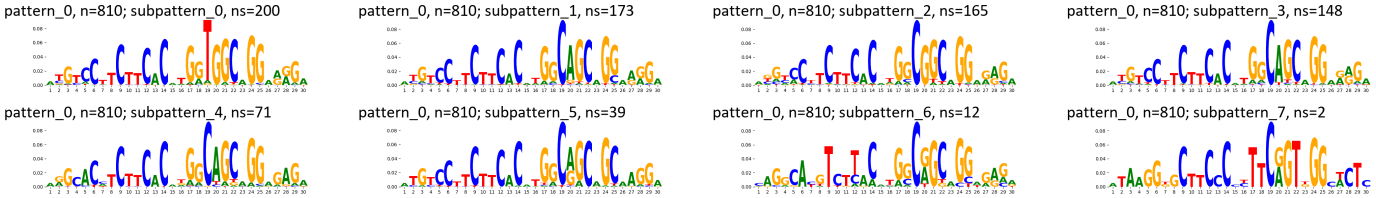

TF-MoDisCO pattern_0 n=810, PWM

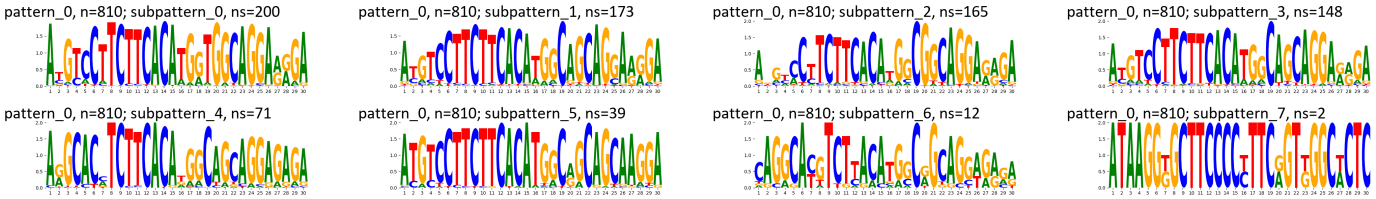

Supplementary Figure 945: TF-MoDisCO subpatterns for the ZNF267 transcription factor in HEK293 (accession ChipExo models).

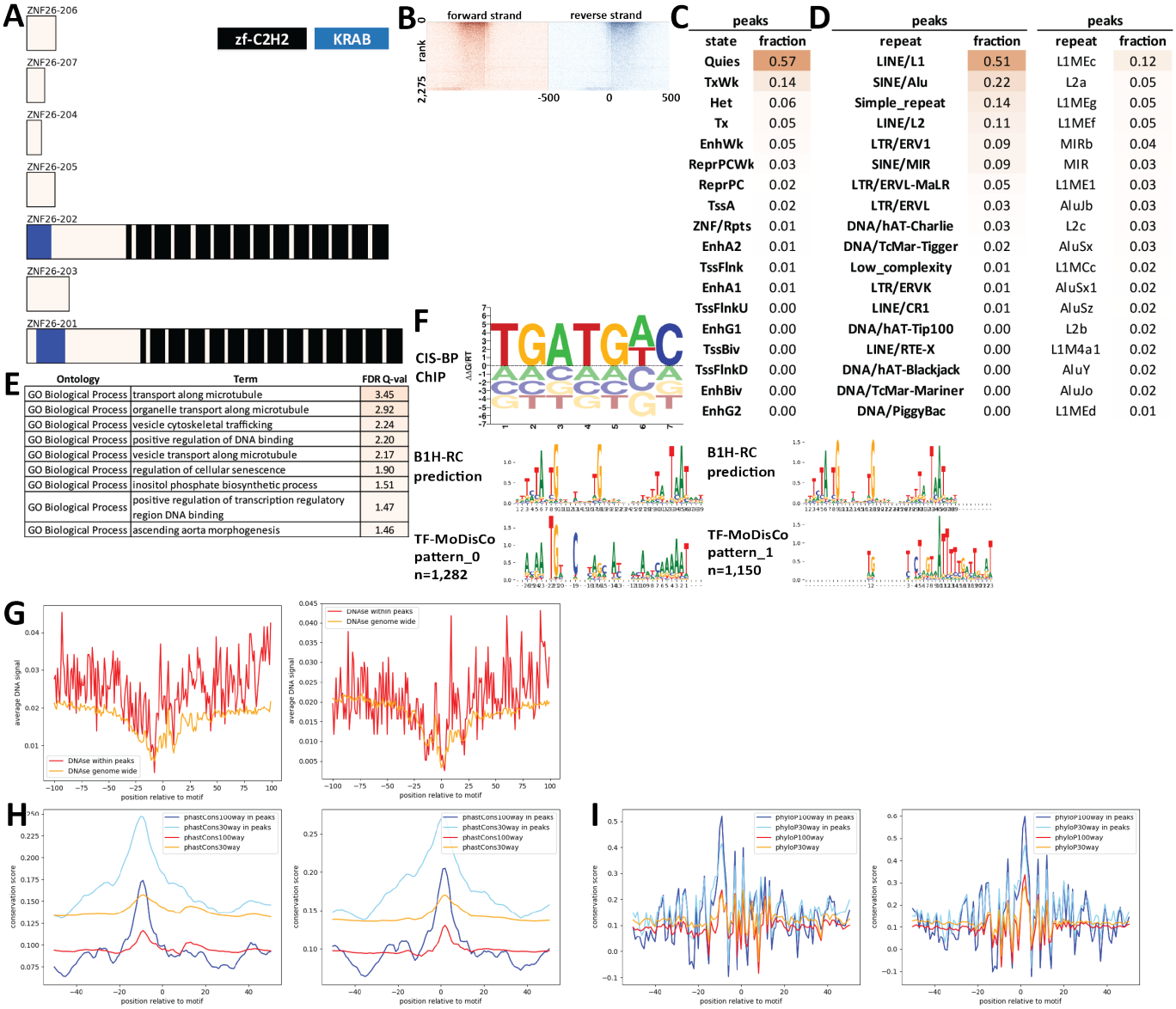

Supplementary Figure 946: Properties and genomic distribution of motifs identified for the ZNF26 transcription factor in HEK293 (accession ENCSR028EGI).

TF-MoDisCO pattern_0 n=1282, CWM

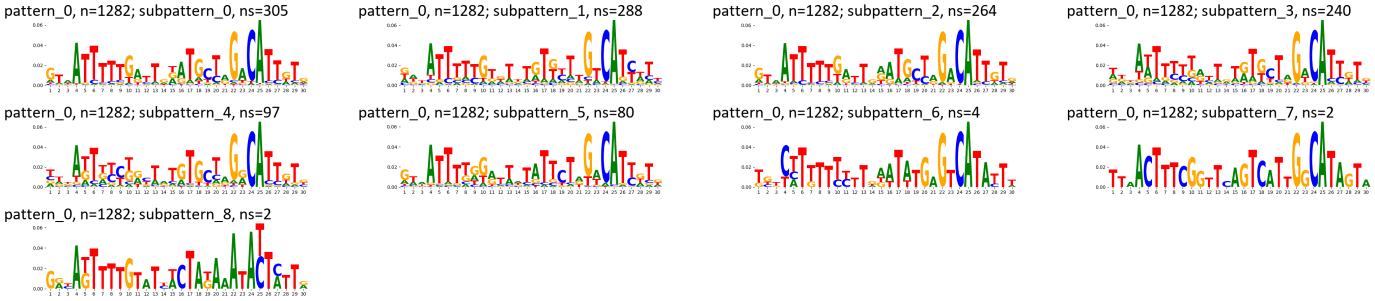

TF-MoDisCO pattern_0 n=1282, PWM

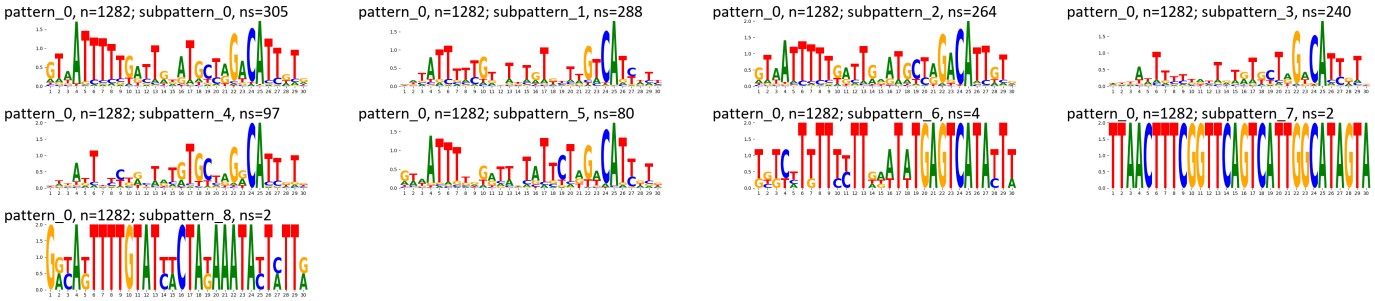

TF-MoDisCO pattern_1 n=1150, CWM

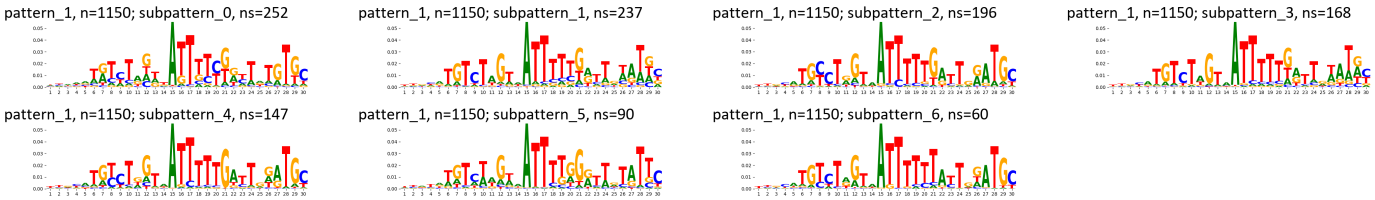

TF-MoDisCO pattern_1 n=1150, PWM

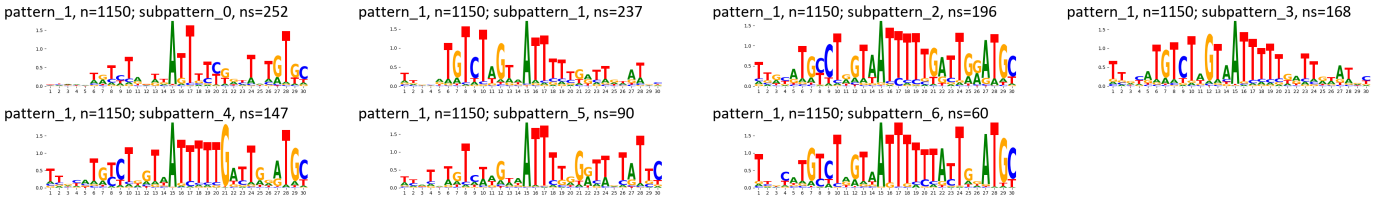

Supplementary Figure 947: TF-MoDisCO subpatterns for the ZNF26 transcription factor in HEK293 (accession ENCSR028EGI).

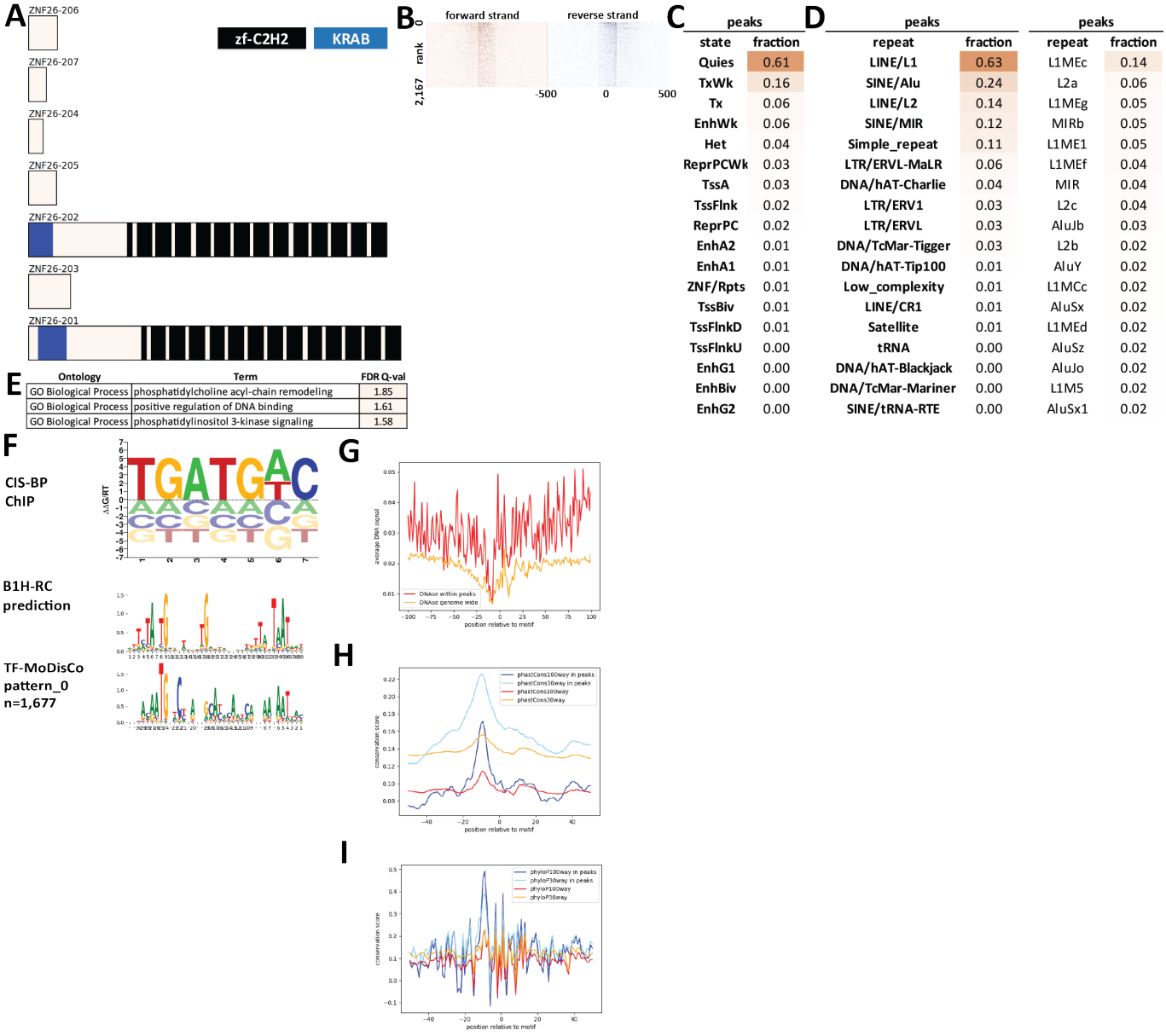

C

peaks	
state	fraction
Quies	0.61
TxWk	0.16
Tx	0.06
EnhWk	0.06
Het	0.04
ReprPCWk	0.03
TssA	0.03
TssFlnk	0.02
ReprPC	0.02
EnhA2	0.01
EnhA1	0.01
ZNF/Rpts	0.01
TssBiv	0.01
TssFlnkD	0.01
TssFlnkU	0.00
EnhG1	0.00
EnhBiv	0.00
EnhG2	0.00

D

peaks		peaks	
repeat	fraction	repeat	fraction
LINE/L1	0.63	L1MEc	0.14
SINE/Alu	0.24	L2a	0.06
LINE/L2	0.14	L1MEg	0.05
SINE/MIR	0.12	MIRb	0.05
Simple_repeat	0.11	L1ME1	0.05
LTR/ERVL-MaLR	0.06	L1MEf	0.04
DNA/hAT-Charlie	0.04	MIR	0.04
LTR/ERV1	0.03	L2c	0.04
LTR/ERVL	0.03	AluJb	0.03
DNA/TcMar-Tigger	0.03	L2b	0.02
DNA/hAT-Tip100	0.01	AluY	0.02
Low_complexity	0.01	L1MCc	0.02
LINE/CR1	0.01	AluSx	0.02
Satellite	0.01	L1MEd	0.02
tRNA	0.00	AluSz	0.02
DNA/hAT-Blackjack	0.00	AluJo	0.02
DNA/TcMar-Mariner	0.00	L1M5	0.02
SINE/tRNA-RTE	0.00	AluSx1	0.02

E

Ontology	Term	FDR Q-val
GO Biological Process	phosphatidylcholine acyl-chain remodeling	1.85
GO Biological Process	positive regulation of DNA binding	1.61
GO Biological Process	phosphatidylinositol 3-kinase signaling	1.58

Supplementary Figure 948: Properties and genomic distribution of motifs identified for the ZNF26 transcription factor in HEK293 (accession ChipExo models).

TF-MoDisCO pattern_0 n=1677, CWM

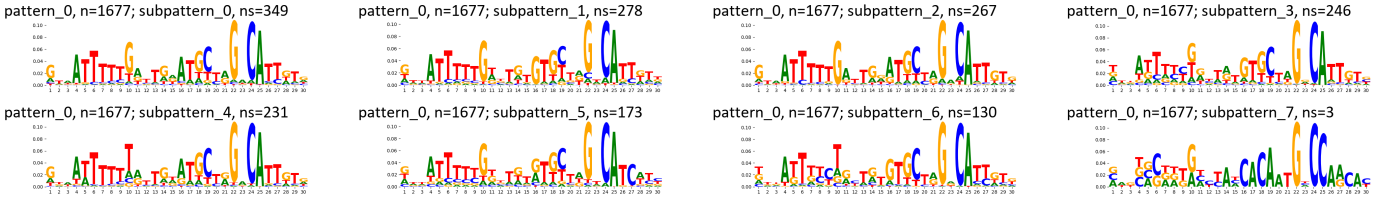

TF-MoDisCO pattern_0 n=1677, PWM

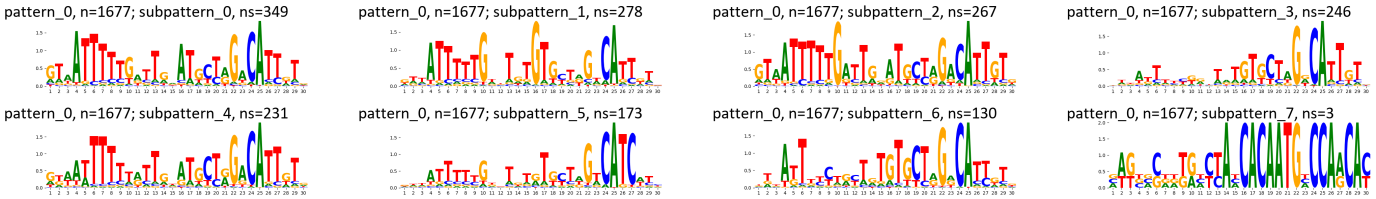

Supplementary Figure 949: TF-MoDisCO subpatterns for the ZNF26 transcription factor in HEK293 (accession ChipExo models).

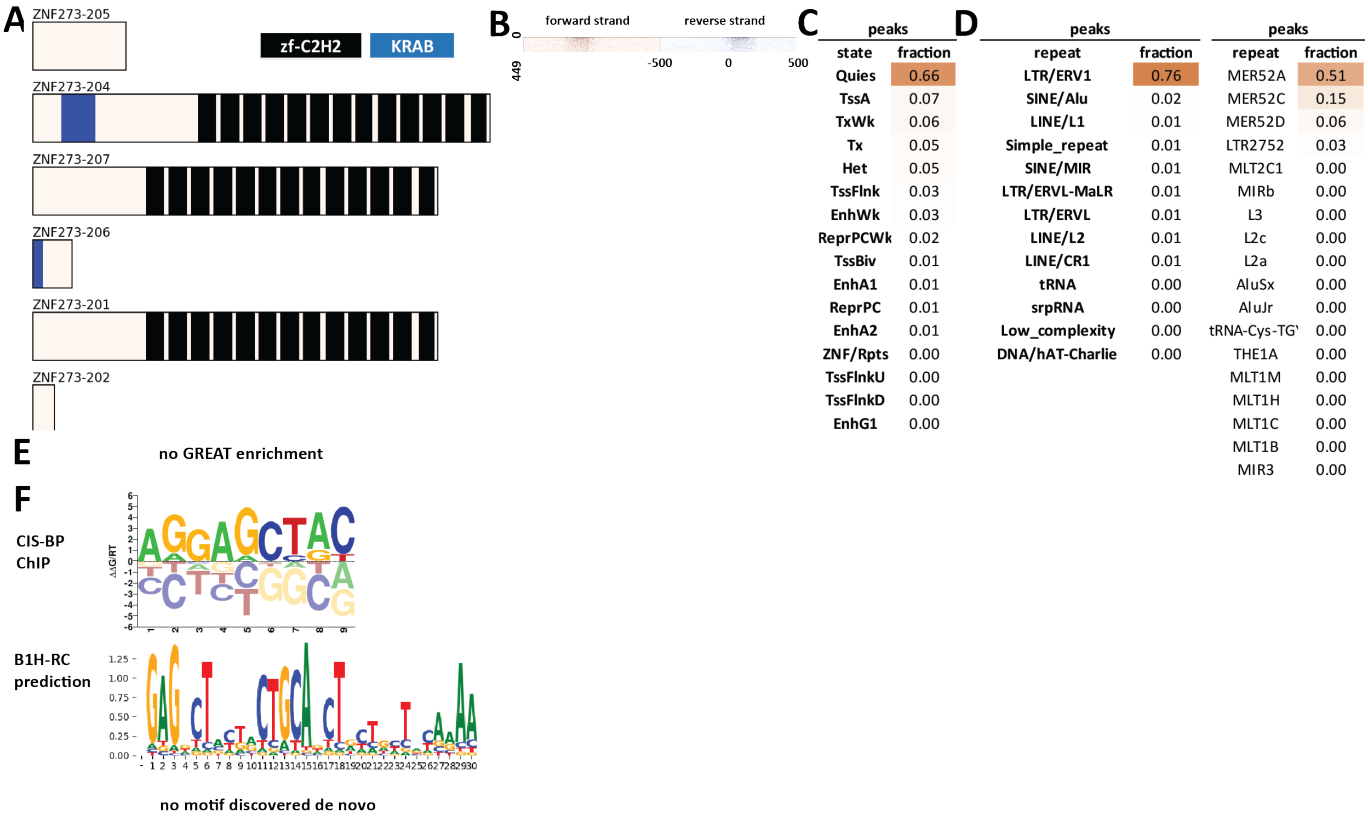

Supplementary Figure 950: Properties and genomic distribution of motifs identified for the ZNF273 transcription factor in HEK293 (accession Hughes NB models).

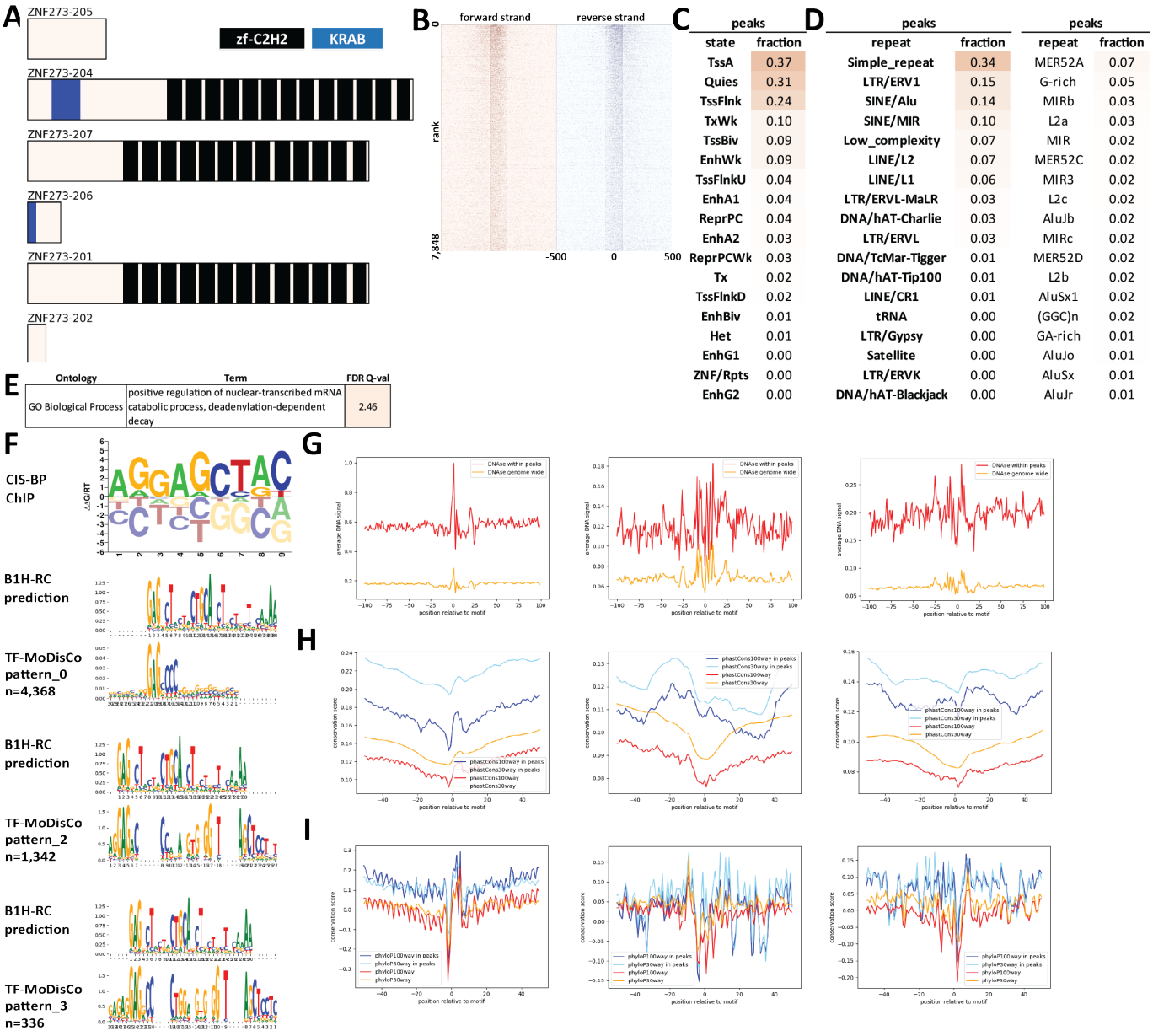

Supplementary Figure 951: Properties and genomic distribution of motifs identified for the ZNF273 transcription factor in HEK293 (accession ChipExo models).

TF-MoDisCO pattern_0 n=4368, CWM

pattern_0, n=4368; subpattern_0, ns=1092

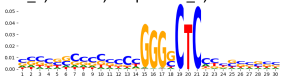

pattern_0, n=4368; subpattern_1, ns=883

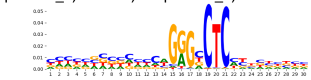

pattern_0, n=4368; subpattern_2, ns=730

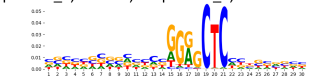

pattern_0, n=4368; subpattern_3, ns=485

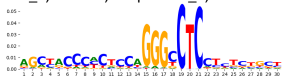

pattern_0, n=4368; subpattern_4, ns=439

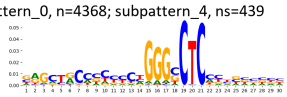

pattern_0, n=4368; subpattern_5, ns=238

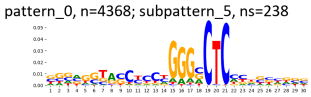

pattern_0, n=4368; subpattern_6, ns=207

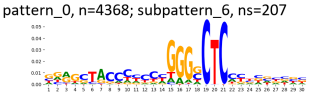

pattern_0, n=4368; subpattern_7, ns=143

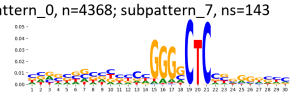

pattern_0, n=4368; subpattern_8, ns=138

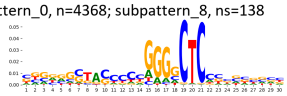

pattern_0, n=4368; subpattern_9, ns=13

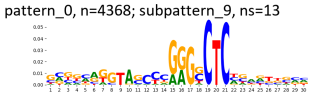

TF-MoDisCO pattern_0 n=4368, PWM

pattern_0, n=4368; subpattern_0, ns=1092

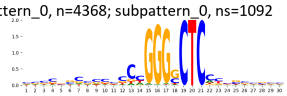

pattern_0, n=4368; subpattern_1, ns=883

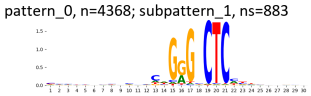

pattern_0, n=4368; subpattern_2, ns=730

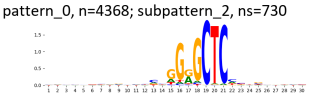

pattern_0, n=4368; subpattern_3, ns=485

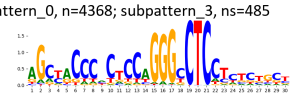

pattern_0, n=4368; subpattern_4, ns=439

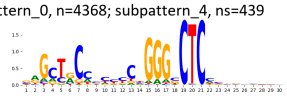

pattern_0, n=4368; subpattern_5, ns=238

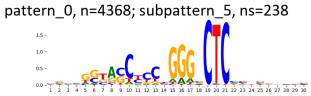

pattern_0, n=4368; subpattern_6, ns=207

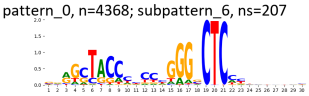

pattern_0, n=4368; subpattern_7, ns=143

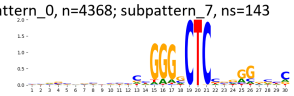

pattern_0, n=4368; subpattern_8, ns=138

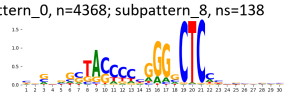

pattern_0, n=4368; subpattern_9, ns=13

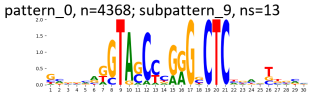

TF-MoDisCO pattern_2 n=1342, CWM

pattern_2, n=1342; subpattern_0, ns=330

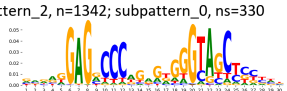

pattern_2, n=1342; subpattern_1, ns=292

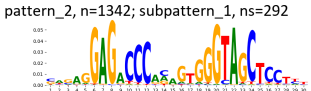

pattern_2, n=1342; subpattern_2, ns=286

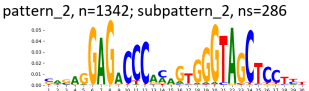

pattern_2, n=1342; subpattern_3, ns=203

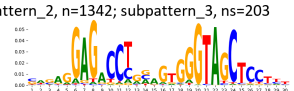

pattern_2, n=1342; subpattern_4, ns=189

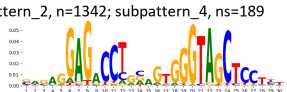

pattern_2, n=1342; subpattern_5, ns=31

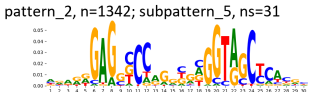

pattern_2, n=1342; subpattern_6, ns=11

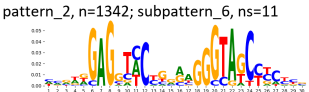

TF-MoDisCO pattern_2 n=1342, PWM

pattern_2, n=1342; subpattern_0, ns=330

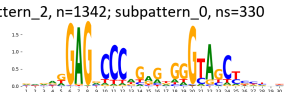

pattern_2, n=1342; subpattern_1, ns=292

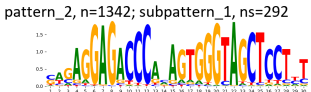

pattern_2, n=1342; subpattern_2, ns=286

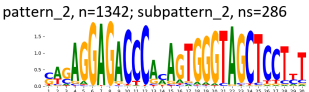

pattern_2, n=1342; subpattern_3, ns=203

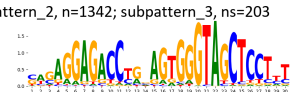

pattern_2, n=1342; subpattern_4, ns=189

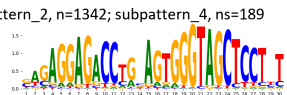

pattern_2, n=1342; subpattern_5, ns=31

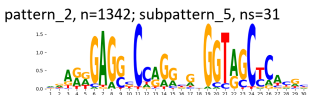

pattern_2, n=1342; subpattern_6, ns=11

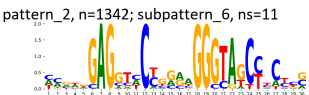

TF-MoDisCO pattern_3 n=336, CWM

pattern_3, n=336; subpattern_0, ns=130

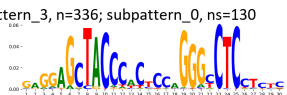

pattern_3, n=336; subpattern_1, ns=117

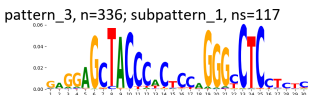

pattern_3, n=336; subpattern_2, ns=52

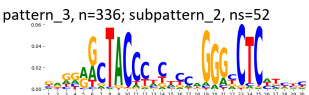

pattern_3, n=336; subpattern_3, ns=21

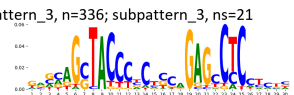

pattern_3, n=336; subpattern_4, ns=16

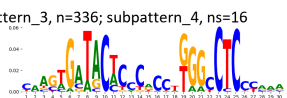

TF-MoDisCO pattern_3 n=336, PWM

pattern_3, n=336; subpattern_0, ns=130

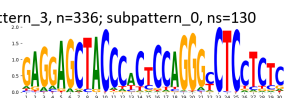

pattern_3, n=336; subpattern_1, ns=117

pattern_3, n=336; subpattern_2, ns=52

pattern_3, n=336; subpattern_3, ns=21

pattern_3, n=336; subpattern_4, ns=16

Supplementary Figure 952: TF-MoDisCO subpatterns for the ZNF273 transcription factor in HEK293 (accession ChipExo models).

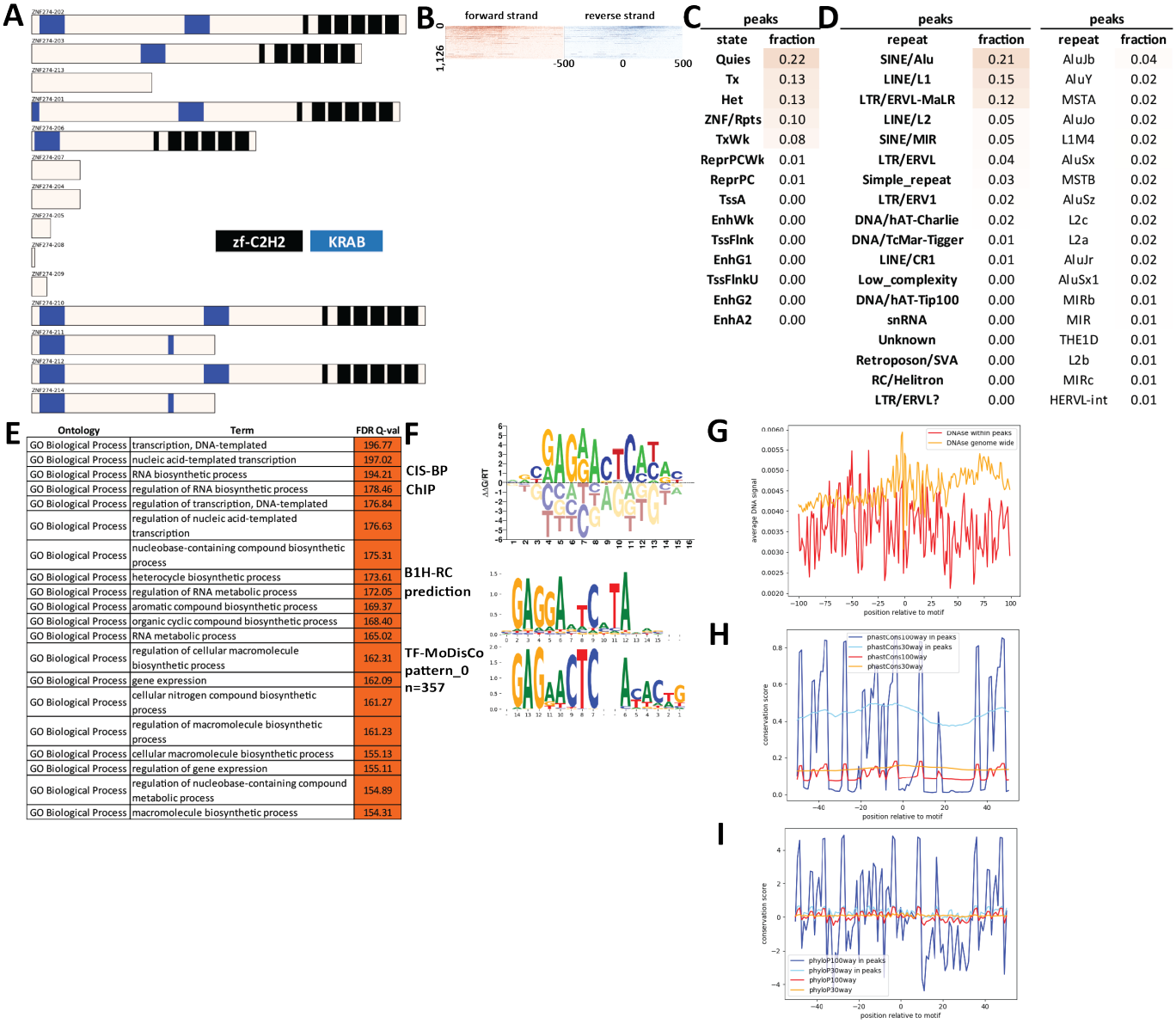

Supplementary Figure 953: Properties and genomic distribution of motifs identified for the ZNF274 transcription factor in GM08714 (accession ENCSR000EUI).

TF-MoDisCO pattern_0 n=357, CWM

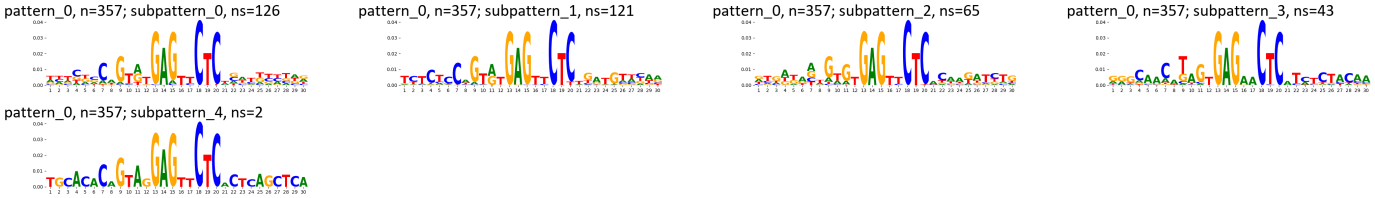

TF-MoDisCO pattern_0 n=357, PWM

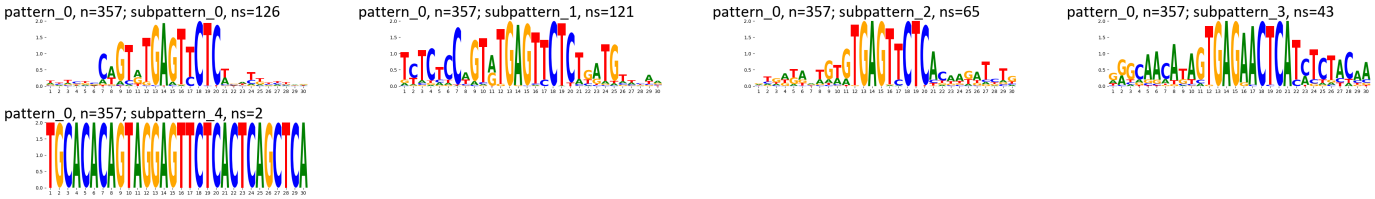

Supplementary Figure 954: TF-MoDisCO subpatterns for the ZNF274 transcription factor in GM08714 (accession ENCSR000EUI).

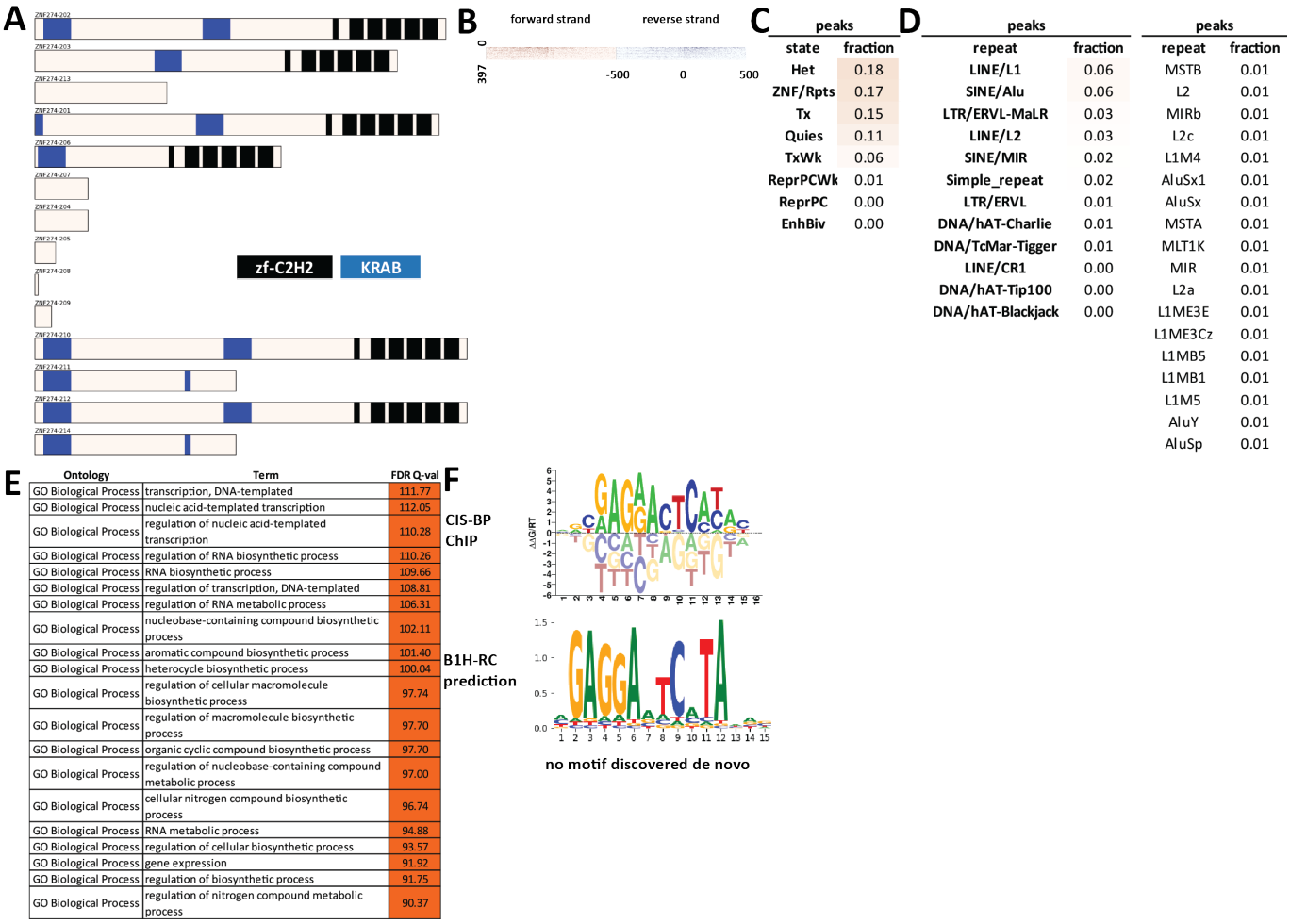

Supplementary Figure 955: Properties and genomic distribution of motifs identified for the ZNF274 transcription factor in GM12878 (accession ENCSR000EUK).

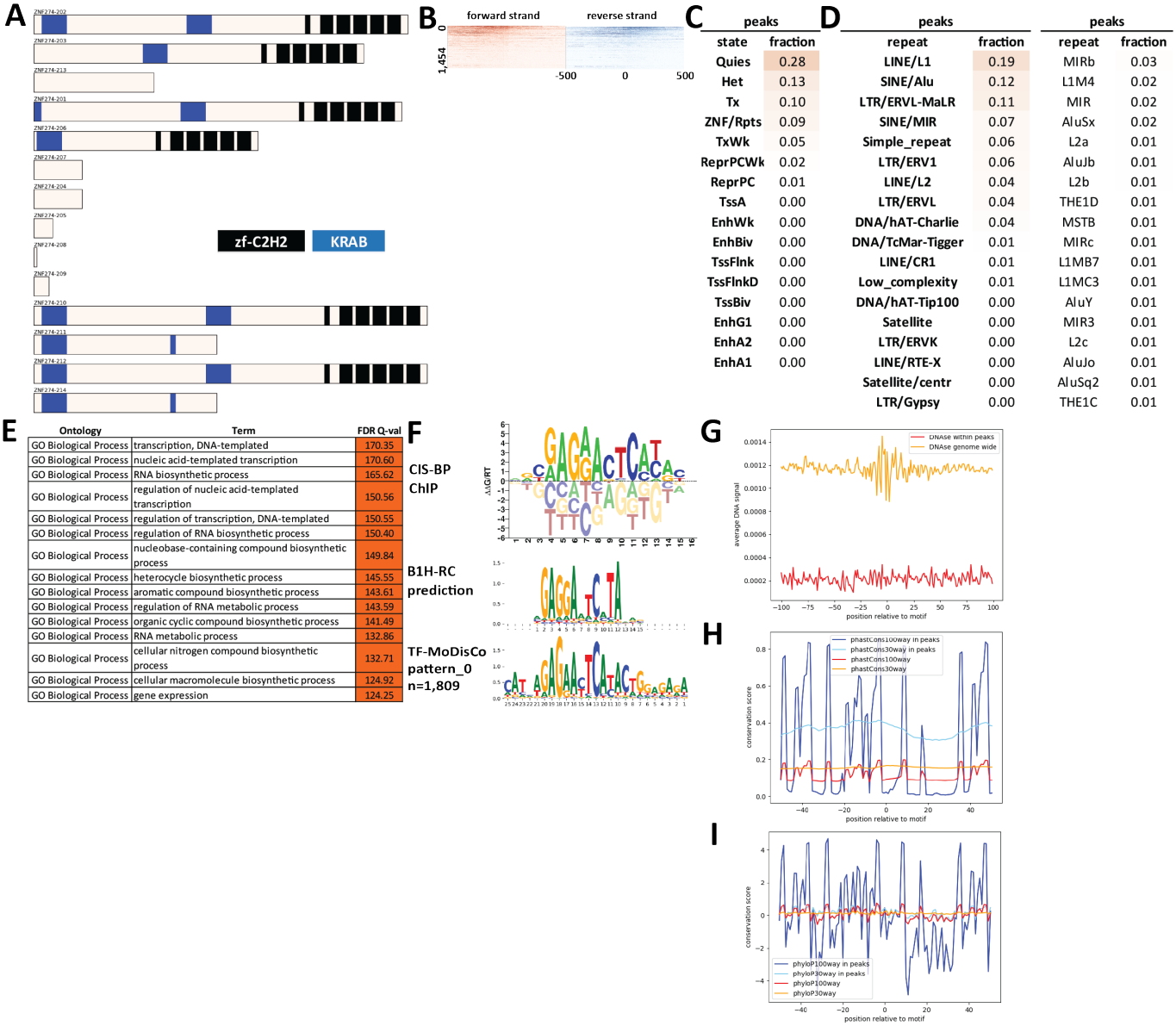

Supplementary Figure 956: Properties and genomic distribution of motifs identified for the ZNF274 transcription factor in H1 (accession ENCSR000EUN).

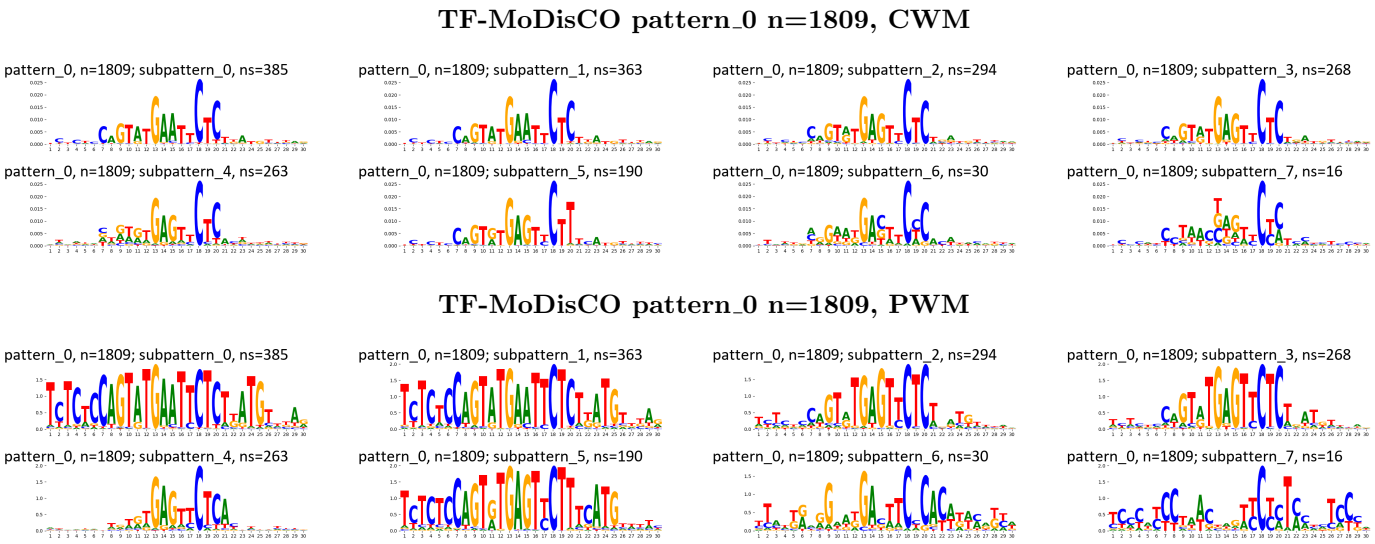

Supplementary Figure 957: TF-MoDisCO subpatterns for the ZNF274 transcription factor in H1 (accession ENCSR000EUN).

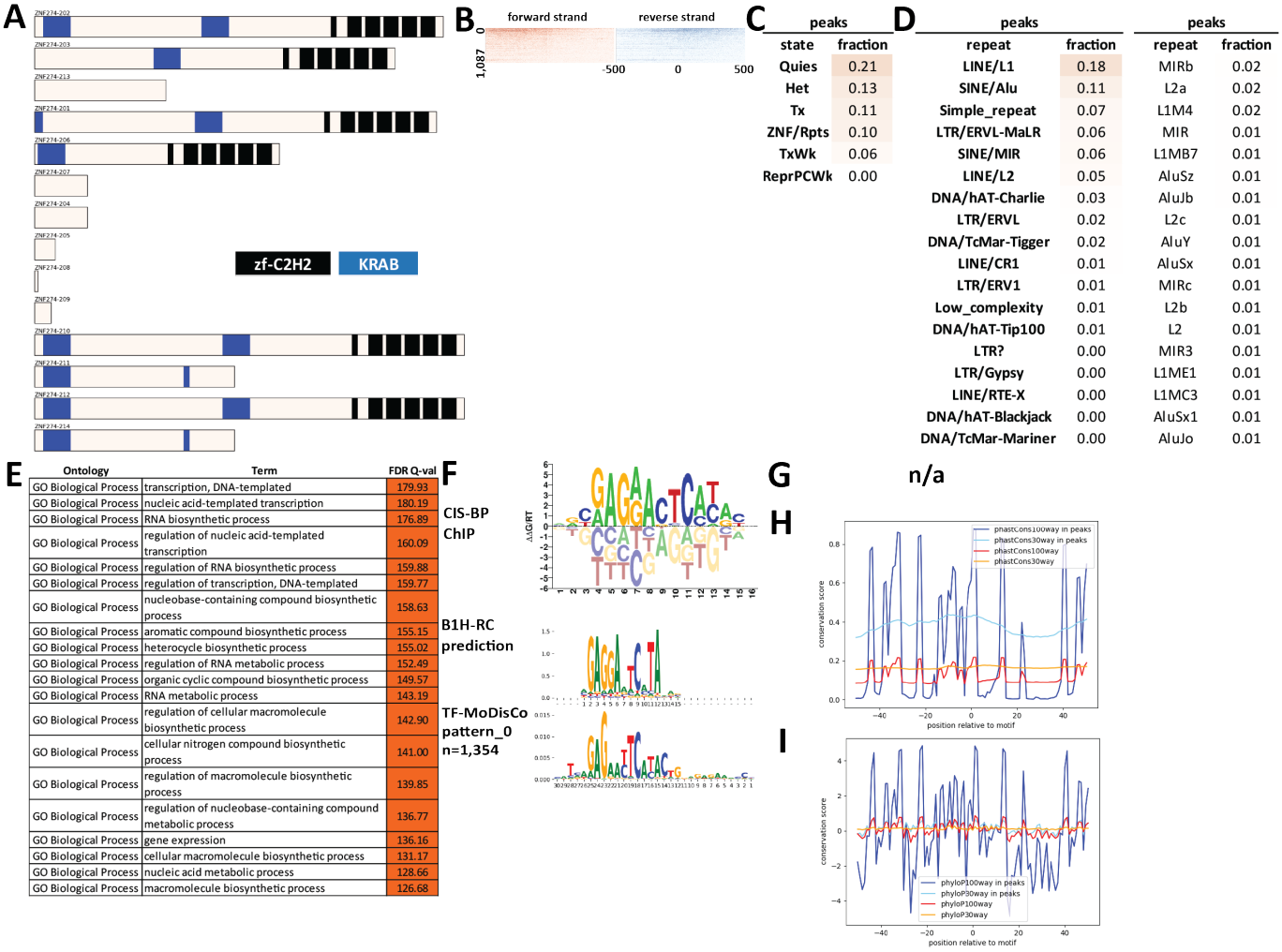

peaks	
state	fraction
Quies	0.21
Het	0.13
Tx	0.11
ZNF/Rpts	0.10
TxWk	0.06
ReprPCWk	0.00

peaks		peaks	
repeat	fraction	repeat	fraction
LINE/L1	0.18	MIRb	0.02
SINE/Alu	0.11	L2a	0.02
Simple_repeat	0.07	L1M4	0.02
LTR/ERVL-MaLR	0.06	MIR	0.01
SINE/MIR	0.06	L1MB7	0.01
LINE/L2	0.05	AluSz	0.01
DNA/hAT-Charlie	0.03	AluJb	0.01
LTR/ERVL	0.02	L2c	0.01
DNA/TcMar-Tigger	0.02	AluY	0.01
LINE/CR1	0.01	AluSx	0.01
LTR/ERV1	0.01	MIRc	0.01
Low_complexity	0.01	L2b	0.01
DNA/hAT-Tip100	0.01	L2	0.01
LTR?	0.00	MIR3	0.01
LTR/Gypsy	0.00	L1ME1	0.01
LINE/RTE-X	0.00	L1MC3	0.01
DNA/hAT-Blackjack	0.00	AluSx1	0.01
DNA/TcMar-Mariner	0.00	AluJo	0.01

Ontology	Term	FDR Q-val
GO Biological Process	transcription, DNA-templated	179.93
GO Biological Process	nucleic acid-templated transcription	180.19
GO Biological Process	RNA biosynthetic process	176.89
GO Biological Process	regulation of nucleic acid-templated transcription	160.09
GO Biological Process	regulation of RNA biosynthetic process	159.88
GO Biological Process	regulation of transcription, DNA-templated	159.77
GO Biological Process	nucleobase-containing compound biosynthetic process	158.63
GO Biological Process	aromatic compound biosynthetic process	155.15
GO Biological Process	heterocycle biosynthetic process	155.02
GO Biological Process	regulation of RNA metabolic process	152.49
GO Biological Process	organic cyclic compound biosynthetic process	149.57
GO Biological Process	RNA metabolic process	143.19
GO Biological Process	regulation of cellular macromolecule biosynthetic process	142.90
GO Biological Process	cellular nitrogen compound biosynthetic process	141.00
GO Biological Process	regulation of macromolecule biosynthetic process	139.85
GO Biological Process	regulation of nucleobase-containing compound metabolic process	136.77
GO Biological Process	gene expression	136.16
GO Biological Process	cellular macromolecule biosynthetic process	131.17
GO Biological Process	nucleic acid metabolic process	128.66
GO Biological Process	macromolecule biosynthetic process	126.68

Supplementary Figure 958: Properties and genomic distribution of motifs identified for the ZNF274 transcription factor in HCT116 (accession ENCSR101FJM).

TF-MoDisCO pattern_0 n=1354, CWM

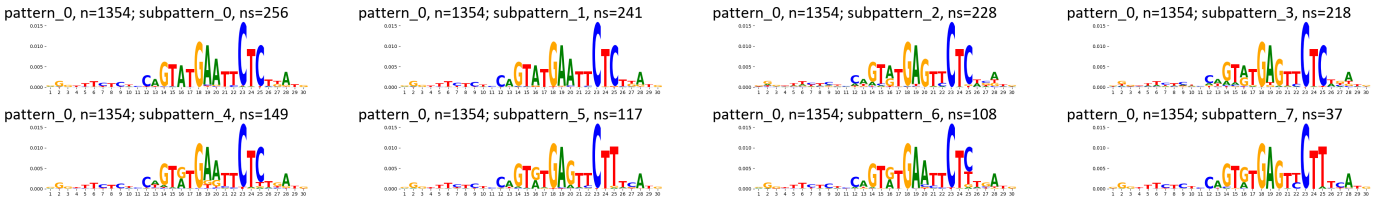

TF-MoDisCO pattern_0 n=1354, PWM

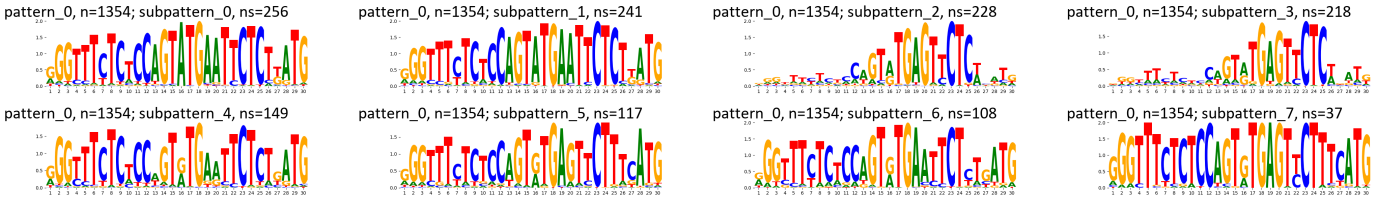

Supplementary Figure 959: TF-MoDisCO subpatterns for the ZNF274 transcription factor in HCT116 (accession ENCSR101FJM).

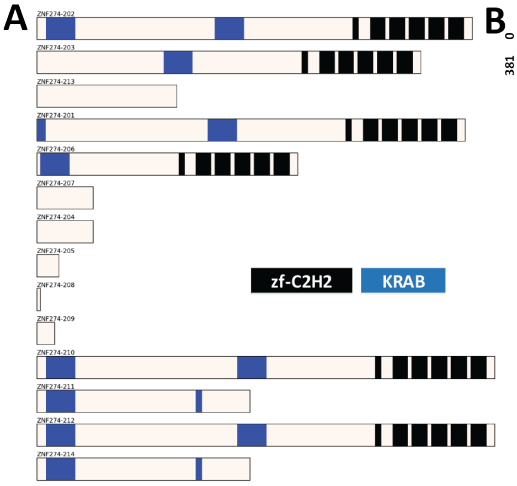

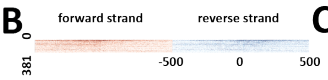

C

peaks	
state	fraction
ZNF/Rpts	0.23
Het	0.22
Quies	0.15
Tx	0.10
TxWk	0.06
ReprPCWk	0.01
ReprPC	0.01
EnhWk	0.01
TssFlnkU	0.00
TssFlnkD	0.00
TssA	0.00
EnhG1	0.00

D

peaks		peaks	
repeat	fraction	repeat	fraction
LINE/L1	0.09	L2b	0.02
LINE/L2	0.04	MIR	0.02
SINE/MIR	0.03	L1MB4	0.01
SINE/Alu	0.03	MIRb	0.01
LTR/ERVL-MaLR	0.03	L2c	0.01
Simple_repeat	0.03	L2	0.01
DNA/hAT-Charlie	0.02	L1M4	0.01
LINE/CR1	0.01	AluJb	0.01
DNA/hAT-Tip100	0.01	L3b	0.01
LTR/ERVL	0.00	L1ME1	0.01
LTR/ERV1	0.00	MLT1C	0.01
DNA?	0.00	MLT1A1	0.01
DNA/hAT-Blackjack	0.00	MIRc	0.01
DNA/TcMar-Tigger	0.00	MER5B	0.01
DNA/TcMar-Mariner	0.00	L1ME3Cz	0.01
DNA	0.00	L1ME3A	0.01
		L1ME3	0.01
		L1M5	0.01

E

Ontology	Term	FDR Q-val
GO Biological Process	transcription, DNA-templated	110.76
GO Biological Process	nucleic acid-templated transcription	111.04
GO Biological Process	RNA biosynthetic process	108.49
GO Biological Process	nucleobase-containing compound biosynthetic process	99.13
GO Biological Process	heterocycle biosynthetic process	97.13
GO Biological Process	aromatic compound biosynthetic process	96.62
GO Biological Process	RNA metabolic process	94.27
GO Biological Process	organic cyclic compound biosynthetic process	94.04
GO Biological Process	regulation of transcription, DNA-templated	93.46
GO Biological Process	regulation of nucleic acid-templated transcription	93.06
GO Biological Process	regulation of RNA biosynthetic process	92.96
GO Biological Process	gene expression	92.75
GO Biological Process	cellular nitrogen compound biosynthetic process	90.47
GO Biological Process	regulation of RNA metabolic process	89.28
GO Biological Process	nucleic acid metabolic process	86.55
GO Biological Process	regulation of cellular macromolecule biosynthetic process	85.38
GO Biological Process	regulation of macromolecule biosynthetic process	83.36
GO Biological Process	regulation of nucleobase-containing compound metabolic process	82.69
GO Biological Process	cellular macromolecule biosynthetic process	81.17
GO Biological Process	macromolecule biosynthetic process	79.36

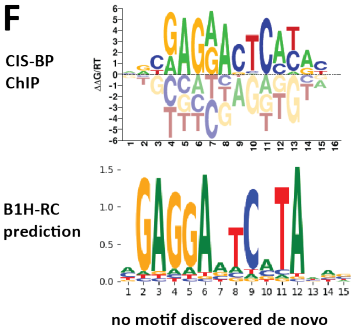

Supplementary Figure 960: Properties and genomic distribution of motifs identified for the ZNF274 transcription factor in HEK293 (accession ENCSR000FCI).

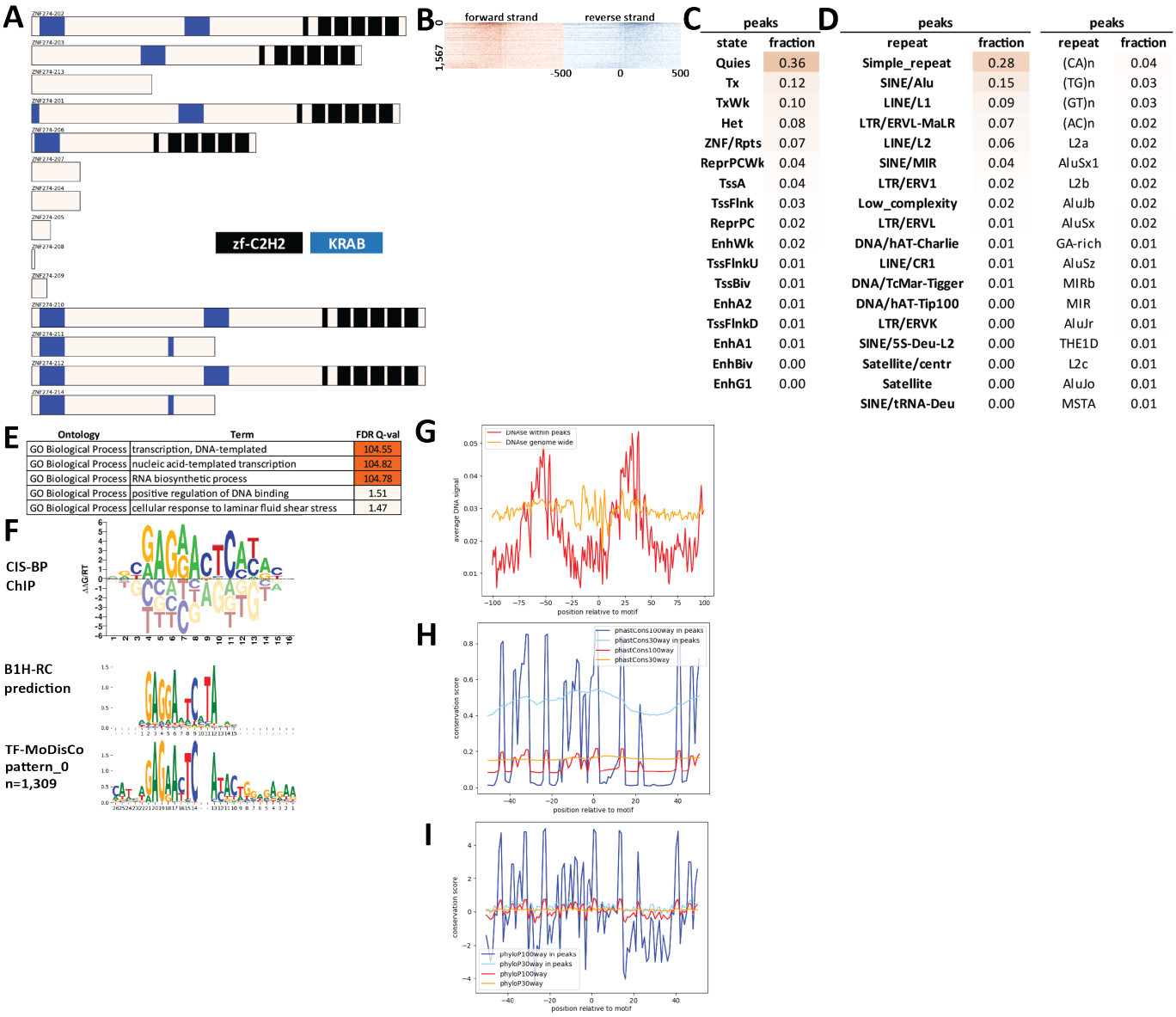

Supplementary Figure 961: Properties and genomic distribution of motifs identified for the ZNF274 transcription factor in HEK293 (accession ENCSR178QVJ).

TF-MoDisCO pattern_0 n=1309, CWM

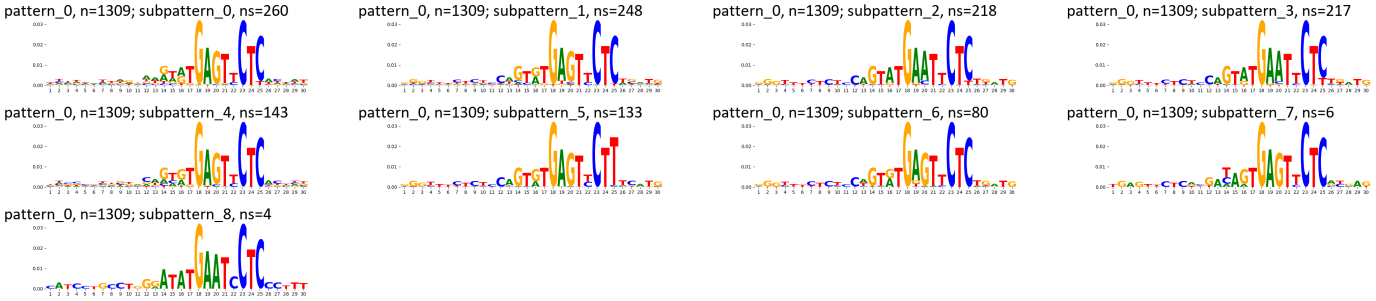

TF-MoDisCO pattern_0 n=1309, PWM

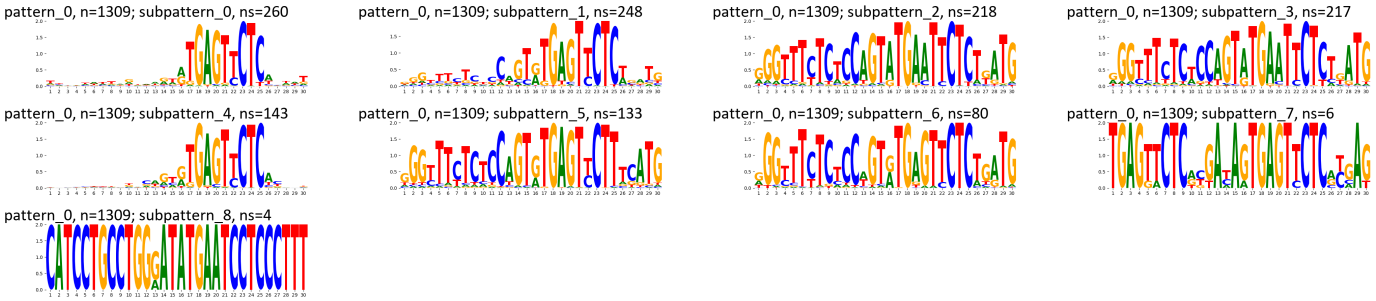

Supplementary Figure 962: TF-MoDisCO subpatterns for the ZNF274 transcription factor in HEK293 (accession ENCSR178QVJ).

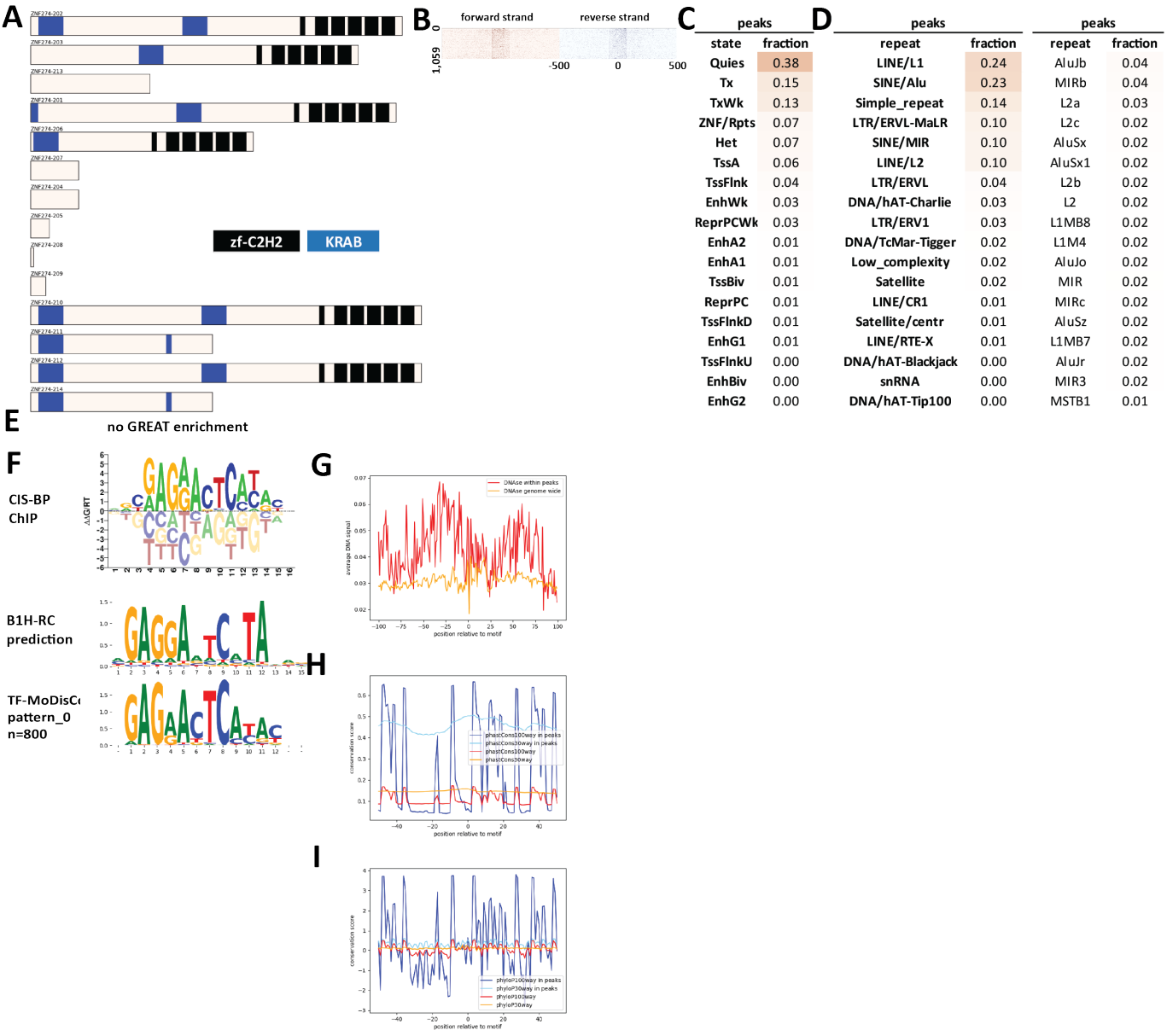

Supplementary Figure 963: Properties and genomic distribution of motifs identified for the ZNF274 transcription factor in HEK293 (accession ChipExo models).

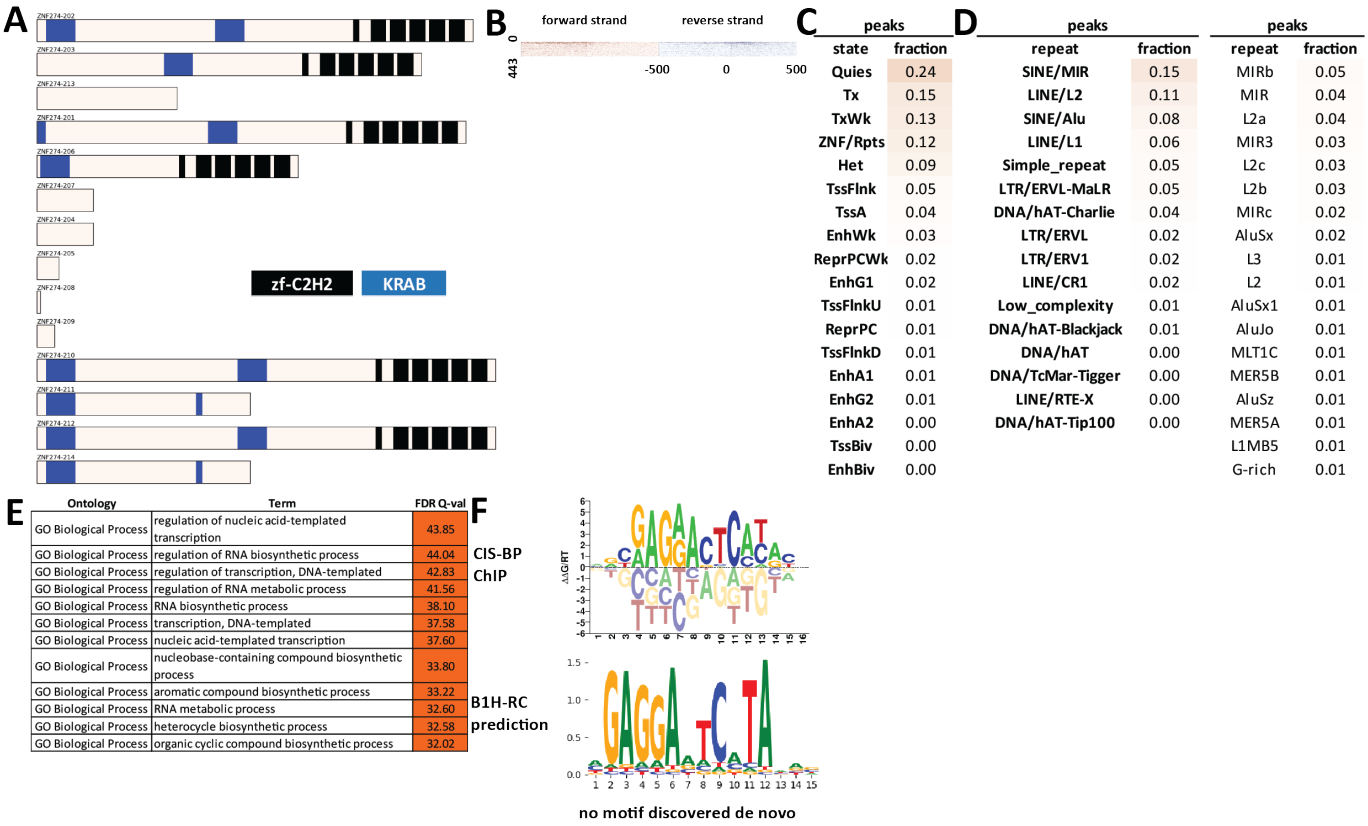

Supplementary Figure 964: Properties and genomic distribution of motifs identified for the ZNF274 transcription factor in HeLa-S3 (accession ENCSR000EVG).

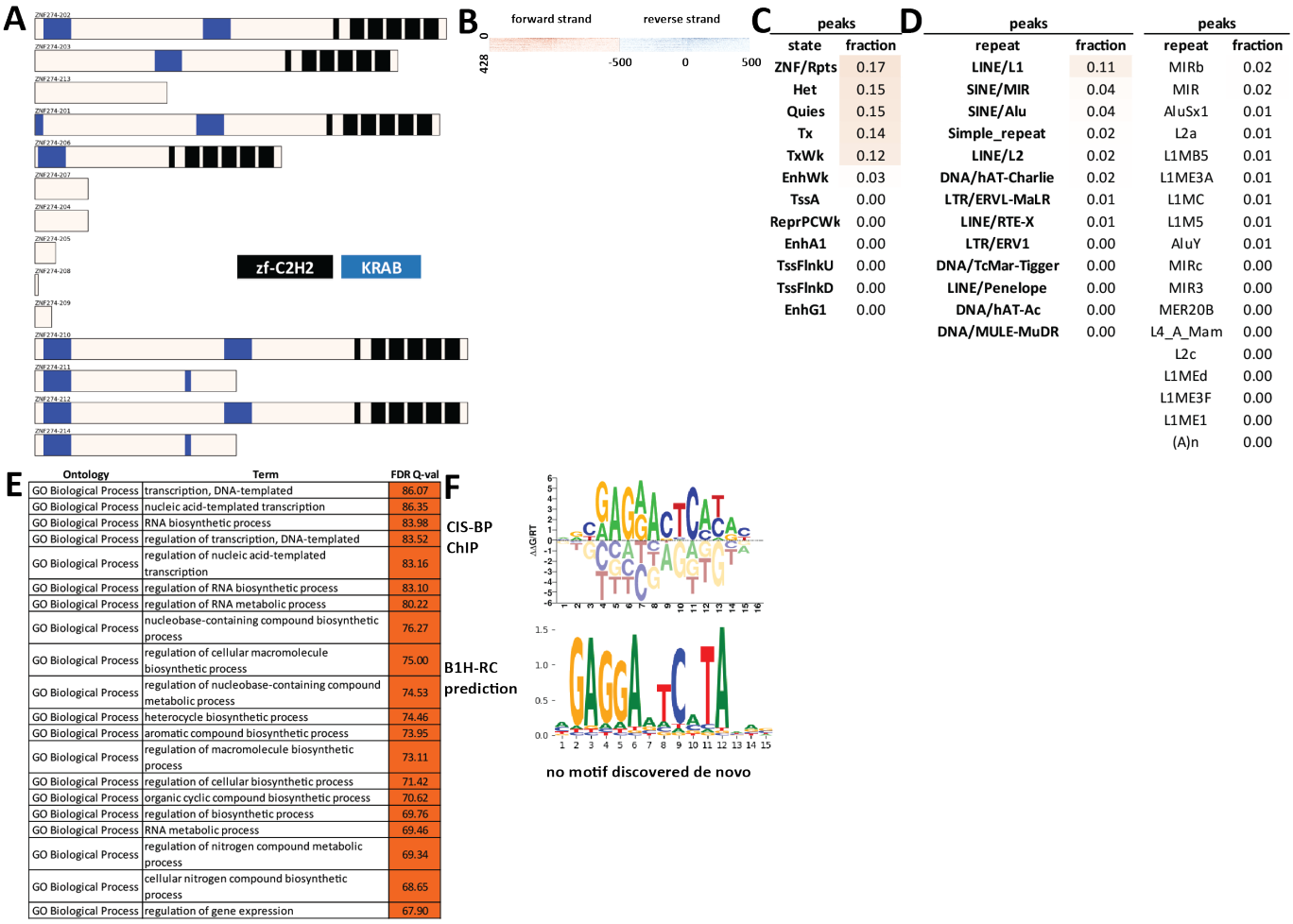

Supplementary Figure 965: Properties and genomic distribution of motifs identified for the ZNF274 transcription factor in HepG2 (accession ENCSR000EVR).

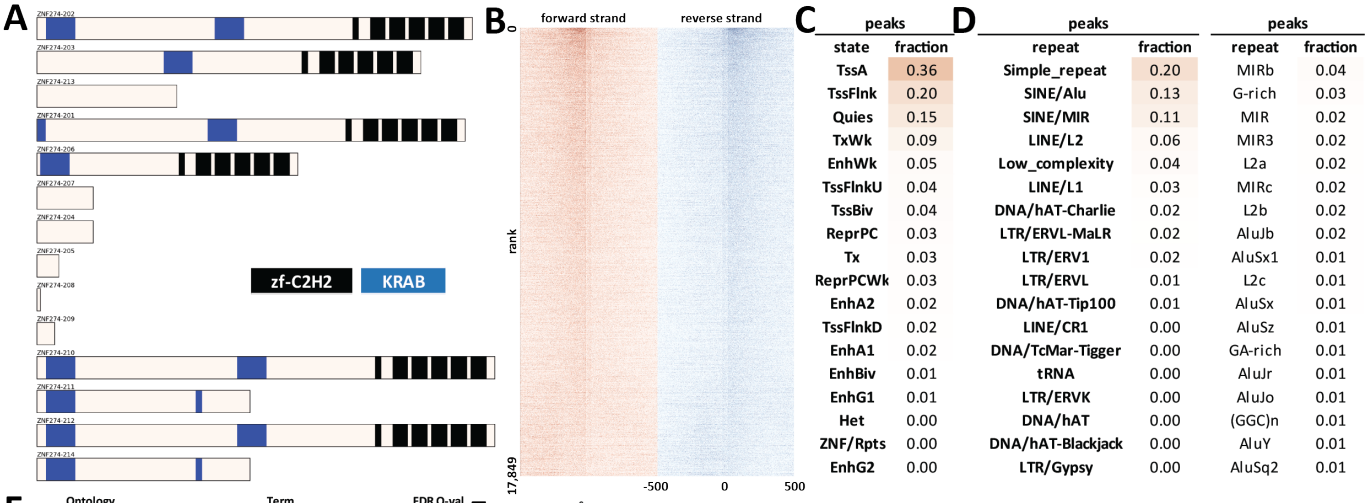

peaks	
state	fraction
TssA	0.36
TssFlnk	0.20
Quies	0.15
TxWk	0.09
EnhWk	0.05
TssFlnkU	0.04
TssBiv	0.04
ReprPC	0.03
Tx	0.03
ReprPCWk	0.03
EnhA2	0.02
TssFlnkD	0.02
EnhA1	0.02
EnhBiv	0.01
EnhG1	0.01
Het	0.00
ZNF/Rpts	0.00
EnhG2	0.00

peaks		peaks	
repeat	fraction	repeat	fraction
Simple_repeat	0.20	MIRb	0.04
SINE/Alu	0.13	G-rich	0.03
SINE/MIR	0.11	MIR	0.02
LINE/L2	0.06	MIR3	0.02
Low_complexity	0.04	L2a	0.02
LINE/L1	0.03	MIRc	0.02
DNA/hAT-Charlie	0.02	L2b	0.02
LTR/ERVL-MaLR	0.02	AluJb	0.02
LTR/ERV1	0.02	AluSx1	0.01
LTR/ERVL	0.01	L2c	0.01
DNA/hAT-Tip100	0.01	AluSx	0.01
LINE/CR1	0.00	AluSz	0.01
DNA/TcMar-Tigger	0.00	GA-rich	0.01
tRNA	0.00	AluJr	0.01
LTR/ERVK	0.00	AluJo	0.01
DNA/hAT	0.00	(GGC)n	0.01
DNA/hAT-Blackjack	0.00	AluY	0.01
LTR/Gypsy	0.00	AluSq2	0.01

E

Ontology	Term	FDR Q-val
GO Biological Process	regulation of transcription from RNA polymerase II promoter in response to stress	57.97
GO Biological Process	regulation of DNA-templated transcription in response to stress	49.70
GO Biological Process	regulation of intrinsic apoptotic signaling pathway	49.34
GO Biological Process	negative regulation of intrinsic apoptotic signaling pathway	42.99
GO Biological Process	endoplasmic reticulum unfolded protein response	41.94
GO Biological Process	cellular response to topologically incorrect protein	38.39
GO Biological Process	regulation of nuclease activity	36.50
GO Biological Process	cellular response to unfolded protein	34.71
GO Biological Process	nuclear-transcribed mRNA catabolic process	34.45
GO Biological Process	platelet-derived growth factor receptor signaling pathway	32.78
GO Biological Process	regulation of transcription from RNA polymerase II promoter in response to hypoxia	32.66
GO Biological Process	nuclear-transcribed mRNA catabolic process, nonsense-mediated decay	28.91
GO Biological Process	mitochondrial translational termination	26.81
GO Biological Process	translational elongation	25.59
GO Biological Process	regulation of necrotic cell death	25.59
GO Biological Process	regulation of cellular amino acid metabolic process	25.14
GO Biological Process	mitochondrial translational elongation	24.65
GO Biological Process	DNA-templated transcription, elongation	24.55
GO Biological Process	cotranslational protein targeting to membrane	24.06
GO Biological Process	cellular protein complex disassembly	22.75
Human Phenotype	Exercise intolerance	12.04
Human Phenotype	Abnormal CSF metabolite level	10.71
Human Phenotype	Laryngomalacia	5.28
Human Phenotype	Increased muscle lipid content	4.97
Human Phenotype	Increased intramyocellular lipid droplets	4.58

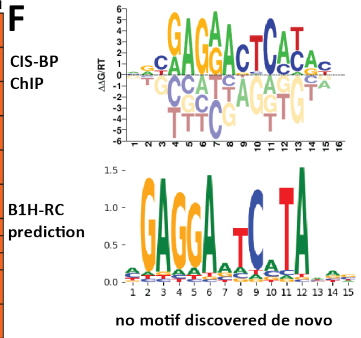

Supplementary Figure 966: Properties and genomic distribution of motifs identified for the ZNF274 transcription factor in HepG2 (accession ENCSR871VNN).

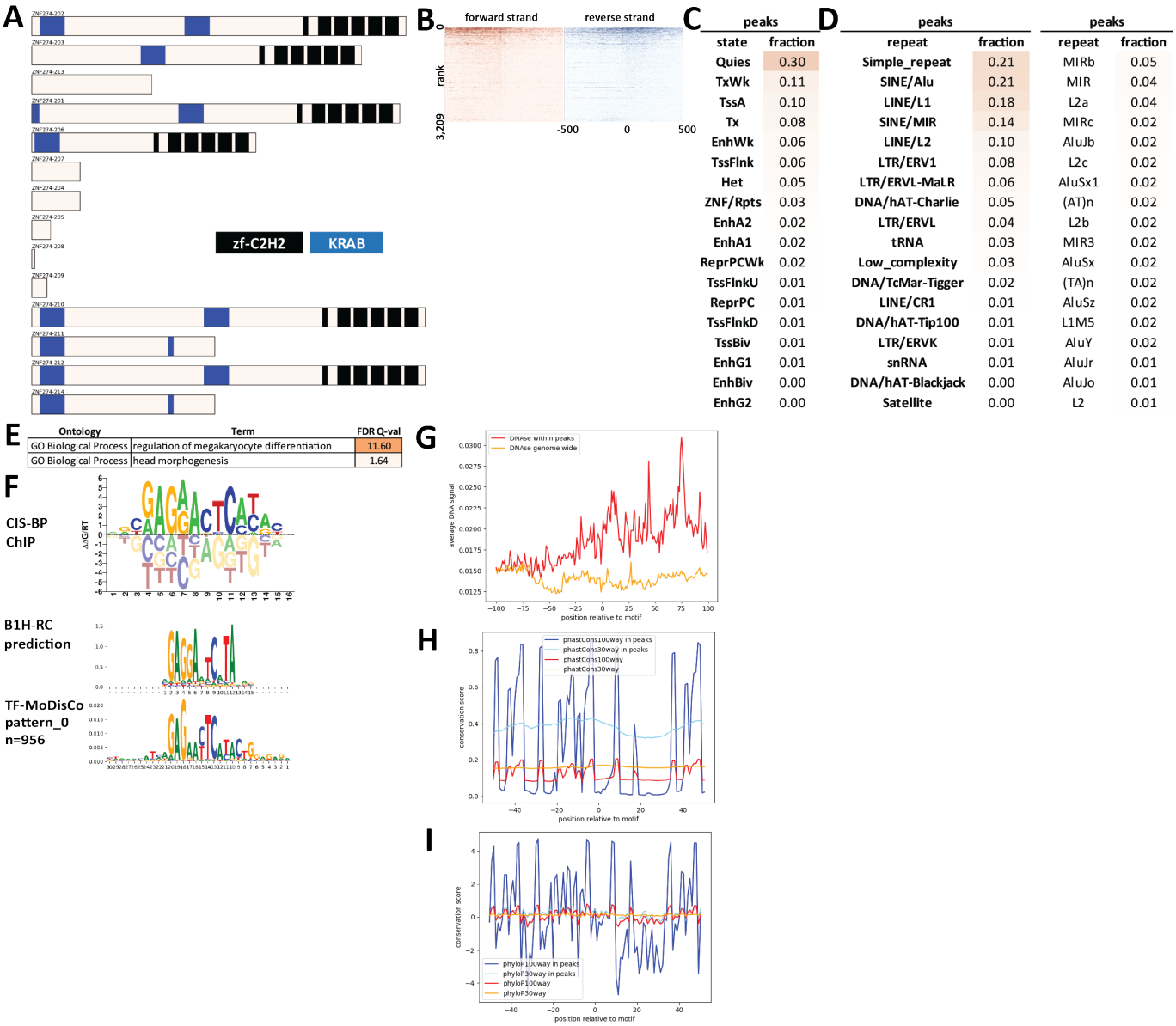

Supplementary Figure 967: Properties and genomic distribution of motifs identified for the ZNF274 transcription factor in K562 (accession ENCSR000EVX).

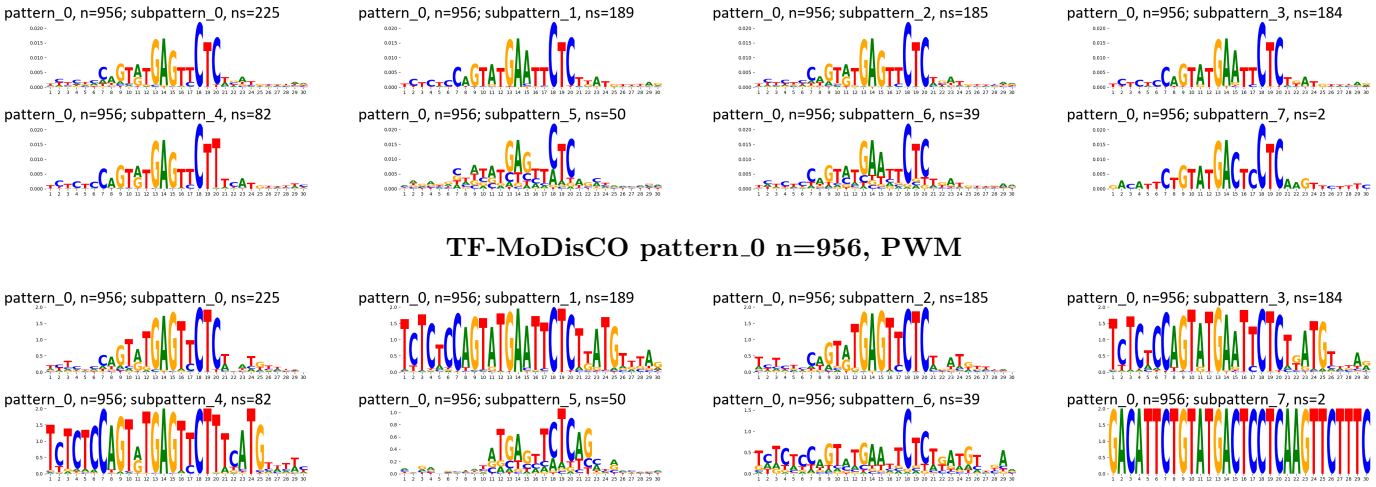

Supplementary Figure 968: TF-MoDisCO subpatterns for the ZNF274 transcription factor in K562 (accession ENCSR000EVX).

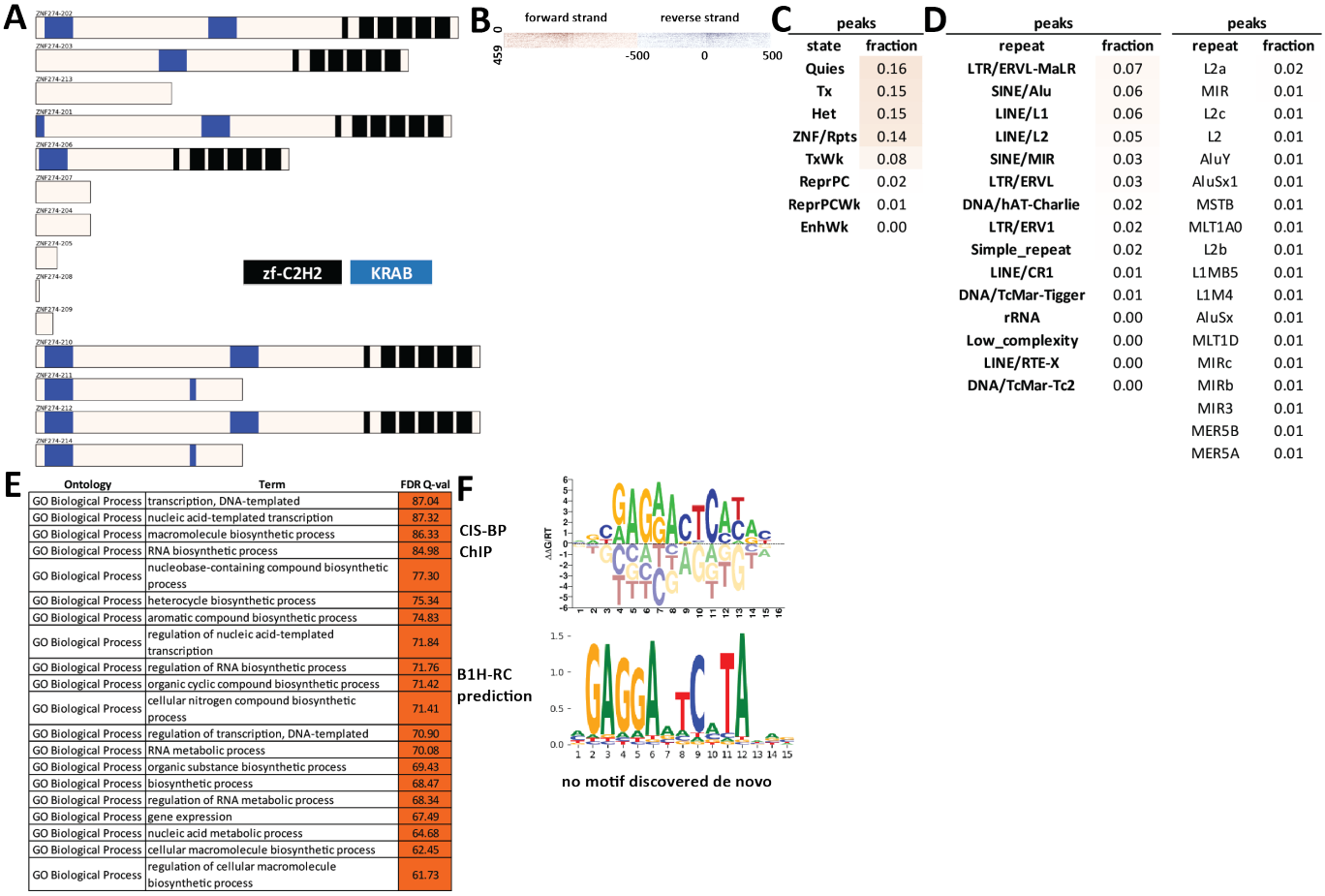

C

peaks	
state	fraction
Quies	0.16
Tx	0.15
Het	0.15
ZNF/Rpts	0.14
TxWk	0.08
ReprPC	0.02
ReprPCWk	0.01
EnhWk	0.00

D

peaks		peaks	
repeat	fraction	repeat	fraction
LTR/ERVL-MaLR	0.07	L2a	0.02
SINE/Alu	0.06	MIR	0.01
LINE/L1	0.06	L2c	0.01
LINE/L2	0.05	L2	0.01
SINE/MIR	0.03	AluY	0.01
LTR/ERVL	0.03	AluSx1	0.01
DNA/hAT-Charlie	0.02	MSTB	0.01
LTR/ERV1	0.02	MLT1A0	0.01
Simple_repeat	0.02	L2b	0.01
LINE/CR1	0.01	L1MB5	0.01
DNA/TcMar-Tigger	0.01	L1M4	0.01
rRNA	0.00	AluSx	0.01
Low_complexity	0.00	MLT1D	0.01
LINE/RTE-X	0.00	MIRc	0.01
DNA/TcMar-Tc2	0.00	MIRb	0.01
		MIR3	0.01
		MER5B	0.01
		MER5A	0.01

E

Ontology	Term	FDR Q-val
GO Biological Process	transcription, DNA-templated	87.04
GO Biological Process	nucleic acid-templated transcription	87.32
GO Biological Process	macromolecule biosynthetic process	86.33
GO Biological Process	RNA biosynthetic process	84.98
GO Biological Process	nucleobase-containing compound biosynthetic process	77.30
GO Biological Process	heterocycle biosynthetic process	75.34
GO Biological Process	aromatic compound biosynthetic process	74.83
GO Biological Process	regulation of nucleic acid-templated transcription	71.84
GO Biological Process	regulation of RNA biosynthetic process	71.76
GO Biological Process	organic cyclic compound biosynthetic process	71.42
GO Biological Process	cellular nitrogen compound biosynthetic process	71.41
GO Biological Process	regulation of transcription, DNA-templated	70.90
GO Biological Process	RNA metabolic process	70.08
GO Biological Process	organic substance biosynthetic process	69.43
GO Biological Process	biosynthetic process	68.47
GO Biological Process	regulation of RNA metabolic process	68.34
GO Biological Process	gene expression	67.49
GO Biological Process	nucleic acid metabolic process	64.68
GO Biological Process	cellular macromolecule biosynthetic process	62.45
GO Biological Process	regulation of cellular macromolecule biosynthetic process	61.73

Supplementary Figure 969: Properties and genomic distribution of motifs identified for the ZNF274 transcription factor in K562 (accession ENCSR000EWE).

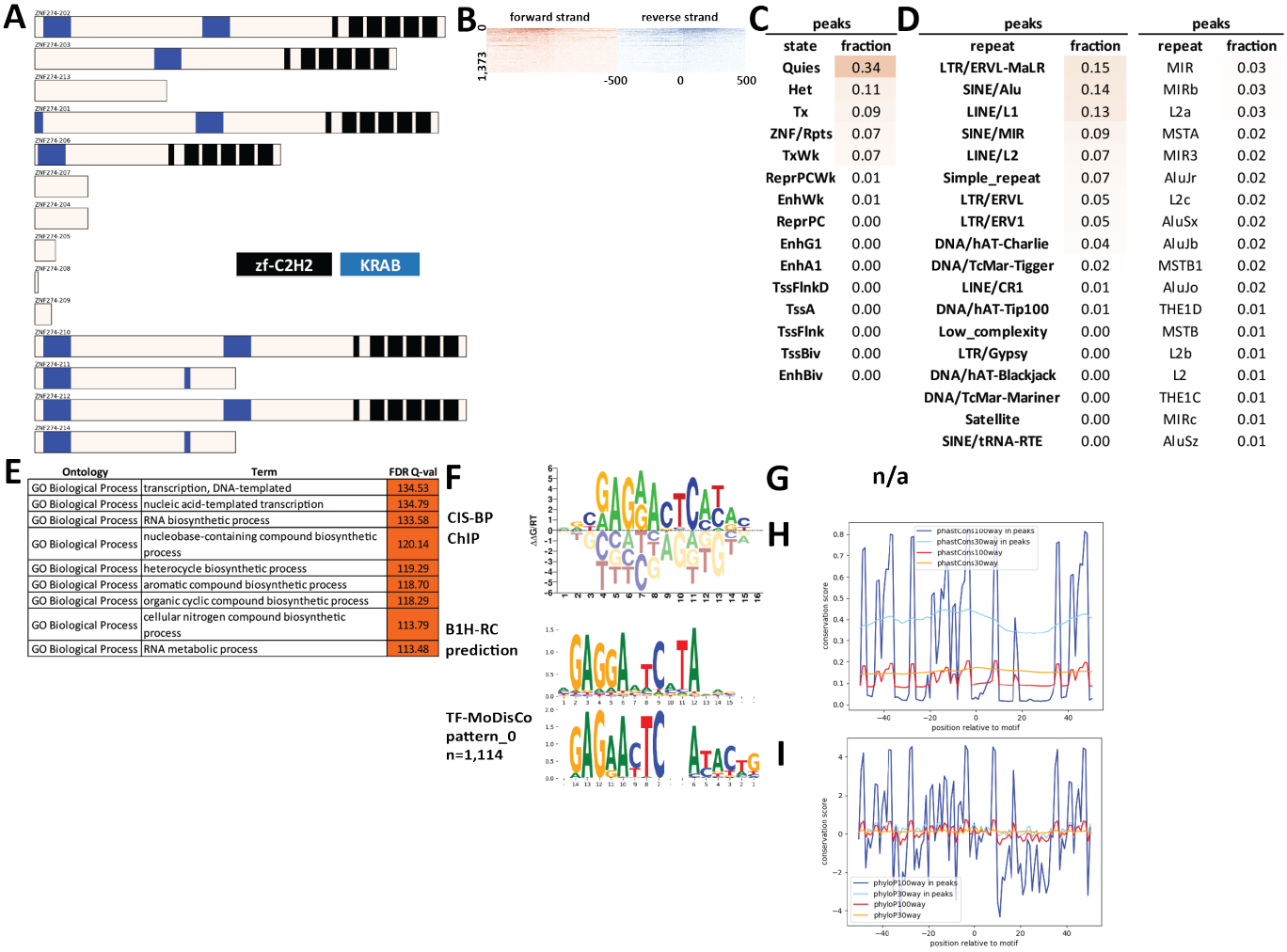

Supplementary Figure 970: Properties and genomic distribution of motifs identified for the ZNF274 transcription factor in NT2D1 (accession ENCSR000EWY).

TF-MoDisCO pattern_0 n=1114, CWM

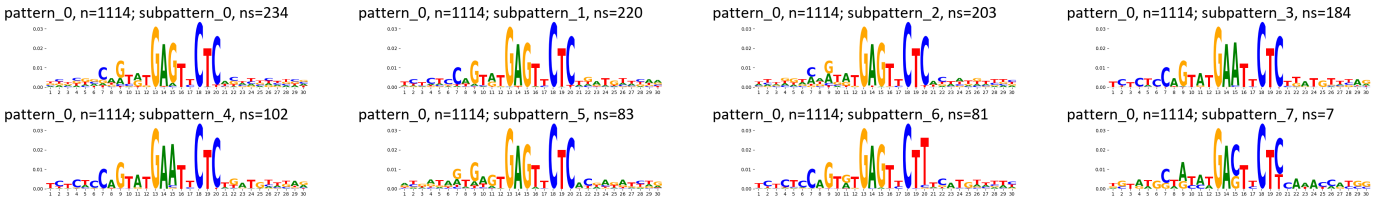

TF-MoDisCO pattern_0 n=1114, PWM

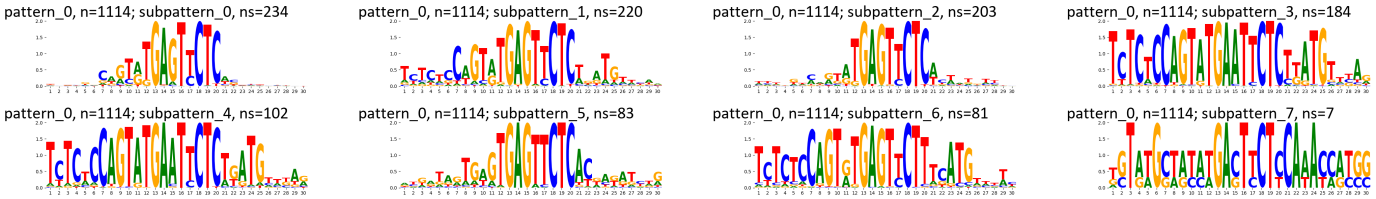

Supplementary Figure 971: TF-MoDisCO subpatterns for the ZNF274 transcription factor in NT2D1 (accession ENCSR000EWY).

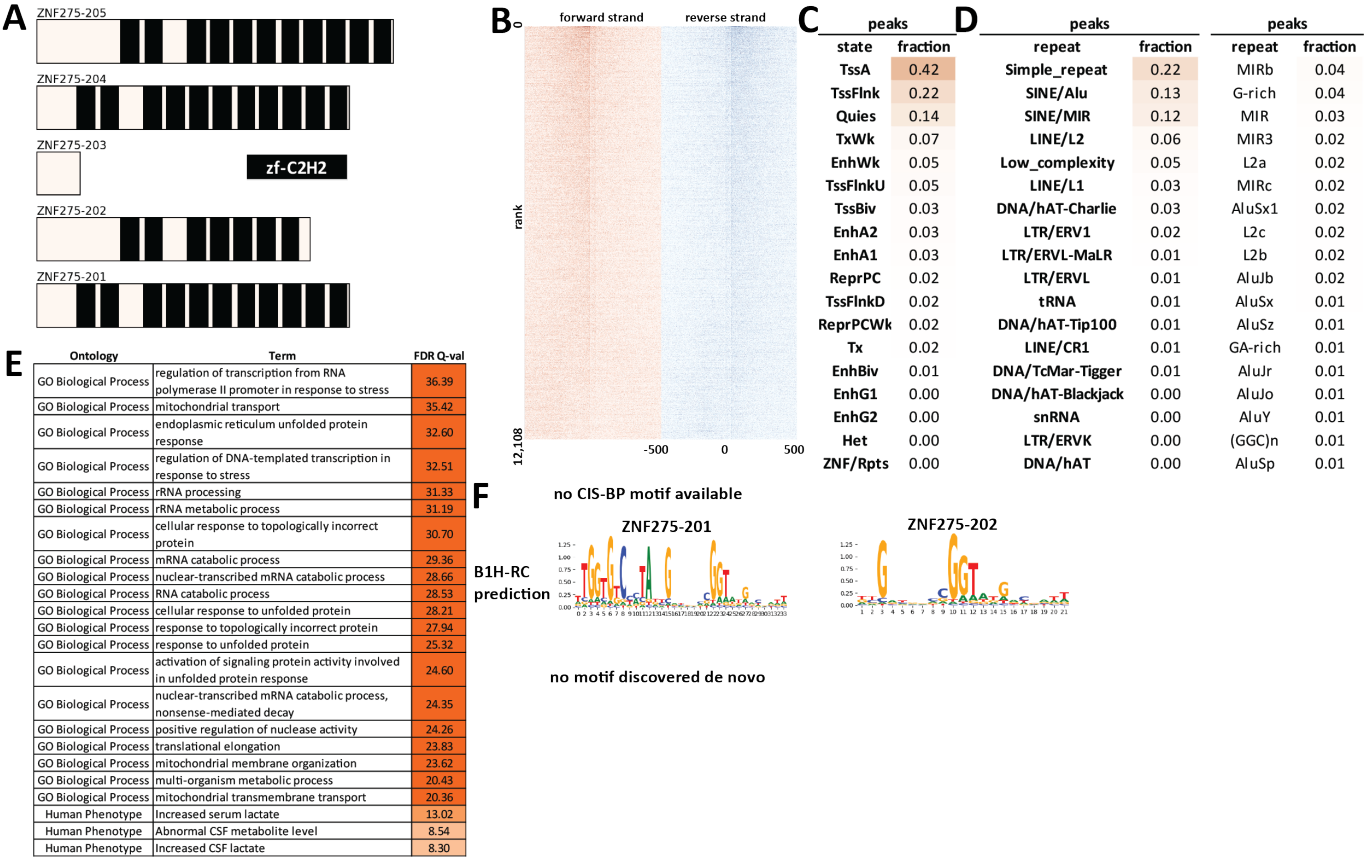

Supplementary Figure 972: Properties and genomic distribution of motifs identified for the ZNF275 transcription factor in HepG2 (accession ENCSR590BHJ).

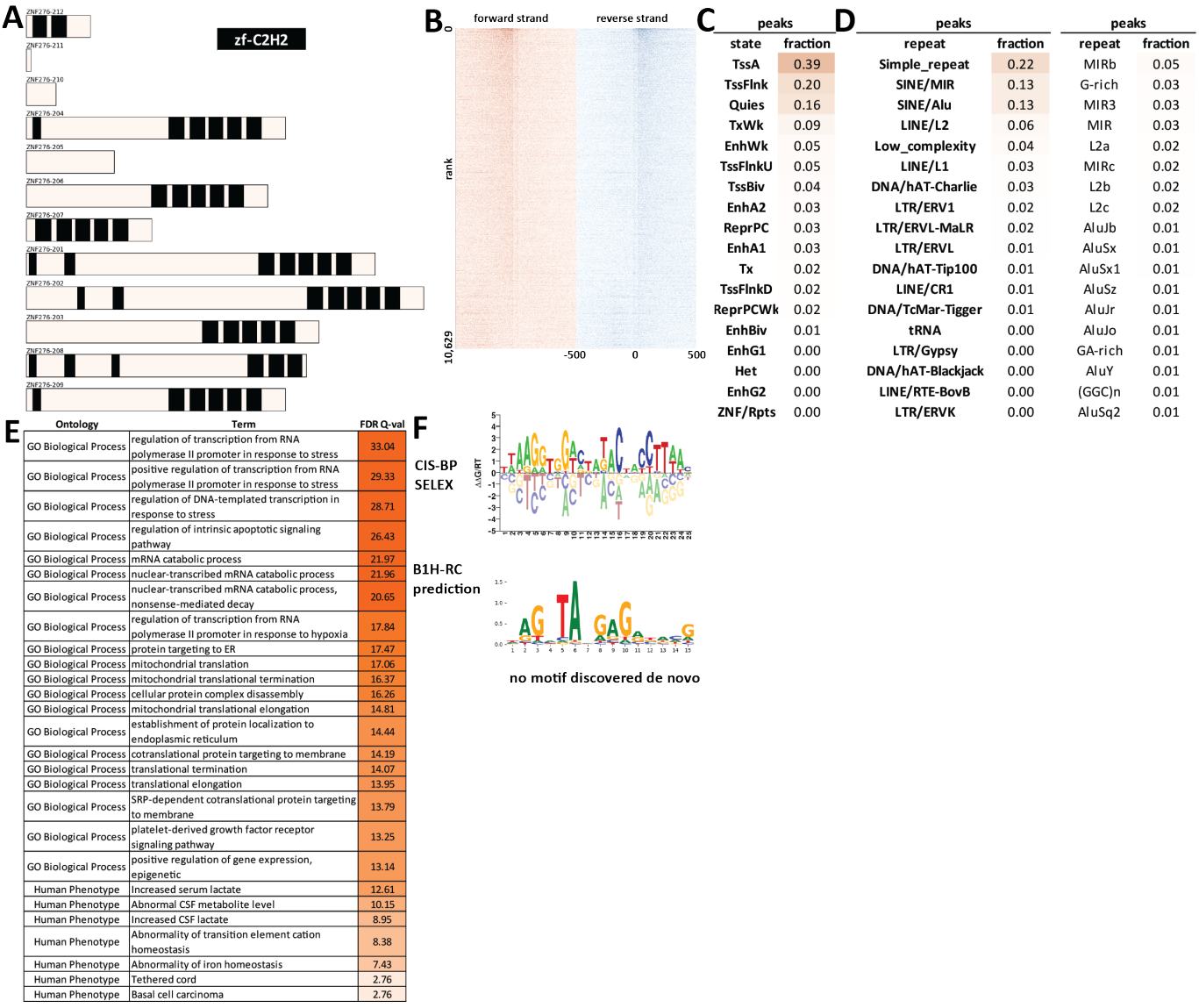

Supplementary Figure 973: Properties and genomic distribution of motifs identified for the ZNF276 transcription factor in HepG2 (accession ENCSR076KLJ).

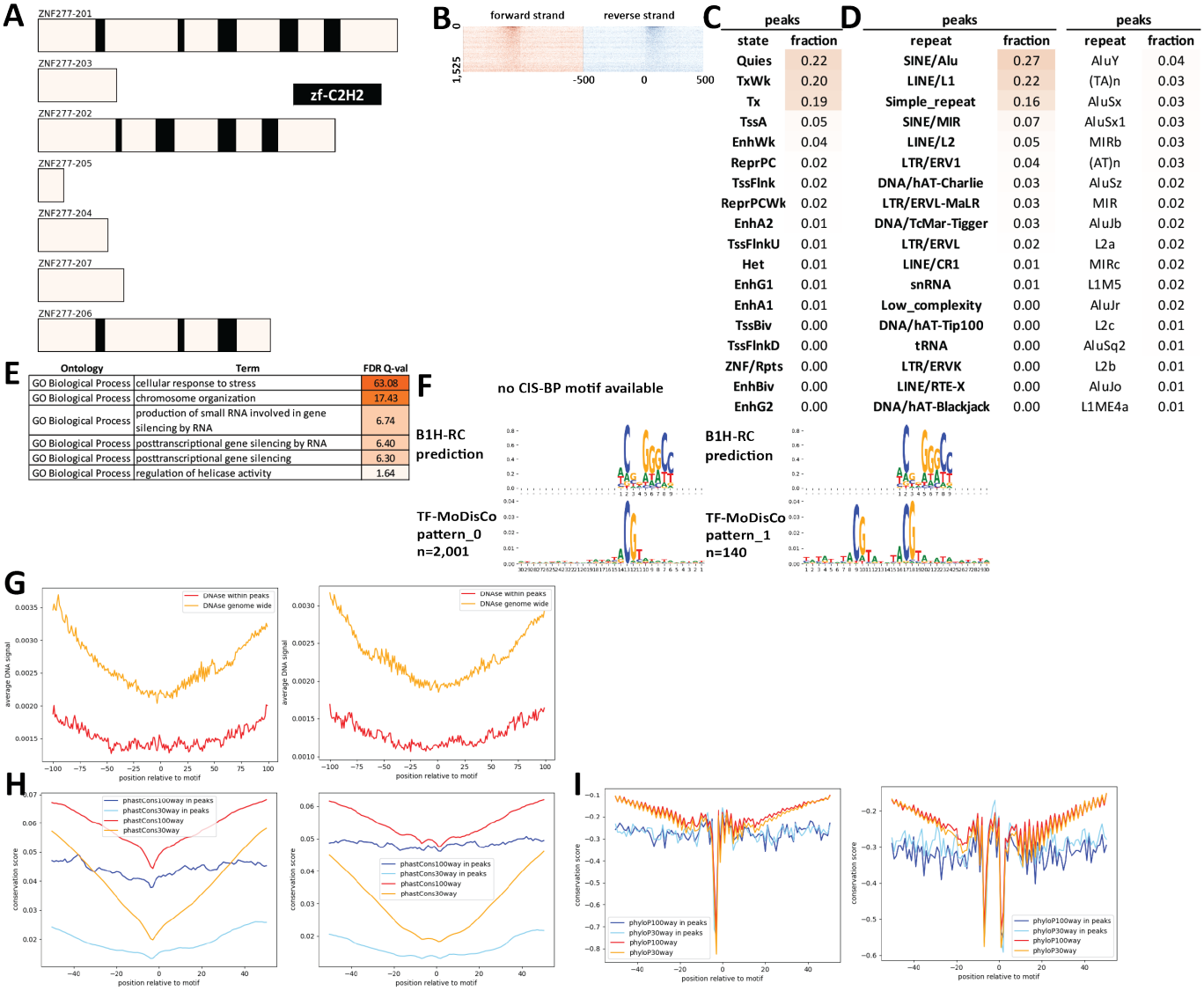

peaks	
state	fraction
Quies	0.22
TxWk	0.20
Tx	0.19
TssA	0.05
EnhWk	0.04
ReprPC	0.02
TssFlnk	0.02
ReprPCWk	0.02
EnhA2	0.01
TssFlnkU	0.01
Het	0.01
EnhG1	0.01
EnhA1	0.01
TssBiv	0.00
TssFlnkD	0.00
ZNF/Rpts	0.00
EnhBiv	0.00
EnhG2	0.00

peaks		peaks	
repeat	fraction	repeat	fraction
SINE/Alu	0.27	AluY	0.04
LINE/L1	0.22	(TA)n	0.03
Simple_repeat	0.16	AluSx	0.03
SINE/MIR	0.07	AluSx1	0.03
LINE/L2	0.05	MIRb	0.03
LTR/ERV1	0.04	(AT)n	0.03
DNA/hAT-Charlie	0.03	AluSz	0.02
LTR/ERVL-MaLR	0.03	MIR	0.02
DNA/TcMar-Tigger	0.03	AluJb	0.02
LTR/ERVL	0.02	L2a	0.02
LINE/CR1	0.01	MIRc	0.02
snRNA	0.01	L1M5	0.02
Low_complexity	0.00	AluJr	0.02
DNA/hAT-Tip100	0.00	L2c	0.01
tRNA	0.00	AluSq2	0.01
LTR/ERVK	0.00	L2b	0.01
LINE/RTE-X	0.00	AluJo	0.01
DNA/hAT-Blackjack	0.00	L1ME4a	0.01

Ontology	Term	FDR Q-val
GO Biological Process	cellular response to stress	63.08
GO Biological Process	chromosome organization	17.43
GO Biological Process	production of small RNA involved in gene silencing by RNA	6.74
GO Biological Process	posttranscriptional gene silencing by RNA	6.40
GO Biological Process	posttranscriptional gene silencing	6.30
GO Biological Process	regulation of helicase activity	1.64

Supplementary Figure 974: Properties and genomic distribution of motifs identified for the ZNF277 transcription factor in K562 (accession ENCSR358PJI).

TF-MoDisCO pattern_0 n=2001, CWM

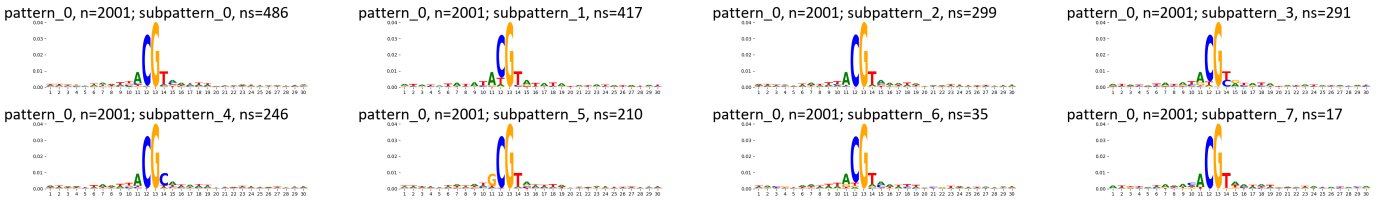

TF-MoDisCO pattern_0 n=2001, PWM

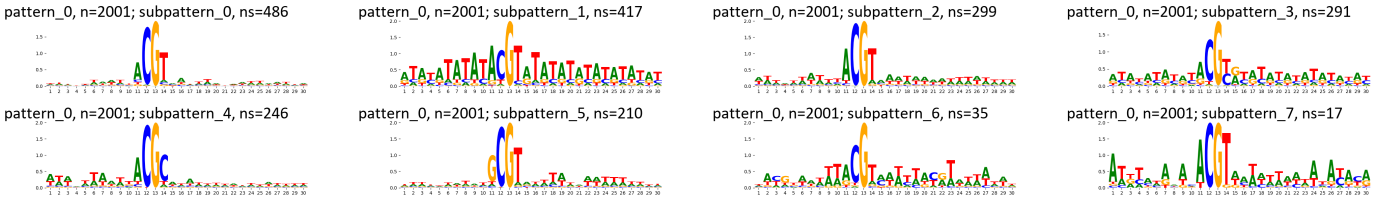

TF-MoDisCO pattern_1 n=140, CWM

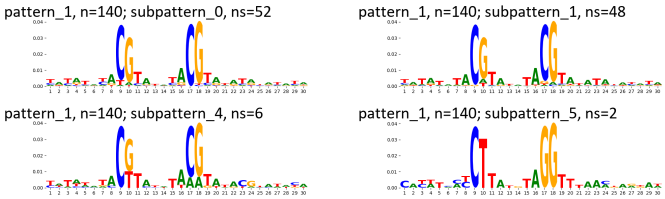

TF-MoDisCO pattern_1 n=140, PWM

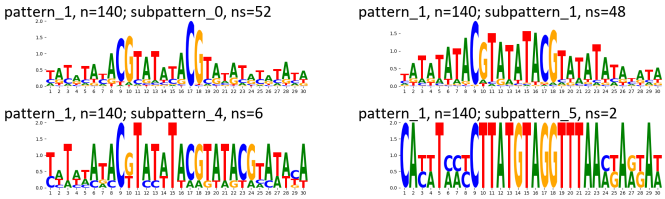

Supplementary Figure 975: TF-MoDisCO subpatterns for the ZNF277 transcription factor in K562 (accession ENCSR358PJI).

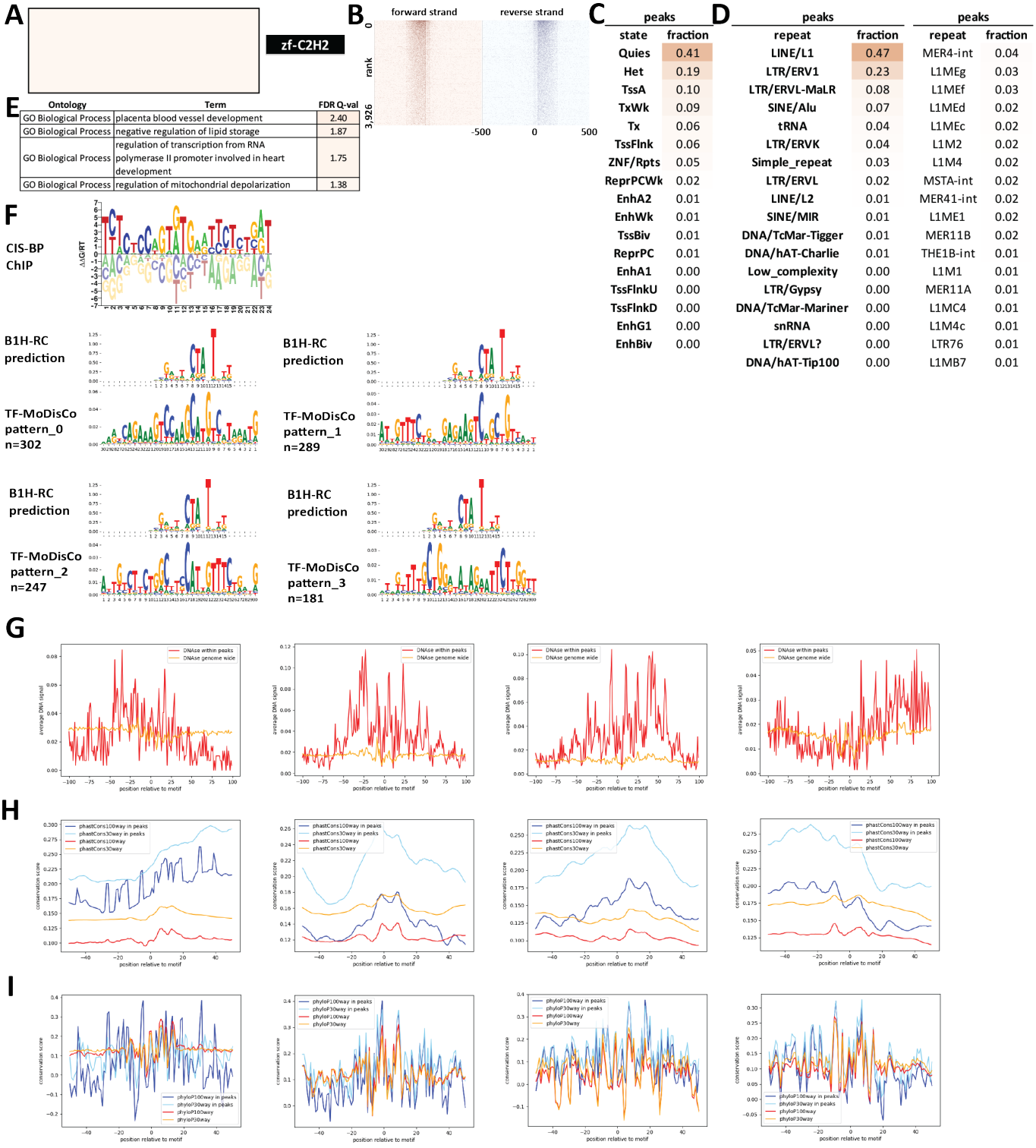

Supplementary Figure 976: Properties and genomic distribution of motifs identified for the ZNF280A transcription factor in HEK293 (accession Hughes GR models).

TF-MoDisCO pattern_0 n=302, CWM

pattern_0, n=302; subpattern_0, ns=94

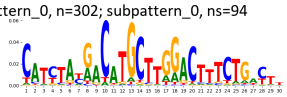

pattern_0, n=302; subpattern_1, ns=82

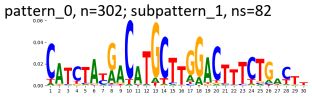

pattern_0, n=302; subpattern_2, ns=56

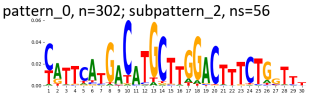

pattern_0, n=302; subpattern_3, ns=55

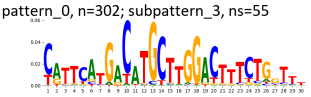

pattern_0, n=302; subpattern_4, ns=6

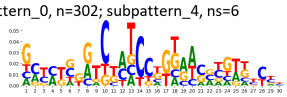

pattern_0, n=302; subpattern_5, ns=4

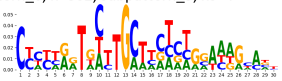

pattern_0, n=302; subpattern_6, ns=3

pattern_0, n=302; subpattern_7, ns=2

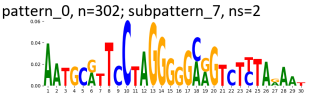

TF-MoDisCO pattern_0 n=302, PWM

pattern_0, n=302; subpattern_0, ns=94

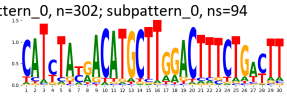

pattern_0, n=302; subpattern_1, ns=82

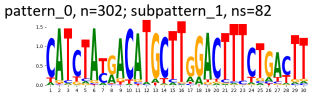

pattern_0, n=302; subpattern_2, ns=56

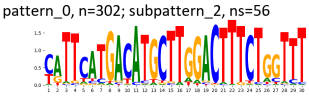

pattern_0, n=302; subpattern_3, ns=55

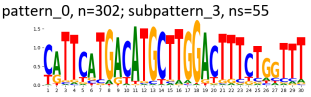

pattern_0, n=302; subpattern_4, ns=6

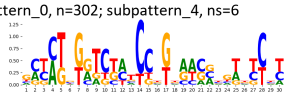

pattern_0, n=302; subpattern_5, ns=4

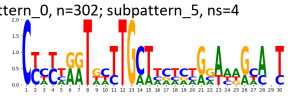

pattern_0, n=302; subpattern_6, ns=3

pattern_0, n=302; subpattern_7, ns=2

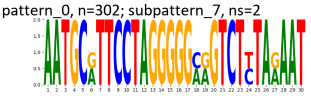

TF-MoDisCO pattern_1 n=289, CWM

pattern_1, n=289; subpattern_0, ns=129

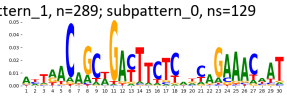

pattern_1, n=289; subpattern_1, ns=126

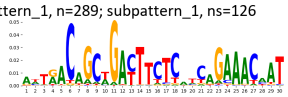

pattern_1, n=289; subpattern_2, ns=30

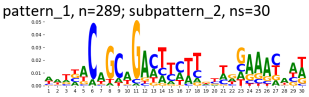

pattern_1, n=289; subpattern_3, ns=4

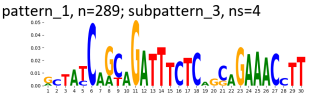

TF-MoDisCO pattern_1 n=289, PWM

pattern_1, n=289; subpattern_0, ns=129

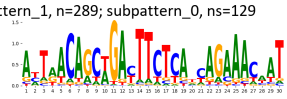

pattern_1, n=289; subpattern_1, ns=126

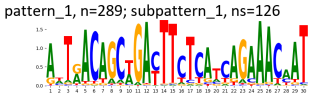

pattern_1, n=289; subpattern_2, ns=30

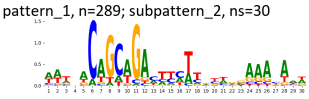

pattern_1, n=289; subpattern_3, ns=4

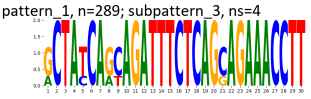

TF-MoDisCO pattern_2 n=247, CWM

pattern_2, n=247; subpattern_0, ns=106

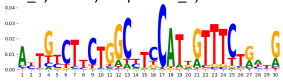

pattern_2, n=247; subpattern_1, ns=84

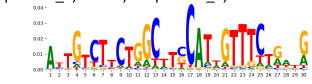

pattern_2, n=247; subpattern_2, ns=53

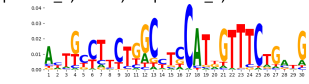

pattern_2, n=247; subpattern_3, ns=2

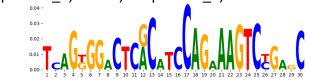

pattern_2, n=247; subpattern_4, ns=2

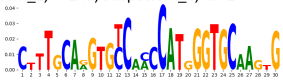

TF-MoDisCO pattern_2 n=247, PWM

pattern_2, n=247; subpattern_0, ns=106

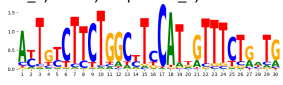

pattern_2, n=247; subpattern_1, ns=84

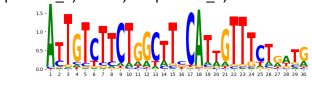

pattern_2, n=247; subpattern_2, ns=53

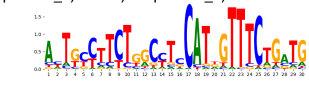

pattern_2, n=247; subpattern_3, ns=2

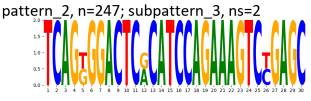

pattern_2, n=247; subpattern_4, ns=2

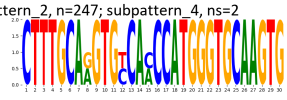

TF-MoDisCO pattern_3 n=181, CWM

pattern_3, n=181; subpattern_0, ns=68

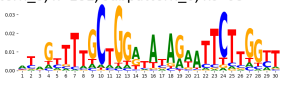

pattern_3, n=181; subpattern_1, ns=61

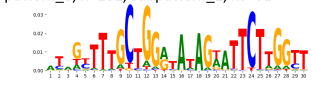

pattern_3, n=181; subpattern_2, ns=33

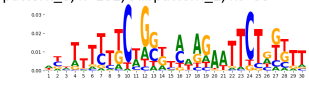

pattern_3, n=181; subpattern_3, ns=19

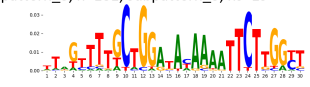

TF-MoDisCO pattern_3 n=181, PWM

pattern_3, n=181; subpattern_0, ns=68

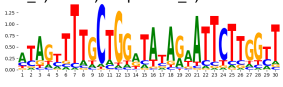

pattern_3, n=181; subpattern_1, ns=61

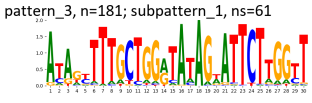

pattern_3, n=181; subpattern_2, ns=33

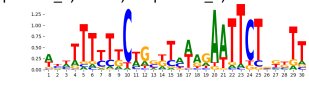

pattern_3, n=181; subpattern_3, ns=19

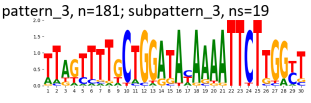

Supplementary Figure 977: TF-MoDisCO subpatterns for the ZNF280A transcription factor in HEK293 (accession Hughes GR models).

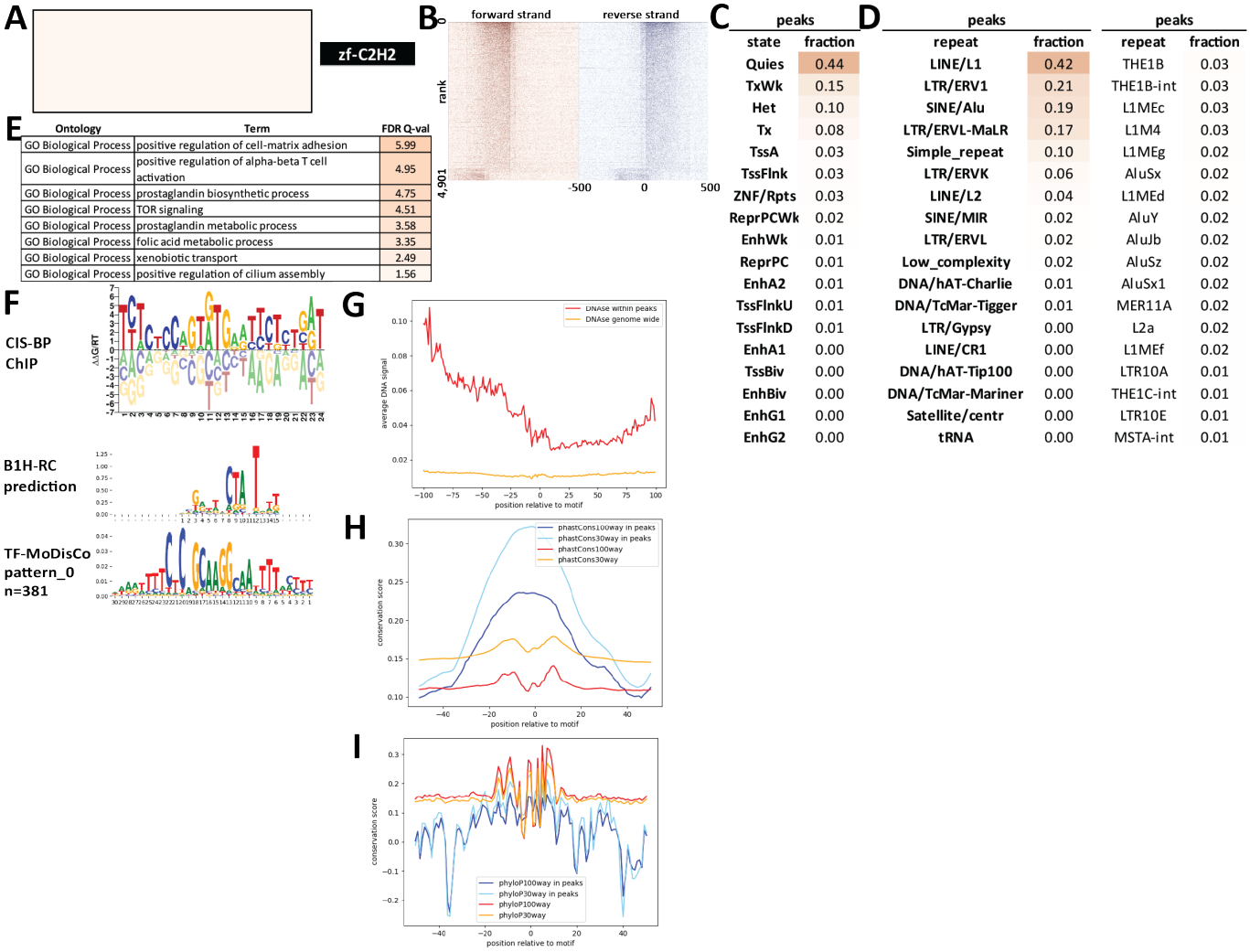

Ontology	Term	FDR Q-val
GO Biological Process	positive regulation of cell-matrix adhesion	5.99
GO Biological Process	positive regulation of alpha-beta T cell activation	4.95
GO Biological Process	prostaglandin biosynthetic process	4.75
GO Biological Process	TOR signaling	4.51
GO Biological Process	prostaglandin metabolic process	3.58
GO Biological Process	folic acid metabolic process	3.35
GO Biological Process	xenobiotic transport	2.49
GO Biological Process	positive regulation of cilium assembly	1.56

peaks	
state	fraction
Quies	0.44
TxWk	0.15
Het	0.10
Tx	0.08
TssA	0.03
TssFlnk	0.03
ZNF/Rpts	0.03
ReprPCWk	0.02
EnhWk	0.01
ReprPC	0.01
EnhA2	0.01
TssFlnkU	0.01
TssFlnkD	0.01
EnhA1	0.00
TssBiv	0.00
EnhBiv	0.00
EnhG1	0.00
EnhG2	0.00

peaks		peaks	
repeat	fraction	repeat	fraction
LINE/L1	0.42	THE1B	0.03
LTR/ERV1	0.21	THE1B-int	0.03
SINE/Alu	0.19	L1MEc	0.03
LTR/ERVL-MaLR	0.17	L1M4	0.03
Simple_repeat	0.10	L1MEg	0.02
LTR/ERVK	0.06	AluSx	0.02
LINE/L2	0.04	L1MEd	0.02
SINE/MIR	0.02	AluY	0.02
LTR/ERVL	0.02	AluJb	0.02
Low_complexity	0.02	AluSz	0.02
DNA/hAT-Charlie	0.01	AluSx1	0.02
DNA/TcMar-Tigger	0.01	MER11A	0.02
LTR/Gypsy	0.00	L2a	0.02
LINE/CR1	0.00	L1MEf	0.02
DNA/hAT-Tip100	0.00	LTR10A	0.01
DNA/TcMar-Mariner	0.00	THE1C-int	0.01
Satellite/centr	0.00	LTR10E	0.01
tRNA	0.00	MSTA-int	0.01

Supplementary Figure 978: Properties and genomic distribution of motifs identified for the ZNF280A transcription factor in K562 (accession ENCSR370NFS).

A

B

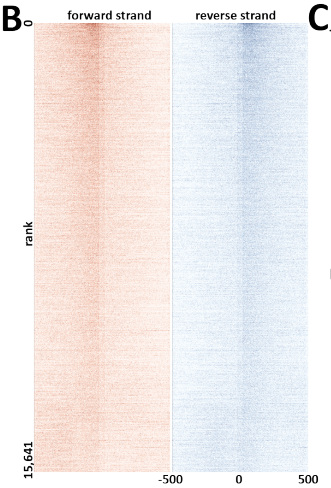

C

peaks	
state	fraction
TssA	0.36
TssFlnk	0.19
Quies	0.16
TxWk	0.09
TssBiv	0.04
TssFlnkU	0.04
EnhWk	0.04
Tx	0.03
ReprPC	0.03
ReprPCWk	0.03
EnhA2	0.02
TssFlnkD	0.02
EnhA1	0.02
EnhG1	0.01
EnhBiv	0.01
Het	0.00
EnhG2	0.00
ZNF/Rpts	0.00

D

peaks		peaks	
repeat	fraction	repeat	fraction
Simple_repeat	0.17	MIRb	0.03
SINE/Alu	0.12	G-rich	0.03
SINE/MIR	0.10	MIR3	0.02
LINE/L2	0.05	L2a	0.02
Low_complexity	0.04	MIR	0.02
LINE/L1	0.03	MIRc	0.02
LTR/ERVL-MaLR	0.02	L2b	0.02
LTR/ERV1	0.02	AluSx1	0.02
DNA/hAT-Charlie	0.02	AluSx	0.01
LTR/ERVL	0.01	AluJb	0.01
DNA/hAT-Tip100	0.01	L2c	0.01
LTR/ERVK	0.01	AluSz	0.01
LINE/CR1	0.00	AluY	0.01
tRNA	0.00	GA-rich	0.01
DNA/TcMar-Tigger	0.00	AluJr	0.01
Retroposon/SVA	0.00	AluJo	0.01
LTR/Gypsy	0.00	AluSq2	0.01
DNA/hAT-Blackjack	0.00	AluSp	0.01

E

Ontology	Term	FDR Q-val
GO Biological Process	regulation of transcription from RNA polymerase II promoter in response to stress	46.03
GO Biological Process	regulation of DNA-templated transcription in response to stress	40.83
GO Biological Process	regulation of intrinsic apoptotic signaling pathway	40.74
GO Biological Process	negative regulation of intrinsic apoptotic signaling pathway	36.35
GO Biological Process	DNA-templated transcription, elongation	30.53
GO Biological Process	regulation of transcription from RNA polymerase II promoter in response to hypoxia	28.61
GO Biological Process	endoplasmic reticulum unfolded protein response	27.43
GO Biological Process	transcription elongation from RNA polymerase II promoter	25.78
GO Biological Process	cellular response to topologically incorrect protein	25.14
GO Biological Process	regulation of hematopoietic progenitor cell differentiation	24.97
GO Biological Process	regulation of cellular amino acid metabolic process	24.30
GO Biological Process	cellular response to epidermal growth factor stimulus	23.71
GO Biological Process	cellular response to unfolded protein	22.64
GO Biological Process	response to epidermal growth factor	22.25
GO Biological Process	cellular protein complex disassembly	20.95
GO Biological Process	translational elongation	20.74
GO Biological Process	mitochondrial translational termination	20.50
GO Biological Process	regulation of hematopoietic stem cell differentiation	20.48
GO Biological Process	anaphase-promoting complex-dependent catabolic process	20.43
GO Biological Process	mitochondrial translational elongation	20.34
Human Phenotype	Increased serum lactate	14.75
Human Phenotype	External ophthalmoplegia	7.98
Human Phenotype	Abnormality of glycolysis	3.25
Human Phenotype	Increased serum pyruvate	2.53

F

no CIS-BP motif available

B1H-RC prediction

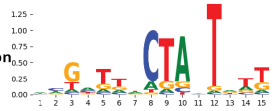

no motif discovered de novo

Supplementary Figure 979: Properties and genomic distribution of motifs identified for the ZNF280B transcription factor in HepG2 (accession ENCSR940EZR).

A

B

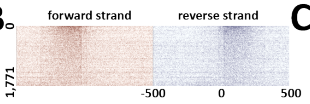

C

peaks	
state	fraction
Quies	0.36
TxWk	0.12
TssA	0.10
Tx	0.07
Het	0.06
TssFlnk	0.03
EnhA2	0.02
EnhWk	0.02
ZNF/Rpts	0.02
ReprPCWk	0.02
EnhA1	0.01
TssFlnkU	0.01
ReprPC	0.01
EnhG1	0.01
TssFlnkD	0.01
EnhG2	0.00
TssBiv	0.00
EnhBiv	0.00

D

peaks		peaks	
repeat	fraction	repeat	fraction
LINE/L1	0.31	MER41B	0.04
LTR/ERV1	0.28	L1M4	0.02
SINE/Alu	0.13	L2a	0.02
Simple_repeat	0.06	MER41A	0.02
LTR/ERVL-MaLR	0.05	LTR76	0.02
LINE/L2	0.05	L1M2	0.02
LTR/ERVK	0.04	AluSx1	0.01
SINE/MIR	0.03	AluJb	0.01
DNA/hAT-Charlie	0.02	MIRb	0.01
LTR/ERVL	0.02	MER11A	0.01
DNA/TcMar-Tigger	0.02	L1M1	0.01
snRNA	0.02	L1MEg	0.01
Low_complexity	0.01	L1MB7	0.01
LINE/CR1	0.01	AluSx	0.01
Retroposon/SVA	0.00	L2c	0.01
LTR/ERVL?	0.00	AluSp	0.01
LINE/RTE-X	0.00	MER41-int	0.01
DNA/hAT-Tip100	0.00	AluJr	0.01

E

Ontology	Term	FDR Q-val
GO Biological Process	regulation of synaptic vesicle transport	3.15

F

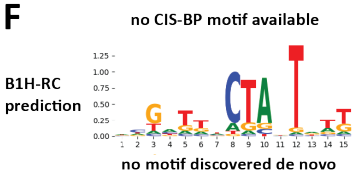

Supplementary Figure 980: Properties and genomic distribution of motifs identified for the ZNF280B transcription factor in K562 (accession ENCSR775FSH).

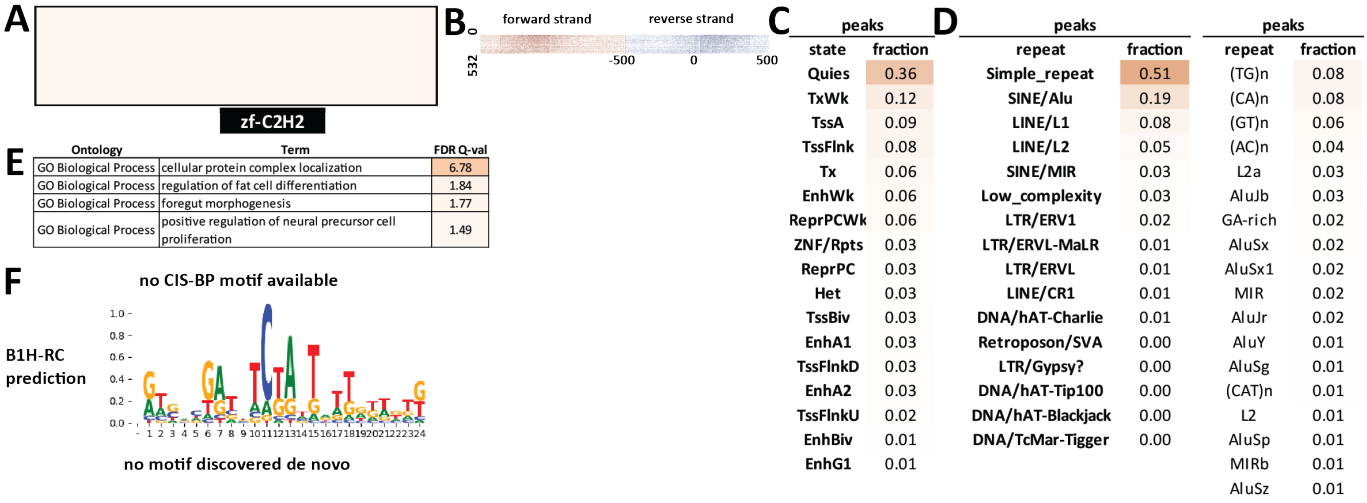

Supplementary Figure 981: Properties and genomic distribution of motifs identified for the ZNF280C transcription factor in HEK293 (accession ENCSR076KZW).

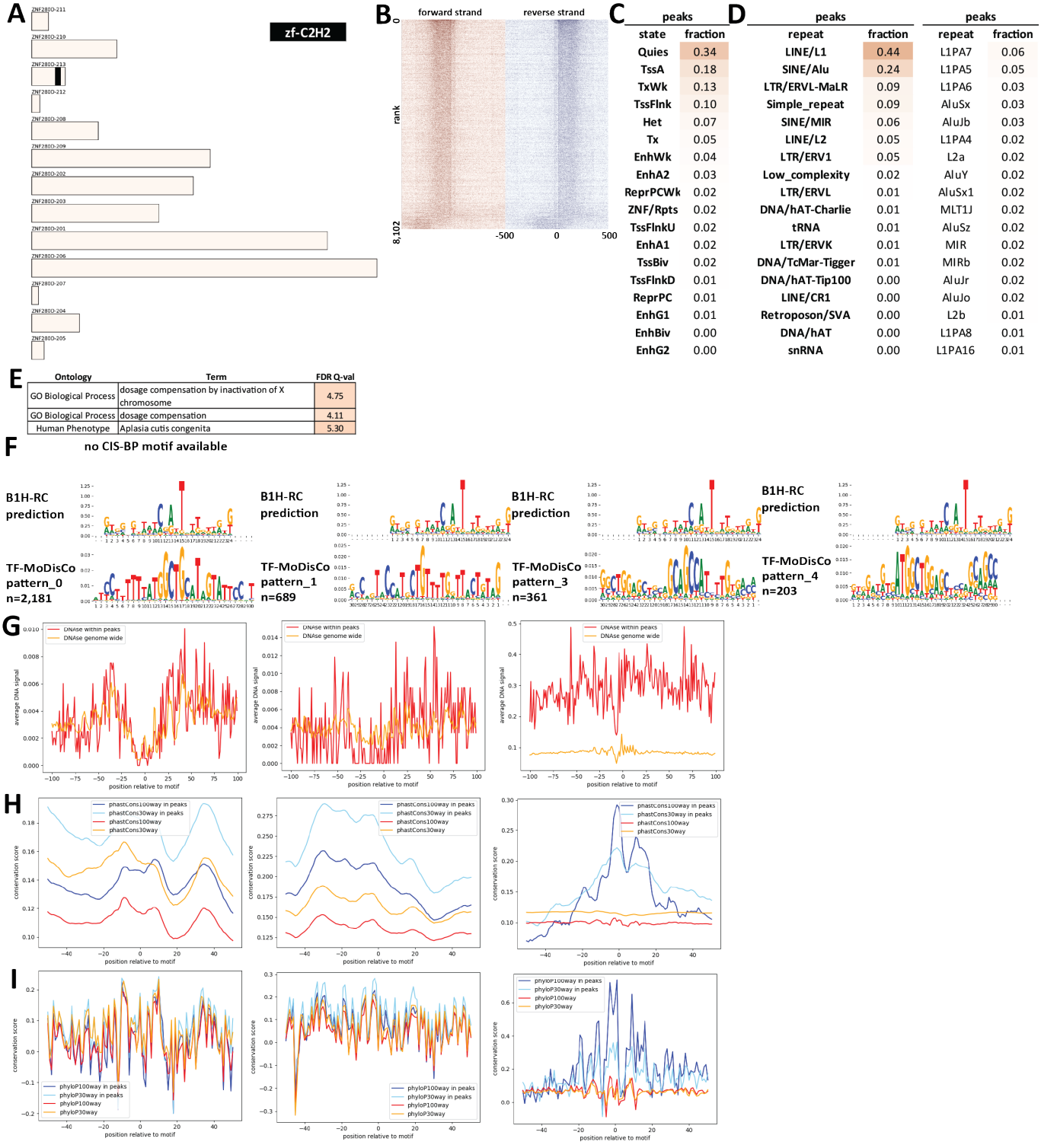

Supplementary Figure 982: Properties and genomic distribution of motifs identified for the ZNF280D transcription factor in HEK293 (accession ENCSR451CYX).

TF-MoDisCO pattern_0 n=2181, CWM

pattern_0, n=2181; subpattern_0, ns=626

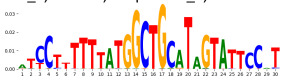

pattern_0, n=2181; subpattern_1, ns=552

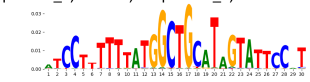

pattern_0, n=2181; subpattern_2, ns=251

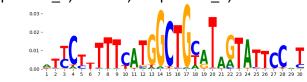

pattern_0, n=2181; subpattern_3, ns=245

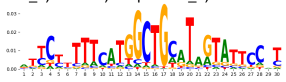

pattern_0, n=2181; subpattern_4, ns=220

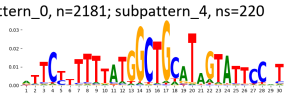

pattern_0, n=2181; subpattern_5, ns=155

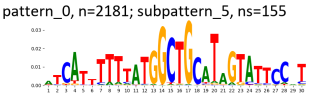

pattern_0, n=2181; subpattern_6, ns=112

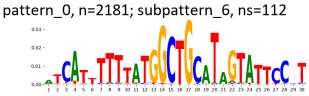

pattern_0, n=2181; subpattern_7, ns=18

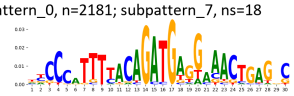

pattern_0, n=2181; subpattern_8, ns=2

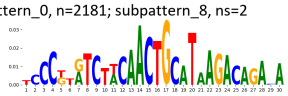

TF-MoDisCO pattern_0 n=2181, PWM

pattern_0, n=2181; subpattern_0, ns=626

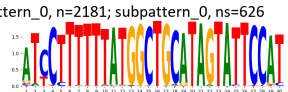

pattern_0, n=2181; subpattern_1, ns=552

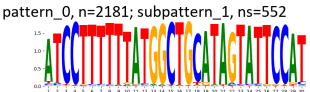

pattern_0, n=2181; subpattern_2, ns=251

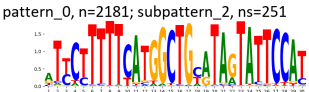

pattern_0, n=2181; subpattern_3, ns=245

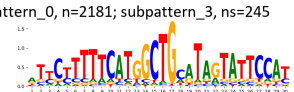

pattern_0, n=2181; subpattern_4, ns=220

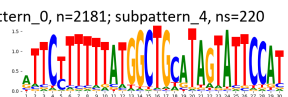

pattern_0, n=2181; subpattern_5, ns=155

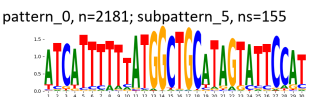

pattern_0, n=2181; subpattern_6, ns=112

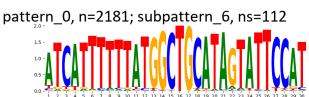

pattern_0, n=2181; subpattern_7, ns=18

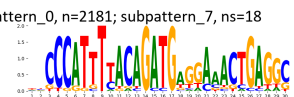

pattern_0, n=2181; subpattern_8, ns=2

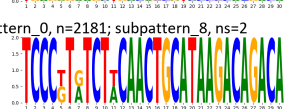

TF-MoDisCO pattern_1 n=689, CWM

pattern_1, n=689; subpattern_0, ns=186

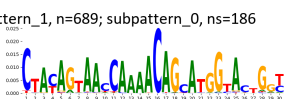

pattern_1, n=689; subpattern_1, ns=180

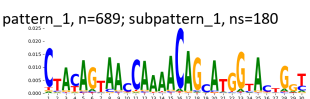

pattern_1, n=689; subpattern_2, ns=176

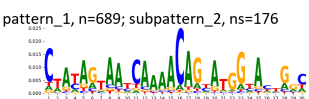

pattern_1, n=689; subpattern_3, ns=129

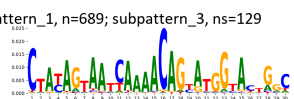

pattern_1, n=689; subpattern_4, ns=7

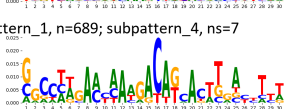

pattern_1, n=689; subpattern_5, ns=5

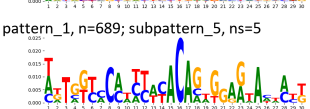

pattern_1, n=689; subpattern_6, ns=4

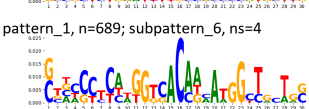

pattern_1, n=689; subpattern_7, ns=2

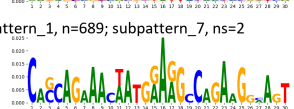

TF-MoDisCO pattern_1 n=689, PWM

pattern_1, n=689; subpattern_0, ns=186

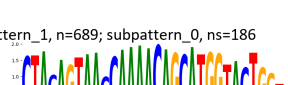

pattern_1, n=689; subpattern_1, ns=180

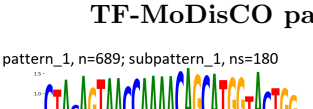

pattern_1, n=689; subpattern_2, ns=176

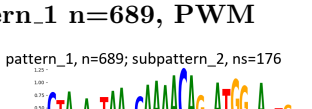

pattern_1, n=689; subpattern_3, ns=129

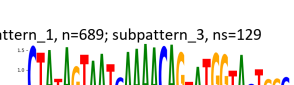

pattern_1, n=689; subpattern_4, ns=7

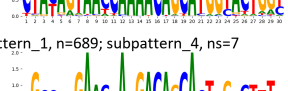

pattern_1, n=689; subpattern_5, ns=5

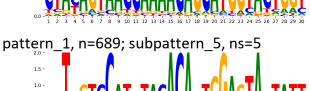

pattern_1, n=689; subpattern_6, ns=4



pattern_1, n=689; subpattern_7, ns=2

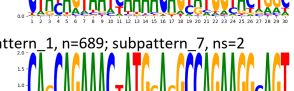

TF-MoDisCO pattern_3 n=361, CWM

pattern_3, n=361; subpattern_0, ns=89



pattern_3, n=361; subpattern_1, ns=85



pattern_3, n=361; subpattern_2, ns=74

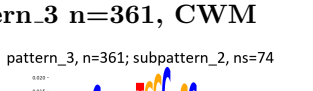

pattern_3, n=361; subpattern_3, ns=58

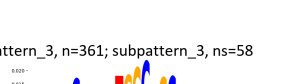

pattern_3, n=361; subpattern_4, ns=52

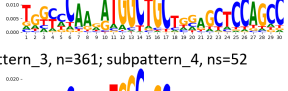

pattern_3, n=361; subpattern_5, ns=3

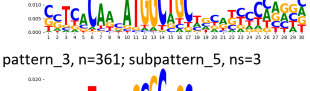

TF-MoDisCO pattern_3 n=361, PWM

pattern_3, n=361; subpattern_0, ns=89

pattern_3, n=361; subpattern_1, ns=85

pattern_3, n=361; subpattern_2, ns=74

pattern_3, n=361; subpattern_3, ns=58

pattern_3, n=361; subpattern_4, ns=52

pattern_3, n=361; subpattern_5, ns=3

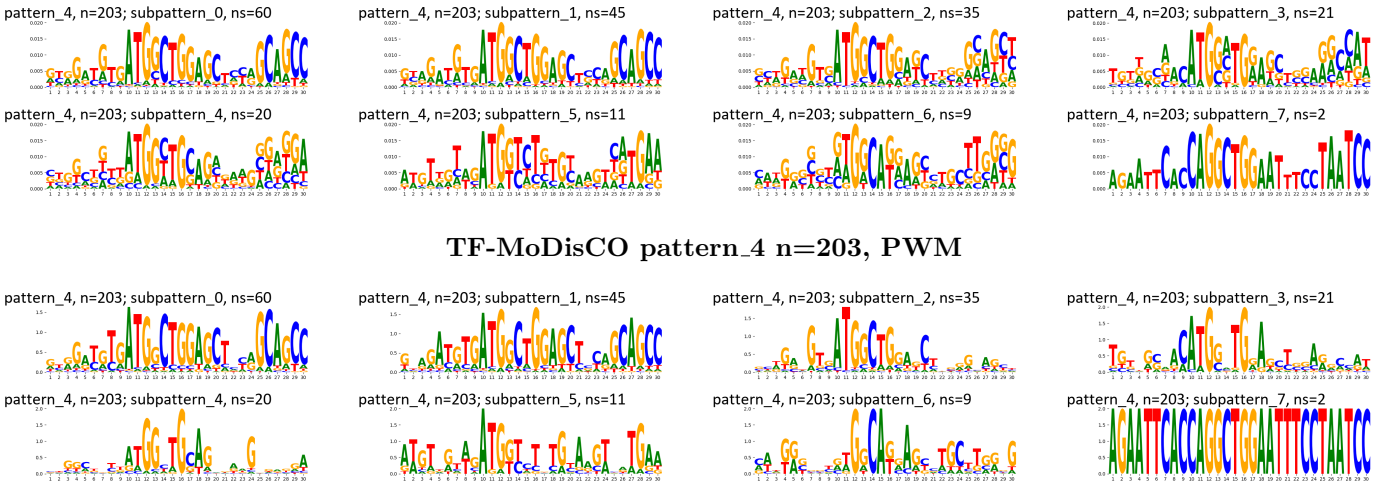

Supplementary Figure 983: TF-MoDisCO subpatterns for the ZNF280D transcription factor in HEK293 (accession ENCSR451CYX).



peaks	
state	fraction
TssA	0.24
Quies	0.22
TssFlnk	0.16
TxWk	0.13
EnhWk	0.08
TssFlnkU	0.04
Tx	0.04
EnhA2	0.03
EnhA1	0.03
ReprPCWk	0.02
TssFlnkD	0.02
TssBiv	0.02
ReprPC	0.02
Het	0.01
EnhG1	0.01
EnhBiv	0.01
ZNF/Rpts	0.00
EnhG2	0.00

peaks		peaks	
repeat	fraction	repeat	fraction
SINE/Alu	0.29	MIRb	0.06
Simple_repeat	0.17	MIR	0.04
SINE/MIR	0.16	L2a	0.04
LINE/L1	0.11	AluJb	0.04
LINE/L2	0.10	AluSx	0.03
LTR/ERV1	0.05	L2b	0.03
LTR/ERVL-MaLR	0.05	MIR3	0.03
DNA/hAT-Charlie	0.04	MIRc	0.03
Low_complexity	0.03	AluSx1	0.03
LTR/ERVL	0.02	L2c	0.03
DNA/TcMar-Tigger	0.01	AluJr	0.02
LINE/CR1	0.01	AluJo	0.02
DNA/hAT-Tip100	0.01	AluSz	0.02
LTR/ERVK	0.01	AluY	0.02
tRNA	0.01	G-rich	0.02
DNA/hAT-Blackjack	0.00	AluSq2	0.01
LTR/Gypsy	0.00	AluSp	0.01
LINE/RTE-BovB	0.00	AluSg	0.01

Ontology	Term	FDR Q-val
GO Biological Process	regulation of transcription from RNA polymerase II promoter in response to stress	60.46
GO Biological Process	regulation of DNA-templated transcription in response to stress	56.96
GO Biological Process	regulation of intrinsic apoptotic signaling pathway	45.80
GO Biological Process	cellular response to insulin stimulus	44.82
GO Biological Process	mRNA catabolic process	40.83
GO Biological Process	endoplasmic reticulum unfolded protein response	39.51
GO Biological Process	nuclear-transcribed mRNA catabolic process	39.41
GO Biological Process	nuclear-transcribed mRNA catabolic process, nonsense-mediated decay	38.79
GO Biological Process	IRE1-mediated unfolded protein response	36.05
GO Biological Process	viral gene expression	34.45
GO Biological Process	cellular response to topologically incorrect protein	33.93
GO Biological Process	multi-organism metabolic process	32.96
GO Biological Process	cotranslational protein targeting to membrane	32.79
GO Biological Process	cellular response to unfolded protein	32.77
GO Biological Process	regulation of transcription from RNA polymerase II promoter in response to hypoxia	32.76
GO Biological Process	viral transcription	32.56
GO Biological Process	cellular response to epidermal growth factor stimulus	30.96
GO Biological Process	protein targeting to ER	30.88
GO Biological Process	response to epidermal growth factor	29.73
GO Biological Process	SRP-dependent cotranslational protein targeting to membrane	28.19

Supplementary Figure 984: Properties and genomic distribution of motifs identified for the ZNF280D transcription factor in HepG2 (accession ENCSR233FJO).

TF-MoDisCO pattern_0 n=2841, CWM

pattern_0, n=2841; subpattern_0, ns=707

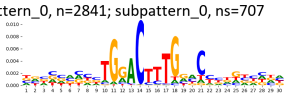

pattern_0, n=2841; subpattern_1, ns=634

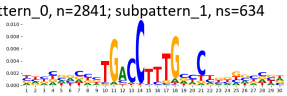

pattern_0, n=2841; subpattern_2, ns=597

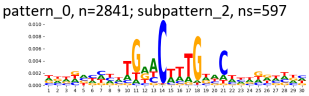

pattern_0, n=2841; subpattern_3, ns=546

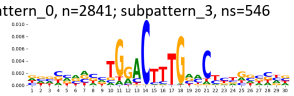

pattern_0, n=2841; subpattern_4, ns=278

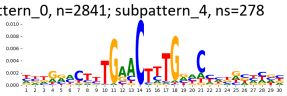

pattern_0, n=2841; subpattern_5, ns=43

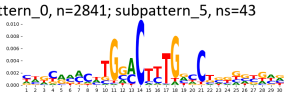

pattern_0, n=2841; subpattern_6, ns=27

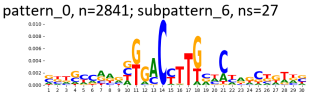

pattern_0, n=2841; subpattern_7, ns=7

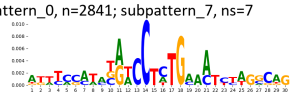

pattern_0, n=2841; subpattern_8, ns=2

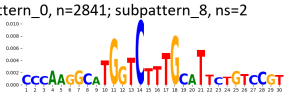

TF-MoDisCO pattern_0 n=2841, PWM

pattern_0, n=2841; subpattern_0, ns=707

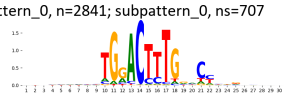

pattern_0, n=2841; subpattern_1, ns=634

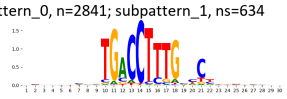

pattern_0, n=2841; subpattern_2, ns=597

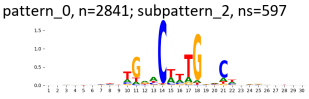

pattern_0, n=2841; subpattern_3, ns=546

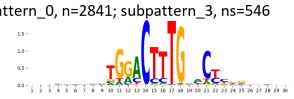

pattern_0, n=2841; subpattern_4, ns=278

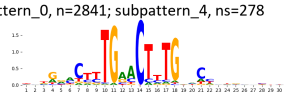

pattern_0, n=2841; subpattern_5, ns=43

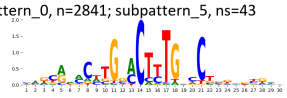

pattern_0, n=2841; subpattern_6, ns=27

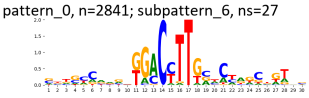

pattern_0, n=2841; subpattern_7, ns=7

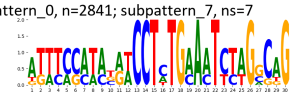

pattern_0, n=2841; subpattern_8, ns=2

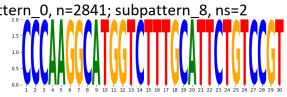

TF-MoDisCO pattern_1 n=1007, CWM

pattern_1, n=1007; subpattern_0, ns=230

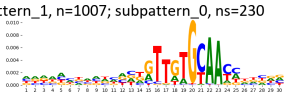

pattern_1, n=1007; subpattern_1, ns=198

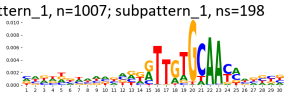

pattern_1, n=1007; subpattern_2, ns=196

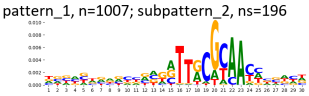

pattern_1, n=1007; subpattern_3, ns=179

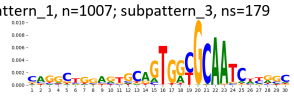

pattern_1, n=1007; subpattern_4, ns=107

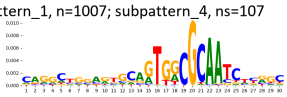

pattern_1, n=1007; subpattern_5, ns=67

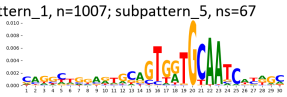

pattern_1, n=1007; subpattern_6, ns=26

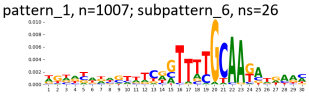

pattern_1, n=1007; subpattern_7, ns=2

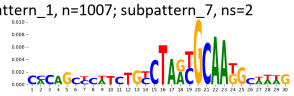

pattern_1, n=1007; subpattern_8, ns=2

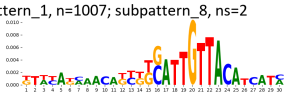

TF-MoDisCO pattern_1 n=1007, PWM

pattern_1, n=1007; subpattern_0, ns=230

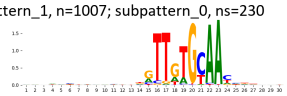

pattern_1, n=1007; subpattern_1, ns=198

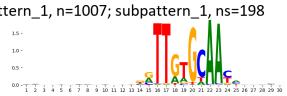

pattern_1, n=1007; subpattern_2, ns=196

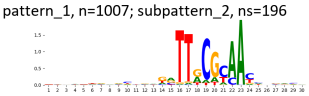

pattern_1, n=1007; subpattern_3, ns=179

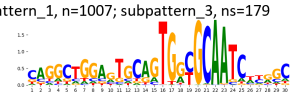

pattern_1, n=1007; subpattern_4, ns=107

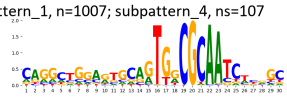

pattern_1, n=1007; subpattern_5, ns=67

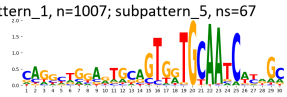

pattern_1, n=1007; subpattern_6, ns=26

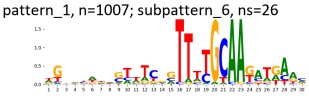

pattern_1, n=1007; subpattern_7, ns=2

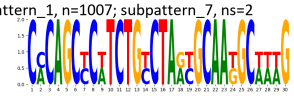

pattern_1, n=1007; subpattern_8, ns=2

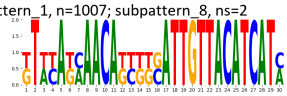

TF-MoDisCO pattern_8 n=407, CWM

pattern_8, n=407; subpattern_0, ns=157

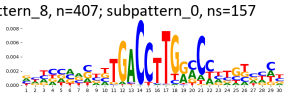

pattern_8, n=407; subpattern_1, ns=86

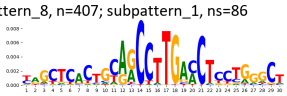

pattern_8, n=407; subpattern_2, ns=76

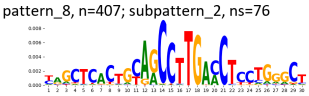

pattern_8, n=407; subpattern_3, ns=59

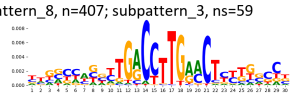

pattern_8, n=407; subpattern_4, ns=25

pattern_8, n=407; subpattern_5, ns=2

pattern_8, n=407; subpattern_6, ns=2

TF-MoDisCO pattern_8 n=407, PWM

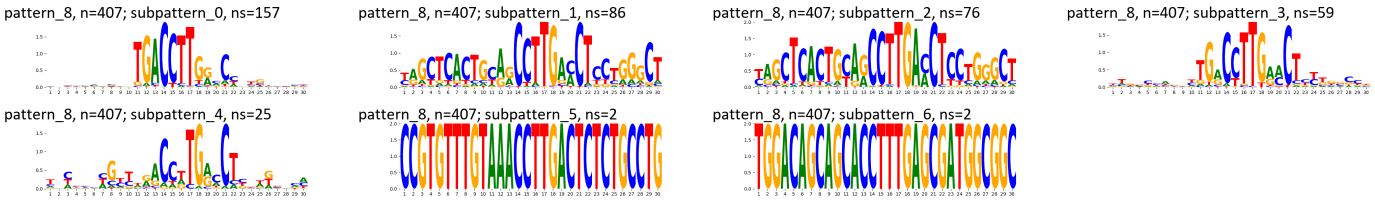

Supplementary Figure 985: TF-MoDisCO subpatterns for the ZNF280D transcription factor in HepG2 (accession ENCSR233FJO).

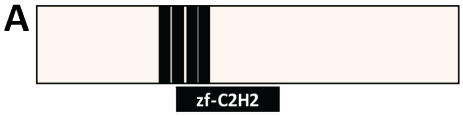

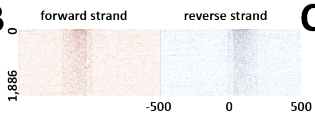

C

peaks	
state	fraction
TssA	0.41
TssFlnk	0.14
EnhWk	0.10
EnhA1	0.09
TssBiv	0.08
Quies	0.07
EnhA2	0.05
TssFlnkU	0.05
TxWk	0.04
TssFlnkD	0.03
ReprPC	0.02
EnhBiv	0.02
ReprPCWk	0.01
Tx	0.01
EnhG1	0.01
EnhG2	0.01

D

peaks		peaks	
repeat	fraction	repeat	fraction
Simple_repeat	0.15	G-rich	0.04
Low_complexity	0.05	GA-rich	0.01
SINE/MIR	0.03	MIR3	0.01
LINE/L2	0.02	MIRb	0.01
LINE/L1	0.01	MIRc	0.01
DNA/hAT-Charlie	0.00	L2b	0.01
SINE/Alu	0.00	MIR	0.00
LTR/ERVL-MaLR	0.00	L2a	0.00
LTR/ERV1	0.00	(TG)n	0.00
LTR/ERVL	0.00	(CCCT)n	0.00
LINE/CR1	0.00	(GT)n	0.00
Unknown	0.00	(GGC)n	0.00
DNA/TcMar-Tigger	0.00	(CTCC)n	0.00
Satellite	0.00	(CCT)n	0.00
SINE/tRNA-RTE	0.00	(TCC)n	0.00
SINE/5S-Deu-L2	0.00	(TC)n	0.00
LTR/Gypsy	0.00	(GCC)n	0.00
LTR/ERVK	0.00	MIR1_Amn	0.00

E

Ontology	Term	FDR Q-val
GO Biological Process	negative regulation of cellular amide metabolic process	13.44
GO Biological Process	negative regulation of translation	13.36
GO Biological Process	posttranscriptional regulation of gene expression	12.15
GO Biological Process	regulation of gene expression, epigenetic	11.85
GO Biological Process	regulation of translation	10.26
GO Biological Process	histone modification	9.81
GO Biological Process	gene silencing by miRNA	8.16
GO Biological Process	regulation of mRNA stability	7.14
GO Biological Process	mRNA stabilization	6.95
GO Biological Process	posttranscriptional gene silencing by RNA	6.64
GO Biological Process	heterochromatin organization	6.57
GO Biological Process	RNA stabilization	6.47
GO Biological Process	regulation of RNA stability	6.26
GO Biological Process	regulation of chromatin organization	5.64
GO Biological Process	negative regulation of hyaluronan biosynthetic process	4.20
GO Biological Process	regulation of histone modification	3.84
GO Biological Process	histone deacetylation	3.84
GO Biological Process	protein deacetylation	3.76
GO Biological Process	negative regulation of intrinsic apoptotic signaling pathway	3.73
GO Biological Process	regulation of protein deacetylation	3.60
Human Phenotype	Renal malrotation	4.09
Human Phenotype	Abnormality of adipose tissue	2.12
Human Phenotype	Distal lower limb amyotrophy	1.61

F

CIS-BP SELEX

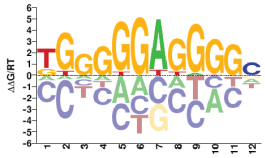

B1H-RC prediction

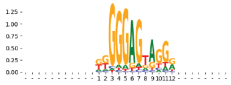

TF-MoDisCo pattern_0 n=1,284

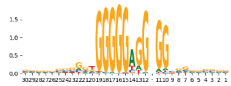

G

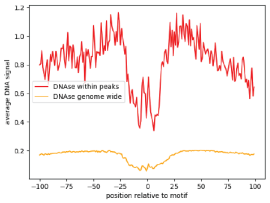

H

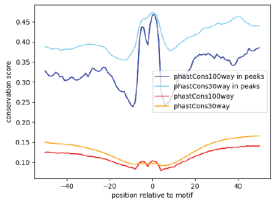

I

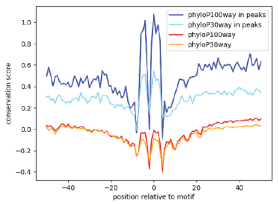

Supplementary Figure 986: Properties and genomic distribution of motifs identified for the ZNF281 transcription factor in HEK293 (accession Hughes GR models).

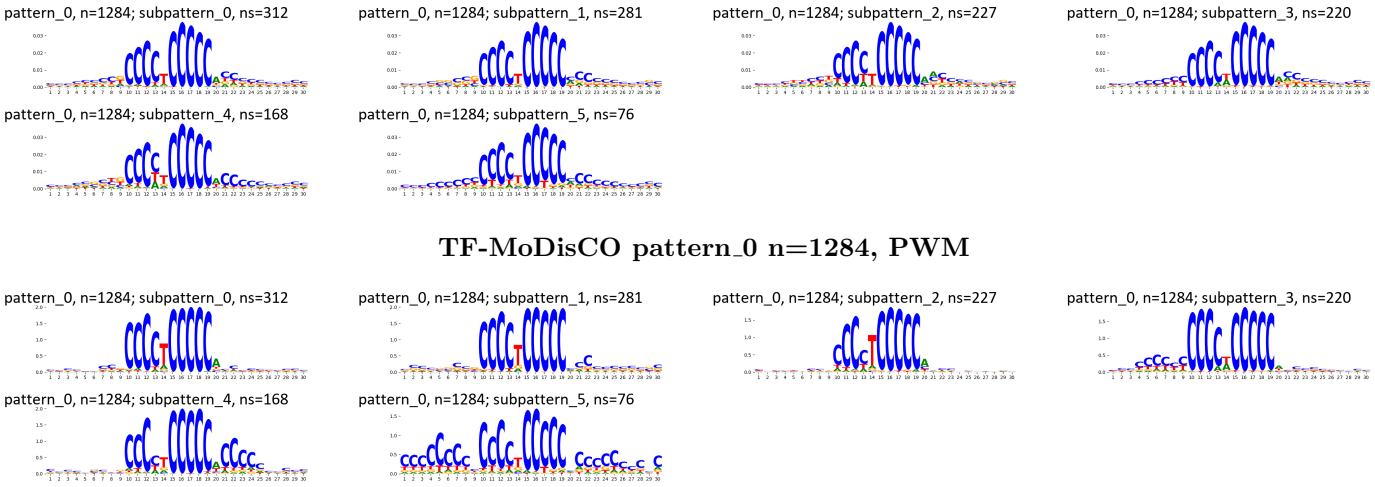

Supplementary Figure 987: TF-MoDisCO subpatterns for the ZNF281 transcription factor in HEK293 (accession Hughes GR models).

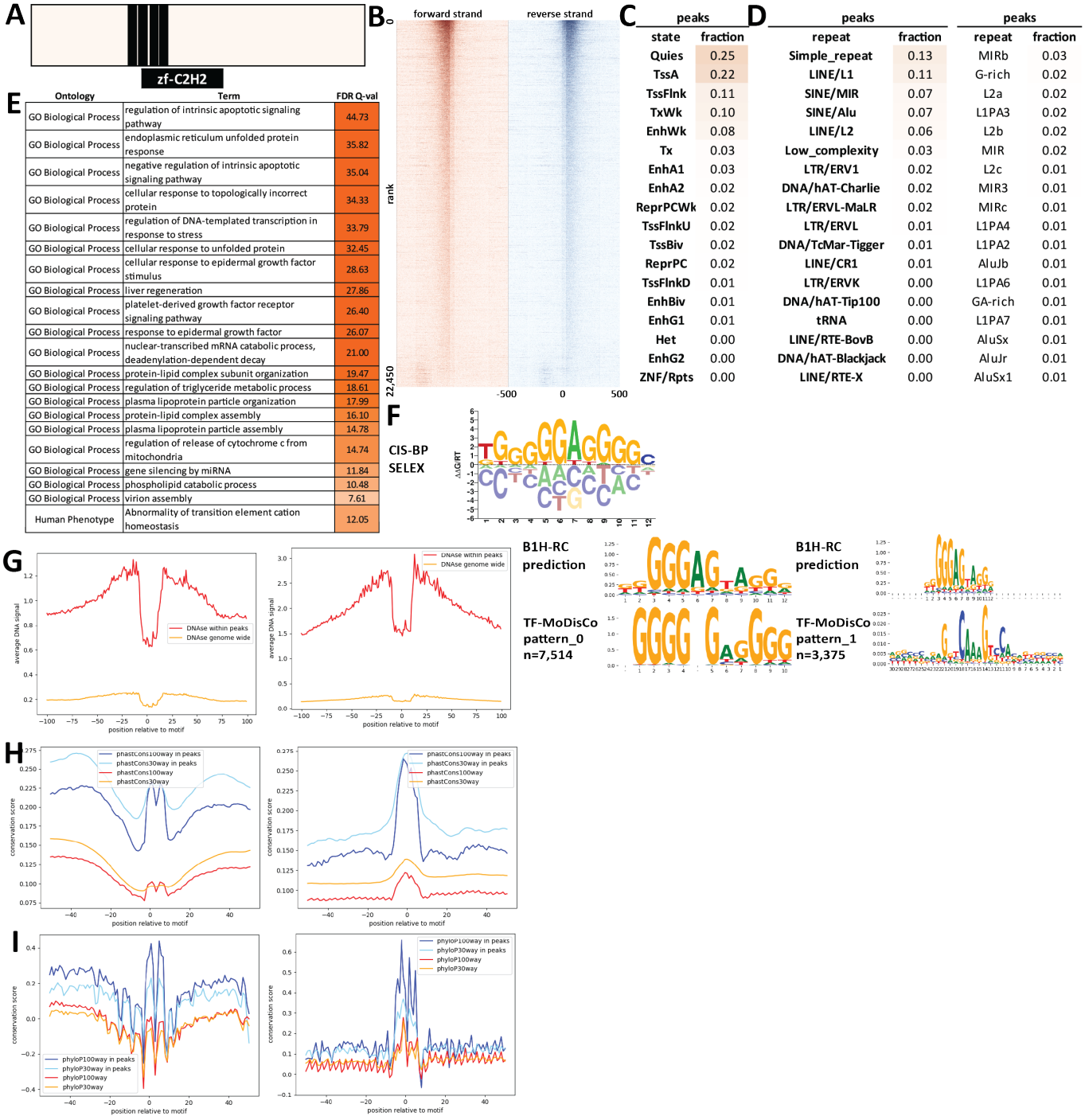

Supplementary Figure 988: Properties and genomic distribution of motifs identified for the ZNF281 transcription factor in HepG2 (accession ENCSR403MJY).

TF-MoDisCO pattern_0 n=7514, CWM

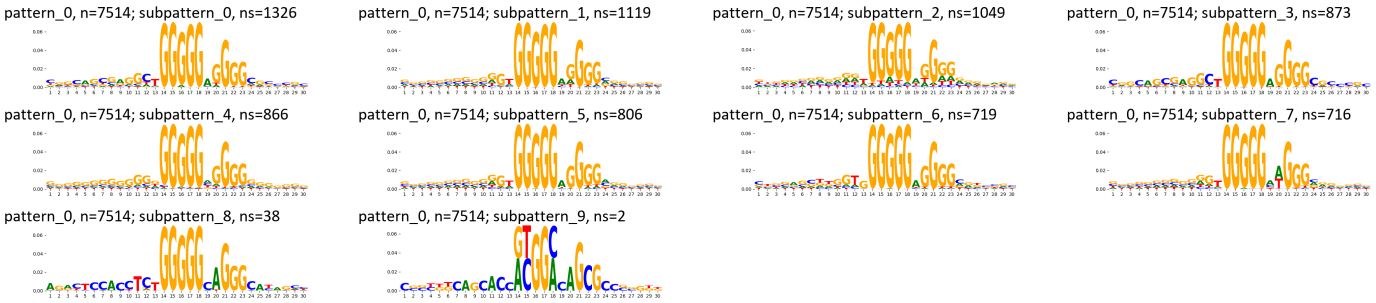

TF-MoDisCO pattern_0 n=7514, PWM

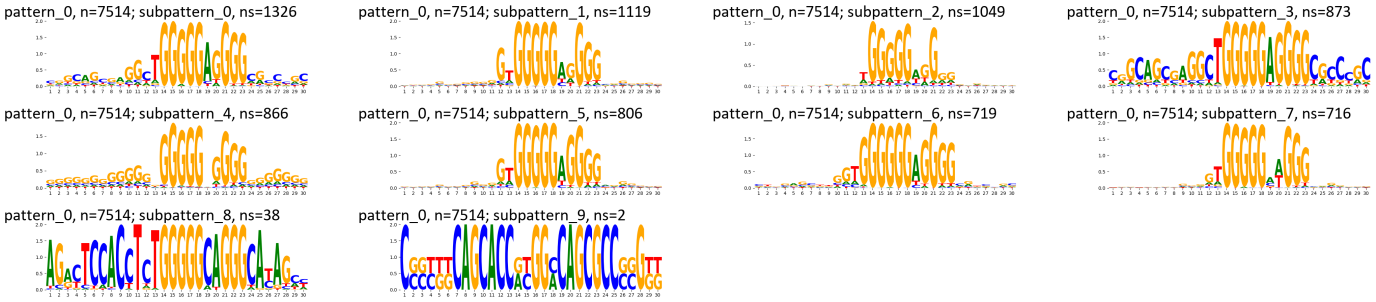

TF-MoDisCO pattern_1 n=3375, CWM

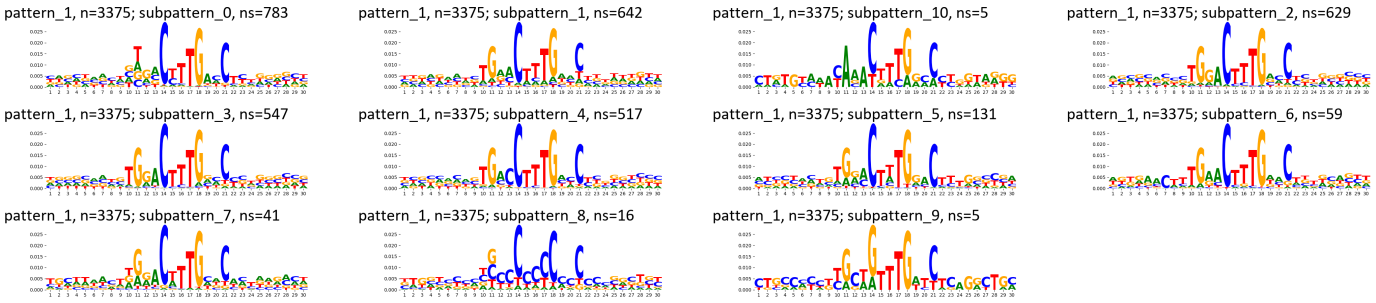

TF-MoDisCO pattern_1 n=3375, PWM

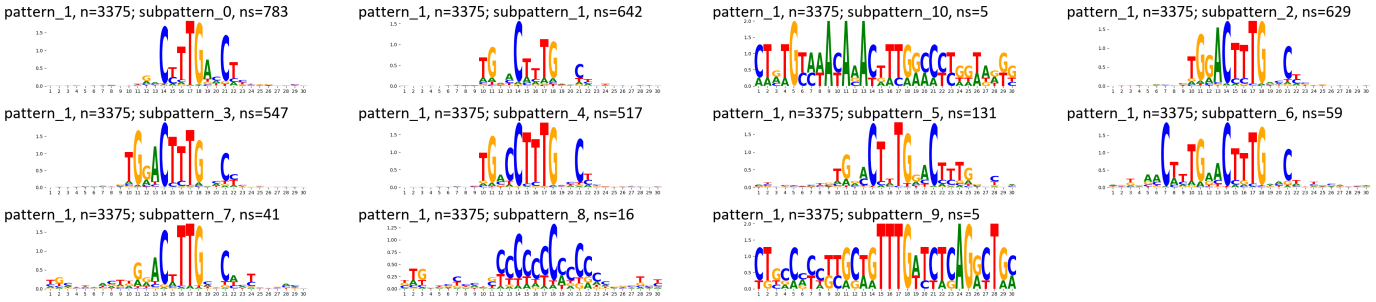

Supplementary Figure 989: TF-MoDisCO subpatterns for the ZNF281 transcription factor in HepG2 (accession ENCSR403MJY).

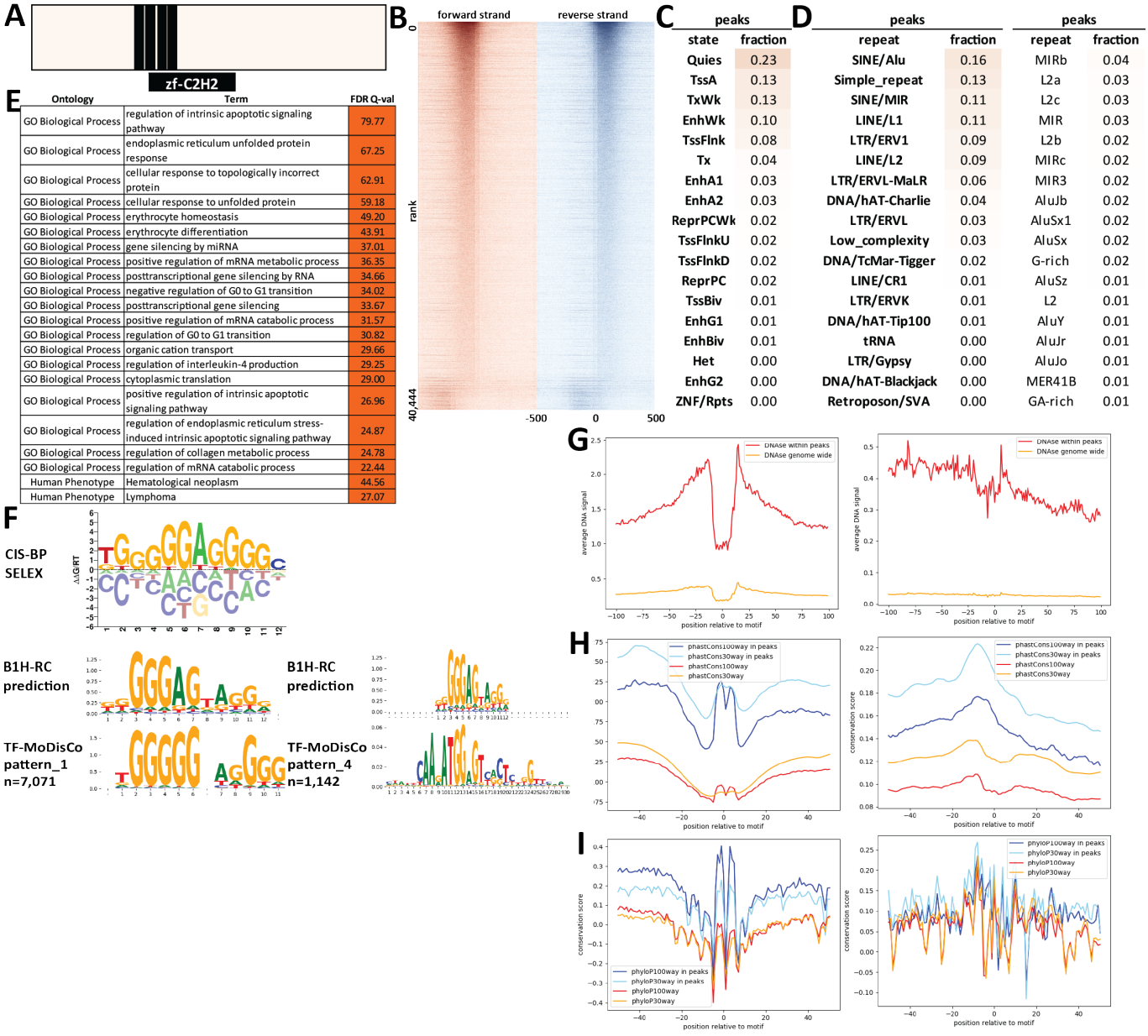

Supplementary Figure 990: Properties and genomic distribution of motifs identified for the ZNF281 transcription factor in K562 (accession ENCSR214EKV).

TF-MoDisCO pattern_1 n=7071, CWM

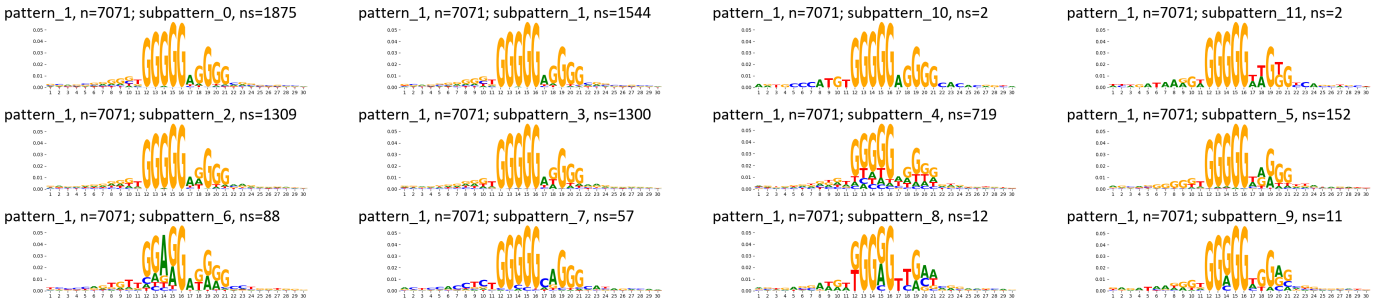

TF-MoDisCO pattern_1 n=7071, PWM

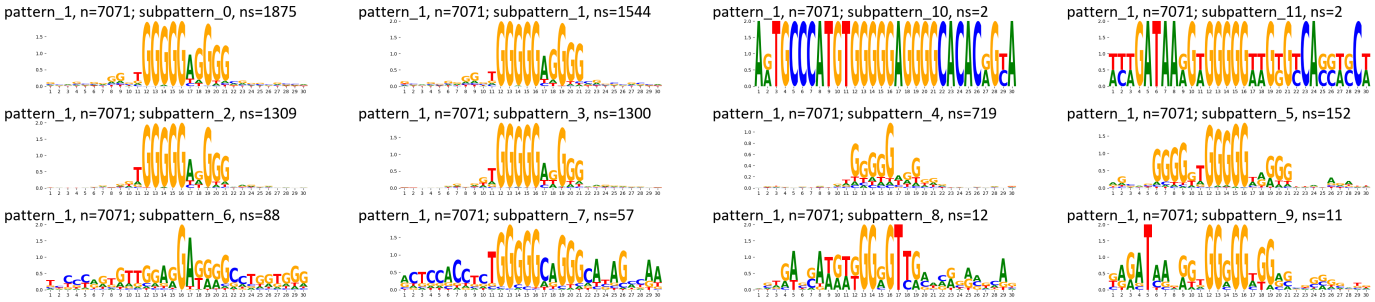

TF-MoDisCO pattern_4 n=1142, CWM

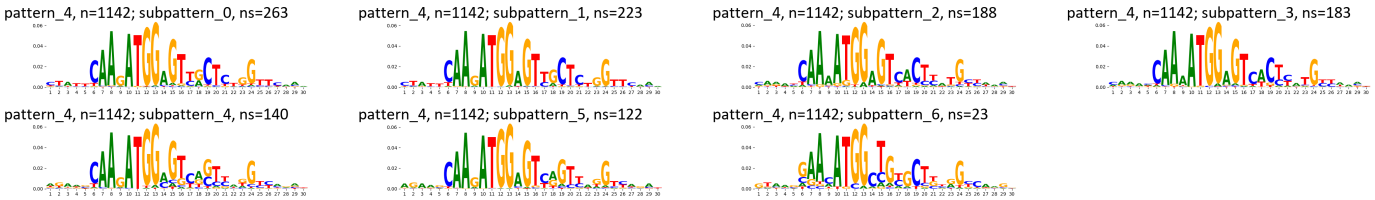

TF-MoDisCO pattern_4 n=1142, PWM

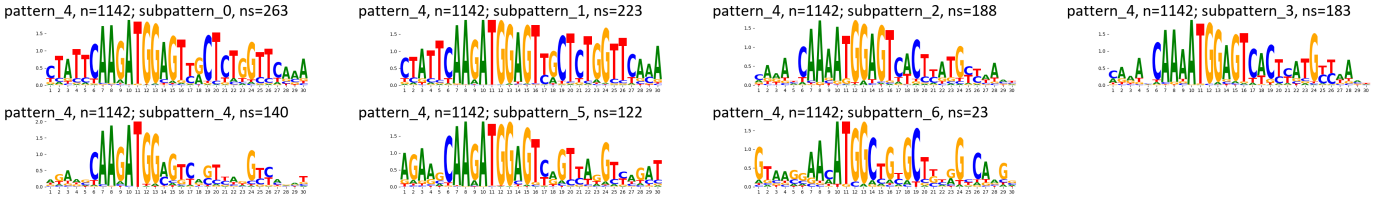

Supplementary Figure 991: TF-MoDisCO subpatterns for the ZNF281 transcription factor in K562 (accession ENCSR214EKV).

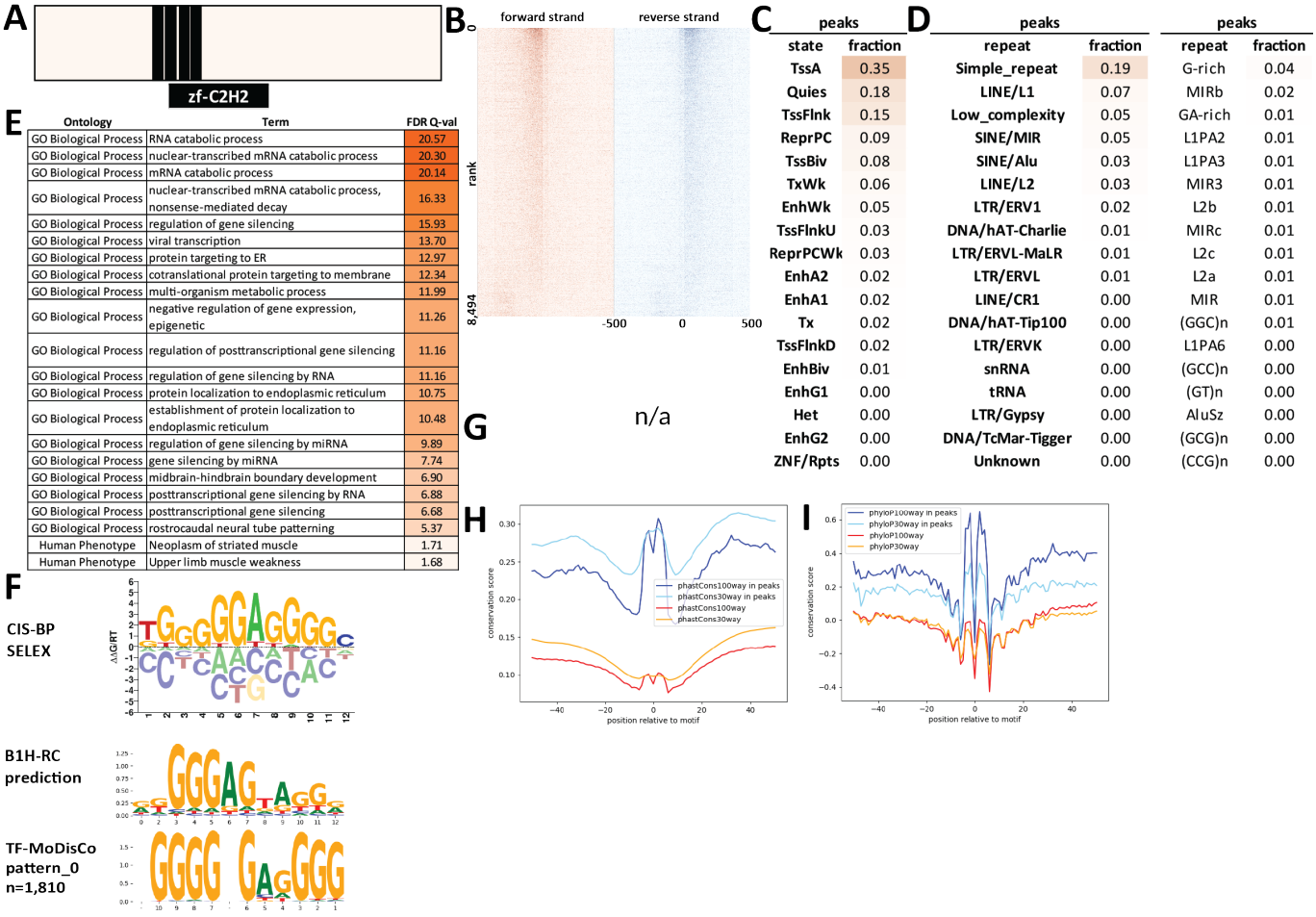

Supplementary Figure 992: Properties and genomic distribution of motifs identified for the ZNF281 transcription factor in WTC11 (accession ENCSR032DGZ).

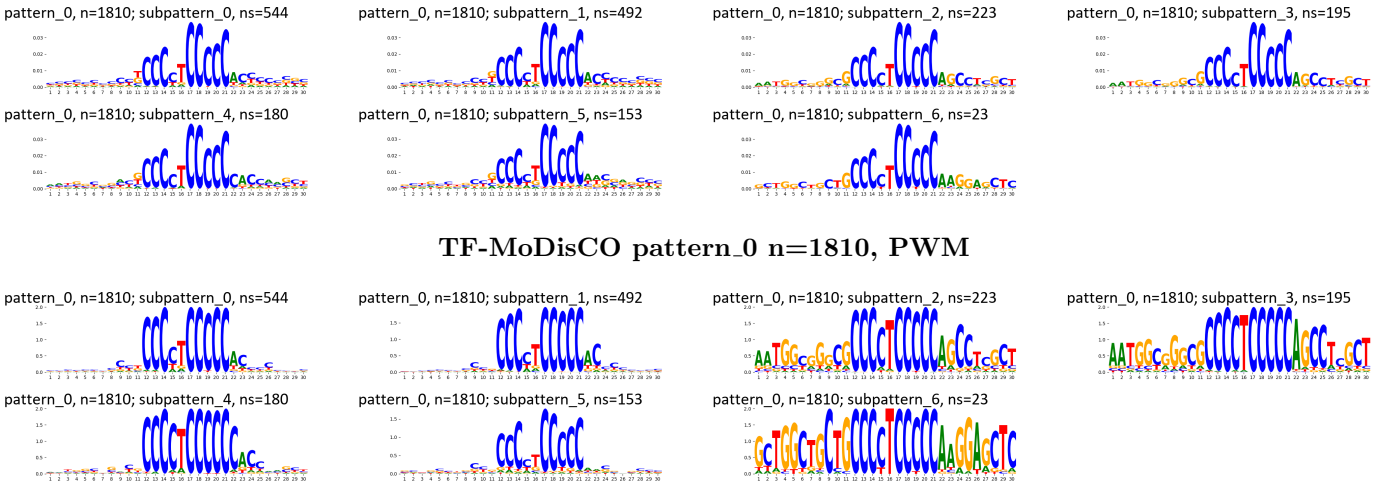

Supplementary Figure 993: TF-MoDisCO subpatterns for the ZNF281 transcription factor in WTC11 (accession ENCSR032DGZ).

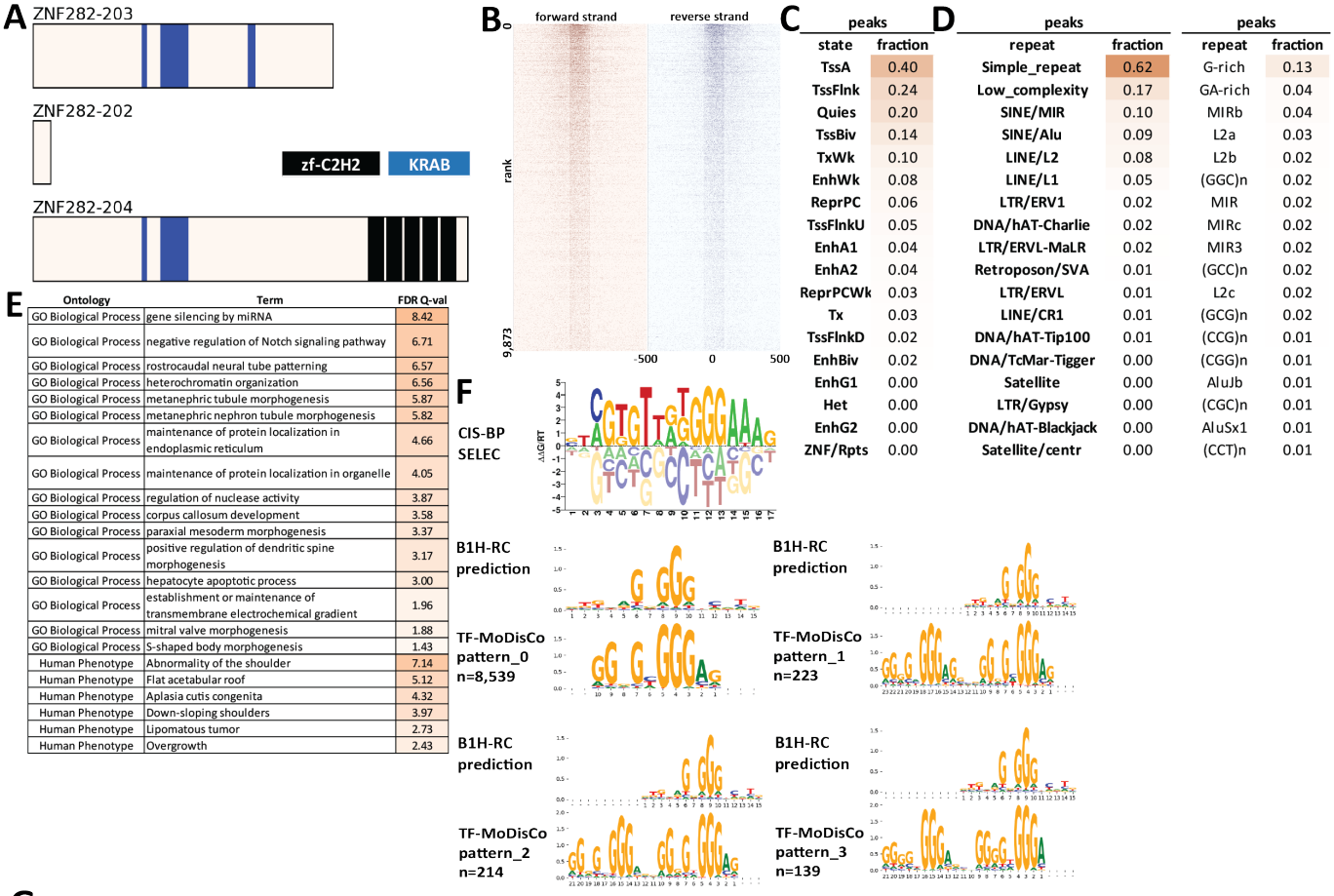

Supplementary Figure 994: Properties and genomic distribution of motifs identified for the ZNF282 transcription factor in HEK293 (accession ChipExo models).

TF-MoDisCO pattern_0 n=8539, CWM

pattern_0, n=8539; subpattern_0, ns=1460

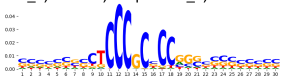

pattern_0, n=8539; subpattern_1, ns=1408

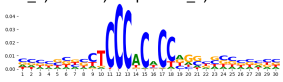

pattern_0, n=8539; subpattern_2, ns=1342

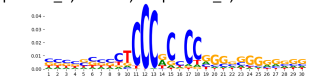

pattern_0, n=8539; subpattern_3, ns=989

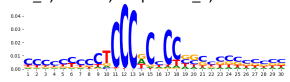

pattern_0, n=8539; subpattern_4, ns=982

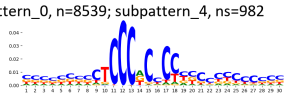

pattern_0, n=8539; subpattern_5, ns=926

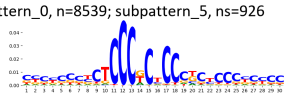

pattern_0, n=8539; subpattern_6, ns=823

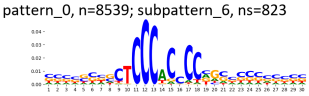

pattern_0, n=8539; subpattern_7, ns=323

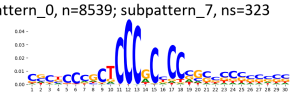

pattern_0, n=8539; subpattern_8, ns=286

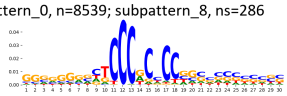

TF-MoDisCO pattern_0 n=8539, PWM

pattern_0, n=8539; subpattern_0, ns=1460

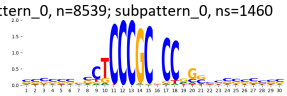

pattern_0, n=8539; subpattern_1, ns=1408

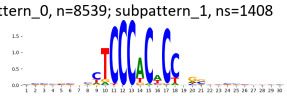

pattern_0, n=8539; subpattern_2, ns=1342

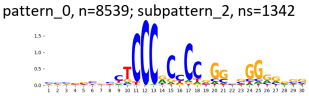

pattern_0, n=8539; subpattern_3, ns=989

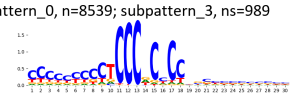

pattern_0, n=8539; subpattern_4, ns=982

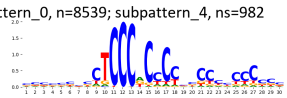

pattern_0, n=8539; subpattern_5, ns=926

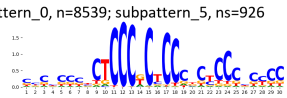

pattern_0, n=8539; subpattern_6, ns=823

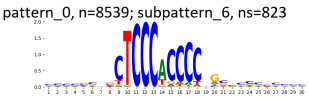

pattern_0, n=8539; subpattern_7, ns=323

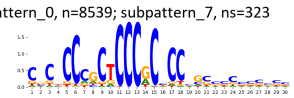

pattern_0, n=8539; subpattern_8, ns=286

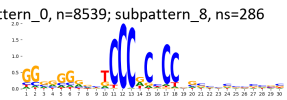

TF-MoDisCO pattern_1 n=223, CWM

pattern_1, n=223; subpattern_0, ns=62

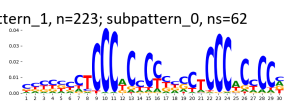

pattern_1, n=223; subpattern_1, ns=53

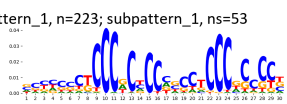

pattern_1, n=223; subpattern_2, ns=45

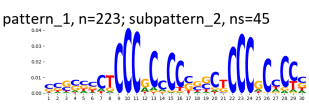

pattern_1, n=223; subpattern_3, ns=35

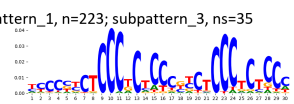

pattern_1, n=223; subpattern_4, ns=28

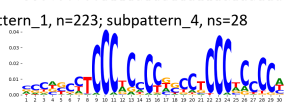

TF-MoDisCO pattern_1 n=223, PWM

pattern_1, n=223; subpattern_0, ns=62

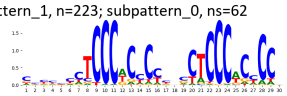

pattern_1, n=223; subpattern_1, ns=53

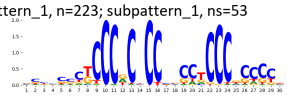

pattern_1, n=223; subpattern_2, ns=45

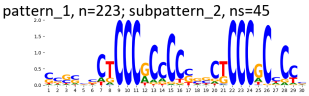

pattern_1, n=223; subpattern_3, ns=35

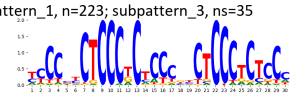

pattern_1, n=223; subpattern_4, ns=28

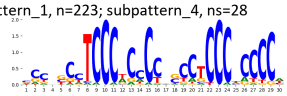

TF-MoDisCO pattern_2 n=214, CWM

pattern_2, n=214; subpattern_0, ns=60

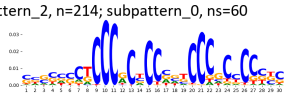

pattern_2, n=214; subpattern_1, ns=53

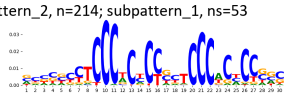

pattern_2, n=214; subpattern_2, ns=49

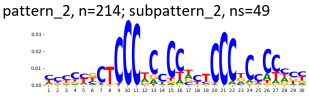

pattern_2, n=214; subpattern_3, ns=36

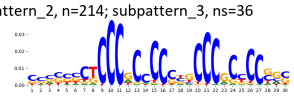

pattern_2, n=214; subpattern_4, ns=16

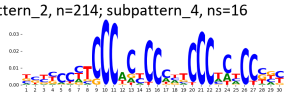

TF-MoDisCO pattern_2 n=214, PWM

pattern_2, n=214; subpattern_0, ns=60

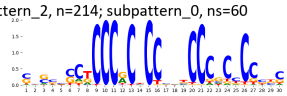

pattern_2, n=214; subpattern_1, ns=53

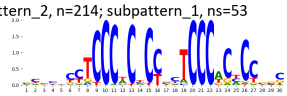

pattern_2, n=214; subpattern_2, ns=49

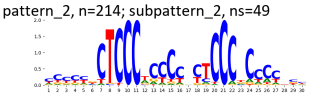

pattern_2, n=214; subpattern_3, ns=36

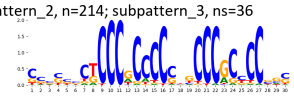

pattern_2, n=214; subpattern_4, ns=16

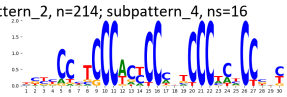

TF-MoDisCO pattern_3 n=139, CWM

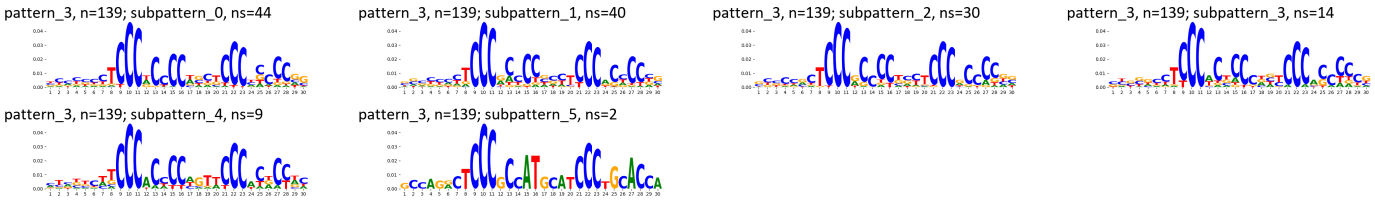

TF-MoDisCO pattern_3 n=139, PWM

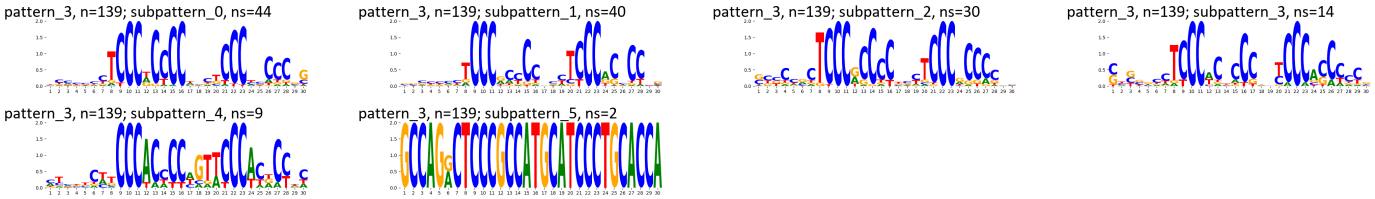

Supplementary Figure 995: TF-MoDisCO subpatterns for the ZNF282 transcription factor in HEK293 (accession ChipExo models).

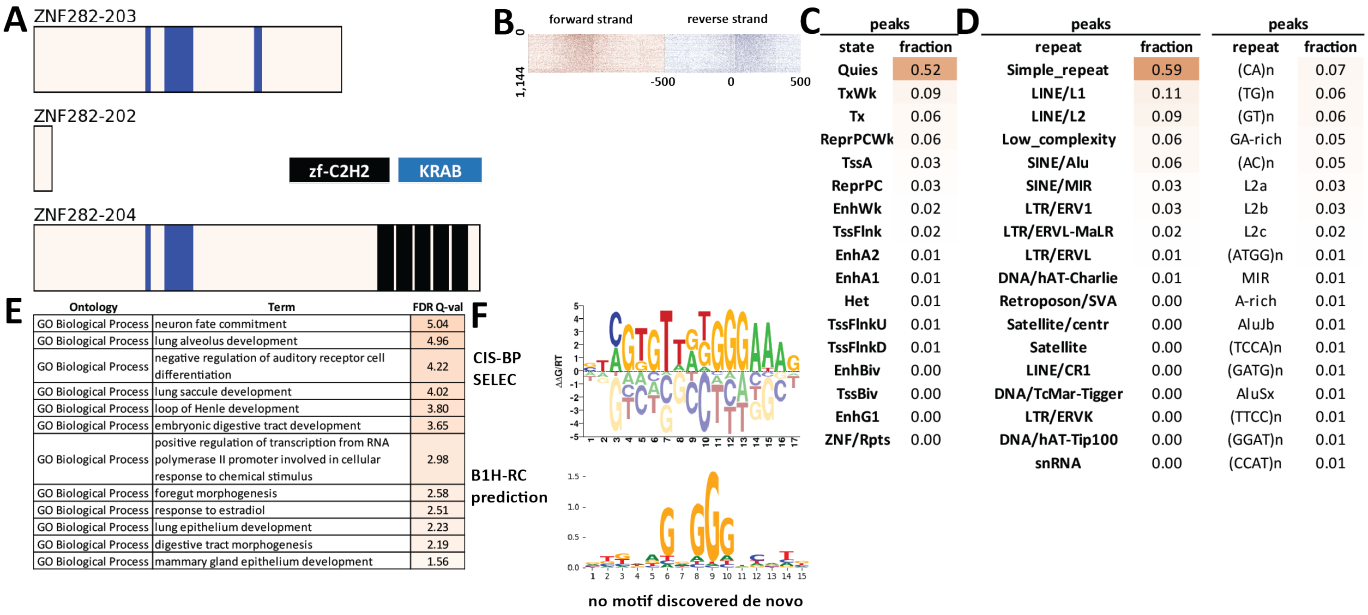

peaks	
state	fraction
Quies	0.52
TxWk	0.09
Tx	0.06
ReprPCWk	0.06
TssA	0.03
ReprPC	0.03
EnhWk	0.02
TssFlnk	0.02
EnhA2	0.01
EnhA1	0.01
Het	0.01
TssFlnkU	0.01
TssFlnkD	0.01
EnhBiv	0.00
TssBiv	0.00
EnhG1	0.00
ZNF/Rpts	0.00

peaks		peaks	
repeat	fraction	repeat	fraction
Simple_repeat	0.59	(CA)n	0.07
LINE/L1	0.11	(TG)n	0.06
LINE/L2	0.09	(GT)n	0.06
Low_complexity	0.06	GA-rich	0.05
SINE/Alu	0.06	(AC)n	0.05
SINE/MIR	0.03	L2a	0.03
LTR/ERV1	0.03	L2b	0.03
LTR/ERVL-MaLR	0.02	L2c	0.02
LTR/ERVL	0.01	(ATGG)n	0.01
DNA/hAT-Charlie	0.01	MIR	0.01
Retroposon/SVA	0.00	A-rich	0.01
Satellite/centr	0.00	AluJb	0.01
Satellite	0.00	(TCCA)n	0.01
LINE/CR1	0.00	(GATG)n	0.01
DNA/TcMar-Tigger	0.00	AluSx	0.01
LTR/ERVK	0.00	(TTCC)n	0.01
DNA/hAT-Tip100	0.00	(GGAT)n	0.01
snRNA	0.00	(CCAT)n	0.01

Ontology	Term	FDR Q-val
GO Biological Process	neuron fate commitment	5.04
GO Biological Process	lung alveolus development	4.96
GO Biological Process	negative regulation of auditory receptor cell differentiation	4.22
GO Biological Process	lung saccule development	4.02
GO Biological Process	loop of Henle development	3.80
GO Biological Process	embryonic digestive tract development	3.65
GO Biological Process	positive regulation of transcription from RNA polymerase II promoter involved in cellular response to chemical stimulus	2.98
GO Biological Process	foregut morphogenesis	2.58
GO Biological Process	response to estradiol	2.51
GO Biological Process	lung epithelium development	2.23
GO Biological Process	digestive tract morphogenesis	2.19
GO Biological Process	mammary gland epithelium development	1.56

Supplementary Figure 996: Properties and genomic distribution of motifs identified for the ZNF282 transcription factor in HepG2 (accession ENCSR752NDX).

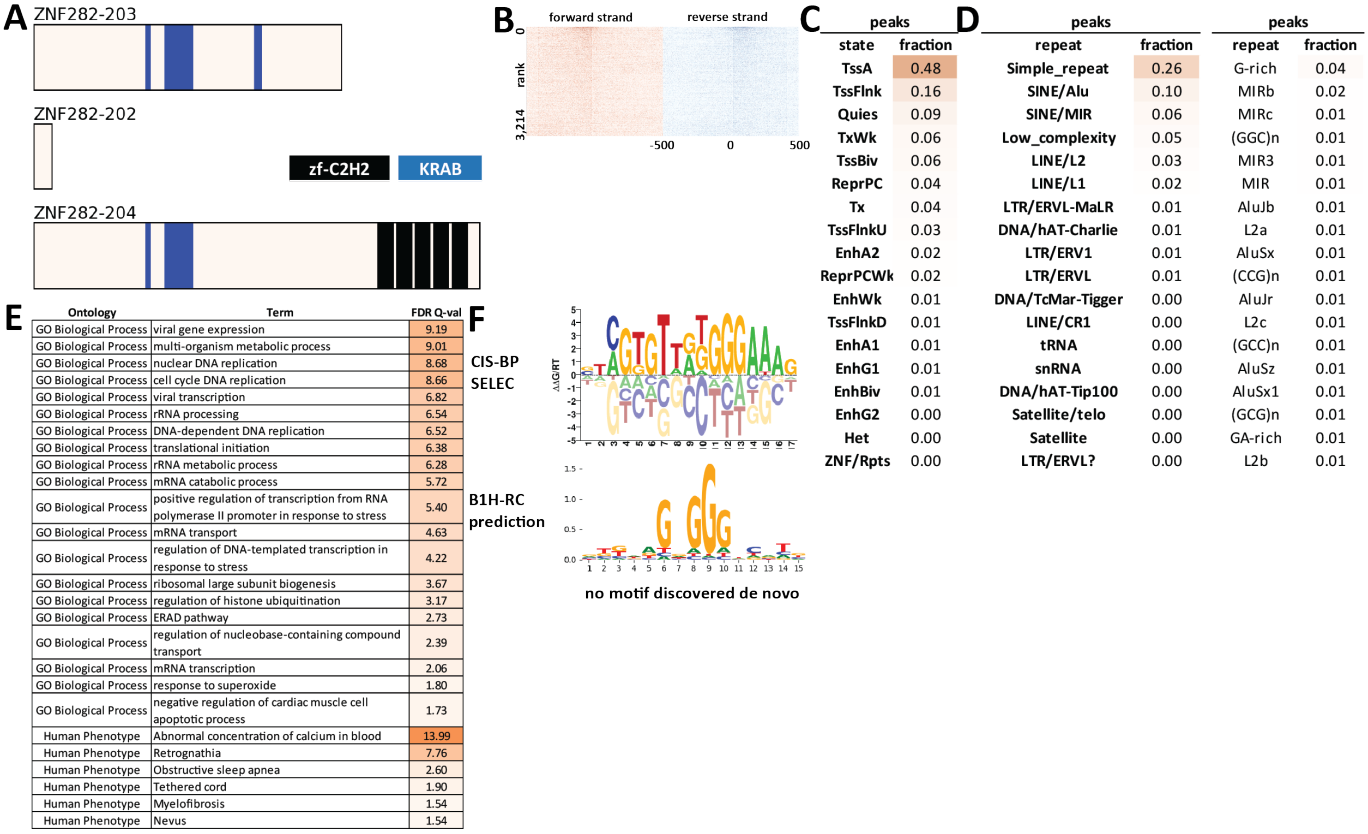

C

peaks	
state	fraction
TssA	0.48
TssFlnk	0.16
Quies	0.09
TxWk	0.06
TssBiv	0.06
ReprPC	0.04
Tx	0.04
TssFlnkU	0.03
EnhA2	0.02
ReprPCWk	0.02
EnhWk	0.01
TssFlnkD	0.01
EnhA1	0.01
EnhG1	0.01
EnhBiv	0.01
EnhG2	0.00
Het	0.00
ZNF/Rpts	0.00

D

peaks		peaks	
repeat	fraction	repeat	fraction
Simple_repeat	0.26	G-rich	0.04
SINE/Alu	0.10	MIRb	0.02
SINE/MIR	0.06	MIRc	0.01
Low_complexity	0.05	(GGC)n	0.01
LINE/L2	0.03	MIR3	0.01
LINE/L1	0.02	MIR	0.01
LTR/ERVL-MaLR	0.01	AluJb	0.01
DNA/hAT-Charlie	0.01	L2a	0.01
LTR/ERV1	0.01	AluSx	0.01
LTR/ERVL	0.01	(CCG)n	0.01
DNA/TcMar-Tigger	0.00	AluJr	0.01
LINE/CR1	0.00	L2c	0.01
tRNA	0.00	(GCC)n	0.01
snRNA	0.00	AluSz	0.01
DNA/hAT-Tip100	0.00	AluSx1	0.01
Satellite/telo	0.00	(GCG)n	0.01
Satellite	0.00	GA-rich	0.01
LTR/ERVL?	0.00	L2b	0.01

E

Ontology	Term	FDR Q-val
GO Biological Process	viral gene expression	9.19
GO Biological Process	multi-organism metabolic process	9.01
GO Biological Process	nuclear DNA replication	8.68
GO Biological Process	cell cycle DNA replication	8.66
GO Biological Process	viral transcription	6.82
GO Biological Process	rRNA processing	6.54
GO Biological Process	DNA-dependent DNA replication	6.52
GO Biological Process	translational initiation	6.38
GO Biological Process	rRNA metabolic process	6.28
GO Biological Process	mRNA catabolic process	5.72
GO Biological Process	positive regulation of transcription from RNA polymerase II promoter in response to stress	5.40
GO Biological Process	mRNA transport	4.63
GO Biological Process	regulation of DNA-templated transcription in response to stress	4.22
GO Biological Process	ribosomal large subunit biogenesis	3.67
GO Biological Process	regulation of histone ubiquitination	3.17
GO Biological Process	ERAD pathway	2.73
GO Biological Process	regulation of nucleobase-containing compound transport	2.39
GO Biological Process	mRNA transcription	2.06
GO Biological Process	response to superoxide	1.80
GO Biological Process	negative regulation of cardiac muscle cell apoptotic process	1.73
Human Phenotype	Abnormal concentration of calcium in blood	13.99
Human Phenotype	Retrognathia	7.76
Human Phenotype	Obstructive sleep apnea	2.60
Human Phenotype	Tethered cord	1.90
Human Phenotype	Myelofibrosis	1.54
Human Phenotype	Nevus	1.54

Supplementary Figure 997: Properties and genomic distribution of motifs identified for the ZNF282 transcription factor in K562 (accession ENCSR229KXQ).

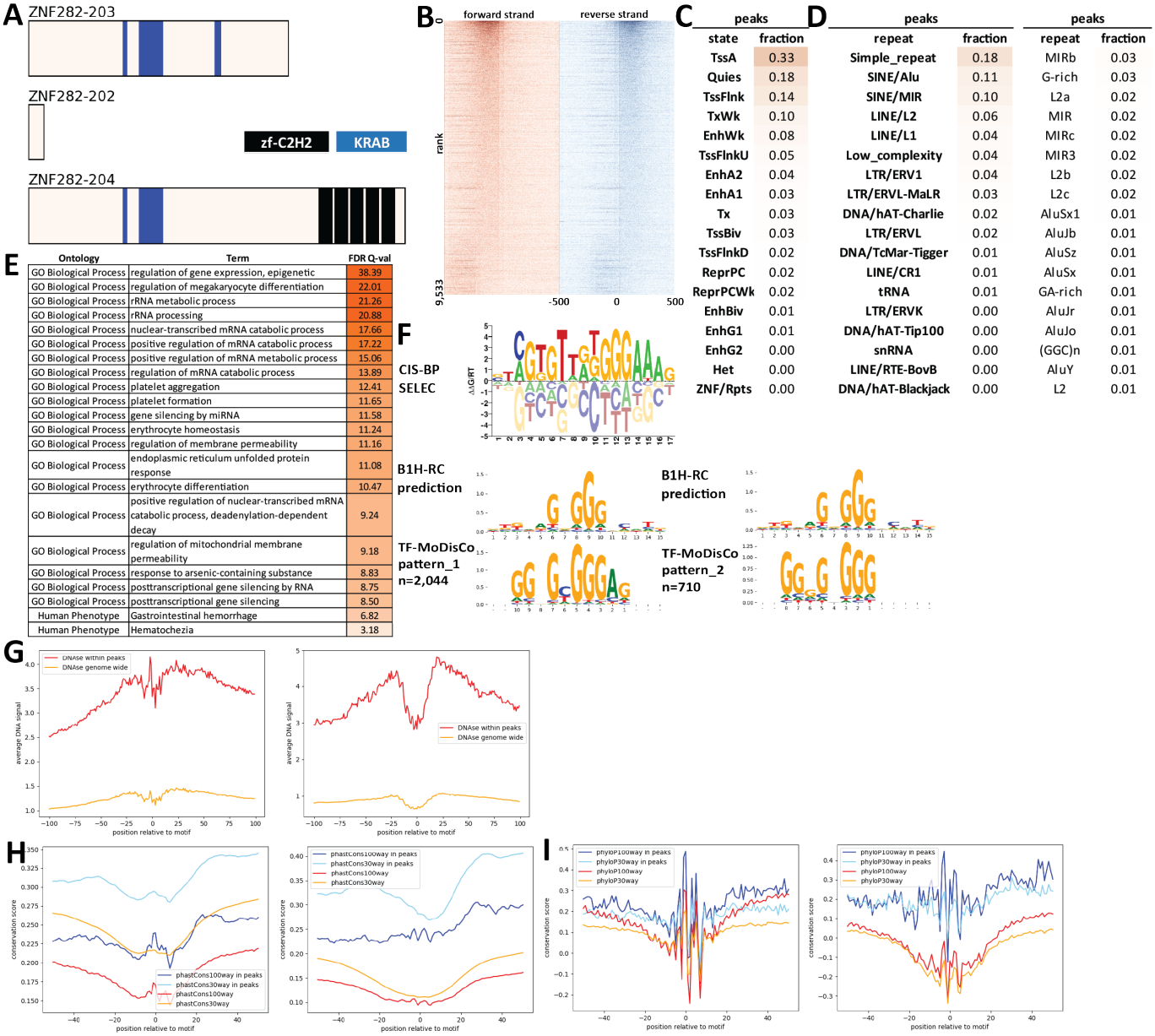

Supplementary Figure 998: Properties and genomic distribution of motifs identified for the ZNF282 transcription factor in K562 (accession ENCSR742TMU).

TF-MoDisCO pattern_1 n=2044, CWM

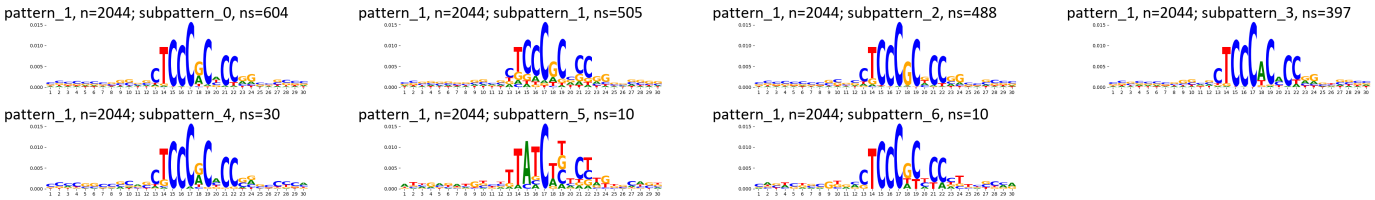

TF-MoDisCO pattern_1 n=2044, PWM

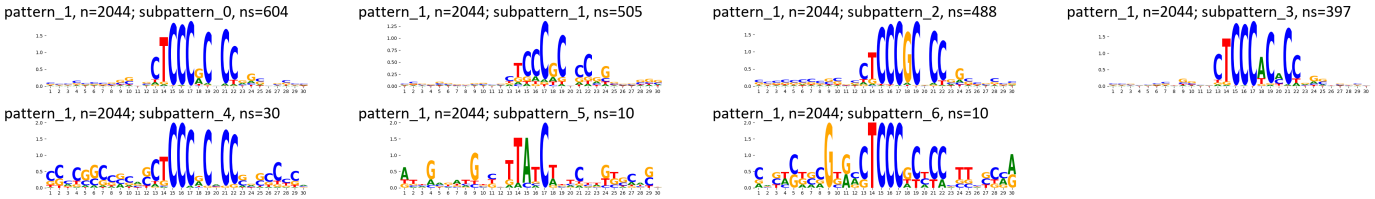

TF-MoDisCO pattern_2 n=710, CWM

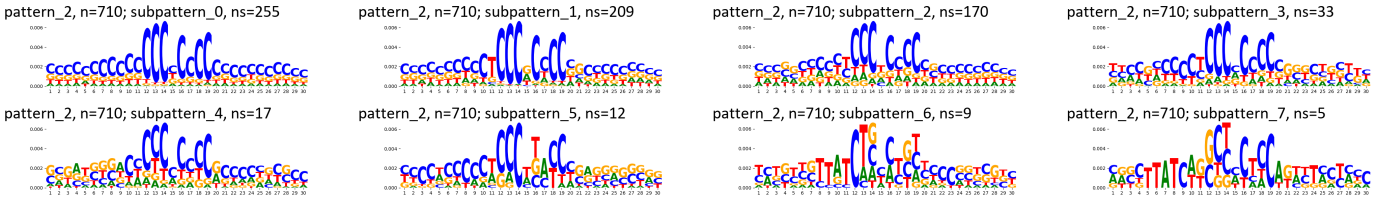

TF-MoDisCO pattern_2 n=710, PWM

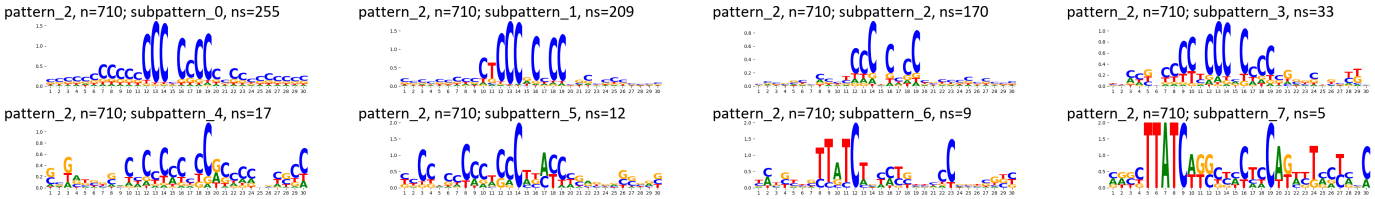

Supplementary Figure 999: TF-MoDisCO subpatterns for the ZNF282 transcription factor in K562 (accession ENCSR742TMU).

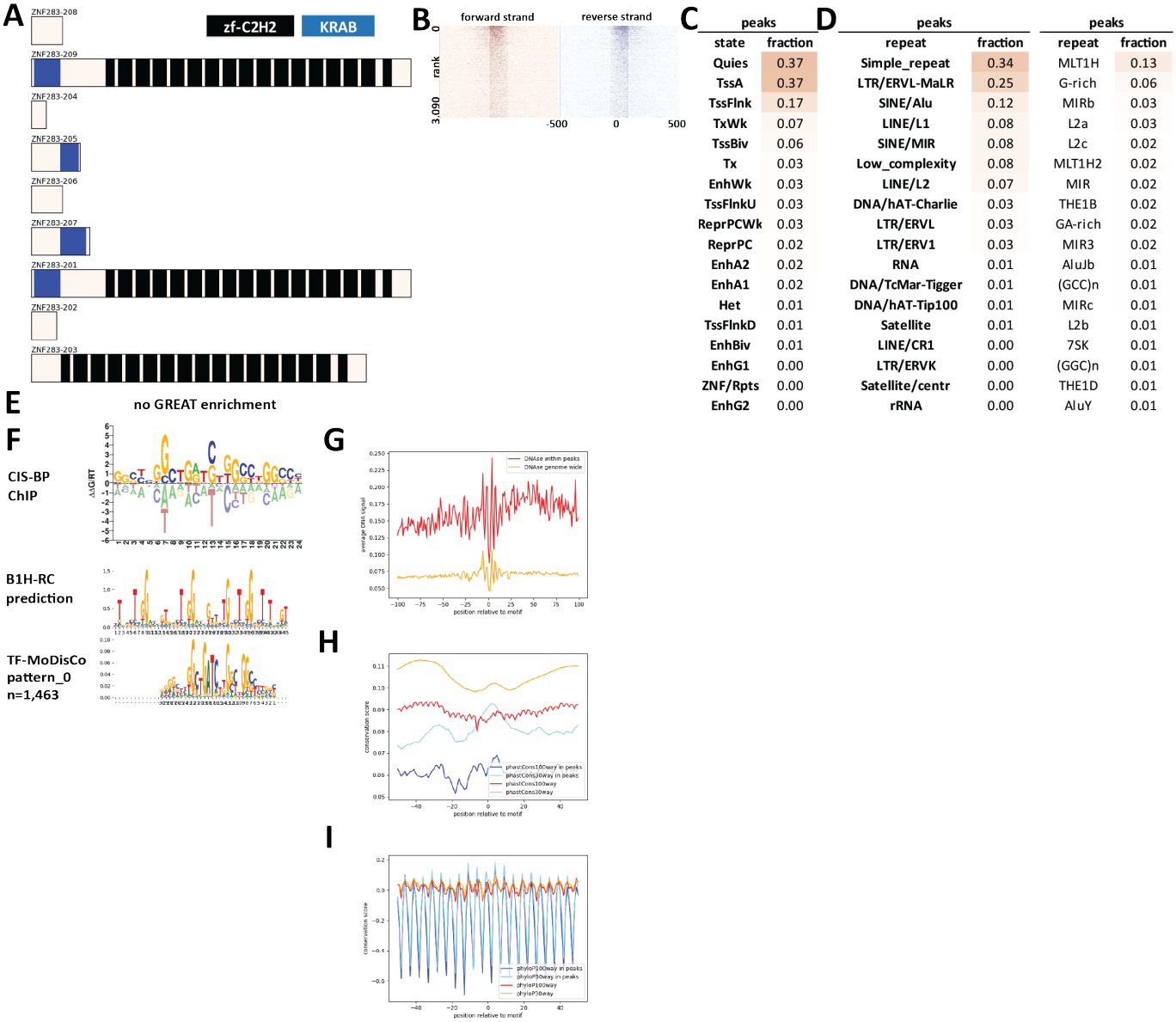

C

peaks	
state	fraction
Quies	0.37
TssA	0.37
TssFlnk	0.17
TxWk	0.07
TssBiv	0.06
Tx	0.03
EnhWk	0.03
TssFlnkU	0.03
ReprPCWk	0.03
ReprPC	0.02
EnhA2	0.02
EnhA1	0.02
Het	0.01
TssFlnkD	0.01
EnhBiv	0.01
EnhG1	0.00
ZNF/Rpts	0.00
EnhG2	0.00

D

peaks		peaks	
repeat	fraction	repeat	fraction
Simple_repeat	0.34	MLT1H	0.13
LTR/ERVL-MaLR	0.25	G-rich	0.06
SINE/Alu	0.12	MIRb	0.03
LINE/L1	0.08	L2a	0.03
SINE/MIR	0.08	L2c	0.02
Low_complexity	0.08	MLT1H2	0.02
LINE/L2	0.07	MIR	0.02
DNA/hAT-Charlie	0.03	THE1B	0.02
LTR/ERVL	0.03	GA-rich	0.02
LTR/ERV1	0.03	MIR3	0.02
RNA	0.01	AluJb	0.01
DNA/TcMar-Tigger	0.01	(GCC)n	0.01
DNA/hAT-Tip100	0.01	MIRc	0.01
Satellite	0.01	L2b	0.01
LINE/CR1	0.00	7SK	0.01
LTR/ERVK	0.00	(GGC)n	0.01
Satellite/centr	0.00	THE1D	0.01
rRNA	0.00	AluY	0.01

Supplementary Figure 1000: Properties and genomic distribution of motifs identified for the ZNF283 transcription factor in HEK293 (accession ChipExo models).

TF-MoDisCO pattern_0 n=1463, CWM

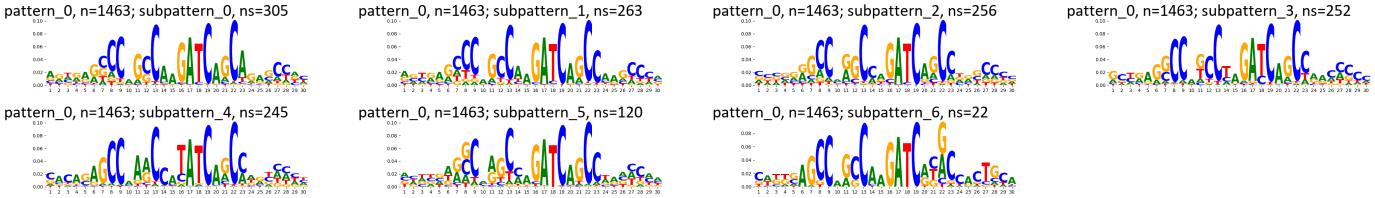

TF-MoDisCO pattern_0 n=1463, PWM

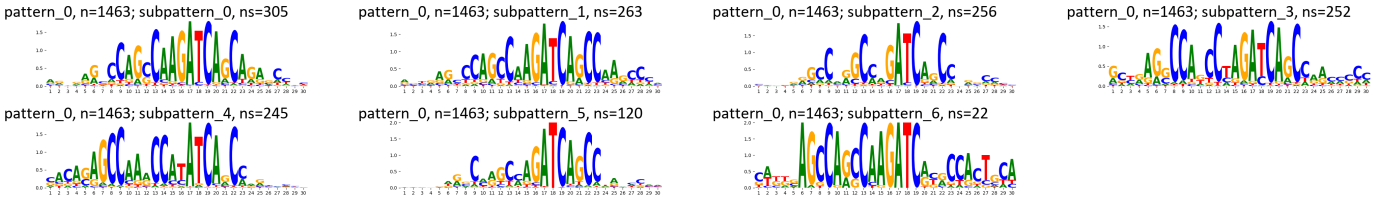

Supplementary Figure 1001: TF-MoDisCO subpatterns for the ZNF283 transcription factor in HEK293 (accession ChipExo models).

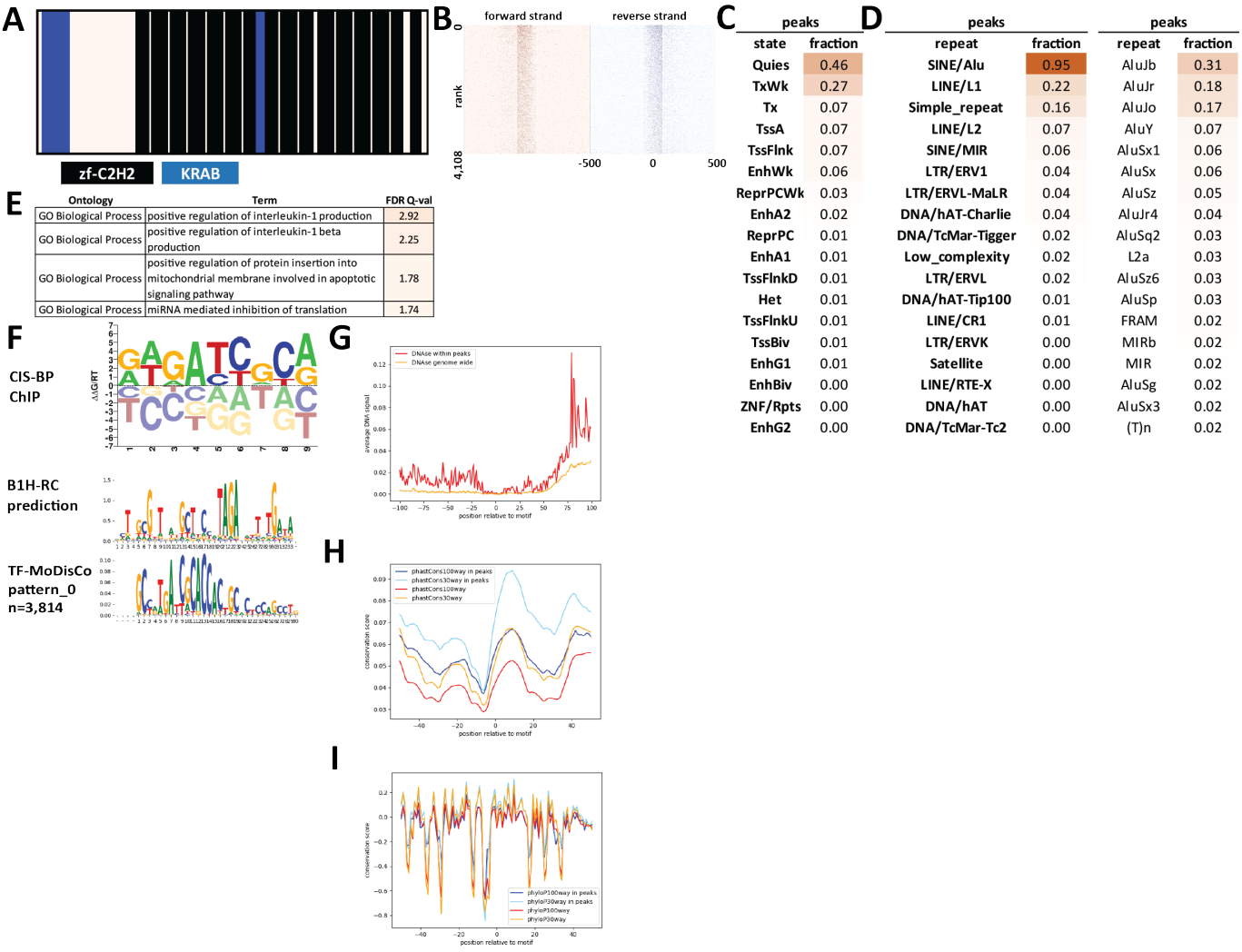

Ontology	Term	FDR Q-val
GO Biological Process	positive regulation of interleukin-1 production	2.92
GO Biological Process	positive regulation of interleukin-1 beta production	2.25
GO Biological Process	positive regulation of protein insertion into mitochondrial membrane involved in apoptotic signaling pathway	1.78
GO Biological Process	miRNA mediated inhibition of translation	1.74

peaks

state	fraction
Quies	0.46
TxWk	0.27
Tx	0.07
TssA	0.07
TssFlnk	0.07
EnhWk	0.06
ReprPCWk	0.03
EnhA2	0.02
ReprPC	0.01
EnhA1	0.01
TssFlnkD	0.01
Het	0.01
TssFlnkU	0.01
TssBiv	0.01
EnhG1	0.01
EnhBiv	0.00
ZNF/Rpts	0.00
EnhG2	0.00

peaks

repeat	fraction
SINE/Alu	0.95
LINE/L1	0.22
Simple_repeat	0.16
LINE/L2	0.07
SINE/MIR	0.06
LTR/ERV1	0.04
LTR/ERVL-MaLR	0.04
DNA/hAT-Charlie	0.04
DNA/TcMar-Tigger	0.02
Low_complexity	0.02
LTR/ERVL	0.02
DNA/hAT-Tip100	0.01
LINE/CR1	0.01
LTR/ERVK	0.00
Satellite	0.00
LINE/RTE-X	0.00
DNA/hAT	0.00
DNA/TcMar-Tc2	0.00

peaks

repeat	fraction
AluJb	0.31
AluJr	0.18
AluJo	0.17
AluY	0.07
AluSx1	0.06
AluSx	0.06
AluSz	0.05
AluJr4	0.04
AluSq2	0.03
L2a	0.03
AluSz6	0.03
AluSp	0.03
FRAM	0.02
MIRb	0.02
MIR	0.02
AluSg	0.02
AluSx3	0.02
(T)n	0.02

Supplementary Figure 1002: Properties and genomic distribution of motifs identified for the ZNF284 transcription factor in HEK293 (accession ChipExo models).

TF-MoDisCO pattern_0 n=3814, CWM

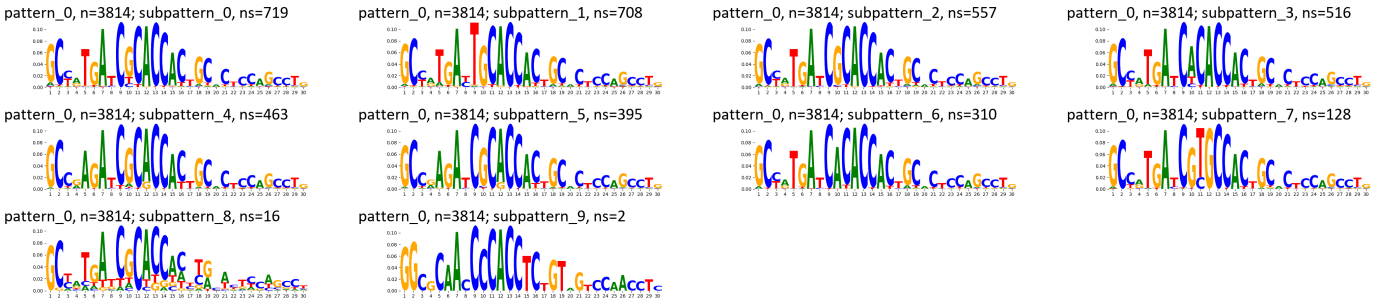

TF-MoDisCO pattern_0 n=3814, PWM

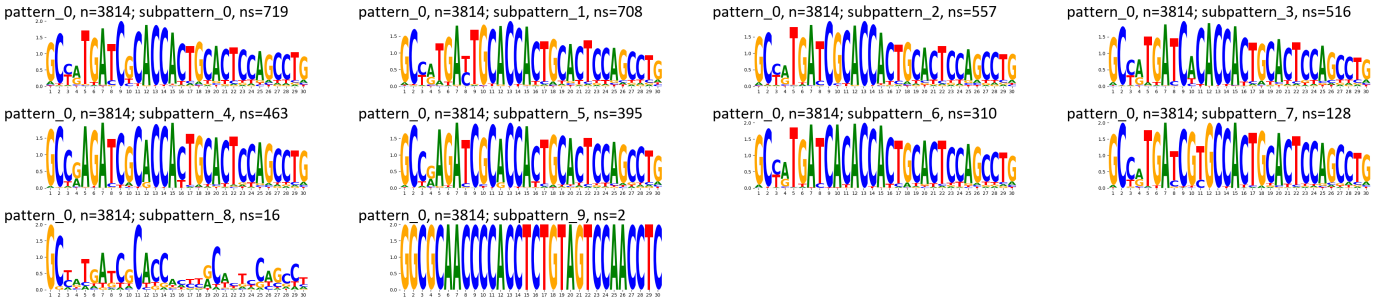

Supplementary Figure 1003: TF-MoDisCO subpatterns for the ZNF284 transcription factor in HEK293 (accession ChipExo models).

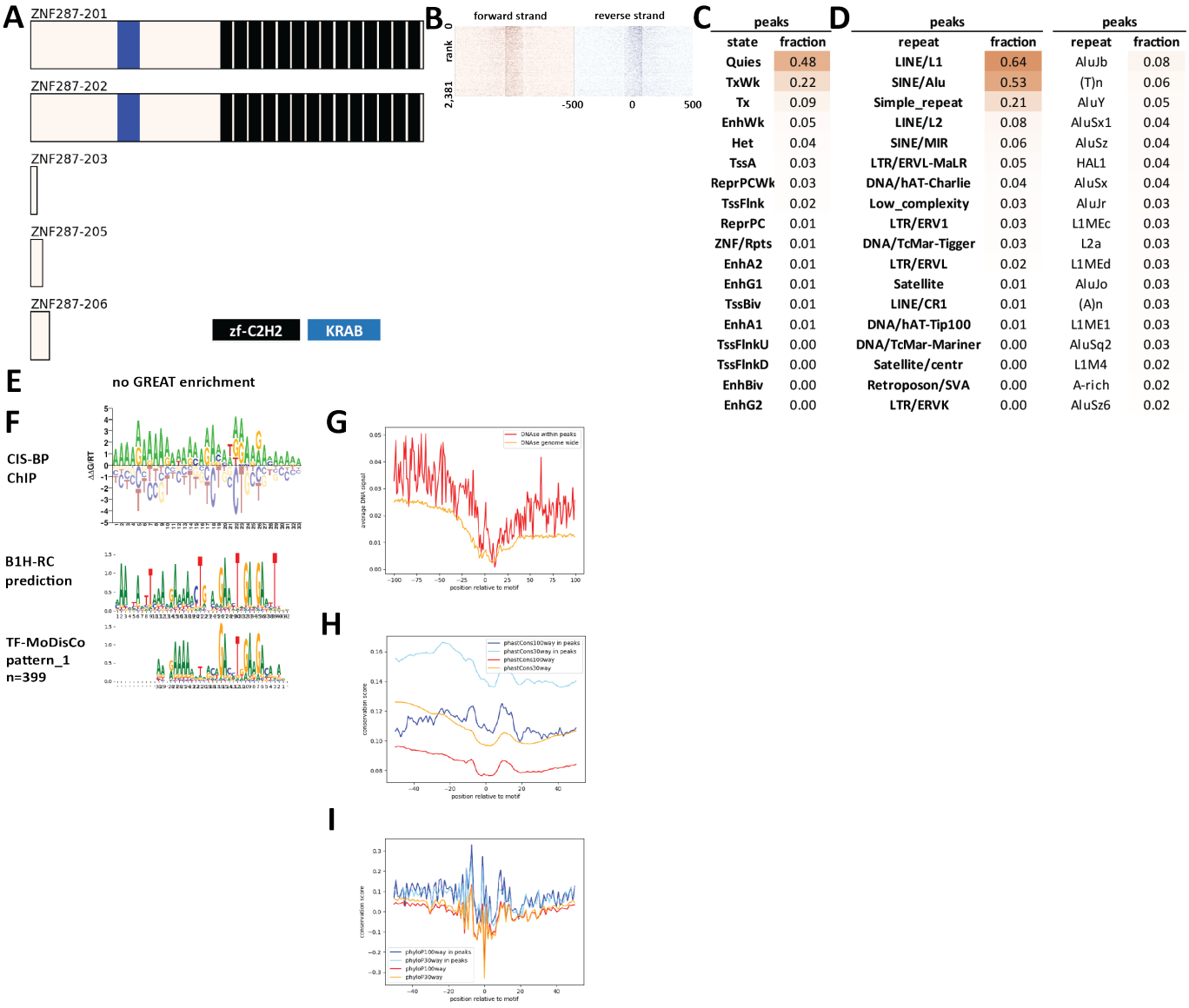

C

peaks	
state	fraction
Quies	0.48
TxWk	0.22
Tx	0.09
EnhWk	0.05
Het	0.04
TssA	0.03
ReprPCWk	0.03
TssFlnk	0.02
ReprPC	0.01
ZNF/Rpts	0.01
EnhA2	0.01
EnhG1	0.01
TssBiv	0.01
EnhA1	0.01
TssFlnkU	0.00
TssFlnkD	0.00
EnhBiv	0.00
EnhG2	0.00

D

peaks		peaks	
repeat	fraction	repeat	fraction
LINE/L1	0.64	AluJb	0.08
SINE/Alu	0.53	(T)n	0.06
Simple_repeat	0.21	AluY	0.05
LINE/L2	0.08	AluSx1	0.04
SINE/MIR	0.06	AluSz	0.04
LTR/ERVL-MaLR	0.05	HAL1	0.04
DNA/hAT-Charlie	0.04	AluSx	0.04
Low_complexity	0.03	AluJr	0.03
LTR/ERV1	0.03	L1MEc	0.03
DNA/TcMar-Tigger	0.03	L2a	0.03
LTR/ERVL	0.02	L1MEd	0.03
Satellite	0.01	AluJo	0.03
LINE/CR1	0.01	(A)n	0.03
DNA/hAT-Tip100	0.01	L1ME1	0.03
DNA/TcMar-Mariner	0.00	AluSq2	0.03
Satellite/centr	0.00	L1M4	0.02
Retroposon/SVA	0.00	A-rich	0.02
LTR/ERVK	0.00	AluSz6	0.02

Supplementary Figure 1004: Properties and genomic distribution of motifs identified for the ZNF287 transcription factor in HEK293 (accession ChipExo models).

TF-MoDisCO pattern_1 n=399, CWM

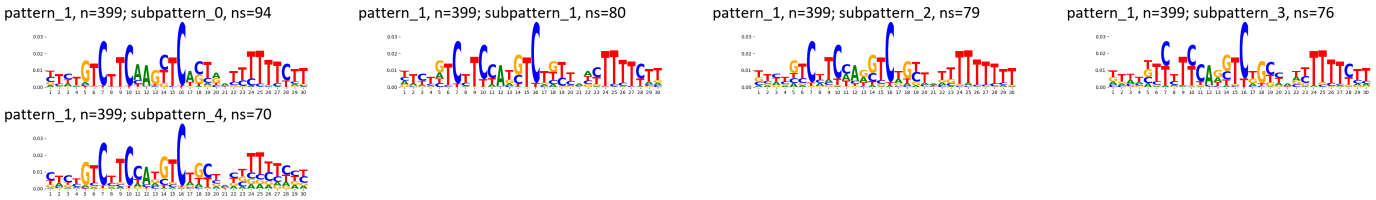

TF-MoDisCO pattern_1 n=399, PWM

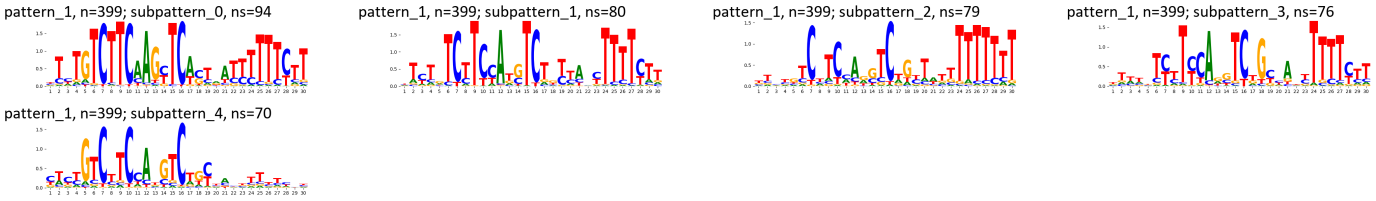

Supplementary Figure 1005: TF-MoDisCO subpatterns for the ZNF287 transcription factor in HEK293 (accession ChipExo models).

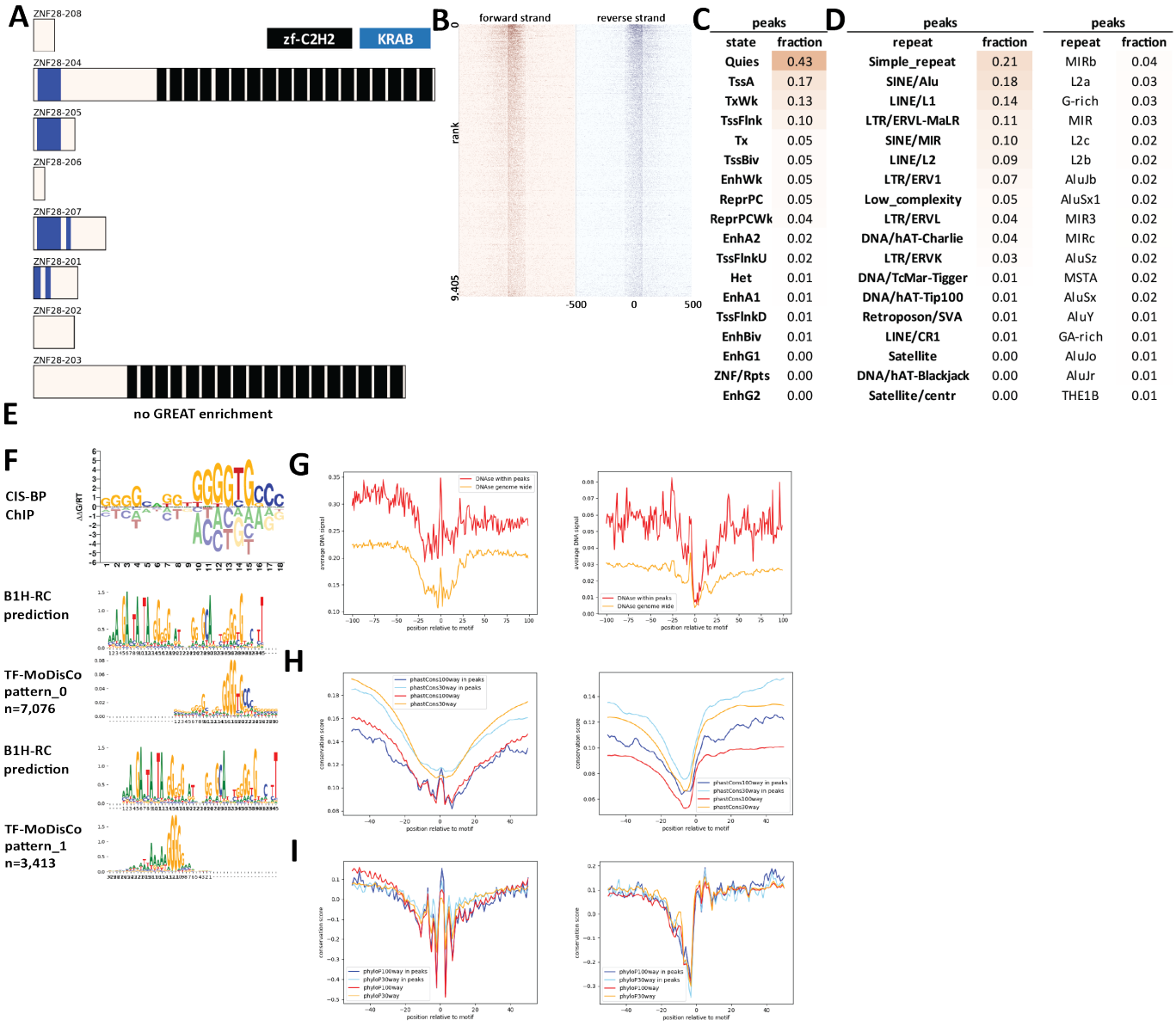

peaks	
state	fraction
Quies	0.43
TssA	0.17
TxWk	0.13
TssFlnk	0.10
Tx	0.05
TssBiv	0.05
EnhWk	0.05
ReprPC	0.05
ReprPCWk	0.04
EnhA2	0.02
TssFlnkU	0.02
Het	0.01
EnhA1	0.01
TssFlnkD	0.01
EnhBiv	0.01
EnhG1	0.00
ZNF/Rpts	0.00
EnhG2	0.00

peaks	
repeat	fraction
Simple_repeat	0.21
SINE/Alu	0.18
LINE/L1	0.14
LTR/ERVL-MaLR	0.11
SINE/MIR	0.10
LINE/L2	0.09
LTR/ERV1	0.07
Low_complexity	0.05
LTR/ERVL	0.04
DNA/hAT-Charlie	0.04
LTR/ERVK	0.03
DNA/TcMar-Tigger	0.01
DNA/hAT-Tip100	0.01
Retroposon/SVA	0.01
LINE/CR1	0.01
Satellite	0.00
DNA/hAT-Blackjack	0.00
Satellite/centr	0.00

peaks	
repeat	fraction
MIRb	0.04
L2a	0.03
G-rich	0.03
MIR	0.03
L2c	0.02
L2b	0.02
AluJb	0.02
AluSx1	0.02
MIR3	0.02
MIRc	0.02
AluSz	0.02
MSTA	0.02
AluSx	0.02
AluY	0.01
GA-rich	0.01
AluJo	0.01
AluJr	0.01
THE1B	0.01

Supplementary Figure 1006: Properties and genomic distribution of motifs identified for the ZNF28 transcription factor in HEK293 (accession ChipExo models).

TF-MoDisCO pattern_0 n=7076, CWM

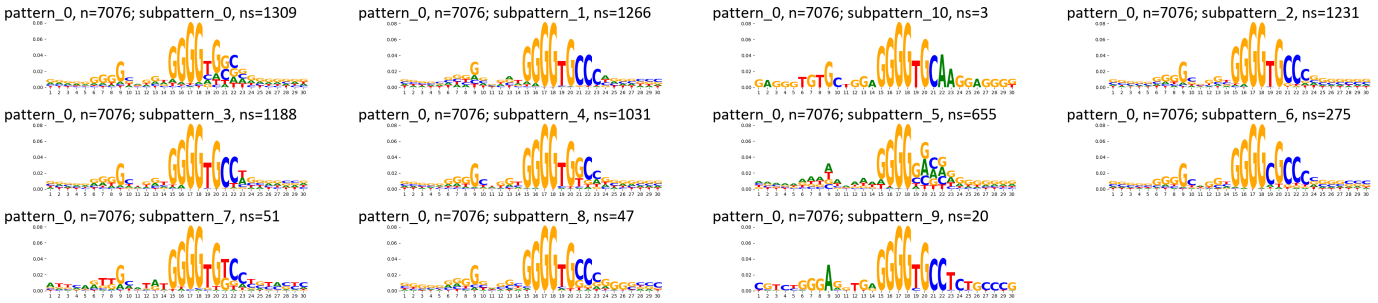

TF-MoDisCO pattern_0 n=7076, PWM

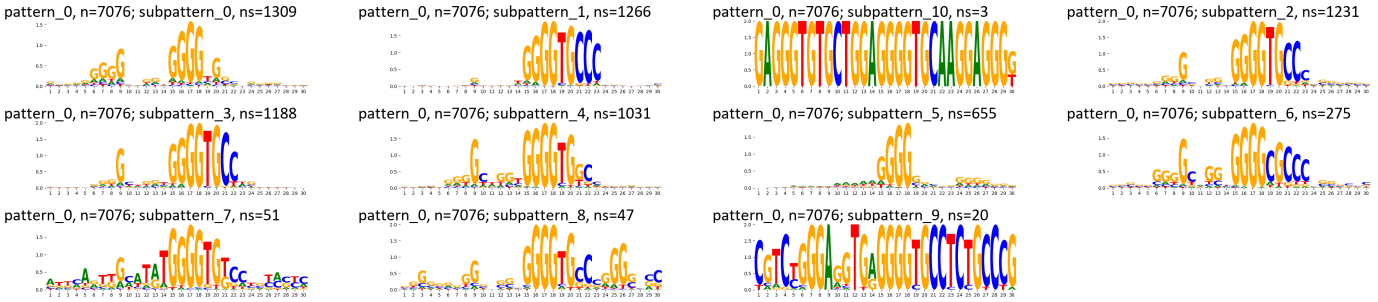

TF-MoDisCO pattern_1 n=3413, CWM

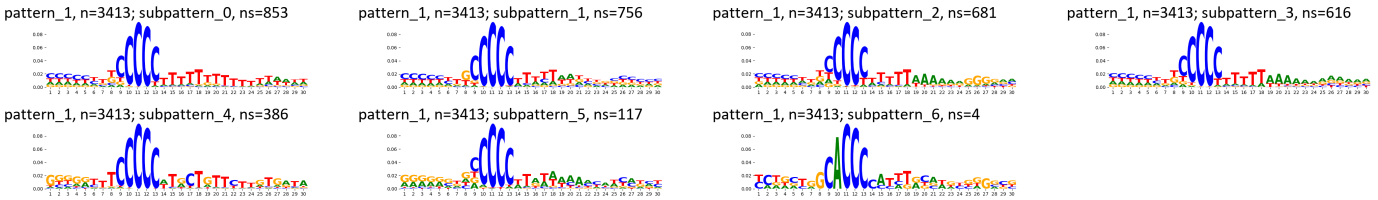

TF-MoDisCO pattern_1 n=3413, PWM

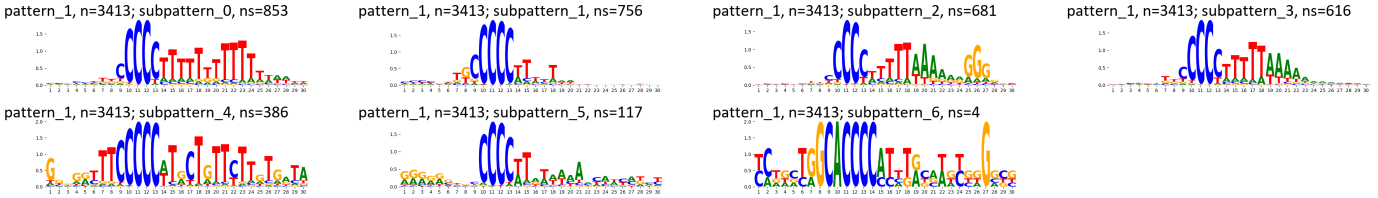

Supplementary Figure 1007: TF-MoDisCO subpatterns for the ZNF28 transcription factor in HEK293 (accession ChipExo models).

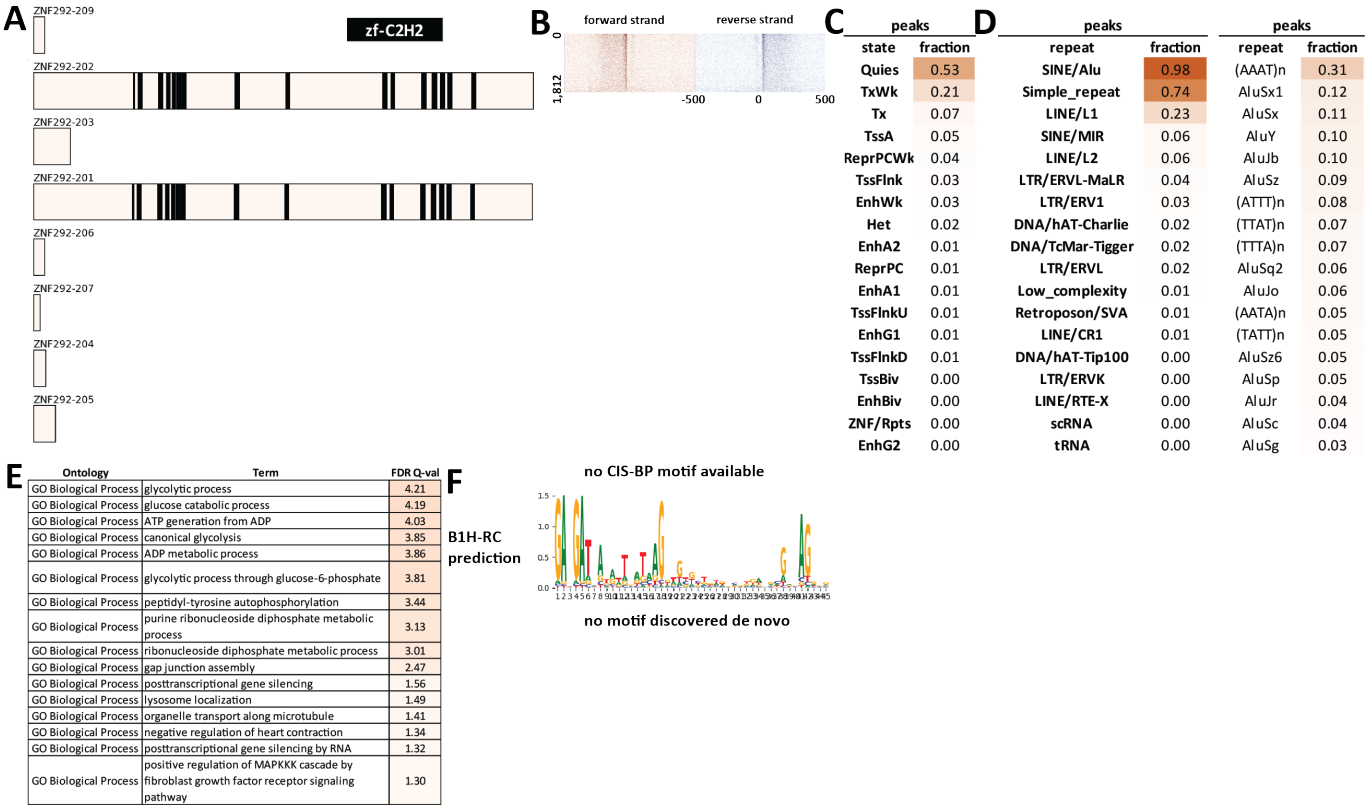

Supplementary Figure 1008: Properties and genomic distribution of motifs identified for the ZNF292 transcription factor in HEK293 (accession ENCSR228PGT).

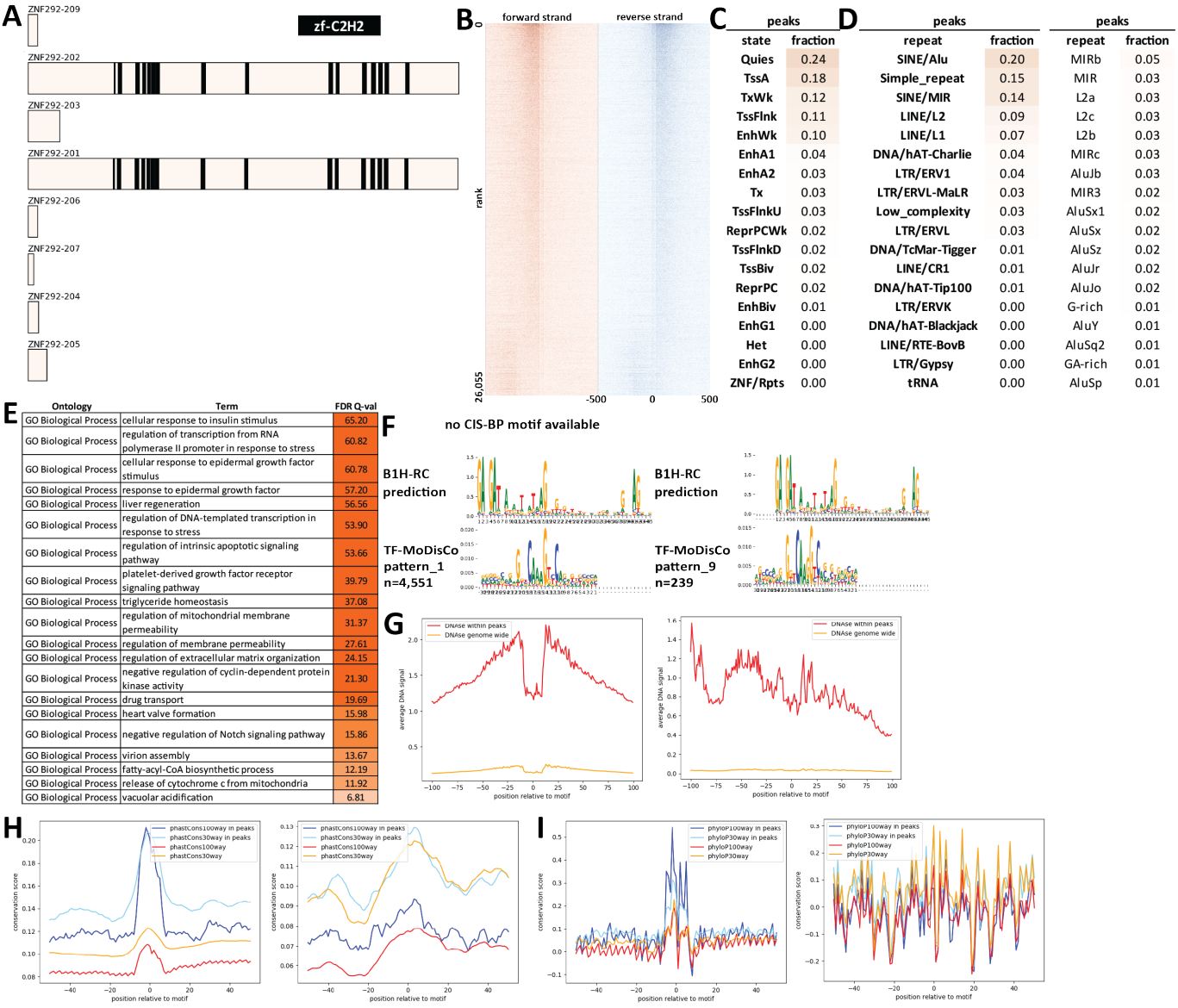

peaks	
state	fraction
Quies	0.24
TssA	0.18
TxWk	0.12
TssFlnk	0.11
EnhWk	0.10
EnhA1	0.04
EnhA2	0.03
Tx	0.03
TssFlnkU	0.03
ReprPCWk	0.02
TssFlnkD	0.02
TssBiv	0.02
ReprPC	0.02
EnhBiv	0.01
EnhG1	0.00
Het	0.00
EnhG2	0.00
ZNF/Rpts	0.00

peaks		peaks	
repeat	fraction	repeat	fraction
SINE/Alu	0.20	MIRb	0.05
Simple_repeat	0.15	MIR	0.03
SINE/MIR	0.14	L2a	0.03
LINE/L2	0.09	L2c	0.03
LINE/L1	0.07	L2b	0.03
DNA/hAT-Charlie	0.04	MIRc	0.03
LTR/ERV1	0.04	AluJb	0.03
LTR/ERVL-MaLR	0.03	MIR3	0.02
Low_complexity	0.03	AluSx1	0.02
LTR/ERVL	0.03	AluSx	0.02
DNA/TcMar-Tigger	0.01	AluSz	0.02
LINE/CR1	0.01	AluJr	0.02
DNA/hAT-Tip100	0.01	AluJo	0.02
LTR/ERVK	0.00	G-rich	0.01
DNA/hAT-Blackjack	0.00	AluY	0.01
LINE/RTE-BovB	0.00	AluSq2	0.01
LTR/Gypsy	0.00	GA-rich	0.01
tRNA	0.00	AluSp	0.01

Ontology	Term	FDR Q-val
GO Biological Process	cellular response to insulin stimulus	65.20
GO Biological Process	regulation of transcription from RNA polymerase II promoter in response to stress	60.82
GO Biological Process	cellular response to epidermal growth factor stimulus	60.78
GO Biological Process	response to epidermal growth factor	57.20
GO Biological Process	liver regeneration	56.56
GO Biological Process	regulation of DNA-templated transcription in response to stress	53.90
GO Biological Process	regulation of intrinsic apoptotic signaling pathway	53.66
GO Biological Process	platelet-derived growth factor receptor signaling pathway	39.79
GO Biological Process	triglyceride homeostasis	37.08
GO Biological Process	regulation of mitochondrial membrane permeability	31.37
GO Biological Process	regulation of membrane permeability	27.61
GO Biological Process	regulation of extracellular matrix organization	24.15
GO Biological Process	negative regulation of cyclin-dependent protein kinase activity	21.30
GO Biological Process	drug transport	19.69
GO Biological Process	heart valve formation	15.98
GO Biological Process	negative regulation of Notch signaling pathway	15.86
GO Biological Process	virion assembly	13.67
GO Biological Process	fatty-acyl-CoA biosynthetic process	12.19
GO Biological Process	release of cytochrome c from mitochondria	11.92
GO Biological Process	vacuolar acidification	6.81

Supplementary Figure 1009: Properties and genomic distribution of motifs identified for the ZNF292 transcription factor in HepG2 (accession ENCSR853BYT).

TF-MoDisCO pattern_1 n=4551, CWM

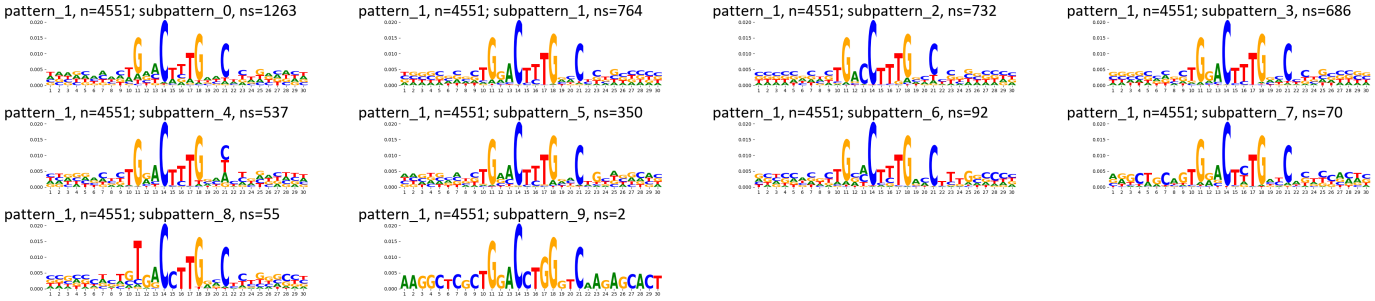

TF-MoDisCO pattern_1 n=4551, PWM

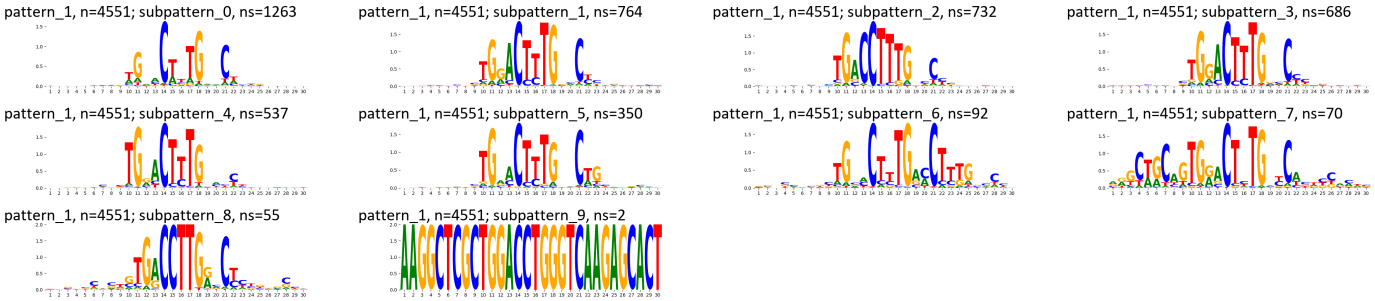

TF-MoDisCO pattern_9 n=239, CWM

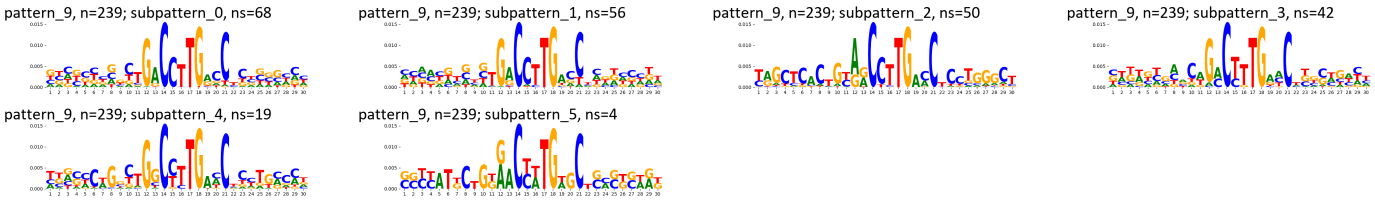

TF-MoDisCO pattern_9 n=239, PWM

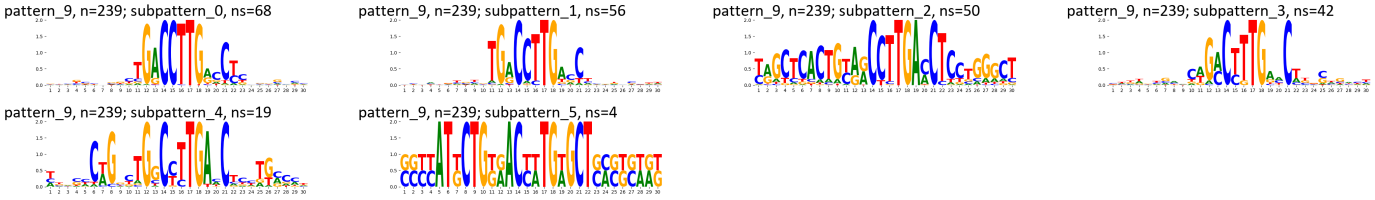

Supplementary Figure 1010: TF-MoDisCO subpatterns for the ZNF292 transcription factor in HepG2 (accession ENCSR853BYT).

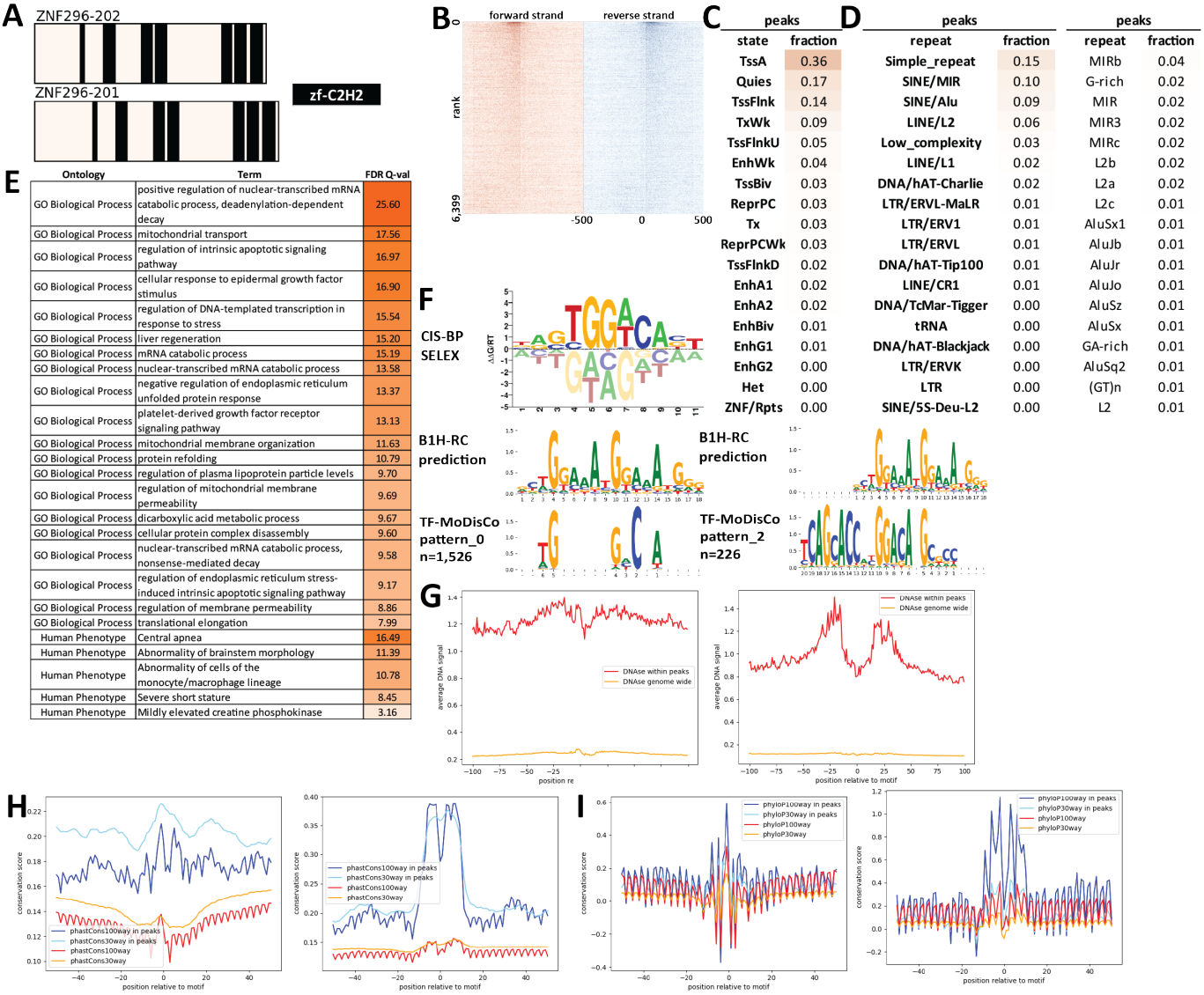

Supplementary Figure 1011: Properties and genomic distribution of motifs identified for the ZNF296 transcription factor in HepG2 (accession ENCSR862LJQ).

TF-MoDisCO pattern_0 n=1526, CWM

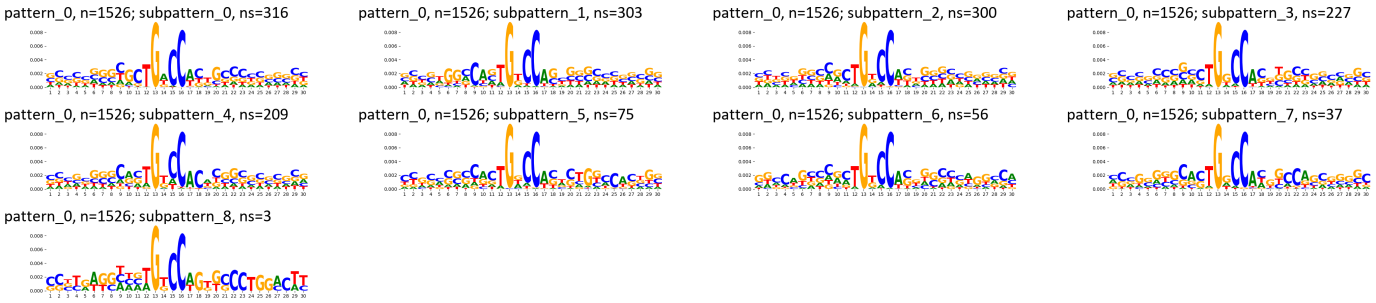

TF-MoDisCO pattern_0 n=1526, PWM

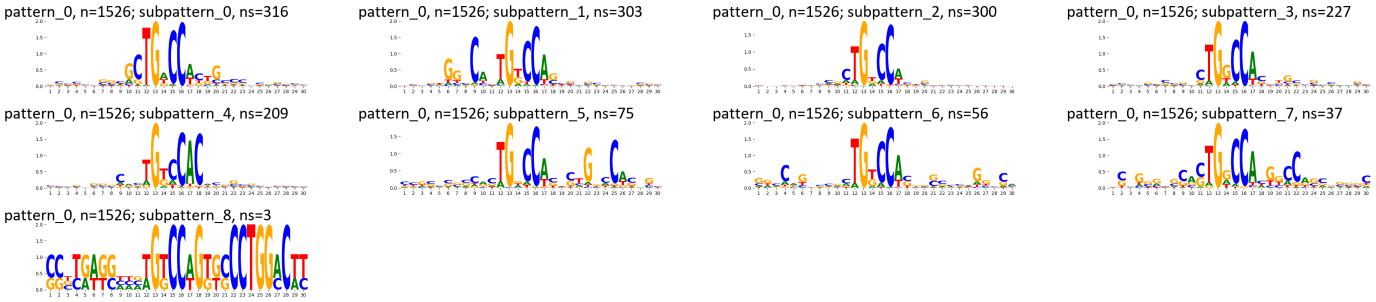

TF-MoDisCO pattern_2 n=226, CWM

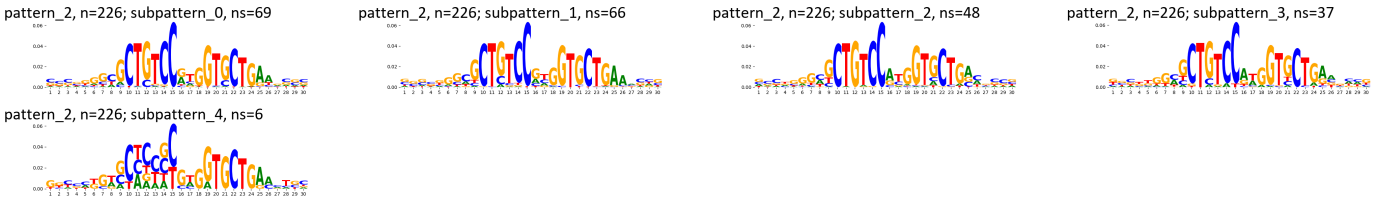

TF-MoDisCO pattern_2 n=226, PWM

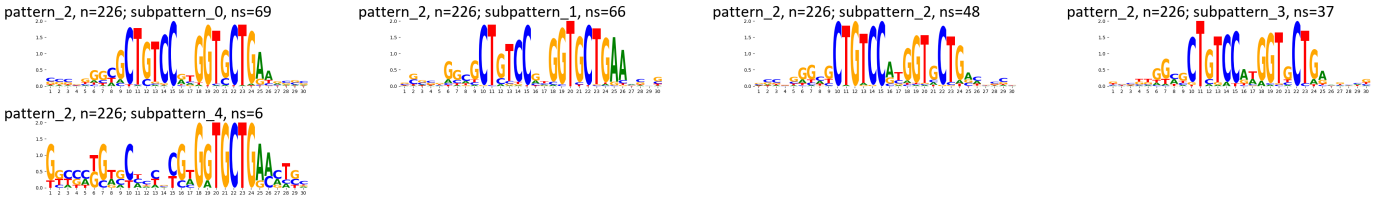

Supplementary Figure 1012: TF-MoDisCO subpatterns for the ZNF296 transcription factor in HepG2 (accession ENCSR862LJQ).

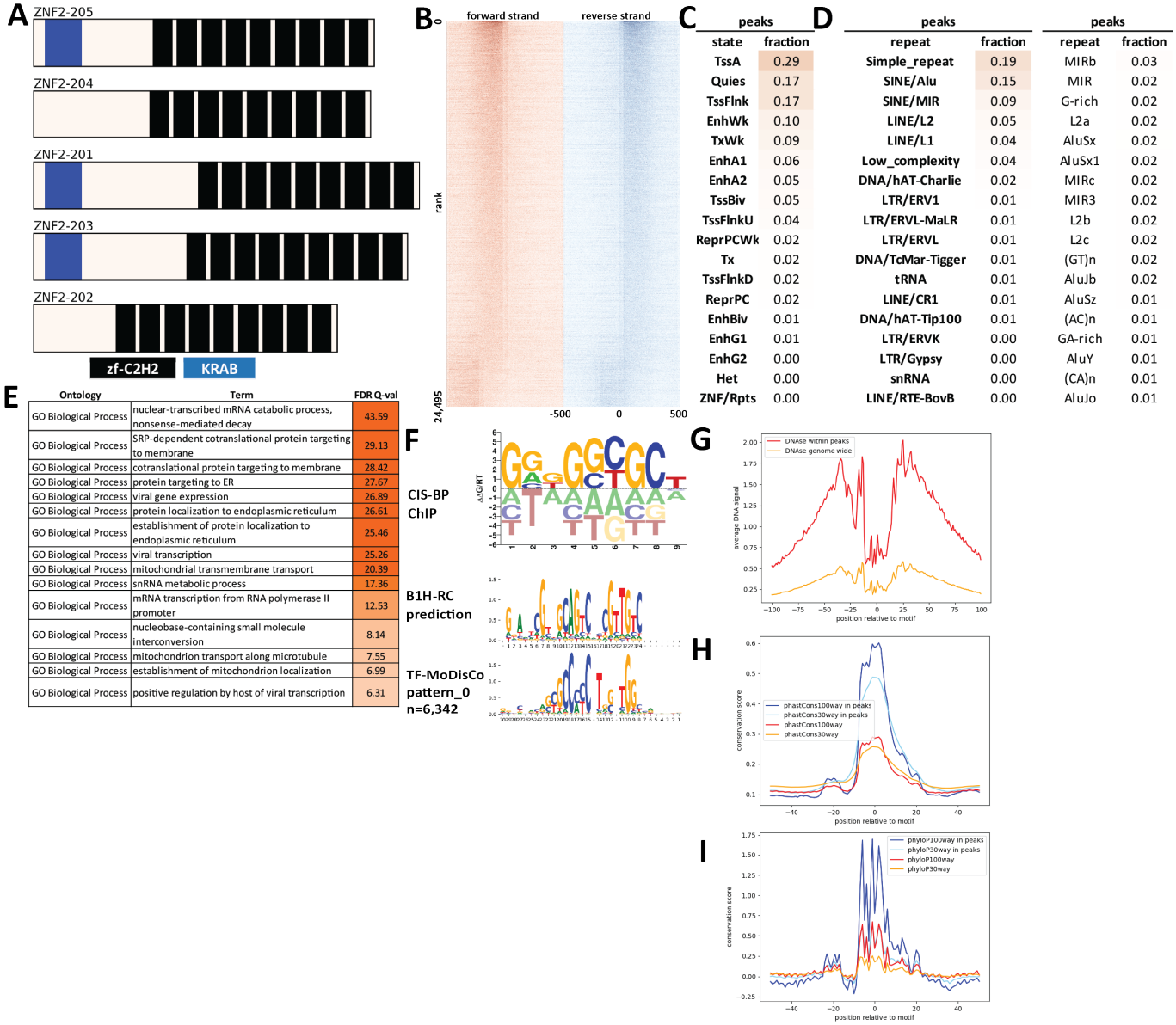

Supplementary Figure 1013: Properties and genomic distribution of motifs identified for the ZNF2 transcription factor in HEK293 (accession ENCSR011CKE).

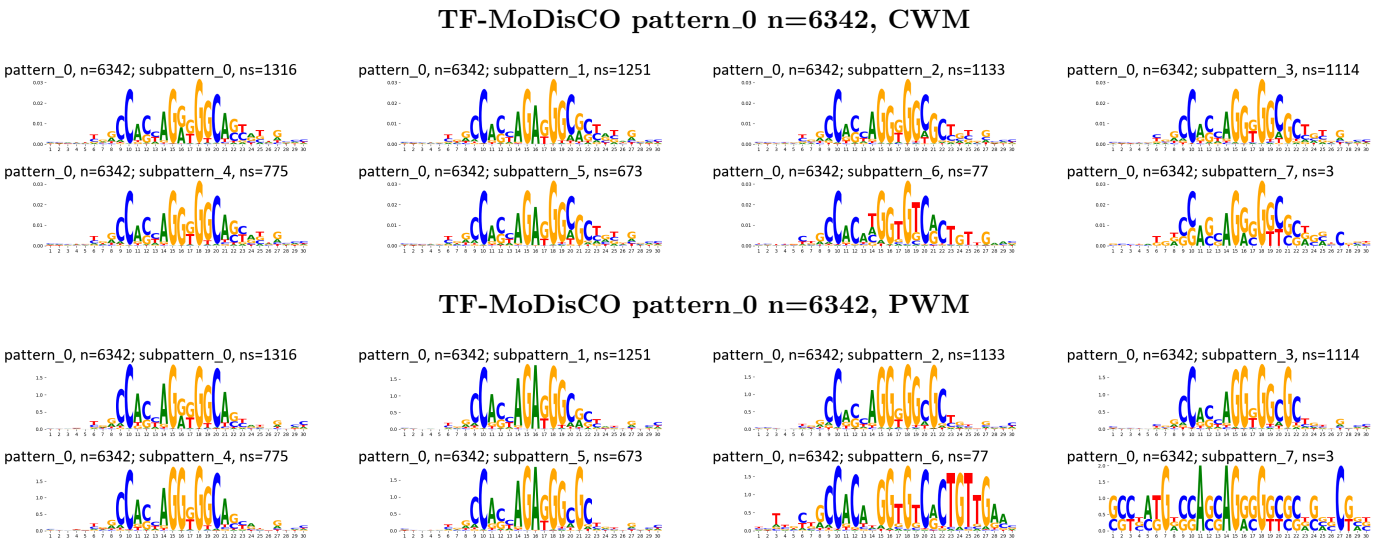

Supplementary Figure 1014: TF-MoDisCO subpatterns for the ZNF2 transcription factor in HEK293 (accession ENCSR011CKE).

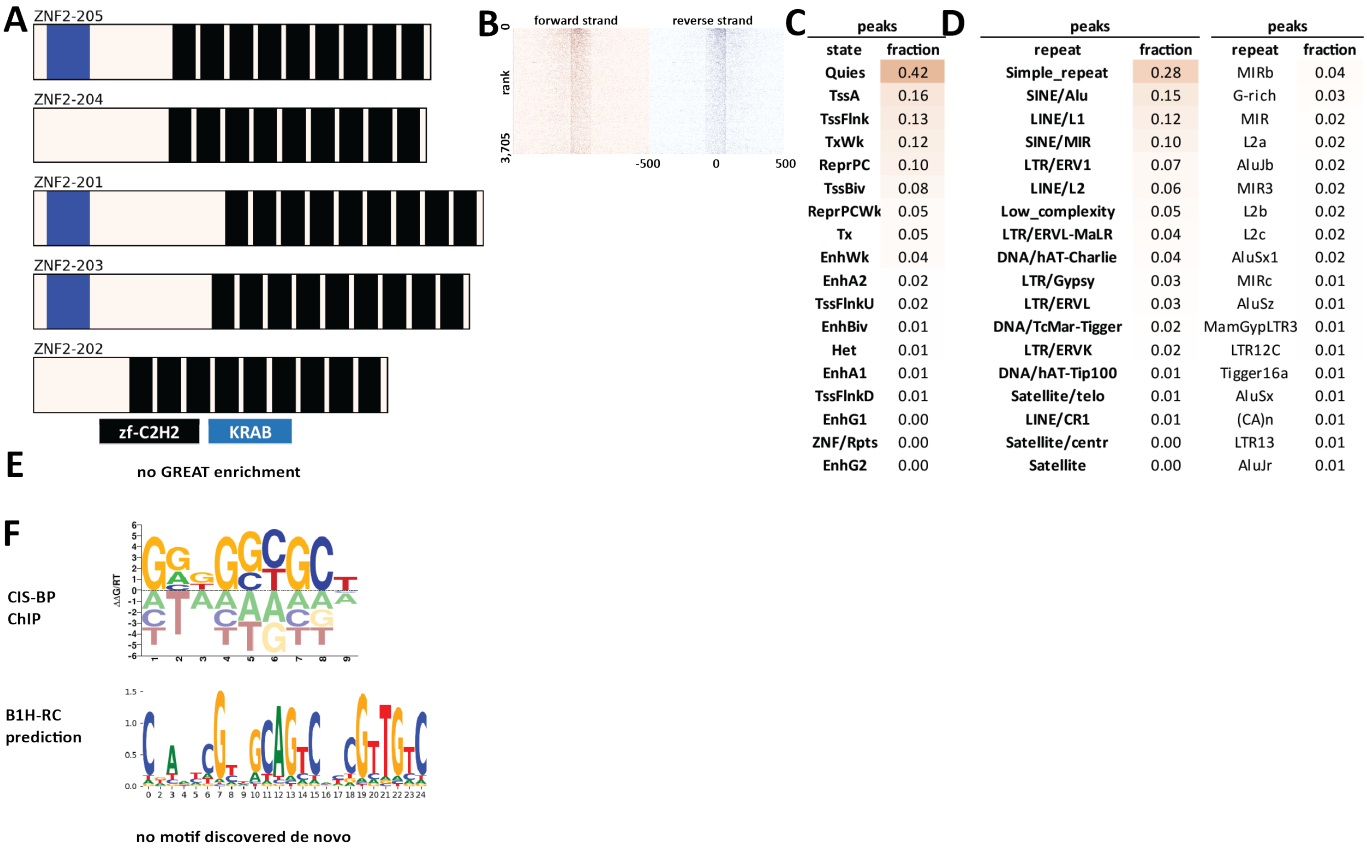

peaks	
state	fraction
Quies	0.42
TssA	0.16
TssFlnk	0.13
TxWk	0.12
ReprPC	0.10
TssBiv	0.08
ReprPCWk	0.05
Tx	0.05
EnhWk	0.04
EnhA2	0.02
TssFlnkU	0.02
EnhBiv	0.01
Het	0.01
EnhA1	0.01
TssFlnkD	0.01
EnhG1	0.00
ZNF/Rpts	0.00
EnhG2	0.00

peaks	
repeat	fraction
Simple_repeat	0.28
SINE/Alu	0.15
LINE/L1	0.12
SINE/MIR	0.10
LTR/ERV1	0.07
LINE/L2	0.06
Low_complexity	0.05
LTR/ERVL-MaLR	0.04
DNA/hAT-Charlie	0.04
LTR/Gypsy	0.03
LTR/ERVL	0.03
DNA/TcMar-Tigger	0.02
LTR/ERVK	0.02
DNA/hAT-Tip100	0.01
Satellite/telo	0.01
LINE/CR1	0.01
Satellite/centr	0.00
Satellite	0.00

peaks	
repeat	fraction
MIRb	0.04
G-rich	0.03
MIR	0.02
L2a	0.02
AluJb	0.02
MIR3	0.02
L2b	0.02
L2c	0.02
AluSx1	0.02
MIRc	0.01
AluSz	0.01
MamGypLTR3	0.01
LTR12C	0.01
Tigger16a	0.01
AluSx	0.01
(CA)n	0.01
LTR13	0.01
AluJr	0.01

Supplementary Figure 1015: Properties and genomic distribution of motifs identified for the ZNF2 transcription factor in HEK293 (accession ChipExo models).

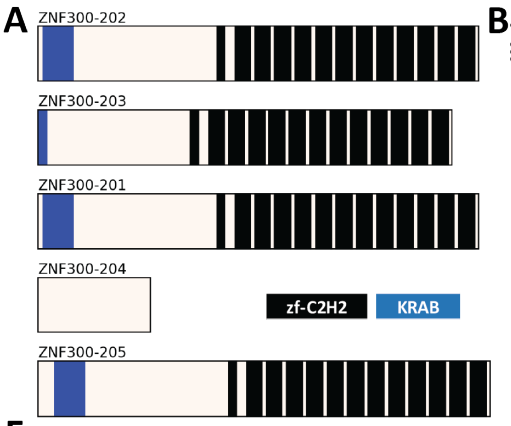

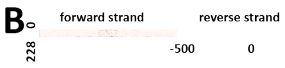

C

peaks	
state	fraction
Quies	0.43
TxWk	0.08
Tx	0.03
ReprPCWk	0.03
ReprPC	0.03
EnhWk	0.02
TssA	0.02
Het	0.02
EnhA2	0.02
ZNF/Rpts	0.01
TssFlnkU	0.01
TssFlnk	0.01
TssBiv	0.00
EnhG1	0.00
EnhA1	0.00

D

peaks		peaks	
repeat	fraction	repeat	fraction
Simple_repeat	0.29	Charlie1a	0.07
SINE/Alu	0.15	MIRb	0.02
LINE/L1	0.11	L2b	0.02
DNA/hAT-Charlie	0.09	AluYj4	0.02
LINE/L2	0.06	AluSz	0.02
SINE/MIR	0.05	AluJb	0.02
LTR/ERV1	0.04	L2a	0.02
LTR/ERVL-MaLR	0.04	(GT)n	0.02
Satellite	0.03	MIR	0.01
LTR/ERVL	0.03	LTR10A	0.01
Low_complexity	0.02	L2	0.01
DNA/TcMar-Tigger	0.01	L1MD1	0.01
Satellite/centr	0.01	GA-rich	0.01
Satellite/acro	0.01	BSR/Beta	0.01
LINE/RTE-X	0.01	AluSx1	0.01
DNA/hAT-Tip100	0.01	(TGGAA)n	0.01
snRNA	0.00	(TCTC)n	0.01
rRNA	0.00	(GA)n	0.01

E

no GREAT enrichment

F

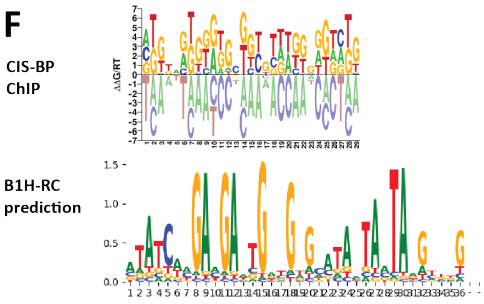

no motif discovered de novo

Supplementary Figure 1016: Properties and genomic distribution of motifs identified for the ZNF300 transcription factor in HEK293 (accession ChipExo models).

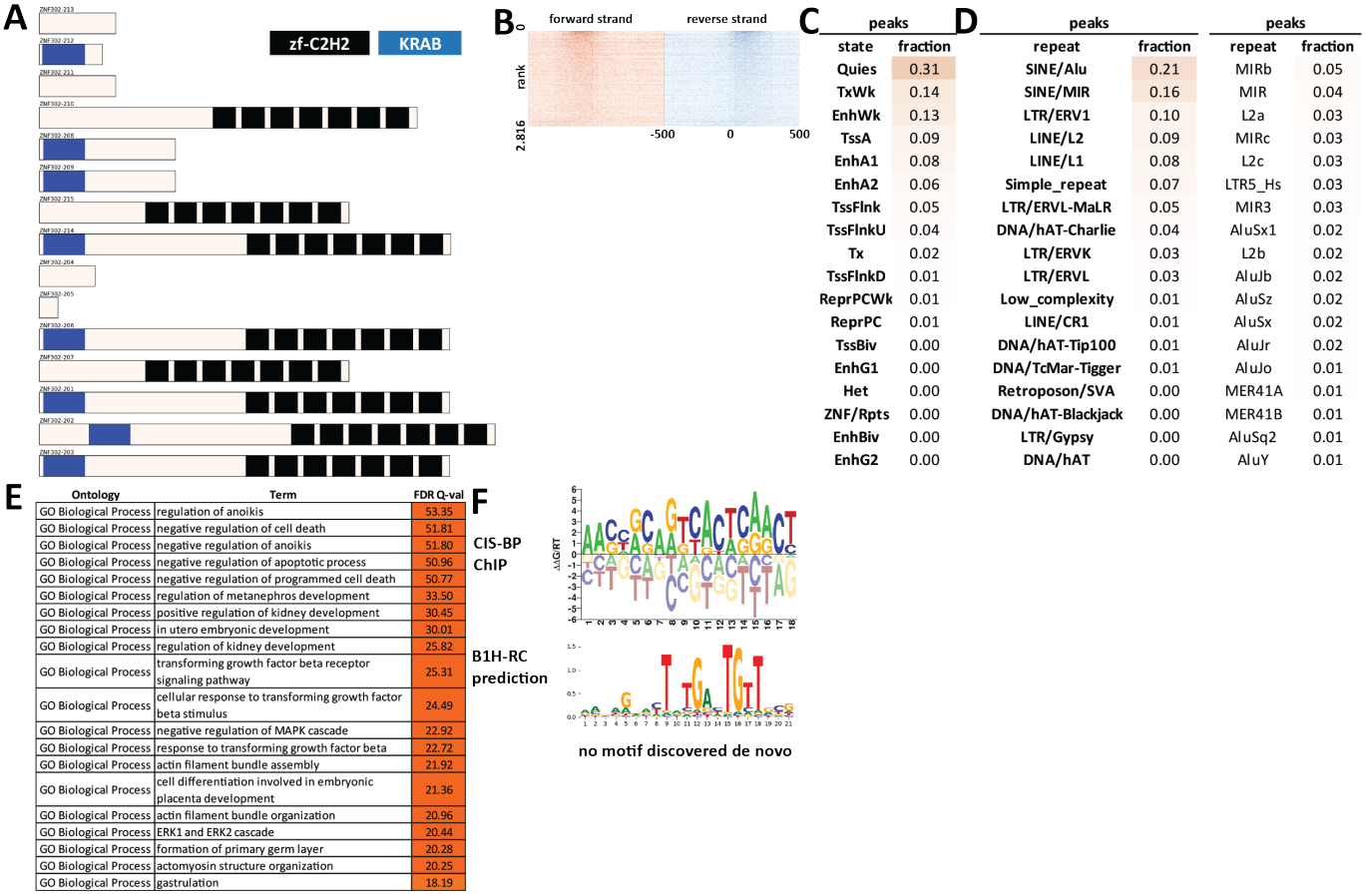

C

peaks	
state	fraction
Quies	0.31
TxWk	0.14
EnhWk	0.13
TssA	0.09
EnhA1	0.08
EnhA2	0.06
TssFlnk	0.05
TssFlnkU	0.04
Tx	0.02
TssFlnkD	0.01
ReprPCWk	0.01
ReprPC	0.01
TssBiv	0.00
EnhG1	0.00
Het	0.00
ZNF/Rpts	0.00
EnhBiv	0.00
EnhG2	0.00

D

peaks		peaks	
repeat	fraction	repeat	fraction
SINE/Alu	0.21	MIRb	0.05
SINE/MIR	0.16	MIR	0.04
LTR/ERV1	0.10	L2a	0.03
LINE/L2	0.09	MIRc	0.03
LINE/L1	0.08	L2c	0.03
Simple_repeat	0.07	LTR5_Hs	0.03
LTR/ERVL-MaLR	0.05	MIR3	0.03
DNA/hAT-Charlie	0.04	AluSx1	0.02
LTR/ERVK	0.03	L2b	0.02
LTR/ERVL	0.03	AluJb	0.02
Low_complexity	0.01	AluSz	0.02
LINE/CR1	0.01	AluSx	0.02
DNA/hAT-Tip100	0.01	AluJr	0.02
DNA/TcMar-Tigger	0.01	AluJo	0.01
Retroposon/SVA	0.00	MER41A	0.01
DNA/hAT-Blackjack	0.00	MER41B	0.01
LTR/Gypsy	0.00	AluSq2	0.01
DNA/hAT	0.00	AluY	0.01

E

Ontology	Term	FDR Q-val
GO Biological Process	regulation of anoikis	53.35
GO Biological Process	negative regulation of cell death	51.81
GO Biological Process	negative regulation of anoikis	51.80
GO Biological Process	negative regulation of apoptotic process	50.96
GO Biological Process	negative regulation of programmed cell death	50.77
GO Biological Process	regulation of metanephros development	33.50
GO Biological Process	positive regulation of kidney development	30.45
GO Biological Process	in utero embryonic development	30.01
GO Biological Process	regulation of kidney development	25.82
GO Biological Process	transforming growth factor beta receptor signaling pathway	25.31
GO Biological Process	cellular response to transforming growth factor beta stimulus	24.49
GO Biological Process	negative regulation of MAPK cascade	22.92
GO Biological Process	response to transforming growth factor beta	22.72
GO Biological Process	actin filament bundle assembly	21.92
GO Biological Process	cell differentiation involved in embryonic placenta development	21.36
GO Biological Process	actin filament bundle organization	20.96
GO Biological Process	ERK1 and ERK2 cascade	20.44
GO Biological Process	formation of primary germ layer	20.28
GO Biological Process	actomyosin structure organization	20.25
GO Biological Process	gastrulation	18.19

Supplementary Figure 1017: Properties and genomic distribution of motifs identified for the ZNF302 transcription factor in A549 (accession ENCSR590IHT).

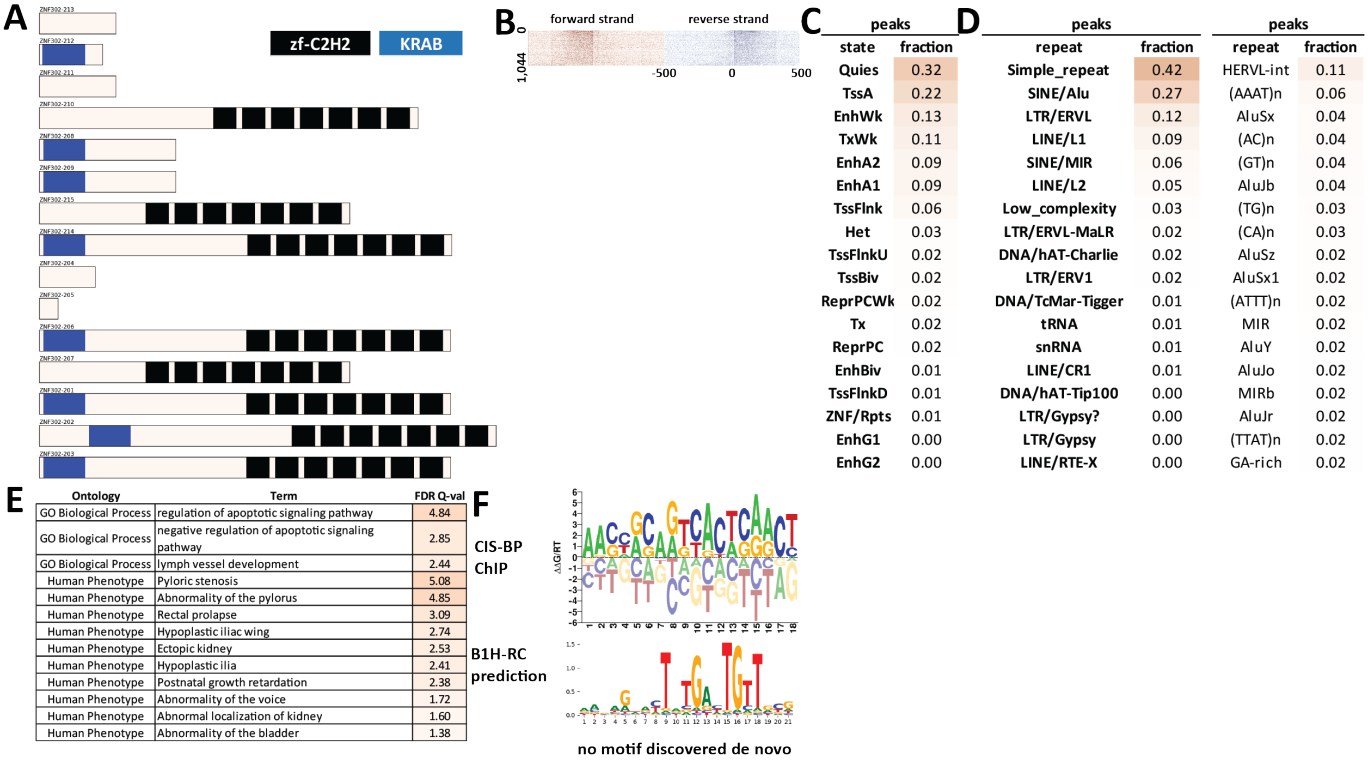

Supplementary Figure 1018: Properties and genomic distribution of motifs identified for the ZNF302 transcription factor in HEK293 (accession ENCSR513MGG).

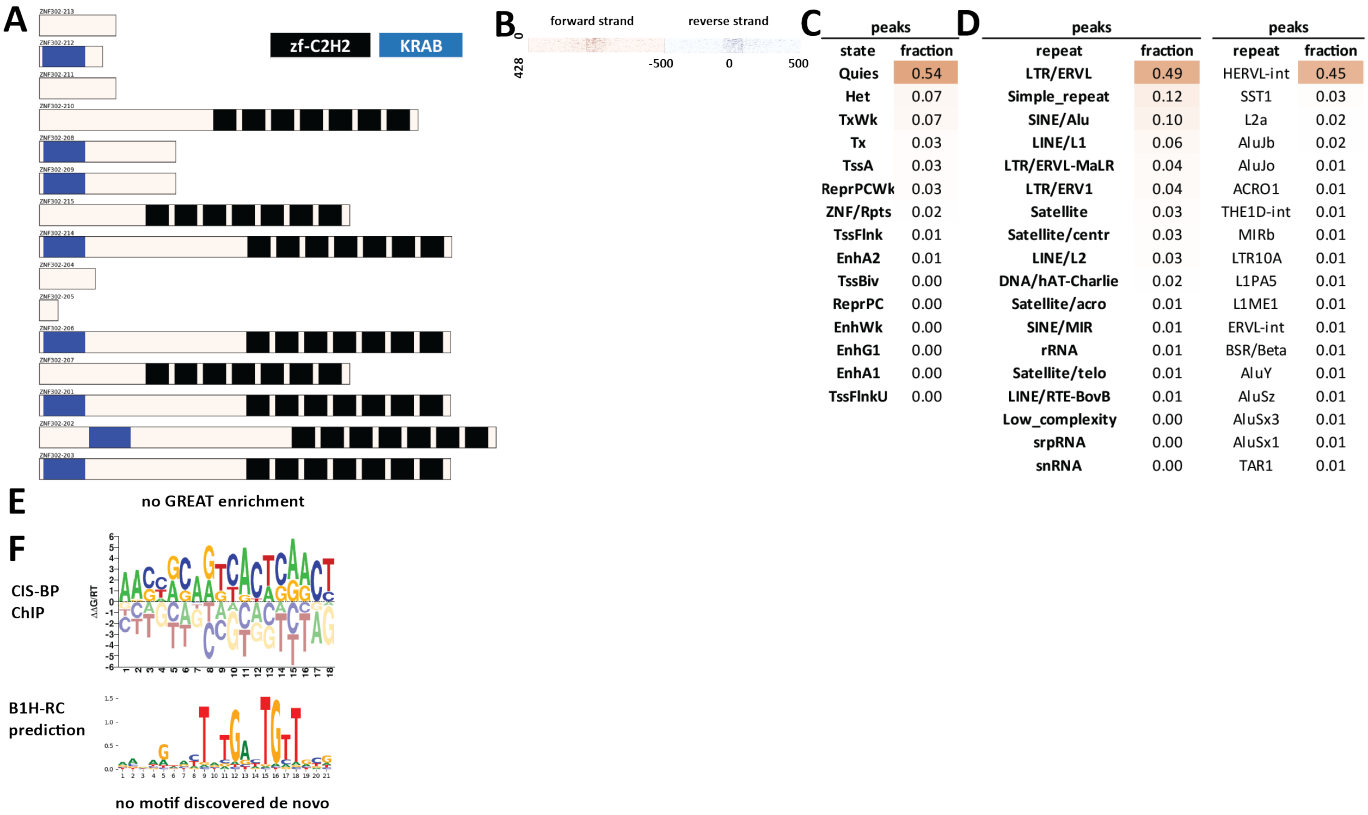

Supplementary Figure 1019: Properties and genomic distribution of motifs identified for the ZNF302 transcription factor in HEK293 (accession ChipExo models).

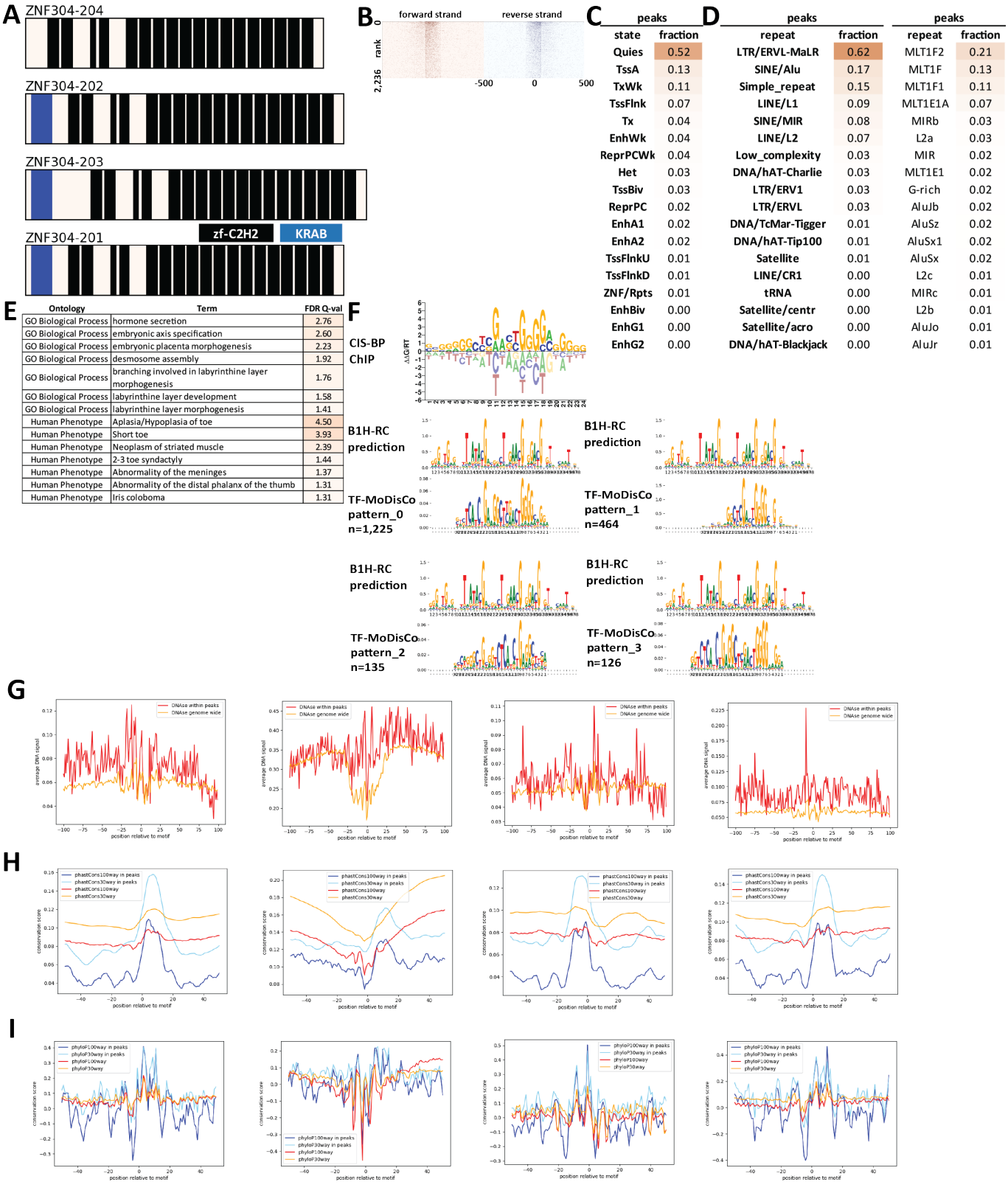

Supplementary Figure 1020: Properties and genomic distribution of motifs identified for the ZNF304 transcription factor in HEK293 (accession ChipExo models).

TF-MoDisCO pattern_0 n=1225, CWM

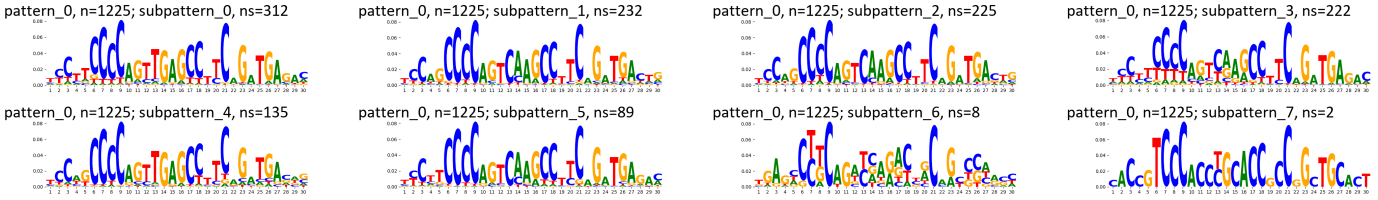

TF-MoDisCO pattern_0 n=1225, PWM

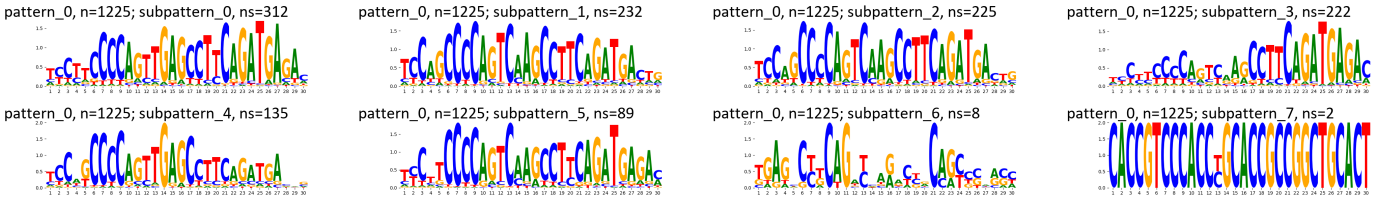

TF-MoDisCO pattern_1 n=464, CWM

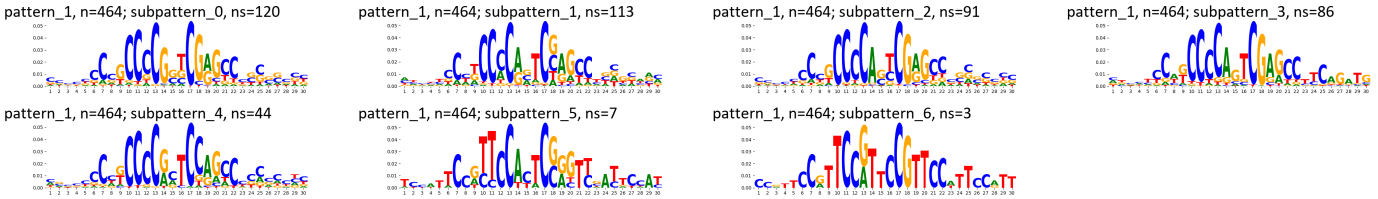

TF-MoDisCO pattern_1 n=464, PWM

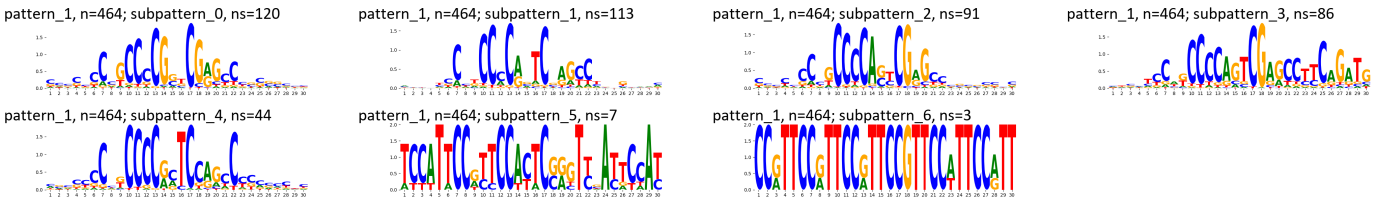

TF-MoDisCO pattern_2 n=135, CWM

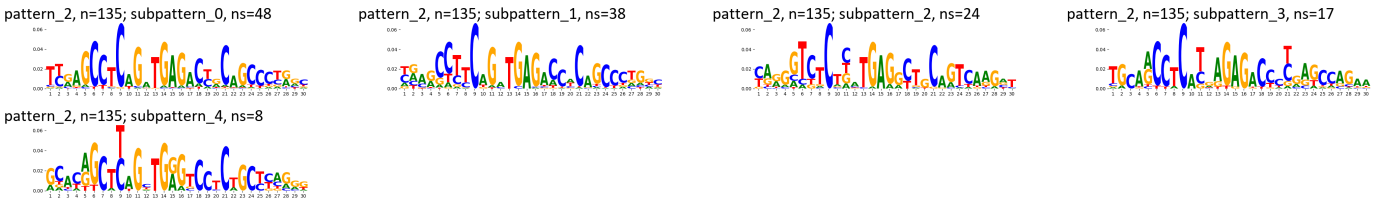

TF-MoDisCO pattern_2 n=135, PWM

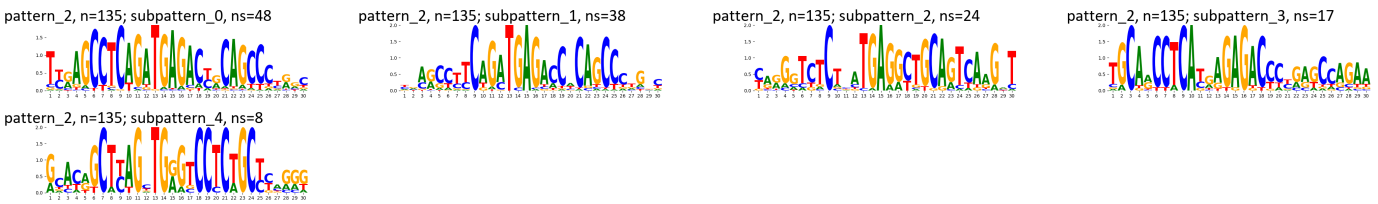

TF-MoDisCO pattern_3 n=126, CWM

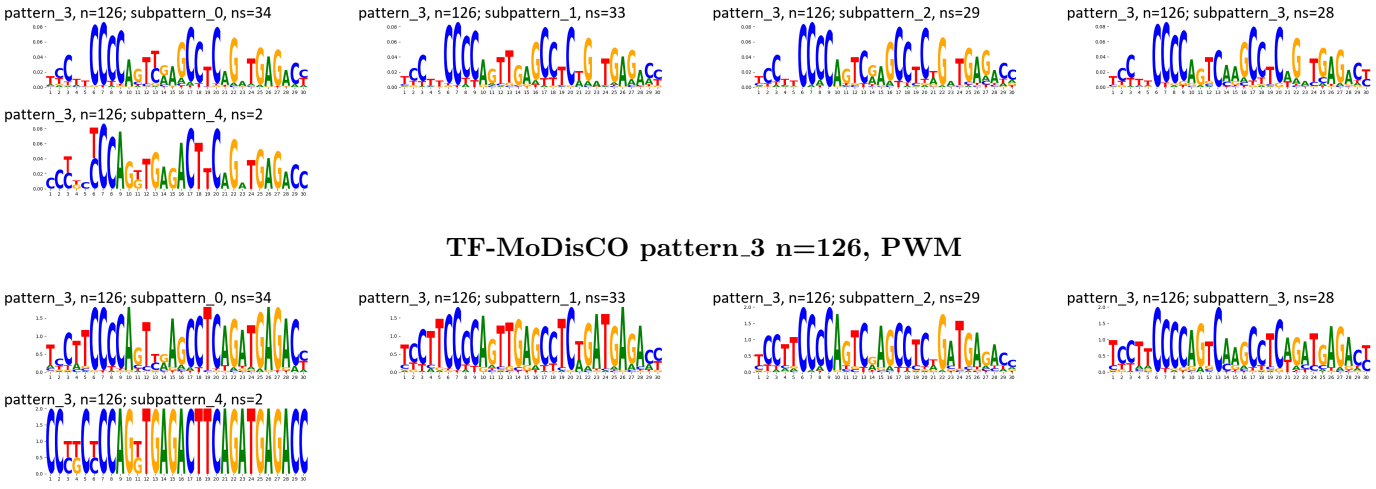

TF-MoDisCO pattern_3 n=126, PWM

Supplementary Figure 1021: TF-MoDisCO subpatterns for the ZNF304 transcription factor in HEK293 (accession ChipExo models).

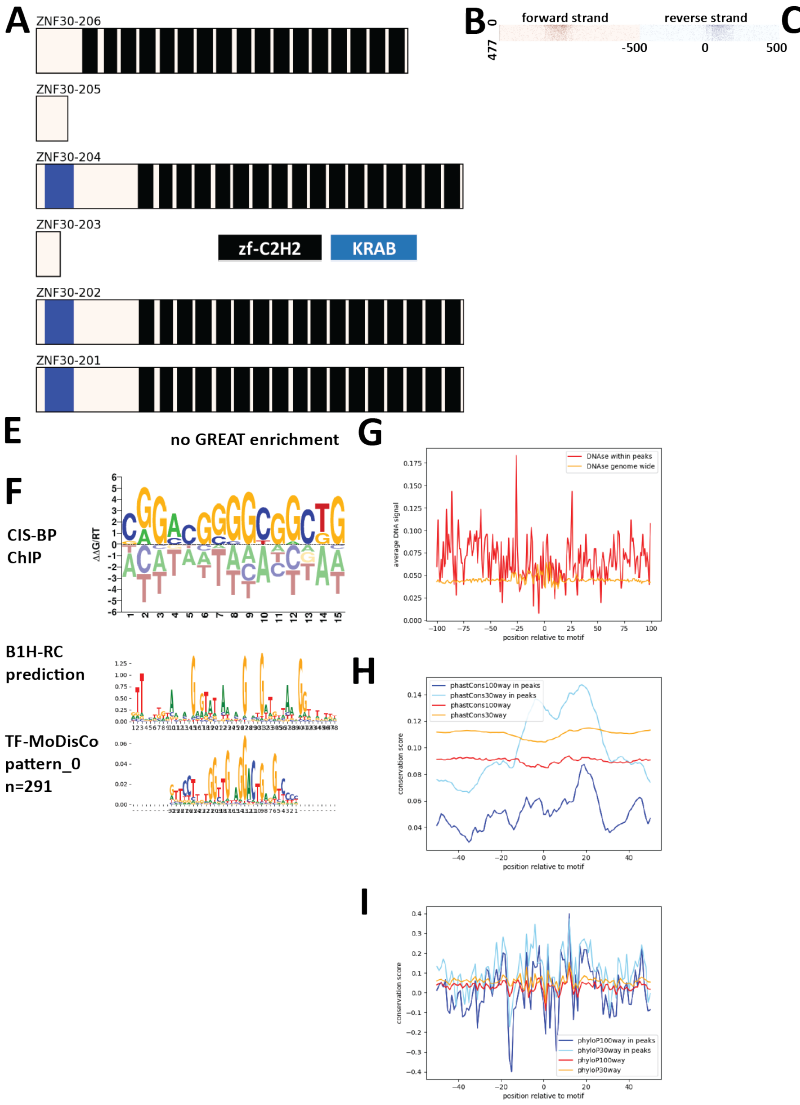

C

peaks	
state	fraction
Quies	0.47
TssA	0.13
TxWk	0.10
EnhWk	0.08
Tx	0.07
TssFlnk	0.05
EnhA1	0.04
ReprPCWk	0.03
Het	0.03
TssFlnkU	0.02
EnhA2	0.02
ReprPC	0.01
TssBiv	0.01
ZNF/Rpts	0.01
EnhG1	0.01
EnhG2	0.00

D

peaks		peaks	
repeat	fraction	repeat	fraction
LTR/ERVL-MaLR	0.44	MLT1E2	0.22
SINE/Alu	0.05	MLT1E3	0.08
LINE/L1	0.04	MLT1E1A	0.07
SINE/MIR	0.04	MLT1F2	0.02
LTR/ERV1	0.03	MLT1E1	0.02
LINE/L2	0.03	MIRb	0.01
Simple_repeat	0.02	AluJr	0.01
DNA/hAT-Charlie	0.01	MLT1E	0.01
DNA/TcMar-Tigger	0.01	MIRc	0.01
LTR/ERVL	0.01	AluJb	0.01
Low_complexity	0.01	MIR3	0.01
tRNA	0.00	LTR76	0.01
LTR/ERV1?	0.00	L2a	0.01
LINE/CR1	0.00	L2	0.01
DNA/hAT-Tip100	0.00	L2b	0.01
DNA/TcMar-Tc2	0.00	MLT1F	0.00
Retroposon/SVA	0.00	MLT1C	0.00
LTR?	0.00	MIR	0.00

Supplementary Figure 1022: Properties and genomic distribution of motifs identified for the ZNF30 transcription factor in HEK293 (accession Hughes GR models).

TF-MoDisCO pattern_0 n=291, CWM

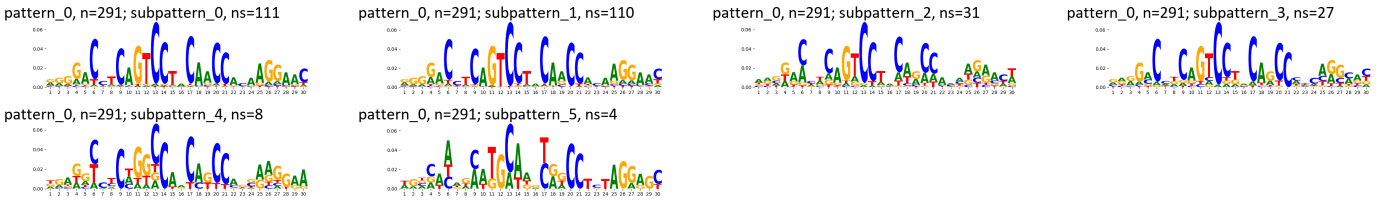

TF-MoDisCO pattern_0 n=291, PWM

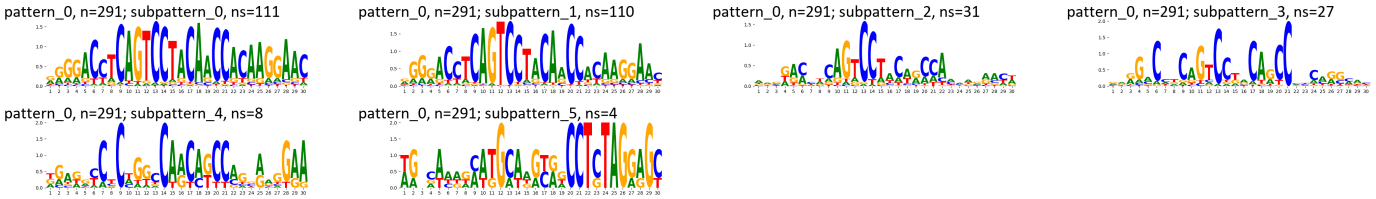

Supplementary Figure 1023: TF-MoDisCO subpatterns for the ZNF30 transcription factor in HEK293 (accession Hughes GR models).

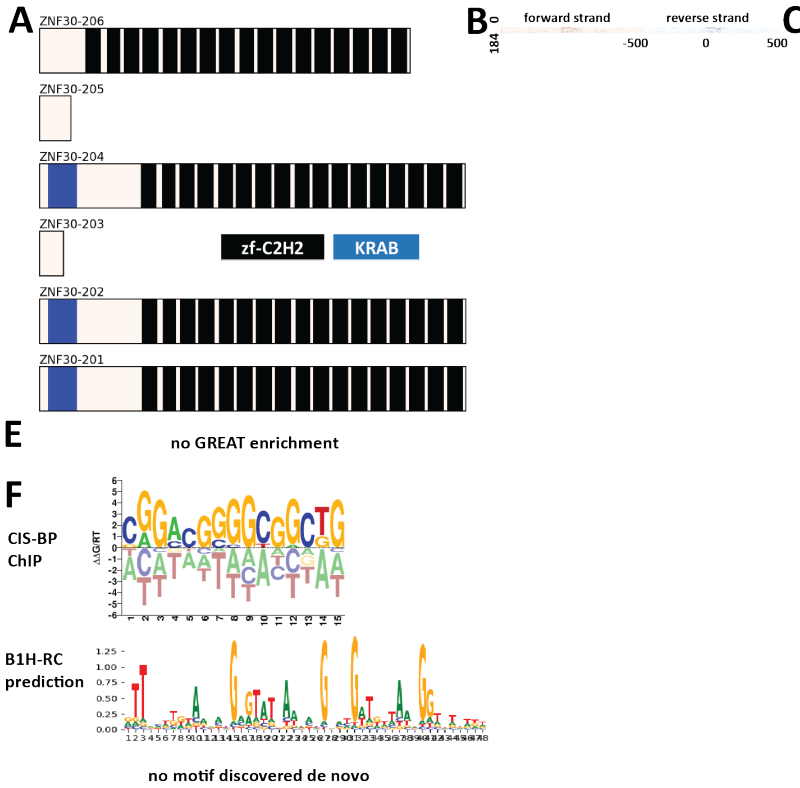

C

peaks	
state	fraction
Quies	0.30
TssA	0.19
ReprPCWk	0.04
TssFlnk	0.04
TssBiv	0.04
ZNF/Rpts	0.03
TxWk	0.03
Het	0.03
ReprPC	0.02
EnhA2	0.02
Tx	0.01
EnhWk	0.01
EnhG1	0.01
EnhA1	0.01

D

peaks		peaks	
repeat	fraction	repeat	fraction
Simple_repeat	0.32	SST1	0.04
LTR/ERV1	0.09	LTR10A	0.02
SINE/Alu	0.09	LSAU	0.02
LINE/L1	0.08	G-rich	0.02
Satellite	0.06	BSR/Beta	0.02
Satellite/centr	0.05	MIRb	0.02
Low_complexity	0.04	MER50	0.02
LINE/L2	0.03	MER21B	0.02
SINE/MIR	0.03	LSU-rRNA_Hs	0.02
LTR/ERVL-MaLR	0.03	L2c	0.02
LTR/ERVL	0.03	(TCTC)n	0.02
tRNA	0.02	(G)n	0.02
rRNA	0.02	SVA_E	0.01
DNA/TcMar-Tigger	0.02	MLT1J-int	0.01
Satellite/acro	0.01	MIR3	0.01
Retroposon/SVA	0.01	MER2	0.01
DNA/hAT-Tip100	0.01	LTR41B	0.01
DNA/hAT-Charlie	0.01	LTR12C	0.01

Supplementary Figure 1024: Properties and genomic distribution of motifs identified for the ZNF30 transcription factor in HEK293 (accession ChipExo models).

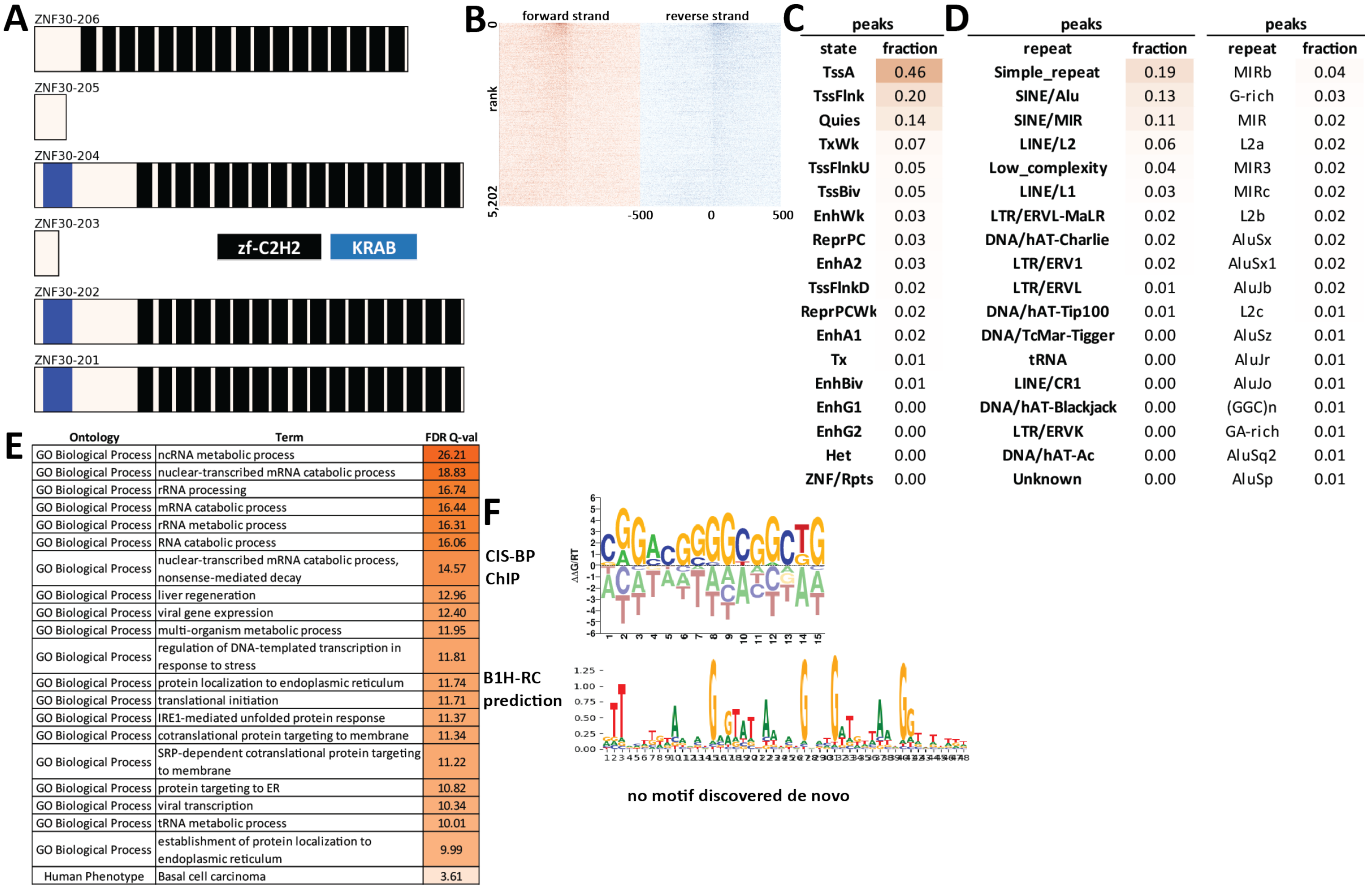

Supplementary Figure 1025: Properties and genomic distribution of motifs identified for the ZNF30 transcription factor in HepG2 (accession ENCSR891KNP).

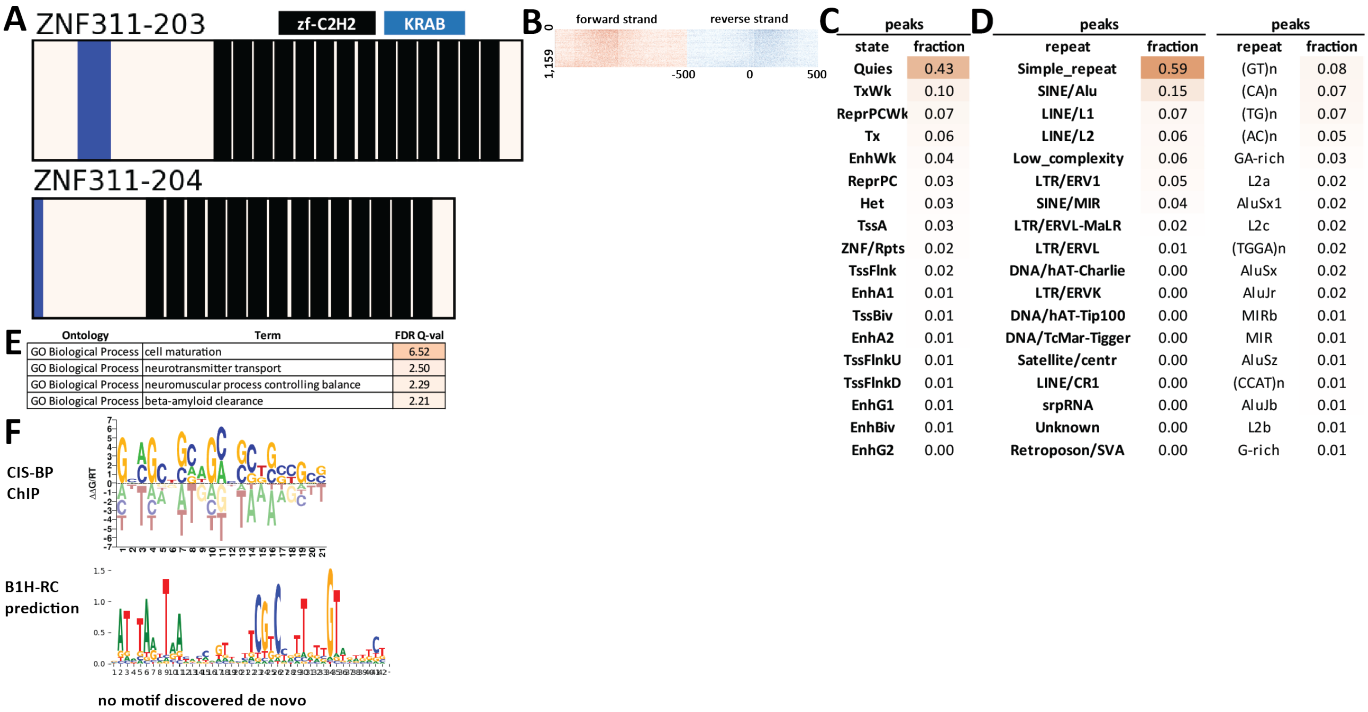

C

peaks	
state	fraction
Quies	0.43
TxWk	0.10
ReprPCWk	0.07
Tx	0.06
EnhWk	0.04
ReprPC	0.03
Het	0.03
TssA	0.03
ZNF/Rpts	0.02
TssFlnk	0.02
EnhA1	0.01
TssBiv	0.01
EnhA2	0.01
TssFlnkU	0.01
TssFlnkD	0.01
EnhG1	0.01
EnhBiv	0.01
EnhG2	0.00

D

peaks		peaks	
repeat	fraction	repeat	fraction
Simple_repeat	0.59	(GT)n	0.08
SINE/Alu	0.15	(CA)n	0.07
LINE/L1	0.07	(TG)n	0.07
LINE/L2	0.06	(AC)n	0.05
Low_complexity	0.06	GA-rich	0.03
LTR/ERV1	0.05	L2a	0.02
SINE/MIR	0.04	AluSx1	0.02
LTR/ERVL-MaLR	0.02	L2c	0.02
LTR/ERVL	0.01	(TGGA)n	0.02
DNA/hAT-Charlie	0.00	AluSx	0.02
LTR/ERVK	0.00	AluJr	0.02
DNA/hAT-Tip100	0.00	MIRb	0.01
DNA/TcMar-Tigger	0.00	MIR	0.01
Satellite/centr	0.00	AluSz	0.01
LINE/CR1	0.00	(CCAT)n	0.01
srpRNA	0.00	AluJb	0.01
Unknown	0.00	L2b	0.01
Retroposon/SVA	0.00	G-rich	0.01

E

Ontology	Term	FDR Q-val
GO Biological Process	cell maturation	6.52
GO Biological Process	neurotransmitter transport	2.50
GO Biological Process	neuromuscular process controlling balance	2.29
GO Biological Process	beta-amyloid clearance	2.21

Supplementary Figure 1026: Properties and genomic distribution of motifs identified for the ZNF311 transcription factor in HEK293 (accession ENCSR096LSN).

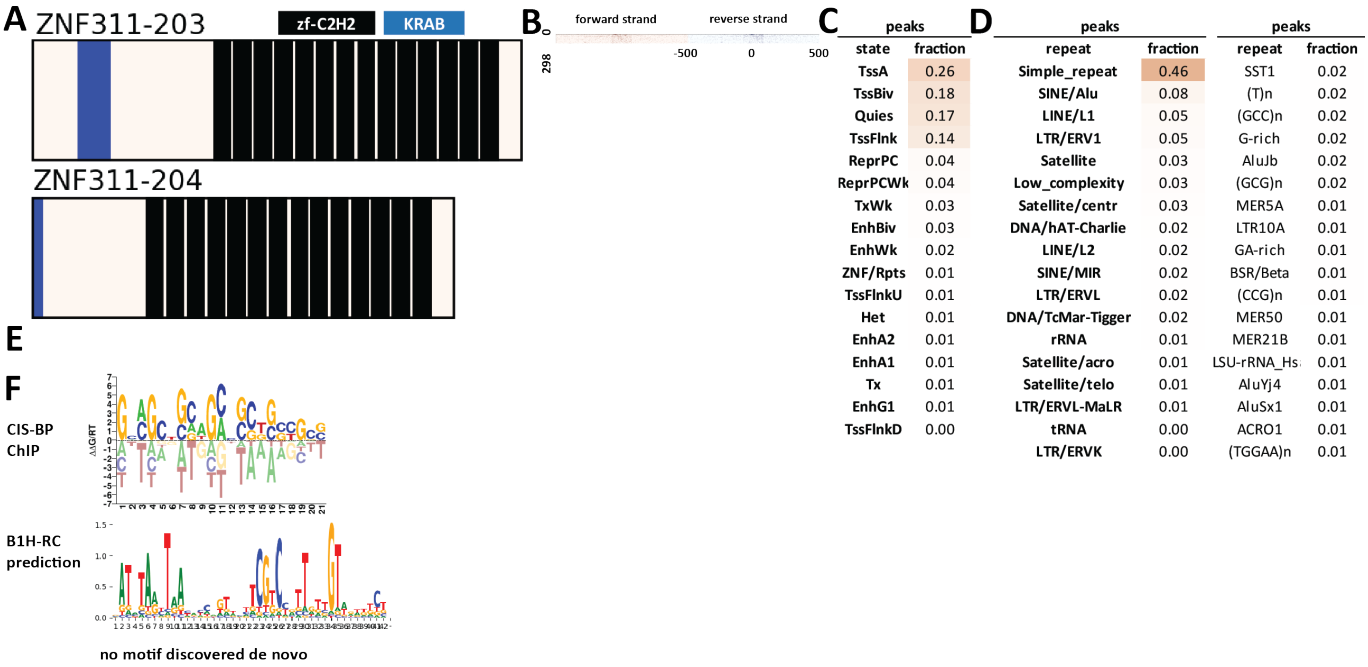

peaks	
state	fraction
TssA	0.26
TssBiv	0.18
Quies	0.17
TssFlnk	0.14
ReprPC	0.04
ReprPCWk	0.04
TxWk	0.03
EnhBiv	0.03
EnhWk	0.02
ZNF/Rpts	0.01
TssFlnkU	0.01
Het	0.01
EnhA2	0.01
EnhA1	0.01
Tx	0.01
EnhG1	0.01
TssFlnkD	0.00

peaks		peaks	
repeat	fraction	repeat	fraction
Simple_repeat	0.46	SST1	0.02
SINE/Alu	0.08	(T)n	0.02
LINE/L1	0.05	(GCC)n	0.02
LTR/ERV1	0.05	G-rich	0.02
Satellite	0.03	AluJb	0.02
Low_complexity	0.03	(GCG)n	0.02
Satellite/centr	0.03	MER5A	0.01
DNA/hAT-Charlie	0.02	LTR10A	0.01
LINE/L2	0.02	GA-rich	0.01
SINE/MIR	0.02	BSR/Beta	0.01
LTR/ERVL	0.02	(CCG)n	0.01
DNA/TcMar-Tigger	0.02	MER50	0.01
rRNA	0.01	MER21B	0.01
Satellite/acro	0.01	LSU-rRNA_Hs	0.01
Satellite/telo	0.01	AluYj4	0.01
LTR/ERVL-MaLR	0.01	AluSx1	0.01
tRNA	0.00	ACRO1	0.01
LTR/ERVK	0.00	(TGGAA)n	0.01

Supplementary Figure 1027: Properties and genomic distribution of motifs identified for the ZNF311 transcription factor in HEK293 (accession ChipExo models).

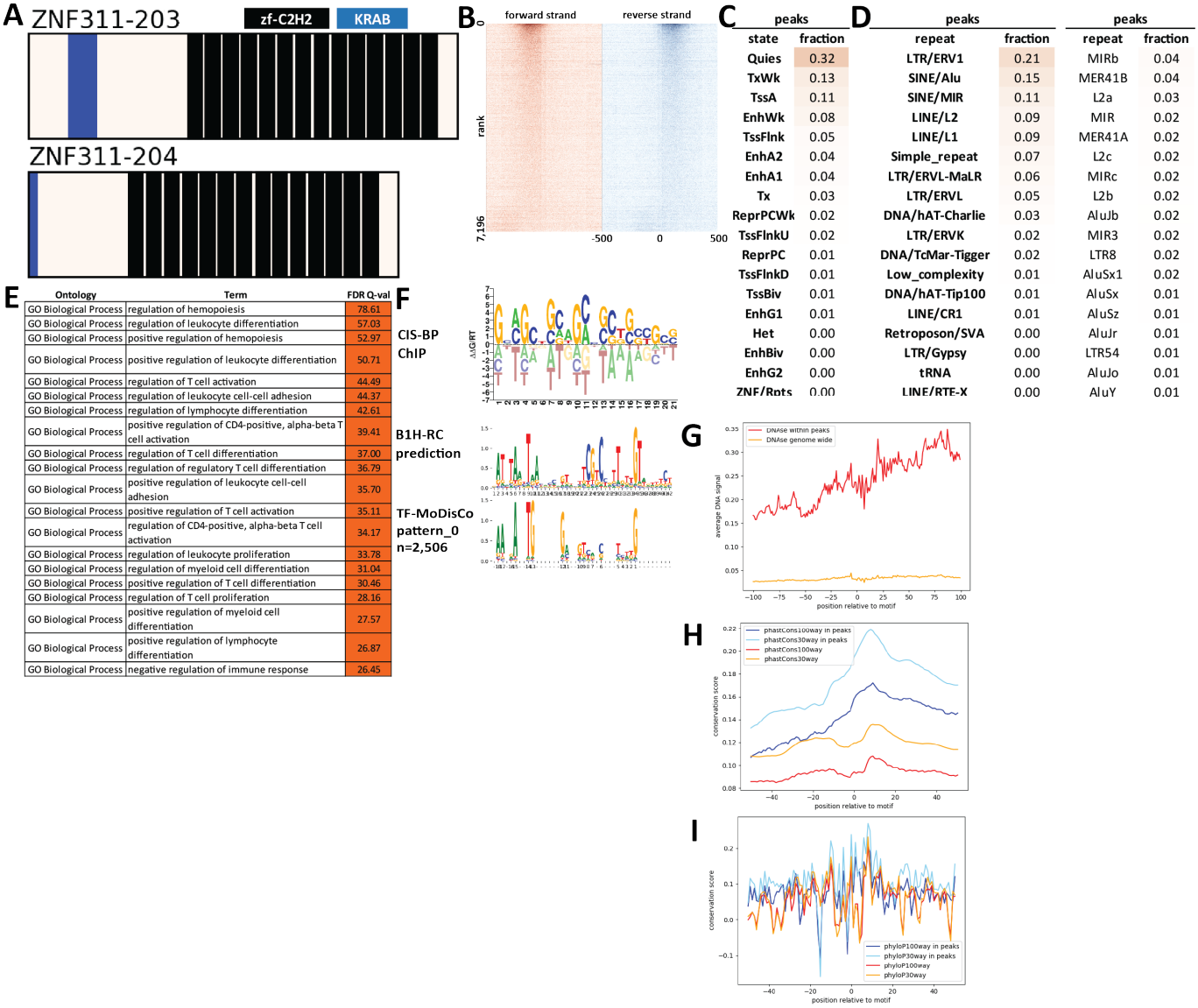

Supplementary Figure 1028: Properties and genomic distribution of motifs identified for the ZNF311 transcription factor in K562 (accession ENCSR388ZRV).

TF-MoDisCO pattern_0 n=2506, CWM

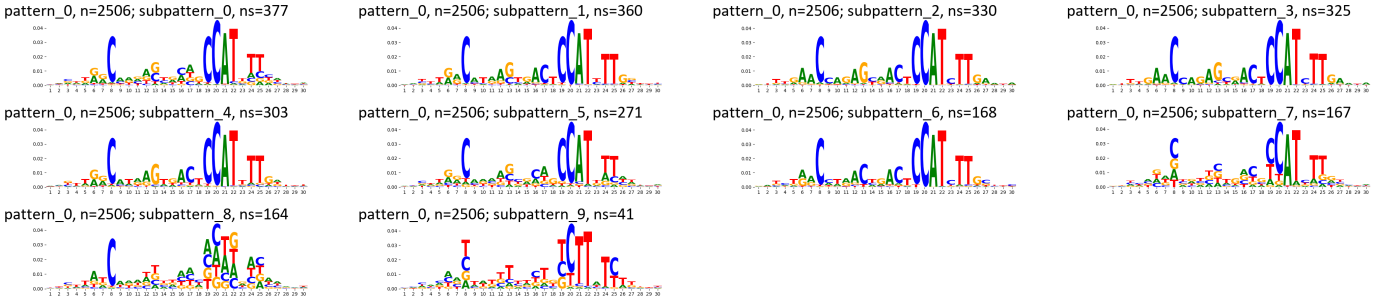

TF-MoDisCO pattern_0 n=2506, PWM

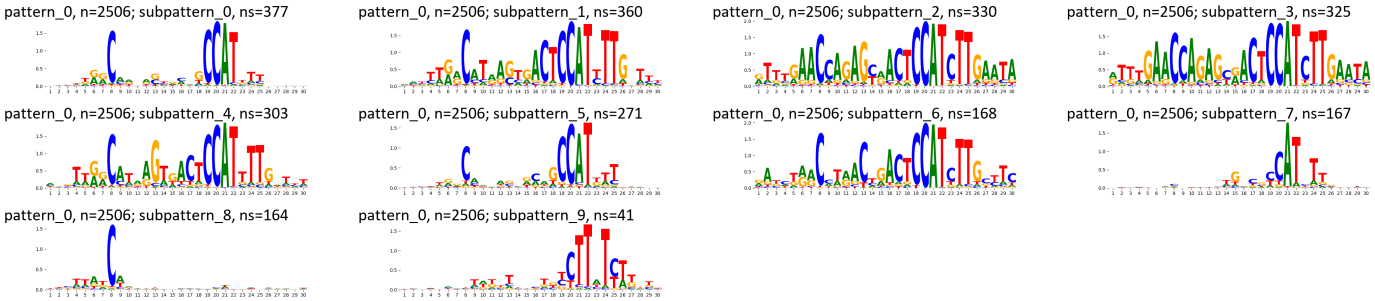

Supplementary Figure 1029: TF-MoDisCO subpatterns for the ZNF311 transcription factor in K562 (accession ENCSR388ZRV).

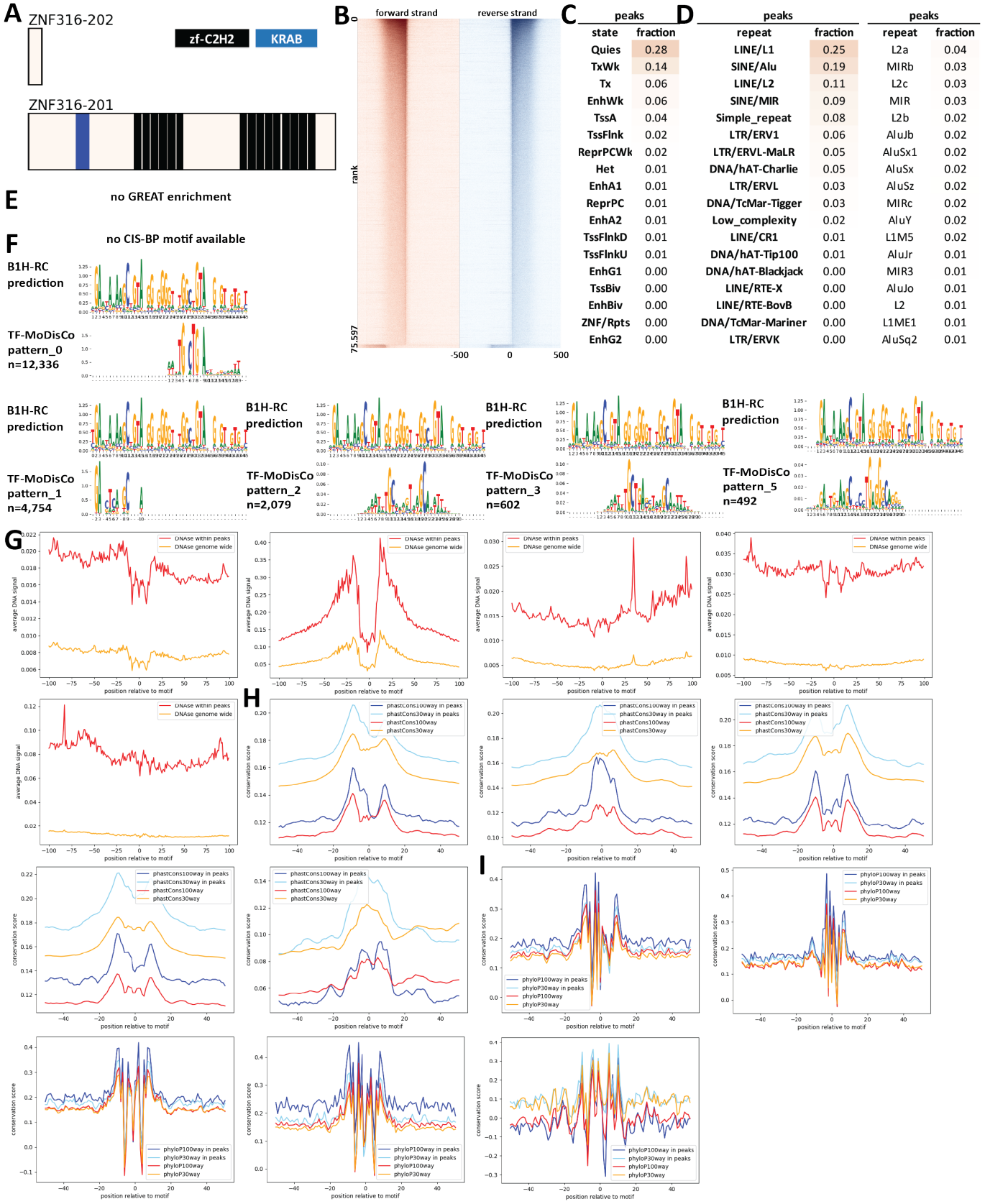

Supplementary Figure 1030: Properties and genomic distribution of motifs identified for the ZNF316 transcription factor in K562 (accession ENCSR167KBO).

TF-MoDisCO pattern_0 n=12336, CWM

pattern_0, n=12336; subpattern_0, ns=2558

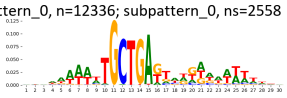

pattern_0, n=12336; subpattern_1, ns=2059

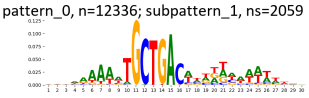

pattern_0, n=12336; subpattern_2, ns=2058

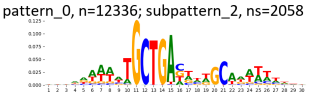

pattern_0, n=12336; subpattern_3, ns=1676

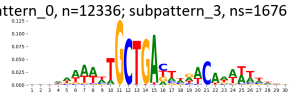

pattern_0, n=12336; subpattern_4, ns=1014

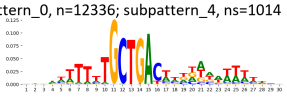

pattern_0, n=12336; subpattern_5, ns=983

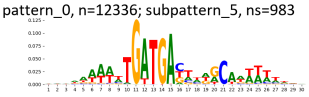

pattern_0, n=12336; subpattern_6, ns=841

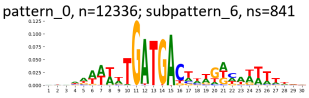

pattern_0, n=12336; subpattern_7, ns=812

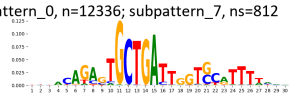

pattern_0, n=12336; subpattern_8, ns=262

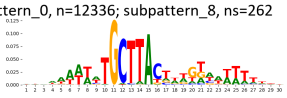

pattern_0, n=12336; subpattern_9, ns=73

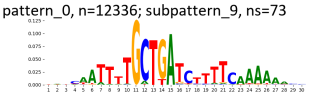

TF-MoDisCO pattern_0 n=12336, PWM

pattern_0, n=12336; subpattern_0, ns=2558

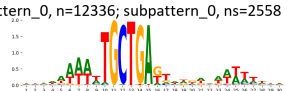

pattern_0, n=12336; subpattern_1, ns=2059

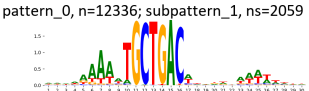

pattern_0, n=12336; subpattern_2, ns=2058

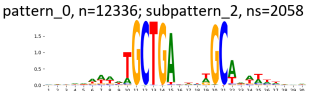

pattern_0, n=12336; subpattern_3, ns=1676

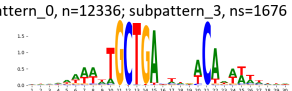

pattern_0, n=12336; subpattern_4, ns=1014

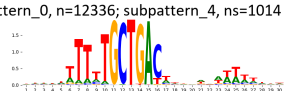

pattern_0, n=12336; subpattern_5, ns=983

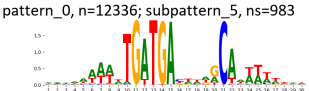

pattern_0, n=12336; subpattern_6, ns=841

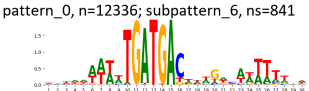

pattern_0, n=12336; subpattern_7, ns=812

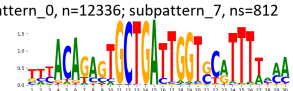

pattern_0, n=12336; subpattern_8, ns=262

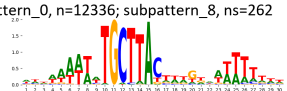

pattern_0, n=12336; subpattern_9, ns=73

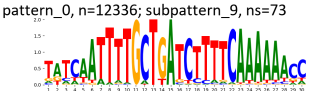

TF-MoDisCO pattern_1 n=4754, CWM

pattern_1, n=4754; subpattern_0, ns=1053

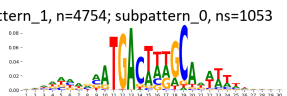

pattern_1, n=4754; subpattern_1, ns=786

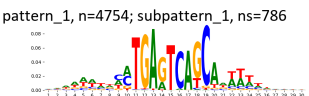

pattern_1, n=4754; subpattern_2, ns=759

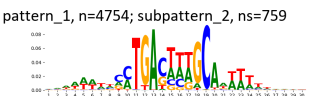

pattern_1, n=4754; subpattern_3, ns=749

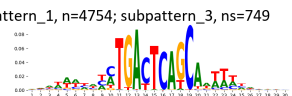

pattern_1, n=4754; subpattern_4, ns=668

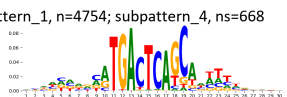

pattern_1, n=4754; subpattern_5, ns=444



pattern_1, n=4754; subpattern_6, ns=285

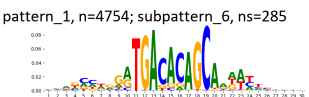

pattern_1, n=4754; subpattern_7, ns=10

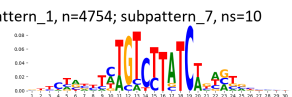

TF-MoDisCO pattern_1 n=4754, PWM

pattern_1, n=4754; subpattern_0, ns=1053

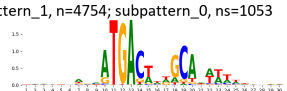

pattern_1, n=4754; subpattern_1, ns=786

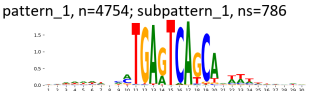

pattern_1, n=4754; subpattern_2, ns=759

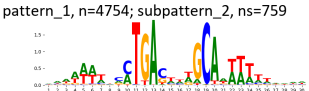

pattern_1, n=4754; subpattern_3, ns=749

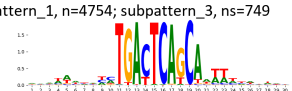

pattern_1, n=4754; subpattern_4, ns=668

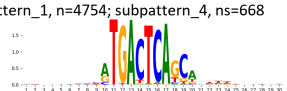

pattern_1, n=4754; subpattern_5, ns=444

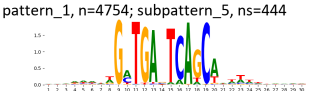

pattern_1, n=4754; subpattern_6, ns=285

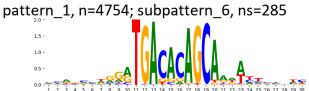

pattern_1, n=4754; subpattern_7, ns=10



TF-MoDisCO pattern_2 n=2079, CWM

pattern_2, n=2079; subpattern_0, ns=433

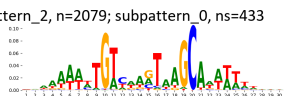

pattern_2, n=2079; subpattern_1, ns=374

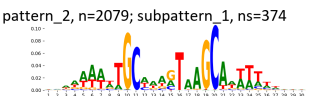

pattern_2, n=2079; subpattern_2, ns=345

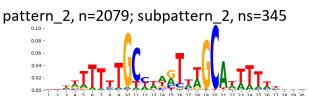

pattern_2, n=2079; subpattern_3, ns=300

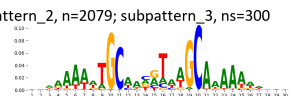

pattern_2, n=2079; subpattern_4, ns=298

pattern_2, n=2079; subpattern_5, ns=259

pattern_2, n=2079; subpattern_6, ns=40

pattern_2, n=2079; subpattern_7, ns=30

TF-MoDisCO pattern_2 n=2079, PWM

pattern_2, n=2079; subpattern_0, ns=433

pattern_2, n=2079; subpattern_1, ns=374

pattern_2, n=2079; subpattern_2, ns=345

pattern_2, n=2079; subpattern_3, ns=300

pattern_2, n=2079; subpattern_4, ns=298

pattern_2, n=2079; subpattern_5, ns=259

pattern_2, n=2079; subpattern_6, ns=40

pattern_2, n=2079; subpattern_7, ns=30

TF-MoDisCO pattern_3 n=602, CWM

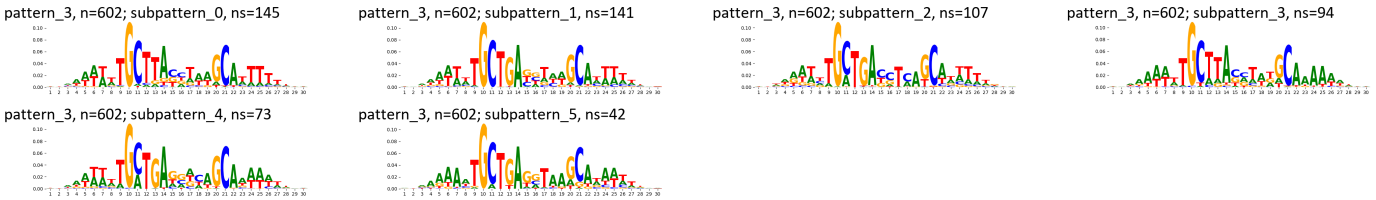

TF-MoDisCO pattern_3 n=602, PWM

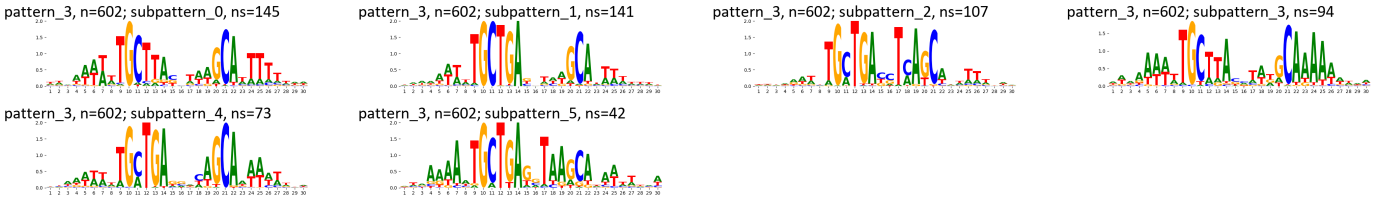

TF-MoDisCO pattern_5 n=492, CWM



TF-MoDisCO pattern_5 n=492, PWM

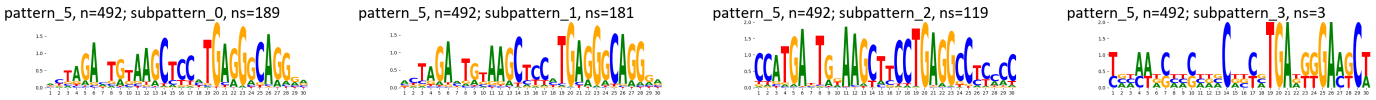

Supplementary Figure 1031: TF-MoDisCO subpatterns for the ZNF316 transcription factor in K562 (accession ENCSR167KBO).

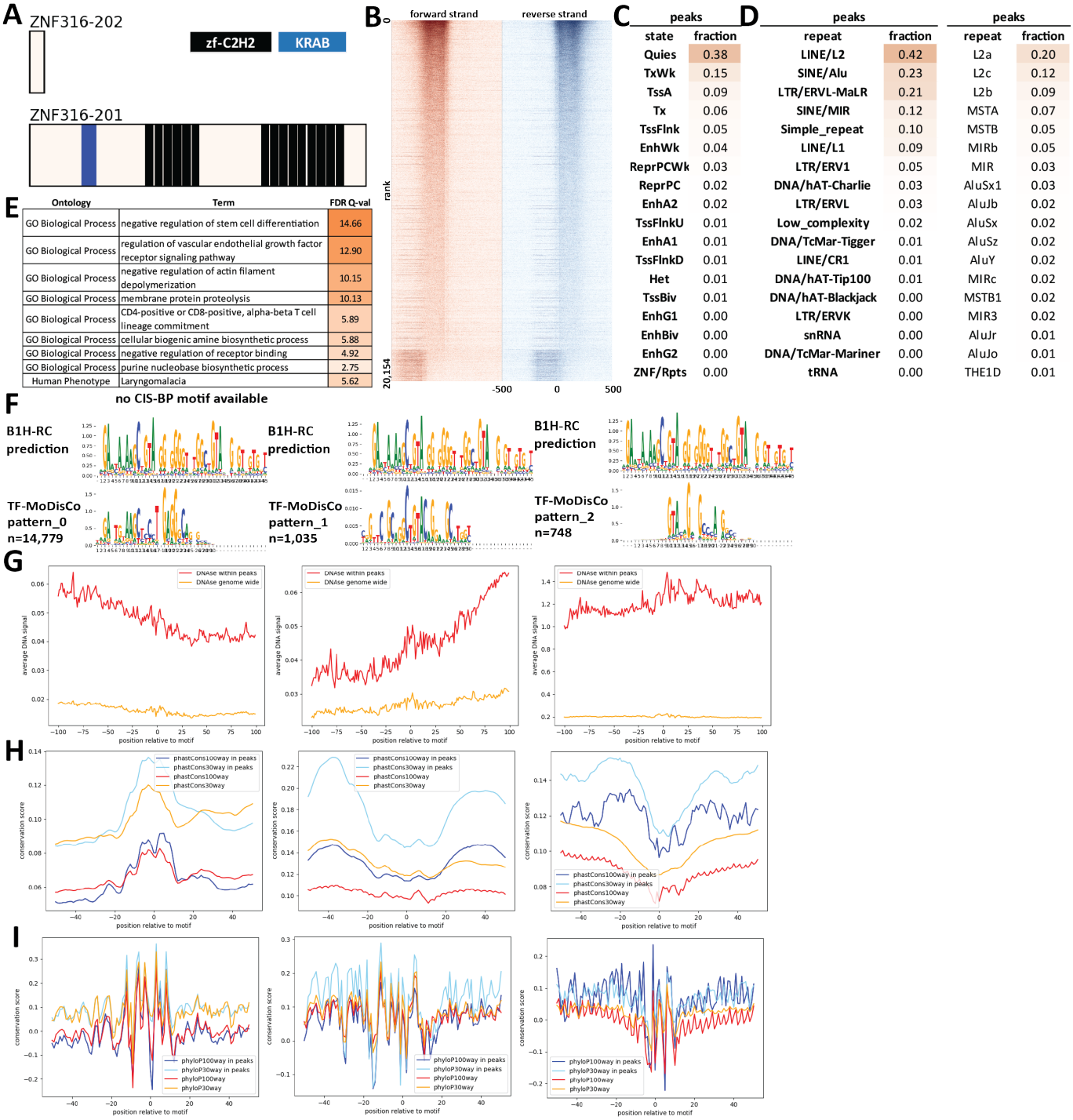

Supplementary Figure 1032: Properties and genomic distribution of motifs identified for the ZNF316 transcription factor in K562 (accession ENCSR200JYP).

TF-MoDisCO pattern_0 n=14799, CWM

pattern_0, n=14799; subpattern_0, ns=3829

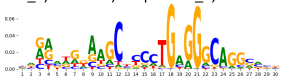

pattern_0, n=14799; subpattern_1, ns=3130

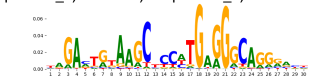

pattern_0, n=14799; subpattern_10, ns=2

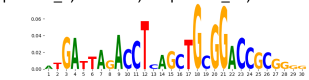

pattern_0, n=14799; subpattern_11, ns=2

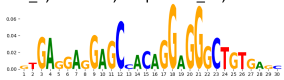

pattern_0, n=14799; subpattern_2, ns=2959

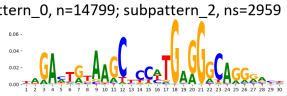

pattern_0, n=14799; subpattern_3, ns=1350

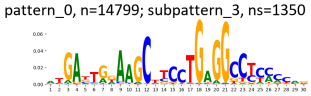

pattern_0, n=14799; subpattern_4, ns=1237

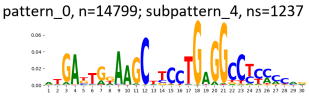

pattern_0, n=14799; subpattern_5, ns=1015

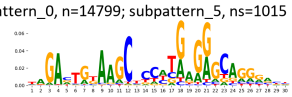

pattern_0, n=14799; subpattern_6, ns=563

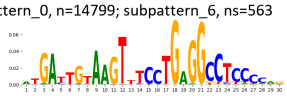

pattern_0, n=14799; subpattern_7, ns=512

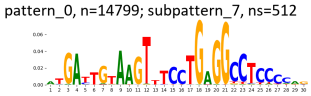

pattern_0, n=14799; subpattern_8, ns=170

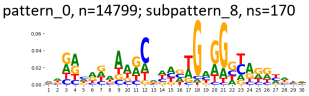

pattern_0, n=14799; subpattern_9, ns=30

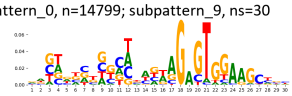

TF-MoDisCO pattern_0 n=14799, PWM

pattern_0, n=14799; subpattern_0, ns=3829

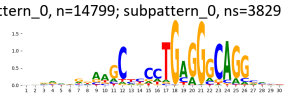

pattern_0, n=14799; subpattern_1, ns=3130

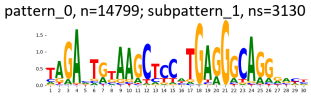

pattern_0, n=14799; subpattern_10, ns=2

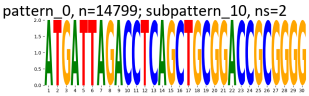

pattern_0, n=14799; subpattern_11, ns=2

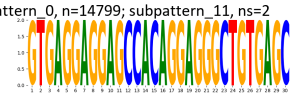

pattern_0, n=14799; subpattern_2, ns=2959

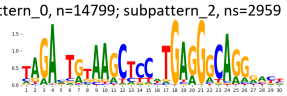

pattern_0, n=14799; subpattern_3, ns=1350

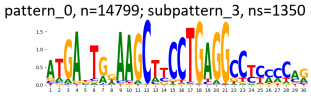

pattern_0, n=14799; subpattern_4, ns=1237

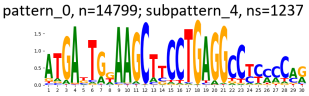

pattern_0, n=14799; subpattern_5, ns=1015

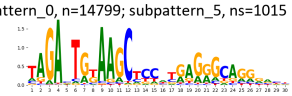

pattern_0, n=14799; subpattern_6, ns=563

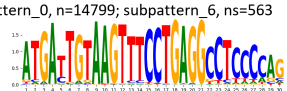

pattern_0, n=14799; subpattern_7, ns=512

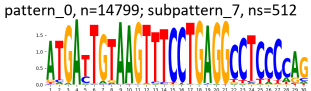

pattern_0, n=14799; subpattern_8, ns=170

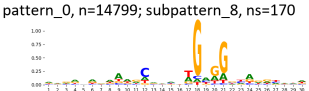

pattern_0, n=14799; subpattern_9, ns=30

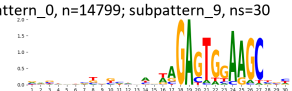

TF-MoDisCO pattern_1 n=1035, CWM

pattern_1, n=1035; subpattern_0, ns=324

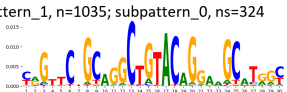

pattern_1, n=1035; subpattern_1, ns=277

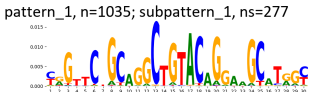

pattern_1, n=1035; subpattern_2, ns=177

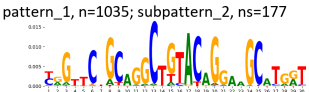

pattern_1, n=1035; subpattern_3, ns=129

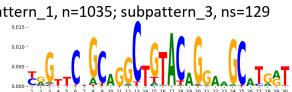

pattern_1, n=1035; subpattern_4, ns=98

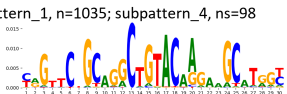

pattern_1, n=1035; subpattern_5, ns=17

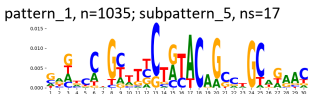

pattern_1, n=1035; subpattern_6, ns=9

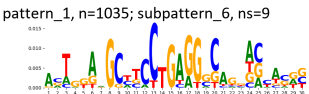

pattern_1, n=1035; subpattern_7, ns=4

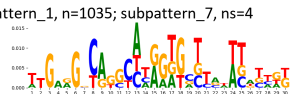

TF-MoDisCO pattern_1 n=1035, PWM

pattern_1, n=1035; subpattern_0, ns=324

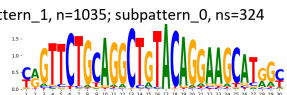

pattern_1, n=1035; subpattern_1, ns=277



pattern_1, n=1035; subpattern_2, ns=177

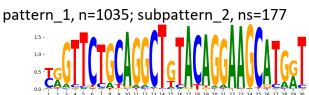

pattern_1, n=1035; subpattern_3, ns=129

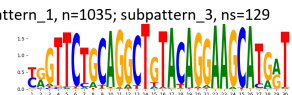

pattern_1, n=1035; subpattern_4, ns=98

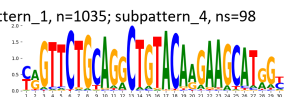

pattern_1, n=1035; subpattern_5, ns=17

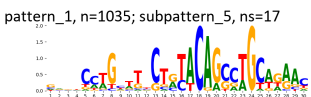

pattern_1, n=1035; subpattern_6, ns=9

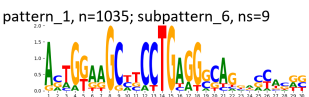

pattern_1, n=1035; subpattern_7, ns=4



TF-MoDisCO pattern_2 n=748, CWM

pattern_2, n=748; subpattern_0, ns=246

pattern_2, n=748; subpattern_1, ns=231

pattern_2, n=748; subpattern_2, ns=191

pattern_2, n=748; subpattern_3, ns=52

pattern_2, n=748; subpattern_4, ns=23

pattern_2, n=748; subpattern_5, ns=3

pattern_2, n=748; subpattern_6, ns=2

TF-MoDisCO pattern_2 n=748, PWM

pattern_2, n=748; subpattern_0, ns=246

pattern_2, n=748; subpattern_1, ns=231

pattern_2, n=748; subpattern_2, ns=191

pattern_2, n=748; subpattern_3, ns=52

pattern_2, n=748; subpattern_4, ns=23

pattern_2, n=748; subpattern_5, ns=3

pattern_2, n=748; subpattern_6, ns=2

Supplementary Figure 1033: TF-MoDisCO subpatterns for the ZNF316 transcription factor in K562 (accession ENCSR200JYP).

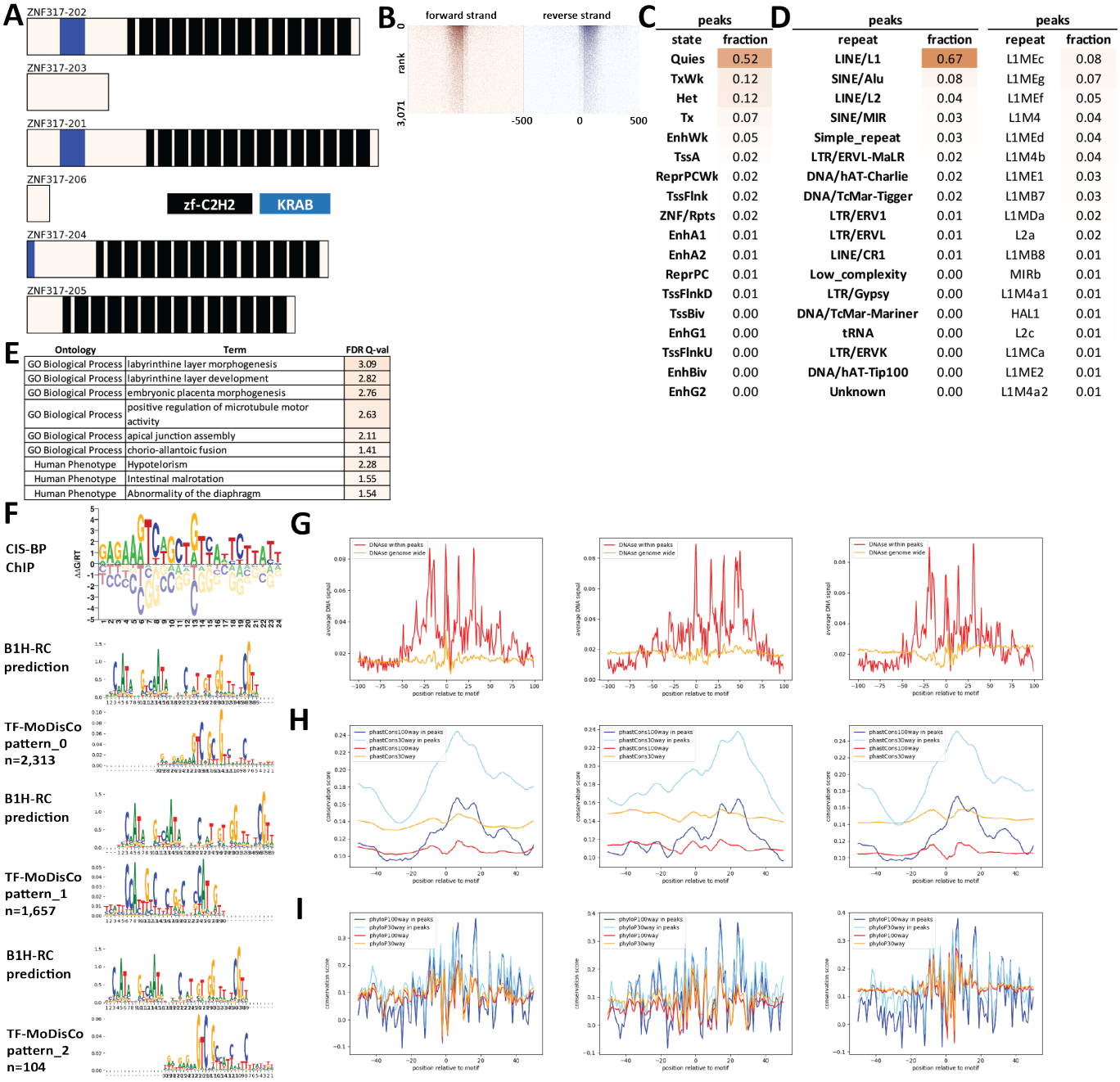

C

peaks	
state	fraction
Quies	0.52
TxWk	0.12
Het	0.12
Tx	0.07
EnhWk	0.05
TssA	0.02
ReprPCWk	0.02
TssFlnk	0.02
ZNF/Rpts	0.02
EnhA1	0.01
EnhA2	0.01
ReprPC	0.01
TssFlnkD	0.01
TssBiv	0.00
EnhG1	0.00
TssFlnkU	0.00
EnhBiv	0.00
EnhG2	0.00

D

peaks		peaks	
repeat	fraction	repeat	fraction
LINE/L1	0.67	L1MEc	0.08
SINE/Alu	0.08	L1MEg	0.07
LINE/L2	0.04	L1MEf	0.05
SINE/MIR	0.03	L1M4	0.04
Simple_repeat	0.03	L1MEd	0.04
LTR/ERVL-MaLR	0.02	L1M4b	0.04
DNA/hAT-Charlie	0.02	L1ME1	0.03
DNA/TcMar-Tigger	0.02	L1MB7	0.03
LTR/ERV1	0.01	L1MDa	0.02
LTR/ERVL	0.01	L2a	0.02
LINE/CR1	0.01	L1MB8	0.01
Low_complexity	0.00	MIRb	0.01
LTR/Gypsy	0.00	L1M4a1	0.01
DNA/TcMar-Mariner	0.00	HAL1	0.01
tRNA	0.00	L2c	0.01
LTR/ERVK	0.00	L1MCa	0.01
DNA/hAT-Tip100	0.00	L1ME2	0.01
Unknown	0.00	L1M4a2	0.01

E

Ontology	Term	FDR Q-val
GO Biological Process	labyrinthine layer morphogenesis	3.09
GO Biological Process	labyrinthine layer development	2.82
GO Biological Process	embryonic placenta morphogenesis	2.76
GO Biological Process	positive regulation of microtubule motor activity	2.63
GO Biological Process	apical junction assembly	2.11
GO Biological Process	chorio-allantoic fusion	1.41
Human Phenotype	Hypotelorism	2.28
Human Phenotype	Intestinal malrotation	1.55
Human Phenotype	Abnormality of the diaphragm	1.54

Supplementary Figure 1034: Properties and genomic distribution of motifs identified for the ZNF317 transcription factor in HEK293 (accession Hughes NB models).

TF-MoDisCO pattern_0 n=2313, CWM

pattern_0, n=2313; subpattern_0, ns=584

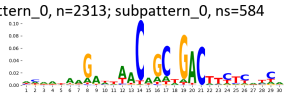

pattern_0, n=2313; subpattern_1, ns=509

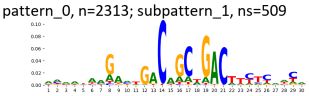

pattern_0, n=2313; subpattern_2, ns=411

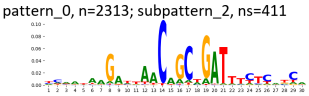

pattern_0, n=2313; subpattern_3, ns=393

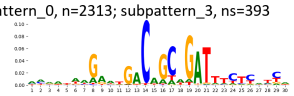

pattern_0, n=2313; subpattern_4, ns=340

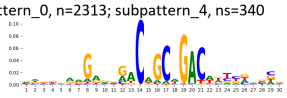

pattern_0, n=2313; subpattern_5, ns=65

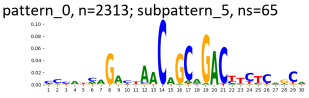

pattern_0, n=2313; subpattern_6, ns=11

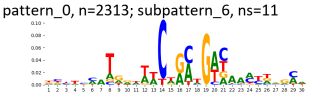

TF-MoDisCO pattern_0 n=2313, PWM

pattern_0, n=2313; subpattern_0, ns=584

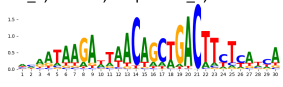

pattern_0, n=2313; subpattern_1, ns=509

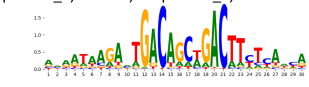

pattern_0, n=2313; subpattern_2, ns=411

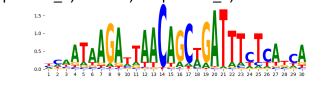

pattern_0, n=2313; subpattern_3, ns=393

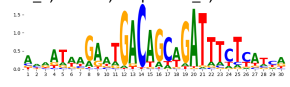

pattern_0, n=2313; subpattern_4, ns=340

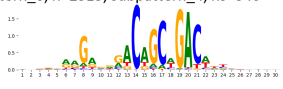

pattern_0, n=2313; subpattern_5, ns=65

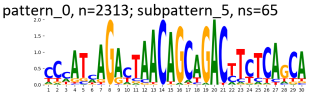

pattern_0, n=2313; subpattern_6, ns=11

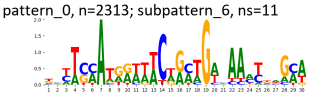

TF-MoDisCO pattern_1 n=1657, CWM

pattern_1, n=1657; subpattern_0, ns=379

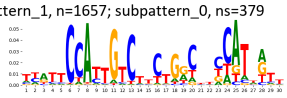

pattern_1, n=1657; subpattern_1, ns=295

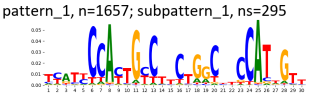

pattern_1, n=1657; subpattern_2, ns=281

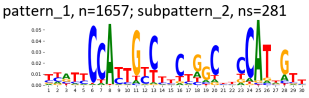

pattern_1, n=1657; subpattern_3, ns=181

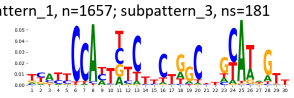

pattern_1, n=1657; subpattern_4, ns=181

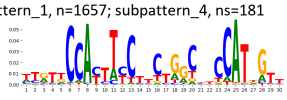

pattern_1, n=1657; subpattern_5, ns=145

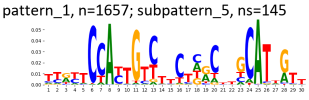

pattern_1, n=1657; subpattern_6, ns=130

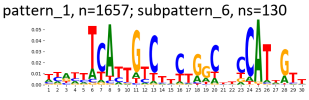

pattern_1, n=1657; subpattern_7, ns=65

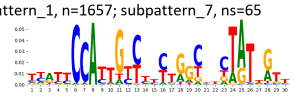

TF-MoDisCO pattern_1 n=1657, PWM

pattern_1, n=1657; subpattern_0, ns=379

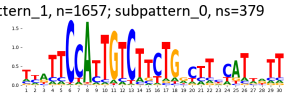

pattern_1, n=1657; subpattern_1, ns=295

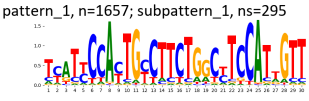

pattern_1, n=1657; subpattern_2, ns=281

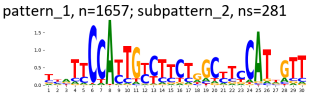

pattern_1, n=1657; subpattern_3, ns=181

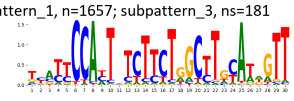

pattern_1, n=1657; subpattern_4, ns=181

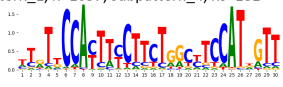

pattern_1, n=1657; subpattern_5, ns=145

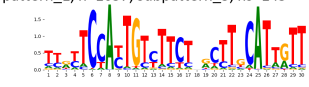

pattern_1, n=1657; subpattern_6, ns=130

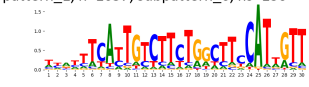

pattern_1, n=1657; subpattern_7, ns=65

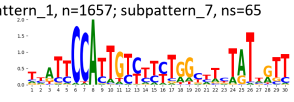

TF-MoDisCO pattern_2 n=104, CWM

pattern_2, n=104; subpattern_0, ns=34

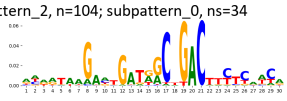

pattern_2, n=104; subpattern_1, ns=23

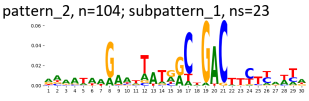

pattern_2, n=104; subpattern_2, ns=18

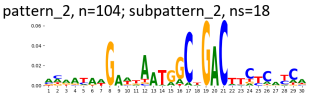

pattern_2, n=104; subpattern_3, ns=16

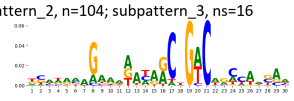

pattern_2, n=104; subpattern_4, ns=13

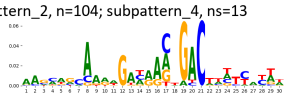

TF-MoDisCO pattern_2 n=104, PWM

pattern_2, n=104; subpattern_0, ns=34

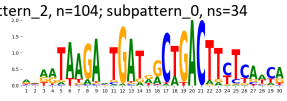

pattern_2, n=104; subpattern_1, ns=23

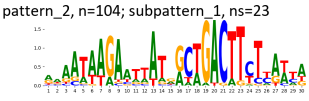

pattern_2, n=104; subpattern_2, ns=18

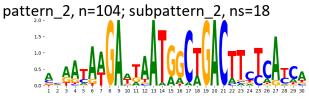

pattern_2, n=104; subpattern_3, ns=16

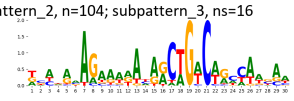

pattern_2, n=104; subpattern_4, ns=13

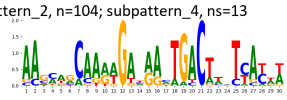

Supplementary Figure 1035: TF-MoDisCO subpatterns for the ZNF317 transcription factor in HEK293 (accession Hughes NB models).

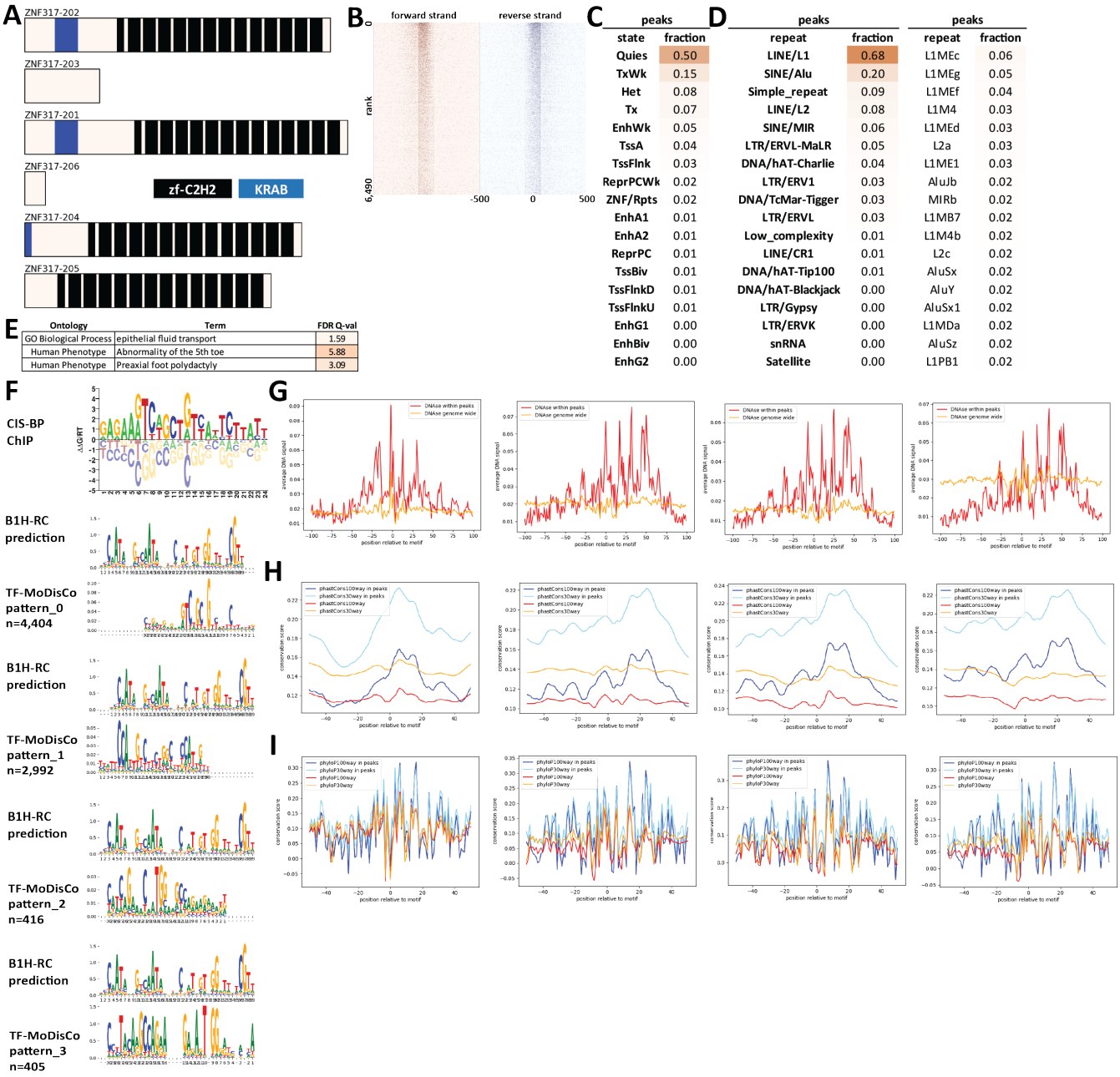

Supplementary Figure 1036: Properties and genomic distribution of motifs identified for the ZNF317 transcription factor in HEK293 (accession ChipExo models).

TF-MoDisCO pattern_0 n=4404, CWM

pattern_0, n=4404; subpattern_0, ns=1004

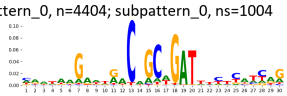

pattern_0, n=4404; subpattern_1, ns=709

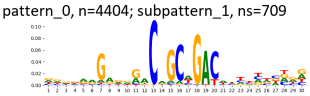

pattern_0, n=4404; subpattern_2, ns=607

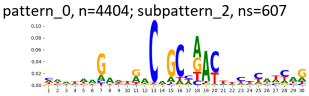

pattern_0, n=4404; subpattern_3, ns=528

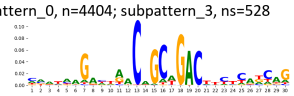

pattern_0, n=4404; subpattern_4, ns=416

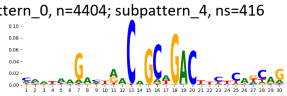

pattern_0, n=4404; subpattern_5, ns=367

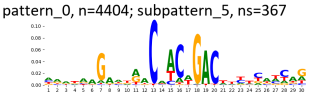

pattern_0, n=4404; subpattern_6, ns=337

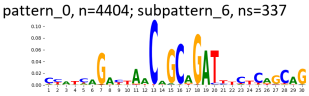

pattern_0, n=4404; subpattern_7, ns=263

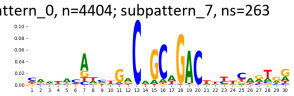

pattern_0, n=4404; subpattern_8, ns=160

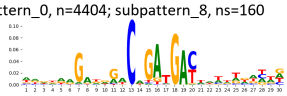

pattern_0, n=4404; subpattern_9, ns=13

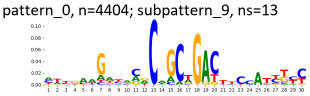

TF-MoDisCO pattern_0 n=4404, PWM

pattern_0, n=4404; subpattern_0, ns=1004

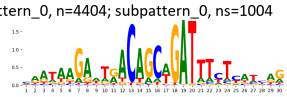

pattern_0, n=4404; subpattern_1, ns=709

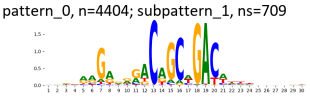

pattern_0, n=4404; subpattern_2, ns=607

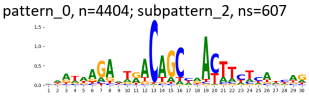

pattern_0, n=4404; subpattern_3, ns=528

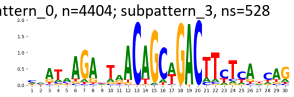

pattern_0, n=4404; subpattern_4, ns=416

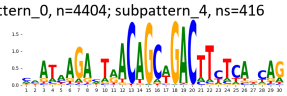

pattern_0, n=4404; subpattern_5, ns=367

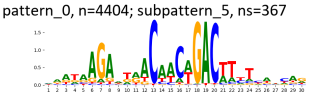

pattern_0, n=4404; subpattern_6, ns=337

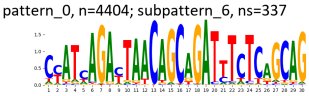

pattern_0, n=4404; subpattern_7, ns=263

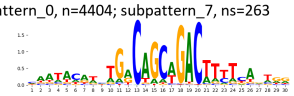

pattern_0, n=4404; subpattern_8, ns=160

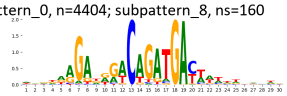

pattern_0, n=4404; subpattern_9, ns=13

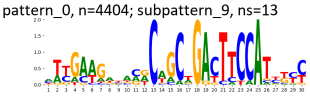

TF-MoDisCO pattern_1 n=2992, CWM

pattern_1, n=2992; subpattern_0, ns=750

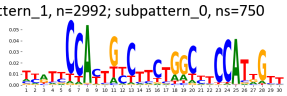

pattern_1, n=2992; subpattern_1, ns=652

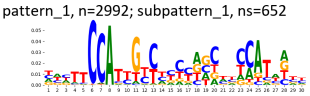

pattern_1, n=2992; subpattern_2, ns=531

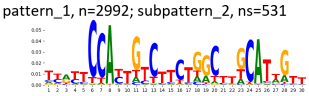

pattern_1, n=2992; subpattern_3, ns=431

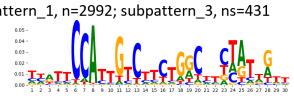

pattern_1, n=2992; subpattern_4, ns=325

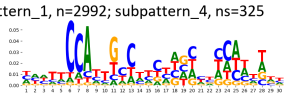

pattern_1, n=2992; subpattern_5, ns=141

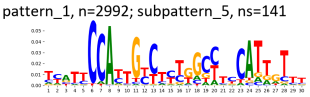

pattern_1, n=2992; subpattern_6, ns=132

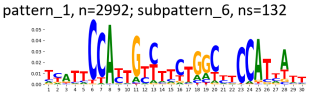

pattern_1, n=2992; subpattern_7, ns=20

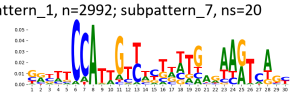

pattern_1, n=2992; subpattern_8, ns=10

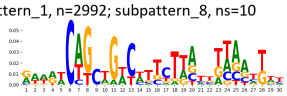

TF-MoDisCO pattern_1 n=2992, PWM

pattern_1, n=2992; subpattern_0, ns=750

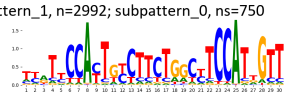

pattern_1, n=2992; subpattern_1, ns=652

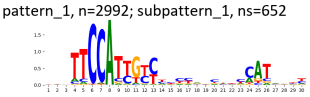

pattern_1, n=2992; subpattern_2, ns=531

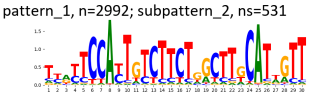

pattern_1, n=2992; subpattern_3, ns=431

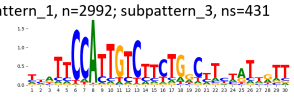

pattern_1, n=2992; subpattern_4, ns=325

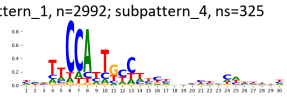

pattern_1, n=2992; subpattern_5, ns=141

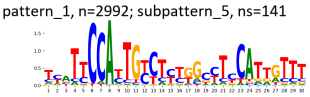

pattern_1, n=2992; subpattern_6, ns=132

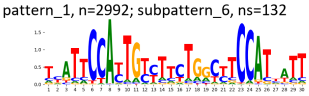

pattern_1, n=2992; subpattern_7, ns=20

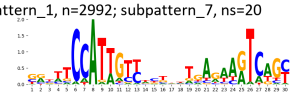

pattern_1, n=2992; subpattern_8, ns=10

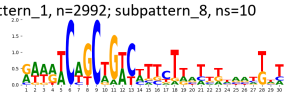

TF-MoDisCO pattern_2 n=416, CWM

pattern_2, n=416; subpattern_0, ns=113

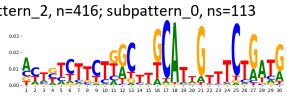

pattern_2, n=416; subpattern_1, ns=88

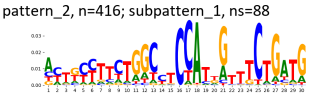

pattern_2, n=416; subpattern_2, ns=73

pattern_2, n=416; subpattern_3, ns=71

pattern_2, n=416; subpattern_4, ns=40

pattern_2, n=416; subpattern_5, ns=31

TF-MoDisCO pattern_2 n=416, PWM

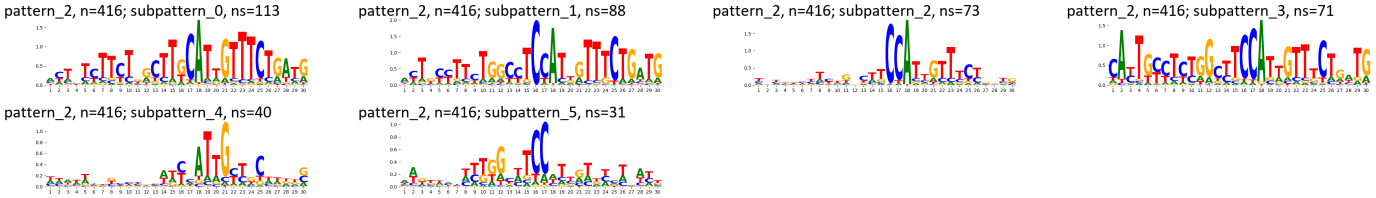

TF-MoDisCO pattern_3 n=405, CWM

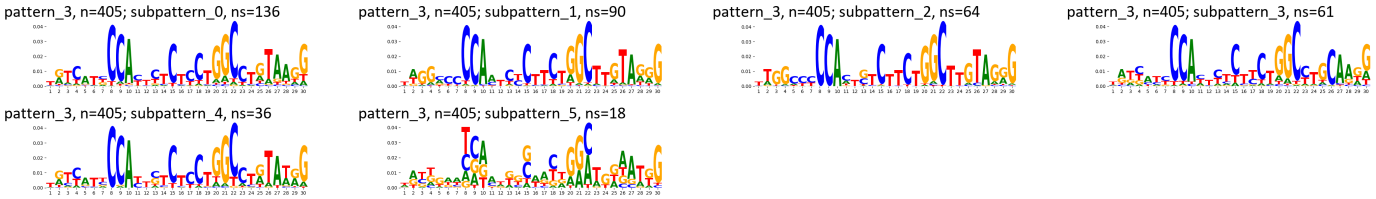

TF-MoDisCO pattern_3 n=405, PWM

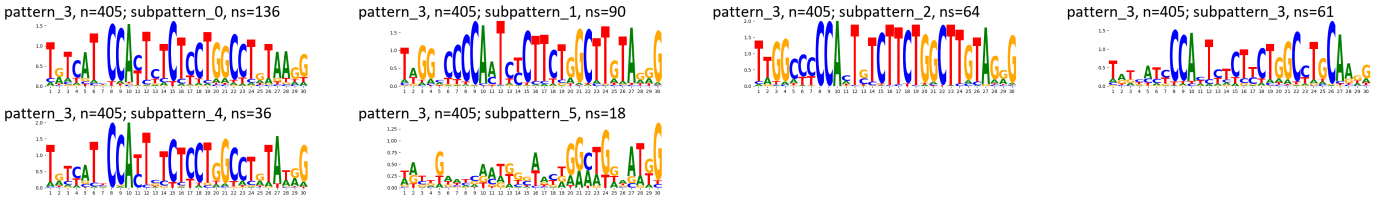

Supplementary Figure 1037: TF-MoDisCO subpatterns for the ZNF317 transcription factor in HEK293 (accession ChipExo models).

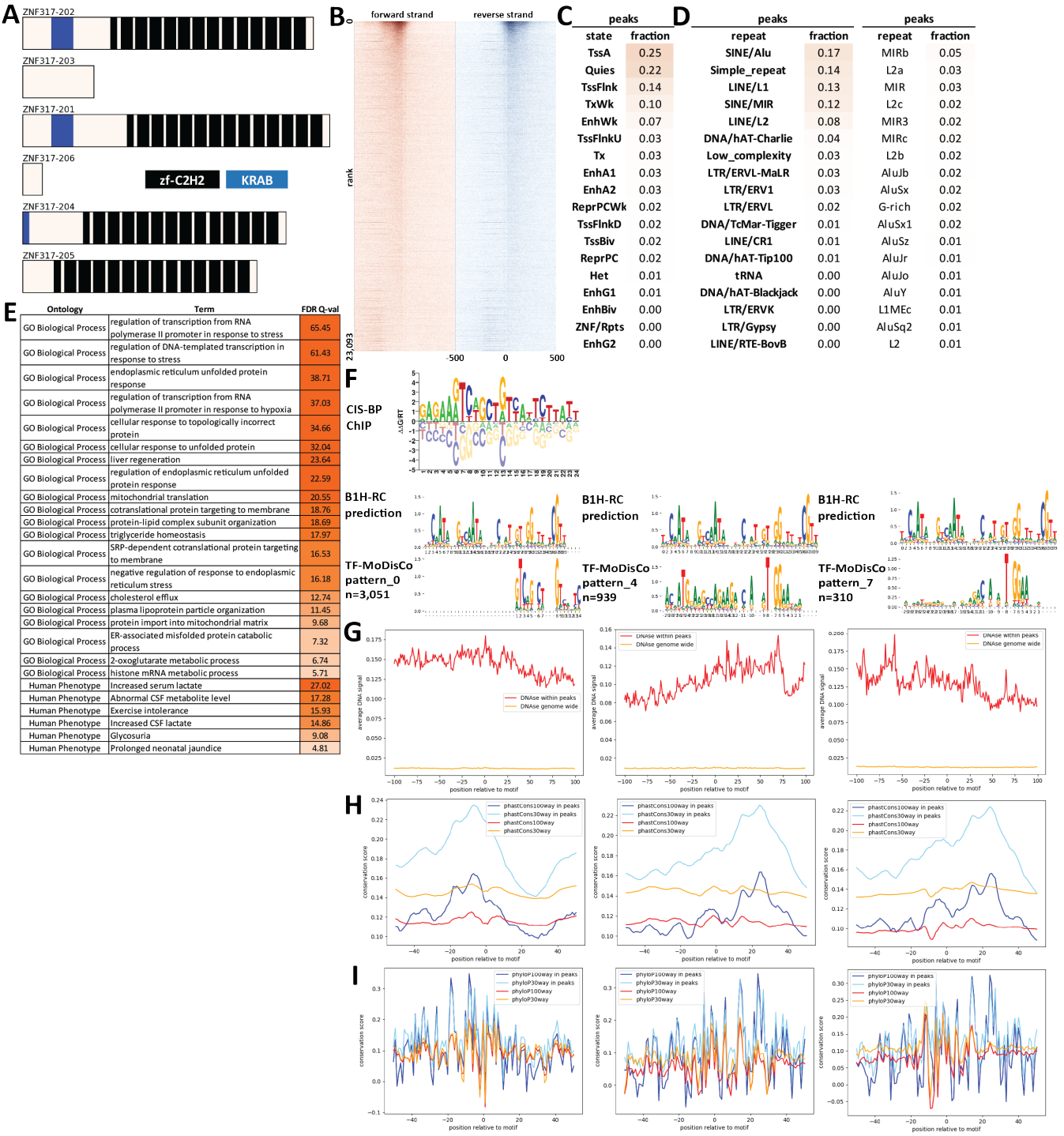

Supplementary Figure 1038: Properties and genomic distribution of motifs identified for the ZNF317 transcription factor in HepG2 (accession ENCSR016OHL).

TF-MoDisCO pattern_0 n=3051, CWM

pattern_0, n=3051; subpattern_0, ns=658

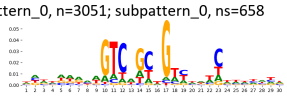

pattern_0, n=3051; subpattern_1, ns=549

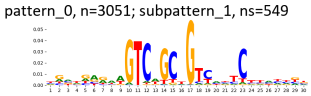

pattern_0, n=3051; subpattern_2, ns=430

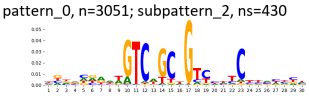

pattern_0, n=3051; subpattern_3, ns=403

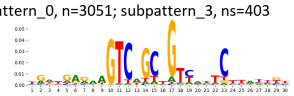

pattern_0, n=3051; subpattern_4, ns=348

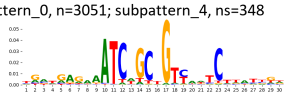

pattern_0, n=3051; subpattern_5, ns=315

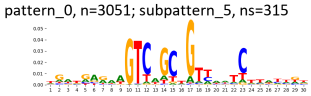

pattern_0, n=3051; subpattern_6, ns=286

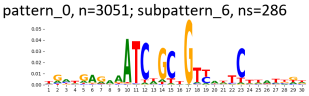

pattern_0, n=3051; subpattern_7, ns=62

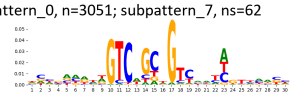

TF-MoDisCO pattern_0 n=3051, PWM

pattern_0, n=3051; subpattern_0, ns=658

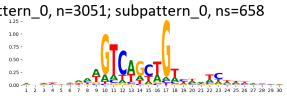

pattern_0, n=3051; subpattern_1, ns=549

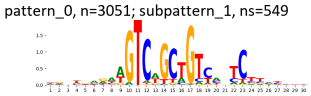

pattern_0, n=3051; subpattern_2, ns=430

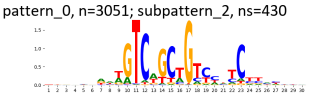

pattern_0, n=3051; subpattern_3, ns=403

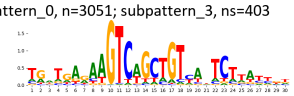

pattern_0, n=3051; subpattern_4, ns=348

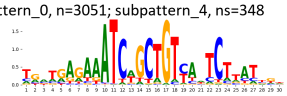

pattern_0, n=3051; subpattern_5, ns=315

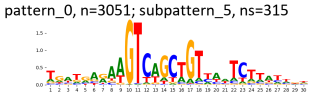

pattern_0, n=3051; subpattern_6, ns=286

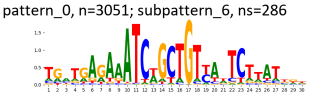

pattern_0, n=3051; subpattern_7, ns=62

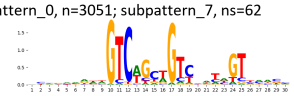

TF-MoDisCO pattern_4 n=939, CWM

pattern_4, n=939; subpattern_0, ns=258

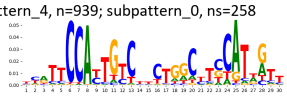

pattern_4, n=939; subpattern_1, ns=204

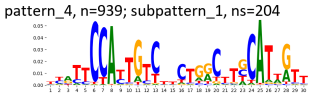

pattern_4, n=939; subpattern_2, ns=167

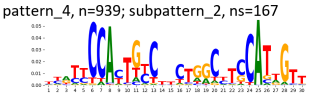

pattern_4, n=939; subpattern_3, ns=158

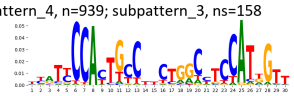

pattern_4, n=939; subpattern_4, ns=149

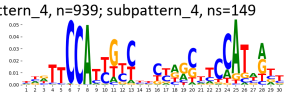

pattern_4, n=939; subpattern_5, ns=3

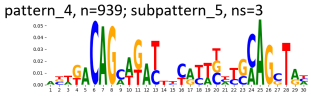

TF-MoDisCO pattern_4 n=939, PWM

pattern_4, n=939; subpattern_0, ns=258

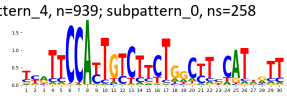

pattern_4, n=939; subpattern_1, ns=204

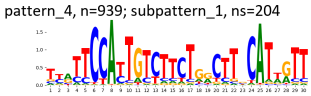

pattern_4, n=939; subpattern_2, ns=167

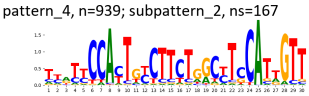

pattern_4, n=939; subpattern_3, ns=158

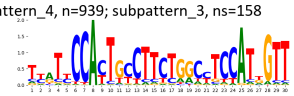

pattern_4, n=939; subpattern_4, ns=149

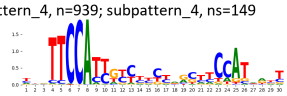

pattern_4, n=939; subpattern_5, ns=3

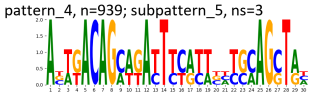

TF-MoDisCO pattern_7 n=310, CWM

pattern_7, n=310; subpattern_0, ns=70

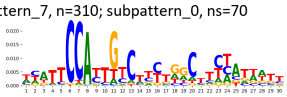

pattern_7, n=310; subpattern_1, ns=65

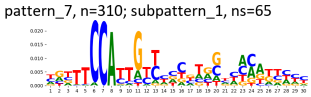

pattern_7, n=310; subpattern_2, ns=60

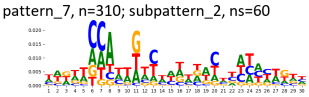

pattern_7, n=310; subpattern_3, ns=52

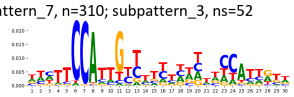

pattern_7, n=310; subpattern_4, ns=35

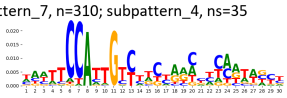

pattern_7, n=310; subpattern_5, ns=22

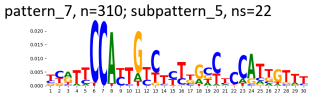

pattern_7, n=310; subpattern_6, ns=4

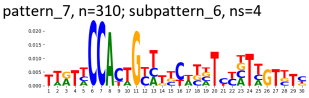

pattern_7, n=310; subpattern_7, ns=2

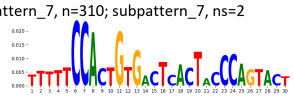

TF-MoDisCO pattern_7 n=310, PWM

pattern_7, n=310; subpattern_0, ns=70

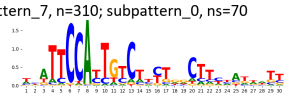

pattern_7, n=310; subpattern_1, ns=65

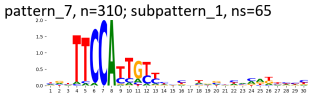

pattern_7, n=310; subpattern_2, ns=60

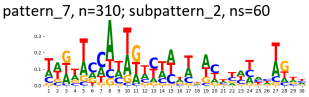

pattern_7, n=310; subpattern_3, ns=52

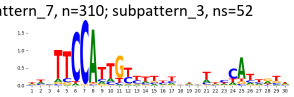

pattern_7, n=310; subpattern_4, ns=35

pattern_7, n=310; subpattern_5, ns=22

pattern_7, n=310; subpattern_6, ns=4

pattern_7, n=310; subpattern_7, ns=2

Supplementary Figure 1039: TF-MoDisCO subpatterns for the ZNF317 transcription factor in HepG2 (accession ENCSR016OHL).

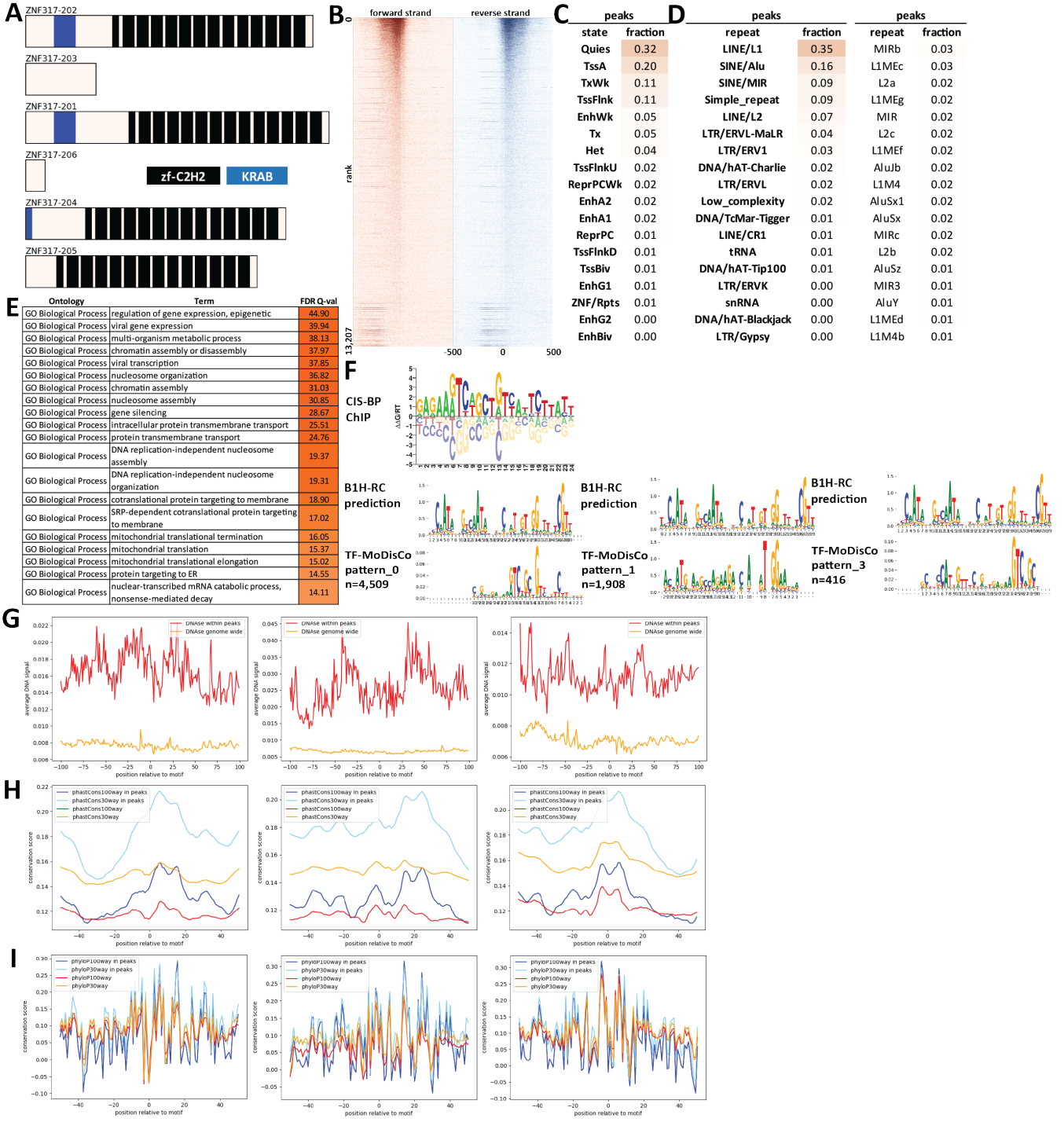

Supplementary Figure 1040: Properties and genomic distribution of motifs identified for the ZNF317 transcription factor in K562 (accession ENCSR976MXN).

TF-MoDisCO pattern_0 n=4509, CWM

pattern_0, n=4509; subpattern_0, ns=824

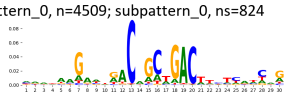

pattern_0, n=4509; subpattern_1, ns=718

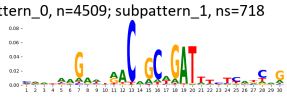

pattern_0, n=4509; subpattern_2, ns=550

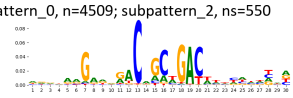

pattern_0, n=4509; subpattern_3, ns=505

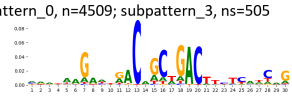

pattern_0, n=4509; subpattern_4, ns=470

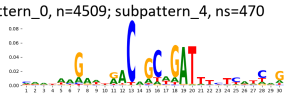

pattern_0, n=4509; subpattern_5, ns=411

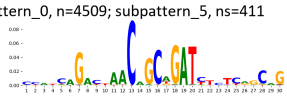

pattern_0, n=4509; subpattern_6, ns=350

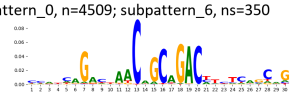

pattern_0, n=4509; subpattern_7, ns=331

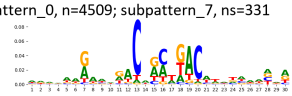

pattern_0, n=4509; subpattern_8, ns=239

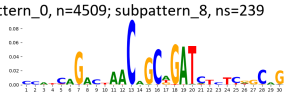

pattern_0, n=4509; subpattern_9, ns=111

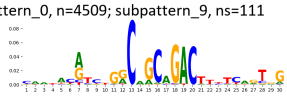

TF-MoDisCO pattern_0 n=4509, PWM

pattern_0, n=4509; subpattern_0, ns=824

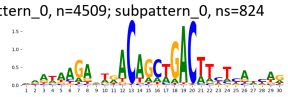

pattern_0, n=4509; subpattern_1, ns=718

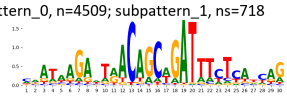

pattern_0, n=4509; subpattern_2, ns=550

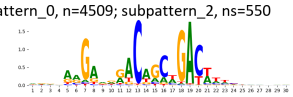

pattern_0, n=4509; subpattern_3, ns=505

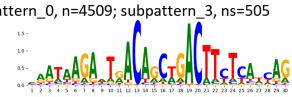

pattern_0, n=4509; subpattern_4, ns=470

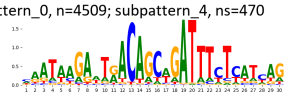

pattern_0, n=4509; subpattern_5, ns=411

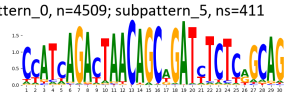

pattern_0, n=4509; subpattern_6, ns=350

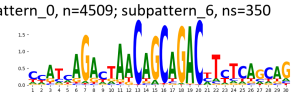

pattern_0, n=4509; subpattern_7, ns=331

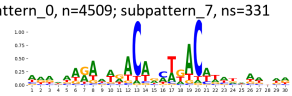

pattern_0, n=4509; subpattern_8, ns=239

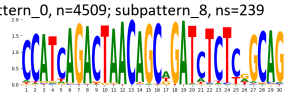

pattern_0, n=4509; subpattern_9, ns=111

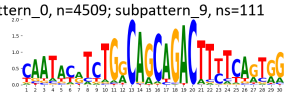

TF-MoDisCO pattern_1 n=1908, CWM

pattern_1, n=1908; subpattern_0, ns=601

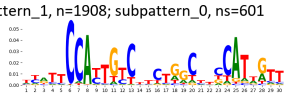

pattern_1, n=1908; subpattern_1, ns=563

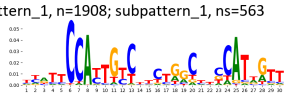

pattern_1, n=1908; subpattern_2, ns=201

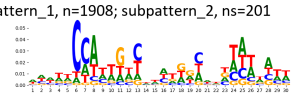

pattern_1, n=1908; subpattern_3, ns=168

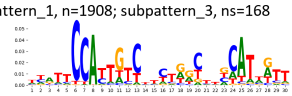

pattern_1, n=1908; subpattern_4, ns=153

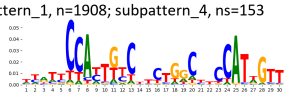

pattern_1, n=1908; subpattern_5, ns=116

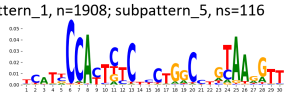

pattern_1, n=1908; subpattern_6, ns=106

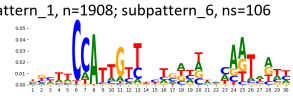

TF-MoDisCO pattern_1 n=1908, PWM

pattern_1, n=1908; subpattern_0, ns=601

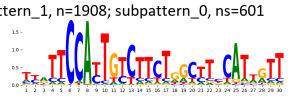

pattern_1, n=1908; subpattern_1, ns=563

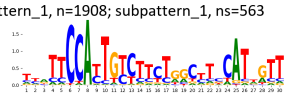

pattern_1, n=1908; subpattern_2, ns=201

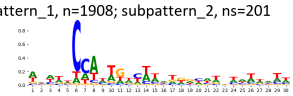

pattern_1, n=1908; subpattern_3, ns=168

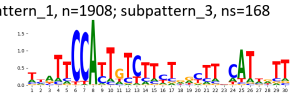

pattern_1, n=1908; subpattern_4, ns=153

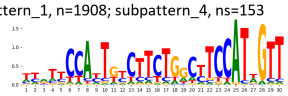

pattern_1, n=1908; subpattern_5, ns=116

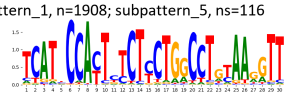

pattern_1, n=1908; subpattern_6, ns=106

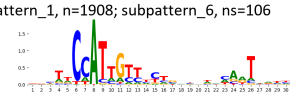

TF-MoDisCO pattern_3 n=416, CWM

pattern_3, n=416; subpattern_0, ns=124

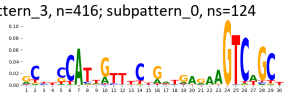

pattern_3, n=416; subpattern_1, ns=105

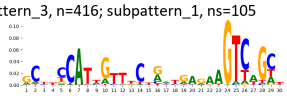

pattern_3, n=416; subpattern_2, ns=99

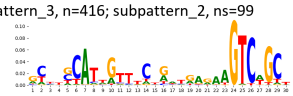

pattern_3, n=416; subpattern_3, ns=86

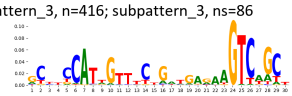

pattern_3, n=416; subpattern_4, ns=2

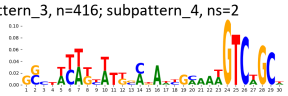

TF-MoDisCO pattern_3 n=416, PWM

pattern_3, n=416; subpattern_0, ns=124

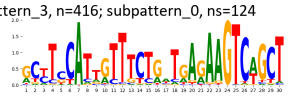

pattern_3, n=416; subpattern_1, ns=105

pattern_3, n=416; subpattern_2, ns=99

pattern_3, n=416; subpattern_3, ns=86

pattern_3, n=416; subpattern_4, ns=2

Supplementary Figure 1041: TF-MoDisCO subpatterns for the ZNF317 transcription factor in K562 (accession ENCSR976MXN).

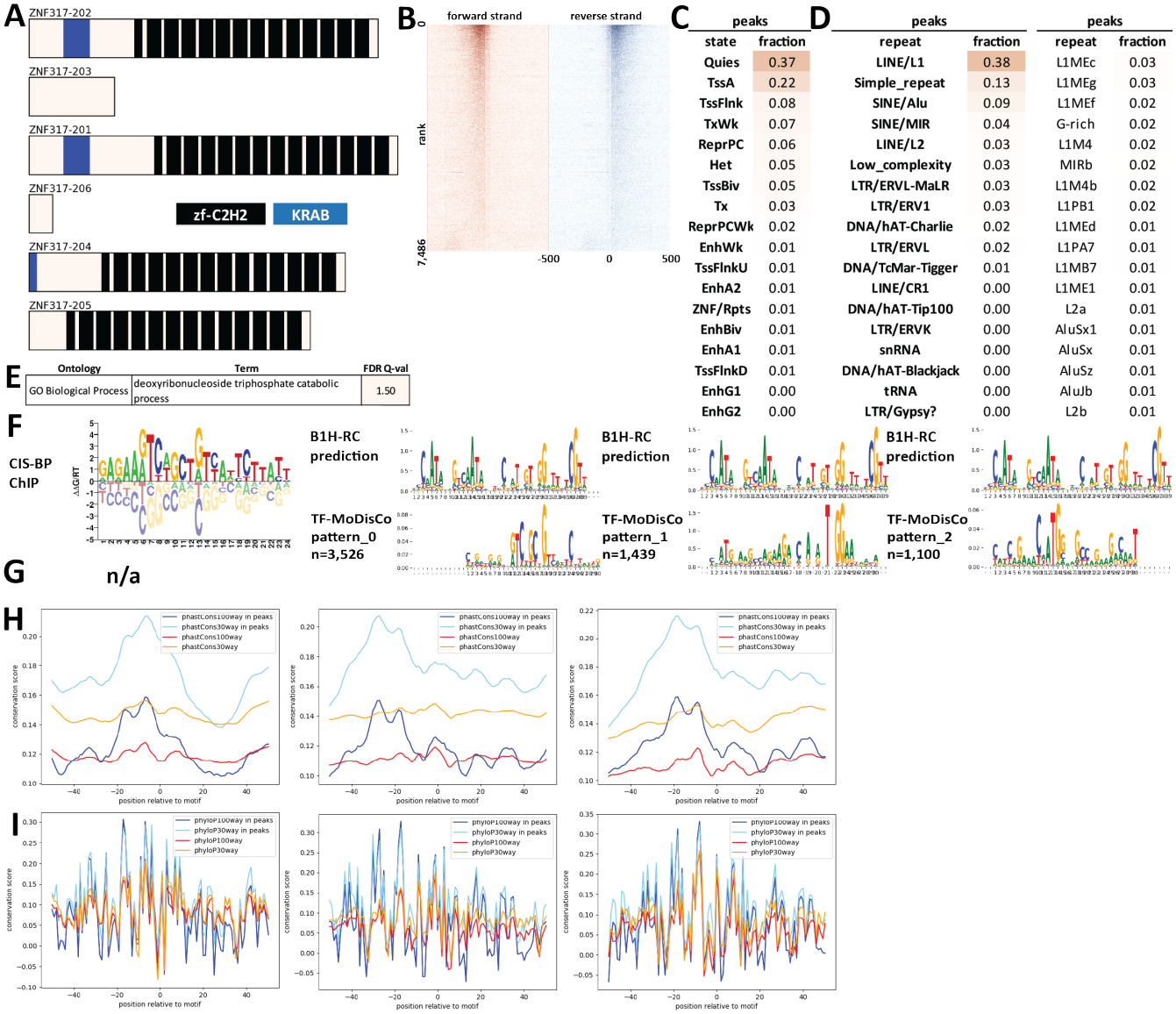

Supplementary Figure 1042: Properties and genomic distribution of motifs identified for the ZNF317 transcription factor in WTC11 (accession ENCSR795KRU).

TF-MoDiSCO pattern_0 n=3526, CWM

pattern_0, n=3526; subpattern_0, ns=753

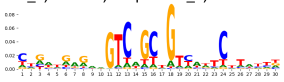

pattern_0, n=3526; subpattern_1, ns=656

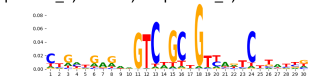

pattern_0, n=3526; subpattern_10, ns=4

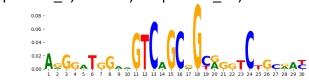

pattern_0, n=3526; subpattern_2, ns=637

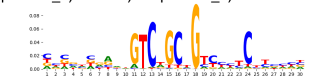

pattern_0, n=3526; subpattern_3, ns=498

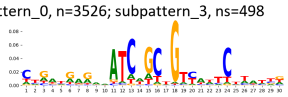

pattern_0, n=3526; subpattern_4, ns=460

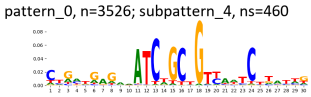

pattern_0, n=3526; subpattern_5, ns=271

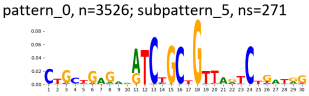

pattern_0, n=3526; subpattern_6, ns=121

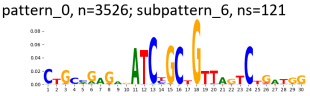

pattern_0, n=3526; subpattern_7, ns=67

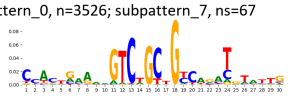

pattern_0, n=3526; subpattern_8, ns=53

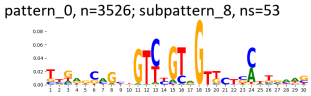

pattern_0, n=3526; subpattern_9, ns=6

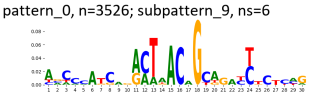

TF-MoDiSCO pattern_0 n=3526, PWM

pattern_0, n=3526; subpattern_0, ns=753

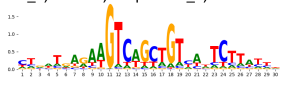

pattern_0, n=3526; subpattern_1, ns=656

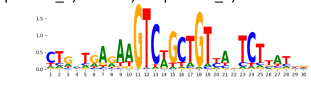

pattern_0, n=3526; subpattern_10, ns=4

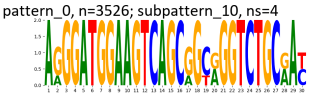

pattern_0, n=3526; subpattern_2, ns=637

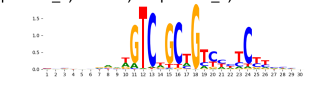

pattern_0, n=3526; subpattern_3, ns=498

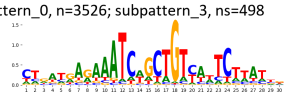

pattern_0, n=3526; subpattern_4, ns=460

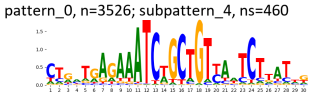

pattern_0, n=3526; subpattern_5, ns=271

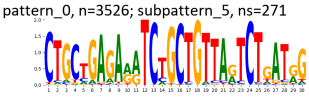

pattern_0, n=3526; subpattern_6, ns=121

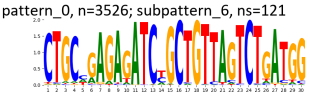

pattern_0, n=3526; subpattern_7, ns=67

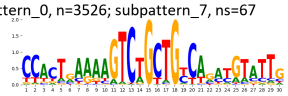

pattern_0, n=3526; subpattern_8, ns=53

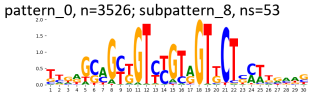

pattern_0, n=3526; subpattern_9, ns=6

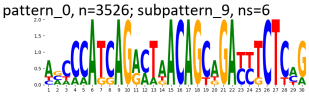

TF-MoDiSCO pattern_1 n=1439, CWM

pattern_1, n=1439; subpattern_0, ns=290

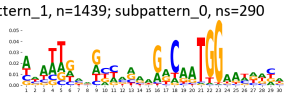

pattern_1, n=1439; subpattern_1, ns=273

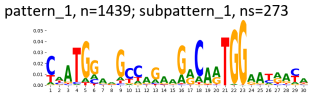

pattern_1, n=1439; subpattern_2, ns=261

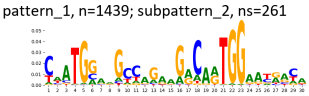

pattern_1, n=1439; subpattern_3, ns=163

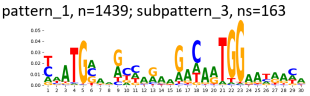

pattern_1, n=1439; subpattern_4, ns=132

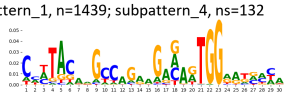

pattern_1, n=1439; subpattern_5, ns=131

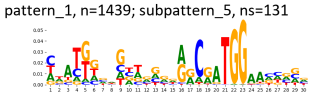

pattern_1, n=1439; subpattern_6, ns=109

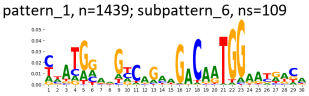

pattern_1, n=1439; subpattern_7, ns=80

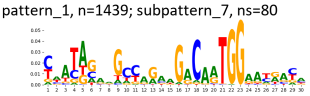

TF-MoDiSCO pattern_1 n=1439, PWM

pattern_1, n=1439; subpattern_0, ns=290

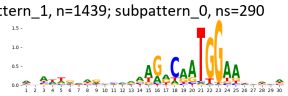

pattern_1, n=1439; subpattern_1, ns=273

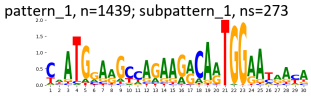

pattern_1, n=1439; subpattern_2, ns=261

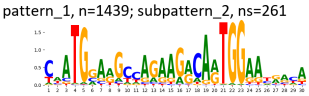

pattern_1, n=1439; subpattern_3, ns=163

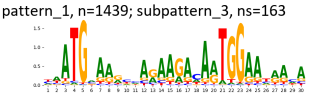

pattern_1, n=1439; subpattern_4, ns=132

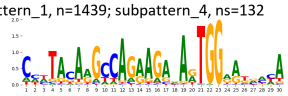

pattern_1, n=1439; subpattern_5, ns=131

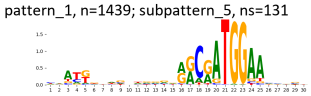

pattern_1, n=1439; subpattern_6, ns=109

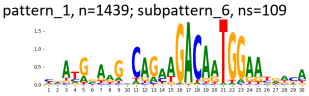

pattern_1, n=1439; subpattern_7, ns=80

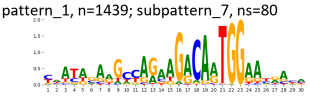

TF-MoDiSCO pattern_2 n=1100, CWM

pattern_2, n=1100; subpattern_0, ns=272

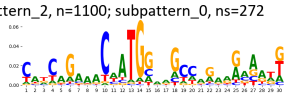

pattern_2, n=1100; subpattern_1, ns=250

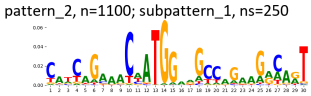

pattern_2, n=1100; subpattern_2, ns=226

pattern_2, n=1100; subpattern_3, ns=179

pattern_2, n=1100; subpattern_4, ns=164

pattern_2, n=1100; subpattern_5, ns=7

pattern_2, n=1100; subpattern_6, ns=2

TF-MoDiSCO pattern_2 n=1100, PWM

pattern_2, n=1100; subpattern_0, ns=272

pattern_2, n=1100; subpattern_1, ns=250

pattern_2, n=1100; subpattern_2, ns=226

pattern_2, n=1100; subpattern_3, ns=179

pattern_2, n=1100; subpattern_4, ns=164

pattern_2, n=1100; subpattern_5, ns=7

pattern_2, n=1100; subpattern_6, ns=2

Supplementary Figure 1043: TF-MoDisCO subpatterns for the ZNF317 transcription factor in WTC11 (accession ENCSR795KRU).

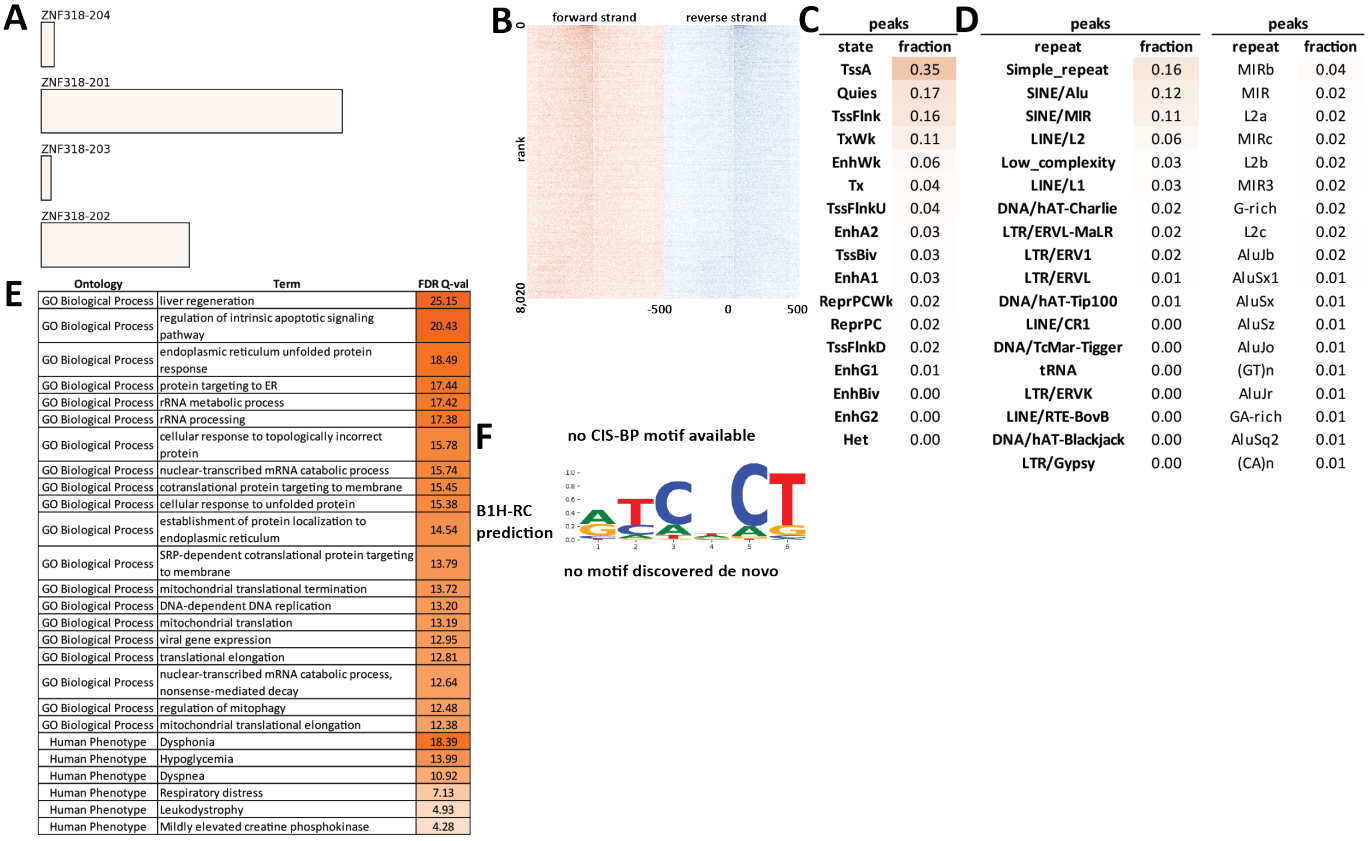

Supplementary Figure 1044: Properties and genomic distribution of motifs identified for the ZNF318 transcription factor in HepG2 (accession ENCSR832PID).

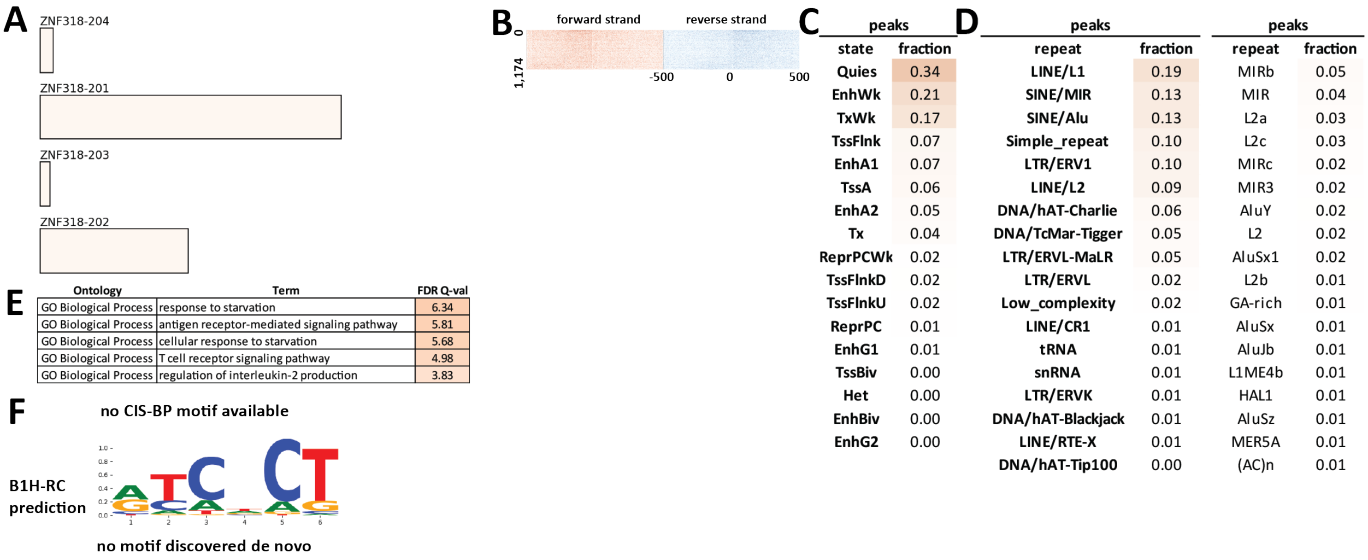

peaks	
state	fraction
Quies	0.34
EnhWk	0.21
TxWk	0.17
TssFlnk	0.07
EnhA1	0.07
TssA	0.06
EnhA2	0.05
Tx	0.04
ReprPCWk	0.02
TssFlnkD	0.02
TssFlnkU	0.02
ReprPC	0.01
EnhG1	0.01
TssBiv	0.00
Het	0.00
EnhBiv	0.00
EnhG2	0.00

peaks	
repeat	fraction
LINE/L1	0.19
SINE/MIR	0.13
SINE/Alu	0.13
Simple_repeat	0.10
LTR/ERV1	0.10
LINE/L2	0.09
DNA/hAT-Charlie	0.06
DNA/TcMar-Tigger	0.05
LTR/ERVL-MaLR	0.05
LTR/ERVL	0.02
Low_complexity	0.02
LINE/CR1	0.01
tRNA	0.01
snRNA	0.01
LTR/ERVK	0.01
DNA/hAT-Blackjack	0.01
LINE/RTE-X	0.01
DNA/hAT-Tip100	0.00

peaks	
repeat	fraction
MIRb	0.05
MIR	0.04
L2a	0.03
L2c	0.03
MIRc	0.02
MIR3	0.02
AluY	0.02
L2	0.02
AluSx1	0.02
L2b	0.01
GA-rich	0.01
AluSx	0.01
AluJb	0.01
L1ME4b	0.01
HAL1	0.01
AluSz	0.01
MER5A	0.01
(AC)n	0.01

Ontology	Term	FDR Q-val
GO Biological Process	response to starvation	6.34
GO Biological Process	antigen receptor-mediated signaling pathway	5.81
GO Biological Process	cellular response to starvation	5.68
GO Biological Process	T cell receptor signaling pathway	4.98
GO Biological Process	regulation of interleukin-2 production	3.83

Supplementary Figure 1045: Properties and genomic distribution of motifs identified for the ZNF318 transcription factor in K562 (accession ENCSR334HSW).

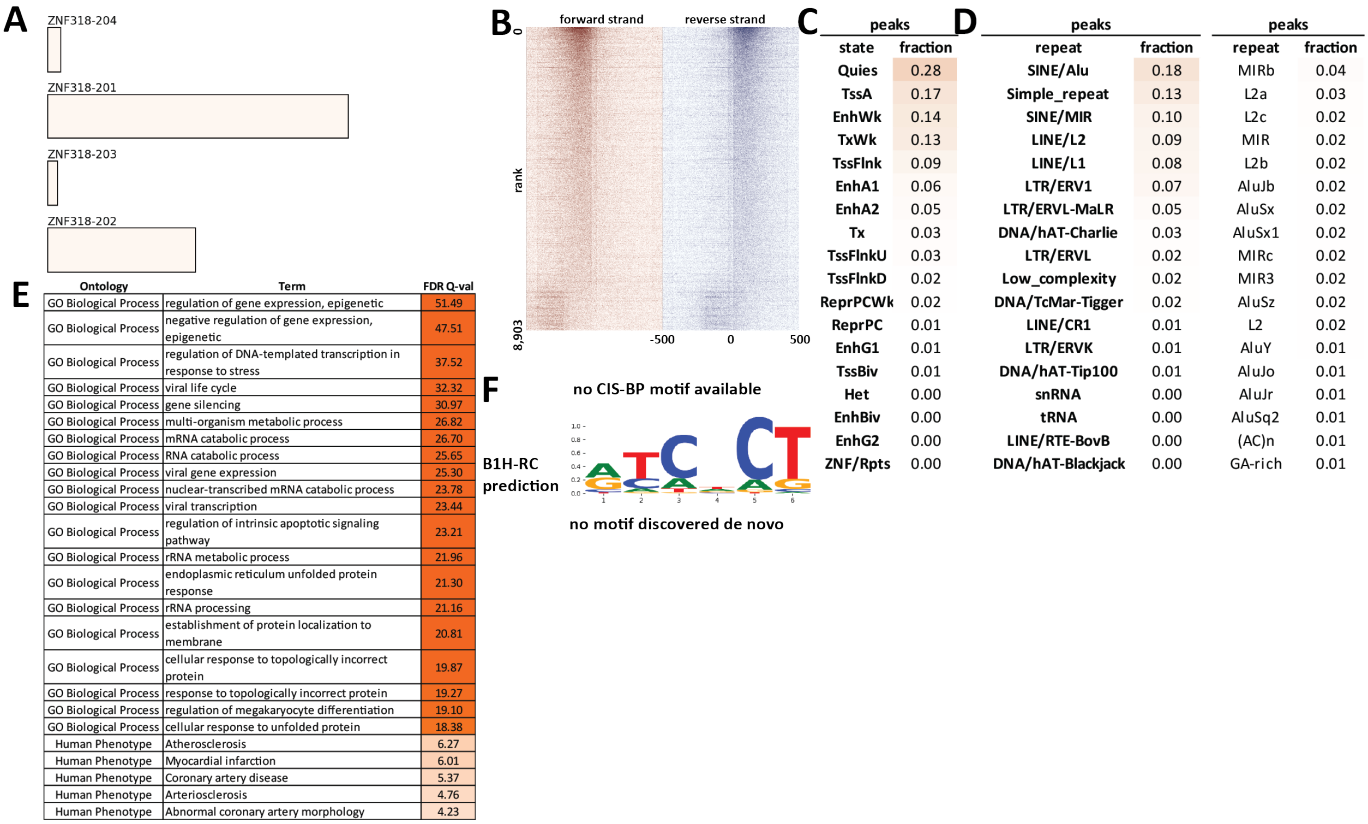

C

peaks	
state	fraction
Quies	0.28
TssA	0.17
EnhWk	0.14
TxWk	0.13
TssFlnk	0.09
EnhA1	0.06
EnhA2	0.05
Tx	0.03
TssFlnkU	0.03
TssFlnkD	0.02
ReprPCWk	0.02
ReprPC	0.01
EnhG1	0.01
TssBiv	0.01
Het	0.00
EnhBiv	0.00
EnhG2	0.00
ZNF/Rpts	0.00

D

peaks		peaks	
repeat	fraction	repeat	fraction
SINE/Alu	0.18	MIRb	0.04
Simple_repeat	0.13	L2a	0.03
SINE/MIR	0.10	L2c	0.02
LINE/L2	0.09	MIR	0.02
LINE/L1	0.08	L2b	0.02
LTR/ERV1	0.07	AluJb	0.02
LTR/ERVL-MaLR	0.05	AluSx	0.02
DNA/hAT-Charlie	0.03	AluSx1	0.02
LTR/ERVL	0.02	MIRc	0.02
Low_complexity	0.02	MIR3	0.02
DNA/TcMar-Tigger	0.02	AluSz	0.02
LINE/CR1	0.01	L2	0.02
LTR/ERVK	0.01	AluY	0.01
DNA/hAT-Tip100	0.01	AluJo	0.01
snRNA	0.00	AluJr	0.01
tRNA	0.00	AluSq2	0.01
LINE/RTE-BovB	0.00	(AC)n	0.01
DNA/hAT-Blackjack	0.00	GA-rich	0.01

E

Ontology	Term	FDR Q-val
GO Biological Process	regulation of gene expression, epigenetic	51.49
GO Biological Process	negative regulation of gene expression, epigenetic	47.51
GO Biological Process	regulation of DNA-templated transcription in response to stress	37.52
GO Biological Process	viral life cycle	32.32
GO Biological Process	gene silencing	30.97
GO Biological Process	multi-organism metabolic process	26.82
GO Biological Process	mRNA catabolic process	26.70
GO Biological Process	RNA catabolic process	25.65
GO Biological Process	viral gene expression	25.30
GO Biological Process	nuclear-transcribed mRNA catabolic process	23.78
GO Biological Process	viral transcription	23.44
GO Biological Process	regulation of intrinsic apoptotic signaling pathway	23.21
GO Biological Process	rRNA metabolic process	21.96
GO Biological Process	endoplasmic reticulum unfolded protein response	21.30
GO Biological Process	rRNA processing	21.16
GO Biological Process	establishment of protein localization to membrane	20.81
GO Biological Process	cellular response to topologically incorrect protein	19.87
GO Biological Process	response to topologically incorrect protein	19.27
GO Biological Process	regulation of megakaryocyte differentiation	19.10
GO Biological Process	cellular response to unfolded protein	18.38
Human Phenotype	Atherosclerosis	6.27
Human Phenotype	Myocardial infarction	6.01
Human Phenotype	Coronary artery disease	5.37
Human Phenotype	Arteriosclerosis	4.76
Human Phenotype	Abnormal coronary artery morphology	4.23

Supplementary Figure 1046: Properties and genomic distribution of motifs identified for the ZNF318 transcription factor in K562 (accession ENCSR352BJL).

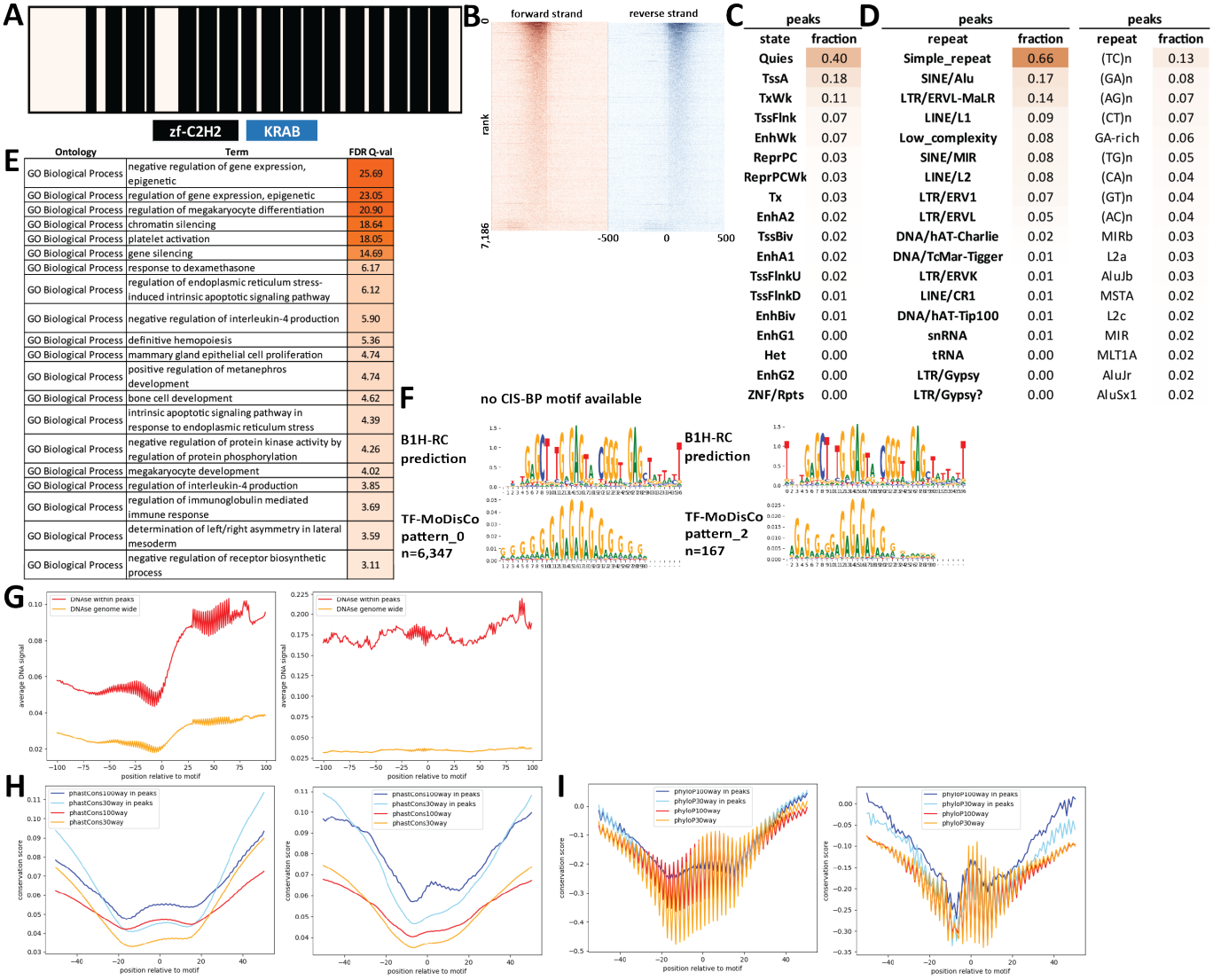

Supplementary Figure 1047: Properties and genomic distribution of motifs identified for the ZNF319 transcription factor in K562 (accession ENCSR231PDA).

TF-MoDisCO pattern_0 n=6347, CWM

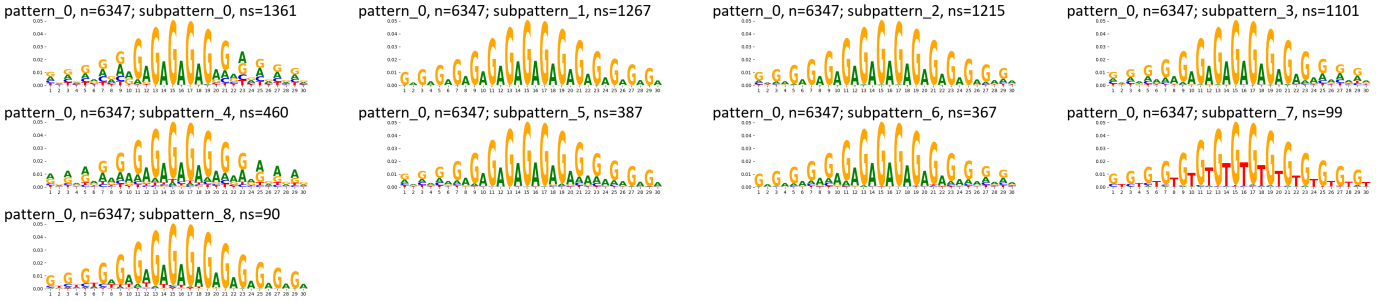

TF-MoDisCO pattern_0 n=6347, PWM

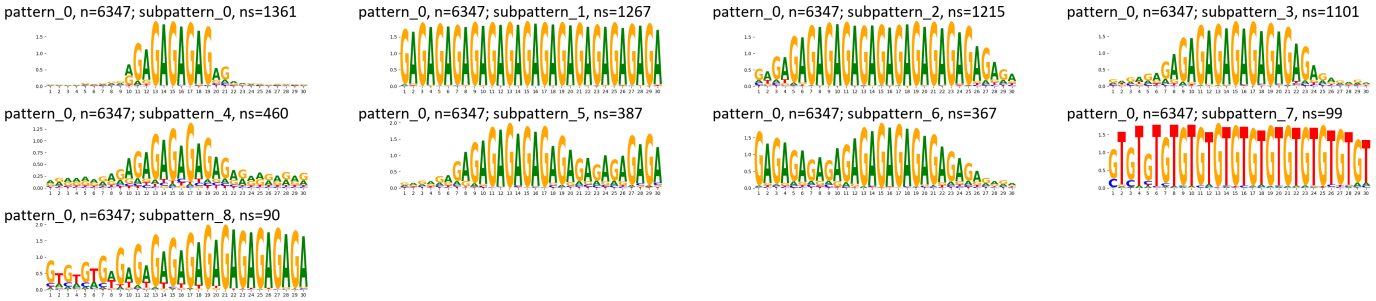

TF-MoDisCO pattern_2 n=167, CWM

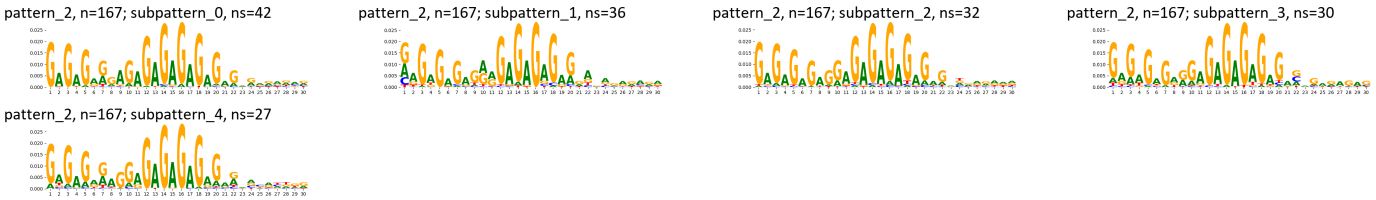

TF-MoDisCO pattern_2 n=167, PWM

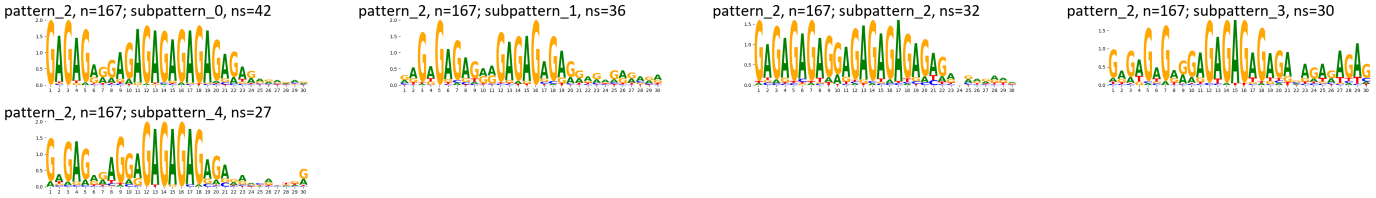

Supplementary Figure 1048: TF-MoDisCO subpatterns for the ZNF319 transcription factor in K562 (accession ENCSR231PDA).

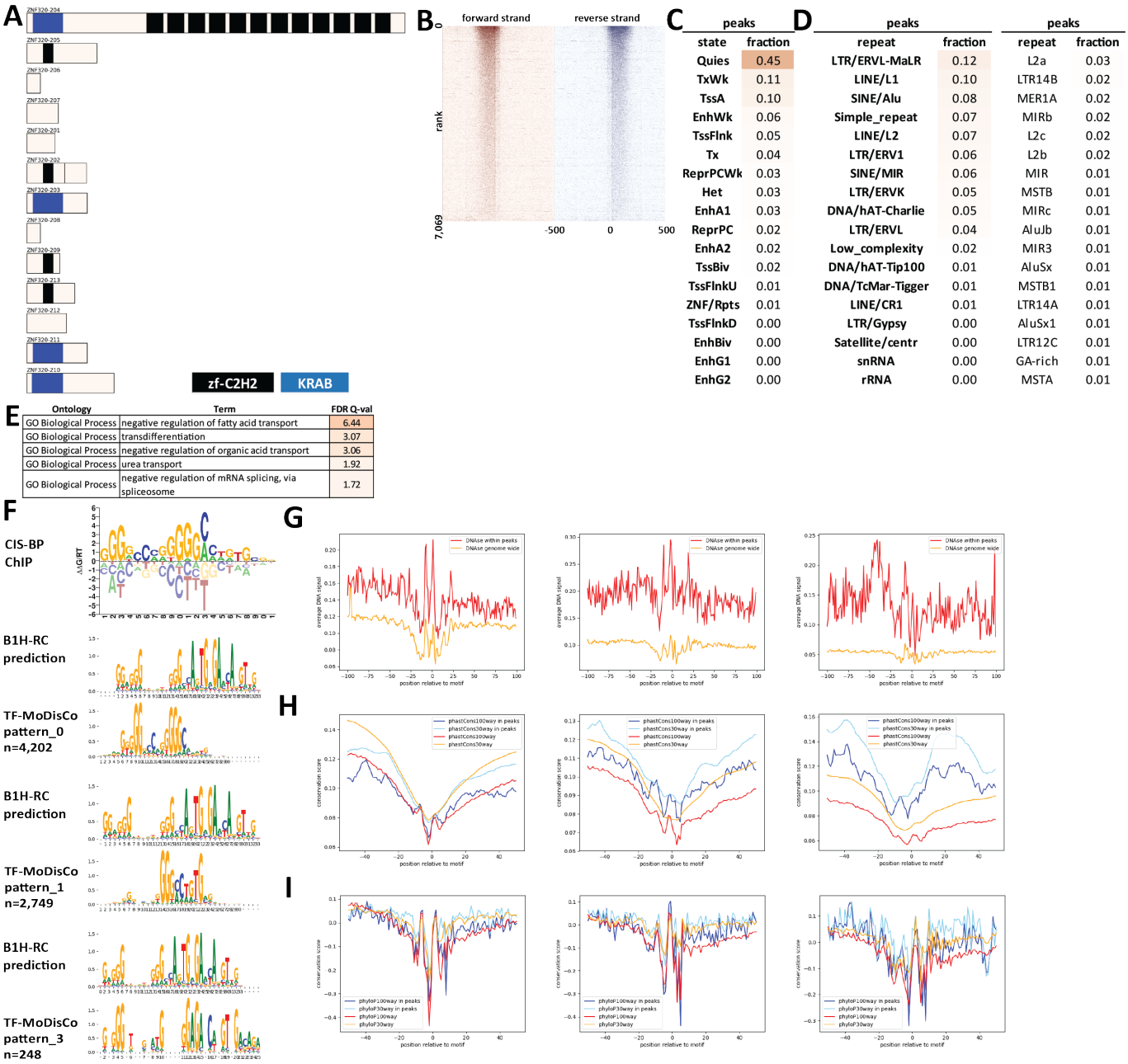

C

peaks	
state	fraction
Quies	0.45
TxWk	0.11
TssA	0.10
EnhWk	0.06
TssFlnk	0.05
Tx	0.04
ReprPCWk	0.03
Het	0.03
EnhA1	0.03
ReprPC	0.02
EnhA2	0.02
TssBiv	0.02
TssFlnkU	0.01
ZNF/Rpts	0.01
TssFlnkD	0.00
EnhBiv	0.00
EnhG1	0.00
EnhG2	0.00

D

peaks		peaks	
repeat	fraction	repeat	fraction
LTR/ERVL-MaLR	0.12	L2a	0.03
LINE/L1	0.10	LTR14B	0.02
SINE/Alu	0.08	MER1A	0.02
Simple_repeat	0.07	MIRb	0.02
LINE/L2	0.07	L2c	0.02
LTR/ERV1	0.06	L2b	0.02
SINE/MIR	0.06	MIR	0.01
LTR/ERVK	0.05	MSTB	0.01
DNA/hAT-Charlie	0.05	MIRc	0.01
LTR/ERVL	0.04	AluJb	0.01
Low_complexity	0.02	MIR3	0.01
DNA/hAT-Tip100	0.01	AluSx	0.01
DNA/TcMar-Tigger	0.01	MSTB1	0.01
LINE/CR1	0.01	LTR14A	0.01
LTR/Gypsy	0.00	AluSx1	0.01
Satellite/centr	0.00	LTR12C	0.01
snRNA	0.00	GA-rich	0.01
rRNA	0.00	MSTA	0.01

E

Ontology	Term	FDR Q-val
GO Biological Process	negative regulation of fatty acid transport	6.44
GO Biological Process	transdifferentiation	3.07
GO Biological Process	negative regulation of organic acid transport	3.06
GO Biological Process	urea transport	1.92
GO Biological Process	negative regulation of mRNA splicing, via spliceosome	1.72

Supplementary Figure 1049: Properties and genomic distribution of motifs identified for the ZNF320 transcription factor in HEK293 (accession Hughes GR models).

TF-MoDisCO pattern_0 n=4202, CWM

pattern_0, n=4202; subpattern_0, ns=891

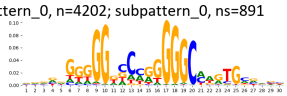

pattern_0, n=4202; subpattern_1, ns=759

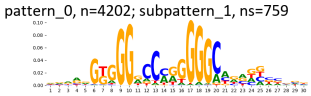

pattern_0, n=4202; subpattern_2, ns=547

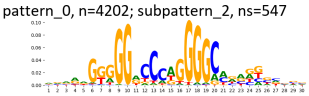

pattern_0, n=4202; subpattern_3, ns=490

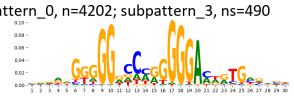

pattern_0, n=4202; subpattern_4, ns=431

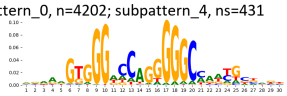

pattern_0, n=4202; subpattern_5, ns=333

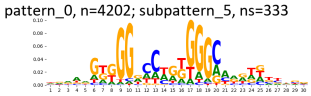

pattern_0, n=4202; subpattern_6, ns=274

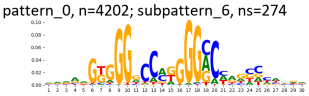

pattern_0, n=4202; subpattern_7, ns=242

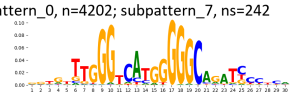

pattern_0, n=4202; subpattern_8, ns=231

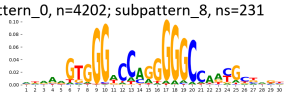

pattern_0, n=4202; subpattern_9, ns=4

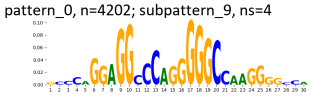

TF-MoDisCO pattern_0 n=4202, PWM

pattern_0, n=4202; subpattern_0, ns=891

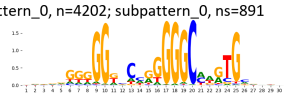

pattern_0, n=4202; subpattern_1, ns=759

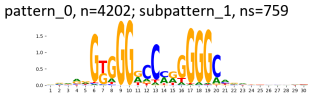

pattern_0, n=4202; subpattern_2, ns=547

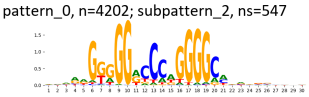

pattern_0, n=4202; subpattern_3, ns=490

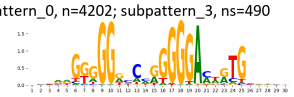

pattern_0, n=4202; subpattern_4, ns=431

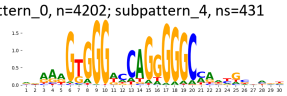

pattern_0, n=4202; subpattern_5, ns=333

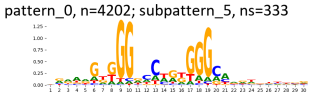

pattern_0, n=4202; subpattern_6, ns=274

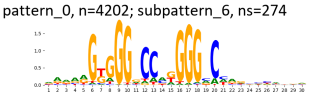

pattern_0, n=4202; subpattern_7, ns=242

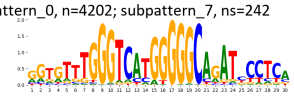

pattern_0, n=4202; subpattern_8, ns=231

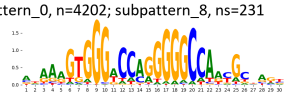

pattern_0, n=4202; subpattern_9, ns=4

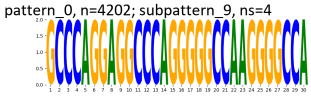

TF-MoDisCO pattern_1 n=2749, CWM

pattern_1, n=2749; subpattern_0, ns=724

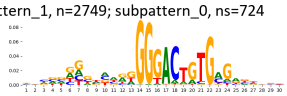

pattern_1, n=2749; subpattern_1, ns=507

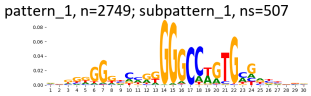

pattern_1, n=2749; subpattern_2, ns=467

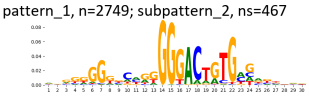

pattern_1, n=2749; subpattern_3, ns=379

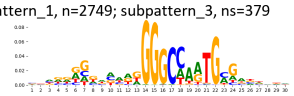

pattern_1, n=2749; subpattern_4, ns=336

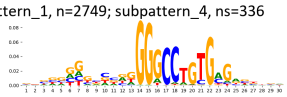

pattern_1, n=2749; subpattern_5, ns=129

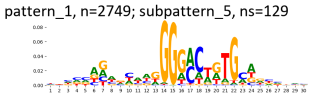

pattern_1, n=2749; subpattern_6, ns=81

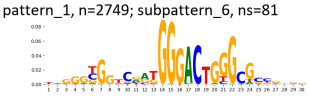

pattern_1, n=2749; subpattern_7, ns=64

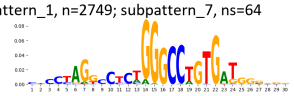

pattern_1, n=2749; subpattern_8, ns=43

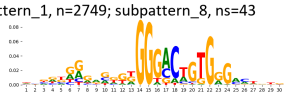

pattern_1, n=2749; subpattern_9, ns=19

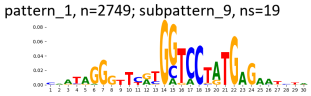

TF-MoDisCO pattern_1 n=2749, PWM

pattern_1, n=2749; subpattern_0, ns=724

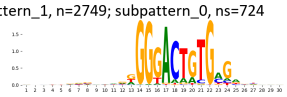

pattern_1, n=2749; subpattern_1, ns=507

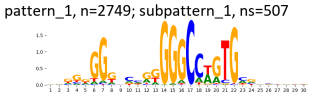

pattern_1, n=2749; subpattern_2, ns=467

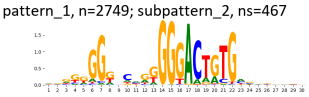

pattern_1, n=2749; subpattern_3, ns=379

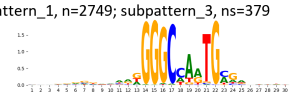

pattern_1, n=2749; subpattern_4, ns=336

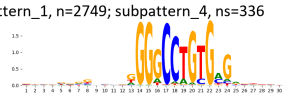

pattern_1, n=2749; subpattern_5, ns=129

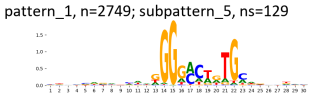

pattern_1, n=2749; subpattern_6, ns=81

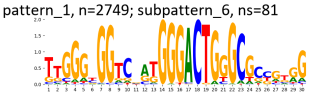

pattern_1, n=2749; subpattern_7, ns=64

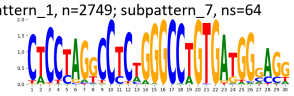

pattern_1, n=2749; subpattern_8, ns=43

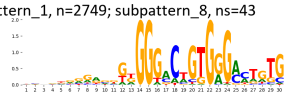

pattern_1, n=2749; subpattern_9, ns=19

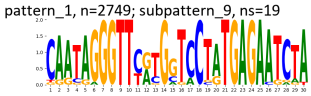

TF-MoDisCO pattern_3 n=248, CWM

pattern_3, n=248; subpattern_0, ns=78

pattern_3, n=248; subpattern_1, ns=72

pattern_3, n=248; subpattern_2, ns=35

pattern_3, n=248; subpattern_3, ns=32

pattern_3, n=248; subpattern_4, ns=27

pattern_3, n=248; subpattern_5, ns=2

pattern_3, n=248; subpattern_6, ns=2

TF-MoDisCO pattern_3 n=248, PWM

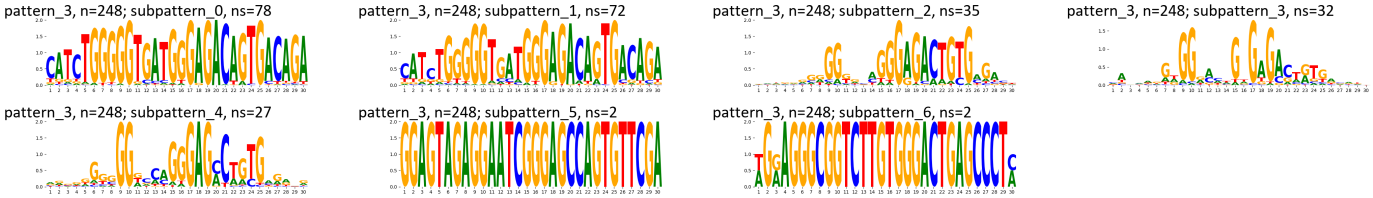

Supplementary Figure 1050: TF-MoDisCO subpatterns for the ZNF320 transcription factor in HEK293 (accession Hughes GR models).

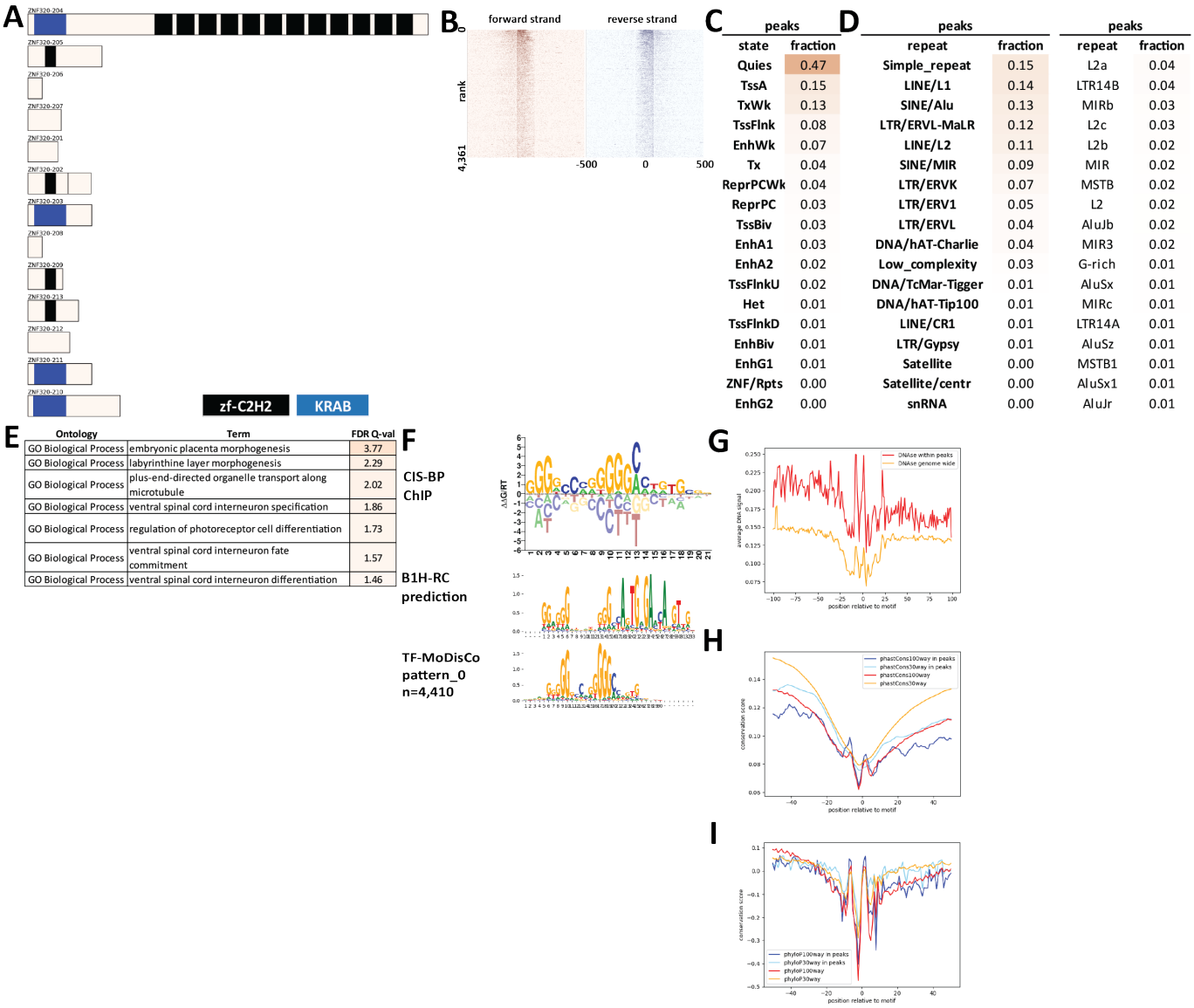

peaks	
state	fraction
Quies	0.47
TssA	0.15
TxWk	0.13
TssFlnk	0.08
EnhWk	0.07
Tx	0.04
ReprPCWk	0.04
ReprPC	0.03
TssBiv	0.03
EnhA1	0.03
EnhA2	0.02
TssFlnkU	0.02
Het	0.01
TssFlnkD	0.01
EnhBiv	0.01
EnhG1	0.01
ZNF/Rpts	0.00
EnhG2	0.00

peaks	
repeat	fraction
Simple_repeat	0.15
LINE/L1	0.14
SINE/Alu	0.13
LTR/ERVL-MaLR	0.12
LINE/L2	0.11
SINE/MIR	0.09
LTR/ERVK	0.07
LTR/ERV1	0.05
LTR/ERVL	0.04
DNA/hAT-Charlie	0.04
Low_complexity	0.03
DNA/TcMar-Tigger	0.01
DNA/hAT-Tip100	0.01
LINE/CR1	0.01
LTR/Gypsy	0.01
Satellite	0.00
Satellite/centr	0.00
snRNA	0.00

peaks	
repeat	fraction
L2a	0.04
LTR14B	0.04
MIRb	0.03
L2c	0.03
L2b	0.02
MIR	0.02
MSTB	0.02
L2	0.02
AluJb	0.02
MIR3	0.02
G-rich	0.01
AluSx	0.01
MIRc	0.01
LTR14A	0.01
AluSz	0.01
MSTB1	0.01
AluSx1	0.01
AluJr	0.01

Ontology	Term	FDR Q-val
GO Biological Process	embryonic placenta morphogenesis	3.77
GO Biological Process	labyrinthine layer morphogenesis	2.29
GO Biological Process	plus-end-directed organelle transport along microtubule	2.02
GO Biological Process	ventral spinal cord interneuron specification	1.86
GO Biological Process	regulation of photoreceptor cell differentiation	1.73
GO Biological Process	ventral spinal cord interneuron fate commitment	1.57
GO Biological Process	ventral spinal cord interneuron differentiation	1.46

Supplementary Figure 1051: Properties and genomic distribution of motifs identified for the ZNF320 transcription factor in HEK293 (accession ChipExo models).

TF-MoDisCO pattern_0 n=4410, CWM

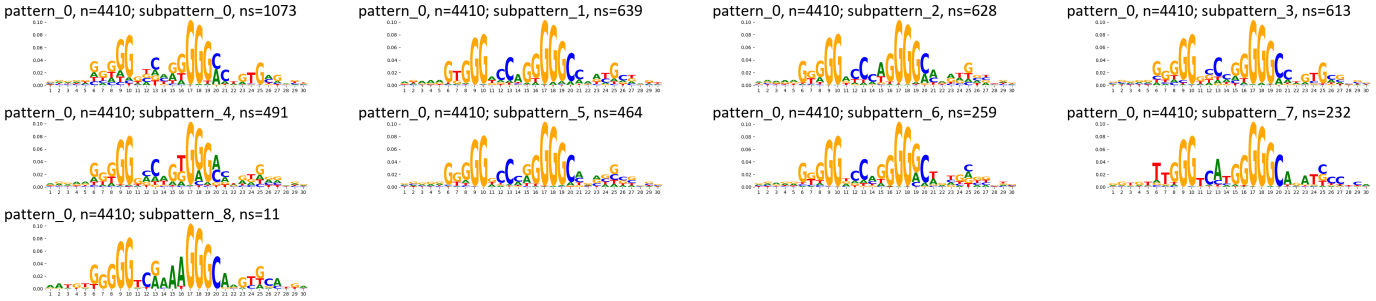

TF-MoDisCO pattern_0 n=4410, PWM

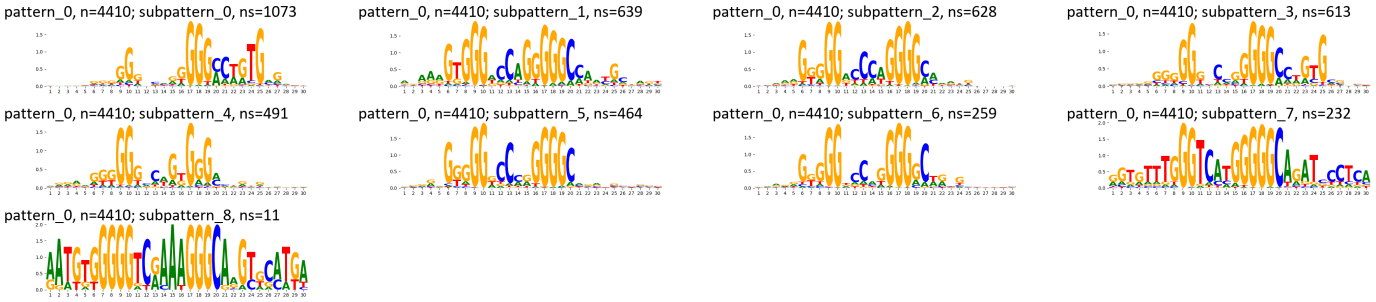

Supplementary Figure 1052: TF-MoDisCO subpatterns for the ZNF320 transcription factor in HEK293 (accession ChipExo models).

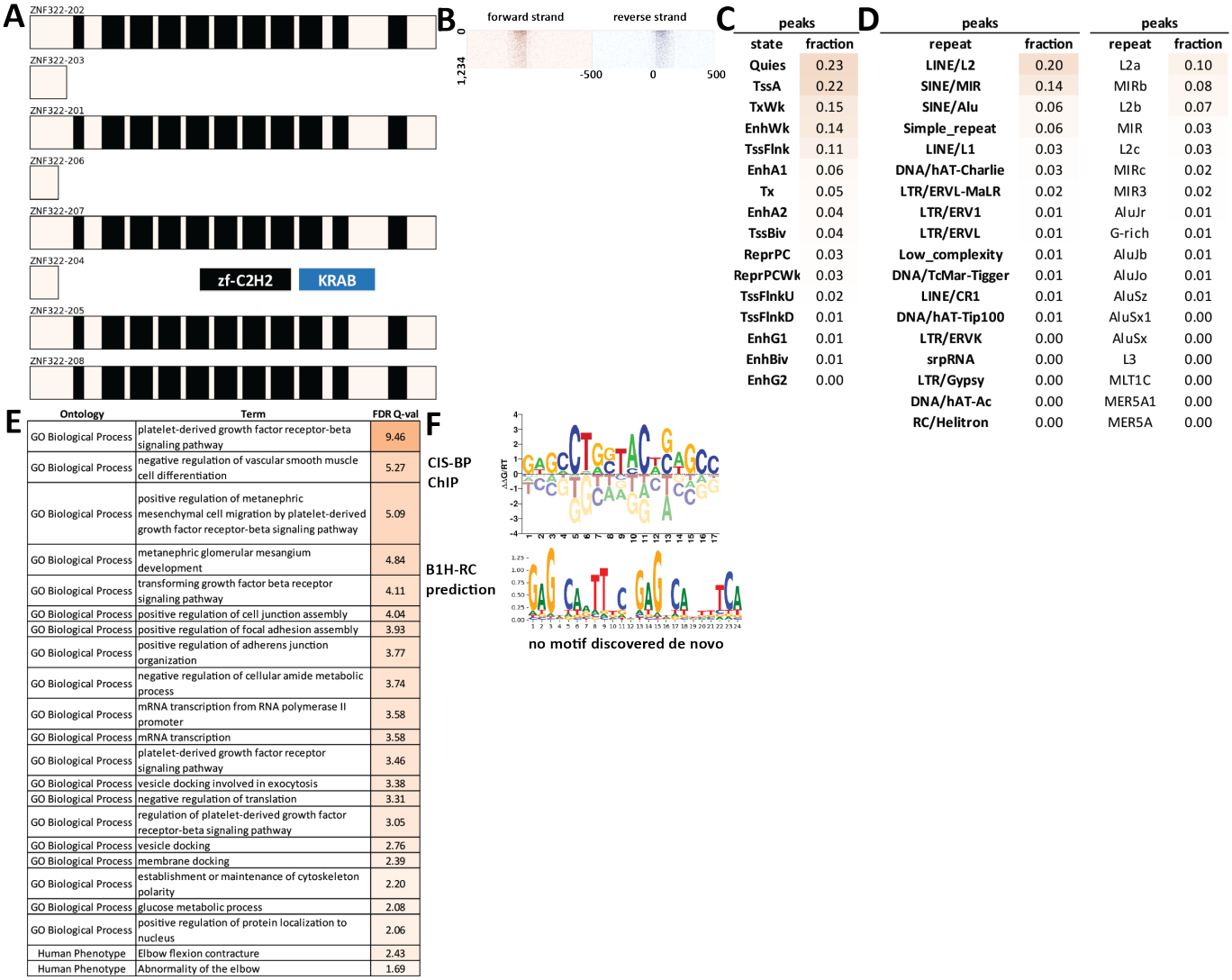

C

peaks	
state	fraction
Quies	0.23
TssA	0.22
TxWk	0.15
EnhWk	0.14
TssFlnk	0.11
EnhA1	0.06
Tx	0.05
EnhA2	0.04
TssBiv	0.04
ReprPC	0.03
ReprPCWk	0.03
TssFlnkU	0.02
TssFlnkD	0.01
EnhG1	0.01
EnhBiv	0.01
EnhG2	0.00

D

peaks		peaks	
repeat	fraction	repeat	fraction
LINE/L2	0.20	L2a	0.10
SINE/MIR	0.14	MIRb	0.08
SINE/Alu	0.06	L2b	0.07
Simple_repeat	0.06	MIR	0.03
LINE/L1	0.03	L2c	0.03
DNA/hAT-Charlie	0.03	MIRc	0.02
LTR/ERVL-MaLR	0.02	MIR3	0.02
LTR/ERV1	0.01	AluJr	0.01
LTR/ERVL	0.01	G-rich	0.01
Low_complexity	0.01	AluJb	0.01
DNA/TcMar-Tigger	0.01	AluJo	0.01
LINE/CR1	0.01	AluSz	0.01
DNA/hAT-Tip100	0.01	AluSx1	0.00
LTR/ERVK	0.00	AluSx	0.00
srpRNA	0.00	L3	0.00
LTR/Gypsy	0.00	MLT1C	0.00
DNA/hAT-Ac	0.00	MER5A1	0.00
RC/Helitron	0.00	MER5A	0.00

E

Ontology	Term	FDR Q-val
GO Biological Process	platelet-derived growth factor receptor-beta signaling pathway	9.46
GO Biological Process	negative regulation of vascular smooth muscle cell differentiation	5.27
GO Biological Process	positive regulation of metanephric mesenchymal cell migration by platelet-derived growth factor receptor-beta signaling pathway	5.09
GO Biological Process	metanephric glomerular mesangium development	4.84
GO Biological Process	transforming growth factor beta receptor signaling pathway	4.11
GO Biological Process	positive regulation of cell junction assembly	4.04
GO Biological Process	positive regulation of focal adhesion assembly	3.93
GO Biological Process	positive regulation of adherens junction organization	3.77
GO Biological Process	negative regulation of cellular amide metabolic process	3.74
GO Biological Process	mRNA transcription from RNA polymerase II promoter	3.58
GO Biological Process	mRNA transcription	3.58
GO Biological Process	platelet-derived growth factor receptor signaling pathway	3.46
GO Biological Process	vesicle docking involved in exocytosis	3.38
GO Biological Process	negative regulation of translation	3.31
GO Biological Process	regulation of platelet-derived growth factor receptor-beta signaling pathway	3.05
GO Biological Process	vesicle docking	2.76
GO Biological Process	membrane docking	2.39
GO Biological Process	establishment or maintenance of cytoskeleton polarity	2.20
GO Biological Process	glucose metabolic process	2.08
GO Biological Process	positive regulation of protein localization to nucleus	2.06
Human Phenotype	Elbow flexion contracture	2.43
Human Phenotype	Abnormality of the elbow	1.69

Supplementary Figure 1053: Properties and genomic distribution of motifs identified for the ZNF322 transcription factor in HEK293 (accession Hughes GR models).

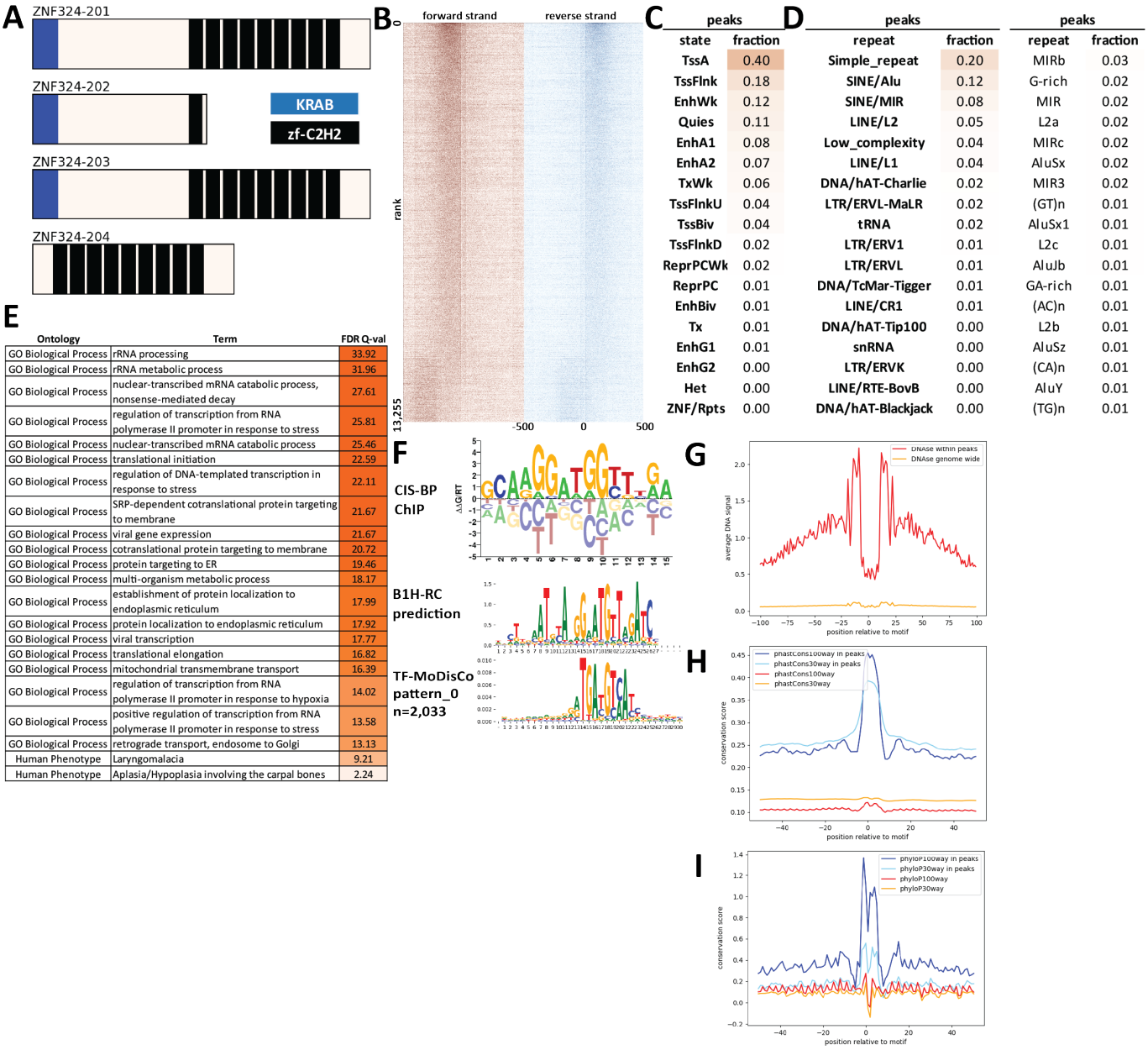

Supplementary Figure 1054: Properties and genomic distribution of motifs identified for the ZNF324 transcription factor in HEK293 (accession ENCSR768HOH).

TF-MoDisCO pattern_0 n=2033, CWM

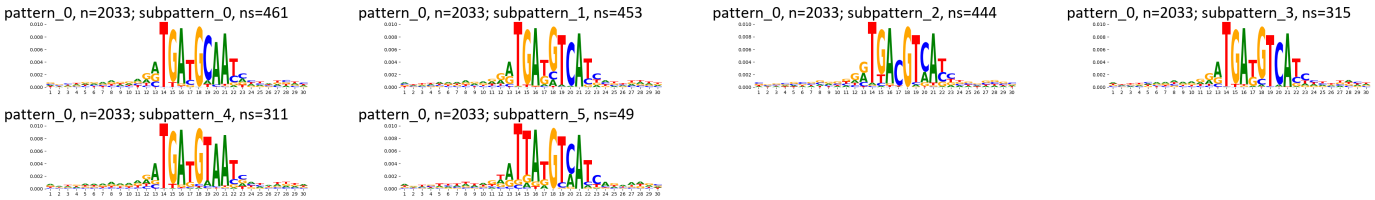

TF-MoDisCO pattern_0 n=2033, PWM

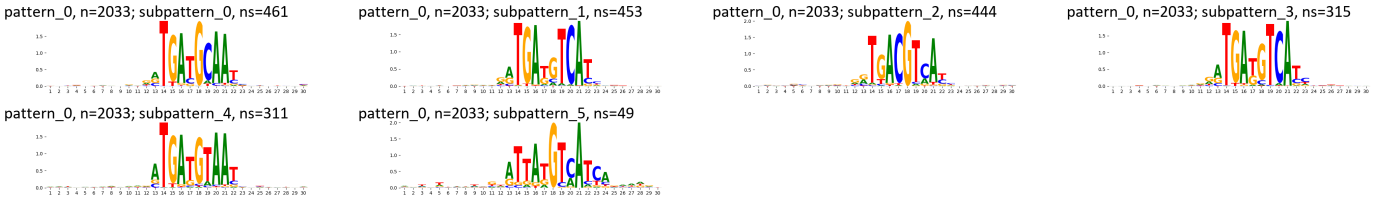

Supplementary Figure 1055: TF-MoDisCO subpatterns for the ZNF324 transcription factor in HEK293 (accession ENCSR768HOH).

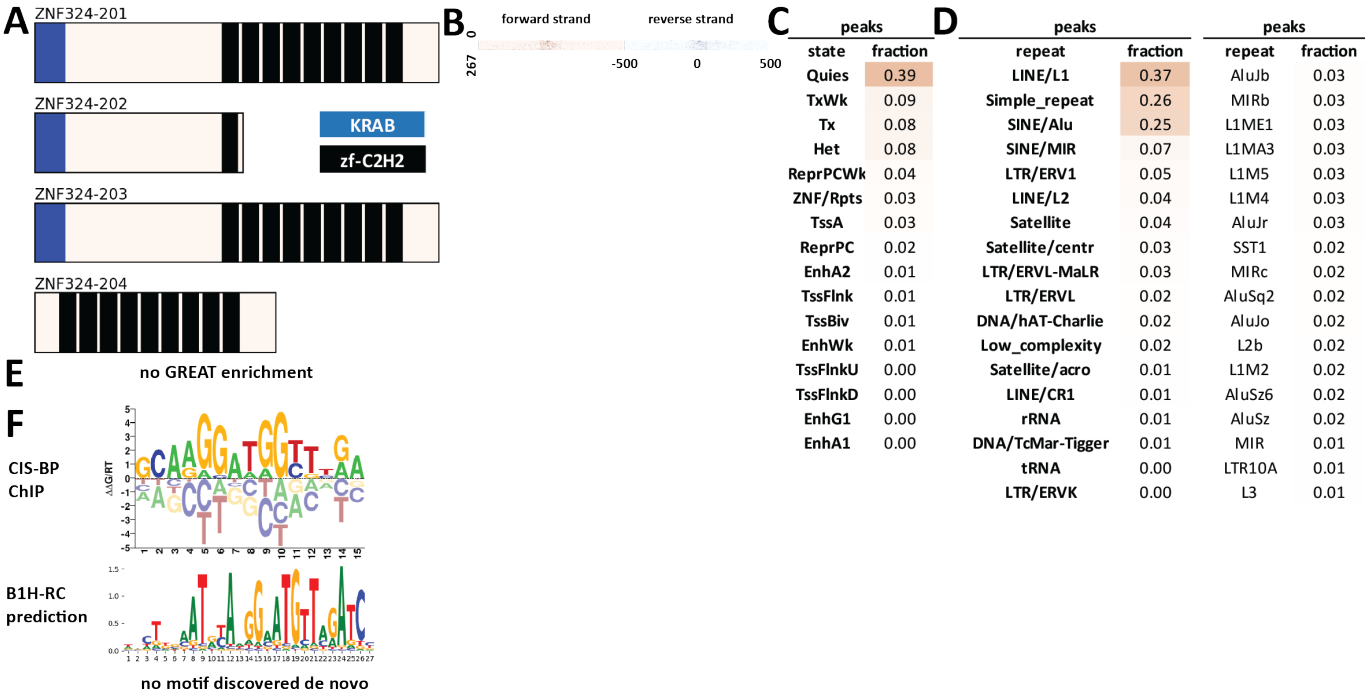

Supplementary Figure 1056: Properties and genomic distribution of motifs identified for the ZNF324 transcription factor in HEK293 (accession ChipExo models).

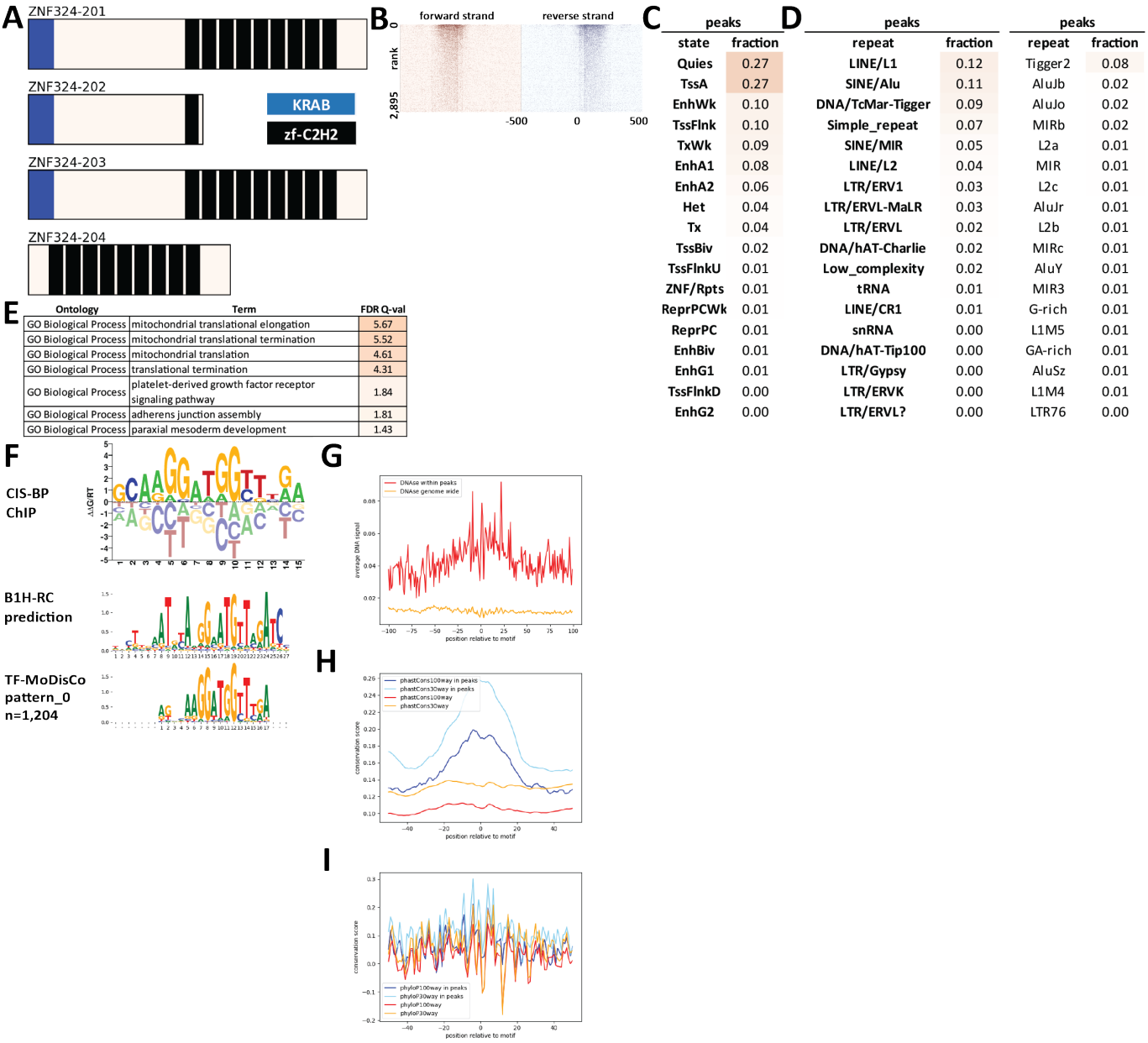

C

peaks	
state	fraction
Quies	0.27
TssA	0.27
EnhWk	0.10
TssFlnk	0.10
TxWk	0.09
EnhA1	0.08
EnhA2	0.06
Het	0.04
Tx	0.04
TssBiv	0.02
TssFlnkU	0.01
ZNF/Rpts	0.01
ReprPCWk	0.01
ReprPC	0.01
EnhBiv	0.01
EnhG1	0.01
TssFlnkD	0.00
EnhG2	0.00

D

peaks		peaks	
repeat	fraction	repeat	fraction
LINE/L1	0.12	Tigger2	0.08
SINE/Alu	0.11	AluJb	0.02
DNA/TcMar-Tigger	0.09	AluJo	0.02
Simple_repeat	0.07	MIRb	0.02
SINE/MIR	0.05	L2a	0.01
LINE/L2	0.04	MIR	0.01
LTR/ERV1	0.03	L2c	0.01
LTR/ERVL-MaLR	0.03	AluJr	0.01
LTR/ERVL	0.02	L2b	0.01
DNA/hAT-Charlie	0.02	MIRc	0.01
Low_complexity	0.02	AluY	0.01
tRNA	0.01	MIR3	0.01
LINE/CR1	0.01	G-rich	0.01
snRNA	0.00	L1M5	0.01
DNA/hAT-Tip100	0.00	GA-rich	0.01
LTR/Gypsy	0.00	AluSz	0.01
LTR/ERVK	0.00	L1M4	0.01
LTR/ERVL?	0.00	LTR76	0.00

E

Ontology	Term	FDR Q-val
GO Biological Process	mitochondrial translational elongation	5.67
GO Biological Process	mitochondrial translational termination	5.52
GO Biological Process	mitochondrial translation	4.61
GO Biological Process	translational termination	4.31
GO Biological Process	platelet-derived growth factor receptor signaling pathway	1.84
GO Biological Process	adherens junction assembly	1.81
GO Biological Process	paraxial mesoderm development	1.43

Supplementary Figure 1057: Properties and genomic distribution of motifs identified for the ZNF324 transcription factor in HEK293 (accession Hughes GR models).

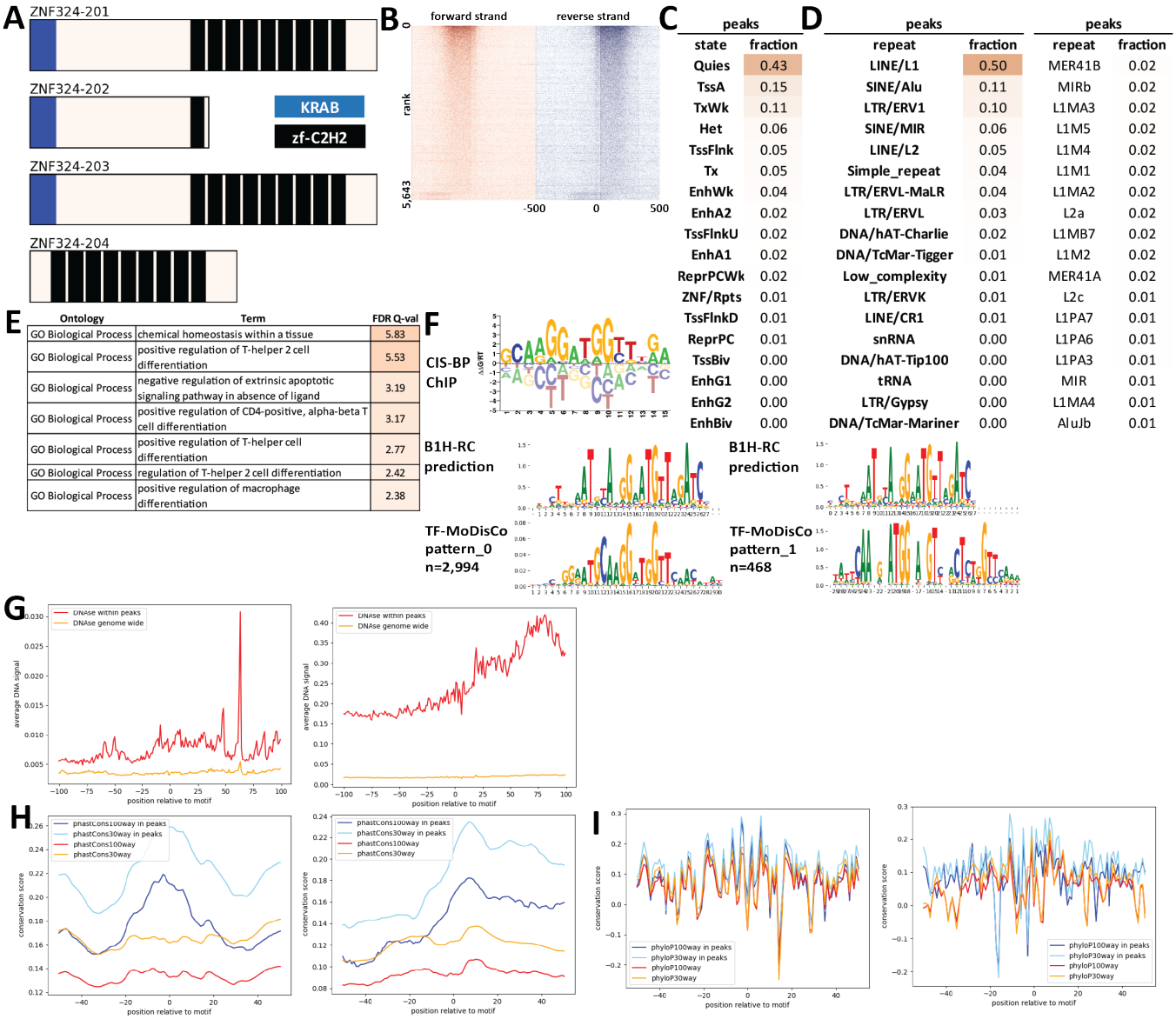

Supplementary Figure 1058: Properties and genomic distribution of motifs identified for the ZNF324 transcription factor in K562 (accession ENCSR712KVZ).

TF-MoDisCO pattern_0 n=2994, CWM

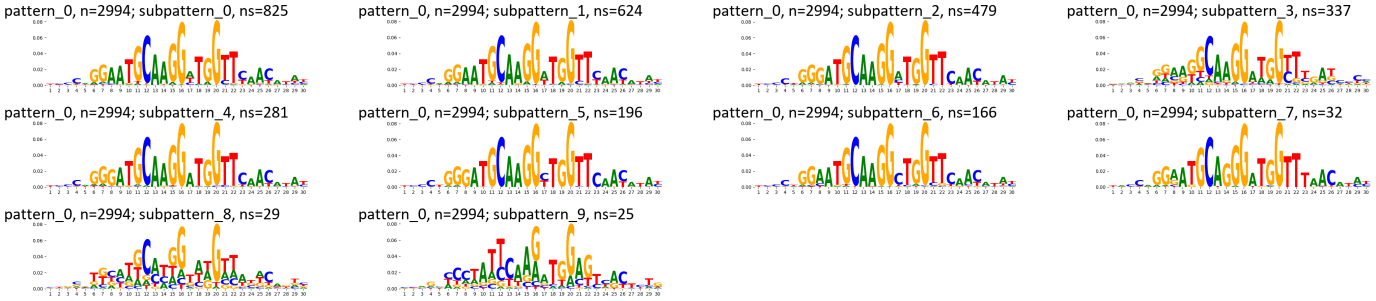

TF-MoDisCO pattern_0 n=2994, PWM

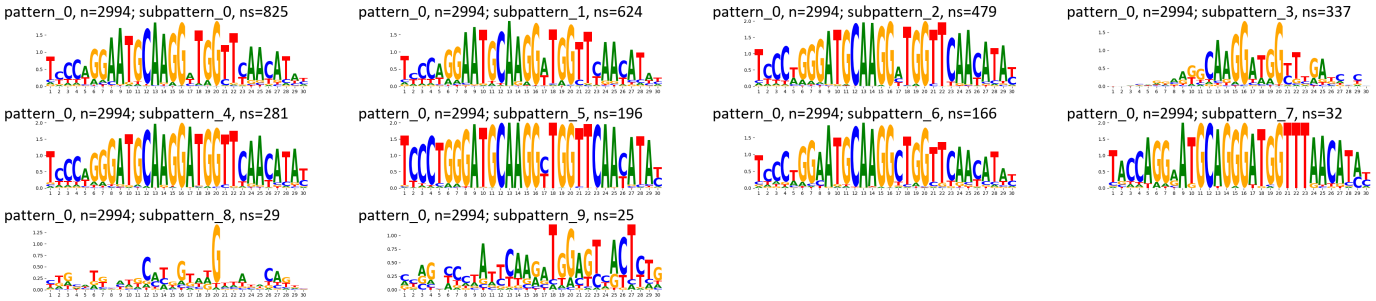

TF-MoDisCO pattern_1 n=468, CWM

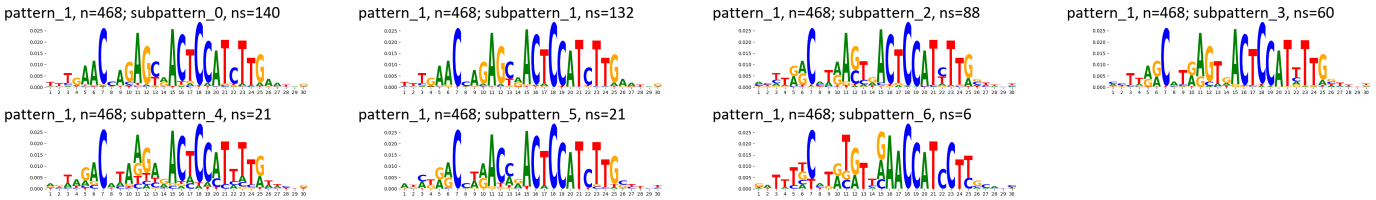

TF-MoDisCO pattern_1 n=468, PWM

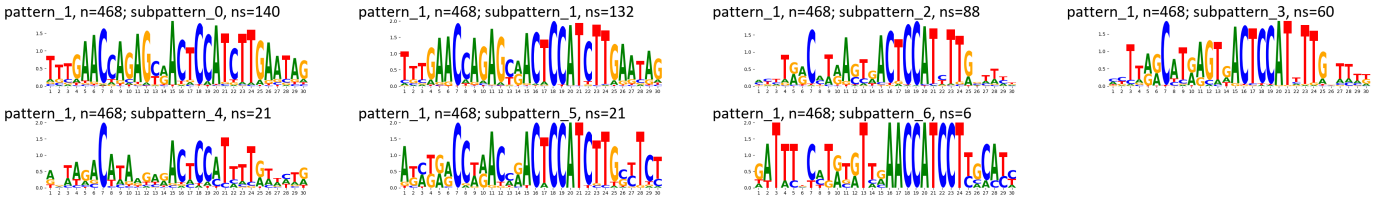

Supplementary Figure 1059: TF-MoDisCO subpatterns for the ZNF324 transcription factor in K562 (accession ENCSR712KVZ).

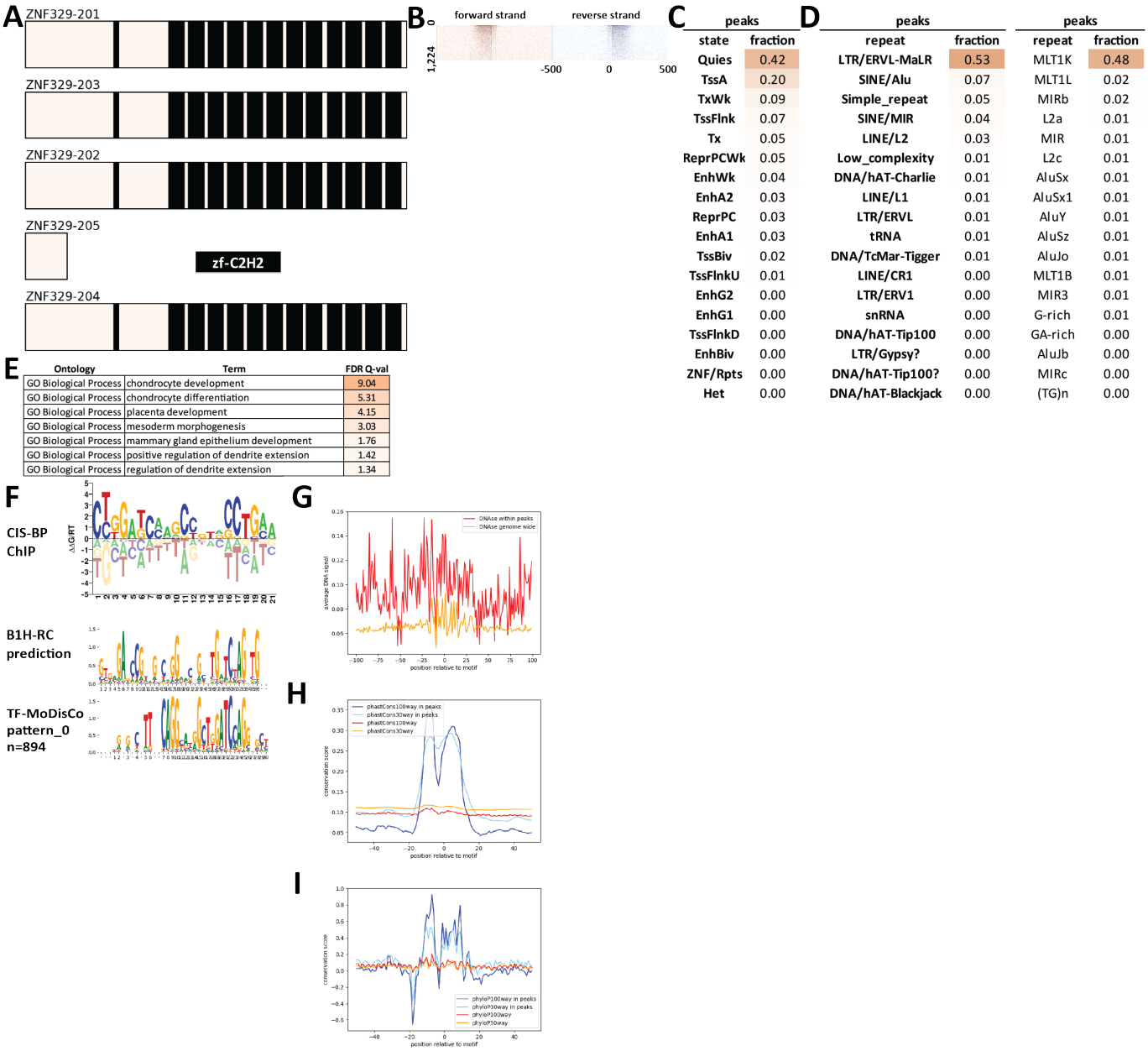

C

peaks	
state	fraction
Quies	0.42
TssA	0.20
TxWk	0.09
TssFlnk	0.07
Tx	0.05
ReprPCWk	0.05
EnhWk	0.04
EnhA2	0.03
ReprPC	0.03
EnhA1	0.03
TssBiv	0.02
TssFlnkU	0.01
EnhG2	0.00
EnhG1	0.00
TssFlnkD	0.00
EnhBiv	0.00
ZNF/Rpts	0.00
Het	0.00

D

peaks		peaks	
repeat	fraction	repeat	fraction
LTR/ERVL-MaLR	0.53	MLT1K	0.48
SINE/Alu	0.07	MLT1L	0.02
Simple_repeat	0.05	MIRb	0.02
SINE/MIR	0.04	L2a	0.01
LINE/L2	0.03	MIR	0.01
Low_complexity	0.01	L2c	0.01
DNA/hAT-Charlie	0.01	AluSx	0.01
LINE/L1	0.01	AluSx1	0.01
LTR/ERVL	0.01	AluY	0.01
tRNA	0.01	AluSz	0.01
DNA/TcMar-Tigger	0.01	AluJo	0.01
LINE/CR1	0.00	MLT1B	0.01
LTR/ERV1	0.00	MIR3	0.01
snRNA	0.00	G-rich	0.01
DNA/hAT-Tip100	0.00	GA-rich	0.00
LTR/Gypsy?	0.00	AluJb	0.00
DNA/hAT-Tip100?	0.00	MIRc	0.00
DNA/hAT-Blackjack	0.00	(TG)n	0.00

E

Ontology	Term	FDR Q-val
GO Biological Process	chondrocyte development	9.04
GO Biological Process	chondrocyte differentiation	5.31
GO Biological Process	placenta development	4.15
GO Biological Process	mesoderm morphogenesis	3.03
GO Biological Process	mammary gland epithelium development	1.76
GO Biological Process	positive regulation of dendrite extension	1.42
GO Biological Process	regulation of dendrite extension	1.34

Supplementary Figure 1060: Properties and genomic distribution of motifs identified for the ZNF329 transcription factor in HEK293 (accession Hughes GR models).

TF-MoDisCO pattern_0 n=894, CWM

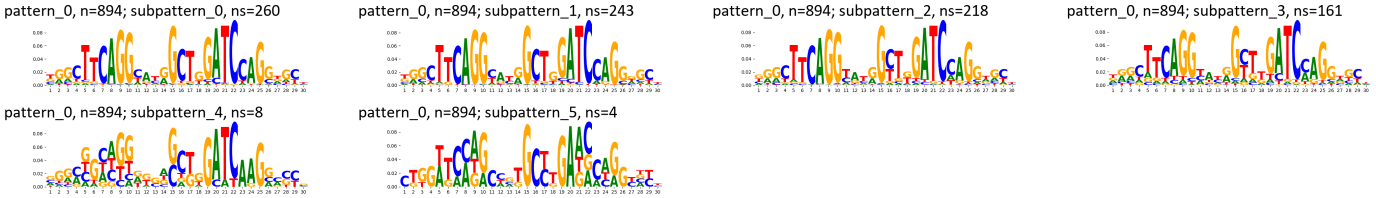

TF-MoDisCO pattern_0 n=894, PWM

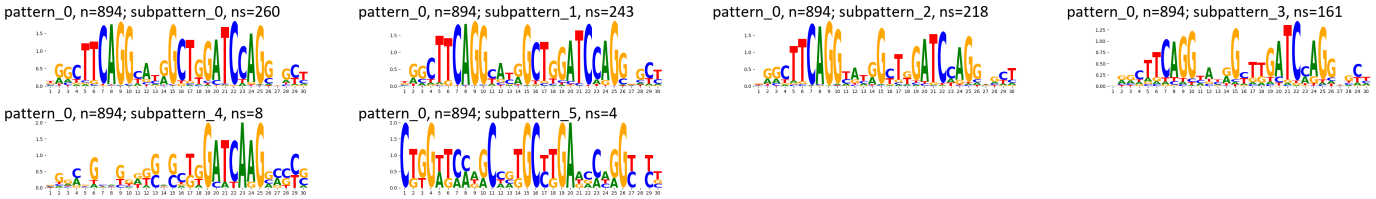

Supplementary Figure 1061: TF-MoDisCO subpatterns for the ZNF329 transcription factor in HEK293 (accession Hughes GR models).

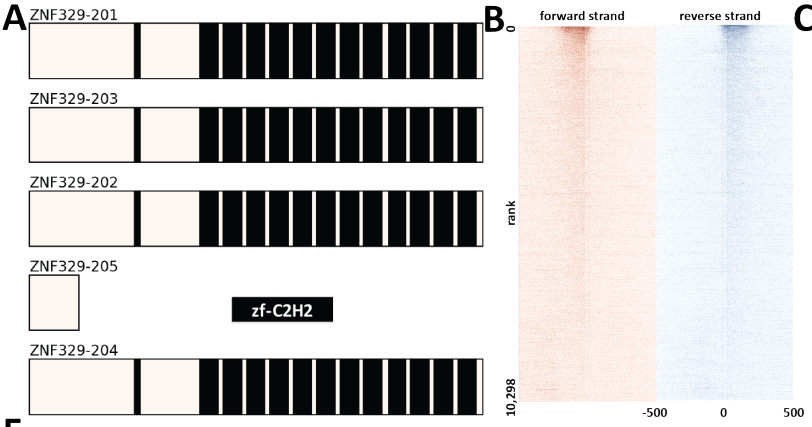

C

peaks	
state	fraction
TssA	0.42
TssFlnk	0.19
Quies	0.16
TxWk	0.07
TssBiv	0.04
TssFlnkU	0.04
EnhWk	0.03
ReprPC	0.03
ReprPCWk	0.02
EnhA2	0.02
Tx	0.02
EnhA1	0.02
TssFlnkD	0.01
EnhBiv	0.01
EnhG1	0.00
Het	0.00
EnhG2	0.00
ZNF/Rpts	0.00

D

peaks		peaks	
repeat	fraction	repeat	fraction
Simple_repeat	0.25	MLT1K	0.07
SINE/Alu	0.10	G-rich	0.04
SINE/MIR	0.09	MIRb	0.03
LTR/ERVL-MaLR	0.09	L2a	0.02
Low_complexity	0.05	MIR	0.02
LINE/L2	0.05	MIRc	0.02
DNA/hAT-Charlie	0.02	MIR3	0.02
LINE/L1	0.02	L2b	0.01
LTR/ERV1	0.01	L2c	0.01
LTR/ERVL	0.01	AluSx	0.01
LINE/CR1	0.01	(GGC)n	0.01
tRNA	0.01	AluJb	0.01
DNA/hAT-Tip100	0.00	AluSx1	0.01
DNA/TcMar-Tigger	0.00	(GCC)n	0.01
DNA/hAT-Blackjack	0.00	AluSz	0.01
snRNA	0.00	GA-rich	0.01
LTR/ERVK	0.00	AluJo	0.01
DNA/hAT	0.00	AluY	0.01

E

Ontology	Term	FDR Q-val
GO Biological Process	rRNA processing	26.44
GO Biological Process	rRNA metabolic process	25.62
GO Biological Process	IRE1-mediated unfolded protein response	22.24
GO Biological Process	cellular response to topologically incorrect protein	20.61
GO Biological Process	response to topologically incorrect protein	19.94
GO Biological Process	cellular response to unfolded protein	18.63
GO Biological Process	response to unfolded protein	17.60
GO Biological Process	regulation of DNA-templated transcription in response to stress	15.28
GO Biological Process	regulation of transcription from RNA polymerase II promoter in response to stress	14.87
GO Biological Process	regulation of nuclease activity	14.40
GO Biological Process	mitochondrial translational elongation	14.21
GO Biological Process	mitochondrial transmembrane transport	13.88
GO Biological Process	mitochondrial translational termination	13.78
GO Biological Process	mitochondrial translation	13.44
GO Biological Process	viral gene expression	12.57
GO Biological Process	regulation of triglyceride biosynthetic process	12.52
GO Biological Process	nuclear-transcribed mRNA catabolic process, nonsense-mediated decay	12.33
GO Biological Process	spliceosomal snRNP assembly	12.16
GO Biological Process	translational elongation	11.87
GO Biological Process	protein targeting to ER	11.73
Human Phenotype	Increased serum lactate	8.77

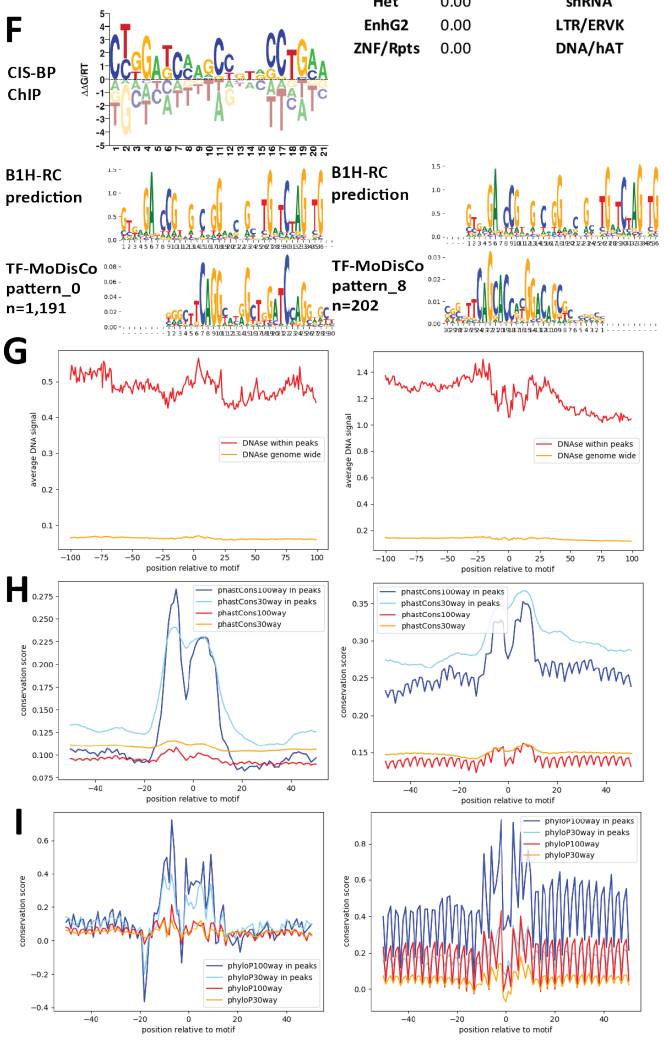

Supplementary Figure 1062: Properties and genomic distribution of motifs identified for the ZNF329 transcription factor in HepG2 (accession ENCSR681KXT).

TF-MoDisCO pattern_0 n=1191, CWM

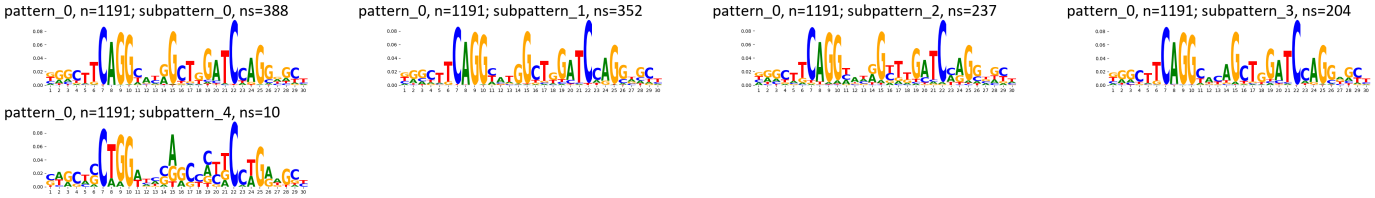

TF-MoDisCO pattern_0 n=1191, PWM

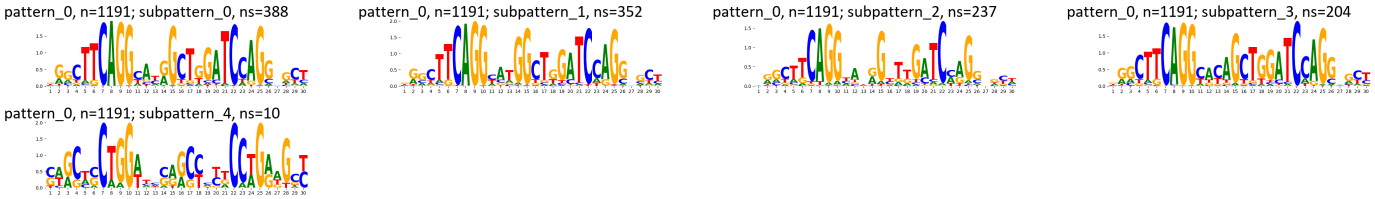

TF-MoDisCO pattern_8 n=202, CWM

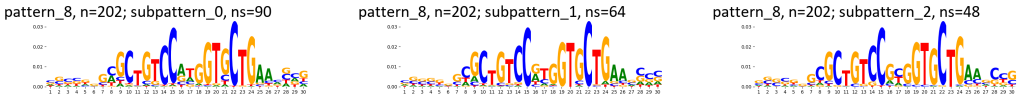

TF-MoDisCO pattern_8 n=202, PWM

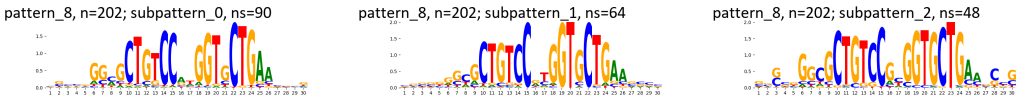

Supplementary Figure 1063: TF-MoDisCO subpatterns for the ZNF329 transcription factor in HepG2 (accession ENCSR681KXT).

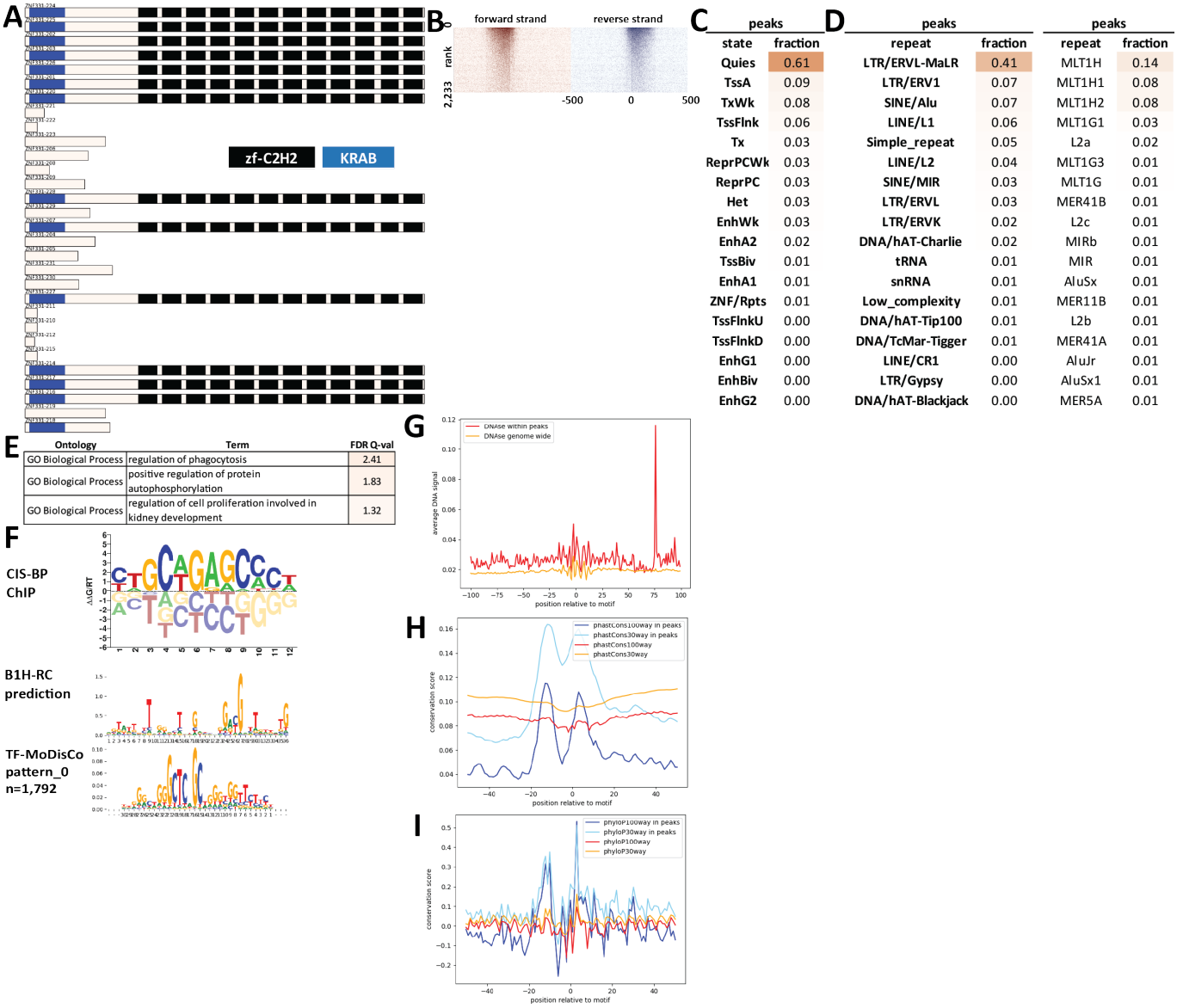

Supplementary Figure 1064: Properties and genomic distribution of motifs identified for the ZNF331 transcription factor in GM23338 (accession ENCSR918LRB).

TF-MoDisCO pattern_0 n=1792, CWM

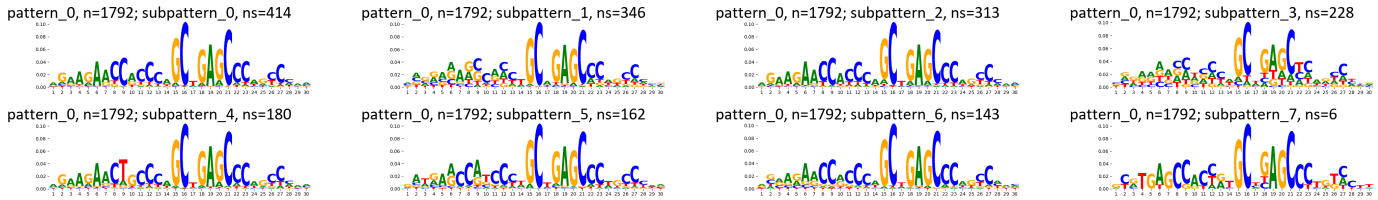

TF-MoDisCO pattern_0 n=1792, PWM

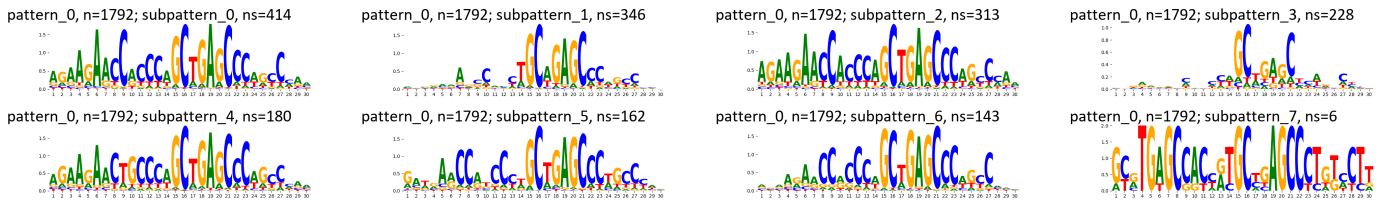

Supplementary Figure 1065: TF-MoDisCO subpatterns for the ZNF331 transcription factor in GM23338 (accession ENCSR918LRB).

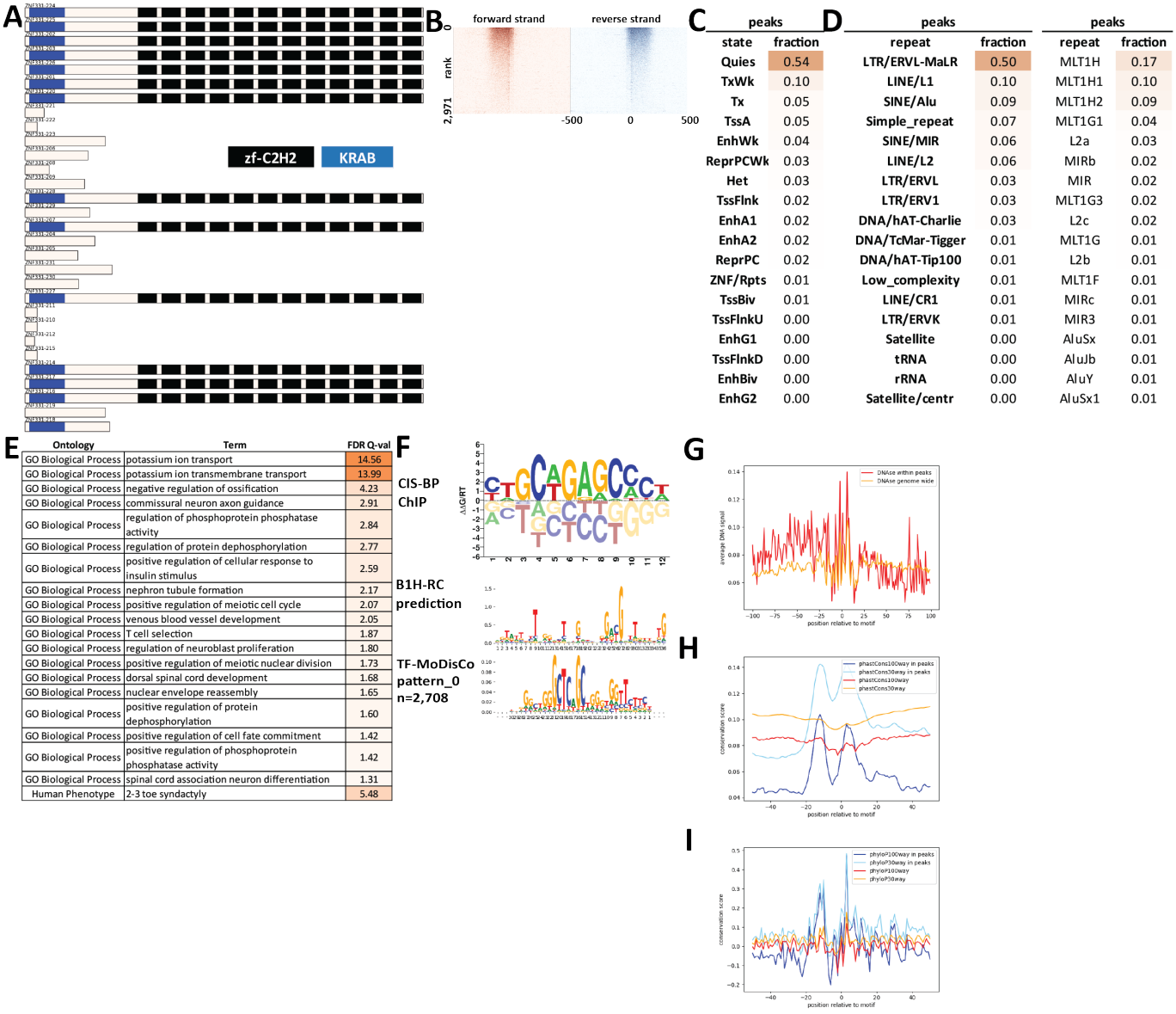

C

peaks	
state	fraction
Quies	0.54
TxWk	0.10
Tx	0.05
TssA	0.05
EnhWk	0.04
ReprPCWk	0.03
Het	0.03
TssFlnk	0.02
EnhA1	0.02
EnhA2	0.02
ReprPC	0.02
ZNF/Rpts	0.01
TssBiv	0.01
TssFlnkU	0.00
EnhG1	0.00
TssFlnkD	0.00
EnhBiv	0.00
EnhG2	0.00

D

peaks		peaks	
repeat	fraction	repeat	fraction
LTR/ERVL-MaLR	0.50	MLT1H	0.17
LINE/L1	0.10	MLT1H1	0.10
SINE/Alu	0.09	MLT1H2	0.09
Simple_repeat	0.07	MLT1G1	0.04
SINE/MIR	0.06	L2a	0.03
LINE/L2	0.06	MIRb	0.02
LTR/ERVL	0.03	MIR	0.02
LTR/ERV1	0.03	MLT1G3	0.02
DNA/hAT-Charlie	0.03	L2c	0.02
DNA/TcMar-Tigger	0.01	MLT1G	0.01
DNA/hAT-Tip100	0.01	L2b	0.01
Low_complexity	0.01	MLT1F	0.01
LINE/CR1	0.01	MIRc	0.01
LTR/ERVK	0.01	MIR3	0.01
Satellite	0.00	AluSx	0.01
tRNA	0.00	AluJb	0.01
rRNA	0.00	AluY	0.01
Satellite/centr	0.00	AluSx1	0.01

E

Ontology	Term	FDR Q-val
GO Biological Process	potassium ion transport	14.56
GO Biological Process	potassium ion transmembrane transport	13.99
GO Biological Process	negative regulation of ossification	4.23
GO Biological Process	commissural neuron axon guidance	2.91
GO Biological Process	regulation of phosphoprotein phosphatase activity	2.84
GO Biological Process	regulation of protein dephosphorylation	2.77
GO Biological Process	positive regulation of cellular response to insulin stimulus	2.59
GO Biological Process	nephron tubule formation	2.17
GO Biological Process	positive regulation of meiotic cell cycle	2.07
GO Biological Process	venous blood vessel development	2.05
GO Biological Process	T cell selection	1.87
GO Biological Process	regulation of neuroblast proliferation	1.80
GO Biological Process	positive regulation of meiotic nuclear division	1.73
GO Biological Process	dorsal spinal cord development	1.68
GO Biological Process	nuclear envelope reassembly	1.65
GO Biological Process	positive regulation of protein dephosphorylation	1.60
GO Biological Process	positive regulation of cell fate commitment	1.42
GO Biological Process	positive regulation of phosphoprotein phosphatase activity	1.42
GO Biological Process	spinal cord association neuron differentiation	1.31
Human Phenotype	2-3 toe syndactyly	5.48

Supplementary Figure 1066: Properties and genomic distribution of motifs identified for the ZNF331 transcription factor in HEK293 (accession Hughes GR models).

TF-MoDisCO pattern_0 n=2708, CWM

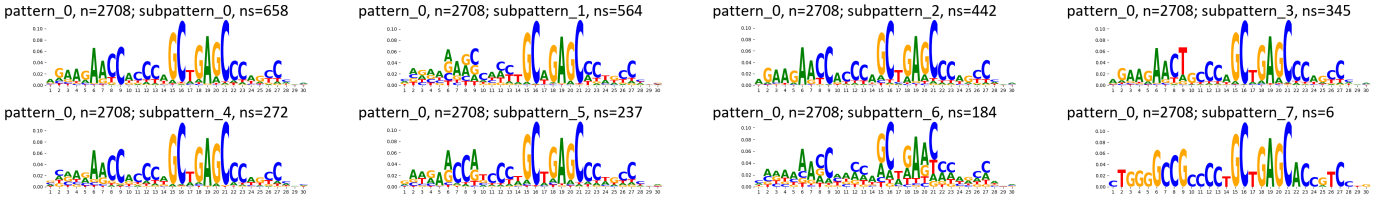

TF-MoDisCO pattern_0 n=2708, PWM

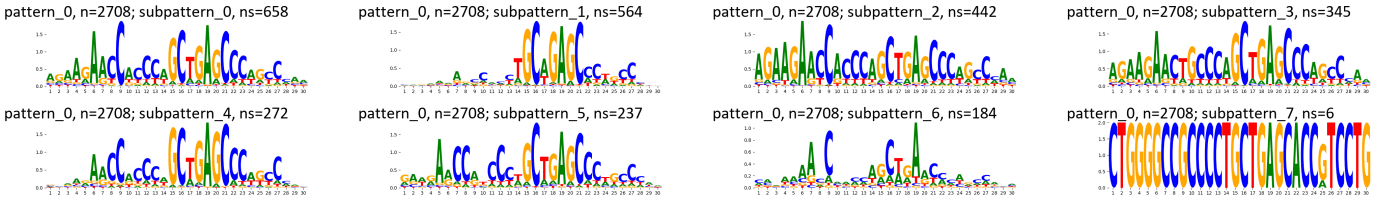

Supplementary Figure 1067: TF-MoDisCO subpatterns for the ZNF331 transcription factor in HEK293 (accession Hughes GR models).

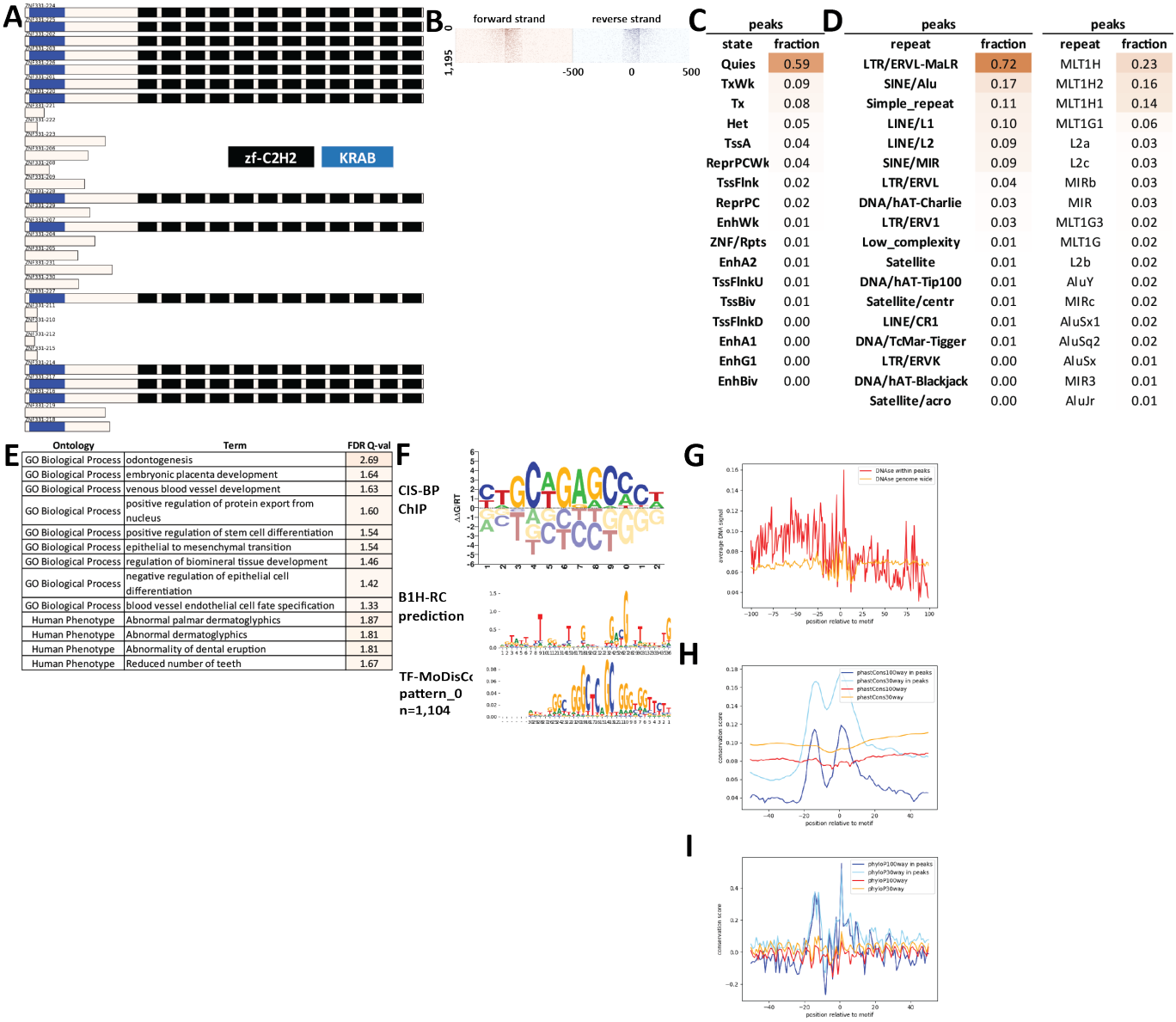

Supplementary Figure 1068: Properties and genomic distribution of motifs identified for the ZNF331 transcription factor in HEK293 (accession ChipExo models).

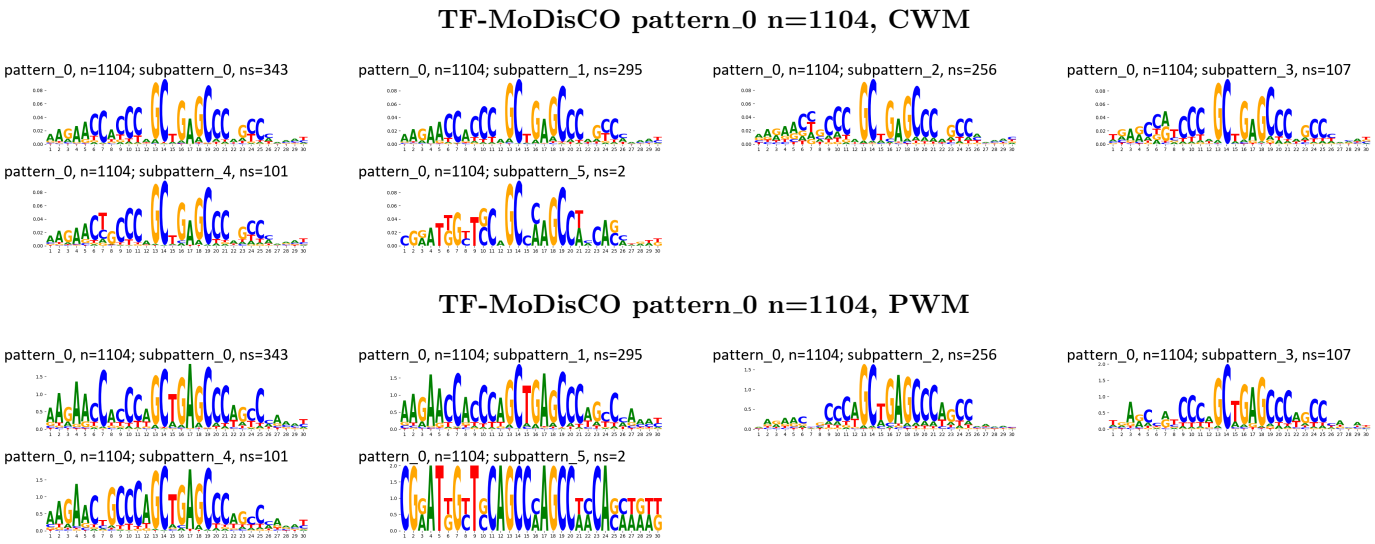

Supplementary Figure 1069: TF-MoDisCO subpatterns for the ZNF331 transcription factor in HEK293 (accession ChipExo models).

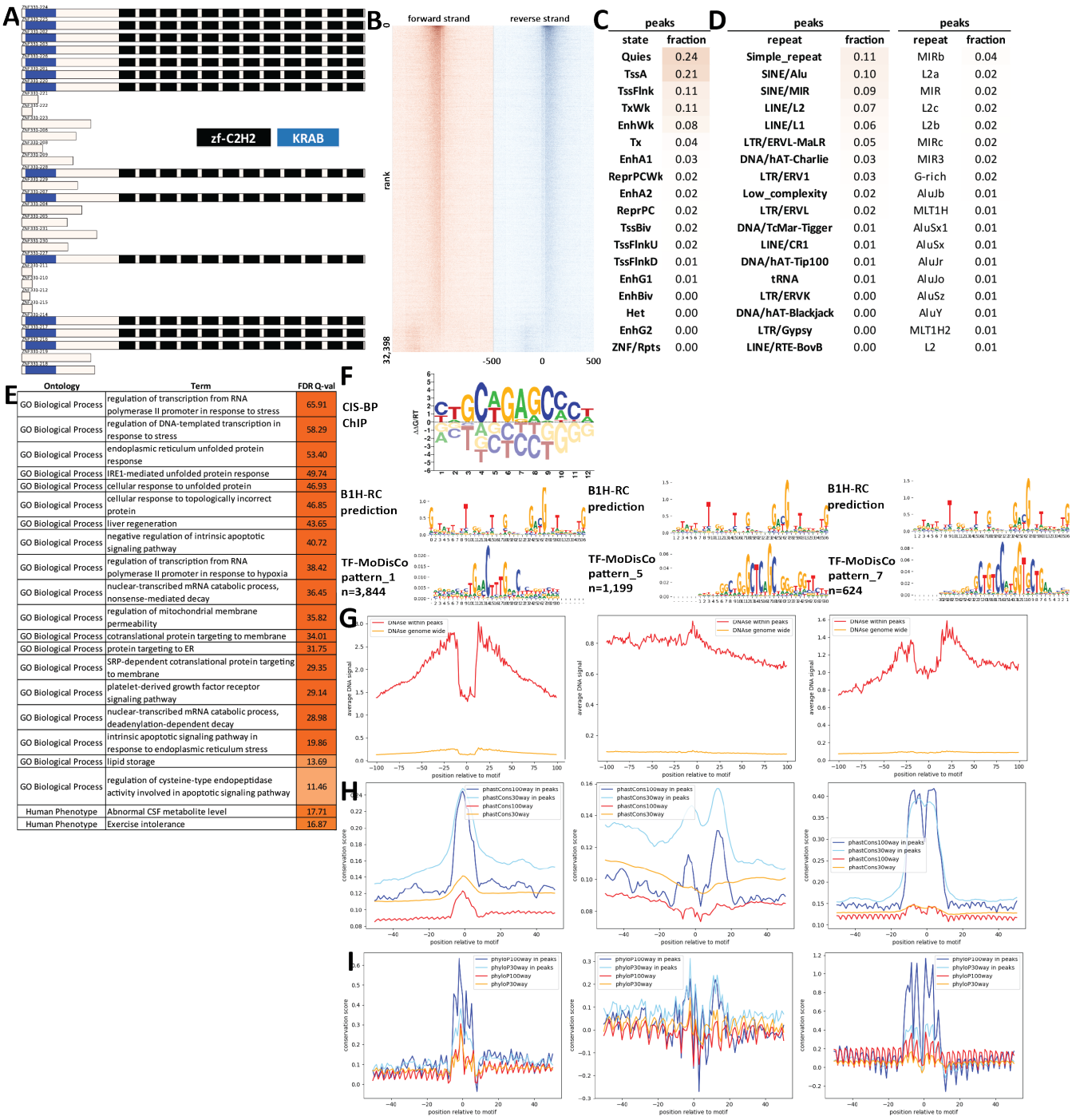

Supplementary Figure 1070: Properties and genomic distribution of motifs identified for the ZNF331 transcription factor in HepG2 (accession ENCSR369TCR).

TF-MoDisCO pattern_1 n=3844, CWM

pattern_1, n=3844; subpattern_0, ns=1028

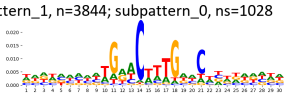

pattern_1, n=3844; subpattern_1, ns=834

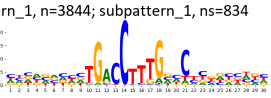

pattern_1, n=3844; subpattern_2, ns=740

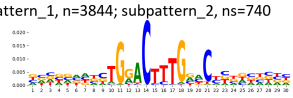

pattern_1, n=3844; subpattern_3, ns=690

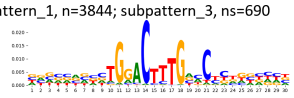

pattern_1, n=3844; subpattern_4, ns=347

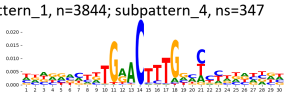

pattern_1, n=3844; subpattern_5, ns=205

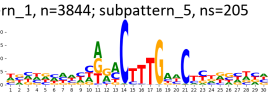

TF-MoDisCO pattern_1 n=3844, PWM

pattern_1, n=3844; subpattern_0, ns=1028

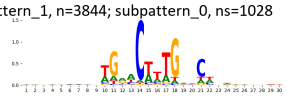

pattern_1, n=3844; subpattern_1, ns=834

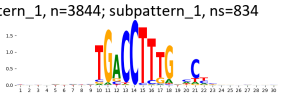

pattern_1, n=3844; subpattern_2, ns=740

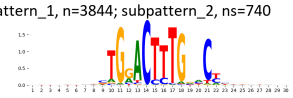

pattern_1, n=3844; subpattern_3, ns=690

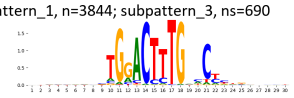

pattern_1, n=3844; subpattern_4, ns=347

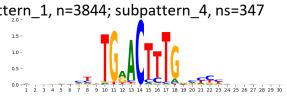

pattern_1, n=3844; subpattern_5, ns=205

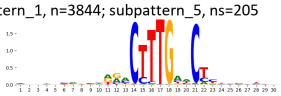

TF-MoDisCO pattern_5 n=1199, CWM

pattern_5, n=1199; subpattern_0, ns=348

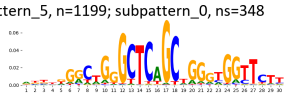

pattern_5, n=1199; subpattern_1, ns=327

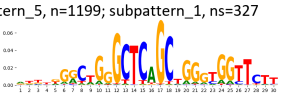

pattern_5, n=1199; subpattern_2, ns=177

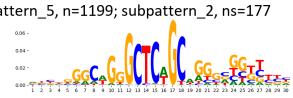

pattern_5, n=1199; subpattern_3, ns=173

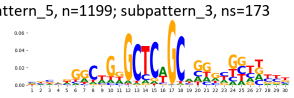

pattern_5, n=1199; subpattern_4, ns=117

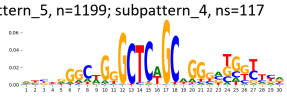

pattern_5, n=1199; subpattern_5, ns=57

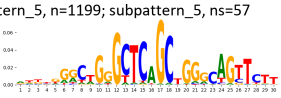

TF-MoDisCO pattern_5 n=1199, PWM

pattern_5, n=1199; subpattern_0, ns=348

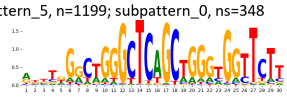

pattern_5, n=1199; subpattern_1, ns=327

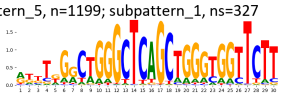

pattern_5, n=1199; subpattern_2, ns=177

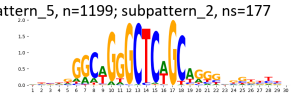

pattern_5, n=1199; subpattern_3, ns=173

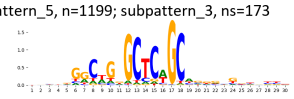

pattern_5, n=1199; subpattern_4, ns=117

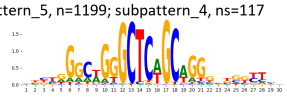

pattern_5, n=1199; subpattern_5, ns=57

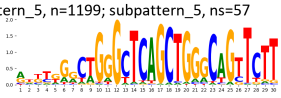

TF-MoDisCO pattern_7 n=624, CWM

pattern_7, n=624; subpattern_0, ns=245

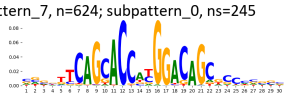

pattern_7, n=624; subpattern_1, ns=167

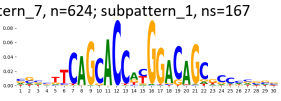

pattern_7, n=624; subpattern_2, ns=123

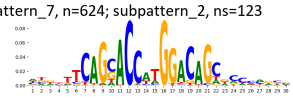

pattern_7, n=624; subpattern_3, ns=85

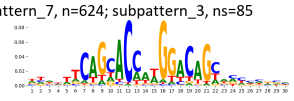

pattern_7, n=624; subpattern_4, ns=4

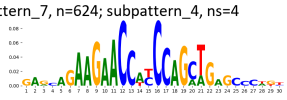

TF-MoDisCO pattern_7 n=624, PWM

pattern_7, n=624; subpattern_0, ns=245

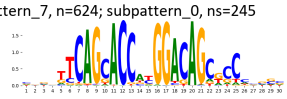

pattern_7, n=624; subpattern_1, ns=167

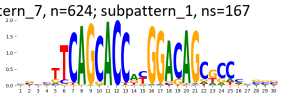

pattern_7, n=624; subpattern_2, ns=123

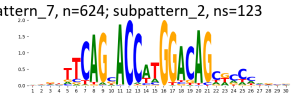

pattern_7, n=624; subpattern_3, ns=85

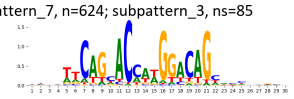

pattern_7, n=624; subpattern_4, ns=4

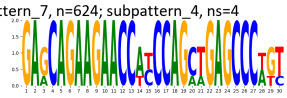

Supplementary Figure 1071: TF-MoDisCO subpatterns for the ZNF331 transcription factor in HepG2 (accession ENCSR369TCR).

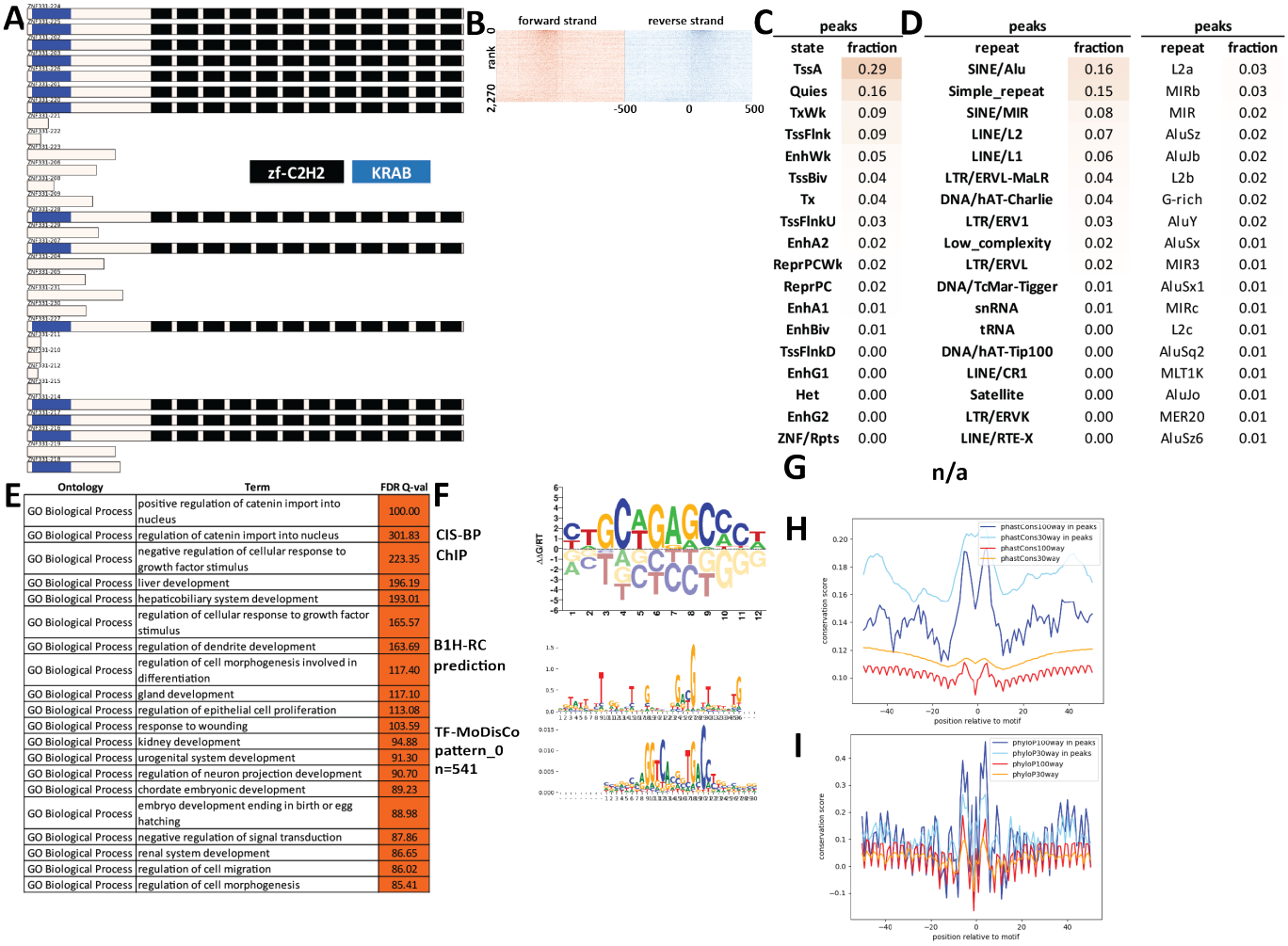

peaks	
state	fraction
TssA	0.29
Quies	0.16
TxWk	0.09
TssFlnk	0.09
EnhWk	0.05
TssBiv	0.04
Tx	0.04
TssFlnkU	0.03
EnhA2	0.02
ReprPCWk	0.02
ReprPC	0.02
EnhA1	0.01
EnhBiv	0.01
TssFlnkD	0.00
EnhG1	0.00
Het	0.00
EnhG2	0.00
ZNF/Rpts	0.00

peaks		peaks	
repeat	fraction	repeat	fraction
SINE/Alu	0.16	L2a	0.03
Simple_repeat	0.15	MIRb	0.03
SINE/MIR	0.08	MIR	0.02
LINE/L2	0.07	AluSz	0.02
LINE/L1	0.06	AluJb	0.02
LTR/ERVL-MaLR	0.04	L2b	0.02
DNA/hAT-Charlie	0.04	G-rich	0.02
LTR/ERV1	0.03	AluY	0.02
Low_complexity	0.02	AluSx	0.01
LTR/ERVL	0.02	MIR3	0.01
DNA/TcMar-Tigger	0.01	AluSx1	0.01
snRNA	0.01	MIRc	0.01
tRNA	0.00	L2c	0.01
DNA/hAT-Tip100	0.00	AluSq2	0.01
LINE/CR1	0.00	MLT1K	0.01
Satellite	0.00	AluJo	0.01
LTR/ERVK	0.00	MER20	0.01
LINE/RTE-X	0.00	AluSz6	0.01

Ontology	Term	FDR Q-val
GO Biological Process	positive regulation of catenin import into nucleus	100.00
GO Biological Process	regulation of catenin import into nucleus	301.83
GO Biological Process	negative regulation of cellular response to growth factor stimulus	223.35
GO Biological Process	liver development	196.19
GO Biological Process	hepaticobiliary system development	193.01
GO Biological Process	regulation of cellular response to growth factor stimulus	165.57
GO Biological Process	regulation of dendrite development	163.69
GO Biological Process	regulation of cell morphogenesis involved in differentiation	117.40
GO Biological Process	gland development	117.10
GO Biological Process	regulation of epithelial cell proliferation	113.08
GO Biological Process	response to wounding	103.59
GO Biological Process	kidney development	94.88
GO Biological Process	urogenital system development	91.30
GO Biological Process	regulation of neuron projection development	90.70
GO Biological Process	chordate embryonic development	89.23
GO Biological Process	embryo development ending in birth or egg hatching	88.98
GO Biological Process	negative regulation of signal transduction	87.86
GO Biological Process	renal system development	86.65
GO Biological Process	regulation of cell migration	86.02
GO Biological Process	regulation of cell morphogenesis	85.41

Supplementary Figure 1072: Properties and genomic distribution of motifs identified for the ZNF331 transcription factor in MCF-7 (accession ENCSR860XVO).

TF-MoDisCO pattern_0 n=541, CWM

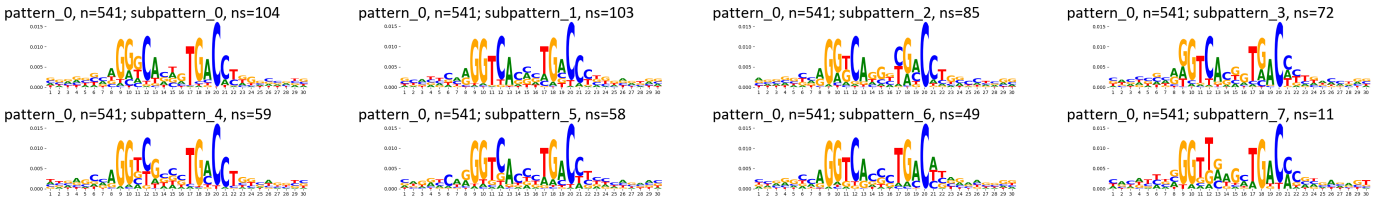

TF-MoDisCO pattern_0 n=541, PWM

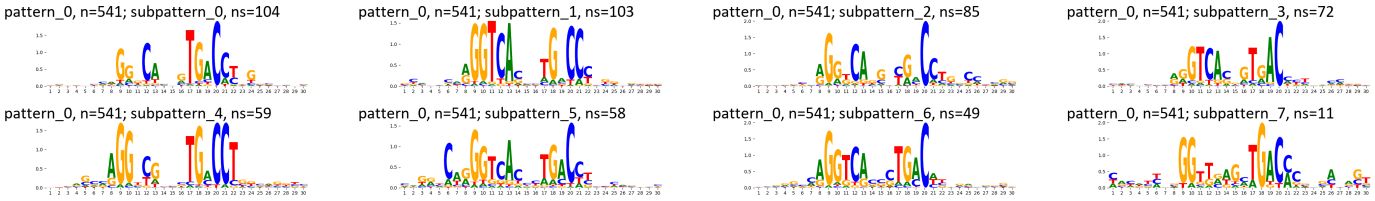

Supplementary Figure 1073: TF-MoDisCO subpatterns for the ZNF331 transcription factor in MCF-7 (accession ENCSR860XVO).

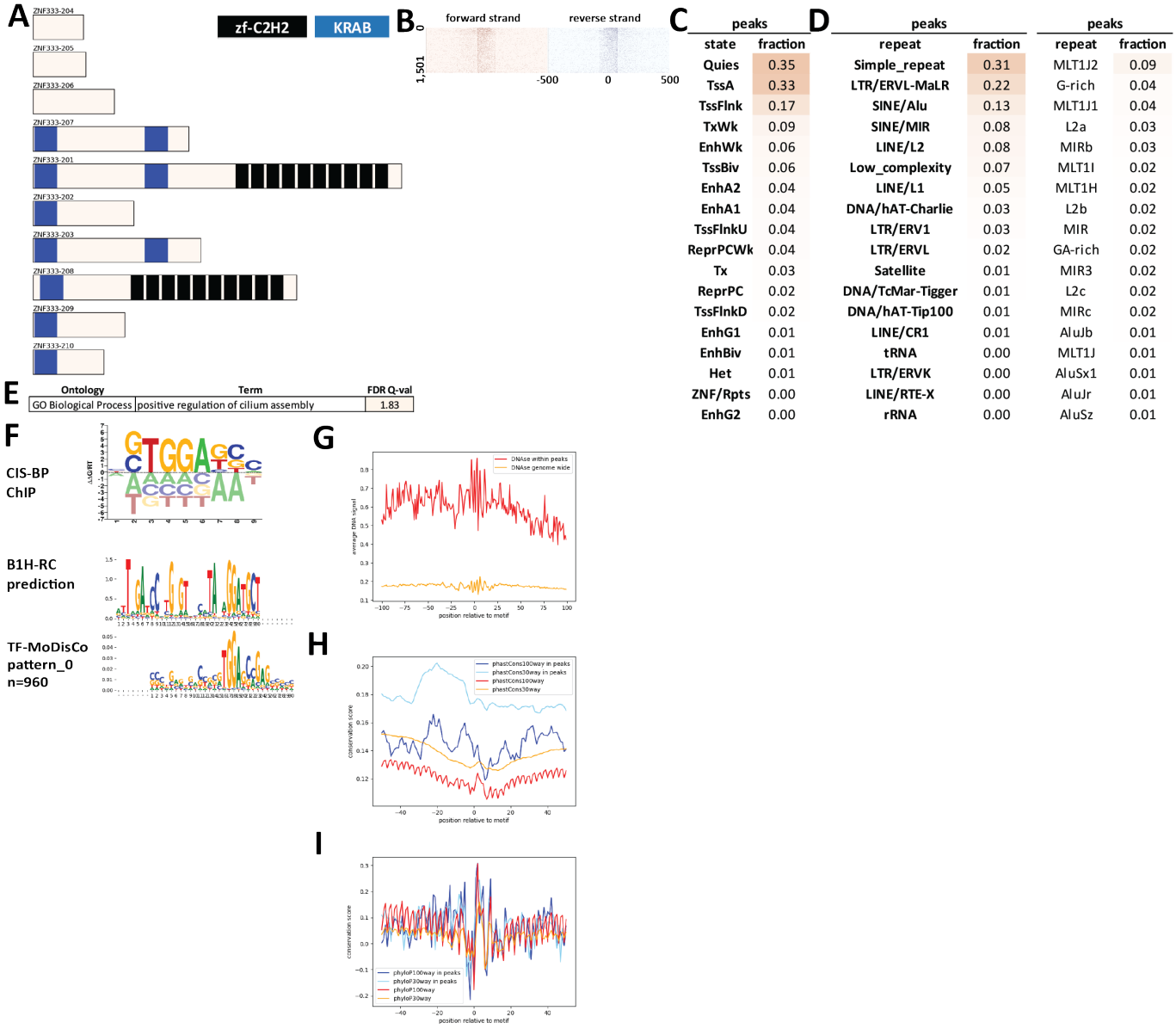

peaks	
state	fraction
Quies	0.35
TssA	0.33
TssFlnk	0.17
TxWk	0.09
EnhWk	0.06
TssBiv	0.06
EnhA2	0.04
EnhA1	0.04
TssFlnkU	0.04
ReprPCWk	0.04
Tx	0.03
ReprPC	0.02
TssFlnkD	0.02
EnhG1	0.01
EnhBiv	0.01
Het	0.01
ZNF/Rpts	0.00
EnhG2	0.00

peaks	
repeat	fraction
Simple_repeat	0.31
LTR/ERVL-MaLR	0.22
SINE/Alu	0.13
SINE/MIR	0.08
LINE/L2	0.08
Low_complexity	0.07
LINE/L1	0.05
DNA/hAT-Charlie	0.03
LTR/ERV1	0.03
LTR/ERVL	0.02
Satellite	0.01
DNA/TcMar-Tigger	0.01
DNA/hAT-Tip100	0.01
LINE/CR1	0.01
tRNA	0.00
LTR/ERVK	0.00
LINE/RTE-X	0.00
rRNA	0.00

peaks	
repeat	fraction
MLT1J2	0.09
G-rich	0.04
MLT1J1	0.04
L2a	0.03
MIRb	0.03
MLT1I	0.02
MLT1H	0.02
L2b	0.02
MIR	0.02
GA-rich	0.02
MIR3	0.02
L2c	0.02
MIRc	0.02
AluJb	0.01
MLT1J	0.01
AluSx1	0.01
AluJr	0.01
AluSz	0.01

Supplementary Figure 1074: Properties and genomic distribution of motifs identified for the ZNF333 transcription factor in HEK293 (accession ChipExo models).

TF-MoDisCO pattern_0 n=960, CWM

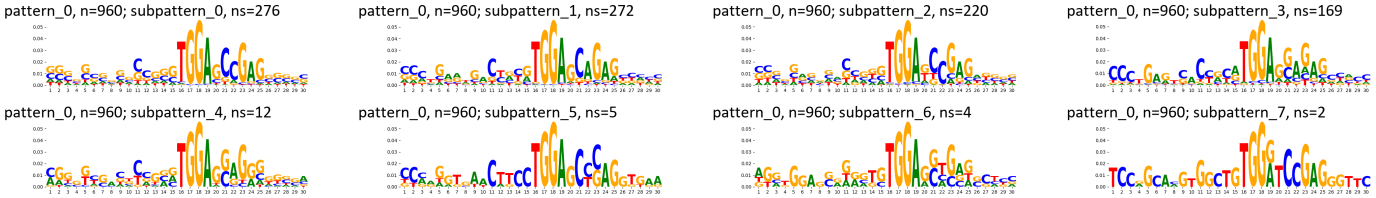

TF-MoDisCO pattern_0 n=960, PWM

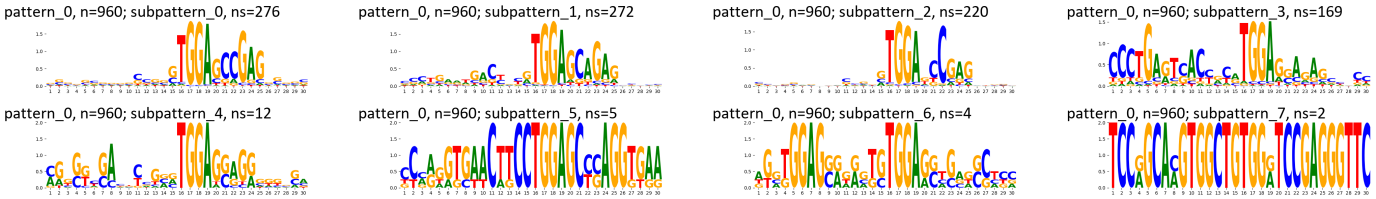

Supplementary Figure 1075: TF-MoDisCO subpatterns for the ZNF333 transcription factor in HEK293 (accession ChipExo models).

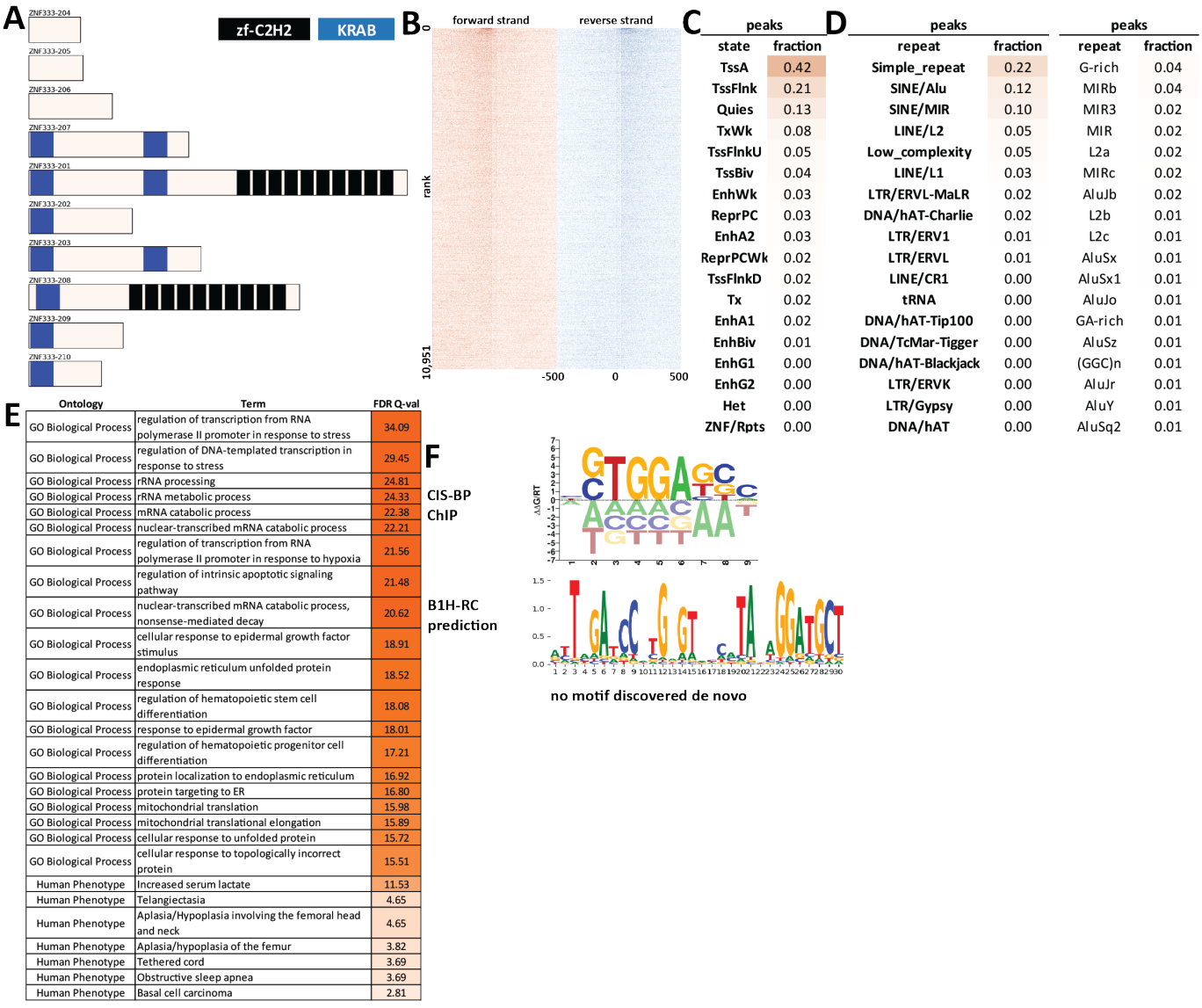

peaks	
state	fraction
TssA	0.42
TssFlnk	0.21
Quies	0.13
TxWk	0.08
TssFlnkU	0.05
TssBiv	0.04
EnhWk	0.03
ReprPC	0.03
EnhA2	0.03
ReprPCWk	0.02
TssFlnkD	0.02
Tx	0.02
EnhA1	0.02
EnhBiv	0.01
EnhG1	0.00
EnhG2	0.00
Het	0.00
ZNF/Rpts	0.00

peaks		peaks	
repeat	fraction	repeat	fraction
Simple_repeat	0.22	G-rich	0.04
SINE/Alu	0.12	MIRb	0.04
SINE/MIR	0.10	MIR3	0.02
LINE/L2	0.05	MIR	0.02
Low_complexity	0.05	L2a	0.02
LINE/L1	0.03	MIRc	0.02
LTR/ERVL-MaLR	0.02	AluJb	0.02
DNA/hAT-Charlie	0.02	L2b	0.01
LTR/ERV1	0.01	L2c	0.01
LTR/ERVL	0.01	AluSx	0.01
LINE/CR1	0.00	AluSx1	0.01
tRNA	0.00	AluJo	0.01
DNA/hAT-Tip100	0.00	GA-rich	0.01
DNA/TcMar-Tigger	0.00	AluSz	0.01
DNA/hAT-Blackjack	0.00	(GGC)n	0.01
LTR/ERVK	0.00	AluJr	0.01
LTR/Gypsy	0.00	AluY	0.01
DNA/hAT	0.00	AluSq2	0.01

Ontology	Term	FDR Q-val
GO Biological Process	regulation of transcription from RNA polymerase II promoter in response to stress	34.09
GO Biological Process	regulation of DNA-templated transcription in response to stress	29.45
GO Biological Process	rRNA processing	24.81
GO Biological Process	rRNA metabolic process	24.33
GO Biological Process	mRNA catabolic process	22.38
GO Biological Process	nuclear-transcribed mRNA catabolic process	22.21
GO Biological Process	regulation of transcription from RNA polymerase II promoter in response to hypoxia	21.56
GO Biological Process	regulation of intrinsic apoptotic signaling pathway	21.48
GO Biological Process	nuclear-transcribed mRNA catabolic process, nonsense-mediated decay	20.62
GO Biological Process	cellular response to epidermal growth factor stimulus	18.91
GO Biological Process	endoplasmic reticulum unfolded protein response	18.52
GO Biological Process	regulation of hematopoietic stem cell differentiation	18.08
GO Biological Process	response to epidermal growth factor	18.01
GO Biological Process	regulation of hematopoietic progenitor cell differentiation	17.21
GO Biological Process	protein localization to endoplasmic reticulum	16.92
GO Biological Process	protein targeting to ER	16.80
GO Biological Process	mitochondrial translation	15.98
GO Biological Process	mitochondrial translational elongation	15.89
GO Biological Process	cellular response to unfolded protein	15.72
GO Biological Process	cellular response to topologically incorrect protein	15.51
Human Phenotype	Increased serum lactate	11.53
Human Phenotype	Telangiectasia	4.65
Human Phenotype	Aplasia/Hypoplasia involving the femoral head and neck	4.65
Human Phenotype	Aplasia/hypoplasia of the femur	3.82
Human Phenotype	Tethered cord	3.69
Human Phenotype	Obstructive sleep apnea	3.69
Human Phenotype	Basal cell carcinoma	2.81

Supplementary Figure 1076: Properties and genomic distribution of motifs identified for the ZNF333 transcription factor in HepG2 (accession ENCSR505UNL).

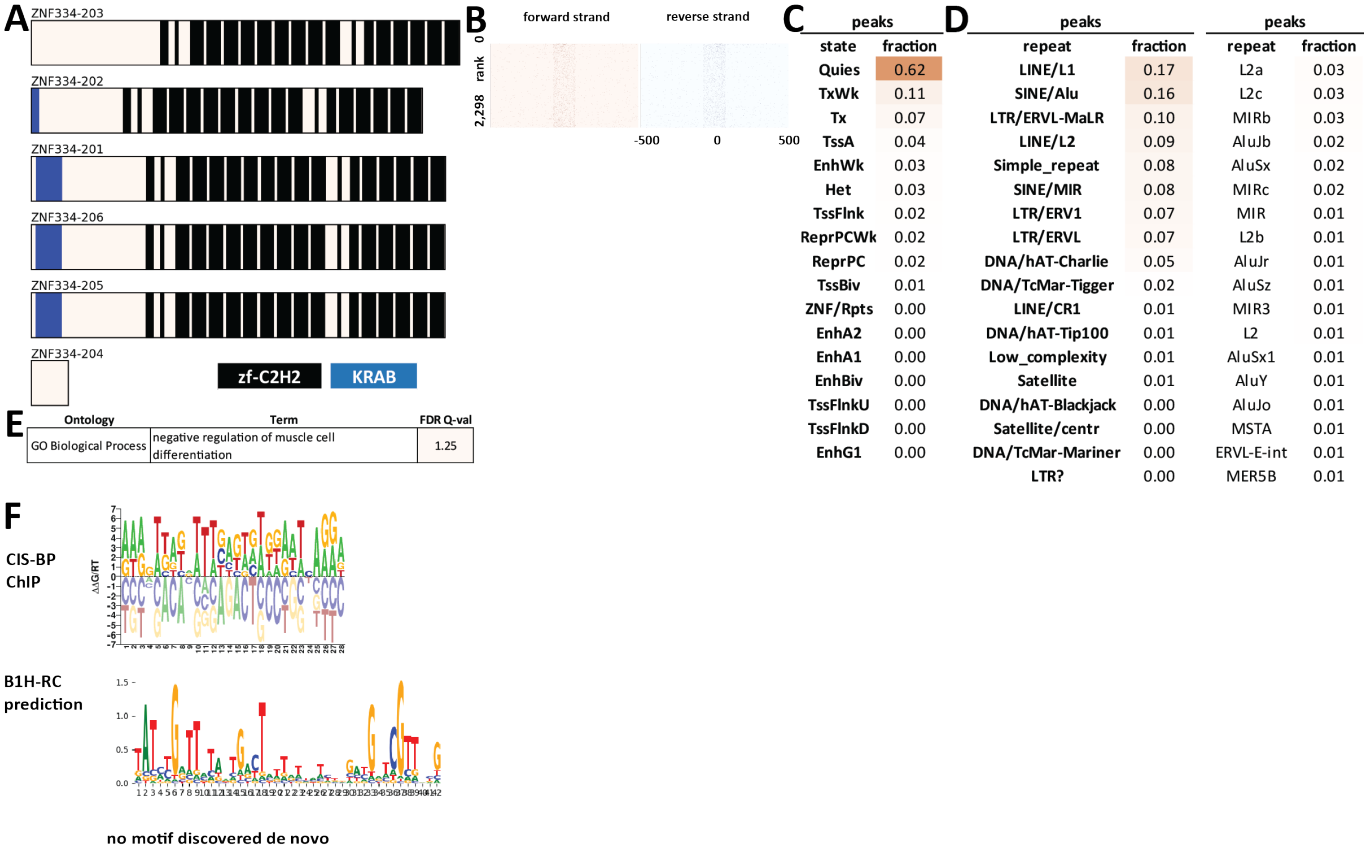

Supplementary Figure 1077: Properties and genomic distribution of motifs identified for the ZNF334 transcription factor in HEK293 (accession ChipExo models).

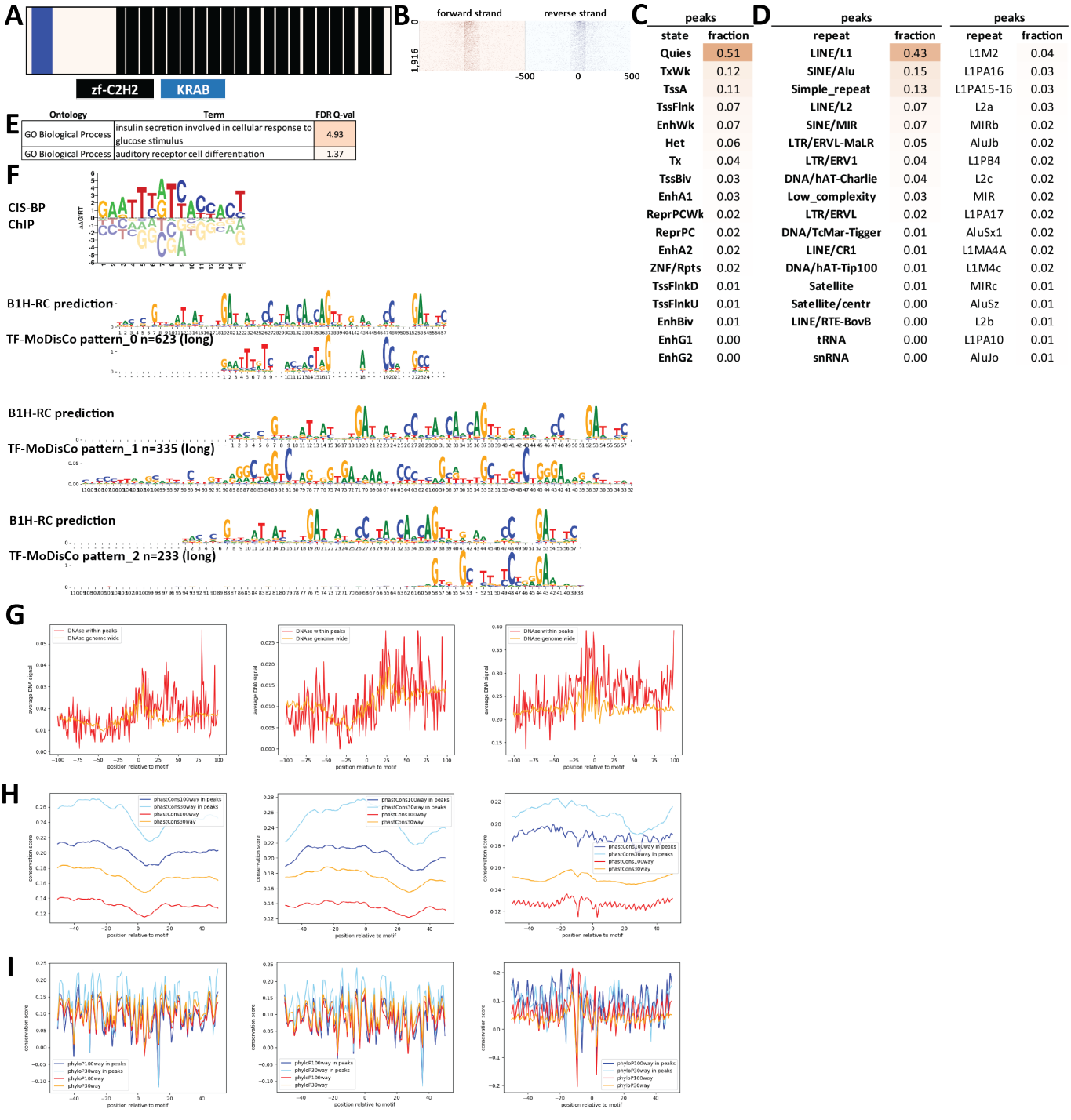

Supplementary Figure 1078: Properties and genomic distribution of motifs identified for the ZNF337 transcription factor in HEK293 (accession ChipExo models).

TF-MoDisCO pattern_0 n=623, CWM

pattern_0, n=623; subpattern_0, ns=174

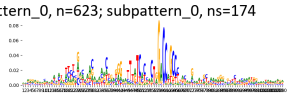

pattern_0, n=623; subpattern_1, ns=158

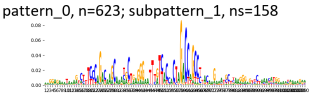

pattern_0, n=623; subpattern_2, ns=150

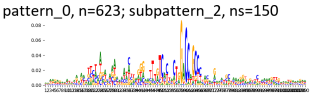

pattern_0, n=623; subpattern_3, ns=122

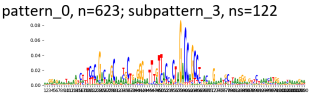

pattern_0, n=623; subpattern_4, ns=13

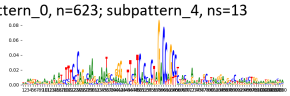

pattern_0, n=623; subpattern_5, ns=4

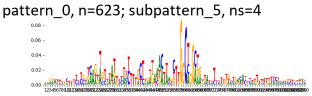

pattern_0, n=623; subpattern_6, ns=2

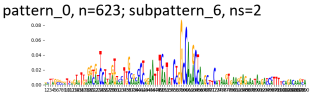

TF-MoDisCO pattern_0 n=623, PWM

pattern_0, n=623; subpattern_0, ns=174

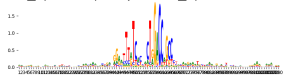

pattern_0, n=623; subpattern_1, ns=158

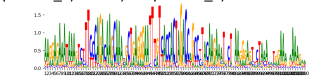

pattern_0, n=623; subpattern_2, ns=150

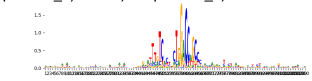

pattern_0, n=623; subpattern_3, ns=122

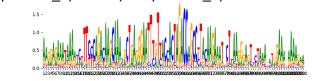

pattern_0, n=623; subpattern_4, ns=13

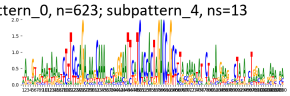

pattern_0, n=623; subpattern_5, ns=4

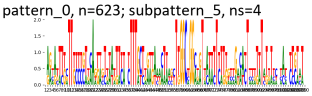

pattern_0, n=623; subpattern_6, ns=2

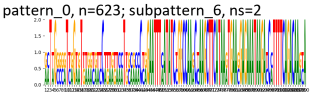

TF-MoDisCO pattern_1 n=335, CWM

pattern_1, n=335; subpattern_0, ns=122

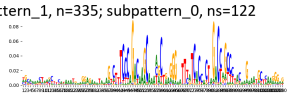

pattern_1, n=335; subpattern_1, ns=122

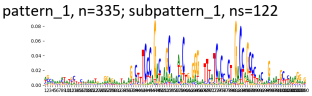

pattern_1, n=335; subpattern_2, ns=52

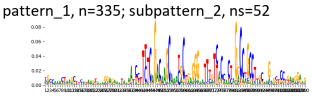

pattern_1, n=335; subpattern_3, ns=34

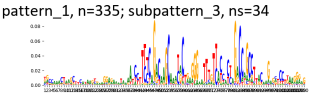

pattern_1, n=335; subpattern_4, ns=3

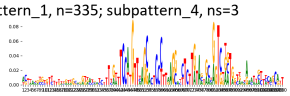

pattern_1, n=335; subpattern_5, ns=2

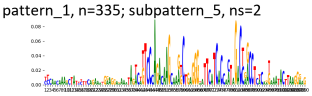

TF-MoDisCO pattern_1 n=335, PWM

pattern_1, n=335; subpattern_0, ns=122

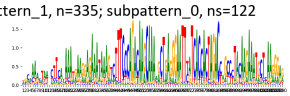

pattern_1, n=335; subpattern_1, ns=122

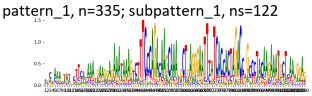

pattern_1, n=335; subpattern_2, ns=52

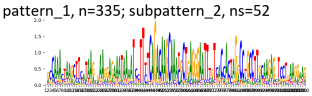

pattern_1, n=335; subpattern_3, ns=34

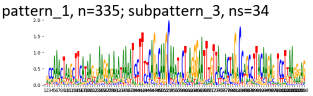

pattern_1, n=335; subpattern_4, ns=3

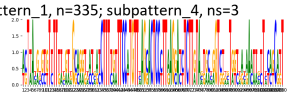

pattern_1, n=335; subpattern_5, ns=2

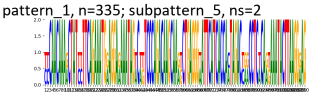

TF-MoDisCO pattern_1 n=233, CWM

pattern_2, n=233; subpattern_0, ns=66

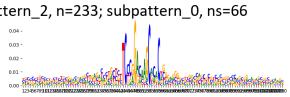

pattern_2, n=233; subpattern_1, ns=55

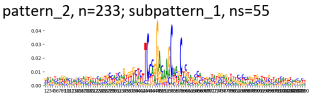

pattern_2, n=233; subpattern_2, ns=53

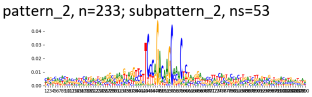

pattern_2, n=233; subpattern_3, ns=49

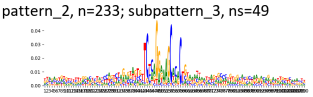

pattern_2, n=233; subpattern_4, ns=7

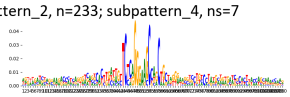

pattern_2, n=233; subpattern_5, ns=3

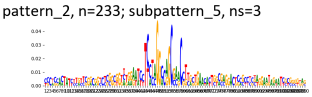

TF-MoDisCO pattern_1 n=233, PWM

pattern_2, n=233; subpattern_0, ns=66

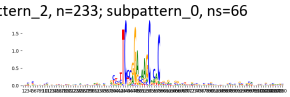

pattern_2, n=233; subpattern_1, ns=55

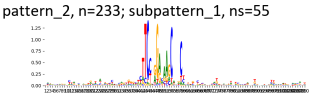

pattern_2, n=233; subpattern_2, ns=53

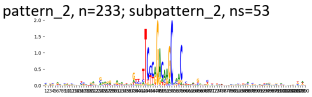

pattern_2, n=233; subpattern_3, ns=49

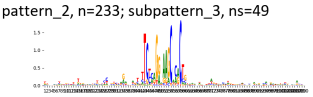

pattern_2, n=233; subpattern_4, ns=7

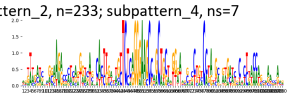

pattern_2, n=233; subpattern_5, ns=3



Supplementary Figure 1079: TF-MoDisCO subpatterns for the ZNF337 transcription factor in HEK293 (accession ChipExo models).

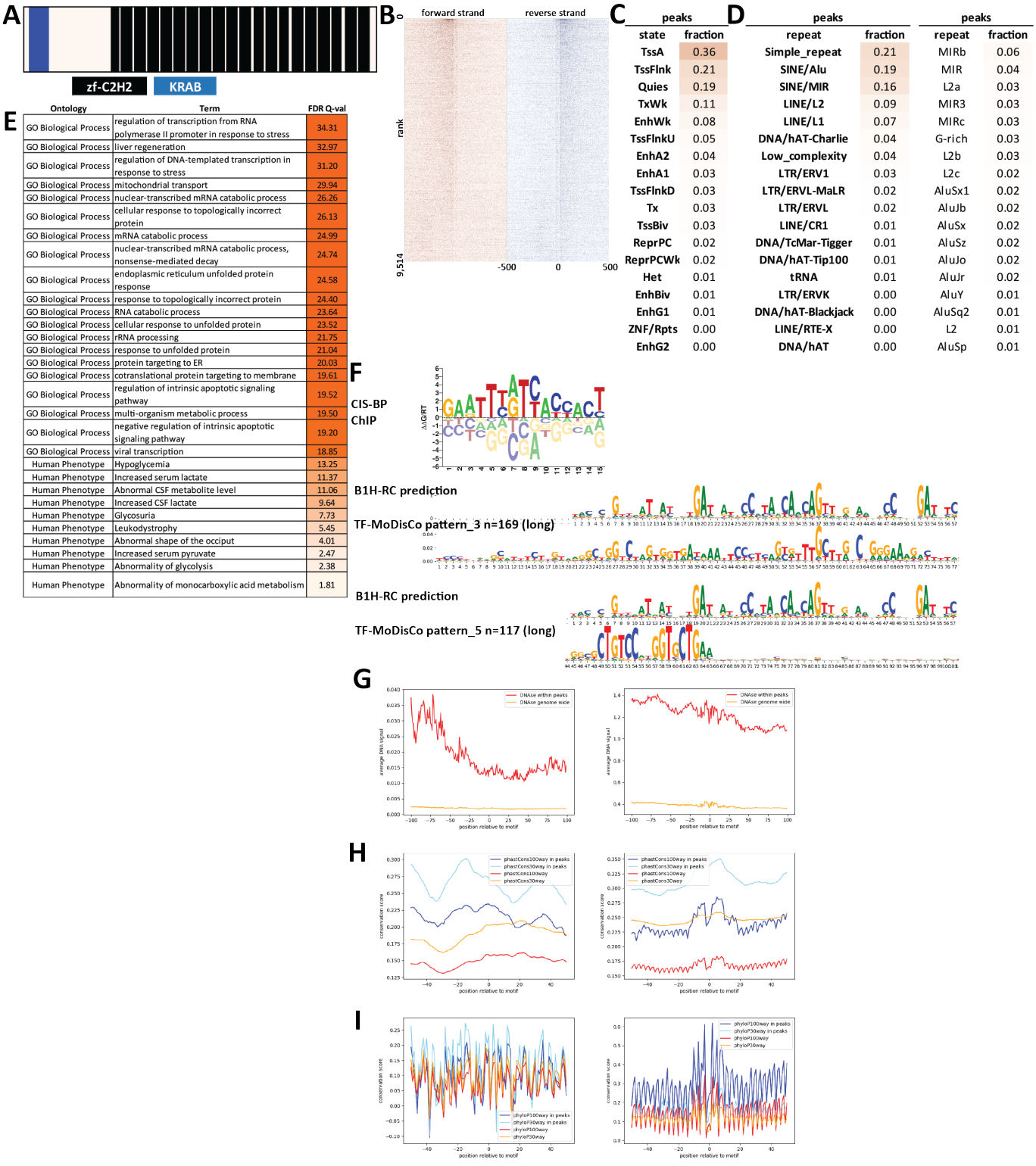

Supplementary Figure 1080: Properties and genomic distribution of motifs identified for the ZNF337 transcription factor in HepG2 (accession ENCSR759KXQ).

TF-MoDisCO pattern_3 n=169, CWM

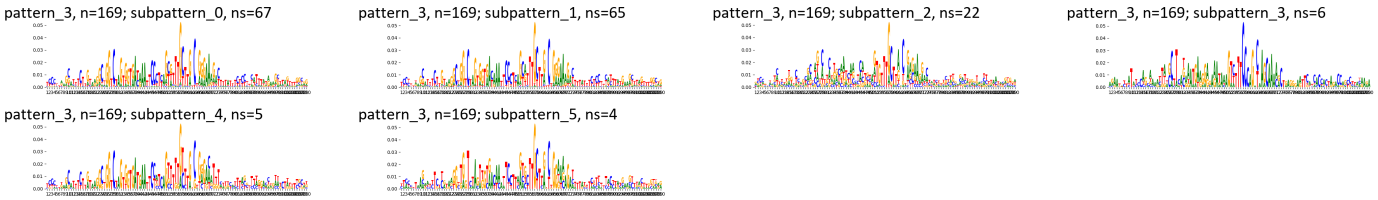

TF-MoDisCO pattern_3 n=169, PWM

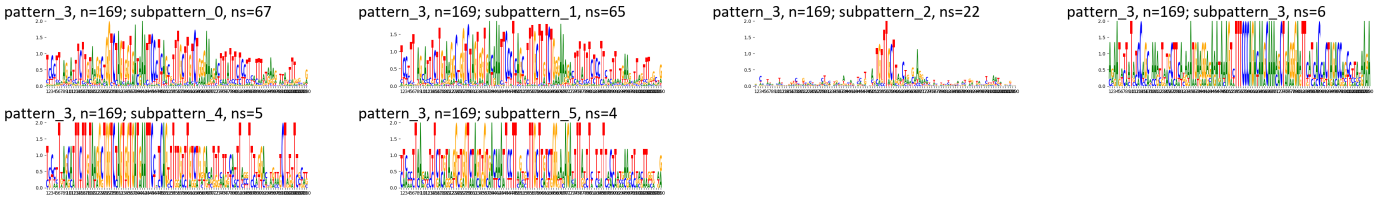

TF-MoDisCO pattern_5 n=117, CWM

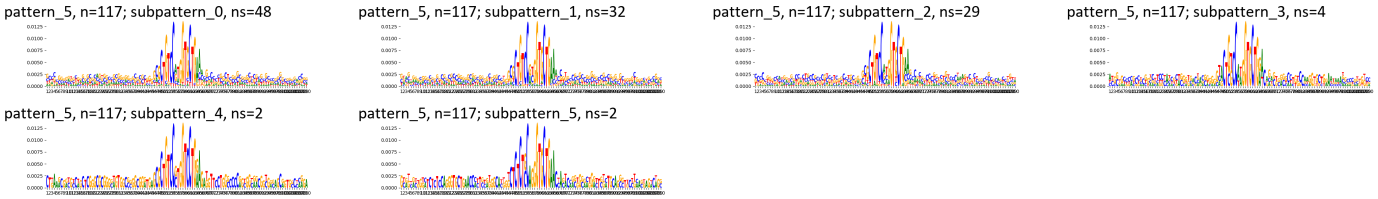

TF-MoDisCO pattern_5 n=117, PWM

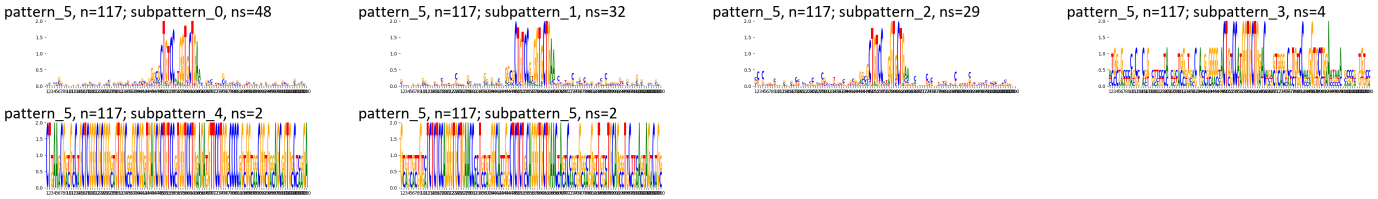

Supplementary Figure 1081: TF-MoDisCO subpatterns for the ZNF337 transcription factor in HepG2 (accession ENCSR759KXQ).

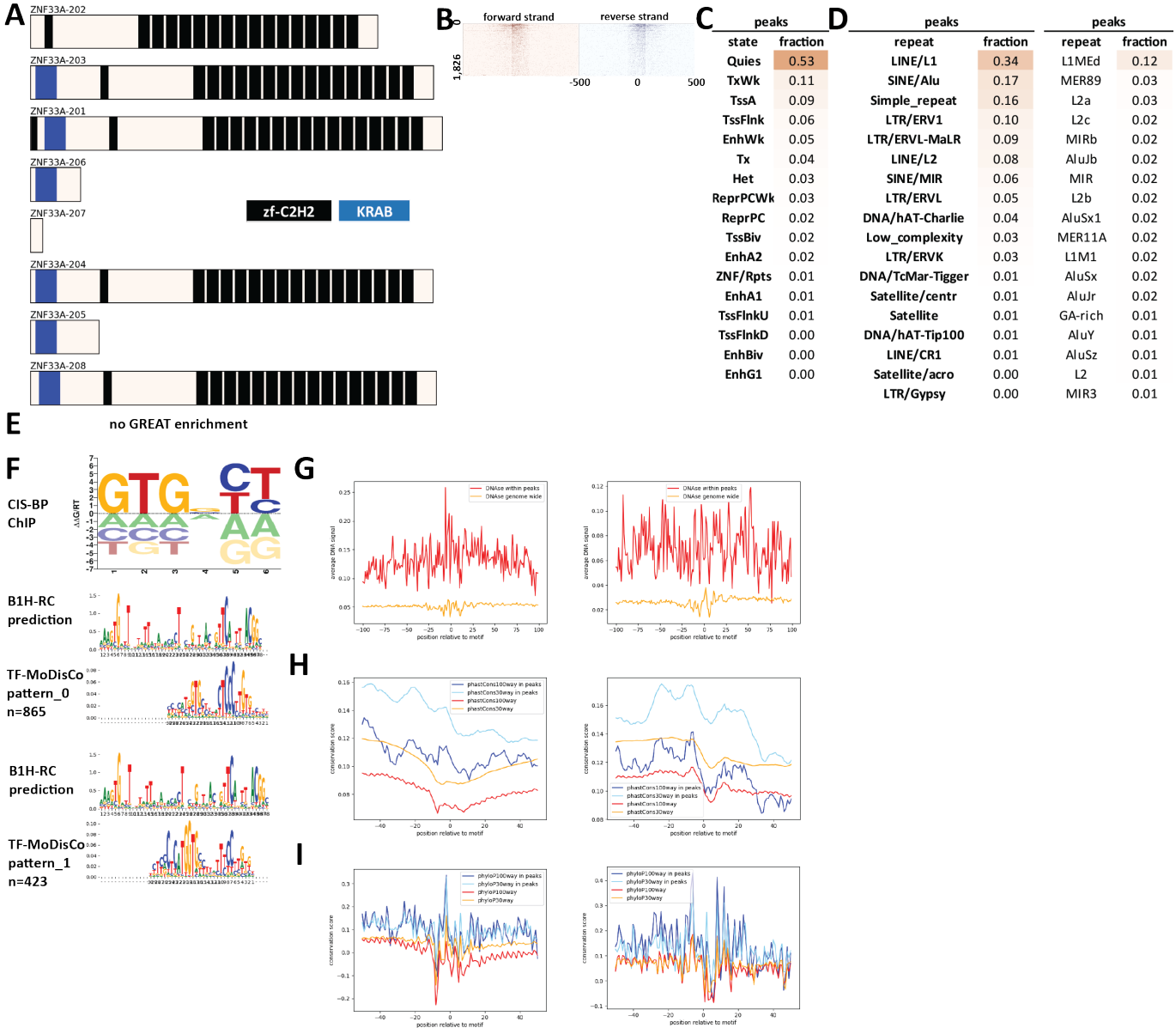

Supplementary Figure 1082: Properties and genomic distribution of motifs identified for the ZNF33A transcription factor in HEK293 (accession ChipExo models).

TF-MoDisCO pattern_0 n=865, CWM

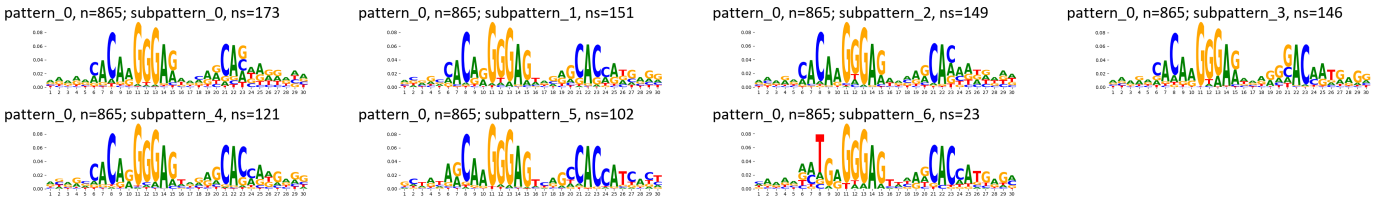

TF-MoDisCO pattern_0 n=865, PWM

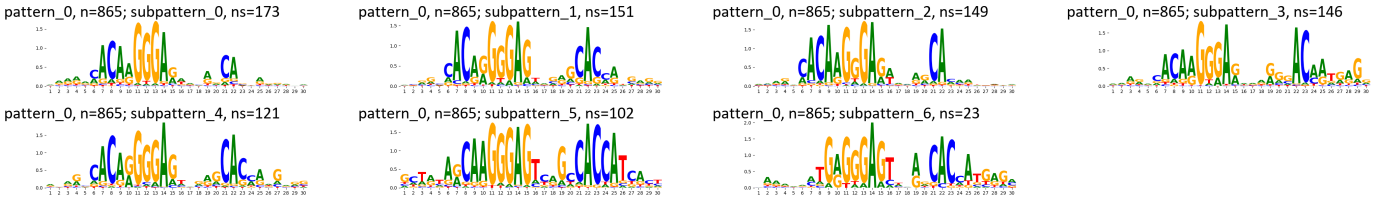

TF-MoDisCO pattern_1 n=423, CWM

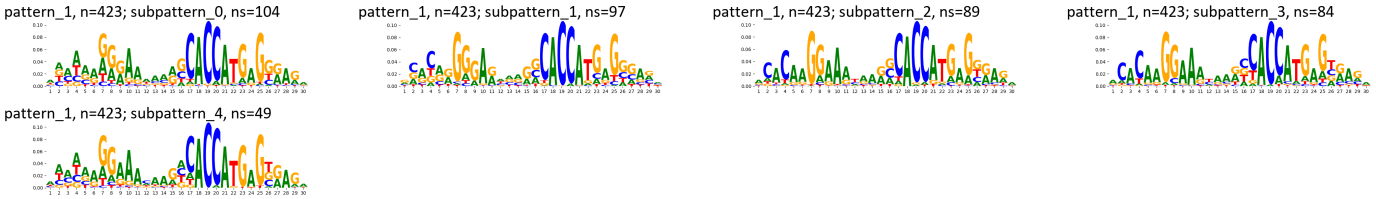

TF-MoDisCO pattern_1 n=423, PWM

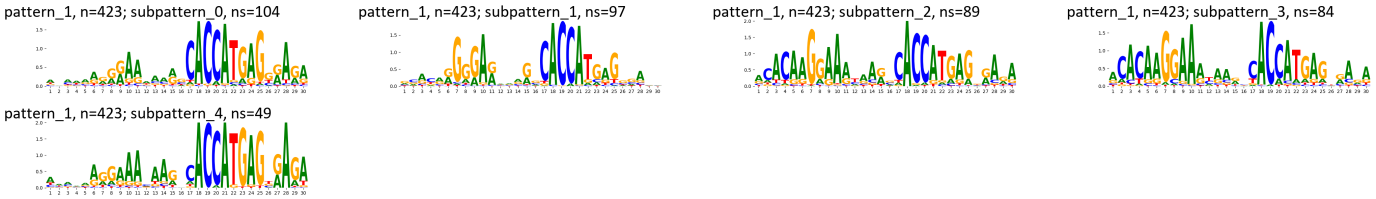

Supplementary Figure 1083: TF-MoDisCO subpatterns for the ZNF33A transcription factor in HEK293 (accession ChipExo models).

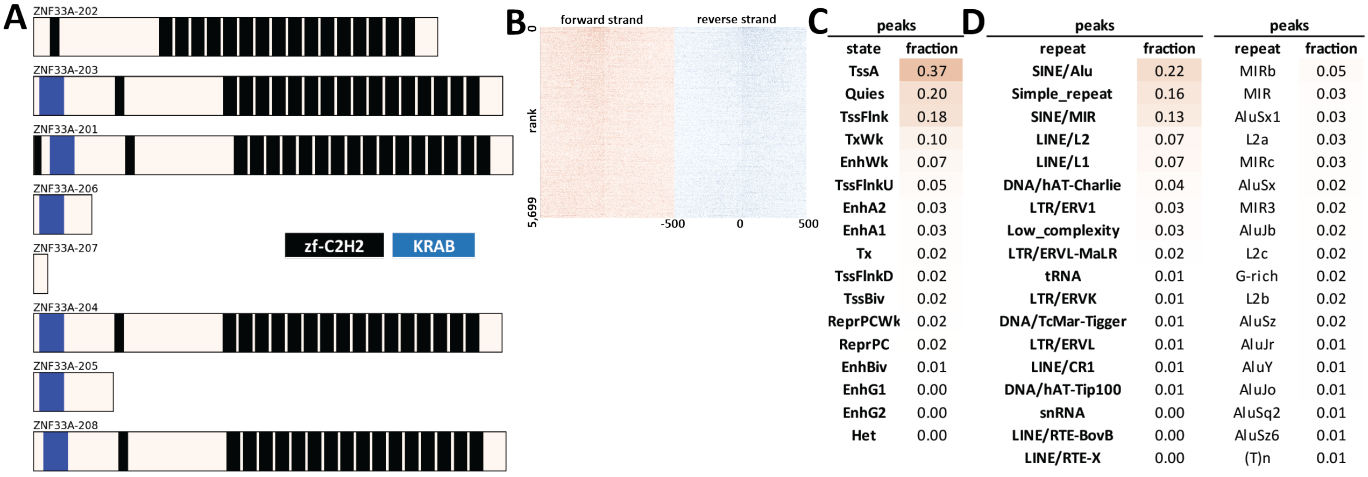

C

peaks	
state	fraction
TssA	0.37
Quies	0.20
TssFlnk	0.18
TxWk	0.10
EnhWk	0.07
TssFlnkU	0.05
EnhA2	0.03
EnhA1	0.03
Tx	0.02
TssFlnkD	0.02
TssBiv	0.02
ReprPCWk	0.02
ReprPC	0.02
EnhBiv	0.01
EnhG1	0.00
EnhG2	0.00
Het	0.00

D

peaks		peaks	
repeat	fraction	repeat	fraction
SINE/Alu	0.22	MIRb	0.05
Simple_repeat	0.16	MIR	0.03
SINE/MIR	0.13	AluSx1	0.03
LINE/L2	0.07	L2a	0.03
LINE/L1	0.07	MIRc	0.03
DNA/hAT-Charlie	0.04	AluSx	0.02
LTR/ERV1	0.03	MIR3	0.02
Low_complexity	0.03	AluJb	0.02
LTR/ERVL-MaLR	0.02	L2c	0.02
tRNA	0.01	G-rich	0.02
LTR/ERVK	0.01	L2b	0.02
DNA/TcMar-Tigger	0.01	AluSz	0.02
LTR/ERVL	0.01	AluJr	0.01
LINE/CR1	0.01	AluY	0.01
DNA/hAT-Tip100	0.01	AluJo	0.01
snRNA	0.00	AluSq2	0.01
LINE/RTE-BovB	0.00	AluSz6	0.01
LINE/RTE-X	0.00	(T)n	0.01

E

Ontology	Term	FDR Q-val
GO Biological Process	ncRNA metabolic process	29.39
GO Biological Process	rRNA processing	22.89
GO Biological Process	rRNA metabolic process	21.85
GO Biological Process	ncRNA processing	21.76
GO Biological Process	regulation of DNA-templated transcription in response to stress	21.27
GO Biological Process	ribosome biogenesis	18.44
GO Biological Process	nuclear-transcribed mRNA catabolic process, nonsense-mediated decay	18.16
GO Biological Process	regulation of gene expression, epigenetic	16.68
GO Biological Process	viral gene expression	15.94
GO Biological Process	RNA catabolic process	15.82
GO Biological Process	regulation of transcription from RNA polymerase II promoter in response to hypoxia	15.83
GO Biological Process	cotranslational protein targeting to membrane	15.66
GO Biological Process	establishment of protein localization to endoplasmic reticulum	15.43
GO Biological Process	protein targeting to ER	15.41
GO Biological Process	nuclear-transcribed mRNA catabolic process	15.33
GO Biological Process	viral transcription	15.32
GO Biological Process	protein localization to endoplasmic reticulum	15.06
GO Biological Process	mRNA catabolic process	14.67
GO Biological Process	multi-organism metabolic process	13.62
GO Biological Process	SRP-dependent cotranslational protein targeting to membrane	13.36
Human Phenotype	Lactic acidosis	8.78
Human Phenotype	Increased serum lactate	8.48
Human Phenotype	Increased CSF lactate	6.52

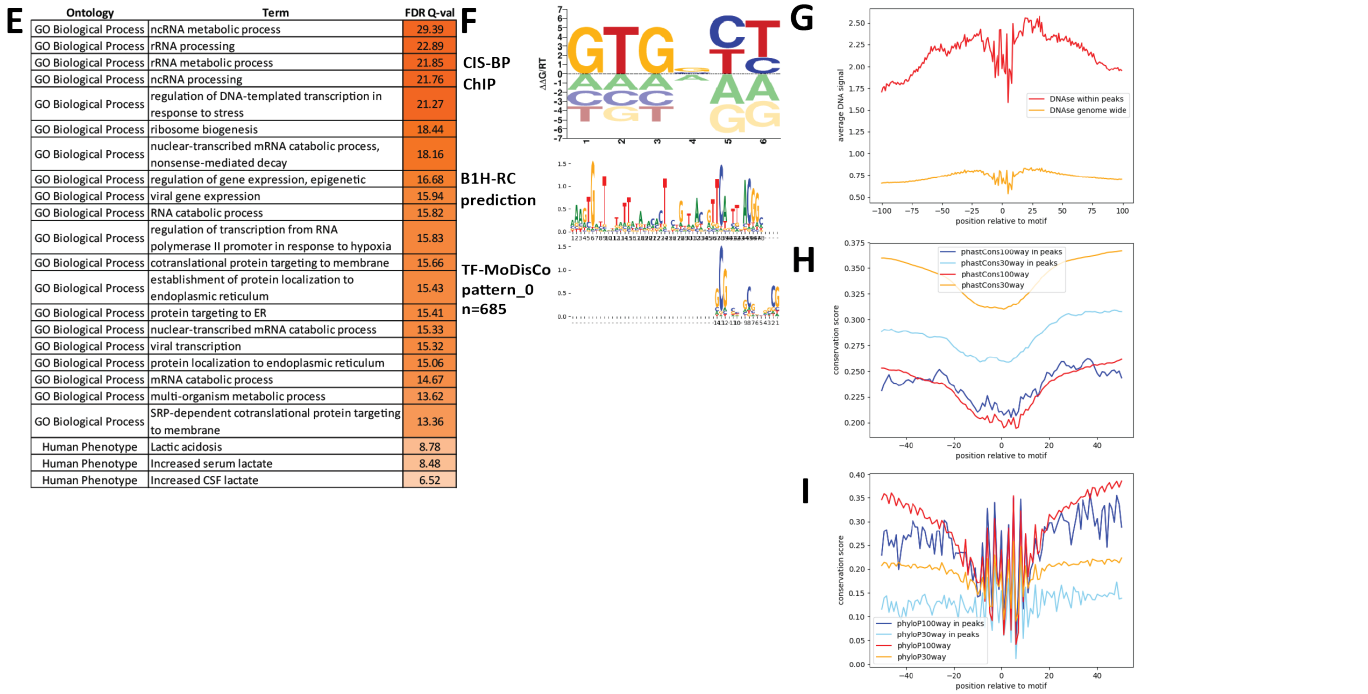

Supplementary Figure 1084: Properties and genomic distribution of motifs identified for the ZNF33A transcription factor in HepG2 (accession ENCSR110BYN).

TF-MoDisCO pattern_0 n=685, CWM

pattern_0, n=685; subpattern_0, ns=136

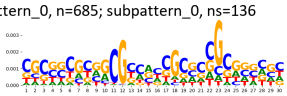

pattern_0, n=685; subpattern_1, ns=125

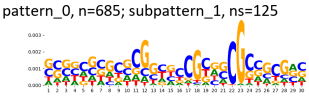

pattern_0, n=685; subpattern_2, ns=88

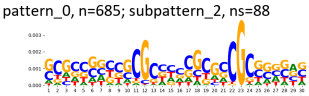

pattern_0, n=685; subpattern_3, ns=87

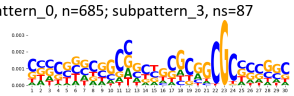

pattern_0, n=685; subpattern_4, ns=85

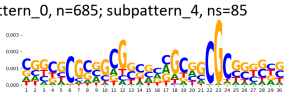

pattern_0, n=685; subpattern_5, ns=50

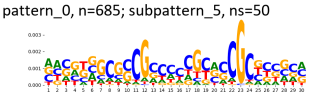

pattern_0, n=685; subpattern_6, ns=50

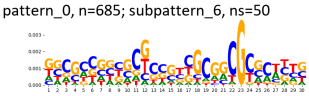

pattern_0, n=685; subpattern_7, ns=38

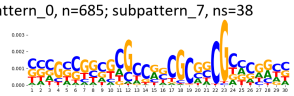

pattern_0, n=685; subpattern_8, ns=26

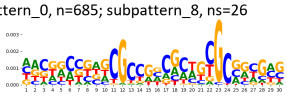

TF-MoDisCO pattern_0 n=685, PWM

pattern_0, n=685; subpattern_0, ns=136

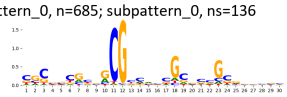

pattern_0, n=685; subpattern_1, ns=125

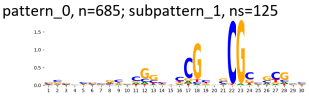

pattern_0, n=685; subpattern_2, ns=88

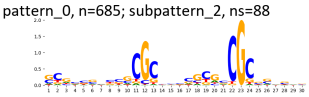

pattern_0, n=685; subpattern_3, ns=87

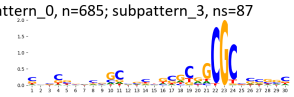

pattern_0, n=685; subpattern_4, ns=85

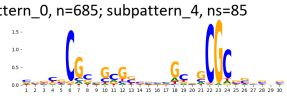

pattern_0, n=685; subpattern_5, ns=50

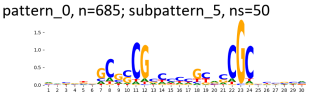

pattern_0, n=685; subpattern_6, ns=50

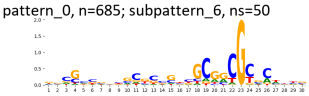

pattern_0, n=685; subpattern_7, ns=38

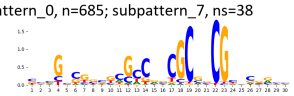

pattern_0, n=685; subpattern_8, ns=26

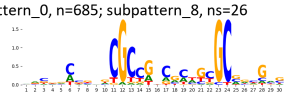

Supplementary Figure 1085: TF-MoDisCO subpatterns for the ZNF33A transcription factor in HepG2 (accession ENCSR110BYN).

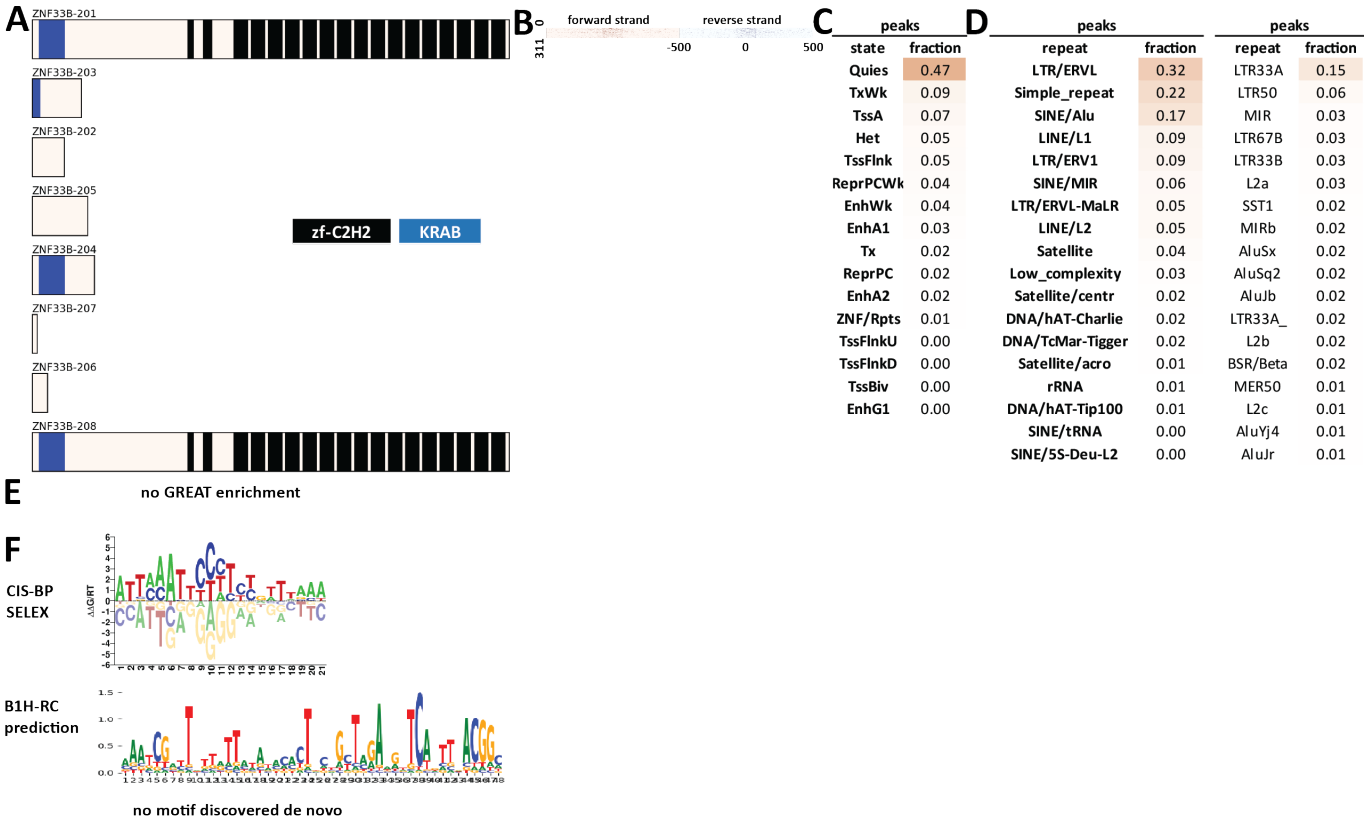

Supplementary Figure 1086: Properties and genomic distribution of motifs identified for the ZNF33B transcription factor in HEK293 (accession ChipExo models).

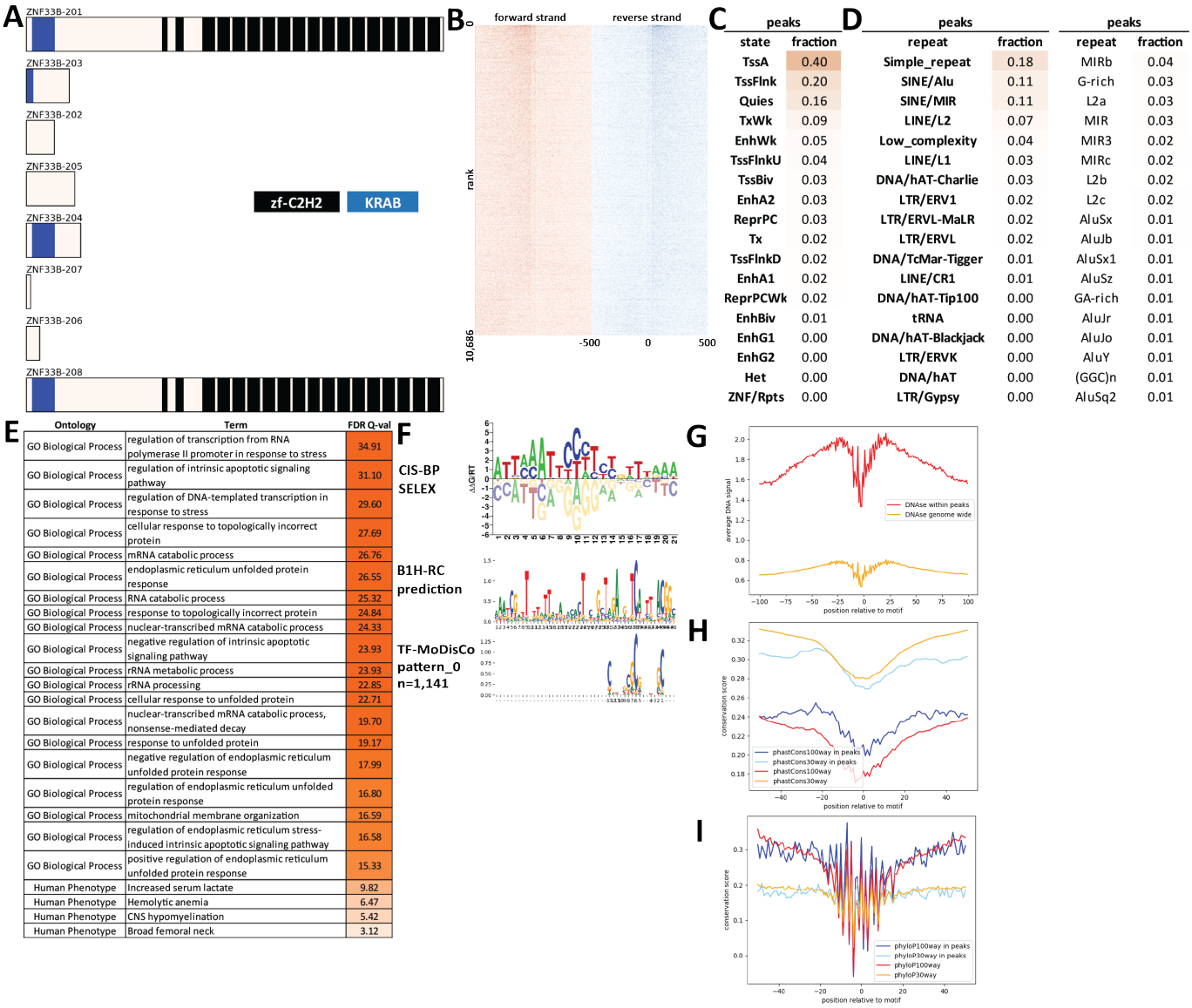

peaks	
state	fraction
TssA	0.40
TssFlnk	0.20
Quies	0.16
TxWk	0.09
EnhWk	0.05
TssFlnkU	0.04
TssBiv	0.03
EnhA2	0.03
ReprPC	0.03
Tx	0.02
TssFlnkD	0.02
EnhA1	0.02
ReprPCWk	0.02
EnhBiv	0.01
EnhG1	0.00
EnhG2	0.00
Het	0.00
ZNF/Rpts	0.00

peaks		peaks	
repeat	fraction	repeat	fraction
Simple_repeat	0.18	MIRb	0.04
SINE/Alu	0.11	G-rich	0.03
SINE/MIR	0.11	L2a	0.03
LINE/L2	0.07	MIR	0.03
Low_complexity	0.04	MIR3	0.02
LINE/L1	0.03	MIRc	0.02
DNA/hAT-Charlie	0.03	L2b	0.02
LTR/ERV1	0.02	L2c	0.02
LTR/ERVL-MaLR	0.02	AluSx	0.01
LTR/ERVL	0.02	AluJb	0.01
DNA/TcMar-Tigger	0.01	AluSx1	0.01
LINE/CR1	0.01	AluSz	0.01
DNA/hAT-Tip100	0.00	GA-rich	0.01
tRNA	0.00	AluJr	0.01
DNA/hAT-Blackjack	0.00	AluJo	0.01
LTR/ERVK	0.00	AluY	0.01
DNA/hAT	0.00	(GGC)n	0.01
LTR/Gypsy	0.00	AluSq2	0.01

Ontology	Term	FDR Q-val
GO Biological Process	regulation of transcription from RNA polymerase II promoter in response to stress	34.91
GO Biological Process	regulation of intrinsic apoptotic signaling pathway	31.10
GO Biological Process	regulation of DNA-templated transcription in response to stress	29.60
GO Biological Process	cellular response to topologically incorrect protein	27.69
GO Biological Process	mRNA catabolic process	26.76
GO Biological Process	endoplasmic reticulum unfolded protein response	26.55
GO Biological Process	RNA catabolic process	25.32
GO Biological Process	response to topologically incorrect protein	24.84
GO Biological Process	nuclear-transcribed mRNA catabolic process	24.33
GO Biological Process	negative regulation of intrinsic apoptotic signaling pathway	23.93
GO Biological Process	rRNA metabolic process	23.93
GO Biological Process	rRNA processing	22.85
GO Biological Process	cellular response to unfolded protein	22.71
GO Biological Process	nuclear-transcribed mRNA catabolic process, nonsense-mediated decay	19.70
GO Biological Process	response to unfolded protein	19.17
GO Biological Process	negative regulation of endoplasmic reticulum unfolded protein response	17.99
GO Biological Process	regulation of endoplasmic reticulum unfolded protein response	16.80
GO Biological Process	mitochondrial membrane organization	16.59
GO Biological Process	regulation of endoplasmic reticulum stress-induced intrinsic apoptotic signaling pathway	16.58
GO Biological Process	positive regulation of endoplasmic reticulum unfolded protein response	15.33
Human Phenotype	Increased serum lactate	9.82
Human Phenotype	Hemolytic anemia	6.47
Human Phenotype	CNS hypomyelination	5.42
Human Phenotype	Broad femoral neck	3.12

Supplementary Figure 1087: Properties and genomic distribution of motifs identified for the ZNF33B transcription factor in HepG2 (accession ENCSR052FXA).

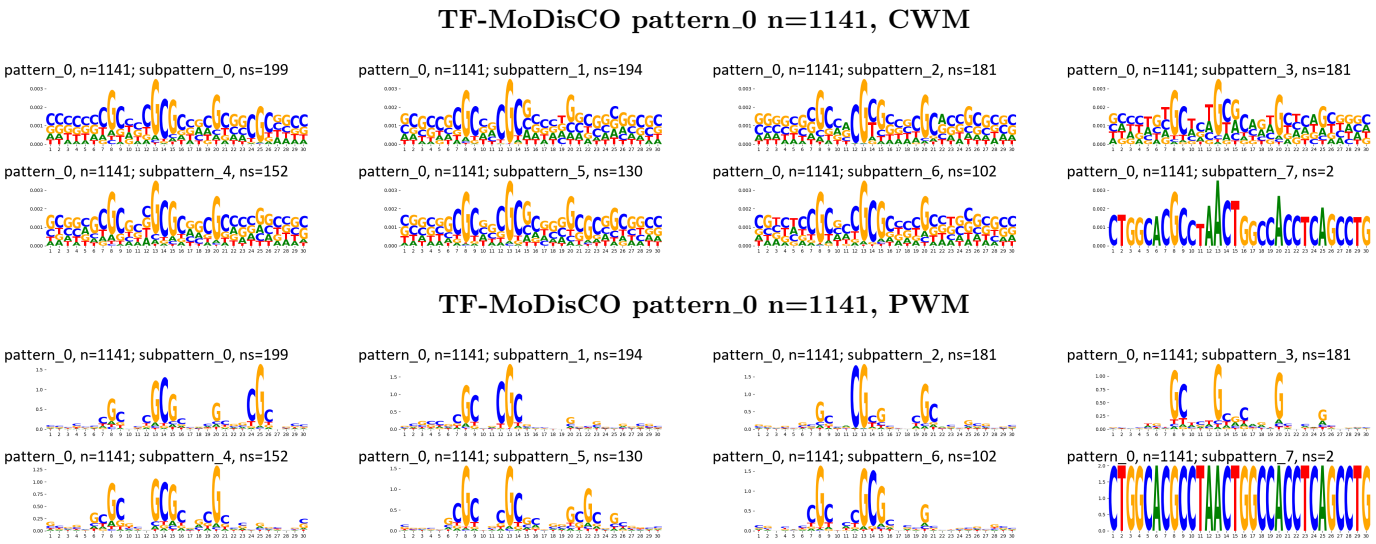

Supplementary Figure 1088: TF-MoDisCO subpatterns for the ZNF33B transcription factor in HepG2 (accession ENCSR052FXA).

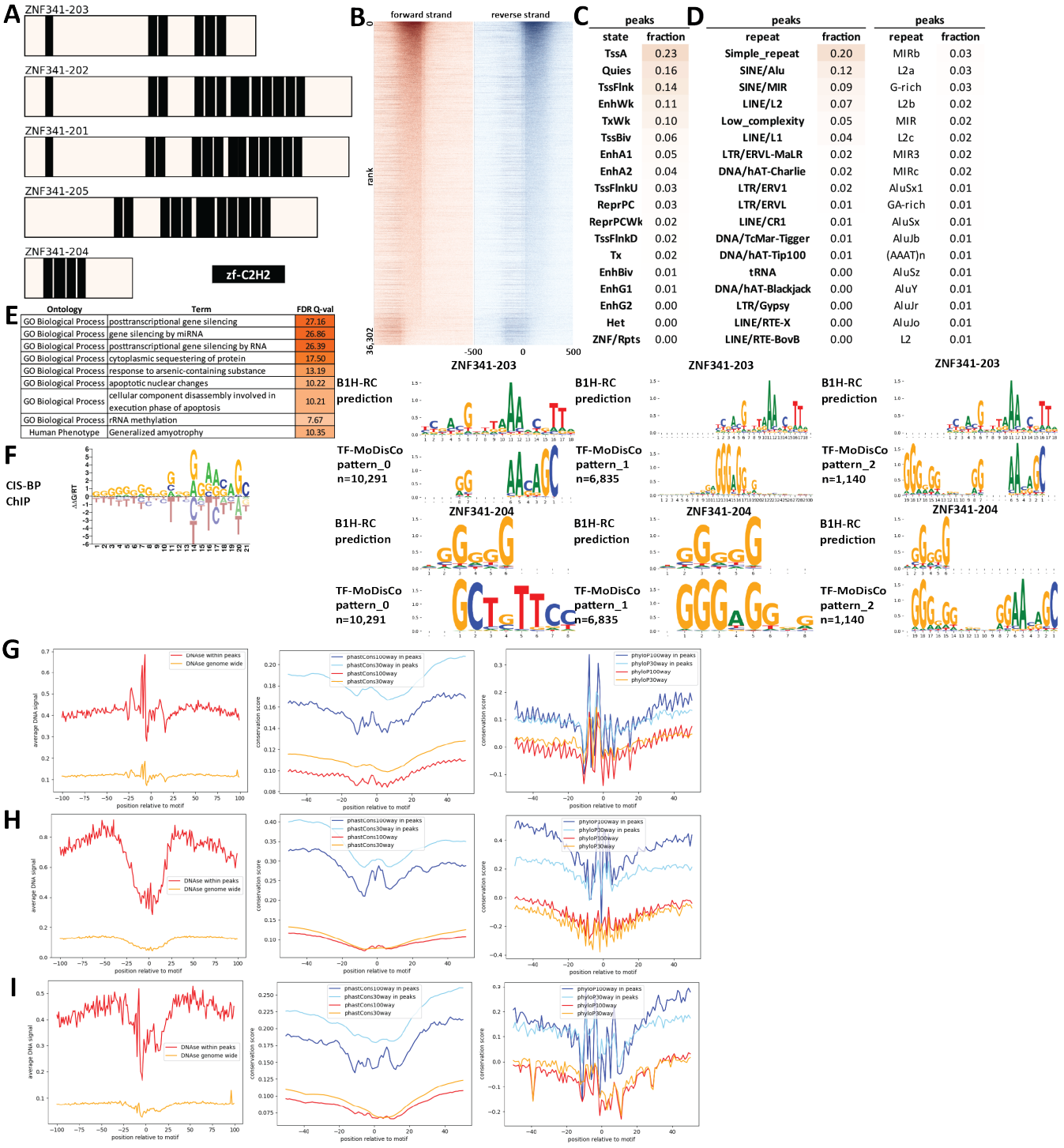

Ontology	Term	FDR Q-val
GO Biological Process	posttranscriptional gene silencing	27.16
GO Biological Process	gene silencing by miRNA	26.86
GO Biological Process	posttranscriptional gene silencing by RNA	26.39
GO Biological Process	cytoplasmic sequestering of protein	17.50
GO Biological Process	response to arsenic-containing substance	13.19
GO Biological Process	apoptotic nuclear changes	10.22
GO Biological Process	cellular component disassembly involved in execution phase of apoptosis	10.21
GO Biological Process	rRNA methylation	7.67
Human Phenotype	Generalized amyotrophy	10.35

peaks	
state	fraction
TssA	0.23
Quies	0.16
TssFlnk	0.14
EnhWk	0.11
TxWk	0.10
TssBiv	0.06
EnhA1	0.05
EnhA2	0.04
TssFlnkU	0.03
ReprPC	0.03
ReprPCWk	0.02
TssFlnkD	0.02
Tx	0.02
EnhBiv	0.01
EnhG1	0.01
EnhG2	0.00
Het	0.00
ZNF/Rpts	0.00

peaks		peaks	
repeat	fraction	repeat	fraction
Simple_repeat	0.20	MIRb	0.03
SINE/Alu	0.12	L2a	0.03
SINE/MIR	0.09	G-rich	0.03
LINE/L2	0.07	L2b	0.02
Low_complexity	0.05	MIR	0.02
LINE/L1	0.04	L2c	0.02
LTR/ERVL-MaLR	0.02	MIR3	0.02
DNA/hAT-Charlie	0.02	MIRc	0.02
LTR/ERV1	0.02	AluSx1	0.01
LTR/ERVL	0.01	GA-rich	0.01
LINE/CR1	0.01	AluSx	0.01
DNA/TcMar-Tigger	0.01	AluJb	0.01
DNA/hAT-Tip100	0.01	(AAAT)n	0.01
tRNA	0.00	AluSz	0.01
DNA/hAT-Blackjack	0.00	AluY	0.01
LTR/Gypsy	0.00	AluJr	0.01
LINE/RTE-X	0.00	AluJo	0.01
LINE/RTE-BovB	0.00	L2	0.01

Supplementary Figure 1089: Properties and genomic distribution of motifs identified for the ZNF341 transcription factor in HEK293 (accession ENCSR185FOY).

TF-MoDisCO pattern_0 n=10291, CWM

pattern_0, n=10291; subpattern_0, ns=2278

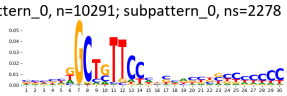

pattern_0, n=10291; subpattern_1, ns=1926

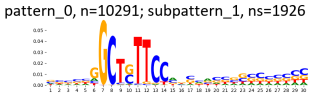

pattern_0, n=10291; subpattern_10, ns=56

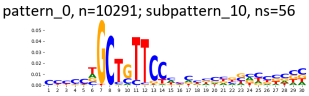

pattern_0, n=10291; subpattern_11, ns=16

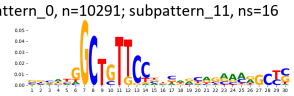

pattern_0, n=10291; subpattern_12, ns=7

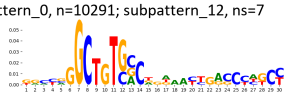

pattern_0, n=10291; subpattern_13, ns=6

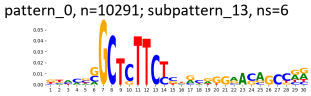

pattern_0, n=10291; subpattern_2, ns=1768

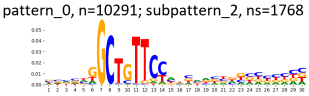

pattern_0, n=10291; subpattern_3, ns=1632

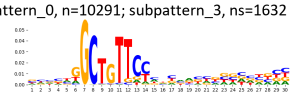

pattern_0, n=10291; subpattern_4, ns=1167

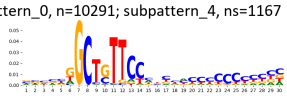

pattern_0, n=10291; subpattern_5, ns=911

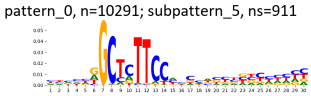

pattern_0, n=10291; subpattern_6, ns=215

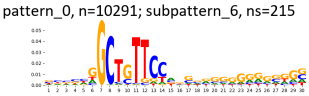

pattern_0, n=10291; subpattern_7, ns=143

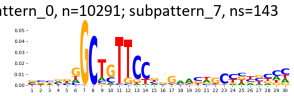

pattern_0, n=10291; subpattern_8, ns=104

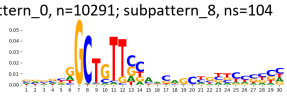

pattern_0, n=10291; subpattern_9, ns=62

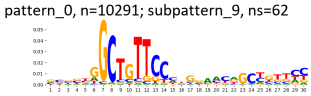

TF-MoDisCO pattern_0 n=10291, PWM

pattern_0, n=10291; subpattern_0, ns=2278

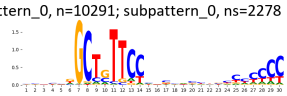

pattern_0, n=10291; subpattern_1, ns=1926

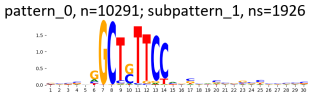

pattern_0, n=10291; subpattern_10, ns=56

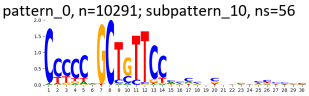

pattern_0, n=10291; subpattern_11, ns=16

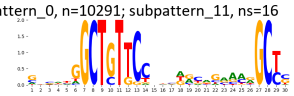

pattern_0, n=10291; subpattern_12, ns=7

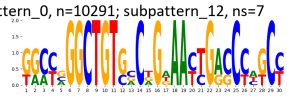

pattern_0, n=10291; subpattern_13, ns=6

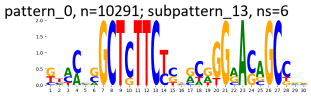

pattern_0, n=10291; subpattern_2, ns=1768

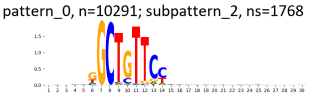

pattern_0, n=10291; subpattern_3, ns=1632

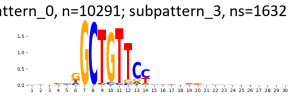

pattern_0, n=10291; subpattern_4, ns=1167

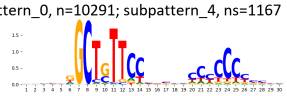

pattern_0, n=10291; subpattern_5, ns=911

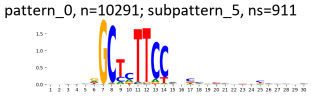

pattern_0, n=10291; subpattern_6, ns=215

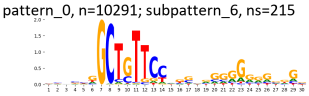

pattern_0, n=10291; subpattern_7, ns=143

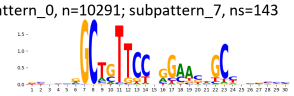

pattern_0, n=10291; subpattern_8, ns=104

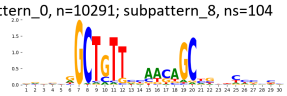

pattern_0, n=10291; subpattern_9, ns=62

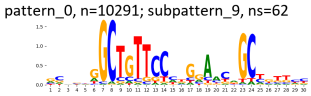

TF-MoDisCO pattern_1 n=6835, CWM

pattern_1, n=6835; subpattern_0, ns=950

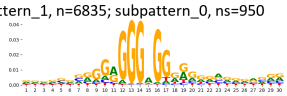

pattern_1, n=6835; subpattern_1, ns=905

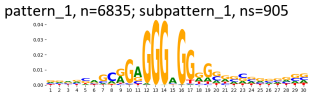

pattern_1, n=6835; subpattern_10, ns=136

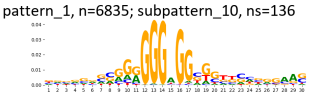

pattern_1, n=6835; subpattern_11, ns=91

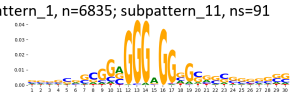

pattern_1, n=6835; subpattern_12, ns=88

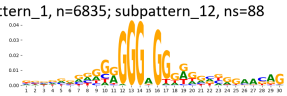

pattern_1, n=6835; subpattern_13, ns=61

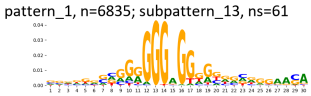

pattern_1, n=6835; subpattern_14, ns=45

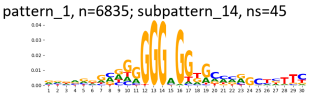

pattern_1, n=6835; subpattern_15, ns=33

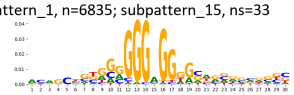

pattern_1, n=6835; subpattern_16, ns=21

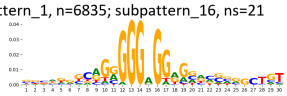

pattern_1, n=6835; subpattern_17, ns=21

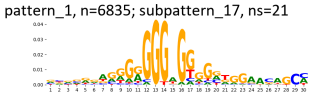

pattern_1, n=6835; subpattern_18, ns=19

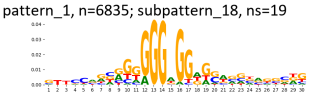

pattern_1, n=6835; subpattern_19, ns=17

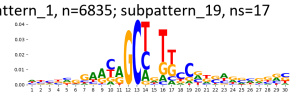

pattern_1, n=6835; subpattern_2, ns=874

pattern_1, n=6835; subpattern_20, ns=15

pattern_1, n=6835; subpattern_21, ns=5

pattern_1, n=6835; subpattern_3, ns=801

pattern_1, n=6835; subpattern_4, ns=761

pattern_1, n=6835; subpattern_5, ns=649

pattern_1, n=6835; subpattern_6, ns=503

pattern_1, n=6835; subpattern_7, ns=323

pattern_1, n=6835; subpattern_8, ns=315

pattern_1, n=6835; subpattern_9, ns=202

TF-MoDisCO pattern_1 n=6835, PWM

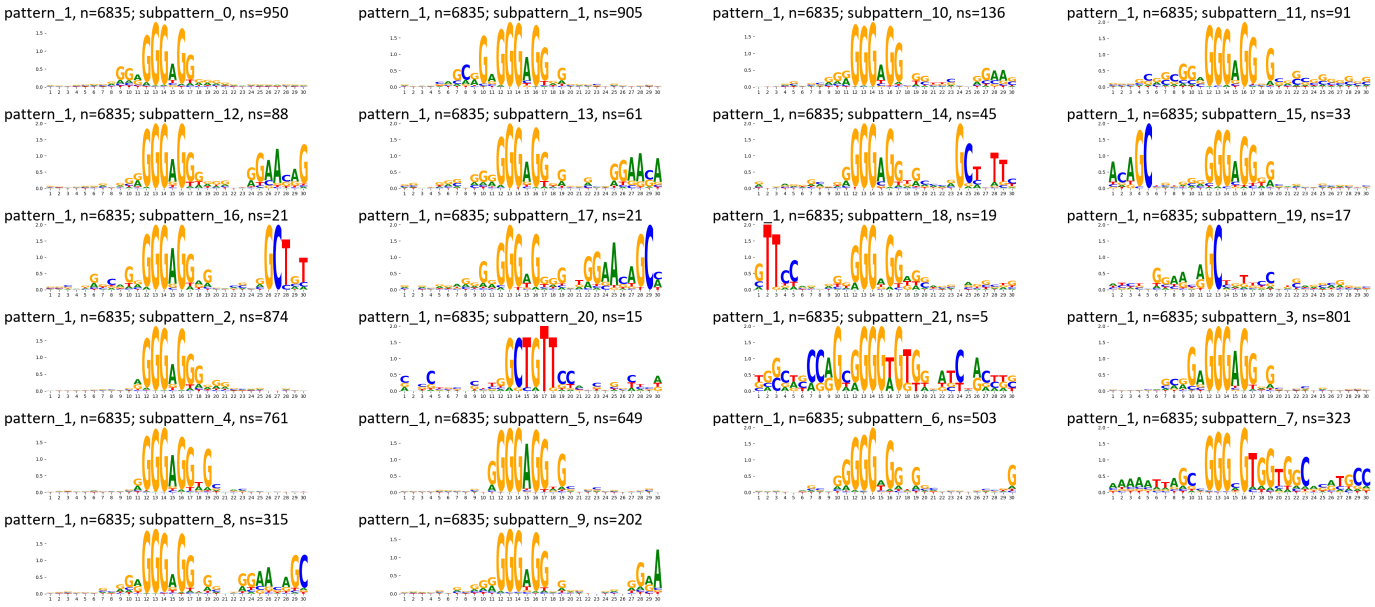

TF-MoDisCO pattern_2 n=1140, CWM

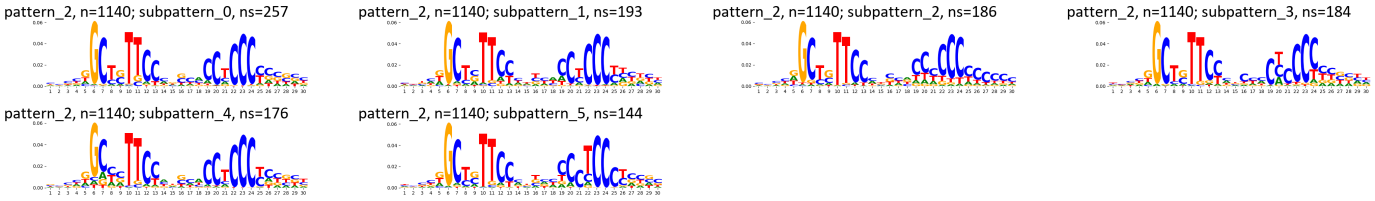

TF-MoDisCO pattern_2 n=1140, PWM

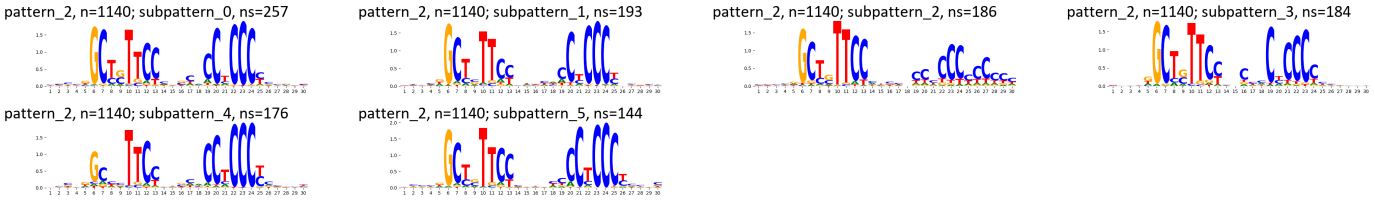

Supplementary Figure 1090: TF-MoDisCO subpatterns for the ZNF341 transcription factor in HEK293 (accession ENCSR185FOY).

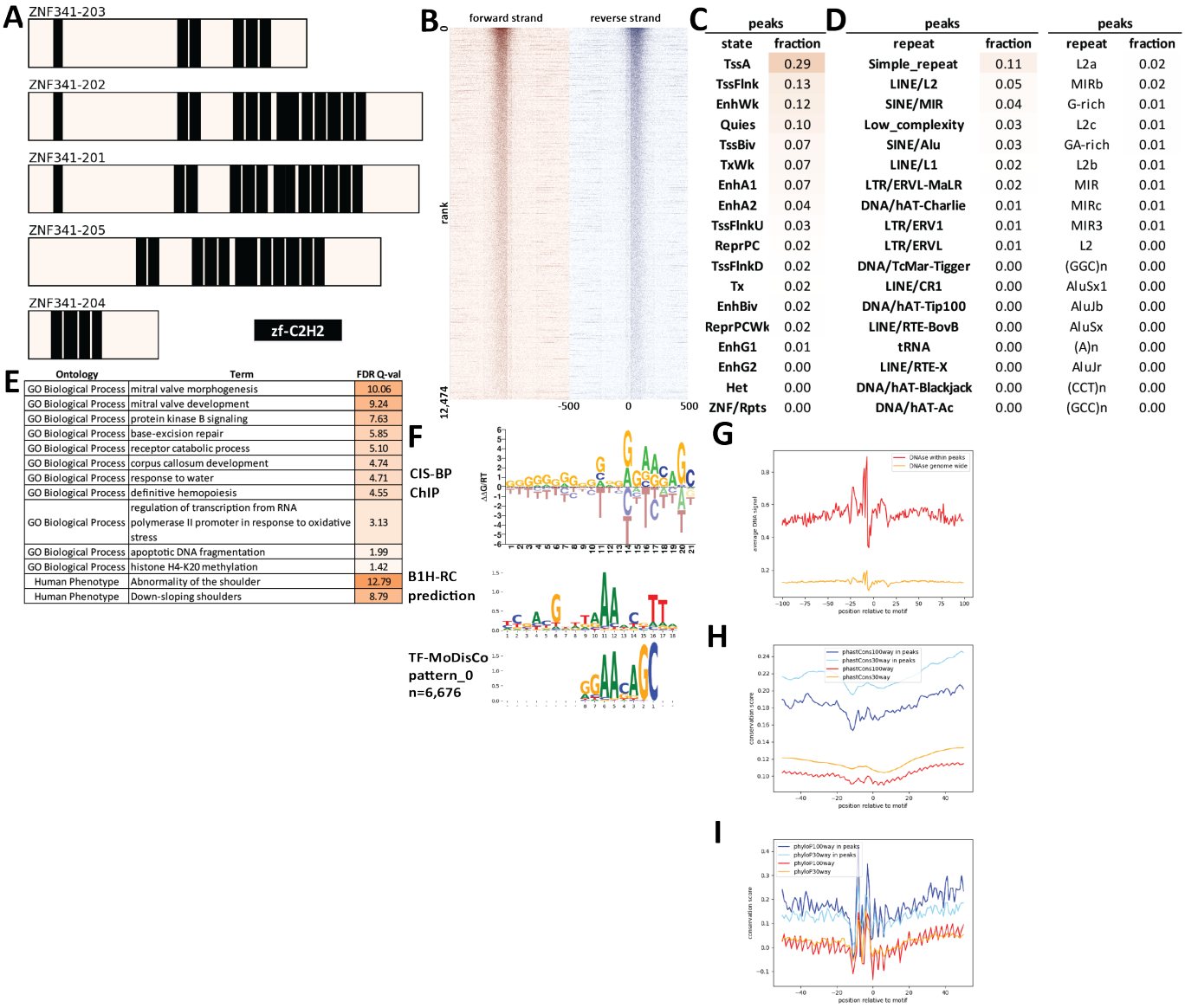

Supplementary Figure 1091: Properties and genomic distribution of motifs identified for the ZNF341 transcription factor in HEK293 (accession Hughes GR models).

TF-MoDisCO pattern_0 n=6676, CWM

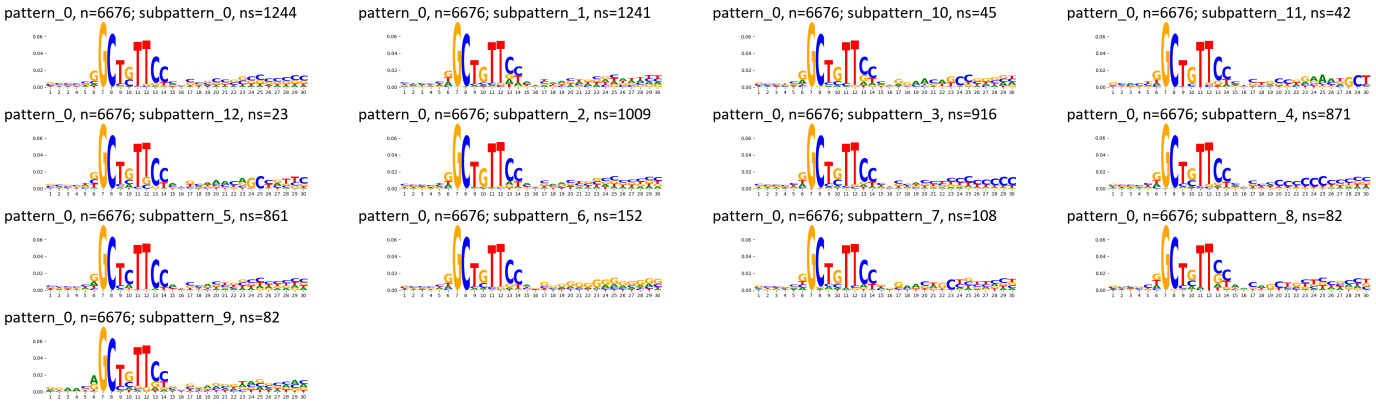

TF-MoDisCO pattern_0 n=6676, PWM

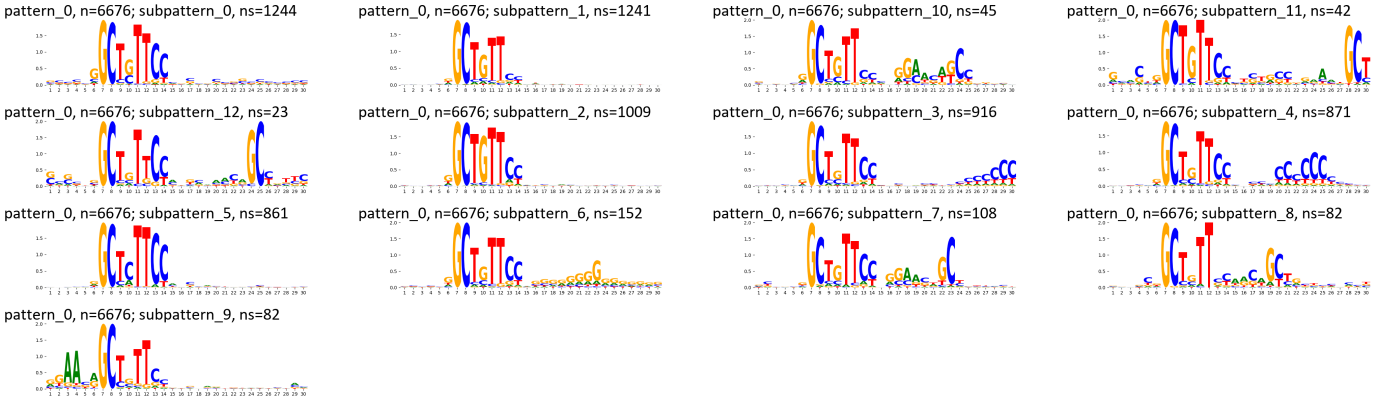

Supplementary Figure 1092: TF-MoDisCO subpatterns for the ZNF341 transcription factor in HEK293 (accession Hughes GR models).

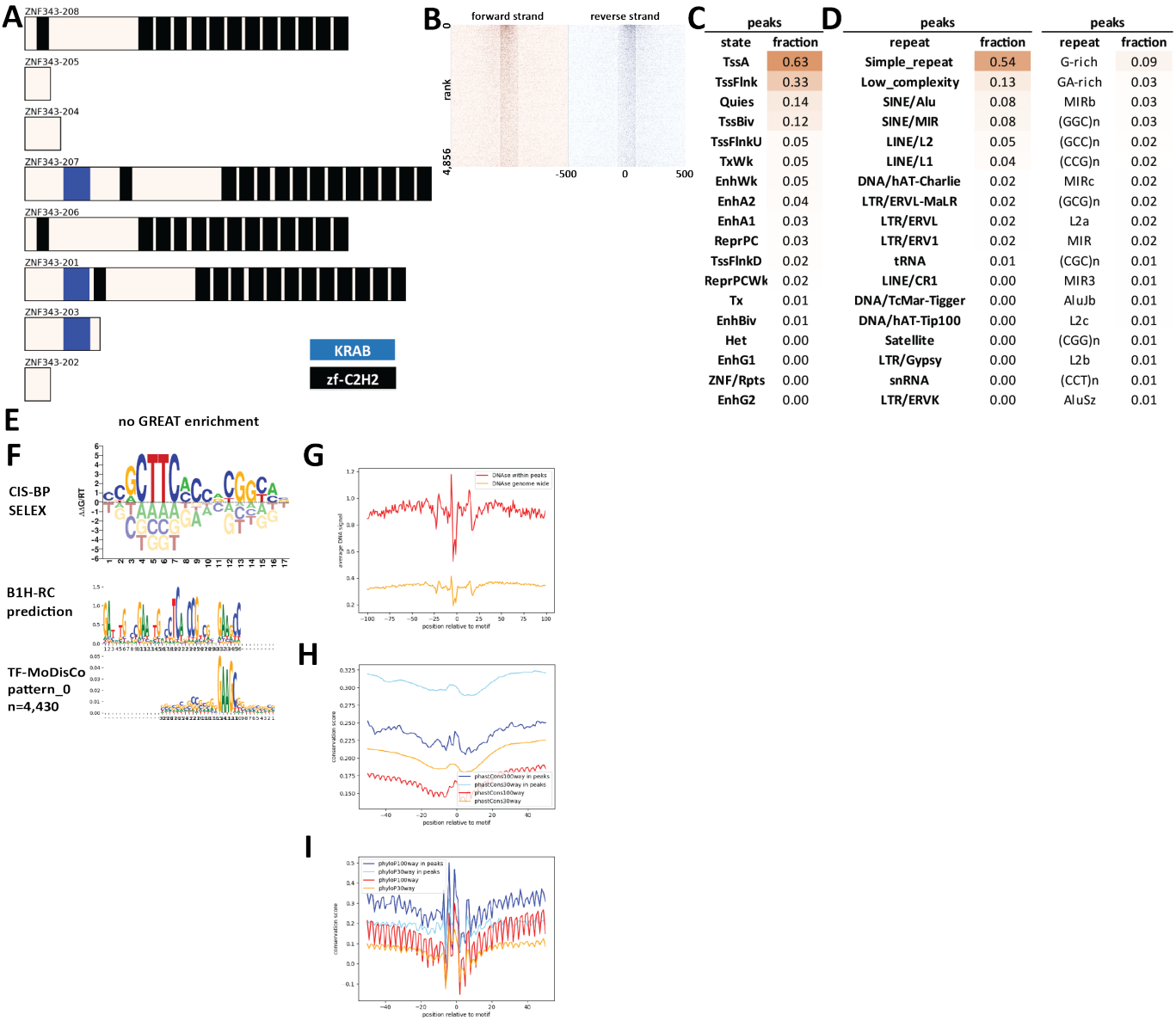

C	peaks	
	state	fraction
	TssA	0.63
	TssFlnk	0.33
	Quies	0.14
	TssBiv	0.12
	TssFlnkU	0.05
	TxWk	0.05
	EnhWk	0.05
	EnhA2	0.04
	EnhA1	0.03
	ReprPC	0.03
	TssFlnkD	0.02
	ReprPCWk	0.02
	Tx	0.01
	EnhBiv	0.01
	Het	0.00
	EnhG1	0.00
	ZNF/Rpts	0.00
	EnhG2	0.00

D	peaks		peaks	
	repeat	fraction	repeat	fraction
	Simple_repeat	0.54	G-rich	0.09
	Low_complexity	0.13	GA-rich	0.03
	SINE/Alu	0.08	MIRb	0.03
	SINE/MIR	0.08	(GGC)n	0.03
	LINE/L2	0.05	(GCC)n	0.02
	LINE/L1	0.04	(CCG)n	0.02
	DNA/hAT-Charlie	0.02	MIRc	0.02
	LTR/ERVL-MaLR	0.02	(GCG)n	0.02
	LTR/ERVL	0.02	L2a	0.02
	LTR/ERV1	0.02	MIR	0.02
	tRNA	0.01	(CGC)n	0.01
	LINE/CR1	0.00	MIR3	0.01
	DNA/TcMar-Tigger	0.00	AluJb	0.01
	DNA/hAT-Tip100	0.00	L2c	0.01
	Satellite	0.00	(CGG)n	0.01
	LTR/Gypsy	0.00	L2b	0.01
	snRNA	0.00	(CCT)n	0.01
	LTR/ERVK	0.00	AluSz	0.01

Supplementary Figure 1093: Properties and genomic distribution of motifs identified for the ZNF343 transcription factor in HEK293 (accession ChipExo models).

TF-MoDisCO pattern_0 n=4430, CWM

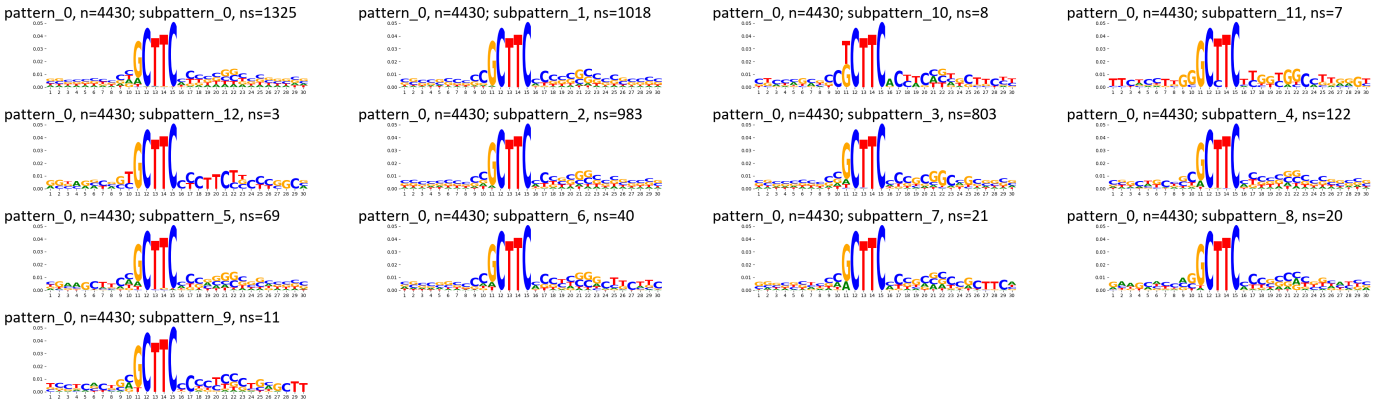

TF-MoDisCO pattern_0 n=4430, PWM

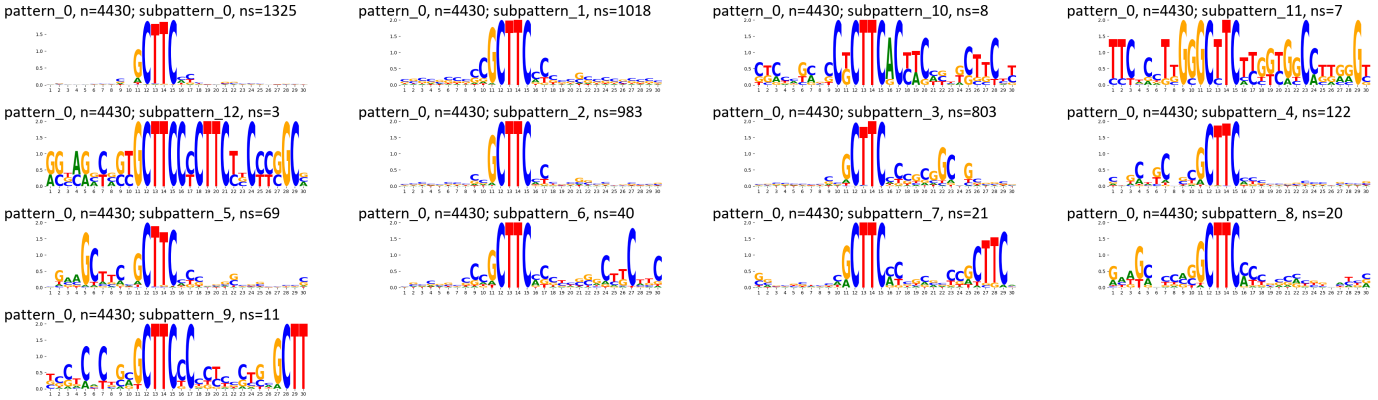

Supplementary Figure 1094: TF-MoDisCO subpatterns for the ZNF343 transcription factor in HEK293 (accession ChipExo models).

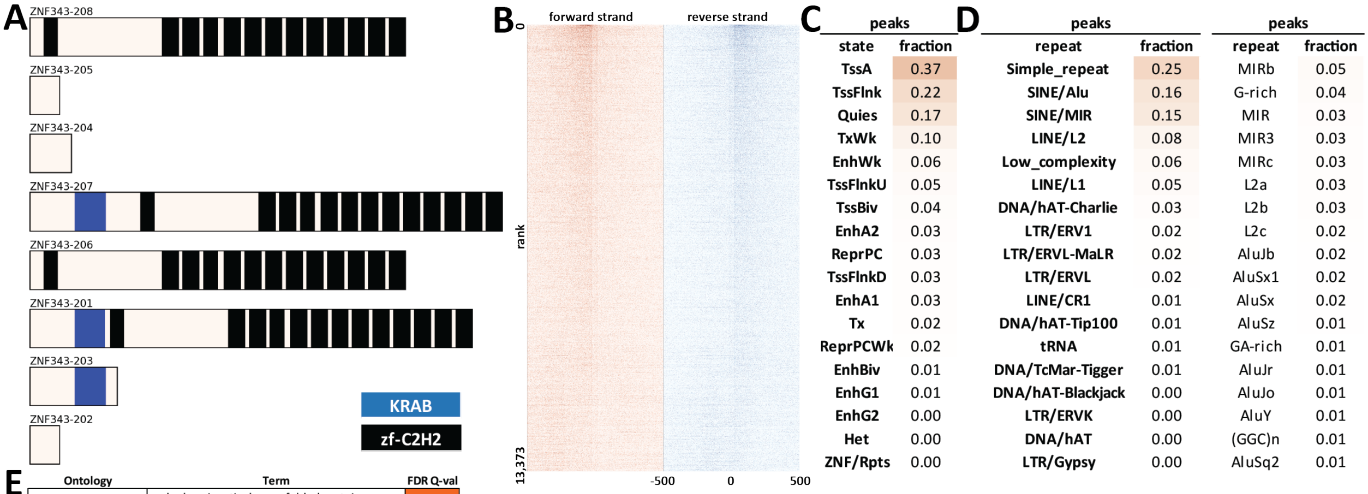

C

peaks	
state	fraction
TssA	0.37
TssFlnk	0.22
Quies	0.17
TxWk	0.10
EnhWk	0.06
TssFlnkU	0.05
TssBiv	0.04
EnhA2	0.03
ReprPC	0.03
TssFlnkD	0.03
EnhA1	0.03
Tx	0.02
ReprPCWk	0.02
EnhBiv	0.01
EnhG1	0.01
EnhG2	0.00
Het	0.00
ZNF/Rpts	0.00

D

peaks		peaks	
repeat	fraction	repeat	fraction
Simple_repeat	0.25	MIRb	0.05
SINE/Alu	0.16	G-rich	0.04
SINE/MIR	0.15	MIR	0.03
LINE/L2	0.08	MIR3	0.03
Low_complexity	0.06	MIRc	0.03
LINE/L1	0.05	L2a	0.03
DNA/hAT-Charlie	0.03	L2b	0.03
LTR/ERV1	0.02	L2c	0.02
LTR/ERVL-MaLR	0.02	AluJb	0.02
LTR/ERVL	0.02	AluSx1	0.02
LINE/CR1	0.01	AluSx	0.02
DNA/hAT-Tip100	0.01	AluSz	0.01
tRNA	0.01	GA-rich	0.01
DNA/TcMar-Tigger	0.01	AluJr	0.01
DNA/hAT-Blackjack	0.00	AluJo	0.01
LTR/ERVK	0.00	AluY	0.01
DNA/hAT	0.00	(GGC)n	0.01
LTR/Gypsy	0.00	AluSq2	0.01

E

Ontology	Term	FDR Q-val
GO Biological Process	endoplasmic reticulum unfolded protein response	35.84
GO Biological Process	IRE1-mediated unfolded protein response	34.21
GO Biological Process	mRNA catabolic process	33.20
GO Biological Process	RNA catabolic process	33.01
GO Biological Process	nuclear-transcribed mRNA catabolic process	32.96
GO Biological Process	cellular response to topologically incorrect protein	32.70
GO Biological Process	cellular response to unfolded protein	30.32
GO Biological Process	response to topologically incorrect protein	28.02
GO Biological Process	regulation of intrinsic apoptotic signaling pathway	27.07
GO Biological Process	regulation of DNA-templated transcription in response to stress	26.28
GO Biological Process	response to unfolded protein	25.32
GO Biological Process	negative regulation of intrinsic apoptotic signaling pathway	23.97
GO Biological Process	liver regeneration	23.01
GO Biological Process	nuclear-transcribed mRNA catabolic process, nonsense-mediated decay	21.81
GO Biological Process	protein targeting to ER	21.68
GO Biological Process	nuclear-transcribed mRNA catabolic process, deadenylation-dependent decay	20.04
GO Biological Process	RNA phosphodiester bond hydrolysis	19.02
GO Biological Process	protein-lipid complex assembly	18.42
GO Biological Process	cotranslational protein targeting to membrane	17.94
GO Biological Process	DNA-templated transcription, elongation	17.70
Human Phenotype	Increased serum lactate	14.62
Human Phenotype	Abnormal CSF metabolite level	13.55
Human Phenotype	Exercise intolerance	13.23
Human Phenotype	Increased CSF lactate	12.89
Human Phenotype	Abnormality of transition element cation homeostasis	12.17
Human Phenotype	Increased serum ferritin	9.97
Human Phenotype	Abnormality of mitochondrial metabolism	9.51
Human Phenotype	Abnormality of the mitochondrion	8.97
Human Phenotype	Abnormality of iron homeostasis	8.85
Human Phenotype	Glycosuria	7.93
Human Phenotype	Decreased circulating low-density lipoprotein levels	6.89
Human Phenotype	Cytochrome C oxidase-negative muscle fibers	5.03

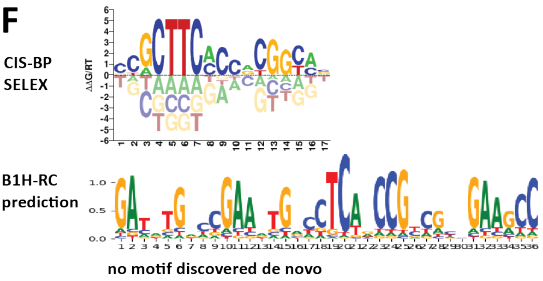

Supplementary Figure 1095: Properties and genomic distribution of motifs identified for the ZNF343 transcription factor in HepG2 (accession ENCSR938VRO).

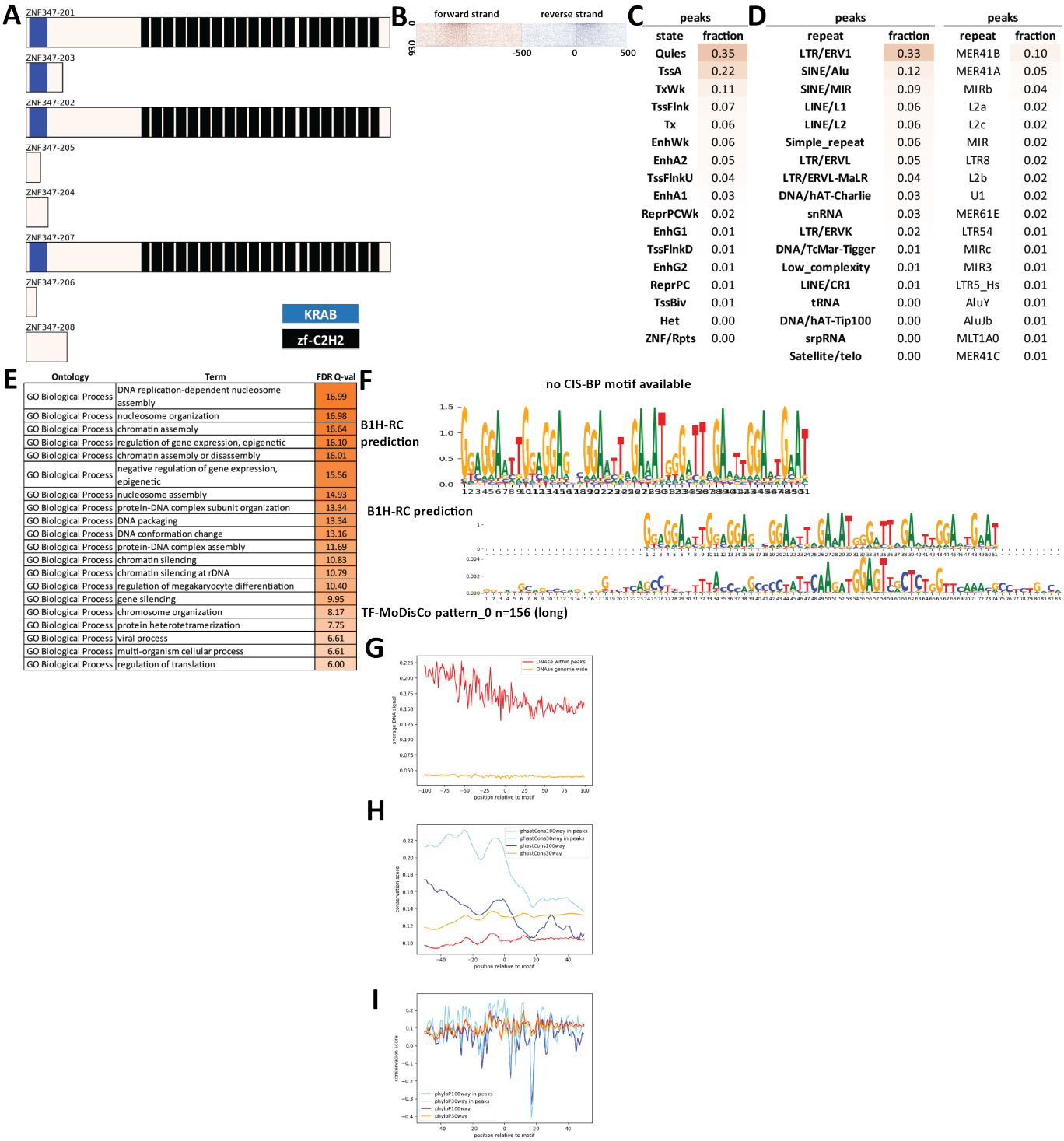

Supplementary Figure 1096: Properties and genomic distribution of motifs identified for the ZNF347 transcription factor in K562 (accession ENCSR590FLL).

TF-MoDisCO pattern_0 n=152, CWM

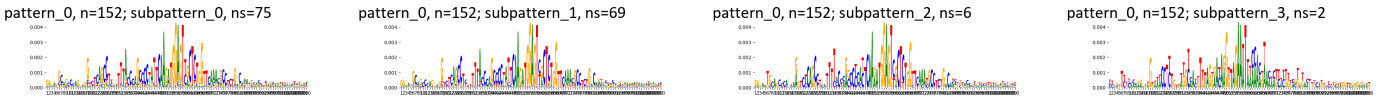

TF-MoDisCO pattern_0 n=152, PWM



Supplementary Figure 1097: TF-MoDisCO subpatterns for the ZNF347 transcription factor in K562 (accession ENCSR590FLL).

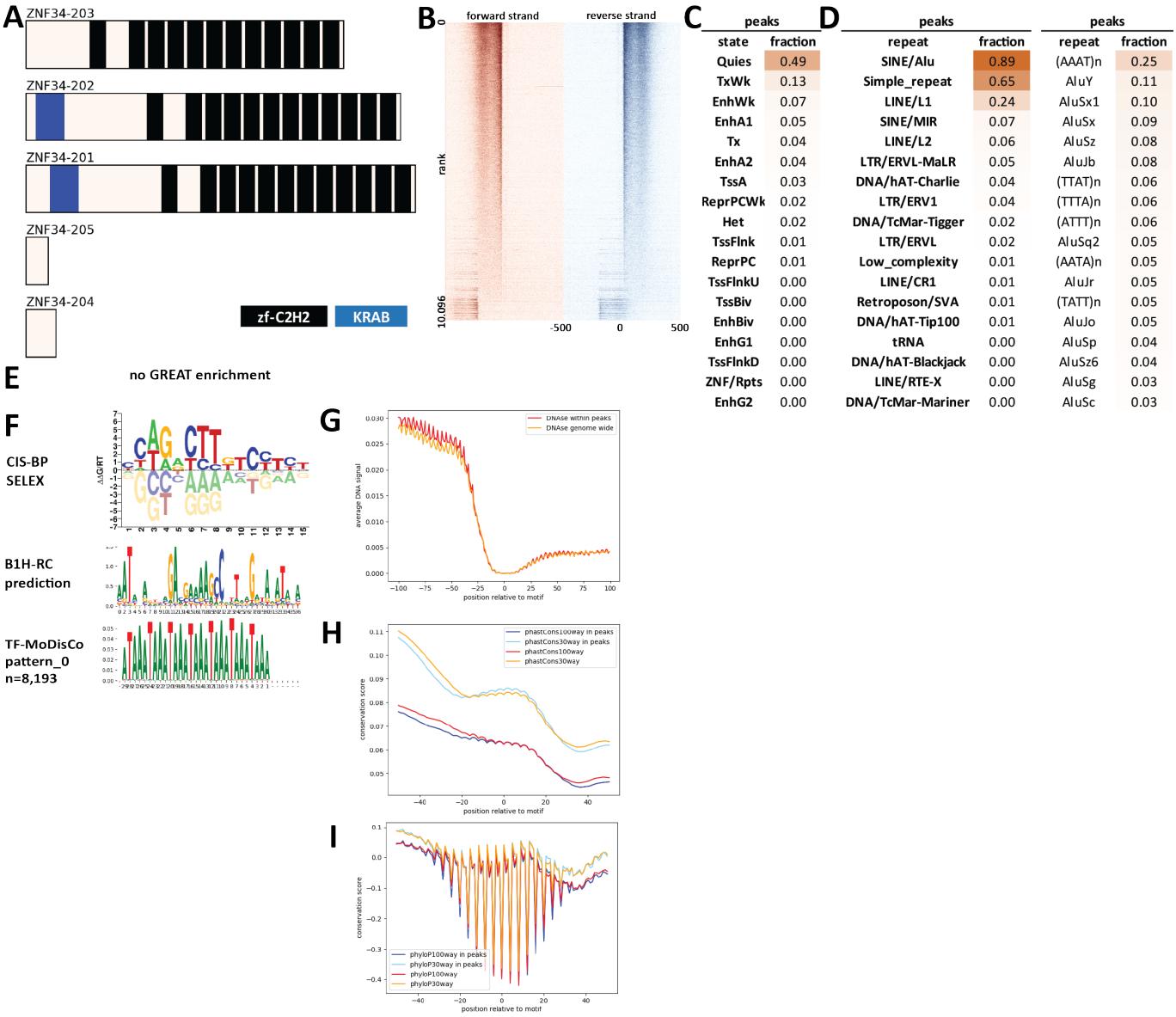

C

peaks	
state	fraction
Quies	0.49
TxWk	0.13
EnhWk	0.07
EnhA1	0.05
Tx	0.04
EnhA2	0.04
TssA	0.03
ReprPCWk	0.02
Het	0.02
TssFlnk	0.01
ReprPC	0.01
TssFlnkU	0.00
TssBiv	0.00
EnhBiv	0.00
EnhG1	0.00
TssFlnkD	0.00
ZNF/Rpts	0.00
EnhG2	0.00

D

peaks		peaks	
repeat	fraction	repeat	fraction
SINE/Alu	0.89	(AAAT)n	0.25
Simple_repeat	0.65	AluY	0.11
LINE/L1	0.24	AluSx1	0.10
SINE/MIR	0.07	AluSx	0.09
LINE/L2	0.06	AluSz	0.08
LTR/ERVL-MaLR	0.05	AluJb	0.08
DNA/hAT-Charlie	0.04	(TTAT)n	0.06
LTR/ERV1	0.04	(TTTA)n	0.06
DNA/TcMar-Tigger	0.02	(ATTT)n	0.06
LTR/ERVL	0.02	AluSq2	0.05
Low_complexity	0.01	(AATA)n	0.05
LINE/CR1	0.01	AluJr	0.05
Retroposon/SVA	0.01	(TATT)n	0.05
DNA/hAT-Tip100	0.01	AluJo	0.05
tRNA	0.00	AluSp	0.04
DNA/hAT-Blackjack	0.00	AluSz6	0.04
LINE/RTE-X	0.00	AluSg	0.03
DNA/TcMar-Mariner	0.00	AluSc	0.03

Supplementary Figure 1098: Properties and genomic distribution of motifs identified for the ZNF34 transcription factor in HEK293 (accession ENCSR727PIC).

TF-MoDisCO pattern_0 n=8193, CWM

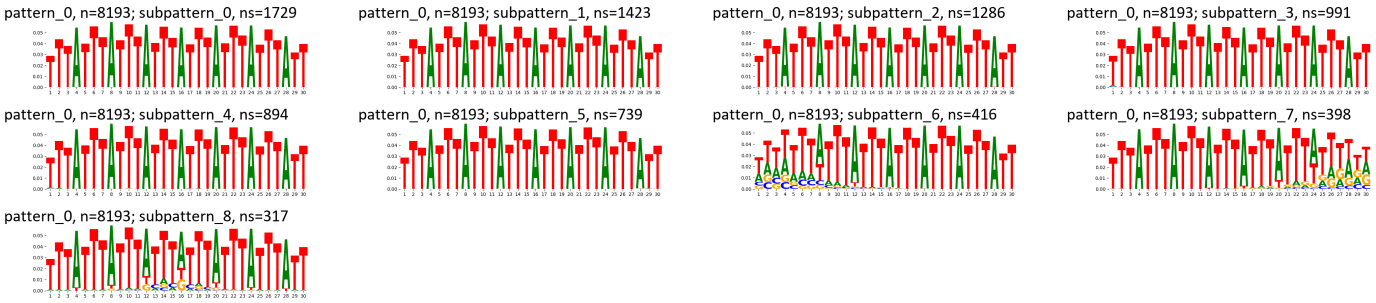

TF-MoDisCO pattern_0 n=8193, PWM

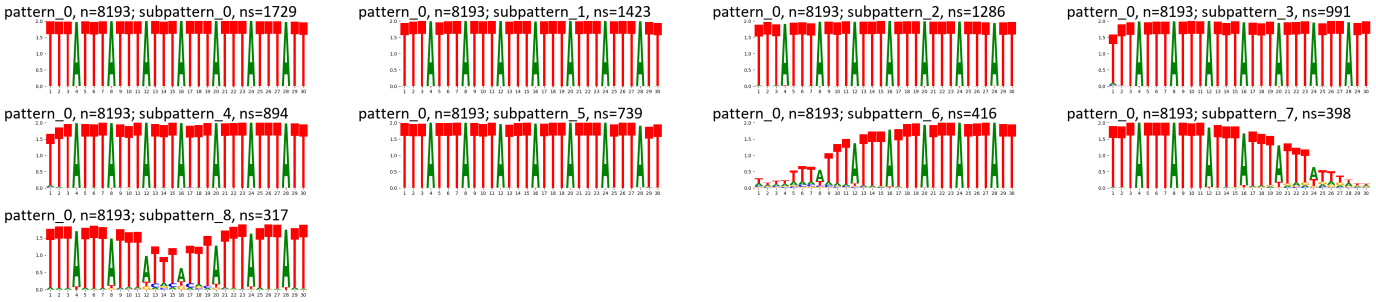

Supplementary Figure 1099: TF-MoDisCO subpatterns for the ZNF34 transcription factor in HEK293 (accession ENCSR727PIC).

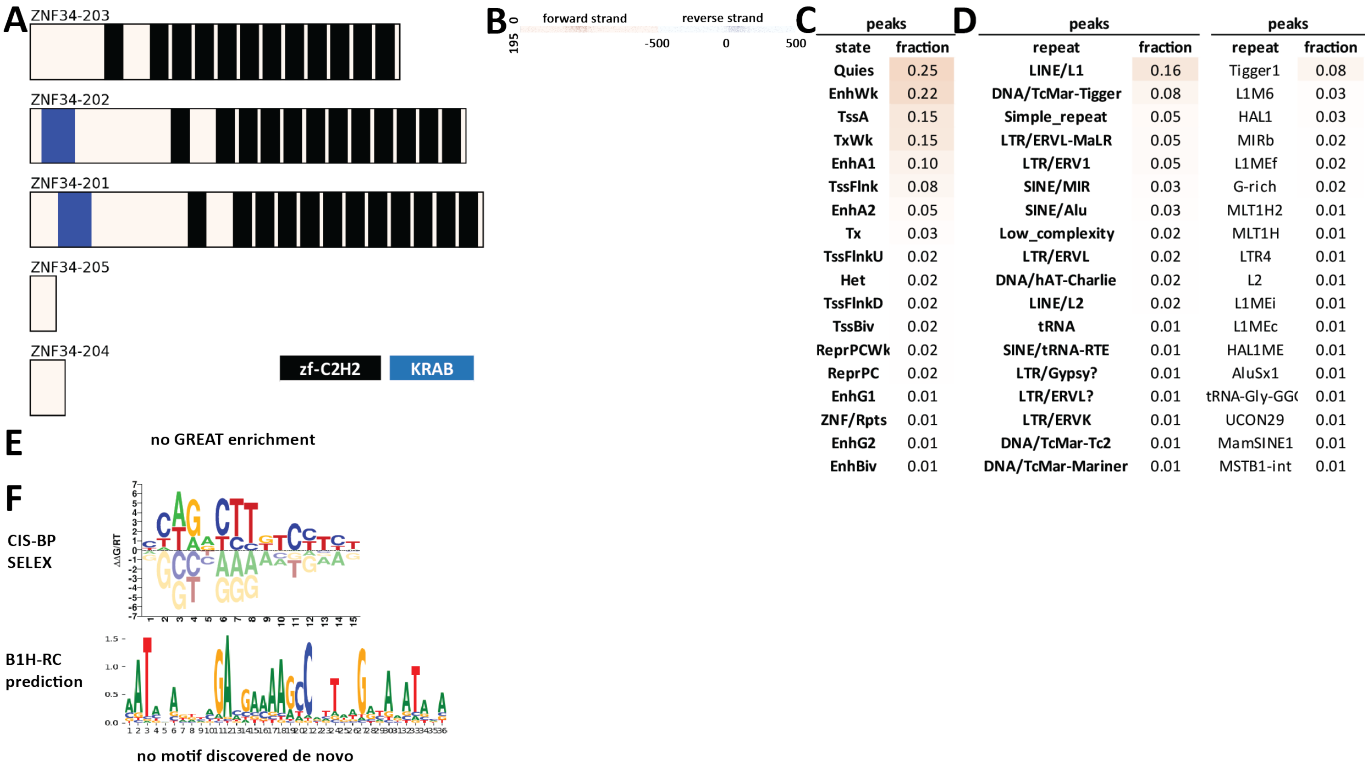

Supplementary Figure 1100: Properties and genomic distribution of motifs identified for the ZNF34 transcription factor in HEK293 (accession Hughes GR models).

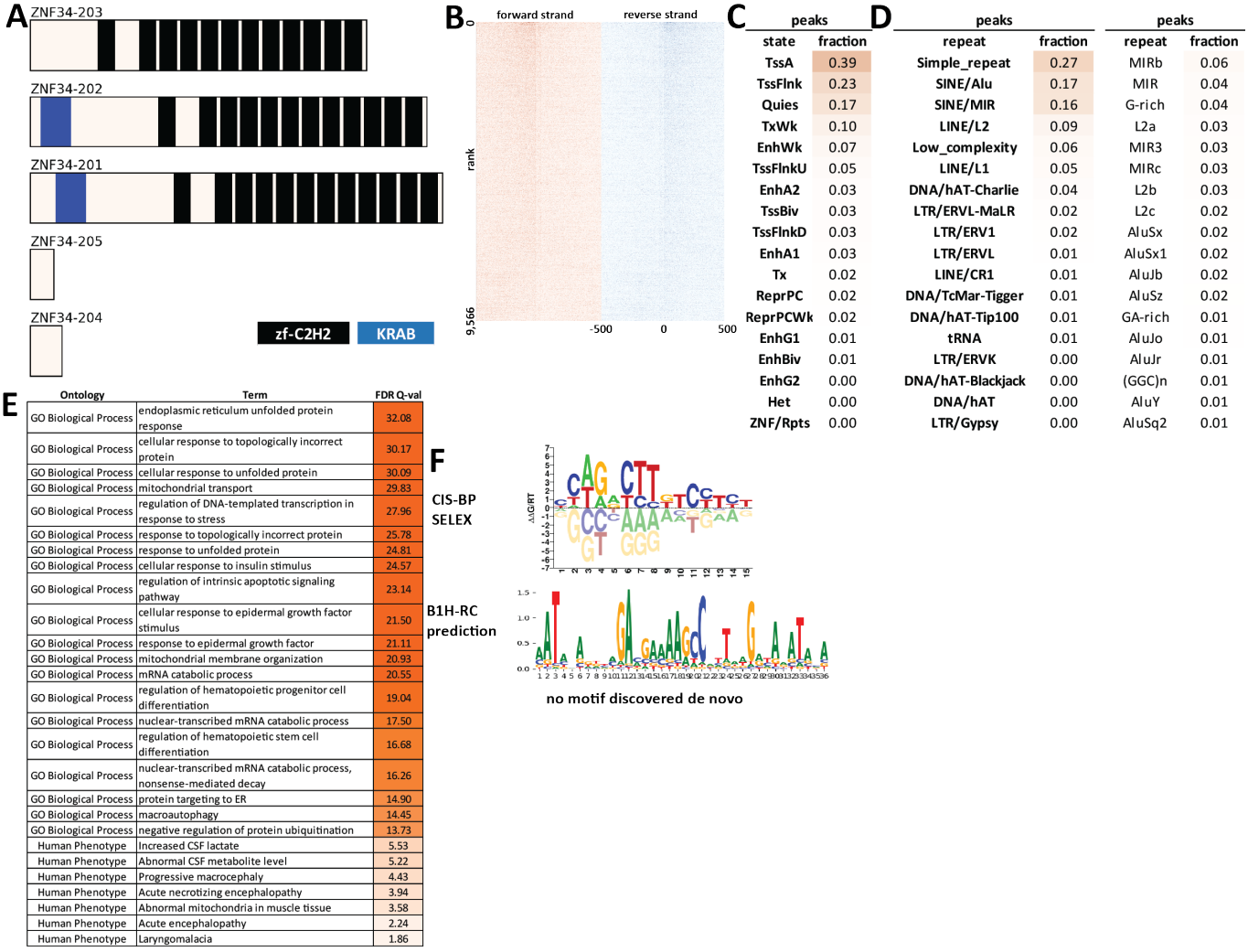

C

peaks	
state	fraction
TssA	0.39
TssFlnk	0.23
Quies	0.17
TxWk	0.10
EnhWk	0.07
TssFlnkU	0.05
EnhA2	0.03
TssBiv	0.03
TssFlnkD	0.03
EnhA1	0.03
Tx	0.02
ReprPC	0.02
ReprPCWk	0.02
EnhG1	0.01
EnhBiv	0.01
EnhG2	0.00
Het	0.00
ZNF/Rpts	0.00

D

peaks		peaks	
repeat	fraction	repeat	fraction
Simple_repeat	0.27	MIRb	0.06
SINE/Alu	0.17	MIR	0.04
SINE/MIR	0.16	G-rich	0.04
LINE/L2	0.09	L2a	0.03
Low_complexity	0.06	MIR3	0.03
LINE/L1	0.05	MIRc	0.03
DNA/hAT-Charlie	0.04	L2b	0.03
LTR/ERVL-MaLR	0.02	L2c	0.02
LTR/ERV1	0.02	AluSx	0.02
LTR/ERVL	0.01	AluSx1	0.02
LINE/CR1	0.01	AluJb	0.02
DNA/TcMar-Tigger	0.01	AluSz	0.02
DNA/hAT-Tip100	0.01	GA-rich	0.01
tRNA	0.01	AluJo	0.01
LTR/ERVK	0.00	AluJr	0.01
DNA/hAT-Blackjack	0.00	(GGC)n	0.01
DNA/hAT	0.00	AluY	0.01
LTR/Gypsy	0.00	AluSq2	0.01

E

Ontology	Term	FDR Q-val
GO Biological Process	endoplasmic reticulum unfolded protein response	32.08
GO Biological Process	cellular response to topologically incorrect protein	30.17
GO Biological Process	cellular response to unfolded protein	30.09
GO Biological Process	mitochondrial transport	29.83
GO Biological Process	regulation of DNA-templated transcription in response to stress	27.96
GO Biological Process	response to topologically incorrect protein	25.78
GO Biological Process	response to unfolded protein	24.81
GO Biological Process	cellular response to insulin stimulus	24.57
GO Biological Process	regulation of intrinsic apoptotic signaling pathway	23.14
GO Biological Process	cellular response to epidermal growth factor stimulus	21.50
GO Biological Process	response to epidermal growth factor	21.11
GO Biological Process	mitochondrial membrane organization	20.93
GO Biological Process	mRNA catabolic process	20.55
GO Biological Process	regulation of hematopoietic progenitor cell differentiation	19.04
GO Biological Process	nuclear-transcribed mRNA catabolic process	17.50
GO Biological Process	regulation of hematopoietic stem cell differentiation	16.68
GO Biological Process	nuclear-transcribed mRNA catabolic process, nonsense-mediated decay	16.26
GO Biological Process	protein targeting to ER	14.90
GO Biological Process	macroautophagy	14.45
GO Biological Process	negative regulation of protein ubiquitination	13.73
Human Phenotype	Increased CSF lactate	5.53
Human Phenotype	Abnormal CSF metabolite level	5.22
Human Phenotype	Progressive macrocephaly	4.43
Human Phenotype	Acute necrotizing encephalopathy	3.94
Human Phenotype	Abnormal mitochondria in muscle tissue	3.58
Human Phenotype	Acute encephalopathy	2.24
Human Phenotype	Laryngomalacia	1.86

Supplementary Figure 1101: Properties and genomic distribution of motifs identified for the ZNF34 transcription factor in HepG2 (accession ENCSR904JEY).

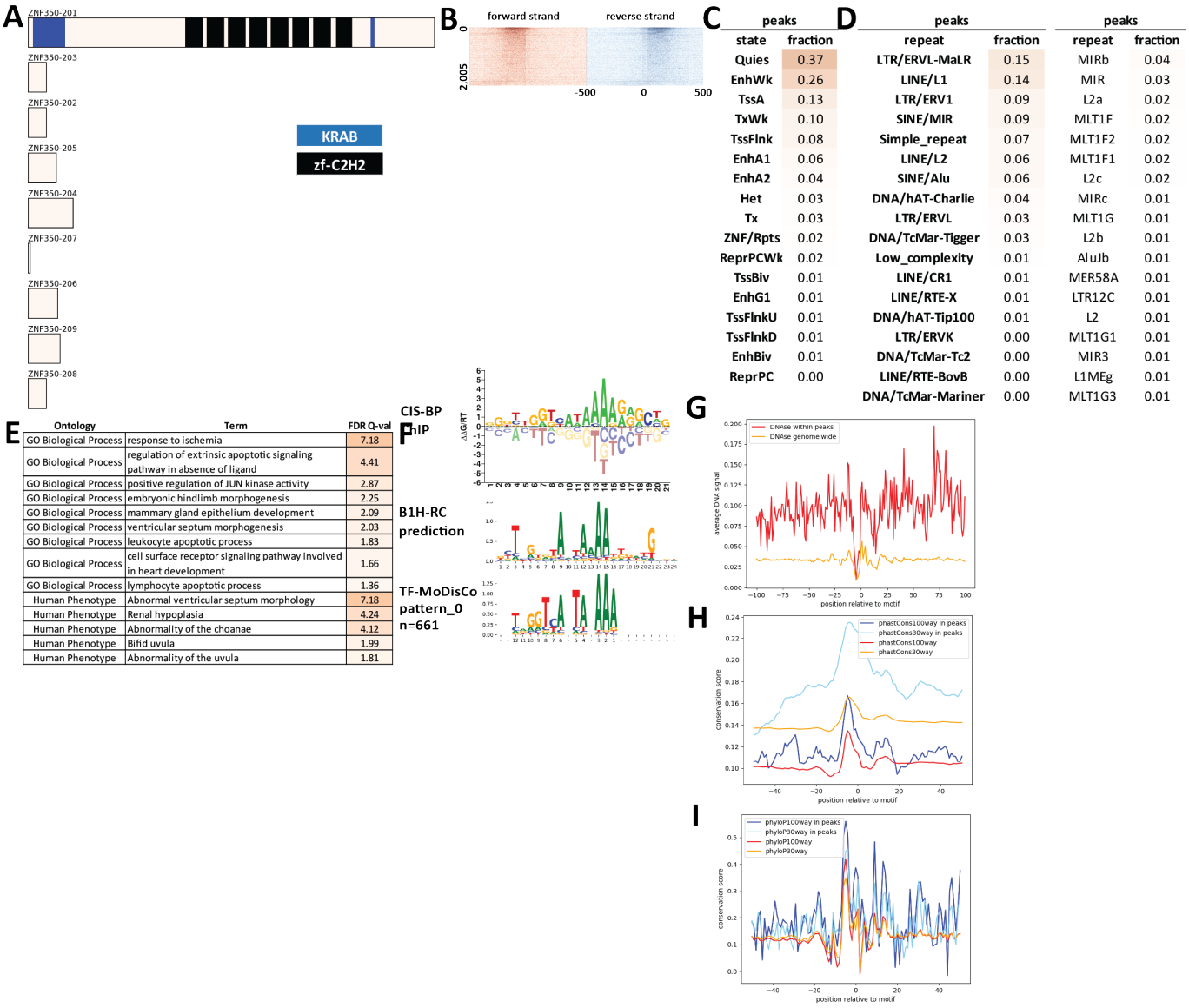

Supplementary Figure 1102: Properties and genomic distribution of motifs identified for the ZNF350 transcription factor in HEK293 (accession ENCSR854ORP).

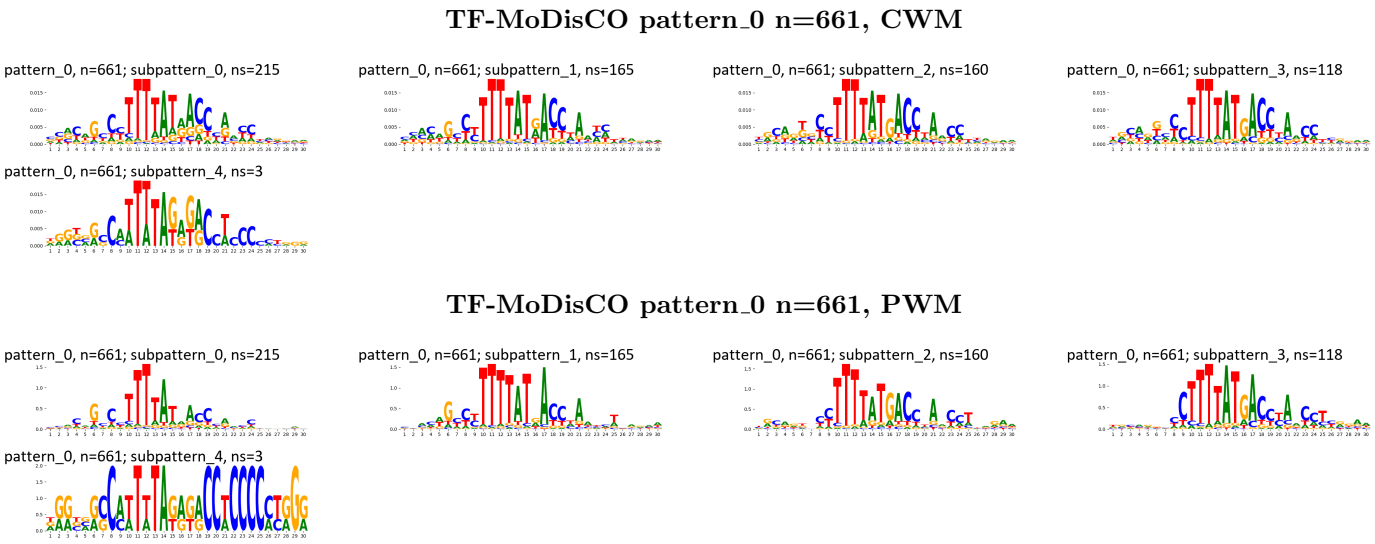

Supplementary Figure 1103: TF-MoDisCO subpatterns for the ZNF350 transcription factor in HEK293 (accession ENCSR854ORP).

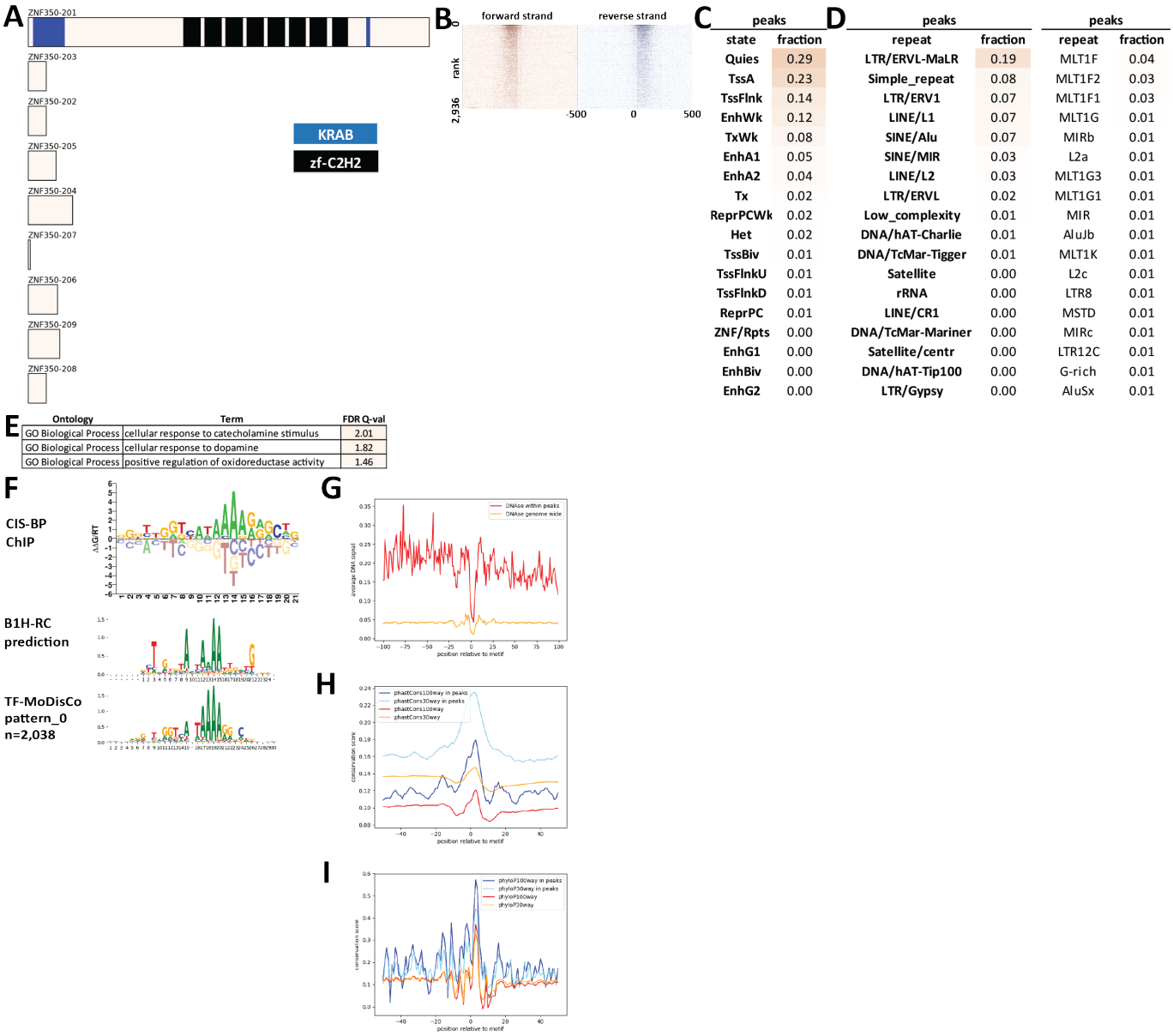

Supplementary Figure 1104: Properties and genomic distribution of motifs identified for the ZNF350 transcription factor in HEK293 (accession Hughes GR models).

TF-MoDisCO pattern_0 n=2038, CWM

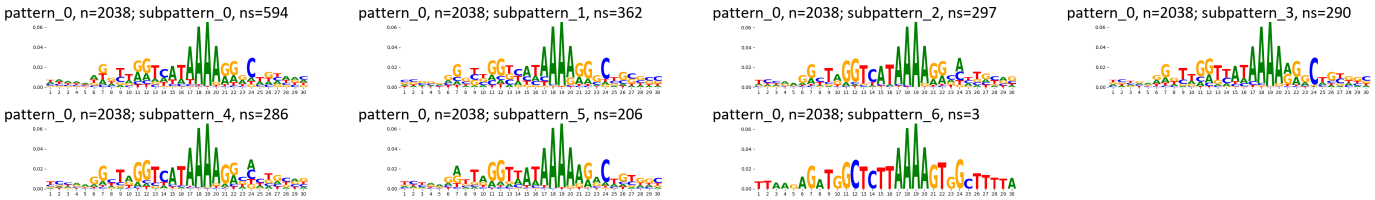

TF-MoDisCO pattern_0 n=2038, PWM

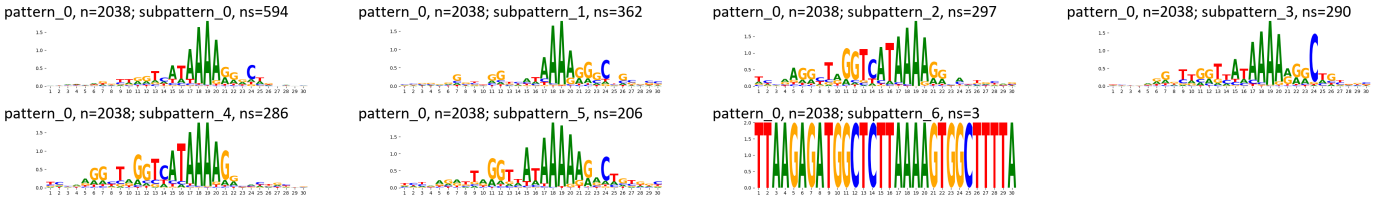

Supplementary Figure 1105: TF-MoDisCO subpatterns for the ZNF350 transcription factor in HEK293 (accession Hughes GR models).

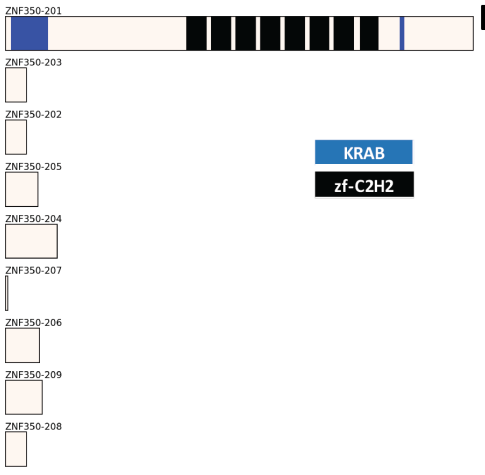

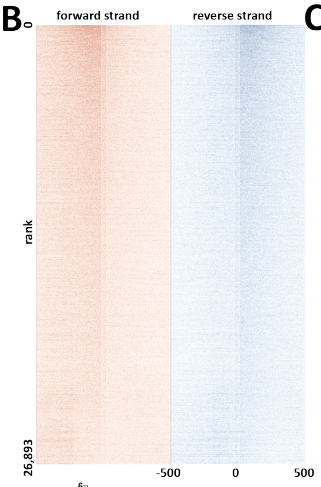

C

peaks	
state	fraction
TssA	0.29
TssFlnk	0.19
Quies	0.17
TxWk	0.10
EnhWk	0.07
TssFlnkU	0.04
EnhA2	0.03
EnhA1	0.03
Tx	0.03
TssBiv	0.03
TssFlnkD	0.02
ReprPCWk	0.02
ReprPC	0.02
EnhBiv	0.01
EnhG1	0.01
EnhG2	0.00
Het	0.00
ZNF/Rpts	0.00

D

peaks		peaks	
repeat	fraction	repeat	fraction
SINE/Alu	0.21	MIRb	0.05
Simple_repeat	0.18	MIR	0.03
SINE/MIR	0.15	L2a	0.03
LINE/L2	0.08	MIR3	0.03
LINE/L1	0.05	MIRc	0.03
Low_complexity	0.04	G-rich	0.03
DNA/hAT-Charlie	0.03	L2b	0.02
LTR/ERV1	0.02	AluSx1	0.02
LTR/ERVL-MaLR	0.02	AluJb	0.02
LTR/ERVL	0.02	AluSx	0.02
DNA/hAT-Tip100	0.01	L2c	0.02
LINE/CR1	0.01	AluSz	0.02
DNA/TcMar-Tigger	0.01	AluJr	0.02
tRNA	0.01	AluJo	0.01
LTR/ERVK	0.00	AluY	0.01
DNA/hAT-Blackjack	0.00	AluSq2	0.01
LTR/Gypsy	0.00	GA-rich	0.01
DNA/hAT	0.00	AluSp	0.01

E

Ontology	Term	FDR Q-val
GO Biological Process	regulation of transcription from RNA polymerase II promoter in response to stress	78.45
GO Biological Process	endoplasmic reticulum unfolded protein response	77.14
GO Biological Process	IRE1-mediated unfolded protein response	71.39
GO Biological Process	cellular response to topologically incorrect protein	70.53
GO Biological Process	regulation of DNA-templated transcription in response to stress	70.09
GO Biological Process	cellular response to unfolded protein	67.09
GO Biological Process	regulation of intrinsic apoptotic signaling pathway	65.35
GO Biological Process	response to topologically incorrect protein	63.53
GO Biological Process	positive regulation of transcription from RNA polymerase II promoter in response to stress	62.02
GO Biological Process	rRNA processing	61.66
GO Biological Process	rRNA metabolic process	61.60
GO Biological Process	response to unfolded protein	57.37
GO Biological Process	positive regulation of nuclease activity	52.85
GO Biological Process	nuclear-transcribed mRNA catabolic process	52.45
GO Biological Process	negative regulation of intrinsic apoptotic signaling pathway	52.35
GO Biological Process	liver regeneration	44.02
GO Biological Process	protein targeting to ER	43.37
GO Biological Process	regulation of cellular amino acid metabolic process	42.24
GO Biological Process	regulation of nuclease activity	40.55
GO Biological Process	nuclear-transcribed mRNA catabolic process, nonsense-mediated decay	39.62
Human Phenotype	Increased serum lactate	32.33
Human Phenotype	Abnormal CSF metabolite level	23.17
Human Phenotype	Abnormality of mitochondrial metabolism	20.87
Human Phenotype	Abnormality of the mitochondrion	20.61
Human Phenotype	Increased CSF lactate	19.56
Human Phenotype	Exercise intolerance	17.10
Human Phenotype	Abnormality of transition element cation homeostasis	16.34
Human Phenotype	Global brain atrophy	4.62

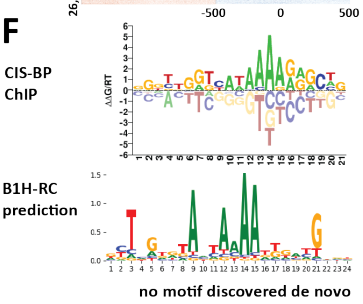

Supplementary Figure 1106: Properties and genomic distribution of motifs identified for the ZNF350 transcription factor in HepG2 (accession ENCSR842SRB).

A

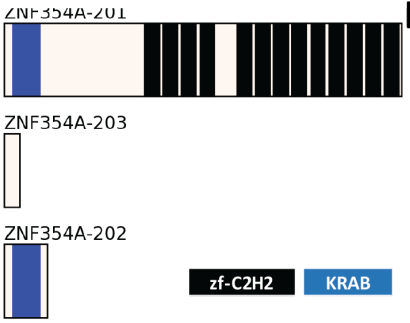

B

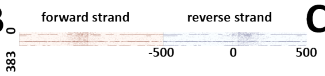

C

peaks	
state	fraction
Quies	0.37
TxWk	0.19
Het	0.15
Tx	0.11
ReprPCWk	0.06
ZNF/Rpts	0.03
EnhWk	0.03
EnhA1	0.01
TssFlnk	0.01
TssFlnkU	0.01
TssA	0.01
ReprPC	0.01
EnhBiv	0.01
TssBiv	0.00
EnhA2	0.00

D

peaks		peaks	
repeat	fraction	repeat	fraction
LINE/L1	0.86	L1MEc	0.19
SINE/Alu	0.11	L1MEf	0.08
LINE/L2	0.02	L1MDa	0.07
DNA/hAT-Charlie	0.02	L1ME1	0.06
SINE/MIR	0.01	L1M4	0.05
LTR/ERVL-MaLR	0.01	L1MEd	0.05
LTR/ERVL	0.01	L1MEg	0.04
DNA/TcMar-Tigger	0.01	L1MD1	0.03
Simple_repeat	0.01	L1MB7	0.03
LTR/ERV1	0.01	L1M4a2	0.02
rRNA	0.00	L1M4a1	0.02
LINE/RTE-X	0.00	AluSx	0.02
LINE/RTE-BovB	0.00	AluJb	0.02
LINE/CR1	0.00	L1ME3B	0.01
DNA/hAT?	0.00	L1MB3	0.01
DNA/hAT-Tip100	0.00	L1MEi	0.01
		L1ME3A	0.01
		L1ME2z	0.01

E

Ontology	Term	FDR Q-val
GO Biological Process	mitochondrial ATP synthesis coupled electron transport	7.57
GO Biological Process	ATP synthesis coupled electron transport	7.40
GO Biological Process	ATP metabolic process	7.18
GO Biological Process	oxidative phosphorylation	7.20
GO Biological Process	purine ribonucleoside monophosphate metabolic process	6.06
GO Biological Process	purine nucleoside monophosphate metabolic process	6.07
GO Biological Process	ribonucleoside monophosphate metabolic process	6.01
GO Biological Process	purine ribonucleoside triphosphate metabolic process	5.81
GO Biological Process	ribose phosphate metabolic process	5.82
GO Biological Process	nucleotide metabolic process	5.83
GO Biological Process	nucleoside phosphate metabolic process	5.78
GO Biological Process	nucleoside monophosphate metabolic process	5.71
GO Biological Process	organophosphate metabolic process	5.68
GO Biological Process	nucleobase-containing small molecule metabolic process	5.69
GO Biological Process	ribonucleoside triphosphate metabolic process	5.68
GO Biological Process	purine ribonucleoside metabolic process	5.66
GO Biological Process	purine nucleoside triphosphate metabolic process	5.63
GO Biological Process	purine nucleoside metabolic process	5.61
GO Biological Process	ribonucleoside metabolic process	5.53
GO Biological Process	purine-containing compound metabolic process	5.49
Human Phenotype	Leber optic atrophy	48.40
Human Phenotype	Central retinal vessel vascular tortuosity	48.40
Human Phenotype	Hemianopia	48.40
Human Phenotype	Stroke-like episode	27.50
Human Phenotype	Centrocecal scotoma	25.88
Human Phenotype	Optic neuropathy	24.85
Human Phenotype	Wolff-Parkinson-White syndrome	23.13
Human Phenotype	Episodic vomiting	22.02
Human Phenotype	Mitochondrial myopathy	21.18
Human Phenotype	Retinal vascular tortuosity	20.15
Human Phenotype	Ragged-red muscle fibers	20.16
Human Phenotype	Abnormal retinal artery morphology	16.55
Human Phenotype	Bilateral sensorineural hearing impairment	15.76
Human Phenotype	Arterial tortuosity	15.78
Human Phenotype	Vascular tortuosity	15.52
Human Phenotype	Abnormality of head blood vessel	15.29
Human Phenotype	Muscle abnormality related to mitochondrial dysfunction	15.25
Human Phenotype	Migraine	15.14
Human Phenotype	Scotoma	14.66
Human Phenotype	Hemiparesis	14.64

F

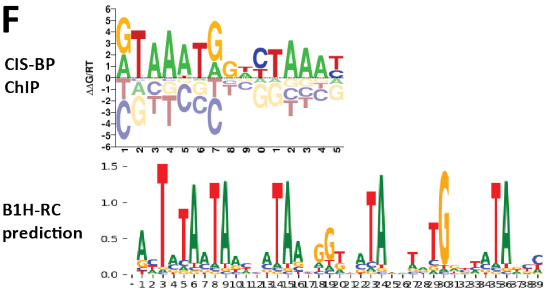

Supplementary Figure 1107: Properties and genomic distribution of motifs identified for the ZNF354A transcription factor in HEK293 (accession Hughes GR models).

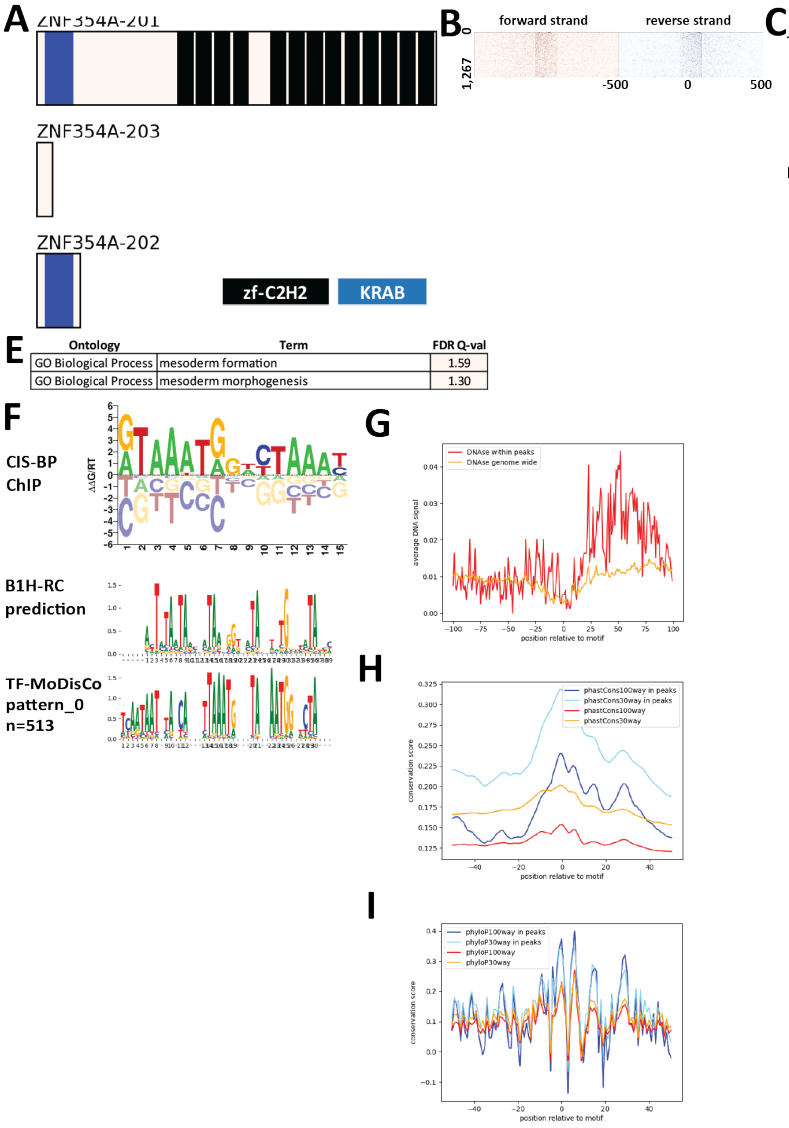

C

peaks	
state	fraction
Quies	0.50
TxWk	0.14
Het	0.09
Tx	0.07
ReprPCWk	0.04
EnhWk	0.04
TssA	0.03
EnhA2	0.02
TssFlnk	0.02
ZNF/Rpts	0.02
EnhA1	0.01
ReprPC	0.01
TssBiv	0.01
EnhG1	0.00
TssFlnkD	0.00
TssFlnkU	0.00
EnhBiv	0.00

D

peaks		peaks	
repeat	fraction	repeat	fraction
LINE/L1	0.87	L1MEc	0.13
SINE/Alu	0.27	L1MEf	0.08
Simple_repeat	0.10	L1MDa	0.04
SINE/MIR	0.04	L1MEd	0.04
LINE/L2	0.04	L1ME1	0.04
LTR/ERVL-MaLR	0.03	L1M4	0.04
DNA/hAT-Charlie	0.03	AluJb	0.04
LTR/ERV1	0.03	L1MD1	0.03
LTR/ERVL	0.03	L1MEg	0.03
DNA/TcMar-Tigger	0.03	L1MB7	0.03
Satellite	0.01	AluJr	0.02
snRNA	0.01	AluJo	0.02
Low_complexity	0.01	AluSx1	0.02
Satellite/centr	0.01	AluY	0.02
Satellite/acro	0.00	AluSz	0.02
DNA/hAT-Tip100	0.00	AluSx	0.02
DNA/TcMar-Mariner	0.00	MIRb	0.02
DNA/PiggyBac	0.00	L1ME2	0.02

Supplementary Figure 1108: Properties and genomic distribution of motifs identified for the ZNF354A transcription factor in HEK293 (accession ChipExo models).

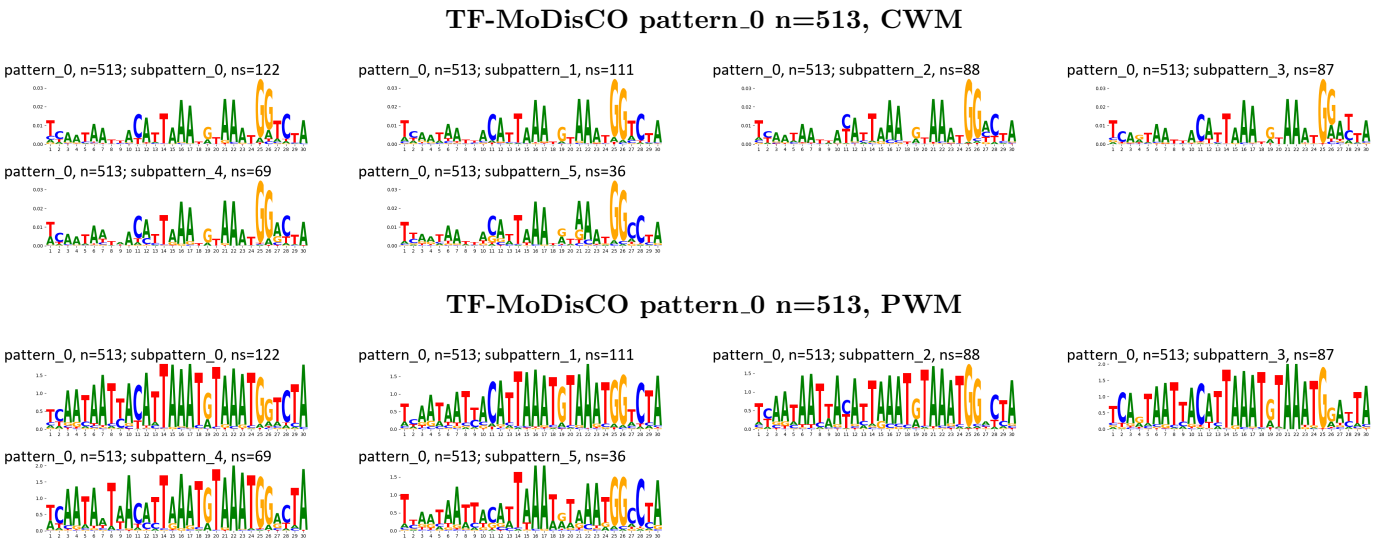

Supplementary Figure 1109: TF-MoDisCO subpatterns for the ZNF354A transcription factor in HEK293 (accession ChipExo models).

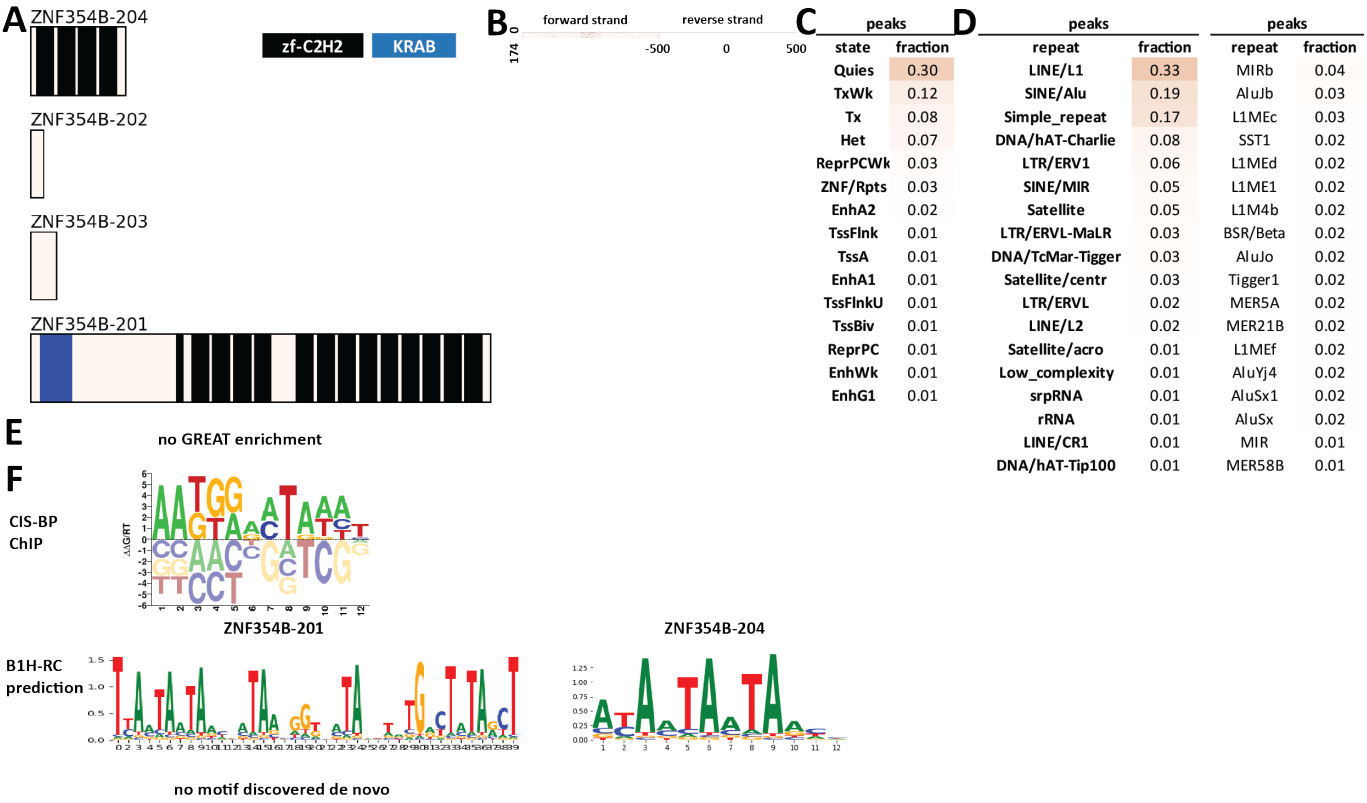

Supplementary Figure 1110: Properties and genomic distribution of motifs identified for the ZNF354B transcription factor in HEK293 (accession ChipExo models).

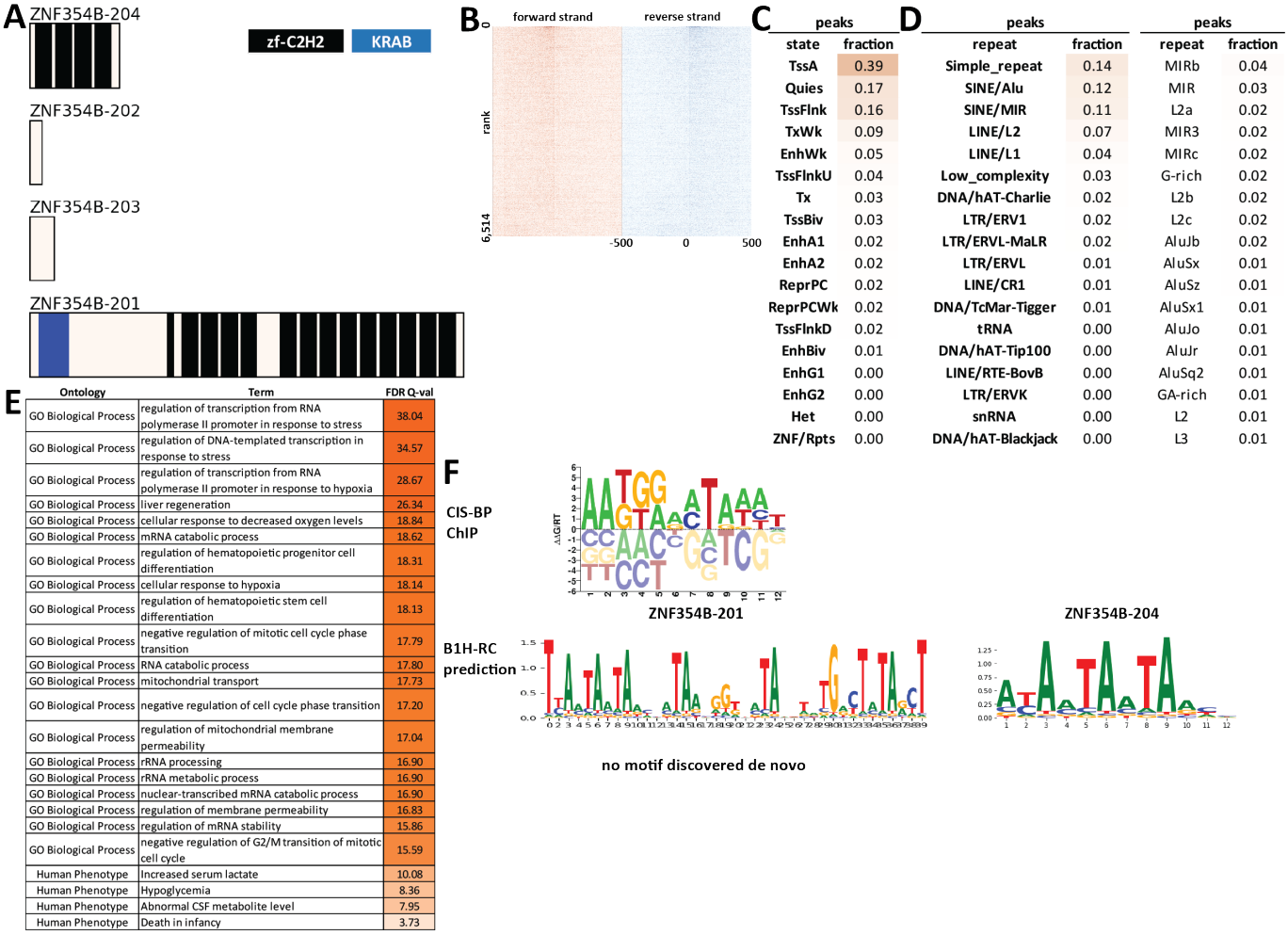

Supplementary Figure 1111: Properties and genomic distribution of motifs identified for the ZNF354B transcription factor in HepG2 (accession ENCSR124QQJ).

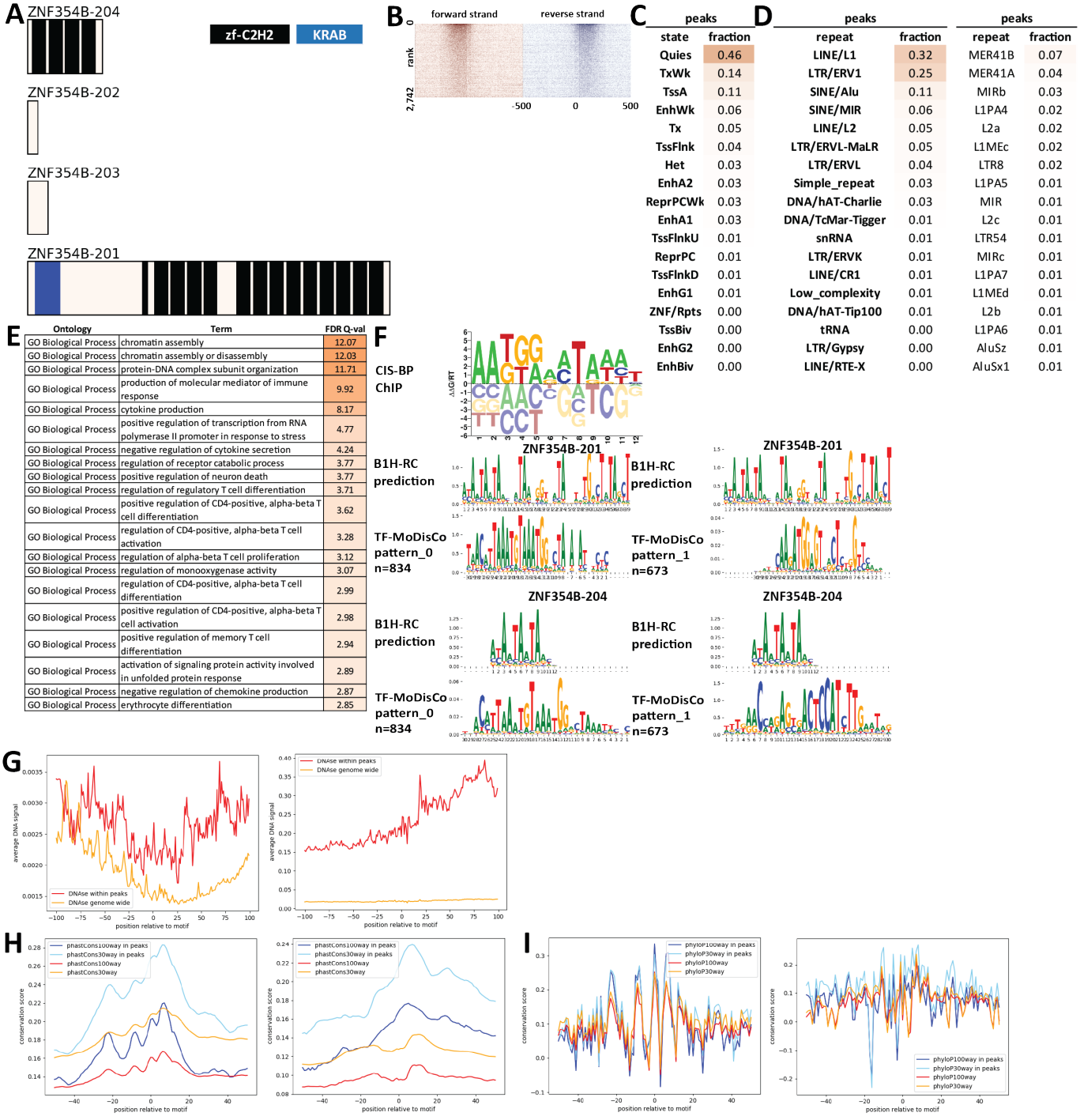

C

peaks	
state	fraction
Quies	0.46
TxWk	0.14
TssA	0.11
EnhWk	0.06
Tx	0.05
TssFlnk	0.04
Het	0.03
EnhA2	0.03
ReprPCWk	0.03
EnhA1	0.03
TssFlnkU	0.01
ReprPC	0.01
TssFlnkD	0.01
EnhG1	0.01
ZNF/Rpts	0.00
TssBiv	0.00
EnhG2	0.00
EnhBiv	0.00

D

peaks		peaks	
repeat	fraction	repeat	fraction
LINE/L1	0.32	MER41B	0.07
LTR/ERV1	0.25	MER41A	0.04
SINE/Alu	0.11	MIRb	0.03
SINE/MIR	0.06	L1PA4	0.02
LINE/L2	0.05	L2a	0.02
LTR/ERVL-MaLR	0.05	L1MEc	0.02
LTR/ERVL	0.04	LTR8	0.02
Simple_repeat	0.03	L1PA5	0.01
DNA/hAT-Charlie	0.03	MIR	0.01
DNA/TcMar-Tigger	0.01	L2c	0.01
snRNA	0.01	LTR54	0.01
LTR/ERVK	0.01	MIRc	0.01
LINE/CR1	0.01	L1PA7	0.01
Low_complexity	0.01	L1MEd	0.01
DNA/hAT-Tip100	0.01	L2b	0.01
tRNA	0.00	L1PA6	0.01
LTR/Gypsy	0.00	AluSz	0.01
LINE/RTE-X	0.00	AluSx1	0.01

E

Ontology	Term	FDR Q-val
GO Biological Process	chromatin assembly	12.07
GO Biological Process	chromatin assembly or disassembly	12.03
GO Biological Process	protein-DNA complex subunit organization	11.71
GO Biological Process	production of molecular mediator of immune response	9.92
GO Biological Process	cytokine production	8.17
GO Biological Process	positive regulation of transcription from RNA polymerase II promoter in response to stress	4.77
GO Biological Process	negative regulation of cytokine secretion	4.24
GO Biological Process	regulation of receptor catabolic process	3.77
GO Biological Process	positive regulation of neuron death	3.77
GO Biological Process	regulation of regulatory T cell differentiation	3.71
GO Biological Process	positive regulation of CD4-positive, alpha-beta T cell differentiation	3.62
GO Biological Process	regulation of CD4-positive, alpha-beta T cell activation	3.28
GO Biological Process	regulation of alpha-beta T cell proliferation	3.12
GO Biological Process	regulation of monooxygenase activity	3.07
GO Biological Process	regulation of CD4-positive, alpha-beta T cell differentiation	2.99
GO Biological Process	positive regulation of CD4-positive, alpha-beta T cell activation	2.98
GO Biological Process	positive regulation of memory T cell differentiation	2.94
GO Biological Process	activation of signaling protein activity involved in unfolded protein response	2.89
GO Biological Process	negative regulation of chemokine production	2.87
GO Biological Process	erythrocyte differentiation	2.85

Supplementary Figure 1112: Properties and genomic distribution of motifs identified for the ZNF354B transcription factor in K562 (accession ENCSR044IXA).

TF-MoDisCO pattern_0 n=834, CWM

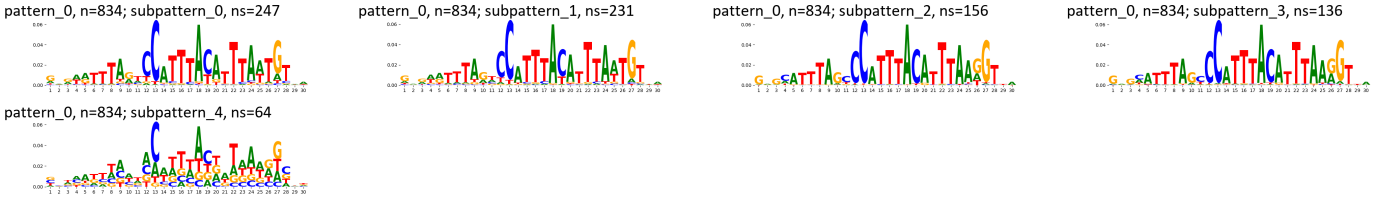

TF-MoDisCO pattern_0 n=834, PWM

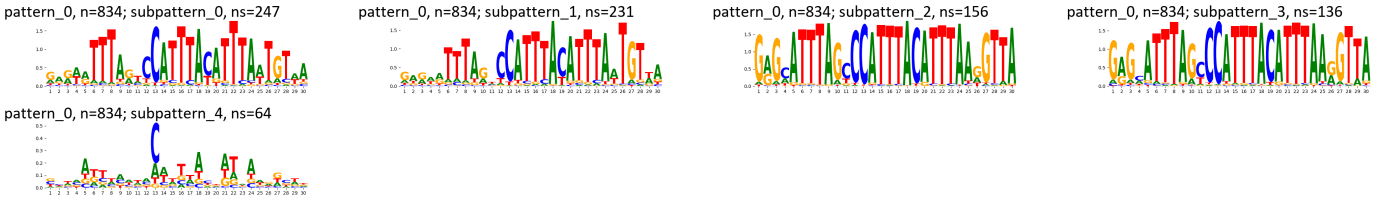

TF-MoDisCO pattern_1 n=673, CWM

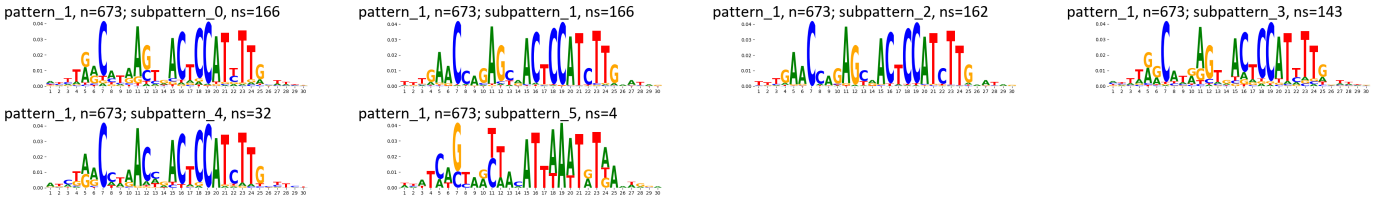

TF-MoDisCO pattern_1 n=673, PWM

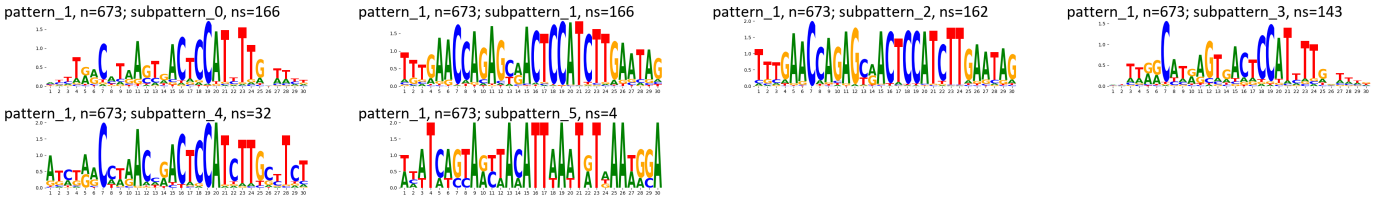

Supplementary Figure 1113: TF-MoDisCO subpatterns for the ZNF354B transcription factor in K562 (accession ENCSR044IXA).

A

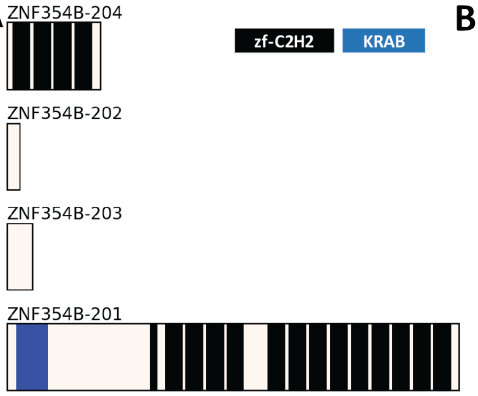

B

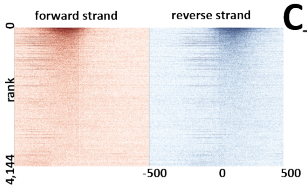

C

peaks	
state	fraction
Quies	0.38
TxWk	0.13
TssA	0.11
TssFlnk	0.06
EnhWk	0.06
Tx	0.03
EnhA2	0.03
EnhA1	0.02
ReprPCWk	0.02
TssFlnkU	0.01
ReprPC	0.01
TssFlnkD	0.01
TssBiv	0.01
Het	0.01
EnhG1	0.00
EnhBiv	0.00
ZNF/Rpts	0.00
EnhG2	0.00

D

peaks		peaks	
repeat	fraction	repeat	fraction
LTR/ERV1	0.26	MER41B	0.07
SINE/Alu	0.20	MIRb	0.05
LINE/L1	0.13	MER41A	0.04
Simple_repeat	0.12	L2a	0.03
LTR/ERVL-MaLR	0.11	MIR	0.02
SINE/MIR	0.11	AluJb	0.02
LINE/L2	0.08	AluSx	0.02
DNA/hAT-Charlie	0.05	LTR8	0.02
LTR/ERVL	0.05	MIRc	0.02
DNA/TcMar-Tigger	0.03	AluSx1	0.02
Low_complexity	0.02	L2c	0.02
LTR/ERVK	0.01	L2b	0.02
LINE/CR1	0.01	MIR3	0.02
DNA/hAT-Tip100	0.01	AluY	0.02
DNA/TcMar-Mariner	0.00	AluSz	0.02
Retroposon/SVA	0.00	MLT1J	0.02
LTR/Gypsy	0.00	G-rich	0.01
DNA/hAT-Blackjack	0.00	AluJr	0.01

E

Ontology	Term	FDR Q-val
GO Biological Process	production of molecular mediator of immune response	24.14
GO Biological Process	leukocyte migration	18.07
GO Biological Process	cellular response to leukemia inhibitory factor	8.84
GO Biological Process	bud elongation involved in lung branching	6.80
GO Biological Process	pH reduction	6.69
GO Biological Process	positive regulation of CD4-positive, alpha-beta T cell activation	5.63
GO Biological Process	cellular response to topologically incorrect protein	5.04
GO Biological Process	endoplasmic reticulum unfolded protein response	4.94
GO Biological Process	regulation of CD4-positive, alpha-beta T cell activation	4.73
GO Biological Process	positive regulation of adaptive immune response	4.53
GO Biological Process	cytokine production involved in immune response	4.50
GO Biological Process	positive regulation of adaptive immune response based on somatic recombination of immune receptors built from immunoglobulin superfamily domains	4.20
GO Biological Process	JAK-STAT cascade	3.91
GO Biological Process	iron ion transport	3.59
GO Biological Process	lysosome organization	3.54
GO Biological Process	CD4-positive, alpha-beta T cell cytokine production	3.48
GO Biological Process	cellular response to increased oxygen levels	3.35
GO Biological Process	branch elongation of an epithelium	2.98
GO Biological Process	regulation of platelet-derived growth factor receptor signaling pathway	2.27
GO Biological Process	positive regulation of osteoclast differentiation	2.12

F

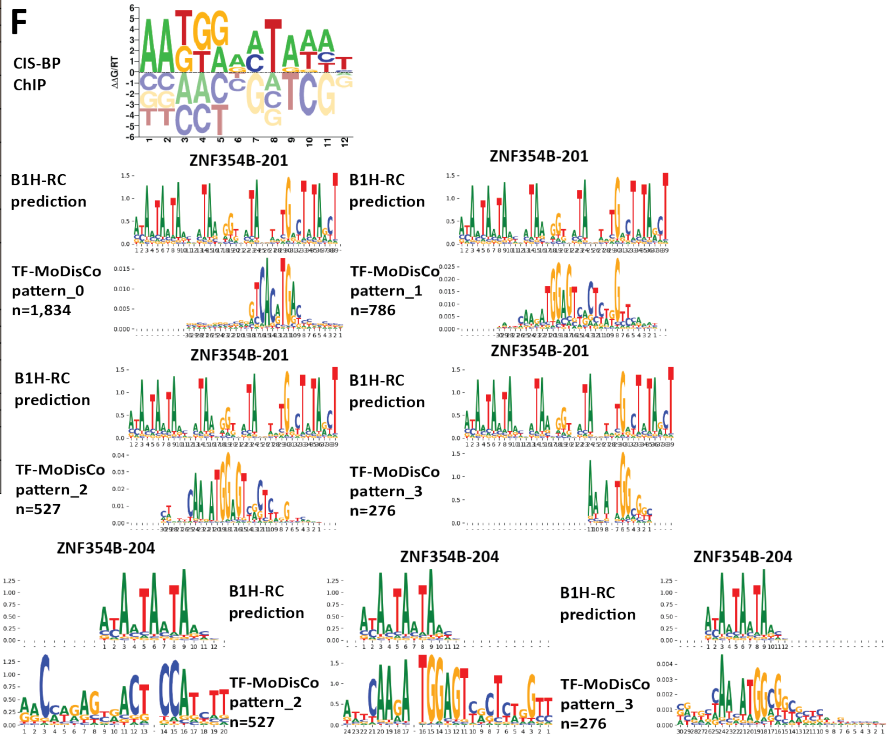

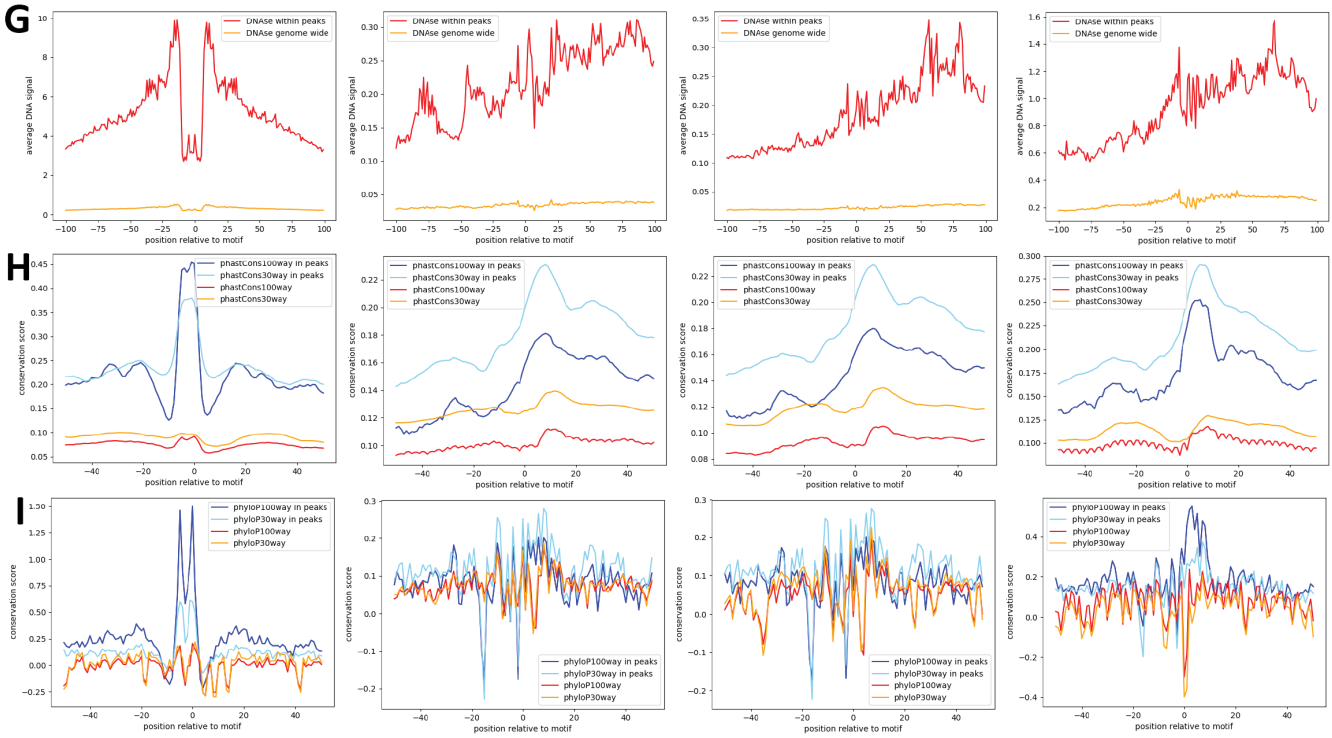

Supplementary Figure 1114: Properties and genomic distribution of motifs identified for the ZNF354B transcription factor in K562 (accession ENCSR674SCQ).

TF-MoDisCO pattern_0 n=1834, CWM

pattern_0, n=1834; subpattern_0, ns=439

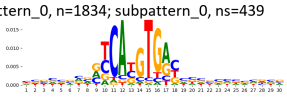

pattern_0, n=1834; subpattern_1, ns=434

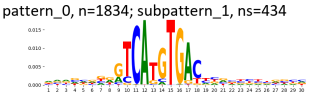

pattern_0, n=1834; subpattern_10, ns=11

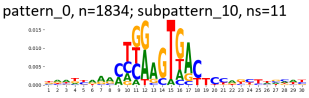

pattern_0, n=1834; subpattern_11, ns=10

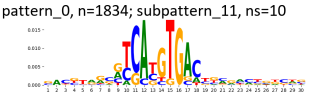

pattern_0, n=1834; subpattern_2, ns=351

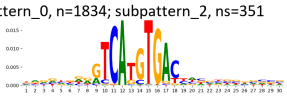

pattern_0, n=1834; subpattern_3, ns=268

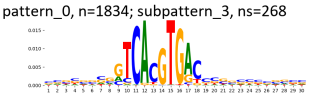

pattern_0, n=1834; subpattern_4, ns=187

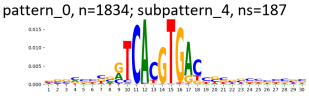

pattern_0, n=1834; subpattern_5, ns=42

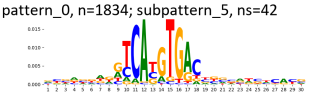

pattern_0, n=1834; subpattern_6, ns=32

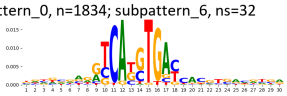

pattern_0, n=1834; subpattern_7, ns=27

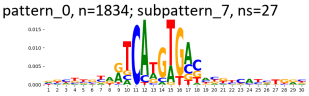

pattern_0, n=1834; subpattern_8, ns=19

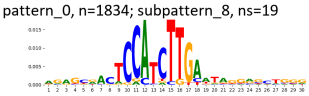

pattern_0, n=1834; subpattern_9, ns=14

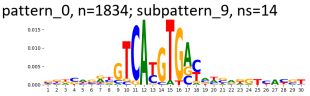

TF-MoDisCO pattern_0 n=1834, PWM

pattern_0, n=1834; subpattern_0, ns=439

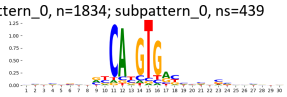

pattern_0, n=1834; subpattern_1, ns=434

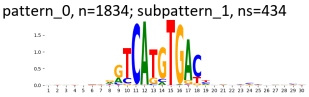

pattern_0, n=1834; subpattern_10, ns=11

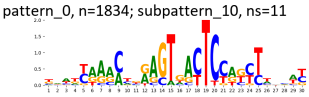

pattern_0, n=1834; subpattern_11, ns=10

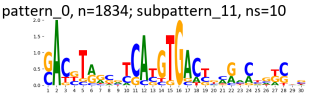

pattern_0, n=1834; subpattern_2, ns=351

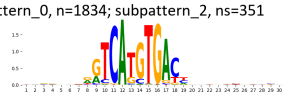

pattern_0, n=1834; subpattern_3, ns=268

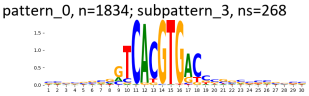

pattern_0, n=1834; subpattern_4, ns=187

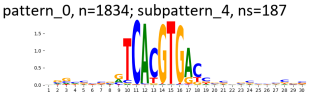

pattern_0, n=1834; subpattern_5, ns=42

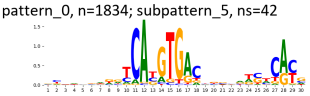

pattern_0, n=1834; subpattern_6, ns=32

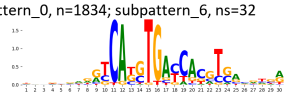

pattern_0, n=1834; subpattern_7, ns=27

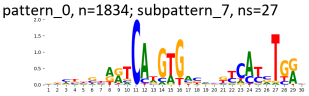

pattern_0, n=1834; subpattern_8, ns=19

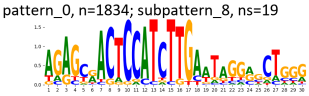

pattern_0, n=1834; subpattern_9, ns=14

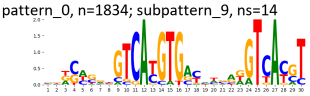

TF-MoDisCO pattern_1 n=786, CWM

pattern_1, n=786; subpattern_0, ns=204

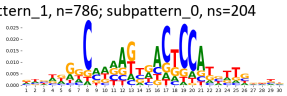

pattern_1, n=786; subpattern_1, ns=151

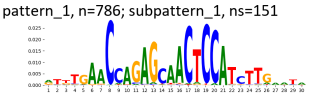

pattern_1, n=786; subpattern_2, ns=122

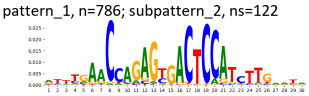

pattern_1, n=786; subpattern_3, ns=89

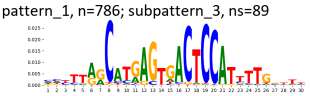

pattern_1, n=786; subpattern_4, ns=84

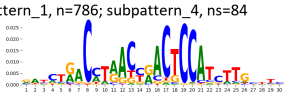

pattern_1, n=786; subpattern_5, ns=84

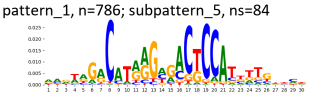

pattern_1, n=786; subpattern_6, ns=32

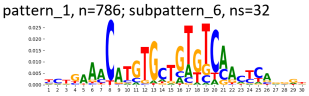

pattern_1, n=786; subpattern_7, ns=20

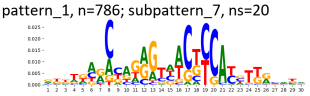

TF-MoDisCO pattern_1 n=786, PWM

pattern_1, n=786; subpattern_0, ns=204

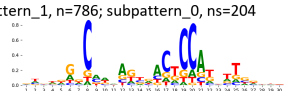

pattern_1, n=786; subpattern_1, ns=151

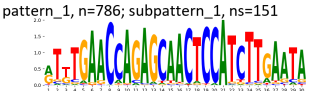

pattern_1, n=786; subpattern_2, ns=122

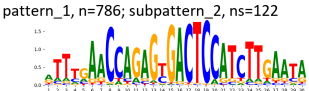

pattern_1, n=786; subpattern_3, ns=89

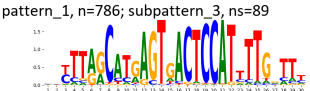

pattern_1, n=786; subpattern_4, ns=84

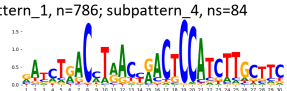

pattern_1, n=786; subpattern_5, ns=84

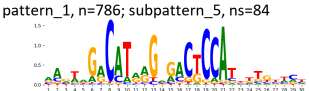

pattern_1, n=786; subpattern_6, ns=32

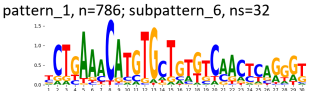

pattern_1, n=786; subpattern_7, ns=20

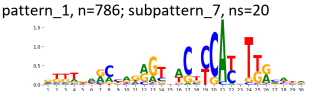

TF-MoDisCO pattern_2 n=527, CWM

pattern_2, n=527; subpattern_0, ns=182

pattern_2, n=527; subpattern_1, ns=132

pattern_2, n=527; subpattern_2, ns=88

pattern_2, n=527; subpattern_3, ns=71

pattern_2, n=527; subpattern_4, ns=28

pattern_2, n=527; subpattern_5, ns=23

pattern_2, n=527; subpattern_6, ns=3

TF-MoDisCO pattern_2 n=527, PWM

pattern_2, n=527; subpattern_0, ns=182

pattern_2, n=527; subpattern_1, ns=132

pattern_2, n=527; subpattern_2, ns=88

pattern_2, n=527; subpattern_3, ns=71

pattern_2, n=527; subpattern_4, ns=28

pattern_2, n=527; subpattern_5, ns=23

pattern_2, n=527; subpattern_6, ns=3

TF-MoDisCO pattern_3 n=276, CWM

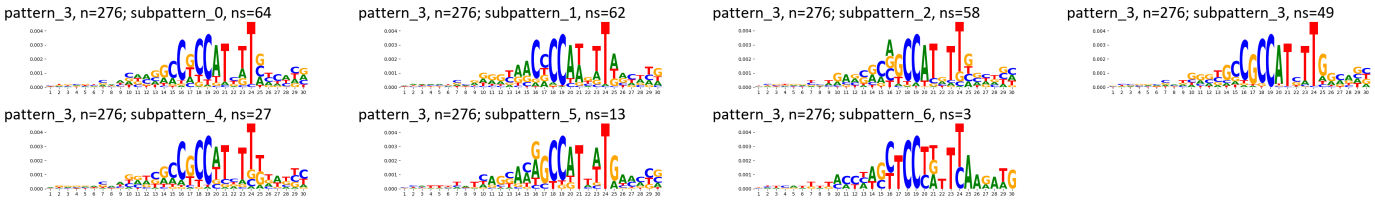

TF-MoDisCO pattern_3 n=276, PWM

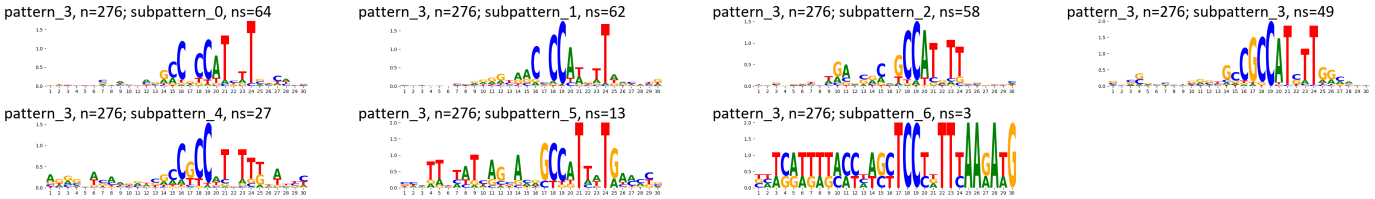

Supplementary Figure 1115: TF-MoDisCO subpatterns for the ZNF354B transcription factor in K562 (accession ENCSR674SCQ).

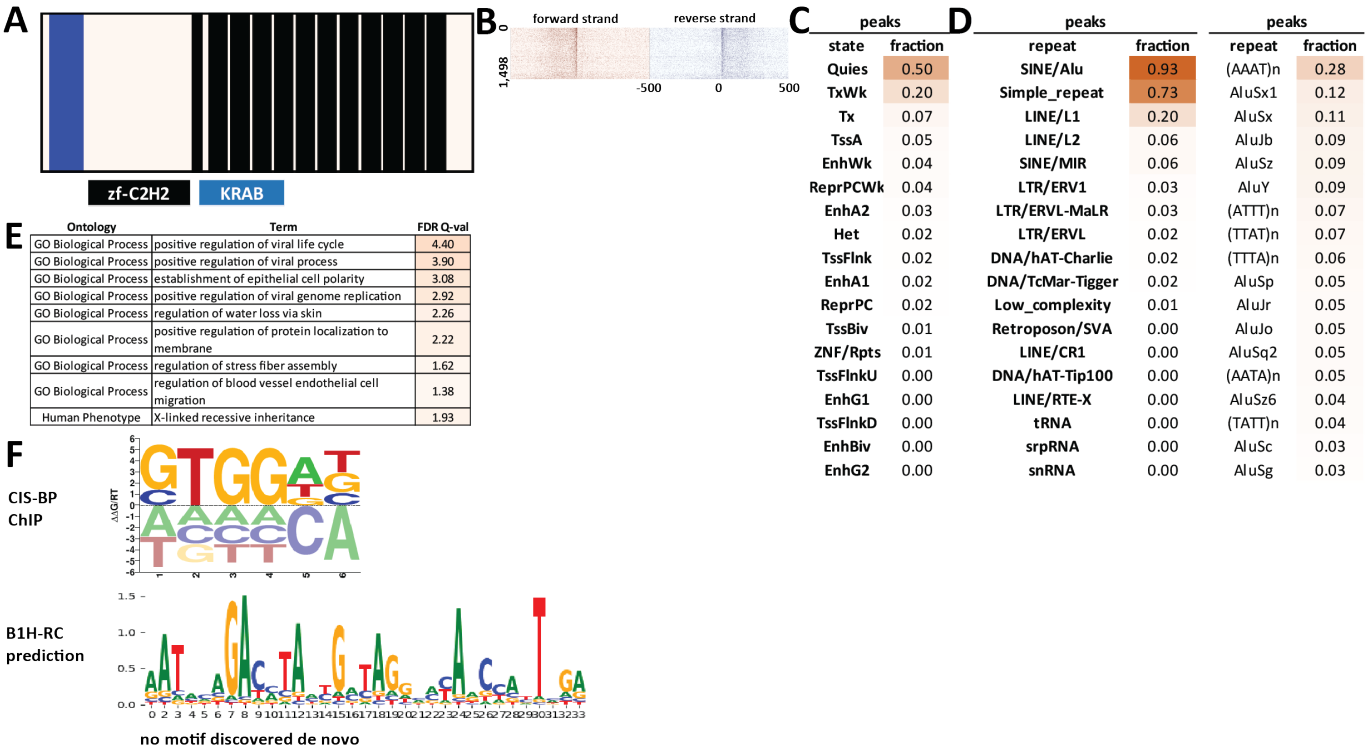

Supplementary Figure 1116: Properties and genomic distribution of motifs identified for the ZNF354C transcription factor in HEK293 (accession ENCSR289NSN).

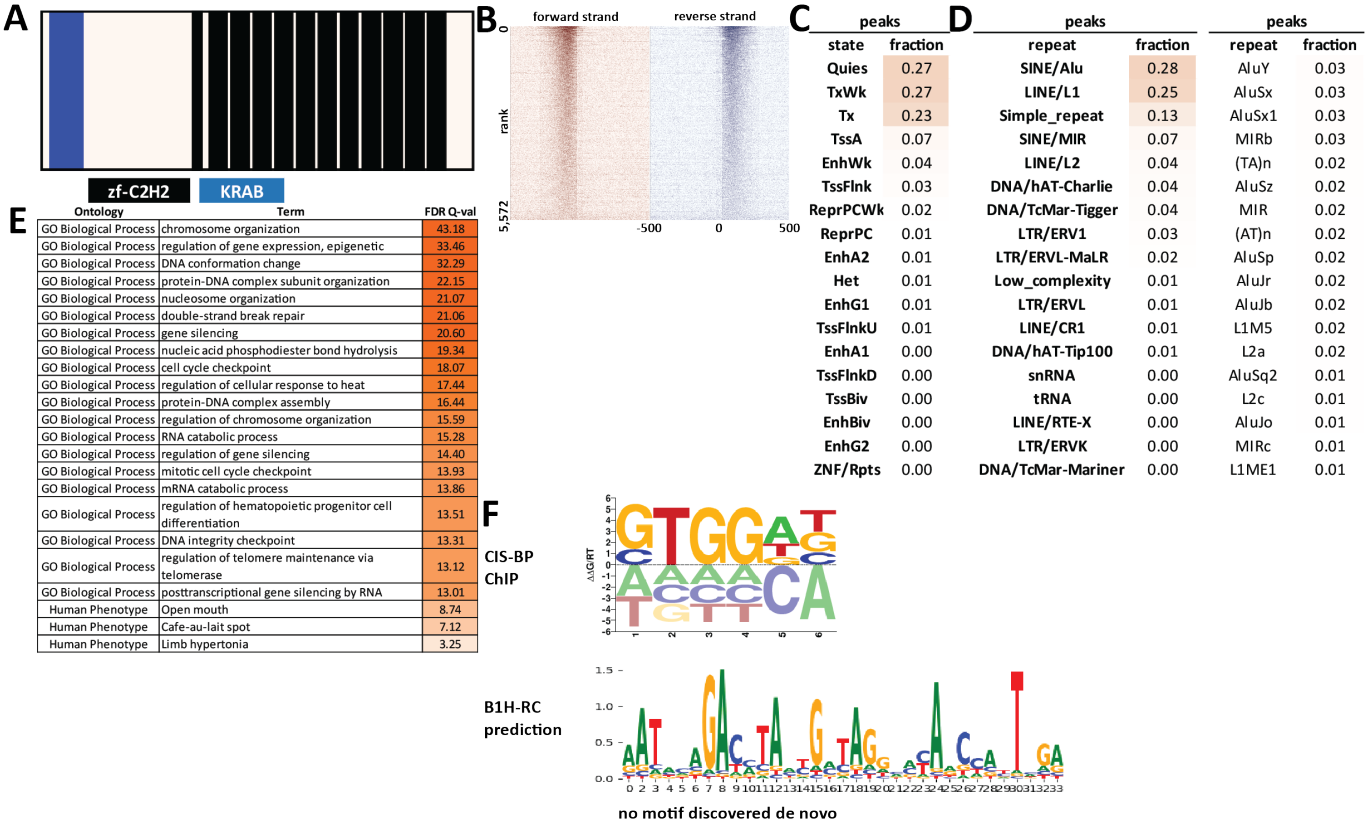

Supplementary Figure 1117: Properties and genomic distribution of motifs identified for the ZNF354C transcription factor in K562 (accession ENCSR506SSQ).

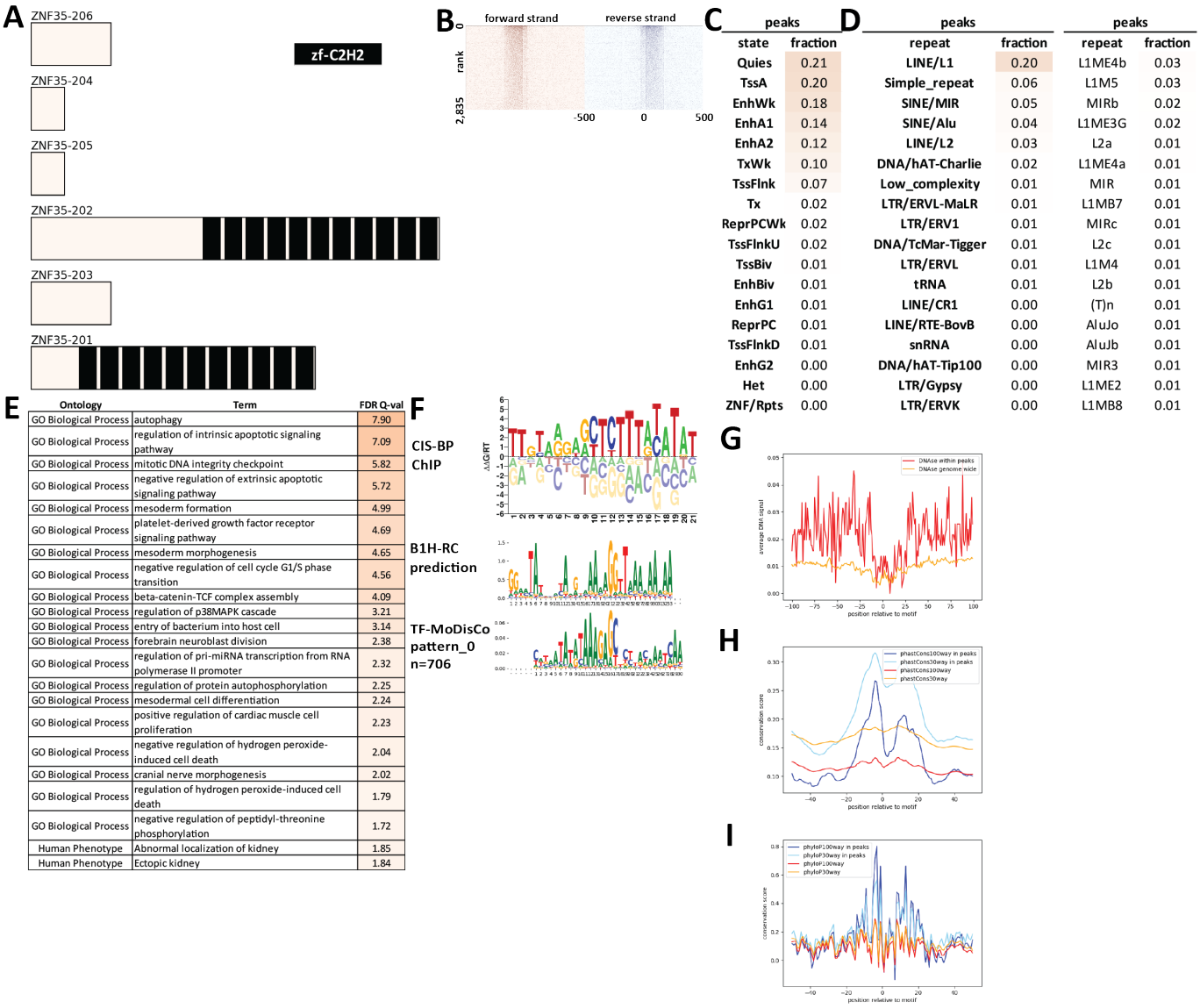

peaks	
state	fraction
Quies	0.21
TssA	0.20
EnhWk	0.18
EnhA1	0.14
EnhA2	0.12
TxWk	0.10
TssFlnk	0.07
Tx	0.02
ReprPCWk	0.02
TssFlnkU	0.02
TssBiv	0.01
EnhBiv	0.01
EnhG1	0.01
ReprPC	0.01
TssFlnkD	0.01
EnhG2	0.00
Het	0.00
ZNF/Rpts	0.00

peaks		peaks	
repeat	fraction	repeat	fraction
LINE/L1	0.20	L1ME4b	0.03
Simple_repeat	0.06	L1M5	0.03
SINE/MIR	0.05	MIRb	0.02
SINE/Alu	0.04	L1ME3G	0.02
LINE/L2	0.03	L2a	0.01
DNA/hAT-Charlie	0.02	L1ME4a	0.01
Low_complexity	0.01	MIR	0.01
LTR/ERVL-MaLR	0.01	L1MB7	0.01
LTR/ERV1	0.01	MIRc	0.01
DNA/TcMar-Tigger	0.01	L2c	0.01
LTR/ERVL	0.01	L1M4	0.01
tRNA	0.01	L2b	0.01
LINE/CR1	0.00	(T)n	0.01
LINE/RTE-BovB	0.00	AluJo	0.01
snRNA	0.00	AluJb	0.01
DNA/hAT-Tip100	0.00	MIR3	0.01
LTR/Gypsy	0.00	L1ME2	0.01
LTR/ERVK	0.00	L1MB8	0.01

Ontology	Term	FDR Q-val
GO Biological Process	autophagy	7.90
GO Biological Process	regulation of intrinsic apoptotic signaling pathway	7.09
GO Biological Process	mitotic DNA integrity checkpoint	5.82
GO Biological Process	negative regulation of extrinsic apoptotic signaling pathway	5.72
GO Biological Process	mesoderm formation	4.99
GO Biological Process	platelet-derived growth factor receptor signaling pathway	4.69
GO Biological Process	mesoderm morphogenesis	4.65
GO Biological Process	negative regulation of cell cycle G1/S phase transition	4.56
GO Biological Process	beta-catenin-TCF complex assembly	4.09
GO Biological Process	regulation of p38MAPK cascade	3.21
GO Biological Process	entry of bacterium into host cell	3.14
GO Biological Process	forebrain neuroblast division	2.38
GO Biological Process	regulation of pri-miRNA transcription from RNA polymerase II promoter	2.32
GO Biological Process	regulation of protein autophosphorylation	2.25
GO Biological Process	mesodermal cell differentiation	2.24
GO Biological Process	positive regulation of cardiac muscle cell proliferation	2.23
GO Biological Process	negative regulation of hydrogen peroxide-induced cell death	2.04
GO Biological Process	cranial nerve morphogenesis	2.02
GO Biological Process	regulation of hydrogen peroxide-induced cell death	1.79
GO Biological Process	negative regulation of peptidyl-threonine phosphorylation	1.72
Human Phenotype	Abnormal localization of kidney	1.85
Human Phenotype	Ectopic kidney	1.84

Supplementary Figure 1118: Properties and genomic distribution of motifs identified for the ZNF35 transcription factor in HEK293 (accession Hughes NB models).

TF-MoDisCO pattern_0 n=706, CWM

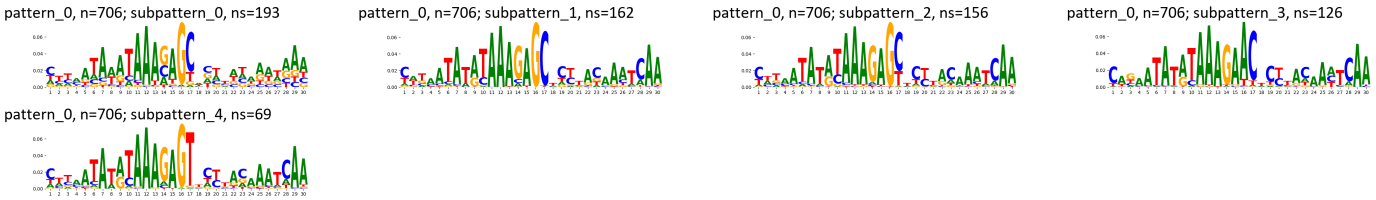

TF-MoDisCO pattern_0 n=706, PWM

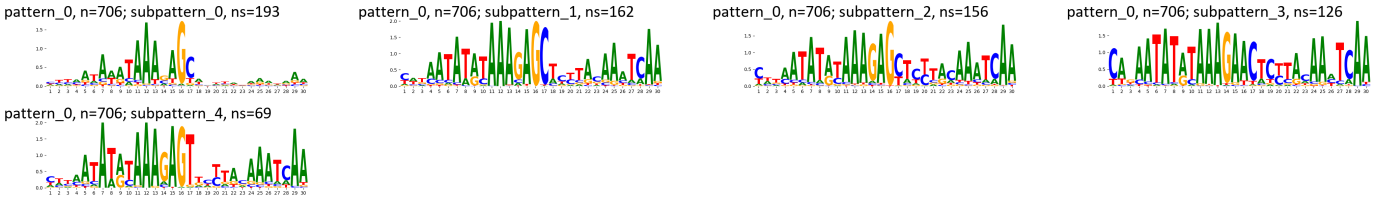

Supplementary Figure 1119: TF-MoDisCO subpatterns for the ZNF35 transcription factor in HEK293 (accession Hughes NB models).

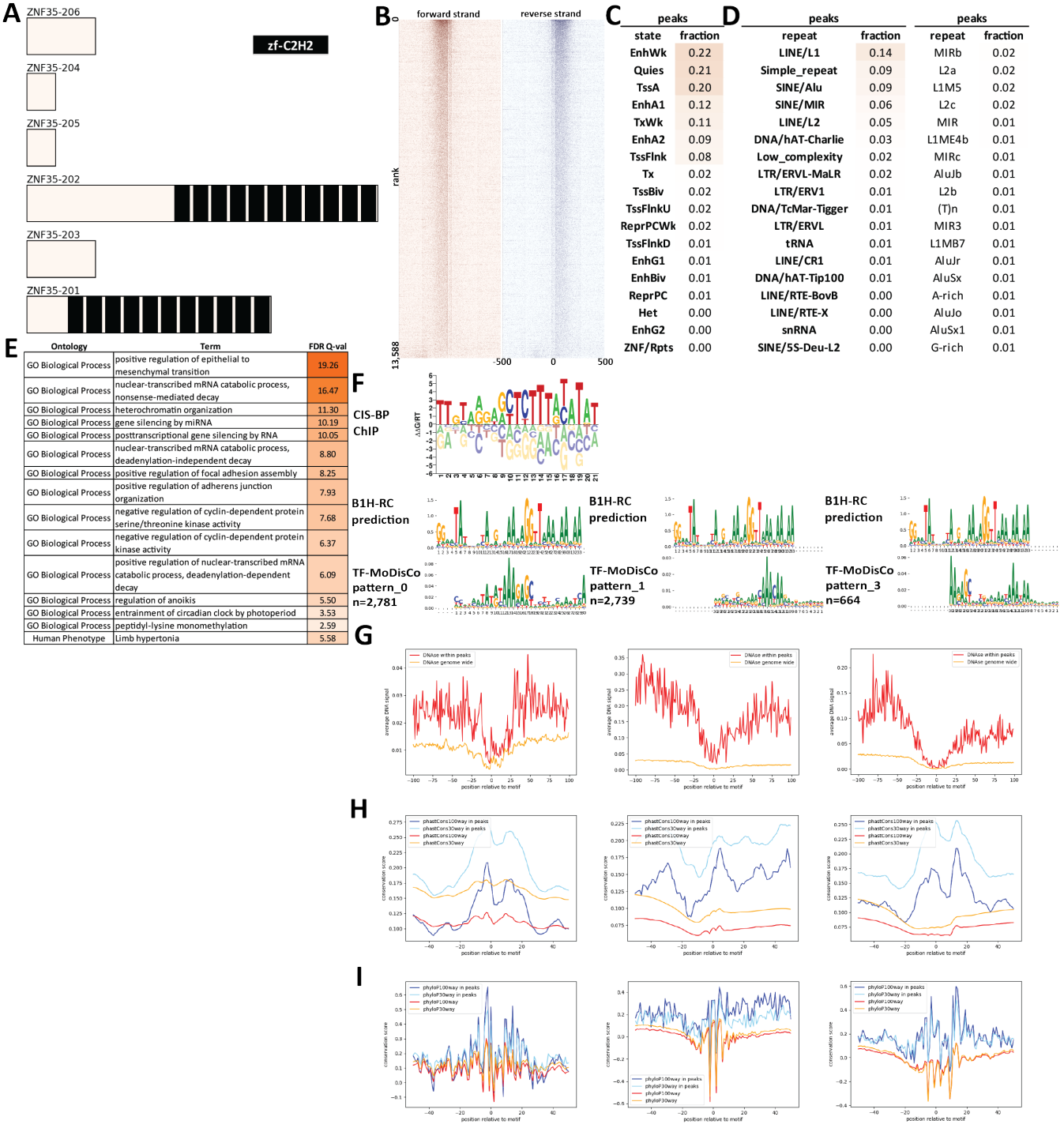

Supplementary Figure 1120: Properties and genomic distribution of motifs identified for the ZNF35 transcription factor in HEK293 (accession Hughes GR models).

TF-MoDisCO pattern_0 n=2781, CWM

pattern_0, n=2781; subpattern_0, ns=609

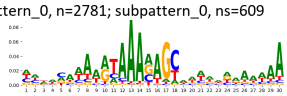

pattern_0, n=2781; subpattern_1, ns=585

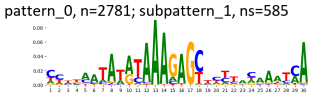

pattern_0, n=2781; subpattern_2, ns=495

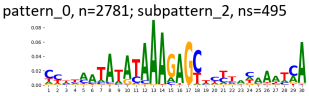

pattern_0, n=2781; subpattern_3, ns=442

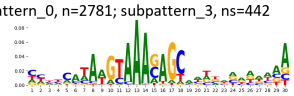

pattern_0, n=2781; subpattern_4, ns=296

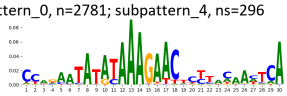

pattern_0, n=2781; subpattern_5, ns=284

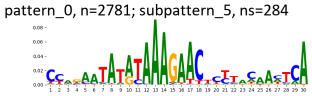

pattern_0, n=2781; subpattern_6, ns=70

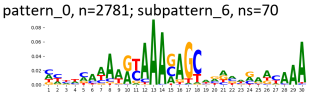

TF-MoDisCO pattern_0 n=2781, PWM

pattern_0, n=2781; subpattern_0, ns=609

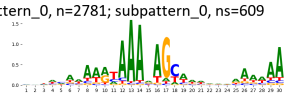

pattern_0, n=2781; subpattern_1, ns=585

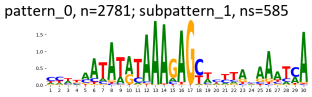

pattern_0, n=2781; subpattern_2, ns=495

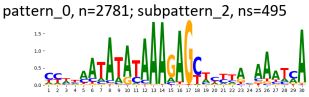

pattern_0, n=2781; subpattern_3, ns=442

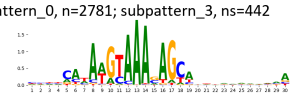

pattern_0, n=2781; subpattern_4, ns=296

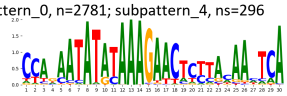

pattern_0, n=2781; subpattern_5, ns=284

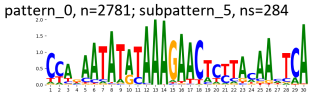

pattern_0, n=2781; subpattern_6, ns=70

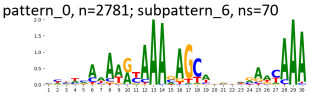

TF-MoDisCO pattern_1 n=2739, CWM

pattern_1, n=2739; subpattern_0, ns=720

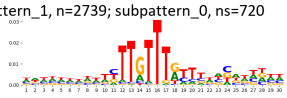

pattern_1, n=2739; subpattern_1, ns=543

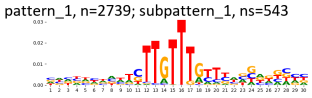

pattern_1, n=2739; subpattern_2, ns=465

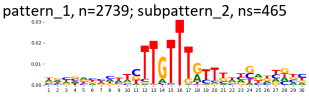

pattern_1, n=2739; subpattern_3, ns=421

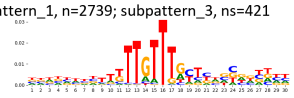

pattern_1, n=2739; subpattern_4, ns=259

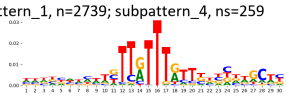

pattern_1, n=2739; subpattern_5, ns=242

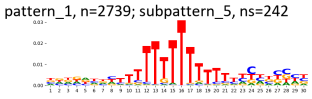

pattern_1, n=2739; subpattern_6, ns=84

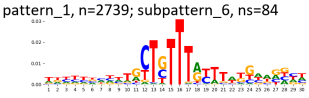

pattern_1, n=2739; subpattern_7, ns=3

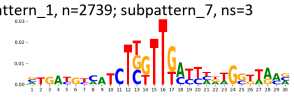

pattern_1, n=2739; subpattern_8, ns=2

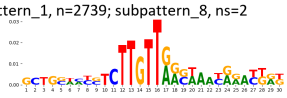

TF-MoDisCO pattern_1 n=2739, PWM

pattern_1, n=2739; subpattern_0, ns=720

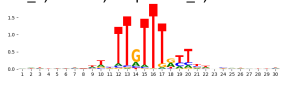

pattern_1, n=2739; subpattern_1, ns=543

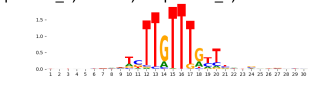

pattern_1, n=2739; subpattern_2, ns=465

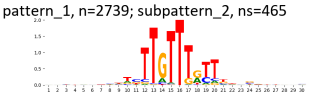

pattern_1, n=2739; subpattern_3, ns=421

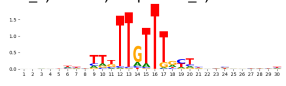

pattern_1, n=2739; subpattern_4, ns=259

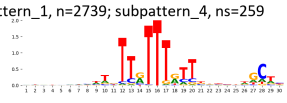

pattern_1, n=2739; subpattern_5, ns=242

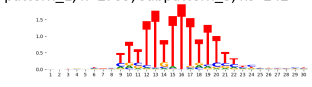

pattern_1, n=2739; subpattern_6, ns=84

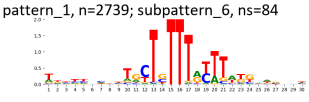

pattern_1, n=2739; subpattern_7, ns=3

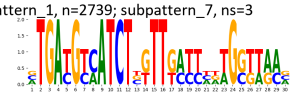

pattern_1, n=2739; subpattern_8, ns=2

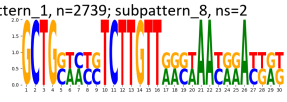

TF-MoDisCO pattern_3 n=664, CWM

pattern_3, n=664; subpattern_0, ns=211

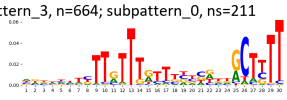

pattern_3, n=664; subpattern_1, ns=171

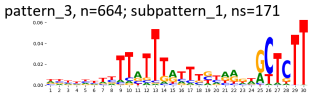

pattern_3, n=664; subpattern_2, ns=107

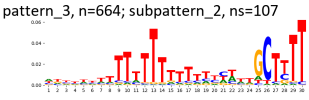

pattern_3, n=664; subpattern_3, ns=98

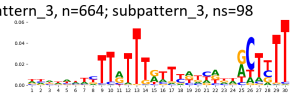

pattern_3, n=664; subpattern_4, ns=77

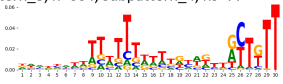

TF-MoDisCO pattern_3 n=664, PWM

pattern_3, n=664; subpattern_0, ns=211

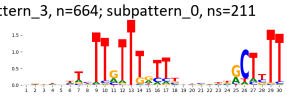

pattern_3, n=664; subpattern_1, ns=171

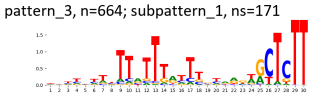

pattern_3, n=664; subpattern_2, ns=107

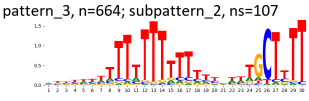

pattern_3, n=664; subpattern_3, ns=98

pattern_3, n=664; subpattern_4, ns=77

Supplementary Figure 1121: TF-MoDisCO subpatterns for the ZNF35 transcription factor in HEK293 (accession Hughes GR models).

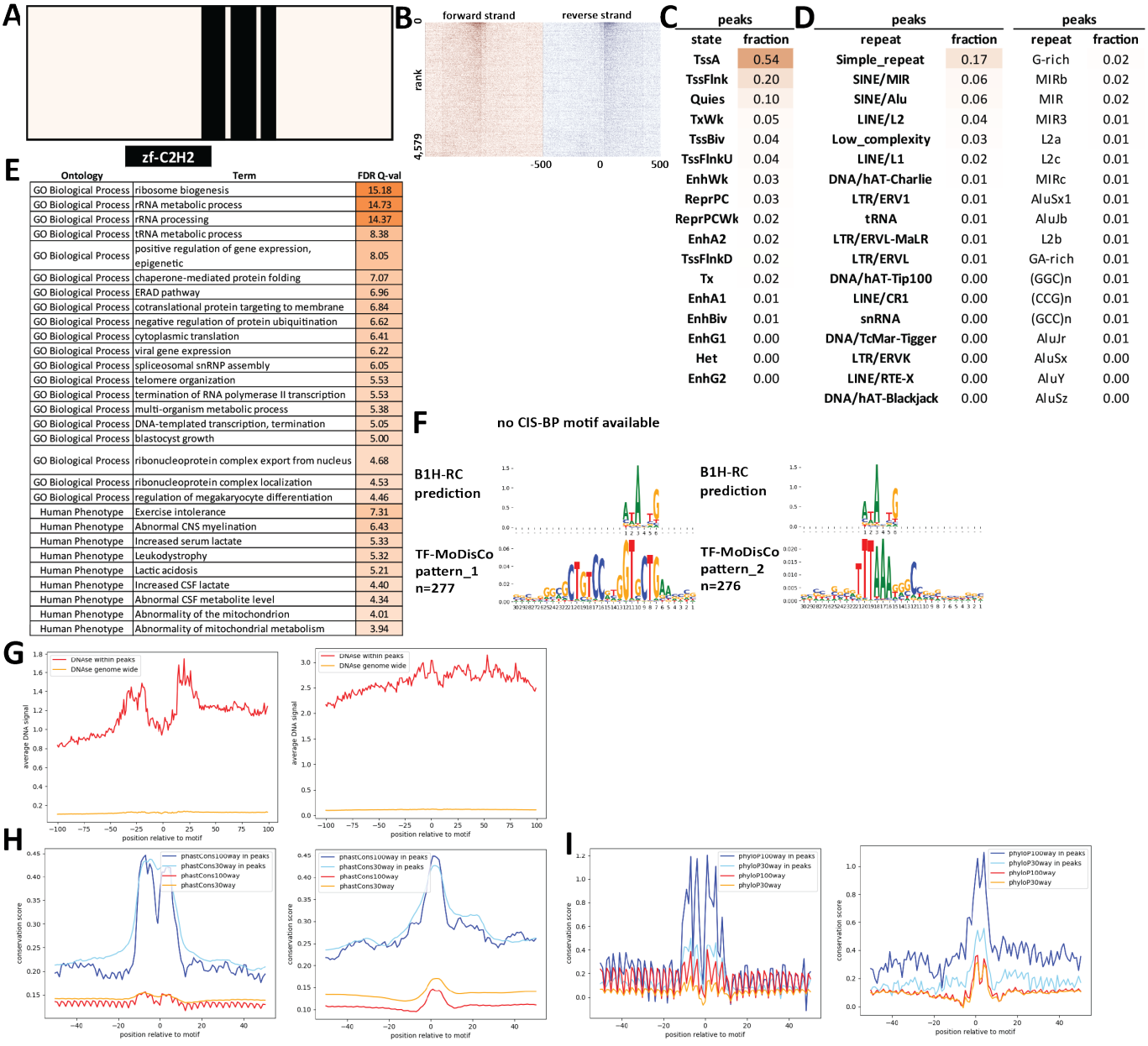

Supplementary Figure 1122: Properties and genomic distribution of motifs identified for the ZNF367 transcription factor in HepG2 (accession ENCSR048WVW).

TF-MoDisCO pattern_1 n=277, CWM

pattern_1, n=277; subpattern_0, ns=149

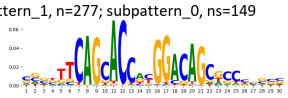

pattern_1, n=277; subpattern_1, ns=126

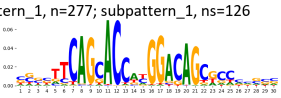

pattern_1, n=277; subpattern_2, ns=2

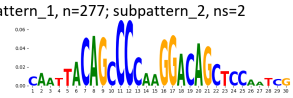

TF-MoDisCO pattern_1 n=277, PWM

pattern_1, n=277; subpattern_0, ns=149

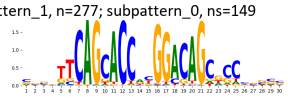

pattern_1, n=277; subpattern_1, ns=126

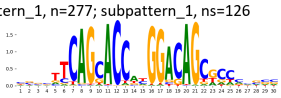

pattern_1, n=277; subpattern_2, ns=2

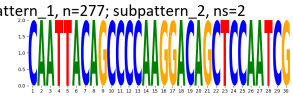

TF-MoDisCO pattern_2 n=276, CWM

pattern_2, n=276; subpattern_0, ns=78

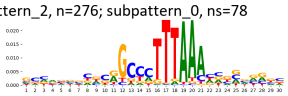

pattern_2, n=276; subpattern_1, ns=70

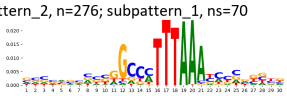

pattern_2, n=276; subpattern_2, ns=54

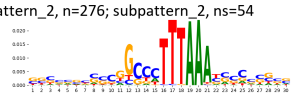

pattern_2, n=276; subpattern_3, ns=50

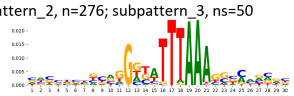

pattern_2, n=276; subpattern_4, ns=19

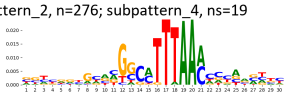

pattern_2, n=276; subpattern_5, ns=5

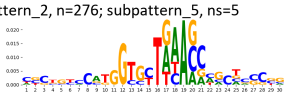

TF-MoDisCO pattern_2 n=276, PWM

pattern_2, n=276; subpattern_0, ns=78

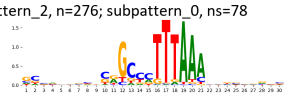

pattern_2, n=276; subpattern_1, ns=70

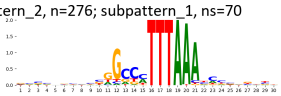

pattern_2, n=276; subpattern_2, ns=54

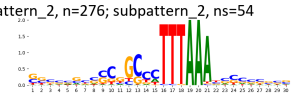

pattern_2, n=276; subpattern_3, ns=50

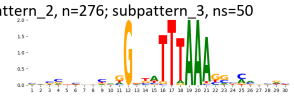

pattern_2, n=276; subpattern_4, ns=19

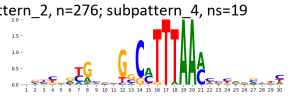

pattern_2, n=276; subpattern_5, ns=5

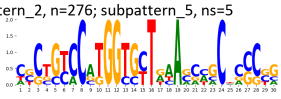

Supplementary Figure 1123: TF-MoDisCO subpatterns for the ZNF367 transcription factor in HepG2 (accession ENCSR048WVW).



Supplementary Figure 1124: Properties and genomic distribution of motifs identified for the ZNF37A transcription factor in HEK293 (accession ENCSR371LLY).

TF-MoDisCO pattern_0 n=539, CWM

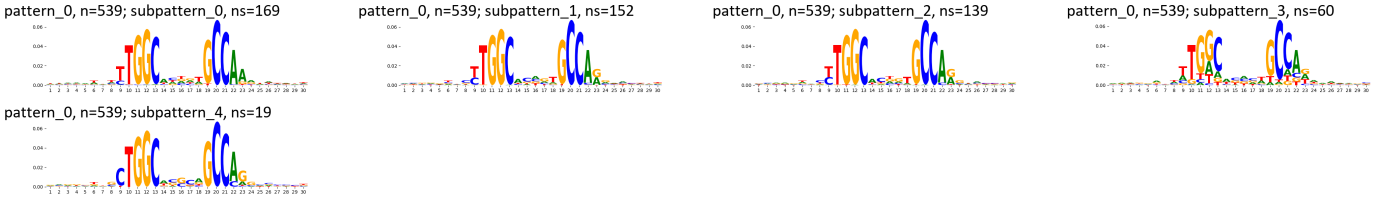

TF-MoDisCO pattern_0 n=539, PWM

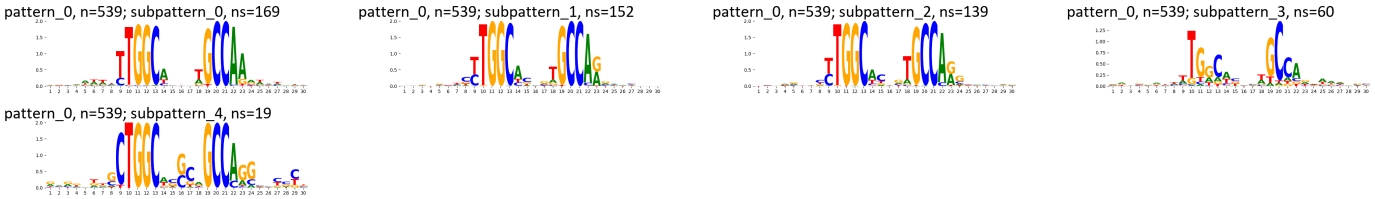

TF-MoDisCO pattern_1 n=400, CWM

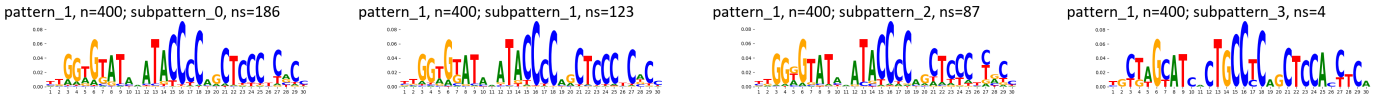

TF-MoDisCO pattern_1 n=400, PWM

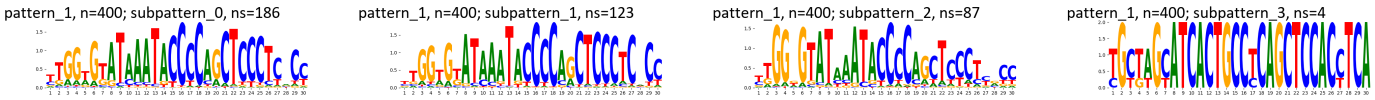

TF-MoDisCO pattern_2 n=293, CWM

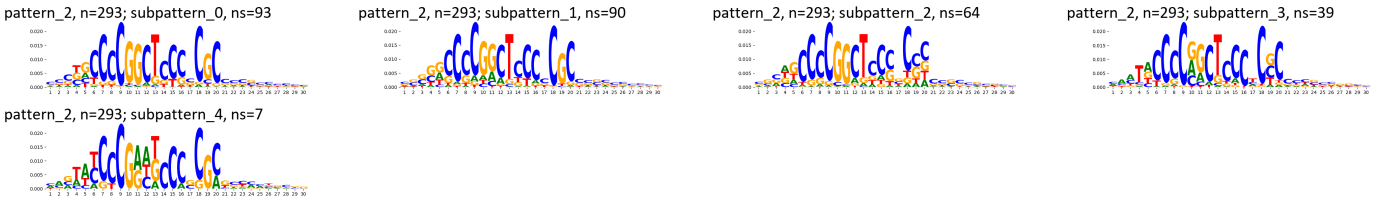

TF-MoDisCO pattern_2 n=293, PWM

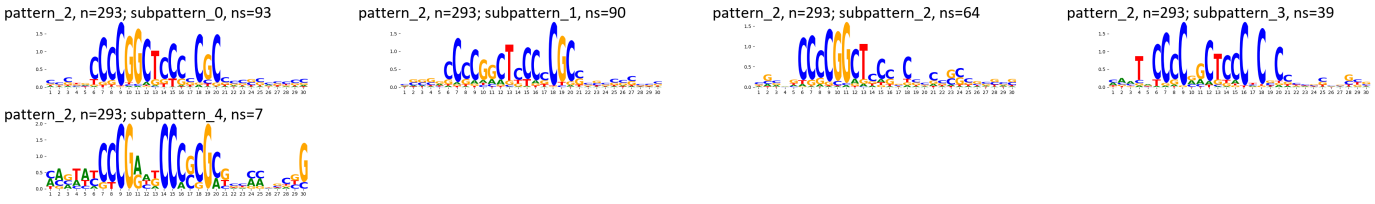

Supplementary Figure 1125: TF-MoDisCO subpatterns for the ZNF37A transcription factor in HEK293 (accession ENCSR371LLY).

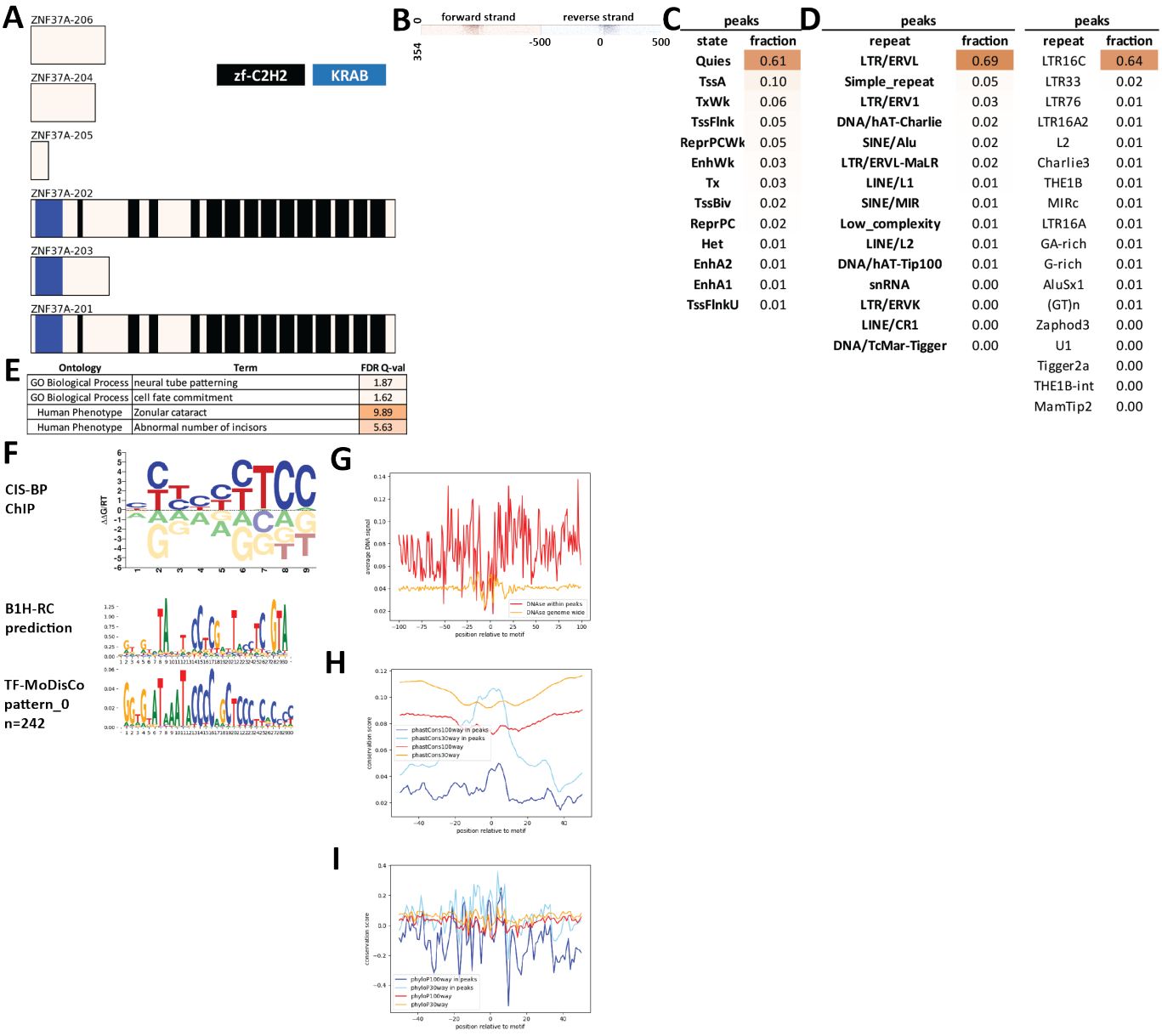

Supplementary Figure 1126: Properties and genomic distribution of motifs identified for the ZNF37A transcription factor in HEK293 (accession Hughes GR models).

TF-MoDisCO pattern_0 n=242, CWM

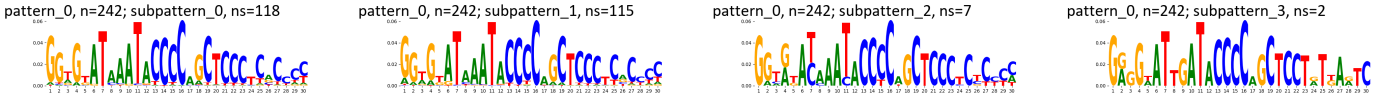

TF-MoDisCO pattern_0 n=242, PWM

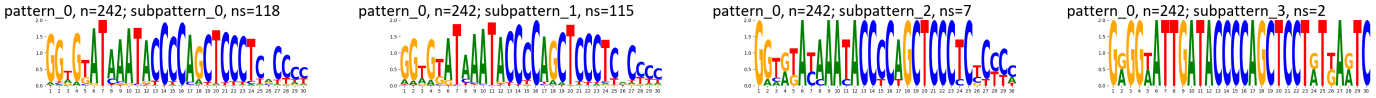

Supplementary Figure 1127: TF-MoDisCO subpatterns for the ZNF37A transcription factor in HEK293 (accession Hughes GR models).

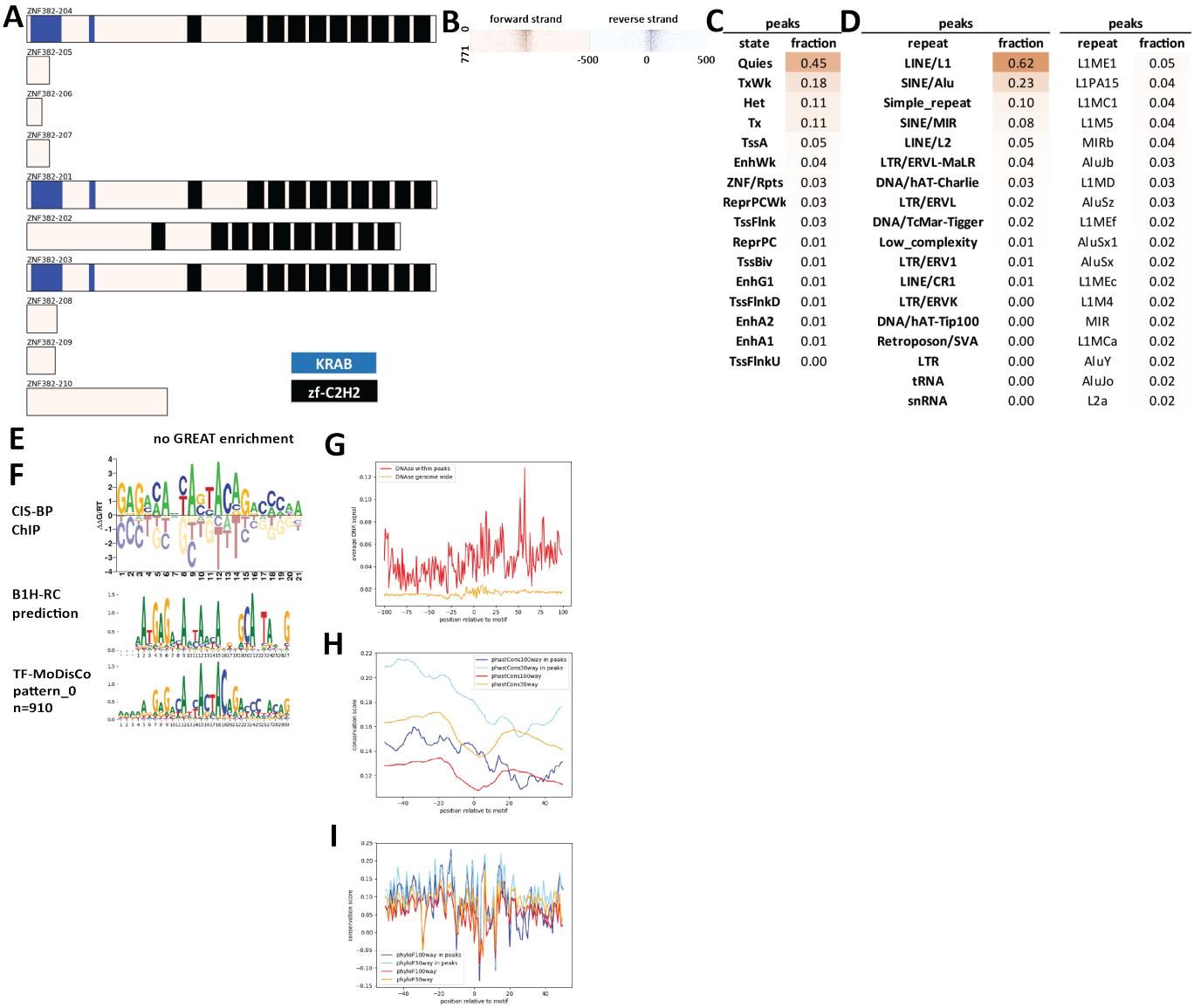

Supplementary Figure 1128: Properties and genomic distribution of motifs identified for the ZNF382 transcription factor in HEK293 (accession Hughes NB models).

TF-MoDisCO pattern_0 n=910, CWM

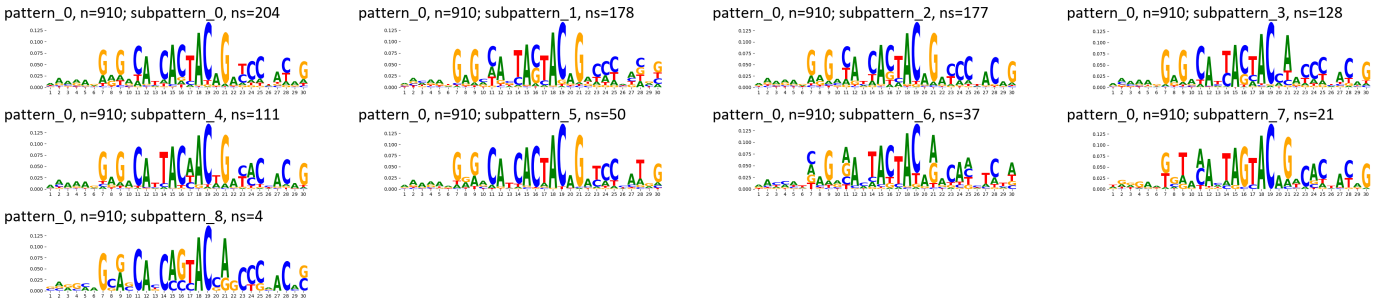

TF-MoDisCO pattern_0 n=910, PWM

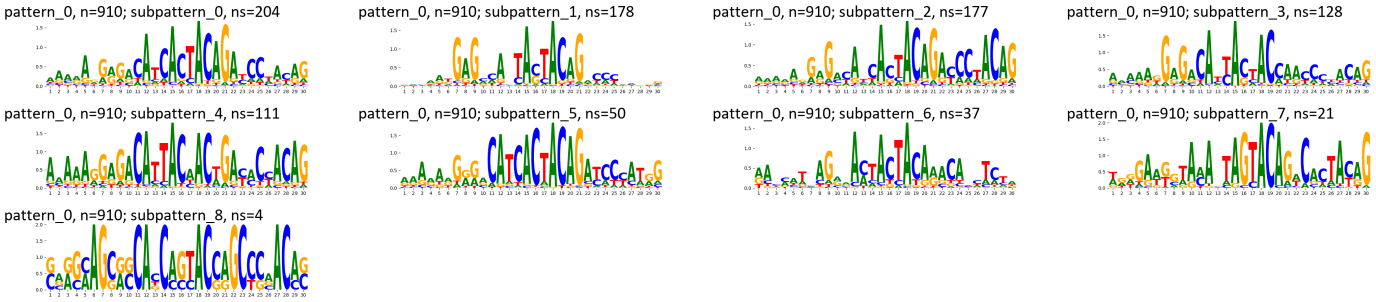

Supplementary Figure 1129: TF-MoDisCO subpatterns for the ZNF382 transcription factor in HEK293 (accession Hughes NB models).

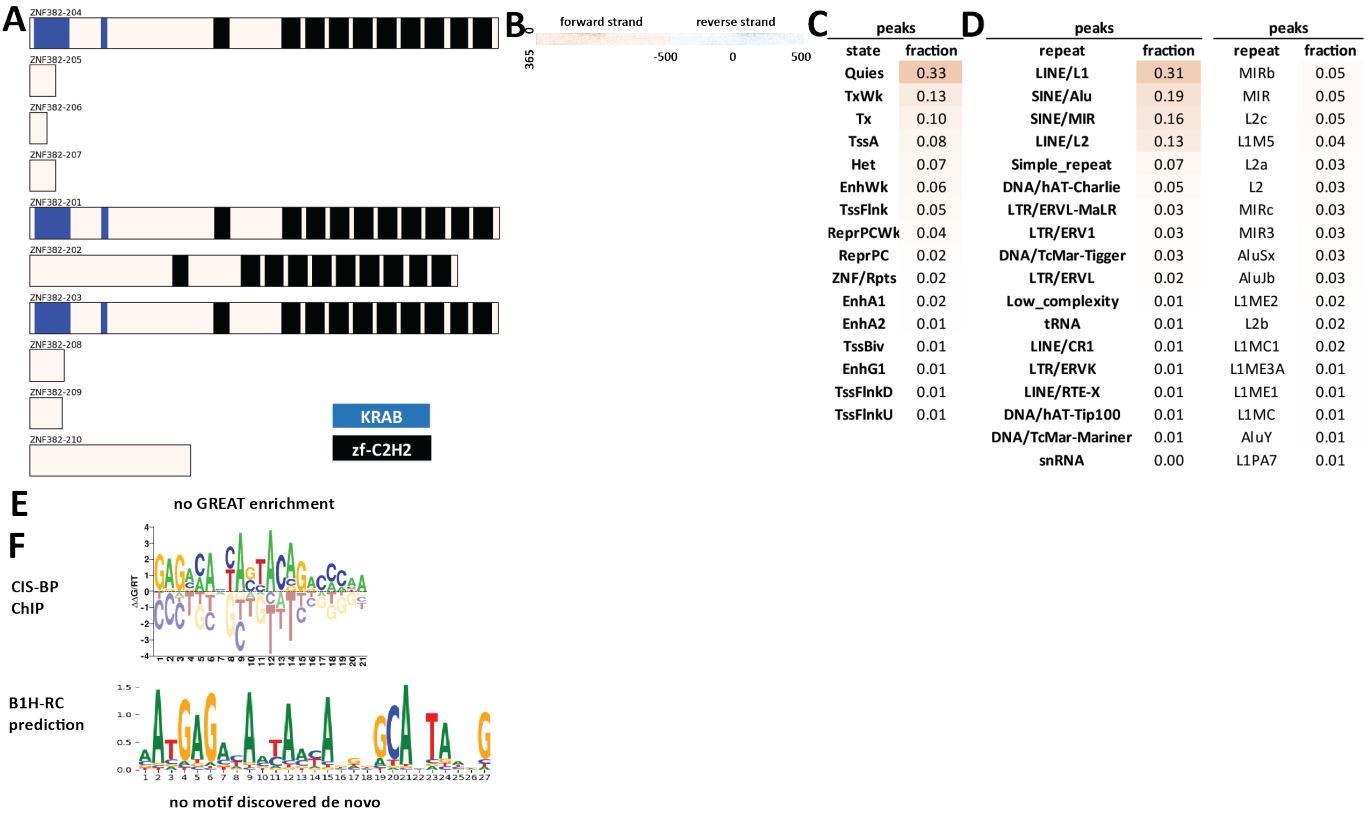

peaks	
state	fraction
Quies	0.33
TxWk	0.13
Tx	0.10
TssA	0.08
Het	0.07
EnhWk	0.06
TssFlnk	0.05
ReprPCWk	0.04
ReprPC	0.02
ZNF/Rpts	0.02
EnhA1	0.02
EnhA2	0.01
TssBiv	0.01
EnhG1	0.01
TssFlnkD	0.01
TssFlnkU	0.01

peaks	
repeat	fraction
LINE/L1	0.31
SINE/Alu	0.19
SINE/MIR	0.16
LINE/L2	0.13
Simple_repeat	0.07
DNA/hAT-Charlie	0.05
LTR/ERVL-MaLR	0.03
LTR/ERV1	0.03
DNA/TcMar-Tigger	0.03
LTR/ERVL	0.02
Low_complexity	0.01
tRNA	0.01
LINE/CR1	0.01
LTR/ERVK	0.01
LINE/RTE-X	0.01
DNA/hAT-Tip100	0.01
DNA/TcMar-Mariner	0.01
snRNA	0.00

peaks	
repeat	fraction
MIRb	0.05
MIR	0.05
L2c	0.05
L1M5	0.04
L2a	0.03
L2	0.03
MIRc	0.03
MIR3	0.03
AluSx	0.03
AluJb	0.03
L1ME2	0.02
L2b	0.02
L1MC1	0.02
L1ME3A	0.01
L1ME1	0.01
L1MC	0.01
AluY	0.01
L1PA7	0.01

Supplementary Figure 1130: Properties and genomic distribution of motifs identified for the ZNF382 transcription factor in HepG2 (accession ENCSR014HQD).

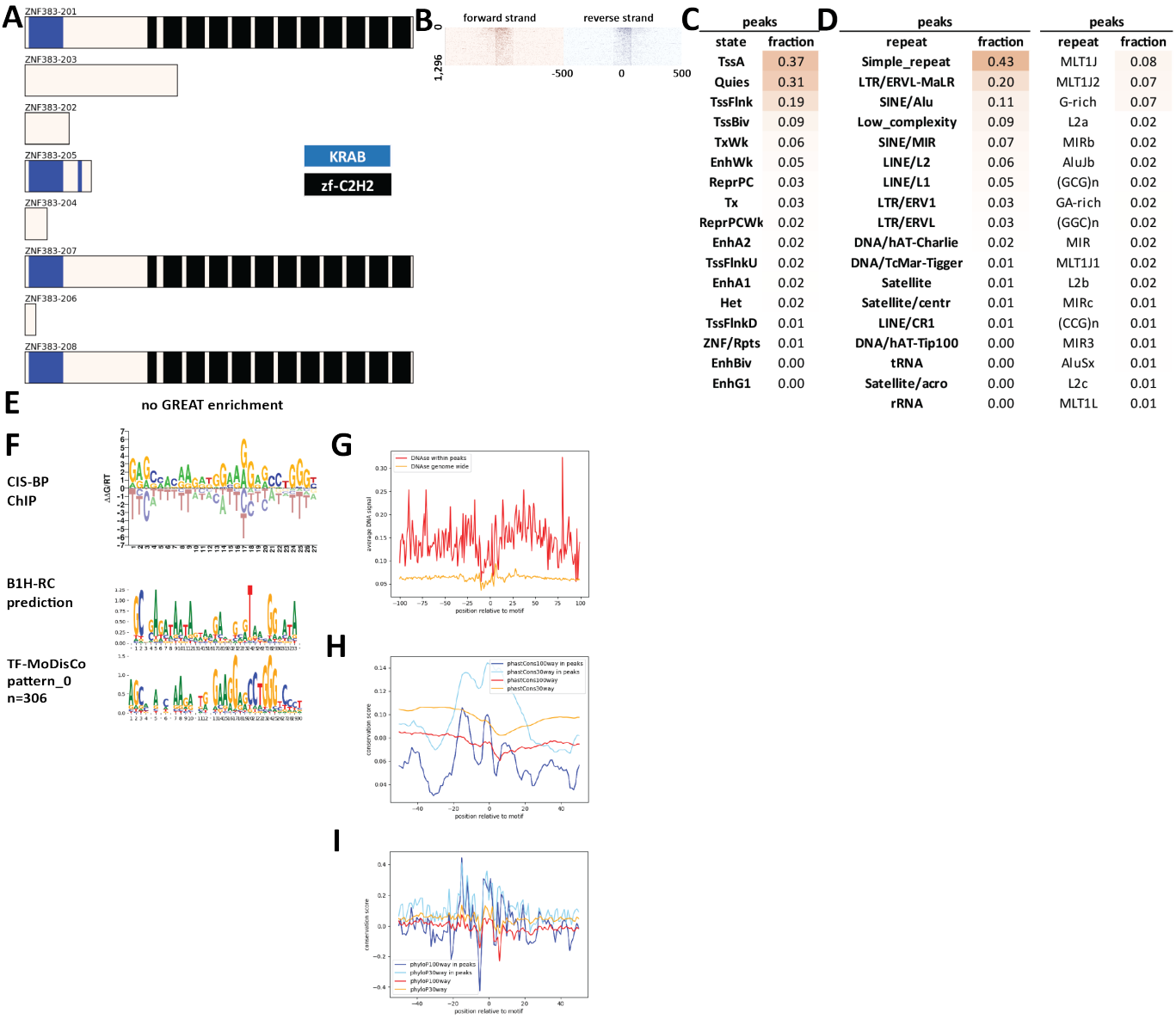

Supplementary Figure 1131: Properties and genomic distribution of motifs identified for the ZNF383 transcription factor in HEK293 (accession ChipExo models).

TF-MoDisCO pattern_0 n=306, CWM

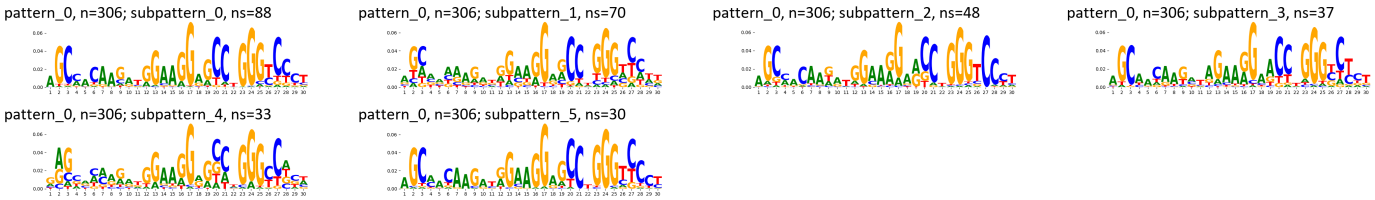

TF-MoDisCO pattern_0 n=306, PWM

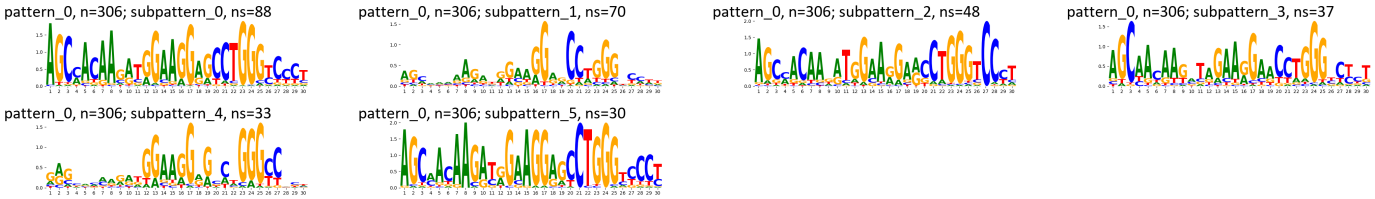

Supplementary Figure 1132: TF-MoDisCO subpatterns for the ZNF383 transcription factor in HEK293 (accession ChipExo models).

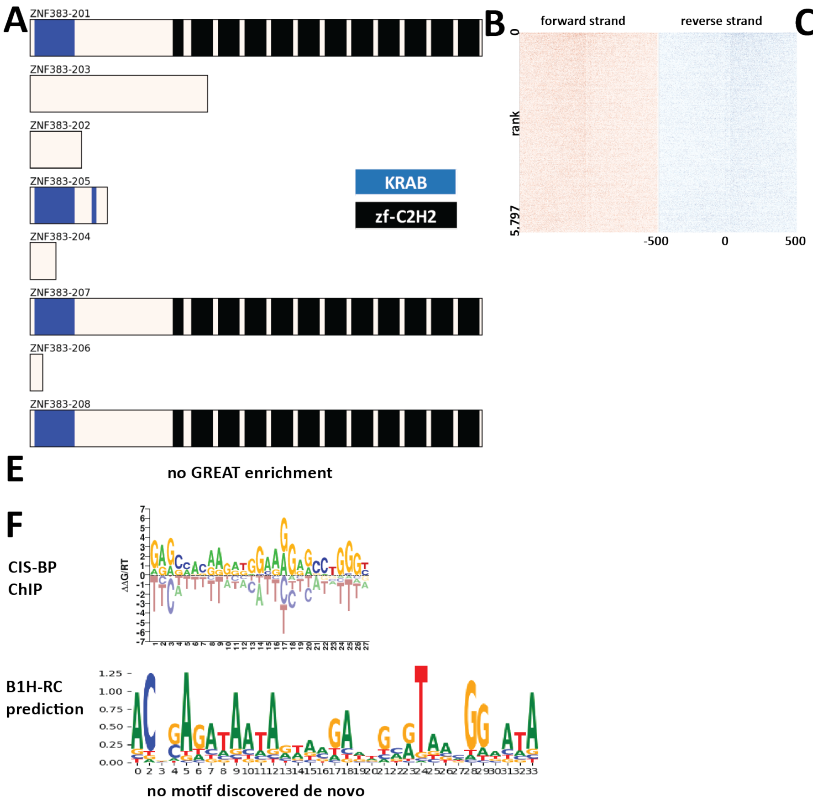

C

peaks	
state	fraction
TssA	0.38
TssFlnk	0.22
Quies	0.18
TxWk	0.11
EnhWk	0.07
TssFlnkU	0.05
EnhA2	0.04
TssFlnkD	0.03
EnhA1	0.03
TssBiv	0.03
Tx	0.03
ReprPC	0.02
ReprPCWk	0.02
EnhG1	0.01
EnhBiv	0.01
Het	0.00
EnhG2	0.00
ZNF/Rpts	0.00

D

peaks		peaks	
repeat	fraction	repeat	fraction
Simple_repeat	0.23	MIRb	0.06
SINE/Alu	0.18	MIR	0.04
SINE/MIR	0.18	L2a	0.04
LINE/L2	0.10	MIR3	0.03
LINE/L1	0.05	MIRc	0.03
Low_complexity	0.05	G-rich	0.03
DNA/hAT-Charlie	0.04	L2b	0.03
LTR/ERV1	0.02	L2c	0.02
LTR/ERVL-MaLR	0.02	AluSx1	0.02
LTR/ERVL	0.02	AluSx	0.02
LINE/CR1	0.01	AluJb	0.02
DNA/TcMar-Tigger	0.01	AluSz	0.02
tRNA	0.01	AluJo	0.01
DNA/hAT-Tip100	0.01	AluJr	0.01
DNA/hAT	0.00	AluY	0.01
LTR/ERVK	0.00	L2	0.01
LINE/RTE-BovB	0.00	GA-rich	0.01
DNA/hAT-Blackjack	0.00	AluSp	0.01

Supplementary Figure 1133: Properties and genomic distribution of motifs identified for the ZNF383 transcription factor in HepG2 (accession ENCSR264LQX).

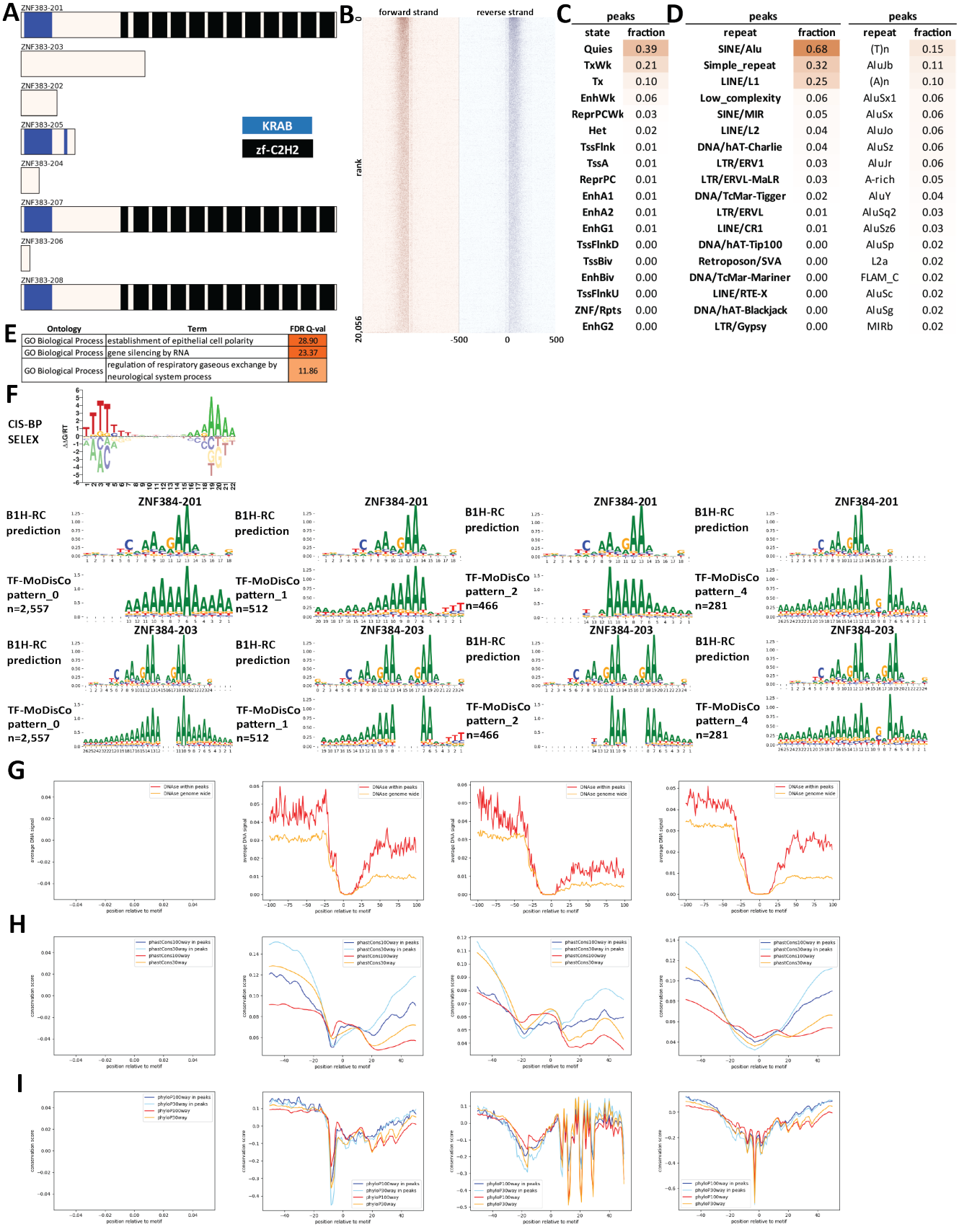

Supplementary Figure 1134: Properties and genomic distribution of motifs identified for the ZNF384 transcription factor in HEK293 (accession Hughes GR models).

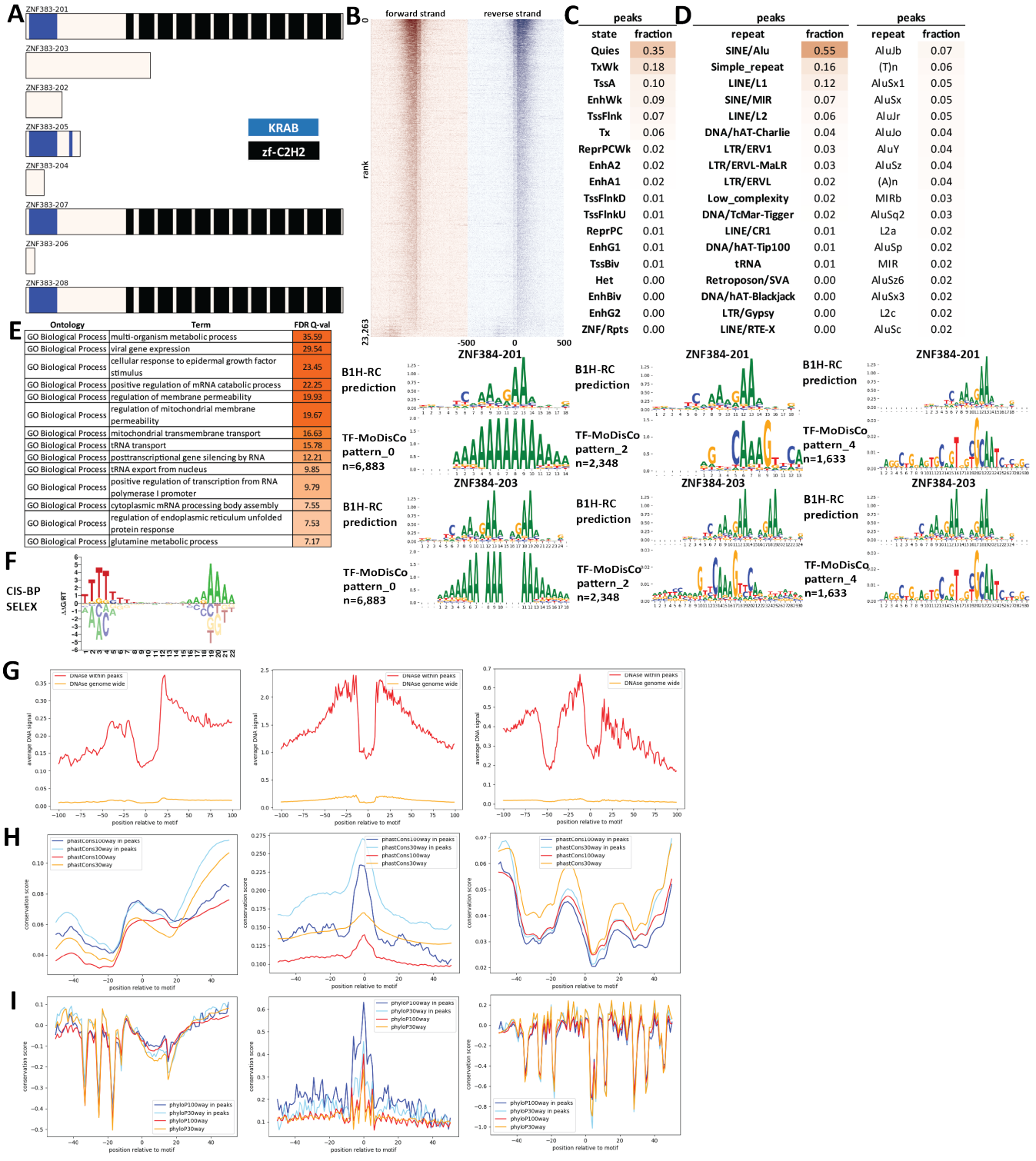

Supplementary Figure 1135: Properties and genomic distribution of motifs identified for the ZNF384 transcription factor in HepG2 (accession ENCSR101FJU).

TF-MoDisCO pattern_0 n=6883, CWM

pattern_0, n=6883; subpattern_0, ns=2127

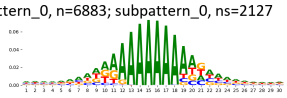

pattern_0, n=6883; subpattern_1, ns=1748

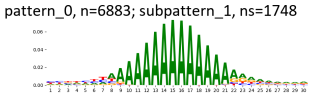

pattern_0, n=6883; subpattern_2, ns=1420

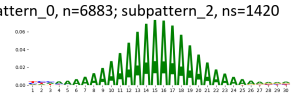

pattern_0, n=6883; subpattern_3, ns=1119

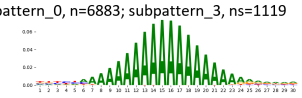

pattern_0, n=6883; subpattern_4, ns=372

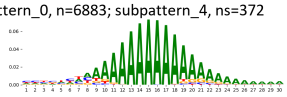

pattern_0, n=6883; subpattern_5, ns=97

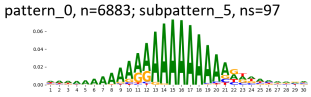

TF-MoDisCO pattern_0 n=6883, PWM

pattern_0, n=6883; subpattern_0, ns=2127

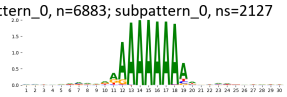

pattern_0, n=6883; subpattern_1, ns=1748

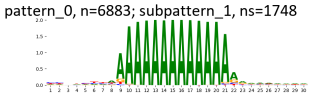

pattern_0, n=6883; subpattern_2, ns=1420

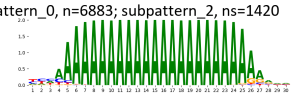

pattern_0, n=6883; subpattern_3, ns=1119

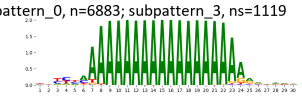

pattern_0, n=6883; subpattern_4, ns=372

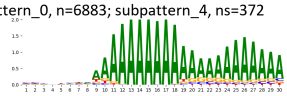

pattern_0, n=6883; subpattern_5, ns=97

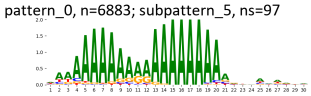

TF-MoDisCO pattern_2 n=2348, CWM

pattern_2, n=2348; subpattern_0, ns=744

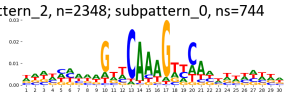

pattern_2, n=2348; subpattern_1, ns=567

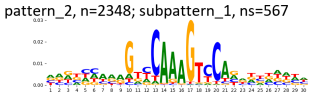

pattern_2, n=2348; subpattern_2, ns=366

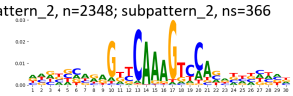

pattern_2, n=2348; subpattern_3, ns=301

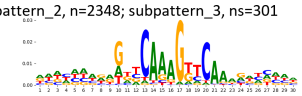

pattern_2, n=2348; subpattern_4, ns=279

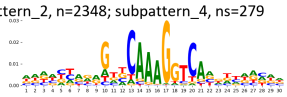

pattern_2, n=2348; subpattern_5, ns=52

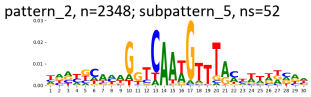

pattern_2, n=2348; subpattern_6, ns=33

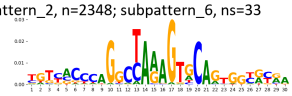

pattern_2, n=2348; subpattern_7, ns=4

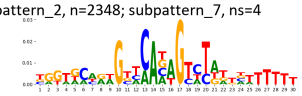

pattern_2, n=2348; subpattern_8, ns=2

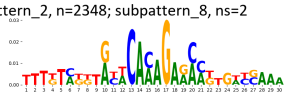

TF-MoDisCO pattern_2 n=2348, PWM

pattern_2, n=2348; subpattern_0, ns=744

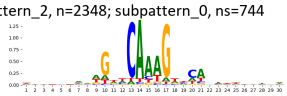

pattern_2, n=2348; subpattern_1, ns=567

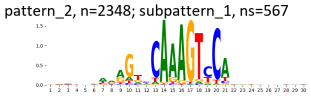

pattern_2, n=2348; subpattern_2, ns=366

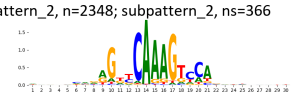

pattern_2, n=2348; subpattern_3, ns=301

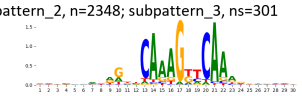

pattern_2, n=2348; subpattern_4, ns=279

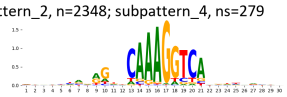

pattern_2, n=2348; subpattern_5, ns=52

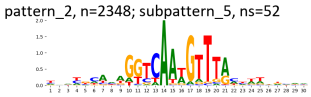

pattern_2, n=2348; subpattern_6, ns=33

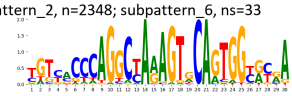

pattern_2, n=2348; subpattern_7, ns=4

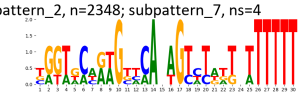

pattern_2, n=2348; subpattern_8, ns=2

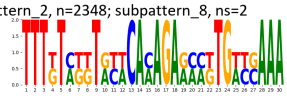

TF-MoDisCO pattern_4 n=1633, CWM

pattern_4, n=1633; subpattern_0, ns=431

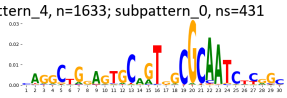

pattern_4, n=1633; subpattern_1, ns=338

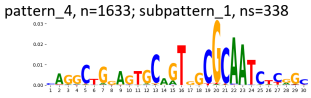

pattern_4, n=1633; subpattern_2, ns=328

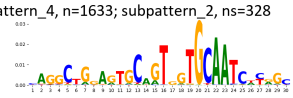

pattern_4, n=1633; subpattern_3, ns=296

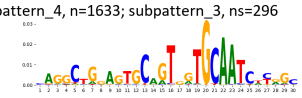

pattern_4, n=1633; subpattern_4, ns=168

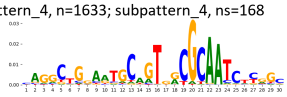

pattern_4, n=1633; subpattern_5, ns=37

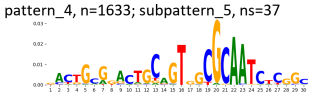

pattern_4, n=1633; subpattern_6, ns=25

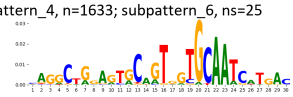

pattern_4, n=1633; subpattern_7, ns=10

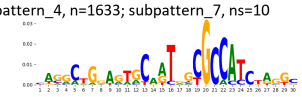

TF-MoDisCO pattern_4 n=1633, PWM

pattern_4, n=1633; subpattern_0, ns=431

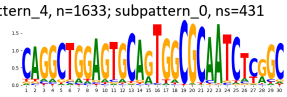

pattern_4, n=1633; subpattern_1, ns=338

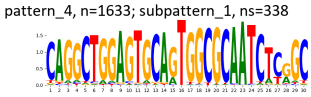

pattern_4, n=1633; subpattern_2, ns=328

pattern_4, n=1633; subpattern_3, ns=296

pattern_4, n=1633; subpattern_4, ns=168

pattern_4, n=1633; subpattern_5, ns=37

pattern_4, n=1633; subpattern_6, ns=25

pattern_4, n=1633; subpattern_7, ns=10

Supplementary Figure 1136: TF-MoDisCO subpatterns for the ZNF384 transcription factor in HepG2 (accession ENCSR101FJU).

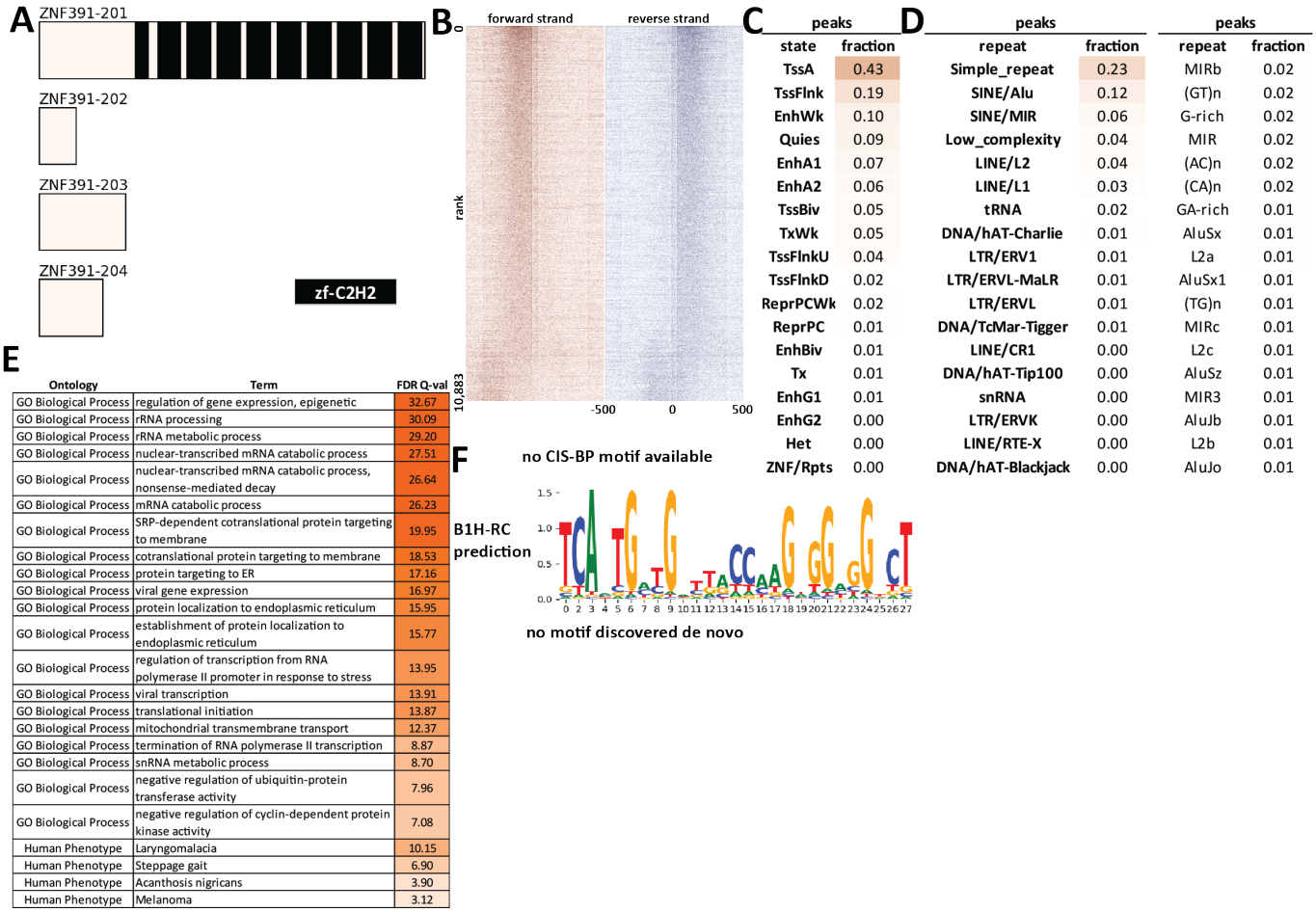

Supplementary Figure 1137: Properties and genomic distribution of motifs identified for the ZNF391 transcription factor in HEK293 (accession ENCSR210MET).

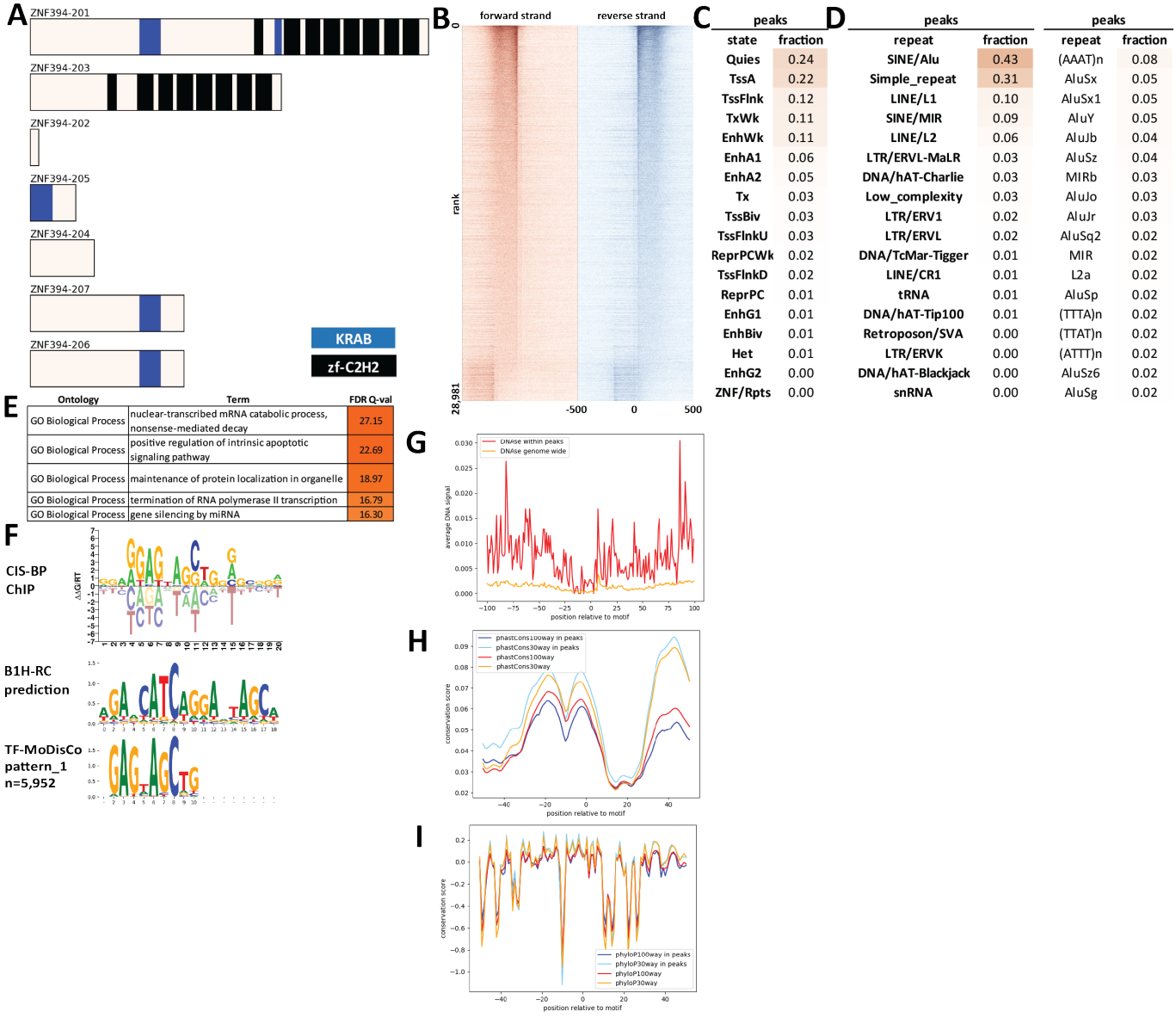

Supplementary Figure 1138: Properties and genomic distribution of motifs identified for the ZNF394 transcription factor in HEK293 (accession ENCSR125DNC).

TF-MoDisCO pattern_1 n=5952, CWM

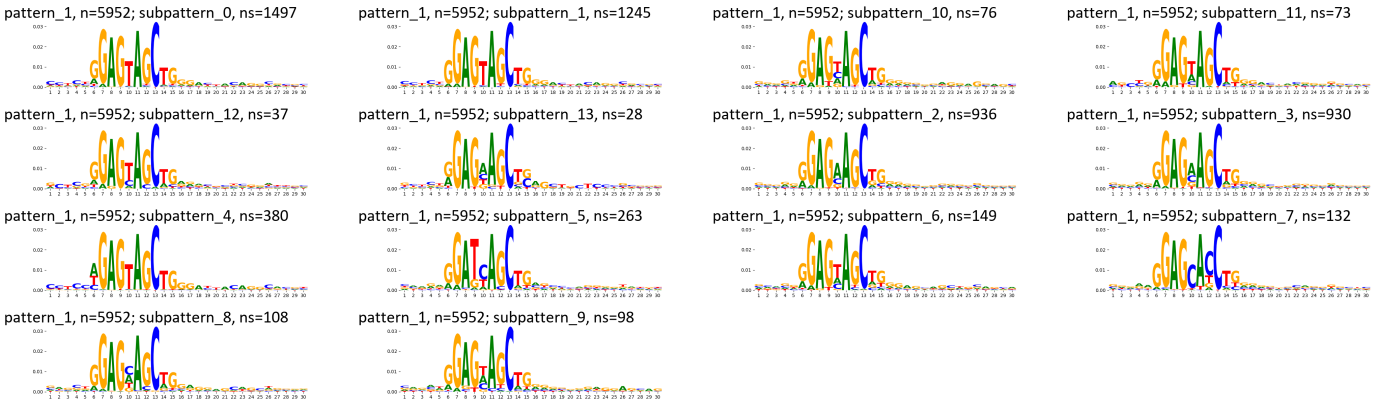

TF-MoDisCO pattern_1 n=5952, PWM

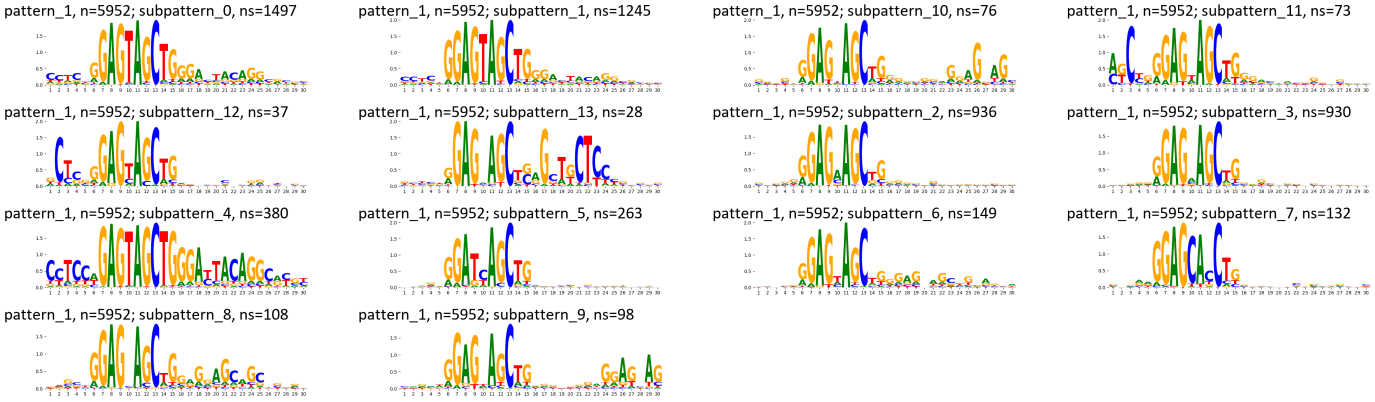

Supplementary Figure 1139: TF-MoDisCO subpatterns for the ZNF394 transcription factor in HEK293 (accession ENCSR125DNC).

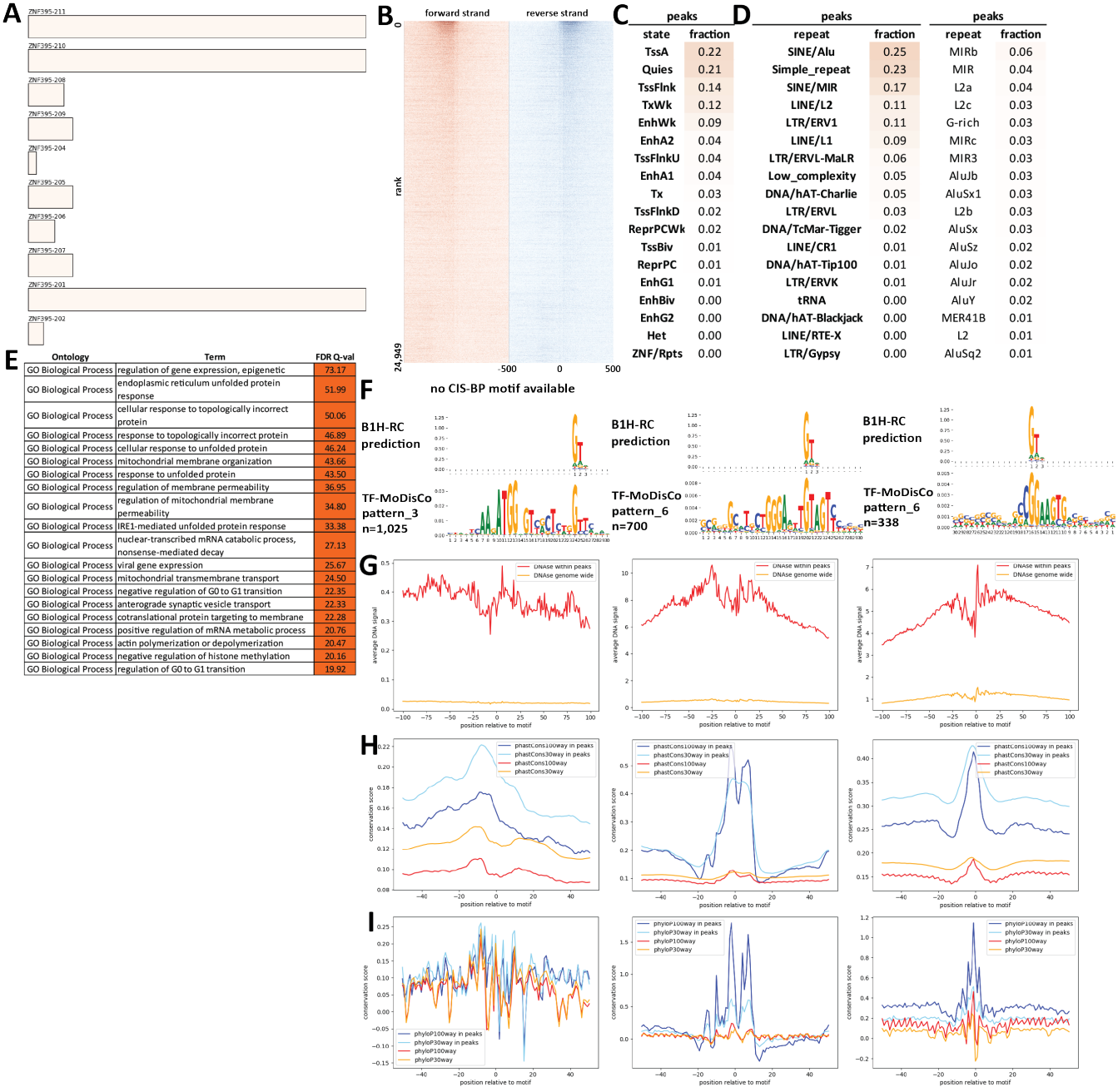

C

peaks	
state	fraction
TssA	0.22
Quies	0.21
TssFlnk	0.14
TxWk	0.12
EnhWk	0.09
EnhA2	0.04
TssFlnkU	0.04
EnhA1	0.04
Tx	0.03
TssFlnkD	0.02
ReprPCWk	0.02
TssBiv	0.01
ReprPC	0.01
EnhG1	0.01
EnhBiv	0.00
EnhG2	0.00
Het	0.00
ZNF/Rpts	0.00

D

peaks		peaks	
repeat	fraction	repeat	fraction
SINE/Alu	0.25	MIRb	0.06
Simple_repeat	0.23	MIR	0.04
SINE/MIR	0.17	L2a	0.04
LINE/L2	0.11	L2c	0.03
LTR/ERV1	0.11	G-rich	0.03
LINE/L1	0.09	MIRc	0.03
LTR/ERVL-MaLR	0.06	MIR3	0.03
Low_complexity	0.05	AluJb	0.03
DNA/hAT-Charlie	0.05	AluSx1	0.03
LTR/ERVL	0.03	L2b	0.03
DNA/TcMar-Tigger	0.02	AluSx	0.03
LINE/CR1	0.01	AluSz	0.02
DNA/hAT-Tip100	0.01	AluJo	0.02
LTR/ERVK	0.01	AluJr	0.02
tRNA	0.00	AluY	0.02
DNA/hAT-Blackjack	0.00	MER41B	0.01
LINE/RTE-X	0.00	L2	0.01
LTR/Gypsy	0.00	AluSq2	0.01

E

Ontology	Term	FDR Q-val
GO Biological Process	regulation of gene expression, epigenetic	73.17
GO Biological Process	endoplasmic reticulum unfolded protein response	51.99
GO Biological Process	cellular response to topologically incorrect protein	50.06
GO Biological Process	response to topologically incorrect protein	46.89
GO Biological Process	cellular response to unfolded protein	46.24
GO Biological Process	mitochondrial membrane organization	43.66
GO Biological Process	response to unfolded protein	43.50
GO Biological Process	regulation of membrane permeability	36.95
GO Biological Process	regulation of mitochondrial membrane permeability	34.80
GO Biological Process	IRE1-mediated unfolded protein response	33.38
GO Biological Process	nuclear-transcribed mRNA catabolic process, nonsense-mediated decay	27.13
GO Biological Process	viral gene expression	25.67
GO Biological Process	mitochondrial transmembrane transport	24.50
GO Biological Process	negative regulation of G0 to G1 transition	22.35
GO Biological Process	anterograde synaptic vesicle transport	22.33
GO Biological Process	cotranslational protein targeting to membrane	22.28
GO Biological Process	positive regulation of mRNA metabolic process	20.76
GO Biological Process	actin polymerization or depolymerization	20.47
GO Biological Process	negative regulation of histone methylation	20.16
GO Biological Process	regulation of G0 to G1 transition	19.92

Supplementary Figure 1140: Properties and genomic distribution of motifs identified for the ZNF395 transcription factor in K562 (accession ENCSR462QZZ).

TF-MoDisCO pattern_10 n=338, CWM

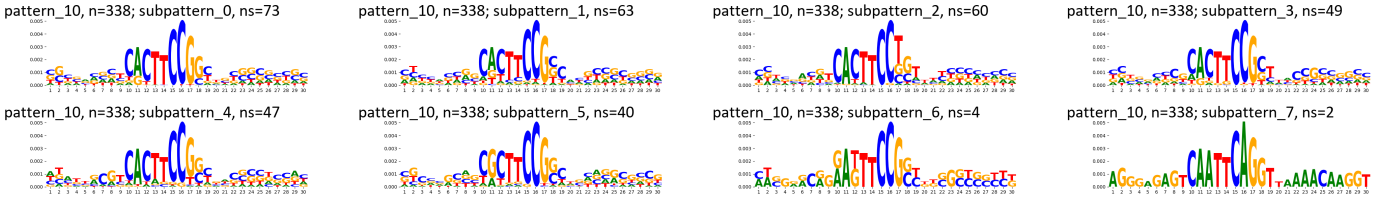

TF-MoDisCO pattern_10 n=338, PWM

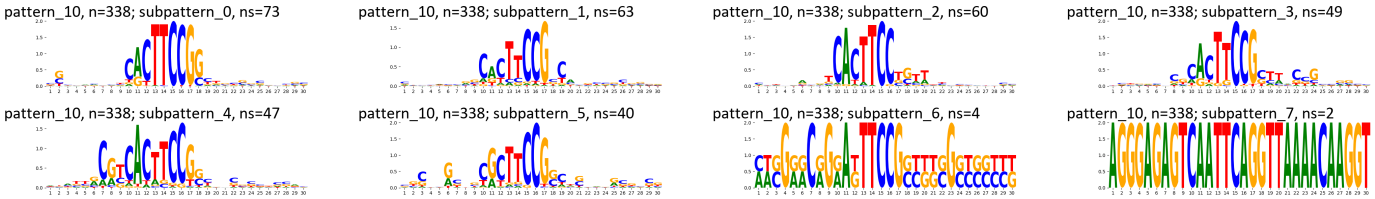

TF-MoDisCO pattern_3 n=1025, CWM

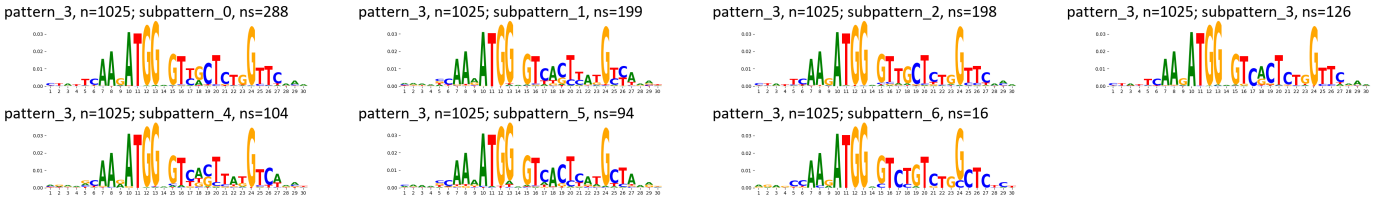

TF-MoDisCO pattern_3 n=1025, PWM

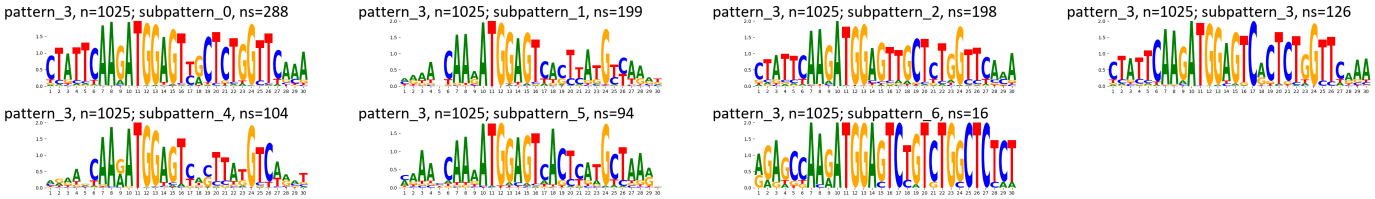

TF-MoDisCO pattern_6 n=700, CWM

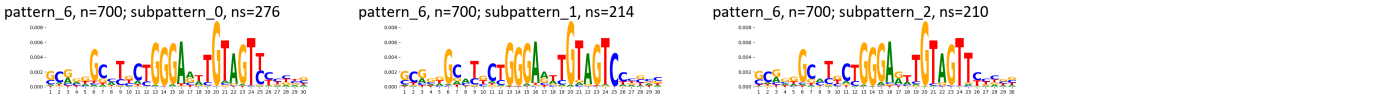

TF-MoDisCO pattern_6 n=700, PWM

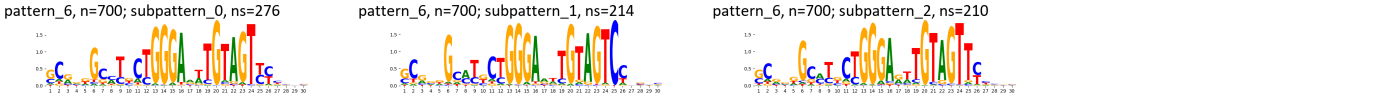

Supplementary Figure 1141: TF-MoDisCO subpatterns for the ZNF395 transcription factor in K562 (accession ENCSR462QZZ).

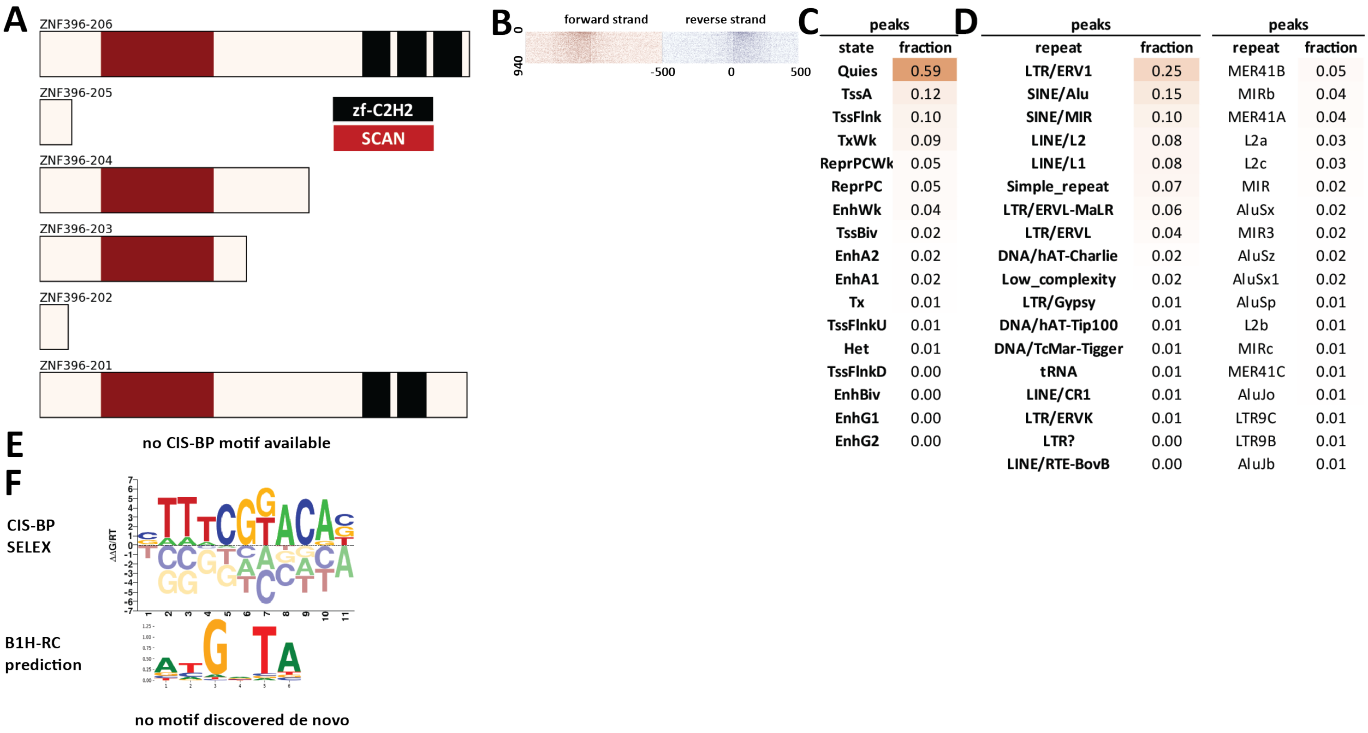

peaks	
state	fraction
Quies	0.59
TssA	0.12
TssFlnk	0.10
TxWk	0.09
ReprPCWk	0.05
ReprPC	0.05
EnhWk	0.04
TssBiv	0.02
EnhA2	0.02
EnhA1	0.02
Tx	0.01
TssFlnkU	0.01
Het	0.01
TssFlnkD	0.00
EnhBiv	0.00
EnhG1	0.00
EnhG2	0.00

peaks	
repeat	fraction
LTR/ERV1	0.25
SINE/Alu	0.15
SINE/MIR	0.10
LINE/L2	0.08
LINE/L1	0.08
Simple_repeat	0.07
LTR/ERVL-MaLR	0.06
LTR/ERVL	0.04
DNA/hAT-Charlie	0.02
Low_complexity	0.02
LTR/Gypsy	0.01
DNA/hAT-Tip100	0.01
DNA/TcMar-Tigger	0.01
tRNA	0.01
LINE/CR1	0.01
LTR/ERVK	0.01
LTR?	0.00
LINE/RTE-BovB	0.00

peaks	
repeat	fraction
MER41B	0.05
MIRb	0.04
MER41A	0.04
L2a	0.03
L2c	0.03
MIR	0.02
AluSx	0.02
MIR3	0.02
AluSz	0.02
AluSx1	0.02
AluSp	0.01
L2b	0.01
MIRc	0.01
MER41C	0.01
AluJo	0.01
LTR9C	0.01
LTR9B	0.01
AluJb	0.01

Supplementary Figure 1142: Properties and genomic distribution of motifs identified for the ZNF396 transcription factor in WTC11 (accession ENCSR422ODX).

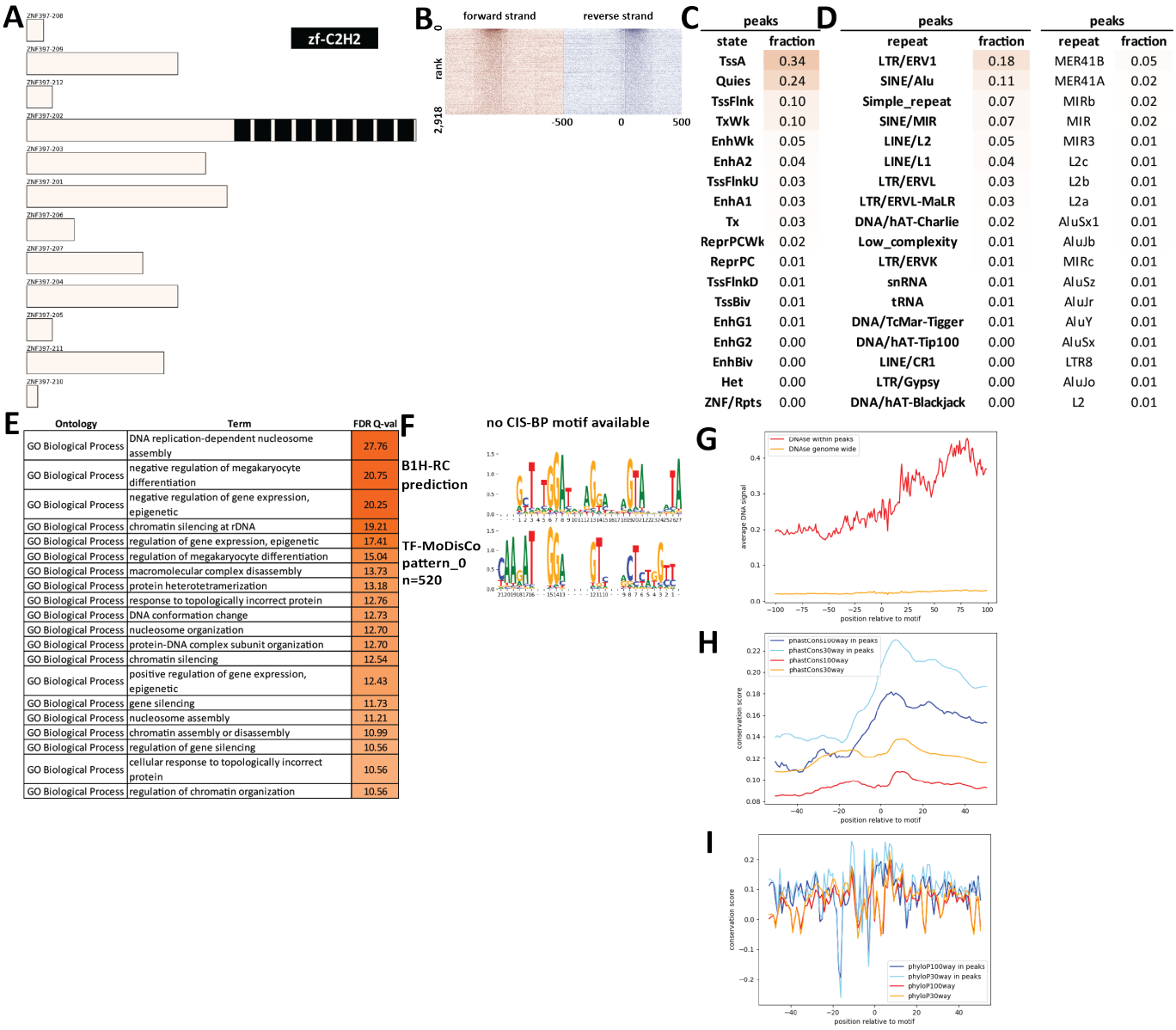

peaks	
state	fraction
TssA	0.34
Quies	0.24
TssFlnk	0.10
TxWk	0.10
EnhWk	0.05
EnhA2	0.04
TssFlnkU	0.03
EnhA1	0.03
Tx	0.03
ReprPCWk	0.02
ReprPC	0.01
TssFlnkD	0.01
TssBiv	0.01
EnhG1	0.01
EnhG2	0.00
EnhBiv	0.00
Het	0.00
ZNF/Rpts	0.00

peaks		peaks	
repeat	fraction	repeat	fraction
LTR/ERV1	0.18	MER41B	0.05
SINE/Alu	0.11	MER41A	0.02
Simple_repeat	0.07	MIRb	0.02
SINE/MIR	0.07	MIR	0.02
LINE/L2	0.05	MIR3	0.01
LINE/L1	0.04	L2c	0.01
LTR/ERVL	0.03	L2b	0.01
LTR/ERVL-MaLR	0.03	L2a	0.01
DNA/hAT-Charlie	0.02	AluSx1	0.01
Low_complexity	0.01	AluJb	0.01
LTR/ERVK	0.01	MIRc	0.01
snRNA	0.01	AluSz	0.01
tRNA	0.01	AluJr	0.01
DNA/TcMar-Tigger	0.01	AluY	0.01
DNA/hAT-Tip100	0.00	AluSx	0.01
LINE/CR1	0.00	LTR8	0.01
LTR/Gypsy	0.00	AluJo	0.01
DNA/hAT-Blackjack	0.00	L2	0.01

Ontology	Term	FDR Q-val
GO Biological Process	DNA replication-dependent nucleosome assembly	27.76
GO Biological Process	negative regulation of megakaryocyte differentiation	20.75
GO Biological Process	negative regulation of gene expression, epigenetic	20.25
GO Biological Process	chromatin silencing at rDNA	19.21
GO Biological Process	regulation of gene expression, epigenetic	17.41
GO Biological Process	regulation of megakaryocyte differentiation	15.04
GO Biological Process	macromolecular complex disassembly	13.73
GO Biological Process	protein heterotetramerization	13.18
GO Biological Process	response to topologically incorrect protein	12.76
GO Biological Process	DNA conformation change	12.73
GO Biological Process	nucleosome organization	12.70
GO Biological Process	protein-DNA complex subunit organization	12.70
GO Biological Process	chromatin silencing	12.54
GO Biological Process	positive regulation of gene expression, epigenetic	12.43
GO Biological Process	gene silencing	11.73
GO Biological Process	nucleosome assembly	11.21
GO Biological Process	chromatin assembly or disassembly	10.99
GO Biological Process	regulation of gene silencing	10.56
GO Biological Process	cellular response to topologically incorrect protein	10.56
GO Biological Process	regulation of chromatin organization	10.56

Supplementary Figure 1143: Properties and genomic distribution of motifs identified for the ZNF397 transcription factor in K562 (accession ENCSR508EEX).

TF-MoDisCO pattern_0 n=520, CWM

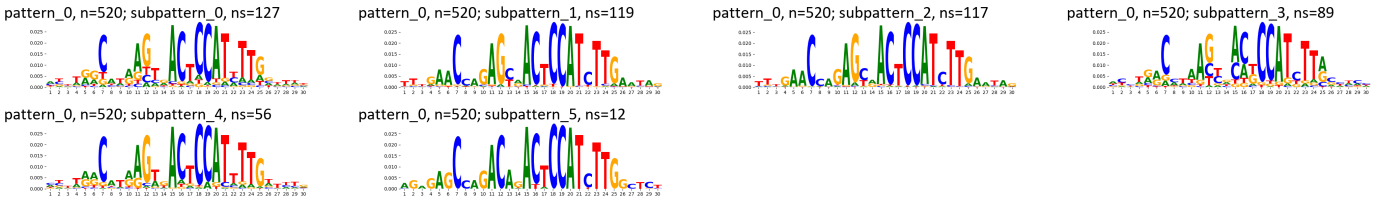

TF-MoDisCO pattern_0 n=520, PWM

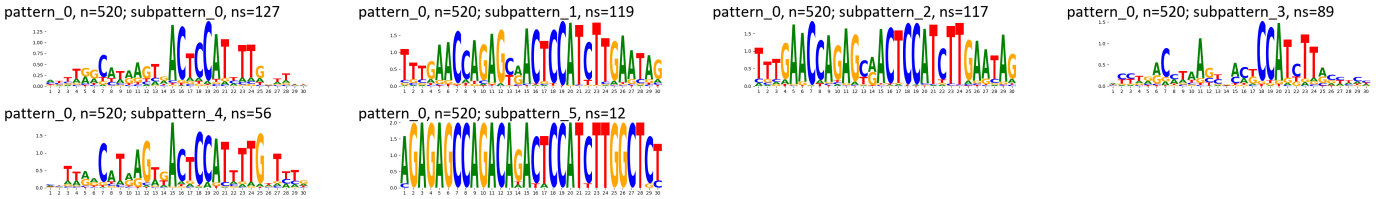

Supplementary Figure 1144: TF-MoDisCO subpatterns for the ZNF397 transcription factor in K562 (accession ENCSR508EEX).

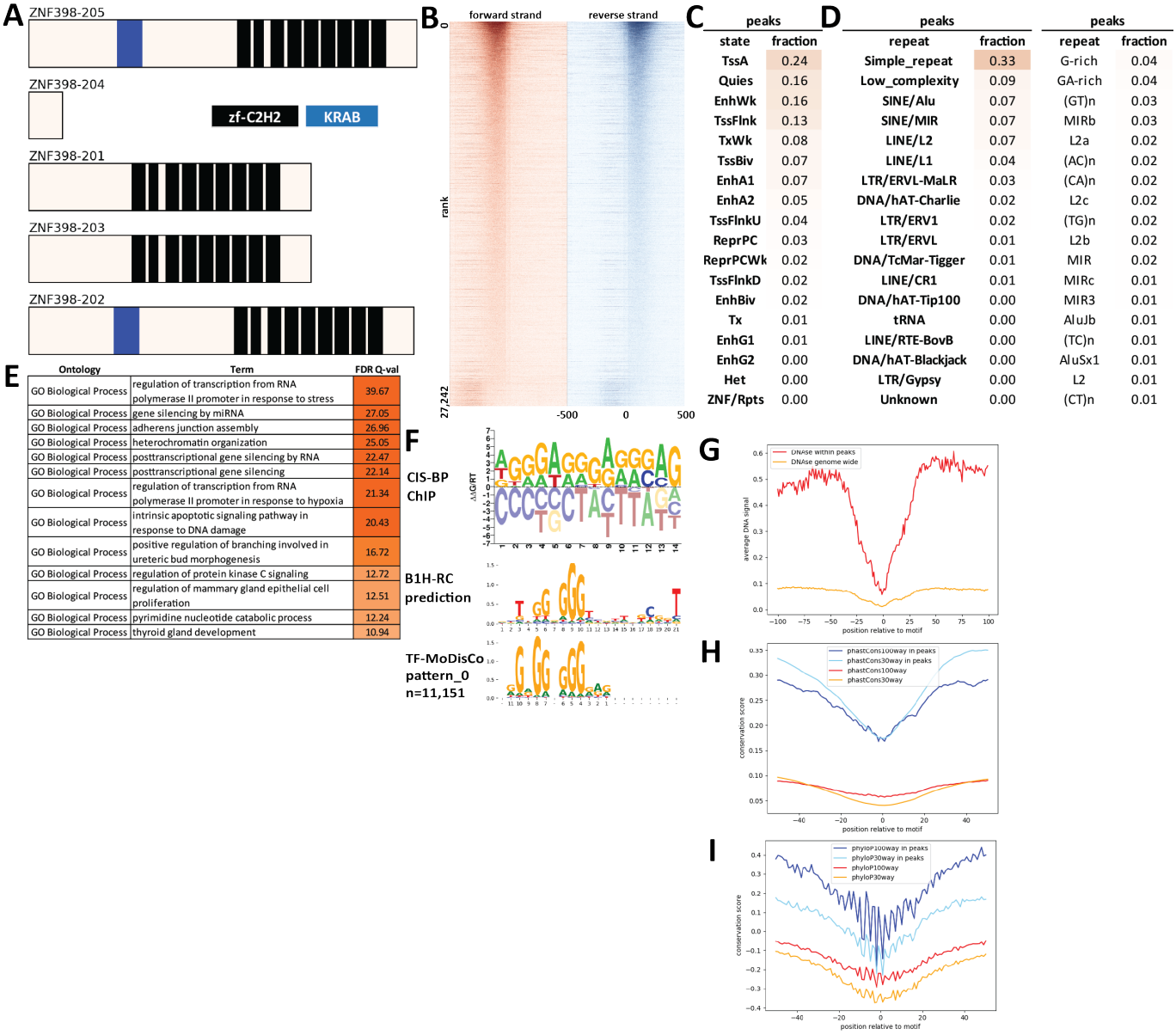

Supplementary Figure 1145: Properties and genomic distribution of motifs identified for the ZNF398 transcription factor in HEK293 (accession ENCSR676ZEF).

TF-MoDisCO pattern_0 n=11151, CWM

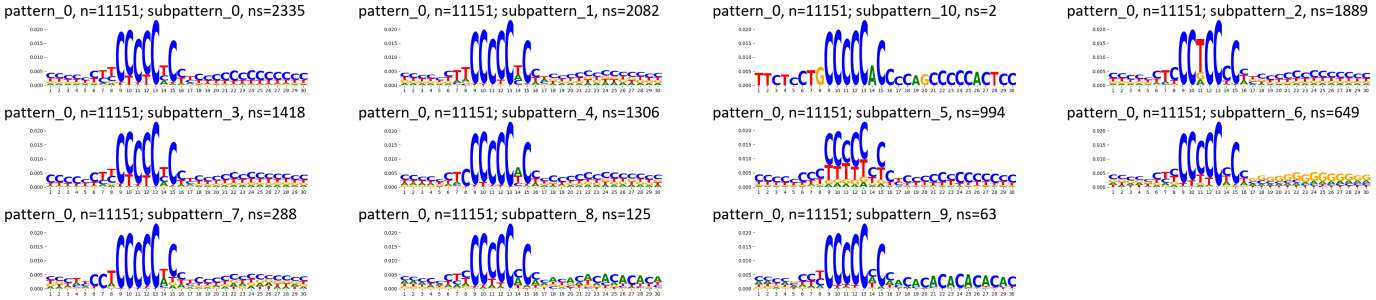

TF-MoDisCO pattern_0 n=11151, PWM

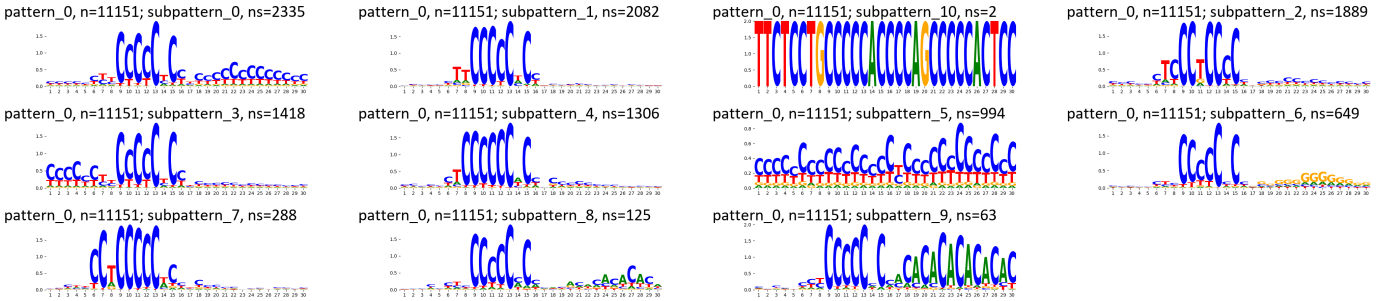

Supplementary Figure 1146: TF-MoDisCO subpatterns for the ZNF398 transcription factor in HEK293 (accession ENCSR676ZEF).

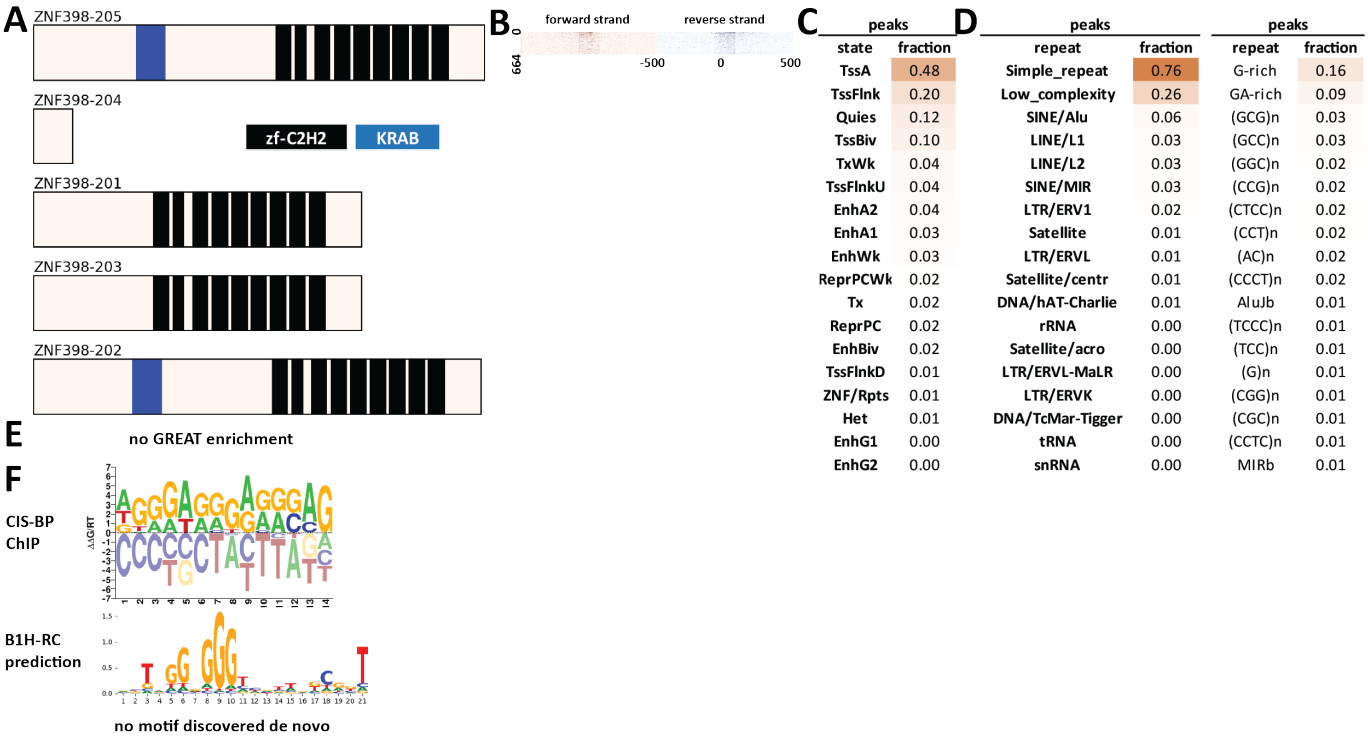

Supplementary Figure 1147: Properties and genomic distribution of motifs identified for the ZNF398 transcription factor in HEK293 (accession ChipExo models).

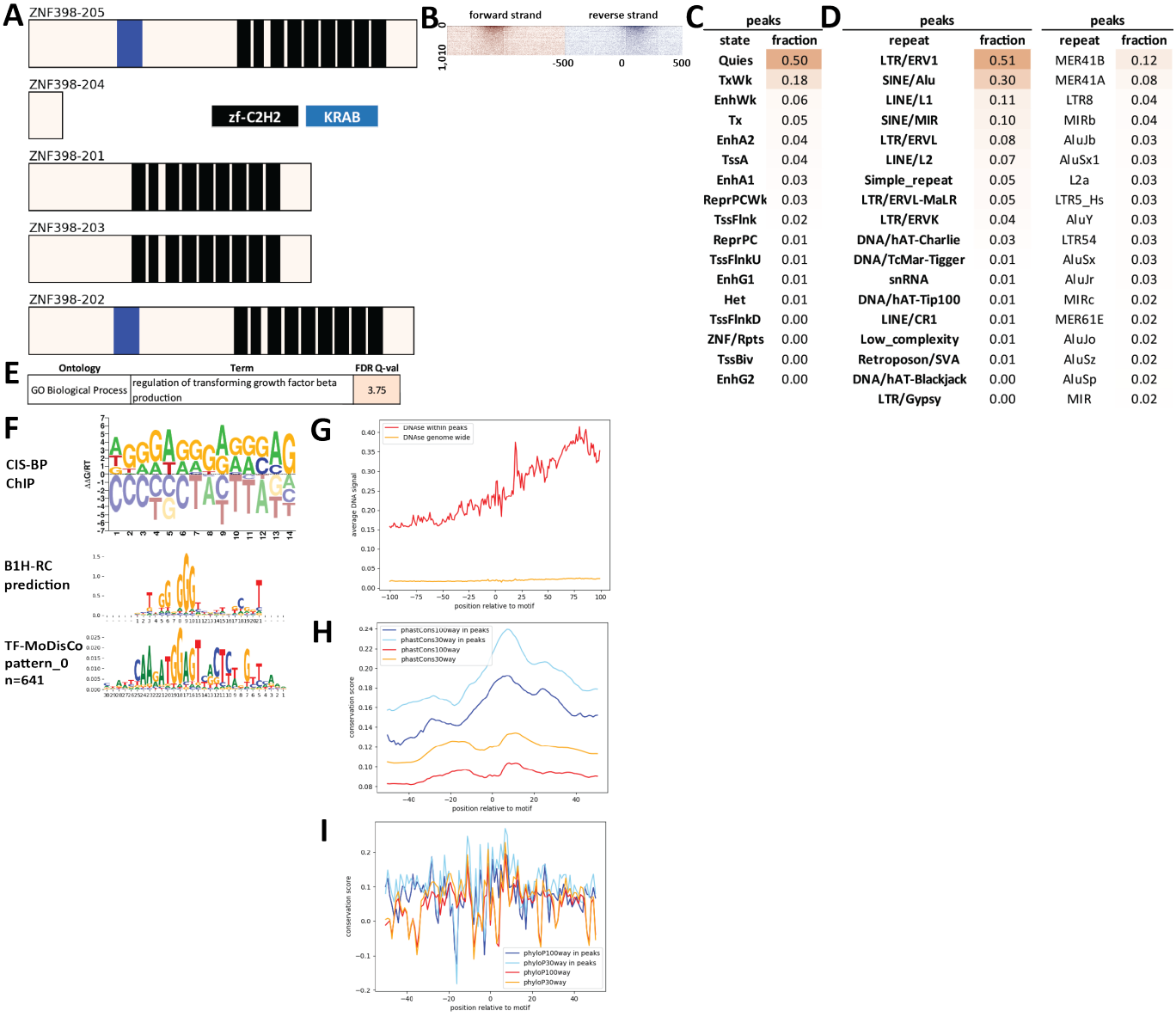

Supplementary Figure 1148: Properties and genomic distribution of motifs identified for the ZNF398 transcription factor in K562 (accession ENCSR948JND).

TF-MoDisCO pattern_0 n=641, CWM

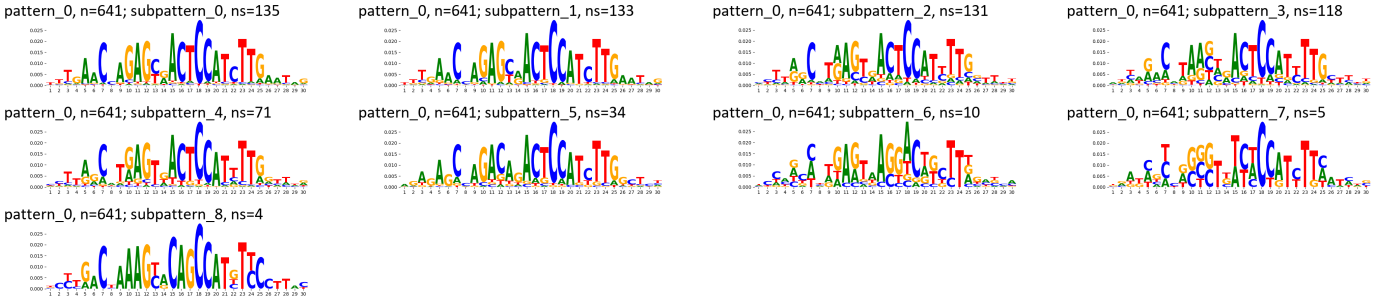

TF-MoDisCO pattern_0 n=641, PWM

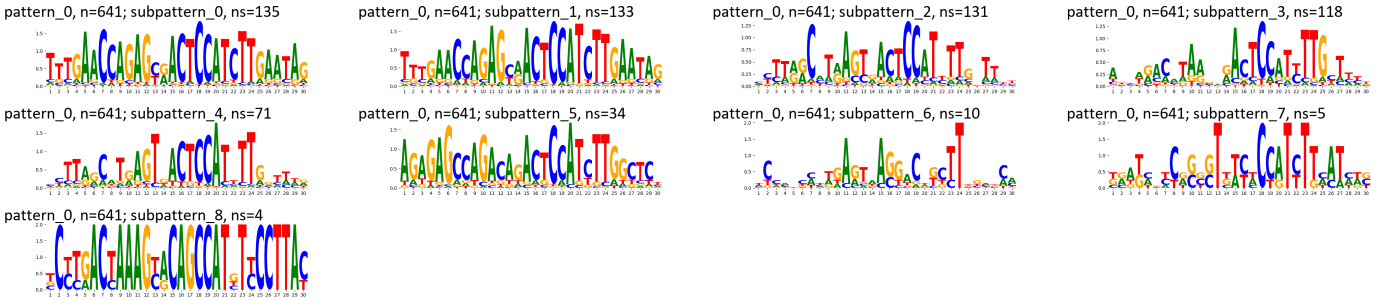

Supplementary Figure 1149: TF-MoDisCO subpatterns for the ZNF398 transcription factor in K562 (accession ENCSR948JND).

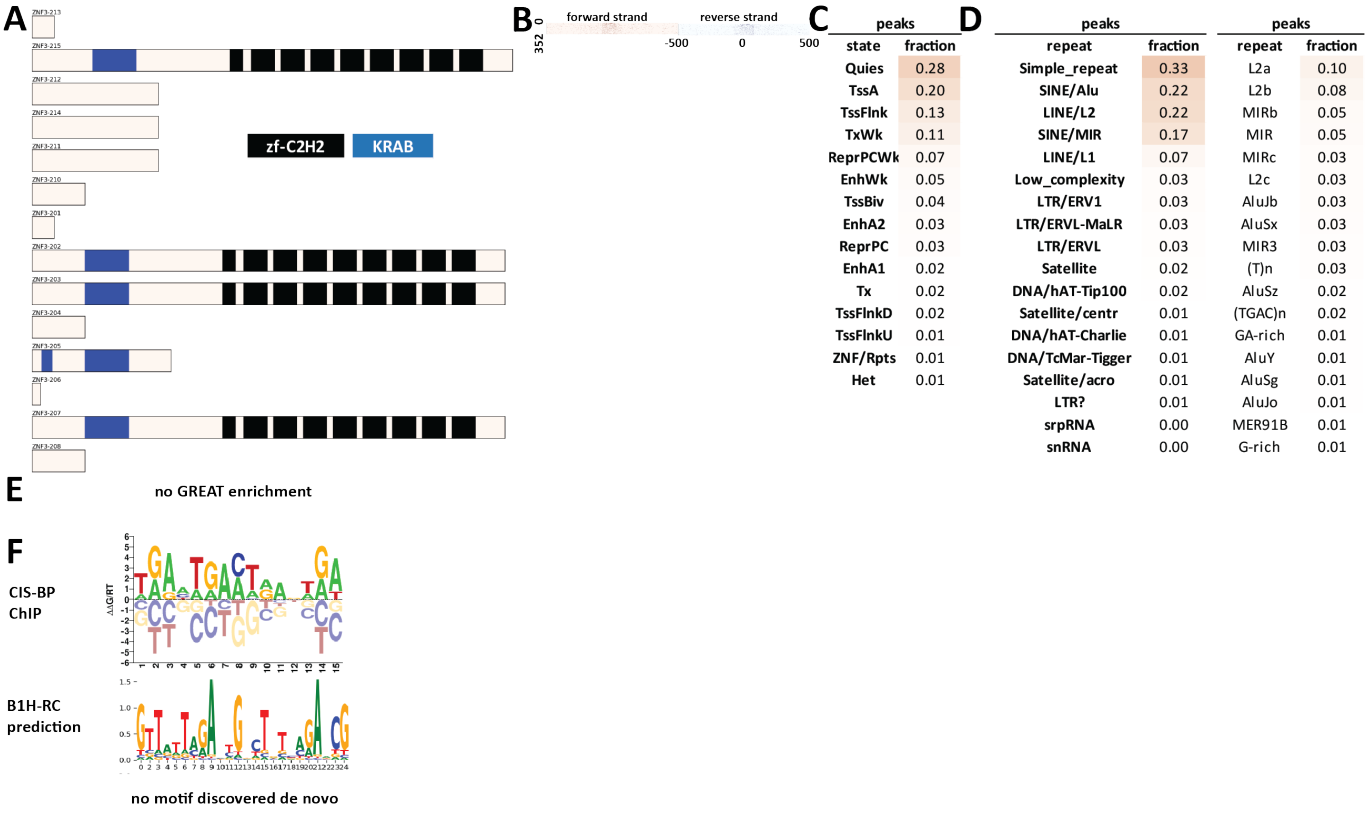

peaks	
state	fraction
Quies	0.28
TssA	0.20
TssFlnk	0.13
TxWk	0.11
ReprPCWk	0.07
EnhWk	0.05
TssBiv	0.04
EnhA2	0.03
ReprPC	0.03
EnhA1	0.02
Tx	0.02
TssFlnkD	0.02
TssFlnkU	0.01
ZNF/Rpts	0.01
Het	0.01

peaks	
repeat	fraction
Simple_repeat	0.33
SINE/Alu	0.22
LINE/L2	0.22
SINE/MIR	0.17
LINE/L1	0.07
Low_complexity	0.03
LTR/ERV1	0.03
LTR/ERVL-MaLR	0.03
LTR/ERVL	0.03
Satellite	0.02
DNA/hAT-Tip100	0.02
Satellite/centr	0.01
DNA/hAT-Charlie	0.01
DNA/TcMar-Tigger	0.01
Satellite/acro	0.01
LTR?	0.01
srpRNA	0.00
snRNA	0.00

peaks	
repeat	fraction
L2a	0.10
L2b	0.08
MIRb	0.05
MIR	0.05
MIRc	0.03
L2c	0.03
AluJb	0.03
AluSx	0.03
MIR3	0.03
(T)n	0.03
AluSz	0.02
(TGAC)n	0.02
GA-rich	0.01
AluY	0.01
AluSg	0.01
AluJo	0.01
MER91B	0.01
G-rich	0.01

Supplementary Figure 1150: Properties and genomic distribution of motifs identified for the ZNF3 transcription factor in HEK293 (accession ChipExo models).

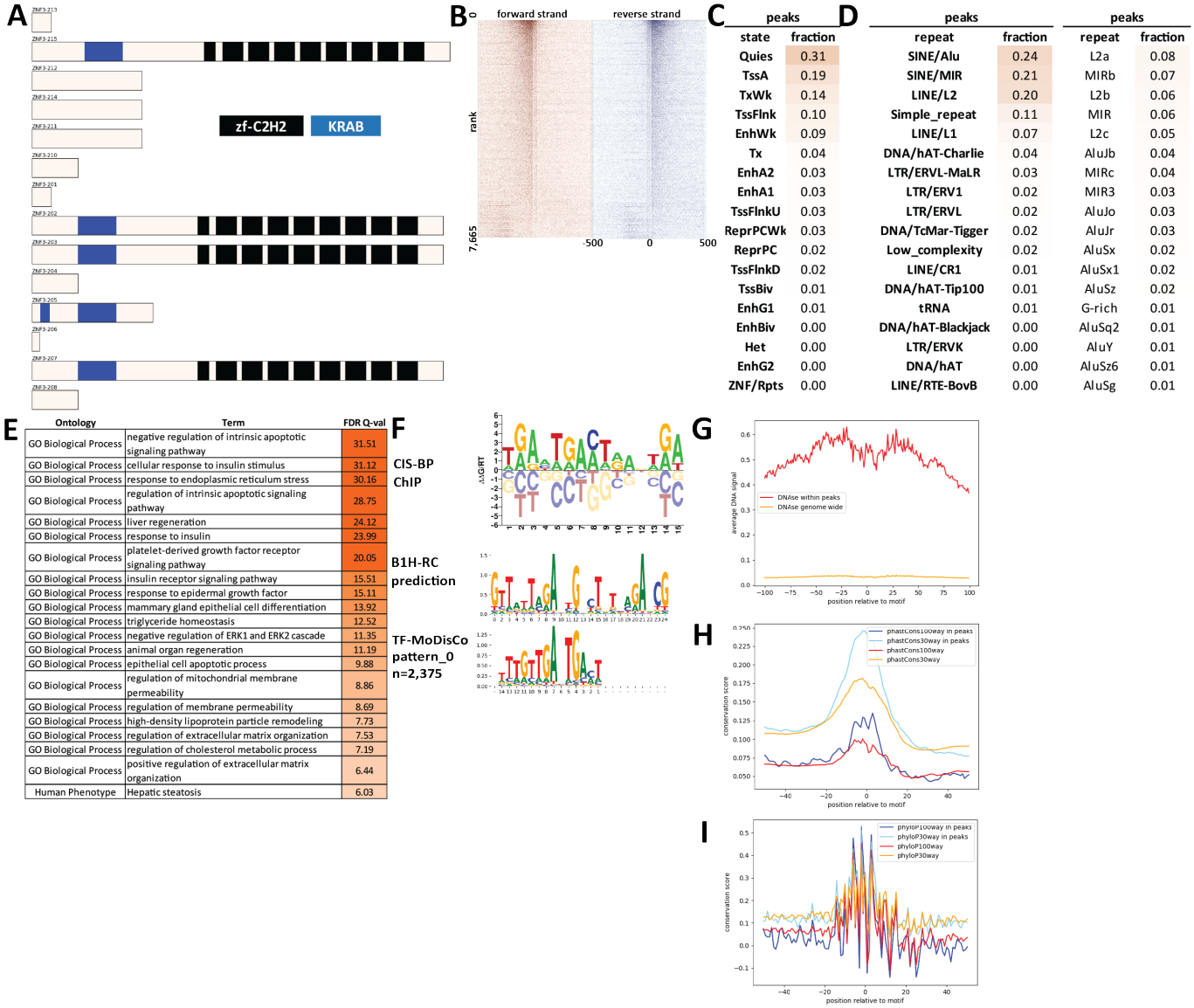

Supplementary Figure 1151: Properties and genomic distribution of motifs identified for the ZNF3 transcription factor in HepG2 (accession ENCSR182QWU).

TF-MoDisCO pattern_0 n=2375, CWM

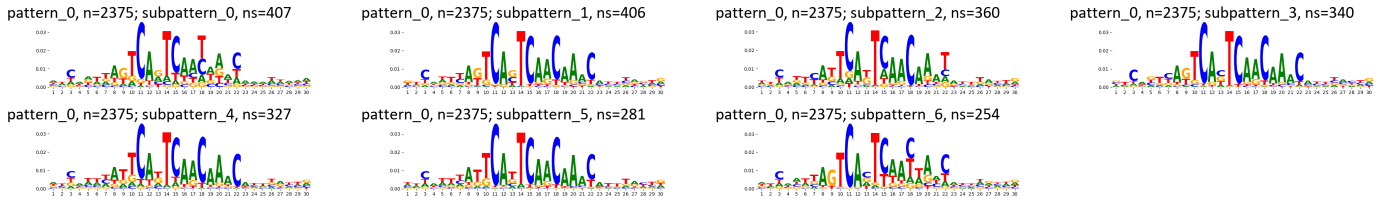

TF-MoDisCO pattern_0 n=2375, PWM

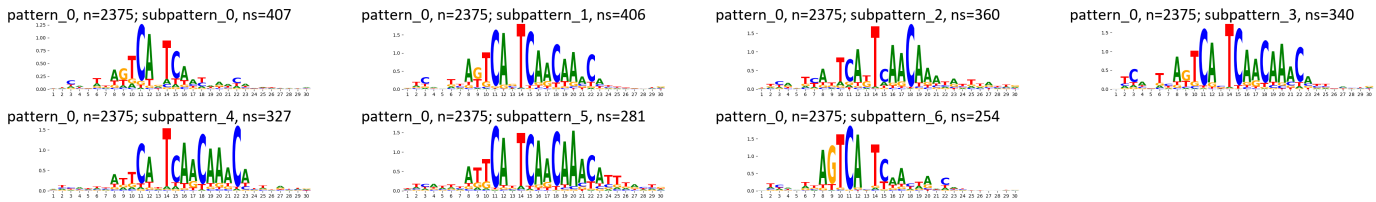

Supplementary Figure 1152: TF-MoDisCO subpatterns for the ZNF3 transcription factor in HepG2 (accession ENCSR182QWU).

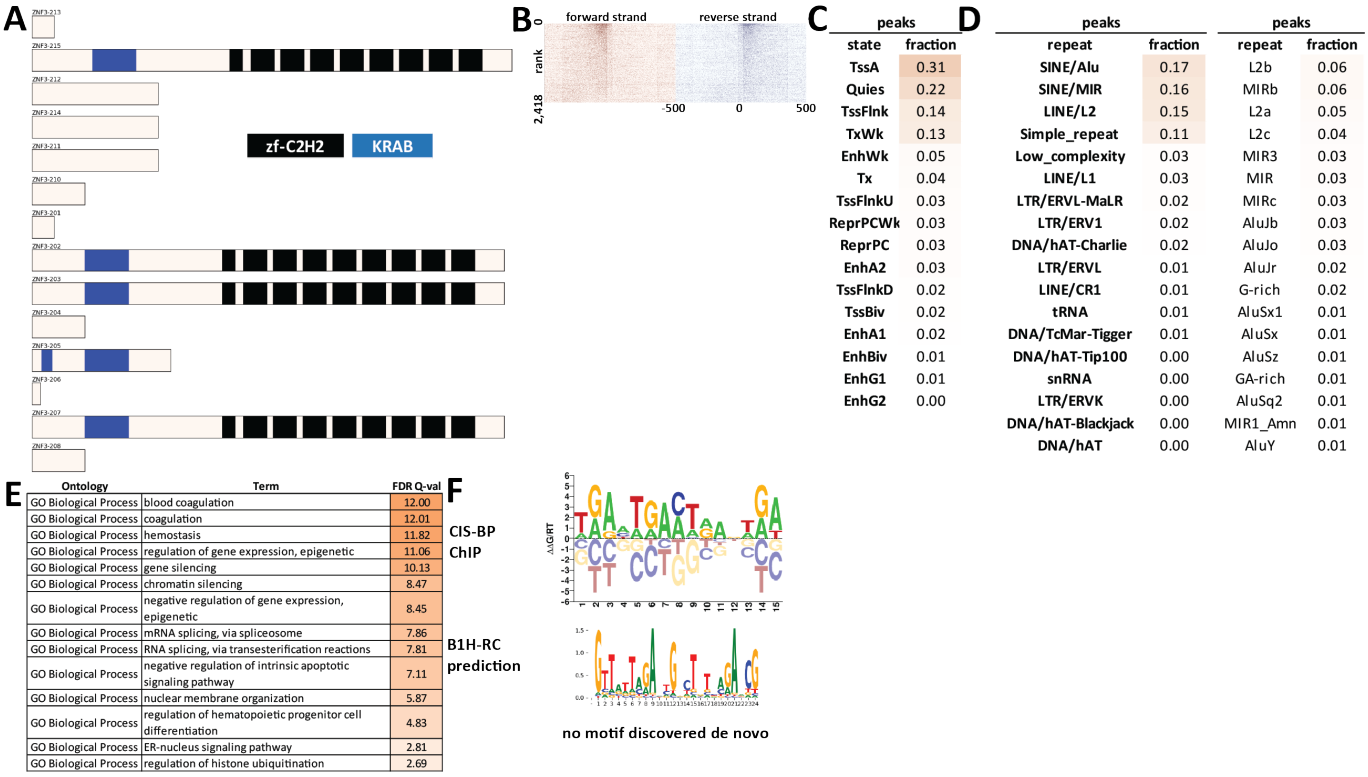

Supplementary Figure 1153: Properties and genomic distribution of motifs identified for the ZNF3 transcription factor in K562 (accession ENCSR195QFV).

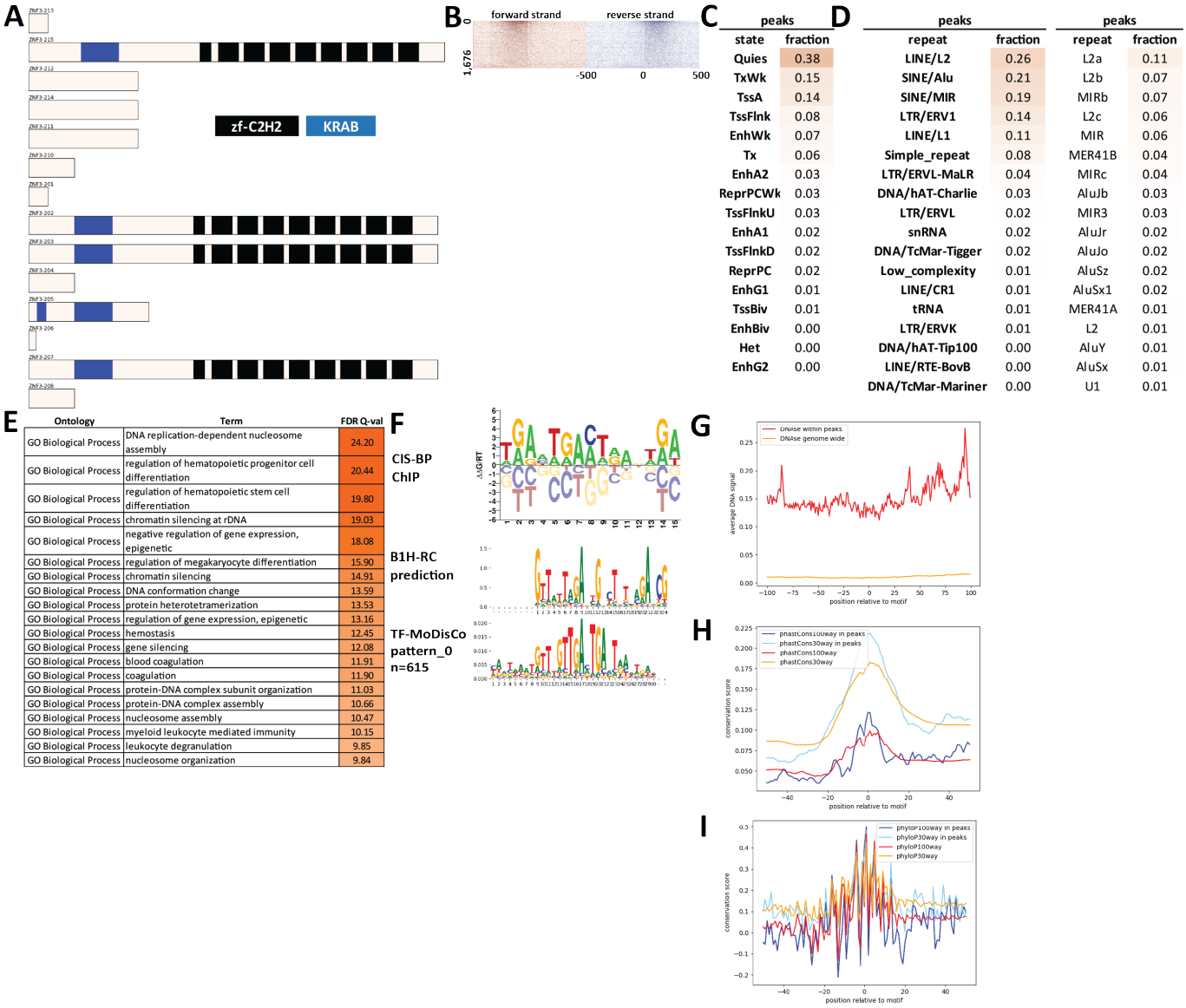

Supplementary Figure 1154: Properties and genomic distribution of motifs identified for the ZNF3 transcription factor in K562 (accession ENCSR934RJP).

TF-MoDisCO pattern_0 n=615, CWM

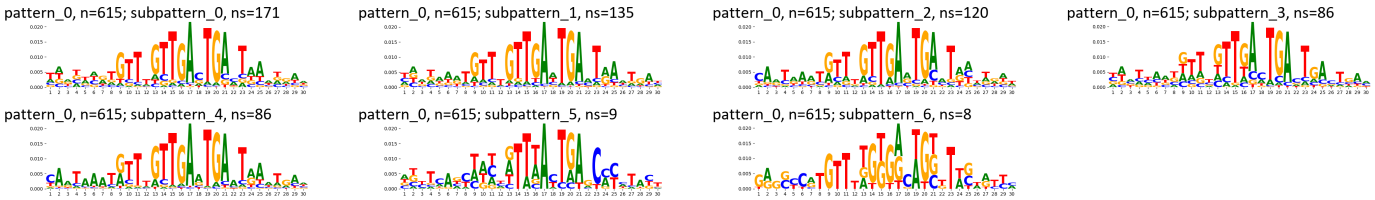

TF-MoDisCO pattern_0 n=615, PWM

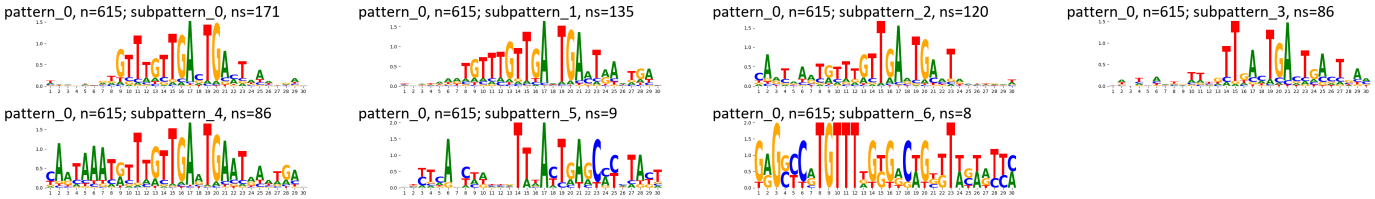

Supplementary Figure 1155: TF-MoDisCO subpatterns for the ZNF3 transcription factor in K562 (accession ENCSR934RJP).

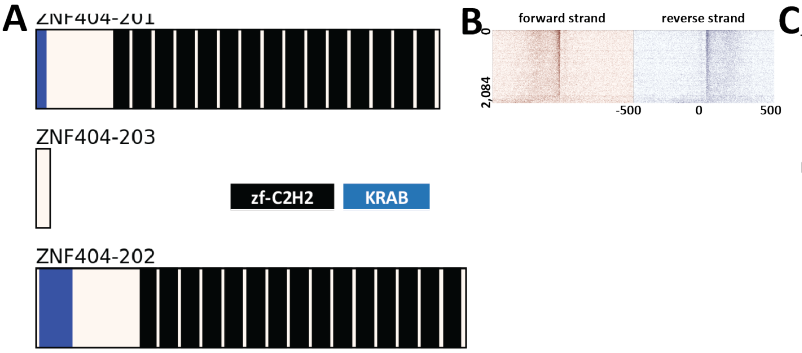

C

peaks	
state	fraction
Quies	0.50
TxWk	0.18
TssA	0.08
Tx	0.06
ReprPCWk	0.04
EnhWk	0.04
TssFlnk	0.03
EnhA1	0.03
EnhA2	0.02
Het	0.02
TssFlnkU	0.02
ReprPC	0.01
TssBiv	0.01
EnhBiv	0.01
TssFlnkD	0.00
ZNF/Rpts	0.00
EnhG1	0.00
EnhG2	0.00

D

peaks		peaks	
repeat	fraction	repeat	fraction
SINE/Alu	0.92	(AAAT)n	0.27
Simple_repeat	0.68	AluSx1	0.11
LINE/L1	0.20	AluSx	0.11
SINE/MIR	0.07	AluY	0.09
LINE/L2	0.06	AluJb	0.09
LTR/ERVL-MaLR	0.04	AluSz	0.08
LTR/ERV1	0.04	(ATTT)n	0.07
DNA/hAT-Charlie	0.03	(TTAT)n	0.06
DNA/TcMar-Tigger	0.02	AluJr	0.06
LTR/ERVL	0.01	(TTTA)n	0.05
Low_complexity	0.01	AluSq2	0.05
LINE/CR1	0.01	AluJo	0.05
LTR/ERVK	0.00	AluSp	0.05
DNA/hAT-Tip100	0.00	(AATA)n	0.04
DNA/hAT-Blackjack	0.00	AluSz6	0.04
tRNA	0.00	(TATT)n	0.04
Retroposon/SVA	0.00	AluSg	0.03
snRNA	0.00	AluSc	0.03

E

Ontology	Term	FDR Q-val
GO Biological Process	antigen receptor-mediated signaling pathway	5.10
GO Biological Process	regulation of mRNA stability	3.67
GO Biological Process	regulation of RNA stability	3.35
GO Biological Process	T cell receptor signaling pathway	3.26
GO Biological Process	peptidyl-tyrosine autophosphorylation	3.13
GO Biological Process	positive regulation of multicellular organism growth	2.91
GO Biological Process	myelination in peripheral nervous system	2.56
GO Biological Process	Schwann cell development	2.51
GO Biological Process	establishment of epithelial cell polarity	2.20
GO Biological Process	B cell receptor signaling pathway	1.95
GO Biological Process	epithelial cell-cell adhesion	1.93
GO Biological Process	Schwann cell differentiation	1.85
GO Biological Process	regulation of T cell receptor signaling pathway	1.54
GO Biological Process	long-chain fatty acid biosynthetic process	1.32
Human Phenotype	Laryngomalacia	1.46

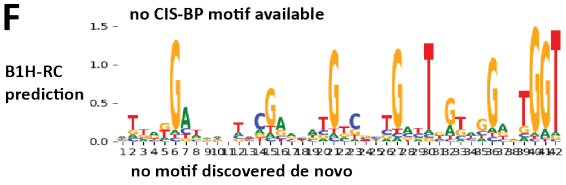

Supplementary Figure 1156: Properties and genomic distribution of motifs identified for the ZNF404 transcription factor in HEK293 (accession ENCSR669GUM).

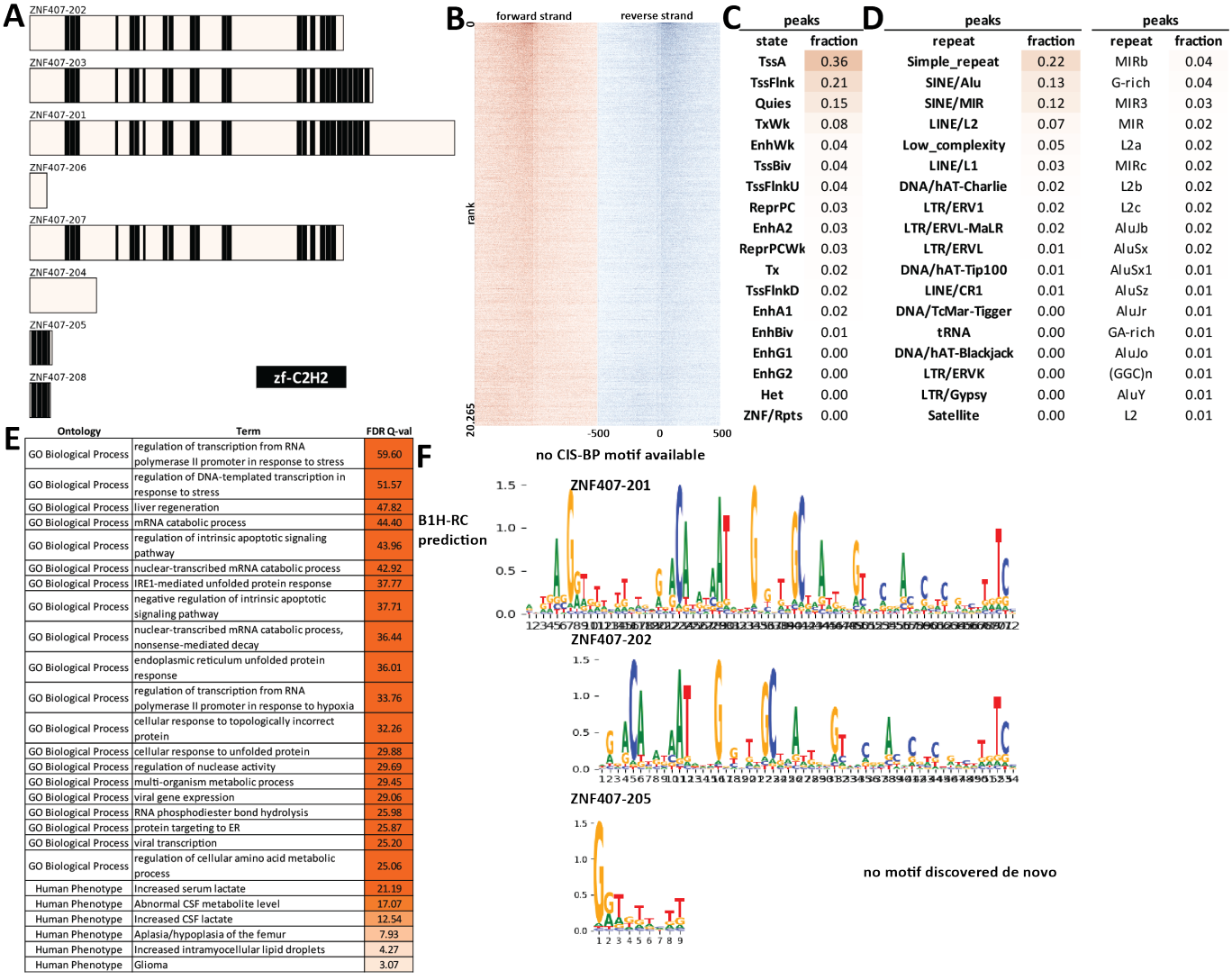

peaks	
state	fraction
TssA	0.36
TssFlnk	0.21
Quies	0.15
TxWk	0.08
EnhWk	0.04
TssBiv	0.04
TssFlnkU	0.04
ReprPC	0.03
EnhA2	0.03
ReprPCWk	0.03
Tx	0.02
TssFlnkD	0.02
EnhA1	0.02
EnhBiv	0.01
EnhG1	0.00
EnhG2	0.00
Het	0.00
ZNF/Rpts	0.00

peaks		peaks	
repeat	fraction	repeat	fraction
Simple_repeat	0.22	MIRb	0.04
SINE/Alu	0.13	G-rich	0.04
SINE/MIR	0.12	MIR3	0.03
LINE/L2	0.07	MIR	0.02
Low_complexity	0.05	L2a	0.02
LINE/L1	0.03	MIRc	0.02
DNA/hAT-Charlie	0.02	L2b	0.02
LTR/ERV1	0.02	L2c	0.02
LTR/ERVL-MaLR	0.02	AluJb	0.02
LTR/ERVL	0.01	AluSx	0.02
DNA/hAT-Tip100	0.01	AluSx1	0.01
LINE/CR1	0.01	AluSz	0.01
DNA/TcMar-Tigger	0.00	AluJr	0.01
tRNA	0.00	GA-rich	0.01
DNA/hAT-Blackjack	0.00	AluJo	0.01
LTR/ERVK	0.00	(GGC)n	0.01
LTR/Gypsy	0.00	AluY	0.01
Satellite	0.00	L2	0.01

Ontology	Term	FDR Q-val
GO Biological Process	regulation of transcription from RNA polymerase II promoter in response to stress	59.60
GO Biological Process	regulation of DNA-templated transcription in response to stress	51.57
GO Biological Process	liver regeneration	47.82
GO Biological Process	mRNA catabolic process	44.40
GO Biological Process	regulation of intrinsic apoptotic signaling pathway	43.96
GO Biological Process	nuclear-transcribed mRNA catabolic process	42.92
GO Biological Process	IRE1-mediated unfolded protein response	37.77
GO Biological Process	negative regulation of intrinsic apoptotic signaling pathway	37.71
GO Biological Process	nuclear-transcribed mRNA catabolic process, nonsense-mediated decay	36.44
GO Biological Process	endoplasmic reticulum unfolded protein response	36.01
GO Biological Process	regulation of transcription from RNA polymerase II promoter in response to hypoxia	33.76
GO Biological Process	cellular response to topologically incorrect protein	32.26
GO Biological Process	cellular response to unfolded protein	29.88
GO Biological Process	regulation of nuclease activity	29.69
GO Biological Process	multi-organism metabolic process	29.45
GO Biological Process	viral gene expression	29.06
GO Biological Process	RNA phosphodiester bond hydrolysis	25.98
GO Biological Process	protein targeting to ER	25.87
GO Biological Process	viral transcription	25.20
GO Biological Process	regulation of cellular amino acid metabolic process	25.06
Human Phenotype	Increased serum lactate	21.19
Human Phenotype	Abnormal CSF metabolite level	17.07
Human Phenotype	Increased CSF lactate	12.54
Human Phenotype	Aplasia/hypoplasia of the femur	7.93
Human Phenotype	Increased intramyocellular lipid droplets	4.27
Human Phenotype	Glioma	3.07

Supplementary Figure 1157: Properties and genomic distribution of motifs identified for the ZNF407 transcription factor in HepG2 (accession ENCSR005WGY).

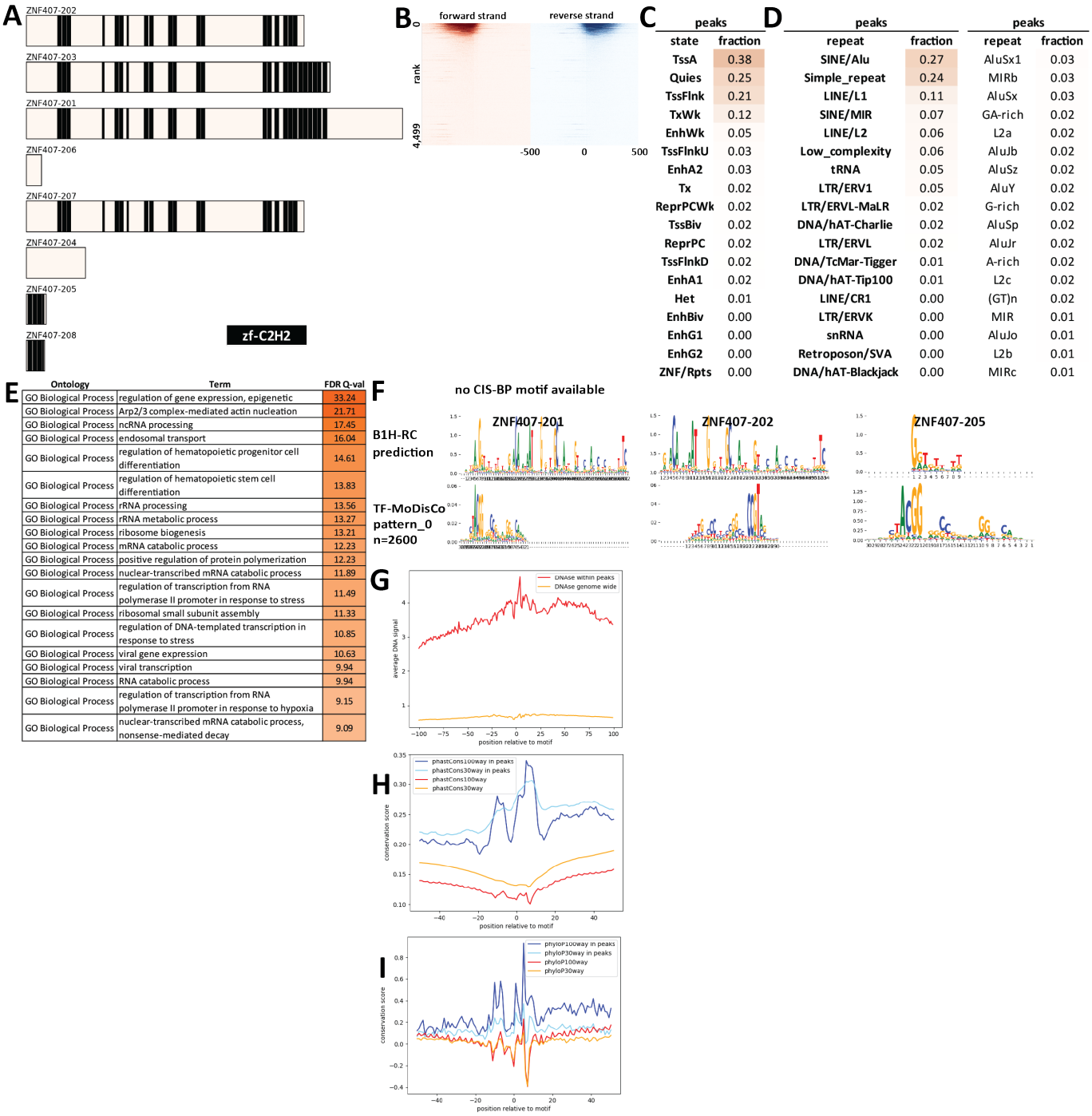

peaks	
state	fraction
TssA	0.38
Quies	0.25
TssFlnk	0.21
TxWk	0.12
EnhWk	0.05
TssFlnkU	0.03
EnhA2	0.03
Tx	0.02
ReprPCWk	0.02
TssBiv	0.02
ReprPC	0.02
TssFlnkD	0.02
EnhA1	0.02
Het	0.01
EnhBiv	0.00
EnhG1	0.00
EnhG2	0.00
ZNF/Rpts	0.00

peaks		peaks	
repeat	fraction	repeat	fraction
SINE/Alu	0.27	AluSx1	0.03
Simple_repeat	0.24	MIRb	0.03
LINE/L1	0.11	AluSx	0.03
SINE/MIR	0.07	GA-rich	0.02
LINE/L2	0.06	L2a	0.02
Low_complexity	0.06	AluJb	0.02
tRNA	0.05	AluSz	0.02
LTR/ERV1	0.05	AluY	0.02
LTR/ERVL-MaLR	0.02	G-rich	0.02
DNA/hAT-Charlie	0.02	AluSp	0.02
LTR/ERVL	0.02	AluJr	0.02
DNA/TcMar-Tigger	0.01	A-rich	0.02
DNA/hAT-Tip100	0.01	L2c	0.02
LINE/CR1	0.00	(GT)n	0.02
LTR/ERVK	0.00	MIR	0.01
snRNA	0.00	AluJo	0.01
Retroposon/SVA	0.00	L2b	0.01
DNA/hAT-Blackjack	0.00	MIRc	0.01

Ontology	Term	FDR Q-val
GO Biological Process	regulation of gene expression, epigenetic	33.24
GO Biological Process	Arp2/3 complex-mediated actin nucleation	21.71
GO Biological Process	ncRNA processing	17.45
GO Biological Process	endosomal transport	16.04
GO Biological Process	regulation of hematopoietic progenitor cell differentiation	14.61
GO Biological Process	regulation of hematopoietic stem cell differentiation	13.83
GO Biological Process	rRNA processing	13.56
GO Biological Process	rRNA metabolic process	13.27
GO Biological Process	ribosome biogenesis	13.21
GO Biological Process	mRNA catabolic process	12.23
GO Biological Process	positive regulation of protein polymerization	12.23
GO Biological Process	nuclear-transcribed mRNA catabolic process	11.89
GO Biological Process	regulation of transcription from RNA polymerase II promoter in response to stress	11.49
GO Biological Process	ribosomal small subunit assembly	11.33
GO Biological Process	regulation of DNA-templated transcription in response to stress	10.85
GO Biological Process	viral gene expression	10.63
GO Biological Process	viral transcription	9.94
GO Biological Process	RNA catabolic process	9.94
GO Biological Process	regulation of transcription from RNA polymerase II promoter in response to hypoxia	9.15
GO Biological Process	nuclear-transcribed mRNA catabolic process, nonsense-mediated decay	9.09

Supplementary Figure 1158: Properties and genomic distribution of motifs identified for the ZNF407 transcription factor in K562 (accession ENCSR011NOZ).

TF-MoDisCO pattern_0 n=2600, CWM

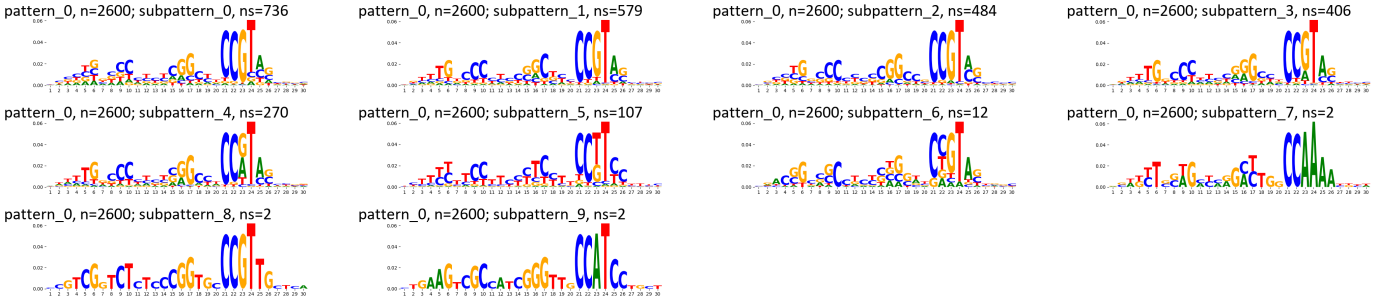

TF-MoDisCO pattern_0 n=2600, PWM

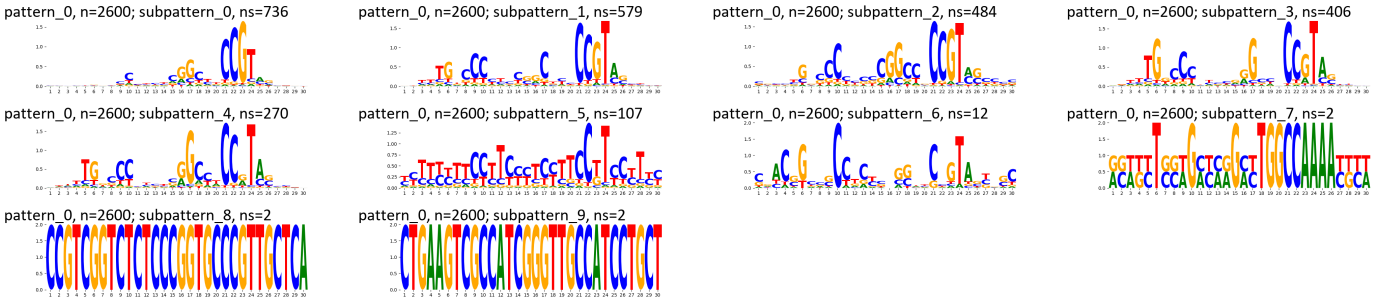

Supplementary Figure 1159: TF-MoDisCO subpatterns for the ZNF407 transcription factor in K562 (accession ENCSR011NOZ).

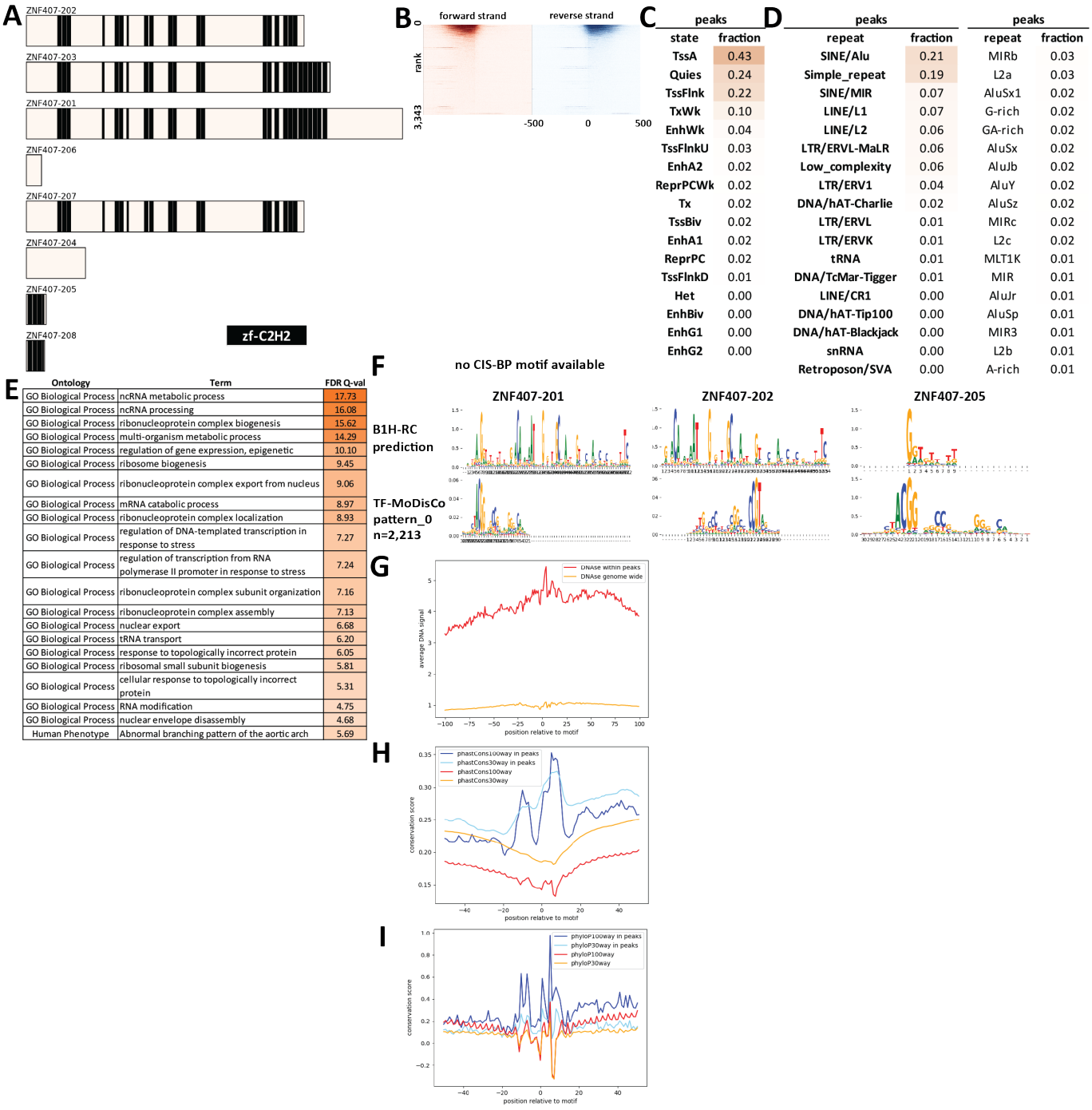

peaks	
state	fraction
TssA	0.43
Quies	0.24
TssFlnk	0.22
TxWk	0.10
EnhWk	0.04
TssFlnkU	0.03
EnhA2	0.02
ReprPCWk	0.02
Tx	0.02
TssBiv	0.02
EnhA1	0.02
ReprPC	0.02
TssFlnkD	0.01
Het	0.00
EnhBiv	0.00
EnhG1	0.00
EnhG2	0.00

peaks		peaks	
repeat	fraction	repeat	fraction
SINE/Alu	0.21	MIRb	0.03
Simple_repeat	0.19	L2a	0.03
SINE/MIR	0.07	AluSx1	0.02
LINE/L1	0.07	G-rich	0.02
LINE/L2	0.06	GA-rich	0.02
LTR/ERVL-MaLR	0.06	AluSx	0.02
Low_complexity	0.06	AluJb	0.02
LTR/ERV1	0.04	AluY	0.02
DNA/hAT-Charlie	0.02	AluSz	0.02
LTR/ERVL	0.01	MIRc	0.02
LTR/ERVK	0.01	L2c	0.02
tRNA	0.01	MLT1K	0.01
DNA/TcMar-Tigger	0.01	MIR	0.01
LINE/CR1	0.00	AluJr	0.01
DNA/hAT-Tip100	0.00	AluSp	0.01
DNA/hAT-Blackjack	0.00	MIR3	0.01
snRNA	0.00	L2b	0.01
Retroposon/SVA	0.00	A-rich	0.01

Ontology	Term	FDR Q-val
GO Biological Process	ncRNA metabolic process	17.73
GO Biological Process	ncRNA processing	16.08
GO Biological Process	ribonucleoprotein complex biogenesis	15.62
GO Biological Process	multi-organism metabolic process	14.29
GO Biological Process	regulation of gene expression, epigenetic	10.10
GO Biological Process	ribosome biogenesis	9.45
GO Biological Process	ribonucleoprotein complex export from nucleus	9.06
GO Biological Process	mRNA catabolic process	8.97
GO Biological Process	ribonucleoprotein complex localization	8.93
GO Biological Process	regulation of DNA-templated transcription in response to stress	7.27
GO Biological Process	regulation of transcription from RNA polymerase II promoter in response to stress	7.24
GO Biological Process	ribonucleoprotein complex subunit organization	7.16
GO Biological Process	ribonucleoprotein complex assembly	7.13
GO Biological Process	nuclear export	6.68
GO Biological Process	tRNA transport	6.20
GO Biological Process	response to topologically incorrect protein	6.05
GO Biological Process	ribosomal small subunit biogenesis	5.81
GO Biological Process	cellular response to topologically incorrect protein	5.31
GO Biological Process	RNA modification	4.75
GO Biological Process	nuclear envelope disassembly	4.68
Human Phenotype	Abnormal branching pattern of the aortic arch	5.69

Supplementary Figure 1160: Properties and genomic distribution of motifs identified for the ZNF407 transcription factor in K562 (accession ENCSR439OCL).

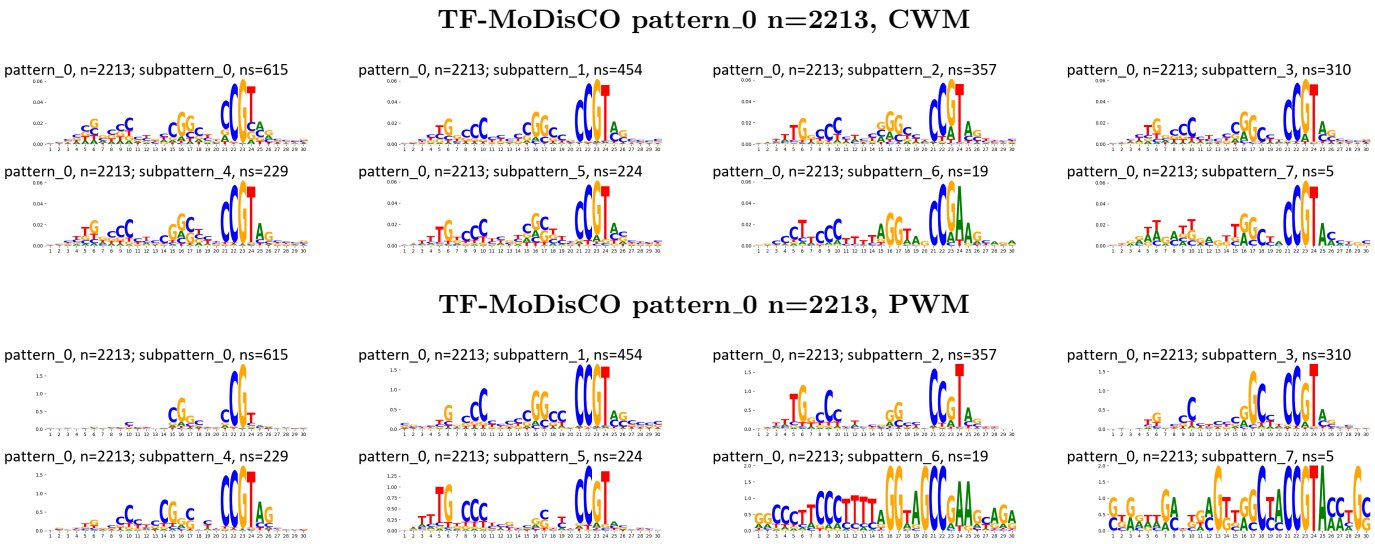

Supplementary Figure 1161: TF-MoDisCO subpatterns for the ZNF407 transcription factor in K562 (accession ENCSR439OCL).

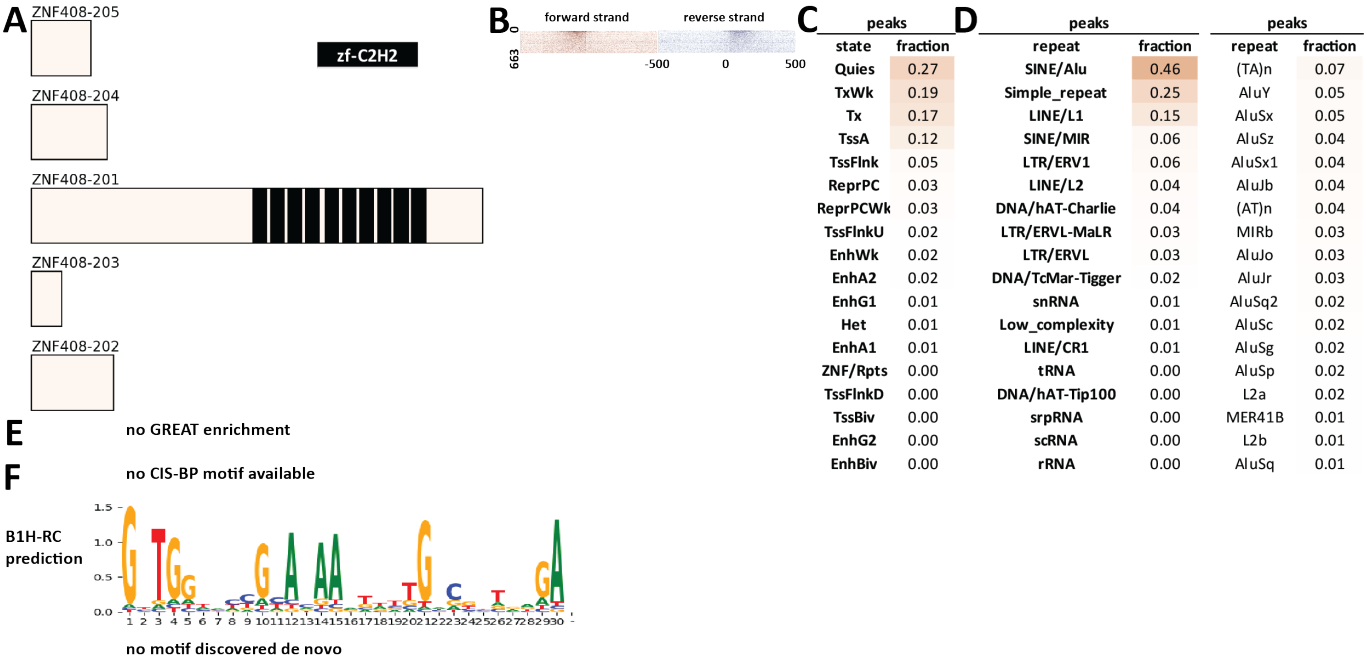

peaks	
state	fraction
Quies	0.27
TxWk	0.19
Tx	0.17
TssA	0.12
TssFlnk	0.05
ReprPC	0.03
ReprPCWk	0.03
TssFlnkU	0.02
EnhWk	0.02
EnhA2	0.02
EnhG1	0.01
Het	0.01
EnhA1	0.01
ZNF/Rpts	0.00
TssFlnkD	0.00
TssBiv	0.00
EnhG2	0.00
EnhBiv	0.00

peaks		peaks	
repeat	fraction	repeat	fraction
SINE/Alu	0.46	(TA)n	0.07
Simple_repeat	0.25	AluY	0.05
LINE/L1	0.15	AluSx	0.05
SINE/MIR	0.06	AluSz	0.04
LTR/ERV1	0.06	AluSx1	0.04
LINE/L2	0.04	AluJb	0.04
DNA/hAT-Charlie	0.04	(AT)n	0.04
LTR/ERVL-MaLR	0.03	MIRb	0.03
LTR/ERVL	0.03	AluJo	0.03
DNA/TcMar-Tigger	0.02	AluJr	0.03
snRNA	0.01	AluSq2	0.02
Low_complexity	0.01	AluSc	0.02
LINE/CR1	0.01	AluSg	0.02
tRNA	0.00	AluSp	0.02
DNA/hAT-Tip100	0.00	L2a	0.02
srpRNA	0.00	MER41B	0.01
scRNA	0.00	L2b	0.01
rRNA	0.00	AluSq	0.01

Supplementary Figure 1162: Properties and genomic distribution of motifs identified for the ZNF408 transcription factor in K562 (accession ENCSR758PLU).

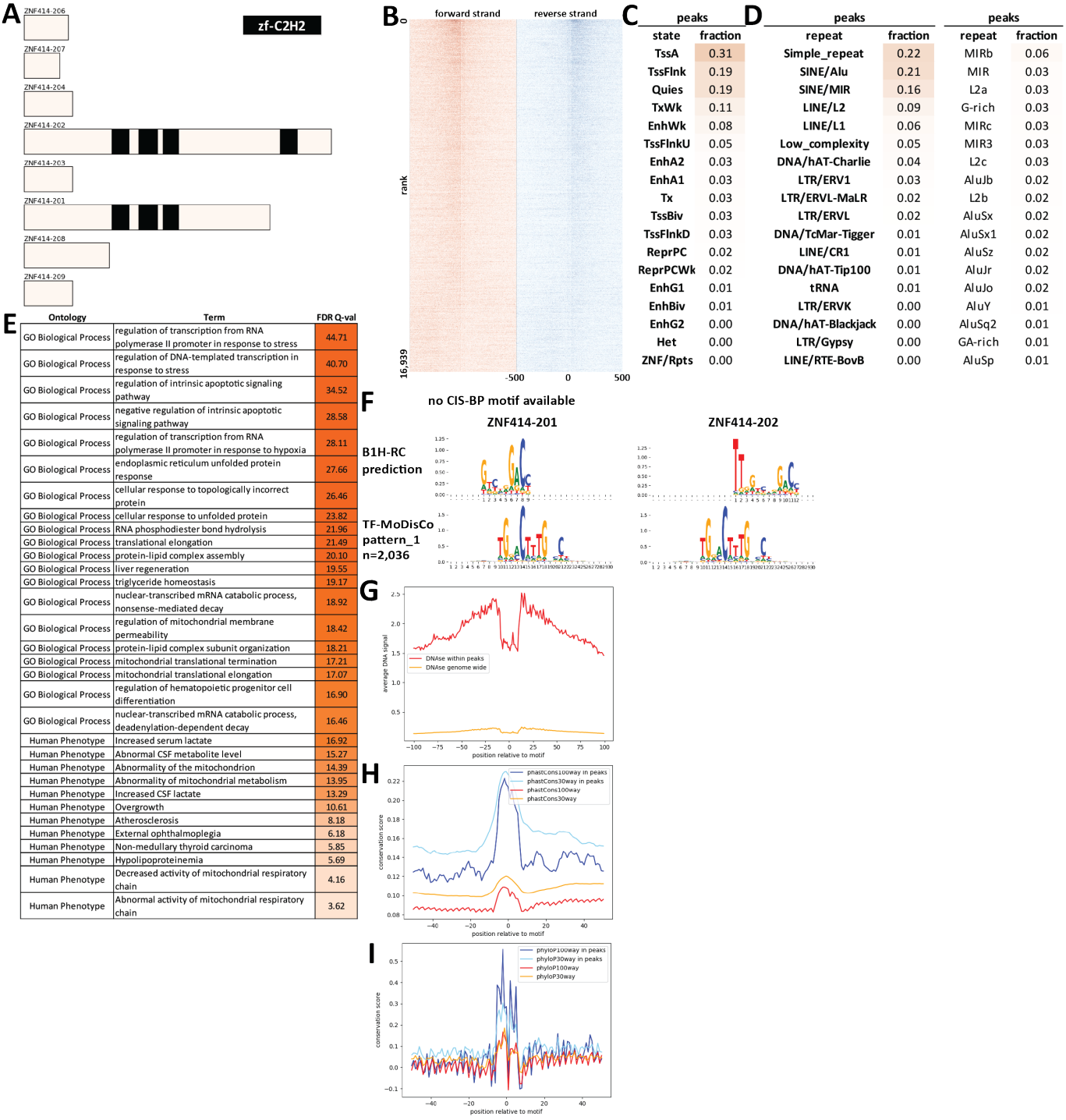

C

peaks	
state	fraction
TssA	0.31
TssFlnk	0.19
Quies	0.19
TxWk	0.11
EnhWk	0.08
TssFlnkU	0.05
EnhA2	0.03
EnhA1	0.03
Tx	0.03
TssBiv	0.03
TssFlnkD	0.03
ReprPC	0.02
ReprPCWk	0.02
EnhG1	0.01
EnhBiv	0.01
EnhG2	0.00
Het	0.00
ZNF/Rpts	0.00

D

peaks		peaks	
repeat	fraction	repeat	fraction
Simple_repeat	0.22	MIRb	0.06
SINE/Alu	0.21	MIR	0.03
SINE/MIR	0.16	L2a	0.03
LINE/L2	0.09	G-rich	0.03
LINE/L1	0.06	MIRc	0.03
Low_complexity	0.05	MIR3	0.03
DNA/hAT-Charlie	0.04	L2c	0.03
LTR/ERV1	0.03	AluJb	0.02
LTR/ERVL-MaLR	0.02	L2b	0.02
LTR/ERVL	0.02	AluSx	0.02
DNA/TcMar-Tigger	0.01	AluSx1	0.02
LINE/CR1	0.01	AluSz	0.02
DNA/hAT-Tip100	0.01	AluJr	0.02
tRNA	0.01	AluJo	0.02
LTR/ERVK	0.00	AluY	0.01
DNA/hAT-Blackjack	0.00	AluSq2	0.01
LTR/Gypsy	0.00	GA-rich	0.01
LINE/RTE-BovB	0.00	AluSp	0.01

E

Ontology	Term	FDR Q-val
GO Biological Process	regulation of transcription from RNA polymerase II promoter in response to stress	44.71
GO Biological Process	regulation of DNA-templated transcription in response to stress	40.70
GO Biological Process	regulation of intrinsic apoptotic signaling pathway	34.52
GO Biological Process	negative regulation of intrinsic apoptotic signaling pathway	28.58
GO Biological Process	regulation of transcription from RNA polymerase II promoter in response to hypoxia	28.11
GO Biological Process	endoplasmic reticulum unfolded protein response	27.66
GO Biological Process	cellular response to topologically incorrect protein	26.46
GO Biological Process	cellular response to unfolded protein	23.82
GO Biological Process	RNA phosphodiester bond hydrolysis	21.96
GO Biological Process	translational elongation	21.49
GO Biological Process	protein-lipid complex assembly	20.10
GO Biological Process	liver regeneration	19.55
GO Biological Process	triglyceride homeostasis	19.17
GO Biological Process	nuclear-transcribed mRNA catabolic process, nonsense-mediated decay	18.92
GO Biological Process	regulation of mitochondrial membrane permeability	18.42
GO Biological Process	protein-lipid complex subunit organization	18.21
GO Biological Process	mitochondrial translational termination	17.21
GO Biological Process	mitochondrial translational elongation	17.07
GO Biological Process	regulation of hematopoietic progenitor cell differentiation	16.90
GO Biological Process	nuclear-transcribed mRNA catabolic process, deadenylation-dependent decay	16.46
Human Phenotype	Increased serum lactate	16.92
Human Phenotype	Abnormal CSF metabolite level	15.27
Human Phenotype	Abnormality of the mitochondrion	14.39
Human Phenotype	Abnormality of mitochondrial metabolism	13.95
Human Phenotype	Increased CSF lactate	13.29
Human Phenotype	Overgrowth	10.61
Human Phenotype	Atherosclerosis	8.18
Human Phenotype	External ophthalmoplegia	6.18
Human Phenotype	Non-medullary thyroid carcinoma	5.85
Human Phenotype	Hypolipoproteinemia	5.69
Human Phenotype	Decreased activity of mitochondrial respiratory chain	4.16
Human Phenotype	Abnormal activity of mitochondrial respiratory chain	3.62

Supplementary Figure 1163: Properties and genomic distribution of motifs identified for the ZNF414 transcription factor in HepG2 (accession ENCSR224NQI).

TF-MoDisCO pattern_1 n=2036, CWM

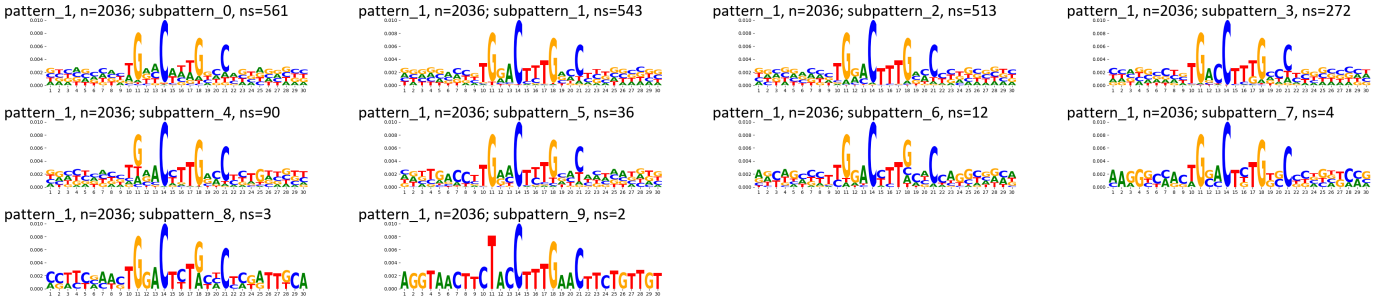

TF-MoDisCO pattern_1 n=2036, PWM

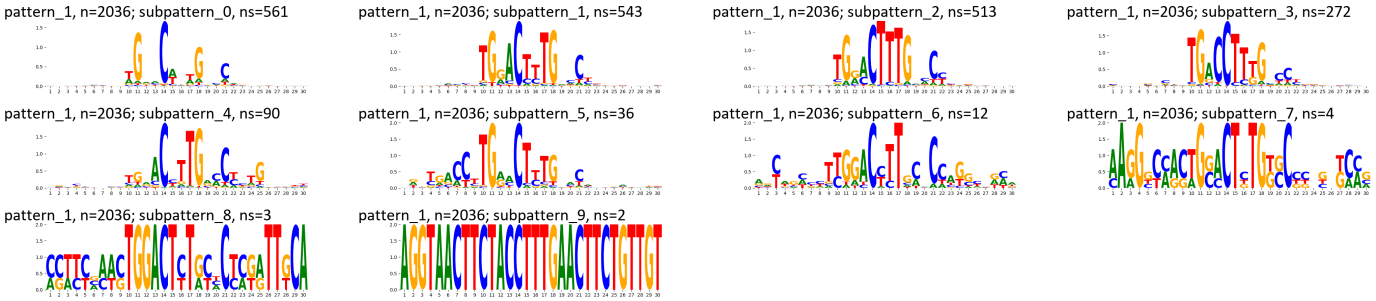

Supplementary Figure 1164: TF-MoDisCO subpatterns for the ZNF414 transcription factor in HepG2 (accession ENCSR224NQI).

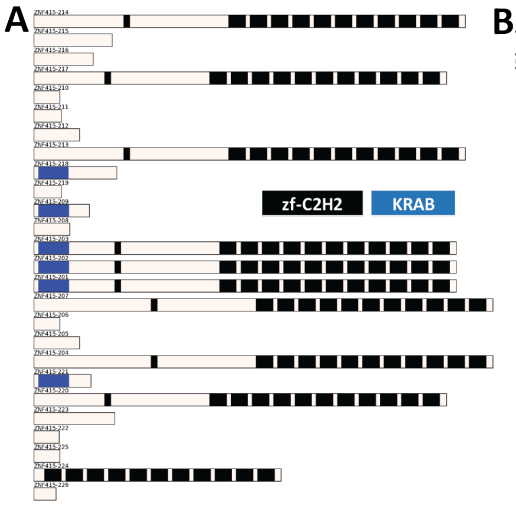

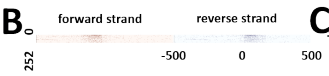

C

peaks	
state	fraction
TssA	0.41
TssFlnk	0.17
Quies	0.15
EnhWk	0.09
TxWk	0.08
TssBiv	0.07
EnhA1	0.06
EnhA2	0.04
TssFlnkU	0.03
ReprPC	0.02
Tx	0.01
TssFlnkD	0.01
ReprPCWk	0.01
EnhG1	0.01
EnhBiv	0.01

D

peaks		peaks	
repeat	fraction	repeat	fraction
Simple_repeat	0.14	MIR	0.03
SINE/Alu	0.08	G-rich	0.02
SINE/MIR	0.05	AluJb	0.02
Low_complexity	0.03	MIRb	0.02
LINE/L2	0.03	L2c	0.02
LTR/ERVL-MaLR	0.03	AluJr	0.02
LINE/L1	0.02	AluJo	0.02
LTR/ERVL	0.02	MLT1H1	0.01
LTR/ERV1	0.01	MER21A	0.01
DNA/TcMar-Tigger	0.01	L2b	0.01
tRNA	0.00	GA-rich	0.01
RNA	0.00	(T)n	0.01
LTR/Gypsy	0.00	(GAGCCA)n	0.01
LINE/CR1	0.00	(CGG)n	0.01
DNA/hAT-Charlie	0.00	tRNA-Ser-TCC	0.00
DNA	0.00	Tigger3a	0.00
		Tigger19b	0.00
		MamGyp-int	0.00

E

no GREAT enrichment

F

CIS-BP ChIP

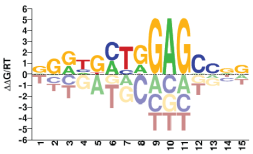

B1H-RC prediction

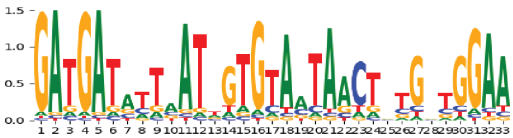

no motif discovered de novo

Supplementary Figure 1165: Properties and genomic distribution of motifs identified for the ZNF415 transcription factor in HEK293 (accession Hughes NB models).

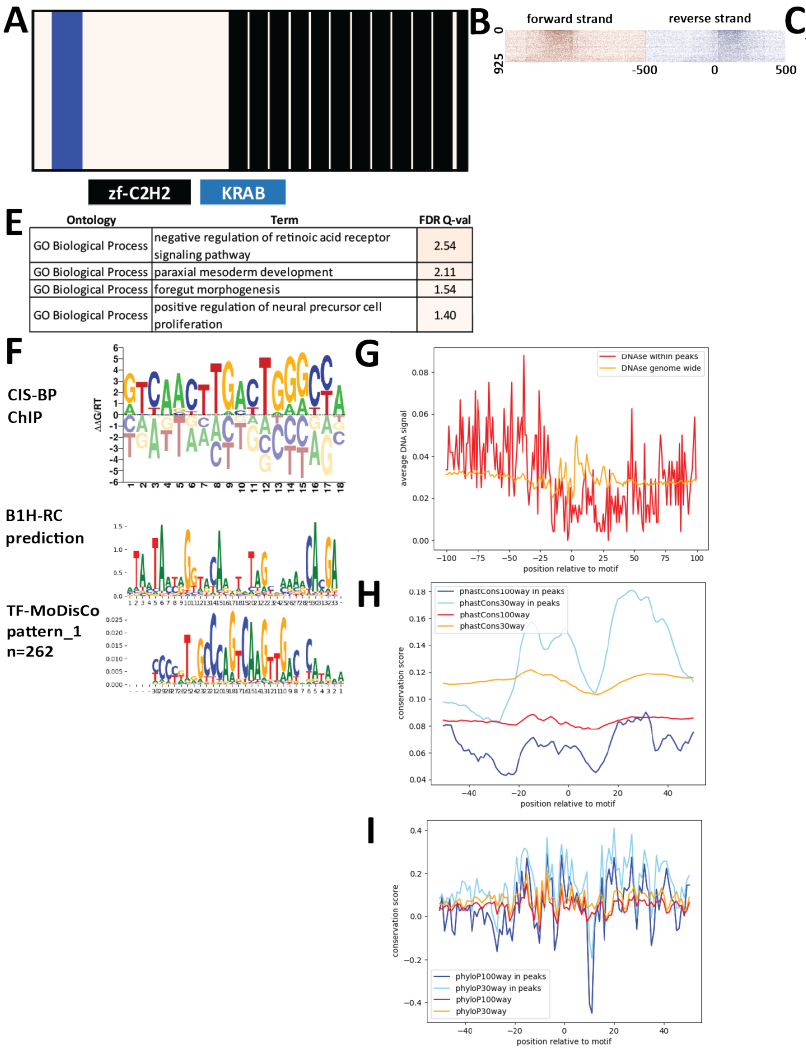

E

Ontology	Term	FDR Q-val
GO Biological Process	negative regulation of retinoic acid receptor signaling pathway	2.54
GO Biological Process	paraxial mesoderm development	2.11
GO Biological Process	foregut morphogenesis	1.54
GO Biological Process	positive regulation of neural precursor cell proliferation	1.40

C

peaks	
state	fraction
Quies	0.37
TssA	0.21
TssFlnk	0.11
TxWk	0.10
EnhWk	0.07
Het	0.04
TssBiv	0.04
EnhA2	0.04
EnhA1	0.04
ReprPCWk	0.03
TssFlnkU	0.03
Tx	0.02
TssFlnkD	0.02
ZNF/Rpts	0.02
ReprPC	0.01
EnhBiv	0.01
EnhG1	0.01
EnhG2	0.00

D

peaks		peaks		peaks	
repeat	fraction	repeat	fraction	repeat	fraction
Simple_repeat	0.30	MLT2B4	0.12	AluJb	0.03
LTR/ERVL	0.28	MLT2B1	0.07	AluSx	0.03
SINE/Alu	0.22	(GT)n	0.06	AluSx1	0.02
LINE/L1	0.07	MLT2B2	0.04	MIRb	0.02
LTR/ERV1	0.07	(AC)n	0.04	MIR	0.02
LINE/L2	0.07	(TG)n	0.03	AluY	0.02
SINE/MIR	0.05	L2a	0.03	AluSz	0.02
LTR/ERVL-MaLR	0.04	AluJb	0.03	AluJo	0.02
Low_complexity	0.03	AluSx	0.03	L2	0.01
DNA/hAT-Charlie	0.02	(CA)n	0.02	AluJr	0.01
DNA/TcMar-Tigger	0.01	AluSx1	0.02		
tRNA	0.01	MIRb	0.02		
LINE/CR1	0.01	MIR	0.02		
DNA/hAT-Tip100	0.00	AluY	0.02		
Retroposon/SVA	0.00	AluSz	0.02		
LTR/Gypsy?	0.00	AluJo	0.02		
LTR/ERVK	0.00	L2	0.01		
DNA/hAT-Blackjack	0.00	AluJr	0.01		

Supplementary Figure 1166: Properties and genomic distribution of motifs identified for the ZNF416 transcription factor in HEK293 (accession ENCSR604CNJ).

TF-MoDisCO pattern_1 n=262, CWM

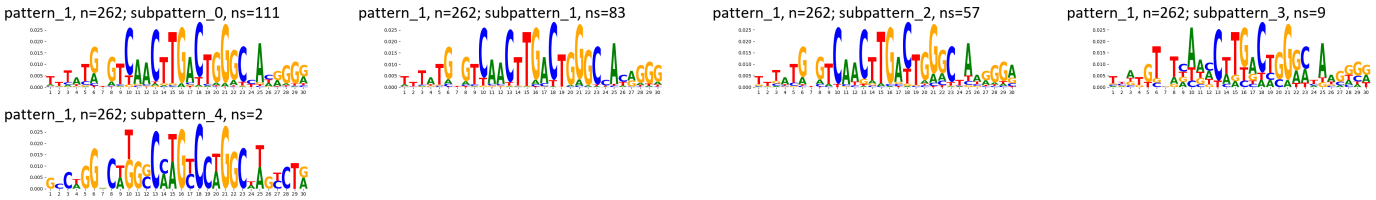

TF-MoDisCO pattern_1 n=262, PWM

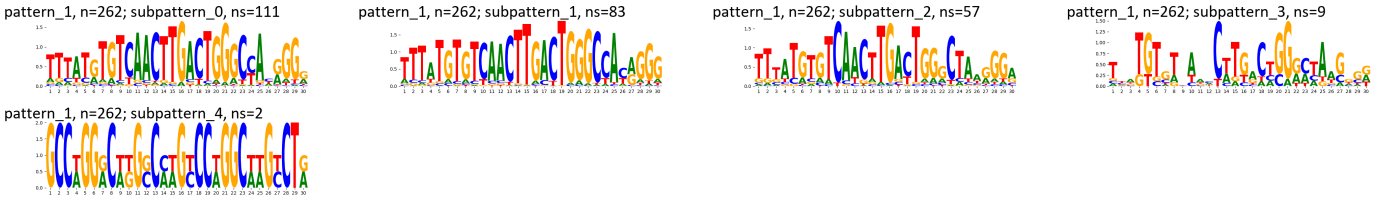

Supplementary Figure 1167: TF-MoDisCO subpatterns for the ZNF416 transcription factor in HEK293 (accession ENCSR604CNJ).

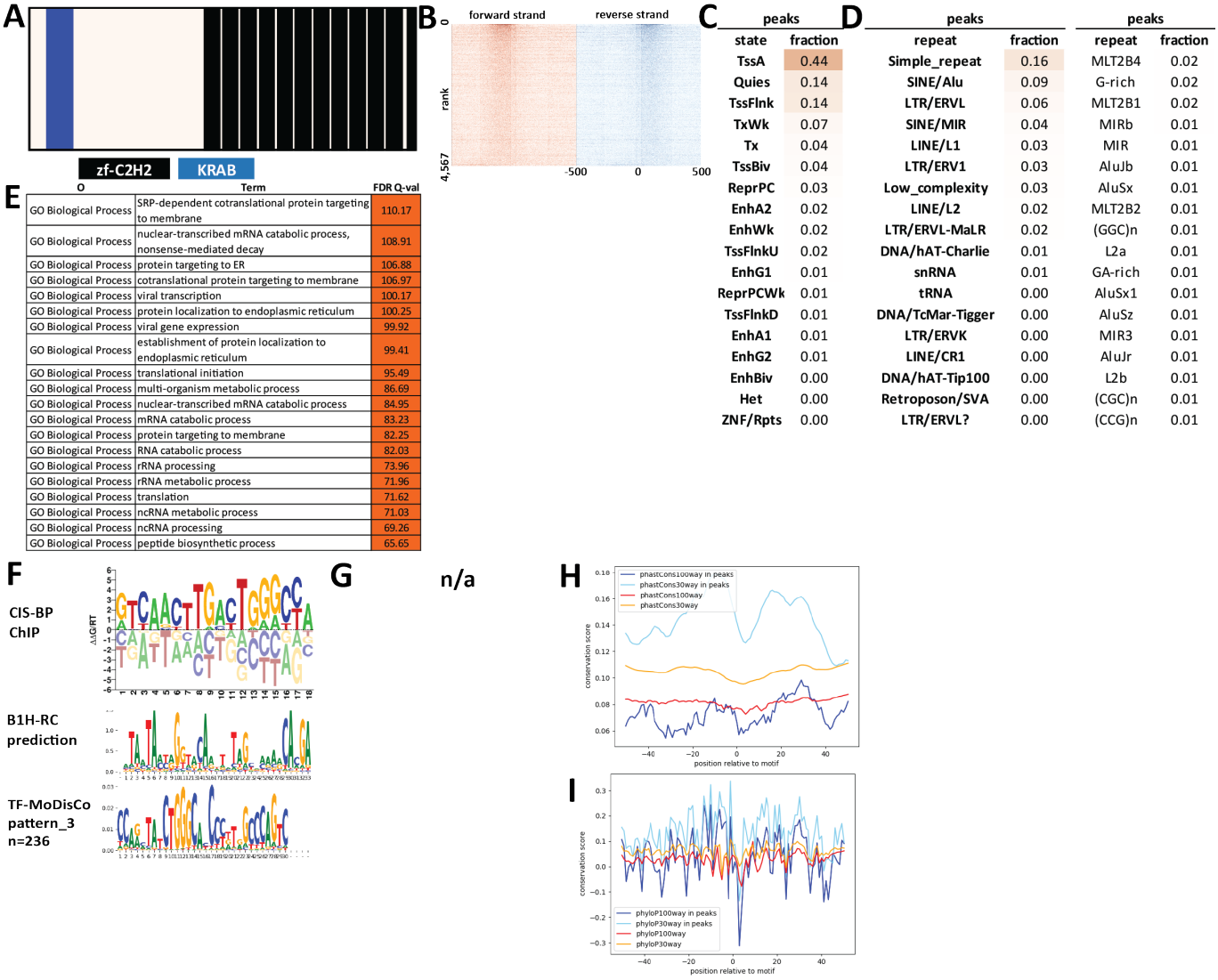

Supplementary Figure 1168: Properties and genomic distribution of motifs identified for the ZNF416 transcription factor in WTC11 (accession ENCSR288NNJ).

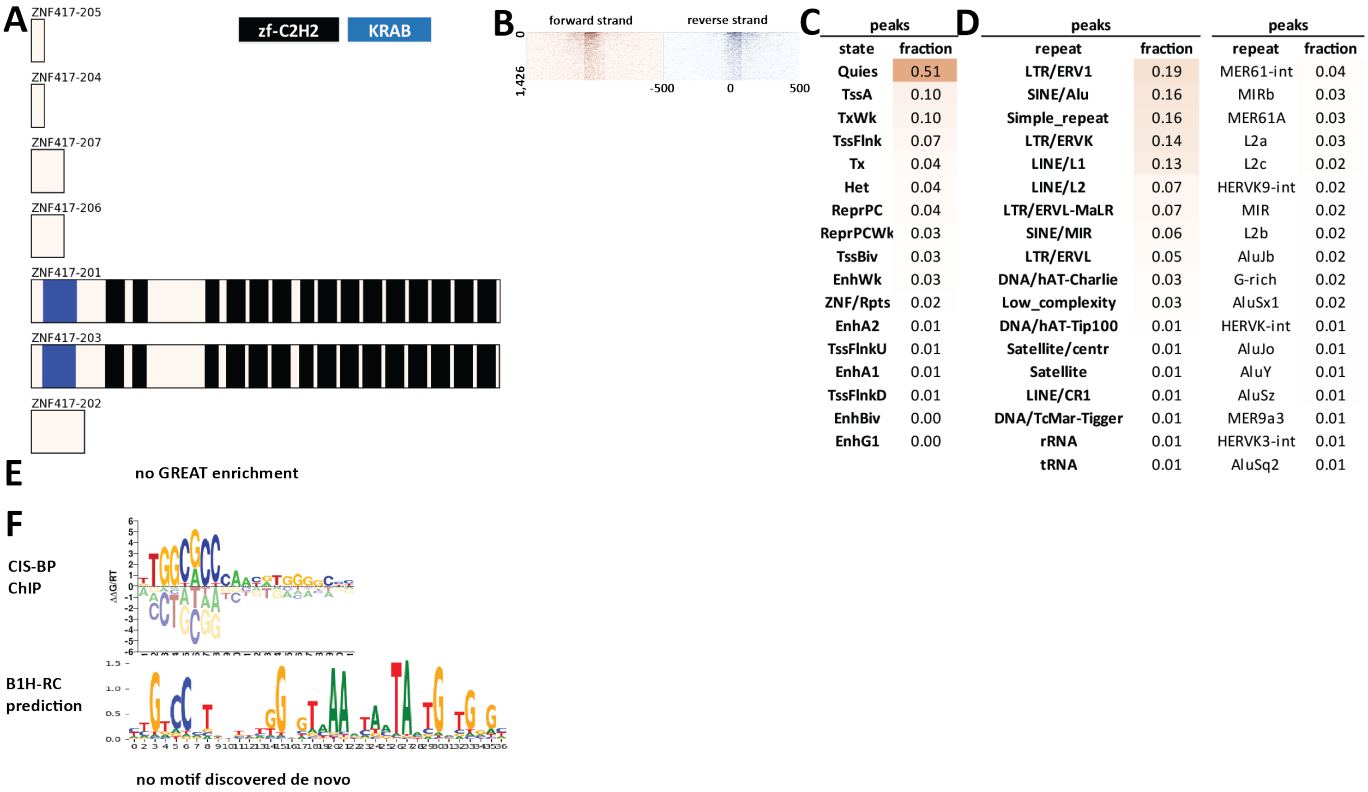

peaks	
state	fraction
Quies	0.51
TssA	0.10
TxWk	0.10
TssFlnk	0.07
Tx	0.04
Het	0.04
ReprPC	0.04
ReprPCWk	0.03
TssBiv	0.03
EnhWk	0.03
ZNF/Rpts	0.02
EnhA2	0.01
TssFlnkU	0.01
EnhA1	0.01
TssFlnkD	0.01
EnhBiv	0.00
EnhG1	0.00

peaks		peaks	
repeat	fraction	repeat	fraction
LTR/ERV1	0.19	MER61-int	0.04
SINE/Alu	0.16	MIRb	0.03
Simple_repeat	0.16	MER61A	0.03
LTR/ERVK	0.14	L2a	0.03
LINE/L1	0.13	L2c	0.02
LINE/L2	0.07	HERVK9-int	0.02
LTR/ERVL-MaLR	0.07	MIR	0.02
SINE/MIR	0.06	L2b	0.02
LTR/ERVL	0.05	AluJb	0.02
DNA/hAT-Charlie	0.03	G-rich	0.02
Low_complexity	0.03	AluSx1	0.02
DNA/hAT-Tip100	0.01	HERVK-int	0.01
Satellite/centr	0.01	AluJo	0.01
Satellite	0.01	AluY	0.01
LINE/CR1	0.01	AluSz	0.01
DNA/TcMar-Tigger	0.01	MER9a3	0.01
rRNA	0.01	HERVK3-int	0.01
tRNA	0.01	AluSq2	0.01

Supplementary Figure 1169: Properties and genomic distribution of motifs identified for the ZNF417 transcription factor in HEK293 (accession ChipExo models).

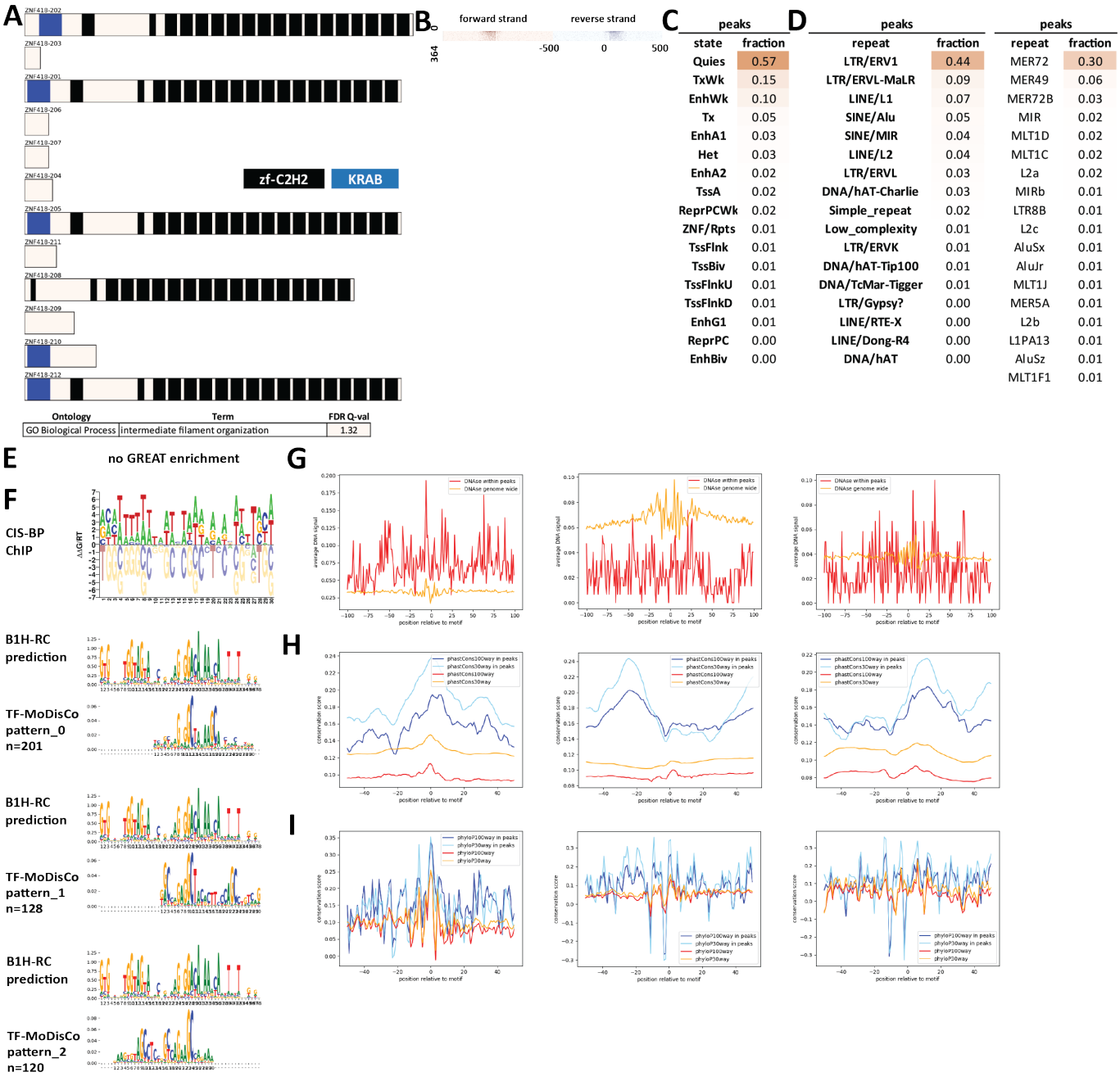

Supplementary Figure 1170: Properties and genomic distribution of motifs identified for the ZNF418 transcription factor in HEK293 (accession Hughes GR models).

TF-MoDisCO pattern_0 n=201, CWM

pattern_0, n=201; subpattern_0, ns=57

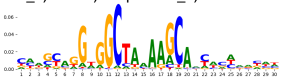

pattern_0, n=201; subpattern_1, ns=45

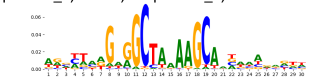

pattern_0, n=201; subpattern_2, ns=35

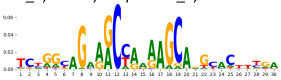

pattern_0, n=201; subpattern_3, ns=29

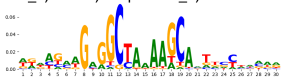

pattern_0, n=201; subpattern_4, ns=28

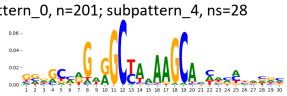

pattern_0, n=201; subpattern_5, ns=7

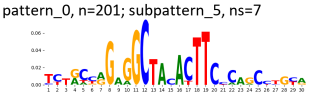

TF-MoDisCO pattern_0 n=201, PWM

pattern_0, n=201; subpattern_0, ns=57

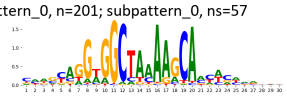

pattern_0, n=201; subpattern_1, ns=45

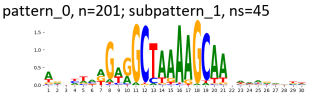

pattern_0, n=201; subpattern_2, ns=35

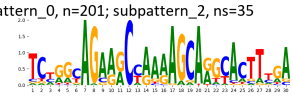

pattern_0, n=201; subpattern_3, ns=29

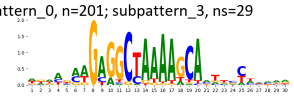

pattern_0, n=201; subpattern_4, ns=28

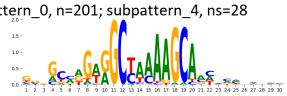

pattern_0, n=201; subpattern_5, ns=7

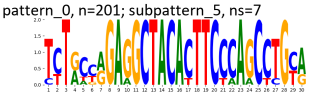

TF-MoDisCO pattern_1 n=128, CWM

pattern_1, n=128; subpattern_0, ns=49

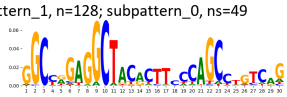

pattern_1, n=128; subpattern_1, ns=46

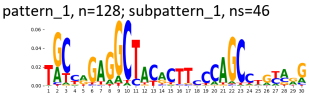

pattern_1, n=128; subpattern_2, ns=33

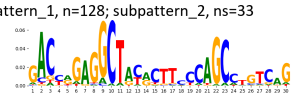

TF-MoDisCO pattern_1 n=128, PWM

pattern_1, n=128; subpattern_0, ns=49

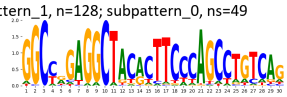

pattern_1, n=128; subpattern_1, ns=46

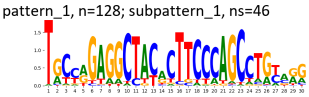

pattern_1, n=128; subpattern_2, ns=33

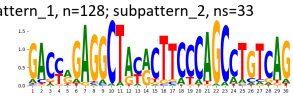

TF-MoDisCO pattern_2 n=120, CWM

pattern_2, n=120; subpattern_0, ns=41

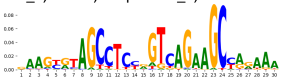

pattern_2, n=120; subpattern_1, ns=40

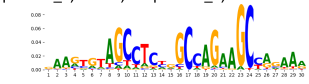

pattern_2, n=120; subpattern_2, ns=39

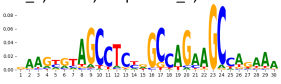

TF-MoDisCO pattern_2 n=120, PWM

pattern_2, n=120; subpattern_0, ns=41

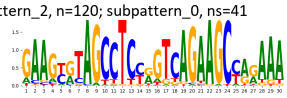

pattern_2, n=120; subpattern_1, ns=40

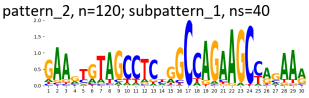

pattern_2, n=120; subpattern_2, ns=39

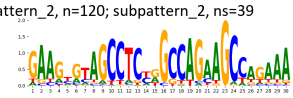

Supplementary Figure 1171: TF-MoDisCO subpatterns for the ZNF418 transcription factor in HEK293 (accession Hughes GR models).

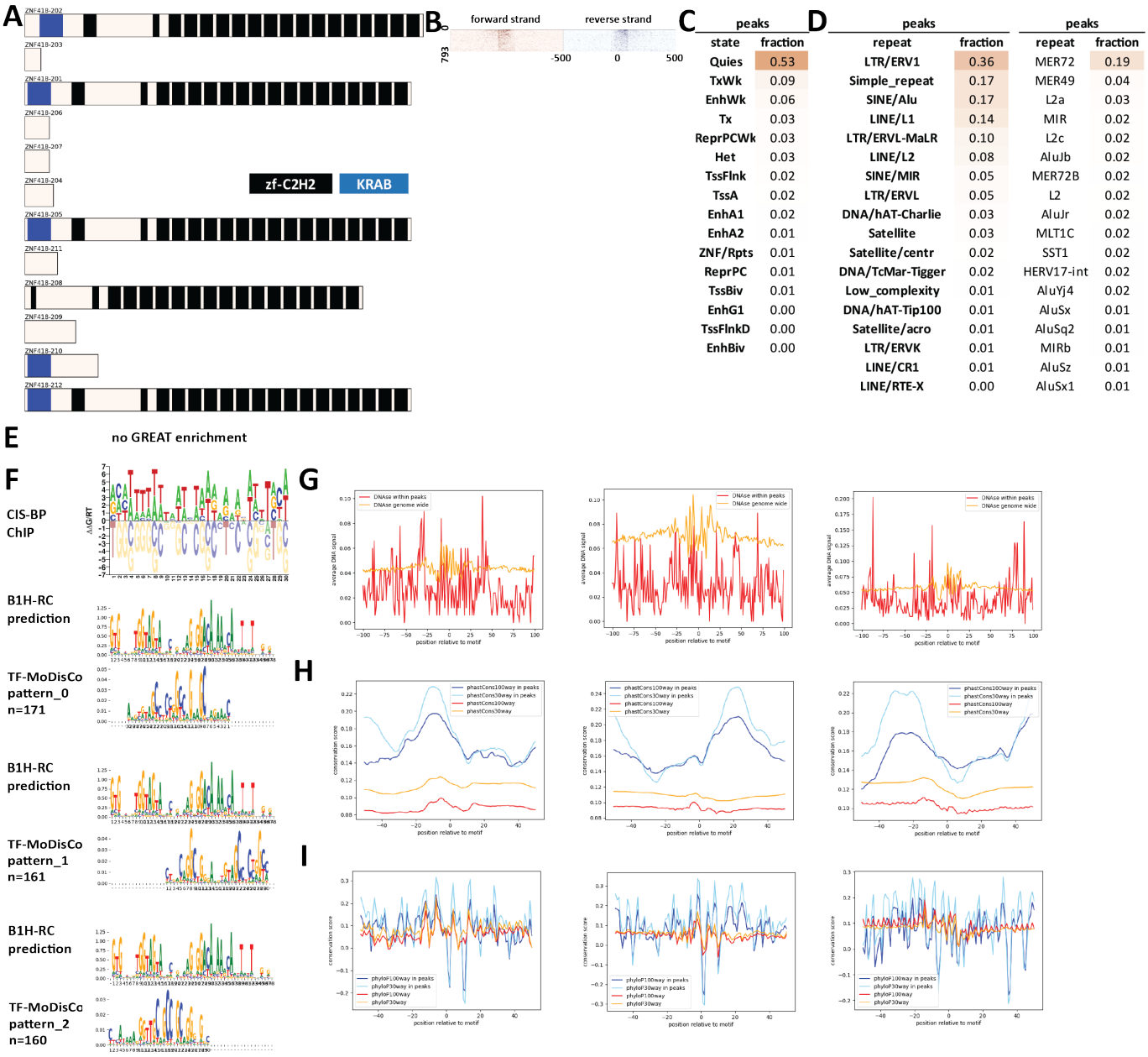

Supplementary Figure 1172: Properties and genomic distribution of motifs identified for the ZNF418 transcription factor in HEK293 (accession ChipExo models).

TF-MoDisCO pattern_0 n=171, CWM

pattern_0, n=171; subpattern_0, ns=53

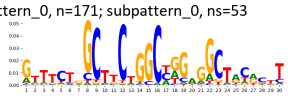

pattern_0, n=171; subpattern_1, ns=34

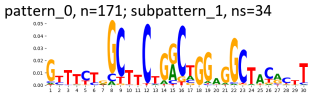

pattern_0, n=171; subpattern_2, ns=33

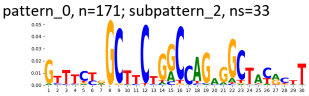

pattern_0, n=171; subpattern_3, ns=29

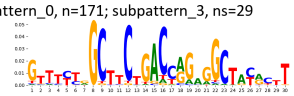

pattern_0, n=171; subpattern_4, ns=18

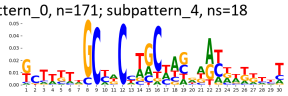

pattern_0, n=171; subpattern_5, ns=4

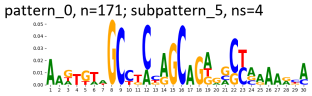

TF-MoDisCO pattern_0 n=171, PWM

pattern_0, n=171; subpattern_0, ns=53

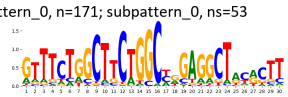

pattern_0, n=171; subpattern_1, ns=34

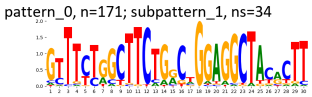

pattern_0, n=171; subpattern_2, ns=33

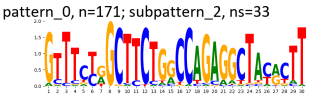

pattern_0, n=171; subpattern_3, ns=29

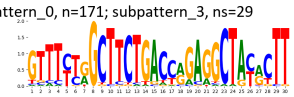

pattern_0, n=171; subpattern_4, ns=18

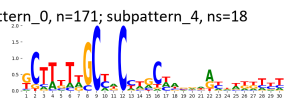

pattern_0, n=171; subpattern_5, ns=4

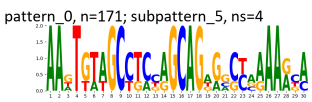

TF-MoDisCO pattern_1 n=161, CWM

pattern_1, n=161; subpattern_0, ns=64

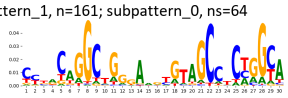

pattern_1, n=161; subpattern_1, ns=50

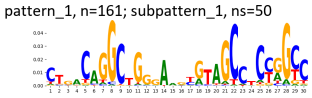

pattern_1, n=161; subpattern_2, ns=47

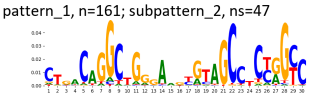

TF-MoDisCO pattern_1 n=161, PWM

pattern_1, n=161; subpattern_0, ns=64

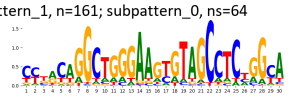

pattern_1, n=161; subpattern_1, ns=50

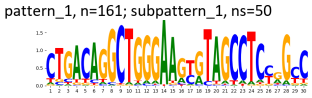

pattern_1, n=161; subpattern_2, ns=47

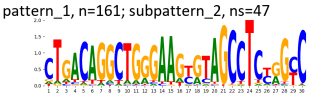

TF-MoDisCO pattern_2 n=160, CWM

pattern_2, n=160; subpattern_0, ns=67

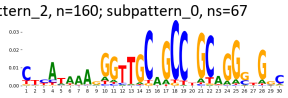

pattern_2, n=160; subpattern_1, ns=45

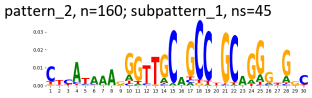

pattern_2, n=160; subpattern_2, ns=36

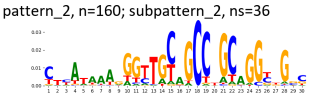

pattern_2, n=160; subpattern_3, ns=12

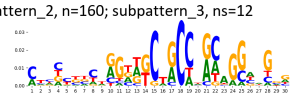

TF-MoDisCO pattern_2 n=160, PWM

pattern_2, n=160; subpattern_0, ns=67

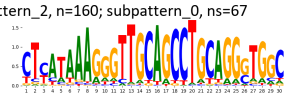

pattern_2, n=160; subpattern_1, ns=45

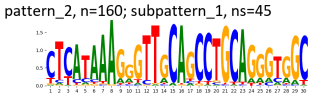

pattern_2, n=160; subpattern_2, ns=36

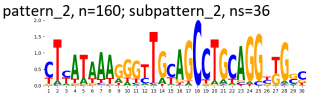

pattern_2, n=160; subpattern_3, ns=12

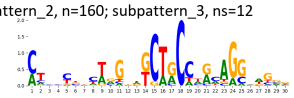

Supplementary Figure 1173: TF-MoDisCO subpatterns for the ZNF418 transcription factor in HEK293 (accession ChipExo models).

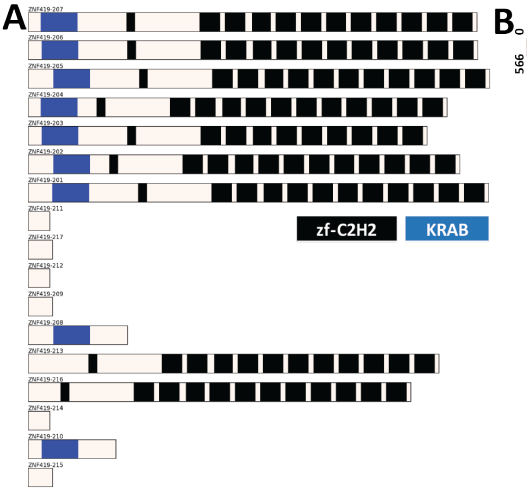

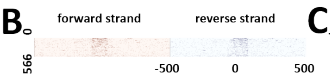

C

peaks	
state	fraction
Quies	0.35
TxWk	0.07
Tx	0.05
TssA	0.04
Het	0.04
ReprPCWk	0.03
ZNF/Rpts	0.03
TssFlnk	0.02
ReprPC	0.02
EnhWk	0.01
EnhA2	0.01
EnhA1	0.01
TssBiv	0.01
EnhG1	0.00
EnhBiv	0.00

D

peaks		peaks	
repeat	fraction	repeat	fraction
Simple_repeat	0.20	HERVK22-int	0.07
SINE/Alu	0.12	SST1	0.02
LINE/L1	0.11	L2a	0.02
LTR/ERVK	0.08	AluYj4	0.02
LTR/ERV1	0.06	AluJb	0.02
LTR/ERVL-MaLR	0.05	MIRb	0.01
LINE/L2	0.05	L2c	0.01
Satellite	0.04	AluJo	0.01
LTR/ERVL	0.04	L2	0.01
Satellite/centr	0.02	ACRO1	0.01
SINE/MIR	0.02	MER5A	0.01
DNA/hAT-Charlie	0.02	L1MB8	0.01
Low_complexity	0.02	GA-rich	0.01
Satellite/acro	0.01	LSU-rRNA_Hs	0.01
rRNA	0.01	L2b	0.01
DNA/TcMar-Tigger	0.01	L1MDa	0.01
Satellite/telo	0.01	BSR/Beta	0.01
DNA/hAT-Tip100	0.01	(GT)n	0.01

E

no GREAT enrichment

F

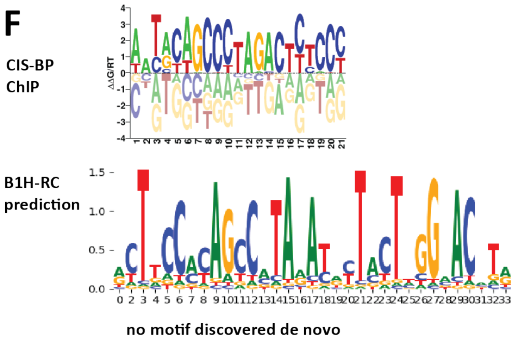

Supplementary Figure 1174: Properties and genomic distribution of motifs identified for the ZNF419 transcription factor in HEK293 (accession ChipExo models).

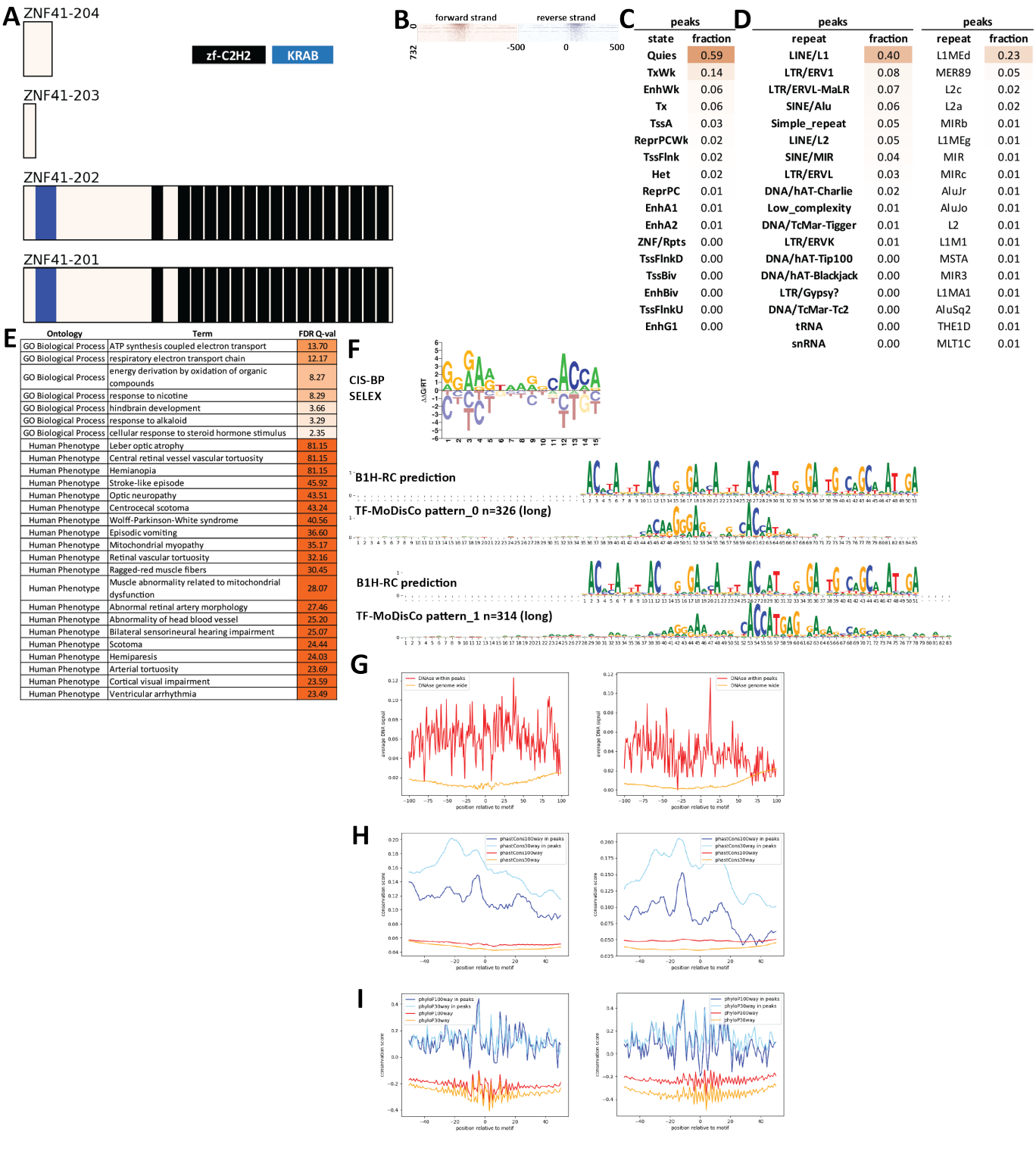

Supplementary Figure 1175: Properties and genomic distribution of motifs identified for the ZNF41 transcription factor in HEK293 (accession Hughes NB models).

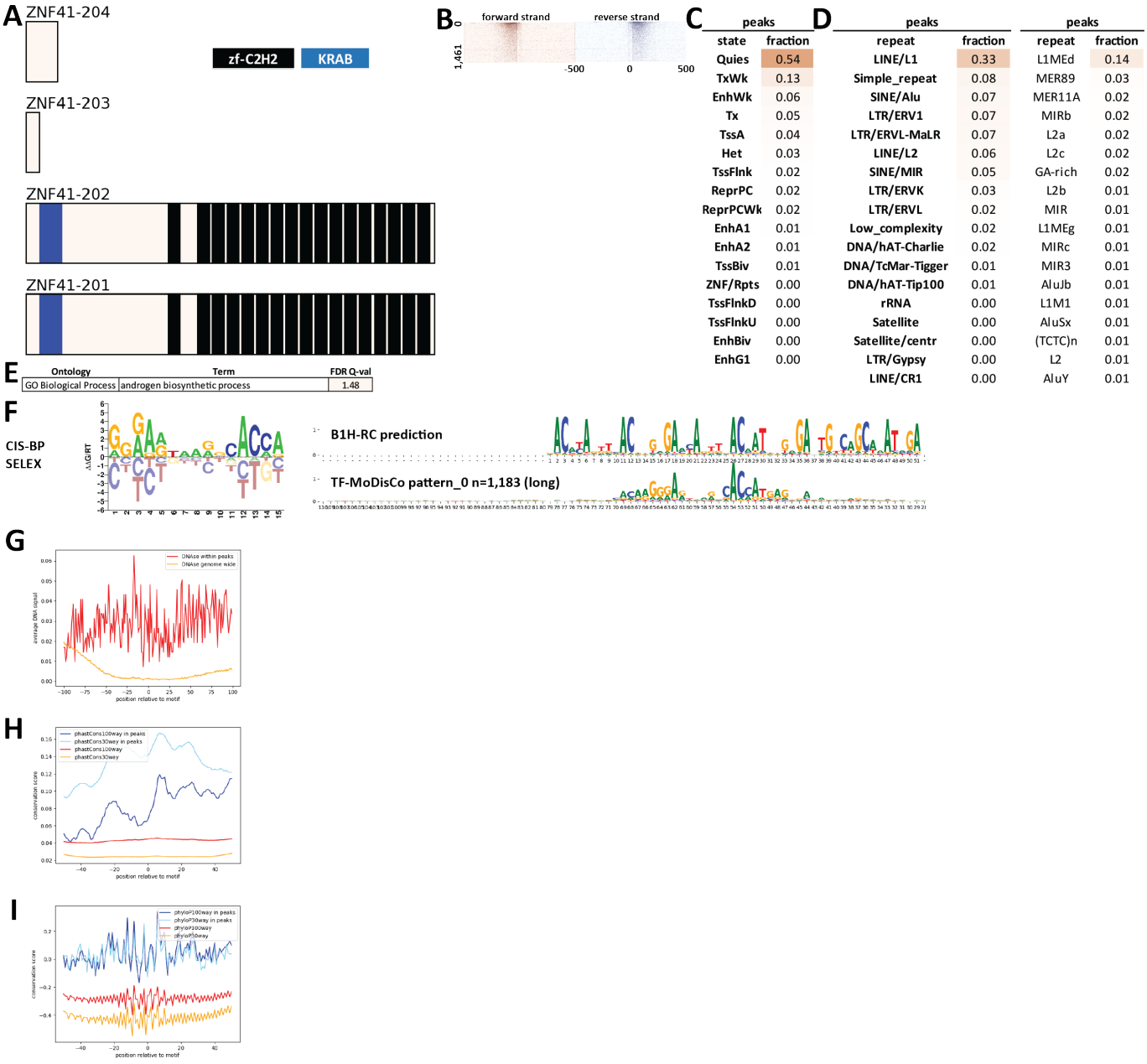

peaks	
state	fraction
Quies	0.54
TxWk	0.13
EnhWk	0.06
Tx	0.05
TssA	0.04
Het	0.03
TssFlnk	0.02
ReprPC	0.02
ReprPCWk	0.02
EnhA1	0.01
EnhA2	0.01
TssBiv	0.01
ZNF/Rpts	0.00
TssFlnkD	0.00
TssFlnkU	0.00
EnhBiv	0.00
EnhG1	0.00

peaks	
repeat	fraction
LINE/L1	0.33
Simple_repeat	0.08
SINE/Alu	0.07
LTR/ERV1	0.07
LTR/ERVL-MaLR	0.07
LINE/L2	0.06
SINE/MIR	0.05
LTR/ERVK	0.03
LTR/ERVL	0.02
Low_complexity	0.02
DNA/hAT-Charlie	0.02
DNA/TcMar-Tigger	0.01
DNA/hAT-Tip100	0.01
rRNA	0.00
Satellite	0.00
Satellite/centr	0.00
LTR/Gypsy	0.00
LINE/CR1	0.00

peaks	
repeat	fraction
L1MEd	0.14
MER89	0.03
MER11A	0.02
MIRb	0.02
L2a	0.02
L2c	0.02
GA-rich	0.02
L2b	0.01
MIR	0.01
L1MEg	0.01
MIRc	0.01
MIR3	0.01
AluJb	0.01
L1M1	0.01
AluSx	0.01
(TCTC)n	0.01
L2	0.01
AluY	0.01

Supplementary Figure 1176: Properties and genomic distribution of motifs identified for the ZNF41 transcription factor in HEK293 (accession Hughes GR models).

TF-MoDisCO pattern_0 n=894, CWM

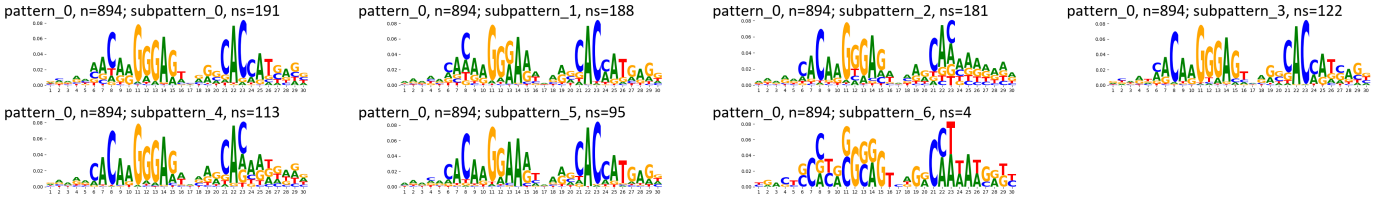

TF-MoDisCO pattern_0 n=894, PWM

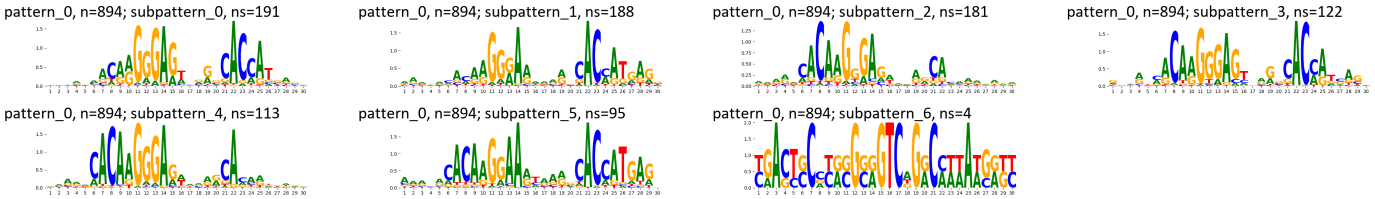

TF-MoDisCO pattern_1 n=471, CWM

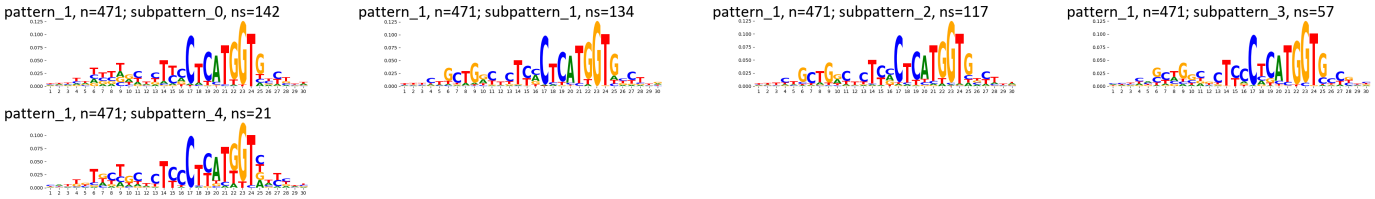

TF-MoDisCO pattern_1 n=471, PWM

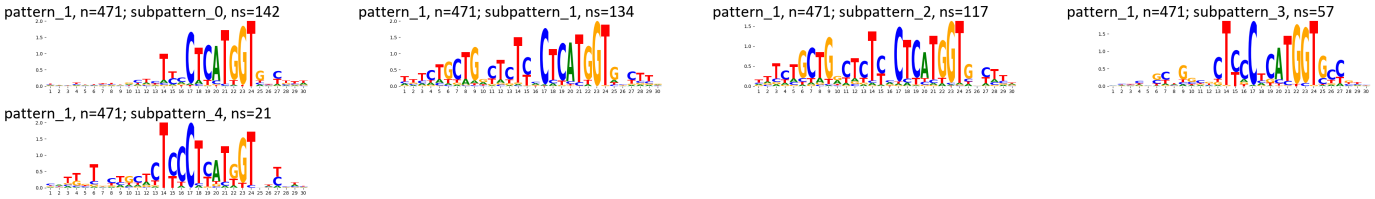

TF-MoDisCO pattern_2 n=165, CWM

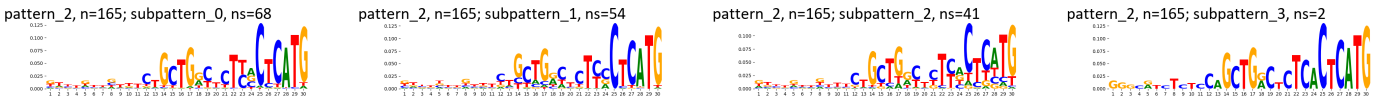

TF-MoDisCO pattern_2 n=165, PWM

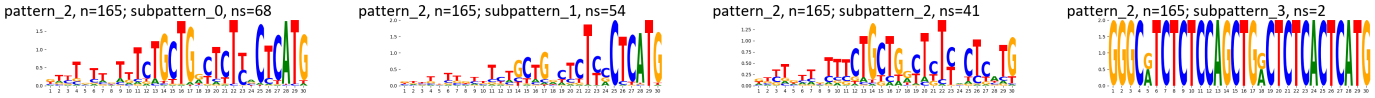

Supplementary Figure 1177: TF-MoDisCO subpatterns for the ZNF41 transcription factor in HEK293 (accession Hughes GR models).

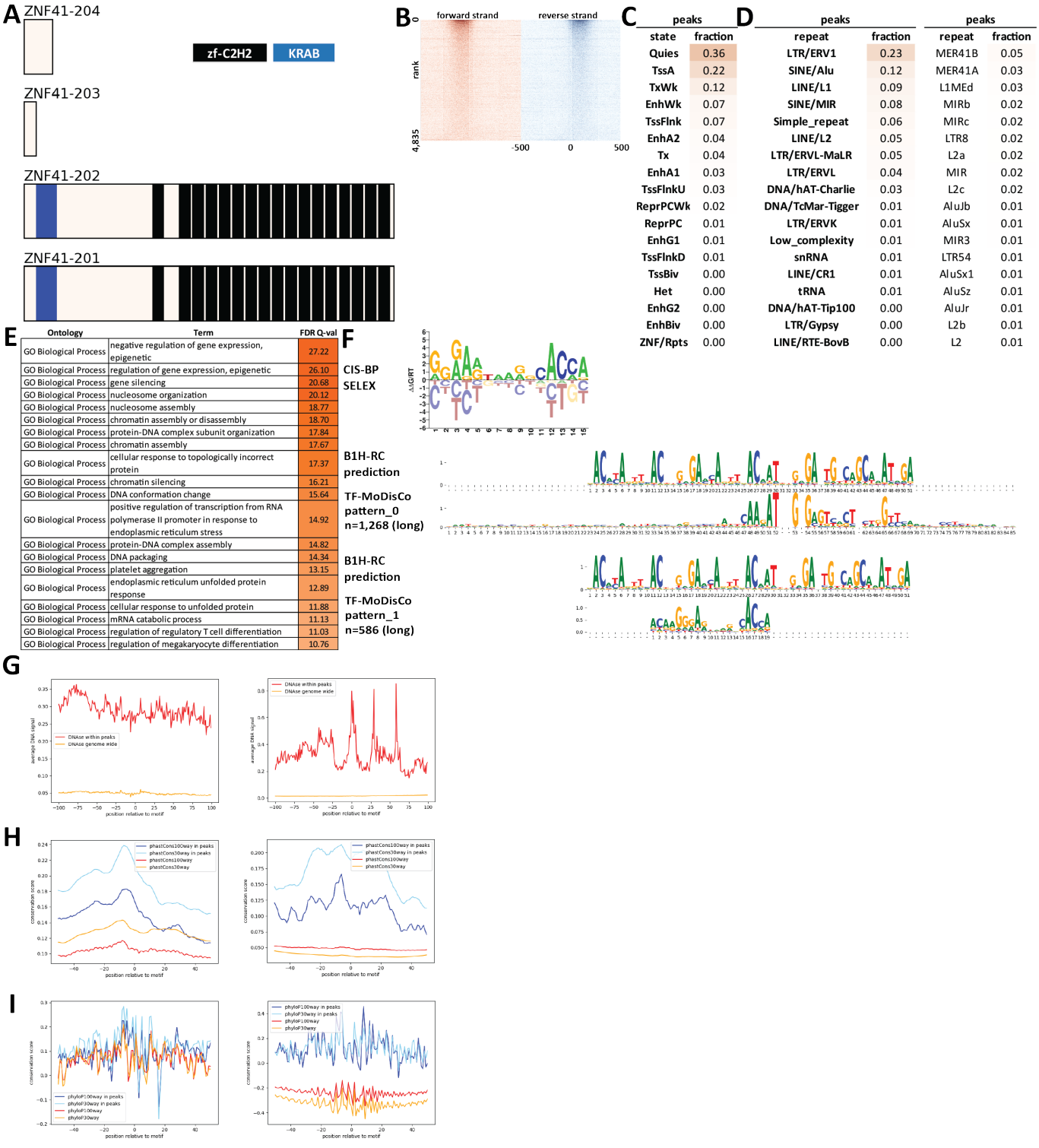

peaks	
state	fraction
Quies	0.36
TssA	0.22
TxWk	0.12
EnhWk	0.07
TssFlnk	0.07
EnhA2	0.04
Tx	0.04
EnhA1	0.03
TssFlnkU	0.03
ReprPCWk	0.02
ReprPC	0.01
EnhG1	0.01
TssFlnkD	0.01
TssBiv	0.00
Het	0.00
EnhG2	0.00
EnhBiv	0.00
ZNF/Rpts	0.00

peaks		peaks	
repeat	fraction	repeat	fraction
LTR/ERV1	0.23	MER41B	0.05
SINE/Alu	0.12	MER41A	0.03
LINE/L1	0.09	L1MEd	0.03
SINE/MIR	0.08	MIRb	0.02
Simple_repeat	0.06	MIRc	0.02
LINE/L2	0.05	LTR8	0.02
LTR/ERVL-MaLR	0.05	L2a	0.02
LTR/ERVL	0.04	MIR	0.02
DNA/hAT-Charlie	0.03	L2c	0.02
DNA/TcMar-Tigger	0.01	AluJb	0.01
LTR/ERVK	0.01	AluSx	0.01
Low_complexity	0.01	MIR3	0.01
snRNA	0.01	LTR54	0.01
LINE/CR1	0.01	AluSx1	0.01
tRNA	0.01	AluSz	0.01
DNA/hAT-Tip100	0.00	AluJr	0.01
LTR/Gypsy	0.00	L2b	0.01
LINE/RTE-BovB	0.00	L2	0.01

Ontology	Term	FDR Q-val
GO Biological Process	negative regulation of gene expression, epigenetic	27.22
GO Biological Process	regulation of gene expression, epigenetic	26.10
GO Biological Process	gene silencing	20.68
GO Biological Process	nucleosome organization	20.12
GO Biological Process	nucleosome assembly	18.77
GO Biological Process	chromatin assembly or disassembly	18.70
GO Biological Process	protein-DNA complex subunit organization	17.84
GO Biological Process	chromatin assembly	17.67
GO Biological Process	cellular response to topologically incorrect protein	17.37
GO Biological Process	chromatin silencing	16.21
GO Biological Process	DNA conformation change	15.64
GO Biological Process	positive regulation of transcription from RNA polymerase II promoter in response to endoplasmic reticulum stress	14.92
GO Biological Process	protein-DNA complex assembly	14.82
GO Biological Process	DNA packaging	14.34
GO Biological Process	platelet aggregation	13.15
GO Biological Process	endoplasmic reticulum unfolded protein response	12.89
GO Biological Process	cellular response to unfolded protein	11.88
GO Biological Process	mRNA catabolic process	11.13
GO Biological Process	regulation of regulatory T cell differentiation	11.03
GO Biological Process	regulation of megakaryocyte differentiation	10.76

Supplementary Figure 1178: Properties and genomic distribution of motifs identified for the ZNF41 transcription factor in K562 (accession ENCSR235PYI).

TF-MoDisCO pattern_0 n=1268, CWM

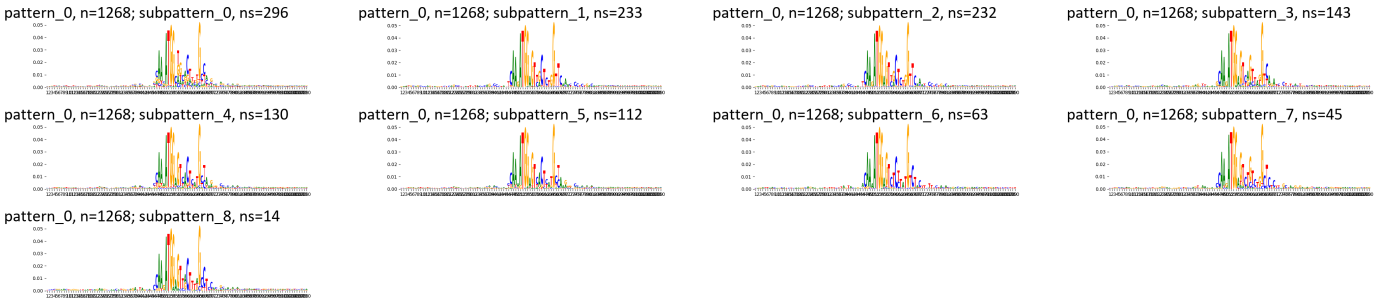

TF-MoDisCO pattern_0 n=1268, PWM

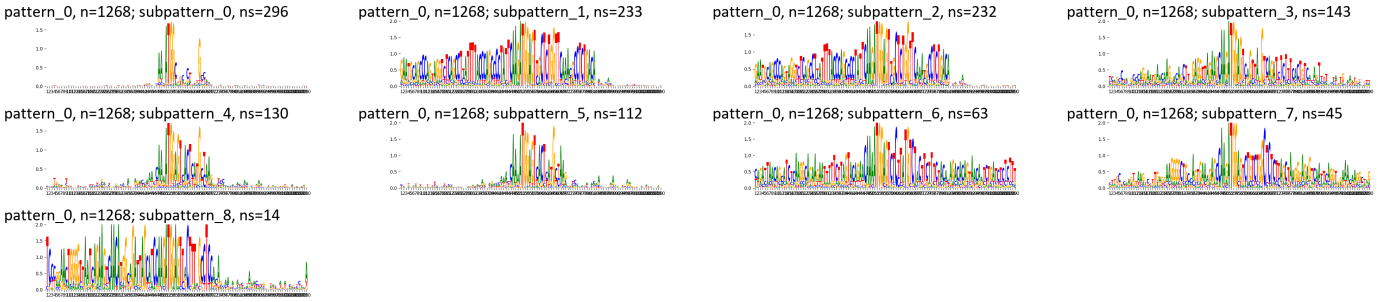

TF-MoDisCO pattern_1 n=586, CWM

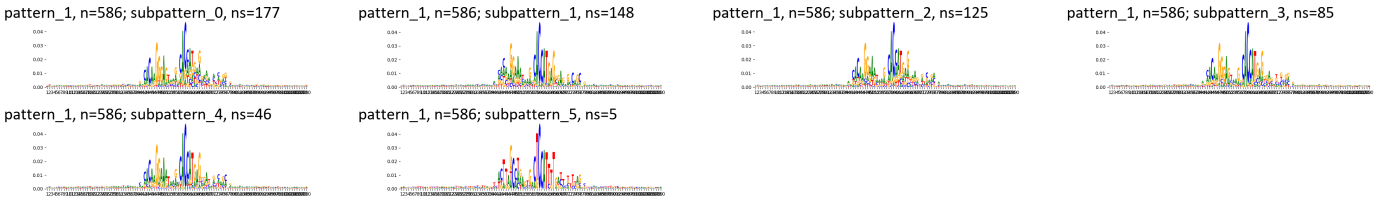

TF-MoDisCO pattern_1 n=586, PWM

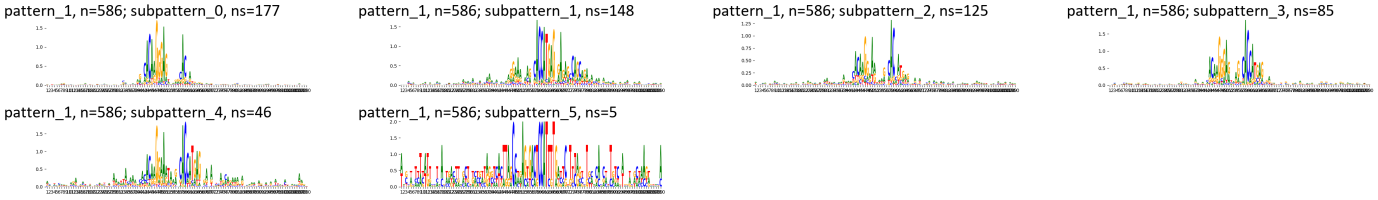

Supplementary Figure 1179: TF-MoDisCO subpatterns for the ZNF41 transcription factor in K562 (accession ENCSR235PYI).

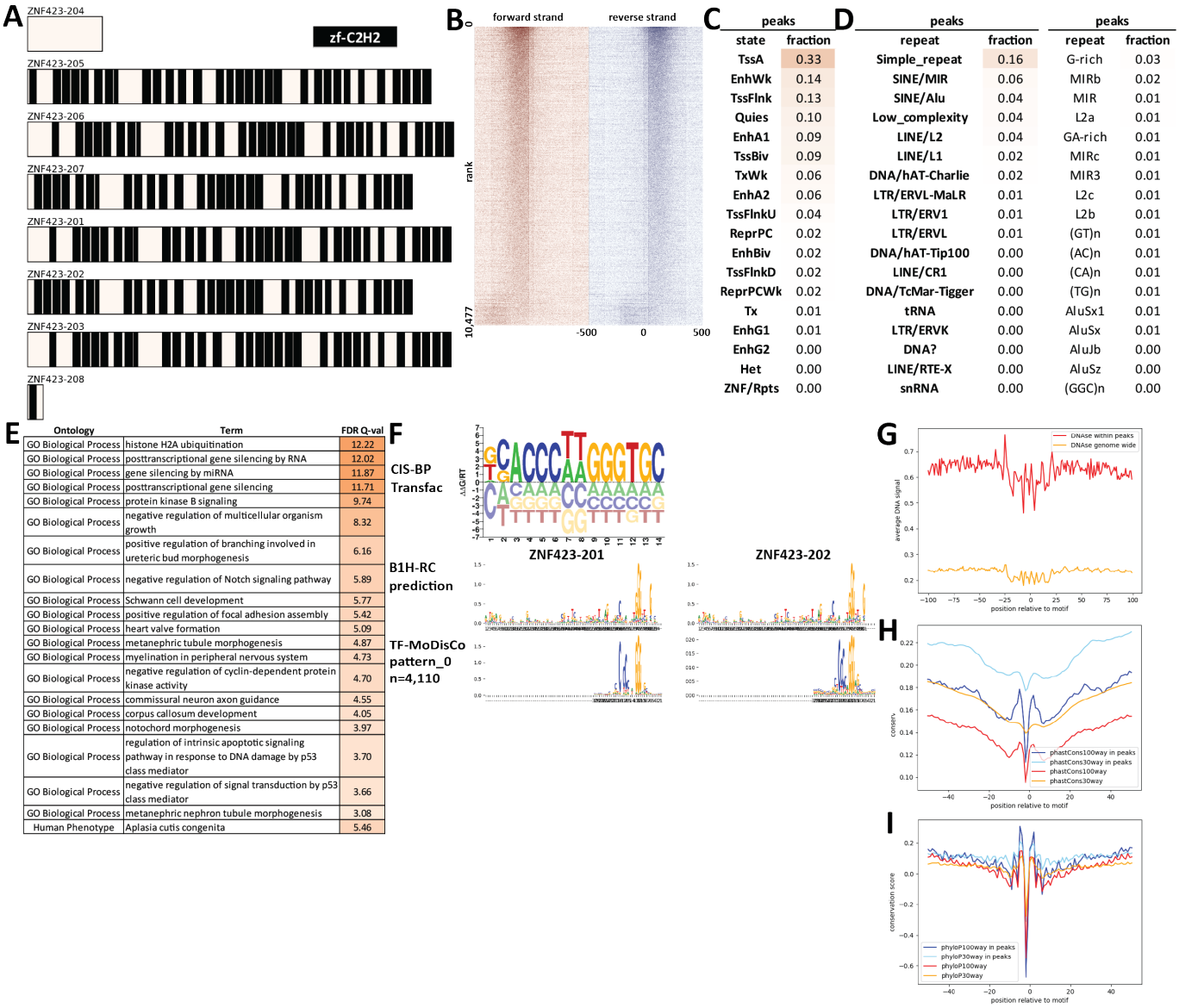

peaks	
state	fraction
TssA	0.33
EnhWk	0.14
TssFlnk	0.13
Quies	0.10
EnhA1	0.09
TssBiv	0.09
TxWk	0.06
EnhA2	0.06
TssFlnkU	0.04
ReprPC	0.02
EnhBiv	0.02
TssFlnkD	0.02
ReprPCWk	0.02
Tx	0.01
EnhG1	0.01
EnhG2	0.00
Het	0.00
ZNF/Rpts	0.00

peaks		peaks	
repeat	fraction	repeat	fraction
Simple_repeat	0.16	G-rich	0.03
SINE/MIR	0.06	MIRb	0.02
SINE/Alu	0.04	MIR	0.01
Low_complexity	0.04	L2a	0.01
LINE/L2	0.04	GA-rich	0.01
LINE/L1	0.02	MIRc	0.01
DNA/hAT-Charlie	0.02	MIR3	0.01
LTR/ERVL-MaLR	0.01	L2c	0.01
LTR/ERV1	0.01	L2b	0.01
LTR/ERVL	0.01	(GT)n	0.01
DNA/hAT-Tip100	0.00	(AC)n	0.01
LINE/CR1	0.00	(CA)n	0.01
DNA/TcMar-Tigger	0.00	(TG)n	0.01
tRNA	0.00	AluSx1	0.01
LTR/ERVK	0.00	AluSx	0.01
DNA?	0.00	AluJb	0.00
LINE/RTE-X	0.00	AluSz	0.00
snRNA	0.00	(GGC)n	0.00

Ontology	Term	FDR Q-val
GO Biological Process	histone H2A ubiquitination	12.22
GO Biological Process	posttranscriptional gene silencing by RNA	12.02
GO Biological Process	gene silencing by miRNA	11.87
GO Biological Process	posttranscriptional gene silencing	11.71
GO Biological Process	protein kinase B signaling	9.74
GO Biological Process	negative regulation of multicellular organism growth	8.32
GO Biological Process	positive regulation of branching involved in ureteric bud morphogenesis	6.16
GO Biological Process	negative regulation of Notch signaling pathway	5.89
GO Biological Process	Schwann cell development	5.77
GO Biological Process	positive regulation of focal adhesion assembly	5.42
GO Biological Process	heart valve formation	5.09
GO Biological Process	metanephric tubule morphogenesis	4.87
GO Biological Process	myelination in peripheral nervous system	4.73
GO Biological Process	negative regulation of cyclin-dependent protein kinase activity	4.70
GO Biological Process	commissural neuron axon guidance	4.55
GO Biological Process	corpus callosum development	4.05
GO Biological Process	notochord morphogenesis	3.97
GO Biological Process	regulation of intrinsic apoptotic signaling pathway in response to DNA damage by p53 class mediator	3.70
GO Biological Process	negative regulation of signal transduction by p53 class mediator	3.66
GO Biological Process	metanephric nephron tubule morphogenesis	3.08
Human Phenotype	Aplasia cutis congenita	5.46

Supplementary Figure 1180: Properties and genomic distribution of motifs identified for the ZNF423 transcription factor in HEK293 (accession ENCSR477OJI).

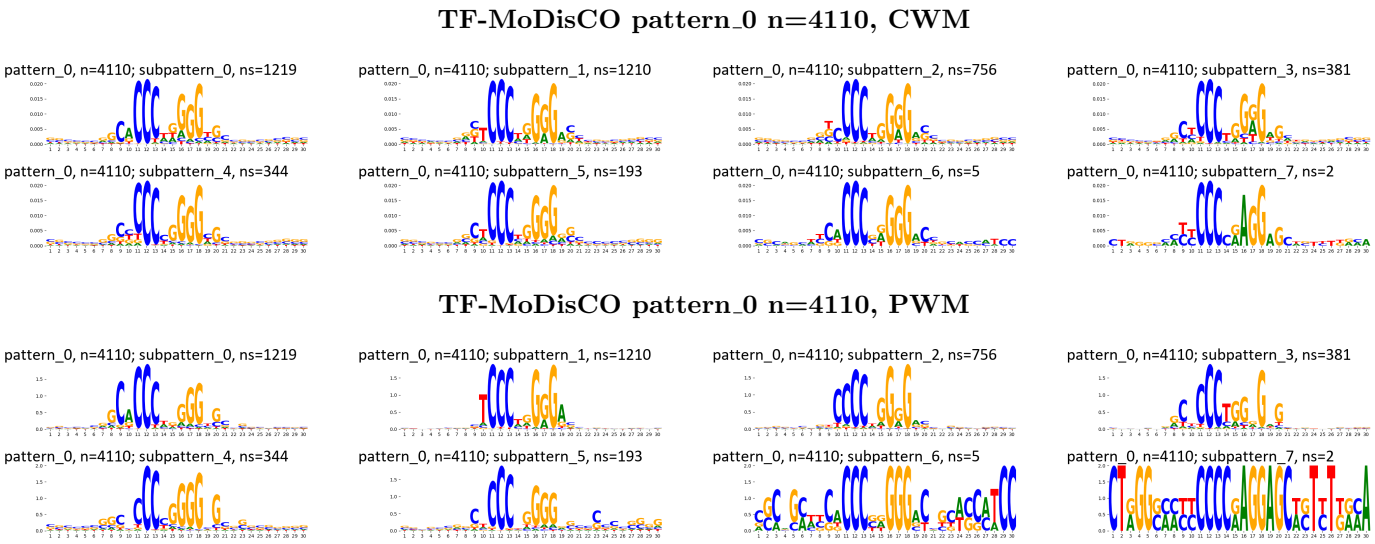

Supplementary Figure 1181: TF-MoDisCO subpatterns for the ZNF423 transcription factor in HEK293 (accession ENCSR477OJI).

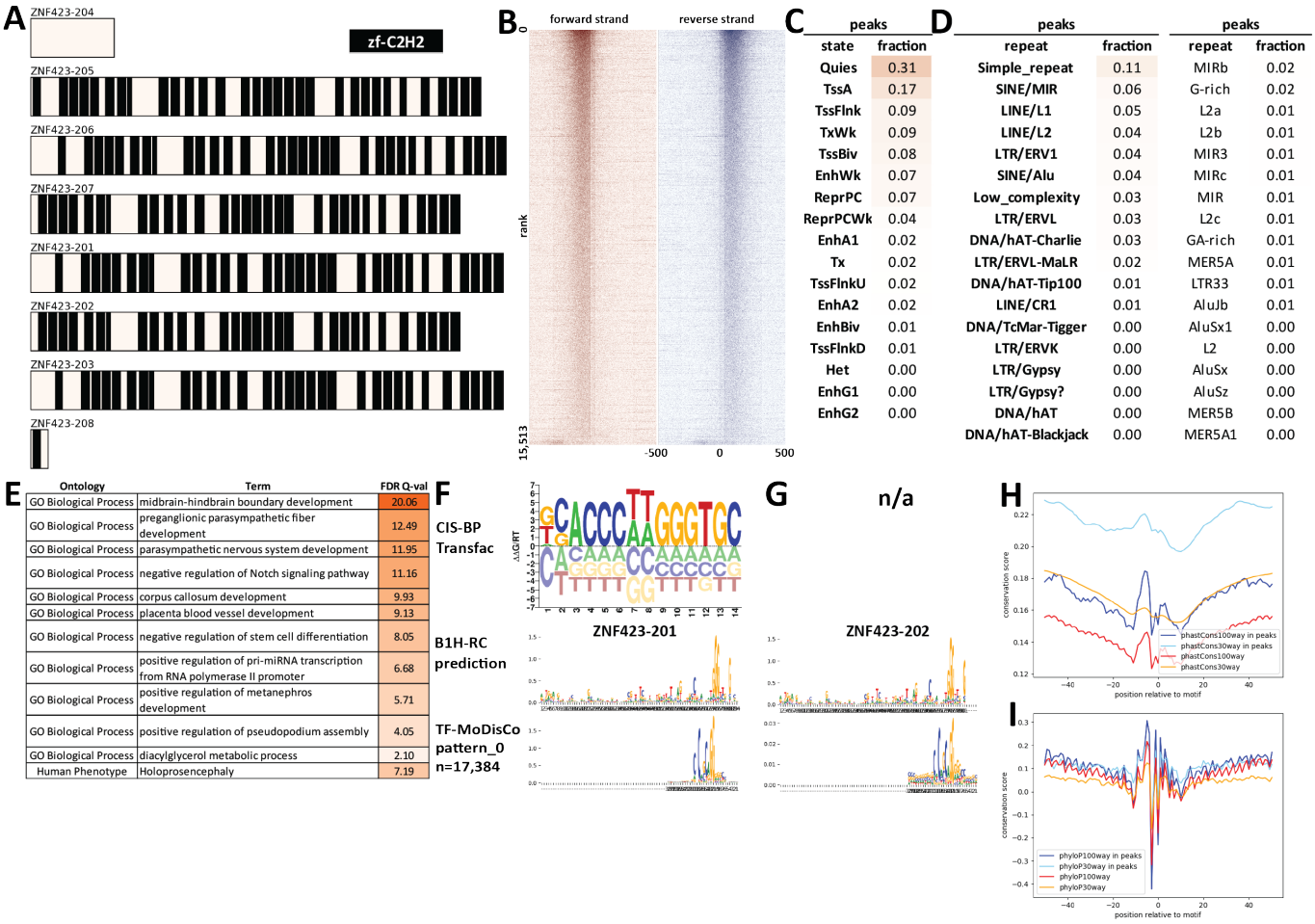

Supplementary Figure 1182: Properties and genomic distribution of motifs identified for the ZNF423 transcription factor in WTC11 (accession ENCSR413CVQ).

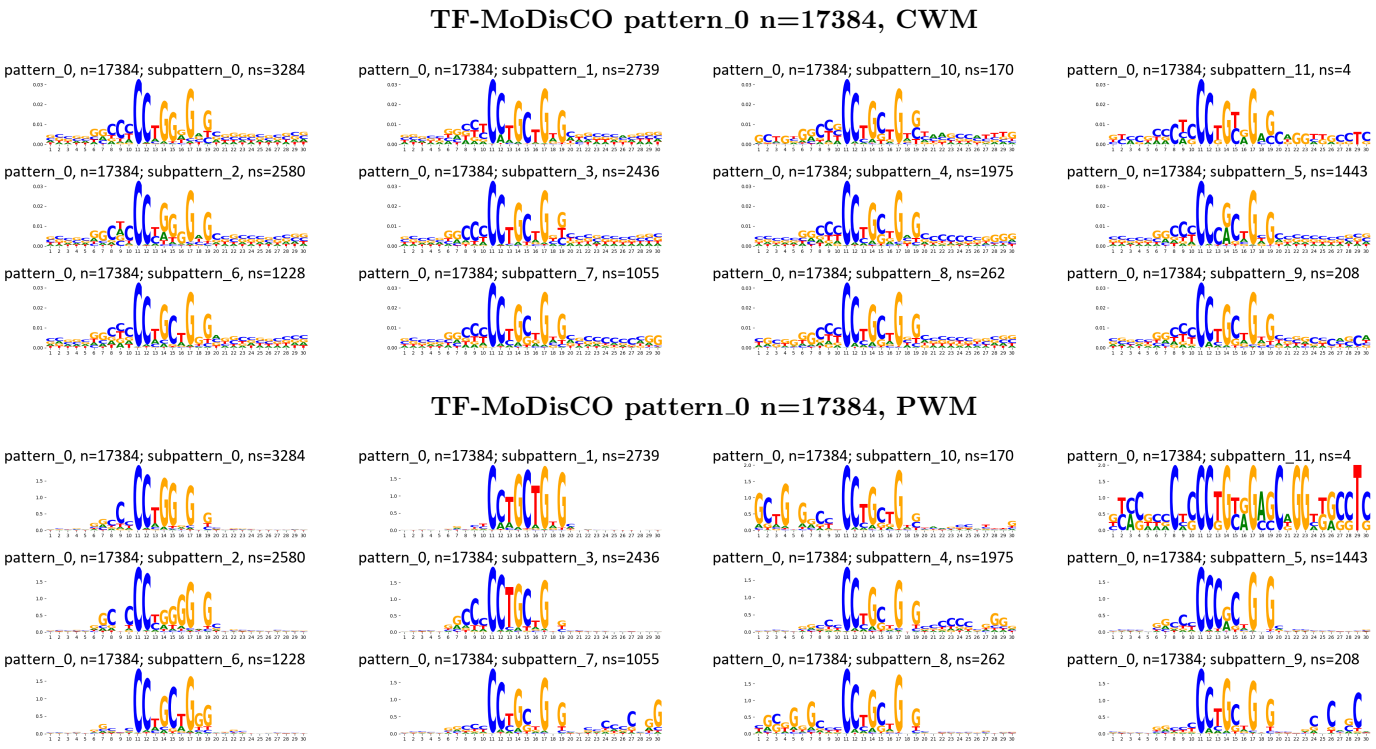

Supplementary Figure 1183: TF-MoDisCO subpatterns for the ZNF423 transcription factor in WTC11 (accession ENCSR413CVQ).

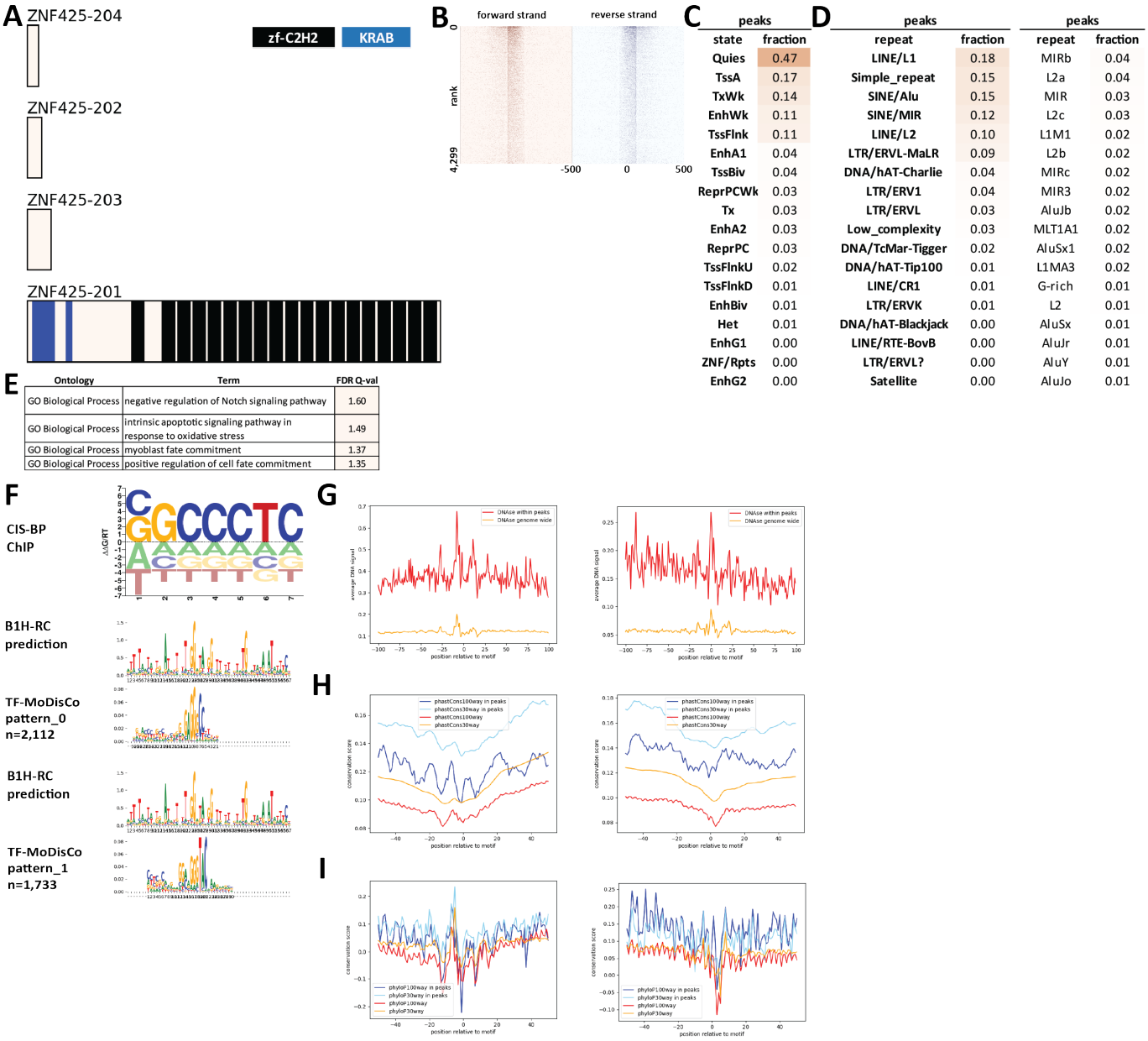

C

peaks	
state	fraction
Quies	0.47
TssA	0.17
TxWk	0.14
EnhWk	0.11
TssFlnk	0.11
EnhA1	0.04
TssBiv	0.04
ReprPCWk	0.03
Tx	0.03
EnhA2	0.03
ReprPC	0.03
TssFlnkU	0.02
TssFlnkD	0.01
EnhBiv	0.01
Het	0.01
EnhG1	0.00
ZNF/Rpts	0.00
EnhG2	0.00

D

peaks		peaks	
repeat	fraction	repeat	fraction
LINE/L1	0.18	MIRb	0.04
Simple_repeat	0.15	L2a	0.04
SINE/Alu	0.15	MIR	0.03
SINE/MIR	0.12	L2c	0.03
LINE/L2	0.10	L1M1	0.02
LTR/ERVL-MaLR	0.09	L2b	0.02
DNA/hAT-Charlie	0.04	MIRc	0.02
LTR/ERV1	0.04	MIR3	0.02
LTR/ERVL	0.03	AluJb	0.02
Low_complexity	0.03	MLT1A1	0.02
DNA/TcMar-Tigger	0.02	AluSx1	0.02
DNA/hAT-Tip100	0.01	L1MA3	0.02
LINE/CR1	0.01	G-rich	0.01
LTR/ERVK	0.01	L2	0.01
DNA/hAT-Blackjack	0.00	AluSx	0.01
LINE/RTE-BovB	0.00	AluJr	0.01
LTR/ERVL?	0.00	AluY	0.01
Satellite	0.00	AluJo	0.01

E

Ontology	Term	FDR Q-val
GO Biological Process	negative regulation of Notch signaling pathway	1.60
GO Biological Process	intrinsic apoptotic signaling pathway in response to oxidative stress	1.49
GO Biological Process	myoblast fate commitment	1.37
GO Biological Process	positive regulation of cell fate commitment	1.35

Supplementary Figure 1184: Properties and genomic distribution of motifs identified for the ZNF425 transcription factor in HEK293 (accession ChipExo models).

TF-MoDisCO pattern_0 n=2112, CWM

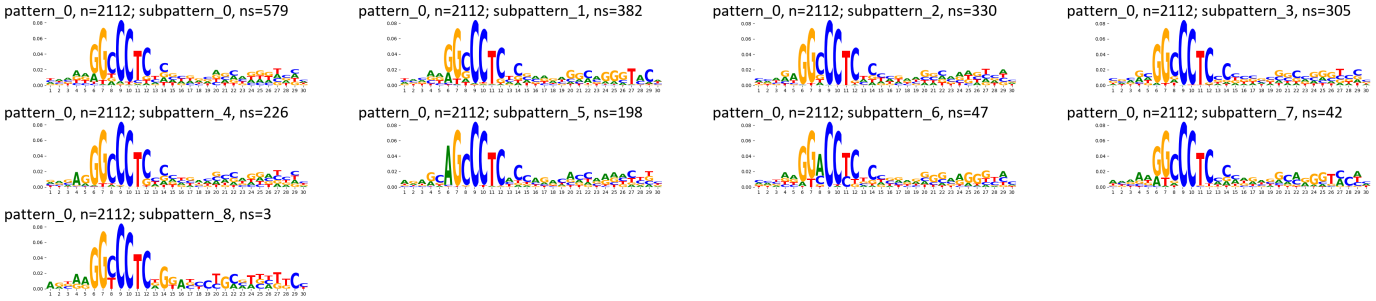

TF-MoDisCO pattern_0 n=2112, PWM

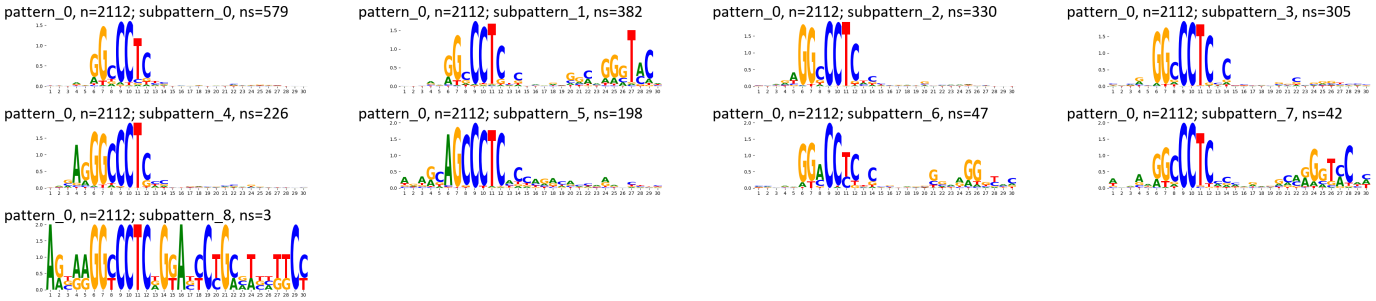

TF-MoDisCO pattern_1 n=1733, CWM

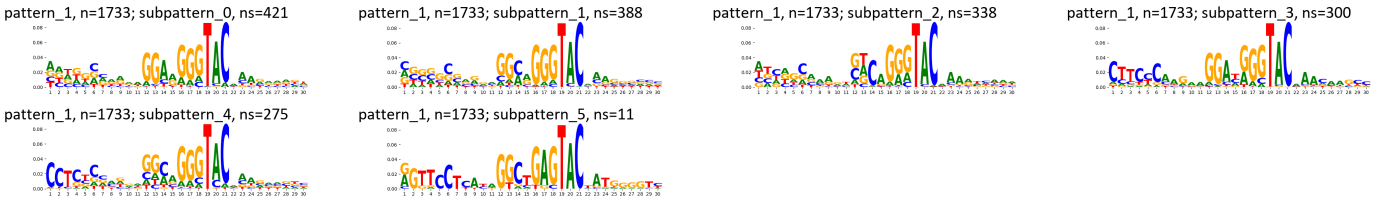

TF-MoDisCO pattern_1 n=1733, PWM

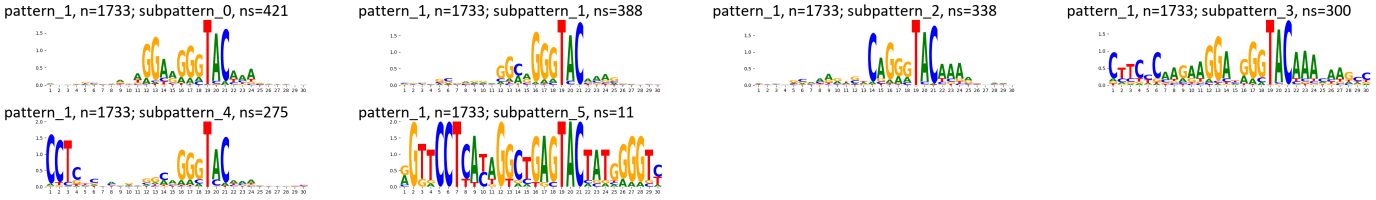

Supplementary Figure 1185: TF-MoDisCO subpatterns for the ZNF425 transcription factor in HEK293 (accession ChipExo models).

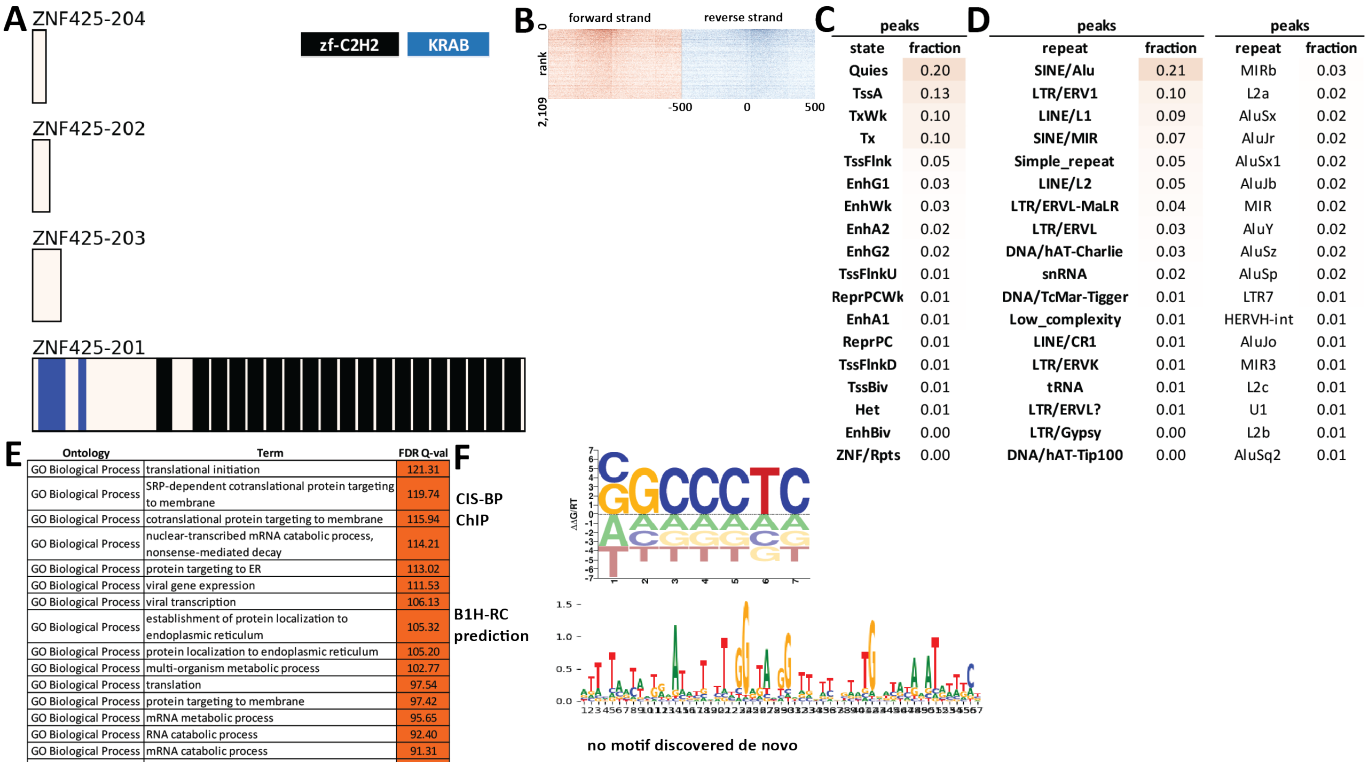

Supplementary Figure 1186: Properties and genomic distribution of motifs identified for the ZNF425 transcription factor in WTC11 (accession ENCSR717QWW).

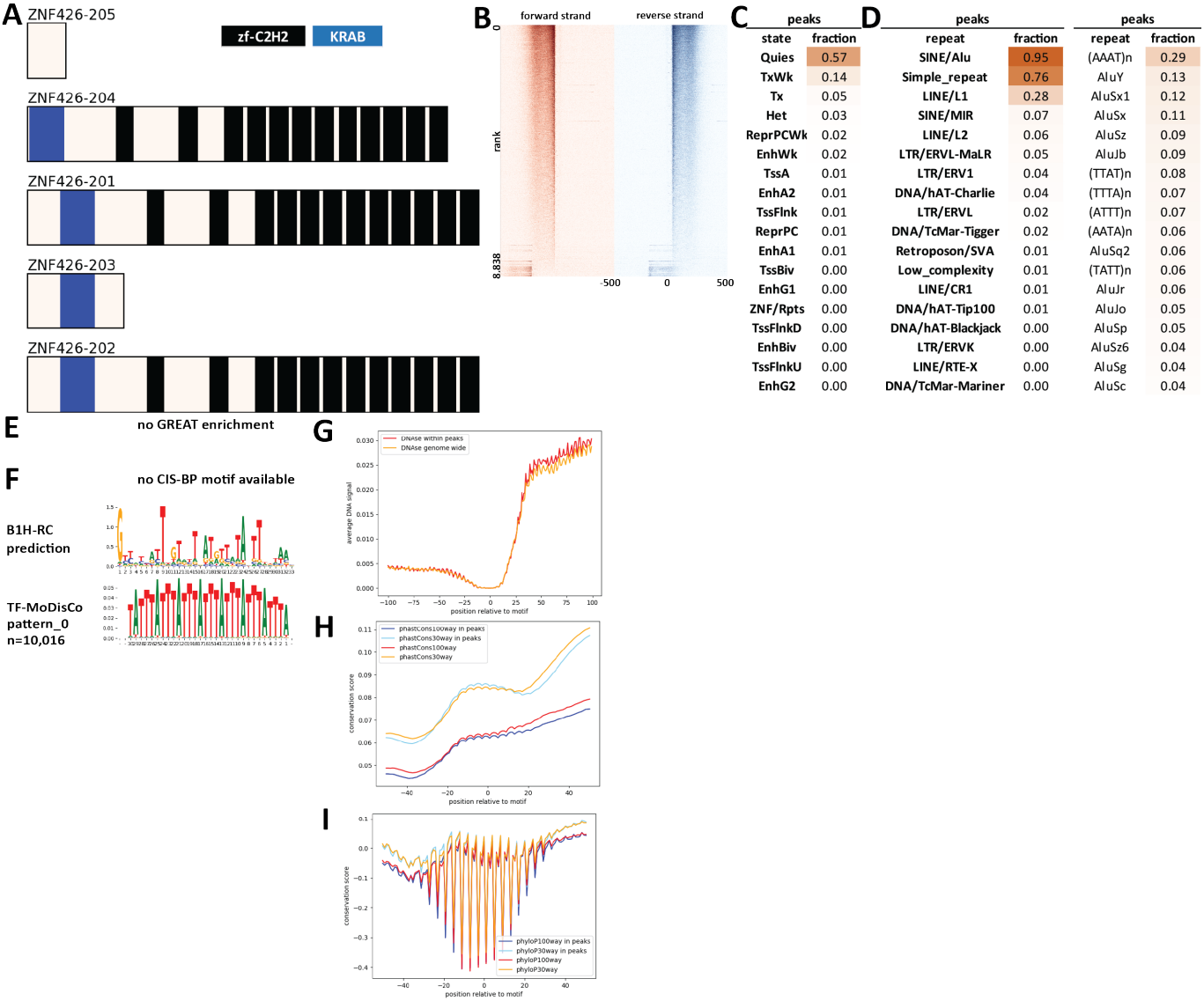

C

peaks	
state	fraction
Quies	0.57
TxWk	0.14
Tx	0.05
Het	0.03
ReprPCWk	0.02
EnhWk	0.02
TssA	0.01
EnhA2	0.01
TssFlnk	0.01
ReprPC	0.01
EnhA1	0.01
TssBiv	0.00
EnhG1	0.00
ZNF/Rpts	0.00
TssFlnkD	0.00
EnhBiv	0.00
TssFlnkU	0.00
EnhG2	0.00

D

peaks		peaks	
repeat	fraction	repeat	fraction
SINE/Alu	0.95	(AAAT)n	0.29
Simple_repeat	0.76	AluY	0.13
LINE/L1	0.28	AluSx1	0.12
SINE/MIR	0.07	AluSx	0.11
LINE/L2	0.06	AluSz	0.09
LTR/ERVL-MaLR	0.05	AluJb	0.09
LTR/ERV1	0.04	(TTAT)n	0.08
DNA/hAT-Charlie	0.04	(TTTA)n	0.07
LTR/ERVL	0.02	(ATTT)n	0.07
DNA/TcMar-Tigger	0.02	(AATA)n	0.06
Retroposon/SVA	0.01	AluSq2	0.06
Low_complexity	0.01	(TATT)n	0.06
LINE/CR1	0.01	AluJr	0.06
DNA/hAT-Tip100	0.01	AluJo	0.05
DNA/hAT-Blackjack	0.00	AluSp	0.05
LTR/ERVK	0.00	AluSz6	0.04
LINE/RTE-X	0.00	AluSg	0.04
DNA/TcMar-Mariner	0.00	AluSc	0.04

Supplementary Figure 1187: Properties and genomic distribution of motifs identified for the ZNF426 transcription factor in HEK293 (accession ENCSR224NFP).

TF-MoDisCO pattern_0 n=10016, CWM

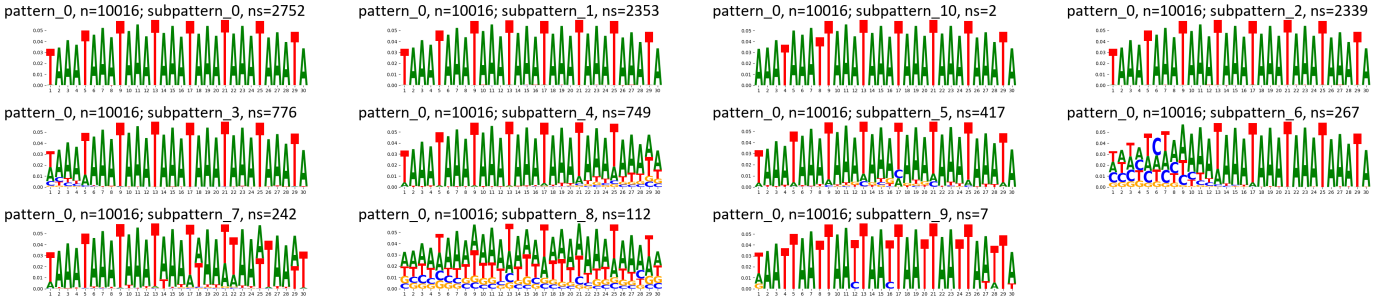

TF-MoDisCO pattern_0 n=10016, PWM

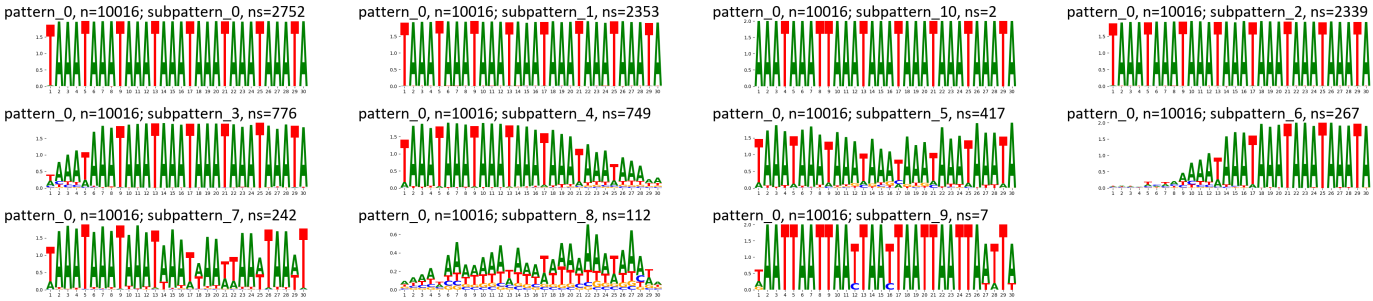

Supplementary Figure 1188: TF-MoDisCO subpatterns for the ZNF426 transcription factor in HEK293 (accession ENCSR224NFP).

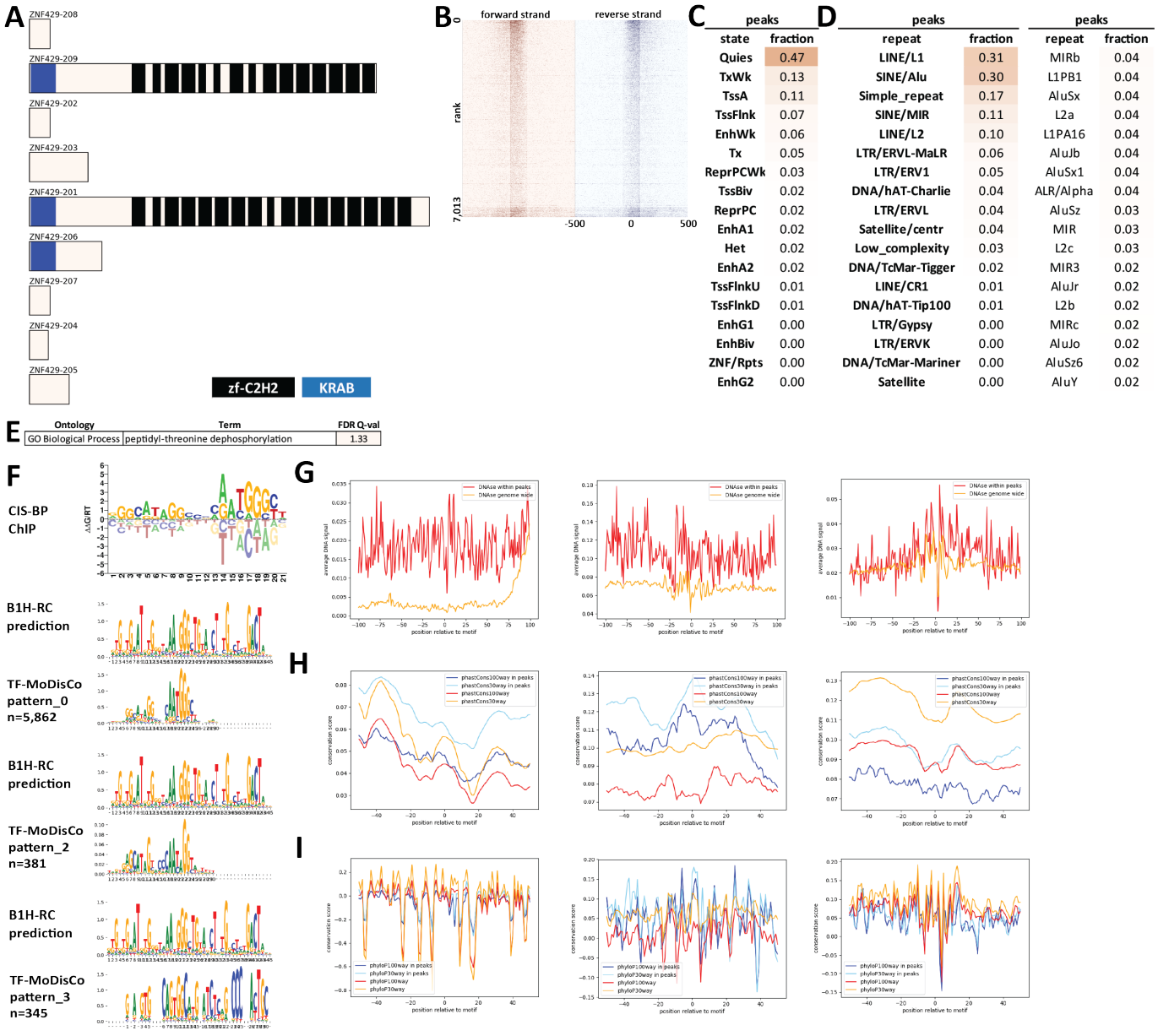

Supplementary Figure 1189: Properties and genomic distribution of motifs identified for the ZNF429 transcription factor in HEK293 (accession ChipExo models).

TF-MoDisCO pattern_0 n=5862, CWM

pattern_0, n=5862; subpattern_0, ns=994

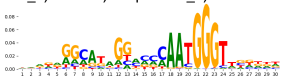

pattern_0, n=5862; subpattern_1, ns=783

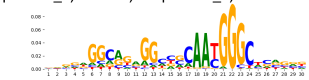

pattern_0, n=5862; subpattern_2, ns=760

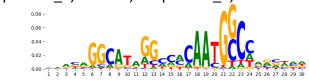

pattern_0, n=5862; subpattern_3, ns=698

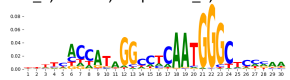

pattern_0, n=5862; subpattern_4, ns=622

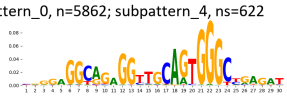

pattern_0, n=5862; subpattern_5, ns=618

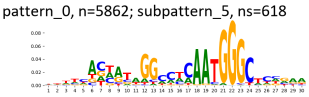

pattern_0, n=5862; subpattern_6, ns=527

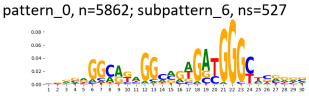

pattern_0, n=5862; subpattern_7, ns=336

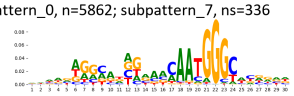

pattern_0, n=5862; subpattern_8, ns=333

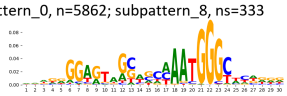

pattern_0, n=5862; subpattern_9, ns=191

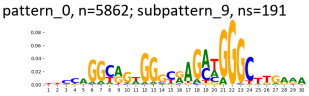

TF-MoDisCO pattern_0 n=5862, PWM

pattern_0, n=5862; subpattern_0, ns=994

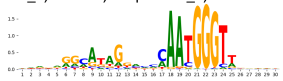

pattern_0, n=5862; subpattern_1, ns=783

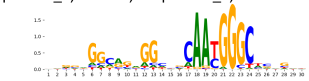

pattern_0, n=5862; subpattern_2, ns=760

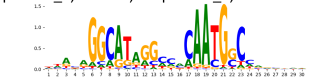

pattern_0, n=5862; subpattern_3, ns=698

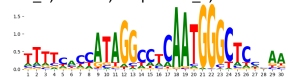

pattern_0, n=5862; subpattern_4, ns=622

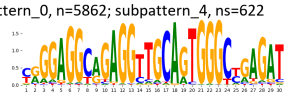

pattern_0, n=5862; subpattern_5, ns=618

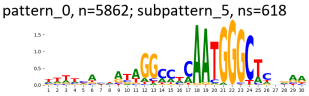

pattern_0, n=5862; subpattern_6, ns=527

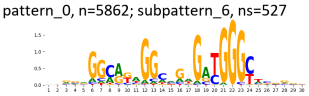

pattern_0, n=5862; subpattern_7, ns=336

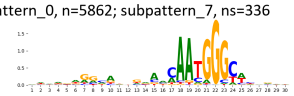

pattern_0, n=5862; subpattern_8, ns=333

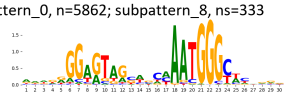

pattern_0, n=5862; subpattern_9, ns=191

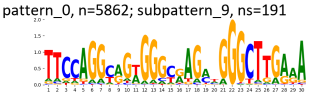

TF-MoDisCO pattern_2 n=381, CWM

pattern_2, n=381; subpattern_0, ns=98

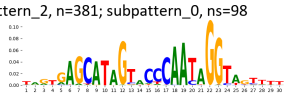

pattern_2, n=381; subpattern_1, ns=96

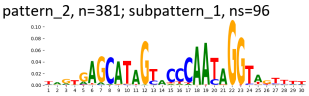

pattern_2, n=381; subpattern_2, ns=72

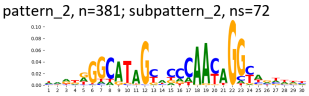

pattern_2, n=381; subpattern_3, ns=68

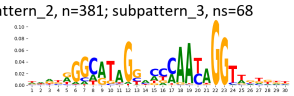

pattern_2, n=381; subpattern_4, ns=45

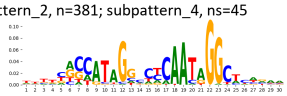

pattern_2, n=381; subpattern_5, ns=2

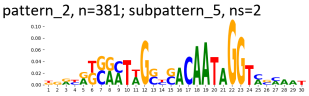

TF-MoDisCO pattern_2 n=381, PWM

pattern_2, n=381; subpattern_0, ns=98

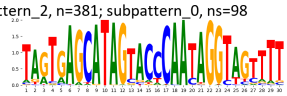

pattern_2, n=381; subpattern_1, ns=96

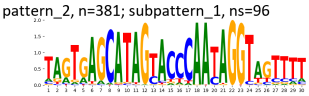

pattern_2, n=381; subpattern_2, ns=72

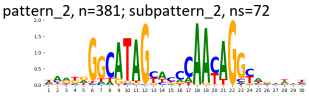

pattern_2, n=381; subpattern_3, ns=68

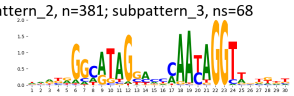

pattern_2, n=381; subpattern_4, ns=45

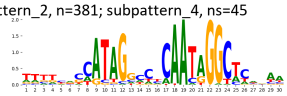

pattern_2, n=381; subpattern_5, ns=2

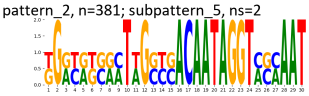

TF-MoDisCO pattern_3 n=345, CWM

pattern_3, n=345; subpattern_0, ns=102

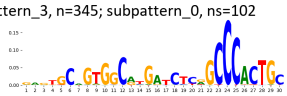

pattern_3, n=345; subpattern_1, ns=93

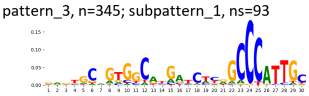

pattern_3, n=345; subpattern_2, ns=78

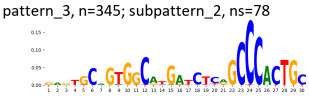

pattern_3, n=345; subpattern_3, ns=57

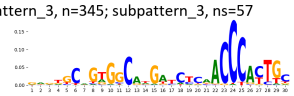

pattern_3, n=345; subpattern_4, ns=15

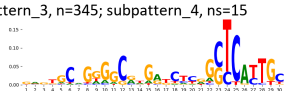

TF-MoDisCO pattern_3 n=345, PWM

pattern_3, n=345; subpattern_0, ns=102

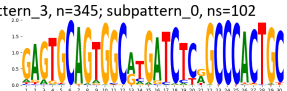

pattern_3, n=345; subpattern_1, ns=93

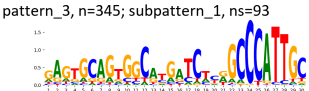

pattern_3, n=345; subpattern_2, ns=78

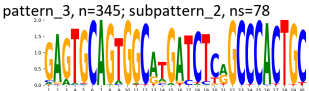

pattern_3, n=345; subpattern_3, ns=57

pattern_3, n=345; subpattern_4, ns=15

Supplementary Figure 1190: TF-MoDisCO subpatterns for the ZNF429 transcription factor in HEK293 (accession ChipExo models).

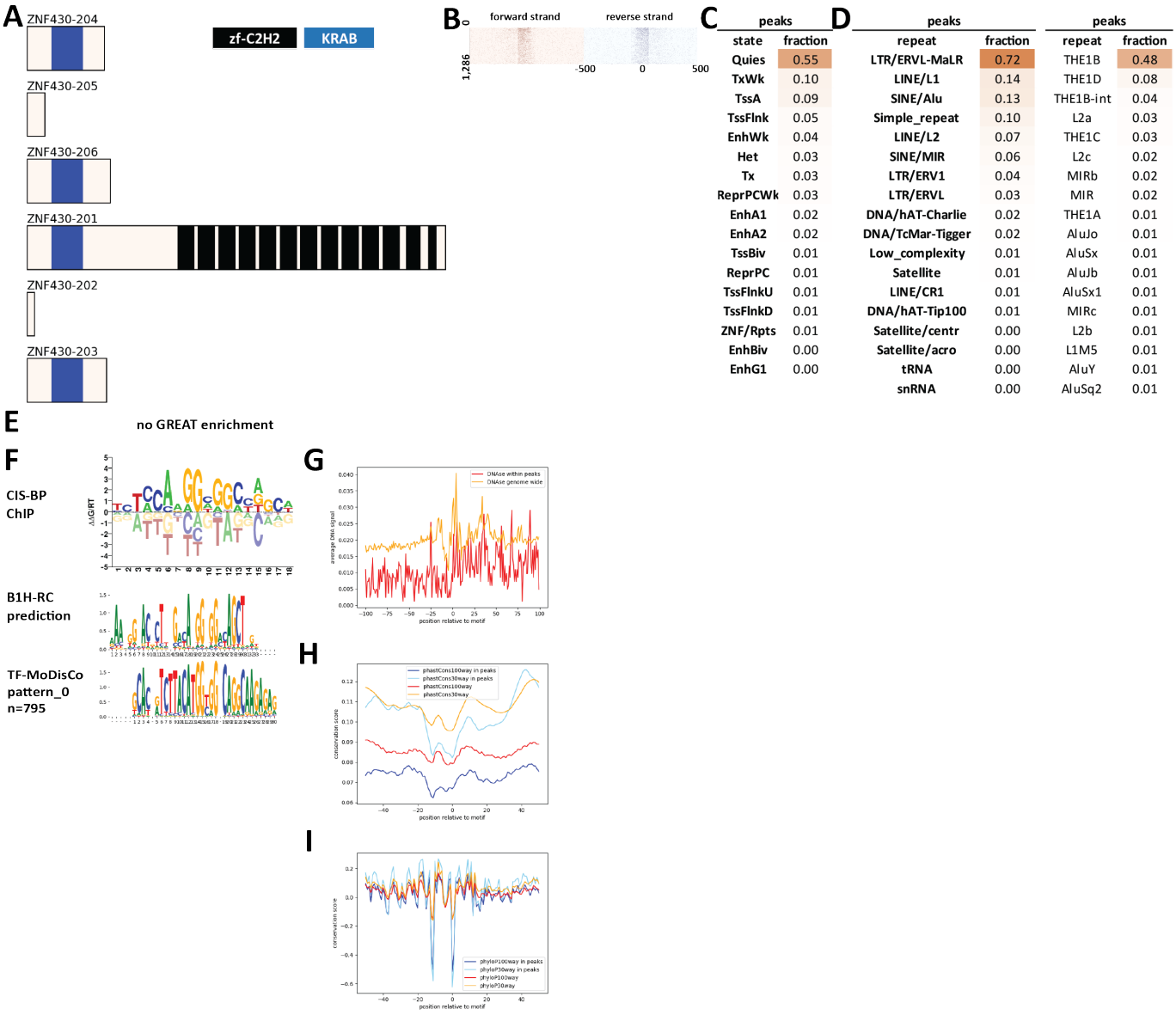

Supplementary Figure 1191: Properties and genomic distribution of motifs identified for the ZNF430 transcription factor in HEK293 (accession ChipExo models).

TF-MoDisCO pattern_0 n=795, CWM

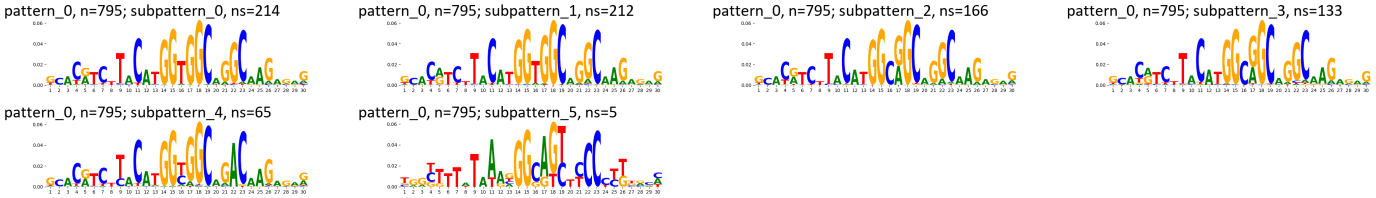

TF-MoDisCO pattern_0 n=795, PWM

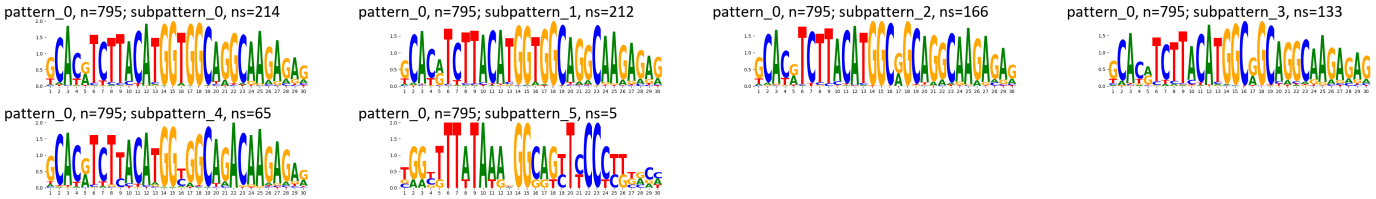

Supplementary Figure 1192: TF-MoDisCO subpatterns for the ZNF430 transcription factor in HEK293 (accession ChipExo models).

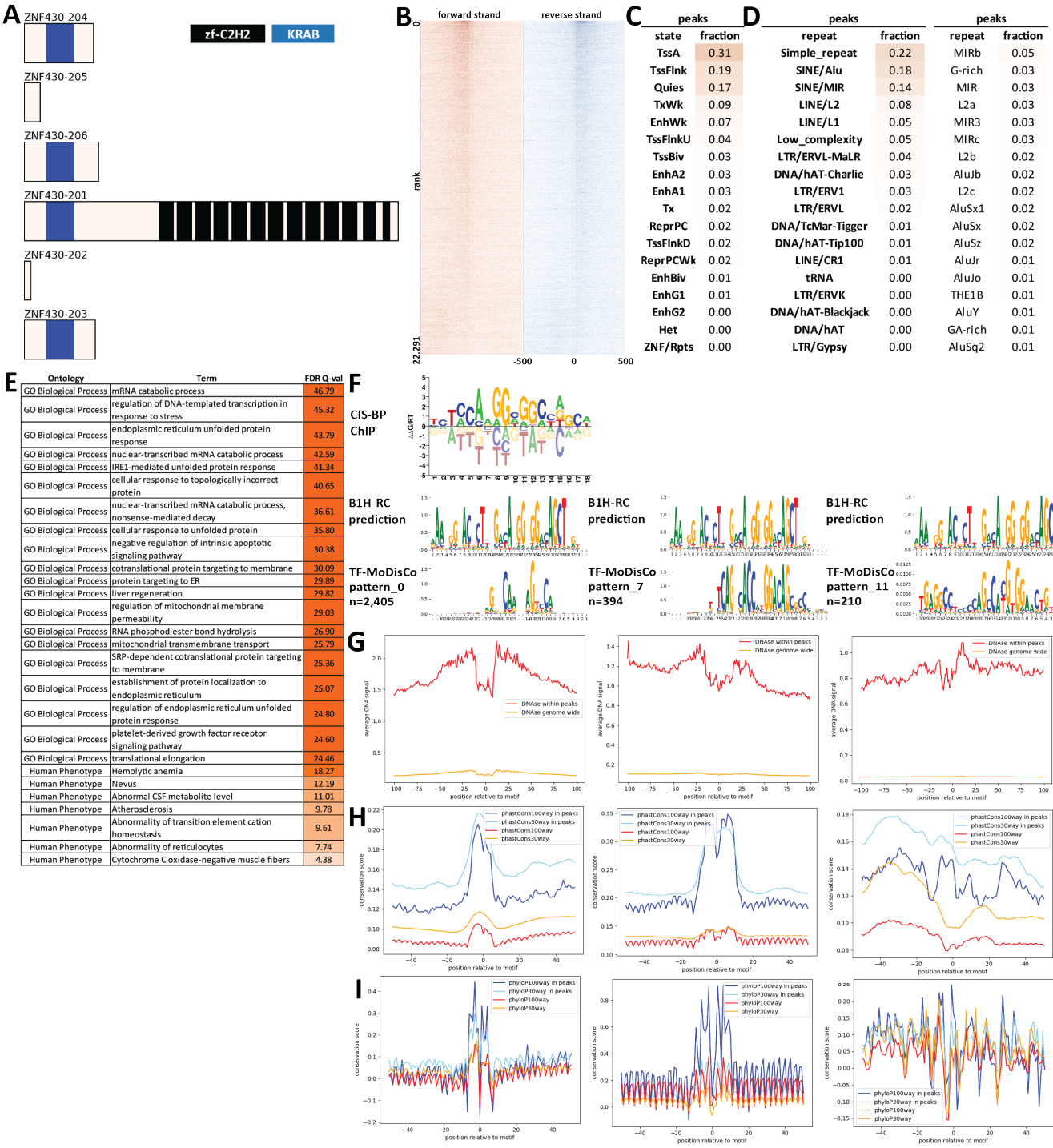

Supplementary Figure 1193: Properties and genomic distribution of motifs identified for the ZNF430 transcription factor in HepG2 (accession ENCSR618END).

TF-MoDisCO pattern_0 n=2405, CWM

pattern_0, n=2405; subpattern_0, ns=684

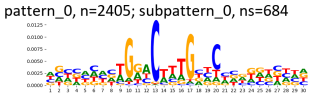

pattern_0, n=2405; subpattern_1, ns=459

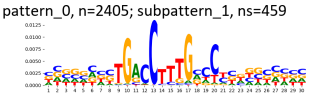

pattern_0, n=2405; subpattern_10, ns=2

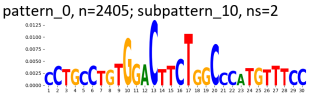

pattern_0, n=2405; subpattern_2, ns=396

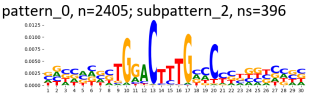

pattern_0, n=2405; subpattern_3, ns=328

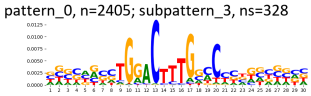

pattern_0, n=2405; subpattern_4, ns=301

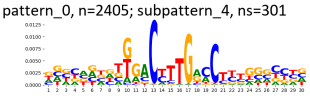

pattern_0, n=2405; subpattern_5, ns=198

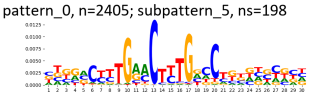

pattern_0, n=2405; subpattern_6, ns=28

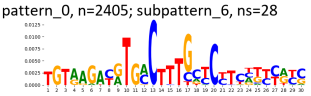

pattern_0, n=2405; subpattern_7, ns=4

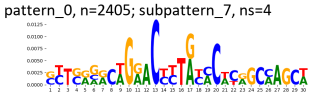

pattern_0, n=2405; subpattern_8, ns=3

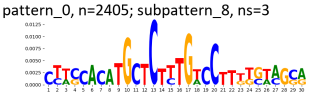

pattern_0, n=2405; subpattern_9, ns=2

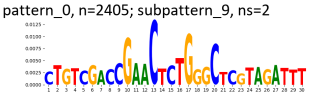

TF-MoDisCO pattern_0 n=2405, PWM

pattern_0, n=2405; subpattern_0, ns=684

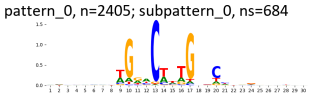

pattern_0, n=2405; subpattern_1, ns=459

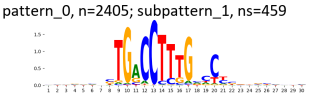

pattern_0, n=2405; subpattern_10, ns=2

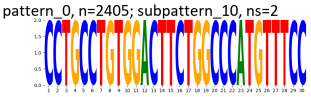

pattern_0, n=2405; subpattern_2, ns=396

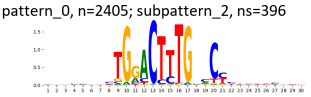

pattern_0, n=2405; subpattern_3, ns=328

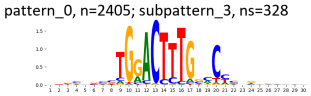

pattern_0, n=2405; subpattern_4, ns=301

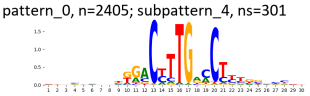

pattern_0, n=2405; subpattern_5, ns=198

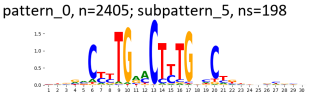

pattern_0, n=2405; subpattern_6, ns=28

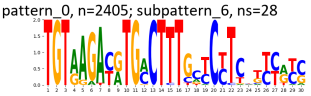

pattern_0, n=2405; subpattern_7, ns=4

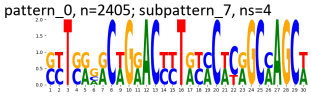

pattern_0, n=2405; subpattern_8, ns=3

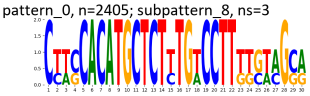

pattern_0, n=2405; subpattern_9, ns=2

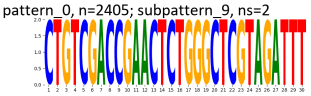

TF-MoDisCO pattern_11 n=210, CWM

pattern_11, n=210; subpattern_0, ns=61

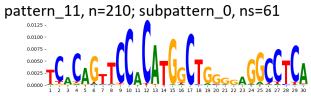

pattern_11, n=210; subpattern_1, ns=51

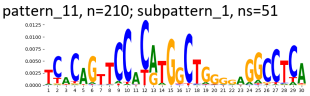

pattern_11, n=210; subpattern_2, ns=36

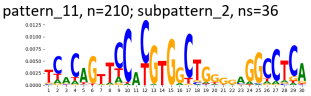

pattern_11, n=210; subpattern_3, ns=33

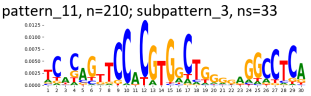

pattern_11, n=210; subpattern_4, ns=24

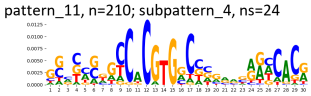

pattern_11, n=210; subpattern_5, ns=5

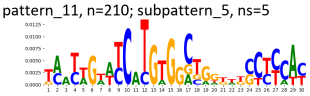

TF-MoDisCO pattern_11 n=210, PWM

pattern_11, n=210; subpattern_0, ns=61

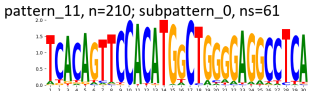

pattern_11, n=210; subpattern_1, ns=51

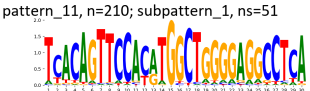

pattern_11, n=210; subpattern_2, ns=36

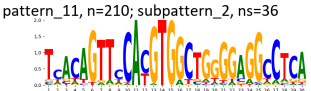

pattern_11, n=210; subpattern_3, ns=33

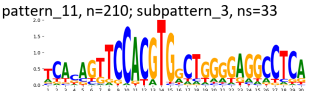

pattern_11, n=210; subpattern_4, ns=24

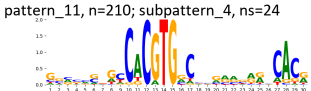

pattern_11, n=210; subpattern_5, ns=5

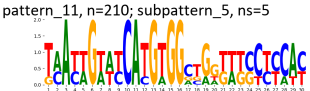

TF-MoDisCO pattern_7 n=394, CWM

pattern_7, n=394; subpattern_0, ns=197

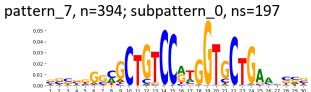

pattern_7, n=394; subpattern_1, ns=143

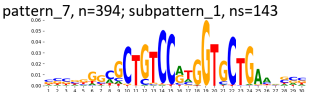

pattern_7, n=394; subpattern_2, ns=33

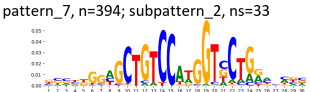

pattern_7, n=394; subpattern_3, ns=21

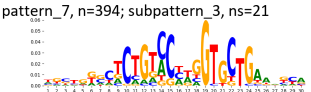

TF-MoDisCO pattern_7 n=394, PWM

pattern_7, n=394; subpattern_0, ns=197

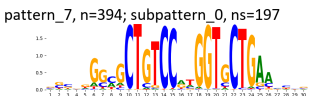

pattern_7, n=394; subpattern_1, ns=143

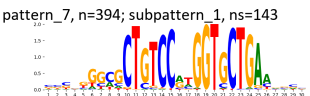

pattern_7, n=394; subpattern_2, ns=33

pattern_7, n=394; subpattern_3, ns=21

Supplementary Figure 1194: TF-MoDisCO subpatterns for the ZNF430 transcription factor in HepG2 (accession ENCSR618END).

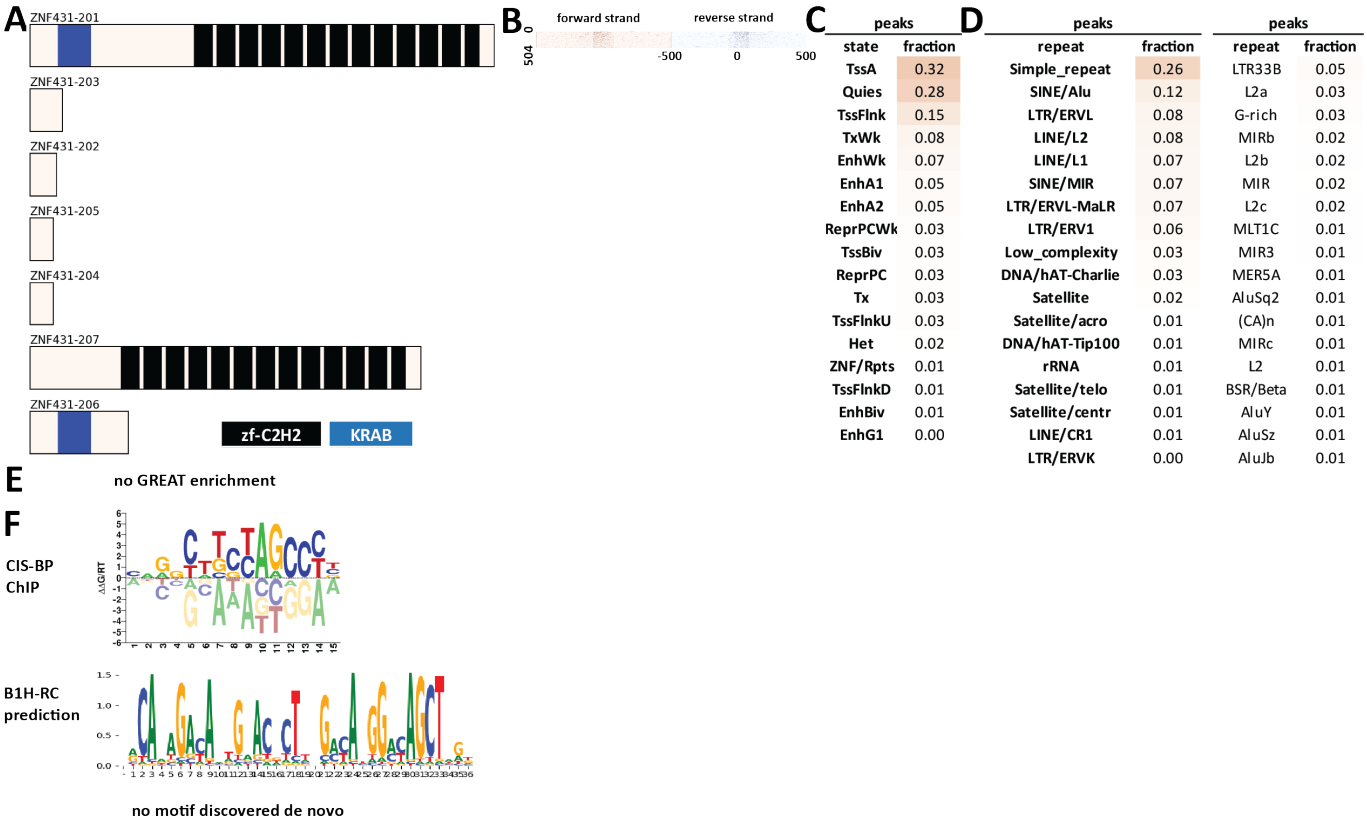

C	peaks	
	state	fraction
	TssA	0.32
	Quies	0.28
	TssFlnk	0.15
	TxWk	0.08
	EnhWk	0.07
	EnhA1	0.05
	EnhA2	0.05
	ReprPCWk	0.03
	TssBiv	0.03
	ReprPC	0.03
	Tx	0.03
	TssFlnkU	0.03
	Het	0.02
	ZNF/Rpts	0.01
	TssFlnkD	0.01
	EnhBiv	0.01
	EnhG1	0.00

D	peaks		peaks	
	repeat	fraction	repeat	fraction
	Simple_repeat	0.26	LTR33B	0.05
	SINE/Alu	0.12	L2a	0.03
	LTR/ERVL	0.08	G-rich	0.03
	LINE/L2	0.08	MIRb	0.02
	LINE/L1	0.07	L2b	0.02
	SINE/MIR	0.07	MIR	0.02
	LTR/ERVL-MaLR	0.07	L2c	0.02
	LTR/ERV1	0.06	MLT1C	0.01
	Low_complexity	0.03	MIR3	0.01
	DNA/hAT-Charlie	0.03	MER5A	0.01
	Satellite	0.02	AluSq2	0.01
	Satellite/acro	0.01	(CA)n	0.01
	DNA/hAT-Tip100	0.01	MIRc	0.01
	rRNA	0.01	L2	0.01
	Satellite/telo	0.01	BSR/Beta	0.01
	Satellite/centr	0.01	AluY	0.01
	LINE/CR1	0.01	AluSz	0.01
	LTR/ERVK	0.00	AluJb	0.01

Supplementary Figure 1195: Properties and genomic distribution of motifs identified for the ZNF431 transcription factor in HEK293 (accession ChipExo models).

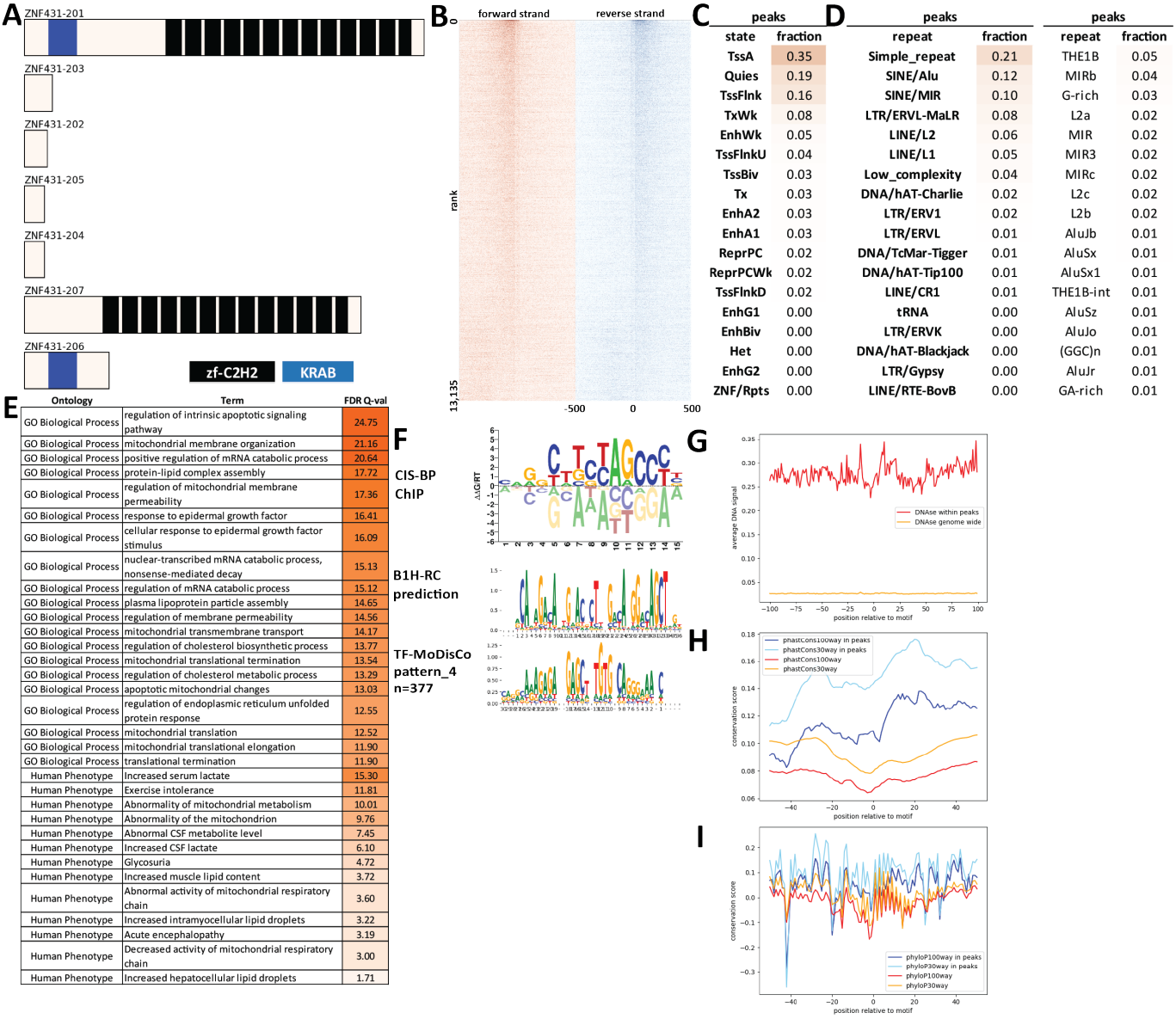

Supplementary Figure 1196: Properties and genomic distribution of motifs identified for the ZNF431 transcription factor in HepG2 (accession ENCSR204ALX).

TF-MoDisCO pattern_4 n=377, CWM

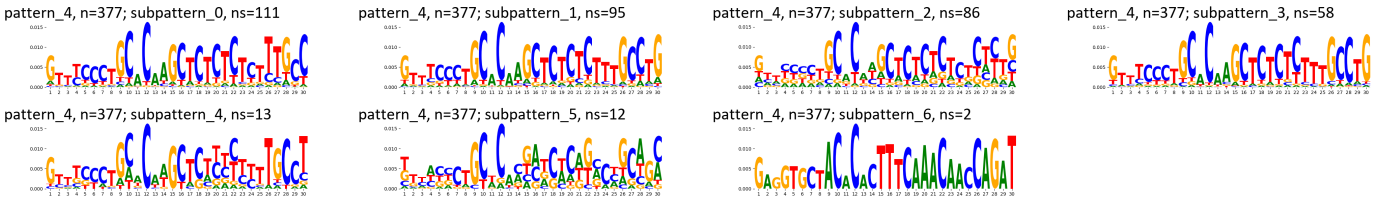

TF-MoDisCO pattern_4 n=377, PWM

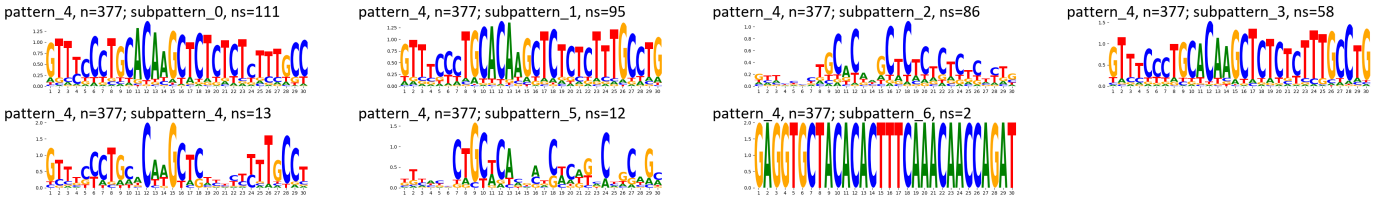

Supplementary Figure 1197: TF-MoDisCO subpatterns for the ZNF431 transcription factor in HepG2 (accession ENCSR204ALX).

A

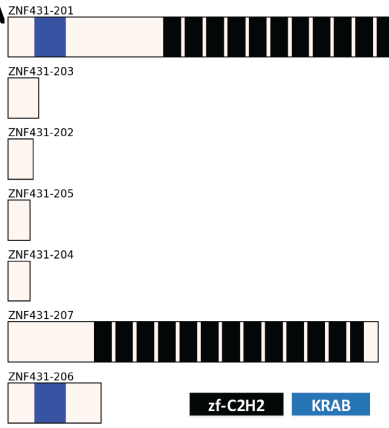

B

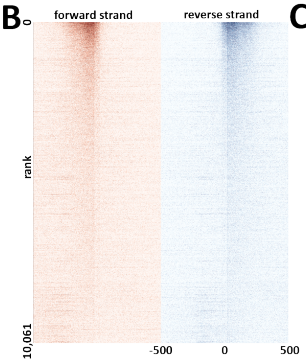

C

peaks	
state	fraction
TssA	0.33
Quies	0.26
TssFlnk	0.15
TxWk	0.08
TssFlnkU	0.03
Tx	0.03
EnhWk	0.03
TssBiv	0.03
EnhA2	0.02
ReprPC	0.02
ReprPCWk	0.02
Het	0.02
TssFlnkD	0.01
EnhA1	0.01
EnhG1	0.01
EnhBiv	0.00
EnhG2	0.00
ZNF/Rpts	0.00

D

peaks		peaks	
repeat	fraction	repeat	fraction
LTR/ERVL-MaLR	0.33	THE1B	0.21
Simple_repeat	0.17	THE1B-int	0.04
SINE/Alu	0.13	MIRb	0.03
LINE/L1	0.10	G-rich	0.02
SINE/MIR	0.09	L2a	0.02
LINE/L2	0.06	MIR	0.02
Low_complexity	0.03	MIRc	0.02
LTR/ERV1	0.03	MIR3	0.02
DNA/hAT-Charlie	0.02	AluSx	0.02
LTR/ERVL	0.02	L2c	0.02
DNA/TcMar-Tigger	0.01	THE1D	0.02
tRNA	0.01	L2b	0.01
LINE/CR1	0.01	MSTA	0.01
DNA/hAT-Tip100	0.00	AluJb	0.01
snRNA	0.00	AluSx1	0.01
DNA/hAT-Blackjack	0.00	AluSz	0.01
LTR/ERVK	0.00	AluY	0.01
LINE/RTE-X	0.00	AluJo	0.01

E

Ontology	Term	FDR Q-val
GO Biological Process	regulation of gene expression, epigenetic	35.12
GO Biological Process	nucleosome organization	24.64
GO Biological Process	mRNA catabolic process	23.52
GO Biological Process	chromatin assembly or disassembly	23.27
GO Biological Process	chromatin assembly	22.19
GO Biological Process	nucleosome assembly	21.24
GO Biological Process	nuclear-transcribed mRNA catabolic process	21.08
GO Biological Process	gene silencing	20.72
GO Biological Process	response to topologically incorrect protein	18.19
GO Biological Process	nuclear-transcribed mRNA catabolic process, nonsense-mediated decay	17.54
GO Biological Process	cotranslational protein targeting to membrane	14.07
GO Biological Process	regulation of megakaryocyte differentiation	13.88
GO Biological Process	viral gene expression	13.59
GO Biological Process	SRP-dependent cotranslational protein targeting to membrane	12.48
GO Biological Process	viral transcription	12.20
GO Biological Process	protein targeting to ER	11.98
GO Biological Process	establishment of protein localization to endoplasmic reticulum	9.34
GO Biological Process	carbohydrate phosphorylation	5.78
GO Biological Process	regulation of nucleobase-containing compound transport	5.35
GO Biological Process	platelet formation	4.52

F

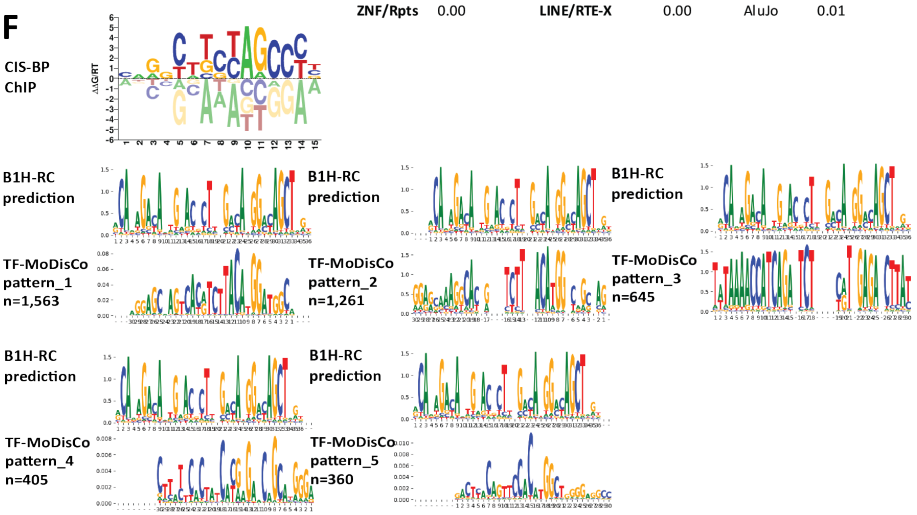



Supplementary Figure 1198: Properties and genomic distribution of motifs identified for the ZNF431 transcription factor in K562 (accession ENCSR609ZLF).

TF-MoDisCO pattern_1 n=1563, CWM

pattern_1, n=1563; subpattern_0, ns=412

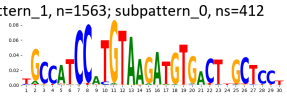

pattern_1, n=1563; subpattern_1, ns=407

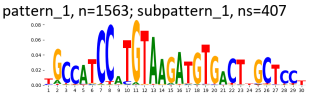

pattern_1, n=1563; subpattern_2, ns=363

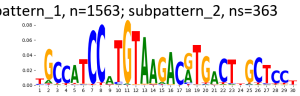

pattern_1, n=1563; subpattern_3, ns=180

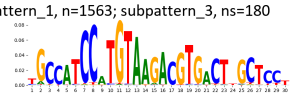

pattern_1, n=1563; subpattern_4, ns=174

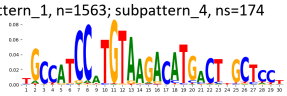

pattern_1, n=1563; subpattern_5, ns=27

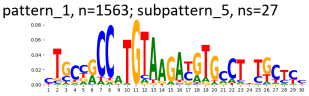

TF-MoDisCO pattern_1 n=1563, PWM

pattern_1, n=1563; subpattern_0, ns=412

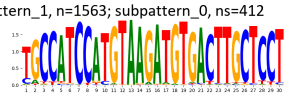

pattern_1, n=1563; subpattern_1, ns=407

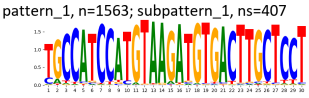

pattern_1, n=1563; subpattern_2, ns=363

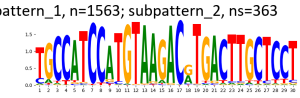

pattern_1, n=1563; subpattern_3, ns=180

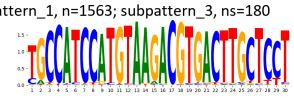

pattern_1, n=1563; subpattern_4, ns=174

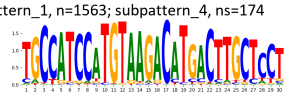

pattern_1, n=1563; subpattern_5, ns=27

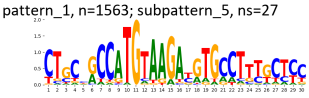

TF-MoDisCO pattern_2 n=1261, CWM

pattern_2, n=1261; subpattern_0, ns=255

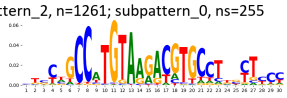

pattern_2, n=1261; subpattern_1, ns=245

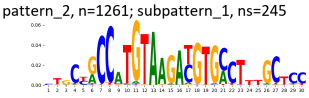

pattern_2, n=1261; subpattern_2, ns=220

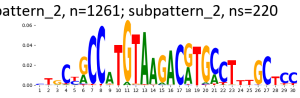

pattern_2, n=1261; subpattern_3, ns=137

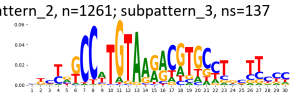

pattern_2, n=1261; subpattern_4, ns=128

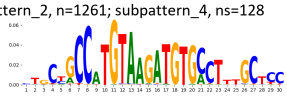

pattern_2, n=1261; subpattern_5, ns=95

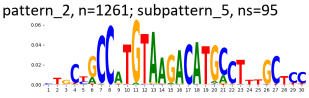

pattern_2, n=1261; subpattern_6, ns=93

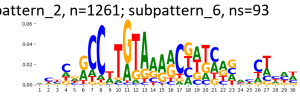

pattern_2, n=1261; subpattern_7, ns=88

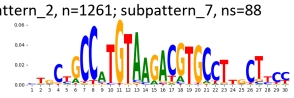

TF-MoDisCO pattern_2 n=1261, PWM

pattern_2, n=1261; subpattern_0, ns=255

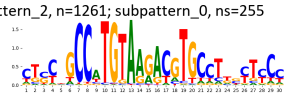

pattern_2, n=1261; subpattern_1, ns=245

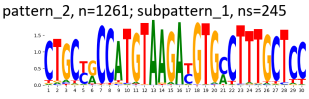

pattern_2, n=1261; subpattern_2, ns=220

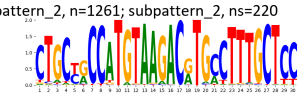

pattern_2, n=1261; subpattern_3, ns=137

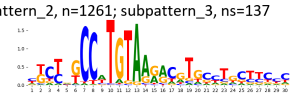

pattern_2, n=1261; subpattern_4, ns=128

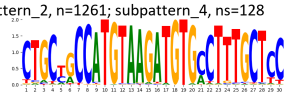

pattern_2, n=1261; subpattern_5, ns=95

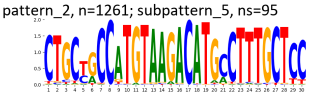

pattern_2, n=1261; subpattern_6, ns=93

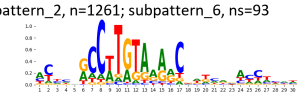

pattern_2, n=1261; subpattern_7, ns=88

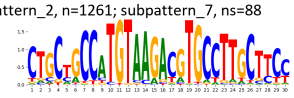

TF-MoDisCO pattern_3 n=645, CWM

pattern_3, n=645; subpattern_0, ns=158

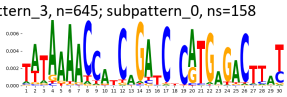

pattern_3, n=645; subpattern_1, ns=153

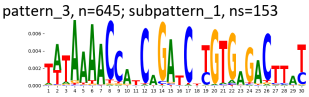

pattern_3, n=645; subpattern_2, ns=138

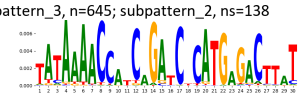

pattern_3, n=645; subpattern_3, ns=81

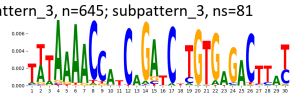

pattern_3, n=645; subpattern_4, ns=73

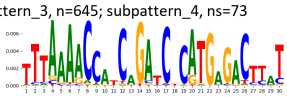

pattern_3, n=645; subpattern_5, ns=40

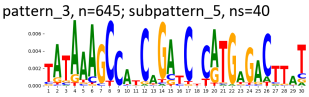

pattern_3, n=645; subpattern_6, ns=2

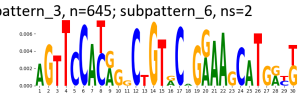

TF-MoDisCO pattern_3 n=645, PWM

pattern_3, n=645; subpattern_0, ns=158

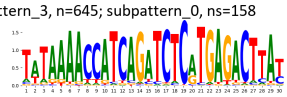

pattern_3, n=645; subpattern_1, ns=153

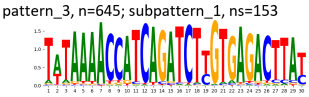

pattern_3, n=645; subpattern_2, ns=138

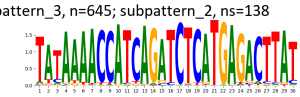

pattern_3, n=645; subpattern_3, ns=81

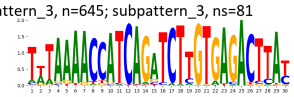

pattern_3, n=645; subpattern_4, ns=73

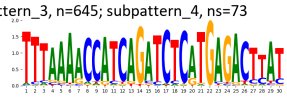

pattern_3, n=645; subpattern_5, ns=40

pattern_3, n=645; subpattern_6, ns=2

TF-MoDisCO pattern_5 n=360, CWM

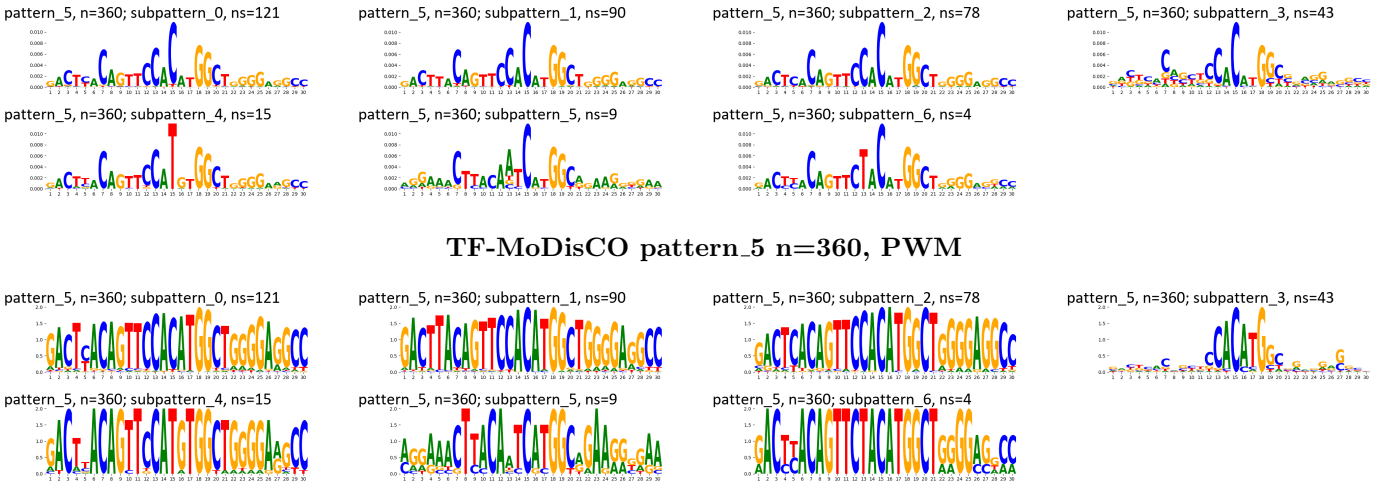

Supplementary Figure 1199: TF-MoDisCO subpatterns for the ZNF431 transcription factor in K562 (accession ENCSR609ZLF).

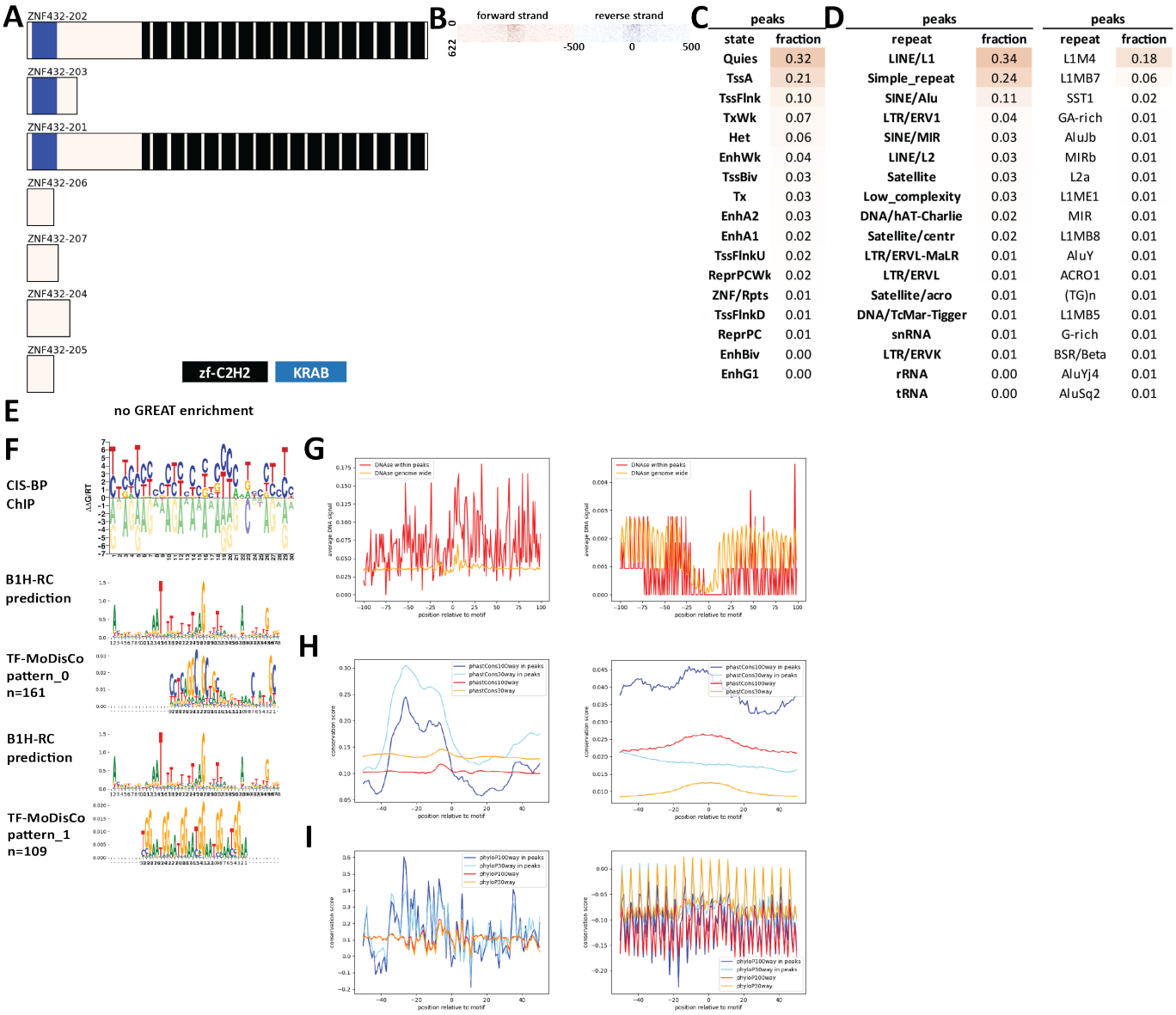

Supplementary Figure 1200: Properties and genomic distribution of motifs identified for the ZNF432 transcription factor in HEK293 (accession ChipExo models).

TF-MoDisCO pattern_0 n=161, CWM

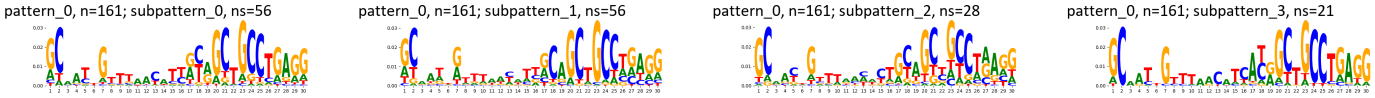

TF-MoDisCO pattern_0 n=161, PWM

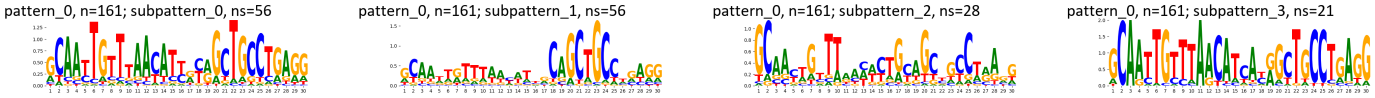

TF-MoDisCO pattern_1 n=109, CWM

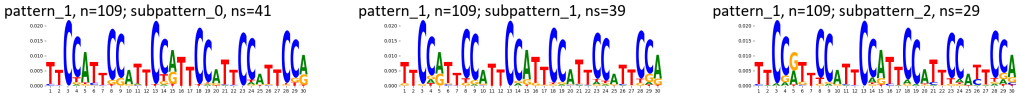

TF-MoDisCO pattern_1 n=109, PWM

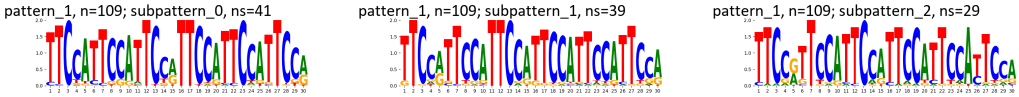

Supplementary Figure 1201: TF-MoDisCO subpatterns for the ZNF432 transcription factor in HEK293 (accession ChipExo models).

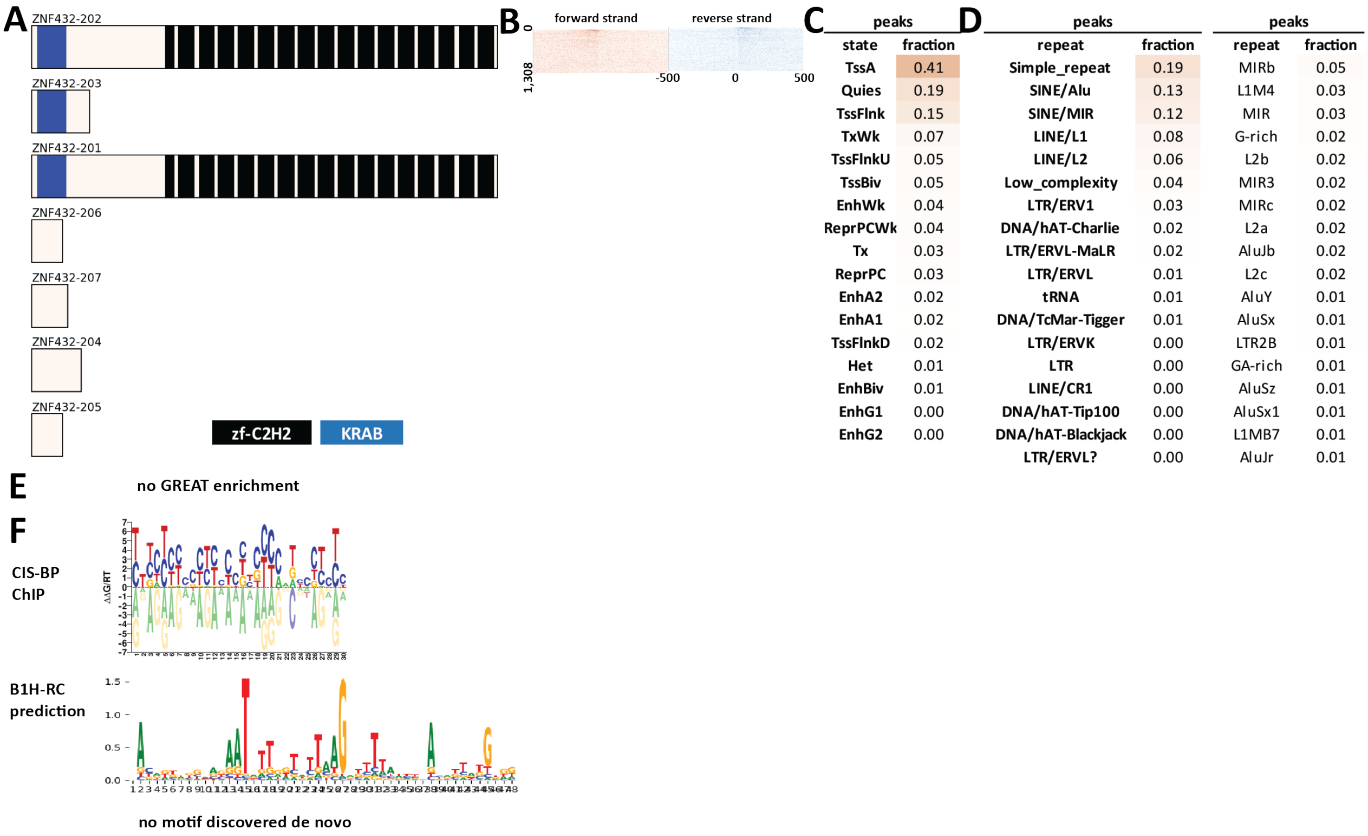

Supplementary Figure 1202: Properties and genomic distribution of motifs identified for the ZNF432 transcription factor in HepG2 (accession ENCSR043VRG).

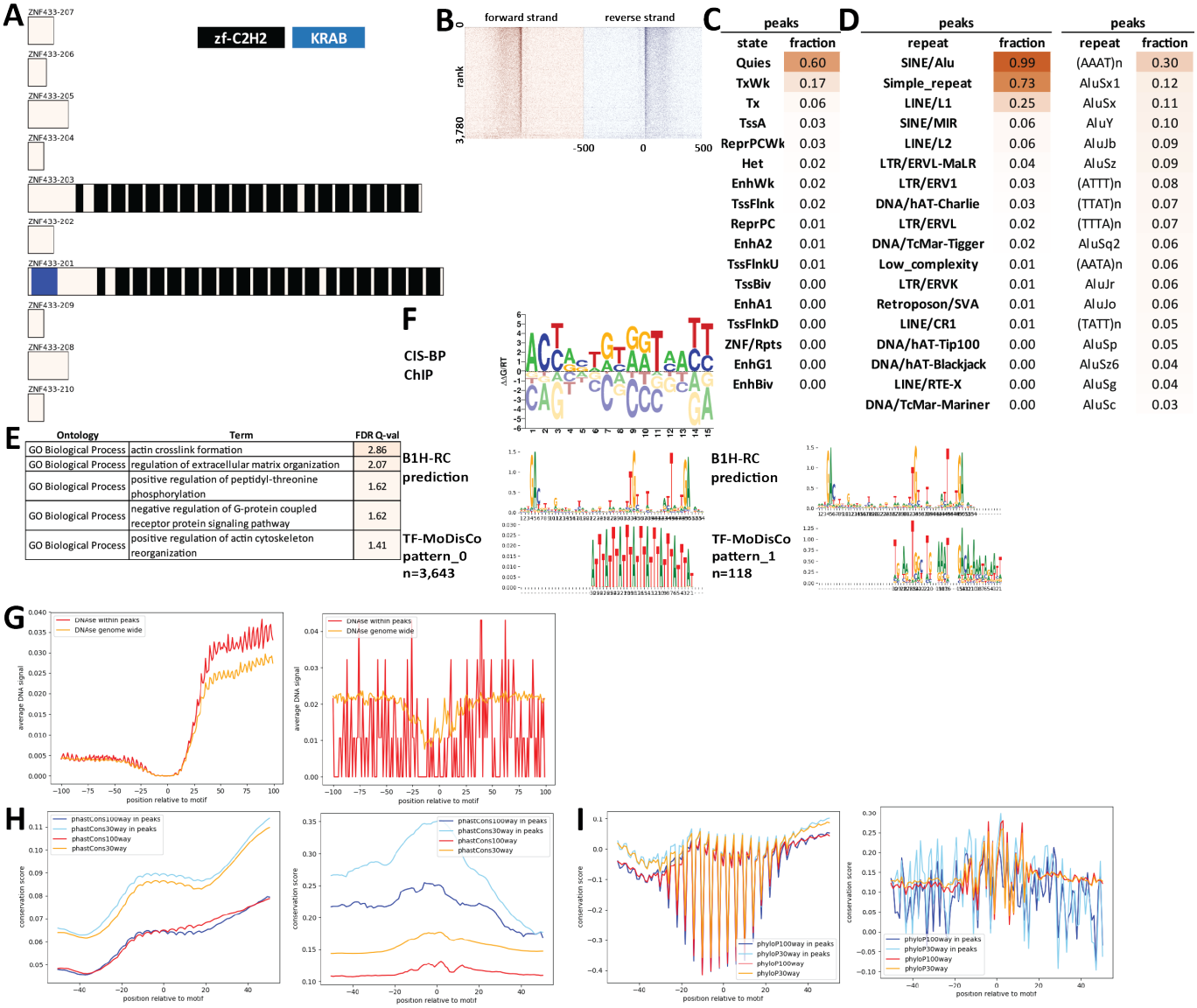

Supplementary Figure 1203: Properties and genomic distribution of motifs identified for the ZNF433 transcription factor in HEK293 (accession ENCSR586BRJ).

TF-MoDisCO pattern_0 n=3643, CWM

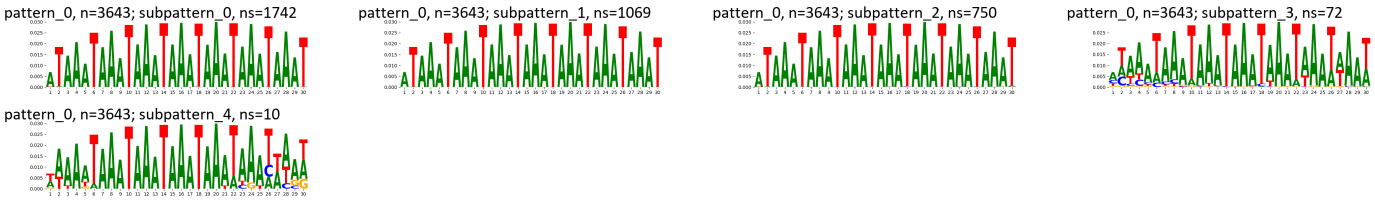

TF-MoDisCO pattern_0 n=3643, PWM

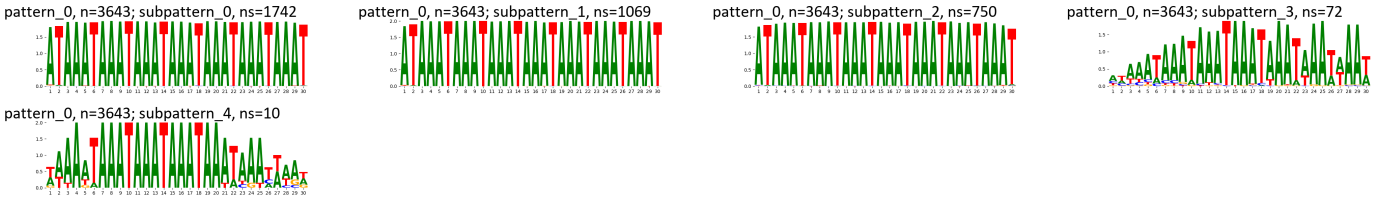

TF-MoDisCO pattern_1 n=118, CWM

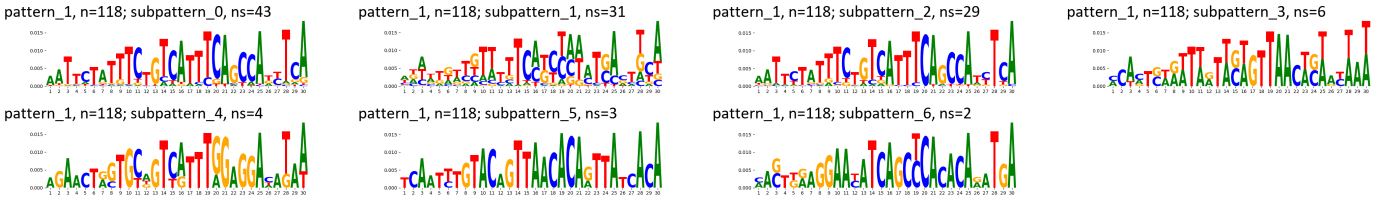

TF-MoDisCO pattern_1 n=118, PWM

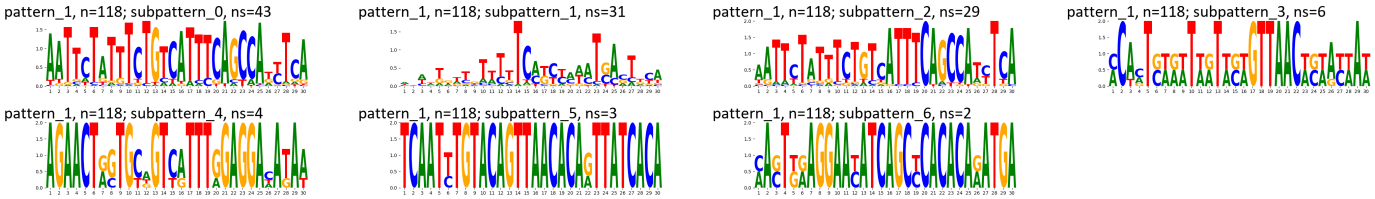

Supplementary Figure 1204: TF-MoDisCO subpatterns for the ZNF433 transcription factor in HEK293 (accession ENCSR586BRJ).

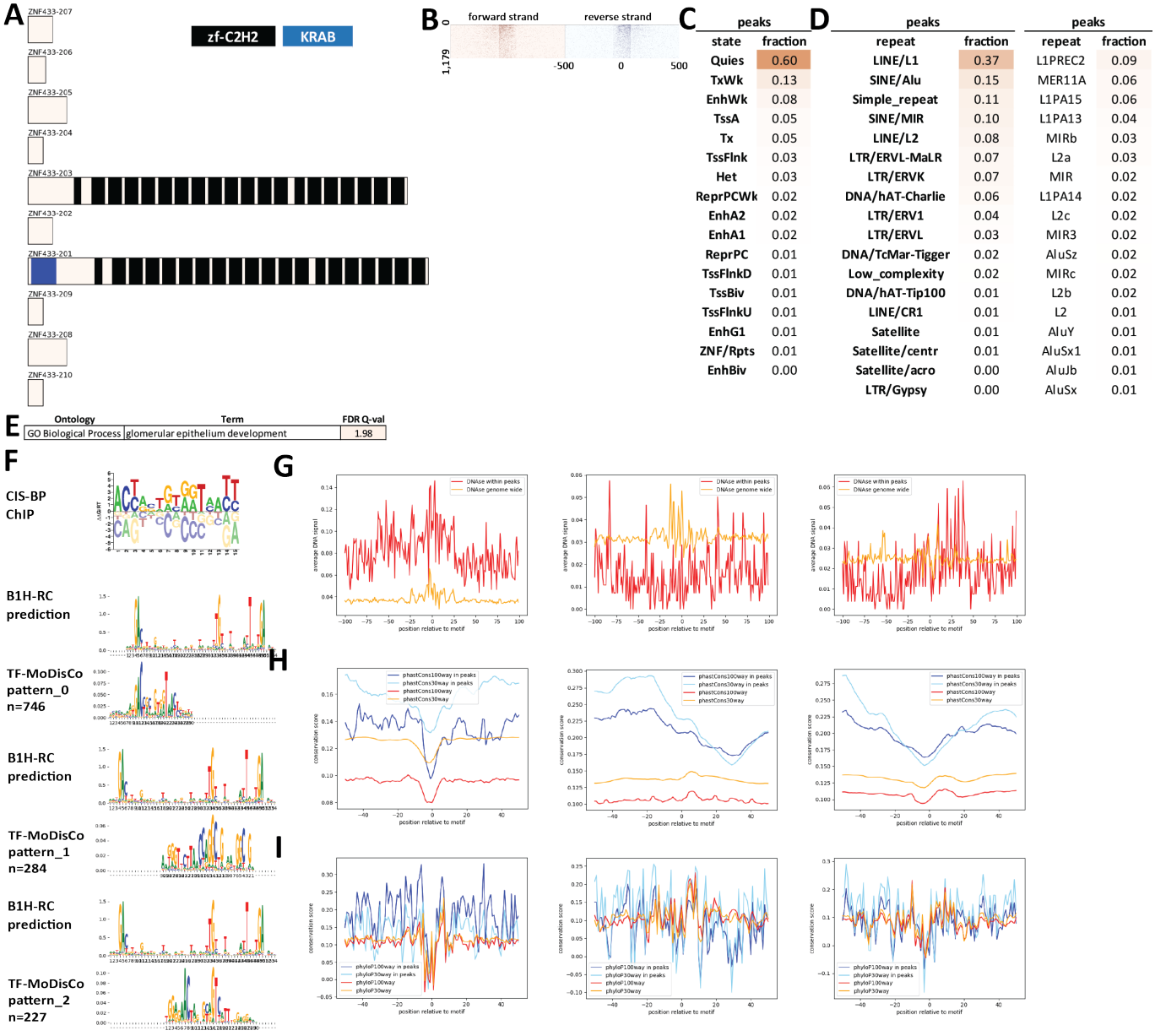

Supplementary Figure 1205: Properties and genomic distribution of motifs identified for the ZNF433 transcription factor in HEK293 (accession ChipExo models).

TF-MoDisCO pattern_0 n=746, CWM

pattern_0, n=746; subpattern_0, ns=196

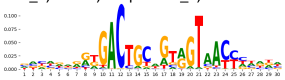

pattern_0, n=746; subpattern_1, ns=176

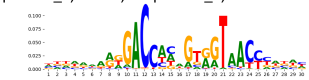

pattern_0, n=746; subpattern_2, ns=156

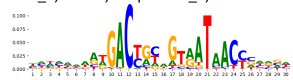

pattern_0, n=746; subpattern_3, ns=100

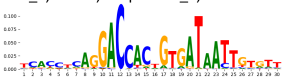

pattern_0, n=746; subpattern_4, ns=75

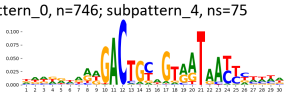

pattern_0, n=746; subpattern_5, ns=43

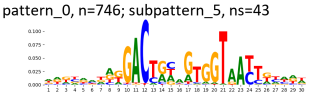

TF-MoDisCO pattern_0 n=746, PWM

pattern_0, n=746; subpattern_0, ns=196

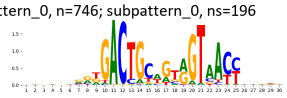

pattern_0, n=746; subpattern_1, ns=176

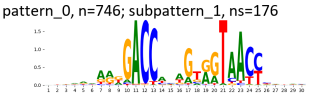

pattern_0, n=746; subpattern_2, ns=156

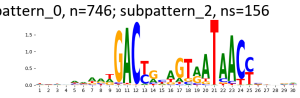

pattern_0, n=746; subpattern_3, ns=100

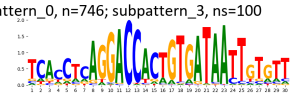

pattern_0, n=746; subpattern_4, ns=75

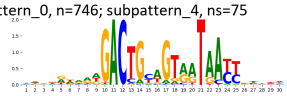

pattern_0, n=746; subpattern_5, ns=43

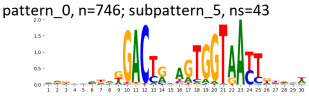

TF-MoDisCO pattern_1 n=284, CWM

pattern_1, n=284; subpattern_0, ns=124

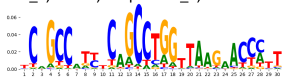

pattern_1, n=284; subpattern_1, ns=70

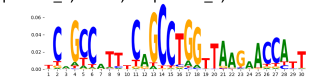

pattern_1, n=284; subpattern_2, ns=51

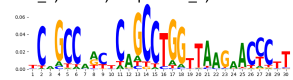

pattern_1, n=284; subpattern_3, ns=26

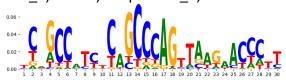

pattern_1, n=284; subpattern_4, ns=4

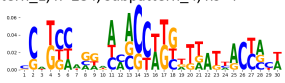

pattern_1, n=284; subpattern_5, ns=4

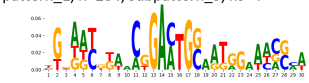

pattern_1, n=284; subpattern_6, ns=3

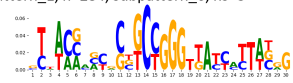

pattern_1, n=284; subpattern_7, ns=2

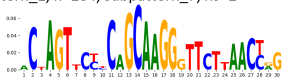

TF-MoDisCO pattern_1 n=284, PWM

pattern_1, n=284; subpattern_0, ns=124

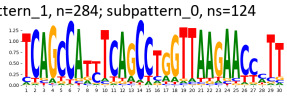

pattern_1, n=284; subpattern_1, ns=70

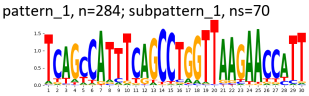

pattern_1, n=284; subpattern_2, ns=51

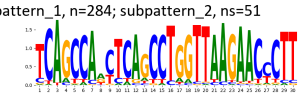

pattern_1, n=284; subpattern_3, ns=26

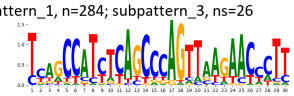

pattern_1, n=284; subpattern_4, ns=4

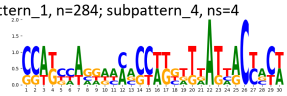

pattern_1, n=284; subpattern_5, ns=4

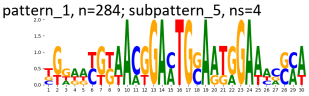

pattern_1, n=284; subpattern_6, ns=3

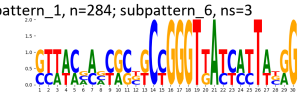

pattern_1, n=284; subpattern_7, ns=2

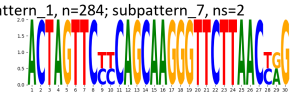

TF-MoDisCO pattern_2 n=227, CWM

pattern_2, n=227; subpattern_0, ns=58

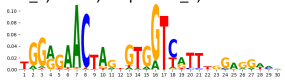

pattern_2, n=227; subpattern_1, ns=58

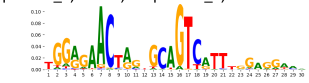

pattern_2, n=227; subpattern_2, ns=47

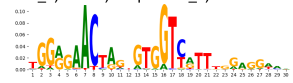

pattern_2, n=227; subpattern_3, ns=33

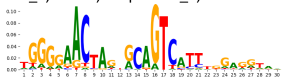

pattern_2, n=227; subpattern_4, ns=31

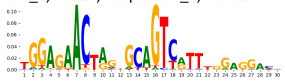

TF-MoDisCO pattern_2 n=227, PWM

pattern_2, n=227; subpattern_0, ns=58

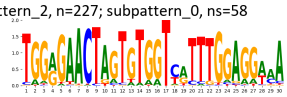

pattern_2, n=227; subpattern_1, ns=58

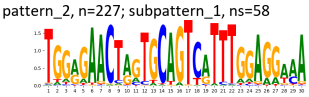

pattern_2, n=227; subpattern_2, ns=47

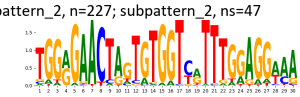

pattern_2, n=227; subpattern_3, ns=33

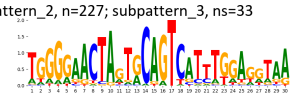

pattern_2, n=227; subpattern_4, ns=31

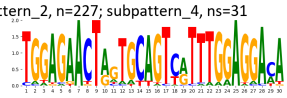

Supplementary Figure 1206: TF-MoDisCO subpatterns for the ZNF433 transcription factor in HEK293 (accession ChipExo models).

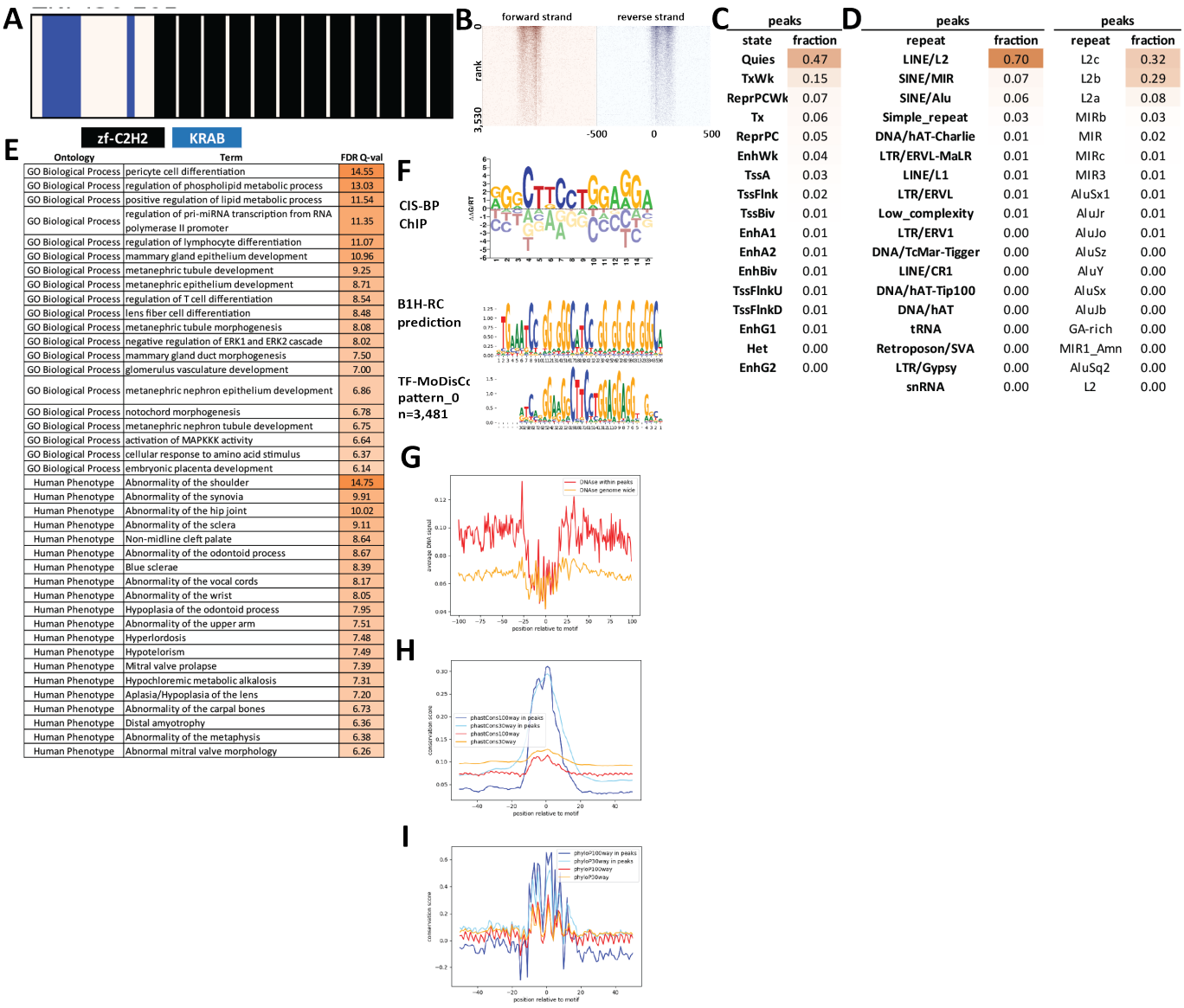

Supplementary Figure 1207: Properties and genomic distribution of motifs identified for the ZNF436 transcription factor in HEK293 (accession Hughes GR models).

TF-MoDisCO pattern_0 n=3481, CWM

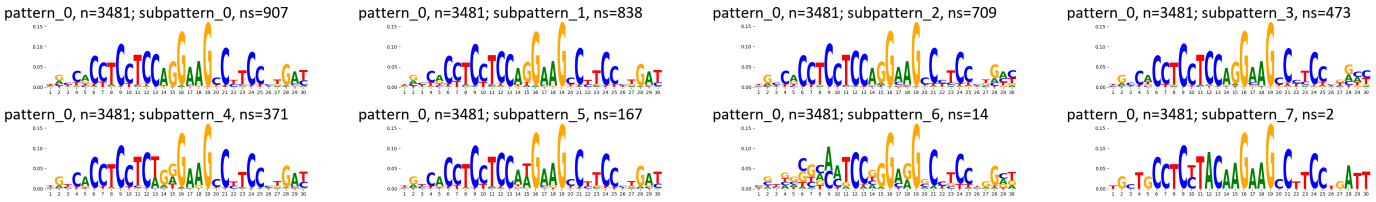

TF-MoDisCO pattern_0 n=3481, PWM

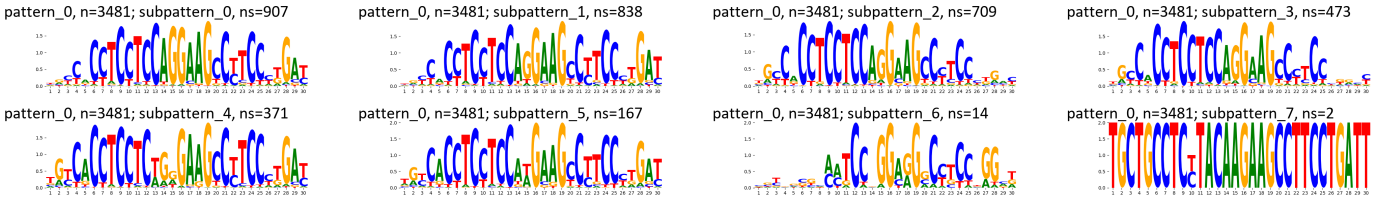

Supplementary Figure 1208: TF-MoDisCO subpatterns for the ZNF436 transcription factor in HEK293 (accession Hughes GR models).

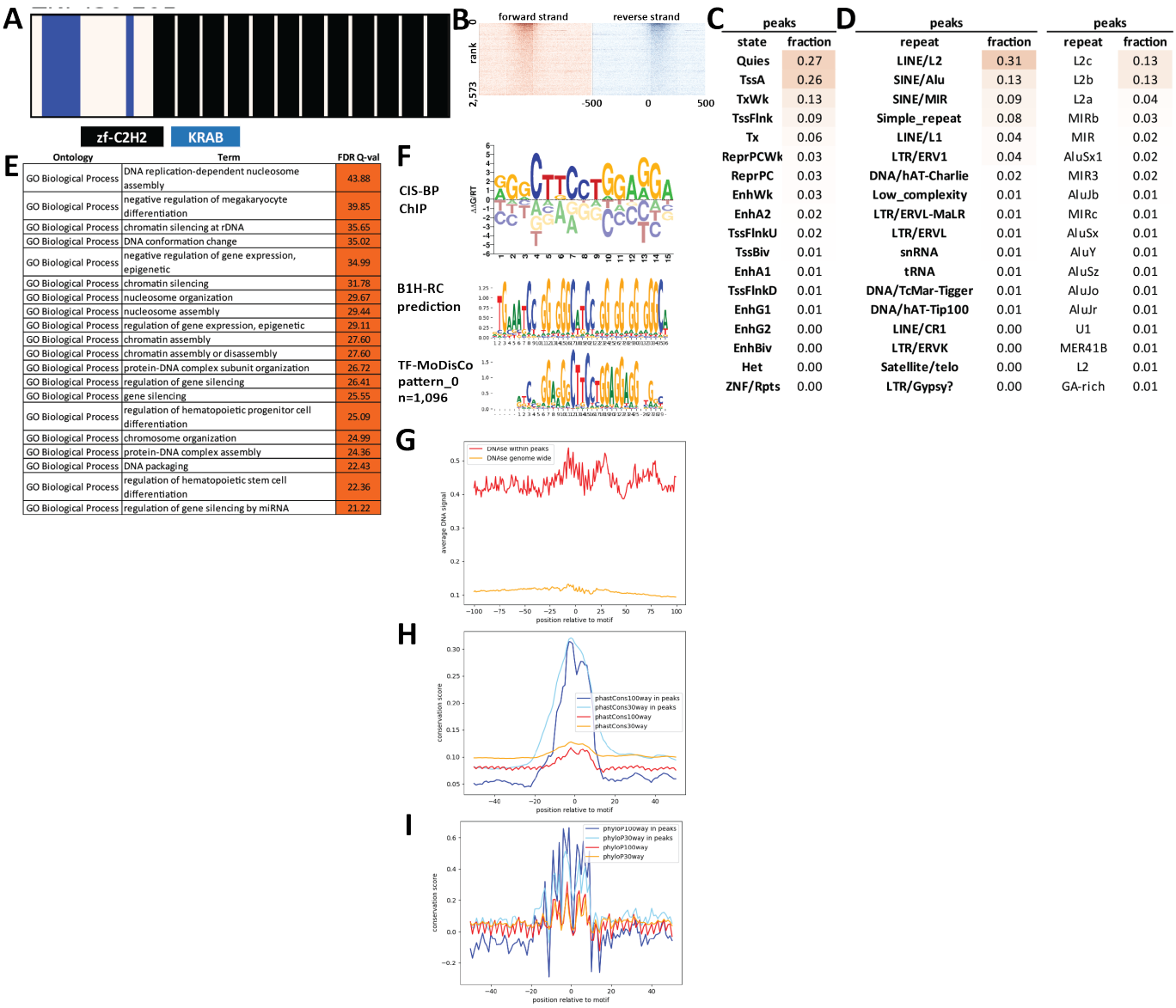

Supplementary Figure 1209: Properties and genomic distribution of motifs identified for the ZNF436 transcription factor in K562 (accession ENCSR335SUD).

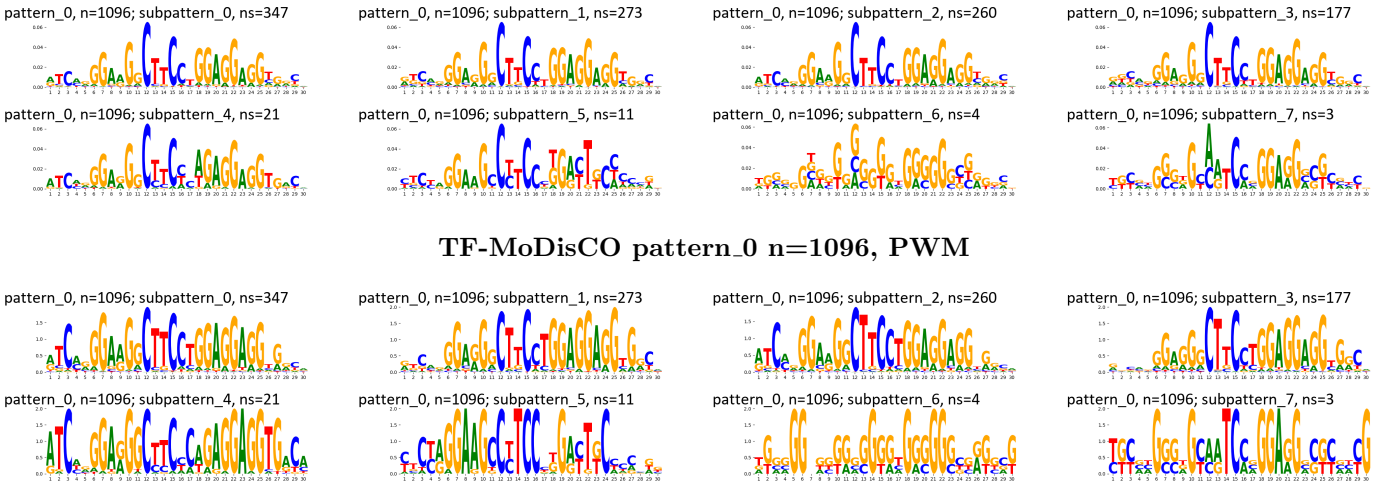

Supplementary Figure 1210: TF-MoDisCO subpatterns for the ZNF436 transcription factor in K562 (accession ENCSR335SUD).

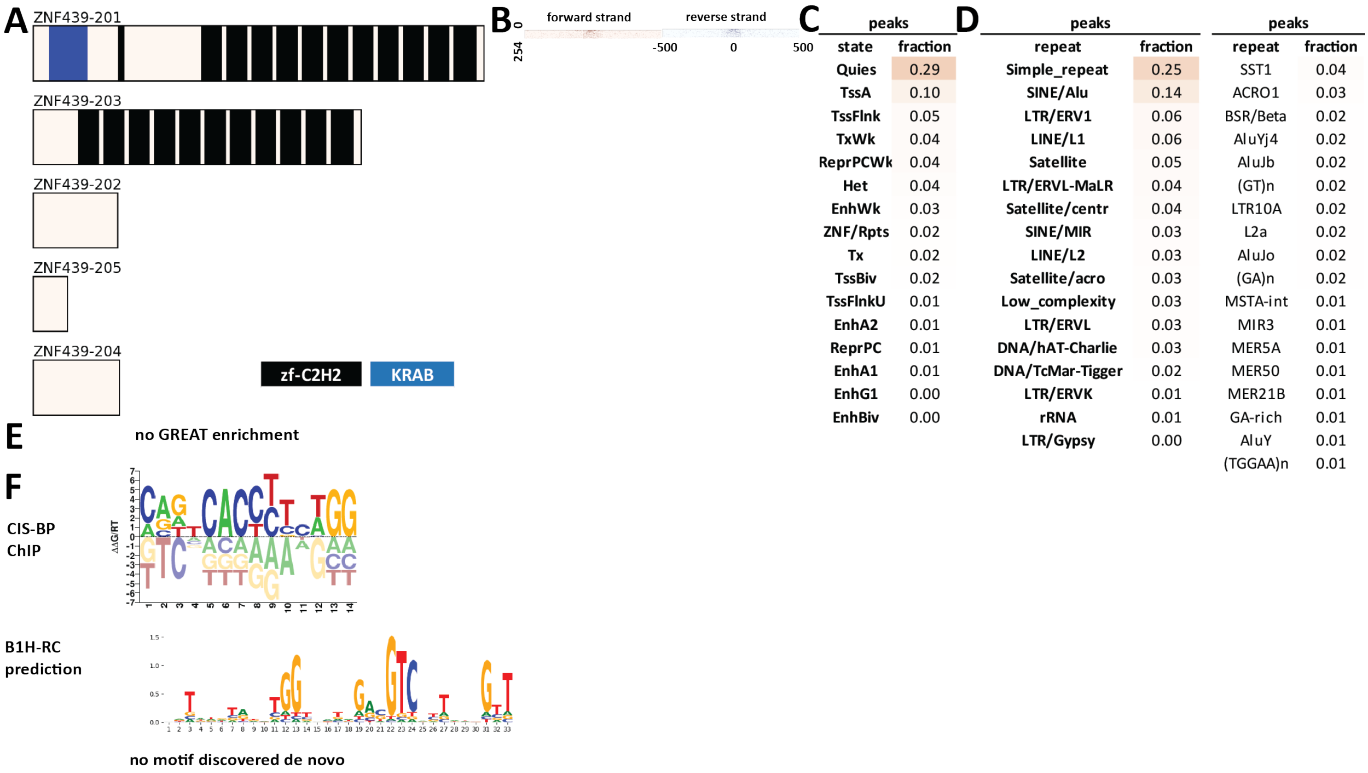

Supplementary Figure 1211: Properties and genomic distribution of motifs identified for the ZNF439 transcription factor in HEK293 (accession ChipExo models).

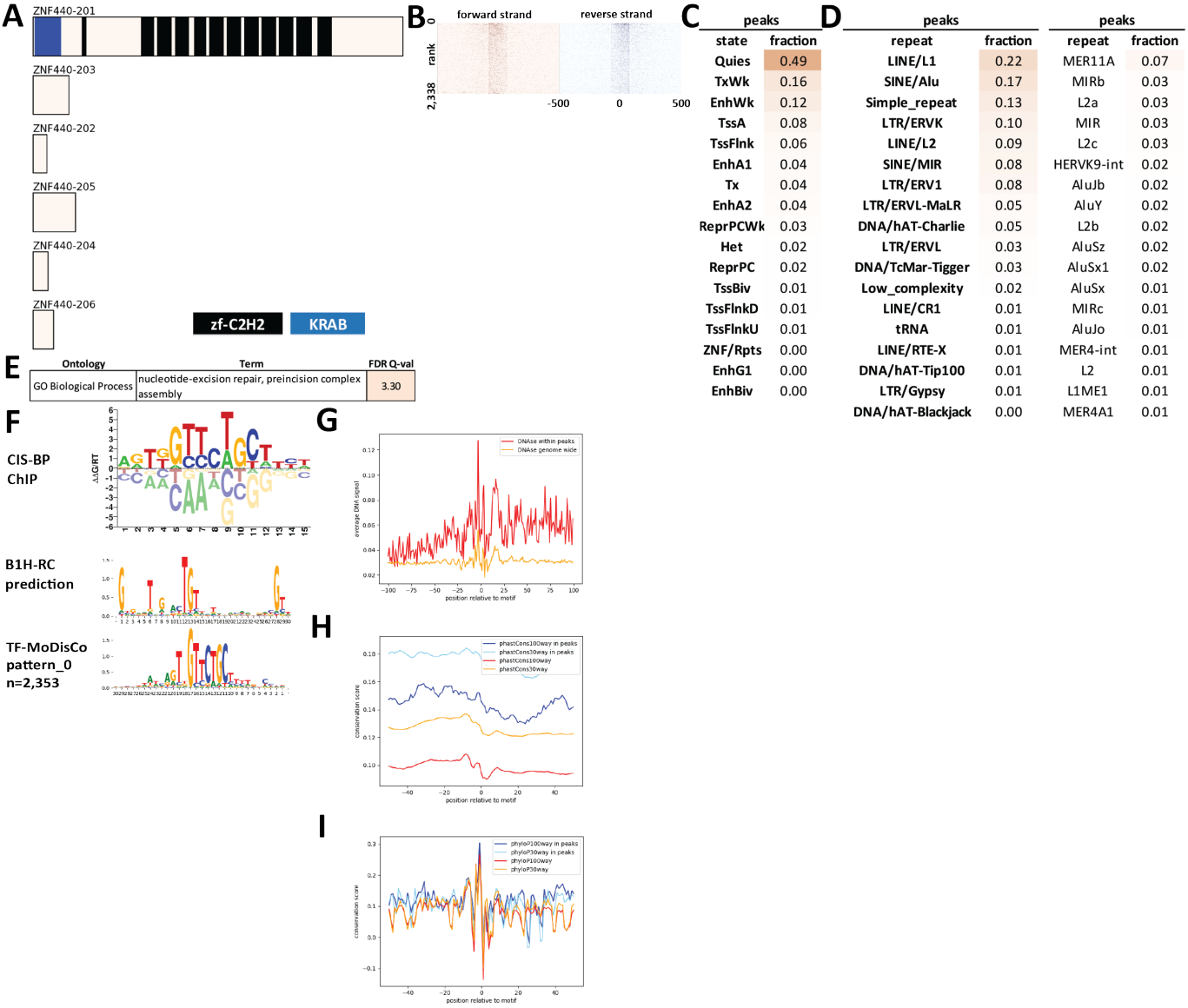

Supplementary Figure 1212: Properties and genomic distribution of motifs identified for the ZNF440 transcription factor in HEK293 (accession ChipExo models).

TF-MoDisCO pattern_0 n=2353, CWM

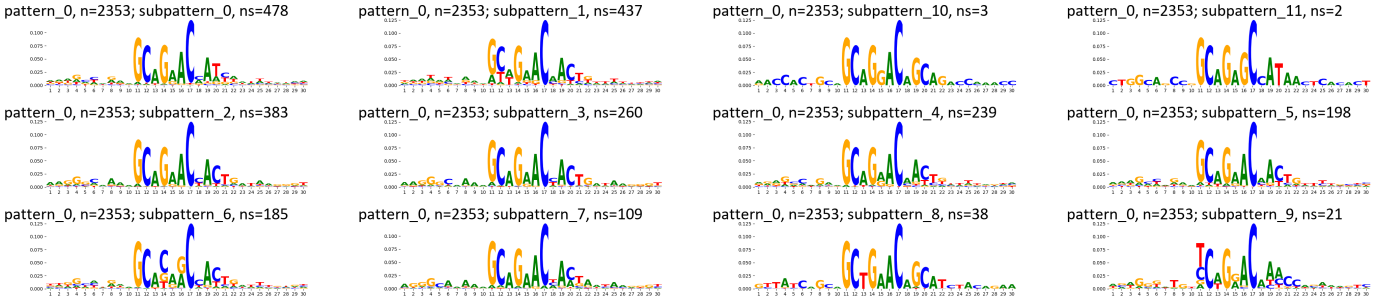

TF-MoDisCO pattern_0 n=2353, PWM

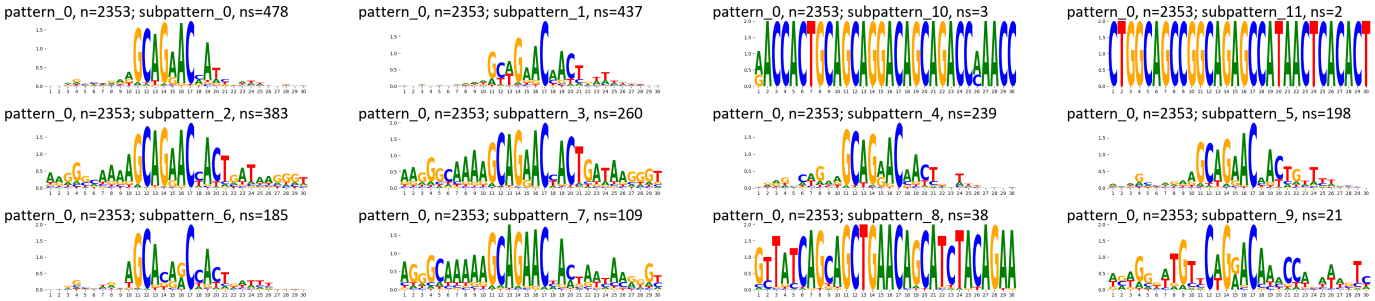

Supplementary Figure 1213: TF-MoDisCO subpatterns for the ZNF440 transcription factor in HEK293 (accession ChipExo models).

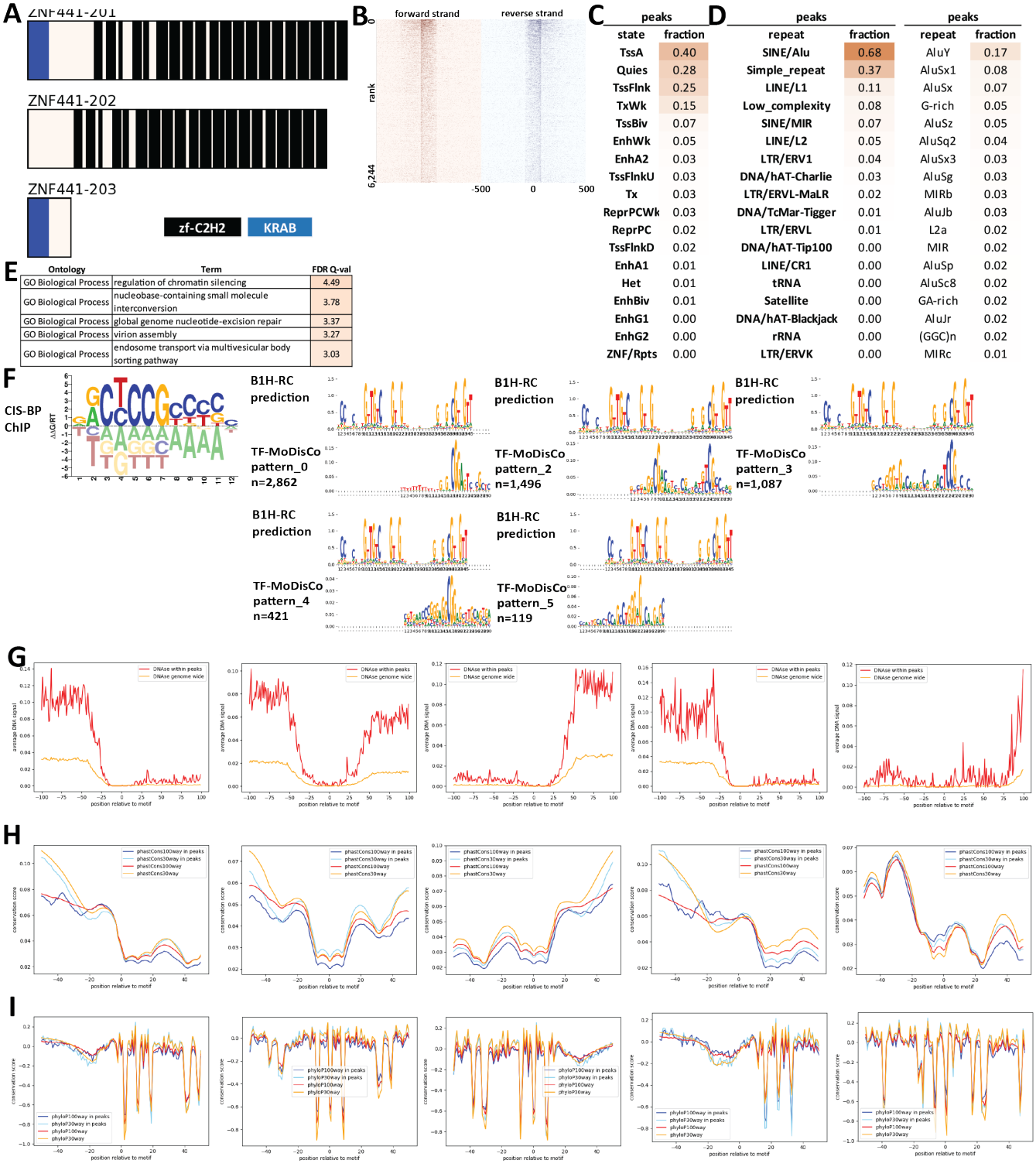

Supplementary Figure 1214: Properties and genomic distribution of motifs identified for the ZNF441 transcription factor in HEK293 (accession ChipExo models).

TF-MoDisCO pattern_2 n=1496, CWM

pattern_2, n=1496; subpattern_0, ns=344

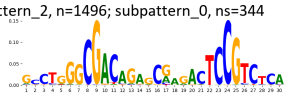

pattern_2, n=1496; subpattern_1, ns=304

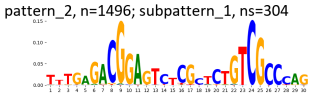

pattern_2, n=1496; subpattern_2, ns=223

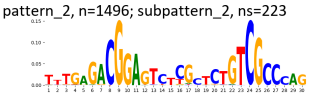

pattern_2, n=1496; subpattern_3, ns=218

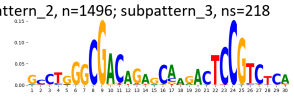

pattern_2, n=1496; subpattern_4, ns=148

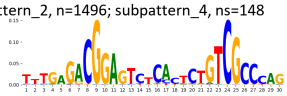

pattern_2, n=1496; subpattern_5, ns=145

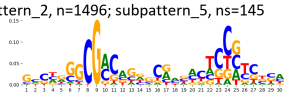

pattern_2, n=1496; subpattern_6, ns=114

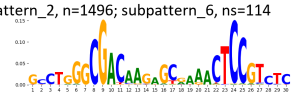

TF-MoDisCO pattern_2 n=1496, PWM

pattern_2, n=1496; subpattern_0, ns=344

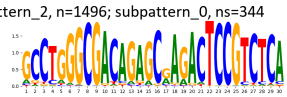

pattern_2, n=1496; subpattern_1, ns=304

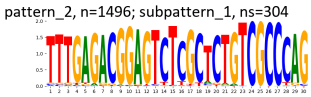

pattern_2, n=1496; subpattern_2, ns=223

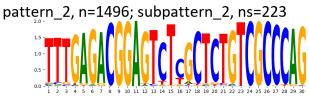

pattern_2, n=1496; subpattern_3, ns=218

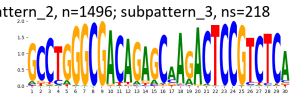

pattern_2, n=1496; subpattern_4, ns=148

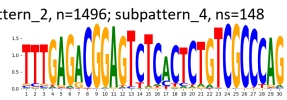

pattern_2, n=1496; subpattern_5, ns=145

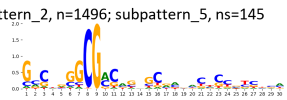

pattern_2, n=1496; subpattern_6, ns=114

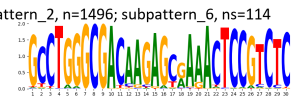

TF-MoDisCO pattern_3 n=1087, CWM

pattern_3, n=1087; subpattern_0, ns=283

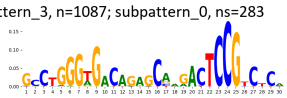

pattern_3, n=1087; subpattern_1, ns=222

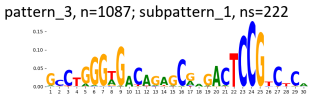

pattern_3, n=1087; subpattern_2, ns=204

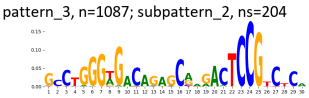

pattern_3, n=1087; subpattern_3, ns=166

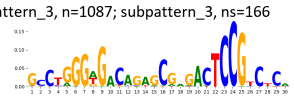

pattern_3, n=1087; subpattern_4, ns=111

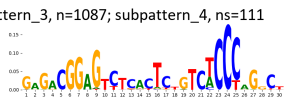

pattern_3, n=1087; subpattern_5, ns=96

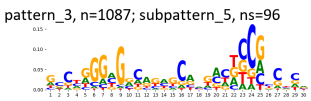

pattern_3, n=1087; subpattern_6, ns=5

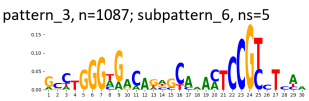

TF-MoDisCO pattern_3 n=1087, PWM

pattern_3, n=1087; subpattern_0, ns=283

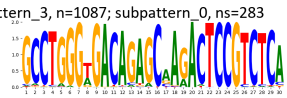

pattern_3, n=1087; subpattern_1, ns=222

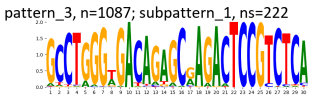

pattern_3, n=1087; subpattern_2, ns=204

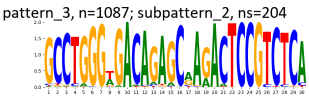

pattern_3, n=1087; subpattern_3, ns=166

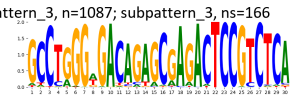

pattern_3, n=1087; subpattern_4, ns=111

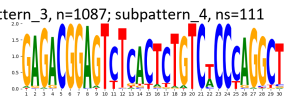

pattern_3, n=1087; subpattern_5, ns=96

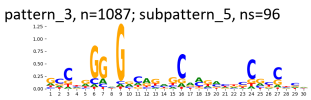

pattern_3, n=1087; subpattern_6, ns=5

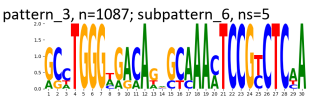

TF-MoDisCO pattern_5 n=421, CWM

pattern_5, n=421; subpattern_0, ns=101

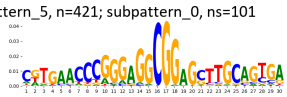

pattern_5, n=421; subpattern_1, ns=81

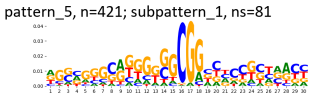

pattern_5, n=421; subpattern_2, ns=75

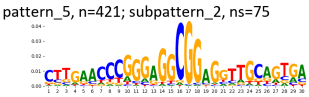

pattern_5, n=421; subpattern_3, ns=66

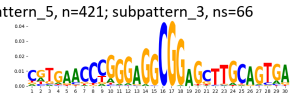

pattern_5, n=421; subpattern_4, ns=48

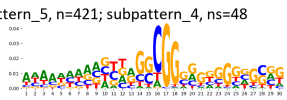

pattern_5, n=421; subpattern_5, ns=34

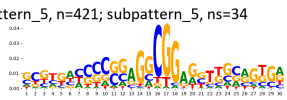

pattern_5, n=421; subpattern_6, ns=8

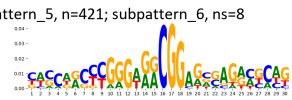

pattern_5, n=421; subpattern_7, ns=6

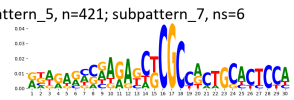

pattern_5, n=421; subpattern_8, ns=2

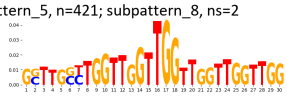

TF-MoDisCO pattern_5 n=421, PWM

pattern_5, n=421; subpattern_0, ns=101

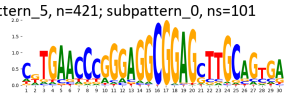

pattern_5, n=421; subpattern_1, ns=81

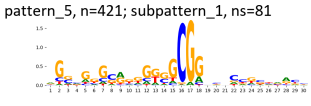

pattern_5, n=421; subpattern_2, ns=75

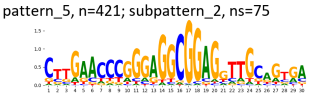

pattern_5, n=421; subpattern_3, ns=66

pattern_5, n=421; subpattern_4, ns=48

pattern_5, n=421; subpattern_5, ns=34

pattern_5, n=421; subpattern_6, ns=8

pattern_5, n=421; subpattern_7, ns=6

pattern_5, n=421; subpattern_8, ns=2

TF-MoDisCO pattern_6 n=119, CWM

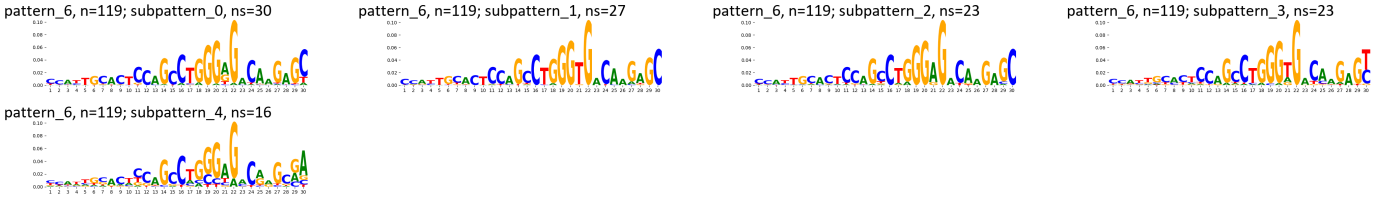

TF-MoDisCO pattern_6 n=119, PWM

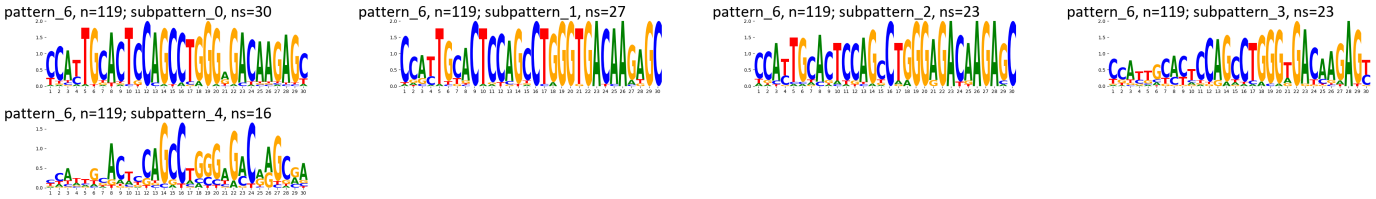

Supplementary Figure 1215: TF-MoDisCO subpatterns for the ZNF441 transcription factor in HEK293 (accession ChipExo models).

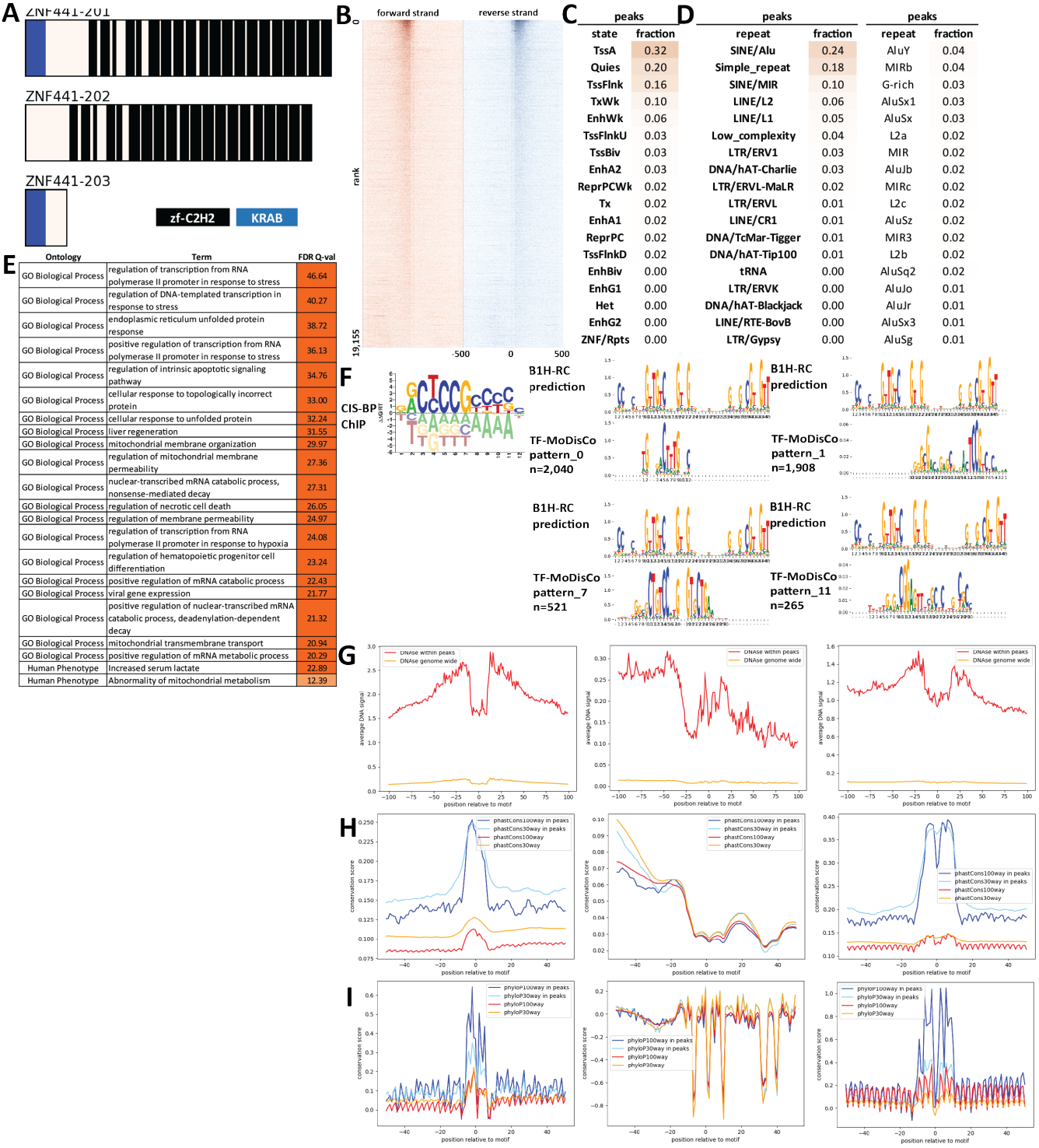

Supplementary Figure 1216: Properties and genomic distribution of motifs identified for the ZNF441 transcription factor in HepG2 (accession ENCSR673GDQ).

TF-MoDisCO pattern_0 n=2040, CWM

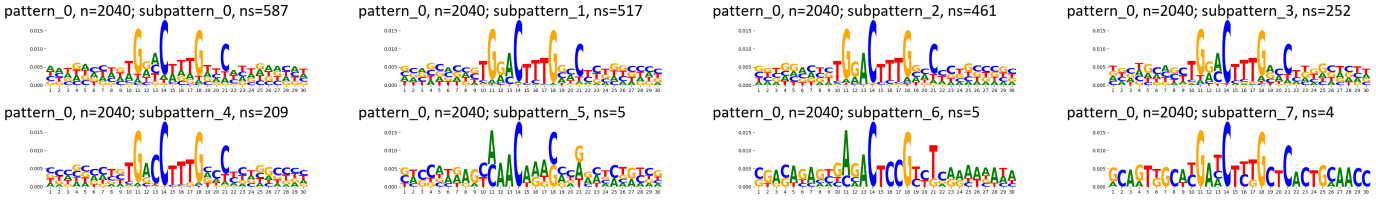

TF-MoDisCO pattern_0 n=2040, PWM

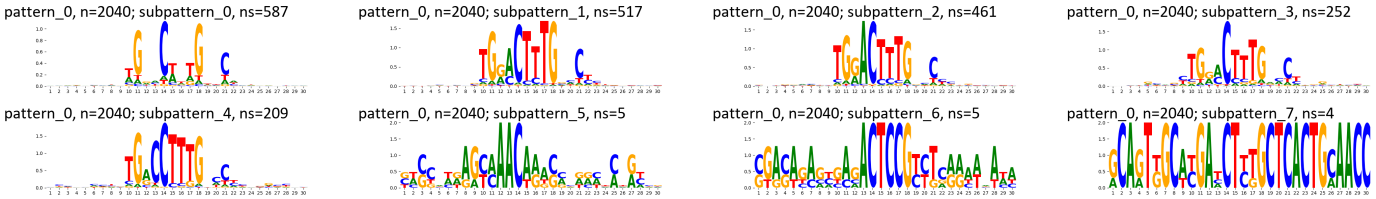

TF-MoDisCO pattern_1 n=1908, CWM

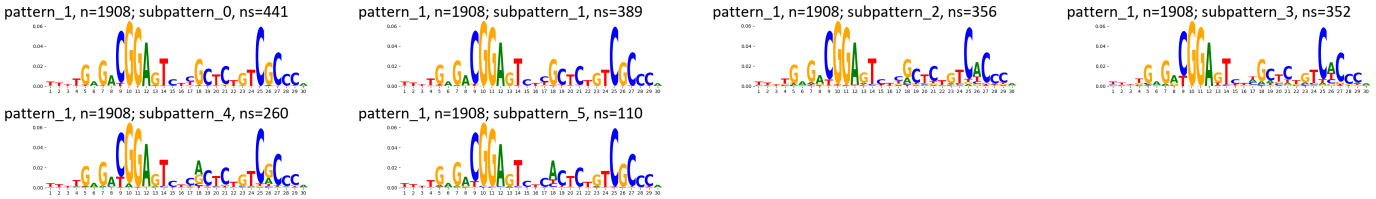

TF-MoDisCO pattern_1 n=1908, PWM

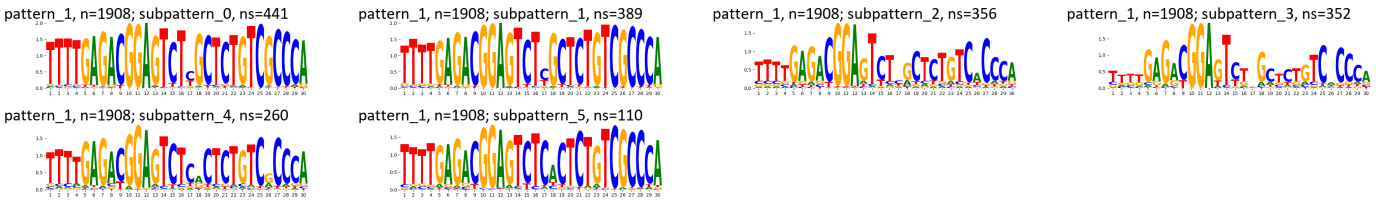

TF-MoDisCO pattern_7 n=521, CWM

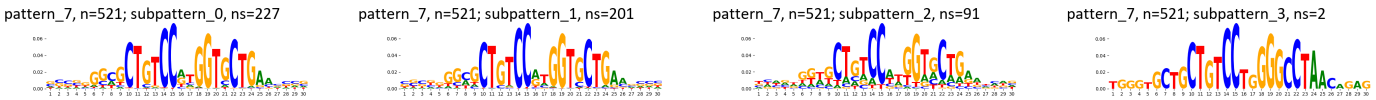

TF-MoDisCO pattern_7 n=521, PWM

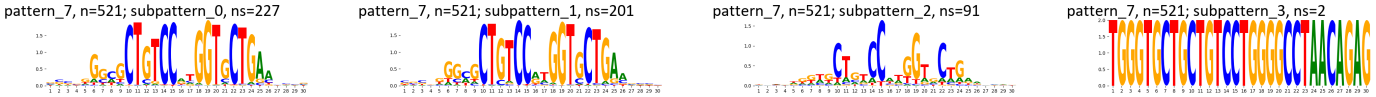

Supplementary Figure 1217: TF-MoDisCO subpatterns for the ZNF441 transcription factor in HepG2 (accession ENCSR673GDQ).

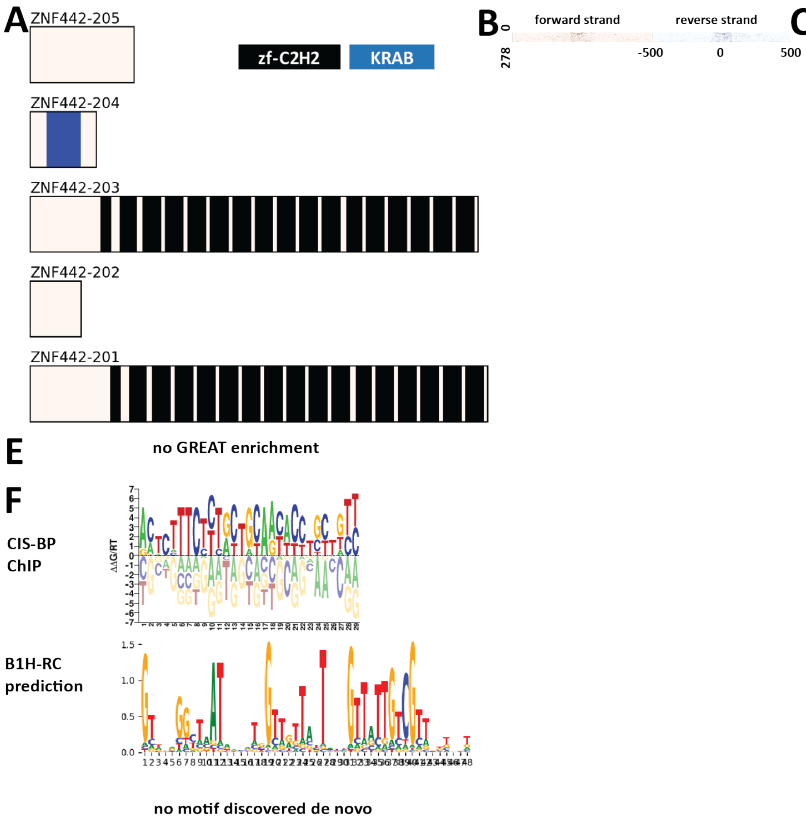

C

peaks	
state	fraction
Quies	0.37
TxWk	0.05
Tx	0.04
Het	0.04
ZNF/Rpts	0.03
ReprPCWk	0.03
EnhWk	0.02
TssA	0.01
EnhA2	0.01
TssBiv	0.01
ReprPC	0.01
TssFlnk	0.00
EnhG1	0.00
EnhA1	0.00

D

peaks		peaks	
repeat	fraction	repeat	fraction
LTR/ERV1	0.28	LTR8B	0.15
Simple_repeat	0.22	SST1	0.03
SINE/Alu	0.14	AluJb	0.03
LINE/L1	0.08	L2a	0.02
LTR/ERVL-MaLR	0.06	LTR8	0.02
LINE/L2	0.05	L2	0.02
Satellite	0.04	BSR/Beta	0.02
SINE/MIR	0.04	AluSx1	0.02
Satellite/centr	0.03	ACRO1	0.02
DNA/hAT-Charlie	0.03	LTR10A	0.01
LTR/ERVL	0.03	AluJo	0.01
Satellite/acro	0.02	(TGGAA)n	0.01
DNA/TcMar-Tigger	0.02	Tigger1	0.01
Low_complexity	0.01	MSTA	0.01
rRNA	0.01	MIRb	0.01
Satellite/telo	0.00	MER50	0.01
SINE/5S-Deu-L2	0.00	MER21B	0.01
Retroposon/SVA	0.00	MER20	0.01

Supplementary Figure 1218: Properties and genomic distribution of motifs identified for the ZNF442 transcription factor in HEK293 (accession ChipExo models).

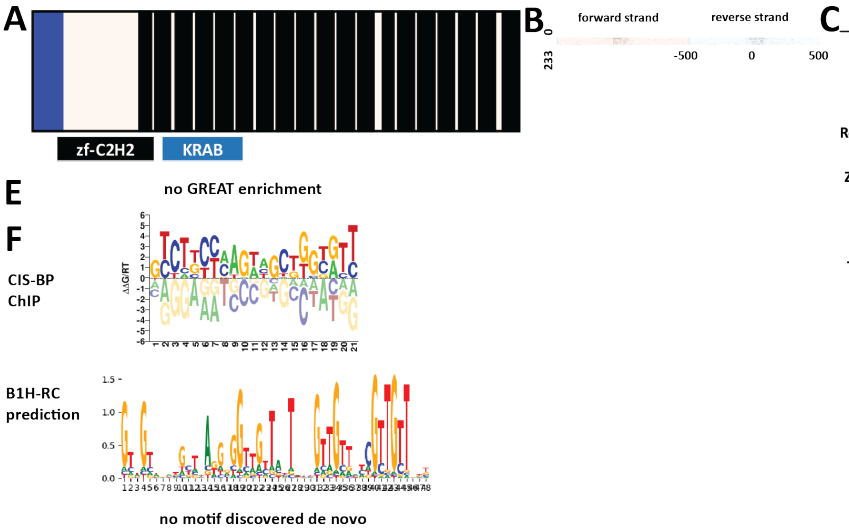

C

peaks	
state	fraction
Quies	0.42
TxWk	0.10
Tx	0.06
ReprPCWk	0.05
Het	0.03
ZNF/Rpts	0.02
EnhG1	0.01
EnhA2	0.01
ReprPC	0.01
TssFlnkU	0.00
TssFlnk	0.00
TssBiv	0.00
EnhA1	0.00

D

peaks		peaks	
repeat	fraction	repeat	fraction
LTR/ERVK	0.37	LTR13	0.35
Simple_repeat	0.15	SST1	0.02
SINE/Alu	0.09	BSR/Beta	0.02
LTR/ERV1	0.06	AluJb	0.02
LINE/L1	0.05	L2a	0.02
Satellite	0.05	MER21B	0.01
Satellite/centr	0.03	LTR10A	0.01
LINE/L2	0.03	HERVK-int	0.01
LTR/ERVL	0.02	GA-rich	0.01
Satellite/acro	0.01	AluYj4	0.01
SINE/MIR	0.01	AluSc8	0.01
Low_complexity	0.01	ACRO1	0.01
LTR/ERVL-MaLR	0.01	(GA)n	0.01
rRNA	0.01	(G)n	0.01
DNA/TcMar-Tigger	0.01	(ATTCC)n	0.01
LINE/CR1	0.00	MLT1J-int	0.01
DNA/hAT-Tip100	0.00	MIRb	0.01
DNA/hAT-Charlie	0.00	MER50	0.01

Supplementary Figure 1219: Properties and genomic distribution of motifs identified for the ZNF443 transcription factor in HEK293 (accession ChipExo models).

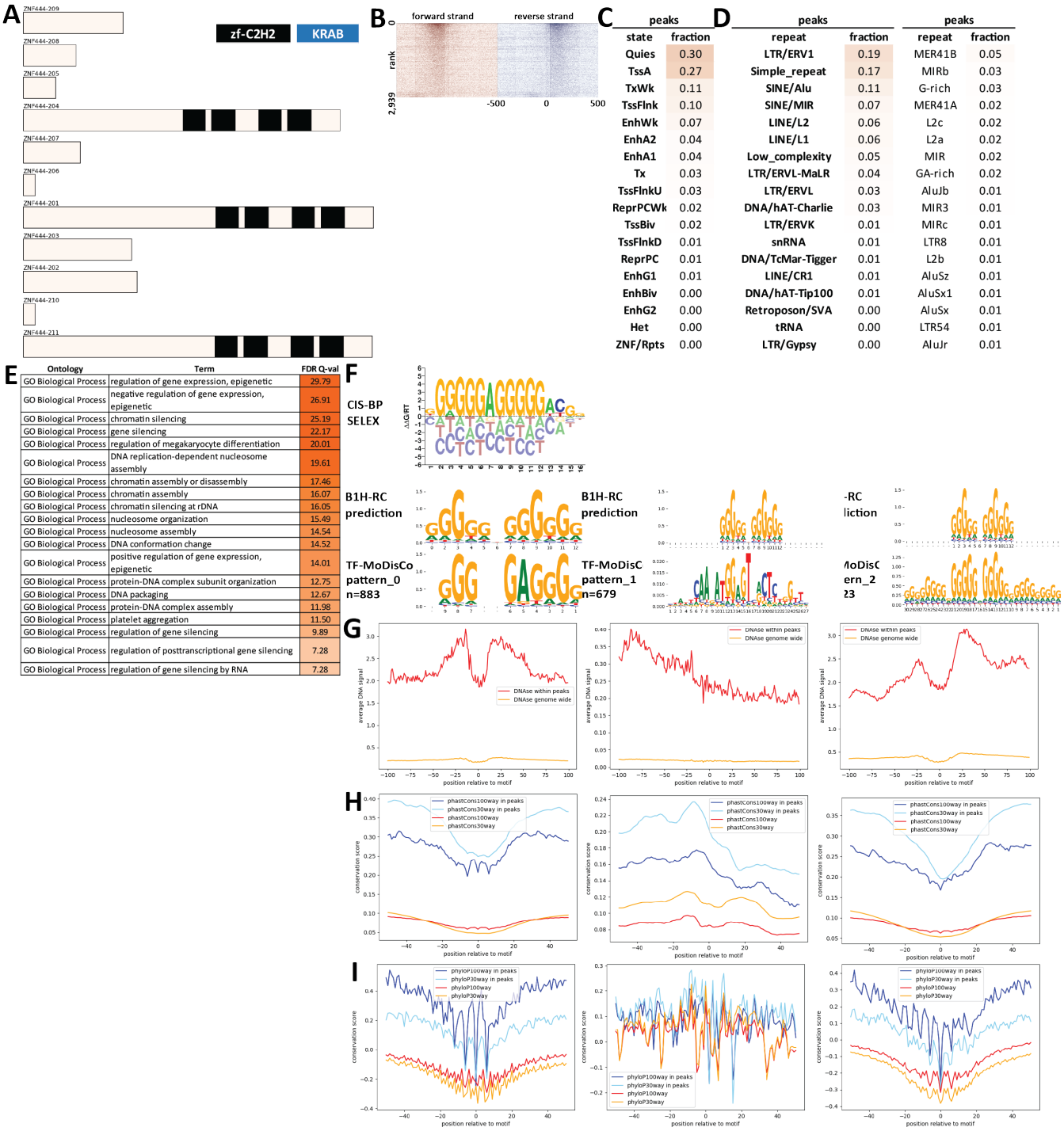

Supplementary Figure 1220: Properties and genomic distribution of motifs identified for the ZNF444 transcription factor in K562 (accession ENCSR164RIC).

TF-MoDisCO pattern_0 n=883, CWM

pattern_0, n=883; subpattern_0, ns=216

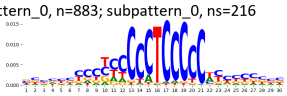

pattern_0, n=883; subpattern_1, ns=214

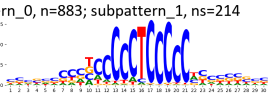

pattern_0, n=883; subpattern_2, ns=144

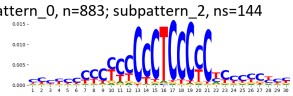

pattern_0, n=883; subpattern_3, ns=137

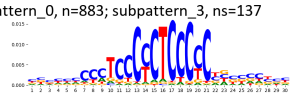

pattern_0, n=883; subpattern_4, ns=117

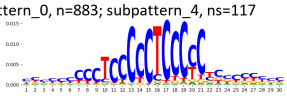

pattern_0, n=883; subpattern_5, ns=55

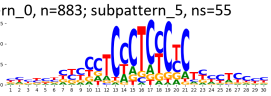

TF-MoDisCO pattern_0 n=883, PWM

pattern_0, n=883; subpattern_0, ns=216

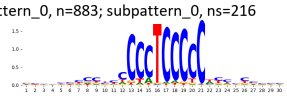

pattern_0, n=883; subpattern_1, ns=214

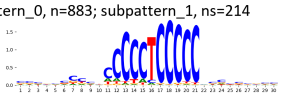

pattern_0, n=883; subpattern_2, ns=144

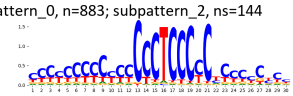

pattern_0, n=883; subpattern_3, ns=137

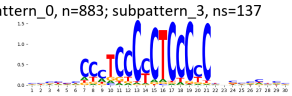

pattern_0, n=883; subpattern_4, ns=117

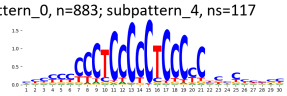

pattern_0, n=883; subpattern_5, ns=55

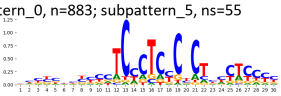

TF-MoDisCO pattern_1 n=679, CWM

pattern_1, n=679; subpattern_0, ns=168

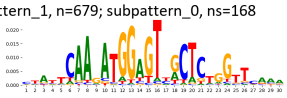

pattern_1, n=679; subpattern_1, ns=152

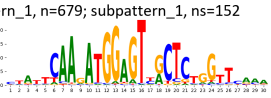

pattern_1, n=679; subpattern_2, ns=140

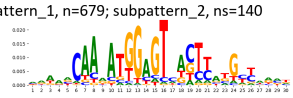

pattern_1, n=679; subpattern_3, ns=117

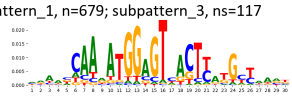

pattern_1, n=679; subpattern_4, ns=72

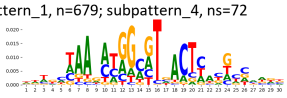

pattern_1, n=679; subpattern_5, ns=22

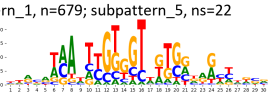

pattern_1, n=679; subpattern_6, ns=6

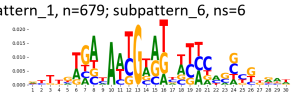

pattern_1, n=679; subpattern_7, ns=2

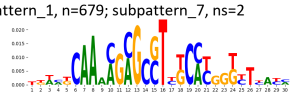

TF-MoDisCO pattern_1 n=679, PWM

pattern_1, n=679; subpattern_0, ns=168

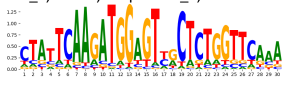

pattern_1, n=679; subpattern_1, ns=152

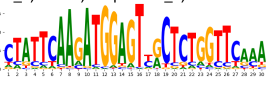

pattern_1, n=679; subpattern_2, ns=140

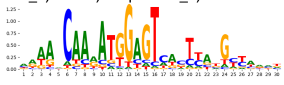

pattern_1, n=679; subpattern_3, ns=117

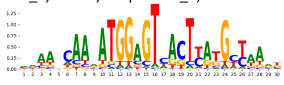

pattern_1, n=679; subpattern_4, ns=72

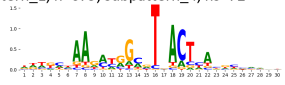

pattern_1, n=679; subpattern_5, ns=22

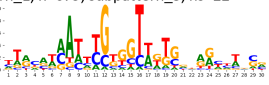

pattern_1, n=679; subpattern_6, ns=6

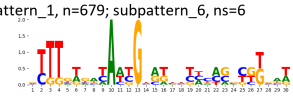

pattern_1, n=679; subpattern_7, ns=2

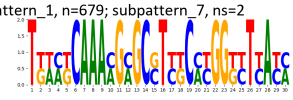

TF-MoDisCO pattern_2 n=323, CWM

pattern_2, n=323; subpattern_0, ns=101

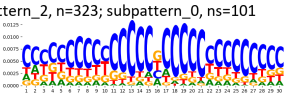

pattern_2, n=323; subpattern_1, ns=93

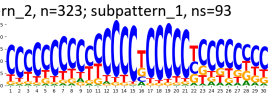

pattern_2, n=323; subpattern_2, ns=49

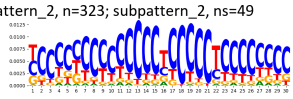

pattern_2, n=323; subpattern_3, ns=31

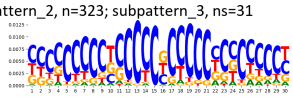

pattern_2, n=323; subpattern_4, ns=24

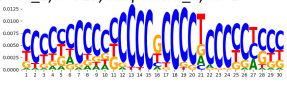

pattern_2, n=323; subpattern_5, ns=22

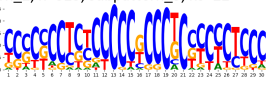

pattern_2, n=323; subpattern_6, ns=3

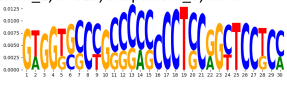

TF-MoDisCO pattern_2 n=323, PWM

pattern_2, n=323; subpattern_0, ns=101

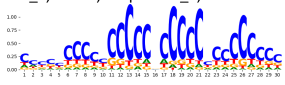

pattern_2, n=323; subpattern_1, ns=93

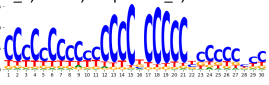

pattern_2, n=323; subpattern_2, ns=49

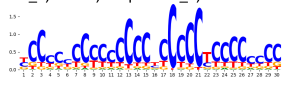

pattern_2, n=323; subpattern_3, ns=31

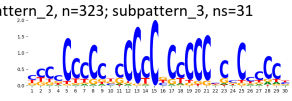

pattern_2, n=323; subpattern_4, ns=24

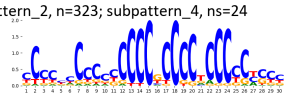

pattern_2, n=323; subpattern_5, ns=22

pattern_2, n=323; subpattern_6, ns=3

Supplementary Figure 1221: TF-MoDisCO subpatterns for the ZNF444 transcription factor in K562 (accession ENCSR164RIC).

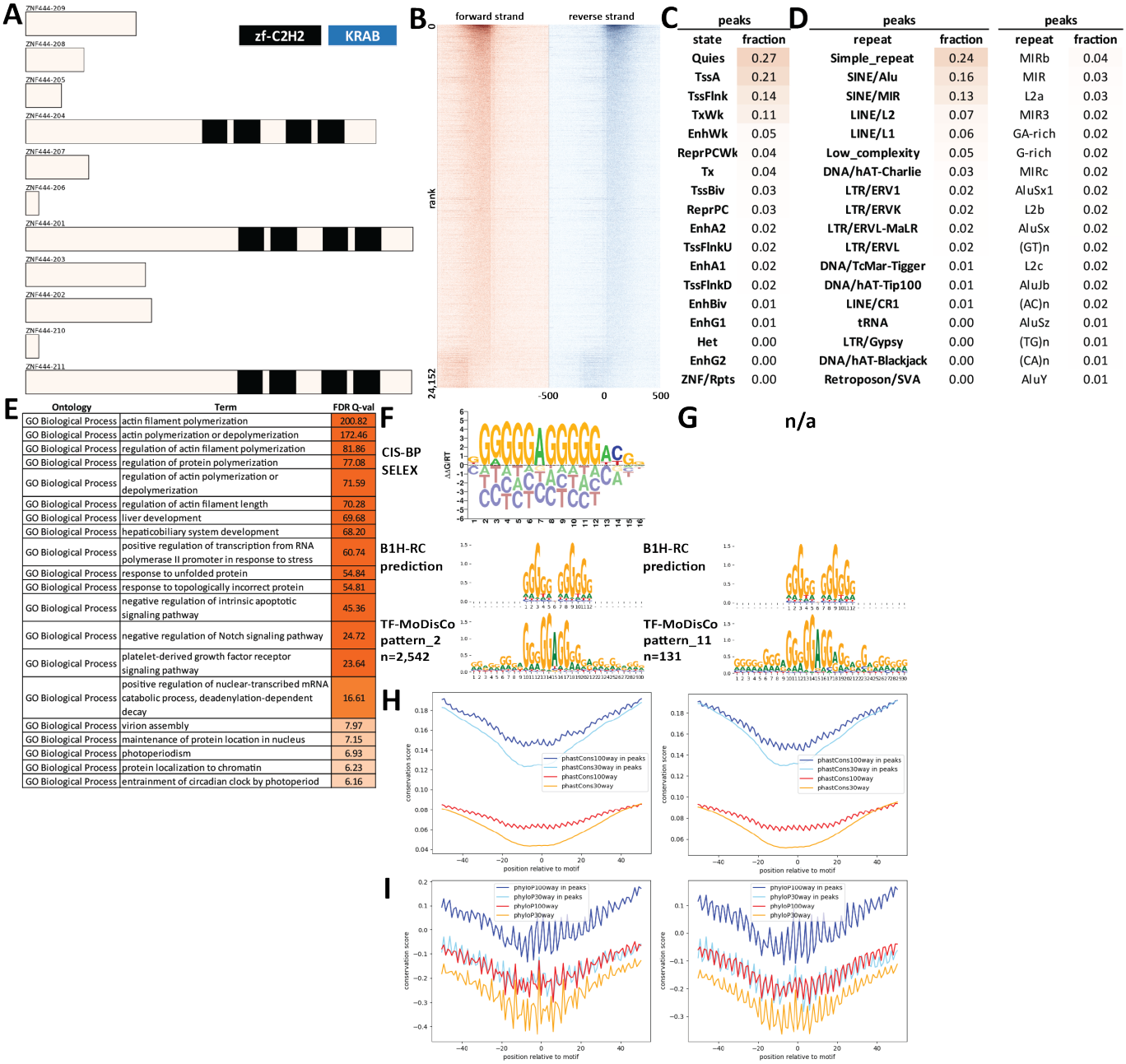

C

peaks	
state	fraction
Quies	0.27
TssA	0.21
TssFlnk	0.14
TxWk	0.11
EnhWk	0.05
ReprPCWk	0.04
Tx	0.04
TssBiv	0.03
ReprPC	0.03
EnhA2	0.02
TssFlnkU	0.02
EnhA1	0.02
TssFlnkD	0.02
EnhBiv	0.01
EnhG1	0.01
Het	0.00
EnhG2	0.00
ZNF/Rpts	0.00

D

peaks		peaks	
repeat	fraction	repeat	fraction
Simple_repeat	0.24	MIRb	0.04
SINE/Alu	0.16	MIR	0.03
SINE/MIR	0.13	L2a	0.03
LINE/L2	0.07	MIR3	0.02
LINE/L1	0.06	GA-rich	0.02
Low_complexity	0.05	G-rich	0.02
DNA/hAT-Charlie	0.03	MIRc	0.02
LTR/ERV1	0.02	AluSx1	0.02
LTR/ERVK	0.02	L2b	0.02
LTR/ERVL-MaLR	0.02	AluSx	0.02
LTR/ERVL	0.02	(GT)n	0.02
DNA/TcMar-Tigger	0.01	L2c	0.02
DNA/hAT-Tip100	0.01	AluJb	0.02
LINE/CR1	0.01	(AC)n	0.02
tRNA	0.00	AluSz	0.01
LTR/Gypsy	0.00	(TG)n	0.01
DNA/hAT-Blackjack	0.00	(CA)n	0.01
Retroposon/SVA	0.00	AluY	0.01

E

Ontology	Term	FDR Q-val
GO Biological Process	actin filament polymerization	200.82
GO Biological Process	actin polymerization or depolymerization	172.46
GO Biological Process	regulation of actin filament polymerization	81.86
GO Biological Process	regulation of protein polymerization	77.08
GO Biological Process	regulation of actin polymerization or depolymerization	71.59
GO Biological Process	regulation of actin filament length	70.28
GO Biological Process	liver development	69.68
GO Biological Process	hepaticobiliary system development	68.20
GO Biological Process	positive regulation of transcription from RNA polymerase II promoter in response to stress	60.74
GO Biological Process	response to unfolded protein	54.84
GO Biological Process	response to topologically incorrect protein	54.81
GO Biological Process	negative regulation of intrinsic apoptotic signaling pathway	45.36
GO Biological Process	negative regulation of Notch signaling pathway	24.72
GO Biological Process	platelet-derived growth factor receptor signaling pathway	23.64
GO Biological Process	positive regulation of nuclear-transcribed mRNA catabolic process, deadenylation-dependent decay	16.61
GO Biological Process	virion assembly	7.97
GO Biological Process	maintenance of protein location in nucleus	7.15
GO Biological Process	photoperiodism	6.93
GO Biological Process	protein localization to chromatin	6.23
GO Biological Process	entrainment of circadian clock by photoperiod	6.16

Supplementary Figure 1222: Properties and genomic distribution of motifs identified for the ZNF444 transcription factor in MCF-7 (accession ENCSR038XIA).

TF-MoDisCO pattern_11 n=131, CWM

pattern_11, n=131; subpattern_0, ns=52

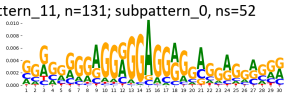

pattern_11, n=131; subpattern_1, ns=41

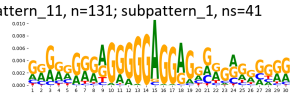

pattern_11, n=131; subpattern_2, ns=17

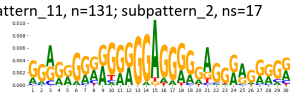

pattern_11, n=131; subpattern_3, ns=11

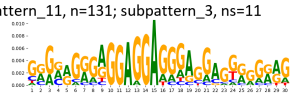

pattern_11, n=131; subpattern_4, ns=10

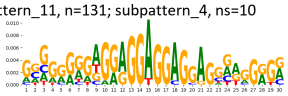

TF-MoDisCO pattern_11 n=131, PWM

pattern_11, n=131; subpattern_0, ns=52

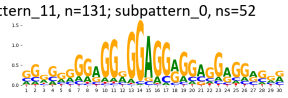

pattern_11, n=131; subpattern_1, ns=41

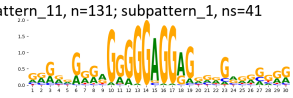

pattern_11, n=131; subpattern_2, ns=17

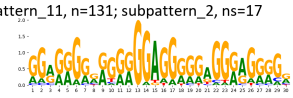

pattern_11, n=131; subpattern_3, ns=11

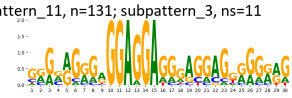

pattern_11, n=131; subpattern_4, ns=10

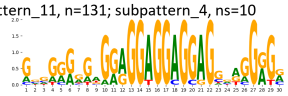

TF-MoDisCO pattern_2 n=2542, CWM

pattern_2, n=2542; subpattern_0, ns=678

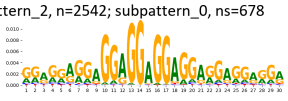

pattern_2, n=2542; subpattern_1, ns=644

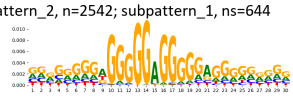

pattern_2, n=2542; subpattern_2, ns=543

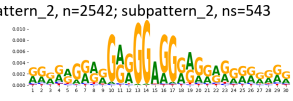

pattern_2, n=2542; subpattern_3, ns=280

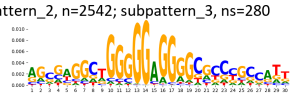

pattern_2, n=2542; subpattern_4, ns=214

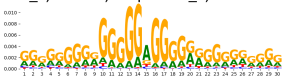

pattern_2, n=2542; subpattern_5, ns=179

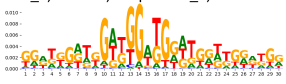

pattern_2, n=2542; subpattern_6, ns=4

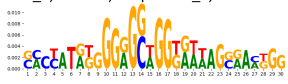

TF-MoDisCO pattern_2 n=2542, PWM

pattern_2, n=2542; subpattern_0, ns=678

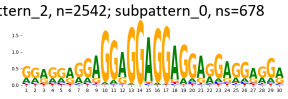

pattern_2, n=2542; subpattern_1, ns=644

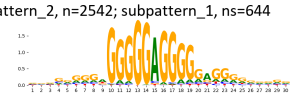

pattern_2, n=2542; subpattern_2, ns=543

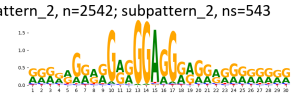

pattern_2, n=2542; subpattern_3, ns=280

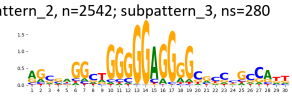

pattern_2, n=2542; subpattern_4, ns=214

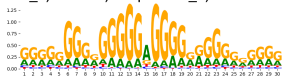

pattern_2, n=2542; subpattern_5, ns=179

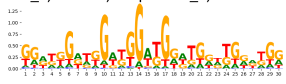

pattern_2, n=2542; subpattern_6, ns=4

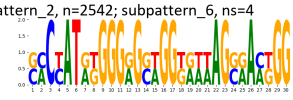

Supplementary Figure 1223: TF-MoDisCO subpatterns for the ZNF444 transcription factor in MCF-7 (accession ENCSR038XIA).

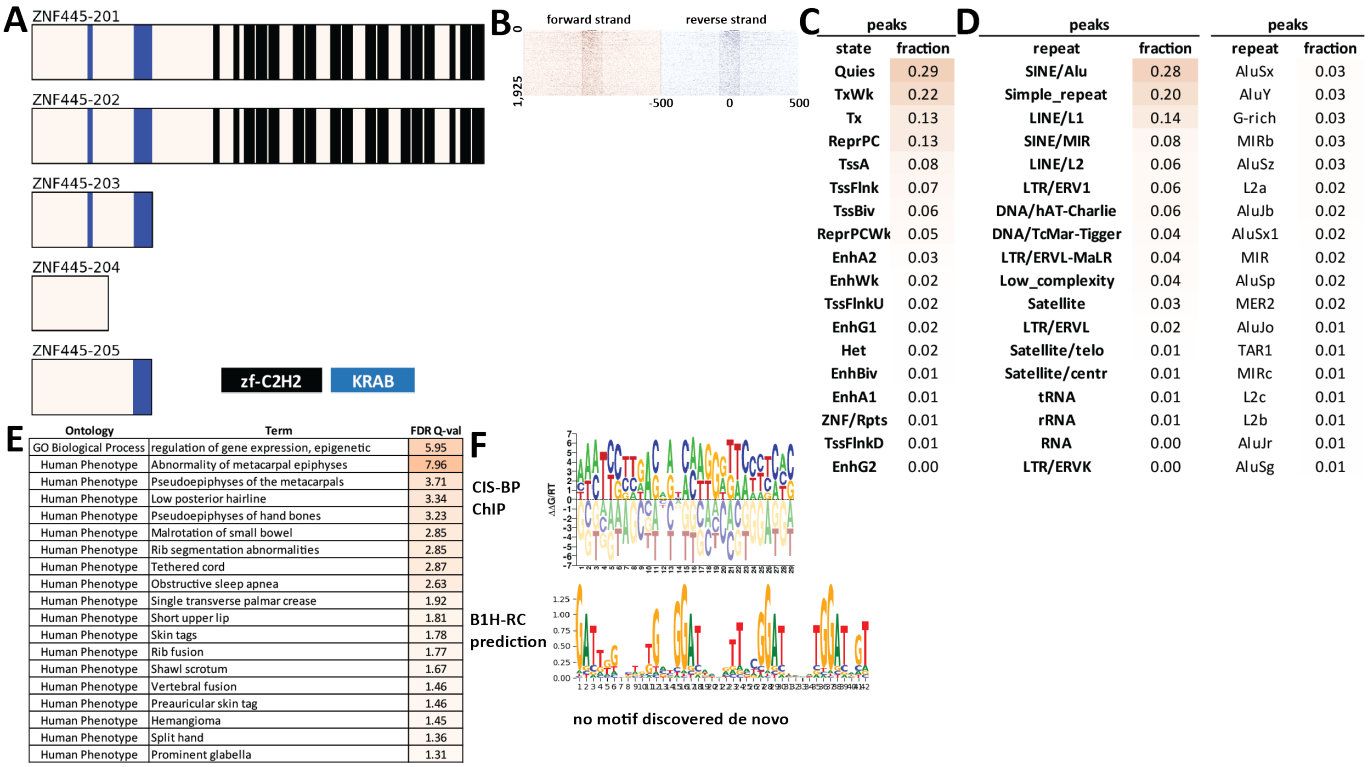

Supplementary Figure 1224: Properties and genomic distribution of motifs identified for the ZNF445 transcription factor in HEK293 (accession ChipExo models).

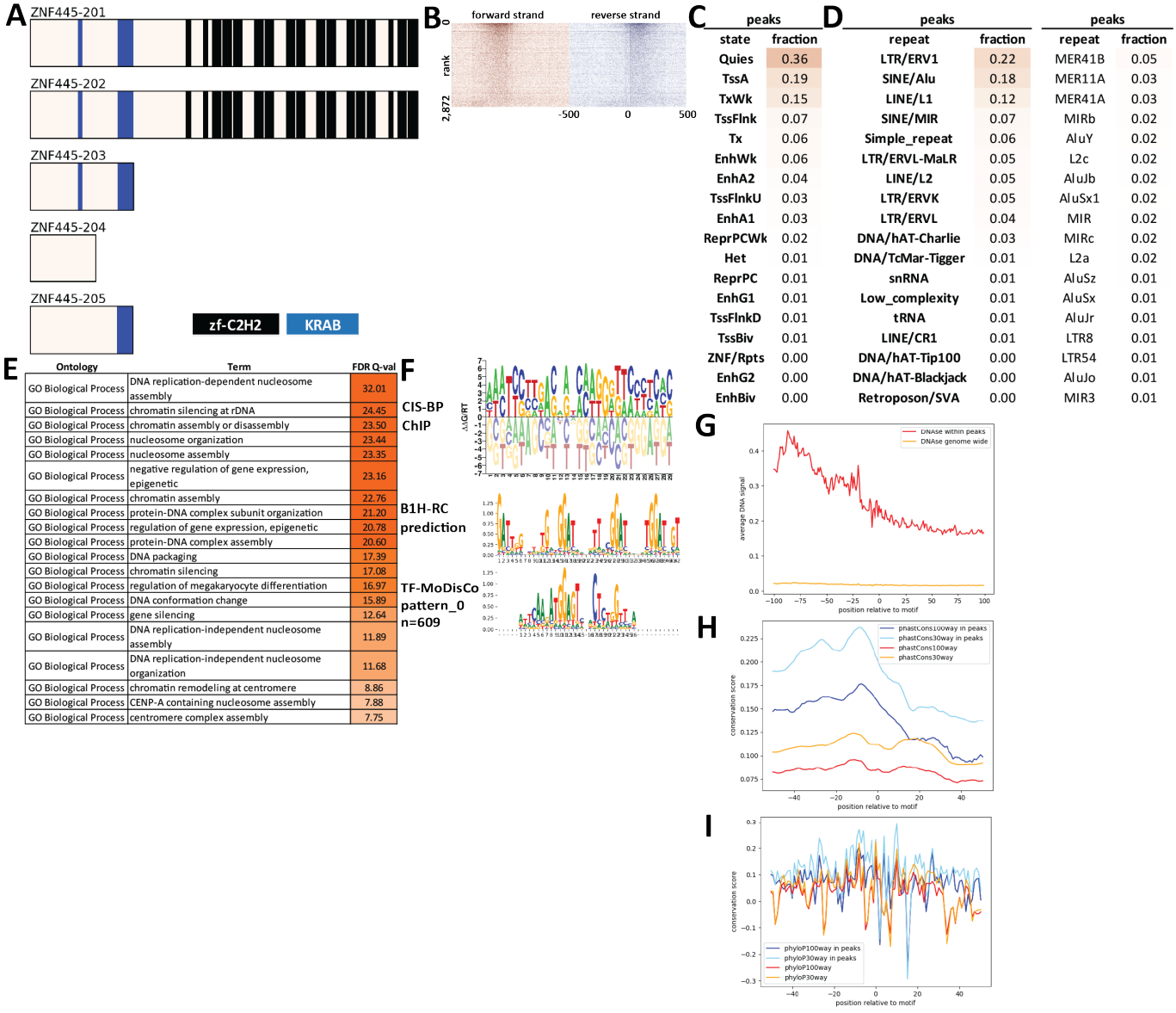

Supplementary Figure 1225: Properties and genomic distribution of motifs identified for the ZNF445 transcription factor in K562 (accession ENCSR883UGG).

TF-MoDisCO pattern_0 n=609, CWM

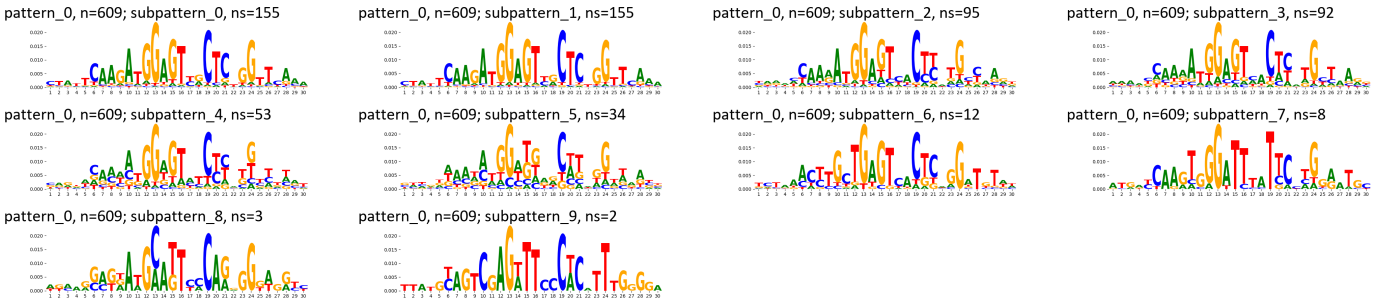

TF-MoDisCO pattern_0 n=609, PWM

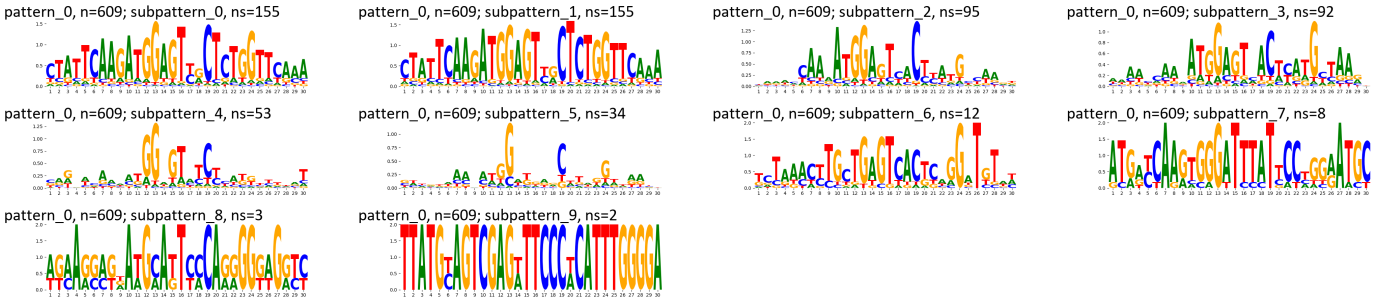

Supplementary Figure 1226: TF-MoDisCO subpatterns for the ZNF445 transcription factor in K562 (accession ENCSR883UGG).

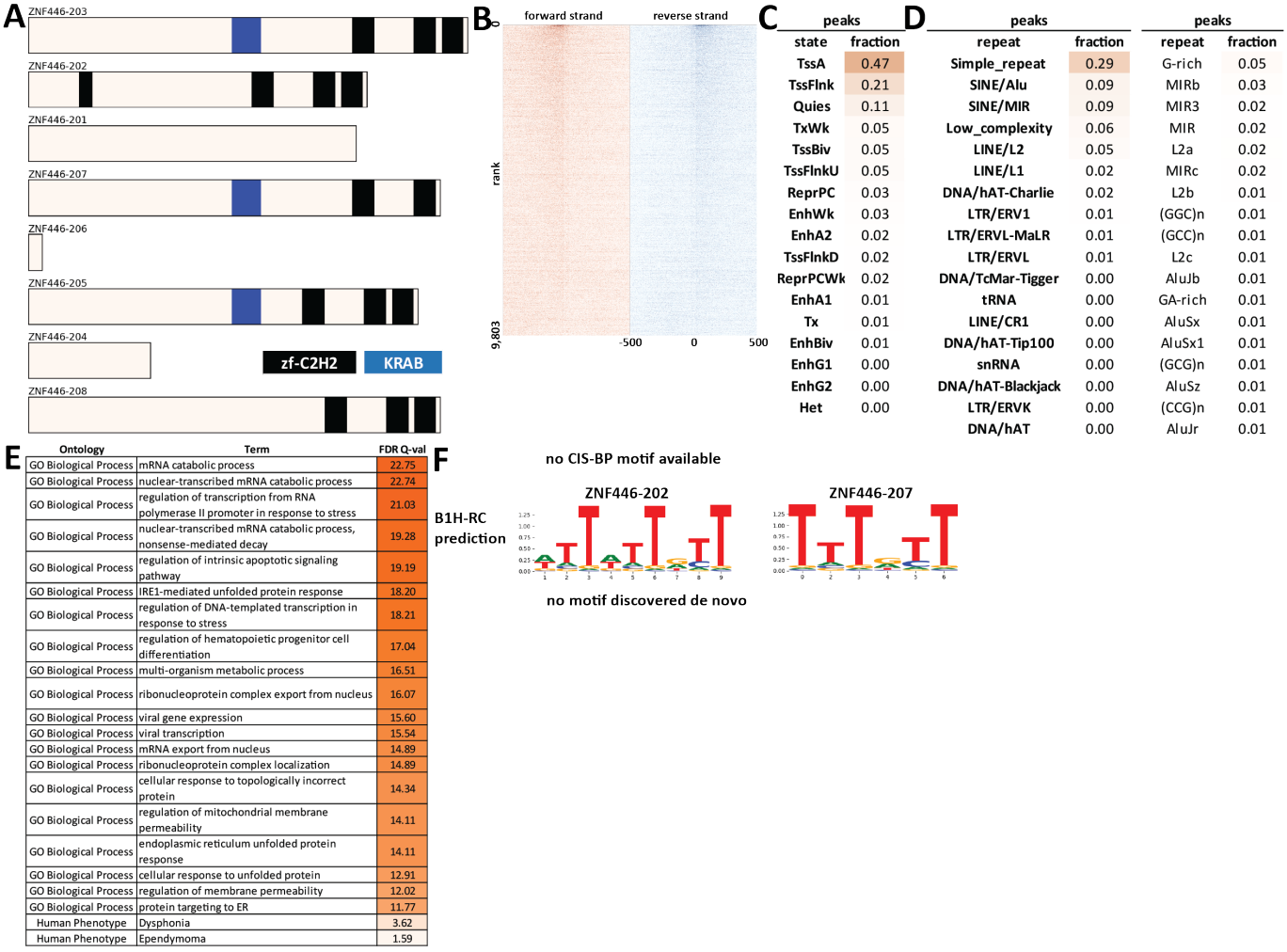

peaks	
state	fraction
TssA	0.47
TssFlnk	0.21
Quies	0.11
TxWk	0.05
TssBiv	0.05
TssFlnkU	0.05
ReprPC	0.03
EnhWk	0.03
EnhA2	0.02
TssFlnkD	0.02
ReprPCWk	0.02
EnhA1	0.01
Tx	0.01
EnhBiv	0.01
EnhG1	0.00
EnhG2	0.00
Het	0.00

peaks		peaks	
repeat	fraction	repeat	fraction
Simple_repeat	0.29	G-rich	0.05
SINE/Alu	0.09	MIRb	0.03
SINE/MIR	0.09	MIR3	0.02
Low_complexity	0.06	MIR	0.02
LINE/L2	0.05	L2a	0.02
LINE/L1	0.02	MIRc	0.02
DNA/hAT-Charlie	0.02	L2b	0.01
LTR/ERV1	0.01	(GGC)n	0.01
LTR/ERVL-MaLR	0.01	(GCC)n	0.01
LTR/ERVL	0.01	L2c	0.01
DNA/TcMar-Tigger	0.00	AluJb	0.01
tRNA	0.00	GA-rich	0.01
LINE/CR1	0.00	AluSx	0.01
DNA/hAT-Tip100	0.00	AluSx1	0.01
snRNA	0.00	(GCG)n	0.01
DNA/hAT-Blackjack	0.00	AluSz	0.01
LTR/ERVK	0.00	(CCG)n	0.01
DNA/hAT	0.00	AluJr	0.01

Ontology	Term	FDR Q-val
GO Biological Process	mRNA catabolic process	22.75
GO Biological Process	nuclear-transcribed mRNA catabolic process	22.74
GO Biological Process	regulation of transcription from RNA polymerase II promoter in response to stress	21.03
GO Biological Process	nuclear-transcribed mRNA catabolic process, nonsense-mediated decay	19.28
GO Biological Process	regulation of intrinsic apoptotic signaling pathway	19.19
GO Biological Process	IRE1-mediated unfolded protein response	18.20
GO Biological Process	regulation of DNA-templated transcription in response to stress	18.21
GO Biological Process	regulation of hematopoietic progenitor cell differentiation	17.04
GO Biological Process	multi-organism metabolic process	16.51
GO Biological Process	ribonucleoprotein complex export from nucleus	16.07
GO Biological Process	viral gene expression	15.60
GO Biological Process	viral transcription	15.54
GO Biological Process	mRNA export from nucleus	14.89
GO Biological Process	ribonucleoprotein complex localization	14.89
GO Biological Process	cellular response to topologically incorrect protein	14.34
GO Biological Process	regulation of mitochondrial membrane permeability	14.11
GO Biological Process	endoplasmic reticulum unfolded protein response	14.11
GO Biological Process	cellular response to unfolded protein	12.91
GO Biological Process	regulation of membrane permeability	12.02
GO Biological Process	protein targeting to ER	11.77
Human Phenotype	Dysphonia	3.62
Human Phenotype	Ependymoma	1.59

Supplementary Figure 1227: Properties and genomic distribution of motifs identified for the ZNF446 transcription factor in HepG2 (accession ENCSR839AJZ).

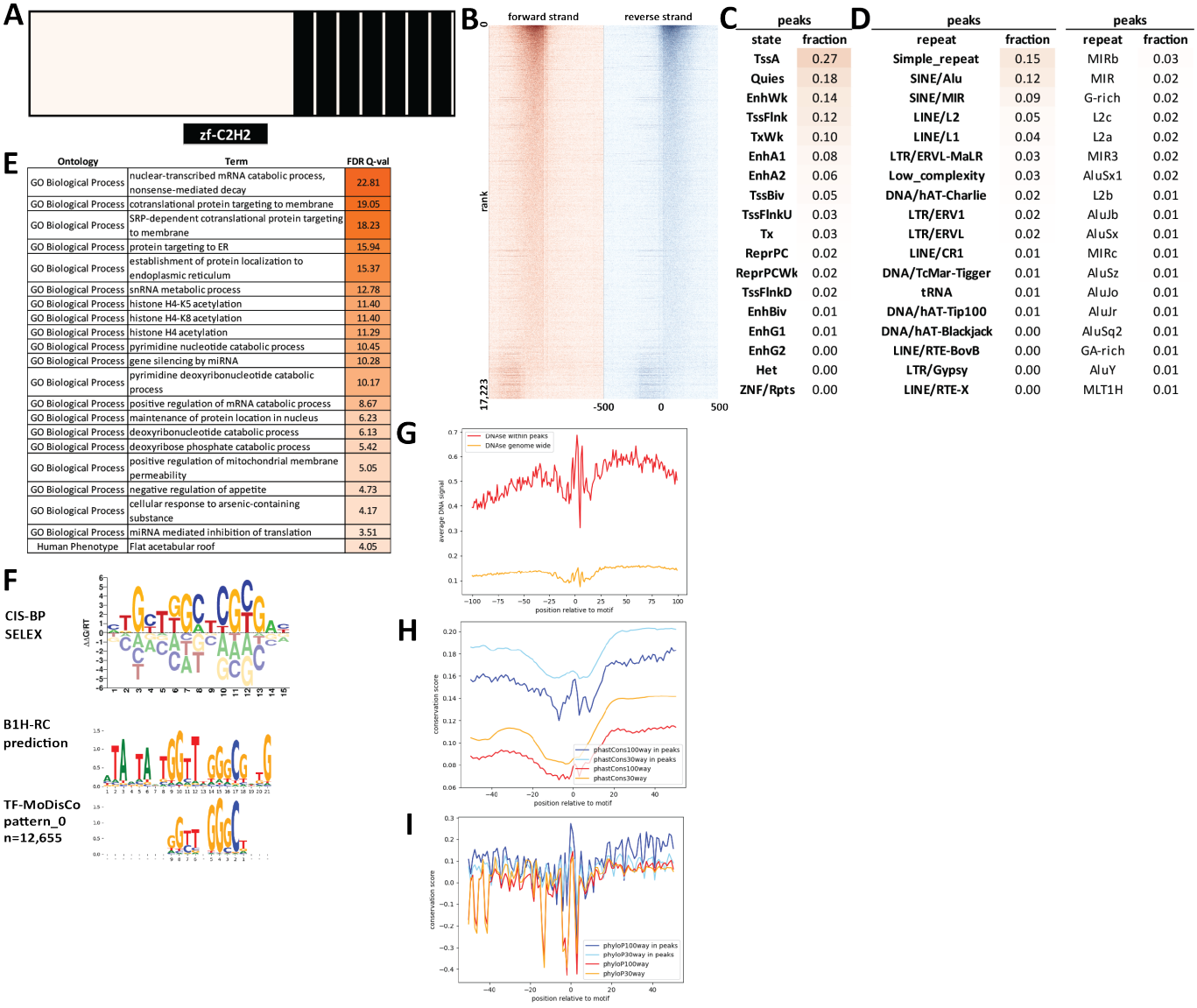

Supplementary Figure 1228: Properties and genomic distribution of motifs identified for the ZNF449 transcription factor in HEK293 (accession ENCSR738SLS).

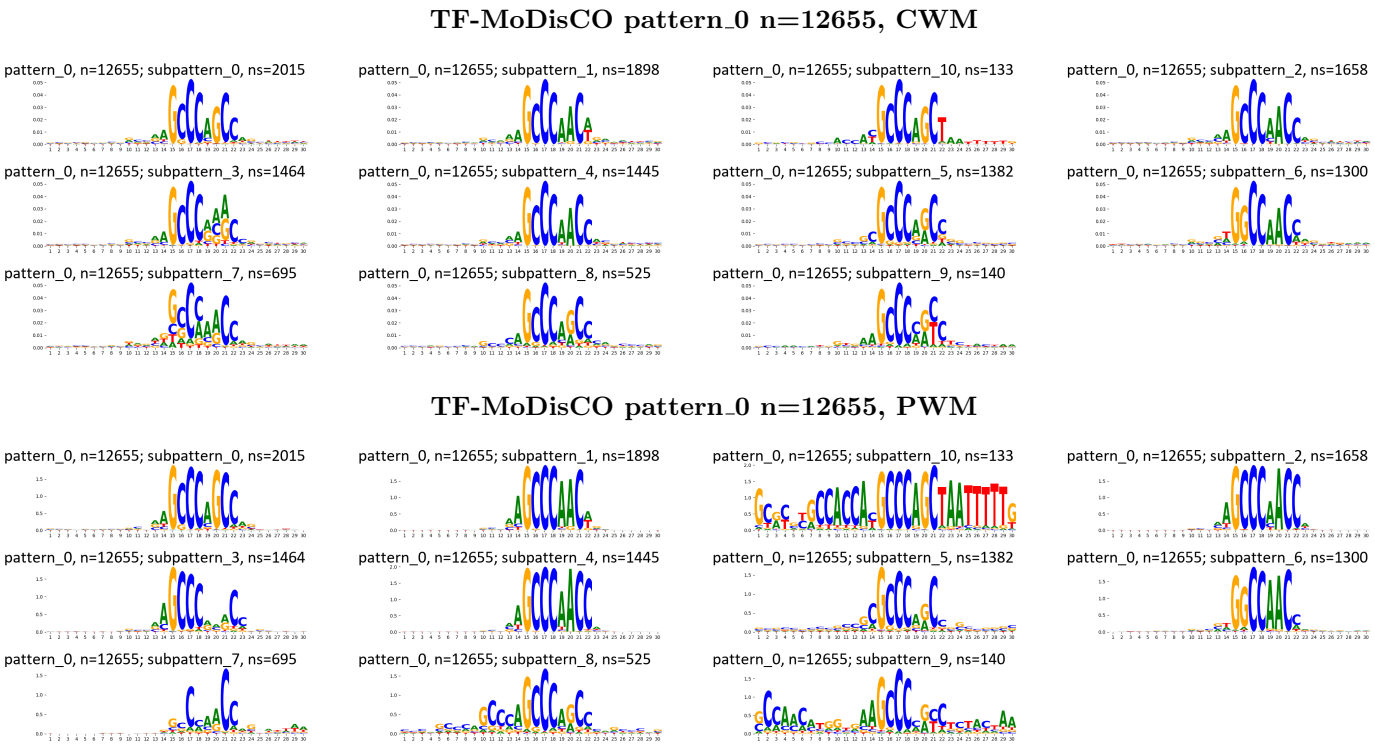

Supplementary Figure 1229: TF-MoDisCO subpatterns for the ZNF449 transcription factor in HEK293 (accession ENCSR738SLS).

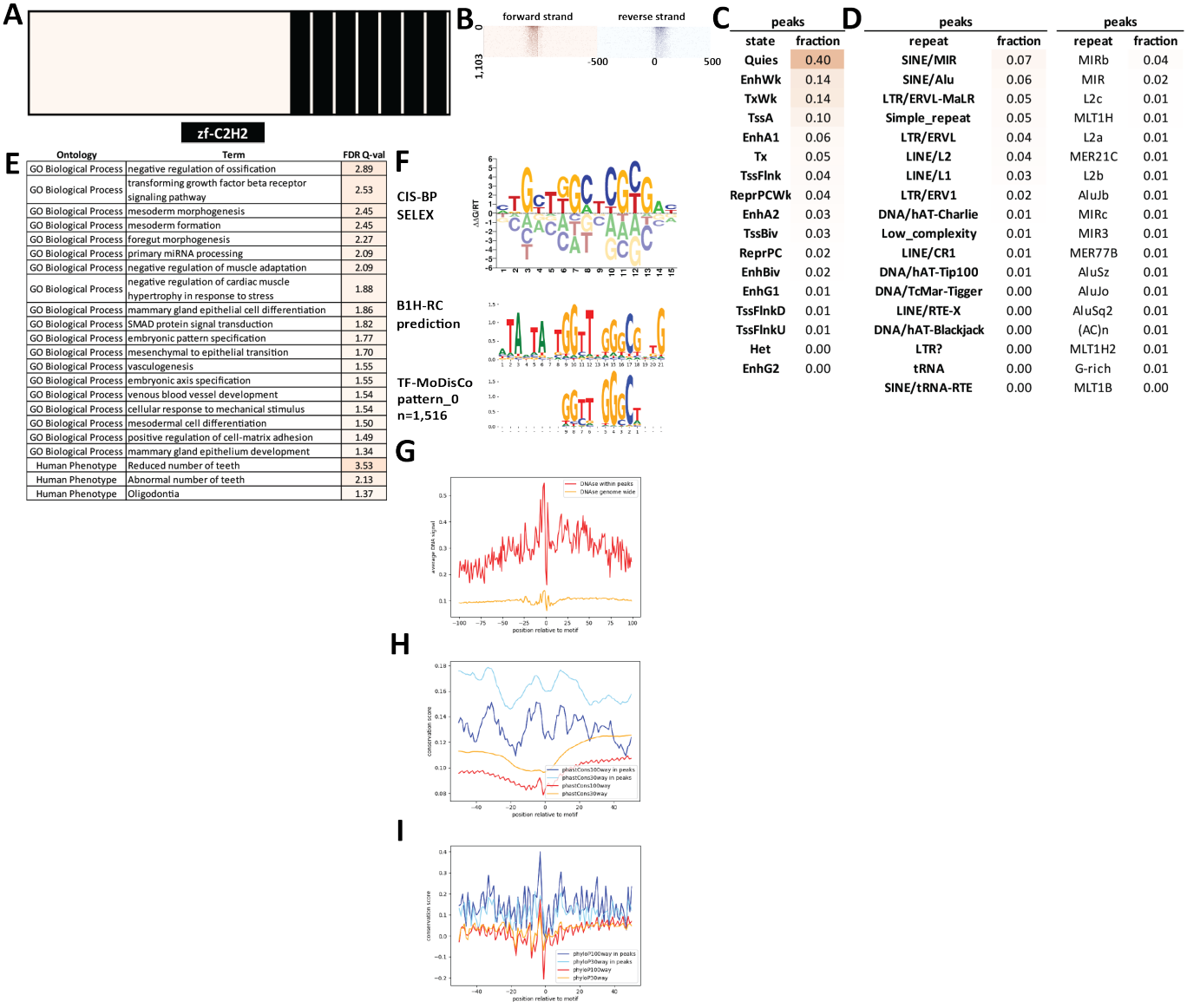

Supplementary Figure 1230: Properties and genomic distribution of motifs identified for the ZNF449 transcription factor in HEK293 (accession Hughes GR models).

TF-MoDisCO pattern_0 n=1516, CWM

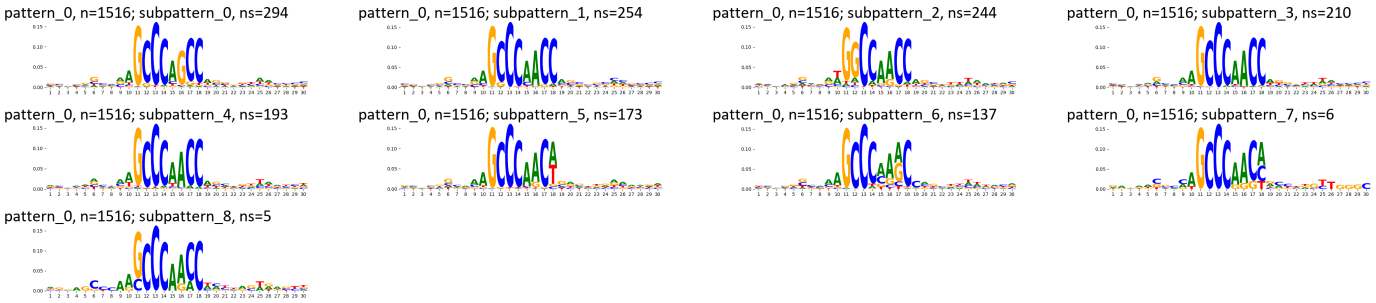

TF-MoDisCO pattern_0 n=1516, PWM

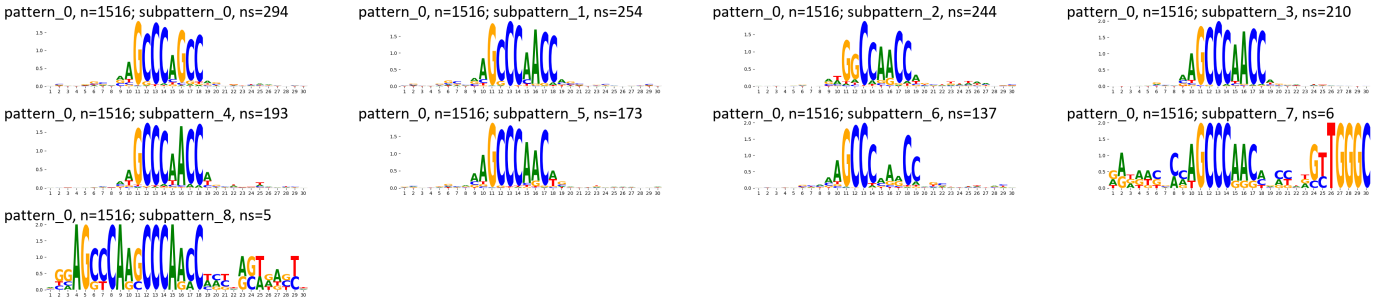

Supplementary Figure 1231: TF-MoDisCO subpatterns for the ZNF449 transcription factor in HEK293 (accession Hughes GR models).

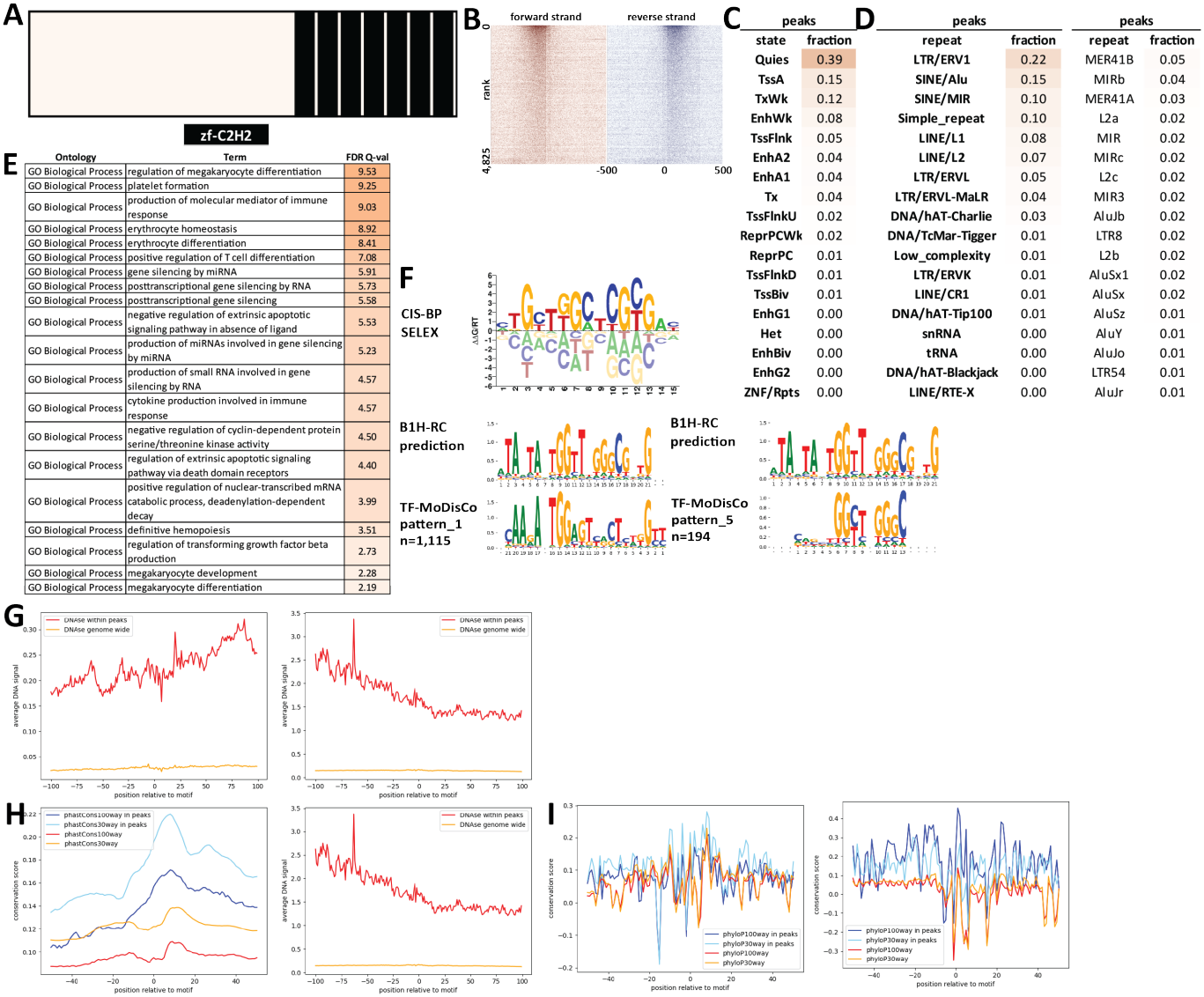

Supplementary Figure 1232: Properties and genomic distribution of motifs identified for the ZNF449 transcription factor in K562 (accession ENCSR659YWQ).

TF-MoDisCO pattern_1 n=1115, CWM

pattern_1, n=1115; subpattern_0, ns=253

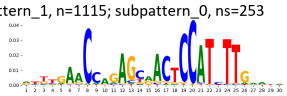

pattern_1, n=1115; subpattern_1, ns=228

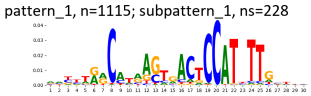

pattern_1, n=1115; subpattern_2, ns=226

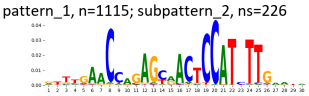

pattern_1, n=1115; subpattern_3, ns=215

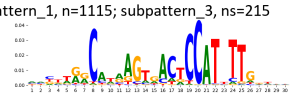

pattern_1, n=1115; subpattern_4, ns=105

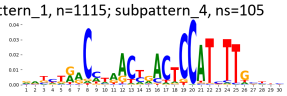

pattern_1, n=1115; subpattern_5, ns=85

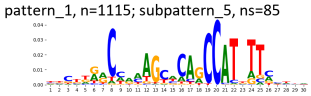

pattern_1, n=1115; subpattern_6, ns=3

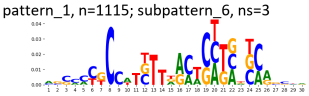

TF-MoDisCO pattern_1 n=1115, CWM

pattern_1, n=1115; subpattern_0, ns=253

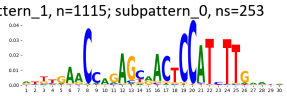

pattern_1, n=1115; subpattern_1, ns=228

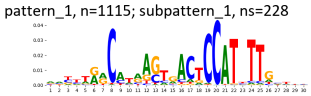

pattern_1, n=1115; subpattern_2, ns=226

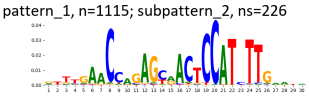

pattern_1, n=1115; subpattern_3, ns=215

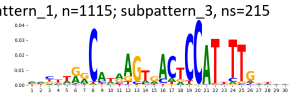

pattern_1, n=1115; subpattern_4, ns=105

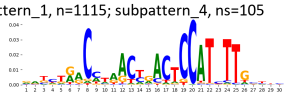

pattern_1, n=1115; subpattern_5, ns=85

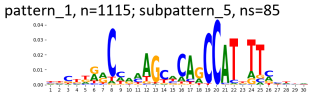

pattern_1, n=1115; subpattern_6, ns=3

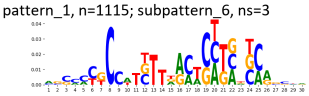

TF-MoDisCO pattern_1 n=1115, PWM

pattern_1, n=1115; subpattern_0, ns=253

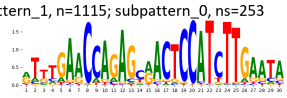

pattern_1, n=1115; subpattern_1, ns=228

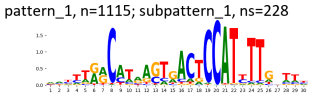

pattern_1, n=1115; subpattern_2, ns=226

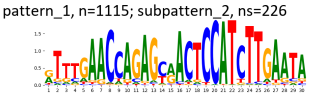

pattern_1, n=1115; subpattern_3, ns=215

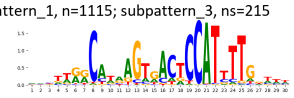

pattern_1, n=1115; subpattern_4, ns=105

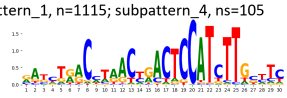

pattern_1, n=1115; subpattern_5, ns=85

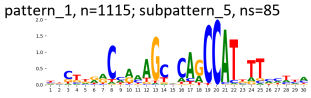

pattern_1, n=1115; subpattern_6, ns=3

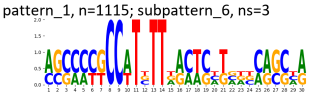

TF-MoDisCO pattern_1 n=1115, PWM

pattern_1, n=1115; subpattern_0, ns=253

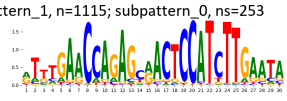

pattern_1, n=1115; subpattern_1, ns=228

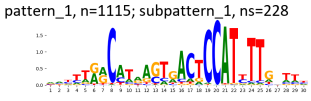

pattern_1, n=1115; subpattern_2, ns=226

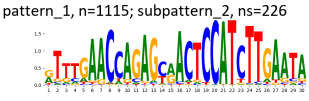

pattern_1, n=1115; subpattern_3, ns=215

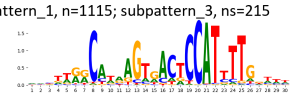

pattern_1, n=1115; subpattern_4, ns=105

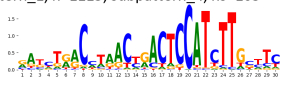

pattern_1, n=1115; subpattern_5, ns=85

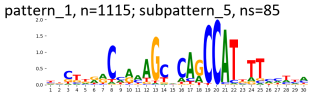

pattern_1, n=1115; subpattern_6, ns=3

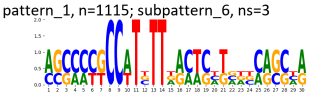

TF-MoDisCO pattern_5 n=194, CWM

pattern_5, n=194; subpattern_0, ns=50

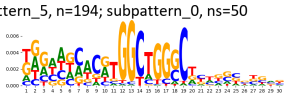

pattern_5, n=194; subpattern_1, ns=44

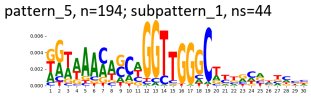

pattern_5, n=194; subpattern_2, ns=41

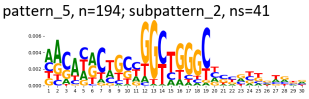

pattern_5, n=194; subpattern_3, ns=36

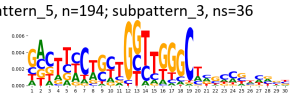

pattern_5, n=194; subpattern_4, ns=20

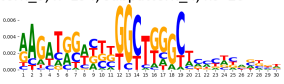

pattern_5, n=194; subpattern_5, ns=3



TF-MoDisCO pattern_5 n=194, PWM

pattern_5, n=194; subpattern_0, ns=50

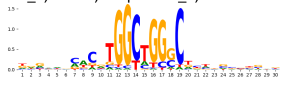

pattern_5, n=194; subpattern_1, ns=44

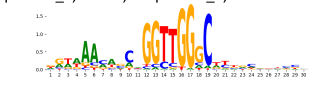

pattern_5, n=194; subpattern_2, ns=41

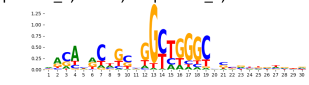

pattern_5, n=194; subpattern_3, ns=36

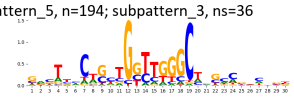

pattern_5, n=194; subpattern_4, ns=20

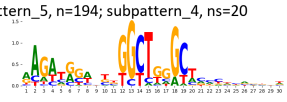

pattern_5, n=194; subpattern_5, ns=3

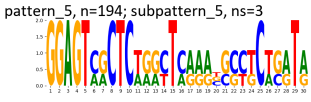

Supplementary Figure 1233: TF-MoDisCO subpatterns for the ZNF449 transcription factor in K562 (accession ENCSR659YWQ).

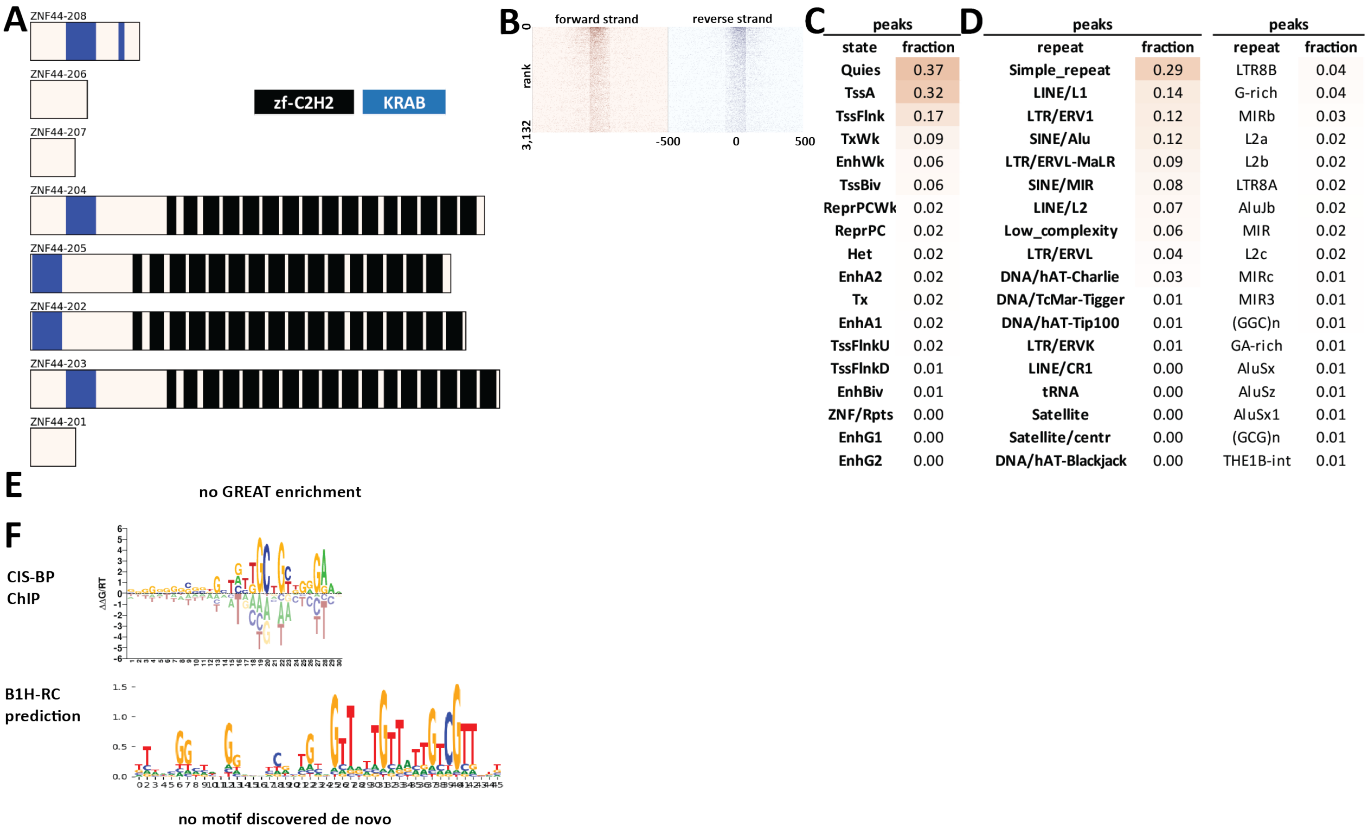

peaks	
state	fraction
Quies	0.37
TssA	0.32
TssFlnk	0.17
TxWk	0.09
EnhWk	0.06
TssBiv	0.06
ReprPCWk	0.02
ReprPC	0.02
Het	0.02
EnhA2	0.02
Tx	0.02
EnhA1	0.02
TssFlnkU	0.02
TssFlnkD	0.01
EnhBiv	0.01
ZNF/Rpts	0.00
EnhG1	0.00
EnhG2	0.00

peaks		peaks	
repeat	fraction	repeat	fraction
Simple_repeat	0.29	LTR8B	0.04
LINE/L1	0.14	G-rich	0.04
LTR/ERV1	0.12	MIRb	0.03
SINE/Alu	0.12	L2a	0.02
LTR/ERVL-MaLR	0.09	L2b	0.02
SINE/MIR	0.08	LTR8A	0.02
LINE/L2	0.07	AluJb	0.02
Low_complexity	0.06	MIR	0.02
LTR/ERVL	0.04	L2c	0.02
DNA/hAT-Charlie	0.03	MIRc	0.01
DNA/TcMar-Tigger	0.01	MIR3	0.01
DNA/hAT-Tip100	0.01	(GGC)n	0.01
LTR/ERVK	0.01	GA-rich	0.01
LINE/CR1	0.00	AluSx	0.01
tRNA	0.00	AluSz	0.01
Satellite	0.00	AluSx1	0.01
Satellite/centr	0.00	(GCG)n	0.01
DNA/hAT-Blackjack	0.00	THE1B-int	0.01

Supplementary Figure 1234: Properties and genomic distribution of motifs identified for the ZNF44 transcription factor in HEK293 (accession ChipExo models).

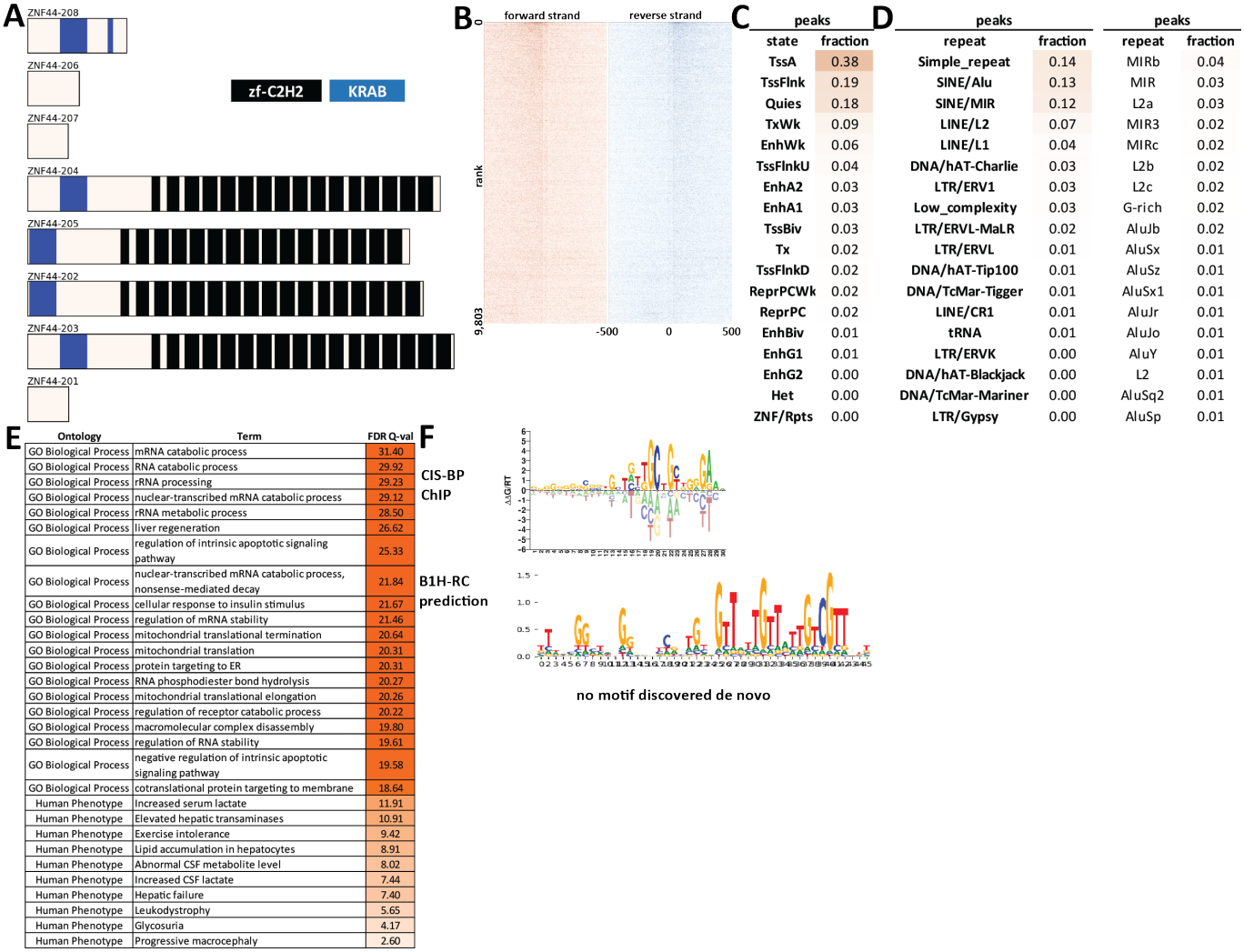

C

peaks	
state	fraction
TssA	0.38
TssFlnk	0.19
Quies	0.18
TxWk	0.09
EnhWk	0.06
TssFlnkU	0.04
EnhA2	0.03
EnhA1	0.03
TssBiv	0.03
Tx	0.02
TssFlnkD	0.02
ReprPCWk	0.02
ReprPC	0.02
EnhBiv	0.01
EnhG1	0.01
EnhG2	0.00
Het	0.00
ZNF/Rpts	0.00

D

peaks		peaks	
repeat	fraction	repeat	fraction
Simple_repeat	0.14	MIRb	0.04
SINE/Alu	0.13	MIR	0.03
SINE/MIR	0.12	L2a	0.03
LINE/L2	0.07	MIR3	0.02
LINE/L1	0.04	MIRc	0.02
DNA/hAT-Charlie	0.03	L2b	0.02
LTR/ERV1	0.03	L2c	0.02
Low_complexity	0.03	G-rich	0.02
LTR/ERVL-MaLR	0.02	AluJb	0.02
LTR/ERVL	0.01	AluSx	0.01
DNA/hAT-Tip100	0.01	AluSz	0.01
DNA/TcMar-Tigger	0.01	AluSx1	0.01
LINE/CR1	0.01	AluJr	0.01
tRNA	0.01	AluJo	0.01
LTR/ERVK	0.00	AluY	0.01
DNA/hAT-Blackjack	0.00	L2	0.01
DNA/TcMar-Mariner	0.00	AluSq2	0.01
LTR/Gypsy	0.00	AluSp	0.01

E

Ontology	Term	FDR Q-val
GO Biological Process	mRNA catabolic process	31.40
GO Biological Process	RNA catabolic process	29.92
GO Biological Process	rRNA processing	29.23
GO Biological Process	nuclear-transcribed mRNA catabolic process	29.12
GO Biological Process	rRNA metabolic process	28.50
GO Biological Process	liver regeneration	26.62
GO Biological Process	regulation of intrinsic apoptotic signaling pathway	25.33
GO Biological Process	nuclear-transcribed mRNA catabolic process, nonsense-mediated decay	21.84
GO Biological Process	cellular response to insulin stimulus	21.67
GO Biological Process	regulation of mRNA stability	21.46
GO Biological Process	mitochondrial translational termination	20.64
GO Biological Process	mitochondrial translation	20.31
GO Biological Process	protein targeting to ER	20.31
GO Biological Process	RNA phosphodiester bond hydrolysis	20.27
GO Biological Process	mitochondrial translational elongation	20.26
GO Biological Process	regulation of receptor catabolic process	20.22
GO Biological Process	macromolecular complex disassembly	19.80
GO Biological Process	regulation of RNA stability	19.61
GO Biological Process	negative regulation of intrinsic apoptotic signaling pathway	19.58
GO Biological Process	cotranslational protein targeting to membrane	18.64
Human Phenotype	Increased serum lactate	11.91
Human Phenotype	Elevated hepatic transaminases	10.91
Human Phenotype	Exercise intolerance	9.42
Human Phenotype	Lipid accumulation in hepatocytes	8.91
Human Phenotype	Abnormal CSF metabolite level	8.02
Human Phenotype	Increased CSF lactate	7.44
Human Phenotype	Hepatic failure	7.40
Human Phenotype	Leukodystrophy	5.65
Human Phenotype	Glycosuria	4.17
Human Phenotype	Progressive macrocephaly	2.60

Supplementary Figure 1235: Properties and genomic distribution of motifs identified for the ZNF44 transcription factor in HepG2 (accession ENCSR914HPP).

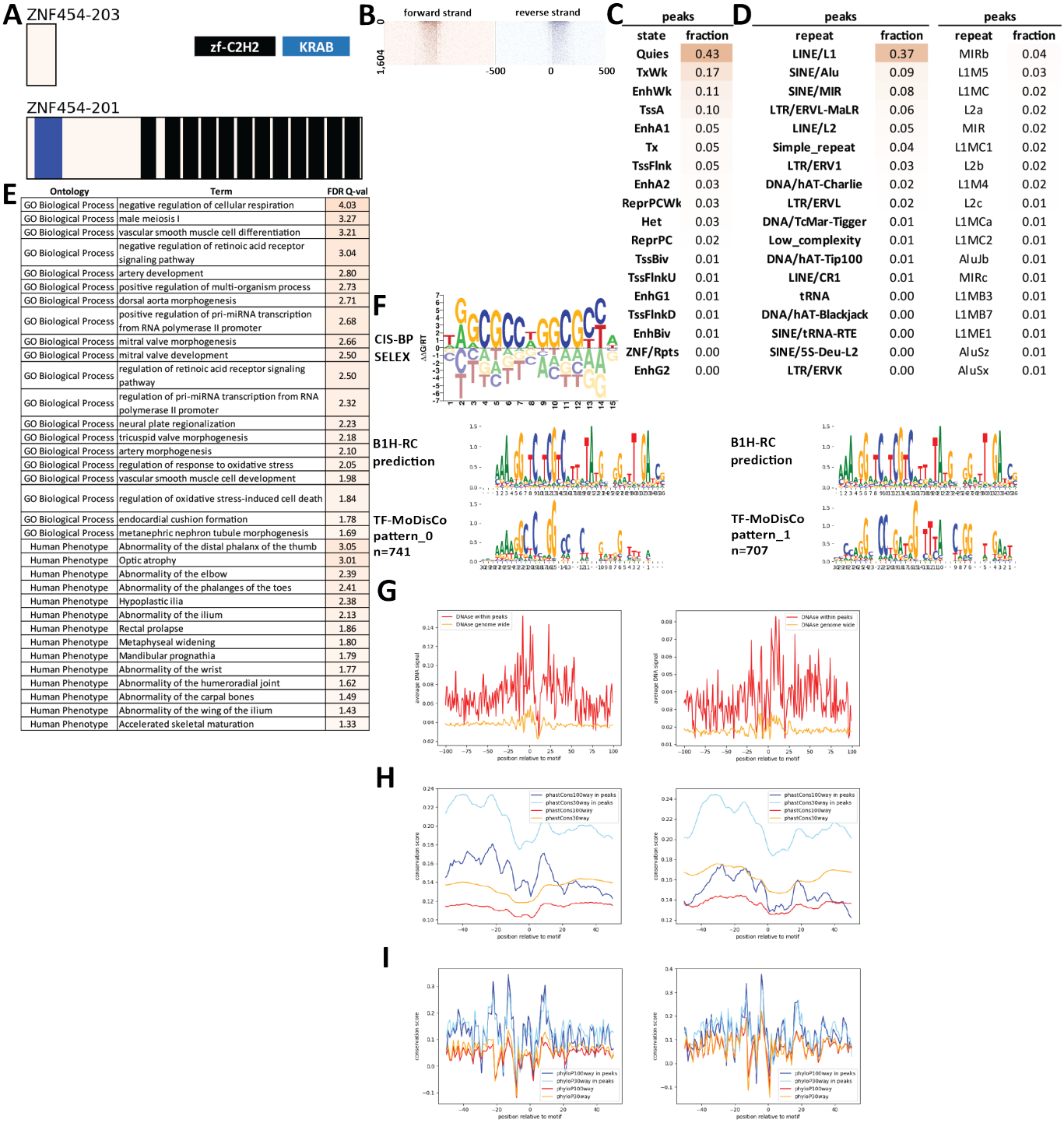

peaks	
state	fraction
Quies	0.43
TxWk	0.17
EnhWk	0.11
TssA	0.10
EnhA1	0.05
Tx	0.05
TssFlnk	0.05
EnhA2	0.03
ReprPCWk	0.03
Het	0.03
ReprPC	0.02
TssBiv	0.01
TssFlnkU	0.01
EnhG1	0.01
TssFlnkD	0.01
EnhBiv	0.01
ZNF/Rpts	0.00
EnhG2	0.00

peaks		peaks	
repeat	fraction	repeat	fraction
LINE/L1	0.37	MIRb	0.04
SINE/Alu	0.09	L1M5	0.03
SINE/MIR	0.08	L1MC	0.02
LTR/ERVL-MaLR	0.06	L2a	0.02
LINE/L2	0.05	MIR	0.02
Simple_repeat	0.04	L1MC1	0.02
LTR/ERV1	0.03	L2b	0.02
DNA/hAT-Charlie	0.02	L1M4	0.02
LTR/ERVL	0.02	L2c	0.01
DNA/TcMar-Tigger	0.01	L1MCa	0.01
Low_complexity	0.01	L1MC2	0.01
DNA/hAT-Tip100	0.01	AluJb	0.01
LINE/CR1	0.01	MIRc	0.01
tRNA	0.00	L1MB3	0.01
DNA/hAT-Blackjack	0.00	L1MB7	0.01
SINE/tRNA-RTE	0.00	L1ME1	0.01
SINE/5S-Deu-L2	0.00	AluSz	0.01
LTR/ERVK	0.00	AluSx	0.01

Ontology	Term	FDR Q-val
GO Biological Process	negative regulation of cellular respiration	4.03
GO Biological Process	male meiosis I	3.27
GO Biological Process	vascular smooth muscle cell differentiation	3.21
GO Biological Process	negative regulation of retinoic acid receptor signaling pathway	3.04
GO Biological Process	artery development	2.80
GO Biological Process	positive regulation of multi-organism process	2.73
GO Biological Process	dorsal aorta morphogenesis	2.71
GO Biological Process	positive regulation of pri-miRNA transcription from RNA polymerase II promoter	2.68
GO Biological Process	mitral valve morphogenesis	2.66
GO Biological Process	mitral valve development	2.50
GO Biological Process	regulation of retinoic acid receptor signaling pathway	2.50
GO Biological Process	regulation of pri-miRNA transcription from RNA polymerase II promoter	2.32
GO Biological Process	neural plate regionalization	2.23
GO Biological Process	tricuspid valve morphogenesis	2.18
GO Biological Process	artery morphogenesis	2.10
GO Biological Process	regulation of response to oxidative stress	2.05
GO Biological Process	vascular smooth muscle cell development	1.98
GO Biological Process	regulation of oxidative stress-induced cell death	1.84
GO Biological Process	endocardial cushion formation	1.78
GO Biological Process	metanephric nephron tubule morphogenesis	1.69
Human Phenotype	Abnormality of the distal phalanx of the thumb	3.05
Human Phenotype	Optic atrophy	3.01
Human Phenotype	Abnormality of the elbow	2.39
Human Phenotype	Abnormality of the phalanges of the toes	2.41
Human Phenotype	Hypoplastic ilia	2.38
Human Phenotype	Abnormality of the ilium	2.13
Human Phenotype	Rectal prolapse	1.86
Human Phenotype	Metaphyseal widening	1.80
Human Phenotype	Mandibular prognathia	1.79
Human Phenotype	Abnormality of the wrist	1.77
Human Phenotype	Abnormality of the humeroradial joint	1.62
Human Phenotype	Abnormality of the carpal bones	1.49
Human Phenotype	Abnormality of the wing of the ilium	1.43
Human Phenotype	Accelerated skeletal maturation	1.33

Supplementary Figure 1236: Properties and genomic distribution of motifs identified for the ZNF454 transcription factor in HEK293 (accession Hughes NB models).

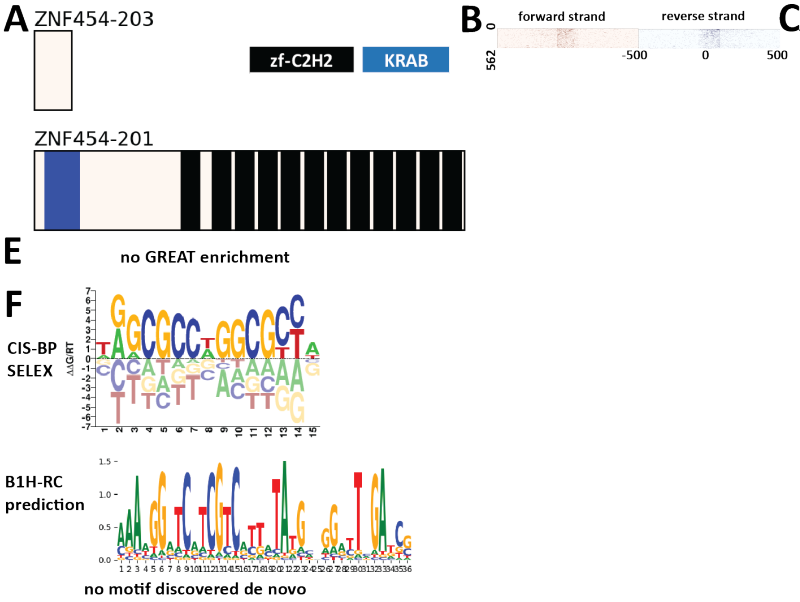

C

peaks	
state	fraction
Quies	0.38
TssA	0.15
TxWk	0.10
Tx	0.06
TssFlnk	0.06
Het	0.04
ReprPCWk	0.03
EnhWk	0.03
TssBiv	0.02
ReprPC	0.01
EnhA2	0.01
ZNF/Rpts	0.01
EnhG1	0.01
EnhA1	0.01
TssFlnkU	0.00
TssFlnkD	0.00
EnhBiv	0.00

D

peaks		peaks	
repeat	fraction	repeat	fraction
LINE/L1	0.41	L1M5	0.05
Simple_repeat	0.21	L1MC	0.02
SINE/Alu	0.20	AluSx	0.02
SINE/MIR	0.06	MIRb	0.02
LINE/L2	0.05	MIR3	0.02
LTR/ERV1	0.03	L2b	0.02
LTR/ERVL-MaLR	0.03	L1MB3	0.02
Satellite	0.03	L1M4	0.02
Low_complexity	0.02	AluJb	0.02
Satellite/centr	0.02	SST1	0.02
LTR/ERVL	0.02	L1MC2	0.02
DNA/hAT-Charlie	0.02	L1MC1	0.02
Satellite/acro	0.01	AluSx1	0.02
DNA/TcMar-Tigger	0.01	AluSq2	0.02
rRNA	0.01	L1MD	0.02
LINE/CR1	0.01	L1MB8	0.02
DNA/hAT-Tip100	0.01	AluSz	0.02
LTR/Gypsy?	0.00	L2a	0.01

Supplementary Figure 1237: Properties and genomic distribution of motifs identified for the ZNF454 transcription factor in HEK293 (accession ChipExo models).

TF-MoDisCO pattern_0 n=221, CWM

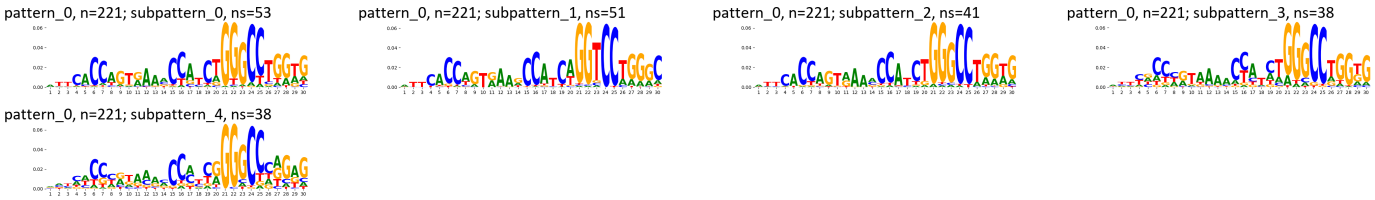

TF-MoDisCO pattern_0 n=221, PWM

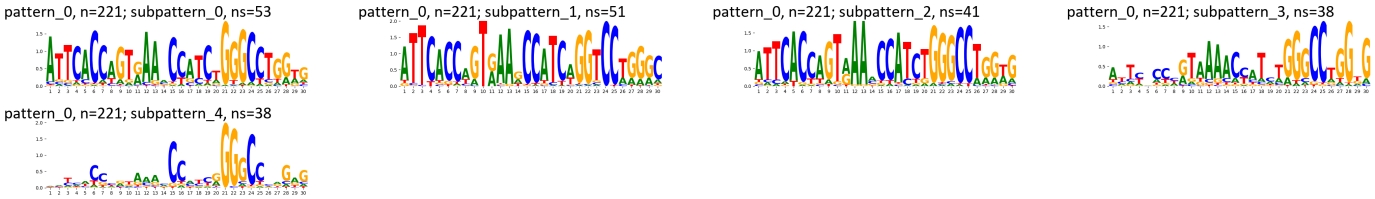

Supplementary Figure 1238: TF-MoDisCO subpatterns for the ZNF454 transcription factor in HEK293 (accession ChipExo models).

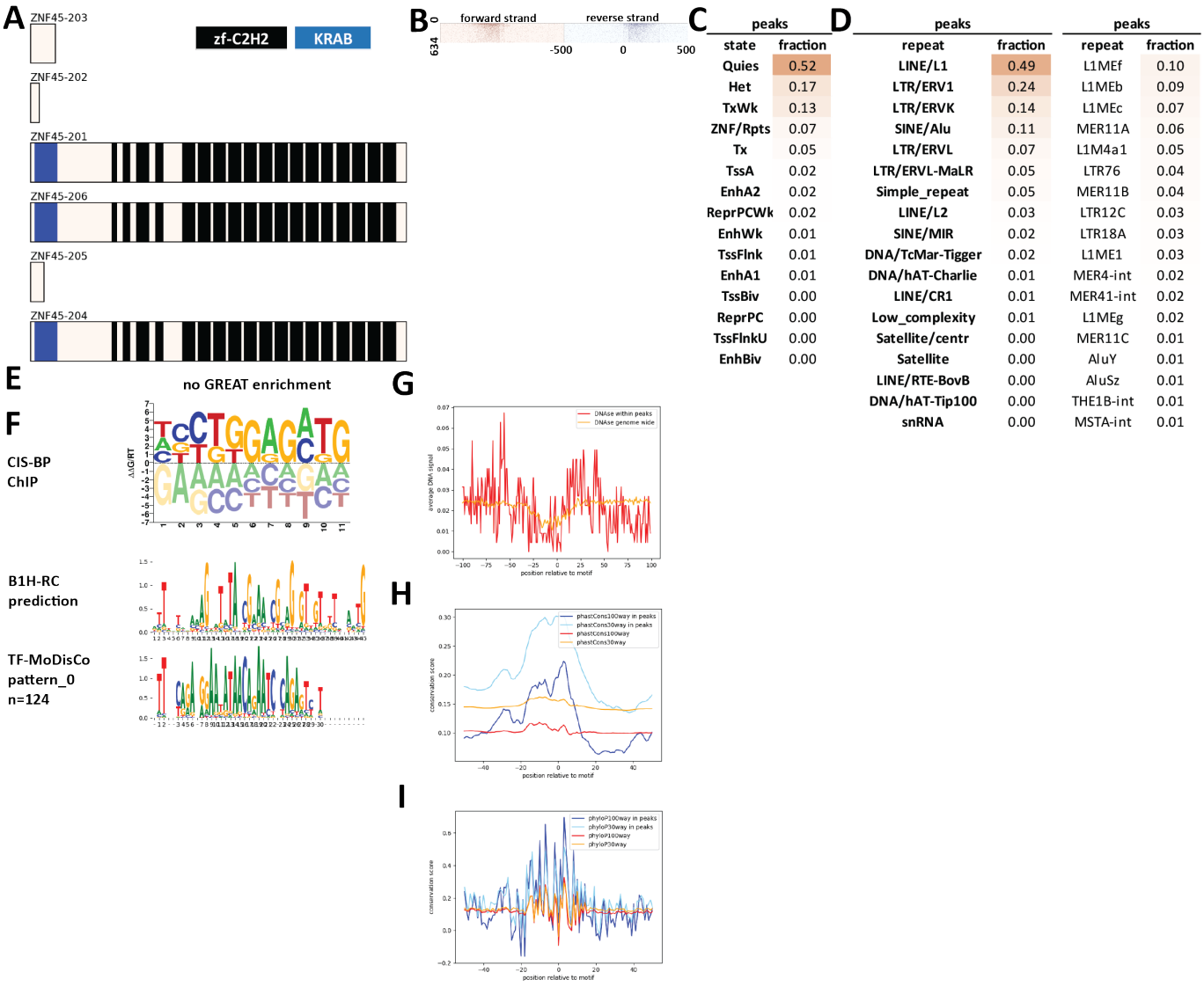

peaks	
state	fraction
Quies	0.52
Het	0.17
TxWk	0.13
ZNF/Rpts	0.07
Tx	0.05
TssA	0.02
EnhA2	0.02
ReprPCWk	0.02
EnhWk	0.01
TssFlnk	0.01
EnhA1	0.01
TssBiv	0.00
ReprPC	0.00
TssFlnkU	0.00
EnhBiv	0.00

peaks		peaks	
repeat	fraction	repeat	fraction
LINE/L1	0.49	L1MEf	0.10
LTR/ERV1	0.24	L1MEb	0.09
LTR/ERVK	0.14	L1MEc	0.07
SINE/Alu	0.11	MER11A	0.06
LTR/ERVL	0.07	L1M4a1	0.05
LTR/ERVL-MaLR	0.05	LTR76	0.04
Simple_repeat	0.05	MER11B	0.04
LINE/L2	0.03	LTR12C	0.03
SINE/MIR	0.02	LTR18A	0.03
DNA/TcMar-Tigger	0.02	L1ME1	0.03
DNA/hAT-Charlie	0.01	MER4-int	0.02
LINE/CR1	0.01	MER41-int	0.02
Low_complexity	0.01	L1MEg	0.02
Satellite/centr	0.00	MER11C	0.01
Satellite	0.00	AluY	0.01
LINE/RTE-BovB	0.00	AluSz	0.01
DNA/hAT-Tip100	0.00	THE1B-int	0.01
snRNA	0.00	MSTA-int	0.01

Supplementary Figure 1239: Properties and genomic distribution of motifs identified for the ZNF45 transcription factor in HEK293 (accession Hughes NB models).

TF-MoDisCO pattern_0 n=124, CWM

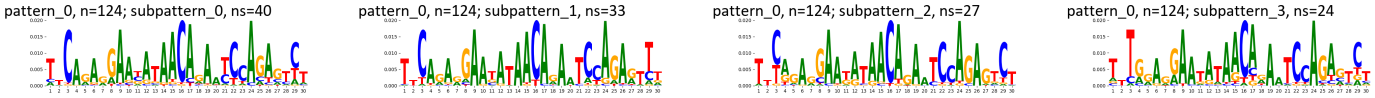

TF-MoDisCO pattern_0 n=124, PWM

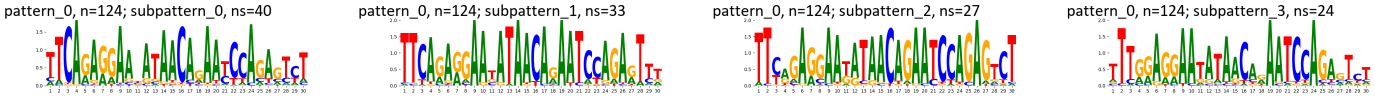

Supplementary Figure 1240: TF-MoDisCO subpatterns for the ZNF45 transcription factor in HEK293 (accession Hughes NB models).

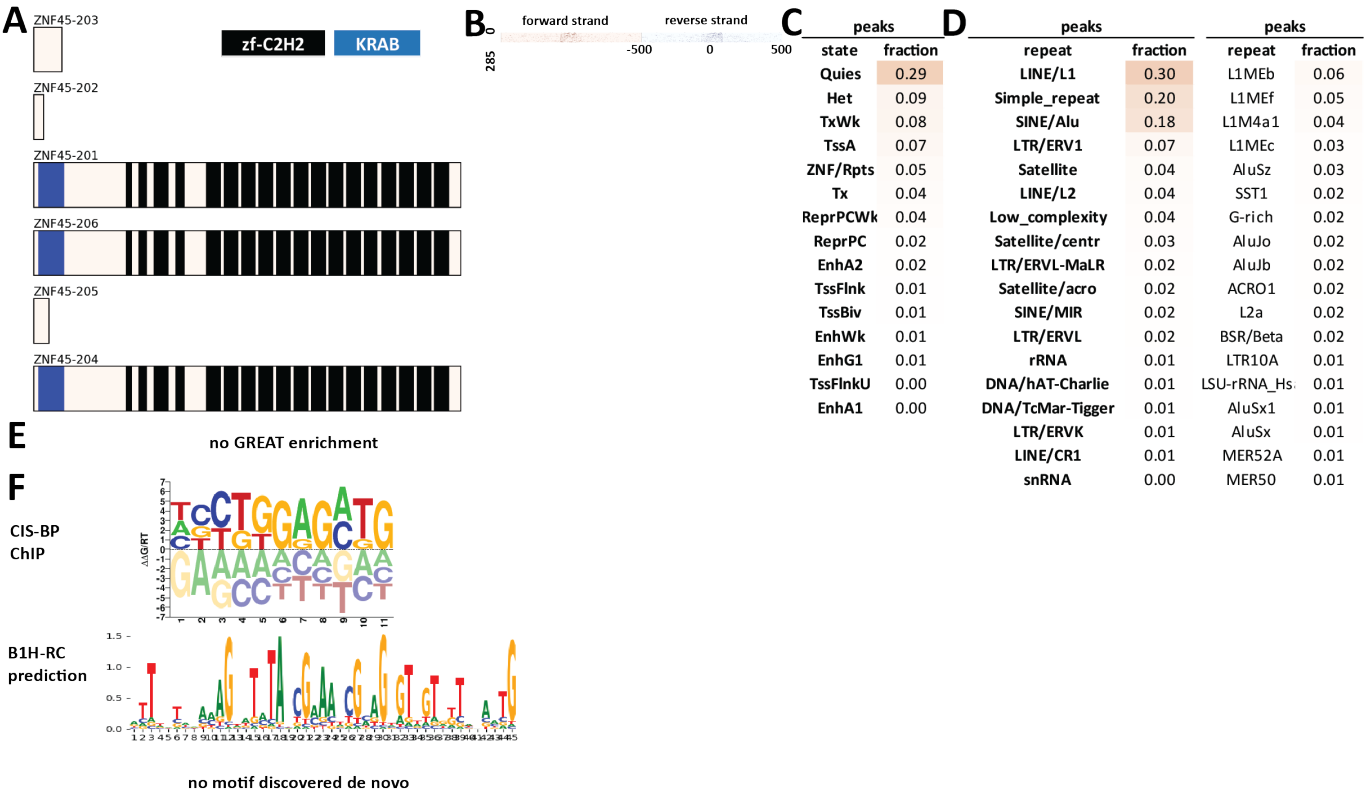

Supplementary Figure 1241: Properties and genomic distribution of motifs identified for the ZNF45 transcription factor in HEK293 (accession ChipExo models).

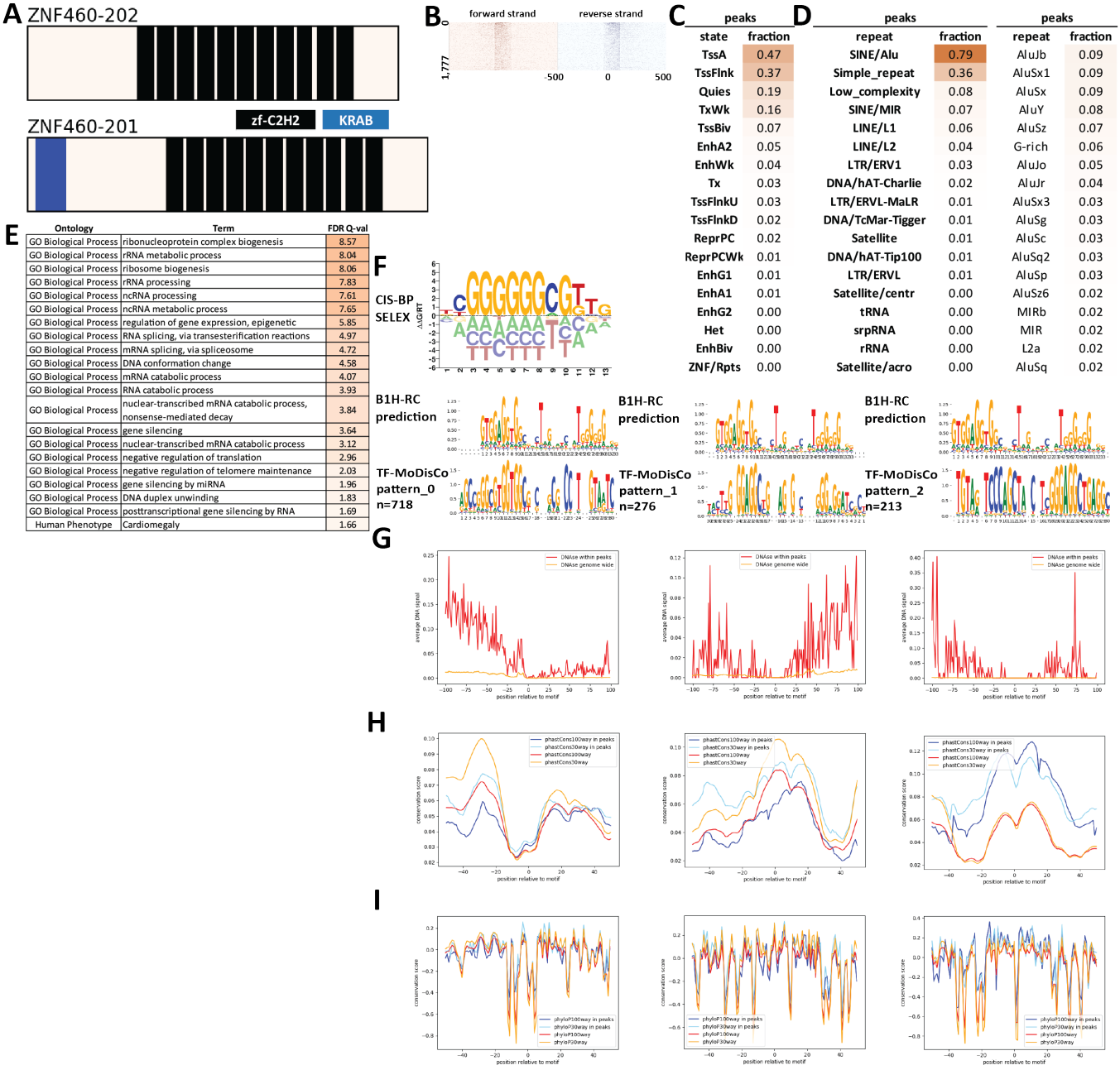

Supplementary Figure 1242: Properties and genomic distribution of motifs identified for the ZNF460 transcription factor in HEK293 (accession ChipExo models).

TF-MoDisCO pattern_0 n=718, CWM

pattern_0, n=718; subpattern_0, ns=178

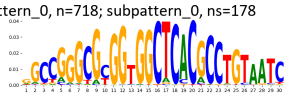

pattern_0, n=718; subpattern_1, ns=170

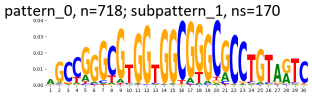

pattern_0, n=718; subpattern_2, ns=144

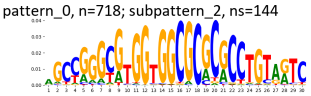

pattern_0, n=718; subpattern_3, ns=98

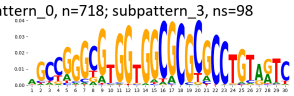

pattern_0, n=718; subpattern_4, ns=67

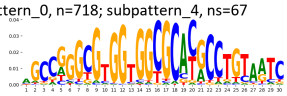

pattern_0, n=718; subpattern_5, ns=61

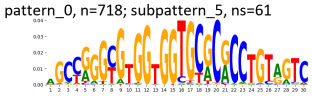

TF-MoDisCO pattern_0 n=718, PWM

pattern_0, n=718; subpattern_0, ns=178

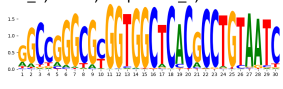

pattern_0, n=718; subpattern_1, ns=170

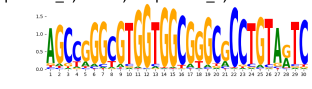

pattern_0, n=718; subpattern_2, ns=144

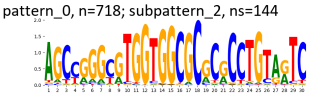

pattern_0, n=718; subpattern_3, ns=98

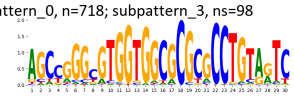

pattern_0, n=718; subpattern_4, ns=67

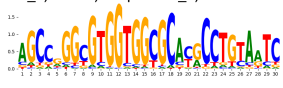

pattern_0, n=718; subpattern_5, ns=61

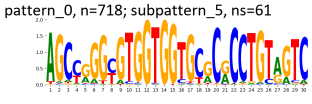

TF-MoDisCO pattern_1 n=276, CWM

pattern_1, n=276; subpattern_0, ns=92

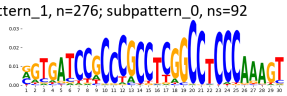

pattern_1, n=276; subpattern_1, ns=79

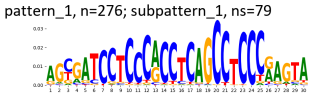

pattern_1, n=276; subpattern_2, ns=76

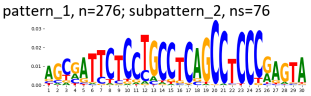

pattern_1, n=276; subpattern_3, ns=27

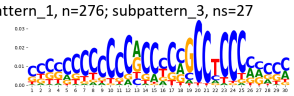

pattern_1, n=276; subpattern_4, ns=2

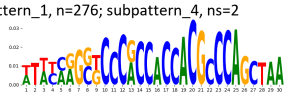

TF-MoDisCO pattern_1 n=276, PWM

pattern_1, n=276; subpattern_0, ns=92

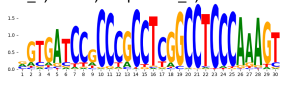

pattern_1, n=276; subpattern_1, ns=79

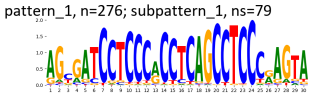

pattern_1, n=276; subpattern_2, ns=76

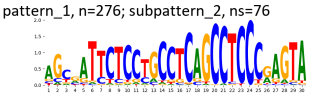

pattern_1, n=276; subpattern_3, ns=27

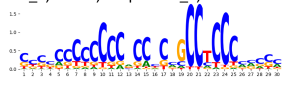

pattern_1, n=276; subpattern_4, ns=2

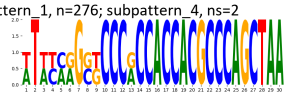

TF-MoDisCO pattern_2 n=213, CWM

pattern_2, n=213; subpattern_0, ns=60

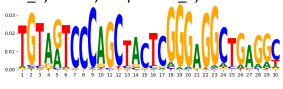

pattern_2, n=213; subpattern_1, ns=55

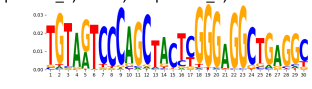

pattern_2, n=213; subpattern_2, ns=38

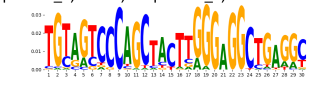

pattern_2, n=213; subpattern_3, ns=29



pattern_2, n=213; subpattern_4, ns=23

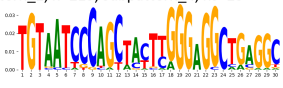

pattern_2, n=213; subpattern_5, ns=8



TF-MoDisCO pattern_2 n=213, PWM

pattern_2, n=213; subpattern_0, ns=60

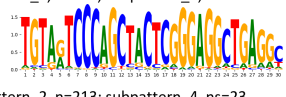

pattern_2, n=213; subpattern_1, ns=55

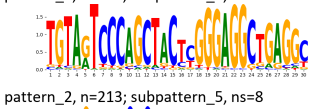

pattern_2, n=213; subpattern_2, ns=38

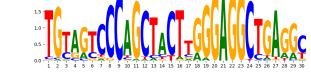

pattern_2, n=213; subpattern_3, ns=29



pattern_2, n=213; subpattern_4, ns=23



pattern_2, n=213; subpattern_5, ns=8



Supplementary Figure 1243: TF-MoDisCO subpatterns for the ZNF460 transcription factor in HEK293 (accession ChipExo models).

A

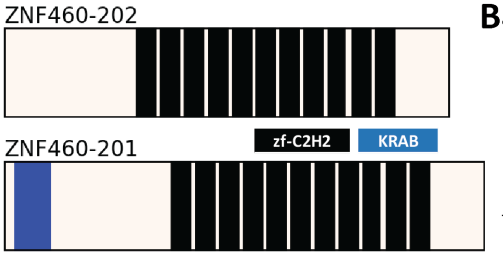

B



C

peaks	
state	fraction
Quies	0.27
TxWk	0.22
TssA	0.12
TssFlnk	0.09
Tx	0.06
EnhWk	0.05
ReprPCWk	0.02
EnhA2	0.02
TssFlnkU	0.01
EnhA1	0.01
TssFlnkD	0.01
ReprPC	0.01
EnhG1	0.01
TssBiv	0.01
Het	0.00
EnhBiv	0.00
EnhG2	0.00
ZNF/Rpts	0.00

D

peaks		peaks	
repeat	fraction	repeat	fraction
SINE/Alu	0.93	AluSx	0.12
LINE/L1	0.15	AluJb	0.11
Simple_repeat	0.11	AluSx1	0.10
SINE/MIR	0.10	AluSz	0.10
LINE/L2	0.08	AluY	0.09
DNA/hAT-Charlie	0.05	AluJr	0.06
LTR/ERV1	0.04	AluJo	0.06
LTR/ERVL-MaLR	0.03	AluSq2	0.06
Low_complexity	0.02	AluSp	0.04
LTR/ERVL	0.02	AluSz6	0.04
DNA/TcMar-Tigger	0.02	AluSg	0.04
DNA/hAT-Tip100	0.01	AluSc	0.04
LINE/CR1	0.01	MIRb	0.04
DNA/hAT-Blackjack	0.00	L2a	0.03
LTR/ERVK	0.00	AluSx3	0.03
tRNA	0.00	MIR	0.03
Retroposon/SVA	0.00	AluSq	0.02
DNA/TcMar-Mariner	0.00	L2b	0.02

E

Ontology	Term	FDR Q-val
GO Biological Process	viral life cycle	84.72
GO Biological Process	regulation of intrinsic apoptotic signaling pathway	60.84
GO Biological Process	mitochondrial transport	57.08
GO Biological Process	mRNA catabolic process	54.13
GO Biological Process	multi-organism metabolic process	53.30
GO Biological Process	regulation of mRNA stability	52.84
GO Biological Process	nuclear-transcribed mRNA catabolic process	51.39
GO Biological Process	cellular response to insulin stimulus	49.23
GO Biological Process	RNA catabolic process	47.49
GO Biological Process	regulation of RNA stability	47.46
GO Biological Process	regulation of hematopoietic progenitor cell differentiation	47.02
GO Biological Process	regulation of transcription from RNA polymerase II promoter in response to stress	46.56
GO Biological Process	nuclear-transcribed mRNA catabolic process, nonsense-mediated decay	45.94
GO Biological Process	negative regulation of intrinsic apoptotic signaling pathway	42.81
GO Biological Process	viral gene expression	42.73
GO Biological Process	regulation of DNA-templated transcription in response to stress	41.47
GO Biological Process	rRNA processing	40.90
GO Biological Process	rRNA metabolic process	39.63
GO Biological Process	interaction with host	39.13
GO Biological Process	macroautophagy	38.76
Human Phenotype	Hypoglycemia	22.28
Human Phenotype	Increased serum ferritin	11.55
Human Phenotype	Leukodystrophy	8.15

F

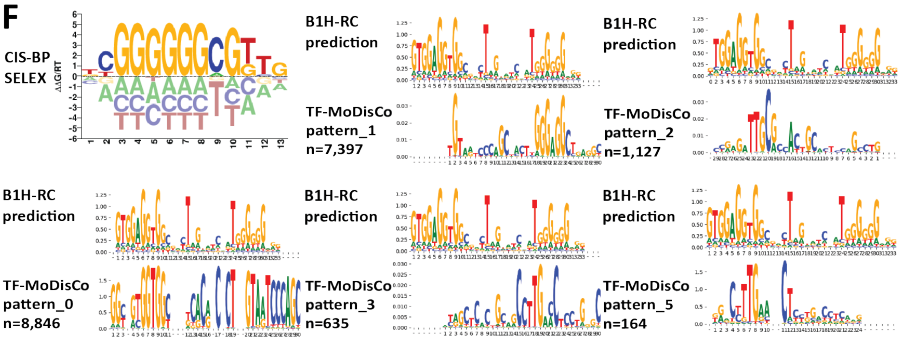

G

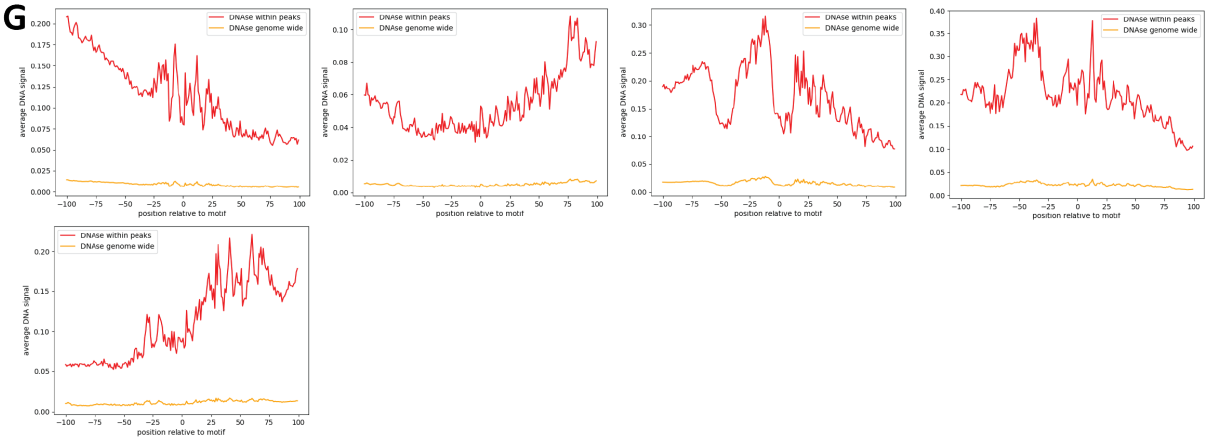

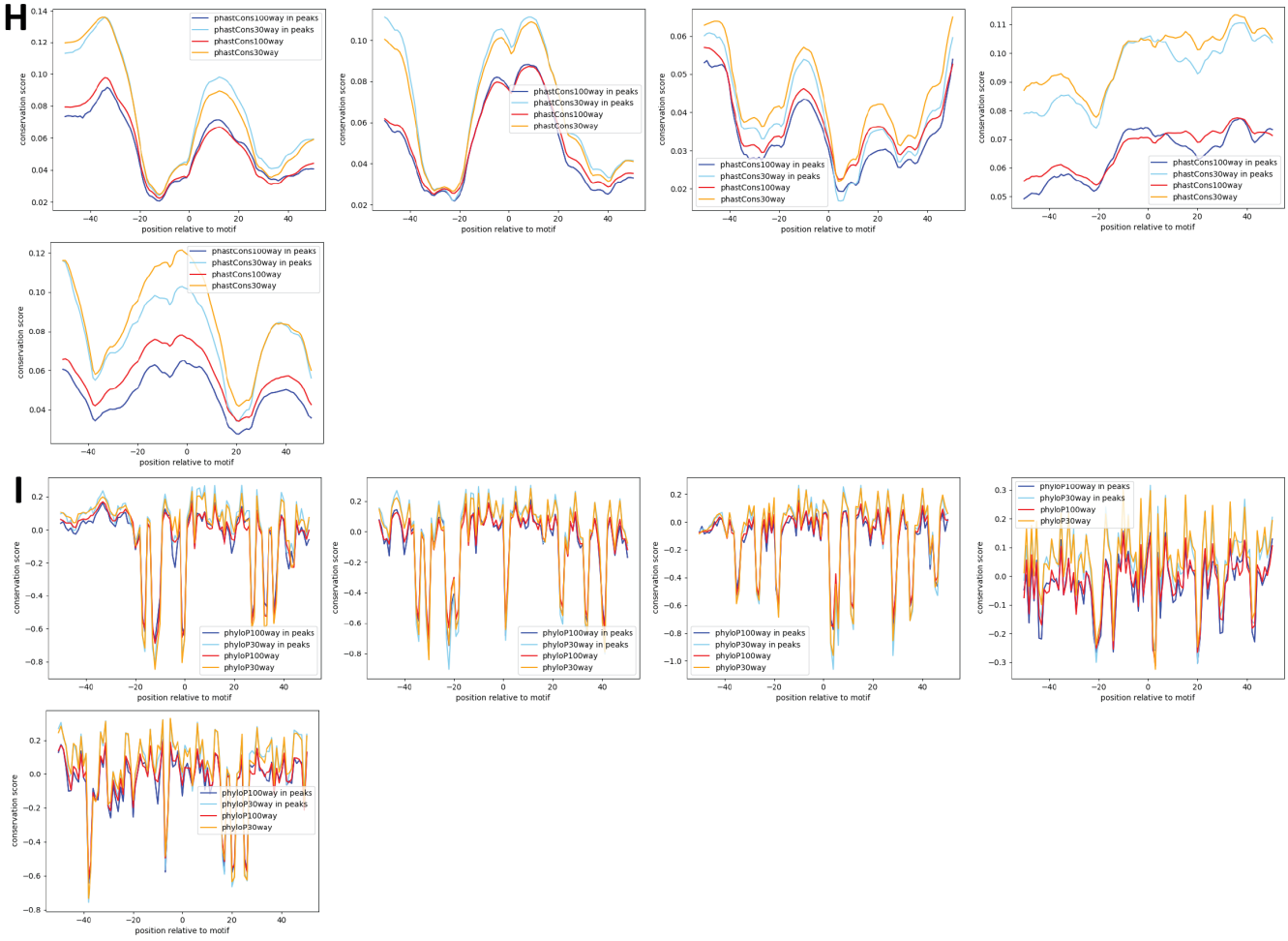

Supplementary Figure 1244: Properties and genomic distribution of motifs identified for the ZNF460 transcription factor in HepG2 (accession ENCSR261UIH).

TF-MoDisCO pattern_0 n=8846, CWM

pattern_0, n=8846; subpattern_0, ns=2095

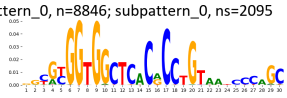

pattern_0, n=8846; subpattern_1, ns=1480

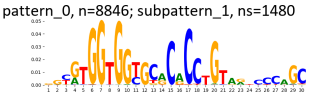

pattern_0, n=8846; subpattern_2, ns=1256

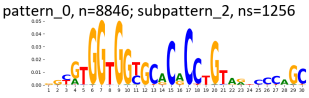

pattern_0, n=8846; subpattern_3, ns=1163

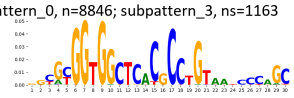

pattern_0, n=8846; subpattern_4, ns=955

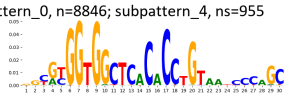

pattern_0, n=8846; subpattern_5, ns=723

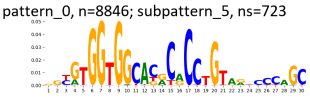

pattern_0, n=8846; subpattern_6, ns=705

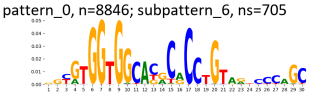

pattern_0, n=8846; subpattern_7, ns=399

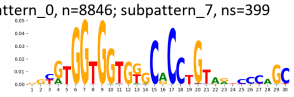

pattern_0, n=8846; subpattern_8, ns=70

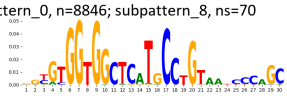

TF-MoDisCO pattern_0 n=8846, PWM

pattern_0, n=8846; subpattern_0, ns=2095

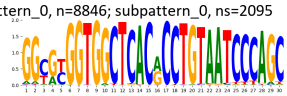

pattern_0, n=8846; subpattern_1, ns=1480

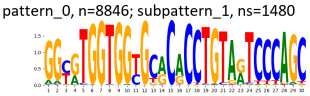

pattern_0, n=8846; subpattern_2, ns=1256

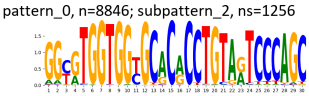

pattern_0, n=8846; subpattern_3, ns=1163

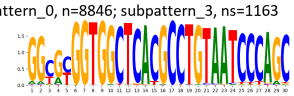

pattern_0, n=8846; subpattern_4, ns=955

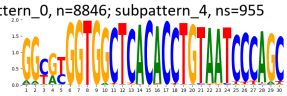

pattern_0, n=8846; subpattern_5, ns=723

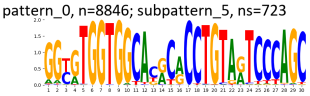

pattern_0, n=8846; subpattern_6, ns=705

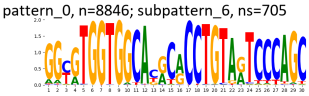

pattern_0, n=8846; subpattern_7, ns=399

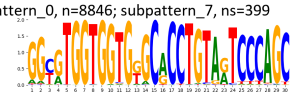

pattern_0, n=8846; subpattern_8, ns=70

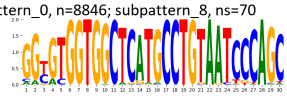

TF-MoDisCO pattern_1 n=7397, CWM

pattern_1, n=7397; subpattern_0, ns=2364

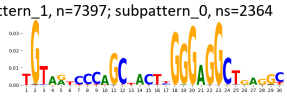

pattern_1, n=7397; subpattern_1, ns=1559

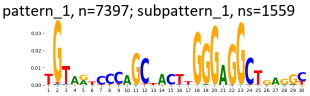

pattern_1, n=7397; subpattern_2, ns=1003

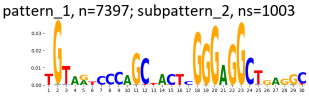

pattern_1, n=7397; subpattern_3, ns=1000

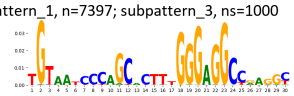

pattern_1, n=7397; subpattern_4, ns=619

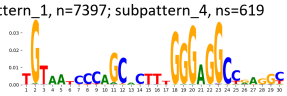

pattern_1, n=7397; subpattern_5, ns=430

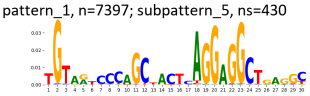

pattern_1, n=7397; subpattern_6, ns=422

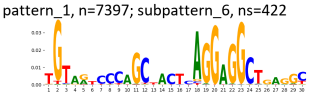

TF-MoDisCO pattern_1 n=7397, PWM

pattern_1, n=7397; subpattern_0, ns=2364

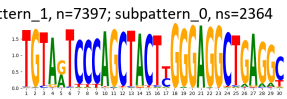

pattern_1, n=7397; subpattern_1, ns=1559

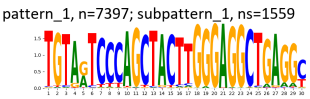

pattern_1, n=7397; subpattern_2, ns=1003

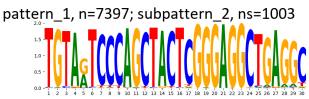

pattern_1, n=7397; subpattern_3, ns=1000

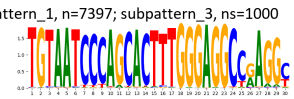

pattern_1, n=7397; subpattern_4, ns=619

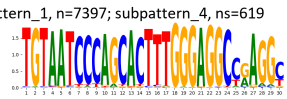

pattern_1, n=7397; subpattern_5, ns=430

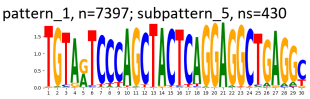

pattern_1, n=7397; subpattern_6, ns=422

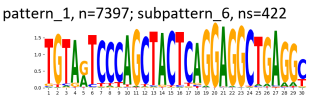

TF-MoDisCO pattern_2 n=1127, CWM

pattern_2, n=1127; subpattern_0, ns=367



pattern_2, n=1127; subpattern_1, ns=357

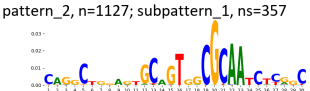

pattern_2, n=1127; subpattern_2, ns=169

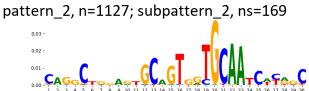

pattern_2, n=1127; subpattern_3, ns=109

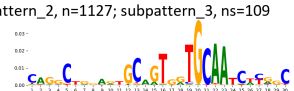

pattern_2, n=1127; subpattern_4, ns=97

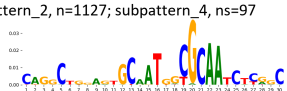

pattern_2, n=1127; subpattern_5, ns=22



pattern_2, n=1127; subpattern_6, ns=6

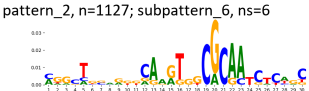

TF-MoDisCO pattern_2 n=1127, PWM

pattern_2, n=1127; subpattern_0, ns=367

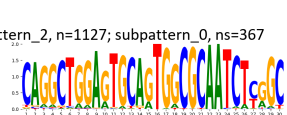

pattern_2, n=1127; subpattern_1, ns=357

pattern_2, n=1127; subpattern_2, ns=169

pattern_2, n=1127; subpattern_3, ns=109

pattern_2, n=1127; subpattern_4, ns=97

pattern_2, n=1127; subpattern_5, ns=22

pattern_2, n=1127; subpattern_6, ns=6

TF-MoDisCO pattern_3 n=635, CWM

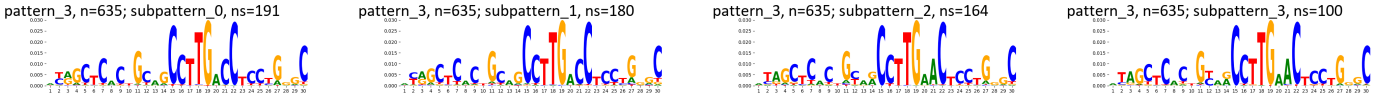

TF-MoDisCO pattern_3 n=635, PWM

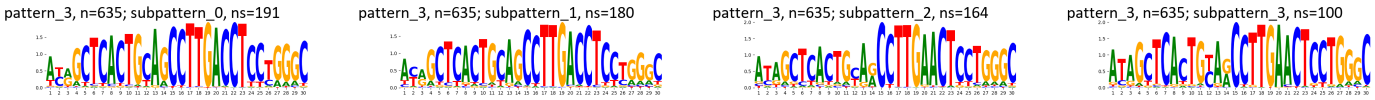

TF-MoDisCO pattern_5 n=164, CWM

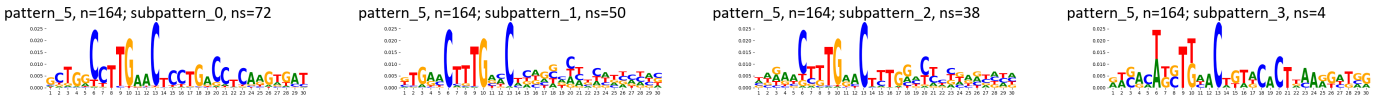

TF-MoDisCO pattern_5 n=164, PWM

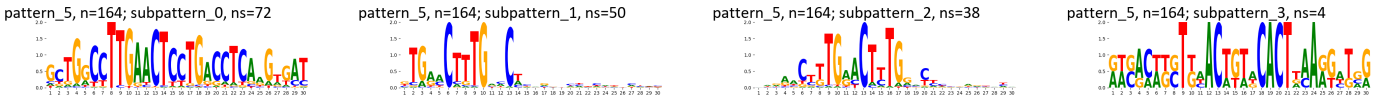

Supplementary Figure 1245: TF-MoDisCO subpatterns for the ZNF460 transcription factor in HepG2 (accession ENCSR261UIH).

A

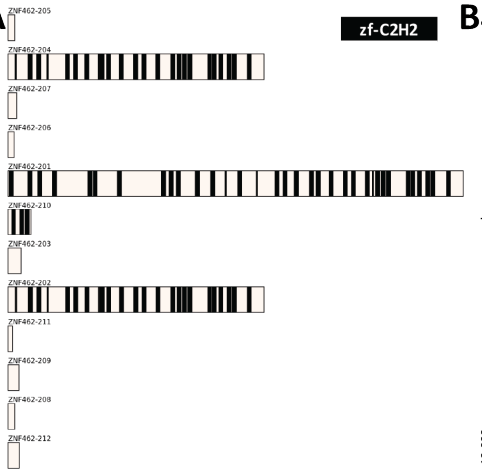

B

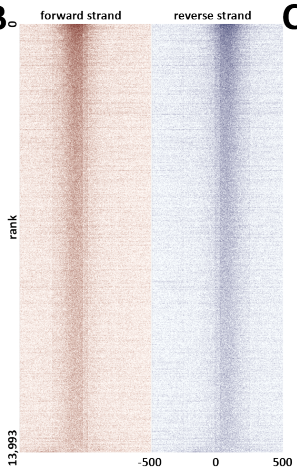

C

peaks	
state	fraction
Quies	0.50
TxWk	0.10
EnhWk	0.08
ReprPCWk	0.02
TssFlnk	0.02
Tx	0.02
EnhA1	0.02
ReprPC	0.02
TssA	0.02
EnhA2	0.01
TssBiv	0.01
Het	0.01
TssFlnkD	0.00
TssFlnkU	0.00
EnhBiv	0.00
EnhG1	0.00
EnhG2	0.00
ZNF/Rpts	0.00

D

peaks		peaks	
repeat	fraction	repeat	fraction
LTR/ERV1	0.10	L2a	0.03
LINE/L2	0.07	L2c	0.02
LINE/L1	0.07	MIRb	0.02
LTR/ERVL-MaLR	0.07	L2b	0.02
LTR/ERVL	0.06	MIR3	0.01
SINE/MIR	0.06	MIR	0.01
DNA/hAT-Charlie	0.04	MER5A	0.01
Simple_repeat	0.04	MER5A1	0.01
SINE/Alu	0.03	MIRc	0.01
LINE/CR1	0.01	L2	0.01
Low_complexity	0.01	MLT1D	0.01
LTR/ERVK	0.01	L3	0.01
DNA/hAT-Tip100	0.01	MER21C	0.01
DNA/TcMar-Tigger	0.01	LTR33	0.01
LTR/Gypsy	0.01	GA-rich	0.00
LTR/Gypsy?	0.00	MER4D	0.00
DNA/hAT-Blackjack	0.00	MER5B	0.00
Unknown	0.00	LTR7	0.00

E

Ontology	Term	FDR Q-val
GO Biological Process	primitive streak formation	5.82
GO Biological Process	cellular response to macrophage colony-stimulating factor stimulus	4.24

F

no CIS-BP motif available

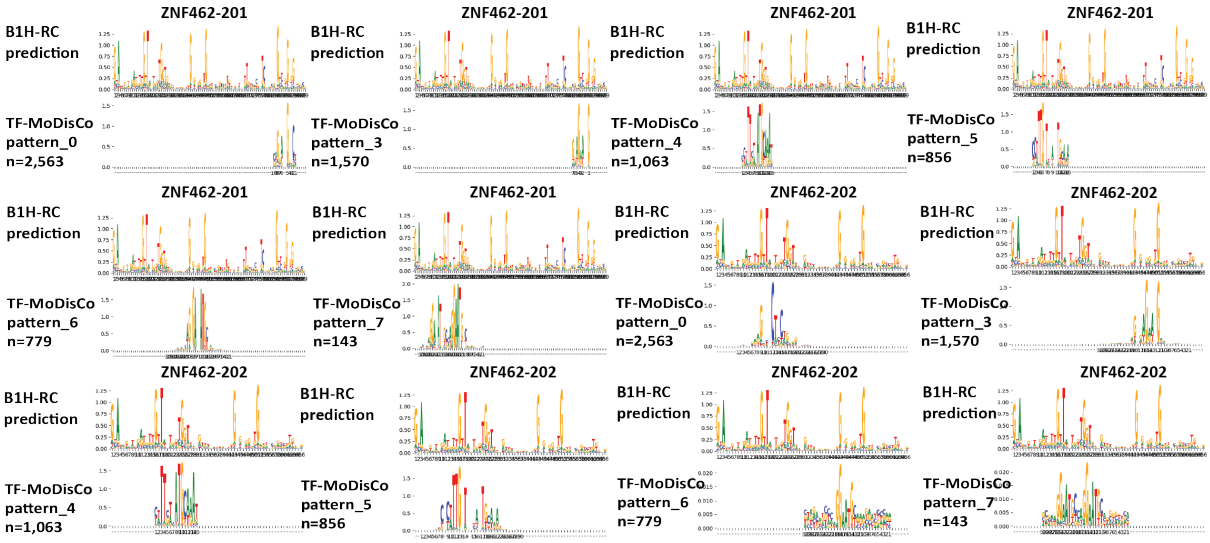

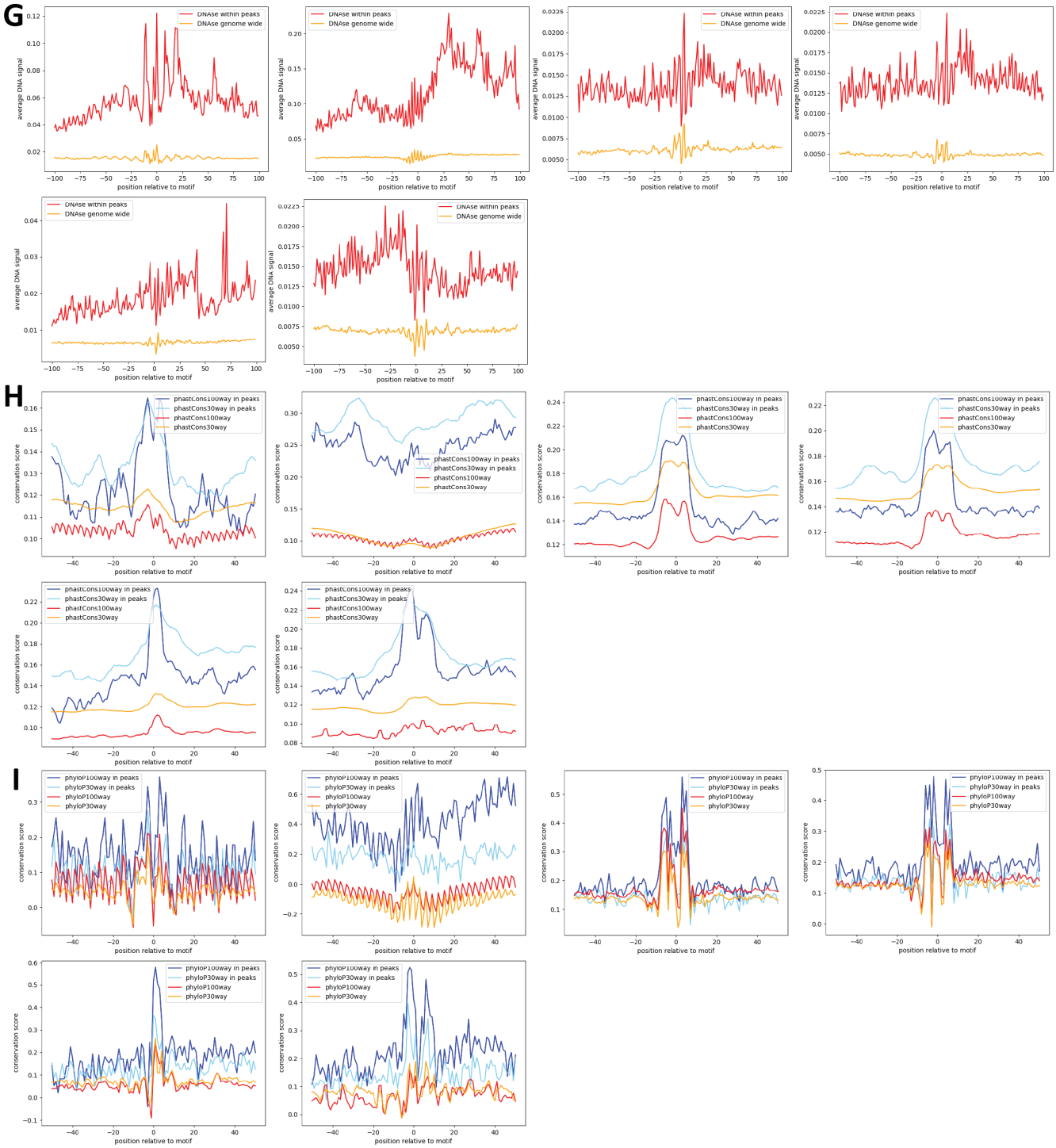

Supplementary Figure 1246: Properties and genomic distribution of motifs identified for the ZNF462 transcription factor in GM23338 (accession ENCSR334UWP).

TF-MoDisCO pattern_0 n=2563, CWM

pattern_0, n=2563; subpattern_0, ns=628

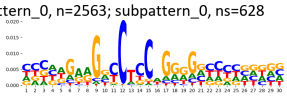

pattern_0, n=2563; subpattern_1, ns=478

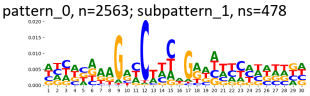

pattern_0, n=2563; subpattern_2, ns=473

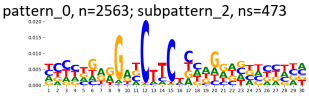

pattern_0, n=2563; subpattern_3, ns=375

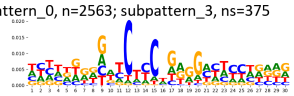

pattern_0, n=2563; subpattern_4, ns=199

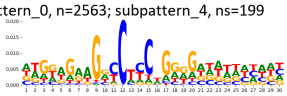

pattern_0, n=2563; subpattern_5, ns=129

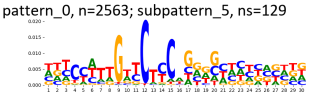

pattern_0, n=2563; subpattern_6, ns=105

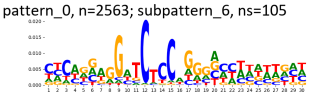

pattern_0, n=2563; subpattern_7, ns=94

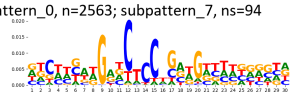

pattern_0, n=2563; subpattern_8, ns=82

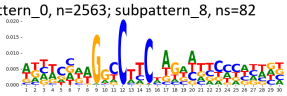

TF-MoDisCO pattern_0 n=2563, PWM

pattern_0, n=2563; subpattern_0, ns=628

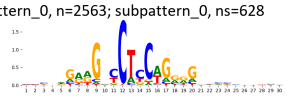

pattern_0, n=2563; subpattern_1, ns=478

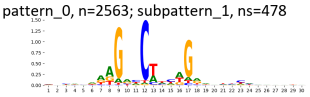

pattern_0, n=2563; subpattern_2, ns=473

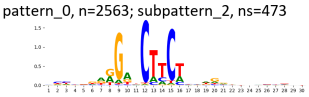

pattern_0, n=2563; subpattern_3, ns=375

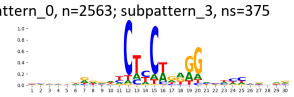

pattern_0, n=2563; subpattern_4, ns=199

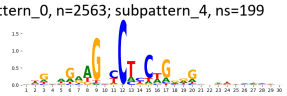

pattern_0, n=2563; subpattern_5, ns=129

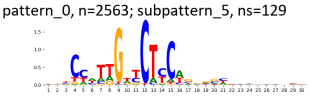

pattern_0, n=2563; subpattern_6, ns=105

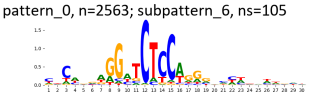

pattern_0, n=2563; subpattern_7, ns=94

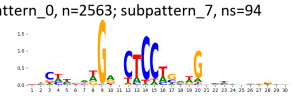

pattern_0, n=2563; subpattern_8, ns=82

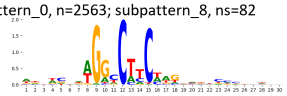

TF-MoDisCO pattern_3 n=1570, CWM

pattern_3, n=1570; subpattern_0, ns=293

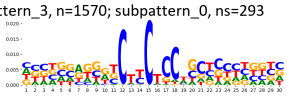

pattern_3, n=1570; subpattern_1, ns=257

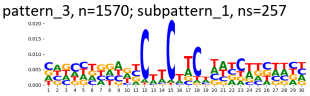

pattern_3, n=1570; subpattern_10, ns=4

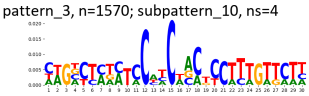

pattern_3, n=1570; subpattern_11, ns=2

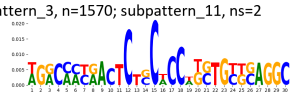

pattern_3, n=1570; subpattern_2, ns=195

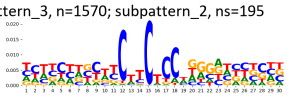

pattern_3, n=1570; subpattern_3, ns=181

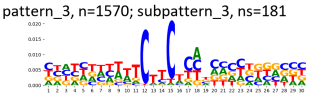

pattern_3, n=1570; subpattern_4, ns=149

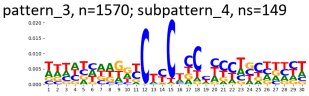

pattern_3, n=1570; subpattern_5, ns=148

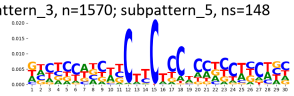

pattern_3, n=1570; subpattern_6, ns=111

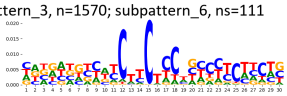

pattern_3, n=1570; subpattern_7, ns=96

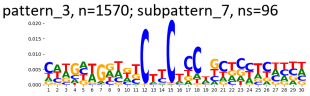

pattern_3, n=1570; subpattern_8, ns=82

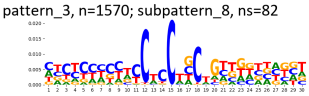

pattern_3, n=1570; subpattern_9, ns=52

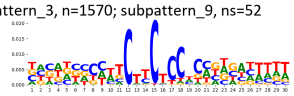

TF-MoDisCO pattern_3 n=1570, PWM

pattern_3, n=1570; subpattern_0, ns=293

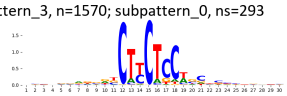

pattern_3, n=1570; subpattern_1, ns=257

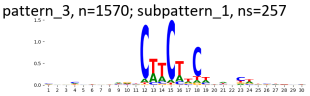

pattern_3, n=1570; subpattern_10, ns=4

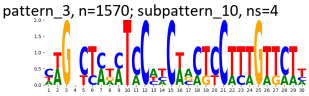

pattern_3, n=1570; subpattern_11, ns=2

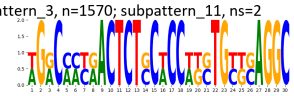

pattern_3, n=1570; subpattern_2, ns=195

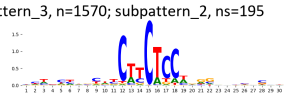

pattern_3, n=1570; subpattern_3, ns=181

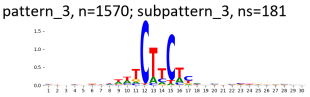

pattern_3, n=1570; subpattern_4, ns=149

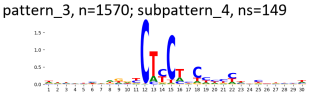

pattern_3, n=1570; subpattern_5, ns=148

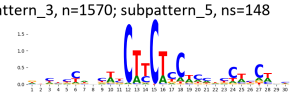

pattern_3, n=1570; subpattern_6, ns=111

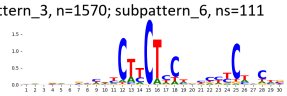

pattern_3, n=1570; subpattern_7, ns=96

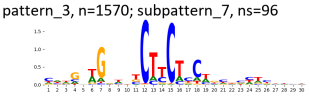

pattern_3, n=1570; subpattern_8, ns=82

pattern_3, n=1570; subpattern_9, ns=52

TF-MoDisCO pattern_4 n=1063, CWM

pattern_4, n=1063; subpattern_0, ns=277

pattern_4, n=1063; subpattern_1, ns=264

pattern_4, n=1063; subpattern_2, ns=186

pattern_4, n=1063; subpattern_3, ns=126

pattern_4, n=1063; subpattern_4, ns=122

pattern_4, n=1063; subpattern_5, ns=88

TF-MoDisCO pattern_4 n=1063, PWM

pattern_4, n=1063; subpattern_0, ns=277

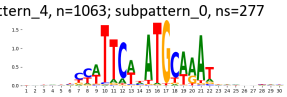

pattern_4, n=1063; subpattern_1, ns=264

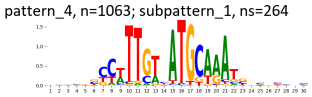

pattern_4, n=1063; subpattern_2, ns=186

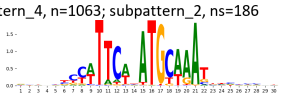

pattern_4, n=1063; subpattern_3, ns=126

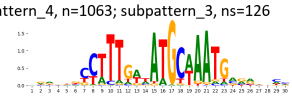

pattern_4, n=1063; subpattern_4, ns=122

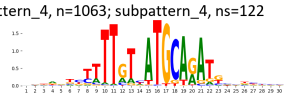

pattern_4, n=1063; subpattern_5, ns=88

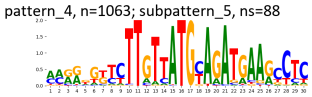

TF-MoDisCO pattern_5 n=856, CWM

pattern_5, n=856; subpattern_0, ns=223

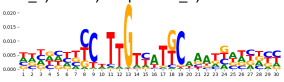

pattern_5, n=856; subpattern_1, ns=205

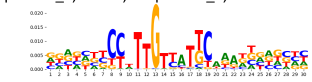

pattern_5, n=856; subpattern_2, ns=120

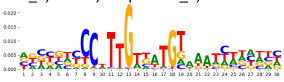

pattern_5, n=856; subpattern_3, ns=120

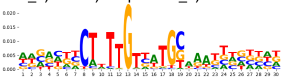

pattern_5, n=856; subpattern_4, ns=117

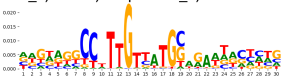

pattern_5, n=856; subpattern_5, ns=71

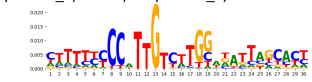

TF-MoDisCO pattern_5 n=856, PWM

pattern_5, n=856; subpattern_0, ns=223

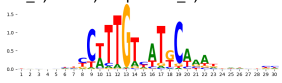

pattern_5, n=856; subpattern_1, ns=205

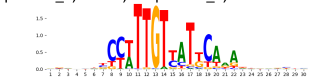

pattern_5, n=856; subpattern_2, ns=120

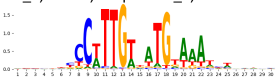

pattern_5, n=856; subpattern_3, ns=120

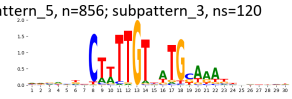

pattern_5, n=856; subpattern_4, ns=117

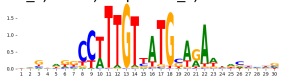

pattern_5, n=856; subpattern_5, ns=71

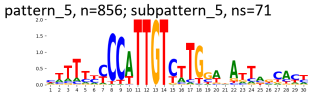

TF-MoDisCO pattern_6 n=779, CWM

pattern_6, n=779; subpattern_0, ns=188

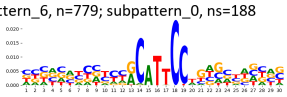

pattern_6, n=779; subpattern_1, ns=146

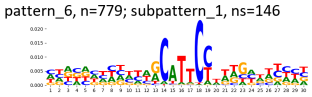

pattern_6, n=779; subpattern_2, ns=142

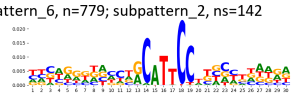

pattern_6, n=779; subpattern_3, ns=121

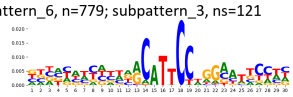

pattern_6, n=779; subpattern_4, ns=102

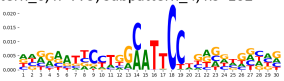

pattern_6, n=779; subpattern_5, ns=78

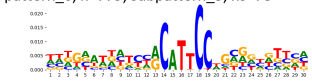

pattern_6, n=779; subpattern_6, ns=2

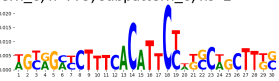

TF-MoDisCO pattern_6 n=779, PWM

pattern_6, n=779; subpattern_0, ns=188

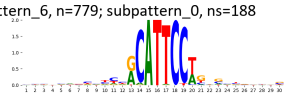

pattern_6, n=779; subpattern_1, ns=146

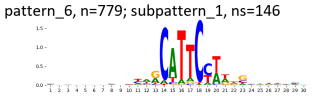

pattern_6, n=779; subpattern_2, ns=142

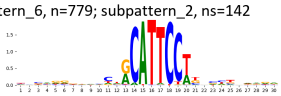

pattern_6, n=779; subpattern_3, ns=121

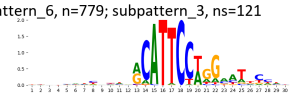

pattern_6, n=779; subpattern_4, ns=102

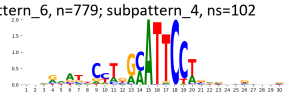

pattern_6, n=779; subpattern_5, ns=78

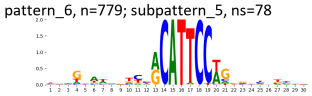

pattern_6, n=779; subpattern_6, ns=2

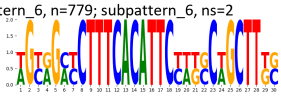

TF-MoDisCO pattern_7 n=143, CWM

pattern_7, n=143; subpattern_0, ns=61

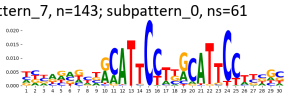

pattern_7, n=143; subpattern_1, ns=39

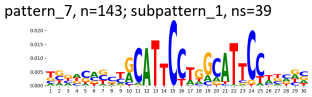

pattern_7, n=143; subpattern_2, ns=32

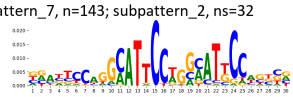

pattern_7, n=143; subpattern_3, ns=6

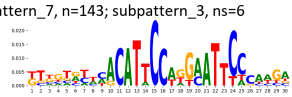

pattern_7, n=143; subpattern_4, ns=5

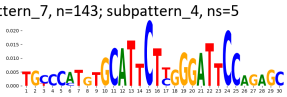

TF-MoDisCO pattern_7 n=143, PWM

pattern_7, n=143; subpattern_0, ns=61

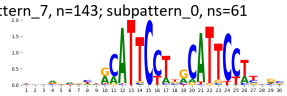

pattern_7, n=143; subpattern_1, ns=39

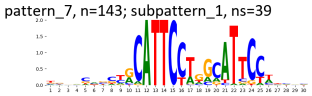

pattern_7, n=143; subpattern_2, ns=32

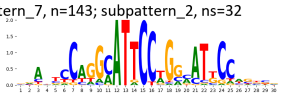

pattern_7, n=143; subpattern_3, ns=6

pattern_7, n=143; subpattern_4, ns=5

Supplementary Figure 1247: TF-MoDisCO subpatterns for the ZNF462 transcription factor in GM23338 (accession ENCSR334UWP).

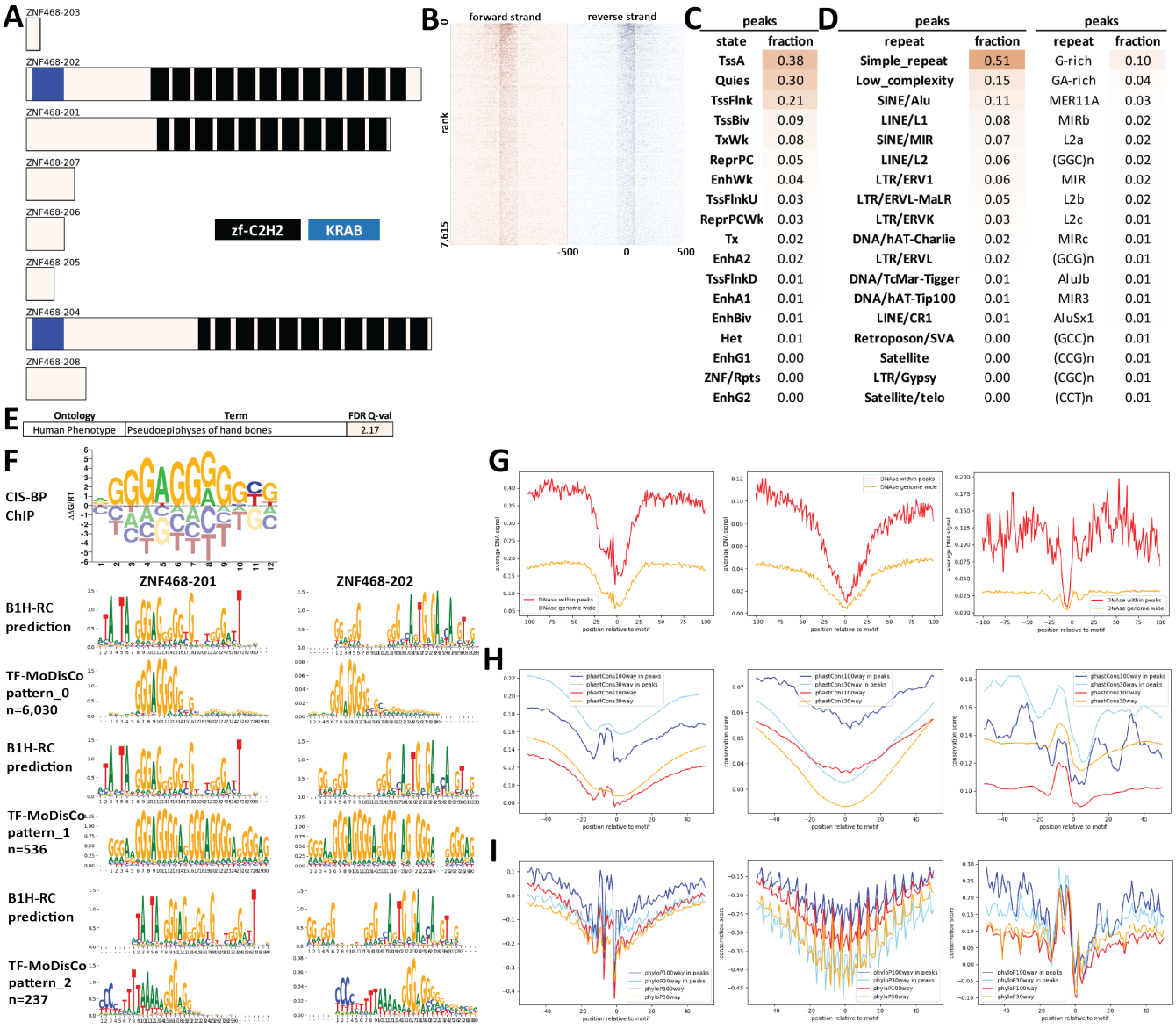

Supplementary Figure 1248: Properties and genomic distribution of motifs identified for the ZNF468 transcription factor in HEK293 (accession ChipExo models).

TF-MoDisCO pattern_0 n=6030, CWM

pattern_0, n=6030; subpattern_0, ns=1311

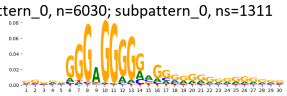

pattern_0, n=6030; subpattern_1, ns=1021

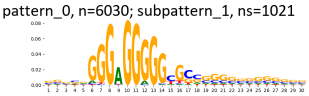

pattern_0, n=6030; subpattern_2, ns=894

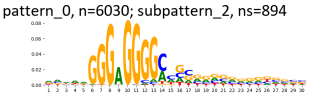

pattern_0, n=6030; subpattern_3, ns=866

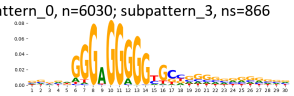

pattern_0, n=6030; subpattern_4, ns=774

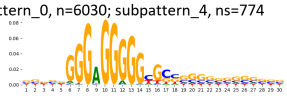

pattern_0, n=6030; subpattern_5, ns=629

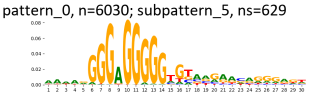

pattern_0, n=6030; subpattern_6, ns=519

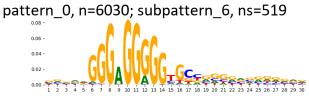

pattern_0, n=6030; subpattern_7, ns=16

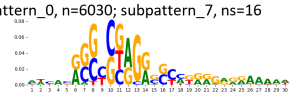

TF-MoDisCO pattern_0 n=6030, PWM

pattern_0, n=6030; subpattern_0, ns=1311

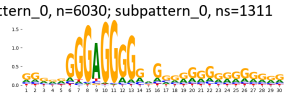

pattern_0, n=6030; subpattern_1, ns=1021

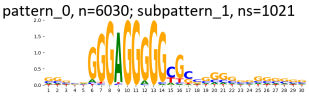

pattern_0, n=6030; subpattern_2, ns=894

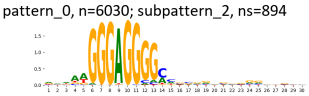

pattern_0, n=6030; subpattern_3, ns=866

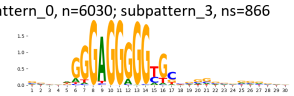

pattern_0, n=6030; subpattern_4, ns=774

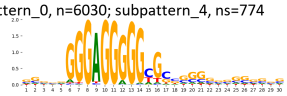

pattern_0, n=6030; subpattern_5, ns=629

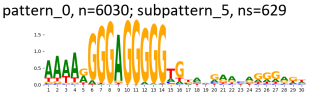

pattern_0, n=6030; subpattern_6, ns=519

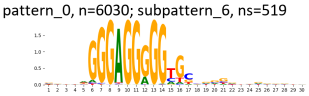

pattern_0, n=6030; subpattern_7, ns=16

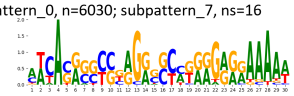

TF-MoDisCO pattern_1 n=536, CWM

pattern_1, n=536; subpattern_0, ns=139

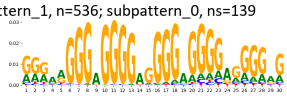

pattern_1, n=536; subpattern_1, ns=125

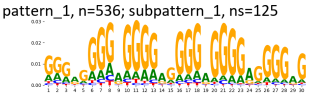

pattern_1, n=536; subpattern_2, ns=102

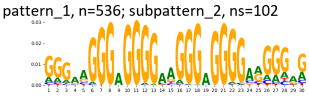

pattern_1, n=536; subpattern_3, ns=70

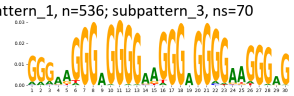

pattern_1, n=536; subpattern_4, ns=62

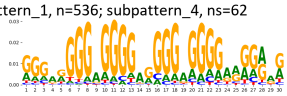

pattern_1, n=536; subpattern_5, ns=38

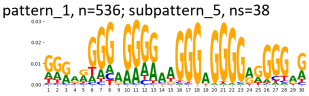

TF-MoDisCO pattern_1 n=536, PWM

pattern_1, n=536; subpattern_0, ns=139

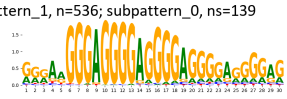

pattern_1, n=536; subpattern_1, ns=125

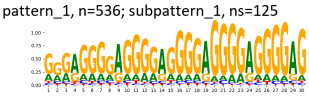

pattern_1, n=536; subpattern_2, ns=102

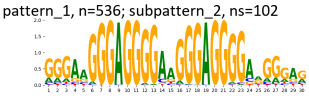

pattern_1, n=536; subpattern_3, ns=70

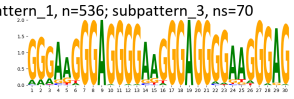

pattern_1, n=536; subpattern_4, ns=62

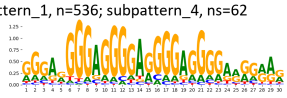

pattern_1, n=536; subpattern_5, ns=38

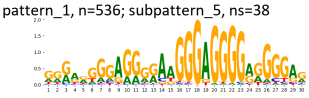

TF-MoDisCO pattern_2 n=237, CWM

pattern_2, n=237; subpattern_0, ns=77

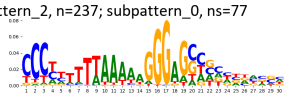

pattern_2, n=237; subpattern_1, ns=60

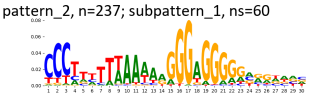

pattern_2, n=237; subpattern_2, ns=52

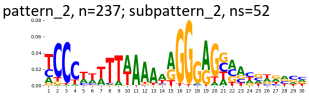

pattern_2, n=237; subpattern_3, ns=40

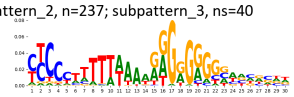

pattern_2, n=237; subpattern_4, ns=8

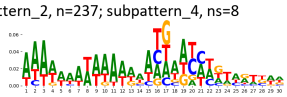

TF-MoDisCO pattern_2 n=237, PWM

pattern_2, n=237; subpattern_0, ns=77

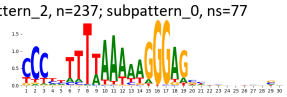

pattern_2, n=237; subpattern_1, ns=60

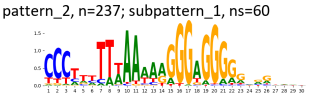

pattern_2, n=237; subpattern_2, ns=52

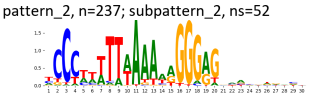

pattern_2, n=237; subpattern_3, ns=40

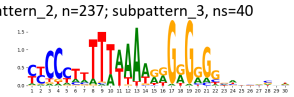

pattern_2, n=237; subpattern_4, ns=8

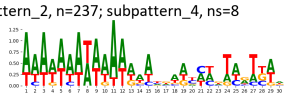

Supplementary Figure 1249: TF-MoDisCO subpatterns for the ZNF468 transcription factor in HEK293 (accession ChipExo models).

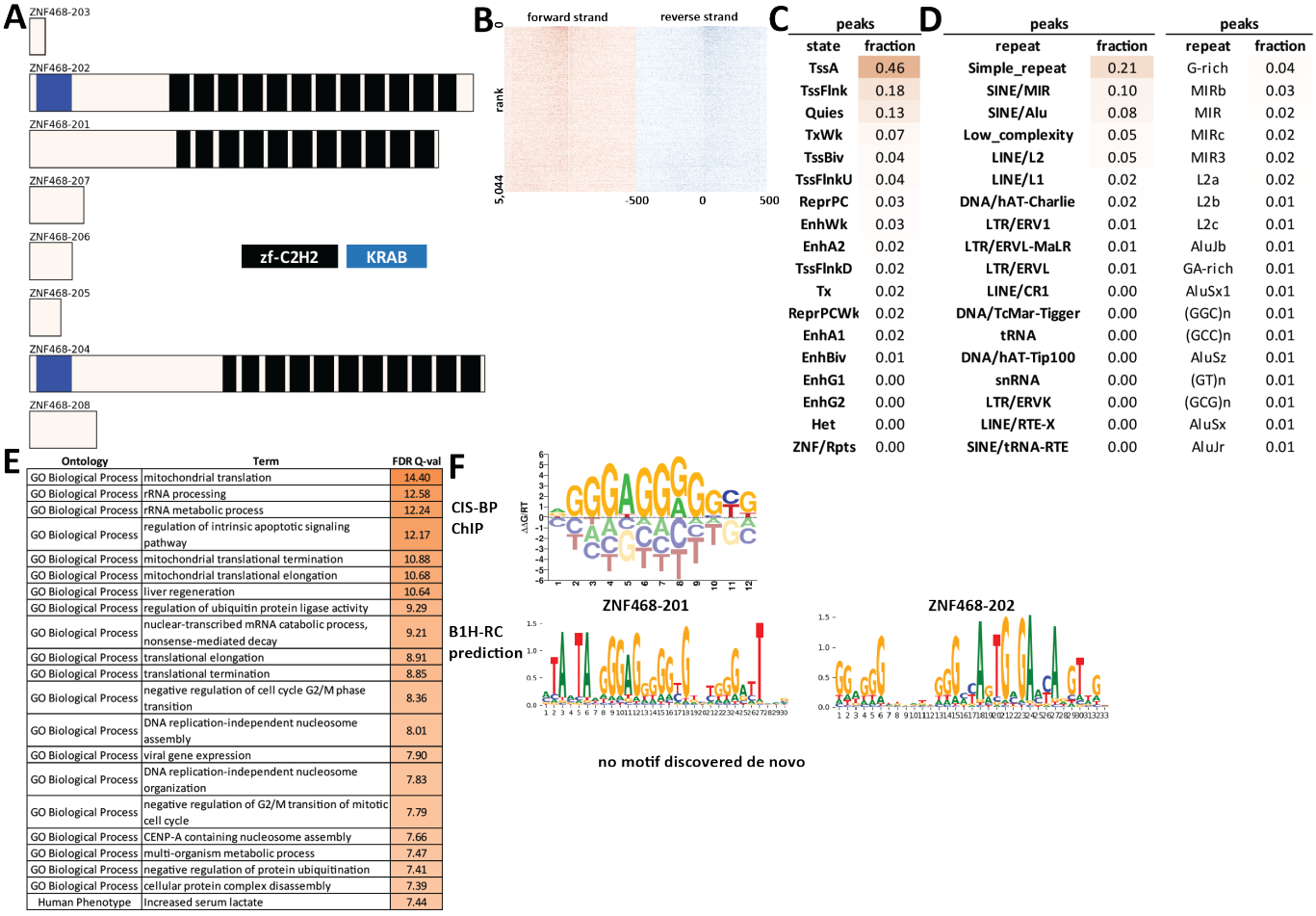

Supplementary Figure 1250: Properties and genomic distribution of motifs identified for the ZNF468 transcription factor in HepG2 (accession ENCSR613YQN).

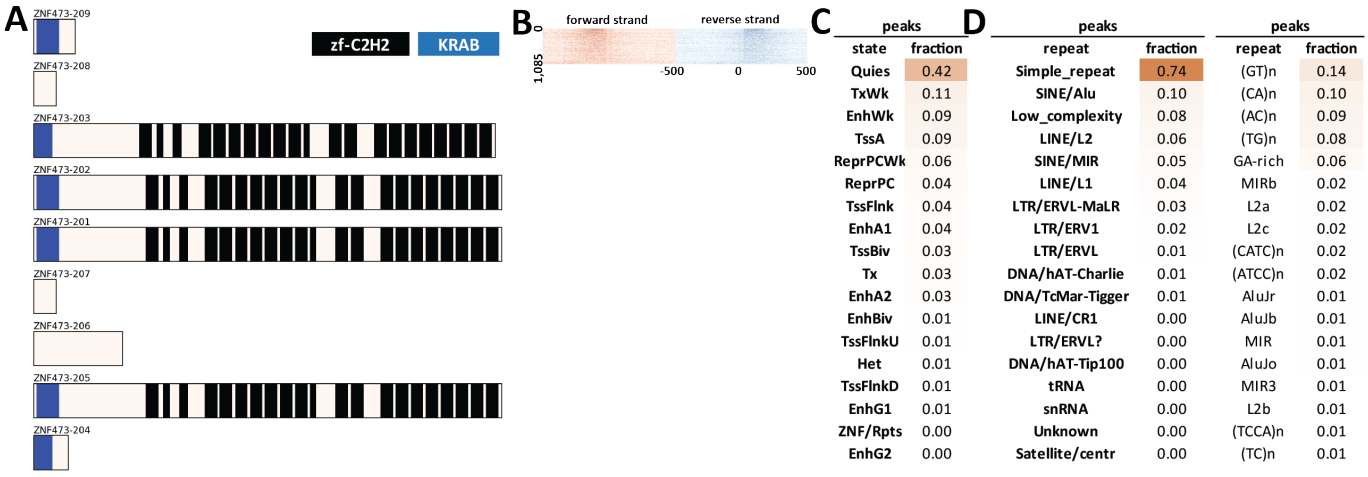

peaks	
state	fraction
Quies	0.42
TxWk	0.11
EnhWk	0.09
TssA	0.09
ReprPCWk	0.06
ReprPC	0.04
TssFlnk	0.04
EnhA1	0.04
TssBiv	0.03
Tx	0.03
EnhA2	0.03
EnhBiv	0.01
TssFlnkU	0.01
Het	0.01
TssFlnkD	0.01
EnhG1	0.01
ZNF/Rpts	0.00
EnhG2	0.00

peaks		peaks	
repeat	fraction	repeat	fraction
Simple_repeat	0.74	(GT)n	0.14
SINE/Alu	0.10	(CA)n	0.10
Low_complexity	0.08	(AC)n	0.09
LINE/L2	0.06	(TG)n	0.08
SINE/MIR	0.05	GA-rich	0.06
LINE/L1	0.04	MIRb	0.02
LTR/ERVL-MaLR	0.03	L2a	0.02
LTR/ERV1	0.02	L2c	0.02
LTR/ERVL	0.01	(CATC)n	0.02
DNA/hAT-Charlie	0.01	(ATCC)n	0.02
DNA/TcMar-Tigger	0.01	AluJr	0.01
LINE/CR1	0.00	AluJb	0.01
LTR/ERVL?	0.00	MIR	0.01
DNA/hAT-Tip100	0.00	AluJo	0.01
tRNA	0.00	MIR3	0.01
snRNA	0.00	L2b	0.01
Unknown	0.00	(TCCA)n	0.01
Satellite/centr	0.00	(TC)n	0.01

E

Ontology	Term	FDR Q-val
GO Biological Process	regulation of fat cell differentiation	5.76
GO Biological Process	positive regulation of gliogenesis	4.84
GO Biological Process	metanephric nephron development	4.78
GO Biological Process	striated muscle cell differentiation	4.04
GO Biological Process	regulation of axon extension involved in axon guidance	3.64
GO Biological Process	regulation of axon extension	3.28
GO Biological Process	paramesonephric duct development	3.11
GO Biological Process	regulation of lymphocyte differentiation	3.01
GO Biological Process	myoblast fusion	3.00
GO Biological Process	regulation of axon guidance	2.59
GO Biological Process	positive regulation of protein localization to plasma membrane	2.30
GO Biological Process	positive regulation of embryonic development	2.16
GO Biological Process	nephron tubule morphogenesis	1.95
GO Biological Process	positive regulation of protein localization to cell periphery	1.91
GO Biological Process	positive regulation of neural precursor cell proliferation	1.82
GO Biological Process	positive regulation of protein localization to membrane	1.82
GO Biological Process	eye photoreceptor cell differentiation	1.58

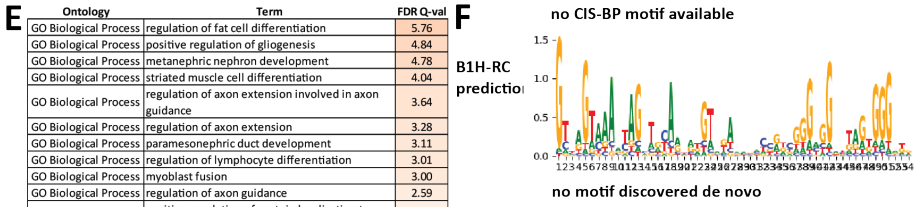

Supplementary Figure 1251: Properties and genomic distribution of motifs identified for the ZNF473 transcription factor in HEK293 (accession ENCSR567XAM).

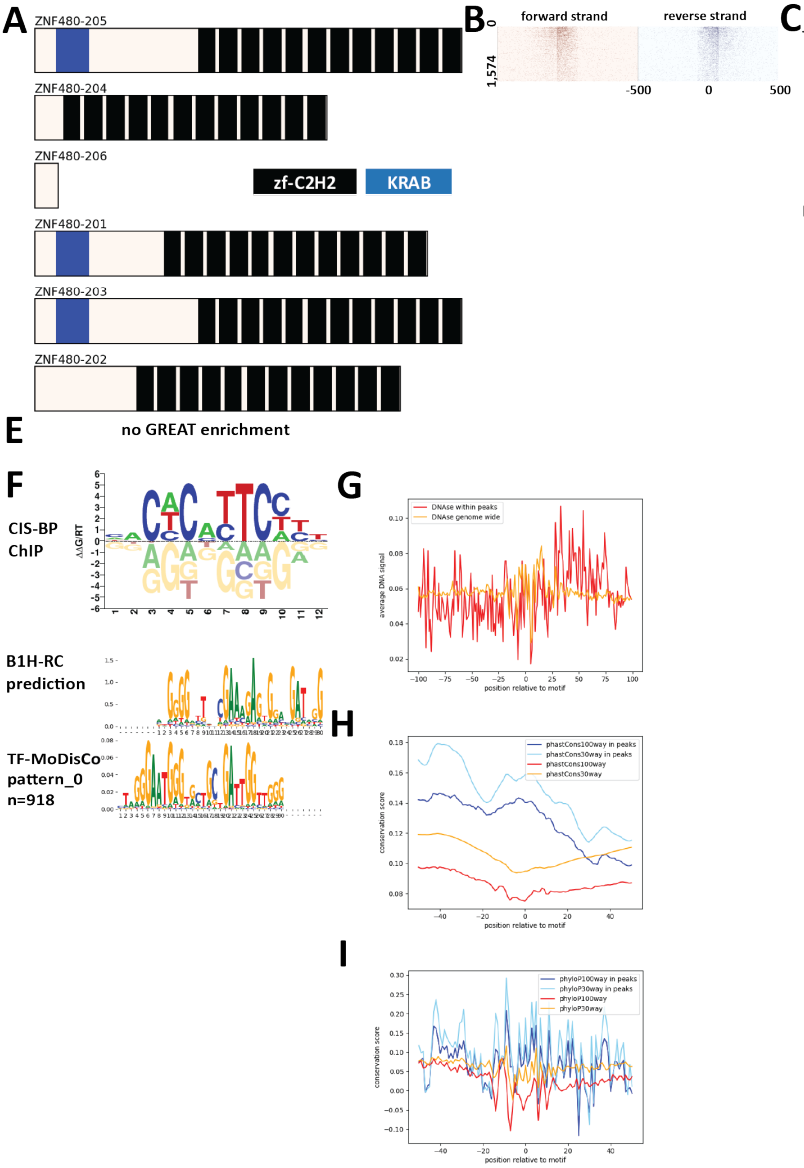

Supplementary Figure 1252: Properties and genomic distribution of motifs identified for the ZNF480 transcription factor in HEK293 (accession ChipExo models).

TF-MoDisCO pattern_0 n=918, CWM

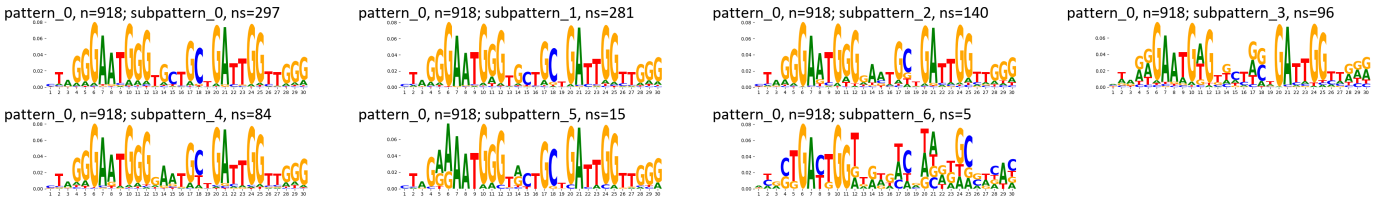

TF-MoDisCO pattern_0 n=918, PWM

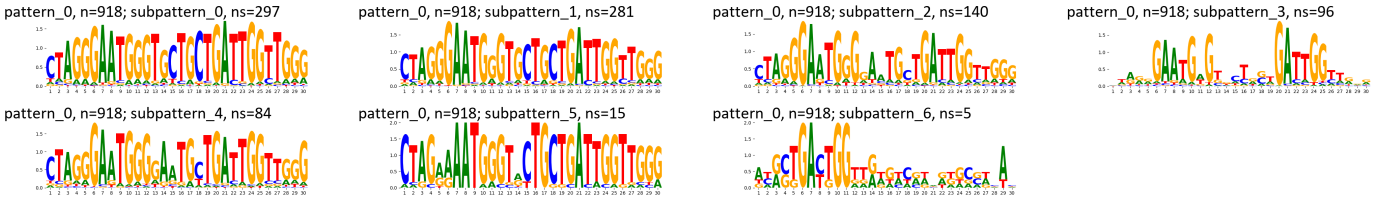

Supplementary Figure 1253: TF-MoDisCO subpatterns for the ZNF480 transcription factor in HEK293 (accession ChipExo models).

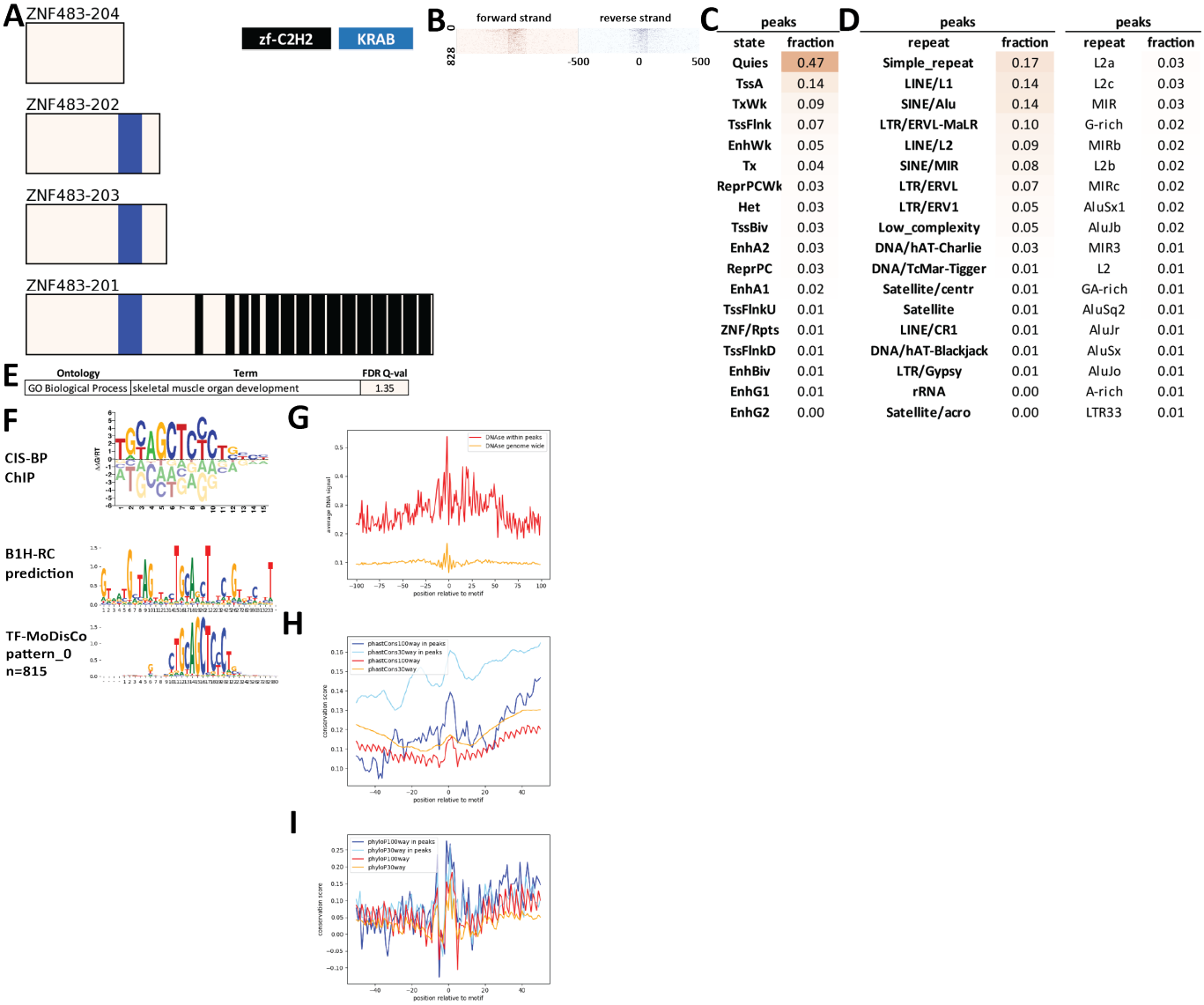

Supplementary Figure 1254: Properties and genomic distribution of motifs identified for the ZNF483 transcription factor in HEK293 (accession ChipExo models).

TF-MoDisCO pattern_0 n=815, CWM

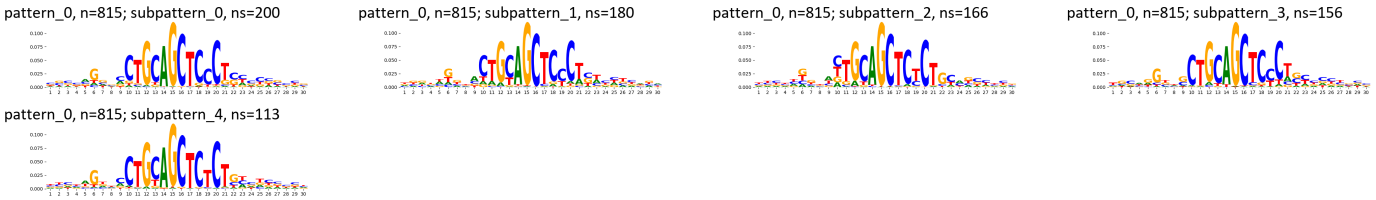

TF-MoDisCO pattern_0 n=815, PWM

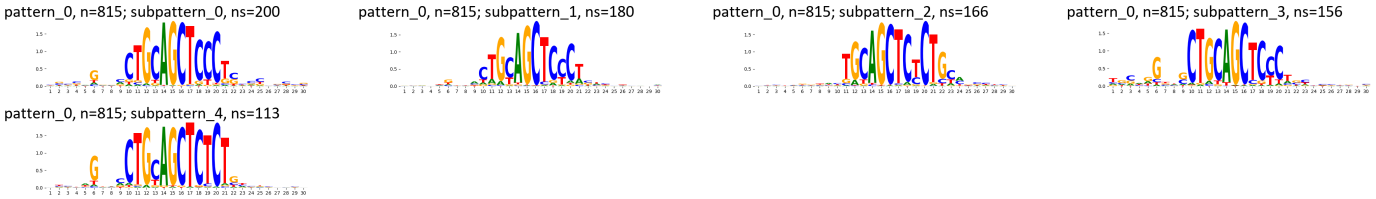

Supplementary Figure 1255: TF-MoDisCO subpatterns for the ZNF483 transcription factor in HEK293 (accession ChipExo models).

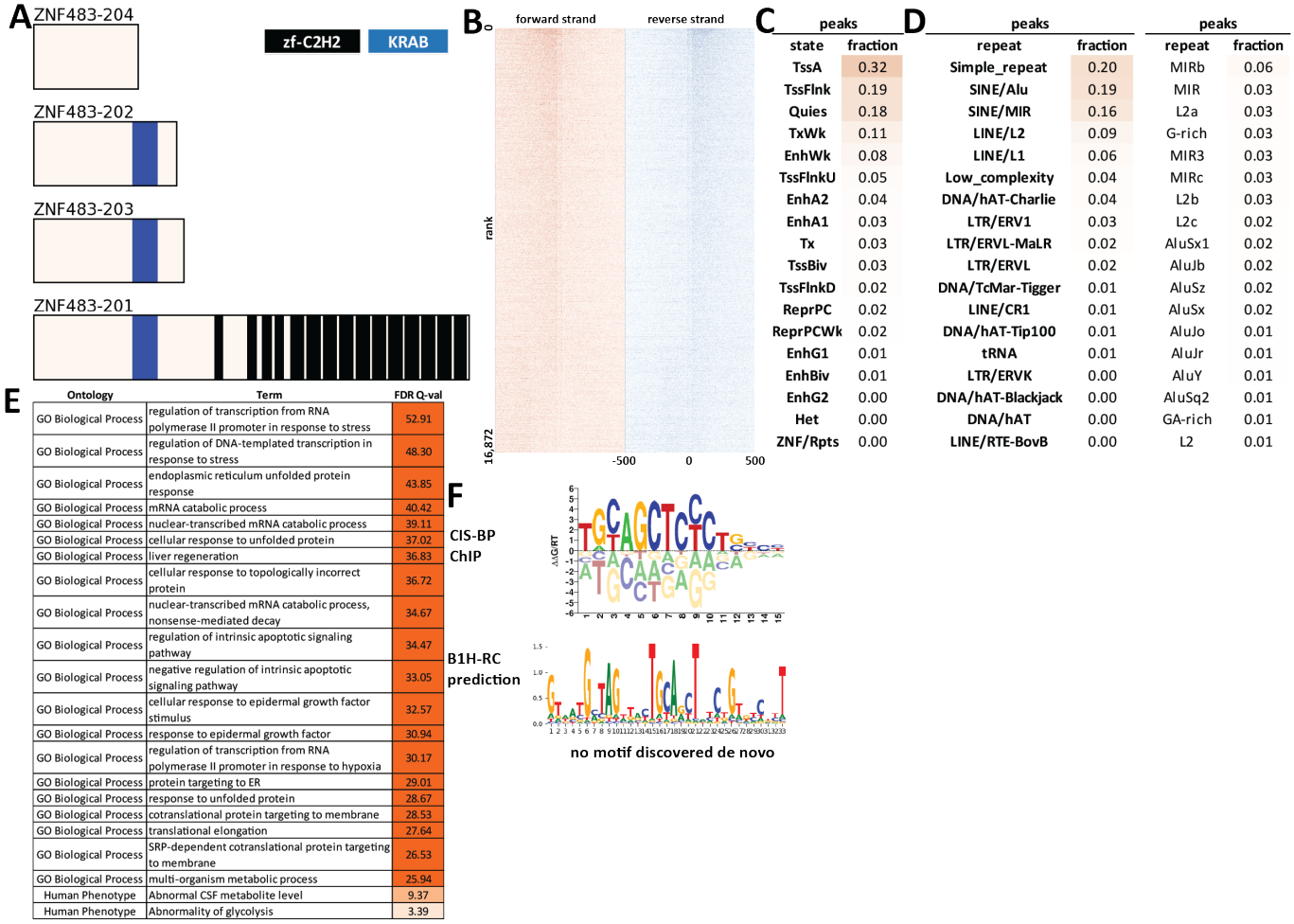

C	peaks	
	state	fraction
	TssA	0.32
	TssFlnk	0.19
	Quies	0.18
	TxWk	0.11
	EnhWk	0.08
	TssFlnkU	0.05
	EnhA2	0.04
	EnhA1	0.03
	Tx	0.03
	TssBiv	0.03
	TssFlnkD	0.02
	ReprPC	0.02
	ReprPCWk	0.02
	EnhG1	0.01
	EnhBiv	0.01
	EnhG2	0.00
	Het	0.00
	ZNF/Rpts	0.00

D	peaks		peaks	
	repeat	fraction	repeat	fraction
	Simple_repeat	0.20	MIRb	0.06
	SINE/Alu	0.19	MIR	0.03
	SINE/MIR	0.16	L2a	0.03
	LINE/L2	0.09	G-rich	0.03
	LINE/L1	0.06	MIR3	0.03
	Low_complexity	0.04	MIRc	0.03
	DNA/hAT-Charlie	0.04	L2b	0.03
	LTR/ERV1	0.03	L2c	0.02
	LTR/ERVL-MaLR	0.02	AluSx1	0.02
	LTR/ERVL	0.02	AluJb	0.02
	DNA/TcMar-Tigger	0.01	AluSz	0.02
	LINE/CR1	0.01	AluSx	0.02
	DNA/hAT-Tip100	0.01	AluJo	0.01
	tRNA	0.01	AluJr	0.01
	LTR/ERVK	0.00	AluY	0.01
	DNA/hAT-Blackjack	0.00	AluSq2	0.01
	DNA/hAT	0.00	GA-rich	0.01
	LINE/RTE-BovB	0.00	L2	0.01

E	Ontology	Term	FDR Q-val
	GO Biological Process	regulation of transcription from RNA polymerase II promoter in response to stress	52.91
	GO Biological Process	regulation of DNA-templated transcription in response to stress	48.30
	GO Biological Process	endoplasmic reticulum unfolded protein response	43.85
	GO Biological Process	mRNA catabolic process	40.42
	GO Biological Process	nuclear-transcribed mRNA catabolic process	39.11
	GO Biological Process	cellular response to unfolded protein	37.02
	GO Biological Process	liver regeneration	36.83
	GO Biological Process	cellular response to topologically incorrect protein	36.72
	GO Biological Process	nuclear-transcribed mRNA catabolic process, nonsense-mediated decay	34.67
	GO Biological Process	regulation of intrinsic apoptotic signaling pathway	34.47
	GO Biological Process	negative regulation of intrinsic apoptotic signaling pathway	33.05
	GO Biological Process	cellular response to epidermal growth factor stimulus	32.57
	GO Biological Process	response to epidermal growth factor	30.94
	GO Biological Process	regulation of transcription from RNA polymerase II promoter in response to hypoxia	30.17
	GO Biological Process	protein targeting to ER	29.01
	GO Biological Process	response to unfolded protein	28.67
	GO Biological Process	cotranslational protein targeting to membrane	28.53
	GO Biological Process	translational elongation	27.64
	GO Biological Process	SRP-dependent cotranslational protein targeting to membrane	26.53
	GO Biological Process	multi-organism metabolic process	25.94
	Human Phenotype	Abnormal CSF metabolite level	9.37
	Human Phenotype	Abnormality of glycolysis	3.39

Supplementary Figure 1256: Properties and genomic distribution of motifs identified for the ZNF483 transcription factor in HepG2 (accession ENCSR436PIH).

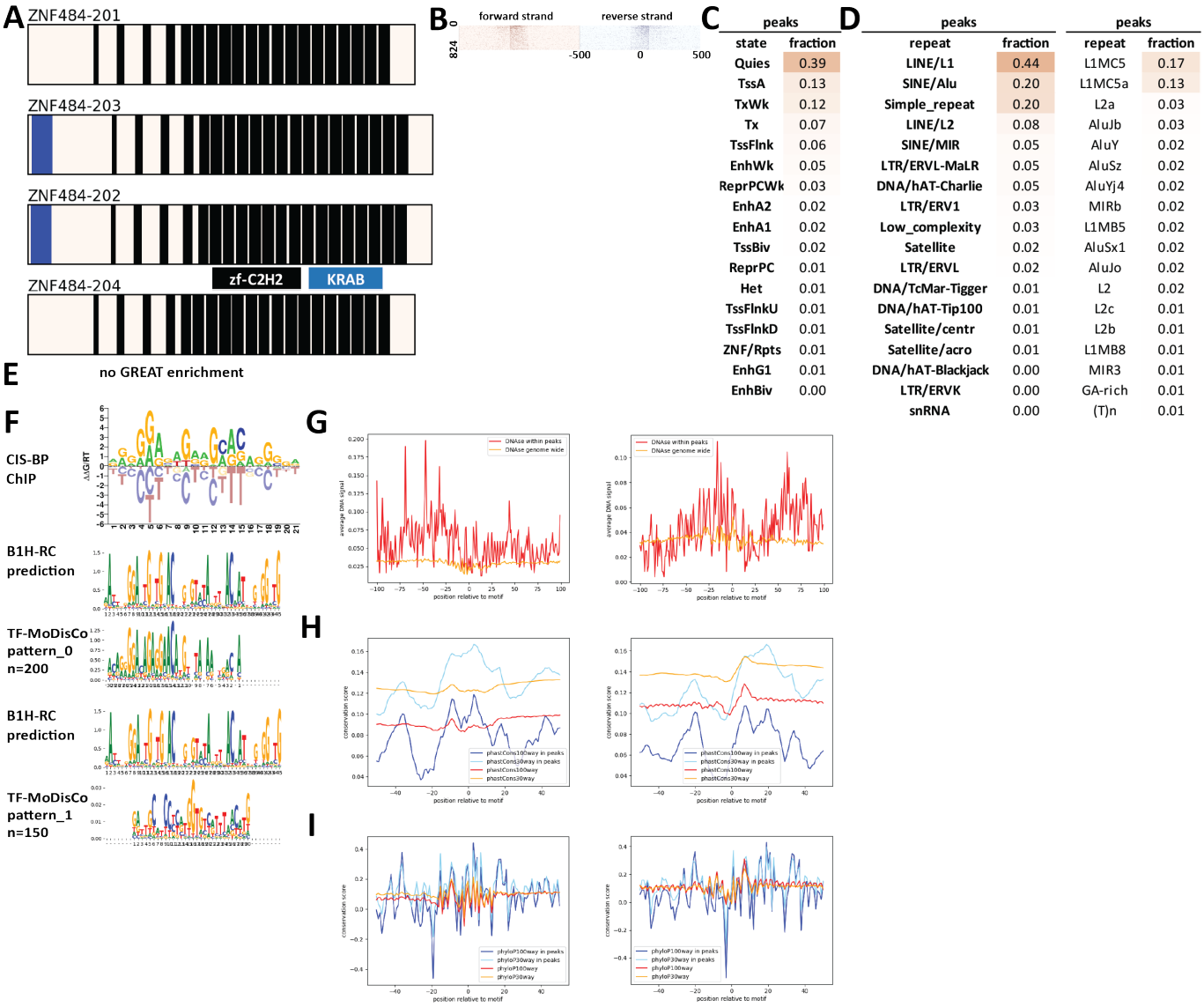

Supplementary Figure 1257: Properties and genomic distribution of motifs identified for the ZNF484 transcription factor in HEK293 (accession ChipExo models).

TF-MoDisCO pattern_0 n=200, CWM

pattern_0, n=200; subpattern_0, ns=72

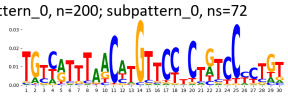

pattern_0, n=200; subpattern_1, ns=59

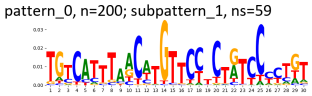

pattern_0, n=200; subpattern_2, ns=47

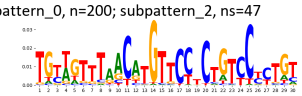

pattern_0, n=200; subpattern_3, ns=20

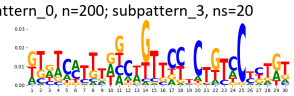

pattern_0, n=200; subpattern_4, ns=2

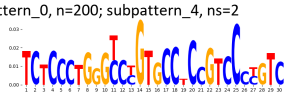

TF-MoDisCO pattern_0 n=200, PWM

pattern_0, n=200; subpattern_0, ns=72

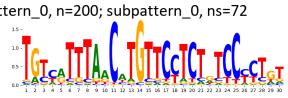

pattern_0, n=200; subpattern_1, ns=59

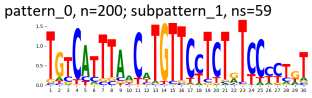

pattern_0, n=200; subpattern_2, ns=47

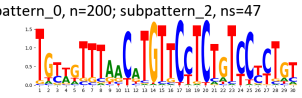

pattern_0, n=200; subpattern_3, ns=20

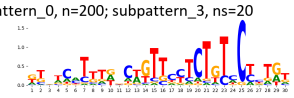

pattern_0, n=200; subpattern_4, ns=2

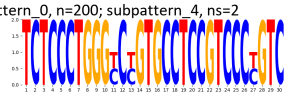

TF-MoDisCO pattern_1 n=150, CWM

pattern_1, n=150; subpattern_0, ns=36

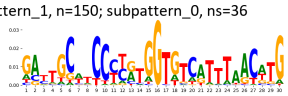

pattern_1, n=150; subpattern_1, ns=35

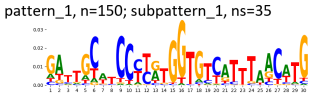

pattern_1, n=150; subpattern_2, ns=27

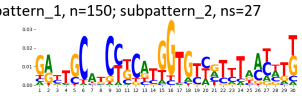

pattern_1, n=150; subpattern_3, ns=25

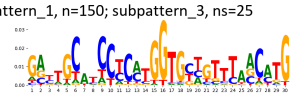

pattern_1, n=150; subpattern_4, ns=14

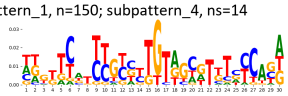

pattern_1, n=150; subpattern_5, ns=13

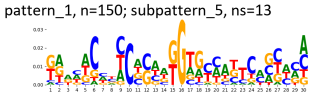

TF-MoDisCO pattern_1 n=150, PWM

pattern_1, n=150; subpattern_0, ns=36

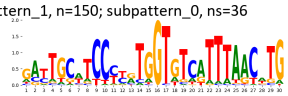

pattern_1, n=150; subpattern_1, ns=35

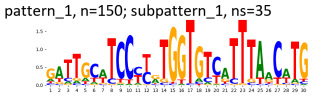

pattern_1, n=150; subpattern_2, ns=27

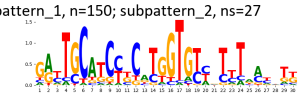

pattern_1, n=150; subpattern_3, ns=25

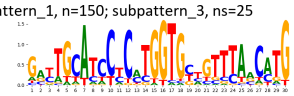

pattern_1, n=150; subpattern_4, ns=14

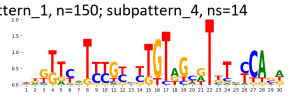

pattern_1, n=150; subpattern_5, ns=13

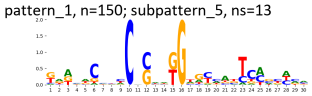

Supplementary Figure 1258: TF-MoDisCO subpatterns for the ZNF484 transcription factor in HEK293 (accession ChipExo models).

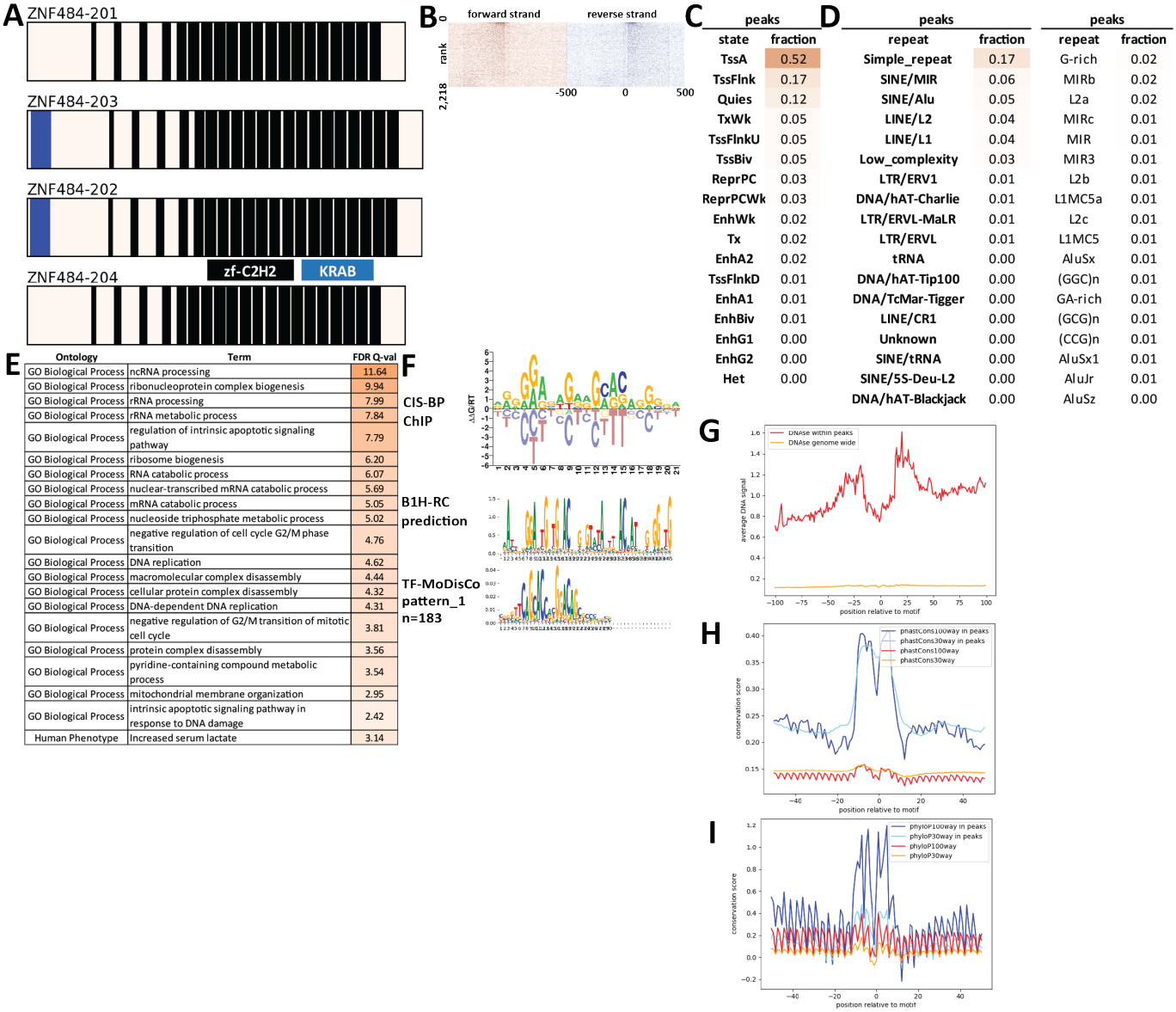

C

peaks	
state	fraction
TssA	0.52
TssFlnk	0.17
Quies	0.12
TxWk	0.05
TssFlnkU	0.05
TssBiv	0.05
ReprPC	0.03
ReprPCWk	0.03
EnhWk	0.02
Tx	0.02
EnhA2	0.02
TssFlnkD	0.01
EnhA1	0.01
EnhBiv	0.01
EnhG1	0.00
EnhG2	0.00
Het	0.00

D

peaks		peaks	
repeat	fraction	repeat	fraction
Simple_repeat	0.17	G-rich	0.02
SINE/MIR	0.06	MIRb	0.02
SINE/Alu	0.05	L2a	0.02
LINE/L2	0.04	MIRc	0.01
LINE/L1	0.04	MIR	0.01
Low_complexity	0.03	MIR3	0.01
LTR/ERV1	0.01	L2b	0.01
DNA/hAT-Charlie	0.01	L1MC5a	0.01
LTR/ERVL-MaLR	0.01	L2c	0.01
LTR/ERVL	0.01	L1MC5	0.01
tRNA	0.00	AluSx	0.01
DNA/hAT-Tip100	0.00	(GGC)n	0.01
DNA/TcMar-Tigger	0.00	GA-rich	0.01
LINE/CR1	0.00	(GCG)n	0.01
Unknown	0.00	(CCG)n	0.01
SINE/tRNA	0.00	AluSx1	0.01
SINE/5S-Deu-L2	0.00	AluJr	0.01
DNA/hAT-Blackjack	0.00	AluSz	0.00

E

Ontology	Term	FDR Q-val
GO Biological Process	ncRNA processing	11.64
GO Biological Process	ribonucleoprotein complex biogenesis	9.94
GO Biological Process	rRNA processing	7.99
GO Biological Process	rRNA metabolic process	7.84
GO Biological Process	regulation of intrinsic apoptotic signaling pathway	7.79
GO Biological Process	ribosome biogenesis	6.20
GO Biological Process	RNA catabolic process	6.07
GO Biological Process	nuclear-transcribed mRNA catabolic process	5.69
GO Biological Process	mRNA catabolic process	5.05
GO Biological Process	nucleoside triphosphate metabolic process	5.02
GO Biological Process	negative regulation of cell cycle G2/M phase transition	4.76
GO Biological Process	DNA replication	4.62
GO Biological Process	macromolecular complex disassembly	4.44
GO Biological Process	cellular protein complex disassembly	4.32
GO Biological Process	DNA-dependent DNA replication	4.31
GO Biological Process	negative regulation of G2/M transition of mitotic cell cycle	3.81
GO Biological Process	protein complex disassembly	3.56
GO Biological Process	pyridine-containing compound metabolic process	3.54
GO Biological Process	mitochondrial membrane organization	2.95
GO Biological Process	intrinsic apoptotic signaling pathway in response to DNA damage	2.42
Human Phenotype	Increased serum lactate	3.14

Supplementary Figure 1259: Properties and genomic distribution of motifs identified for the ZNF484 transcription factor in HepG2 (accession ENCSR471VAY).

TF-MoDisCO pattern_1 n=183, CWM

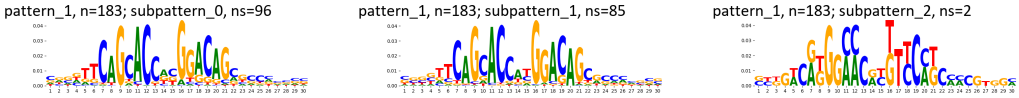

TF-MoDisCO pattern_1 n=183, PWM

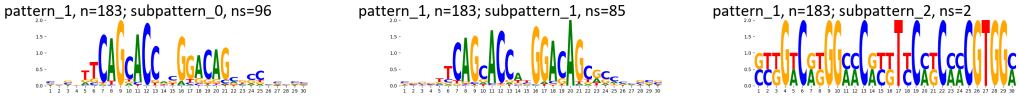

Supplementary Figure 1260: TF-MoDisCO subpatterns for the ZNF484 transcription factor in HepG2 (accession ENCSR471VAY).

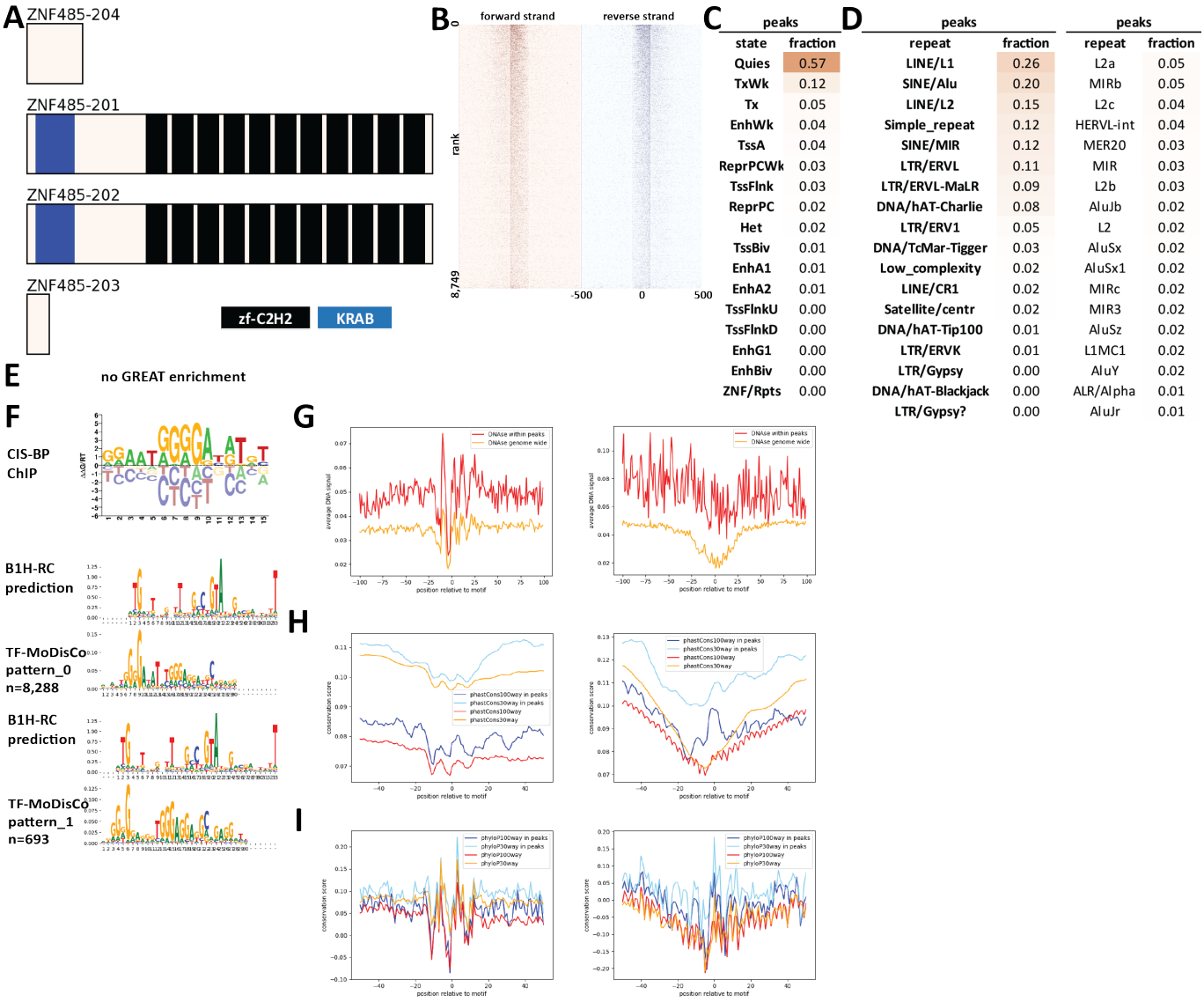

Supplementary Figure 1261: Properties and genomic distribution of motifs identified for the ZNF485 transcription factor in HEK293 (accession ChipExo models).

TF-MoDisCO pattern_0 n=8288, CWM

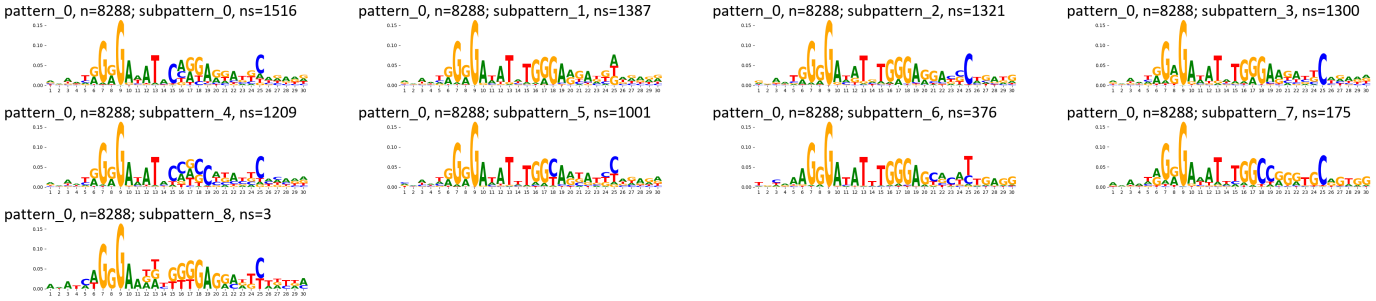

TF-MoDisCO pattern_0 n=8288, PWM

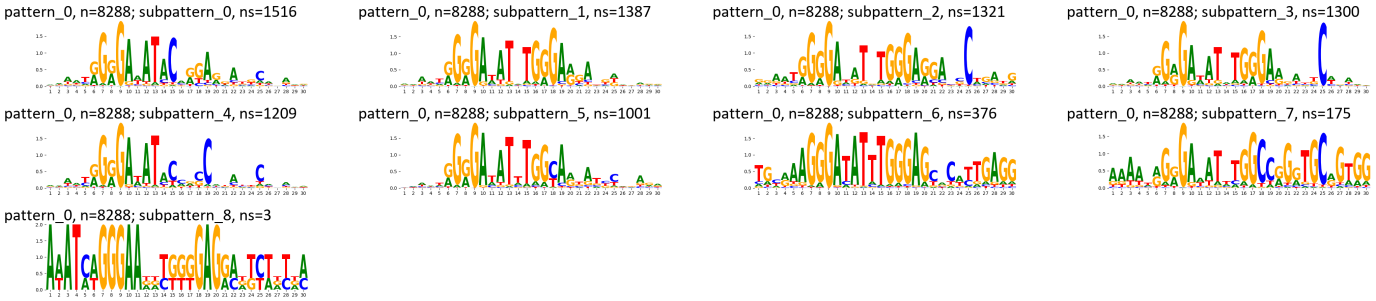

TF-MoDisCO pattern_1 n=693, CWM

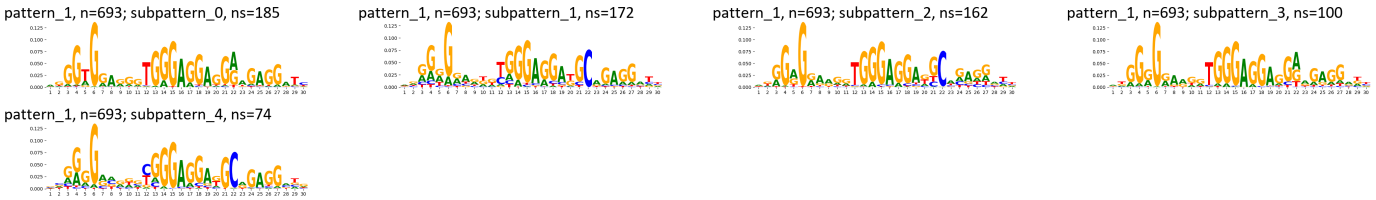

TF-MoDisCO pattern_1 n=693, PWM

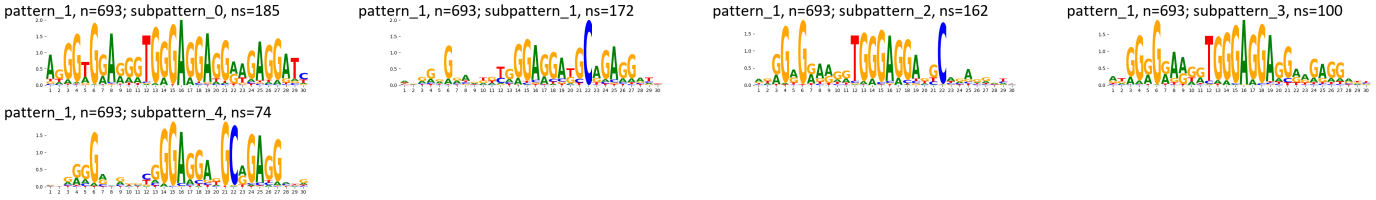

Supplementary Figure 1262: TF-MoDisCO subpatterns for the ZNF485 transcription factor in HEK293 (accession ChipExo models).

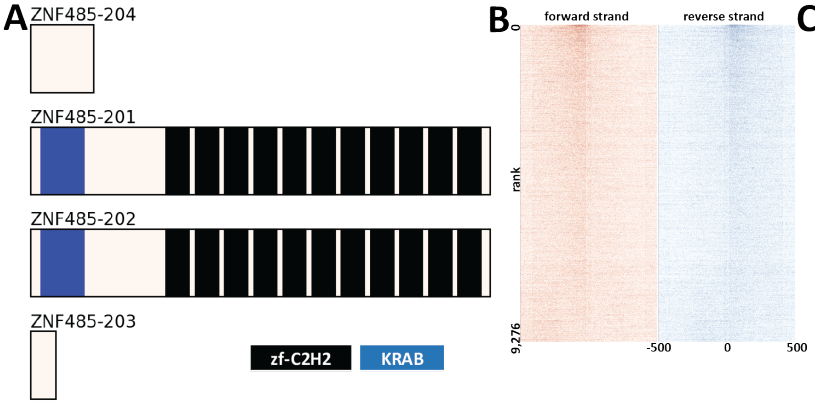

C

peaks	
state	fraction
TssA	0.37
TssFlnk	0.17
Quies	0.15
TxWk	0.10
TssFlnkU	0.04
EnhWk	0.04
TssBiv	0.04
Tx	0.03
ReprPC	0.03
EnhA2	0.03
ReprPCWk	0.02
EnhA1	0.02
TssFlnkD	0.02
EnhG1	0.01
EnhBiv	0.01
EnhG2	0.00
Het	0.00
ZNF/Rpts	0.00

D

peaks		peaks	
repeat	fraction	repeat	fraction
Simple_repeat	0.14	MIRb	0.04
SINE/Alu	0.11	MIR3	0.02
SINE/MIR	0.10	G-rich	0.02
LINE/L2	0.06	L2a	0.02
Low_complexity	0.03	MIR	0.02
LINE/L1	0.02	MIRc	0.02
DNA/hAT-Charlie	0.02	L2b	0.02
LTR/ERVL-MaLR	0.02	AluJb	0.02
LTR/ERV1	0.01	AluSx	0.01
LTR/ERVL	0.01	L2c	0.01
DNA/hAT-Tip100	0.01	AluSx1	0.01
LINE/CR1	0.00	AluSz	0.01
DNA/TcMar-Tigger	0.00	AluJr	0.01
tRNA	0.00	AluJo	0.01
DNA/hAT-Blackjack	0.00	AluSq2	0.01
LTR/Gypsy	0.00	L2	0.01
LTR/ERVK	0.00	MIR1_Amn	0.01
DNA/hAT	0.00	GA-rich	0.01

E

Ontology	Term	FDR Q-val
GO Biological Process	regulation of intrinsic apoptotic signaling pathway	29.28
GO Biological Process	cellular response to epidermal growth factor stimulus	24.19
GO Biological Process	response to epidermal growth factor	22.36
GO Biological Process	nuclear-transcribed mRNA catabolic process	20.28
GO Biological Process	protein targeting to ER	19.34
GO Biological Process	mRNA catabolic process	19.16
GO Biological Process	nuclear-transcribed mRNA catabolic process, nonsense-mediated decay	18.29
GO Biological Process	negative regulation of intrinsic apoptotic signaling pathway	16.92
GO Biological Process	establishment of protein localization to endoplasmic reticulum	16.34
GO Biological Process	cotranslational protein targeting to membrane	15.15
GO Biological Process	protein localization to endoplasmic reticulum	14.80
GO Biological Process	endoplasmic reticulum unfolded protein response	14.36
GO Biological Process	SRP-dependent cotranslational protein targeting to membrane	14.12
GO Biological Process	regulation of mitochondrial membrane permeability	14.12
GO Biological Process	viral transcription	13.10
GO Biological Process	DNA-templated transcription, elongation	13.03
GO Biological Process	viral gene expression	13.01
GO Biological Process	cellular response to unfolded protein	11.49
GO Biological Process	regulation of membrane permeability	10.90
GO Biological Process	mitochondrial translational termination	10.87
Human Phenotype	Increased serum lactate	9.20
Human Phenotype	Nevus	6.60
Human Phenotype	Ectropion	3.05
Human Phenotype	Increased serum pyruvate	2.62
Human Phenotype	Abnormality of glycolysis	2.54
Human Phenotype	Facial diplegia	1.81

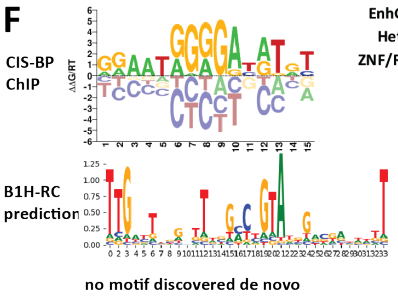

Supplementary Figure 1263: Properties and genomic distribution of motifs identified for the ZNF485 transcription factor in HepG2 (accession ENCSR574UJE).

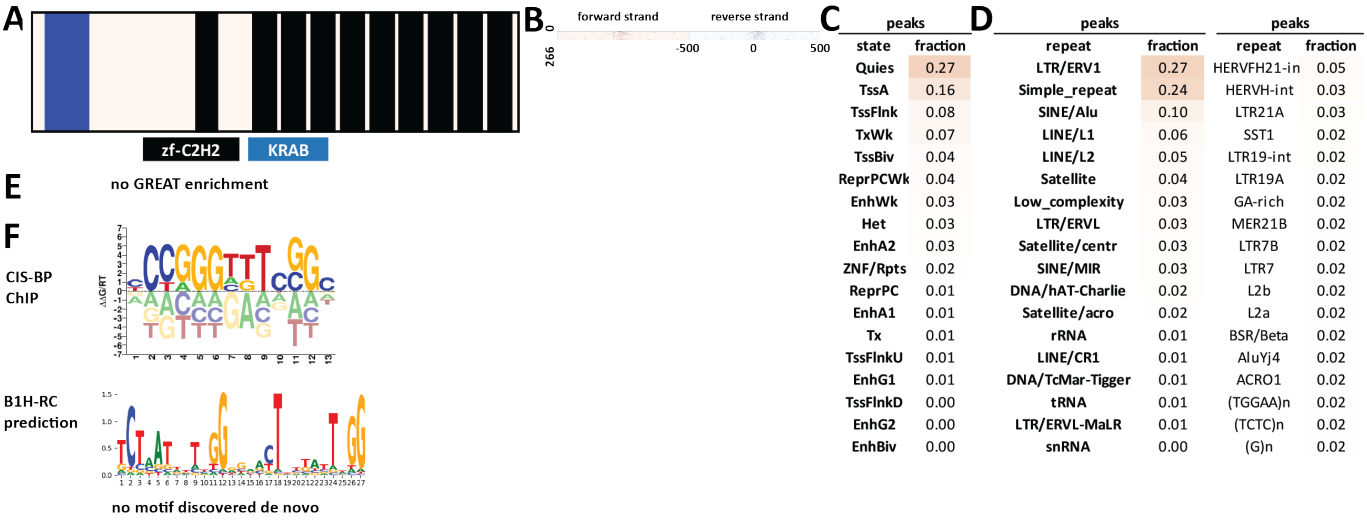

peaks

state	fraction
Quies	0.27
TssA	0.16
TssFlnk	0.08
TxWk	0.07
TssBiv	0.04
ReprPCWk	0.04
EnhWk	0.03
Het	0.03
EnhA2	0.03
ZNF/Rpts	0.02
ReprPC	0.01
EnhA1	0.01
Tx	0.01
TssFlnkU	0.01
EnhG1	0.01
TssFlnkD	0.00
EnhG2	0.00
EnhBiv	0.00

peaks

repeat	fraction
LTR/ERV1	0.27
Simple_repeat	0.24
SINE/Alu	0.10
LINE/L1	0.06
LINE/L2	0.05
Satellite	0.04
Low_complexity	0.03
LTR/ERVL	0.03
Satellite/centr	0.03
SINE/MIR	0.03
DNA/hAT-Charlie	0.02
Satellite/acro	0.02
rRNA	0.01
LINE/CR1	0.01
DNA/TcMar-Tigger	0.01
tRNA	0.01
LTR/ERVL-MaLR	0.01
snRNA	0.00

peaks

repeat	fraction
HERVFH21-in	0.05
HERVH-int	0.03
LTR21A	0.03
SST1	0.02
LTR19-int	0.02
LTR19A	0.02
GA-rich	0.02
MER21B	0.02
LTR7B	0.02
LTR7	0.02
L2b	0.02
L2a	0.02
BSR/Beta	0.02
AluYj4	0.02
ACRO1	0.02
(TGGAA)n	0.02
(TCTC)n	0.02
(G)n	0.02

Supplementary Figure 1264: Properties and genomic distribution of motifs identified for the ZNF486 transcription factor in HEK293 (accession ChipExo models).

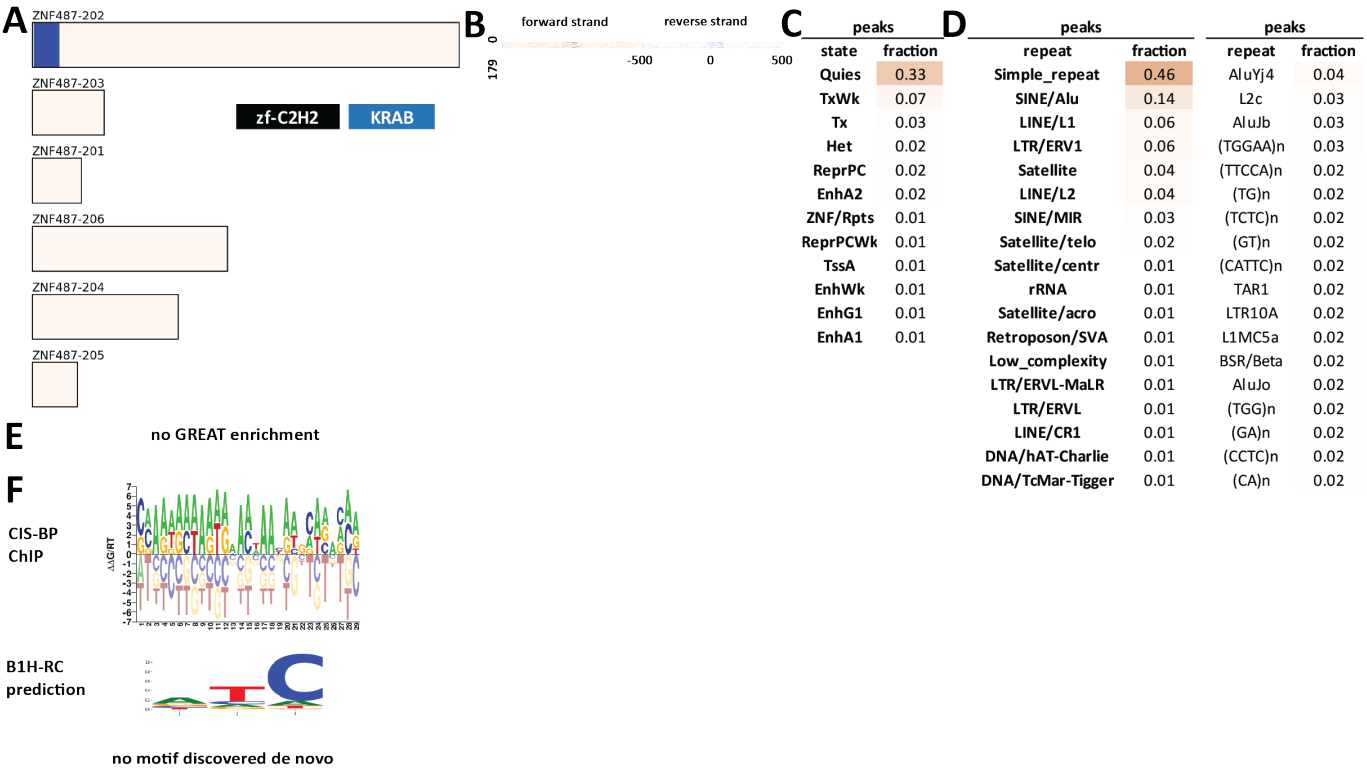

Supplementary Figure 1265: Properties and genomic distribution of motifs identified for the ZNF487 transcription factor in HEK293 (accession ChipExo models).

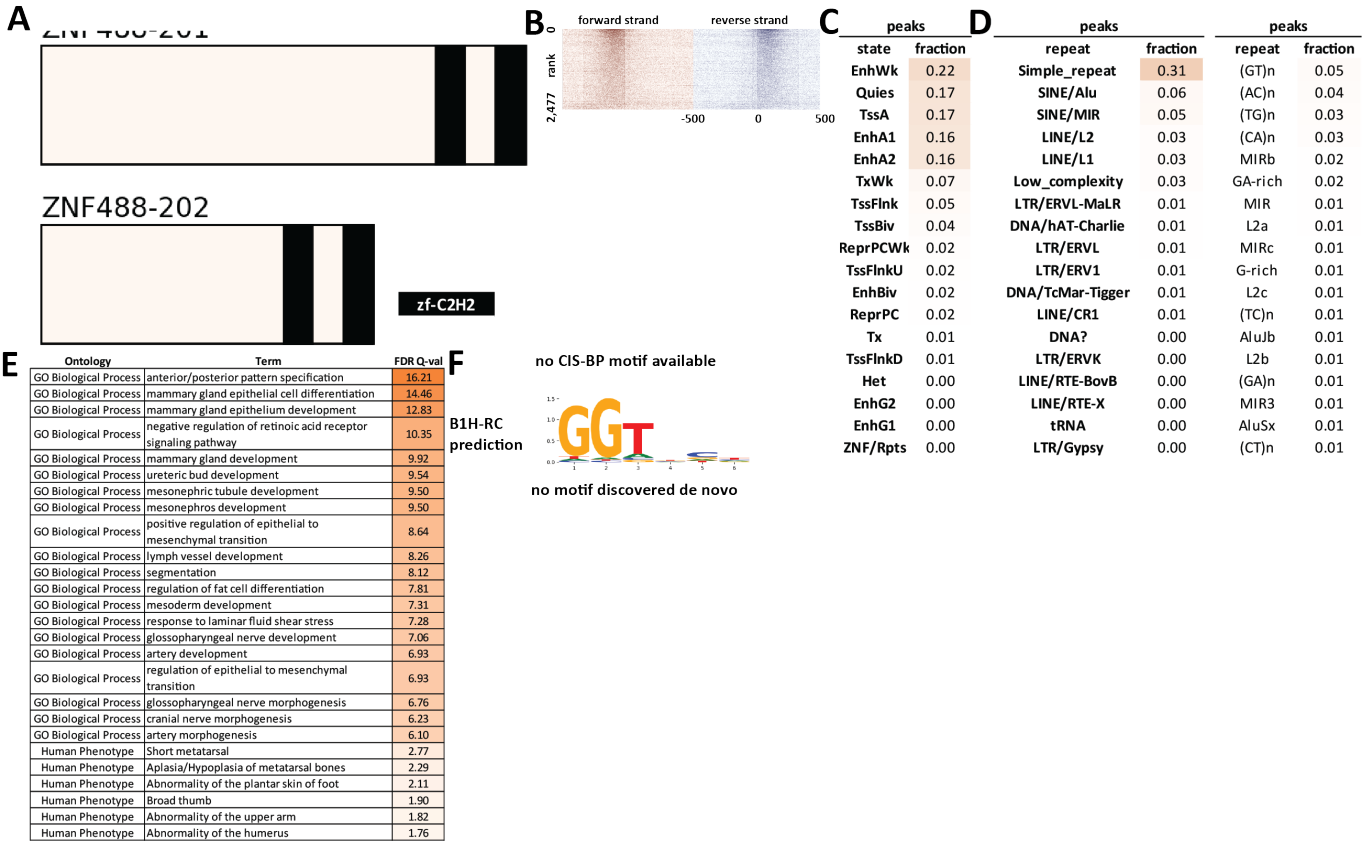

Supplementary Figure 1266: Properties and genomic distribution of motifs identified for the ZNF488 transcription factor in HEK293 (accession ENCSR363XBR).

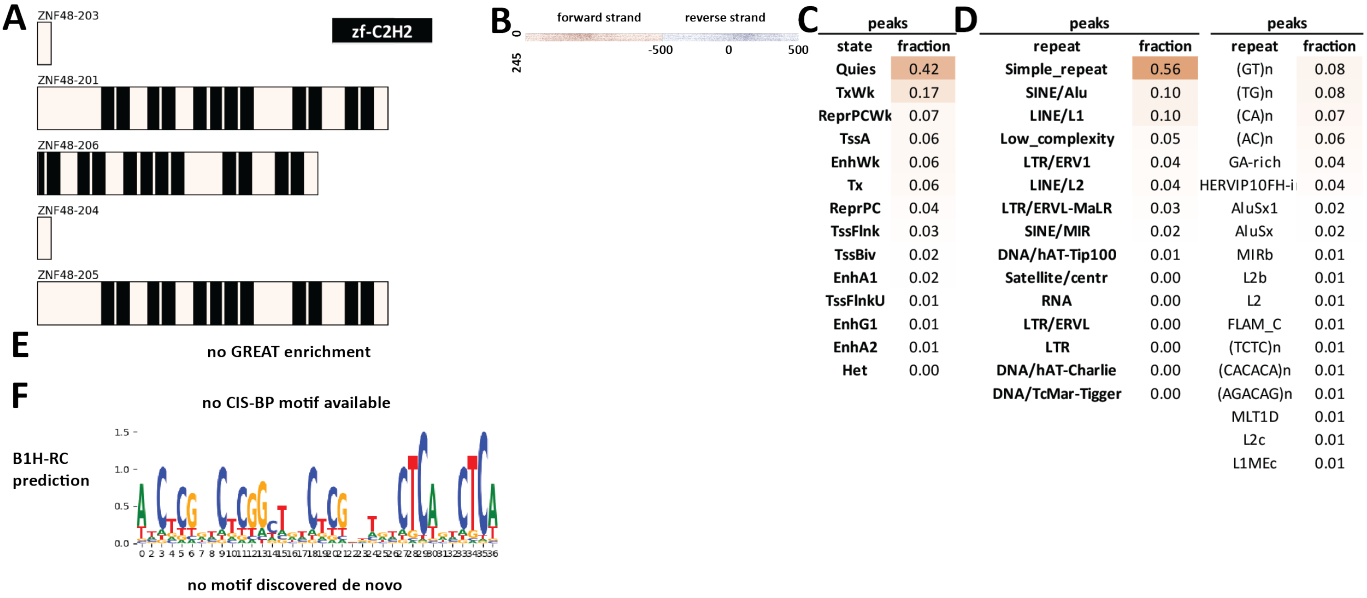

Supplementary Figure 1267: Properties and genomic distribution of motifs identified for the ZNF48 transcription factor in HEK293 (accession ENCSR517DDU).

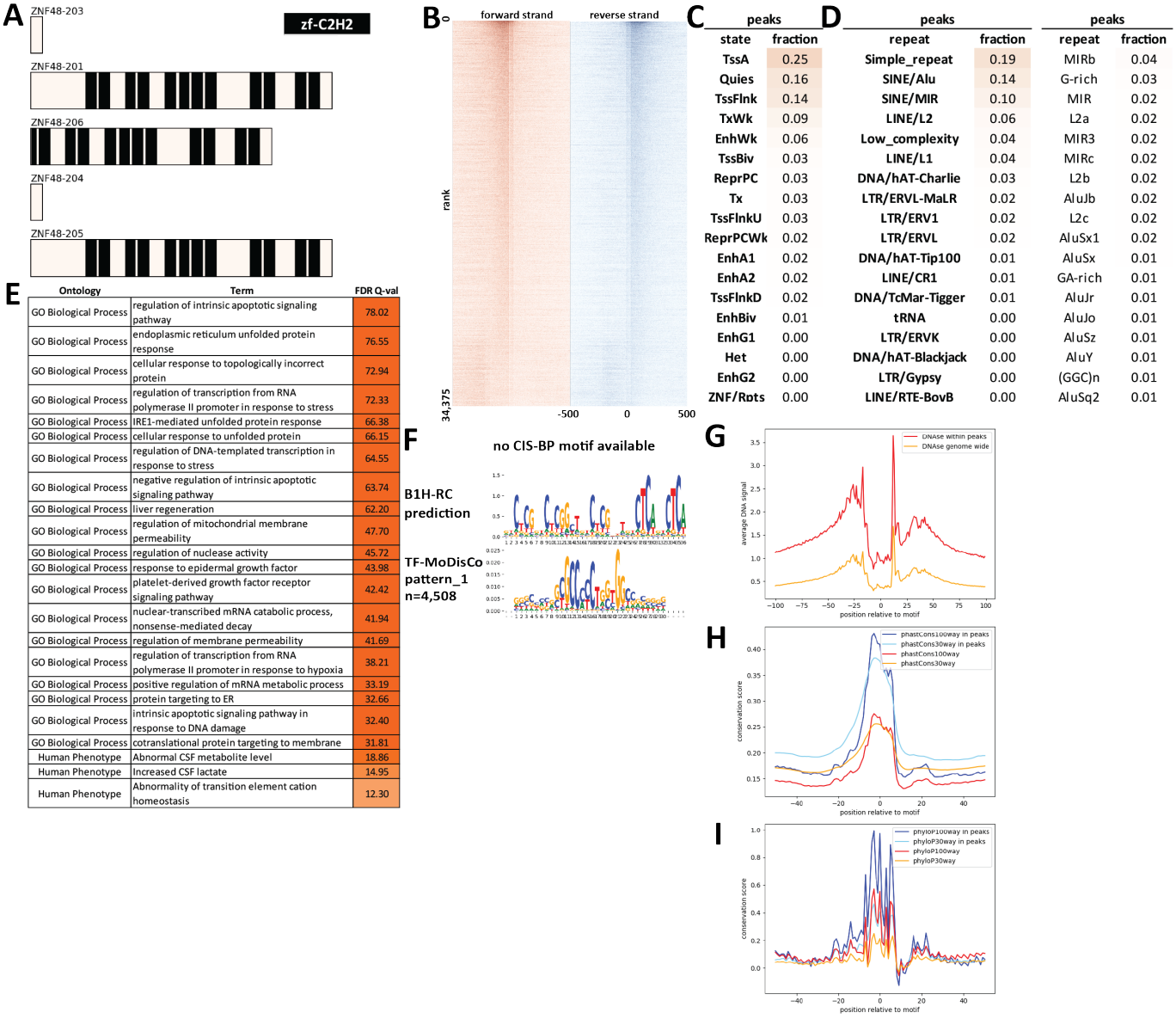

C

peaks	
state	fraction
TssA	0.25
Quies	0.16
TssFlnk	0.14
TxWk	0.09
EnhWk	0.06
TssBiv	0.03
ReprPC	0.03
Tx	0.03
TssFlnkU	0.03
ReprPCWk	0.02
EnhA1	0.02
EnhA2	0.02
TssFlnkD	0.02
EnhBiv	0.01
EnhG1	0.00
Het	0.00
EnhG2	0.00
ZNF/Rpts	0.00

D

peaks		peaks	
repeat	fraction	repeat	fraction
Simple_repeat	0.19	MIRb	0.04
SINE/Alu	0.14	G-rich	0.03
SINE/MIR	0.10	MIR	0.02
LINE/L2	0.06	L2a	0.02
Low_complexity	0.04	MIR3	0.02
LINE/L1	0.04	MIRc	0.02
DNA/hAT-Charlie	0.03	L2b	0.02
LTR/ERVL-MaLR	0.02	AluJb	0.02
LTR/ERV1	0.02	L2c	0.02
LTR/ERVL	0.02	AluSx1	0.02
DNA/hAT-Tip100	0.01	AluSx	0.01
LINE/CR1	0.01	GA-rich	0.01
DNA/TcMar-Tigger	0.01	AluJr	0.01
tRNA	0.00	AluJo	0.01
LTR/ERVK	0.00	AluSz	0.01
DNA/hAT-Blackjack	0.00	AluY	0.01
LTR/Gypsy	0.00	(GGC)n	0.01
LINE/RTE-BovB	0.00	AluSq2	0.01

E

Ontology	Term	FDR Q-val
GO Biological Process	regulation of intrinsic apoptotic signaling pathway	78.02
GO Biological Process	endoplasmic reticulum unfolded protein response	76.55
GO Biological Process	cellular response to topologically incorrect protein	72.94
GO Biological Process	regulation of transcription from RNA polymerase II promoter in response to stress	72.33
GO Biological Process	IRE1-mediated unfolded protein response	66.38
GO Biological Process	cellular response to unfolded protein	66.15
GO Biological Process	regulation of DNA-templated transcription in response to stress	64.55
GO Biological Process	negative regulation of intrinsic apoptotic signaling pathway	63.74
GO Biological Process	liver regeneration	62.20
GO Biological Process	regulation of mitochondrial membrane permeability	47.70
GO Biological Process	regulation of nuclease activity	45.72
GO Biological Process	response to epidermal growth factor	43.98
GO Biological Process	platelet-derived growth factor receptor signaling pathway	42.42
GO Biological Process	nuclear-transcribed mRNA catabolic process, nonsense-mediated decay	41.94
GO Biological Process	regulation of membrane permeability	41.69
GO Biological Process	regulation of transcription from RNA polymerase II promoter in response to hypoxia	38.21
GO Biological Process	positive regulation of mRNA metabolic process	33.19
GO Biological Process	protein targeting to ER	32.66
GO Biological Process	intrinsic apoptotic signaling pathway in response to DNA damage	32.40
GO Biological Process	cotranslational protein targeting to membrane	31.81
Human Phenotype	Abnormal CSF metabolite level	18.86
Human Phenotype	Increased CSF lactate	14.95
Human Phenotype	Abnormality of transition element cation homeostasis	12.30

Supplementary Figure 1268: Properties and genomic distribution of motifs identified for the ZNF48 transcription factor in HepG2 (accession ENCSR415AEB).

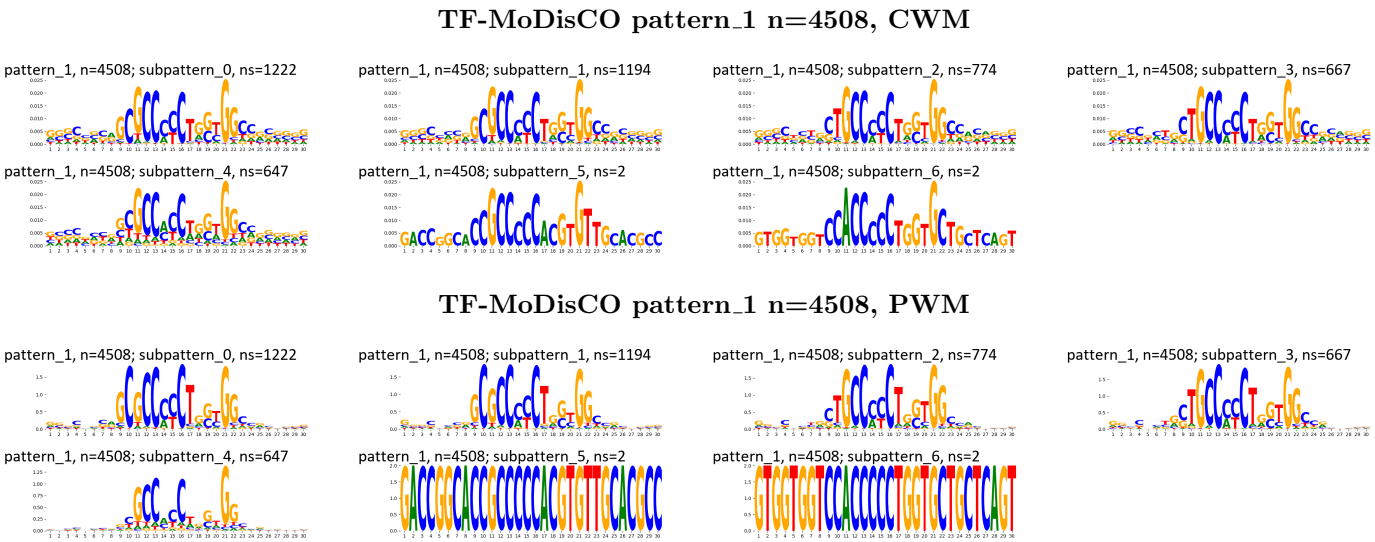

Supplementary Figure 1269: TF-MoDisCO subpatterns for the ZNF48 transcription factor in HepG2 (accession ENCSR415AEB).

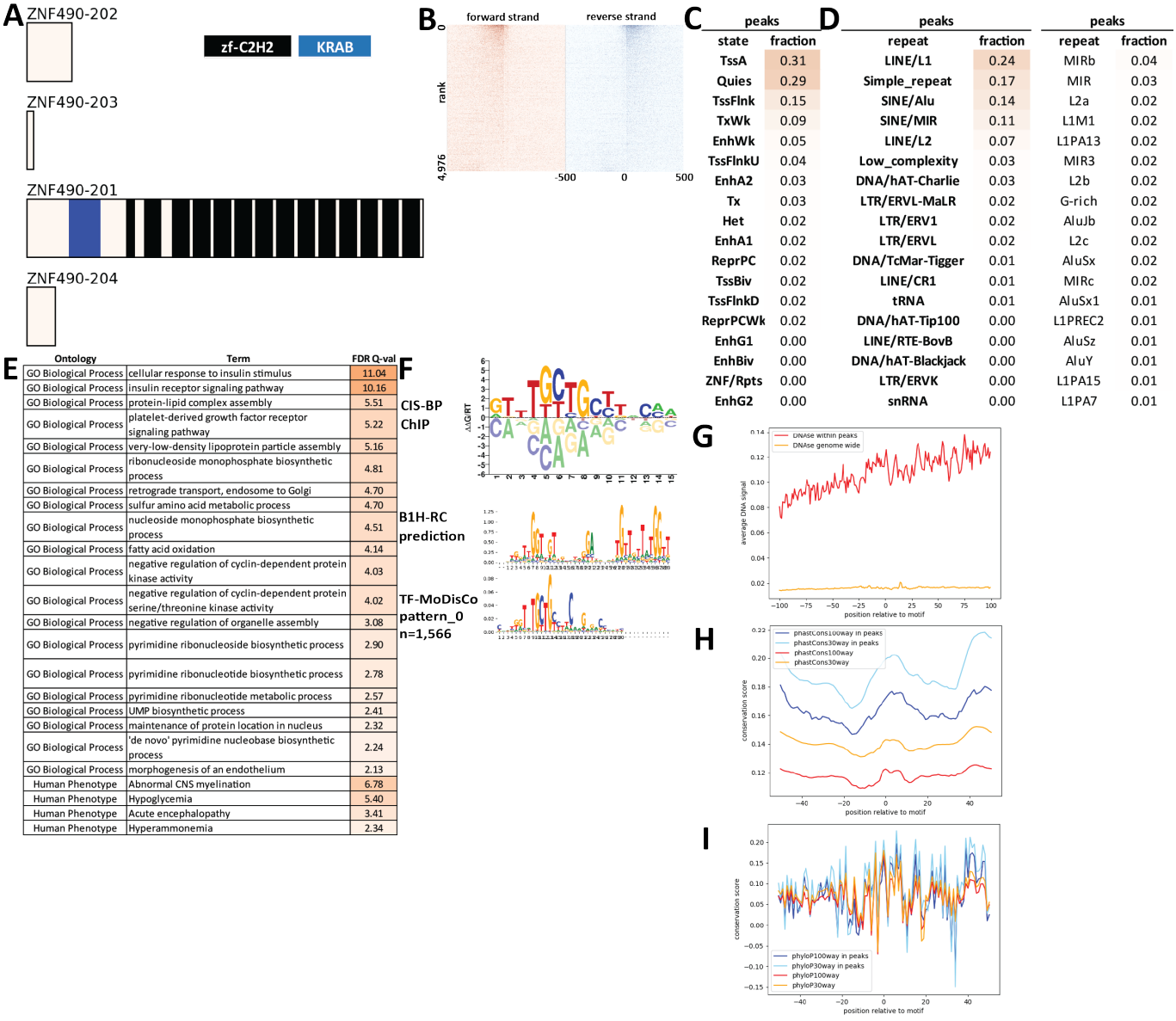

Supplementary Figure 1270: Properties and genomic distribution of motifs identified for the ZNF490 transcription factor in HepG2 (accession ENCSR542PZA).

TF-MoDisCO pattern_0 n=1566, CWM

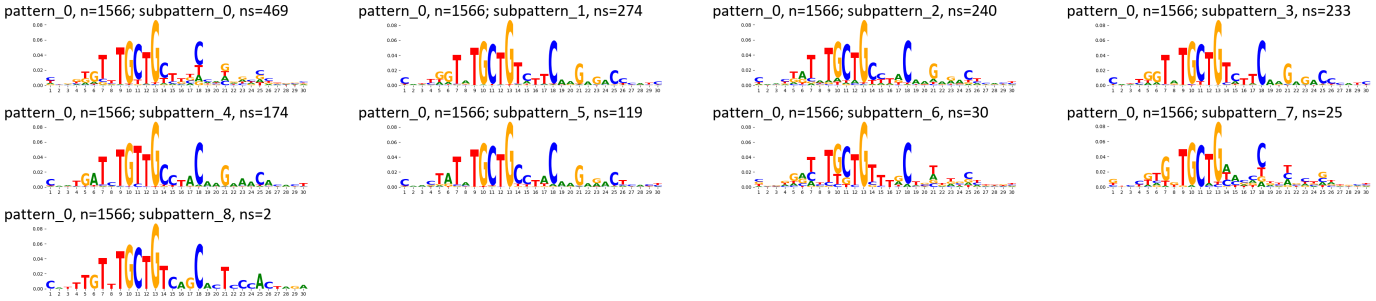

TF-MoDisCO pattern_0 n=1566, PWM

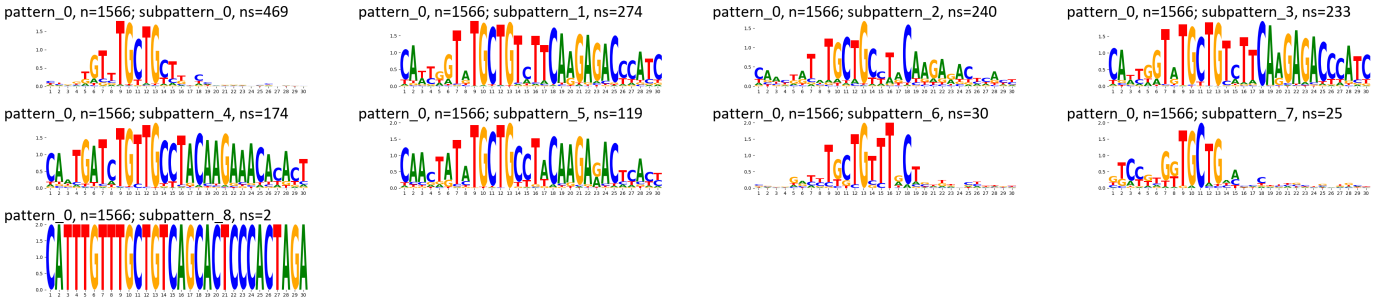

Supplementary Figure 1271: TF-MoDisCO subpatterns for the ZNF490 transcription factor in HepG2 (accession ENCSR542PZA).

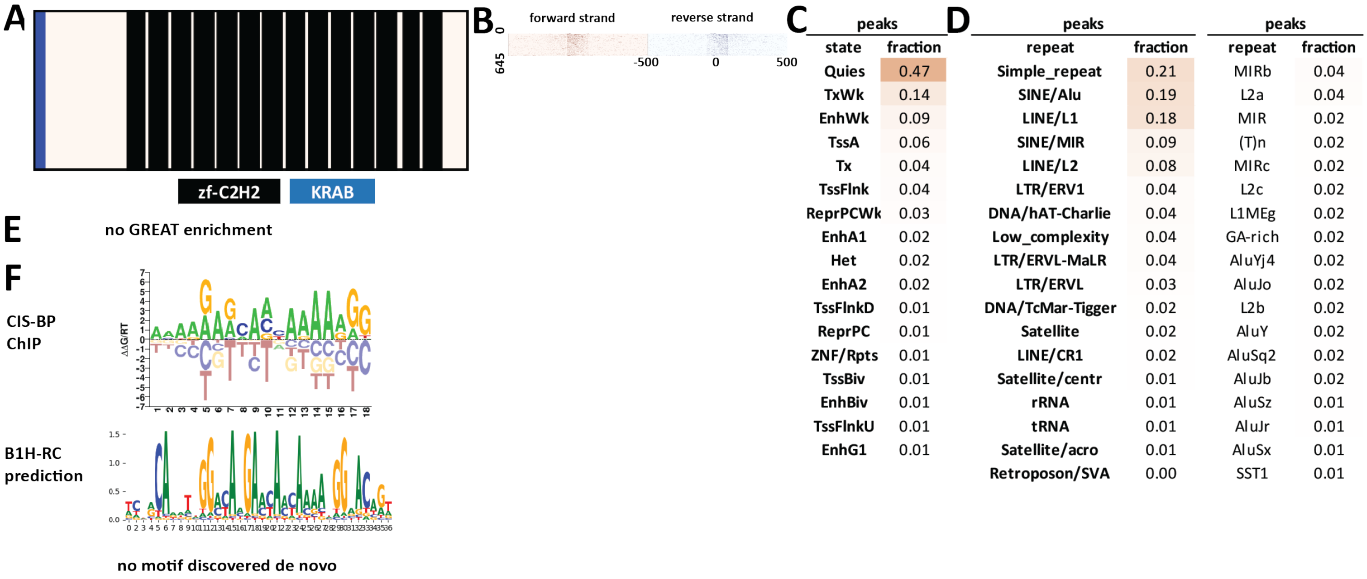

C

peaks	
state	fraction
Quies	0.47
TxWk	0.14
EnhWk	0.09
TssA	0.06
Tx	0.04
TssFlnk	0.04
ReprPCWk	0.03
EnhA1	0.02
Het	0.02
EnhA2	0.02
TssFlnkD	0.01
ReprPC	0.01
ZNF/Rpts	0.01
TssBiv	0.01
EnhBiv	0.01
TssFlnkU	0.01
EnhG1	0.01

D

peaks		peaks	
repeat	fraction	repeat	fraction
Simple_repeat	0.21	MIRb	0.04
SINE/Alu	0.19	L2a	0.04
LINE/L1	0.18	MIR	0.02
SINE/MIR	0.09	(T)n	0.02
LINE/L2	0.08	MIRc	0.02
LTR/ERV1	0.04	L2c	0.02
DNA/hAT-Charlie	0.04	L1MEg	0.02
Low_complexity	0.04	GA-rich	0.02
LTR/ERVL-MaLR	0.04	AluYj4	0.02
LTR/ERVL	0.03	AluJo	0.02
DNA/TcMar-Tigger	0.02	L2b	0.02
Satellite	0.02	AluY	0.02
LINE/CR1	0.02	AluSq2	0.02
Satellite/centr	0.01	AluJb	0.02
rRNA	0.01	AluSz	0.01
tRNA	0.01	AluJr	0.01
Satellite/acro	0.01	AluSx	0.01
Retroposon/SVA	0.00	SST1	0.01

Supplementary Figure 1272: Properties and genomic distribution of motifs identified for the ZNF492 transcription factor in HEK293 (accession ChipExo models).

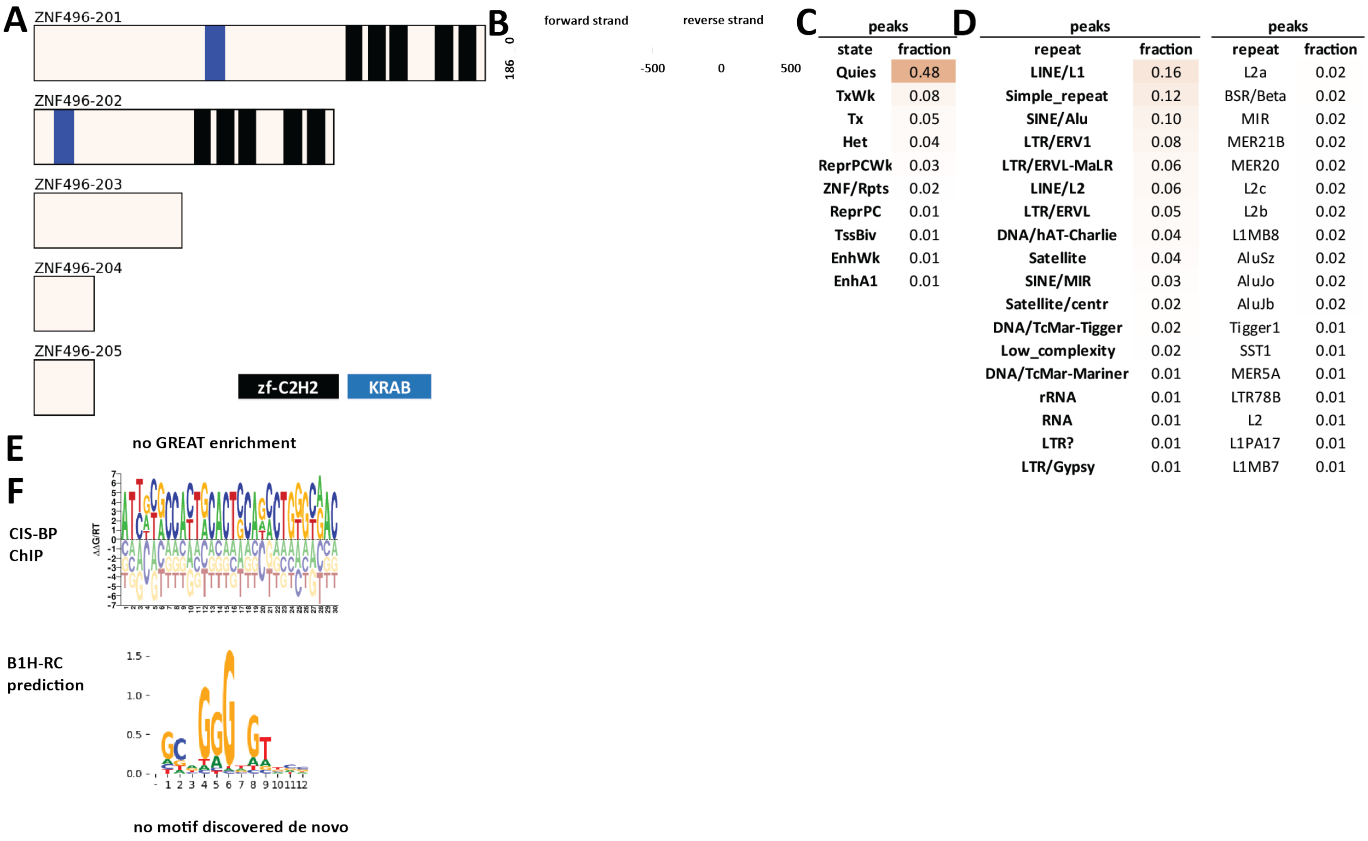

Supplementary Figure 1273: Properties and genomic distribution of motifs identified for the ZNF496 transcription factor in HEK293 (accession ChipExo models).

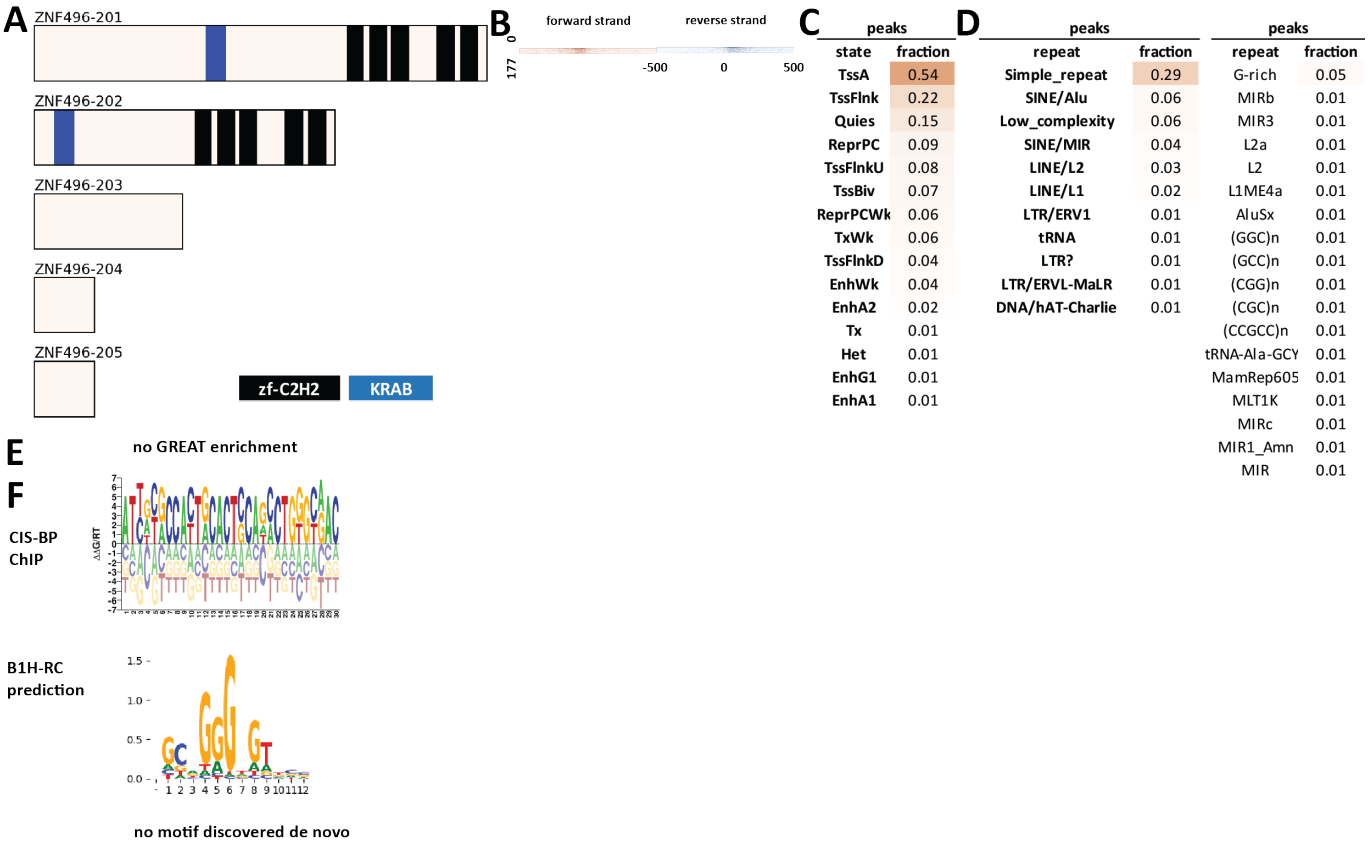

Supplementary Figure 1274: Properties and genomic distribution of motifs identified for the ZNF496 transcription factor in HepG2 (accession ENCSR828TVO).

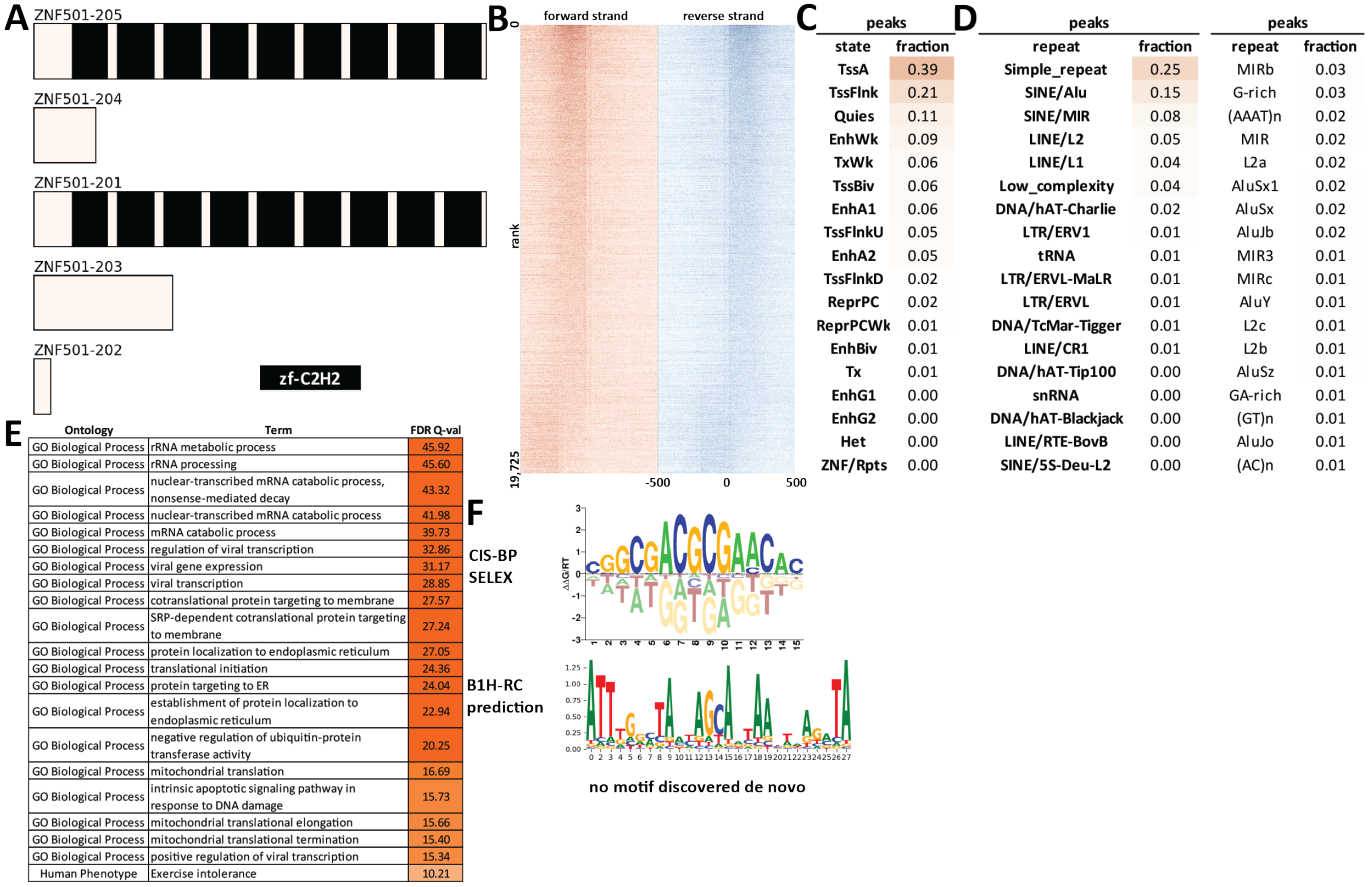

Supplementary Figure 1275: Properties and genomic distribution of motifs identified for the ZNF501 transcription factor in HEK293 (accession ENCSR461ZJT).

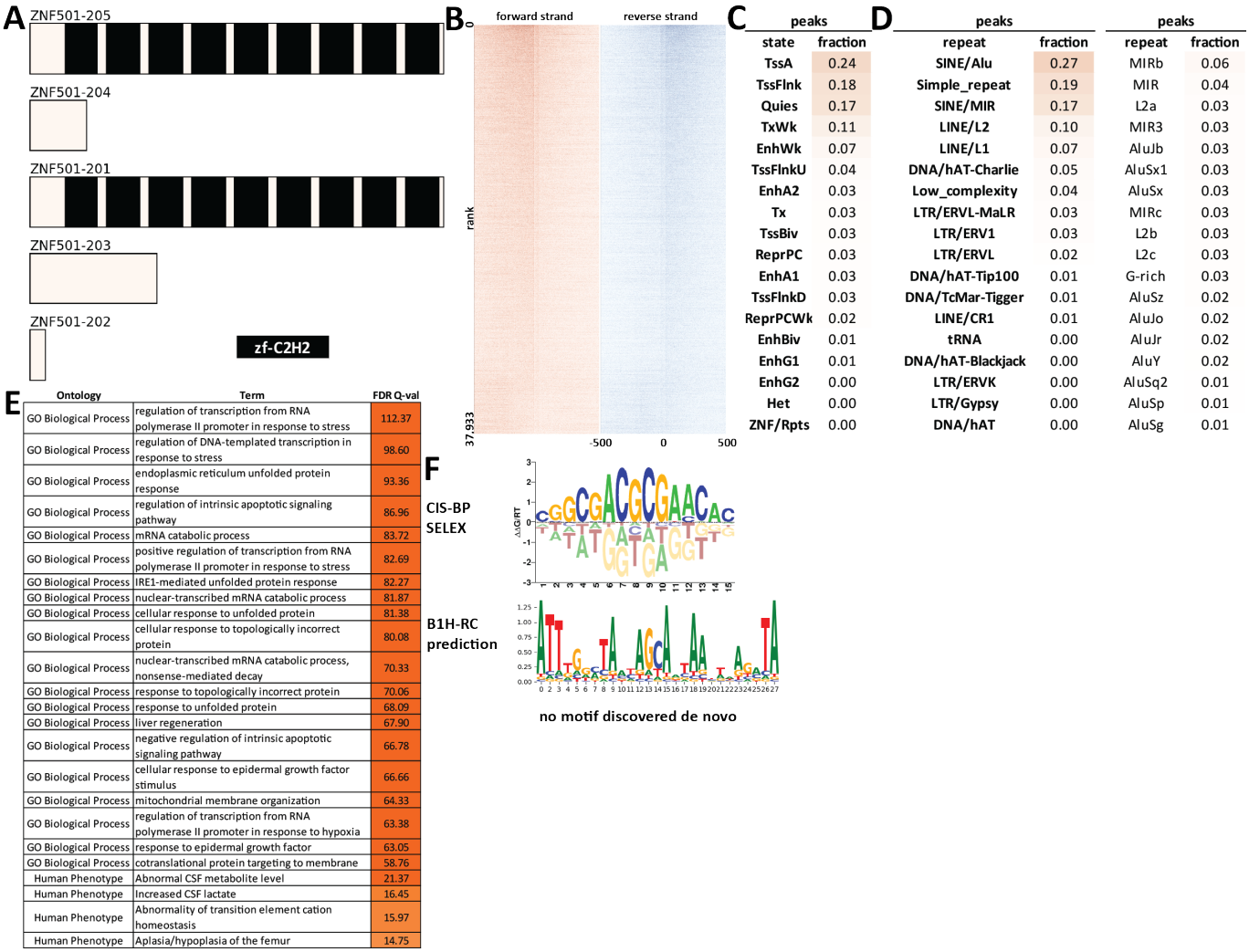

C

peaks	
state	fraction
TssA	0.24
TssFlnk	0.18
Quies	0.17
TxWk	0.11
EnhWk	0.07
TssFlnkU	0.04
EnhA2	0.03
Tx	0.03
TssBiv	0.03
ReprPC	0.03
EnhA1	0.03
TssFlnkD	0.03
ReprPCWk	0.02
EnhBiv	0.01
EnhG1	0.01
EnhG2	0.00
Het	0.00
ZNF/Rpts	0.00

D

peaks		peaks	
repeat	fraction	repeat	fraction
SINE/Alu	0.27	MIRb	0.06
Simple_repeat	0.19	MIR	0.04
SINE/MIR	0.17	L2a	0.03
LINE/L2	0.10	MIR3	0.03
LINE/L1	0.07	AluJb	0.03
DNA/hAT-Charlie	0.05	AluSx1	0.03
Low_complexity	0.04	AluSx	0.03
LTR/ERVL-MaLR	0.03	MIRc	0.03
LTR/ERV1	0.03	L2b	0.03
LTR/ERVL	0.02	L2c	0.03
DNA/hAT-Tip100	0.01	G-rich	0.03
DNA/TcMar-Tigger	0.01	AluSz	0.02
LINE/CR1	0.01	AluJo	0.02
tRNA	0.00	AluJr	0.02
DNA/hAT-Blackjack	0.00	AluY	0.02
LTR/ERVK	0.00	AluSq2	0.01
LTR/Gypsy	0.00	AluSp	0.01
DNA/hAT	0.00	AluSg	0.01

E

Ontology	Term	FDR Q-val
GO Biological Process	regulation of transcription from RNA polymerase II promoter in response to stress	112.37
GO Biological Process	regulation of DNA-templated transcription in response to stress	98.60
GO Biological Process	endoplasmic reticulum unfolded protein response	93.36
GO Biological Process	regulation of intrinsic apoptotic signaling pathway	86.96
GO Biological Process	mRNA catabolic process	83.72
GO Biological Process	positive regulation of transcription from RNA polymerase II promoter in response to stress	82.69
GO Biological Process	IRE1-mediated unfolded protein response	82.27
GO Biological Process	nuclear-transcribed mRNA catabolic process	81.87
GO Biological Process	cellular response to unfolded protein	81.38
GO Biological Process	cellular response to topologically incorrect protein	80.08
GO Biological Process	nuclear-transcribed mRNA catabolic process, nonsense-mediated decay	70.33
GO Biological Process	response to topologically incorrect protein	70.06
GO Biological Process	response to unfolded protein	68.09
GO Biological Process	liver regeneration	67.90
GO Biological Process	negative regulation of intrinsic apoptotic signaling pathway	66.78
GO Biological Process	cellular response to epidermal growth factor stimulus	66.66
GO Biological Process	mitochondrial membrane organization	64.33
GO Biological Process	regulation of transcription from RNA polymerase II promoter in response to hypoxia	63.38
GO Biological Process	response to epidermal growth factor	63.05
GO Biological Process	cotranslational protein targeting to membrane	58.76
Human Phenotype	Abnormal CSF metabolite level	21.37
Human Phenotype	Increased CSF lactate	16.45
Human Phenotype	Abnormality of transition element cation homeostasis	15.97
Human Phenotype	Aplasia/hypoplasia of the femur	14.75

Supplementary Figure 1276: Properties and genomic distribution of motifs identified for the ZNF501 transcription factor in HepG2 (accession ENCSR227PHM).

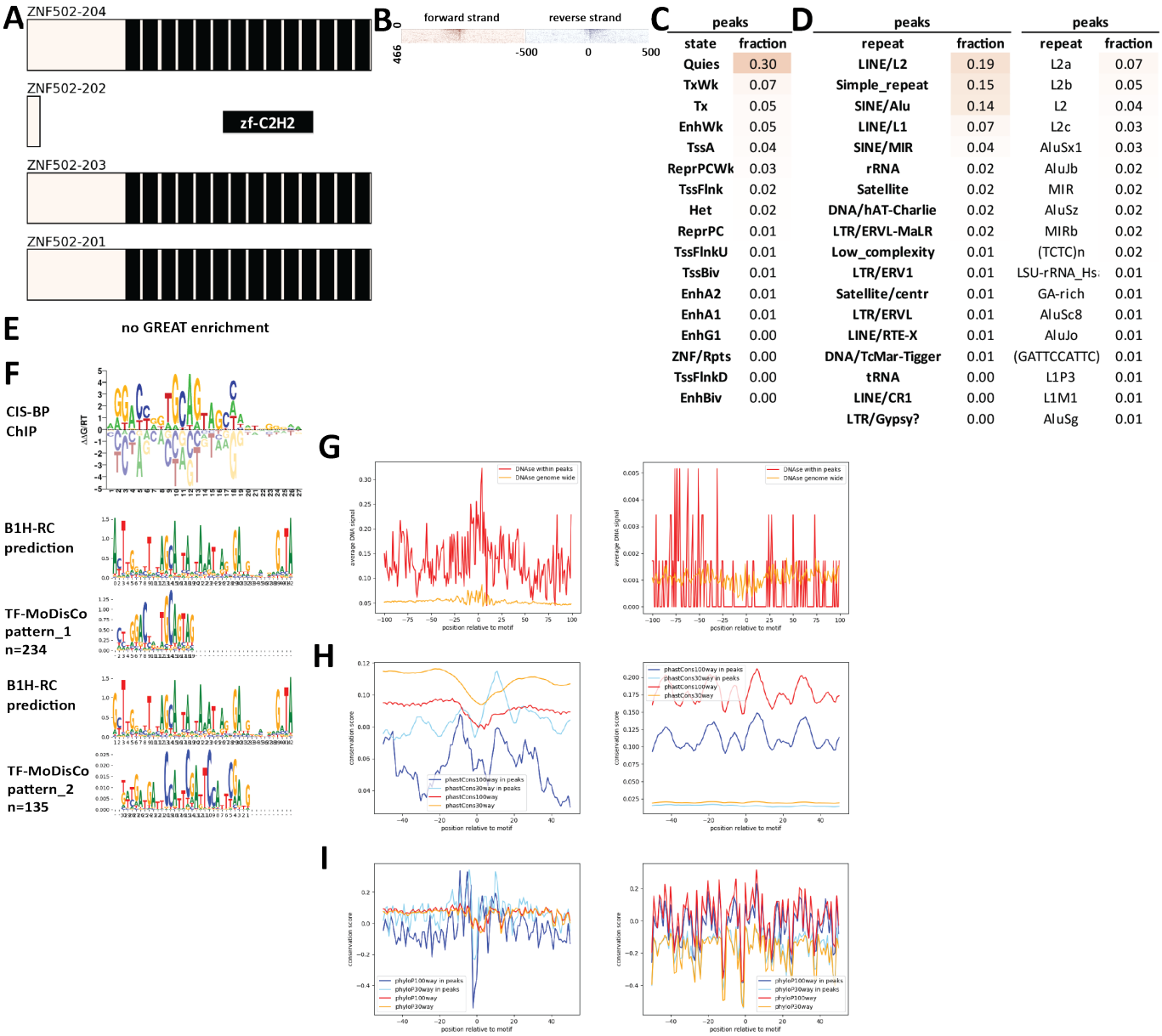

peaks	
state	fraction
Quies	0.30
TxWk	0.07
Tx	0.05
EnhWk	0.05
TssA	0.04
ReprPCWk	0.03
TssFlnk	0.02
Het	0.02
ReprPC	0.01
TssFlnkU	0.01
TssBiv	0.01
EnhA2	0.01
EnhA1	0.01
EnhG1	0.00
ZNF/Rpts	0.00
TssFlnkD	0.00
EnhBiv	0.00

peaks	
repeat	fraction
LINE/L2	0.19
Simple_repeat	0.15
SINE/Alu	0.14
LINE/L1	0.07
SINE/MIR	0.04
rRNA	0.02
Satellite	0.02
DNA/hAT-Charlie	0.02
LTR/ERVL-MaLR	0.02
Low_complexity	0.01
LTR/ERV1	0.01
Satellite/centr	0.01
LTR/ERVL	0.01
LINE/RTE-X	0.01
DNA/TcMar-Tigger	0.01
tRNA	0.00
LINE/CR1	0.00
LTR/Gypsy?	0.00

peaks	
repeat	fraction
L2a	0.07
L2b	0.05
L2	0.04
L2c	0.03
AluSx1	0.03
AluJb	0.02
MIR	0.02
AluSz	0.02
MIRb	0.02
(TCTC)n	0.02
LSU-rRNA_Hs	0.01
GA-rich	0.01
AluSc8	0.01
AluJo	0.01
(GATTCCATTC)	0.01
L1P3	0.01
L1M1	0.01
AluSg	0.01

Supplementary Figure 1277: Properties and genomic distribution of motifs identified for the ZNF502 transcription factor in HEK293 (accession Hughes GR models).

TF-MoDisCO pattern_1 n=234, CWM

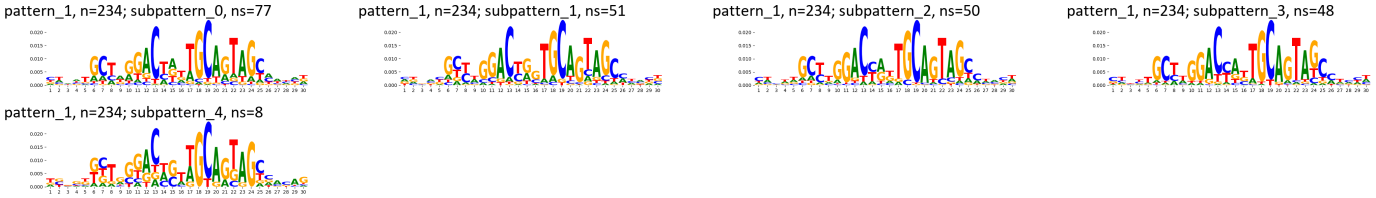

TF-MoDisCO pattern_1 n=234, PWM

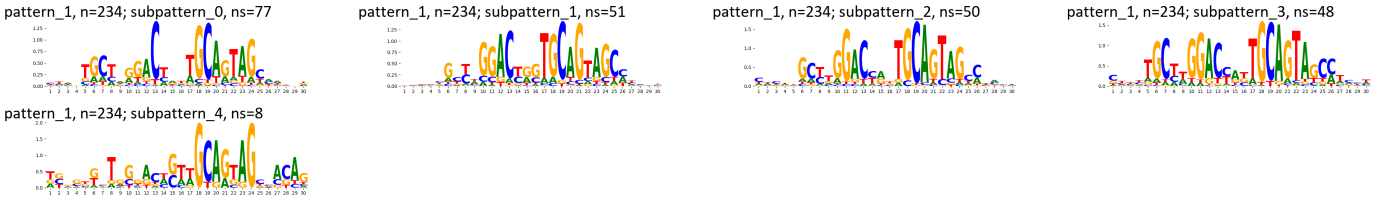

TF-MoDisCO pattern_2 n=135, CWM

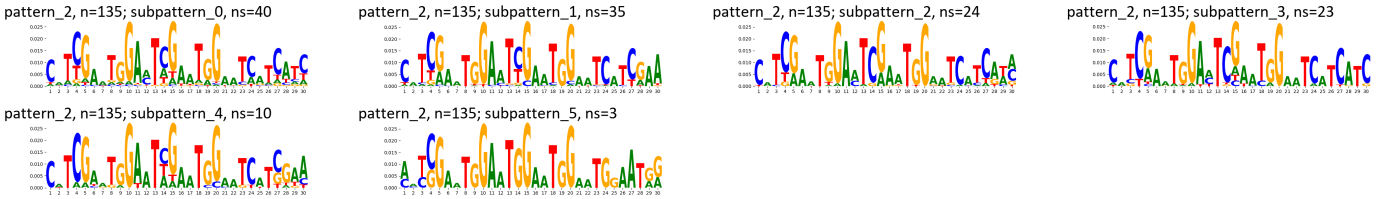

TF-MoDisCO pattern_2 n=135, PWM

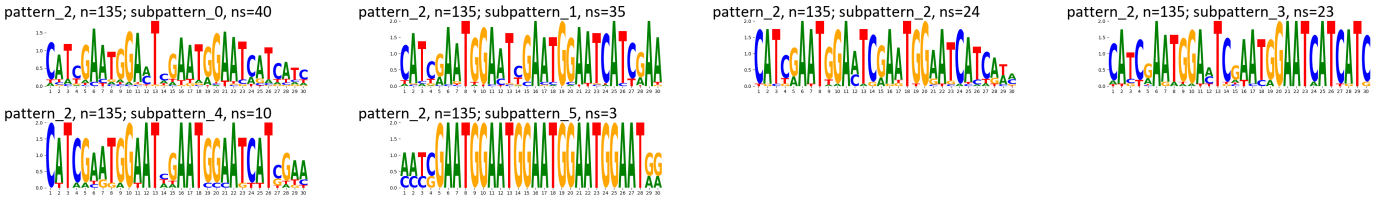

Supplementary Figure 1278: TF-MoDisCO subpatterns for the ZNF502 transcription factor in HEK293 (accession Hughes GR models).

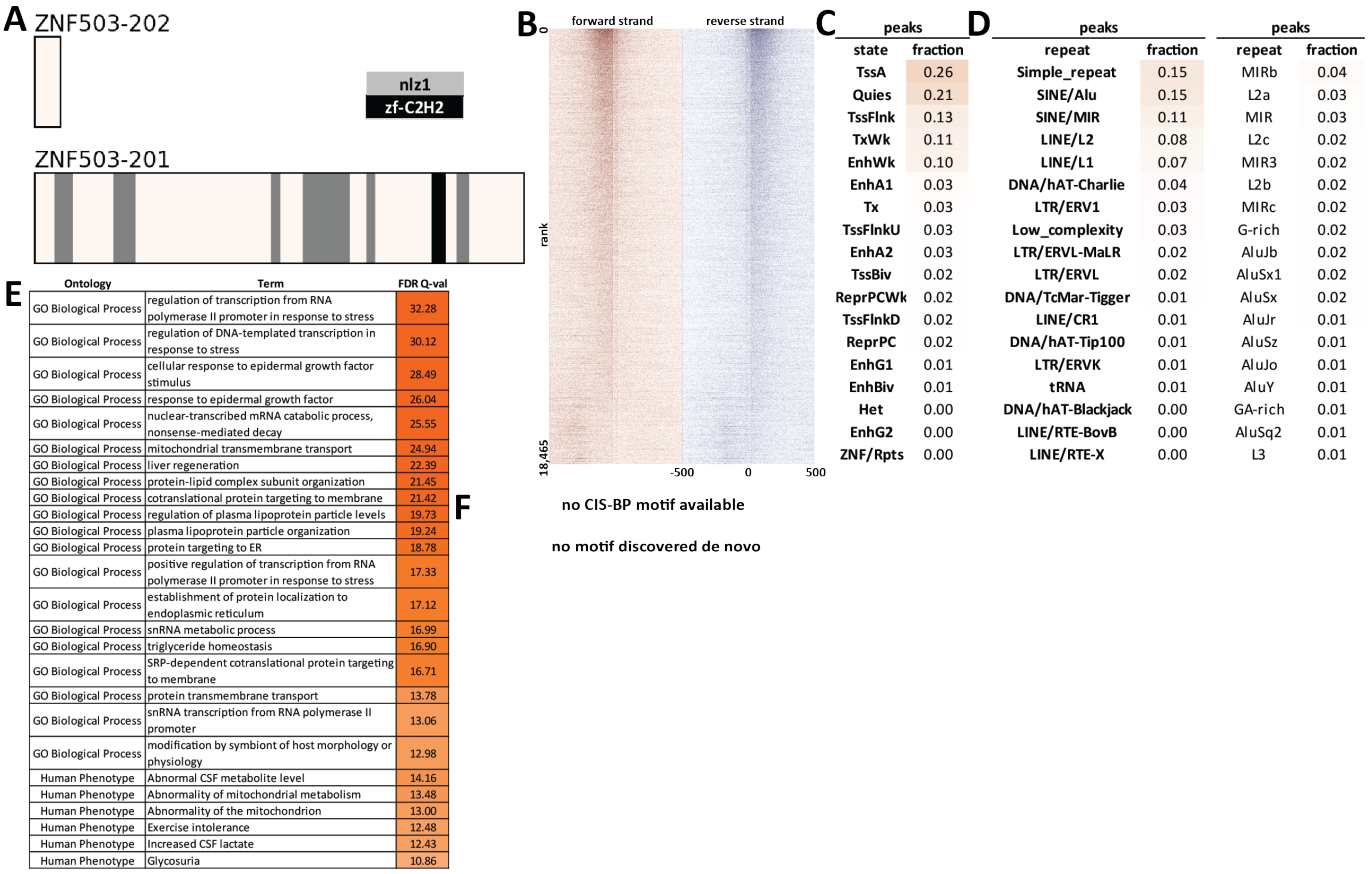

C

peaks	
state	fraction
TssA	0.26
Quies	0.21
TssFlnk	0.13
TxWk	0.11
EnhWk	0.10
EnhA1	0.03
Tx	0.03
TssFlnkU	0.03
EnhA2	0.03
TssBiv	0.02
ReprPCWk	0.02
TssFlnkD	0.02
ReprPC	0.02
EnhG1	0.01
EnhBiv	0.01
Het	0.00
EnhG2	0.00
ZNF/Rpts	0.00

D

peaks		peaks	
repeat	fraction	repeat	fraction
Simple_repeat	0.15	MIRb	0.04
SINE/Alu	0.15	L2a	0.03
SINE/MIR	0.11	MIR	0.03
LINE/L2	0.08	L2c	0.02
LINE/L1	0.07	MIR3	0.02
DNA/hAT-Charlie	0.04	L2b	0.02
LTR/ERV1	0.03	MIRc	0.02
Low_complexity	0.03	G-rich	0.02
LTR/ERVL-MaLR	0.02	AluJb	0.02
LTR/ERVL	0.02	AluSx1	0.02
DNA/TcMar-Tigger	0.01	AluSx	0.02
LINE/CR1	0.01	AluJr	0.01
DNA/hAT-Tip100	0.01	AluSz	0.01
LTR/ERVK	0.01	AluJo	0.01
tRNA	0.01	AluY	0.01
DNA/hAT-Blackjack	0.00	GA-rich	0.01
LINE/RTE-BovB	0.00	AluSq2	0.01
LINE/RTE-X	0.00	L3	0.01

E

Ontology	Term	FDR Q-val
GO Biological Process	regulation of transcription from RNA polymerase II promoter in response to stress	32.28
GO Biological Process	regulation of DNA-templated transcription in response to stress	30.12
GO Biological Process	cellular response to epidermal growth factor stimulus	28.49
GO Biological Process	response to epidermal growth factor	26.04
GO Biological Process	nuclear-transcribed mRNA catabolic process, nonsense-mediated decay	25.55
GO Biological Process	mitochondrial transmembrane transport	24.94
GO Biological Process	liver regeneration	22.39
GO Biological Process	protein-lipid complex subunit organization	21.45
GO Biological Process	cotranslational protein targeting to membrane	21.42
GO Biological Process	regulation of plasma lipoprotein particle levels	19.73
GO Biological Process	plasma lipoprotein particle organization	19.24
GO Biological Process	protein targeting to ER	18.78
GO Biological Process	positive regulation of transcription from RNA polymerase II promoter in response to stress	17.33
GO Biological Process	establishment of protein localization to endoplasmic reticulum	17.12
GO Biological Process	snRNA metabolic process	16.99
GO Biological Process	triglyceride homeostasis	16.90
GO Biological Process	SRP-dependent cotranslational protein targeting to membrane	16.71
GO Biological Process	protein transmembrane transport	13.78
GO Biological Process	snRNA transcription from RNA polymerase II promoter	13.06
GO Biological Process	modification by symbiont of host morphology or physiology	12.98
Human Phenotype	Abnormal CSF metabolite level	14.16
Human Phenotype	Abnormality of mitochondrial metabolism	13.48
Human Phenotype	Abnormality of the mitochondrion	13.00
Human Phenotype	Exercise intolerance	12.48
Human Phenotype	Increased CSF lactate	12.43
Human Phenotype	Glycosuria	10.86

Supplementary Figure 1279: Properties and genomic distribution of motifs identified for the ZNF503 transcription factor in HepG2 (accession ENCSR998YJI).

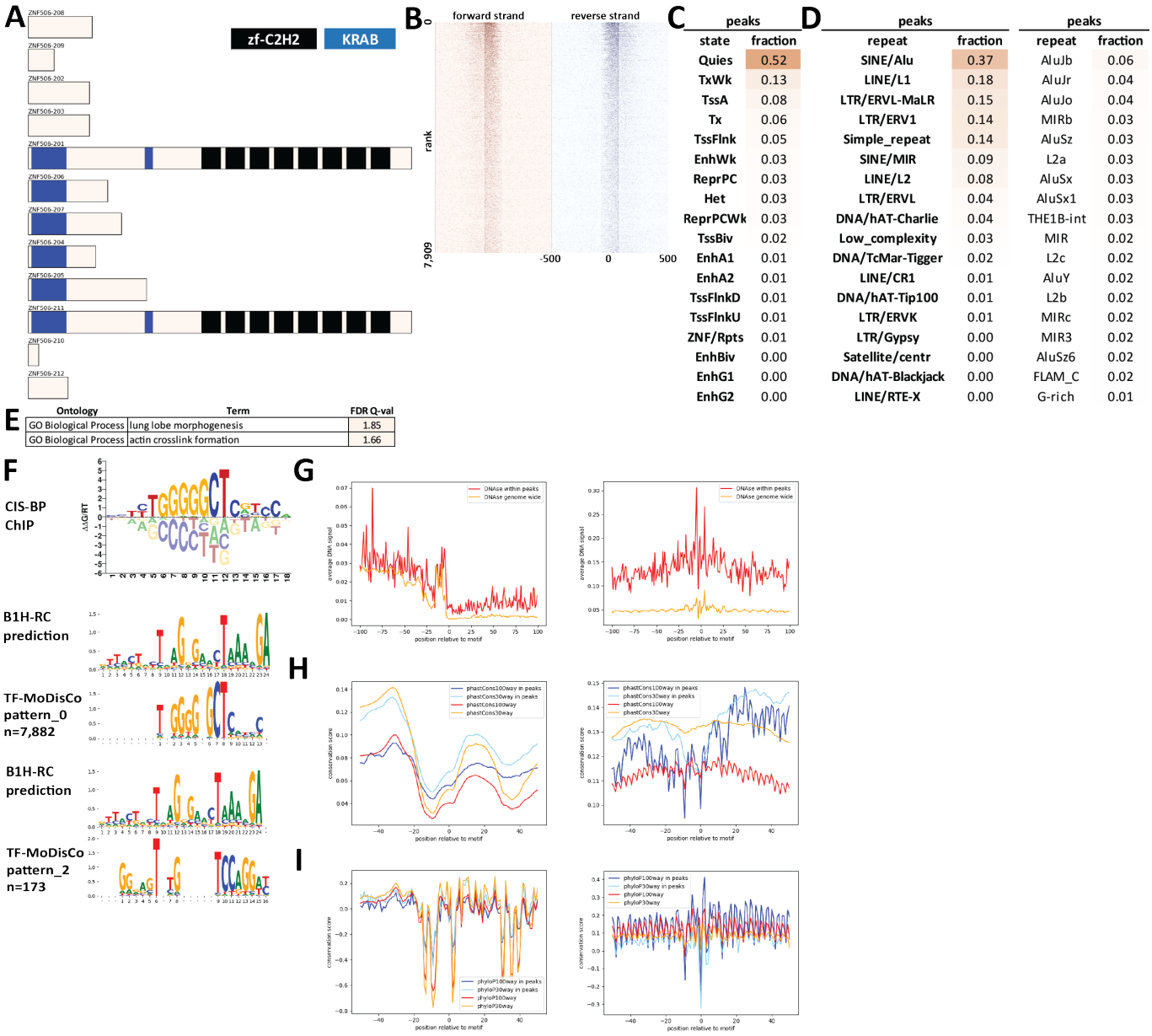

Supplementary Figure 1280: Properties and genomic distribution of motifs identified for the ZNF506 transcription factor in HEK293 (accession ChipExo models).

TF-MoDisCO pattern_0 n=7882, CWM

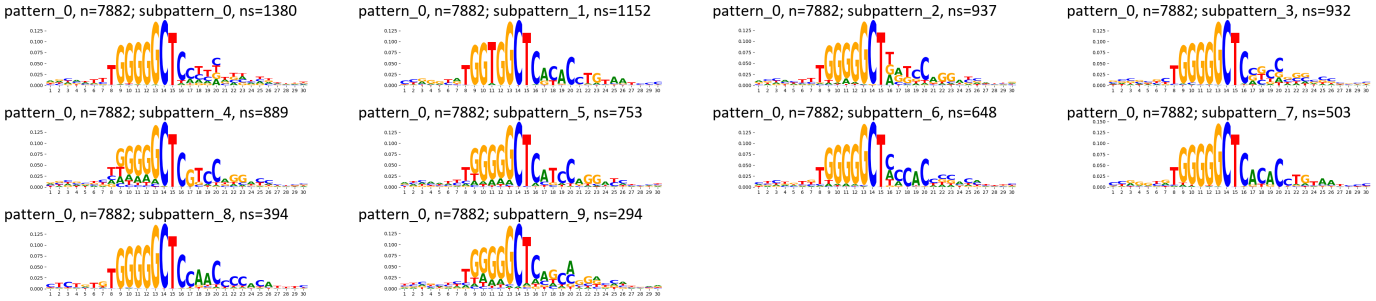

TF-MoDisCO pattern_0 n=7882, PWM

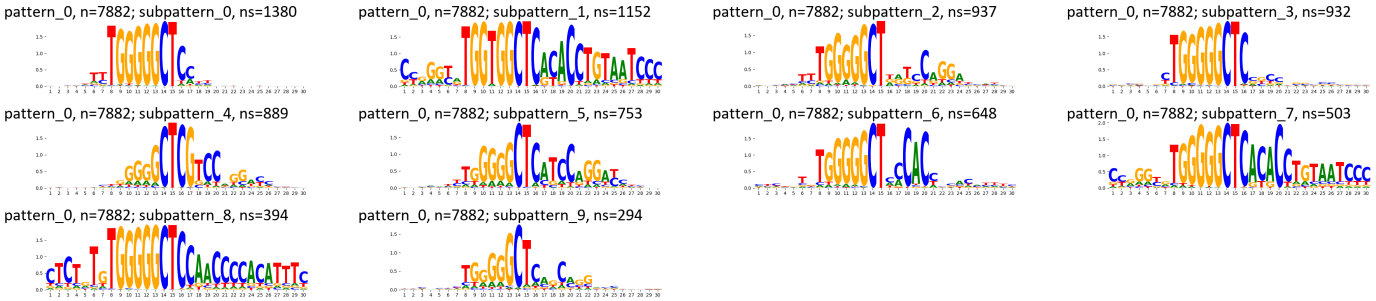

TF-MoDisCO pattern_2 n=173, CWM

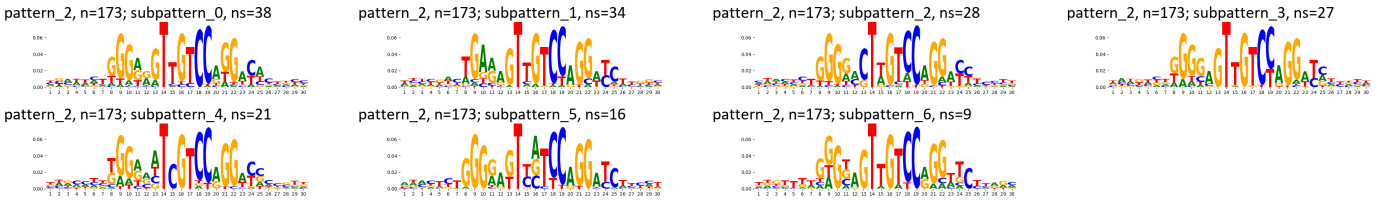

TF-MoDisCO pattern_2 n=173, PWM

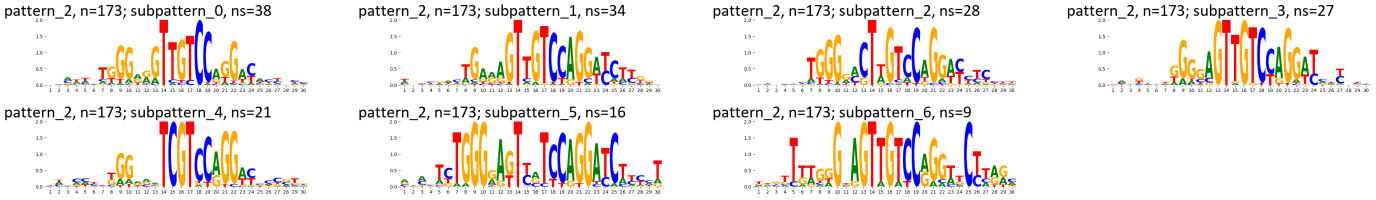

Supplementary Figure 1281: TF-MoDisCO subpatterns for the ZNF506 transcription factor in HEK293 (accession ChipExo models).

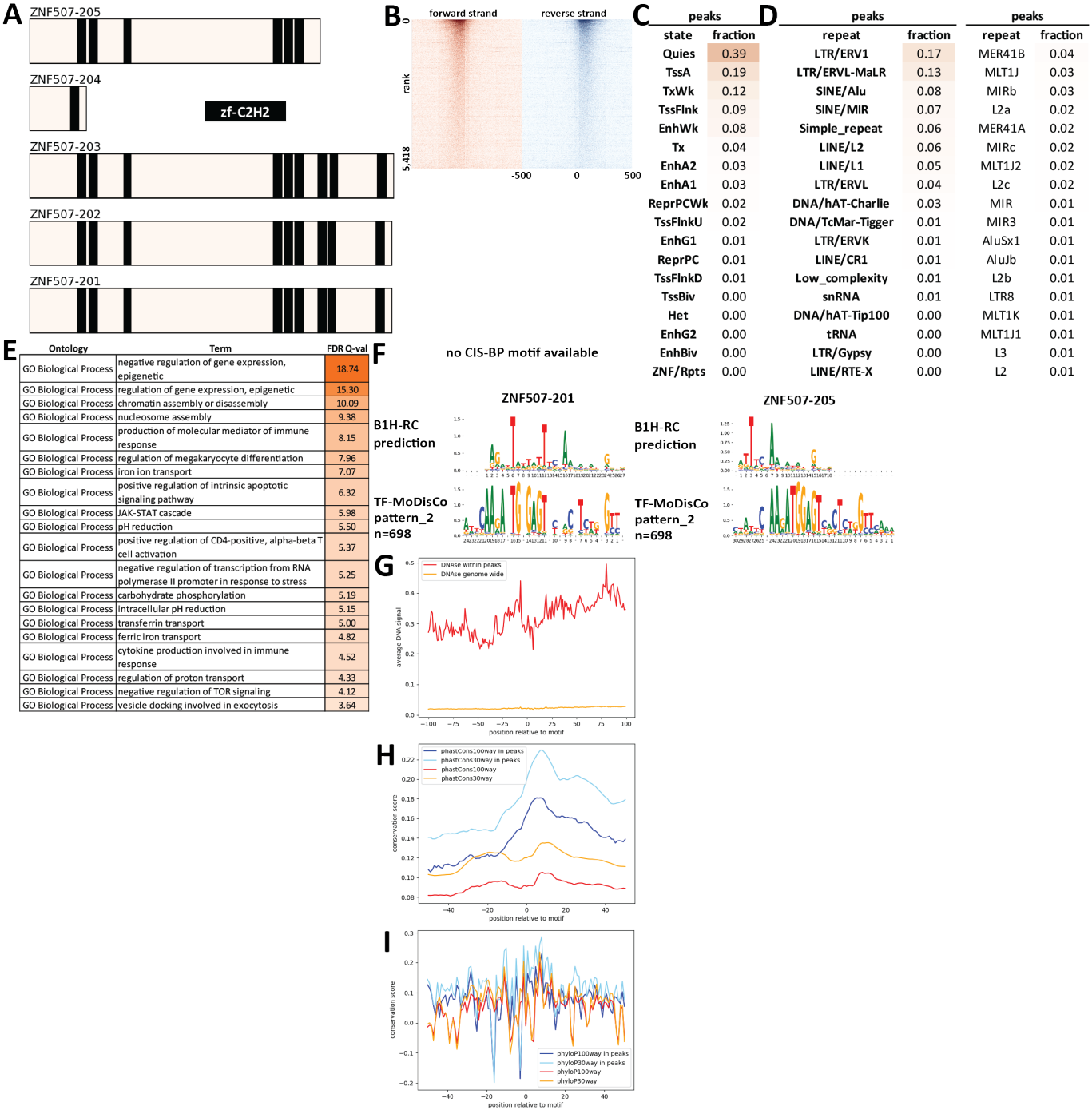

Supplementary Figure 1282: Properties and genomic distribution of motifs identified for the ZNF507 transcription factor in K562 (accession ENCSR577KQD).

TF-MoDisCO pattern_2 n=698, CWM

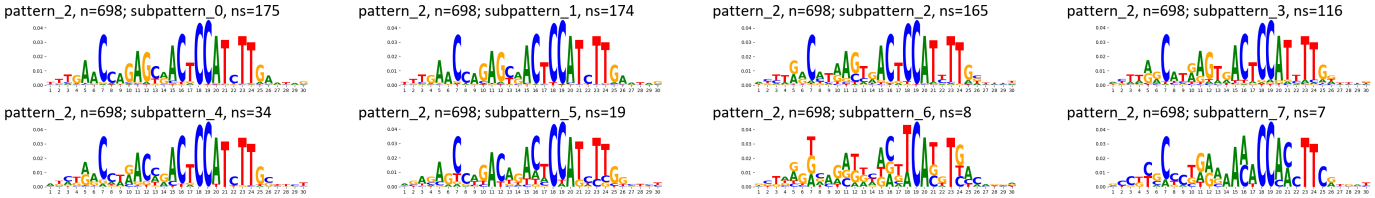

TF-MoDisCO pattern_2 n=698, PWM

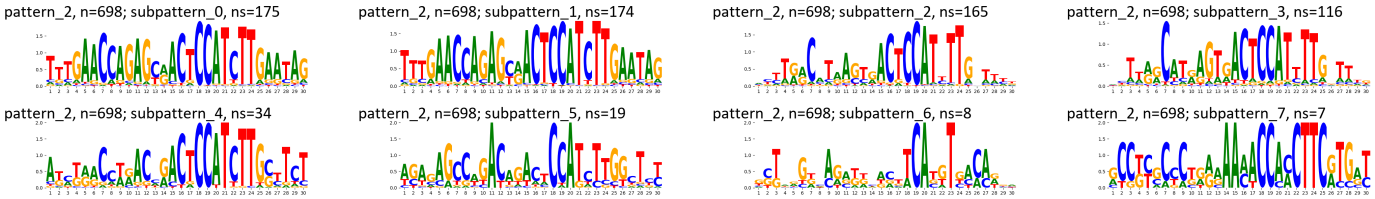

Supplementary Figure 1283: TF-MoDisCO subpatterns for the ZNF507 transcription factor in K562 (accession ENCSR577KQD).

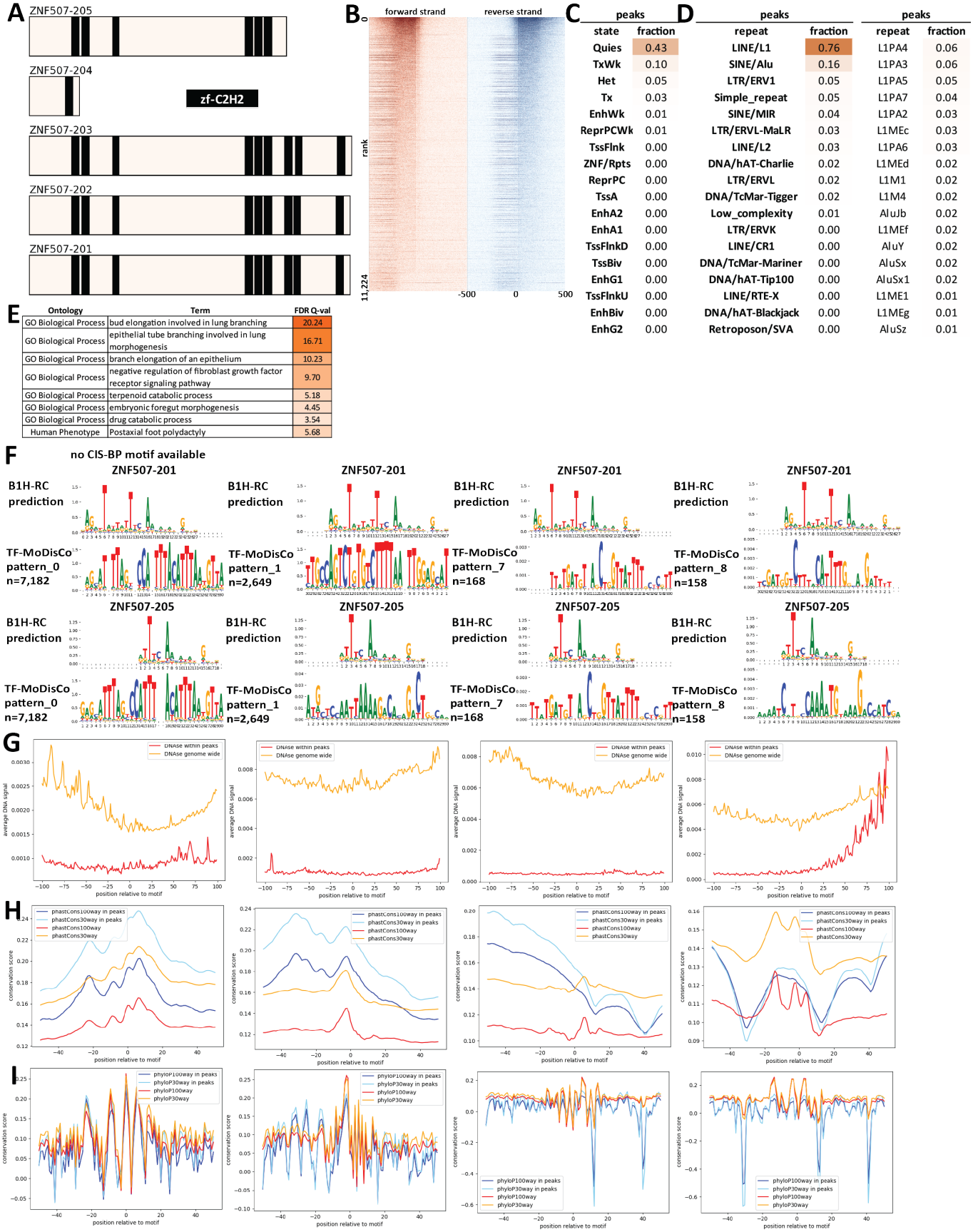

Supplementary Figure 1284: Properties and genomic distribution of motifs identified for the ZNF507 transcription factor in K562 (accession ENCSR598TIR).

TF-MoDisCO pattern_0 n=7182, CWM

pattern_0, n=7182; subpattern_0, n=1426

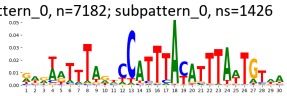

pattern_0, n=7182; subpattern_1, ns=1257

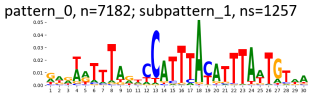

pattern_0, n=7182; subpattern_10, ns=11

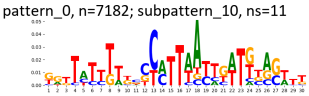

pattern_0, n=7182; subpattern_2, ns=1031

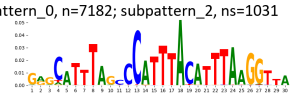

pattern_0, n=7182; subpattern_3, ns=955

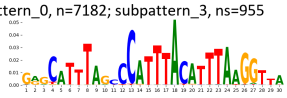

pattern_0, n=7182; subpattern_4, ns=639

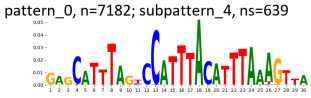

pattern_0, n=7182; subpattern_5, ns=601

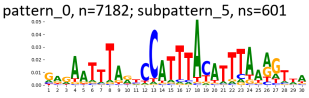

pattern_0, n=7182; subpattern_6, ns=582

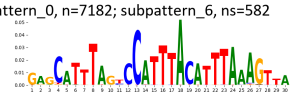

pattern_0, n=7182; subpattern_7, ns=495

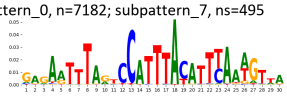

pattern_0, n=7182; subpattern_8, ns=160

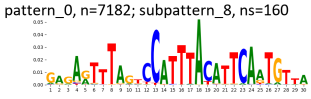

pattern_0, n=7182; subpattern_9, ns=25

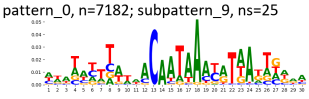

TF-MoDisCO pattern_0 n=7182, PWM

pattern_0, n=7182; subpattern_0, ns=1426

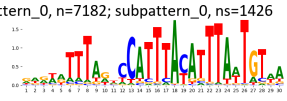

pattern_0, n=7182; subpattern_1, ns=1257

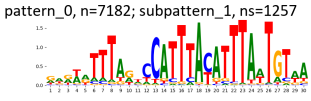

pattern_0, n=7182; subpattern_10, ns=11

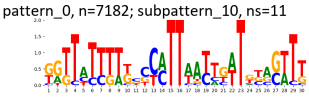

pattern_0, n=7182; subpattern_2, ns=1031

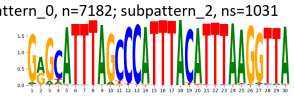

pattern_0, n=7182; subpattern_3, ns=955

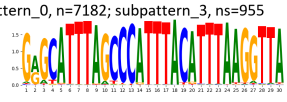

pattern_0, n=7182; subpattern_4, ns=639

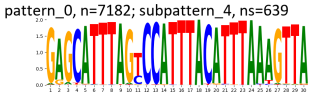

pattern_0, n=7182; subpattern_5, ns=601

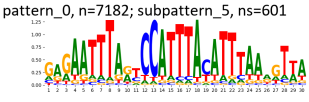

pattern_0, n=7182; subpattern_6, ns=582

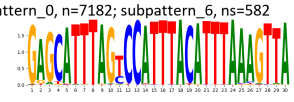

pattern_0, n=7182; subpattern_7, ns=495

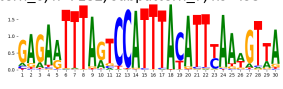

pattern_0, n=7182; subpattern_8, ns=160

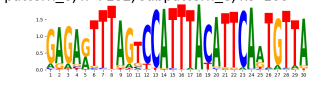

pattern_0, n=7182; subpattern_9, ns=25

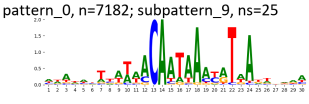

TF-MoDisCO pattern_1 n=2649, CWM

pattern_1, n=2649; subpattern_0, ns=914

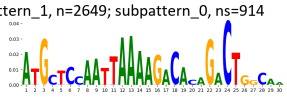

pattern_1, n=2649; subpattern_1, ns=484

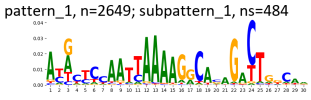

pattern_1, n=2649; subpattern_2, ns=341

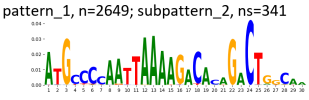

pattern_1, n=2649; subpattern_3, ns=306

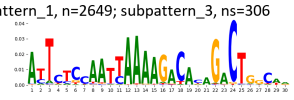

pattern_1, n=2649; subpattern_4, ns=240

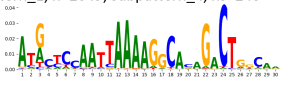

pattern_1, n=2649; subpattern_5, ns=189

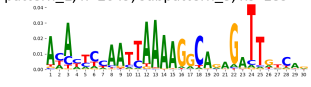

pattern_1, n=2649; subpattern_6, ns=114

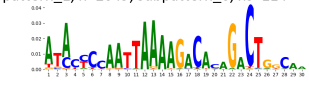

pattern_1, n=2649; subpattern_7, ns=29

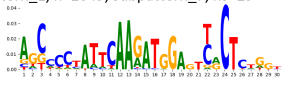

pattern_1, n=2649; subpattern_8, ns=25

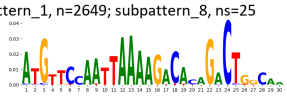

pattern_1, n=2649; subpattern_9, ns=7

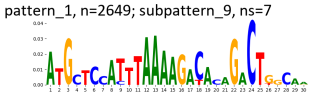

TF-MoDisCO pattern_1 n=2649, PWM

pattern_1, n=2649; subpattern_0, ns=914

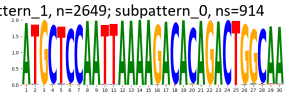

pattern_1, n=2649; subpattern_1, ns=484

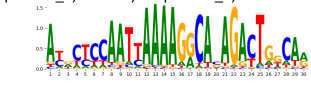

pattern_1, n=2649; subpattern_2, ns=341

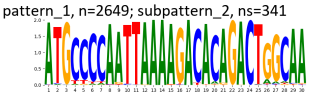

pattern_1, n=2649; subpattern_3, ns=306

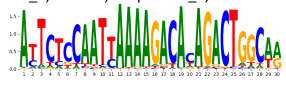

pattern_1, n=2649; subpattern_4, ns=240

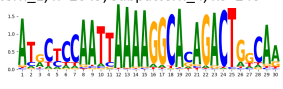

pattern_1, n=2649; subpattern_5, ns=189

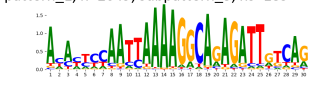

pattern_1, n=2649; subpattern_6, ns=114

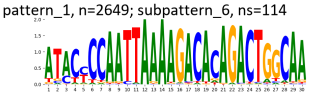

pattern_1, n=2649; subpattern_7, ns=29

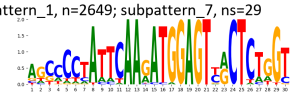

pattern_1, n=2649; subpattern_8, ns=25

pattern_1, n=2649; subpattern_9, ns=7

TF-MoDisCO pattern_7 n=168, CWM

pattern_7, n=168; subpattern_0, ns=54

pattern_7, n=168; subpattern_1, ns=41

pattern_7, n=168; subpattern_2, ns=40

pattern_7, n=168; subpattern_3, ns=23

pattern_7, n=168; subpattern_4, ns=8

pattern_7, n=168; subpattern_5, ns=2

TF-MoDisCO pattern_7 n=168, PWM

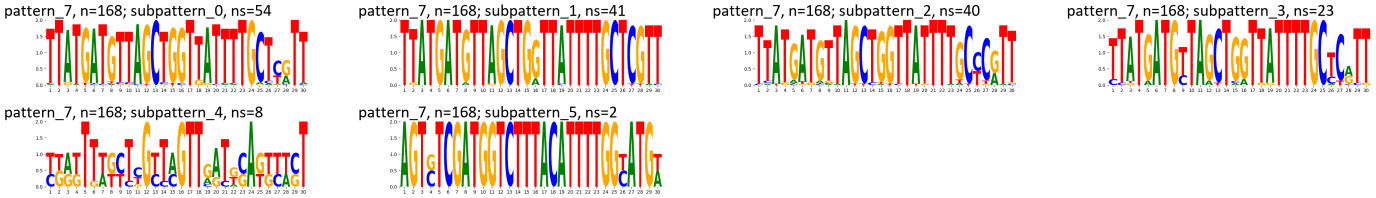

TF-MoDisCO pattern_8 n=158, CWM

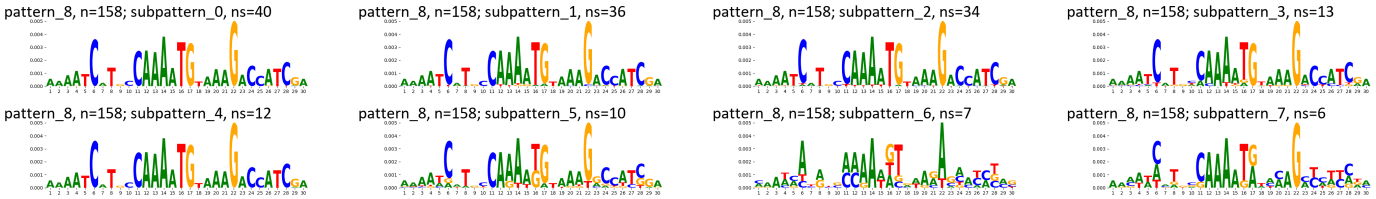

TF-MoDisCO pattern_8 n=158, PWM

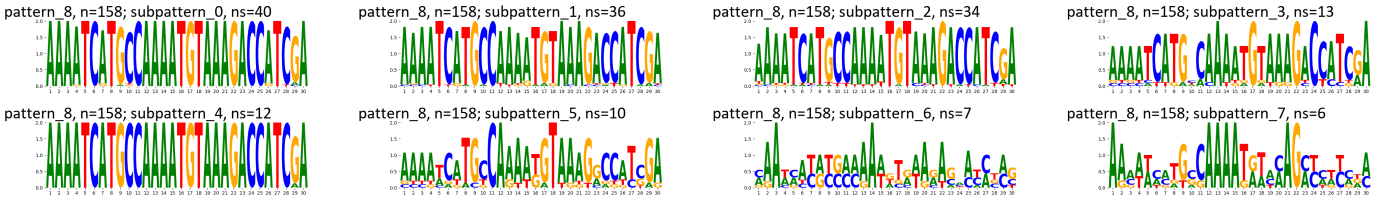

Supplementary Figure 1285: TF-MoDisCO subpatterns for the ZNF507 transcription factor in K562 (accession ENCSR598TIR).

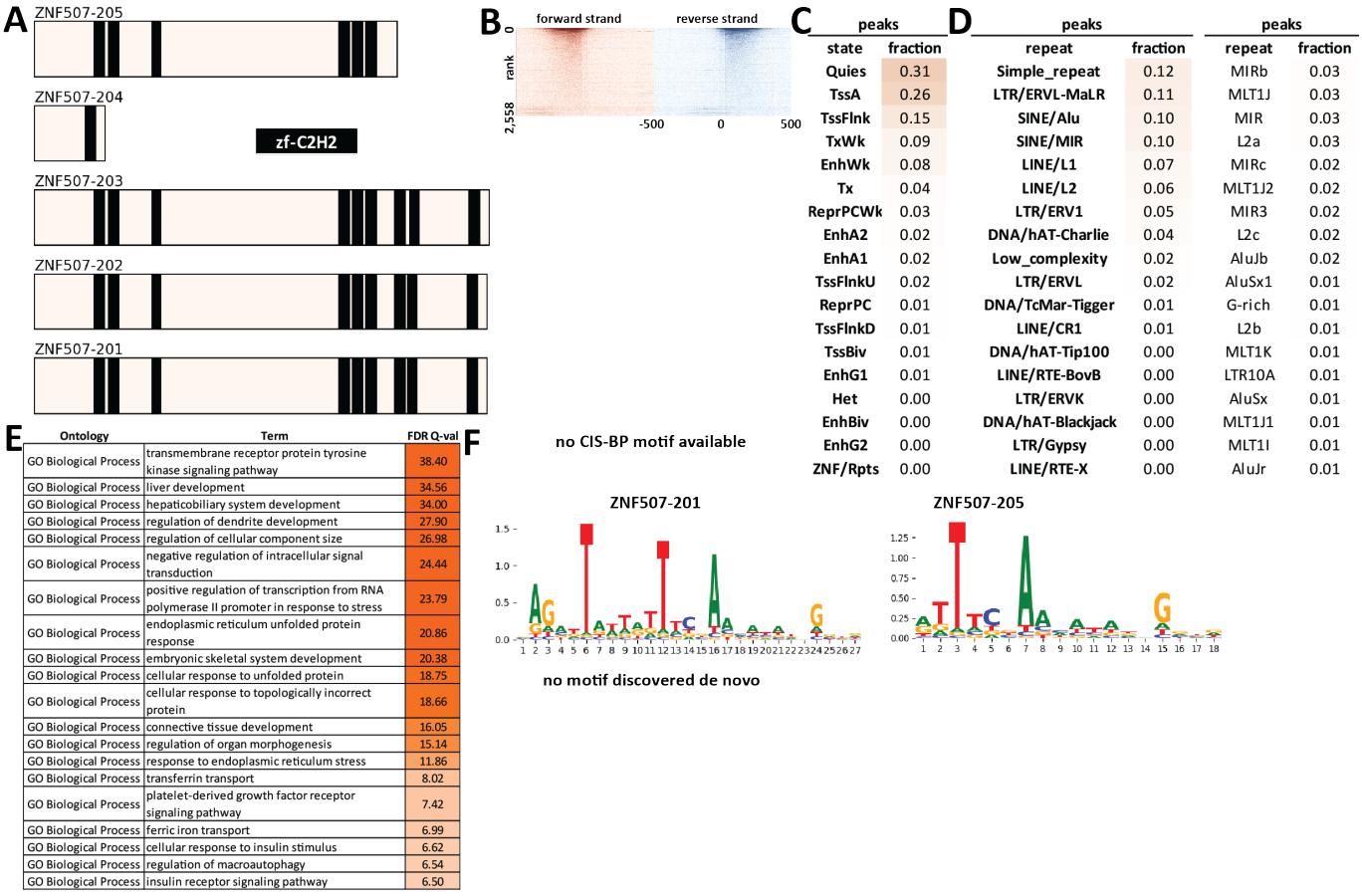

C

peaks	
state	fraction
Quies	0.31
TssA	0.26
TssFlnk	0.15
TxWk	0.09
EnhWk	0.08
Tx	0.04
ReprPCWk	0.03
EnhA2	0.02
EnhA1	0.02
TssFlnkU	0.02
ReprPC	0.01
TssFlnkD	0.01
TssBiv	0.01
EnhG1	0.01
Het	0.00
EnhBiv	0.00
EnhG2	0.00
ZNF/Rpts	0.00

D

peaks		peaks	
repeat	fraction	repeat	fraction
Simple_repeat	0.12	MIRb	0.03
LTR/ERVL-MaLR	0.11	MLT1J	0.03
SINE/Alu	0.10	MIR	0.03
SINE/MIR	0.10	L2a	0.03
LINE/L1	0.07	MIRc	0.02
LINE/L2	0.06	MLT1J2	0.02
LTR/ERV1	0.05	MIR3	0.02
DNA/hAT-Charlie	0.04	L2c	0.02
Low_complexity	0.02	AluJb	0.02
LTR/ERVL	0.02	AluSx1	0.01
DNA/TcMar-Tigger	0.01	G-rich	0.01
LINE/CR1	0.01	L2b	0.01
DNA/hAT-Tip100	0.00	MLT1K	0.01
LINE/RTE-BovB	0.00	LTR10A	0.01
LTR/ERVK	0.00	AluSx	0.01
DNA/hAT-Blackjack	0.00	MLT1J1	0.01
LTR/Gypsy	0.00	MLT1I	0.01
LINE/RTE-X	0.00	AluJr	0.01

E

Ontology	Term	FDR Q-val
GO Biological Process	transmembrane receptor protein tyrosine kinase signaling pathway	38.40
GO Biological Process	liver development	34.56
GO Biological Process	hepaticobiliary system development	34.00
GO Biological Process	regulation of dendrite development	27.90
GO Biological Process	regulation of cellular component size	26.98
GO Biological Process	negative regulation of intracellular signal transduction	24.44
GO Biological Process	positive regulation of transcription from RNA polymerase II promoter in response to stress	23.79
GO Biological Process	endoplasmic reticulum unfolded protein response	20.86
GO Biological Process	embryonic skeletal system development	20.38
GO Biological Process	cellular response to unfolded protein	18.75
GO Biological Process	cellular response to topologically incorrect protein	18.66
GO Biological Process	connective tissue development	16.05
GO Biological Process	regulation of organ morphogenesis	15.14
GO Biological Process	response to endoplasmic reticulum stress	11.86
GO Biological Process	transferrin transport	8.02
GO Biological Process	platelet-derived growth factor receptor signaling pathway	7.42
GO Biological Process	ferric iron transport	6.99
GO Biological Process	cellular response to insulin stimulus	6.62
GO Biological Process	regulation of macroautophagy	6.54
GO Biological Process	insulin receptor signaling pathway	6.50

Supplementary Figure 1286: Properties and genomic distribution of motifs identified for the ZNF507 transcription factor in MCF-7 (accession ENCSR419ODQ).

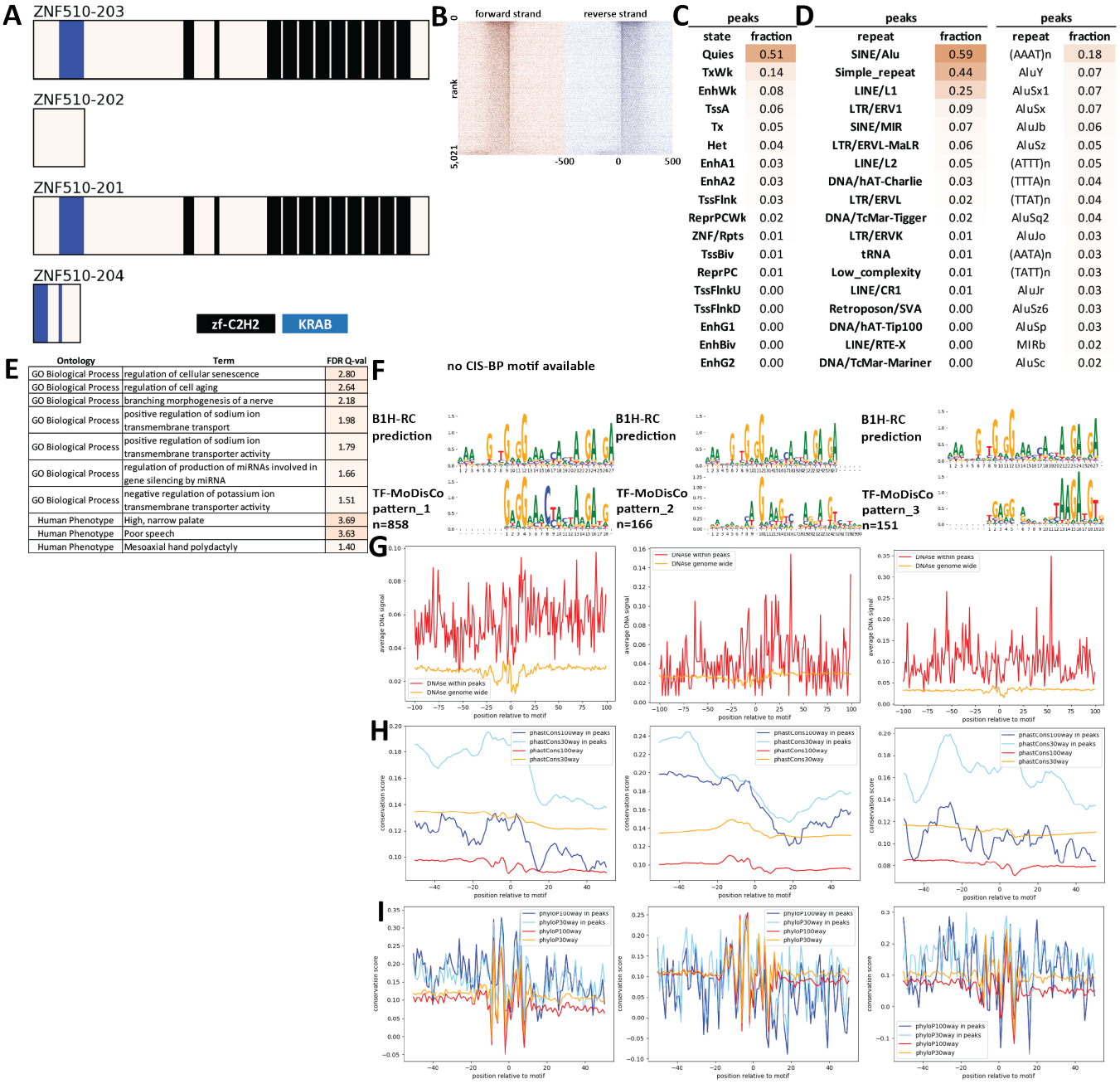

Supplementary Figure 1287: Properties and genomic distribution of motifs identified for the ZNF510 transcription factor in HEK293 (accession ENCSR595FAO).

TF-MoDisCO pattern_1 n=858, CWM

pattern_1, n=858; subpattern_0, ns=210

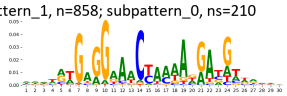

pattern_1, n=858; subpattern_1, ns=204

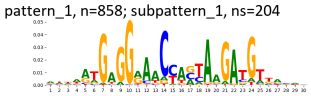

pattern_1, n=858; subpattern_2, ns=204

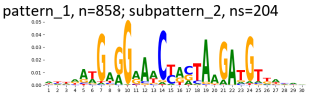

pattern_1, n=858; subpattern_3, ns=119

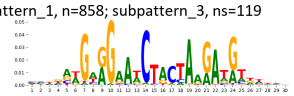

pattern_1, n=858; subpattern_4, ns=113

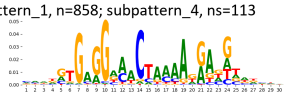

pattern_1, n=858; subpattern_5, ns=5

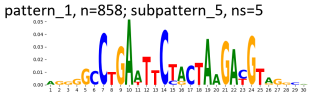

pattern_1, n=858; subpattern_6, ns=3

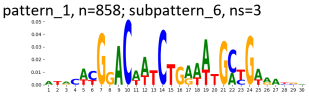

TF-MoDisCO pattern_1 n=858, PWM

pattern_1, n=858; subpattern_0, ns=210

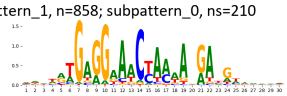

pattern_1, n=858; subpattern_1, ns=204

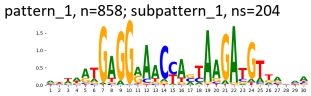

pattern_1, n=858; subpattern_2, ns=204

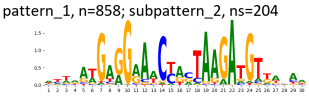

pattern_1, n=858; subpattern_3, ns=119

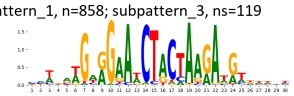

pattern_1, n=858; subpattern_4, ns=113

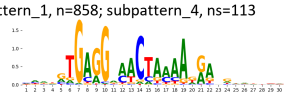

pattern_1, n=858; subpattern_5, ns=5

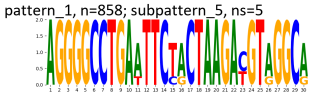

pattern_1, n=858; subpattern_6, ns=3

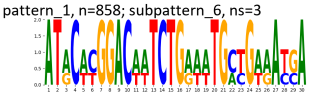

TF-MoDisCO pattern_2 n=166, CWM

pattern_2, n=166; subpattern_0, ns=69

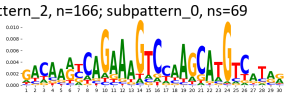

pattern_2, n=166; subpattern_1, ns=43

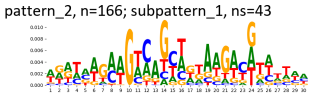

pattern_2, n=166; subpattern_2, ns=28

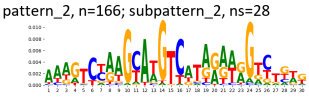

pattern_2, n=166; subpattern_3, ns=11

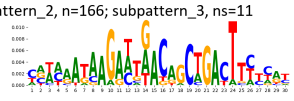

pattern_2, n=166; subpattern_4, ns=9

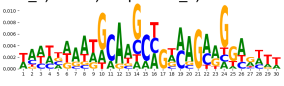

pattern_2, n=166; subpattern_5, ns=4



pattern_2, n=166; subpattern_6, ns=2

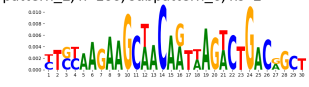

TF-MoDisCO pattern_2 n=166, PWM

pattern_2, n=166; subpattern_0, ns=69

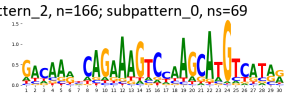

pattern_2, n=166; subpattern_1, ns=43

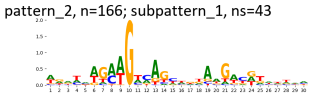

pattern_2, n=166; subpattern_2, ns=28

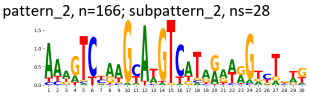

pattern_2, n=166; subpattern_3, ns=11

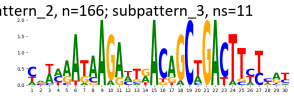

pattern_2, n=166; subpattern_4, ns=9

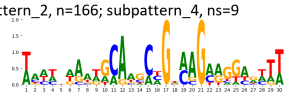

pattern_2, n=166; subpattern_5, ns=4

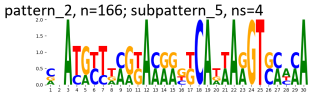

pattern_2, n=166; subpattern_6, ns=2

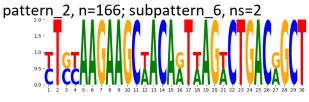

TF-MoDisCO pattern_3 n=151, CWM

pattern_3, n=151; subpattern_0, ns=62

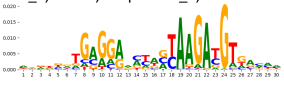

pattern_3, n=151; subpattern_1, ns=52

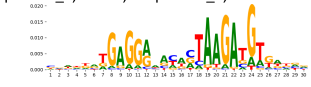

pattern_3, n=151; subpattern_2, ns=16

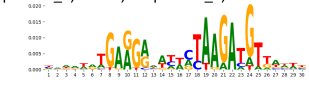

pattern_3, n=151; subpattern_3, ns=11

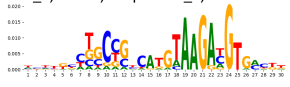

pattern_3, n=151; subpattern_4, ns=10

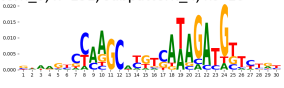

TF-MoDisCO pattern_3 n=151, PWM

pattern_3, n=151; subpattern_0, ns=62

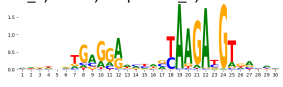

pattern_3, n=151; subpattern_1, ns=52

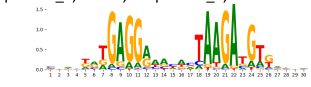

pattern_3, n=151; subpattern_2, ns=16

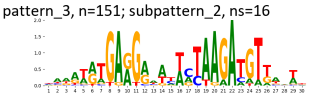

pattern_3, n=151; subpattern_3, ns=11

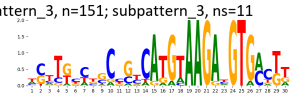

pattern_3, n=151; subpattern_4, ns=10

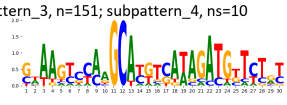

Supplementary Figure 1288: TF-MoDisCO subpatterns for the ZNF510 transcription factor in HEK293 (accession ENCSR595FAO).

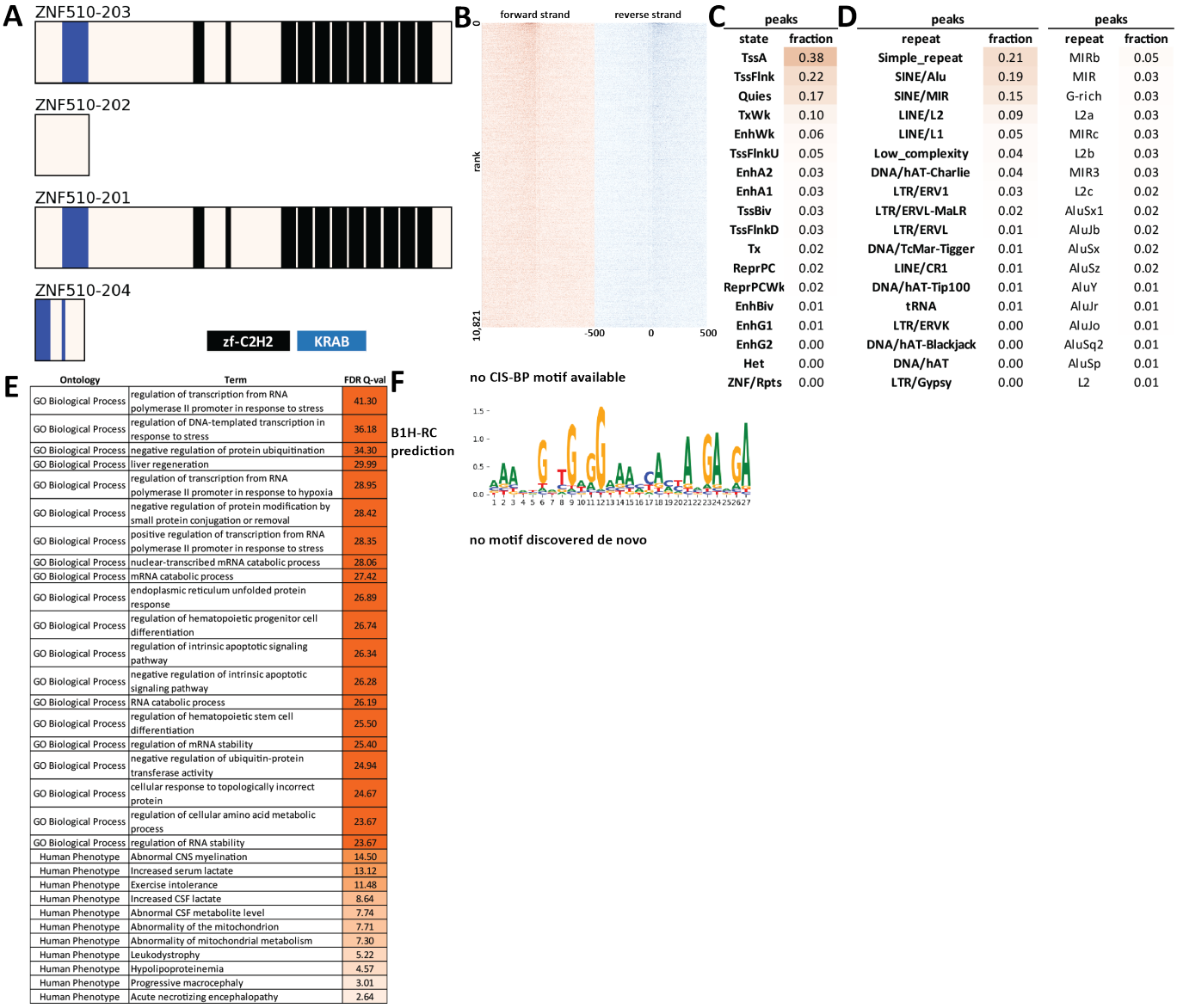

Ontology	Term	FDR Q-val
GO Biological Process	regulation of transcription from RNA polymerase II promoter in response to stress	41.30
GO Biological Process	regulation of DNA-templated transcription in response to stress	36.18
GO Biological Process	negative regulation of protein ubiquitination	34.30
GO Biological Process	liver regeneration	29.99
GO Biological Process	regulation of transcription from RNA polymerase II promoter in response to hypoxia	28.95
GO Biological Process	negative regulation of protein modification by small protein conjugation or removal	28.42
GO Biological Process	positive regulation of transcription from RNA polymerase II promoter in response to stress	28.35
GO Biological Process	nuclear-transcribed mRNA catabolic process	28.06
GO Biological Process	mRNA catabolic process	27.42
GO Biological Process	endoplasmic reticulum unfolded protein response	26.89
GO Biological Process	regulation of hematopoietic progenitor cell differentiation	26.74
GO Biological Process	regulation of intrinsic apoptotic signaling pathway	26.34
GO Biological Process	negative regulation of intrinsic apoptotic signaling pathway	26.28
GO Biological Process	RNA catabolic process	26.19
GO Biological Process	regulation of hematopoietic stem cell differentiation	25.50
GO Biological Process	regulation of mRNA stability	25.40
GO Biological Process	negative regulation of ubiquitin-protein transferase activity	24.94
GO Biological Process	cellular response to topologically incorrect protein	24.67
GO Biological Process	regulation of cellular amino acid metabolic process	23.67
GO Biological Process	regulation of RNA stability	23.67
Human Phenotype	Abnormal CNS myelination	14.50
Human Phenotype	Increased serum lactate	13.12
Human Phenotype	Exercise intolerance	11.48
Human Phenotype	Increased CSF lactate	8.64
Human Phenotype	Abnormal CSF metabolite level	7.74
Human Phenotype	Abnormality of the mitochondrion	7.71
Human Phenotype	Abnormality of mitochondrial metabolism	7.30
Human Phenotype	Leukodystrophy	5.22
Human Phenotype	Hypolipoproteinemia	4.57
Human Phenotype	Progressive macrocephaly	3.01
Human Phenotype	Acute necrotizing encephalopathy	2.64

Supplementary Figure 1289: Properties and genomic distribution of motifs identified for the ZNF510 transcription factor in HepG2 (accession ENCSR695SLS).

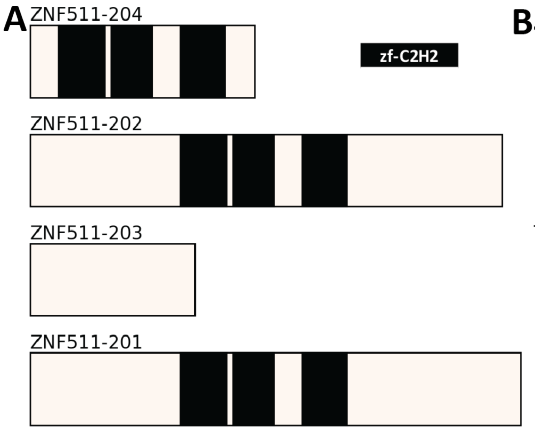



C

peaks	
state	fraction
TssA	0.28
Quies	0.22
TssFlnk	0.15
TxWk	0.12
EnhWk	0.09
EnhA1	0.03
Tx	0.03
TssFlnkU	0.03
EnhA2	0.03
ReprPCWk	0.02
TssFlnkD	0.02
ReprPC	0.02
TssBiv	0.02
EnhG1	0.01
EnhBiv	0.00
Het	0.00
EnhG2	0.00
ZNF/Rpts	0.00

D

peaks		peaks	
repeat	fraction	repeat	fraction
Simple_repeat	0.14	MIRb	0.05
SINE/Alu	0.14	L2a	0.03
SINE/MIR	0.12	MIR	0.03
LINE/L2	0.08	MIR3	0.02
LINE/L1	0.06	L2b	0.02
DNA/hAT-Charlie	0.03	MIRc	0.02
Low_complexity	0.03	L2c	0.02
LTR/ERV1	0.03	G-rich	0.02
LTR/ERVL-MaLR	0.02	AluSx1	0.02
LTR/ERVL	0.02	AluJb	0.02
DNA/TcMar-Tigger	0.01	AluSx	0.01
LINE/CR1	0.01	AluSz	0.01
DNA/hAT-Tip100	0.01	AluJo	0.01
tRNA	0.01	AluJr	0.01
LTR/ERVK	0.00	AluY	0.01
DNA/hAT-Blackjack	0.00	AluSq2	0.01
LINE/RTE-BovB	0.00	GA-rich	0.01
LTR/Gypsy	0.00	AluSp	0.01

E

Ontology	Term	FDR Q-val
GO Biological Process	mRNA catabolic process	50.00
GO Biological Process	nuclear-transcribed mRNA catabolic process	47.69
GO Biological Process	RNA catabolic process	45.32
GO Biological Process	endoplasmic reticulum unfolded protein response	40.90
GO Biological Process	cellular response to epidermal growth factor stimulus	38.67
GO Biological Process	cellular response to topologically incorrect protein	37.82
GO Biological Process	response to epidermal growth factor	37.50
GO Biological Process	nuclear-transcribed mRNA catabolic process, nonsense-mediated decay	37.35
GO Biological Process	cellular response to unfolded protein	36.35
GO Biological Process	response to topologically incorrect protein	33.42
GO Biological Process	regulation of intrinsic apoptotic signaling pathway	33.11
GO Biological Process	response to unfolded protein	31.42
GO Biological Process	multi-organism metabolic process	31.08
GO Biological Process	liver regeneration	30.83
GO Biological Process	viral gene expression	29.82
GO Biological Process	protein targeting to ER	27.66
GO Biological Process	regulation of transcription from RNA polymerase II promoter in response to hypoxia	27.22
GO Biological Process	translational elongation	27.19
GO Biological Process	viral transcription	27.01
GO Biological Process	cotranslational protein targeting to membrane	26.90
Human Phenotype	Skin rash	17.61
Human Phenotype	Abnormal CSF metabolite level	13.09

F

no CIS-BP motif available

no B1H-RC prediction

no motif discovered de novo

Supplementary Figure 1290: Properties and genomic distribution of motifs identified for the ZNF511 transcription factor in HepG2 (accession ENCSR372JXR).

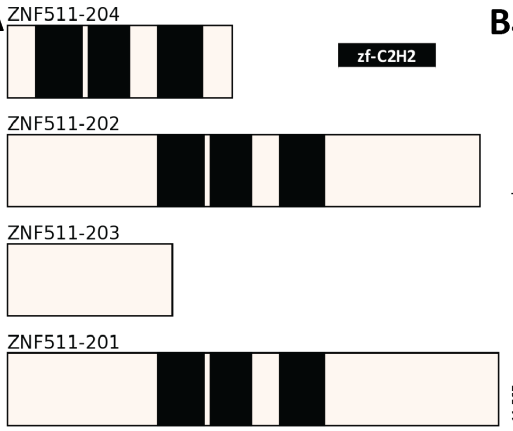

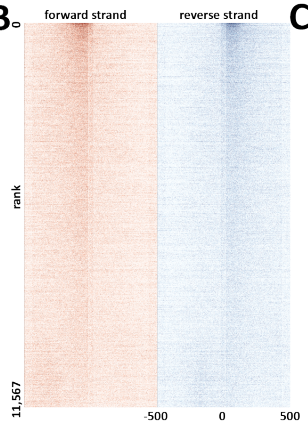

C

peaks	
state	fraction
TssA	0.44
TssFlnk	0.21
Quies	0.12
TxWk	0.06
TssBiv	0.04
TssFlnkU	0.04
ReprPC	0.03
EnhWk	0.03
EnhA2	0.02
ReprPCWk	0.02
Tx	0.02
TssFlnkD	0.02
EnhA1	0.01
EnhBiv	0.01
EnhG1	0.00
EnhG2	0.00
Het	0.00
ZNF/Rpts	0.00

D

peaks		peaks	
repeat	fraction	repeat	fraction
Simple_repeat	0.19	G-rich	0.03
SINE/Alu	0.10	MIRb	0.03
SINE/MIR	0.08	MIR3	0.02
LINE/L2	0.04	MIRc	0.02
Low_complexity	0.04	MIR	0.02
LINE/L1	0.02	L2b	0.01
LTR/ERV1	0.02	L2a	0.01
LTR/ERVL-MaLR	0.01	AluSx	0.01
DNA/hAT-Charlie	0.01	AluSx1	0.01
LTR/ERVL	0.01	L2c	0.01
tRNA	0.01	AluJb	0.01
LINE/CR1	0.00	AluSz	0.01
DNA/TcMar-Tigger	0.00	GA-rich	0.01
DNA/hAT-Tip100	0.00	AluJr	0.01
snRNA	0.00	(GGC)n	0.01
Satellite	0.00	AluY	0.01
LTR/Gypsy	0.00	(GCC)n	0.01
DNA/hAT	0.00	AluSq2	0.01

E

Ontology	Term	FDR Q-val
GO Biological Process	ncRNA processing	42.85
GO Biological Process	regulation of gene expression, epigenetic	37.19
GO Biological Process	multi-organism metabolic process	33.15
GO Biological Process	rRNA processing	32.46
GO Biological Process	rRNA metabolic process	32.06
GO Biological Process	viral gene expression	30.53
GO Biological Process	viral transcription	28.74
GO Biological Process	negative regulation of gene expression, epigenetic	27.91
GO Biological Process	nuclear-transcribed mRNA catabolic process, nonsense-mediated decay	27.71
GO Biological Process	mRNA catabolic process	26.73
GO Biological Process	nuclear-transcribed mRNA catabolic process	23.76
GO Biological Process	cotranslational protein targeting to membrane	23.51
GO Biological Process	regulation of transcription from RNA polymerase II promoter in response to stress	23.26
GO Biological Process	regulation of hematopoietic progenitor cell differentiation	22.63
GO Biological Process	gene silencing	22.12
GO Biological Process	SRP-dependent cotranslational protein targeting to membrane	21.67
GO Biological Process	protein targeting to ER	21.47
GO Biological Process	ribonucleoprotein complex export from nucleus	21.38
GO Biological Process	positive regulation of gene expression, epigenetic	21.10
GO Biological Process	regulation of DNA-templated transcription in response to stress	20.68
Human Phenotype	Increased serum lactate	13.15
Human Phenotype	Abnormal CSF metabolite level	8.99
Human Phenotype	Exercise intolerance	8.39
Human Phenotype	Increased CSF lactate	7.59
Human Phenotype	Basal cell carcinoma	6.00
Human Phenotype	Increased muscle lipid content	4.52

F

no CIS-BP motif available

no B1H-RC prediction

no motif discovered de novo

Supplementary Figure 1291: Properties and genomic distribution of motifs identified for the ZNF511 transcription factor in K562 (accession ENCSR652OGX).

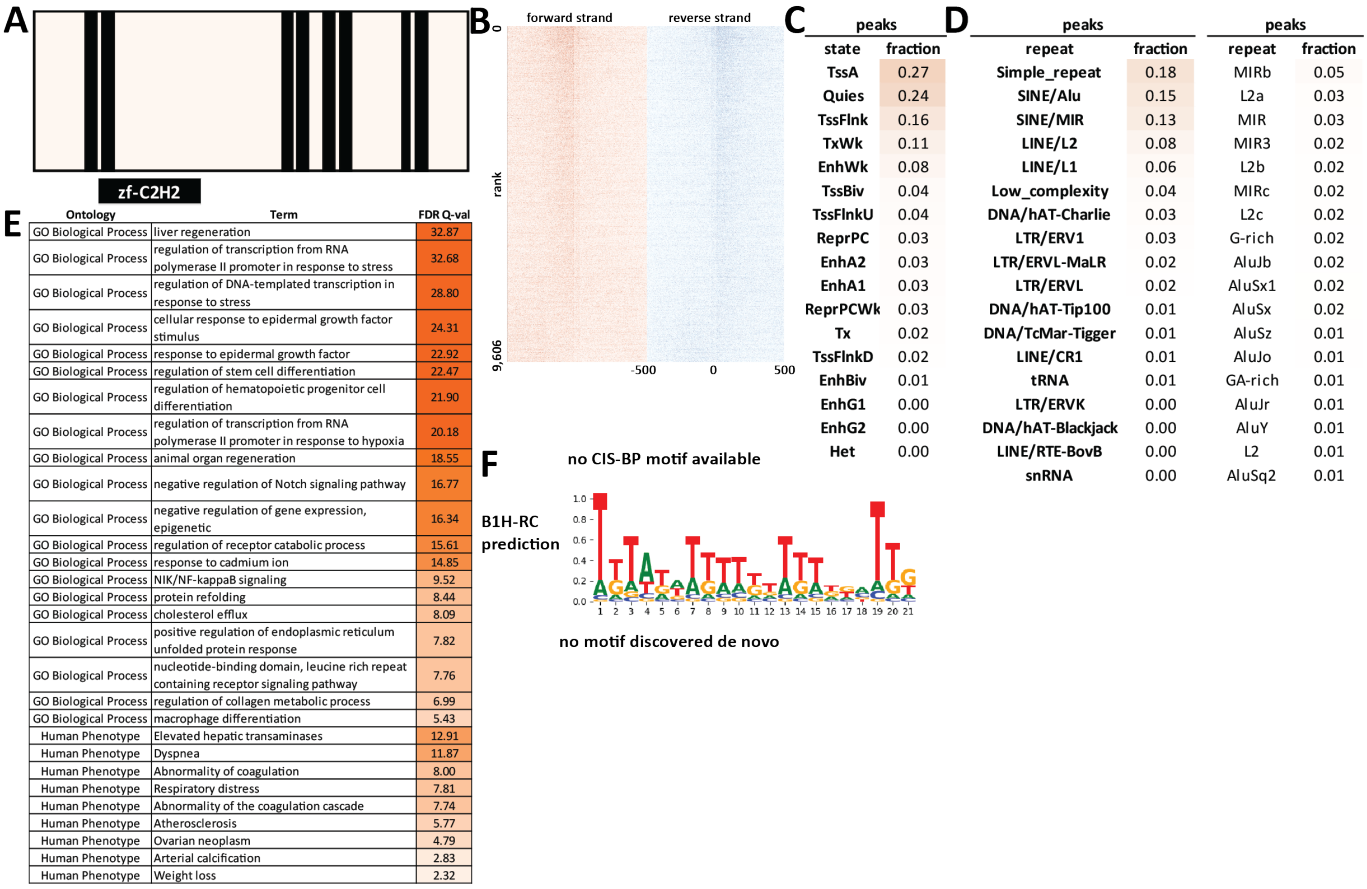

Supplementary Figure 1292: Properties and genomic distribution of motifs identified for the ZNF512B transcription factor in HepG2 (accession ENCSR801SNX).

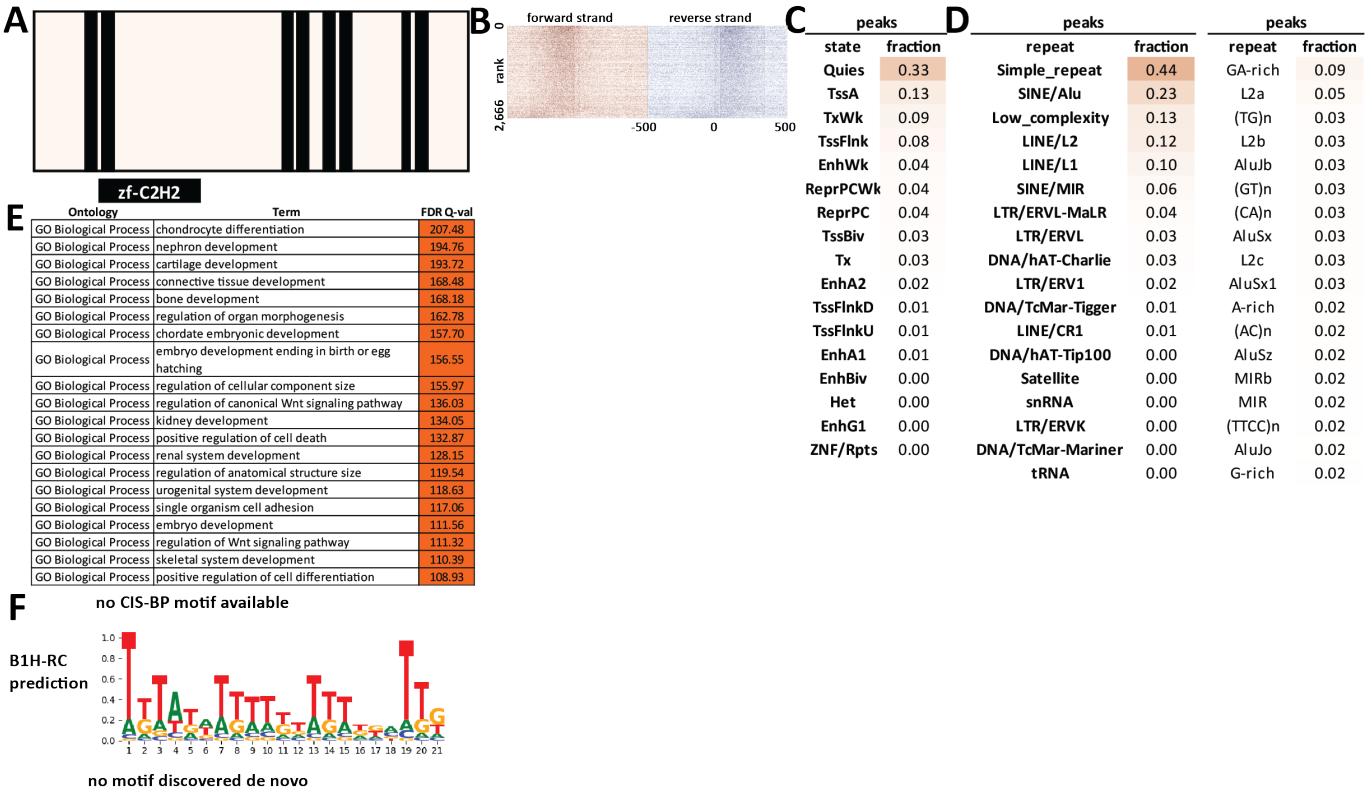

Supplementary Figure 1293: Properties and genomic distribution of motifs identified for the ZNF512B transcription factor in MCF-7 (accession ENCSR555DCF).

A



B

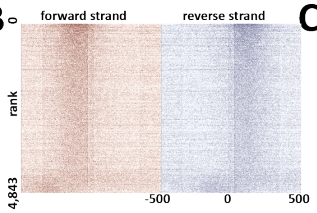

C

peaks	
state	fraction
Quies	0.30
TssA	0.21
TssFlnk	0.11
TxWk	0.08
TssBiv	0.04
EnhWk	0.04
ReprPCWk	0.03
ReprPC	0.03
Tx	0.02
TssFlnkU	0.02
EnhA2	0.02
TssFlnkD	0.01
EnhA1	0.01
EnhBiv	0.01
Het	0.00
EnhG1	0.00
ZNF/Rpts	0.00
EnhG2	0.00

D

peaks		peaks	
repeat	fraction	repeat	fraction
Simple_repeat	0.46	GA-rich	0.09
SINE/Alu	0.25	L2a	0.04
Low_complexity	0.14	AluJb	0.04
LINE/L1	0.09	A-rich	0.03
LINE/L2	0.08	(TG)n	0.03
SINE/MIR	0.05	AluSx1	0.03
LTR/ERVL-MaLR	0.03	(GT)n	0.03
DNA/hAT-Charlie	0.02	AluSz	0.02
LTR/ERVL	0.02	AluSx	0.02
LTR/ERV1	0.01	(TTTC)n	0.02
LINE/CR1	0.00	(CA)n	0.02
DNA/TcMar-Tigger	0.00	(TTCC)n	0.02
tRNA	0.00	G-rich	0.02
DNA/hAT-Tip100	0.00	(AC)n	0.02
snRNA	0.00	AluJr	0.02
Satellite	0.00	AluY	0.02
Retroposon/SVA	0.00	L2c	0.01
DNA/TcMar-Mariner	0.00	MIR	0.01

E

Ontology	Term	FDR Q-val
GO Biological Process	liver regeneration	302.79
GO Biological Process	positive regulation of catenin import into nucleus	251.75
GO Biological Process	regulation of catenin import into nucleus	221.54
GO Biological Process	chondrocyte development	171.87
GO Biological Process	glomerulus development	135.34
GO Biological Process	positive regulation of cell morphogenesis involved in differentiation	131.68
GO Biological Process	nephron development	128.34
GO Biological Process	chondrocyte differentiation	124.08
GO Biological Process	embryonic skeletal system development	120.82
GO Biological Process	regulation of cellular component size	114.67
GO Biological Process	cartilage development	111.49
GO Biological Process	chordate embryonic development	108.11
GO Biological Process	regulation of organ morphogenesis	107.29
GO Biological Process	embryo development ending in birth or egg hatching	106.93
GO Biological Process	positive regulation of cell death	100.11
GO Biological Process	positive regulation of apoptotic process	97.41
GO Biological Process	positive regulation of programmed cell death	95.95
GO Biological Process	connective tissue development	93.11
GO Biological Process	bone development	90.27
GO Biological Process	kidney development	79.69

F

no CIS-BP motif available

B1H-RC prediction

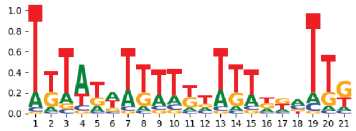

no motif discovered de novo

Supplementary Figure 1294: Properties and genomic distribution of motifs identified for the ZNF512B transcription factor in MCF-7 (accession ENCSR761LRR).

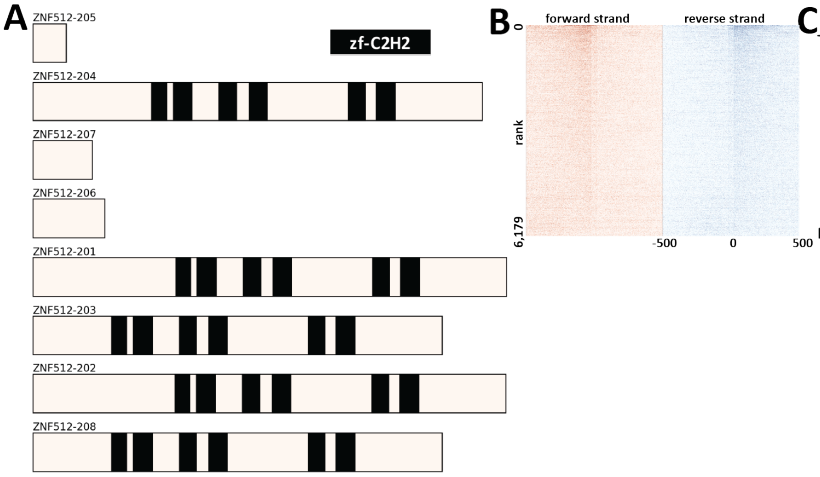

C

peaks	
state	fraction
Quies	0.29
TssA	0.25
TssFlnk	0.14
TxWk	0.10
EnhWk	0.05
TssBiv	0.03
TssFlnkU	0.03
ReprPCWk	0.03
ReprPC	0.03
Tx	0.02
EnhA2	0.02
EnhA1	0.02
TssFlnkD	0.02
EnhBiv	0.01
EnhG1	0.00
Het	0.00
EnhG2	0.00
ZNF/Rpts	0.00

D

peaks		peaks	
repeat	fraction	repeat	fraction
Simple_repeat	0.33	GA-rich	0.07
SINE/Alu	0.28	MIRb	0.04
Low_complexity	0.13	AluJb	0.04
SINE/MIR	0.10	A-rich	0.03
LINE/L1	0.09	L2a	0.03
LINE/L2	0.08	AluSx	0.03
LTR/ERVL-MaLR	0.03	(TTTC)n	0.03
DNA/hAT-Charlie	0.03	AluSx1	0.03
LTR/ERV1	0.03	AluSz	0.03
LTR/ERVL	0.02	MIR	0.02
DNA/TcMar-Tigger	0.01	AluJr	0.02
DNA/hAT-Tip100	0.01	AluJo	0.02
LINE/CR1	0.01	G-rich	0.02
tRNA	0.00	L2c	0.02
DNA/hAT-Blackjack	0.00	MIRc	0.02
LTR/ERVK	0.00	L2b	0.02
Retroposon/SVA	0.00	MIR3	0.02
LINE/RTE-BovB	0.00	AluSq2	0.02

E

Ontology	Term	FDR Q-val
GO Biological Process	negative regulation of PERK-mediated unfolded protein response	27.29
GO Biological Process	negative regulation of endoplasmic reticulum unfolded protein response	26.81
GO Biological Process	liver regeneration	24.61
GO Biological Process	regulation of receptor catabolic process	23.34
GO Biological Process	negative regulation of intrinsic apoptotic signaling pathway	19.72
GO Biological Process	response to endoplasmic reticulum stress	19.47
GO Biological Process	regulation of endoplasmic reticulum unfolded protein response	16.27
GO Biological Process	vitamin transmembrane transport	13.73
GO Biological Process	intrinsic apoptotic signaling pathway in response to endoplasmic reticulum stress	11.79
GO Biological Process	animal organ regeneration	11.45
GO Biological Process	negative regulation of cyclin-dependent protein serine/threonine kinase activity	9.45
GO Biological Process	cellular senescence	9.11
GO Biological Process	negative regulation of cyclin-dependent protein kinase activity	9.05
GO Biological Process	cellular response to epidermal growth factor stimulus	8.89
GO Biological Process	negative regulation of T cell proliferation	8.50
GO Biological Process	regulation of mitochondrial membrane potential	7.51
GO Biological Process	protection from non-homologous end joining at telomere	7.03
GO Biological Process	actin filament bundle organization	6.33
GO Biological Process	regulation of mitochondrial membrane permeability	5.89
GO Biological Process	negative regulation of pri-miRNA transcription from RNA polymerase II promoter	5.74
Human Phenotype	Hemolytic anemia	10.53
Human Phenotype	Bronchomalacia	8.09

F

no CIS-BP motif available

B1H-RC prediction

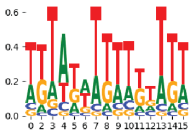

no motif discovered de novo

Supplementary Figure 1295: Properties and genomic distribution of motifs identified for the ZNF512 transcription factor in HepG2 (accession ENCSR264SRY).

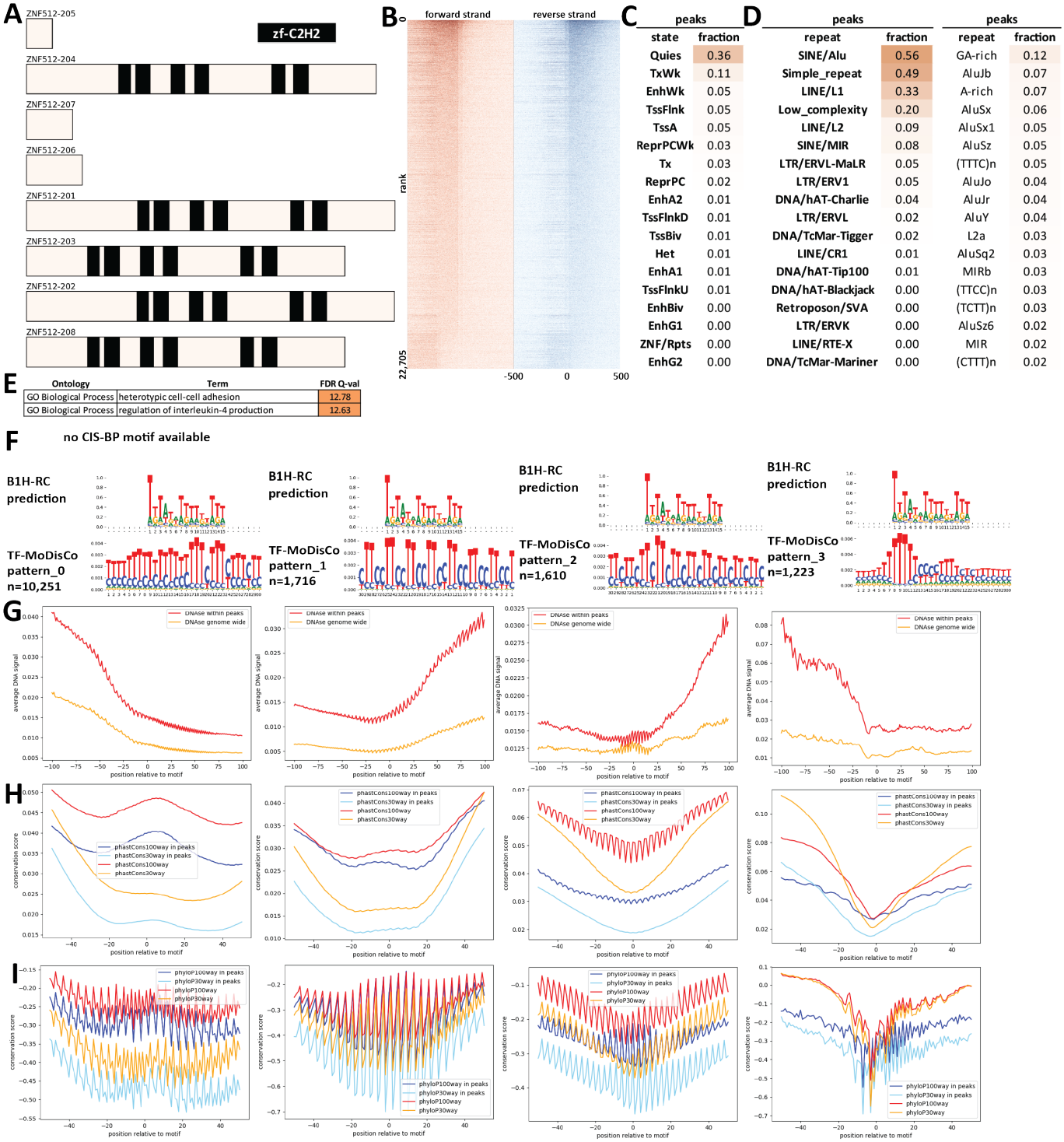

Supplementary Figure 1296: Properties and genomic distribution of motifs identified for the ZNF512 transcription factor in K562 (accession ENCSR591CCL).

TF-MoDisCO pattern_0 n=10251, CWM

pattern_0, n=10251; subpattern_0, ns=2227

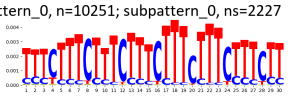

pattern_0, n=10251; subpattern_1, ns=2041

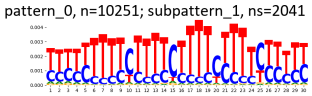

pattern_0, n=10251; subpattern_2, ns=1852

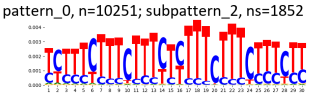

pattern_0, n=10251; subpattern_3, ns=1142

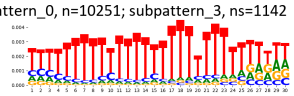

pattern_0, n=10251; subpattern_4, ns=1092

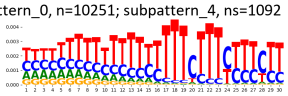

pattern_0, n=10251; subpattern_5, ns=896

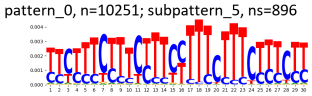

pattern_0, n=10251; subpattern_6, ns=528

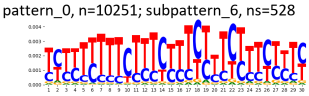

pattern_0, n=10251; subpattern_7, ns=473

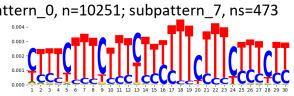

TF-MoDisCO pattern_0 n=10251, PWM

pattern_0, n=10251; subpattern_0, ns=2227

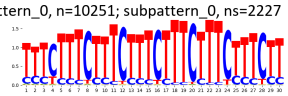

pattern_0, n=10251; subpattern_1, ns=2041

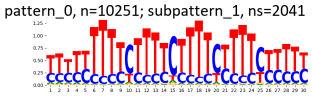

pattern_0, n=10251; subpattern_2, ns=1852

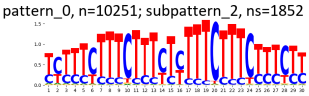

pattern_0, n=10251; subpattern_3, ns=1142

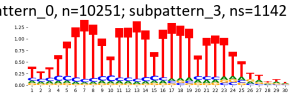

pattern_0, n=10251; subpattern_4, ns=1092

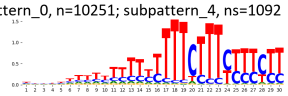

pattern_0, n=10251; subpattern_5, ns=896

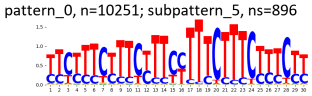

pattern_0, n=10251; subpattern_6, ns=528

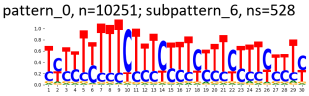

pattern_0, n=10251; subpattern_7, ns=473

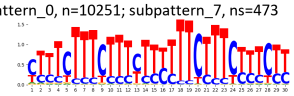

TF-MoDisCO pattern_1 n=1716, CWM

pattern_1, n=1716; subpattern_0, ns=346

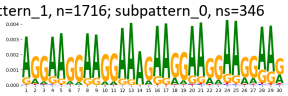

pattern_1, n=1716; subpattern_1, ns=341

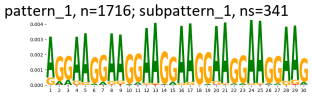

pattern_1, n=1716; subpattern_2, ns=321

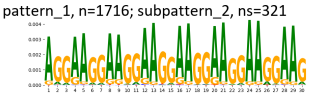

pattern_1, n=1716; subpattern_3, ns=241

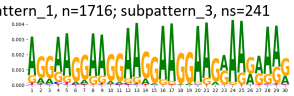

pattern_1, n=1716; subpattern_4, ns=188

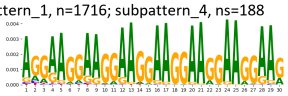

pattern_1, n=1716; subpattern_5, ns=143

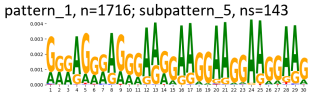

pattern_1, n=1716; subpattern_6, ns=96

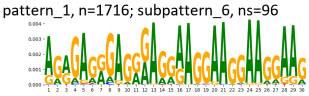

pattern_1, n=1716; subpattern_7, ns=40

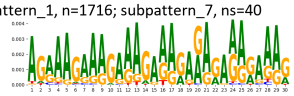

TF-MoDisCO pattern_1 n=1716, PWM

pattern_1, n=1716; subpattern_0, ns=346

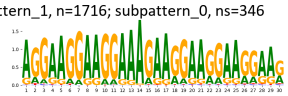

pattern_1, n=1716; subpattern_1, ns=341

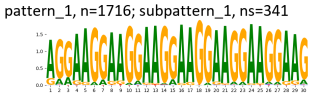

pattern_1, n=1716; subpattern_2, ns=321

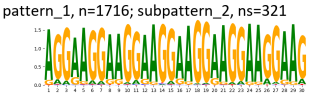

pattern_1, n=1716; subpattern_3, ns=241

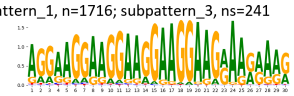

pattern_1, n=1716; subpattern_4, ns=188

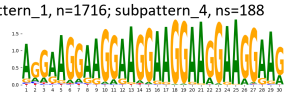

pattern_1, n=1716; subpattern_5, ns=143

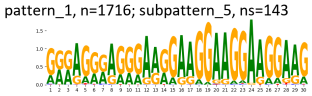

pattern_1, n=1716; subpattern_6, ns=96

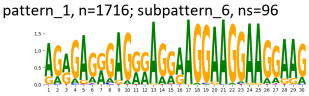

pattern_1, n=1716; subpattern_7, ns=40

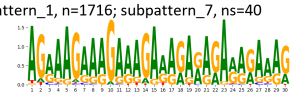

TF-MoDisCO pattern_2 n=1610, CWM

pattern_2, n=1610; subpattern_0, ns=342

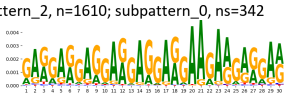

pattern_2, n=1610; subpattern_1, ns=323

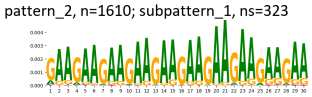

pattern_2, n=1610; subpattern_2, ns=314

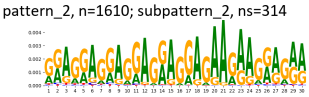

pattern_2, n=1610; subpattern_3, ns=256

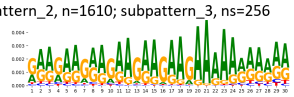

pattern_2, n=1610; subpattern_4, ns=180

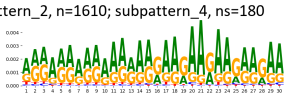

pattern_2, n=1610; subpattern_5, ns=159

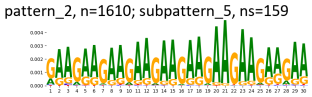

pattern_2, n=1610; subpattern_6, ns=34

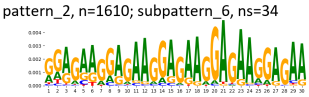

pattern_2, n=1610; subpattern_7, ns=2

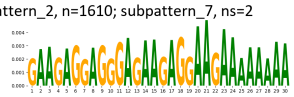

TF-MoDisCO pattern_2 n=1610, PWM

pattern_2, n=1610; subpattern_0, ns=342

pattern_2, n=1610; subpattern_1, ns=323

pattern_2, n=1610; subpattern_2, ns=314

pattern_2, n=1610; subpattern_3, ns=256

pattern_2, n=1610; subpattern_4, ns=180

pattern_2, n=1610; subpattern_5, ns=159

pattern_2, n=1610; subpattern_6, ns=34

pattern_2, n=1610; subpattern_7, ns=2

TF-MoDisCO pattern_3 n=1223, CWM

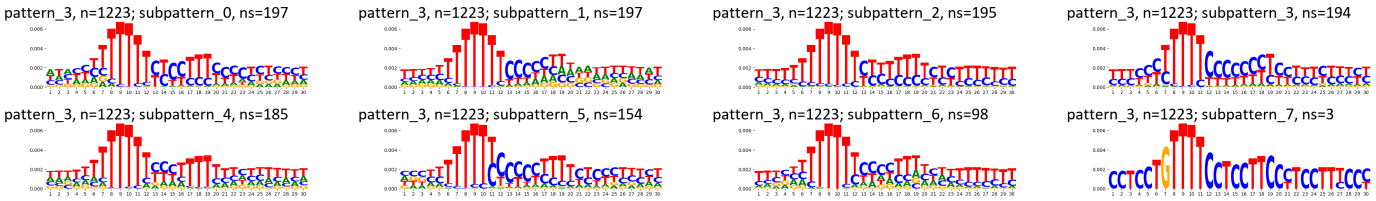

TF-MoDisCO pattern_3 n=1223, PWM

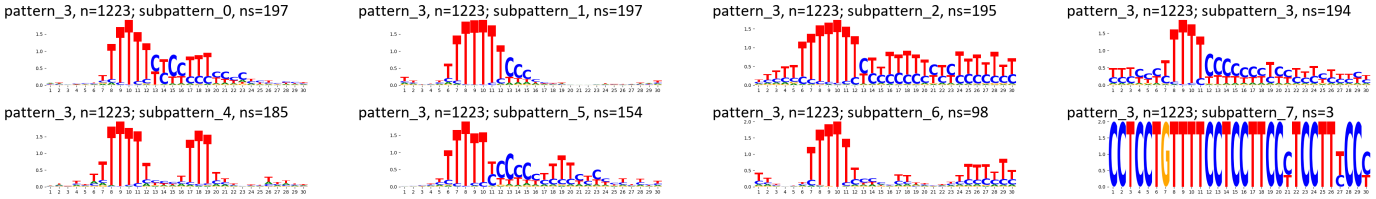

Supplementary Figure 1297: TF-MoDisCO subpatterns for the ZNF512 transcription factor in K562 (accession ENCSR591CCL).

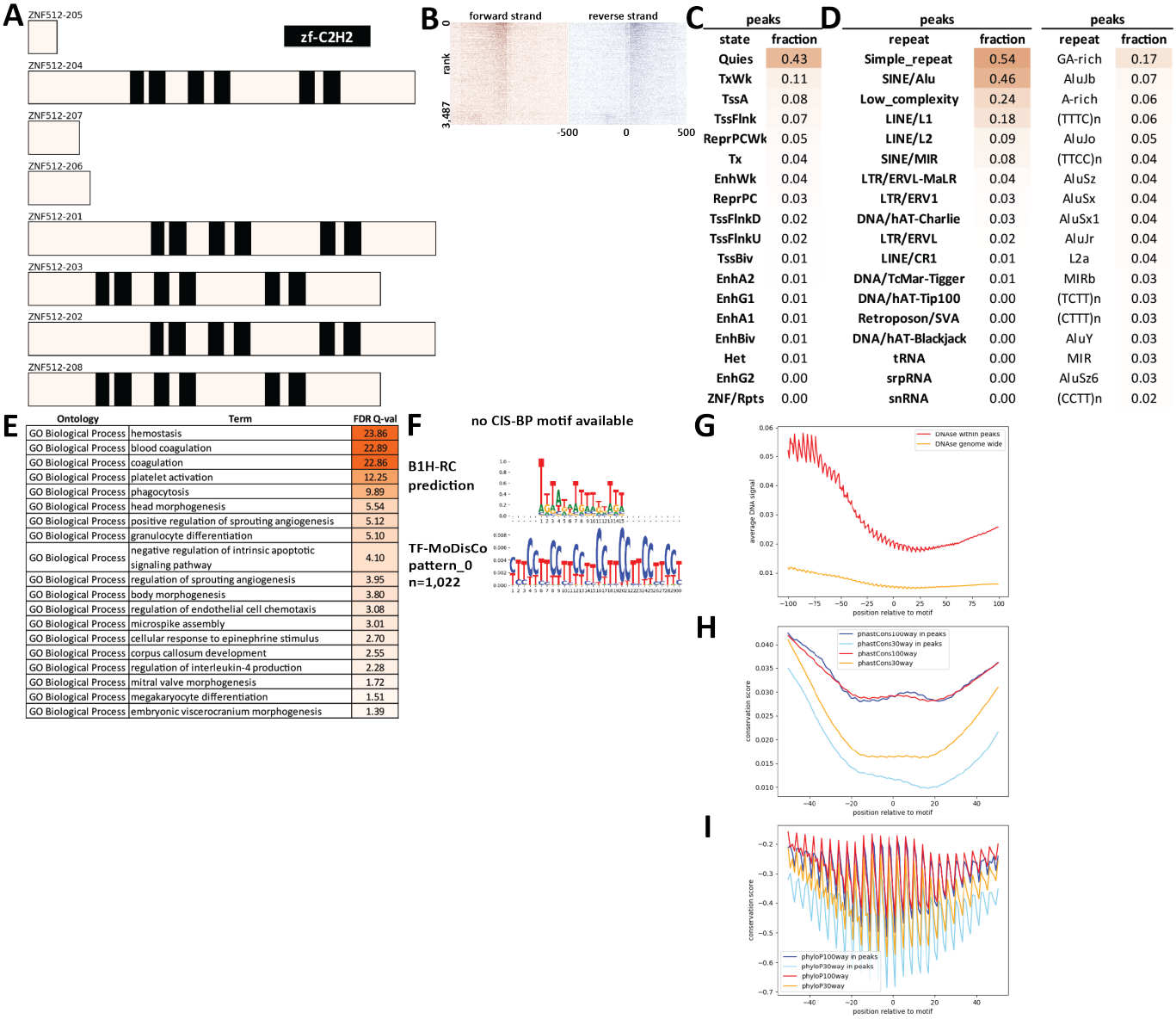

peaks	
state	fraction
Quies	0.43
TxWk	0.11
TssA	0.08
TssFlnk	0.07
ReprPCWk	0.05
Tx	0.04
EnhWk	0.04
ReprPC	0.03
TssFlnkD	0.02
TssFlnkU	0.02
TssBiv	0.01
EnhA2	0.01
EnhG1	0.01
EnhA1	0.01
EnhBiv	0.01
Het	0.01
EnhG2	0.00
ZNF/Rpts	0.00

peaks		peaks	
repeat	fraction	repeat	fraction
Simple_repeat	0.54	GA-rich	0.17
SINE/Alu	0.46	AluJb	0.07
Low_complexity	0.24	A-rich	0.06
LINE/L1	0.18	(TTTC)n	0.06
LINE/L2	0.09	AluJo	0.05
SINE/MIR	0.08	(TTCC)n	0.04
LTR/ERVL-MaLR	0.04	AluSz	0.04
LTR/ERV1	0.03	AluSx	0.04
DNA/hAT-Charlie	0.03	AluSx1	0.04
LTR/ERVL	0.02	AluJr	0.04
LINE/CR1	0.01	L2a	0.04
DNA/TcMar-Tigger	0.01	MIRb	0.03
DNA/hAT-Tip100	0.00	(TCTT)n	0.03
Retroposon/SVA	0.00	(CTTT)n	0.03
DNA/hAT-Blackjack	0.00	AluY	0.03
tRNA	0.00	MIR	0.03
srpRNA	0.00	AluSz6	0.03
snRNA	0.00	(CCTT)n	0.02

Ontology	Term	FDR Q-val
GO Biological Process	hemostasis	23.86
GO Biological Process	blood coagulation	22.89
GO Biological Process	coagulation	22.86
GO Biological Process	platelet activation	12.25
GO Biological Process	phagocytosis	9.89
GO Biological Process	head morphogenesis	5.54
GO Biological Process	positive regulation of sprouting angiogenesis	5.12
GO Biological Process	granulocyte differentiation	5.10
GO Biological Process	negative regulation of intrinsic apoptotic signaling pathway	4.10
GO Biological Process	regulation of sprouting angiogenesis	3.95
GO Biological Process	body morphogenesis	3.80
GO Biological Process	regulation of endothelial cell chemotaxis	3.08
GO Biological Process	microspike assembly	3.01
GO Biological Process	cellular response to epinephrine stimulus	2.70
GO Biological Process	corpus callosum development	2.55
GO Biological Process	regulation of interleukin-4 production	2.28
GO Biological Process	mitral valve morphogenesis	1.72
GO Biological Process	megakaryocyte differentiation	1.51
GO Biological Process	embryonic viscerocranium morphogenesis	1.39

Supplementary Figure 1298: Properties and genomic distribution of motifs identified for the ZNF512 transcription factor in K562 (accession ENCSR696URR).

TF-MoDisCO pattern_0 n=1022, CWM

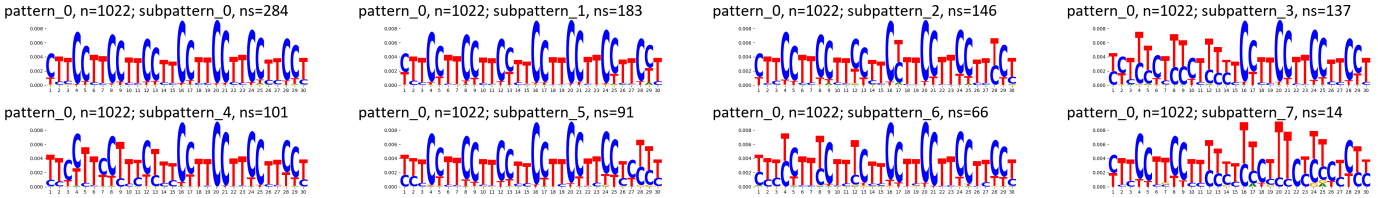

TF-MoDisCO pattern_0 n=1022, PWM

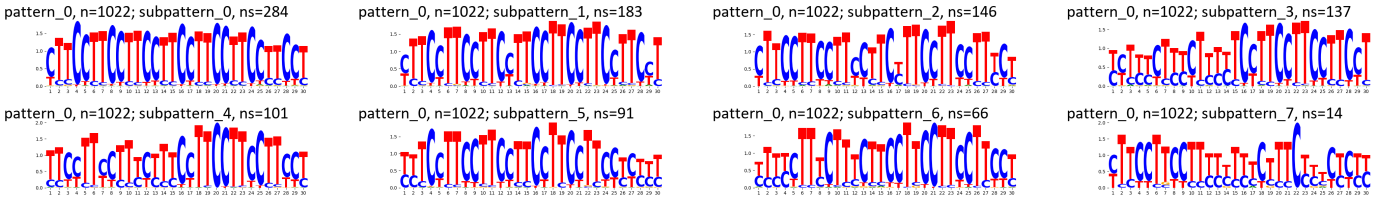

Supplementary Figure 1299: TF-MoDisCO subpatterns for the ZNF512 transcription factor in K562 (accession ENCSR696URR).

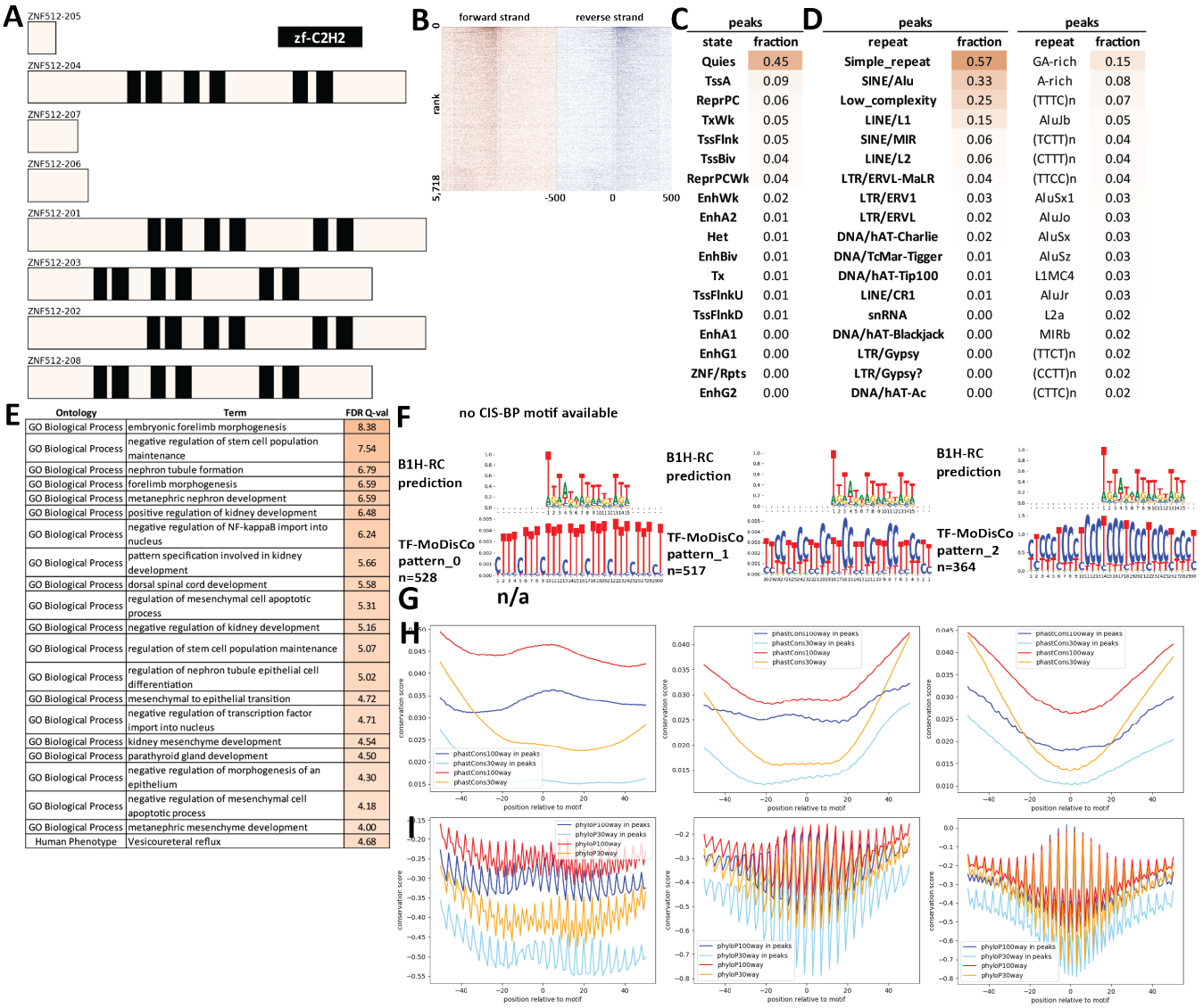

Supplementary Figure 1300: Properties and genomic distribution of motifs identified for the ZNF512 transcription factor in WTC11 (accession ENCSR634WRC).

TF-MoDisCO pattern_0 n=528, CWM

pattern_0, n=528; subpattern_0, ns=142

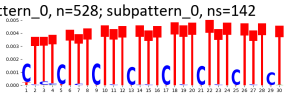

pattern_0, n=528; subpattern_1, ns=138

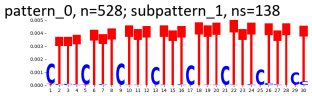

pattern_0, n=528; subpattern_2, ns=108

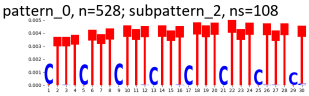

pattern_0, n=528; subpattern_3, ns=91

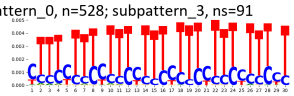

pattern_0, n=528; subpattern_4, ns=49

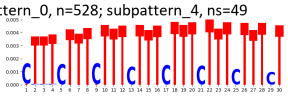

TF-MoDisCO pattern_0 n=528, PWM

pattern_0, n=528; subpattern_0, ns=142

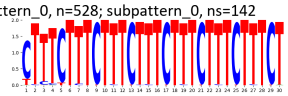

pattern_0, n=528; subpattern_1, ns=138

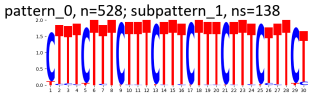

pattern_0, n=528; subpattern_2, ns=108

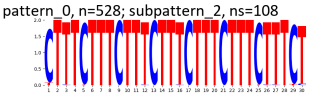

pattern_0, n=528; subpattern_3, ns=91

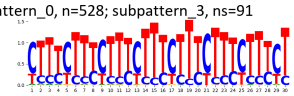

pattern_0, n=528; subpattern_4, ns=49

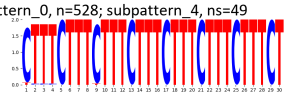

TF-MoDisCO pattern_1 n=517, CWM

pattern_1, n=517; subpattern_0, ns=147

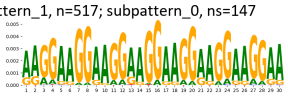

pattern_1, n=517; subpattern_1, ns=87

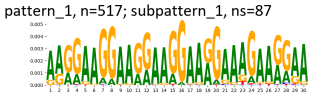

pattern_1, n=517; subpattern_2, ns=78

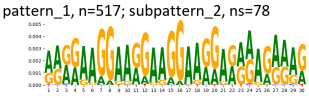

pattern_1, n=517; subpattern_3, ns=64

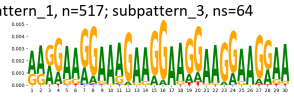

pattern_1, n=517; subpattern_4, ns=56

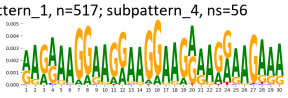

pattern_1, n=517; subpattern_5, ns=37

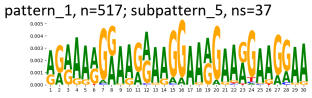

pattern_1, n=517; subpattern_6, ns=28

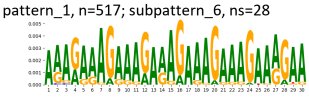

pattern_1, n=517; subpattern_7, ns=20

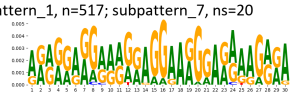

TF-MoDisCO pattern_1 n=517, PWM

pattern_1, n=517; subpattern_0, ns=147

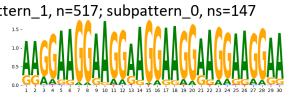

pattern_1, n=517; subpattern_1, ns=87

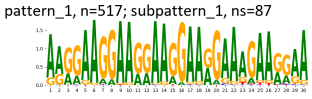

pattern_1, n=517; subpattern_2, ns=78

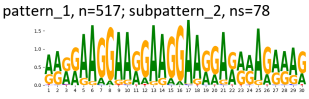

pattern_1, n=517; subpattern_3, ns=64

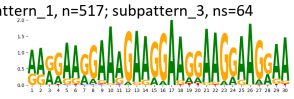

pattern_1, n=517; subpattern_4, ns=56



pattern_1, n=517; subpattern_5, ns=37

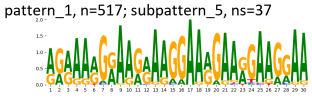

pattern_1, n=517; subpattern_6, ns=28

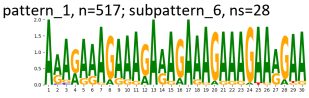

pattern_1, n=517; subpattern_7, ns=20

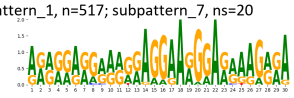

TF-MoDisCO pattern_2 n=364, CWM

pattern_2, n=364; subpattern_0, ns=154

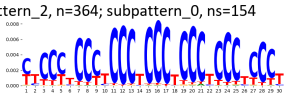

pattern_2, n=364; subpattern_1, ns=91

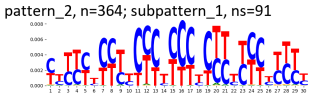

pattern_2, n=364; subpattern_2, ns=82

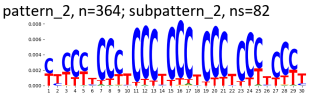

pattern_2, n=364; subpattern_3, ns=35

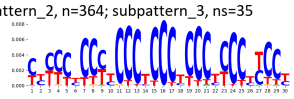

pattern_2, n=364; subpattern_4, ns=2

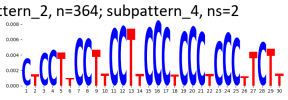

TF-MoDisCO pattern_2 n=364, PWM

pattern_2, n=364; subpattern_0, ns=154

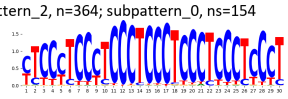

pattern_2, n=364; subpattern_1, ns=91

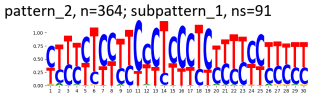

pattern_2, n=364; subpattern_2, ns=82

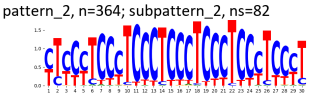

pattern_2, n=364; subpattern_3, ns=35

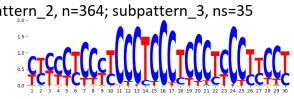

pattern_2, n=364; subpattern_4, ns=2

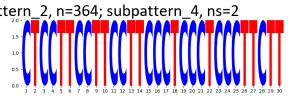

Supplementary Figure 1301: TF-MoDisCO subpatterns for the ZNF512 transcription factor in WTC11 (accession ENCSR634WRC).

A

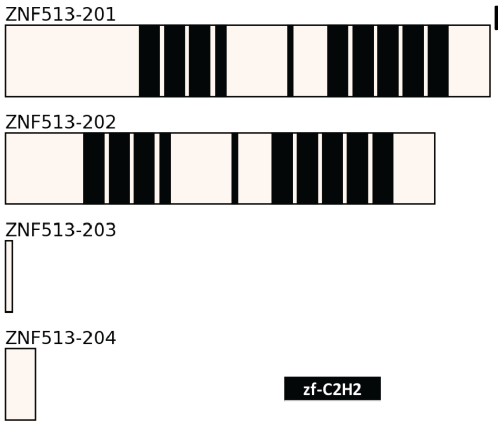

B

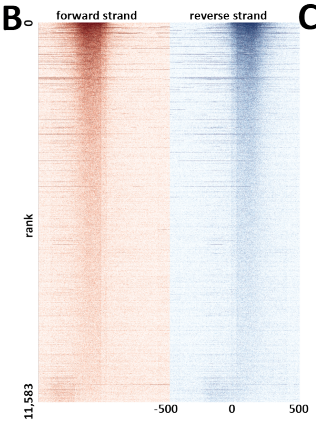

C

peaks	
state	fraction
Quies	0.31
TssA	0.19
EnhWk	0.10
TxWk	0.10
TssFlnk	0.08
Tx	0.05
EnhA1	0.05
EnhA2	0.04
TssBiv	0.03
ReprPCWk	0.03
ReprPC	0.02
TssFlnkU	0.02
TssFlnkD	0.01
EnhG1	0.01
EnhBiv	0.01
Het	0.01
EnhG2	0.00
ZNF/Rpts	0.00

D

peaks		peaks	
repeat	fraction	repeat	fraction
Simple_repeat	0.51	GA-rich	0.08
SINE/MIR	0.18	MIR	0.07
SINE/Alu	0.14	MIRb	0.07
Low_complexity	0.10	(TGA)n	0.03
LINE/L1	0.07	(ATC)n	0.03
LINE/L2	0.06	(ATG)n	0.03
LTR/ERVL-MaLR	0.03	(TCA)n	0.03
DNA/hAT-Charlie	0.03	(TCC)n	0.03
DNA/TcMar-Tigger	0.03	(CAT)n	0.02
LTR/ERVL	0.01	L2a	0.02
LTR/ERV1	0.01	(CCT)n	0.02
tRNA	0.01	(GAT)n	0.02
LINE/CR1	0.01	MIRc	0.02
DNA/hAT-Tip100	0.01	(CTC)n	0.02
LTR/Gypsy	0.00	AluJb	0.02
snRNA	0.00	L2c	0.02
LTR/ERVK	0.00	G-rich	0.02
LINE/RTE-X	0.00	(TTC)n	0.02

E

Ontology	Term	FDR Q-val
GO Biological Process	nucleosome disassembly	8.25
GO Biological Process	protein-DNA complex disassembly	6.67
GO Biological Process	positive regulation of mesonephros development	6.51
GO Biological Process	positive regulation of epithelial cell differentiation involved in kidney development	3.47
GO Biological Process	deoxyribonucleoside monophosphate metabolic process	2.93
GO Biological Process	deoxyribonucleoside monophosphate biosynthetic process	1.85
Human Phenotype	Advanced eruption of teeth	4.63
Human Phenotype	Natal tooth	3.50
Human Phenotype	[illegible]	1.73

F

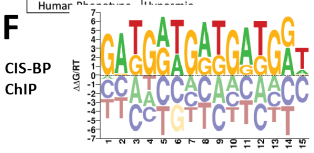

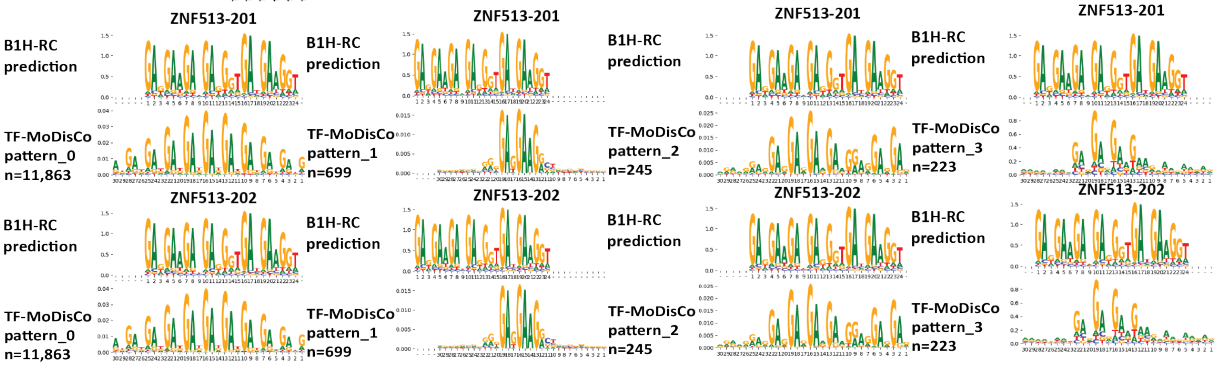

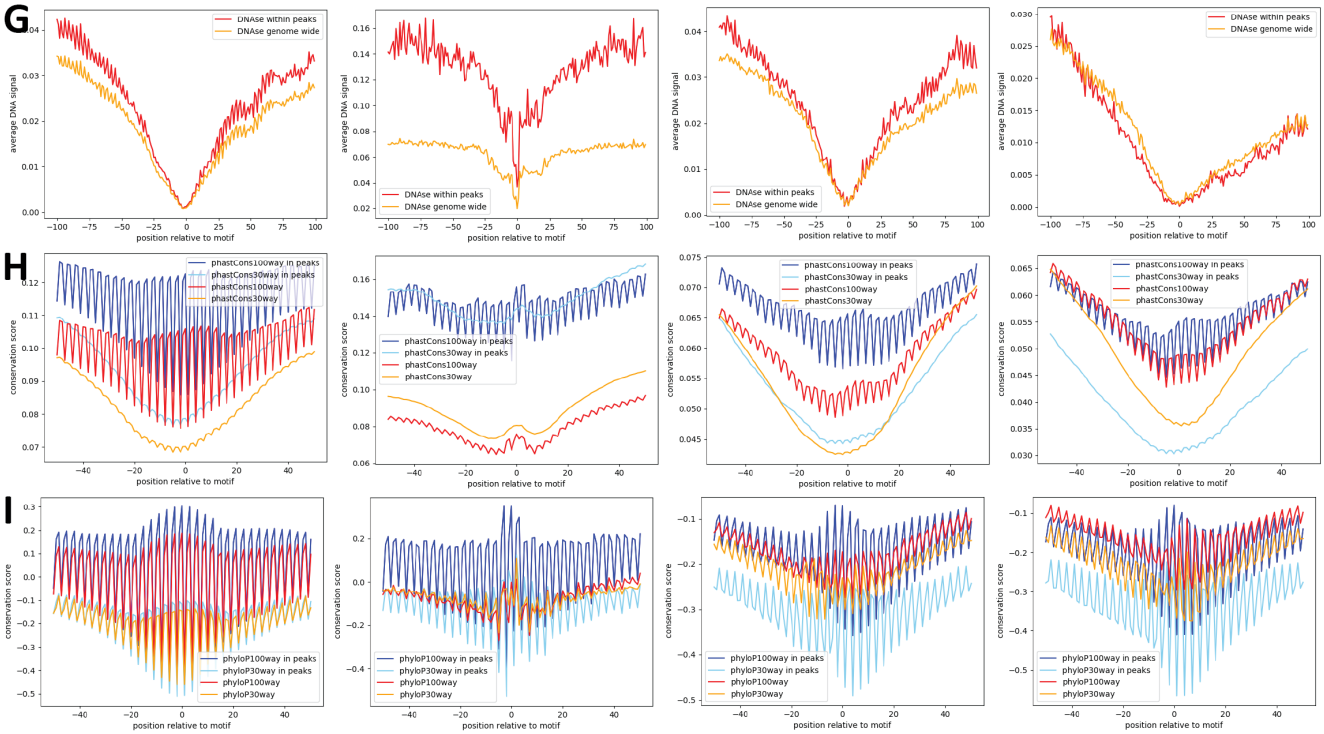

Supplementary Figure 1302: Properties and genomic distribution of motifs identified for the ZNF513 transcription factor in HEK293 (accession ENCSR503DPC).

TF-MoDisCO pattern_0 n=11863, CWM

pattern_0, n=11863; subpattern_0, ns=1775

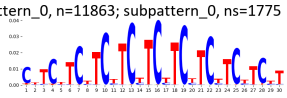

pattern_0, n=11863; subpattern_1, ns=1610

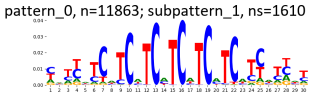

pattern_0, n=11863; subpattern_10, ns=53

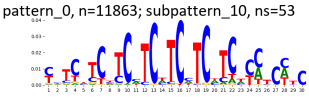

pattern_0, n=11863; subpattern_2, ns=1552

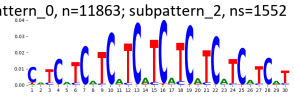

pattern_0, n=11863; subpattern_3, ns=1140

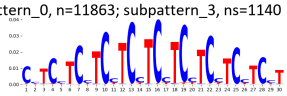

pattern_0, n=11863; subpattern_4, ns=1114

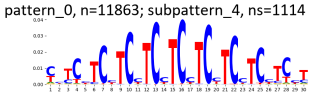

pattern_0, n=11863; subpattern_5, ns=1100

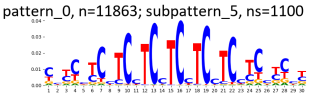

pattern_0, n=11863; subpattern_6, ns=1044

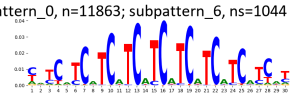

pattern_0, n=11863; subpattern_7, ns=1018

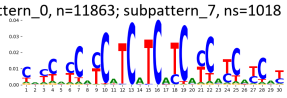

pattern_0, n=11863; subpattern_8, ns=845

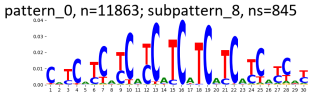

pattern_0, n=11863; subpattern_9, ns=612

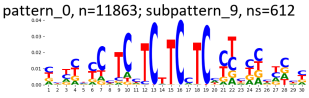

TF-MoDisCO pattern_0 n=11863, PWM

pattern_0, n=11863; subpattern_0, ns=1775

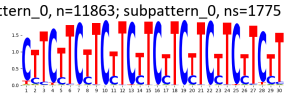

pattern_0, n=11863; subpattern_1, ns=1610

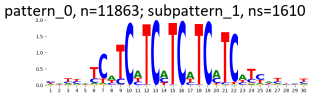

pattern_0, n=11863; subpattern_10, ns=53

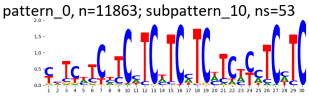

pattern_0, n=11863; subpattern_2, ns=1552

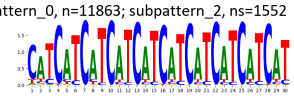

pattern_0, n=11863; subpattern_3, ns=1140

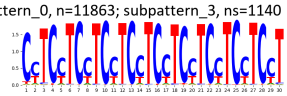

pattern_0, n=11863; subpattern_4, ns=1114

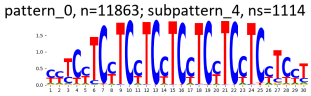

pattern_0, n=11863; subpattern_5, ns=1100

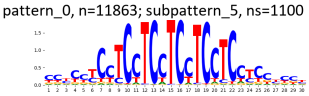

pattern_0, n=11863; subpattern_6, ns=1044

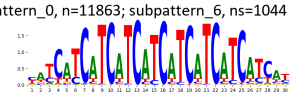

pattern_0, n=11863; subpattern_7, ns=1018

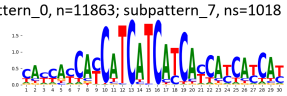

pattern_0, n=11863; subpattern_8, ns=845

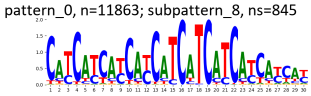

pattern_0, n=11863; subpattern_9, ns=612

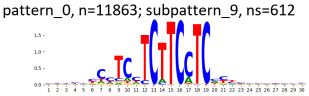

TF-MoDisCO pattern_1 n=699, CWM

pattern_1, n=699; subpattern_0, ns=121

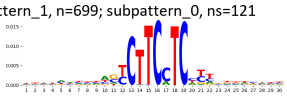

pattern_1, n=699; subpattern_1, ns=115

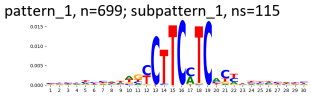

pattern_1, n=699; subpattern_2, ns=114

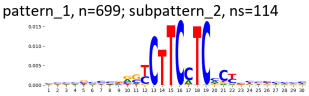

pattern_1, n=699; subpattern_3, ns=106

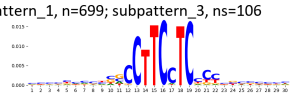

pattern_1, n=699; subpattern_4, ns=101

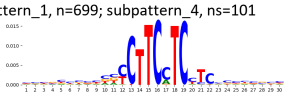

pattern_1, n=699; subpattern_5, ns=72

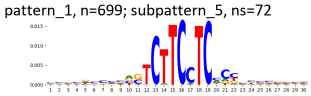

pattern_1, n=699; subpattern_6, ns=70

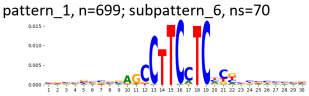

TF-MoDisCO pattern_1 n=699, PWM

pattern_1, n=699; subpattern_0, ns=121

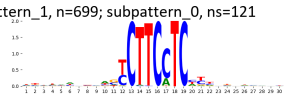

pattern_1, n=699; subpattern_1, ns=115

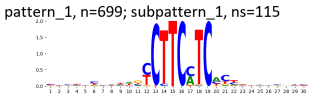

pattern_1, n=699; subpattern_2, ns=114

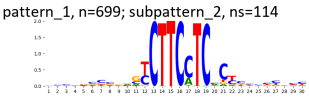

pattern_1, n=699; subpattern_3, ns=106

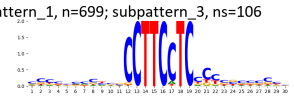

pattern_1, n=699; subpattern_4, ns=101

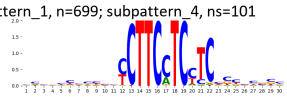

pattern_1, n=699; subpattern_5, ns=72

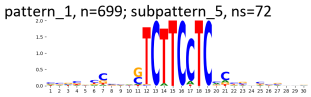

pattern_1, n=699; subpattern_6, ns=70

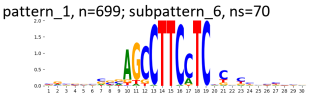

TF-MoDisCO pattern_2 n=245, CWM

pattern_2, n=245; subpattern_0, ns=48

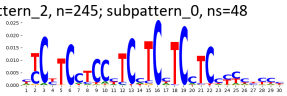

pattern_2, n=245; subpattern_1, ns=47

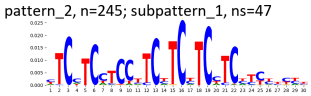

pattern_2, n=245; subpattern_2, ns=46

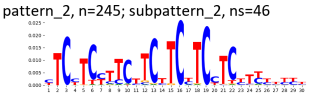

pattern_2, n=245; subpattern_3, ns=30

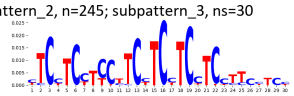

pattern_2, n=245; subpattern_4, ns=28

pattern_2, n=245; subpattern_5, ns=20

pattern_2, n=245; subpattern_6, ns=15

pattern_2, n=245; subpattern_7, ns=11

TF-MoDisCO pattern_2 n=245, PWM

pattern_2, n=245; subpattern_0, ns=48

pattern_2, n=245; subpattern_1, ns=47

pattern_2, n=245; subpattern_2, ns=46

pattern_2, n=245; subpattern_3, ns=30

pattern_2, n=245; subpattern_4, ns=28

pattern_2, n=245; subpattern_5, ns=20

pattern_2, n=245; subpattern_6, ns=15

pattern_2, n=245; subpattern_7, ns=11

TF-MoDisCO pattern_3 n=223, CWM

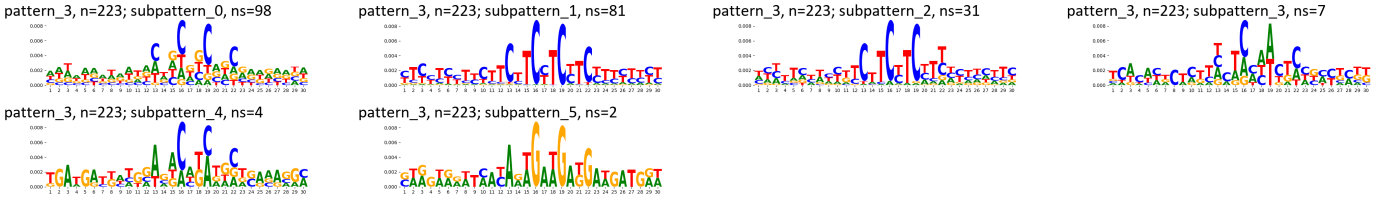

TF-MoDisCO pattern_3 n=223, PWM

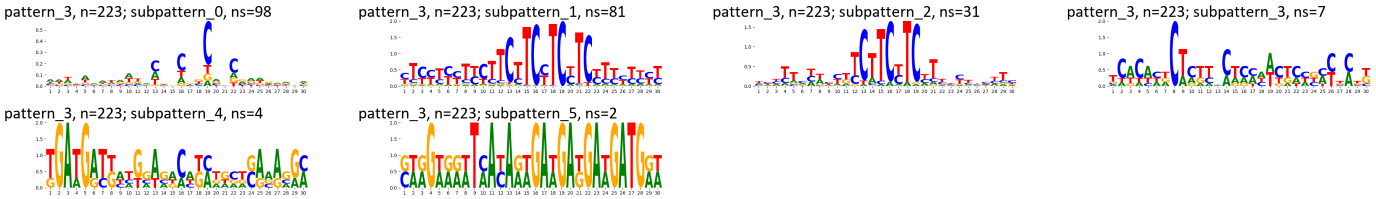

Supplementary Figure 1303: TF-MoDisCO subpatterns for the ZNF513 transcription factor in HEK293 (accession ENCSR503DPC).

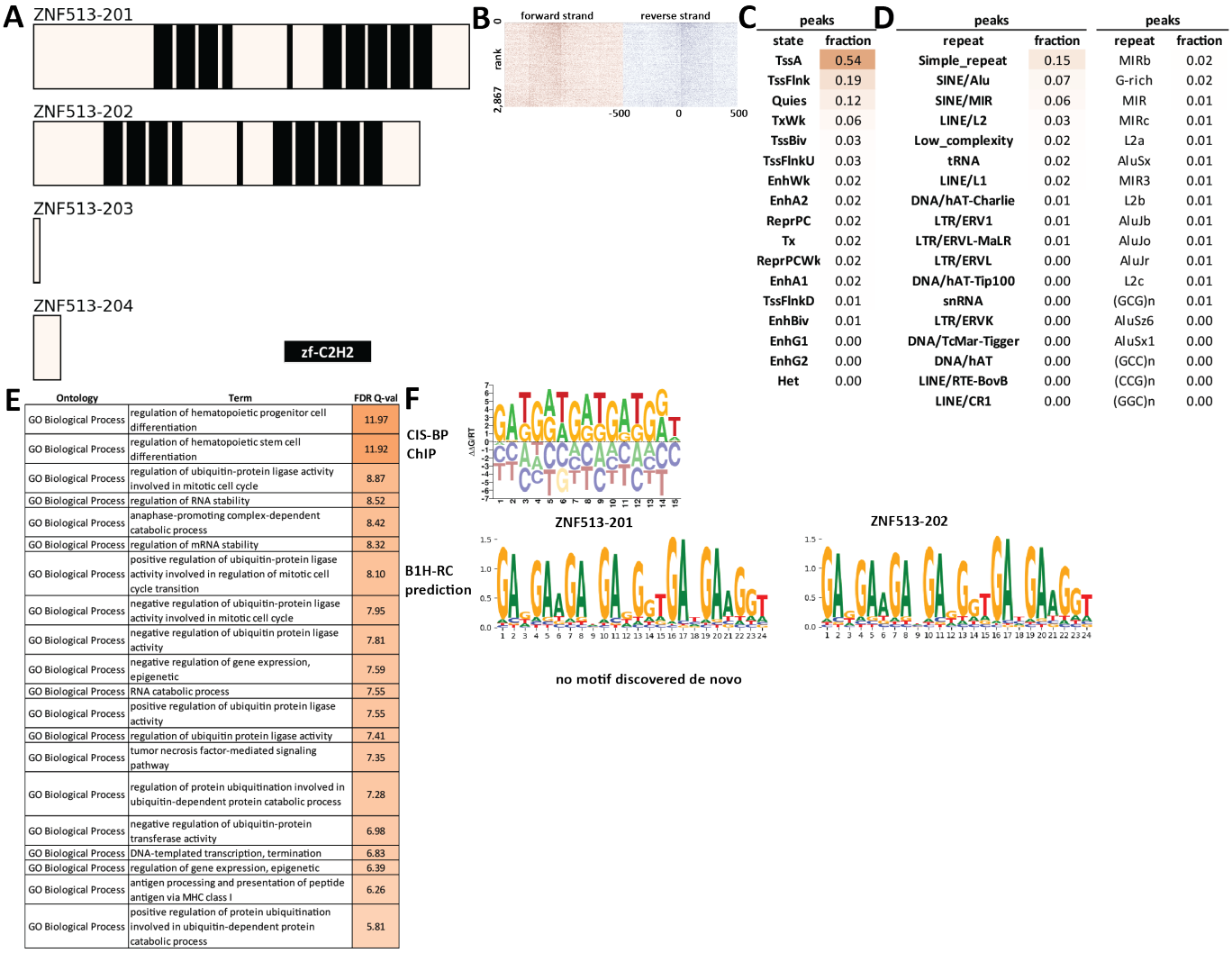

Supplementary Figure 1304: Properties and genomic distribution of motifs identified for the ZNF513 transcription factor in HepG2 (accession ENCSR171KUL).

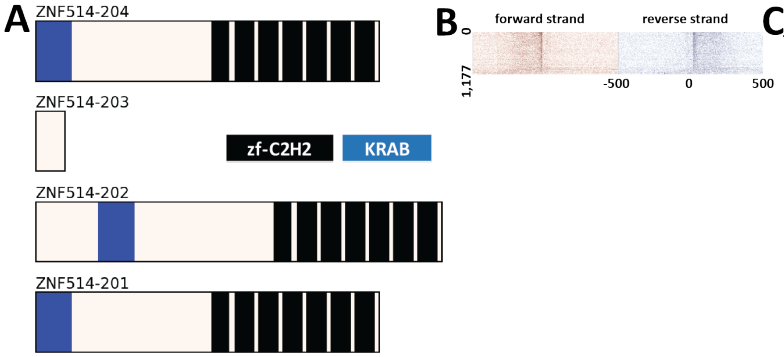

C

peaks	
state	fraction
Quies	0.51
TxWk	0.20
Tx	0.06
ReprPCWk	0.06
EnhWk	0.04
TssA	0.04
TssFlnk	0.02
ReprPC	0.02
Het	0.02
EnhA2	0.01
EnhA1	0.01
TssBiv	0.01
TssFlnkU	0.01
ZNF/Rpts	0.00
TssFlnkD	0.00
EnhBiv	0.00
EnhG1	0.00
EnhG2	0.00

D

peaks		peaks	
repeat	fraction	repeat	fraction
SINE/Alu	0.77	(AAAT)n	0.22
Simple_repeat	0.73	AluSx	0.10
LINE/L1	0.17	AluSx1	0.09
SINE/MIR	0.06	AluJb	0.08
LINE/L2	0.05	AluSz	0.07
LTR/ERVL-MaLR	0.03	(ATTT)n	0.06
Low_complexity	0.03	AluJo	0.06
LTR/ERV1	0.03	AluY	0.06
LTR/ERVL	0.03	AluJr	0.05
DNA/hAT-Charlie	0.02	(TTAT)n	0.05
DNA/TcMar-Tigger	0.02	(TTTA)n	0.04
LTR/ERVK	0.01	AluSq2	0.04
Retroposon/SVA	0.00	(GT)n	0.04
LINE/RTE-X	0.00	AluSz6	0.03
DNA/hAT-Tip100	0.00	AluSp	0.03
LINE/CR1	0.00	(AATA)n	0.03
rRNA	0.00	(TATT)n	0.03
DNA/hAT-Blackjack	0.00	(CA)n	0.03

E

Ontology	Term	FDR Q-val
GO Biological Process	positive regulation of binding	4.12
GO Biological Process	establishment of epithelial cell polarity	3.50
GO Biological Process	positive regulation of T cell receptor signaling pathway	3.13
GO Biological Process	mammary gland epithelium development	2.42
GO Biological Process	nuclear migration	2.09
GO Biological Process	membrane depolarization	1.94
GO Biological Process	positive regulation of interleukin-13 secretion	1.85
GO Biological Process	regulation of stress fiber assembly	1.83
GO Biological Process	regulation of actin filament bundle assembly	1.66
GO Biological Process	thymic T cell selection	1.61
GO Biological Process	trachea cartilage development	1.52
GO Biological Process	positive regulation of transcription initiation from RNA polymerase II promoter	1.43
GO Biological Process	cardiac vascular smooth muscle cell differentiation	1.41
Human Phenotype	Prominent fingertip pads	1.62

F

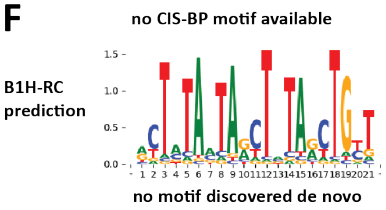

Supplementary Figure 1305: Properties and genomic distribution of motifs identified for the ZNF514 transcription factor in HEK293 (accession ENCSR897RVP).

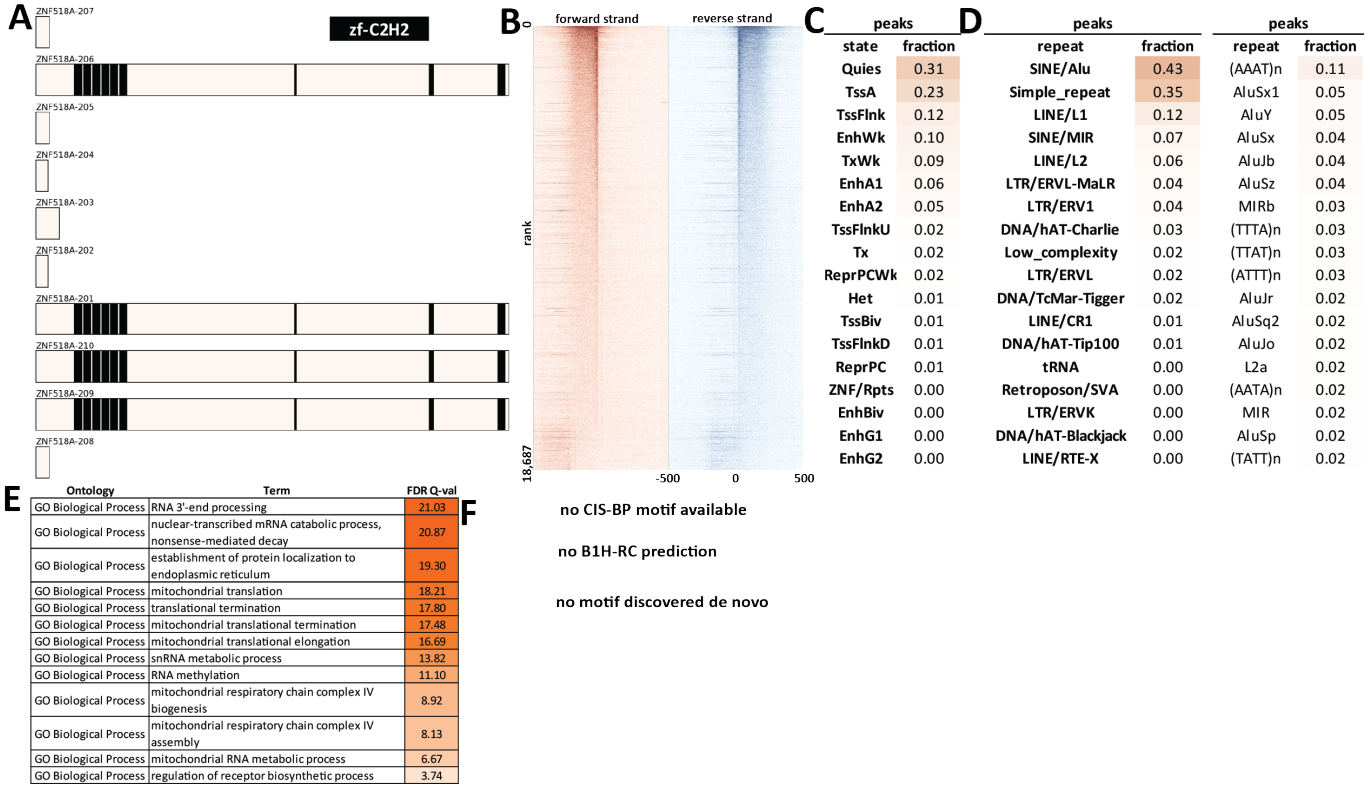

C

peaks	
state	fraction
Quies	0.31
TssA	0.23
TssFlnk	0.12
EnhWk	0.10
TxWk	0.09
EnhA1	0.06
EnhA2	0.05
TssFlnkU	0.02
Tx	0.02
ReprPCWk	0.02
Het	0.01
TssBiv	0.01
TssFlnkD	0.01
ReprPC	0.01
ZNF/Rpts	0.00
EnhBiv	0.00
EnhG1	0.00
EnhG2	0.00

D

peaks		peaks	
repeat	fraction	repeat	fraction
SINE/Alu	0.43	(AAAT)n	0.11
Simple_repeat	0.35	AluSx1	0.05
LINE/L1	0.12	AluY	0.05
SINE/MIR	0.07	AluSx	0.04
LINE/L2	0.06	AluJb	0.04
LTR/ERVL-MaLR	0.04	AluSz	0.04
LTR/ERV1	0.04	MIRb	0.03
DNA/hAT-Charlie	0.03	(TTTA)n	0.03
Low_complexity	0.02	(TTAT)n	0.03
LTR/ERVL	0.02	(ATTT)n	0.03
DNA/TcMar-Tigger	0.02	AluJr	0.02
LINE/CR1	0.01	AluSq2	0.02
DNA/hAT-Tip100	0.01	AluJo	0.02
tRNA	0.00	L2a	0.02
Retroposon/SVA	0.00	(AATA)n	0.02
LTR/ERVK	0.00	MIR	0.02
DNA/hAT-Blackjack	0.00	AluSp	0.02
LINE/RTE-X	0.00	(TATT)n	0.02

E

Ontology	Term	FDR Q-val
GO Biological Process	RNA 3'-end processing	21.03
GO Biological Process	nuclear-transcribed mRNA catabolic process, nonsense-mediated decay	20.87
GO Biological Process	establishment of protein localization to endoplasmic reticulum	19.30
GO Biological Process	mitochondrial translation	18.21
GO Biological Process	translational termination	17.80
GO Biological Process	mitochondrial translational termination	17.48
GO Biological Process	mitochondrial translational elongation	16.69
GO Biological Process	snRNA metabolic process	13.82
GO Biological Process	RNA methylation	11.10
GO Biological Process	mitochondrial respiratory chain complex IV biogenesis	8.92
GO Biological Process	mitochondrial respiratory chain complex IV assembly	8.13
GO Biological Process	mitochondrial RNA metabolic process	6.67
GO Biological Process	regulation of receptor biosynthetic process	3.74

Supplementary Figure 1306: Properties and genomic distribution of motifs identified for the ZNF518A transcription factor in HEK293 (accession ENCSR159GFL).

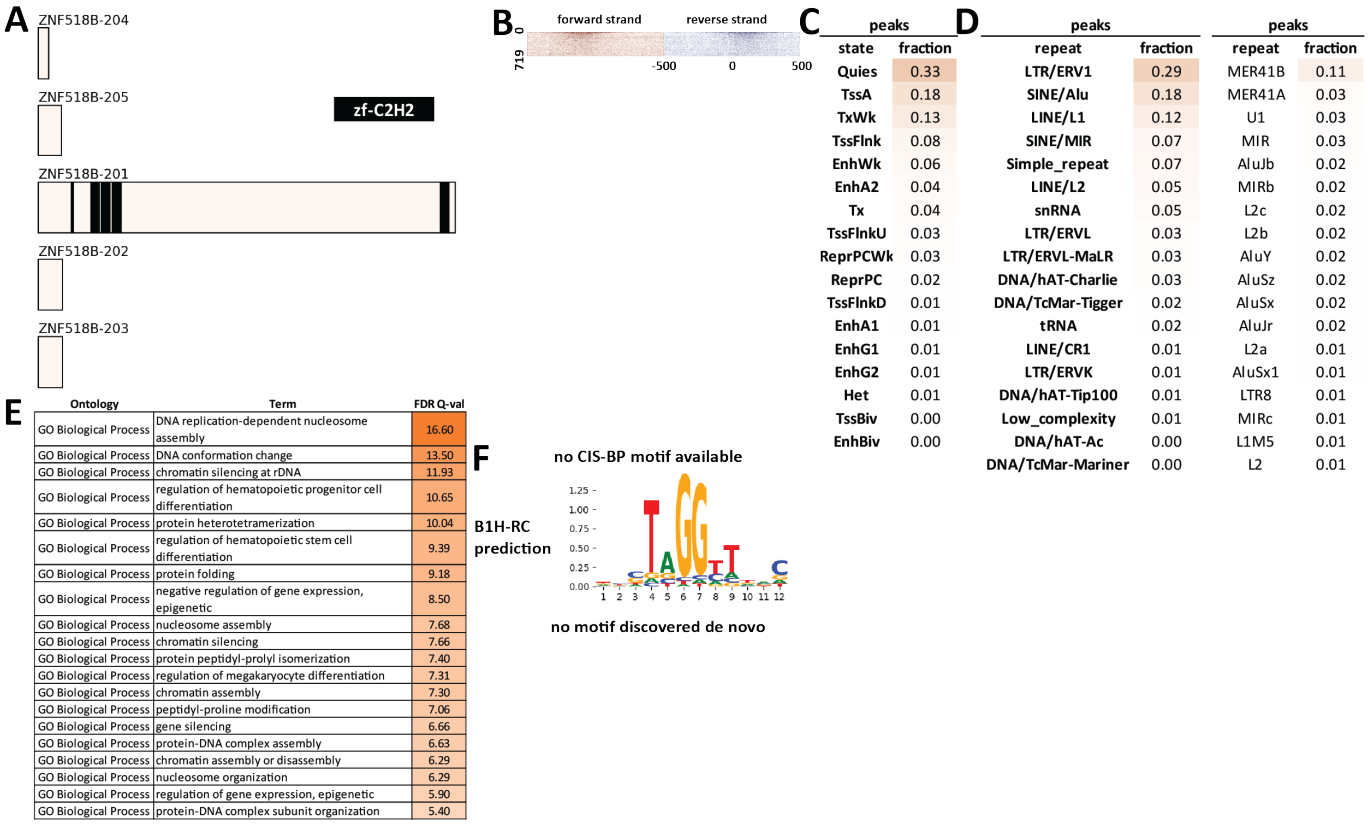

C

peaks	
state	fraction
Quies	0.33
TssA	0.18
TxWk	0.13
TssFlnk	0.08
EnhWk	0.06
EnhA2	0.04
Tx	0.04
TssFlnkU	0.03
ReprPCWk	0.03
ReprPC	0.02
TssFlnkD	0.01
EnhA1	0.01
EnhG1	0.01
EnhG2	0.01
Het	0.01
TssBiv	0.00
EnhBiv	0.00

D

peaks		peaks	
repeat	fraction	repeat	fraction
LTR/ERV1	0.29	MER41B	0.11
SINE/Alu	0.18	MER41A	0.03
LINE/L1	0.12	U1	0.03
SINE/MIR	0.07	MIR	0.03
Simple_repeat	0.07	AluJb	0.02
LINE/L2	0.05	MIRb	0.02
snRNA	0.05	L2c	0.02
LTR/ERVL	0.03	L2b	0.02
LTR/ERVL-MaLR	0.03	AluY	0.02
DNA/hAT-Charlie	0.03	AluSz	0.02
DNA/TcMar-Tigger	0.02	AluSx	0.02
tRNA	0.02	AluJr	0.02
LINE/CR1	0.01	L2a	0.01
LTR/ERVK	0.01	AluSx1	0.01
DNA/hAT-Tip100	0.01	LTR8	0.01
Low_complexity	0.01	MIRc	0.01
DNA/hAT-Ac	0.00	L1M5	0.01
DNA/TcMar-Mariner	0.00	L2	0.01

E

Ontology	Term	FDR Q-val
GO Biological Process	DNA replication-dependent nucleosome assembly	16.60
GO Biological Process	DNA conformation change	13.50
GO Biological Process	chromatin silencing at rDNA	11.93
GO Biological Process	regulation of hematopoietic progenitor cell differentiation	10.65
GO Biological Process	protein heterotetramerization	10.04
GO Biological Process	regulation of hematopoietic stem cell differentiation	9.39
GO Biological Process	protein folding	9.18
GO Biological Process	negative regulation of gene expression, epigenetic	8.50
GO Biological Process	nucleosome assembly	7.68
GO Biological Process	chromatin silencing	7.66
GO Biological Process	protein peptidyl-prolyl isomerization	7.40
GO Biological Process	regulation of megakaryocyte differentiation	7.31
GO Biological Process	chromatin assembly	7.30
GO Biological Process	peptidyl-proline modification	7.06
GO Biological Process	gene silencing	6.66
GO Biological Process	protein-DNA complex assembly	6.63
GO Biological Process	chromatin assembly or disassembly	6.29
GO Biological Process	nucleosome organization	6.29
GO Biological Process	regulation of gene expression, epigenetic	5.90
GO Biological Process	protein-DNA complex subunit organization	5.40

Supplementary Figure 1307: Properties and genomic distribution of motifs identified for the ZNF518B transcription factor in K562 (accession ENCSR597CHL).

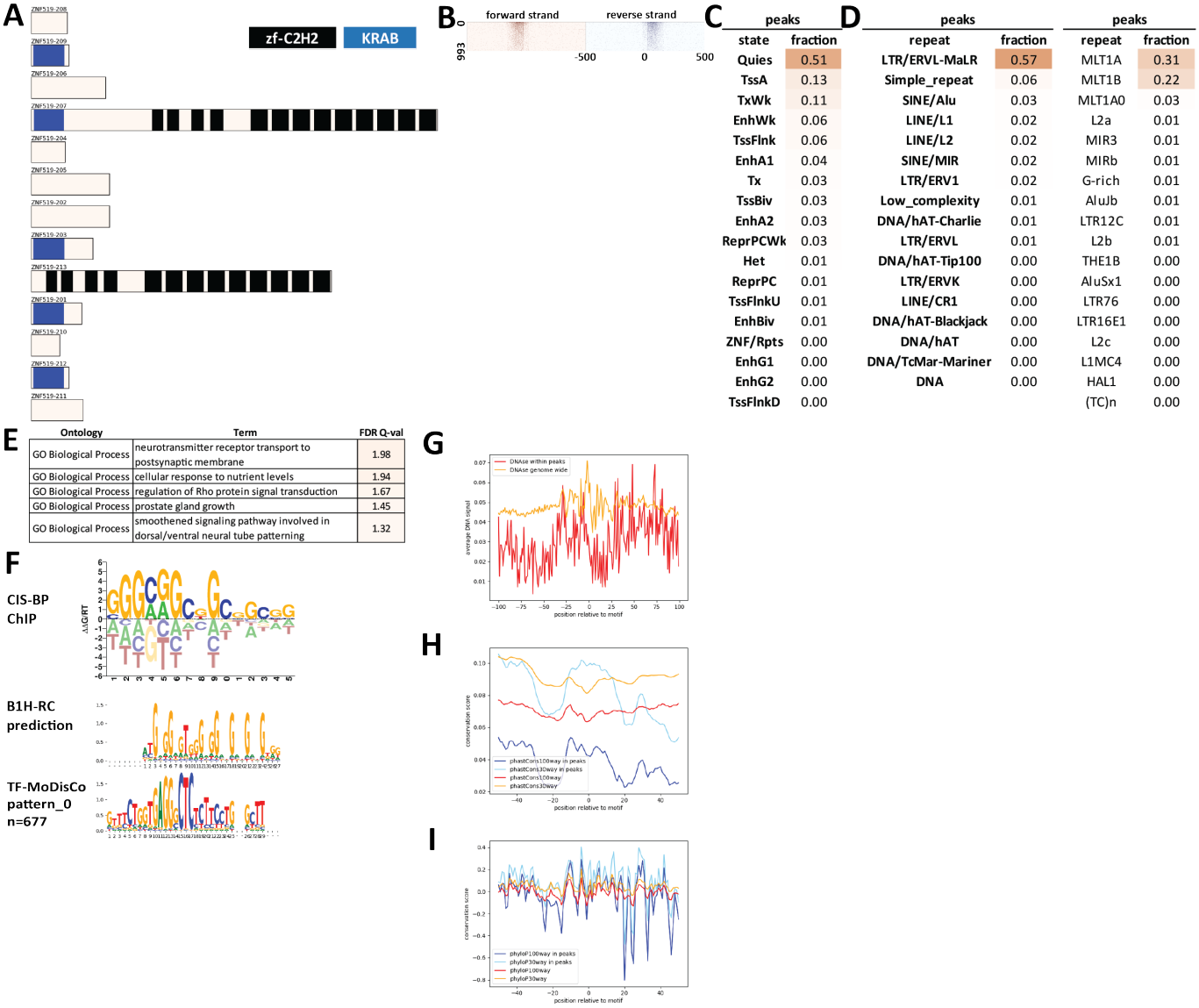

C

peaks	
state	fraction
Quies	0.51
TssA	0.13
TxWk	0.11
EnhWk	0.06
TssFlnk	0.06
EnhA1	0.04
Tx	0.03
TssBiv	0.03
EnhA2	0.03
ReprPCWk	0.03
Het	0.01
ReprPC	0.01
TssFlnkU	0.01
EnhBiv	0.01
ZNF/Rpts	0.00
EnhG1	0.00
EnhG2	0.00
TssFlnkD	0.00

D

peaks		peaks	
repeat	fraction	repeat	fraction
LTR/ERVL-MaLR	0.57	MLT1A	0.31
Simple_repeat	0.06	MLT1B	0.22
SINE/Alu	0.03	MLT1A0	0.03
LINE/L1	0.02	L2a	0.01
LINE/L2	0.02	MIR3	0.01
SINE/MIR	0.02	MIRb	0.01
LTR/ERV1	0.02	G-rich	0.01
Low_complexity	0.01	AluJb	0.01
DNA/hAT-Charlie	0.01	LTR12C	0.01
LTR/ERVL	0.01	L2b	0.01
DNA/hAT-Tip100	0.00	THE1B	0.00
LTR/ERVK	0.00	AluSx1	0.00
LINE/CR1	0.00	LTR76	0.00
DNA/hAT-Blackjack	0.00	LTR16E1	0.00
DNA/hAT	0.00	L2c	0.00
DNA/TcMar-Mariner	0.00	L1MC4	0.00
DNA	0.00	HAL1	0.00
		(TC)n	0.00

E

Ontology	Term	FDR Q-val
GO Biological Process	neurotransmitter receptor transport to postsynaptic membrane	1.98
GO Biological Process	cellular response to nutrient levels	1.94
GO Biological Process	regulation of Rho protein signal transduction	1.67
GO Biological Process	prostate gland growth	1.45
GO Biological Process	smoothened signaling pathway involved in dorsal/ventral neural tube patterning	1.32

Supplementary Figure 1308: Properties and genomic distribution of motifs identified for the ZNF519 transcription factor in HEK293 (accession Hughes NB models).

TF-MoDisCO pattern_0 n=677, CWM

pattern_0, n=677; subpattern_0, ns=247

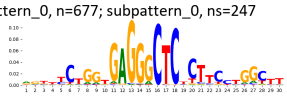

pattern_0, n=677; subpattern_1, ns=245

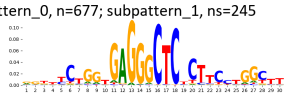

pattern_0, n=677; subpattern_2, ns=107

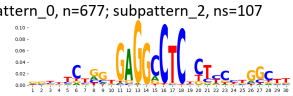

pattern_0, n=677; subpattern_3, ns=76

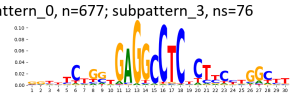

pattern_0, n=677; subpattern_4, ns=2

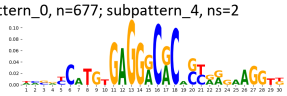

TF-MoDisCO pattern_0 n=677, PWM

pattern_0, n=677; subpattern_0, ns=247

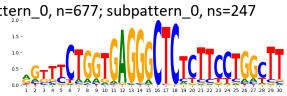

pattern_0, n=677; subpattern_1, ns=245

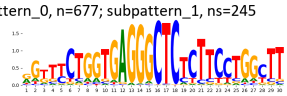

pattern_0, n=677; subpattern_2, ns=107

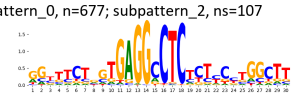

pattern_0, n=677; subpattern_3, ns=76

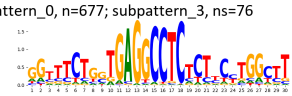

pattern_0, n=677; subpattern_4, ns=2

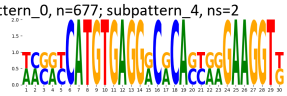

Supplementary Figure 1309: TF-MoDisCO subpatterns for the ZNF519 transcription factor in HEK293 (accession Hughes NB models).

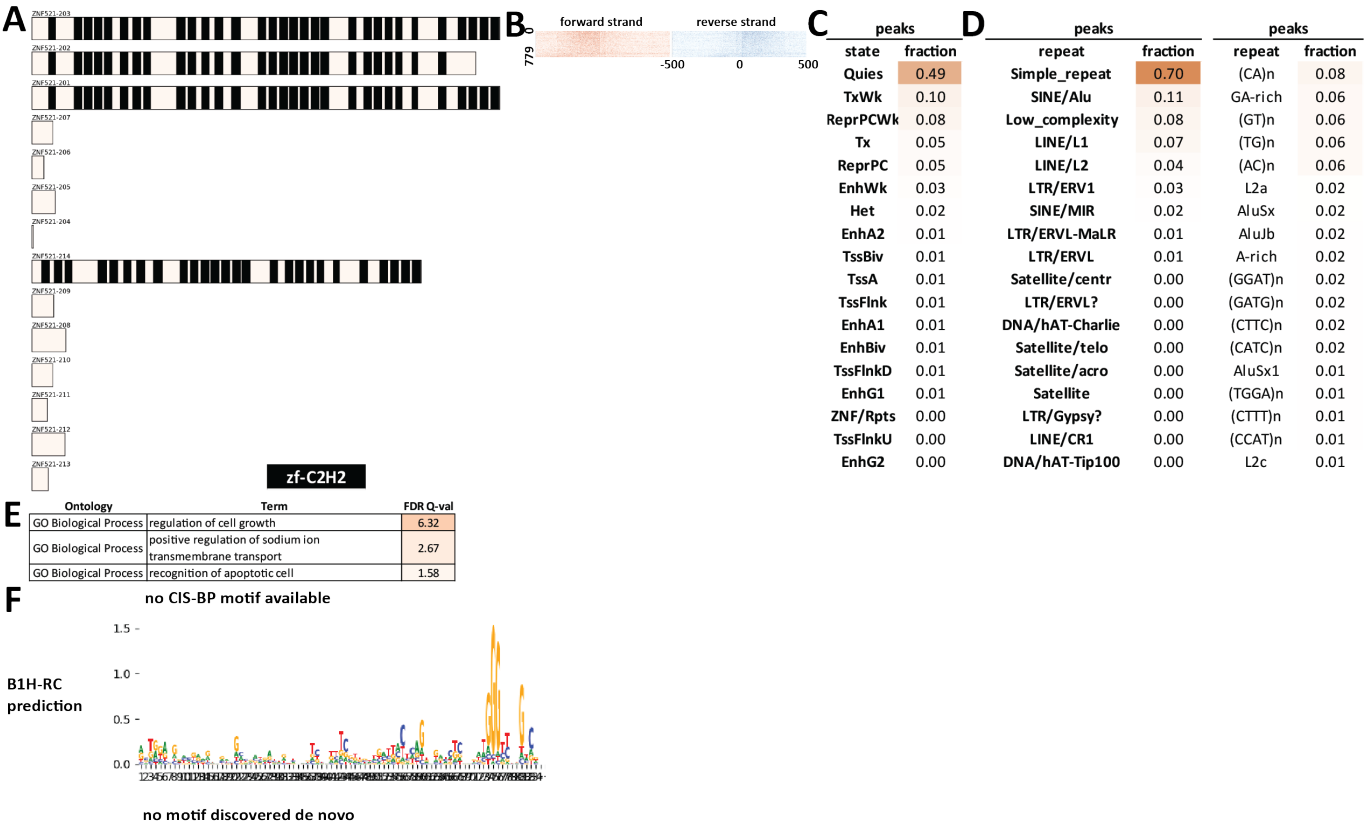

C

peaks	
state	fraction
Quies	0.49
TxWk	0.10
ReprPCWk	0.08
Tx	0.05
ReprPC	0.05
EnhWk	0.03
Het	0.02
EnhA2	0.01
TssBiv	0.01
TssA	0.01
TssFlnk	0.01
EnhA1	0.01
EnhBiv	0.01
TssFlnkD	0.01
EnhG1	0.01
ZNF/Rpts	0.00
TssFlnkU	0.00
EnhG2	0.00

D

peaks		peaks	
repeat	fraction	repeat	fraction
Simple_repeat	0.70	(CA)n	0.08
SINE/Alu	0.11	GA-rich	0.06
Low_complexity	0.08	(GT)n	0.06
LINE/L1	0.07	(TG)n	0.06
LINE/L2	0.04	(AC)n	0.06
LTR/ERV1	0.03	L2a	0.02
SINE/MIR	0.02	AluSx	0.02
LTR/ERVL-MaLR	0.01	AluJb	0.02
LTR/ERVL	0.01	A-rich	0.02
Satellite/centr	0.00	(GGAT)n	0.02
LTR/ERVL?	0.00	(GATG)n	0.02
DNA/hAT-Charlie	0.00	(CTTC)n	0.02
Satellite/telo	0.00	(CATC)n	0.02
Satellite/acro	0.00	AluSx1	0.01
Satellite	0.00	(TGGA)n	0.01
LTR/Gypsy?	0.00	(CTTT)n	0.01
LINE/CR1	0.00	(CCAT)n	0.01
DNA/hAT-Tip100	0.00	L2c	0.01

E

Ontology	Term	FDR Q-val
GO Biological Process	regulation of cell growth	6.32
GO Biological Process	positive regulation of sodium ion transmembrane transport	2.67
GO Biological Process	recognition of apoptotic cell	1.58

Supplementary Figure 1310: Properties and genomic distribution of motifs identified for the ZNF521 transcription factor in HEK293 (accession ENCSR665KYH).

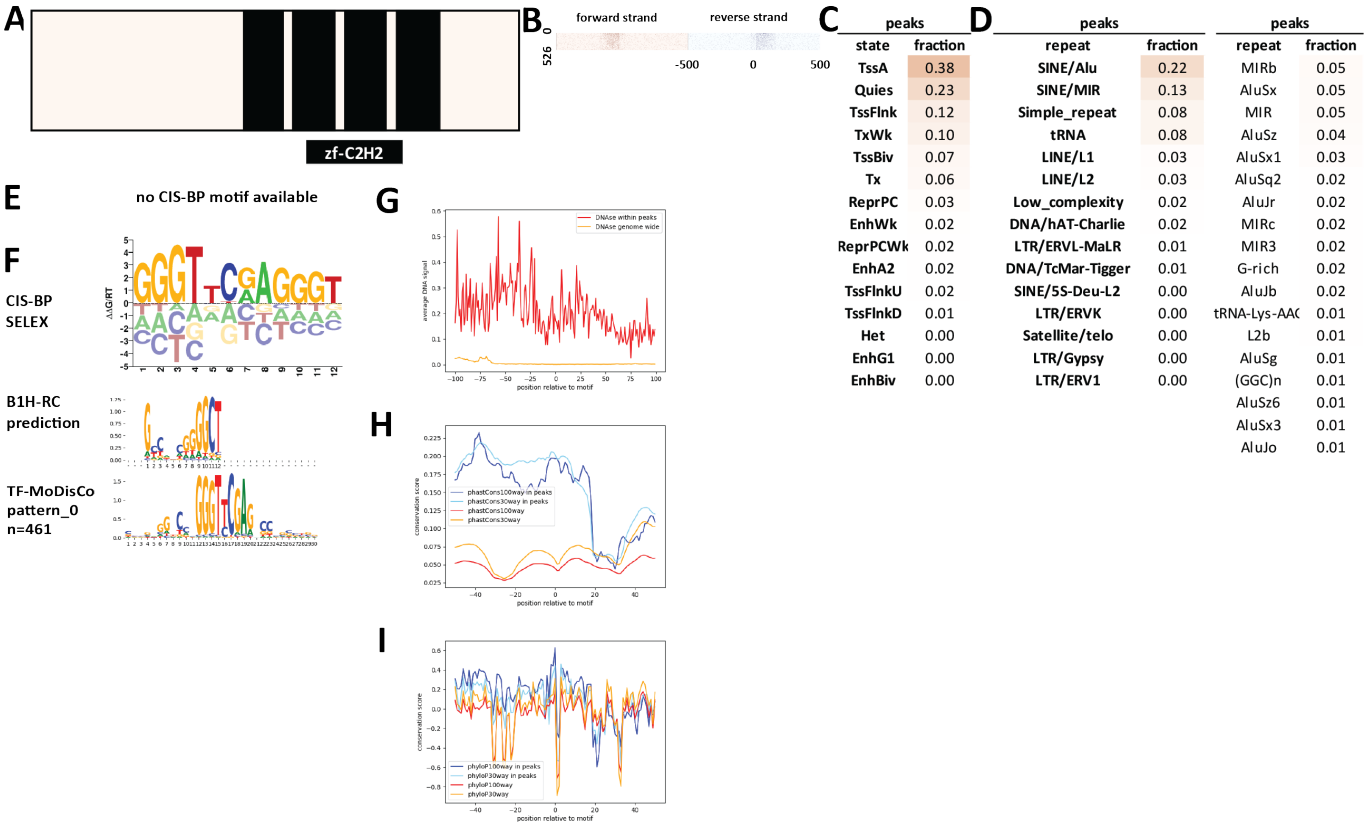

C

peaks	
state	fraction
TssA	0.38
Quies	0.23
TssFlnk	0.12
TxWk	0.10
TssBiv	0.07
Tx	0.06
ReprPC	0.03
EnhWk	0.02
ReprPCWk	0.02
EnhA2	0.02
TssFlnkU	0.02
TssFlnkD	0.01
Het	0.00
EnhG1	0.00
EnhBiv	0.00

D

peaks		peaks	
repeat	fraction	repeat	fraction
SINE/Alu	0.22	MIRb	0.05
SINE/MIR	0.13	AluSx	0.05
Simple_repeat	0.08	MIR	0.05
tRNA	0.08	AluSz	0.04
LINE/L1	0.03	AluSx1	0.03
LINE/L2	0.03	AluSq2	0.02
Low_complexity	0.02	AluJr	0.02
DNA/hAT-Charlie	0.02	MIRc	0.02
LTR/ERVL-MaLR	0.01	MIR3	0.02
DNA/TcMar-Tigger	0.01	G-rich	0.02
SINE/5S-Deu-L2	0.00	AluJb	0.02
LTR/ERVK	0.00	tRNA-Lys-AAC	0.01
Satellite/telo	0.00	L2b	0.01
LTR/Gypsy	0.00	AluSg	0.01
LTR/ERV1	0.00	(GGC)n	0.01
		AluSz6	0.01
		AluSx3	0.01
		AluJo	0.01

Supplementary Figure 1311: Properties and genomic distribution of motifs identified for the ZNF524 transcription factor in HEK293 (accession Hughes GR models).

TF-MoDisCO pattern_0 n=461, CWM

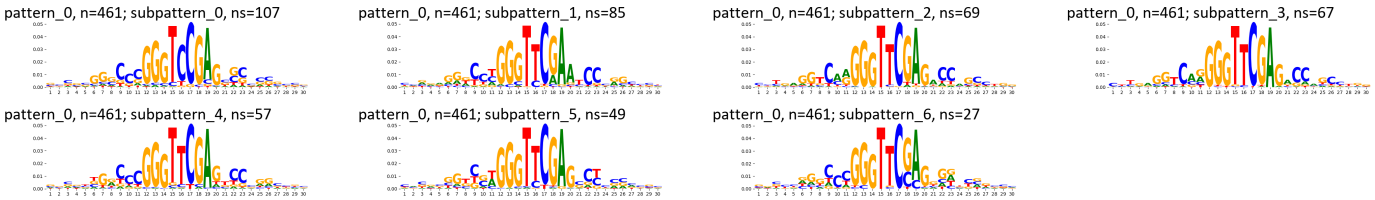

TF-MoDisCO pattern_0 n=461, PWM

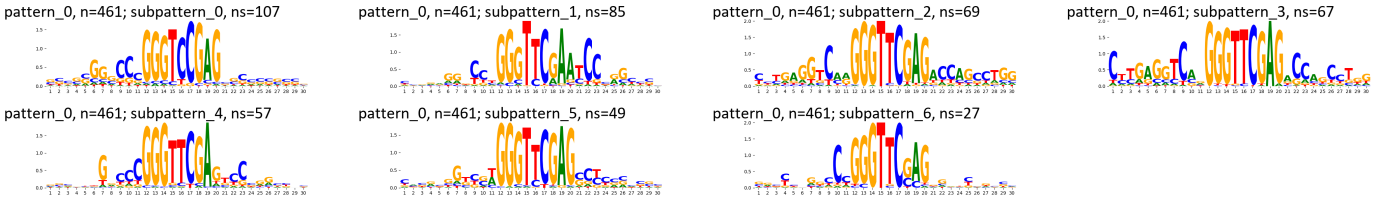

Supplementary Figure 1312: TF-MoDisCO subpatterns for the ZNF524 transcription factor in HEK293 (accession Hughes GR models).

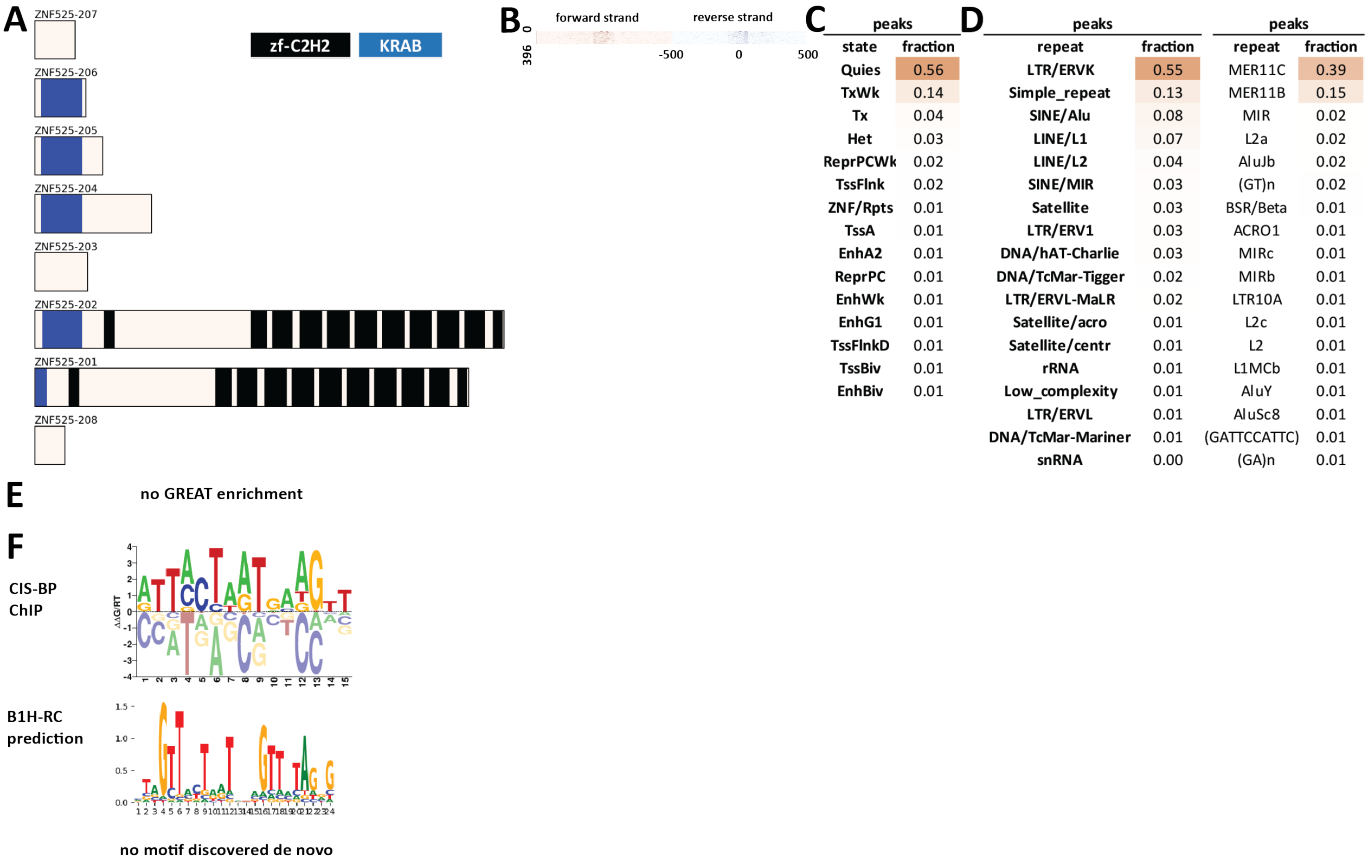

Supplementary Figure 1313: Properties and genomic distribution of motifs identified for the ZNF525 transcription factor in HEK293 (accession ChipExo models).

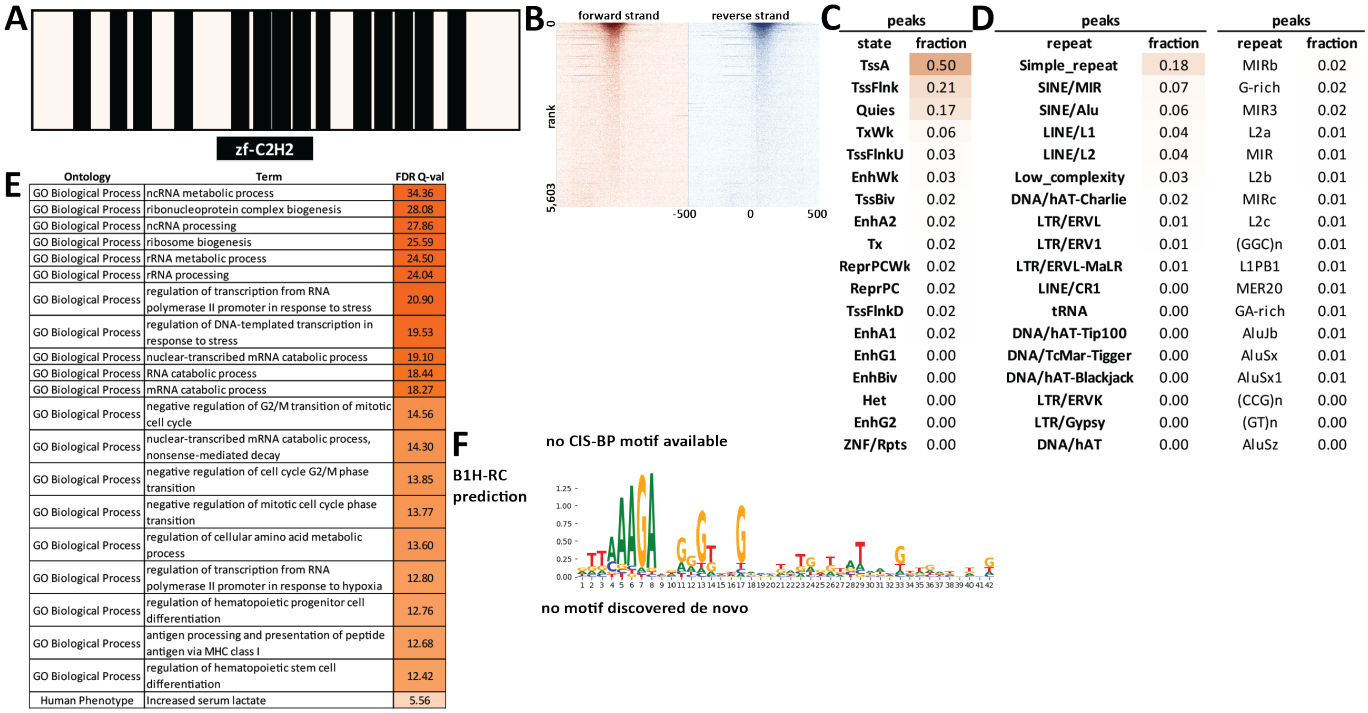

Supplementary Figure 1314: Properties and genomic distribution of motifs identified for the ZNF526 transcription factor in HepG2 (accession ENCSR608XRC).

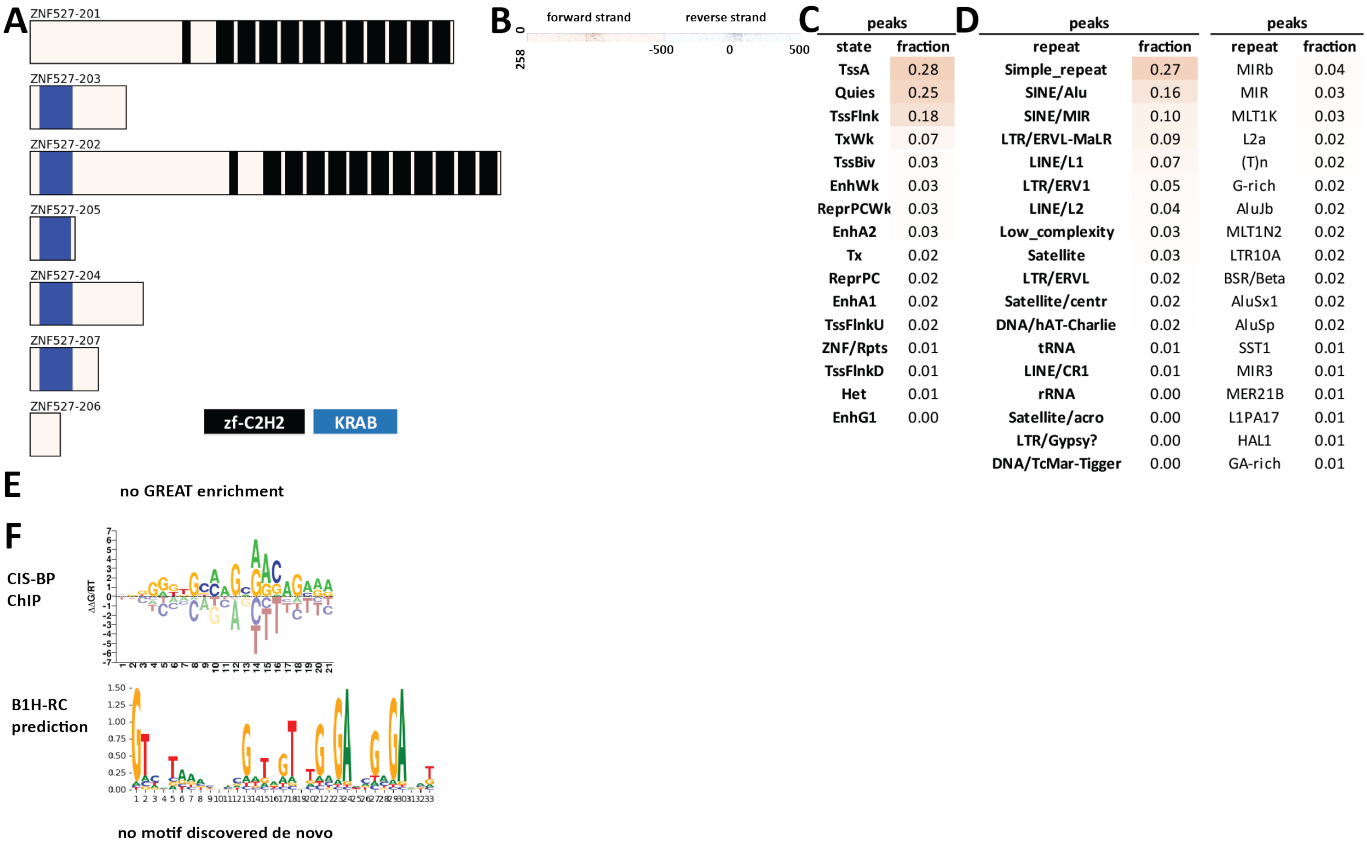

peaks	
state	fraction
TssA	0.28
Quies	0.25
TssFlnk	0.18
TxWk	0.07
TssBiv	0.03
EnhWk	0.03
ReprPCWk	0.03
EnhA2	0.03
Tx	0.02
ReprPC	0.02
EnhA1	0.02
TssFlnkU	0.02
ZNF/Rpts	0.01
TssFlnkD	0.01
Het	0.01
EnhG1	0.00

peaks		peaks	
repeat	fraction	repeat	fraction
Simple_repeat	0.27	MIRb	0.04
SINE/Alu	0.16	MIR	0.03
SINE/MIR	0.10	MLT1K	0.03
LTR/ERVL-MaLR	0.09	L2a	0.02
LINE/L1	0.07	(T)n	0.02
LTR/ERV1	0.05	G-rich	0.02
LINE/L2	0.04	AluJb	0.02
Low_complexity	0.03	MLT1N2	0.02
Satellite	0.03	LTR10A	0.02
LTR/ERVL	0.02	BSR/Beta	0.02
Satellite/centr	0.02	AluSx1	0.02
DNA/hAT-Charlie	0.02	AluSp	0.02
tRNA	0.01	SST1	0.01
LINE/CR1	0.01	MIR3	0.01
rRNA	0.00	MER21B	0.01
Satellite/acro	0.00	L1PA17	0.01
LTR/Gypsy?	0.00	HAL1	0.01
DNA/TcMar-Tigger	0.00	GA-rich	0.01

Supplementary Figure 1315: Properties and genomic distribution of motifs identified for the ZNF527 transcription factor in HEK293 (accession ChipExo models).

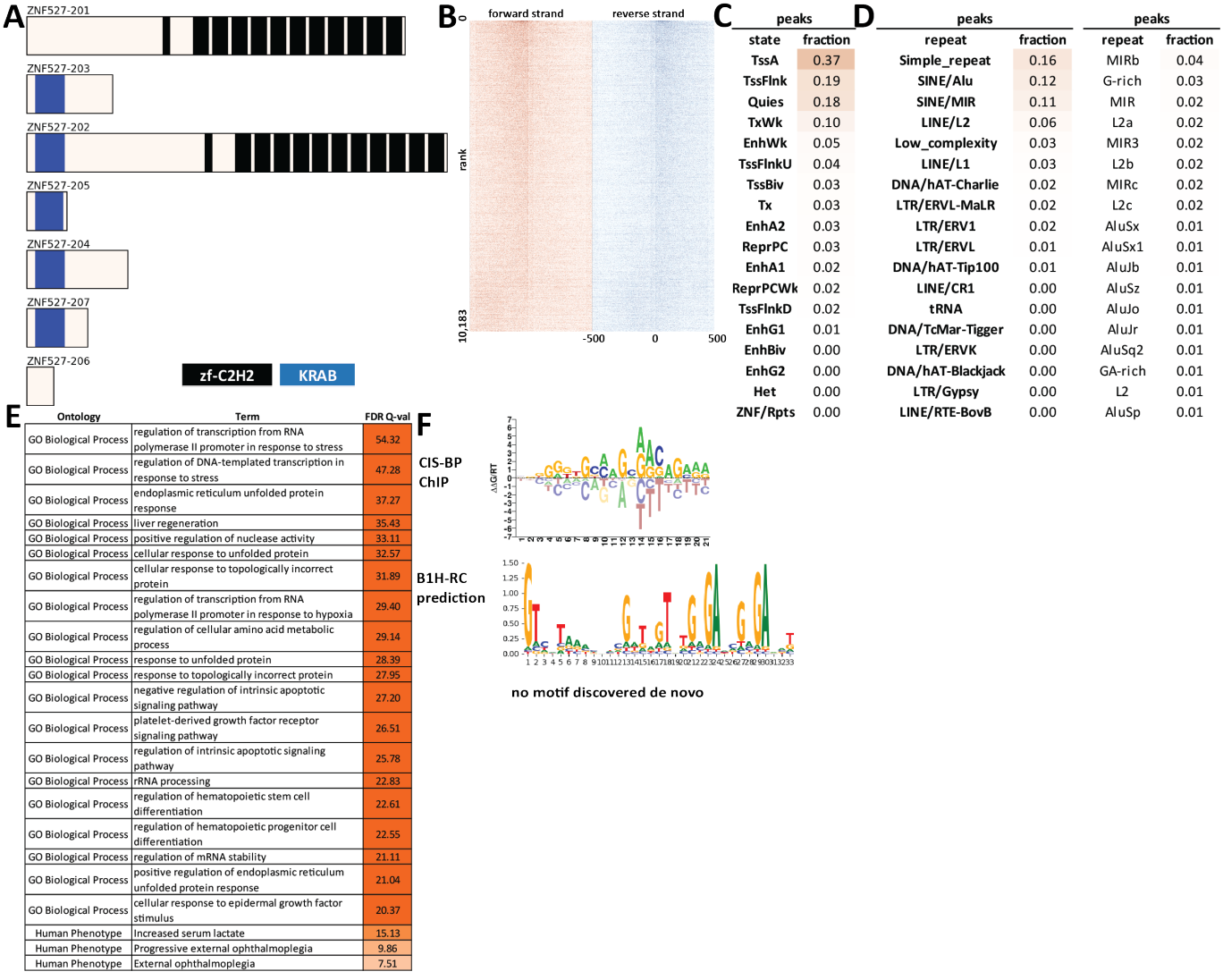

Supplementary Figure 1316: Properties and genomic distribution of motifs identified for the ZNF527 transcription factor in HepG2 (accession ENCSR656RTA).

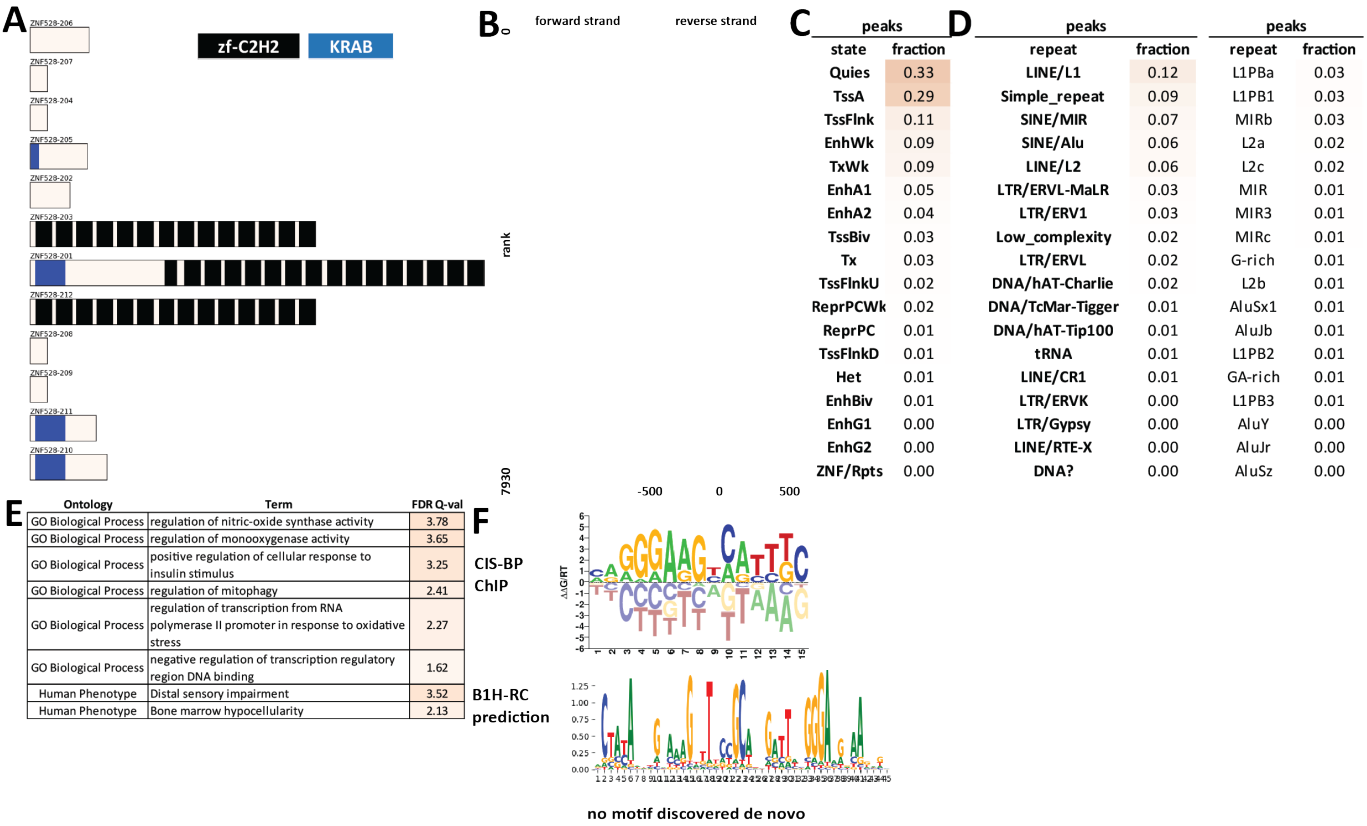

C

peaks	
state	fraction
Quies	0.33
TssA	0.29
TssFlnk	0.11
EnhWk	0.09
TxWk	0.09
EnhA1	0.05
EnhA2	0.04
TssBiv	0.03
Tx	0.03
TssFlnkU	0.02
ReprPCWk	0.02
ReprPC	0.01
TssFlnkD	0.01
Het	0.01
EnhBiv	0.01
EnhG1	0.00
EnhG2	0.00
ZNF/Rpts	0.00

D

peaks		peaks	
repeat	fraction	repeat	fraction
LINE/L1	0.12	L1PBa	0.03
Simple_repeat	0.09	L1PB1	0.03
SINE/MIR	0.07	MIRb	0.03
SINE/Alu	0.06	L2a	0.02
LINE/L2	0.06	L2c	0.02
LTR/ERVL-MaLR	0.03	MIR	0.01
LTR/ERV1	0.03	MIR3	0.01
Low_complexity	0.02	MIRc	0.01
LTR/ERVL	0.02	G-rich	0.01
DNA/hAT-Charlie	0.02	L2b	0.01
DNA/TcMar-Tigger	0.01	AluSx1	0.01
DNA/hAT-Tip100	0.01	AluJb	0.01
tRNA	0.01	L1PB2	0.01
LINE/CR1	0.01	GA-rich	0.01
LTR/ERVK	0.00	L1PB3	0.01
LTR/Gypsy	0.00	AluY	0.00
LINE/RTE-X	0.00	AluJr	0.00
DNA?	0.00	AluSz	0.00

E

Ontology	Term	FDR Q-val
GO Biological Process	regulation of nitric-oxide synthase activity	3.78
GO Biological Process	regulation of monooxygenase activity	3.65
GO Biological Process	positive regulation of cellular response to insulin stimulus	3.25
GO Biological Process	regulation of mitophagy	2.41
GO Biological Process	regulation of transcription from RNA polymerase II promoter in response to oxidative stress	2.27
GO Biological Process	negative regulation of transcription regulatory region DNA binding	1.62
Human Phenotype	Distal sensory impairment	3.52
Human Phenotype	Bone marrow hypocellularity	2.13

Supplementary Figure 1317: Properties and genomic distribution of motifs identified for the ZNF528 transcription factor in HEK293 (accession Hughes GR models).

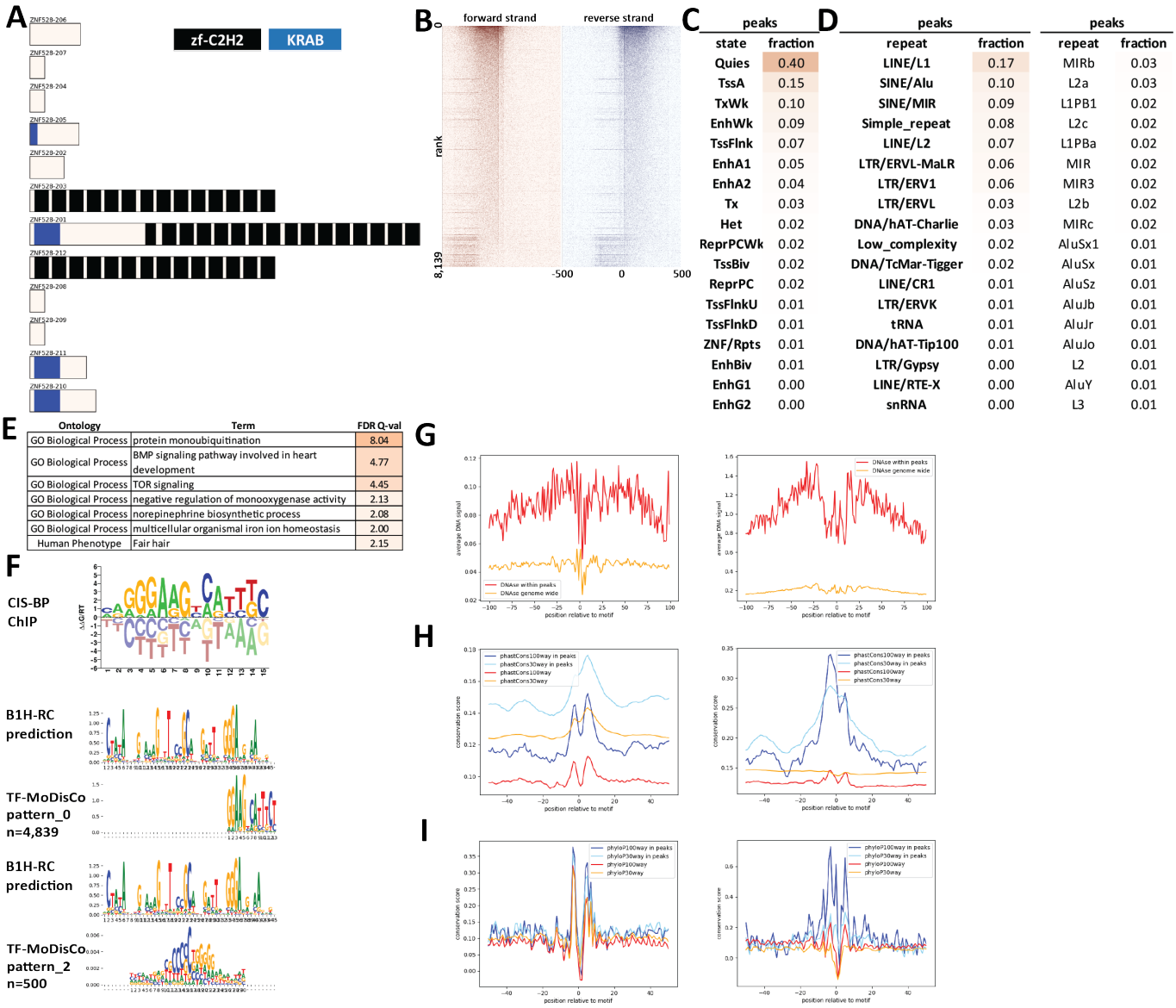

Supplementary Figure 1318: Properties and genomic distribution of motifs identified for the ZNF528 transcription factor in HEK293 (accession Hughes NB models).

TF-MoDisCO pattern_0 n=4839, CWM

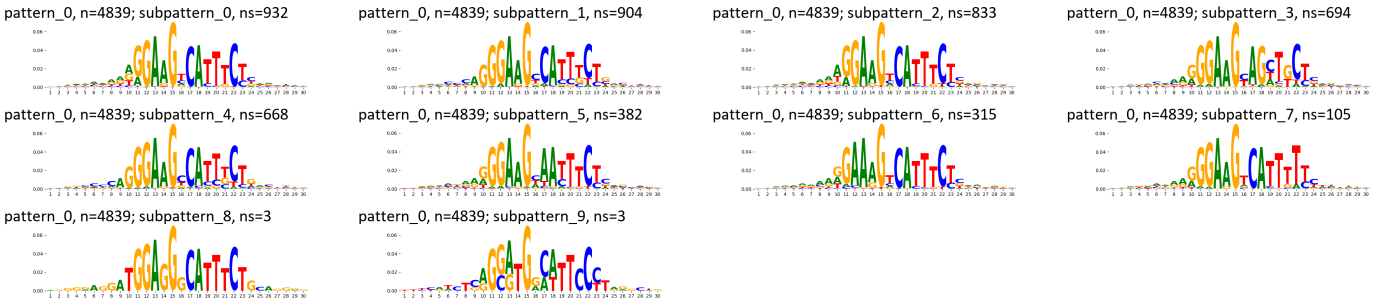

TF-MoDisCO pattern_0 n=4839, PWM

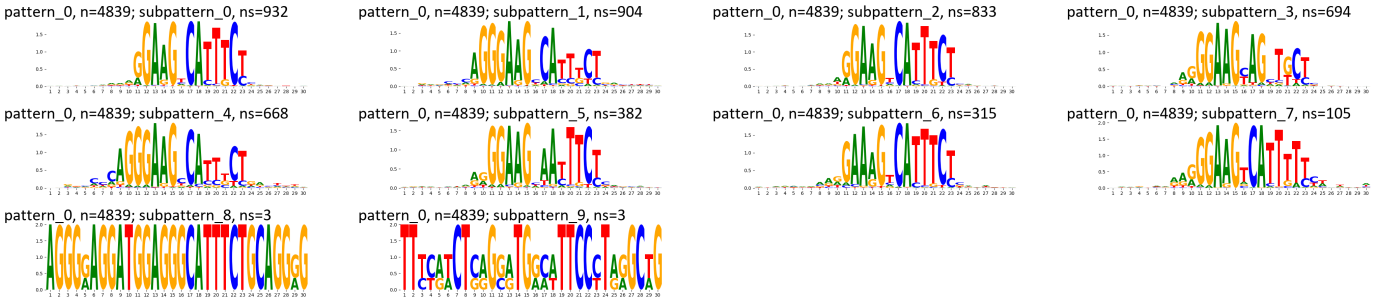

TF-MoDisCO pattern_2 n=500, CWM

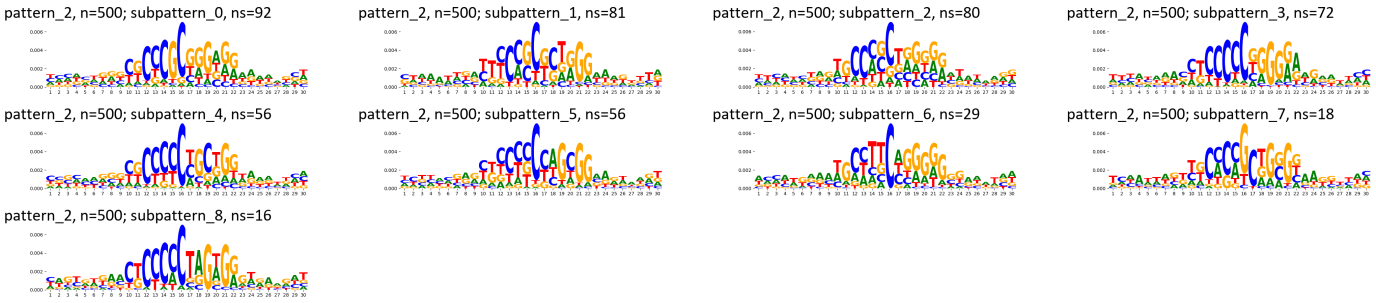

TF-MoDisCO pattern_2 n=500, PWM

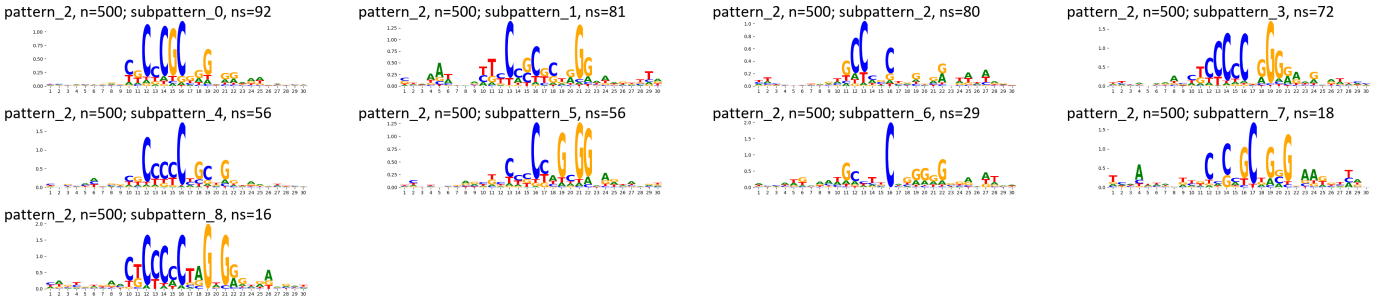

Supplementary Figure 1319: TF-MoDisCO subpatterns for the ZNF528 transcription factor in HEK293 (accession Hughes NB models).

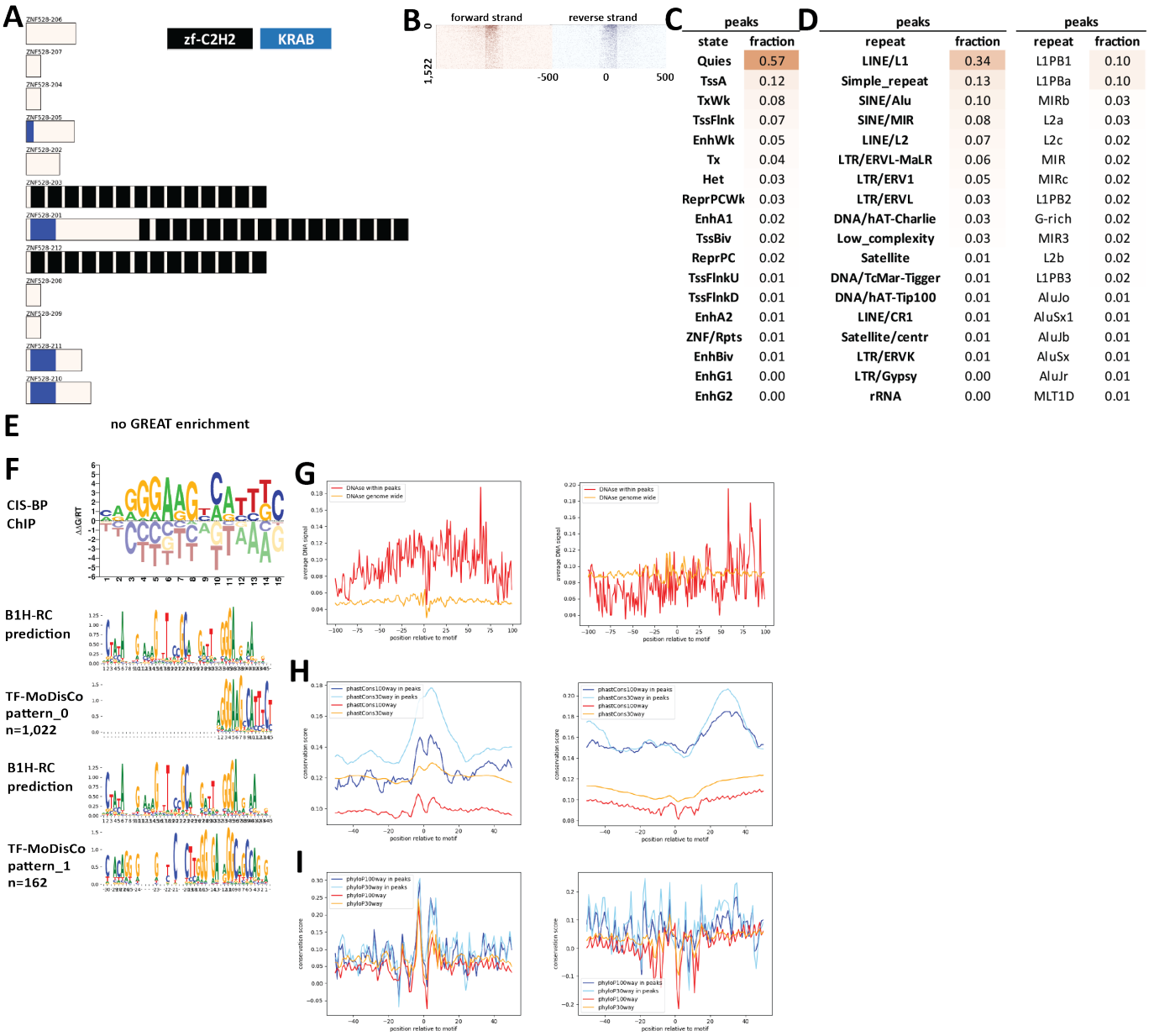

Supplementary Figure 1320: Properties and genomic distribution of motifs identified for the ZNF528 transcription factor in HEK293 (accession ChipExo models).

TF-MoDisCO pattern_0 n=1022, CWM

pattern_0, n=1022; subpattern_0, ns=294

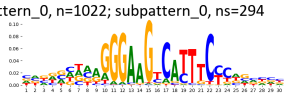

pattern_0, n=1022; subpattern_1, ns=238

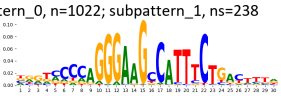

pattern_0, n=1022; subpattern_2, ns=230

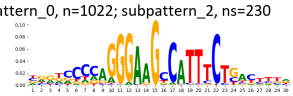

pattern_0, n=1022; subpattern_3, ns=143

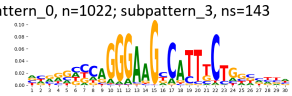

pattern_0, n=1022; subpattern_4, ns=111

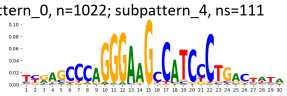

pattern_0, n=1022; subpattern_5, ns=6

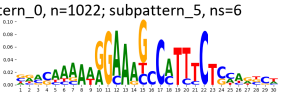

TF-MoDisCO pattern_0 n=1022, PWM

pattern_0, n=1022; subpattern_0, ns=294

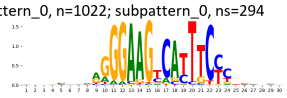

pattern_0, n=1022; subpattern_1, ns=238

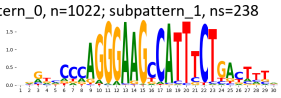

pattern_0, n=1022; subpattern_2, ns=230

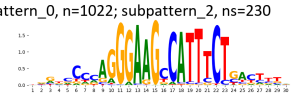

pattern_0, n=1022; subpattern_3, ns=143

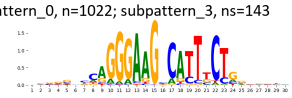

pattern_0, n=1022; subpattern_4, ns=111

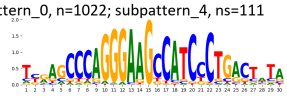

pattern_0, n=1022; subpattern_5, ns=6

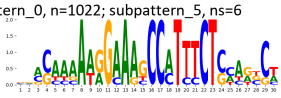

TF-MoDisCO pattern_1 n=162, CWM

pattern_1, n=162; subpattern_0, ns=62

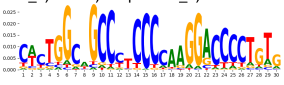

pattern_1, n=162; subpattern_1, ns=51

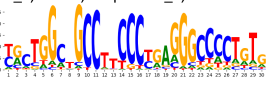

pattern_1, n=162; subpattern_2, ns=49

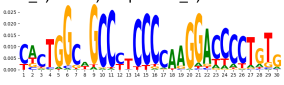

TF-MoDisCO pattern_1 n=162, PWM

pattern_1, n=162; subpattern_0, ns=62

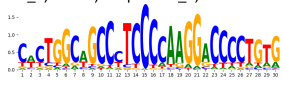

pattern_1, n=162; subpattern_1, ns=51

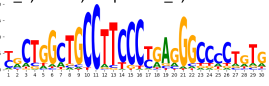

pattern_1, n=162; subpattern_2, ns=49

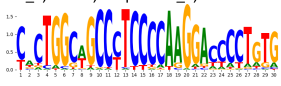

Supplementary Figure 1321: TF-MoDisCO subpatterns for the ZNF528 transcription factor in HEK293 (accession ChipExo models).

A

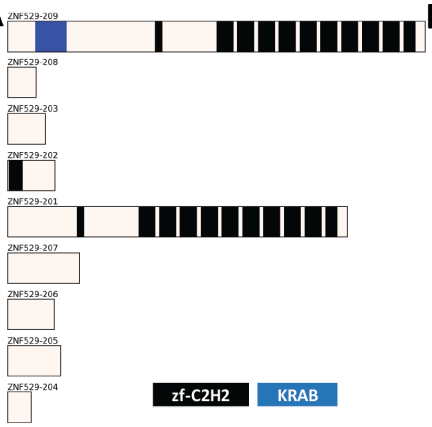

B

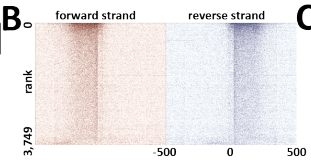

C

peaks

state	fraction
Quies	0.52
TxWk	0.15
Het	0.07
EnhWk	0.07
Tx	0.04
EnhA1	0.04
EnhA2	0.03
TssA	0.03
ReprPCWk	0.02
TssFlnk	0.02
ZNF/Rpts	0.01
ReprPC	0.01
TssBiv	0.01
TssFlnkU	0.00
TssFlnkD	0.00
EnhBiv	0.00
EnhG1	0.00
EnhG2	0.00

D

peaks

repeat	fraction
LINE/L1	0.51
SINE/Alu	0.40
Simple_repeat	0.28
LTR/ERV1	0.09
SINE/MIR	0.05
LTR/ERVL-MaLR	0.04
LINE/L2	0.04
LTR/ERVK	0.02
DNA/hAT-Charlie	0.02
LTR/ERVL	0.02
DNA/TcMar-Tigger	0.01
Low_complexity	0.01
LINE/CR1	0.01
DNA/hAT-Tip100	0.00
tRNA	0.00
Retroposon/SVA	0.00
LINE/RTE-X	0.00
DNA/hAT-Blackjack	0.00

peaks

repeat	fraction
(AAAT)n	0.11
L1MD2	0.05
AluSx	0.04
AluY	0.04
AluJb	0.04
AluSx1	0.04
AluSz	0.04
L1PA7	0.03
(TTTA)n	0.03
L1PA13	0.03
(ATTT)n	0.02
L1MC4a	0.02
AluJo	0.02
L1MD3	0.02
AluJr	0.02
AluSq2	0.02
L1PA5	0.02
L1PA10	0.02

E

Ontology	Term	FDR Q-val
GO Biological Process	negative regulation of Ras protein signal transduction	3.25
GO Biological Process	negative regulation of heart contraction	2.65
GO Biological Process	transdifferentiation	2.60
GO Biological Process	striated muscle hypertrophy	2.59
GO Biological Process	epithelial cell morphogenesis	2.39
GO Biological Process	cardiac muscle hypertrophy	2.21
GO Biological Process	myoblast fate commitment	2.00
GO Biological Process	regulation of transforming growth factor beta production	1.81
GO Biological Process	mitochondrion transport along microtubule	1.73
GO Biological Process	establishment of mitochondrion localization	1.73
GO Biological Process	mitochondrion localization	1.71
GO Biological Process	epithelial cell differentiation involved in prostate gland development	1.60
GO Biological Process	negative regulation of Rho protein signal transduction	1.38
GO Biological Process	striated muscle cell proliferation	1.36
Human Phenotype	Short chin	1.84

F

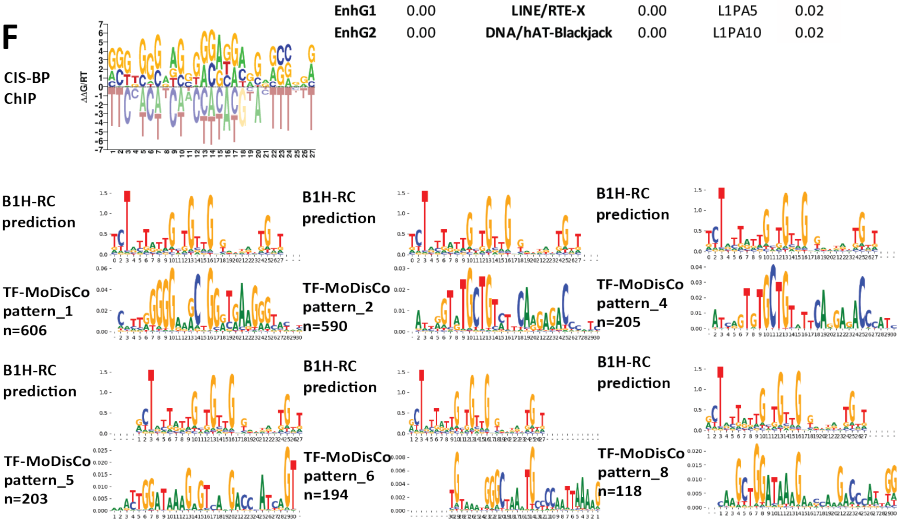

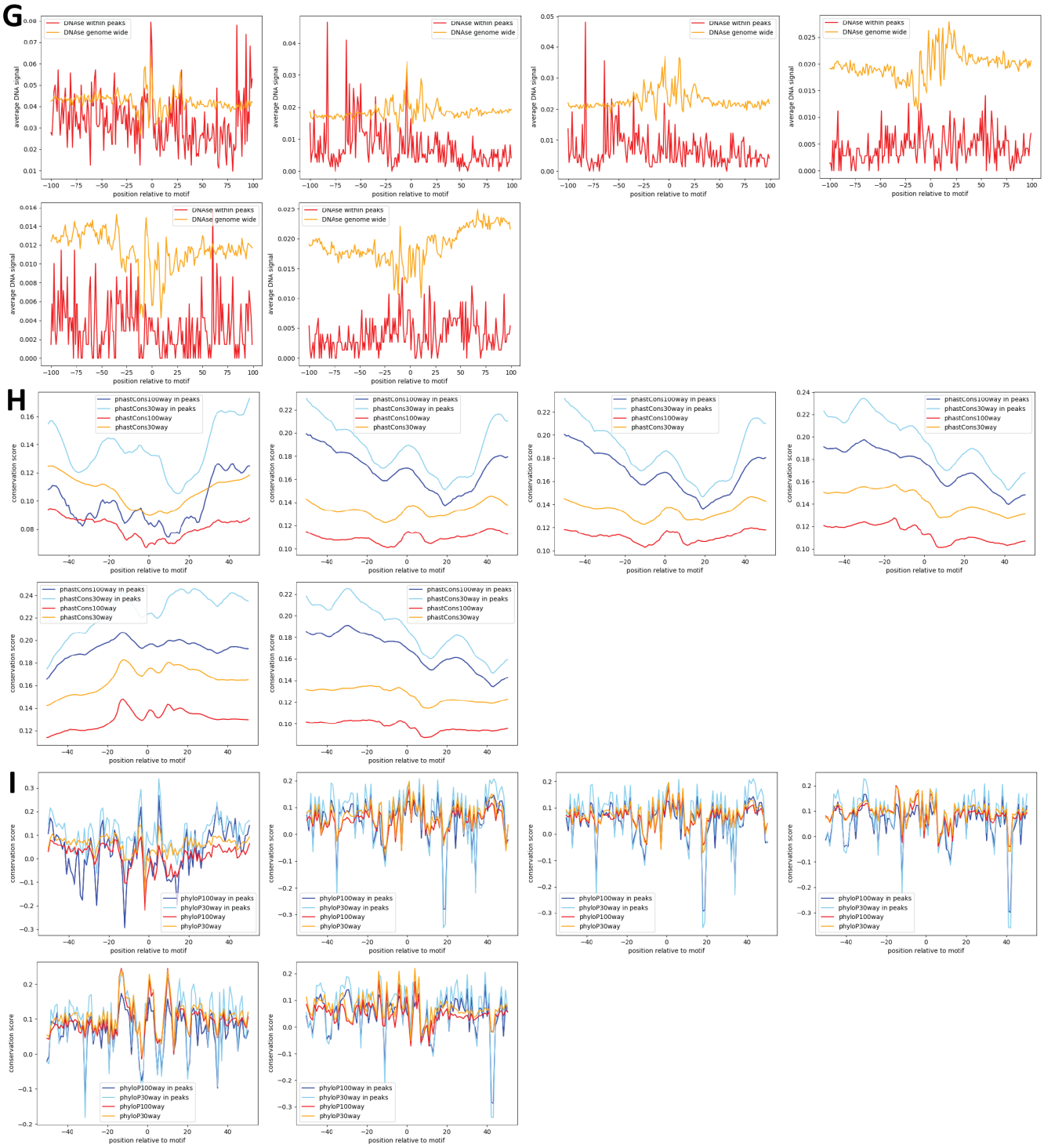

Supplementary Figure 1322: Properties and genomic distribution of motifs identified for the ZNF529 transcription factor in HEK293 (accession ENCSR754SOI).

TF-MoDisCO pattern_1 n=606, CWM

pattern_1, n=606; subpattern_0, ns=214

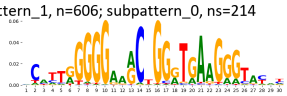

pattern_1, n=606; subpattern_1, ns=205

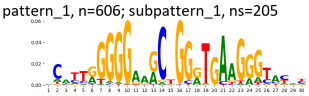

pattern_1, n=606; subpattern_2, ns=102

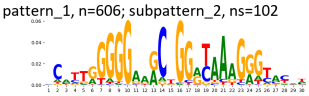

pattern_1, n=606; subpattern_3, ns=75

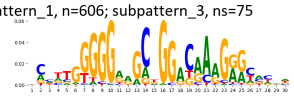

pattern_1, n=606; subpattern_4, ns=10

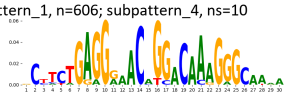

TF-MoDisCO pattern_1 n=606, PWM

pattern_1, n=606; subpattern_0, ns=214

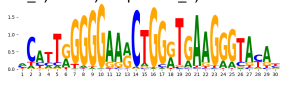

pattern_1, n=606; subpattern_1, ns=205

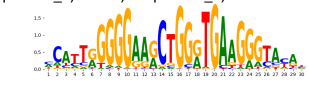

pattern_1, n=606; subpattern_2, ns=102

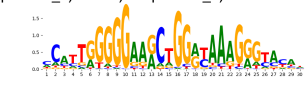

pattern_1, n=606; subpattern_3, ns=75

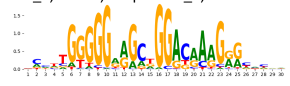

pattern_1, n=606; subpattern_4, ns=10

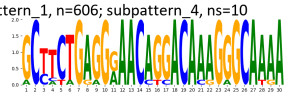

TF-MoDisCO pattern_2 n=590, CWM

pattern_2, n=590; subpattern_0, ns=183

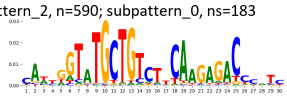

pattern_2, n=590; subpattern_1, ns=173

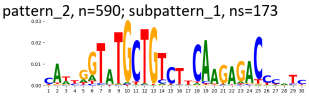

pattern_2, n=590; subpattern_2, ns=165

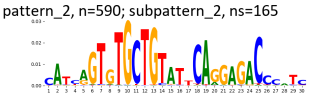

pattern_2, n=590; subpattern_3, ns=52

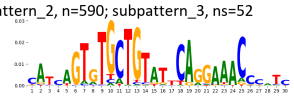

pattern_2, n=590; subpattern_4, ns=5

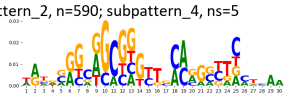

pattern_2, n=590; subpattern_5, ns=4

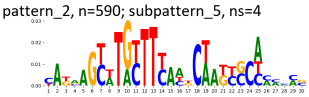

pattern_2, n=590; subpattern_6, ns=4

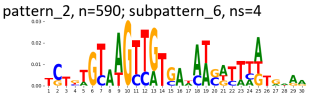

pattern_2, n=590; subpattern_7, ns=4

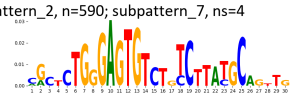

TF-MoDisCO pattern_2 n=590, PWM

pattern_2, n=590; subpattern_0, ns=183

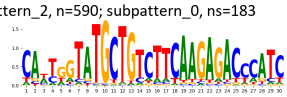

pattern_2, n=590; subpattern_1, ns=173

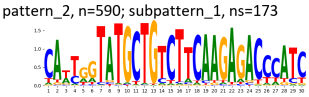

pattern_2, n=590; subpattern_2, ns=165

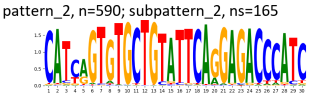

pattern_2, n=590; subpattern_3, ns=52

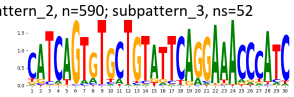

pattern_2, n=590; subpattern_4, ns=5



pattern_2, n=590; subpattern_5, ns=4

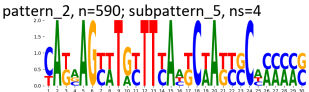

pattern_2, n=590; subpattern_6, ns=4

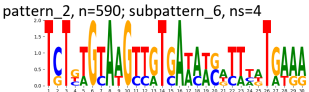

pattern_2, n=590; subpattern_7, ns=4

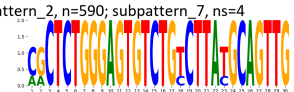

TF-MoDisCO pattern_4 n=205, CWM

pattern_4, n=205; subpattern_0, ns=64

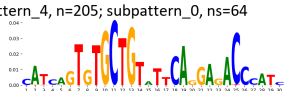

pattern_4, n=205; subpattern_1, ns=39

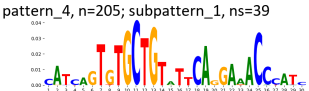

pattern_4, n=205; subpattern_2, ns=39

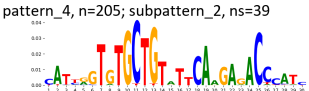

pattern_4, n=205; subpattern_3, ns=30

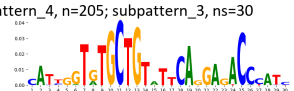

pattern_4, n=205; subpattern_4, ns=26

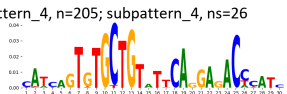

pattern_4, n=205; subpattern_5, ns=7

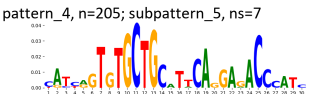

TF-MoDisCO pattern_4 n=205, PWM

pattern_4, n=205; subpattern_0, ns=64

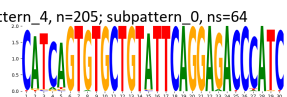

pattern_4, n=205; subpattern_1, ns=39

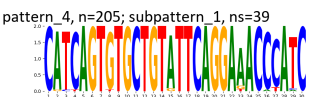

pattern_4, n=205; subpattern_2, ns=39

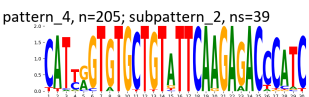

pattern_4, n=205; subpattern_3, ns=30



pattern_4, n=205; subpattern_4, ns=26



pattern_4, n=205; subpattern_5, ns=7

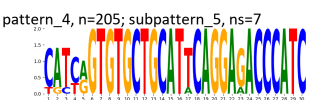

TF-MoDisCO pattern_5 n=203, CWM

pattern_5, n=203; subpattern_0, ns=89

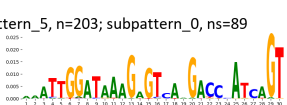

pattern_5, n=203; subpattern_1, ns=65

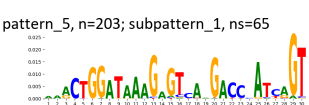

pattern_5, n=203; subpattern_2, ns=35

pattern_5, n=203; subpattern_3, ns=14

TF-MoDisCO pattern_5 n=203, PWM

pattern_5, n=203; subpattern_0, ns=89

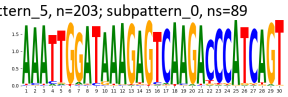

pattern_5, n=203; subpattern_1, ns=65

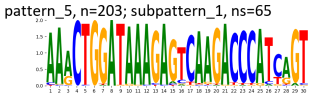

pattern_5, n=203; subpattern_2, ns=35

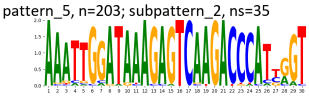

pattern_5, n=203; subpattern_3, ns=14

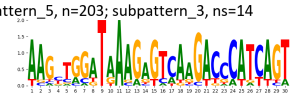

TF-MoDisCO pattern_6 n=194, CWM

pattern_6, n=194; subpattern_0, ns=69

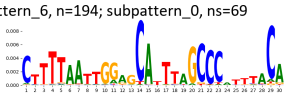

pattern_6, n=194; subpattern_1, ns=46

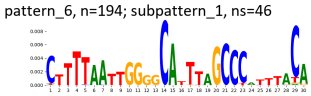

pattern_6, n=194; subpattern_2, ns=24

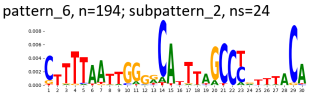

pattern_6, n=194; subpattern_3, ns=22

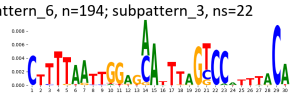

pattern_6, n=194; subpattern_4, ns=20

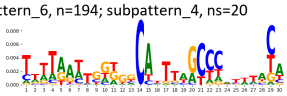

pattern_6, n=194; subpattern_5, ns=13

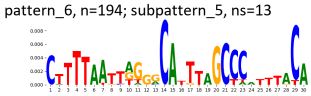

TF-MoDisCO pattern_6 n=194, PWM

pattern_6, n=194; subpattern_0, ns=69

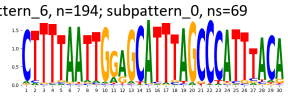

pattern_6, n=194; subpattern_1, ns=46

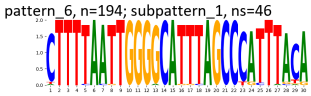

pattern_6, n=194; subpattern_2, ns=24

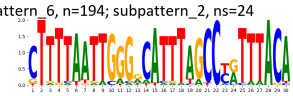

pattern_6, n=194; subpattern_3, ns=22

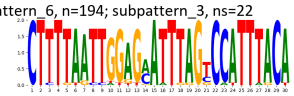

pattern_6, n=194; subpattern_4, ns=20

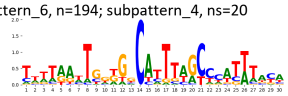

pattern_6, n=194; subpattern_5, ns=13

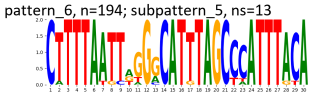

TF-MoDisCO pattern_8 n=118, CWM

pattern_8, n=118; subpattern_0, ns=47

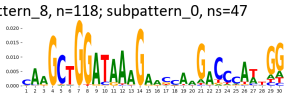

pattern_8, n=118; subpattern_1, ns=41

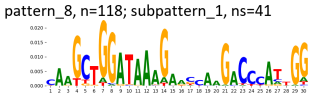

pattern_8, n=118; subpattern_2, ns=22

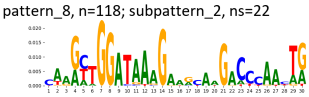

pattern_8, n=118; subpattern_3, ns=8

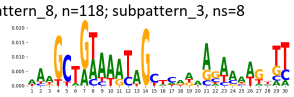

TF-MoDisCO pattern_8 n=118, PWM

pattern_8, n=118; subpattern_0, ns=47

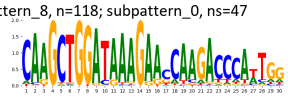

pattern_8, n=118; subpattern_1, ns=41

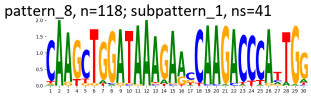

pattern_8, n=118; subpattern_2, ns=22

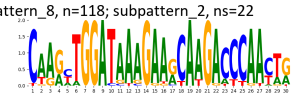

pattern_8, n=118; subpattern_3, ns=8

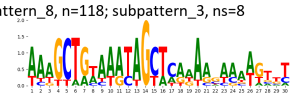

Supplementary Figure 1323: TF-MoDisCO subpatterns for the ZNF529 transcription factor in HEK293 (accession ENCSR754SOI).

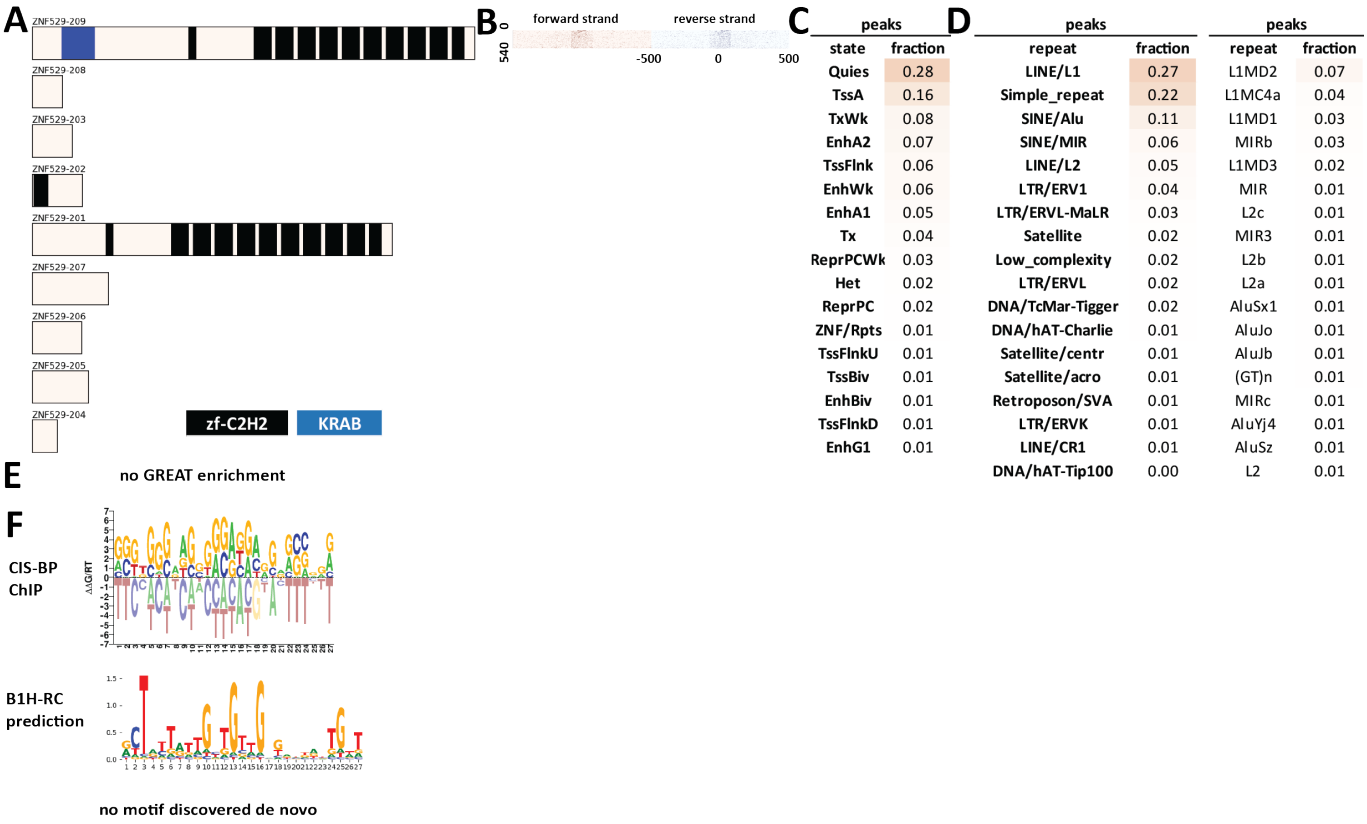

C

peaks	
state	fraction
Quies	0.28
TssA	0.16
TxWk	0.08
EnhA2	0.07
TssFlnk	0.06
EnhWk	0.06
EnhA1	0.05
Tx	0.04
ReprPCWk	0.03
Het	0.02
ReprPC	0.02
ZNF/Rpts	0.01
TssFlnkU	0.01
TssBiv	0.01
EnhBiv	0.01
TssFlnkD	0.01
EnhG1	0.01

D

peaks		peaks	
repeat	fraction	repeat	fraction
LINE/L1	0.27	L1MD2	0.07
Simple_repeat	0.22	L1MC4a	0.04
SINE/Alu	0.11	L1MD1	0.03
SINE/MIR	0.06	MIRb	0.03
LINE/L2	0.05	L1MD3	0.02
LTR/ERV1	0.04	MIR	0.01
LTR/ERVL-MaLR	0.03	L2c	0.01
Satellite	0.02	MIR3	0.01
Low_complexity	0.02	L2b	0.01
LTR/ERVL	0.02	L2a	0.01
DNA/TcMar-Tigger	0.02	AluSx1	0.01
DNA/hAT-Charlie	0.01	AluJo	0.01
Satellite/centr	0.01	AluJb	0.01
Satellite/acro	0.01	(GT)n	0.01
Retroposon/SVA	0.01	MIRc	0.01
LTR/ERVK	0.01	AluYj4	0.01
LINE/CR1	0.01	AluSz	0.01
DNA/hAT-Tip100	0.00	L2	0.01

Supplementary Figure 1324: Properties and genomic distribution of motifs identified for the ZNF529 transcription factor in HEK293 (accession ChipExo models).

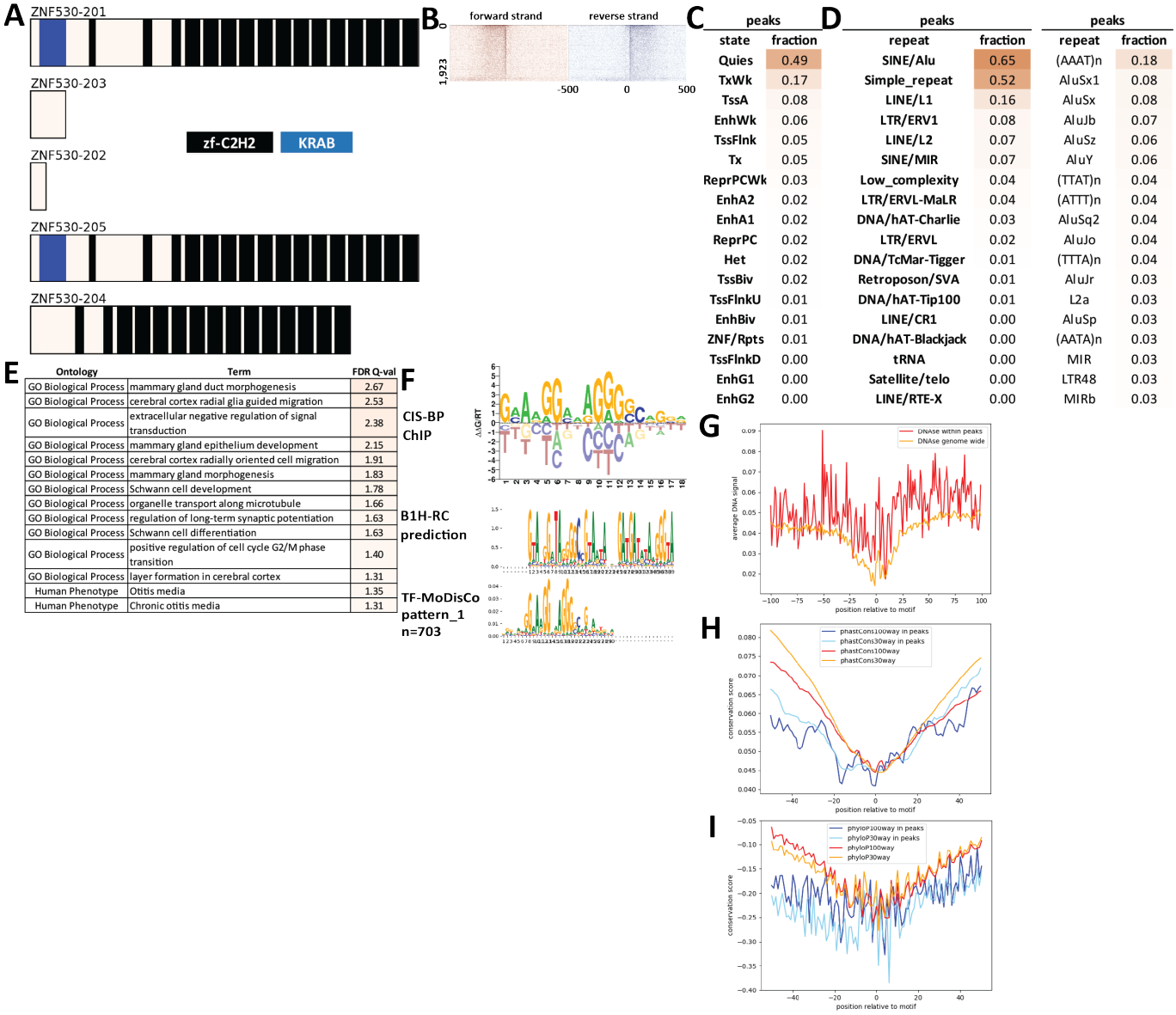

peaks	
state	fraction
Quies	0.49
TxWk	0.17
TssA	0.08
EnhWk	0.06
TssFlnk	0.05
Tx	0.05
ReprPCWk	0.03
EnhA2	0.02
EnhA1	0.02
ReprPC	0.02
Het	0.02
TssBiv	0.02
TssFlnkU	0.01
EnhBiv	0.01
ZNF/Rpts	0.01
TssFlnkD	0.00
EnhG1	0.00
EnhG2	0.00

peaks		peaks	
repeat	fraction	repeat	fraction
SINE/Alu	0.65	(AAAT)n	0.18
Simple_repeat	0.52	AluSx1	0.08
LINE/L1	0.16	AluSx	0.08
LTR/ERV1	0.08	AluJb	0.07
LINE/L2	0.07	AluSz	0.06
SINE/MIR	0.07	AluY	0.06
Low_complexity	0.04	(TTAT)n	0.04
LTR/ERVL-MaLR	0.04	(ATTT)n	0.04
DNA/hAT-Charlie	0.03	AluSq2	0.04
LTR/ERVL	0.02	AluJo	0.04
DNA/TcMar-Tigger	0.01	(TTTA)n	0.04
Retroposon/SVA	0.01	AluJr	0.03
DNA/hAT-Tip100	0.01	L2a	0.03
LINE/CR1	0.00	AluSp	0.03
DNA/hAT-Blackjack	0.00	(AATA)n	0.03
tRNA	0.00	MIR	0.03
Satellite/telo	0.00	LTR48	0.03
LINE/RTE-X	0.00	MIRb	0.03

Ontology	Term	FDR Q-val
GO Biological Process	mammary gland duct morphogenesis	2.67
GO Biological Process	cerebral cortex radial glia guided migration	2.53
GO Biological Process	extracellular negative regulation of signal transduction	2.38
GO Biological Process	mammary gland epithelium development	2.15
GO Biological Process	cerebral cortex radially oriented cell migration	1.91
GO Biological Process	mammary gland morphogenesis	1.83
GO Biological Process	Schwann cell development	1.78
GO Biological Process	organelle transport along microtubule	1.66
GO Biological Process	regulation of long-term synaptic potentiation	1.63
GO Biological Process	Schwann cell differentiation	1.63
GO Biological Process	positive regulation of cell cycle G2/M phase transition	1.40
GO Biological Process	layer formation in cerebral cortex	1.31
Human Phenotype	Otitis media	1.35
Human Phenotype	Chronic otitis media	1.31

Supplementary Figure 1325: Properties and genomic distribution of motifs identified for the ZNF530 transcription factor in HEK293 (accession ENCSR701RXW).

TF-MoDisCO pattern_1 n=703, CWM

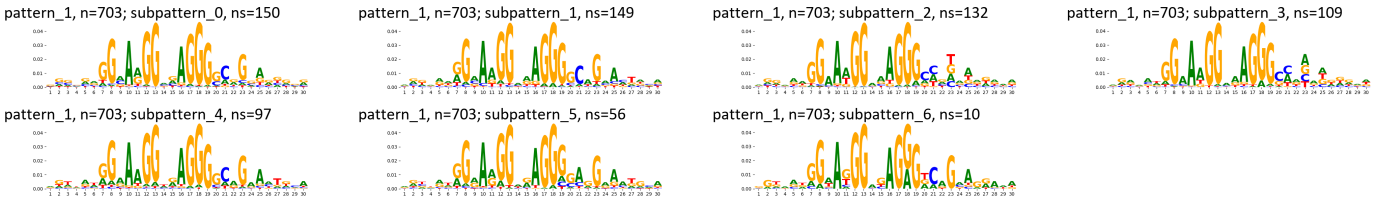

TF-MoDisCO pattern_1 n=703, PWM

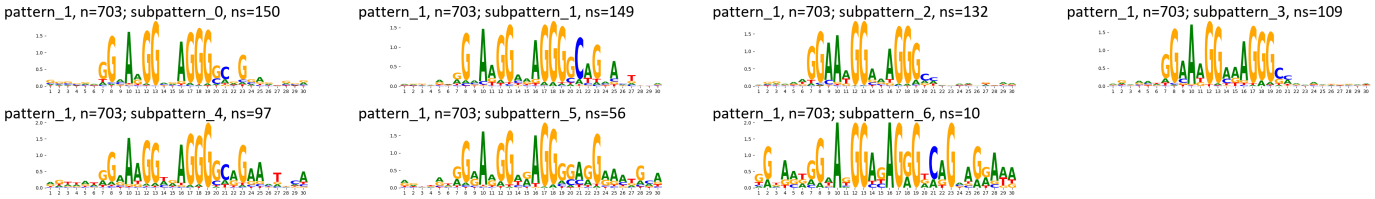

Supplementary Figure 1326: TF-MoDisCO subpatterns for the ZNF530 transcription factor in HEK293 (accession ENCSR701RXW).

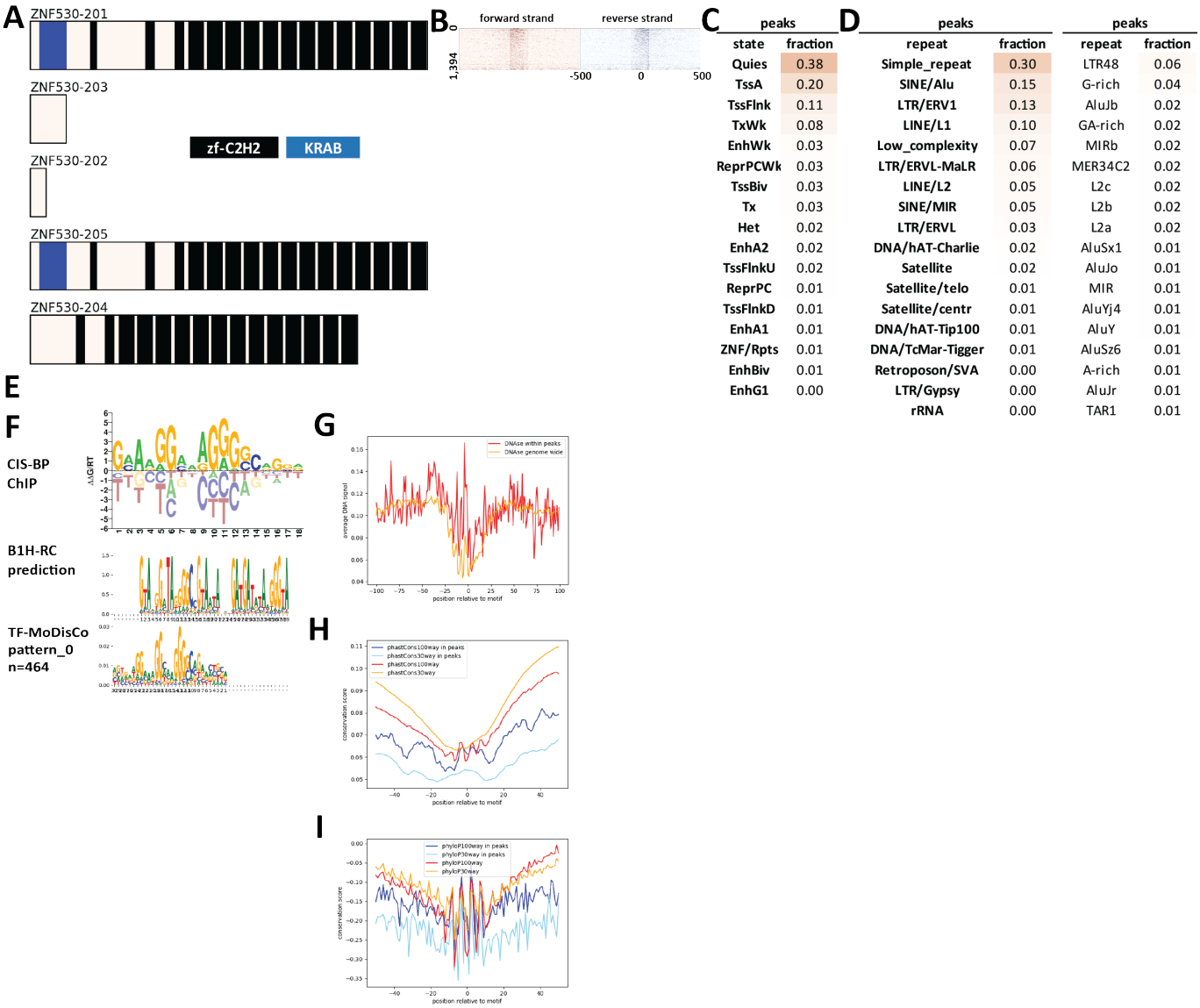

Supplementary Figure 1327: Properties and genomic distribution of motifs identified for the ZNF530 transcription factor in HEK293 (accession ChipExo models).

TF-MoDisCO pattern_0 n=464, CWM

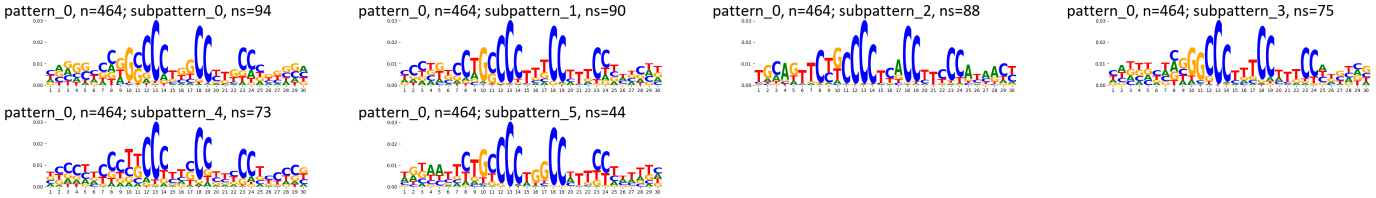

TF-MoDisCO pattern_0 n=464, PWM

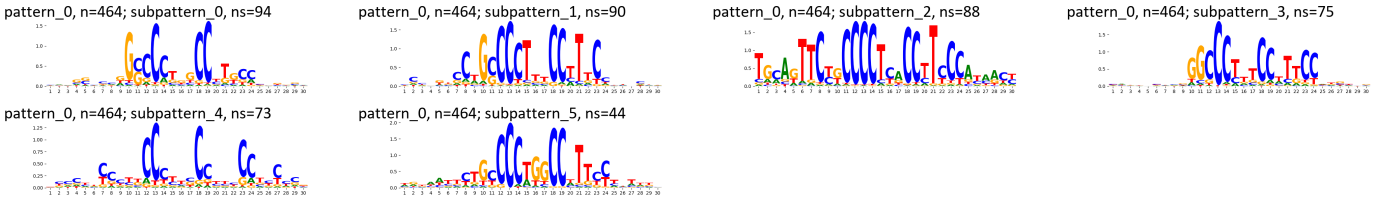

Supplementary Figure 1328: TF-MoDisCO subpatterns for the ZNF530 transcription factor in HEK293 (accession ChipExo models).

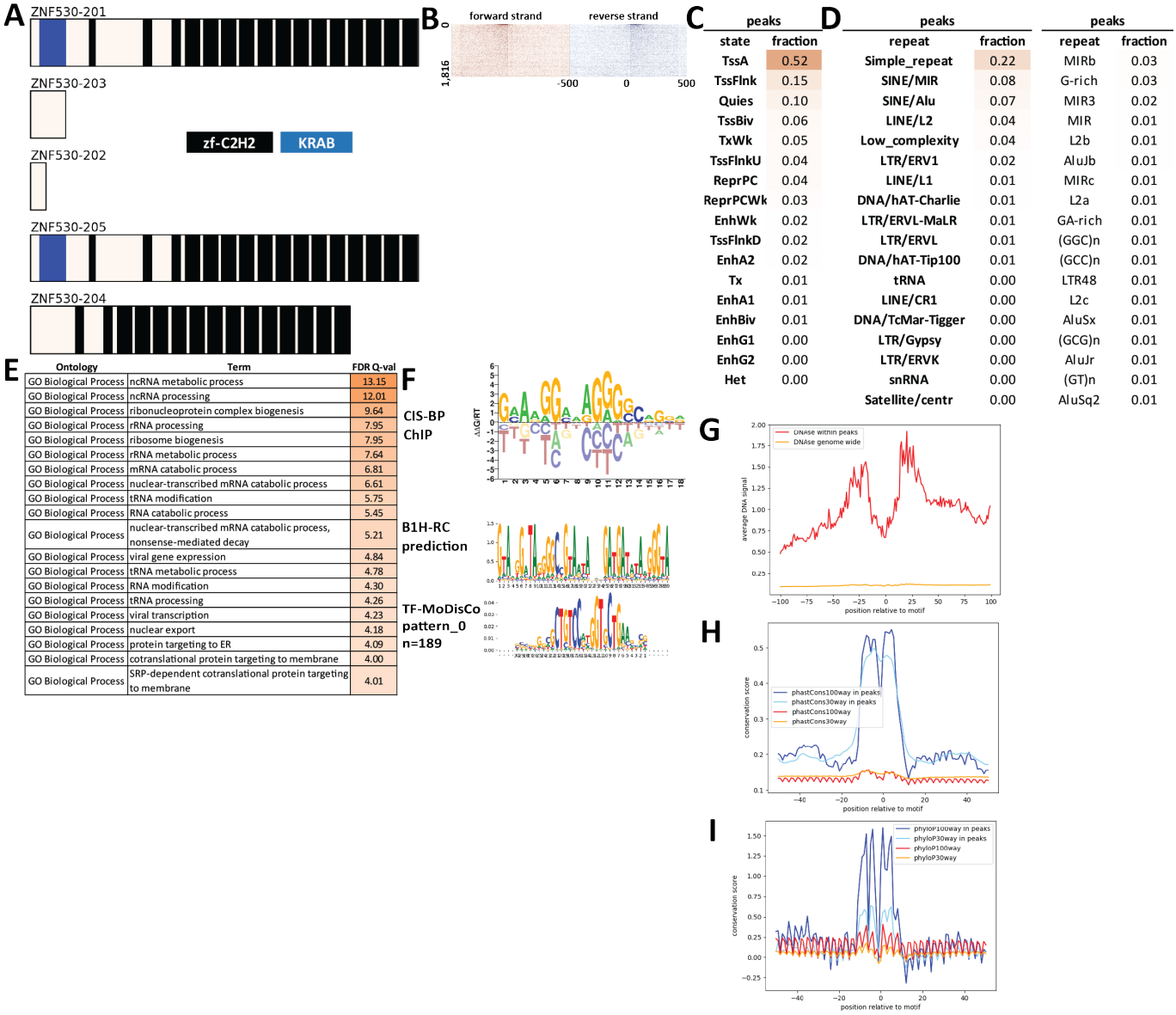

C

peaks	
state	fraction
TssA	0.52
TssFlnk	0.15
Quies	0.10
TssBiv	0.06
TxWk	0.05
TssFlnkU	0.04
ReprPC	0.04
ReprPCWk	0.03
EnhWk	0.02
TssFlnkD	0.02
EnhA2	0.02
Tx	0.01
EnhA1	0.01
EnhBiv	0.01
EnhG1	0.00
EnhG2	0.00
Het	0.00

D

peaks		peaks	
repeat	fraction	repeat	fraction
Simple_repeat	0.22	MIRb	0.03
SINE/MIR	0.08	G-rich	0.03
SINE/Alu	0.07	MIR3	0.02
LINE/L2	0.04	MIR	0.01
Low_complexity	0.04	L2b	0.01
LTR/ERV1	0.02	AluJb	0.01
LINE/L1	0.01	MIRc	0.01
DNA/hAT-Charlie	0.01	L2a	0.01
LTR/ERVL-MaLR	0.01	GA-rich	0.01
LTR/ERVL	0.01	(GGC)n	0.01
DNA/hAT-Tip100	0.01	(GCC)n	0.01
tRNA	0.00	LTR48	0.01
LINE/CR1	0.00	L2c	0.01
DNA/TcMar-Tigger	0.00	AluSx	0.01
LTR/Gypsy	0.00	(GCG)n	0.01
LTR/ERVK	0.00	AluJr	0.01
snRNA	0.00	(GT)n	0.01
Satellite/centr	0.00	AluSq2	0.01

E

Ontology	Term	FDR Q-val
GO Biological Process	ncRNA metabolic process	13.15
GO Biological Process	ncRNA processing	12.01
GO Biological Process	ribonucleoprotein complex biogenesis	9.64
GO Biological Process	rRNA processing	7.95
GO Biological Process	ribosome biogenesis	7.95
GO Biological Process	rRNA metabolic process	7.64
GO Biological Process	mRNA catabolic process	6.81
GO Biological Process	nuclear-transcribed mRNA catabolic process	6.61
GO Biological Process	tRNA modification	5.75
GO Biological Process	RNA catabolic process	5.45
GO Biological Process	nuclear-transcribed mRNA catabolic process, nonsense-mediated decay	5.21
GO Biological Process	viral gene expression	4.84
GO Biological Process	tRNA metabolic process	4.78
GO Biological Process	RNA modification	4.30
GO Biological Process	tRNA processing	4.26
GO Biological Process	viral transcription	4.23
GO Biological Process	nuclear export	4.18
GO Biological Process	protein targeting to ER	4.09
GO Biological Process	cotranslational protein targeting to membrane	4.00
GO Biological Process	SRP-dependent cotranslational protein targeting to membrane	4.01

Supplementary Figure 1329: Properties and genomic distribution of motifs identified for the ZNF530 transcription factor in HepG2 (accession ENCSR013DKM).

TF-MoDisCO pattern_0 n=189, CWM

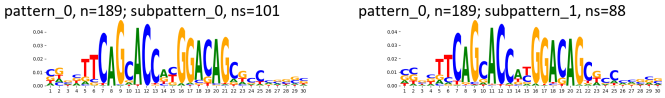

TF-MoDisCO pattern_0 n=189, PWM

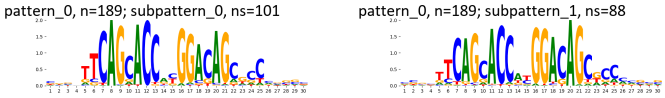

Supplementary Figure 1330: TF-MoDisCO subpatterns for the ZNF530 transcription factor in HepG2 (accession ENCSR013DKM).

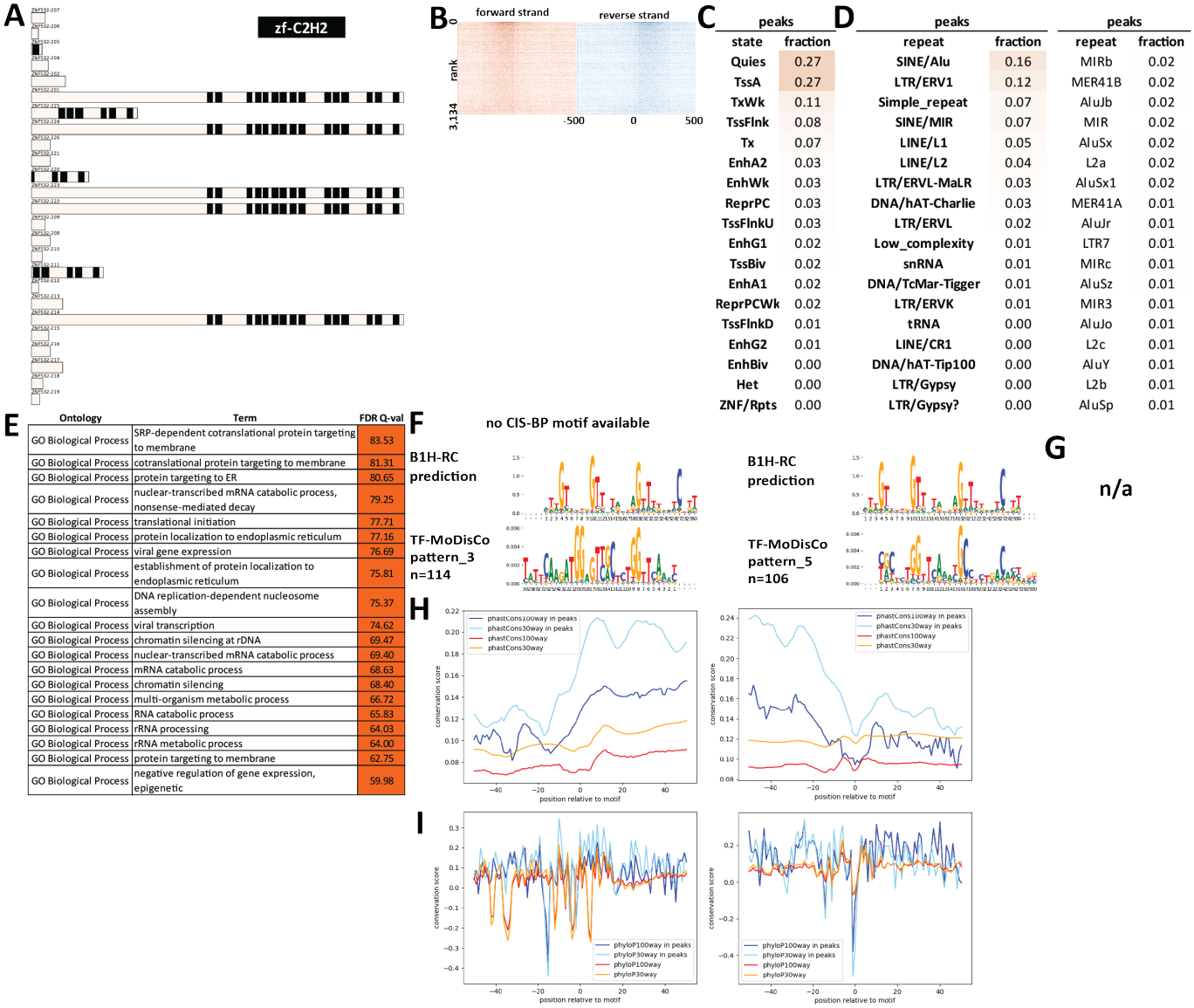

Supplementary Figure 1331: Properties and genomic distribution of motifs identified for the ZNF532 transcription factor in WTC11 (accession ENCSR444BFV).

TF-MoDisCO pattern_3 n=114, CWM

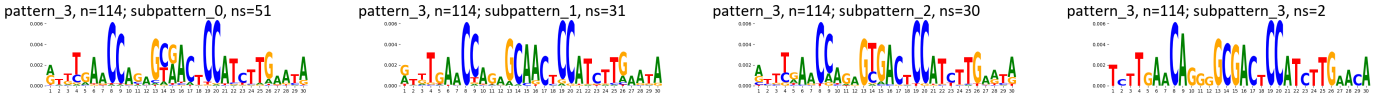

TF-MoDisCO pattern_3 n=114, PWM

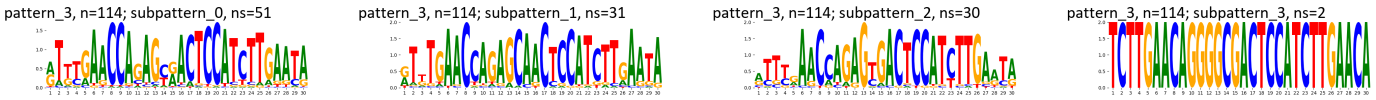

TF-MoDisCO pattern_5 n=106, CWM

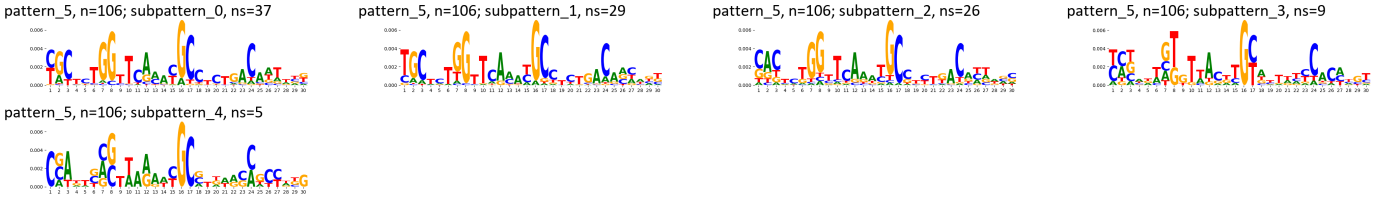

TF-MoDisCO pattern_5 n=106, PWM

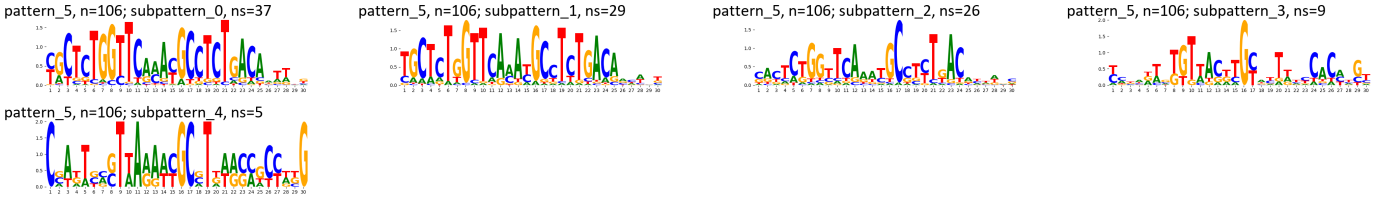

Supplementary Figure 1332: TF-MoDisCO subpatterns for the ZNF532 transcription factor in WTC11 (accession ENCSR444BFV).

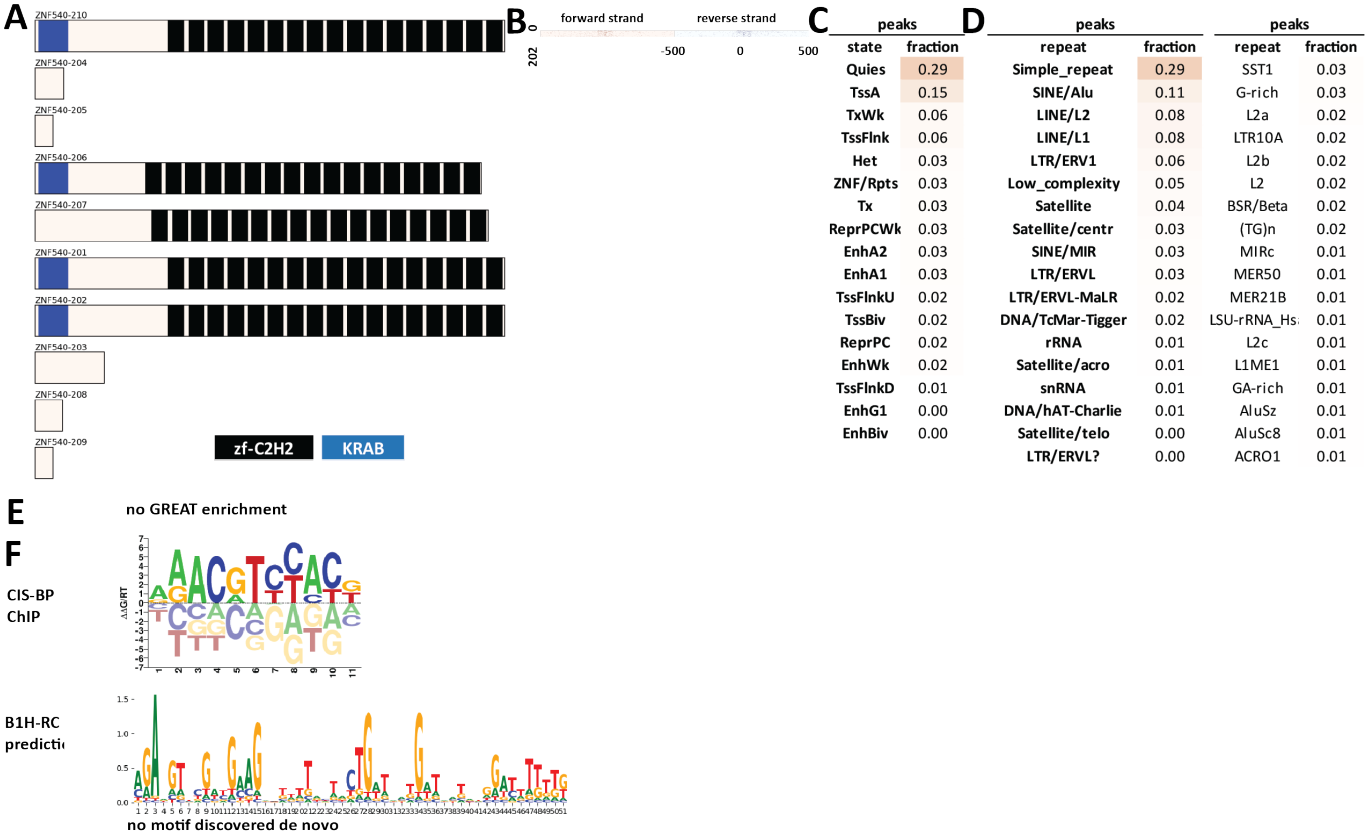

peaks	
state	fraction
Quies	0.29
TssA	0.15
TxWk	0.06
TssFlnk	0.06
Het	0.03
ZNF/Rpts	0.03
Tx	0.03
ReprPCWk	0.03
EnhA2	0.03
EnhA1	0.03
TssFlnkU	0.02
TssBiv	0.02
ReprPC	0.02
EnhWk	0.02
TssFlnkD	0.01
EnhG1	0.00
EnhBiv	0.00

peaks		peaks	
repeat	fraction	repeat	fraction
Simple_repeat	0.29	SST1	0.03
SINE/Alu	0.11	G-rich	0.03
LINE/L2	0.08	L2a	0.02
LINE/L1	0.08	LTR10A	0.02
LTR/ERV1	0.06	L2b	0.02
Low_complexity	0.05	L2	0.02
Satellite	0.04	BSR/Beta	0.02
Satellite/centr	0.03	(TG)n	0.02
SINE/MIR	0.03	MIRc	0.01
LTR/ERVL	0.03	MER50	0.01
LTR/ERVL-MaLR	0.02	MER21B	0.01
DNA/TcMar-Tigger	0.02	LSU-rRNA_Hs	0.01
rRNA	0.01	L2c	0.01
Satellite/acro	0.01	L1ME1	0.01
snRNA	0.01	GA-rich	0.01
DNA/hAT-Charlie	0.01	AluSz	0.01
Satellite/telo	0.00	AluSc8	0.01
LTR/ERVL?	0.00	ACRO1	0.01

Supplementary Figure 1333: Properties and genomic distribution of motifs identified for the ZNF540 transcription factor in HEK293 (accession ChipExo models).

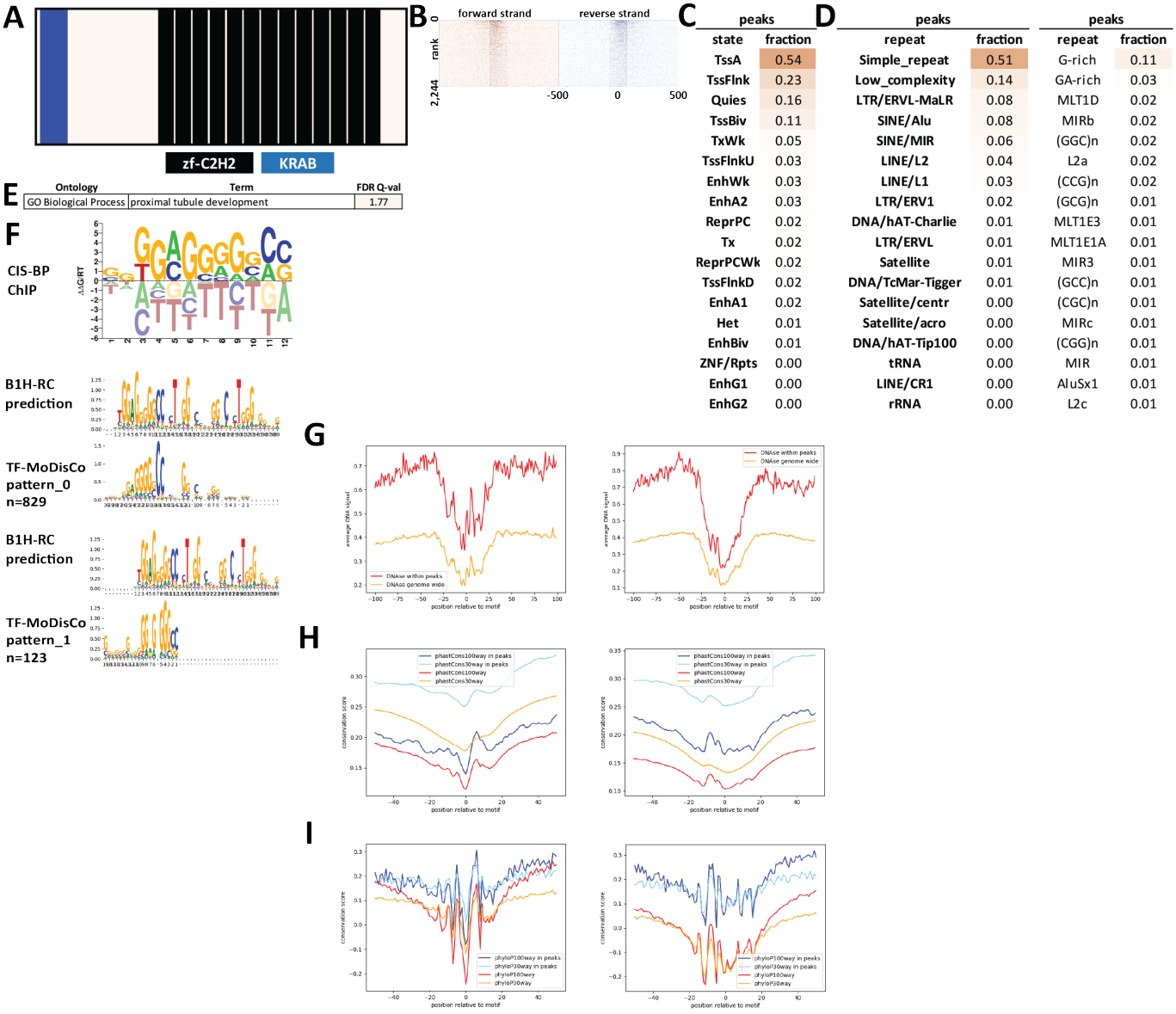

Supplementary Figure 1334: Properties and genomic distribution of motifs identified for the ZNF543 transcription factor in HEK293 (accession ChipExo models).

TF-MoDisCO pattern_0 n=829, CWM

pattern_0, n=829; subpattern_0, ns=173

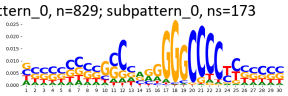

pattern_0, n=829; subpattern_1, ns=139

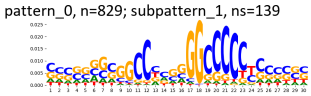

pattern_0, n=829; subpattern_2, ns=113

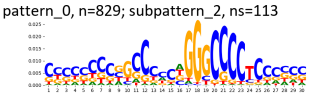

pattern_0, n=829; subpattern_3, ns=113

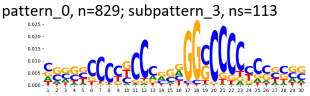

pattern_0, n=829; subpattern_4, ns=98

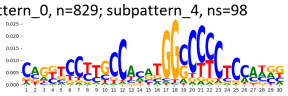

pattern_0, n=829; subpattern_5, ns=96

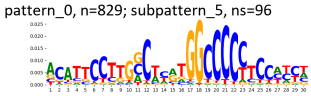

pattern_0, n=829; subpattern_6, ns=52

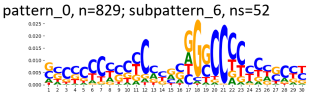

pattern_0, n=829; subpattern_7, ns=45

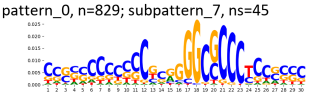

TF-MoDisCO pattern_0 n=829, PWM

pattern_0, n=829; subpattern_0, ns=173

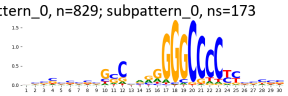

pattern_0, n=829; subpattern_1, ns=139

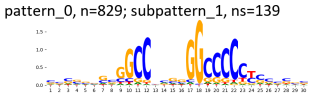

pattern_0, n=829; subpattern_2, ns=113

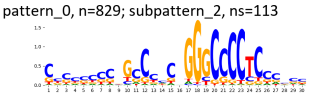

pattern_0, n=829; subpattern_3, ns=113

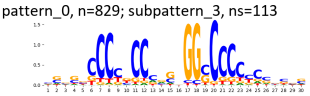

pattern_0, n=829; subpattern_4, ns=98

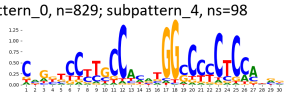

pattern_0, n=829; subpattern_5, ns=96

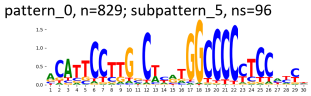

pattern_0, n=829; subpattern_6, ns=52

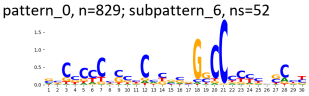

pattern_0, n=829; subpattern_7, ns=45

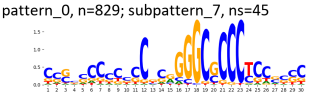

TF-MoDisCO pattern_1 n=123, CWM

pattern_1, n=123; subpattern_0, ns=30

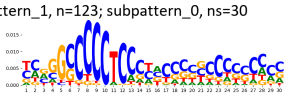

pattern_1, n=123; subpattern_1, ns=26

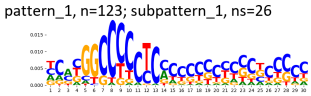

pattern_1, n=123; subpattern_2, ns=20

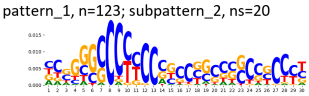

pattern_1, n=123; subpattern_3, ns=17

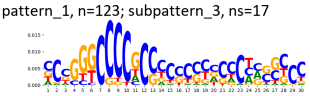

pattern_1, n=123; subpattern_4, ns=15

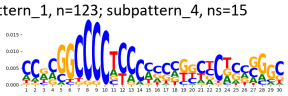

pattern_1, n=123; subpattern_5, ns=10

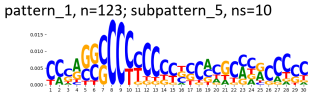

pattern_1, n=123; subpattern_6, ns=5

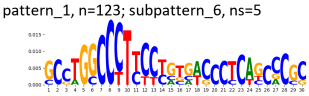

TF-MoDisCO pattern_1 n=123, PWM

pattern_1, n=123; subpattern_0, ns=30

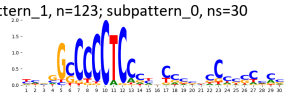

pattern_1, n=123; subpattern_1, ns=26

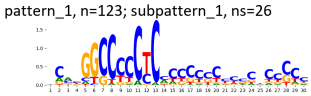

pattern_1, n=123; subpattern_2, ns=20

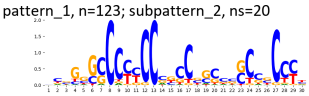

pattern_1, n=123; subpattern_3, ns=17

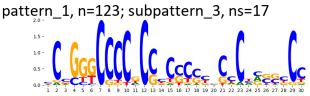

pattern_1, n=123; subpattern_4, ns=15

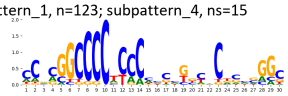

pattern_1, n=123; subpattern_5, ns=10

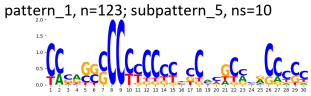

pattern_1, n=123; subpattern_6, ns=5

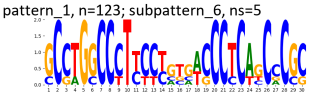

Supplementary Figure 1335: TF-MoDisCO subpatterns for the ZNF543 transcription factor in HEK293 (accession ChipExo models).

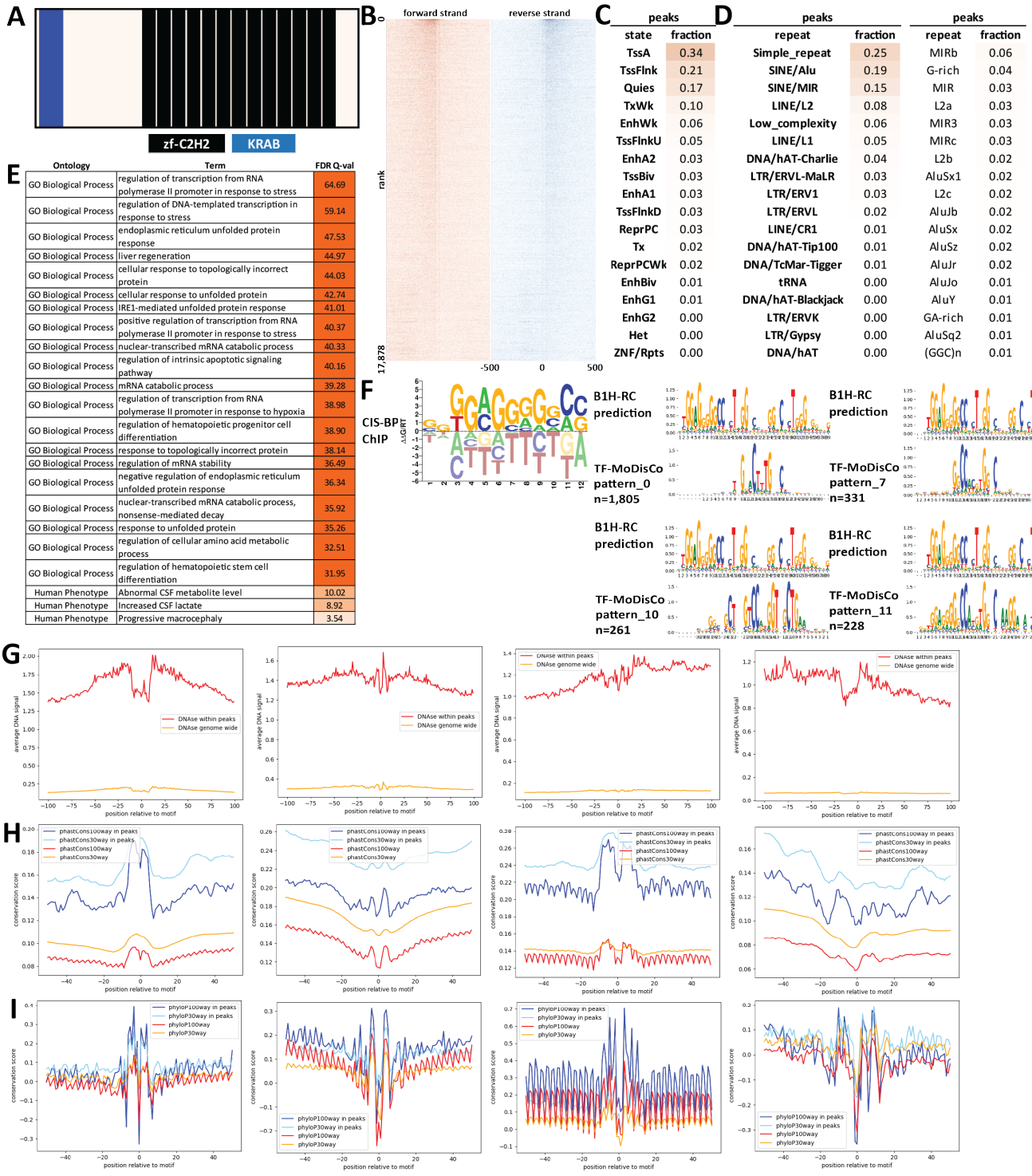

Supplementary Figure 1336: Properties and genomic distribution of motifs identified for the ZNF543 transcription factor in HepG2 (accession ENCSR584DEL).

TF-MoDisCO pattern_0 n=1805, CWM

pattern_0, n=1805; subpattern_0, ns=532

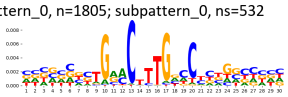

pattern_0, n=1805; subpattern_1, ns=495

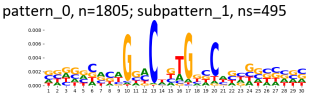

pattern_0, n=1805; subpattern_2, ns=462

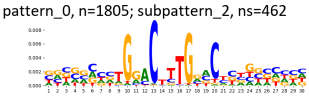

pattern_0, n=1805; subpattern_3, ns=151

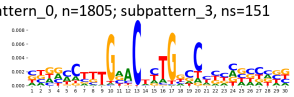

pattern_0, n=1805; subpattern_4, ns=61

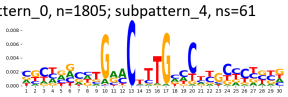

pattern_0, n=1805; subpattern_5, ns=57

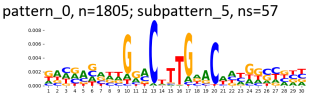

pattern_0, n=1805; subpattern_6, ns=41

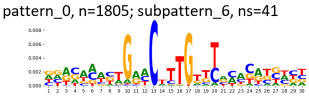

pattern_0, n=1805; subpattern_7, ns=6

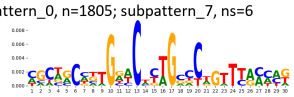

TF-MoDisCO pattern_0 n=1805, PWM

pattern_0, n=1805; subpattern_0, ns=532

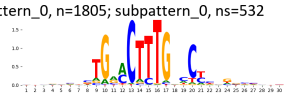

pattern_0, n=1805; subpattern_1, ns=495

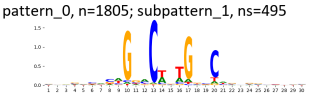

pattern_0, n=1805; subpattern_2, ns=462

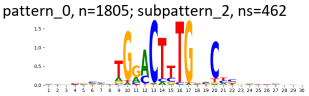

pattern_0, n=1805; subpattern_3, ns=151

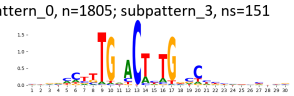

pattern_0, n=1805; subpattern_4, ns=61

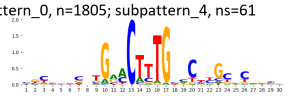

pattern_0, n=1805; subpattern_5, ns=57

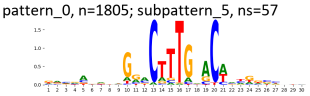

pattern_0, n=1805; subpattern_6, ns=41

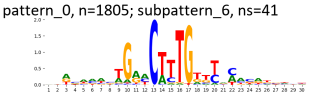

pattern_0, n=1805; subpattern_7, ns=6

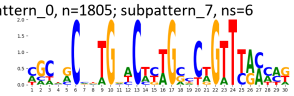

TF-MoDisCO pattern_10 n=261, CWM

pattern_10, n=261; subpattern_0, ns=101

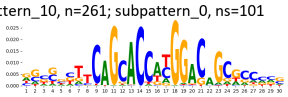

pattern_10, n=261; subpattern_1, ns=94

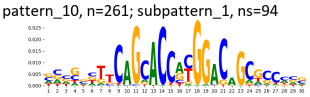

pattern_10, n=261; subpattern_2, ns=40

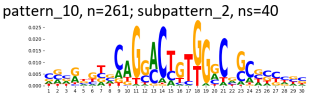

pattern_10, n=261; subpattern_3, ns=26

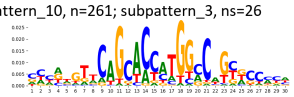

TF-MoDisCO pattern_10 n=261, PWM

pattern_10, n=261; subpattern_0, ns=101

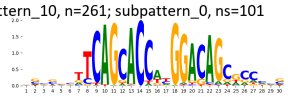

pattern_10, n=261; subpattern_1, ns=94

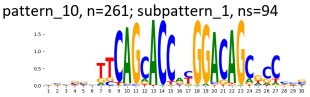

pattern_10, n=261; subpattern_2, ns=40

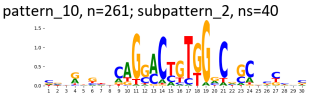

pattern_10, n=261; subpattern_3, ns=26

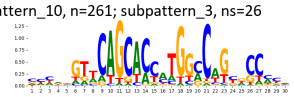

TF-MoDisCO pattern_11 n=228, CWM

pattern_11, n=228; subpattern_0, ns=68

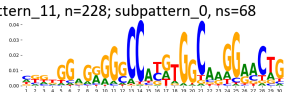

pattern_11, n=228; subpattern_1, ns=62

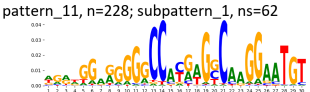

pattern_11, n=228; subpattern_2, ns=49

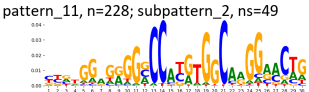

pattern_11, n=228; subpattern_3, ns=49

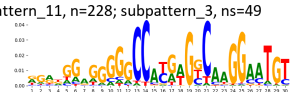

TF-MoDisCO pattern_11 n=228, PWM

pattern_11, n=228; subpattern_0, ns=68

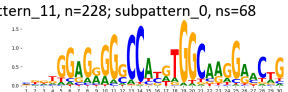

pattern_11, n=228; subpattern_1, ns=62

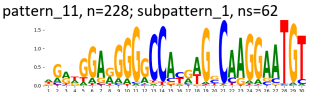

pattern_11, n=228; subpattern_2, ns=49

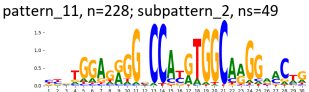

pattern_11, n=228; subpattern_3, ns=49

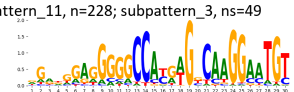

TF-MoDisCO pattern_7 n=331, CWM

pattern_7, n=331; subpattern_0, ns=85

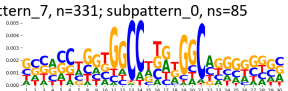

pattern_7, n=331; subpattern_1, ns=64

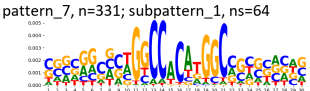

pattern_7, n=331; subpattern_2, ns=64

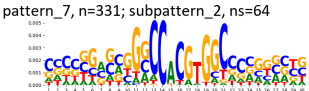

pattern_7, n=331; subpattern_3, ns=35

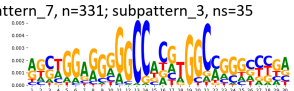

pattern_7, n=331; subpattern_4, ns=31

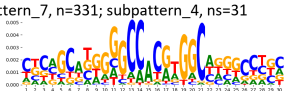

pattern_7, n=331; subpattern_5, ns=27

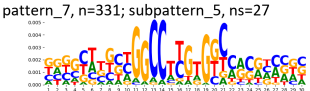

pattern_7, n=331; subpattern_6, ns=23

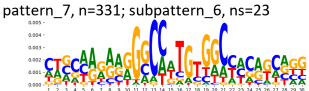

pattern_7, n=331; subpattern_7, ns=2

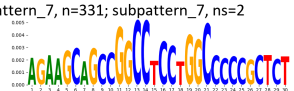

TF-MoDisCO pattern_7 n=331, PWM

pattern_7, n=331; subpattern_0, ns=85

pattern_7, n=331; subpattern_1, ns=64

pattern_7, n=331; subpattern_2, ns=64

pattern_7, n=331; subpattern_3, ns=35

pattern_7, n=331; subpattern_4, ns=31

pattern_7, n=331; subpattern_5, ns=27

pattern_7, n=331; subpattern_6, ns=23

pattern_7, n=331; subpattern_7, ns=2

Supplementary Figure 1337: TF-MoDisCO subpatterns for the ZNF543 transcription factor in HepG2 (accession ENCSR584DEL).

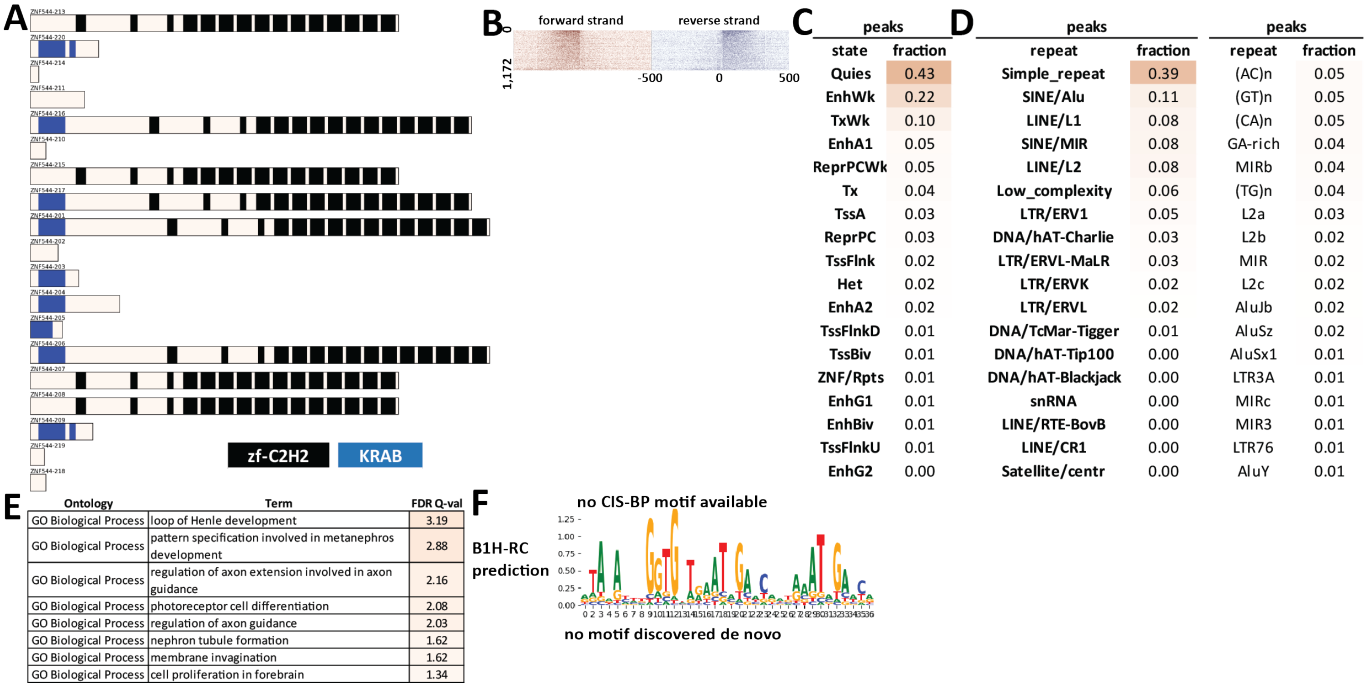

Supplementary Figure 1338: Properties and genomic distribution of motifs identified for the ZNF544 transcription factor in HEK293 (accession ENCSR167XFW).

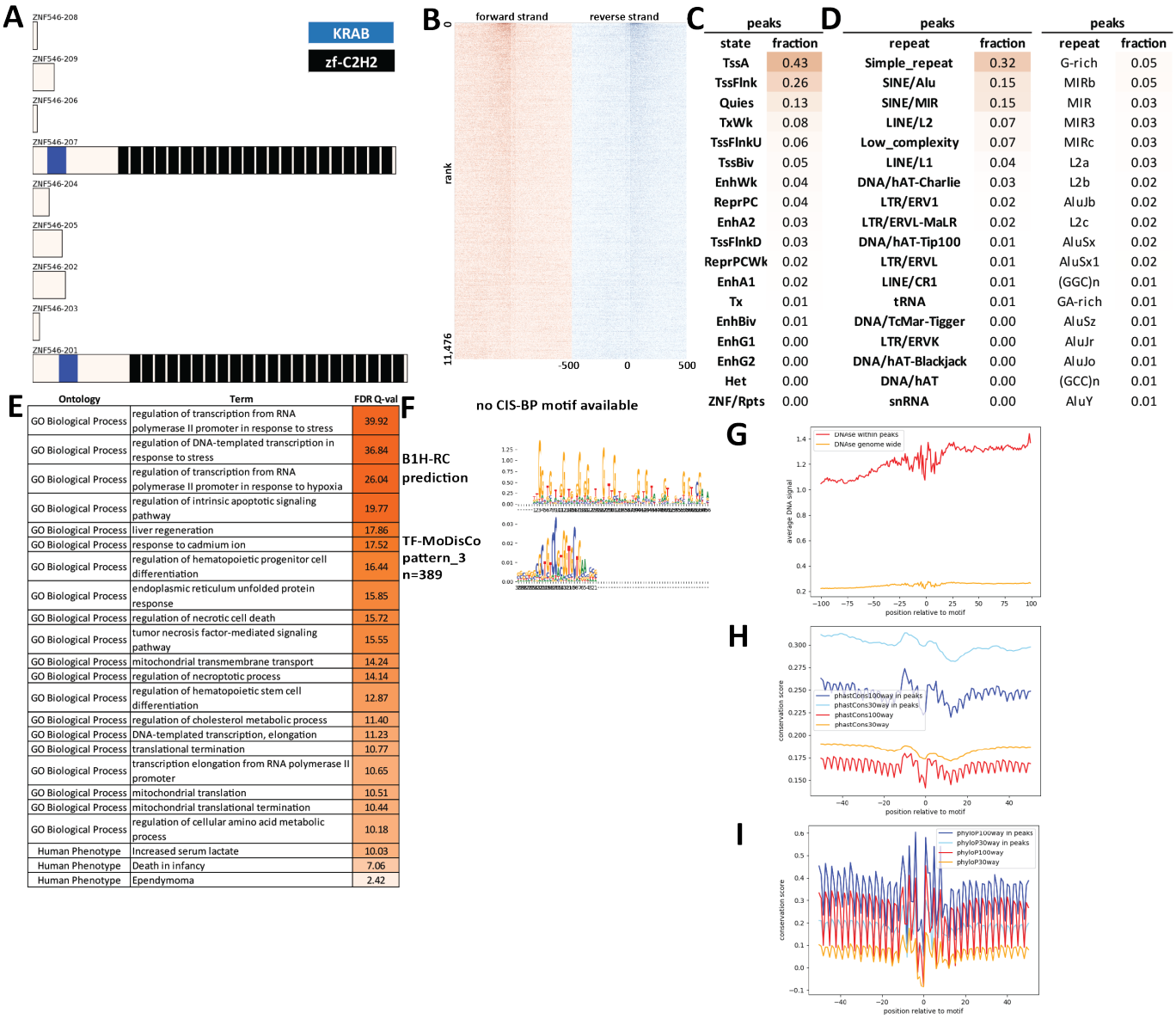

Supplementary Figure 1339: Properties and genomic distribution of motifs identified for the ZNF546 transcription factor in HepG2 (accession ENCSR782WWY).

TF-MoDisCO pattern_3 n=389, CWM

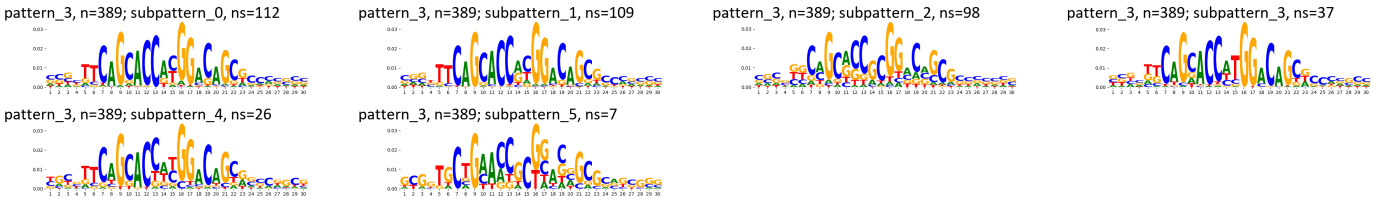

TF-MoDisCO pattern_3 n=389, PWM

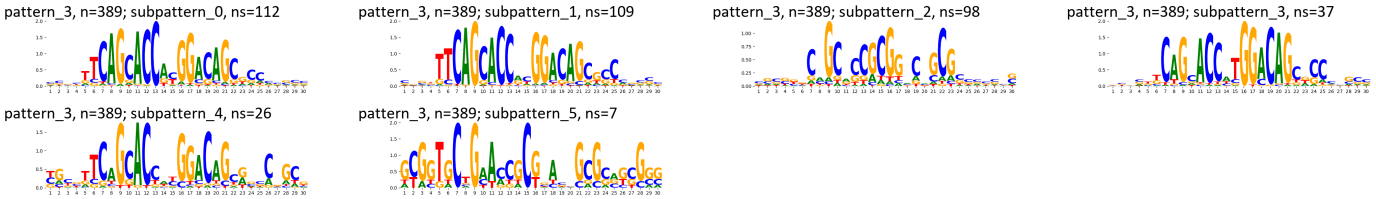

Supplementary Figure 1340: TF-MoDisCO subpatterns for the ZNF546 transcription factor in HepG2 (accession ENCSR782WWY).

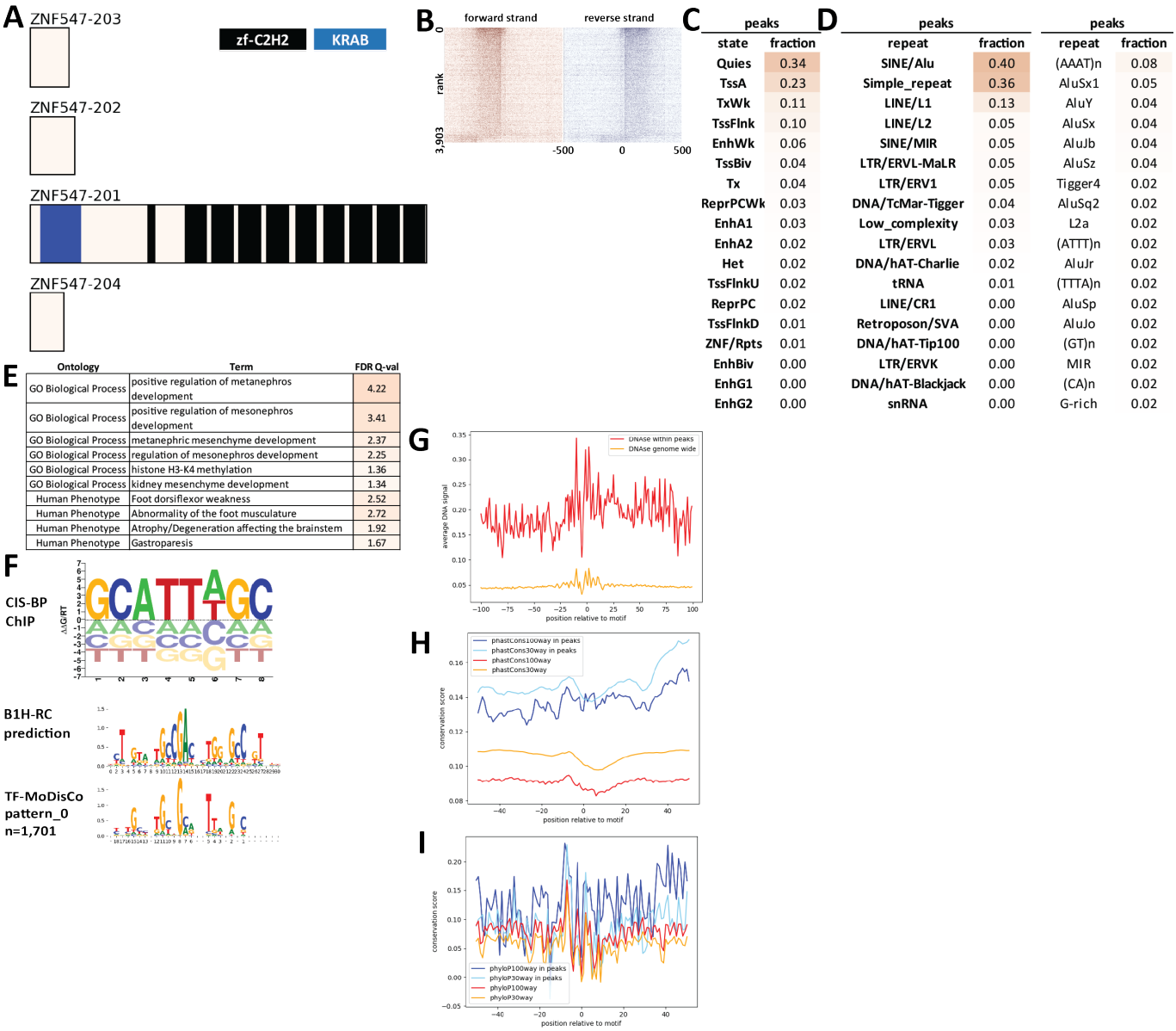

Supplementary Figure 1341: Properties and genomic distribution of motifs identified for the ZNF547 transcription factor in HEK293 (accession ENCSR909TSW).

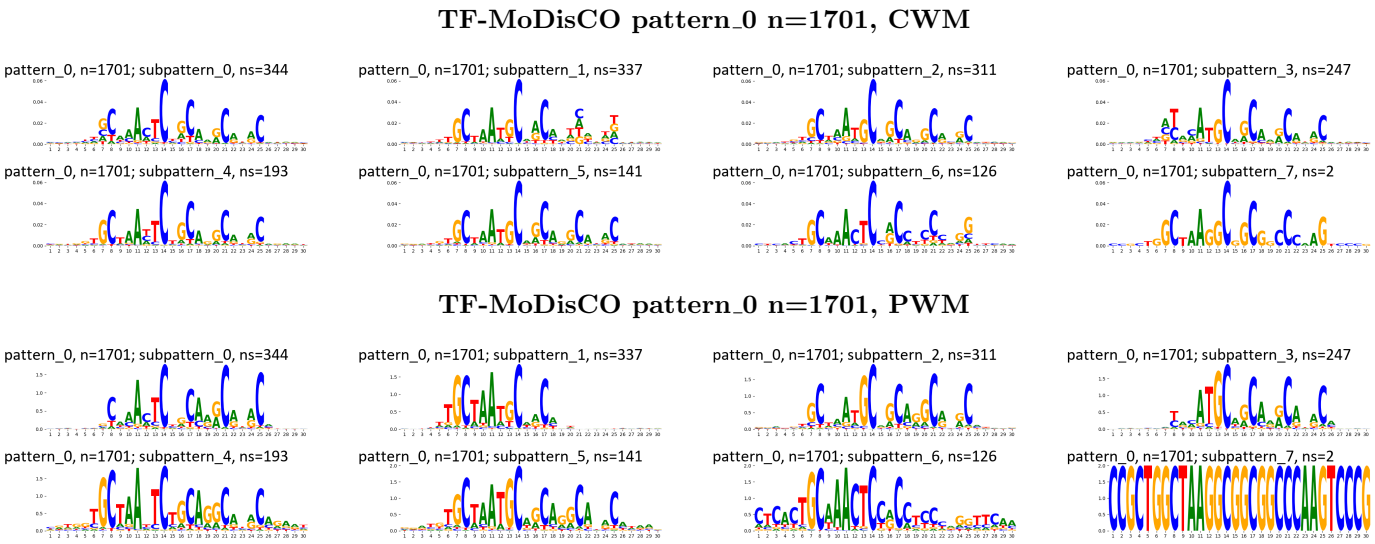

Supplementary Figure 1342: TF-MoDisCO subpatterns for the ZNF547 transcription factor in HEK293 (accession ENCSR909TSW).

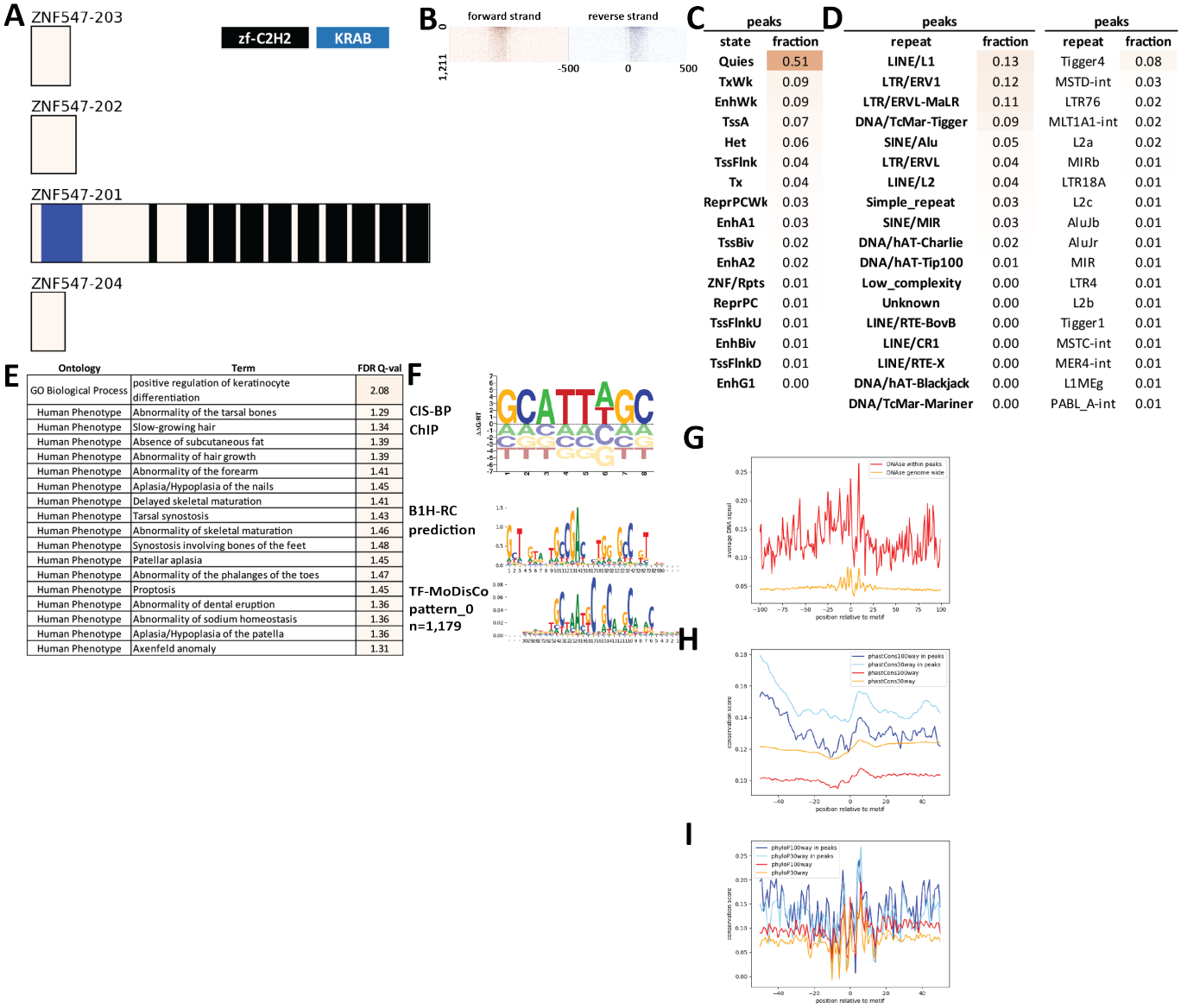

Supplementary Figure 1343: Properties and genomic distribution of motifs identified for the ZNF547 transcription factor in HEK293 (accession Hughes GR models).

TF-MoDisCO pattern_0 n=1179, CWM

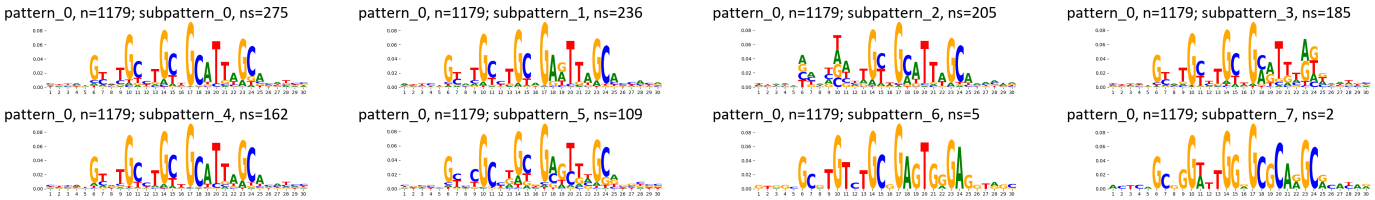

TF-MoDisCO pattern_0 n=1179, PWM

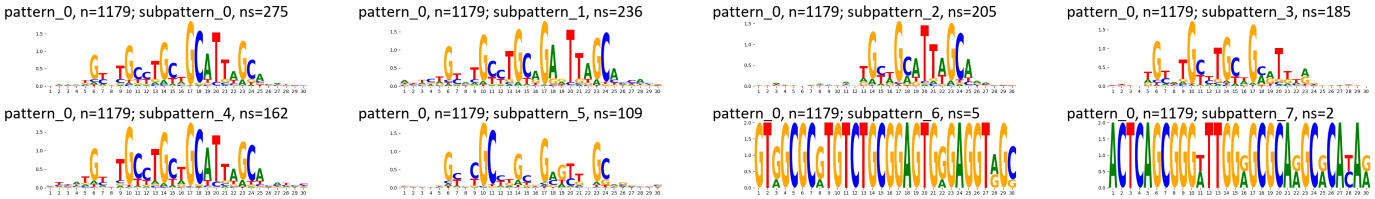

Supplementary Figure 1344: TF-MoDisCO subpatterns for the ZNF547 transcription factor in HEK293 (accession Hughes GR models).

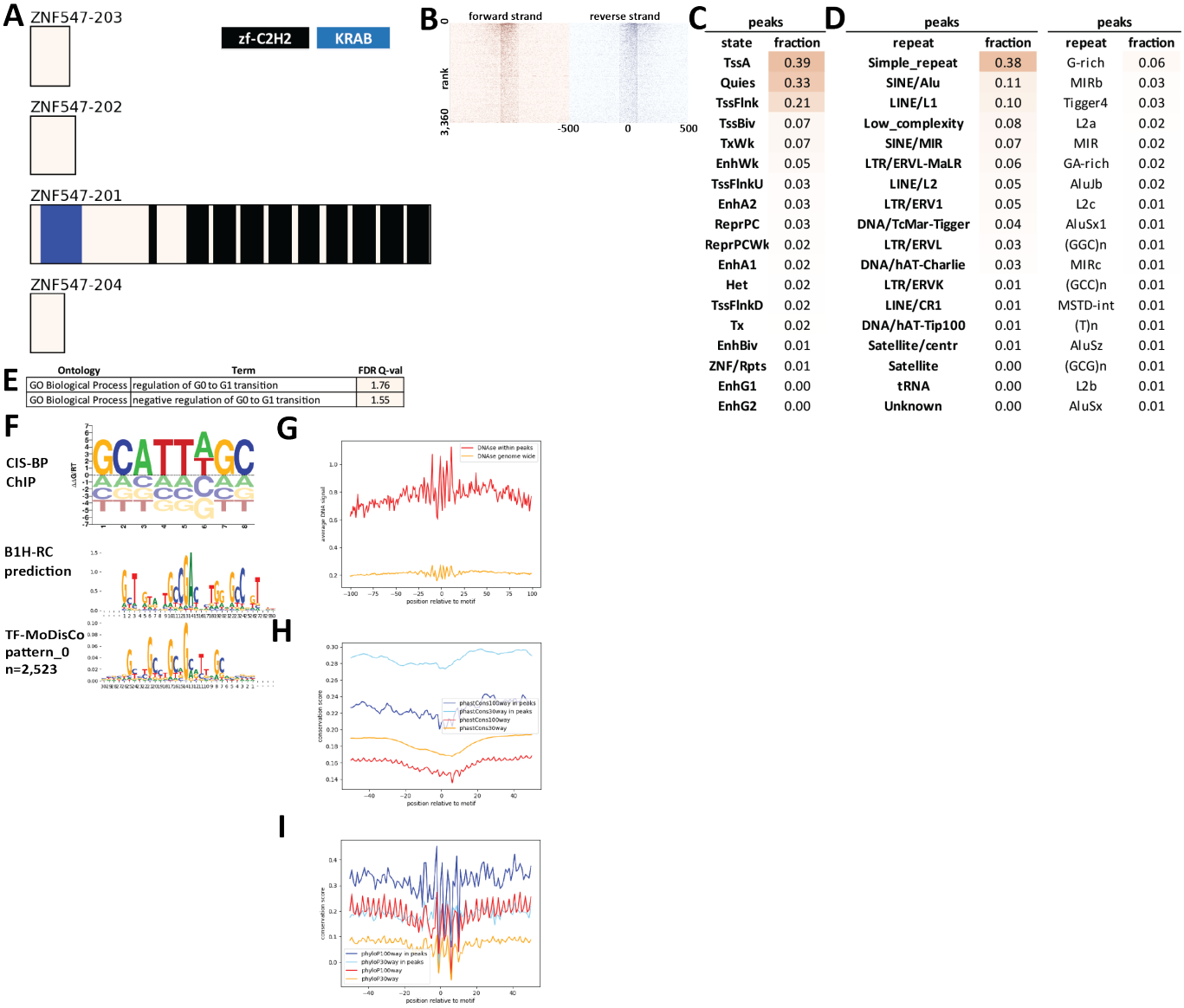

Supplementary Figure 1345: Properties and genomic distribution of motifs identified for the ZNF547 transcription factor in HEK293 (accession ChipExo models).

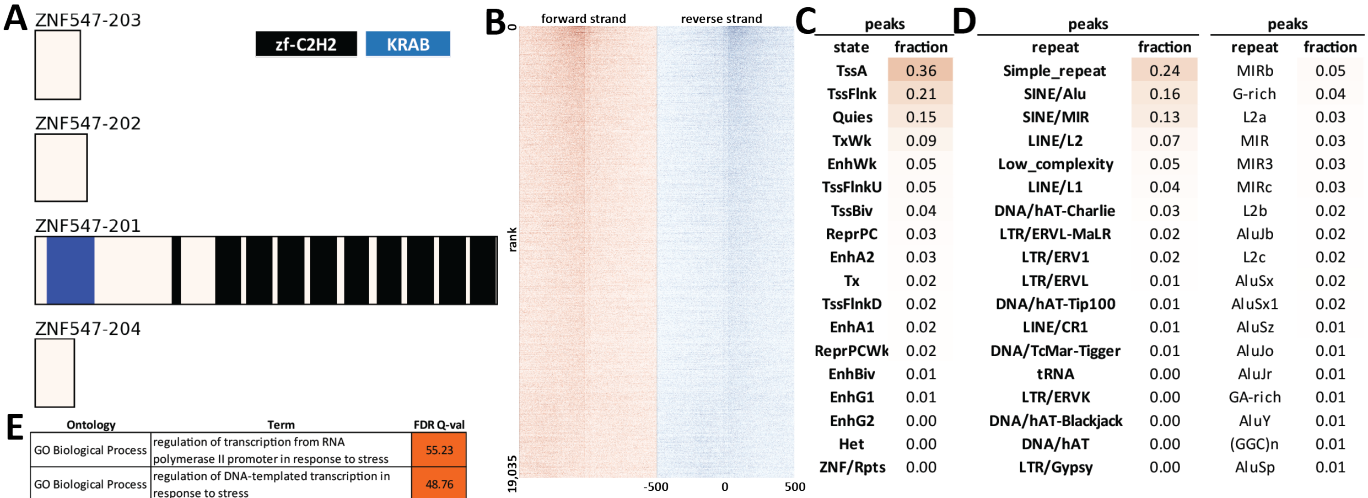

Supplementary Figure 1346: Properties and genomic distribution of motifs identified for the ZNF547 transcription factor in HepG2 (accession ENCSR964ZJC).

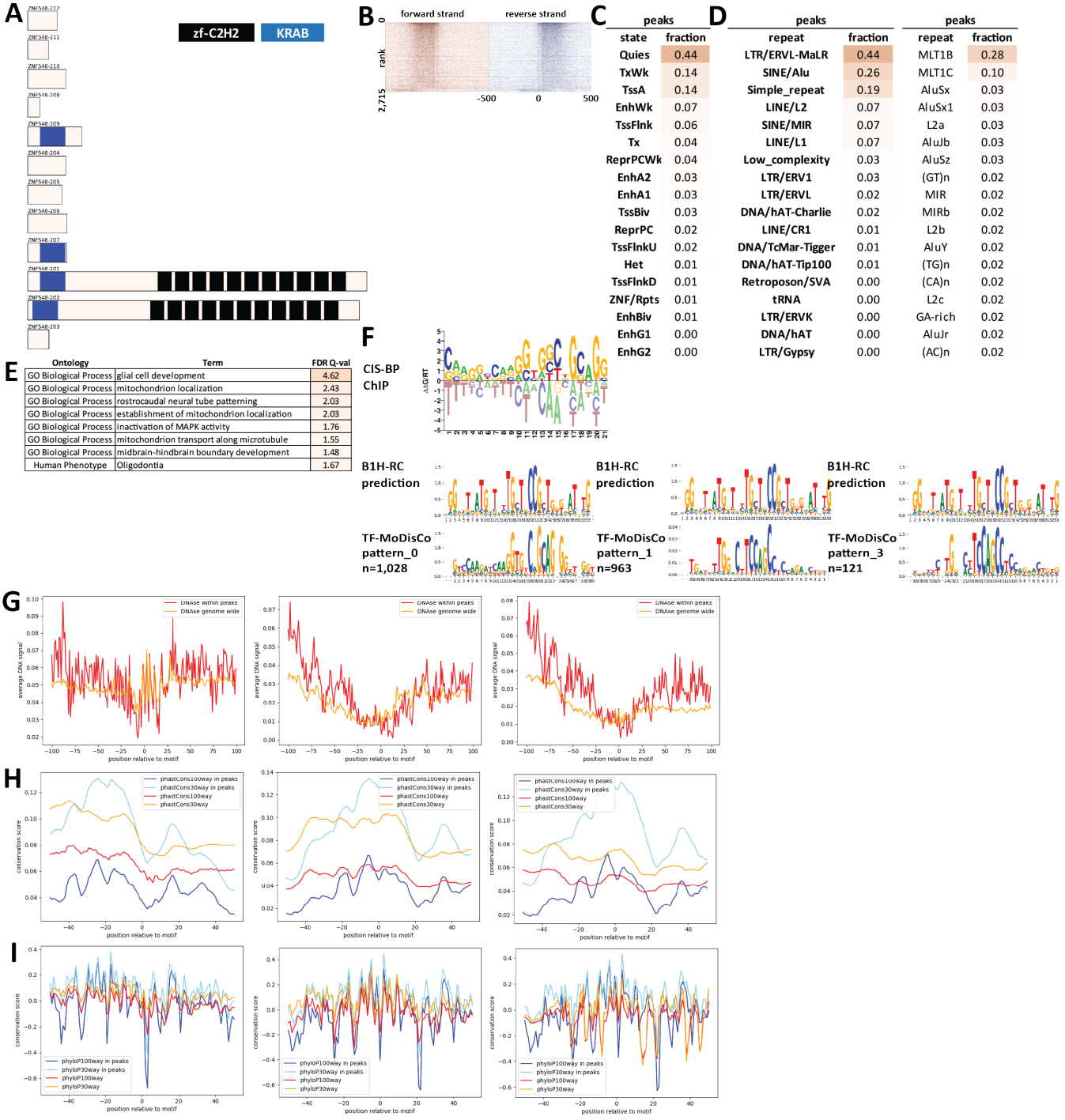

Supplementary Figure 1347: Properties and genomic distribution of motifs identified for the ZNF548 transcription factor in HEK293 (accession ENCSR892ZTO).

TF-MoDisCO pattern_0 n=1028, CWM

pattern_0, n=1028; subpattern_0, ns=290

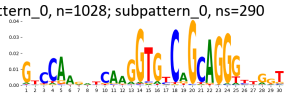

pattern_0, n=1028; subpattern_1, ns=282

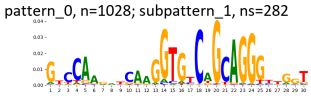

pattern_0, n=1028; subpattern_2, ns=216

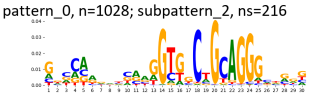

pattern_0, n=1028; subpattern_3, ns=212

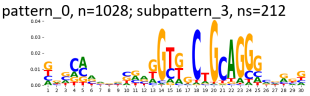

pattern_0, n=1028; subpattern_4, ns=26

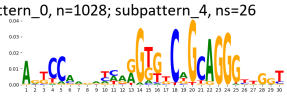

pattern_0, n=1028; subpattern_5, ns=2

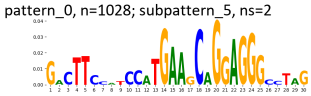

TF-MoDisCO pattern_0 n=1028, PWM

pattern_0, n=1028; subpattern_0, ns=290

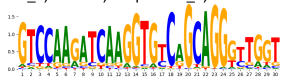

pattern_0, n=1028; subpattern_1, ns=282

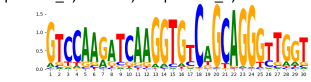

pattern_0, n=1028; subpattern_2, ns=216

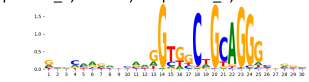

pattern_0, n=1028; subpattern_3, ns=212

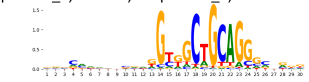

pattern_0, n=1028; subpattern_4, ns=26

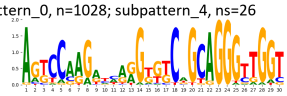

pattern_0, n=1028; subpattern_5, ns=2

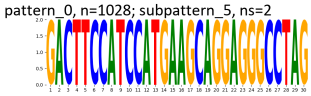

TF-MoDisCO pattern_1 n=963, CWM

pattern_1, n=963; subpattern_0, ns=405

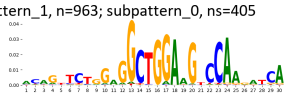

pattern_1, n=963; subpattern_1, ns=355

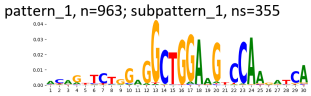

pattern_1, n=963; subpattern_2, ns=70

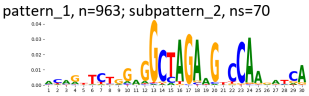

pattern_1, n=963; subpattern_3, ns=52

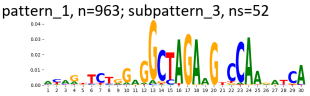

pattern_1, n=963; subpattern_4, ns=44

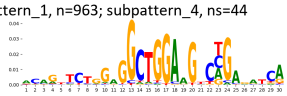

pattern_1, n=963; subpattern_5, ns=37

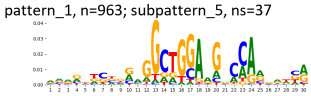

TF-MoDisCO pattern_1 n=963, PWM

pattern_1, n=963; subpattern_0, ns=405

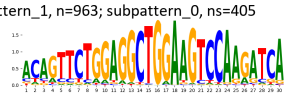

pattern_1, n=963; subpattern_1, ns=355

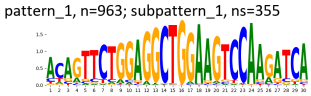

pattern_1, n=963; subpattern_2, ns=70

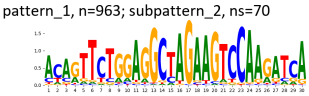

pattern_1, n=963; subpattern_3, ns=52

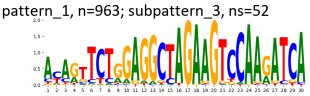

pattern_1, n=963; subpattern_4, ns=44

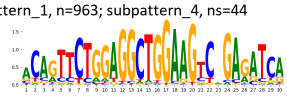

pattern_1, n=963; subpattern_5, ns=37

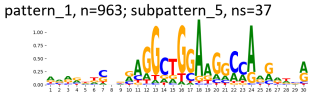

TF-MoDisCO pattern_3 n=121, CWM

pattern_3, n=121; subpattern_0, ns=43

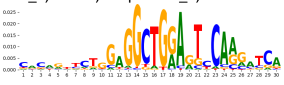

pattern_3, n=121; subpattern_1, ns=42

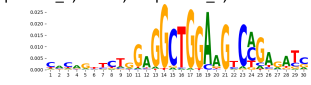

pattern_3, n=121; subpattern_2, ns=36

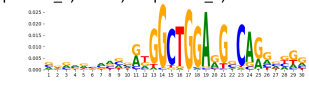

TF-MoDisCO pattern_3 n=121, PWM

pattern_3, n=121; subpattern_0, ns=43

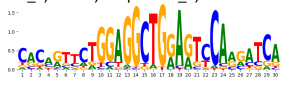

pattern_3, n=121; subpattern_1, ns=42

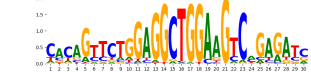

pattern_3, n=121; subpattern_2, ns=36

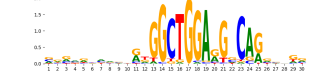

Supplementary Figure 1348: TF-MoDisCO subpatterns for the ZNF548 transcription factor in HEK293 (accession ENCSR892ZTO).

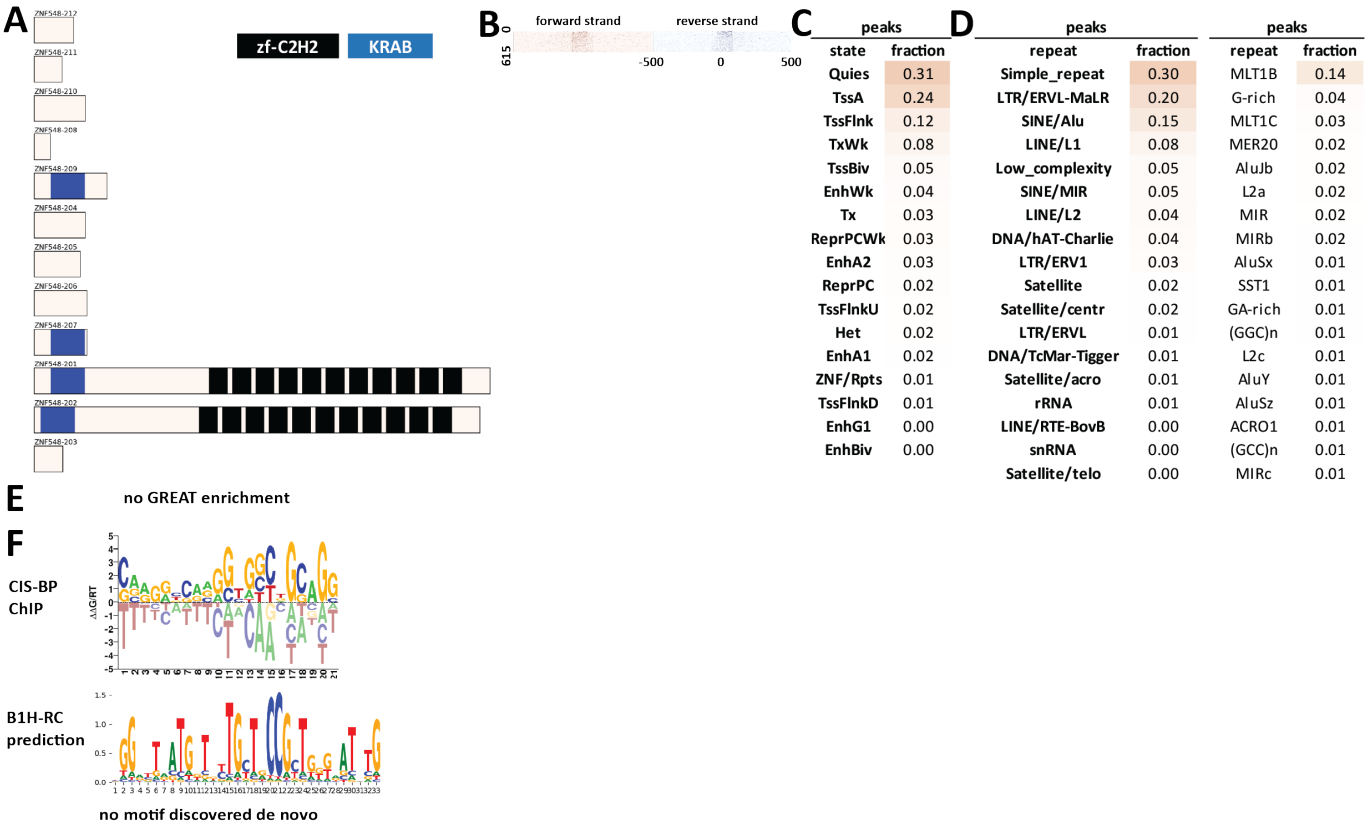

Supplementary Figure 1349: Properties and genomic distribution of motifs identified for the ZNF548 transcription factor in HEK293 (accession ChipExo models).

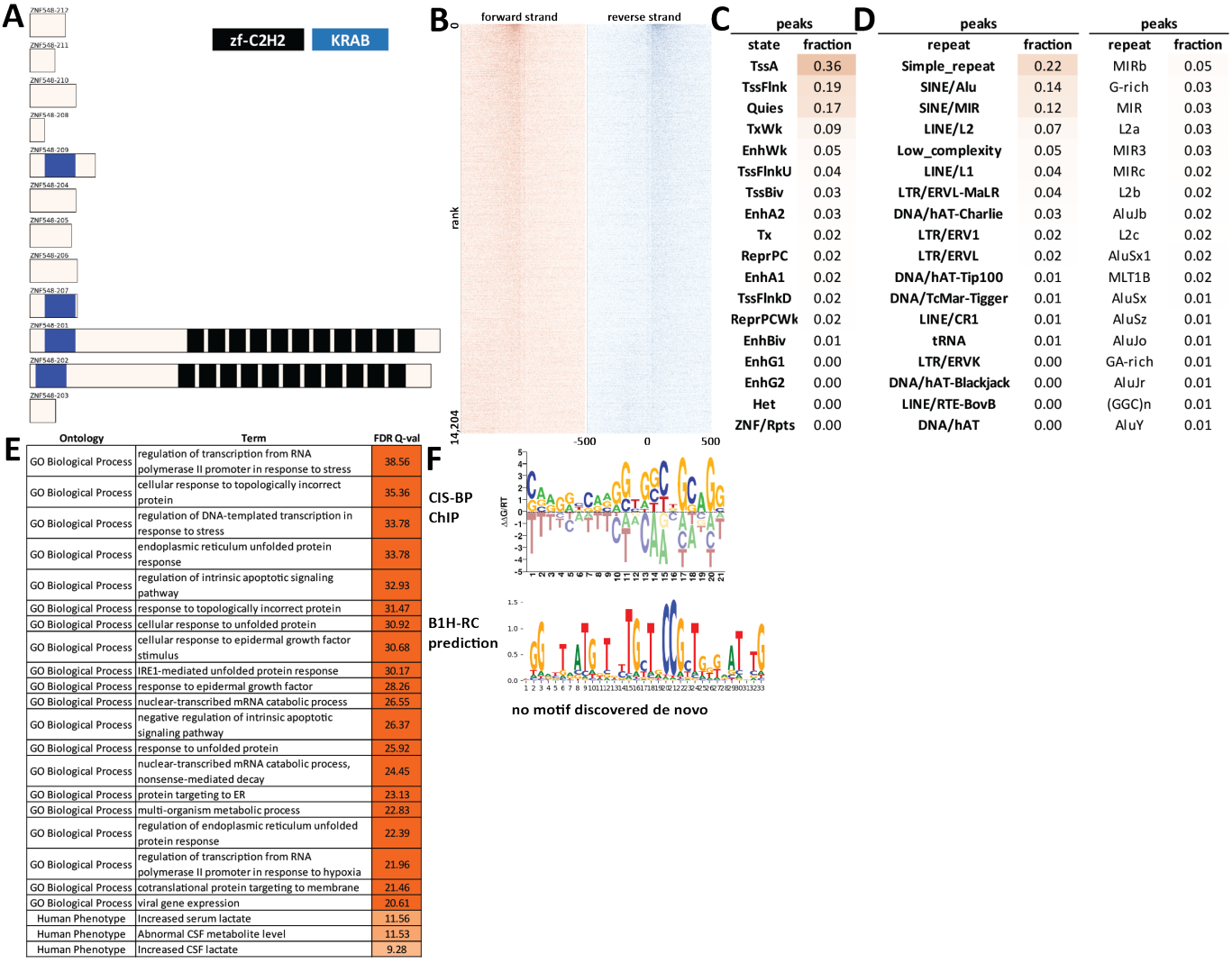

C

peaks	
state	fraction
TssA	0.36
TssFlnk	0.19
Quies	0.17
TxWk	0.09
EnhWk	0.05
TssFlnkU	0.04
TssBiv	0.03
EnhA2	0.03
Tx	0.02
ReprPC	0.02
EnhA1	0.02
TssFlnkD	0.02
ReprPCWk	0.02
EnhBiv	0.01
EnhG1	0.00
EnhG2	0.00
Het	0.00
ZNF/Rpts	0.00

D

peaks		peaks	
repeat	fraction	repeat	fraction
Simple_repeat	0.22	MIRb	0.05
SINE/Alu	0.14	G-rich	0.03
SINE/MIR	0.12	MIR	0.03
LINE/L2	0.07	L2a	0.03
Low_complexity	0.05	MIR3	0.03
LINE/L1	0.04	MIRc	0.02
LTR/ERVL-MaLR	0.04	L2b	0.02
DNA/hAT-Charlie	0.03	AluJb	0.02
LTR/ERV1	0.02	L2c	0.02
LTR/ERVL	0.02	AluSx1	0.02
DNA/hAT-Tip100	0.01	MLT1B	0.02
DNA/TcMar-Tigger	0.01	AluSx	0.01
LINE/CR1	0.01	AluSz	0.01
tRNA	0.01	AluJo	0.01
LTR/ERVK	0.00	GA-rich	0.01
DNA/hAT-Blackjack	0.00	AluJr	0.01
LINE/RTE-BovB	0.00	(GGC)n	0.01
DNA/hAT	0.00	AluY	0.01

E

Ontology	Term	FDR Q-val
GO Biological Process	regulation of transcription from RNA polymerase II promoter in response to stress	38.56
GO Biological Process	cellular response to topologically incorrect protein	35.36
GO Biological Process	regulation of DNA-templated transcription in response to stress	33.78
GO Biological Process	endoplasmic reticulum unfolded protein response	33.78
GO Biological Process	regulation of intrinsic apoptotic signaling pathway	32.93
GO Biological Process	response to topologically incorrect protein	31.47
GO Biological Process	cellular response to unfolded protein	30.92
GO Biological Process	cellular response to epidermal growth factor stimulus	30.68
GO Biological Process	IRE1-mediated unfolded protein response	30.17
GO Biological Process	response to epidermal growth factor	28.26
GO Biological Process	nuclear-transcribed mRNA catabolic process	26.55
GO Biological Process	negative regulation of intrinsic apoptotic signaling pathway	26.37
GO Biological Process	response to unfolded protein	25.92
GO Biological Process	nuclear-transcribed mRNA catabolic process, nonsense-mediated decay	24.45
GO Biological Process	protein targeting to ER	23.13
GO Biological Process	multi-organism metabolic process	22.83
GO Biological Process	regulation of endoplasmic reticulum unfolded protein response	22.39
GO Biological Process	regulation of transcription from RNA polymerase II promoter in response to hypoxia	21.96
GO Biological Process	cotranslational protein targeting to membrane	21.46
GO Biological Process	viral gene expression	20.61
Human Phenotype	Increased serum lactate	11.56
Human Phenotype	Abnormal CSF metabolite level	11.53
Human Phenotype	Increased CSF lactate	9.28

Supplementary Figure 1350: Properties and genomic distribution of motifs identified for the ZNF548 transcription factor in HepG2 (accession ENCSR756UNW).

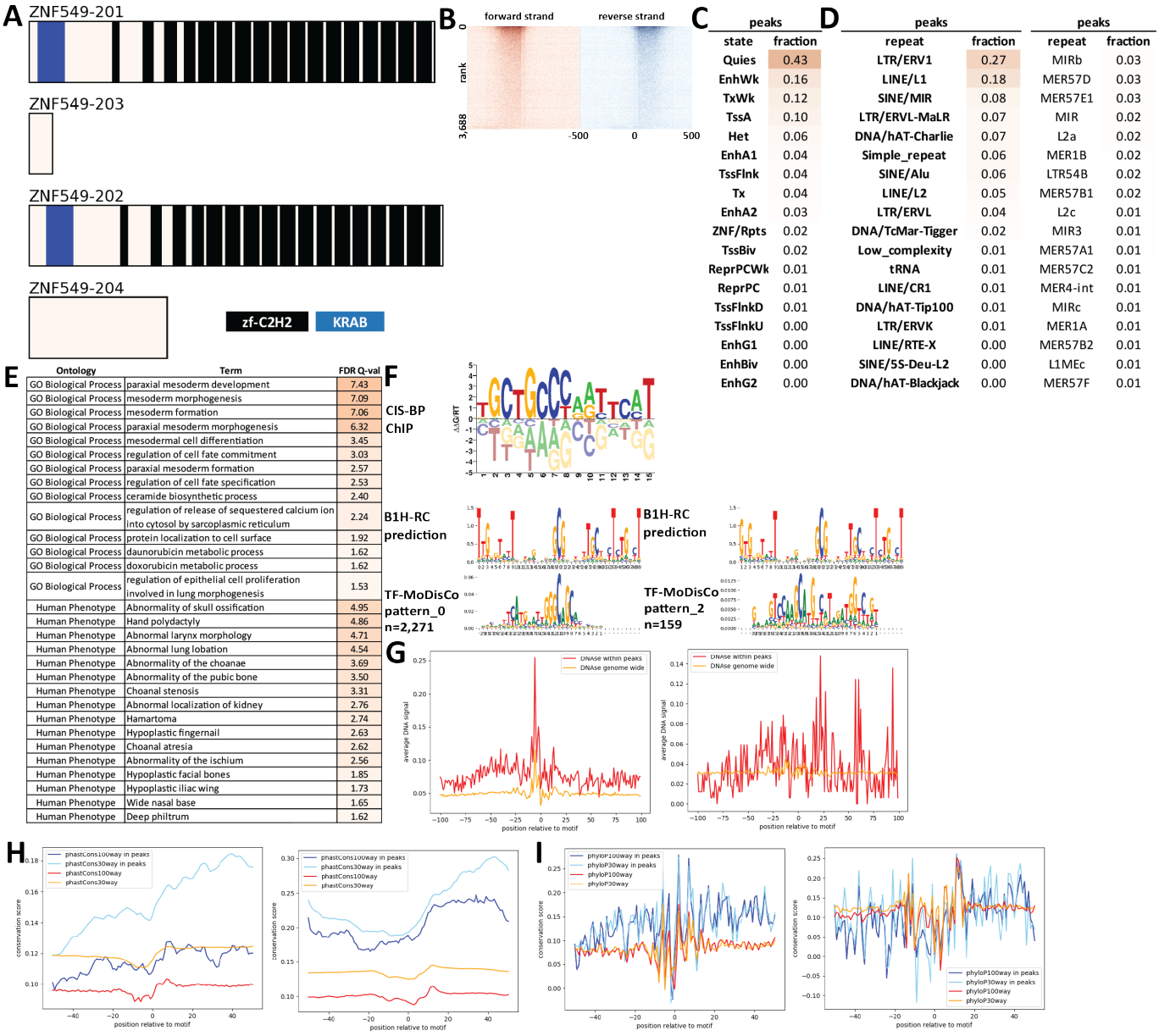

Supplementary Figure 1351: Properties and genomic distribution of motifs identified for the ZNF549 transcription factor in HEK293 (accession ENCSR185QFX).

TF-MoDisCO pattern_0 n=2271, CWM

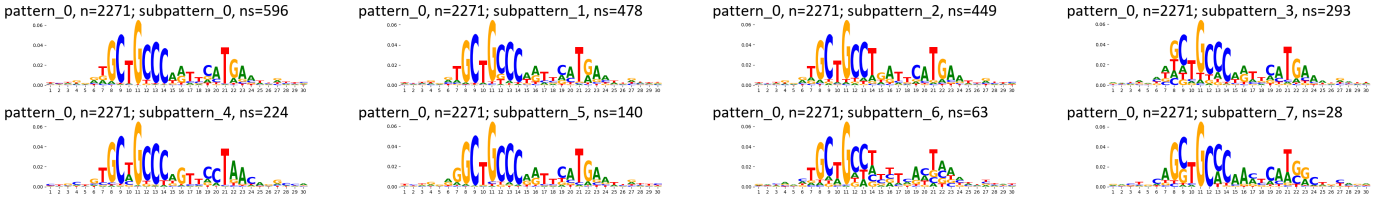

TF-MoDisCO pattern_0 n=2271, PWM

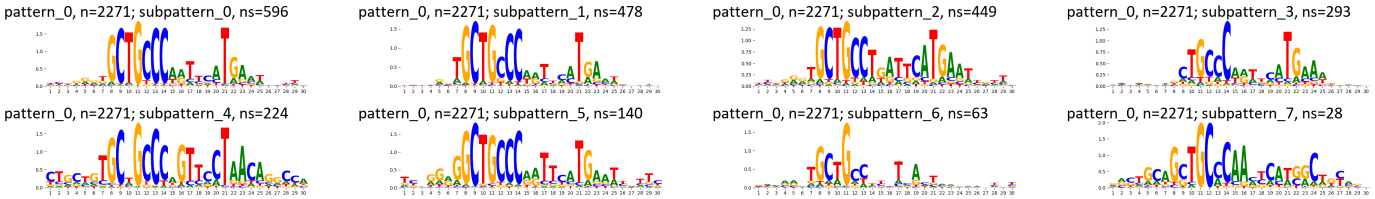

TF-MoDisCO pattern_2 n=159, CWM

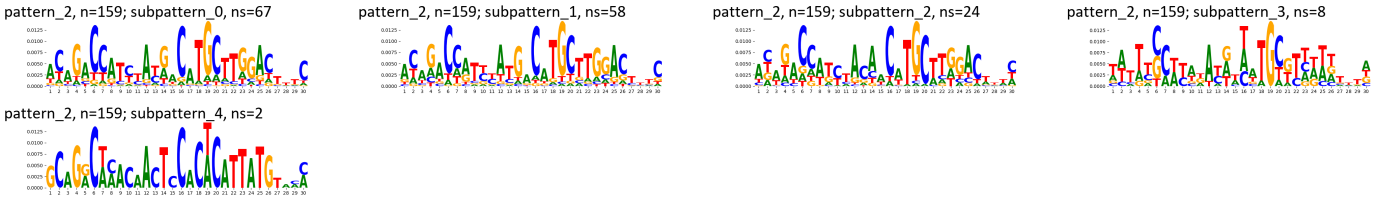

TF-MoDisCO pattern_2 n=159, PWM

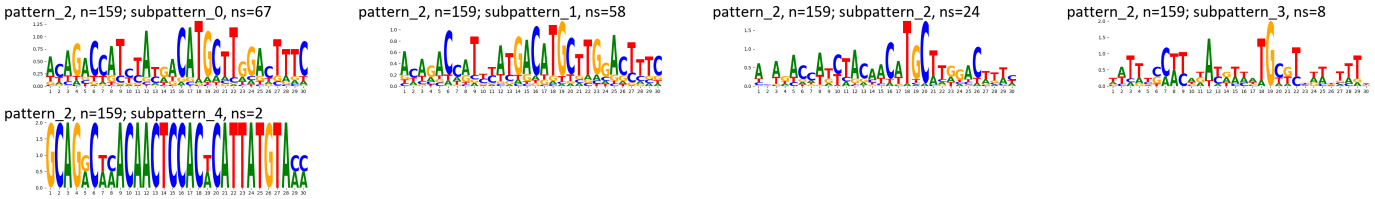

Supplementary Figure 1352: TF-MoDisCO subpatterns for the ZNF549 transcription factor in HEK293 (accession ENCSR185QFX).

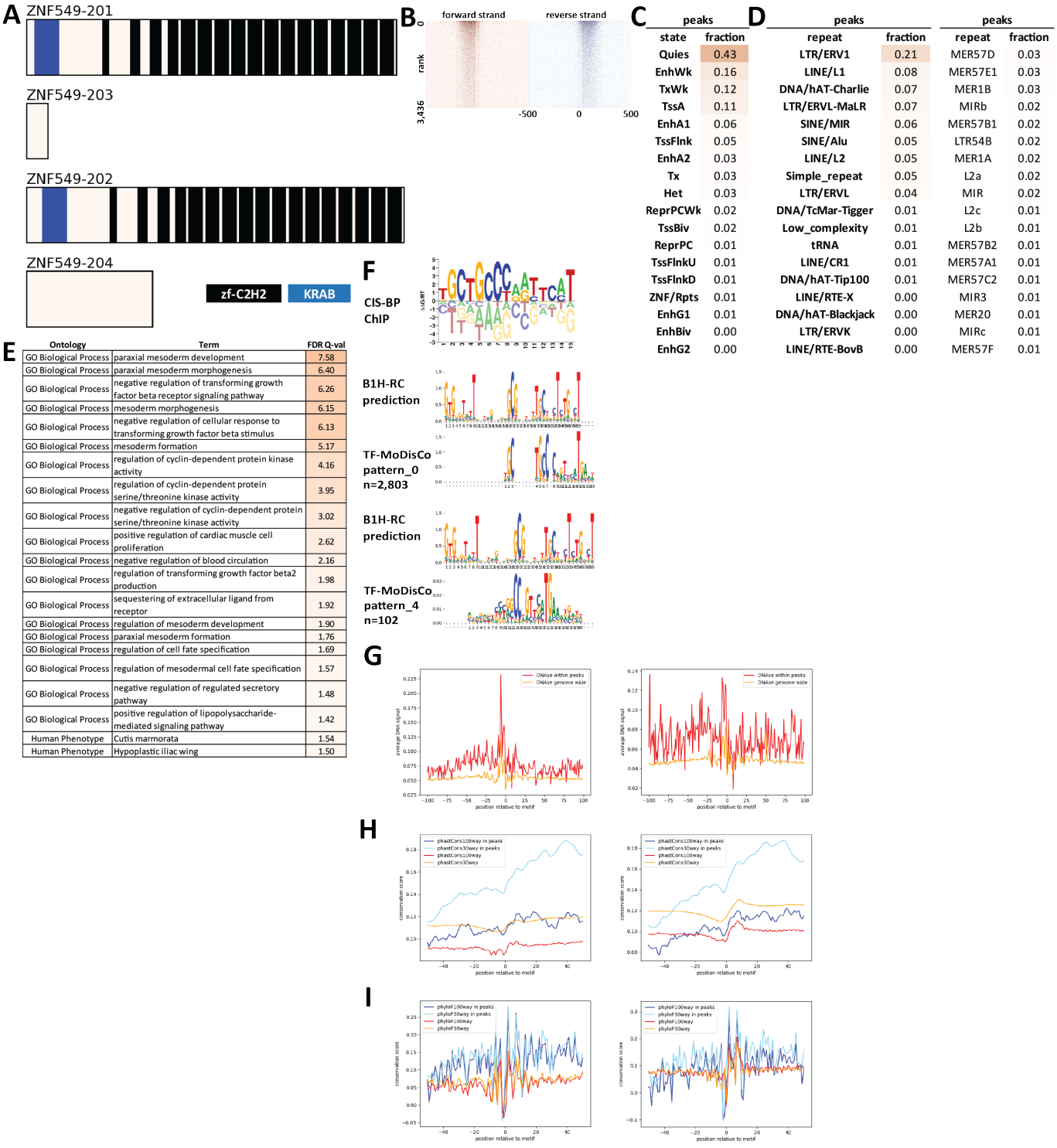

Supplementary Figure 1353: Properties and genomic distribution of motifs identified for the ZNF549 transcription factor in HEK293 (accession Hughes GR models).

TF-MoDisCO pattern_0 n=2803, CWM

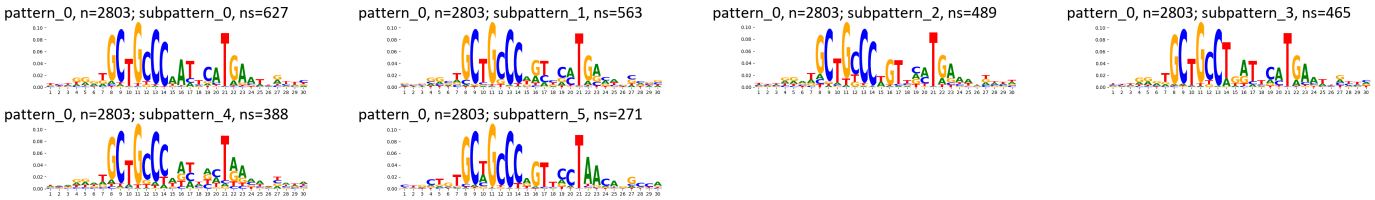

TF-MoDisCO pattern_0 n=2803, PWM

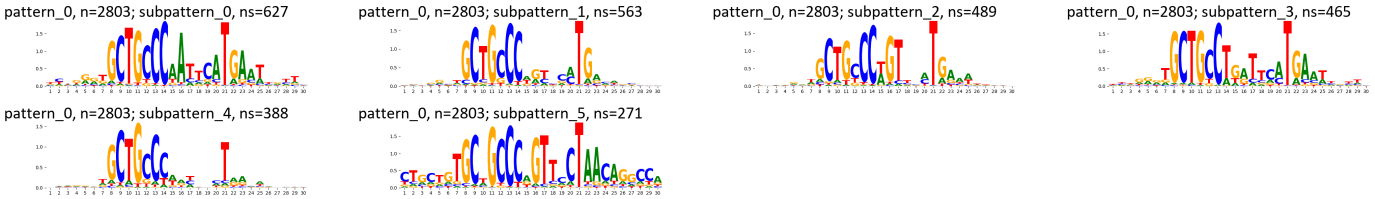

TF-MoDisCO pattern_4 n=102, CWM

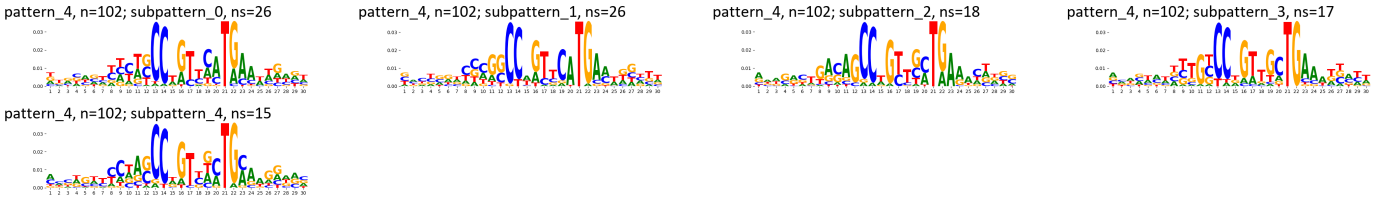

TF-MoDisCO pattern_4 n=102, PWM

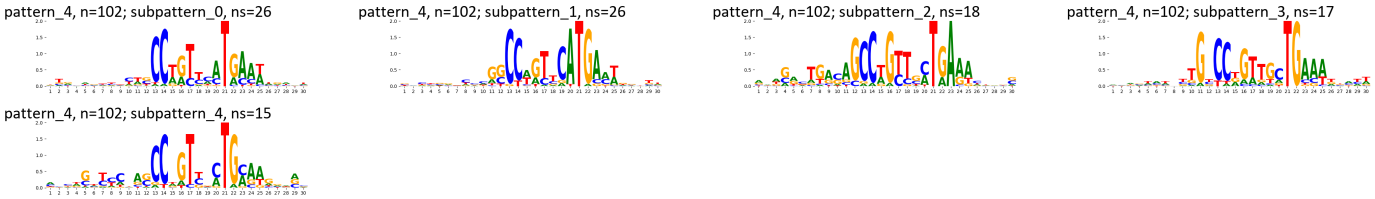

Supplementary Figure 1354: TF-MoDisCO subpatterns for the ZNF549 transcription factor in HEK293 (accession Hughes GR models).

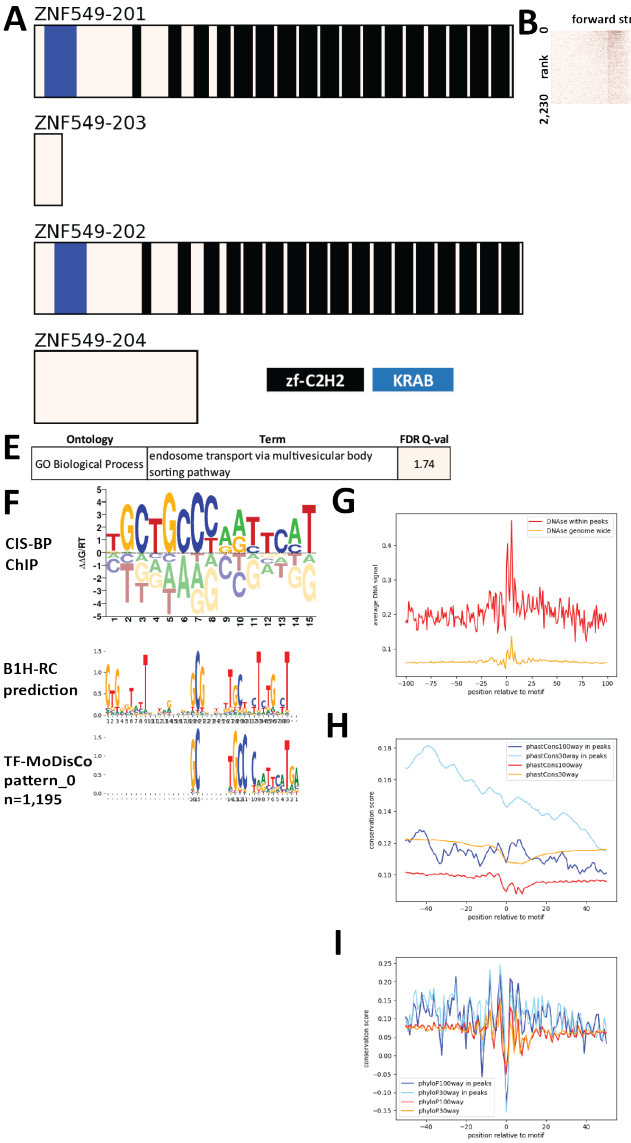

C

peaks	
state	fraction
Quies	0.38
TssA	0.31
TssFlnk	0.16
TxWk	0.08
EnhWk	0.05
TssBiv	0.05
Tx	0.03
EnhA2	0.02
Het	0.02
ReprPCWk	0.02
ReprPC	0.02
TssFlnkU	0.02
EnhA1	0.01
TssFlnkD	0.01
ZNF/Rpts	0.01
EnhBiv	0.00
EnhG1	0.00
EnhG2	0.00

D

peaks		peaks	
repeat	fraction	repeat	fraction
Simple_repeat	0.28	MER57D	0.04
LTR/ERV1	0.25	G-rich	0.04
SINE/Alu	0.13	MER57E1	0.04
LINE/L1	0.12	MIRb	0.03
SINE/MIR	0.08	MER1B	0.03
DNA/hAT-Charlie	0.07	LTR54B	0.02
LINE/L2	0.06	L2a	0.02
Low_complexity	0.06	MER57B1	0.02
LTR/ERVL-MaLR	0.05	MIR	0.02
LTR/ERVL	0.03	AluSx1	0.02
DNA/TcMar-Tigger	0.02	L2c	0.02
tRNA	0.01	MIRc	0.02
Satellite	0.01	MER57A1	0.01
DNA/hAT-Tip100	0.01	AluJb	0.01
LINE/CR1	0.01	MER57C2	0.01
Satellite/centr	0.00	AluSx	0.01
Satellite/acro	0.00	L2	0.01
snRNA	0.00	(T)n	0.01

Supplementary Figure 1355: Properties and genomic distribution of motifs identified for the ZNF549 transcription factor in HEK293 (accession ChipExo models).

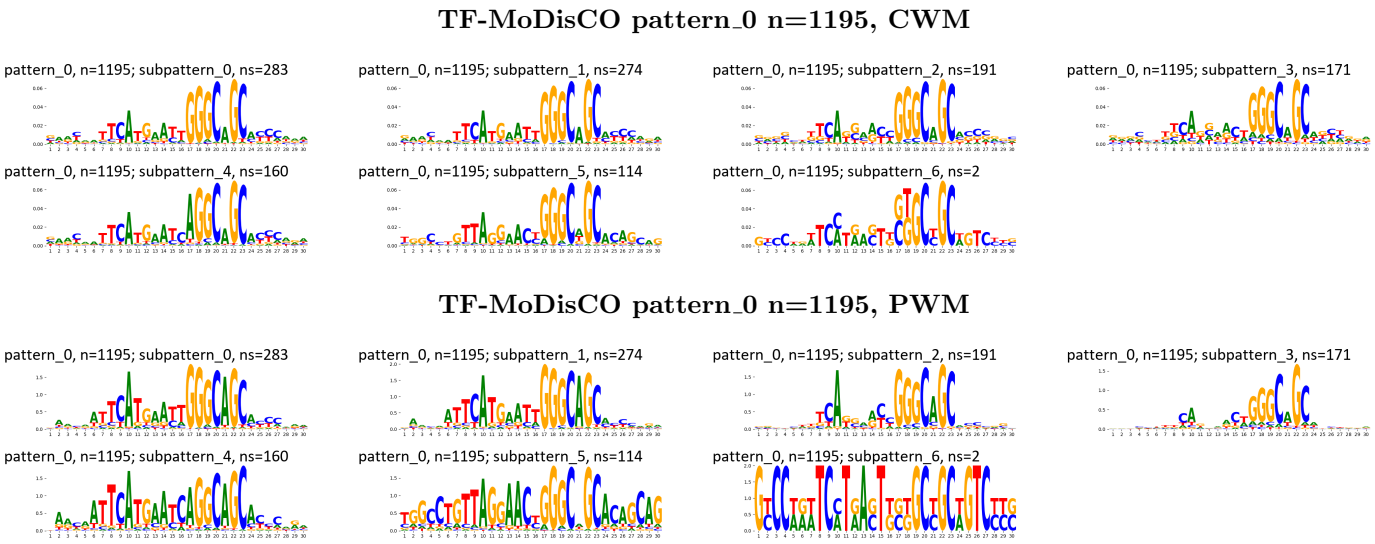

Supplementary Figure 1356: TF-MoDisCO subpatterns for the ZNF549 transcription factor in HEK293 (accession ChipExo models).

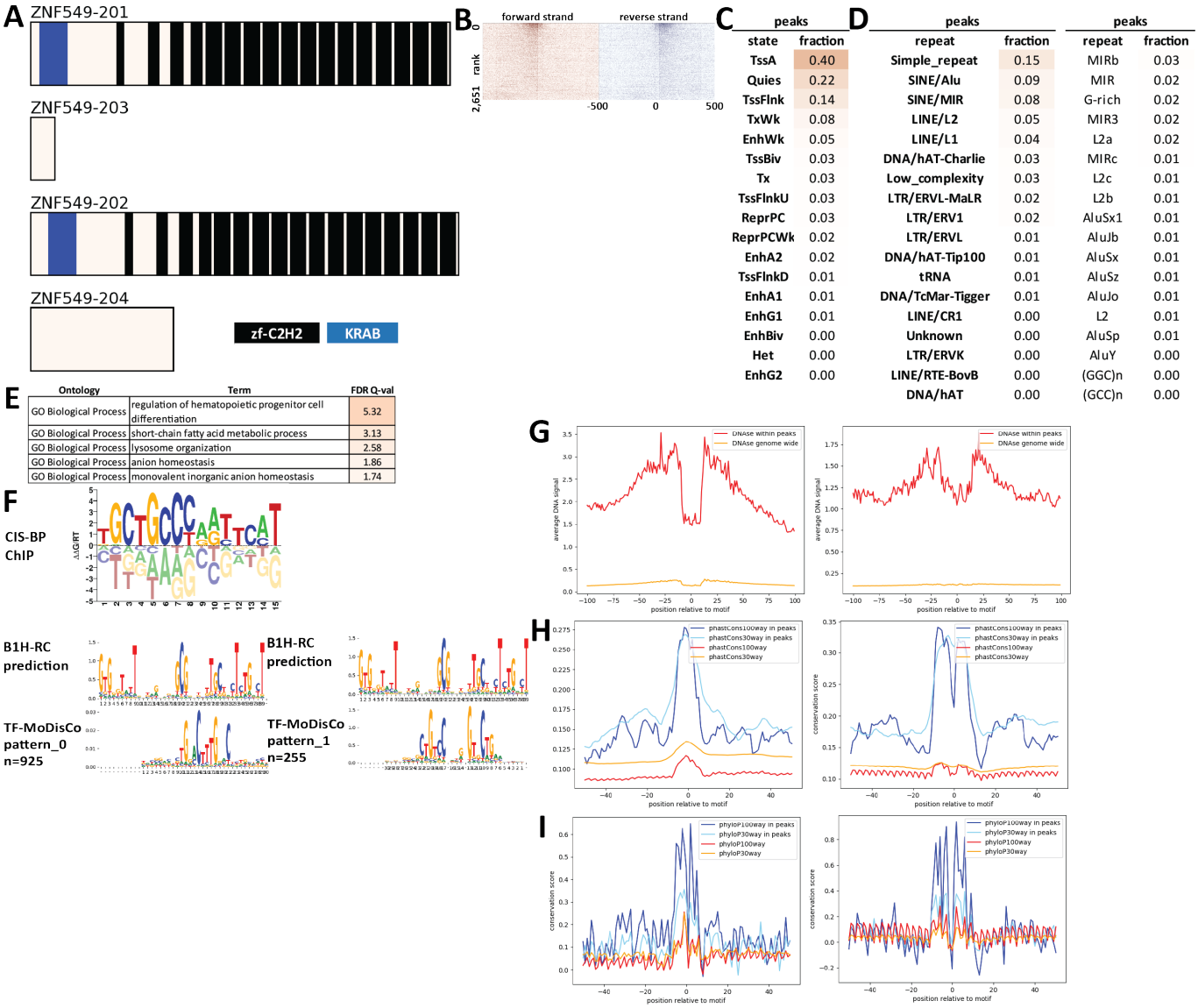

Supplementary Figure 1357: Properties and genomic distribution of motifs identified for the ZNF549 transcription factor in HepG2 (accession ENCSR545ACM).

TF-MoDisCO pattern_0 n=925, CWM

pattern_0, n=925; subpattern_0, ns=367

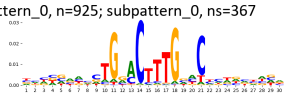

pattern_0, n=925; subpattern_1, ns=338

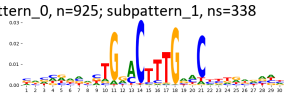

pattern_0, n=925; subpattern_2, ns=123

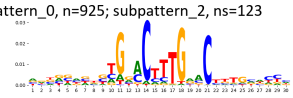

pattern_0, n=925; subpattern_3, ns=60

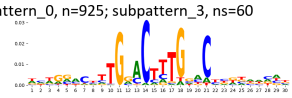

pattern_0, n=925; subpattern_4, ns=37

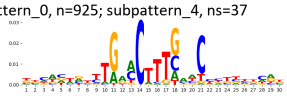

TF-MoDisCO pattern_0 n=925, PWM

pattern_0, n=925; subpattern_0, ns=367

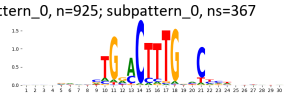

pattern_0, n=925; subpattern_1, ns=338

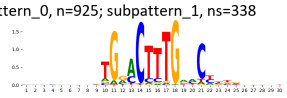

pattern_0, n=925; subpattern_2, ns=123

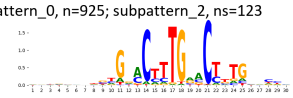

pattern_0, n=925; subpattern_3, ns=60

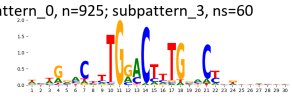

pattern_0, n=925; subpattern_4, ns=37

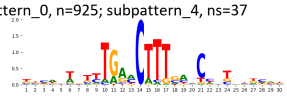

TF-MoDisCO pattern_1 n=255, CWM

pattern_1, n=255; subpattern_0, ns=97

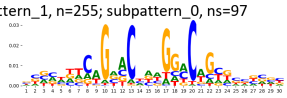

pattern_1, n=255; subpattern_1, ns=77

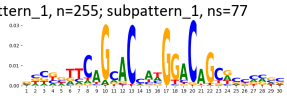

pattern_1, n=255; subpattern_2, ns=69

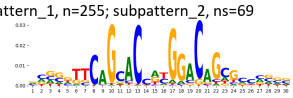

pattern_1, n=255; subpattern_3, ns=12

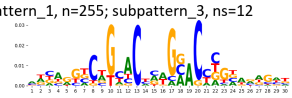

TF-MoDisCO pattern_1 n=255, PWM

pattern_1, n=255; subpattern_0, ns=97

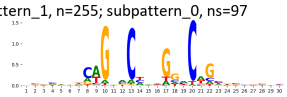

pattern_1, n=255; subpattern_1, ns=77

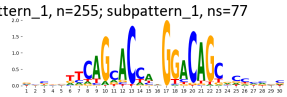

pattern_1, n=255; subpattern_2, ns=69

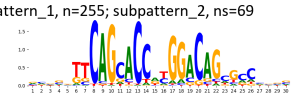

pattern_1, n=255; subpattern_3, ns=12

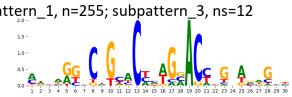

Supplementary Figure 1358: TF-MoDisCO subpatterns for the ZNF549 transcription factor in HepG2 (accession ENCSR545ACM).

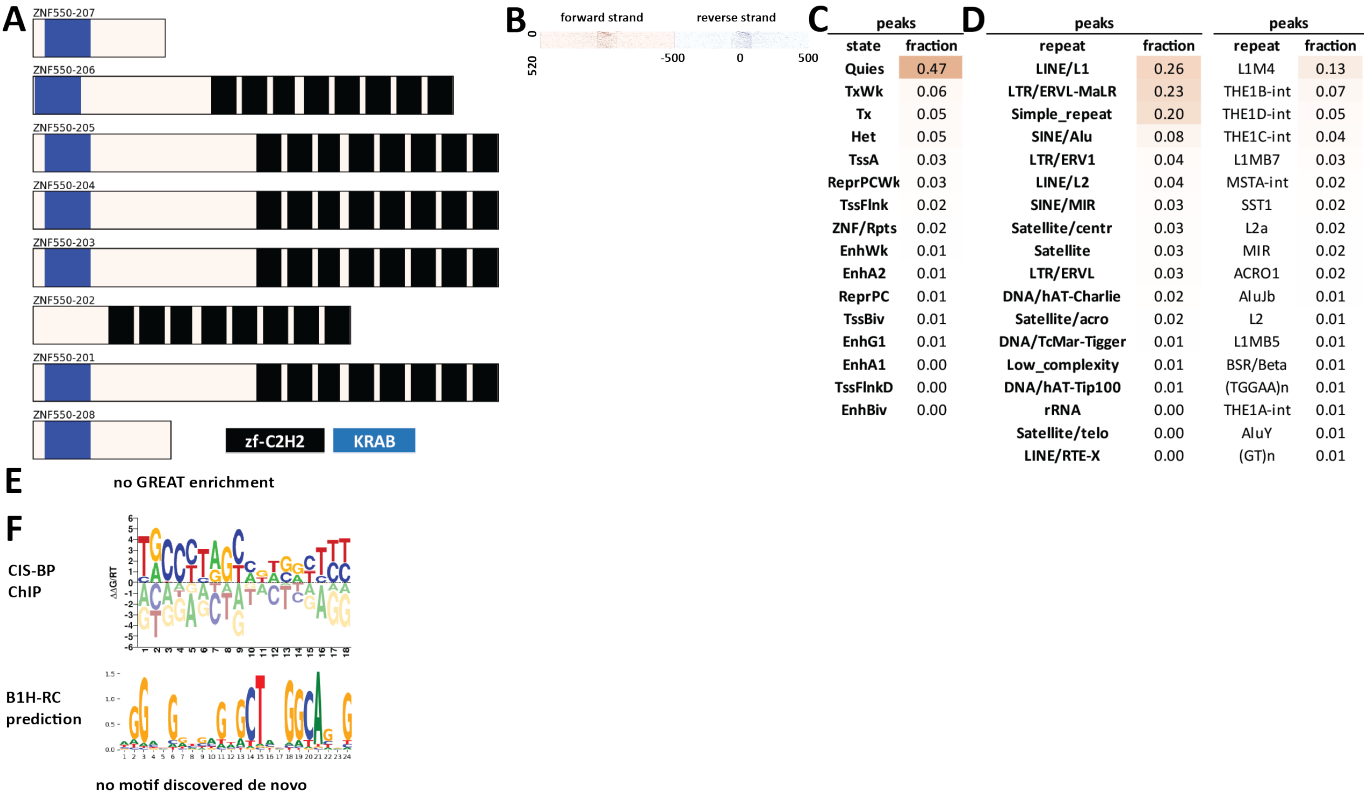

Supplementary Figure 1359: Properties and genomic distribution of motifs identified for the ZNF550 transcription factor in HEK293 (accession ChipExo models).

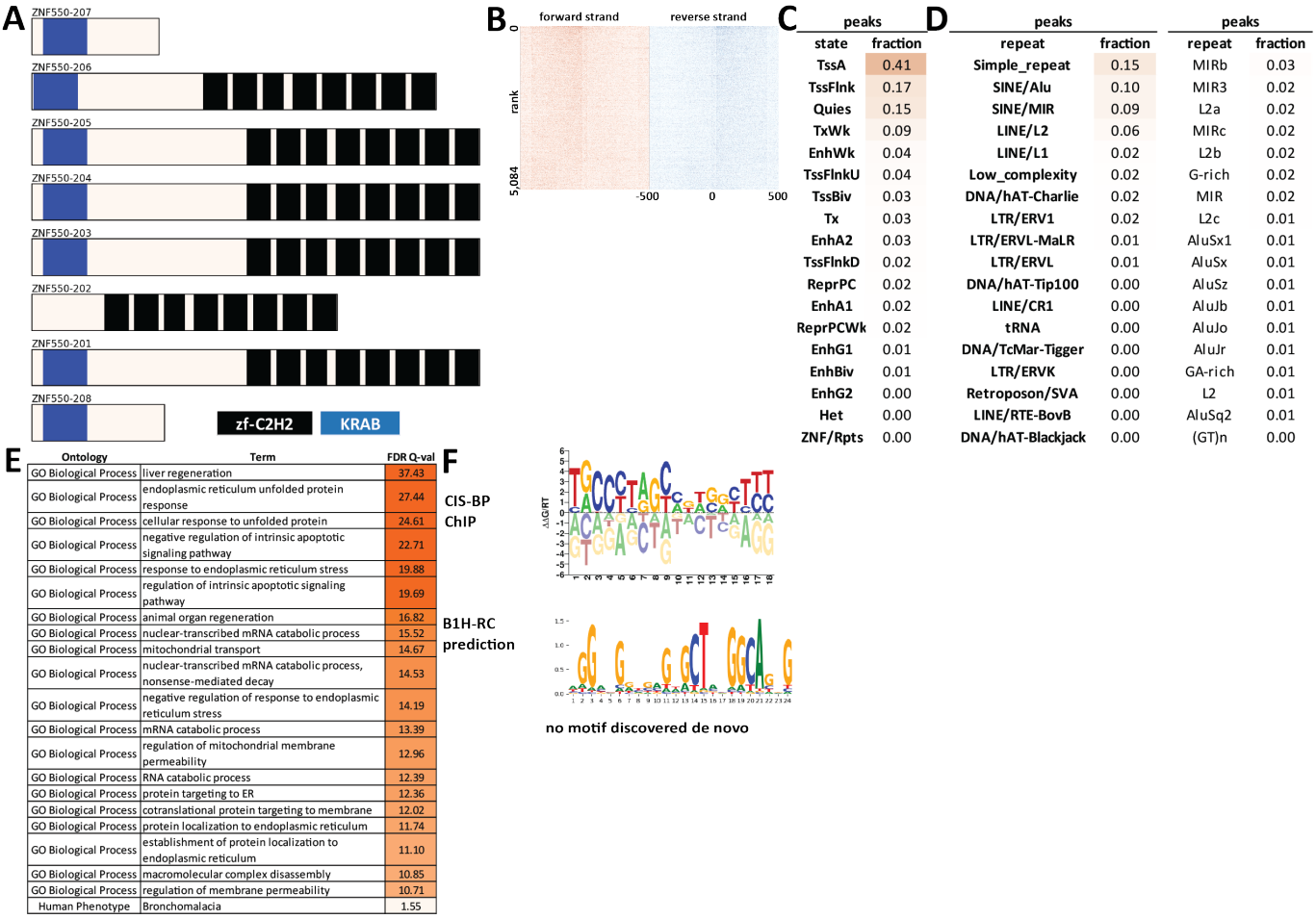

Supplementary Figure 1360: Properties and genomic distribution of motifs identified for the ZNF550 transcription factor in HepG2 (accession ENCSR198BHH).

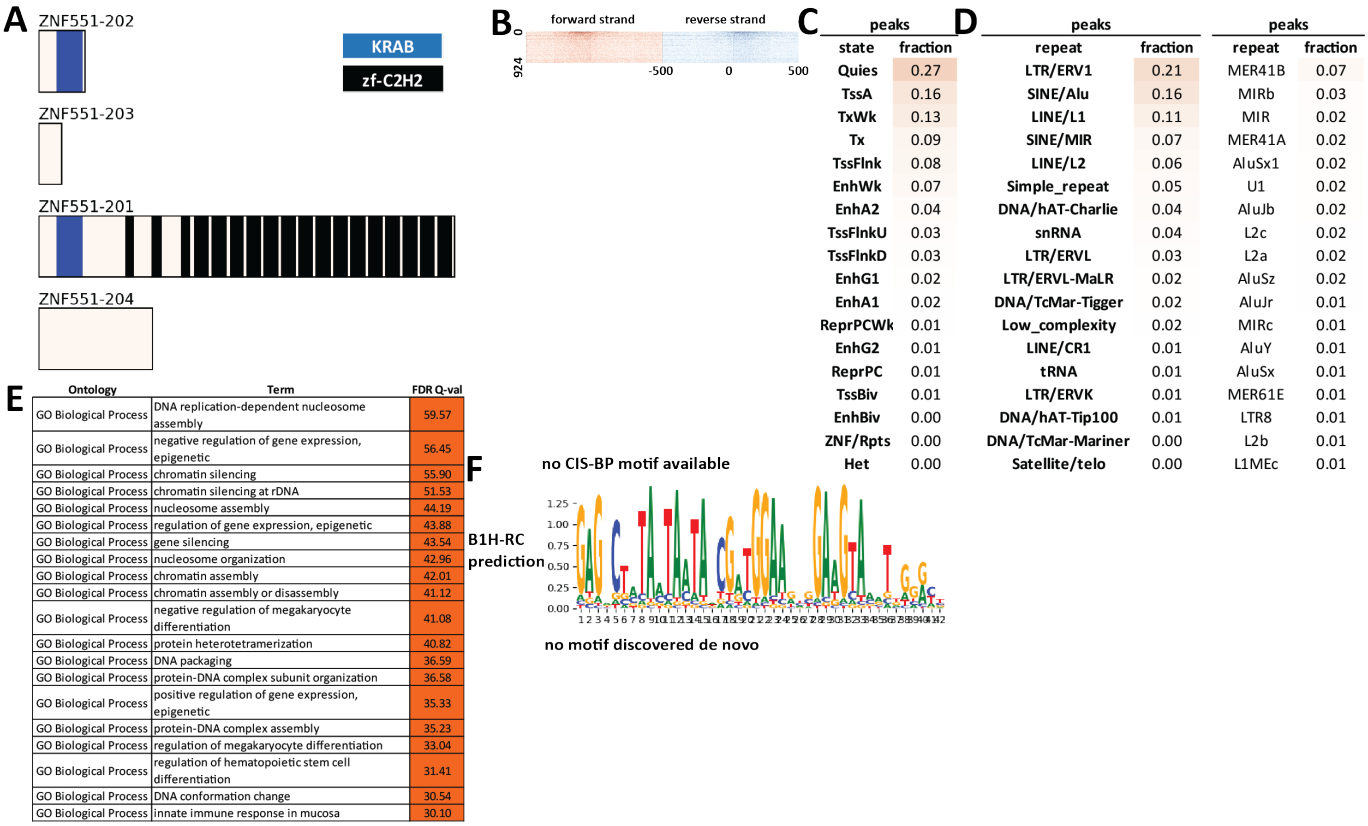

Supplementary Figure 1361: Properties and genomic distribution of motifs identified for the ZNF551 transcription factor in K562 (accession ENCSR451UQX).

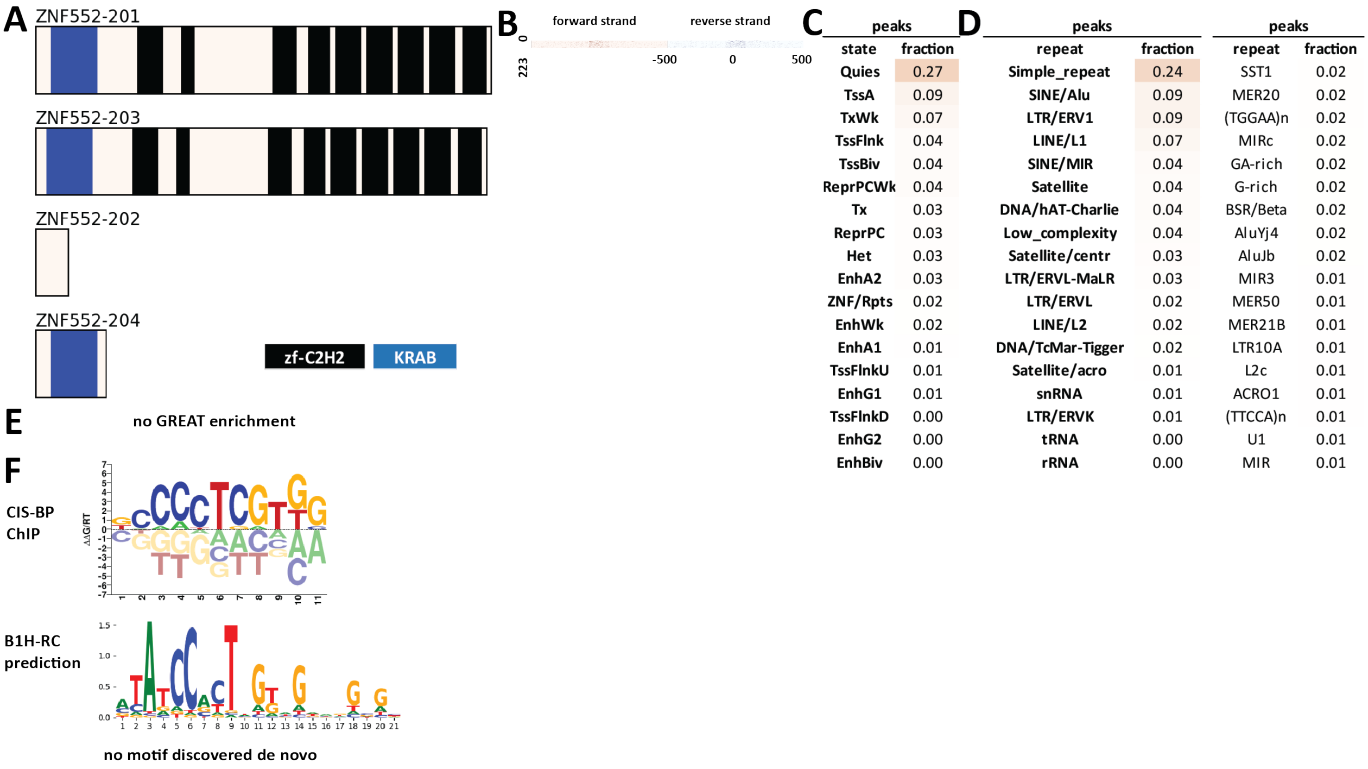

C

peaks	
state	fraction
Quies	0.27
TssA	0.09
TxWk	0.07
TssFlnk	0.04
TssBiv	0.04
ReprPCWk	0.04
Tx	0.03
ReprPC	0.03
Het	0.03
EnhA2	0.03
ZNF/Rpts	0.02
EnhWk	0.02
EnhA1	0.01
TssFlnkU	0.01
EnhG1	0.01
TssFlnkD	0.00
EnhG2	0.00
EnhBiv	0.00

D

peaks		peaks	
repeat	fraction	repeat	fraction
Simple_repeat	0.24	SST1	0.02
SINE/Alu	0.09	MER20	0.02
LTR/ERV1	0.09	(TGGAA)n	0.02
LINE/L1	0.07	MIRc	0.02
SINE/MIR	0.04	GA-rich	0.02
Satellite	0.04	G-rich	0.02
DNA/hAT-Charlie	0.04	BSR/Beta	0.02
Low_complexity	0.04	AluYj4	0.02
Satellite/centr	0.03	AluJb	0.02
LTR/ERVL-MaLR	0.03	MIR3	0.01
LTR/ERVL	0.02	MER50	0.01
LINE/L2	0.02	MER21B	0.01
DNA/TcMar-Tigger	0.02	LTR10A	0.01
Satellite/acro	0.01	L2c	0.01
snRNA	0.01	ACRO1	0.01
LTR/ERVK	0.01	(TTCCA)n	0.01
tRNA	0.00	U1	0.01
rRNA	0.00	MIR	0.01

Supplementary Figure 1362: Properties and genomic distribution of motifs identified for the ZNF552 transcription factor in HEK293 (accession ChipExo models).

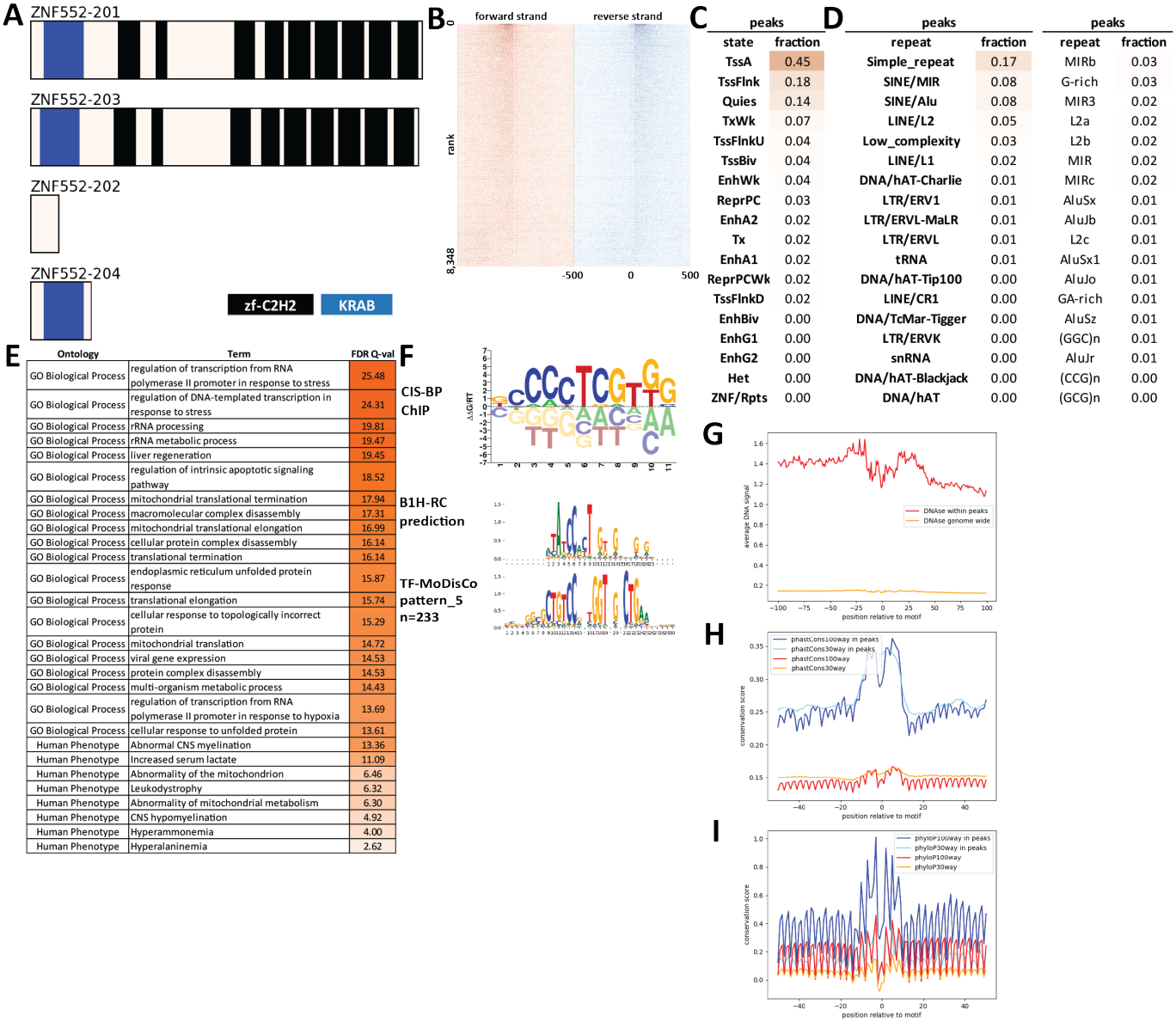

peaks	
state	fraction
TssA	0.45
TssFlnk	0.18
Quies	0.14
TxWk	0.07
TssFlnkU	0.04
TssBiv	0.04
EnhWk	0.04
ReprPC	0.03
EnhA2	0.02
Tx	0.02
EnhA1	0.02
ReprPCWk	0.02
TssFlnkD	0.02
EnhBiv	0.00
EnhG1	0.00
EnhG2	0.00
Het	0.00
ZNF/Rpts	0.00

peaks		peaks	
repeat	fraction	repeat	fraction
Simple_repeat	0.17	MIRb	0.03
SINE/MIR	0.08	G-rich	0.03
SINE/Alu	0.08	MIR3	0.02
LINE/L2	0.05	L2a	0.02
Low_complexity	0.03	L2b	0.02
LINE/L1	0.02	MIR	0.02
DNA/hAT-Charlie	0.01	MIRc	0.02
LTR/ERV1	0.01	AluSx	0.01
LTR/ERVL-MaLR	0.01	AluJb	0.01
LTR/ERVL	0.01	L2c	0.01
tRNA	0.01	AluSx1	0.01
DNA/hAT-Tip100	0.00	AluJo	0.01
LINE/CR1	0.00	GA-rich	0.01
DNA/TcMar-Tigger	0.00	AluSz	0.01
LTR/ERVK	0.00	(GGC)n	0.01
snRNA	0.00	AluJr	0.01
DNA/hAT-Blackjack	0.00	(CCG)n	0.00
DNA/hAT	0.00	(GCG)n	0.00

Ontology	Term	FDR Q-val
GO Biological Process	regulation of transcription from RNA polymerase II promoter in response to stress	25.48
GO Biological Process	regulation of DNA-templated transcription in response to stress	24.31
GO Biological Process	rRNA processing	19.81
GO Biological Process	rRNA metabolic process	19.47
GO Biological Process	liver regeneration	19.45
GO Biological Process	regulation of intrinsic apoptotic signaling pathway	18.52
GO Biological Process	mitochondrial translational termination	17.94
GO Biological Process	macromolecular complex disassembly	17.31
GO Biological Process	mitochondrial translational elongation	16.99
GO Biological Process	cellular protein complex disassembly	16.14
GO Biological Process	translational termination	16.14
GO Biological Process	endoplasmic reticulum unfolded protein response	15.87
GO Biological Process	translational elongation	15.74
GO Biological Process	cellular response to topologically incorrect protein	15.29
GO Biological Process	mitochondrial translation	14.72
GO Biological Process	viral gene expression	14.53
GO Biological Process	protein complex disassembly	14.53
GO Biological Process	multi-organism metabolic process	14.43
GO Biological Process	regulation of transcription from RNA polymerase II promoter in response to hypoxia	13.69
GO Biological Process	cellular response to unfolded protein	13.61
Human Phenotype	Abnormal CNS myelination	13.36
Human Phenotype	Increased serum lactate	11.09
Human Phenotype	Abnormality of the mitochondrion	6.46
Human Phenotype	Leukodystrophy	6.32
Human Phenotype	Abnormality of mitochondrial metabolism	6.30
Human Phenotype	CNS hypomyelination	4.92
Human Phenotype	Hyperammonemia	4.00
Human Phenotype	Hyperalaninemia	2.62

Supplementary Figure 1363: Properties and genomic distribution of motifs identified for the ZNF552 transcription factor in HepG2 (accession ENCSR448RAP).

TF-MoDisCO pattern_5 n=233, CWM

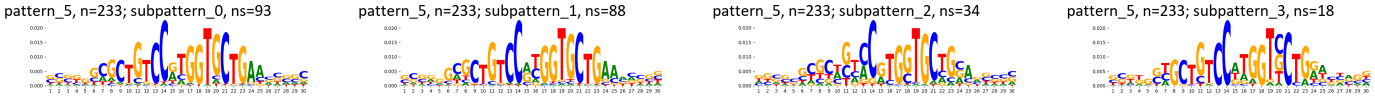

TF-MoDisCO pattern_5 n=233, PWM



Supplementary Figure 1364: TF-MoDisCO subpatterns for the ZNF552 transcription factor in HepG2 (accession ENCSR448RAP).

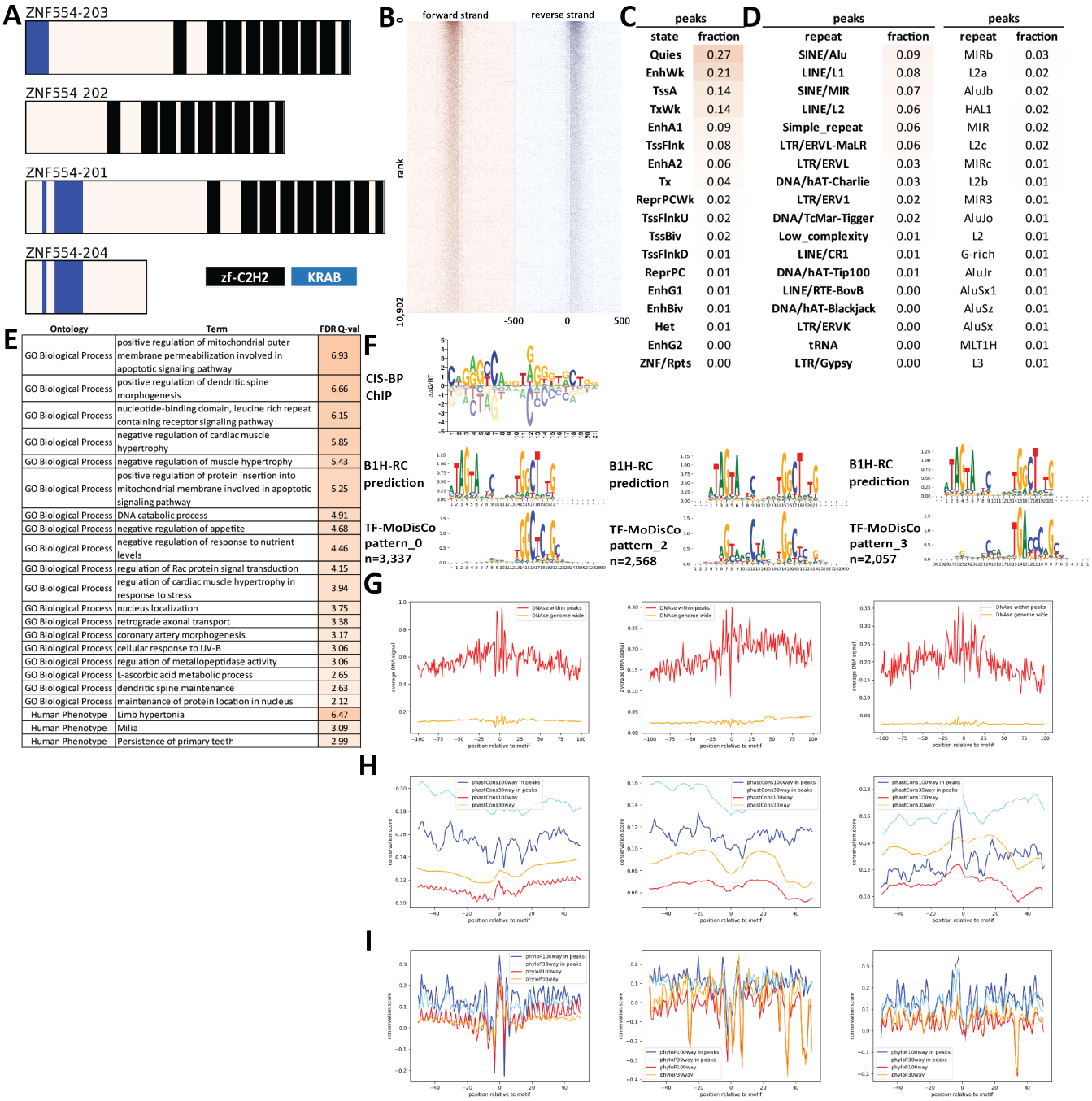

Supplementary Figure 1365: Properties and genomic distribution of motifs identified for the ZNF554 transcription factor in HEK293 (accession Hughes GR models).

TF-MoDisCO pattern_0 n=3337, CWM

pattern_0, n=3337; subpattern_0, ns=894

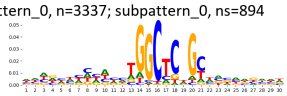

pattern_0, n=3337; subpattern_1, ns=820

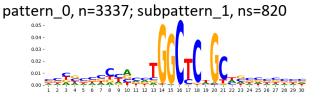

pattern_0, n=3337; subpattern_2, ns=760

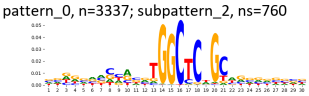

pattern_0, n=3337; subpattern_3, ns=690

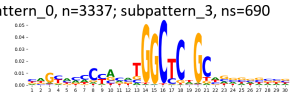

pattern_0, n=3337; subpattern_4, ns=61

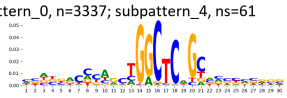

pattern_0, n=3337; subpattern_5, ns=53

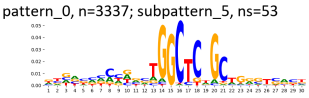

pattern_0, n=3337; subpattern_6, ns=45

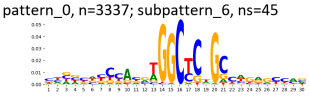

pattern_0, n=3337; subpattern_7, ns=11

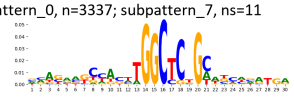

pattern_0, n=3337; subpattern_8, ns=3

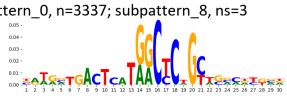

TF-MoDisCO pattern_0 n=3337, PWM

pattern_0, n=3337; subpattern_0, ns=894

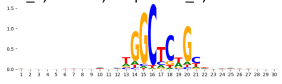

pattern_0, n=3337; subpattern_1, ns=820

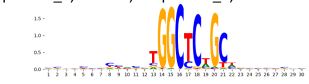

pattern_0, n=3337; subpattern_2, ns=760

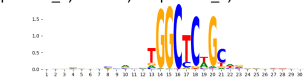

pattern_0, n=3337; subpattern_3, ns=690

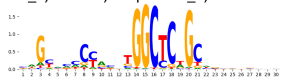

pattern_0, n=3337; subpattern_4, ns=61

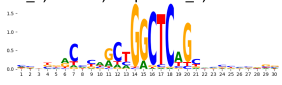

pattern_0, n=3337; subpattern_5, ns=53

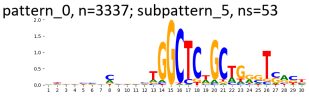

pattern_0, n=3337; subpattern_6, ns=45

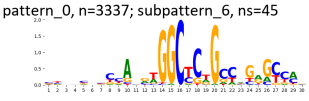

pattern_0, n=3337; subpattern_7, ns=11

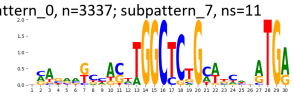

pattern_0, n=3337; subpattern_8, ns=3

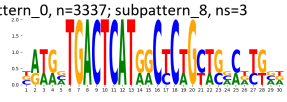

TF-MoDisCO pattern_2 n=2568, CWM

pattern_2, n=2568; subpattern_0, ns=689

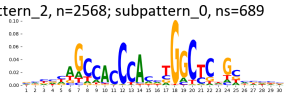

pattern_2, n=2568; subpattern_1, ns=657

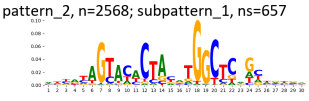

pattern_2, n=2568; subpattern_2, ns=590

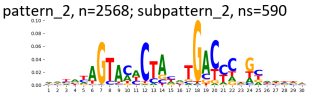

pattern_2, n=2568; subpattern_3, ns=514

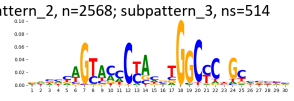

pattern_2, n=2568; subpattern_4, ns=53

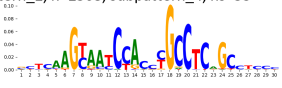

pattern_2, n=2568; subpattern_5, ns=27

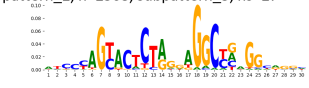

pattern_2, n=2568; subpattern_6, ns=20

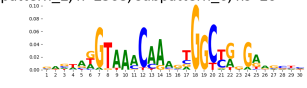

pattern_2, n=2568; subpattern_7, ns=18

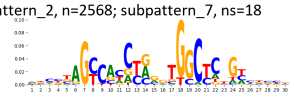

TF-MoDisCO pattern_2 n=2568, PWM

pattern_2, n=2568; subpattern_0, ns=689

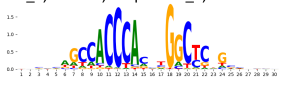

pattern_2, n=2568; subpattern_1, ns=657

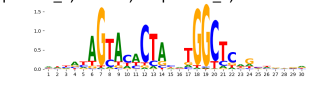

pattern_2, n=2568; subpattern_2, ns=590

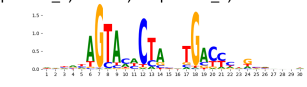

pattern_2, n=2568; subpattern_3, ns=514

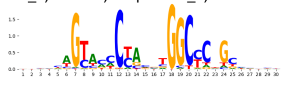

pattern_2, n=2568; subpattern_4, ns=53

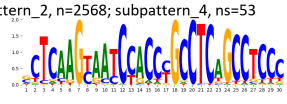

pattern_2, n=2568; subpattern_5, ns=27

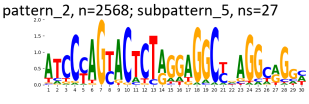

pattern_2, n=2568; subpattern_6, ns=20

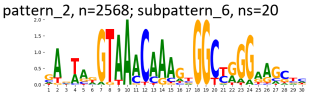

pattern_2, n=2568; subpattern_7, ns=18

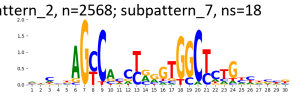

TF-MoDisCO pattern_3 n=2057, CWM

pattern_3, n=2057; subpattern_0, ns=560

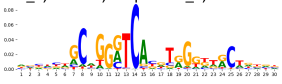

pattern_3, n=2057; subpattern_1, ns=538

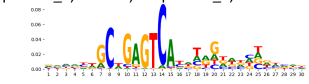

pattern_3, n=2057; subpattern_2, ns=421

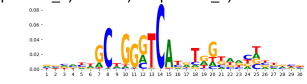

pattern_3, n=2057; subpattern_3, ns=348

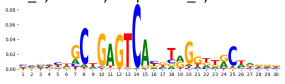

pattern_3, n=2057; subpattern_4, ns=187

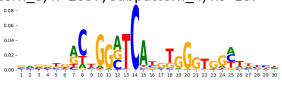

pattern_3, n=2057; subpattern_5, ns=3

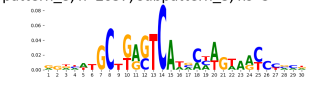

TF-MoDisCO pattern_3 n=2057, PWM

pattern_3, n=2057; subpattern_0, ns=560

pattern_3, n=2057; subpattern_1, ns=538

pattern_3, n=2057; subpattern_2, ns=421

pattern_3, n=2057; subpattern_3, ns=348

pattern_3, n=2057; subpattern_4, ns=187

pattern_3, n=2057; subpattern_5, ns=3

Supplementary Figure 1366: TF-MoDisCO subpatterns for the ZNF554 transcription factor in HEK293 (accession Hughes GR models).

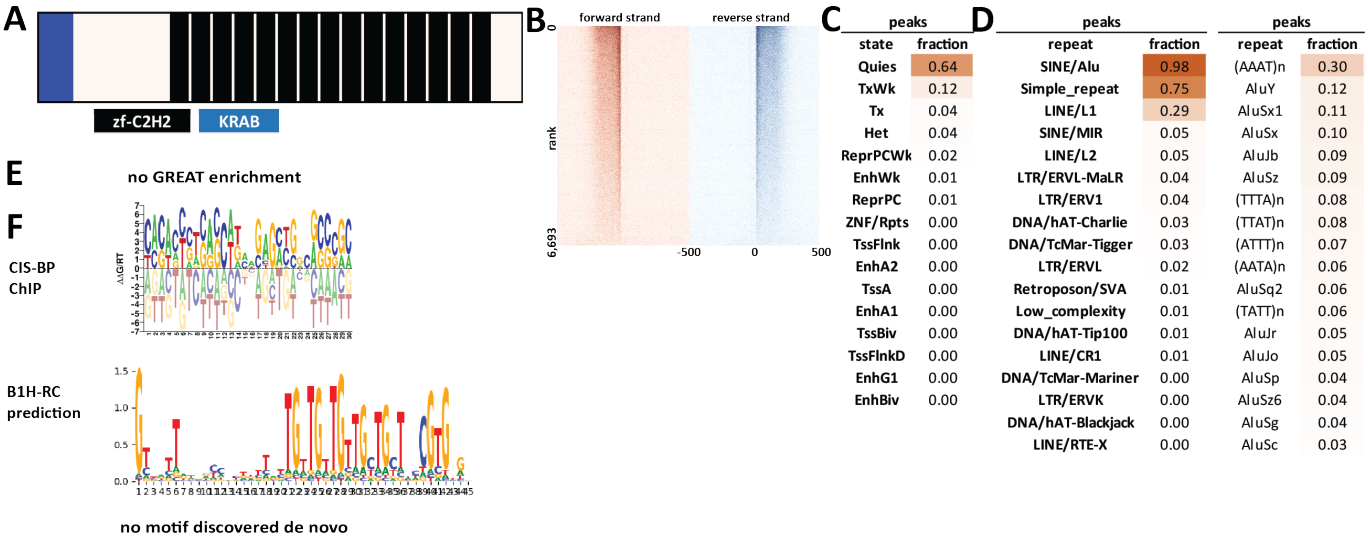

Supplementary Figure 1367: Properties and genomic distribution of motifs identified for the ZNF555 transcription factor in HEK293 (accession ENCSR767XSF).

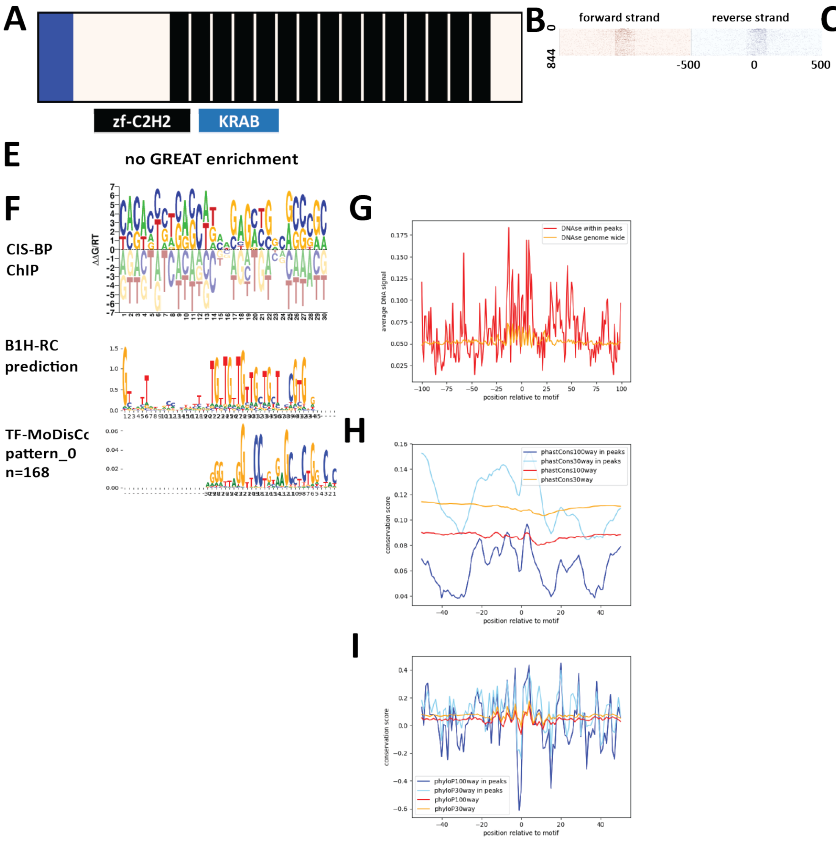

C

peaks	
state	fraction
Quies	0.39
TssA	0.17
TxWk	0.09
TssFlnk	0.08
Tx	0.04
ReprPCWk	0.04
ReprPC	0.03
EnhWk	0.03
TssBiv	0.03
EnhA2	0.02
Het	0.01
TssFlnkU	0.01
EnhA1	0.01
TssFlnkD	0.01
ZNF/Rpts	0.00
EnhG1	0.00
EnhG2	0.00

D

peaks		peaks	
repeat	fraction	repeat	fraction
Simple_repeat	0.29	Tigger17a	0.19
DNA/TcMar-Tigger	0.23	L2a	0.03
SINE/Alu	0.16	(GT)n	0.02
LINE/L1	0.11	AluY	0.02
LINE/L2	0.06	(CA)n	0.02
SINE/MIR	0.04	L2c	0.02
DNA/hAT-Charlie	0.03	AluSx1	0.02
LTR/ERVL	0.02	AluYj4	0.02
LTR/ERV1	0.02	AluSz	0.02
Low_complexity	0.02	AluJb	0.02
Satellite	0.02	TAR1	0.01
LTR/ERVL-MaLR	0.02	MIR	0.01
Satellite/telo	0.01	AluSx	0.01
snRNA	0.01	MIRb	0.01
Satellite/centr	0.01	G-rich	0.01
DNA/hAT-Tip100	0.01	L2	0.01
Satellite/acro	0.01	(TG)n	0.01
rRNA	0.00	L2b	0.01

Supplementary Figure 1368: Properties and genomic distribution of motifs identified for the ZNF555 transcription factor in HEK293 (accession ChipExo models).

TF-MoDisCO pattern_0 n=168, CWM

pattern_0, n=168; subpattern_0, ns=84

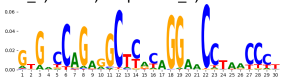

pattern_0, n=168; subpattern_1, ns=61

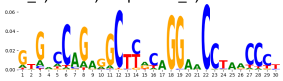

pattern_0, n=168; subpattern_2, ns=23

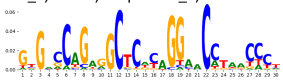

TF-MoDisCO pattern_0 n=168, PWM

pattern_0, n=168; subpattern_0, ns=84

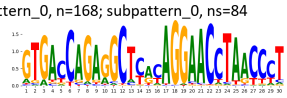

pattern_0, n=168; subpattern_1, ns=61

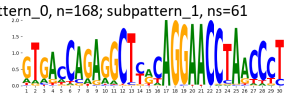

pattern_0, n=168; subpattern_2, ns=23

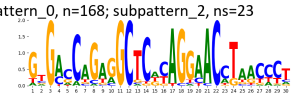

Supplementary Figure 1369: TF-MoDisCO subpatterns for the ZNF555 transcription factor in HEK293 (accession ChipExo models).

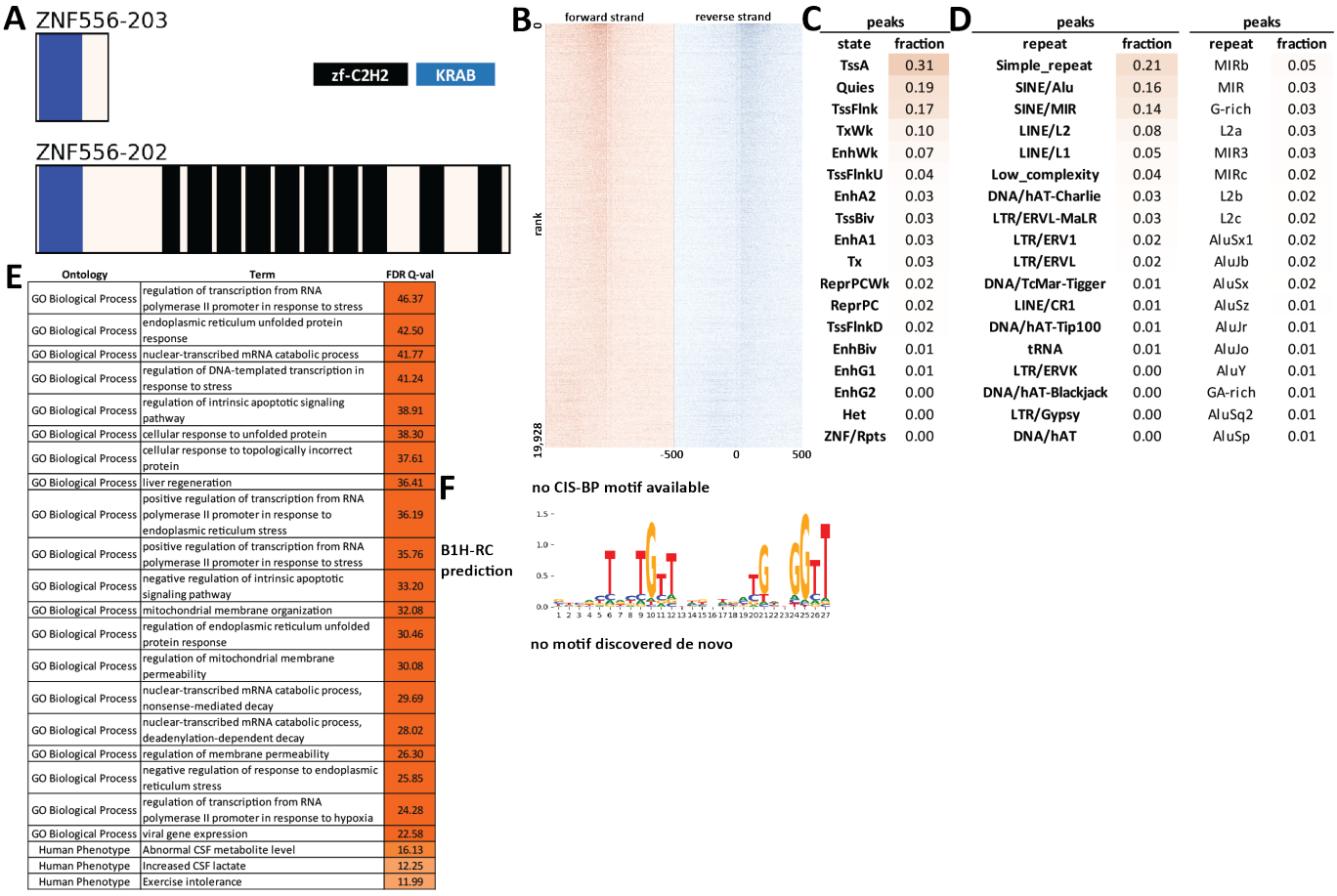

C

peaks	
state	fraction
TssA	0.31
Quies	0.19
TssFlnk	0.17
TxWk	0.10
EnhWk	0.07
TssFlnkU	0.04
EnhA2	0.03
TssBiv	0.03
EnhA1	0.03
Tx	0.03
ReprPCWk	0.02
ReprPC	0.02
TssFlnkD	0.02
EnhBiv	0.01
EnhG1	0.01
EnhG2	0.00
Het	0.00
ZNF/Rpts	0.00

D

peaks		peaks	
repeat	fraction	repeat	fraction
Simple_repeat	0.21	MIRb	0.05
SINE/Alu	0.16	MIR	0.03
SINE/MIR	0.14	G-rich	0.03
LINE/L2	0.08	L2a	0.03
LINE/L1	0.05	MIR3	0.03
Low_complexity	0.04	MIRc	0.02
DNA/hAT-Charlie	0.03	L2b	0.02
LTR/ERVL-MaLR	0.03	L2c	0.02
LTR/ERV1	0.02	AluSx1	0.02
LTR/ERVL	0.02	AluJb	0.02
DNA/TcMar-Tigger	0.01	AluSx	0.02
LINE/CR1	0.01	AluSz	0.01
DNA/hAT-Tip100	0.01	AluJr	0.01
tRNA	0.01	AluJo	0.01
LTR/ERVK	0.00	AluY	0.01
DNA/hAT-Blackjack	0.00	GA-rich	0.01
LTR/Gypsy	0.00	AluSq2	0.01
DNA/hAT	0.00	AluSp	0.01

E

Ontology	Term	FDR Q-val
GO Biological Process	regulation of transcription from RNA polymerase II promoter in response to stress	46.37
GO Biological Process	endoplasmic reticulum unfolded protein response	42.50
GO Biological Process	nuclear-transcribed mRNA catabolic process	41.77
GO Biological Process	regulation of DNA-templated transcription in response to stress	41.24
GO Biological Process	regulation of intrinsic apoptotic signaling pathway	38.91
GO Biological Process	cellular response to unfolded protein	38.30
GO Biological Process	cellular response to topologically incorrect protein	37.61
GO Biological Process	liver regeneration	36.41
GO Biological Process	positive regulation of transcription from RNA polymerase II promoter in response to endoplasmic reticulum stress	36.19
GO Biological Process	positive regulation of transcription from RNA polymerase II promoter in response to stress	35.76
GO Biological Process	negative regulation of intrinsic apoptotic signaling pathway	33.20
GO Biological Process	mitochondrial membrane organization	32.08
GO Biological Process	regulation of endoplasmic reticulum unfolded protein response	30.46
GO Biological Process	regulation of mitochondrial membrane permeability	30.08
GO Biological Process	nuclear-transcribed mRNA catabolic process, nonsense-mediated decay	29.69
GO Biological Process	nuclear-transcribed mRNA catabolic process, deadenylation-dependent decay	28.02
GO Biological Process	regulation of membrane permeability	26.30
GO Biological Process	negative regulation of response to endoplasmic reticulum stress	25.85
GO Biological Process	regulation of transcription from RNA polymerase II promoter in response to hypoxia	24.28
GO Biological Process	viral gene expression	22.58
Human Phenotype	Abnormal CSF metabolite level	16.13
Human Phenotype	Increased CSF lactate	12.25
Human Phenotype	Exercise intolerance	11.99

Supplementary Figure 1370: Properties and genomic distribution of motifs identified for the ZNF556 transcription factor in HepG2 (accession ENCSR644WQN).

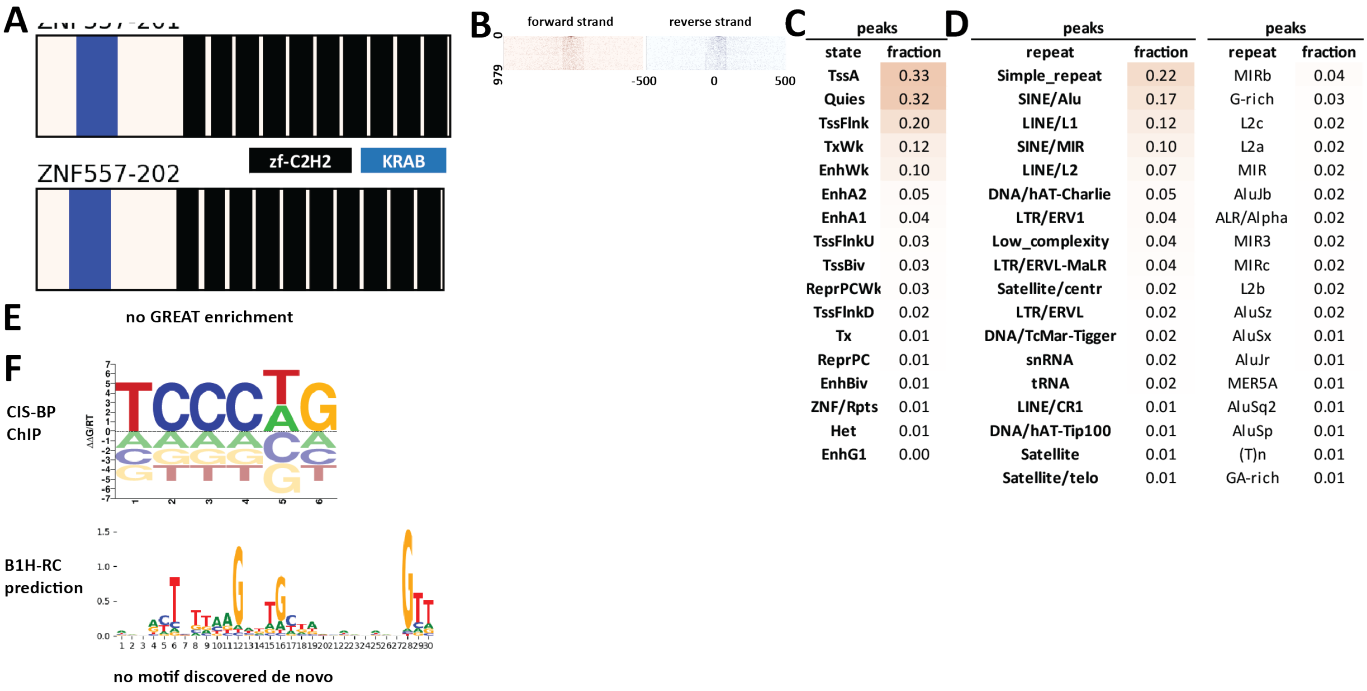

peaks	
state	fraction
TssA	0.33
Quies	0.32
TssFlnk	0.20
TxWk	0.12
EnhWk	0.10
EnhA2	0.05
EnhA1	0.04
TssFlnkU	0.03
TssBiv	0.03
ReprPCWk	0.03
TssFlnkD	0.02
Tx	0.01
ReprPC	0.01
EnhBiv	0.01
ZNF/Rpts	0.01
Het	0.01
EnhG1	0.00

peaks		peaks	
repeat	fraction	repeat	fraction
Simple_repeat	0.22	MIRb	0.04
SINE/Alu	0.17	G-rich	0.03
LINE/L1	0.12	L2c	0.02
SINE/MIR	0.10	L2a	0.02
LINE/L2	0.07	MIR	0.02
DNA/hAT-Charlie	0.05	AluJb	0.02
LTR/ERV1	0.04	ALR/Alpha	0.02
Low_complexity	0.04	MIR3	0.02
LTR/ERVL-MaLR	0.04	MIRc	0.02
Satellite/centr	0.02	L2b	0.02
LTR/ERVL	0.02	AluSz	0.02
DNA/TcMar-Tigger	0.02	AluSx	0.01
snRNA	0.02	AluJr	0.01
tRNA	0.02	MER5A	0.01
LINE/CR1	0.01	AluSq2	0.01
DNA/hAT-Tip100	0.01	AluSp	0.01
Satellite	0.01	(T)n	0.01
Satellite/telo	0.01	GA-rich	0.01

Supplementary Figure 1371: Properties and genomic distribution of motifs identified for the ZNF557 transcription factor in HEK293 (accession ChipExo models).

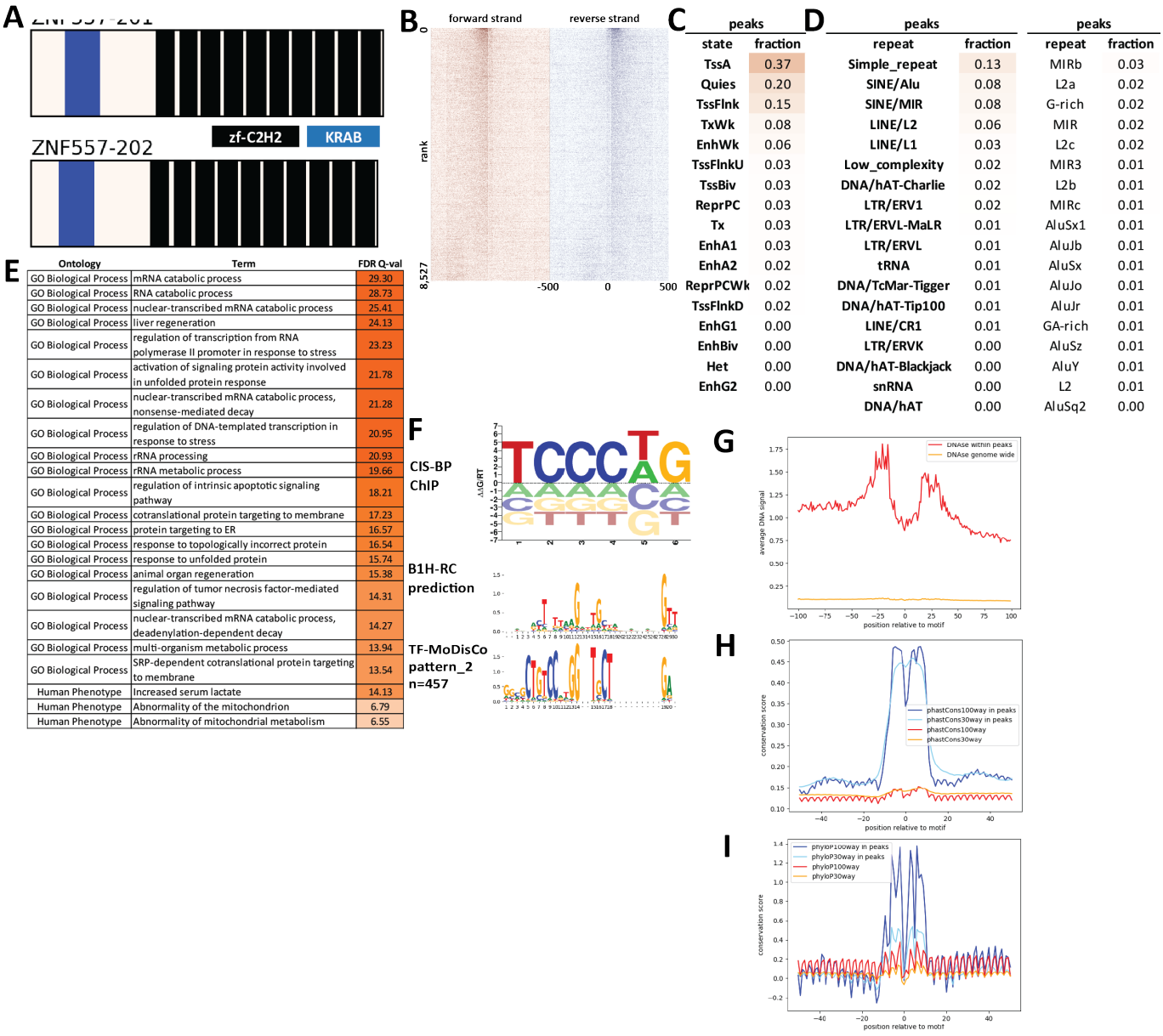

Supplementary Figure 1372: Properties and genomic distribution of motifs identified for the ZNF557 transcription factor in HepG2 (accession ENCSR325VYA).

TF-MoDisCO pattern_2 n=457, CWM

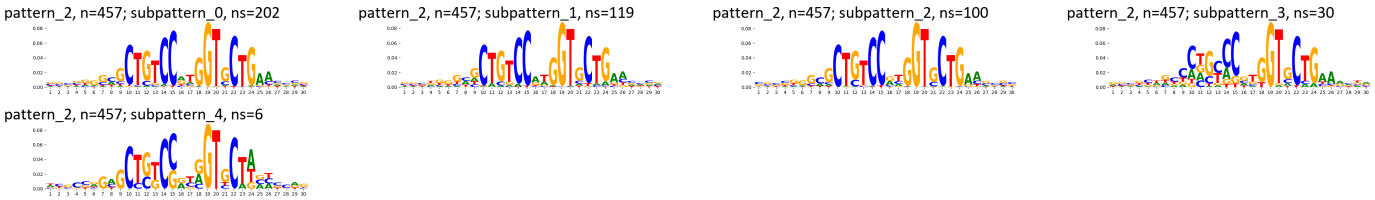

TF-MoDisCO pattern_2 n=457, PWM

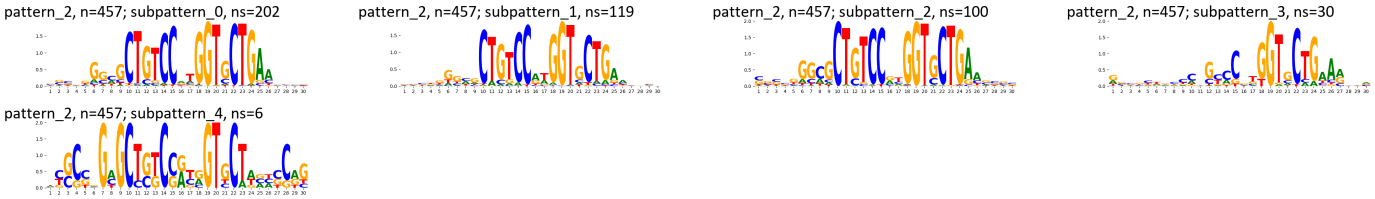

Supplementary Figure 1373: TF-MoDisCO subpatterns for the ZNF557 transcription factor in HepG2 (accession ENCSR325VYA).

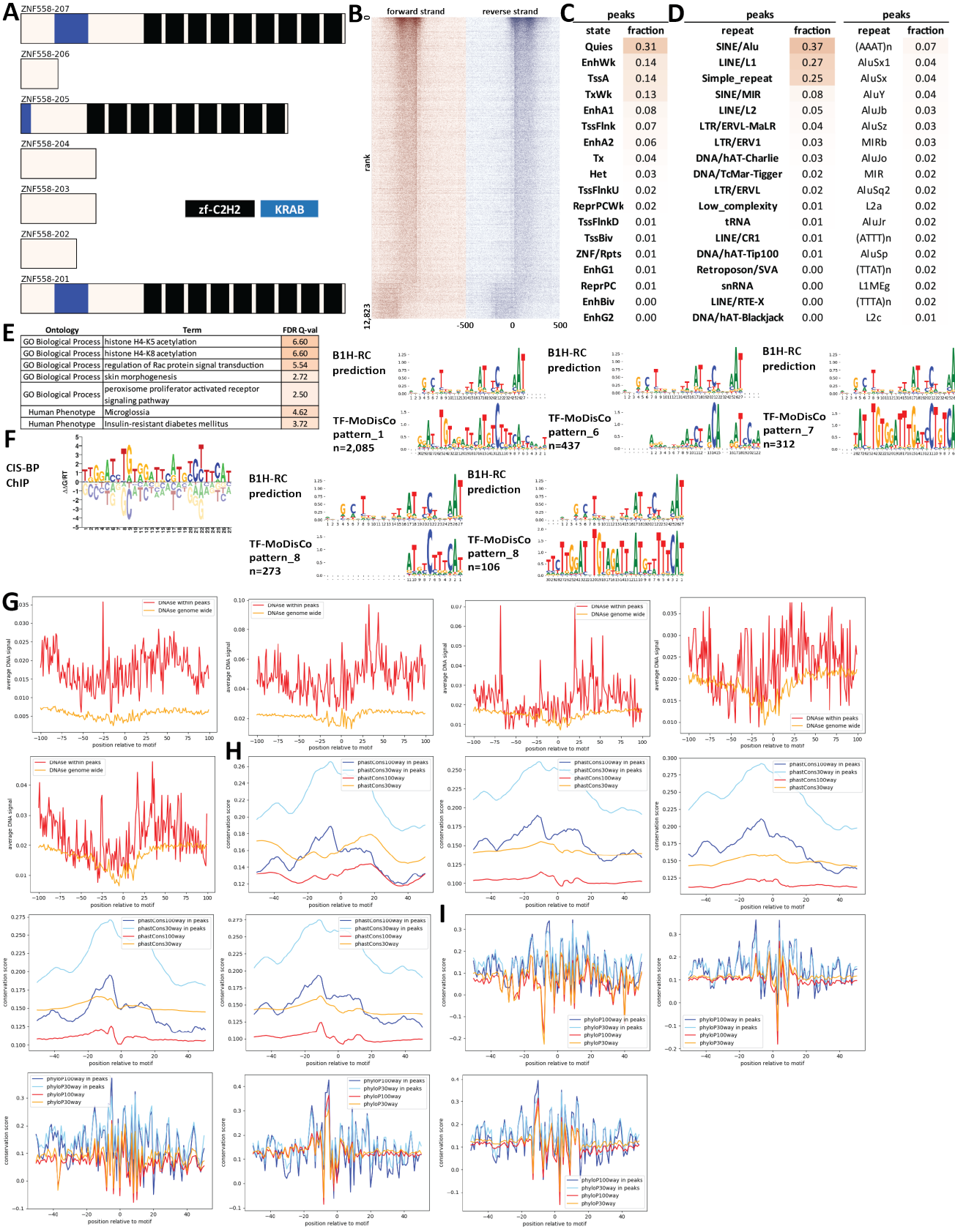

Supplementary Figure 1374: Properties and genomic distribution of motifs identified for the ZNF558 transcription factor in HEK293 (accession ENCSR447ZTA).

TF-MoDisCO pattern_1 n=2085, CWM

pattern_1, n=2085; subpattern_0, ns=461

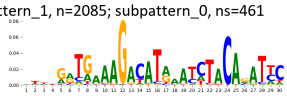

pattern_1, n=2085; subpattern_1, ns=430

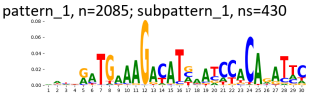

pattern_1, n=2085; subpattern_2, ns=317

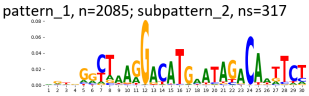

pattern_1, n=2085; subpattern_3, ns=316

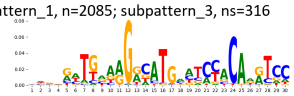

pattern_1, n=2085; subpattern_4, ns=236

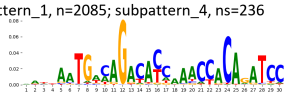

pattern_1, n=2085; subpattern_5, ns=219

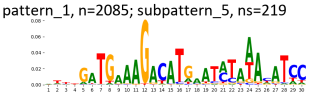

pattern_1, n=2085; subpattern_6, ns=106

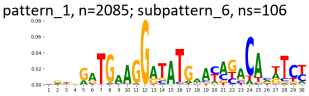

TF-MoDisCO pattern_1 n=2085, PWM

pattern_1, n=2085; subpattern_0, ns=461

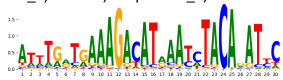

pattern_1, n=2085; subpattern_1, ns=430

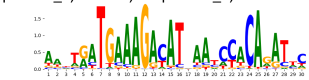

pattern_1, n=2085; subpattern_2, ns=317

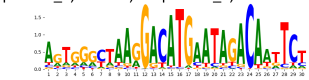

pattern_1, n=2085; subpattern_3, ns=316

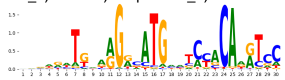

pattern_1, n=2085; subpattern_4, ns=236

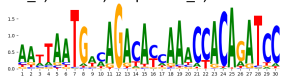

pattern_1, n=2085; subpattern_5, ns=219

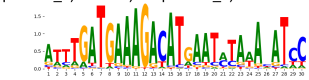

pattern_1, n=2085; subpattern_6, ns=106

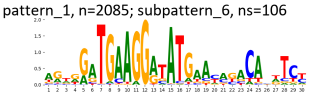

TF-MoDisCO pattern_10 n=106, CWM

pattern_10, n=106; subpattern_0, ns=41

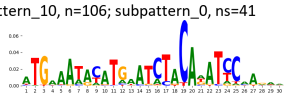

pattern_10, n=106; subpattern_1, ns=30

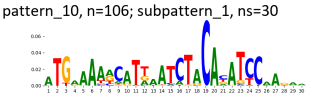

pattern_10, n=106; subpattern_2, ns=18

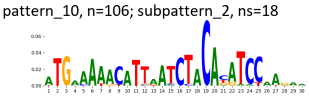

pattern_10, n=106; subpattern_3, ns=17

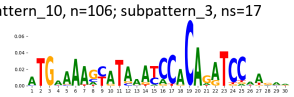

TF-MoDisCO pattern_10 n=106, PWM

pattern_10, n=106; subpattern_0, ns=41

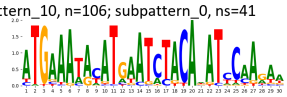

pattern_10, n=106; subpattern_1, ns=30

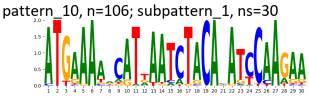

pattern_10, n=106; subpattern_2, ns=18

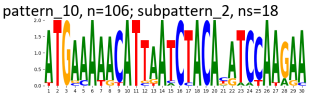

pattern_10, n=106; subpattern_3, ns=17

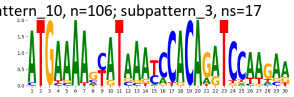

TF-MoDisCO pattern_6 n=437, CWM

pattern_6, n=437; subpattern_0, ns=70

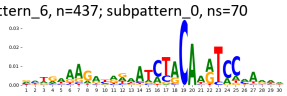

pattern_6, n=437; subpattern_1, ns=70

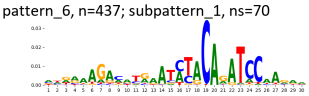

pattern_6, n=437; subpattern_2, ns=67

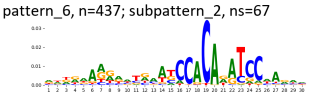

pattern_6, n=437; subpattern_3, ns=65

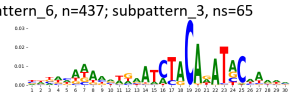

pattern_6, n=437; subpattern_4, ns=63

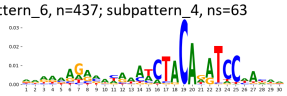

pattern_6, n=437; subpattern_5, ns=50

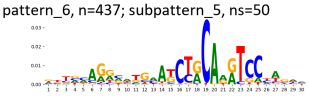

pattern_6, n=437; subpattern_6, ns=44

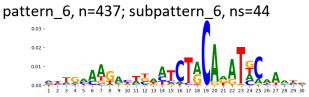

pattern_6, n=437; subpattern_7, ns=5

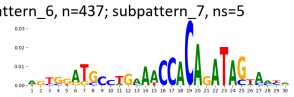

pattern_6, n=437; subpattern_8, ns=3

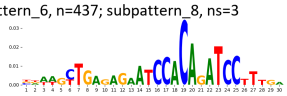

TF-MoDisCO pattern_6 n=437, PWM

pattern_6, n=437; subpattern_0, ns=70

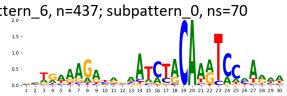

pattern_6, n=437; subpattern_1, ns=70

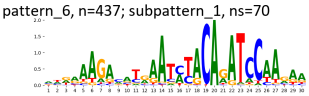

pattern_6, n=437; subpattern_2, ns=67

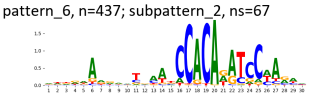

pattern_6, n=437; subpattern_3, ns=65

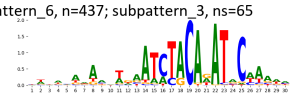

pattern_6, n=437; subpattern_4, ns=63

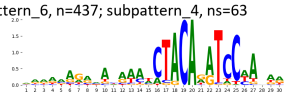

pattern_6, n=437; subpattern_5, ns=50

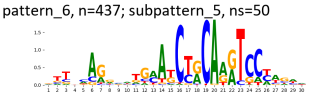

pattern_6, n=437; subpattern_6, ns=44

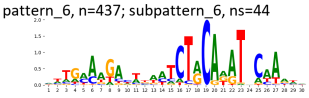

pattern_6, n=437; subpattern_7, ns=5

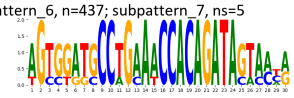

pattern_6, n=437; subpattern_8, ns=3

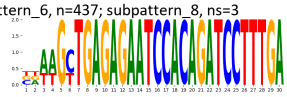

TF-MoDisCO pattern_7 n=312, CWM

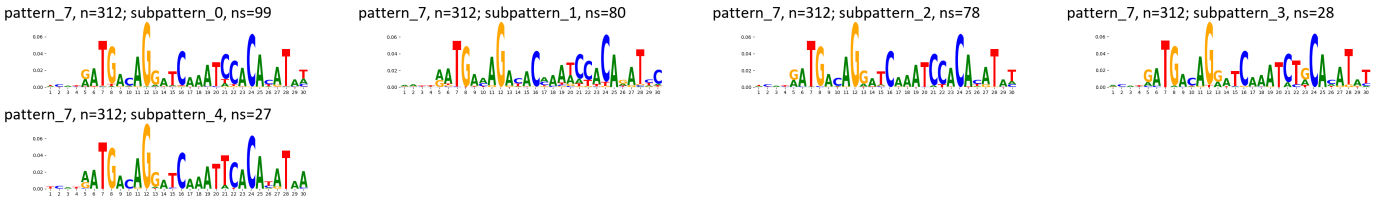

TF-MoDisCO pattern_7 n=312, PWM

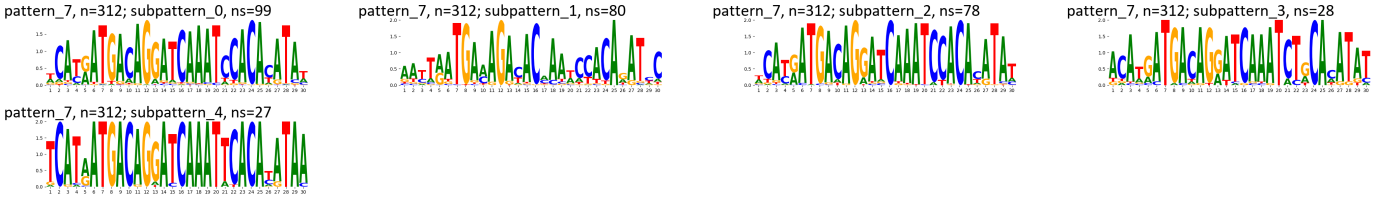

TF-MoDisCO pattern_8 n=273, CWM

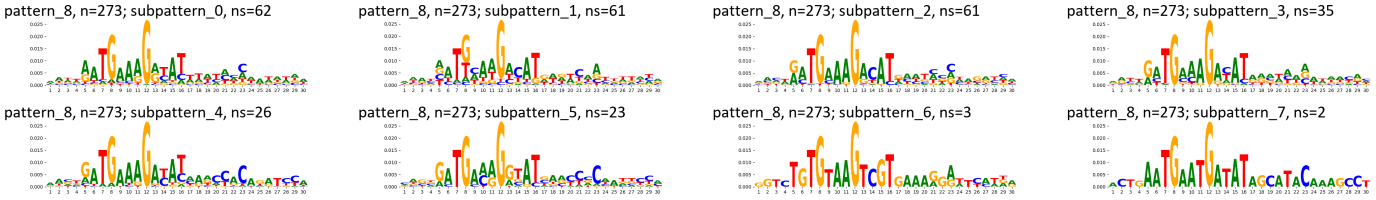

TF-MoDisCO pattern_8 n=273, PWM

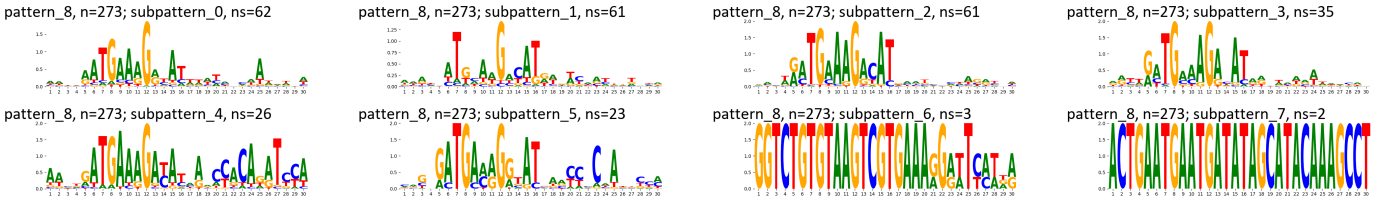

Supplementary Figure 1375: TF-MoDisCO subpatterns for the ZNF558 transcription factor in HEK293 (accession ENCSR447ZTA).

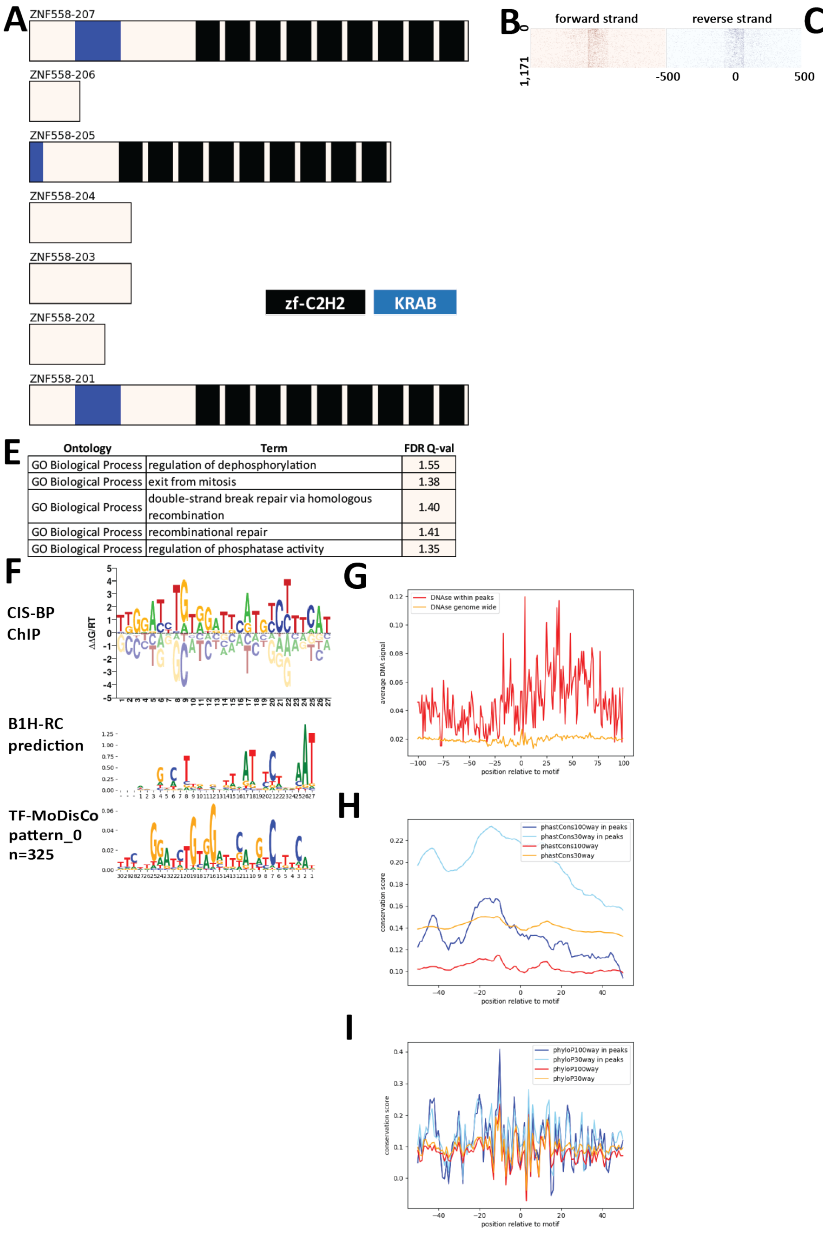

C

peaks	
state	fraction
Quies	0.44
TssA	0.16
TxWk	0.14
TssFlnk	0.08
Tx	0.06
Het	0.05
EnhWk	0.05
EnhA2	0.03
ReprPCWk	0.02
EnhA1	0.02
ZNF/Rpts	0.02
TssBiv	0.01
TssFlnkU	0.01
ReprPC	0.01
TssFlnkD	0.01
EnhG1	0.01
EnhBiv	0.00

D

peaks		peaks	
repeat	fraction	repeat	fraction
LINE/L1	0.41	L1MEg	0.05
SINE/Alu	0.21	L1M4	0.04
Simple_repeat	0.15	L2a	0.03
LTR/ERVL-MaLR	0.09	MLT1C	0.03
LTR/ERV1	0.07	L1MCa	0.03
SINE/MIR	0.06	AluJb	0.03
LINE/L2	0.06	L1MEf	0.02
Low_complexity	0.03	AluSx	0.02
LTR/ERVL	0.03	MIRb	0.02
DNA/hAT-Charlie	0.03	G-rich	0.02
DNA/TcMar-Tigger	0.02	AluY	0.02
Satellite/centr	0.01	AluSz	0.02
Satellite	0.01	AluSx1	0.02
LINE/CR1	0.00	L1MEd	0.02
rRNA	0.00	L1MEc	0.02
Satellite/acro	0.00	AluJr	0.02
Retroposon/SVA	0.00	MIRc	0.02
DNA/hAT-Tip100	0.00	AluJo	0.02

E

Ontology	Term	FDR Q-val
GO Biological Process	regulation of dephosphorylation	1.55
GO Biological Process	exit from mitosis	1.38
GO Biological Process	double-strand break repair via homologous recombination	1.40
GO Biological Process	recombinational repair	1.41
GO Biological Process	regulation of phosphatase activity	1.35

Supplementary Figure 1376: Properties and genomic distribution of motifs identified for the ZNF558 transcription factor in HEK293 (accession ChipExo models).

TF-MoDisCO pattern_0 n=325, CWM

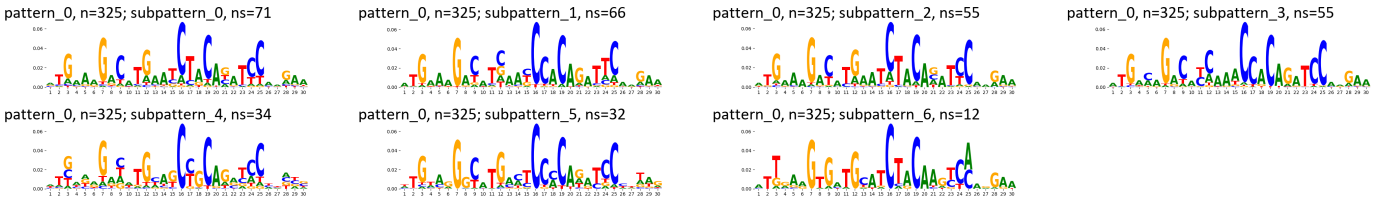

TF-MoDisCO pattern_0 n=325, PWM

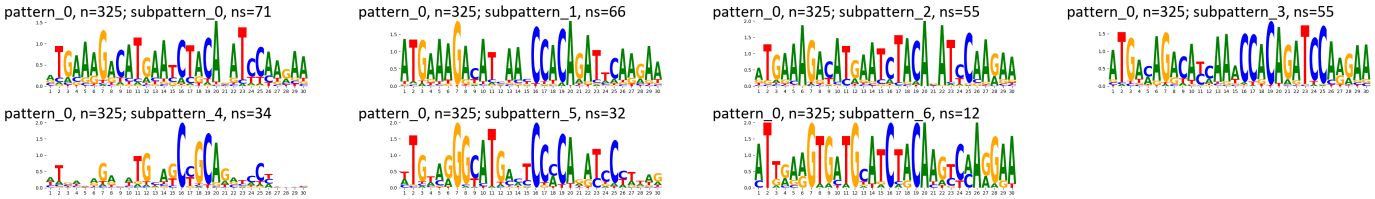

Supplementary Figure 1377: TF-MoDisCO subpatterns for the ZNF558 transcription factor in HEK293 (accession ChipExo models).

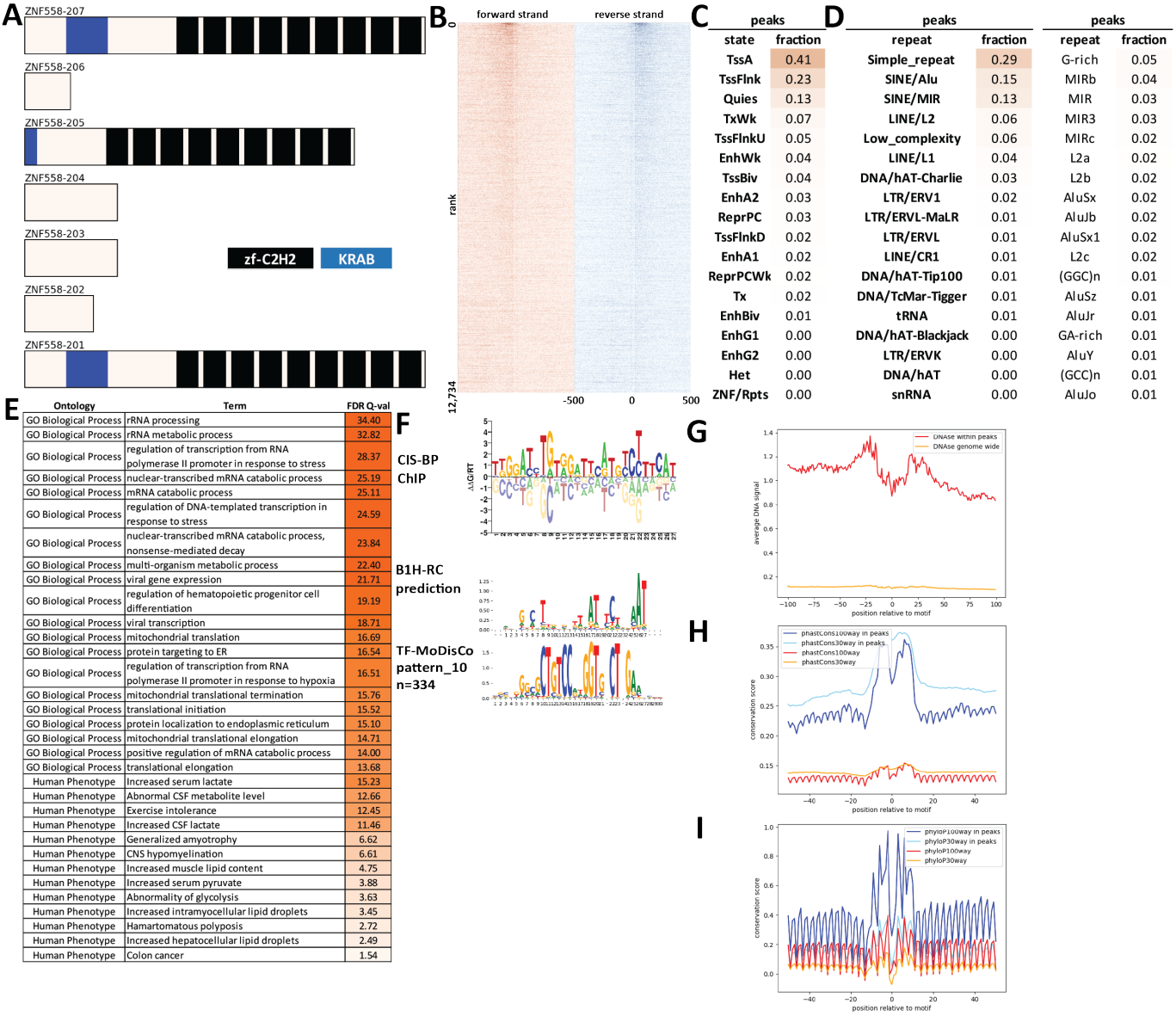

peaks	
state	fraction
TssA	0.41
TssFlnk	0.23
Quies	0.13
TxWk	0.07
TssFlnkU	0.05
EnhWk	0.04
TssBiv	0.04
EnhA2	0.03
ReprPC	0.03
TssFlnkD	0.02
EnhA1	0.02
ReprPCWk	0.02
Tx	0.02
EnhBiv	0.01
EnhG1	0.00
EnhG2	0.00
Het	0.00
ZNF/Rpts	0.00

peaks	
repeat	fraction
Simple_repeat	0.29
SINE/Alu	0.15
SINE/MIR	0.13
LINE/L2	0.06
Low_complexity	0.06
LINE/L1	0.04
DNA/hAT-Charlie	0.03
LTR/ERV1	0.02
LTR/ERVL-MaLR	0.01
LTR/ERVL	0.01
LINE/CR1	0.01
DNA/hAT-Tip100	0.01
DNA/TcMar-Tigger	0.01
tRNA	0.01
DNA/hAT-Blackjack	0.00
LTR/ERVK	0.00
DNA/hAT	0.00
snRNA	0.00

peaks	
repeat	fraction
G-rich	0.05
MIRb	0.04
MIR	0.03
MIR3	0.03
MIRc	0.02
L2a	0.02
L2b	0.02
AluSx	0.02
AluJb	0.02
AluSx1	0.02
L2c	0.02
(GGC)n	0.01
AluSz	0.01
AluJr	0.01
GA-rich	0.01
AluY	0.01
(GCC)n	0.01
AluJo	0.01

Ontology	Term	FDR Q-val
GO Biological Process	rRNA processing	34.40
GO Biological Process	rRNA metabolic process	32.82
GO Biological Process	regulation of transcription from RNA polymerase II promoter in response to stress	28.37
GO Biological Process	nuclear-transcribed mRNA catabolic process	25.19
GO Biological Process	mRNA catabolic process	25.11
GO Biological Process	regulation of DNA-templated transcription in response to stress	24.59
GO Biological Process	nuclear-transcribed mRNA catabolic process, nonsense-mediated decay	23.84
GO Biological Process	multi-organism metabolic process	22.40
GO Biological Process	viral gene expression	21.71
GO Biological Process	regulation of hematopoietic progenitor cell differentiation	19.19
GO Biological Process	viral transcription	18.71
GO Biological Process	mitochondrial translation	16.69
GO Biological Process	protein targeting to ER	16.54
GO Biological Process	regulation of transcription from RNA polymerase II promoter in response to hypoxia	16.51
GO Biological Process	mitochondrial translational termination	15.76
GO Biological Process	translational initiation	15.52
GO Biological Process	protein localization to endoplasmic reticulum	15.10
GO Biological Process	mitochondrial translational elongation	14.71
GO Biological Process	positive regulation of mRNA catabolic process	14.00
GO Biological Process	translational elongation	13.68
Human Phenotype	Increased serum lactate	15.23
Human Phenotype	Abnormal CSF metabolite level	12.66
Human Phenotype	Exercise intolerance	12.45
Human Phenotype	Increased CSF lactate	11.46
Human Phenotype	Generalized amyotrophy	6.62
Human Phenotype	CNS hypomyelination	6.61
Human Phenotype	Increased muscle lipid content	4.75
Human Phenotype	Increased serum pyruvate	3.88
Human Phenotype	Abnormality of glycolysis	3.63
Human Phenotype	Increased intramyocellular lipid droplets	3.45
Human Phenotype	Hamartomatous polyposis	2.72
Human Phenotype	Increased hepatocellular lipid droplets	2.49
Human Phenotype	Colon cancer	1.54

Supplementary Figure 1378: Properties and genomic distribution of motifs identified for the ZNF558 transcription factor in HepG2 (accession ENCSR154YWK).

TF-MoDisCO pattern_10 n=324, CWM

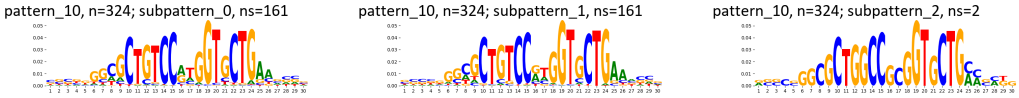

TF-MoDisCO pattern_10 n=324, PWM

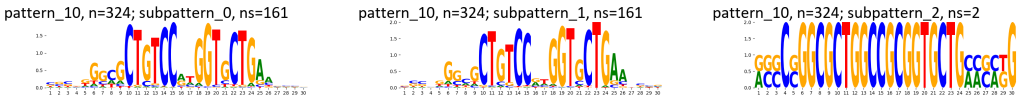

Supplementary Figure 1379: TF-MoDisCO subpatterns for the ZNF558 transcription factor in HepG2 (accession ENCSR154YWK).

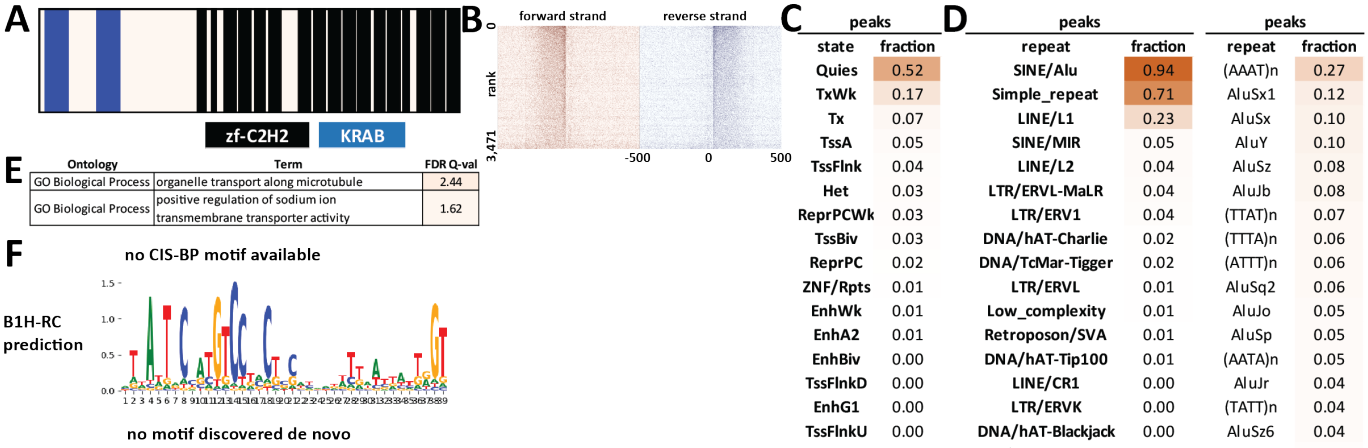

Supplementary Figure 1380: Properties and genomic distribution of motifs identified for the ZNF560 transcription factor in HEK293 (accession ENCSR538RDA).

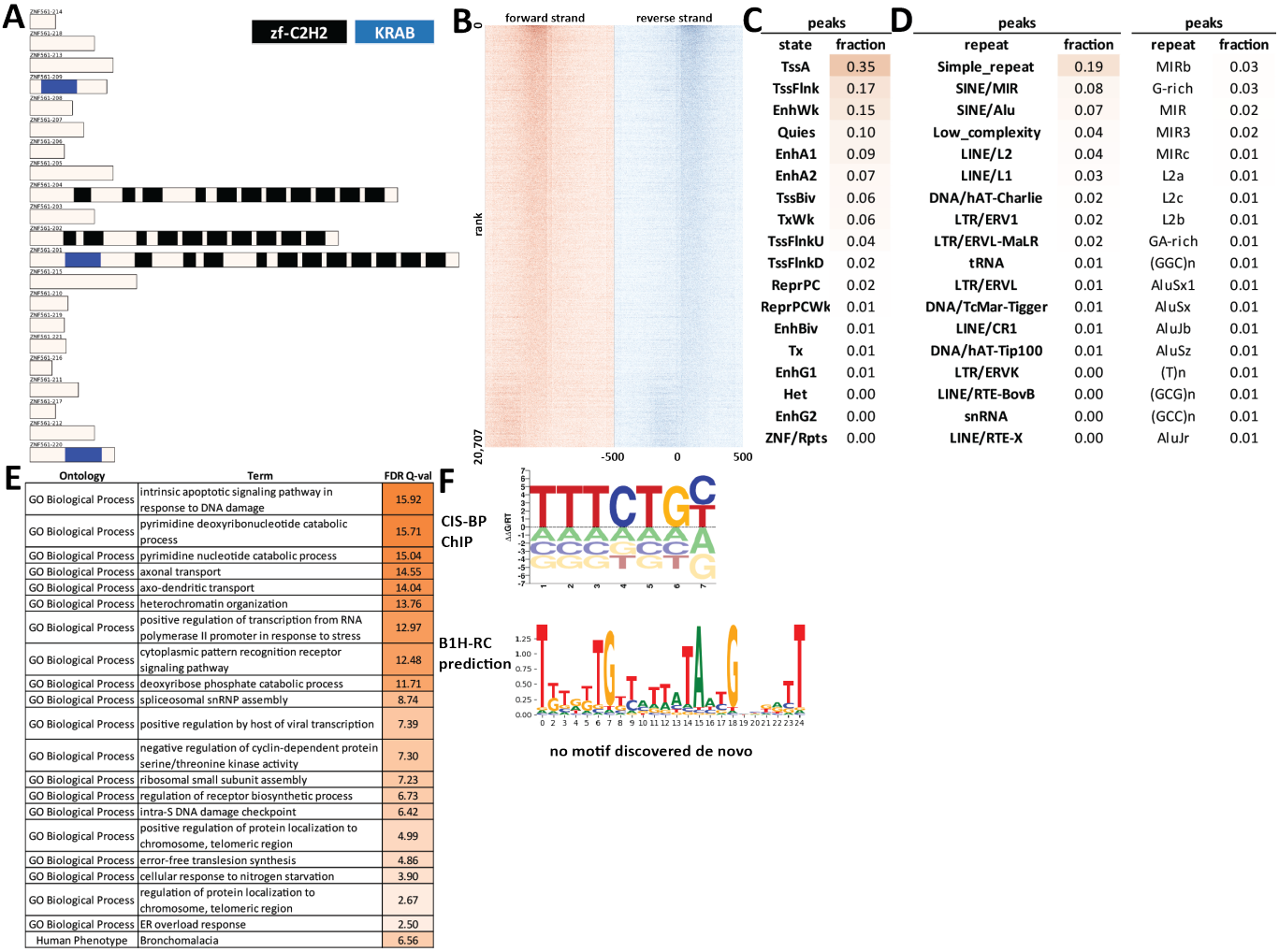

Supplementary Figure 1381: Properties and genomic distribution of motifs identified for the ZNF561 transcription factor in HEK293 (accession ENCSR125ULS).

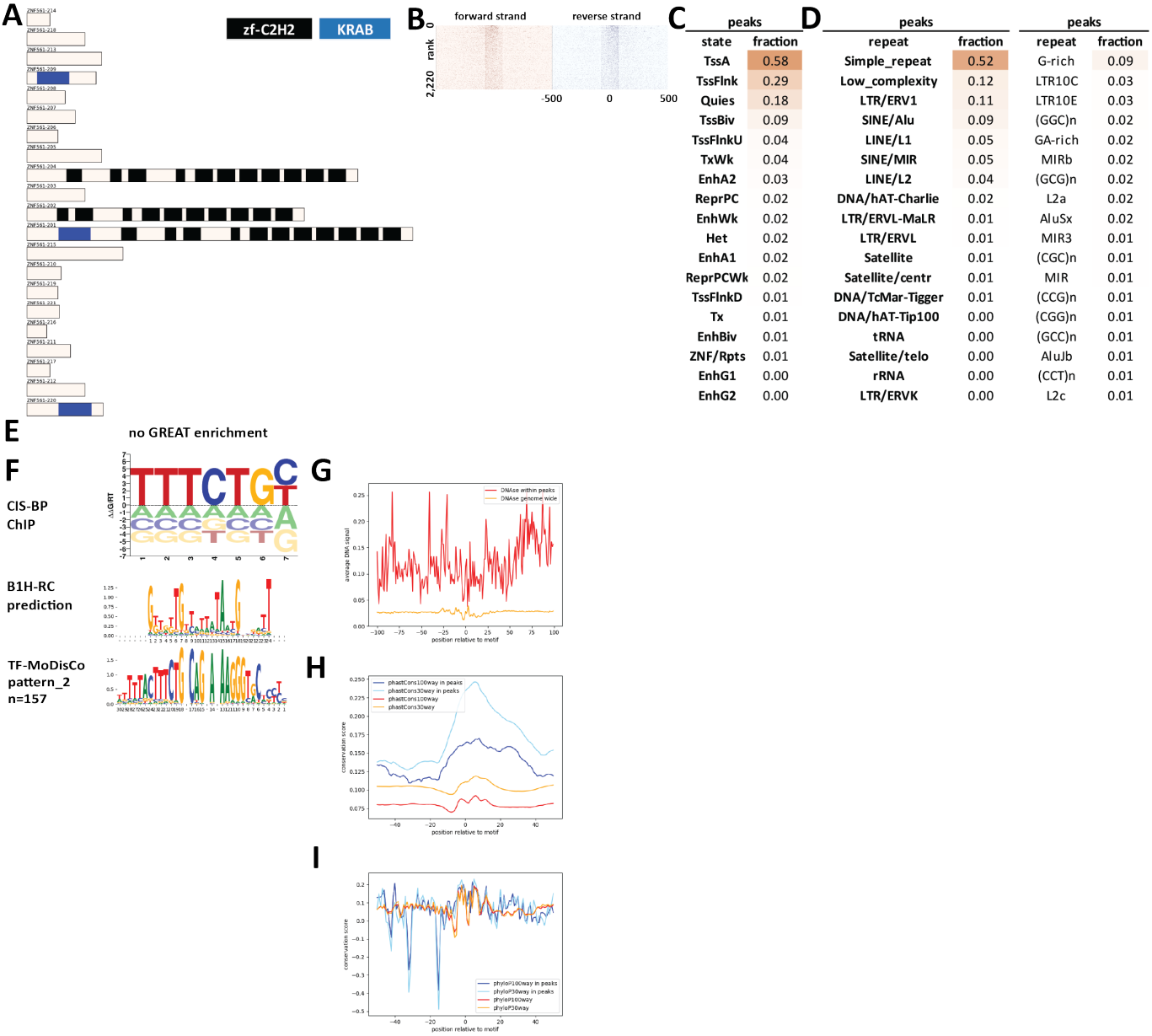

Supplementary Figure 1382: Properties and genomic distribution of motifs identified for the ZNF561 transcription factor in HEK293 (accession ChipExo models).

TF-MoDisCO pattern_2 n=157, CWM

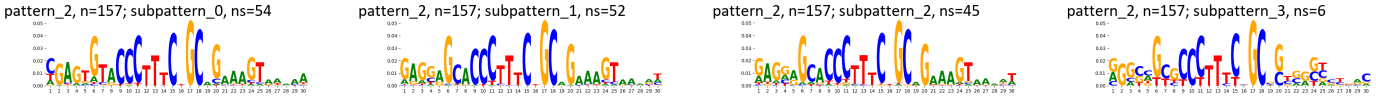

TF-MoDisCO pattern_2 n=157, PWM

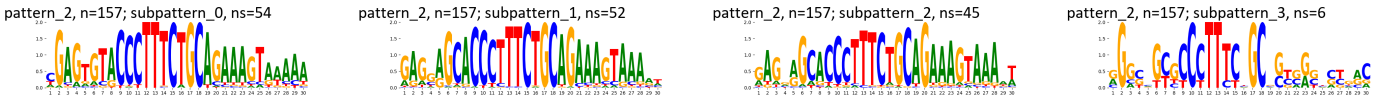

Supplementary Figure 1383: TF-MoDisCO subpatterns for the ZNF561 transcription factor in HEK293 (accession ChipExo models).

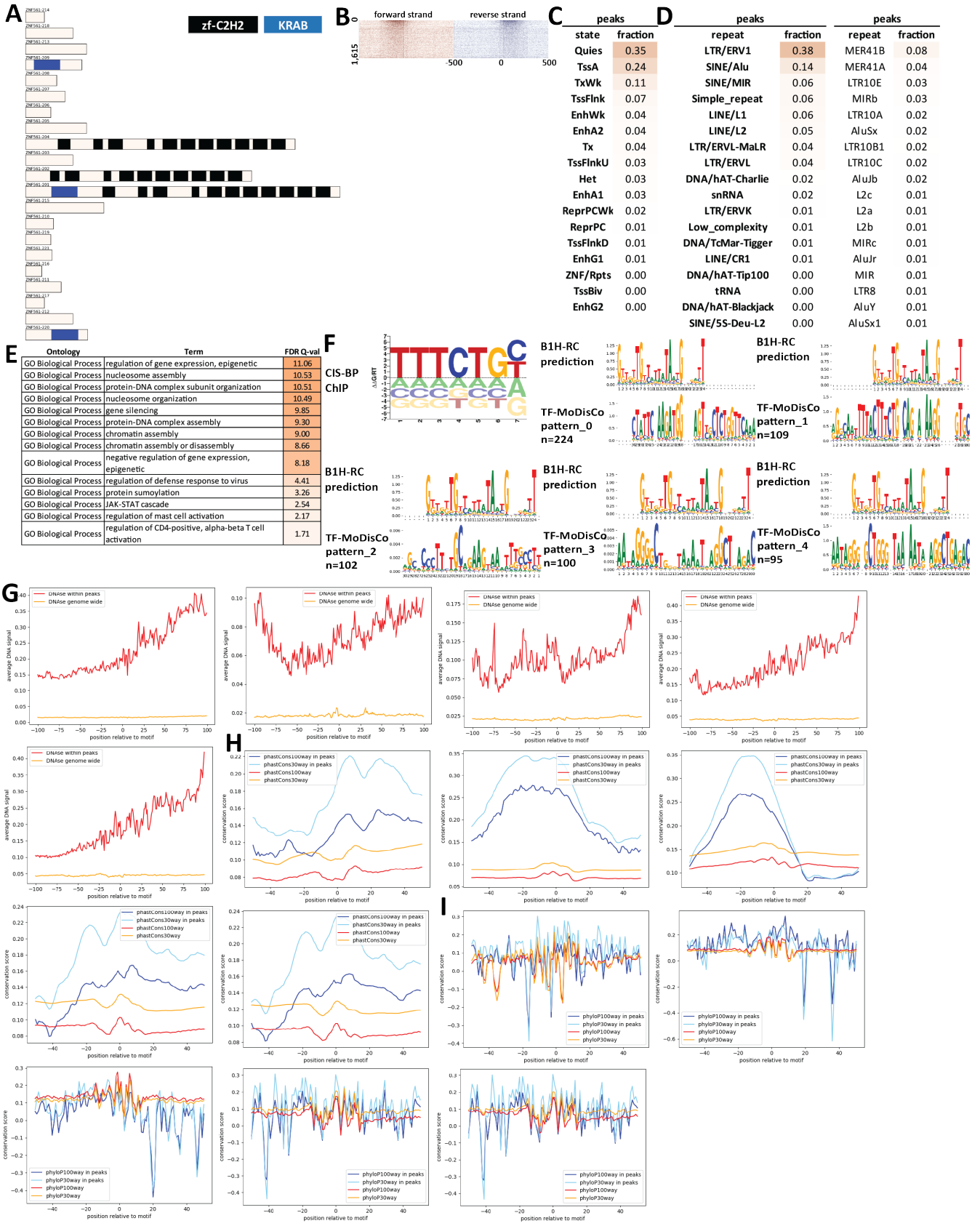

Supplementary Figure 1384: Properties and genomic distribution of motifs identified for the ZNF561 transcription factor in K562 (accession ENCSR350GZC).

TF-MoDisCO pattern_0 n=224, CWM

pattern_0, n=224; subpattern_0, ns=116

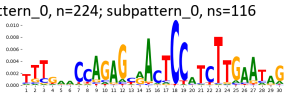

pattern_0, n=224; subpattern_1, ns=100

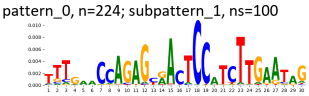

pattern_0, n=224; subpattern_2, ns=3

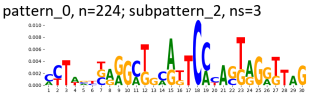

pattern_0, n=224; subpattern_3, ns=3

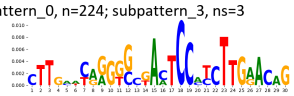

pattern_0, n=224; subpattern_4, ns=2

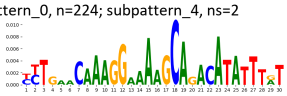

TF-MoDisCO pattern_0 n=224, PWM

pattern_0, n=224; subpattern_0, ns=116

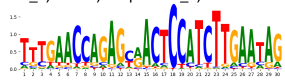

pattern_0, n=224; subpattern_1, ns=100

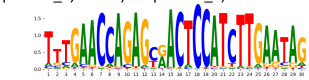

pattern_0, n=224; subpattern_2, ns=3

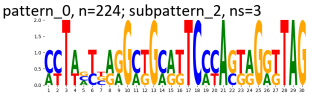

pattern_0, n=224; subpattern_3, ns=3

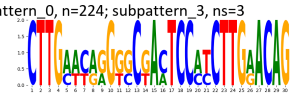

pattern_0, n=224; subpattern_4, ns=2

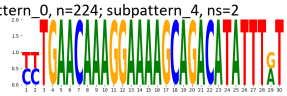

TF-MoDisCO pattern_1 n=109, CWM

pattern_1, n=109; subpattern_0, ns=47

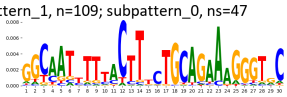

pattern_1, n=109; subpattern_1, ns=30

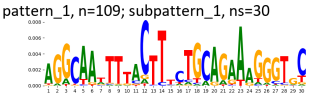

pattern_1, n=109; subpattern_2, ns=30

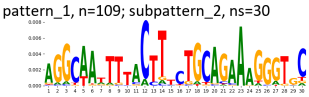

pattern_1, n=109; subpattern_3, ns=2

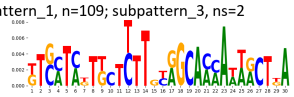

TF-MoDisCO pattern_1 n=109, PWM

pattern_1, n=109; subpattern_0, ns=47

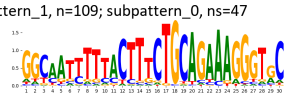

pattern_1, n=109; subpattern_1, ns=30

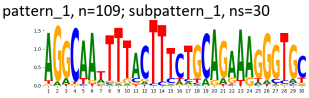

pattern_1, n=109; subpattern_2, ns=30

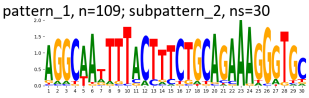

pattern_1, n=109; subpattern_3, ns=2

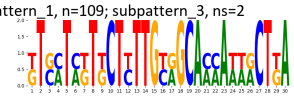

TF-MoDisCO pattern_2 n=102, CWM

pattern_2, n=102; subpattern_0, ns=28

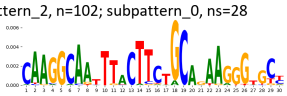

pattern_2, n=102; subpattern_1, ns=26

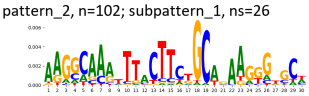

pattern_2, n=102; subpattern_2, ns=21

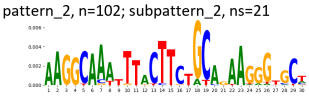

pattern_2, n=102; subpattern_3, ns=13

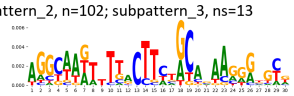

pattern_2, n=102; subpattern_4, ns=10

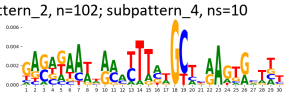

pattern_2, n=102; subpattern_5, ns=2

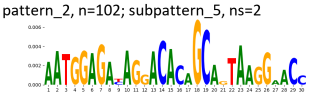

pattern_2, n=102; subpattern_6, ns=2

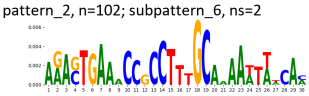

TF-MoDisCO pattern_2 n=102, PWM

pattern_2, n=102; subpattern_0, ns=28

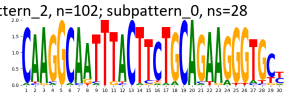

pattern_2, n=102; subpattern_1, ns=26

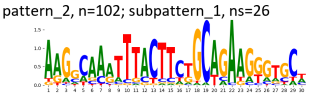

pattern_2, n=102; subpattern_2, ns=21

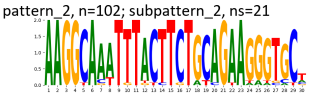

pattern_2, n=102; subpattern_3, ns=13

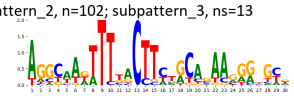

pattern_2, n=102; subpattern_4, ns=10

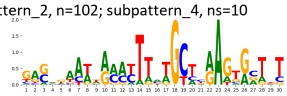

pattern_2, n=102; subpattern_5, ns=2

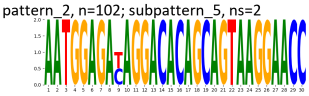

pattern_2, n=102; subpattern_6, ns=2

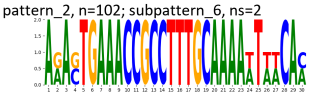

TF-MoDisCO pattern_3 n=100, CWM

pattern_3, n=100; subpattern_0, ns=38

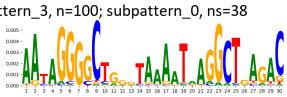

pattern_3, n=100; subpattern_1, ns=34

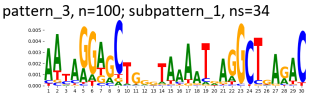

pattern_3, n=100; subpattern_2, ns=15

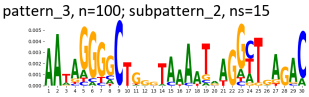

pattern_3, n=100; subpattern_3, ns=13

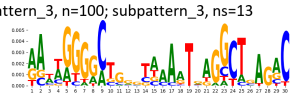

TF-MoDisCO pattern_3 n=100, PWM

pattern_3, n=100; subpattern_0, ns=38

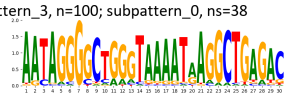

pattern_3, n=100; subpattern_1, ns=34

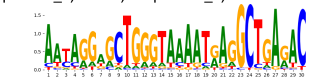

pattern_3, n=100; subpattern_2, ns=15

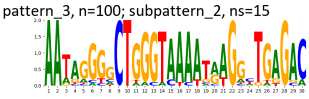

pattern_3, n=100; subpattern_3, ns=13

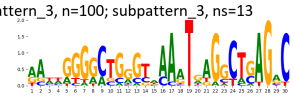

TF-MoDisCO pattern_4 n=95, CWM

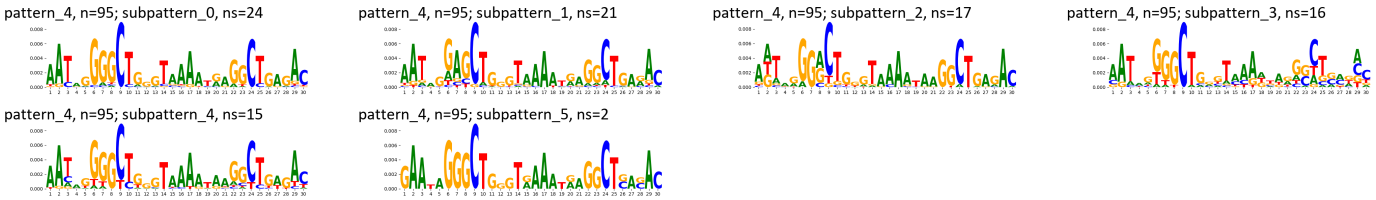

TF-MoDisCO pattern_4 n=95, PWM

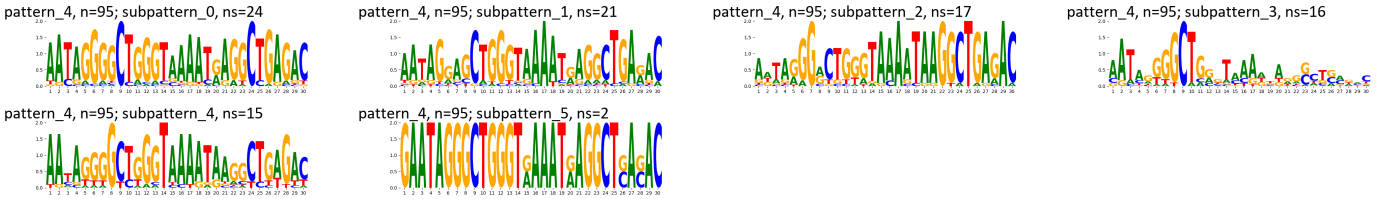

Supplementary Figure 1385: TF-MoDisCO subpatterns for the ZNF561 transcription factor in K562 (accession ENCSR350GZC).

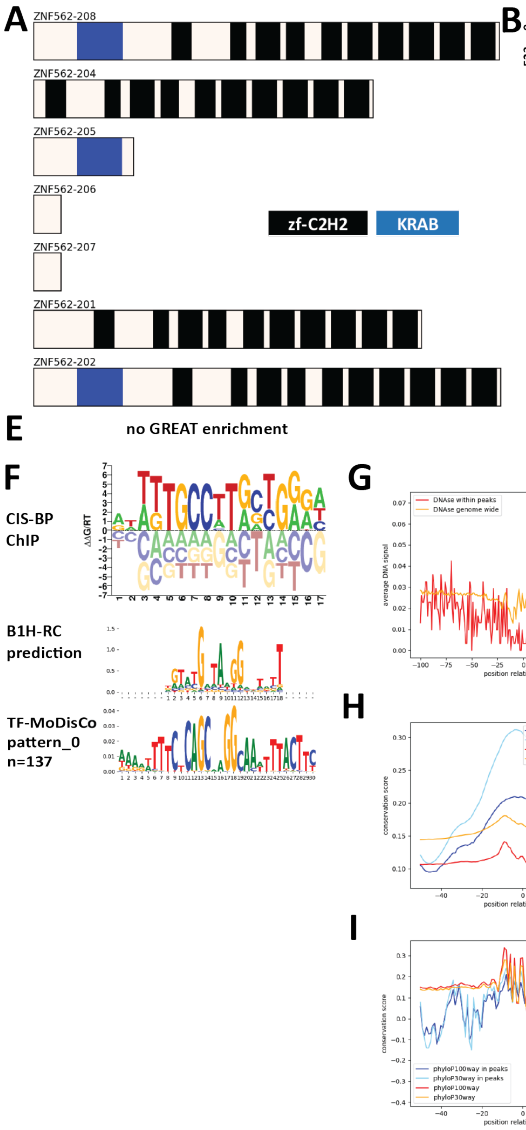

C

peaks	
state	fraction
Quies	0.47
Het	0.13
TxWk	0.11
Tx	0.07
ZNF/Rpts	0.04
ReprPCWk	0.02
EnhA2	0.02
TssFlnk	0.01
ReprPC	0.01
TssA	0.01
EnhWk	0.01
EnhG1	0.01
TssFlnkD	0.00
TssBiv	0.00
TssFlnkU	0.00
EnhBiv	0.00
EnhA1	0.00

D

peaks		peaks	
repeat	fraction	repeat	fraction
LTR/ERV1	0.75	LTR10A	0.21
SINE/Alu	0.20	LTR10B1	0.09
LINE/L1	0.13	LTR10E	0.08
Simple_repeat	0.11	LTR10B2	0.06
LINE/L2	0.06	AluSx	0.05
LTR/ERVL-MaLR	0.05	LTR10G	0.05
SINE/MIR	0.04	LTR10B	0.04
LTR/ERVL	0.03	HERVIP10B3-i	0.04
DNA/hAT-Charlie	0.03	LTR10F	0.03
Satellite	0.02	AluJb	0.03
DNA/TcMar-Tigger	0.02	HERVIP10FH-i	0.02
Satellite/centr	0.02	HERVIP10F-in	0.02
Satellite/acro	0.01	L2c	0.02
Low_complexity	0.01	MER51-int	0.02
LINE/CR1	0.01	AluY	0.02
rRNA	0.01	MIRb	0.02
DNA/hAT-Tip100	0.01	L2b	0.02
Satellite/telo	0.00	L2a	0.02

Supplementary Figure 1386: Properties and genomic distribution of motifs identified for the ZNF562 transcription factor in HEK293 (accession ChipExo models).

TF-MoDisCO pattern_0 n=137, CWM

pattern_0, n=137; subpattern_0, ns=45

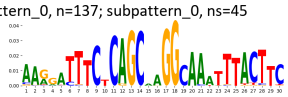

pattern_0, n=137; subpattern_1, ns=42

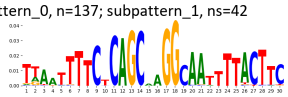

pattern_0, n=137; subpattern_2, ns=33

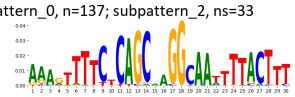

pattern_0, n=137; subpattern_3, ns=17

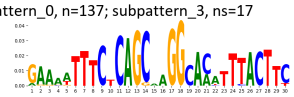

TF-MoDisCO pattern_0 n=137, PWM

pattern_0, n=137; subpattern_0, ns=45

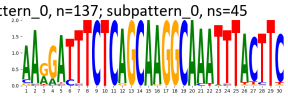

pattern_0, n=137; subpattern_1, ns=42

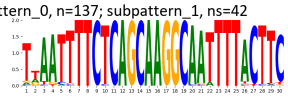

pattern_0, n=137; subpattern_2, ns=33

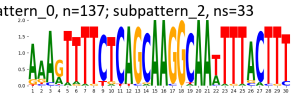

pattern_0, n=137; subpattern_3, ns=17

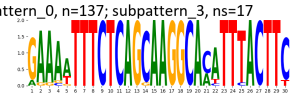

Supplementary Figure 1387: TF-MoDisCO subpatterns for the ZNF562 transcription factor in HEK293 (accession ChipExo models).

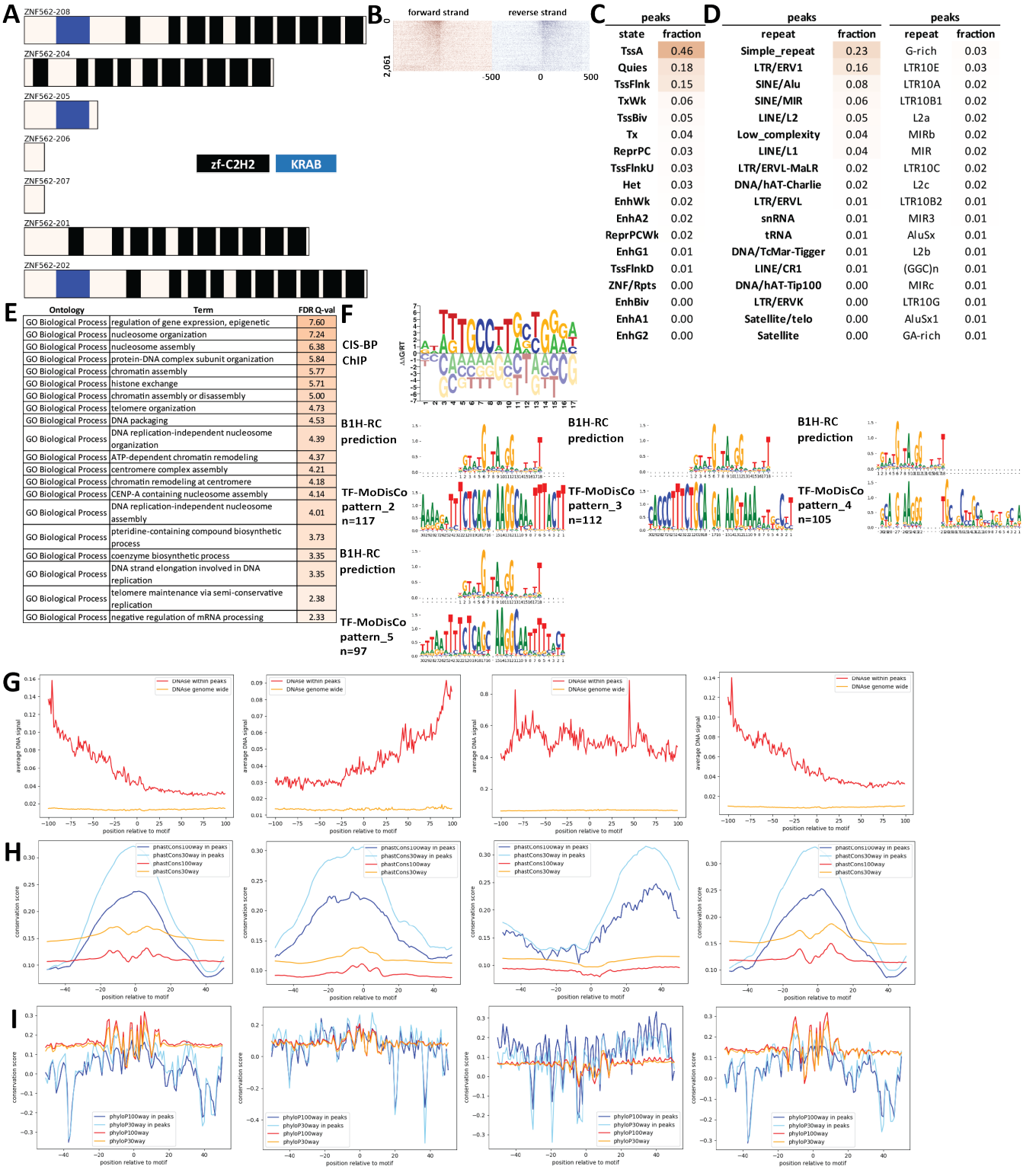

Supplementary Figure 1388: Properties and genomic distribution of motifs identified for the ZNF562 transcription factor in HepG2 (accession ENCSR727IJD).

TF-MoDisCO pattern_2 n=117, CWM

pattern_2, n=117; subpattern_0, ns=38

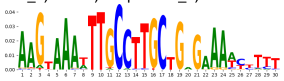

pattern_2, n=117; subpattern_1, ns=27

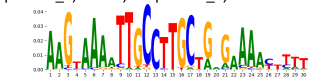

pattern_2, n=117; subpattern_2, ns=25

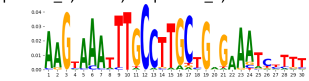

pattern_2, n=117; subpattern_3, ns=14

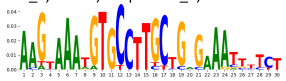

pattern_2, n=117; subpattern_4, ns=13

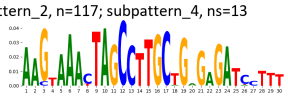

TF-MoDisCO pattern_2 n=117, PWM

pattern_2, n=117; subpattern_0, ns=38

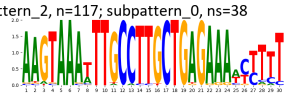

pattern_2, n=117; subpattern_1, ns=27

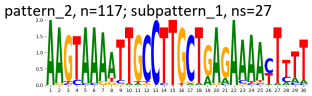

pattern_2, n=117; subpattern_2, ns=25

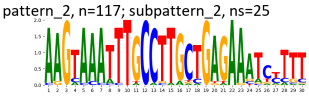

pattern_2, n=117; subpattern_3, ns=14

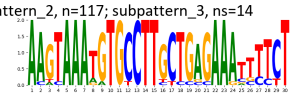

pattern_2, n=117; subpattern_4, ns=13

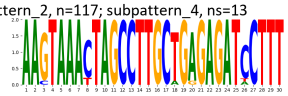

TF-MoDisCO pattern_3 n=112, CWM

pattern_3, n=112; subpattern_0, ns=50

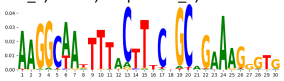

pattern_3, n=112; subpattern_1, ns=49

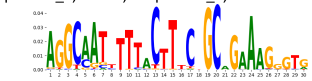

pattern_3, n=112; subpattern_2, ns=11

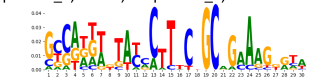

pattern_3, n=112; subpattern_3, ns=2

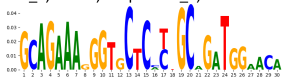

TF-MoDisCO pattern_3 n=112, PWM

pattern_3, n=112; subpattern_0, ns=50

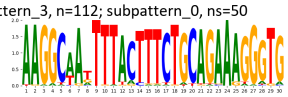

pattern_3, n=112; subpattern_1, ns=49

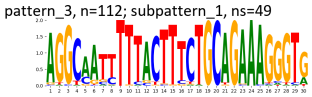

pattern_3, n=112; subpattern_2, ns=11

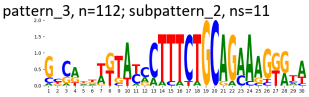

pattern_3, n=112; subpattern_3, ns=2

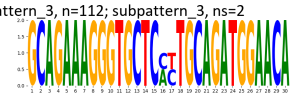

TF-MoDisCO pattern_4 n=104, CWM

pattern_4, n=104; subpattern_0, ns=35

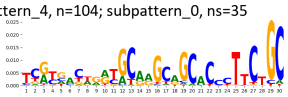

pattern_4, n=104; subpattern_1, ns=25

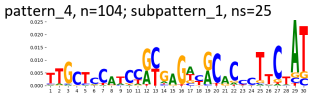

pattern_4, n=104; subpattern_2, ns=23

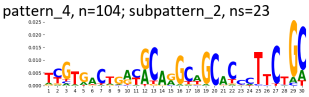

pattern_4, n=104; subpattern_3, ns=12

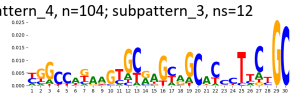

pattern_4, n=104; subpattern_4, ns=9

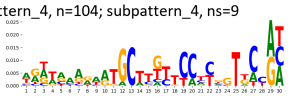

TF-MoDisCO pattern_4 n=104, PWM

pattern_4, n=104; subpattern_0, ns=35

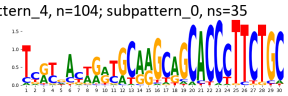

pattern_4, n=104; subpattern_1, ns=25

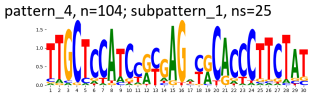

pattern_4, n=104; subpattern_2, ns=23

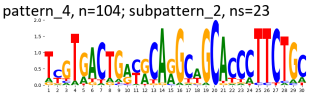

pattern_4, n=104; subpattern_3, ns=12

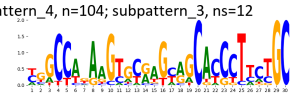

pattern_4, n=104; subpattern_4, ns=9

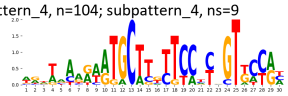

TF-MoDisCO pattern_6 n=97, CWM

pattern_6, n=97; subpattern_0, ns=33

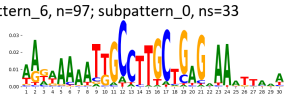

pattern_6, n=97; subpattern_1, ns=25

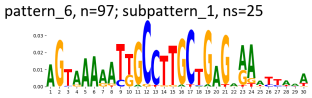

pattern_6, n=97; subpattern_2, ns=25

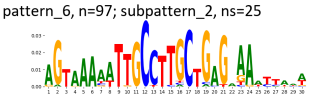

pattern_6, n=97; subpattern_3, ns=14

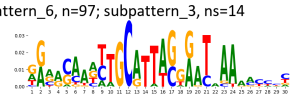

TF-MoDisCO pattern_6 n=97, PWM

pattern_6, n=97; subpattern_0, ns=33

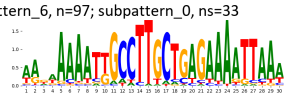

pattern_6, n=97; subpattern_1, ns=25

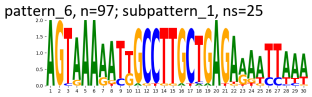

pattern_6, n=97; subpattern_2, ns=25

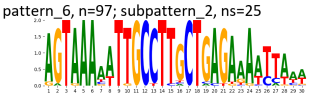

pattern_6, n=97; subpattern_3, ns=14

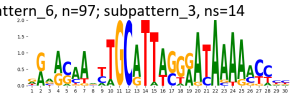

Supplementary Figure 1389: TF-MoDisCO subpatterns for the ZNF562 transcription factor in HepG2 (accession ENCSR727IJD).

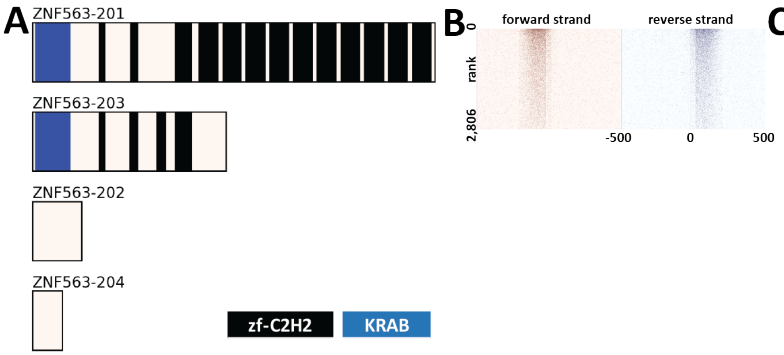

C

peaks	
state	fraction
Quies	0.50
TxWk	0.13
TssA	0.08
EnhWk	0.08
Tx	0.06
TssFlnk	0.05
TssBiv	0.04
ReprPC	0.04
ReprPCWk	0.03
EnhA1	0.02
EnhA2	0.01
Het	0.01
TssFlnkU	0.01
EnhBiv	0.01
EnhG1	0.00
TssFlnkD	0.00
ZNF/Rpts	0.00
EnhG2	0.00

D

peaks		peaks	
repeat	fraction	repeat	fraction
LINE/L1	0.14	L1M1	0.04
Simple_repeat	0.07	L1MA3	0.03
SINE/MIR	0.07	MIRb	0.03
LINE/L2	0.06	L2c	0.02
SINE/Alu	0.05	MIR	0.02
LTR/ERVL-MaLR	0.04	L2a	0.02
LTR/ERVL	0.04	L2b	0.01
DNA/hAT-Charlie	0.04	MIRc	0.01
LTR/ERV1	0.03	L2	0.01
DNA/TcMar-Tigger	0.01	MIR3	0.01
Low_complexity	0.01	MER5A	0.01
LINE/CR1	0.01	L1MA2	0.01
DNA/hAT-Tip100	0.01	L3	0.01
DNA/hAT-Blackjack	0.00	G-rich	0.01
LTR/Gypsy	0.00	AluJb	0.01
LTR/ERVK	0.00	AluSx1	0.01
LINE/RTE-BovB	0.00	AluJr	0.01
LINE/RTE-X	0.00	AluJo	0.01

E

Ontology	Term	FDR Q-val
GO Biological Process	mesoderm formation	4.19
GO Biological Process	paraxial mesoderm development	3.93
GO Biological Process	paraxial mesoderm morphogenesis	3.51
GO Biological Process	negative regulation of cardiac muscle hypertrophy in response to stress	3.19
GO Biological Process	signal transduction involved in regulation of gene expression	2.48
GO Biological Process	determination of heart left/right asymmetry	2.35
GO Biological Process	autophagosome organization	2.35
GO Biological Process	autophagosome assembly	2.12
GO Biological Process	interleukin-10 production	2.00
GO Biological Process	response to muscle inactivity	1.67
GO Biological Process	regulation of lipoprotein particle clearance	1.64
GO Biological Process	osteoblast development	1.58
GO Biological Process	positive regulation of pri-miRNA transcription from RNA polymerase II promoter	1.58
GO Biological Process	regulation of transcription from RNA polymerase II promoter involved in heart development	1.57
GO Biological Process	dorsal aorta morphogenesis	1.46
GO Biological Process	regulation of microvillus assembly	1.40

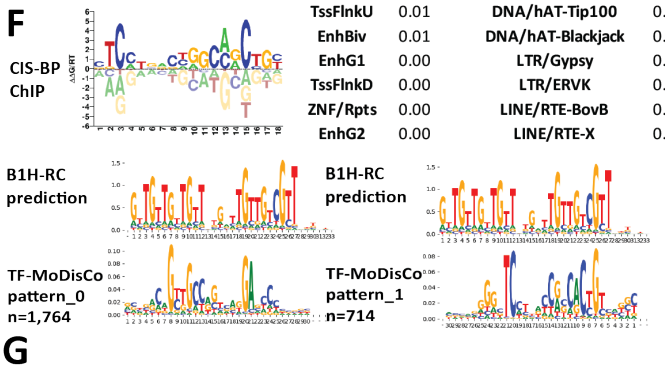

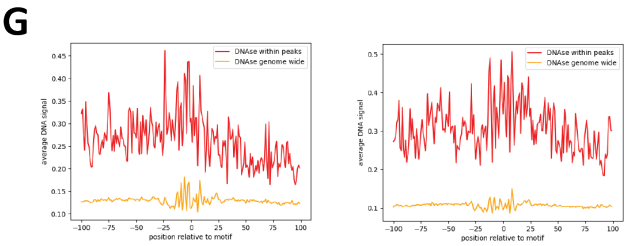

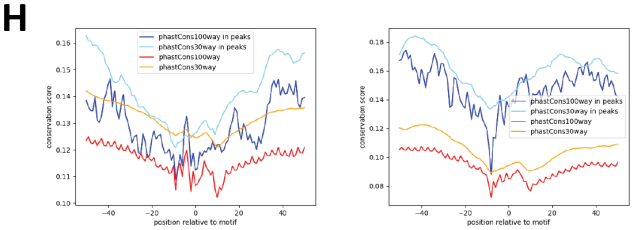

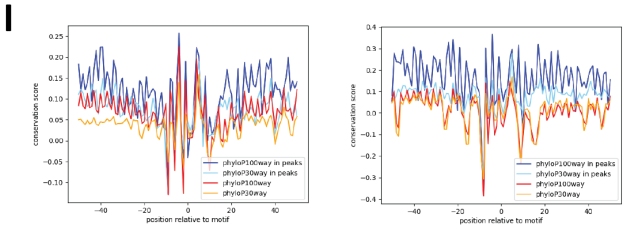

Supplementary Figure 1390: Properties and genomic distribution of motifs identified for the ZNF563 transcription factor in HEK293 (accession Hughes GR models).

TF-MoDisCO pattern_0 n=1764, CWM

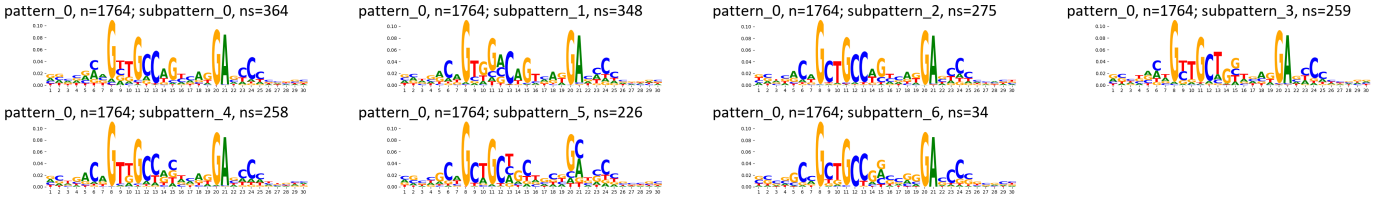

TF-MoDisCO pattern_0 n=1764, PWM

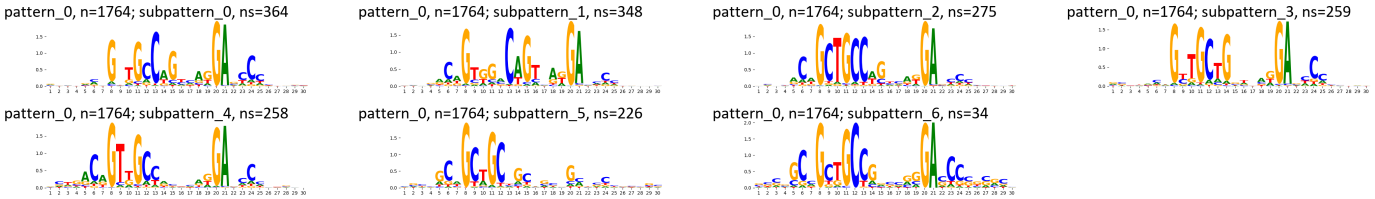

TF-MoDisCO pattern_1 n=714, CWM

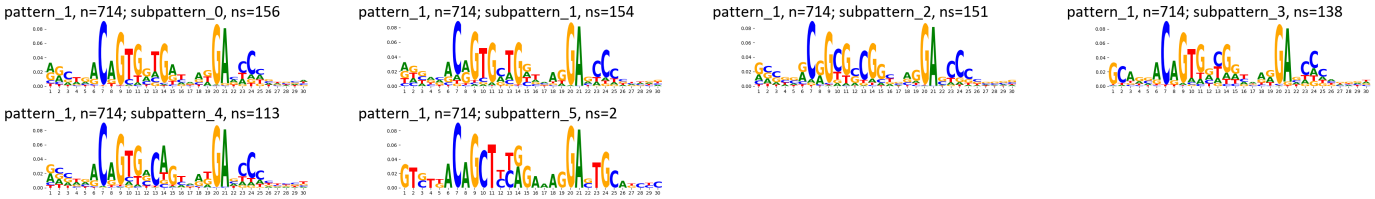

TF-MoDisCO pattern_1 n=714, PWM

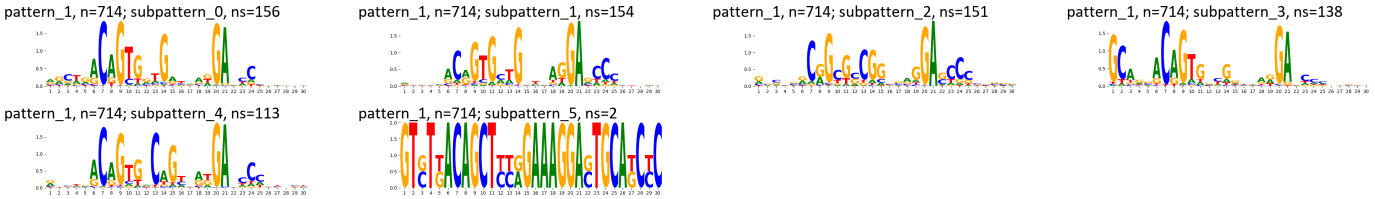

Supplementary Figure 1391: TF-MoDisCO subpatterns for the ZNF563 transcription factor in HEK293 (accession Hughes GR models).

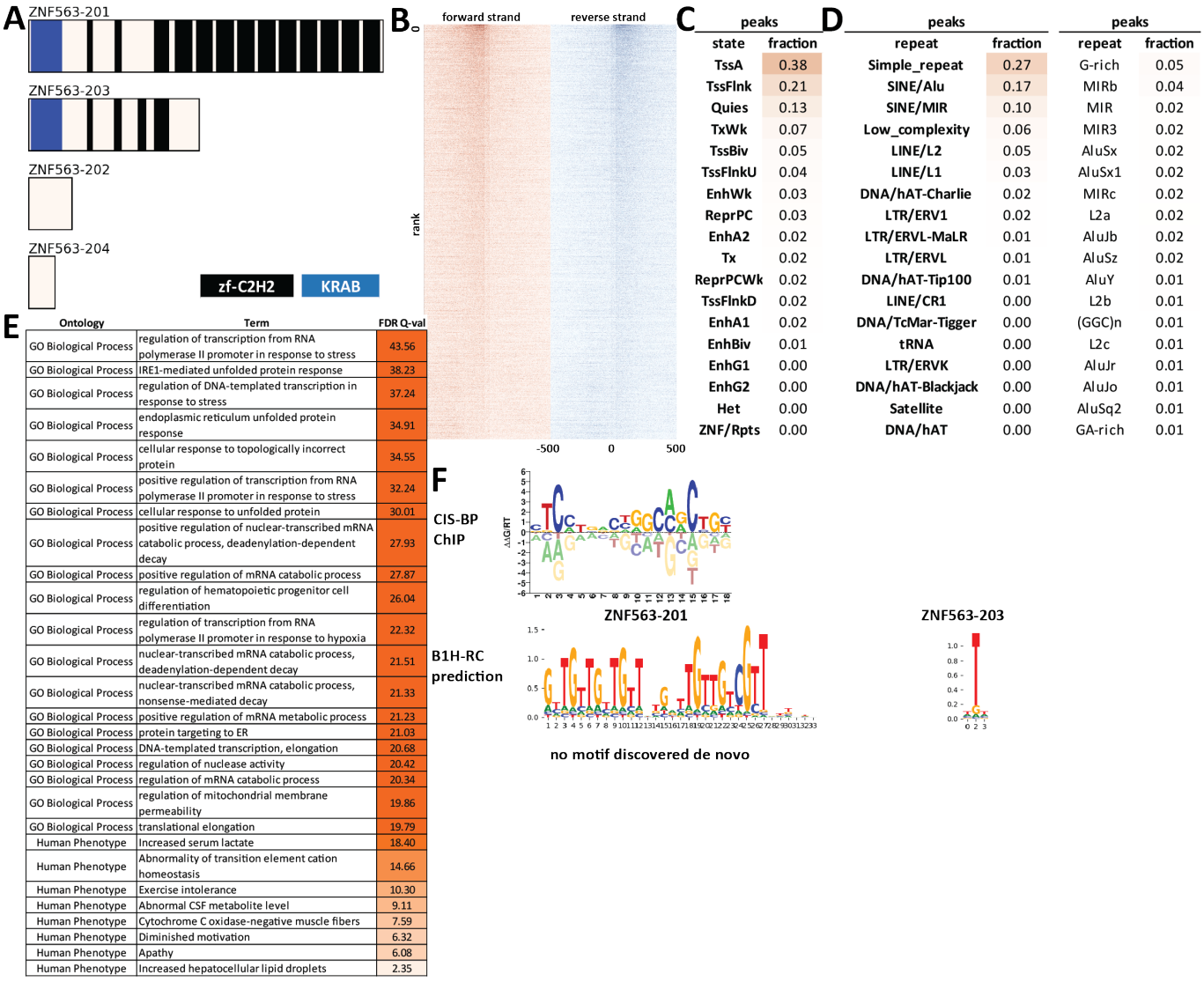

C

peaks	
state	fraction
TssA	0.38
TssFlnk	0.21
Quies	0.13
TxWk	0.07
TssBiv	0.05
TssFlnkU	0.04
EnhWk	0.03
ReprPC	0.03
EnhA2	0.02
Tx	0.02
ReprPCWk	0.02
TssFlnkD	0.02
EnhA1	0.02
EnhBiv	0.01
EnhG1	0.00
EnhG2	0.00
Het	0.00
ZNF/Rpts	0.00

D

peaks		peaks	
repeat	fraction	repeat	fraction
Simple_repeat	0.27	G-rich	0.05
SINE/Alu	0.17	MIRb	0.04
SINE/MIR	0.10	MIR	0.02
Low_complexity	0.06	MIR3	0.02
LINE/L2	0.05	AluSx	0.02
LINE/L1	0.03	AluSx1	0.02
DNA/hAT-Charlie	0.02	MIRc	0.02
LTR/ERV1	0.02	L2a	0.02
LTR/ERVL-MaLR	0.01	AluJb	0.02
LTR/ERVL	0.01	AluSz	0.02
DNA/hAT-Tip100	0.01	AluY	0.01
LINE/CR1	0.00	L2b	0.01
DNA/TcMar-Tigger	0.00	(GGC)n	0.01
tRNA	0.00	L2c	0.01
LTR/ERVK	0.00	AluJr	0.01
DNA/hAT-Blackjack	0.00	AluJo	0.01
Satellite	0.00	AluSq2	0.01
DNA/hAT	0.00	GA-rich	0.01

E

Ontology	Term	FDR Q-val
GO Biological Process	regulation of transcription from RNA polymerase II promoter in response to stress	43.56
GO Biological Process	IRE1-mediated unfolded protein response	38.23
GO Biological Process	regulation of DNA-templated transcription in response to stress	37.24
GO Biological Process	endoplasmic reticulum unfolded protein response	34.91
GO Biological Process	cellular response to topologically incorrect protein	34.55
GO Biological Process	positive regulation of transcription from RNA polymerase II promoter in response to stress	32.24
GO Biological Process	cellular response to unfolded protein	30.01
GO Biological Process	positive regulation of nuclear-transcribed mRNA catabolic process, deadenylation-dependent decay	27.93
GO Biological Process	positive regulation of mRNA catabolic process	27.87
GO Biological Process	regulation of hematopoietic progenitor cell differentiation	26.04
GO Biological Process	regulation of transcription from RNA polymerase II promoter in response to hypoxia	22.32
GO Biological Process	nuclear-transcribed mRNA catabolic process, deadenylation-dependent decay	21.51
GO Biological Process	nuclear-transcribed mRNA catabolic process, nonsense-mediated decay	21.33
GO Biological Process	positive regulation of mRNA metabolic process	21.23
GO Biological Process	protein targeting to ER	21.03
GO Biological Process	DNA-templated transcription, elongation	20.68
GO Biological Process	regulation of nuclease activity	20.42
GO Biological Process	regulation of mRNA catabolic process	20.34
GO Biological Process	regulation of mitochondrial membrane permeability	19.86
GO Biological Process	translational elongation	19.79
Human Phenotype	Increased serum lactate	18.40
Human Phenotype	Abnormality of transition element cation homeostasis	14.66
Human Phenotype	Exercise intolerance	10.30
Human Phenotype	Abnormal CSF metabolite level	9.11
Human Phenotype	Cytochrome C oxidase-negative muscle fibers	7.59
Human Phenotype	Diminished motivation	6.32
Human Phenotype	Apathy	6.08
Human Phenotype	Increased hepatocellular lipid droplets	2.35

Supplementary Figure 1392: Properties and genomic distribution of motifs identified for the ZNF563 transcription factor in HepG2 (accession ENCSR977FRK).

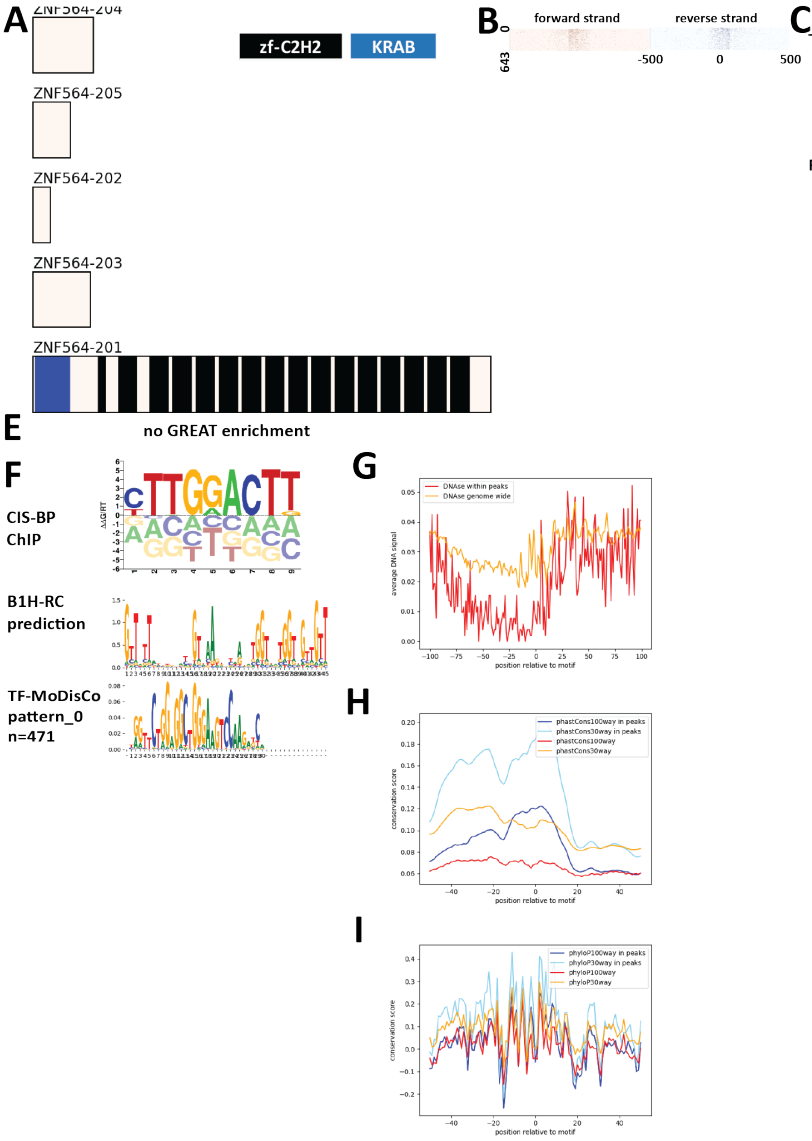

C

peaks	
state	fraction
Quies	0.64
TxWk	0.11
Tx	0.05
TssA	0.04
ReprPCWk	0.03
TssFlnk	0.02
EnhWk	0.02
TssBiv	0.01
Het	0.01
ReprPC	0.01
EnhA1	0.01
ZNF/Rpts	0.01
EnhG1	0.00
TssFlnkU	0.00
EnhBiv	0.00
EnhA2	0.00

D

peaks		peaks	
repeat	fraction	repeat	fraction
LTR/ERVL-MaLR	0.83	MSTD	0.40
SINE/Alu	0.23	MLT1A0	0.18
LINE/L1	0.15	MSTB2	0.06
Simple_repeat	0.12	MLT1A1	0.05
LINE/L2	0.08	MSTC	0.04
SINE/MIR	0.07	MLT1A	0.03
LTR/ERVL	0.07	L2a	0.03
DNA/hAT-Charlie	0.03	AluSx1	0.03
DNA/TcMar-Tigger	0.02	MLT2D	0.03
LTR/ERV1	0.02	MIRb	0.02
Low_complexity	0.02	AluJb	0.02
Satellite	0.01	L2b	0.02
Satellite/centr	0.01	MIR	0.02
DNA/hAT-Tip100	0.01	AluSx	0.02
Satellite/acro	0.00	MSTD-int	0.02
LINE/CR1	0.00	L2c	0.02
LTR/ERVK	0.00	AluY	0.02
DNA/TcMar-Tc2	0.00	AluSz	0.02

Supplementary Figure 1393: Properties and genomic distribution of motifs identified for the ZNF564 transcription factor in HEK293 (accession ChipExo models).

TF-MoDisCO pattern_0 n=471, CWM

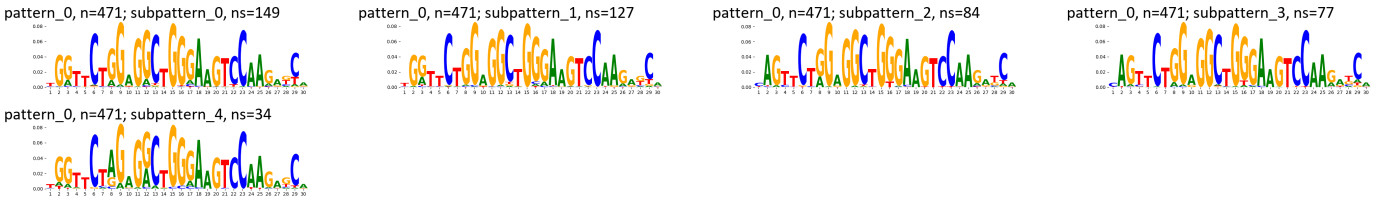

TF-MoDisCO pattern_0 n=471, PWM

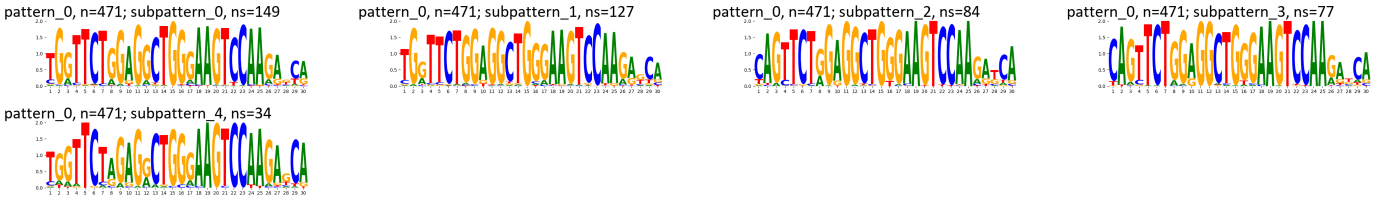

Supplementary Figure 1394: TF-MoDisCO subpatterns for the ZNF564 transcription factor in HEK293 (accession ChipExo models).

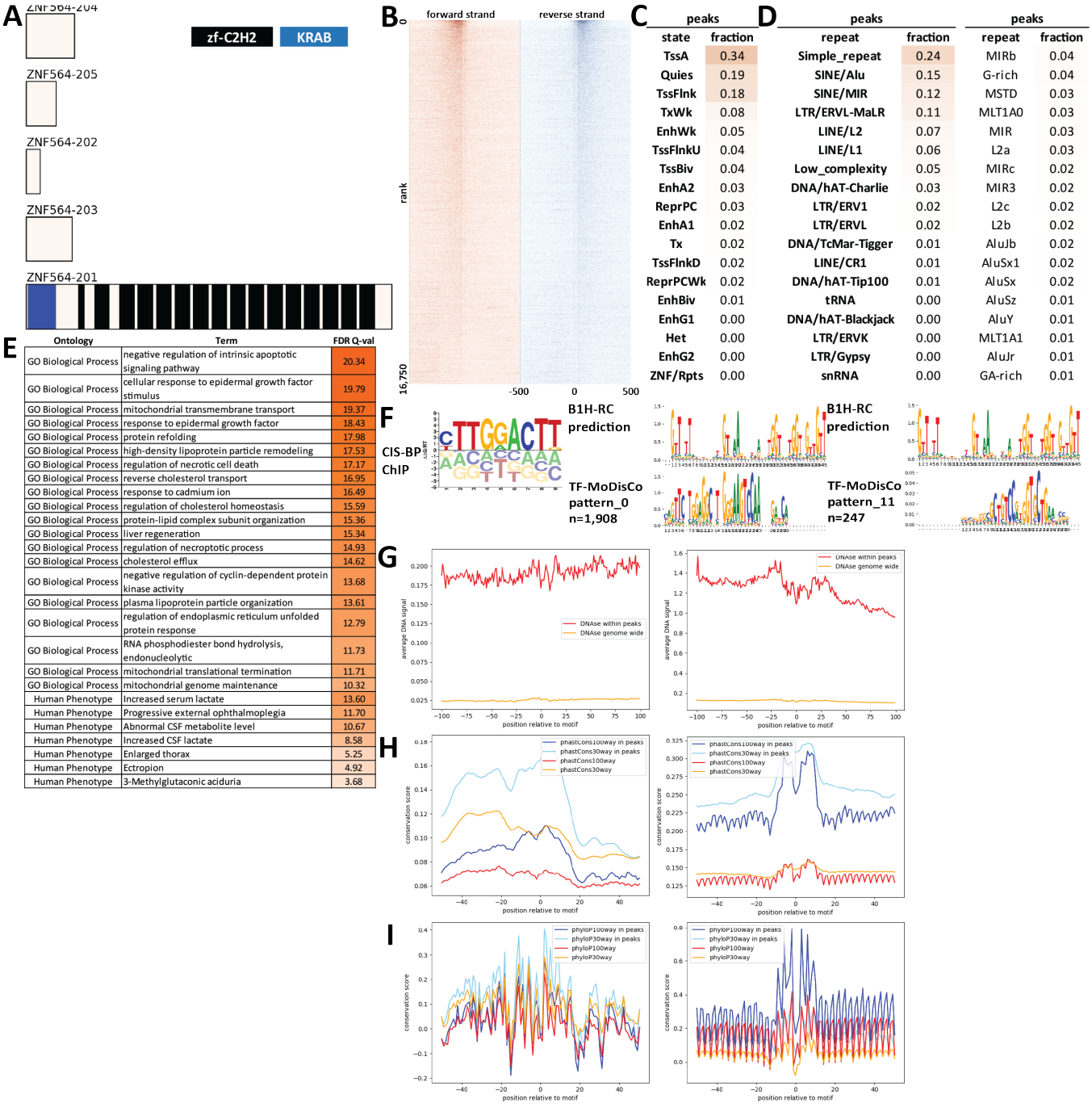

Supplementary Figure 1395: Properties and genomic distribution of motifs identified for the ZNF564 transcription factor in HepG2 (accession ENCSR397EOT).

TF-MoDisCO pattern_0 n=1908, CWM

pattern_0, n=1908; subpattern_0, ns=506

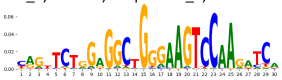

pattern_0, n=1908; subpattern_1, ns=447

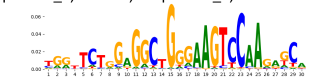

pattern_0, n=1908; subpattern_2, ns=421

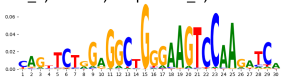

pattern_0, n=1908; subpattern_3, ns=320

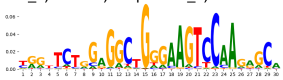

pattern_0, n=1908; subpattern_4, ns=211

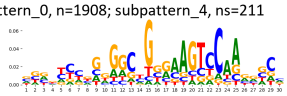

pattern_0, n=1908; subpattern_5, ns=3

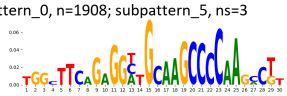

TF-MoDisCO pattern_0 n=1908, PWM

pattern_0, n=1908; subpattern_0, ns=506

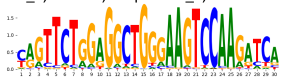

pattern_0, n=1908; subpattern_1, ns=447

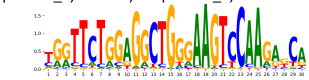

pattern_0, n=1908; subpattern_2, ns=421

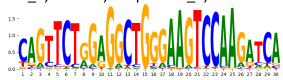

pattern_0, n=1908; subpattern_3, ns=320

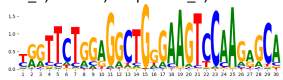

pattern_0, n=1908; subpattern_4, ns=211

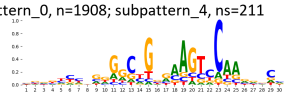

pattern_0, n=1908; subpattern_5, ns=3

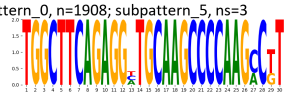

TF-MoDisCO pattern_11 n=247, CWM

pattern_11, n=247; subpattern_0, ns=129

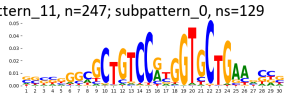

pattern_11, n=247; subpattern_1, ns=118

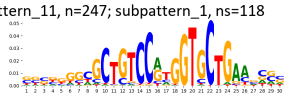

TF-MoDisCO pattern_11 n=247, PWM

pattern_11, n=247; subpattern_0, ns=129

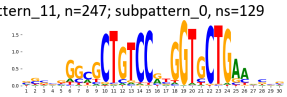

pattern_11, n=247; subpattern_1, ns=118

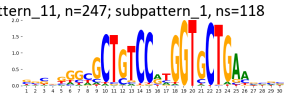

Supplementary Figure 1396: TF-MoDisCO subpatterns for the ZNF564 transcription factor in HepG2 (accession ENCSR397EOT).

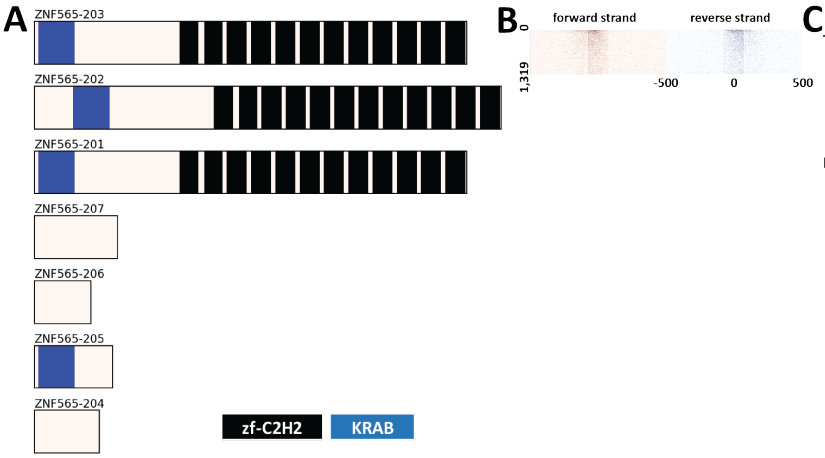

C

peaks	
state	fraction
Quies	0.54
TssA	0.19
TxWk	0.07
TssFlnk	0.07
ReprPCWk	0.04
Tx	0.04
Het	0.03
EnhWk	0.02
ReprPC	0.02
TssBiv	0.01
EnhA2	0.01
TssFlnkU	0.01
ZNF/Rpts	0.01
EnhA1	0.01
TssFlnkD	0.00
EnhBiv	0.00
EnhG1	0.00

D

peaks		peaks	
repeat	fraction	repeat	fraction
LTR/ERVL-MaLR	0.59	MLT1G1	0.15
Simple_repeat	0.18	MLT1G	0.12
SINE/Alu	0.13	MLT1G3	0.10
LINE/L1	0.09	MLT1F	0.08
SINE/MIR	0.07	MLT1F1	0.05
LINE/L2	0.05	MIRb	0.03
Low_complexity	0.03	L2a	0.02
LTR/ERV1	0.03	MLT1H1	0.02
DNA/hAT-Charlie	0.02	G-rich	0.02
LTR/ERVL	0.02	MIR	0.02
Satellite	0.01	AluJo	0.02
DNA/TcMar-Tigger	0.01	AluY	0.01
DNA/hAT-Tip100	0.01	MLT1H2	0.01
Satellite/centr	0.00	MIR3	0.01
snRNA	0.00	L1M7	0.01
LTR/ERVK	0.00	AluJb	0.01
tRNA	0.00	L2c	0.01
LTR/Gypsy?	0.00	AluSx1	0.01

E

Ontology	Term	FDR Q-val
GO Biological Process	platelet-derived growth factor receptor-beta signaling pathway	4.44
GO Biological Process	middle ear morphogenesis	2.03
GO Biological Process	negative regulation of vascular smooth muscle cell differentiation	1.97
GO Biological Process	embryonic placenta development	1.59

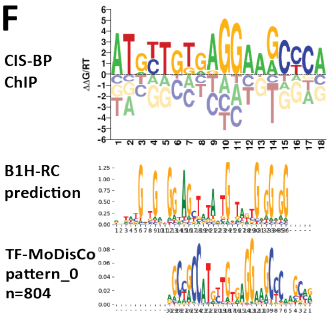

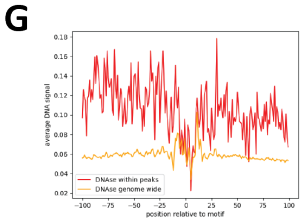

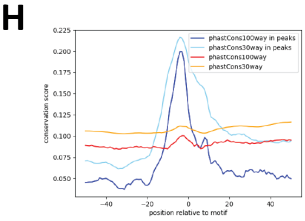

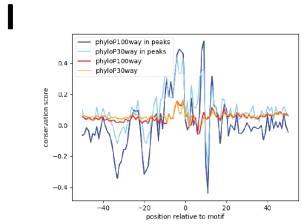

Supplementary Figure 1397: Properties and genomic distribution of motifs identified for the ZNF565 transcription factor in HEK293 (accession ChipExo models).

TF-MoDisCO pattern_0 n=804, CWM

pattern_0, n=804; subpattern_0, ns=201

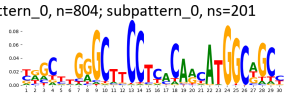

pattern_0, n=804; subpattern_1, ns=177

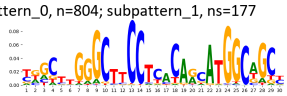

pattern_0, n=804; subpattern_2, ns=142

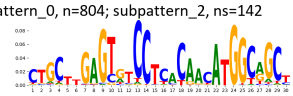

pattern_0, n=804; subpattern_3, ns=141

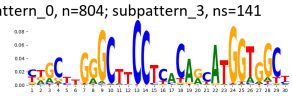

pattern_0, n=804; subpattern_4, ns=129

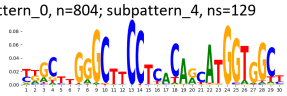

pattern_0, n=804; subpattern_5, ns=14

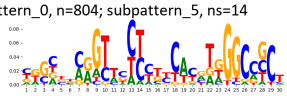

TF-MoDisCO pattern_0 n=804, PWM

pattern_0, n=804; subpattern_0, ns=201

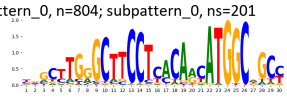

pattern_0, n=804; subpattern_1, ns=177

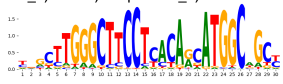

pattern_0, n=804; subpattern_2, ns=142

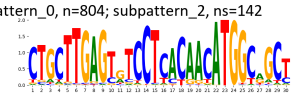

pattern_0, n=804; subpattern_3, ns=141

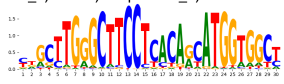

pattern_0, n=804; subpattern_4, ns=129

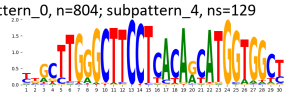

pattern_0, n=804; subpattern_5, ns=14

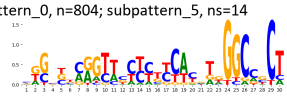

Supplementary Figure 1398: TF-MoDisCO subpatterns for the ZNF565 transcription factor in HEK293 (accession ChipExo models).

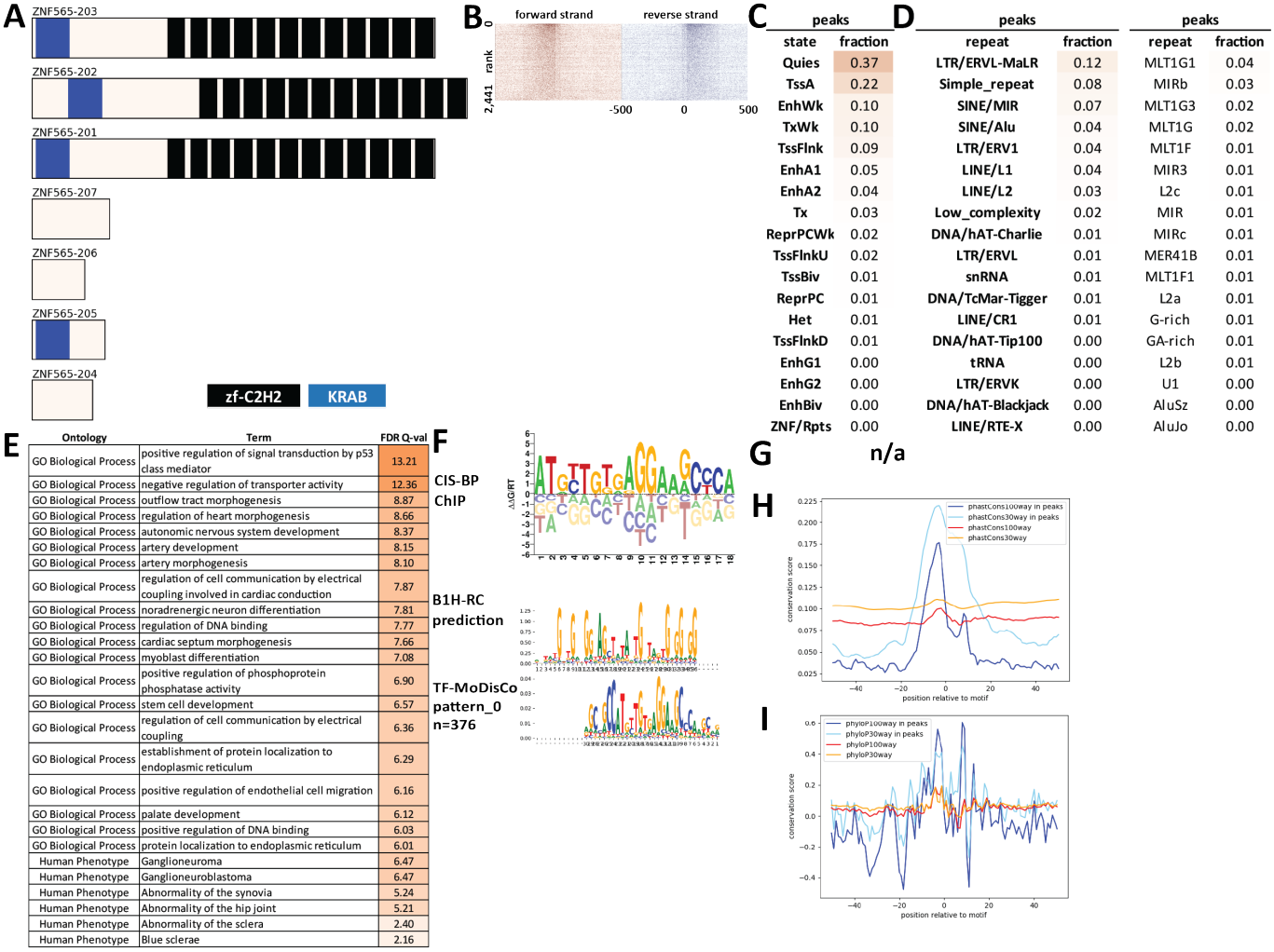

Supplementary Figure 1399: Properties and genomic distribution of motifs identified for the ZNF565 transcription factor in SK-N-SH (accession ENCSR754ALX).

TF-MoDisCO pattern_0 n=376, CWM

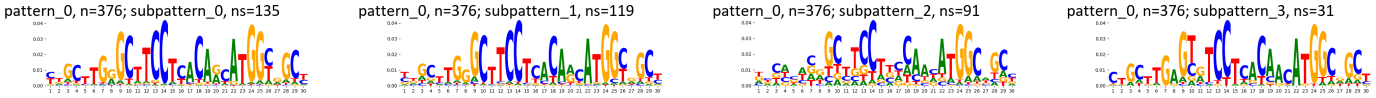

TF-MoDisCO pattern_0 n=376, PWM

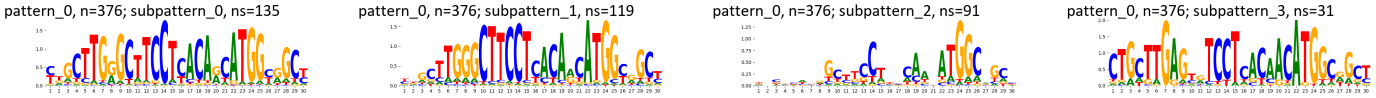

Supplementary Figure 1400: TF-MoDisCO subpatterns for the ZNF565 transcription factor in SK-N-SH (accession ENCSR754ALX).

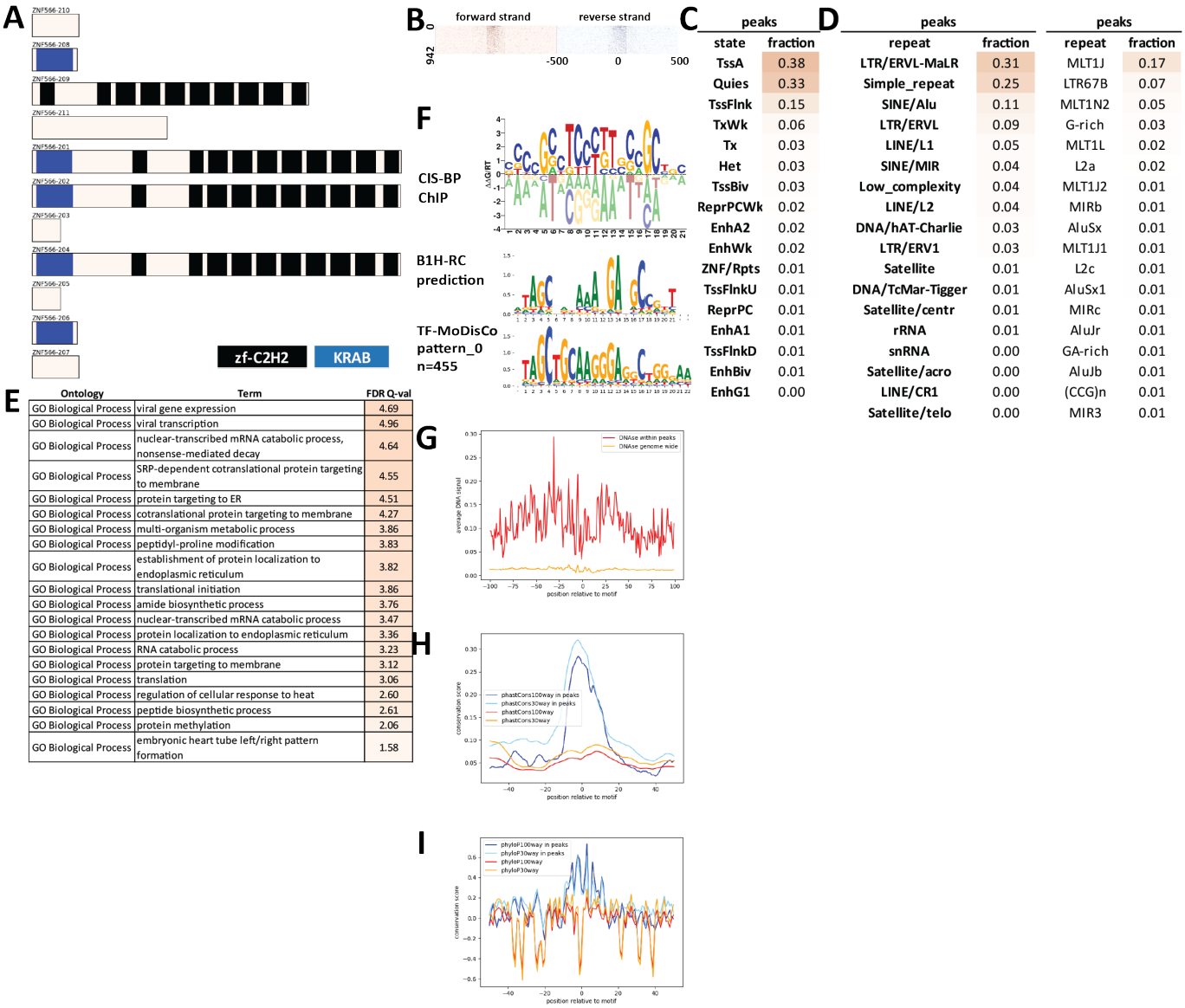

C

peaks	
state	fraction
TssA	0.38
Quies	0.33
TssFlnk	0.15
TxWk	0.06
Tx	0.03
Het	0.03
TssBiv	0.03
ReprPCWk	0.02
EnhA2	0.02
EnhWk	0.02
ZNF/Rpts	0.01
TssFlnkU	0.01
ReprPC	0.01
EnhA1	0.01
TssFlnkD	0.01
EnhBiv	0.01
EnhG1	0.00

D

peaks		peaks	
repeat	fraction	repeat	fraction
LTR/ERVL-MaLR	0.31	MLT1J	0.17
Simple_repeat	0.25	LTR67B	0.07
SINE/Alu	0.11	MLT1N2	0.05
LTR/ERVL	0.09	G-rich	0.03
LINE/L1	0.05	MLT1L	0.02
SINE/MIR	0.04	L2a	0.02
Low_complexity	0.04	MLT1J2	0.01
LINE/L2	0.04	MIRb	0.01
DNA/hAT-Charlie	0.03	AluSx	0.01
LTR/ERV1	0.03	MLT1J1	0.01
Satellite	0.01	L2c	0.01
DNA/TcMar-Tigger	0.01	AluSx1	0.01
Satellite/centr	0.01	MIRc	0.01
rRNA	0.01	AluJr	0.01
snRNA	0.00	GA-rich	0.01
Satellite/acro	0.00	AluJb	0.01
LINE/CR1	0.00	(CCG)n	0.01
Satellite/telo	0.00	MIR3	0.01

E

Ontology	Term	FDR Q-val
GO Biological Process	viral gene expression	4.69
GO Biological Process	viral transcription	4.96
GO Biological Process	nuclear-transcribed mRNA catabolic process, nonsense-mediated decay	4.64
GO Biological Process	SRP-dependent cotranslational protein targeting to membrane	4.55
GO Biological Process	protein targeting to ER	4.51
GO Biological Process	cotranslational protein targeting to membrane	4.27
GO Biological Process	multi-organism metabolic process	3.86
GO Biological Process	peptidyl-proline modification	3.83
GO Biological Process	establishment of protein localization to endoplasmic reticulum	3.82
GO Biological Process	translational initiation	3.86
GO Biological Process	amide biosynthetic process	3.76
GO Biological Process	nuclear-transcribed mRNA catabolic process	3.47
GO Biological Process	protein localization to endoplasmic reticulum	3.36
GO Biological Process	RNA catabolic process	3.23
GO Biological Process	protein targeting to membrane	3.12
GO Biological Process	translation	3.06
GO Biological Process	regulation of cellular response to heat	2.60
GO Biological Process	peptide biosynthetic process	2.61
GO Biological Process	protein methylation	2.06
GO Biological Process	embryonic heart tube left/right pattern formation	1.58

Supplementary Figure 1401: Properties and genomic distribution of motifs identified for the ZNF566 transcription factor in HEK293 (accession ChipExo models).

TF-MoDisCO pattern_0 n=455, CWM

pattern_0, n=455; subpattern_0, ns=91

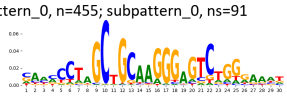

pattern_0, n=455; subpattern_1, ns=84

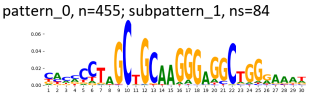

pattern_0, n=455; subpattern_2, ns=81

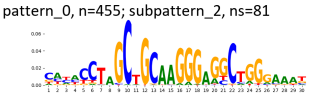

pattern_0, n=455; subpattern_3, ns=78

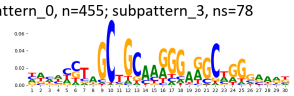

pattern_0, n=455; subpattern_4, ns=53

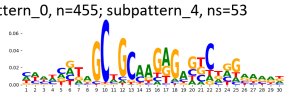

pattern_0, n=455; subpattern_5, ns=43

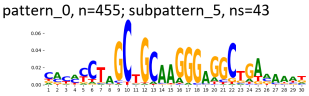

pattern_0, n=455; subpattern_6, ns=25

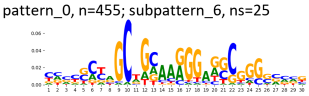

TF-MoDisCO pattern_0 n=455, PWM

pattern_0, n=455; subpattern_0, ns=91

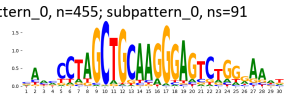

pattern_0, n=455; subpattern_1, ns=84

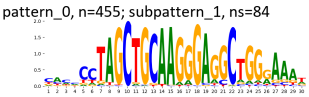

pattern_0, n=455; subpattern_2, ns=81

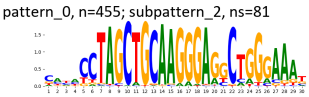

pattern_0, n=455; subpattern_3, ns=78

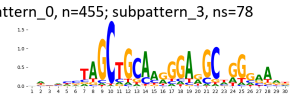

pattern_0, n=455; subpattern_4, ns=53

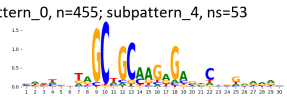

pattern_0, n=455; subpattern_5, ns=43

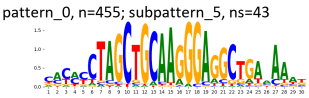

pattern_0, n=455; subpattern_6, ns=25

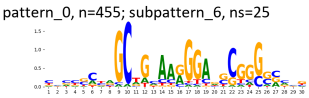

Supplementary Figure 1402: TF-MoDisCO subpatterns for the ZNF566 transcription factor in HEK293 (accession ChipExo models).

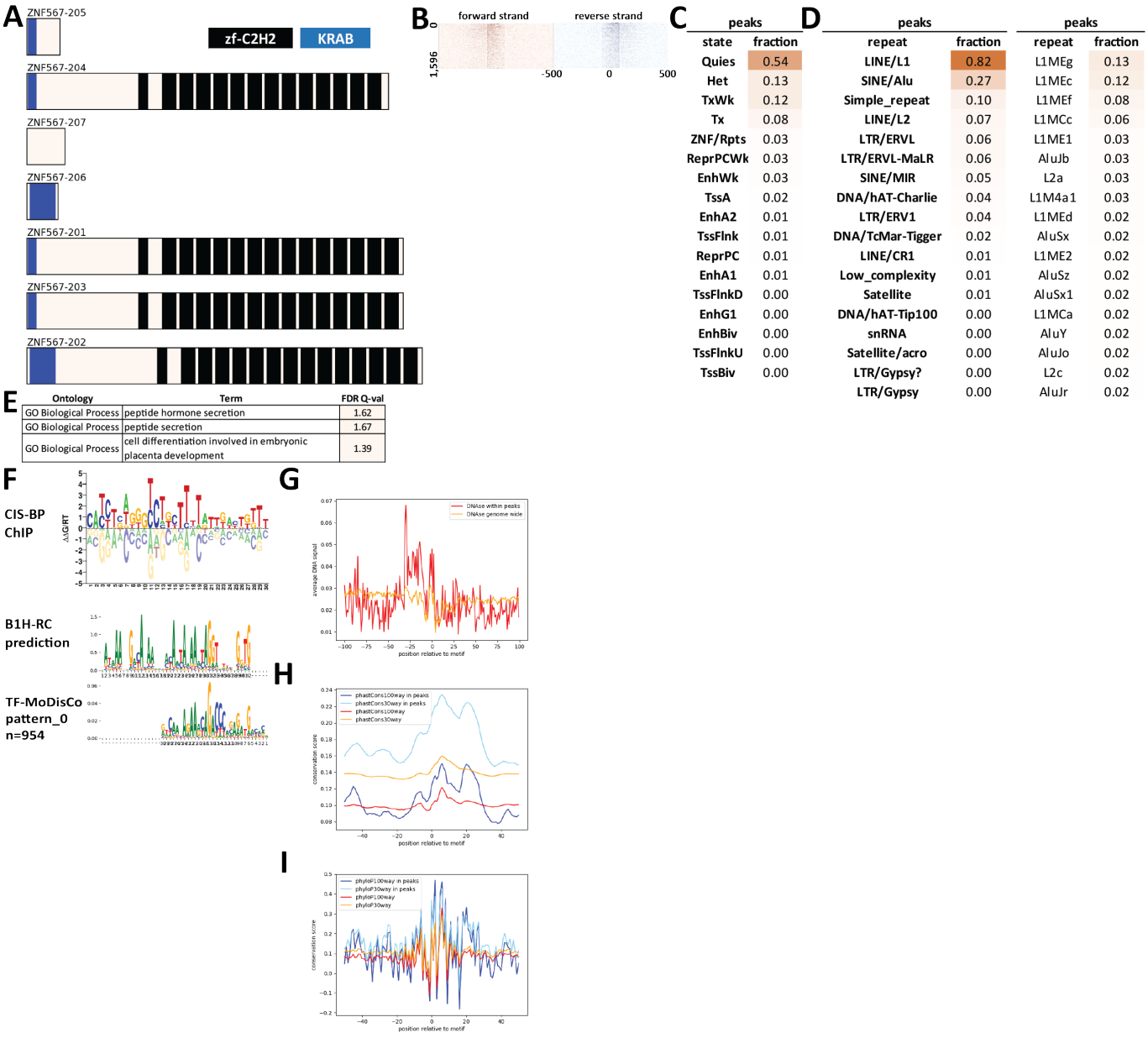

Supplementary Figure 1403: Properties and genomic distribution of motifs identified for the ZNF567 transcription factor in HEK293 (accession ChipExo models).

TF-MoDisCO pattern_0 n=954, CWM

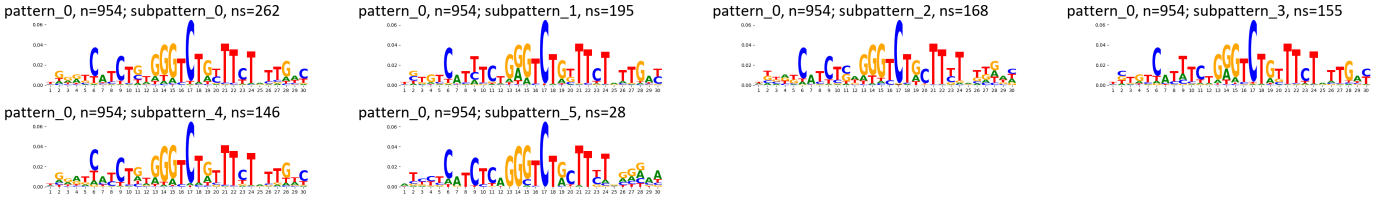

TF-MoDisCO pattern_0 n=954, PWM

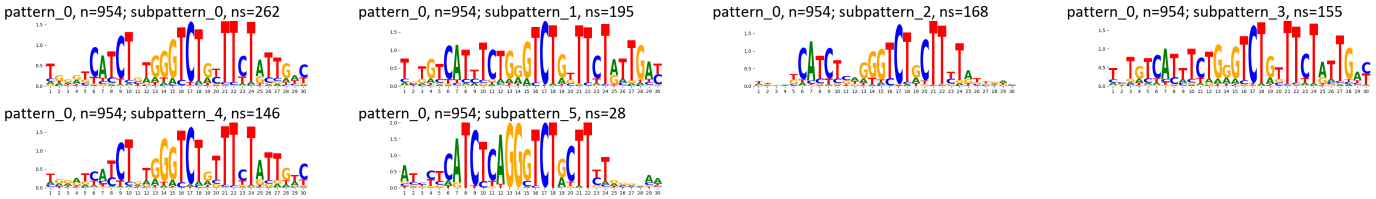

Supplementary Figure 1404: TF-MoDisCO subpatterns for the ZNF567 transcription factor in HEK293 (accession ChipExo models).

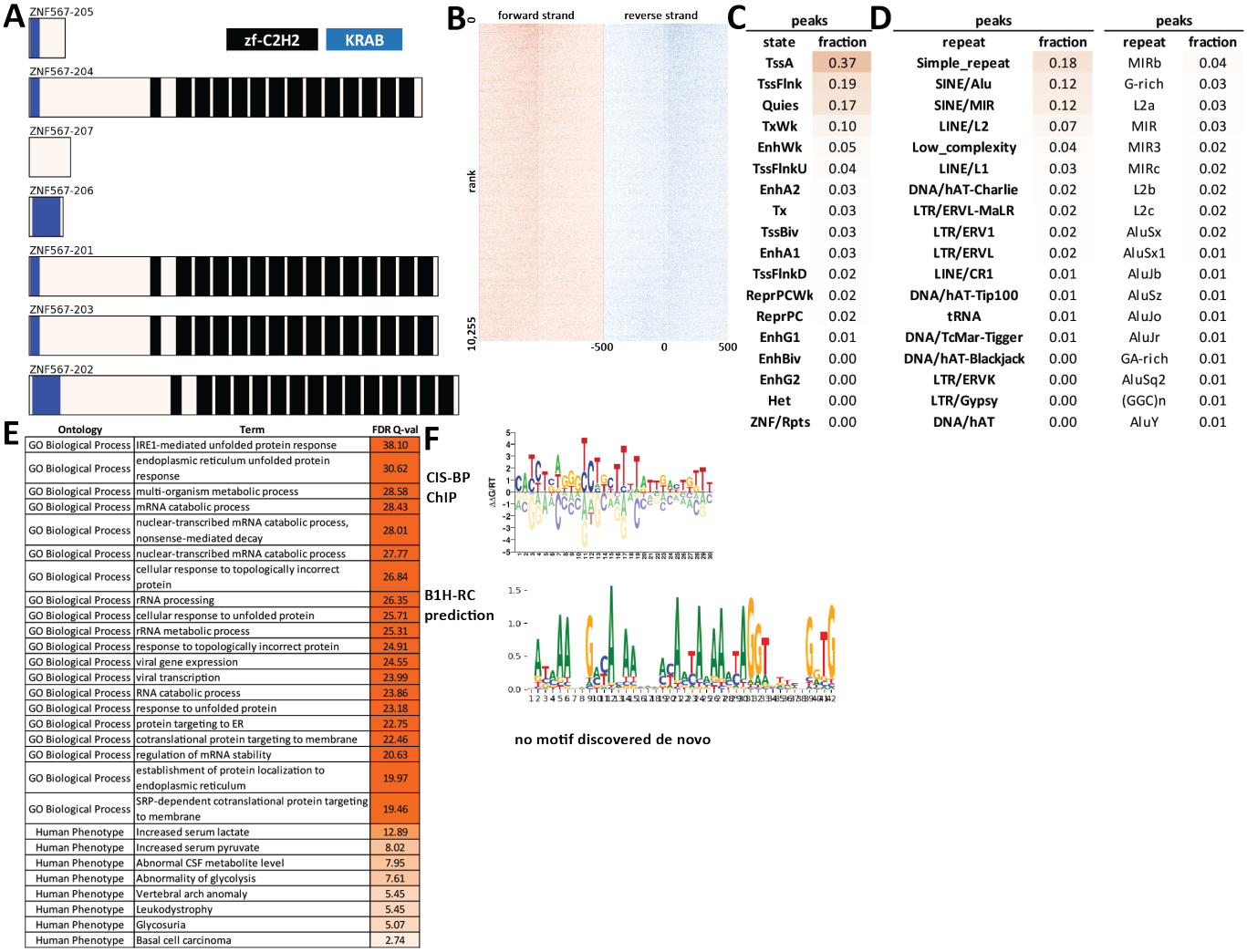

C

peaks	
state	fraction
TssA	0.37
TssFlnk	0.19
Quies	0.17
TxWk	0.10
EnhWk	0.05
TssFlnkU	0.04
EnhA2	0.03
Tx	0.03
TssBiv	0.03
EnhA1	0.03
TssFlnkD	0.02
ReprPCWk	0.02
ReprPC	0.02
EnhG1	0.01
EnhBiv	0.00
EnhG2	0.00
Het	0.00
ZNF/Rpts	0.00

D

peaks		peaks	
repeat	fraction	repeat	fraction
Simple_repeat	0.18	MIRb	0.04
SINE/Alu	0.12	G-rich	0.03
SINE/MIR	0.12	L2a	0.03
LINE/L2	0.07	MIR	0.03
Low_complexity	0.04	MIR3	0.02
LINE/L1	0.03	MIRc	0.02
DNA/hAT-Charlie	0.02	L2b	0.02
LTR/ERVL-MaLR	0.02	L2c	0.02
LTR/ERV1	0.02	AluSx	0.02
LTR/ERVL	0.02	AluSx1	0.01
LINE/CR1	0.01	AluJb	0.01
DNA/hAT-Tip100	0.01	AluSz	0.01
tRNA	0.01	AluJo	0.01
DNA/TcMar-Tigger	0.01	AluJr	0.01
DNA/hAT-Blackjack	0.00	GA-rich	0.01
LTR/ERVK	0.00	AluSq2	0.01
LTR/Gypsy	0.00	(GGC)n	0.01
DNA/hAT	0.00	AluY	0.01

E

Ontology	Term	FDR Q-val
GO Biological Process	IRE1-mediated unfolded protein response	38.10
GO Biological Process	endoplasmic reticulum unfolded protein response	30.62
GO Biological Process	multi-organism metabolic process	28.58
GO Biological Process	mRNA catabolic process	28.43
GO Biological Process	nuclear-transcribed mRNA catabolic process, nonsense-mediated decay	28.01
GO Biological Process	nuclear-transcribed mRNA catabolic process	27.77
GO Biological Process	cellular response to topologically incorrect protein	26.84
GO Biological Process	rRNA processing	26.35
GO Biological Process	cellular response to unfolded protein	25.71
GO Biological Process	rRNA metabolic process	25.31
GO Biological Process	response to topologically incorrect protein	24.91
GO Biological Process	viral gene expression	24.55
GO Biological Process	viral transcription	23.99
GO Biological Process	RNA catabolic process	23.86
GO Biological Process	response to unfolded protein	23.18
GO Biological Process	protein targeting to ER	22.75
GO Biological Process	cotranslational protein targeting to membrane	22.46
GO Biological Process	regulation of mRNA stability	20.63
GO Biological Process	establishment of protein localization to endoplasmic reticulum	19.97
GO Biological Process	SRP-dependent cotranslational protein targeting to membrane	19.46
Human Phenotype	Increased serum lactate	12.89
Human Phenotype	Increased serum pyruvate	8.02
Human Phenotype	Abnormal CSF metabolite level	7.95
Human Phenotype	Abnormality of glycolysis	7.61
Human Phenotype	Vertebral arch anomaly	5.45
Human Phenotype	Leukodystrophy	5.45
Human Phenotype	Glycosuria	5.07
Human Phenotype	Basal cell carcinoma	2.74

Supplementary Figure 1405: Properties and genomic distribution of motifs identified for the ZNF567 transcription factor in HepG2 (accession ENCSR231NMZ).

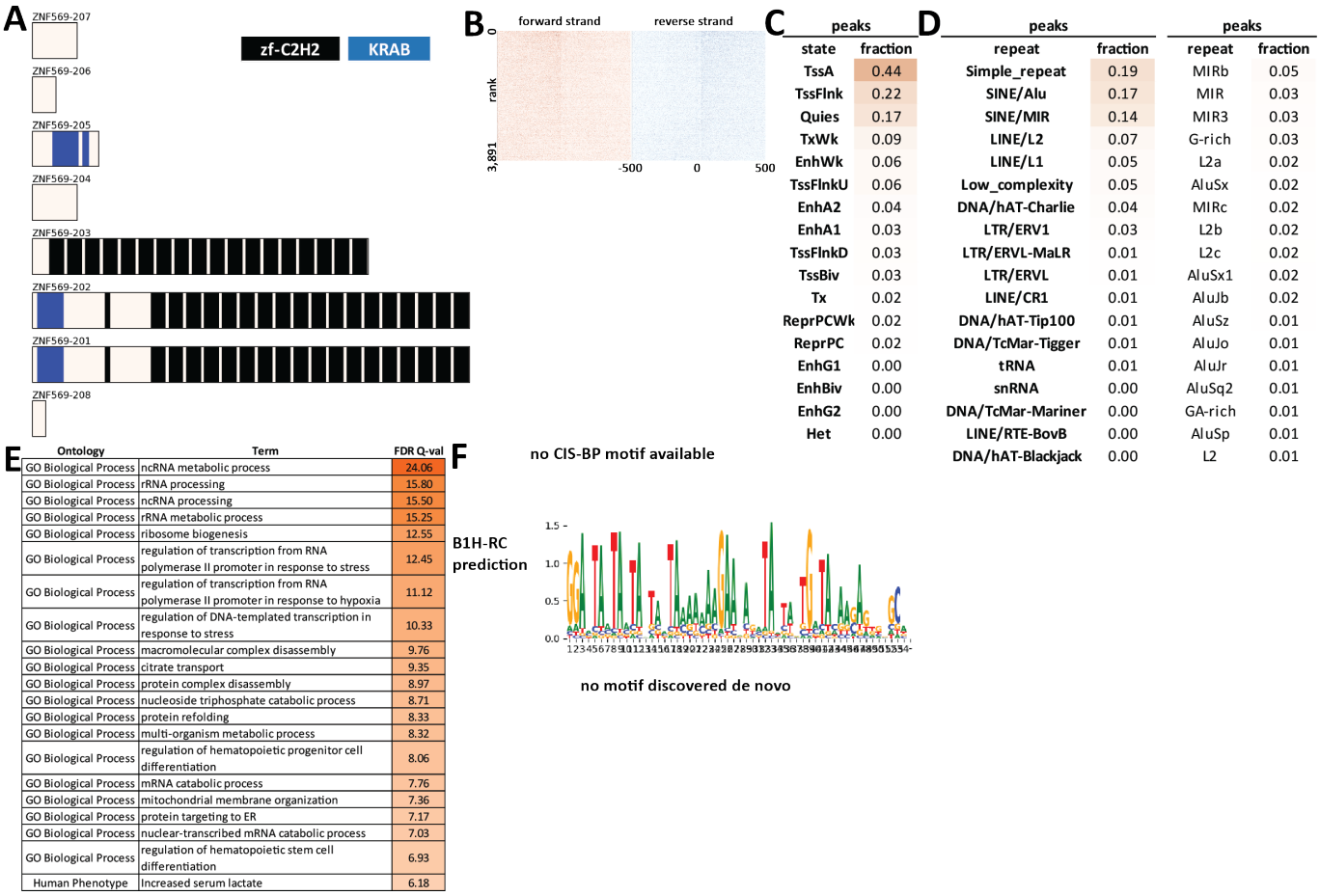

Supplementary Figure 1406: Properties and genomic distribution of motifs identified for the ZNF569 transcription factor in HepG2 (accession ENCSR225SLE).

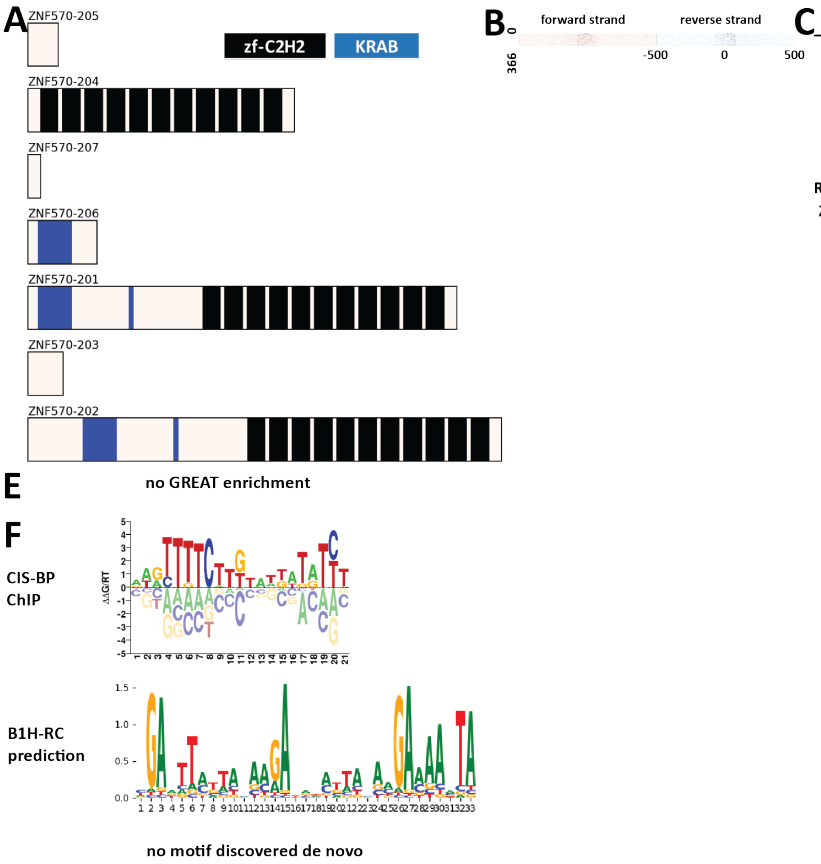

C

peaks	
state	fraction
Quies	0.42
TxWk	0.15
Tx	0.10
Het	0.04
EnhWk	0.04
ReprPCWk	0.03
ZNF/Rpts	0.02
EnhA2	0.02
TssFlnk	0.02
TssA	0.02
EnhA1	0.01
EnhBiv	0.01
TssFlnkU	0.01
TssBiv	0.01
ReprPC	0.01
EnhG1	0.01
TssFlnkD	0.00

D

peaks		peaks	
repeat	fraction	repeat	fraction
LINE/L1	0.46	HAL1	0.09
SINE/Alu	0.29	AluJb	0.05
Simple_repeat	0.15	AluY	0.04
LTR/ERV1	0.04	AluSx	0.03
LINE/L2	0.04	L1M5	0.02
SINE/MIR	0.04	L1M4	0.02
DNA/hAT-Charlie	0.04	L1MEc	0.02
LTR/ERVL-MaLR	0.03	L1MDa	0.02
LTR/ERVL	0.02	L1M7	0.02
Satellite	0.02	AluSz	0.02
Low_complexity	0.02	AluSq2	0.02
DNA/TcMar-Tigger	0.02	MIRb	0.02
Satellite/centr	0.01	AluJr	0.02
Satellite/acro	0.01	L1MEg	0.01
snRNA	0.01	L1MEf	0.01
LINE/CR1	0.01	AluSp	0.01
DNA/hAT-Tip100	0.01	AluJo	0.01
rRNA	0.00	A-rich	0.01

Supplementary Figure 1407: Properties and genomic distribution of motifs identified for the ZNF570 transcription factor in HEK293 (accession ChipExo models).

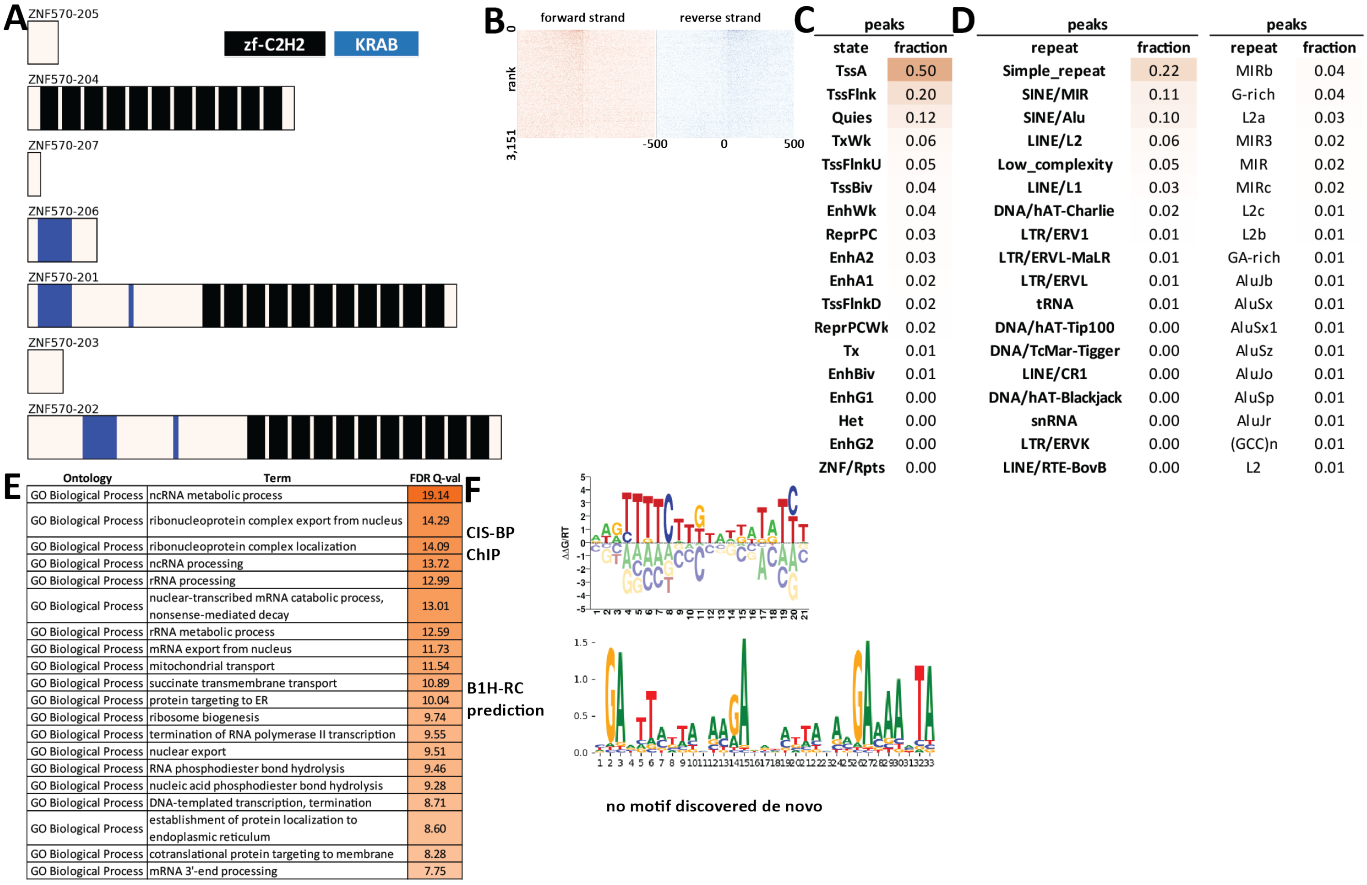

Supplementary Figure 1408: Properties and genomic distribution of motifs identified for the ZNF570 transcription factor in HepG2 (accession ENCSR055ZIA).

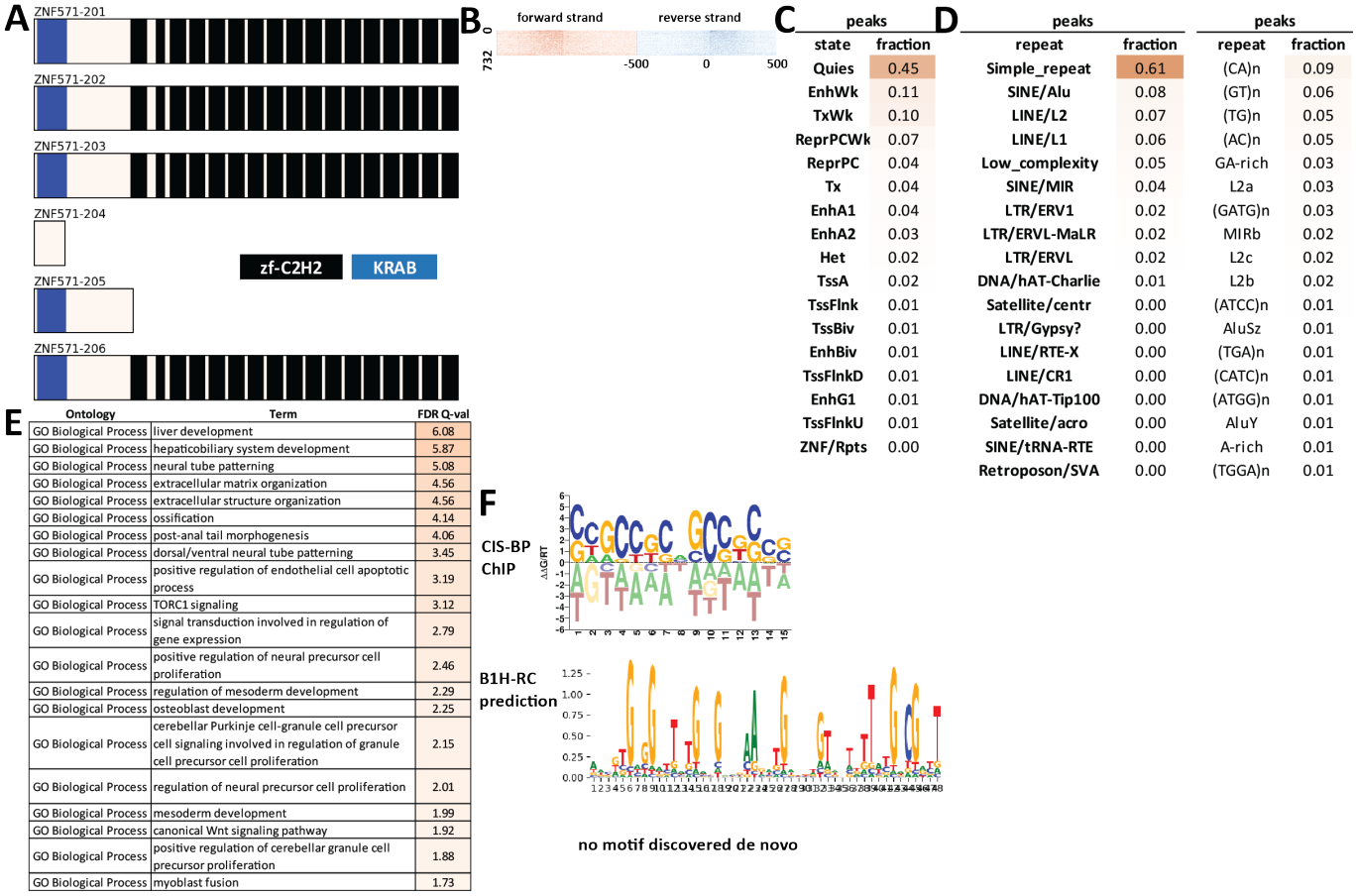

Supplementary Figure 1409: Properties and genomic distribution of motifs identified for the ZNF571 transcription factor in HEK293 (accession ENCSR421QXA).

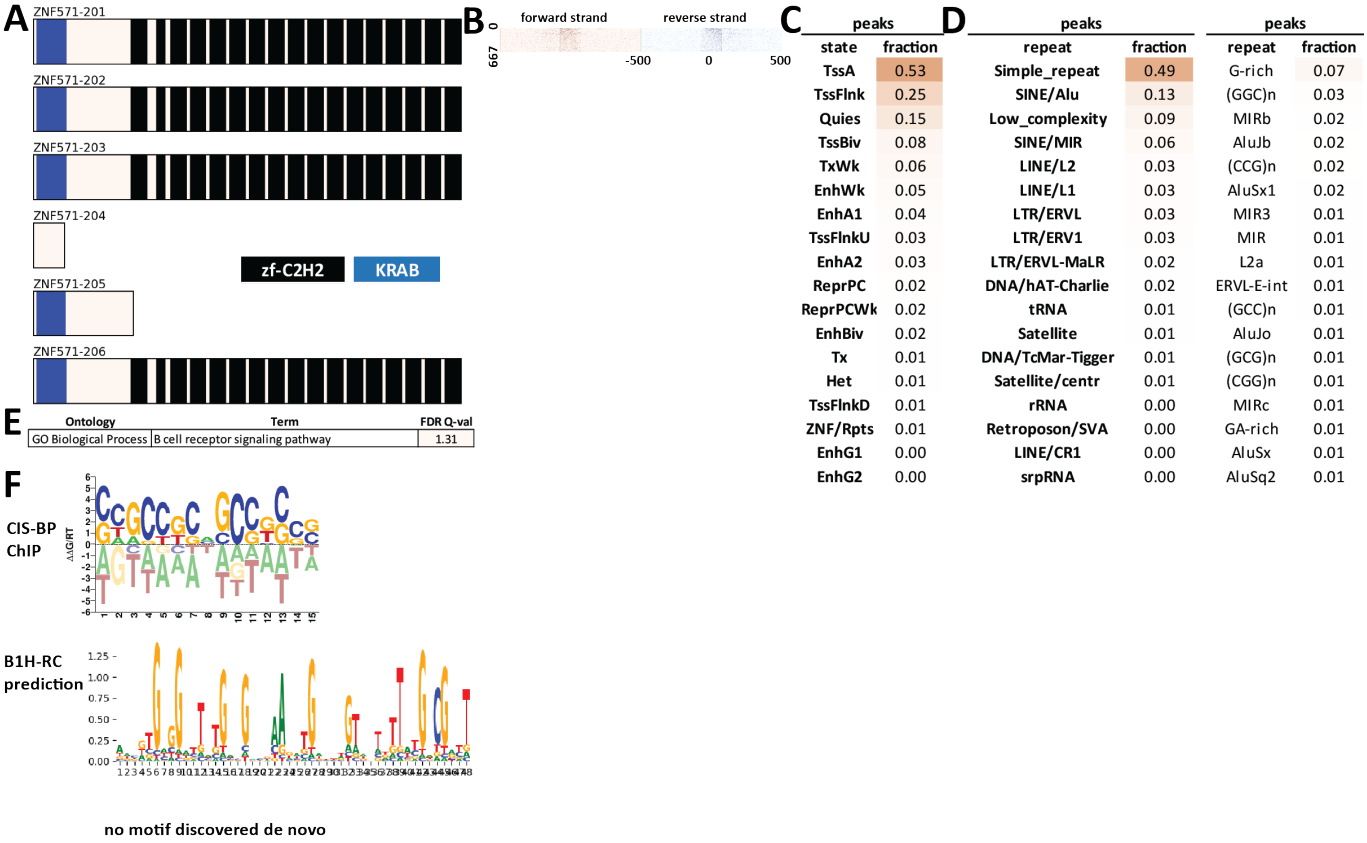

C

peaks	
state	fraction
TssA	0.53
TssFlnk	0.25
Quies	0.15
TssBiv	0.08
TxWk	0.06
EnhWk	0.05
EnhA1	0.04
TssFlnkU	0.03
EnhA2	0.03
ReprPC	0.02
ReprPCWk	0.02
EnhBiv	0.02
Tx	0.01
Het	0.01
TssFlnkD	0.01
ZNF/Rpts	0.01
EnhG1	0.00
EnhG2	0.00

D

peaks		peaks	
repeat	fraction	repeat	fraction
Simple_repeat	0.49	G-rich	0.07
SINE/Alu	0.13	(GGC)n	0.03
Low_complexity	0.09	MIRb	0.02
SINE/MIR	0.06	AluJb	0.02
LINE/L2	0.03	(CCG)n	0.02
LINE/L1	0.03	AluSx1	0.02
LTR/ERVL	0.03	MIR3	0.01
LTR/ERV1	0.03	MIR	0.01
LTR/ERVL-MaLR	0.02	L2a	0.01
DNA/hAT-Charlie	0.02	ERVL-E-int	0.01
tRNA	0.01	(GCC)n	0.01
Satellite	0.01	AluJo	0.01
DNA/TcMar-Tigger	0.01	(GCG)n	0.01
Satellite/centr	0.01	(CGG)n	0.01
rRNA	0.00	MIRc	0.01
Retroposon/SVA	0.00	GA-rich	0.01
LINE/CR1	0.00	AluSx	0.01
srpRNA	0.00	AluSq2	0.01

Supplementary Figure 1410: Properties and genomic distribution of motifs identified for the ZNF571 transcription factor in HEK293 (accession ChipExo models).

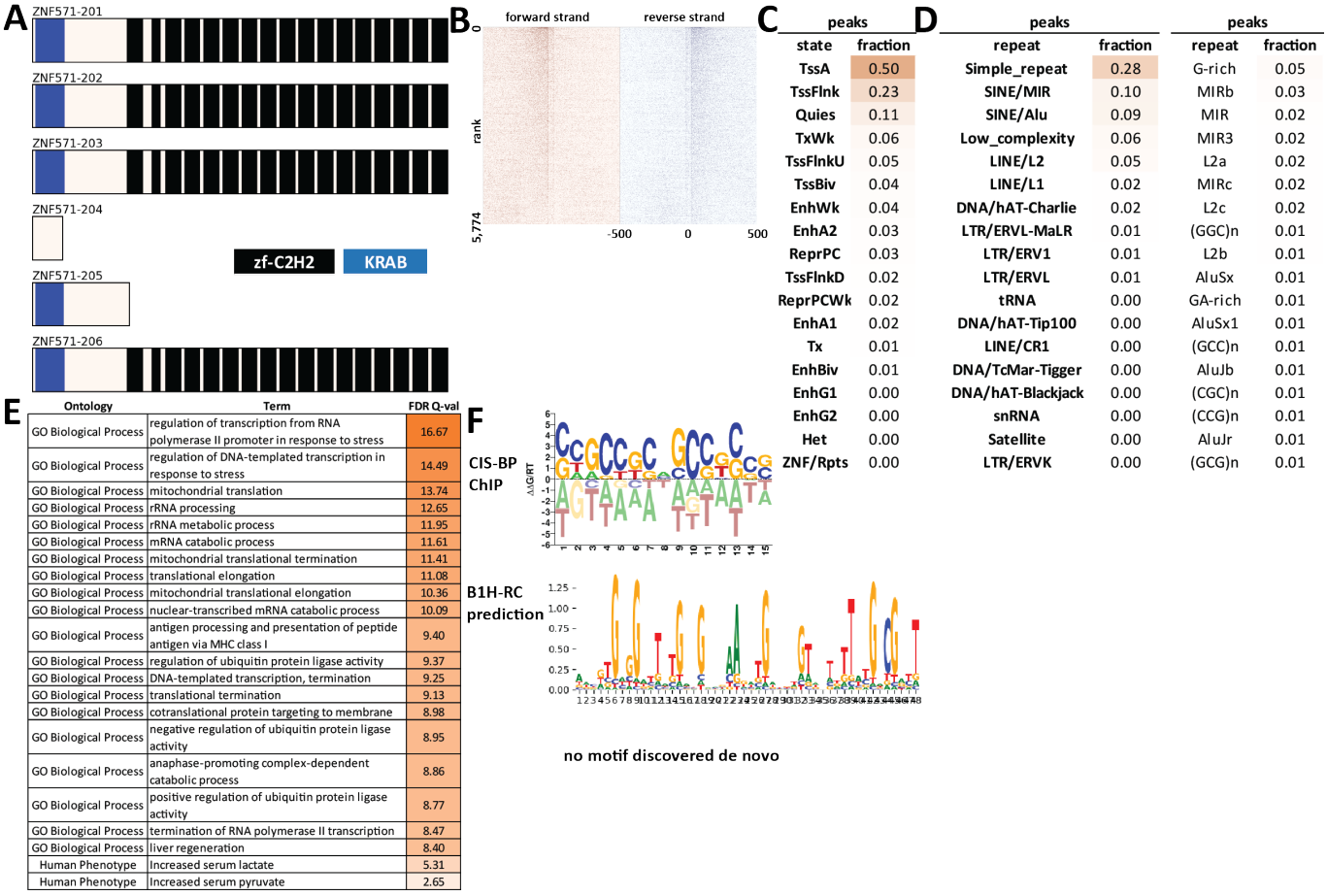

Supplementary Figure 1411: Properties and genomic distribution of motifs identified for the ZNF571 transcription factor in HepG2 (accession ENCSR697CNF).

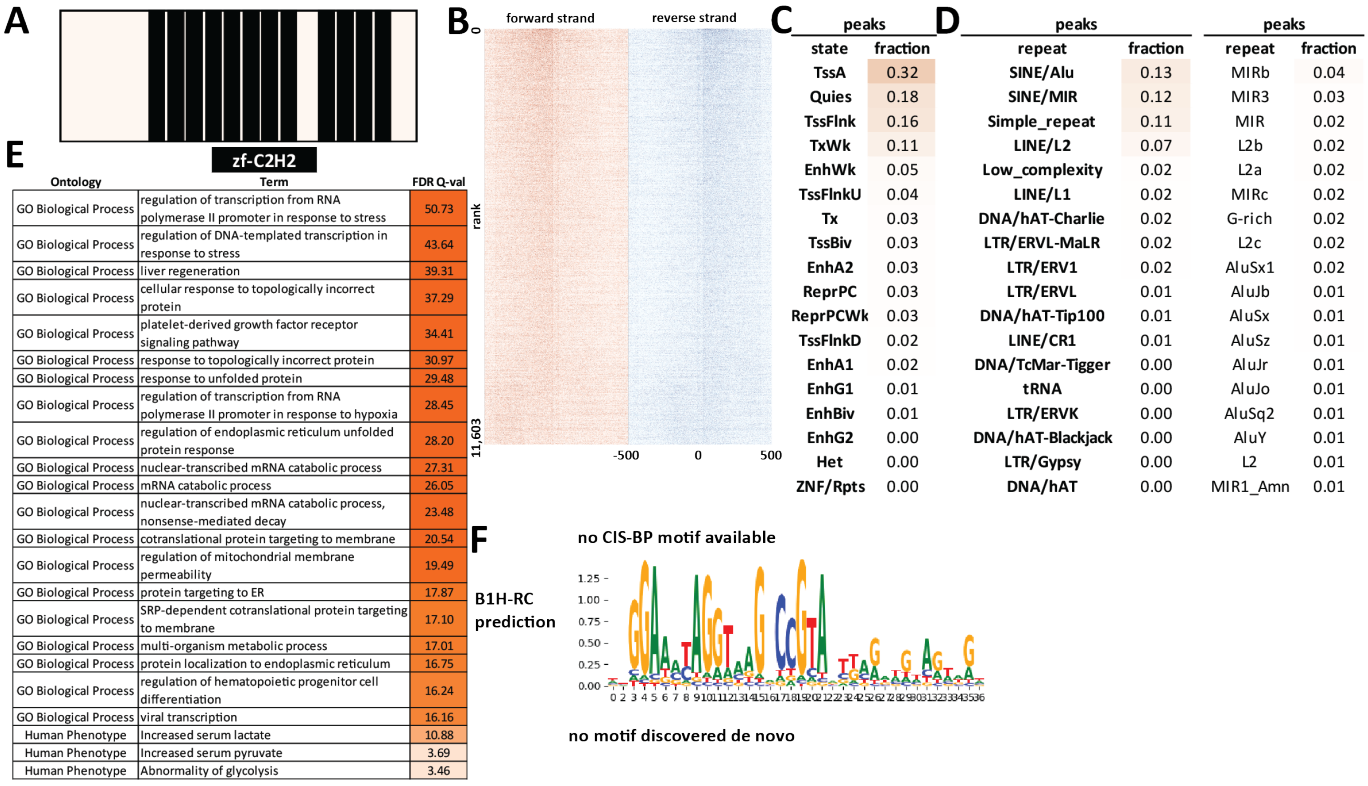

C

peaks	
state	fraction
TssA	0.32
Quies	0.18
TssFlnk	0.16
TxWk	0.11
EnhWk	0.05
TssFlnkU	0.04
Tx	0.03
TssBiv	0.03
EnhA2	0.03
ReprPC	0.03
ReprPCWk	0.03
TssFlnkD	0.02
EnhA1	0.02
EnhG1	0.01
EnhBiv	0.01
EnhG2	0.00
Het	0.00
ZNF/Rpts	0.00

D

peaks		peaks	
repeat	fraction	repeat	fraction
SINE/Alu	0.13	MIRb	0.04
SINE/MIR	0.12	MIR3	0.03
Simple_repeat	0.11	MIR	0.02
LINE/L2	0.07	L2b	0.02
Low_complexity	0.02	L2a	0.02
LINE/L1	0.02	MIRc	0.02
DNA/hAT-Charlie	0.02	G-rich	0.02
LTR/ERVL-MaLR	0.02	L2c	0.02
LTR/ERV1	0.02	AluSx1	0.02
LTR/ERVL	0.01	AluJb	0.01
DNA/hAT-Tip100	0.01	AluSx	0.01
LINE/CR1	0.01	AluSz	0.01
DNA/TcMar-Tigger	0.00	AluJr	0.01
tRNA	0.00	AluJo	0.01
LTR/ERVK	0.00	AluSq2	0.01
DNA/hAT-Blackjack	0.00	AluY	0.01
LTR/Gypsy	0.00	L2	0.01
DNA/hAT	0.00	MIR1_Amn	0.01

E

Ontology	Term	FDR Q-val
GO Biological Process	regulation of transcription from RNA polymerase II promoter in response to stress	50.73
GO Biological Process	regulation of DNA-templated transcription in response to stress	43.64
GO Biological Process	liver regeneration	39.31
GO Biological Process	cellular response to topologically incorrect protein	37.29
GO Biological Process	platelet-derived growth factor receptor signaling pathway	34.41
GO Biological Process	response to topologically incorrect protein	30.97
GO Biological Process	response to unfolded protein	29.48
GO Biological Process	regulation of transcription from RNA polymerase II promoter in response to hypoxia	28.45
GO Biological Process	regulation of endoplasmic reticulum unfolded protein response	28.20
GO Biological Process	nuclear-transcribed mRNA catabolic process	27.31
GO Biological Process	mRNA catabolic process	26.05
GO Biological Process	nuclear-transcribed mRNA catabolic process, nonsense-mediated decay	23.48
GO Biological Process	cotranslational protein targeting to membrane	20.54
GO Biological Process	regulation of mitochondrial membrane permeability	19.49
GO Biological Process	protein targeting to ER	17.87
GO Biological Process	SRP-dependent cotranslational protein targeting to membrane	17.10
GO Biological Process	multi-organism metabolic process	17.01
GO Biological Process	protein localization to endoplasmic reticulum	16.75
GO Biological Process	regulation of hematopoietic progenitor cell differentiation	16.24
GO Biological Process	viral transcription	16.16
Human Phenotype	Increased serum lactate	10.88
Human Phenotype	Increased serum pyruvate	3.69
Human Phenotype	Abnormality of glycolysis	3.46

Supplementary Figure 1412: Properties and genomic distribution of motifs identified for the ZNF572 transcription factor in HepG2 (accession ENCSR663CTC).

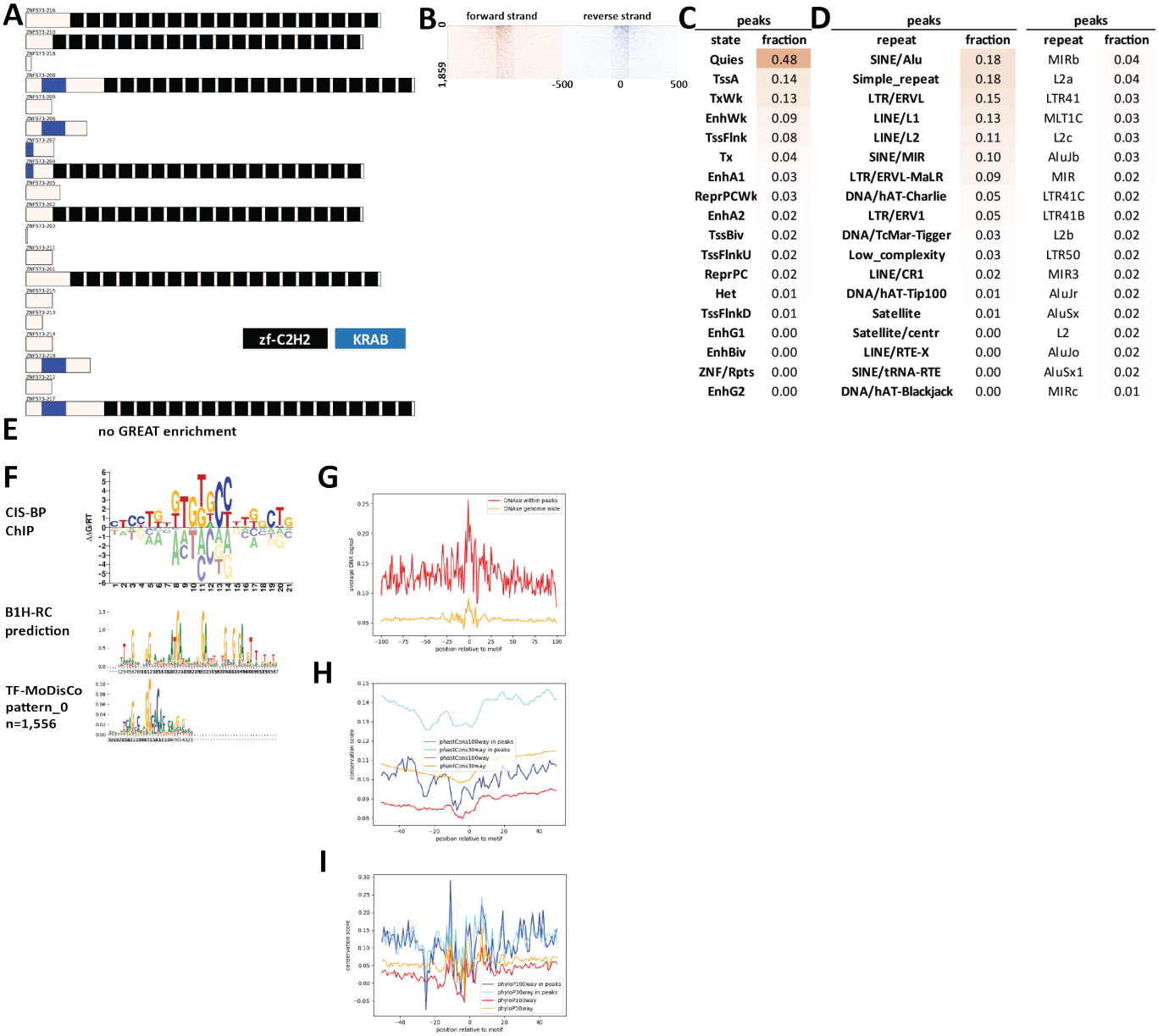

peaks	
state	fraction
Quies	0.48
TssA	0.14
TxWk	0.13
EnhWk	0.09
TssFlnk	0.08
Tx	0.04
EnhA1	0.03
ReprPCWk	0.03
EnhA2	0.02
TssBiv	0.02
TssFlnkU	0.02
ReprPC	0.02
Het	0.01
TssFlnkD	0.01
EnhG1	0.00
EnhBiv	0.00
ZNF/Rpts	0.00
EnhG2	0.00

peaks		peaks	
repeat	fraction	repeat	fraction
SINE/Alu	0.18	MIRb	0.04
Simple_repeat	0.18	L2a	0.04
LTR/ERVL	0.15	LTR41	0.03
LINE/L1	0.13	MLT1C	0.03
LINE/L2	0.11	L2c	0.03
SINE/MIR	0.10	AluJb	0.03
LTR/ERVL-MaLR	0.09	MIR	0.02
DNA/hAT-Charlie	0.05	LTR41C	0.02
LTR/ERV1	0.05	LTR41B	0.02
DNA/TcMar-Tigger	0.03	L2b	0.02
Low_complexity	0.03	LTR50	0.02
LINE/CR1	0.02	MIR3	0.02
DNA/hAT-Tip100	0.01	AluJr	0.02
Satellite	0.01	AluSx	0.02
Satellite/centr	0.00	L2	0.02
LINE/RTE-X	0.00	AluJo	0.02
SINE/tRNA-RTE	0.00	AluSx1	0.02
DNA/hAT-Blackjack	0.00	MIRc	0.01

Supplementary Figure 1413: Properties and genomic distribution of motifs identified for the ZNF573 transcription factor in HEK293 (accession ChipExo models).

TF-MoDisCO pattern_0 n=1556, CWM

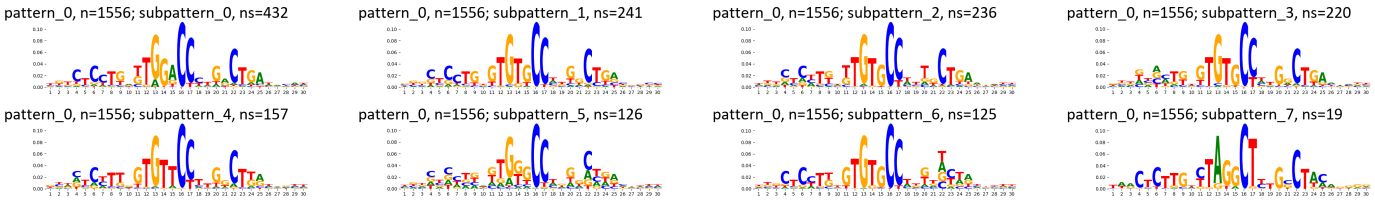

TF-MoDisCO pattern_0 n=1556, PWM

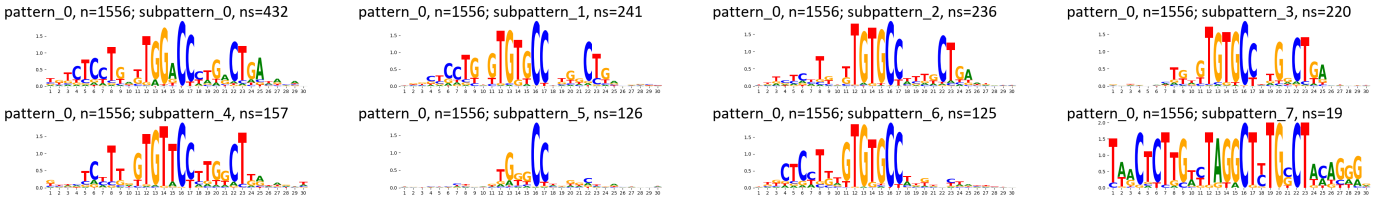

Supplementary Figure 1414: TF-MoDisCO subpatterns for the ZNF573 transcription factor in HEK293 (accession ChipExo models).

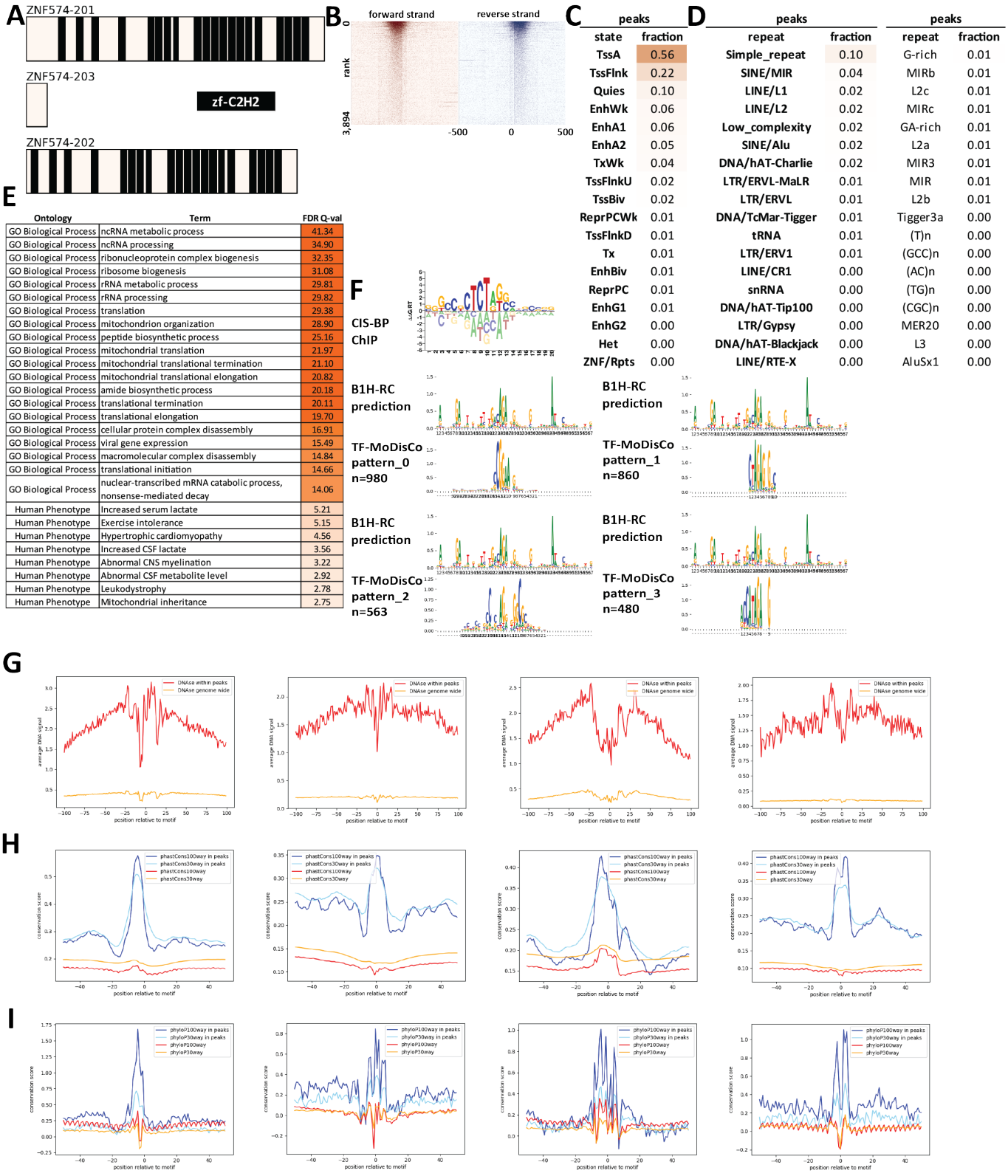

Supplementary Figure 1415: Properties and genomic distribution of motifs identified for the ZNF574 transcription factor in HEK293 (accession Hughes NB models).

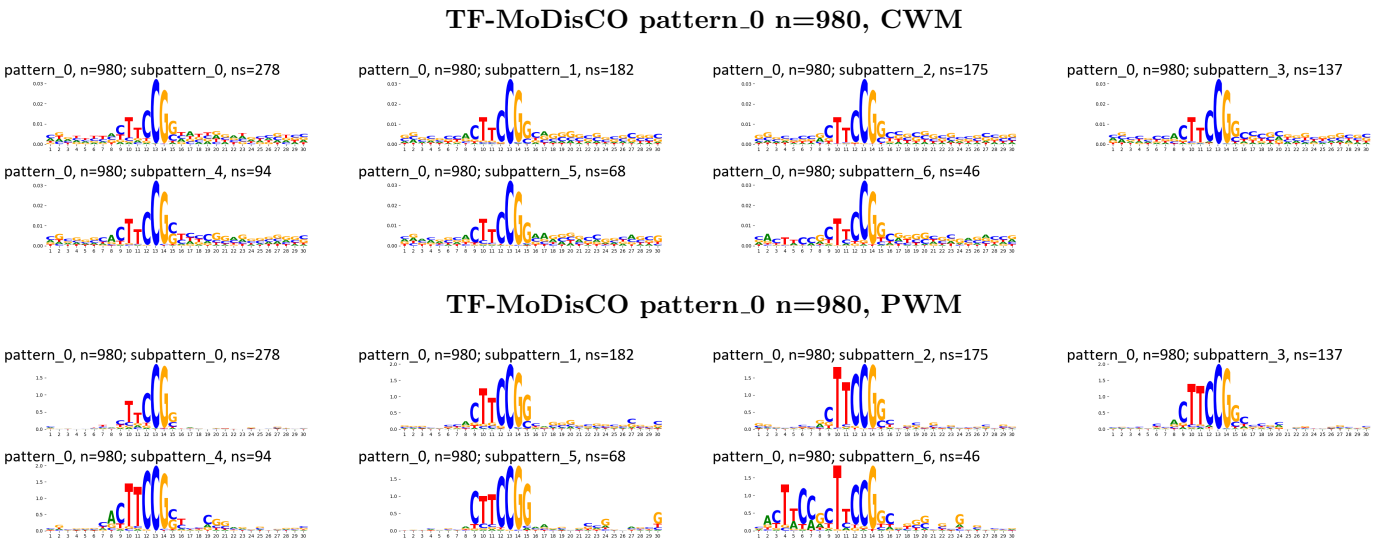

Supplementary Figure 1416: TF-MoDisCO subpatterns for the ZNF574 transcription factor in HEK293 (accession Hughes NB models).

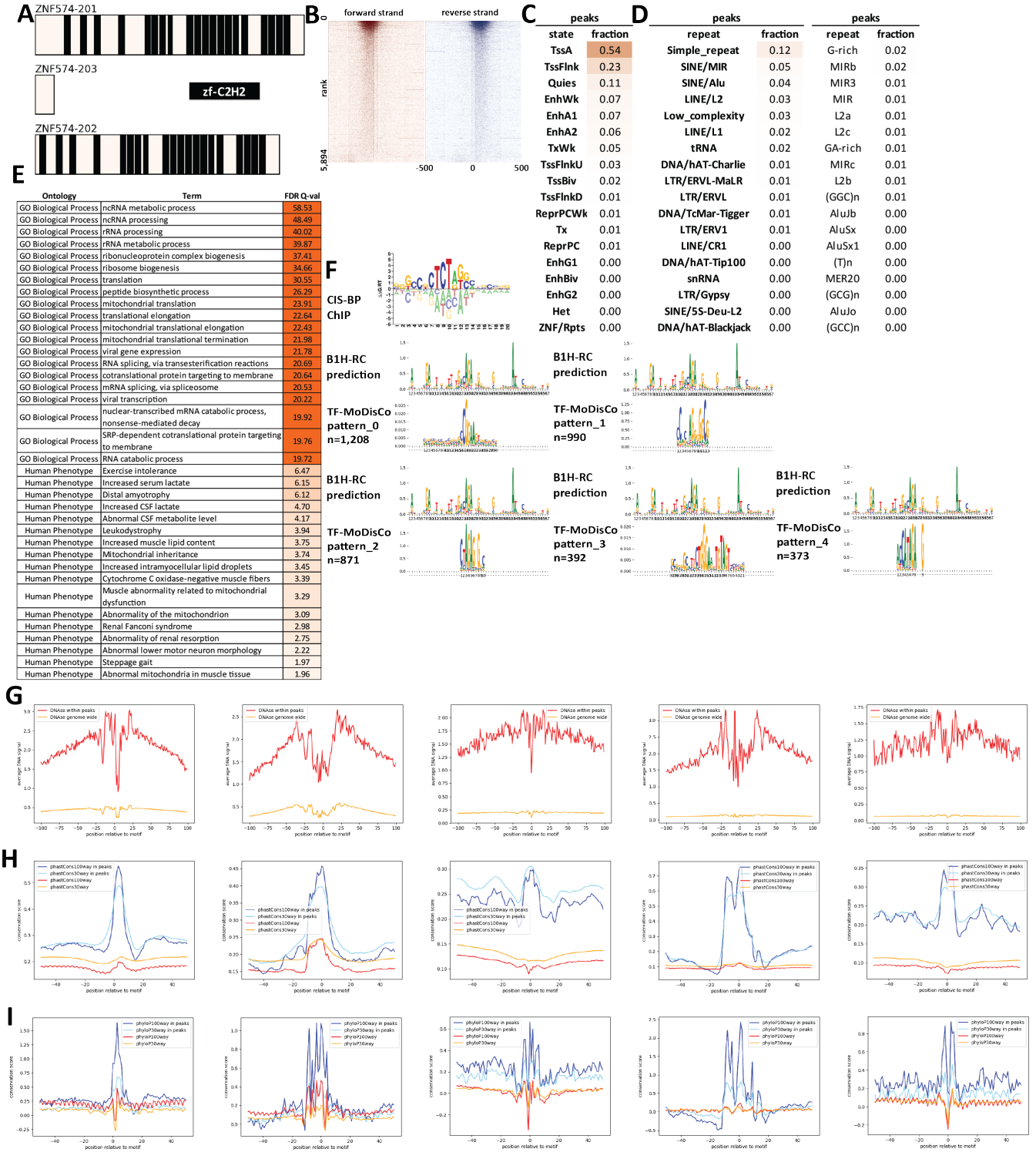

Supplementary Figure 1417: Properties and genomic distribution of motifs identified for the ZNF574 transcription factor in HEK293 (accession Hughes GR models).

TF-MoDisCO pattern_0 n=1208, CWM

pattern_0, n=1208; subpattern_0, ns=226

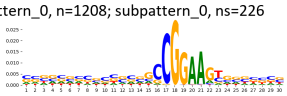

pattern_0, n=1208; subpattern_1, ns=200

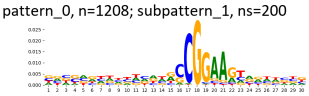

pattern_0, n=1208; subpattern_10, ns=8

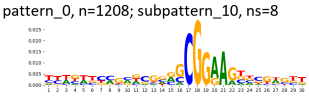

pattern_0, n=1208; subpattern_11, ns=5

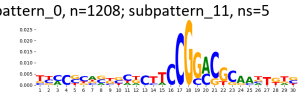

pattern_0, n=1208; subpattern_2, ns=182

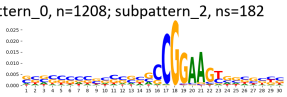

pattern_0, n=1208; subpattern_3, ns=164

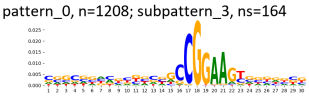

pattern_0, n=1208; subpattern_4, ns=142

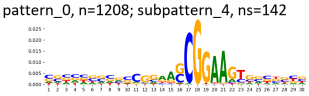

pattern_0, n=1208; subpattern_5, ns=116

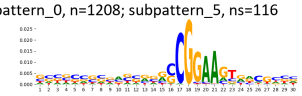

pattern_0, n=1208; subpattern_6, ns=100

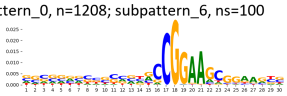

pattern_0, n=1208; subpattern_7, ns=37

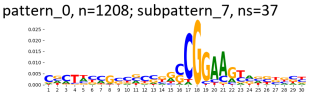

pattern_0, n=1208; subpattern_8, ns=16

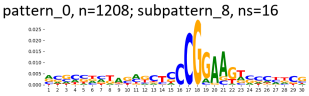

pattern_0, n=1208; subpattern_9, ns=12

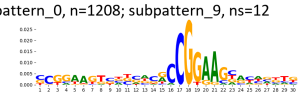

TF-MoDisCO pattern_0 n=1208, PWM

pattern_0, n=1208; subpattern_0, ns=226

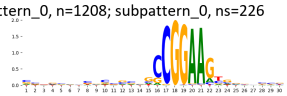

pattern_0, n=1208; subpattern_1, ns=200

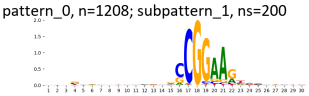

pattern_0, n=1208; subpattern_10, ns=8

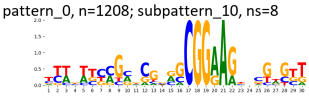

pattern_0, n=1208; subpattern_11, ns=5

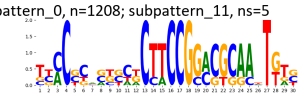

pattern_0, n=1208; subpattern_2, ns=182

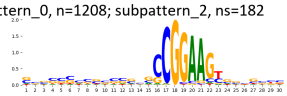

pattern_0, n=1208; subpattern_3, ns=164

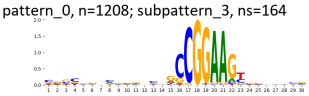

pattern_0, n=1208; subpattern_4, ns=142

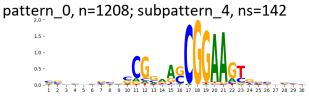

pattern_0, n=1208; subpattern_5, ns=116

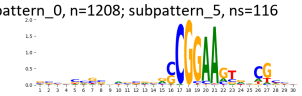

pattern_0, n=1208; subpattern_6, ns=100

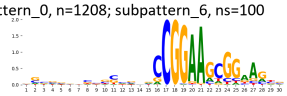

pattern_0, n=1208; subpattern_7, ns=37

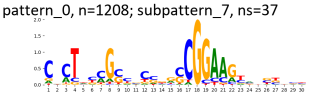

pattern_0, n=1208; subpattern_8, ns=16

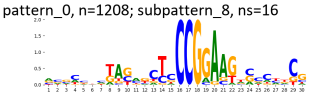

pattern_0, n=1208; subpattern_9, ns=12

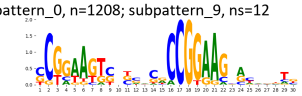

TF-MoDisCO pattern_1 n=990, CWM

pattern_1, n=990; subpattern_0, ns=268

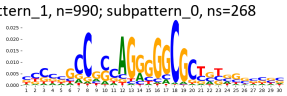

pattern_1, n=990; subpattern_1, ns=222

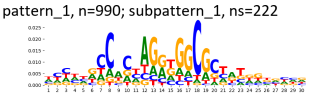

pattern_1, n=990; subpattern_2, ns=202

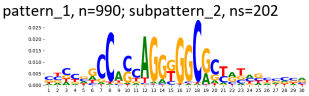

pattern_1, n=990; subpattern_3, ns=135

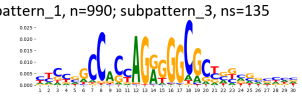

pattern_1, n=990; subpattern_4, ns=110

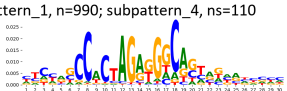

pattern_1, n=990; subpattern_5, ns=53

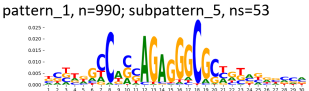

TF-MoDisCO pattern_1 n=990, PWM

pattern_1, n=990; subpattern_0, ns=268

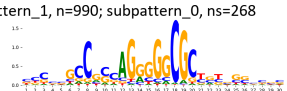

pattern_1, n=990; subpattern_1, ns=222

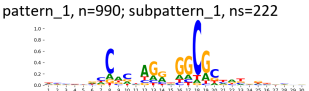

pattern_1, n=990; subpattern_2, ns=202

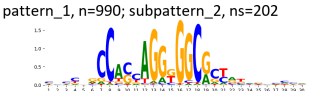

pattern_1, n=990; subpattern_3, ns=135

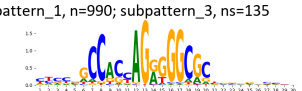

pattern_1, n=990; subpattern_4, ns=110

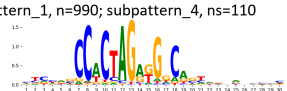

pattern_1, n=990; subpattern_5, ns=53

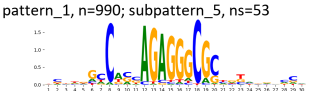

TF-MoDisCO pattern_2 n=871, CWM

pattern_2, n=871; subpattern_0, ns=216

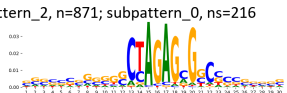

pattern_2, n=871; subpattern_1, ns=191

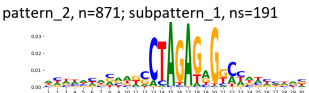

pattern_2, n=871; subpattern_2, ns=190

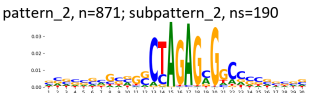

pattern_2, n=871; subpattern_3, ns=121

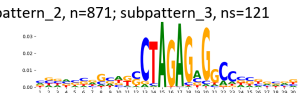

pattern_2, n=871; subpattern_4, ns=74

pattern_2, n=871; subpattern_5, ns=73

pattern_2, n=871; subpattern_6, ns=4

pattern_2, n=871; subpattern_7, ns=2

TF-MoDisCO pattern_2 n=871, PWM

pattern_2, n=871; subpattern_0, ns=216

pattern_2, n=871; subpattern_1, ns=191

pattern_2, n=871; subpattern_2, ns=190

pattern_2, n=871; subpattern_3, ns=121

pattern_2, n=871; subpattern_4, ns=74

pattern_2, n=871; subpattern_5, ns=73

pattern_2, n=871; subpattern_6, ns=4

pattern_2, n=871; subpattern_7, ns=2

TF-MoDisCO pattern_3 n=392, CWM

pattern_3, n=392; subpattern_0, ns=116

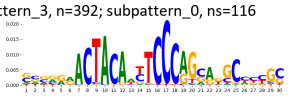

pattern_3, n=392; subpattern_1, ns=112

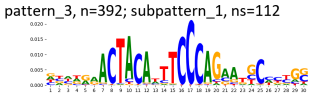

pattern_3, n=392; subpattern_2, ns=101

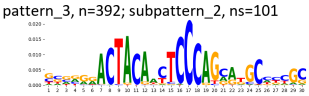

pattern_3, n=392; subpattern_3, ns=60

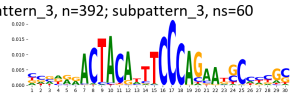

pattern_3, n=392; subpattern_4, ns=3

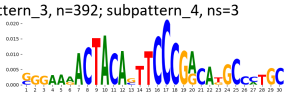

TF-MoDisCO pattern_3 n=392, PWM

pattern_3, n=392; subpattern_0, ns=116

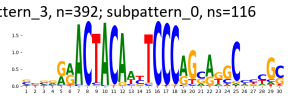

pattern_3, n=392; subpattern_1, ns=112

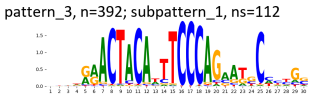

pattern_3, n=392; subpattern_2, ns=101

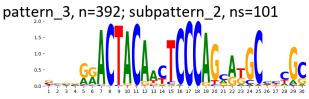

pattern_3, n=392; subpattern_3, ns=60

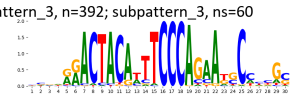

pattern_3, n=392; subpattern_4, ns=3

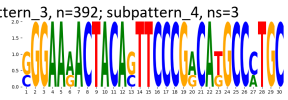

TF-MoDisCO pattern_4 n=373, CWM

pattern_4, n=373; subpattern_0, ns=122

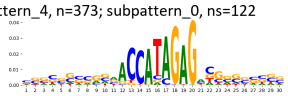

pattern_4, n=373; subpattern_1, ns=82

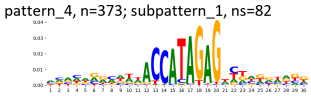

pattern_4, n=373; subpattern_2, ns=71

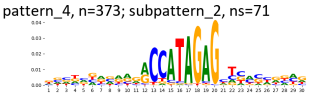

pattern_4, n=373; subpattern_3, ns=57

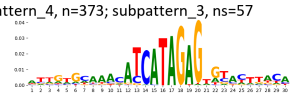

pattern_4, n=373; subpattern_4, ns=37

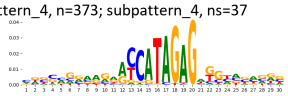

pattern_4, n=373; subpattern_5, ns=2

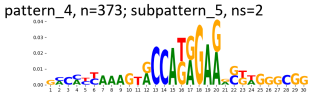

pattern_4, n=373; subpattern_6, ns=2

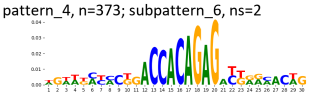

TF-MoDisCO pattern_4 n=373, PWM

pattern_4, n=373; subpattern_0, ns=122

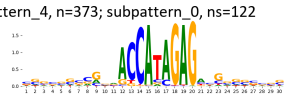

pattern_4, n=373; subpattern_1, ns=82

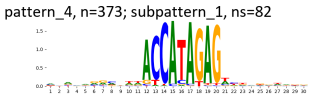

pattern_4, n=373; subpattern_2, ns=71

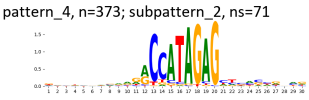

pattern_4, n=373; subpattern_3, ns=57

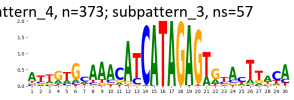

pattern_4, n=373; subpattern_4, ns=37

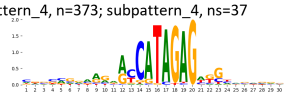

pattern_4, n=373; subpattern_5, ns=2

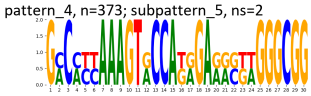

pattern_4, n=373; subpattern_6, ns=2

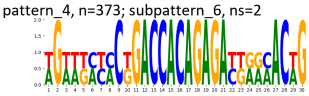

Supplementary Figure 1418: TF-MoDisCO subpatterns for the ZNF574 transcription factor in HEK293 (accession Hughes GR models).

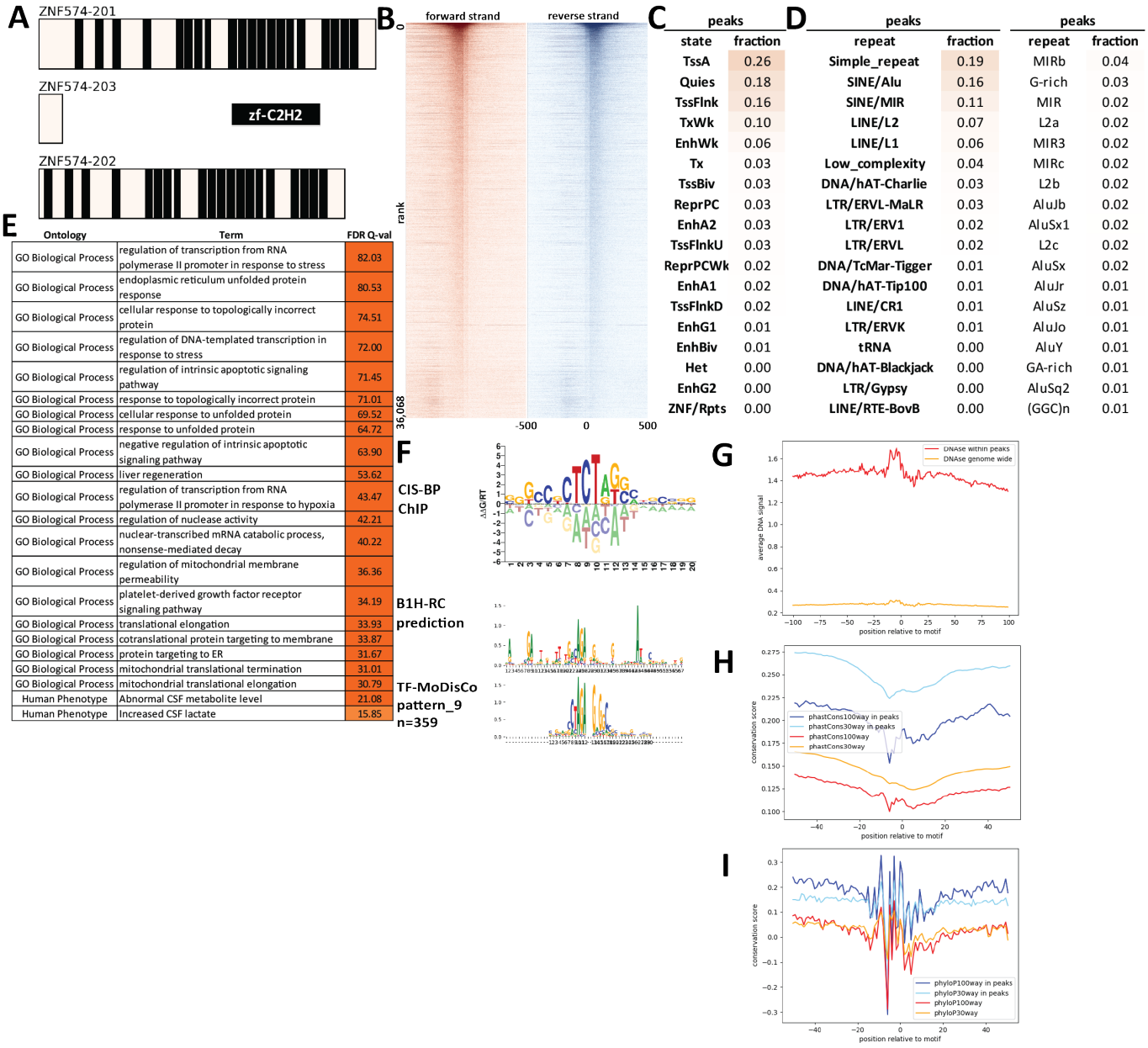

Supplementary Figure 1419: Properties and genomic distribution of motifs identified for the ZNF574 transcription factor in HepG2 (accession ENCSR886YJI).

TF-MoDisCO pattern_9 n=359, CWM

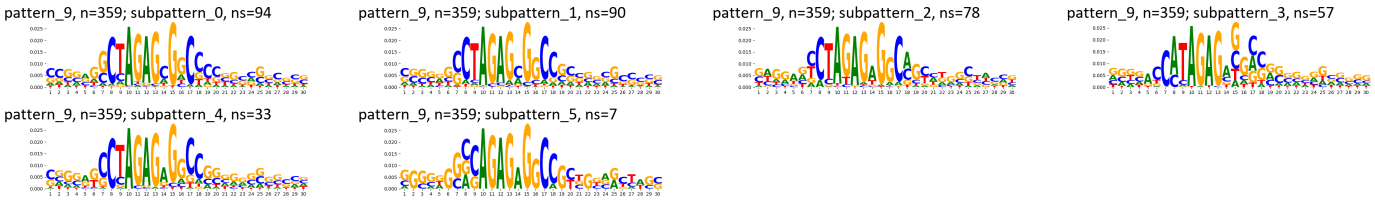

TF-MoDisCO pattern_9 n=359, PWM

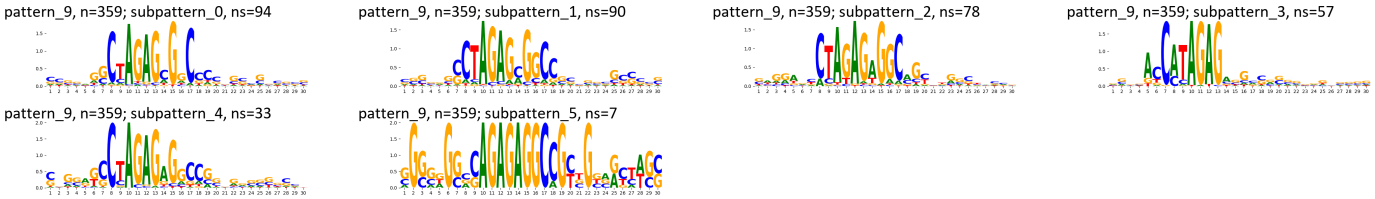

Supplementary Figure 1420: TF-MoDisCO subpatterns for the ZNF574 transcription factor in HepG2 (accession ENCSR886YJI).

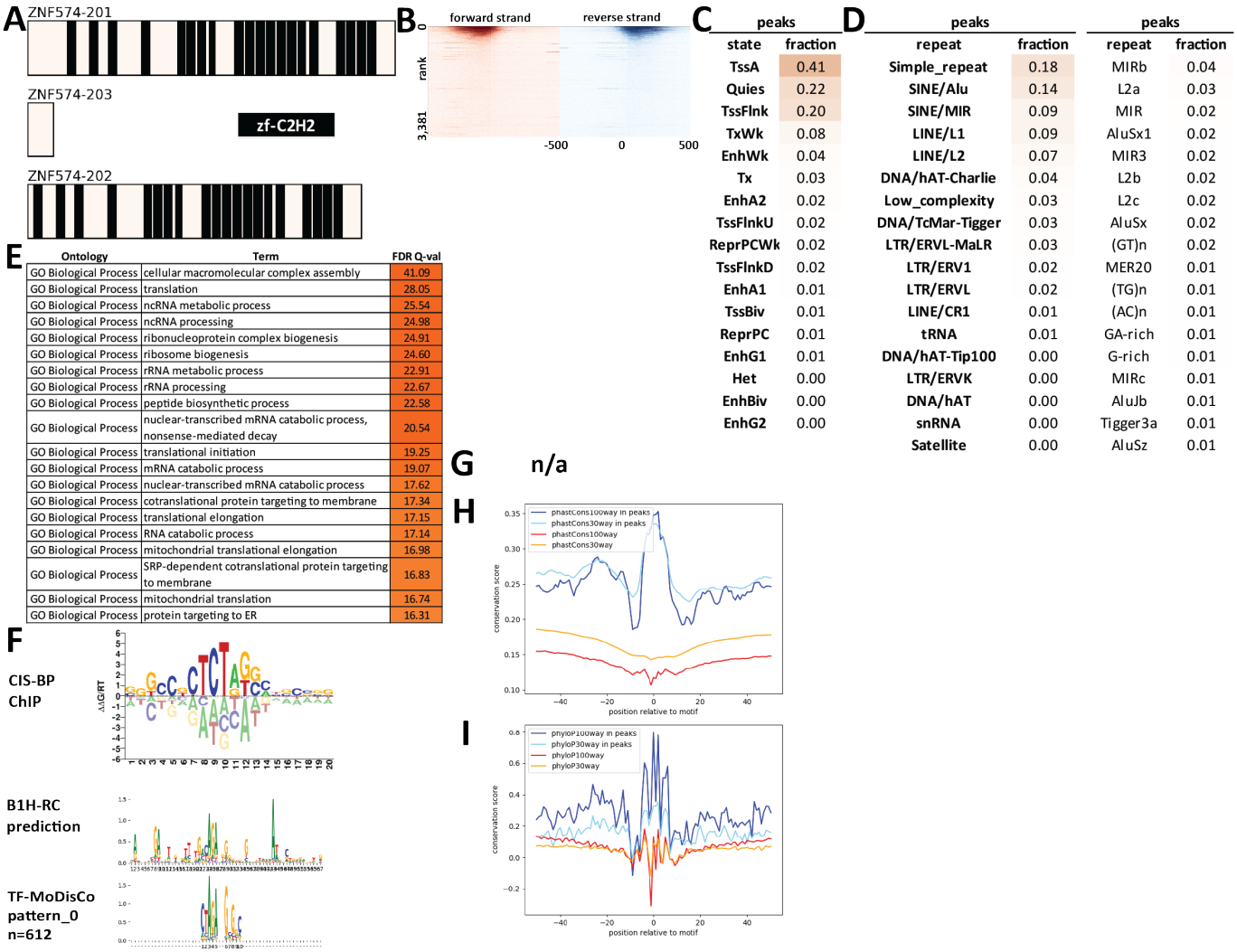

peaks	
state	fraction
TssA	0.41
Quies	0.22
TssFlnk	0.20
TxWk	0.08
EnhWk	0.04
Tx	0.03
EnhA2	0.02
TssFlnkU	0.02
ReprPCWk	0.02
TssFlnkD	0.02
EnhA1	0.01
TssBiv	0.01
ReprPC	0.01
EnhG1	0.01
Het	0.00
EnhBiv	0.00
EnhG2	0.00

peaks		peaks	
repeat	fraction	repeat	fraction
Simple_repeat	0.18	MIRb	0.04
SINE/Alu	0.14	L2a	0.03
SINE/MIR	0.09	MIR	0.02
LINE/L1	0.09	AluSx1	0.02
LINE/L2	0.07	MIR3	0.02
DNA/hAT-Charlie	0.04	L2b	0.02
Low_complexity	0.03	L2c	0.02
DNA/TcMar-Tigger	0.03	AluSx	0.02
LTR/ERVL-MaLR	0.03	(GT)n	0.02
LTR/ERV1	0.02	MER20	0.01
LTR/ERVL	0.02	(TG)n	0.01
LINE/CR1	0.01	(AC)n	0.01
tRNA	0.01	GA-rich	0.01
DNA/hAT-Tip100	0.00	G-rich	0.01
LTR/ERVK	0.00	MIRc	0.01
DNA/hAT	0.00	AluJb	0.01
snRNA	0.00	Tigger3a	0.01
Satellite	0.00	AluSz	0.01

Ontology	Term	FDR Q-val
GO Biological Process	cellular macromolecular complex assembly	41.09
GO Biological Process	translation	28.05
GO Biological Process	ncRNA metabolic process	25.54
GO Biological Process	ncRNA processing	24.98
GO Biological Process	ribonucleoprotein complex biogenesis	24.91
GO Biological Process	ribosome biogenesis	24.60
GO Biological Process	rRNA metabolic process	22.91
GO Biological Process	rRNA processing	22.67
GO Biological Process	peptide biosynthetic process	22.58
GO Biological Process	nuclear-transcribed mRNA catabolic process, nonsense-mediated decay	20.54
GO Biological Process	translational initiation	19.25
GO Biological Process	mRNA catabolic process	19.07
GO Biological Process	nuclear-transcribed mRNA catabolic process	17.62
GO Biological Process	cotranslational protein targeting to membrane	17.34
GO Biological Process	translational elongation	17.15
GO Biological Process	RNA catabolic process	17.14
GO Biological Process	mitochondrial translational elongation	16.98
GO Biological Process	SRP-dependent cotranslational protein targeting to membrane	16.83
GO Biological Process	mitochondrial translation	16.74
GO Biological Process	protein targeting to ER	16.31

Supplementary Figure 1421: Properties and genomic distribution of motifs identified for the ZNF574 transcription factor in MCF-7 (accession ENCSR402JAC).

TF-MoDisCO pattern_0 n=612, CWM

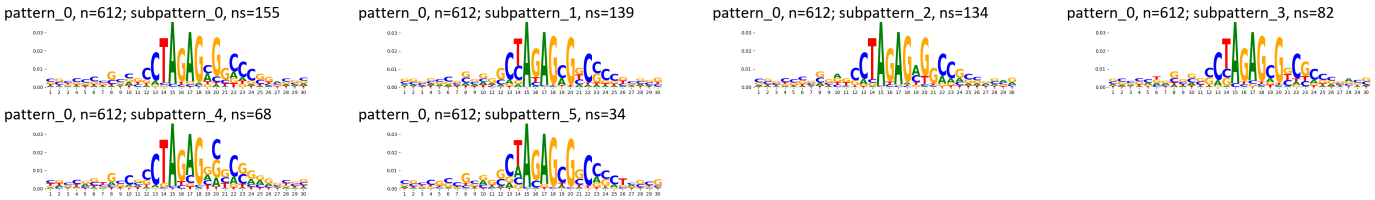

TF-MoDisCO pattern_0 n=612, PWM

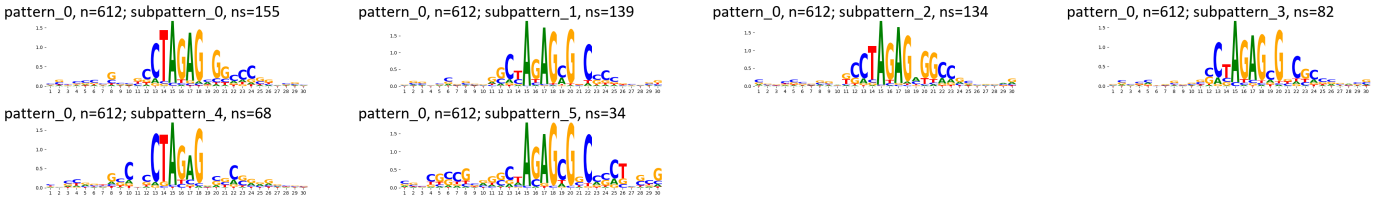

Supplementary Figure 1422: TF-MoDisCO subpatterns for the ZNF574 transcription factor in MCF-7 (accession ENCSR402JAC).

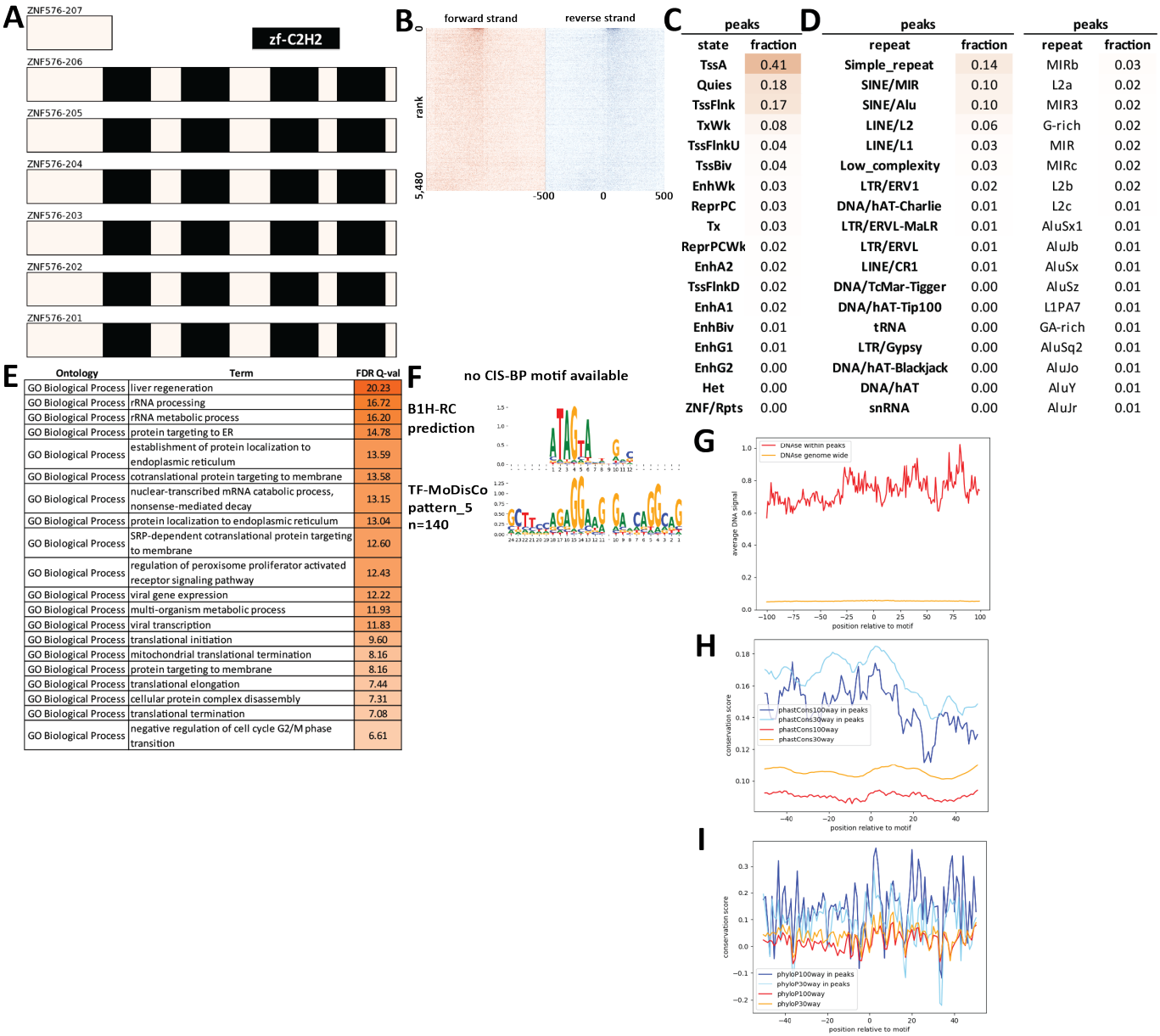

peaks	
state	fraction
TssA	0.41
Quies	0.18
TssFlnk	0.17
TxWk	0.08
TssFlnkU	0.04
TssBiv	0.04
EnhWk	0.03
ReprPC	0.03
Tx	0.03
ReprPCWk	0.02
EnhA2	0.02
TssFlnkD	0.02
EnhA1	0.02
EnhBiv	0.01
EnhG1	0.01
EnhG2	0.00
Het	0.00
ZNF/Rpts	0.00

peaks		peaks	
repeat	fraction	repeat	fraction
Simple_repeat	0.14	MIRb	0.03
SINE/MIR	0.10	L2a	0.02
SINE/Alu	0.10	MIR3	0.02
LINE/L2	0.06	G-rich	0.02
LINE/L1	0.03	MIR	0.02
Low_complexity	0.03	MIRc	0.02
LTR/ERV1	0.02	L2b	0.02
DNA/hAT-Charlie	0.01	L2c	0.01
LTR/ERVL-MaLR	0.01	AluSx1	0.01
LTR/ERVL	0.01	AluJb	0.01
LINE/CR1	0.01	AluSx	0.01
DNA/TcMar-Tigger	0.00	AluSz	0.01
DNA/hAT-Tip100	0.00	L1PA7	0.01
tRNA	0.00	GA-rich	0.01
LTR/Gypsy	0.00	AluSq2	0.01
DNA/hAT-Blackjack	0.00	AluJo	0.01
DNA/hAT	0.00	AluY	0.01
snRNA	0.00	AluJr	0.01

Ontology	Term	FDR Q-val
GO Biological Process	liver regeneration	20.23
GO Biological Process	rRNA processing	16.72
GO Biological Process	rRNA metabolic process	16.20
GO Biological Process	protein targeting to ER	14.78
GO Biological Process	establishment of protein localization to endoplasmic reticulum	13.59
GO Biological Process	cotranslational protein targeting to membrane	13.58
GO Biological Process	nuclear-transcribed mRNA catabolic process, nonsense-mediated decay	13.15
GO Biological Process	protein localization to endoplasmic reticulum	13.04
GO Biological Process	SRP-dependent cotranslational protein targeting to membrane	12.60
GO Biological Process	regulation of peroxisome proliferator activated receptor signaling pathway	12.43
GO Biological Process	viral gene expression	12.22
GO Biological Process	multi-organism metabolic process	11.93
GO Biological Process	viral transcription	11.83
GO Biological Process	translational initiation	9.60
GO Biological Process	mitochondrial translational termination	8.16
GO Biological Process	protein targeting to membrane	8.16
GO Biological Process	translational elongation	7.44
GO Biological Process	cellular protein complex disassembly	7.31
GO Biological Process	translational termination	7.08
GO Biological Process	negative regulation of cell cycle G2/M phase transition	6.61

Supplementary Figure 1423: Properties and genomic distribution of motifs identified for the ZNF576 transcription factor in HepG2 (accession ENCSR253HUM).

TF-MoDisCO pattern_5 n=140, CWM

pattern_5, n=140; subpattern_0, ns=57

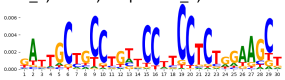

pattern_5, n=140; subpattern_1, ns=55

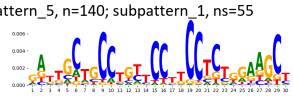

pattern_5, n=140; subpattern_2, ns=17

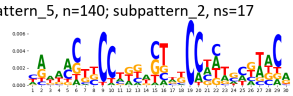

pattern_5, n=140; subpattern_3, ns=8

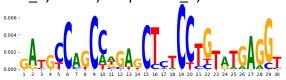

pattern_5, n=140; subpattern_4, ns=3

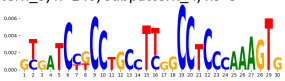

TF-MoDisCO pattern_5 n=140, PWM

pattern_5, n=140; subpattern_0, ns=57

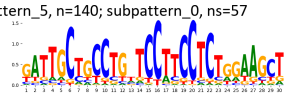

pattern_5, n=140; subpattern_1, ns=55

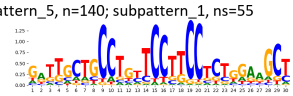

pattern_5, n=140; subpattern_2, ns=17

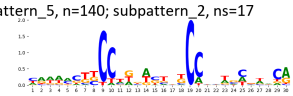

pattern_5, n=140; subpattern_3, ns=8

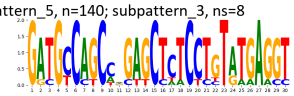

pattern_5, n=140; subpattern_4, ns=3

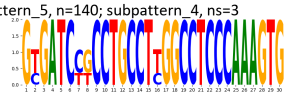

Supplementary Figure 1424: TF-MoDisCO subpatterns for the ZNF576 transcription factor in HepG2 (accession ENCSR253HUM).

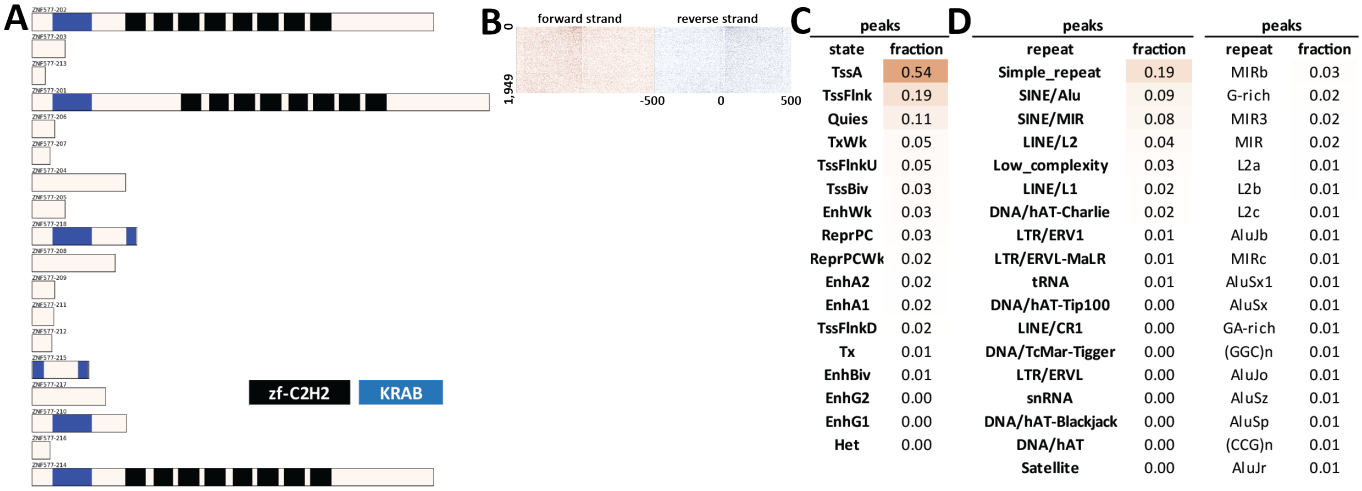

C

peaks

state	fraction
TssA	0.54
TssFlnk	0.19
Quies	0.11
TxWk	0.05
TssFlnkU	0.05
TssBiv	0.03
EnhWk	0.03
ReprPC	0.03
ReprPCWk	0.02
EnhA2	0.02
EnhA1	0.02
TssFlnkD	0.02
Tx	0.01
EnhBiv	0.01
EnhG2	0.00
EnhG1	0.00
Het	0.00

D

peaks

repeat	fraction
Simple_repeat	0.19
SINE/Alu	0.09
SINE/MIR	0.08
LINE/L2	0.04
Low_complexity	0.03
LINE/L1	0.02
DNA/hAT-Charlie	0.02
LTR/ERV1	0.01
LTR/ERVL-MaLR	0.01
tRNA	0.01
DNA/hAT-Tip100	0.00
LINE/CR1	0.00
DNA/TcMar-Tigger	0.00
LTR/ERVL	0.00
snRNA	0.00
DNA/hAT-Blackjack	0.00
DNA/hAT	0.00
Satellite	0.00

peaks

repeat	fraction
MIRb	0.03
G-rich	0.02
MIR3	0.02
MIR	0.02
L2a	0.01
L2b	0.01
L2c	0.01
AluJb	0.01
MIRc	0.01
AluSx1	0.01
AluSx	0.01
GA-rich	0.01
(GGC)n	0.01
AluJo	0.01
AluSz	0.01
AluSp	0.01
(CCG)n	0.01
AluJr	0.01

E

Ontology	Term	FDR Q-val
GO Biological Process	mRNA catabolic process	9.33
GO Biological Process	RNA catabolic process	9.14
GO Biological Process	nuclear-transcribed mRNA catabolic process	9.00
GO Biological Process	ncRNA metabolic process	8.95
GO Biological Process	nuclear-transcribed mRNA catabolic process, nonsense-mediated decay	8.65
GO Biological Process	protein targeting to ER	8.53
GO Biological Process	regulation of transcription from RNA polymerase II promoter in response to stress	8.30
GO Biological Process	negative regulation of protein ubiquitination	8.06
GO Biological Process	establishment of protein localization to endoplasmic reticulum	7.61
GO Biological Process	regulation of gene expression, epigenetic	7.44
GO Biological Process	regulation of DNA-templated transcription in response to stress	7.22
GO Biological Process	SRP-dependent cotranslational protein targeting to membrane	7.00
GO Biological Process	translation	6.98
GO Biological Process	cotranslational protein targeting to membrane	6.96
GO Biological Process	regulation of ubiquitin-protein ligase activity involved in mitotic cell cycle	6.93
GO Biological Process	negative regulation of protein modification by small protein conjugation or removal	6.80
GO Biological Process	protein localization to endoplasmic reticulum	6.66
GO Biological Process	negative regulation of ubiquitin-protein ligase activity involved in mitotic cell cycle	6.44
GO Biological Process	negative regulation of ubiquitin-protein transferase activity	6.39
GO Biological Process	response to endoplasmic reticulum stress	6.26

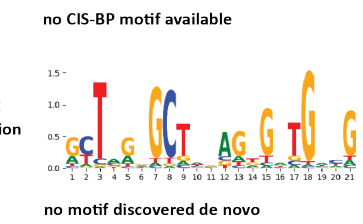

Supplementary Figure 1425: Properties and genomic distribution of motifs identified for the ZNF577 transcription factor in HepG2 (accession ENCSR436RQS).

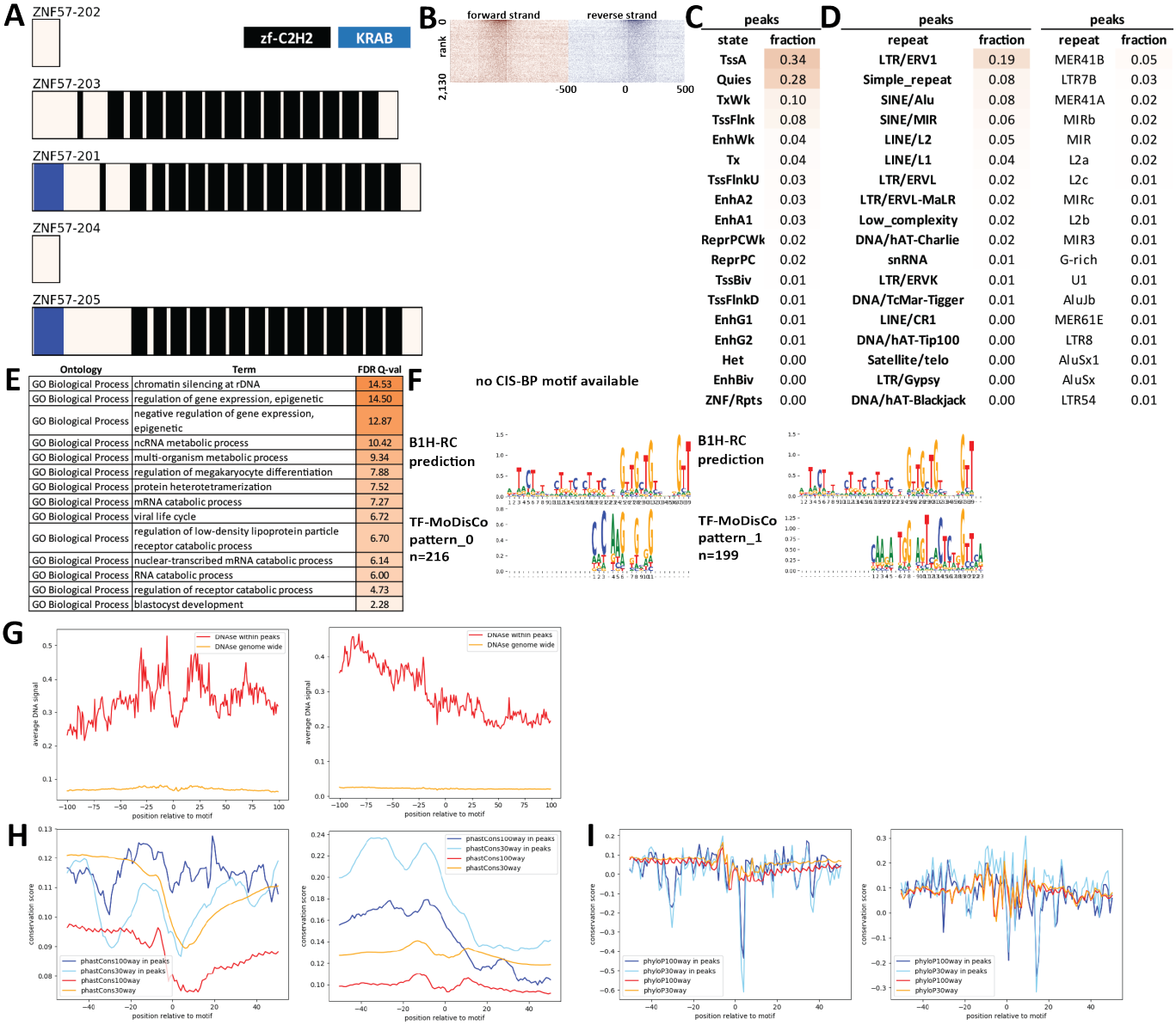

peaks	
state	fraction
TssA	0.34
Quies	0.28
TxWk	0.10
TssFlnk	0.08
EnhWk	0.04
Tx	0.04
TssFlnkU	0.03
EnhA2	0.03
EnhA1	0.03
ReprPCWk	0.02
ReprPC	0.02
TssBiv	0.01
TssFlnkD	0.01
EnhG1	0.01
EnhG2	0.01
Het	0.00
EnhBiv	0.00
ZNF/Rpts	0.00

peaks		peaks	
repeat	fraction	repeat	fraction
LTR/ERV1	0.19	MER41B	0.05
Simple_repeat	0.08	LTR7B	0.03
SINE/Alu	0.08	MER41A	0.02
SINE/MIR	0.06	MIRb	0.02
LINE/L2	0.05	MIR	0.02
LINE/L1	0.04	L2a	0.02
LTR/ERVL	0.02	L2c	0.01
LTR/ERVL-MaLR	0.02	MIRc	0.01
Low_complexity	0.02	L2b	0.01
DNA/hAT-Charlie	0.02	MIR3	0.01
snRNA	0.01	G-rich	0.01
LTR/ERVK	0.01	U1	0.01
DNA/TcMar-Tigger	0.01	AluJb	0.01
LINE/CR1	0.00	MER61E	0.01
DNA/hAT-Tip100	0.00	LTR8	0.01
Satellite/telo	0.00	AluSx1	0.01
LTR/Gypsy	0.00	AluSx	0.01
DNA/hAT-Blackjack	0.00	LTR54	0.01

Ontology	Term	FDR Q-val
GO Biological Process	chromatin silencing at rDNA	14.53
GO Biological Process	regulation of gene expression, epigenetic	14.50
GO Biological Process	negative regulation of gene expression, epigenetic	12.87
GO Biological Process	ncRNA metabolic process	10.42
GO Biological Process	multi-organism metabolic process	9.34
GO Biological Process	regulation of megakaryocyte differentiation	7.88
GO Biological Process	protein heterotetramerization	7.52
GO Biological Process	mRNA catabolic process	7.27
GO Biological Process	viral life cycle	6.72
GO Biological Process	regulation of low-density lipoprotein particle receptor catabolic process	6.70
GO Biological Process	nuclear-transcribed mRNA catabolic process	6.14
GO Biological Process	RNA catabolic process	6.00
GO Biological Process	regulation of receptor catabolic process	4.73
GO Biological Process	blastocyst development	2.28

Supplementary Figure 1426: Properties and genomic distribution of motifs identified for the ZNF57 transcription factor in K562 (accession ENCSR918EFA).

TF-MoDisCO pattern_0 n=216, CWM

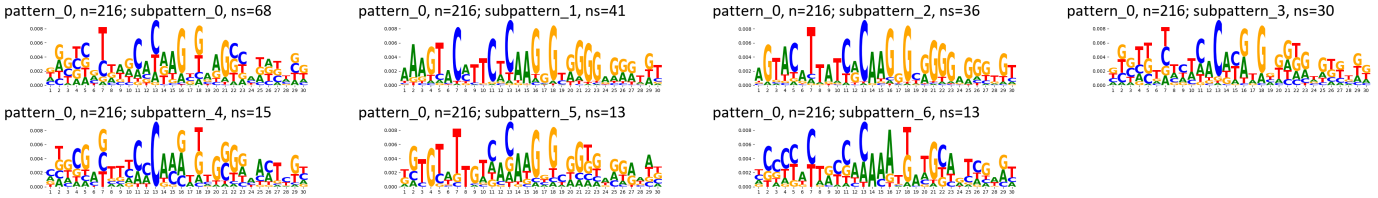

TF-MoDisCO pattern_0 n=216, PWM

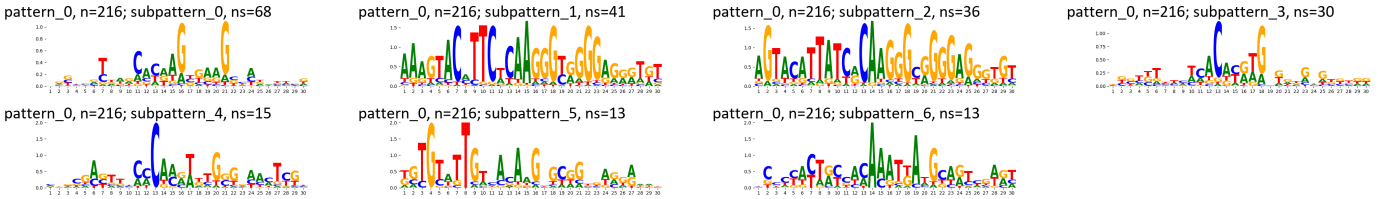

TF-MoDisCO pattern_1 n=199, CWM

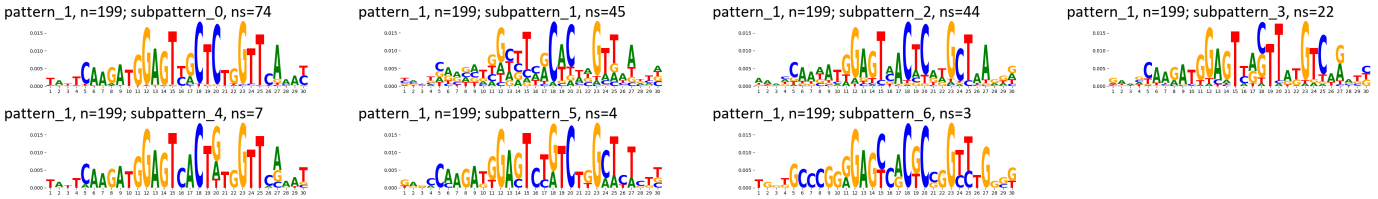

TF-MoDisCO pattern_1 n=199, PWM

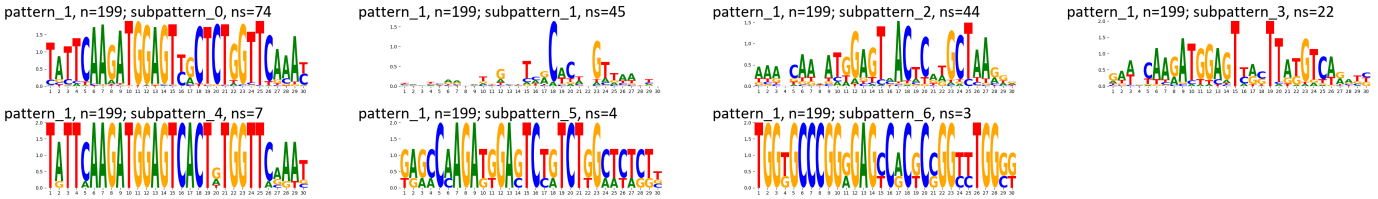

Supplementary Figure 1427: TF-MoDisCO subpatterns for the ZNF57 transcription factor in K562 (accession ENCSR918EFA).

A

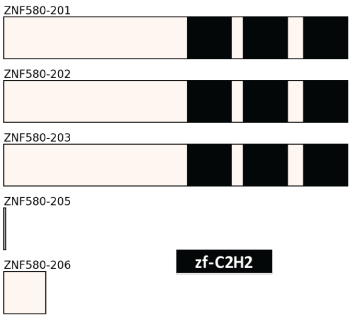

B

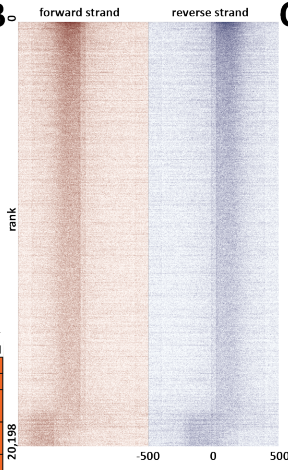

C

peaks

state	fraction
Quies	0.23
TssA	0.23
EnhWk	0.13
TxWk	0.13
TssFlnk	0.11
EnhA1	0.07
EnhA2	0.06
Tx	0.03
TssBiv	0.02
ReprPCWk	0.02
TssFlnkU	0.02
ReprPC	0.01
TssFlnkD	0.01
Het	0.01
EnhBiv	0.01
EnhG1	0.01
ZNF/Rpts	0.00
EnhG2	0.00

D

peaks

repeat	fraction
SINE/Alu	0.25
LINE/L1	0.23
Simple_repeat	0.17
SINE/MIR	0.12
LINE/L2	0.06
LTR/ERVL-MaLR	0.03
Low_complexity	0.02
DNA/hAT-Charlie	0.02
LTR/ERV1	0.02
LTR/ERVL	0.01
tRNA	0.01
LINE/CR1	0.01
DNA/TcMar-Tigger	0.01
DNA/hAT-Tip100	0.01
snRNA	0.00
DNA/hAT-Blackjack	0.00
LINE/RTE-X	0.00
LTR/ERVK	0.00

peaks

repeat	fraction
MIRb	0.04
MIR	0.04
AluSx	0.03
AluSx1	0.03
AluSz	0.02
AluJb	0.02
L2a	0.02
L1PA5	0.02
(AAAT)n	0.02
MIRc	0.02
L1PA7	0.02
AluY	0.02
L2c	0.02
AluJr	0.02
AluJo	0.02
MIR3	0.01
L2b	0.01
AluSq2	0.01

E

Ontology	Term	FDR Q-val
GO Biological Process	nuclear-transcribed mRNA catabolic process	42.49
GO Biological Process	mRNA catabolic process	41.58
GO Biological Process	nuclear-transcribed mRNA catabolic process, nonsense-mediated decay	35.47
GO Biological Process	regulation of transcription from RNA polymerase II promoter in response to stress	26.45
GO Biological Process	SRP-dependent cotranslational protein targeting to membrane	22.51
GO Biological Process	cotranslational protein targeting to membrane	21.50
GO Biological Process	viral transcription	19.17
GO Biological Process	establishment of protein localization to endoplasmic reticulum	18.81
GO Biological Process	protein targeting to ER	18.76
GO Biological Process	signal transduction involved in mitotic G1 DNA damage checkpoint	15.38
GO Biological Process	DNA damage response, signal transduction by p53 class mediator resulting in cell cycle arrest	15.13
GO Biological Process	positive regulation of transcription from RNA polymerase II promoter in response to stress	11.37
GO Biological Process	gene silencing by miRNA	11.25
GO Biological Process	histone ubiquitination	10.88
GO Biological Process	positive regulation of nuclear-transcribed mRNA catabolic process, deadenylation-dependent decay	10.44
GO Biological Process	DNA damage response, detection of DNA damage	10.33
GO Biological Process	positive regulation of mRNA catabolic process	9.61
GO Biological Process	positive regulation of transcription from RNA polymerase II promoter in response to endoplasmic reticulum stress	8.96
GO Biological Process	maintenance of protein localization in organelle	7.98
GO Biological Process	negative regulation of cell aging	7.84
Human Phenotype	Neonatal death	6.51

F

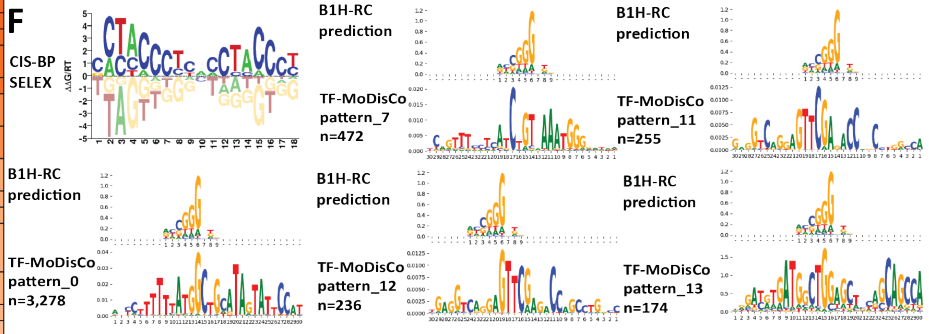

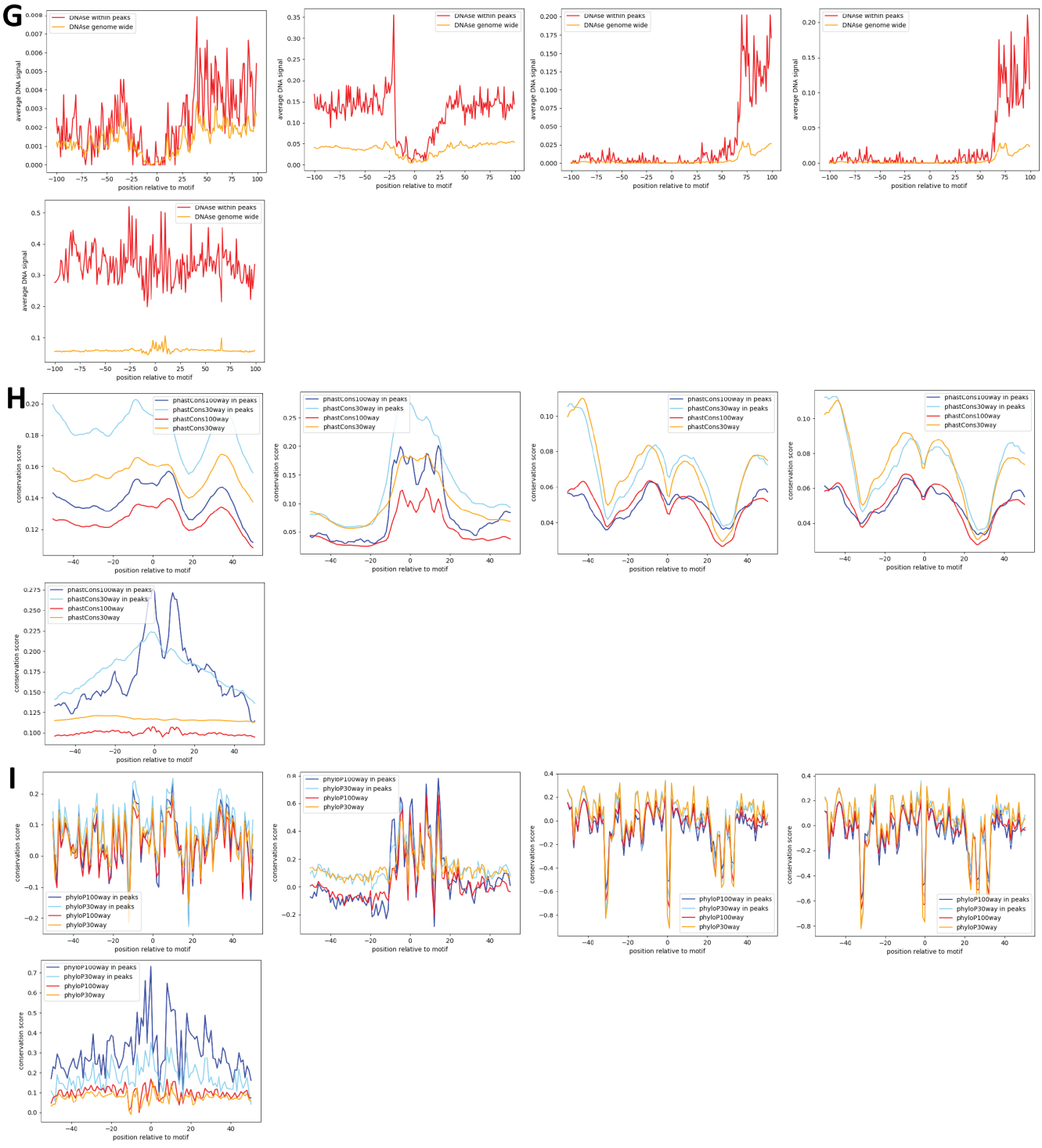

Supplementary Figure 1428: Properties and genomic distribution of motifs identified for the ZNF580 transcription factor in HEK293 (accession ENCSR668HOP).

TF-MoDiSCO pattern_0 n=3278, CWM

pattern_0, n=3278; subpattern_0, ns=894

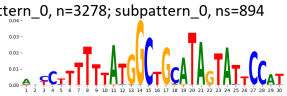

pattern_0, n=3278; subpattern_1, ns=617

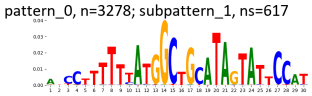

pattern_0, n=3278; subpattern_2, ns=527

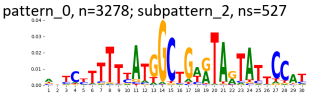

pattern_0, n=3278; subpattern_3, ns=416

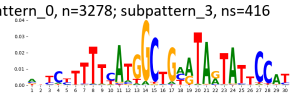

pattern_0, n=3278; subpattern_4, ns=367

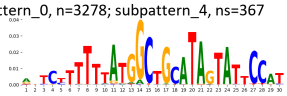

pattern_0, n=3278; subpattern_5, ns=231

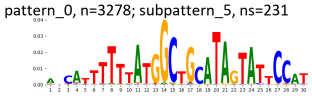

pattern_0, n=3278; subpattern_6, ns=226

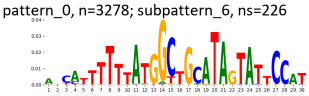

TF-MoDiSCO pattern_0 n=3278, PWM

pattern_0, n=3278; subpattern_0, ns=894

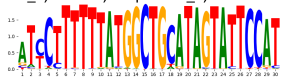

pattern_0, n=3278; subpattern_1, ns=617

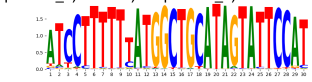

pattern_0, n=3278; subpattern_2, ns=527

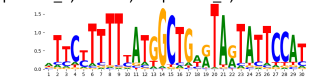

pattern_0, n=3278; subpattern_3, ns=416

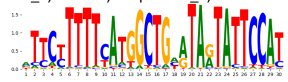

pattern_0, n=3278; subpattern_4, ns=367

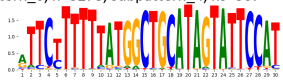

pattern_0, n=3278; subpattern_5, ns=231

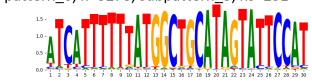

pattern_0, n=3278; subpattern_6, ns=226

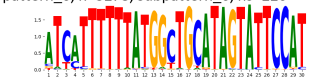

TF-MoDiSCO pattern_11 n=255, CWM

pattern_11, n=255; subpattern_0, ns=83

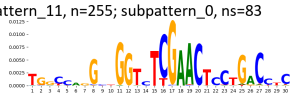

pattern_11, n=255; subpattern_1, ns=70

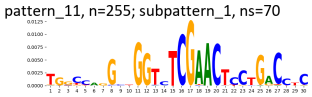

pattern_11, n=255; subpattern_2, ns=70

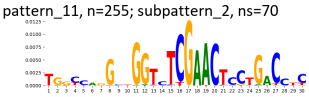

pattern_11, n=255; subpattern_3, ns=20

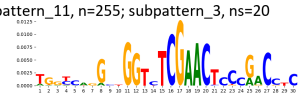

pattern_11, n=255; subpattern_4, ns=9

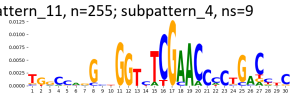

pattern_11, n=255; subpattern_5, ns=3

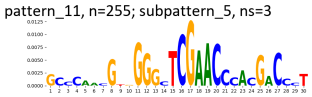

TF-MoDiSCO pattern_11 n=255, PWM

pattern_11, n=255; subpattern_0, ns=83

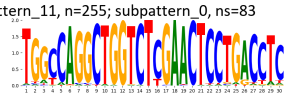

pattern_11, n=255; subpattern_1, ns=70

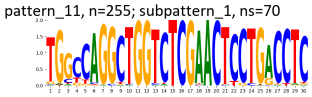

pattern_11, n=255; subpattern_2, ns=70

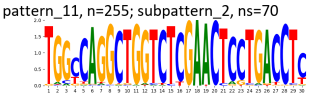

pattern_11, n=255; subpattern_3, ns=20

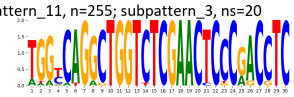

pattern_11, n=255; subpattern_4, ns=9

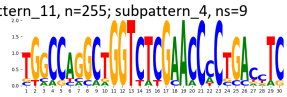

pattern_11, n=255; subpattern_5, ns=3

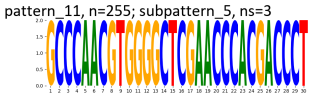

TF-MoDiSCO pattern_12 n=236, CWM

pattern_12, n=236; subpattern_0, ns=68

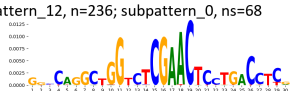

pattern_12, n=236; subpattern_1, ns=63

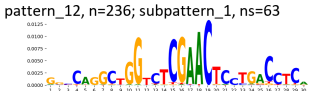

pattern_12, n=236; subpattern_2, ns=43

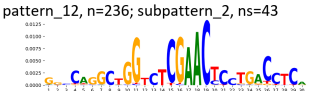

pattern_12, n=236; subpattern_3, ns=33

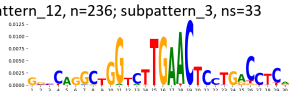

pattern_12, n=236; subpattern_4, ns=25

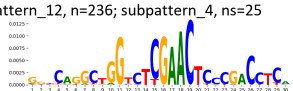

pattern_12, n=236; subpattern_5, ns=4

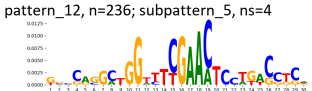

TF-MoDiSCO pattern_12 n=236, PWM

pattern_12, n=236; subpattern_0, ns=68

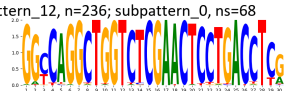

pattern_12, n=236; subpattern_1, ns=63

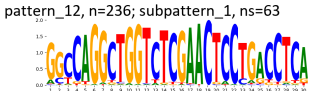

pattern_12, n=236; subpattern_2, ns=43

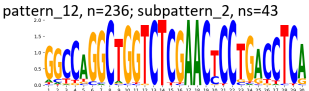

pattern_12, n=236; subpattern_3, ns=33

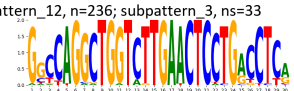

pattern_12, n=236; subpattern_4, ns=25

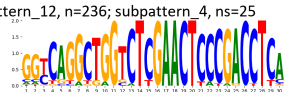

pattern_12, n=236; subpattern_5, ns=4

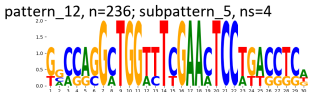

TF-MoDiSCO pattern_13 n=174, CWM

pattern_13, n=174; subpattern_0, ns=84

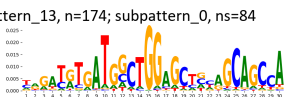

pattern_13, n=174; subpattern_1, ns=57

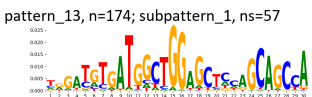

pattern_13, n=174; subpattern_2, ns=30

pattern_13, n=174; subpattern_3, ns=3

TF-MoDisCO pattern_13 n=174, PWM

pattern_13, n=174; subpattern_0, ns=84

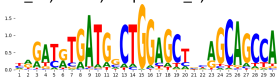

pattern_13, n=174; subpattern_1, ns=57

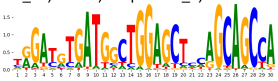

pattern_13, n=174; subpattern_2, ns=30

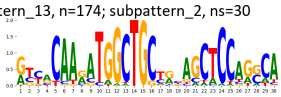

pattern_13, n=174; subpattern_3, ns=3

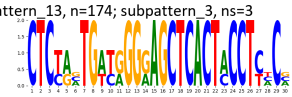

TF-MoDisCO pattern_7 n=472, CWM

pattern_7, n=472; subpattern_0, ns=206

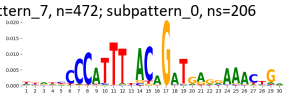

pattern_7, n=472; subpattern_1, ns=178

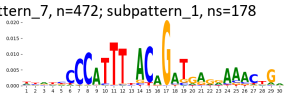

pattern_7, n=472; subpattern_2, ns=88

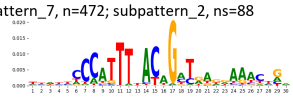

TF-MoDisCO pattern_7 n=472, PWM

pattern_7, n=472; subpattern_0, ns=206

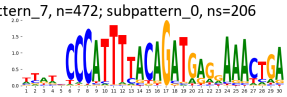

pattern_7, n=472; subpattern_1, ns=178

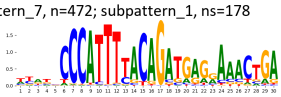

pattern_7, n=472; subpattern_2, ns=88

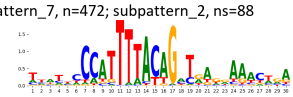

Supplementary Figure 1429: TF-MoDisCO subpatterns for the ZNF580 transcription factor in HEK293 (accession ENCSR668HOP).

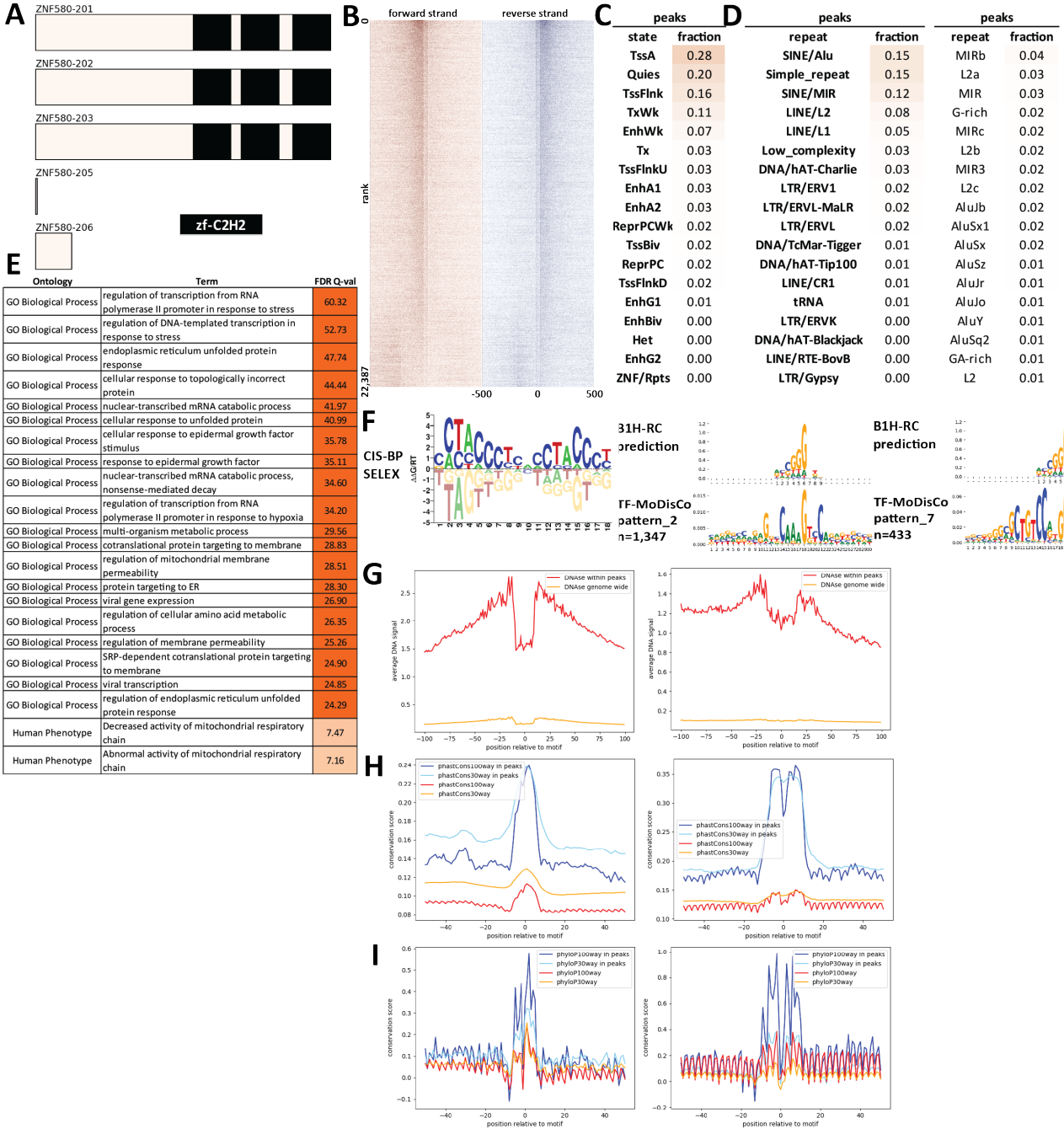

Supplementary Figure 1430: Properties and genomic distribution of motifs identified for the ZNF580 transcription factor in HepG2 (accession ENCSR173CTF).

TF-MoDisCO pattern_2 n=1347, CWM

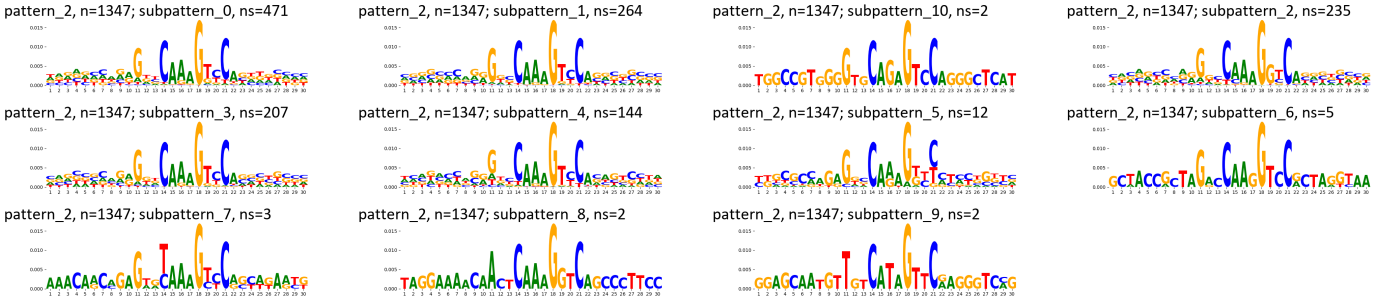

TF-MoDisCO pattern_2 n=1347, PWM

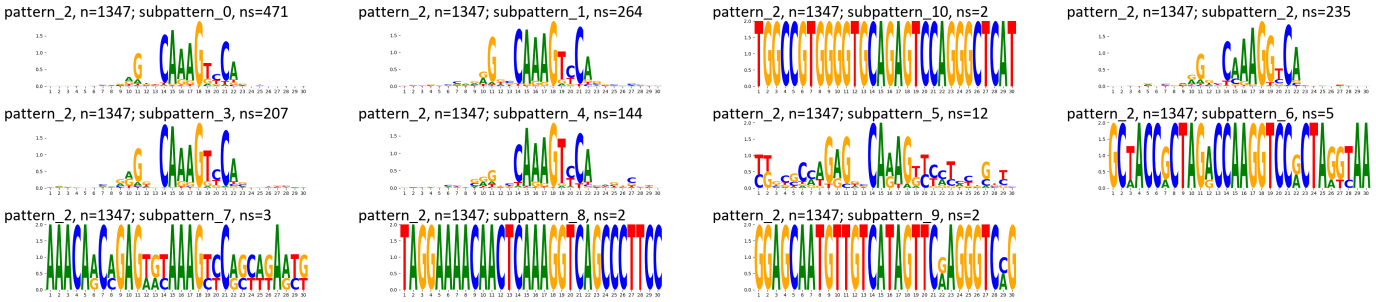

TF-MoDisCO pattern_7 n=433, CWM

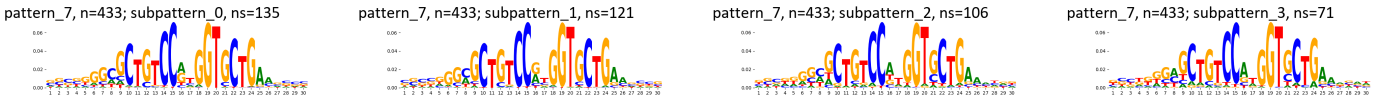

TF-MoDisCO pattern_7 n=433, PWM

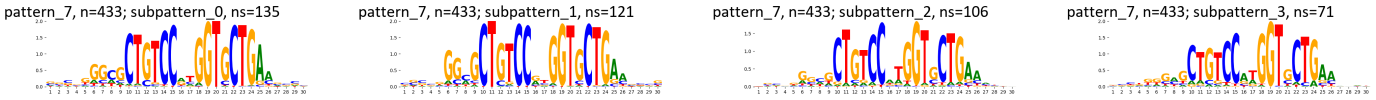

Supplementary Figure 1431: TF-MoDisCO subpatterns for the ZNF580 transcription factor in HepG2 (accession ENCSR173CTF).

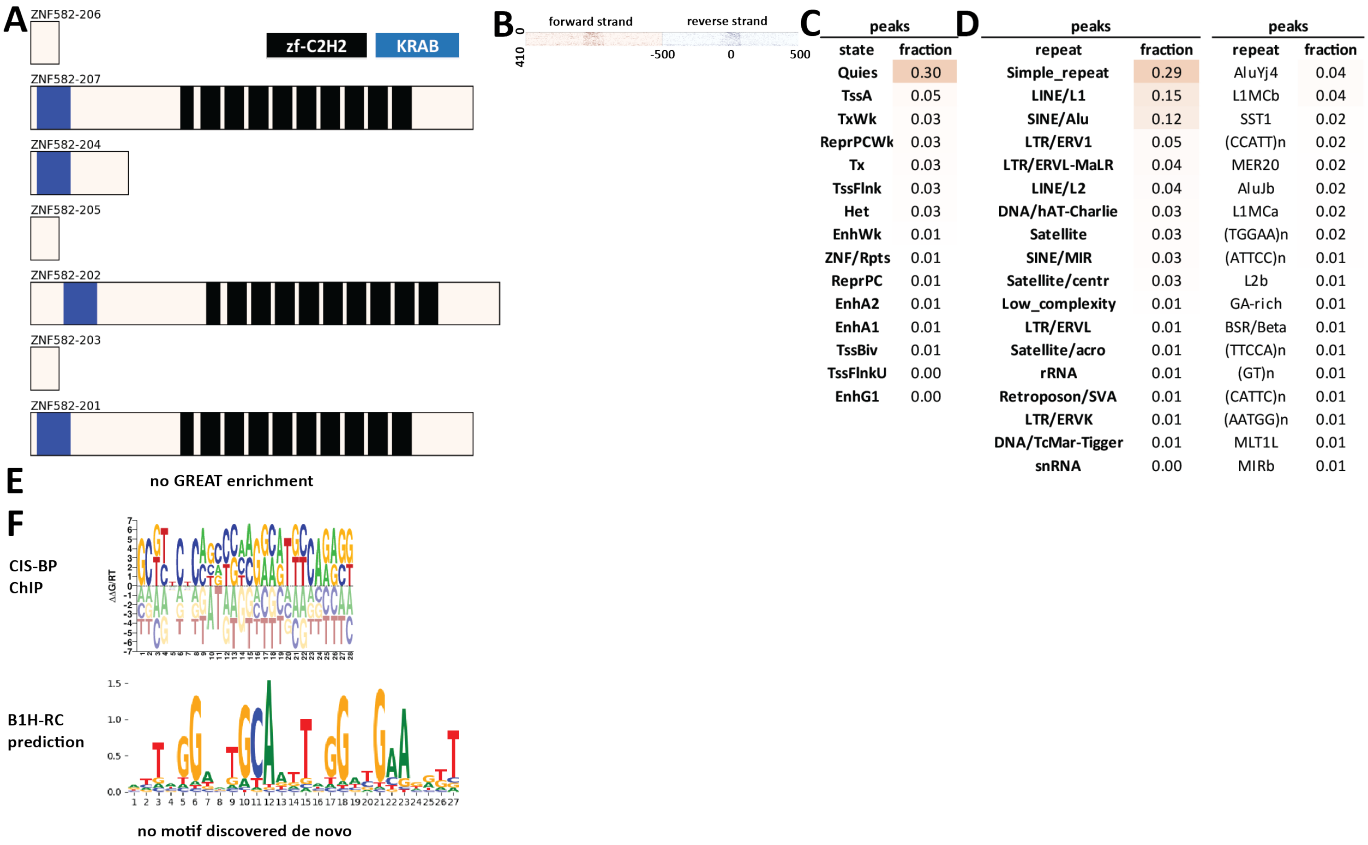

Supplementary Figure 1432: Properties and genomic distribution of motifs identified for the ZNF582 transcription factor in HEK293 (accession ChipExo models).

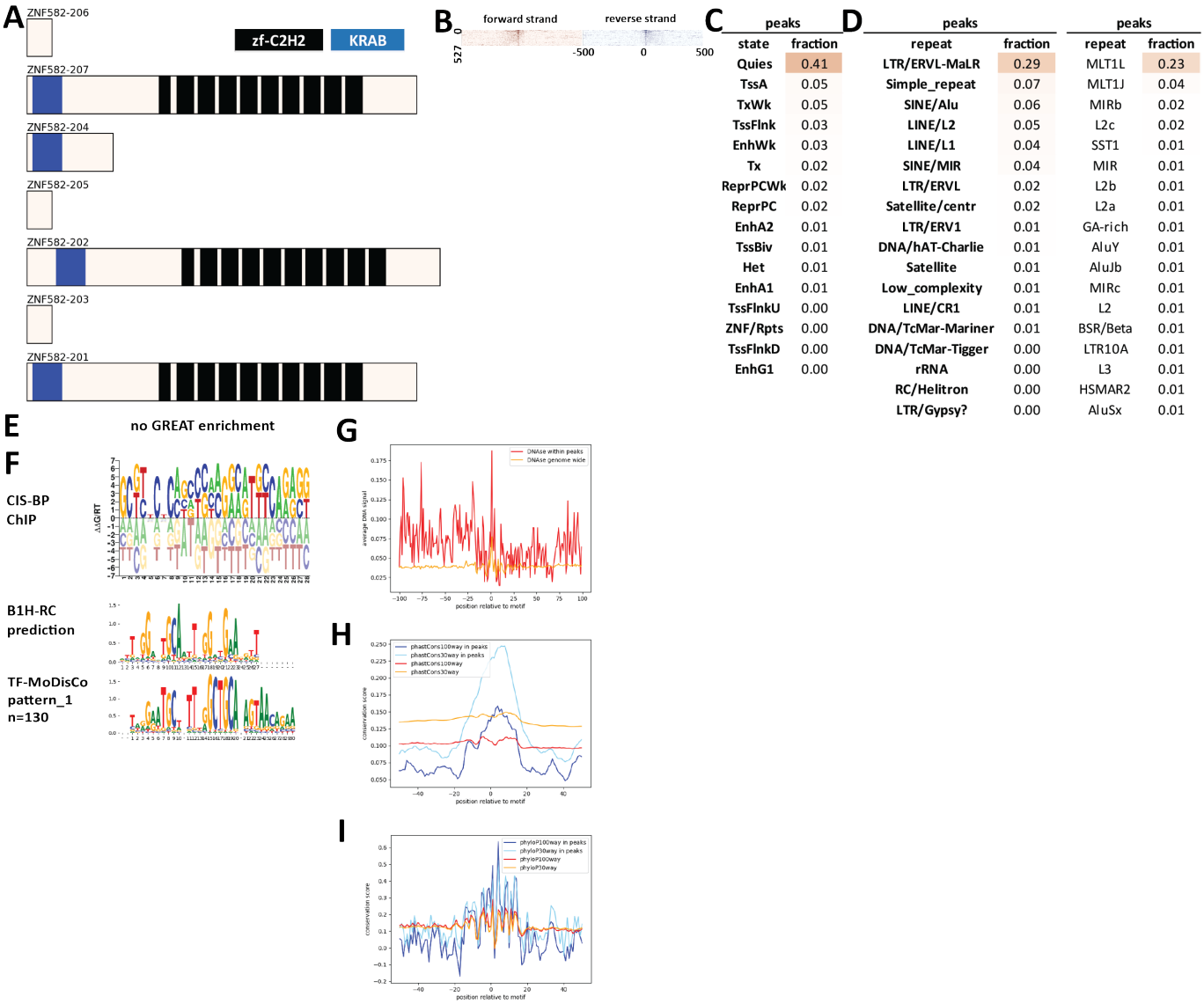

C

peaks	
state	fraction
Quies	0.41
TssA	0.05
TxWk	0.05
TssFlnk	0.03
EnhWk	0.03
Tx	0.02
ReprPCWk	0.02
ReprPC	0.02
EnhA2	0.01
TssBiv	0.01
Het	0.01
EnhA1	0.01
TssFlnkU	0.00
ZNF/Rpts	0.00
TssFlnkD	0.00
EnhG1	0.00

D

peaks		peaks	
repeat	fraction	repeat	fraction
LTR/ERVL-MaLR	0.29	MLT1L	0.23
Simple_repeat	0.07	MLT1J	0.04
SINE/Alu	0.06	MIRb	0.02
LINE/L2	0.05	L2c	0.02
LINE/L1	0.04	SST1	0.01
SINE/MIR	0.04	MIR	0.01
LTR/ERVL	0.02	L2b	0.01
Satellite/centr	0.02	L2a	0.01
LTR/ERV1	0.01	GA-rich	0.01
DNA/hAT-Charlie	0.01	AluY	0.01
Satellite	0.01	AluJb	0.01
Low_complexity	0.01	MIRc	0.01
LINE/CR1	0.01	L2	0.01
DNA/TcMar-Mariner	0.01	BSR/Beta	0.01
DNA/TcMar-Tigger	0.00	LTR10A	0.01
rRNA	0.00	L3	0.01
RC/Helitron	0.00	HSMAR2	0.01
LTR/Gypsy?	0.00	AluSx	0.01

Supplementary Figure 1433: Properties and genomic distribution of motifs identified for the ZNF582 transcription factor in HEK293 (accession Hughes GR models).

TF-MoDisCO pattern_1 n=130, CWM

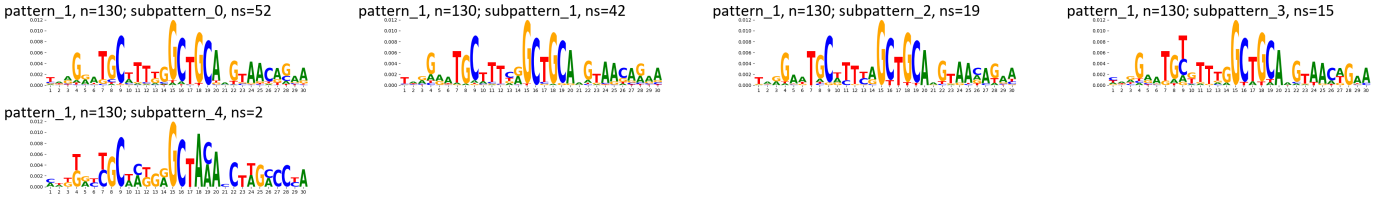

TF-MoDisCO pattern_1 n=130, PWM

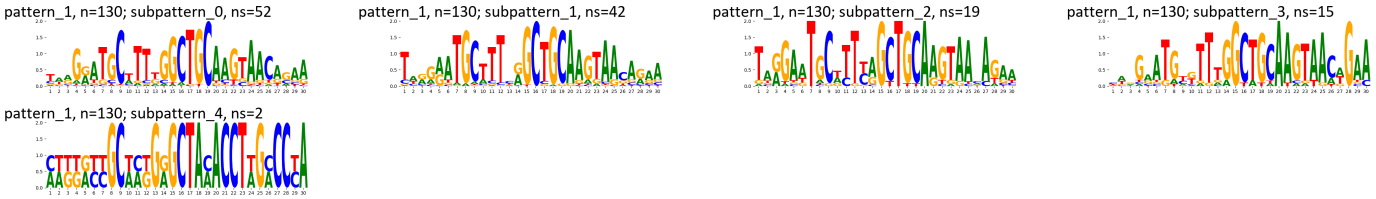

Supplementary Figure 1434: TF-MoDisCO subpatterns for the ZNF582 transcription factor in HEK293 (accession Hughes GR models).

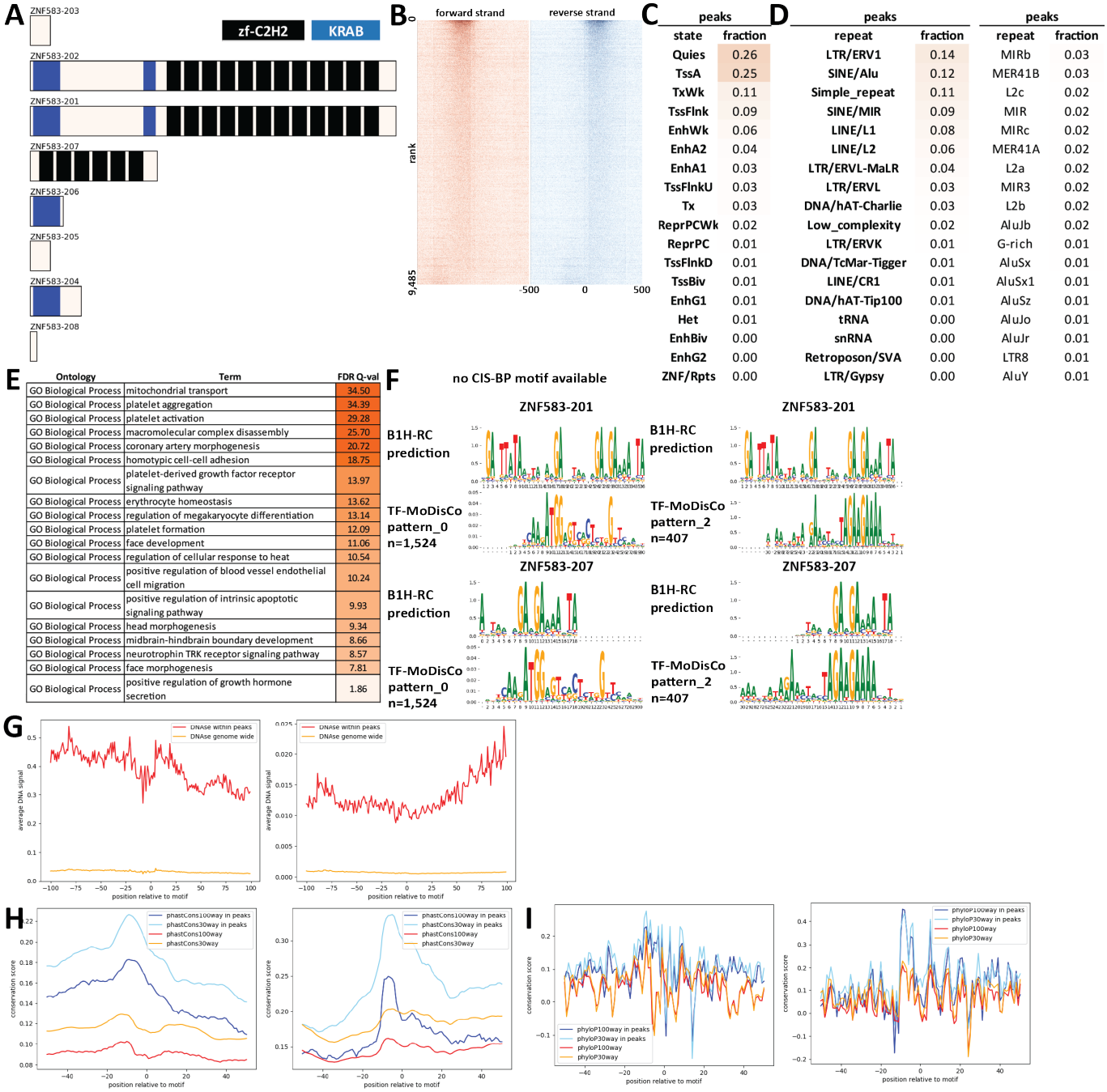

peaks	
state	fraction
Quies	0.26
TssA	0.25
TxWk	0.11
TssFlnk	0.09
EnhWk	0.06
EnhA2	0.04
EnhA1	0.03
TssFlnkU	0.03
Tx	0.03
ReprPCWk	0.02
ReprPC	0.01
TssFlnkD	0.01
TssBiv	0.01
EnhG1	0.01
Het	0.01
EnhBiv	0.00
EnhG2	0.00
ZNF/Rpts	0.00

peaks		peaks	
repeat	fraction	repeat	fraction
LTR/ERV1	0.14	MIRb	0.03
SINE/Alu	0.12	MER41B	0.03
Simple_repeat	0.11	L2c	0.02
SINE/MIR	0.09	MIR	0.02
LINE/L1	0.08	MIRc	0.02
LINE/L2	0.06	MER41A	0.02
LTR/ERVL-MaLR	0.04	L2a	0.02
LTR/ERVL	0.03	MIR3	0.02
DNA/hAT-Charlie	0.03	L2b	0.02
Low_complexity	0.02	AluJb	0.02
LTR/ERVK	0.01	G-rich	0.01
DNA/TcMar-Tigger	0.01	AluSx	0.01
LINE/CR1	0.01	AluSx1	0.01
DNA/hAT-Tip100	0.01	AluSz	0.01
tRNA	0.00	AluJo	0.01
snRNA	0.00	AluJr	0.01
Retroposon/SVA	0.00	LTR8	0.01
LTR/Gypsy	0.00	AluY	0.01

Ontology	Term	FDR Q-val
GO Biological Process	mitochondrial transport	34.50
GO Biological Process	platelet aggregation	34.39
GO Biological Process	platelet activation	29.28
GO Biological Process	macromolecular complex disassembly	25.70
GO Biological Process	coronary artery morphogenesis	20.72
GO Biological Process	homotypic cell-cell adhesion	18.75
GO Biological Process	platelet-derived growth factor receptor signaling pathway	13.97
GO Biological Process	erythrocyte homeostasis	13.62
GO Biological Process	regulation of megakaryocyte differentiation	13.14
GO Biological Process	platelet formation	12.09
GO Biological Process	face development	11.06
GO Biological Process	regulation of cellular response to heat	10.54
GO Biological Process	positive regulation of blood vessel endothelial cell migration	10.24
GO Biological Process	positive regulation of intrinsic apoptotic signaling pathway	9.93
GO Biological Process	head morphogenesis	9.34
GO Biological Process	midbrain-hindbrain boundary development	8.66
GO Biological Process	neurotrophin TRK receptor signaling pathway	8.57
GO Biological Process	face morphogenesis	7.81
GO Biological Process	positive regulation of growth hormone secretion	1.86

Supplementary Figure 1435: Properties and genomic distribution of motifs identified for the ZNF583 transcription factor in K562 (accession ENCSR775EQV).

TF-MoDisCO pattern_0 n=1524, CWM

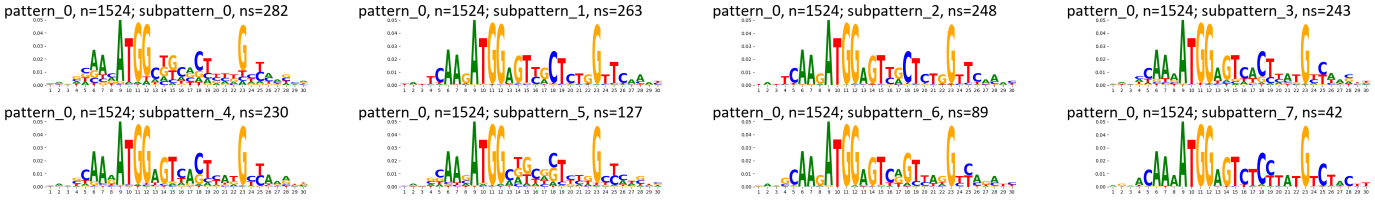

TF-MoDisCO pattern_0 n=1524, PWM

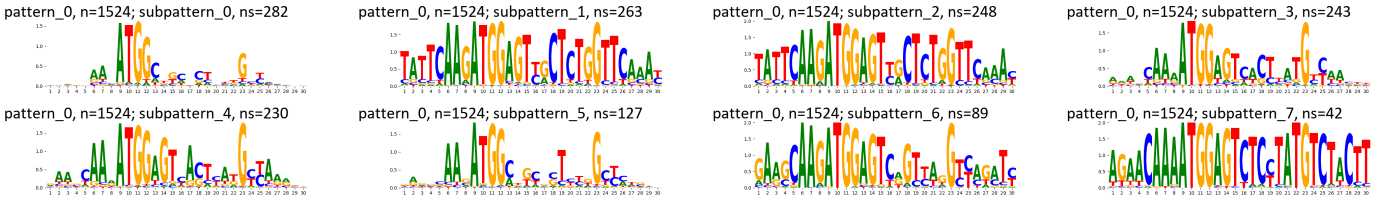

TF-MoDisCO pattern_2 n=407, CWM

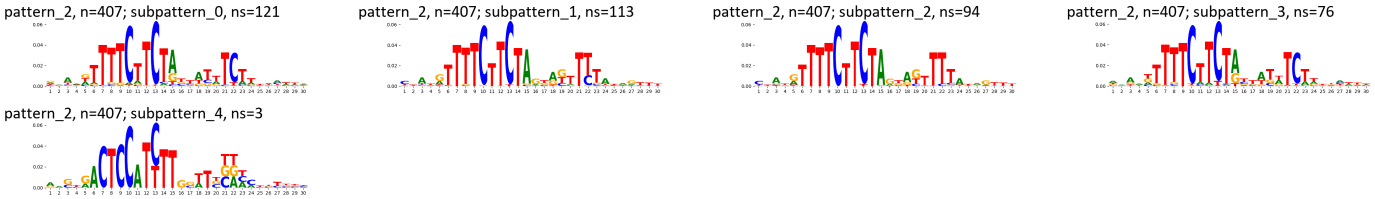

TF-MoDisCO pattern_2 n=407, PWM

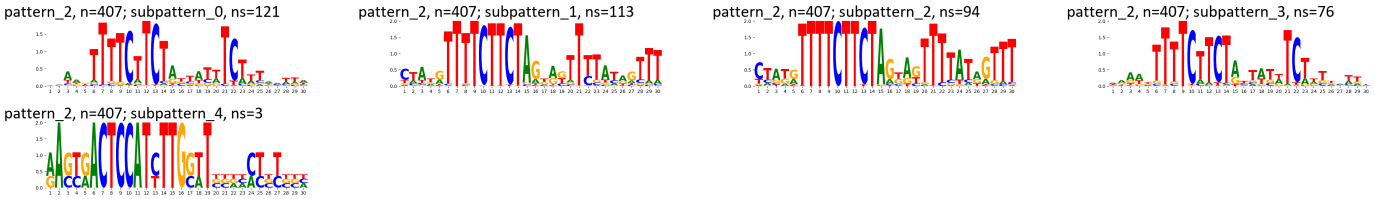

Supplementary Figure 1436: TF-MoDisCO subpatterns for the ZNF583 transcription factor in K562 (accession ENCSR775EQV).

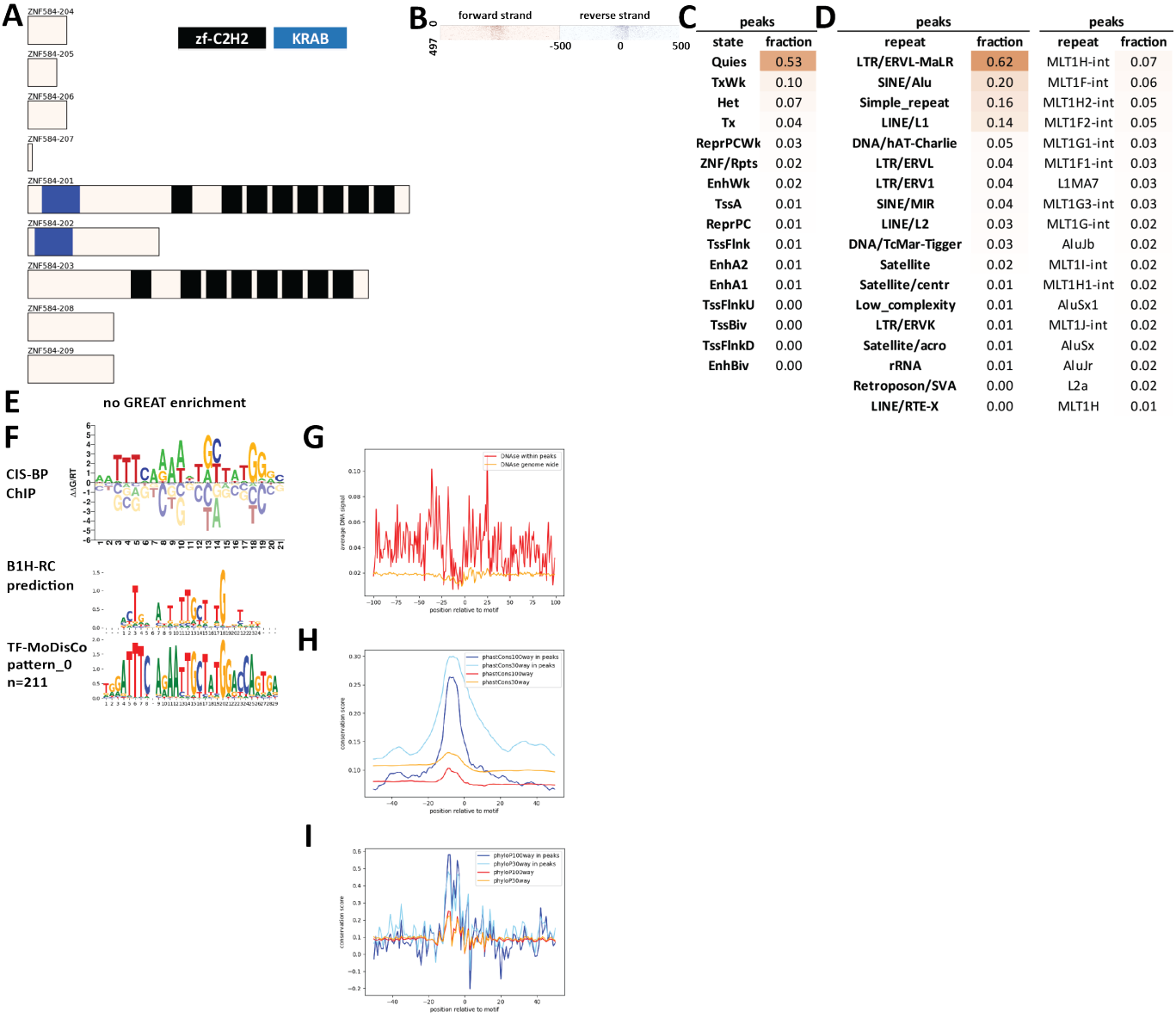

Supplementary Figure 1437: Properties and genomic distribution of motifs identified for the ZNF584 transcription factor in HEK293 (accession ChipExo models).

TF-MoDisCO pattern_0 n=211, CWM



TF-MoDisCO pattern_0 n=211, PWM

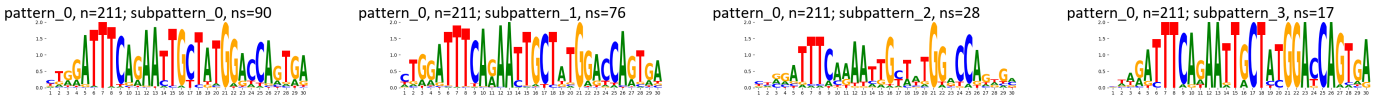

Supplementary Figure 1438: TF-MoDisCO subpatterns for the ZNF584 transcription factor in HEK293 (accession ChipExo models).

A

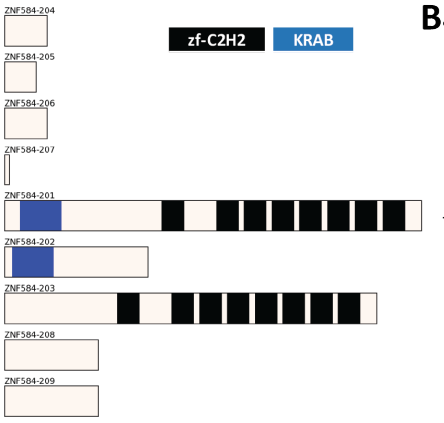

B

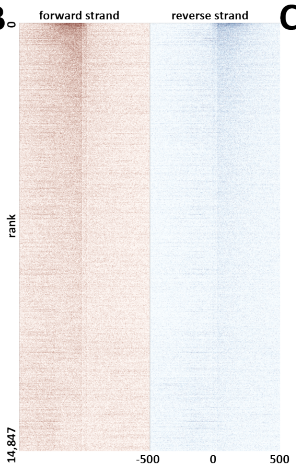

C

peaks	
state	fraction
Quies	0.27
TssA	0.14
TxWk	0.13
EnhWk	0.10
TssFlnk	0.08
EnhA1	0.04
EnhA2	0.04
Tx	0.03
TssFlnkU	0.03
ReprPCWk	0.02
TssFlnkD	0.01
ReprPC	0.01
TssBiv	0.01
EnhG1	0.01
Het	0.00
EnhBiv	0.00
EnhG2	0.00
ZNF/Rpts	0.00

D

peaks		peaks	
repeat	fraction	repeat	fraction
SINE/Alu	0.24	MIRb	0.06
Simple_repeat	0.18	L2a	0.05
SINE/MIR	0.17	MIR	0.04
LINE/L2	0.12	L2c	0.03
LTR/ERV1	0.12	MIR3	0.03
LINE/L1	0.10	MIRc	0.03
LTR/ERVL-MaLR	0.08	AluJb	0.03
DNA/hAT-Charlie	0.05	L2b	0.03
LTR/ERVL	0.05	AluSx1	0.03
Low_complexity	0.03	AluSx	0.02
DNA/TcMar-Tigger	0.02	AluSz	0.02
LINE/CR1	0.02	AluJr	0.02
DNA/hAT-Tip100	0.01	MER41B	0.02
LTR/ERVK	0.01	G-rich	0.02
DNA/hAT-Blackjack	0.00	AluJo	0.02
LINE/RTE-X	0.00	L2	0.02
tRNA	0.00	AluY	0.01
LTR/Gypsy	0.00	AluSq2	0.01

E

Ontology	Term	FDR Q-val
GO Biological Process	platelet activation	50.25
GO Biological Process	cellular response to topologically incorrect protein	40.00
GO Biological Process	negative regulation of tumor necrosis factor superfamily cytokine production	37.63
GO Biological Process	response to topologically incorrect protein	36.74
GO Biological Process	negative regulation of tumor necrosis factor production	36.29
GO Biological Process	cellular response to unfolded protein	35.66
GO Biological Process	response to unfolded protein	32.86
GO Biological Process	mitochondrial membrane organization	28.62
GO Biological Process	erythrocyte homeostasis	27.43
GO Biological Process	erythrocyte differentiation	25.59
GO Biological Process	myeloid cell homeostasis	25.52
GO Biological Process	negative regulation of collagen biosynthetic process	22.75
GO Biological Process	regulation of mitochondrial membrane permeability	22.07
GO Biological Process	positive regulation of blood vessel endothelial cell migration	21.24
GO Biological Process	regulation of membrane permeability	20.64
GO Biological Process	regulation of megakaryocyte differentiation	17.20
GO Biological Process	regulation of podosome assembly	17.15
GO Biological Process	platelet-derived growth factor receptor signaling pathway	15.97
GO Biological Process	cotranslational protein targeting to membrane	15.24
GO Biological Process	cytokine production involved in immune response	14.78

F

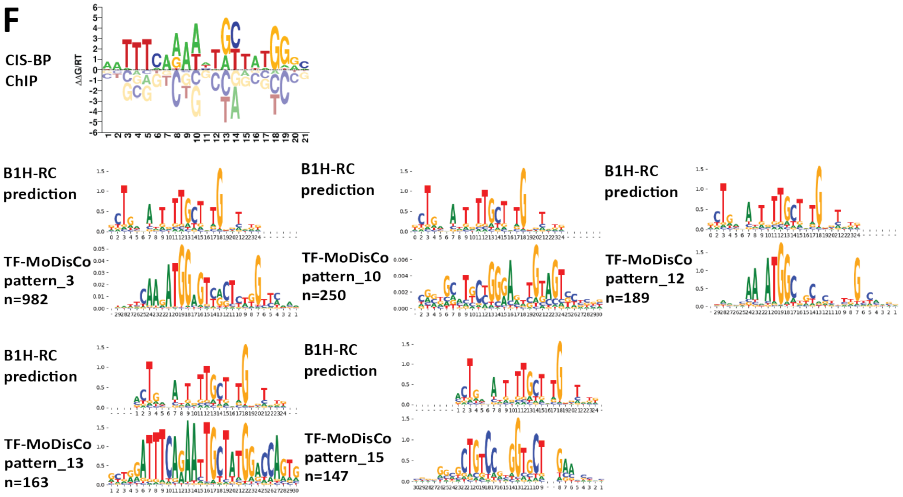

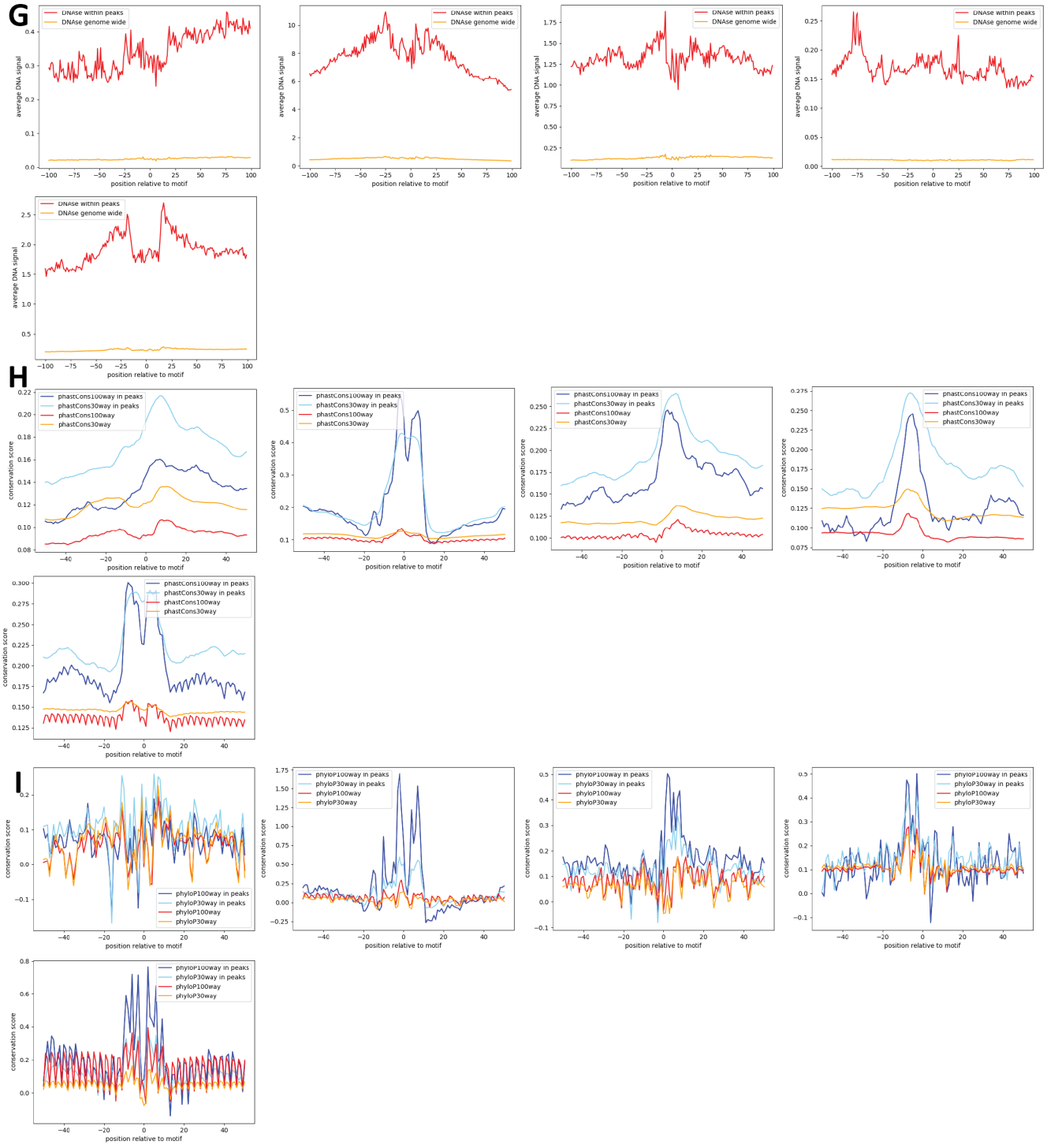

Supplementary Figure 1439: Properties and genomic distribution of motifs identified for the ZNF584 transcription factor in K562 (accession ENCSR149ZBI).

TF-MoDiSCO pattern_10 n=250, CWM

pattern_10, n=250; subpattern_0, ns=109

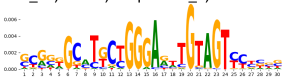

pattern_10, n=250; subpattern_1, ns=49

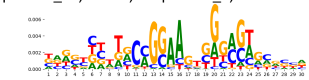

pattern_10, n=250; subpattern_2, ns=30

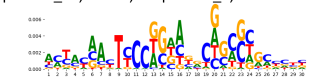

pattern_10, n=250; subpattern_3, ns=21

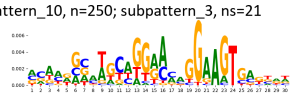

pattern_10, n=250; subpattern_4, ns=17

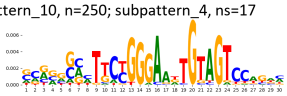

pattern_10, n=250; subpattern_5, ns=13

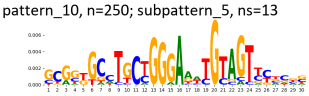

pattern_10, n=250; subpattern_6, ns=9

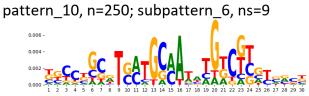

pattern_10, n=250; subpattern_7, ns=2

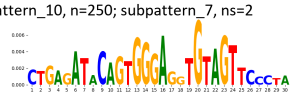

TF-MoDiSCO pattern_10 n=250, PWM

pattern_10, n=250; subpattern_0, ns=109

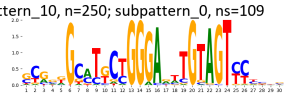

pattern_10, n=250; subpattern_1, ns=49

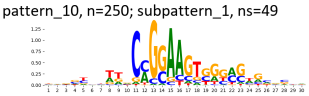

pattern_10, n=250; subpattern_2, ns=30

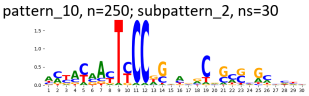

pattern_10, n=250; subpattern_3, ns=21

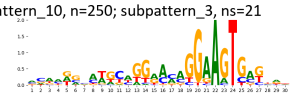

pattern_10, n=250; subpattern_4, ns=17

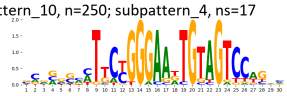

pattern_10, n=250; subpattern_5, ns=13

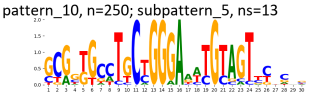

pattern_10, n=250; subpattern_6, ns=9

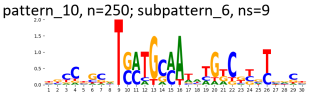

pattern_10, n=250; subpattern_7, ns=2

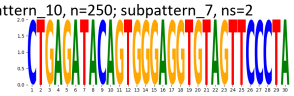

TF-MoDiSCO pattern_12 n=189, CWM

pattern_12, n=189; subpattern_0, ns=49

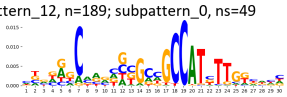

pattern_12, n=189; subpattern_1, ns=46

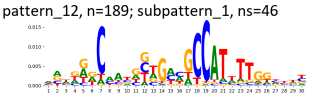

pattern_12, n=189; subpattern_2, ns=39

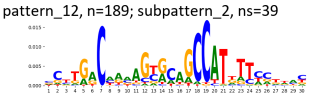

pattern_12, n=189; subpattern_3, ns=35

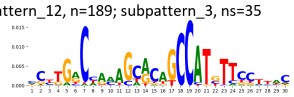

pattern_12, n=189; subpattern_4, ns=15

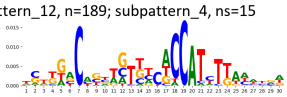

pattern_12, n=189; subpattern_5, ns=3

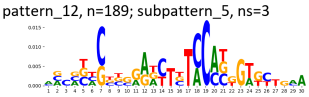

pattern_12, n=189; subpattern_6, ns=2

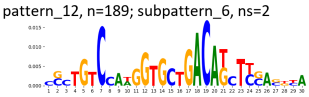

TF-MoDiSCO pattern_12 n=189, PWM

pattern_12, n=189; subpattern_0, ns=49

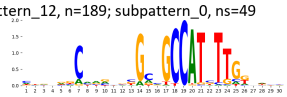

pattern_12, n=189; subpattern_1, ns=46

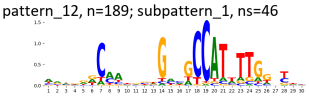

pattern_12, n=189; subpattern_2, ns=39

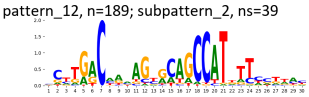

pattern_12, n=189; subpattern_3, ns=35

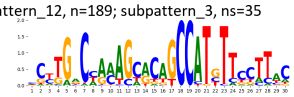

pattern_12, n=189; subpattern_4, ns=15

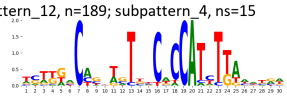

pattern_12, n=189; subpattern_5, ns=3

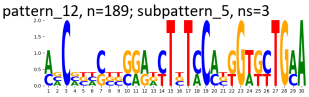

pattern_12, n=189; subpattern_6, ns=2

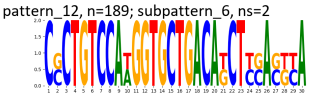

TF-MoDiSCO pattern_13 n=163, CWM

pattern_13, n=163; subpattern_0, ns=89

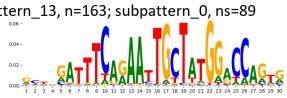

pattern_13, n=163; subpattern_1, ns=74

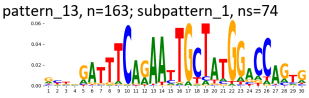

TF-MoDiSCO pattern_13 n=163, PWM

pattern_13, n=163; subpattern_0, ns=89

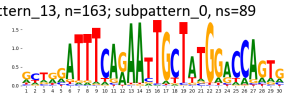

pattern_13, n=163; subpattern_1, ns=74

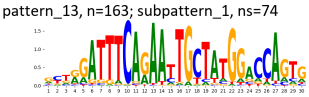

TF-MoDiSCO pattern_14 n=147, CWM

pattern_14, n=147; subpattern_0, ns=48

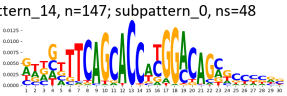

pattern_14, n=147; subpattern_1, ns=46

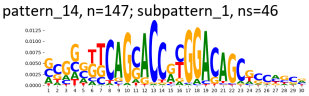

pattern_14, n=147; subpattern_2, ns=16

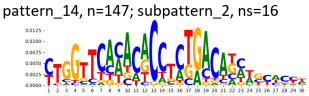

pattern_14, n=147; subpattern_3, ns=14

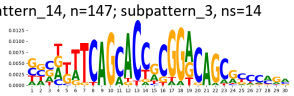

pattern_14, n=147; subpattern_4, ns=7

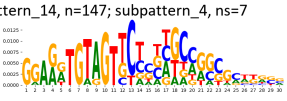

pattern_14, n=147; subpattern_5, ns=6

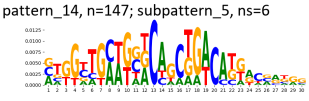

pattern_14, n=147; subpattern_6, ns=5

pattern_14, n=147; subpattern_7, ns=3

pattern_14, n=147; subpattern_8, ns=2

TF-MoDisCO pattern_14 n=147, PWM

pattern_14, n=147; subpattern_0, ns=48

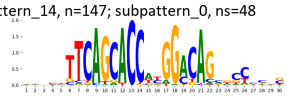

pattern_14, n=147; subpattern_1, ns=46

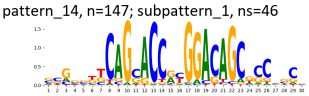

pattern_14, n=147; subpattern_2, ns=16

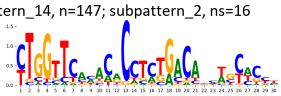

pattern_14, n=147; subpattern_3, ns=14

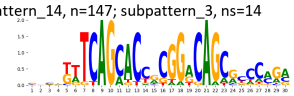

pattern_14, n=147; subpattern_4, ns=7

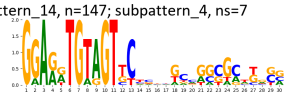

pattern_14, n=147; subpattern_5, ns=6

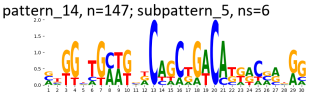

pattern_14, n=147; subpattern_6, ns=5

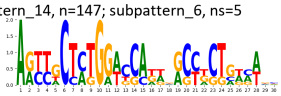

pattern_14, n=147; subpattern_7, ns=3

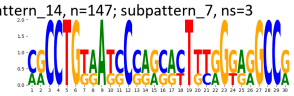

pattern_14, n=147; subpattern_8, ns=2

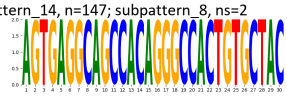

TF-MoDisCO pattern_3 n=982, CWM

pattern_3, n=982; subpattern_0, ns=263

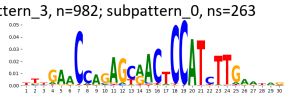

pattern_3, n=982; subpattern_1, ns=235

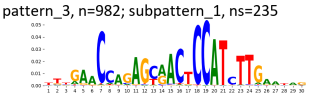

pattern_3, n=982; subpattern_2, ns=172

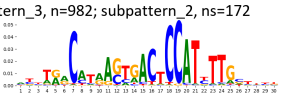

pattern_3, n=982; subpattern_3, ns=148

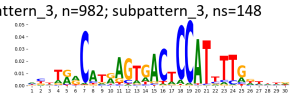

pattern_3, n=982; subpattern_4, ns=132

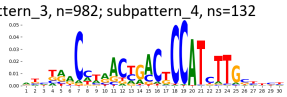

pattern_3, n=982; subpattern_5, ns=17

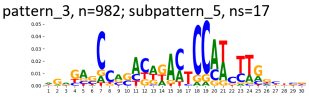

pattern_3, n=982; subpattern_6, ns=13

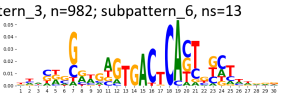

pattern_3, n=982; subpattern_7, ns=2

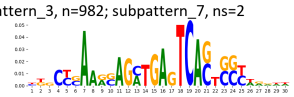

TF-MoDisCO pattern_3 n=982, PWM

pattern_3, n=982; subpattern_0, ns=263

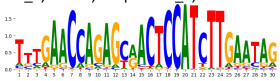

pattern_3, n=982; subpattern_1, ns=235

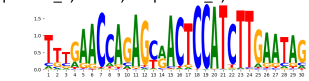

pattern_3, n=982; subpattern_2, ns=172

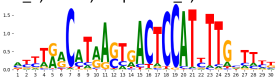

pattern_3, n=982; subpattern_3, ns=148

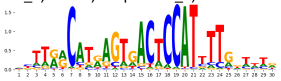

pattern_3, n=982; subpattern_4, ns=132

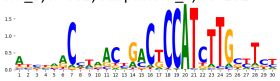

pattern_3, n=982; subpattern_5, ns=17

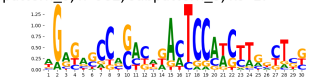

pattern_3, n=982; subpattern_6, ns=13

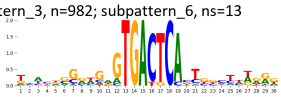

pattern_3, n=982; subpattern_7, ns=2

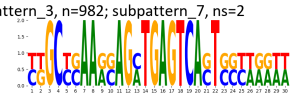

Supplementary Figure 1440: TF-MoDisCO subpatterns for the ZNF584 transcription factor in K562 (accession ENCSR149ZBI).

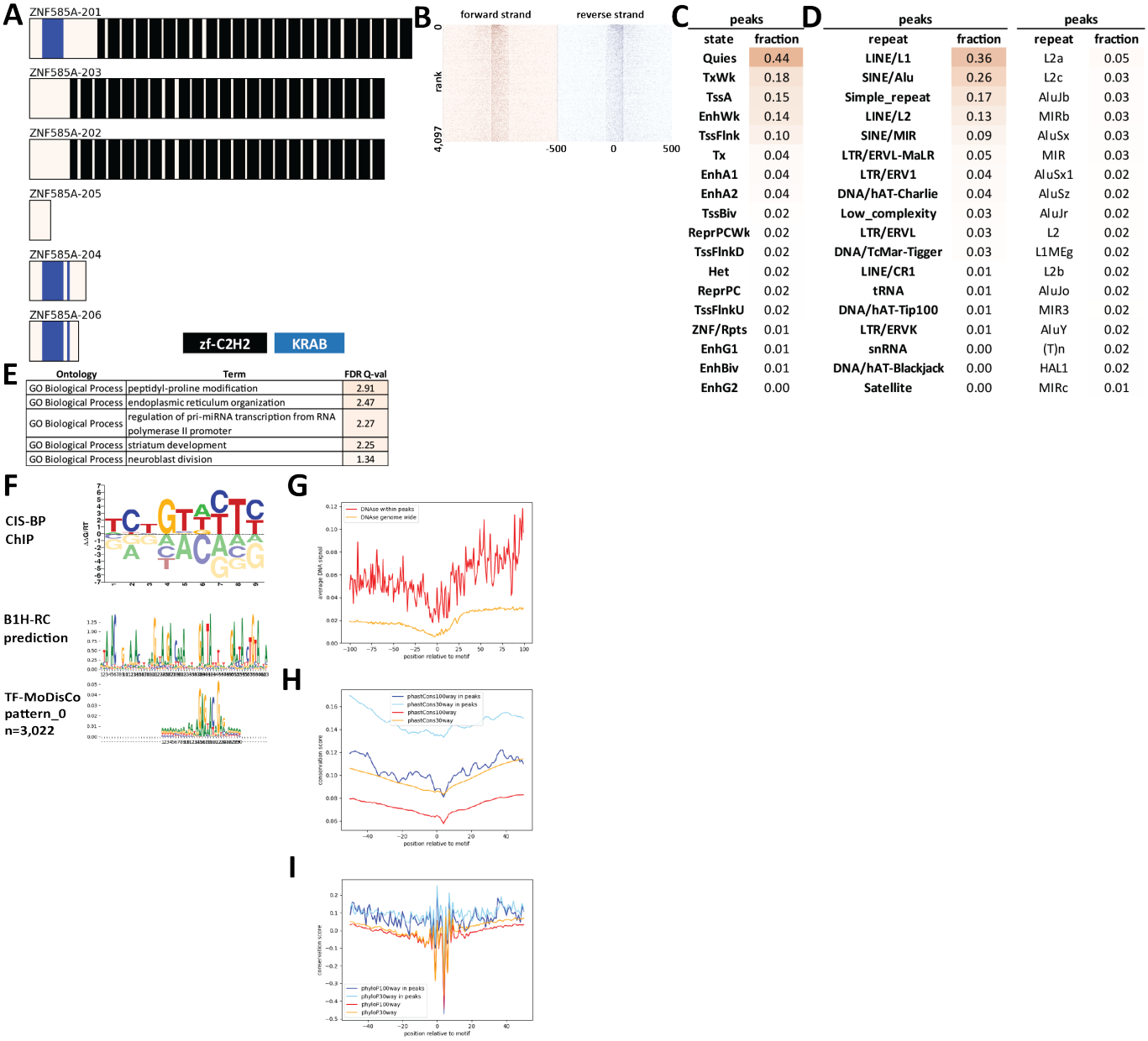

Supplementary Figure 1441: Properties and genomic distribution of motifs identified for the ZNF585A transcription factor in HEK293 (accession ChipExo models).

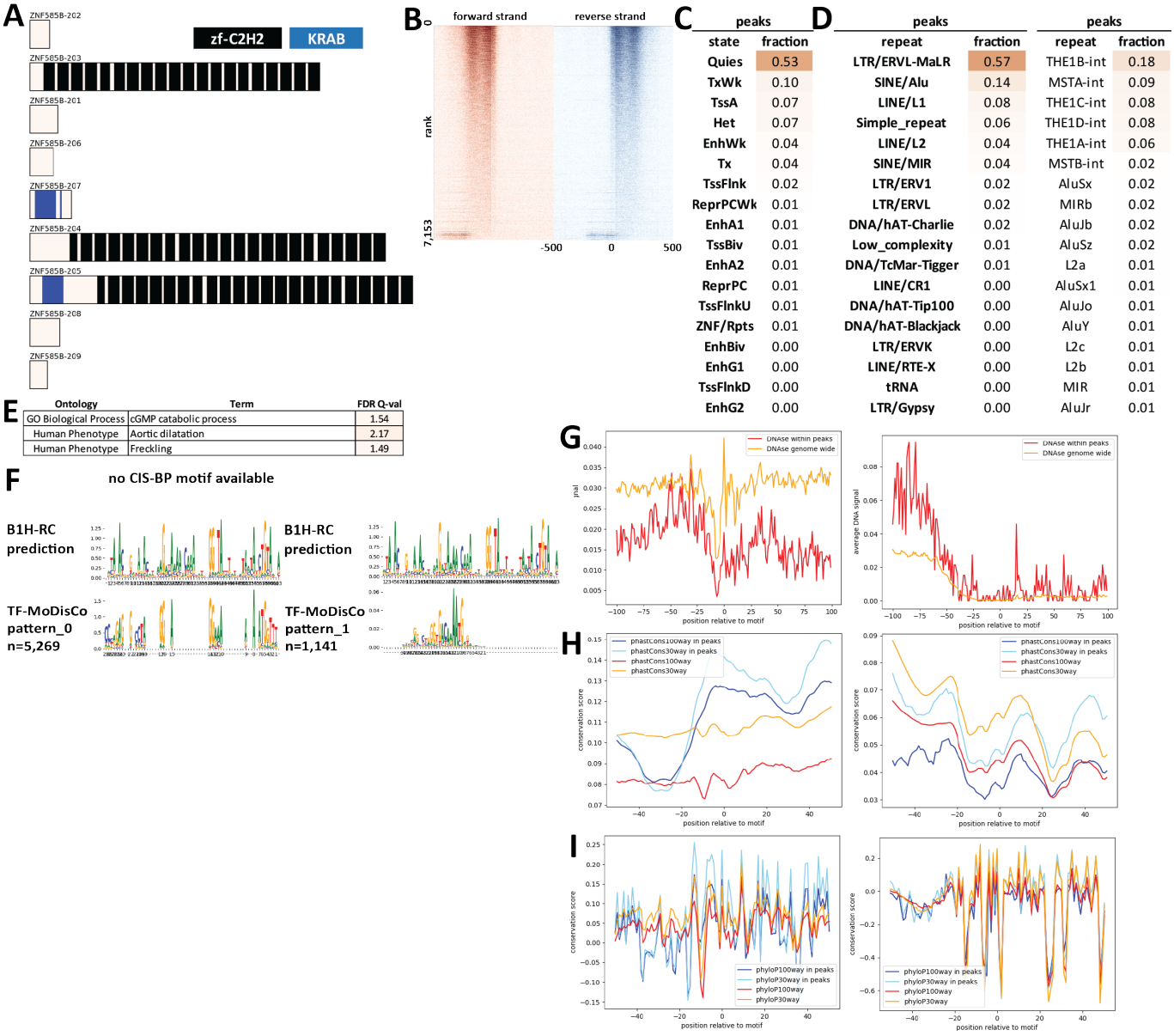

Supplementary Figure 1442: Properties and genomic distribution of motifs identified for the ZNF585B transcription factor in HEK293 (accession ENCSR011XCI).

TF-MoDisCO pattern_0 n=5269, CWM

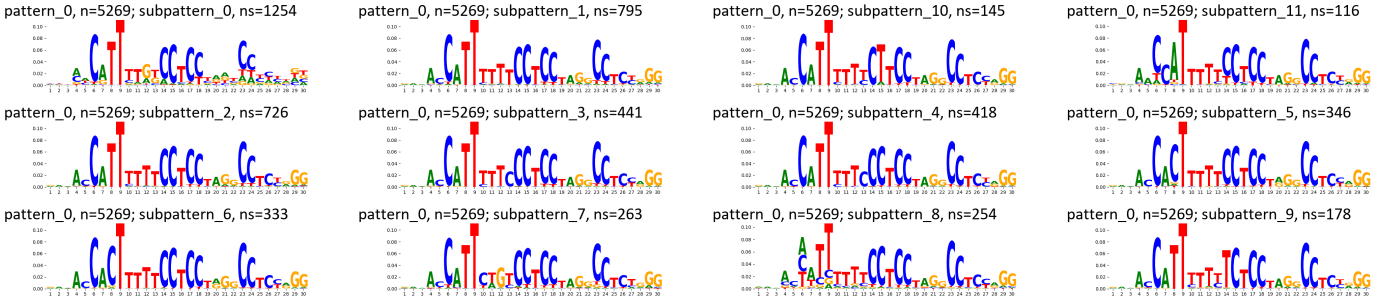

TF-MoDisCO pattern_0 n=5269, PWM

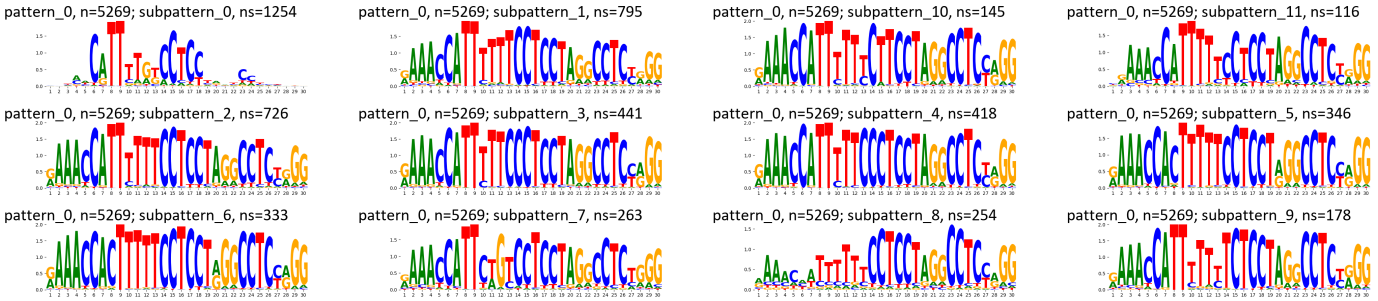

TF-MoDisCO pattern_1 n=1141, CWM

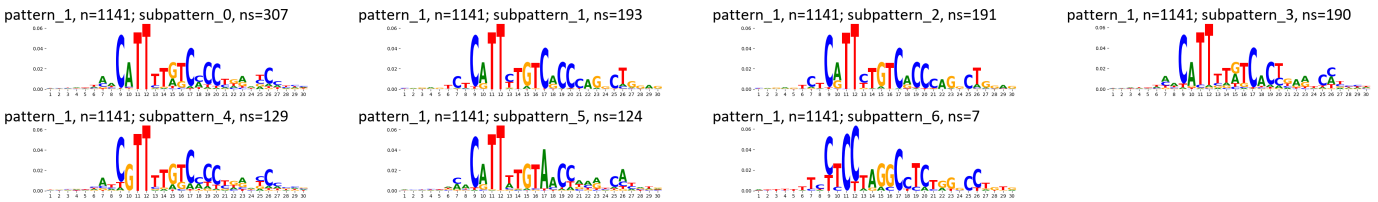

TF-MoDisCO pattern_1 n=1141, PWM

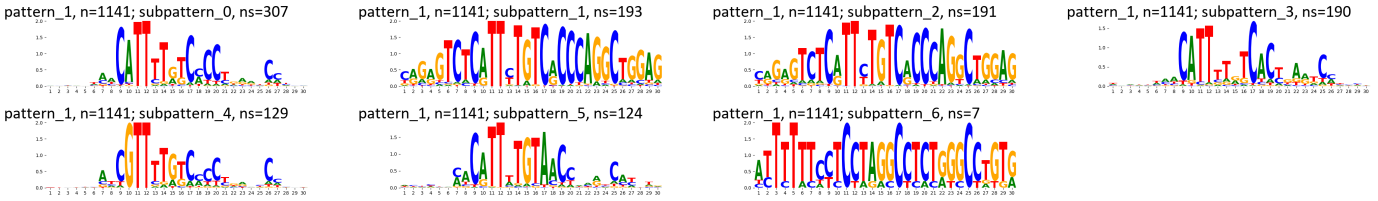

Supplementary Figure 1443: TF-MoDisCO subpatterns for the ZNF585B transcription factor in HEK293 (accession ENCSR011XCI).

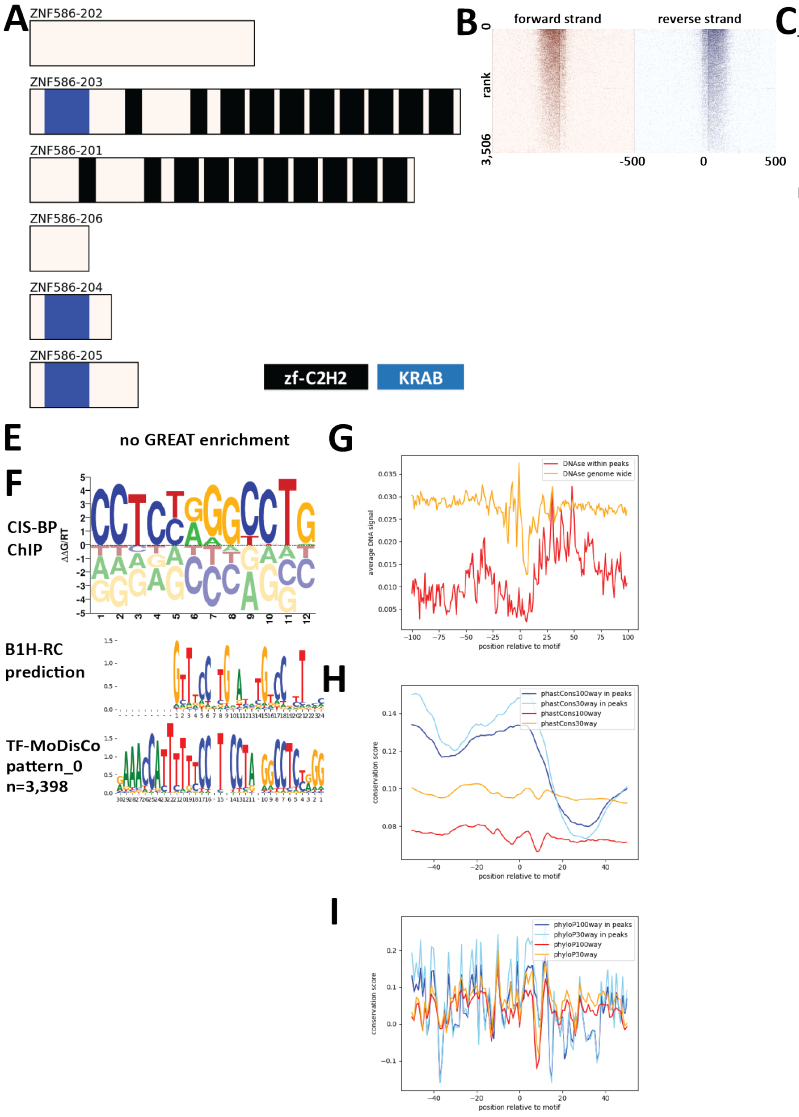

C

peaks	
state	fraction
Quies	0.64
Het	0.12
TxWk	0.06
Tx	0.03
EnhWk	0.01
ReprPCWk	0.01
TssA	0.01
ZNF/Rpts	0.01
EnhA1	0.00
TssFlnk	0.00
ReprPC	0.00
TssBiv	0.00
TssFlnkU	0.00
TssFlnkD	0.00
EnhG1	0.00
EnhA2	0.00
EnhG2	0.00

D

peaks		peaks	
repeat	fraction	repeat	fraction
LTR/ERVL-MaLR	0.89	THE1B-int	0.30
LINE/L1	0.03	MSTA-int	0.15
SINE/Alu	0.02	THE1C-int	0.13
SINE/MIR	0.01	THE1D-int	0.12
LINE/L2	0.01	THE1A-int	0.10
Simple_repeat	0.01	MSTB-int	0.04
LTR/ERV1	0.01	MSTB1-int	0.01
LTR/ERVL	0.01	THE1-int	0.01
DNA/hAT-Charlie	0.00	MIRb	0.01
DNA/TcMar-Tigger	0.00	MSTD-int	0.01
Low_complexity	0.00	MSTC-int	0.00
LINE/CR1	0.00	MST-int	0.00
DNA/hAT-Tip100	0.00	L2a	0.00
LTR/Gypsy?	0.00	AluJo	0.00
DNA/hAT-Blackjack	0.00	AluJb	0.00
tRNA	0.00	MIR	0.00
rRNA	0.00	L2b	0.00
SINE/tRNA-RTE	0.00	AluSx	0.00

Supplementary Figure 1444: Properties and genomic distribution of motifs identified for the ZNF586 transcription factor in HEK293 (accession Hughes GR models).

TF-MoDisCO pattern_0 n=3398, CWM

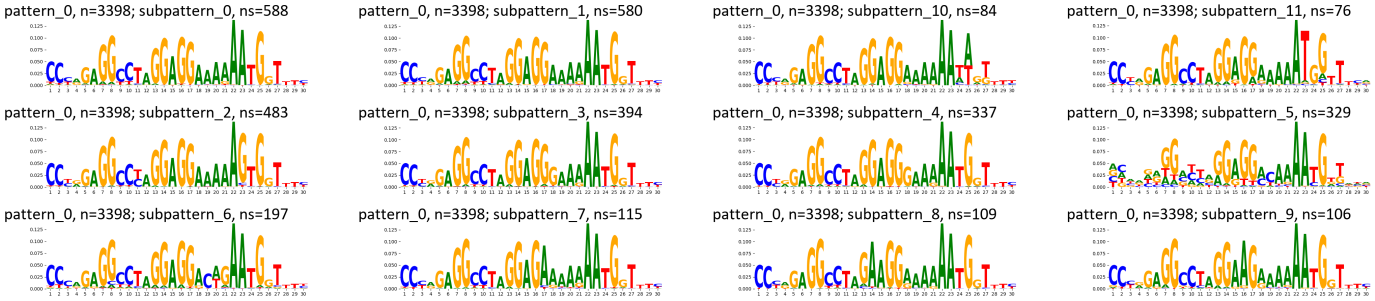

TF-MoDisCO pattern_0 n=3398, PWM

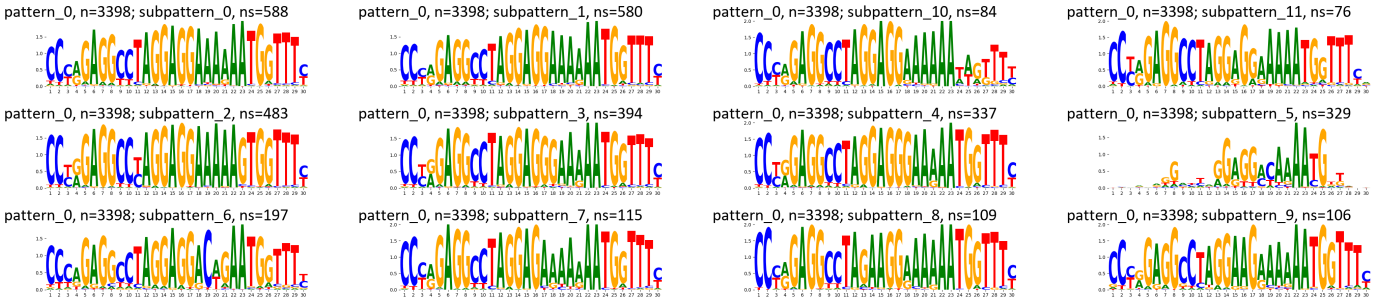

Supplementary Figure 1445: TF-MoDisCO subpatterns for the ZNF586 transcription factor in HEK293 (accession Hughes GR models).

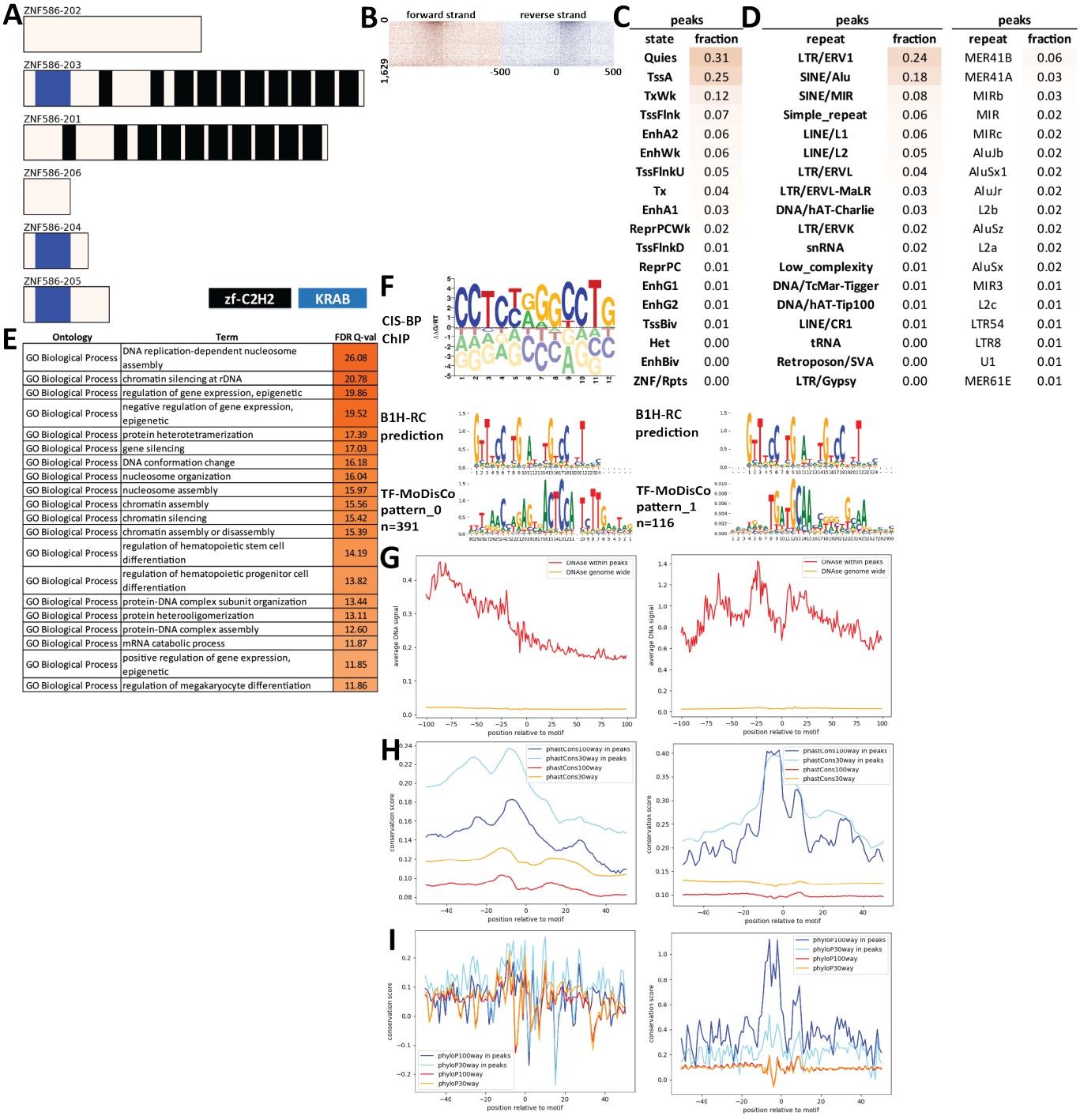

peaks	
state	fraction
Quies	0.31
TssA	0.25
TxWk	0.12
TssFlnk	0.07
EnhA2	0.06
EnhWk	0.06
TssFlnkU	0.05
Tx	0.04
EnhA1	0.03
ReprPCWk	0.02
TssFlnkD	0.01
ReprPC	0.01
EnhG1	0.01
EnhG2	0.01
TssBiv	0.01
Het	0.00
EnhBiv	0.00
ZNF/Rpts	0.00

peaks	
repeat	fraction
LTR/ERV1	0.24
SINE/Alu	0.18
SINE/MIR	0.08
Simple_repeat	0.06
LINE/L1	0.06
LINE/L2	0.05
LTR/ERVL	0.04
LTR/ERVL-MaLR	0.03
DNA/hAT-Charlie	0.03
LTR/ERVK	0.02
snRNA	0.02
Low_complexity	0.01
DNA/TcMar-Tigger	0.01
DNA/hAT-Tip100	0.01
LINE/CR1	0.01
tRNA	0.00
Retroposon/SVA	0.00
LTR/Gypsy	0.00

peaks	
repeat	fraction
MER41B	0.06
MER41A	0.03
MIRb	0.03
MIR	0.02
MIRc	0.02
AluJb	0.02
AluSx1	0.02
AluJr	0.02
L2b	0.02
AluSz	0.02
L2a	0.02
AluSx	0.02
MIR3	0.01
L2c	0.01
LTR54	0.01
LTR8	0.01
U1	0.01
MER61E	0.01

E

Ontology	Term	FDR Q-val
GO Biological Process	DNA replication-dependent nucleosome assembly	26.08
GO Biological Process	chromatin silencing at rDNA	20.78
GO Biological Process	regulation of gene expression, epigenetic	19.86
GO Biological Process	negative regulation of gene expression, epigenetic	19.52
GO Biological Process	protein heterotetramerization	17.39
GO Biological Process	gene silencing	17.03
GO Biological Process	DNA conformation change	16.18
GO Biological Process	nucleosome organization	16.04
GO Biological Process	nucleosome assembly	15.97
GO Biological Process	chromatin assembly	15.56
GO Biological Process	chromatin silencing	15.42
GO Biological Process	chromatin assembly or disassembly	15.39
GO Biological Process	regulation of hematopoietic stem cell differentiation	14.19
GO Biological Process	regulation of hematopoietic progenitor cell differentiation	13.82
GO Biological Process	protein-DNA complex subunit organization	13.44
GO Biological Process	protein heterooligomerization	13.11
GO Biological Process	protein-DNA complex assembly	12.60
GO Biological Process	mRNA catabolic process	11.87
GO Biological Process	positive regulation of gene expression, epigenetic	11.85
GO Biological Process	regulation of megakaryocyte differentiation	11.86

Supplementary Figure 1446: Properties and genomic distribution of motifs identified for the ZNF586 transcription factor in K562 (accession ENCSR236JZN).

TF-MoDisCO pattern_0 n=391, CWM

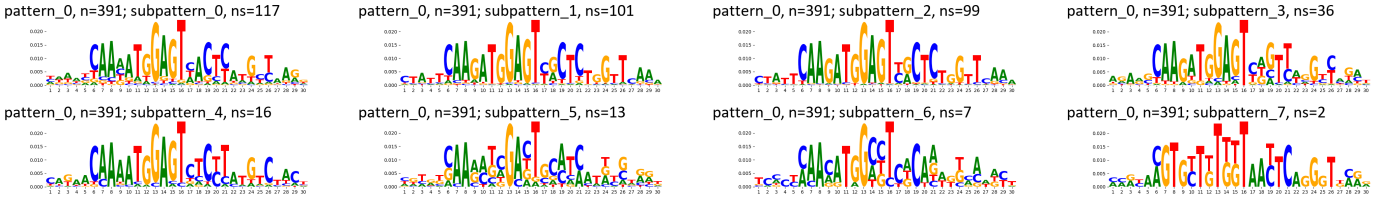

TF-MoDisCO pattern_0 n=391, PWM

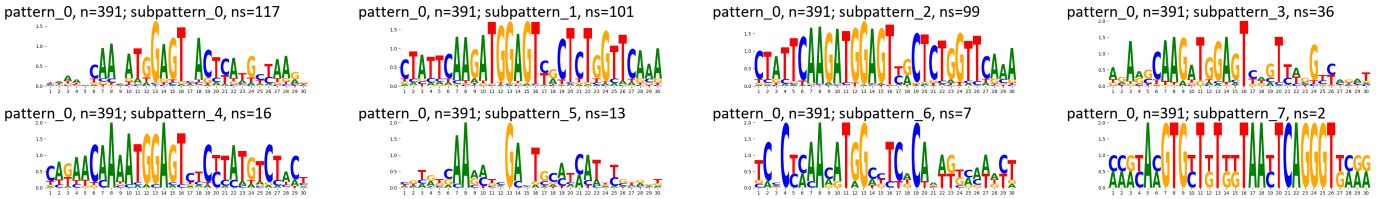

TF-MoDisCO pattern_1 n=116, CWM

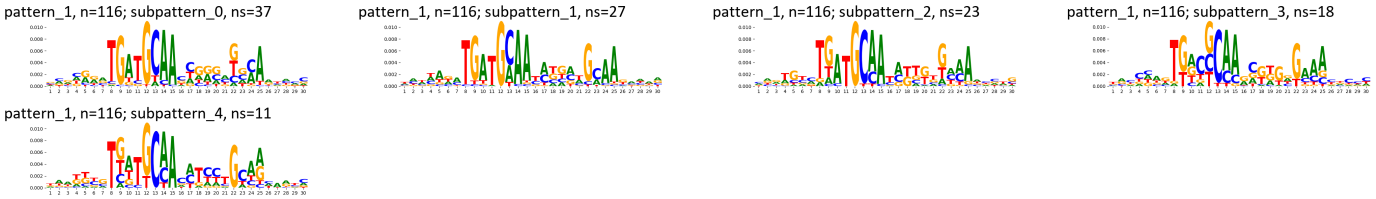

TF-MoDisCO pattern_1 n=116, PWM

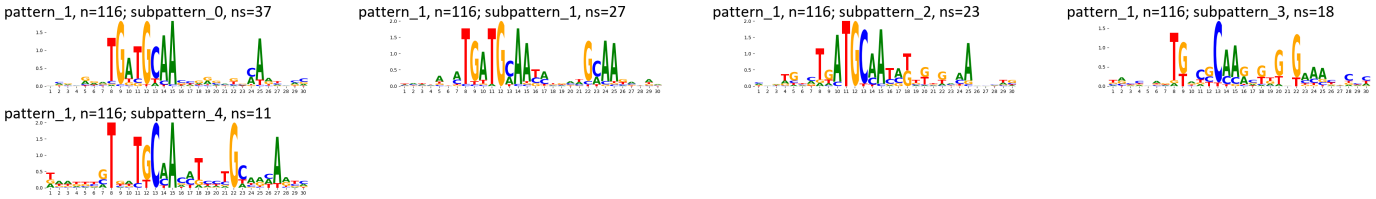

Supplementary Figure 1447: TF-MoDisCO subpatterns for the ZNF586 transcription factor in K562 (accession ENCSR236JZN).

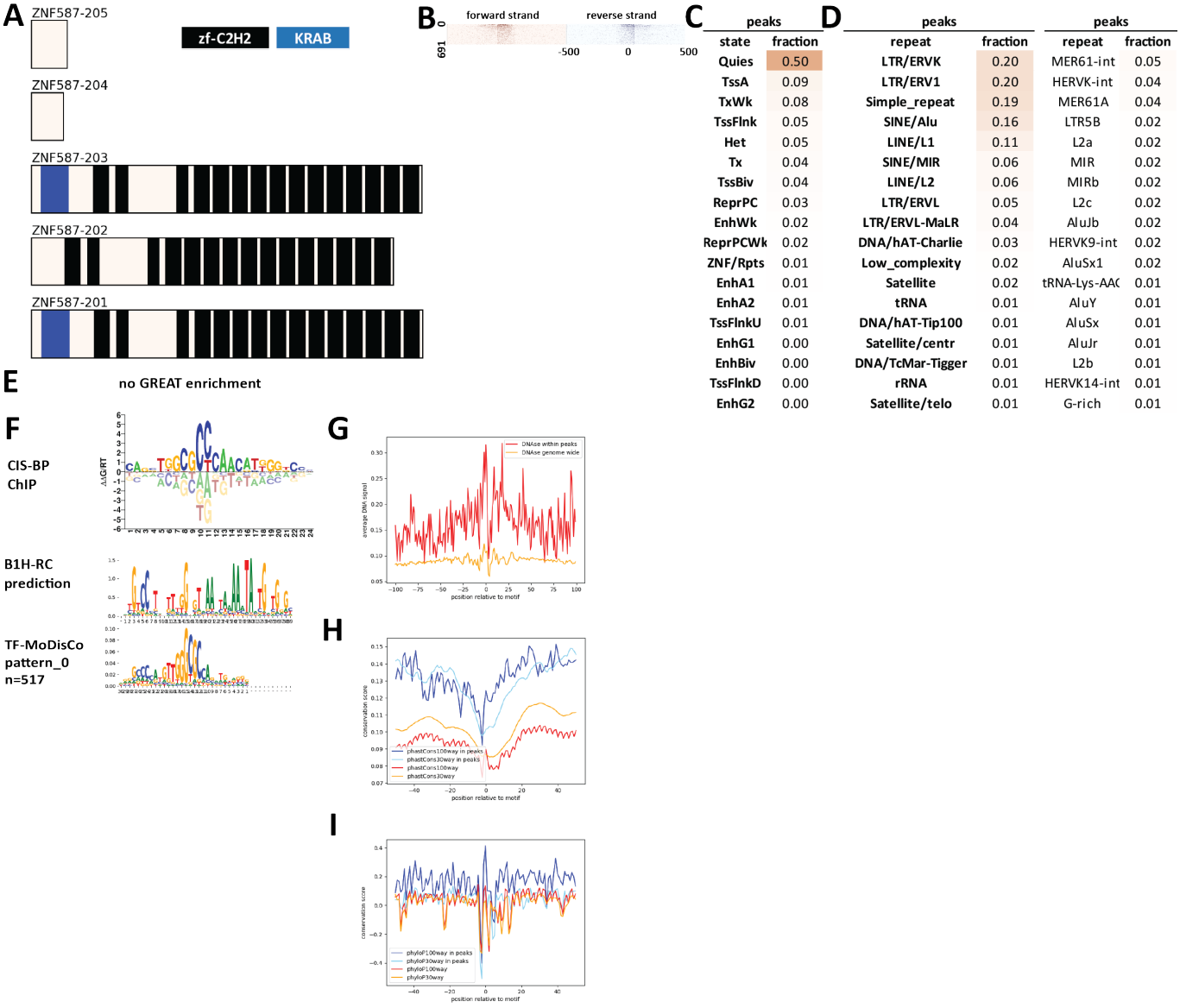

C

peaks	
state	fraction
Quies	0.50
TssA	0.09
TxWk	0.08
TssFlnk	0.05
Het	0.05
Tx	0.04
TssBiv	0.04
ReprPC	0.03
EnhWk	0.02
ReprPCWk	0.02
ZNF/Rpts	0.01
EnhA1	0.01
EnhA2	0.01
TssFlnkU	0.01
EnhG1	0.00
EnhBiv	0.00
TssFlnkD	0.00
EnhG2	0.00

D

peaks		peaks	
repeat	fraction	repeat	fraction
LTR/ERVK	0.20	MER61-int	0.05
LTR/ERV1	0.20	HERVK-int	0.04
Simple_repeat	0.19	MER61A	0.04
SINE/Alu	0.16	LTR5B	0.02
LINE/L1	0.11	L2a	0.02
SINE/MIR	0.06	MIR	0.02
LINE/L2	0.06	MIRb	0.02
LTR/ERVL	0.05	L2c	0.02
LTR/ERVL-MaLR	0.04	AluJb	0.02
DNA/hAT-Charlie	0.03	HERVK9-int	0.02
Low_complexity	0.02	AluSx1	0.02
Satellite	0.02	tRNA-Lys-AAC	0.01
tRNA	0.01	AluY	0.01
DNA/hAT-Tip100	0.01	AluSx	0.01
Satellite/centr	0.01	AluJr	0.01
DNA/TcMar-Tigger	0.01	L2b	0.01
rRNA	0.01	HERVK14-int	0.01
Satellite/telo	0.01	G-rich	0.01

Supplementary Figure 1448: Properties and genomic distribution of motifs identified for the ZNF587 transcription factor in HEK293 (accession ChipExo models).

TF-MoDisCO pattern_0 n=517, CWM

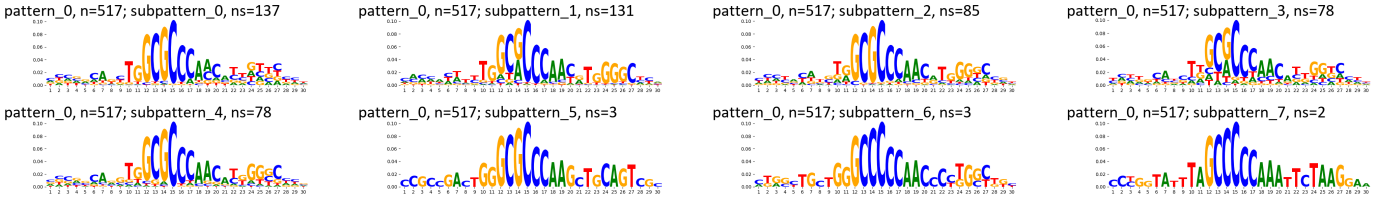

TF-MoDisCO pattern_0 n=517, PWM

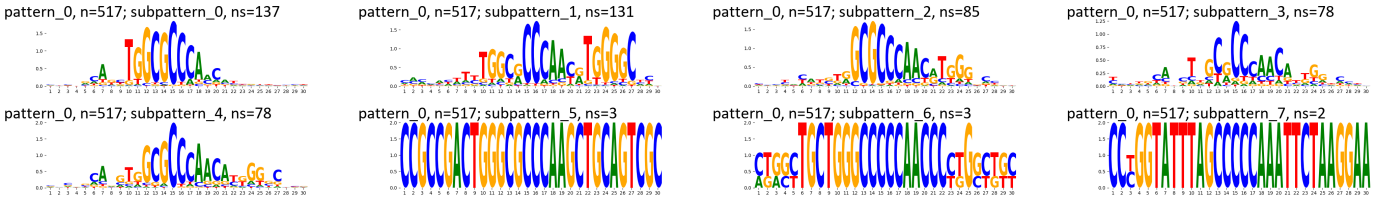

Supplementary Figure 1449: TF-MoDisCO subpatterns for the ZNF587 transcription factor in HEK293 (accession ChipExo models).

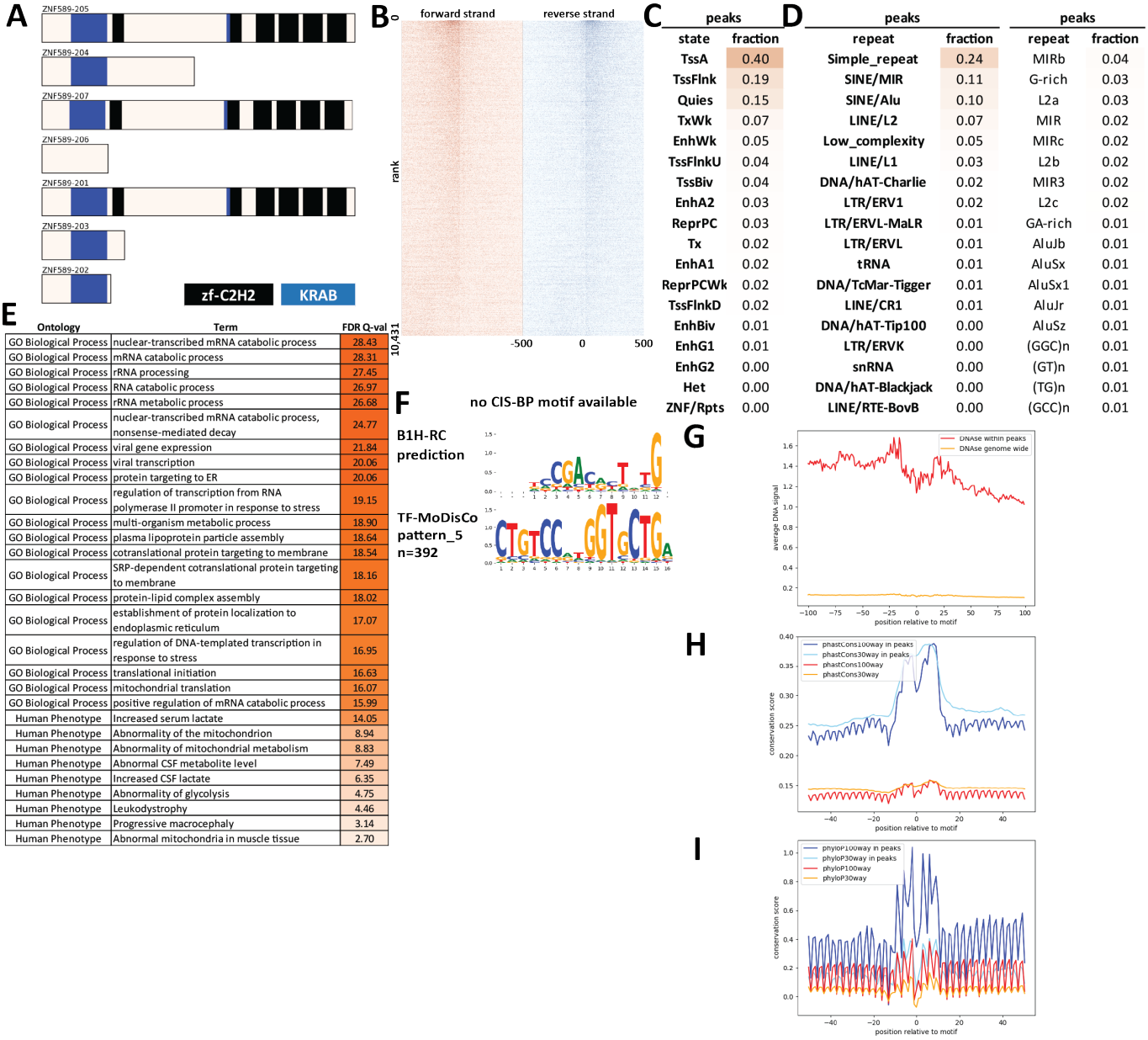

peaks	
state	fraction
TssA	0.40
TssFlnk	0.19
Quies	0.15
TxWk	0.07
EnhWk	0.05
TssFlnkU	0.04
TssBiv	0.04
EnhA2	0.03
ReprPC	0.03
Tx	0.02
EnhA1	0.02
ReprPCWk	0.02
TssFlnkD	0.02
EnhBiv	0.01
EnhG1	0.01
EnhG2	0.00
Het	0.00
ZNF/Rpts	0.00

peaks		peaks	
repeat	fraction	repeat	fraction
Simple_repeat	0.24	MIRb	0.04
SINE/MIR	0.11	G-rich	0.03
SINE/Alu	0.10	L2a	0.03
LINE/L2	0.07	MIR	0.02
Low_complexity	0.05	MIRc	0.02
LINE/L1	0.03	L2b	0.02
DNA/hAT-Charlie	0.02	MIR3	0.02
LTR/ERV1	0.02	L2c	0.02
LTR/ERVL-MaLR	0.01	GA-rich	0.01
LTR/ERVL	0.01	AluJb	0.01
tRNA	0.01	AluSx	0.01
DNA/TcMar-Tigger	0.01	AluSx1	0.01
LINE/CR1	0.01	AluJr	0.01
DNA/hAT-Tip100	0.00	AluSz	0.01
LTR/ERVK	0.00	(GGC)n	0.01
snRNA	0.00	(GT)n	0.01
DNA/hAT-Blackjack	0.00	(TG)n	0.01
LINE/RTE-BovB	0.00	(GCC)n	0.01

Ontology	Term	FDR Q-val
GO Biological Process	nuclear-transcribed mRNA catabolic process	28.43
GO Biological Process	mRNA catabolic process	28.31
GO Biological Process	rRNA processing	27.45
GO Biological Process	RNA catabolic process	26.97
GO Biological Process	rRNA metabolic process	26.68
GO Biological Process	nuclear-transcribed mRNA catabolic process, nonsense-mediated decay	24.77
GO Biological Process	viral gene expression	21.84
GO Biological Process	viral transcription	20.06
GO Biological Process	protein targeting to ER	20.06
GO Biological Process	regulation of transcription from RNA polymerase II promoter in response to stress	19.15
GO Biological Process	multi-organism metabolic process	18.90
GO Biological Process	plasma lipoprotein particle assembly	18.64
GO Biological Process	cotranslational protein targeting to membrane	18.54
GO Biological Process	SRP-dependent cotranslational protein targeting to membrane	18.16
GO Biological Process	protein-lipid complex assembly	18.02
GO Biological Process	establishment of protein localization to endoplasmic reticulum	17.07
GO Biological Process	regulation of DNA-templated transcription in response to stress	16.95
GO Biological Process	translational initiation	16.63
GO Biological Process	mitochondrial translation	16.07
GO Biological Process	positive regulation of mRNA catabolic process	15.99
Human Phenotype	Increased serum lactate	14.05
Human Phenotype	Abnormality of the mitochondrion	8.94
Human Phenotype	Abnormality of mitochondrial metabolism	8.83
Human Phenotype	Abnormal CSF metabolite level	7.49
Human Phenotype	Increased CSF lactate	6.35
Human Phenotype	Abnormality of glycolysis	4.75
Human Phenotype	Leukodystrophy	4.46
Human Phenotype	Progressive macrocephaly	3.14
Human Phenotype	Abnormal mitochondria in muscle tissue	2.70

Supplementary Figure 1450: Properties and genomic distribution of motifs identified for the ZNF589 transcription factor in HepG2 (accession ENCSR827ZGB).

TF-MoDisCO pattern_5 n=392, CWM

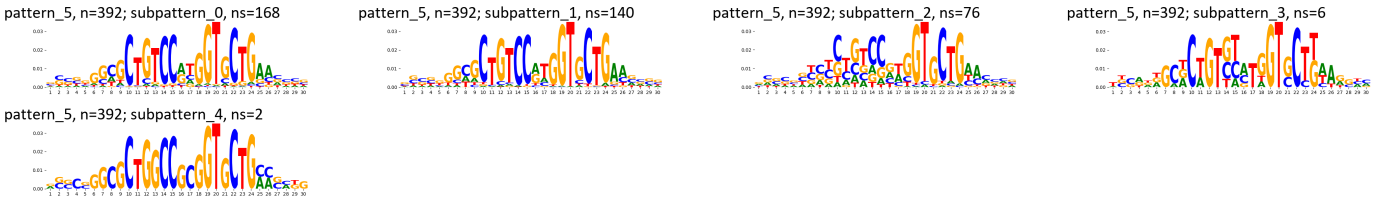

TF-MoDisCO pattern_5 n=392, PWM

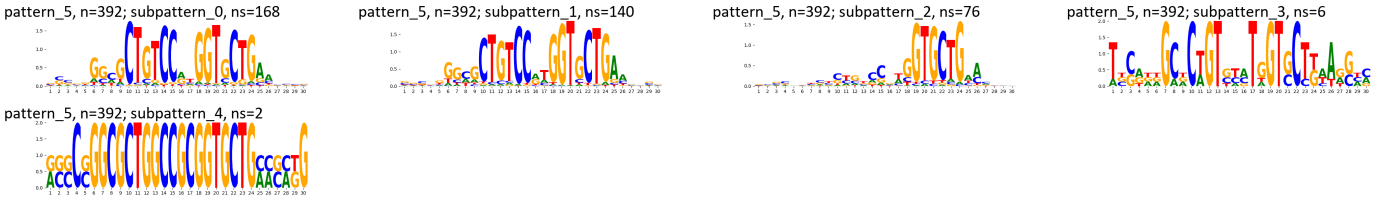

Supplementary Figure 1451: TF-MoDisCO subpatterns for the ZNF589 transcription factor in HepG2 (accession ENCSR827ZGB).

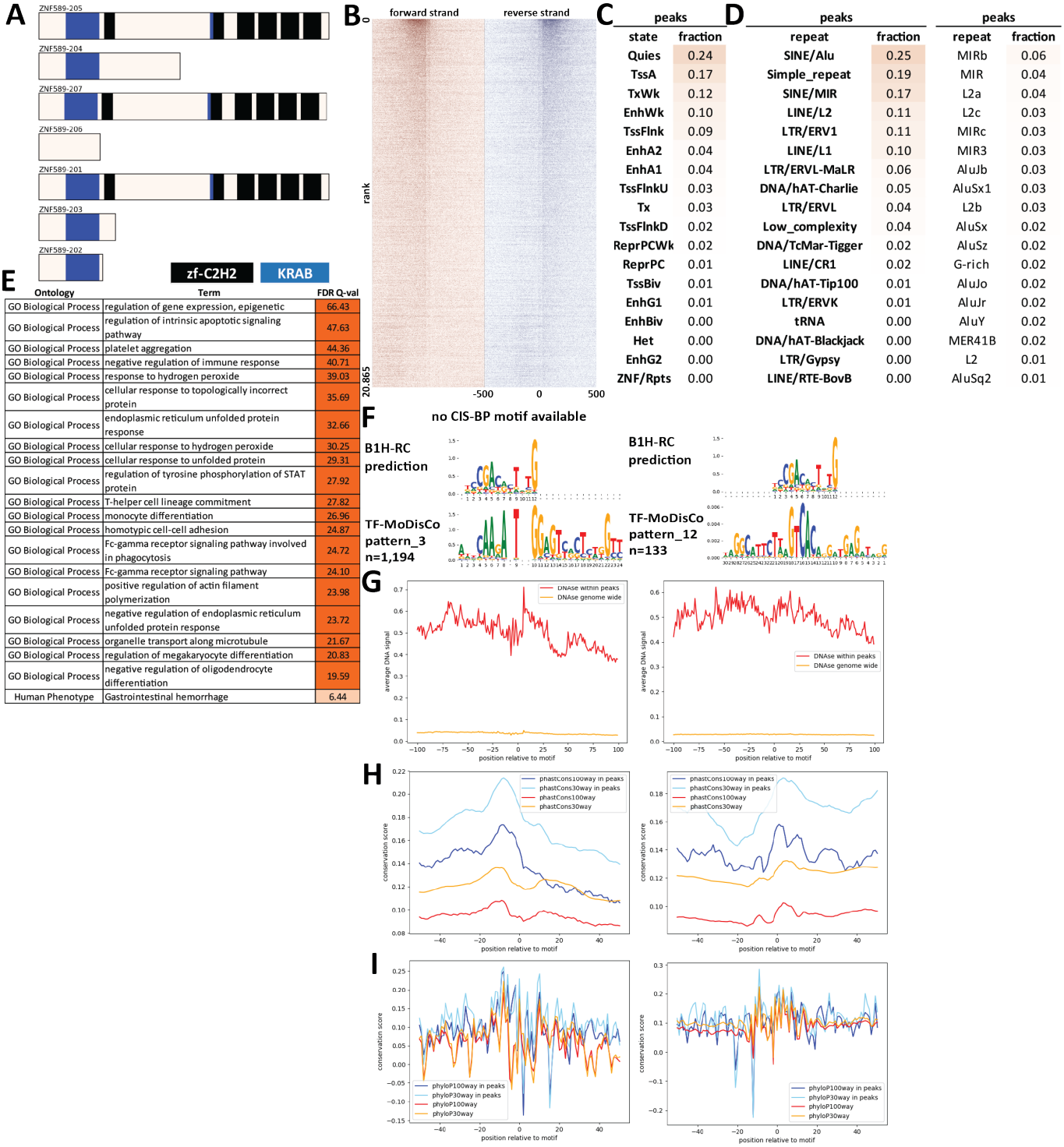

C

peaks	
state	fraction
Quies	0.24
TssA	0.17
TxWk	0.12
EnhWk	0.10
TssFlnk	0.09
EnhA2	0.04
EnhA1	0.04
TssFlnkU	0.03
Tx	0.03
TssFlnkD	0.02
ReprPCWk	0.02
ReprPC	0.01
TssBiv	0.01
EnhG1	0.01
EnhBiv	0.00
Het	0.00
EnhG2	0.00
ZNF/Rpts	0.00

D

peaks		peaks	
repeat	fraction	repeat	fraction
SINE/Alu	0.25	MIRb	0.06
Simple_repeat	0.19	MIR	0.04
SINE/MIR	0.17	L2a	0.04
LINE/L2	0.11	L2c	0.03
LTR/ERV1	0.11	MIRc	0.03
LINE/L1	0.10	MIR3	0.03
LTR/ERVL-MaLR	0.06	AluJb	0.03
DNA/hAT-Charlie	0.05	AluSx1	0.03
LTR/ERVL	0.04	L2b	0.03
Low_complexity	0.04	AluSx	0.02
DNA/TcMar-Tigger	0.02	AluSz	0.02
LINE/CR1	0.02	G-rich	0.02
DNA/hAT-Tip100	0.01	AluJo	0.02
LTR/ERVK	0.01	AluJr	0.02
tRNA	0.00	AluY	0.02
DNA/hAT-Blackjack	0.00	MER41B	0.02
LTR/Gypsy	0.00	L2	0.01
LINE/RTE-BovB	0.00	AluSq2	0.01

E

Ontology	Term	FDR Q-val
GO Biological Process	regulation of gene expression, epigenetic	66.43
GO Biological Process	regulation of intrinsic apoptotic signaling pathway	47.63
GO Biological Process	platelet aggregation	44.36
GO Biological Process	negative regulation of immune response	40.71
GO Biological Process	response to hydrogen peroxide	39.03
GO Biological Process	cellular response to topologically incorrect protein	35.69
GO Biological Process	endoplasmic reticulum unfolded protein response	32.66
GO Biological Process	cellular response to hydrogen peroxide	30.25
GO Biological Process	cellular response to unfolded protein	29.31
GO Biological Process	regulation of tyrosine phosphorylation of STAT protein	27.92
GO Biological Process	T-helper cell lineage commitment	27.82
GO Biological Process	monocyte differentiation	26.96
GO Biological Process	homotypic cell-cell adhesion	24.87
GO Biological Process	Fc-gamma receptor signaling pathway involved in phagocytosis	24.72
GO Biological Process	Fc-gamma receptor signaling pathway	24.10
GO Biological Process	positive regulation of actin filament polymerization	23.98
GO Biological Process	negative regulation of endoplasmic reticulum unfolded protein response	23.72
GO Biological Process	organelle transport along microtubule	21.67
GO Biological Process	regulation of megakaryocyte differentiation	20.83
GO Biological Process	negative regulation of oligodendrocyte differentiation	19.59
Human Phenotype	Gastrointestinal hemorrhage	6.44

Supplementary Figure 1452: Properties and genomic distribution of motifs identified for the ZNF589 transcription factor in K562 (accession ENCSR603XLW).

TF-MoDisCO pattern_12 n=133, CWM

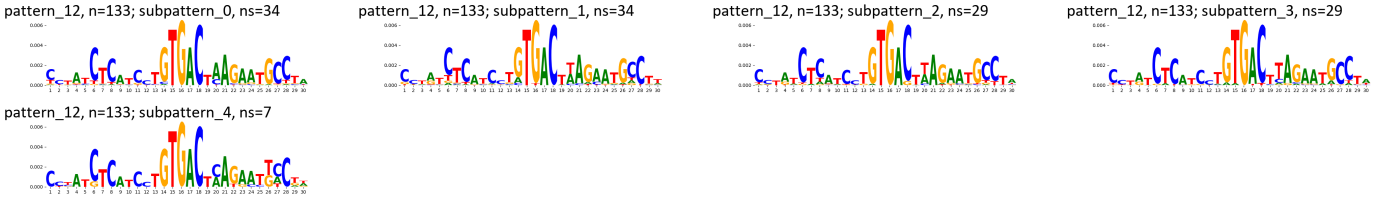

TF-MoDisCO pattern_12 n=133, PWM

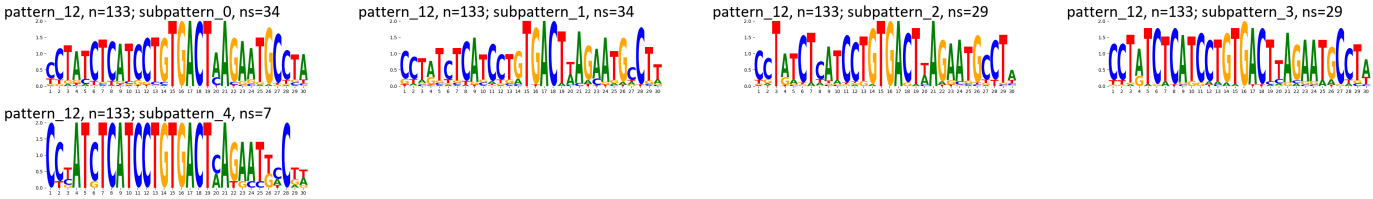

TF-MoDisCO pattern_3 n=1194, CWM

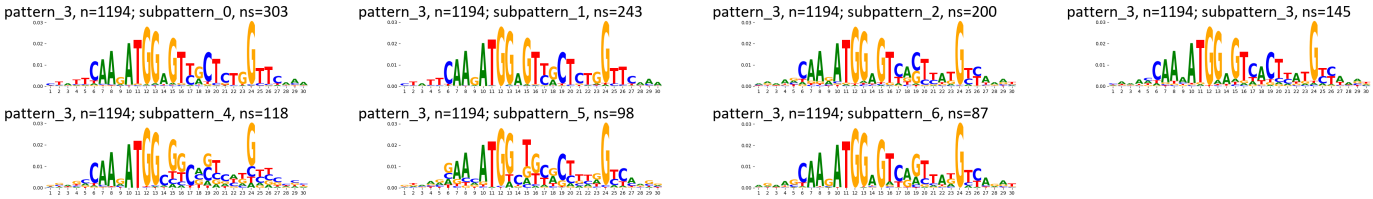

TF-MoDisCO pattern_3 n=1194, PWM

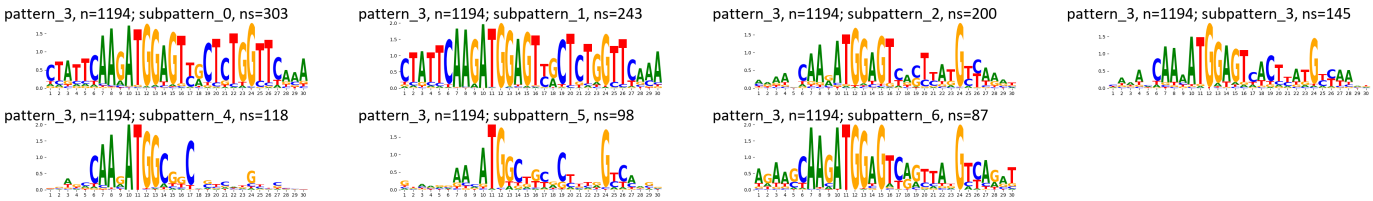

Supplementary Figure 1453: TF-MoDisCO subpatterns for the ZNF589 transcription factor in K562 (accession ENCSR603XLW).

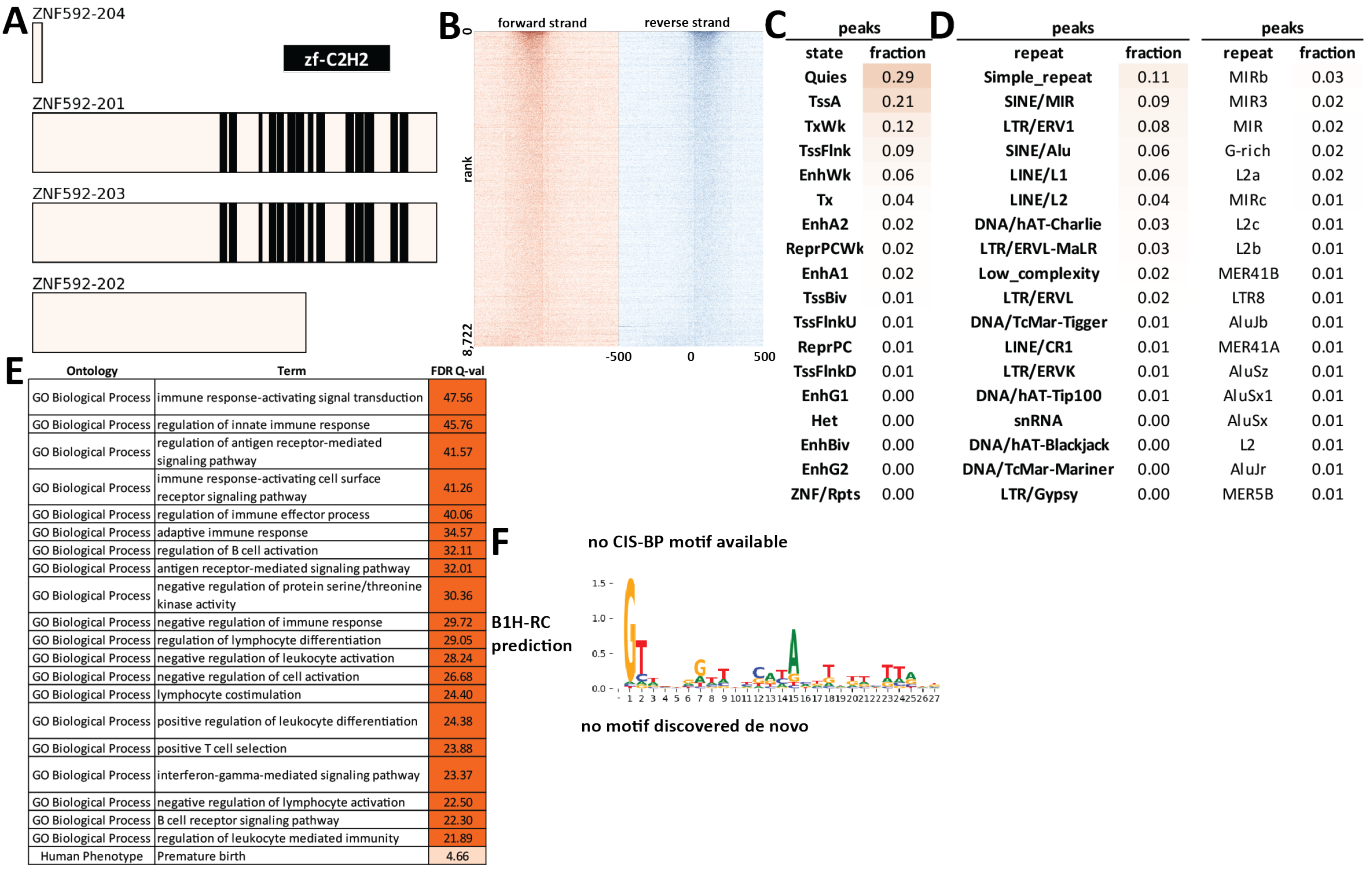

Supplementary Figure 1454: Properties and genomic distribution of motifs identified for the ZNF592 transcription factor in GM12878 (accession ENCSR173ZVL).

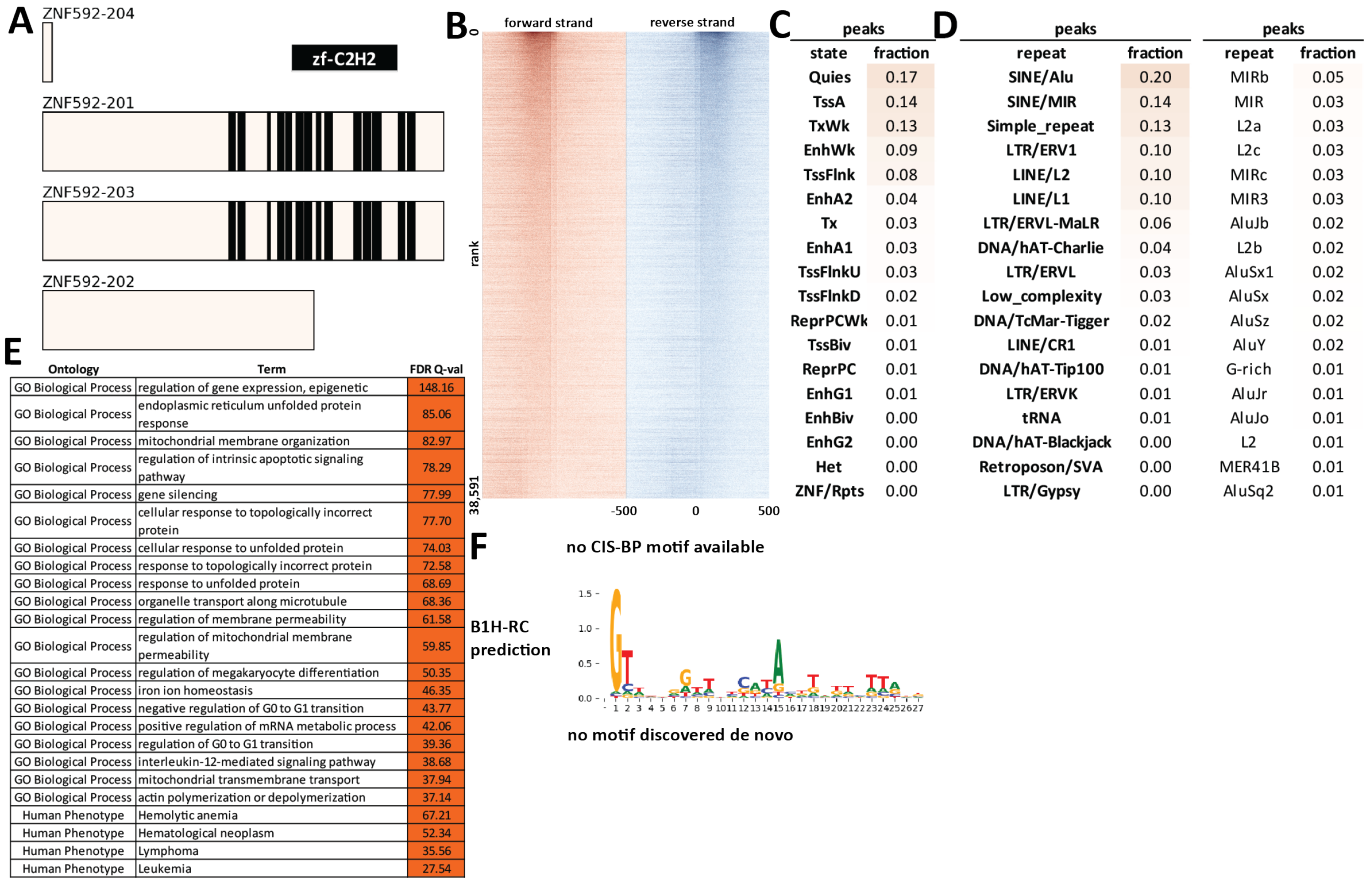

Supplementary Figure 1455: Properties and genomic distribution of motifs identified for the ZNF592 transcription factor in K562 (accession ENCSR249BHQ).

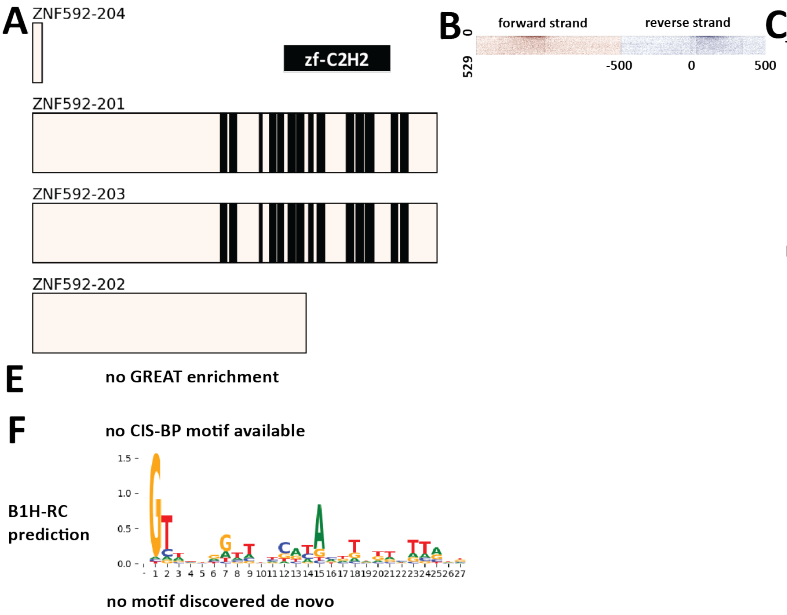

C

peaks	
state	fraction
Quies	0.34
TssA	0.18
TxWk	0.11
TssFlnk	0.07
EnhWk	0.05
Tx	0.04
EnhA2	0.03
ReprPCWk	0.03
EnhA1	0.02
TssFlnkU	0.02
ReprPC	0.02
TssFlnkD	0.01
TssBiv	0.01
EnhG1	0.01
Het	0.00

D

peaks		peaks	
repeat	fraction	repeat	fraction
Simple_repeat	0.24	L2a	0.06
SINE/Alu	0.18	MER41B	0.05
LTR/ERV1	0.15	MER41A	0.04
LINE/L2	0.12	MIRb	0.04
LINE/L1	0.10	(TG)n	0.03
SINE/MIR	0.09	MIR	0.02
LTR/ERVL	0.04	L2c	0.02
Low_complexity	0.04	GA-rich	0.02
LTR/ERVL-MaLR	0.04	L2b	0.02
DNA/hAT-Charlie	0.02	AluSx1	0.02
DNA/TcMar-Tigger	0.01	AluSx	0.02
LINE/CR1	0.01	(CA)n	0.02
DNA/hAT-Tip100	0.01	(AC)n	0.02
Satellite/centr	0.00	AluJo	0.02
Satellite	0.00	MIRc	0.02
Retroposon/SVA	0.00	AluSz	0.02
LTR?	0.00	AluSq2	0.02
LTR/ERVK	0.00	AluJb	0.02

Supplementary Figure 1456: Properties and genomic distribution of motifs identified for the ZNF592 transcription factor in MCF-7 (accession ENCSR028NUR).

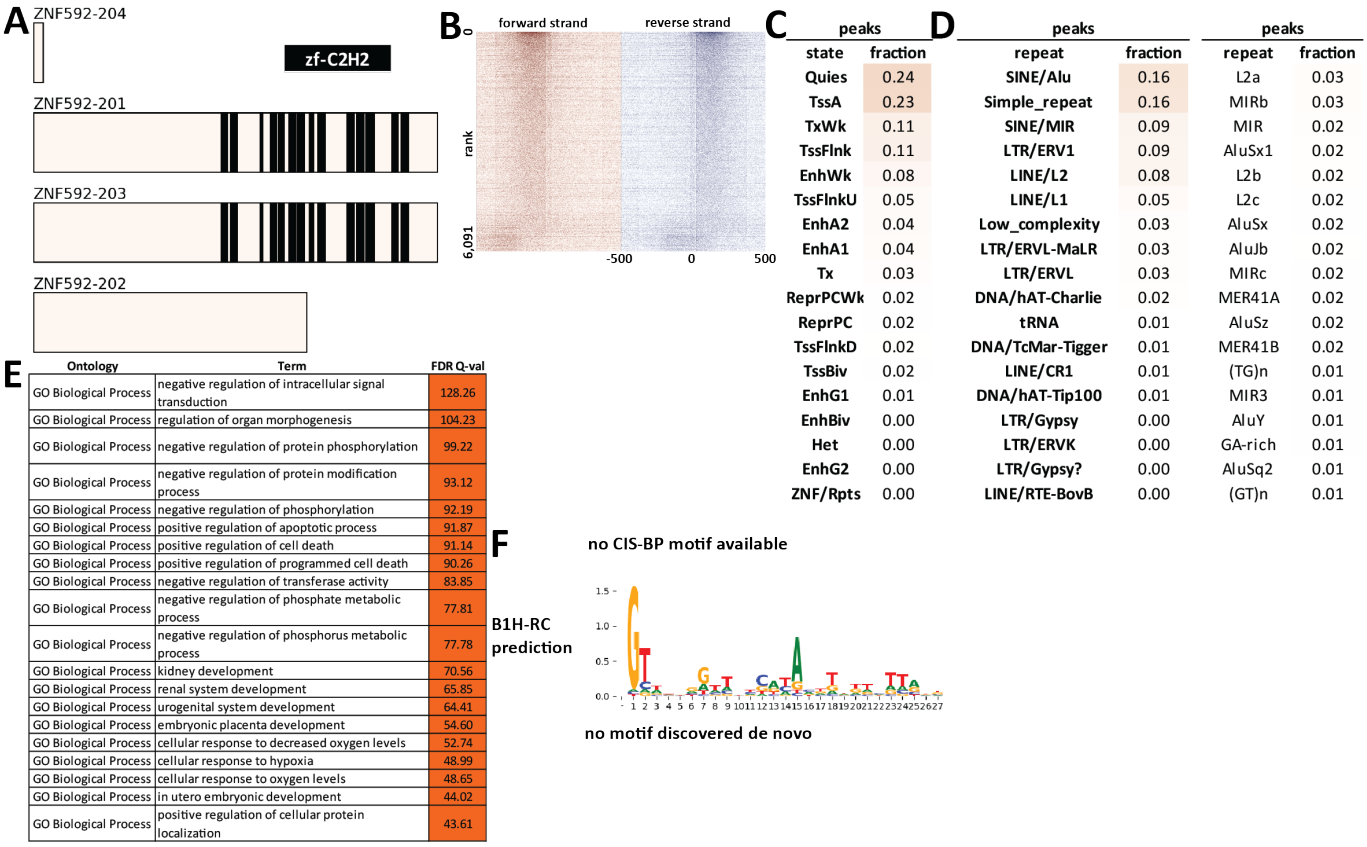

Supplementary Figure 1457: Properties and genomic distribution of motifs identified for the ZNF592 transcription factor in MCF-7 (accession ENCSR701AQS).

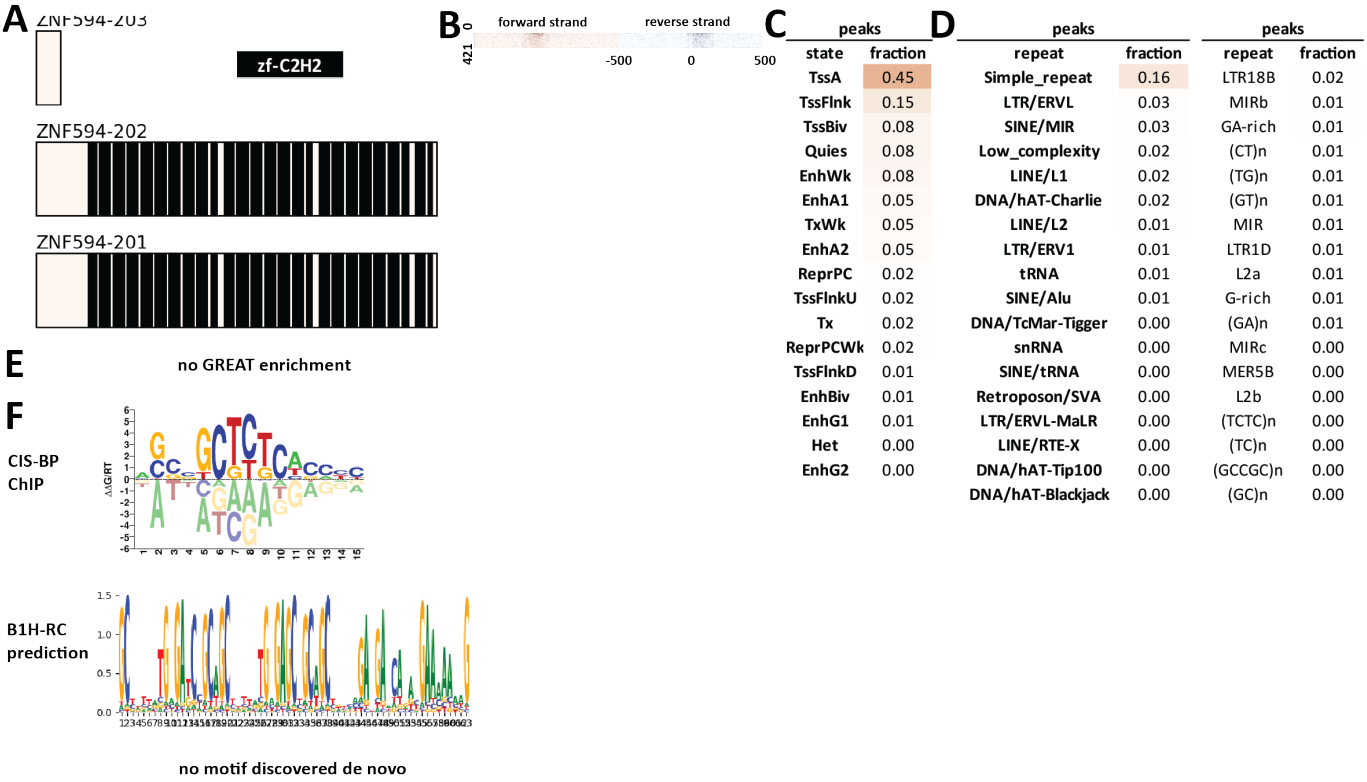

C

peaks	
state	fraction
TssA	0.45
TssFlnk	0.15
TssBiv	0.08
Quies	0.08
EnhWk	0.08
EnhA1	0.05
TxWk	0.05
EnhA2	0.05
ReprPC	0.02
TssFlnkU	0.02
Tx	0.02
ReprPCWk	0.02
TssFlnkD	0.01
EnhBiv	0.01
EnhG1	0.01
Het	0.00
EnhG2	0.00

D

peaks		peaks	
repeat	fraction	repeat	fraction
Simple_repeat	0.16	LTR18B	0.02
LTR/ERVL	0.03	MIRb	0.01
SINE/MIR	0.03	GA-rich	0.01
Low_complexity	0.02	(CT)n	0.01
LINE/L1	0.02	(TG)n	0.01
DNA/hAT-Charlie	0.02	(GT)n	0.01
LINE/L2	0.01	MIR	0.01
LTR/ERV1	0.01	LTR1D	0.01
tRNA	0.01	L2a	0.01
SINE/Alu	0.01	G-rich	0.01
DNA/TcMar-Tigger	0.00	(GA)n	0.01
snRNA	0.00	MIRc	0.00
SINE/tRNA	0.00	MER5B	0.00
Retroposon/SVA	0.00	L2b	0.00
LTR/ERVL-MaLR	0.00	(TCTC)n	0.00
LINE/RTE-X	0.00	(TC)n	0.00
DNA/hAT-Tip100	0.00	(GCCGC)n	0.00
DNA/hAT-Blackjack	0.00	(GC)n	0.00

Supplementary Figure 1458: Properties and genomic distribution of motifs identified for the ZNF594 transcription factor in HEK293 (accession Hughes GR models).

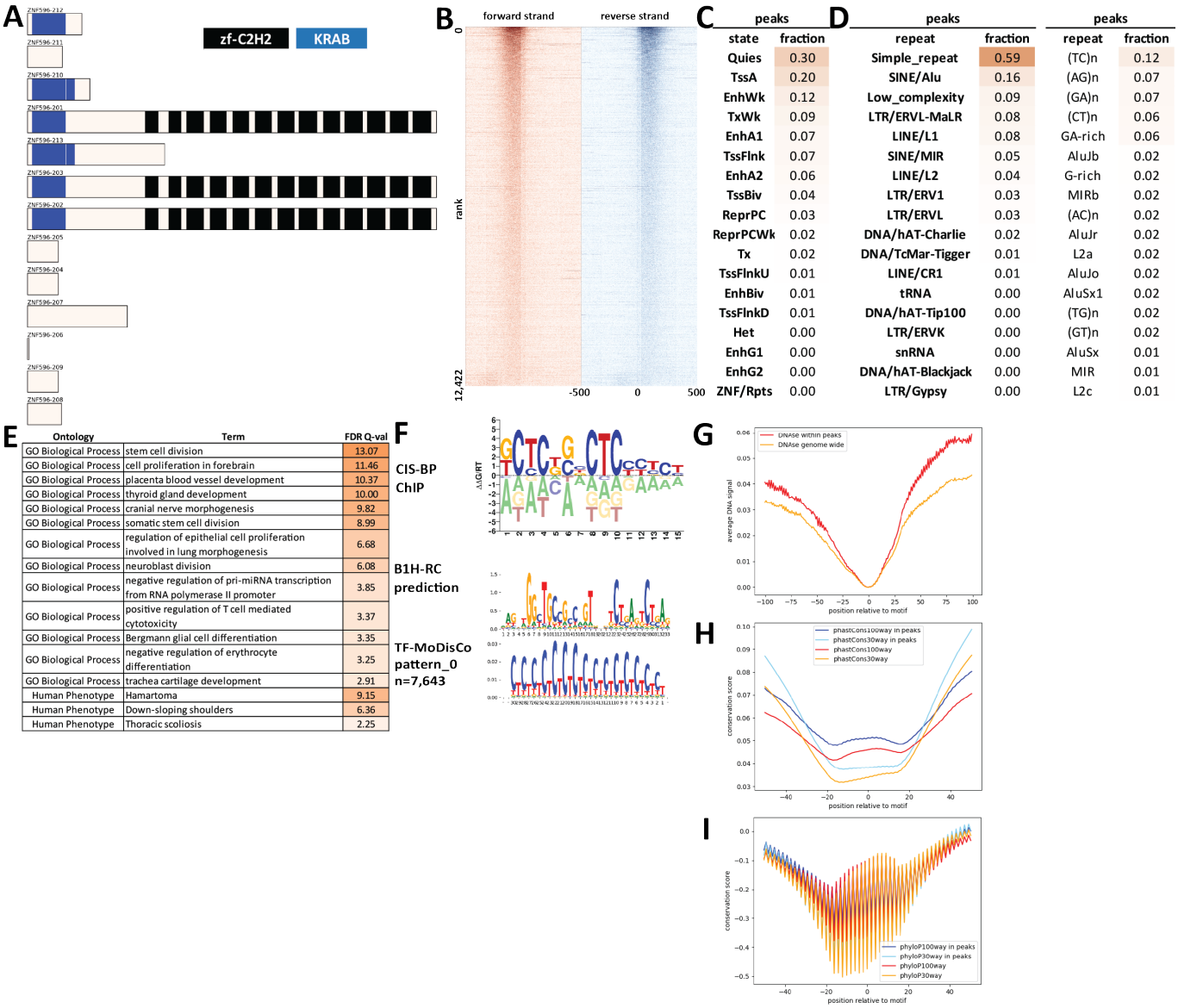

Supplementary Figure 1459: Properties and genomic distribution of motifs identified for the ZNF596 transcription factor in HEK293 (accession ENCSR344SBD).

TF-MoDisCO pattern_0 n=7643, CWM

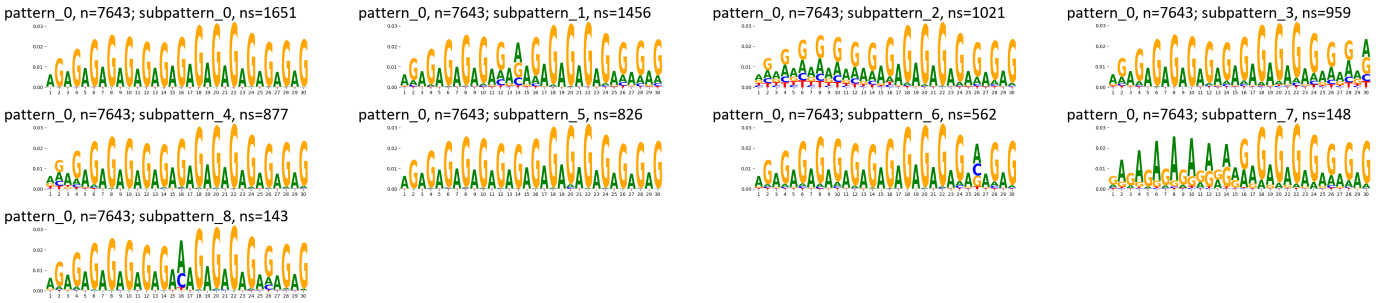

TF-MoDisCO pattern_0 n=7643, PWM

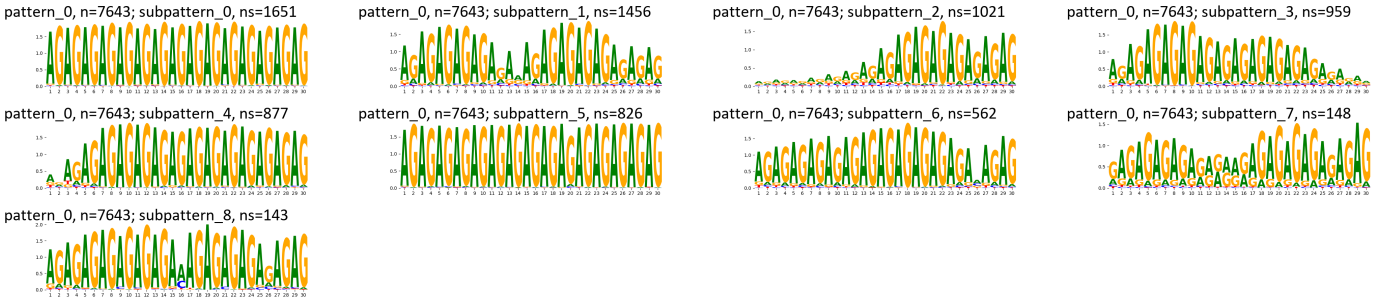

Supplementary Figure 1460: TF-MoDisCO subpatterns for the ZNF596 transcription factor in HEK293 (accession ENCSR344SBD).

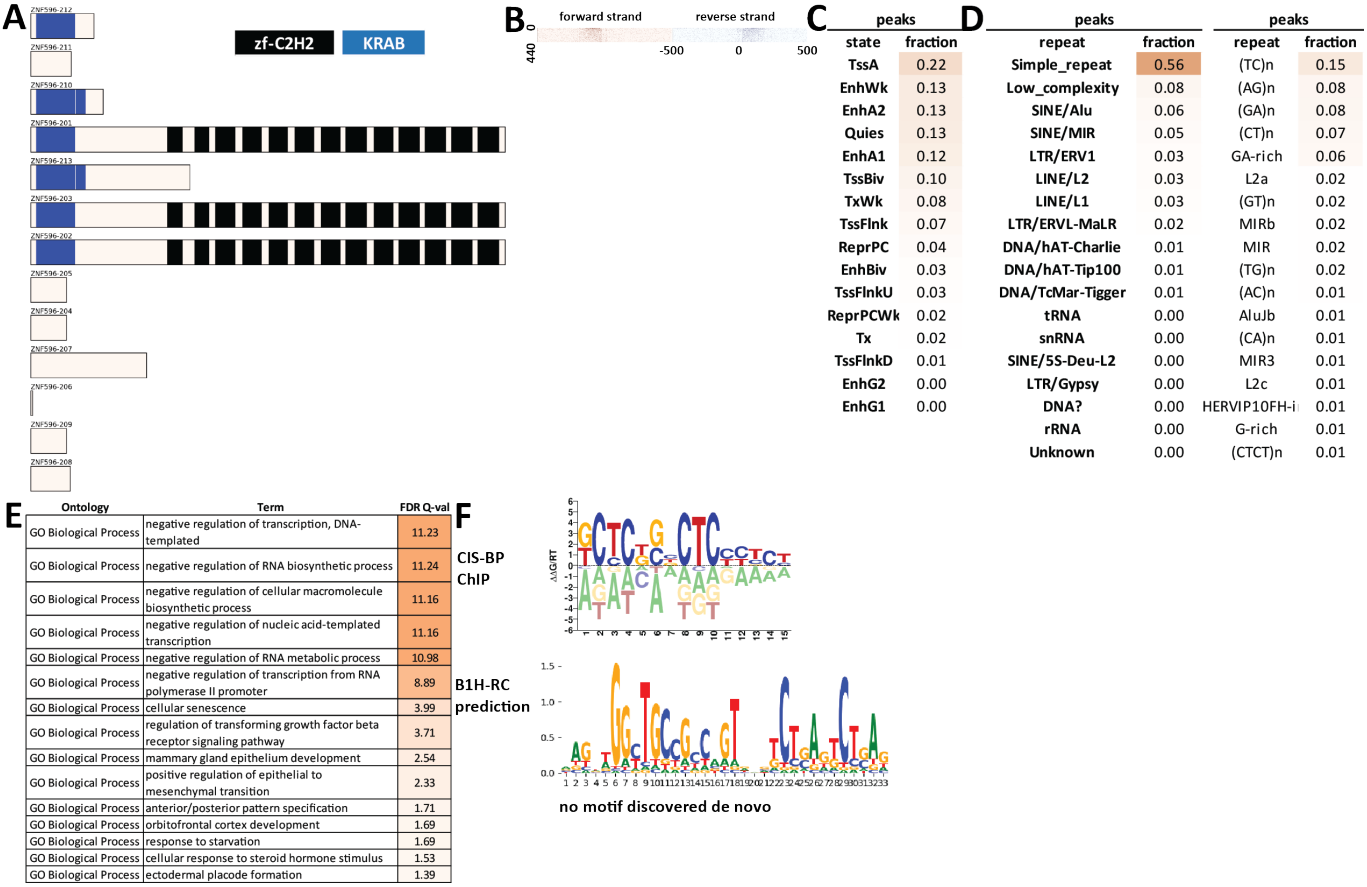

Supplementary Figure 1461: Properties and genomic distribution of motifs identified for the ZNF596 transcription factor in HEK293 (accession Hughes GR models).

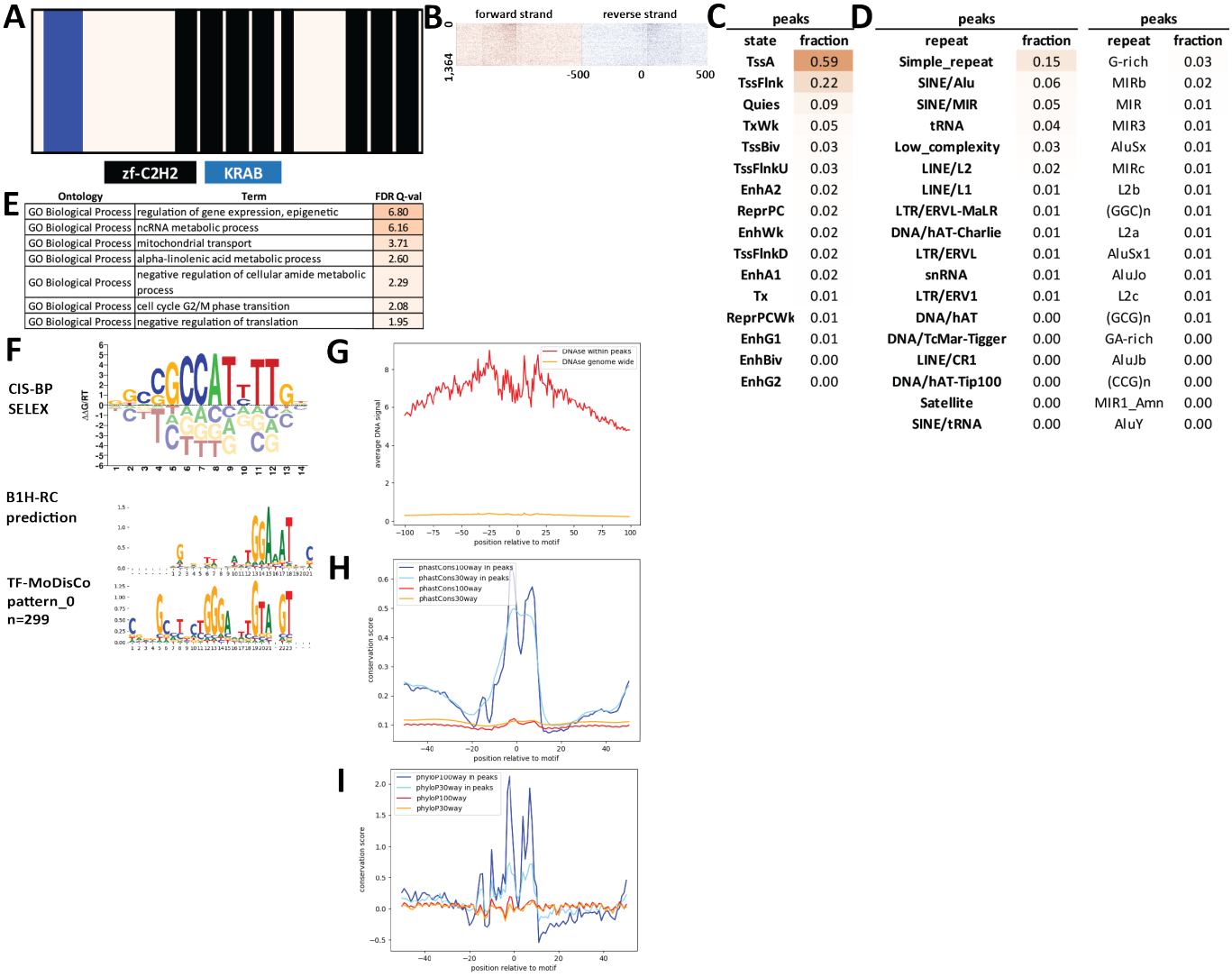

Supplementary Figure 1462: Properties and genomic distribution of motifs identified for the ZNF597 transcription factor in HepG2 (accession ENCSR669PVF).

TF-MoDisCO pattern_0 n=299, CWM

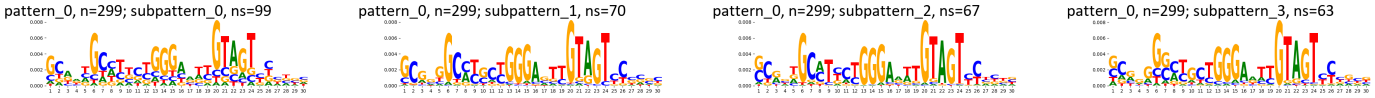

TF-MoDisCO pattern_0 n=299, PWM

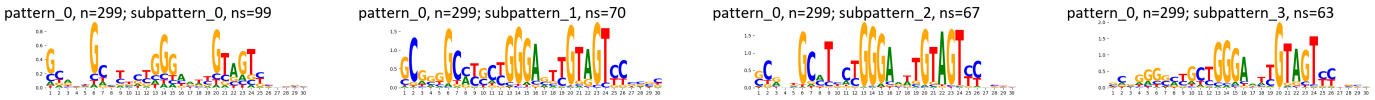

Supplementary Figure 1463: TF-MoDisCO subpatterns for the ZNF597 transcription factor in HepG2 (accession ENCSR669PVF).

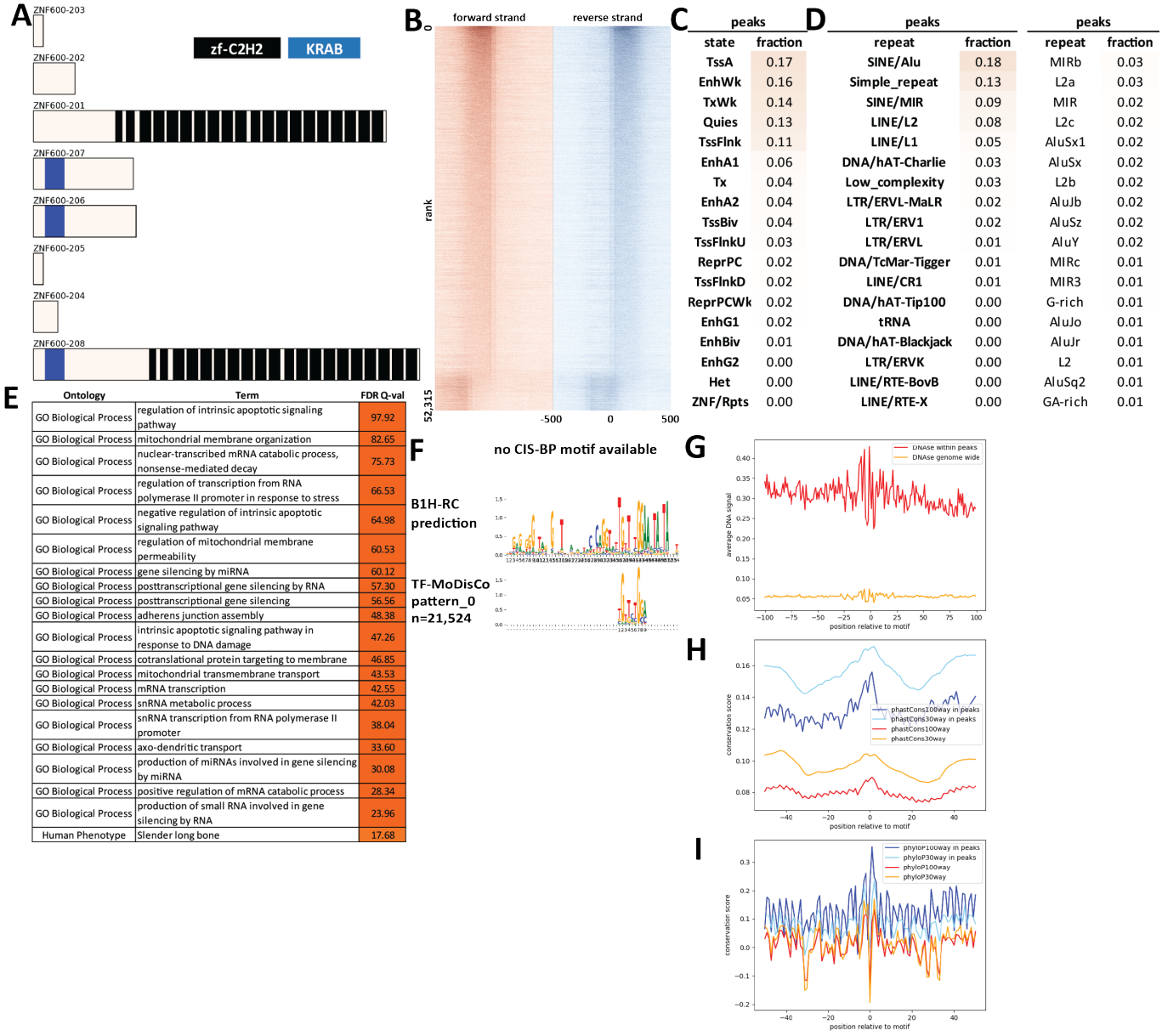

Supplementary Figure 1464: Properties and genomic distribution of motifs identified for the ZNF600 transcription factor in HEK293 (accession ENCSR017QBI).

TF-MoDisCO pattern_0 n=21524, CWM

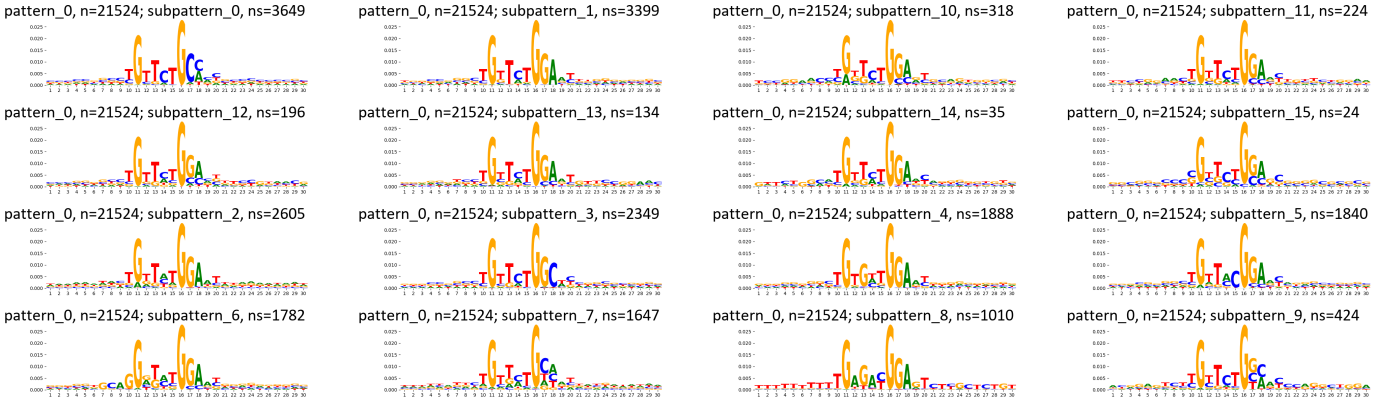

TF-MoDisCO pattern_0 n=21524, PWM

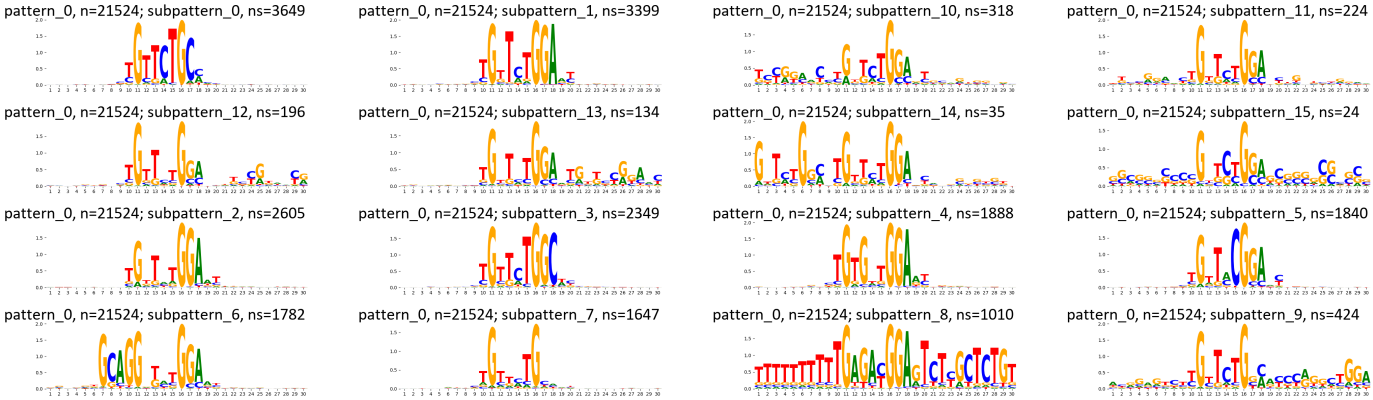

Supplementary Figure 1465: TF-MoDisCO subpatterns for the ZNF600 transcription factor in HEK293 (accession ENCSR017QBI).

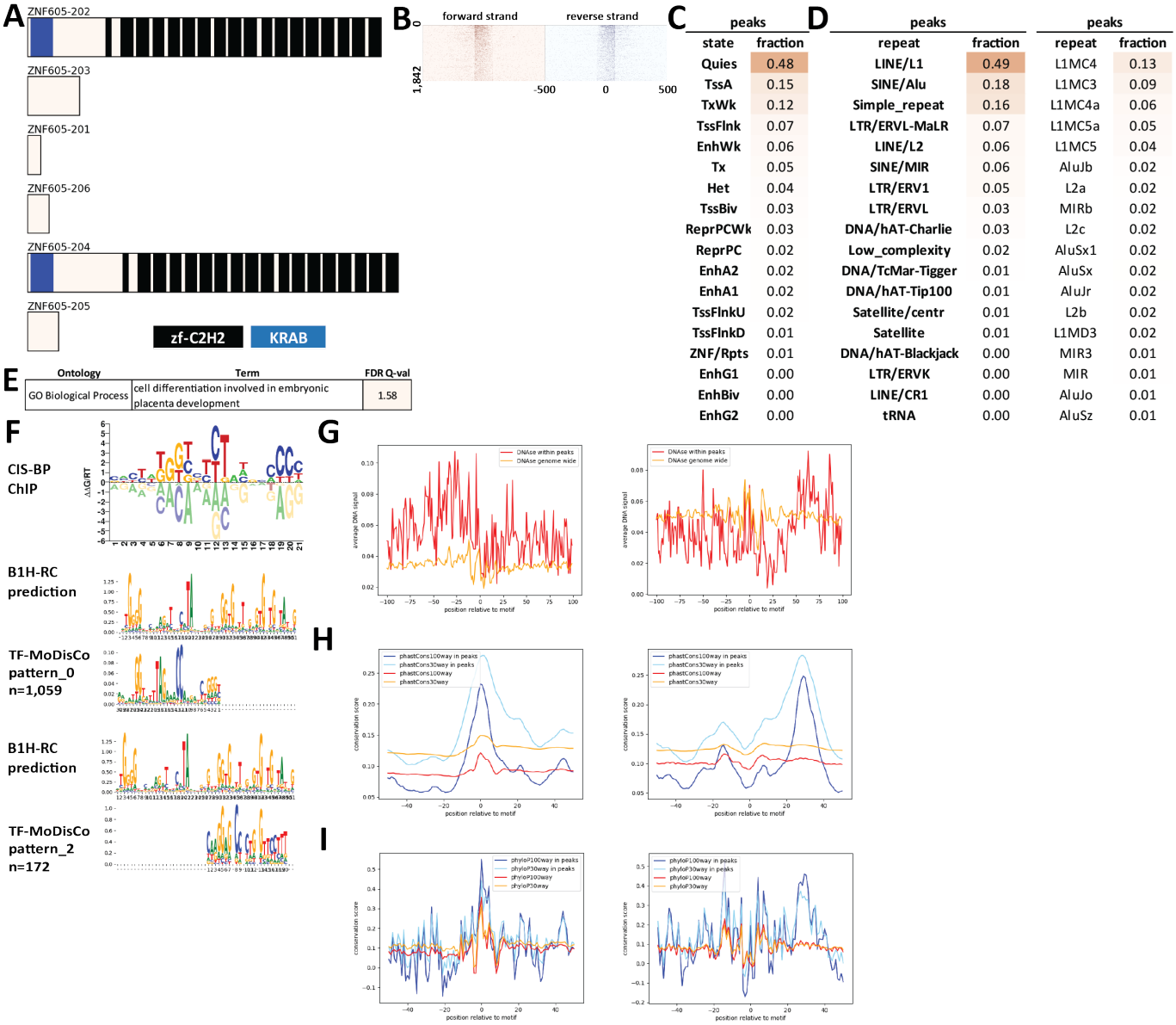

Supplementary Figure 1466: Properties and genomic distribution of motifs identified for the ZNF605 transcription factor in HEK293 (accession ChipExo models).

TF-MoDisCO pattern_0 n=1059, CWM

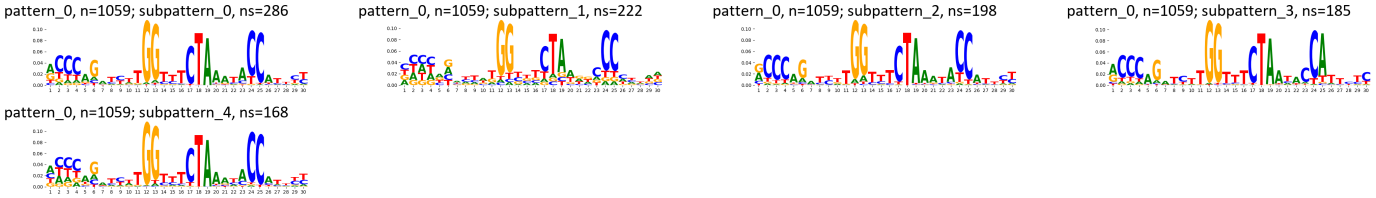

TF-MoDisCO pattern_0 n=1059, PWM

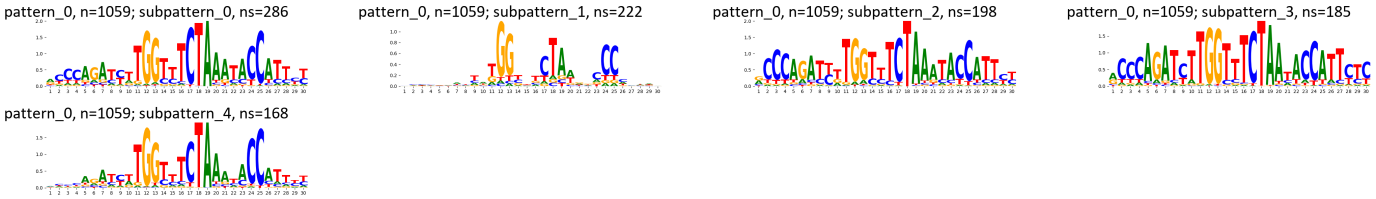

TF-MoDisCO pattern_2 n=172, CWM

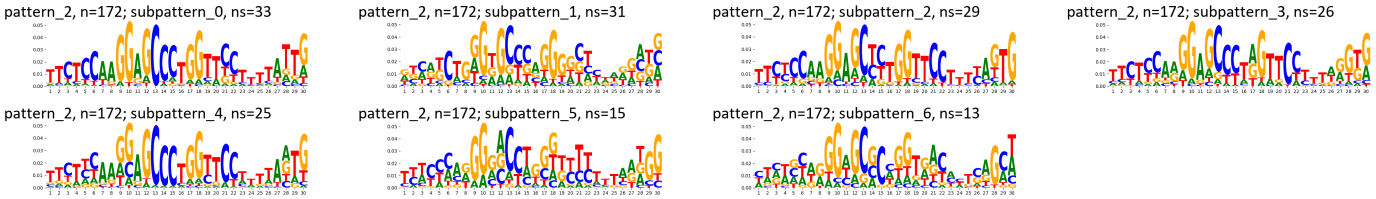

TF-MoDisCO pattern_2 n=172, PWM

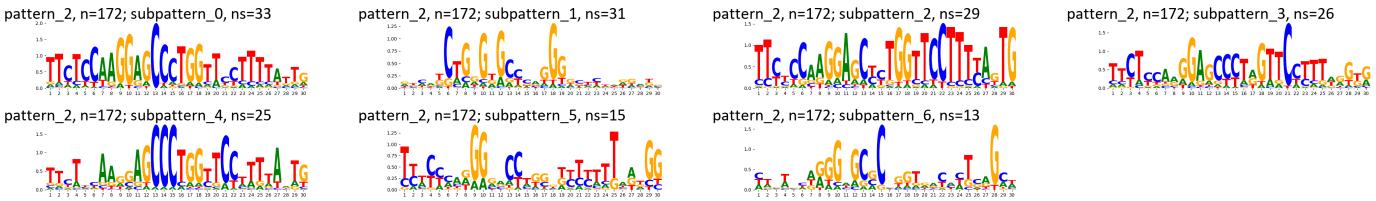

Supplementary Figure 1467: TF-MoDisCO subpatterns for the ZNF605 transcription factor in HEK293 (accession ChipExo models).

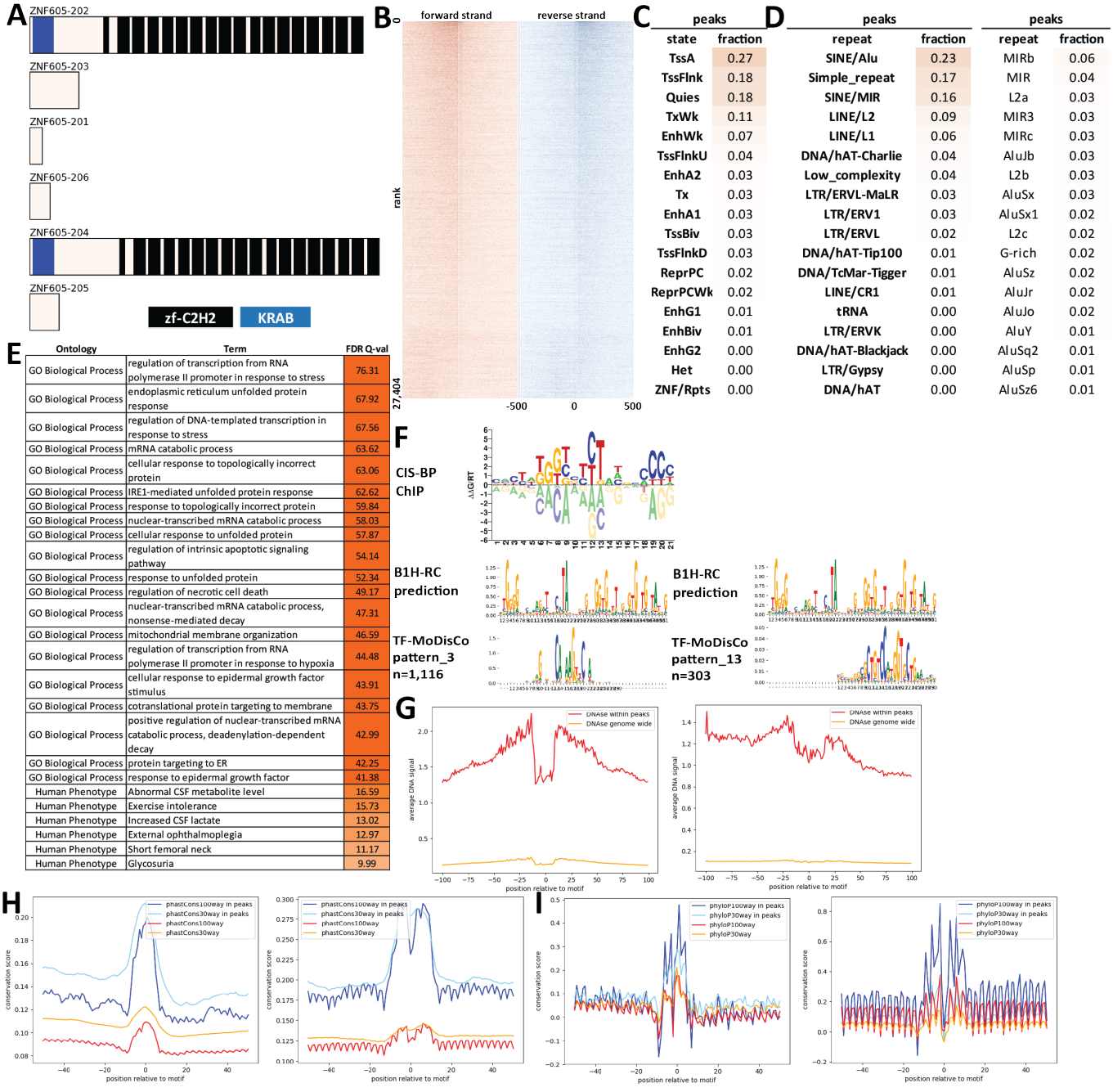

C

peaks	
state	fraction
TssA	0.27
TssFlnk	0.18
Quies	0.18
TxWk	0.11
EnhWk	0.07
TssFlnkU	0.04
EnhA2	0.03
Tx	0.03
EnhA1	0.03
TssBiv	0.03
TssFlnkD	0.03
ReprPC	0.02
ReprPCWk	0.02
EnhG1	0.01
EnhBiv	0.01
EnhG2	0.00
Het	0.00
ZNF/Rpts	0.00

D

peaks		peaks	
repeat	fraction	repeat	fraction
SINE/Alu	0.23	MIRb	0.06
Simple_repeat	0.17	MIR	0.04
SINE/MIR	0.16	L2a	0.03
LINE/L2	0.09	MIR3	0.03
LINE/L1	0.06	MIRc	0.03
DNA/hAT-Charlie	0.04	AluJb	0.03
Low_complexity	0.04	L2b	0.03
LTR/ERVL-MaLR	0.03	AluSx	0.03
LTR/ERV1	0.03	AluSx1	0.02
LTR/ERVL	0.02	L2c	0.02
DNA/hAT-Tip100	0.01	G-rich	0.02
DNA/TcMar-Tigger	0.01	AluSz	0.02
LINE/CR1	0.01	AluJr	0.02
tRNA	0.00	AluJo	0.02
LTR/ERVK	0.00	AluY	0.01
DNA/hAT-Blackjack	0.00	AluSq2	0.01
LTR/Gypsy	0.00	AluSp	0.01
DNA/hAT	0.00	AluSz6	0.01

E

Ontology	Term	FDR Q-val
GO Biological Process	regulation of transcription from RNA polymerase II promoter in response to stress	76.31
GO Biological Process	endoplasmic reticulum unfolded protein response	67.92
GO Biological Process	regulation of DNA-templated transcription in response to stress	67.56
GO Biological Process	mRNA catabolic process	63.62
GO Biological Process	cellular response to topologically incorrect protein	63.06
GO Biological Process	IRE1-mediated unfolded protein response	62.62
GO Biological Process	response to topologically incorrect protein	59.84
GO Biological Process	nuclear-transcribed mRNA catabolic process	58.03
GO Biological Process	cellular response to unfolded protein	57.87
GO Biological Process	regulation of intrinsic apoptotic signaling pathway	54.14
GO Biological Process	response to unfolded protein	52.34
GO Biological Process	regulation of necrotic cell death	49.17
GO Biological Process	nuclear-transcribed mRNA catabolic process, nonsense-mediated decay	47.31
GO Biological Process	mitochondrial membrane organization	46.59
GO Biological Process	regulation of transcription from RNA polymerase II promoter in response to hypoxia	44.48
GO Biological Process	cellular response to epidermal growth factor stimulus	43.91
GO Biological Process	cotranslational protein targeting to membrane	43.75
GO Biological Process	positive regulation of nuclear-transcribed mRNA catabolic process, deadenylation-dependent decay	42.99
GO Biological Process	protein targeting to ER	42.25
GO Biological Process	response to epidermal growth factor	41.38
Human Phenotype	Abnormal CSF metabolite level	16.59
Human Phenotype	Exercise intolerance	15.73
Human Phenotype	Increased CSF lactate	13.02
Human Phenotype	External ophthalmoplegia	12.97
Human Phenotype	Short femoral neck	11.17
Human Phenotype	Glycosuria	9.99

Supplementary Figure 1468: Properties and genomic distribution of motifs identified for the ZNF605 transcription factor in HepG2 (accession ENCSR903JFF).

TF-MoDisCO pattern_13 n=303, CWM

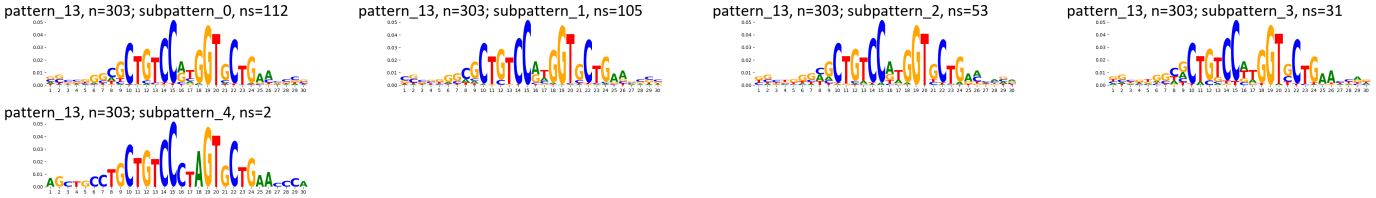

TF-MoDisCO pattern_13 n=303, PWM

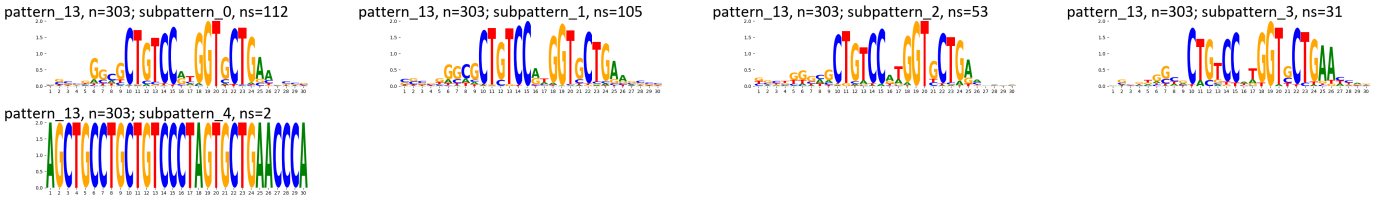

TF-MoDisCO pattern_3 n=1116, CWM

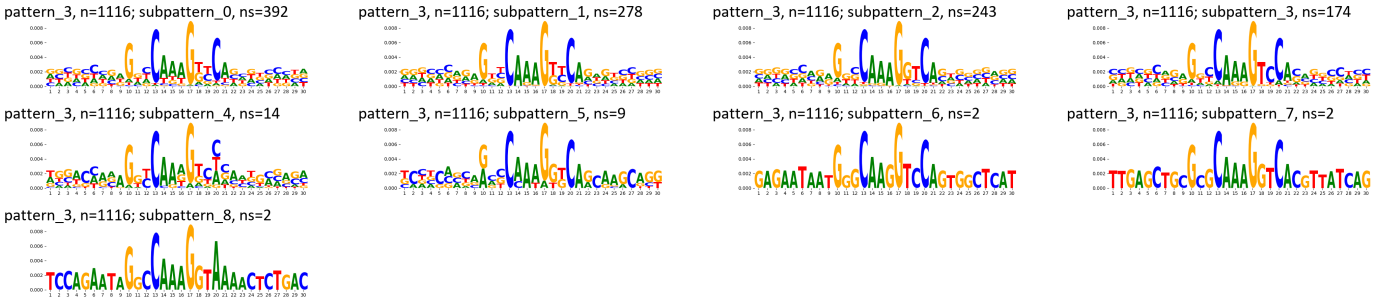

TF-MoDisCO pattern_3 n=1116, PWM

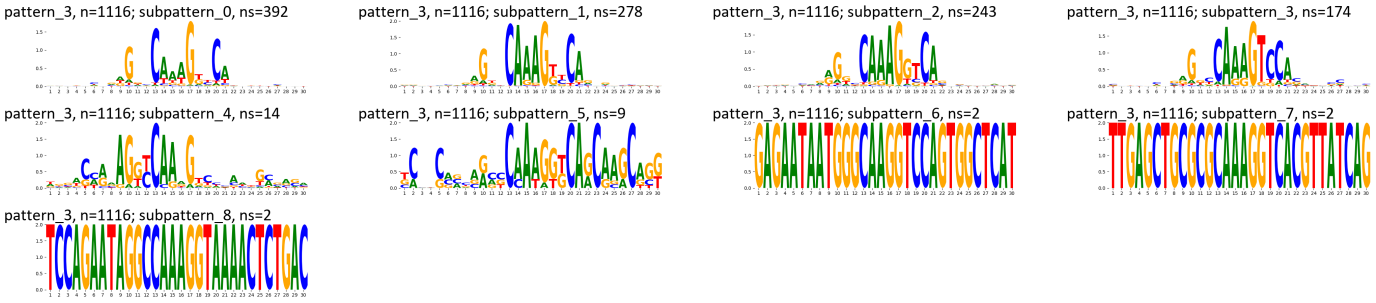

Supplementary Figure 1469: TF-MoDisCO subpatterns for the ZNF605 transcription factor in HepG2 (accession ENCSR903JFF).

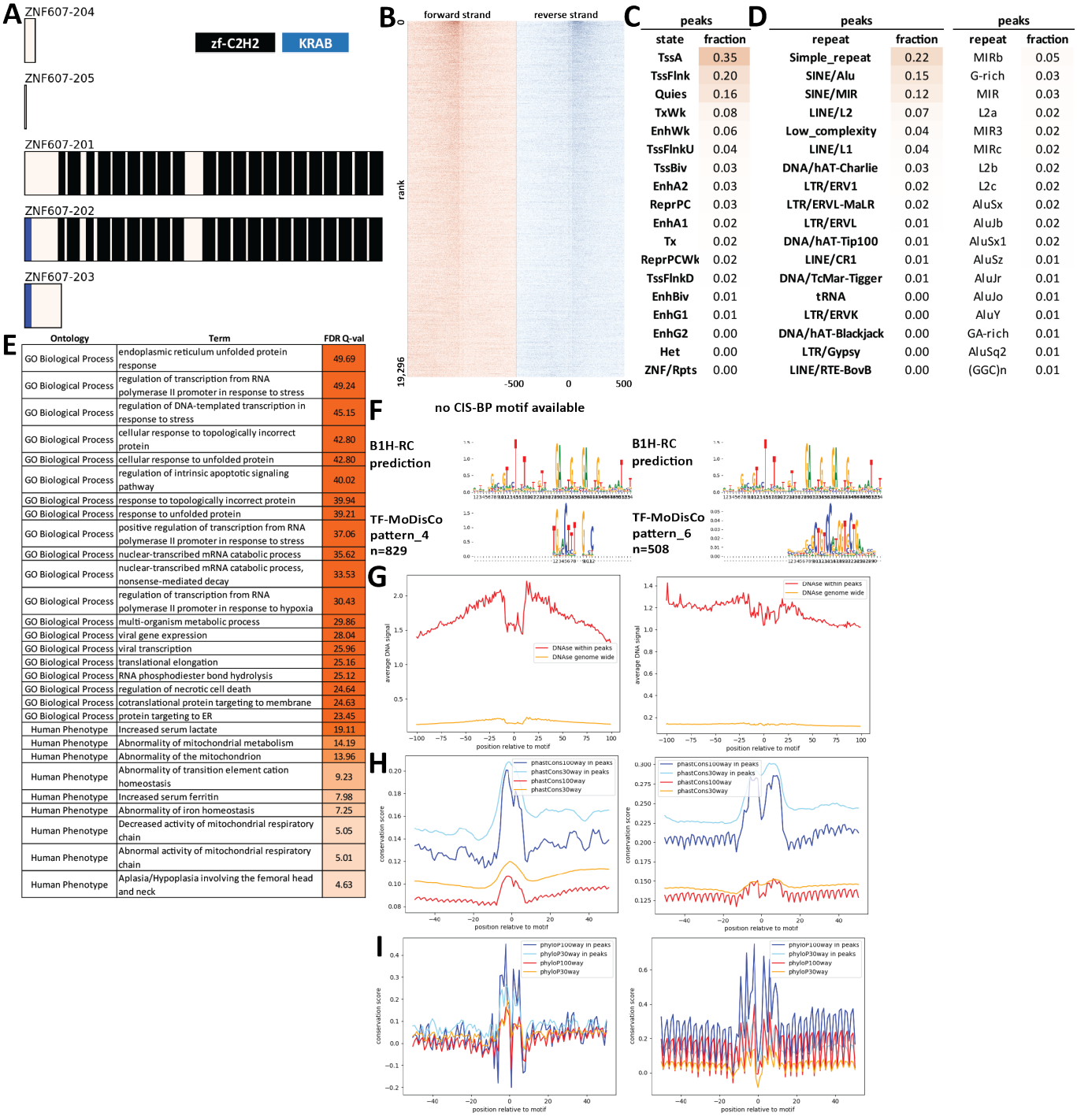

Supplementary Figure 1470: Properties and genomic distribution of motifs identified for the ZNF607 transcription factor in HepG2 (accession ENCSR788SXN).

TF-MoDisCO pattern_4 n=829, CWM

pattern_4, n=829; subpattern_0, ns=270

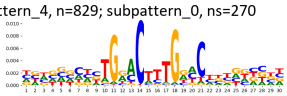

pattern_4, n=829; subpattern_1, ns=145

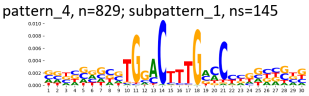

pattern_4, n=829; subpattern_2, ns=136

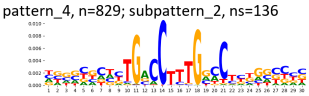

pattern_4, n=829; subpattern_3, ns=136

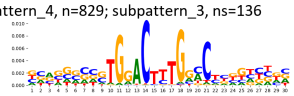

pattern_4, n=829; subpattern_4, ns=93

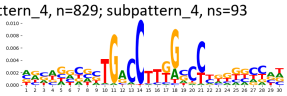

pattern_4, n=829; subpattern_5, ns=41

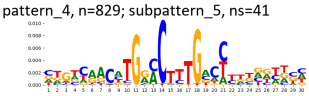

pattern_4, n=829; subpattern_6, ns=4

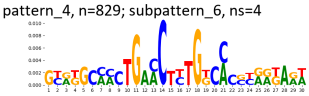

pattern_4, n=829; subpattern_7, ns=2

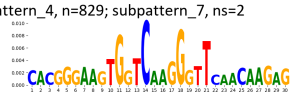

pattern_4, n=829; subpattern_8, ns=2

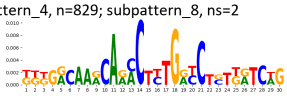

TF-MoDisCO pattern_4 n=829, PWM

pattern_4, n=829; subpattern_0, ns=270

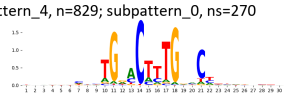

pattern_4, n=829; subpattern_1, ns=145

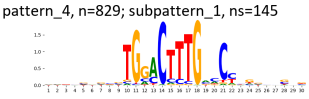

pattern_4, n=829; subpattern_2, ns=136

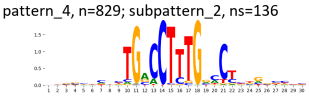

pattern_4, n=829; subpattern_3, ns=136

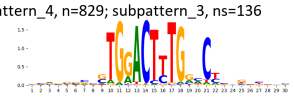

pattern_4, n=829; subpattern_4, ns=93

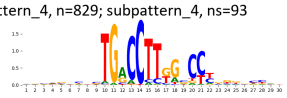

pattern_4, n=829; subpattern_5, ns=41

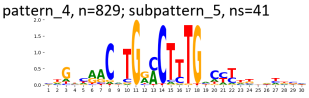

pattern_4, n=829; subpattern_6, ns=4

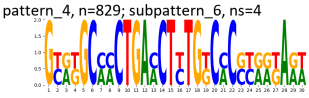

pattern_4, n=829; subpattern_7, ns=2

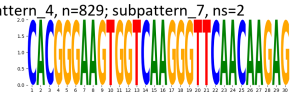

pattern_4, n=829; subpattern_8, ns=2

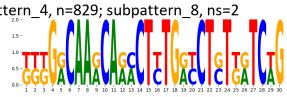

TF-MoDisCO pattern_6 n=508, CWM

pattern_6, n=508; subpattern_0, ns=203

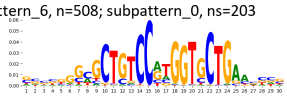

pattern_6, n=508; subpattern_1, ns=183

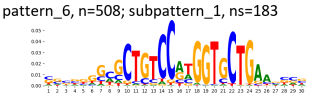

pattern_6, n=508; subpattern_2, ns=80

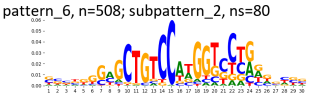

pattern_6, n=508; subpattern_3, ns=42

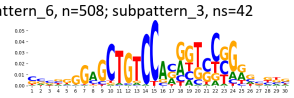

TF-MoDisCO pattern_6 n=508, PWM

pattern_6, n=508; subpattern_0, ns=203

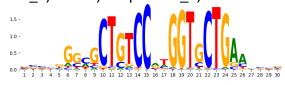

pattern_6, n=508; subpattern_1, ns=183

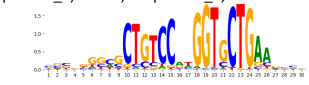

pattern_6, n=508; subpattern_2, ns=80

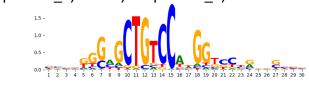

pattern_6, n=508; subpattern_3, ns=42

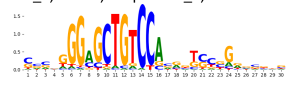

Supplementary Figure 1471: TF-MoDisCO subpatterns for the ZNF607 transcription factor in HepG2 (accession ENCSR788SXN).

A

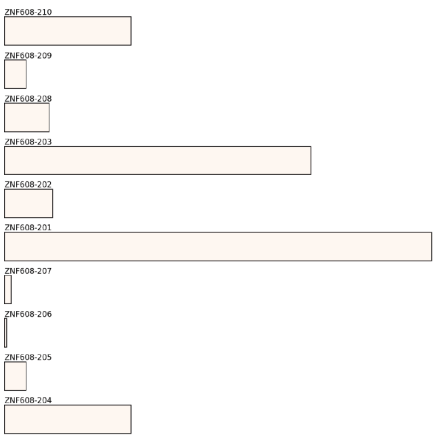

B

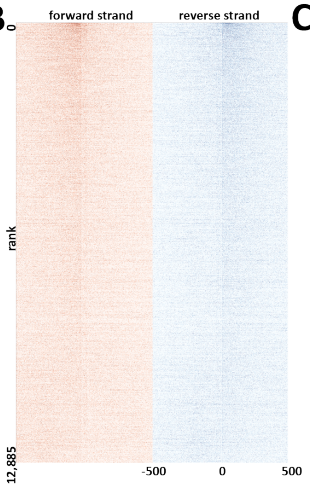

C

peaks	
state	fraction
TssA	0.39
TssFlnk	0.20
Quies	0.15
TxWk	0.08
EnhWk	0.05
TssFlnkU	0.04
TssBiv	0.04
EnhA2	0.03
ReprPC	0.03
TssFlnkD	0.02
EnhA1	0.02
ReprPCWk	0.02
Tx	0.02
EnhBiv	0.01
EnhG1	0.01
EnhG2	0.00
Het	0.00
ZNF/Rpts	0.00

D

peaks		peaks	
repeat	fraction	repeat	fraction
Simple_repeat	0.24	MIRb	0.04
SINE/Alu	0.15	G-rich	0.04
SINE/MIR	0.11	MIR	0.02
LINE/L2	0.06	L2a	0.02
Low_complexity	0.05	MIRc	0.02
LINE/L1	0.03	MIR3	0.02
DNA/hAT-Charlie	0.03	AluSx1	0.02
LTR/ERV1	0.02	L2b	0.02
LTR/ERVL-MaLR	0.02	AluSx	0.02
LTR/ERVL	0.01	L2c	0.02
LINE/CR1	0.01	AluJb	0.02
DNA/hAT-Tip100	0.01	AluSz	0.01
DNA/TcMar-Tigger	0.01	AluJr	0.01
tRNA	0.00	GA-rich	0.01
DNA/hAT-Blackjack	0.00	AluJo	0.01
LTR/ERVK	0.00	(GGC)n	0.01
DNA/hAT	0.00	AluY	0.01
LINE/RTE-BovB	0.00	AluSq2	0.01

E

Ontology	Term	FDR Q-val
GO Biological Process	regulation of transcription from RNA polymerase II promoter in response to stress	34.99
GO Biological Process	endoplasmic reticulum unfolded protein response	30.55
GO Biological Process	regulation of DNA-templated transcription in response to stress	30.11
GO Biological Process	cellular response to unfolded protein	26.45
GO Biological Process	regulation of intrinsic apoptotic signaling pathway	22.47
GO Biological Process	regulation of necrotic cell death	22.25
GO Biological Process	response to unfolded protein	22.25
GO Biological Process	mitochondrial membrane organization	22.05
GO Biological Process	mitochondrial translational termination	21.31
GO Biological Process	translational elongation	20.68
GO Biological Process	mitochondrial translational elongation	20.61
GO Biological Process	translational termination	20.41
GO Biological Process	regulation of necroptotic process	20.25
GO Biological Process	mitochondrial translation	20.17
GO Biological Process	cellular protein complex disassembly	18.75
GO Biological Process	regulation of mitochondrial membrane permeability	18.19
GO Biological Process	cotranslational protein targeting to membrane	18.18
GO Biological Process	multi-organism metabolic process	18.17
GO Biological Process	nuclear-transcribed mRNA catabolic process, nonsense-mediated decay	17.93
GO Biological Process	regulation of transcription from RNA polymerase II promoter in response to hypoxia	17.78
Human Phenotype	Increased serum lactate	17.02
Human Phenotype	Abnormal CSF metabolite level	16.71
Human Phenotype	Increased CSF lactate	13.46
Human Phenotype	Abnormality of the mitochondrion	8.31
Human Phenotype	Abnormality of mitochondrial metabolism	8.33
Human Phenotype	Leukodystrophy	5.85
Human Phenotype	Acute encephalopathy	2.80

F

no CIS-BP motif available

B1H-RC prediction



no motif discovered de novo

Supplementary Figure 1472: Properties and genomic distribution of motifs identified for the ZNF608 transcription factor in HepG2 (accession ENCSR277VXX).

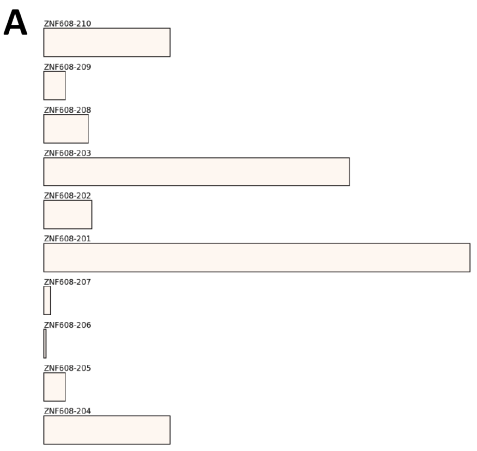

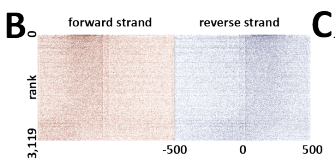

C

peaks	
state	fraction
Quies	0.37
EnhWk	0.14
TxWk	0.12
TssA	0.11
EnhA1	0.06
EnhA2	0.05
TssFlnk	0.04
Tx	0.03
TssFlnkU	0.03
TssFlnkD	0.01
EnhG1	0.01
ReprPC	0.01
TssBiv	0.01
ReprPCWk	0.01
EnhG2	0.00
Het	0.00
EnhBiv	0.00
ZNF/Rpts	0.00

D

peaks		peaks	
repeat	fraction	repeat	fraction
SINE/MIR	0.12	MIRb	0.04
SINE/Alu	0.10	MIR	0.03
Simple_repeat	0.10	L2c	0.03
LTR/ERV1	0.08	L2a	0.03
LINE/L2	0.08	MIR3	0.02
LINE/L1	0.07	MIRc	0.02
LTR/ERVL-MaLR	0.04	MER41B	0.02
DNA/hAT-Charlie	0.04	L2b	0.02
LTR/ERVL	0.03	L3	0.01
LINE/CR1	0.02	AluSz	0.01
Low_complexity	0.02	AluSx	0.01
DNA/TcMar-Tigger	0.02	AluSx1	0.01
snRNA	0.01	MER41A	0.01
DNA/hAT-Tip100	0.01	AluJb	0.01
LTR/ERVK	0.00	(AC)n	0.01
LINE/RTE-BovB	0.00	AluJr	0.01
LINE/RTE-X	0.00	A-rich	0.01
Unknown	0.00	L2	0.01

E

Ontology	Term	FDR Q-val
GO Biological Process	regulation of heart morphogenesis	18.71
GO Biological Process	semaphorin-plexin signaling pathway	17.55
GO Biological Process	outflow tract morphogenesis	13.60
GO Biological Process	positive regulation of epithelial cell migration	12.91
GO Biological Process	regulation of cell-substrate adhesion	12.75
GO Biological Process	stem cell differentiation	12.54
GO Biological Process	regulation of extrinsic apoptotic signaling pathway via death domain receptors	12.49
GO Biological Process	positive regulation of angiogenesis	11.66
GO Biological Process	negative regulation of osteoblast differentiation	11.22
GO Biological Process	positive regulation of vasculature development	10.92
GO Biological Process	regulation of cell-matrix adhesion	10.57
GO Biological Process	cell cycle arrest	10.12
GO Biological Process	cellular response to decreased oxygen levels	9.85
GO Biological Process	negative regulation of cell junction assembly	9.84
GO Biological Process	regulation of extrinsic apoptotic signaling pathway	9.70
GO Biological Process	cellular response to hypoxia	9.44
GO Biological Process	negative regulation of focal adhesion assembly	9.39
GO Biological Process	cellular response to oxygen levels	9.38
GO Biological Process	platelet degranulation	9.20
GO Biological Process	positive regulation of endothelial cell migration	9.03

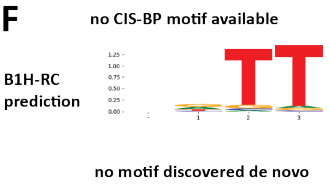

Supplementary Figure 1473: Properties and genomic distribution of motifs identified for the ZNF608 transcription factor in SK-N-SH (accession ENCSR837YGS).

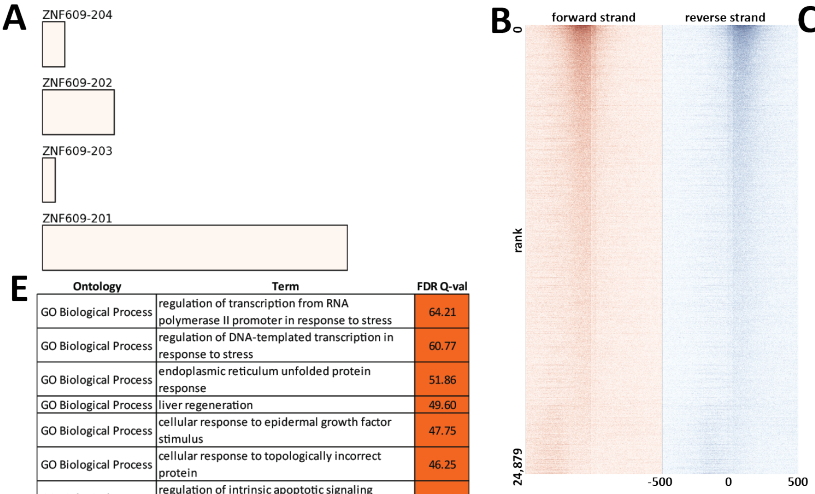

C

peaks	
state	fraction
Quies	0.22
TssA	0.21
TxWk	0.12
TssFlnk	0.11
EnhWk	0.10
Tx	0.04
EnhA1	0.04
EnhA2	0.03
TssFlnkU	0.03
TssBiv	0.02
ReprPC	0.02
ReprPCWk	0.02
TssFlnkD	0.02
EnhG1	0.01
EnhBiv	0.01
Het	0.00
EnhG2	0.00
ZNF/Rpts	0.00

D

peaks		peaks	
repeat	fraction	repeat	fraction
SINE/Alu	0.15	MIRb	0.05
Simple_repeat	0.15	L2a	0.03
SINE/MIR	0.13	MIR	0.03
LINE/L2	0.09	L2b	0.03
LINE/L1	0.06	L2c	0.03
DNA/hAT-Charlie	0.04	MIRc	0.02
LTR/ERV1	0.03	MIR3	0.02
Low_complexity	0.03	AluJb	0.02
LTR/ERVL-MaLR	0.03	G-rich	0.02
LTR/ERVL	0.02	AluSx	0.02
DNA/TcMar-Tigger	0.01	AluSx1	0.02
LINE/CR1	0.01	AluSz	0.01
DNA/hAT-Tip100	0.01	AluJr	0.01
LTR/ERVK	0.01	AluJo	0.01
DNA/hAT-Blackjack	0.00	AluY	0.01
tRNA	0.00	L2	0.01
LINE/RTE-BovB	0.00	L3	0.01
LINE/RTE-X	0.00	AluSq2	0.01

E

Ontology	Term	FDR Q-val
GO Biological Process	regulation of transcription from RNA polymerase II promoter in response to stress	64.21
GO Biological Process	regulation of DNA-templated transcription in response to stress	60.77
GO Biological Process	endoplasmic reticulum unfolded protein response	51.86
GO Biological Process	liver regeneration	49.60
GO Biological Process	cellular response to epidermal growth factor stimulus	47.75
GO Biological Process	cellular response to topologically incorrect protein	46.25
GO Biological Process	regulation of intrinsic apoptotic signaling pathway	45.43
GO Biological Process	cellular response to unfolded protein	44.43
GO Biological Process	negative regulation of intrinsic apoptotic signaling pathway	41.48
GO Biological Process	secondary alcohol metabolic process	35.74
GO Biological Process	triglyceride homeostasis	35.58
GO Biological Process	platelet-derived growth factor receptor signaling pathway	34.22
GO Biological Process	regulation of transcription from RNA polymerase II promoter in response to hypoxia	31.22
GO Biological Process	nuclear-transcribed mRNA catabolic process, deadenylation-dependent decay	29.22
GO Biological Process	high-density lipoprotein particle remodeling	28.26
GO Biological Process	regulation of mitochondrial membrane permeability	27.33
GO Biological Process	nuclear-transcribed mRNA catabolic process, nonsense-mediated decay	27.09
GO Biological Process	regulation of membrane permeability	26.89
GO Biological Process	protein-lipid complex subunit organization	25.20
GO Biological Process	protein targeting to ER	25.13
Human Phenotype	Aplasia/hypoplasia of the femur	18.52
Human Phenotype	Abnormality of mitochondrial metabolism	17.09
Human Phenotype	Abnormality of monocarboxylic acid metabolism	13.64
Human Phenotype	Aplasia/Hypoplasia involving the femoral head and neck	11.77
Human Phenotype	Short femoral neck	11.62

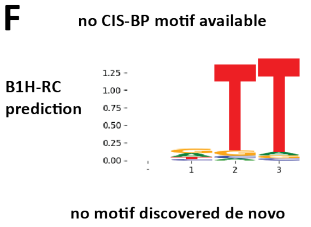

Supplementary Figure 1474: Properties and genomic distribution of motifs identified for the ZNF609 transcription factor in HepG2 (accession ENCSR407BPU).

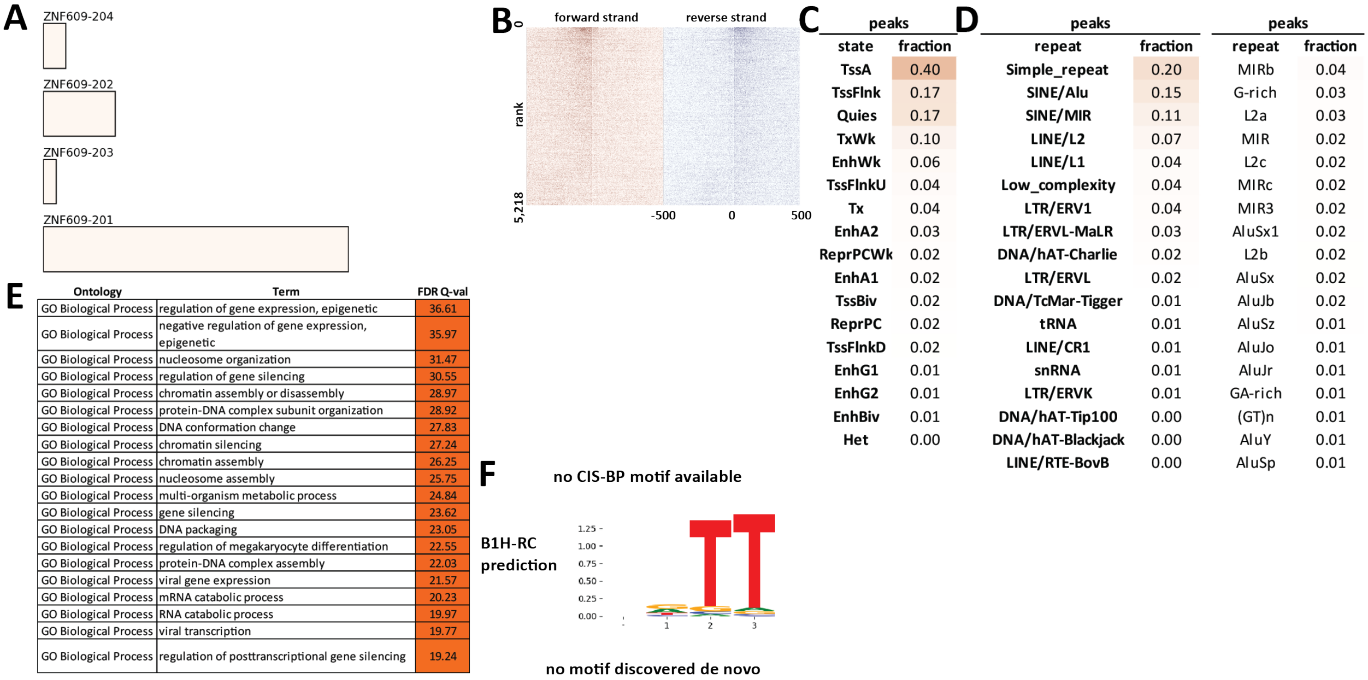

C

peaks	
state	fraction
TssA	0.40
TssFlnk	0.17
Quies	0.17
TxWk	0.10
EnhWk	0.06
TssFlnkU	0.04
Tx	0.04
EnhA2	0.03
ReprPCWk	0.02
EnhA1	0.02
TssBiv	0.02
ReprPC	0.02
TssFlnkD	0.02
EnhG1	0.01
EnhG2	0.01
EnhBiv	0.01
Het	0.00

D

peaks		peaks	
repeat	fraction	repeat	fraction
Simple_repeat	0.20	MIRb	0.04
SINE/Alu	0.15	G-rich	0.03
SINE/MIR	0.11	L2a	0.03
LINE/L2	0.07	MIR	0.02
LINE/L1	0.04	L2c	0.02
Low_complexity	0.04	MIRc	0.02
LTR/ERV1	0.04	MIR3	0.02
LTR/ERVL-MaLR	0.03	AluSx1	0.02
DNA/hAT-Charlie	0.02	L2b	0.02
LTR/ERVL	0.02	AluSx	0.02
DNA/TcMar-Tigger	0.01	AluJb	0.02
tRNA	0.01	AluSz	0.01
LINE/CR1	0.01	AluJo	0.01
snRNA	0.01	AluJr	0.01
LTR/ERVK	0.01	GA-rich	0.01
DNA/hAT-Tip100	0.00	(GT)n	0.01
DNA/hAT-Blackjack	0.00	AluY	0.01
LINE/RTE-BovB	0.00	AluSp	0.01

E

Ontology	Term	FDR Q-val
GO Biological Process	regulation of gene expression, epigenetic	36.61
GO Biological Process	negative regulation of gene expression, epigenetic	35.97
GO Biological Process	nucleosome organization	31.47
GO Biological Process	regulation of gene silencing	30.55
GO Biological Process	chromatin assembly or disassembly	28.97
GO Biological Process	protein-DNA complex subunit organization	28.92
GO Biological Process	DNA conformation change	27.83
GO Biological Process	chromatin silencing	27.24
GO Biological Process	chromatin assembly	26.25
GO Biological Process	nucleosome assembly	25.75
GO Biological Process	multi-organism metabolic process	24.84
GO Biological Process	gene silencing	23.62
GO Biological Process	DNA packaging	23.05
GO Biological Process	regulation of megakaryocyte differentiation	22.55
GO Biological Process	protein-DNA complex assembly	22.03
GO Biological Process	viral gene expression	21.57
GO Biological Process	mRNA catabolic process	20.23
GO Biological Process	RNA catabolic process	19.97
GO Biological Process	viral transcription	19.77
GO Biological Process	regulation of posttranscriptional gene silencing	19.24

Supplementary Figure 1475: Properties and genomic distribution of motifs identified for the ZNF609 transcription factor in K562 (accession ENCSR940PYZ).

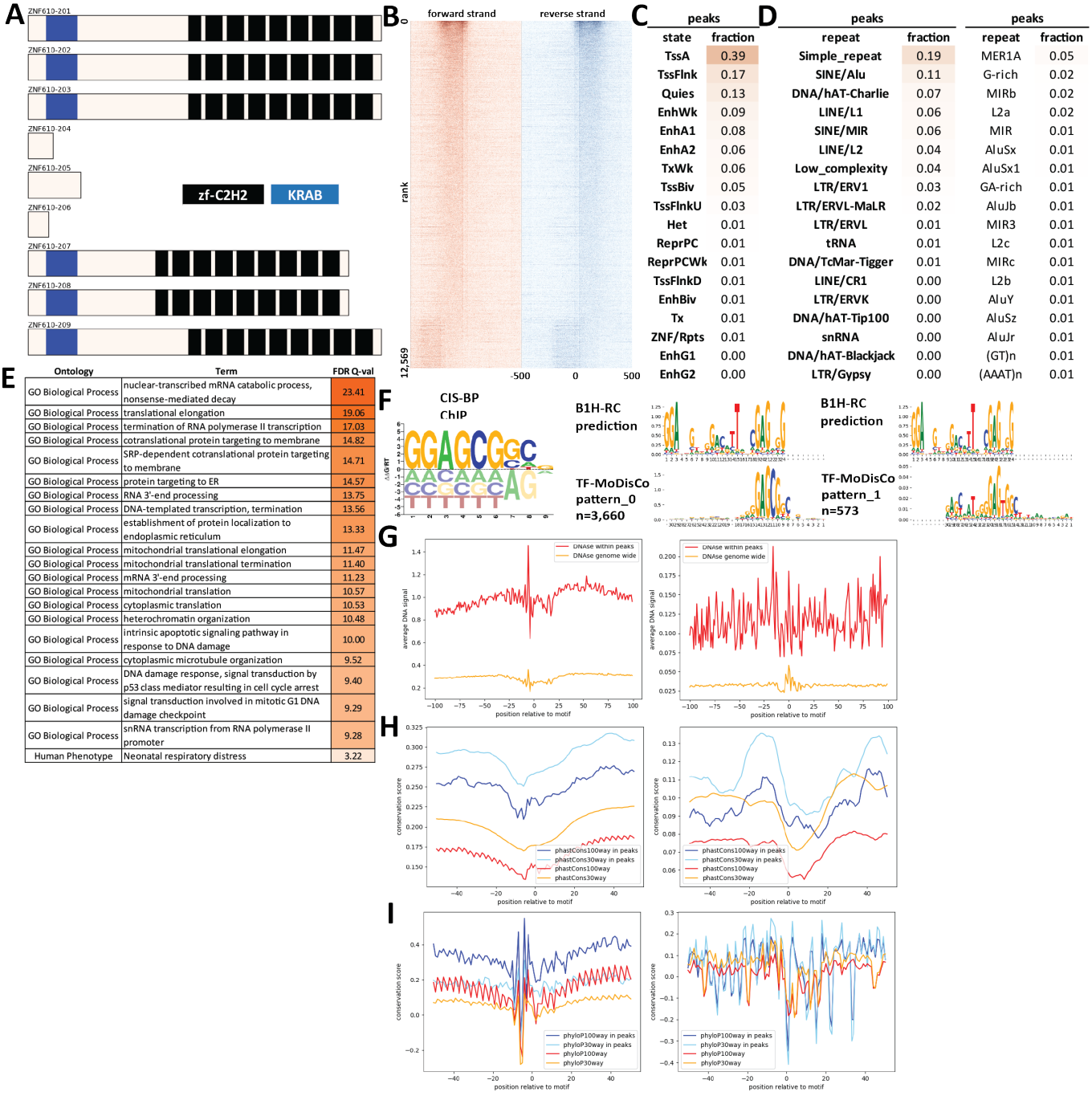

C

peaks	
state	fraction
TssA	0.39
TssFlnk	0.17
Quies	0.13
EnhWk	0.09
EnhA1	0.08
EnhA2	0.06
TxWk	0.06
TssBiv	0.05
TssFlnkU	0.03
Het	0.01
ReprPC	0.01
ReprPCWk	0.01
TssFlnkD	0.01
EnhBiv	0.01
Tx	0.01
ZNF/Rpts	0.01
EnhG1	0.00
EnhG2	0.00

D

peaks		peaks	
repeat	fraction	repeat	fraction
Simple_repeat	0.19	MER1A	0.05
SINE/Alu	0.11	G-rich	0.02
DNA/hAT-Charlie	0.07	MIRb	0.02
LINE/L1	0.06	L2a	0.02
SINE/MIR	0.06	MIR	0.01
LINE/L2	0.04	AluSx	0.01
Low_complexity	0.04	AluSx1	0.01
LTR/ERV1	0.03	GA-rich	0.01
LTR/ERVL-MaLR	0.02	AluJb	0.01
LTR/ERVL	0.01	MIR3	0.01
tRNA	0.01	L2c	0.01
DNA/TcMar-Tigger	0.01	MIRc	0.01
LINE/CR1	0.00	L2b	0.01
LTR/ERVK	0.00	AluY	0.01
DNA/hAT-Tip100	0.00	AluSz	0.01
snRNA	0.00	AluJr	0.01
DNA/hAT-Blackjack	0.00	(GT)n	0.01
LTR/Gypsy	0.00	(AAAT)n	0.01

E

Ontology	Term	FDR Q-val
GO Biological Process	nuclear-transcribed mRNA catabolic process, nonsense-mediated decay	23.41
GO Biological Process	translational elongation	19.06
GO Biological Process	termination of RNA polymerase II transcription	17.03
GO Biological Process	cotranslational protein targeting to membrane	14.82
GO Biological Process	SRP-dependent cotranslational protein targeting to membrane	14.71
GO Biological Process	protein targeting to ER	14.57
GO Biological Process	RNA 3'-end processing	13.75
GO Biological Process	DNA-templated transcription, termination	13.56
GO Biological Process	establishment of protein localization to endoplasmic reticulum	13.33
GO Biological Process	mitochondrial translational elongation	11.47
GO Biological Process	mitochondrial translational termination	11.40
GO Biological Process	mRNA 3'-end processing	11.23
GO Biological Process	mitochondrial translation	10.57
GO Biological Process	cytoplasmic translation	10.53
GO Biological Process	heterochromatin organization	10.48
GO Biological Process	intrinsic apoptotic signaling pathway in response to DNA damage	10.00
GO Biological Process	cytoplasmic microtubule organization	9.52
GO Biological Process	DNA damage response, signal transduction by p53 class mediator resulting in cell cycle arrest	9.40
GO Biological Process	signal transduction involved in mitotic G1 DNA damage checkpoint	9.29
GO Biological Process	snRNA transcription from RNA polymerase II promoter	9.28
Human Phenotype	Neonatal respiratory distress	3.22

Supplementary Figure 1476: Properties and genomic distribution of motifs identified for the ZNF610 transcription factor in HEK293 (accession ENCSR691TXI).

TF-MoDisCO pattern_0 n=3660, CWM

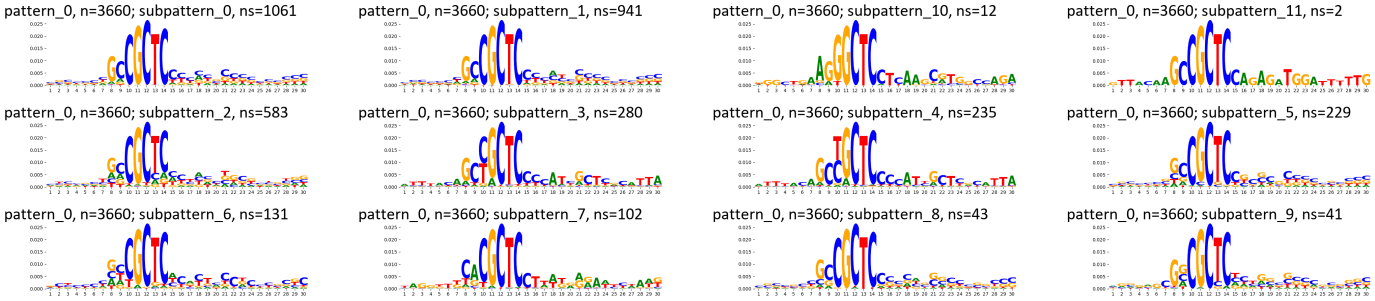

TF-MoDisCO pattern_0 n=3660, PWM

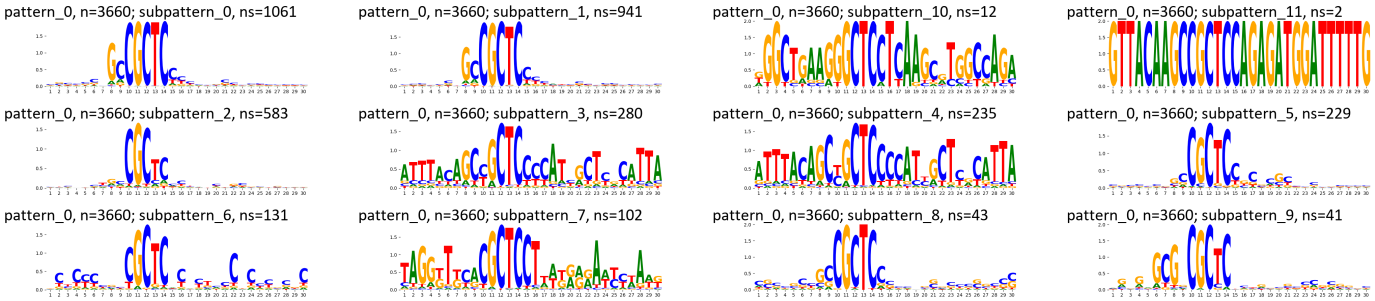

TF-MoDisCO pattern_1 n=573, CWM

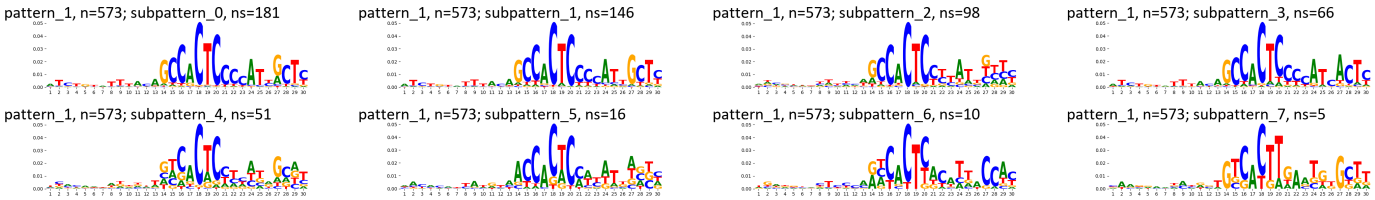

TF-MoDisCO pattern_1 n=573, PWM

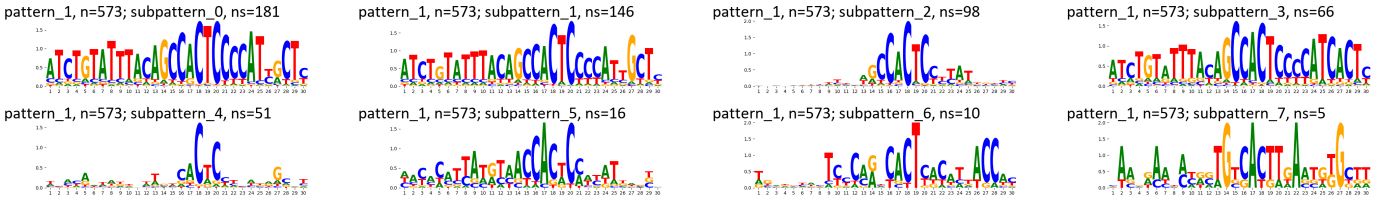

Supplementary Figure 1477: TF-MoDisCO subpatterns for the ZNF610 transcription factor in HEK293 (accession ENCSR691TXI).

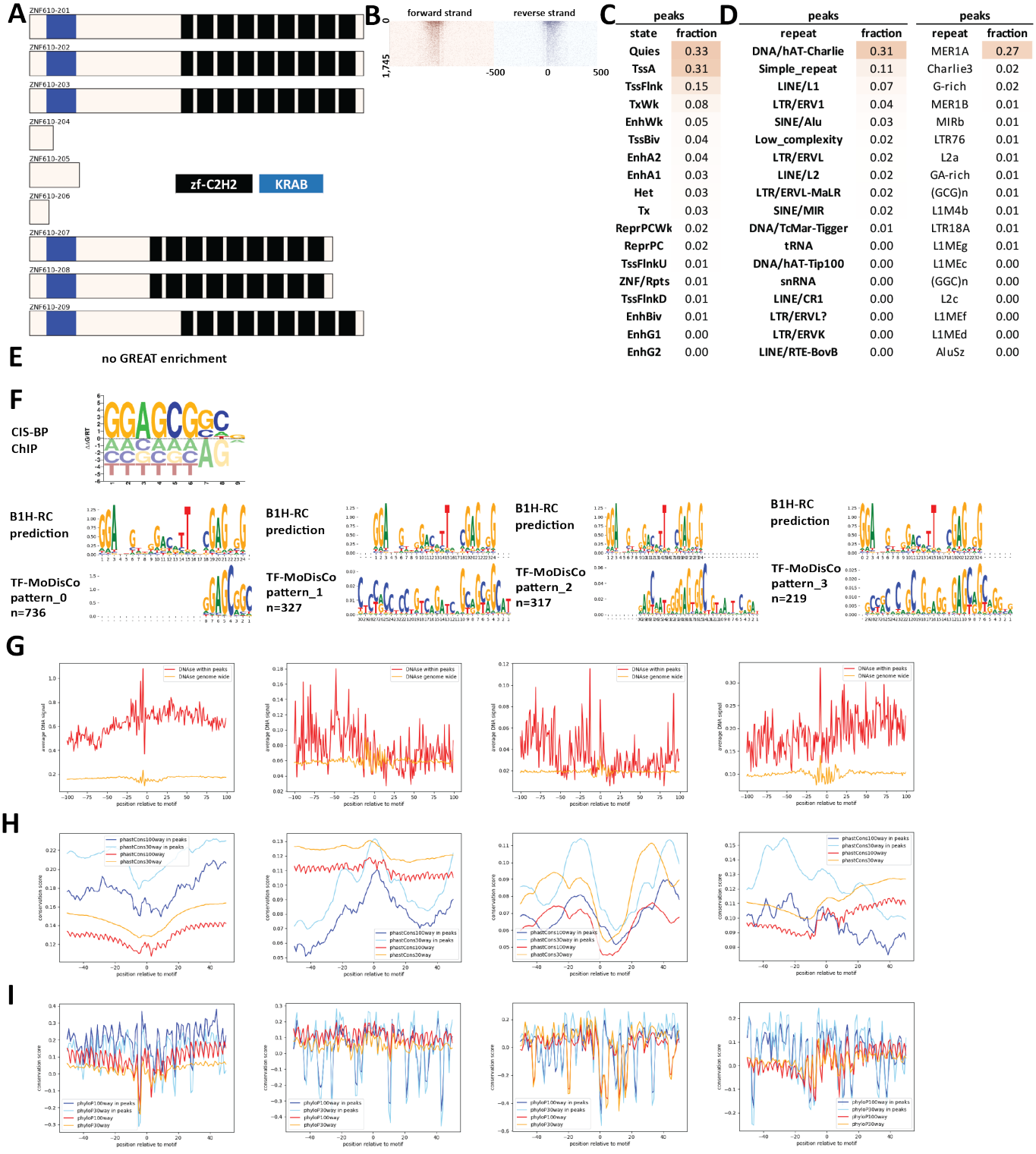

Supplementary Figure 1478: Properties and genomic distribution of motifs identified for the ZNF610 transcription factor in HEK293 (accession Hughes GR models).

TF-MoDisCO pattern_0 n=736, CWM

pattern_0, n=736; subpattern_0, ns=243

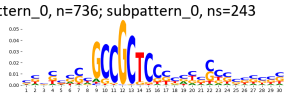

pattern_0, n=736; subpattern_1, ns=167

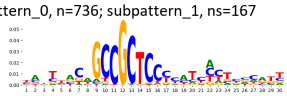

pattern_0, n=736; subpattern_2, ns=142

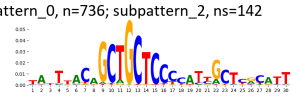

pattern_0, n=736; subpattern_3, ns=125

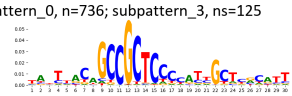

pattern_0, n=736; subpattern_4, ns=48

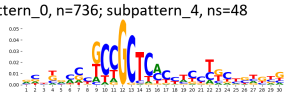

pattern_0, n=736; subpattern_5, ns=11

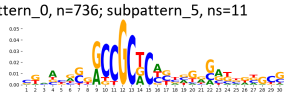

TF-MoDisCO pattern_0 n=736, PWM

pattern_0, n=736; subpattern_0, ns=243

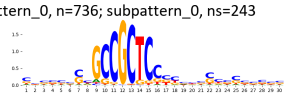

pattern_0, n=736; subpattern_1, ns=167

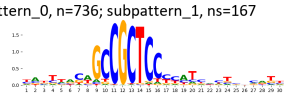

pattern_0, n=736; subpattern_2, ns=142

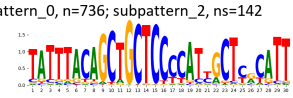

pattern_0, n=736; subpattern_3, ns=125

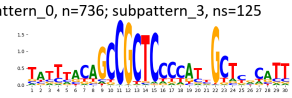

pattern_0, n=736; subpattern_4, ns=48

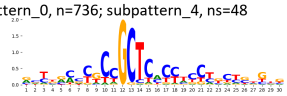

pattern_0, n=736; subpattern_5, ns=11

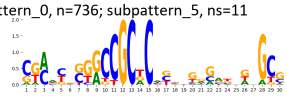

TF-MoDisCO pattern_1 n=327, CWM

pattern_1, n=327; subpattern_0, ns=75

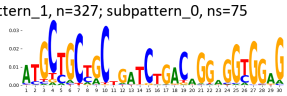

pattern_1, n=327; subpattern_1, ns=62

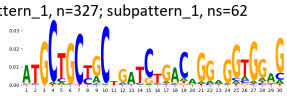

pattern_1, n=327; subpattern_2, ns=54

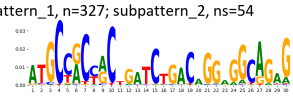

pattern_1, n=327; subpattern_3, ns=53

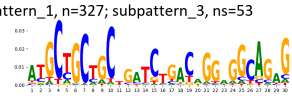

pattern_1, n=327; subpattern_4, ns=43

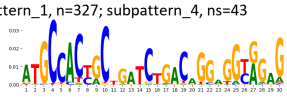

pattern_1, n=327; subpattern_5, ns=40

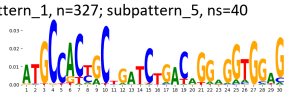

TF-MoDisCO pattern_1 n=327, PWM

pattern_1, n=327; subpattern_0, ns=75

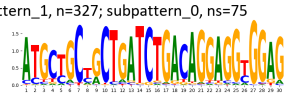

pattern_1, n=327; subpattern_1, ns=62

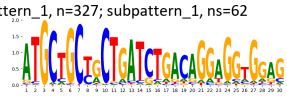

pattern_1, n=327; subpattern_2, ns=54

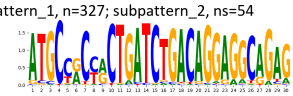

pattern_1, n=327; subpattern_3, ns=53

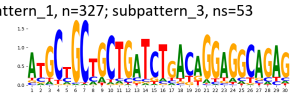

pattern_1, n=327; subpattern_4, ns=43

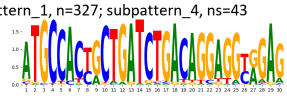

pattern_1, n=327; subpattern_5, ns=40

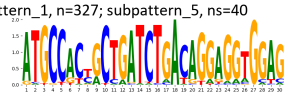

TF-MoDisCO pattern_2 n=317, CWM

pattern_2, n=317; subpattern_0, ns=102

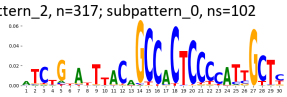

pattern_2, n=317; subpattern_1, ns=102

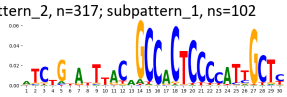

pattern_2, n=317; subpattern_2, ns=64

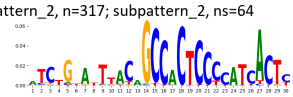

pattern_2, n=317; subpattern_3, ns=47

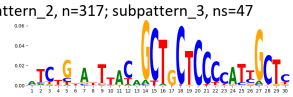

pattern_2, n=317; subpattern_4, ns=2

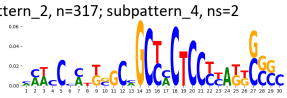

TF-MoDisCO pattern_2 n=317, PWM

pattern_2, n=317; subpattern_0, ns=102

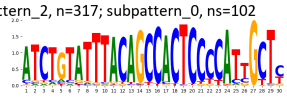

pattern_2, n=317; subpattern_1, ns=102

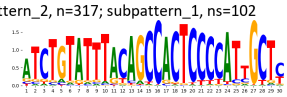

pattern_2, n=317; subpattern_2, ns=64

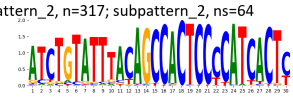

pattern_2, n=317; subpattern_3, ns=47

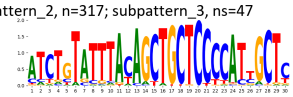

pattern_2, n=317; subpattern_4, ns=2

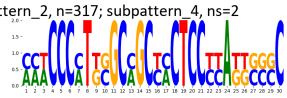

TF-MoDisCO pattern_3 n=219, CWM

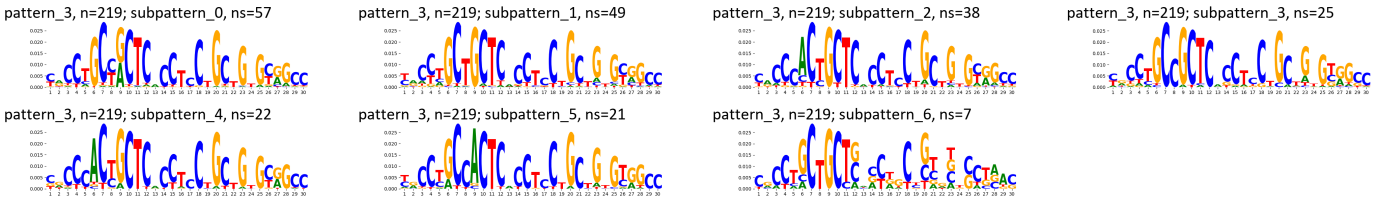

TF-MoDisCO pattern_3 n=219, PWM

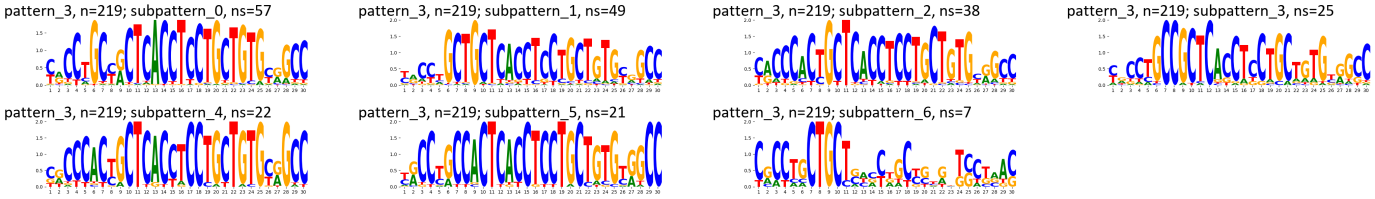

Supplementary Figure 1479: TF-MoDisCO subpatterns for the ZNF610 transcription factor in HEK293 (accession Hughes GR models).

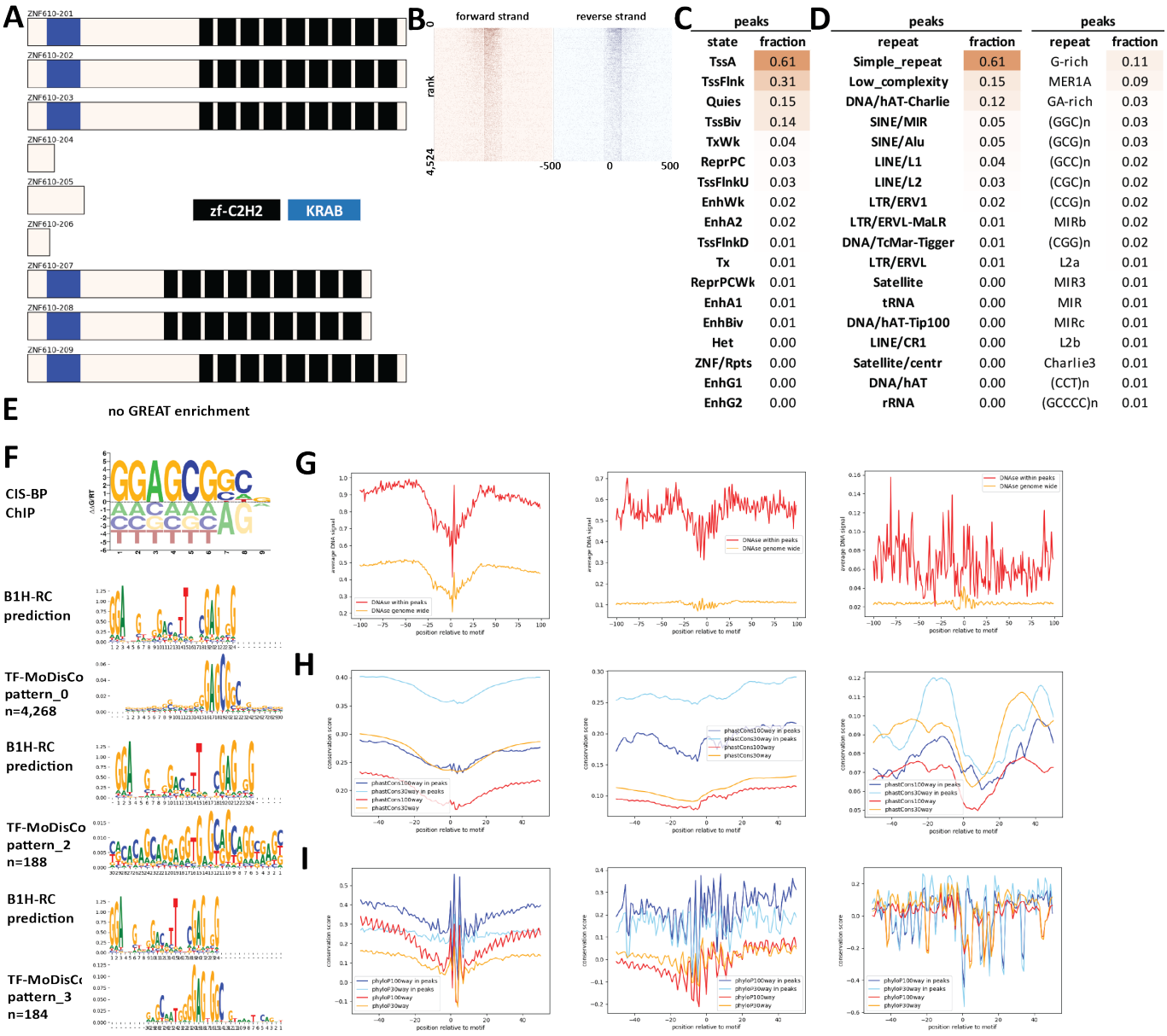

Supplementary Figure 1480: Properties and genomic distribution of motifs identified for the ZNF610 transcription factor in HEK293 (accession ChipExo models).

TF-MoDisCO pattern_0 n=4268, CWM

pattern_0, n=4268; subpattern_0, ns=1087

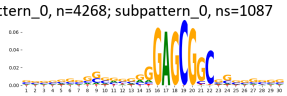

pattern_0, n=4268; subpattern_1, ns=806

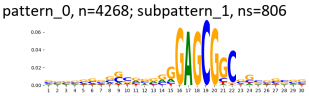

pattern_0, n=4268; subpattern_10, ns=77

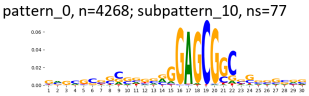

pattern_0, n=4268; subpattern_11, ns=28

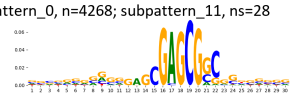

pattern_0, n=4268; subpattern_2, ns=588

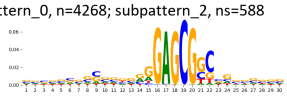

pattern_0, n=4268; subpattern_3, ns=353

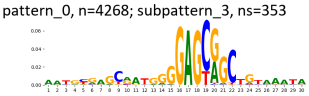

pattern_0, n=4268; subpattern_4, ns=329

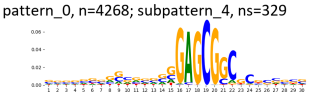

pattern_0, n=4268; subpattern_5, ns=319

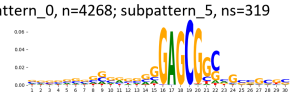

pattern_0, n=4268; subpattern_6, ns=264

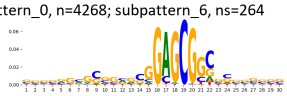

pattern_0, n=4268; subpattern_7, ns=217

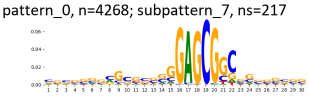

pattern_0, n=4268; subpattern_8, ns=111

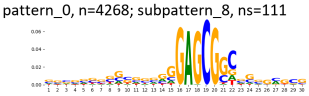

pattern_0, n=4268; subpattern_9, ns=89

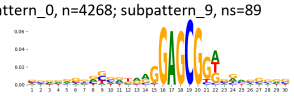

TF-MoDisCO pattern_0 n=4268, PWM

pattern_0, n=4268; subpattern_0, ns=1087

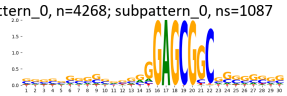

pattern_0, n=4268; subpattern_1, ns=806

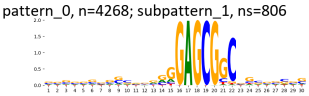

pattern_0, n=4268; subpattern_10, ns=77

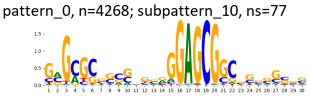

pattern_0, n=4268; subpattern_11, ns=28

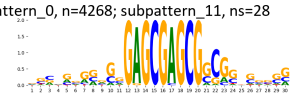

pattern_0, n=4268; subpattern_2, ns=588

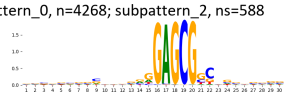

pattern_0, n=4268; subpattern_3, ns=353

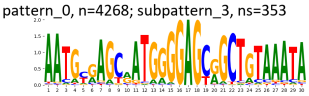

pattern_0, n=4268; subpattern_4, ns=329

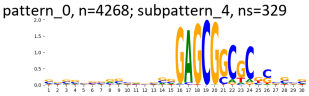

pattern_0, n=4268; subpattern_5, ns=319

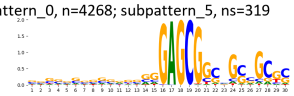

pattern_0, n=4268; subpattern_6, ns=264

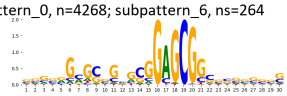

pattern_0, n=4268; subpattern_7, ns=217

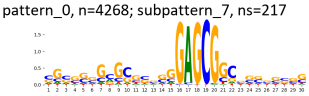

pattern_0, n=4268; subpattern_8, ns=111

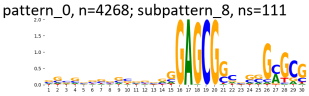

pattern_0, n=4268; subpattern_9, ns=89

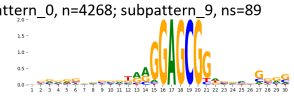

TF-MoDisCO pattern_2 n=188, CWM

pattern_2, n=188; subpattern_0, ns=59

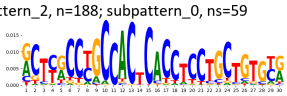

pattern_2, n=188; subpattern_1, ns=48

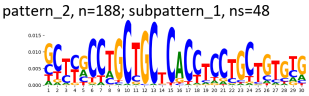

pattern_2, n=188; subpattern_2, ns=39

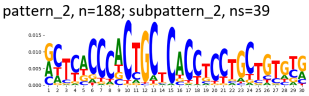

pattern_2, n=188; subpattern_3, ns=21

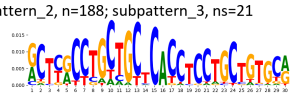

pattern_2, n=188; subpattern_4, ns=18

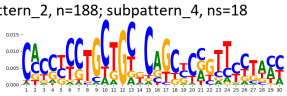

pattern_2, n=188; subpattern_5, ns=3

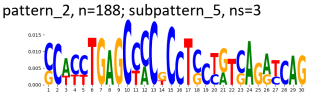

TF-MoDisCO pattern_2 n=188, PWM

pattern_2, n=188; subpattern_0, ns=59

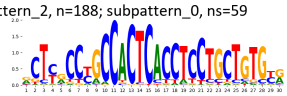

pattern_2, n=188; subpattern_1, ns=48

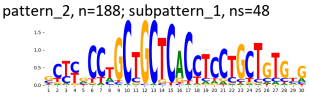

pattern_2, n=188; subpattern_2, ns=39

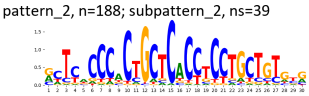

pattern_2, n=188; subpattern_3, ns=21

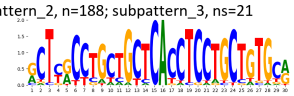

pattern_2, n=188; subpattern_4, ns=18

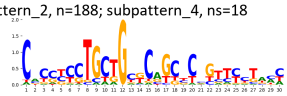

pattern_2, n=188; subpattern_5, ns=3

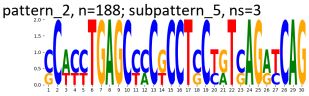

TF-MoDisCO pattern_3 n=184, CWM

pattern_3, n=184; subpattern_0, ns=88

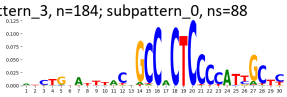

pattern_3, n=184; subpattern_1, ns=83

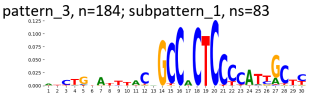

pattern_3, n=184; subpattern_2, ns=13

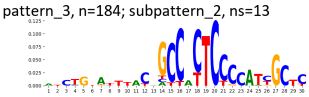

TF-MoDisCO pattern_3 n=184, PWM

pattern_3, n=184; subpattern_0, ns=88

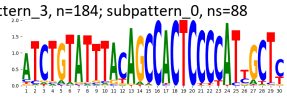

pattern_3, n=184; subpattern_1, ns=83

pattern_3, n=184; subpattern_2, ns=13

Supplementary Figure 1481: TF-MoDisCO subpatterns for the ZNF610 transcription factor in HEK293 (accession ChipExo models).

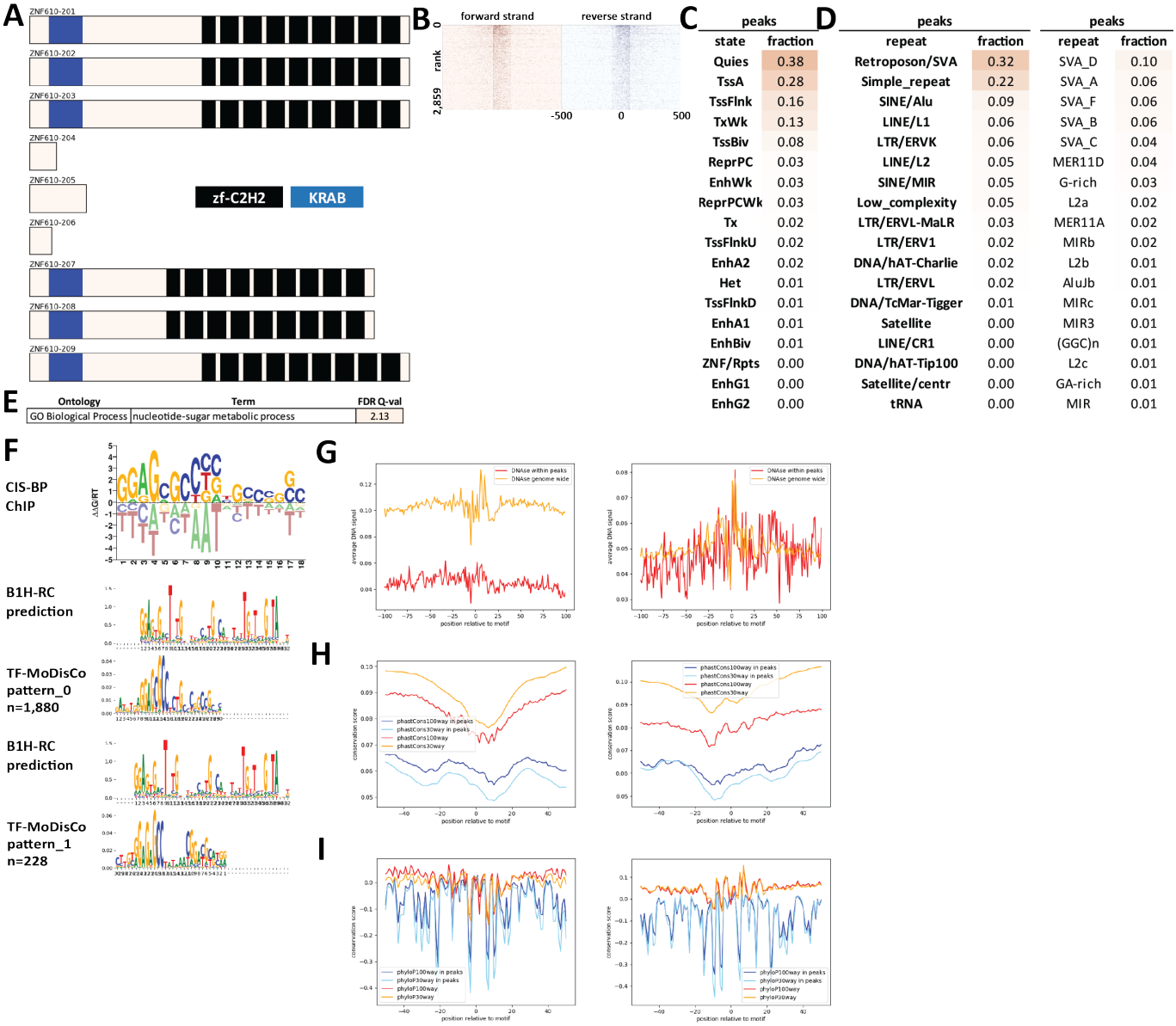

Supplementary Figure 1482: Properties and genomic distribution of motifs identified for the ZNF611 transcription factor in HEK293 (accession ChipExo models).

TF-MoDisCO pattern_0 n=1880, CWM

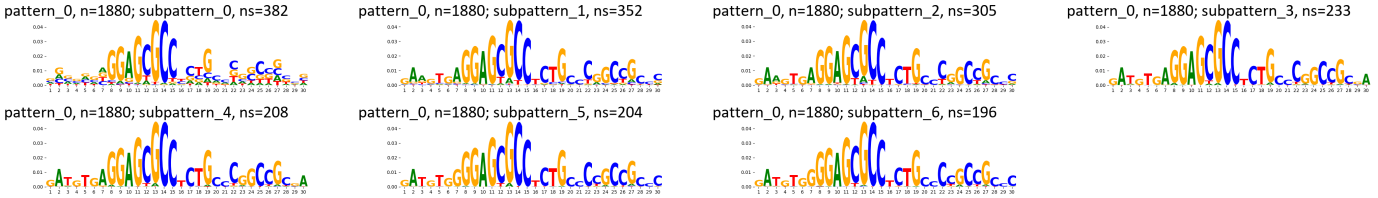

TF-MoDisCO pattern_0 n=1880, PWM

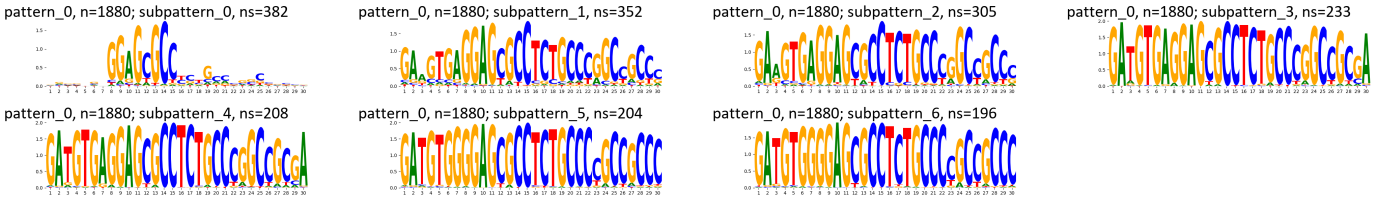

TF-MoDisCO pattern_1 n=228, CWM

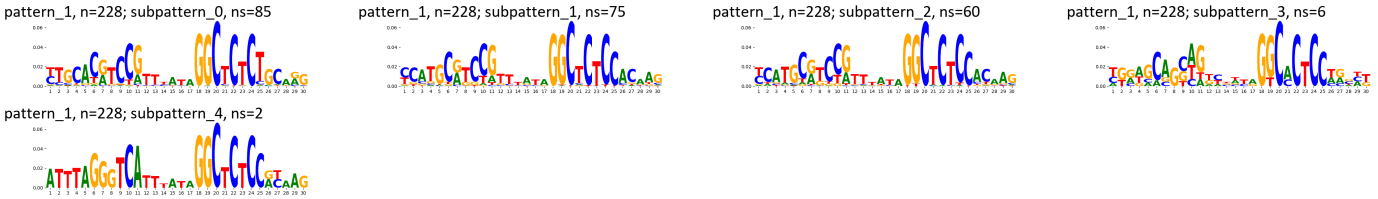

TF-MoDisCO pattern_1 n=228, PWM

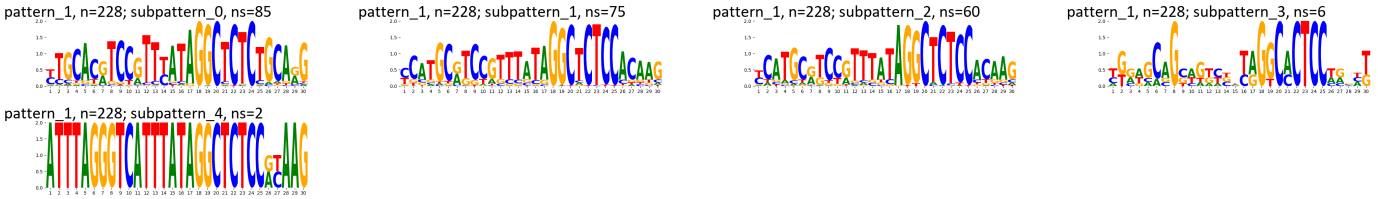

Supplementary Figure 1483: TF-MoDisCO subpatterns for the ZNF611 transcription factor in HEK293 (accession ChipExo models).

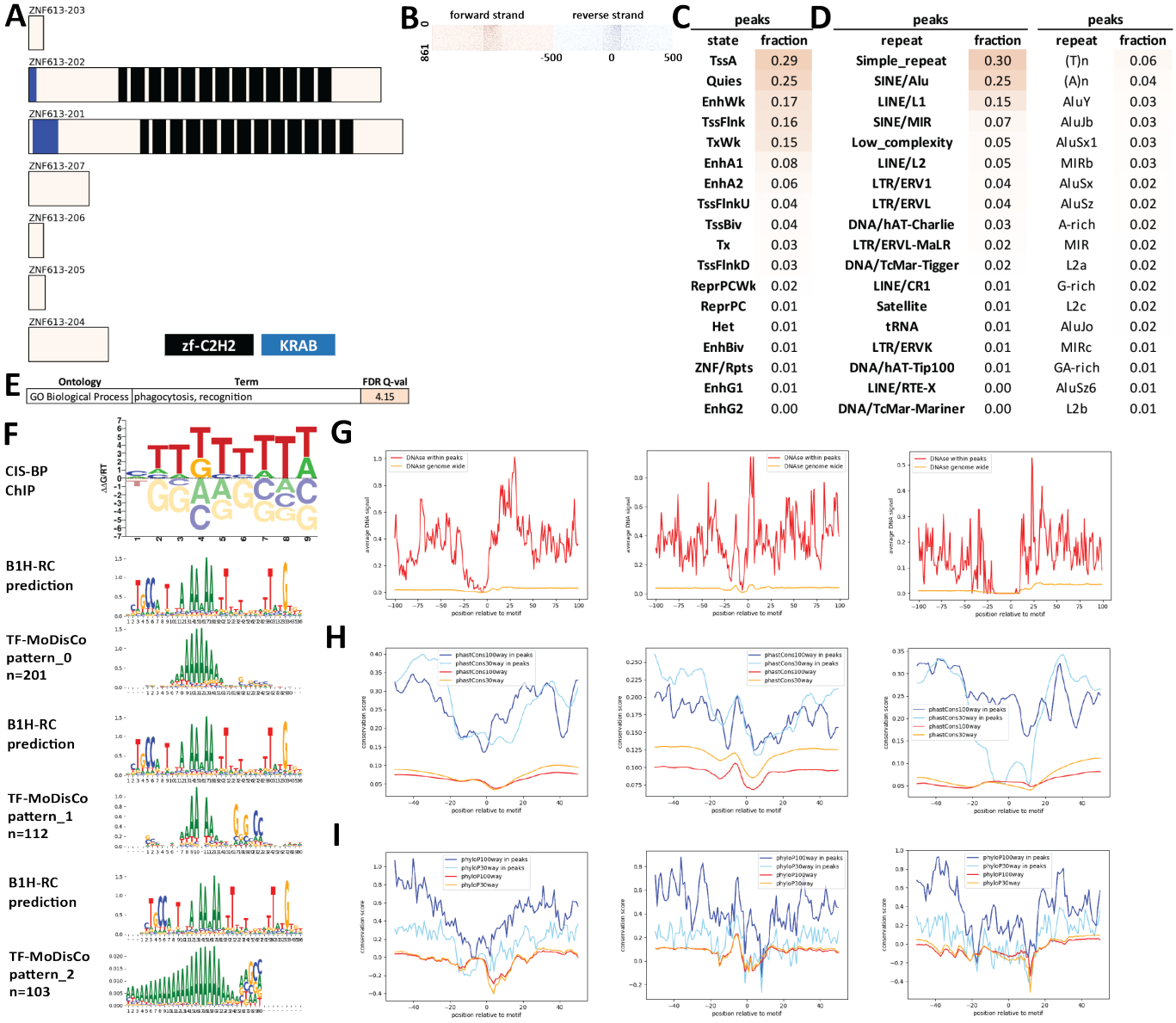

Supplementary Figure 1484: Properties and genomic distribution of motifs identified for the ZNF613 transcription factor in HEK293 (accession ChipExo models).

TF-MoDisCO pattern_0 n=201, CWM

pattern_0, n=201; subpattern_0, ns=51

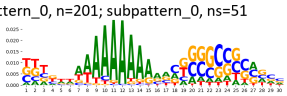

pattern_0, n=201; subpattern_1, ns=49

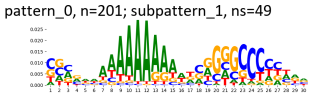

pattern_0, n=201; subpattern_2, ns=46

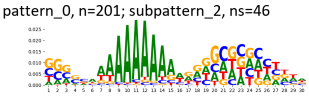

pattern_0, n=201; subpattern_3, ns=33

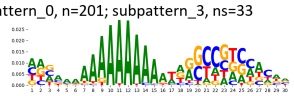

pattern_0, n=201; subpattern_4, ns=22

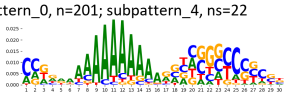

TF-MoDisCO pattern_0 n=201, PWM

pattern_0, n=201; subpattern_0, ns=51

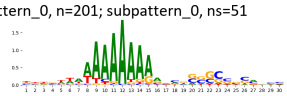

pattern_0, n=201; subpattern_1, ns=49

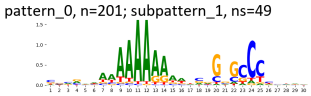

pattern_0, n=201; subpattern_2, ns=46

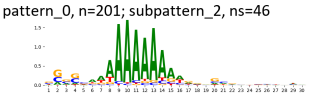

pattern_0, n=201; subpattern_3, ns=33

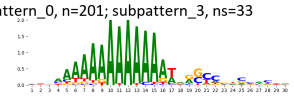

pattern_0, n=201; subpattern_4, ns=22

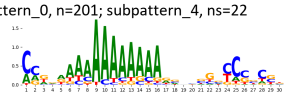

TF-MoDisCO pattern_1 n=112, CWM

pattern_1, n=112; subpattern_0, ns=28

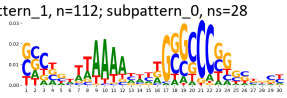

pattern_1, n=112; subpattern_1, ns=25

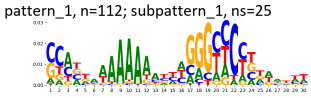

pattern_1, n=112; subpattern_2, ns=23

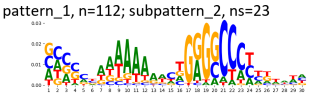

pattern_1, n=112; subpattern_3, ns=20

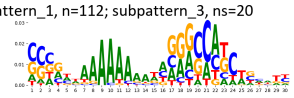

pattern_1, n=112; subpattern_4, ns=16

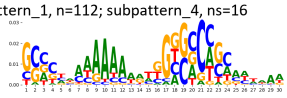

TF-MoDisCO pattern_1 n=112, PWM

pattern_1, n=112; subpattern_0, ns=28

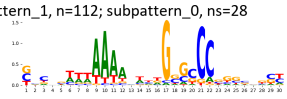

pattern_1, n=112; subpattern_1, ns=25

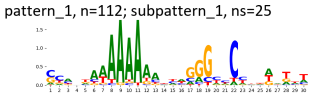

pattern_1, n=112; subpattern_2, ns=23

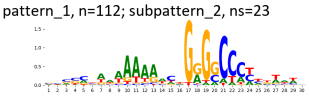

pattern_1, n=112; subpattern_3, ns=20

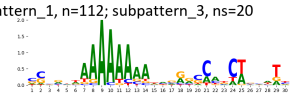

pattern_1, n=112; subpattern_4, ns=16

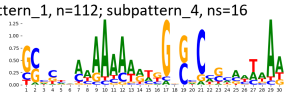

TF-MoDisCO pattern_2 n=103, CWM

pattern_2, n=103; subpattern_0, ns=41

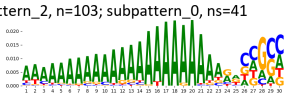

pattern_2, n=103; subpattern_1, ns=32

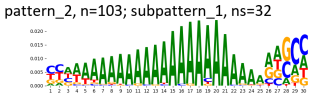

pattern_2, n=103; subpattern_2, ns=30

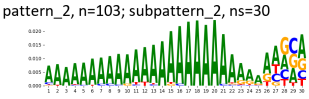

TF-MoDisCO pattern_2 n=103, PWM

pattern_2, n=103; subpattern_0, ns=41

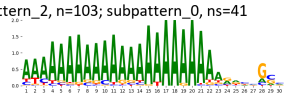

pattern_2, n=103; subpattern_1, ns=32

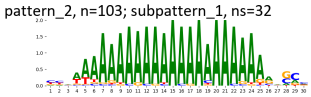

pattern_2, n=103; subpattern_2, ns=30

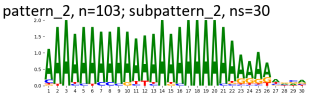

Supplementary Figure 1485: TF-MoDisCO subpatterns for the ZNF613 transcription factor in HEK293 (accession ChipExo models).

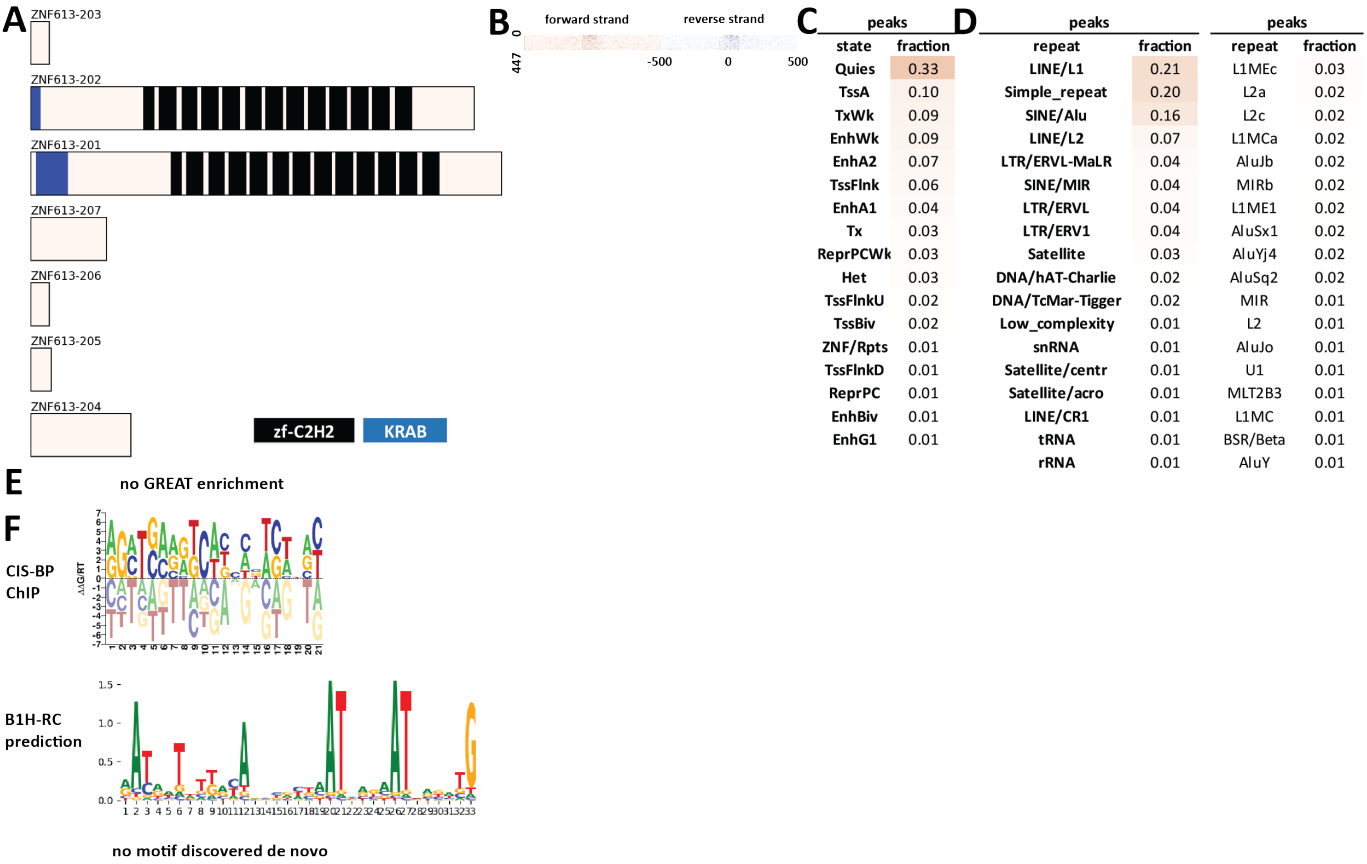

Supplementary Figure 1486: Properties and genomic distribution of motifs identified for the ZNF614 transcription factor in HEK293 (accession ChipExo models).

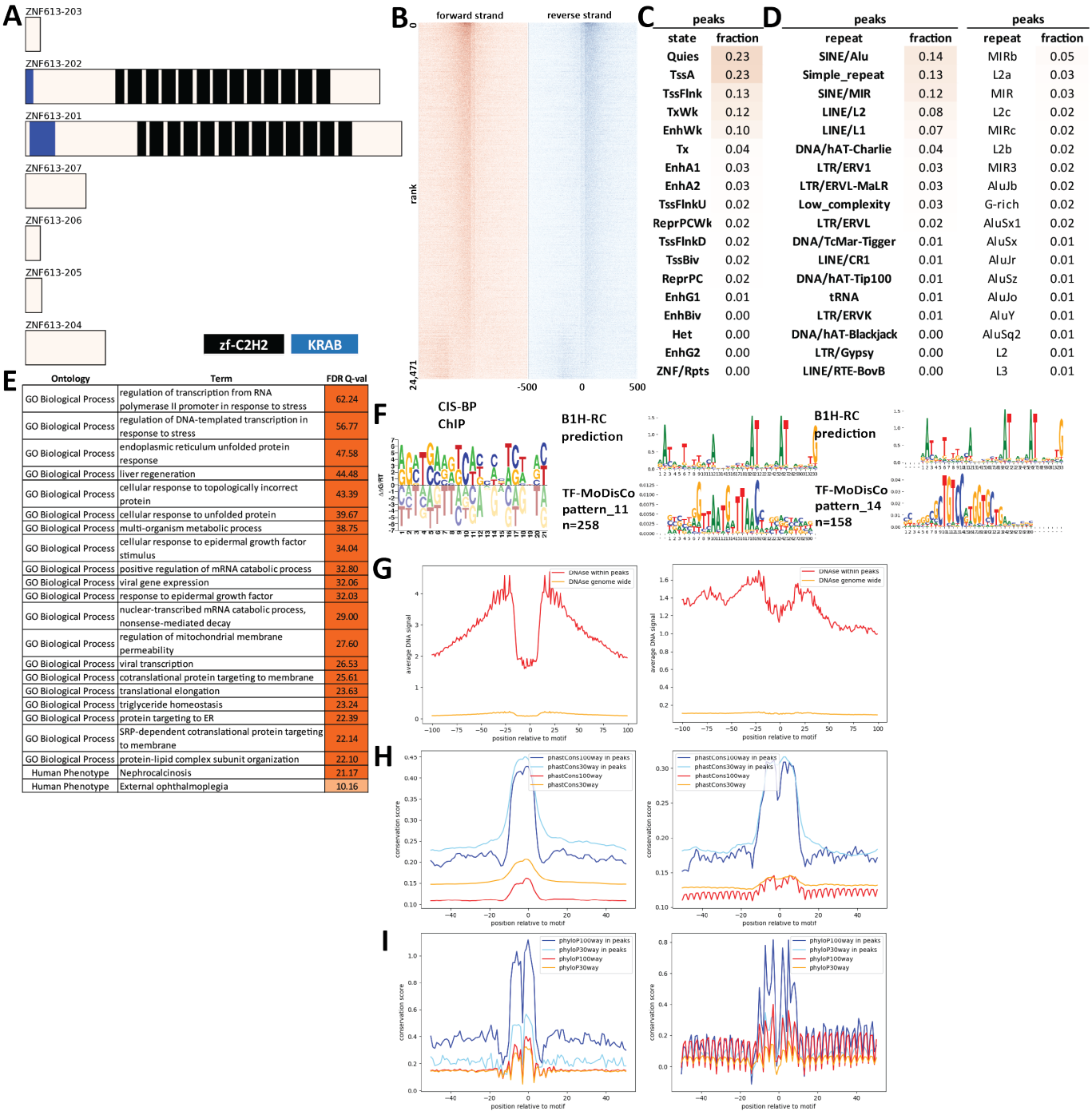

peaks	
state	fraction
Quies	0.23
TssA	0.23
TssFlnk	0.13
TxWk	0.12
EnhWk	0.10
Tx	0.04
EnhA1	0.03
EnhA2	0.03
TssFlnkU	0.02
ReprPCWk	0.02
TssFlnkD	0.02
TssBiv	0.02
ReprPC	0.02
EnhG1	0.01
EnhBiv	0.00
Het	0.00
EnhG2	0.00
ZNF/Rpts	0.00

peaks		peaks	
repeat	fraction	repeat	fraction
SINE/Alu	0.14	MIRb	0.05
Simple_repeat	0.13	L2a	0.03
SINE/MIR	0.12	MIR	0.03
LINE/L2	0.08	L2c	0.02
LINE/L1	0.07	MIRc	0.02
DNA/hAT-Charlie	0.04	L2b	0.02
LTR/ERV1	0.03	MIR3	0.02
LTR/ERVL-MaLR	0.03	AluJb	0.02
Low_complexity	0.03	G-rich	0.02
LTR/ERVL	0.02	AluSx1	0.02
DNA/TcMar-Tigger	0.01	AluSx	0.01
LINE/CR1	0.01	AluJr	0.01
DNA/hAT-Tip100	0.01	AluSz	0.01
tRNA	0.01	AluJo	0.01
LTR/ERVK	0.01	AluY	0.01
DNA/hAT-Blackjack	0.00	AluSq2	0.01
LTR/Gypsy	0.00	L2	0.01
LINE/RTE-BovB	0.00	L3	0.01

Ontology	Term	FDR Q-val
GO Biological Process	regulation of transcription from RNA polymerase II promoter in response to stress	62.24
GO Biological Process	regulation of DNA-templated transcription in response to stress	56.77
GO Biological Process	endoplasmic reticulum unfolded protein response	47.58
GO Biological Process	liver regeneration	44.48
GO Biological Process	cellular response to topologically incorrect protein	43.39
GO Biological Process	cellular response to unfolded protein	39.67
GO Biological Process	multi-organism metabolic process	38.75
GO Biological Process	cellular response to epidermal growth factor stimulus	34.04
GO Biological Process	positive regulation of mRNA catabolic process	32.80
GO Biological Process	viral gene expression	32.06
GO Biological Process	response to epidermal growth factor	32.03
GO Biological Process	nuclear-transcribed mRNA catabolic process, nonsense-mediated decay	29.00
GO Biological Process	regulation of mitochondrial membrane permeability	27.60
GO Biological Process	viral transcription	26.53
GO Biological Process	cotranslational protein targeting to membrane	25.61
GO Biological Process	translational elongation	23.63
GO Biological Process	triglyceride homeostasis	23.24
GO Biological Process	protein targeting to ER	22.39
GO Biological Process	SRP-dependent cotranslational protein targeting to membrane	22.14
GO Biological Process	protein-lipid complex subunit organization	22.10
Human Phenotype	Nephrocalcinosis	21.17
Human Phenotype	External ophthalmoplegia	10.16

Supplementary Figure 1487: Properties and genomic distribution of motifs identified for the ZNF614 transcription factor in HepG2 (accession ENCSR011CIR).

TF-MoDisCO pattern_11 n=258, CWM

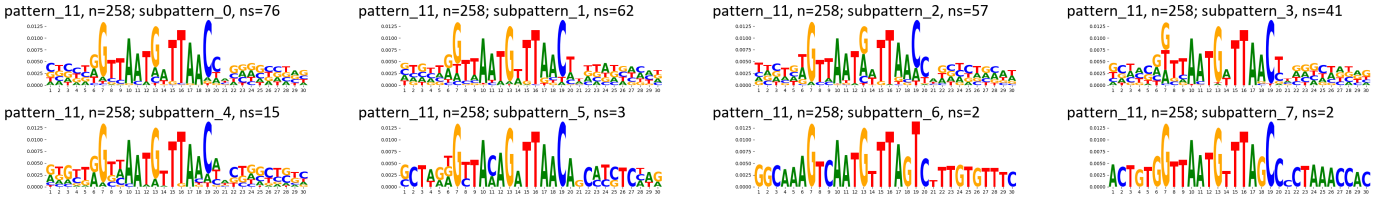

TF-MoDisCO pattern_11 n=258, PWM

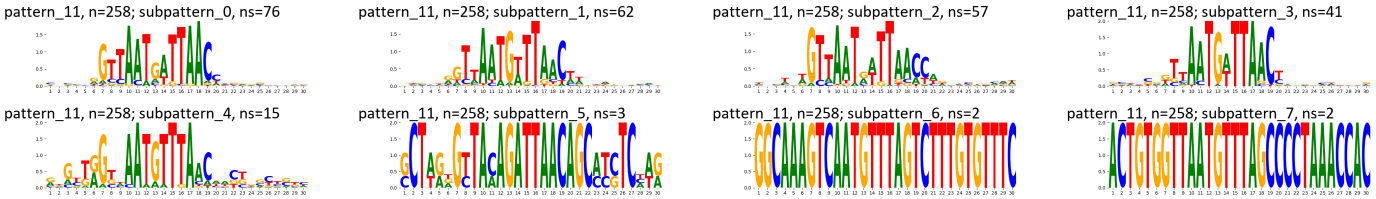

TF-MoDisCO pattern_14 n=158, CWM

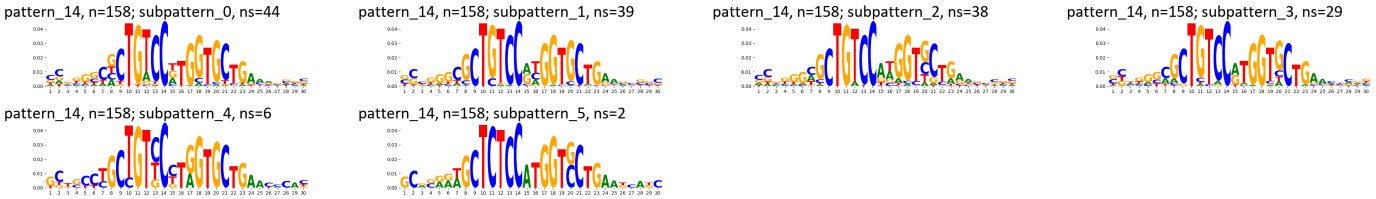

TF-MoDisCO pattern_14 n=158, PWM

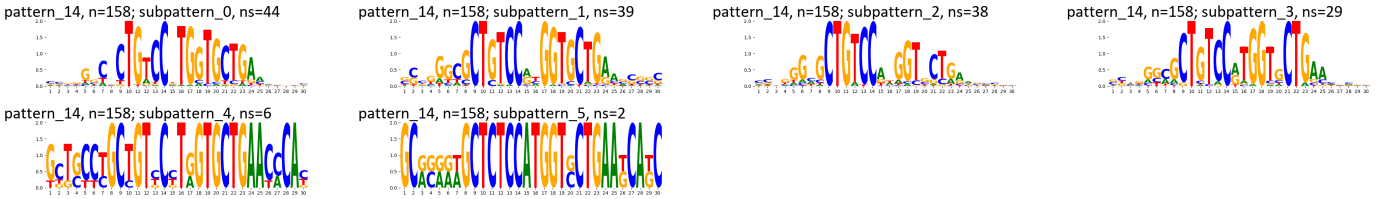

Supplementary Figure 1488: TF-MoDisCO subpatterns for the ZNF614 transcription factor in HepG2 (accession ENCSR011CIR).

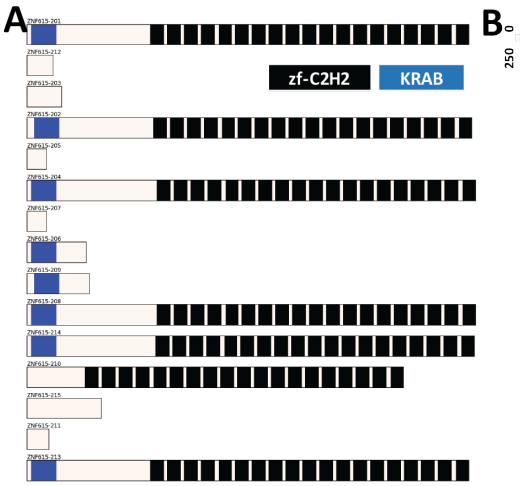



C

peaks	
state	fraction
Quies	0.34
TxWk	0.07
Het	0.06
ReprPCWk	0.04
Tx	0.04
EnhA2	0.02
ZNF/Rpts	0.02
TssFlnk	0.02
TssA	0.02
EnhWk	0.02
ReprPC	0.01
TssBiv	0.00
EnhG1	0.00
EnhA1	0.00

D

peaks		peaks	
repeat	fraction	repeat	fraction
LINE/L1	0.30	L1MC3	0.19
Simple_repeat	0.16	L1MB8	0.02
SINE/Alu	0.13	AluYj4	0.02
LTR/ERVL-MaLR	0.06	L2c	0.02
LTR/ERV1	0.06	BSR/Beta	0.02
LTR/ERVL	0.06	ACRO1	0.02
LINE/L2	0.05	U1	0.02
Satellite	0.04	MIR	0.02
SINE/MIR	0.03	MER68B	0.02
DNA/hAT-Charlie	0.02	MER5A	0.02
snRNA	0.02	AluJb	0.02
Satellite/acro	0.02	MER21B	0.01
DNA/TcMar-Tigger	0.02	LTR10A	0.01
Low_complexity	0.01	L2a	0.01
Satellite/centr	0.01	L2	0.01
DNA/hAT-Tip100	0.01	L1MEd	0.01
DNA/hAT	0.01	(TGGAA)n	0.01
Retroposon/SVA	0.00	MLT1D	0.01

E

no GREAT enrichment

F

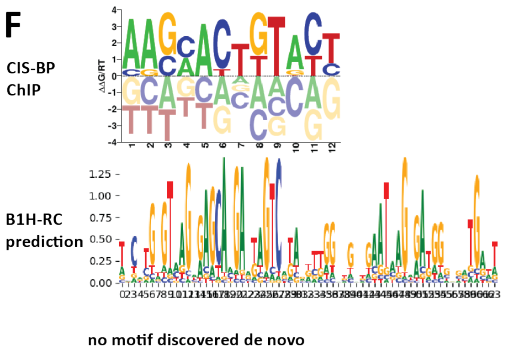

no motif discovered de novo

Supplementary Figure 1489: Properties and genomic distribution of motifs identified for the ZNF615 transcription factor in HEK293 (accession ChipExo models).

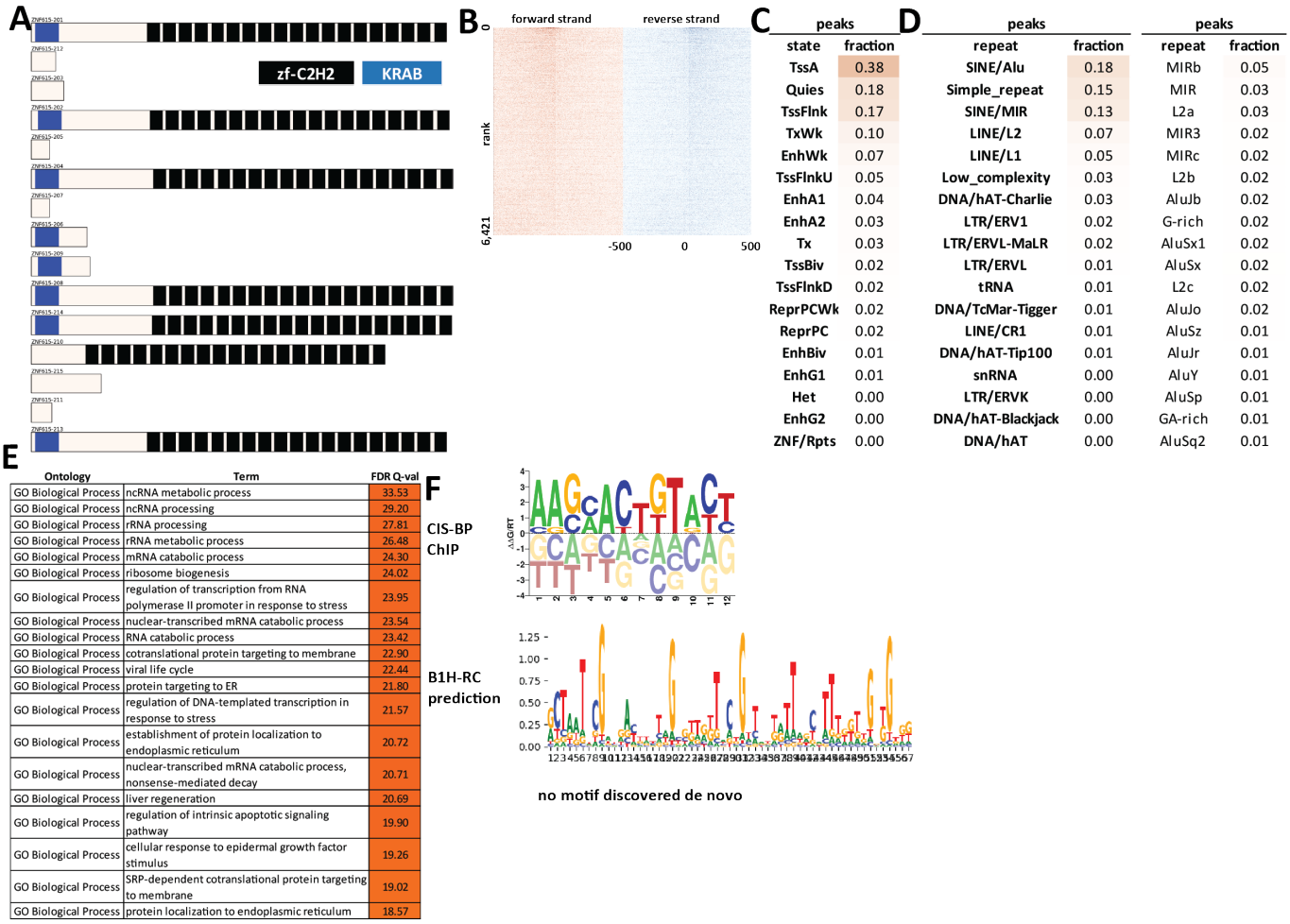

Supplementary Figure 1490: Properties and genomic distribution of motifs identified for the ZNF615 transcription factor in HepG2 (accession ENCSR286LPH).

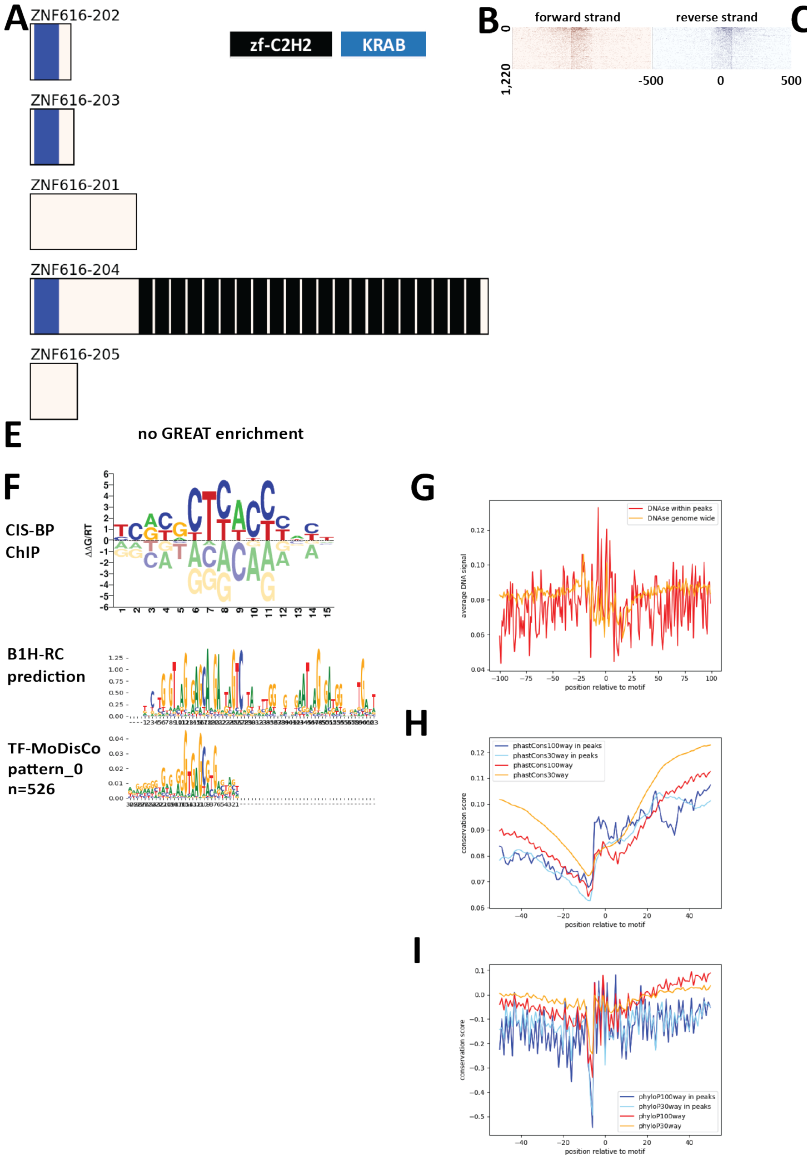

C

peaks	
state	fraction
Quies	0.48
TxWk	0.14
TssA	0.08
Tx	0.07
EnhWk	0.05
Het	0.05
TssFlnk	0.04
ReprPC	0.03
ReprPCWk	0.03
TssBiv	0.03
ZNF/Rpts	0.01
EnhG1	0.01
EnhA2	0.01
TssFlnkU	0.01
EnhA1	0.01
EnhBiv	0.01
TssFlnkD	0.01
EnhG2	0.00

D

peaks		peaks	
repeat	fraction	repeat	fraction
SINE/Alu	0.26	AluJb	0.04
LTR/ERV1	0.21	MIRb	0.04
Simple_repeat	0.17	MER61-int	0.03
LINE/L1	0.14	L2a	0.03
LINE/L2	0.09	AluSx1	0.03
SINE/MIR	0.09	MER52-int	0.03
LTR/ERVL-MaLR	0.06	LTR25-int	0.03
DNA/hAT-Charlie	0.04	L2c	0.03
Low_complexity	0.04	AluY	0.03
LTR/ERVL	0.04	L2b	0.02
DNA/TcMar-Tigger	0.02	MIR	0.02
LINE/CR1	0.01	HUERS-P3-in	0.02
Satellite	0.01	AluSz	0.02
DNA/hAT-Tip100	0.01	HUERS-P3b-ir	0.02
DNA/TcMar-Mariner	0.01	GA-rich	0.02
Satellite/centr	0.01	AluJo	0.02
Satellite/acro	0.01	AluJr	0.02
LTR/Gypsy	0.00	MER52A	0.01

Supplementary Figure 1491: Properties and genomic distribution of motifs identified for the ZNF616 transcription factor in HEK293 (accession ChipExo models).

TF-MoDisCO pattern_0 n=526, CWM

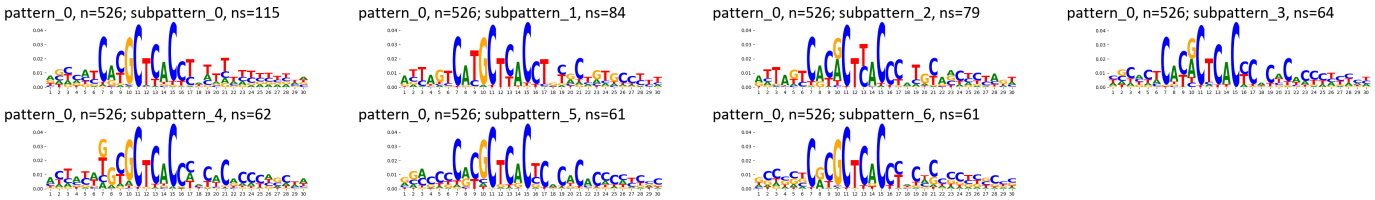

TF-MoDisCO pattern_0 n=526, PWM

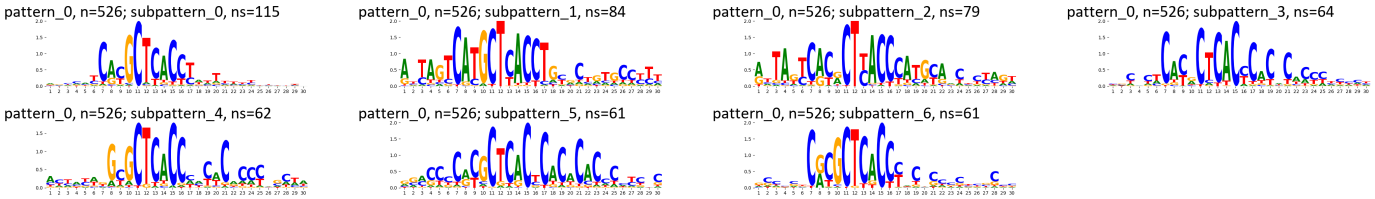

Supplementary Figure 1492: TF-MoDisCO subpatterns for the ZNF616 transcription factor in HEK293 (accession ChipExo models).

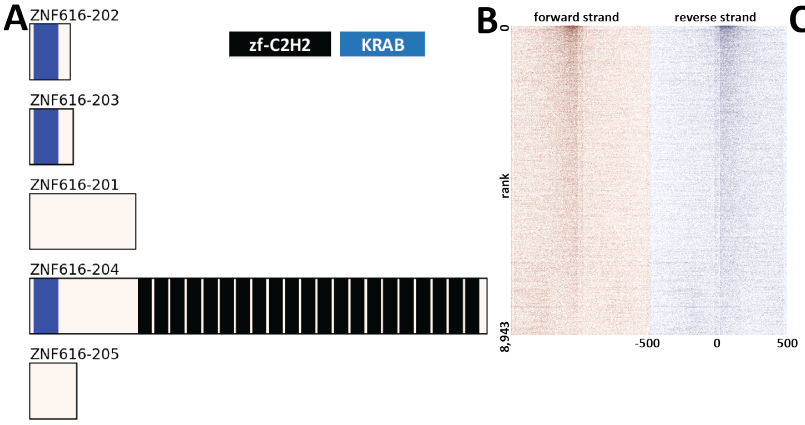

C

peaks	
state	fraction
TssA	0.46
TssFlnk	0.20
Quies	0.13
TxWk	0.06
TssBiv	0.04
TssFlnkU	0.04
EnhWk	0.03
ReprPC	0.03
EnhA2	0.02
EnhA1	0.02
ReprPCWk	0.02
TssFlnkD	0.02
Tx	0.02
EnhBiv	0.01
EnhG1	0.00
Het	0.00
EnhG2	0.00
ZNF/Rpts	0.00

D

peaks		peaks	
repeat	fraction	repeat	fraction
Simple_repeat	0.25	G-rich	0.04
SINE/MIR	0.08	MIRb	0.03
SINE/Alu	0.07	L2a	0.02
Low_complexity	0.05	MIR3	0.02
LINE/L2	0.04	MIR	0.02
LTR/ERV1	0.02	MIRc	0.01
LINE/L1	0.02	L2b	0.01
DNA/hAT-Charlie	0.01	L2c	0.01
LTR/ERVL-MaLR	0.01	AluJb	0.01
LTR/ERVL	0.01	(GGC)n	0.01
DNA/hAT-Tip100	0.00	GA-rich	0.01
LINE/CR1	0.00	(CCG)n	0.01
tRNA	0.00	(GCC)n	0.01
DNA/hAT-Blackjack	0.00	AluSx	0.01
DNA/TcMar-Tigger	0.00	AluSx1	0.01
LTR/ERVK	0.00	(GCG)n	0.01
snRNA	0.00	AluSz	0.01
LINE/RTE-BovB	0.00	AluJr	0.01

E

Ontology	Term	FDR Q-val
GO Biological Process	regulation of transcription from RNA polymerase II promoter in response to stress	26.09
GO Biological Process	regulation of DNA-templated transcription in response to stress	23.52
GO Biological Process	rRNA processing	22.12
GO Biological Process	rRNA metabolic process	21.68
GO Biological Process	regulation of intrinsic apoptotic signaling pathway	19.00
GO Biological Process	regulation of transcription from RNA polymerase II promoter in response to hypoxia	18.12
GO Biological Process	negative regulation of intrinsic apoptotic signaling pathway	16.83
GO Biological Process	cellular response to topologically incorrect protein	16.32
GO Biological Process	cellular response to unfolded protein	15.92
GO Biological Process	translational elongation	15.87
GO Biological Process	liver regeneration	15.66
GO Biological Process	mitochondrial translational termination	14.70
GO Biological Process	mitochondrial translational elongation	14.26
GO Biological Process	translational termination	13.00
GO Biological Process	protein targeting to ER	12.22
GO Biological Process	mitochondrial translation	12.05
GO Biological Process	anaphase-promoting complex-dependent catabolic process	12.05
GO Biological Process	nuclear-transcribed mRNA catabolic process, nonsense-mediated decay	10.71
GO Biological Process	translational initiation	10.67
GO Biological Process	cotranslational protein targeting to membrane	10.62
Human Phenotype	Increased serum lactate	12.78
Human Phenotype	Exercise intolerance	12.16
Human Phenotype	Nevus	7.84
Human Phenotype	Abnormality of glycolysis	7.33
Human Phenotype	Increased serum pyruvate	7.09
Human Phenotype	Abnormal CSF metabolite level	5.10
Human Phenotype	Increased CSF lactate	5.04
Human Phenotype	Death in infancy	4.80
Human Phenotype	CNS hypomyelination	4.33
Human Phenotype	Glycosuria	3.61

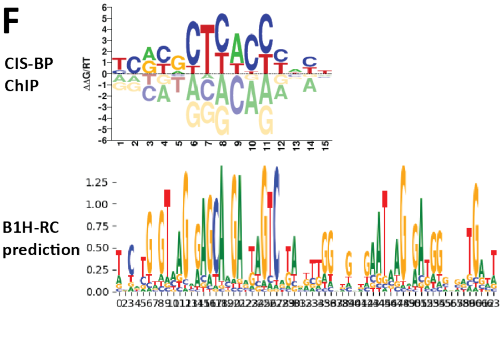

Supplementary Figure 1493: Properties and genomic distribution of motifs identified for the ZNF616 transcription factor in HepG2 (accession ENCSR654PQY).

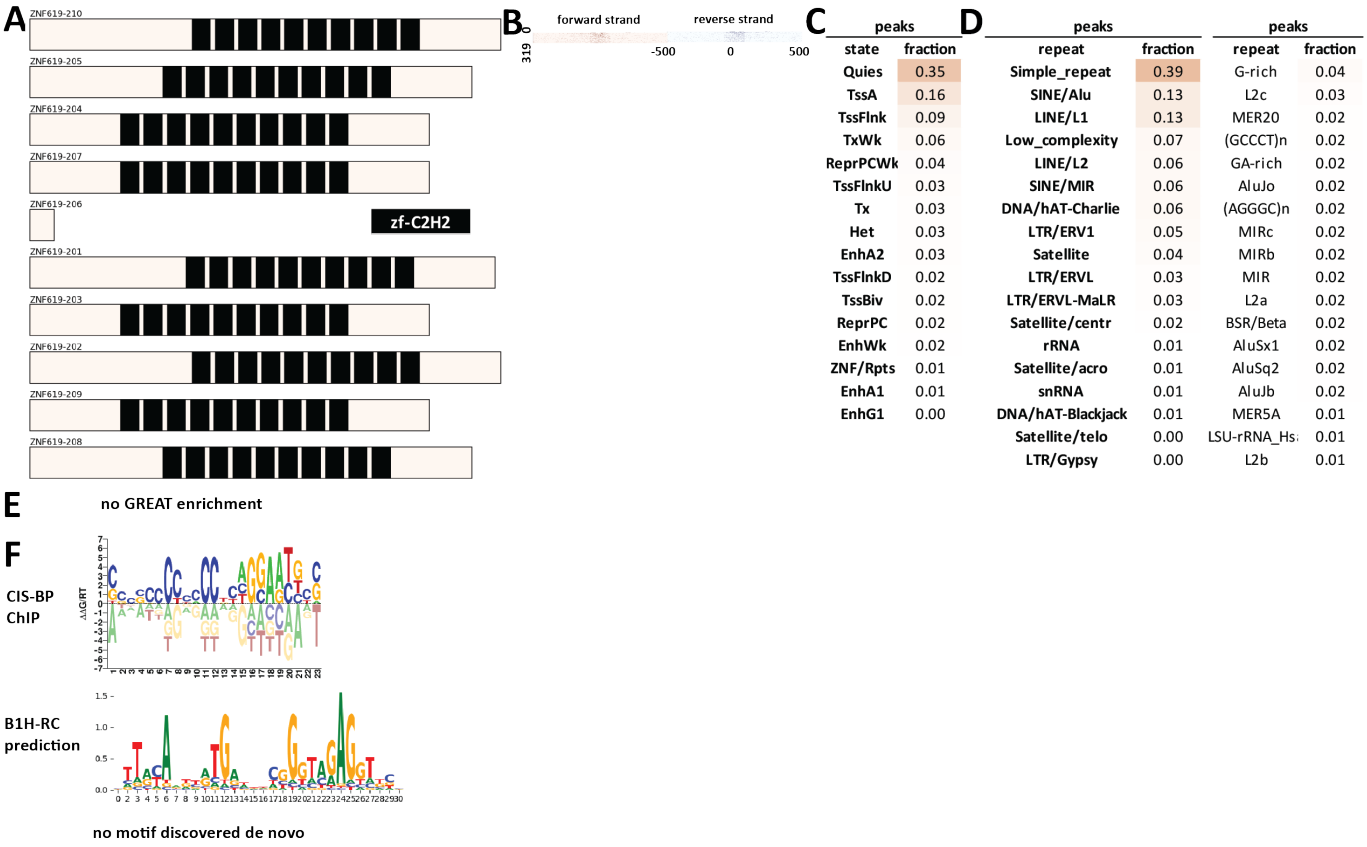

C	peaks	
	state	fraction
	Quies	0.35
	TssA	0.16
	TssFlnk	0.09
	TxWk	0.06
	ReprPCWk	0.04
	TssFlnkU	0.03
	Tx	0.03
	Het	0.03
	EnhA2	0.03
	TssFlnkD	0.02
	TssBiv	0.02
	ReprPC	0.02
	EnhWk	0.02
	ZNF/Rpts	0.01
	EnhA1	0.01
	EnhG1	0.00

D	peaks		peaks	
	repeat	fraction	repeat	fraction
	Simple_repeat	0.39	G-rich	0.04
	SINE/Alu	0.13	L2c	0.03
	LINE/L1	0.13	MER20	0.02
	Low_complexity	0.07	(GCCCT)n	0.02
	LINE/L2	0.06	GA-rich	0.02
	SINE/MIR	0.06	AluJo	0.02
	DNA/hAT-Charlie	0.06	(AGGGC)n	0.02
	LTR/ERV1	0.05	MIRc	0.02
	Satellite	0.04	MIRb	0.02
	LTR/ERVL	0.03	MIR	0.02
	LTR/ERVL-MaLR	0.03	L2a	0.02
	Satellite/centr	0.02	BSR/Beta	0.02
	rRNA	0.01	AluSx1	0.02
	Satellite/acro	0.01	AluSq2	0.02
	snRNA	0.01	AluJb	0.02
	DNA/hAT-Blackjack	0.01	MER5A	0.01
	Satellite/telo	0.00	LSU-rRNA_Hs	0.01
	LTR/Gypsy	0.00	L2b	0.01

Supplementary Figure 1494: Properties and genomic distribution of motifs identified for the ZNF619 transcription factor in HEK293 (accession ChipExo models).

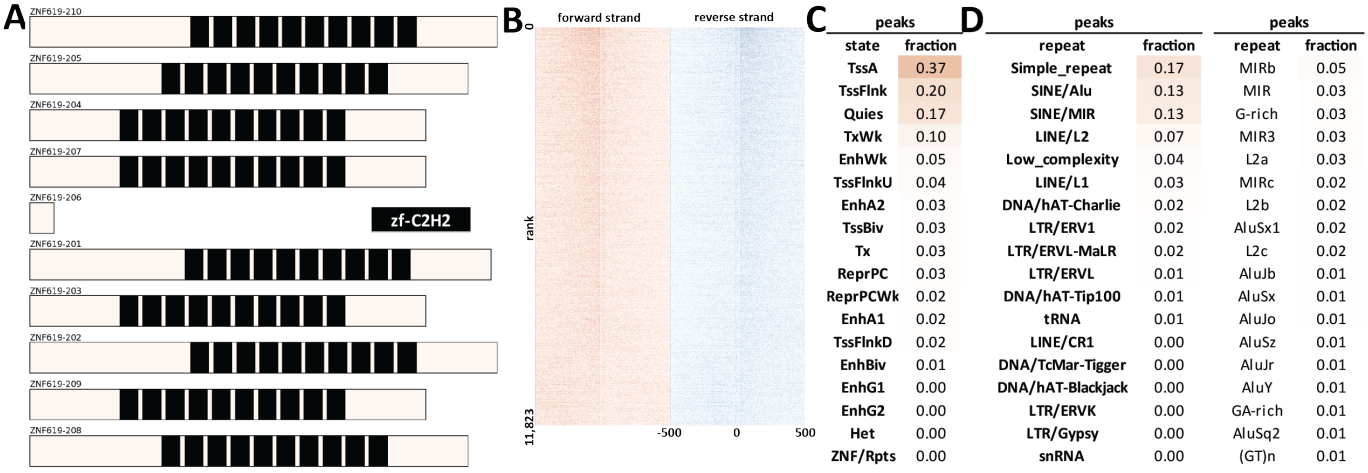

C

peaks	
state	fraction
TssA	0.37
TssFlnk	0.20
Quies	0.17
TxWk	0.10
EnhWk	0.05
TssFlnkU	0.04
EnhA2	0.03
TssBiv	0.03
Tx	0.03
ReprPC	0.03
ReprPCWk	0.02
EnhA1	0.02
TssFlnkD	0.02
EnhBiv	0.01
EnhG1	0.00
EnhG2	0.00
Het	0.00
ZNF/Rpts	0.00

D

peaks		peaks	
repeat	fraction	repeat	fraction
Simple_repeat	0.17	MIRb	0.05
SINE/Alu	0.13	MIR	0.03
SINE/MIR	0.13	G-rich	0.03
LINE/L2	0.07	MIR3	0.03
Low_complexity	0.04	L2a	0.03
LINE/L1	0.03	MIRc	0.02
DNA/hAT-Charlie	0.02	L2b	0.02
LTR/ERV1	0.02	AluSx1	0.02
LTR/ERVL-MaLR	0.02	L2c	0.02
LTR/ERVL	0.01	AluJb	0.01
DNA/hAT-Tip100	0.01	AluSx	0.01
tRNA	0.01	AluJo	0.01
LINE/CR1	0.00	AluSz	0.01
DNA/TcMar-Tigger	0.00	AluJr	0.01
DNA/hAT-Blackjack	0.00	AluY	0.01
LTR/ERVK	0.00	GA-rich	0.01
LTR/Gypsy	0.00	AluSq2	0.01
snRNA	0.00	(GT)n	0.01

E

Ontology	Term	FDR Q-val
GO Biological Process	regulation of transcription from RNA polymerase II promoter in response to stress	34.34
GO Biological Process	liver regeneration	32.83
GO Biological Process	nuclear-transcribed mRNA catabolic process, nonsense-mediated decay	32.71
GO Biological Process	mRNA catabolic process	30.68
GO Biological Process	rRNA processing	30.22
GO Biological Process	nuclear-transcribed mRNA catabolic process	30.23
GO Biological Process	rRNA metabolic process	29.83
GO Biological Process	regulation of DNA-templated transcription in response to stress	29.29
GO Biological Process	regulation of cellular amino acid metabolic process	25.20
GO Biological Process	macromolecular complex disassembly	23.55
GO Biological Process	viral transcription	22.37
GO Biological Process	mitochondrial translational termination	22.25
GO Biological Process	protein complex disassembly	22.15
GO Biological Process	multi-organism metabolic process	21.93
GO Biological Process	viral gene expression	21.83
GO Biological Process	cellular protein complex disassembly	21.39
GO Biological Process	mitochondrial translational elongation	21.05
GO Biological Process	translational elongation	20.47
GO Biological Process	translational termination	20.05
GO Biological Process	cotranslational protein targeting to membrane	19.74
Human Phenotype	Increased serum lactate	16.05
Human Phenotype	Exercise intolerance	14.27
Human Phenotype	Lipid accumulation in hepatocytes	9.18
Human Phenotype	Glycosuria	8.68
Human Phenotype	Dysphonia	7.27
Human Phenotype	Delayed epiphyseal ossification	5.90

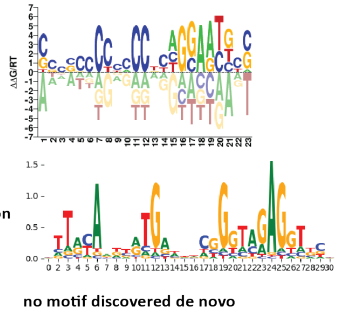

Supplementary Figure 1495: Properties and genomic distribution of motifs identified for the ZNF619 transcription factor in HepG2 (accession ENCSR613RDS).

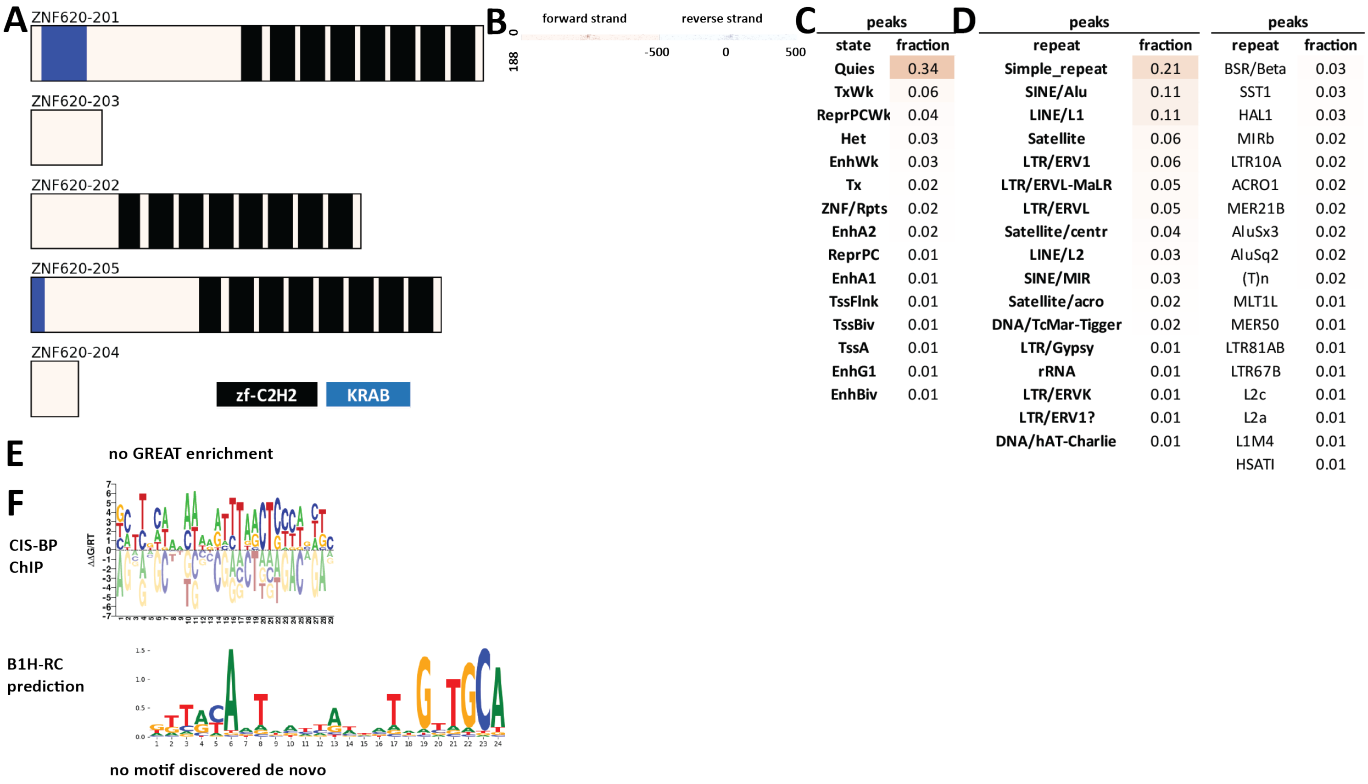

Supplementary Figure 1496: Properties and genomic distribution of motifs identified for the ZNF620 transcription factor in HEK293 (accession ChipExo models).

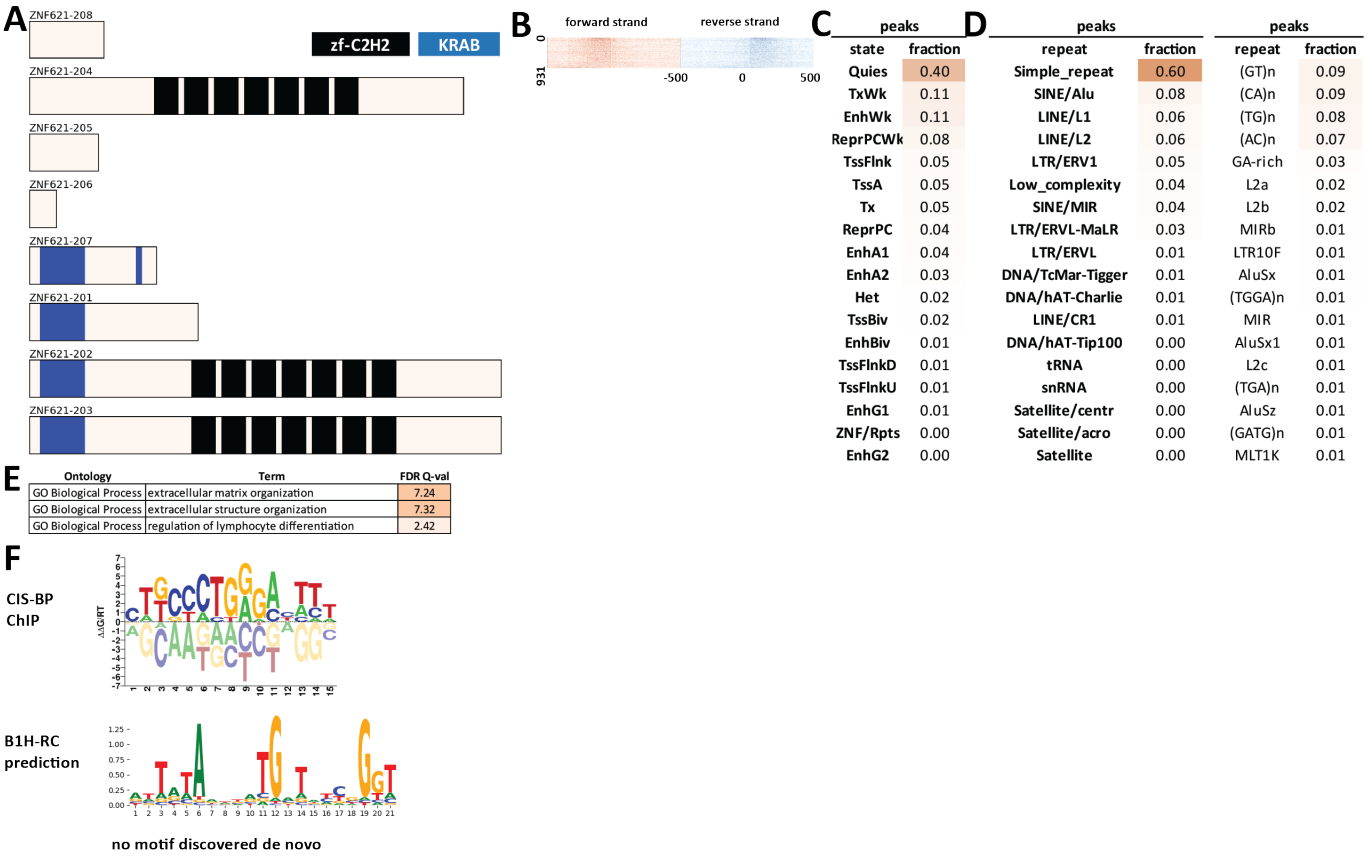

peaks	
state	fraction
Quies	0.40
TxWk	0.11
EnhWk	0.11
ReprPCWk	0.08
TssFlnk	0.05
TssA	0.05
Tx	0.05
ReprPC	0.04
EnhA1	0.04
EnhA2	0.03
Het	0.02
TssBiv	0.02
EnhBiv	0.01
TssFlnkD	0.01
TssFlnkU	0.01
EnhG1	0.01
ZNF/Rpts	0.00
EnhG2	0.00

peaks	
repeat	fraction
Simple_repeat	0.60
SINE/Alu	0.08
LINE/L1	0.06
LINE/L2	0.06
LTR/ERV1	0.05
Low_complexity	0.04
SINE/MIR	0.04
LTR/ERVL-MaLR	0.03
LTR/ERVL	0.01
DNA/TcMar-Tigger	0.01
DNA/hAT-Charlie	0.01
LINE/CR1	0.01
DNA/hAT-Tip100	0.00
tRNA	0.00
snRNA	0.00
Satellite/centr	0.00
Satellite/acro	0.00
Satellite	0.00

peaks	
repeat	fraction
(GT)n	0.09
(CA)n	0.09
(TG)n	0.08
(AC)n	0.07
GA-rich	0.03
L2a	0.02
L2b	0.02
MIRb	0.01
LTR10F	0.01
AluSx	0.01
(TGGA)n	0.01
MIR	0.01
AluSx1	0.01
L2c	0.01
(TGA)n	0.01
AluSz	0.01
(GATG)n	0.01
MLT1K	0.01

Ontology	Term	FDR Q-val
GO Biological Process	extracellular matrix organization	7.24
GO Biological Process	extracellular structure organization	7.32
GO Biological Process	regulation of lymphocyte differentiation	2.42

Supplementary Figure 1497: Properties and genomic distribution of motifs identified for the ZNF621 transcription factor in HEK293 (accession ENCSR858FAN).

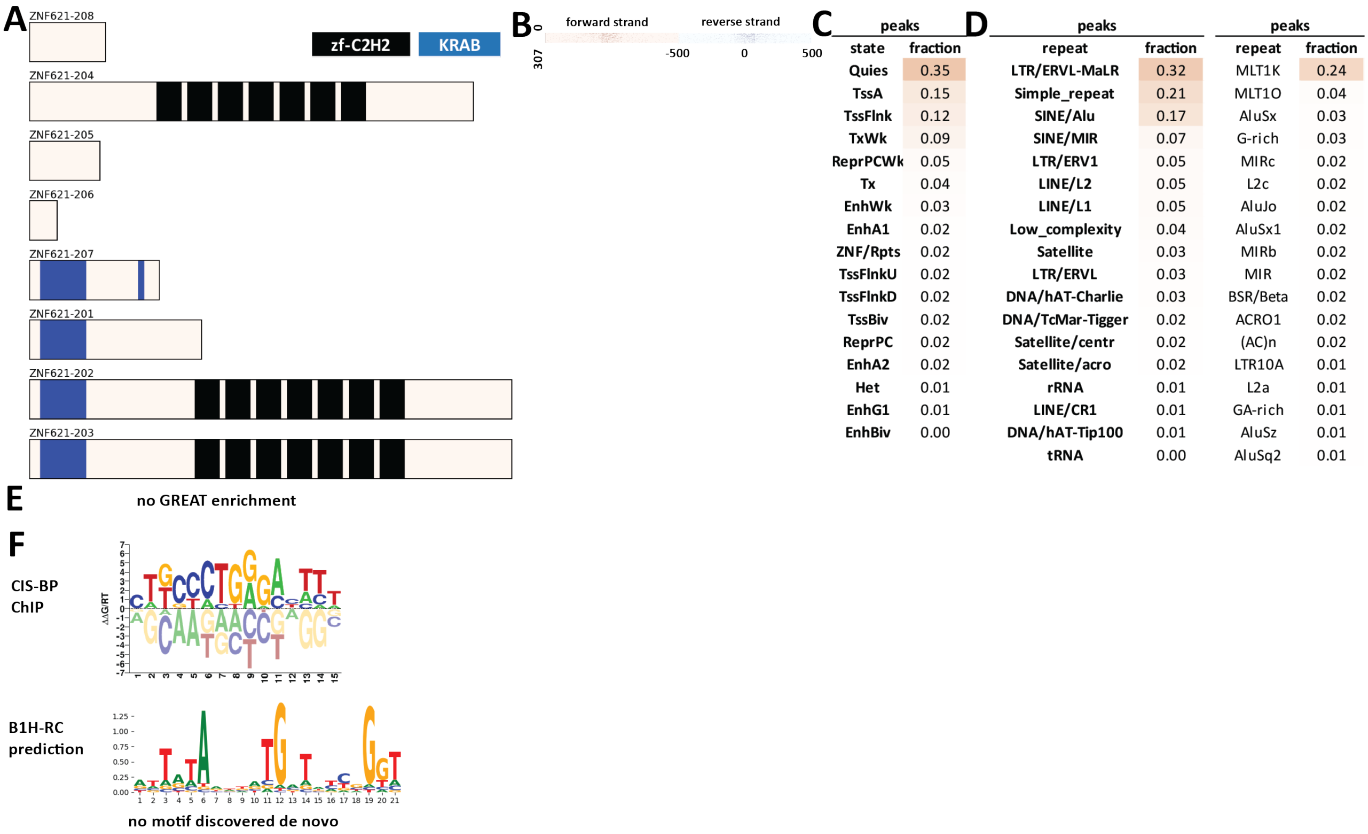

Supplementary Figure 1498: Properties and genomic distribution of motifs identified for the ZNF621 transcription factor in HEK293 (accession ChipExo models).

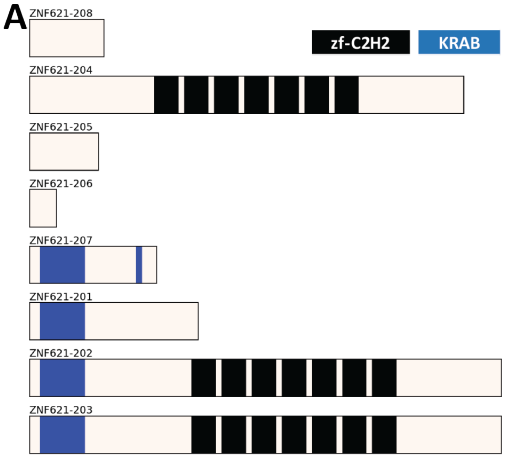

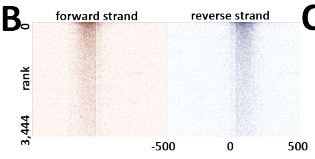

C

peaks	
state	fraction
TssA	0.30
Quies	0.25
TssFlnk	0.22
EnhWk	0.12
TxWk	0.08
EnhA1	0.05
EnhA2	0.04
TssBiv	0.02
ReprPCWk	0.02
Tx	0.02
TssFlnkU	0.01
ReprPC	0.01
TssFlnkD	0.01
Het	0.01
EnhG1	0.01
EnhBiv	0.00
ZNF/Rpts	0.00
EnhG2	0.00

D

peaks		peaks	
repeat	fraction	repeat	fraction
LTR/ERVL-MaLR	0.14	MLT1K	0.08
Simple_repeat	0.08	MLT1O	0.02
LTR/ERV1	0.05	G-rich	0.01
SINE/Alu	0.03	LTR45B	0.01
LINE/L1	0.03	L2a	0.01
SINE/MIR	0.03	MIRb	0.01
LINE/L2	0.03	L2c	0.01
LTR/ERVL	0.03	L2b	0.01
Low_complexity	0.02	MIR3	0.01
DNA/hAT-Charlie	0.01	GA-rich	0.01
LTR/ERVK	0.01	MIRc	0.01
DNA/hAT-Tip100	0.00	MIR	0.01
LINE/CR1	0.00	AluJo	0.00
DNA/TcMar-Tigger	0.00	AluJb	0.00
tRNA	0.00	MLT1H	0.00
LINE/RTE-X	0.00	MLT1N2	0.00
SINE/tRNA-RTE	0.00	MLT1J	0.00
LTR/Gypsy?	0.00	MER50	0.00

E

Ontology	Term	FDR Q-val
GO Biological Process	secondary alcohol metabolic process	4.30
GO Biological Process	mitochondrial membrane organization	4.28
GO Biological Process	negative regulation of chromatin organization	3.15
GO Biological Process	interstrand cross-link repair	3.03
GO Biological Process	alcohol biosynthetic process	2.25
Human Phenotype	Abnormality of adipose tissue	1.54

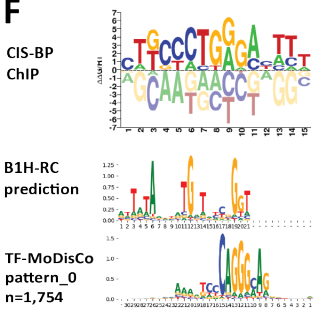

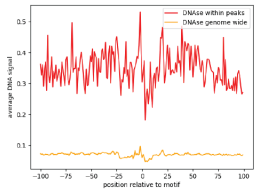

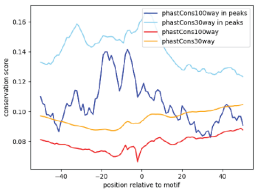

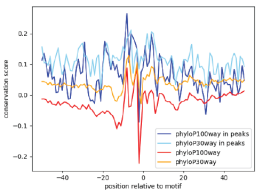

Supplementary Figure 1499: Properties and genomic distribution of motifs identified for the ZNF621 transcription factor in HEK293 (accession Hughes NB models).

TF-MoDisCO pattern_0 n=1754, CWM

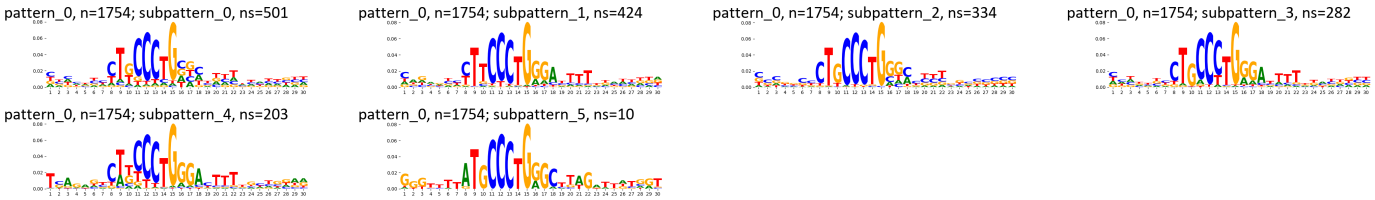

TF-MoDisCO pattern_0 n=1754, PWM

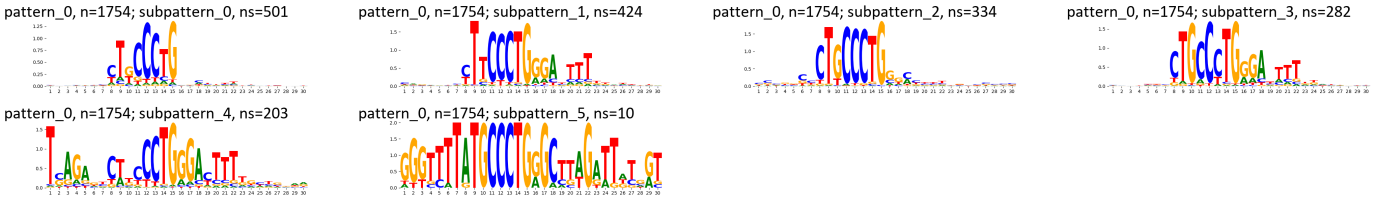

Supplementary Figure 1500: TF-MoDisCO subpatterns for the ZNF621 transcription factor in HEK293 (accession Hughes NB models).

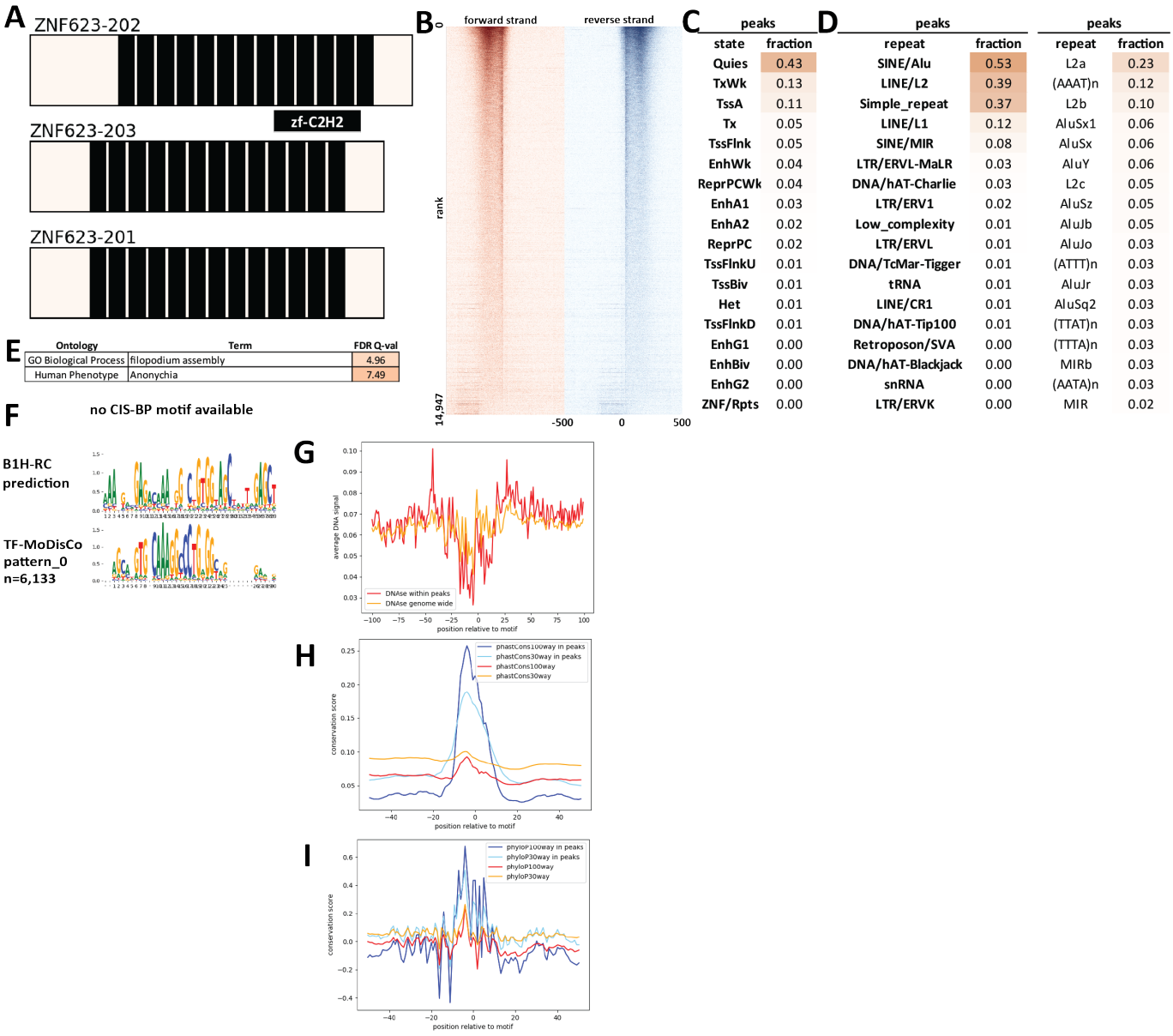

Supplementary Figure 1501: Properties and genomic distribution of motifs identified for the ZNF623 transcription factor in HEK293 (accession ENCSR022IZK).

TF-MoDisCO pattern_0 n=6133, CWM

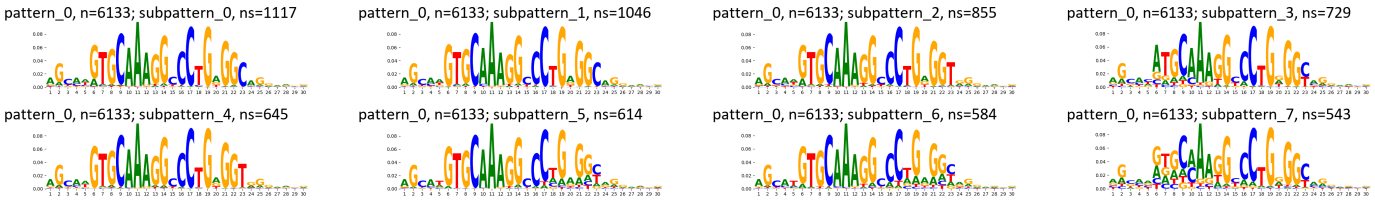

TF-MoDisCO pattern_0 n=6133, PWM

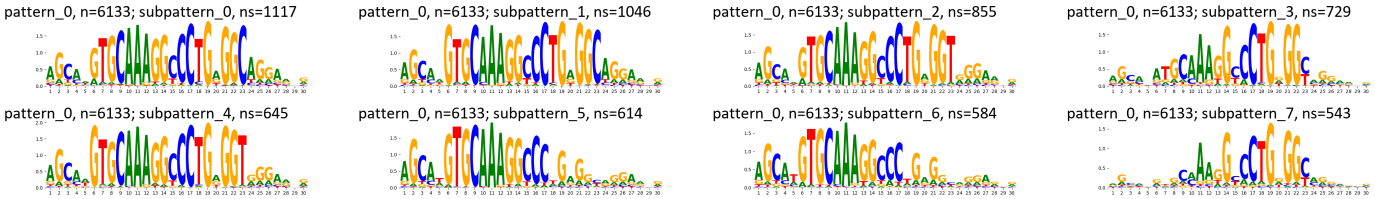

Supplementary Figure 1502: TF-MoDisCO subpatterns for the ZNF623 transcription factor in HEK293 (accession ENCSR022IZK).

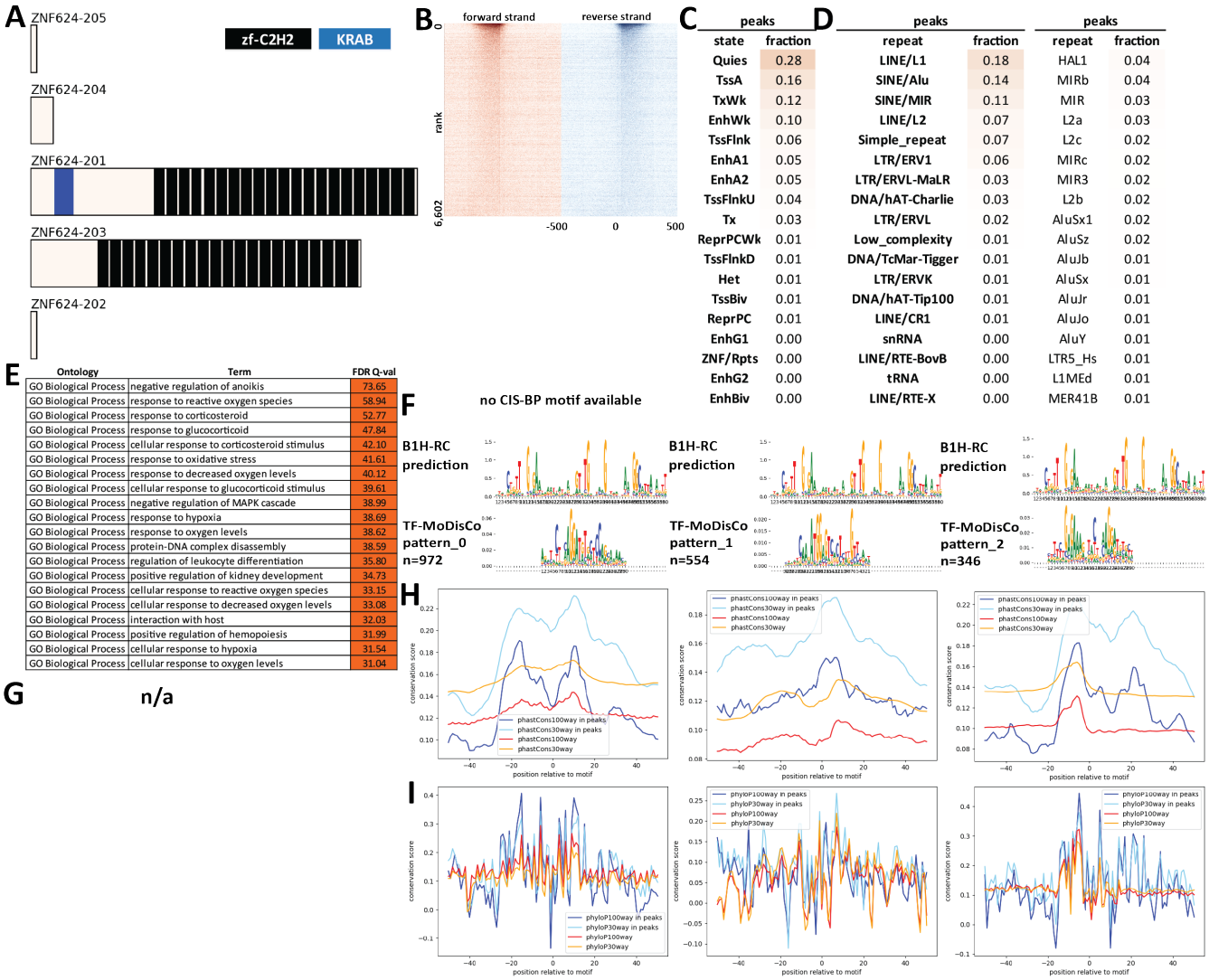

Supplementary Figure 1503: Properties and genomic distribution of motifs identified for the ZNF624 transcription factor in A549 (accession ENCSR419VVI).

TF-MoDisCO pattern_0 n=972, CWM

pattern_0, n=972; subpattern_0, ns=200

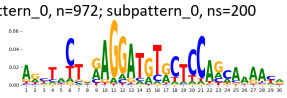

pattern_0, n=972; subpattern_1, ns=161

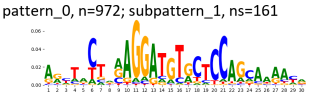

pattern_0, n=972; subpattern_2, ns=141

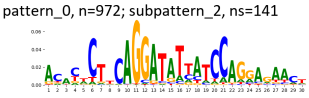

pattern_0, n=972; subpattern_3, ns=137

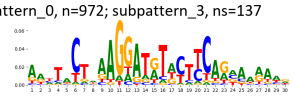

pattern_0, n=972; subpattern_4, ns=111

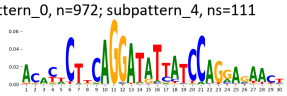

pattern_0, n=972; subpattern_5, ns=107

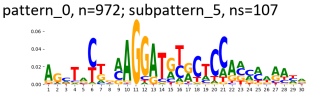

pattern_0, n=972; subpattern_6, ns=102

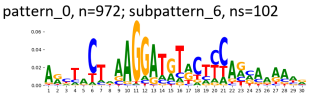

pattern_0, n=972; subpattern_7, ns=7

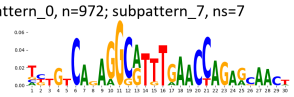

pattern_0, n=972; subpattern_8, ns=6

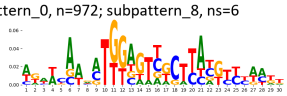

TF-MoDisCO pattern_0 n=972, PWM

pattern_0, n=972; subpattern_0, ns=200

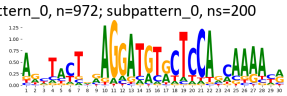

pattern_0, n=972; subpattern_1, ns=161

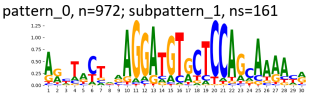

pattern_0, n=972; subpattern_2, ns=141

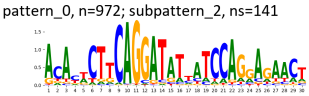

pattern_0, n=972; subpattern_3, ns=137

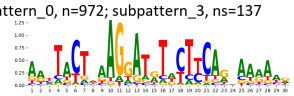

pattern_0, n=972; subpattern_4, ns=111

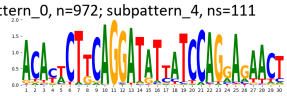

pattern_0, n=972; subpattern_5, ns=107

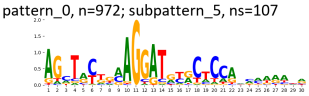

pattern_0, n=972; subpattern_6, ns=102

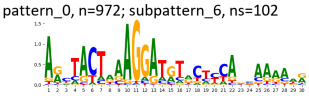

pattern_0, n=972; subpattern_7, ns=7

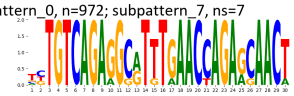

pattern_0, n=972; subpattern_8, ns=6

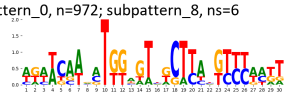

TF-MoDisCO pattern_1 n=554, CWM

pattern_1, n=554; subpattern_0, ns=135

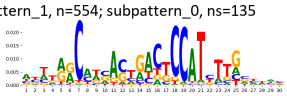

pattern_1, n=554; subpattern_1, ns=126

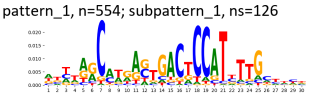

pattern_1, n=554; subpattern_2, ns=82

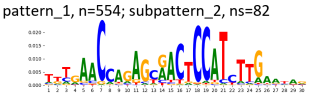

pattern_1, n=554; subpattern_3, ns=74

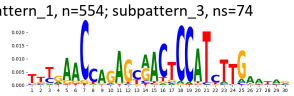

pattern_1, n=554; subpattern_4, ns=59

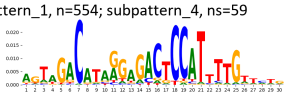

pattern_1, n=554; subpattern_5, ns=44

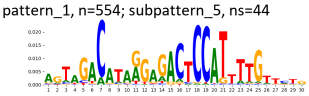

pattern_1, n=554; subpattern_6, ns=34

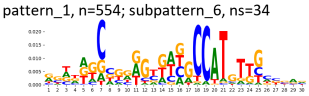

TF-MoDisCO pattern_1 n=554, PWM

pattern_1, n=554; subpattern_0, ns=135

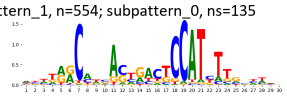

pattern_1, n=554; subpattern_1, ns=126

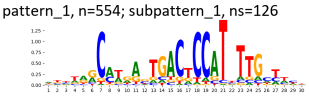

pattern_1, n=554; subpattern_2, ns=82

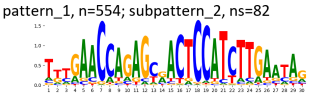

pattern_1, n=554; subpattern_3, ns=74

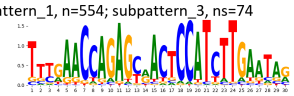

pattern_1, n=554; subpattern_4, ns=59

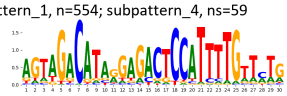

pattern_1, n=554; subpattern_5, ns=44

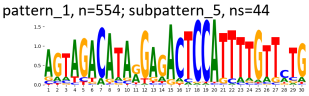

pattern_1, n=554; subpattern_6, ns=34

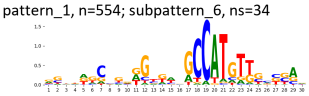

TF-MoDisCO pattern_2 n=346, CWM

pattern_2, n=346; subpattern_0, ns=97

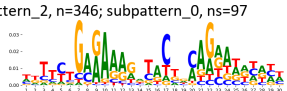

pattern_2, n=346; subpattern_1, ns=74

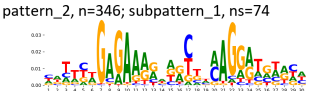

pattern_2, n=346; subpattern_2, ns=70

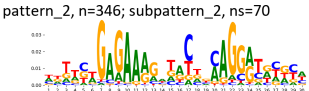

pattern_2, n=346; subpattern_3, ns=53

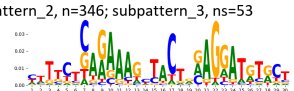

pattern_2, n=346; subpattern_4, ns=45

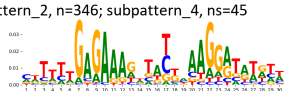

pattern_2, n=346; subpattern_5, ns=7

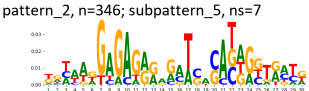

TF-MoDisCO pattern_2 n=346, PWM

pattern_2, n=346; subpattern_0, ns=97

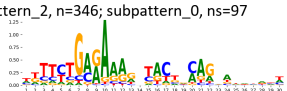

pattern_2, n=346; subpattern_1, ns=74

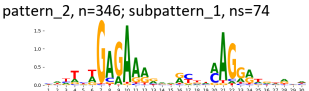

pattern_2, n=346; subpattern_2, ns=70

pattern_2, n=346; subpattern_3, ns=53

pattern_2, n=346; subpattern_4, ns=45

pattern_2, n=346; subpattern_5, ns=7

Supplementary Figure 1504: TF-MoDisCO subpatterns for the ZNF624 transcription factor in A549 (accession ENCSR419VVI).

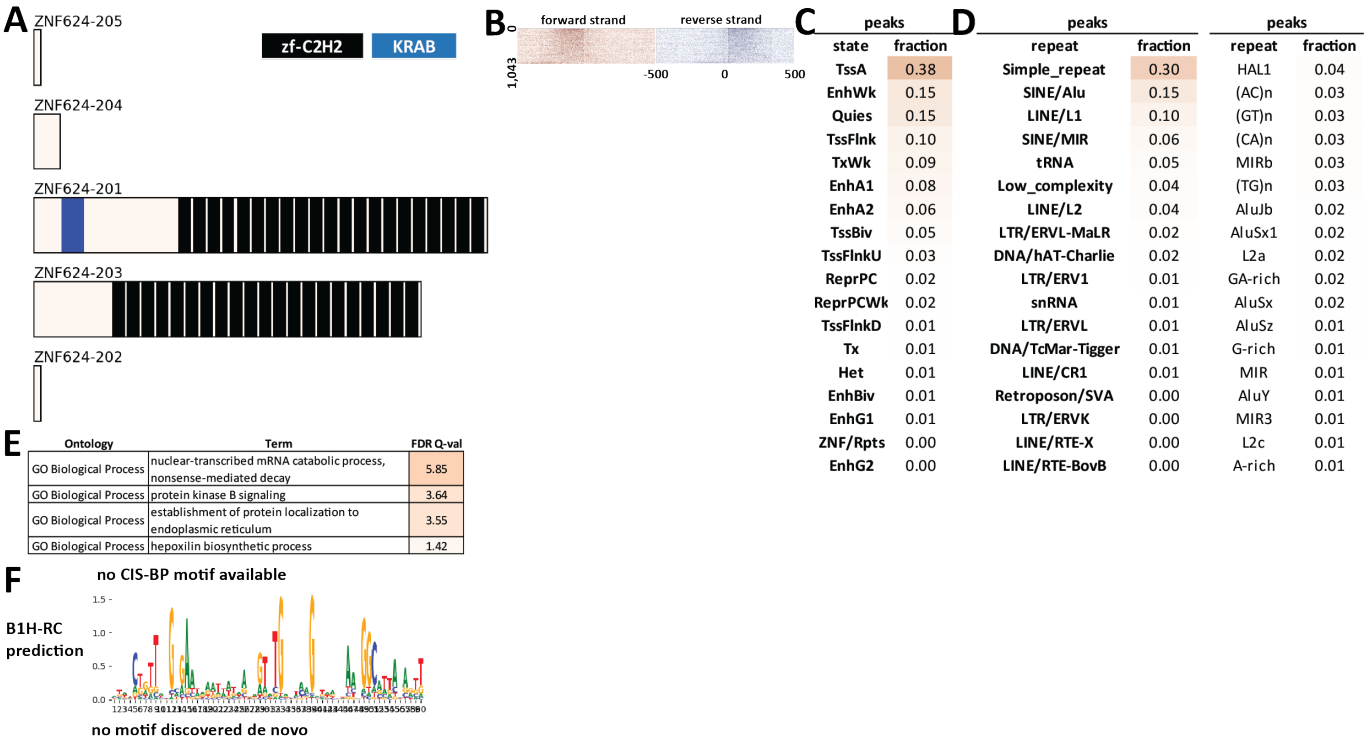

Supplementary Figure 1505: Properties and genomic distribution of motifs identified for the ZNF624 transcription factor in HEK293 (accession ENCSR878DES).

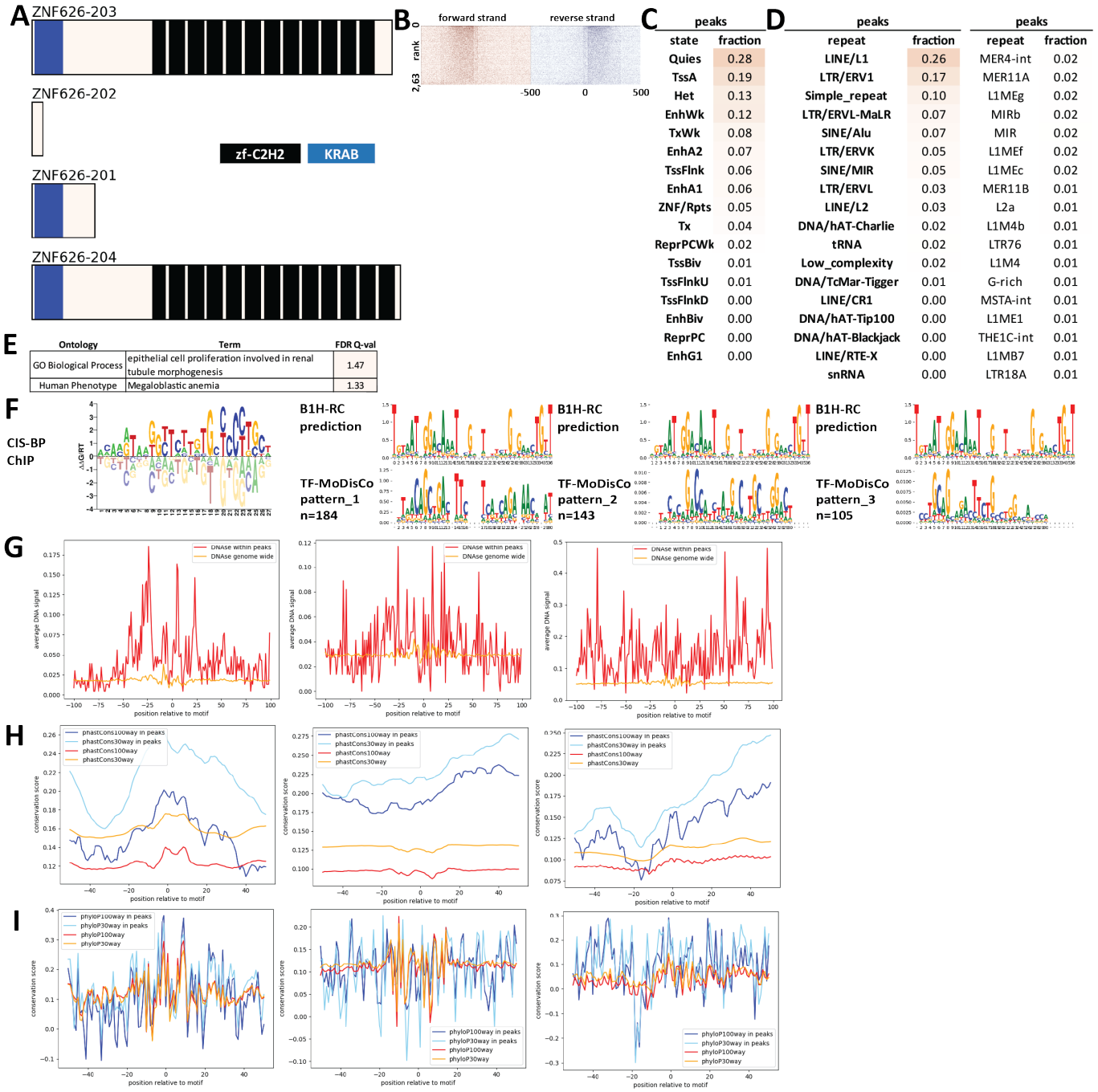

Supplementary Figure 1506: Properties and genomic distribution of motifs identified for the ZNF626 transcription factor in HEK293 (accession ENCSR588MQZ).

TF-MoDisCO pattern_1 n=184, CWM

pattern_1, n=184; subpattern_0, ns=73

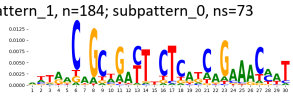

pattern_1, n=184; subpattern_1, ns=73

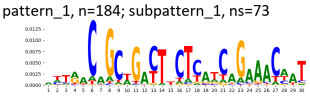

pattern_1, n=184; subpattern_2, ns=34

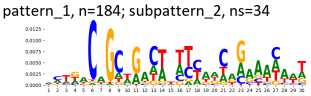

pattern_1, n=184; subpattern_3, ns=2

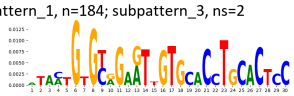

pattern_1, n=184; subpattern_4, ns=2

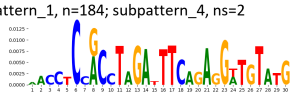

TF-MoDisCO pattern_1 n=184, PWM

pattern_1, n=184; subpattern_0, ns=73

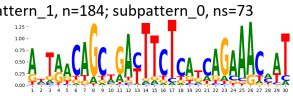

pattern_1, n=184; subpattern_1, ns=73

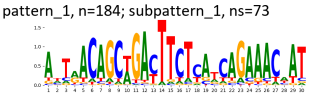

pattern_1, n=184; subpattern_2, ns=34

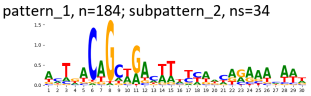

pattern_1, n=184; subpattern_3, ns=2

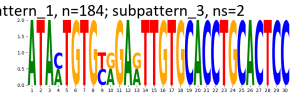

pattern_1, n=184; subpattern_4, ns=2

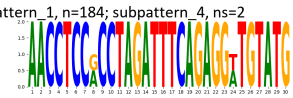

TF-MoDisCO pattern_2 n=143, CWM

pattern_2, n=143; subpattern_0, ns=66

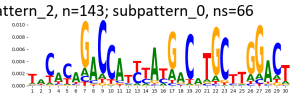

pattern_2, n=143; subpattern_1, ns=56

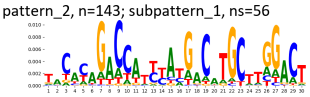

pattern_2, n=143; subpattern_2, ns=21

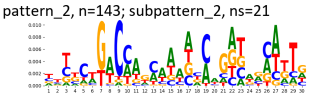

TF-MoDisCO pattern_2 n=143, PWM

pattern_2, n=143; subpattern_0, ns=66

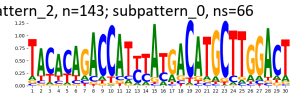

pattern_2, n=143; subpattern_1, ns=56

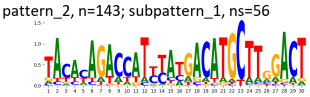

pattern_2, n=143; subpattern_2, ns=21

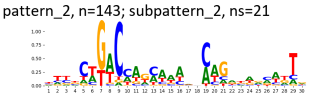

TF-MoDisCO pattern_3 n=105, CWM

pattern_3, n=105; subpattern_0, ns=44

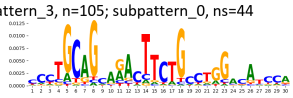

pattern_3, n=105; subpattern_1, ns=35

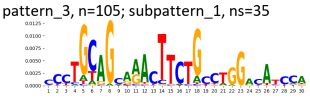

pattern_3, n=105; subpattern_2, ns=21

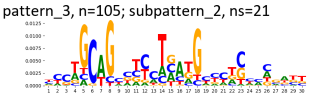

pattern_3, n=105; subpattern_3, ns=5

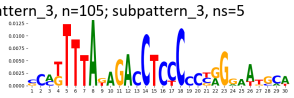

TF-MoDisCO pattern_3 n=105, PWM

pattern_3, n=105; subpattern_0, ns=44

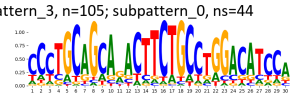

pattern_3, n=105; subpattern_1, ns=35

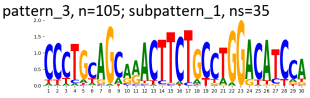

pattern_3, n=105; subpattern_2, ns=21

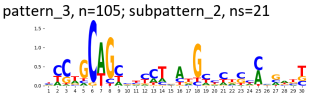

pattern_3, n=105; subpattern_3, ns=5

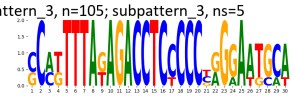

Supplementary Figure 1507: TF-MoDisCO subpatterns for the ZNF626 transcription factor in HEK293 (accession ENCSR588MQZ).

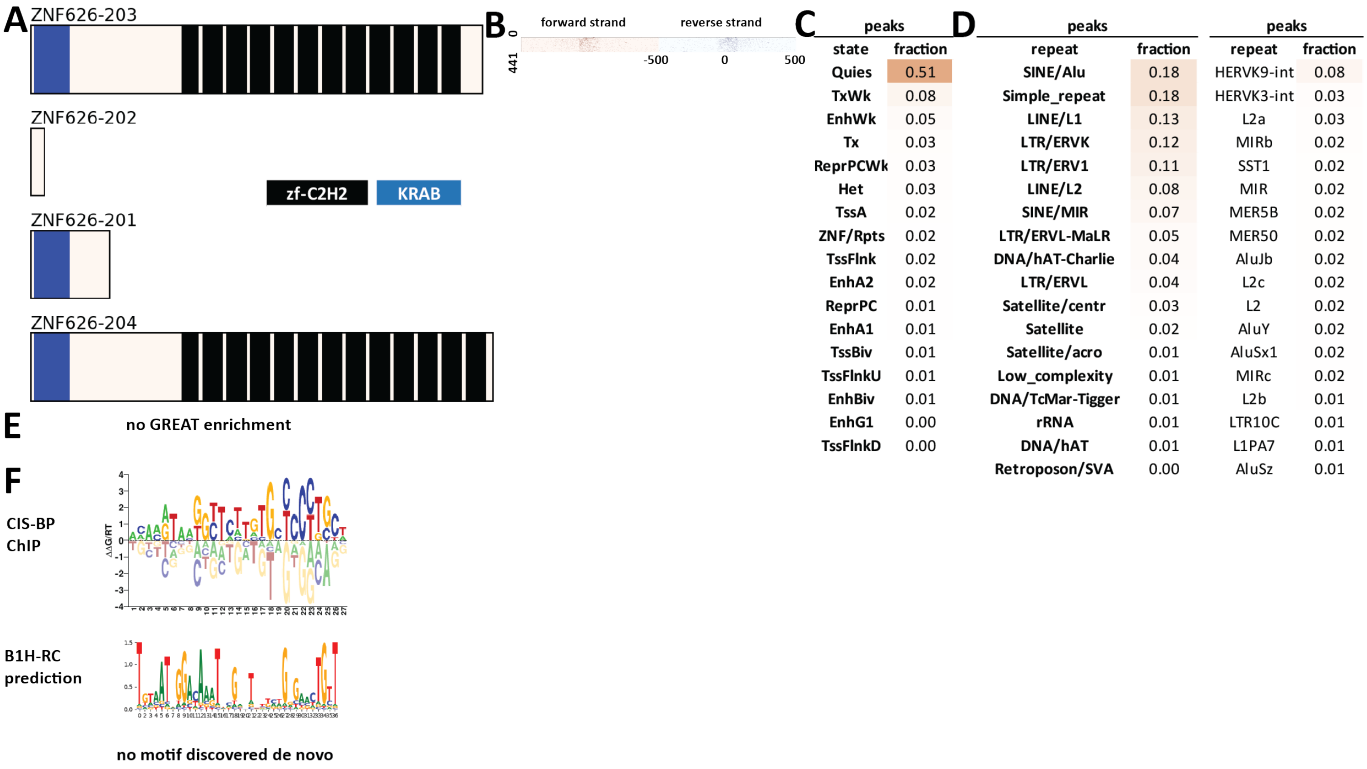

Supplementary Figure 1508: Properties and genomic distribution of motifs identified for the ZNF626 transcription factor in HEK293 (accession ChipExo models).

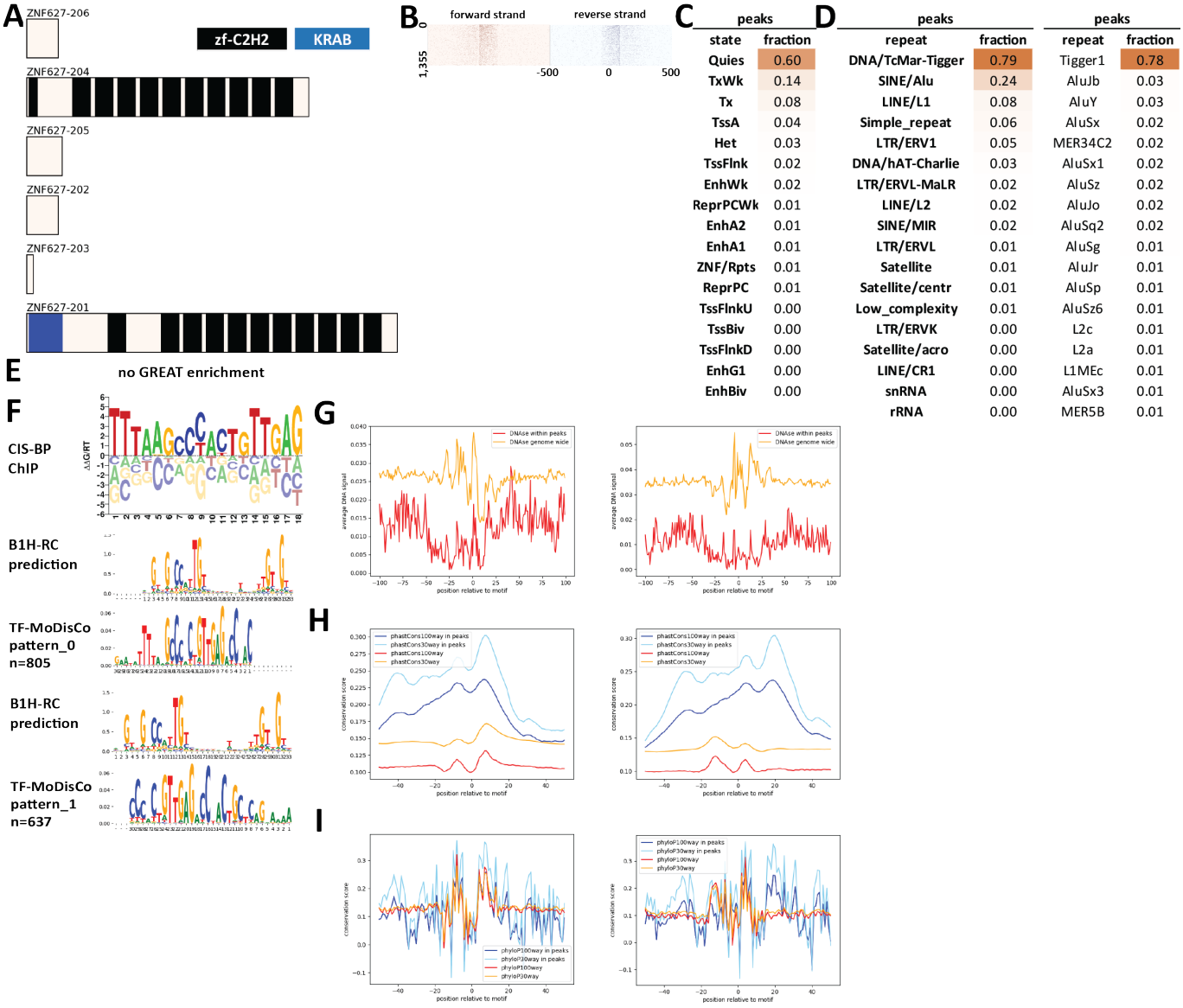

Supplementary Figure 1509: Properties and genomic distribution of motifs identified for the ZNF627 transcription factor in HEK293 (accession ChipExo models).

TF-MoDisCO pattern_0 n=805, CWM

pattern_0, n=805; subpattern_0, ns=342

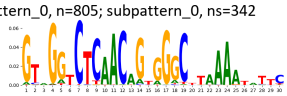

pattern_0, n=805; subpattern_1, ns=291

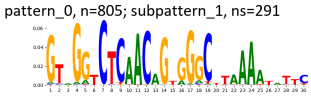

pattern_0, n=805; subpattern_2, ns=61

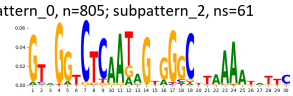

pattern_0, n=805; subpattern_3, ns=55

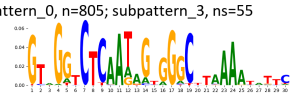

pattern_0, n=805; subpattern_4, ns=53

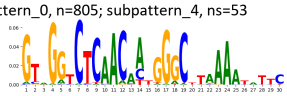

pattern_0, n=805; subpattern_5, ns=3

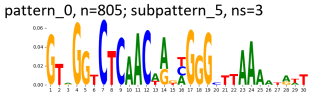

TF-MoDisCO pattern_0 n=805, PWM

pattern_0, n=805; subpattern_0, ns=342

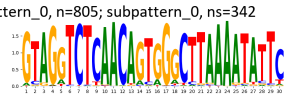

pattern_0, n=805; subpattern_1, ns=291

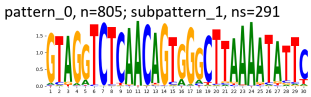

pattern_0, n=805; subpattern_2, ns=61

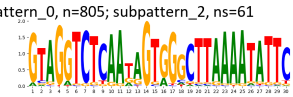

pattern_0, n=805; subpattern_3, ns=55

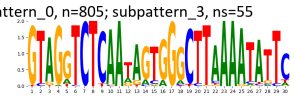

pattern_0, n=805; subpattern_4, ns=53

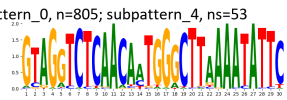

pattern_0, n=805; subpattern_5, ns=3

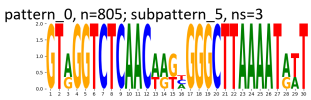

TF-MoDisCO pattern_1 n=637, CWM

pattern_1, n=637; subpattern_0, ns=278

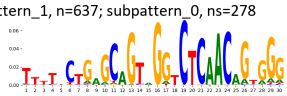

pattern_1, n=637; subpattern_1, ns=250

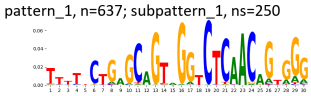

pattern_1, n=637; subpattern_2, ns=51

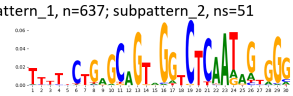

pattern_1, n=637; subpattern_3, ns=37

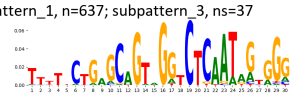

pattern_1, n=637; subpattern_4, ns=21

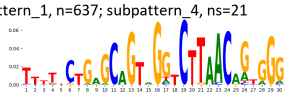

TF-MoDisCO pattern_1 n=637, PWM

pattern_1, n=637; subpattern_0, ns=278

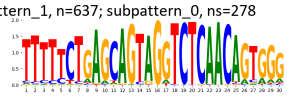

pattern_1, n=637; subpattern_1, ns=250

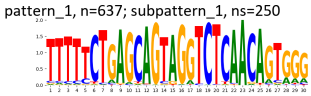

pattern_1, n=637; subpattern_2, ns=51

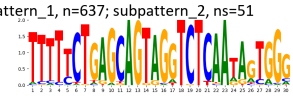

pattern_1, n=637; subpattern_3, ns=37

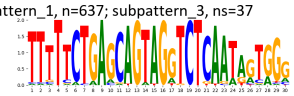

pattern_1, n=637; subpattern_4, ns=21

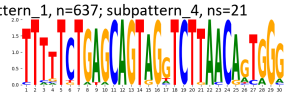

Supplementary Figure 1510: TF-MoDisCO subpatterns for the ZNF627 transcription factor in HEK293 (accession ChipExo models).

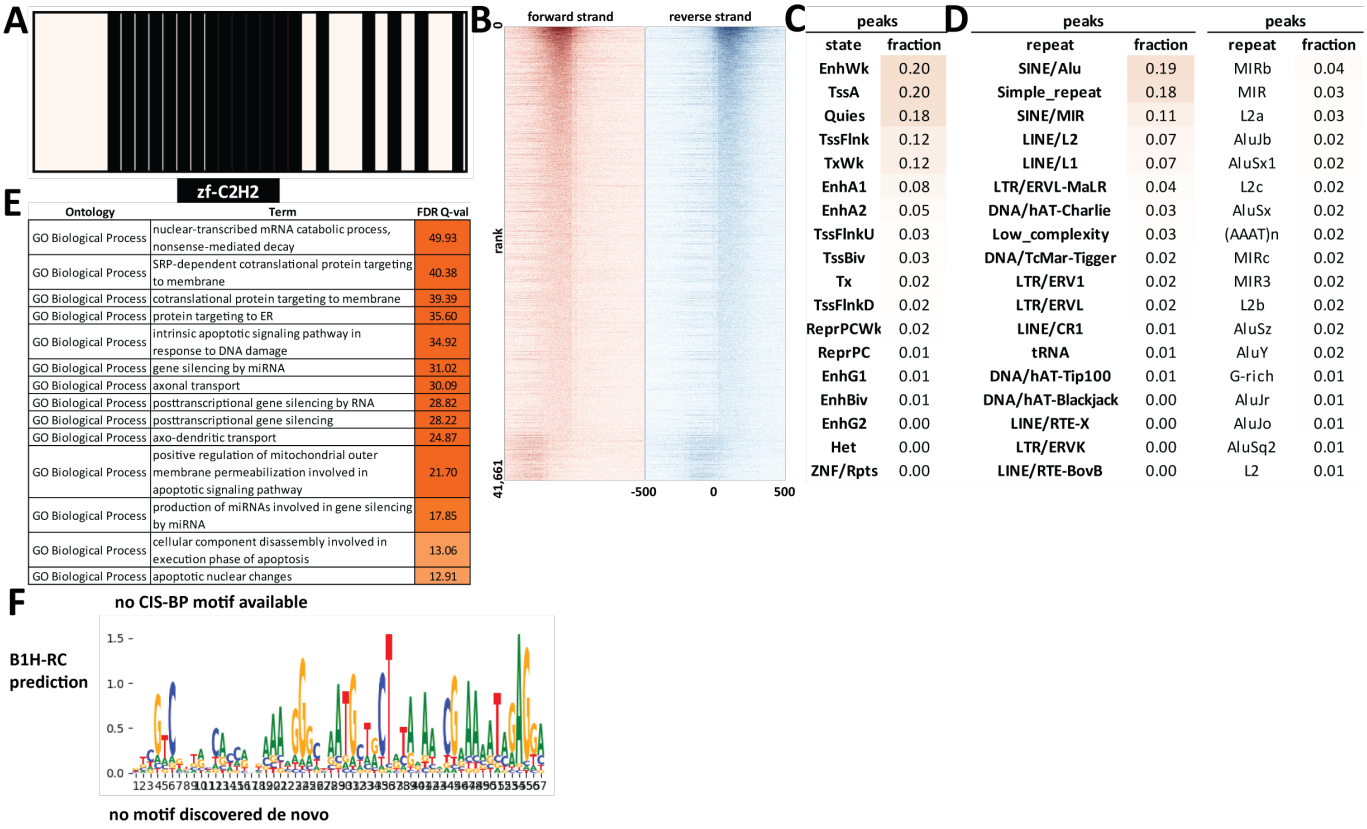

Supplementary Figure 1511: Properties and genomic distribution of motifs identified for the ZNF629 transcription factor in HEK293 (accession ENCSR351NON).

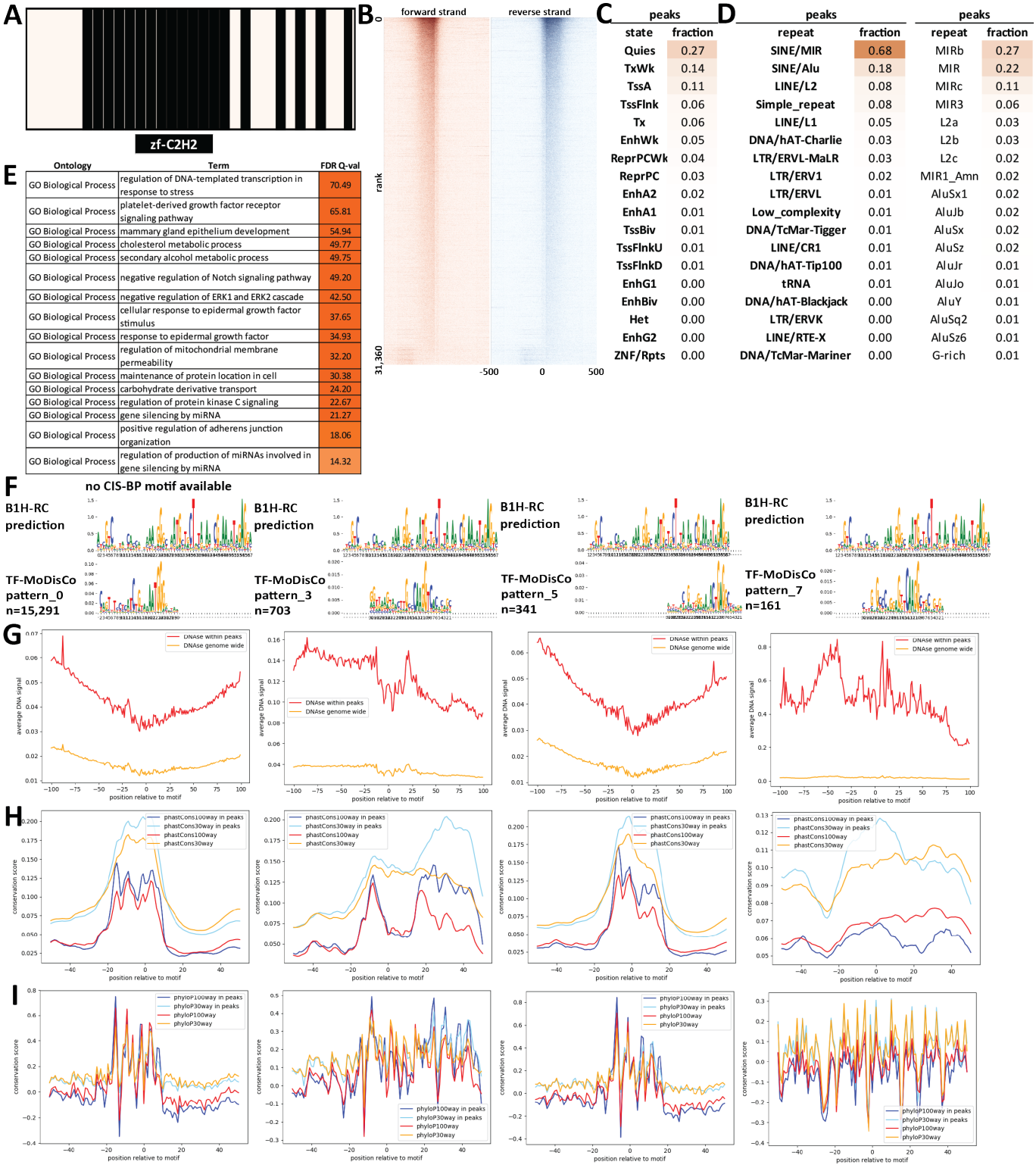

Supplementary Figure 1512: Properties and genomic distribution of motifs identified for the ZNF629 transcription factor in HepG2 (accession ENCSR363ASY).

TF-MoDisCO pattern_0 n=15291, CWM

pattern_0, n=15291; subpattern_0, ns=2776

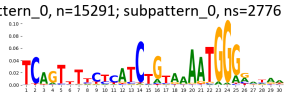

pattern_0, n=15291; subpattern_1, ns=2255

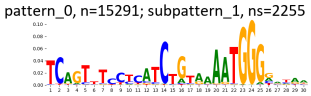

pattern_0, n=15291; subpattern_2, ns=2139

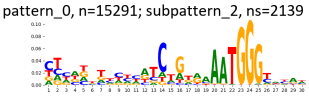

pattern_0, n=15291; subpattern_3, ns=2131

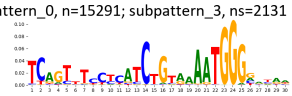

pattern_0, n=15291; subpattern_4, ns=1623

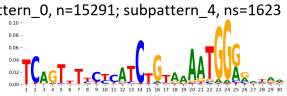

pattern_0, n=15291; subpattern_5, ns=1611

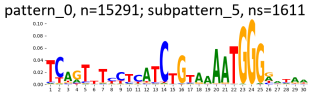

pattern_0, n=15291; subpattern_6, ns=1571

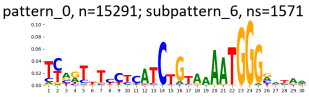

pattern_0, n=15291; subpattern_7, ns=875

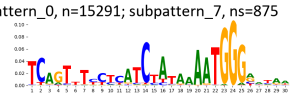

pattern_0, n=15291; subpattern_8, ns=310

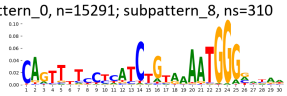

TF-MoDisCO pattern_0 n=15291, PWM

pattern_0, n=15291; subpattern_0, ns=2776

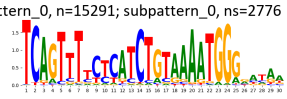

pattern_0, n=15291; subpattern_1, ns=2255

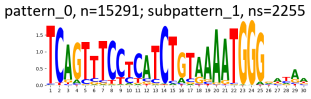

pattern_0, n=15291; subpattern_2, ns=2139

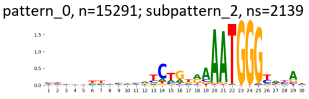

pattern_0, n=15291; subpattern_3, ns=2131

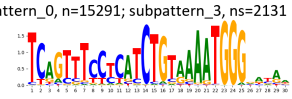

pattern_0, n=15291; subpattern_4, ns=1623

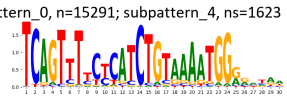

pattern_0, n=15291; subpattern_5, ns=1611

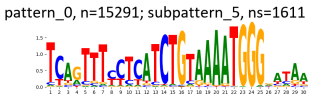

pattern_0, n=15291; subpattern_6, ns=1571

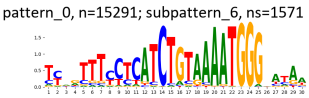

pattern_0, n=15291; subpattern_7, ns=875

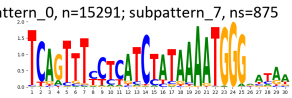

pattern_0, n=15291; subpattern_8, ns=310

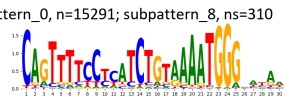

TF-MoDisCO pattern_3 n=703, CWM

pattern_3, n=703; subpattern_0, ns=179

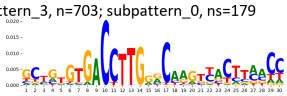

pattern_3, n=703; subpattern_1, ns=178

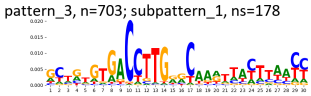

pattern_3, n=703; subpattern_2, ns=160

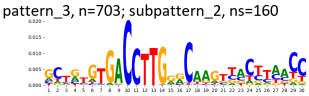

pattern_3, n=703; subpattern_3, ns=69

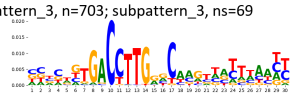

pattern_3, n=703; subpattern_4, ns=68

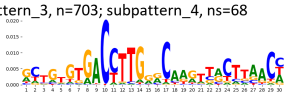

pattern_3, n=703; subpattern_5, ns=31

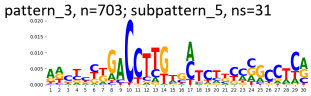

pattern_3, n=703; subpattern_6, ns=18

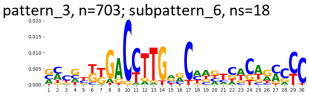

TF-MoDisCO pattern_3 n=703, PWM

pattern_3, n=703; subpattern_0, ns=179

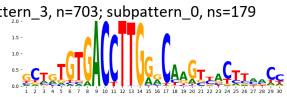

pattern_3, n=703; subpattern_1, ns=178

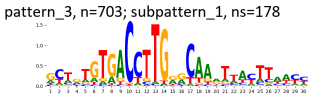

pattern_3, n=703; subpattern_2, ns=160

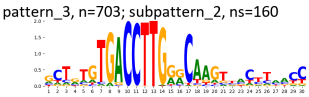

pattern_3, n=703; subpattern_3, ns=69

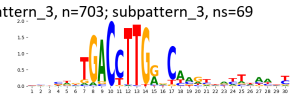

pattern_3, n=703; subpattern_4, ns=68

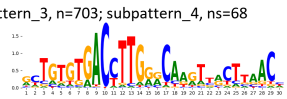

pattern_3, n=703; subpattern_5, ns=31

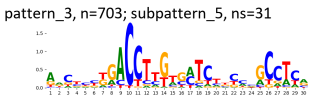

pattern_3, n=703; subpattern_6, ns=18

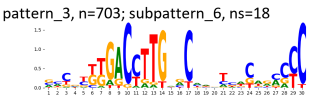

TF-MoDisCO pattern_5 n=341, CWM

pattern_5, n=341; subpattern_0, ns=102

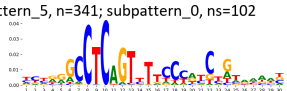

pattern_5, n=341; subpattern_1, ns=86

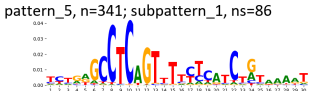

pattern_5, n=341; subpattern_2, ns=59

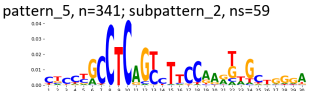

pattern_5, n=341; subpattern_3, ns=50

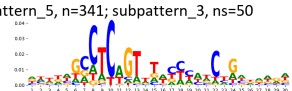

pattern_5, n=341; subpattern_4, ns=33

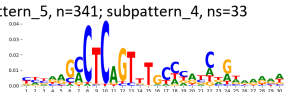

pattern_5, n=341; subpattern_5, ns=7

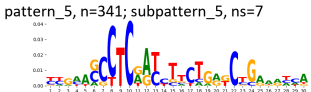

pattern_5, n=341; subpattern_6, ns=4

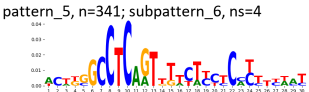

TF-MoDisCO pattern_5 n=341, PWM

pattern_5, n=341; subpattern_0, ns=102

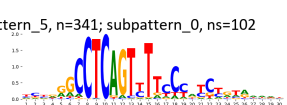

pattern_5, n=341; subpattern_1, ns=86

pattern_5, n=341; subpattern_2, ns=59

pattern_5, n=341; subpattern_3, ns=50

pattern_5, n=341; subpattern_4, ns=33

pattern_5, n=341; subpattern_5, ns=7

pattern_5, n=341; subpattern_6, ns=4

TF-MoDisCO pattern_7 n=161, CWM

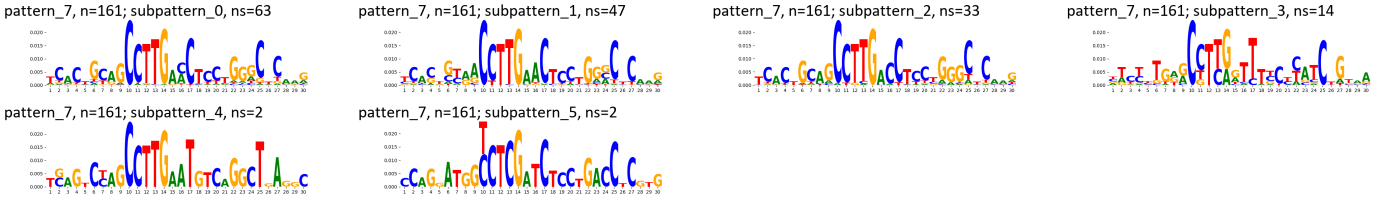

TF-MoDisCO pattern_7 n=161, PWM

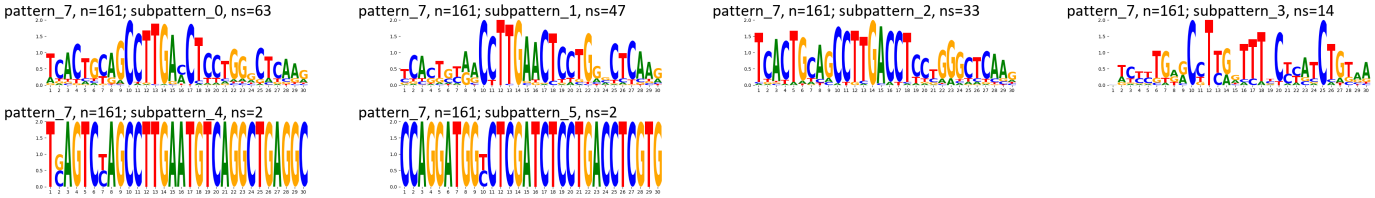

Supplementary Figure 1513: TF-MoDisCO subpatterns for the ZNF629 transcription factor in HepG2 (accession ENCSR363ASY).

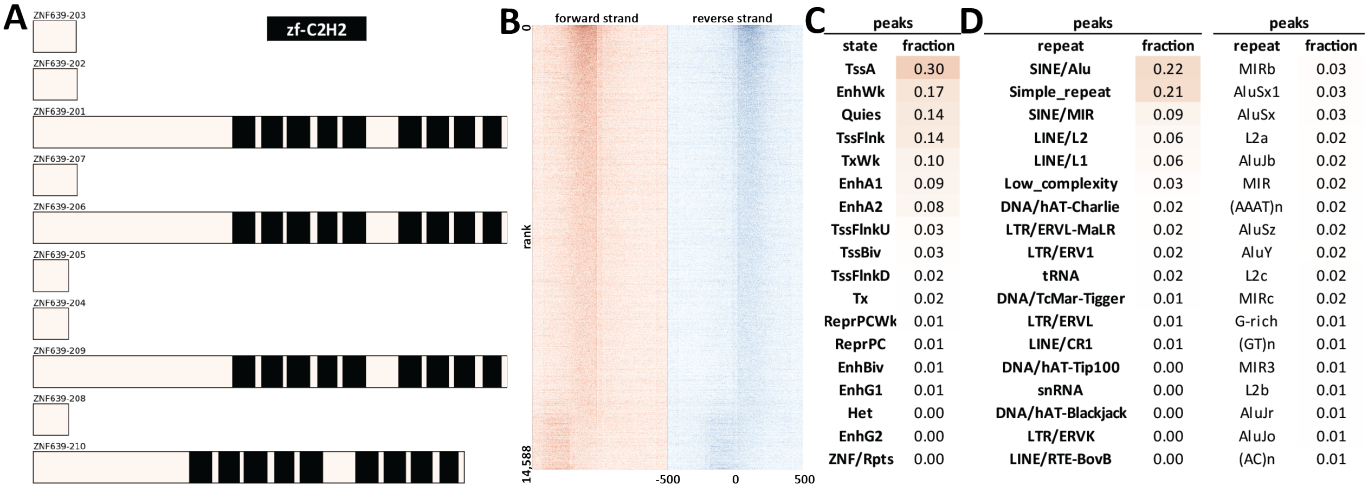

C

peaks	
state	fraction
TssA	0.30
EnhWk	0.17
Quies	0.14
TssFlnk	0.14
TxWk	0.10
EnhA1	0.09
EnhA2	0.08
TssFlnkU	0.03
TssBiv	0.03
TssFlnkD	0.02
Tx	0.02
ReprPCWk	0.01
ReprPC	0.01
EnhBiv	0.01
EnhG1	0.01
Het	0.00
EnhG2	0.00
ZNF/Rpts	0.00

D

peaks		peaks	
repeat	fraction	repeat	fraction
SINE/Alu	0.22	MIRb	0.03
Simple_repeat	0.21	AluSx1	0.03
SINE/MIR	0.09	AluSx	0.03
LINE/L2	0.06	L2a	0.02
LINE/L1	0.06	AluJb	0.02
Low_complexity	0.03	MIR	0.02
DNA/hAT-Charlie	0.02	(AAAT)n	0.02
LTR/ERVL-MaLR	0.02	AluSz	0.02
LTR/ERV1	0.02	AluY	0.02
tRNA	0.02	L2c	0.02
DNA/TcMar-Tigger	0.01	MIRc	0.02
LTR/ERVL	0.01	G-rich	0.01
LINE/CR1	0.01	(GT)n	0.01
DNA/hAT-Tip100	0.00	MIR3	0.01
snRNA	0.00	L2b	0.01
DNA/hAT-Blackjack	0.00	AluJr	0.01
LTR/ERVK	0.00	AluJo	0.01
LINE/RTE-BovB	0.00	(AC)n	0.01

E

Ontology	Term	FDR Q-val
GO Biological Process	ncRNA processing	57.12
GO Biological Process	ribosome biogenesis	51.43
GO Biological Process	rRNA processing	46.00
GO Biological Process	rRNA metabolic process	45.56
GO Biological Process	nuclear-transcribed mRNA catabolic process, nonsense-mediated decay	39.36
GO Biological Process	nuclear-transcribed mRNA catabolic process	35.84
GO Biological Process	mRNA catabolic process	34.47
GO Biological Process	translational initiation	30.80
GO Biological Process	viral gene expression	29.91
GO Biological Process	SRP-dependent cotranslational protein targeting to membrane	27.10
GO Biological Process	cotranslational protein targeting to membrane	25.33
GO Biological Process	protein targeting to ER	24.16
GO Biological Process	multi-organism metabolic process	23.54
GO Biological Process	viral transcription	22.38
GO Biological Process	establishment of protein localization to endoplasmic reticulum	22.01
GO Biological Process	regulation of transcription from RNA polymerase II promoter in response to stress	21.69
GO Biological Process	protein localization to endoplasmic reticulum	20.70
GO Biological Process	regulation of DNA-templated transcription in response to stress	19.61
GO Biological Process	ribosomal small subunit biogenesis	15.59
GO Biological Process	retrograde transport, endosome to Golgi	13.13

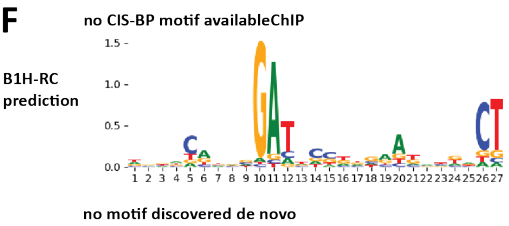

Supplementary Figure 1514: Properties and genomic distribution of motifs identified for the ZNF639 transcription factor in HEK293 (accession ENCSR080CST).

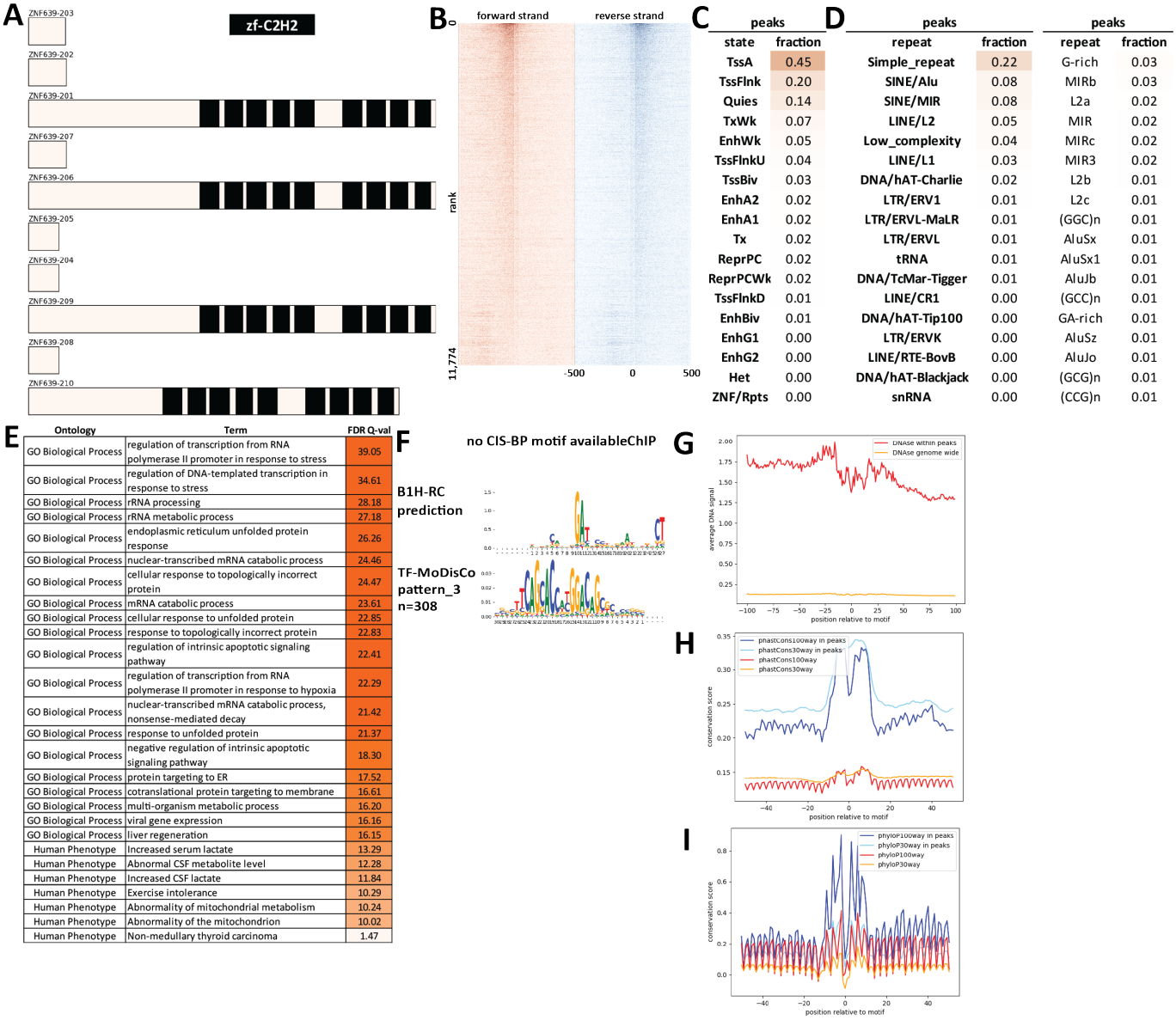

Supplementary Figure 1515: Properties and genomic distribution of motifs identified for the ZNF639 transcription factor in HepG2 (accession ENCSR665UFC).

TF-MoDisCO pattern_7 n=308, CWM

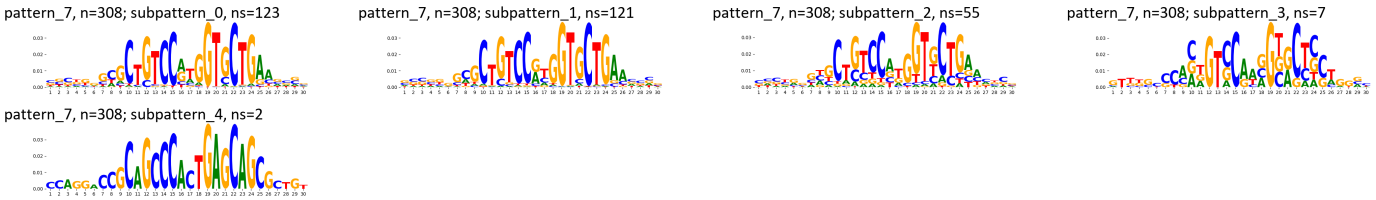

TF-MoDisCO pattern_7 n=308, PWM

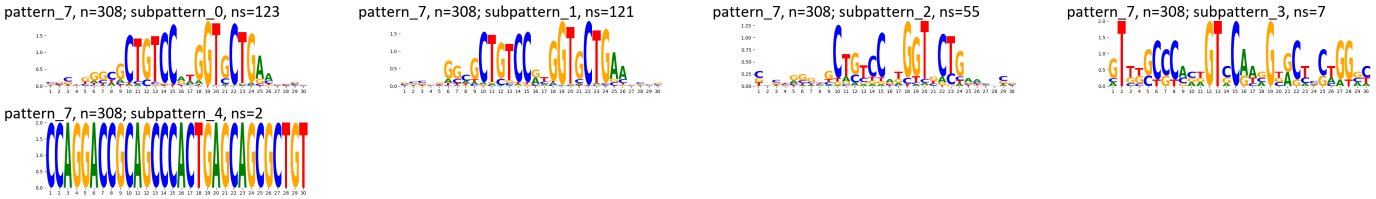

Supplementary Figure 1516: TF-MoDisCO subpatterns for the ZNF639 transcription factor in HepG2 (accession ENCSR665UFC).

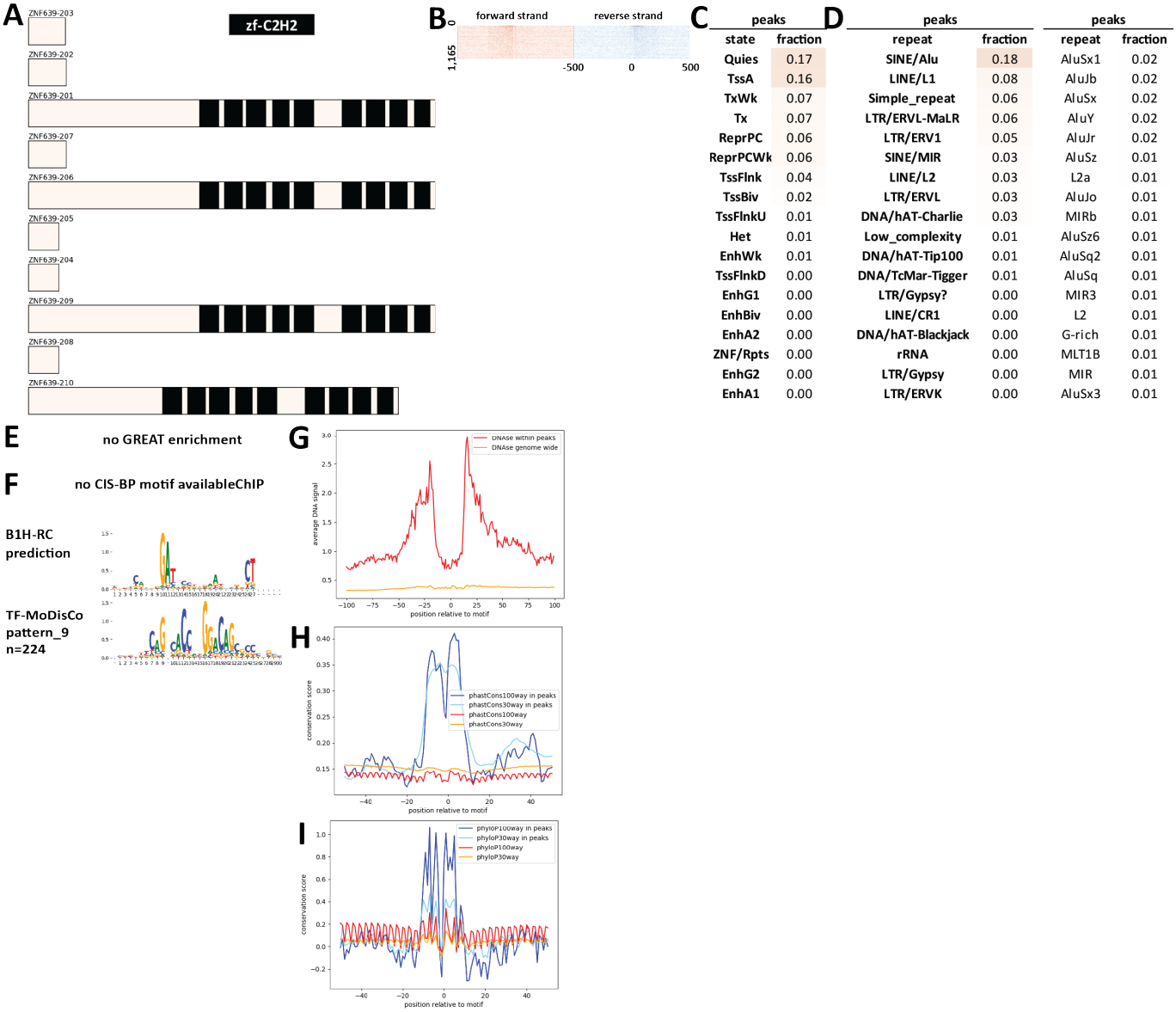

peaks	
state	fraction
Quies	0.17
TssA	0.16
TxWk	0.07
Tx	0.07
ReprPC	0.06
ReprPCWk	0.06
TssFlnk	0.04
TssBiv	0.02
TssFlnkU	0.01
Het	0.01
EnhWk	0.01
TssFlnkD	0.00
EnhG1	0.00
EnhBiv	0.00
EnhA2	0.00
ZNF/Rpts	0.00
EnhG2	0.00
EnhA1	0.00

peaks	
repeat	fraction
SINE/Alu	0.18
LINE/L1	0.08
Simple_repeat	0.06
LTR/ERVL-MaLR	0.06
LTR/ERV1	0.05
SINE/MIR	0.03
LINE/L2	0.03
LTR/ERVL	0.03
DNA/hAT-Charlie	0.03
Low_complexity	0.01
DNA/hAT-Tip100	0.01
DNA/TcMar-Tigger	0.01
LTR/Gypsy?	0.00
LINE/CR1	0.00
DNA/hAT-Blackjack	0.00
rRNA	0.00
LTR/Gypsy	0.00
LTR/ERVK	0.00

peaks	
repeat	fraction
AluSx1	0.02
AluJb	0.02
AluSx	0.02
AluY	0.02
AluJr	0.02
AluSz	0.01
L2a	0.01
AluJo	0.01
MIRb	0.01
AluSz6	0.01
AluSq2	0.01
AluSq	0.01
MIR3	0.01
L2	0.01
G-rich	0.01
MLT1B	0.01
MIR	0.01
AluSx3	0.01

Supplementary Figure 1517: Properties and genomic distribution of motifs identified for the ZNF639 transcription factor in K562 (accession ENCSR258PSN).

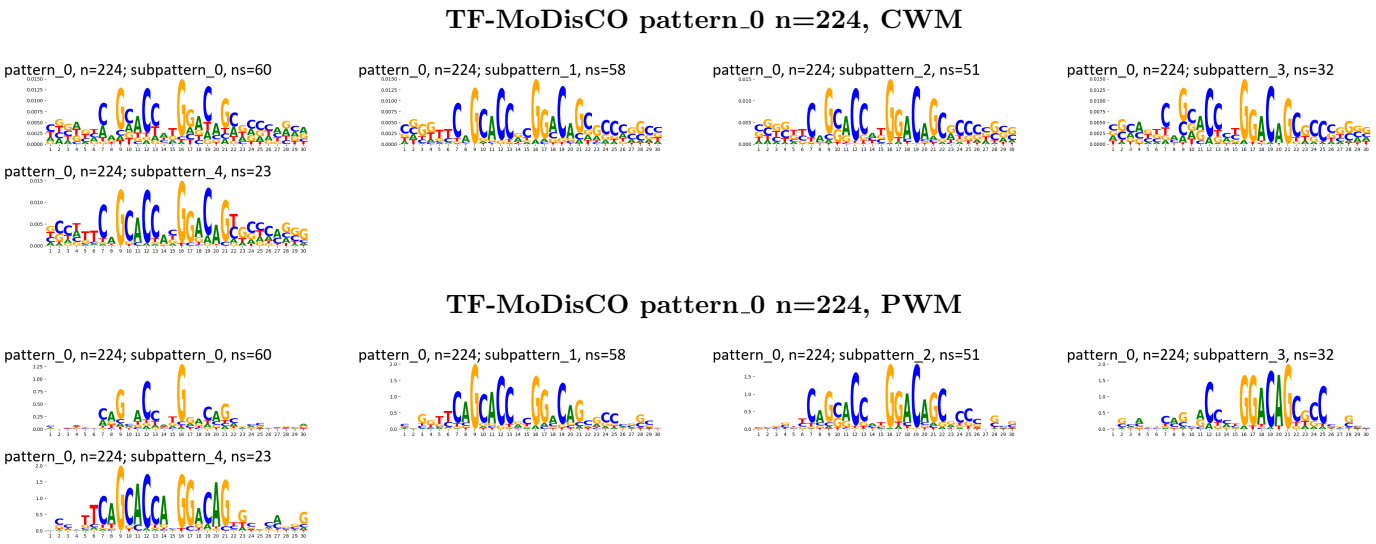

Supplementary Figure 1518: TF-MoDisCO subpatterns for the ZNF639 transcription factor in K562 (accession ENCSR258PSN).

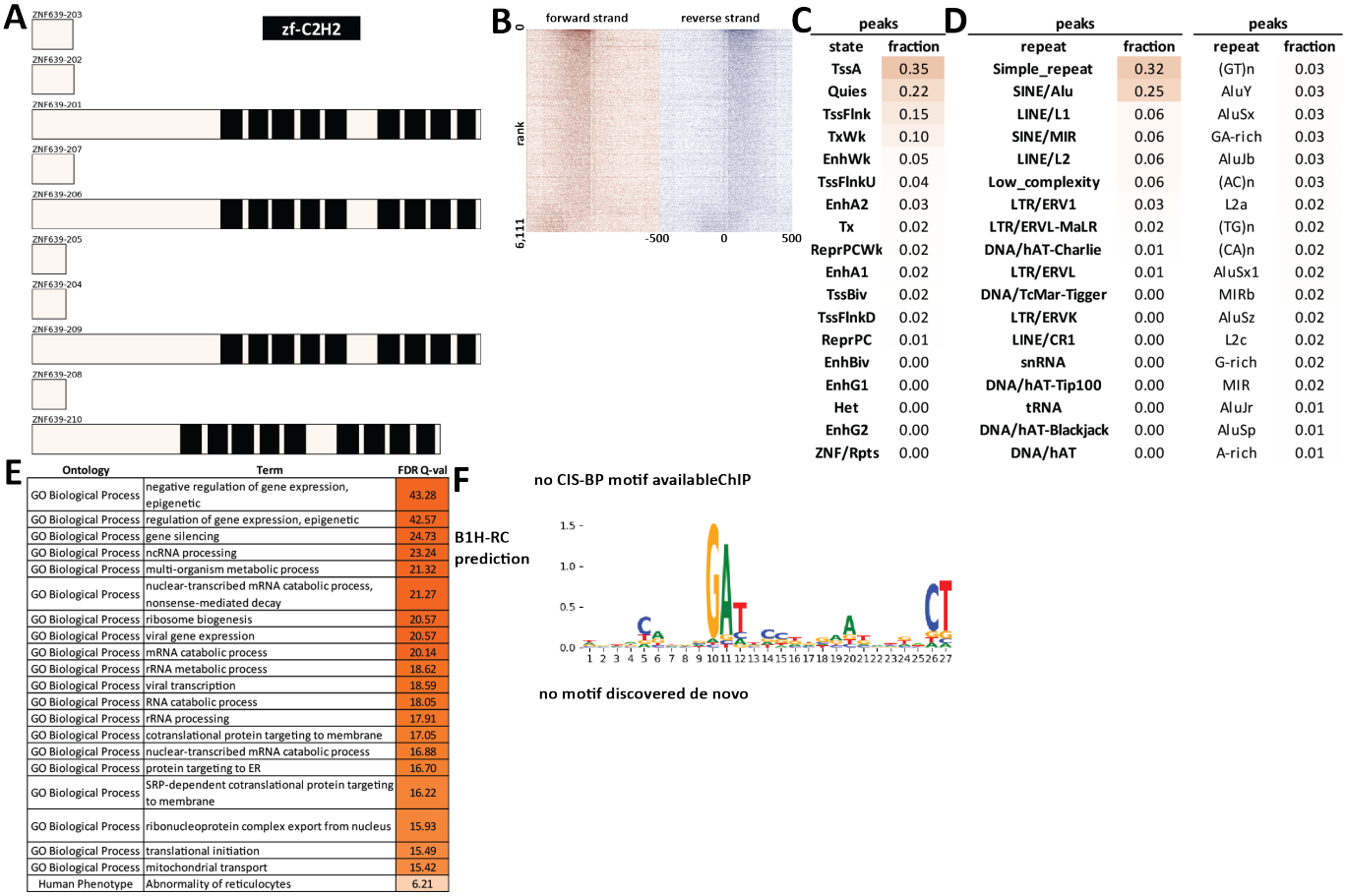

Supplementary Figure 1519: Properties and genomic distribution of motifs identified for the ZNF639 transcription factor in K562 (accession ENCSR497VFH).

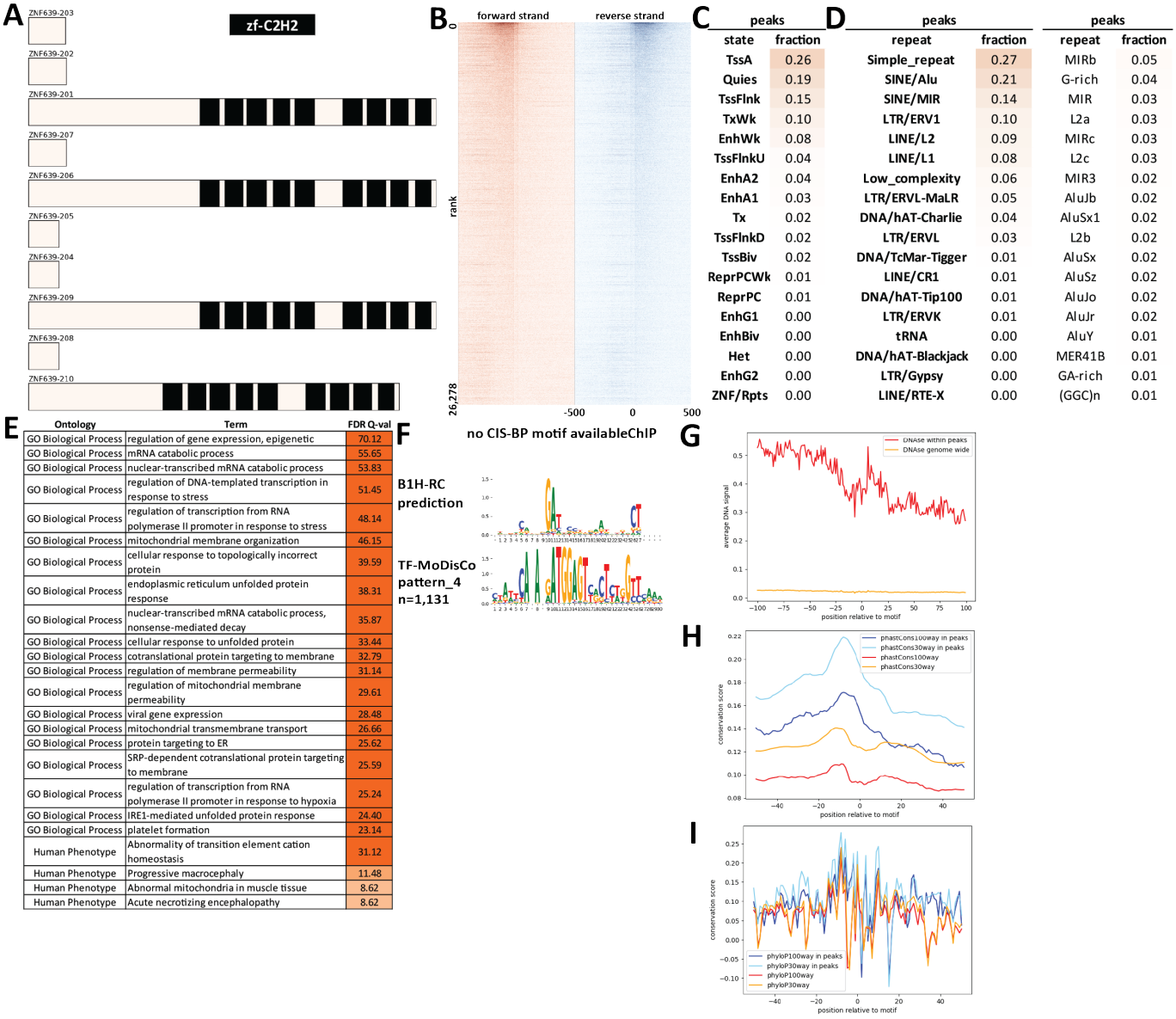

peaks	
state	fraction
TssA	0.26
Quies	0.19
TssFlnk	0.15
TxWk	0.10
EnhWk	0.08
TssFlnkU	0.04
EnhA2	0.04
EnhA1	0.03
Tx	0.02
TssFlnkD	0.02
TssBiv	0.02
ReprPCWk	0.01
ReprPC	0.01
EnhG1	0.00
EnhBiv	0.00
Het	0.00
EnhG2	0.00
ZNF/Rpts	0.00

peaks		peaks	
repeat	fraction	repeat	fraction
Simple_repeat	0.27	MIRb	0.05
SINE/Alu	0.21	G-rich	0.04
SINE/MIR	0.14	MIR	0.03
LTR/ERV1	0.10	L2a	0.03
LINE/L2	0.09	MIRc	0.03
LINE/L1	0.08	L2c	0.03
Low_complexity	0.06	MIR3	0.02
LTR/ERVL-MaLR	0.05	AluJb	0.02
DNA/hAT-Charlie	0.04	AluSx1	0.02
LTR/ERVL	0.03	L2b	0.02
DNA/TcMar-Tigger	0.01	AluSx	0.02
LINE/CR1	0.01	AluSz	0.02
DNA/hAT-Tip100	0.01	AluJo	0.02
LTR/ERVK	0.01	AluJr	0.02
tRNA	0.00	AluY	0.01
DNA/hAT-Blackjack	0.00	MER41B	0.01
LTR/Gypsy	0.00	GA-rich	0.01
LINE/RTE-X	0.00	(GGC)n	0.01

Ontology	Term	FDR Q-val
GO Biological Process	regulation of gene expression, epigenetic	70.12
GO Biological Process	mRNA catabolic process	55.65
GO Biological Process	nuclear-transcribed mRNA catabolic process	53.83
GO Biological Process	regulation of DNA-templated transcription in response to stress	51.45
GO Biological Process	regulation of transcription from RNA polymerase II promoter in response to stress	48.14
GO Biological Process	mitochondrial membrane organization	46.15
GO Biological Process	cellular response to topologically incorrect protein	39.59
GO Biological Process	endoplasmic reticulum unfolded protein response	38.31
GO Biological Process	nuclear-transcribed mRNA catabolic process, nonsense-mediated decay	35.87
GO Biological Process	cellular response to unfolded protein	33.44
GO Biological Process	cotranslational protein targeting to membrane	32.79
GO Biological Process	regulation of membrane permeability	31.14
GO Biological Process	regulation of mitochondrial membrane permeability	29.61
GO Biological Process	viral gene expression	28.48
GO Biological Process	mitochondrial transmembrane transport	26.66
GO Biological Process	protein targeting to ER	25.62
GO Biological Process	SRP-dependent cotranslational protein targeting to membrane	25.59
GO Biological Process	regulation of transcription from RNA polymerase II promoter in response to hypoxia	25.24
GO Biological Process	IRE1-mediated unfolded protein response	24.40
GO Biological Process	platelet formation	23.14
Human Phenotype	Abnormality of transition element cation homeostasis	31.12
Human Phenotype	Progressive macrocephaly	11.48
Human Phenotype	Abnormal mitochondria in muscle tissue	8.62
Human Phenotype	Acute necrotizing encephalopathy	8.62

Supplementary Figure 1520: Properties and genomic distribution of motifs identified for the ZNF639 transcription factor in K562 (accession ENCSR845BCL).

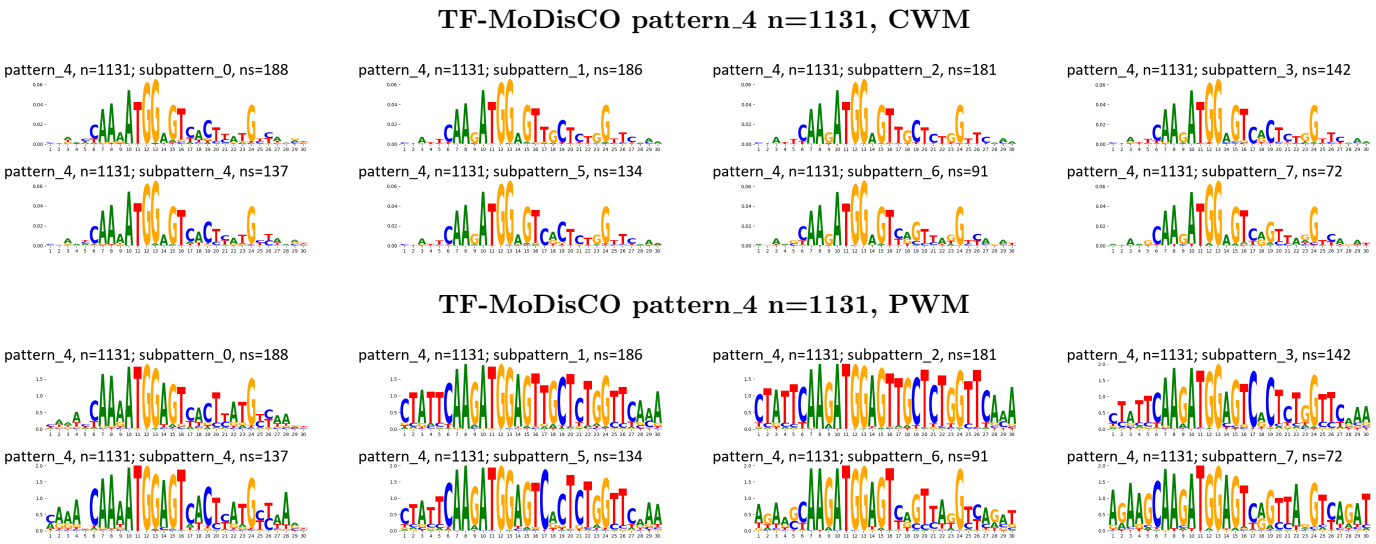

Supplementary Figure 1521: TF-MoDisCO subpatterns for the ZNF639 transcription factor in K562 (accession ENCSR845BCL).

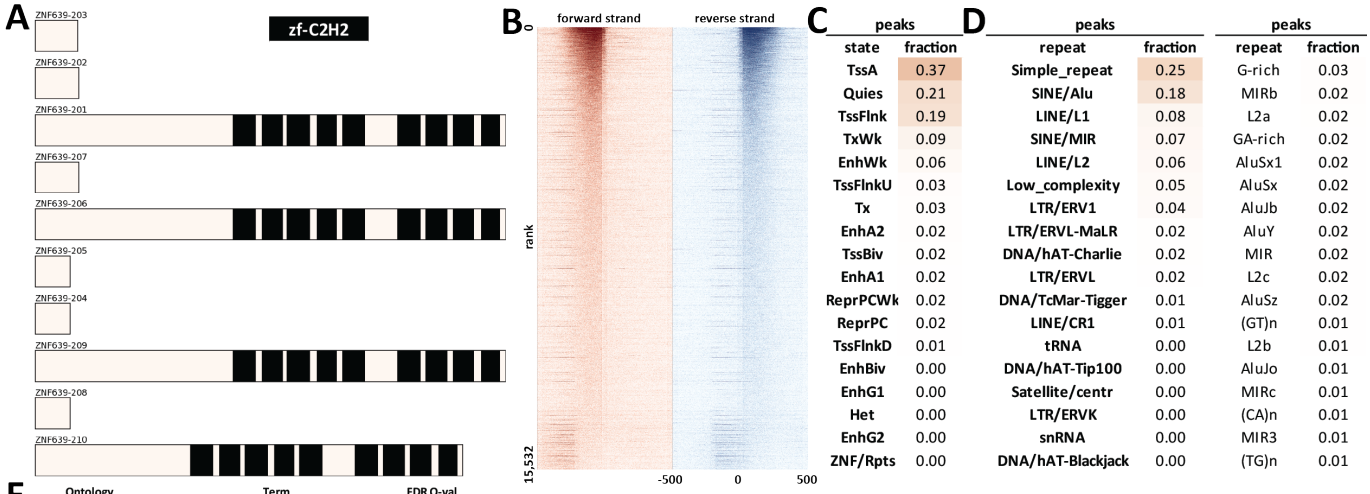

Supplementary Figure 1522: Properties and genomic distribution of motifs identified for the ZNF639 transcription factor in K562 (accession ENCSR949NVY).

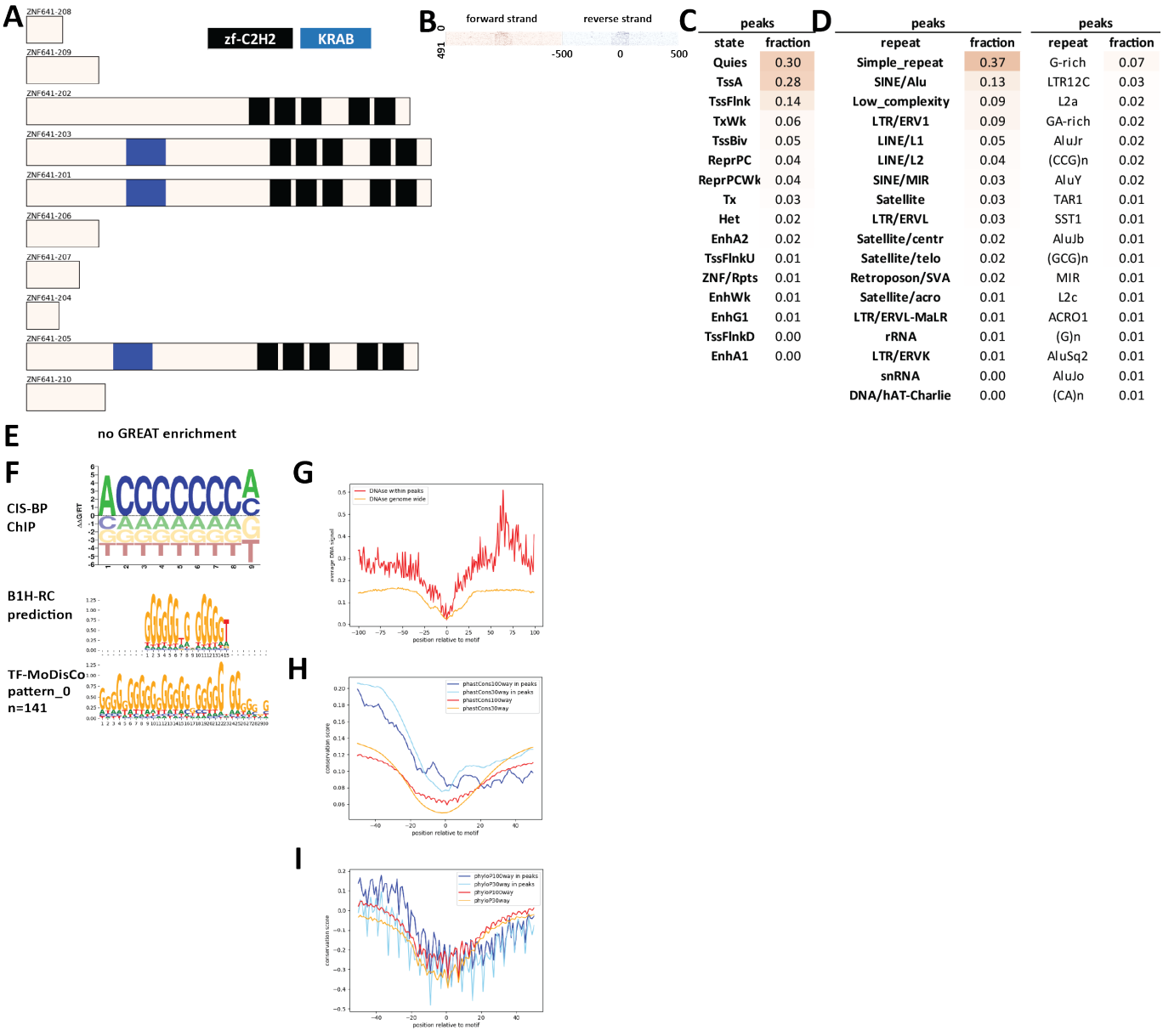

Supplementary Figure 1523: Properties and genomic distribution of motifs identified for the ZNF641 transcription factor in HEK293 (accession ChipExo models).

TF-MoDisCO pattern_0 n=141, CWM

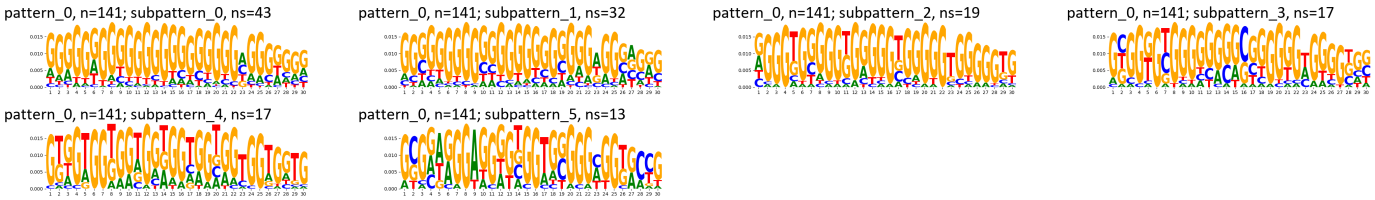

TF-MoDisCO pattern_0 n=141, PWM

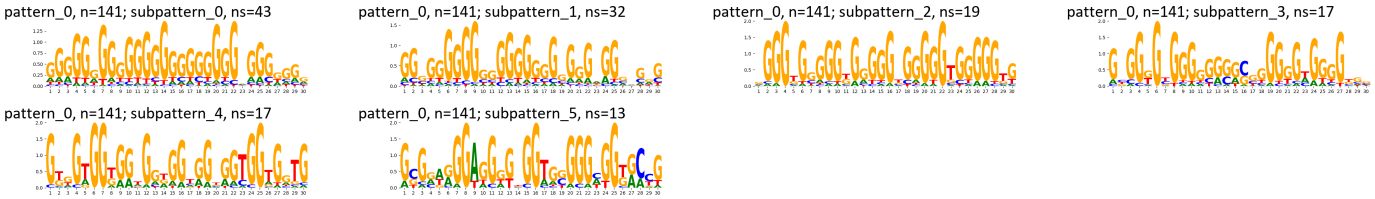

Supplementary Figure 1524: TF-MoDisCO subpatterns for the ZNF641 transcription factor in HEK293 (accession ChipExo models).

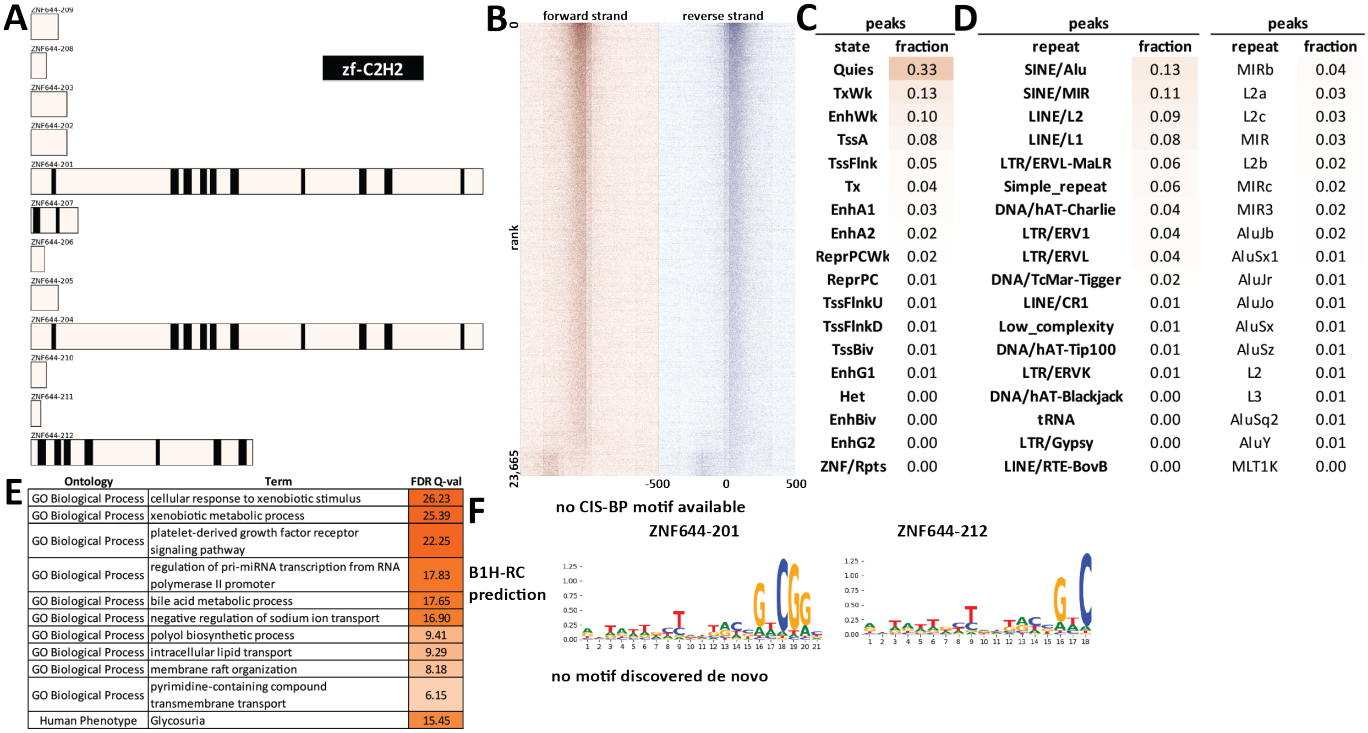

Supplementary Figure 1525: Properties and genomic distribution of motifs identified for the ZNF644 transcription factor in HepG2 (accession ENCSR578CXC).

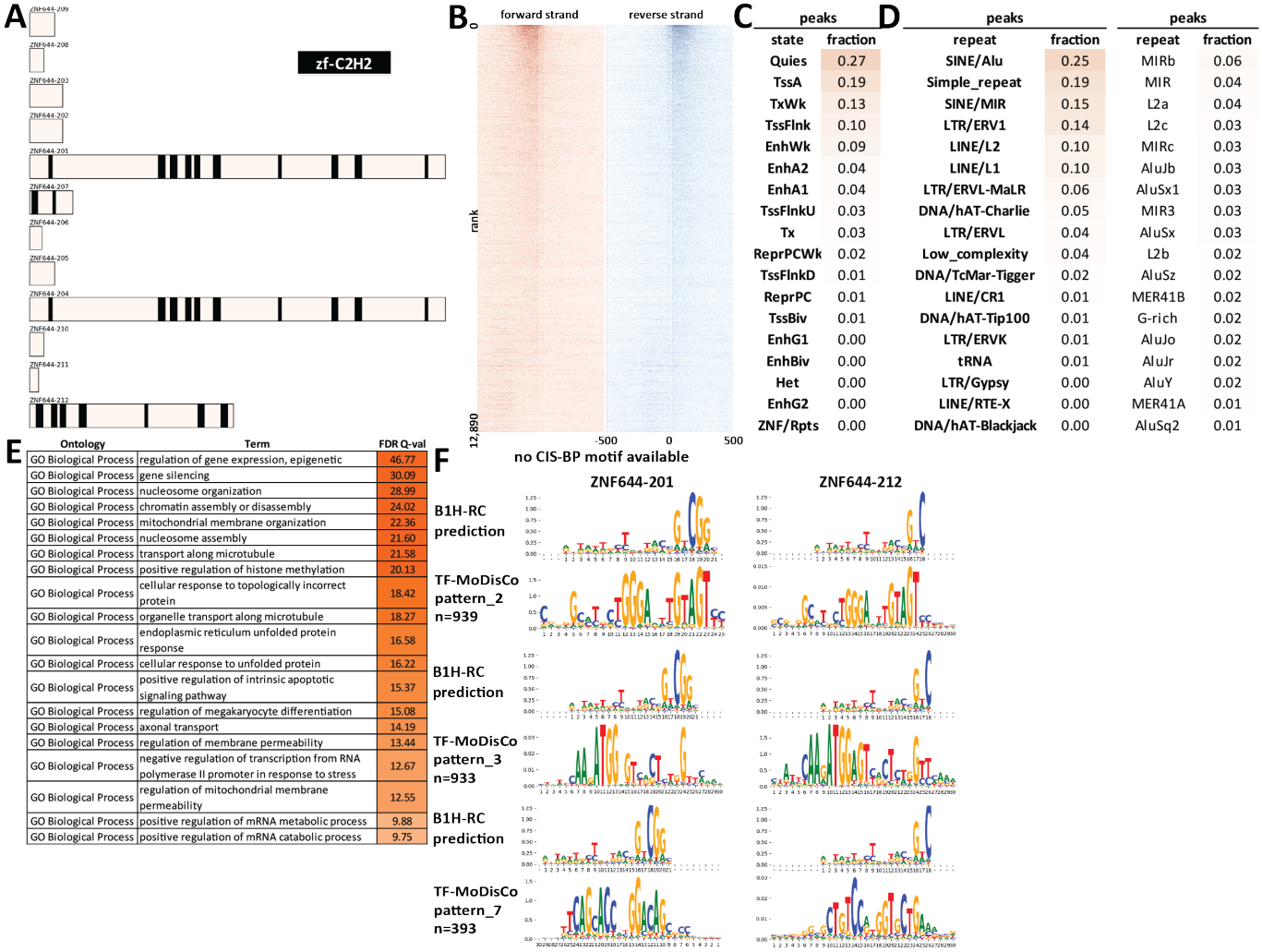

peaks	
state	fraction
Quies	0.27
TssA	0.19
TxWk	0.13
TssFlnk	0.10
EnhWk	0.09
EnhA2	0.04
EnhA1	0.04
TssFlnkU	0.03
Tx	0.03
ReprPCWk	0.02
TssFlnkD	0.01
ReprPC	0.01
TssBiv	0.01
EnhG1	0.00
EnhBiv	0.00
Het	0.00
EnhG2	0.00
ZNF/Rpts	0.00

peaks		peaks	
repeat	fraction	repeat	fraction
SINE/Alu	0.25	MIRb	0.06
Simple_repeat	0.19	MIR	0.04
SINE/MIR	0.15	L2a	0.04
LTR/ERV1	0.14	L2c	0.03
LINE/L2	0.10	MIRc	0.03
LINE/L1	0.10	AluJb	0.03
LTR/ERVL-MaLR	0.06	AluSx1	0.03
DNA/hAT-Charlie	0.05	MIR3	0.03
LTR/ERVL	0.04	AluSx	0.03
Low_complexity	0.04	L2b	0.02
DNA/TcMar-Tigger	0.02	AluSz	0.02
LINE/CR1	0.01	MER41B	0.02
DNA/hAT-Tip100	0.01	G-rich	0.02
LTR/ERVK	0.01	AluJo	0.02
tRNA	0.01	AluJr	0.02
LTR/Gypsy	0.00	AluY	0.02
LINE/RTE-X	0.00	MER41A	0.01
DNA/hAT-Blackjack	0.00	AluSq2	0.01

Ontology	Term	FDR Q-val
GO Biological Process	regulation of gene expression, epigenetic	46.77
GO Biological Process	gene silencing	30.09
GO Biological Process	nucleosome organization	28.99
GO Biological Process	chromatin assembly or disassembly	24.02
GO Biological Process	mitochondrial membrane organization	22.36
GO Biological Process	nucleosome assembly	21.60
GO Biological Process	transport along microtubule	21.58
GO Biological Process	positive regulation of histone methylation	20.13
GO Biological Process	cellular response to topologically incorrect protein	18.42
GO Biological Process	organelle transport along microtubule	18.27
GO Biological Process	endoplasmic reticulum unfolded protein response	16.58
GO Biological Process	cellular response to unfolded protein	16.22
GO Biological Process	positive regulation of intrinsic apoptotic signaling pathway	15.37
GO Biological Process	regulation of megakaryocyte differentiation	15.08
GO Biological Process	axonal transport	14.19
GO Biological Process	regulation of membrane permeability	13.44
GO Biological Process	negative regulation of transcription from RNA polymerase II promoter in response to stress	12.67
GO Biological Process	regulation of mitochondrial membrane permeability	12.55
GO Biological Process	positive regulation of mRNA metabolic process	9.88
GO Biological Process	positive regulation of mRNA catabolic process	9.75

Supplementary Figure 1526: Properties and genomic distribution of motifs identified for the ZNF644 transcription factor in K562 (accession ENCSR729HVR).

TF-MoDisCO pattern_2 n=939, CWM

pattern_2, n=939; subpattern_0, ns=425

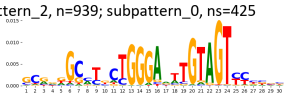

pattern_2, n=939; subpattern_1, ns=324

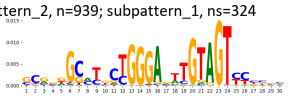

pattern_2, n=939; subpattern_2, ns=188

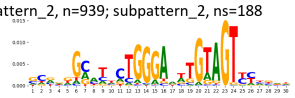

pattern_2, n=939; subpattern_3, ns=2

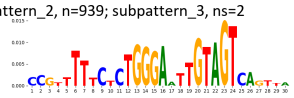

TF-MoDisCO pattern_2 n=939, PWM

pattern_2, n=939; subpattern_0, ns=425

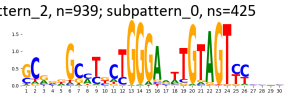

pattern_2, n=939; subpattern_1, ns=324

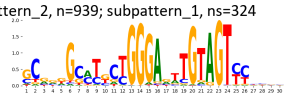

pattern_2, n=939; subpattern_2, ns=188

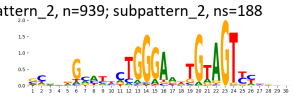

pattern_2, n=939; subpattern_3, ns=2

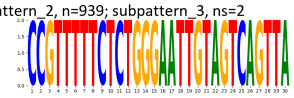

TF-MoDisCO pattern_3 n=933, CWM

pattern_3, n=933; subpattern_0, ns=235

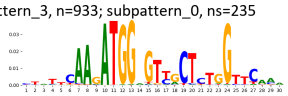

pattern_3, n=933; subpattern_1, ns=221

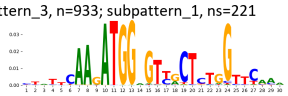

pattern_3, n=933; subpattern_2, ns=150

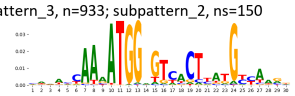

pattern_3, n=933; subpattern_3, ns=139

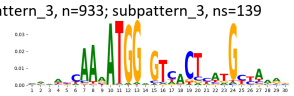

pattern_3, n=933; subpattern_4, ns=110

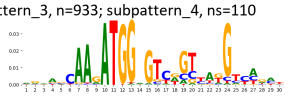

pattern_3, n=933; subpattern_5, ns=78

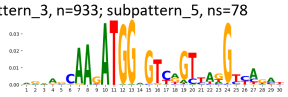

TF-MoDisCO pattern_3 n=933, PWM

pattern_3, n=933; subpattern_0, ns=235

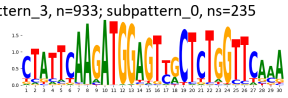

pattern_3, n=933; subpattern_1, ns=221

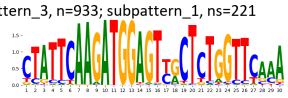

pattern_3, n=933; subpattern_2, ns=150

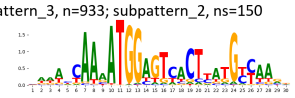

pattern_3, n=933; subpattern_3, ns=139

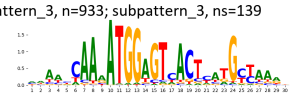

pattern_3, n=933; subpattern_4, ns=110

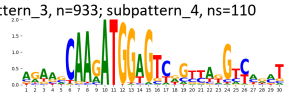

pattern_3, n=933; subpattern_5, ns=78

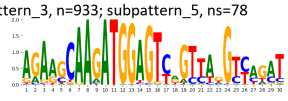

TF-MoDisCO pattern_7 n=393, CWM

pattern_7, n=393; subpattern_0, ns=185

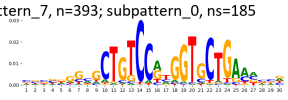

pattern_7, n=393; subpattern_1, ns=158

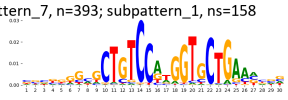

pattern_7, n=393; subpattern_2, ns=16

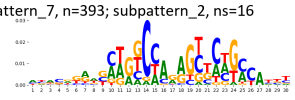

pattern_7, n=393; subpattern_3, ns=14

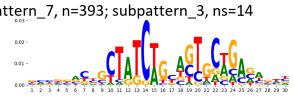

pattern_7, n=393; subpattern_4, ns=8

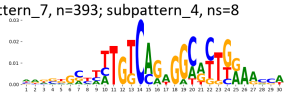

pattern_7, n=393; subpattern_5, ns=5

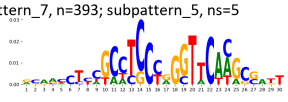

pattern_7, n=393; subpattern_6, ns=3

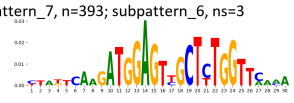

pattern_7, n=393; subpattern_7, ns=2

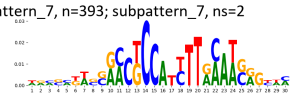

pattern_7, n=393; subpattern_8, ns=2

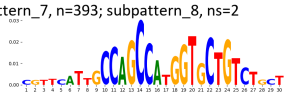

TF-MoDisCO pattern_7 n=393, PWM

pattern_7, n=393; subpattern_0, ns=185

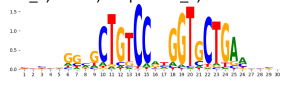

pattern_7, n=393; subpattern_1, ns=158

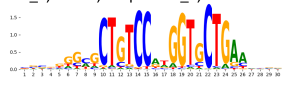

pattern_7, n=393; subpattern_2, ns=16

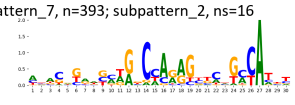

pattern_7, n=393; subpattern_3, ns=14

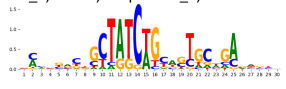

pattern_7, n=393; subpattern_4, ns=8



pattern_7, n=393; subpattern_5, ns=5



pattern_7, n=393; subpattern_6, ns=3

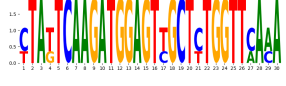

pattern_7, n=393; subpattern_7, ns=2

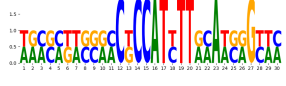

pattern_7, n=393; subpattern_8, ns=2

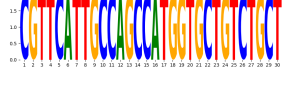

Supplementary Figure 1527: TF-MoDisCO subpatterns for the ZNF644 transcription factor in K562 (accession ENCSR729HVR).

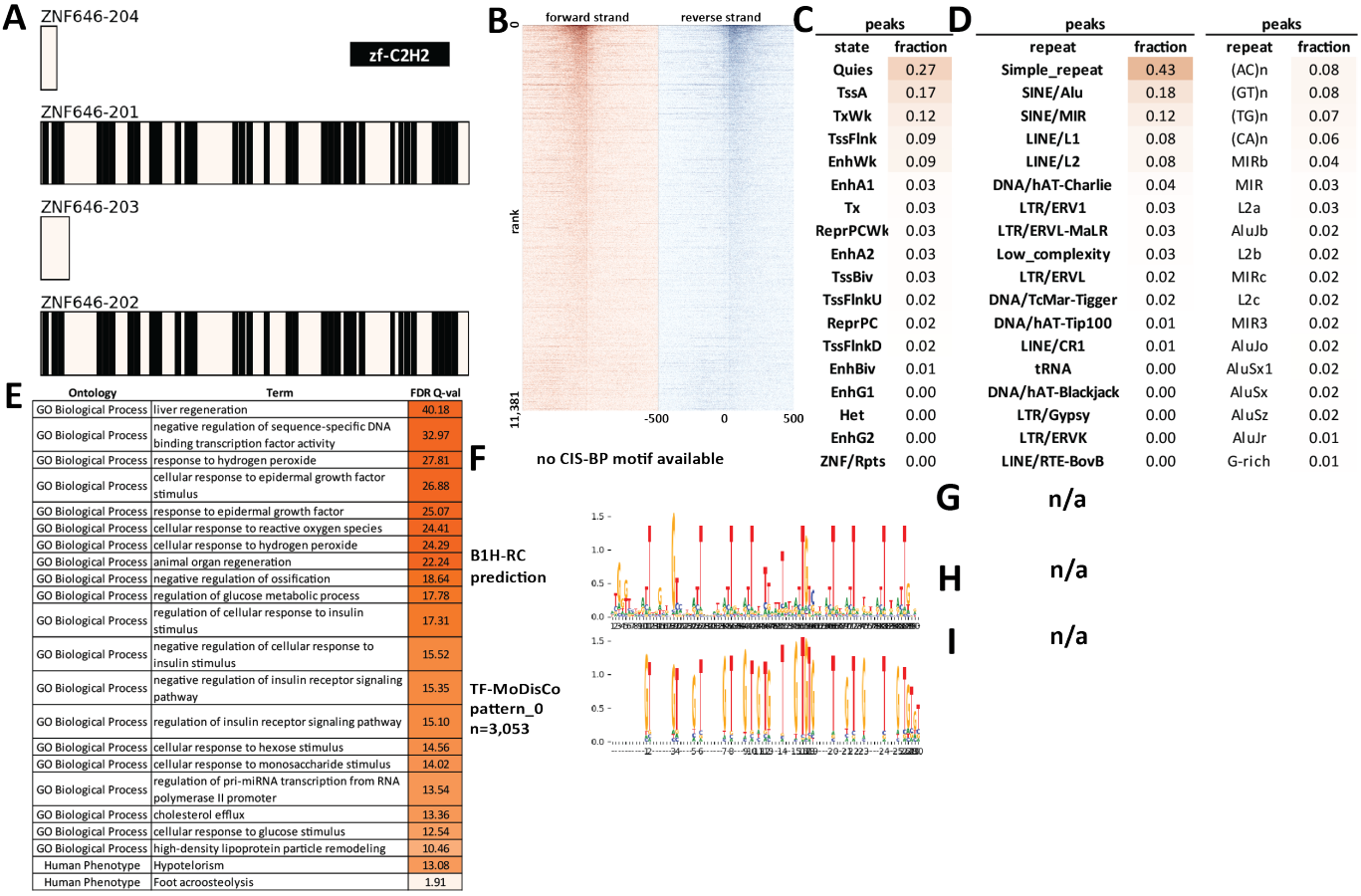

Supplementary Figure 1528: Properties and genomic distribution of motifs identified for the ZNF646 transcription factor in HepG2 (accession ENCSR488ZNK).

TF-MoDisCO pattern_0 n=3053, CWM

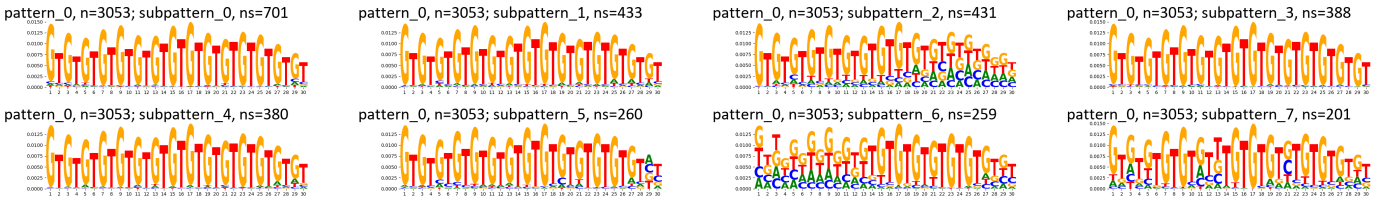

TF-MoDisCO pattern_0 n=3053, PWM

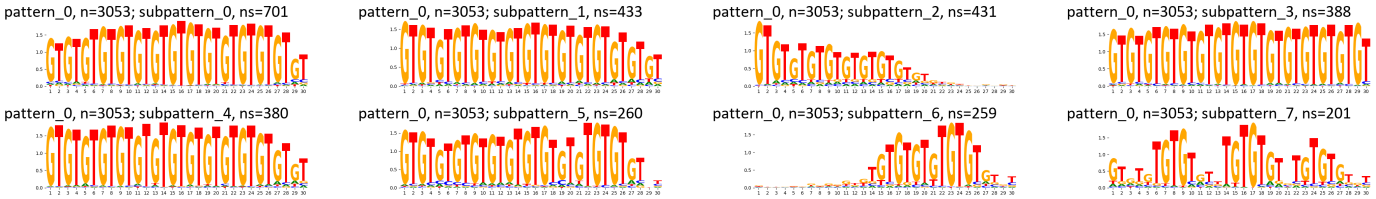

Supplementary Figure 1529: TF-MoDisCO subpatterns for the ZNF646 transcription factor in HepG2 (accession ENCSR488ZNK).

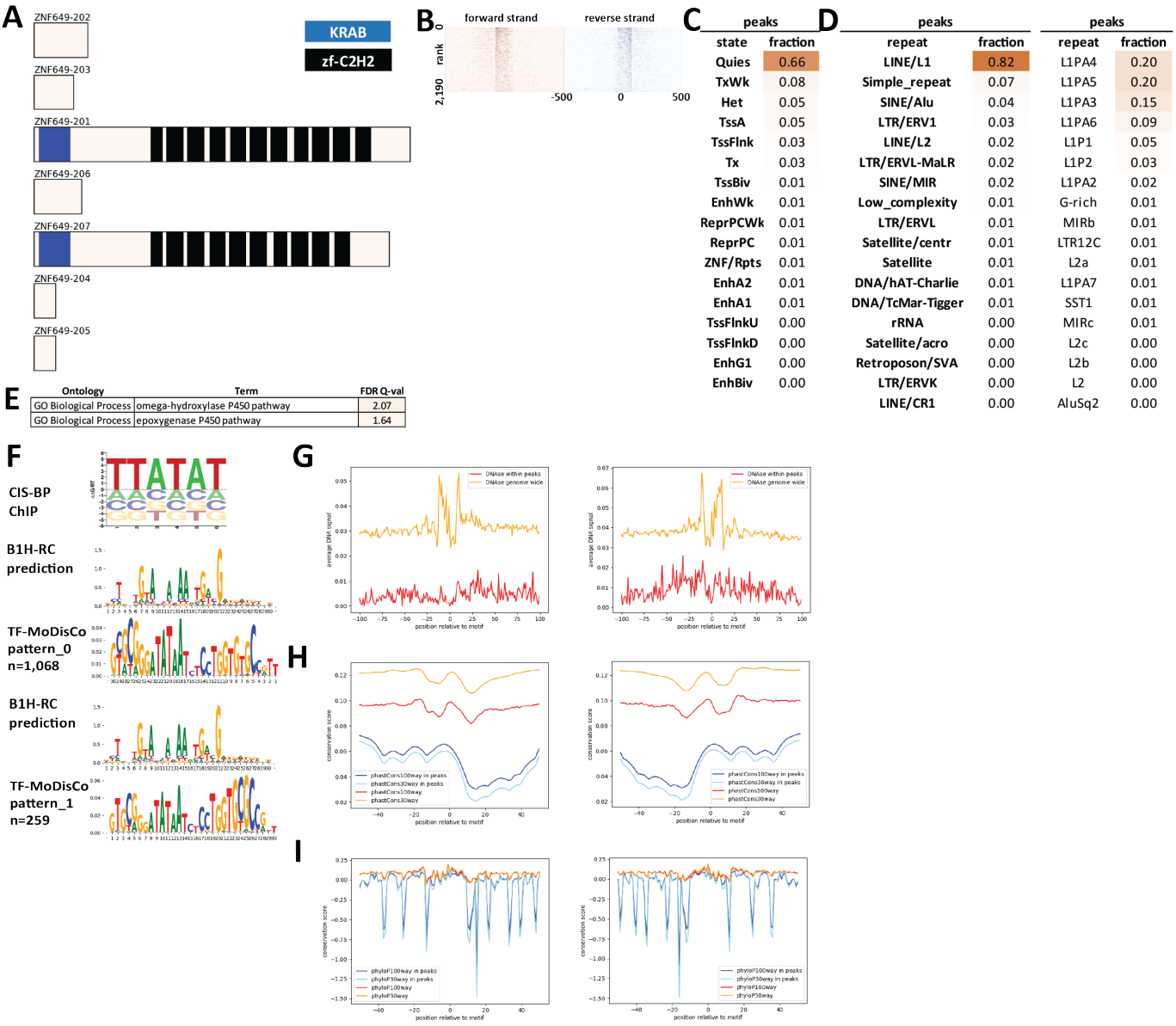

Supplementary Figure 1530: Properties and genomic distribution of motifs identified for the ZNF649 transcription factor in HEK293 (accession ChipExo models).

TF-MoDisCO pattern_0 n=1068, CWM

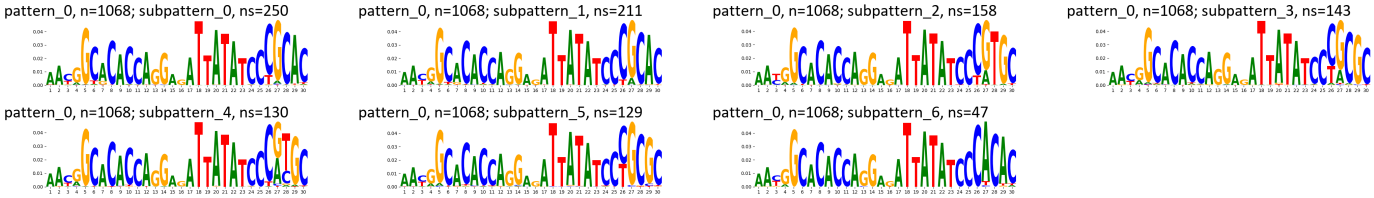

TF-MoDisCO pattern_0 n=1068, PWM

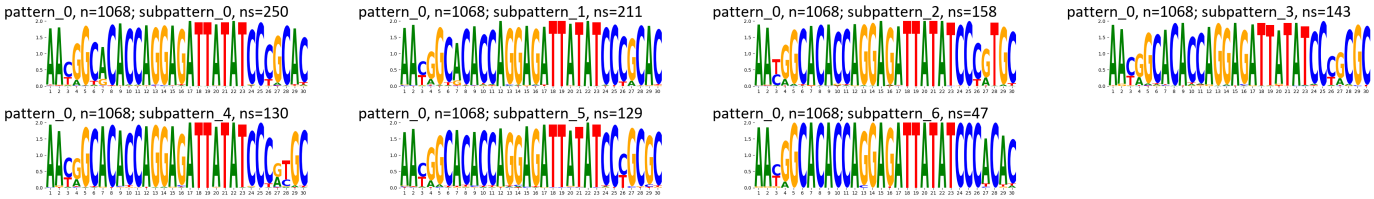

TF-MoDisCO pattern_1 n=259, CWM



TF-MoDisCO pattern_1 n=259, PWM

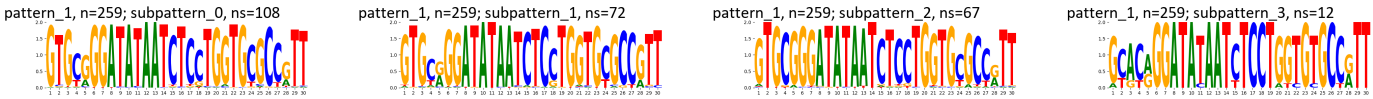

Supplementary Figure 1531: TF-MoDisCO subpatterns for the ZNF649 transcription factor in HEK293 (accession ChipExo models).

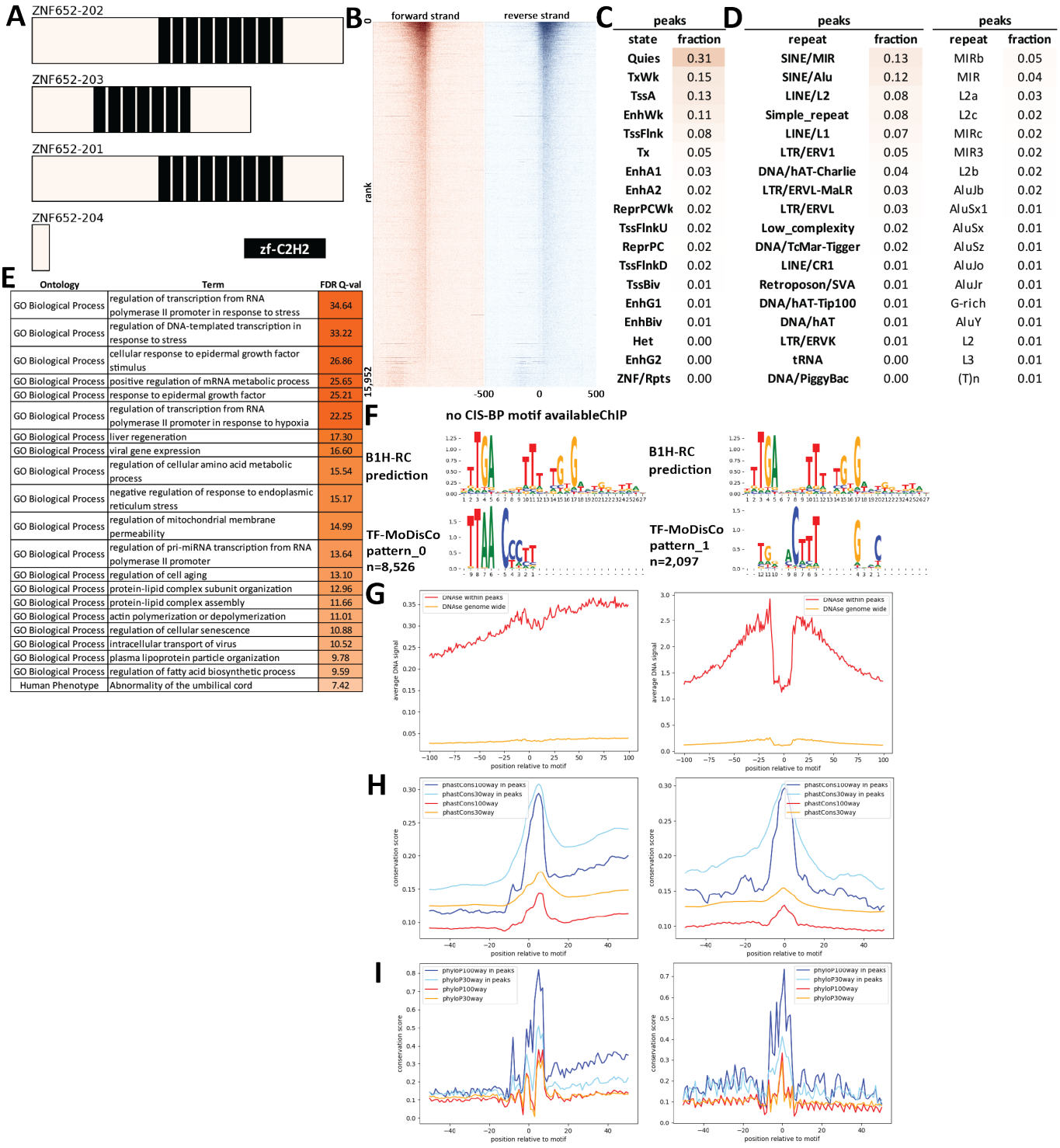

Supplementary Figure 1532: Properties and genomic distribution of motifs identified for the ZNF652 transcription factor in HepG2 (accession ENCSR502GAX).

TF-MoDisCO pattern_0 n=8526, CWM

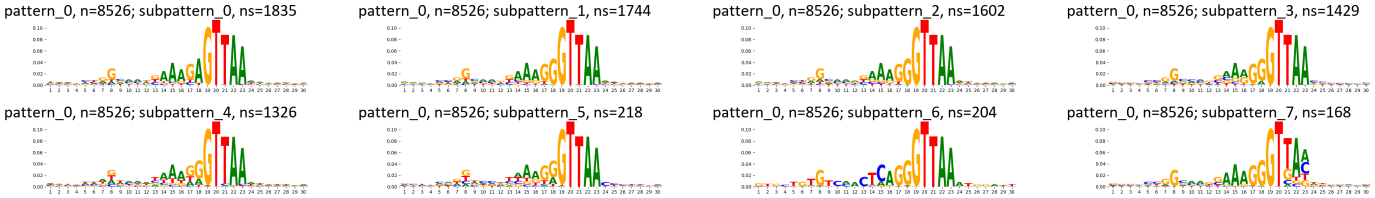

TF-MoDisCO pattern_0 n=8526, PWM

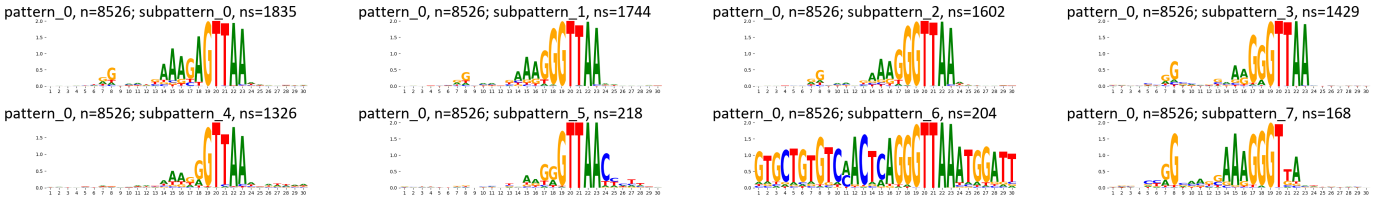

TF-MoDisCO pattern_1 n=2097, CWM

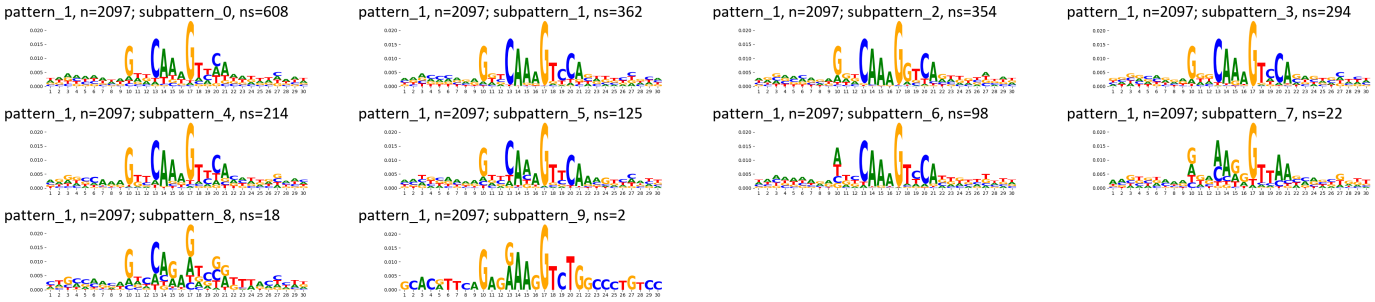

TF-MoDisCO pattern_1 n=2097, PWM

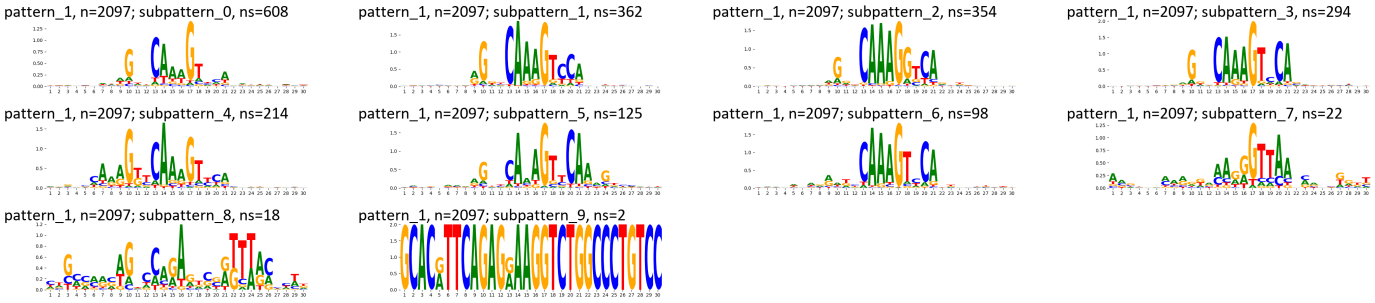

Supplementary Figure 1533: TF-MoDisCO subpatterns for the ZNF652 transcription factor in HepG2 (accession ENCSR502GAX).

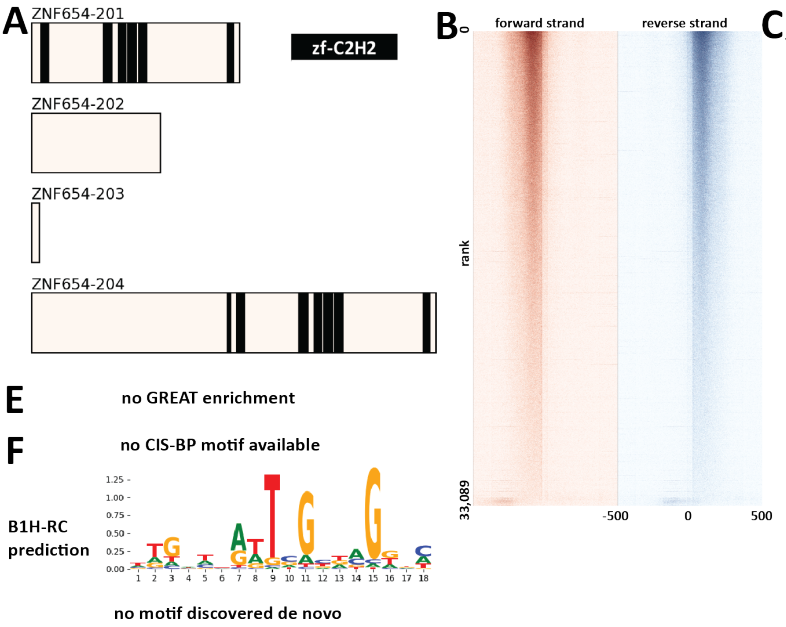

C

peaks	
state	fraction
Quies	0.40
TxWk	0.15
TssFlnk	0.06
EnhWk	0.05
Tx	0.05
TssA	0.04
ReprPCWk	0.04
EnhA2	0.02
ReprPC	0.02
EnhA1	0.01
TssBiv	0.01
Het	0.01
TssFlnkD	0.01
TssFlnkU	0.00
EnhG1	0.00
EnhBiv	0.00
ZNF/Rpts	0.00
EnhG2	0.00

D

peaks		peaks	
repeat	fraction	repeat	fraction
SINE/Alu	0.21	(AAAT)n	0.04
Simple_repeat	0.16	MIRb	0.03
LINE/L1	0.10	AluSx1	0.02
SINE/MIR	0.08	AluSx	0.02
LINE/L2	0.06	L2a	0.02
DNA/hAT-Charlie	0.05	MIR	0.02
LTR/ERVL	0.03	AluJb	0.02
LTR/ERV1	0.03	AluY	0.02
LTR/ERVL-MaLR	0.03	MIR3	0.02
Low_complexity	0.01	AluSz	0.02
DNA/TcMar-Tigger	0.01	L2c	0.02
DNA/hAT-Tip100	0.01	AluJo	0.01
LINE/CR1	0.01	AluJr	0.01
LTR/ERVK	0.01	MIRc	0.01
LTR/Gypsy	0.00	L2b	0.01
tRNA	0.00	AluSq2	0.01
DNA/hAT-Blackjack	0.00	MER20	0.01
Unknown	0.00	AluSp	0.01

Supplementary Figure 1534: Properties and genomic distribution of motifs identified for the ZNF654 transcription factor in HEK293 (accession ENCSR504VDV).

A

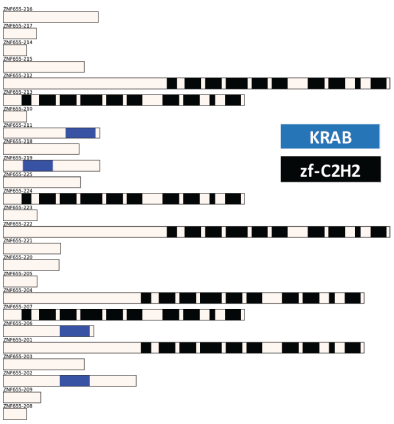

B

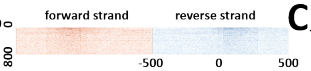

C

peaks	
state	fraction
Quies	0.25
TssA	0.25
TxWk	0.10
TssFlnk	0.08
EnhWk	0.05
EnhA2	0.05
Tx	0.05
ReprPC	0.03
ReprPCWk	0.03
TssFlnkU	0.02
EnhA1	0.02
EnhG1	0.01
TssFlnkD	0.01
Het	0.01
TssBiv	0.01
EnhG2	0.01
EnhBiv	0.00

D

peaks		peaks	
repeat	fraction	repeat	fraction
LTR/ERV1	0.16	MER41B	0.05
LINE/L1	0.10	U1	0.02
SINE/MIR	0.07	MIR	0.02
SINE/Alu	0.07	L2a	0.02
Simple_repeat	0.06	MIRb	0.02
LINE/L2	0.05	MIRc	0.02
snRNA	0.04	MER41A	0.02
LTR/ERVL-MaLR	0.03	L2c	0.02
LTR/ERVL	0.03	MIR3	0.01
DNA/TcMar-Tigger	0.03	AluSx1	0.01
DNA/hAT-Charlie	0.02	AluJb	0.01
Low_complexity	0.02	MER61E	0.01
LINE/CR1	0.01	L2b	0.01
tRNA	0.01	LTR62	0.01
DNA/TcMar-Mariner	0.01	L3	0.01
Satellite/centr	0.00	G-rich	0.01
LTR/ERVK	0.00	U5	0.01
LINE/RTE-X	0.00	L2	0.01

E

Ontology	Term	FDR Q-val
GO Biological Process	protein folding	10.79
GO Biological Process	DNA conformation change	10.42
GO Biological Process	chromosome organization	8.64
GO Biological Process	regulation of DNA-templated transcription in response to stress	8.06
GO Biological Process	DNA replication-dependent nucleosome assembly	7.64
GO Biological Process	PERK-mediated unfolded protein response	7.05
GO Biological Process	nucleosome organization	4.88
GO Biological Process	chromatin assembly	4.87
GO Biological Process	nucleosome assembly	4.69
GO Biological Process	chromatin silencing	4.25
GO Biological Process	negative regulation of gene expression, epigenetic	3.98
GO Biological Process	chromatin assembly or disassembly	3.97
GO Biological Process	DNA packaging	3.94
GO Biological Process	protein heterotetramerization	3.59
GO Biological Process	protein-DNA complex subunit organization	3.30
GO Biological Process	protein-DNA complex assembly	2.82
GO Biological Process	regulation of megakaryocyte differentiation	2.05

F

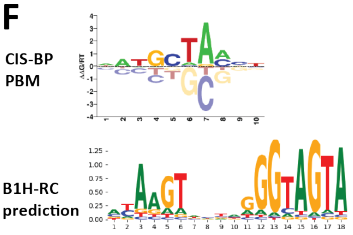

no motif discovered de novo

Supplementary Figure 1535: Properties and genomic distribution of motifs identified for the ZNF655 transcription factor in K562 (accession ENCSR568YNC).

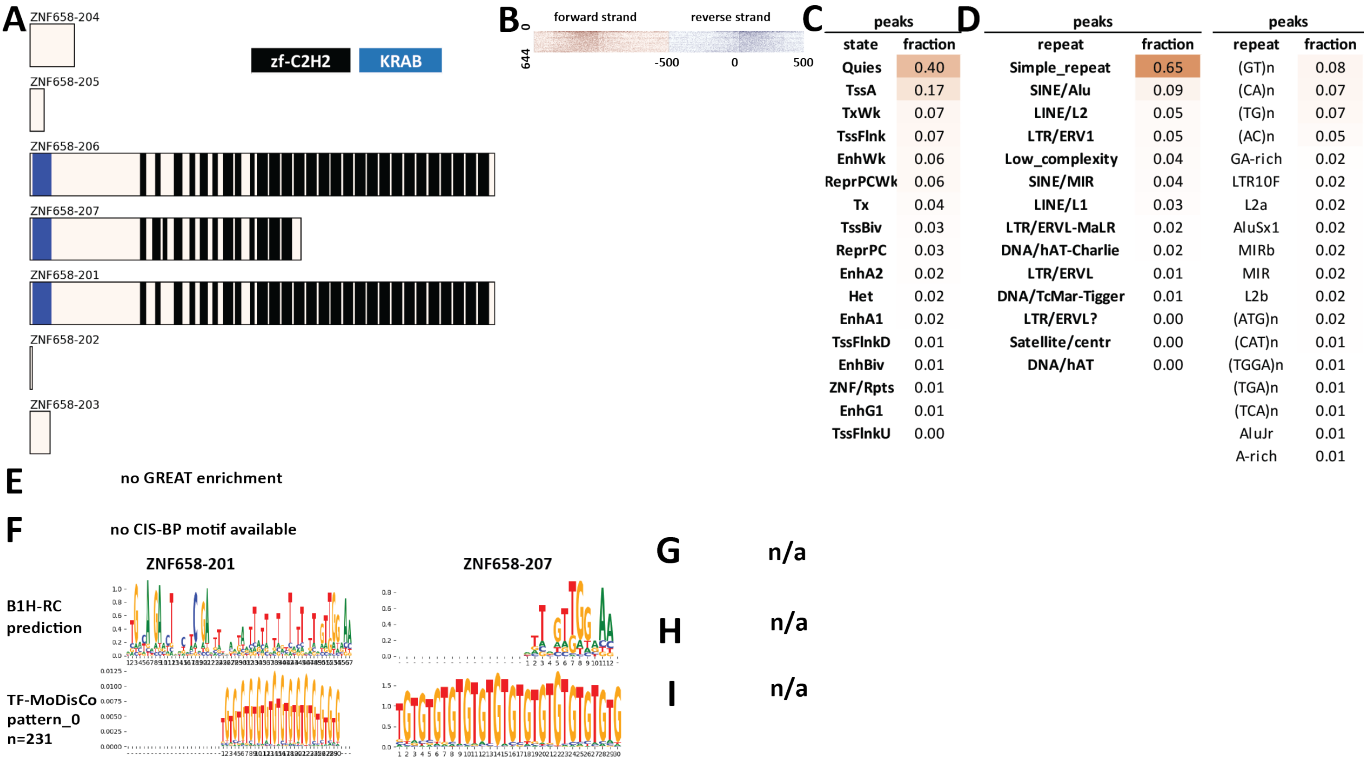

peaks	
state	fraction
Quies	0.40
TssA	0.17
TxWk	0.07
TssFlnk	0.07
EnhWk	0.06
ReprPCWk	0.06
Tx	0.04
TssBiv	0.03
ReprPC	0.03
EnhA2	0.02
Het	0.02
EnhA1	0.02
TssFlnkD	0.01
EnhBiv	0.01
ZNF/Rpts	0.01
EnhG1	0.01
TssFlnkU	0.00

peaks	
repeat	fraction
Simple_repeat	0.65
SINE/Alu	0.09
LINE/L2	0.05
LTR/ERV1	0.05
Low_complexity	0.04
SINE/MIR	0.04
LINE/L1	0.03
LTR/ERVL-MaLR	0.02
DNA/hAT-Charlie	0.02
LTR/ERVL	0.01
DNA/TcMar-Tigger	0.01
LTR/ERVL?	0.00
Satellite/centr	0.00
DNA/hAT	0.00

peaks	
repeat	fraction
(GT)n	0.08
(CA)n	0.07
(TG)n	0.07
(AC)n	0.05
GA-rich	0.02
LTR10F	0.02
L2a	0.02
AluSx1	0.02
MIRb	0.02
MIR	0.02
L2b	0.02
(ATG)n	0.02
(CAT)n	0.01
(TGGA)n	0.01
(TGA)n	0.01
(TCA)n	0.01
AluJr	0.01
A-rich	0.01

Supplementary Figure 1536: Properties and genomic distribution of motifs identified for the ZNF658 transcription factor in HEK293 (accession ENCSR762DQP).

TF-MoDisCO pattern_0 n=231, CWM

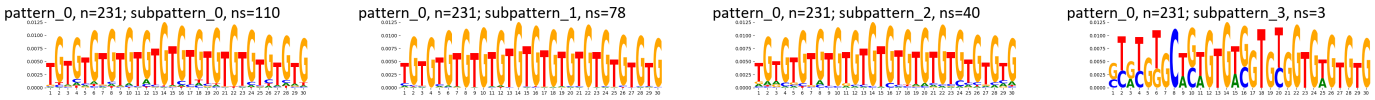

TF-MoDisCO pattern_0 n=231, PWM

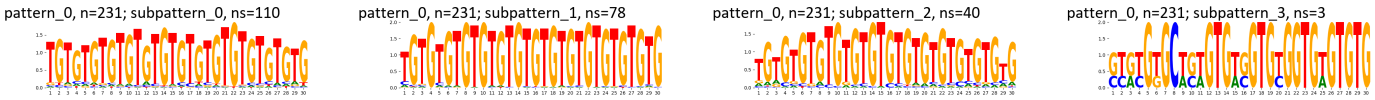

Supplementary Figure 1537: TF-MoDisCO subpatterns for the ZNF658 transcription factor in HEK293 (accession ENCSR762DQP).

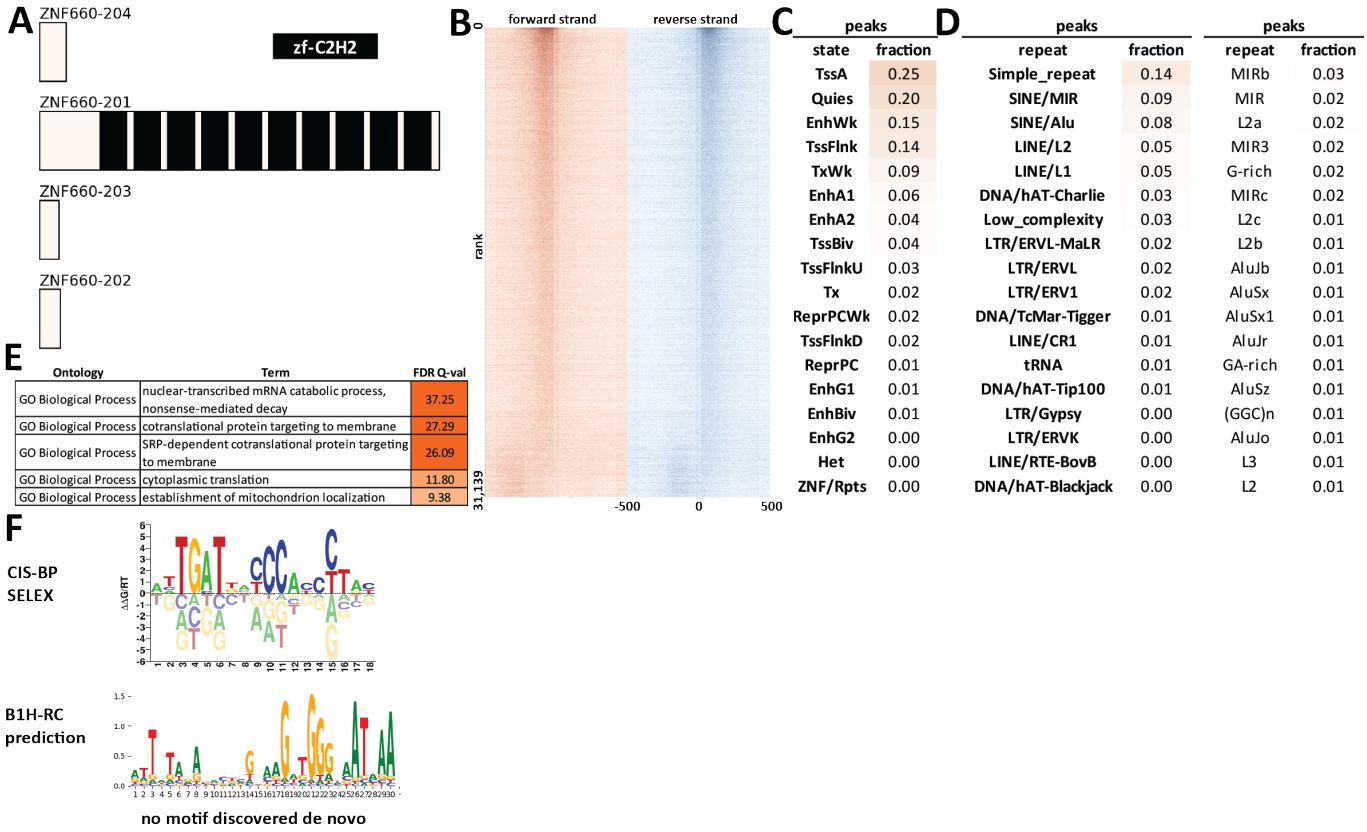

C

peaks	
state	fraction
TssA	0.25
Quies	0.20
EnhWk	0.15
TssFlnk	0.14
TxWk	0.09
EnhA1	0.06
EnhA2	0.04
TssBiv	0.04
TssFlnkU	0.03
Tx	0.02
ReprPCWk	0.02
TssFlnkD	0.02
ReprPC	0.01
EnhG1	0.01
EnhBiv	0.01
EnhG2	0.00
Het	0.00
ZNF/Rpts	0.00

D

peaks		peaks	
repeat	fraction	repeat	fraction
Simple_repeat	0.14	MIRb	0.03
SINE/MIR	0.09	MIR	0.02
SINE/Alu	0.08	L2a	0.02
LINE/L2	0.05	MIR3	0.02
LINE/L1	0.05	G-rich	0.02
DNA/hAT-Charlie	0.03	MIRc	0.02
Low_complexity	0.03	L2c	0.01
LTR/ERVL-MaLR	0.02	L2b	0.01
LTR/ERVL	0.02	AluJb	0.01
LTR/ERV1	0.02	AluSx	0.01
DNA/TcMar-Tigger	0.01	AluSx1	0.01
LINE/CR1	0.01	AluJr	0.01
tRNA	0.01	GA-rich	0.01
DNA/hAT-Tip100	0.01	AluSz	0.01
LTR/Gypsy	0.00	(GGC)n	0.01
LTR/ERVK	0.00	AluJo	0.01
LINE/RTE-BovB	0.00	L3	0.01
DNA/hAT-Blackjack	0.00	L2	0.01

E

Ontology	Term	FDR Q-val
GO Biological Process	nuclear-transcribed mRNA catabolic process, nonsense-mediated decay	37.25
GO Biological Process	cotranslational protein targeting to membrane	27.29
GO Biological Process	SRP-dependent cotranslational protein targeting to membrane	26.09
GO Biological Process	cytoplasmic translation	11.80
GO Biological Process	establishment of mitochondrion localization	9.38

Supplementary Figure 1538: Properties and genomic distribution of motifs identified for the ZNF660 transcription factor in HEK293 (accession ENCSR283DOU).

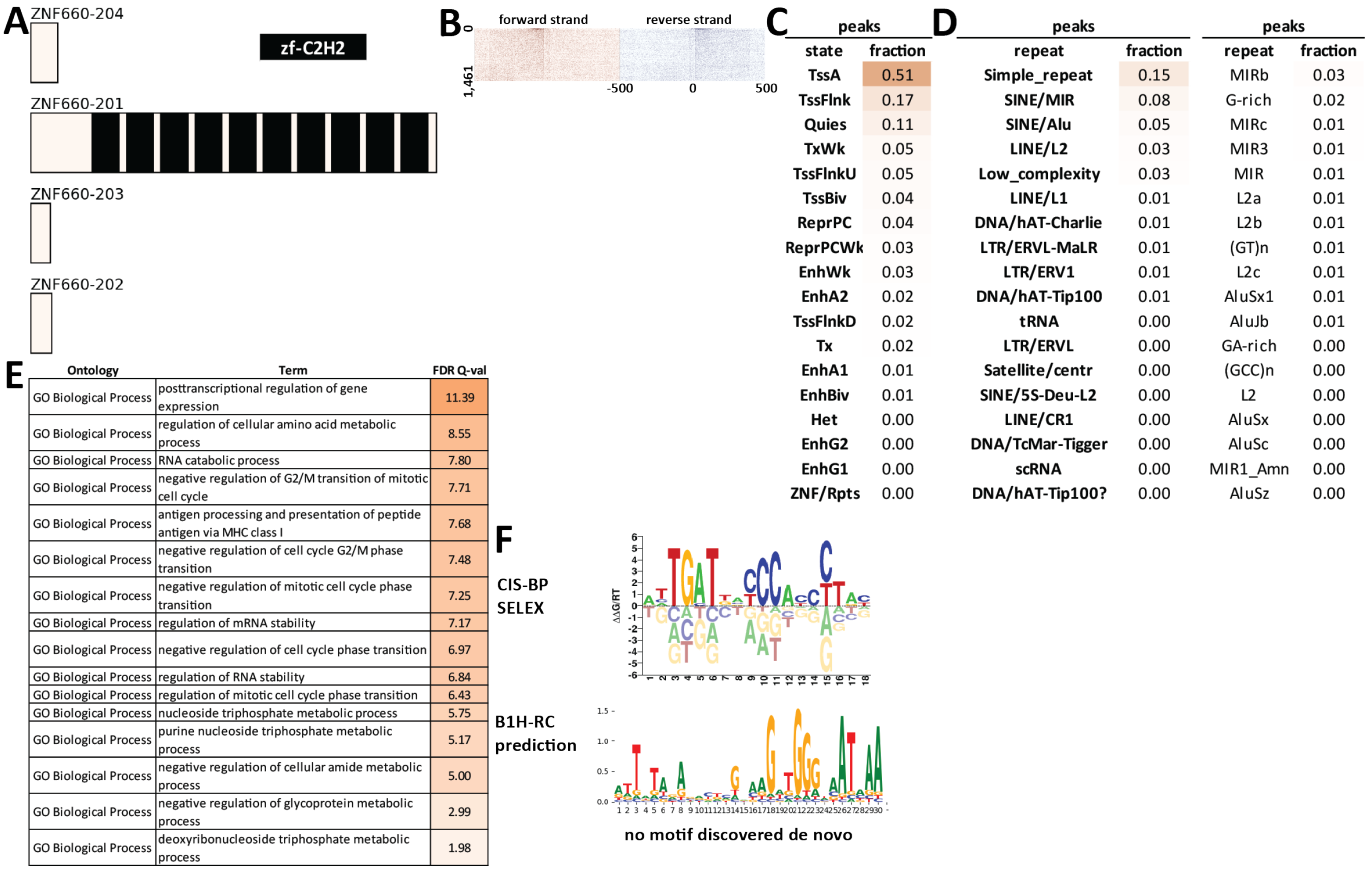

Supplementary Figure 1539: Properties and genomic distribution of motifs identified for the ZNF660 transcription factor in HepG2 (accession ENCSR902AMJ).

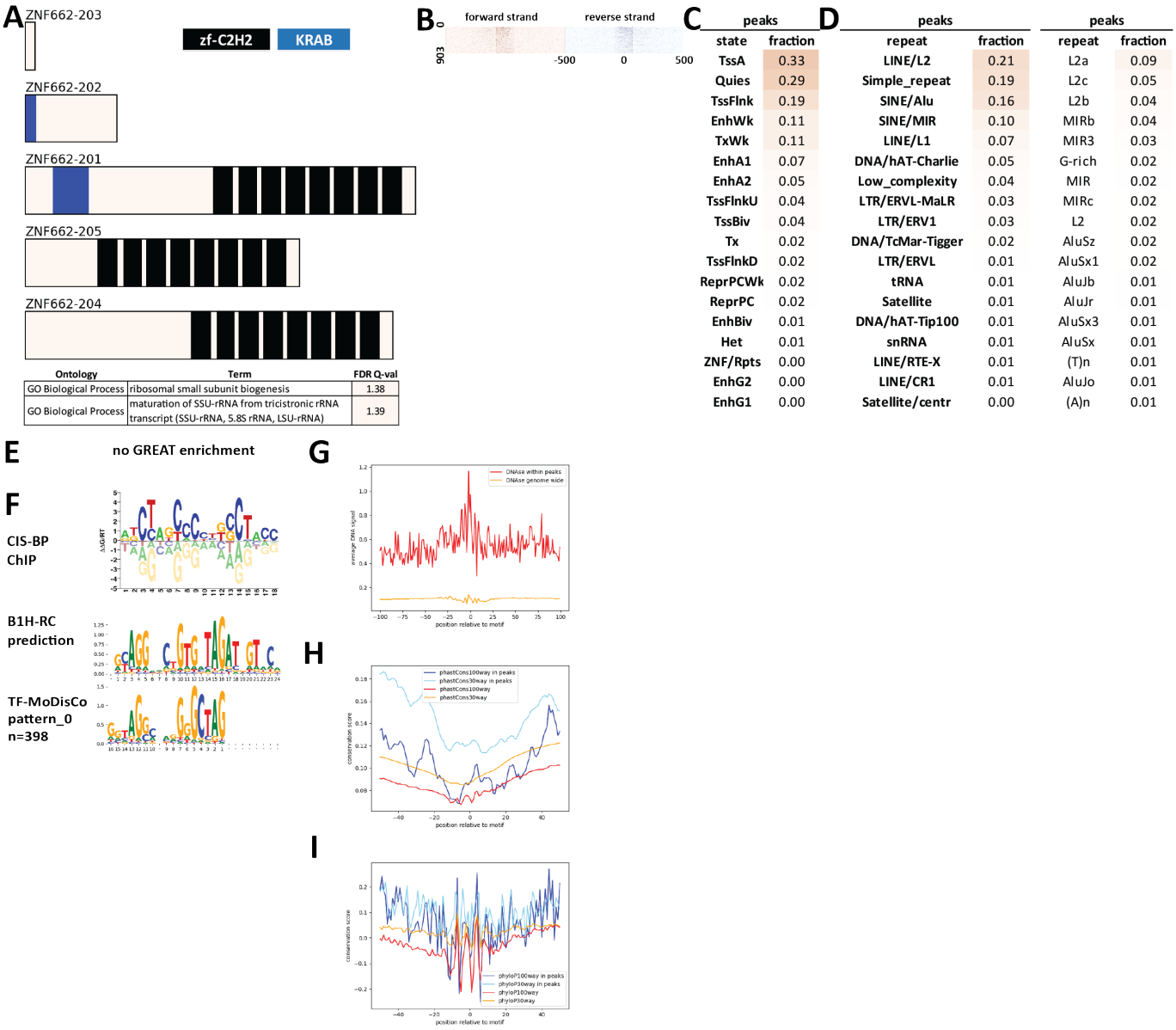

Ontology	Term	FDR Q-val
GO Biological Process	ribosomal small subunit biogenesis	1.38
GO Biological Process	maturation of SSU-rRNA from tricistronic rRNA transcript (SSU-rRNA, 5.8S rRNA, LSU-rRNA)	1.39

C

peaks	
state	fraction
TssA	0.33
Quies	0.29
TssFlnk	0.19
EnhWk	0.11
TxWk	0.11
EnhA1	0.07
EnhA2	0.05
TssFlnkU	0.04
TssBiv	0.04
Tx	0.02
TssFlnkD	0.02
ReprPCWk	0.02
ReprPC	0.02
EnhBiv	0.01
Het	0.01
ZNF/Rpts	0.00
EnhG2	0.00
EnhG1	0.00

D

peaks		peaks	
repeat	fraction	repeat	fraction
LINE/L2	0.21	L2a	0.09
Simple_repeat	0.19	L2c	0.05
SINE/Alu	0.16	L2b	0.04
SINE/MIR	0.10	MIRb	0.04
LINE/L1	0.07	MIR3	0.03
DNA/hAT-Charlie	0.05	G-rich	0.02
Low_complexity	0.04	MIR	0.02
LTR/ERVL-MaLR	0.03	MIRc	0.02
LTR/ERV1	0.03	L2	0.02
DNA/TcMar-Tigger	0.02	AluSz	0.02
LTR/ERVL	0.01	AluSx1	0.02
tRNA	0.01	AluJb	0.01
Satellite	0.01	AluJr	0.01
DNA/hAT-Tip100	0.01	AluSx3	0.01
snRNA	0.01	AluSx	0.01
LINE/RTE-X	0.01	(T)n	0.01
LINE/CR1	0.01	AluJo	0.01
Satellite/centr	0.00	(A)n	0.01

Supplementary Figure 1540: Properties and genomic distribution of motifs identified for the ZNF662 transcription factor in HEK293 (accession ChipExo models).

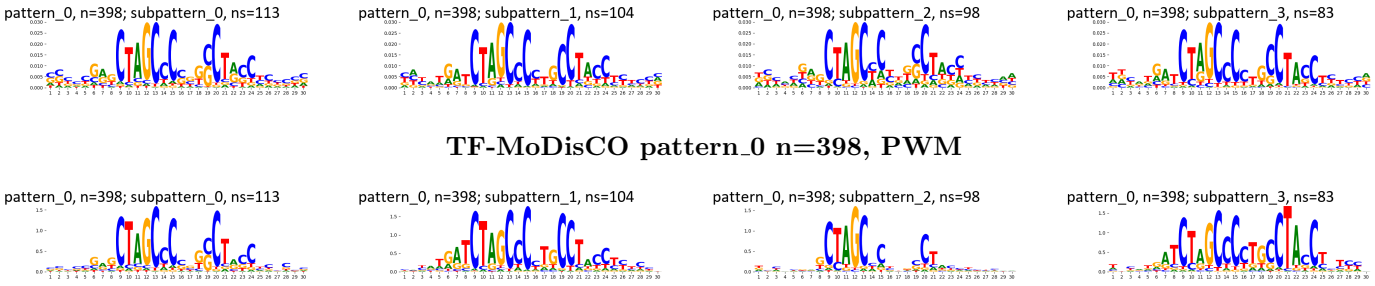

Supplementary Figure 1541: TF-MoDisCO subpatterns for the ZNF662 transcription factor in HEK293 (accession ChipExo models).

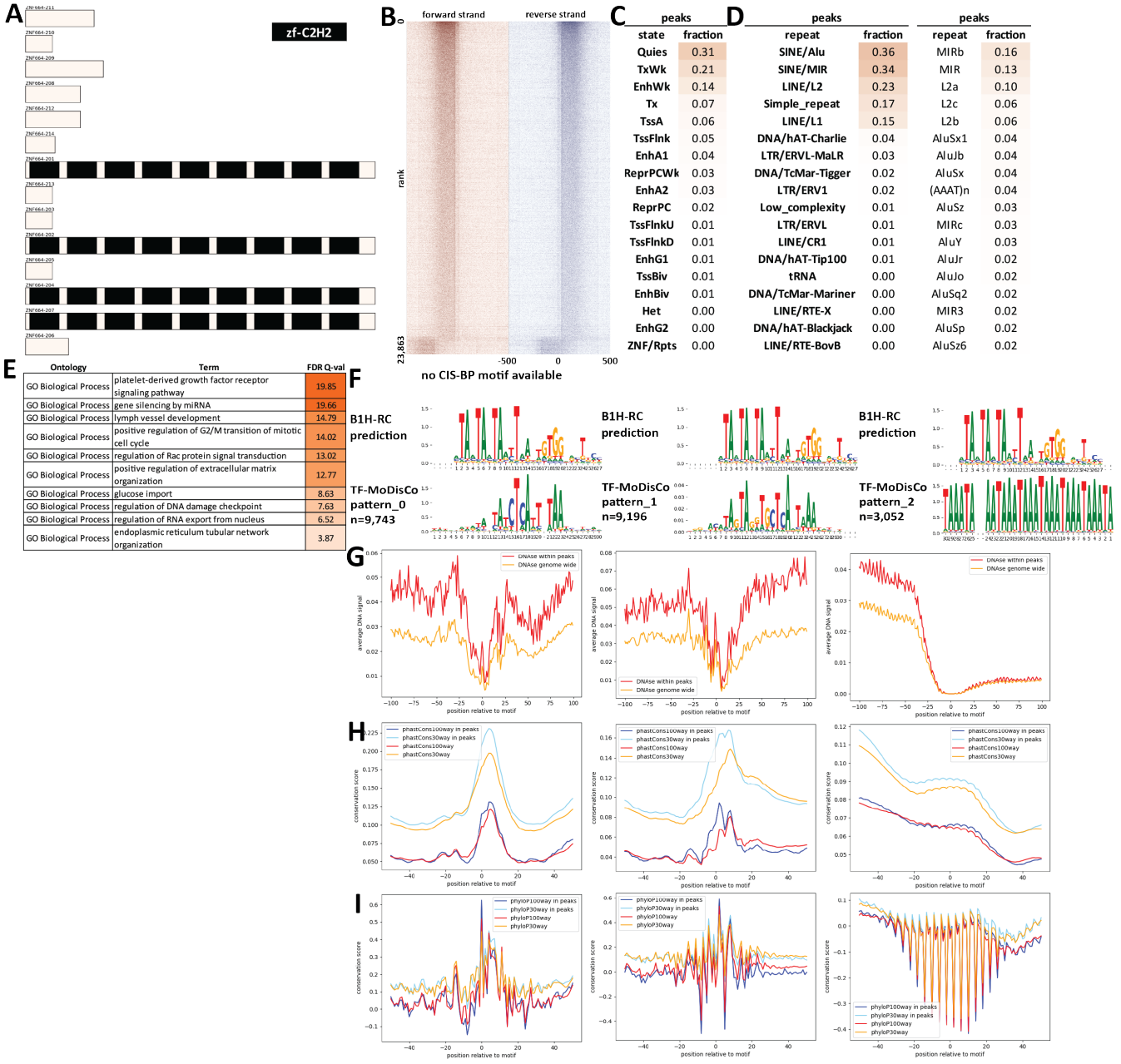

Supplementary Figure 1542: Properties and genomic distribution of motifs identified for the ZNF664 transcription factor in HEK293 (accession ENCSR714LZQ).

TF-MoDisCO pattern_0 n=9743, CWM

pattern_0, n=9743; subpattern_0, ns=2267

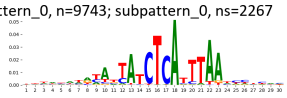

pattern_0, n=9743; subpattern_1, ns=2140

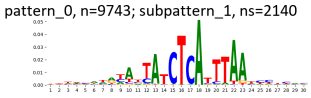

pattern_0, n=9743; subpattern_2, ns=1735

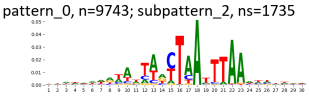

pattern_0, n=9743; subpattern_3, ns=1190

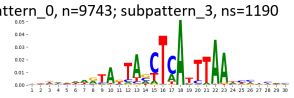

pattern_0, n=9743; subpattern_4, ns=971

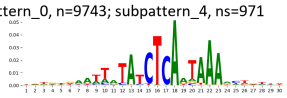

pattern_0, n=9743; subpattern_5, ns=761

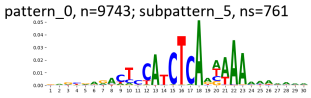

pattern_0, n=9743; subpattern_6, ns=632

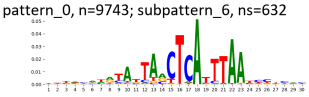

pattern_0, n=9743; subpattern_7, ns=45

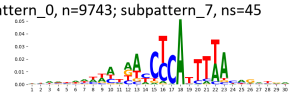

pattern_0, n=9743; subpattern_8, ns=2

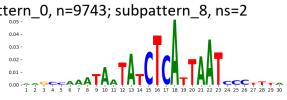

TF-MoDisCO pattern_0 n=9743, PWM

pattern_0, n=9743; subpattern_0, ns=2267

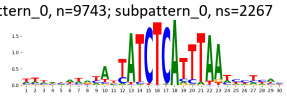

pattern_0, n=9743; subpattern_1, ns=2140

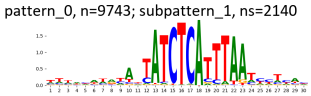

pattern_0, n=9743; subpattern_2, ns=1735

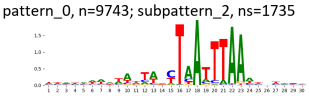

pattern_0, n=9743; subpattern_3, ns=1190

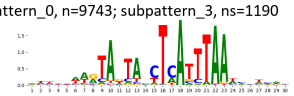

pattern_0, n=9743; subpattern_4, ns=971

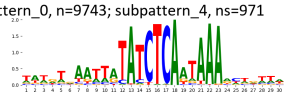

pattern_0, n=9743; subpattern_5, ns=761

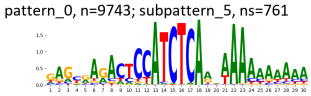

pattern_0, n=9743; subpattern_6, ns=632

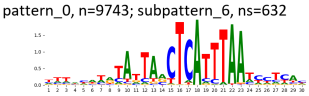

pattern_0, n=9743; subpattern_7, ns=45

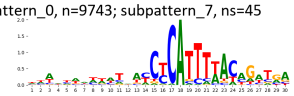

pattern_0, n=9743; subpattern_8, ns=2

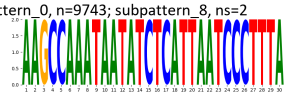

TF-MoDisCO pattern_1 n=9196, CWM

pattern_1, n=9196; subpattern_0, ns=1659

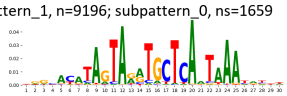

pattern_1, n=9196; subpattern_1, ns=1617

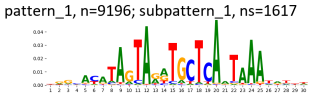

pattern_1, n=9196; subpattern_2, ns=1381

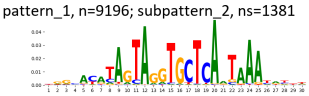

pattern_1, n=9196; subpattern_3, ns=1362

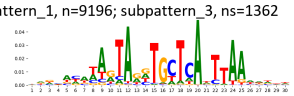

pattern_1, n=9196; subpattern_4, ns=1305

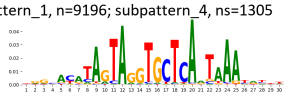

pattern_1, n=9196; subpattern_5, ns=1292

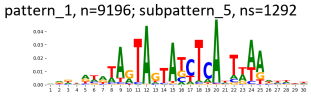

pattern_1, n=9196; subpattern_6, ns=580

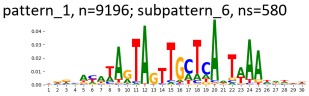

TF-MoDisCO pattern_1 n=9196, PWM

pattern_1, n=9196; subpattern_0, ns=1659

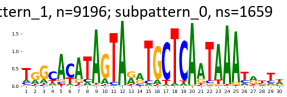

pattern_1, n=9196; subpattern_1, ns=1617

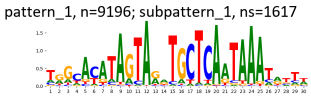

pattern_1, n=9196; subpattern_2, ns=1381

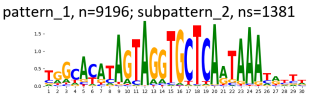

pattern_1, n=9196; subpattern_3, ns=1362

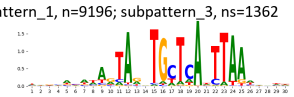

pattern_1, n=9196; subpattern_4, ns=1305

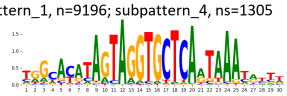

pattern_1, n=9196; subpattern_5, ns=1292

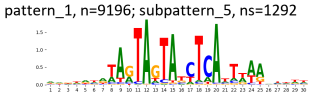

pattern_1, n=9196; subpattern_6, ns=580

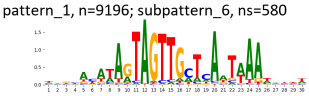

TF-MoDisCO pattern_2 n=3052, CWM

pattern_2, n=3052; subpattern_0, ns=975

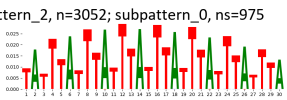

pattern_2, n=3052; subpattern_1, ns=841

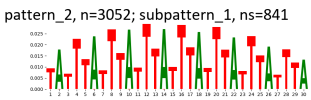

pattern_2, n=3052; subpattern_2, ns=490

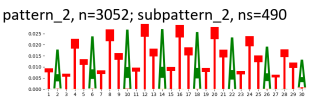

pattern_2, n=3052; subpattern_3, ns=442

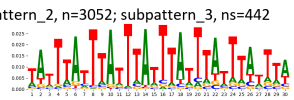

pattern_2, n=3052; subpattern_4, ns=301

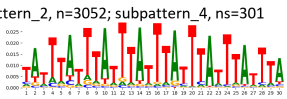

pattern_2, n=3052; subpattern_5, ns=3

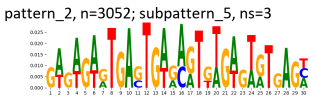

TF-MoDisCO pattern_2 n=3052, PWM

pattern_2, n=3052; subpattern_0, ns=975



pattern_2, n=3052; subpattern_1, ns=841



pattern_2, n=3052; subpattern_2, ns=490

pattern_2, n=3052; subpattern_3, ns=442

pattern_2, n=3052; subpattern_4, ns=301

pattern_2, n=3052; subpattern_5, ns=3

Supplementary Figure 1543: TF-MoDisCO subpatterns for the ZNF664 transcription factor in HEK293 (accession ENCSR714LZQ).

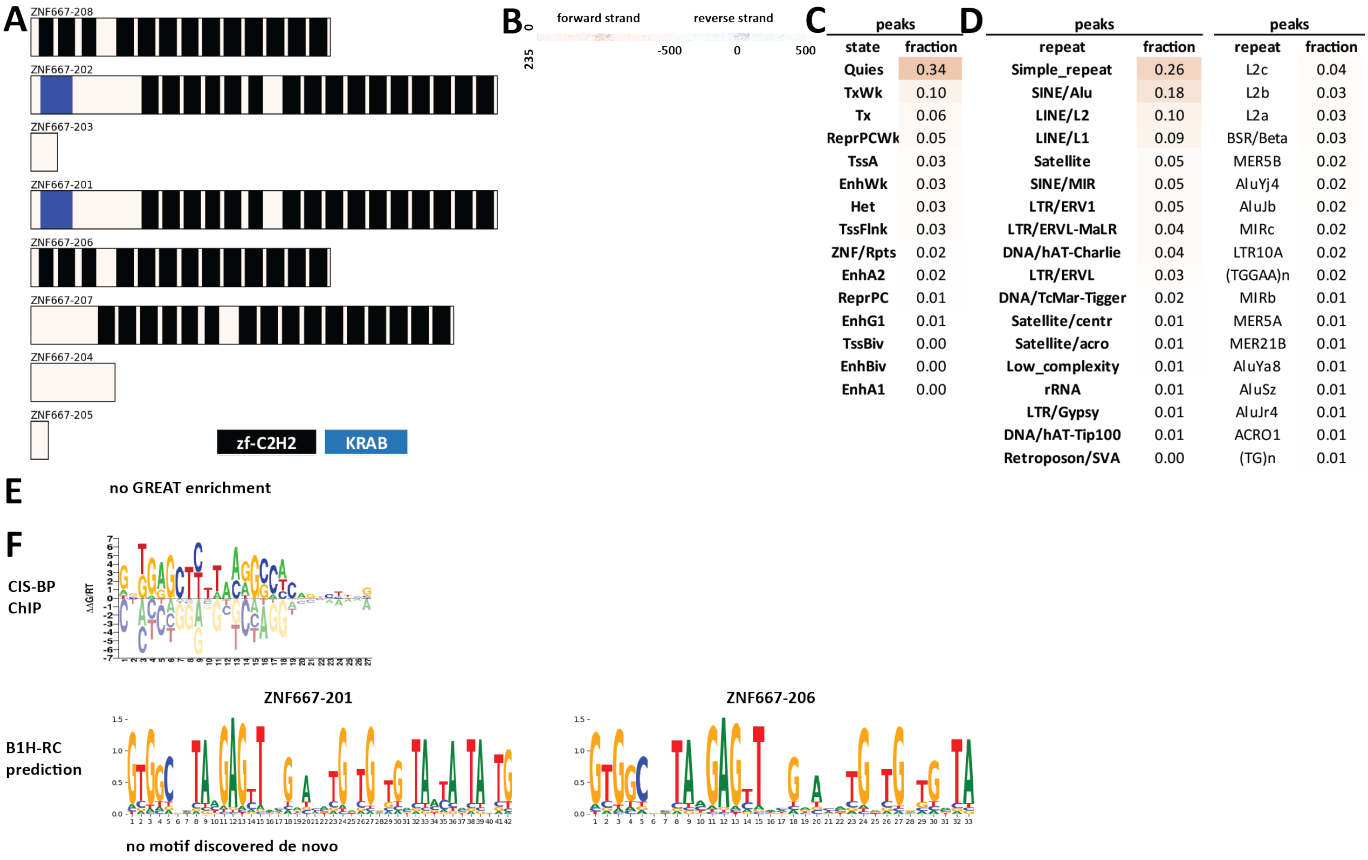

Supplementary Figure 1544: Properties and genomic distribution of motifs identified for the ZNF667 transcription factor in HEK293 (accession ChipExo models).

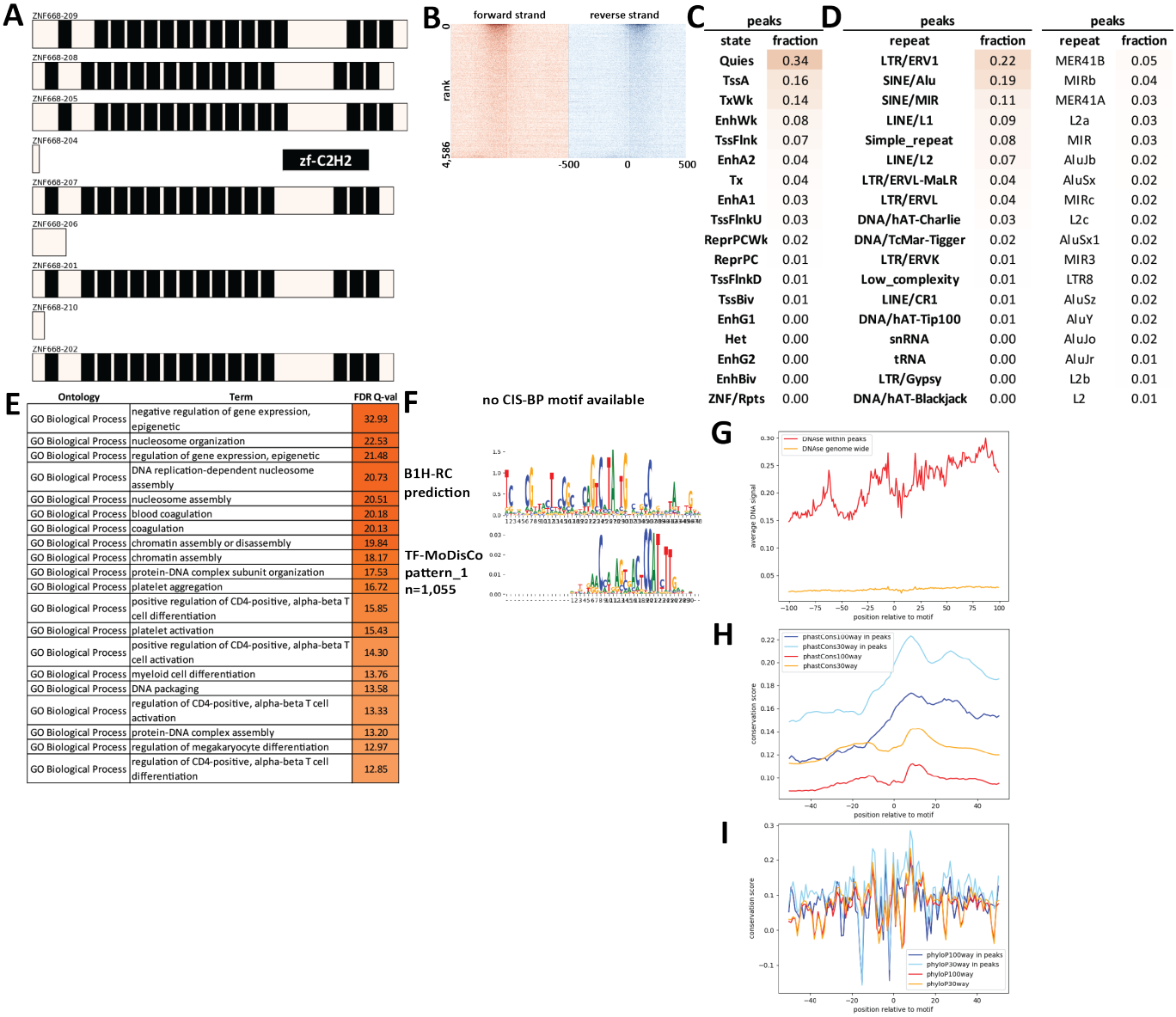

C

peaks	
state	fraction
Quies	0.34
TssA	0.16
TxWk	0.14
EnhWk	0.08
TssFlnk	0.07
EnhA2	0.04
Tx	0.04
EnhA1	0.03
TssFlnkU	0.03
ReprPCWk	0.02
ReprPC	0.01
TssFlnkD	0.01
TssBiv	0.01
EnhG1	0.00
Het	0.00
EnhG2	0.00
EnhBiv	0.00
ZNF/Rpts	0.00

D

peaks		peaks	
repeat	fraction	repeat	fraction
LTR/ERV1	0.22	MER41B	0.05
SINE/Alu	0.19	MIRb	0.04
SINE/MIR	0.11	MER41A	0.03
LINE/L1	0.09	L2a	0.03
Simple_repeat	0.08	MIR	0.03
LINE/L2	0.07	AluJb	0.02
LTR/ERVL-MaLR	0.04	AluSx	0.02
LTR/ERVL	0.04	MIRc	0.02
DNA/hAT-Charlie	0.03	L2c	0.02
DNA/TcMar-Tigger	0.02	AluSx1	0.02
LTR/ERVK	0.01	MIR3	0.02
Low_complexity	0.01	LTR8	0.02
LINE/CR1	0.01	AluSz	0.02
DNA/hAT-Tip100	0.01	AluY	0.02
snRNA	0.00	AluJo	0.02
tRNA	0.00	AluJr	0.01
LTR/Gypsy	0.00	L2b	0.01
DNA/hAT-Blackjack	0.00	L2	0.01

E

Ontology	Term	FDR Q-val
GO Biological Process	negative regulation of gene expression, epigenetic	32.93
GO Biological Process	nucleosome organization	22.53
GO Biological Process	regulation of gene expression, epigenetic	21.48
GO Biological Process	DNA replication-dependent nucleosome assembly	20.73
GO Biological Process	nucleosome assembly	20.51
GO Biological Process	blood coagulation	20.18
GO Biological Process	coagulation	20.13
GO Biological Process	chromatin assembly or disassembly	19.84
GO Biological Process	chromatin assembly	18.17
GO Biological Process	protein-DNA complex subunit organization	17.53
GO Biological Process	platelet aggregation	16.72
GO Biological Process	positive regulation of CD4-positive, alpha-beta T cell differentiation	15.85
GO Biological Process	platelet activation	15.43
GO Biological Process	positive regulation of CD4-positive, alpha-beta T cell activation	14.30
GO Biological Process	myeloid cell differentiation	13.76
GO Biological Process	DNA packaging	13.58
GO Biological Process	regulation of CD4-positive, alpha-beta T cell activation	13.33
GO Biological Process	protein-DNA complex assembly	13.20
GO Biological Process	regulation of megakaryocyte differentiation	12.97
GO Biological Process	regulation of CD4-positive, alpha-beta T cell differentiation	12.85

Supplementary Figure 1545: Properties and genomic distribution of motifs identified for the ZNF668 transcription factor in K562 (accession ENCSR682AAS).

TF-MoDisCO pattern_1 n=1055, CWM

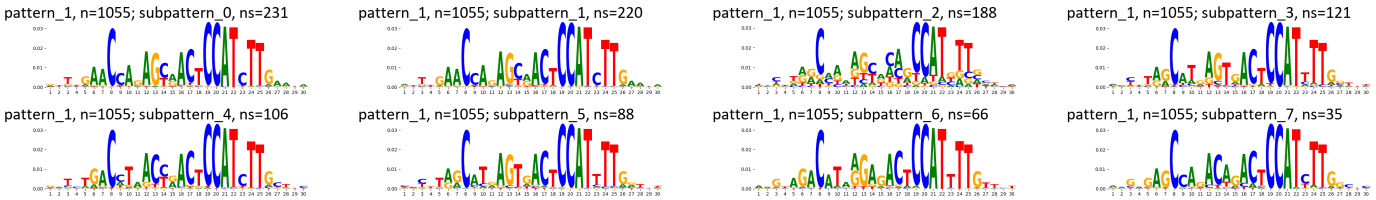

TF-MoDisCO pattern_1 n=1055, PWM

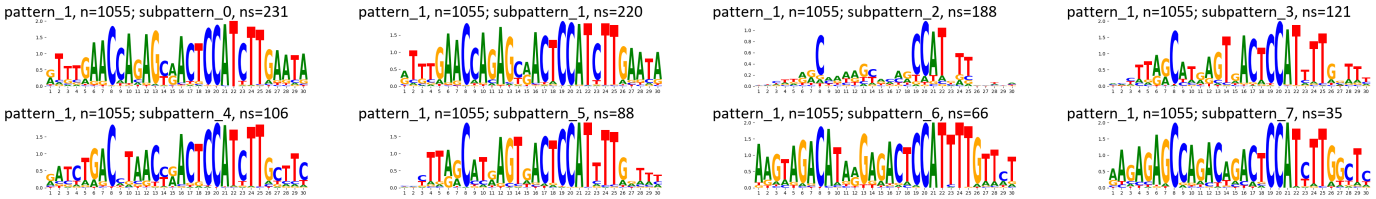

Supplementary Figure 1546: TF-MoDisCO subpatterns for the ZNF668 transcription factor in K562 (accession ENCSR682AAS).

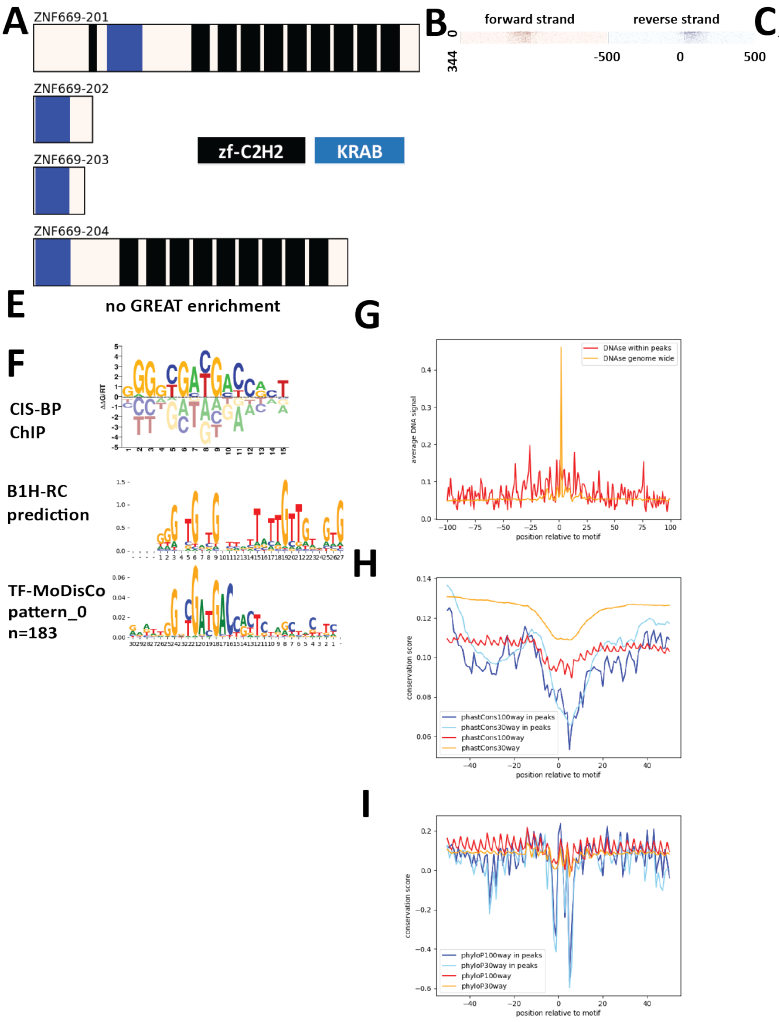

C

peaks	
state	fraction
Quies	0.53
TxWk	0.11
TssA	0.08
Tx	0.07
Het	0.06
EnhWk	0.05
EnhA2	0.04
TssFlnk	0.03
EnhA1	0.03
ReprPCWk	0.02
TssFlnkU	0.01
TssBiv	0.01
ZNF/Rpts	0.01
ReprPC	0.01
EnhG2	0.00
EnhG1	0.00

D

peaks	
repeat	fraction
LTR/ERV1	0.63
LINE/L1	0.12
SINE/Alu	0.04
LTR/ERVL	0.04
LINE/L2	0.04
LTR/ERVL-MaLR	0.03
SINE/MIR	0.03
DNA/hAT-Charlie	0.02
LINE/CR1	0.01
snRNA	0.01
Simple_repeat	0.01
Low_complexity	0.01
DNA/TcMar-Tc2	0.01
DNA/hAT-Tip100	0.00
DNA/TcMar-Tigger	0.00

peaks	
repeat	fraction
HERV9-int	0.10
HERV17-int	0.07
LTR17	0.06
LTR12	0.05
HERV9NC-int	0.04
LTR12F	0.03
LTR12_	0.02
HERV9N-int	0.02
LTR76	0.02
L2a	0.02
LTR18A	0.02
LTR12D	0.02
MIRc	0.01
MER61-int	0.01
LTR12C	0.01
LTR12B	0.01
LTR25-int	0.01
MIRb	0.01

Supplementary Figure 1547: Properties and genomic distribution of motifs identified for the ZNF669 transcription factor in HEK293 (accession Hughes NB models).

TF-MoDisCO pattern_0 n=183, CWM

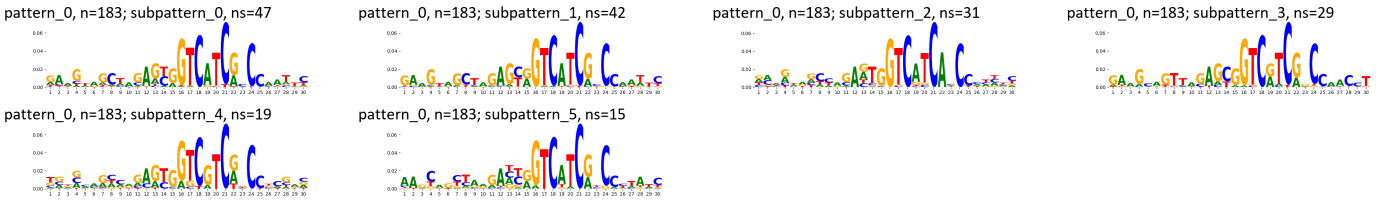

TF-MoDisCO pattern_0 n=183, PWM

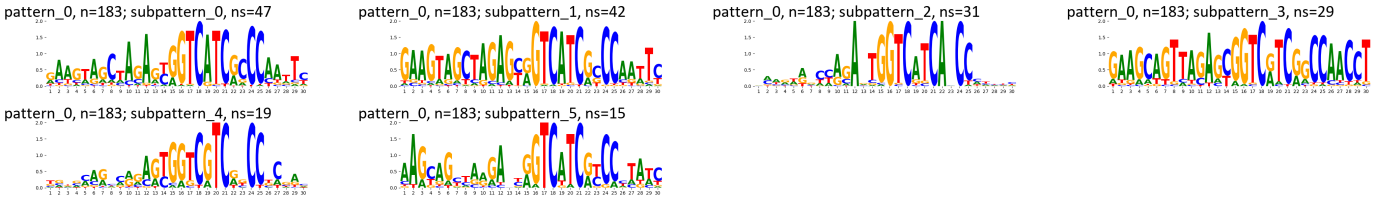

Supplementary Figure 1548: TF-MoDisCO subpatterns for the ZNF669 transcription factor in HEK293 (accession Hughes NB models).

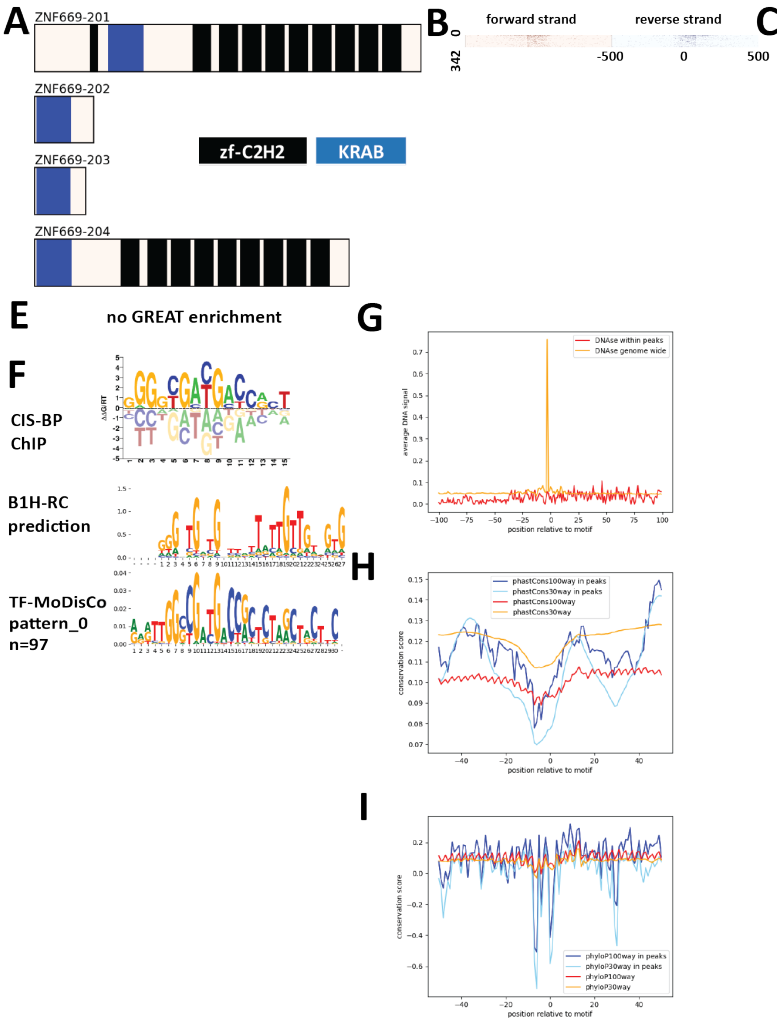

C

peaks	
state	fraction
Quies	0.55
TxWk	0.11
Tx	0.04
ReprPCWk	0.03
TssBiv	0.02
Het	0.02
TssA	0.01
ReprPC	0.01
EnhWk	0.01
EnhA2	0.01
ZNF/Rpts	0.01
TssFlnk	0.01
EnhG1	0.01
TssFlnkU	0.00
EnhA1	0.00

D

peaks		peaks	
repeat	fraction	repeat	fraction
LTR/ERV1	0.81	HERV17-int	0.14
Simple_repeat	0.16	LTR17	0.10
SINE/Alu	0.10	HERV9-int	0.09
LINE/L1	0.08	HERV9NC-int	0.08
LTR/ERVL	0.04	LTR12	0.04
LINE/L2	0.04	LTR12F	0.04
Satellite/centr	0.03	LTR12C	0.04
Satellite	0.03	LTR12D	0.03
SINE/MIR	0.03	HERV9N-int	0.03
LTR/ERVL-MaLR	0.02	SST1	0.03
Low_complexity	0.02	LTR12_	0.02
Satellite/acro	0.01	LTR12B	0.02
DNA/hAT-Charlie	0.01	AluSx1	0.02
DNA/TcMar-Tigger	0.01	MER61-int	0.01
rRNA	0.01	L2a	0.01
Satellite/telo	0.00	HUERS-P3b-ir	0.01
LTR/Gypsy?	0.00	HUERS-P2-in	0.01
LTR/ERVK	0.00	BSR/Beta	0.01

Supplementary Figure 1549: Properties and genomic distribution of motifs identified for the ZNF669 transcription factor in HEK293 (accession ChipExo models).

TF-MoDisCO pattern_0 n=97, CWM

pattern_0, n=97; subpattern_0, ns=41

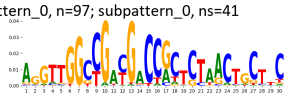

pattern_0, n=97; subpattern_1, ns=29

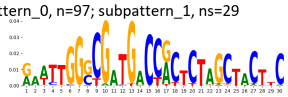

pattern_0, n=97; subpattern_2, ns=27

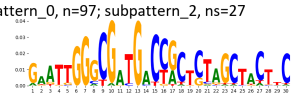

TF-MoDisCO pattern_0 n=97, PWM

pattern_0, n=97; subpattern_0, ns=41

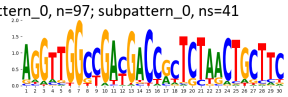

pattern_0, n=97; subpattern_1, ns=29

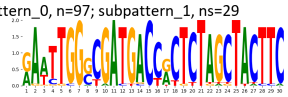

pattern_0, n=97; subpattern_2, ns=27

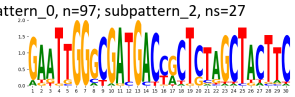

Supplementary Figure 1550: TF-MoDisCO subpatterns for the ZNF669 transcription factor in HEK293 (accession ChipExo models).

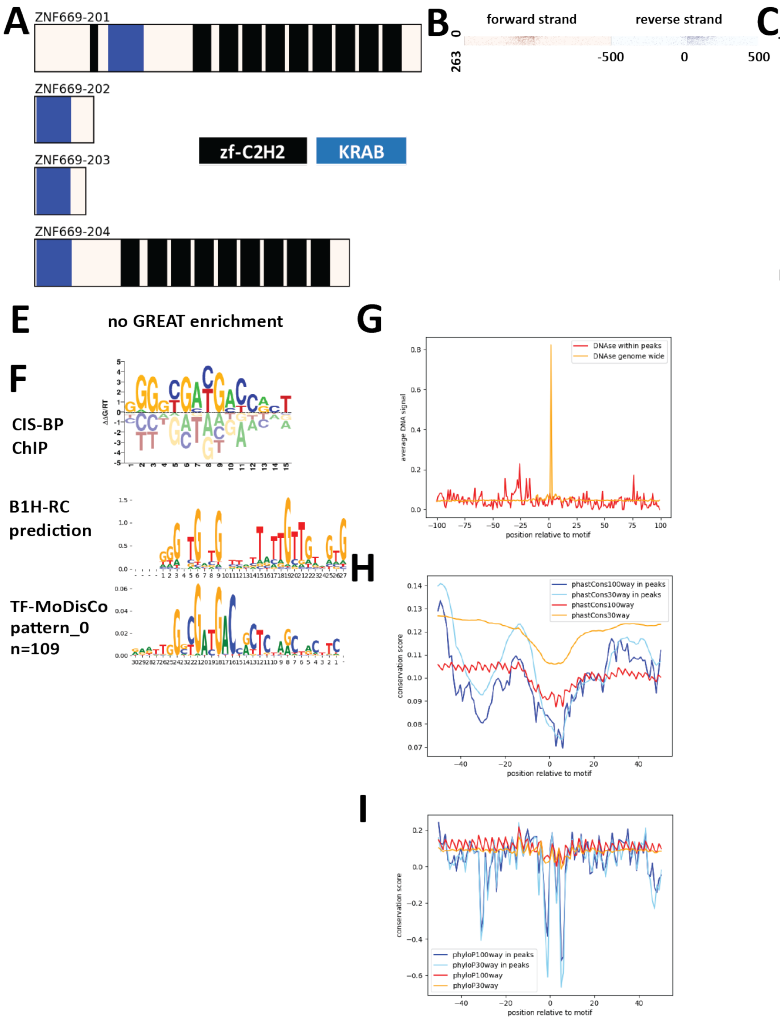

Supplementary Figure 1551: Properties and genomic distribution of motifs identified for the ZNF669 transcription factor in HEK293 (accession Hughes GR models).

TF-MoDisCO pattern_0 n=109, CWM

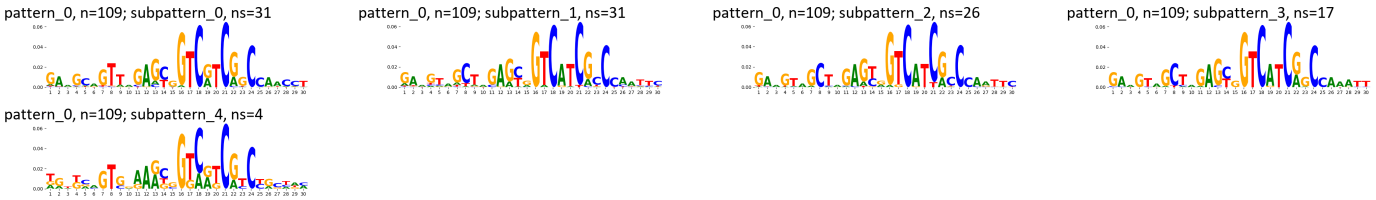

TF-MoDisCO pattern_0 n=109, PWM

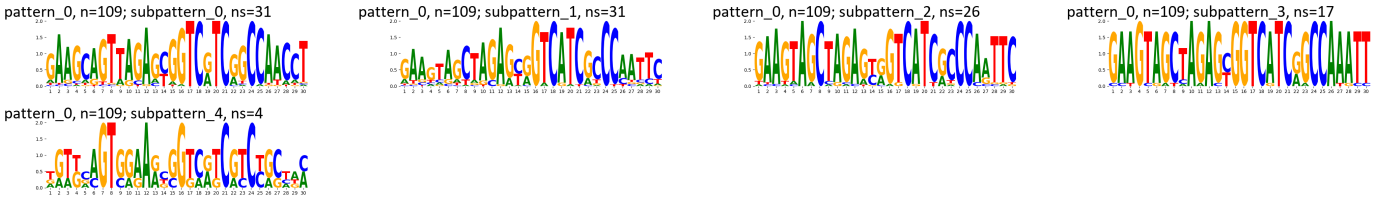

Supplementary Figure 1552: TF-MoDisCO subpatterns for the ZNF669 transcription factor in HEK293 (accession Hughes GR models).

A

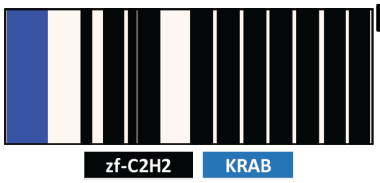

B

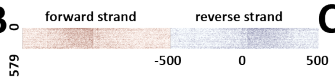

C

peaks	
state	fraction
Quies	0.45
TxWk	0.12
TssA	0.07
TssFlnk	0.05
ReprPCWk	0.05
EnhWk	0.04
Tx	0.03
ReprPC	0.03
EnhA2	0.03
Het	0.02
EnhA1	0.02
TssBiv	0.02
TssFlnkD	0.01
TssFlnkU	0.01
EnhG1	0.01
EnhBiv	0.01
EnhG2	0.00
ZNF/Rpts	0.00

D

peaks		peaks	
repeat	fraction	repeat	fraction
Simple_repeat	0.74	(GT)n	0.12
SINE/Alu	0.16	(CA)n	0.09
LINE/L1	0.07	(AC)n	0.09
Low_complexity	0.05	(TG)n	0.07
SINE/MIR	0.04	(AAAT)n	0.04
LINE/L2	0.04	GA-rich	0.03
LTR/ERV1	0.02	AluSx	0.02
LTR/ERVL-MaLR	0.01	AluJb	0.02
LTR/ERVL	0.01	L2a	0.02
DNA/TcMar-Tigger	0.01	MIR	0.02
LINE/CR1	0.01	AluSz	0.02
DNA/hAT-Tip100	0.01	MIRb	0.01
DNA/hAT-Charlie	0.01	AluSx1	0.01
srpRNA	0.00	A-rich	0.01
Satellite/centr	0.00	AluJo	0.01
LTR/ERVK	0.00	L2	0.01
DNA/TcMar-Tc2	0.00	AluY	0.01
		AluSq2	0.01

E

Ontology	Term	FDR Q-val
GO Biological Process	positive regulation of glial cell differentiation	4.20
GO Biological Process	kidney epithelium development	3.84
GO Biological Process	trachea cartilage development	2.86
GO Biological Process	positive regulation of mesenchymal cell proliferation	2.66
GO Biological Process	mesonephros development	2.61
GO Biological Process	ureteric bud development	2.45
GO Biological Process	mesonephric tubule development	2.44
GO Biological Process	positive regulation of kidney development	2.10
GO Biological Process	regulation of mesenchymal cell proliferation	1.69
GO Biological Process	trachea development	1.52

F

no CIS-BP motif available

B1H-RC prediction

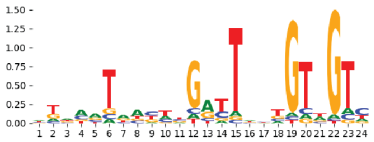

no motif discovered de novo

Supplementary Figure 1553: Properties and genomic distribution of motifs identified for the ZNF670 transcription factor in HEK293 (accession ENCSR233MWH).

A



B

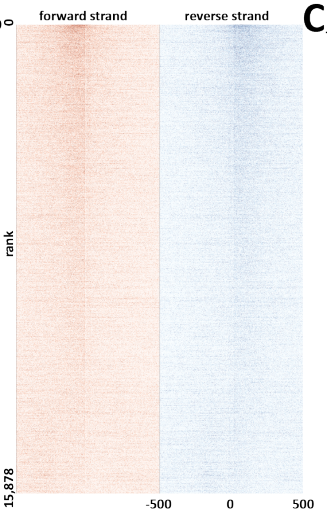

C

peaks	
state	fraction
TssA	0.32
Quies	0.19
TssFlnk	0.18
TxWk	0.10
EnhWk	0.07
TssFlnkU	0.04
EnhA2	0.03
EnhA1	0.03
Tx	0.02
TssBiv	0.02
TssFlnkD	0.02
ReprPC	0.02
ReprPCWk	0.02
EnhG1	0.01
EnhBiv	0.01
EnhG2	0.00
Het	0.00
ZNF/Rpts	0.00

D

peaks		peaks	
repeat	fraction	repeat	fraction
Simple_repeat	0.20	MIRb	0.05
SINE/Alu	0.19	MIR	0.03
SINE/MIR	0.13	L2a	0.03
LINE/L2	0.08	G-rich	0.03
LINE/L1	0.06	MIR3	0.02
Low_complexity	0.04	MIRc	0.02
DNA/hAT-Charlie	0.04	L2c	0.02
LTR/ERV1	0.03	AluSx1	0.02
LTR/ERVL-MaLR	0.02	AluJb	0.02
LTR/ERVL	0.02	L2b	0.02
DNA/TcMar-Tigger	0.01	AluSx	0.02
LINE/CR1	0.01	AluSz	0.02
DNA/hAT-Tip100	0.01	AluJr	0.01
tRNA	0.01	AluJo	0.01
LTR/ERVK	0.00	AluY	0.01
DNA/hAT-Blackjack	0.00	AluSq2	0.01
LINE/RTE-BovB	0.00	GA-rich	0.01
LINE/RTE-X	0.00	AluSp	0.01

E

Ontology	Term	FDR Q-val
GO Biological Process	regulation of transcription from RNA polymerase II promoter in response to stress	45.30
GO Biological Process	regulation of DNA-templated transcription in response to stress	41.29
GO Biological Process	mRNA catabolic process	37.73
GO Biological Process	nuclear-transcribed mRNA catabolic process	35.23
GO Biological Process	rRNA processing	35.20
GO Biological Process	regulation of intrinsic apoptotic signaling pathway	33.89
GO Biological Process	nuclear-transcribed mRNA catabolic process, nonsense-mediated decay	30.16
GO Biological Process	liver regeneration	29.90
GO Biological Process	viral gene expression	28.41
GO Biological Process	multi-organism metabolic process	28.02
GO Biological Process	regulation of necrotic cell death	26.12
GO Biological Process	negative regulation of intrinsic apoptotic signaling pathway	25.08
GO Biological Process	RNA phosphodiester bond hydrolysis	25.03
GO Biological Process	cotranslational protein targeting to membrane	24.97
GO Biological Process	regulation of transcription from RNA polymerase II promoter in response to hypoxia	24.81
GO Biological Process	translational elongation	24.75
GO Biological Process	viral transcription	24.37
GO Biological Process	protein targeting to ER	24.09
GO Biological Process	SRP-dependent cotranslational protein targeting to membrane	23.99
GO Biological Process	cellular response to topologically incorrect protein	22.14
Human Phenotype	Abnormality of transition element cation homeostasis	10.55
Human Phenotype	Abnormality of reticulocytes	8.26

F

no CIS-BP motif available

B1H-RC prediction

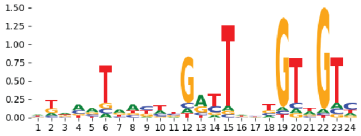

no motif discovered de novo

Supplementary Figure 1554: Properties and genomic distribution of motifs identified for the ZNF670 transcription factor in HepG2 (accession ENCSR699ZES).

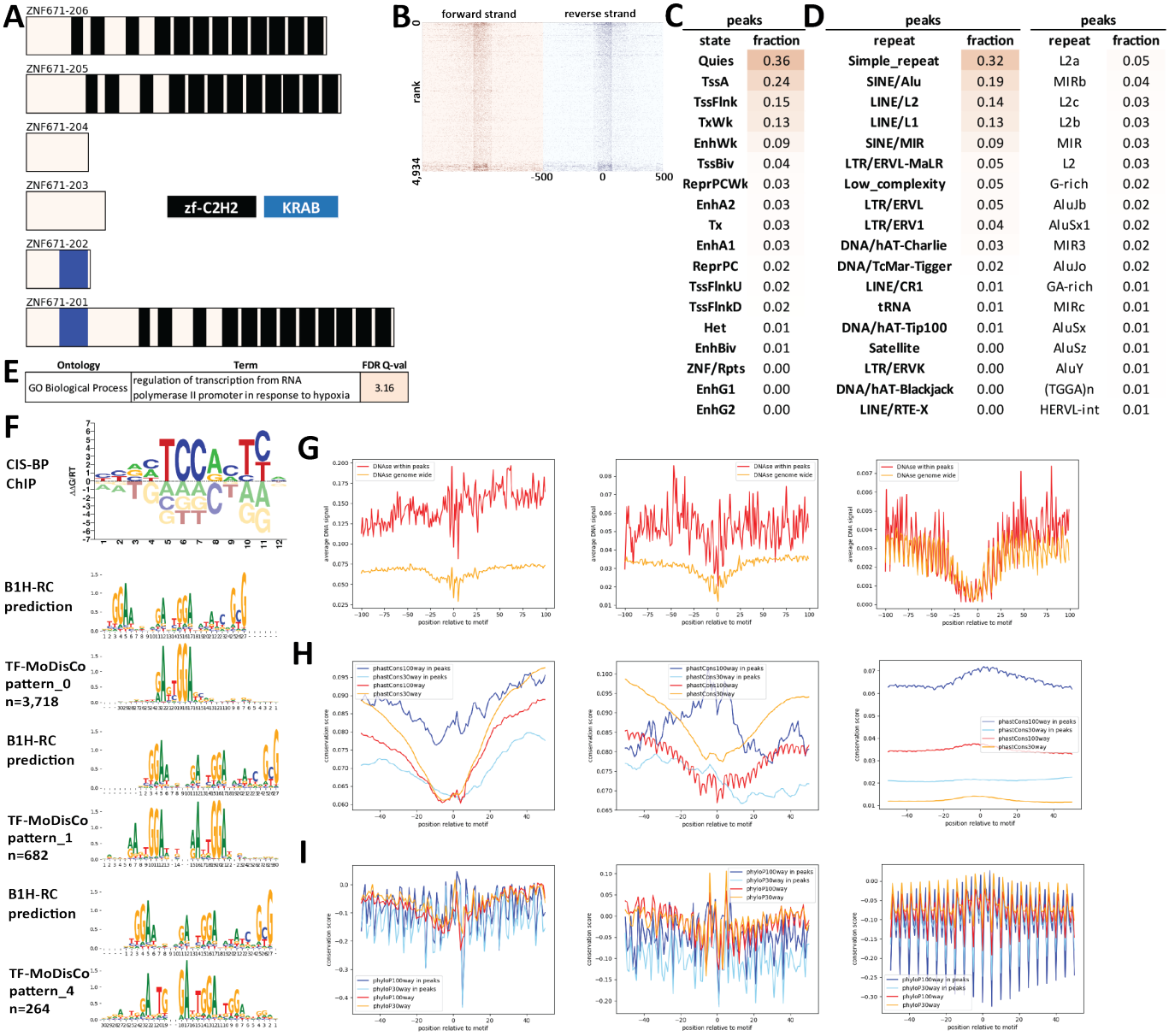

Supplementary Figure 1555: Properties and genomic distribution of motifs identified for the ZNF671 transcription factor in HEK293 (accession ChipExo models).

TF-MoDisCO pattern_0 n=3718, CWM

pattern_0, n=3718; subpattern_0, ns=690

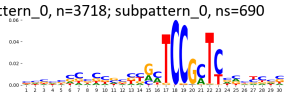

pattern_0, n=3718; subpattern_1, ns=666

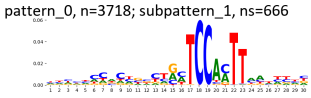

pattern_0, n=3718; subpattern_2, ns=606

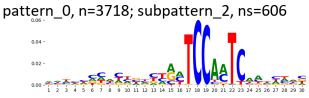

pattern_0, n=3718; subpattern_3, ns=556

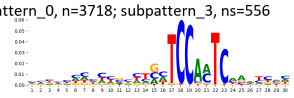

pattern_0, n=3718; subpattern_4, ns=551

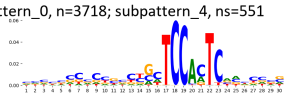

pattern_0, n=3718; subpattern_5, ns=302

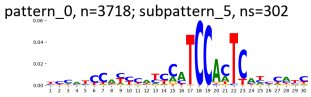

pattern_0, n=3718; subpattern_6, ns=192

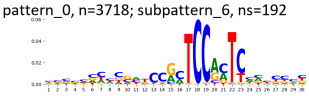

pattern_0, n=3718; subpattern_7, ns=111

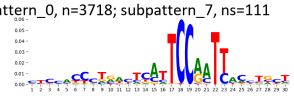

pattern_0, n=3718; subpattern_8, ns=44

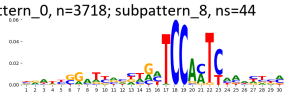

TF-MoDisCO pattern_0 n=3718, PWM

pattern_0, n=3718; subpattern_0, ns=690

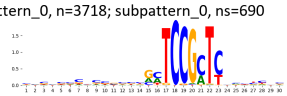

pattern_0, n=3718; subpattern_1, ns=666

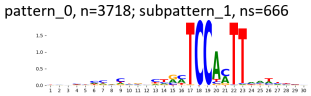

pattern_0, n=3718; subpattern_2, ns=606

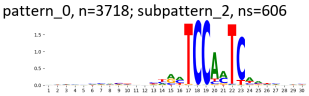

pattern_0, n=3718; subpattern_3, ns=556

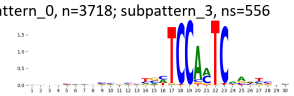

pattern_0, n=3718; subpattern_4, ns=551

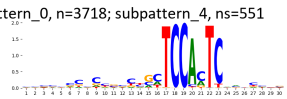

pattern_0, n=3718; subpattern_5, ns=302

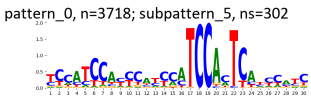

pattern_0, n=3718; subpattern_6, ns=192

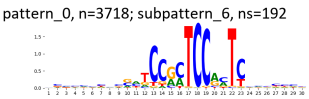

pattern_0, n=3718; subpattern_7, ns=111

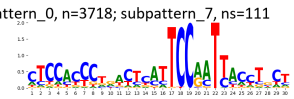

pattern_0, n=3718; subpattern_8, ns=44

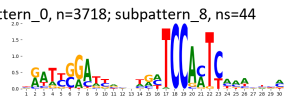

TF-MoDisCO pattern_1 n=682, CWM

pattern_1, n=682; subpattern_0, ns=198

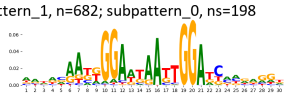

pattern_1, n=682; subpattern_1, ns=164

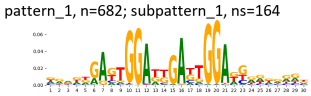

pattern_1, n=682; subpattern_2, ns=135

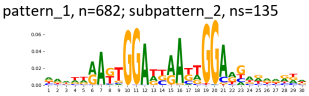

pattern_1, n=682; subpattern_3, ns=98

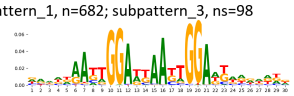

pattern_1, n=682; subpattern_4, ns=77

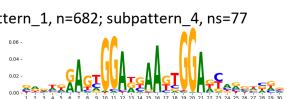

pattern_1, n=682; subpattern_5, ns=10

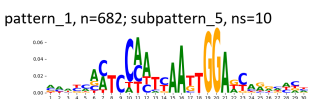

TF-MoDisCO pattern_1 n=682, PWM

pattern_1, n=682; subpattern_0, ns=198

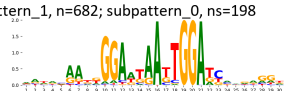

pattern_1, n=682; subpattern_1, ns=164

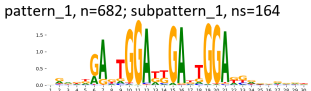

pattern_1, n=682; subpattern_2, ns=135

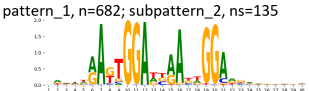

pattern_1, n=682; subpattern_3, ns=98

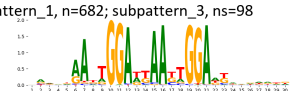

pattern_1, n=682; subpattern_4, ns=77

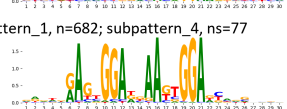

pattern_1, n=682; subpattern_5, ns=10

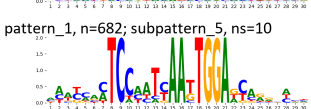

TF-MoDisCO pattern_4 n=264, CWM

pattern_4, n=264; subpattern_0, ns=70

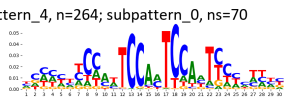

pattern_4, n=264; subpattern_1, ns=69

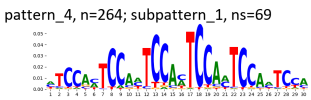

pattern_4, n=264; subpattern_2, ns=51

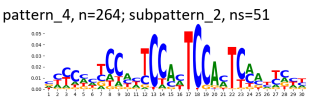

pattern_4, n=264; subpattern_3, ns=38

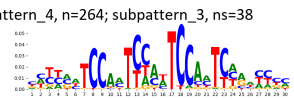

pattern_4, n=264; subpattern_4, ns=18

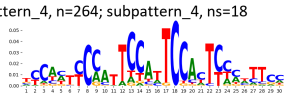

pattern_4, n=264; subpattern_5, ns=18

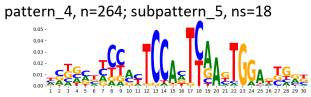

TF-MoDisCO pattern_4 n=264, PWM

pattern_4, n=264; subpattern_0, ns=70

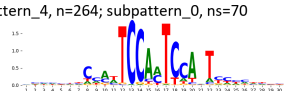

pattern_4, n=264; subpattern_1, ns=69

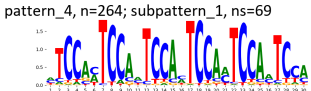

pattern_4, n=264; subpattern_2, ns=51

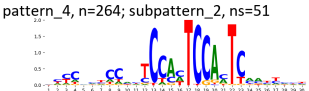

pattern_4, n=264; subpattern_3, ns=38

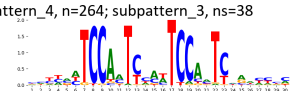

pattern_4, n=264; subpattern_4, ns=18

pattern_4, n=264; subpattern_5, ns=18

Supplementary Figure 1556: TF-MoDisCO subpatterns for the ZNF671 transcription factor in HEK293 (accession ChipExo models).

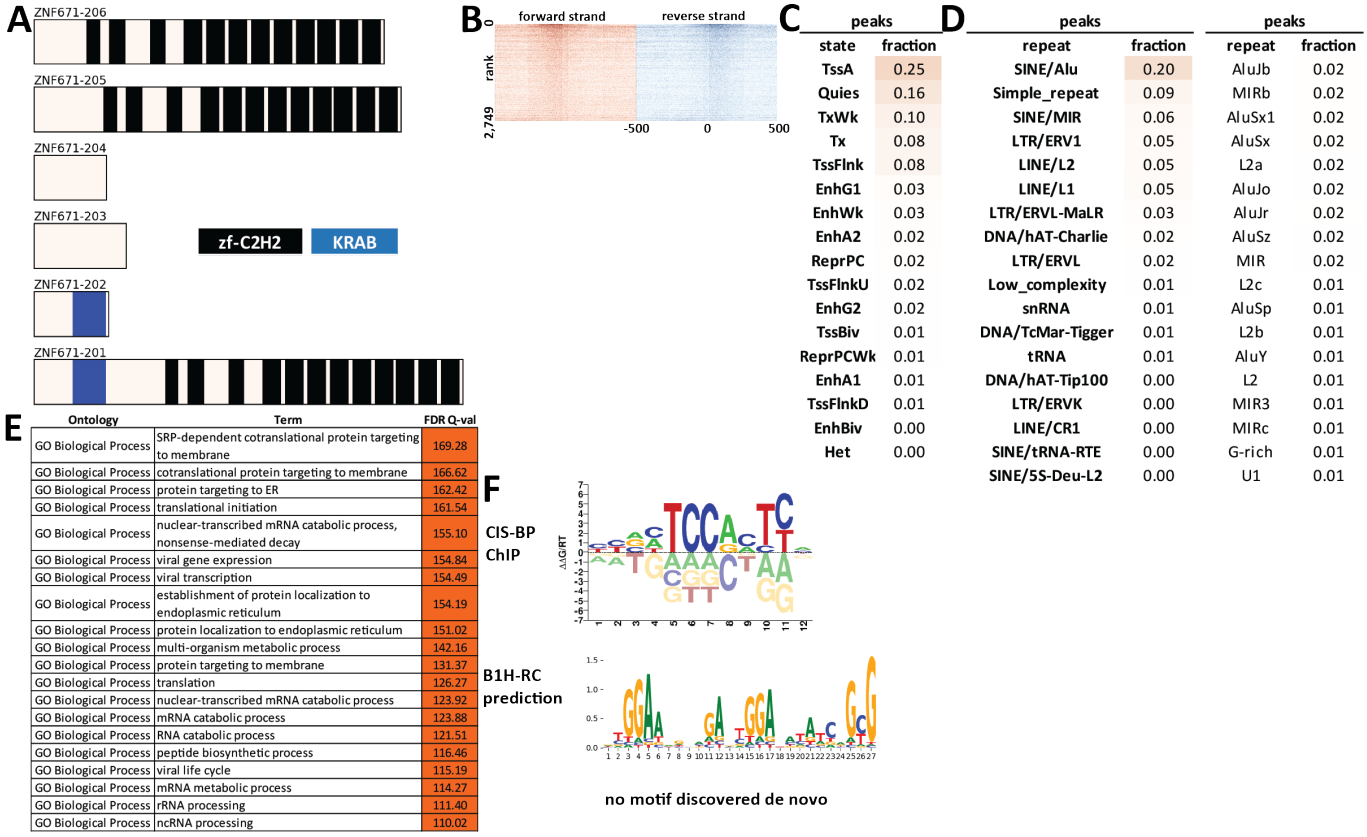

C

peaks	
state	fraction
TssA	0.25
Quies	0.16
TxWk	0.10
Tx	0.08
TssFlnk	0.08
EnhG1	0.03
EnhWk	0.03
EnhA2	0.02
ReprPC	0.02
TssFlnkU	0.02
EnhG2	0.02
TssBiv	0.01
ReprPCWk	0.01
EnhA1	0.01
TssFlnkD	0.01
EnhBiv	0.00
Het	0.00

D

peaks		peaks	
repeat	fraction	repeat	fraction
SINE/Alu	0.20	AluJb	0.02
Simple_repeat	0.09	MIRb	0.02
SINE/MIR	0.06	AluSx1	0.02
LTR/ERV1	0.05	AluSx	0.02
LINE/L2	0.05	L2a	0.02
LINE/L1	0.05	AluJo	0.02
LTR/ERVL-MaLR	0.03	AluJr	0.02
DNA/hAT-Charlie	0.02	AluSz	0.02
LTR/ERVL	0.02	MIR	0.02
Low_complexity	0.01	L2c	0.01
snRNA	0.01	AluSp	0.01
DNA/TcMar-Tigger	0.01	L2b	0.01
tRNA	0.01	AluY	0.01
DNA/hAT-Tip100	0.00	L2	0.01
LTR/ERVK	0.00	MIR3	0.01
LINE/CR1	0.00	MIRc	0.01
SINE/tRNA-RTE	0.00	G-rich	0.01
SINE/5S-Deu-L2	0.00	U1	0.01

E

Ontology	Term	FDR Q-val
GO Biological Process	SRP-dependent cotranslational protein targeting to membrane	169.28
GO Biological Process	cotranslational protein targeting to membrane	166.62
GO Biological Process	protein targeting to ER	162.42
GO Biological Process	translational initiation	161.54
GO Biological Process	nuclear-transcribed mRNA catabolic process, nonsense-mediated decay	155.10
GO Biological Process	viral gene expression	154.84
GO Biological Process	viral transcription	154.49
GO Biological Process	establishment of protein localization to endoplasmic reticulum	154.19
GO Biological Process	protein localization to endoplasmic reticulum	151.02
GO Biological Process	multi-organism metabolic process	142.16
GO Biological Process	protein targeting to membrane	131.37
GO Biological Process	translation	126.27
GO Biological Process	nuclear-transcribed mRNA catabolic process	123.92
GO Biological Process	mRNA catabolic process	123.88
GO Biological Process	RNA catabolic process	121.51
GO Biological Process	peptide biosynthetic process	116.46
GO Biological Process	viral life cycle	115.19
GO Biological Process	mRNA metabolic process	114.27
GO Biological Process	rRNA processing	111.40
GO Biological Process	ncRNA processing	110.02

Supplementary Figure 1557: Properties and genomic distribution of motifs identified for the ZNF671 transcription factor in WTC11 (accession ENCSR260GQA).

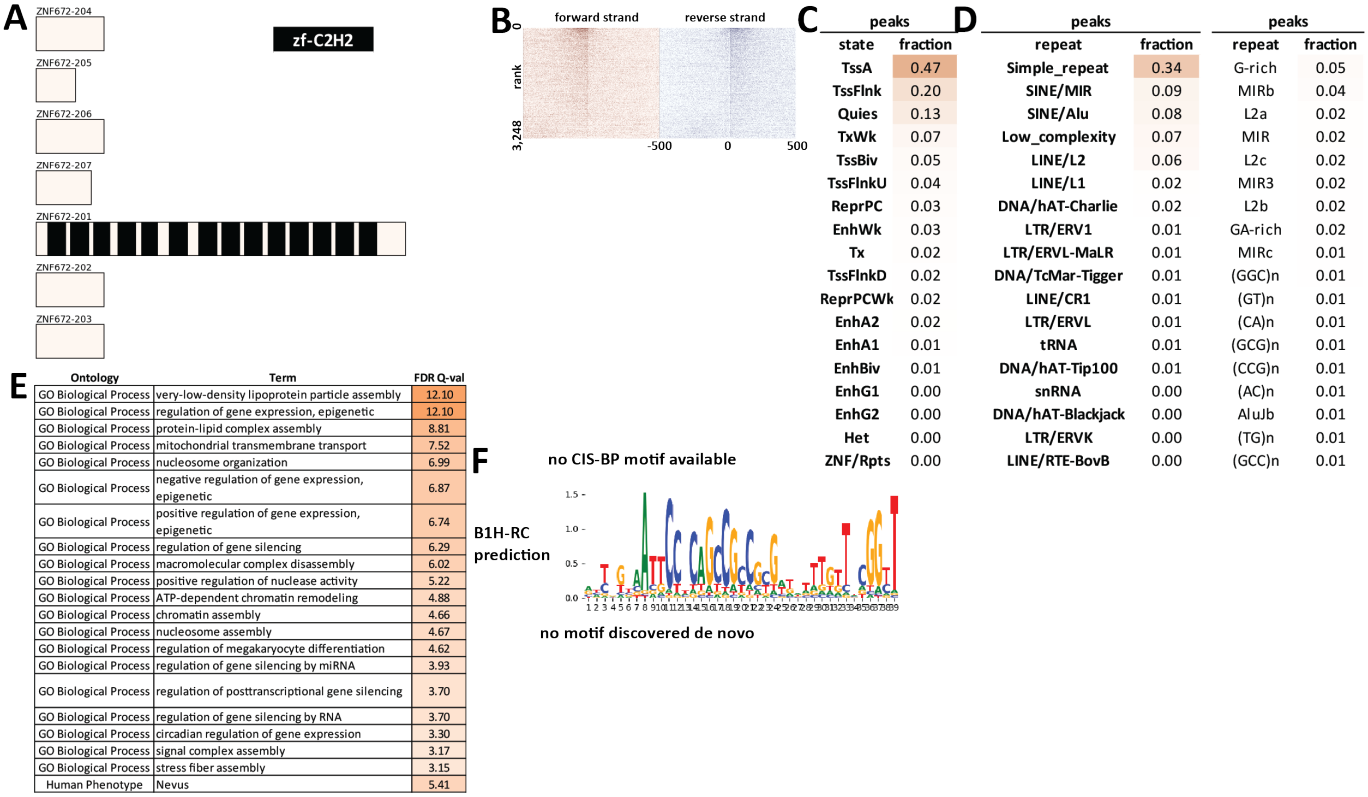

C

peaks	
state	fraction
TssA	0.47
TssFlnk	0.20
Quies	0.13
TxWk	0.07
TssBiv	0.05
TssFlnkU	0.04
ReprPC	0.03
EnhWk	0.03
Tx	0.02
TssFlnkD	0.02
ReprPCWk	0.02
EnhA2	0.02
EnhA1	0.01
EnhBiv	0.01
EnhG1	0.00
EnhG2	0.00
Het	0.00
ZNF/Rpts	0.00

D

peaks		peaks	
repeat	fraction	repeat	fraction
Simple_repeat	0.34	G-rich	0.05
SINE/MIR	0.09	MIRb	0.04
SINE/Alu	0.08	L2a	0.02
Low_complexity	0.07	MIR	0.02
LINE/L2	0.06	L2c	0.02
LINE/L1	0.02	MIR3	0.02
DNA/hAT-Charlie	0.02	L2b	0.02
LTR/ERV1	0.01	GA-rich	0.02
LTR/ERVL-MaLR	0.01	MIRc	0.01
DNA/TcMar-Tigger	0.01	(GGC)n	0.01
LINE/CR1	0.01	(GT)n	0.01
LTR/ERVL	0.01	(CA)n	0.01
tRNA	0.01	(GCG)n	0.01
DNA/hAT-Tip100	0.01	(CCG)n	0.01
snRNA	0.00	(AC)n	0.01
DNA/hAT-Blackjack	0.00	AluJb	0.01
LTR/ERVK	0.00	(TG)n	0.01
LINE/RTE-BovB	0.00	(GCC)n	0.01

E

Ontology	Term	FDR Q-val
GO Biological Process	very-low-density lipoprotein particle assembly	12.10
GO Biological Process	regulation of gene expression, epigenetic	12.10
GO Biological Process	protein-lipid complex assembly	8.81
GO Biological Process	mitochondrial transmembrane transport	7.52
GO Biological Process	nucleosome organization	6.99
GO Biological Process	negative regulation of gene expression, epigenetic	6.87
GO Biological Process	positive regulation of gene expression, epigenetic	6.74
GO Biological Process	regulation of gene silencing	6.29
GO Biological Process	macromolecular complex disassembly	6.02
GO Biological Process	positive regulation of nuclease activity	5.22
GO Biological Process	ATP-dependent chromatin remodeling	4.88
GO Biological Process	chromatin assembly	4.66
GO Biological Process	nucleosome assembly	4.67
GO Biological Process	regulation of megakaryocyte differentiation	4.62
GO Biological Process	regulation of gene silencing by miRNA	3.93
GO Biological Process	regulation of posttranscriptional gene silencing	3.70
GO Biological Process	regulation of gene silencing by RNA	3.70
GO Biological Process	circadian regulation of gene expression	3.30
GO Biological Process	signal complex assembly	3.17
GO Biological Process	stress fiber assembly	3.15
Human Phenotype	Nevus	5.41

Supplementary Figure 1558: Properties and genomic distribution of motifs identified for the ZNF672 transcription factor in HepG2 (accession ENCSR263YXJ).

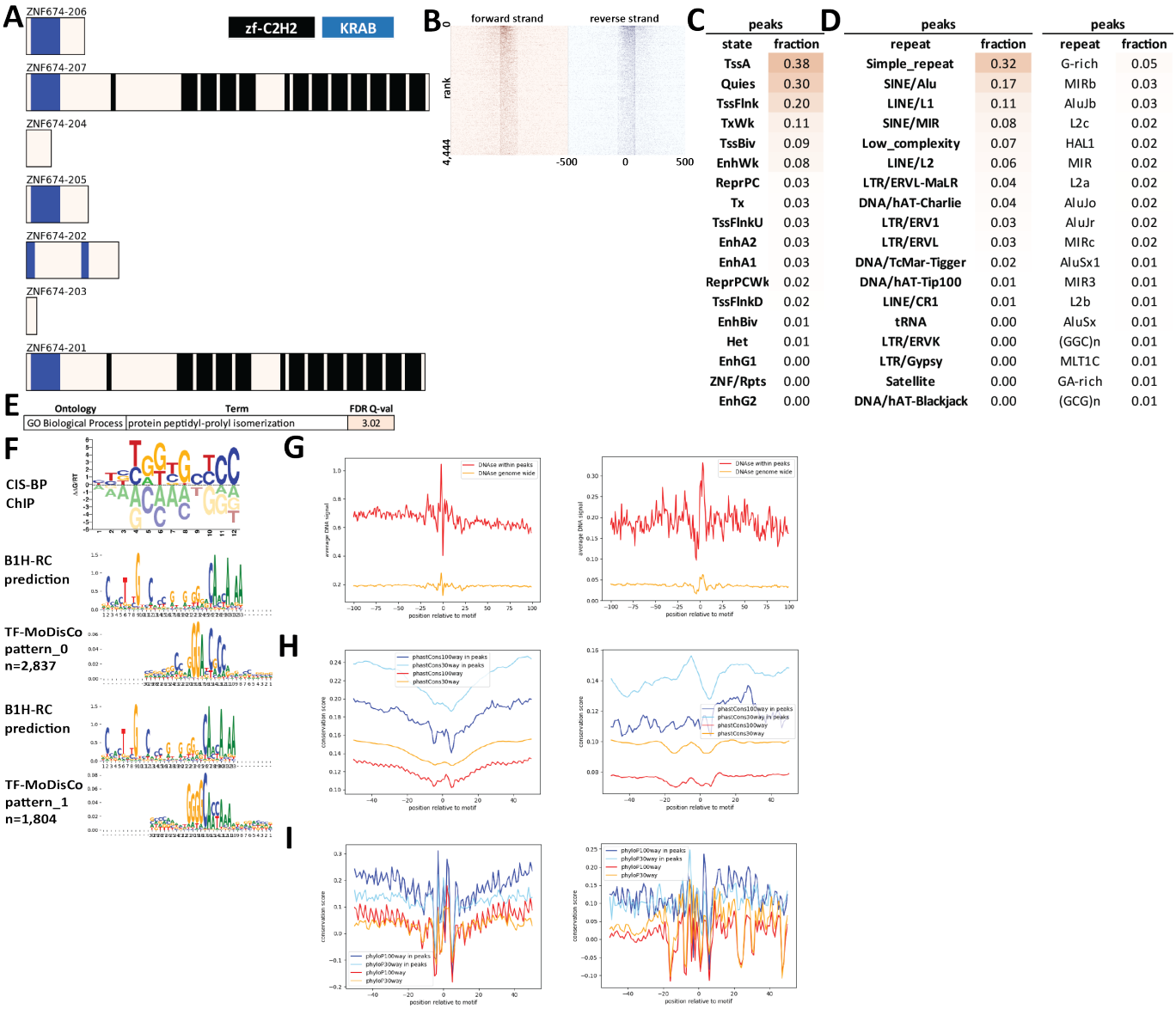

Supplementary Figure 1559: Properties and genomic distribution of motifs identified for the ZNF674 transcription factor in HEK293 (accession ChipExo models).

TF-MoDisCO pattern_0 n=2837, CWM

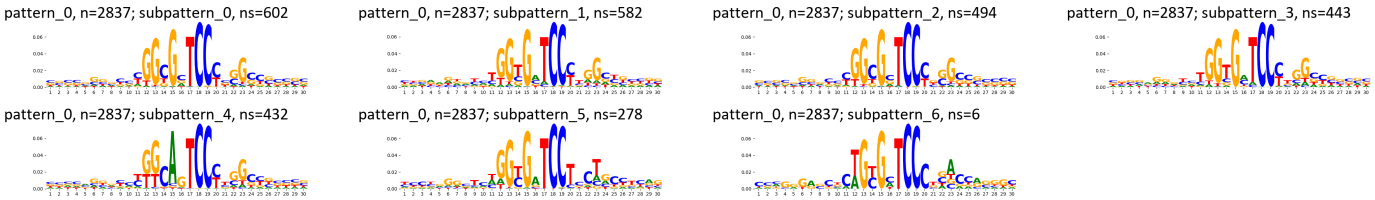

TF-MoDisCO pattern_0 n=2837, PWM

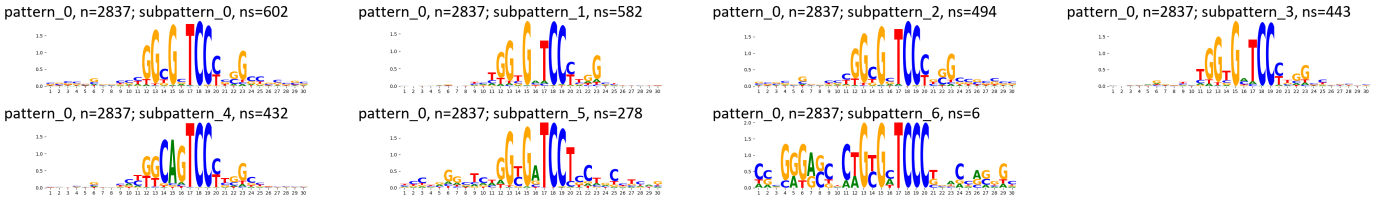

TF-MoDisCO pattern_1 n=1804, CWM

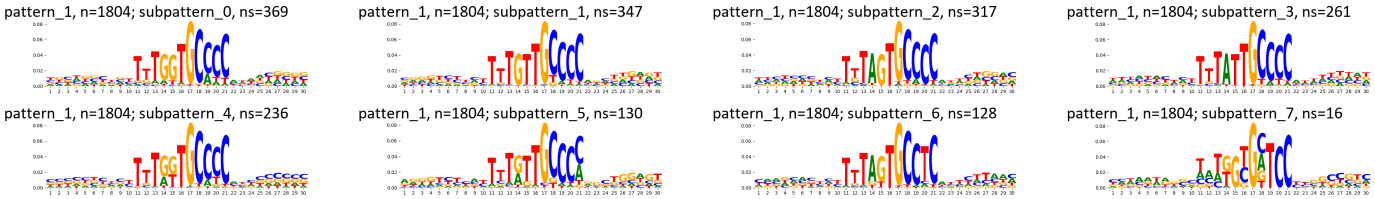

TF-MoDisCO pattern_1 n=1804, PWM

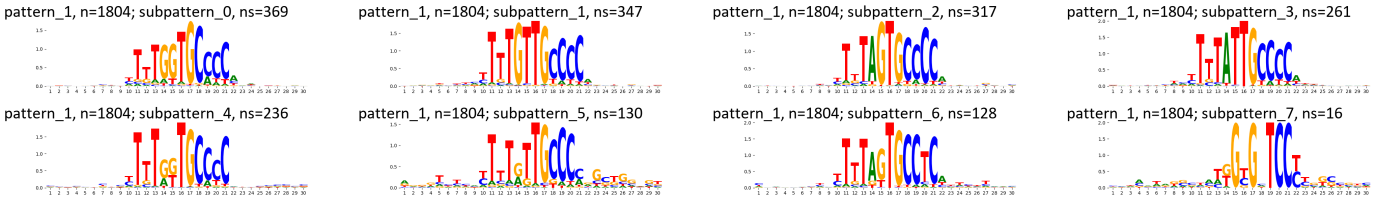

Supplementary Figure 1560: TF-MoDisCO subpatterns for the ZNF674 transcription factor in HEK293 (accession ChipExo models).

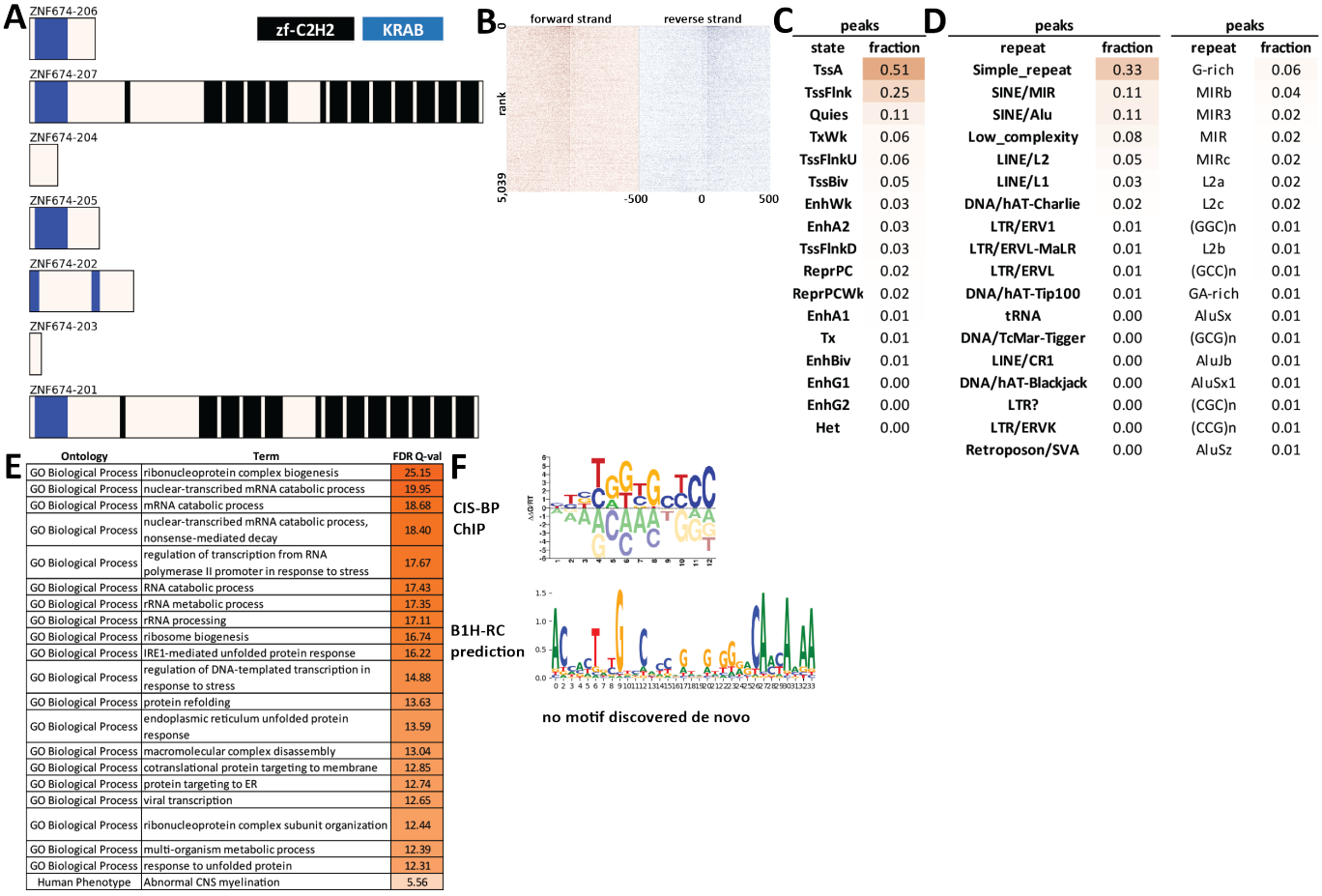

Supplementary Figure 1561: Properties and genomic distribution of motifs identified for the ZNF674 transcription factor in HepG2 (accession ENCSR171BKT).

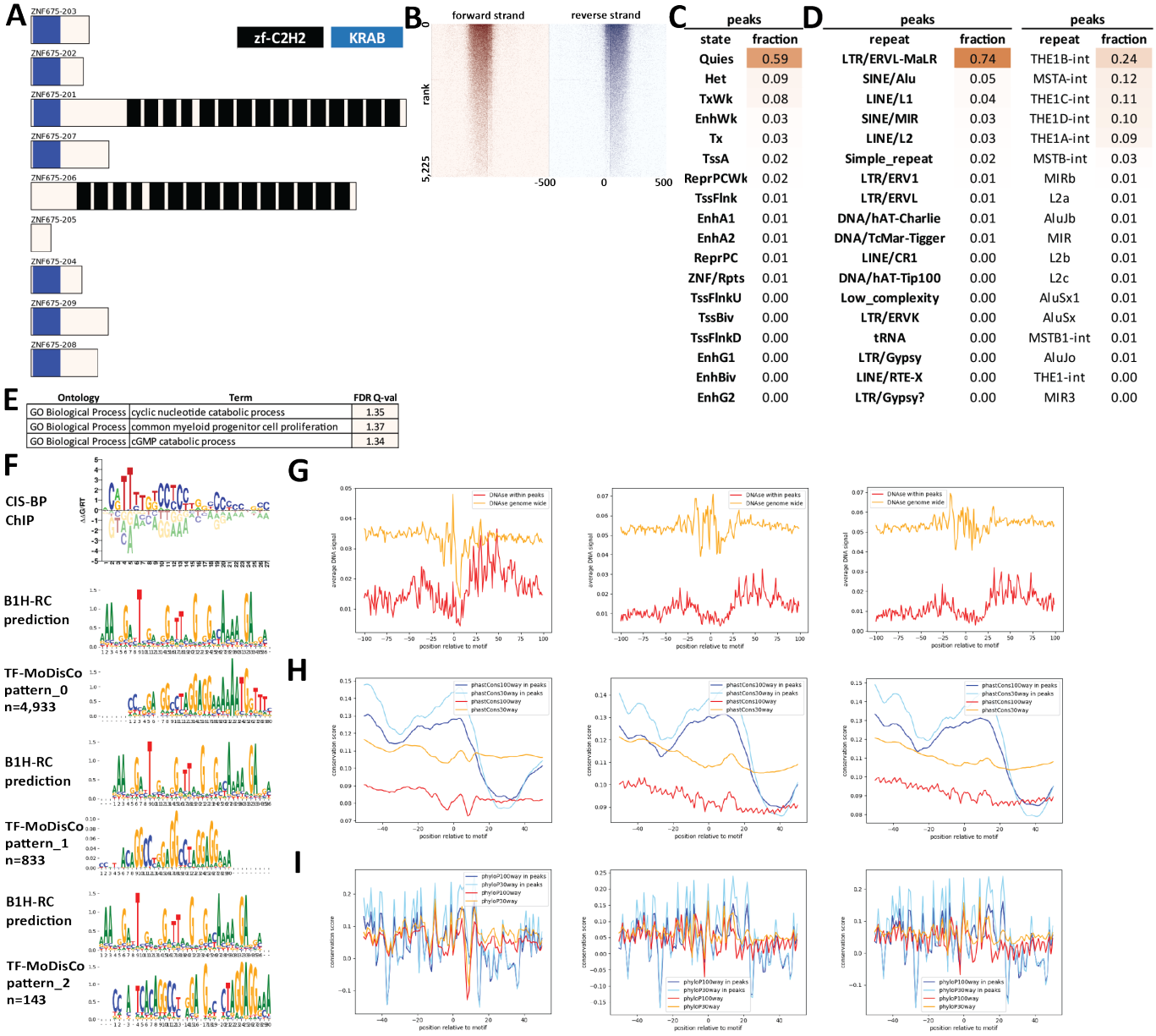

Supplementary Figure 1562: Properties and genomic distribution of motifs identified for the ZNF675 transcription factor in HEK293 (accession Hughes NB models).

TF-MoDisCO pattern_0 n=4933, CWM

pattern_0, n=4933; subpattern_0, ns=1151

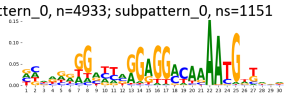

pattern_0, n=4933; subpattern_1, ns=875

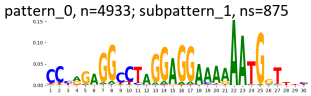

pattern_0, n=4933; subpattern_2, ns=867

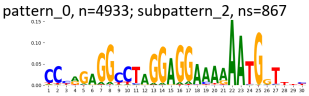

pattern_0, n=4933; subpattern_3, ns=499

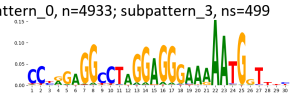

pattern_0, n=4933; subpattern_4, ns=482

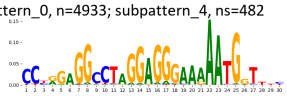

pattern_0, n=4933; subpattern_5, ns=324

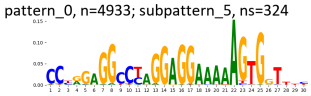

pattern_0, n=4933; subpattern_6, ns=319

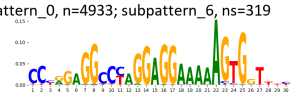

pattern_0, n=4933; subpattern_7, ns=279

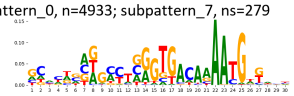

pattern_0, n=4933; subpattern_8, ns=115

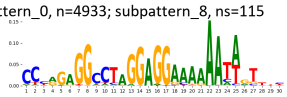

pattern_0, n=4933; subpattern_9, ns=22

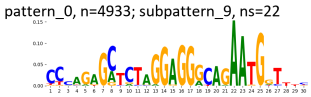

TF-MoDisCO pattern_0 n=4933, PWM

pattern_0, n=4933; subpattern_0, ns=1151

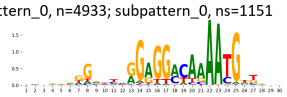

pattern_0, n=4933; subpattern_1, ns=875

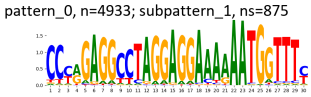

pattern_0, n=4933; subpattern_2, ns=867

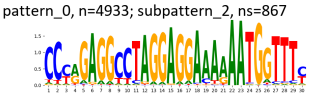

pattern_0, n=4933; subpattern_3, ns=499

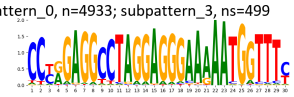

pattern_0, n=4933; subpattern_4, ns=482

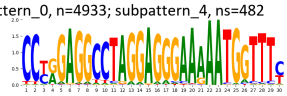

pattern_0, n=4933; subpattern_5, ns=324

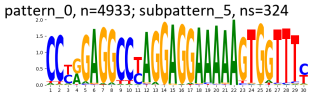

pattern_0, n=4933; subpattern_6, ns=319

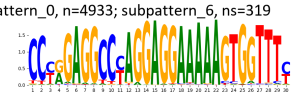

pattern_0, n=4933; subpattern_7, ns=279

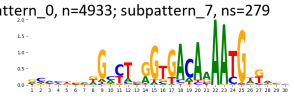

pattern_0, n=4933; subpattern_8, ns=115

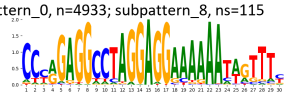

pattern_0, n=4933; subpattern_9, ns=22

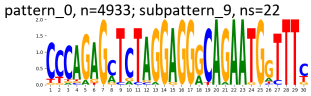

TF-MoDisCO pattern_1 n=883, CWM

pattern_1, n=883; subpattern_0, ns=235

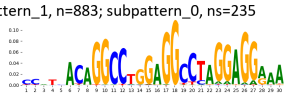

pattern_1, n=883; subpattern_1, ns=201

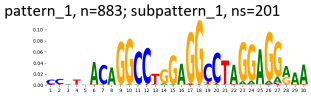

pattern_1, n=883; subpattern_2, ns=196

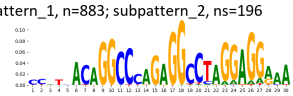

pattern_1, n=883; subpattern_3, ns=158

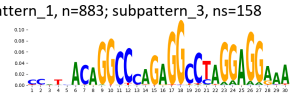

pattern_1, n=883; subpattern_4, ns=67

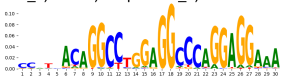

pattern_1, n=883; subpattern_5, ns=26

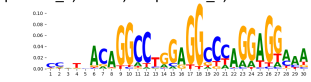

TF-MoDisCO pattern_1 n=883, PWM

pattern_1, n=883; subpattern_0, ns=235

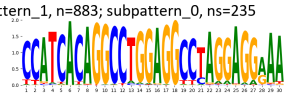

pattern_1, n=883; subpattern_1, ns=201

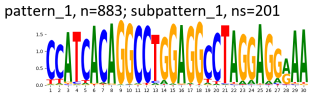

pattern_1, n=883; subpattern_2, ns=196

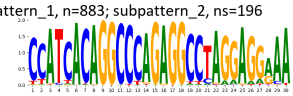

pattern_1, n=883; subpattern_3, ns=158

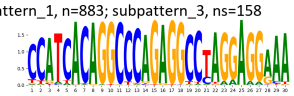

pattern_1, n=883; subpattern_4, ns=67

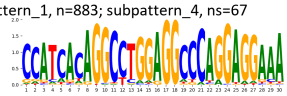

pattern_1, n=883; subpattern_5, ns=26

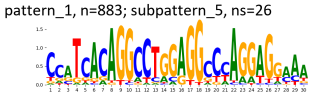

TF-MoDisCO pattern_2 n=143, CWM

pattern_2, n=143; subpattern_0, ns=59

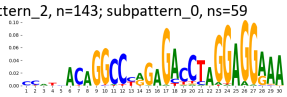

pattern_2, n=143; subpattern_1, ns=43

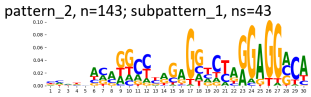

pattern_2, n=143; subpattern_2, ns=41

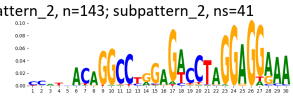

TF-MoDisCO pattern_2 n=143, PWM

pattern_2, n=143; subpattern_0, ns=59

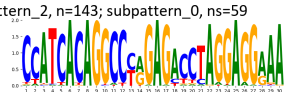

pattern_2, n=143; subpattern_1, ns=43

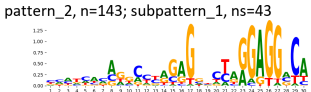

pattern_2, n=143; subpattern_2, ns=41

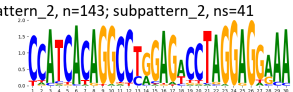

Supplementary Figure 1563: TF-MoDisCO subpatterns for the ZNF675 transcription factor in HEK293 (accession Hughes NB models).

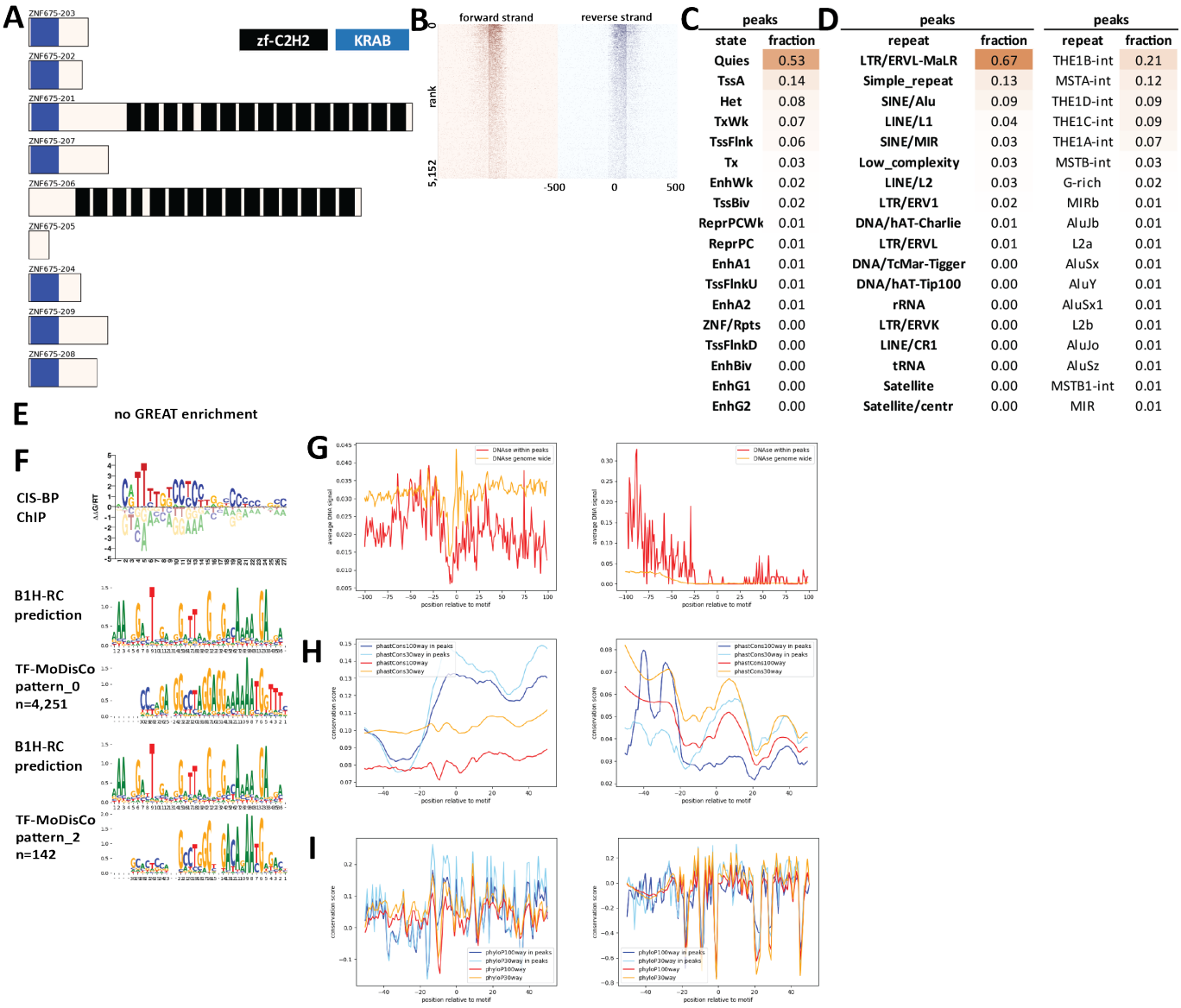

Supplementary Figure 1564: Properties and genomic distribution of motifs identified for the ZNF675 transcription factor in HEK293 (accession ChipExo models).

TF-MoDisCO pattern_0 n=4251, CWM

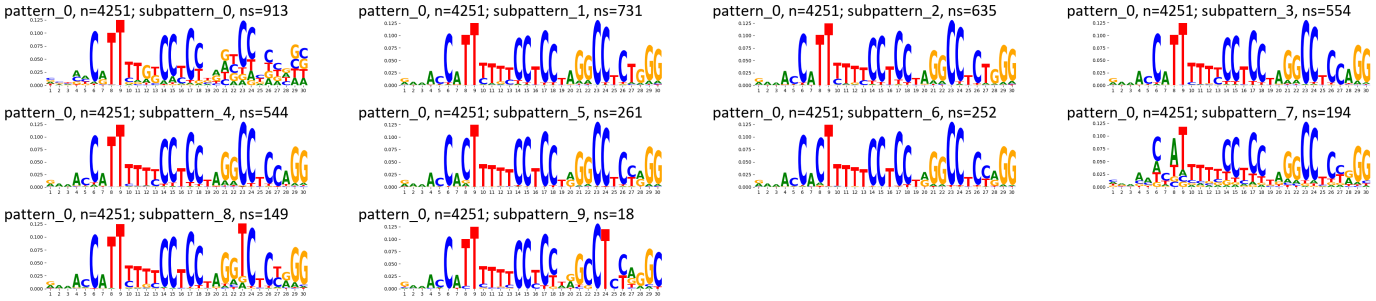

TF-MoDisCO pattern_0 n=4251, PWM

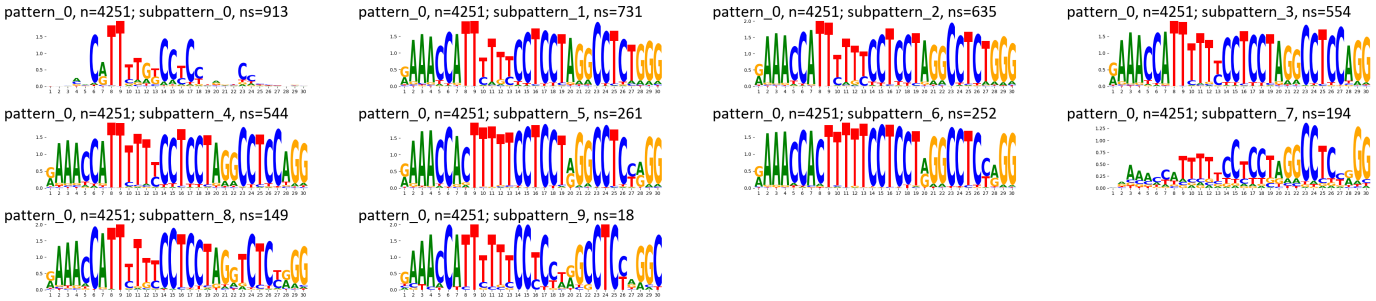

TF-MoDisCO pattern_2 n=142, CWM

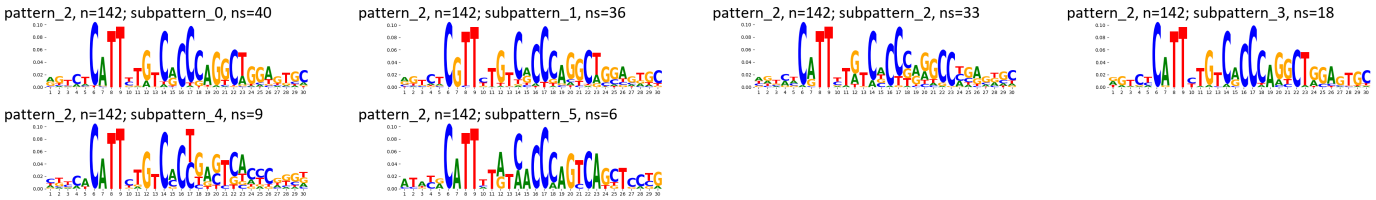

TF-MoDisCO pattern_2 n=142, PWM

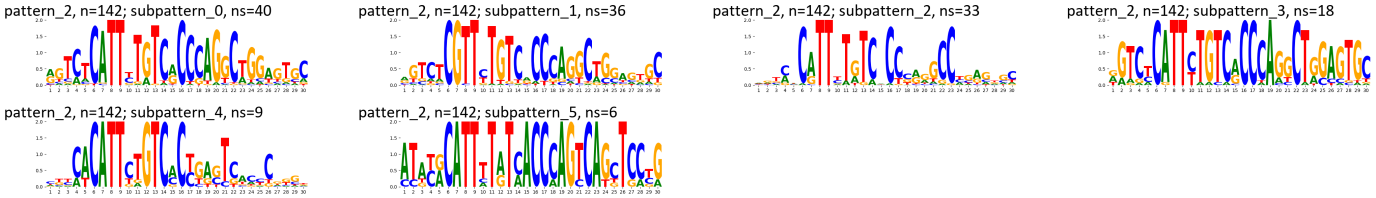

Supplementary Figure 1565: TF-MoDisCO subpatterns for the ZNF675 transcription factor in HEK293 (accession ChipExo models).

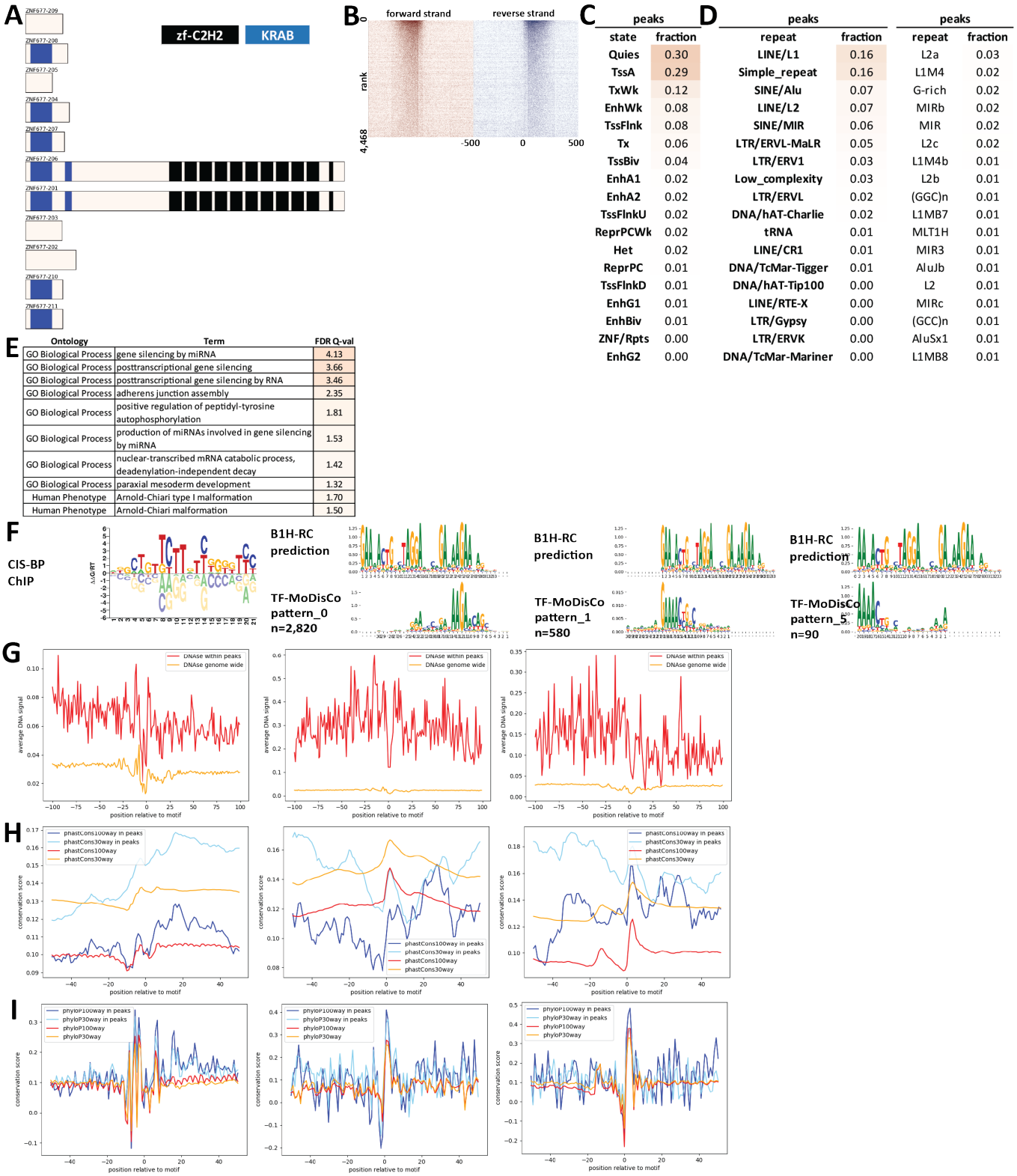

Supplementary Figure 1566: Properties and genomic distribution of motifs identified for the ZNF677 transcription factor in HEK293 (accession ENCSR279KDC).

TF-MoDisCO pattern_0 n=2820, CWM

pattern_0, n=2820; subpattern_0, ns=608

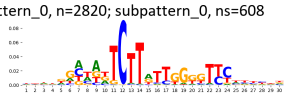

pattern_0, n=2820; subpattern_1, ns=476

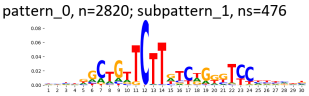

pattern_0, n=2820; subpattern_2, ns=429

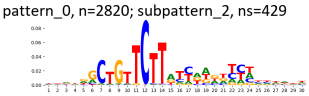

pattern_0, n=2820; subpattern_3, ns=424

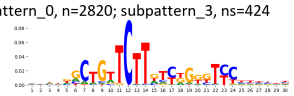

pattern_0, n=2820; subpattern_4, ns=420

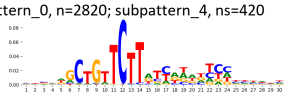

pattern_0, n=2820; subpattern_5, ns=246

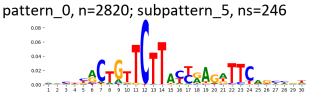

pattern_0, n=2820; subpattern_6, ns=110

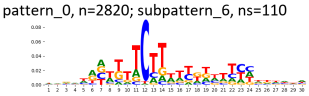

pattern_0, n=2820; subpattern_7, ns=107

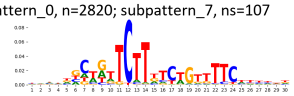

TF-MoDisCO pattern_0 n=2820, PWM

pattern_0, n=2820; subpattern_0, ns=608

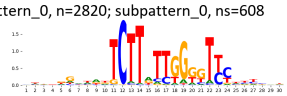

pattern_0, n=2820; subpattern_1, ns=476

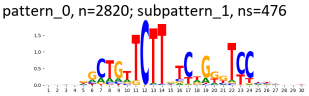

pattern_0, n=2820; subpattern_2, ns=429

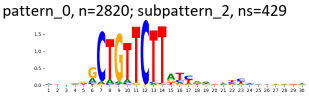

pattern_0, n=2820; subpattern_3, ns=424

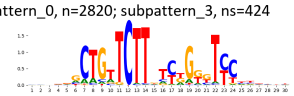

pattern_0, n=2820; subpattern_4, ns=420

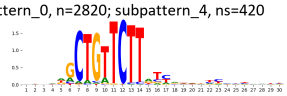

pattern_0, n=2820; subpattern_5, ns=246

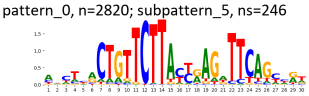

pattern_0, n=2820; subpattern_6, ns=110

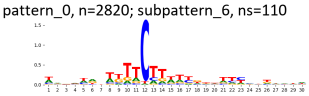

pattern_0, n=2820; subpattern_7, ns=107

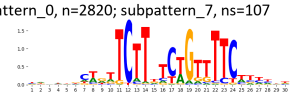

TF-MoDisCO pattern_1 n=580, CWM

pattern_1, n=580; subpattern_0, ns=195

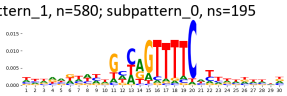

pattern_1, n=580; subpattern_1, ns=186

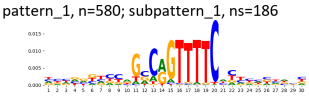

pattern_1, n=580; subpattern_2, ns=183

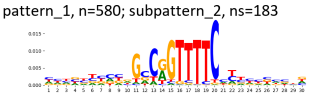

pattern_1, n=580; subpattern_3, ns=8

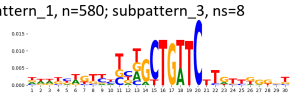

pattern_1, n=580; subpattern_4, ns=4

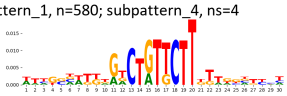

pattern_1, n=580; subpattern_5, ns=2

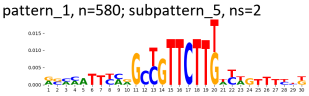

pattern_1, n=580; subpattern_6, ns=2

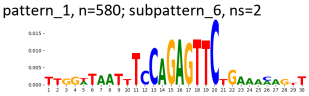

TF-MoDisCO pattern_1 n=580, PWM

pattern_1, n=580; subpattern_0, ns=195

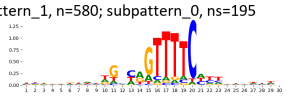

pattern_1, n=580; subpattern_1, ns=186

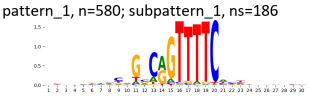

pattern_1, n=580; subpattern_2, ns=183

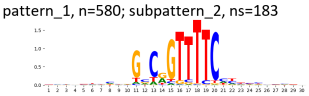

pattern_1, n=580; subpattern_3, ns=8

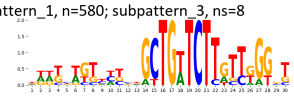

pattern_1, n=580; subpattern_4, ns=4

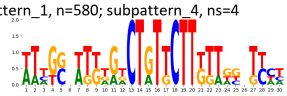

pattern_1, n=580; subpattern_5, ns=2

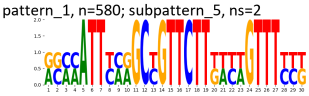

pattern_1, n=580; subpattern_6, ns=2

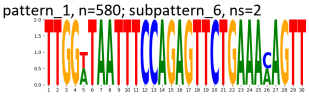

TF-MoDisCO pattern_5 n=90, CWM

pattern_5, n=90; subpattern_0, ns=28

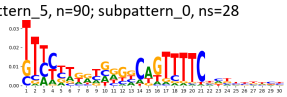

pattern_5, n=90; subpattern_1, ns=25

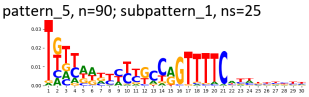

pattern_5, n=90; subpattern_2, ns=18

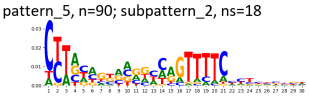

pattern_5, n=90; subpattern_3, ns=14

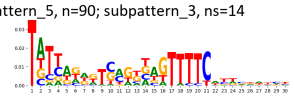

pattern_5, n=90; subpattern_4, ns=5

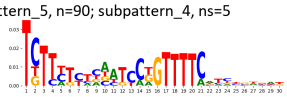

TF-MoDisCO pattern_5 n=90, PWM

pattern_5, n=90; subpattern_0, ns=28

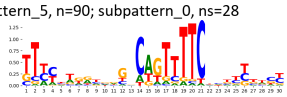

pattern_5, n=90; subpattern_1, ns=25

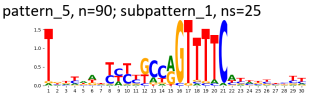

pattern_5, n=90; subpattern_2, ns=18

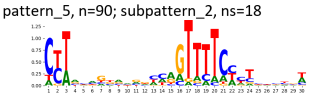

pattern_5, n=90; subpattern_3, ns=14

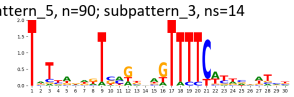

pattern_5, n=90; subpattern_4, ns=5

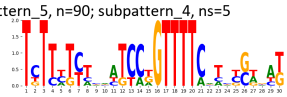

Supplementary Figure 1567: TF-MoDisCO subpatterns for the ZNF677 transcription factor in HEK293 (accession ENCSR279KDC).

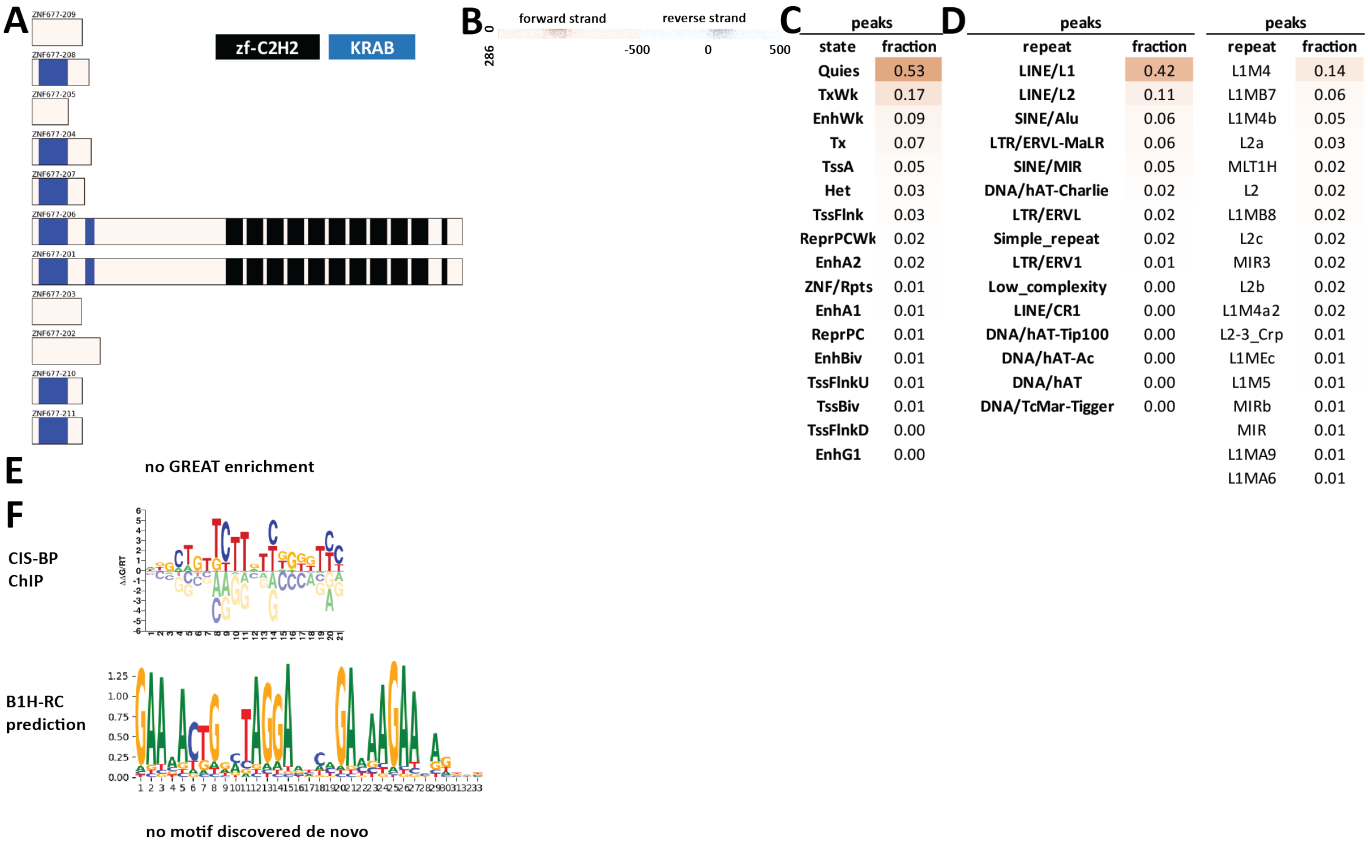

peaks

state	fraction
Quies	0.53
TxWk	0.17
EnhWk	0.09
Tx	0.07
TssA	0.05
Het	0.03
TssFlnk	0.03
ReprPCWk	0.02
EnhA2	0.02
ZNF/Rpts	0.01
EnhA1	0.01
ReprPC	0.01
EnhBiv	0.01
TssFlnkU	0.01
TssBiv	0.01
TssFlnkD	0.00
EnhG1	0.00

peaks

repeat	fraction
LINE/L1	0.42
LINE/L2	0.11
SINE/Alu	0.06
LTR/ERVL-MaLR	0.06
SINE/MIR	0.05
DNA/hAT-Charlie	0.02
LTR/ERVL	0.02
Simple_repeat	0.02
LTR/ERV1	0.01
Low_complexity	0.00
LINE/CR1	0.00
DNA/hAT-Tip100	0.00
DNA/hAT-Ac	0.00
DNA/hAT	0.00
DNA/TcMar-Tigger	0.00

peaks

repeat	fraction
L1M4	0.14
L1MB7	0.06
L1M4b	0.05
L2a	0.03
MLT1H	0.02
L2	0.02
L1MB8	0.02
L2c	0.02
MIR3	0.02
L2b	0.02
L1M4a2	0.02
L2-3_Crp	0.01
L1MEc	0.01
L1M5	0.01
MIRb	0.01
MIR	0.01
L1MA9	0.01
L1MA6	0.01

Supplementary Figure 1568: Properties and genomic distribution of motifs identified for the ZNF677 transcription factor in HEK293 (accession Hughes GR models).

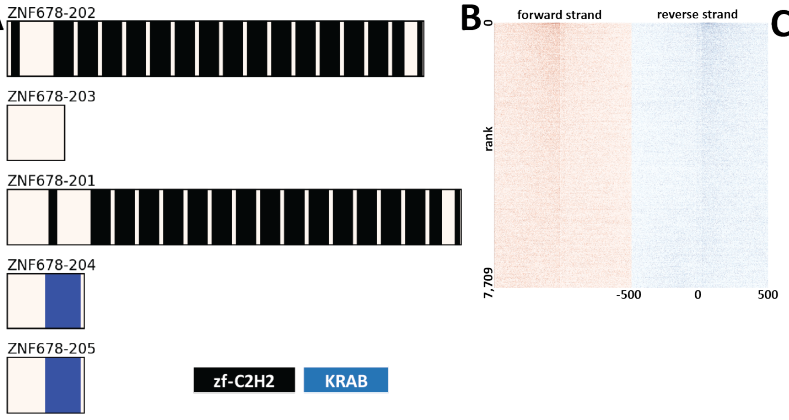

C

peaks	
state	fraction
TssA	0.46
TssFlnk	0.22
Quies	0.12
TxWk	0.07
TssFlnkU	0.05
TssBiv	0.04
EnhWk	0.04
ReprPC	0.03
EnhA2	0.02
TssFlnkD	0.02
ReprPCWk	0.02
EnhA1	0.02
Tx	0.02
EnhBiv	0.01
EnhG1	0.00
EnhG2	0.00
Het	0.00
ZNF/Rpts	0.00

D

peaks		peaks	
repeat	fraction	repeat	fraction
Simple_repeat	0.22	G-rich	0.04
SINE/MIR	0.10	MIRb	0.03
SINE/Alu	0.09	MIR3	0.02
LINE/L2	0.05	MIR	0.02
Low_complexity	0.05	L2a	0.02
LINE/L1	0.03	L2b	0.02
DNA/hAT-Charlie	0.02	MIRc	0.02
LTR/ERV1	0.02	L2c	0.01
LTR/ERVL-MaLR	0.01	AluJb	0.01
LTR/ERVL	0.01	AluSx1	0.01
tRNA	0.01	GA-rich	0.01
LINE/CR1	0.00	AluSx	0.01
DNA/hAT-Tip100	0.00	(GGC)n	0.01
DNA/TcMar-Tigger	0.00	AluJo	0.01
LTR/ERVK	0.00	AluJr	0.01
Satellite	0.00	AluSz	0.01
LINE/RTE-BovB	0.00	(GCC)n	0.01
LTR/Gypsy	0.00	(CCG)n	0.01

E

Ontology	Term	FDR Q-val
GO Biological Process	regulation of transcription from RNA polymerase II promoter in response to stress	28.97
GO Biological Process	regulation of DNA-templated transcription in response to stress	25.38
GO Biological Process	regulation of PERK-mediated unfolded protein response	22.72
GO Biological Process	rRNA metabolic process	20.98
GO Biological Process	rRNA processing	20.62
GO Biological Process	mRNA catabolic process	19.69
GO Biological Process	RNA catabolic process	19.69
GO Biological Process	nuclear-transcribed mRNA catabolic process	18.83
GO Biological Process	regulation of hematopoietic progenitor cell differentiation	18.04
GO Biological Process	regulation of receptor catabolic process	17.16
GO Biological Process	regulation of transcription from RNA polymerase II promoter in response to hypoxia	16.63
GO Biological Process	regulation of intrinsic apoptotic signaling pathway	15.62
GO Biological Process	protein targeting to ER	14.53
GO Biological Process	regulation of mRNA stability	13.89
GO Biological Process	protein localization to endoplasmic reticulum	13.64
GO Biological Process	regulation of hematopoietic stem cell differentiation	13.23
GO Biological Process	regulation of endoplasmic reticulum unfolded protein response	13.02
GO Biological Process	regulation of cellular amino acid metabolic process	12.32
GO Biological Process	establishment of protein localization to endoplasmic reticulum	12.00
GO Biological Process	nuclear-transcribed mRNA catabolic process, nonsense-mediated decay	11.27
Human Phenotype	Increased serum lactate	7.61
Human Phenotype	Abnormality of mitochondrial metabolism	5.72
Human Phenotype	Abnormality of the mitochondrion	5.40
Human Phenotype	Progressive microcephaly	4.51
Human Phenotype	Dysphonia	4.18
Human Phenotype	3-Methylglutaconic aciduria	2.20
Human Phenotype	Basal cell carcinoma	2.10

F

no CIS-BP motif available

B1H-RC prediction

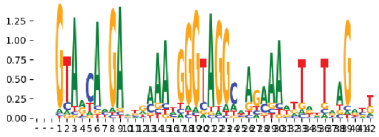

no motif discovered de novo

Supplementary Figure 1569: Properties and genomic distribution of motifs identified for the ZNF678 transcription factor in HepG2 (accession ENCSR946PKH).

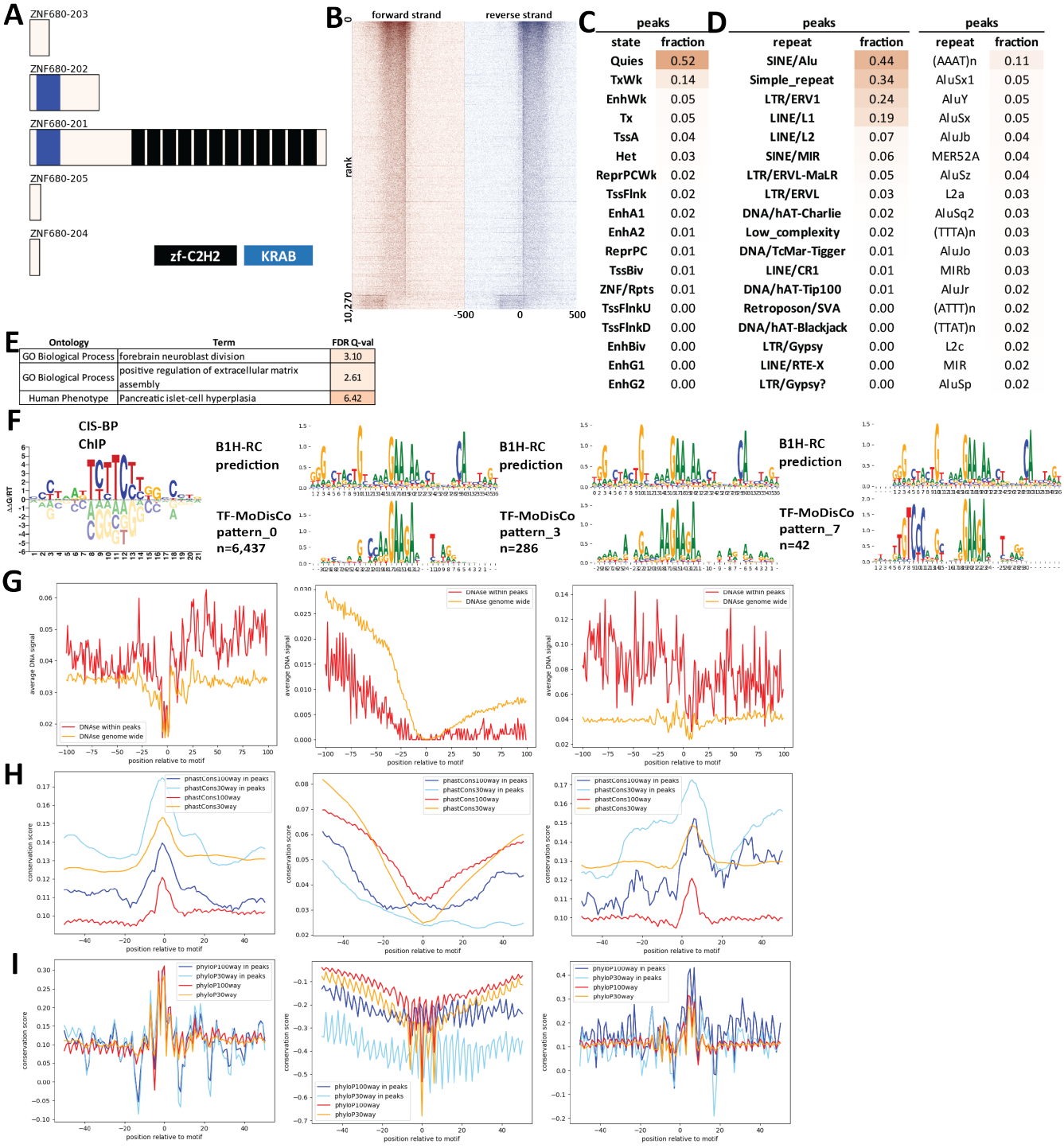

Supplementary Figure 1570: Properties and genomic distribution of motifs identified for the ZNF680 transcription factor in HEK293 (accession ENCSR307CKC).

TF-MoDisCO pattern_0 n=6437, CWM

pattern_0, n=6437; subpattern_0, ns=1399

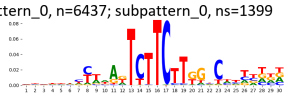

pattern_0, n=6437; subpattern_1, ns=1370

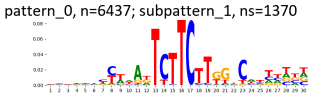

pattern_0, n=6437; subpattern_2, ns=846

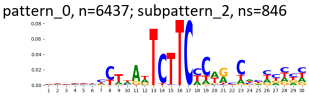

pattern_0, n=6437; subpattern_3, ns=749

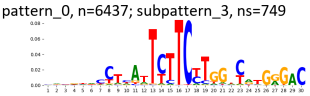

pattern_0, n=6437; subpattern_4, ns=722

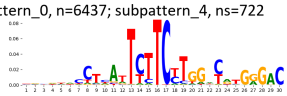

pattern_0, n=6437; subpattern_5, ns=468

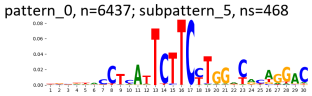

pattern_0, n=6437; subpattern_6, ns=413

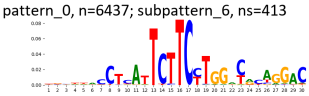

pattern_0, n=6437; subpattern_7, ns=317

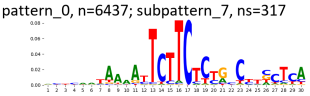

pattern_0, n=6437; subpattern_8, ns=131

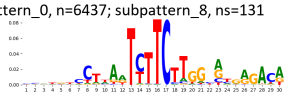

pattern_0, n=6437; subpattern_9, ns=22

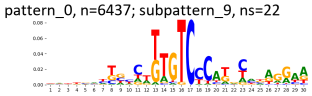

TF-MoDisCO pattern_0 n=6437, PWM

pattern_0, n=6437; subpattern_0, ns=1399

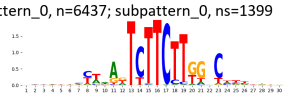

pattern_0, n=6437; subpattern_1, ns=1370

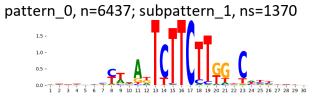

pattern_0, n=6437; subpattern_2, ns=846

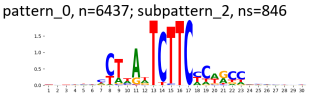

pattern_0, n=6437; subpattern_3, ns=749

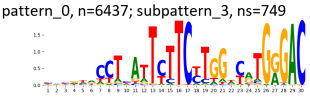

pattern_0, n=6437; subpattern_4, ns=722

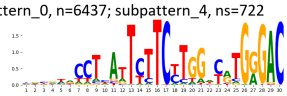

pattern_0, n=6437; subpattern_5, ns=468

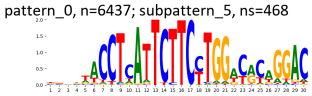

pattern_0, n=6437; subpattern_6, ns=413

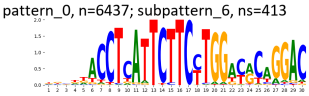

pattern_0, n=6437; subpattern_7, ns=317

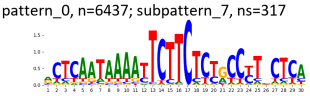

pattern_0, n=6437; subpattern_8, ns=131

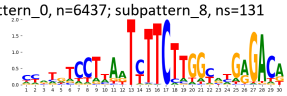

pattern_0, n=6437; subpattern_9, ns=22

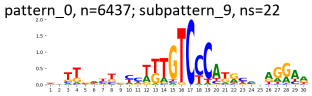

TF-MoDisCO pattern_3 n=286, CWM

pattern_3, n=286; subpattern_0, ns=77

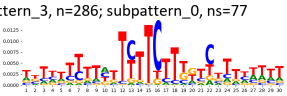

pattern_3, n=286; subpattern_1, ns=71

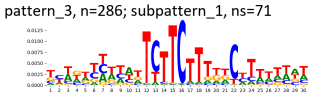

pattern_3, n=286; subpattern_2, ns=56

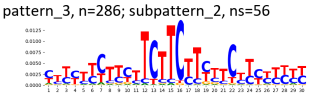

pattern_3, n=286; subpattern_3, ns=52

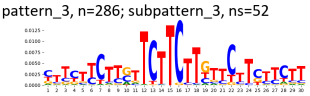

pattern_3, n=286; subpattern_4, ns=23

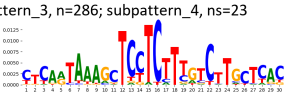

pattern_3, n=286; subpattern_5, ns=7

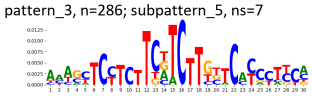

TF-MoDisCO pattern_3 n=286, PWM

pattern_3, n=286; subpattern_0, ns=77

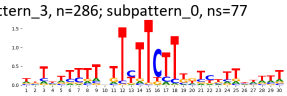

pattern_3, n=286; subpattern_1, ns=71

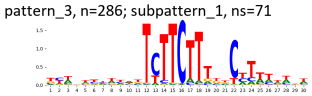

pattern_3, n=286; subpattern_2, ns=56

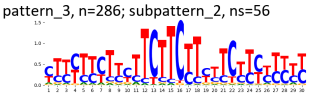

pattern_3, n=286; subpattern_3, ns=52

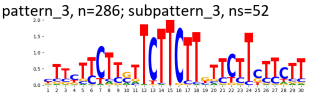

pattern_3, n=286; subpattern_4, ns=23

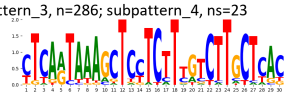

pattern_3, n=286; subpattern_5, ns=7

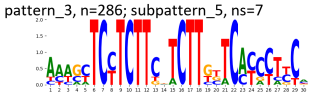

TF-MoDisCO pattern_7 n=42, CWM

pattern_7, n=42; subpattern_0, ns=42

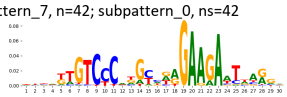

TF-MoDisCO pattern_7 n=42, PWM

pattern_7, n=42; subpattern_0, ns=42

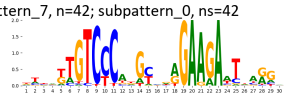

Supplementary Figure 1571: TF-MoDisCO subpatterns for the ZNF680 transcription factor in HEK293 (accession ENCSR307CKC).

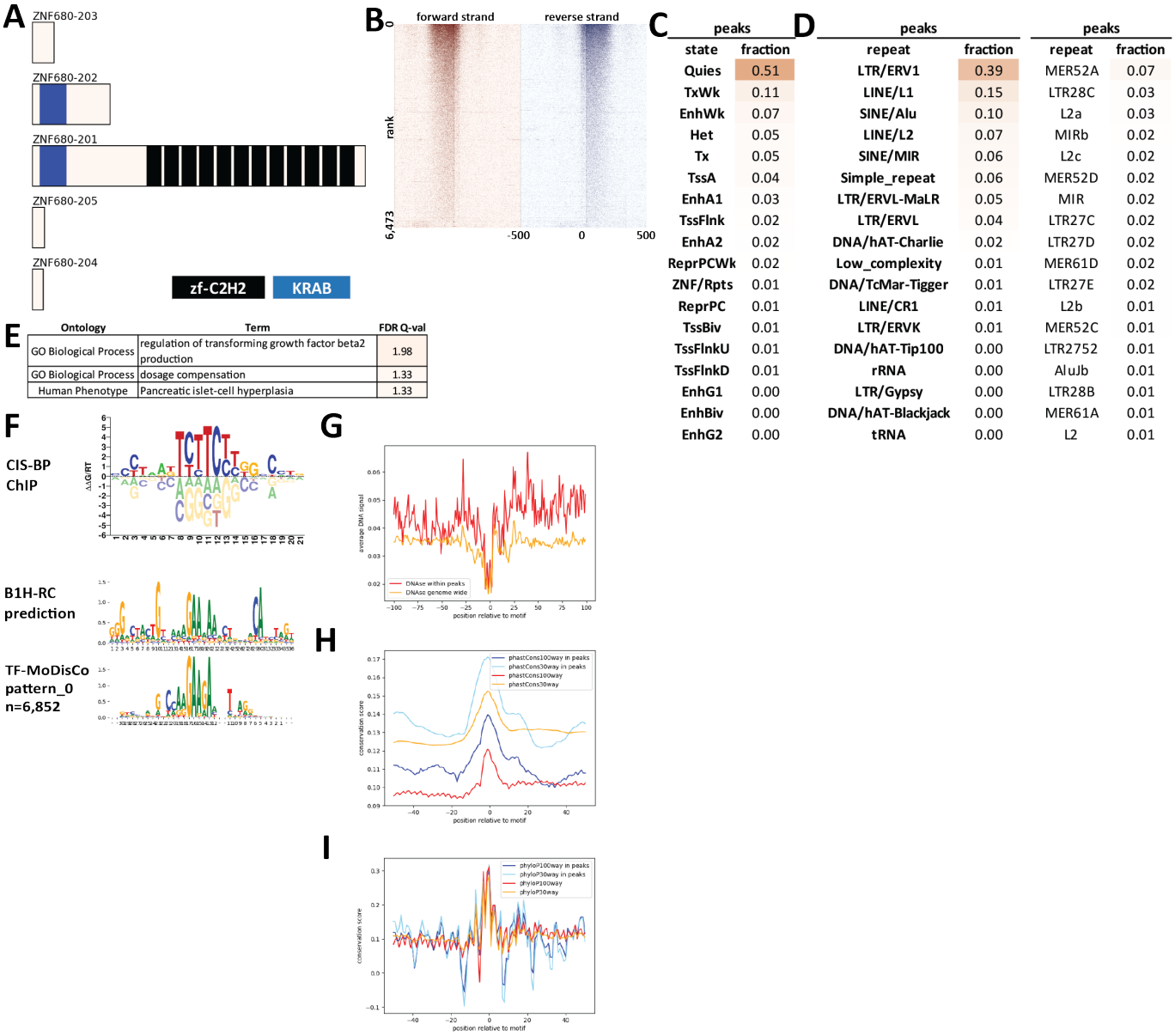

Supplementary Figure 1572: Properties and genomic distribution of motifs identified for the ZNF680 transcription factor in HEK293 (accession Hughes GR models).

TF-MoDisCO pattern_0 n=6852, CWM

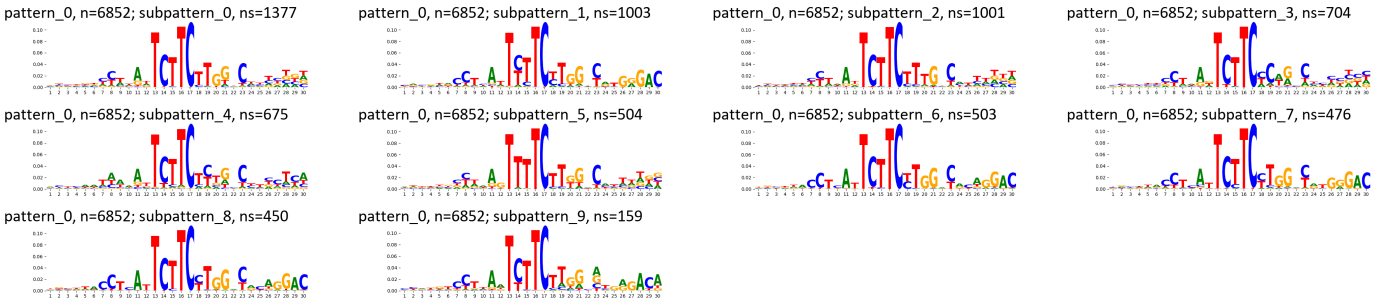

TF-MoDisCO pattern_0 n=6852, PWM

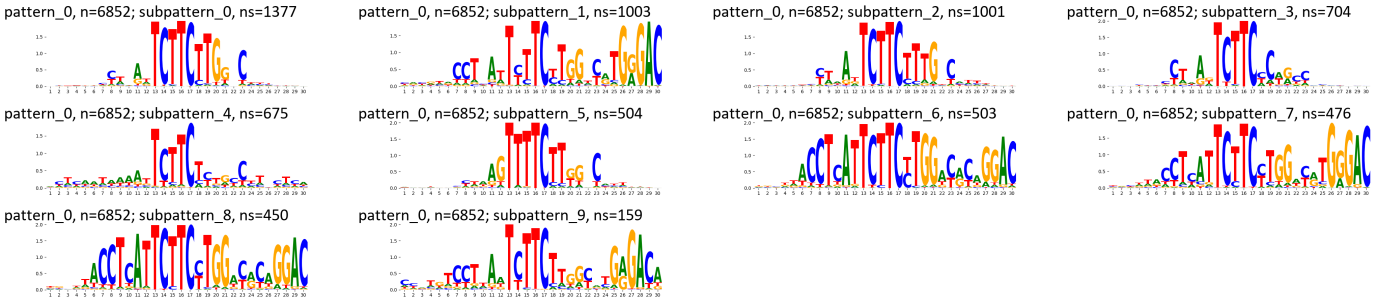

Supplementary Figure 1573: TF-MoDisCO subpatterns for the ZNF680 transcription factor in HEK293 (accession Hughes GR models).

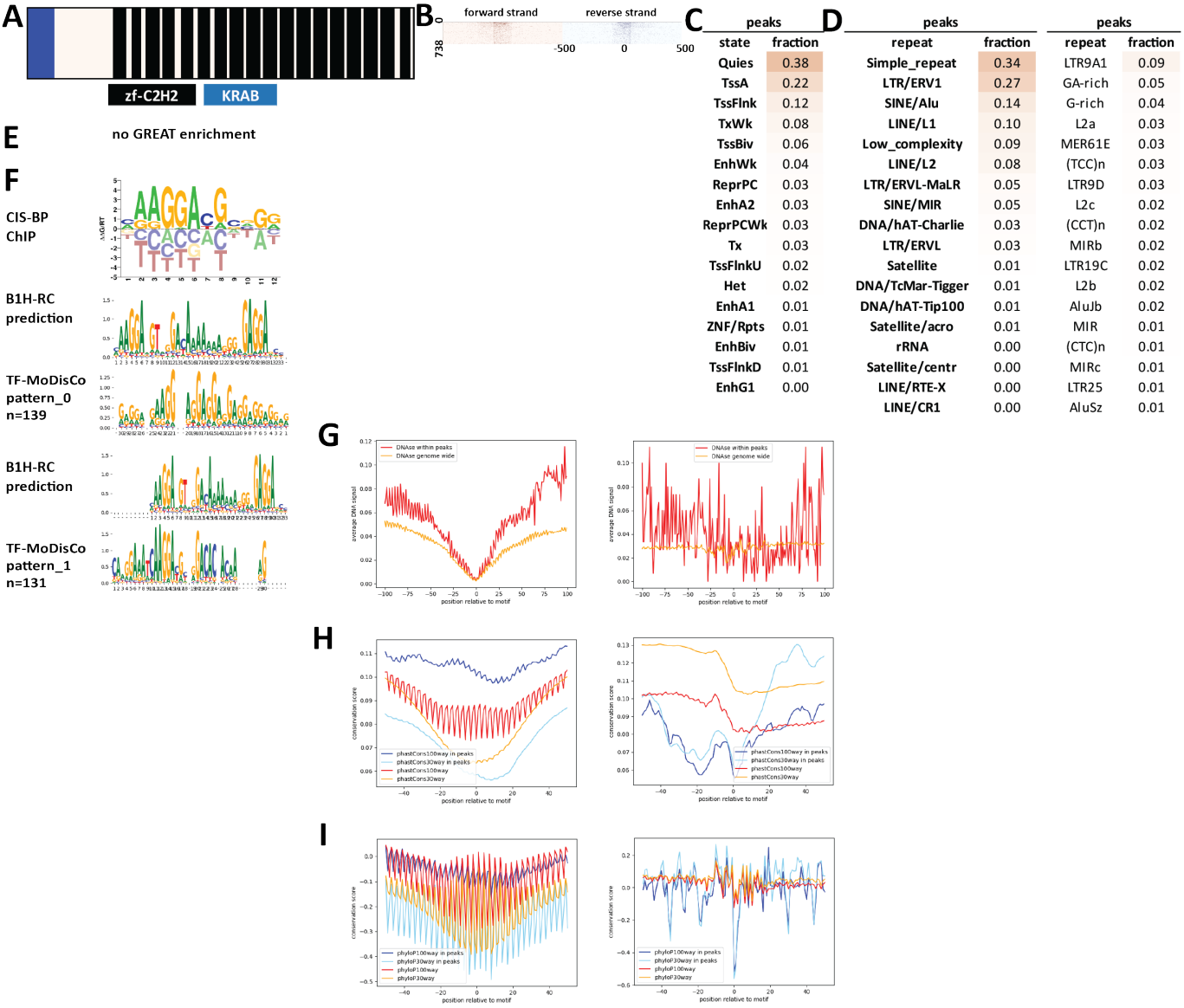

Supplementary Figure 1574: Properties and genomic distribution of motifs identified for the ZNF681 transcription factor in HEK293 (accession ChipExo models).

TF-MoDisCO pattern_0 n=139, CWM

pattern_0, n=139; subpattern_0, ns=33

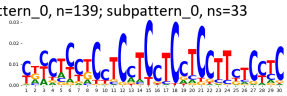

pattern_0, n=139; subpattern_1, ns=32

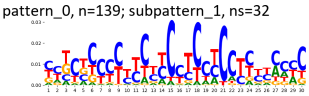

pattern_0, n=139; subpattern_2, ns=30

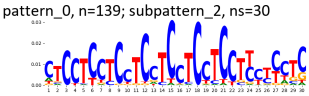

pattern_0, n=139; subpattern_3, ns=26

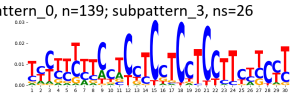

pattern_0, n=139; subpattern_4, ns=18

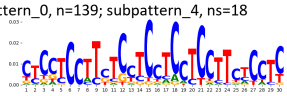

TF-MoDisCO pattern_0 n=139, PWM

pattern_0, n=139; subpattern_0, ns=33

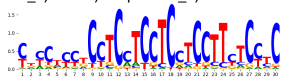

pattern_0, n=139; subpattern_1, ns=32

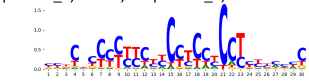

pattern_0, n=139; subpattern_2, ns=30

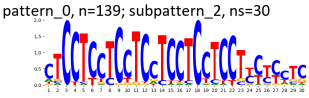

pattern_0, n=139; subpattern_3, ns=26

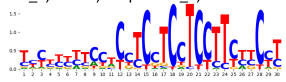

pattern_0, n=139; subpattern_4, ns=18

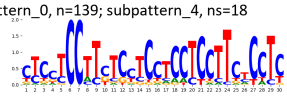

TF-MoDisCO pattern_1 n=131, CWM

pattern_1, n=131; subpattern_0, ns=37

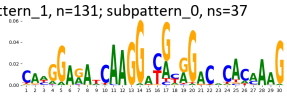

pattern_1, n=131; subpattern_1, ns=29

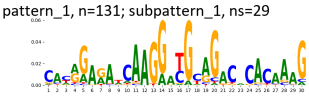

pattern_1, n=131; subpattern_2, ns=21

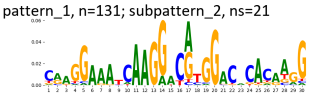

pattern_1, n=131; subpattern_3, ns=14

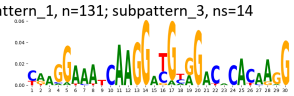

pattern_1, n=131; subpattern_4, ns=13

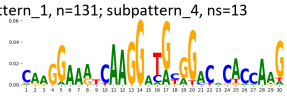

pattern_1, n=131; subpattern_5, ns=11

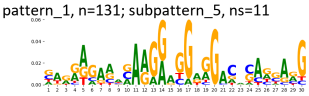

pattern_1, n=131; subpattern_6, ns=6

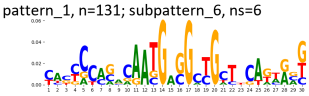

TF-MoDisCO pattern_1 n=131, PWM

pattern_1, n=131; subpattern_0, ns=37

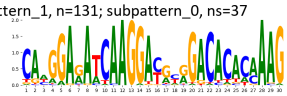

pattern_1, n=131; subpattern_1, ns=29

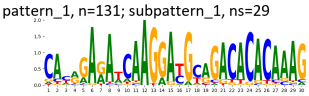

pattern_1, n=131; subpattern_2, ns=21

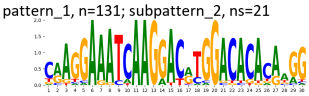

pattern_1, n=131; subpattern_3, ns=14

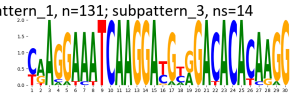

pattern_1, n=131; subpattern_4, ns=13

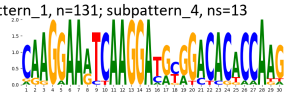

pattern_1, n=131; subpattern_5, ns=11

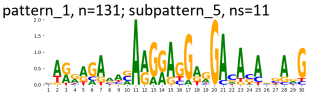

pattern_1, n=131; subpattern_6, ns=6

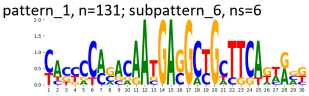

Supplementary Figure 1575: TF-MoDisCO subpatterns for the ZNF681 transcription factor in HEK293 (accession ChipExo models).

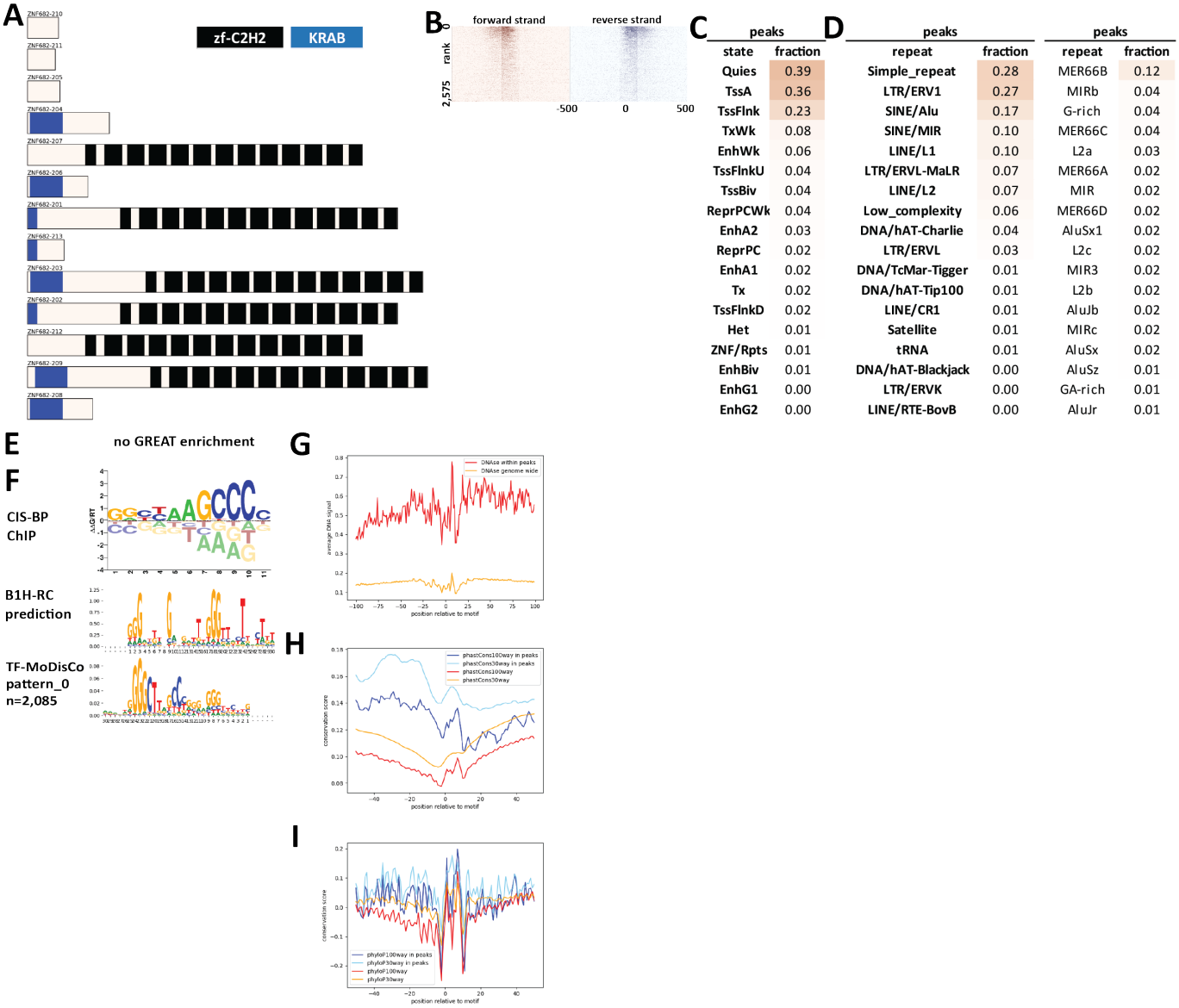

peaks	
state	fraction
Quies	0.39
TssA	0.36
TssFlnk	0.23
TxWk	0.08
EnhWk	0.06
TssFlnkU	0.04
TssBiv	0.04
ReprPCWk	0.04
EnhA2	0.03
ReprPC	0.02
EnhA1	0.02
Tx	0.02
TssFlnkD	0.02
Het	0.01
ZNF/Rpts	0.01
EnhBiv	0.01
EnhG1	0.00
EnhG2	0.00

peaks	
repeat	fraction
Simple_repeat	0.28
LTR/ERV1	0.27
SINE/Alu	0.17
SINE/MIR	0.10
LINE/L1	0.10
LTR/ERVL-MaLR	0.07
LINE/L2	0.07
Low_complexity	0.06
DNA/hAT-Charlie	0.04
LTR/ERVL	0.03
DNA/TcMar-Tigger	0.01
DNA/hAT-Tip100	0.01
LINE/CR1	0.01
Satellite	0.01
tRNA	0.01
DNA/hAT-Blackjack	0.00
LTR/ERVK	0.00
LINE/RTE-BovB	0.00

peaks	
repeat	fraction
MER66B	0.12
MIRb	0.04
G-rich	0.04
MER66C	0.04
L2a	0.03
MER66A	0.02
MIR	0.02
MER66D	0.02
AluSx1	0.02
L2c	0.02
MIR3	0.02
L2b	0.02
AluJb	0.02
MIRc	0.02
AluSx	0.02
AluSz	0.01
GA-rich	0.01
AluJr	0.01

Supplementary Figure 1576: Properties and genomic distribution of motifs identified for the ZNF682 transcription factor in HEK293 (accession ChipExo models).

TF-MoDisCO pattern_0 n=2085, CWM

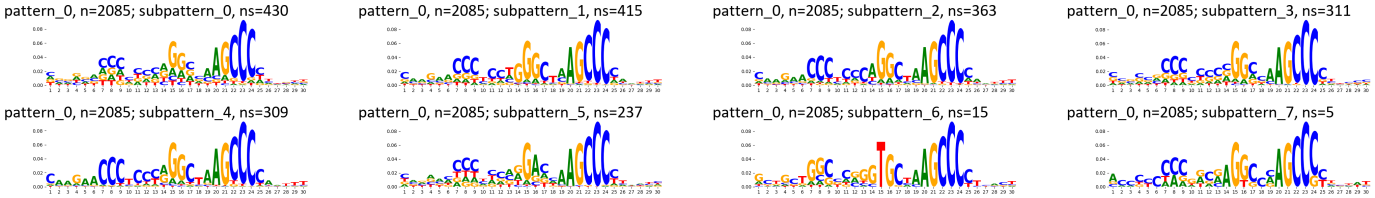

TF-MoDisCO pattern_0 n=2085, PWM

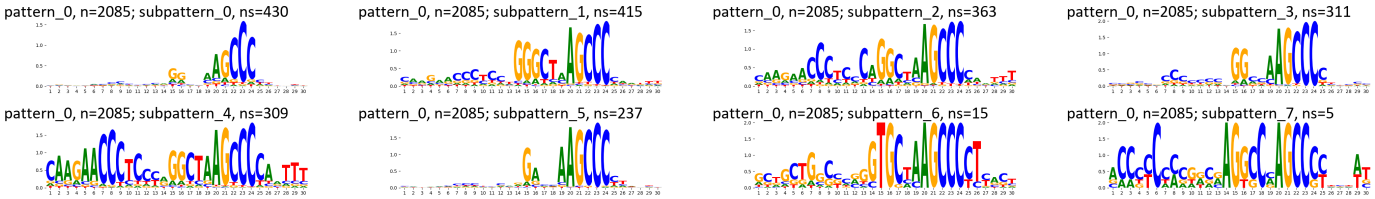

Supplementary Figure 1577: TF-MoDisCO subpatterns for the ZNF682 transcription factor in HEK293 (accession ChipExo models).

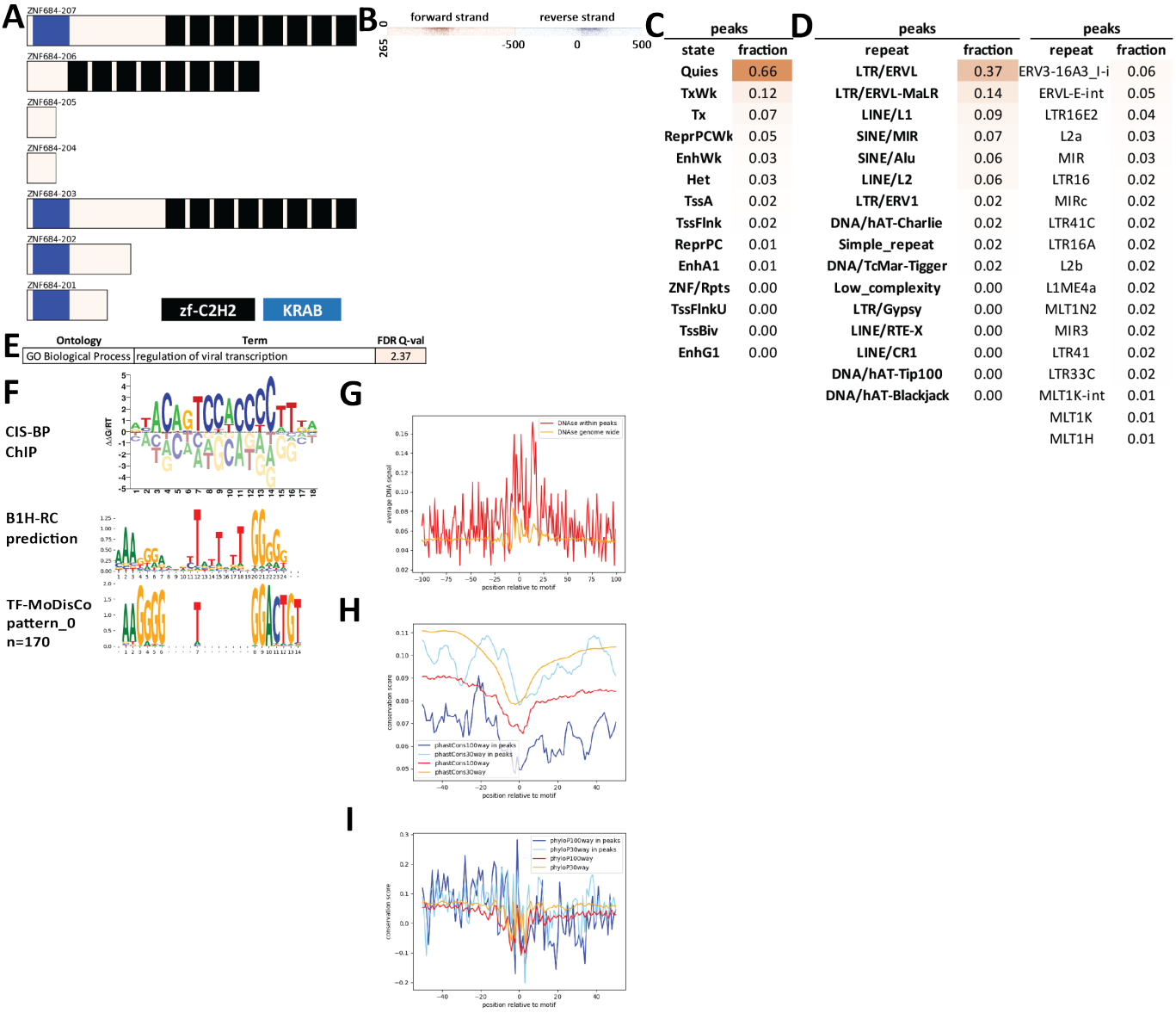

Supplementary Figure 1578: Properties and genomic distribution of motifs identified for the ZNF684 transcription factor in HEK293 (accession Hughes NB models).

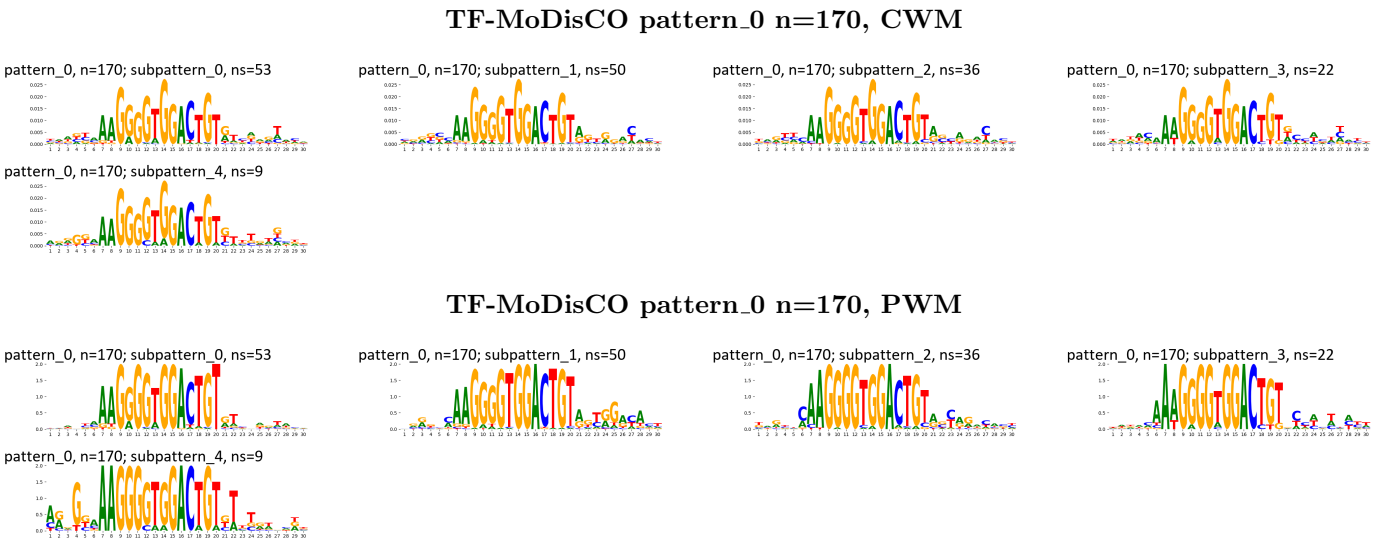

Supplementary Figure 1579: TF-MoDisCO subpatterns for the ZNF684 transcription factor in HEK293 (accession Hughes NB models).

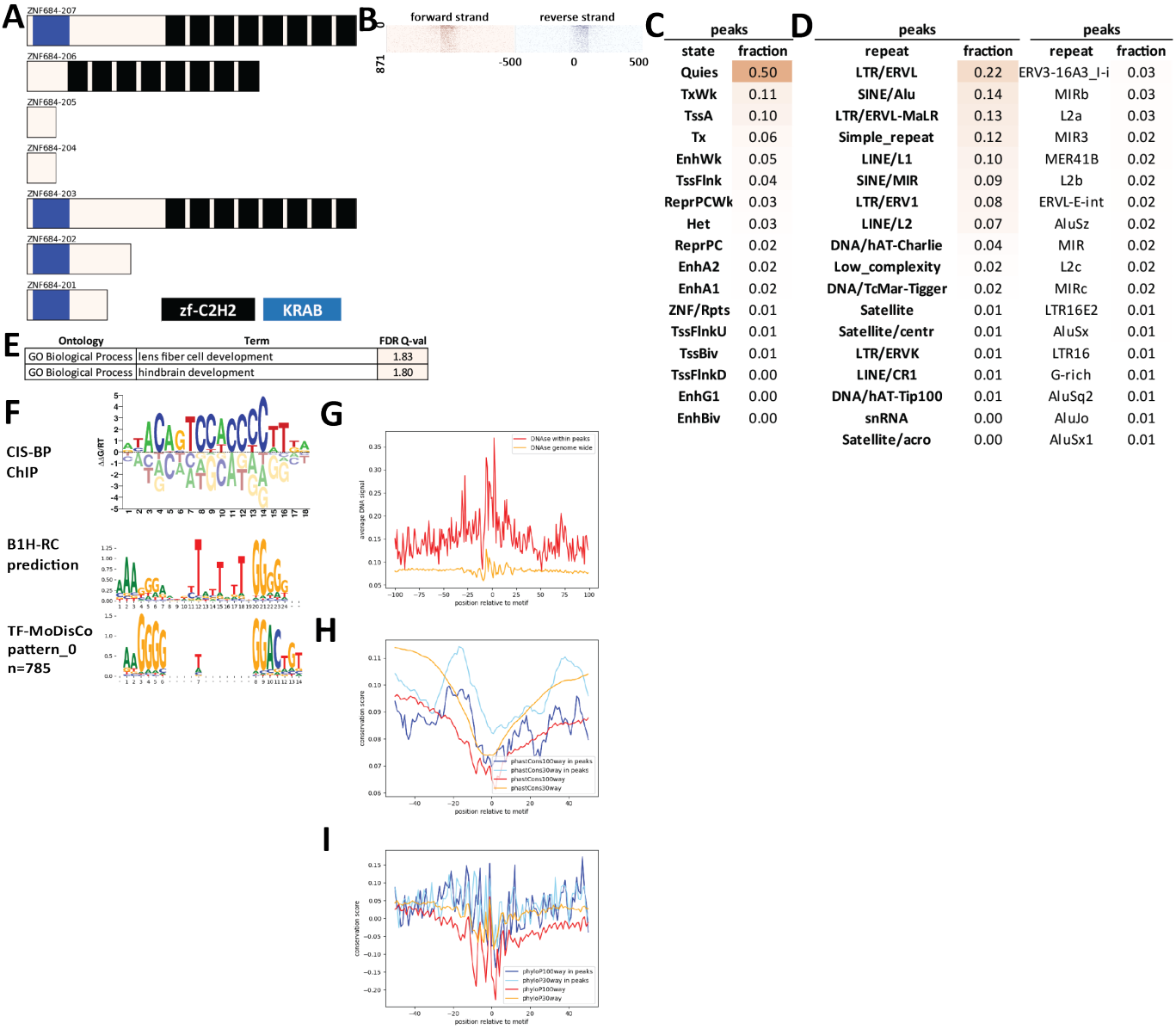

Supplementary Figure 1580: Properties and genomic distribution of motifs identified for the ZNF684 transcription factor in HEK293 (accession ChipExo models).

TF-MoDisCO pattern_0 n=785, CWM

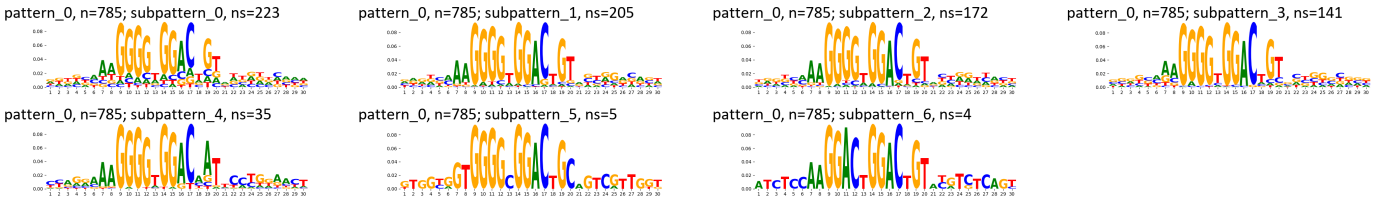

TF-MoDisCO pattern_0 n=785, PWM

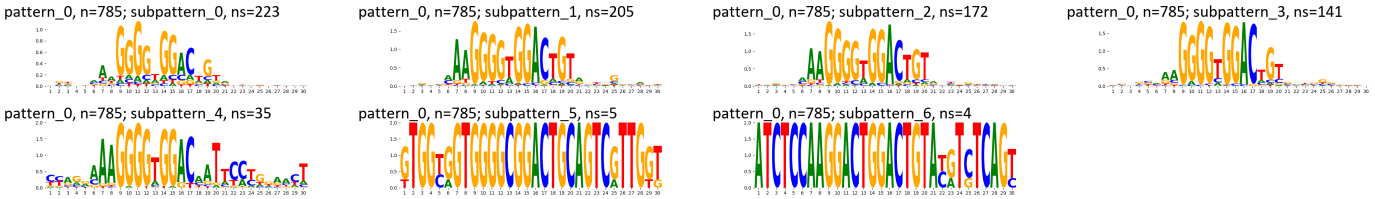

Supplementary Figure 1581: TF-MoDisCO subpatterns for the ZNF684 transcription factor in HEK293 (accession ChipExo models).

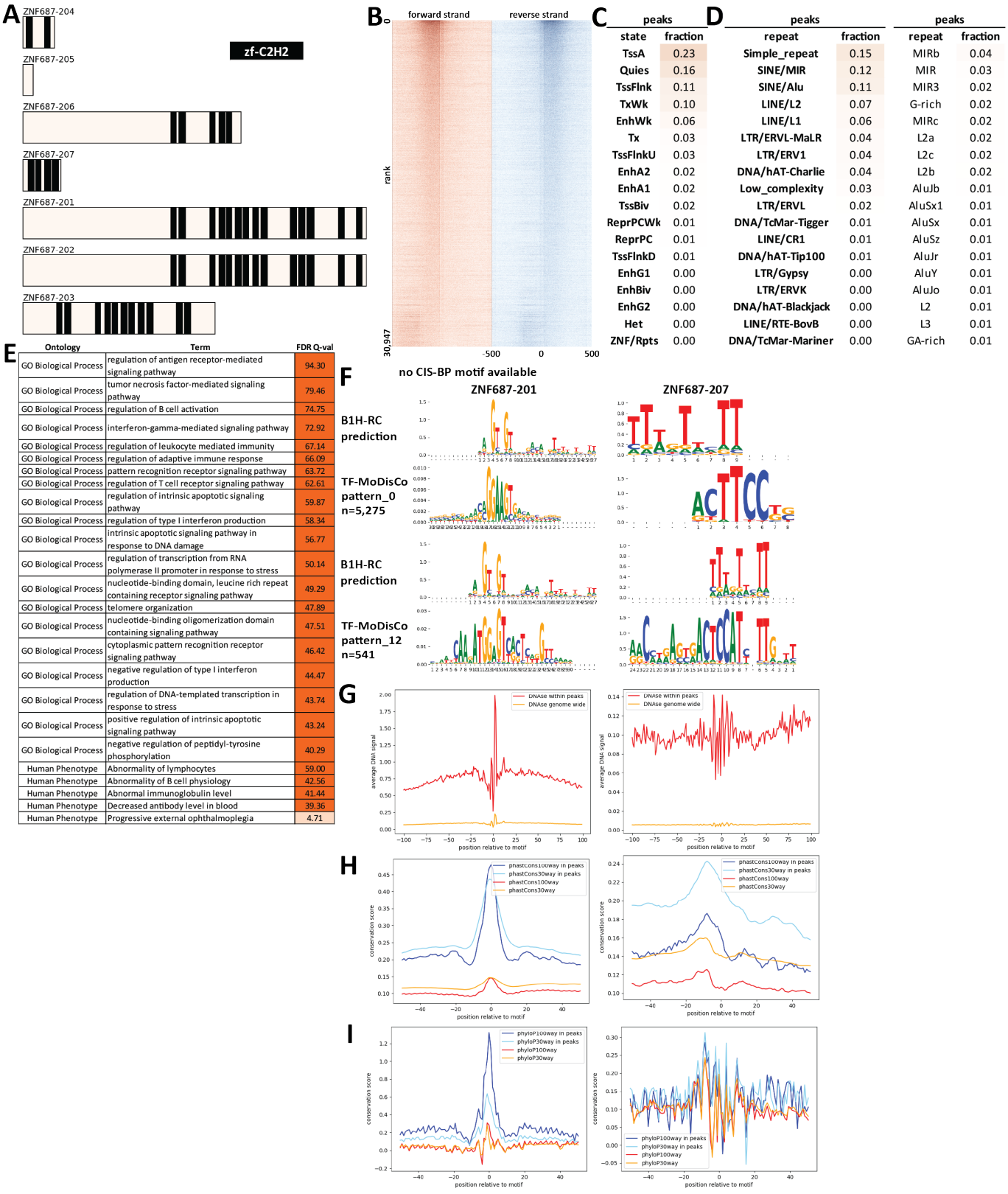

Supplementary Figure 1582: Properties and genomic distribution of motifs identified for the ZNF687 transcription factor in GM12878 (accession ENCSR859FDL).

TF-MoDisCO pattern_0 n=5275, CWM

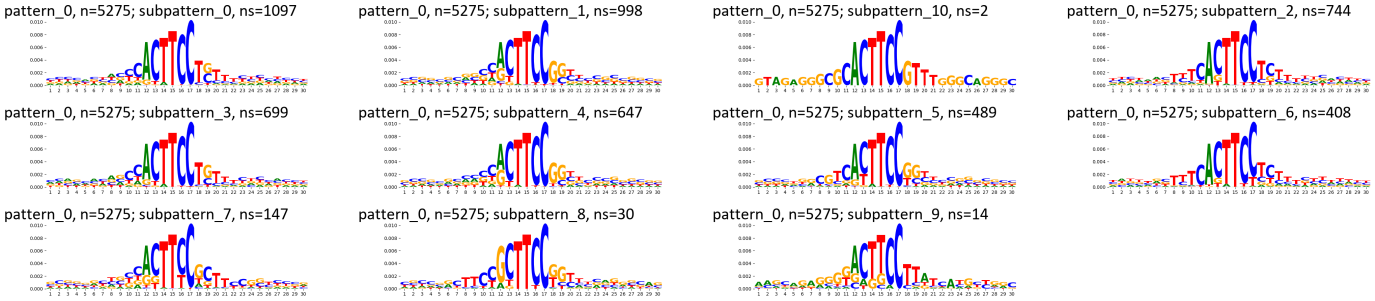

TF-MoDisCO pattern_0 n=5275, PWM

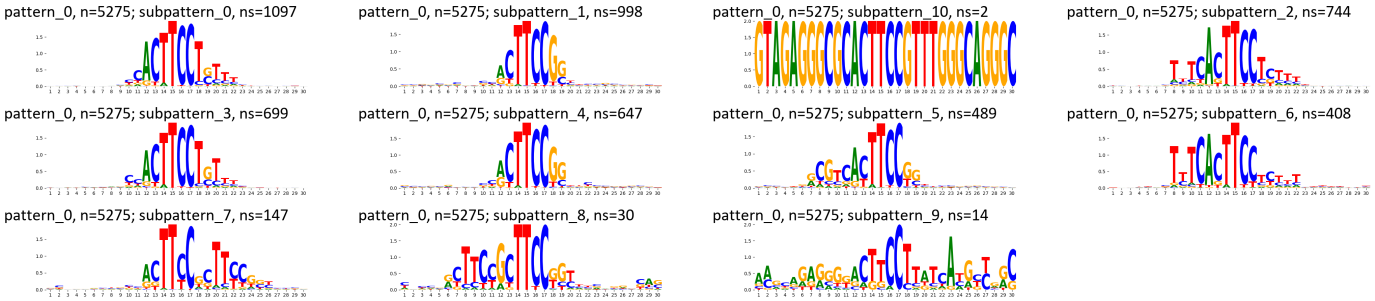

TF-MoDisCO pattern_12 n=541, CWM

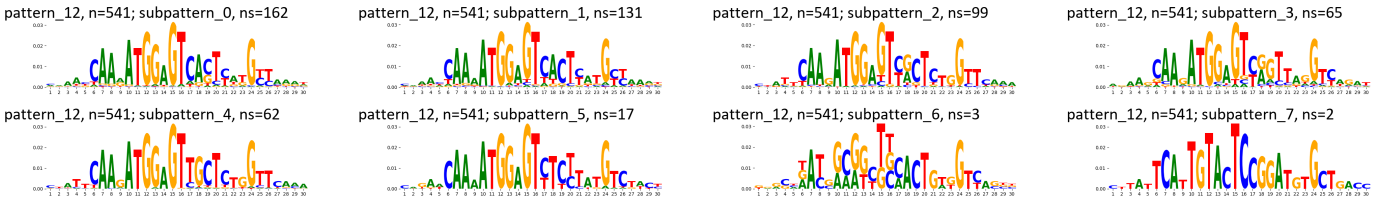

TF-MoDisCO pattern_12 n=541, PWM

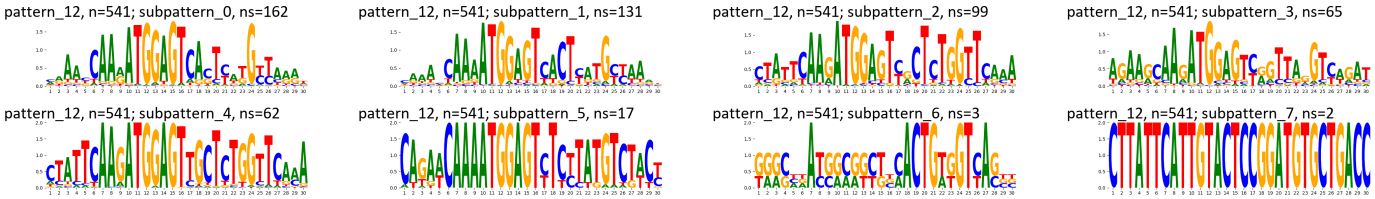

Supplementary Figure 1583: TF-MoDisCO subpatterns for the ZNF687 transcription factor in GM12878 (accession ENCSR859FDL).

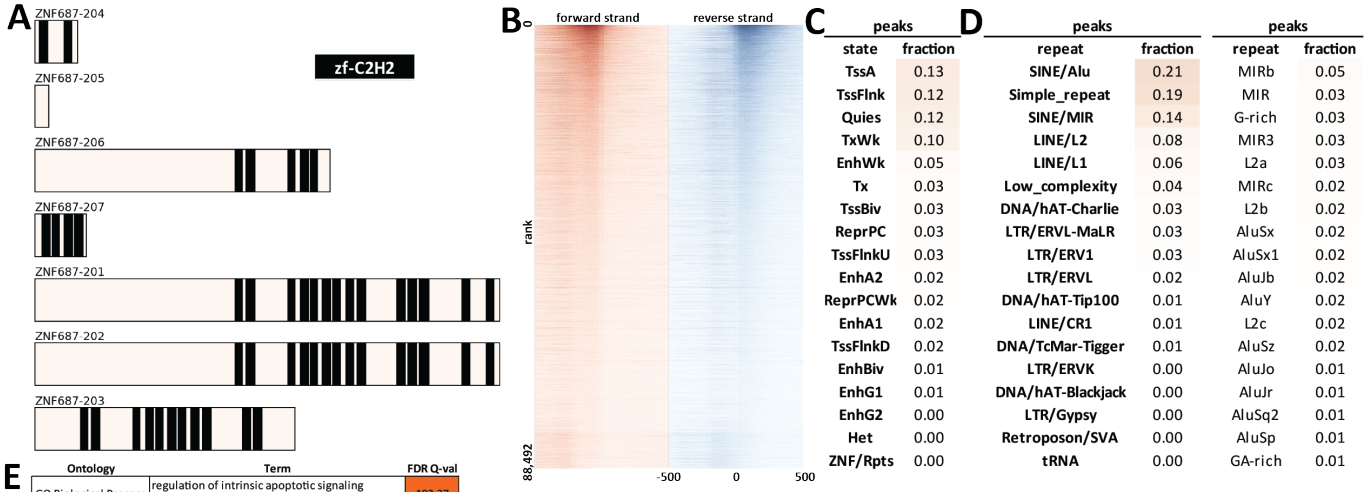

Supplementary Figure 1584: Properties and genomic distribution of motifs identified for the ZNF687 transcription factor in HepG2 (accession ENCSR647PSR).

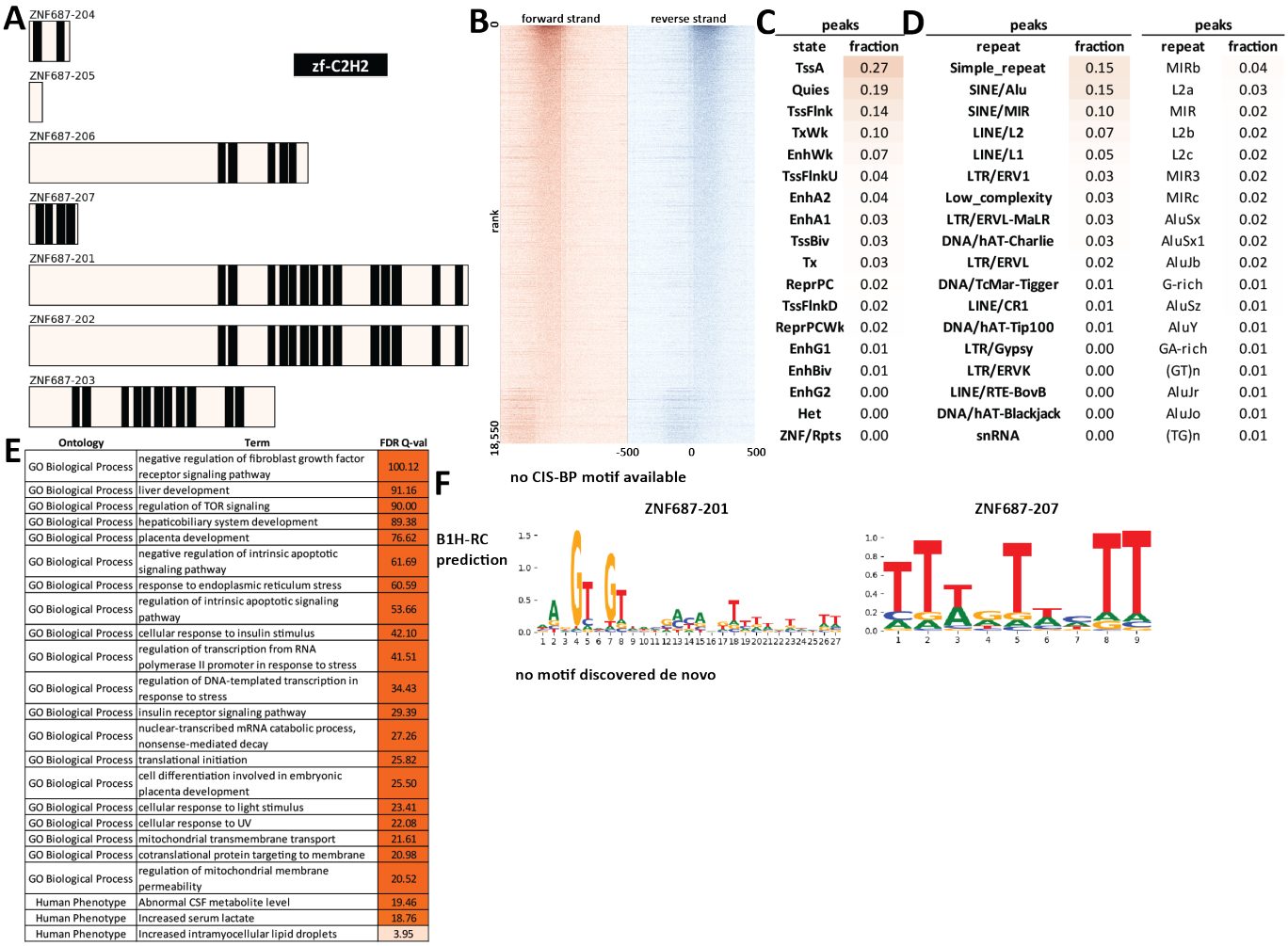

C

peaks	
state	fraction
TssA	0.27
Quies	0.19
TssFlnk	0.14
TxWk	0.10
EnhWk	0.07
TssFlnkU	0.04
EnhA2	0.04
EnhA1	0.03
TssBiv	0.03
Tx	0.03
ReprPC	0.02
TssFlnkD	0.02
ReprPCWk	0.02
EnhG1	0.01
EnhBiv	0.01
EnhG2	0.00
Het	0.00
ZNF/Rpts	0.00

D

peaks		peaks	
repeat	fraction	repeat	fraction
Simple_repeat	0.15	MIRb	0.04
SINE/Alu	0.15	L2a	0.03
SINE/MIR	0.10	MIR	0.02
LINE/L2	0.07	L2b	0.02
LINE/L1	0.05	L2c	0.02
LTR/ERV1	0.03	MIR3	0.02
Low_complexity	0.03	MIRc	0.02
LTR/ERVL-MaLR	0.03	AluSx	0.02
DNA/hAT-Charlie	0.03	AluSx1	0.02
LTR/ERVL	0.02	AluJb	0.02
DNA/TcMar-Tigger	0.01	G-rich	0.01
LINE/CR1	0.01	AluSz	0.01
DNA/hAT-Tip100	0.01	AluY	0.01
LTR/Gypsy	0.00	GA-rich	0.01
LTR/ERVK	0.00	(GT)n	0.01
LINE/RTE-BovB	0.00	AluJr	0.01
DNA/hAT-Blackjack	0.00	AluJo	0.01
snRNA	0.00	(TG)n	0.01

E

Ontology	Term	FDR Q-val
GO Biological Process	negative regulation of fibroblast growth factor receptor signaling pathway	100.12
GO Biological Process	liver development	91.16
GO Biological Process	regulation of TOR signaling	90.00
GO Biological Process	hepaticobiliary system development	89.38
GO Biological Process	placenta development	76.62
GO Biological Process	negative regulation of intrinsic apoptotic signaling pathway	61.69
GO Biological Process	response to endoplasmic reticulum stress	60.59
GO Biological Process	regulation of intrinsic apoptotic signaling pathway	53.66
GO Biological Process	cellular response to insulin stimulus	42.10
GO Biological Process	regulation of transcription from RNA polymerase II promoter in response to stress	41.51
GO Biological Process	regulation of DNA-templated transcription in response to stress	34.43
GO Biological Process	insulin receptor signaling pathway	29.39
GO Biological Process	nuclear-transcribed mRNA catabolic process, nonsense-mediated decay	27.26
GO Biological Process	translational initiation	25.82
GO Biological Process	cell differentiation involved in embryonic placenta development	25.50
GO Biological Process	cellular response to light stimulus	23.41
GO Biological Process	cellular response to UV	22.08
GO Biological Process	mitochondrial transmembrane transport	21.61
GO Biological Process	cotranslational protein targeting to membrane	20.98
GO Biological Process	regulation of mitochondrial membrane permeability	20.52
Human Phenotype	Abnormal CSF metabolite level	19.46
Human Phenotype	Increased serum lactate	18.76
Human Phenotype	Increased intramyocellular lipid droplets	3.95

Supplementary Figure 1585: Properties and genomic distribution of motifs identified for the ZNF687 transcription factor in MCF-7 (accession ENCSR899BKM).

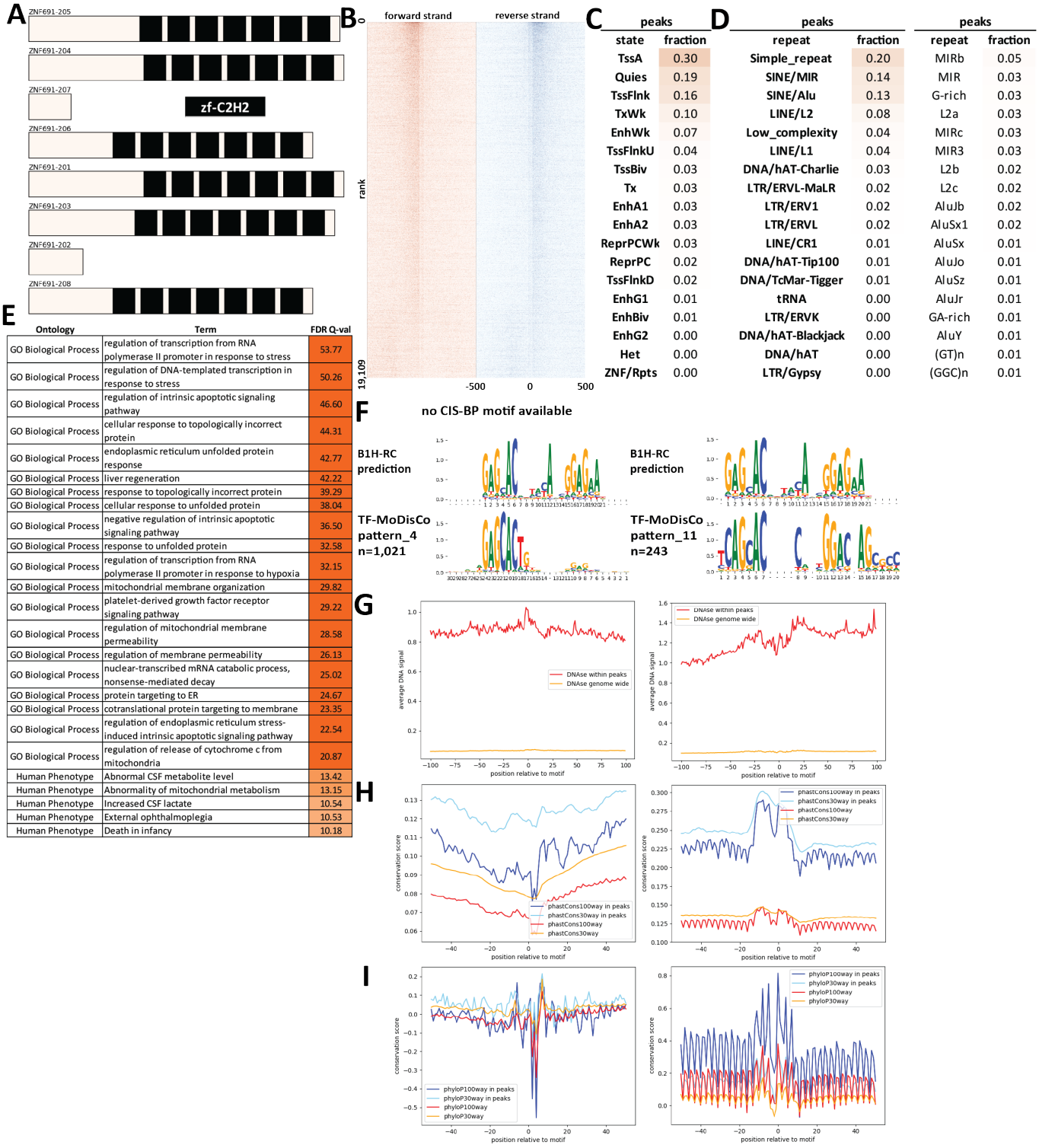

Supplementary Figure 1586: Properties and genomic distribution of motifs identified for the ZNF691 transcription factor in HepG2 (accession ENCSR130ZAR).

TF-MoDisCO pattern_11 n=243, CWM

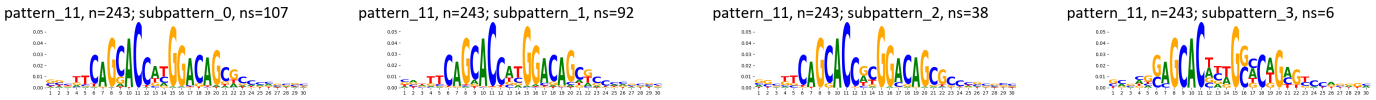

TF-MoDisCO pattern_11 n=243, PWM

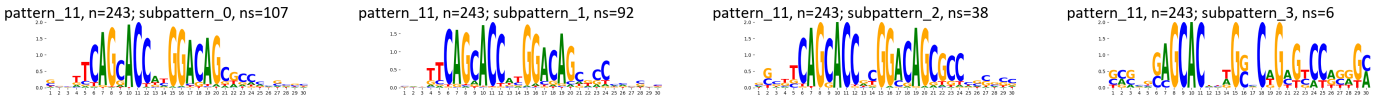

TF-MoDisCO pattern_4 n=1021, CWM

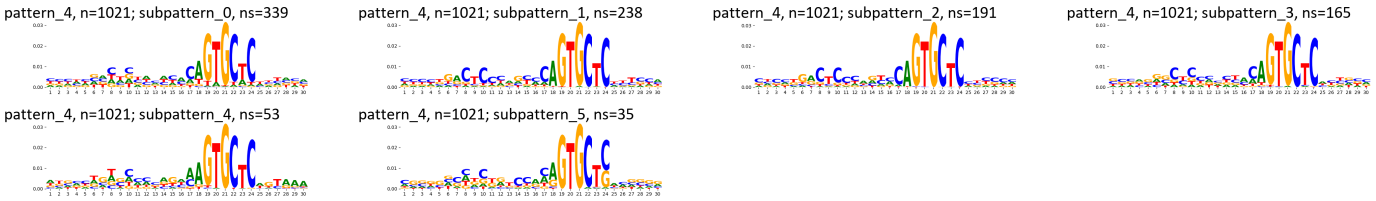

TF-MoDisCO pattern_4 n=1021, PWM

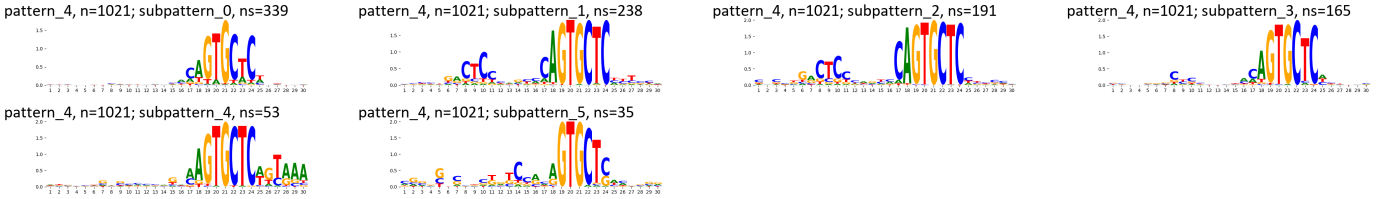

Supplementary Figure 1587: TF-MoDisCO subpatterns for the ZNF691 transcription factor in HepG2 (accession ENCSR130ZAR).

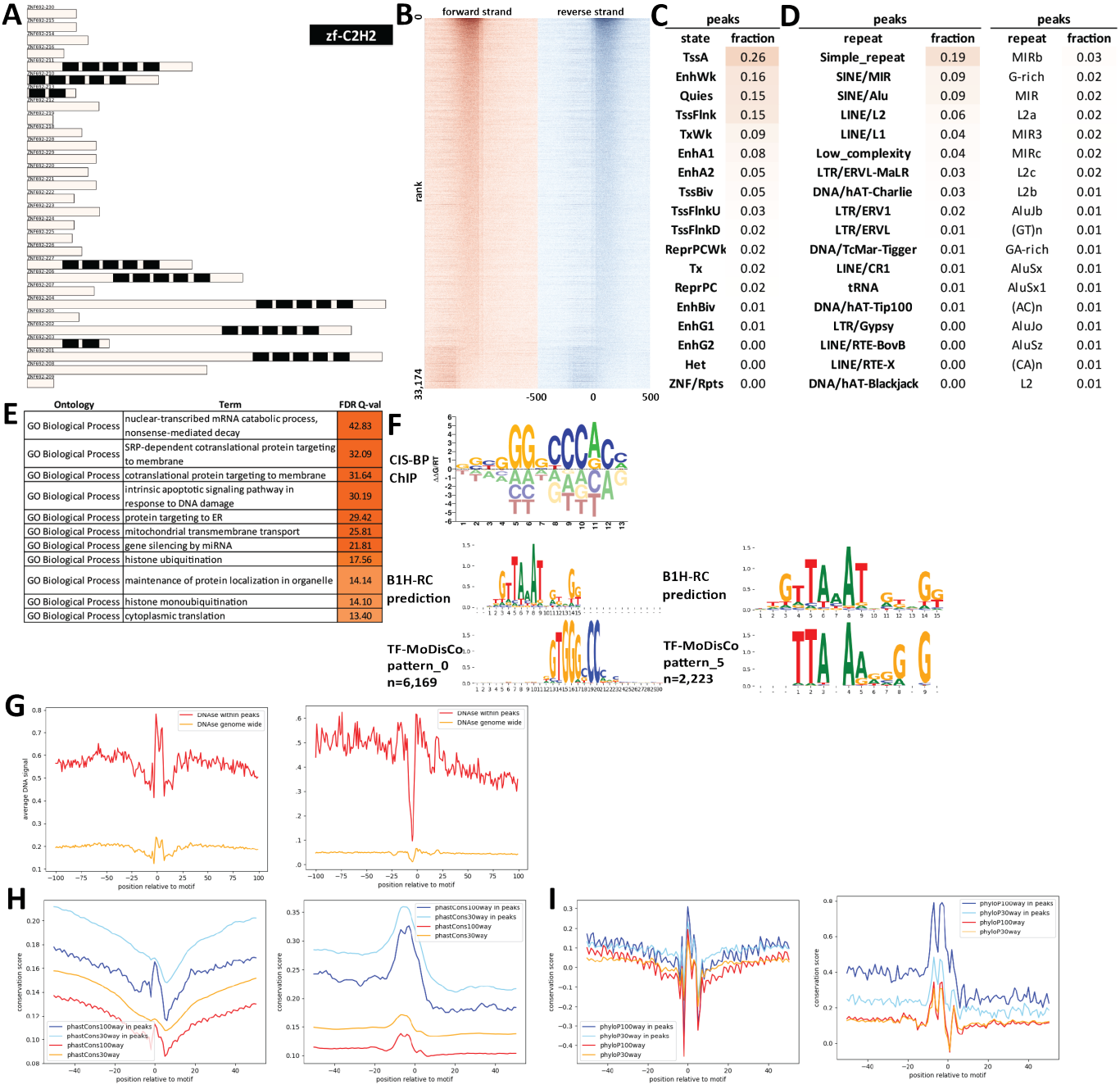

Supplementary Figure 1588: Properties and genomic distribution of motifs identified for the ZNF692 transcription factor in HEK293 (accession ENCSR418MKG).

TF-MoDisCO pattern_0 n=6169, CWM

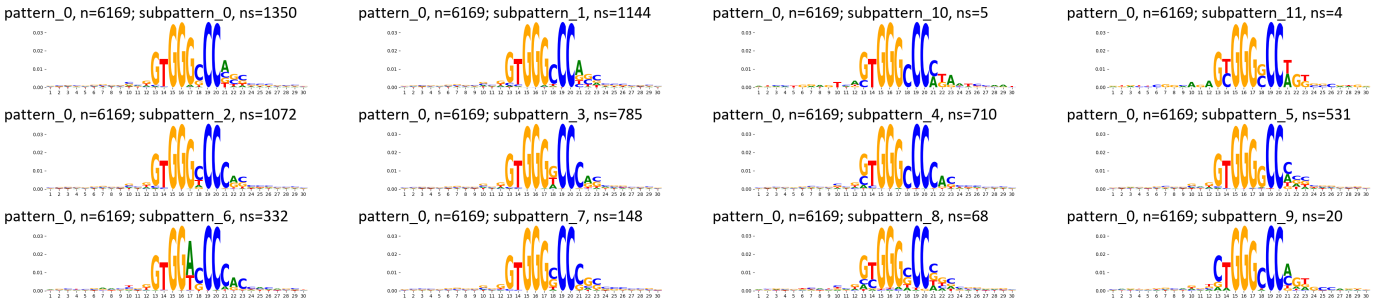

TF-MoDisCO pattern_0 n=6169, PWM

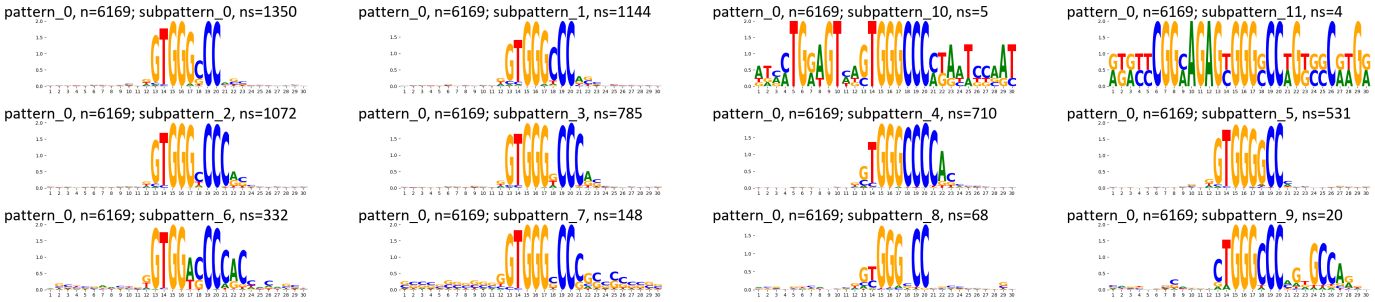

TF-MoDisCO pattern_4 n=2223, CWM

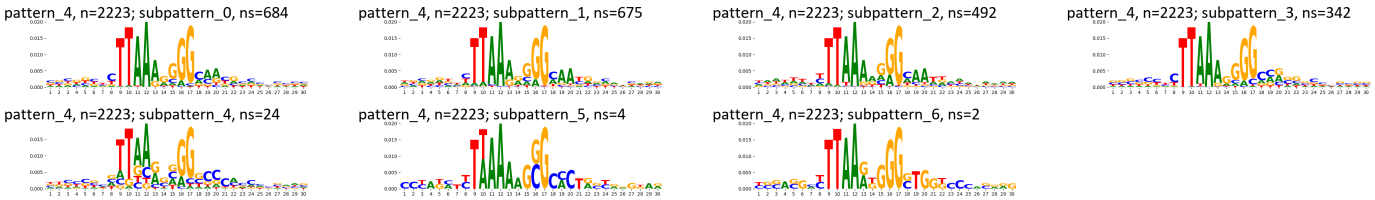

TF-MoDisCO pattern_4 n=2223, PWM

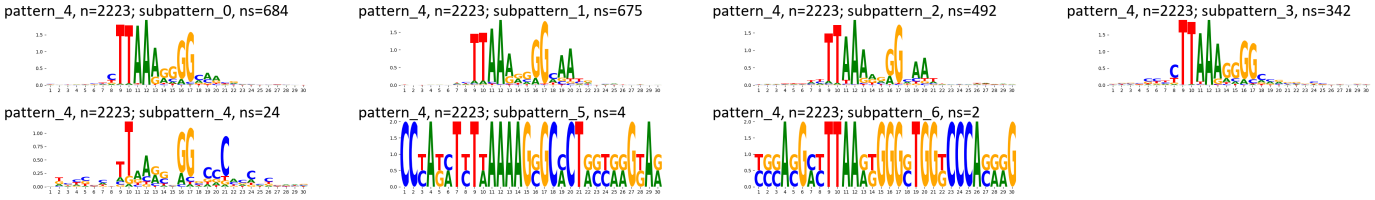

Supplementary Figure 1589: TF-MoDisCO subpatterns for the ZNF692 transcription factor in HEK293 (accession ENCSR418MKG).

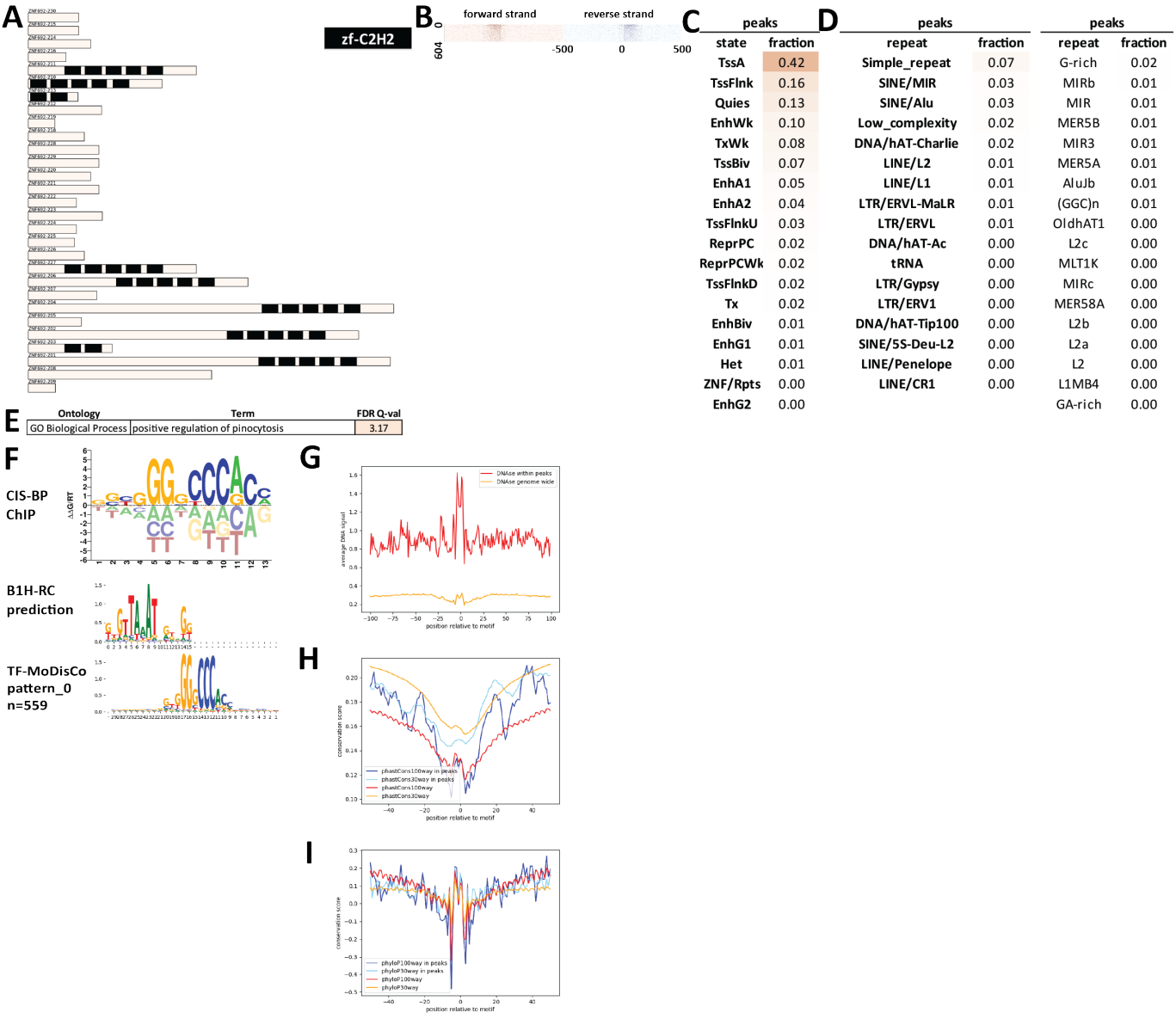

Supplementary Figure 1590: Properties and genomic distribution of motifs identified for the ZNF692 transcription factor in HEK293 (accession Hughes NB models).

TF-MoDisCO pattern_0 n=559, CWM

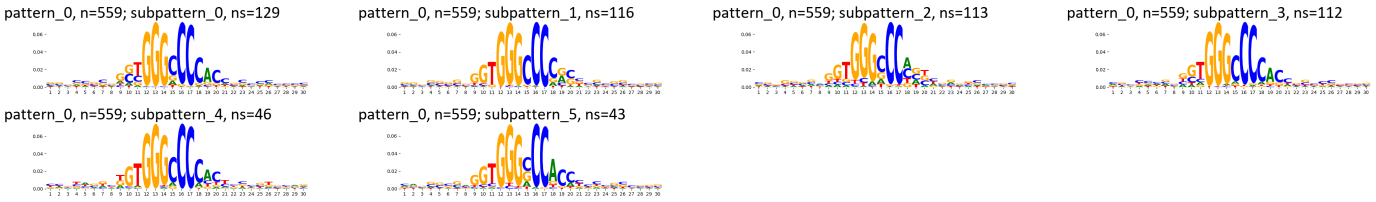

TF-MoDisCO pattern_0 n=559, PWM

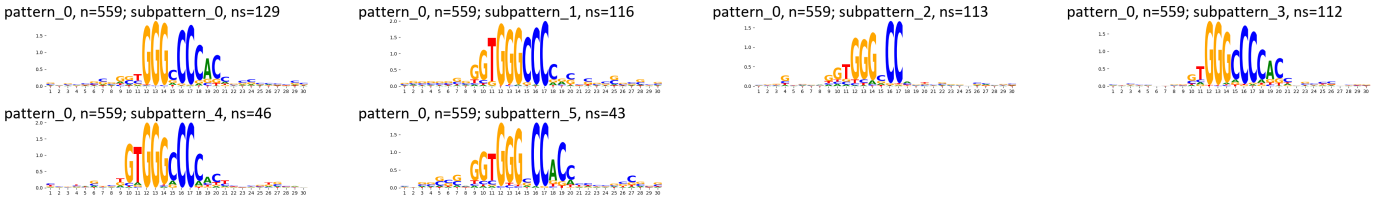

Supplementary Figure 1591: TF-MoDisCO subpatterns for the ZNF692 transcription factor in HEK293 (accession Hughes NB models).

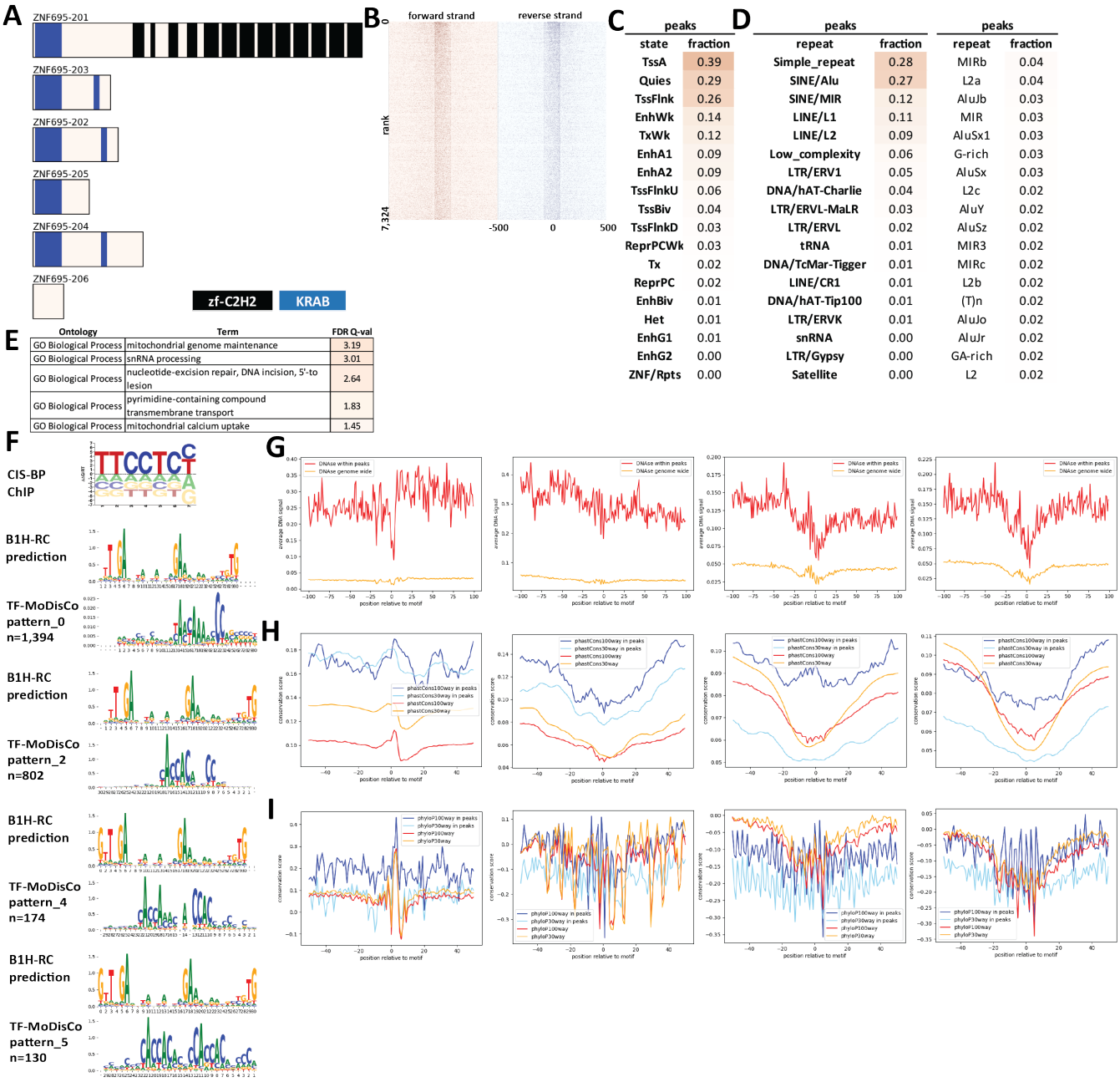

Supplementary Figure 1592: Properties and genomic distribution of motifs identified for the ZNF695 transcription factor in HEK293 (accession ChipExo models).

TF-MoDisCO pattern_0 n=1394, CWM

pattern_0, n=1394; subpattern_0, ns=410

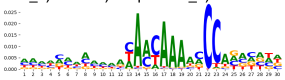

pattern_0, n=1394; subpattern_1, ns=378

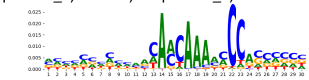

pattern_0, n=1394; subpattern_2, ns=250

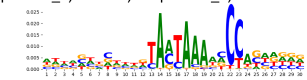

pattern_0, n=1394; subpattern_3, ns=175

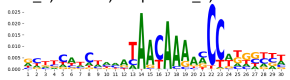

pattern_0, n=1394; subpattern_4, ns=147

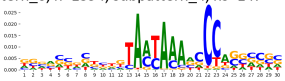

pattern_0, n=1394; subpattern_5, ns=34

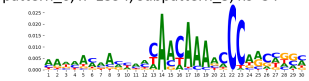

TF-MoDisCO pattern_0 n=1394, PWM

pattern_0, n=1394; subpattern_0, ns=410

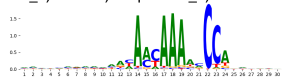

pattern_0, n=1394; subpattern_1, ns=378

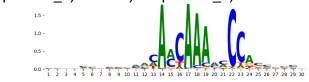

pattern_0, n=1394; subpattern_2, ns=250

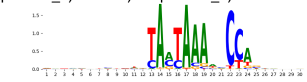

pattern_0, n=1394; subpattern_3, ns=175

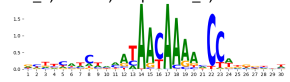

pattern_0, n=1394; subpattern_4, ns=147

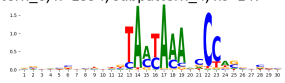

pattern_0, n=1394; subpattern_5, ns=34

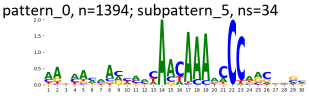

TF-MoDisCO pattern_2 n=802, CWM

pattern_2, n=802; subpattern_0, ns=211

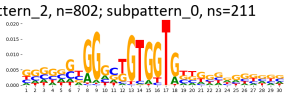

pattern_2, n=802; subpattern_1, ns=193

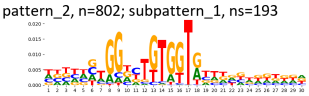

pattern_2, n=802; subpattern_2, ns=128

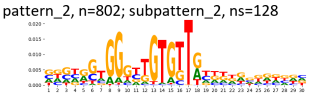

pattern_2, n=802; subpattern_3, ns=119

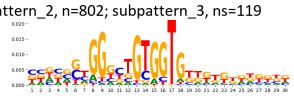

pattern_2, n=802; subpattern_4, ns=86

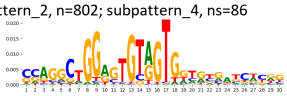

pattern_2, n=802; subpattern_5, ns=65

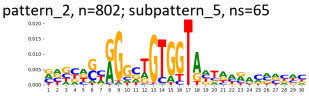

TF-MoDisCO pattern_2 n=802, PWM

pattern_2, n=802; subpattern_0, ns=211

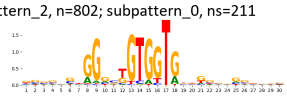

pattern_2, n=802; subpattern_1, ns=193

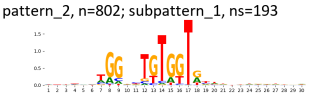

pattern_2, n=802; subpattern_2, ns=128

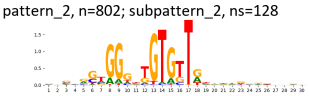

pattern_2, n=802; subpattern_3, ns=119

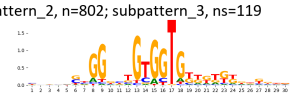

pattern_2, n=802; subpattern_4, ns=86

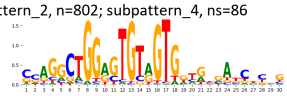

pattern_2, n=802; subpattern_5, ns=65

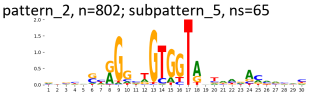

TF-MoDisCO pattern_4 n=174, CWM

pattern_4, n=174; subpattern_0, ns=51

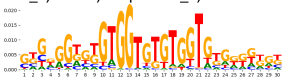

pattern_4, n=174; subpattern_1, ns=46

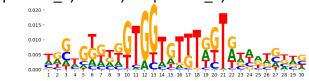

pattern_4, n=174; subpattern_2, ns=39

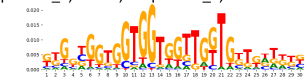

pattern_4, n=174; subpattern_3, ns=36

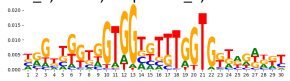

pattern_4, n=174; subpattern_4, ns=2



TF-MoDisCO pattern_4 n=174, PWM

pattern_4, n=174; subpattern_0, ns=51

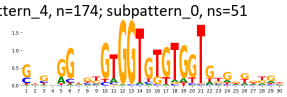

pattern_4, n=174; subpattern_1, ns=46

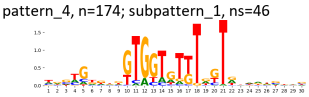

pattern_4, n=174; subpattern_2, ns=39

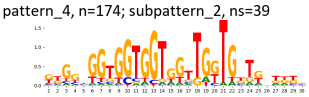

pattern_4, n=174; subpattern_3, ns=36

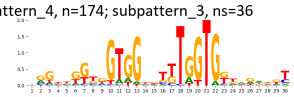

pattern_4, n=174; subpattern_4, ns=2

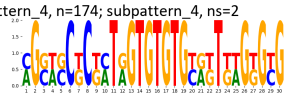

TF-MoDisCO pattern_5 n=130, CWM

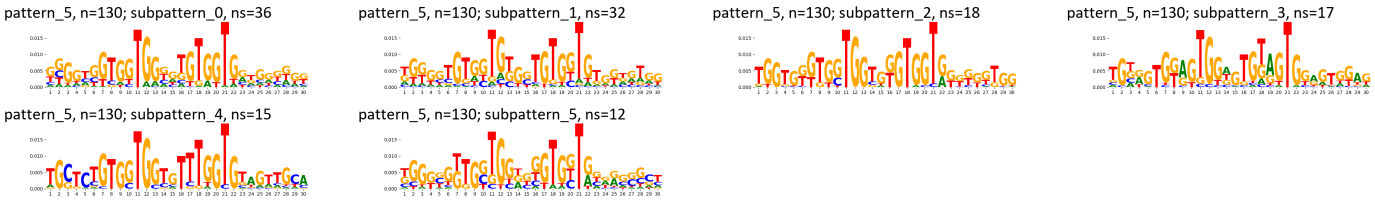

TF-MoDisCO pattern_5 n=130, PWM

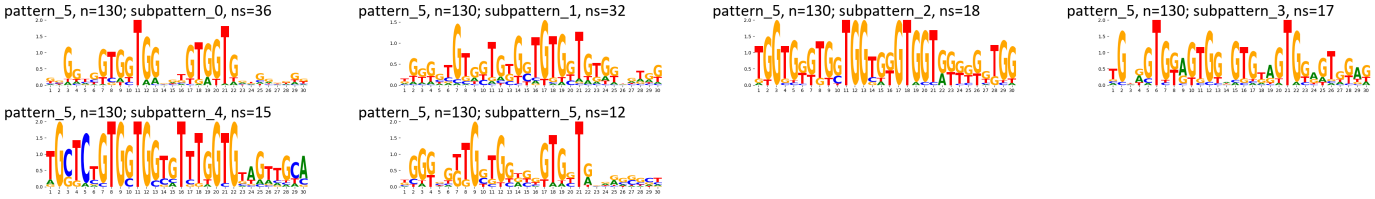

Supplementary Figure 1593: TF-MoDisCO subpatterns for the ZNF695 transcription factor in HEK293 (accession ChipExo models).

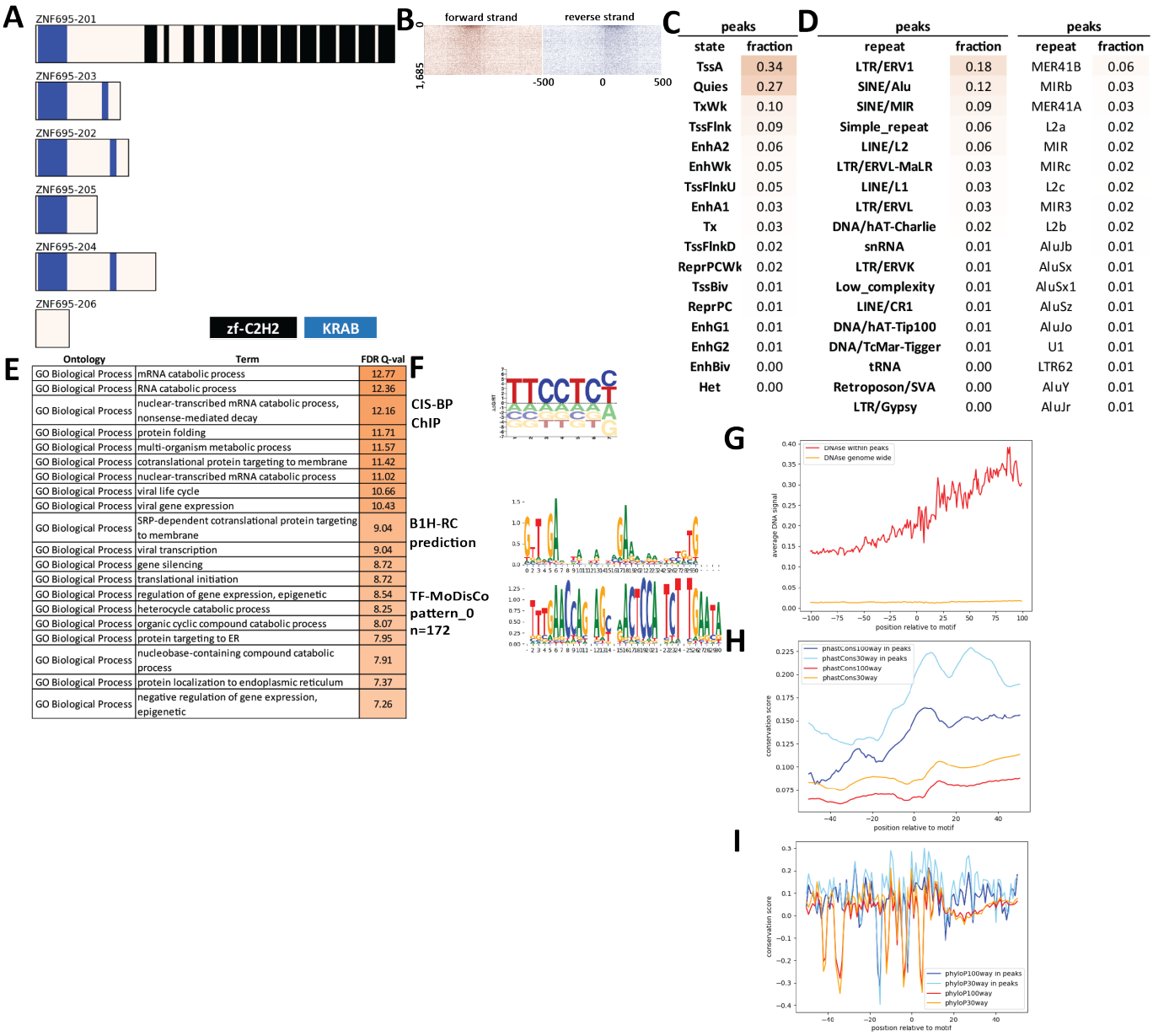

Supplementary Figure 1594: Properties and genomic distribution of motifs identified for the ZNF695 transcription factor in K562 (accession ENCSR187RGF).

TF-MoDisCO pattern_0 n=172, CWM

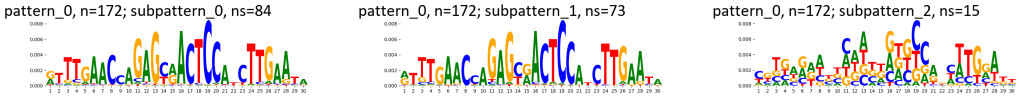

TF-MoDisCO pattern_0 n=172, PWM

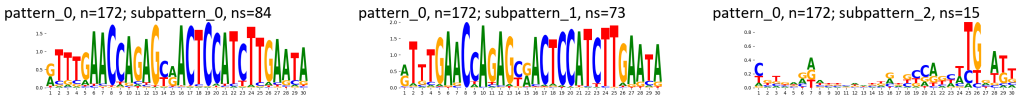

Supplementary Figure 1595: TF-MoDisCO subpatterns for the ZNF695 transcription factor in K562 (accession ENCSR187RGF).

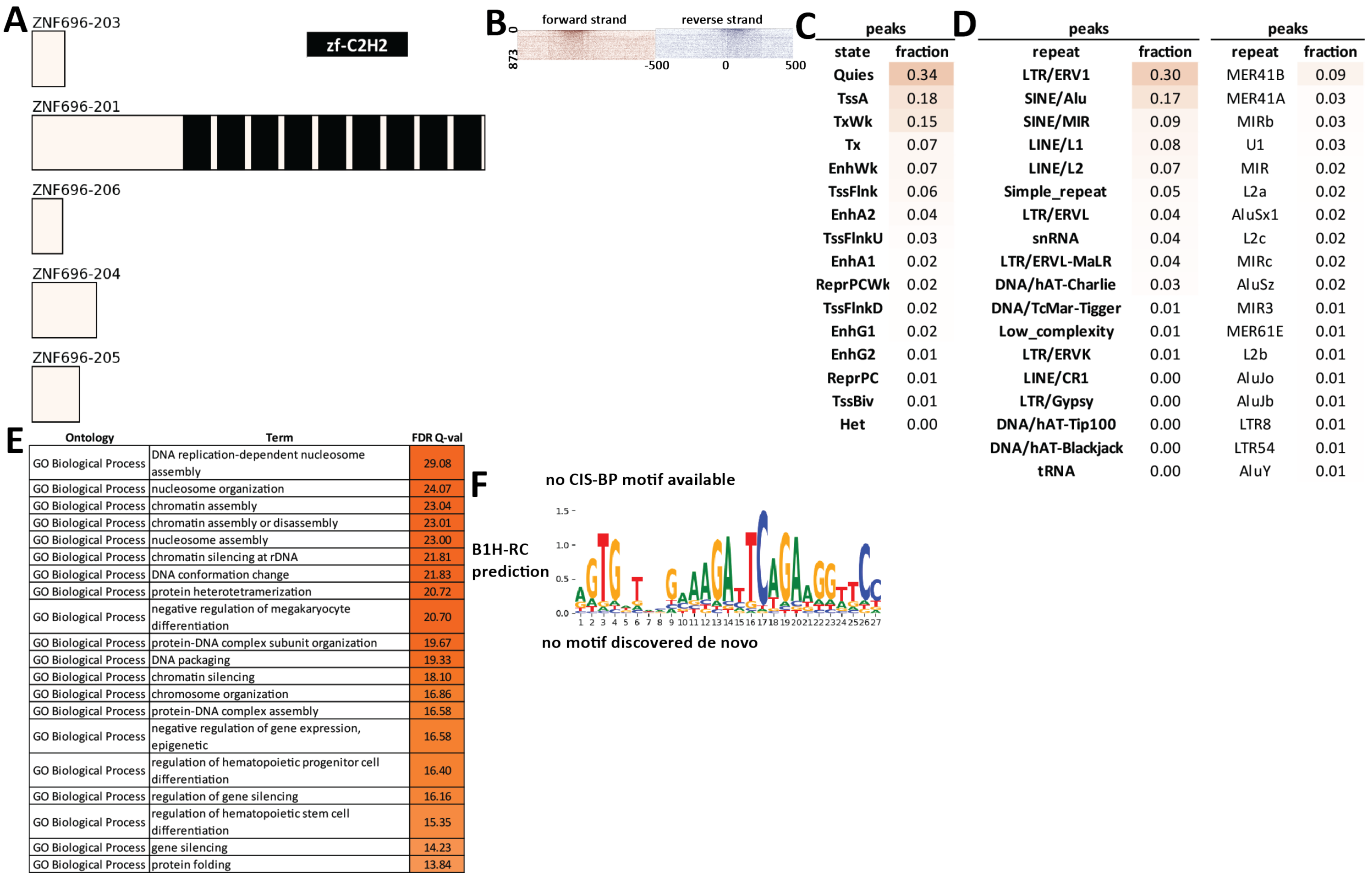

Supplementary Figure 1596: Properties and genomic distribution of motifs identified for the ZNF696 transcription factor in K562 (accession ENCSR276RQG).

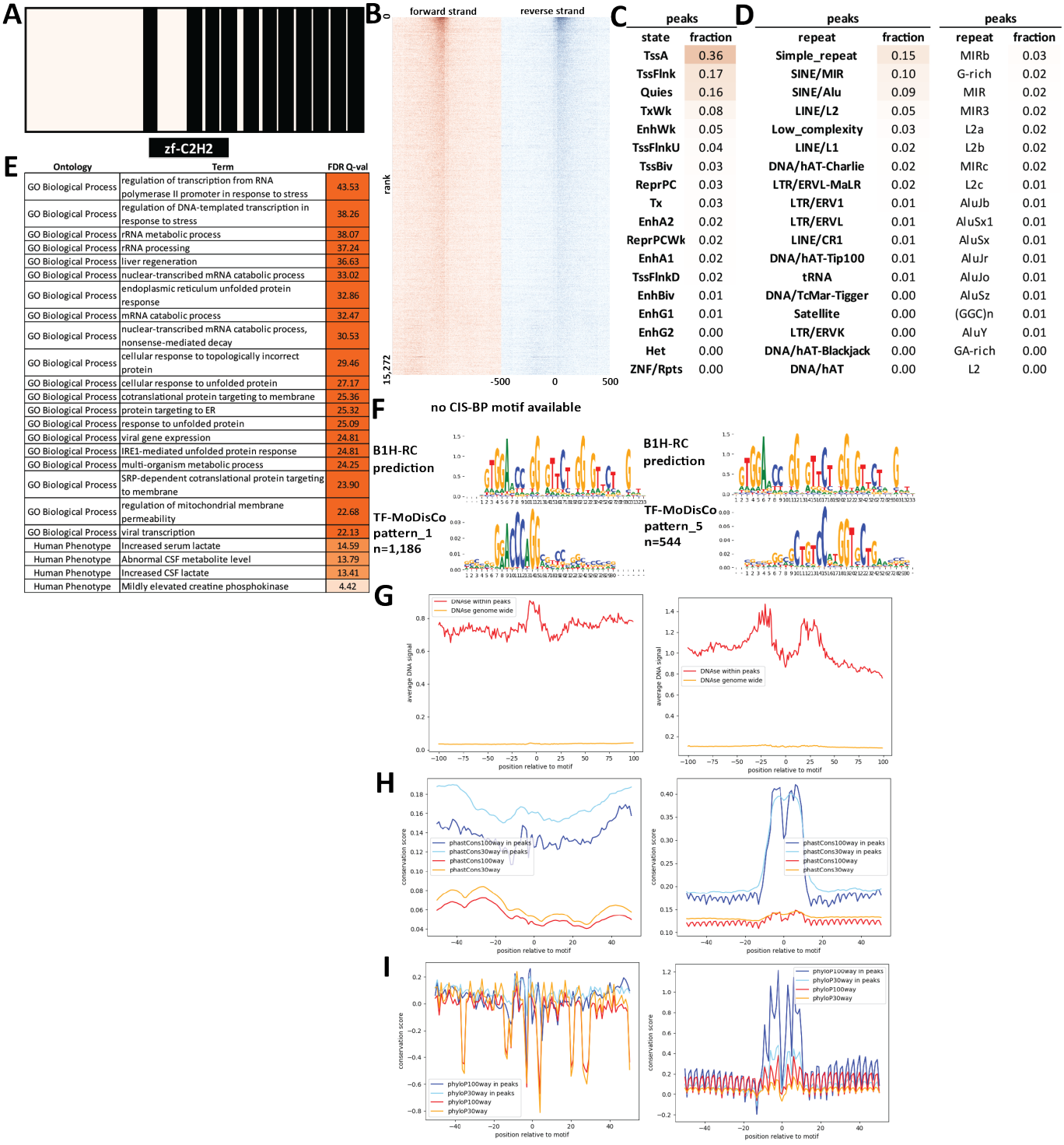

Supplementary Figure 1597: Properties and genomic distribution of motifs identified for the ZNF697 transcription factor in HepG2 (accession ENCSR734WFB).

TF-MoDisCO pattern_1 n=1186, CWM

pattern_1, n=1186; subpattern_0, ns=384

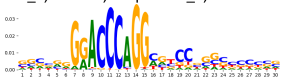

pattern_1, n=1186; subpattern_1, ns=308

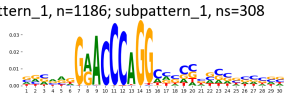

pattern_1, n=1186; subpattern_2, ns=261

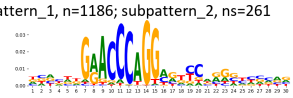

pattern_1, n=1186; subpattern_3, ns=233

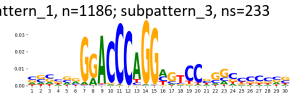

TF-MoDisCO pattern_1 n=1186, PWM

pattern_1, n=1186; subpattern_0, ns=384

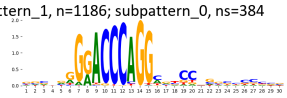

pattern_1, n=1186; subpattern_1, ns=308

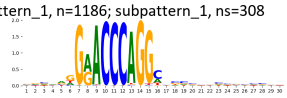

pattern_1, n=1186; subpattern_2, ns=261

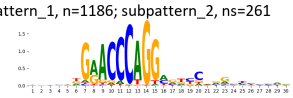

pattern_1, n=1186; subpattern_3, ns=233

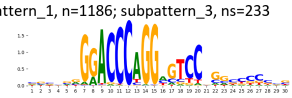

TF-MoDisCO pattern_5 n=544, CWM

pattern_5, n=544; subpattern_0, ns=145

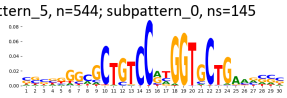

pattern_5, n=544; subpattern_1, ns=137

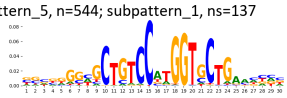

pattern_5, n=544; subpattern_2, ns=132

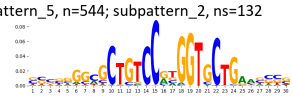

pattern_5, n=544; subpattern_3, ns=130

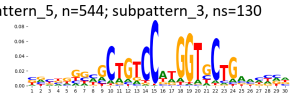

TF-MoDisCO pattern_5 n=544, PWM

pattern_5, n=544; subpattern_0, ns=145

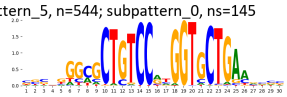

pattern_5, n=544; subpattern_1, ns=137

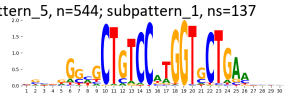

pattern_5, n=544; subpattern_2, ns=132

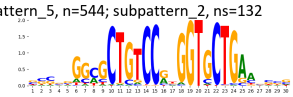

pattern_5, n=544; subpattern_3, ns=130

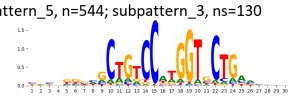

Supplementary Figure 1598: TF-MoDisCO subpatterns for the ZNF697 transcription factor in HepG2 (accession ENCSR734WFB).

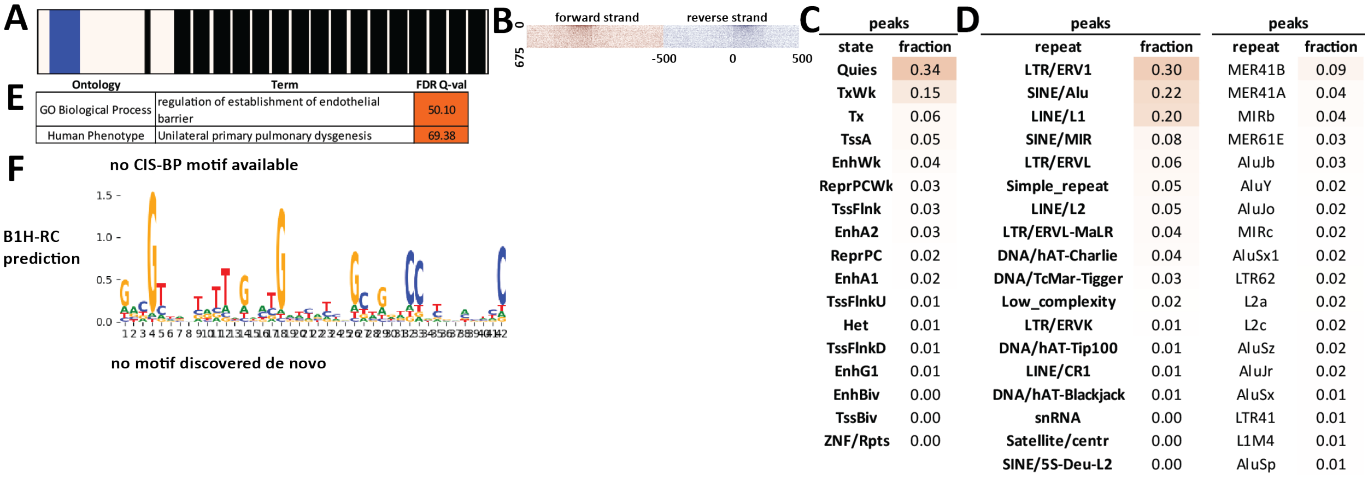

peaks	
state	fraction
Quies	0.34
TxWk	0.15
Tx	0.06
TssA	0.05
EnhWk	0.04
ReprPCWk	0.03
TssFlnk	0.03
EnhA2	0.03
ReprPC	0.02
EnhA1	0.02
TssFlnkU	0.01
Het	0.01
TssFlnkD	0.01
EnhG1	0.01
EnhBiv	0.00
TssBiv	0.00
ZNF/Rpts	0.00

peaks	
repeat	fraction
LTR/ERV1	0.30
SINE/Alu	0.22
LINE/L1	0.20
SINE/MIR	0.08
LTR/ERVL	0.06
Simple_repeat	0.05
LINE/L2	0.05
LTR/ERVL-MaLR	0.04
DNA/hAT-Charlie	0.04
DNA/TcMar-Tigger	0.03
Low_complexity	0.02
LTR/ERVK	0.01
DNA/hAT-Tip100	0.01
LINE/CR1	0.01
DNA/hAT-Blackjack	0.01
snRNA	0.00
Satellite/centr	0.00
SINE/5S-Deu-L2	0.00

peaks	
repeat	fraction
MER41B	0.09
MER41A	0.04
MIRb	0.04
MER61E	0.03
AluJb	0.03
AluY	0.02
AluJo	0.02
MIRc	0.02
AluSx1	0.02
LTR62	0.02
L2a	0.02
L2c	0.02
AluSz	0.02
AluJr	0.02
AluSx	0.01
LTR41	0.01
L1M4	0.01
AluSp	0.01

Supplementary Figure 1599: Properties and genomic distribution of motifs identified for the ZNF699 transcription factor in K562 (accession ENCSR303SHG).

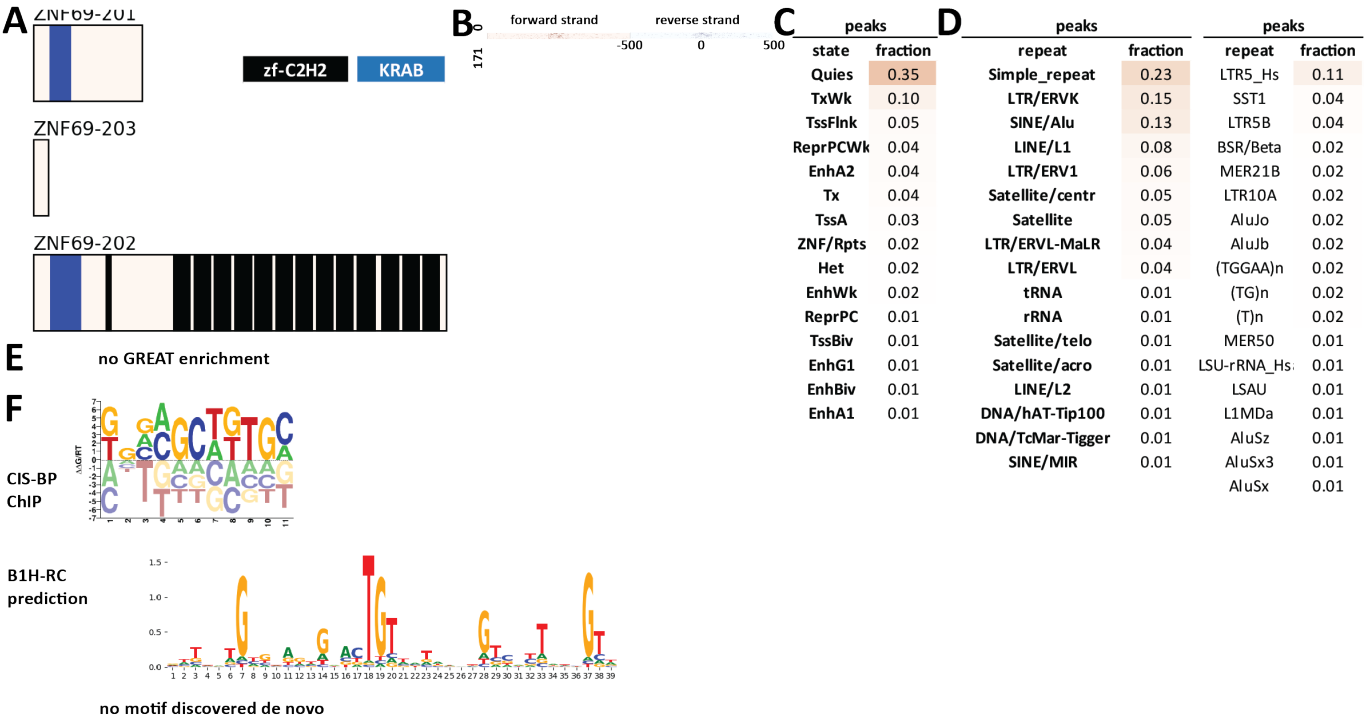

Supplementary Figure 1600: Properties and genomic distribution of motifs identified for the ZNF69 transcription factor in HEK293 (accession ChipExo models).

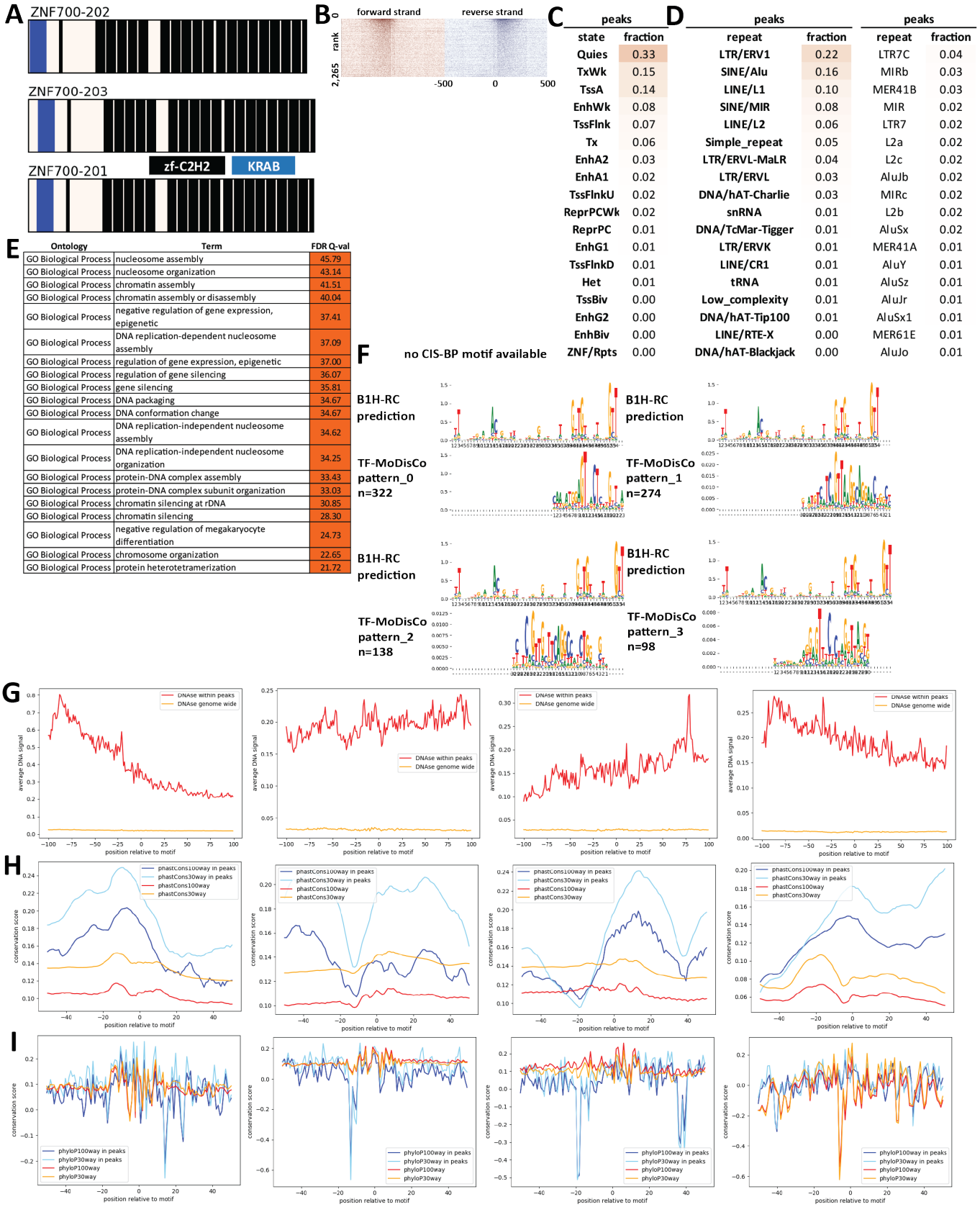

Supplementary Figure 1601: Properties and genomic distribution of motifs identified for the ZNF700 transcription factor in K562 (accession ENCSR959BQO).

TF-MoDisCO pattern_0 n=322, CWM

pattern_0, n=322; subpattern_0, ns=96

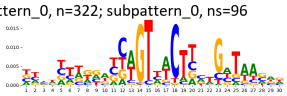

pattern_0, n=322; subpattern_1, ns=75

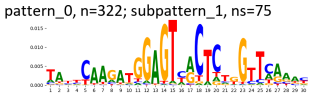

pattern_0, n=322; subpattern_2, ns=65

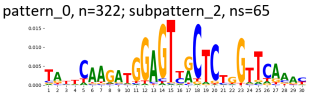

pattern_0, n=322; subpattern_3, ns=59

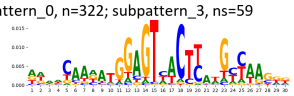

pattern_0, n=322; subpattern_4, ns=25

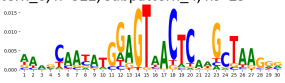

pattern_0, n=322; subpattern_5, ns=2

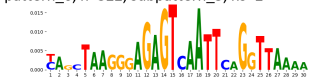

TF-MoDisCO pattern_0 n=322, PWM

pattern_0, n=322; subpattern_0, ns=96

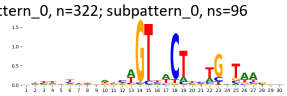

pattern_0, n=322; subpattern_1, ns=75

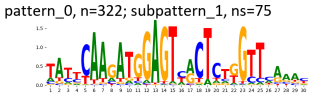

pattern_0, n=322; subpattern_2, ns=65

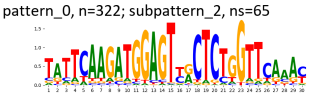

pattern_0, n=322; subpattern_3, ns=59

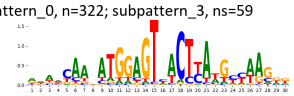

pattern_0, n=322; subpattern_4, ns=25

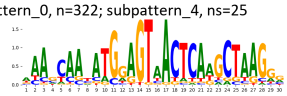

pattern_0, n=322; subpattern_5, ns=2

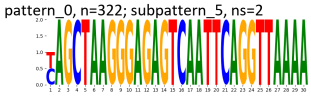

TF-MoDisCO pattern_1 n=274, CWM

pattern_1, n=274; subpattern_0, ns=103

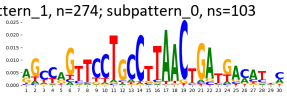

pattern_1, n=274; subpattern_1, ns=52

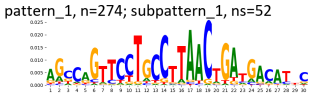

pattern_1, n=274; subpattern_2, ns=39

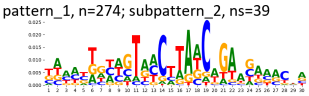

pattern_1, n=274; subpattern_3, ns=38

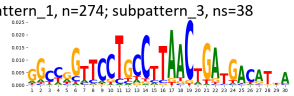

pattern_1, n=274; subpattern_4, ns=29

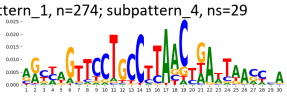

pattern_1, n=274; subpattern_5, ns=13

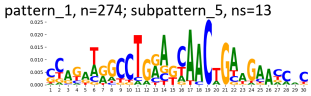

TF-MoDisCO pattern_1 n=274, PWM

pattern_1, n=274; subpattern_0, ns=103

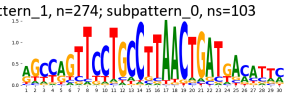

pattern_1, n=274; subpattern_1, ns=52

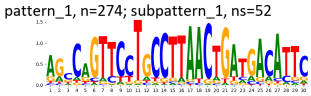

pattern_1, n=274; subpattern_2, ns=39

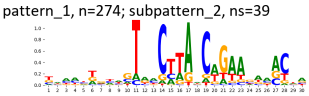

pattern_1, n=274; subpattern_3, ns=38

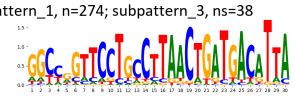

pattern_1, n=274; subpattern_4, ns=29

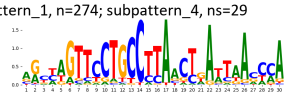

pattern_1, n=274; subpattern_5, ns=13

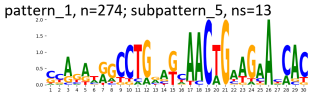

TF-MoDisCO pattern_2 n=138, CWM

pattern_2, n=138; subpattern_0, ns=43

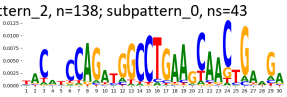

pattern_2, n=138; subpattern_1, ns=34

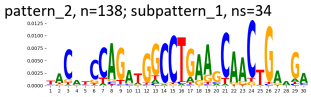

pattern_2, n=138; subpattern_2, ns=20

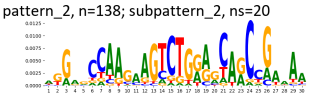

pattern_2, n=138; subpattern_3, ns=17

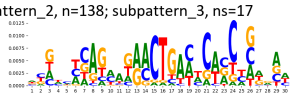

pattern_2, n=138; subpattern_4, ns=14

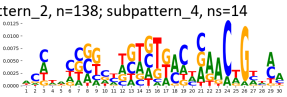

pattern_2, n=138; subpattern_5, ns=10

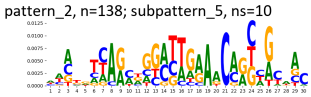

TF-MoDisCO pattern_2 n=138, PWM

pattern_2, n=138; subpattern_0, ns=43

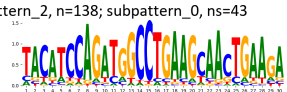

pattern_2, n=138; subpattern_1, ns=34

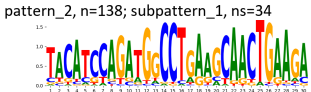

pattern_2, n=138; subpattern_2, ns=20

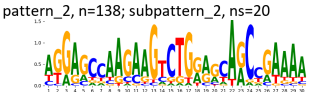

pattern_2, n=138; subpattern_3, ns=17

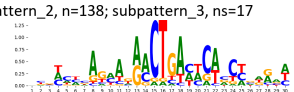

pattern_2, n=138; subpattern_4, ns=14

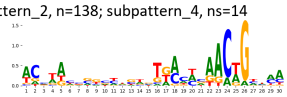

pattern_2, n=138; subpattern_5, ns=10

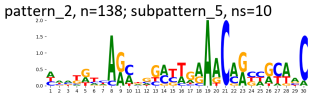

TF-MoDisCO pattern_3 n=98, CWM

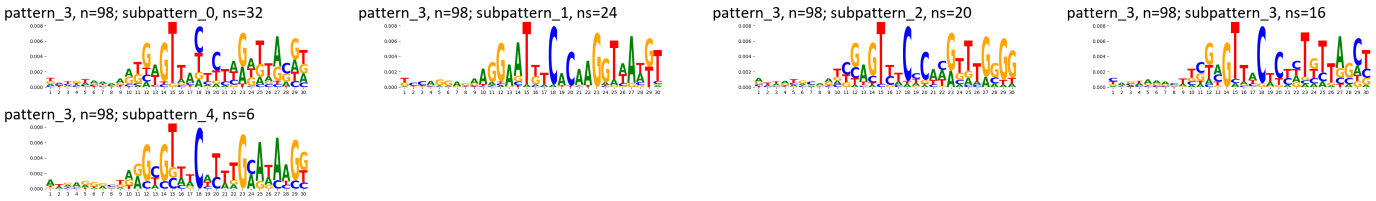

TF-MoDisCO pattern_3 n=98, PWM

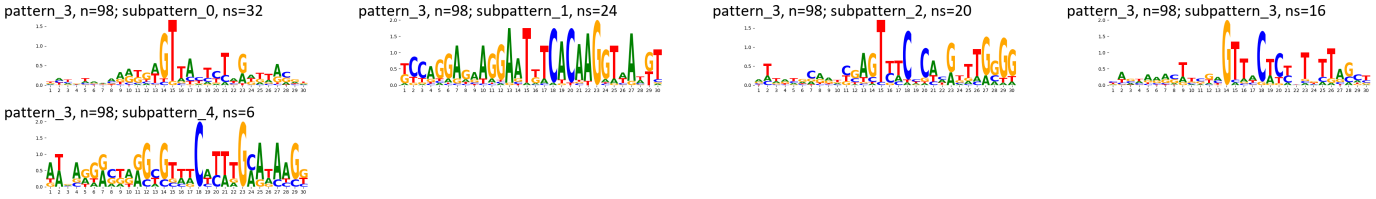

Supplementary Figure 1602: TF-MoDisCO subpatterns for the ZNF700 transcription factor in K562 (accession ENCSR959BQO).

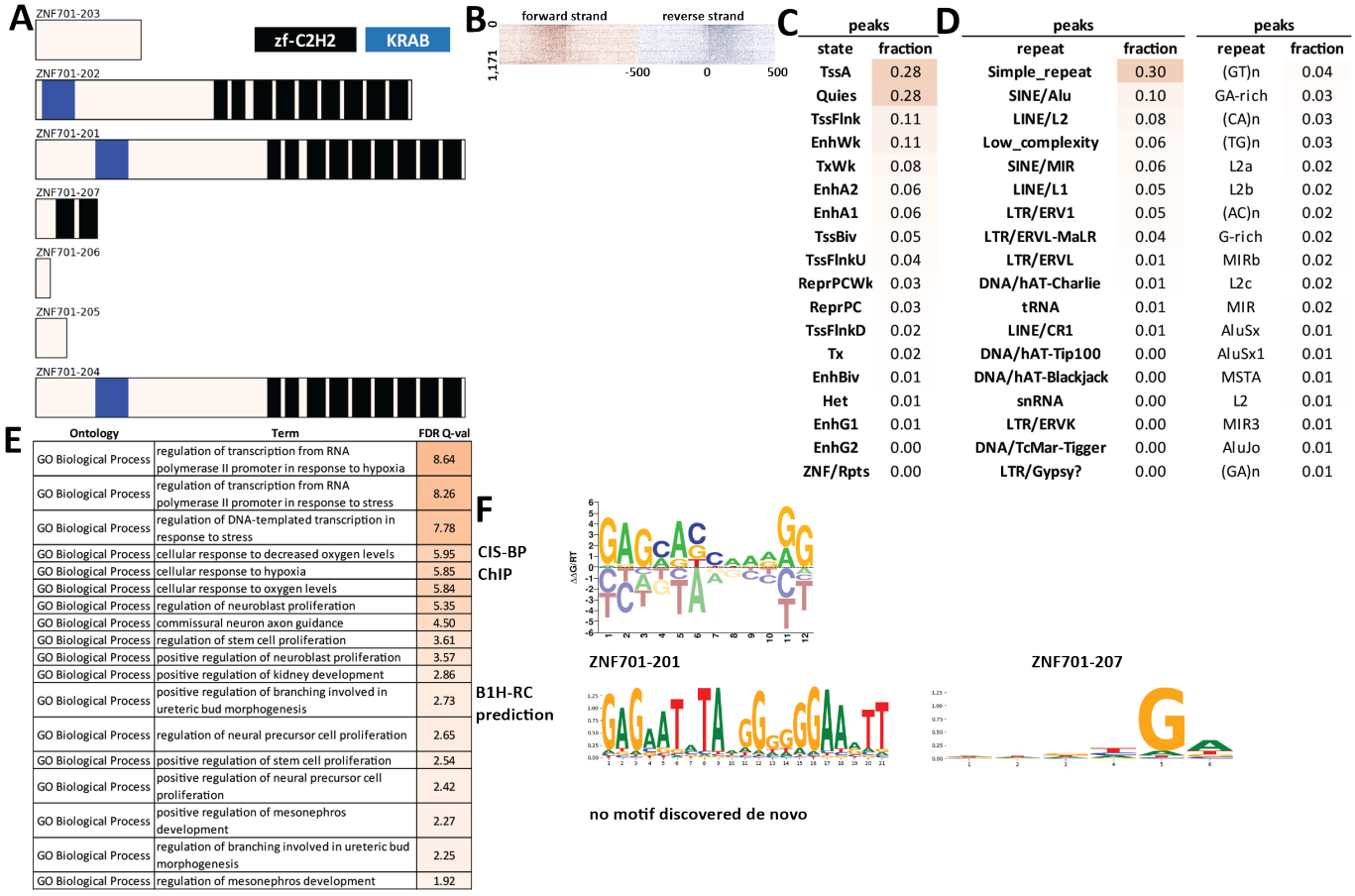

peaks	
state	fraction
TssA	0.28
Quies	0.28
TssFlnk	0.11
EnhWk	0.11
TxWk	0.08
EnhA2	0.06
EnhA1	0.06
TssBiv	0.05
TssFlnkU	0.04
ReprPCWk	0.03
ReprPC	0.03
TssFlnkD	0.02
Tx	0.02
EnhBiv	0.01
Het	0.01
EnhG1	0.01
EnhG2	0.00
ZNF/Rpts	0.00

peaks		peaks	
repeat	fraction	repeat	fraction
Simple_repeat	0.30	(GT)n	0.04
SINE/Alu	0.10	GA-rich	0.03
LINE/L2	0.08	(CA)n	0.03
Low_complexity	0.06	(TG)n	0.03
SINE/MIR	0.06	L2a	0.02
LINE/L1	0.05	L2b	0.02
LTR/ERV1	0.05	(AC)n	0.02
LTR/ERVL-MaLR	0.04	G-rich	0.02
LTR/ERVL	0.01	MIRb	0.02
DNA/hAT-Charlie	0.01	L2c	0.02
tRNA	0.01	MIR	0.02
LINE/CR1	0.01	AluSx	0.01
DNA/hAT-Tip100	0.00	AluSx1	0.01
DNA/hAT-Blackjack	0.00	MSTA	0.01
snRNA	0.00	L2	0.01
LTR/ERVK	0.00	MIR3	0.01
DNA/TcMar-Tigger	0.00	AluJo	0.01
LTR/Gypsy?	0.00	(GA)n	0.01

Ontology	Term	FDR Q-val
GO Biological Process	regulation of transcription from RNA polymerase II promoter in response to hypoxia	8.64
GO Biological Process	regulation of transcription from RNA polymerase II promoter in response to stress	8.26
GO Biological Process	regulation of DNA-templated transcription in response to stress	7.78
GO Biological Process	cellular response to decreased oxygen levels	5.95
GO Biological Process	cellular response to hypoxia	5.85
GO Biological Process	cellular response to oxygen levels	5.84
GO Biological Process	regulation of neuroblast proliferation	5.35
GO Biological Process	commissural neuron axon guidance	4.50
GO Biological Process	regulation of stem cell proliferation	3.61
GO Biological Process	positive regulation of neuroblast proliferation	3.57
GO Biological Process	positive regulation of kidney development	2.86
GO Biological Process	positive regulation of branching involved in ureteric bud morphogenesis	2.73
GO Biological Process	regulation of neural precursor cell proliferation	2.65
GO Biological Process	positive regulation of stem cell proliferation	2.54
GO Biological Process	positive regulation of neural precursor cell proliferation	2.42
GO Biological Process	positive regulation of mesonephros development	2.27
GO Biological Process	regulation of branching involved in ureteric bud morphogenesis	2.25
GO Biological Process	regulation of mesonephros development	1.92

Supplementary Figure 1603: Properties and genomic distribution of motifs identified for the ZNF701 transcription factor in HEK293 (accession ENCSR547TGL).

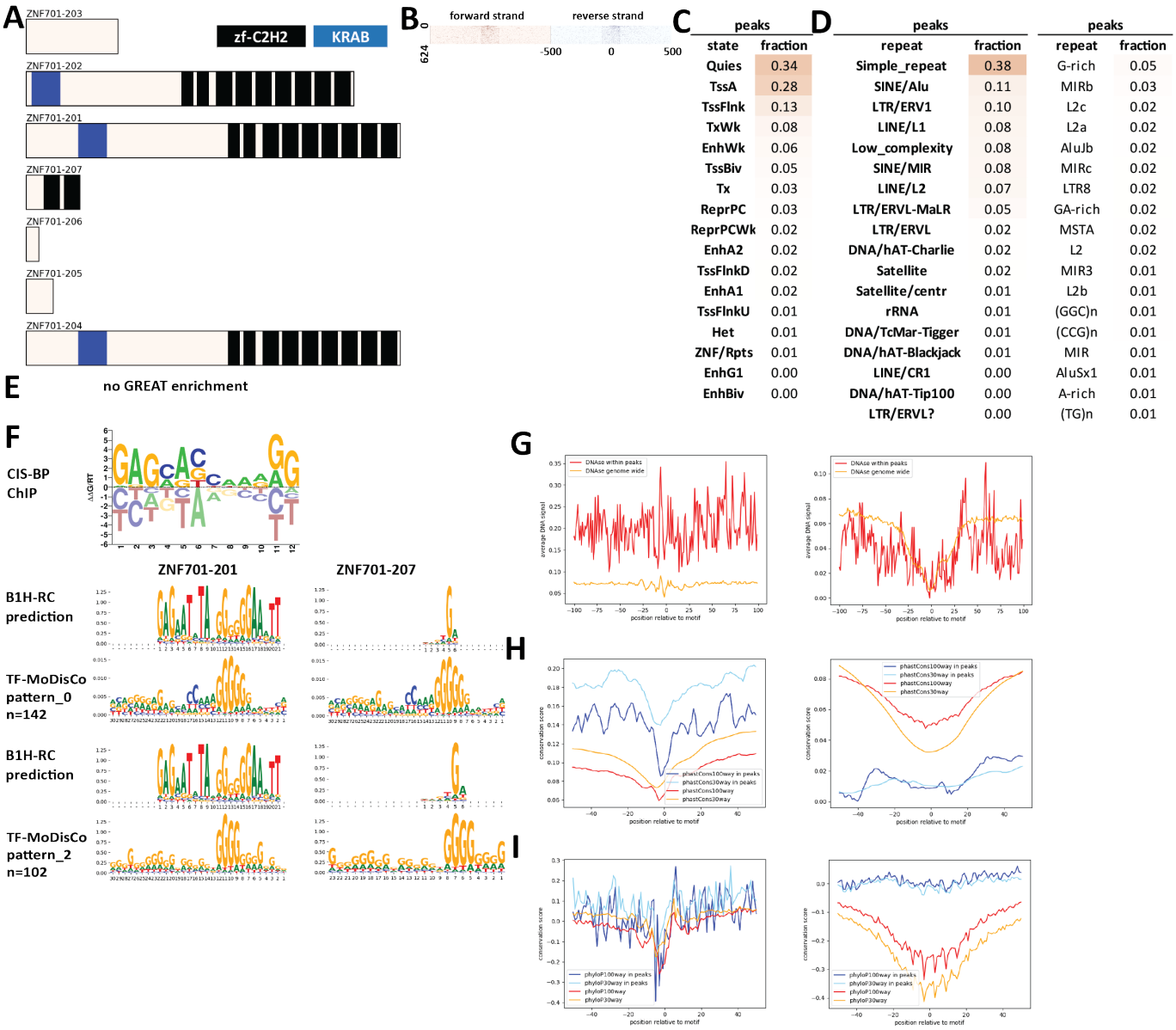

Supplementary Figure 1604: Properties and genomic distribution of motifs identified for the ZNF701 transcription factor in HEK293 (accession ChipExo models).

TF-MoDisCO pattern_0 n=142, CWM

pattern_0, n=142; subpattern_0, ns=52

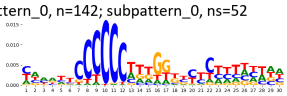

pattern_0, n=142; subpattern_1, ns=36

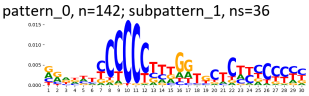

pattern_0, n=142; subpattern_2, ns=29

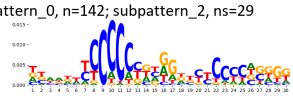

pattern_0, n=142; subpattern_3, ns=17

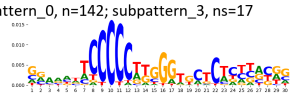

pattern_0, n=142; subpattern_4, ns=6

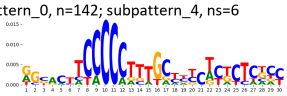

pattern_0, n=142; subpattern_5, ns=2

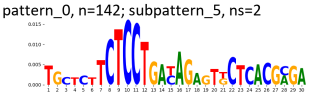

TF-MoDisCO pattern_0 n=142, PWM

pattern_0, n=142; subpattern_0, ns=52

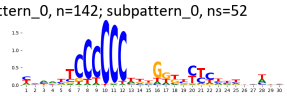

pattern_0, n=142; subpattern_1, ns=36

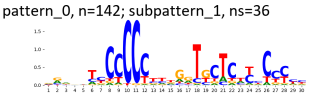

pattern_0, n=142; subpattern_2, ns=29

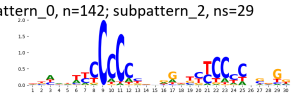

pattern_0, n=142; subpattern_3, ns=17

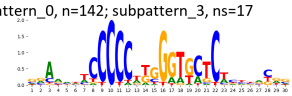

pattern_0, n=142; subpattern_4, ns=6

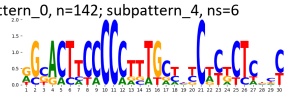

pattern_0, n=142; subpattern_5, ns=2

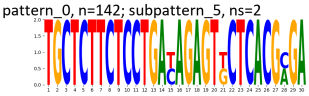

TF-MoDisCO pattern_2 n=102, CWM

pattern_2, n=102; subpattern_0, ns=20

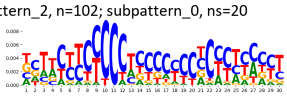

pattern_2, n=102; subpattern_1, ns=19

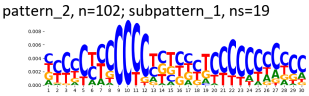

pattern_2, n=102; subpattern_2, ns=19

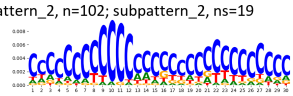

pattern_2, n=102; subpattern_3, ns=17

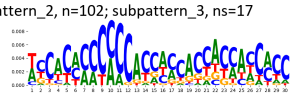

pattern_2, n=102; subpattern_4, ns=9

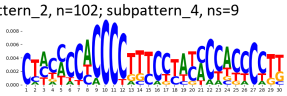

pattern_2, n=102; subpattern_5, ns=7

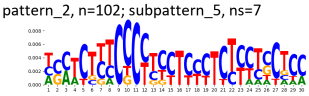

pattern_2, n=102; subpattern_6, ns=6

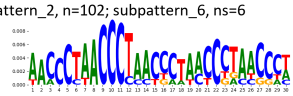

pattern_2, n=102; subpattern_7, ns=5

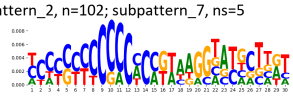

TF-MoDisCO pattern_2 n=102, PWM

pattern_2, n=102; subpattern_0, ns=20

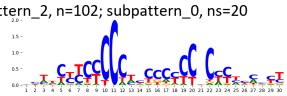

pattern_2, n=102; subpattern_1, ns=19

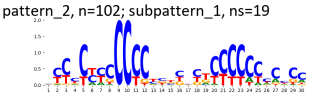

pattern_2, n=102; subpattern_2, ns=19

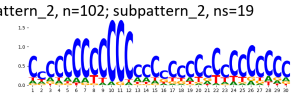

pattern_2, n=102; subpattern_3, ns=17

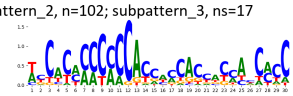

pattern_2, n=102; subpattern_4, ns=9

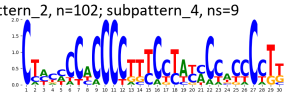

pattern_2, n=102; subpattern_5, ns=7

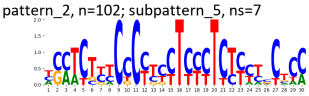

pattern_2, n=102; subpattern_6, ns=6

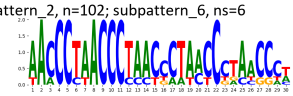

pattern_2, n=102; subpattern_7, ns=5

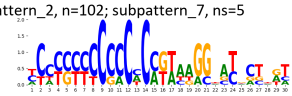

Supplementary Figure 1605: TF-MoDisCO subpatterns for the ZNF701 transcription factor in HEK293 (accession ChipExo models).

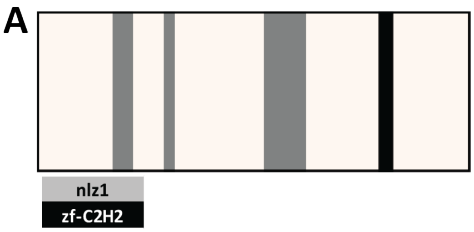

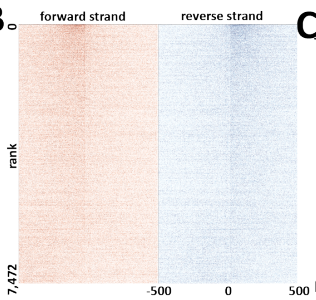

C

peaks	
state	fraction
TssA	0.46
TssFlnkU	0.19
TssFlnk	0.19
EnhA1	0.14
EnhWk	0.10
TssFlnkD	0.07
EnhA2	0.03
TxWk	0.02
TssBiv	0.02
ReprPCWk	0.02
EnhBiv	0.01
EnhG2	0.01
EnhG1	0.01
Quies	0.01
ReprPC	0.01
Tx	0.01
ZNF/Rpts	0.00
Het	0.00

D

B

peaks		peaks	
repeat	fraction	repeat	fraction
Simple_repeat	0.20	MIRb	0.04
SINE/Alu	0.16	G-rich	0.03
SINE/MIR	0.11	MIR	0.02
LINE/L2	0.06	MIR3	0.02
Low_complexity	0.04	L2a	0.02
LINE/L1	0.04	MIRc	0.02
DNA/hAT-Charlie	0.03	AluSx1	0.02
LTR/ERV1	0.02	L2c	0.02
LTR/ERVL-MaLR	0.02	AluSx	0.02
LTR/ERVL	0.01	L2b	0.02
DNA/TcMar-Tigger	0.01	AluJb	0.02
LINE/CR1	0.01	AluSz	0.01
DNA/hAT-Tip100	0.00	AluJr	0.01
tRNA	0.00	AluY	0.01
LTR/ERVK	0.00	AluJo	0.01
DNA/hAT-Blackjack	0.00	AluSq2	0.01
snRNA	0.00	GA-rich	0.01
LTR/Gypsy	0.00	(GGC)n	0.01

E

Ontology	Term	FDR Q-val
GO Biological Process	rRNA processing	21.34
GO Biological Process	rRNA metabolic process	20.45
GO Biological Process	mRNA catabolic process	16.96
GO Biological Process	nuclear-transcribed mRNA catabolic process	16.92
GO Biological Process	cellular response to epidermal growth factor stimulus	13.97
GO Biological Process	nuclear-transcribed mRNA catabolic process, nonsense-mediated decay	12.91
GO Biological Process	cotranslational protein targeting to membrane	11.88
GO Biological Process	translational elongation	11.24
GO Biological Process	chylomicron assembly	9.91
GO Biological Process	mitochondrial translation	9.66
GO Biological Process	translational termination	9.47
GO Biological Process	ribonucleoprotein complex export from nucleus	9.44
GO Biological Process	protein-lipid complex assembly	9.35
GO Biological Process	ribonucleoprotein complex localization	9.26
GO Biological Process	RNA phosphodiester bond hydrolysis	9.05
GO Biological Process	plasma lipoprotein particle assembly	8.66
GO Biological Process	rRNA 3'-end processing	8.37
GO Biological Process	viral gene expression	8.36
GO Biological Process	RNA 3'-end processing	8.36
GO Biological Process	liver regeneration	8.33
Human Phenotype	Increased serum lactate	10.78
Human Phenotype	Abnormality of mitochondrial metabolism	10.86
Human Phenotype	Abnormality of the mitochondrion	10.46
Human Phenotype	Lactic acidosis	10.14
Human Phenotype	Abnormal CSF metabolite level	9.86
Human Phenotype	Increased CSF lactate	8.93
Human Phenotype	Abnormality of lipid metabolism	8.46
Human Phenotype	Hepatic failure	6.23
Human Phenotype	Ectropion	3.56
Human Phenotype	Acute encephalopathy	3.42
Human Phenotype	Abnormal activity of mitochondrial respiratory chain	2.20
Human Phenotype	Thickened ribs	1.99
Human Phenotype	Ependymoma	1.97
Human Phenotype	Non-medullary thyroid carcinoma	1.66

F

no CIS-BP motif available

no B1H-RC prediction

no motif discovered de novo

Supplementary Figure 1606: Properties and genomic distribution of motifs identified for the ZNF703 transcription factor in HepG2 (accession ENCSR400JHG).

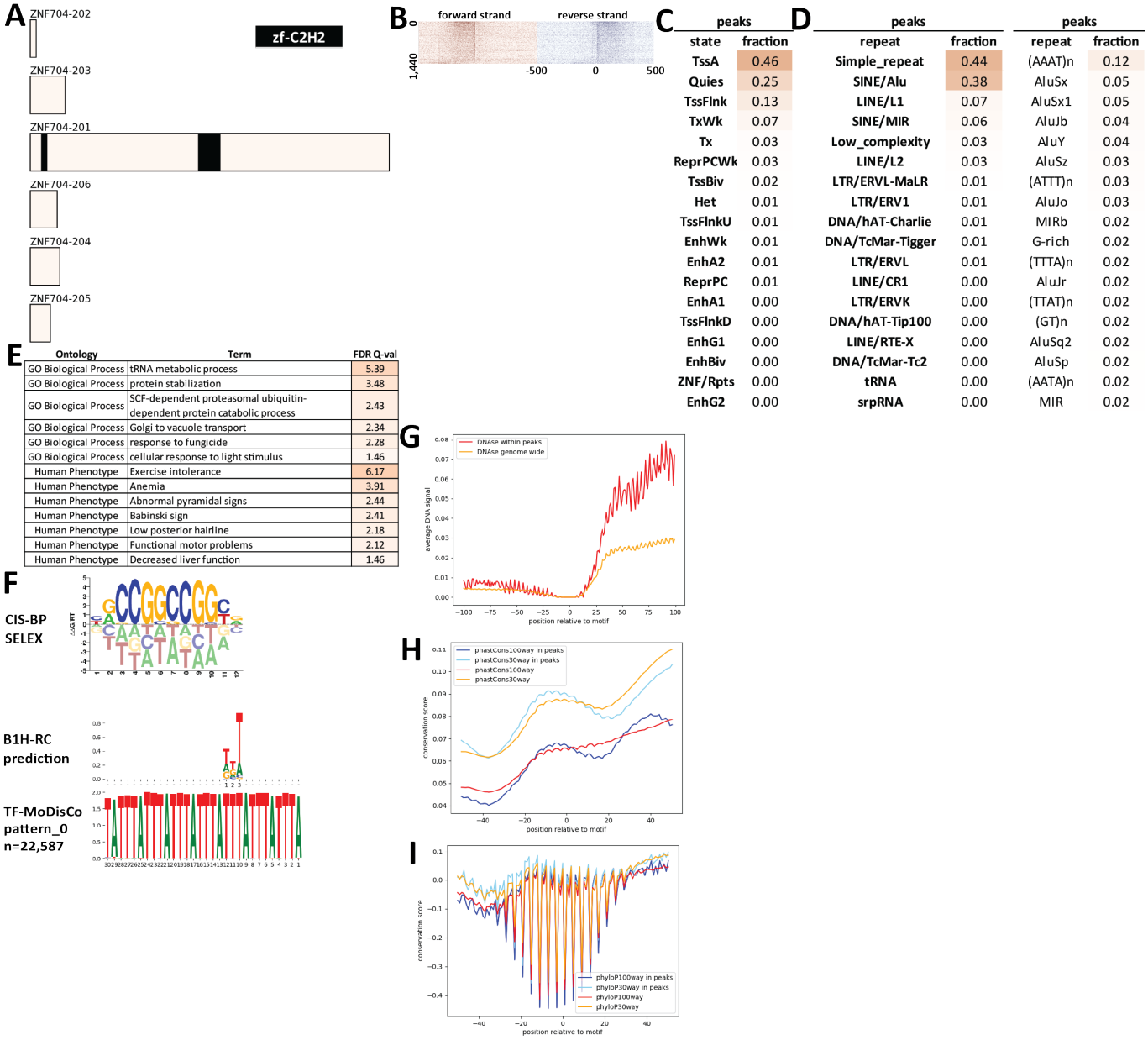

Supplementary Figure 1607: Properties and genomic distribution of motifs identified for the ZNF704 transcription factor in HEK293 (accession ENCSR194KWL).

TF-MoDisCO pattern_0 n=491, CWM

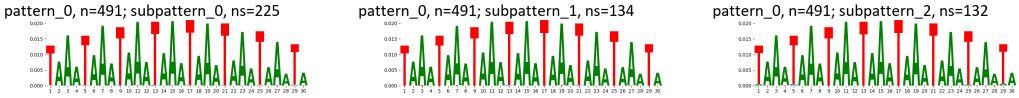

TF-MoDisCO pattern_0 n=491, PWM

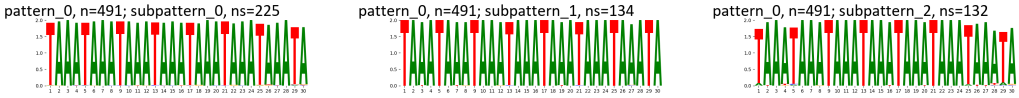

Supplementary Figure 1608: TF-MoDisCO subpatterns for the ZNF704 transcription factor in HEK293 (accession ENCSR194KWL).

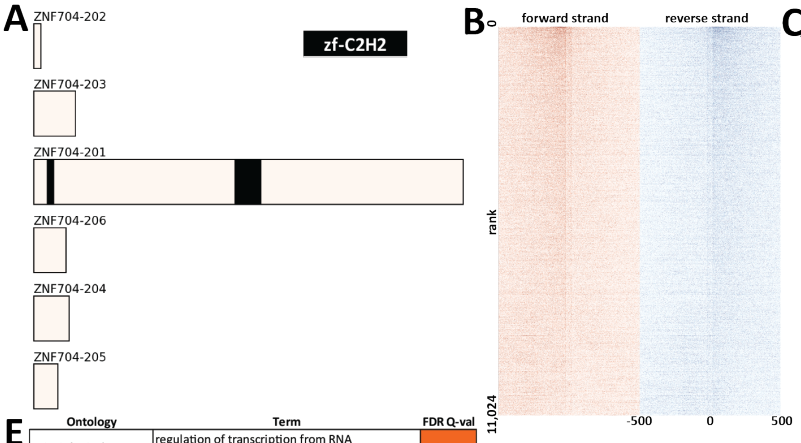

C

peaks	
state	fraction
TssA	0.44
TssFlnk	0.24
Quies	0.13
TxWk	0.07
TssFlnkU	0.05
TssBiv	0.04
EnhWk	0.04
ReprPC	0.03
EnhA2	0.03
TssFlnkD	0.03
EnhA1	0.02
ReprPCWk	0.02
Tx	0.02
EnhBiv	0.01
EnhG1	0.00
EnhG2	0.00
Het	0.00

D

peaks		peaks	
repeat	fraction	repeat	fraction
Simple_repeat	0.23	MIRb	0.04
SINE/Alu	0.14	G-rich	0.04
SINE/MIR	0.12	MIR	0.03
LINE/L2	0.06	MIR3	0.02
Low_complexity	0.05	L2a	0.02
LINE/L1	0.03	MIRc	0.02
DNA/hAT-Charlie	0.02	L2b	0.02
LTR/ERV1	0.02	AluJb	0.02
LTR/ERVL-MaLR	0.01	AluSx	0.02
LTR/ERVL	0.01	AluSx1	0.01
DNA/hAT-Tip100	0.01	L2c	0.01
LINE/CR1	0.01	AluSz	0.01
tRNA	0.00	AluJr	0.01
DNA/TcMar-Tigger	0.00	GA-rich	0.01
DNA/hAT-Blackjack	0.00	AluJo	0.01
LTR/ERVK	0.00	AluY	0.01
DNA/hAT	0.00	AluSp	0.01
Retroposon/SVA	0.00	(GGC)n	0.01

E

Ontology	Term	FDR Q-val
GO Biological Process	regulation of transcription from RNA polymerase II promoter in response to stress	26.41
GO Biological Process	regulation of DNA-templated transcription in response to stress	23.35
GO Biological Process	macromolecular complex disassembly	22.83
GO Biological Process	IRE1-mediated unfolded protein response	22.51
GO Biological Process	protein complex disassembly	21.64
GO Biological Process	response to topologically incorrect protein	21.33
GO Biological Process	regulation of hematopoietic progenitor cell differentiation	19.88
GO Biological Process	regulation of hematopoietic stem cell differentiation	19.76
GO Biological Process	endoplasmic reticulum unfolded protein response	19.64
GO Biological Process	cellular response to topologically incorrect protein	18.99
GO Biological Process	mitochondrial translational termination	17.75
GO Biological Process	nuclear-transcribed mRNA catabolic process, nonsense-mediated decay	17.74
GO Biological Process	regulation of PERK-mediated unfolded protein response	17.61
GO Biological Process	translational elongation	17.60
GO Biological Process	mitochondrial translational elongation	17.40
GO Biological Process	regulation of transcription from RNA polymerase II promoter in response to hypoxia	17.35
GO Biological Process	mitochondrial translation	16.94
GO Biological Process	cellular protein complex disassembly	16.43
GO Biological Process	telomere organization	15.94
GO Biological Process	cellular response to unfolded protein	15.85
Human Phenotype	Increased serum lactate	15.96
Human Phenotype	Increased CSF lactate	15.75
Human Phenotype	Abnormal CSF metabolite level	15.55
Human Phenotype	Glycosuria	9.68
Human Phenotype	Progressive external ophthalmoplegia	8.55

F

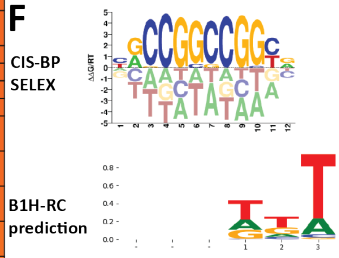

no motif discovered de novo

Supplementary Figure 1609: Properties and genomic distribution of motifs identified for the ZNF704 transcription factor in HepG2 (accession ENCSR523RGJ).

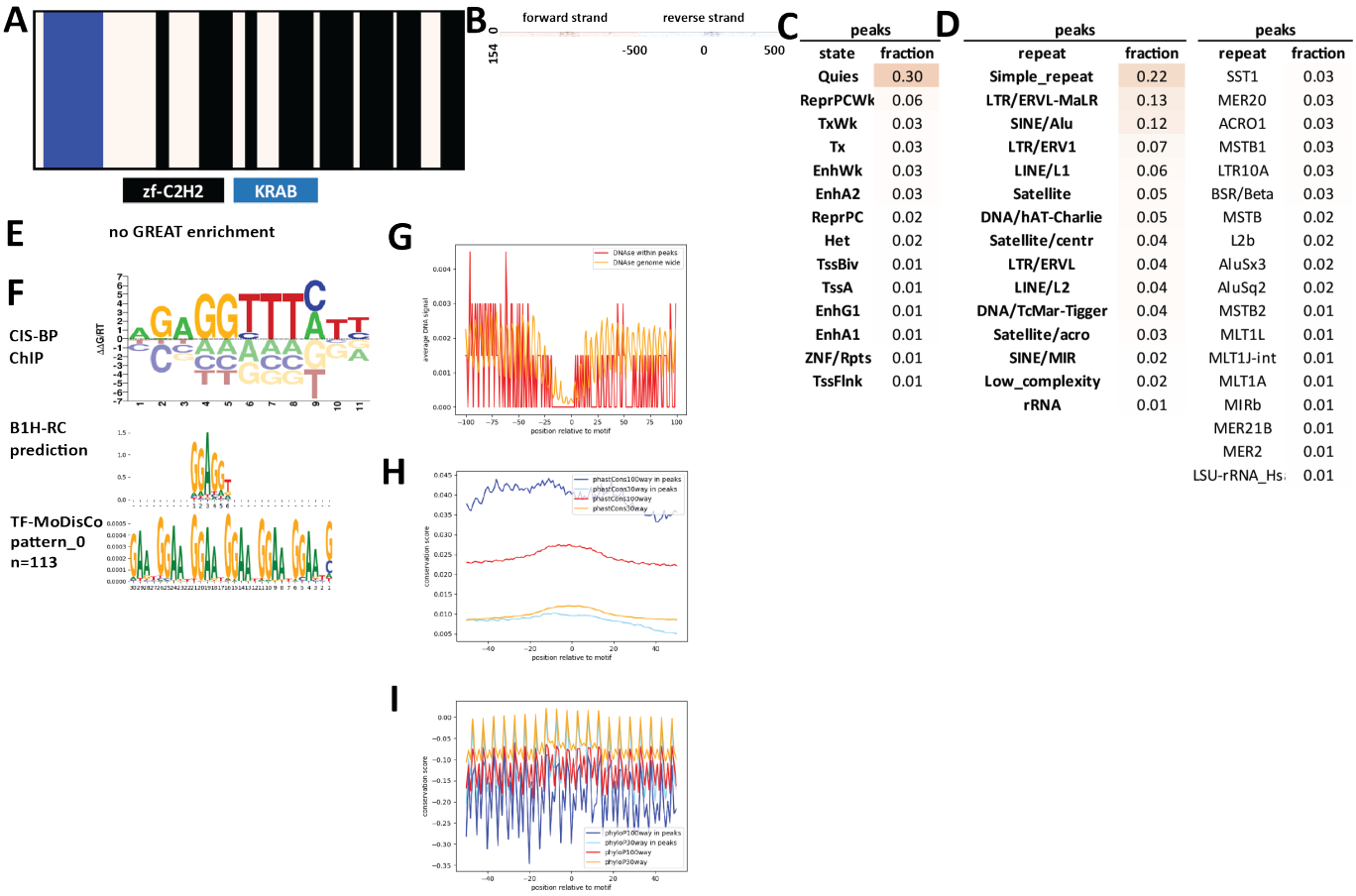

Supplementary Figure 1610: Properties and genomic distribution of motifs identified for the ZNF705G transcription factor in HEK293 (accession ChipExo models).

TF-MoDisCO pattern_0 n=113, CWM

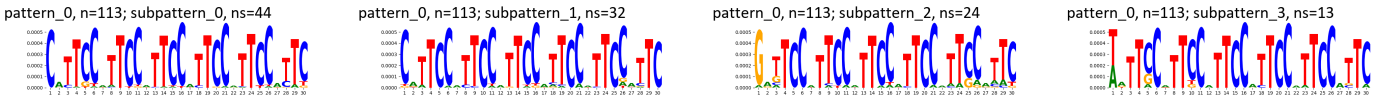

TF-MoDisCO pattern_0 n=113, PWM

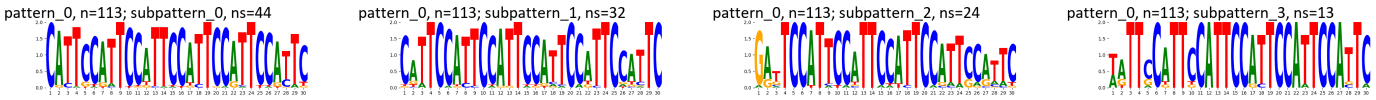

Supplementary Figure 1611: TF-MoDisCO subpatterns for the ZNF705G transcription factor in HEK293 (accession ChipExo models).

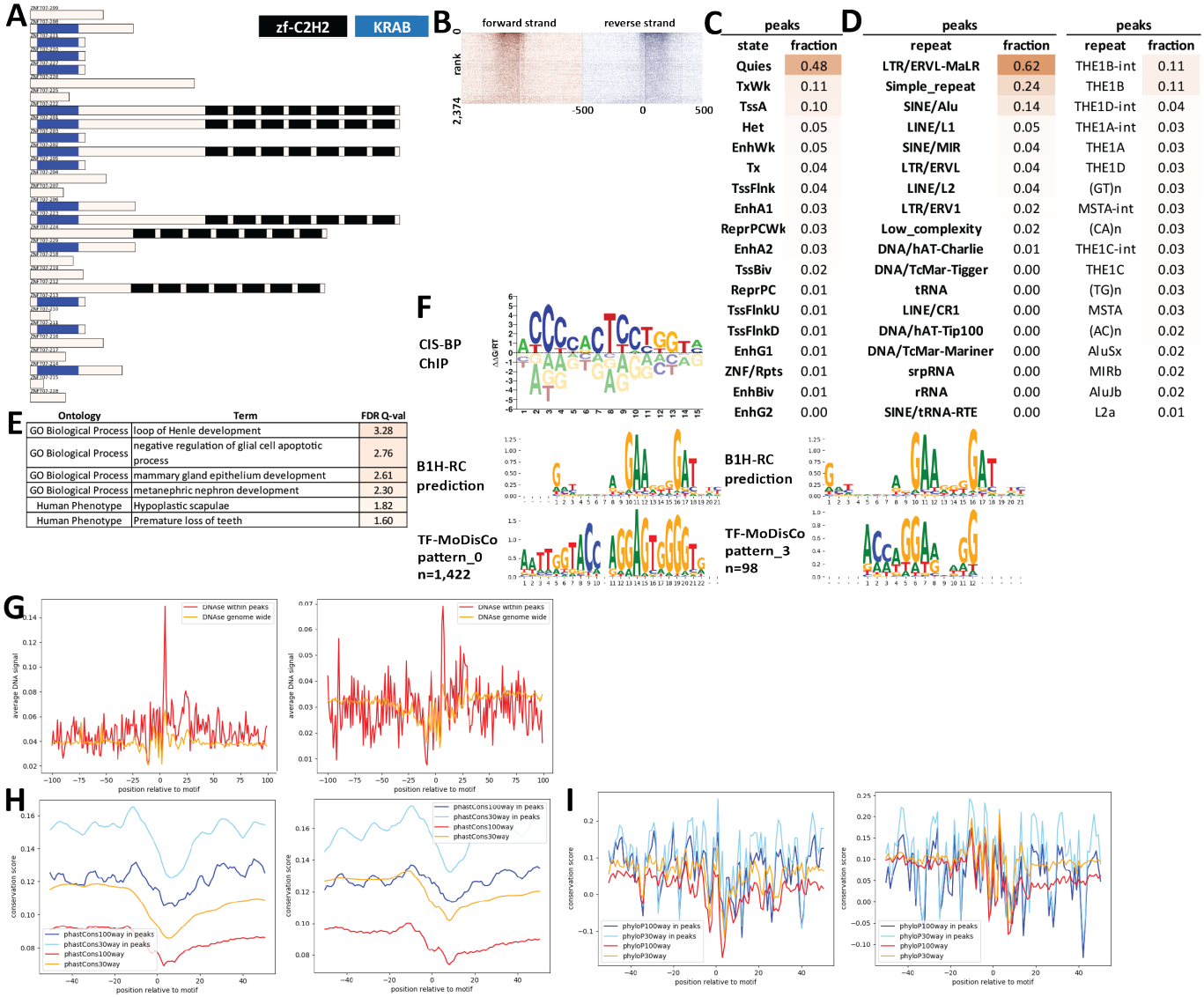

Supplementary Figure 1612: Properties and genomic distribution of motifs identified for the ZNF707 transcription factor in HEK293 (accession ENCSR854IPI).

TF-MoDisCO pattern_0 n=1422, CWM

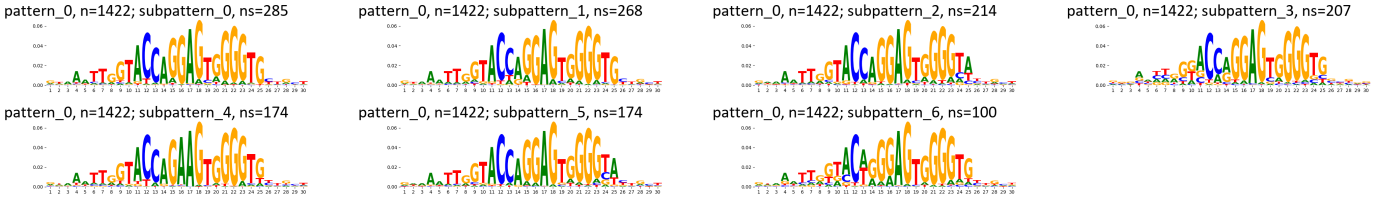

TF-MoDisCO pattern_0 n=1422, PWM

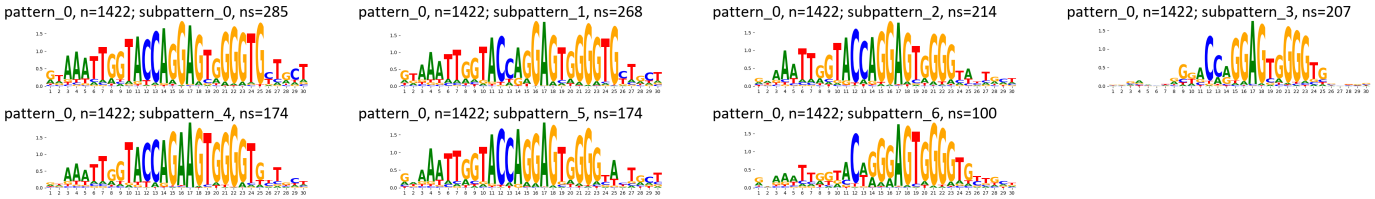

TF-MoDisCO pattern_3 n=98, CWM

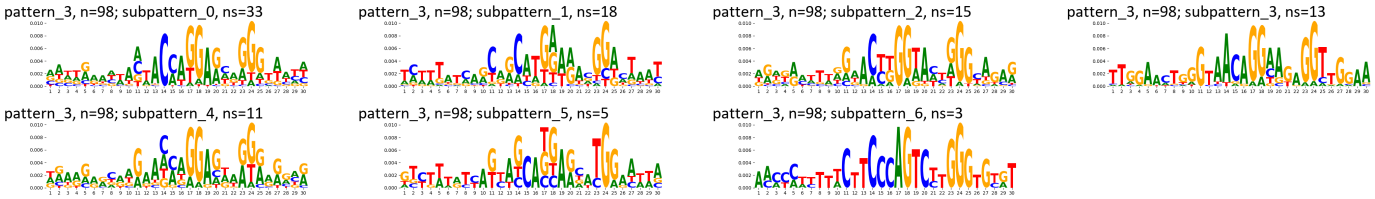

TF-MoDisCO pattern_3 n=98, PWM

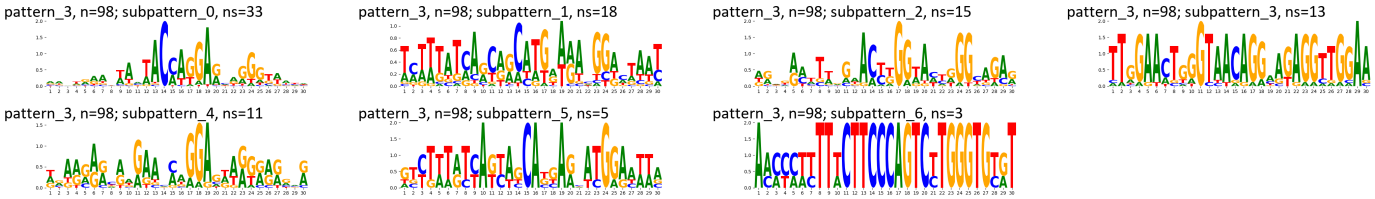

Supplementary Figure 1613: TF-MoDisCO subpatterns for the ZNF707 transcription factor in HEK293 (accession ENCSR854IPI).

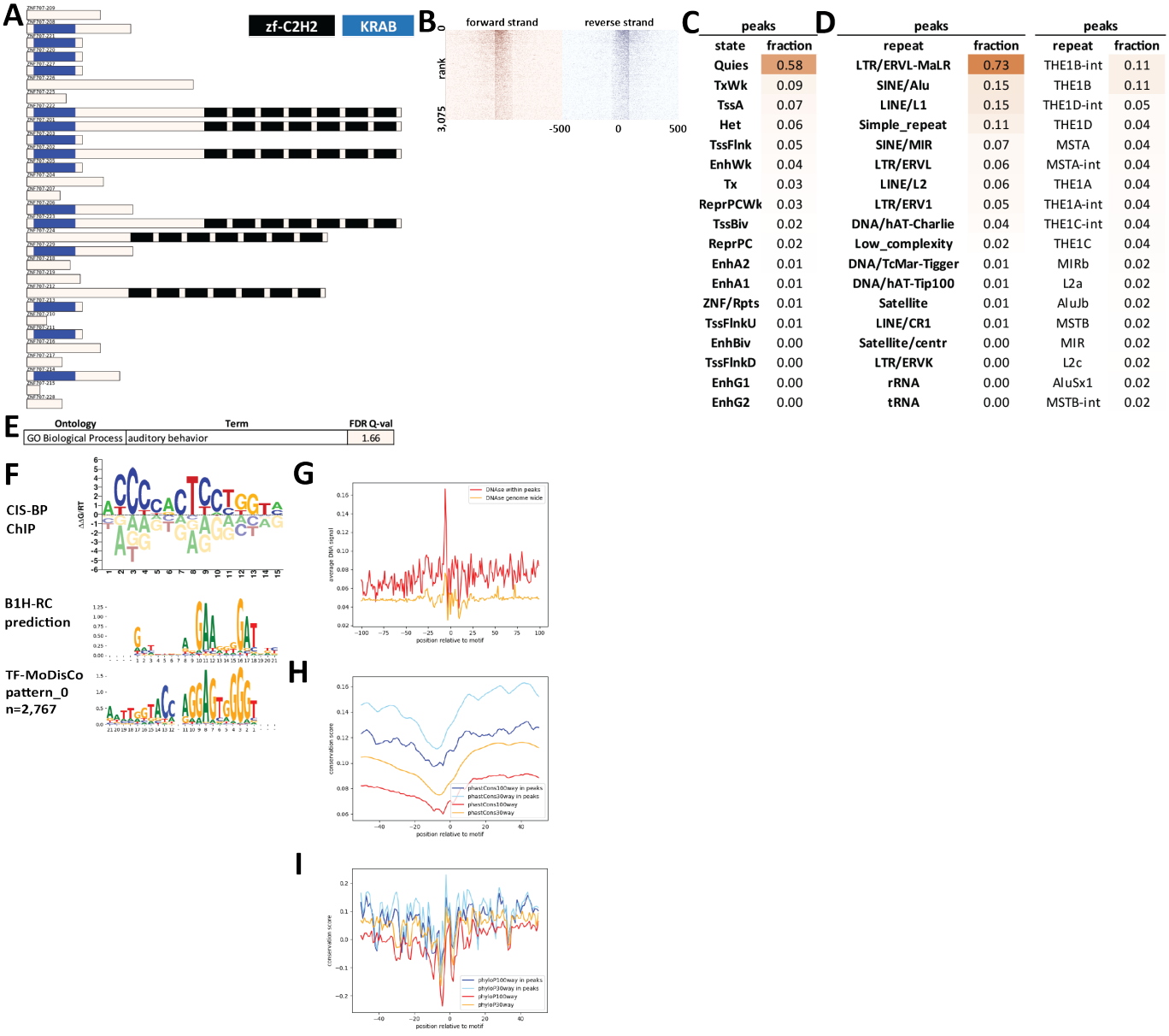

Supplementary Figure 1614: Properties and genomic distribution of motifs identified for the ZNF707 transcription factor in HEK293 (accession ChipExo models).

TF-MoDisCO pattern_0 n=2767, CWM

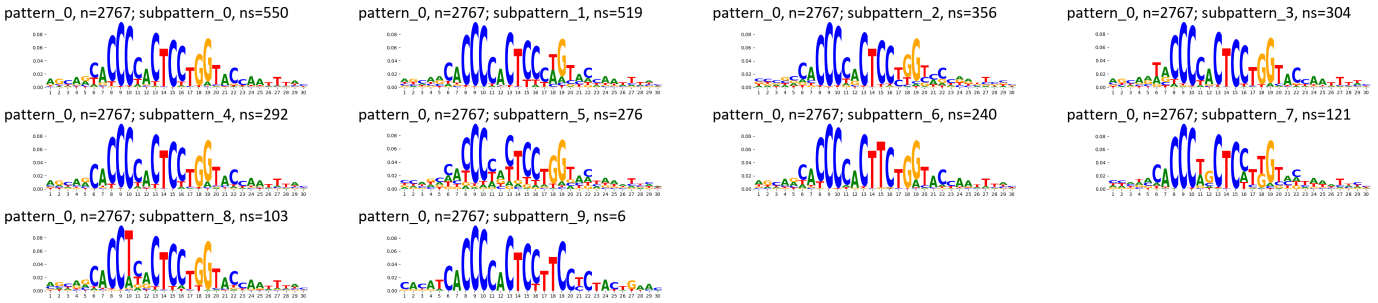

TF-MoDisCO pattern_0 n=2767, PWM

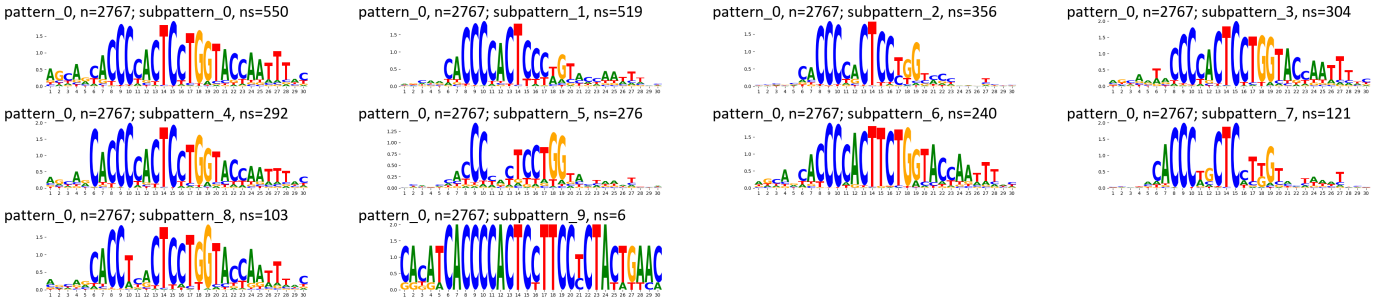

Supplementary Figure 1615: TF-MoDisCO subpatterns for the ZNF707 transcription factor in HEK293 (accession ChipExo models).

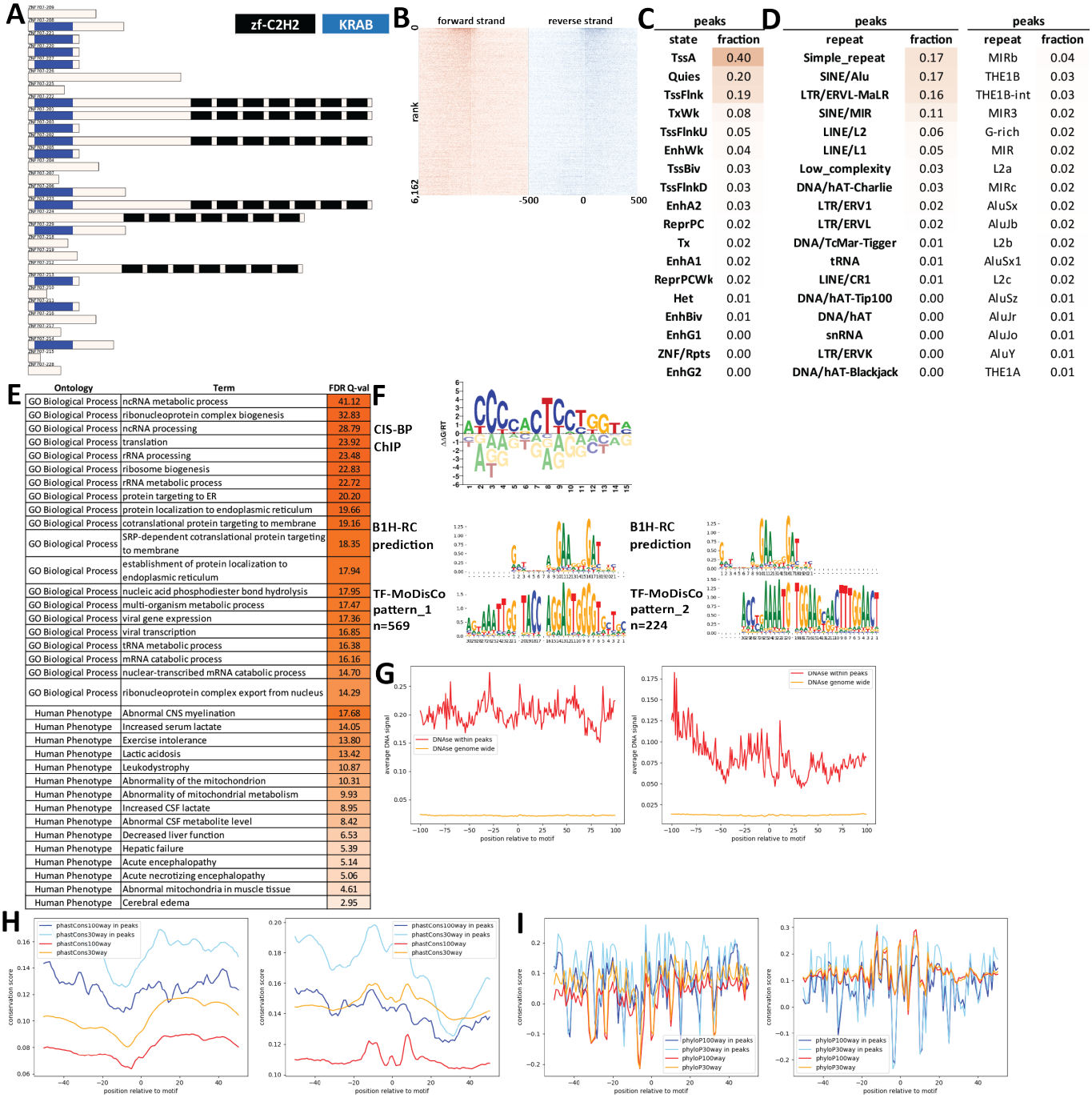

Supplementary Figure 1616: Properties and genomic distribution of motifs identified for the ZNF707 transcription factor in HepG2 (accession ENCSR017XHZ).

TF-MoDisCO pattern_1 n=569, CWM

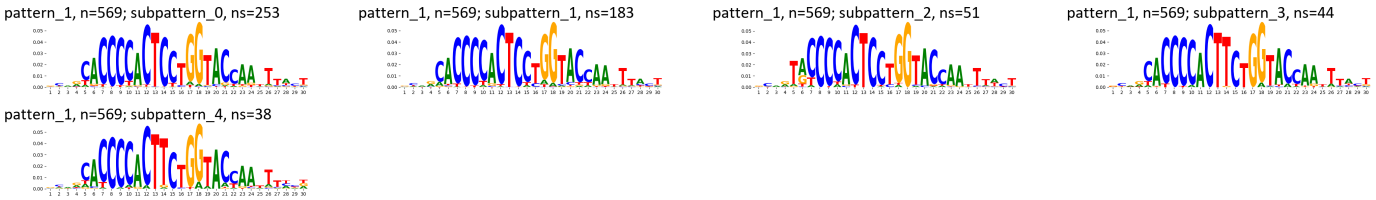

TF-MoDisCO pattern_1 n=569, PWM

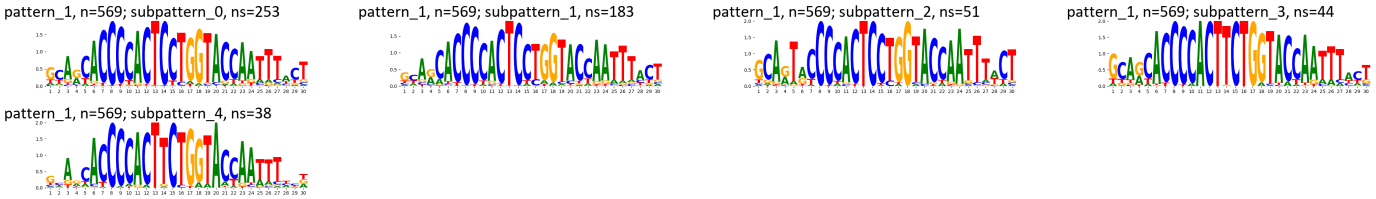

TF-MoDisCO pattern_2 n=224, CWM

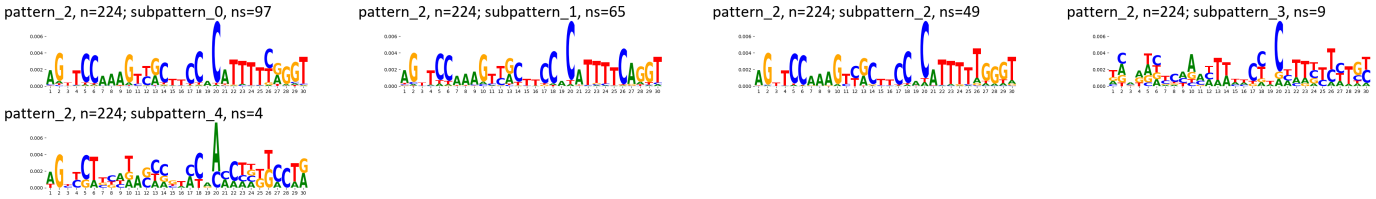

TF-MoDisCO pattern_2 n=224, PWM

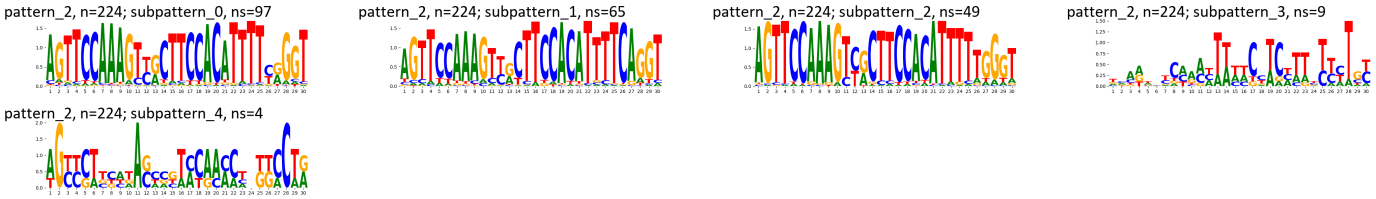

Supplementary Figure 1617: TF-MoDisCO subpatterns for the ZNF707 transcription factor in HepG2 (accession ENCSR017XHZ).

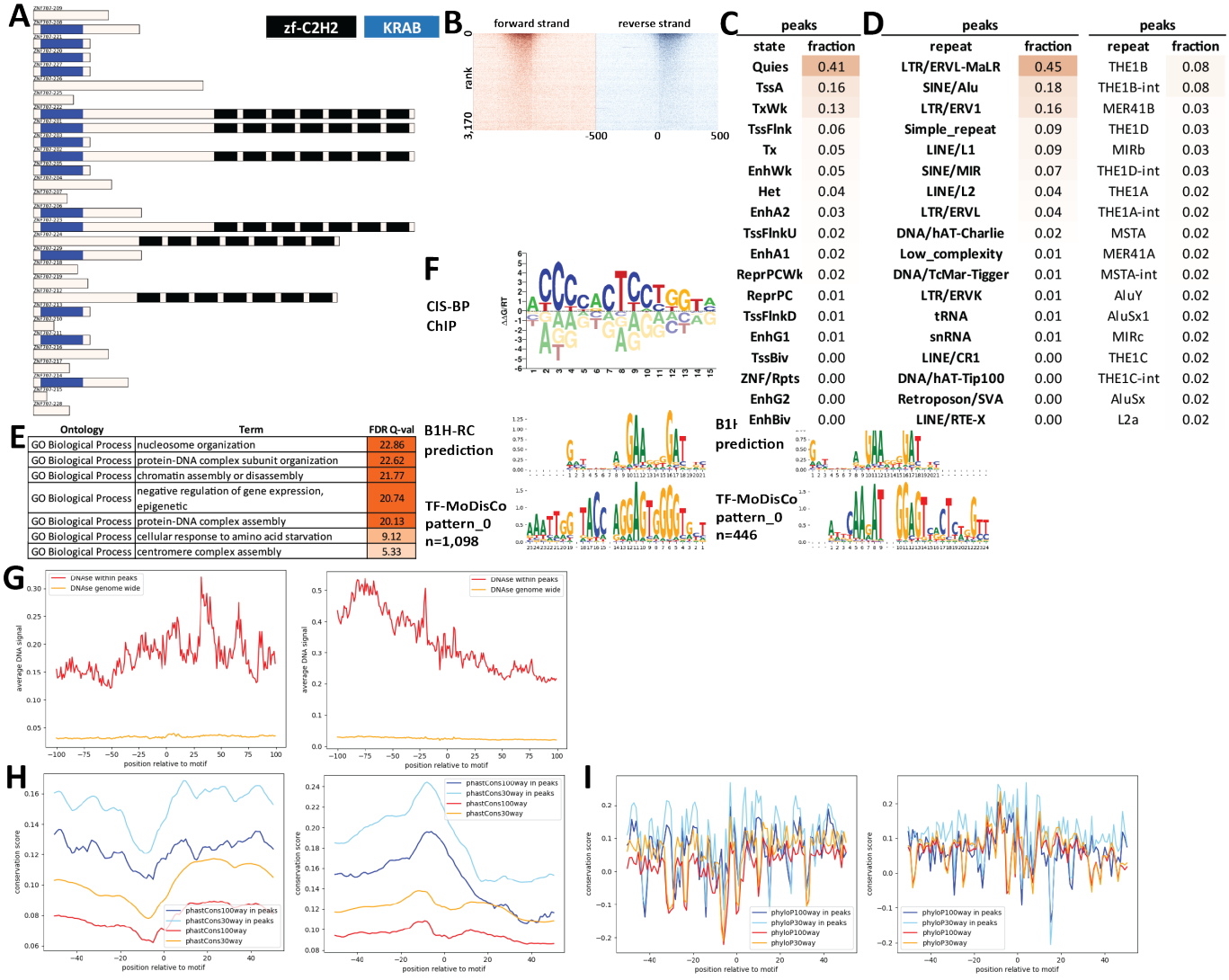

Supplementary Figure 1618: Properties and genomic distribution of motifs identified for the ZNF707 transcription factor in K562 (accession ENCSR077TKJ).

TF-MoDisCO pattern_0 n=1098, CWM

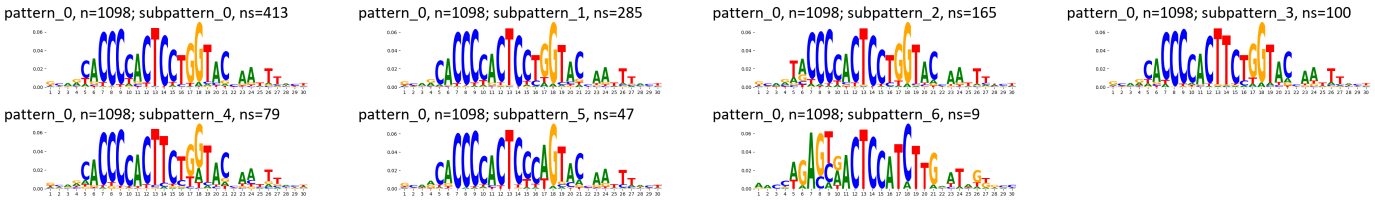

TF-MoDisCO pattern_0 n=1098, PWM

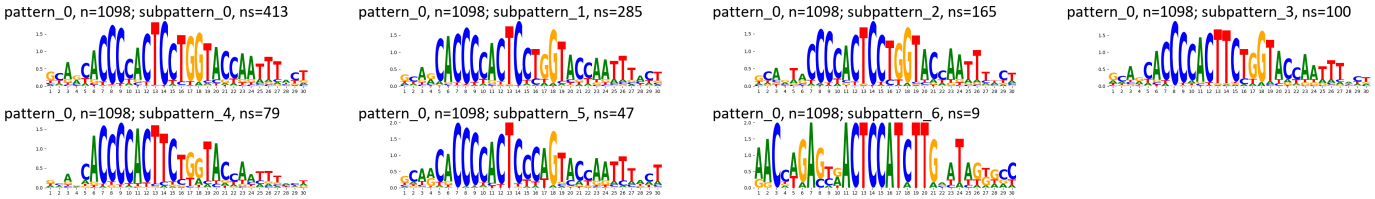

TF-MoDisCO pattern_2 n=446, CWM

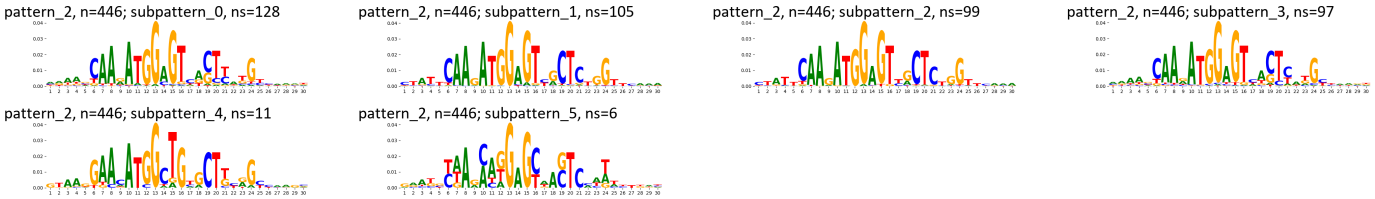

TF-MoDisCO pattern_2 n=446, PWM

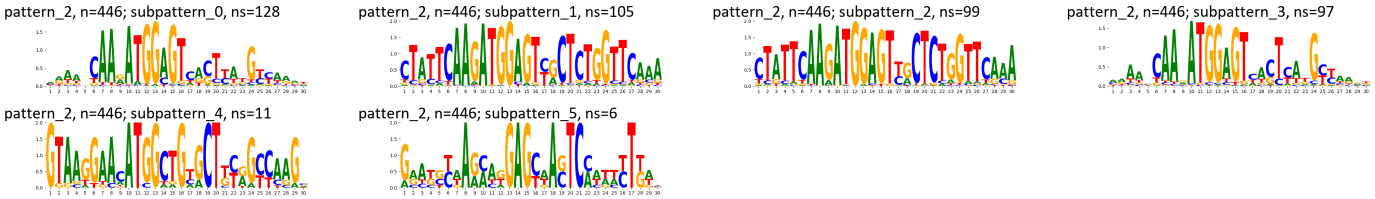

Supplementary Figure 1619: TF-MoDisCO subpatterns for the ZNF707 transcription factor in K562 (accession ENCSR077TKJ).

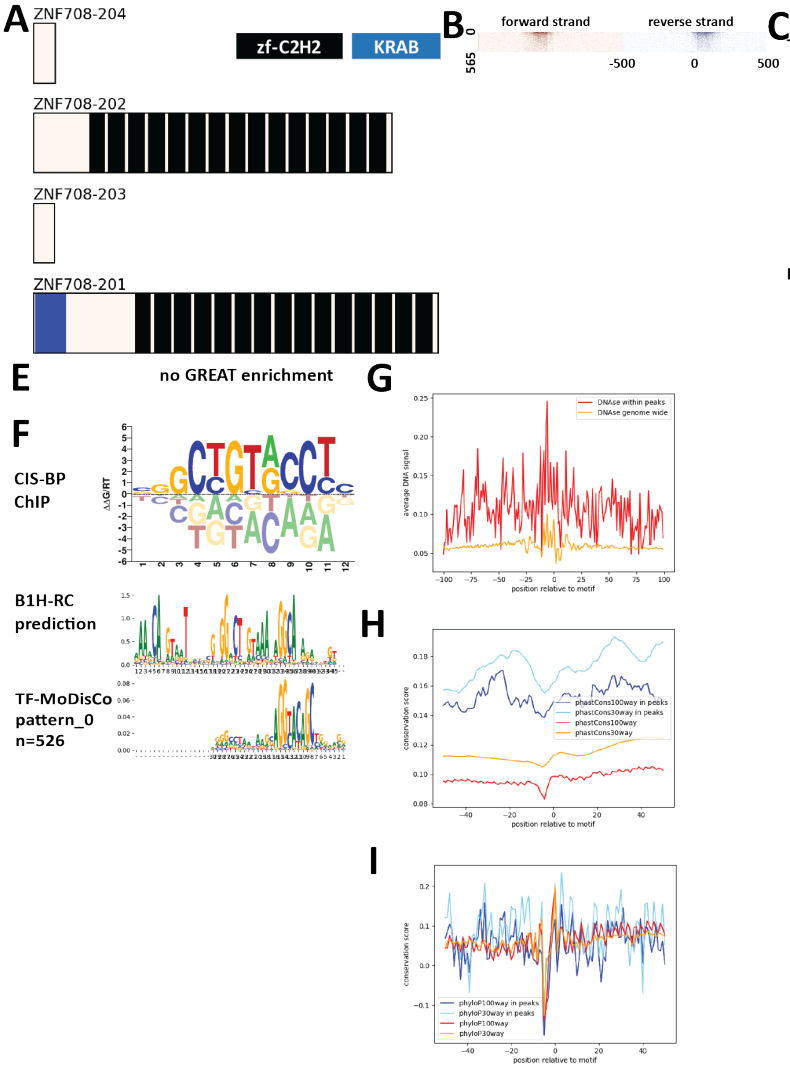

C

peaks	
state	fraction
Quies	0.54
TxWk	0.10
EnhWk	0.09
Het	0.08
TssA	0.06
Tx	0.04
EnhA1	0.03
TssFlnk	0.02
ReprPCWk	0.02
ReprPC	0.01
EnhA2	0.01
ZNF/Rpts	0.01
TssFlnkU	0.01
TssFlnkD	0.01
TssBiv	0.01
EnhBiv	0.00

D

peaks		peaks	
repeat	fraction	repeat	fraction
LTR/ERV1	0.36	MER41-int	0.10
LINE/L1	0.11	MER57-int	0.06
LINE/L2	0.06	LTR25-int	0.04
LTR/ERVL-MaLR	0.05	MER61-int	0.03
SINE/Alu	0.04	HUERS-P1-in	0.03
SINE/MIR	0.03	L2c	0.02
LTR/ERVL	0.02	HERV35I-int	0.02
Simple_repeat	0.02	L2a	0.02
DNA/hAT-Charlie	0.02	HUERS-P3b-ir	0.02
LINE/CR1	0.01	MIRb	0.01
DNA/TcMar-Tigger	0.01	MIR	0.01
DNA/hAT-Tip100	0.01	L2	0.01
LTR/Gypsy	0.00	L1PA8A	0.01
tRNA	0.00	L2b	0.01
Low_complexity	0.00	THE1B-int	0.01
LTR?	0.00	PABL_A-int	0.01
LTR/ERVK	0.00	MLT1J	0.01
LINE/RTE-X	0.00	MIR3	0.01

Supplementary Figure 1620: Properties and genomic distribution of motifs identified for the ZNF708 transcription factor in HEK293 (accession Hughes GR models).

TF-MoDisCO pattern_0 n=526, CWM

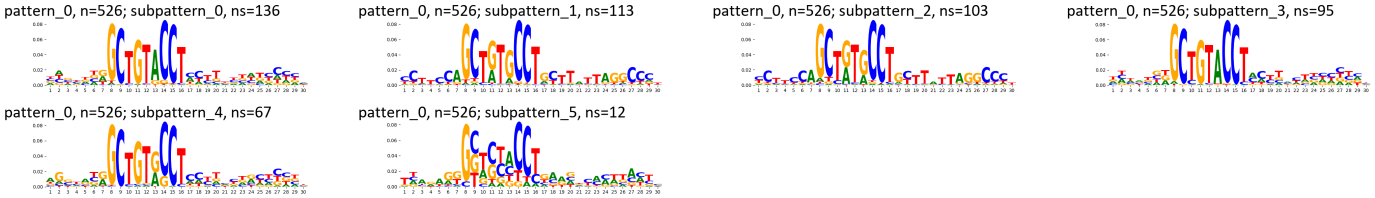

TF-MoDisCO pattern_0 n=526, PWM

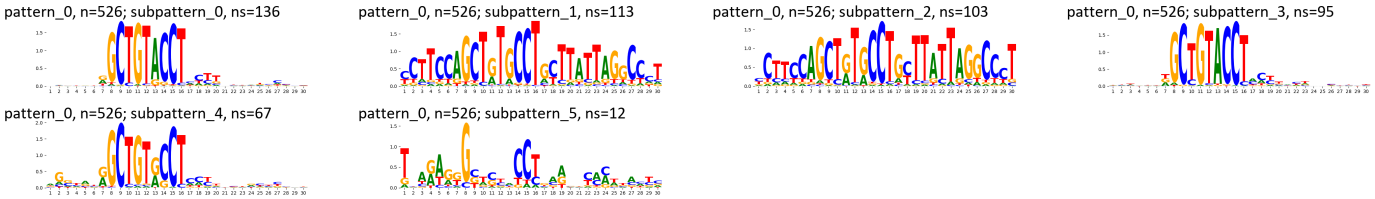

Supplementary Figure 1621: TF-MoDisCO subpatterns for the ZNF708 transcription factor in HEK293 (accession Hughes GR models).

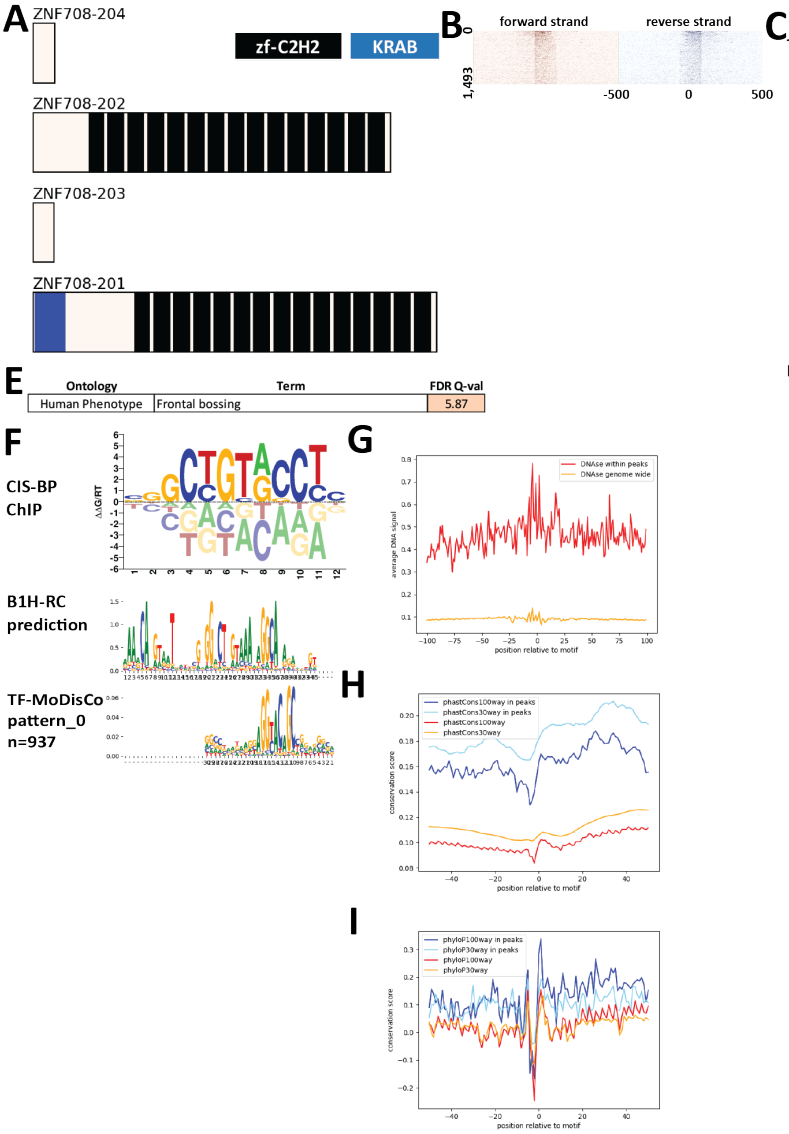

C

peaks	
state	fraction
Quies	0.32
TssA	0.31
TssFlnk	0.15
TxWk	0.09
EnhWk	0.08
TssBiv	0.05
Tx	0.03
EnhA2	0.03
Het	0.03
EnhA1	0.03
TssFlnkU	0.02
ReprPC	0.02
ReprPCWk	0.02
TssFlnkD	0.01
EnhBiv	0.01
ZNF/Rpts	0.01
EnhG1	0.00
EnhG2	0.00

D

peaks		peaks	
repeat	fraction	repeat	fraction
Simple_repeat	0.25	MER41-int	0.04
LTR/ERV1	0.16	G-rich	0.04
SINE/Alu	0.11	MIRb	0.02
LINE/L1	0.10	MER57-int	0.02
LINE/L2	0.06	L2a	0.02
SINE/MIR	0.05	L2c	0.02
Low_complexity	0.05	L2b	0.01
LTR/ERVL-MaLR	0.04	AluJb	0.01
DNA/hAT-Charlie	0.03	LTR25-int	0.01
LTR/ERVL	0.02	AluSx1	0.01
Satellite	0.01	MIR3	0.01
DNA/TcMar-Tigger	0.01	MIR	0.01
Satellite/centr	0.01	MER61-int	0.01
DNA/hAT-Tip100	0.01	HUERS-P1-in	0.01
rRNA	0.01	AluJo	0.01
tRNA	0.00	HERV35I-int	0.01
Satellite/acro	0.00	GA-rich	0.01
LINE/CR1	0.00	AluSx	0.01

Supplementary Figure 1622: Properties and genomic distribution of motifs identified for the ZNF708 transcription factor in HEK293 (accession ChipExo models).

TF-MoDisCO pattern_0 n=937, CWM

pattern_0, n=937; subpattern_0, ns=242

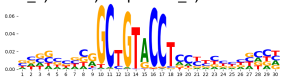

pattern_0, n=937; subpattern_1, ns=225

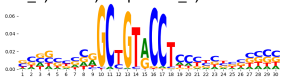

pattern_0, n=937; subpattern_2, ns=172

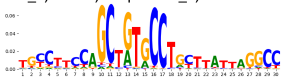

pattern_0, n=937; subpattern_3, ns=161

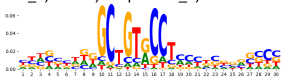

pattern_0, n=937; subpattern_4, ns=137

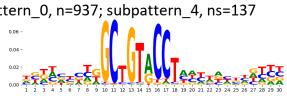

TF-MoDisCO pattern_0 n=937, PWM

pattern_0, n=937; subpattern_0, ns=242

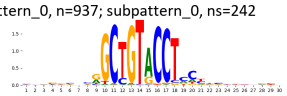

pattern_0, n=937; subpattern_1, ns=225

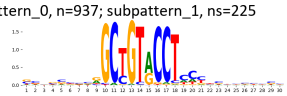

pattern_0, n=937; subpattern_2, ns=172

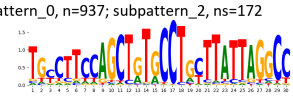

pattern_0, n=937; subpattern_3, ns=161

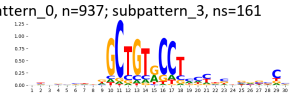

pattern_0, n=937; subpattern_4, ns=137

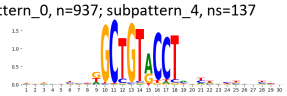

Supplementary Figure 1623: TF-MoDisCO subpatterns for the ZNF708 transcription factor in HEK293 (accession ChipExo models).

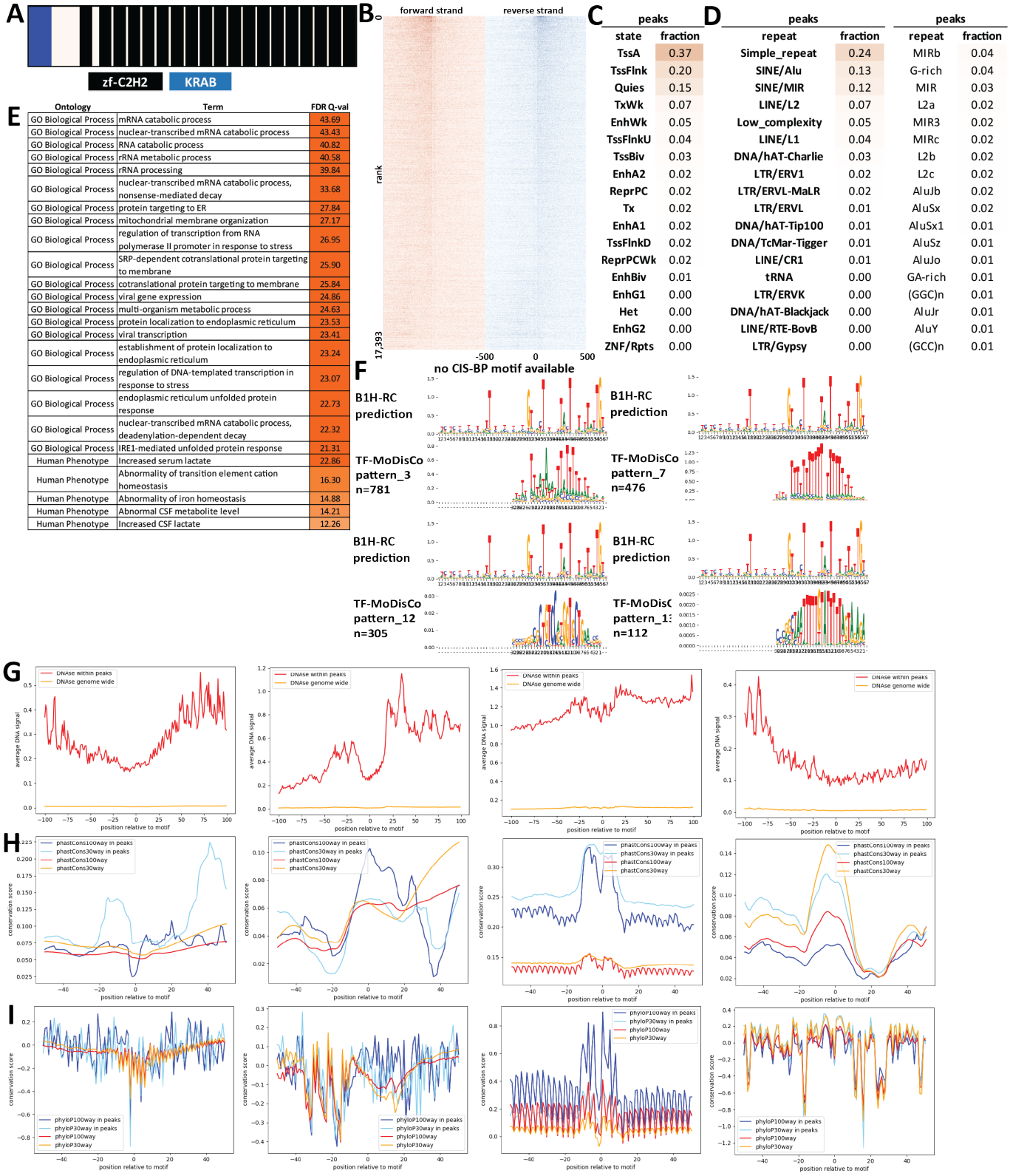

Supplementary Figure 1624: Properties and genomic distribution of motifs identified for the ZNF709 transcription factor in HepG2 (accession ENCSR984IXF).

TF-MoDisCO pattern_12 n=305, CWM

pattern_12, n=305; subpattern_0, ns=145

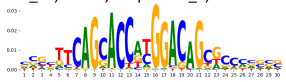

pattern_12, n=305; subpattern_1, ns=140

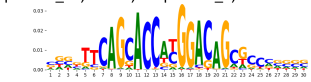

pattern_12, n=305; subpattern_2, ns=17

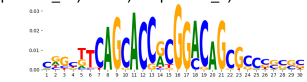

pattern_12, n=305; subpattern_3, ns=3

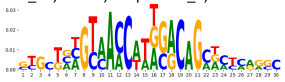

TF-MoDisCO pattern_12 n=305, PWM

pattern_12, n=305; subpattern_0, ns=145

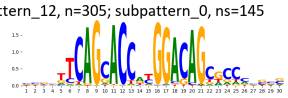

pattern_12, n=305; subpattern_1, ns=140

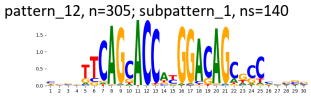

pattern_12, n=305; subpattern_2, ns=17

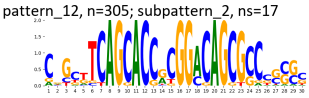

pattern_12, n=305; subpattern_3, ns=3

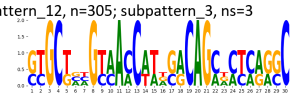

TF-MoDisCO pattern_13 n=112, CWM

pattern_13, n=112; subpattern_0, ns=30

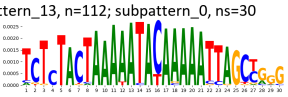

pattern_13, n=112; subpattern_1, ns=30

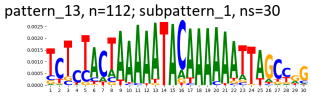

pattern_13, n=112; subpattern_2, ns=24

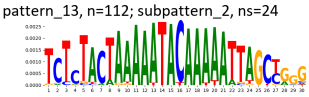

pattern_13, n=112; subpattern_3, ns=17

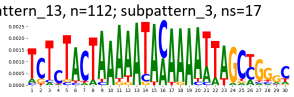

pattern_13, n=112; subpattern_4, ns=11

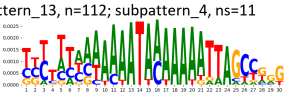

TF-MoDisCO pattern_13 n=112, PWM

pattern_13, n=112; subpattern_0, ns=30

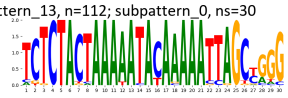

pattern_13, n=112; subpattern_1, ns=30

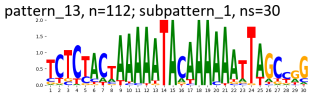

pattern_13, n=112; subpattern_2, ns=24

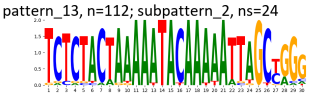

pattern_13, n=112; subpattern_3, ns=17

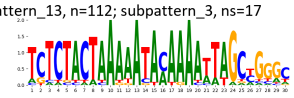

pattern_13, n=112; subpattern_4, ns=11

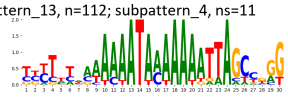

TF-MoDisCO pattern_3 n=781, CWM

pattern_3, n=781; subpattern_0, ns=181

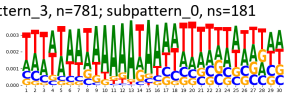

pattern_3, n=781; subpattern_1, ns=152

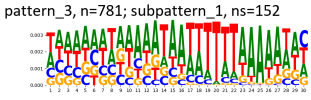

pattern_3, n=781; subpattern_2, ns=108

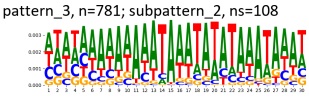

pattern_3, n=781; subpattern_3, ns=97

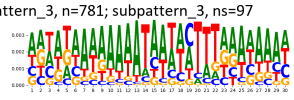

pattern_3, n=781; subpattern_4, ns=96

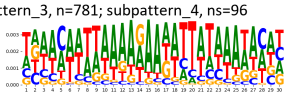

pattern_3, n=781; subpattern_5, ns=57

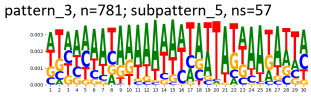

pattern_3, n=781; subpattern_6, ns=54

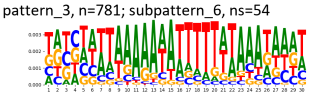

pattern_3, n=781; subpattern_7, ns=36

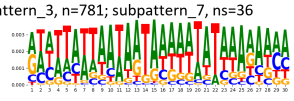

TF-MoDisCO pattern_3 n=781, PWM

pattern_3, n=781; subpattern_0, ns=181

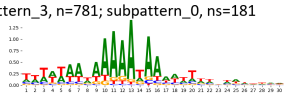

pattern_3, n=781; subpattern_1, ns=152

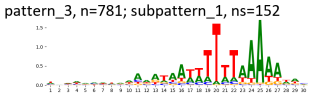

pattern_3, n=781; subpattern_2, ns=108

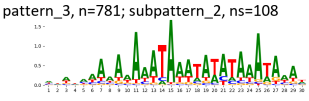

pattern_3, n=781; subpattern_3, ns=97

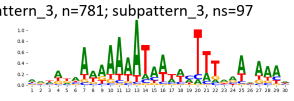

pattern_3, n=781; subpattern_4, ns=96

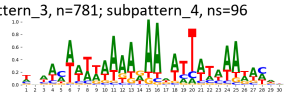

pattern_3, n=781; subpattern_5, ns=57

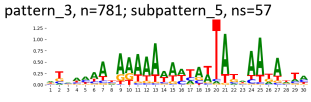

pattern_3, n=781; subpattern_6, ns=54

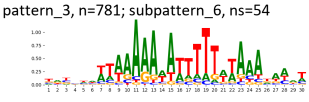

pattern_3, n=781; subpattern_7, ns=36

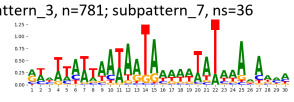

TF-MoDisCO pattern_7 n=476, CWM

pattern_7, n=476; subpattern_0, ns=107

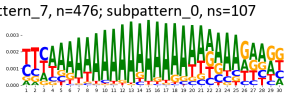

pattern_7, n=476; subpattern_1, ns=105

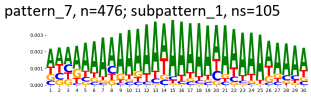

pattern_7, n=476; subpattern_2, ns=84

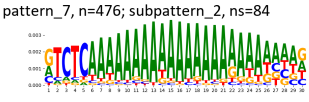

pattern_7, n=476; subpattern_3, ns=82

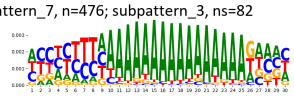

pattern_7, n=476; subpattern_4, ns=61

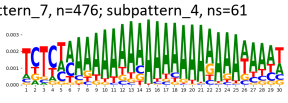

pattern_7, n=476; subpattern_5, ns=32

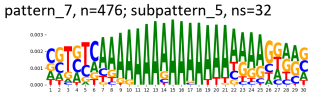

pattern_7, n=476; subpattern_6, ns=5

TF-MoDisCO pattern_7 n=476, PWM

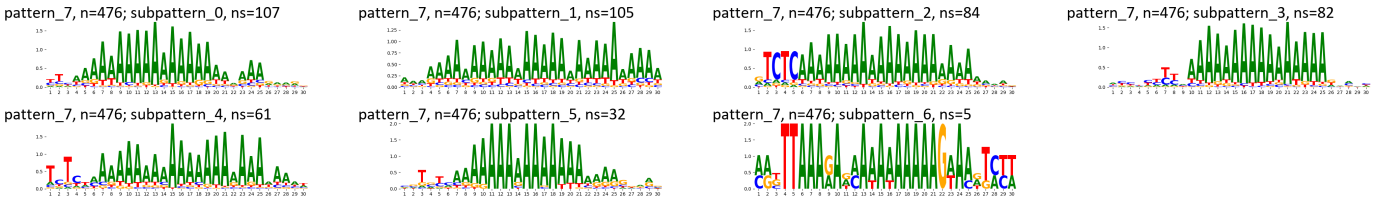

Supplementary Figure 1625: TF-MoDisCO subpatterns for the ZNF709 transcription factor in HepG2 (accession ENCSR984IXF).

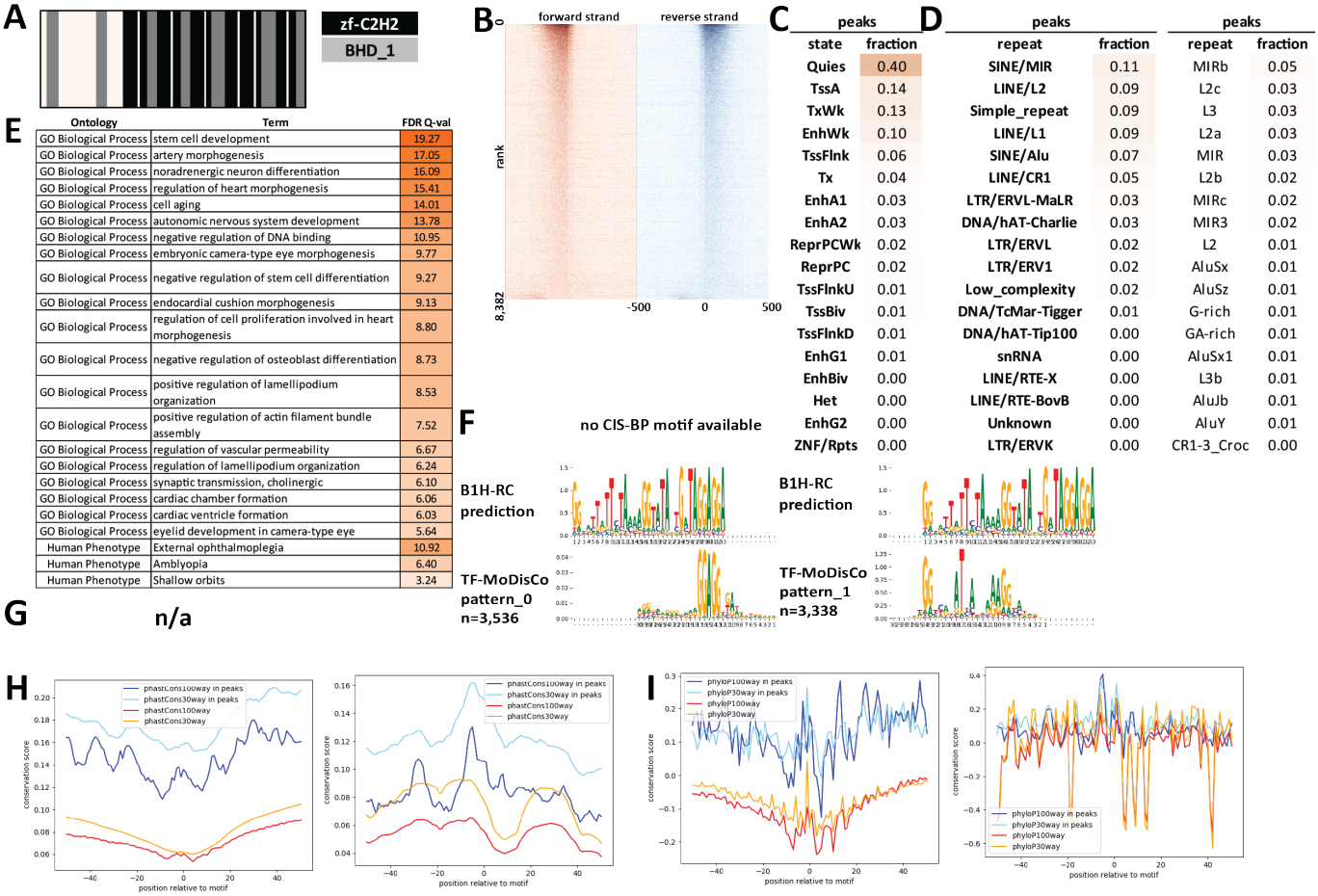

Supplementary Figure 1626: Properties and genomic distribution of motifs identified for the ZNF70 transcription factor in SK-N-SH (accession ENCSR207GYC).

TF-MoDisCO pattern_0 n=3536, CWM

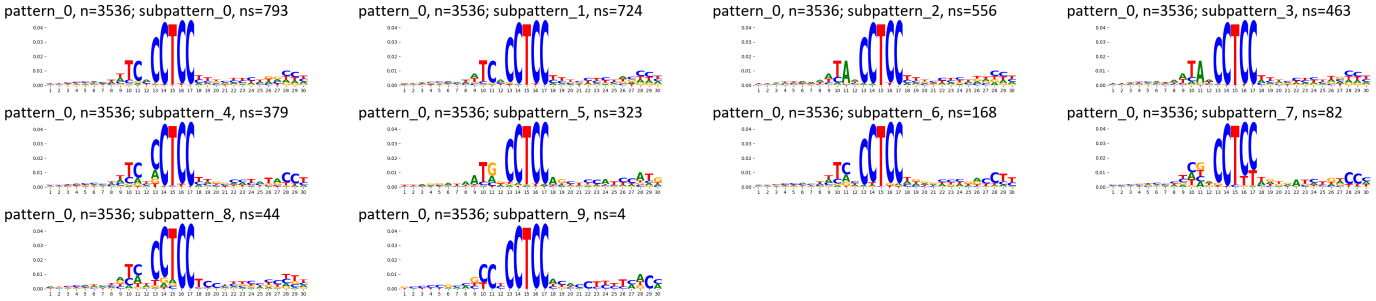

TF-MoDisCO pattern_0 n=3536, PWM

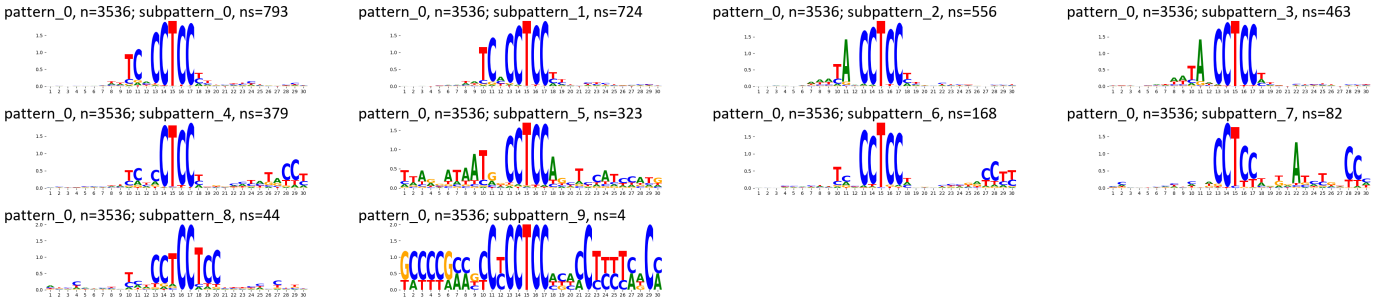

TF-MoDisCO pattern_1 n=3338, CWM

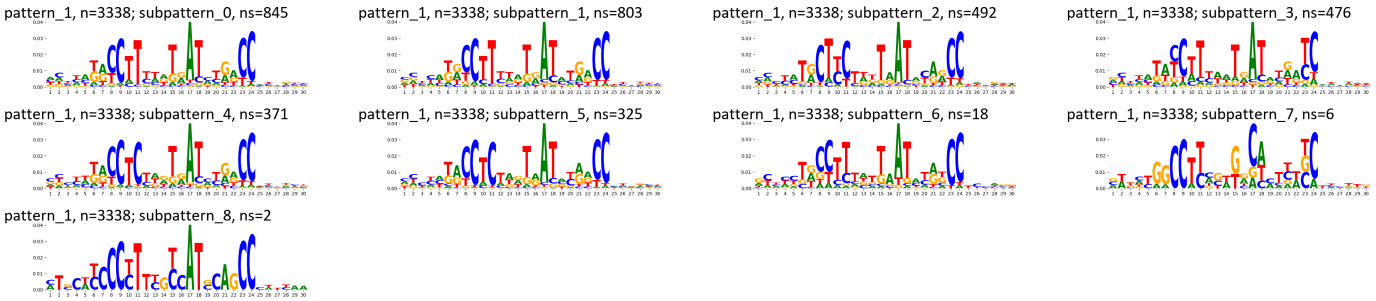

TF-MoDisCO pattern_1 n=3338, PWM

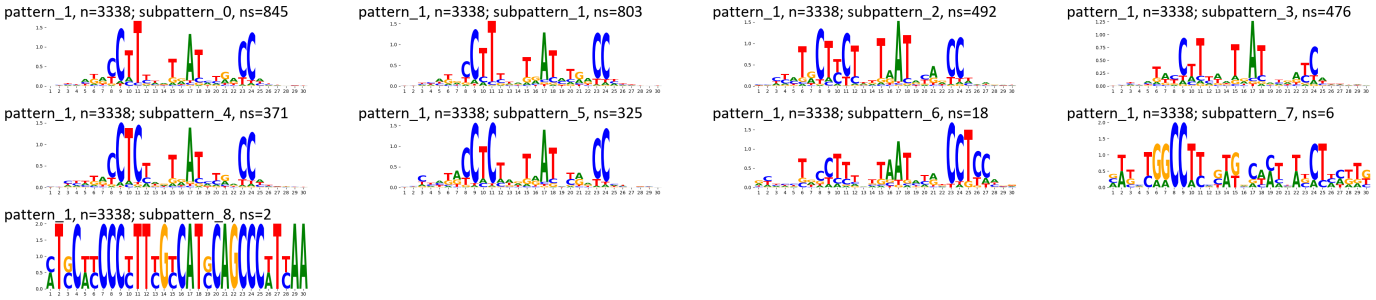

Supplementary Figure 1627: TF-MoDisCO subpatterns for the ZNF70 transcription factor in SK-N-SH (accession ENCSR207GYC).

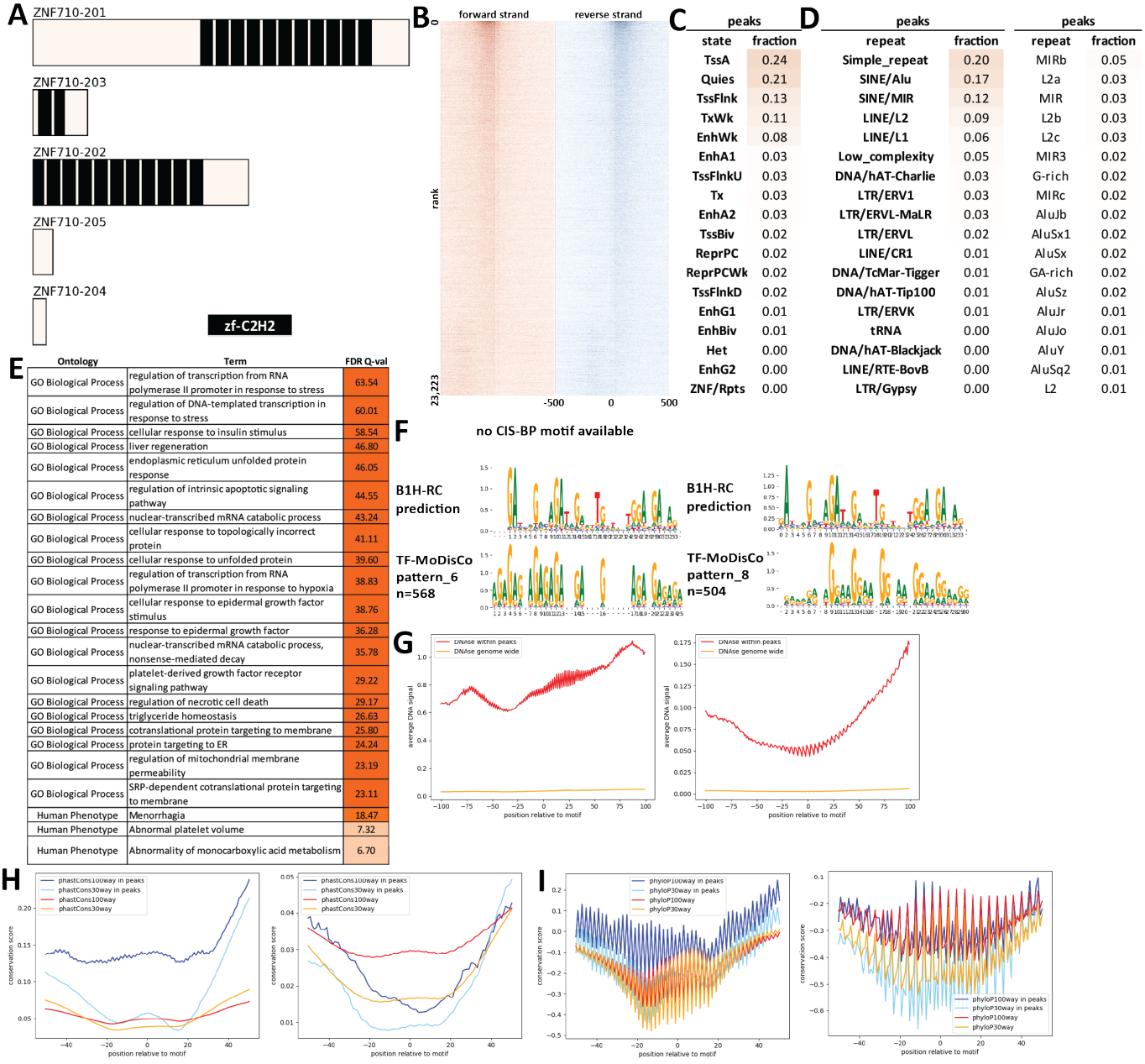

Supplementary Figure 1628: Properties and genomic distribution of motifs identified for the ZNF710 transcription factor in HepG2 (accession ENCSR670UEX).

TF-MoDisCO pattern_6 n=568, CWM

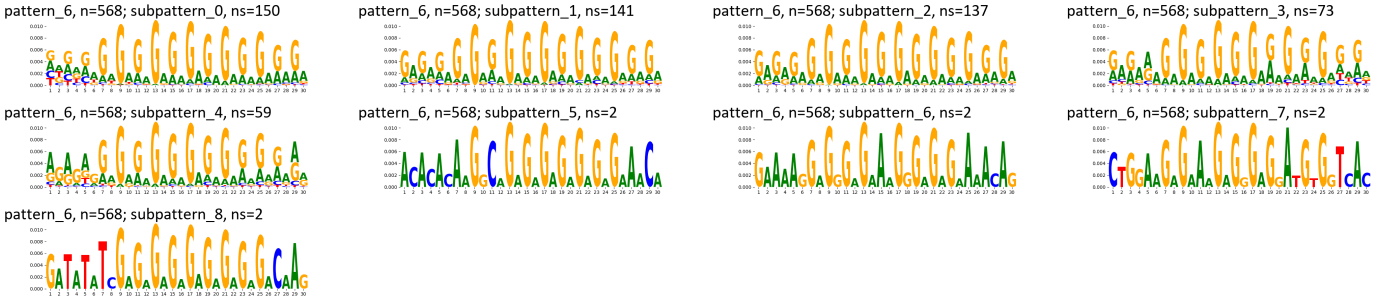

TF-MoDisCO pattern_6 n=568, PWM

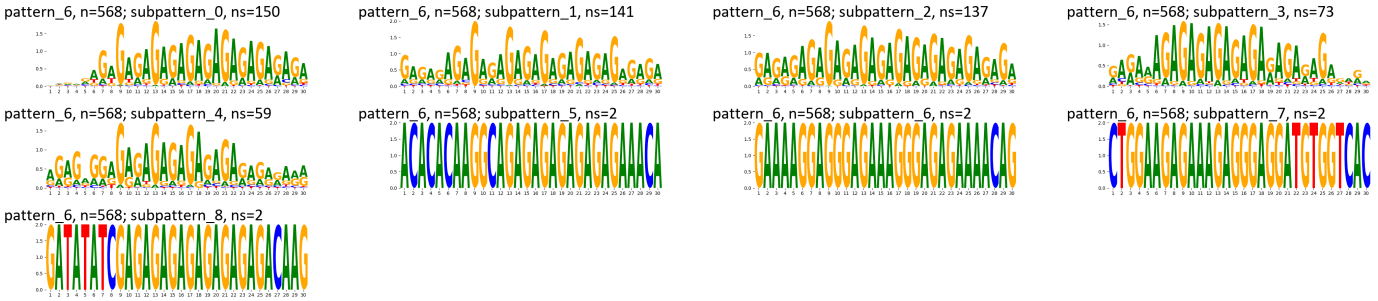

TF-MoDisCO pattern_8 n=504, CWM

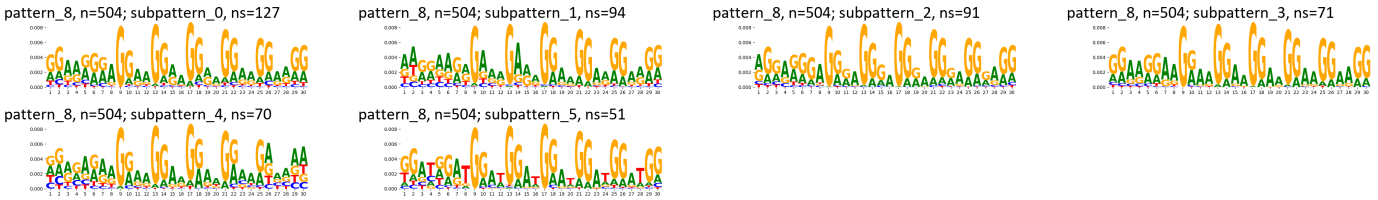

TF-MoDisCO pattern_8 n=504, PWM

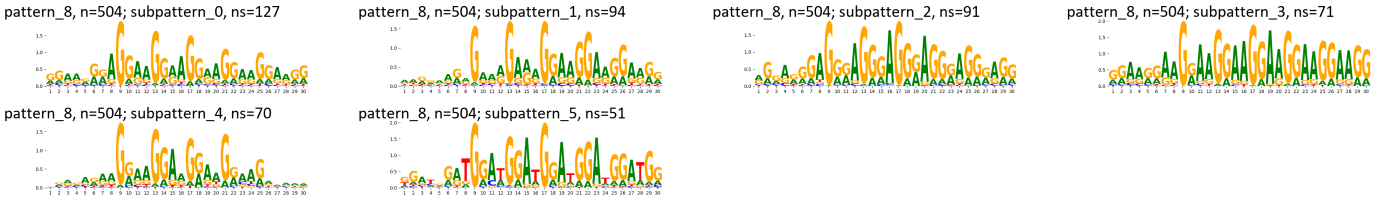

Supplementary Figure 1629: TF-MoDisCO subpatterns for the ZNF710 transcription factor in HepG2 (accession ENCSR670UEX).

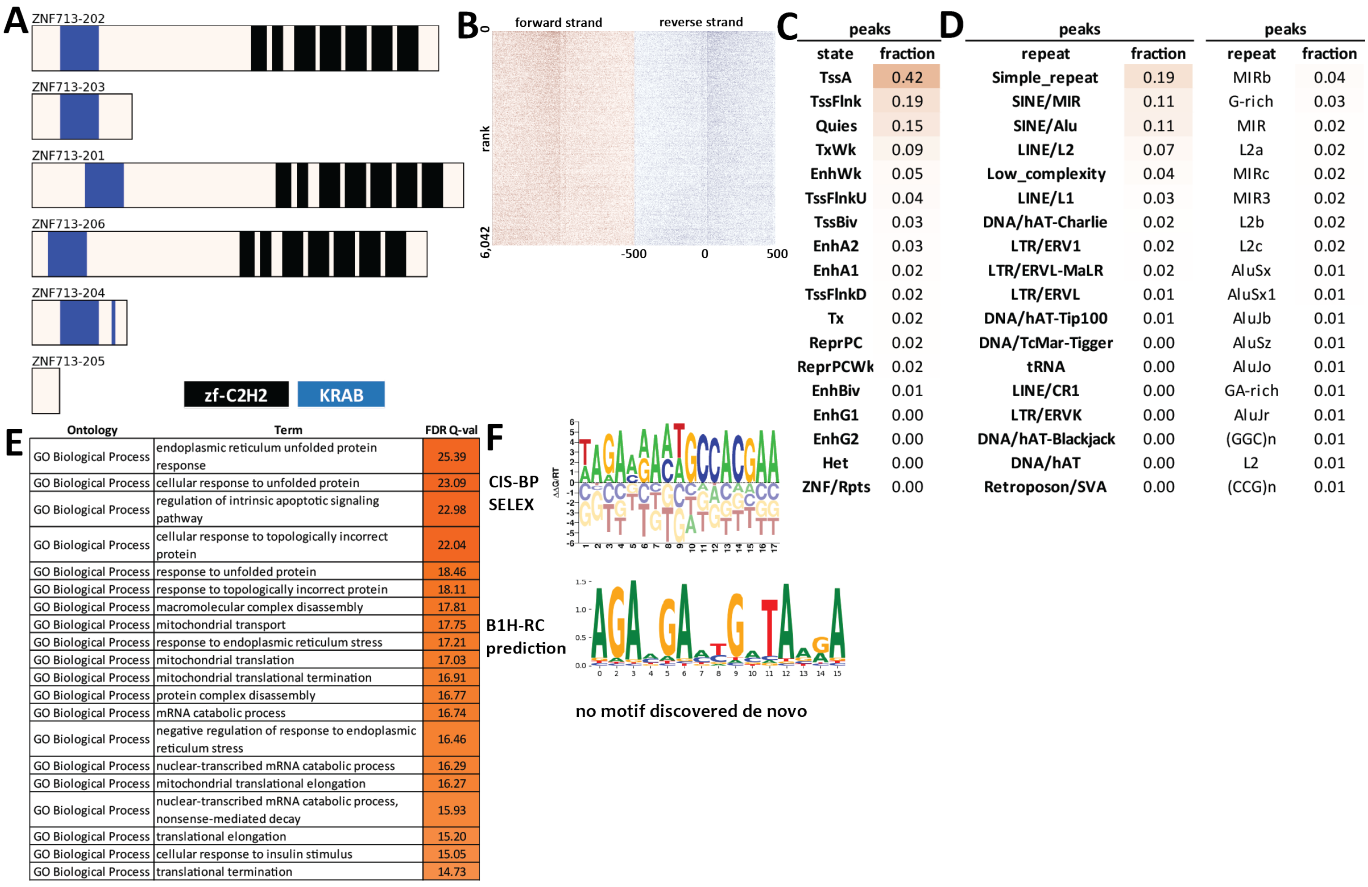

peaks	
state	fraction
TssA	0.42
TssFlnk	0.19
Quies	0.15
TxWk	0.09
EnhWk	0.05
TssFlnkU	0.04
TssBiv	0.03
EnhA2	0.03
EnhA1	0.02
TssFlnkD	0.02
Tx	0.02
ReprPC	0.02
ReprPCWk	0.02
EnhBiv	0.01
EnhG1	0.00
EnhG2	0.00
Het	0.00
ZNF/Rpts	0.00

peaks		peaks	
repeat	fraction	repeat	fraction
Simple_repeat	0.19	MIRb	0.04
SINE/MIR	0.11	G-rich	0.03
SINE/Alu	0.11	MIR	0.02
LINE/L2	0.07	L2a	0.02
Low_complexity	0.04	MIRc	0.02
LINE/L1	0.03	MIR3	0.02
DNA/hAT-Charlie	0.02	L2b	0.02
LTR/ERV1	0.02	L2c	0.02
LTR/ERVL-MaLR	0.02	AluSx	0.01
LTR/ERVL	0.01	AluSx1	0.01
DNA/hAT-Tip100	0.01	AluJb	0.01
DNA/TcMar-Tigger	0.00	AluSz	0.01
tRNA	0.00	AluJo	0.01
LINE/CR1	0.00	GA-rich	0.01
LTR/ERVK	0.00	AluJr	0.01
DNA/hAT-Blackjack	0.00	(GGC)n	0.01
DNA/hAT	0.00	L2	0.01
Retroposon/SVA	0.00	(CCG)n	0.01

Ontology	Term	FDR Q-val
GO Biological Process	endoplasmic reticulum unfolded protein response	25.39
GO Biological Process	cellular response to unfolded protein	23.09
GO Biological Process	regulation of intrinsic apoptotic signaling pathway	22.98
GO Biological Process	cellular response to topologically incorrect protein	22.04
GO Biological Process	response to unfolded protein	18.46
GO Biological Process	response to topologically incorrect protein	18.11
GO Biological Process	macromolecular complex disassembly	17.81
GO Biological Process	mitochondrial transport	17.75
GO Biological Process	response to endoplasmic reticulum stress	17.21
GO Biological Process	mitochondrial translation	17.03
GO Biological Process	mitochondrial translational termination	16.91
GO Biological Process	protein complex disassembly	16.77
GO Biological Process	mRNA catabolic process	16.74
GO Biological Process	negative regulation of response to endoplasmic reticulum stress	16.46
GO Biological Process	nuclear-transcribed mRNA catabolic process	16.29
GO Biological Process	mitochondrial translational elongation	16.27
GO Biological Process	nuclear-transcribed mRNA catabolic process, nonsense-mediated decay	15.93
GO Biological Process	translational elongation	15.20
GO Biological Process	cellular response to insulin stimulus	15.05
GO Biological Process	translational termination	14.73

Supplementary Figure 1630: Properties and genomic distribution of motifs identified for the ZNF713 transcription factor in HepG2 (accession ENCSR513NBU).

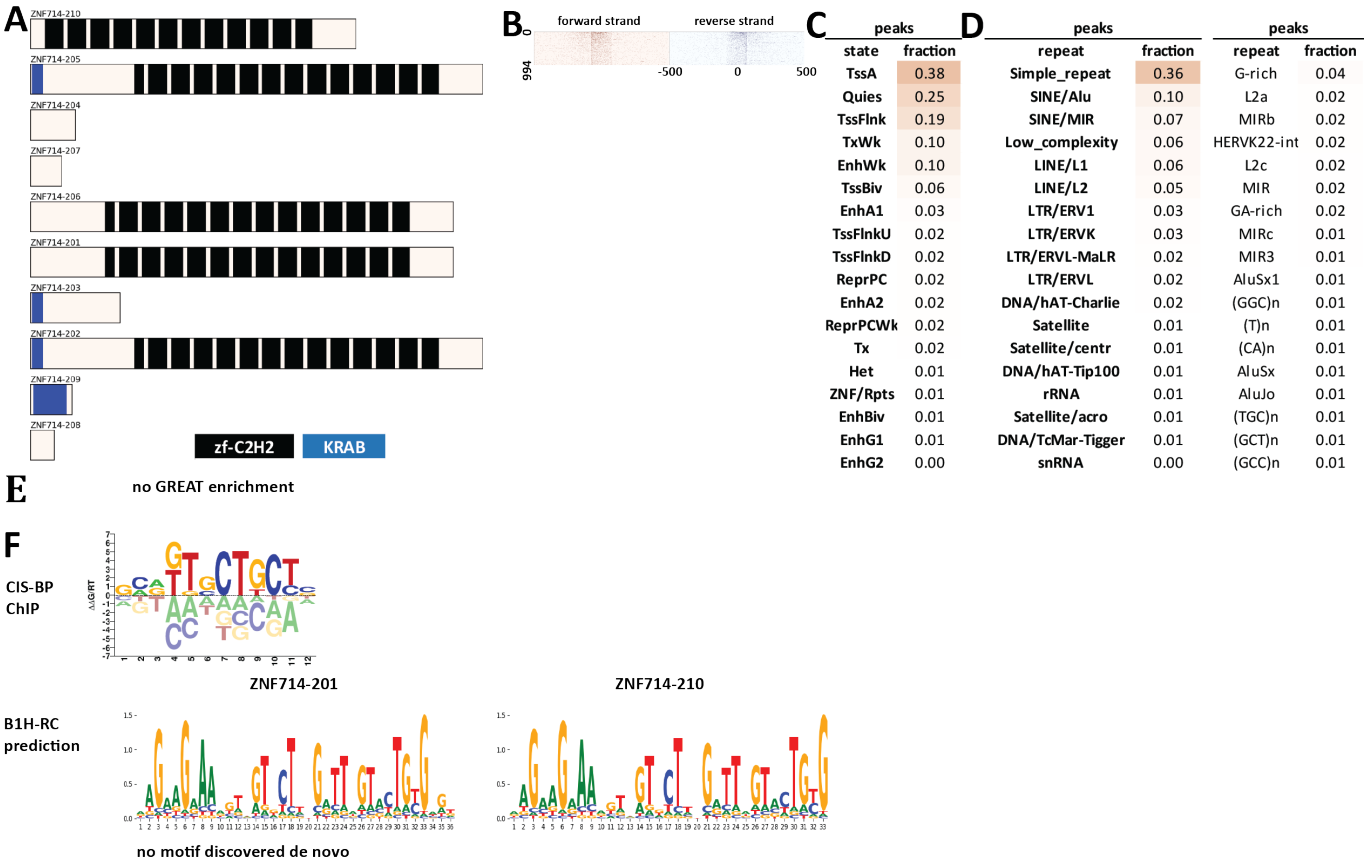

C	peaks	
	state	fraction
	TssA	0.38
	Quies	0.25
	TssFlnk	0.19
	TxWk	0.10
	EnhWk	0.10
	TssBiv	0.06
	EnhA1	0.03
	TssFlnkU	0.02
	TssFlnkD	0.02
	ReprPC	0.02
	EnhA2	0.02
	ReprPCWk	0.02
	Tx	0.02
	Het	0.01
	ZNF/Rpts	0.01
	EnhBiv	0.01
	EnhG1	0.01
	EnhG2	0.00

D	peaks		peaks	
	repeat	fraction	repeat	fraction
	Simple_repeat	0.36	G-rich	0.04
	SINE/Alu	0.10	L2a	0.02
	SINE/MIR	0.07	MIRb	0.02
	Low_complexity	0.06	HERVK22-int	0.02
	LINE/L1	0.06	L2c	0.02
	LINE/L2	0.05	MIR	0.02
	LTR/ERV1	0.03	GA-rich	0.02
	LTR/ERVK	0.03	MIRc	0.01
	LTR/ERVL-MaLR	0.02	MIR3	0.01
	LTR/ERVL	0.02	AluSx1	0.01
	DNA/hAT-Charlie	0.02	(GGC)n	0.01
	Satellite	0.01	(T)n	0.01
	Satellite/centr	0.01	(CA)n	0.01
	DNA/hAT-Tip100	0.01	AluSx	0.01
	rRNA	0.01	AluJo	0.01
	Satellite/acro	0.01	(TGC)n	0.01
	DNA/TcMar-Tigger	0.01	(GCT)n	0.01
	snRNA	0.00	(GCC)n	0.01

Supplementary Figure 1631: Properties and genomic distribution of motifs identified for the ZNF714 transcription factor in HEK293 (accession ChipExo models).

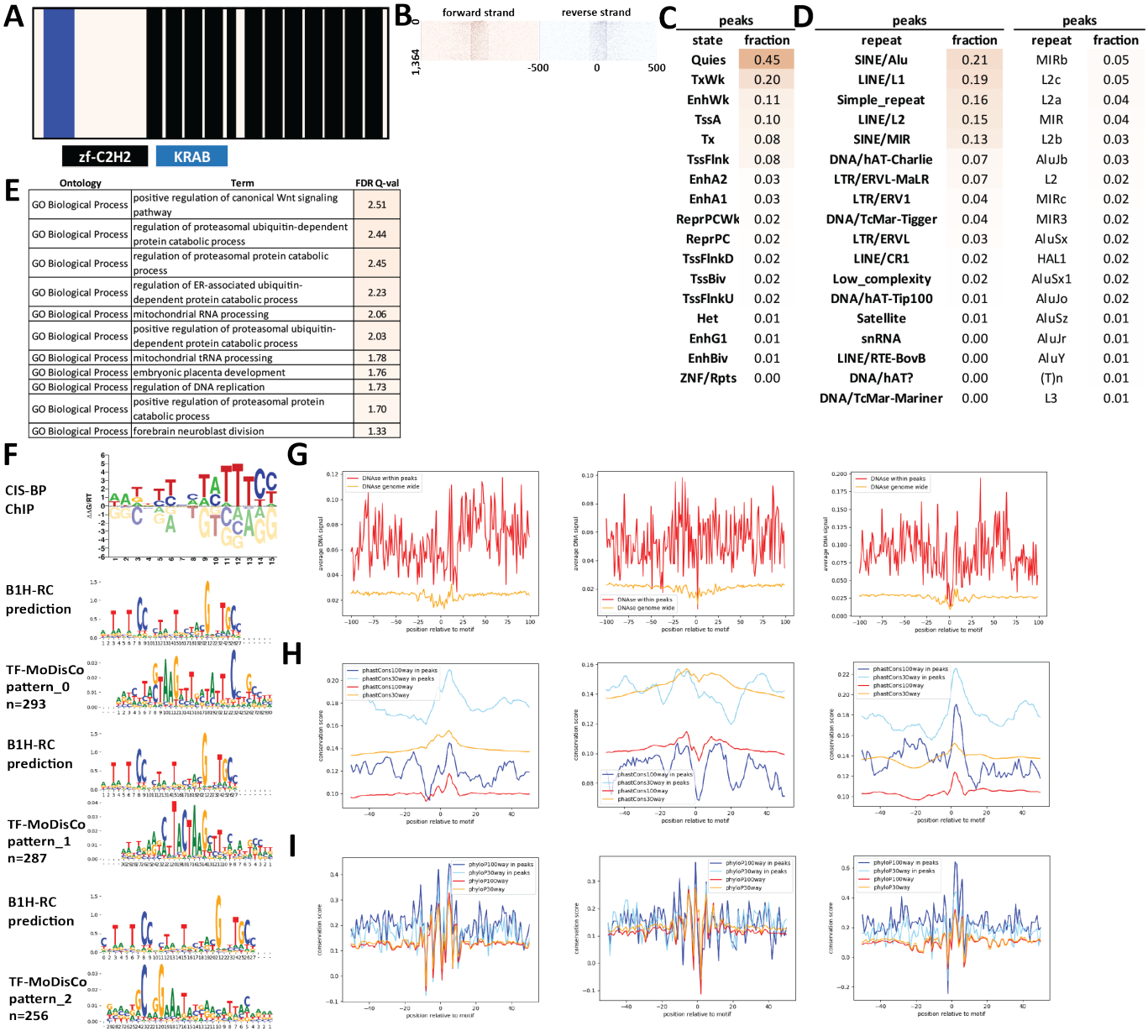

Supplementary Figure 1632: Properties and genomic distribution of motifs identified for the ZNF716 transcription factor in HEK293 (accession ChipExo models).

TF-MoDisCO pattern_0 n=293, CWM

pattern_0, n=293; subpattern_0, ns=70

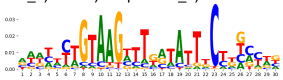

pattern_0, n=293; subpattern_1, ns=63

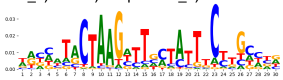

pattern_0, n=293; subpattern_2, ns=63

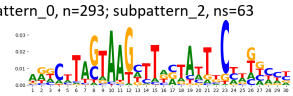

pattern_0, n=293; subpattern_3, ns=63

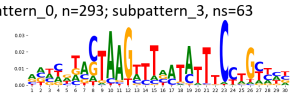

pattern_0, n=293; subpattern_4, ns=34

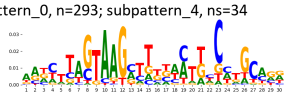

TF-MoDisCO pattern_0 n=293, PWM

pattern_0, n=293; subpattern_0, ns=70

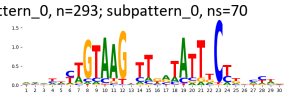

pattern_0, n=293; subpattern_1, ns=63

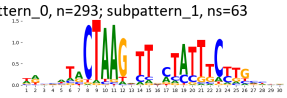

pattern_0, n=293; subpattern_2, ns=63

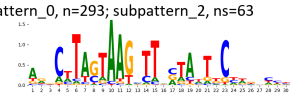

pattern_0, n=293; subpattern_3, ns=63

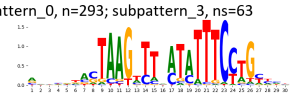

pattern_0, n=293; subpattern_4, ns=34

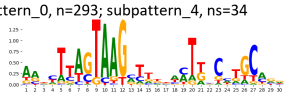

TF-MoDisCO pattern_1 n=287, CWM

pattern_1, n=287; subpattern_0, ns=95

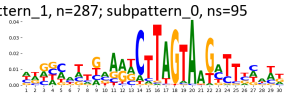

pattern_1, n=287; subpattern_1, ns=79

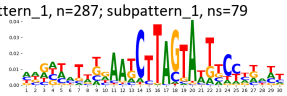

pattern_1, n=287; subpattern_2, ns=52

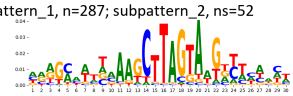

pattern_1, n=287; subpattern_3, ns=41

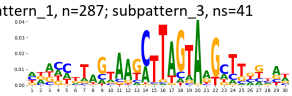

pattern_1, n=287; subpattern_4, ns=13

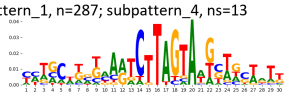

pattern_1, n=287; subpattern_5, ns=7

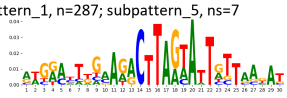

TF-MoDisCO pattern_1 n=287, PWM

pattern_1, n=287; subpattern_0, ns=95

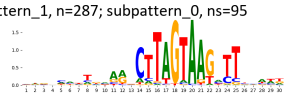

pattern_1, n=287; subpattern_1, ns=79

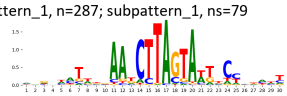

pattern_1, n=287; subpattern_2, ns=52

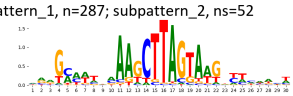

pattern_1, n=287; subpattern_3, ns=41

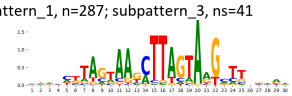

pattern_1, n=287; subpattern_4, ns=13

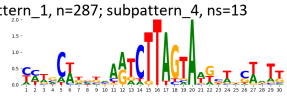

pattern_1, n=287; subpattern_5, ns=7

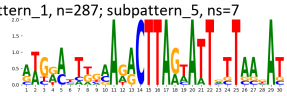

TF-MoDisCO pattern_2 n=256, CWM

pattern_2, n=256; subpattern_0, ns=46

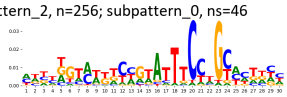

pattern_2, n=256; subpattern_1, ns=42

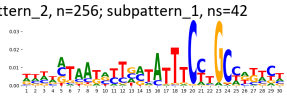

pattern_2, n=256; subpattern_2, ns=42

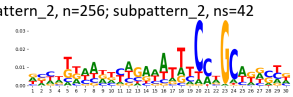

pattern_2, n=256; subpattern_3, ns=40

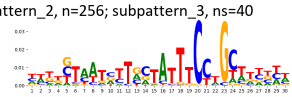

pattern_2, n=256; subpattern_4, ns=34

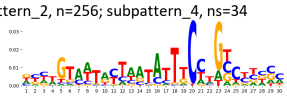

pattern_2, n=256; subpattern_5, ns=32

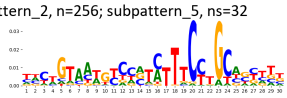

pattern_2, n=256; subpattern_6, ns=20

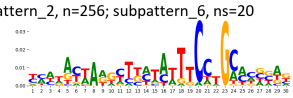

TF-MoDisCO pattern_2 n=256, PWM

pattern_2, n=256; subpattern_0, ns=46

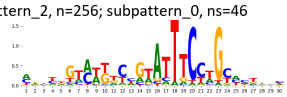

pattern_2, n=256; subpattern_1, ns=42

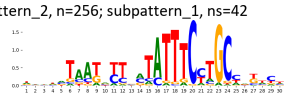

pattern_2, n=256; subpattern_2, ns=42

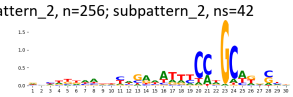

pattern_2, n=256; subpattern_3, ns=40

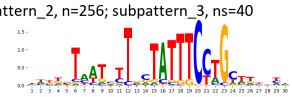

pattern_2, n=256; subpattern_4, ns=34

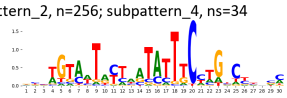

pattern_2, n=256; subpattern_5, ns=32

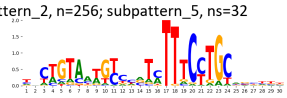

pattern_2, n=256; subpattern_6, ns=20

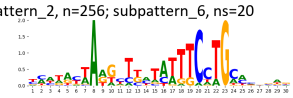

Supplementary Figure 1633: TF-MoDisCO subpatterns for the ZNF716 transcription factor in HEK293 (accession ChipExo models).

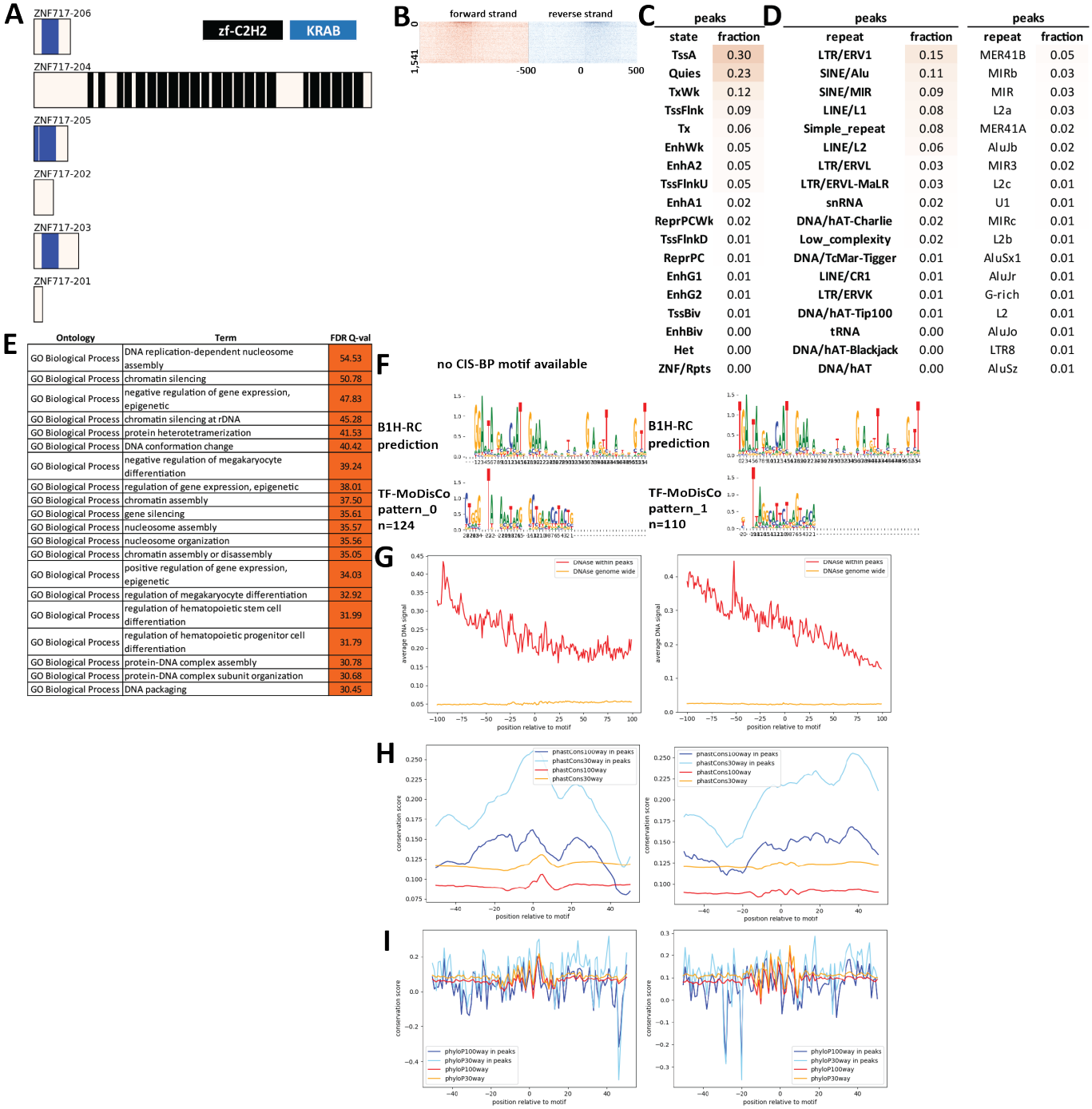

Supplementary Figure 1634: Properties and genomic distribution of motifs identified for the ZNF717 transcription factor in K562 (accession ENCSR987KYK).

TF-MoDisCO pattern_0 n=124, CWM

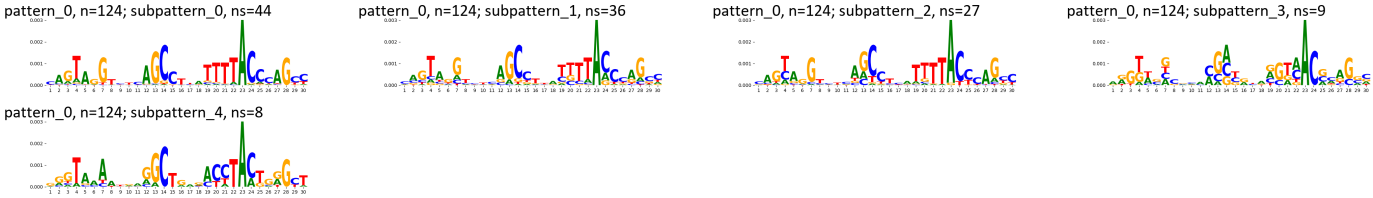

TF-MoDisCO pattern_0 n=124, PWM

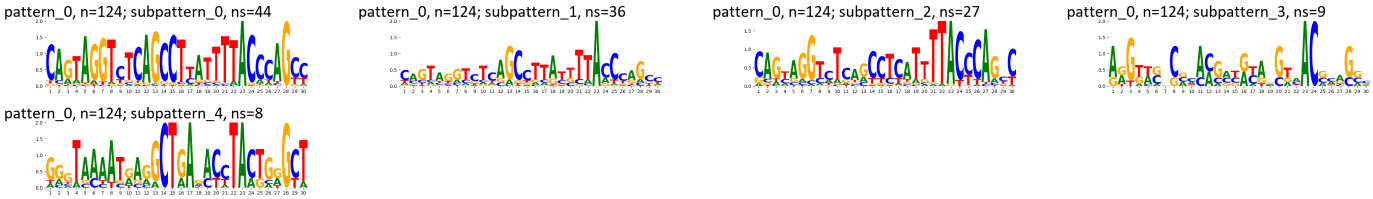

TF-MoDisCO pattern_1 n=110, CWM

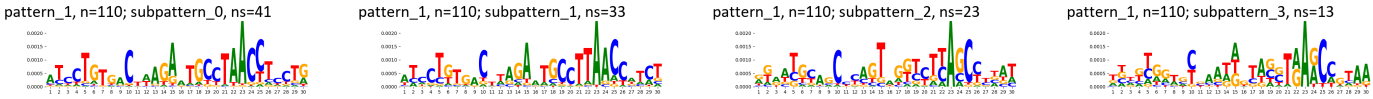

TF-MoDisCO pattern_1 n=110, PWM

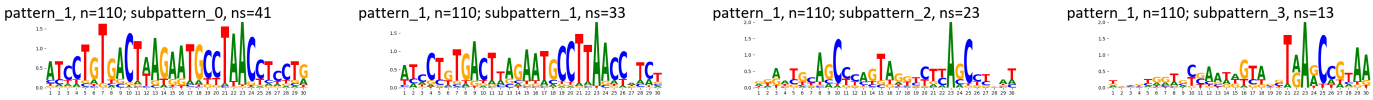

Supplementary Figure 1635: TF-MoDisCO subpatterns for the ZNF717 transcription factor in K562 (accession ENCSR987KYK).

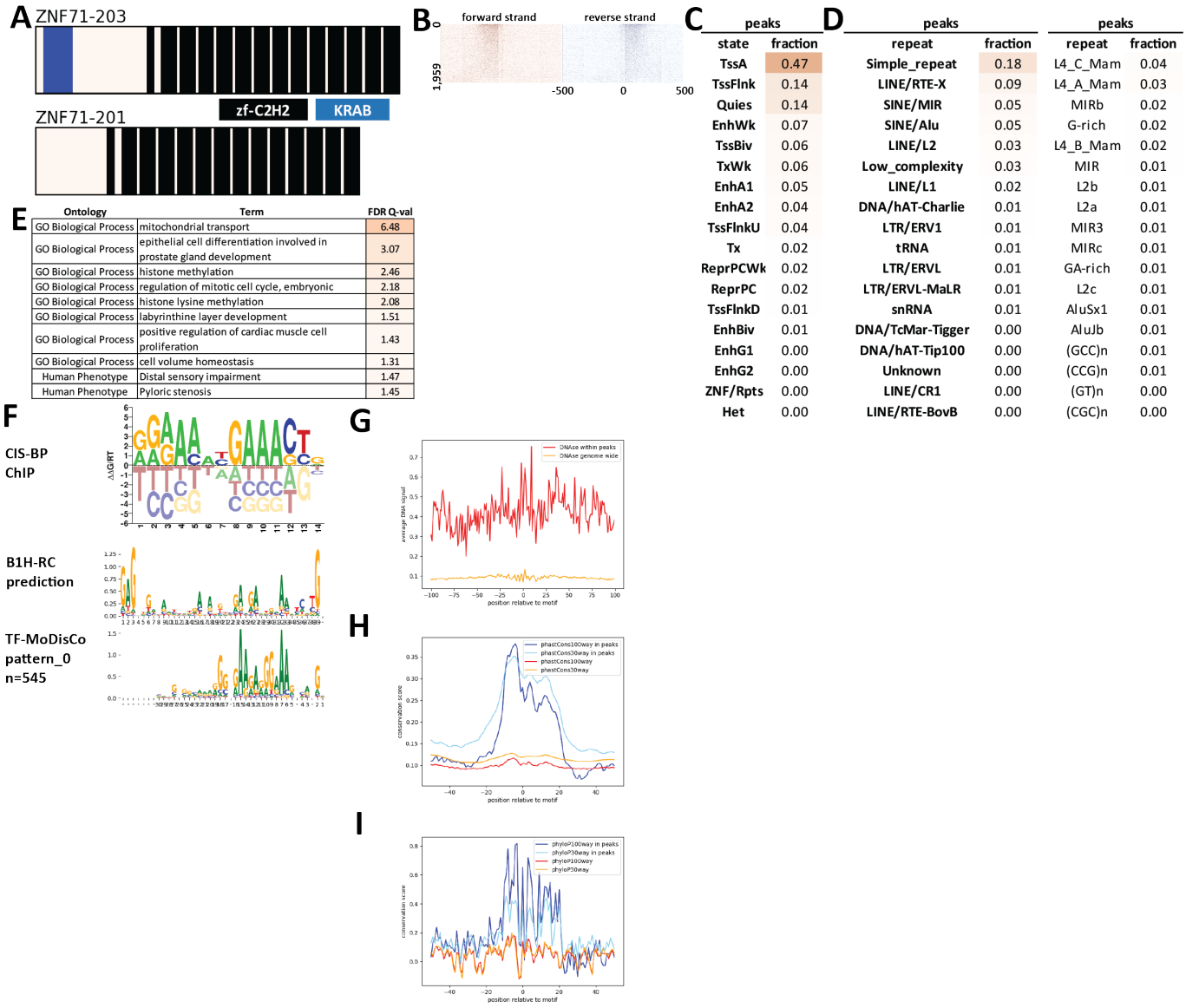

Supplementary Figure 1636: Properties and genomic distribution of motifs identified for the ZNF71 transcription factor in HEK293 (accession Hughes NB models).

TF-MoDisCO pattern_1 n=118, CWM

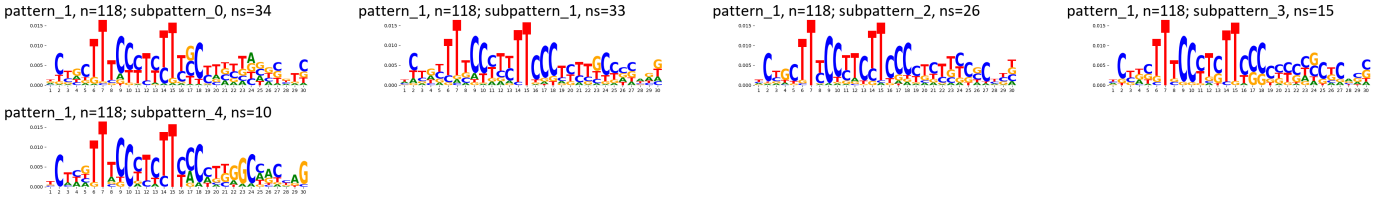

TF-MoDisCO pattern_1 n=118, PWM

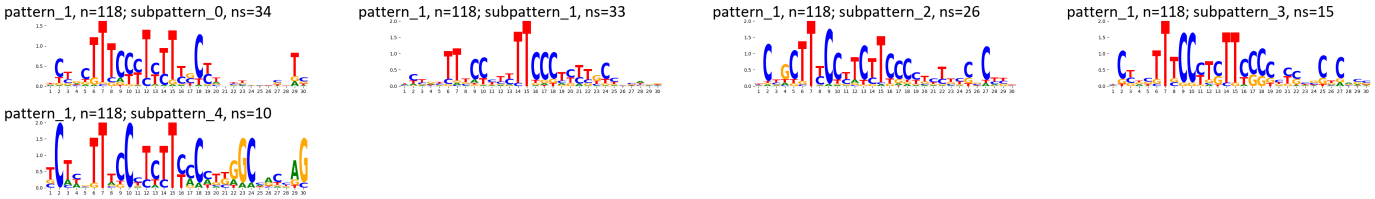

Supplementary Figure 1637: TF-MoDisCO subpatterns for the ZNF71 transcription factor in HEK293 (accession Hughes NB models).

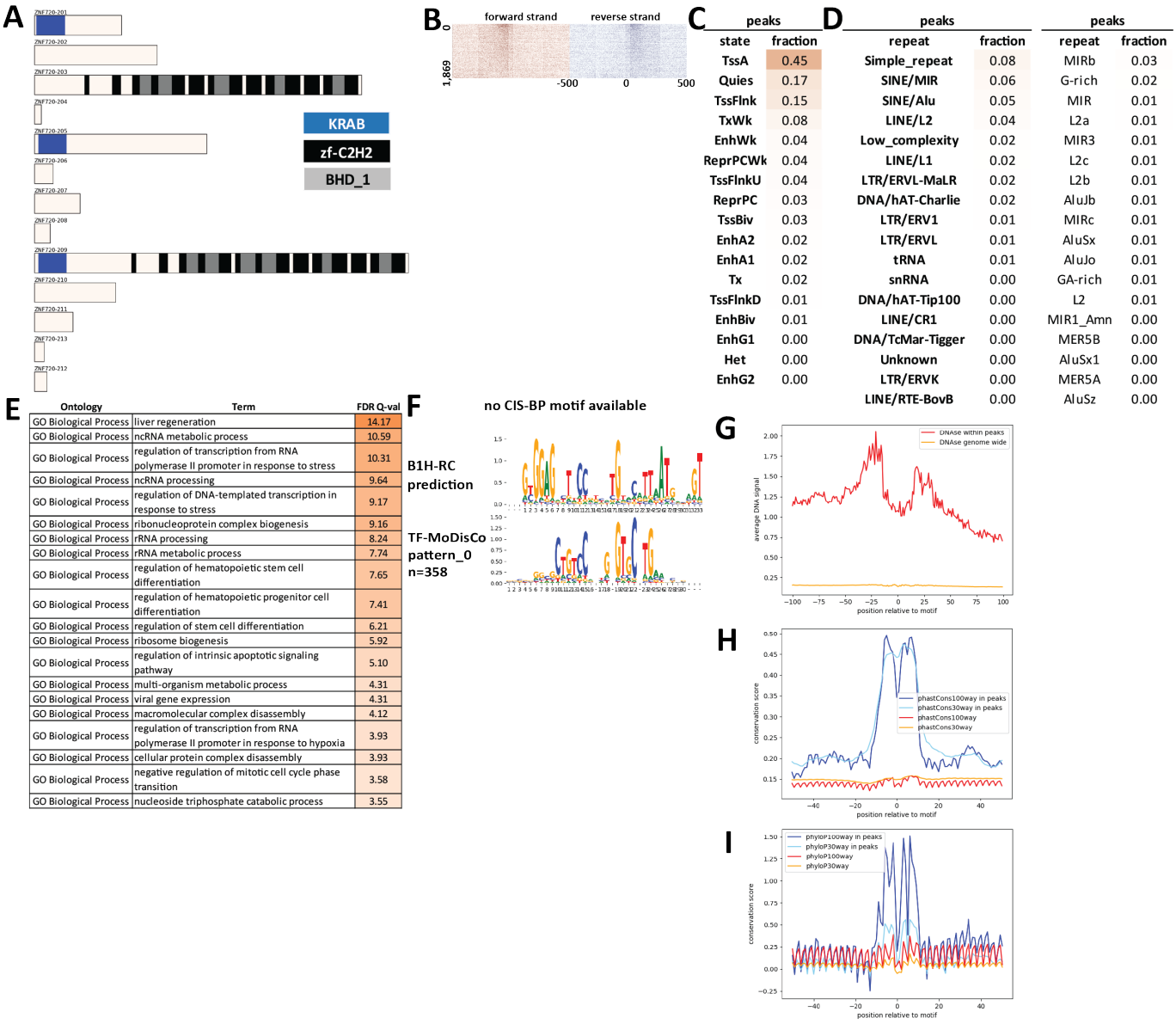

Supplementary Figure 1638: Properties and genomic distribution of motifs identified for the ZNF720 transcription factor in HepG2 (accession ENCSR643XPG).

TF-MoDisCO pattern_0 n=358, CWM

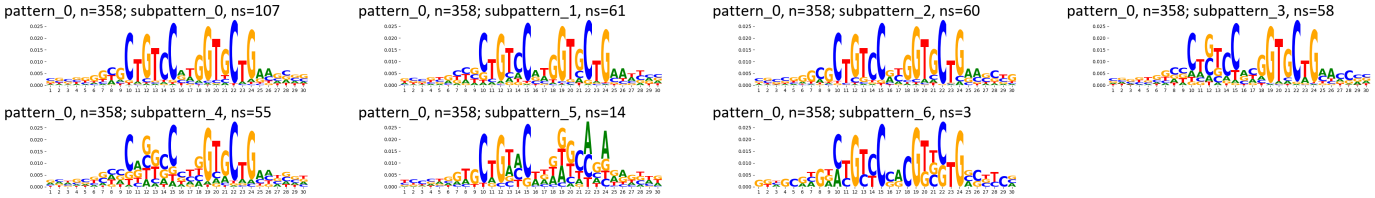

TF-MoDisCO pattern_0 n=358, PWM

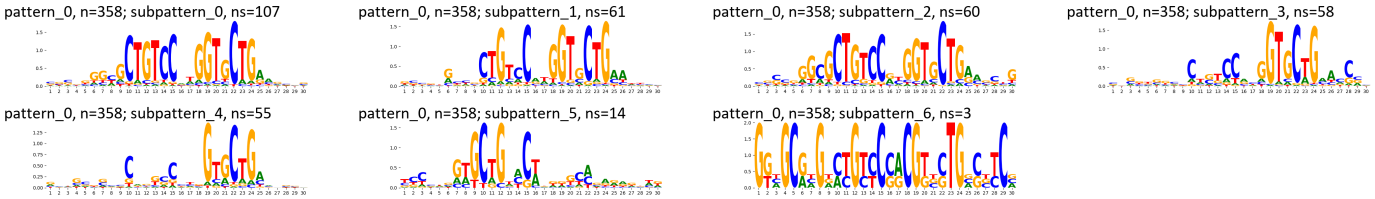

Supplementary Figure 1639: TF-MoDisCO subpatterns for the ZNF720 transcription factor in HepG2 (accession ENCSR643XPG).

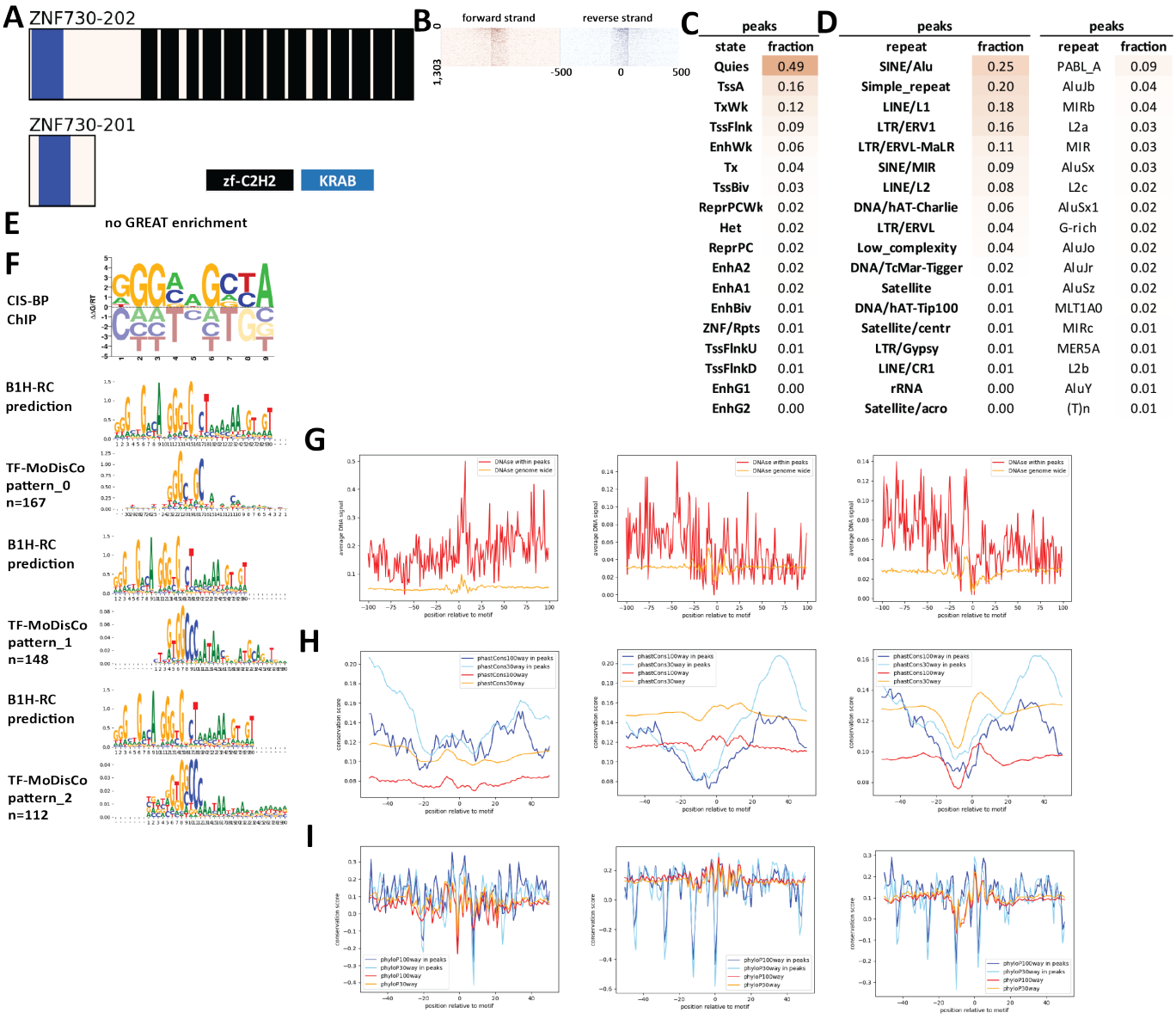

Supplementary Figure 1640: Properties and genomic distribution of motifs identified for the ZNF730 transcription factor in HEK293 (accession ChipExo models).

TF-MoDisCO pattern_0 n=167, CWM

pattern_0, n=167; subpattern_0, ns=46

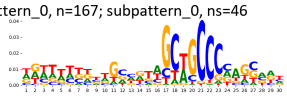

pattern_0, n=167; subpattern_1, ns=40

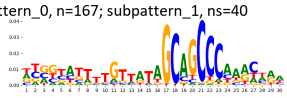

pattern_0, n=167; subpattern_2, ns=28

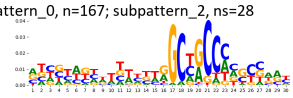

pattern_0, n=167; subpattern_3, ns=27

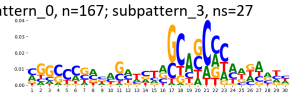

pattern_0, n=167; subpattern_4, ns=24

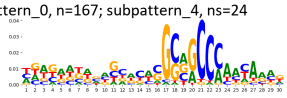

pattern_0, n=167; subpattern_5, ns=2

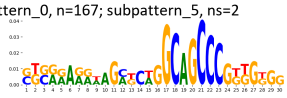

TF-MoDisCO pattern_0 n=167, PWM

pattern_0, n=167; subpattern_0, ns=46

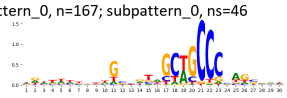

pattern_0, n=167; subpattern_1, ns=40

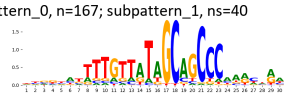

pattern_0, n=167; subpattern_2, ns=28

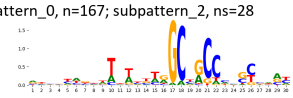

pattern_0, n=167; subpattern_3, ns=27

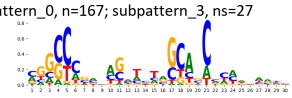

pattern_0, n=167; subpattern_4, ns=24

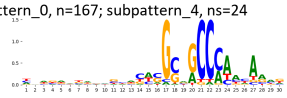

pattern_0, n=167; subpattern_5, ns=2

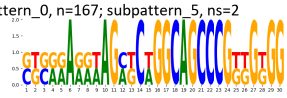

TF-MoDisCO pattern_1 n=148, CWM

pattern_1, n=148; subpattern_0, ns=50

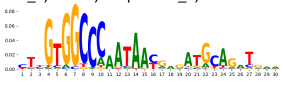

pattern_1, n=148; subpattern_1, ns=49

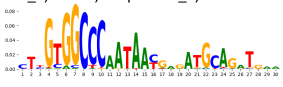

pattern_1, n=148; subpattern_2, ns=23

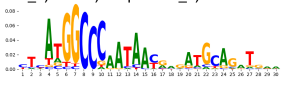

pattern_1, n=148; subpattern_3, ns=17

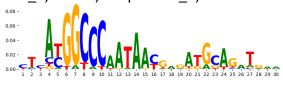

pattern_1, n=148; subpattern_4, ns=9

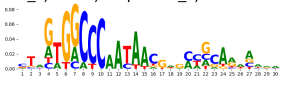

TF-MoDisCO pattern_1 n=148, PWM

pattern_1, n=148; subpattern_0, ns=50

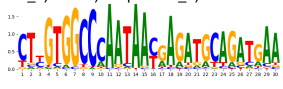

pattern_1, n=148; subpattern_1, ns=49

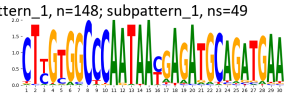

pattern_1, n=148; subpattern_2, ns=23

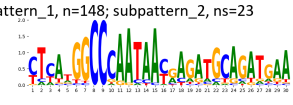

pattern_1, n=148; subpattern_3, ns=17

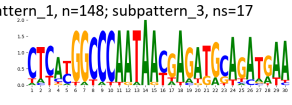

pattern_1, n=148; subpattern_4, ns=9

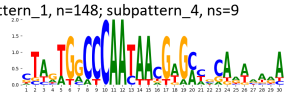

TF-MoDisCO pattern_2 n=112, CWM

pattern_2, n=112; subpattern_0, ns=26

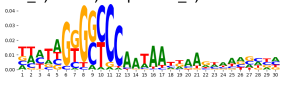

pattern_2, n=112; subpattern_1, ns=25

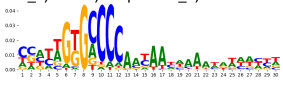

pattern_2, n=112; subpattern_2, ns=22

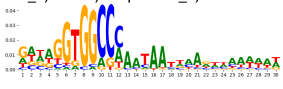

pattern_2, n=112; subpattern_3, ns=20

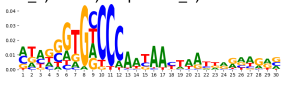

pattern_2, n=112; subpattern_4, ns=19

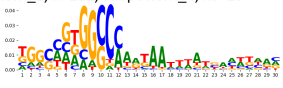

TF-MoDisCO pattern_2 n=112, PWM

pattern_2, n=112; subpattern_0, ns=26

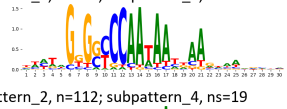

pattern_2, n=112; subpattern_1, ns=25

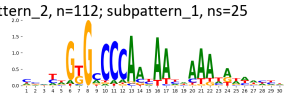

pattern_2, n=112; subpattern_2, ns=22

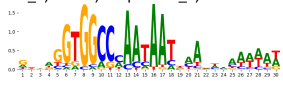

pattern_2, n=112; subpattern_3, ns=20

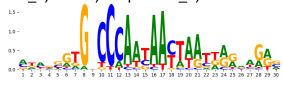

pattern_2, n=112; subpattern_4, ns=19

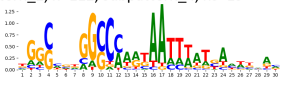

Supplementary Figure 1641: TF-MoDisCO subpatterns for the ZNF730 transcription factor in HEK293 (accession ChipExo models).

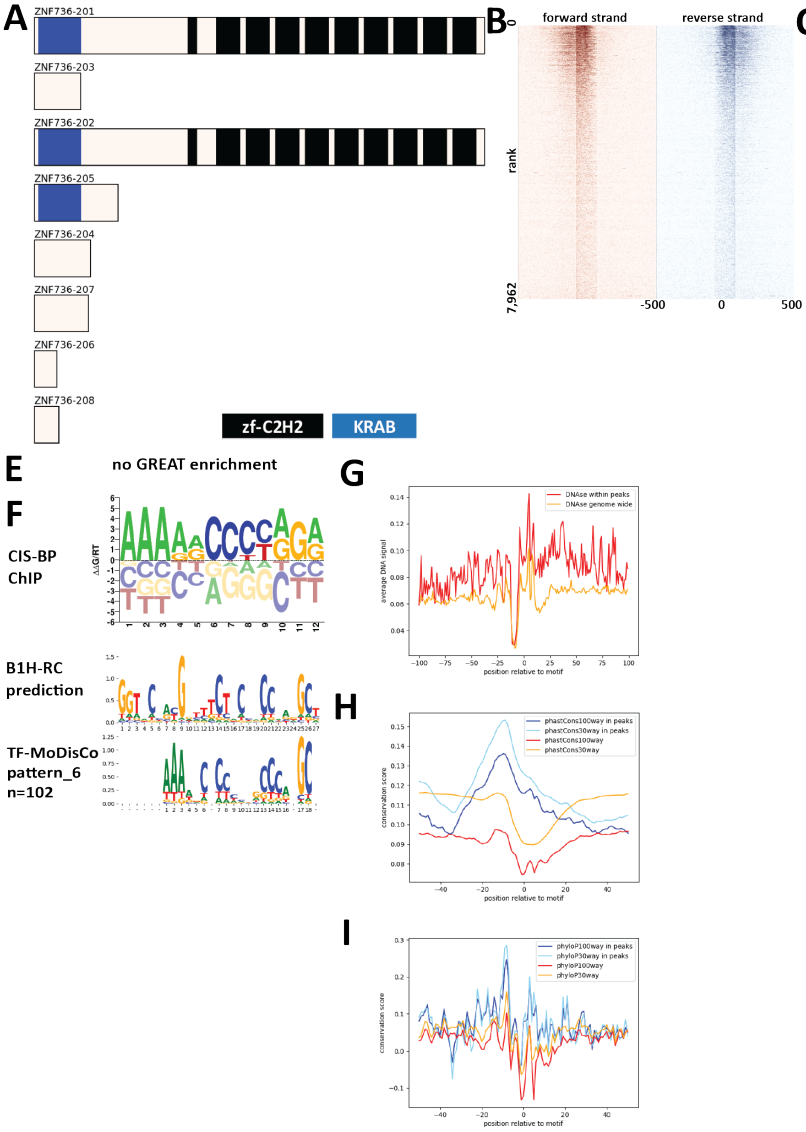

C

peaks	
state	fraction
Quies	0.49
TssA	0.13
TxWk	0.10
TssFlnk	0.07
EnhWk	0.07
Het	0.03
Tx	0.03
ReprPCWk	0.02
TssBiv	0.02
EnhA1	0.02
EnhA2	0.02
ReprPC	0.02
TssFlnkU	0.01
TssFlnkD	0.01
ZNF/Rpts	0.00
EnhBiv	0.00
EnhG1	0.00
EnhG2	0.00

D

peaks		peaks	
repeat	fraction	repeat	fraction
LTR/ERV1	0.39	MER52A	0.08
Simple_repeat	0.15	MIRb	0.03
SINE/Alu	0.12	MER52D	0.03
LINE/L1	0.12	MER52C	0.02
LTR/ERVL-MaLR	0.09	L2a	0.02
SINE/MIR	0.08	LTR28C	0.02
LINE/L2	0.06	MIR	0.02
DNA/hAT-Charlie	0.04	LTR1D	0.02
Low_complexity	0.03	G-rich	0.02
LTR/ERVL	0.03	L2c	0.02
DNA/TcMar-Tigger	0.01	LTR28B	0.02
LTR/ERVK	0.01	MIRc	0.01
DNA/hAT-Tip100	0.01	LTR1D1	0.01
LINE/CR1	0.01	AluJb	0.01
DNA/hAT-Blackjack	0.00	LTR27E	0.01
LTR/Gypsy	0.00	LTR2752	0.01
LINE/RTE-X	0.00	AluY	0.01
Satellite/centr	0.00	LTR27D	0.01

Supplementary Figure 1642: Properties and genomic distribution of motifs identified for the ZNF736 transcription factor in HEK293 (accession ChipExo models).

TF-MoDisCO pattern_6 n=102, CWM

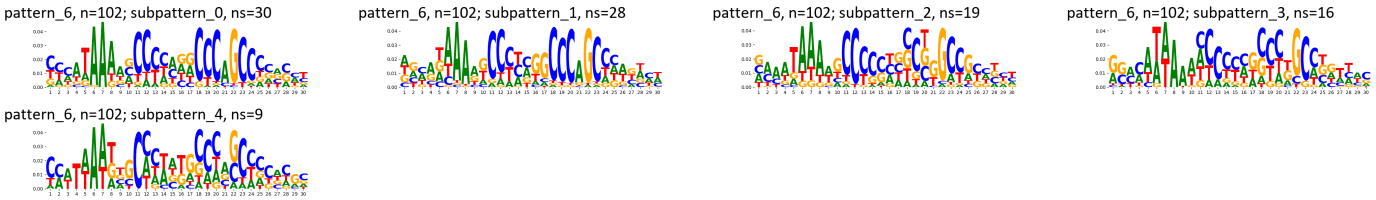

TF-MoDisCO pattern_6 n=102, PWM

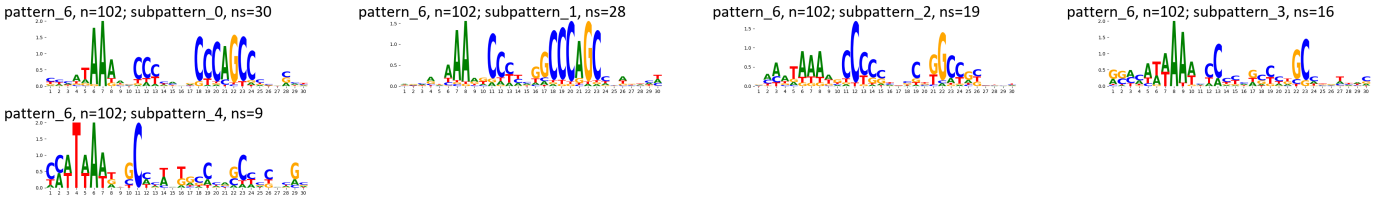

Supplementary Figure 1643: TF-MoDisCO subpatterns for the ZNF736 transcription factor in HEK293 (accession ChipExo models).

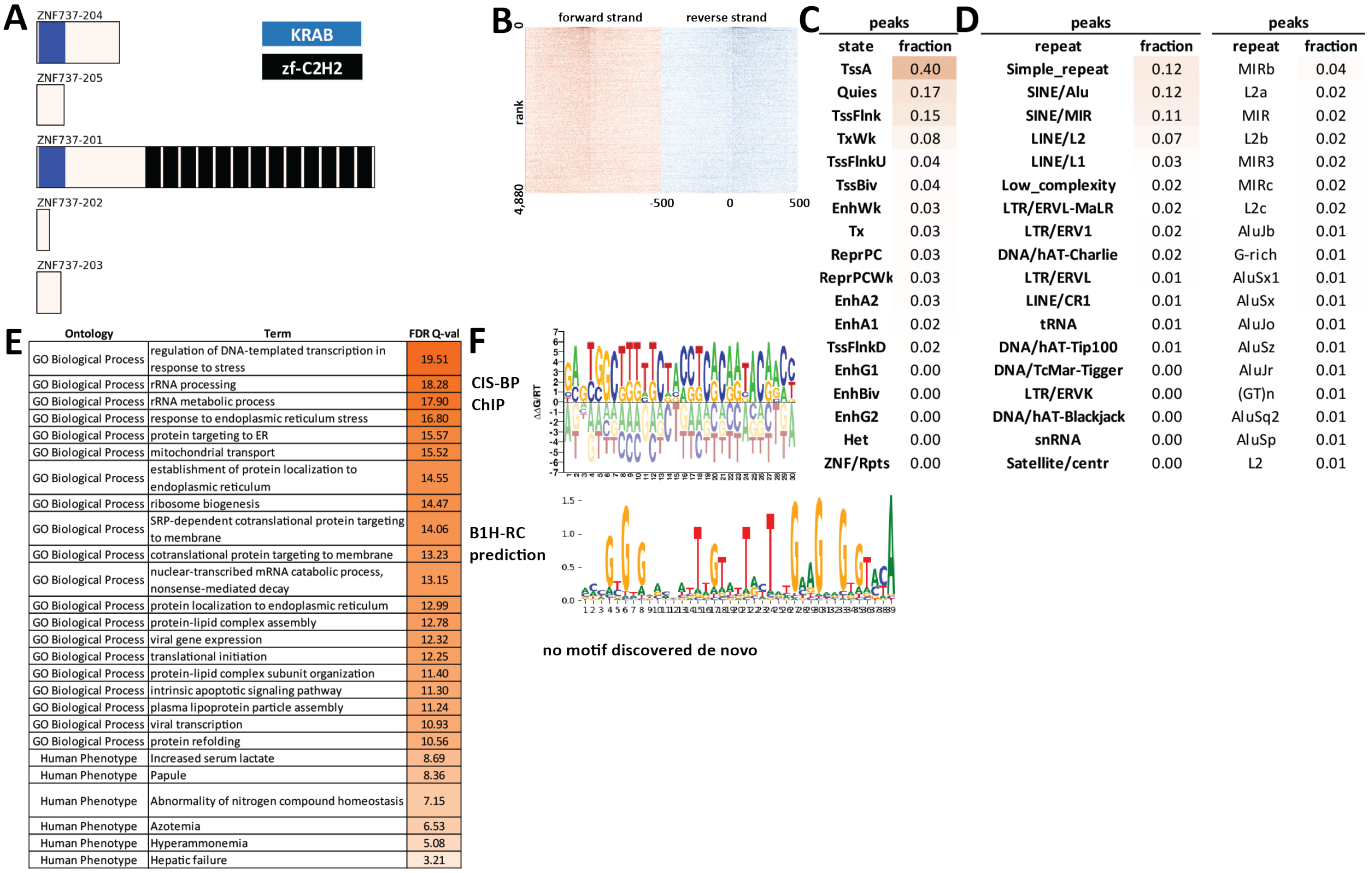

Supplementary Figure 1644: Properties and genomic distribution of motifs identified for the ZNF737 transcription factor in HepG2 (accession ENCSR127IHN).

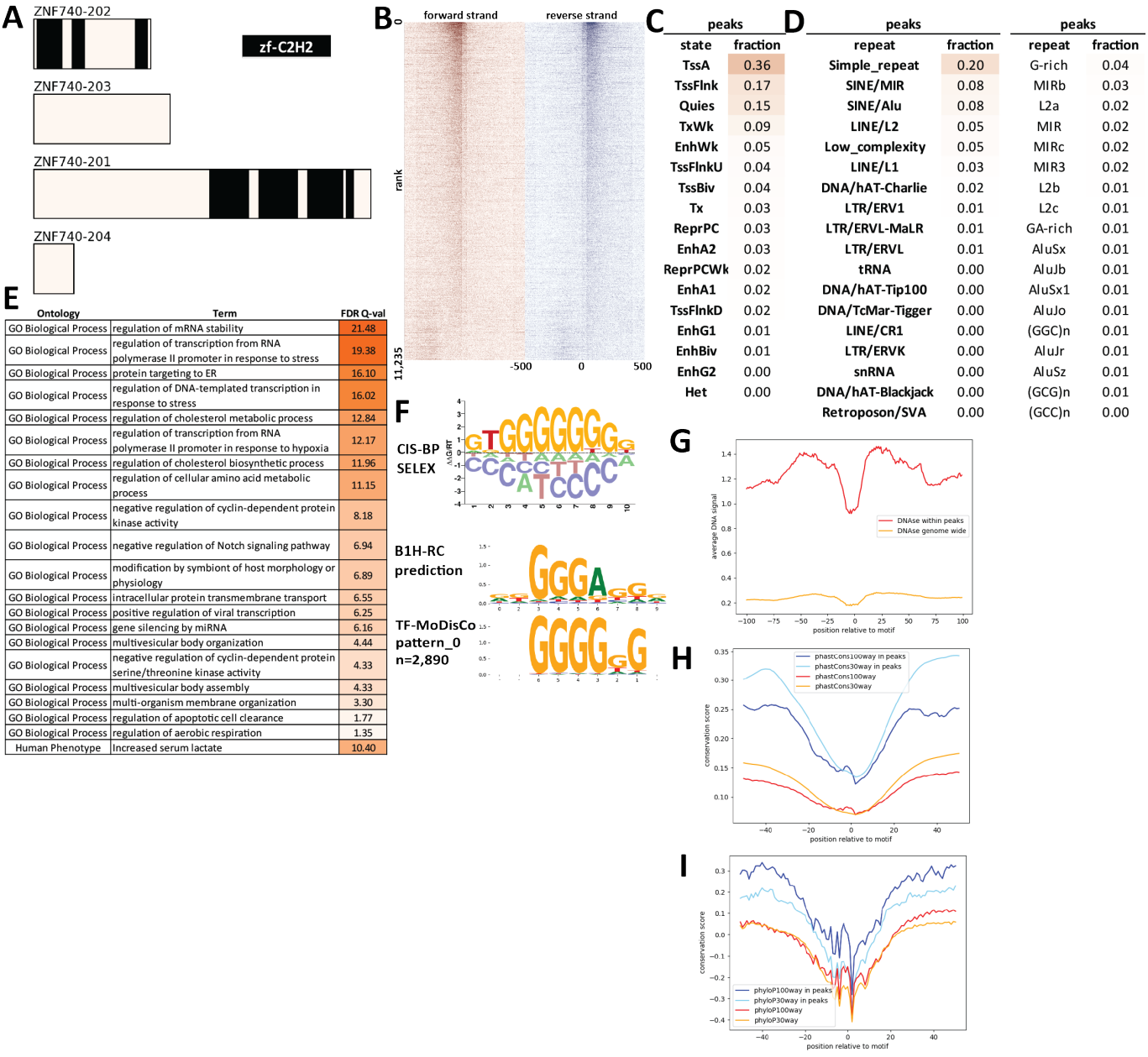

peaks	
state	fraction
TssA	0.36
TssFlnk	0.17
Quies	0.15
TxWk	0.09
EnhWk	0.05
TssFlnkU	0.04
TssBiv	0.04
Tx	0.03
ReprPC	0.03
EnhA2	0.03
ReprPCWk	0.02
EnhA1	0.02
TssFlnkD	0.02
EnhG1	0.01
EnhBiv	0.01
EnhG2	0.00
Het	0.00

peaks		peaks	
repeat	fraction	repeat	fraction
Simple_repeat	0.20	G-rich	0.04
SINE/MIR	0.08	MIRb	0.03
SINE/Alu	0.08	L2a	0.02
LINE/L2	0.05	MIR	0.02
Low_complexity	0.05	MIRc	0.02
LINE/L1	0.03	MIR3	0.02
DNA/hAT-Charlie	0.02	L2b	0.01
LTR/ERV1	0.01	L2c	0.01
LTR/ERVL-MaLR	0.01	GA-rich	0.01
LTR/ERVL	0.01	AluSx	0.01
tRNA	0.00	AluJb	0.01
DNA/hAT-Tip100	0.00	AluSx1	0.01
DNA/TcMar-Tigger	0.00	AluJo	0.01
LINE/CR1	0.00	(GGC)n	0.01
LTR/ERVK	0.00	AluJr	0.01
snRNA	0.00	AluSz	0.01
DNA/hAT-Blackjack	0.00	(GCG)n	0.01
Retroposon/SVA	0.00	(GCC)n	0.00

Ontology	Term	FDR Q-val
GO Biological Process	regulation of mRNA stability	21.48
GO Biological Process	regulation of transcription from RNA polymerase II promoter in response to stress	19.38
GO Biological Process	protein targeting to ER	16.10
GO Biological Process	regulation of DNA-templated transcription in response to stress	16.02
GO Biological Process	regulation of cholesterol metabolic process	12.84
GO Biological Process	regulation of transcription from RNA polymerase II promoter in response to hypoxia	12.17
GO Biological Process	regulation of cholesterol biosynthetic process	11.96
GO Biological Process	regulation of cellular amino acid metabolic process	11.15
GO Biological Process	negative regulation of cyclin-dependent protein kinase activity	8.18
GO Biological Process	negative regulation of Notch signaling pathway	6.94
GO Biological Process	modification by symbiont of host morphology or physiology	6.89
GO Biological Process	intracellular protein transmembrane transport	6.55
GO Biological Process	positive regulation of viral transcription	6.25
GO Biological Process	gene silencing by miRNA	6.16
GO Biological Process	multivesicular body organization	4.44
GO Biological Process	negative regulation of cyclin-dependent protein serine/threonine kinase activity	4.33
GO Biological Process	multivesicular body assembly	4.33
GO Biological Process	multi-organism membrane organization	3.30
GO Biological Process	regulation of apoptotic cell clearance	1.77
GO Biological Process	regulation of aerobic respiration	1.35
Human Phenotype	Increased serum lactate	10.40

Supplementary Figure 1645: Properties and genomic distribution of motifs identified for the ZNF740 transcription factor in HepG2 (accession ENCSR755ZAY).

TF-MoDisCO pattern_0 n=2890, CWM

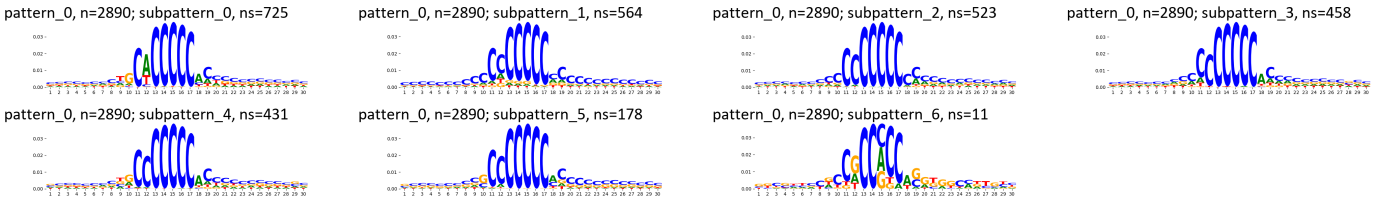

TF-MoDisCO pattern_0 n=2890, PWM

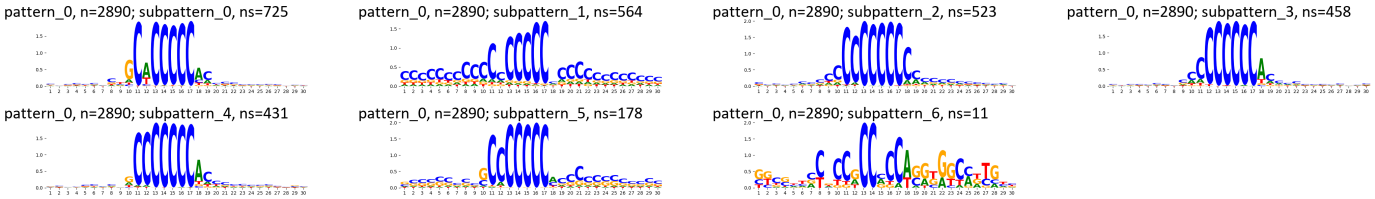

Supplementary Figure 1646: TF-MoDisCO subpatterns for the ZNF740 transcription factor in HepG2 (accession ENCSR755ZAY).

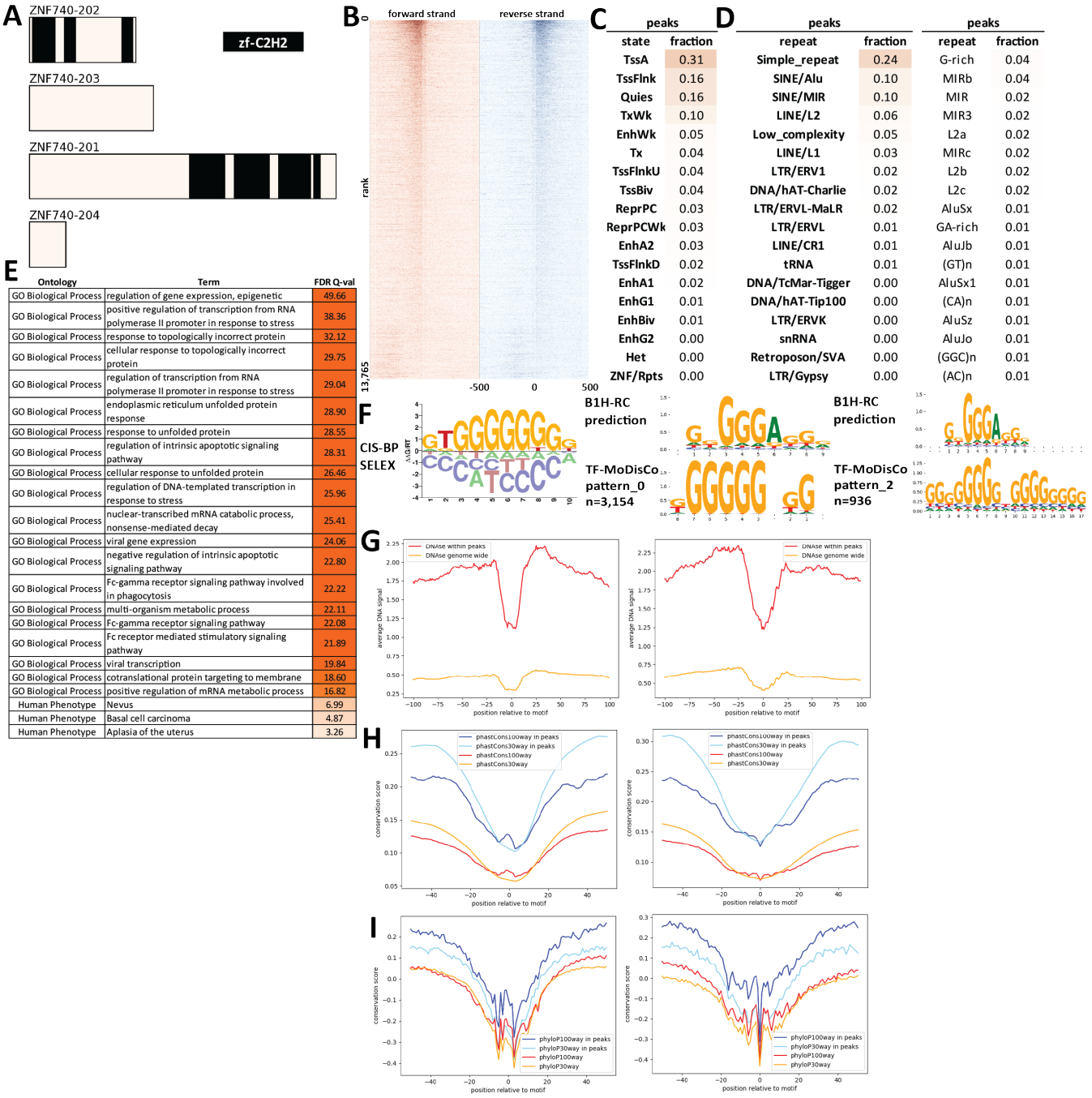

Supplementary Figure 1647: Properties and genomic distribution of motifs identified for the ZNF740 transcription factor in K562 (accession ENCSR427XYP).

TF-MoDisCO pattern_0 n=3154, CWM

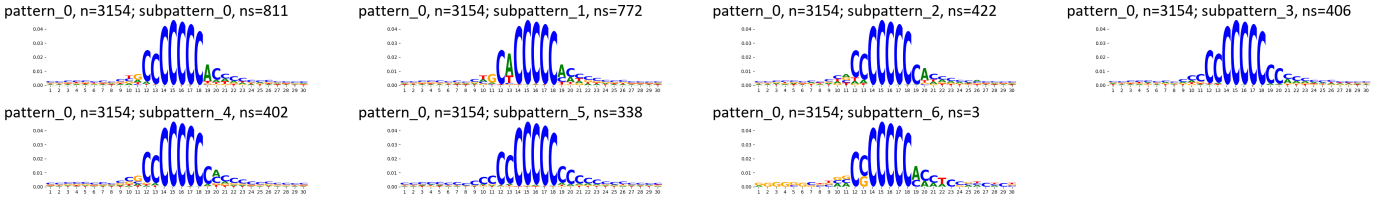

TF-MoDisCO pattern_0 n=3154, PWM

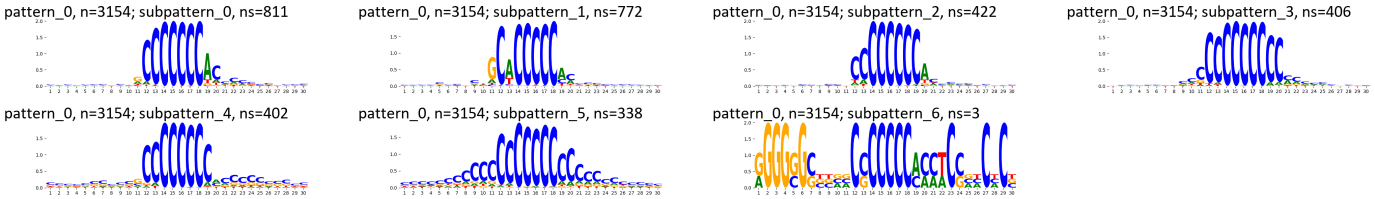

TF-MoDisCO pattern_2 n=936, CWM

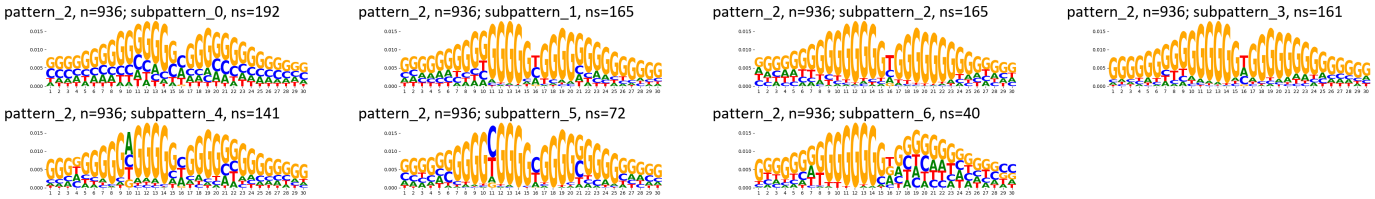

TF-MoDisCO pattern_2 n=936, PWM

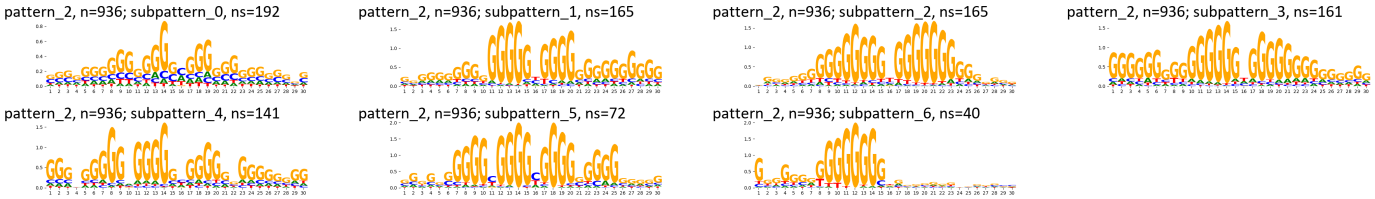

Supplementary Figure 1648: TF-MoDisCO subpatterns for the ZNF740 transcription factor in K562 (accession ENCSR427XYP).

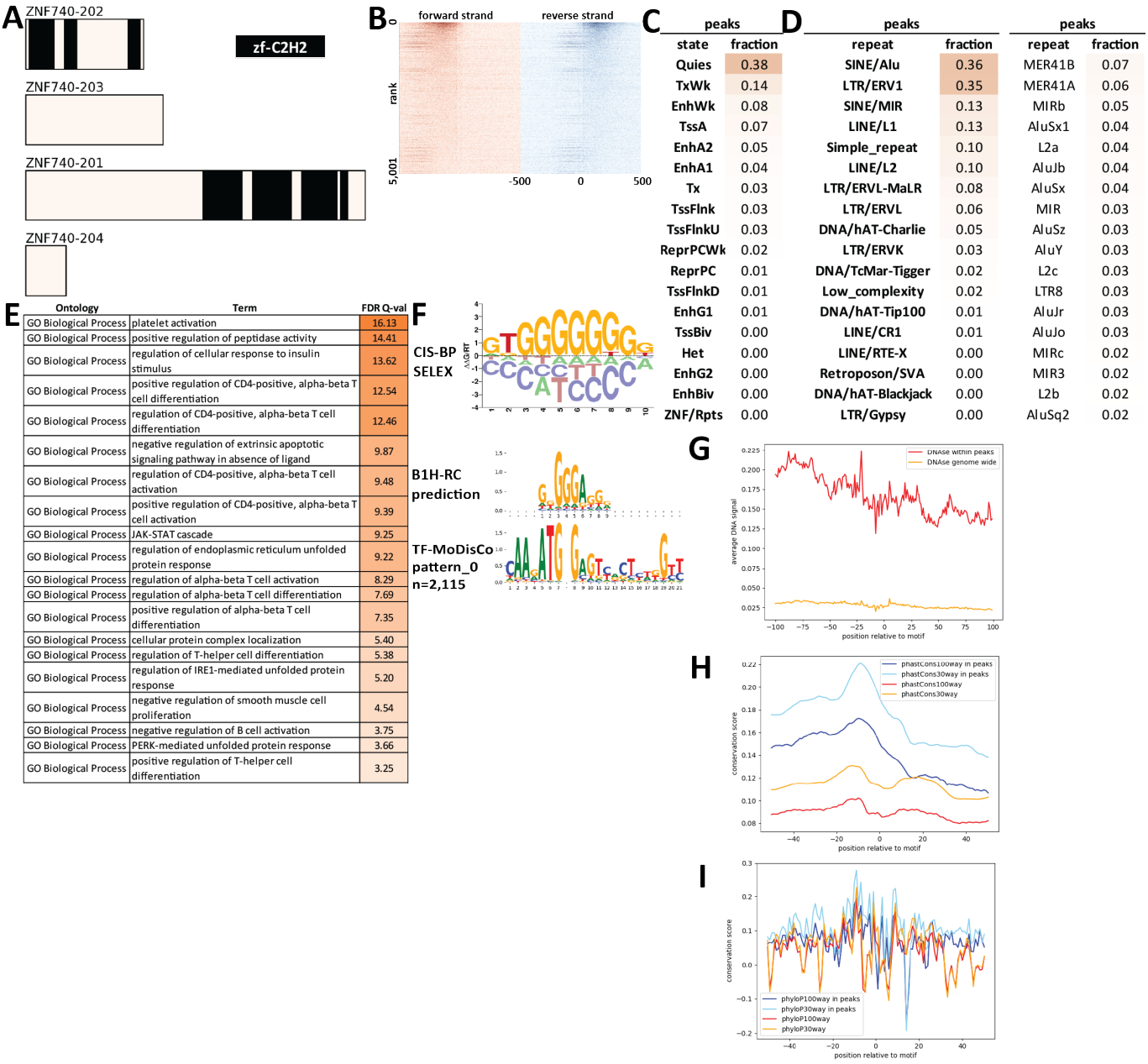

peaks	
state	fraction
Quies	0.38
TxWk	0.14
EnhWk	0.08
TssA	0.07
EnhA2	0.05
EnhA1	0.04
Tx	0.03
TssFlnk	0.03
TssFlnkU	0.03
ReprPCWk	0.02
ReprPC	0.01
TssFlnkD	0.01
EnhG1	0.01
TssBiv	0.00
Het	0.00
EnhG2	0.00
EnhBiv	0.00
ZNF/Rpts	0.00

peaks	
repeat	fraction
SINE/Alu	0.36
LTR/ERV1	0.35
SINE/MIR	0.13
LINE/L1	0.13
Simple_repeat	0.10
LINE/L2	0.10
LTR/ERVL-MaLR	0.08
LTR/ERVL	0.06
DNA/hAT-Charlie	0.05
LTR/ERVK	0.03
DNA/TcMar-Tigger	0.02
Low_complexity	0.02
DNA/hAT-Tip100	0.01
LINE/CR1	0.01
LINE/RTE-X	0.00
Retroposon/SVA	0.00
DNA/hAT-Blackjack	0.00
LTR/Gypsy	0.00

peaks	
repeat	fraction
MER41B	0.07
MER41A	0.06
MIRb	0.05
AluSx1	0.04
L2a	0.04
AluJb	0.04
AluSx	0.04
MIR	0.03
AluSz	0.03
AluY	0.03
L2c	0.03
LTR8	0.03
AluJr	0.03
AluJo	0.03
MIRc	0.02
MIR3	0.02
L2b	0.02
AluSq2	0.02

Ontology	Term	FDR Q-val
GO Biological Process	platelet activation	16.13
GO Biological Process	positive regulation of peptidase activity	14.41
GO Biological Process	regulation of cellular response to insulin stimulus	13.62
GO Biological Process	positive regulation of CD4-positive, alpha-beta T cell differentiation	12.54
GO Biological Process	regulation of CD4-positive, alpha-beta T cell differentiation	12.46
GO Biological Process	negative regulation of extrinsic apoptotic signaling pathway in absence of ligand	9.87
GO Biological Process	regulation of CD4-positive, alpha-beta T cell activation	9.48
GO Biological Process	positive regulation of CD4-positive, alpha-beta T cell activation	9.39
GO Biological Process	JAK-STAT cascade	9.25
GO Biological Process	regulation of endoplasmic reticulum unfolded protein response	9.22
GO Biological Process	regulation of alpha-beta T cell activation	8.29
GO Biological Process	regulation of alpha-beta T cell differentiation	7.69
GO Biological Process	positive regulation of alpha-beta T cell differentiation	7.35
GO Biological Process	cellular protein complex localization	5.40
GO Biological Process	regulation of T-helper cell differentiation	5.38
GO Biological Process	regulation of IRE1-mediated unfolded protein response	5.20
GO Biological Process	negative regulation of smooth muscle cell proliferation	4.54
GO Biological Process	negative regulation of B cell activation	3.75
GO Biological Process	PERK-mediated unfolded protein response	3.66
GO Biological Process	positive regulation of T-helper cell differentiation	3.25

Supplementary Figure 1649: Properties and genomic distribution of motifs identified for the ZNF740 transcription factor in K562 (accession ENCSR532EMP).

TF-MoDisCO pattern_0 n=2115, CWM

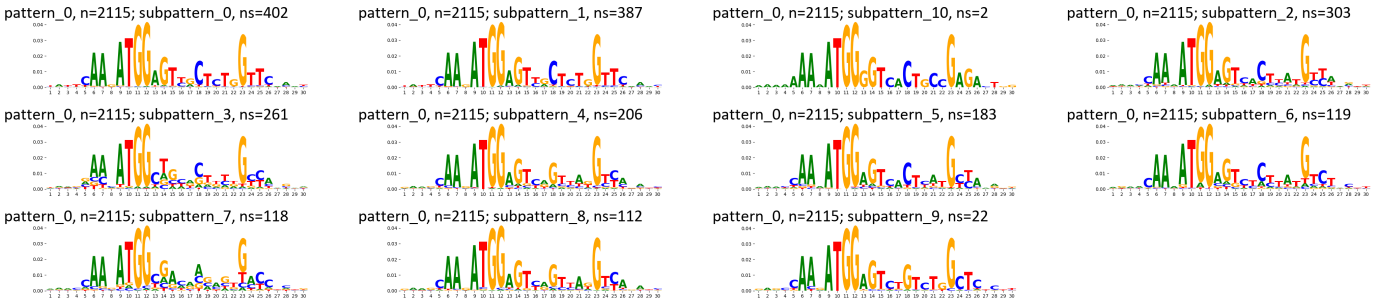

TF-MoDisCO pattern_0 n=2115, PWM

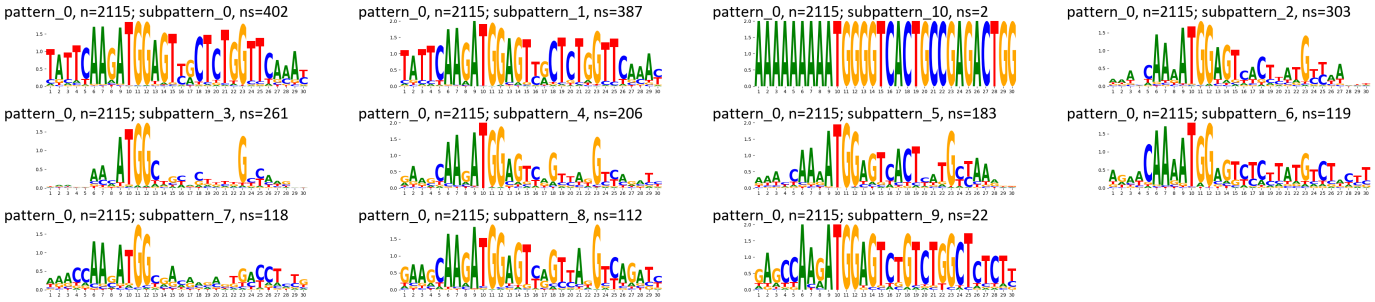

Supplementary Figure 1650: TF-MoDisCO subpatterns for the ZNF740 transcription factor in K562 (accession ENCSR532EMP).

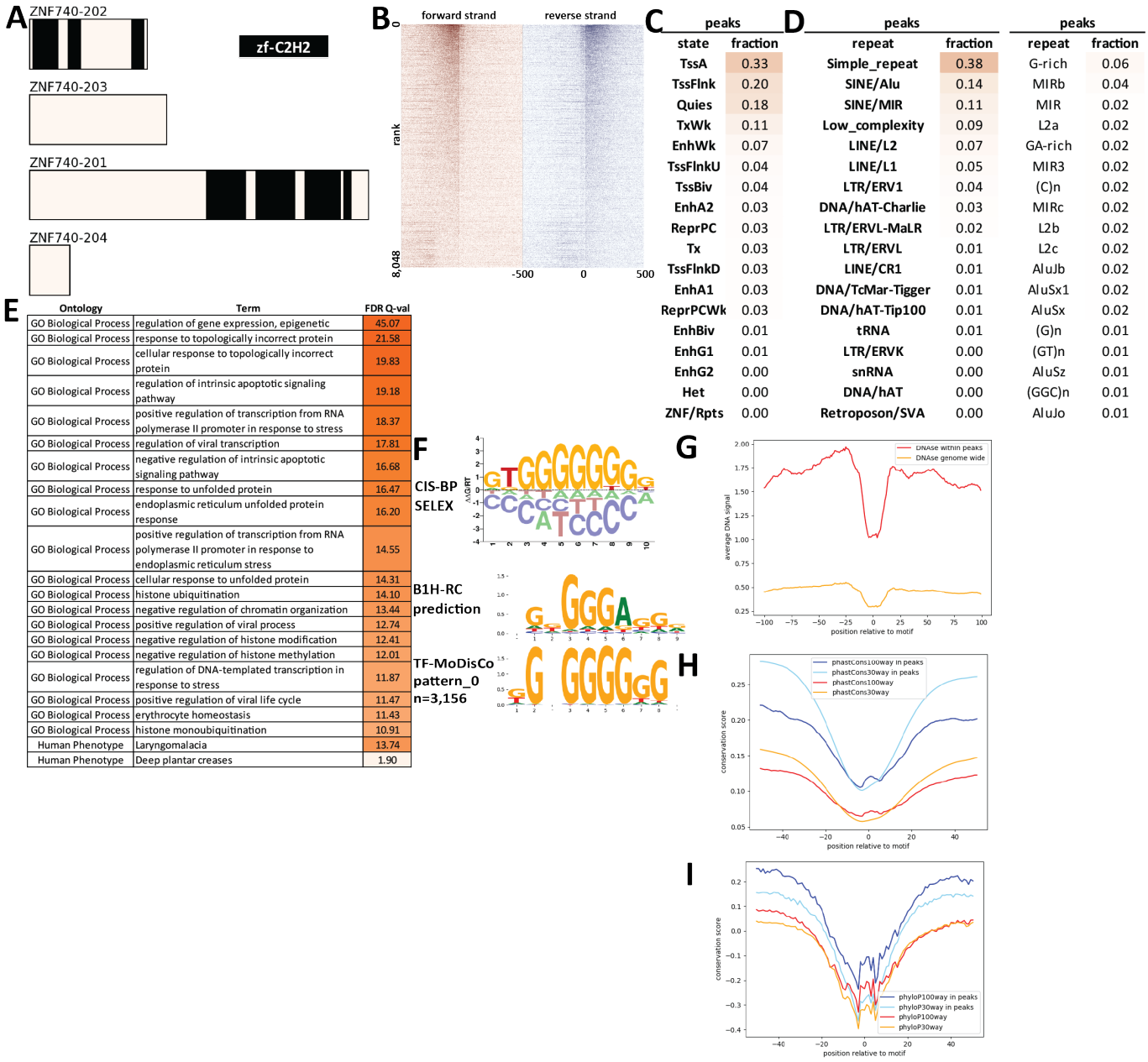

Supplementary Figure 1651: Properties and genomic distribution of motifs identified for the ZNF740 transcription factor in K562 (accession ENCSR737UST).

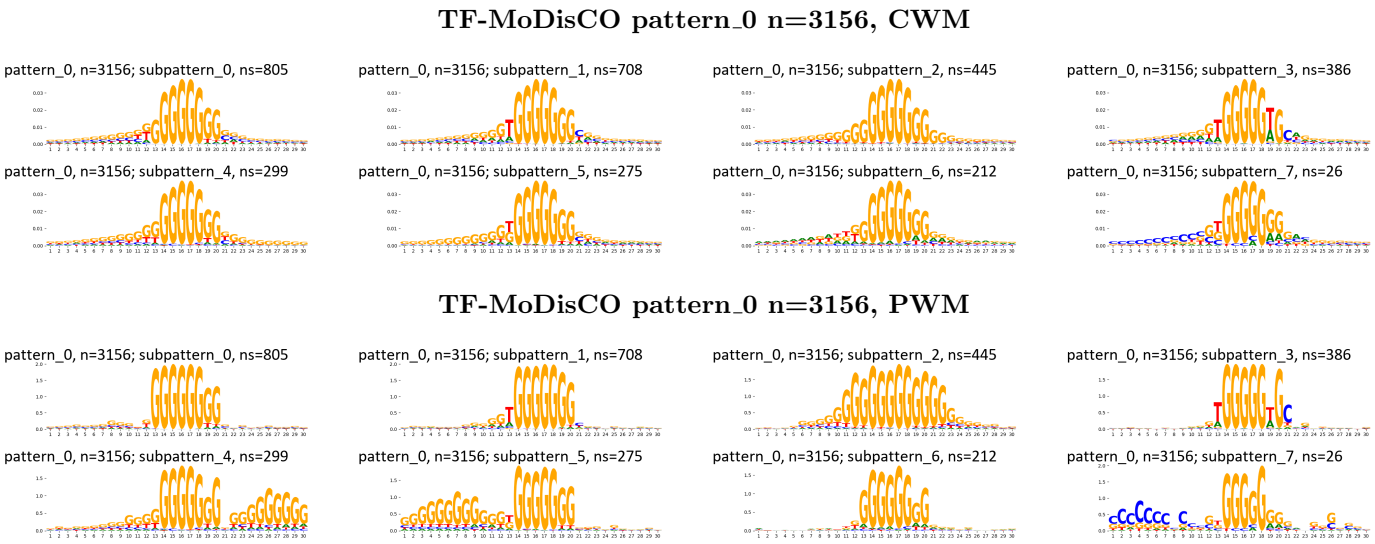

Supplementary Figure 1652: TF-MoDisCO subpatterns for the ZNF740 transcription factor in K562 (accession ENCSR737UST).

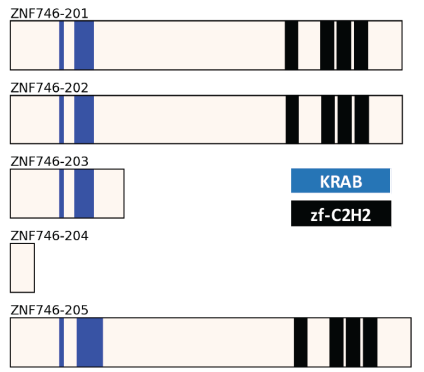

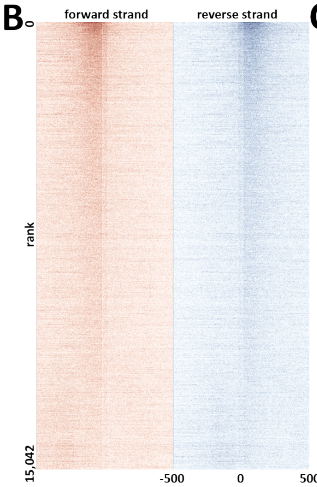

C

peaks	
state	fraction
TssA	0.33
Quies	0.17
TssFlnk	0.16
TxWk	0.09
EnhWk	0.06
TssFlnkU	0.04
EnhA1	0.03
TssBiv	0.03
EnhA2	0.03
ReprPC	0.03
Tx	0.02
TssFlnkD	0.02
ReprPCWk	0.02
EnhBiv	0.01
EnhG1	0.01
EnhG2	0.00
Het	0.00
ZNF/Rpts	0.00

D

peaks		peaks	
repeat	fraction	repeat	fraction
Simple_repeat	0.21	MIRb	0.04
SINE/Alu	0.14	G-rich	0.04
SINE/MIR	0.11	L2a	0.02
LINE/L2	0.07	MIR3	0.02
Low_complexity	0.05	MIR	0.02
LINE/L1	0.03	MIRc	0.02
DNA/hAT-Charlie	0.02	L2b	0.02
LTR/ERV1	0.02	AluJb	0.02
LTR/ERVL-MaLR	0.02	L2c	0.02
LTR/ERVL	0.01	AluSx1	0.02
LINE/CR1	0.01	AluSx	0.02
DNA/hAT-Tip100	0.01	AluSz	0.01
DNA/TcMar-Tigger	0.01	GA-rich	0.01
tRNA	0.00	AluJr	0.01
LTR/ERVK	0.00	AluJo	0.01
DNA/hAT-Blackjack	0.00	AluY	0.01
DNA/hAT	0.00	(GGC)n	0.01
LINE/RTE-BovB	0.00	AluSq2	0.01

E

Ontology	Term	FDR Q-val
GO Biological Process	regulation of intrinsic apoptotic signaling pathway	40.33
GO Biological Process	regulation of transcription from RNA polymerase II promoter in response to stress	36.59
GO Biological Process	endoplasmic reticulum unfolded protein response	36.03
GO Biological Process	liver regeneration	35.42
GO Biological Process	cellular response to topologically incorrect protein	35.39
GO Biological Process	nuclear-transcribed mRNA catabolic process	35.14
GO Biological Process	mRNA catabolic process	34.59
GO Biological Process	positive regulation of transcription from RNA polymerase II promoter in response to stress	33.74
GO Biological Process	response to topologically incorrect protein	32.53
GO Biological Process	regulation of DNA-templated transcription in response to stress	32.18
GO Biological Process	cellular response to unfolded protein	32.03
GO Biological Process	negative regulation of intrinsic apoptotic signaling pathway	32.00
GO Biological Process	response to unfolded protein	28.26
GO Biological Process	nuclear-transcribed mRNA catabolic process, nonsense-mediated decay	28.06
GO Biological Process	cellular response to epidermal growth factor stimulus	26.09
GO Biological Process	regulation of endoplasmic reticulum stress-induced intrinsic apoptotic signaling pathway	25.19
GO Biological Process	response to epidermal growth factor	25.00
GO Biological Process	platelet-derived growth factor receptor signaling pathway	22.42
GO Biological Process	negative regulation of response to endoplasmic reticulum stress	21.34
GO Biological Process	nuclear-transcribed mRNA catabolic process, deadenylation-dependent decay	19.64
Human Phenotype	Abnormality of the odontoid process	8.74
Human Phenotype	CNS hypomyelination	7.36
Human Phenotype	Dysphonia	5.84
Human Phenotype	Abnormality of monocarboxylic acid metabolism	3.40

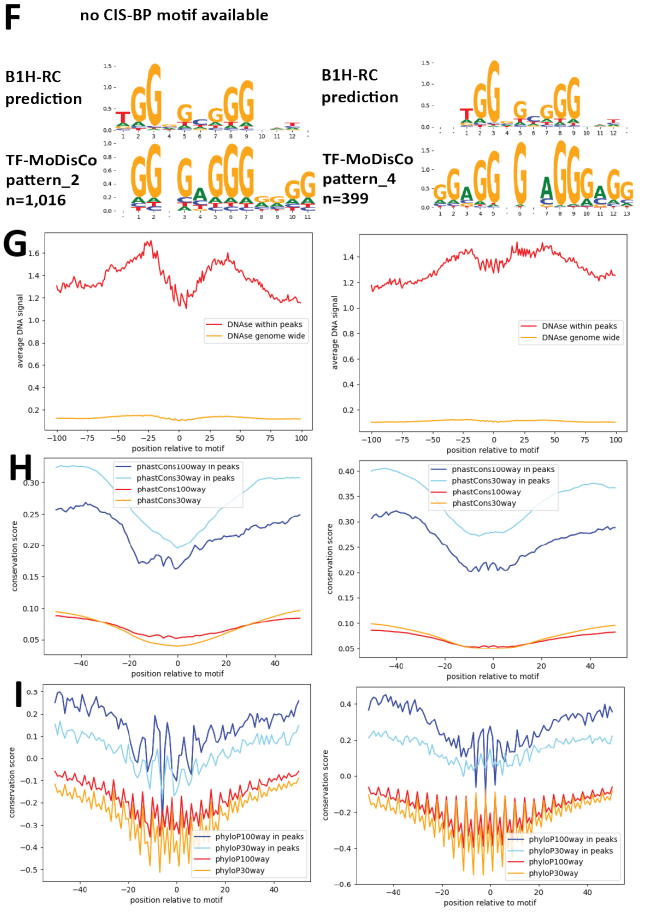

Supplementary Figure 1653: Properties and genomic distribution of motifs identified for the ZNF746 transcription factor in HepG2 (accession ENCSR591MYB).

TF-MoDisCO pattern_2 n=1016, CWM

pattern_2, n=1016; subpattern_0, ns=350

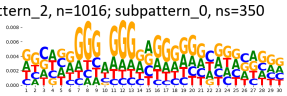

pattern_2, n=1016; subpattern_1, ns=235

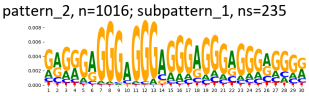

pattern_2, n=1016; subpattern_2, ns=218

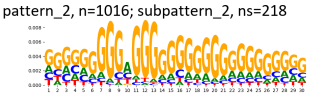

pattern_2, n=1016; subpattern_3, ns=202

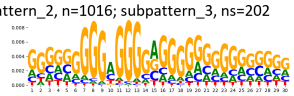

pattern_2, n=1016; subpattern_4, ns=6

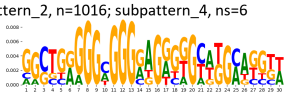

pattern_2, n=1016; subpattern_5, ns=5

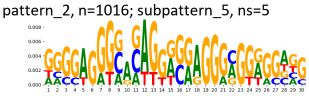

TF-MoDisCO pattern_2 n=1016, PWM

pattern_2, n=1016; subpattern_0, ns=350

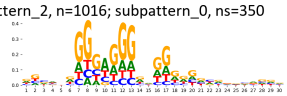

pattern_2, n=1016; subpattern_1, ns=235

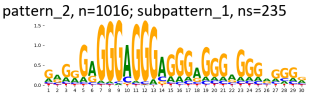

pattern_2, n=1016; subpattern_2, ns=218

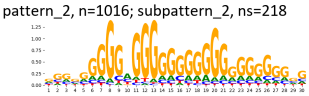

pattern_2, n=1016; subpattern_3, ns=202

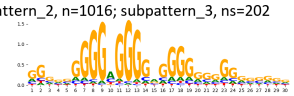

pattern_2, n=1016; subpattern_4, ns=6

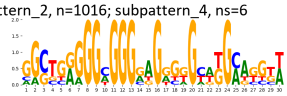

pattern_2, n=1016; subpattern_5, ns=5

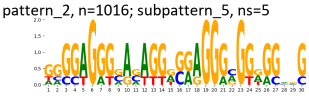

TF-MoDisCO pattern_4 n=399, CWM

pattern_4, n=399; subpattern_0, ns=111

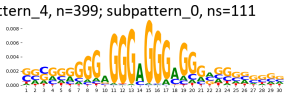

pattern_4, n=399; subpattern_1, ns=101

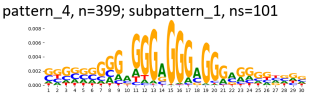

pattern_4, n=399; subpattern_2, ns=68

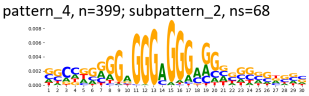

pattern_4, n=399; subpattern_3, ns=52

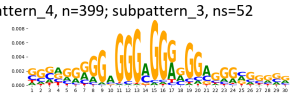

pattern_4, n=399; subpattern_4, ns=42

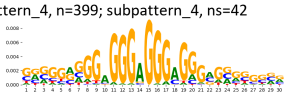

pattern_4, n=399; subpattern_5, ns=10

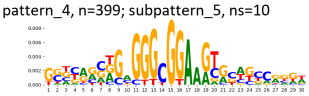

pattern_4, n=399; subpattern_6, ns=10

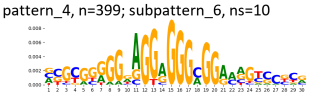

pattern_4, n=399; subpattern_7, ns=5

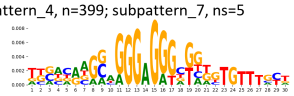

TF-MoDisCO pattern_4 n=399, PWM

pattern_4, n=399; subpattern_0, ns=111

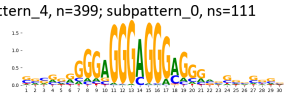

pattern_4, n=399; subpattern_1, ns=101

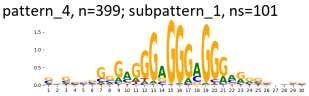

pattern_4, n=399; subpattern_2, ns=68

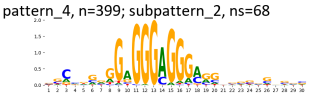

pattern_4, n=399; subpattern_3, ns=52

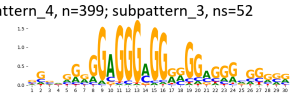

pattern_4, n=399; subpattern_4, ns=42

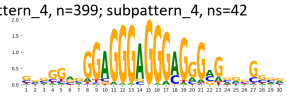

pattern_4, n=399; subpattern_5, ns=10

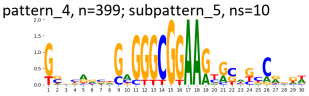

pattern_4, n=399; subpattern_6, ns=10

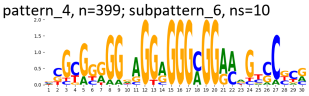

pattern_4, n=399; subpattern_7, ns=5

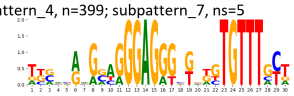

Supplementary Figure 1654: TF-MoDisCO subpatterns for the ZNF746 transcription factor in HepG2 (accession ENCSR591MYB).

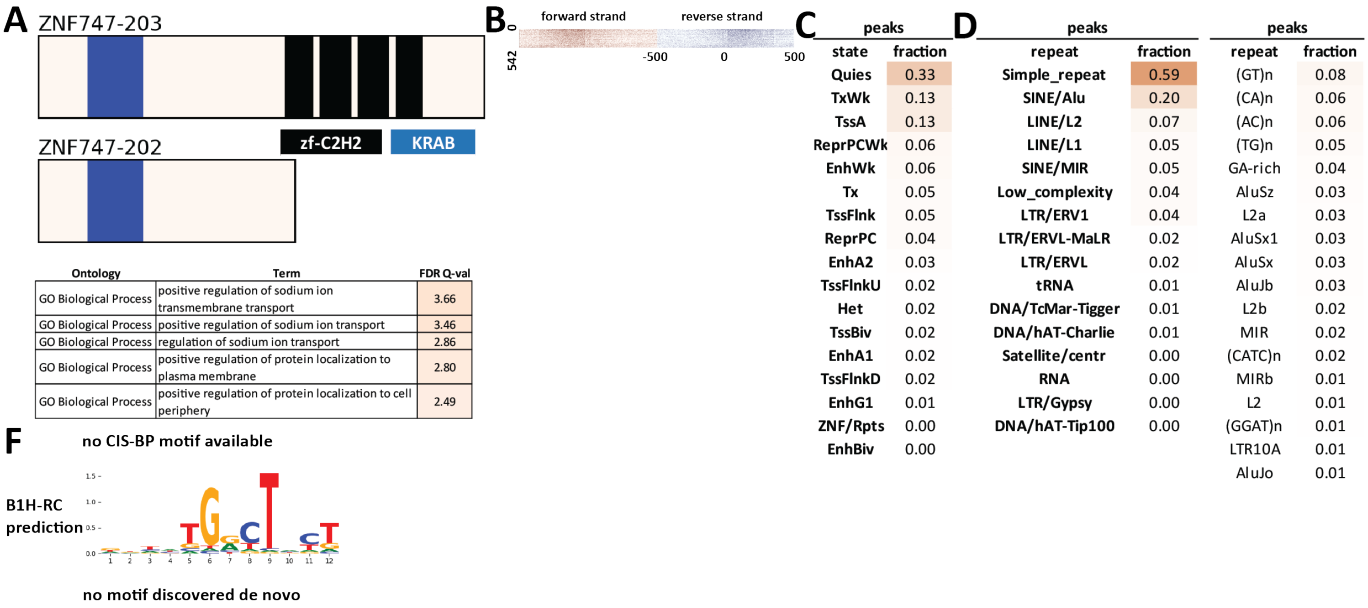

Ontology	Term	FDR Q-val
GO Biological Process	positive regulation of sodium ion transmembrane transport	3.66
GO Biological Process	positive regulation of sodium ion transport	3.46
GO Biological Process	regulation of sodium ion transport	2.86
GO Biological Process	positive regulation of protein localization to plasma membrane	2.80
GO Biological Process	positive regulation of protein localization to cell periphery	2.49

peaks	
state	fraction
Quies	0.33
TxWk	0.13
TssA	0.13
ReprPCWk	0.06
EnhWk	0.06
Tx	0.05
TssFlnk	0.05
ReprPC	0.04
EnhA2	0.03
TssFlnkU	0.02
Het	0.02
TssBiv	0.02
EnhA1	0.02
TssFlnkD	0.02
EnhG1	0.01
ZNF/Rpts	0.00
EnhBiv	0.00

peaks		peaks	
repeat	fraction	repeat	fraction
Simple_repeat	0.59	(GT)n	0.08
SINE/Alu	0.20	(CA)n	0.06
LINE/L2	0.07	(AC)n	0.06
LINE/L1	0.05	(TG)n	0.05
SINE/MIR	0.05	GA-rich	0.04
Low_complexity	0.04	AluSz	0.03
LTR/ERV1	0.04	L2a	0.03
LTR/ERVL-MaLR	0.02	AluSx1	0.03
LTR/ERVL	0.02	AluSx	0.03
tRNA	0.01	AluJb	0.03
DNA/TcMar-Tigger	0.01	L2b	0.02
DNA/hAT-Charlie	0.01	MIR	0.02
Satellite/centr	0.00	(CATC)n	0.02
RNA	0.00	MIRb	0.01
LTR/Gypsy	0.00	L2	0.01
DNA/hAT-Tip100	0.00	(GGAT)n	0.01
		LTR10A	0.01
		AluJo	0.01

Supplementary Figure 1655: Properties and genomic distribution of motifs identified for the ZNF747 transcription factor in HEK293 (accession ENCSR497IAS).

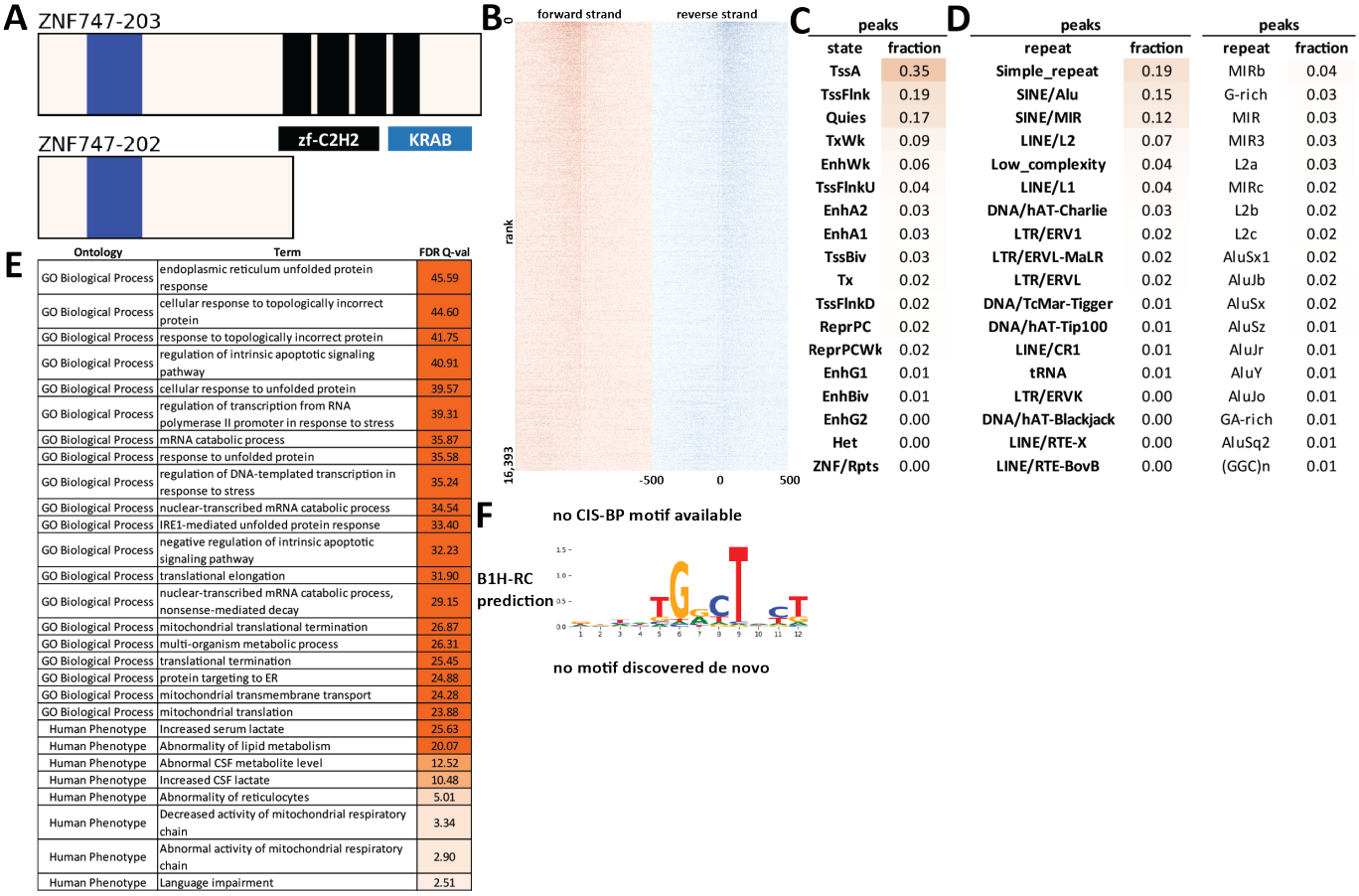

Supplementary Figure 1656: Properties and genomic distribution of motifs identified for the ZNF747 transcription factor in HepG2 (accession ENCSR155IXY).

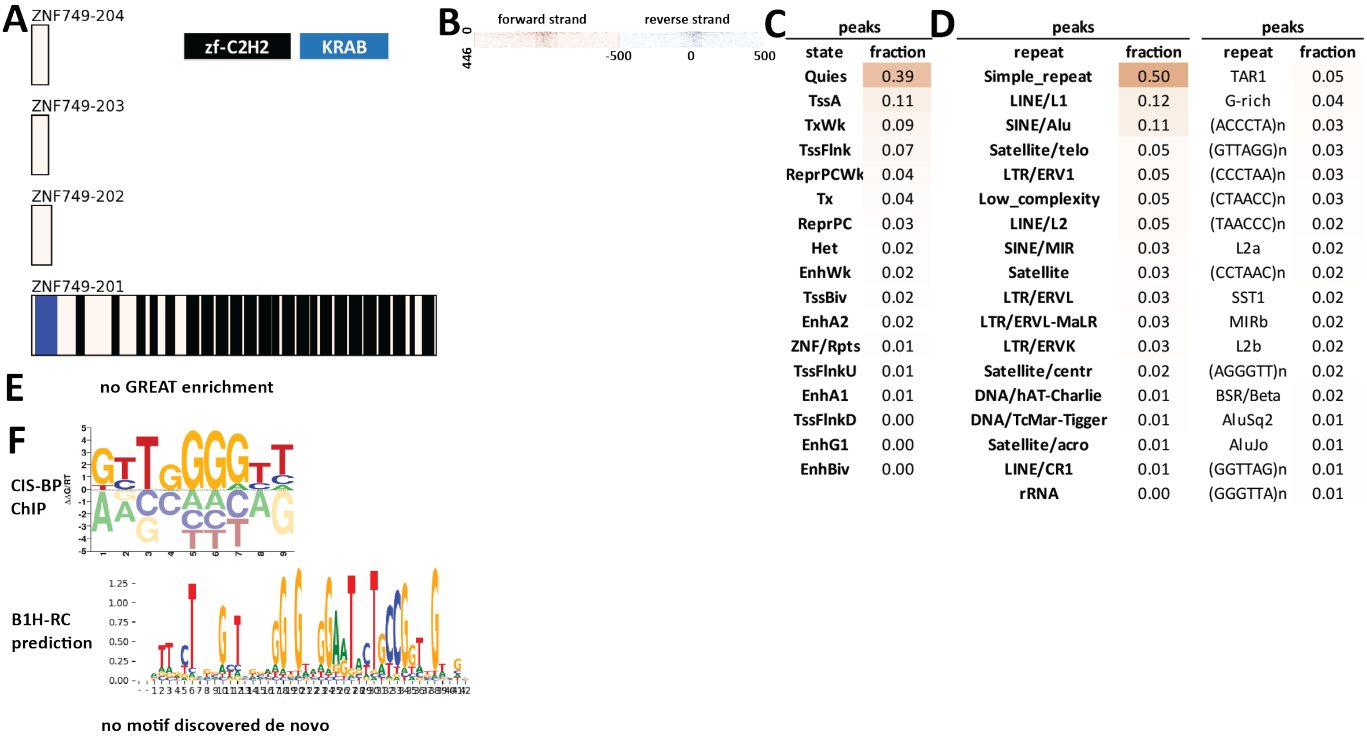

C

peaks	
state	fraction
Quies	0.39
TssA	0.11
TxWk	0.09
TssFlnk	0.07
ReprPCWk	0.04
Tx	0.04
ReprPC	0.03
Het	0.02
EnhWk	0.02
TssBiv	0.02
EnhA2	0.02
ZNF/Rpts	0.01
TssFlnkU	0.01
EnhA1	0.01
TssFlnkD	0.00
EnhG1	0.00
EnhBiv	0.00

D

peaks		peaks	
repeat	fraction	repeat	fraction
Simple_repeat	0.50	TAR1	0.05
LINE/L1	0.12	G-rich	0.04
SINE/Alu	0.11	(ACCCTA)n	0.03
Satellite/telo	0.05	(GTTAGG)n	0.03
LTR/ERV1	0.05	(CCCTAA)n	0.03
Low_complexity	0.05	(CTAACC)n	0.03
LINE/L2	0.05	(TAACCC)n	0.02
SINE/MIR	0.03	L2a	0.02
Satellite	0.03	(CCTAAC)n	0.02
LTR/ERVL	0.03	SST1	0.02
LTR/ERVL-MaLR	0.03	MIRb	0.02
LTR/ERVK	0.03	L2b	0.02
Satellite/centr	0.02	(AGGGTT)n	0.02
DNA/hAT-Charlie	0.01	BSR/Beta	0.02
DNA/TcMar-Tigger	0.01	AluSq2	0.01
Satellite/acro	0.01	AluJo	0.01
LINE/CR1	0.01	(GGTTAG)n	0.01
rRNA	0.00	(GGGTTA)n	0.01

Supplementary Figure 1657: Properties and genomic distribution of motifs identified for the ZNF749 transcription factor in HEK293 (accession ChipExo models).

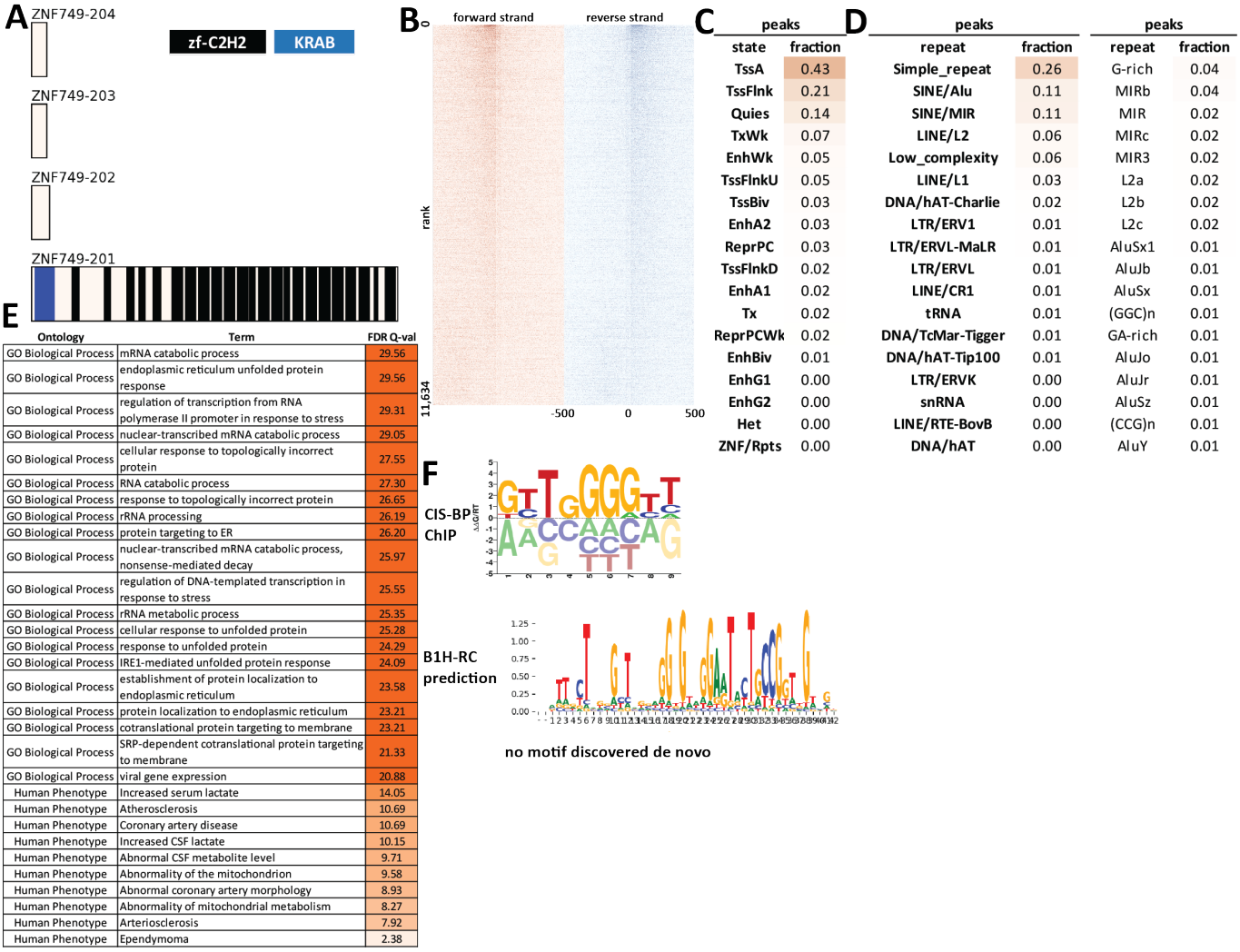

C

peaks	
state	fraction
TssA	0.43
TssFlnk	0.21
Quies	0.14
TxWk	0.07
EnhWk	0.05
TssFlnkU	0.05
TssBiv	0.03
EnhA2	0.03
ReprPC	0.03
TssFlnkD	0.02
EnhA1	0.02
Tx	0.02
ReprPCWk	0.02
EnhBiv	0.01
EnhG1	0.00
EnhG2	0.00
Het	0.00
ZNF/Rpts	0.00

D

peaks		peaks	
repeat	fraction	repeat	fraction
Simple_repeat	0.26	G-rich	0.04
SINE/Alu	0.11	MIRb	0.04
SINE/MIR	0.11	MIR	0.02
LINE/L2	0.06	MIRc	0.02
Low_complexity	0.06	MIR3	0.02
LINE/L1	0.03	L2a	0.02
DNA/hAT-Charlie	0.02	L2b	0.02
LTR/ERV1	0.01	L2c	0.02
LTR/ERVL-MaLR	0.01	AluSx1	0.01
LTR/ERVL	0.01	AluJb	0.01
LINE/CR1	0.01	AluSx	0.01
tRNA	0.01	(GGC)n	0.01
DNA/TcMar-Tigger	0.01	GA-rich	0.01
DNA/hAT-Tip100	0.01	AluJo	0.01
LTR/ERVK	0.00	AluJr	0.01
snRNA	0.00	AluSz	0.01
LINE/RTE-BovB	0.00	(CCG)n	0.01
DNA/hAT	0.00	AluY	0.01

E

Ontology	Term	FDR Q-val
GO Biological Process	mRNA catabolic process	29.56
GO Biological Process	endoplasmic reticulum unfolded protein response	29.56
GO Biological Process	regulation of transcription from RNA polymerase II promoter in response to stress	29.31
GO Biological Process	nuclear-transcribed mRNA catabolic process	29.05
GO Biological Process	cellular response to topologically incorrect protein	27.55
GO Biological Process	RNA catabolic process	27.30
GO Biological Process	response to topologically incorrect protein	26.65
GO Biological Process	rRNA processing	26.19
GO Biological Process	protein targeting to ER	26.20
GO Biological Process	nuclear-transcribed mRNA catabolic process, nonsense-mediated decay	25.97
GO Biological Process	regulation of DNA-templated transcription in response to stress	25.55
GO Biological Process	rRNA metabolic process	25.35
GO Biological Process	cellular response to unfolded protein	25.28
GO Biological Process	response to unfolded protein	24.29
GO Biological Process	IRE1-mediated unfolded protein response	24.09
GO Biological Process	establishment of protein localization to endoplasmic reticulum	23.58
GO Biological Process	protein localization to endoplasmic reticulum	23.21
GO Biological Process	cotranslational protein targeting to membrane	23.21
GO Biological Process	SRP-dependent cotranslational protein targeting to membrane	21.33
GO Biological Process	viral gene expression	20.88
Human Phenotype	Increased serum lactate	14.05
Human Phenotype	Atherosclerosis	10.69
Human Phenotype	Coronary artery disease	10.69
Human Phenotype	Increased CSF lactate	10.15
Human Phenotype	Abnormal CSF metabolite level	9.71
Human Phenotype	Abnormality of the mitochondrion	9.58
Human Phenotype	Abnormal coronary artery morphology	8.93
Human Phenotype	Abnormality of mitochondrial metabolism	8.27
Human Phenotype	Arteriosclerosis	7.92
Human Phenotype	Ependymoma	2.38

Supplementary Figure 1658: Properties and genomic distribution of motifs identified for the ZNF749 transcription factor in HepG2 (accession ENCSR125MLR).

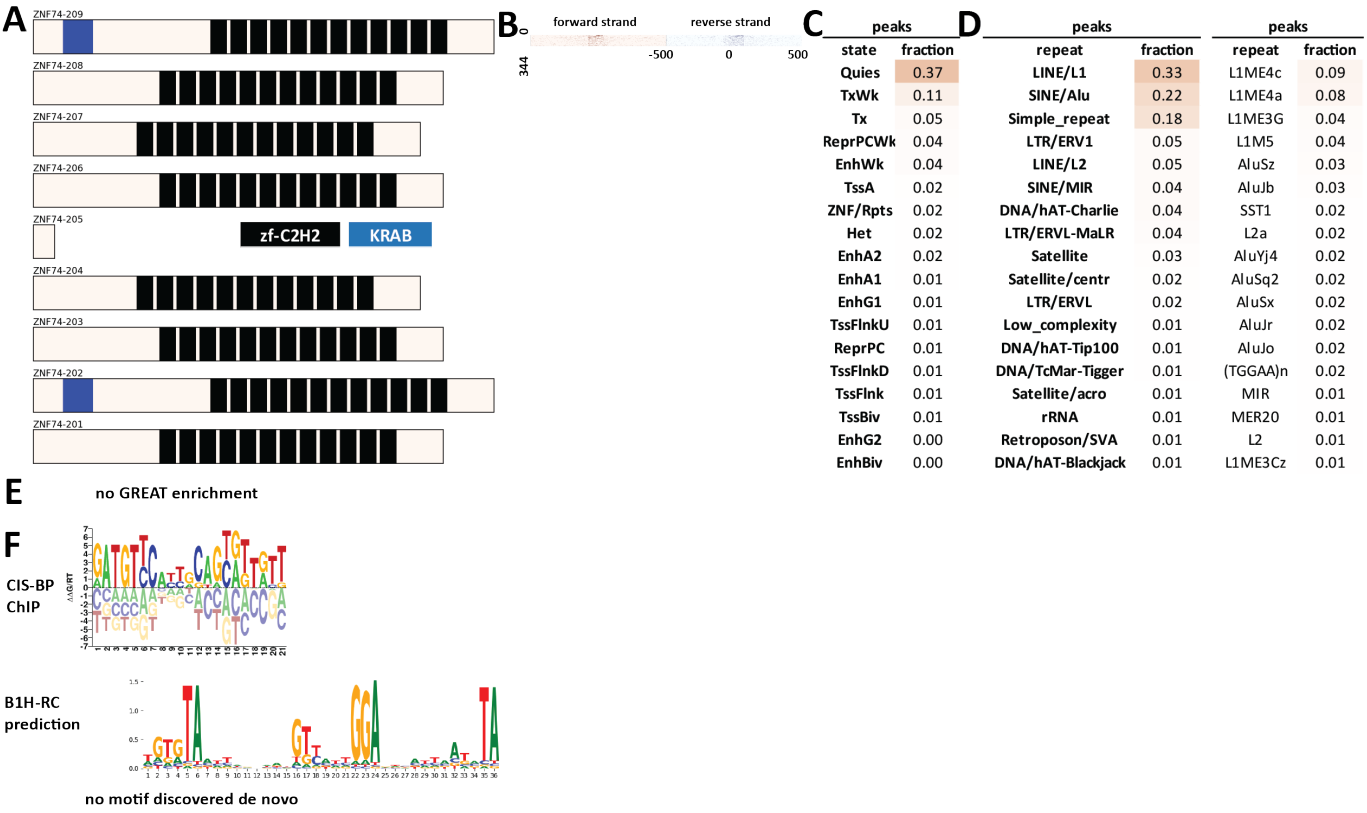

peaks	
state	fraction
Quies	0.37
TxWk	0.11
Tx	0.05
ReprPCWk	0.04
EnhWk	0.04
TssA	0.02
ZNF/Rpts	0.02
Het	0.02
EnhA2	0.02
EnhA1	0.01
EnhG1	0.01
TssFlnkU	0.01
ReprPC	0.01
TssFlnkD	0.01
TssFlnk	0.01
TssBiv	0.01
EnhG2	0.00
EnhBiv	0.00

peaks	
repeat	fraction
LINE/L1	0.33
SINE/Alu	0.22
Simple_repeat	0.18
LTR/ERV1	0.05
LINE/L2	0.05
SINE/MIR	0.04
DNA/hAT-Charlie	0.04
LTR/ERVL-MaLR	0.04
Satellite	0.03
Satellite/centr	0.02
LTR/ERVL	0.02
Low_complexity	0.01
DNA/hAT-Tip100	0.01
DNA/TcMar-Tigger	0.01
Satellite/acro	0.01
rRNA	0.01
Retroposon/SVA	0.01
DNA/hAT-Blackjack	0.01

peaks	
repeat	fraction
L1ME4c	0.09
L1ME4a	0.08
L1ME3G	0.04
L1M5	0.04
AluSz	0.03
AluJb	0.03
SST1	0.02
L2a	0.02
AluYj4	0.02
AluSq2	0.02
AluSx	0.02
AluJr	0.02
AluJo	0.02
(TGGAA)n	0.02
MIR	0.01
MER20	0.01
L2	0.01
L1ME3Cz	0.01

Supplementary Figure 1659: Properties and genomic distribution of motifs identified for the ZNF74 transcription factor in HEK293 (accession ChipExo models).

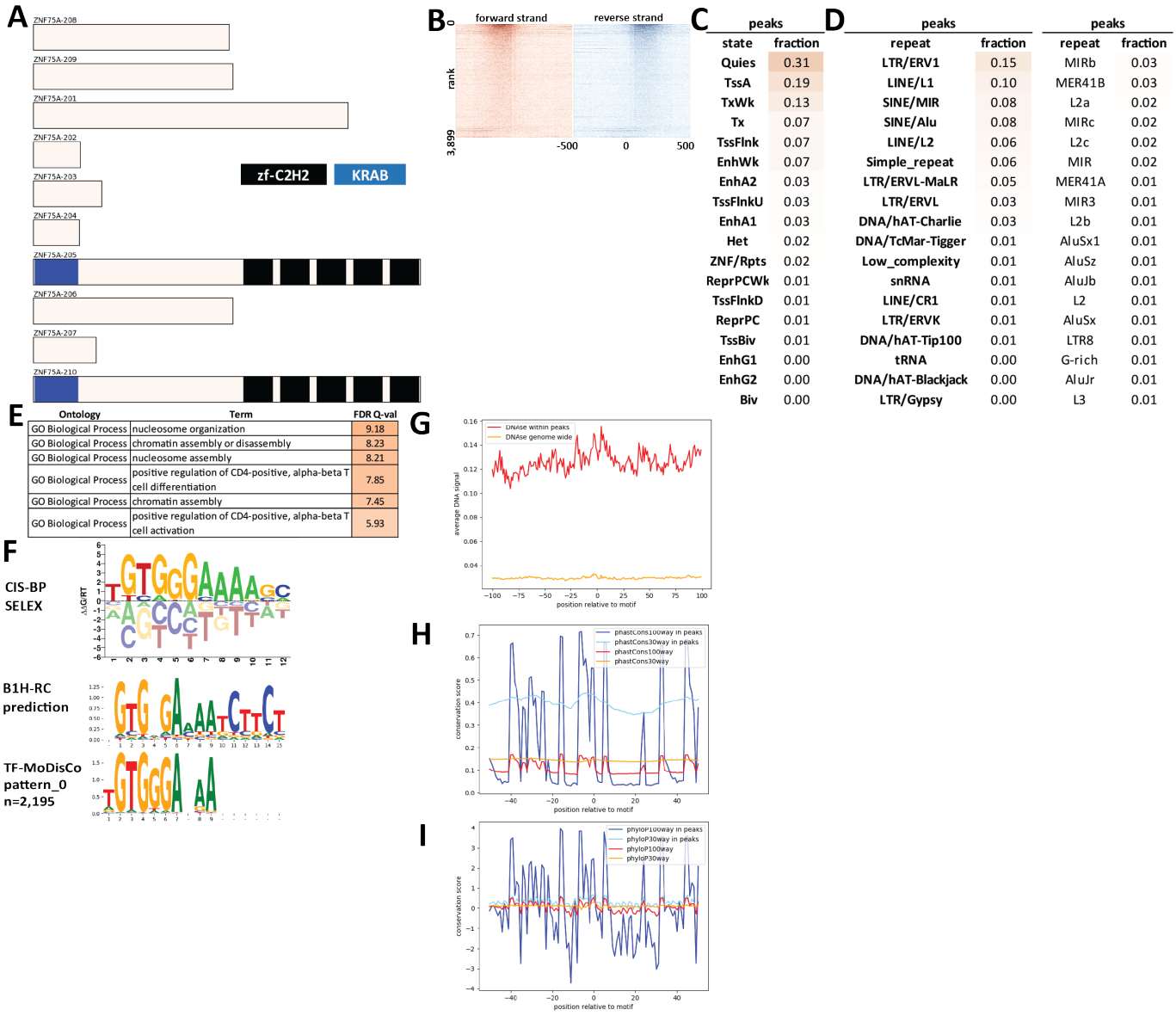

C

peaks	
state	fraction
Quies	0.31
TssA	0.19
TxWk	0.13
Tx	0.07
TssFlnk	0.07
EnhWk	0.07
EnhA2	0.03
TssFlnkU	0.03
EnhA1	0.03
Het	0.02
ZNF/Rpts	0.02
ReprPCWk	0.01
TssFlnkD	0.01
ReprPC	0.01
TssBiv	0.01
EnhG1	0.00
EnhG2	0.00
Biv	0.00

D

peaks		peaks	
repeat	fraction	repeat	fraction
LTR/ERV1	0.15	MIRb	0.03
LINE/L1	0.10	MER41B	0.03
SINE/MIR	0.08	L2a	0.02
SINE/Alu	0.08	MIRc	0.02
LINE/L2	0.06	L2c	0.02
Simple_repeat	0.06	MIR	0.02
LTR/ERVL-MaLR	0.05	MER41A	0.01
LTR/ERVL	0.03	MIR3	0.01
DNA/hAT-Charlie	0.03	L2b	0.01
DNA/TcMar-Tigger	0.01	AluSx1	0.01
Low_complexity	0.01	AluSz	0.01
snRNA	0.01	AluJb	0.01
LINE/CR1	0.01	L2	0.01
LTR/ERVK	0.01	AluSx	0.01
DNA/hAT-Tip100	0.01	LTR8	0.01
tRNA	0.00	G-rich	0.01
DNA/hAT-Blackjack	0.00	AluJr	0.01
LTR/Gypsy	0.00	L3	0.01

E

Ontology	Term	FDR Q-val
GO Biological Process	nucleosome organization	9.18
GO Biological Process	chromatin assembly or disassembly	8.23
GO Biological Process	nucleosome assembly	8.21
GO Biological Process	positive regulation of CD4-positive, alpha-beta T cell differentiation	7.85
GO Biological Process	chromatin assembly	7.45
GO Biological Process	positive regulation of CD4-positive, alpha-beta T cell activation	5.93

Supplementary Figure 1660: Properties and genomic distribution of motifs identified for the ZNF75A transcription factor in K562 (accession ENCSR099MNR).

TF-MoDisCO pattern_0 n=2195, CWM

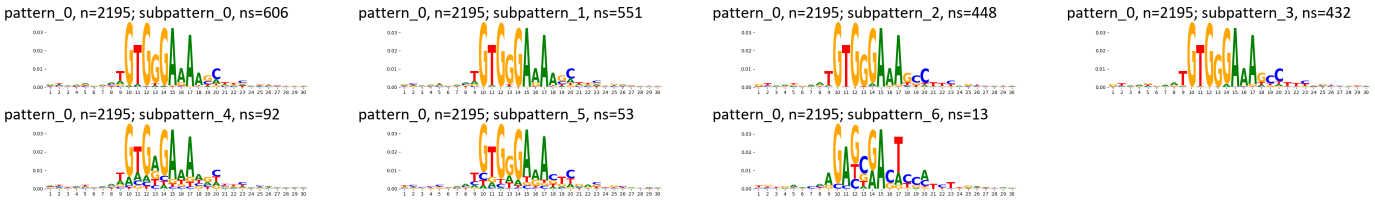

TF-MoDisCO pattern_0 n=2195, PWM

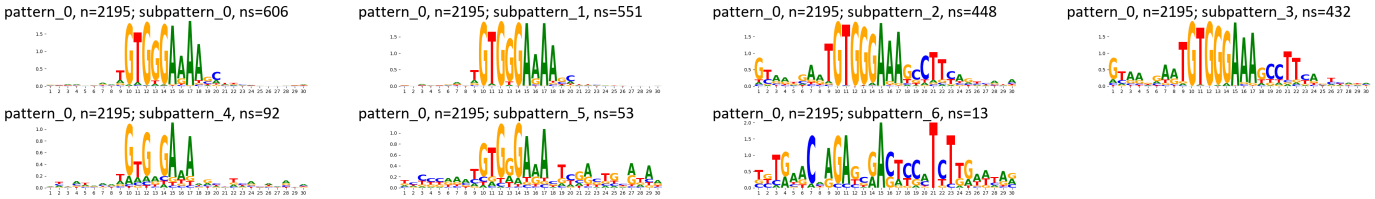

Supplementary Figure 1661: TF-MoDisCO subpatterns for the ZNF75A transcription factor in K562 (accession ENCSR099MNR).

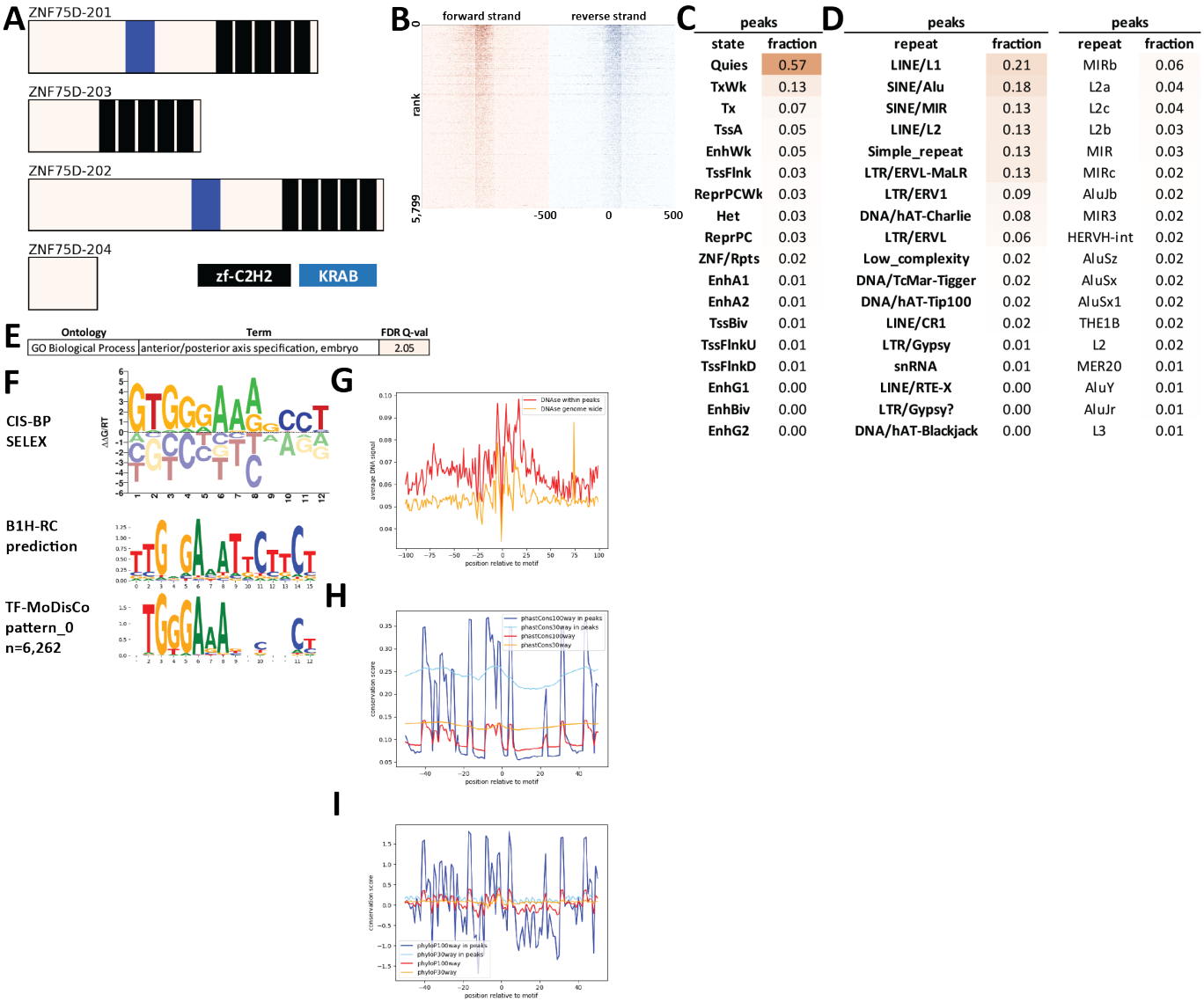

Supplementary Figure 1662: Properties and genomic distribution of motifs identified for the ZNF75D transcription factor in HEK293 (accession ChipExo models).

TF-MoDisCO pattern_0 n=6262, CWM

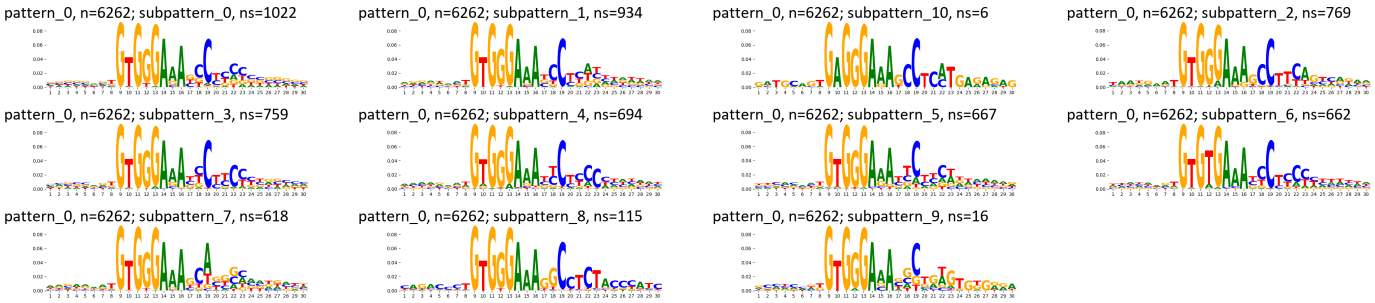

TF-MoDisCO pattern_0 n=6262, PWM

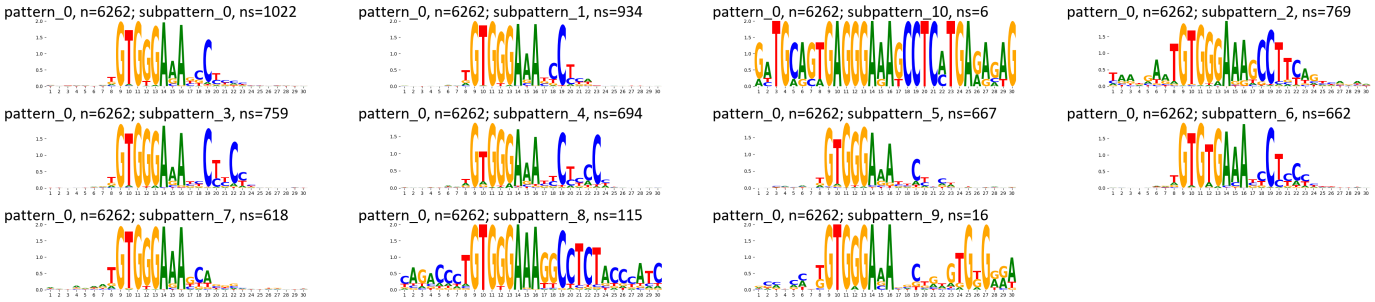

Supplementary Figure 1663: TF-MoDisCO subpatterns for the ZNF75D transcription factor in HEK293 (accession ChipExo models).

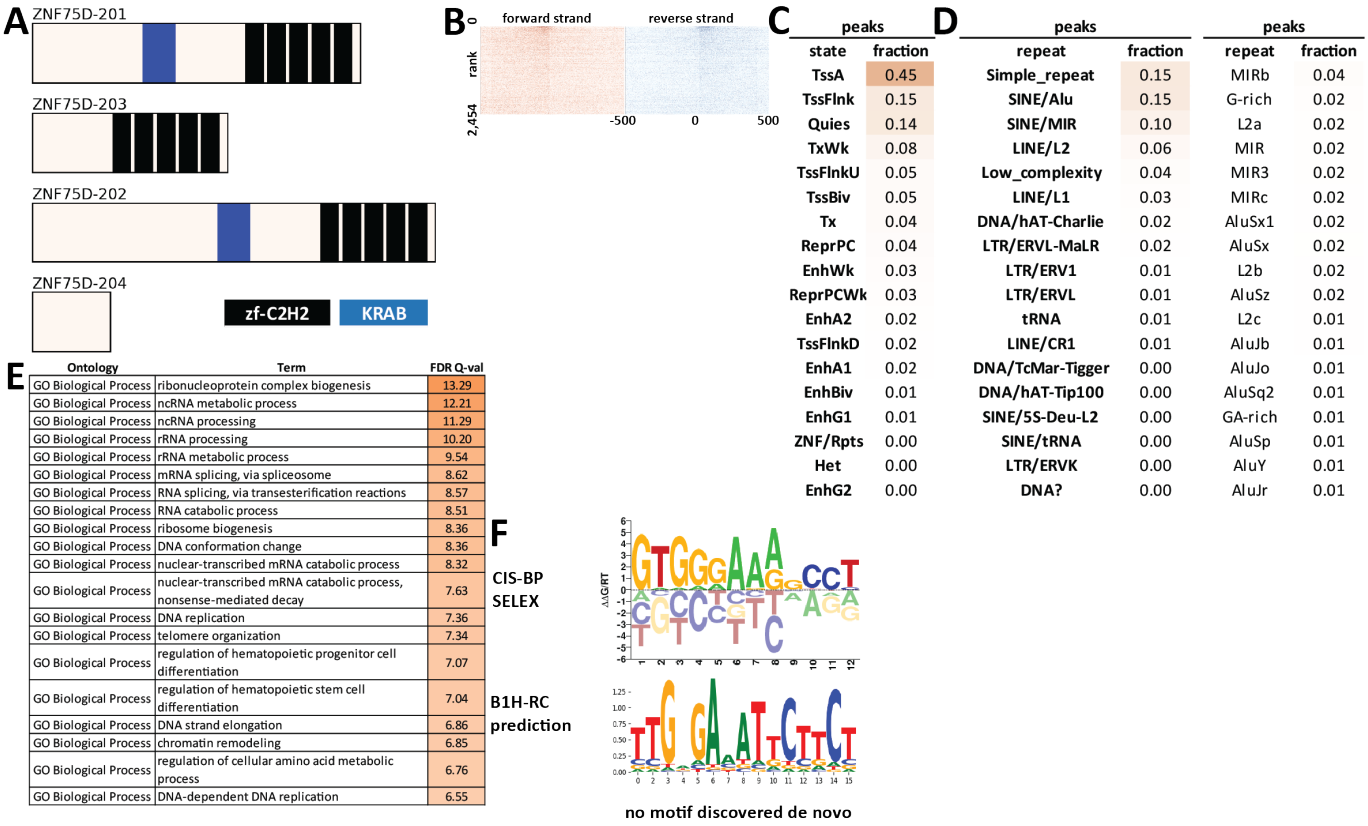

C

peaks	
state	fraction
TssA	0.45
TssFlnk	0.15
Quies	0.14
TxWk	0.08
TssFlnkU	0.05
TssBiv	0.05
Tx	0.04
ReprPC	0.04
EnhWk	0.03
ReprPCWk	0.03
EnhA2	0.02
TssFlnkD	0.02
EnhA1	0.02
EnhBiv	0.01
EnhG1	0.01
ZNF/Rpts	0.00
Het	0.00
EnhG2	0.00

D

peaks		peaks	
repeat	fraction	repeat	fraction
Simple_repeat	0.15	MIRb	0.04
SINE/Alu	0.15	G-rich	0.02
SINE/MIR	0.10	L2a	0.02
LINE/L2	0.06	MIR	0.02
Low_complexity	0.04	MIR3	0.02
LINE/L1	0.03	MIRc	0.02
DNA/hAT-Charlie	0.02	AluSx1	0.02
LTR/ERVL-MaLR	0.02	AluSx	0.02
LTR/ERV1	0.01	L2b	0.02
LTR/ERVL	0.01	AluSz	0.02
tRNA	0.01	L2c	0.01
LINE/CR1	0.01	AluJb	0.01
DNA/TcMar-Tigger	0.00	AluJo	0.01
DNA/hAT-Tip100	0.00	AluSq2	0.01
SINE/5S-Deu-L2	0.00	GA-rich	0.01
SINE/tRNA	0.00	AluSp	0.01
LTR/ERVK	0.00	AluY	0.01
DNA?	0.00	AluJr	0.01

E

Ontology	Term	FDR Q-val
GO Biological Process	ribonucleoprotein complex biogenesis	13.29
GO Biological Process	ncRNA metabolic process	12.21
GO Biological Process	ncRNA processing	11.29
GO Biological Process	rRNA processing	10.20
GO Biological Process	rRNA metabolic process	9.54
GO Biological Process	mRNA splicing, via spliceosome	8.62
GO Biological Process	RNA splicing, via transesterification reactions	8.57
GO Biological Process	RNA catabolic process	8.51
GO Biological Process	ribosome biogenesis	8.36
GO Biological Process	DNA conformation change	8.36
GO Biological Process	nuclear-transcribed mRNA catabolic process	8.32
GO Biological Process	nuclear-transcribed mRNA catabolic process, nonsense-mediated decay	7.63
GO Biological Process	DNA replication	7.36
GO Biological Process	telomere organization	7.34
GO Biological Process	regulation of hematopoietic progenitor cell differentiation	7.07
GO Biological Process	regulation of hematopoietic stem cell differentiation	7.04
GO Biological Process	DNA strand elongation	6.86
GO Biological Process	chromatin remodeling	6.85
GO Biological Process	regulation of cellular amino acid metabolic process	6.76
GO Biological Process	DNA-dependent DNA replication	6.55

Supplementary Figure 1664: Properties and genomic distribution of motifs identified for the ZNF75D transcription factor in HepG2 (accession ENCSR693TYT).

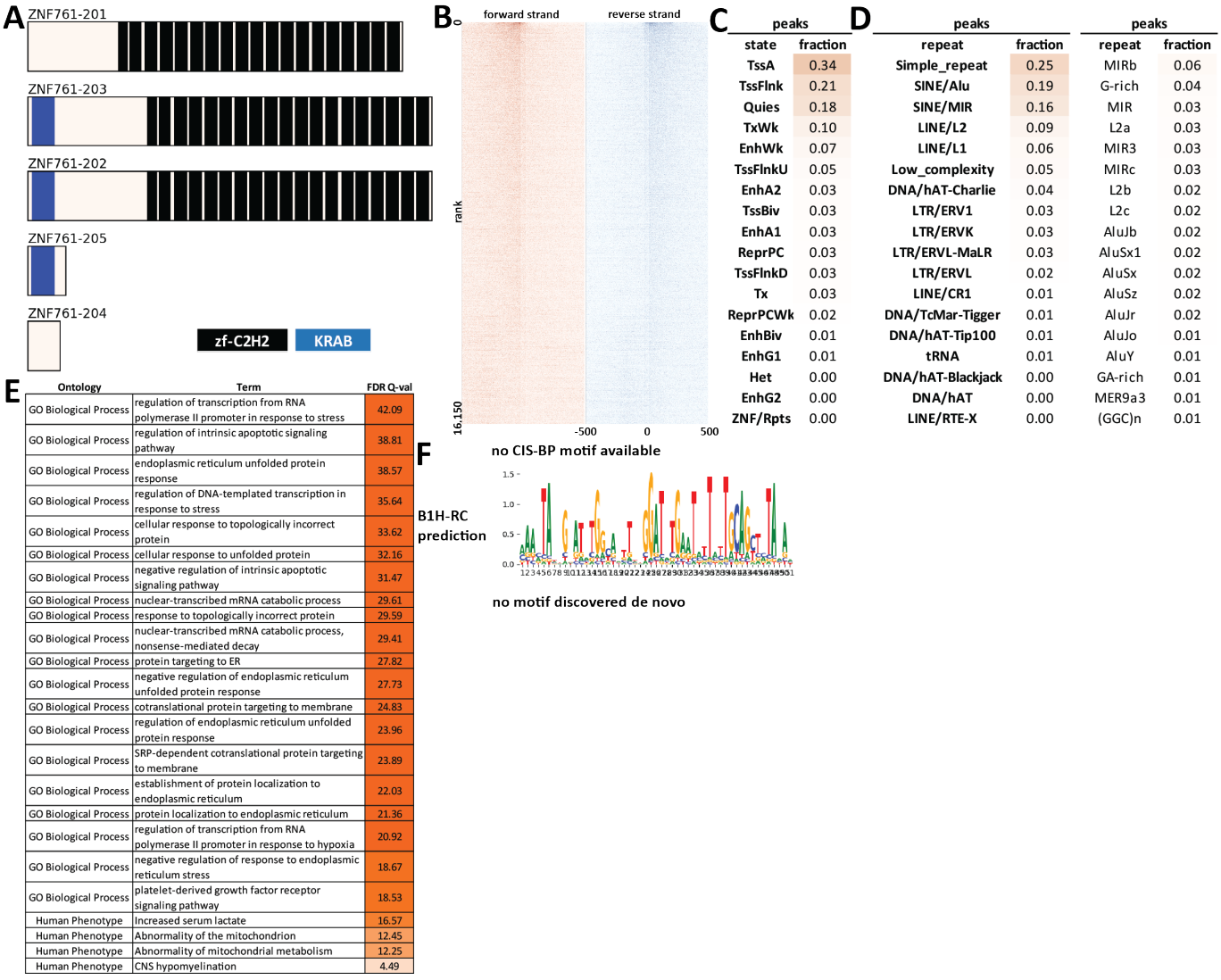

C

peaks	
state	fraction
TssA	0.34
TssFlnk	0.21
Quies	0.18
TxWk	0.10
EnhWk	0.07
TssFlnkU	0.05
EnhA2	0.03
TssBiv	0.03
EnhA1	0.03
ReprPC	0.03
TssFlnkD	0.03
Tx	0.03
ReprPCWk	0.02
EnhBiv	0.01
EnhG1	0.01
Het	0.00
EnhG2	0.00
ZNF/Rpts	0.00

D

peaks		peaks	
repeat	fraction	repeat	fraction
Simple_repeat	0.25	MIRb	0.06
SINE/Alu	0.19	G-rich	0.04
SINE/MIR	0.16	MIR	0.03
LINE/L2	0.09	L2a	0.03
LINE/L1	0.06	MIR3	0.03
Low_complexity	0.05	MIRc	0.03
DNA/hAT-Charlie	0.04	L2b	0.02
LTR/ERV1	0.03	L2c	0.02
LTR/ERVK	0.03	AluJb	0.02
LTR/ERVL-MaLR	0.03	AluSx1	0.02
LTR/ERVL	0.02	AluSx	0.02
LINE/CR1	0.01	AluSz	0.02
DNA/TcMar-Tigger	0.01	AluJr	0.02
DNA/hAT-Tip100	0.01	AluJo	0.01
tRNA	0.01	AluY	0.01
DNA/hAT-Blackjack	0.00	GA-rich	0.01
DNA/hAT	0.00	MER9a3	0.01
LINE/RTE-X	0.00	(GGC)n	0.01

E

Ontology	Term	FDR Q-val
GO Biological Process	regulation of transcription from RNA polymerase II promoter in response to stress	42.09
GO Biological Process	regulation of intrinsic apoptotic signaling pathway	38.81
GO Biological Process	endoplasmic reticulum unfolded protein response	38.57
GO Biological Process	regulation of DNA-templated transcription in response to stress	35.64
GO Biological Process	cellular response to topologically incorrect protein	33.62
GO Biological Process	cellular response to unfolded protein	32.16
GO Biological Process	negative regulation of intrinsic apoptotic signaling pathway	31.47
GO Biological Process	nuclear-transcribed mRNA catabolic process	29.61
GO Biological Process	response to topologically incorrect protein	29.59
GO Biological Process	nuclear-transcribed mRNA catabolic process, nonsense-mediated decay	29.41
GO Biological Process	protein targeting to ER	27.82
GO Biological Process	negative regulation of endoplasmic reticulum unfolded protein response	27.73
GO Biological Process	cotranslational protein targeting to membrane	24.83
GO Biological Process	regulation of endoplasmic reticulum unfolded protein response	23.96
GO Biological Process	SRP-dependent cotranslational protein targeting to membrane	23.89
GO Biological Process	establishment of protein localization to endoplasmic reticulum	22.03
GO Biological Process	protein localization to endoplasmic reticulum	21.36
GO Biological Process	regulation of transcription from RNA polymerase II promoter in response to hypoxia	20.92
GO Biological Process	negative regulation of response to endoplasmic reticulum stress	18.67
GO Biological Process	platelet-derived growth factor receptor signaling pathway	18.53
Human Phenotype	Increased serum lactate	16.57
Human Phenotype	Abnormality of the mitochondrion	12.45
Human Phenotype	Abnormality of mitochondrial metabolism	12.25
Human Phenotype	CNS hypomyelination	4.49

Supplementary Figure 1665: Properties and genomic distribution of motifs identified for the ZNF761 transcription factor in HepG2 (accession ENCSR622AMZ).

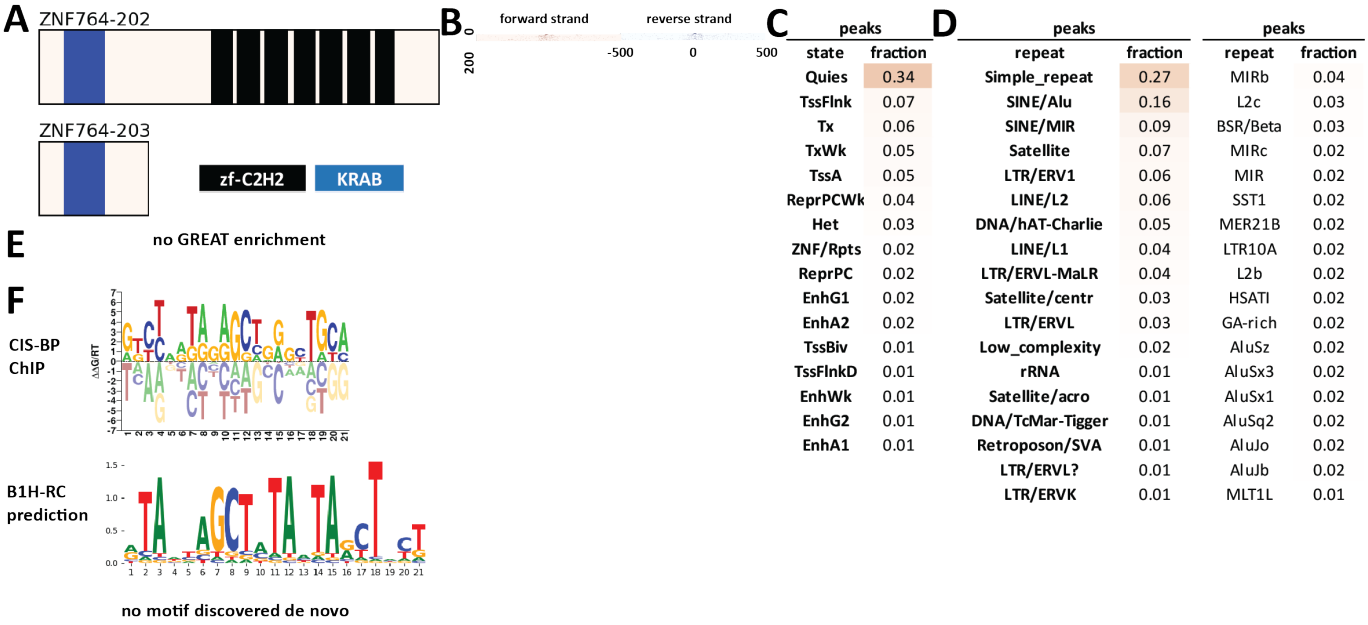

Supplementary Figure 1666: Properties and genomic distribution of motifs identified for the ZNF764 transcription factor in HEK293 (accession ChipExo models).

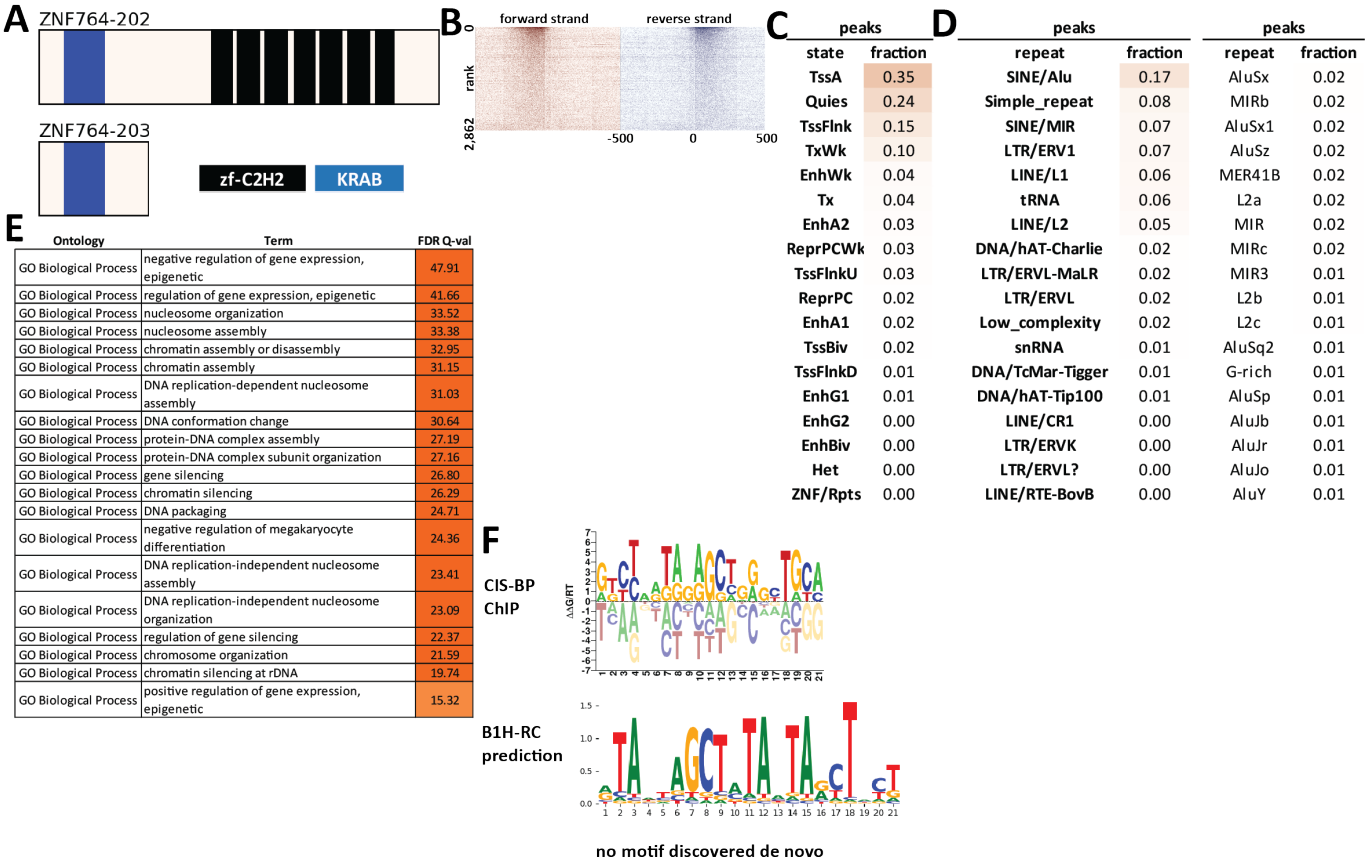

Supplementary Figure 1667: Properties and genomic distribution of motifs identified for the ZNF764 transcription factor in K562 (accession ENCSR023OOE).

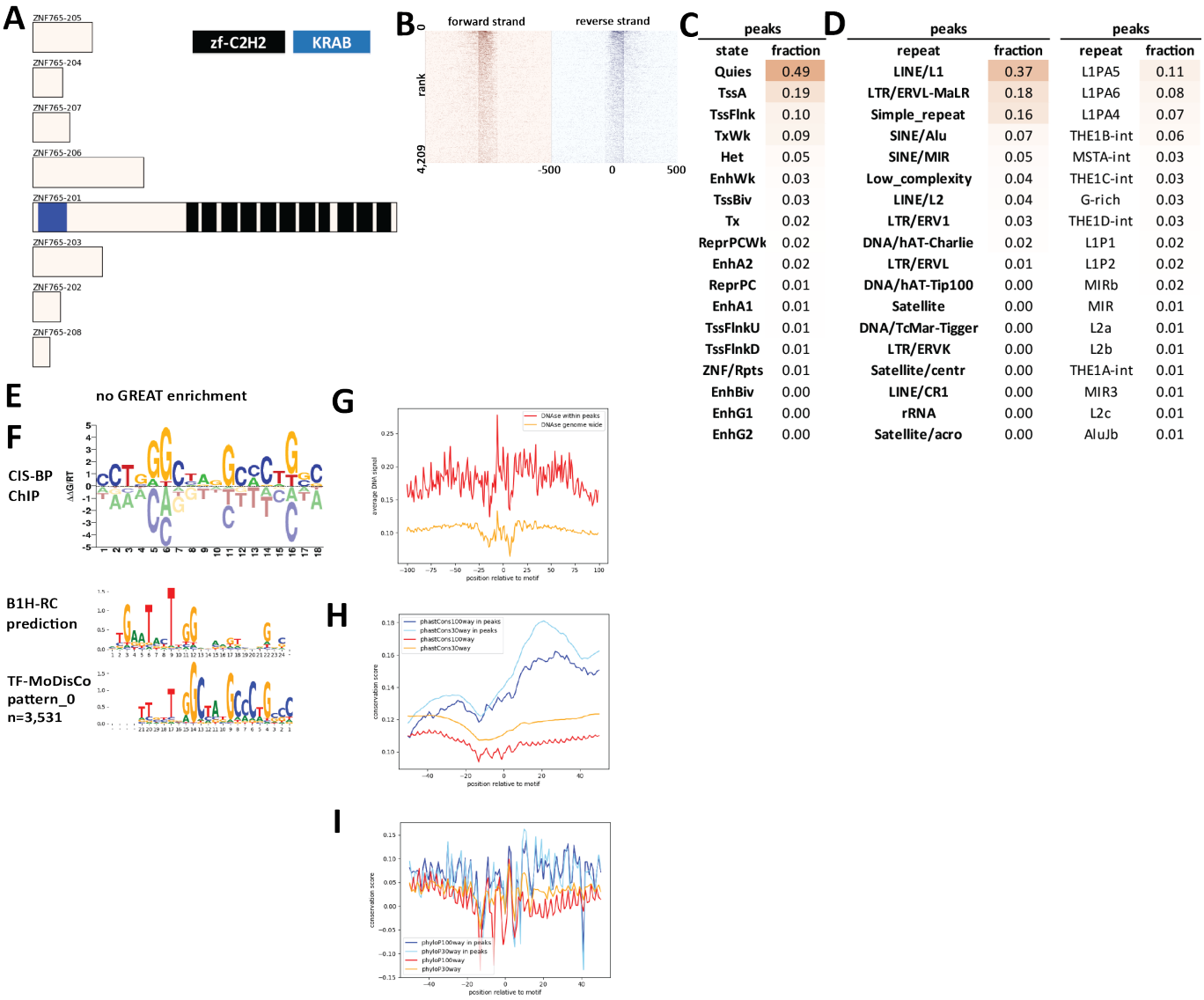

C

peaks	
state	fraction
Quies	0.49
TssA	0.19
TssFlnk	0.10
TxWk	0.09
Het	0.05
EnhWk	0.03
TssBiv	0.03
Tx	0.02
ReprPCWk	0.02
EnhA2	0.02
ReprPC	0.01
EnhA1	0.01
TssFlnkU	0.01
TssFlnkD	0.01
ZNF/Rpts	0.01
EnhBiv	0.00
EnhG1	0.00
EnhG2	0.00

D

peaks		peaks	
repeat	fraction	repeat	fraction
LINE/L1	0.37	L1PA5	0.11
LTR/ERVL-MaLR	0.18	L1PA6	0.08
Simple_repeat	0.16	L1PA4	0.07
SINE/Alu	0.07	THE1B-int	0.06
SINE/MIR	0.05	MSTA-int	0.03
Low_complexity	0.04	THE1C-int	0.03
LINE/L2	0.04	G-rich	0.03
LTR/ERV1	0.03	THE1D-int	0.03
DNA/hAT-Charlie	0.02	L1P1	0.02
LTR/ERVL	0.01	L1P2	0.02
DNA/hAT-Tip100	0.00	MIRb	0.02
Satellite	0.00	MIR	0.01
DNA/TcMar-Tigger	0.00	L2a	0.01
LTR/ERVK	0.00	L2b	0.01
Satellite/centr	0.00	THE1A-int	0.01
LINE/CR1	0.00	MIR3	0.01
rRNA	0.00	L2c	0.01
Satellite/acro	0.00	AluJb	0.01

Supplementary Figure 1668: Properties and genomic distribution of motifs identified for the ZNF765 transcription factor in HEK293 (accession ChipExo models).

TF-MoDisCO pattern_0 n=3531, CWM

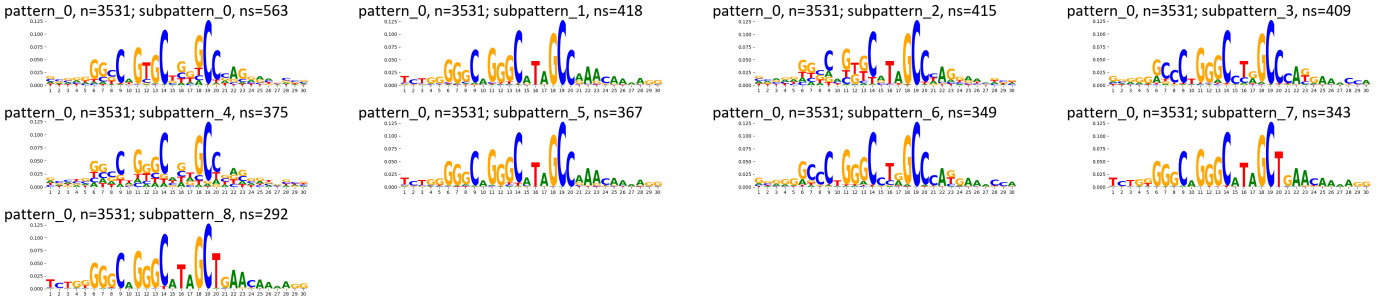

TF-MoDisCO pattern_0 n=3531, PWM

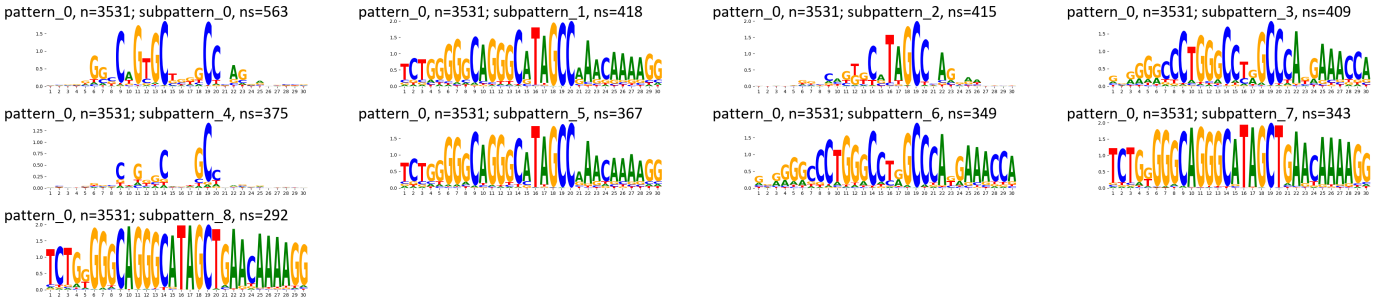

Supplementary Figure 1669: TF-MoDisCO subpatterns for the ZNF765 transcription factor in HEK293 (accession ChipExo models).

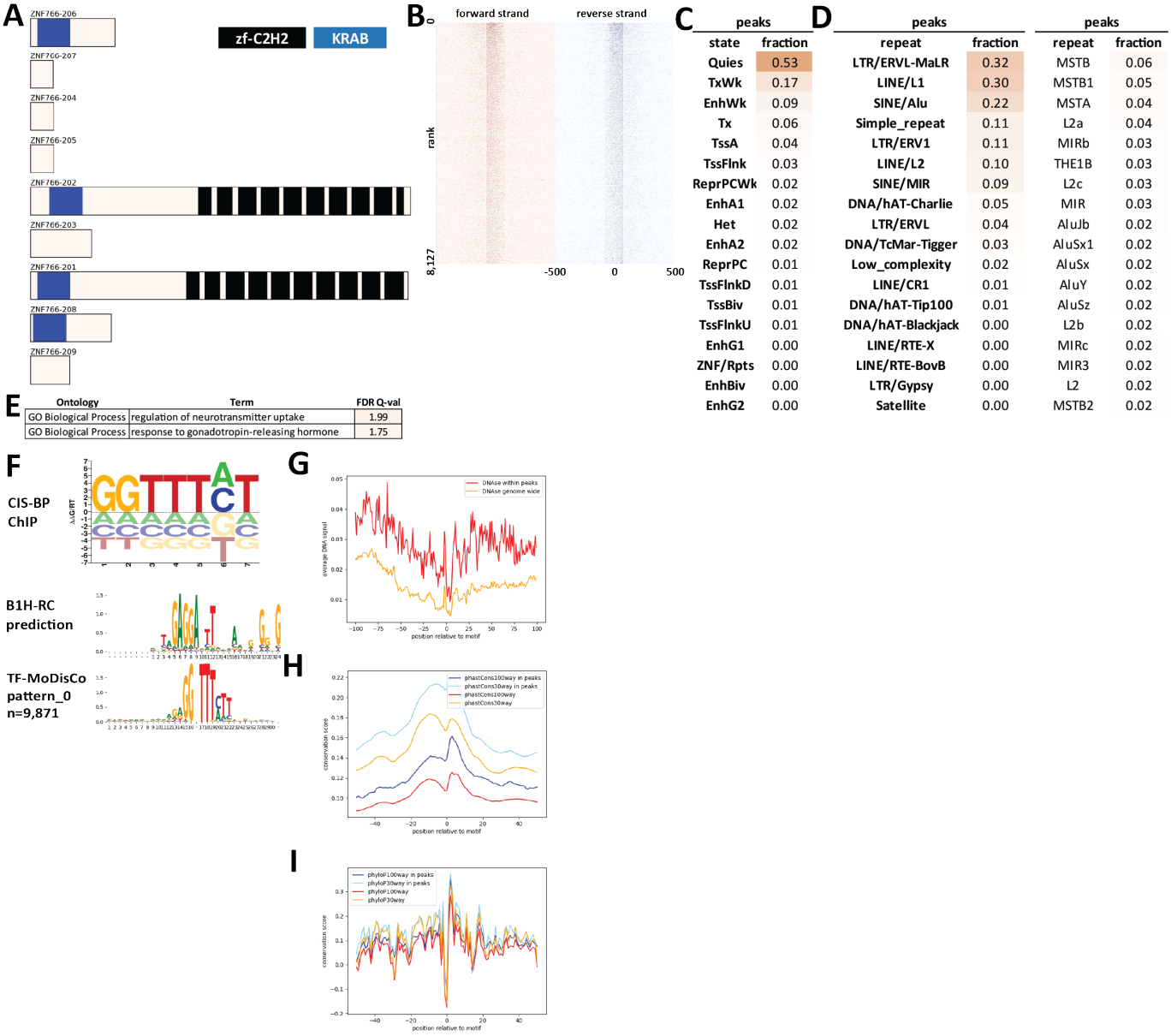

peaks	
state	fraction
Quies	0.53
TxWk	0.17
EnhWk	0.09
Tx	0.06
TssA	0.04
TssFlnk	0.03
ReprPCWk	0.02
EnhA1	0.02
Het	0.02
EnhA2	0.02
ReprPC	0.01
TssFlnkD	0.01
TssBiv	0.01
TssFlnkU	0.01
EnhG1	0.00
ZNF/Rpts	0.00
EnhBiv	0.00
EnhG2	0.00

peaks	
repeat	fraction
LTR/ERVL-MaLR	0.32
LINE/L1	0.30
SINE/Alu	0.22
Simple_repeat	0.11
LTR/ERV1	0.11
LINE/L2	0.10
SINE/MIR	0.09
DNA/hAT-Charlie	0.05
LTR/ERVL	0.04
DNA/TcMar-Tigger	0.03
Low_complexity	0.02
LINE/CR1	0.01
DNA/hAT-Tip100	0.01
DNA/hAT-Blackjack	0.00
LINE/RTE-X	0.00
LINE/RTE-BovB	0.00
LTR/Gypsy	0.00
Satellite	0.00

peaks	
repeat	fraction
MSTB	0.06
MSTB1	0.05
MSTA	0.04
L2a	0.04
MIRb	0.03
THE1B	0.03
L2c	0.03
MIR	0.03
AluJb	0.02
AluSx1	0.02
AluSx	0.02
AluY	0.02
AluSz	0.02
L2b	0.02
MIRc	0.02
MIR3	0.02
L2	0.02
MSTB2	0.02

Supplementary Figure 1670: Properties and genomic distribution of motifs identified for the ZNF766 transcription factor in HEK293 (accession ChipExo models).

TF-MoDisCO pattern_0 n=9871, CWM

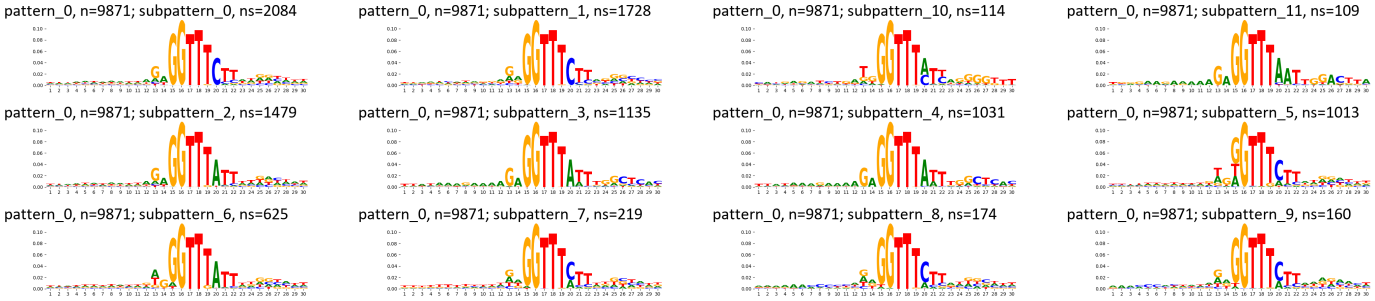

TF-MoDisCO pattern_0 n=9871, PWM

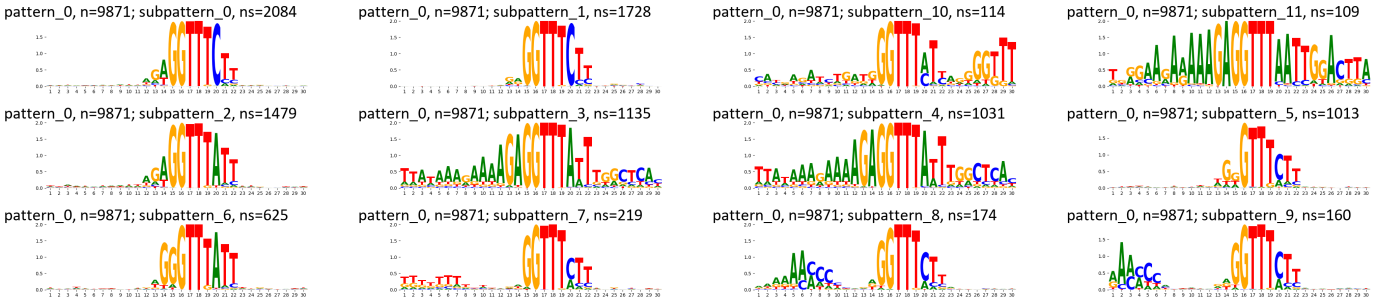

Supplementary Figure 1671: TF-MoDisCO subpatterns for the ZNF766 transcription factor in HEK293 (accession ChipExo models).

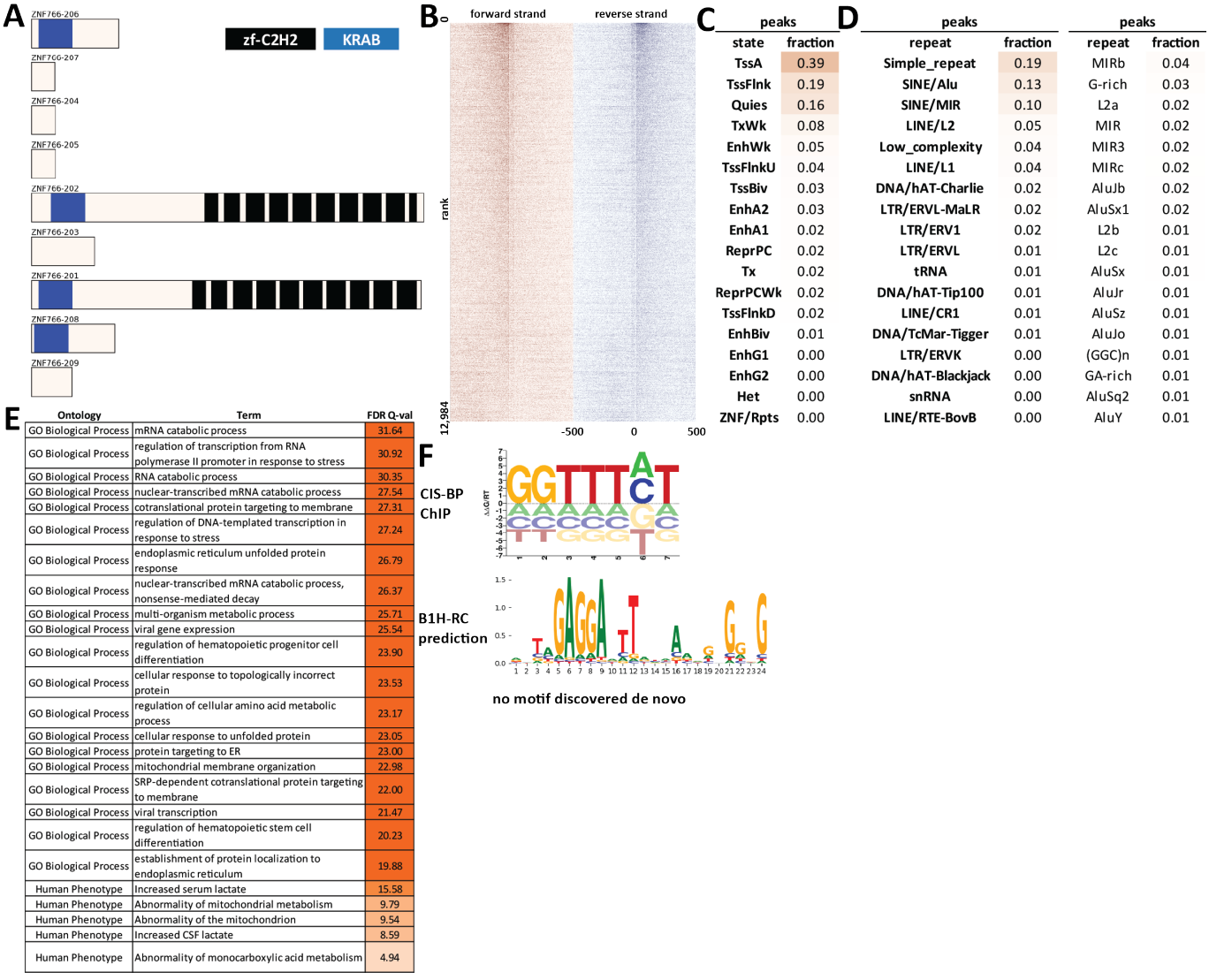

C

peaks	
state	fraction
TssA	0.39
TssFlnk	0.19
Quies	0.16
TxWk	0.08
EnhWk	0.05
TssFlnkU	0.04
TssBiv	0.03
EnhA2	0.03
EnhA1	0.02
ReprPC	0.02
Tx	0.02
ReprPCWk	0.02
TssFlnkD	0.02
EnhBiv	0.01
EnhG1	0.00
EnhG2	0.00
Het	0.00
ZNF/Rpts	0.00

D

peaks		peaks	
repeat	fraction	repeat	fraction
Simple_repeat	0.19	MIRb	0.04
SINE/Alu	0.13	G-rich	0.03
SINE/MIR	0.10	L2a	0.02
LINE/L2	0.05	MIR	0.02
Low_complexity	0.04	MIR3	0.02
LINE/L1	0.04	MIRc	0.02
DNA/hAT-Charlie	0.02	AluJb	0.02
LTR/ERVL-MaLR	0.02	AluSx1	0.02
LTR/ERV1	0.02	L2b	0.01
LTR/ERVL	0.01	L2c	0.01
tRNA	0.01	AluSx	0.01
DNA/hAT-Tip100	0.01	AluJr	0.01
LINE/CR1	0.01	AluSz	0.01
DNA/TcMar-Tigger	0.01	AluJo	0.01
LTR/ERVK	0.00	(GGC)n	0.01
DNA/hAT-Blackjack	0.00	GA-rich	0.01
snRNA	0.00	AluSq2	0.01
LINE/RTE-BovB	0.00	AluY	0.01

E

Ontology	Term	FDR Q-val
GO Biological Process	mRNA catabolic process	31.64
GO Biological Process	regulation of transcription from RNA polymerase II promoter in response to stress	30.92
GO Biological Process	RNA catabolic process	30.35
GO Biological Process	nuclear-transcribed mRNA catabolic process	27.54
GO Biological Process	cotranslational protein targeting to membrane	27.31
GO Biological Process	regulation of DNA-templated transcription in response to stress	27.24
GO Biological Process	endoplasmic reticulum unfolded protein response	26.79
GO Biological Process	nuclear-transcribed mRNA catabolic process, nonsense-mediated decay	26.37
GO Biological Process	multi-organism metabolic process	25.71
GO Biological Process	viral gene expression	25.54
GO Biological Process	regulation of hematopoietic progenitor cell differentiation	23.90
GO Biological Process	cellular response to topologically incorrect protein	23.53
GO Biological Process	regulation of cellular amino acid metabolic process	23.17
GO Biological Process	cellular response to unfolded protein	23.05
GO Biological Process	protein targeting to ER	23.00
GO Biological Process	mitochondrial membrane organization	22.98
GO Biological Process	SRP-dependent cotranslational protein targeting to membrane	22.00
GO Biological Process	viral transcription	21.47
GO Biological Process	regulation of hematopoietic stem cell differentiation	20.23
GO Biological Process	establishment of protein localization to endoplasmic reticulum	19.88
Human Phenotype	Increased serum lactate	15.58
Human Phenotype	Abnormality of mitochondrial metabolism	9.79
Human Phenotype	Abnormality of the mitochondrion	9.54
Human Phenotype	Increased CSF lactate	8.59
Human Phenotype	Abnormality of monocarboxylic acid metabolism	4.94

Supplementary Figure 1672: Properties and genomic distribution of motifs identified for the ZNF766 transcription factor in HepG2 (accession ENCSR869RSW).

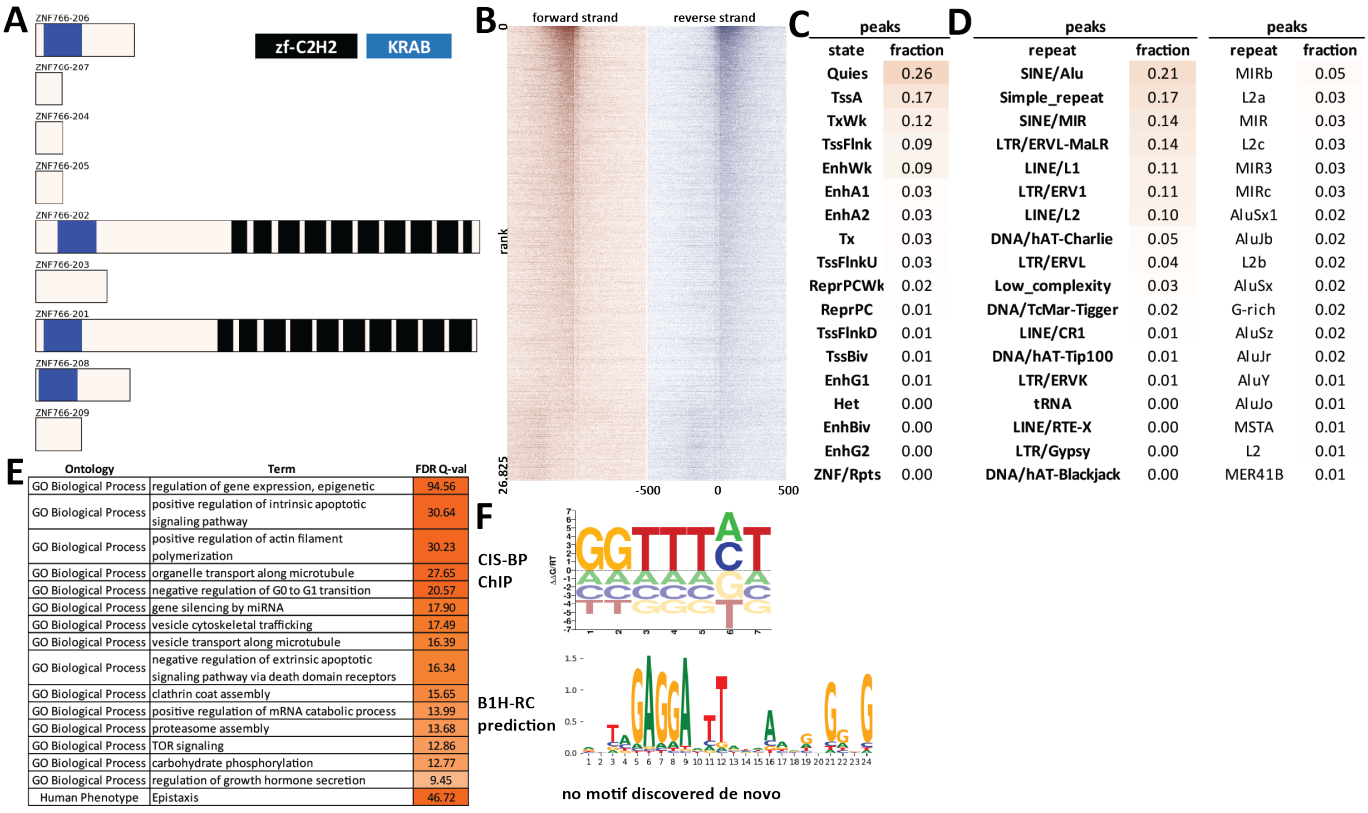

Supplementary Figure 1673: Properties and genomic distribution of motifs identified for the ZNF766 transcription factor in K562 (accession ENCSR194IJN).

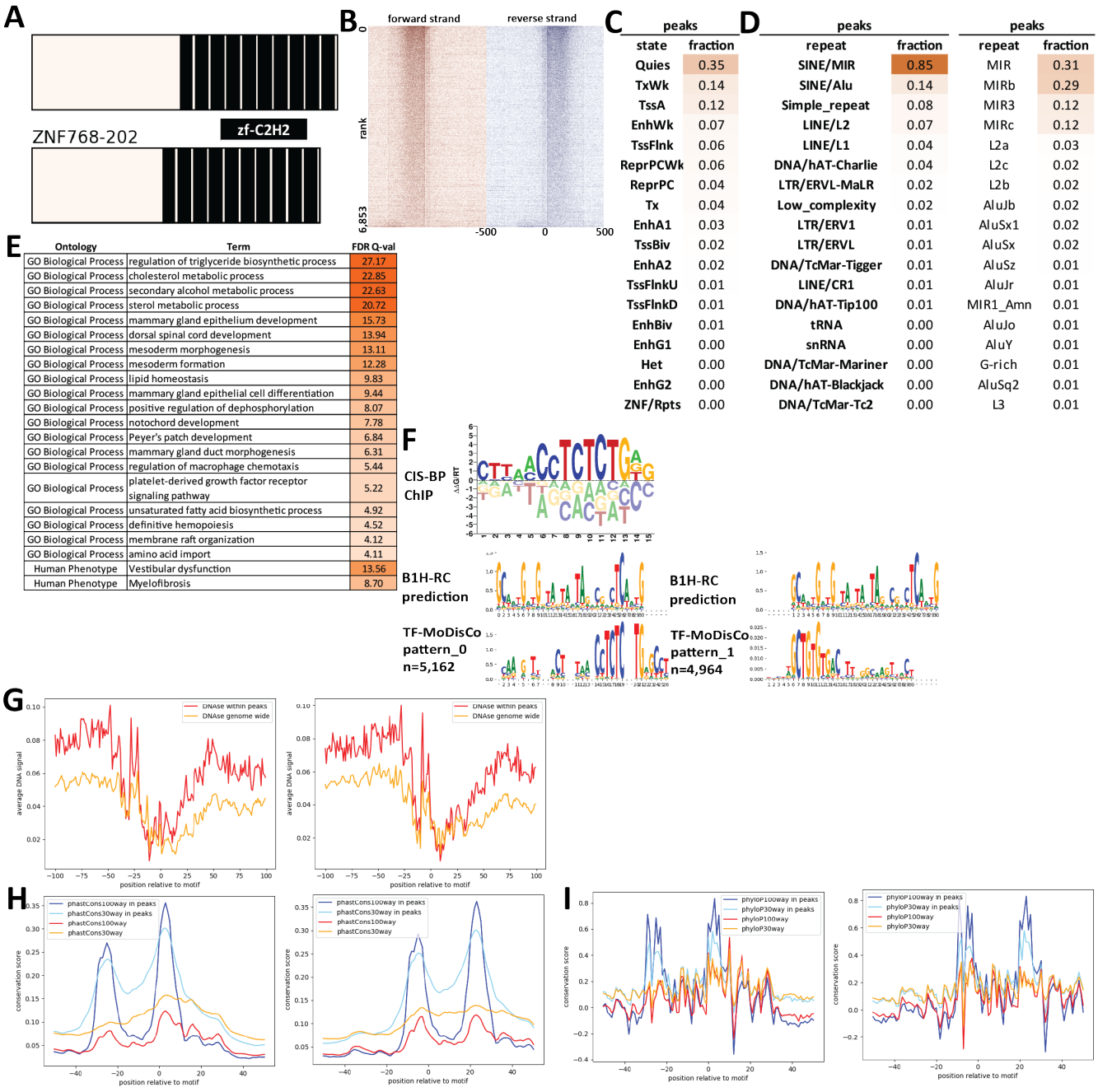

Supplementary Figure 1674: Properties and genomic distribution of motifs identified for the ZNF768 transcription factor in HEK293 (accession ENCSR070HWF).

TF-MoDisCO pattern_0 n=5162, CWM

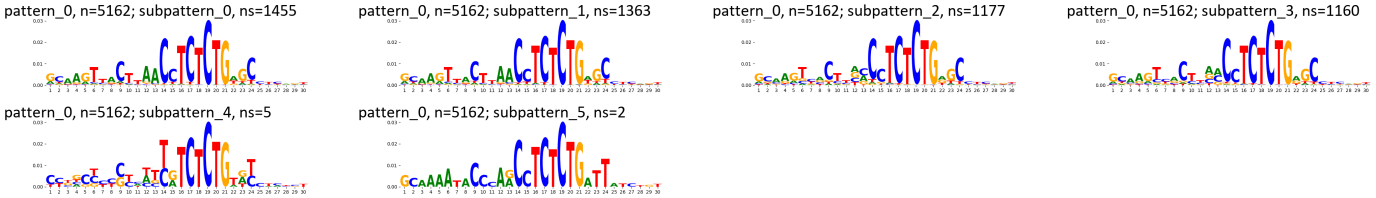

TF-MoDisCO pattern_0 n=5162, PWM

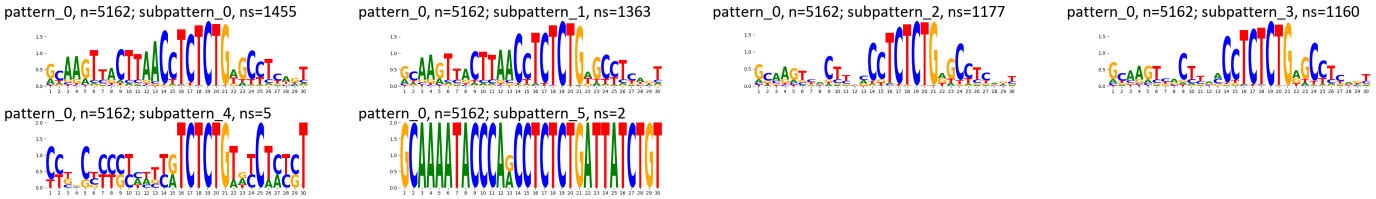

TF-MoDisCO pattern_1 n=4964, CWM

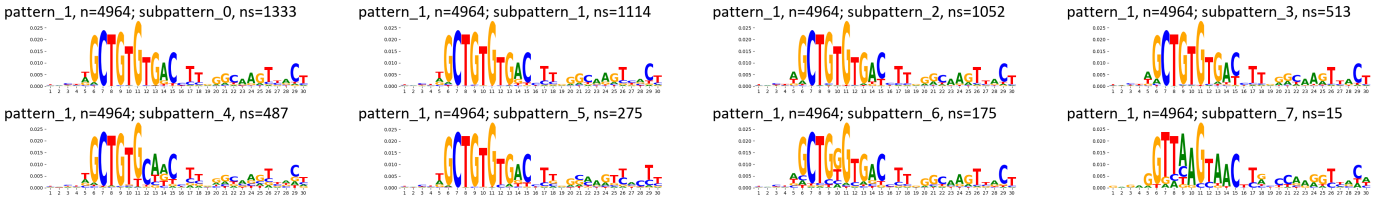

TF-MoDisCO pattern_1 n=4964, PWM

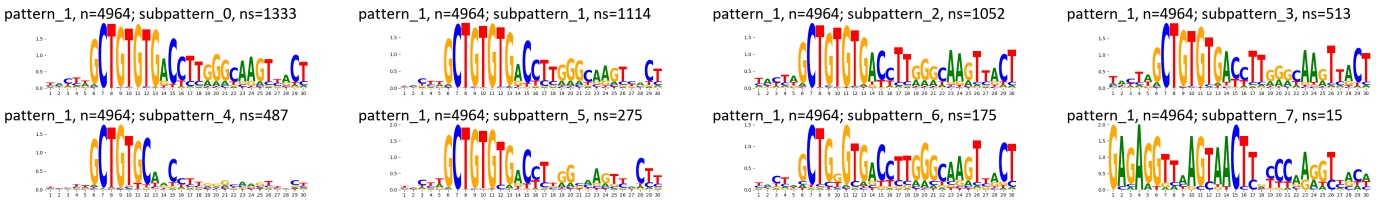

Supplementary Figure 1675: TF-MoDisCO subpatterns for the ZNF768 transcription factor in HEK293 (accession ENCSR070HWF).

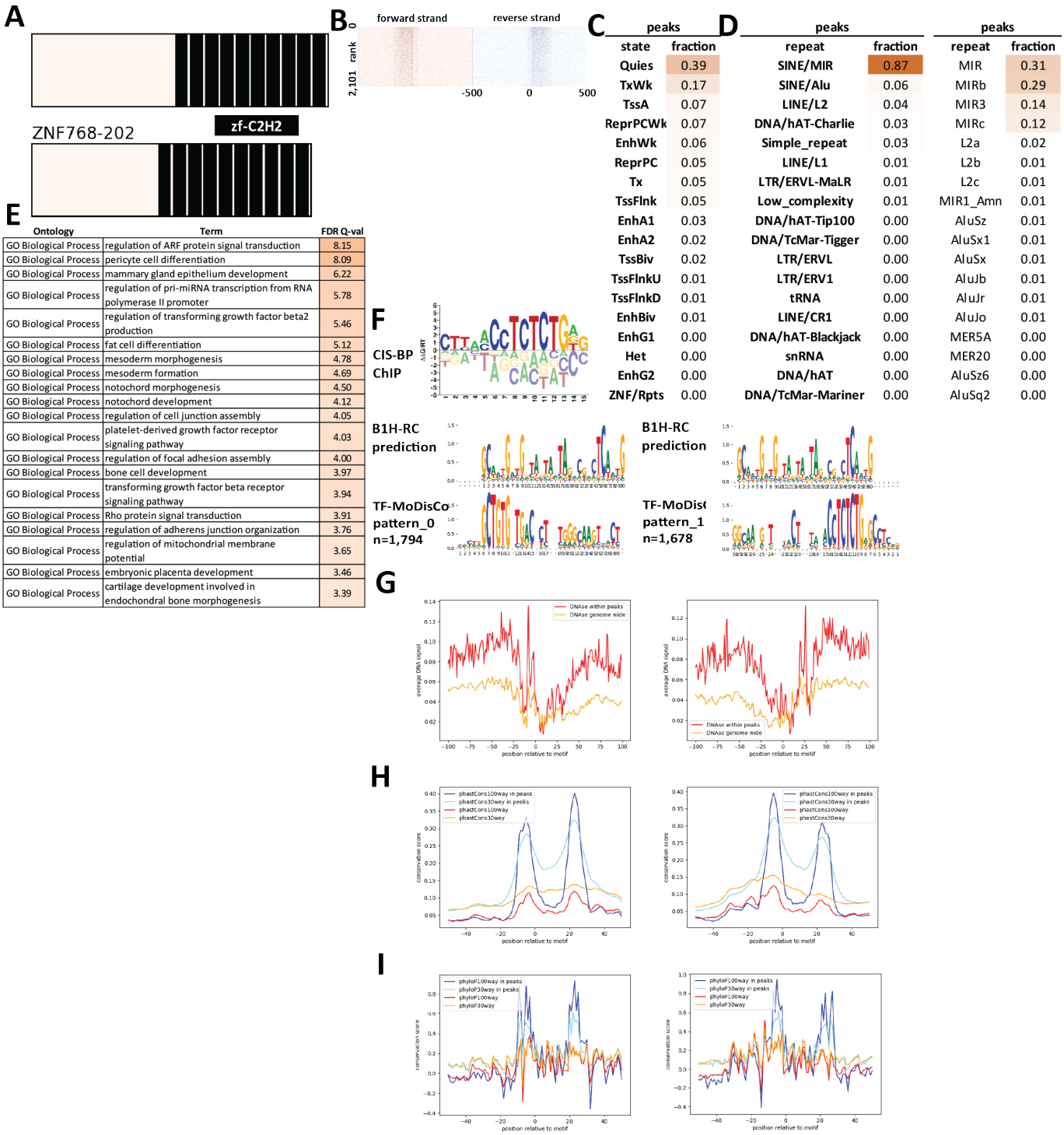

Supplementary Figure 1676: Properties and genomic distribution of motifs identified for the ZNF768 transcription factor in HEK293 (accession Hughes GR models).

TF-MoDisCO pattern_0 n=1794, CWM

pattern_0, n=1794; subpattern_0, ns=536

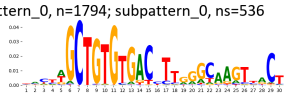

pattern_0, n=1794; subpattern_1, ns=443

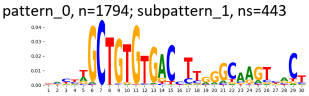

pattern_0, n=1794; subpattern_2, ns=364

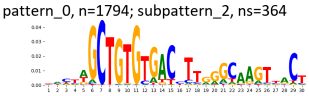

pattern_0, n=1794; subpattern_3, ns=261

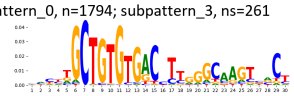

pattern_0, n=1794; subpattern_4, ns=190

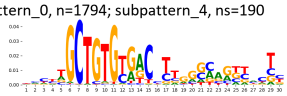

TF-MoDisCO pattern_0 n=1794, PWM

pattern_0, n=1794; subpattern_0, ns=536

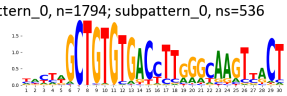

pattern_0, n=1794; subpattern_1, ns=443

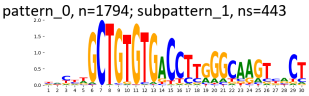

pattern_0, n=1794; subpattern_2, ns=364

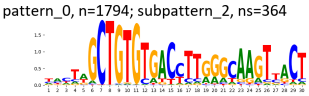

pattern_0, n=1794; subpattern_3, ns=261

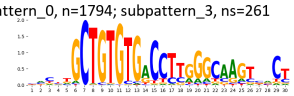

pattern_0, n=1794; subpattern_4, ns=190

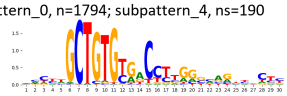

TF-MoDisCO pattern_1 n=1678, CWM

pattern_1, n=1678; subpattern_0, ns=446

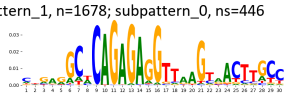

pattern_1, n=1678; subpattern_1, ns=423

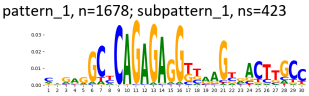

pattern_1, n=1678; subpattern_2, ns=403

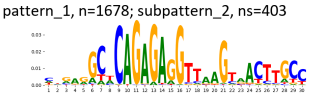

pattern_1, n=1678; subpattern_3, ns=320

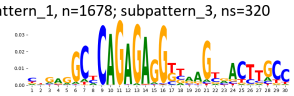

pattern_1, n=1678; subpattern_4, ns=86

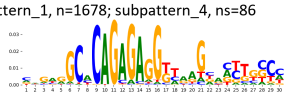

TF-MoDisCO pattern_1 n=1678, PWM

pattern_1, n=1678; subpattern_0, ns=446

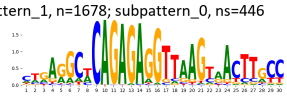

pattern_1, n=1678; subpattern_1, ns=423

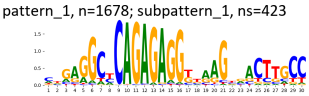

pattern_1, n=1678; subpattern_2, ns=403

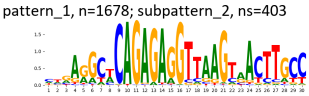

pattern_1, n=1678; subpattern_3, ns=320

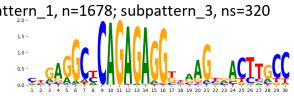

pattern_1, n=1678; subpattern_4, ns=86

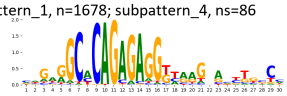

Supplementary Figure 1677: TF-MoDisCO subpatterns for the ZNF768 transcription factor in HEK293 (accession Hughes GR models).

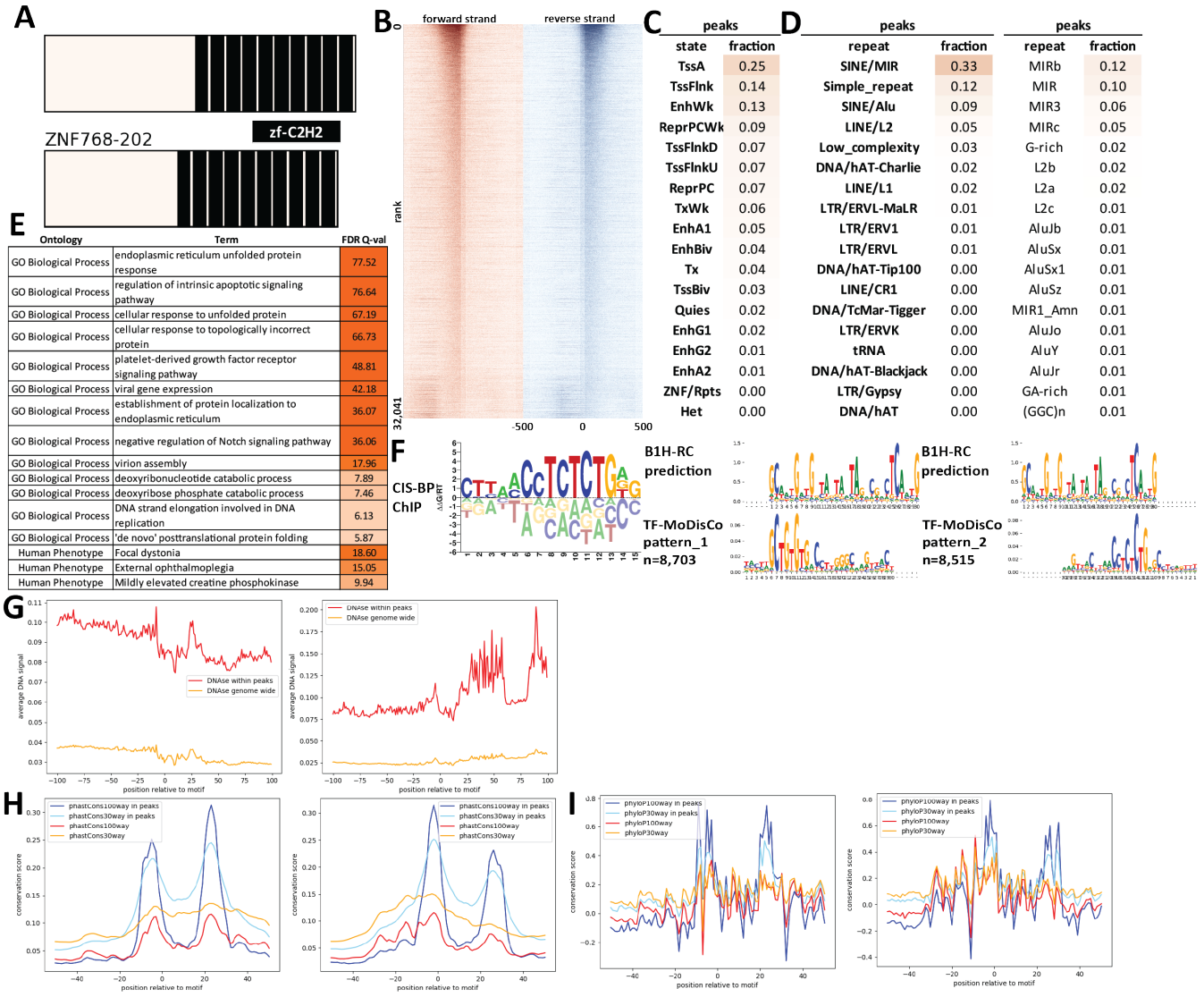

Supplementary Figure 1678: Properties and genomic distribution of motifs identified for the ZNF768 transcription factor in HepG2 (accession ENCSR181ABP).

TF-MoDisCO pattern_1 n=8703, CWM

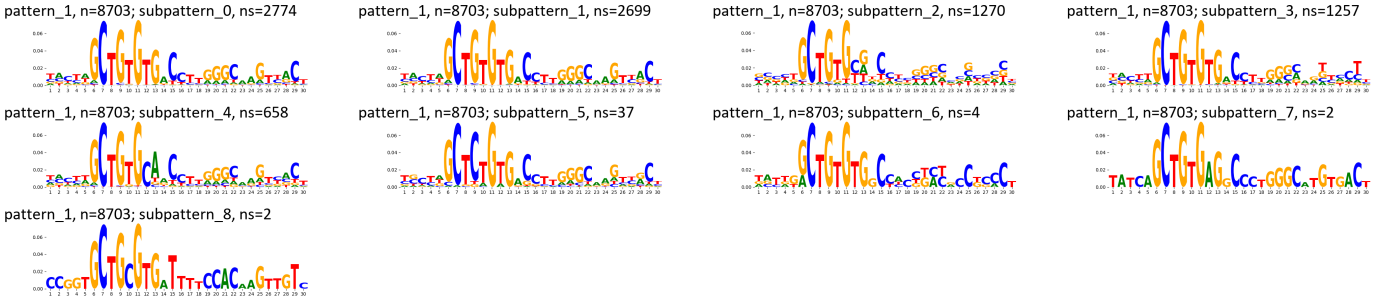

TF-MoDisCO pattern_1 n=8703, PWM

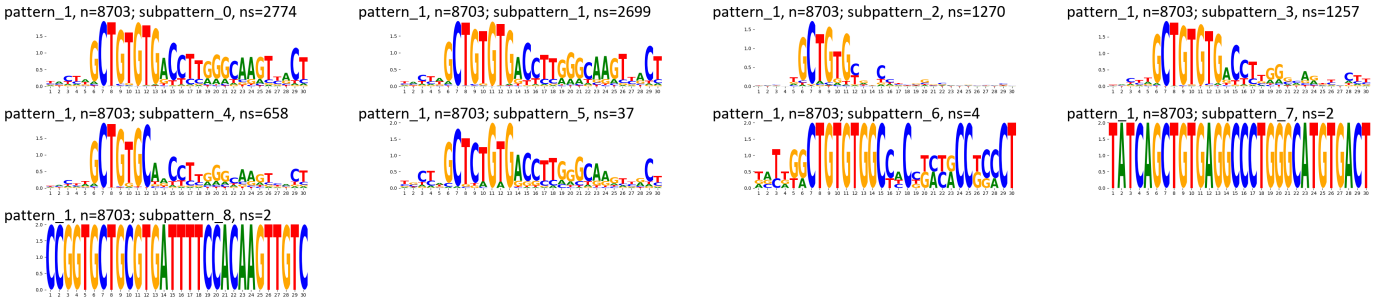

TF-MoDisCO pattern_2 n=8515, CWM

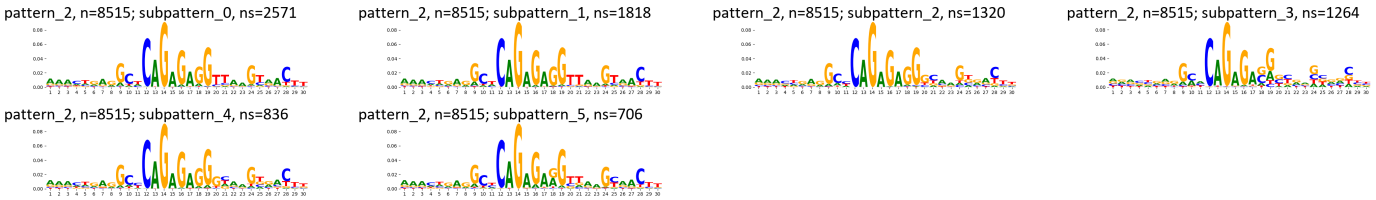

TF-MoDisCO pattern_2 n=8515, PWM

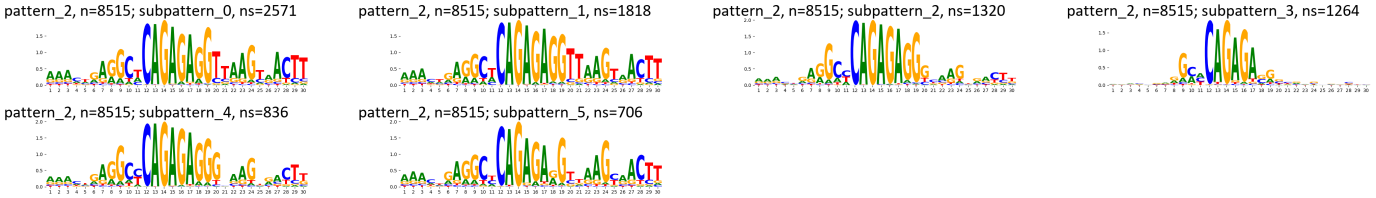

Supplementary Figure 1679: TF-MoDisCO subpatterns for the ZNF768 transcription factor in HepG2 (accession ENCSR181ABP).

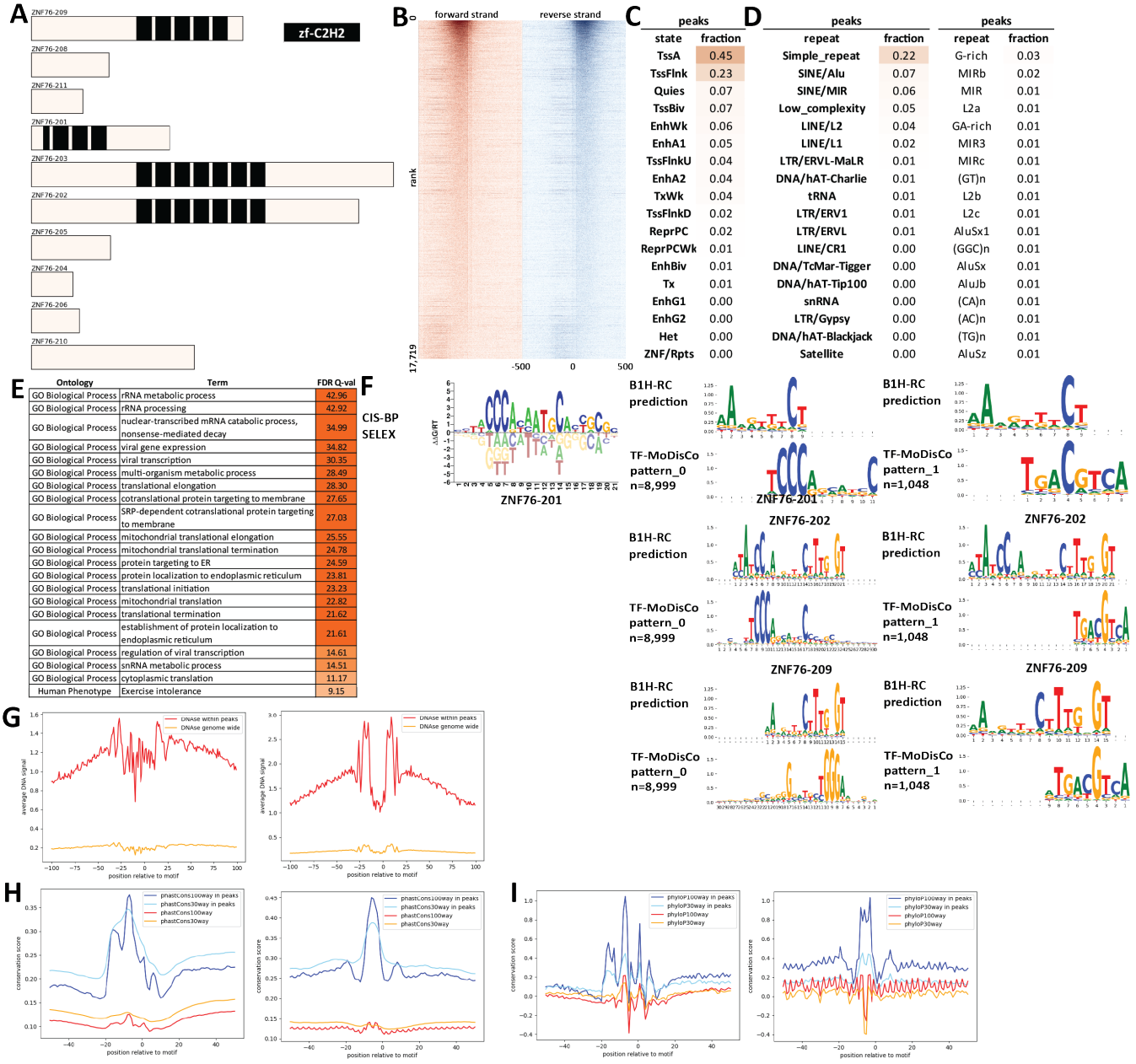

Supplementary Figure 1680: Properties and genomic distribution of motifs identified for the ZNF76 transcription factor in HEK293 (accession ENCSR072LQF).

TF-MoDisCO pattern_0 n=8999, CWM

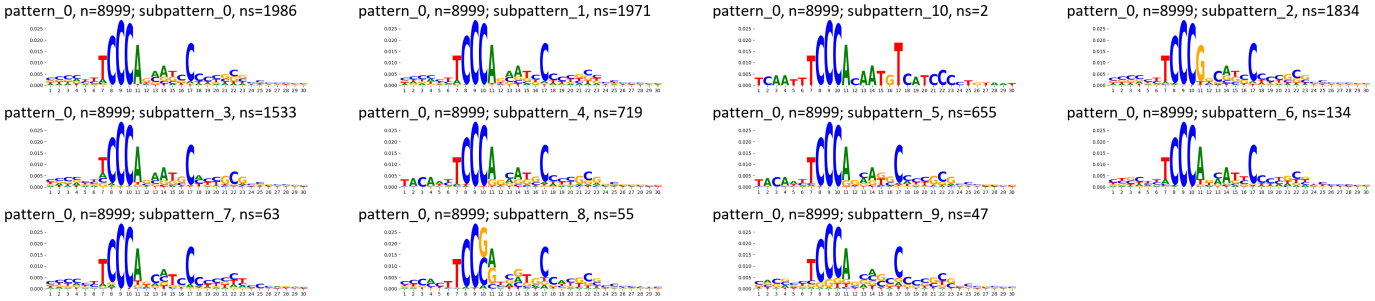

TF-MoDisCO pattern_0 n=8999, PWM

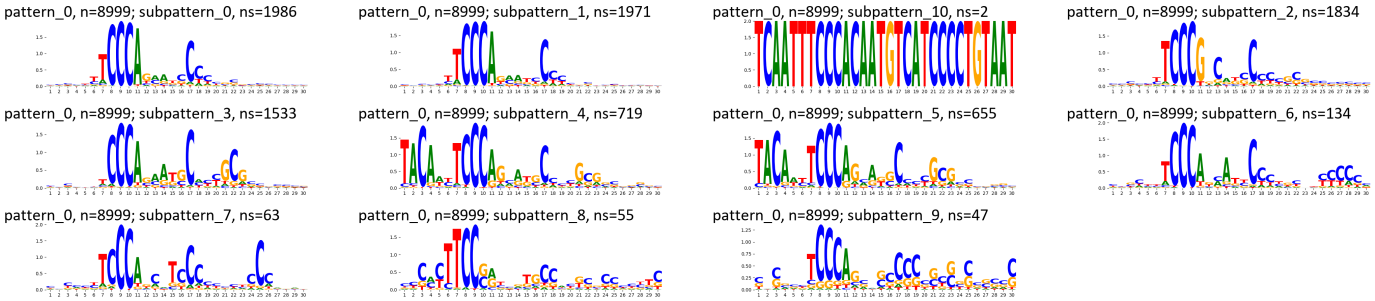

TF-MoDisCO pattern_1 n=1048, CWM

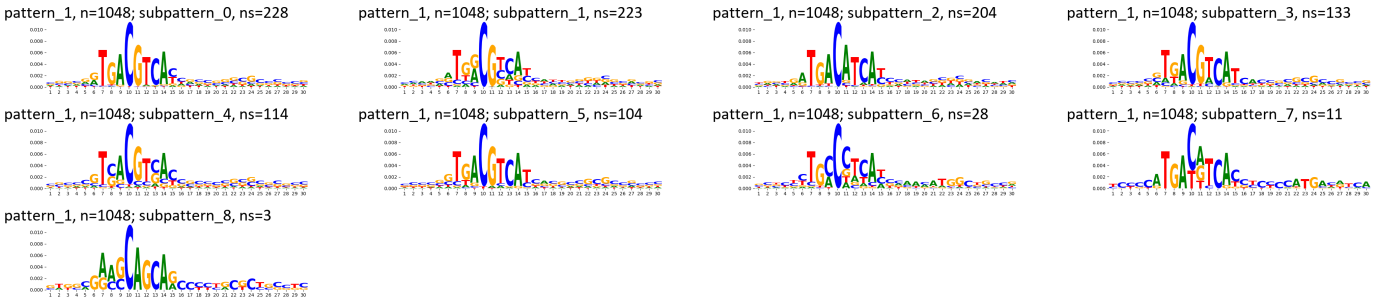

TF-MoDisCO pattern_1 n=1048, PWM

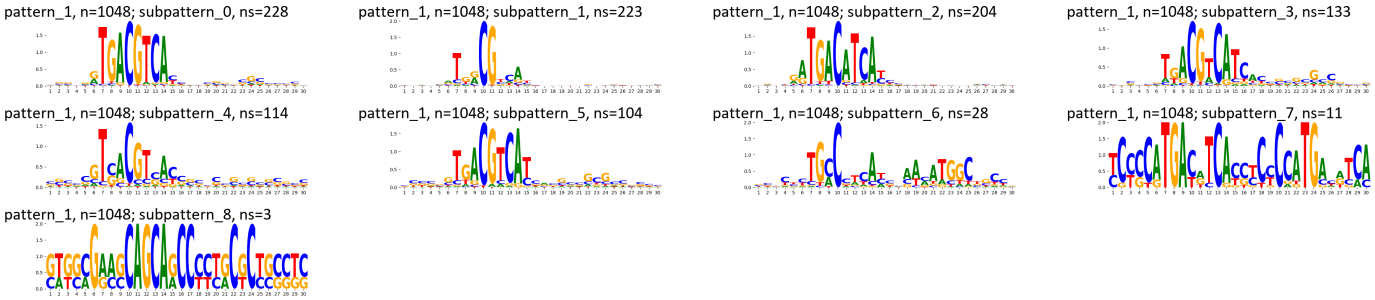

Supplementary Figure 1681: TF-MoDisCO subpatterns for the ZNF76 transcription factor in HEK293 (accession ENCSR072LQF).

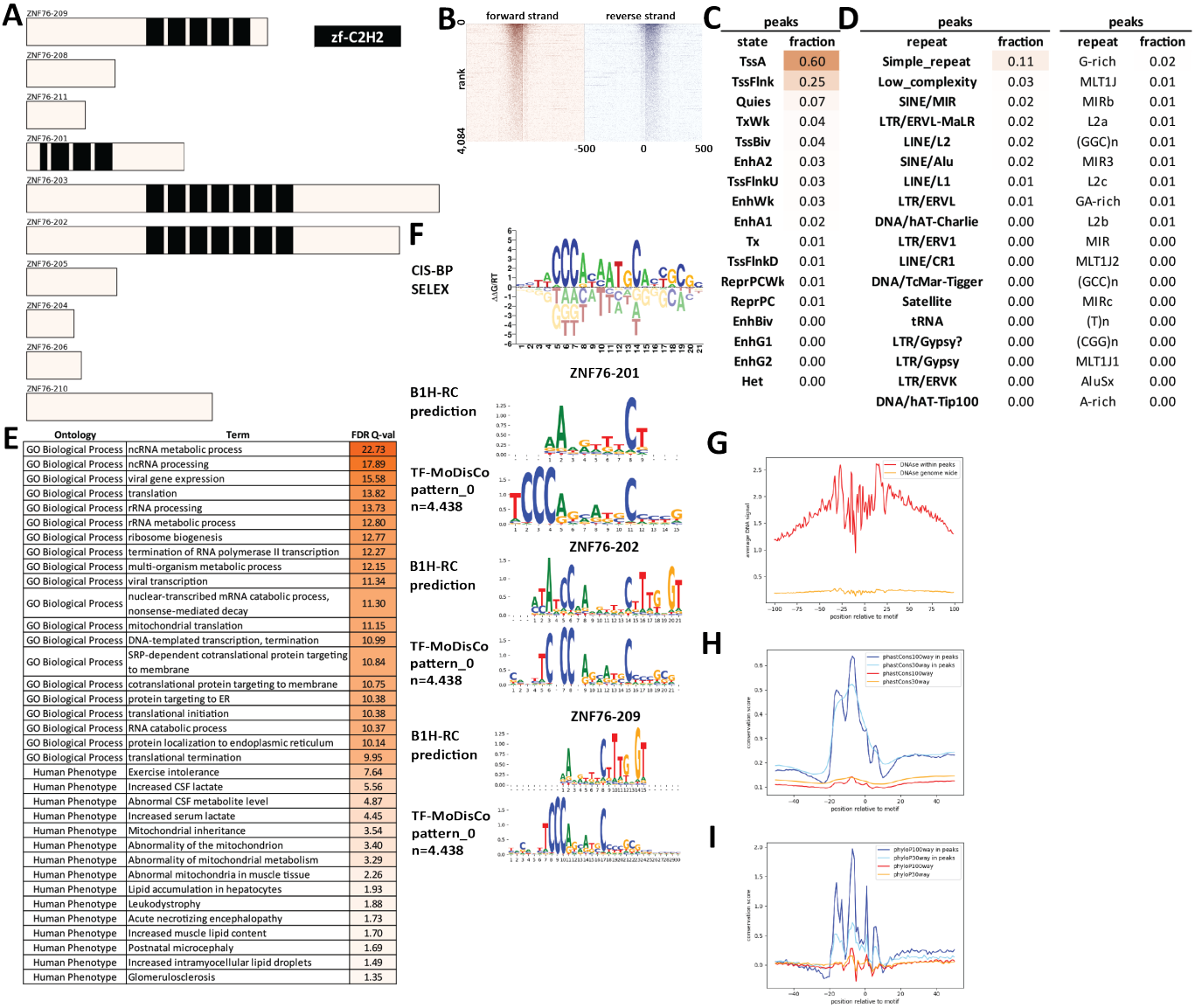

C

peaks	
state	fraction
TssA	0.60
TssFlnk	0.25
Quies	0.07
TxWk	0.04
TssBiv	0.04
EnhA2	0.03
TssFlnkU	0.03
EnhWk	0.03
EnhA1	0.02
Tx	0.01
TssFlnkD	0.01
ReprPCWk	0.01
ReprPC	0.01
EnhBiv	0.00
EnhG1	0.00
EnhG2	0.00
Het	0.00

D

peaks		peaks	
repeat	fraction	repeat	fraction
Simple_repeat	0.11	G-rich	0.02
Low_complexity	0.03	MLT1J	0.01
SINE/MIR	0.02	MIRb	0.01
LTR/ERVL-MaLR	0.02	L2a	0.01
LINE/L2	0.02	(GGC)n	0.01
SINE/Alu	0.02	MIR3	0.01
LINE/L1	0.01	L2c	0.01
LTR/ERVL	0.01	GA-rich	0.01
DNA/hAT-Charlie	0.00	L2b	0.01
LTR/ERV1	0.00	MIR	0.00
LINE/CR1	0.00	MLT1J2	0.00
DNA/TcMar-Tigger	0.00	(GCC)n	0.00
Satellite	0.00	MIRc	0.00
tRNA	0.00	(T)n	0.00
LTR/Gypsy?	0.00	(CGG)n	0.00
LTR/Gypsy	0.00	MLT1J1	0.00
LTR/ERVK	0.00	AluSx	0.00
DNA/hAT-Tip100	0.00	A-rich	0.00

E

Ontology	Term	FDR Q-val
GO Biological Process	ncRNA metabolic process	22.73
GO Biological Process	ncRNA processing	17.89
GO Biological Process	viral gene expression	15.58
GO Biological Process	translation	13.82
GO Biological Process	rRNA processing	13.73
GO Biological Process	rRNA metabolic process	12.80
GO Biological Process	ribosome biogenesis	12.77
GO Biological Process	termination of RNA polymerase II transcription	12.27
GO Biological Process	multi-organism metabolic process	12.15
GO Biological Process	viral transcription	11.34
GO Biological Process	nuclear-transcribed mRNA catabolic process, nonsense-mediated decay	11.30
GO Biological Process	mitochondrial translation	11.15
GO Biological Process	DNA-templated transcription, termination	10.99
GO Biological Process	SRP-dependent cotranslational protein targeting to membrane	10.84
GO Biological Process	cotranslational protein targeting to membrane	10.75
GO Biological Process	protein targeting to ER	10.38
GO Biological Process	translational initiation	10.38
GO Biological Process	RNA catabolic process	10.37
GO Biological Process	protein localization to endoplasmic reticulum	10.14
GO Biological Process	translational termination	9.95
Human Phenotype	Exercise intolerance	7.64
Human Phenotype	Increased CSF lactate	5.56
Human Phenotype	Abnormal CSF metabolite level	4.87
Human Phenotype	Increased serum lactate	4.45
Human Phenotype	Mitochondrial inheritance	3.54
Human Phenotype	Abnormality of the mitochondrion	3.40
Human Phenotype	Abnormality of mitochondrial metabolism	3.29
Human Phenotype	Abnormal mitochondria in muscle tissue	2.26
Human Phenotype	Lipid accumulation in hepatocytes	1.93
Human Phenotype	Leukodystrophy	1.88
Human Phenotype	Acute necrotizing encephalopathy	1.73
Human Phenotype	Increased muscle lipid content	1.70
Human Phenotype	Postnatal microcephaly	1.69
Human Phenotype	Increased intramyocellular lipid droplets	1.49
Human Phenotype	Glomerulosclerosis	1.35

Supplementary Figure 1682: Properties and genomic distribution of motifs identified for the ZNF76 transcription factor in HEK293 (accession Hughes GR models).

TF-MoDisCO pattern_0 n=4438, CWM

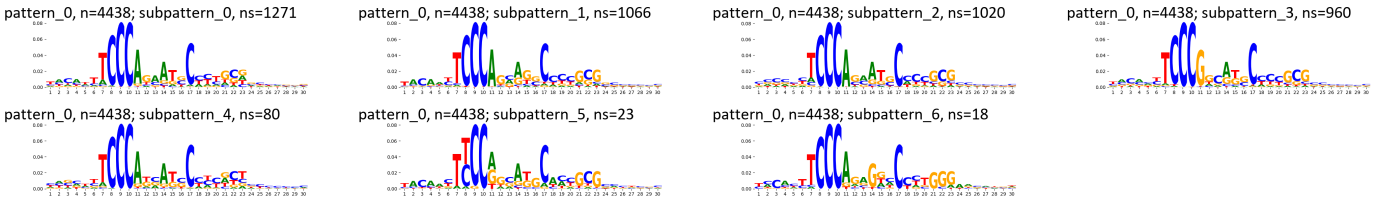

TF-MoDisCO pattern_0 n=4438, PWM

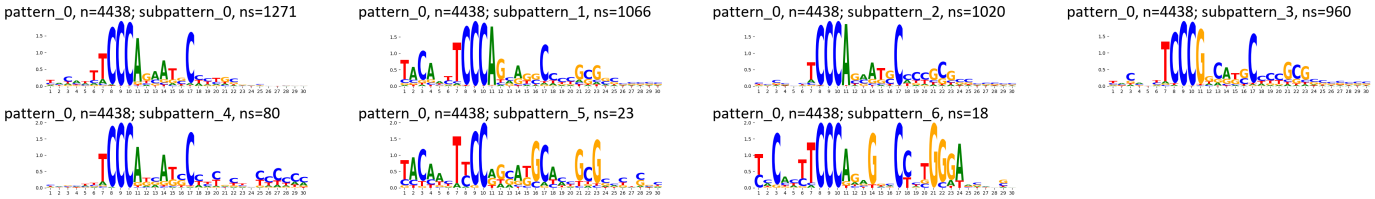

Supplementary Figure 1683: TF-MoDisCO subpatterns for the ZNF76 transcription factor in HEK293 (accession Hughes GR models).

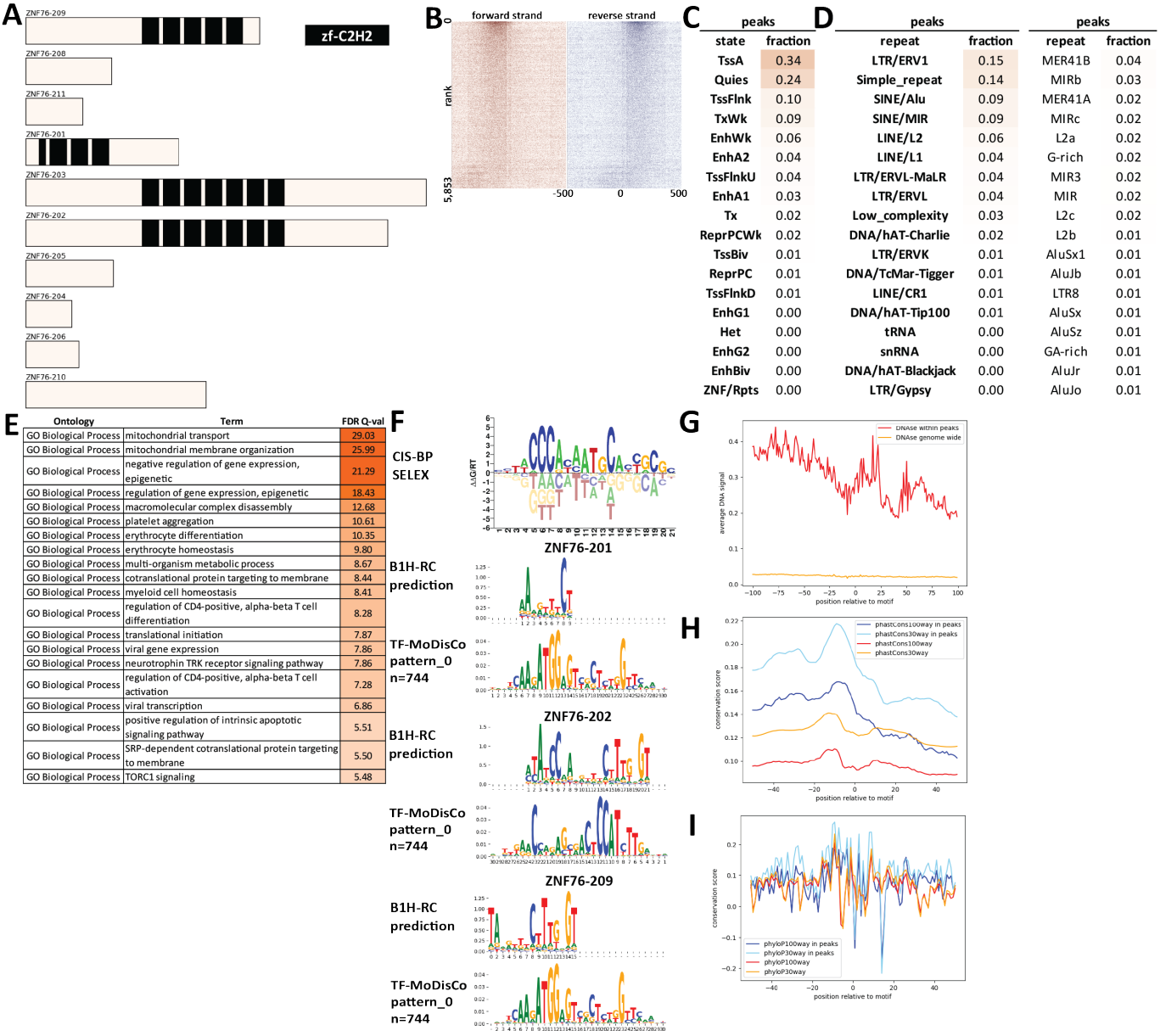

C

peaks	
state	fraction
TssA	0.34
Quies	0.24
TssFlnk	0.10
TxWk	0.09
EnhWk	0.06
EnhA2	0.04
TssFlnkU	0.04
EnhA1	0.03
Tx	0.02
ReprPCWk	0.02
TssBiv	0.01
ReprPC	0.01
TssFlnkD	0.01
EnhG1	0.00
Het	0.00
EnhG2	0.00
EnhBiv	0.00
ZNF/Rpts	0.00

D

peaks		peaks	
repeat	fraction	repeat	fraction
LTR/ERV1	0.15	MER41B	0.04
Simple_repeat	0.14	MIRb	0.03
SINE/Alu	0.09	MER41A	0.02
SINE/MIR	0.09	MIRc	0.02
LINE/L2	0.06	L2a	0.02
LINE/L1	0.04	G-rich	0.02
LTR/ERVL-MaLR	0.04	MIR3	0.02
LTR/ERVL	0.04	MIR	0.02
Low_complexity	0.03	L2c	0.02
DNA/hAT-Charlie	0.02	L2b	0.01
LTR/ERVK	0.01	AluSx1	0.01
DNA/TcMar-Tigger	0.01	AluJb	0.01
LINE/CR1	0.01	LTR8	0.01
DNA/hAT-Tip100	0.01	AluSx	0.01
tRNA	0.00	AluSz	0.01
snRNA	0.00	GA-rich	0.01
DNA/hAT-Blackjack	0.00	AluJr	0.01
LTR/Gypsy	0.00	AluJo	0.01

E

Ontology	Term	FDR Q-val
GO Biological Process	mitochondrial transport	29.03
GO Biological Process	mitochondrial membrane organization	25.99
GO Biological Process	negative regulation of gene expression, epigenetic	21.29
GO Biological Process	regulation of gene expression, epigenetic	18.43
GO Biological Process	macromolecular complex disassembly	12.68
GO Biological Process	platelet aggregation	10.61
GO Biological Process	erythrocyte differentiation	10.35
GO Biological Process	erythrocyte homeostasis	9.80
GO Biological Process	multi-organism metabolic process	8.67
GO Biological Process	cotranslational protein targeting to membrane	8.44
GO Biological Process	myeloid cell homeostasis	8.41
GO Biological Process	regulation of CD4-positive, alpha-beta T cell differentiation	8.28
GO Biological Process	translational initiation	7.87
GO Biological Process	viral gene expression	7.86
GO Biological Process	neurotrophin TRK receptor signaling pathway	7.86
GO Biological Process	regulation of CD4-positive, alpha-beta T cell activation	7.28
GO Biological Process	viral transcription	6.86
GO Biological Process	positive regulation of intrinsic apoptotic signaling pathway	5.51
GO Biological Process	SRP-dependent cotranslational protein targeting to membrane	5.50
GO Biological Process	TORC1 signaling	5.48

Supplementary Figure 1684: Properties and genomic distribution of motifs identified for the ZNF76 transcription factor in K562 (accession ENCSR257AFV).

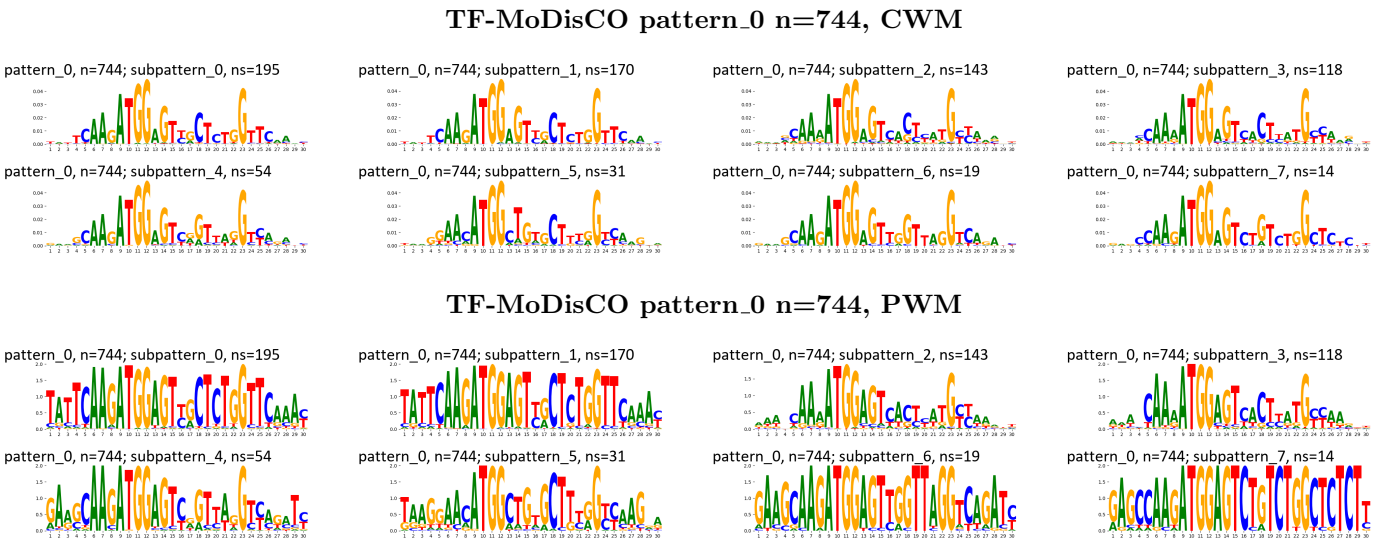

Supplementary Figure 1685: TF-MoDisCO subpatterns for the ZNF76 transcription factor in K562 (accession ENCSR257AFV).

A

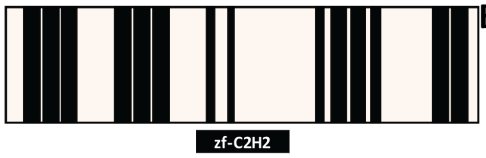

B

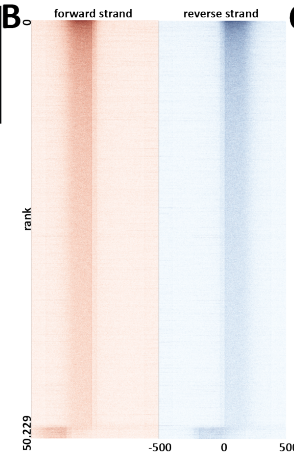

C

peaks	
state	fraction
TxWk	0.23
Quies	0.23
EnhWk	0.08
TssA	0.07
Tx	0.07
TssFlnk	0.05
ReprPCWk	0.03
EnhA2	0.02
EnhA1	0.02
ReprPC	0.02
TssBiv	0.01
TssFlnkU	0.01
EnhG1	0.01
TssFlnkD	0.01
EnhBiv	0.00
Het	0.00
EnhG2	0.00
ZNF/Rpts	0.00

D

peaks		peaks	
repeat	fraction	repeat	fraction
SINE/Alu	0.96	AluJb	0.22
LINE/L1	0.11	AluJr	0.17
Simple_repeat	0.10	AluJo	0.13
SINE/MIR	0.07	AluSx	0.06
LINE/L2	0.06	AluSz	0.06
DNA/hAT-Charlie	0.03	AluSx1	0.06
LTR/ERVL-MaLR	0.03	AluJr4	0.03
LTR/ERV1	0.02	AluSq2	0.03
DNA/TcMar-Tigger	0.02	AluSz6	0.03
Low_complexity	0.02	L2a	0.03
LTR/ERVL	0.01	MIRb	0.02
DNA/hAT-Tip100	0.01	AluSp	0.02
LINE/CR1	0.01	FLAM_C	0.02
Retroposon/SVA	0.00	MIR	0.02
LINE/RTE-X	0.00	AluY	0.02
DNA/hAT-Blackjack	0.00	AluSg	0.02
DNA/TcMar-Tc2	0.00	AluSx3	0.02
tRNA	0.00	AluSc	0.01

E

Ontology	Term	FDR Q-val
GO Biological Process	negative regulation of translation	109.70
GO Biological Process	nuclear-transcribed mRNA catabolic process	99.12
GO Biological Process	regulation of transcription from RNA polymerase II promoter in response to stress	97.15
GO Biological Process	mitochondrial membrane organization	88.15
GO Biological Process	nuclear-transcribed mRNA catabolic process, nonsense-mediated decay	87.58
GO Biological Process	regulation of DNA-templated transcription in response to stress	87.33
GO Biological Process	gene silencing by miRNA	75.40
GO Biological Process	posttranscriptional gene silencing	74.92
GO Biological Process	posttranscriptional gene silencing by RNA	73.28
GO Biological Process	translational initiation	69.03
GO Biological Process	regulation of transcription from RNA polymerase II promoter in response to hypoxia	66.55
GO Biological Process	regulation of mitochondrial membrane permeability	63.87
GO Biological Process	organelle transport along microtubule	62.87
GO Biological Process	maintenance of protein location in cell	61.23
GO Biological Process	gene silencing by RNA	60.13
GO Biological Process	regulation of membrane permeability	56.03
GO Biological Process	regulation of ubiquitin protein ligase activity	54.31
GO Biological Process	viral gene expression	53.61
GO Biological Process	RNA 3'-end processing	47.54
GO Biological Process	regulation of mitochondrial outer membrane permeabilization involved in apoptotic signaling pathway	47.23
Human Phenotype	Low posterior hairline	38.92
Human Phenotype	Cafe-au-lait spot	36.35
Human Phenotype	Microretrognathia	18.68

F

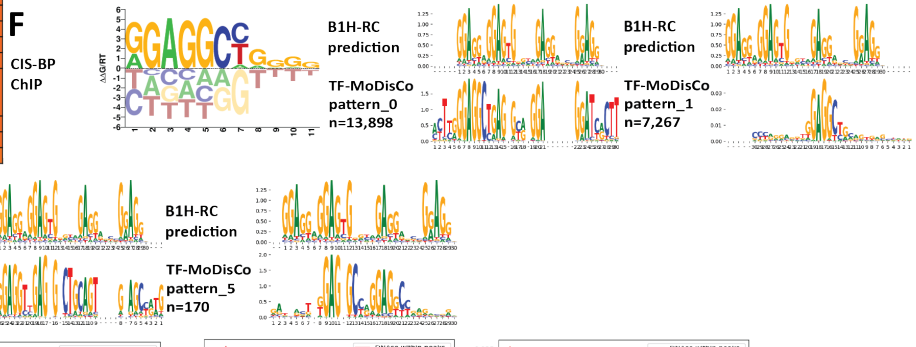

G

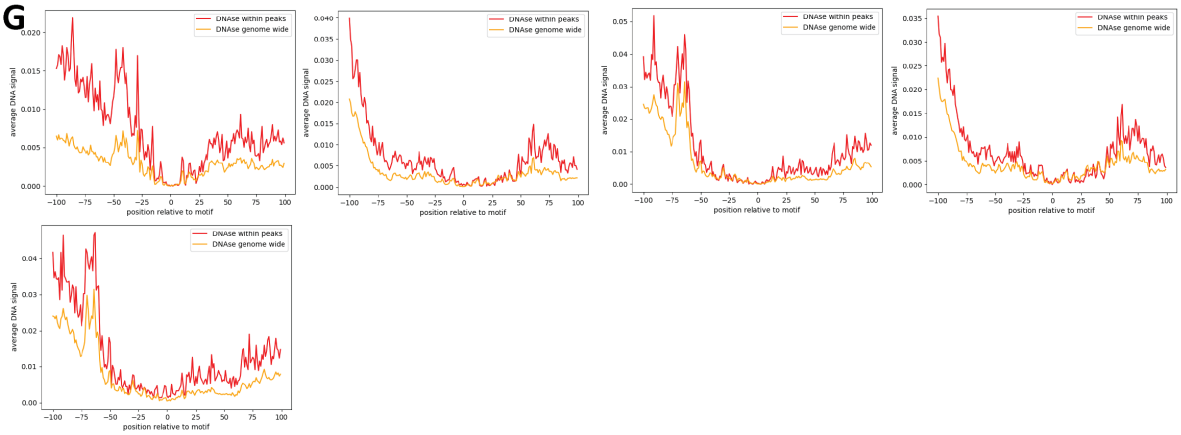

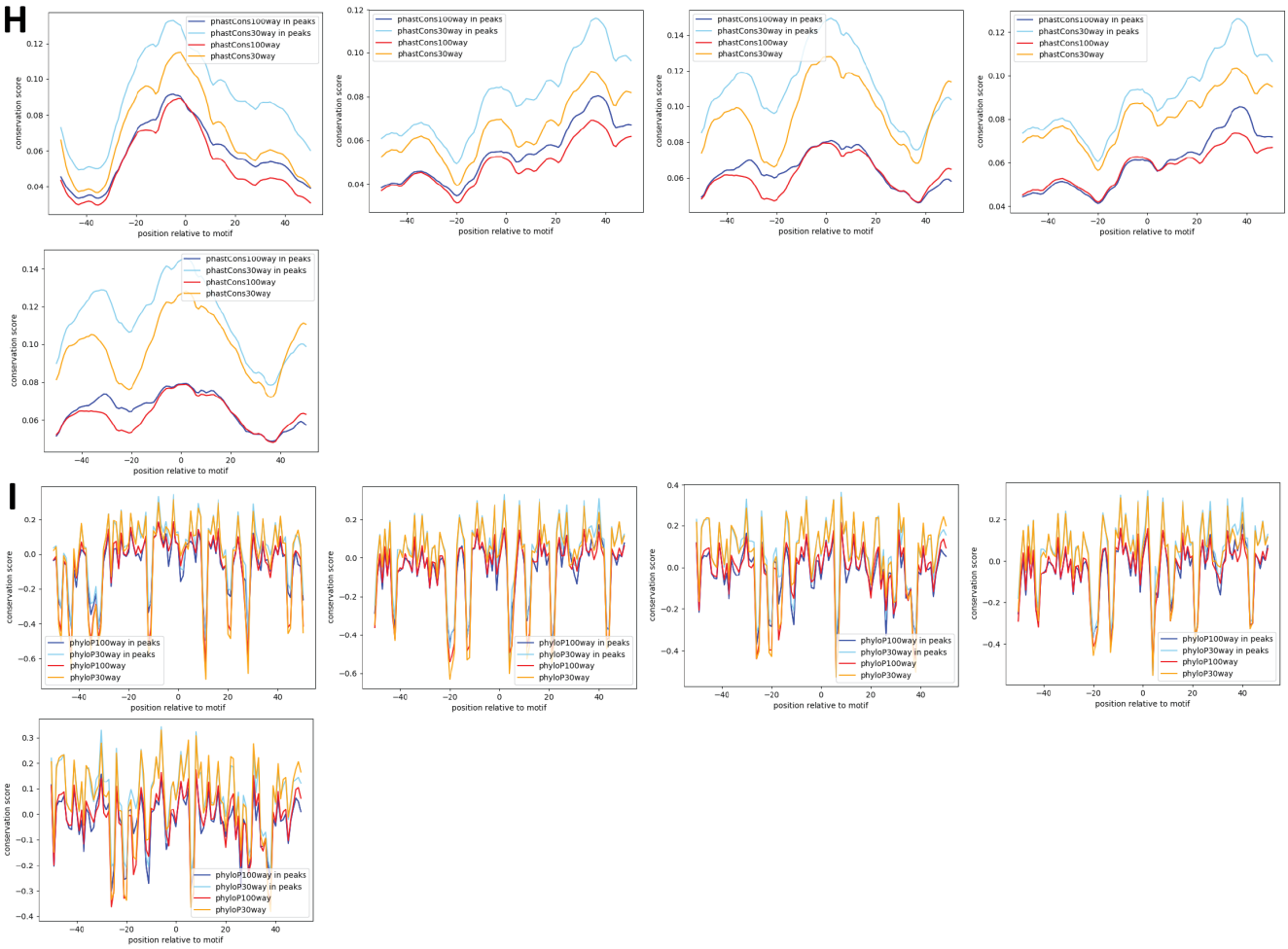

Supplementary Figure 1686: Properties and genomic distribution of motifs identified for the ZNF770 transcription factor in HEK293 (accession ENCSR242BGR).

TF-MoDisCO pattern_0 n=13898, CWM

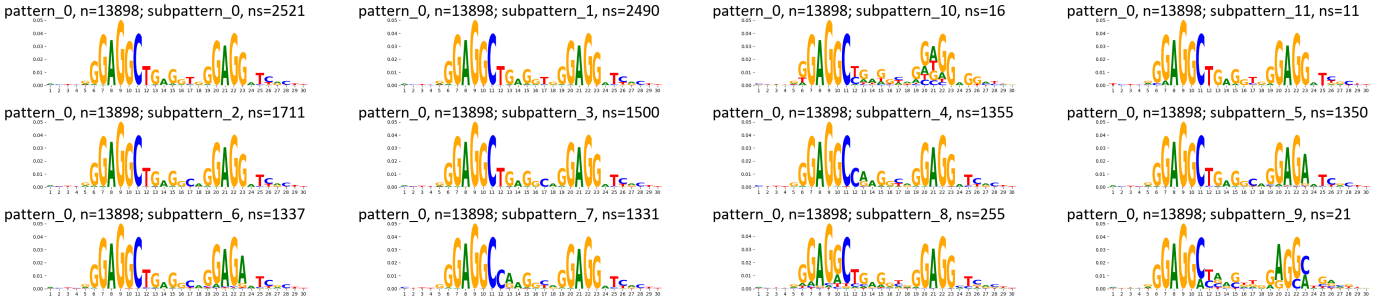

TF-MoDisCO pattern_0 n=13898, PWM

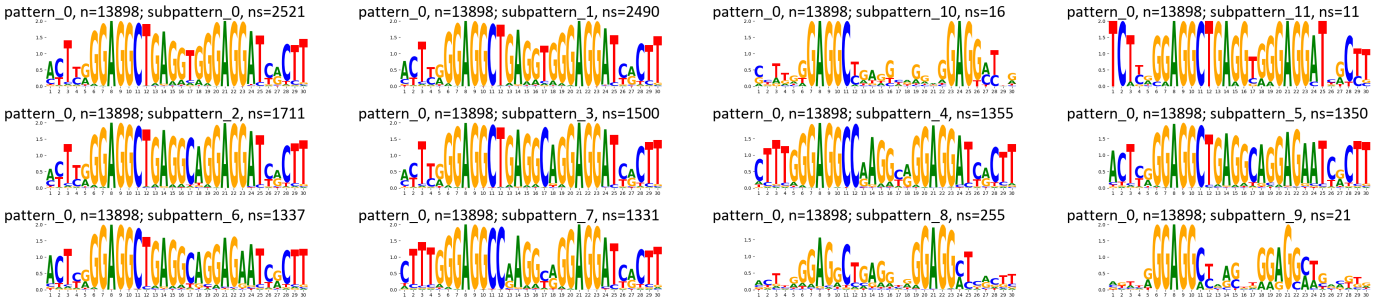

TF-MoDisCO pattern_1 n=7267, CWM

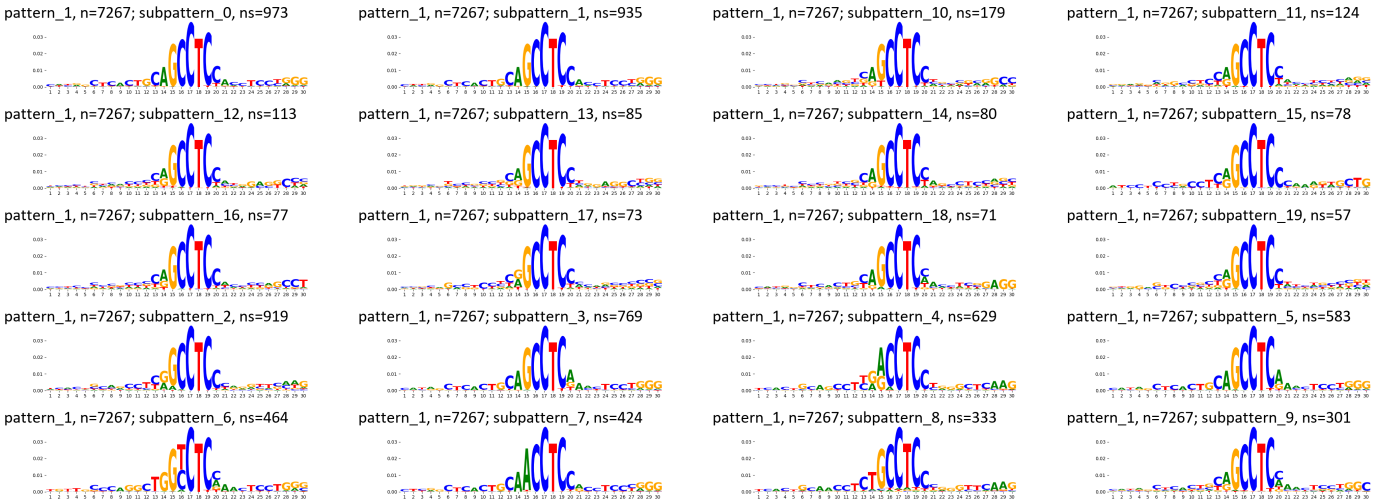

TF-MoDisCO pattern_1 n=7267, CWM

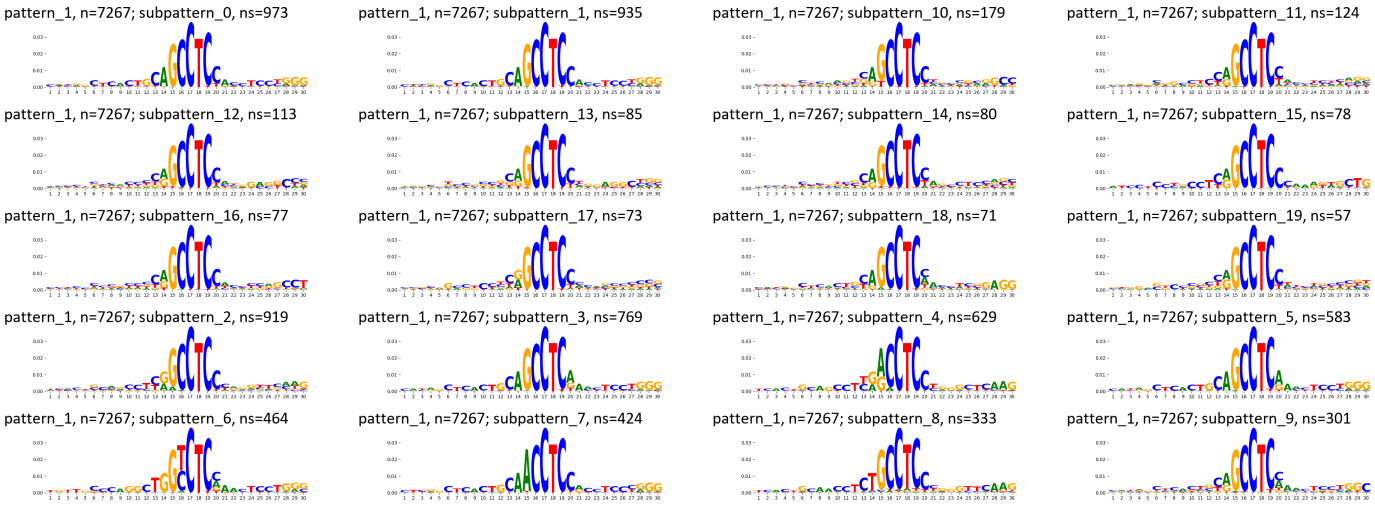

TF-MoDisCO pattern_1 n=7267, PWM

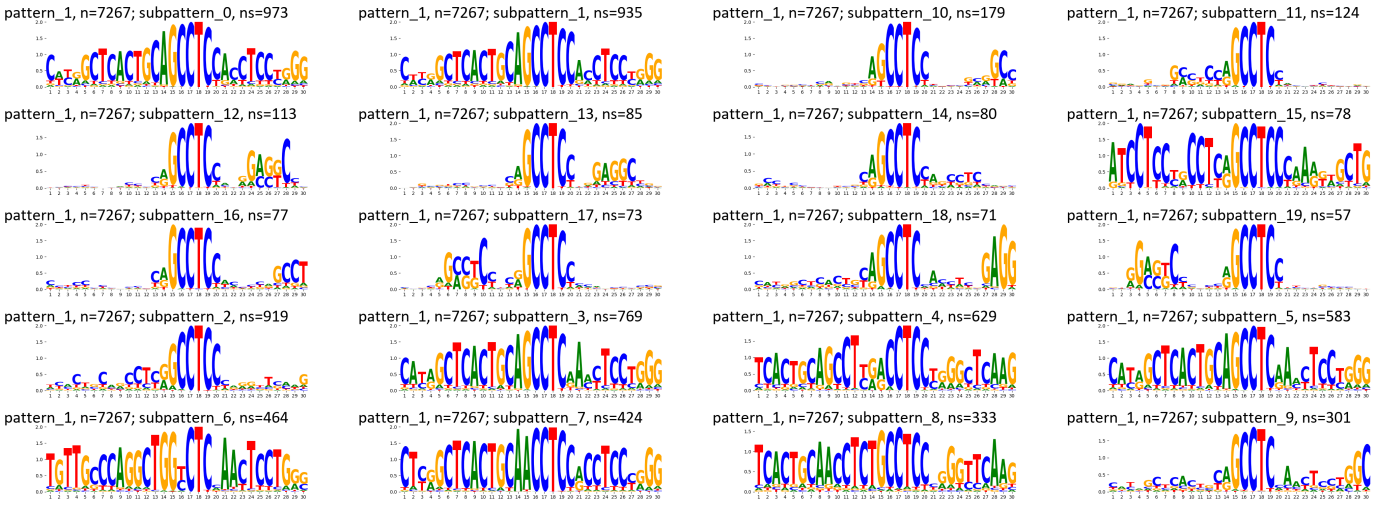

TF-MoDisCO pattern_1 n=7267, PWM

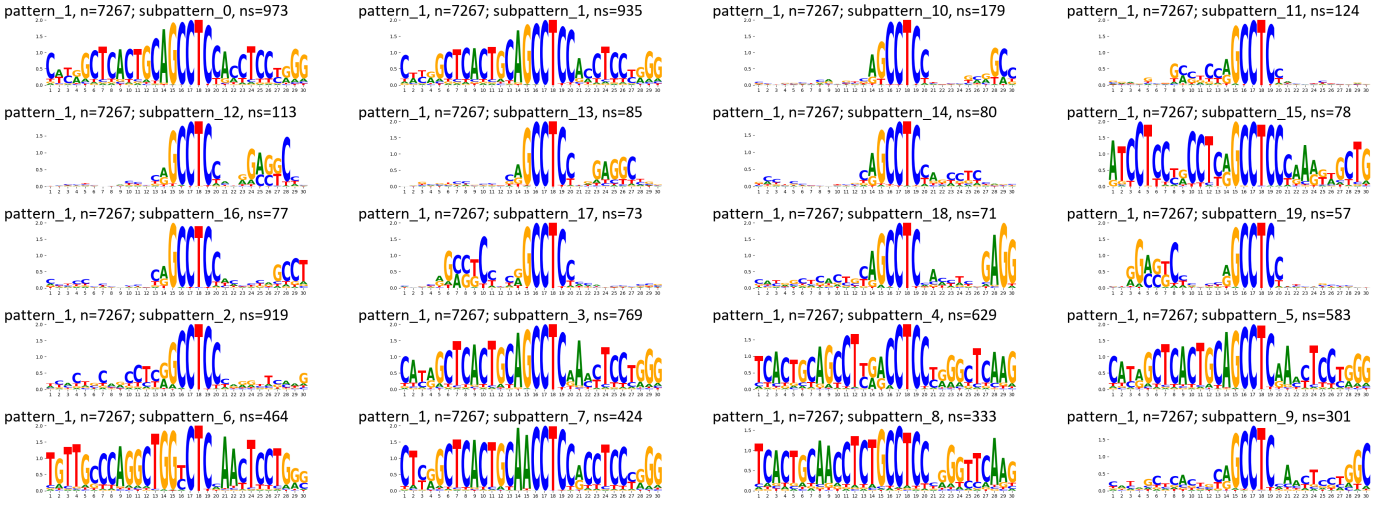

TF-MoDisCO pattern_2 n=600, CWM

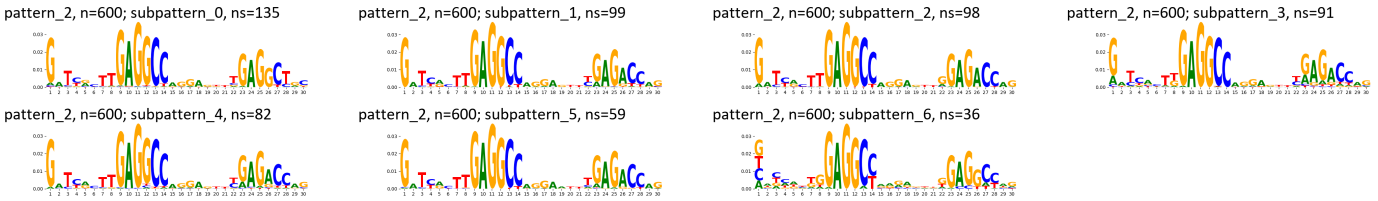

TF-MoDisCO pattern_2 n=600, PWM

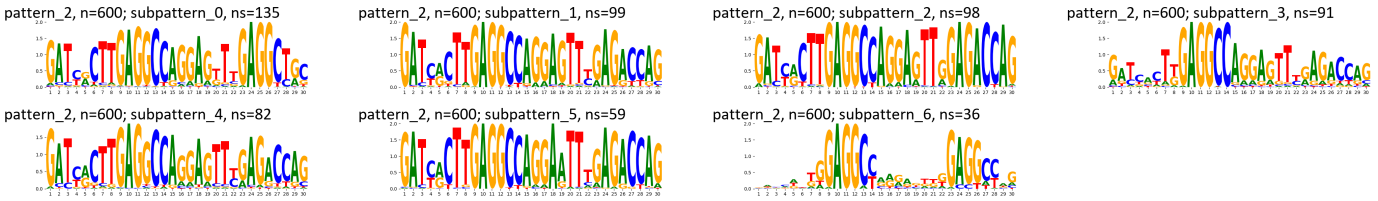

TF-MoDisCO pattern_3 n=384, CWM

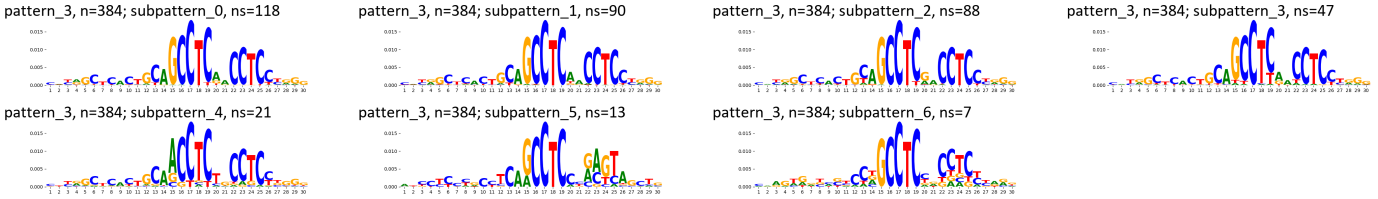

TF-MoDisCO pattern_3 n=384, PWM

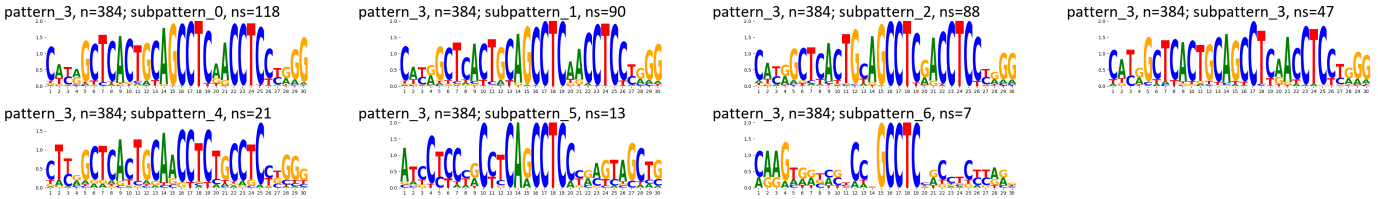

TF-MoDisCO pattern_5 n=170, CWM

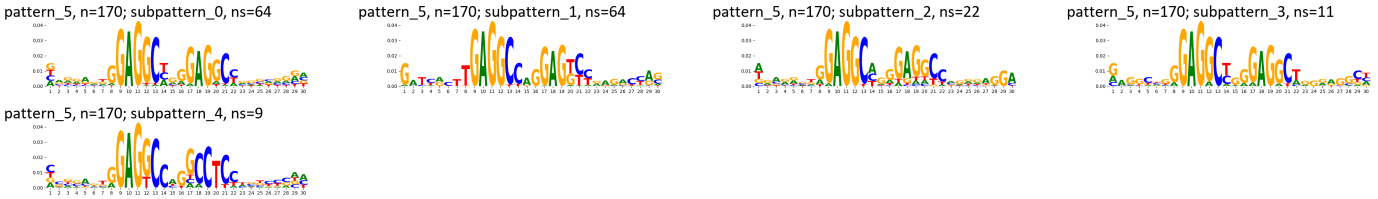

TF-MoDisCO pattern_5 n=170, PWM

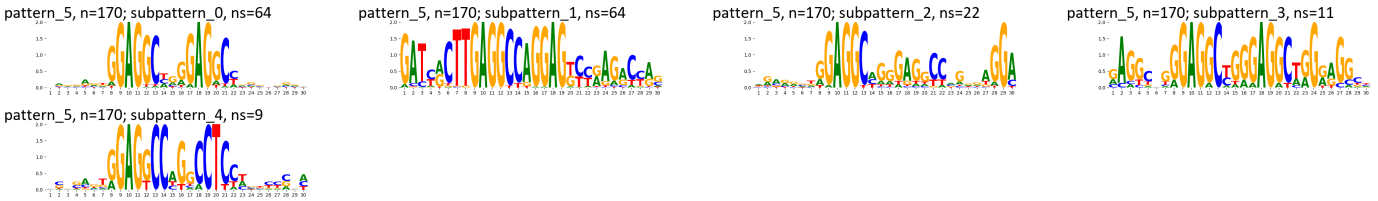

Supplementary Figure 1687: TF-MoDisCO subpatterns for the ZNF770 transcription factor in HEK293 (accession ENCSR242BGR).

A

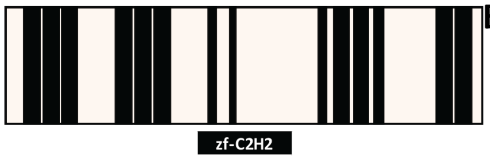

B

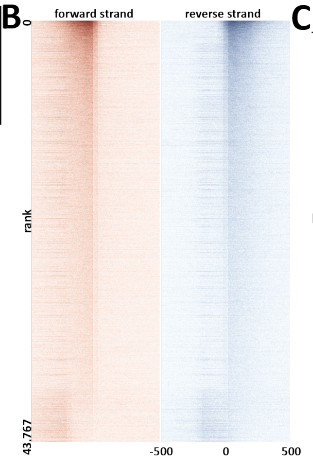

C

peaks	
state	fraction
Quies	0.19
TxWk	0.17
TssA	0.14
TssFlnk	0.09
EnhWk	0.06
Tx	0.05
EnhA2	0.02
ReprPCWk	0.02
TssFlnkU	0.02
EnhA1	0.02
ReprPC	0.01
TssBiv	0.01
TssFlnkD	0.01
EnhG1	0.01
EnhBiv	0.00
Het	0.00
EnhG2	0.00
ZNF/Rpts	0.00

D

peaks		peaks	
repeat	fraction	repeat	fraction
SINE/Alu	0.82	AluJb	0.17
Simple_repeat	0.16	AluJr	0.12
LINE/L1	0.16	AluJo	0.10
SINE/MIR	0.11	AluSx	0.06
LINE/L2	0.09	AluSx1	0.06
DNA/hAT-Charlie	0.05	AluSz	0.05
LTR/ERVL-MaLR	0.04	MIRb	0.04
LTR/ERV1	0.03	L2a	0.04
Low_complexity	0.03	MIR	0.03
DNA/TcMar-Tigger	0.02	AluSq2	0.03
LTR/ERVL	0.02	AluY	0.03
DNA/hAT-Tip100	0.01	AluJr4	0.02
LINE/CR1	0.01	AluSp	0.02
DNA/hAT-Blackjack	0.00	L2c	0.02
Retroposon/SVA	0.00	AluSz6	0.02
tRNA	0.00	L2b	0.02
LINE/RTE-X	0.00	MIRc	0.02
LTR/ERVK	0.00	AluSg	0.02

E

Ontology	Term	FDR Q-val
GO Biological Process	mitochondrial transport	132.12
GO Biological Process	regulation of intrinsic apoptotic signaling pathway	108.93
GO Biological Process	cellular response to insulin stimulus	107.00
GO Biological Process	nuclear-transcribed mRNA catabolic process	100.23
GO Biological Process	mRNA catabolic process	99.14
GO Biological Process	endoplasmic reticulum unfolded protein response	91.29
GO Biological Process	response to topologically incorrect protein	88.12
GO Biological Process	response to unfolded protein	84.38
GO Biological Process	regulation of mRNA stability	83.39
GO Biological Process	mitochondrial membrane organization	82.11
GO Biological Process	macroautophagy	81.65
GO Biological Process	cellular response to unfolded protein	79.38
GO Biological Process	cellular response to topologically incorrect protein	78.98
GO Biological Process	regulation of transcription from RNA polymerase II promoter in response to stress	76.52
GO Biological Process	regulation of mitochondrial membrane permeability	76.34
GO Biological Process	regulation of membrane permeability	75.86
GO Biological Process	IRE1-mediated unfolded protein response	72.38
GO Biological Process	positive regulation of mRNA catabolic process	69.11
GO Biological Process	regulation of DNA-templated transcription in response to stress	66.85
GO Biological Process	nuclear-transcribed mRNA catabolic process, deadenylation-dependent decay	66.76
Human Phenotype	Increased serum lactate	49.19
Human Phenotype	Abnormal CSF metabolite level	36.81

F

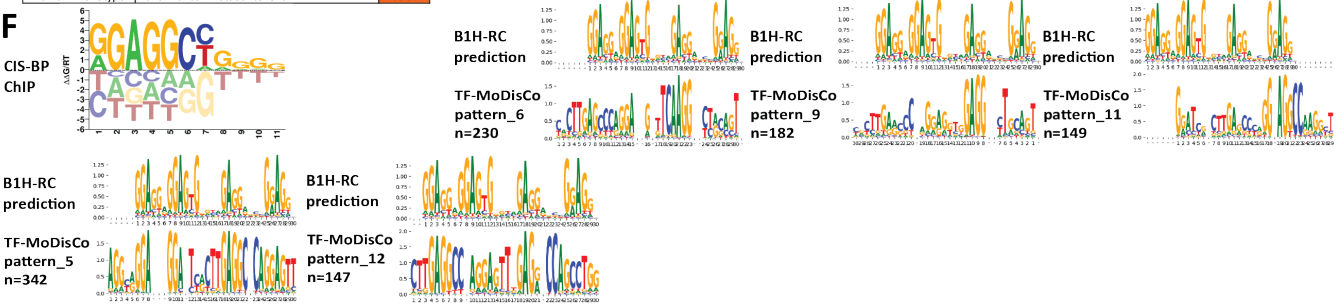

G



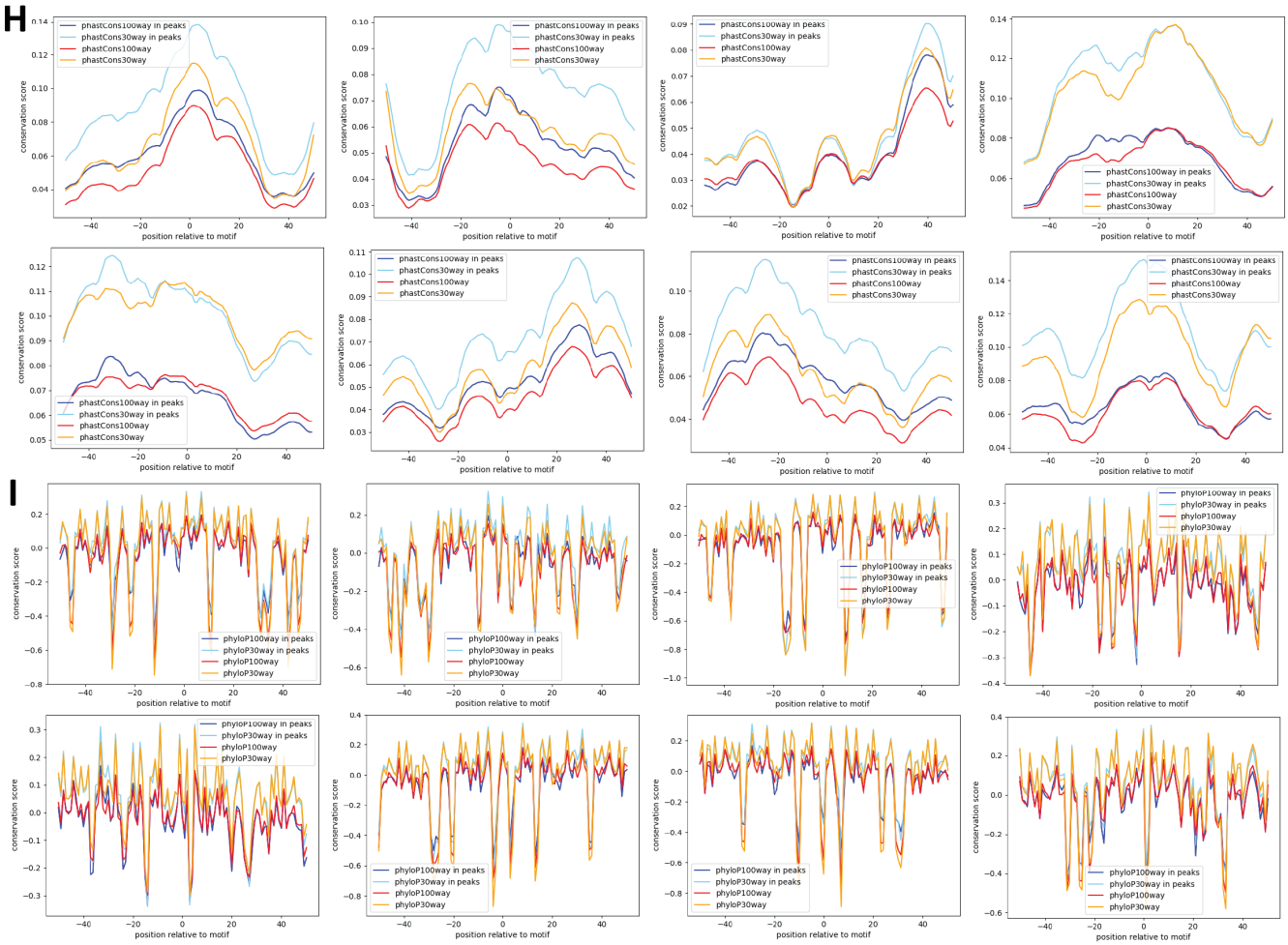

Supplementary Figure 1688: Properties and genomic distribution of motifs identified for the ZNF770 transcription factor in HepG2 (accession ENCSR510GKB).

TF-MoDisCO pattern_0 n=12692, CWM

pattern_0, n=12692; subpattern_0, ns=2244

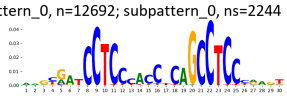

pattern_0, n=12692; subpattern_1, ns=2105

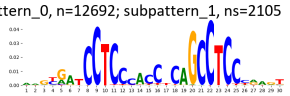

pattern_0, n=12692; subpattern_2, ns=1728

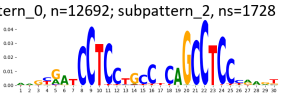

pattern_0, n=12692; subpattern_3, ns=1547

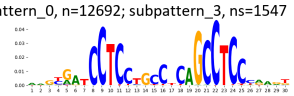

pattern_0, n=12692; subpattern_4, ns=1271

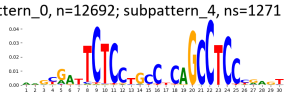

pattern_0, n=12692; subpattern_5, ns=1198

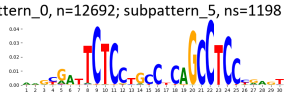

pattern_0, n=12692; subpattern_6, ns=1070

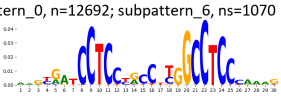

pattern_0, n=12692; subpattern_7, ns=968

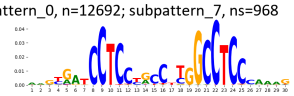

pattern_0, n=12692; subpattern_8, ns=561

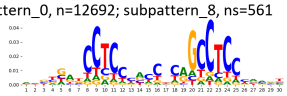

TF-MoDisCO pattern_0 n=12692, PWM

pattern_0, n=12692; subpattern_0, ns=2244

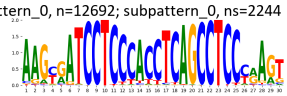

pattern_0, n=12692; subpattern_1, ns=2105

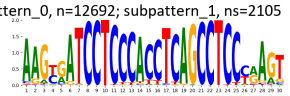

pattern_0, n=12692; subpattern_2, ns=1728

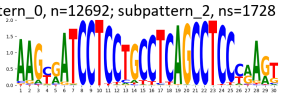

pattern_0, n=12692; subpattern_3, ns=1547

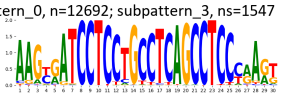

pattern_0, n=12692; subpattern_4, ns=1271

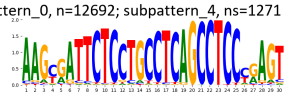

pattern_0, n=12692; subpattern_5, ns=1198

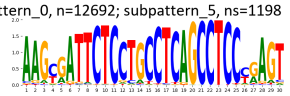

pattern_0, n=12692; subpattern_6, ns=1070

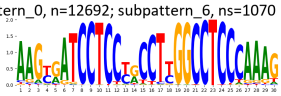

pattern_0, n=12692; subpattern_7, ns=968

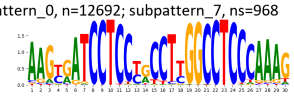

pattern_0, n=12692; subpattern_8, ns=561

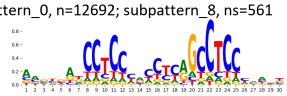

TF-MoDisCO pattern_1 n=1198, CWM

pattern_1, n=1198; subpattern_0, ns=231

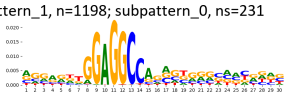

pattern_1, n=1198; subpattern_1, ns=218

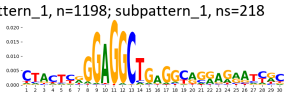

pattern_1, n=1198; subpattern_10, ns=23

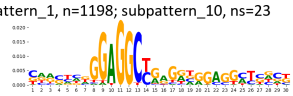

pattern_1, n=1198; subpattern_11, ns=19

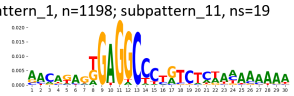

pattern_1, n=1198; subpattern_12, ns=18

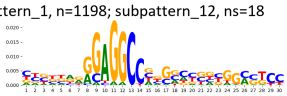

pattern_1, n=1198; subpattern_13, ns=2

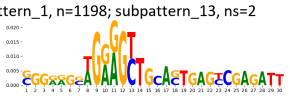

pattern_1, n=1198; subpattern_14, ns=2

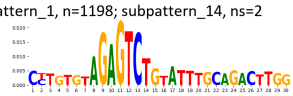

pattern_1, n=1198; subpattern_2, ns=179

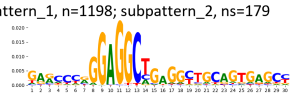

pattern_1, n=1198; subpattern_3, ns=140

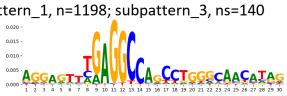

pattern_1, n=1198; subpattern_4, ns=137

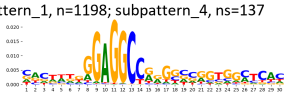

pattern_1, n=1198; subpattern_5, ns=80

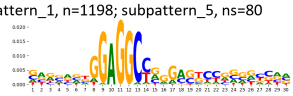

pattern_1, n=1198; subpattern_6, ns=44

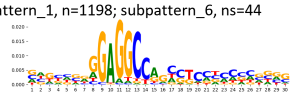

pattern_1, n=1198; subpattern_7, ns=39

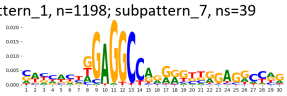

pattern_1, n=1198; subpattern_8, ns=38

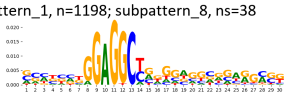

pattern_1, n=1198; subpattern_9, ns=28

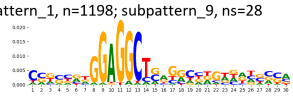

TF-MoDisCO pattern_1 n=1198, PWM

pattern_1, n=1198; subpattern_0, ns=231

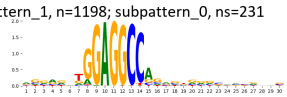

pattern_1, n=1198; subpattern_1, ns=218

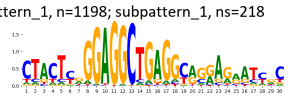

pattern_1, n=1198; subpattern_10, ns=23

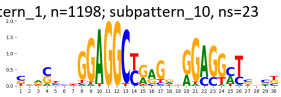

pattern_1, n=1198; subpattern_11, ns=19

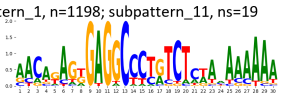

pattern_1, n=1198; subpattern_12, ns=18

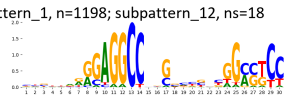

pattern_1, n=1198; subpattern_13, ns=2

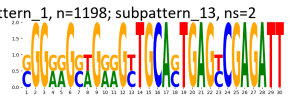

pattern_1, n=1198; subpattern_14, ns=2

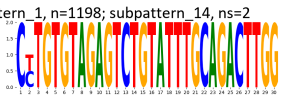

pattern_1, n=1198; subpattern_2, ns=179

pattern_1, n=1198; subpattern_3, ns=140

pattern_1, n=1198; subpattern_4, ns=137

pattern_1, n=1198; subpattern_5, ns=80

pattern_1, n=1198; subpattern_6, ns=44

pattern_1, n=1198; subpattern_7, ns=39

pattern_1, n=1198; subpattern_8, ns=38

pattern_1, n=1198; subpattern_9, ns=28

TF-MoDisCO pattern_11 n=149, CWM

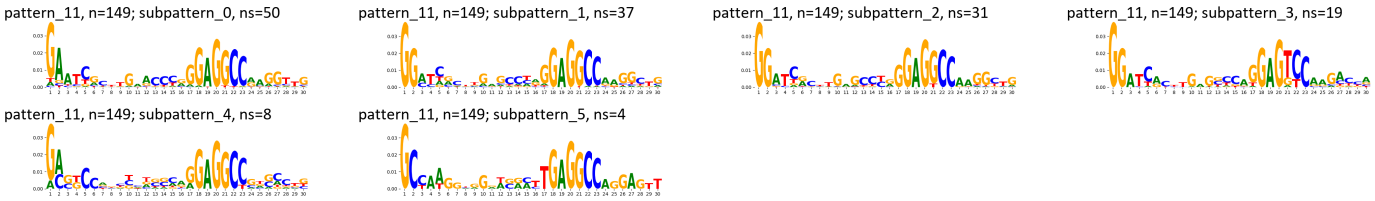

TF-MoDisCO pattern_11 n=149, PWM

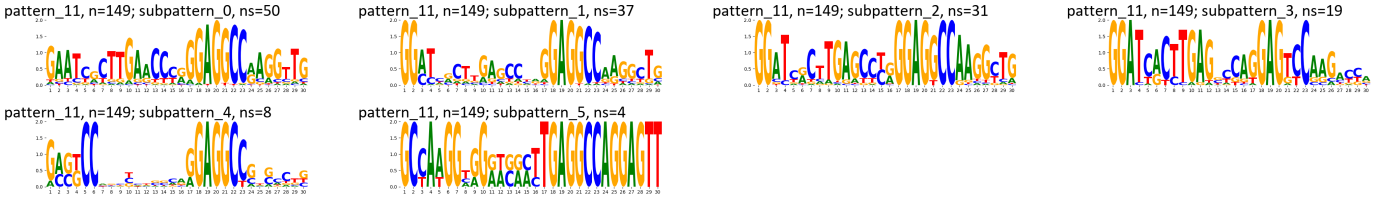

TF-MoDisCO pattern_12 n=147, CWM



TF-MoDisCO pattern_12 n=147, PWM

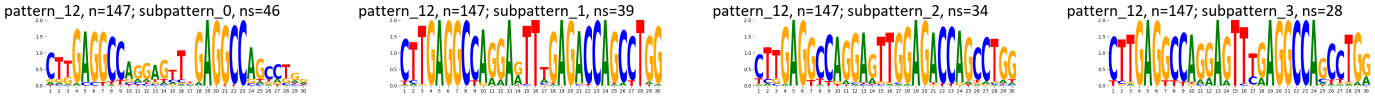

TF-MoDisCO pattern_3 n=439, CWM

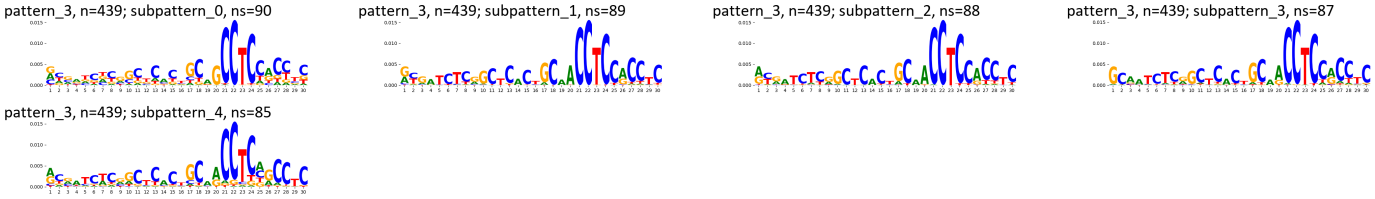

TF-MoDisCO pattern_3 n=439, PWM

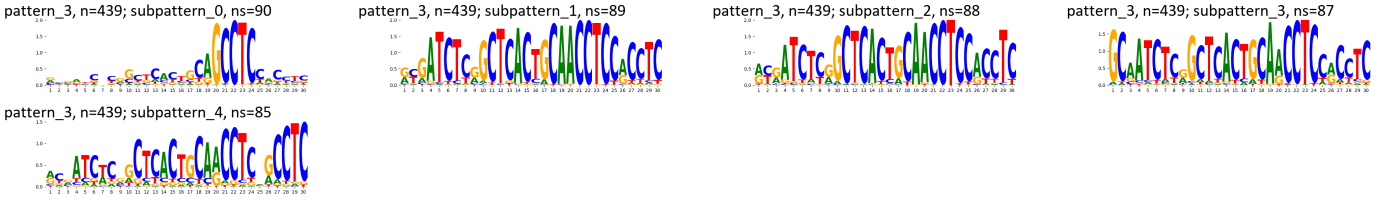

TF-MoDisCO pattern_5 n=342, CWM

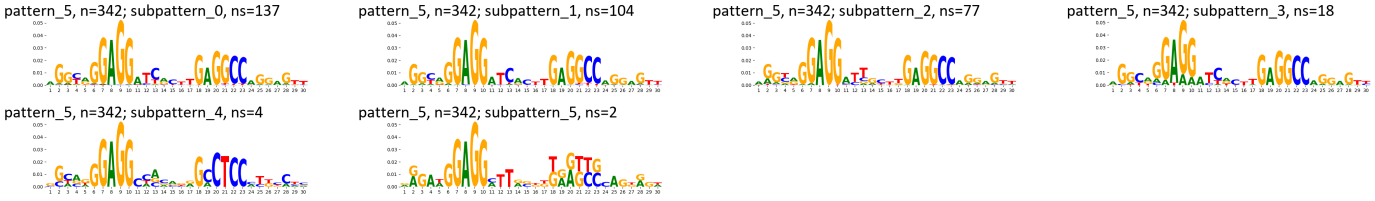

TF-MoDisCO pattern_5 n=342, PWM

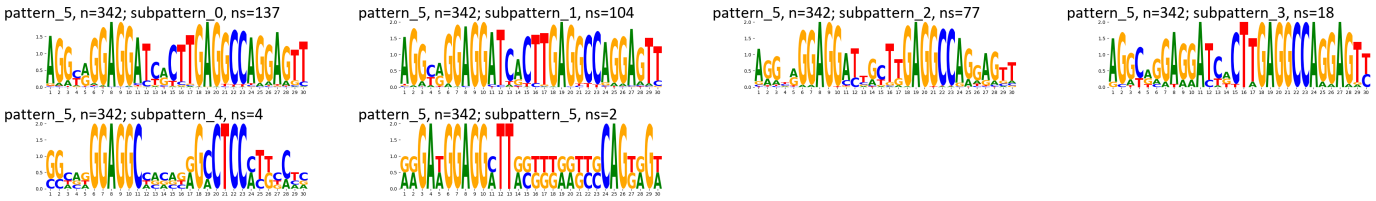

TF-MoDisCO pattern_6 n=230, CWM

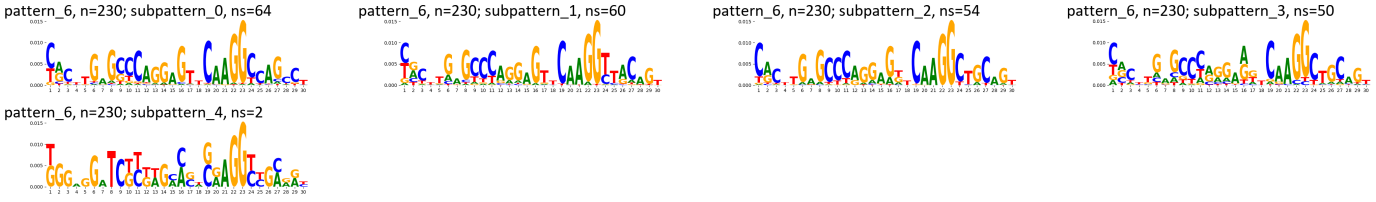

TF-MoDisCO pattern_6 n=230, PWM

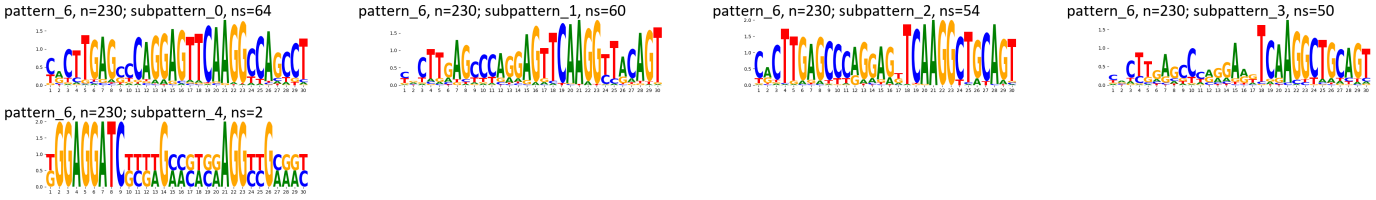

TF-MoDisCO pattern_9 n=182, CWM

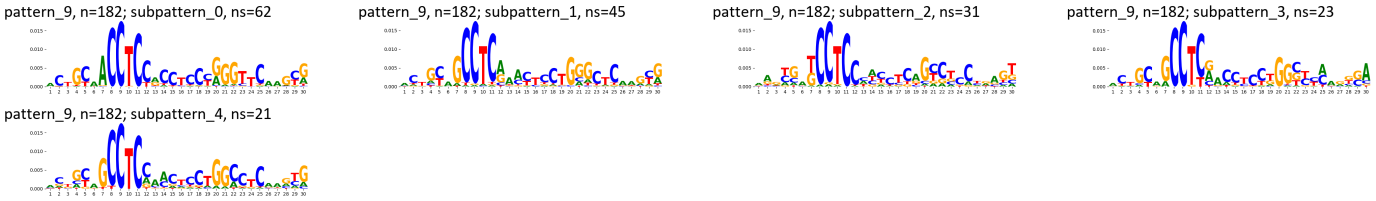

TF-MoDisCO pattern_9 n=182, PWM

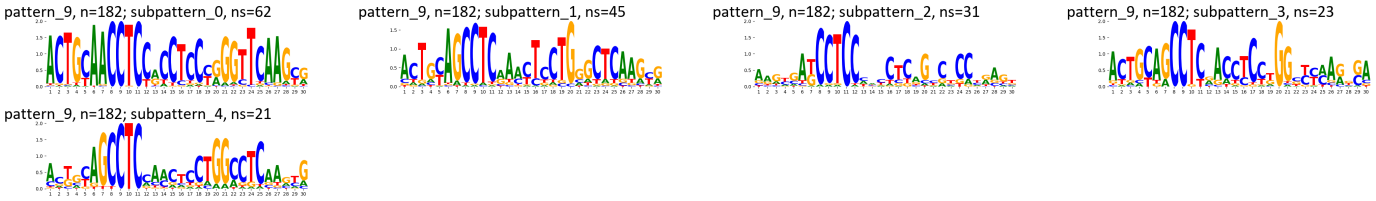

Supplementary Figure 1689: TF-MoDisCO subpatterns for the ZNF770 transcription factor in HepG2 (accession ENCSR510GKB).

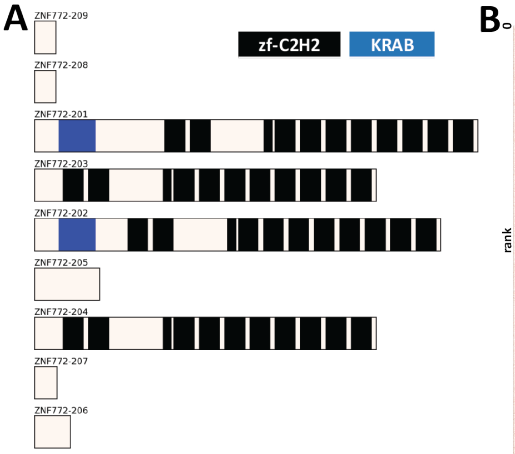

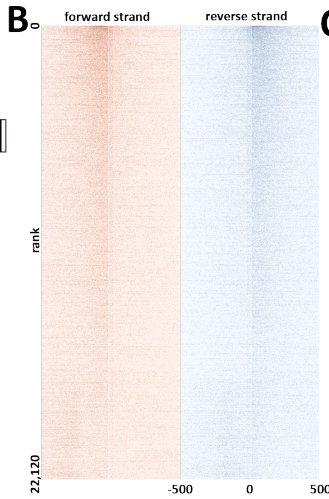

C

peaks	
state	fraction
TssA	0.31
TssFlnk	0.17
Quies	0.17
TxWk	0.10
EnhWk	0.07
TssFlnkU	0.04
EnhA1	0.03
TssBiv	0.03
EnhA2	0.03
Tx	0.03
TssFlnkD	0.02
ReprPC	0.02
ReprPCWk	0.02
EnhG1	0.01
EnhBiv	0.01
EnhG2	0.00
Het	0.00
ZNF/Rpts	0.00

D

peaks		peaks	
repeat	fraction	repeat	fraction
Simple_repeat	0.19	MIRb	0.04
SINE/Alu	0.14	G-rich	0.03
SINE/MIR	0.12	MIR	0.03
LINE/L2	0.07	L2a	0.02
LINE/L1	0.04	MIR3	0.02
Low_complexity	0.04	MIRc	0.02
DNA/hAT-Charlie	0.03	L2b	0.02
LTR/ERV1	0.02	L2c	0.02
LTR/ERVL-MaLR	0.02	AluJb	0.02
LTR/ERVL	0.02	AluSx1	0.02
DNA/hAT-Tip100	0.01	AluSx	0.02
DNA/TcMar-Tigger	0.01	AluSz	0.01
LINE/CR1	0.01	AluJo	0.01
tRNA	0.00	AluJr	0.01
LTR/ERVK	0.00	AluY	0.01
DNA/hAT-Blackjack	0.00	GA-rich	0.01
LINE/RTE-BovB	0.00	AluSq2	0.01
LTR/Gypsy	0.00	L2	0.01

E

Ontology	Term	FDR Q-val
GO Biological Process	regulation of transcription from RNA polymerase II promoter in response to stress	59.04
GO Biological Process	regulation of DNA-templated transcription in response to stress	51.61
GO Biological Process	mRNA catabolic process	50.26
GO Biological Process	nuclear-transcribed mRNA catabolic process	46.58
GO Biological Process	endoplasmic reticulum unfolded protein response	44.50
GO Biological Process	regulation of intrinsic apoptotic signaling pathway	44.25
GO Biological Process	liver regeneration	42.05
GO Biological Process	IRE1-mediated unfolded protein response	41.35
GO Biological Process	cellular response to topologically incorrect protein	40.71
GO Biological Process	positive regulation of nuclease activity	40.31
GO Biological Process	response to topologically incorrect protein	40.23
GO Biological Process	cellular response to unfolded protein	38.51
GO Biological Process	negative regulation of intrinsic apoptotic signaling pathway	37.51
GO Biological Process	regulation of transcription from RNA polymerase II promoter in response to hypoxia	35.31
GO Biological Process	response to epidermal growth factor	33.51
GO Biological Process	nuclear-transcribed mRNA catabolic process, nonsense-mediated decay	32.42
GO Biological Process	translational elongation	31.78
GO Biological Process	mitochondrial translational termination	30.69
GO Biological Process	nuclear-transcribed mRNA catabolic process, deadenylation-dependent decay	30.68
GO Biological Process	mitochondrial translational elongation	29.57
Human Phenotype	Abnormal CSF metabolite level	13.35
Human Phenotype	Exercise intolerance	12.92
Human Phenotype	Abnormality of transition element cation homeostasis	12.71
Human Phenotype	Increased CSF lactate	11.86

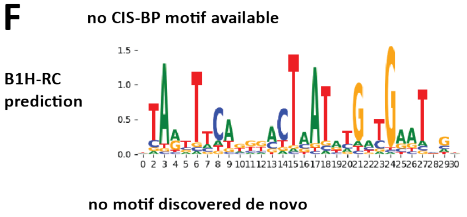

Supplementary Figure 1690: Properties and genomic distribution of motifs identified for the ZNF772 transcription factor in HepG2 (accession ENCSR248WAU).

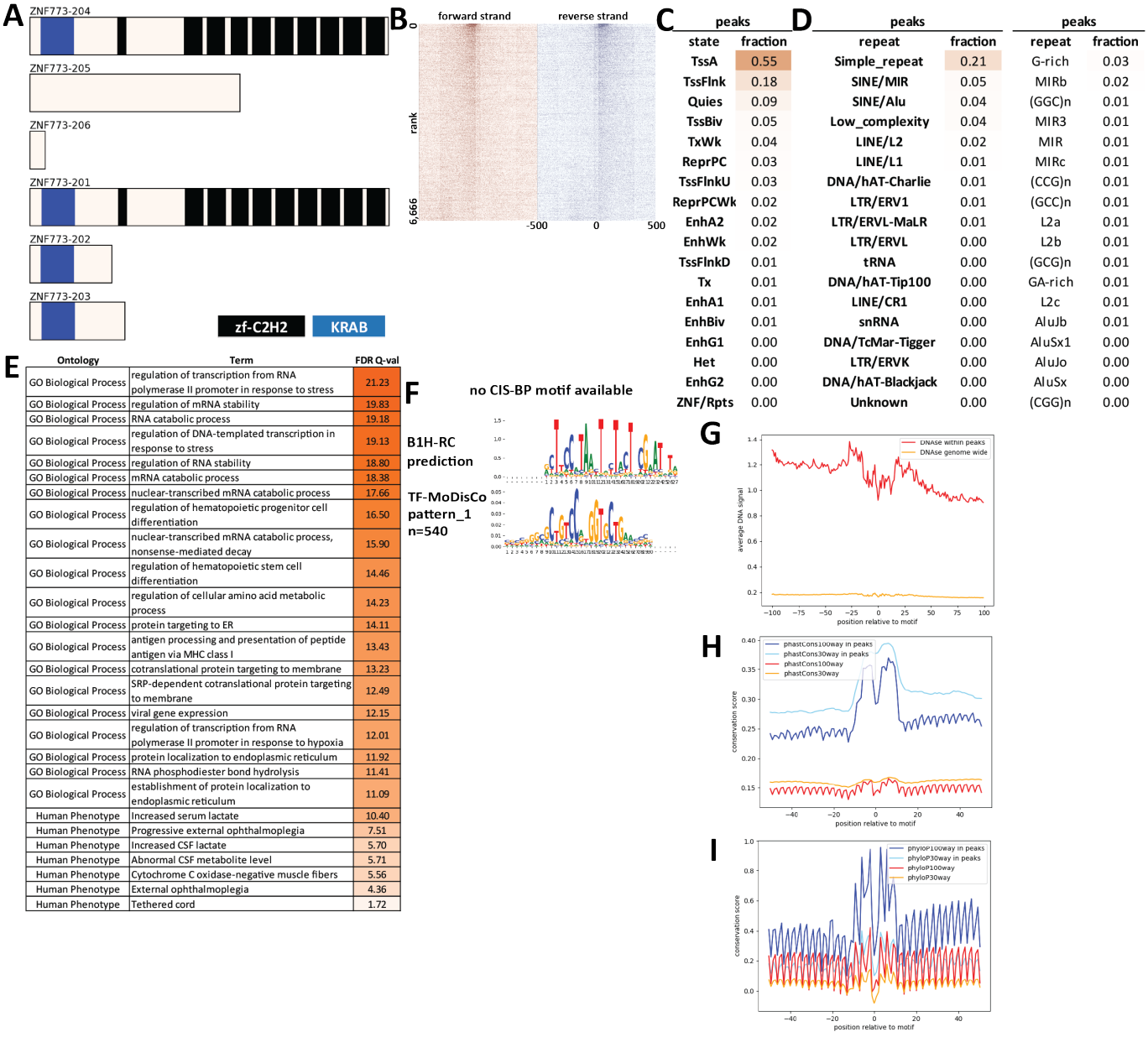

Supplementary Figure 1691: Properties and genomic distribution of motifs identified for the ZNF773 transcription factor in HepG2 (accession ENCSR029ARE).

TF-MoDisCO pattern_1 n=540, CWM

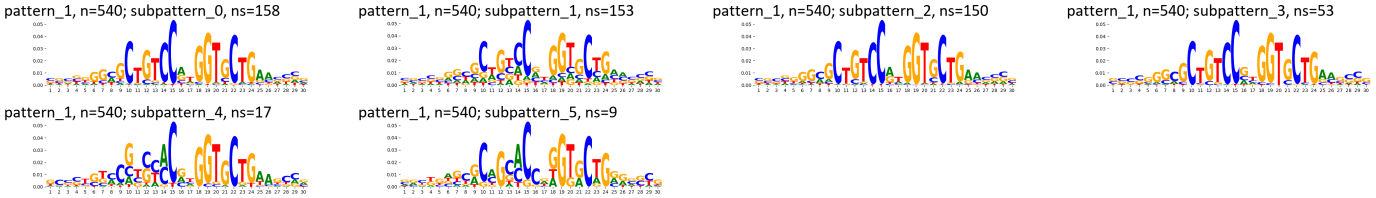

TF-MoDisCO pattern_1 n=540, PWM

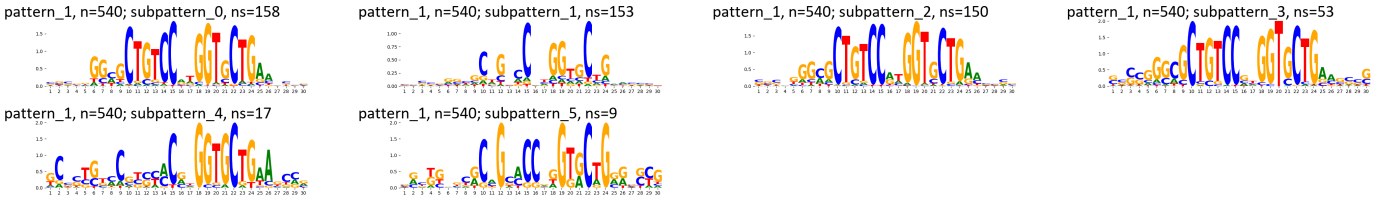

Supplementary Figure 1692: TF-MoDisCO subpatterns for the ZNF773 transcription factor in HepG2 (accession ENCSR029ARE).

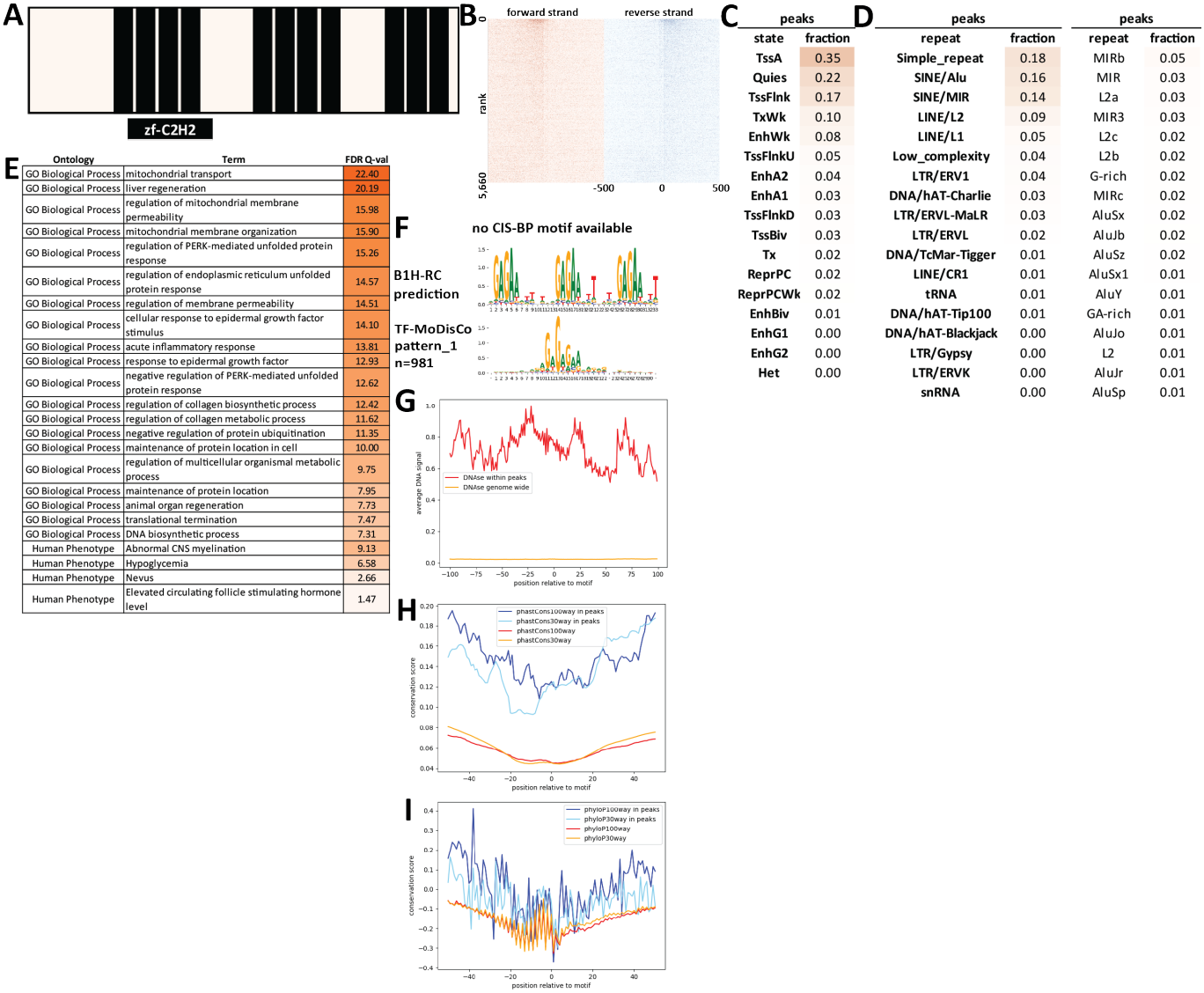

Supplementary Figure 1693: Properties and genomic distribution of motifs identified for the ZNF775 transcription factor in HepG2 (accession ENCSR856QJP).

TF-MoDisCO pattern_1 n=981, CWM

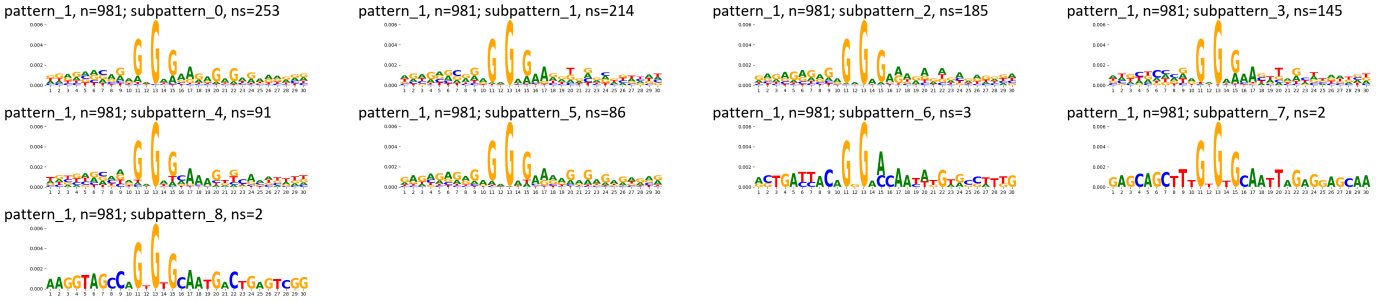

TF-MoDisCO pattern_1 n=981, PWM

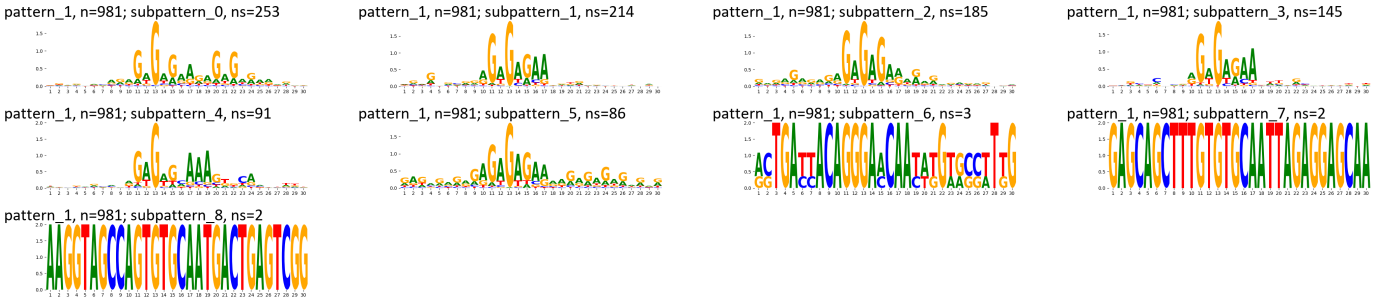

Supplementary Figure 1694: TF-MoDisCO subpatterns for the ZNF775 transcription factor in HepG2 (accession ENCSR856QJP).

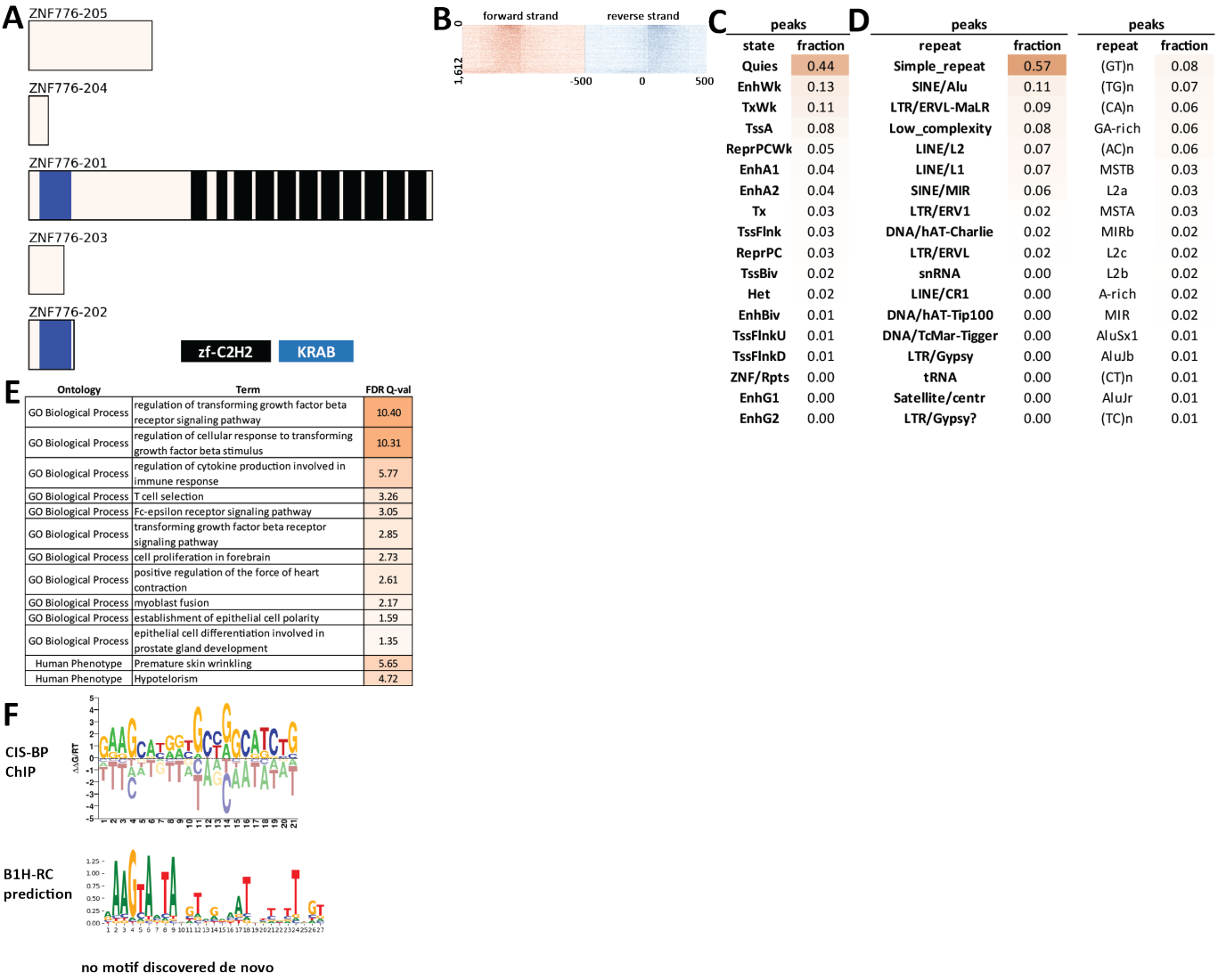

Supplementary Figure 1695: Properties and genomic distribution of motifs identified for the ZNF776 transcription factor in HEK293 (accession ENCSR274LVQ).

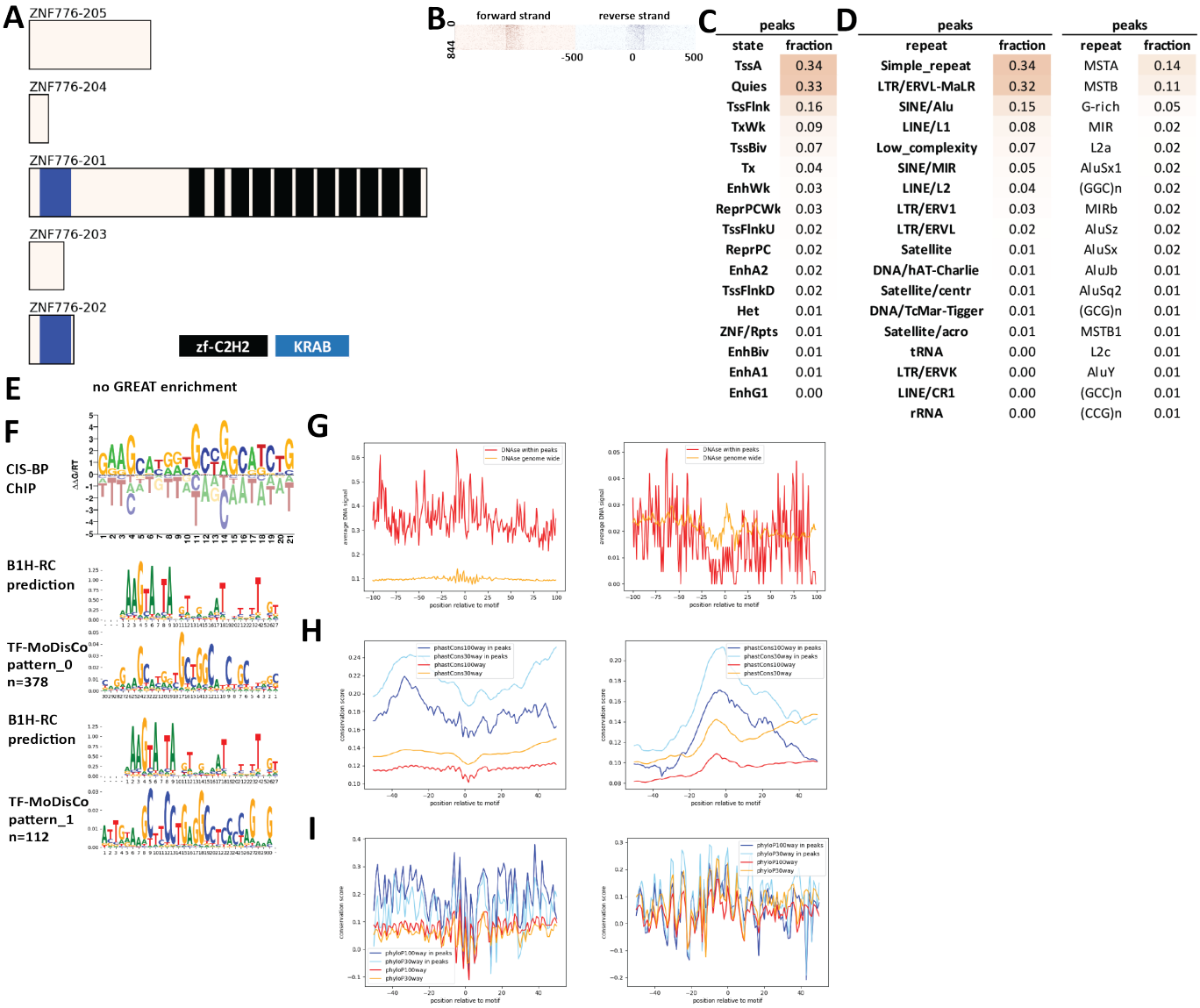

C

peaks	
state	fraction
TssA	0.34
Quies	0.33
TssFlnk	0.16
TxWk	0.09
TssBiv	0.07
Tx	0.04
EnhWk	0.03
ReprPCWk	0.03
TssFlnkU	0.02
ReprPC	0.02
EnhA2	0.02
TssFlnkD	0.02
Het	0.01
ZNF/Rpts	0.01
EnhBiv	0.01
EnhA1	0.01
EnhG1	0.00

D

peaks		peaks	
repeat	fraction	repeat	fraction
Simple_repeat	0.34	MSTA	0.14
LTR/ERVL-MaLR	0.32	MSTB	0.11
SINE/Alu	0.15	G-rich	0.05
LINE/L1	0.08	MIR	0.02
Low_complexity	0.07	L2a	0.02
SINE/MIR	0.05	AluSx1	0.02
LINE/L2	0.04	(GGC)n	0.02
LTR/ERV1	0.03	MIRb	0.02
LTR/ERVL	0.02	AluSz	0.02
Satellite	0.01	AluSx	0.02
DNA/hAT-Charlie	0.01	AluJb	0.01
Satellite/centr	0.01	AluSq2	0.01
DNA/TcMar-Tigger	0.01	(GCG)n	0.01
Satellite/acro	0.01	MSTB1	0.01
tRNA	0.00	L2c	0.01
LTR/ERVK	0.00	AluY	0.01
LINE/CR1	0.00	(GCC)n	0.01
rRNA	0.00	(CCG)n	0.01

Supplementary Figure 1696: Properties and genomic distribution of motifs identified for the ZNF776 transcription factor in HEK293 (accession ChipExo models).

TF-MoDisCO pattern_0 n=378, CWM

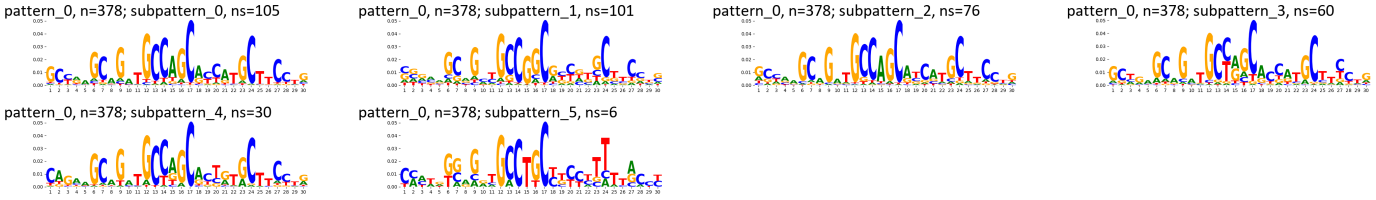

TF-MoDisCO pattern_0 n=378, PWM

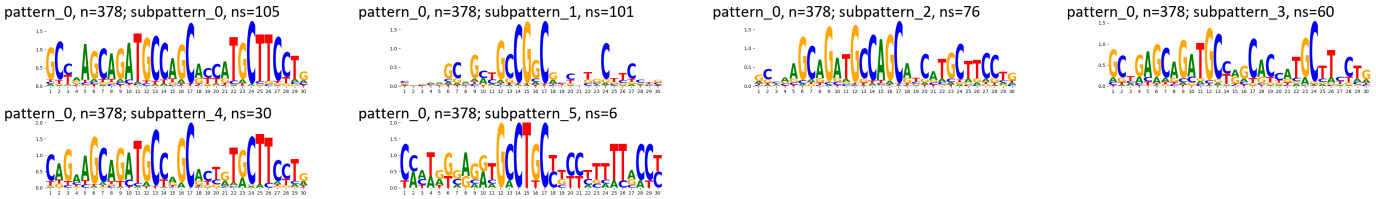

TF-MoDisCO pattern_1 n=112, CWM

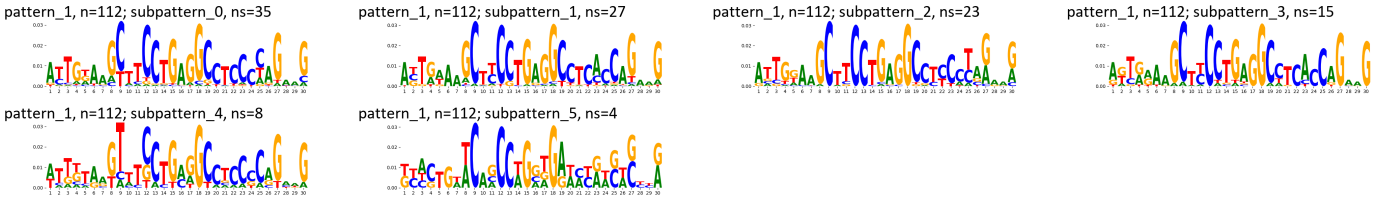

TF-MoDisCO pattern_1 n=112, PWM

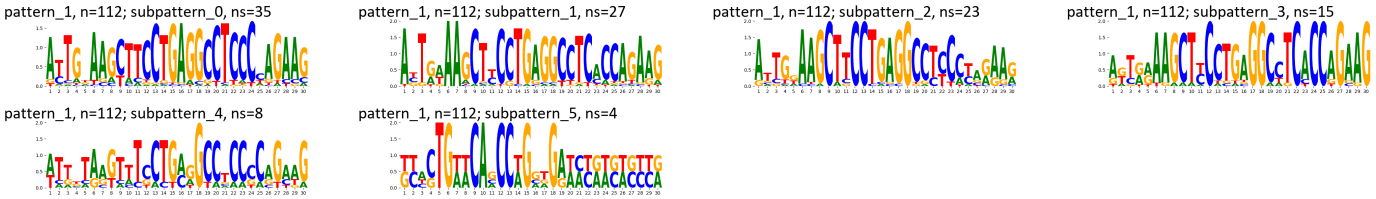

Supplementary Figure 1697: TF-MoDisCO subpatterns for the ZNF776 transcription factor in HEK293 (accession ChipExo models).

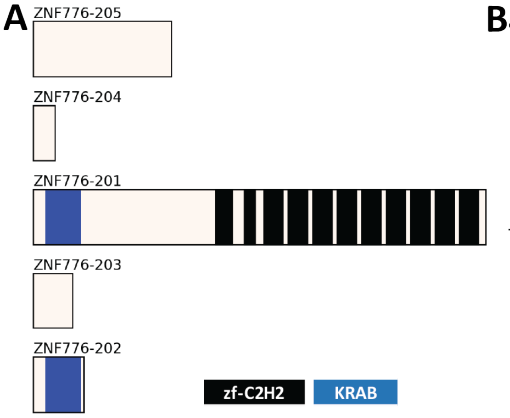

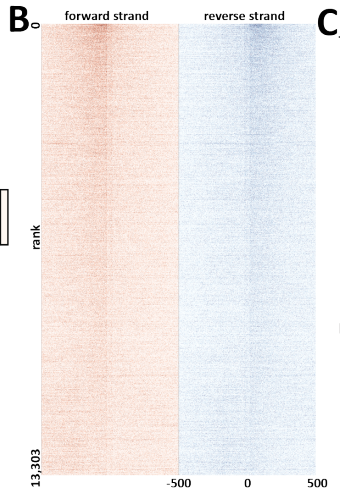

C

peaks	
state	fraction
TssA	0.43
TssFlnk	0.23
Quies	0.11
TxWk	0.07
TssBiv	0.05
TssFlnkU	0.04
ReprPC	0.03
EnhWk	0.03
EnhA2	0.02
Tx	0.02
TssFlnkD	0.02
ReprPCWk	0.02
EnhA1	0.01
EnhBiv	0.01
EnhG1	0.00
EnhG2	0.00
Het	0.00
ZNF/Rpts	0.00

D

peaks		peaks	
repeat	fraction	repeat	fraction
Simple_repeat	0.29	G-rich	0.05
SINE/MIR	0.10	MIRb	0.04
SINE/Alu	0.09	MIR	0.02
Low_complexity	0.06	MIR3	0.02
LINE/L2	0.05	MIRc	0.02
LINE/L1	0.02	L2a	0.02
DNA/hAT-Charlie	0.02	(GGC)n	0.02
LTR/ERVL-MaLR	0.01	L2b	0.02
LTR/ERV1	0.01	L2c	0.01
LTR/ERVL	0.01	AluSx	0.01
LINE/CR1	0.00	AluSx1	0.01
tRNA	0.00	GA-rich	0.01
DNA/hAT-Tip100	0.00	AluJb	0.01
DNA/TcMar-Tigger	0.00	(GCC)n	0.01
DNA/hAT-Blackjack	0.00	(GCG)n	0.01
DNA/hAT	0.00	(CCG)n	0.01
Retroposon/SVA	0.00	AluSz	0.01
LTR/Gypsy	0.00	AluJr	0.01

E

Ontology	Term	FDR Q-val
GO Biological Process	IRE1-mediated unfolded protein response	33.39
GO Biological Process	regulation of transcription from RNA polymerase II promoter in response to stress	32.61
GO Biological Process	activation of signaling protein activity involved in unfolded protein response	32.65
GO Biological Process	endoplasmic reticulum unfolded protein response	32.13
GO Biological Process	liver regeneration	30.01
GO Biological Process	cellular response to topologically incorrect protein	29.14
GO Biological Process	response to topologically incorrect protein	28.80
GO Biological Process	regulation of DNA-templated transcription in response to stress	28.18
GO Biological Process	cellular response to unfolded protein	27.94
GO Biological Process	regulation of intrinsic apoptotic signaling pathway	27.89
GO Biological Process	response to unfolded protein	26.75
GO Biological Process	negative regulation of intrinsic apoptotic signaling pathway	21.16
GO Biological Process	mitochondrial membrane organization	20.77
GO Biological Process	regulation of endoplasmic reticulum unfolded protein response	18.29
GO Biological Process	intrinsic apoptotic signaling pathway in response to endoplasmic reticulum stress	17.83
GO Biological Process	negative regulation of Notch signaling pathway	17.14
GO Biological Process	protein targeting to ER	16.51
GO Biological Process	negative regulation of response to endoplasmic reticulum stress	16.42
GO Biological Process	regulation of mitochondrial membrane permeability	16.13
GO Biological Process	nuclear-transcribed mRNA catabolic process, nonsense-mediated decay	15.90
Human Phenotype	Nevus	13.65
Human Phenotype	Distal upper limb amyotrophy	8.54
Human Phenotype	Progressive external ophthalmoplegia	7.22
Human Phenotype	Hand muscle atrophy	6.69
Human Phenotype	Abnormal CSF metabolite level	6.02
Human Phenotype	Increased CSF lactate	5.56

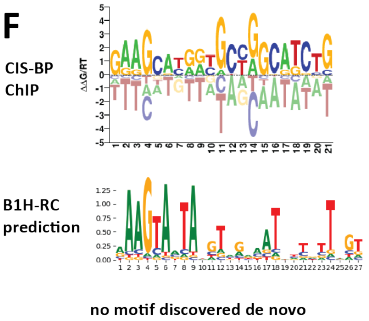

Supplementary Figure 1698: Properties and genomic distribution of motifs identified for the ZNF776 transcription factor in HepG2 (accession ENCSR704ENT).

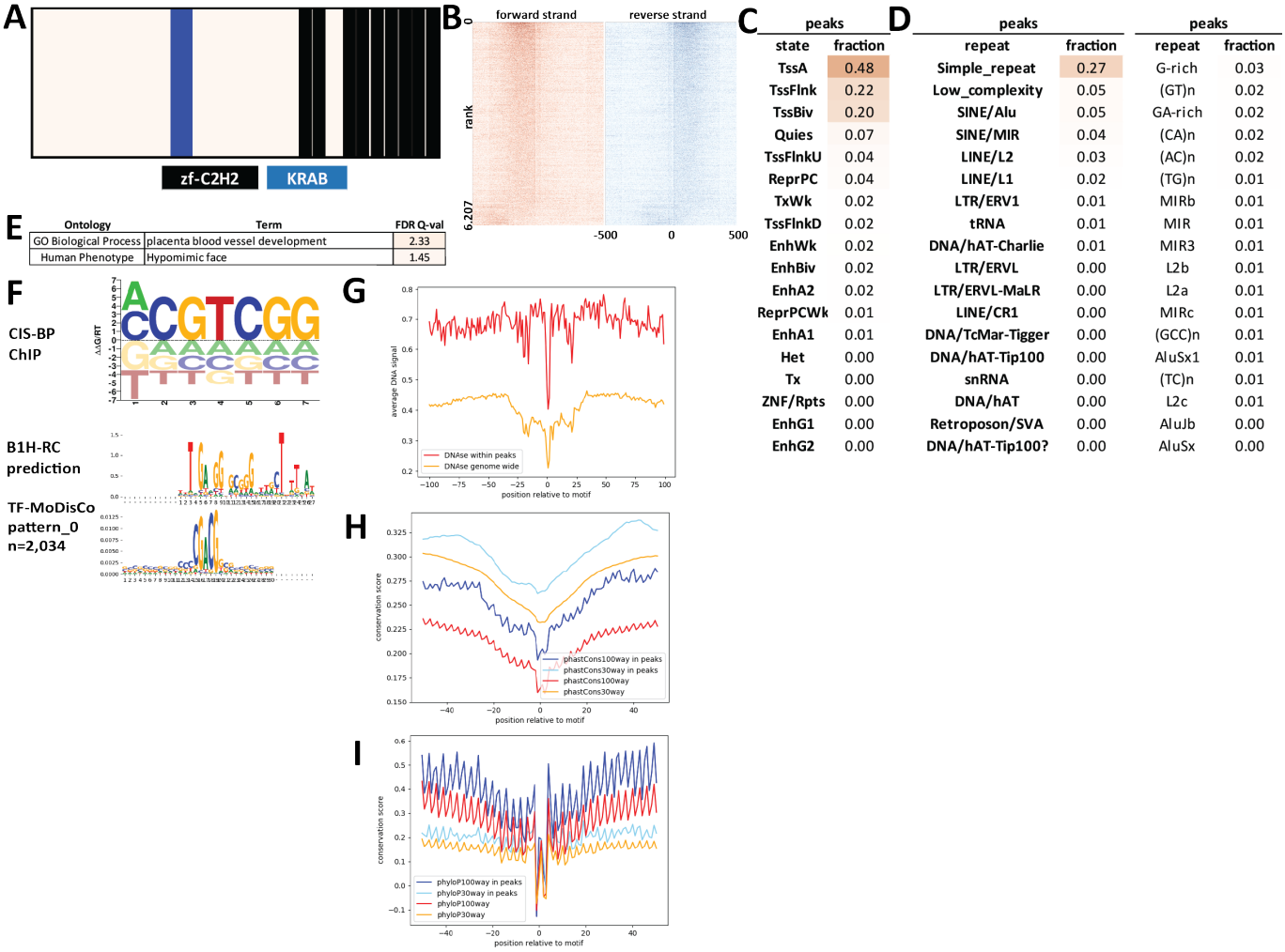

Supplementary Figure 1699: Properties and genomic distribution of motifs identified for the ZNF777 transcription factor in HEK293 (accession ENCSR295BIP).

TF-MoDisCO pattern_0 n=2034, CWM

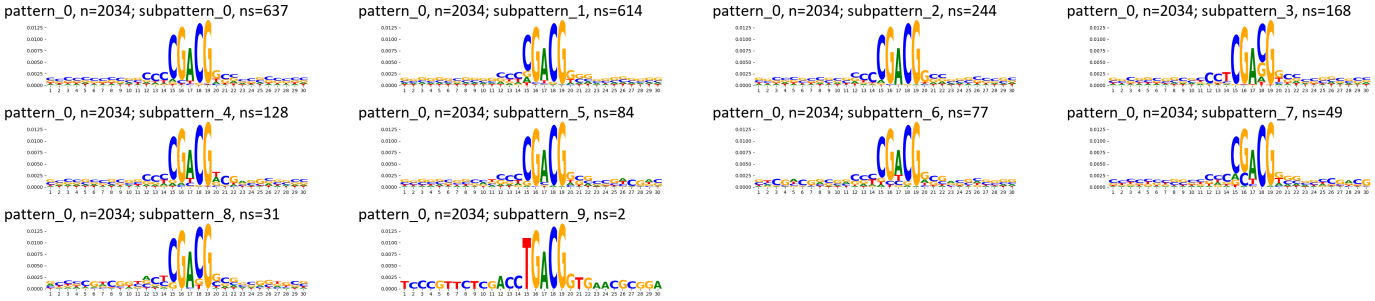

TF-MoDisCO pattern_0 n=2034, PWM

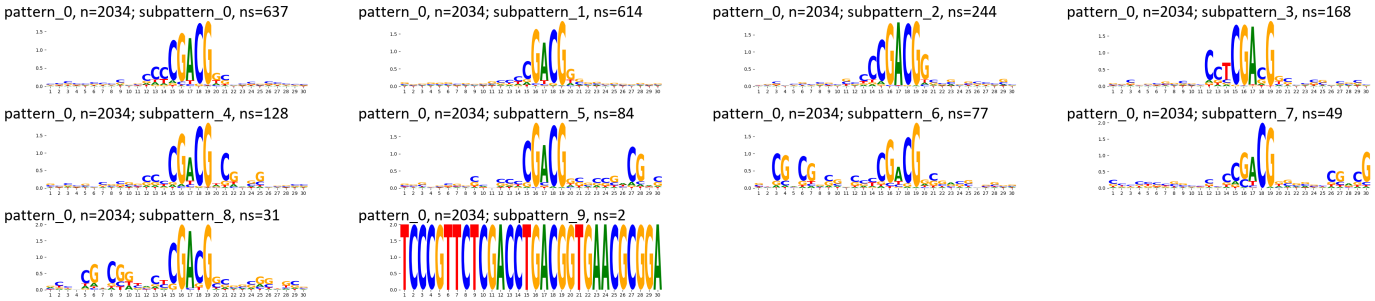

Supplementary Figure 1700: TF-MoDisCO subpatterns for the ZNF777 transcription factor in HEK293 (accession ENCSR295BIP).

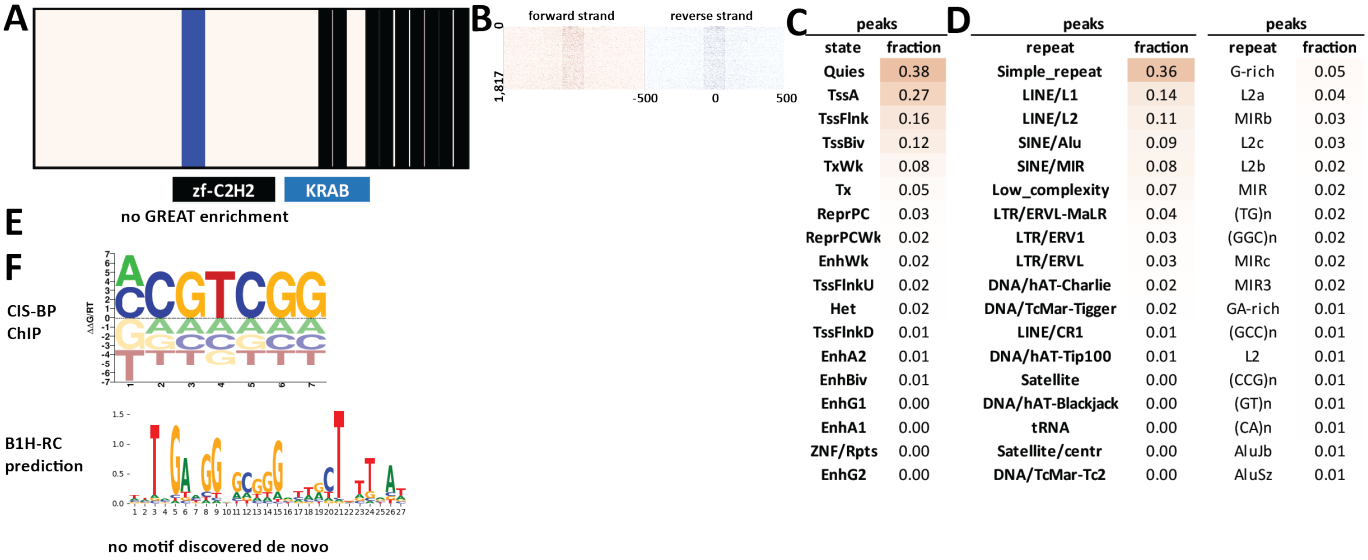

Supplementary Figure 1701: Properties and genomic distribution of motifs identified for the ZNF777 transcription factor in HEK293 (accession ChipExo models).

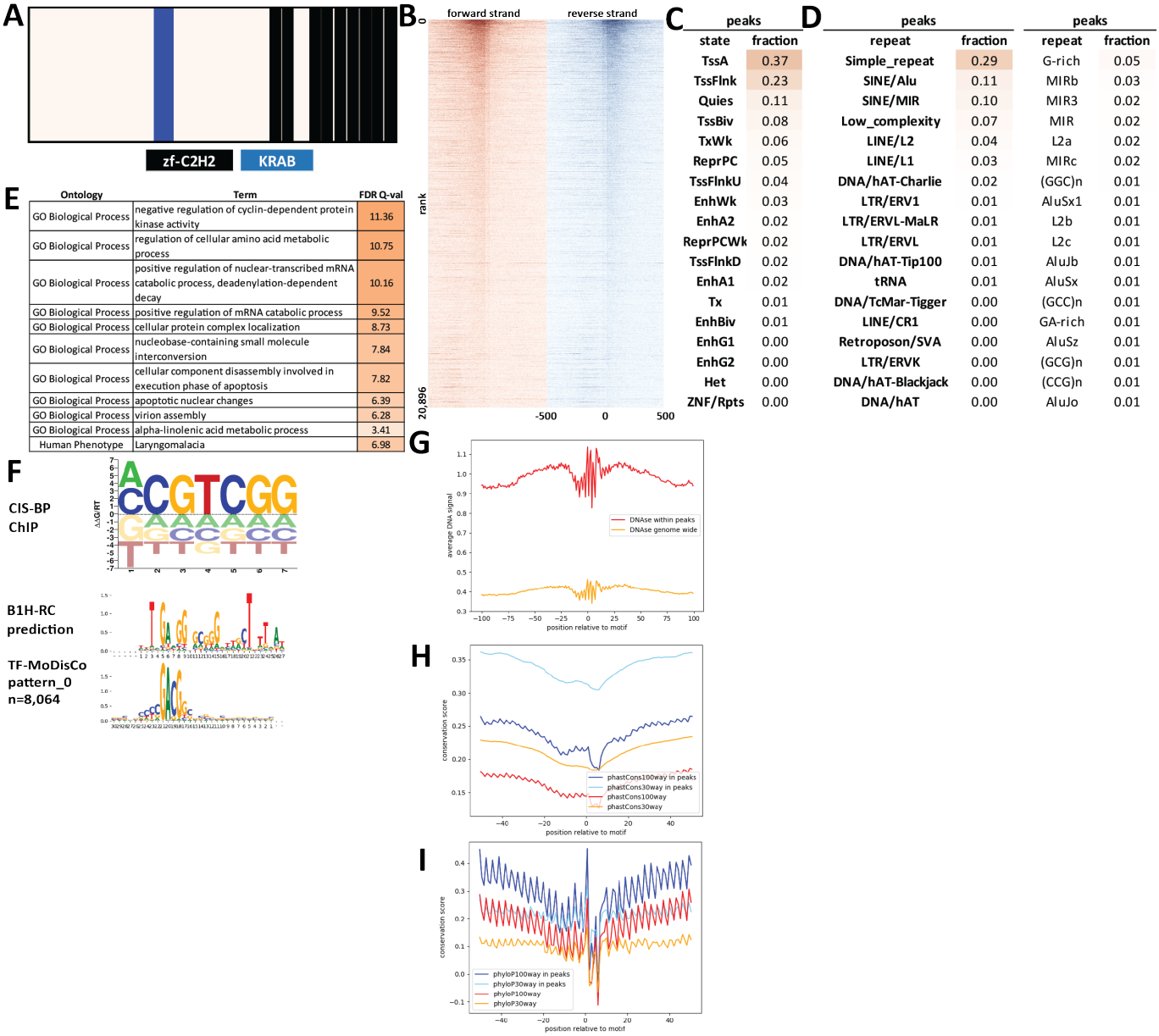

Supplementary Figure 1702: Properties and genomic distribution of motifs identified for the ZNF777 transcription factor in HepG2 (accession ENCSR068ZQR).

TF-MoDisCO pattern_0 n=8064, CWM

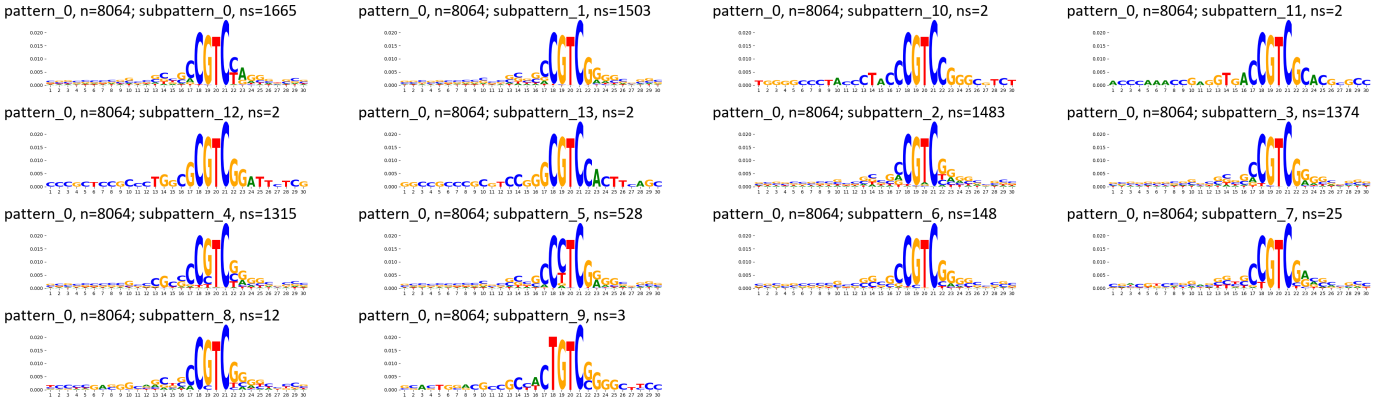

TF-MoDisCO pattern_0 n=8064, PWM

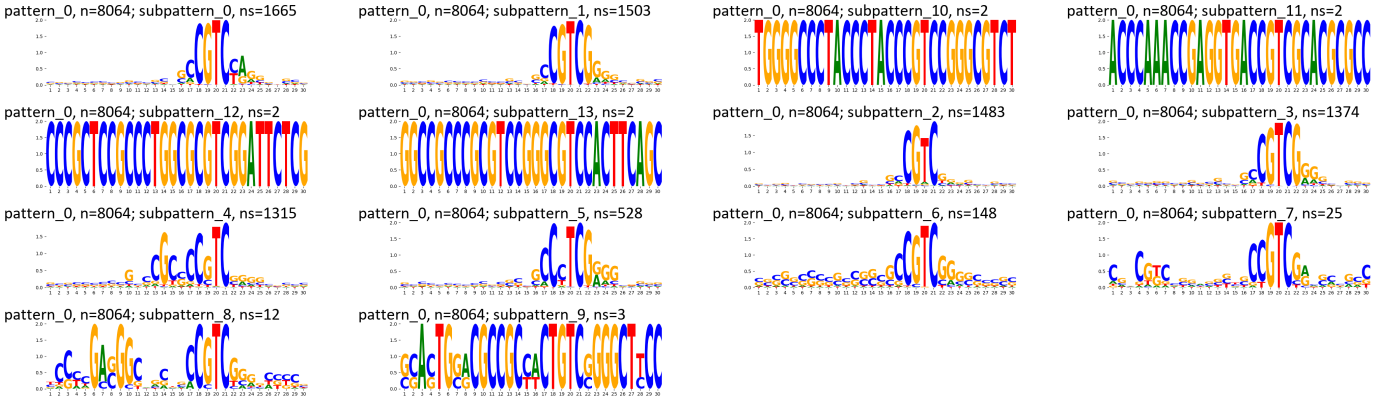

Supplementary Figure 1703: TF-MoDisCO subpatterns for the ZNF777 transcription factor in HepG2 (accession ENCSR068ZQR).

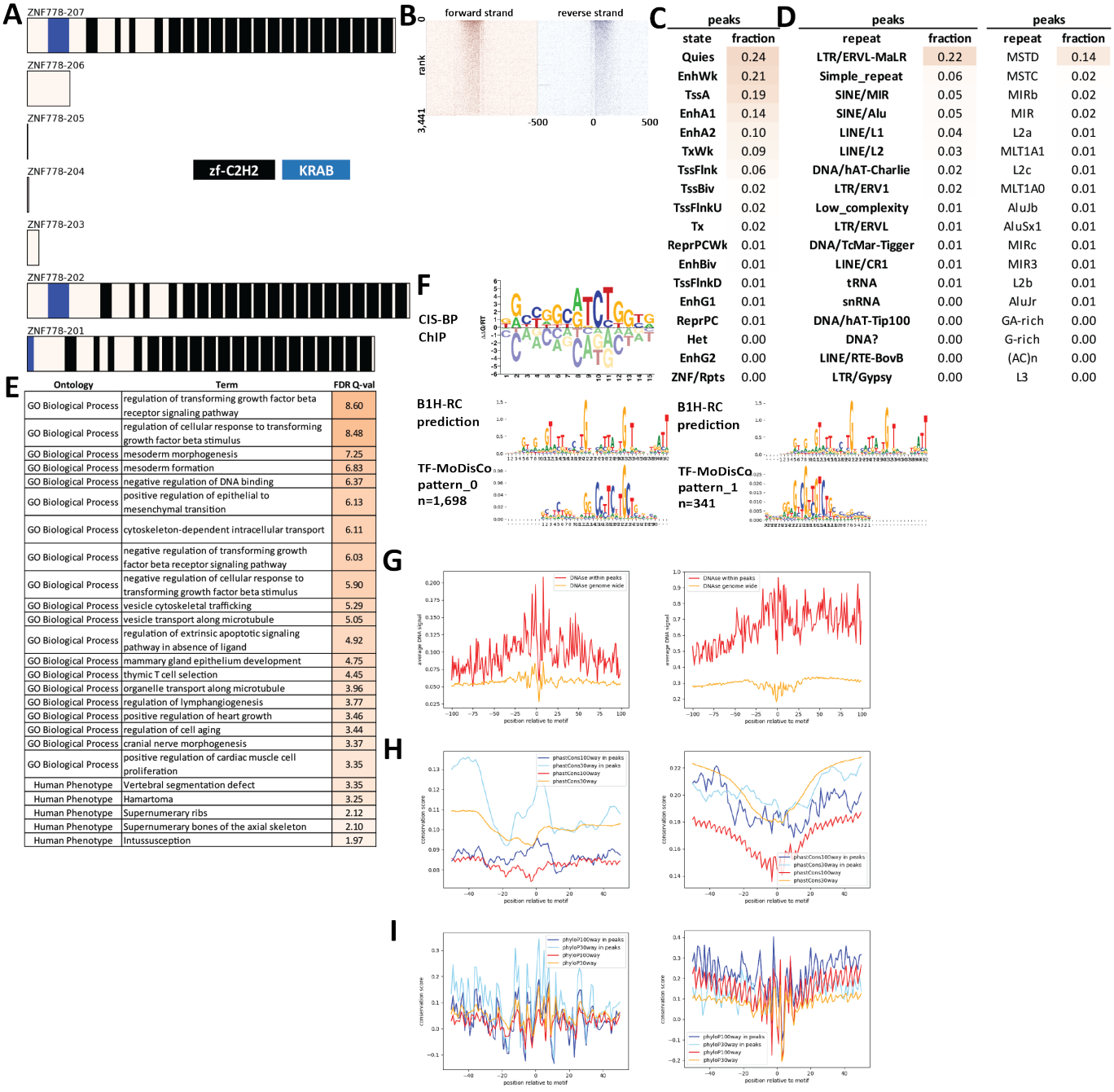

Supplementary Figure 1704: Properties and genomic distribution of motifs identified for the ZNF778 transcription factor in HEK293 (accession Hughes GR models).

TF-MoDisCO pattern_0 n=1698, CWM

pattern_0, n=1698; subpattern_0, ns=387

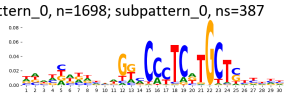

pattern_0, n=1698; subpattern_1, ns=367

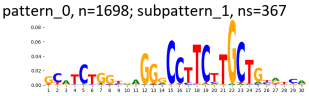

pattern_0, n=1698; subpattern_2, ns=362

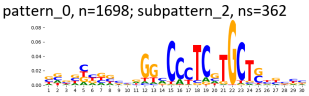

pattern_0, n=1698; subpattern_3, ns=340

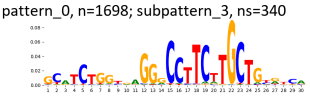

pattern_0, n=1698; subpattern_4, ns=238

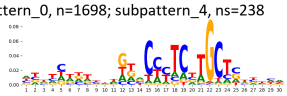

pattern_0, n=1698; subpattern_5, ns=4

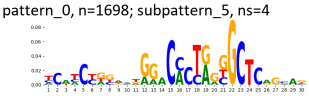

TF-MoDisCO pattern_0 n=1698, PWM

pattern_0, n=1698; subpattern_0, ns=387

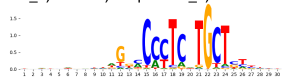

pattern_0, n=1698; subpattern_1, ns=367

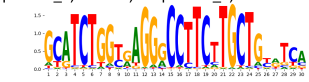

pattern_0, n=1698; subpattern_2, ns=362

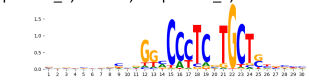

pattern_0, n=1698; subpattern_3, ns=340

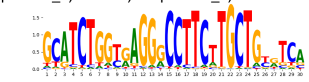

pattern_0, n=1698; subpattern_4, ns=238

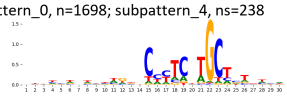

pattern_0, n=1698; subpattern_5, ns=4

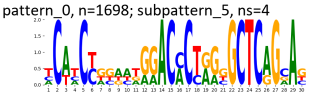

TF-MoDisCO pattern_1 n=341, CWM

pattern_1, n=341; subpattern_0, ns=101

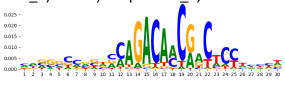

pattern_1, n=341; subpattern_1, ns=98

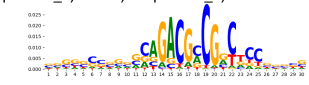

pattern_1, n=341; subpattern_2, ns=92

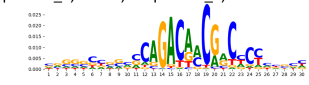

pattern_1, n=341; subpattern_3, ns=35

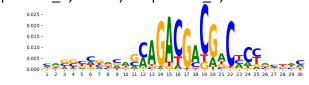

pattern_1, n=341; subpattern_4, ns=12

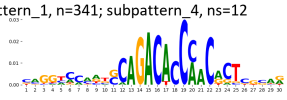

pattern_1, n=341; subpattern_5, ns=3

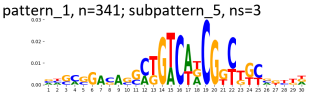

TF-MoDisCO pattern_1 n=341, PWM

pattern_1, n=341; subpattern_0, ns=101

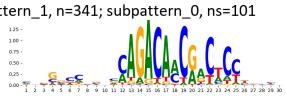

pattern_1, n=341; subpattern_1, ns=98

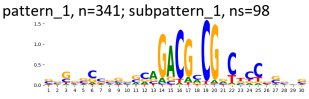

pattern_1, n=341; subpattern_2, ns=92

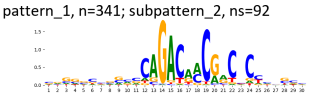

pattern_1, n=341; subpattern_3, ns=35

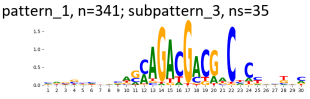

pattern_1, n=341; subpattern_4, ns=12

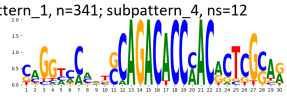

pattern_1, n=341; subpattern_5, ns=3

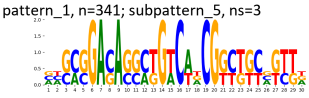

Supplementary Figure 1705: TF-MoDisCO subpatterns for the ZNF778 transcription factor in HEK293 (accession Hughes GR models).

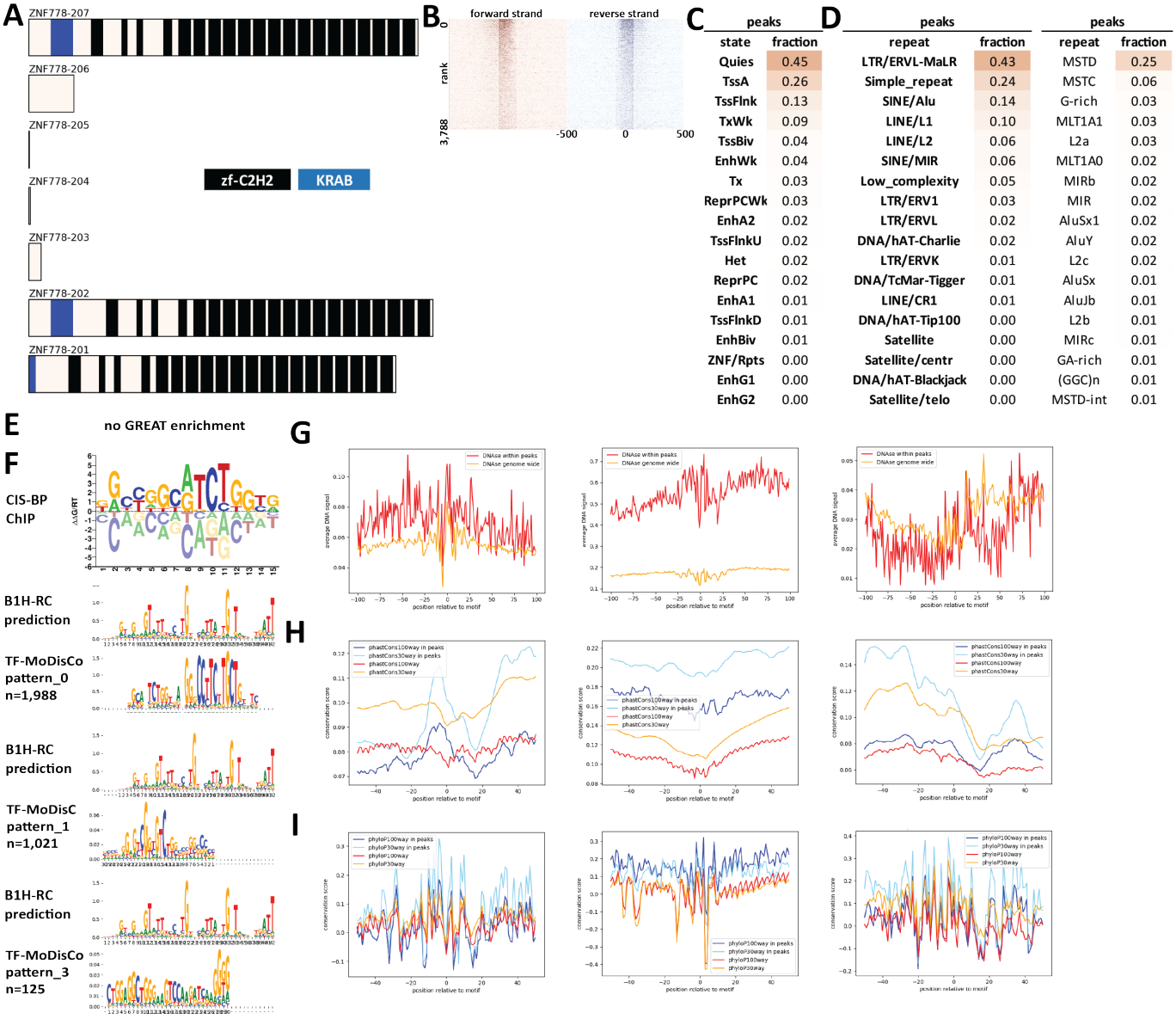

Supplementary Figure 1706: Properties and genomic distribution of motifs identified for the ZNF778 transcription factor in HEK293 (accession ChipExo models).

TF-MoDisCO pattern_0 n=1988, CWM

pattern_0, n=1988; subpattern_0, ns=355

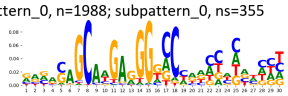

pattern_0, n=1988; subpattern_1, ns=354

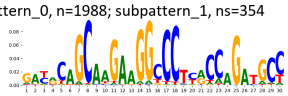

pattern_0, n=1988; subpattern_2, ns=349

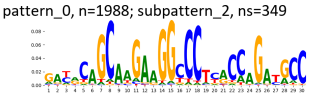

pattern_0, n=1988; subpattern_3, ns=268

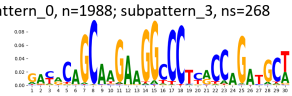

pattern_0, n=1988; subpattern_4, ns=249

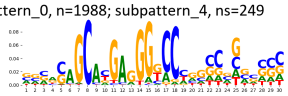

pattern_0, n=1988; subpattern_5, ns=223

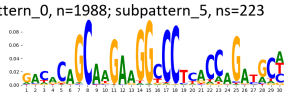

pattern_0, n=1988; subpattern_6, ns=148

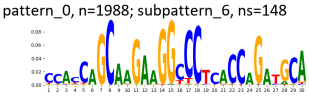

pattern_0, n=1988; subpattern_7, ns=23

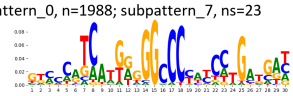

pattern_0, n=1988; subpattern_8, ns=19

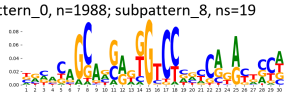

TF-MoDisCO pattern_0 n=1988, PWM

pattern_0, n=1988; subpattern_0, ns=355

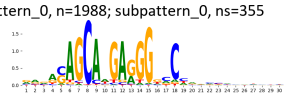

pattern_0, n=1988; subpattern_1, ns=354

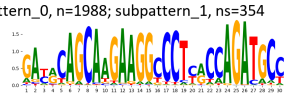

pattern_0, n=1988; subpattern_2, ns=349

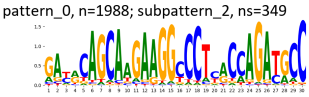

pattern_0, n=1988; subpattern_3, ns=268

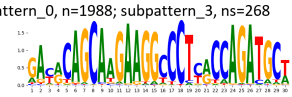

pattern_0, n=1988; subpattern_4, ns=249

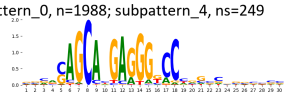

pattern_0, n=1988; subpattern_5, ns=223

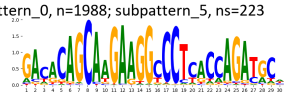

pattern_0, n=1988; subpattern_6, ns=148

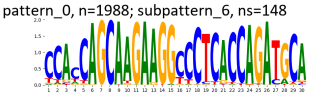

pattern_0, n=1988; subpattern_7, ns=23

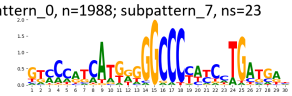

pattern_0, n=1988; subpattern_8, ns=19

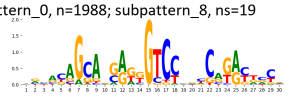

TF-MoDisCO pattern_1 n=1021, CWM

pattern_1, n=1021; subpattern_0, ns=232

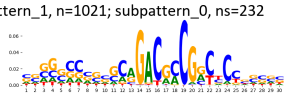

pattern_1, n=1021; subpattern_1, ns=201

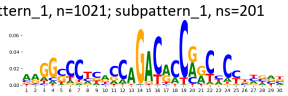

pattern_1, n=1021; subpattern_2, ns=173

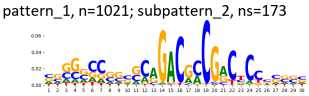

pattern_1, n=1021; subpattern_3, ns=165

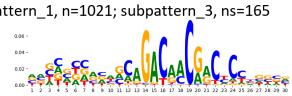

pattern_1, n=1021; subpattern_4, ns=145

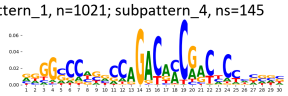

pattern_1, n=1021; subpattern_5, ns=98

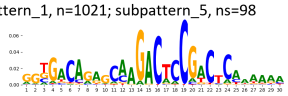

pattern_1, n=1021; subpattern_6, ns=7

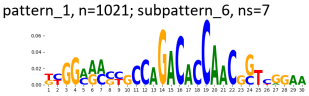

TF-MoDisCO pattern_1 n=1021, PWM

pattern_1, n=1021; subpattern_0, ns=232

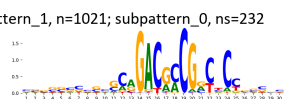

pattern_1, n=1021; subpattern_1, ns=201

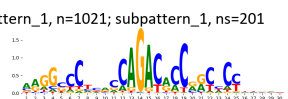

pattern_1, n=1021; subpattern_2, ns=173

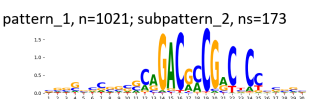

pattern_1, n=1021; subpattern_3, ns=165

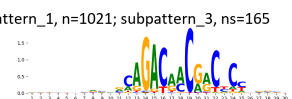

pattern_1, n=1021; subpattern_4, ns=145

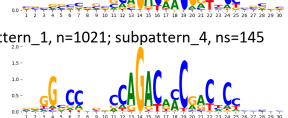

pattern_1, n=1021; subpattern_5, ns=98

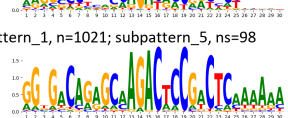

pattern_1, n=1021; subpattern_6, ns=7

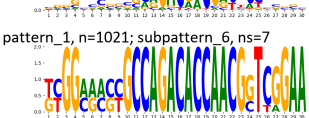

TF-MoDisCO pattern_3 n=125, CWM

pattern_3, n=125; subpattern_0, ns=48

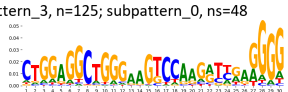

pattern_3, n=125; subpattern_1, ns=32

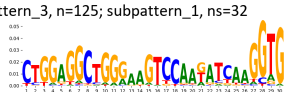

pattern_3, n=125; subpattern_2, ns=29

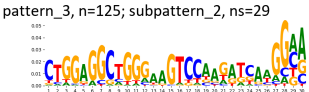

pattern_3, n=125; subpattern_3, ns=16

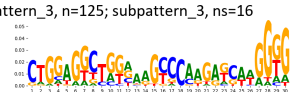

TF-MoDisCO pattern_3 n=125, PWM

pattern_3, n=125; subpattern_0, ns=48

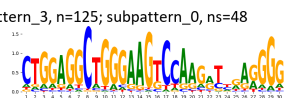

pattern_3, n=125; subpattern_1, ns=32

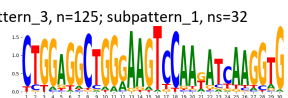

pattern_3, n=125; subpattern_2, ns=29

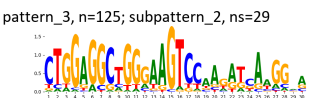

pattern_3, n=125; subpattern_3, ns=16

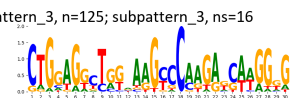

Supplementary Figure 1707: TF-MoDisCO subpatterns for the ZNF778 transcription factor in HEK293 (accession ChipExo models).

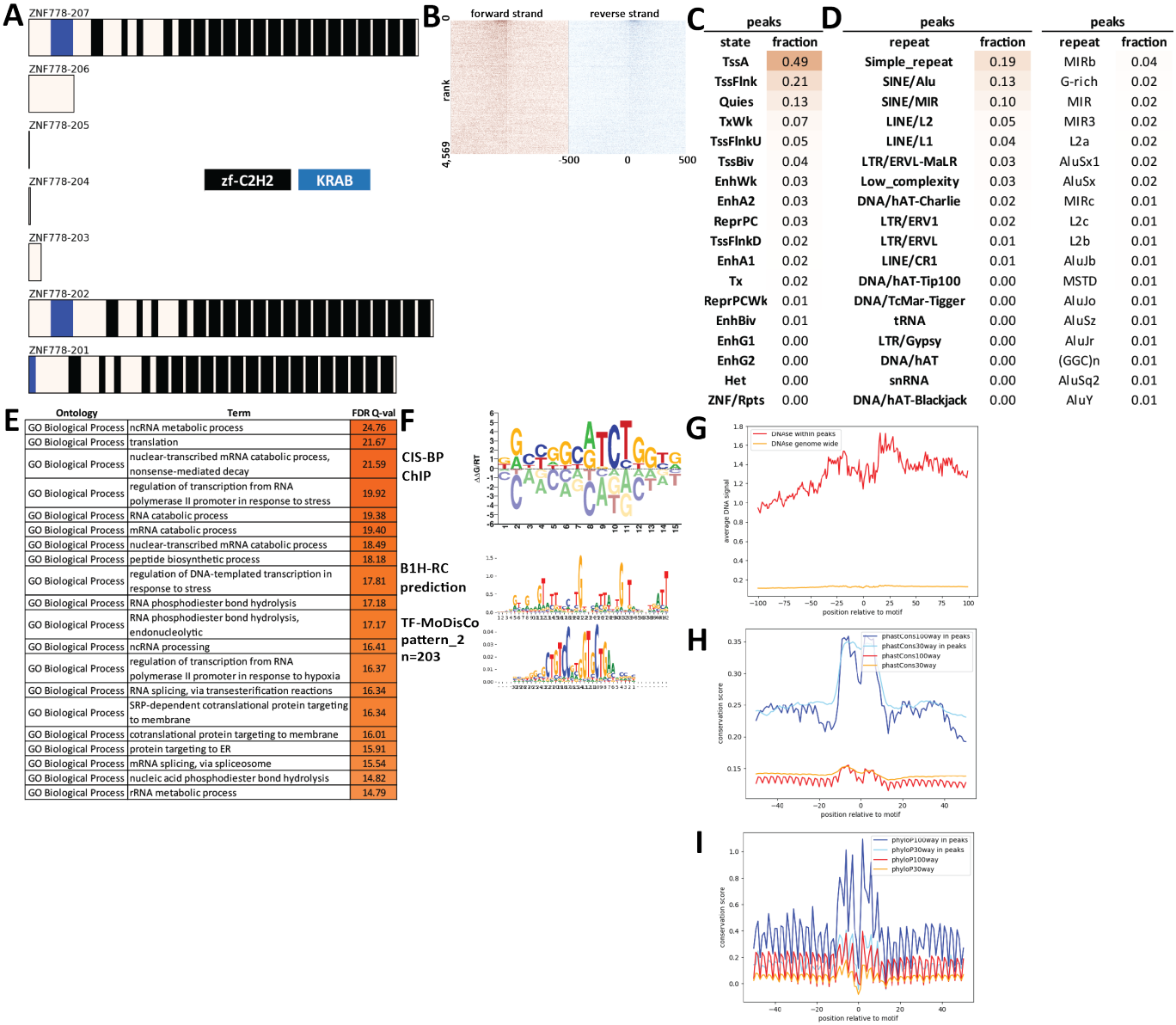

Supplementary Figure 1708: Properties and genomic distribution of motifs identified for the ZNF778 transcription factor in HepG2 (accession ENCSR141ELR).

TF-MoDisCO pattern_2 n=203, CWM

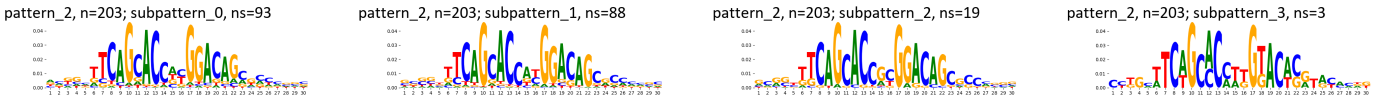

TF-MoDisCO pattern_2 n=203, PWM

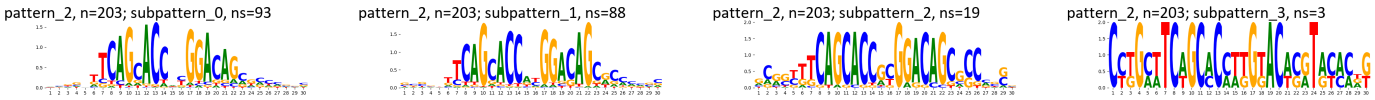

Supplementary Figure 1709: TF-MoDisCO subpatterns for the ZNF778 transcription factor in HepG2 (accession ENCSR141ELR).

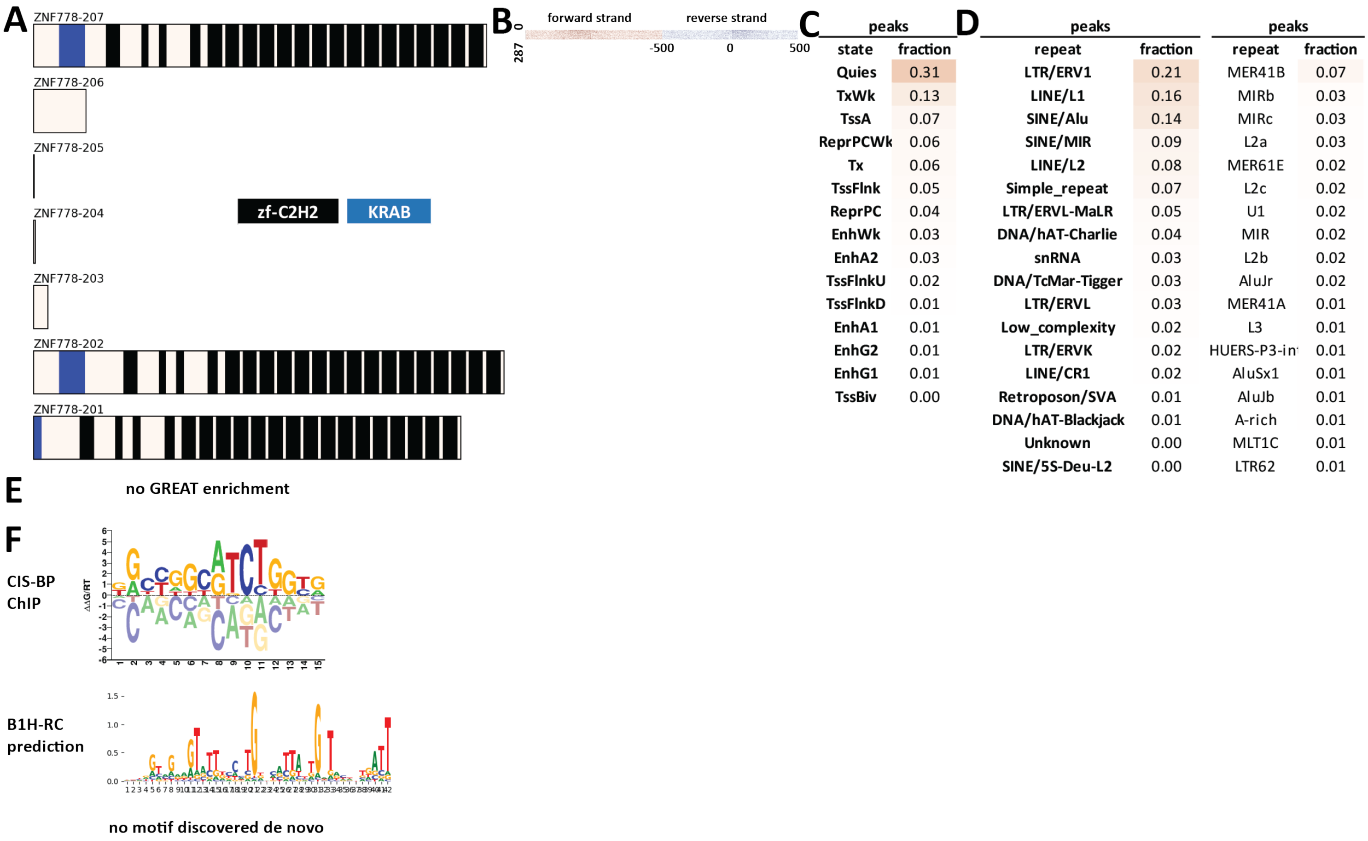

Supplementary Figure 1710: Properties and genomic distribution of motifs identified for the ZNF778 transcription factor in K562 (accession ENCSR110JLQ).

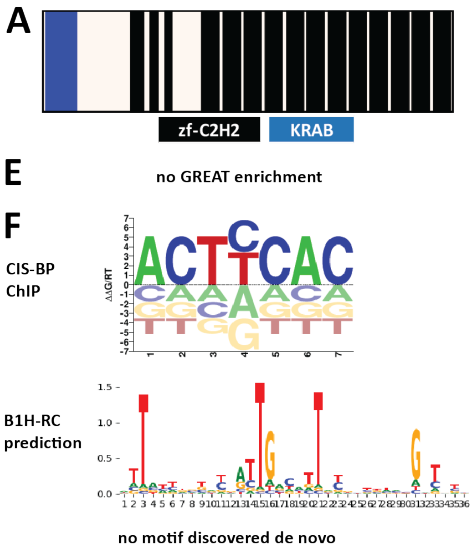

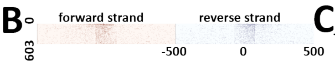

C

peaks	
state	fraction
Quies	0.36
TssA	0.27
TssFlnk	0.11
TxWk	0.09
EnhWk	0.06
Tx	0.04
EnhA2	0.03
ReprPCWk	0.03
EnhA1	0.03
TssBiv	0.02
ReprPC	0.02
Het	0.02
TssFlnkU	0.01
TssFlnkD	0.01
ZNF/Rpts	0.01
EnhBiv	0.01
EnhG1	0.00

D

peaks		peaks	
repeat	fraction	repeat	fraction
Simple_repeat	0.22	L2a	0.06
SINE/Alu	0.17	AluJb	0.03
LINE/L2	0.13	L2c	0.03
LINE/L1	0.10	MIRb	0.03
SINE/MIR	0.08	MER57E1	0.02
LTR/ERV1	0.07	G-rich	0.02
Low_complexity	0.03	MIR	0.02
LTR/ERVL-MaLR	0.03	L2	0.02
LTR/ERVL	0.02	AluSx1	0.02
DNA/TcMar-Tigger	0.02	AluSz	0.02
Satellite	0.02	AluJo	0.02
DNA/hAT-Charlie	0.01	MIRc	0.01
Satellite/centr	0.01	AluY	0.01
Satellite/acro	0.01	L2b	0.01
tRNA	0.00	AluSx	0.01
snRNA	0.00	MIR3	0.01
LINE/CR1	0.00	L1ME1	0.01
rRNA	0.00	AluSq2	0.01

Supplementary Figure 1711: Properties and genomic distribution of motifs identified for the ZNF77 transcription factor in HEK293 (accession ChipExo models).

A



B

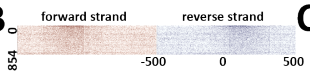

C

peaks	
state	fraction
TssA	0.27
Quies	0.20
TxWk	0.11
Tx	0.09
TssFlnk	0.07
EnhA2	0.05
EnhWk	0.03
ReprPCWk	0.03
TssFlnkU	0.03
EnhG1	0.02
ReprPC	0.02
EnhA1	0.02
TssFlnkD	0.01
EnhG2	0.01
TssBiv	0.01
Het	0.00
EnhBiv	0.00

D

peaks		peaks	
repeat	fraction	repeat	fraction
LTR/ERV1	0.14	MER41B	0.04
SINE/Alu	0.10	MIRb	0.03
LINE/L1	0.09	U1	0.02
Simple_repeat	0.07	MER41A	0.02
SINE/MIR	0.05	L2c	0.02
LINE/L2	0.05	L2b	0.02
snRNA	0.04	L2a	0.01
LTR/ERVL-MaLR	0.02	AluSx1	0.01
LTR/ERVL	0.02	AluSx	0.01
DNA/hAT-Charlie	0.02	MER61E	0.01
DNA/TcMar-Tigger	0.01	MIR	0.01
Low_complexity	0.01	AluY	0.01
tRNA	0.01	AluJo	0.01
DNA/hAT-Tip100	0.01	LTR8	0.01
LTR/ERVK	0.00	L2	0.01
LINE/RTE-X	0.00	MIRc	0.01
LINE/CR1	0.00	MIR3	0.01
DNA/hAT-Blackjack	0.00	L1ME4a	0.01

E

Ontology	Term	FDR Q-val
GO Biological Process	DNA conformation change	12.26
GO Biological Process	protein folding	11.93
GO Biological Process	chromosome organization	8.22
GO Biological Process	oxygen transport	8.20
GO Biological Process	chromatin silencing	8.10
GO Biological Process	protein-DNA complex subunit organization	7.85
GO Biological Process	negative regulation of gene expression, epigenetic	7.85
GO Biological Process	regulation of gene expression, epigenetic	7.80
GO Biological Process	protein localization to endoplasmic reticulum	6.94
GO Biological Process	chromatin assembly	6.80
GO Biological Process	gene silencing	6.71
GO Biological Process	peptidyl-proline modification	6.58
GO Biological Process	nuclear-transcribed mRNA catabolic process, nonsense-mediated decay	6.49
GO Biological Process	cotranslational protein targeting to membrane	6.48
GO Biological Process	SRP-dependent cotranslational protein targeting to membrane	6.21
GO Biological Process	protein-DNA complex assembly	6.17
GO Biological Process	nucleosome organization	5.73
GO Biological Process	chromatin assembly or disassembly	5.68
GO Biological Process	protein targeting to ER	5.46
GO Biological Process	cellular response to topologically incorrect protein	5.22

F

CIS-BP ChIP

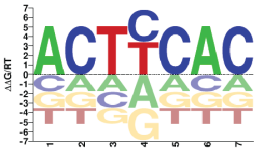

B1H-RC prediction

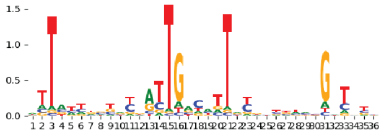

no motif discovered de novo

Supplementary Figure 1712: Properties and genomic distribution of motifs identified for the ZNF77 transcription factor in K562 (accession ENCSR844MAB).

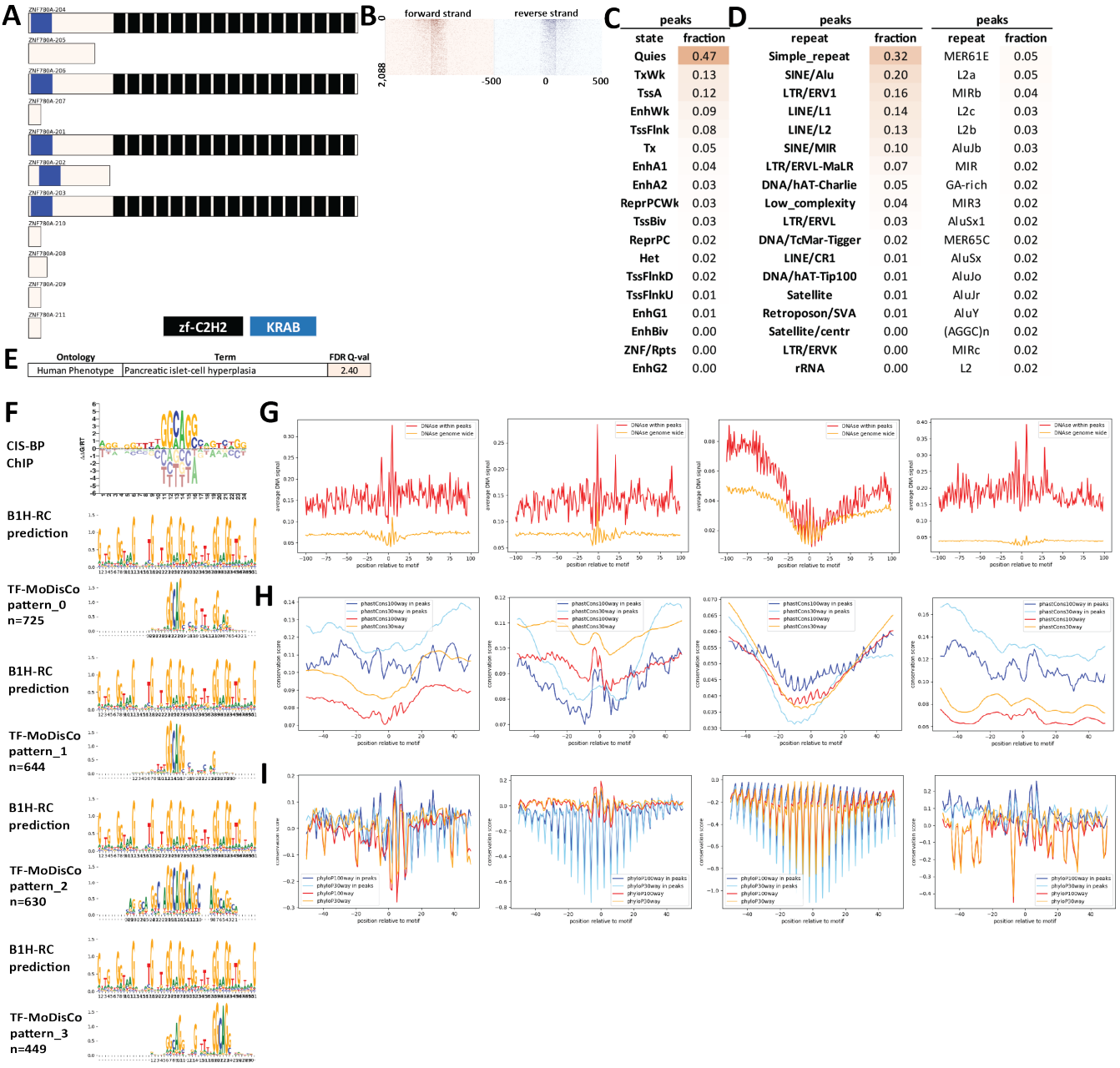

Supplementary Figure 1713: Properties and genomic distribution of motifs identified for the ZNF780A transcription factor in HEK293 (accession ChipExo models).

TF-MoDisCO pattern_0 n=725, CWM

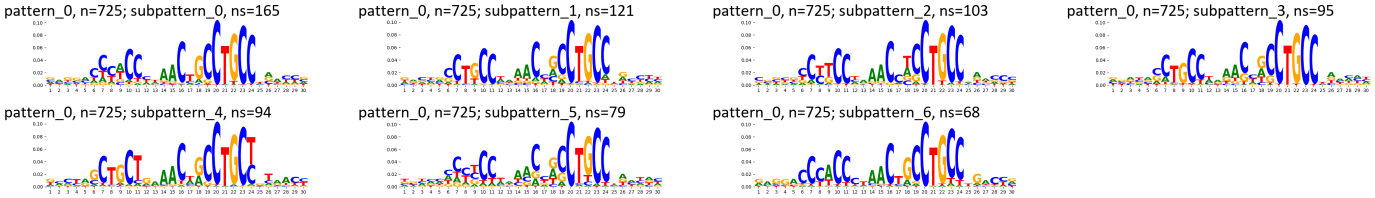

TF-MoDisCO pattern_0 n=725, PWM

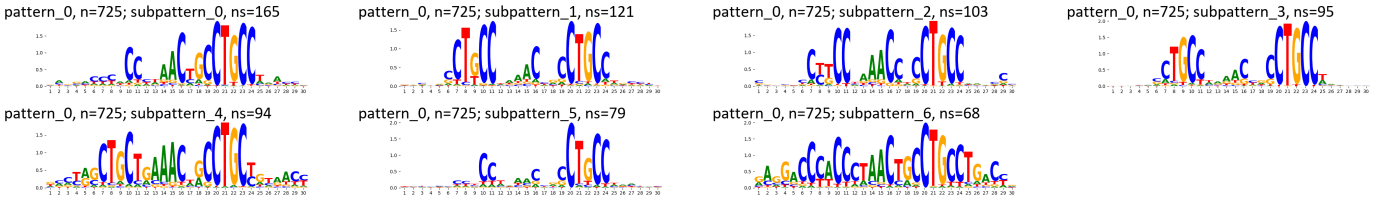

TF-MoDisCO pattern_1 n=644, CWM

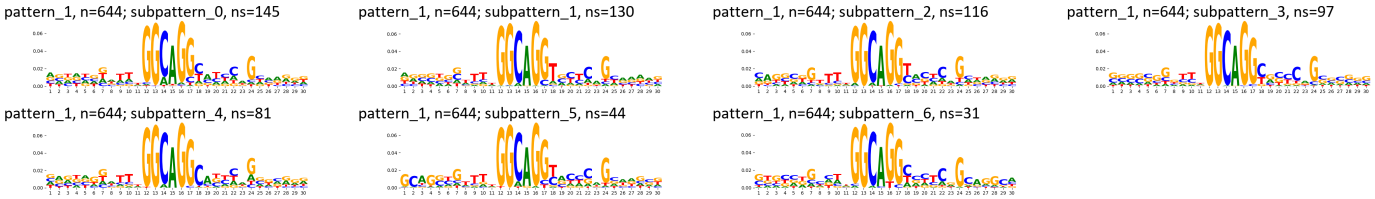

TF-MoDisCO pattern_1 n=644, PWM

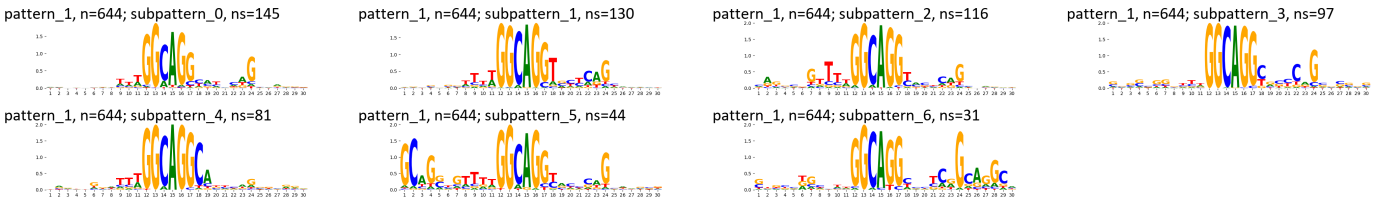

TF-MoDisCO pattern_2 n=630, CWM

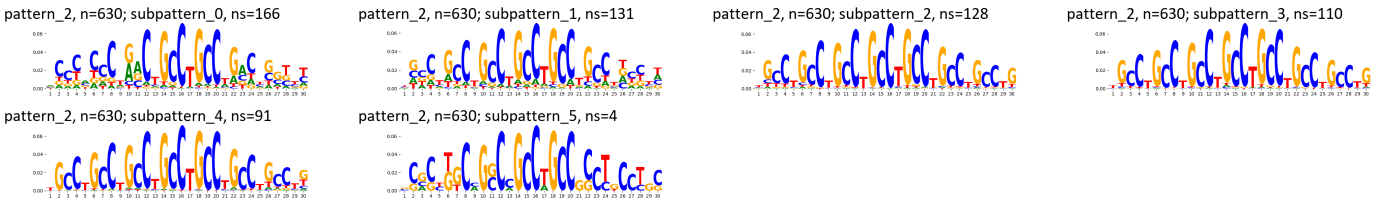

TF-MoDisCO pattern_2 n=630, PWM

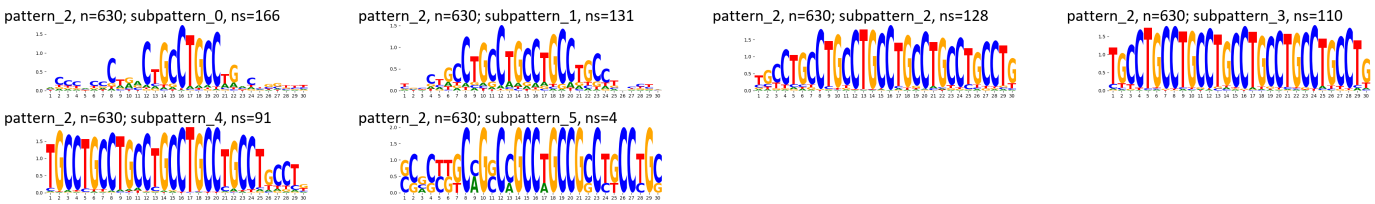

TF-MoDisCO pattern_3 n=449, CWM

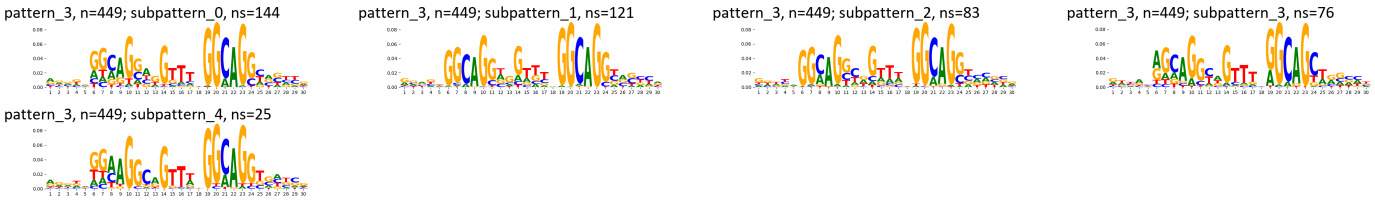

TF-MoDisCO pattern_3 n=449, PWM

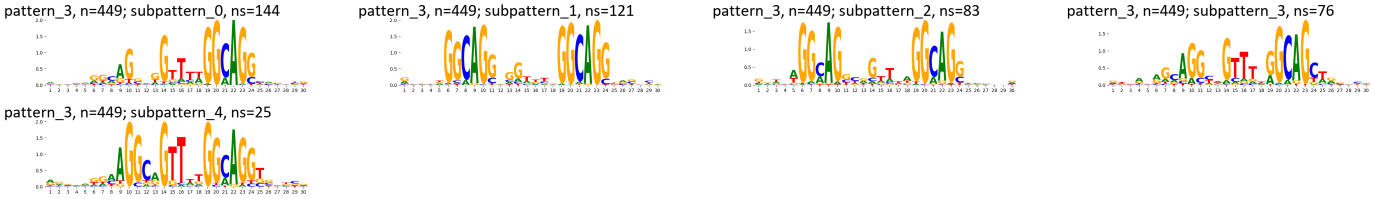

Supplementary Figure 1714: TF-MoDisCO subpatterns for the ZNF780A transcription factor in HEK293 (accession ChipExo models).

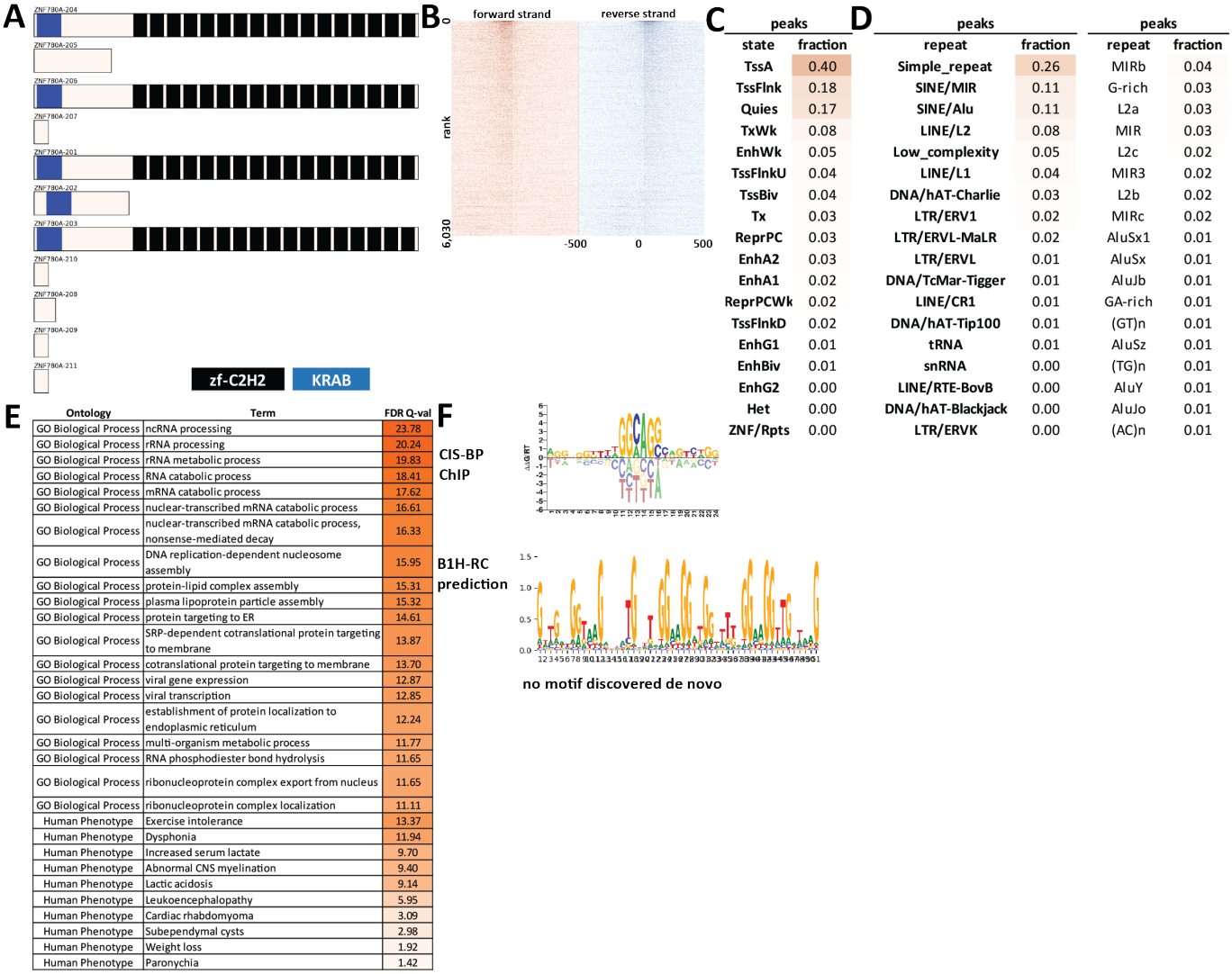

C

peaks	
state	fraction
TssA	0.40
TssFlnk	0.18
Quies	0.17
TxWk	0.08
EnhWk	0.05
TssFlnkU	0.04
TssBiv	0.04
Tx	0.03
ReprPC	0.03
EnhA2	0.03
EnhA1	0.02
ReprPCWk	0.02
TssFlnkD	0.02
EnhG1	0.01
EnhBiv	0.01
EnhG2	0.00
Het	0.00
ZNF/Rpts	0.00

D

peaks		peaks	
repeat	fraction	repeat	fraction
Simple_repeat	0.26	MIRb	0.04
SINE/MIR	0.11	G-rich	0.03
SINE/Alu	0.11	L2a	0.03
LINE/L2	0.08	MIR	0.03
Low_complexity	0.05	L2c	0.02
LINE/L1	0.04	MIR3	0.02
DNA/hAT-Charlie	0.03	L2b	0.02
LTR/ERV1	0.02	MIRc	0.02
LTR/ERVL-MaLR	0.02	AluSx1	0.01
LTR/ERVL	0.01	AluSx	0.01
DNA/TcMar-Tigger	0.01	AluJb	0.01
LINE/CR1	0.01	GA-rich	0.01
DNA/hAT-Tip100	0.01	(GT)n	0.01
tRNA	0.01	AluSz	0.01
snRNA	0.00	(TG)n	0.01
LINE/RTE-BovB	0.00	AluY	0.01
DNA/hAT-Blackjack	0.00	AluJo	0.01
LTR/ERVK	0.00	(AC)n	0.01

E

Ontology	Term	FDR Q-val
GO Biological Process	ncRNA processing	23.78
GO Biological Process	rRNA processing	20.24
GO Biological Process	rRNA metabolic process	19.83
GO Biological Process	RNA catabolic process	18.41
GO Biological Process	mRNA catabolic process	17.62
GO Biological Process	nuclear-transcribed mRNA catabolic process	16.61
GO Biological Process	nuclear-transcribed mRNA catabolic process, nonsense-mediated decay	16.33
GO Biological Process	DNA replication-dependent nucleosome assembly	15.95
GO Biological Process	protein-lipid complex assembly	15.31
GO Biological Process	plasma lipoprotein particle assembly	15.32
GO Biological Process	protein targeting to ER	14.61
GO Biological Process	SRP-dependent cotranslational protein targeting to membrane	13.87
GO Biological Process	cotranslational protein targeting to membrane	13.70
GO Biological Process	viral gene expression	12.87
GO Biological Process	viral transcription	12.85
GO Biological Process	establishment of protein localization to endoplasmic reticulum	12.24
GO Biological Process	multi-organism metabolic process	11.77
GO Biological Process	RNA phosphodiester bond hydrolysis	11.65
GO Biological Process	ribonucleoprotein complex export from nucleus	11.65
GO Biological Process	ribonucleoprotein complex localization	11.11
Human Phenotype	Exercise intolerance	13.37
Human Phenotype	Dysphonia	11.94
Human Phenotype	Increased serum lactate	9.70
Human Phenotype	Abnormal CNS myelination	9.40
Human Phenotype	Lactic acidosis	9.14
Human Phenotype	Leukoencephalopathy	5.95
Human Phenotype	Cardiac rhabdomyoma	3.09
Human Phenotype	Subependymal cysts	2.98
Human Phenotype	Weight loss	1.92
Human Phenotype	Paronychia	1.42

Supplementary Figure 1715: Properties and genomic distribution of motifs identified for the ZNF780A transcription factor in HepG2 (accession ENCSR095JQV).

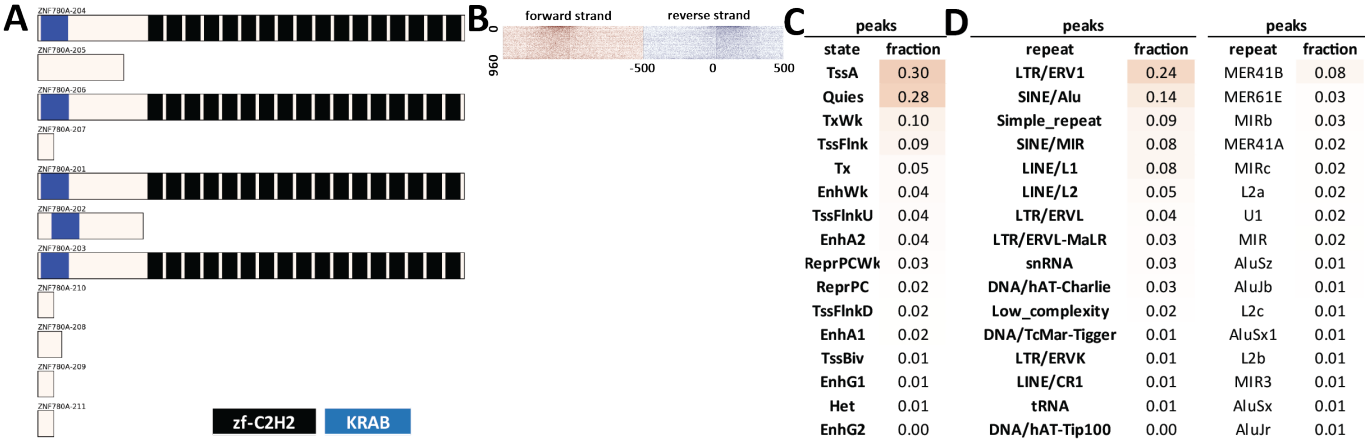

C

peaks	
state	fraction
TssA	0.30
Quies	0.28
TxWk	0.10
TssFlnk	0.09
Tx	0.05
EnhWk	0.04
TssFlnkU	0.04
EnhA2	0.04
ReprPCWk	0.03
ReprPC	0.02
TssFlnkD	0.02
EnhA1	0.02
TssBiv	0.01
EnhG1	0.01
Het	0.01
EnhG2	0.00
EnhBiv	0.00

D

peaks		peaks	
repeat	fraction	repeat	fraction
LTR/ERV1	0.24	MER41B	0.08
SINE/Alu	0.14	MER61E	0.03
Simple_repeat	0.09	MIRb	0.03
SINE/MIR	0.08	MER41A	0.02
LINE/L1	0.08	MIRc	0.02
LINE/L2	0.05	L2a	0.02
LTR/ERVL	0.04	U1	0.02
LTR/ERVL-MaLR	0.03	MIR	0.02
snRNA	0.03	AluSz	0.01
DNA/hAT-Charlie	0.03	AluJb	0.01
Low_complexity	0.02	L2c	0.01
DNA/TcMar-Tigger	0.01	AluSx1	0.01
LTR/ERVK	0.01	L2b	0.01
LINE/CR1	0.01	MIR3	0.01
tRNA	0.01	AluSx	0.01
DNA/hAT-Tip100	0.00	AluJr	0.01
Satellite/centr	0.00	AluJo	0.01
DNA/hAT-Ac	0.00	LTR8	0.01

E

Ontology	Term	FDR Q-val
GO Biological Process	negative regulation of megakaryocyte differentiation	16.02
GO Biological Process	DNA replication-dependent nucleosome assembly	13.69
GO Biological Process	chromatin silencing at rDNA	11.58
GO Biological Process	protein folding	10.24
GO Biological Process	regulation of hematopoietic progenitor cell differentiation	10.18
GO Biological Process	regulation of hematopoietic stem cell differentiation	9.24
GO Biological Process	protein-DNA complex subunit organization	9.12
GO Biological Process	telomere capping	8.49
GO Biological Process	nucleosome organization	8.34
GO Biological Process	negative regulation of gene expression, epigenetic	8.34
GO Biological Process	protein-DNA complex assembly	8.14
GO Biological Process	nucleosome assembly	8.03
GO Biological Process	DNA conformation change	7.75
GO Biological Process	protein heterotetramerization	7.57
GO Biological Process	chromatin assembly	7.50
GO Biological Process	chromatin assembly or disassembly	7.24
GO Biological Process	telomere organization	6.94
GO Biological Process	chromatin silencing	6.83
GO Biological Process	response to topologically incorrect protein	6.05
GO Biological Process	regulation of megakaryocyte differentiation	5.50

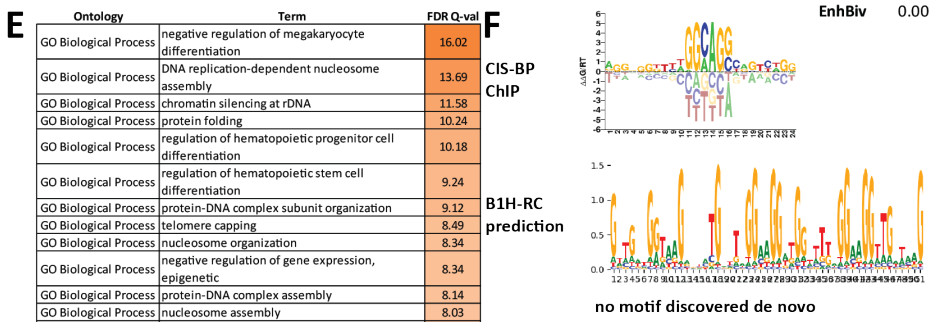

Supplementary Figure 1716: Properties and genomic distribution of motifs identified for the ZNF780A transcription factor in K562 (accession ENCSR214PDW).

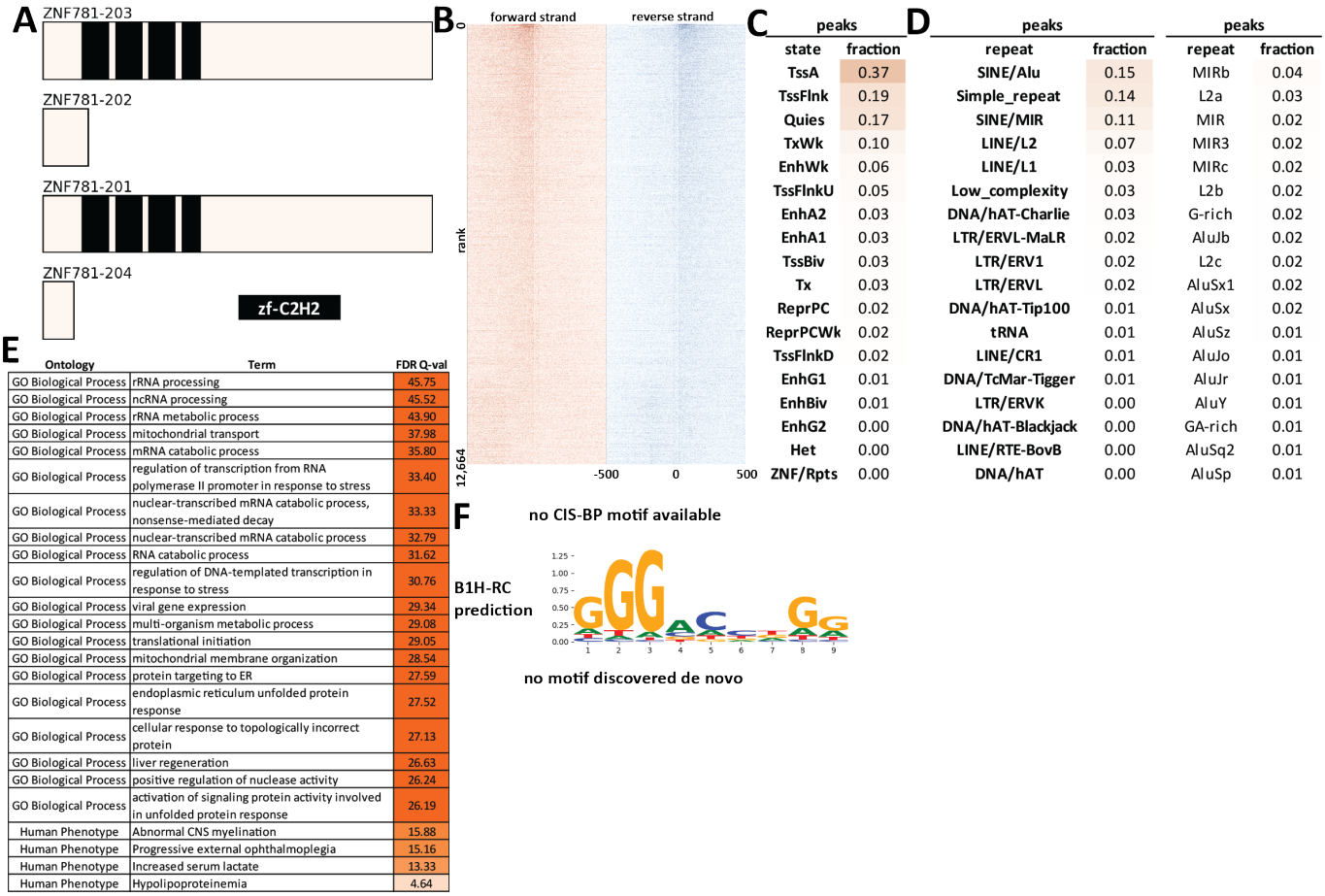

Supplementary Figure 1717: Properties and genomic distribution of motifs identified for the ZNF781 transcription factor in HepG2 (accession ENCSR517HGZ).

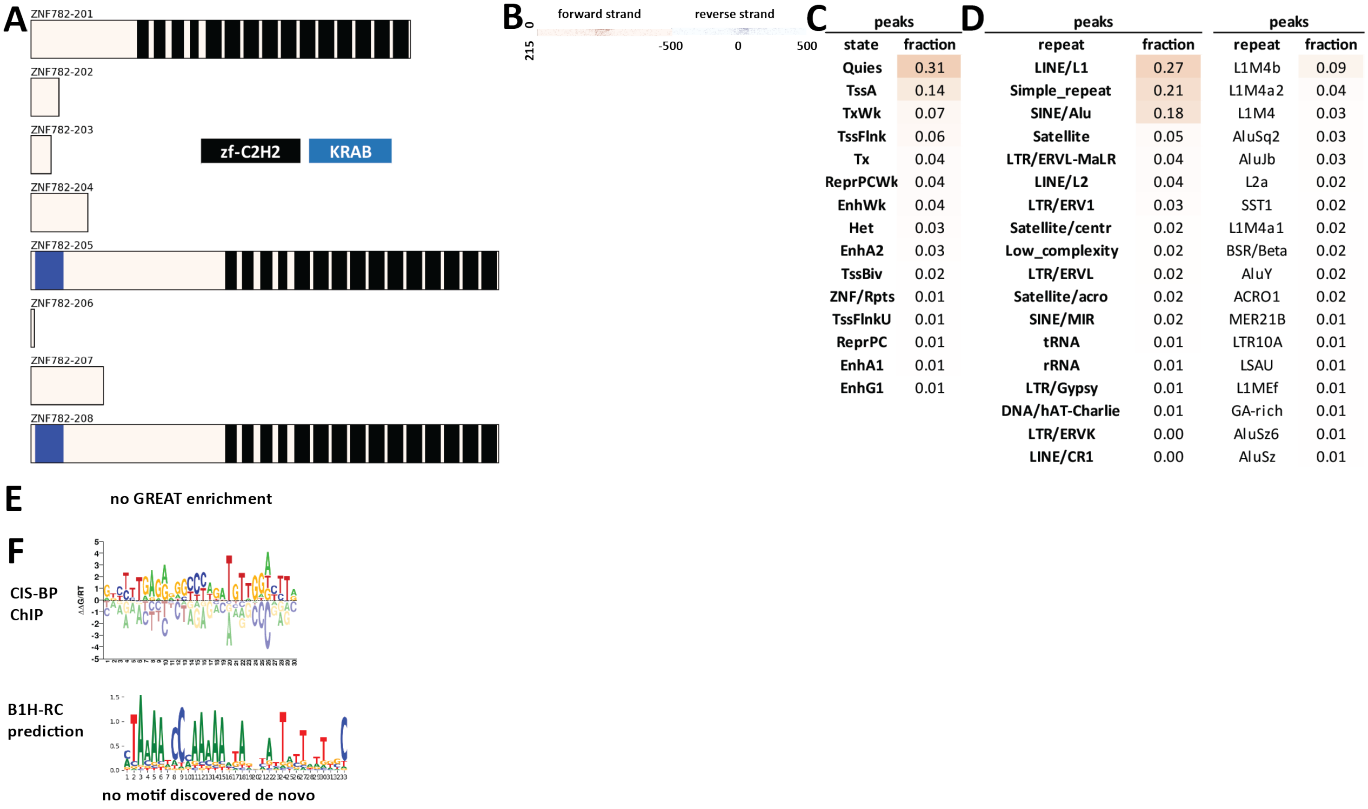

peaks	
state	fraction
Quies	0.31
TssA	0.14
TxWk	0.07
TssFlnk	0.06
Tx	0.04
ReprPCWk	0.04
EnhWk	0.04
Het	0.03
EnhA2	0.03
TssBiv	0.02
ZNF/Rpts	0.01
TssFlnkU	0.01
ReprPC	0.01
EnhA1	0.01
EnhG1	0.01

peaks		peaks	
repeat	fraction	repeat	fraction
LINE/L1	0.27	L1M4b	0.09
Simple_repeat	0.21	L1M4a2	0.04
SINE/Alu	0.18	L1M4	0.03
Satellite	0.05	AluSq2	0.03
LTR/ERVL-MaLR	0.04	AluJb	0.03
LINE/L2	0.04	L2a	0.02
LTR/ERV1	0.03	SST1	0.02
Satellite/centr	0.02	L1M4a1	0.02
Low_complexity	0.02	BSR/Beta	0.02
LTR/ERVL	0.02	AluY	0.02
Satellite/acro	0.02	ACRO1	0.02
SINE/MIR	0.02	MER21B	0.01
tRNA	0.01	LTR10A	0.01
rRNA	0.01	LSAU	0.01
LTR/Gypsy	0.01	L1MEf	0.01
DNA/hAT-Charlie	0.01	GA-rich	0.01
LTR/ERVK	0.00	AluSz6	0.01
LINE/CR1	0.00	AluSz	0.01

Supplementary Figure 1718: Properties and genomic distribution of motifs identified for the ZNF782 transcription factor in HEK293 (accession ChipExo models).

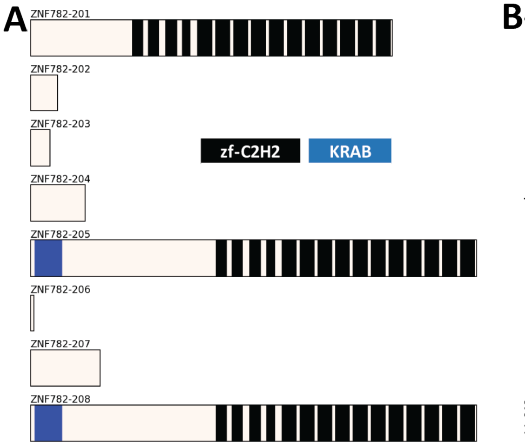



C

peaks	
state	fraction
TssA	0.40
TssFlnk	0.19
Quies	0.15
TxWk	0.08
EnhWk	0.05
TssFlnkU	0.04
TssBiv	0.04
ReprPC	0.03
EnhA2	0.02
Tx	0.02
ReprPCWk	0.02
EnhA1	0.02
TssFlnkD	0.02
EnhBiv	0.01
EnhG1	0.00
EnhG2	0.00
Het	0.00

D

peaks		peaks	
repeat	fraction	repeat	fraction
Simple_repeat	0.20	MIRb	0.04
SINE/Alu	0.10	G-rich	0.03
SINE/MIR	0.10	L2a	0.02
LINE/L2	0.05	MIR	0.02
Low_complexity	0.04	MIR3	0.02
LINE/L1	0.03	L2b	0.02
DNA/hAT-Charlie	0.02	MIRc	0.02
LTR/ERV1	0.02	AluJb	0.01
LTR/ERVL-MaLR	0.02	L2c	0.01
LTR/ERVL	0.01	AluSx1	0.01
DNA/hAT-Tip100	0.01	AluSx	0.01
tRNA	0.00	AluSz	0.01
LINE/CR1	0.00	GA-rich	0.01
DNA/TcMar-Tigger	0.00	(GGC)n	0.01
DNA/hAT-Blackjack	0.00	AluJo	0.01
LINE/RTE-BovB	0.00	AluJr	0.01
LTR/ERVK	0.00	AluSq2	0.01
DNA/hAT	0.00	AluY	0.01

E

Ontology	Term	FDR Q-val
GO Biological Process	endoplasmic reticulum unfolded protein response	37.91
GO Biological Process	positive regulation of nuclease activity	37.62
GO Biological Process	regulation of transcription from RNA polymerase II promoter in response to stress	37.48
GO Biological Process	activation of signaling protein activity involved in unfolded protein response	37.40
GO Biological Process	IRE1-mediated unfolded protein response	36.27
GO Biological Process	cellular response to topologically incorrect protein	35.92
GO Biological Process	cellular response to unfolded protein	34.44
GO Biological Process	regulation of DNA-templated transcription in response to stress	32.93
GO Biological Process	response to topologically incorrect protein	31.20
GO Biological Process	response to unfolded protein	29.76
GO Biological Process	regulation of nuclease activity	28.81
GO Biological Process	regulation of intrinsic apoptotic signaling pathway	28.76
GO Biological Process	regulation of endoplasmic reticulum unfolded protein response	21.25
GO Biological Process	regulation of cellular amino acid metabolic process	19.88
GO Biological Process	protein targeting to ER	16.79
GO Biological Process	regulation of transcription from RNA polymerase II promoter in response to hypoxia	16.00
GO Biological Process	cellular response to epidermal growth factor stimulus	15.89
GO Biological Process	nuclear-transcribed mRNA catabolic process, nonsense-mediated decay	15.22
GO Biological Process	protein localization to endoplasmic reticulum	14.17
GO Biological Process	establishment of protein localization to endoplasmic reticulum	13.90
Human Phenotype	Increased serum lactate	14.75
Human Phenotype	Abnormality of mitochondrial metabolism	9.96
Human Phenotype	Abnormality of the mitochondrion	9.52
Human Phenotype	Lipid accumulation in hepatocytes	9.01
Human Phenotype	Increased CSF lactate	8.99
Human Phenotype	Abnormal CSF metabolite level	8.21
Human Phenotype	Exercise intolerance	8.00
Human Phenotype	Decreased activity of mitochondrial respiratory chain	6.79
Human Phenotype	Cytochrome C oxidase-negative muscle fibers	5.04
Human Phenotype	Increased hepatocellular lipid droplets	3.30
Human Phenotype	Retinopathy	2.36

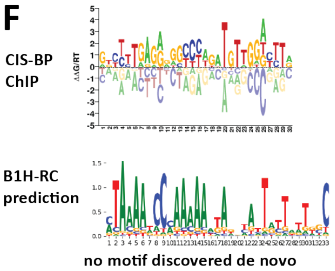

Supplementary Figure 1719: Properties and genomic distribution of motifs identified for the ZNF782 transcription factor in HepG2 (accession ENCSR198RHC).

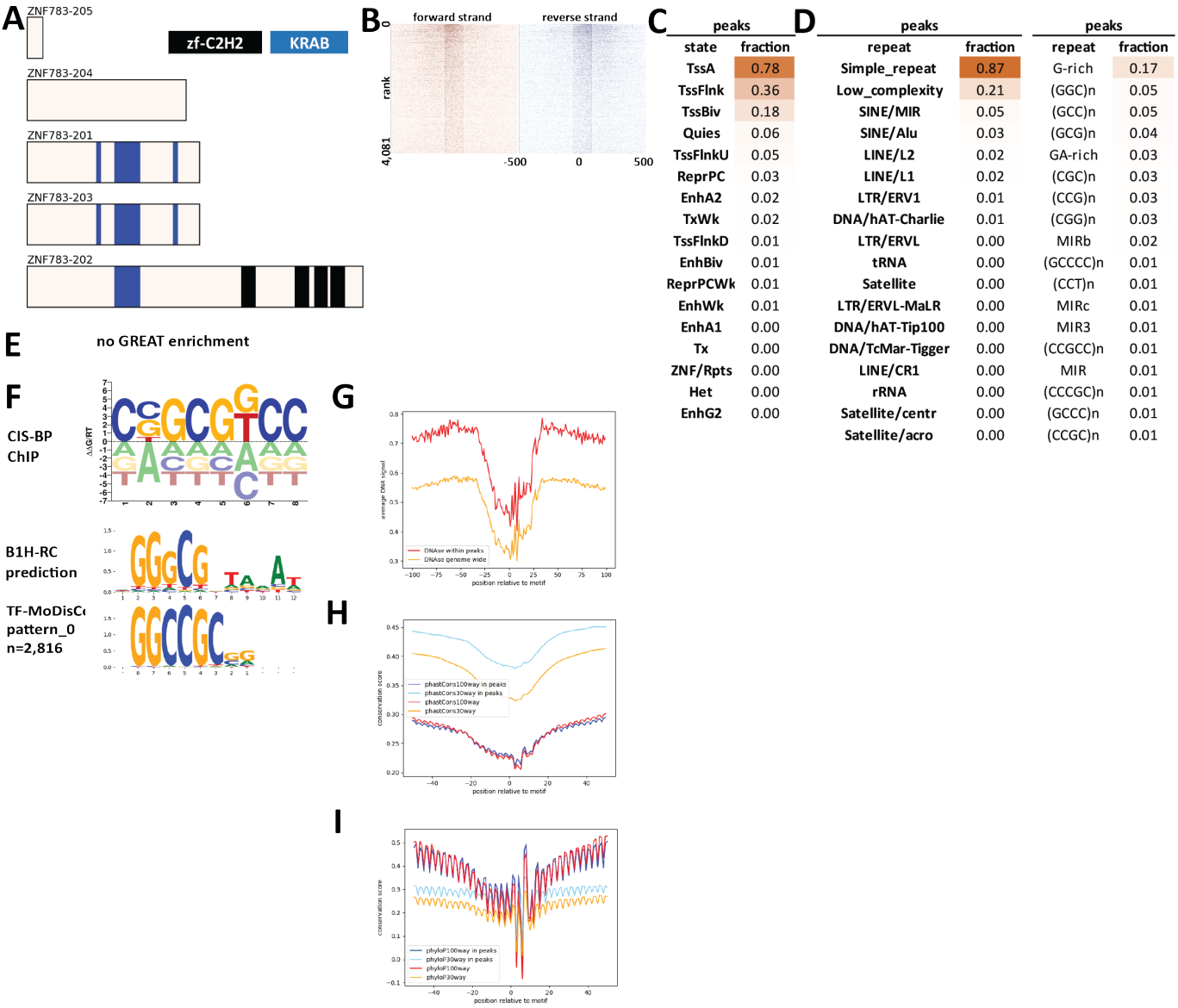

peaks	
state	fraction
TssA	0.78
TssFlnk	0.36
TssBiv	0.18
Quies	0.06
TssFlnkU	0.05
ReprPC	0.03
EnhA2	0.02
TxWk	0.02
TssFlnkD	0.01
EnhBiv	0.01
ReprPCWk	0.01
EnhWk	0.01
EnhA1	0.00
Tx	0.00
ZNF/Rpts	0.00
Het	0.00
EnhG2	0.00

peaks		peaks	
repeat	fraction	repeat	fraction
Simple_repeat	0.87	G-rich	0.17
Low_complexity	0.21	(GGC)n	0.05
SINE/MIR	0.05	(GCC)n	0.05
SINE/Alu	0.03	(GCG)n	0.04
LINE/L2	0.02	GA-rich	0.03
LINE/L1	0.02	(CGC)n	0.03
LTR/ERV1	0.01	(CCG)n	0.03
DNA/hAT-Charlie	0.01	(CGG)n	0.03
LTR/ERVL	0.00	MIRb	0.02
tRNA	0.00	(GCCCC)n	0.01
Satellite	0.00	(CCT)n	0.01
LTR/ERVL-MaLR	0.00	MIRc	0.01
DNA/hAT-Tip100	0.00	MIR3	0.01
DNA/TcMar-Tigger	0.00	(CCGCC)n	0.01
LINE/CR1	0.00	MIR	0.01
rRNA	0.00	(CCCGC)n	0.01
Satellite/centr	0.00	(GCCC)n	0.01
Satellite/acro	0.00	(CCGC)n	0.01

Supplementary Figure 1720: Properties and genomic distribution of motifs identified for the ZNF783 transcription factor in HEK293 (accession ChipExo models).

TF-MoDisCO pattern_0 n=2816, CWM

pattern_0, n=2816; subpattern_0, ns=681

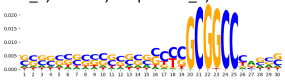

pattern_0, n=2816; subpattern_1, ns=329

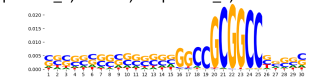

pattern_0, n=2816; subpattern_2, ns=308

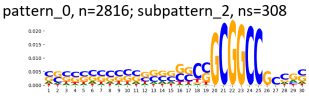

pattern_0, n=2816; subpattern_3, ns=304

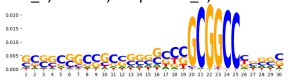

pattern_0, n=2816; subpattern_4, ns=297

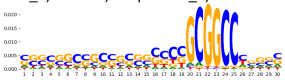

pattern_0, n=2816; subpattern_5, ns=288

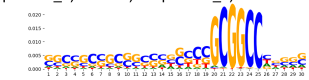

pattern_0, n=2816; subpattern_6, ns=249

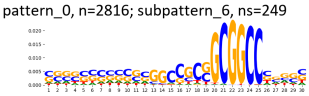

pattern_0, n=2816; subpattern_7, ns=188

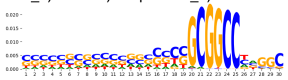

pattern_0, n=2816; subpattern_8, ns=172

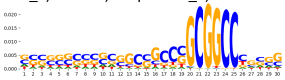

TF-MoDisCO pattern_0 n=2816, PWM

pattern_0, n=2816; subpattern_0, ns=681

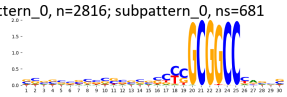

pattern_0, n=2816; subpattern_1, ns=329

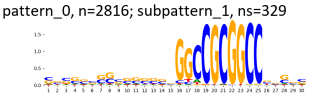

pattern_0, n=2816; subpattern_2, ns=308

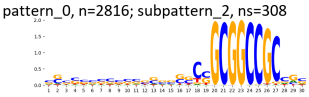

pattern_0, n=2816; subpattern_3, ns=304

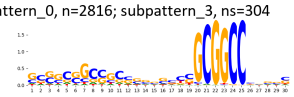

pattern_0, n=2816; subpattern_4, ns=297

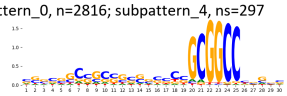

pattern_0, n=2816; subpattern_5, ns=288

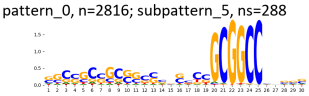

pattern_0, n=2816; subpattern_6, ns=249

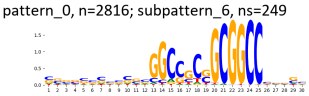

pattern_0, n=2816; subpattern_7, ns=188

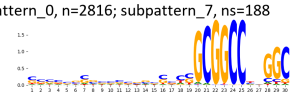

pattern_0, n=2816; subpattern_8, ns=172

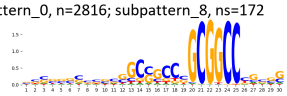

Supplementary Figure 1721: TF-MoDisCO subpatterns for the ZNF783 transcription factor in HEK293 (accession ChipExo models).

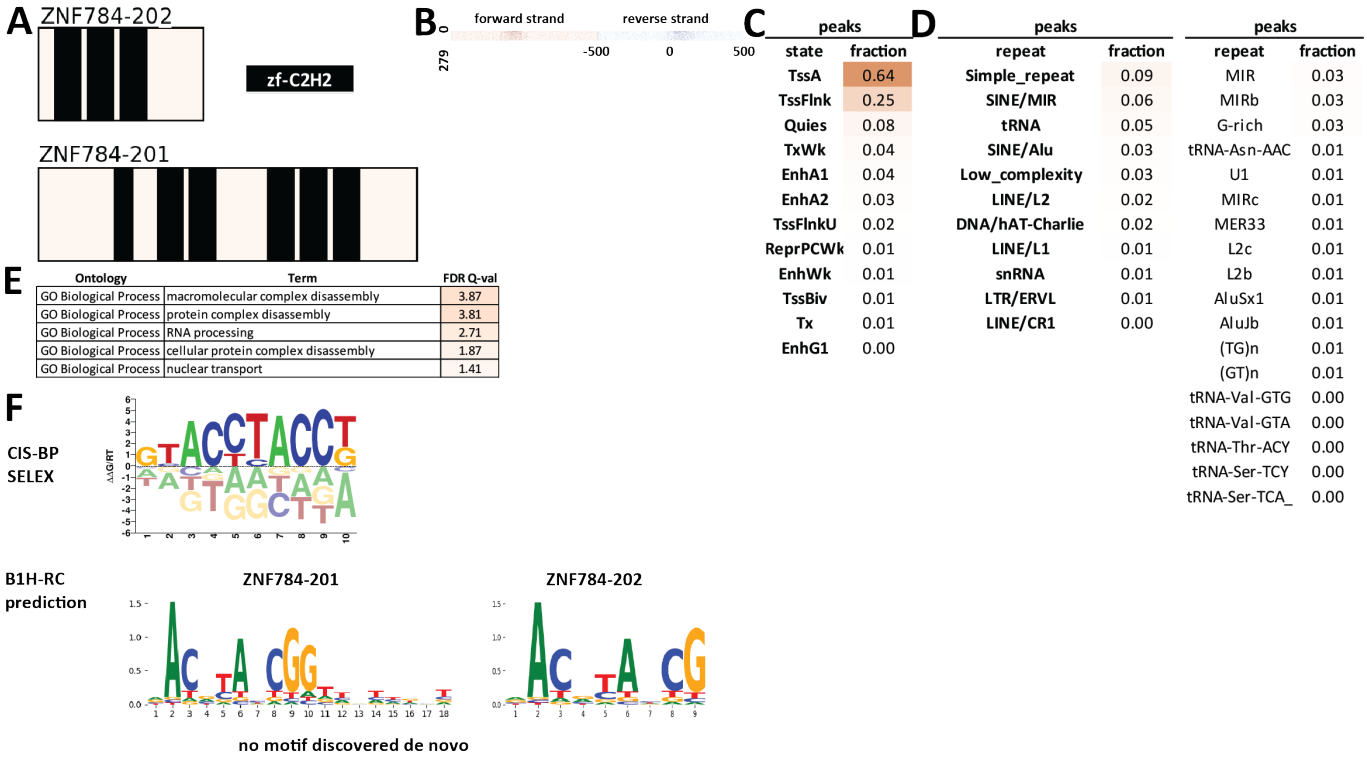

Supplementary Figure 1722: Properties and genomic distribution of motifs identified for the ZNF784 transcription factor in HEK293 (accession Hughes GR models).

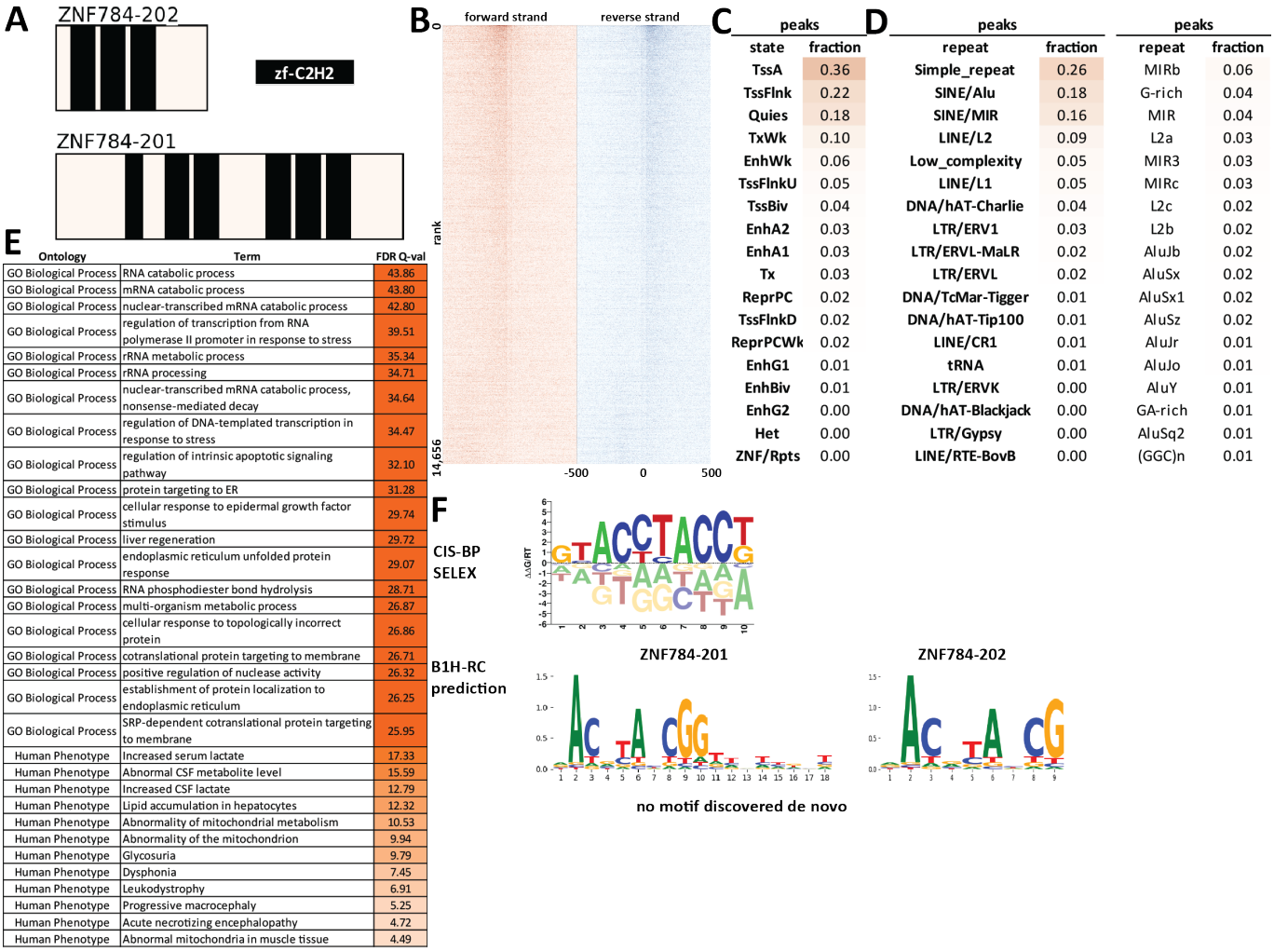

Supplementary Figure 1723: Properties and genomic distribution of motifs identified for the ZNF784 transcription factor in HepG2 (accession ENCSR082QGT).

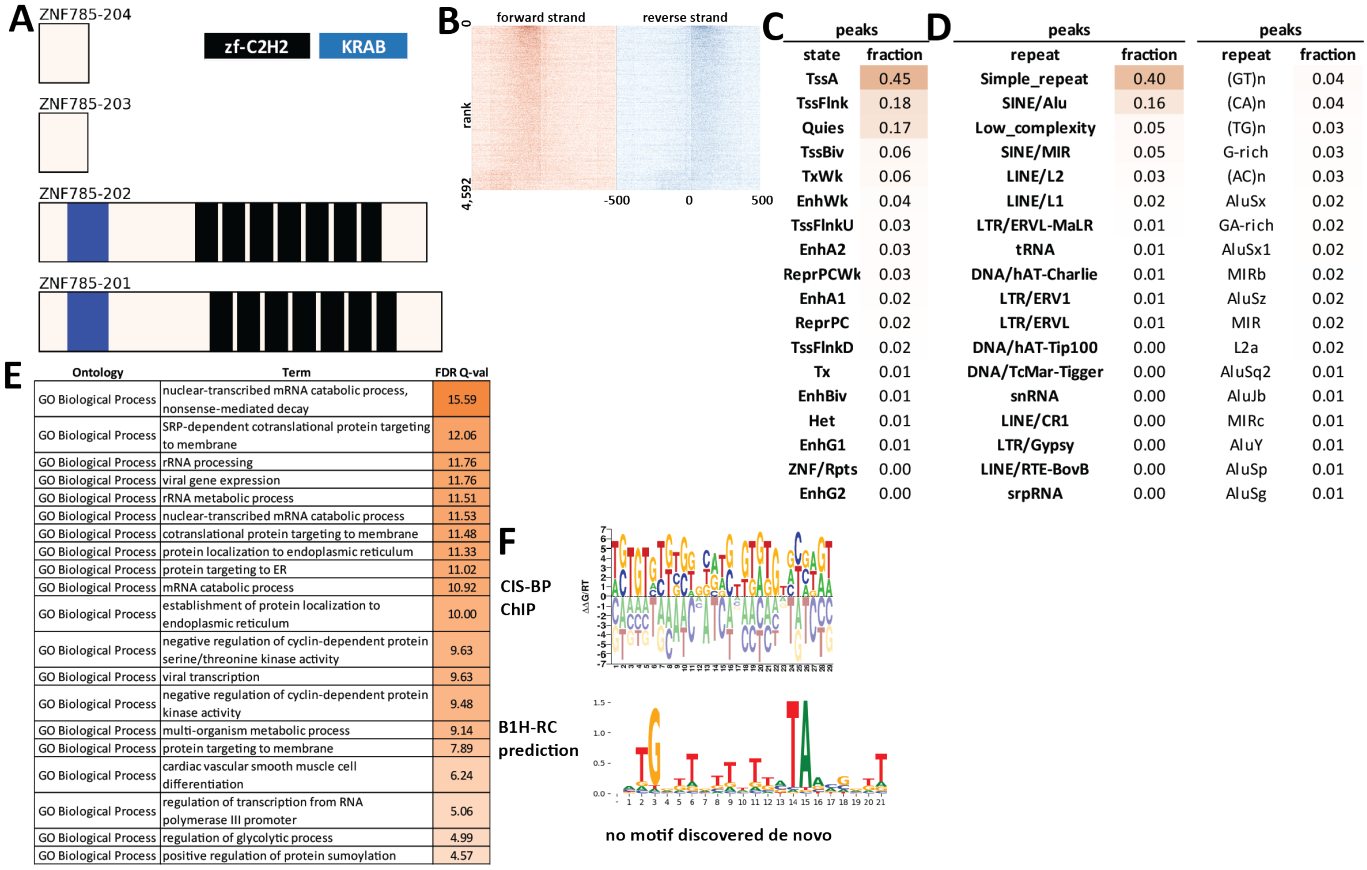

Supplementary Figure 1724: Properties and genomic distribution of motifs identified for the ZNF785 transcription factor in HEK293 (accession ENCSR950ACO).

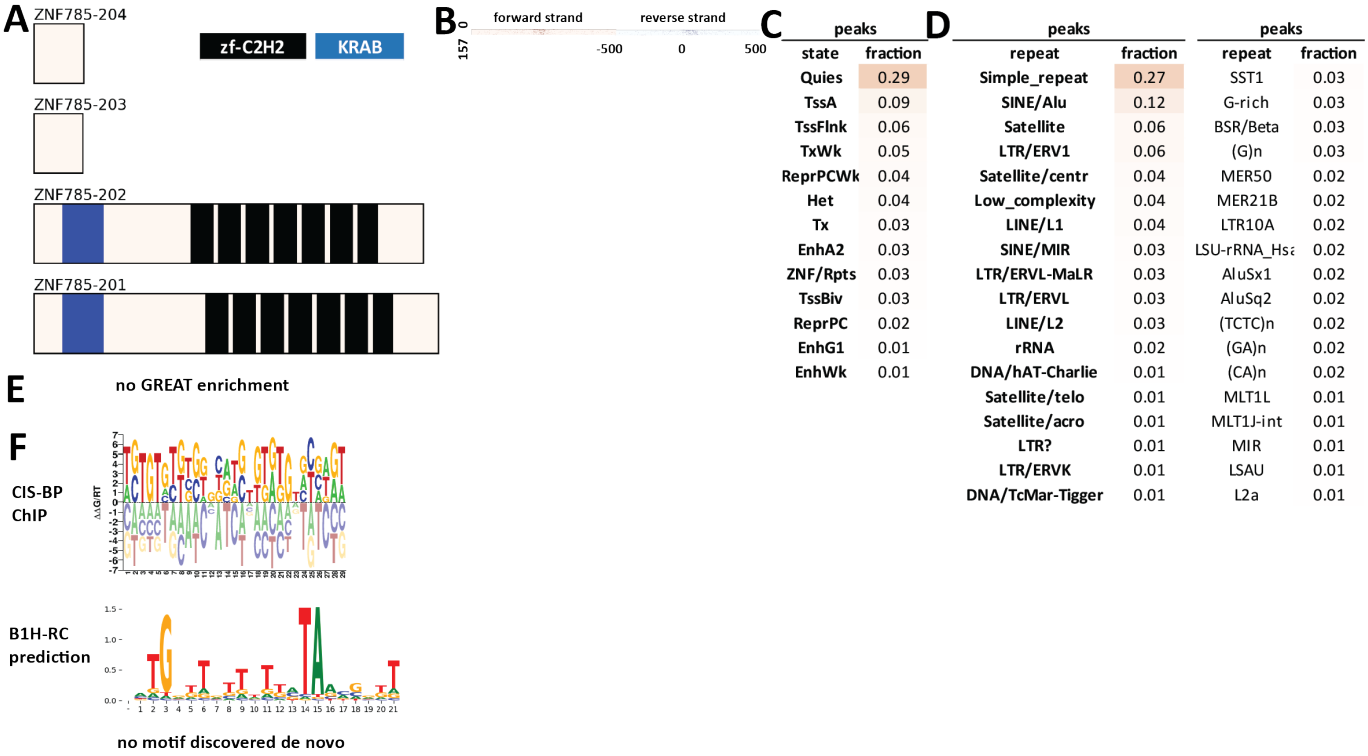

Supplementary Figure 1725: Properties and genomic distribution of motifs identified for the ZNF785 transcription factor in HEK293 (accession ChipExo models).

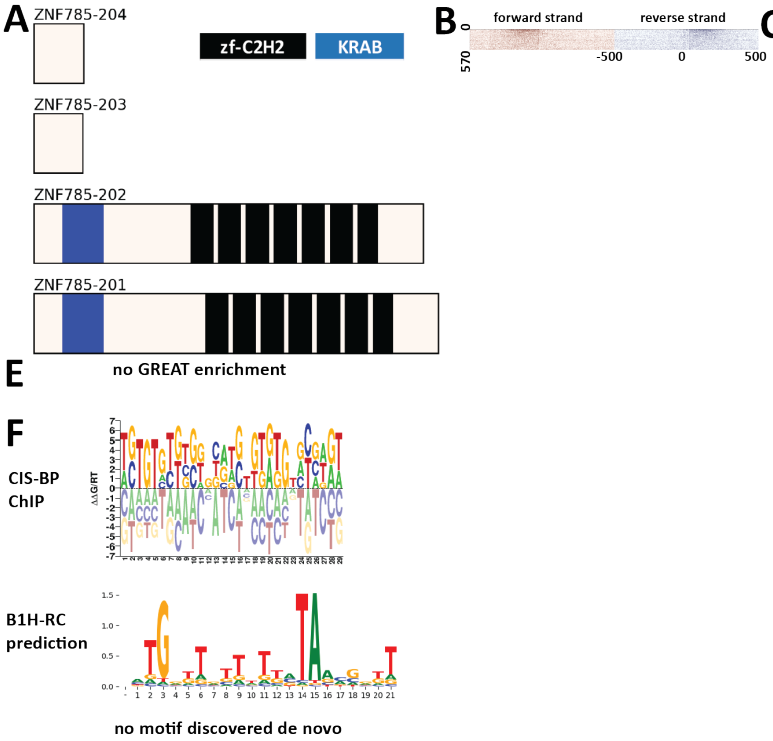

C

peaks	
state	fraction
Quies	0.45
TxWk	0.16
TssA	0.08
Tx	0.06
EnhWk	0.04
ReprPCWk	0.04
EnhA2	0.04
TssFlnk	0.03
ReprPC	0.02
EnhA1	0.01
TssFlnkU	0.01
EnhG1	0.01
TssFlnkD	0.01
ZNF/Rpts	0.00
TssBiv	0.00
Het	0.00
EnhG2	0.00

D

peaks		peaks	
repeat	fraction	repeat	fraction
LTR/ERV1	0.39	MER41B	0.14
SINE/Alu	0.16	MER41A	0.06
LINE/L1	0.15	L2a	0.03
LINE/L2	0.08	MIRb	0.03
SINE/MIR	0.08	L2c	0.03
Simple_repeat	0.07	AluY	0.02
LTR/ERVL	0.06	AluSx1	0.02
LTR/ERVL-MaLR	0.06	MIR	0.02
DNA/hAT-Charlie	0.04	MER61E	0.02
LTR/ERVK	0.01	MIRc	0.02
DNA/TcMar-Tigger	0.01	LTR62	0.02
LINE/CR1	0.01	AluJr	0.02
tRNA	0.01	L2b	0.01
Low_complexity	0.01	L1M5	0.01
DNA/hAT-Tip100	0.01	MIR3	0.01
DNA/hAT-Blackjack	0.01	LTR8	0.01
SINE/5S-Deu-L2	0.00	LTR18B	0.01
LTR/Gypsy	0.00	MER41C	0.01

Supplementary Figure 1726: Properties and genomic distribution of motifs identified for the ZNF785 transcription factor in K562 (accession ENCSR222TVA).

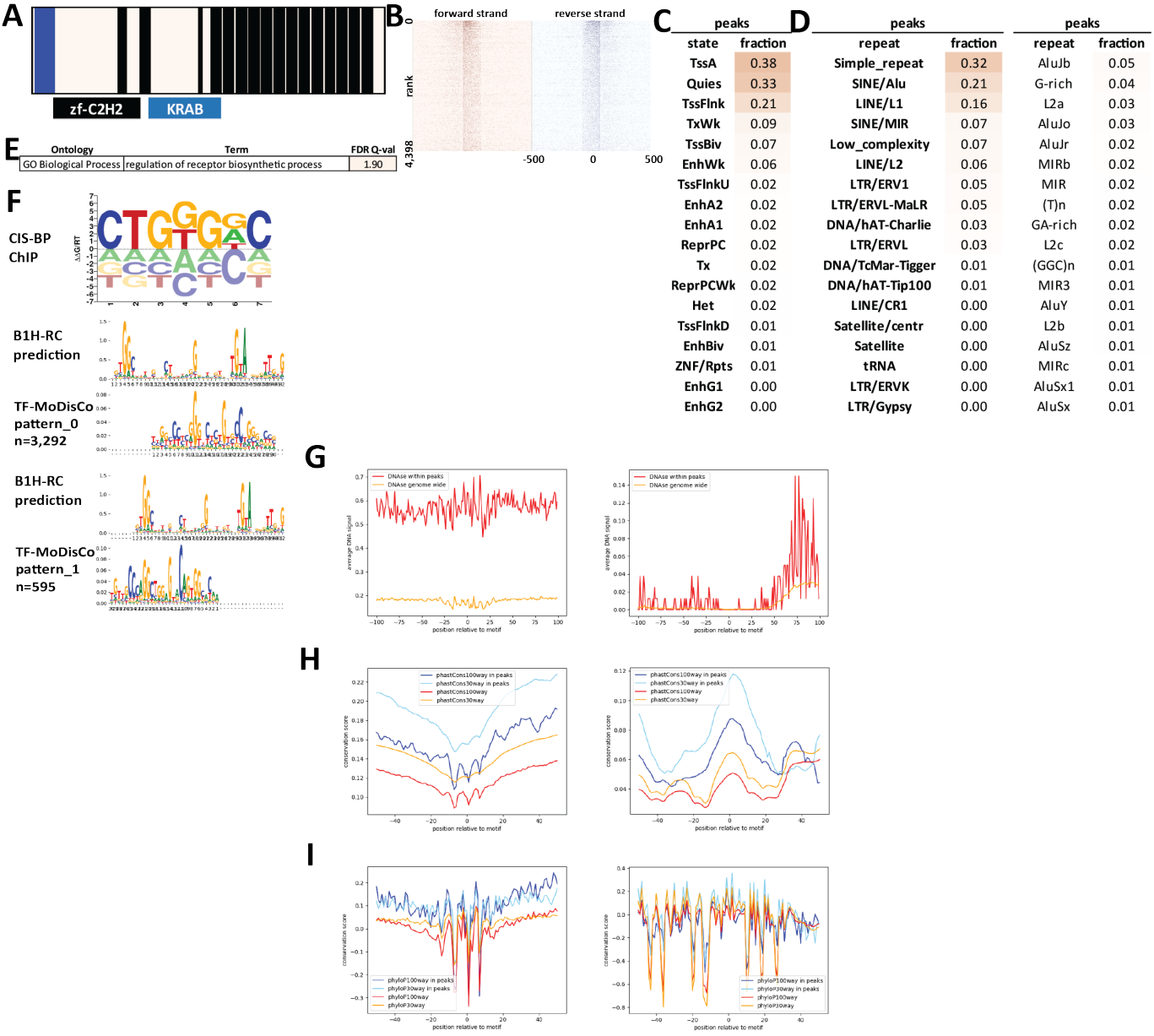

Supplementary Figure 1727: Properties and genomic distribution of motifs identified for the ZNF786 transcription factor in HEK293 (accession ChipExo models).

TF-MoDisCO pattern_0 n=3292, CWM

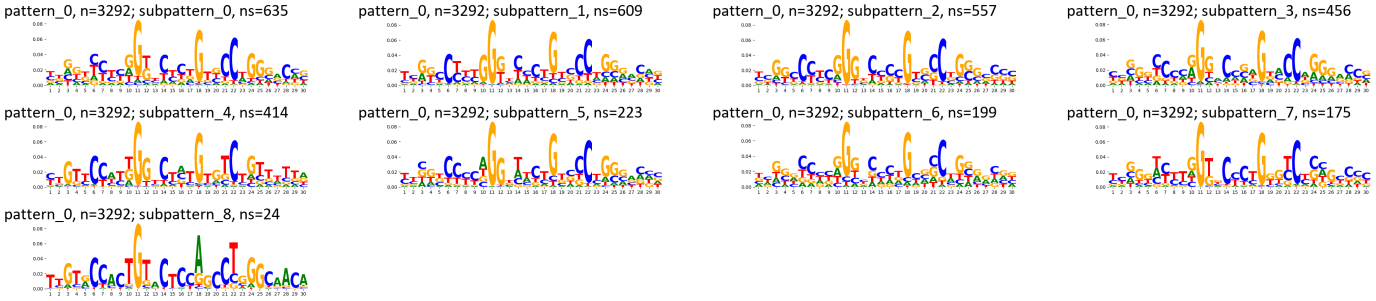

TF-MoDisCO pattern_0 n=3292, PWM

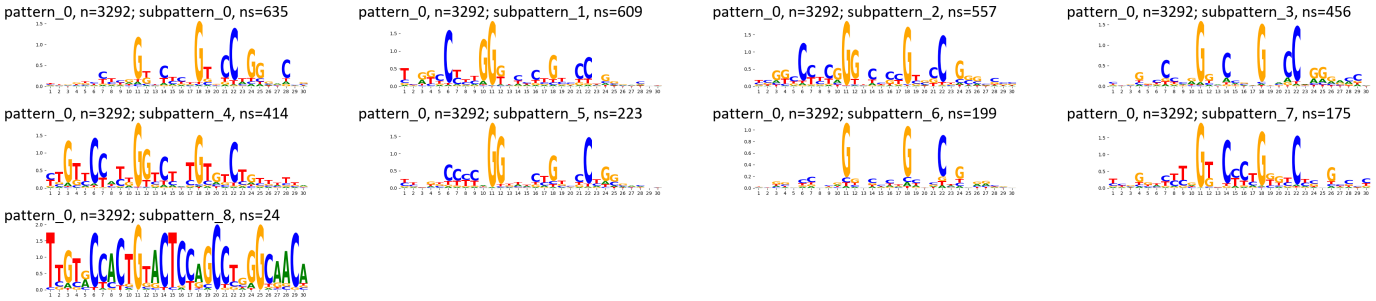

TF-MoDisCO pattern_1 n=595, CWM

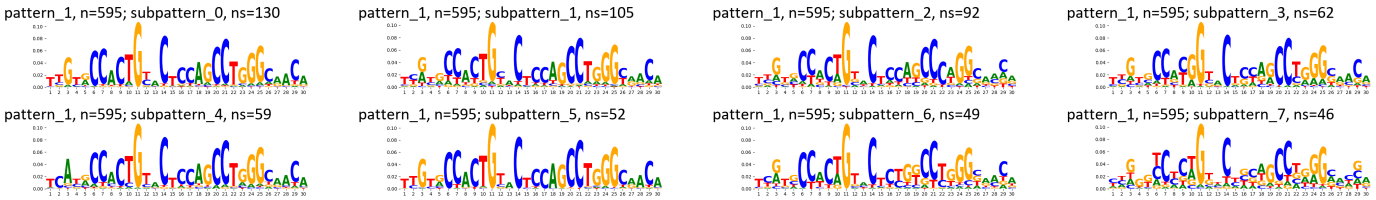

TF-MoDisCO pattern_1 n=595, PWM

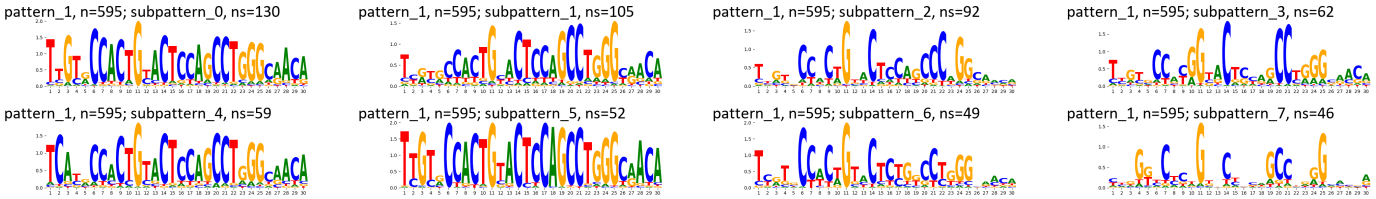

Supplementary Figure 1728: TF-MoDisCO subpatterns for the ZNF786 transcription factor in HEK293 (accession ChipExo models).

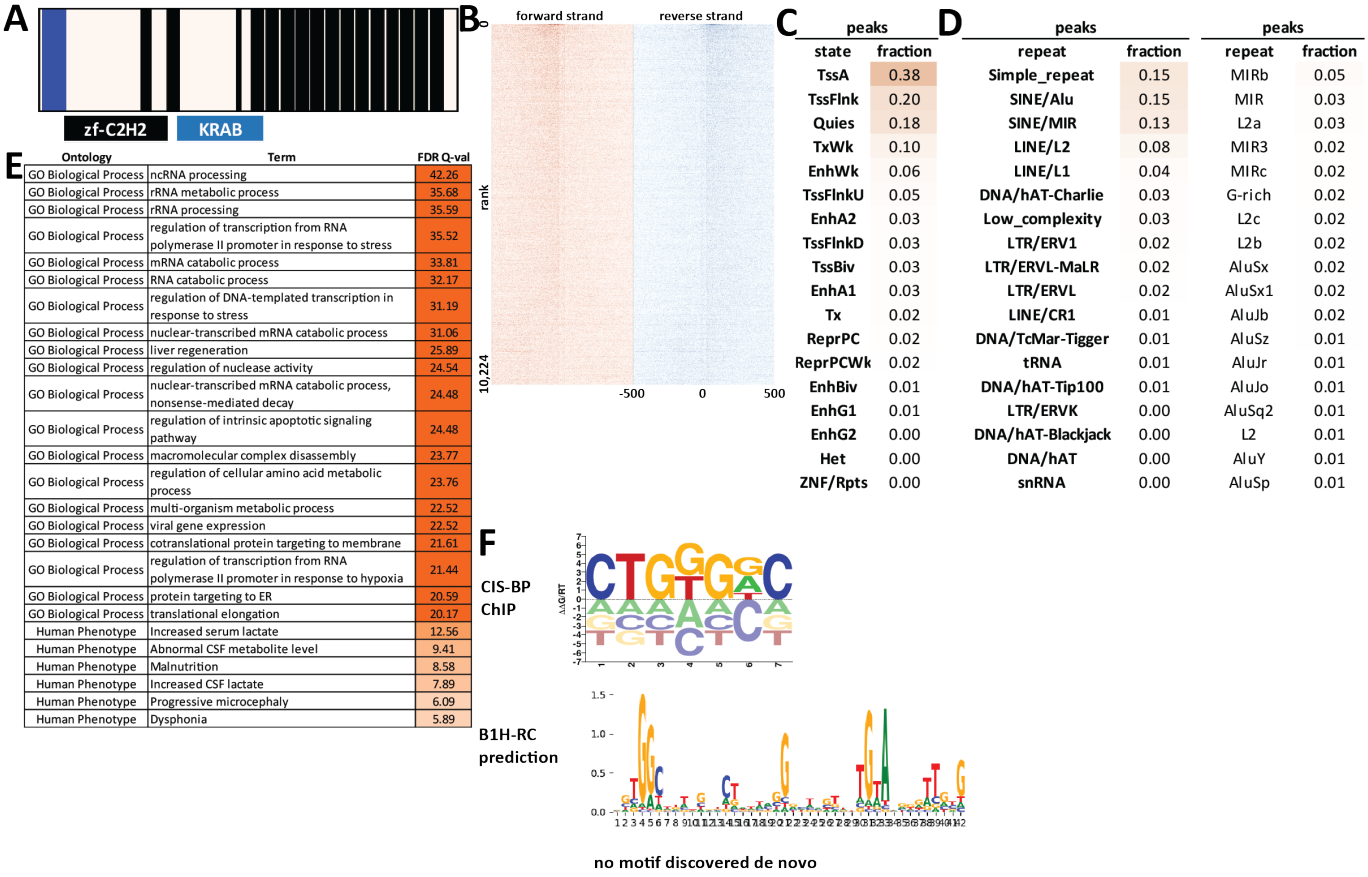

C

peaks	
state	fraction
TssA	0.38
TssFlnk	0.20
Quies	0.18
TxWk	0.10
EnhWk	0.06
TssFlnkU	0.05
EnhA2	0.03
TssFlnkD	0.03
TssBiv	0.03
EnhA1	0.03
Tx	0.02
ReprPC	0.02
ReprPCWk	0.02
EnhBiv	0.01
EnhG1	0.01
EnhG2	0.00
Het	0.00
ZNF/Rpts	0.00

D

peaks		peaks	
repeat	fraction	repeat	fraction
Simple_repeat	0.15	MIRb	0.05
SINE/Alu	0.15	MIR	0.03
SINE/MIR	0.13	L2a	0.03
LINE/L2	0.08	MIR3	0.02
LINE/L1	0.04	MIRc	0.02
DNA/hAT-Charlie	0.03	G-rich	0.02
Low_complexity	0.03	L2c	0.02
LTR/ERV1	0.02	L2b	0.02
LTR/ERVL-MaLR	0.02	AluSx	0.02
LTR/ERVL	0.02	AluSx1	0.02
LINE/CR1	0.01	AluJb	0.02
DNA/TcMar-Tigger	0.01	AluSz	0.01
tRNA	0.01	AluJr	0.01
DNA/hAT-Tip100	0.01	AluJo	0.01
LTR/ERVK	0.00	AluSq2	0.01
DNA/hAT-Blackjack	0.00	L2	0.01
DNA/hAT	0.00	AluY	0.01
snRNA	0.00	AluSp	0.01

E

Ontology	Term	FDR Q-val
GO Biological Process	ncRNA processing	42.26
GO Biological Process	rRNA metabolic process	35.68
GO Biological Process	rRNA processing	35.59
GO Biological Process	regulation of transcription from RNA polymerase II promoter in response to stress	35.52
GO Biological Process	mRNA catabolic process	33.81
GO Biological Process	RNA catabolic process	32.17
GO Biological Process	regulation of DNA-templated transcription in response to stress	31.19
GO Biological Process	nuclear-transcribed mRNA catabolic process	31.06
GO Biological Process	liver regeneration	25.89
GO Biological Process	regulation of nuclease activity	24.54
GO Biological Process	nuclear-transcribed mRNA catabolic process, nonsense-mediated decay	24.48
GO Biological Process	regulation of intrinsic apoptotic signaling pathway	24.48
GO Biological Process	macromolecular complex disassembly	23.77
GO Biological Process	regulation of cellular amino acid metabolic process	23.76
GO Biological Process	multi-organism metabolic process	22.52
GO Biological Process	viral gene expression	22.52
GO Biological Process	cotranslational protein targeting to membrane	21.61
GO Biological Process	regulation of transcription from RNA polymerase II promoter in response to hypoxia	21.44
GO Biological Process	protein targeting to ER	20.59
GO Biological Process	translational elongation	20.17
Human Phenotype	Increased serum lactate	12.56
Human Phenotype	Abnormal CSF metabolite level	9.41
Human Phenotype	Malnutrition	8.58
Human Phenotype	Increased CSF lactate	7.89
Human Phenotype	Progressive microcephaly	6.09
Human Phenotype	Dysphonia	5.89

Supplementary Figure 1729: Properties and genomic distribution of motifs identified for the ZNF786 transcription factor in HepG2 (accession ENCSR206BVQ).

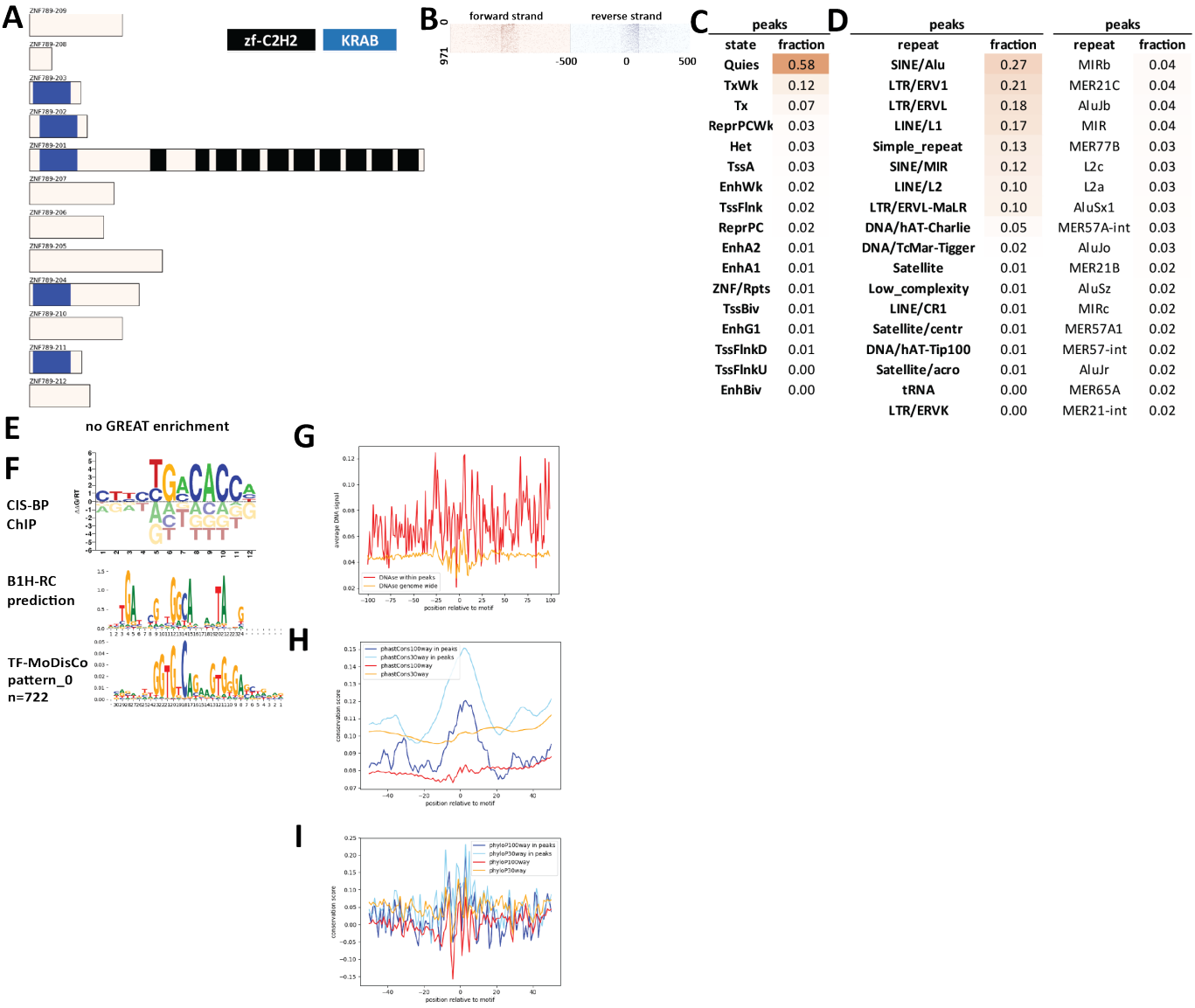

peaks	
state	fraction
Quies	0.58
TxWk	0.12
Tx	0.07
ReprPCWk	0.03
Het	0.03
TssA	0.03
EnhWk	0.02
TssFlnk	0.02
ReprPC	0.02
EnhA2	0.01
EnhA1	0.01
ZNF/Rpts	0.01
TssBiv	0.01
EnhG1	0.01
TssFlnkD	0.01
TssFlnkU	0.00
EnhBiv	0.00

peaks		peaks	
repeat	fraction	repeat	fraction
SINE/Alu	0.27	MIRb	0.04
LTR/ERV1	0.21	MER21C	0.04
LTR/ERVL	0.18	AluJb	0.04
LINE/L1	0.17	MIR	0.04
Simple_repeat	0.13	MER77B	0.03
SINE/MIR	0.12	L2c	0.03
LINE/L2	0.10	L2a	0.03
LTR/ERVL-MaLR	0.10	AluSx1	0.03
DNA/hAT-Charlie	0.05	MER57A-int	0.03
DNA/TcMar-Tigger	0.02	AluJo	0.03
Satellite	0.01	MER21B	0.02
Low_complexity	0.01	AluSz	0.02
LINE/CR1	0.01	MIRc	0.02
Satellite/centr	0.01	MER57A1	0.02
DNA/hAT-Tip100	0.01	MER57-int	0.02
Satellite/acro	0.01	AluJr	0.02
tRNA	0.00	MER65A	0.02
LTR/ERVK	0.00	MER21-int	0.02

Supplementary Figure 1730: Properties and genomic distribution of motifs identified for the ZNF789 transcription factor in HEK293 (accession ChipExo models).

TF-MoDisCO pattern_0 n=722, CWM

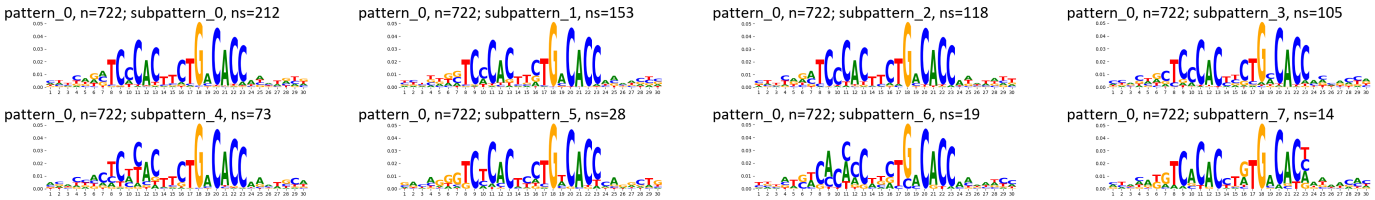

TF-MoDisCO pattern_0 n=722, PWM

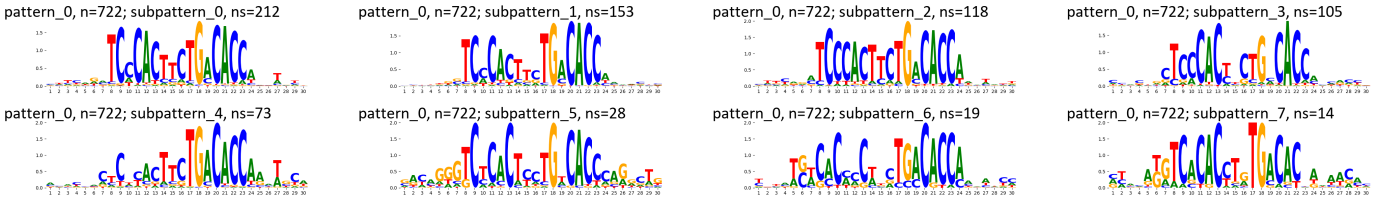

Supplementary Figure 1731: TF-MoDisCO subpatterns for the ZNF789 transcription factor in HEK293 (accession ChipExo models).

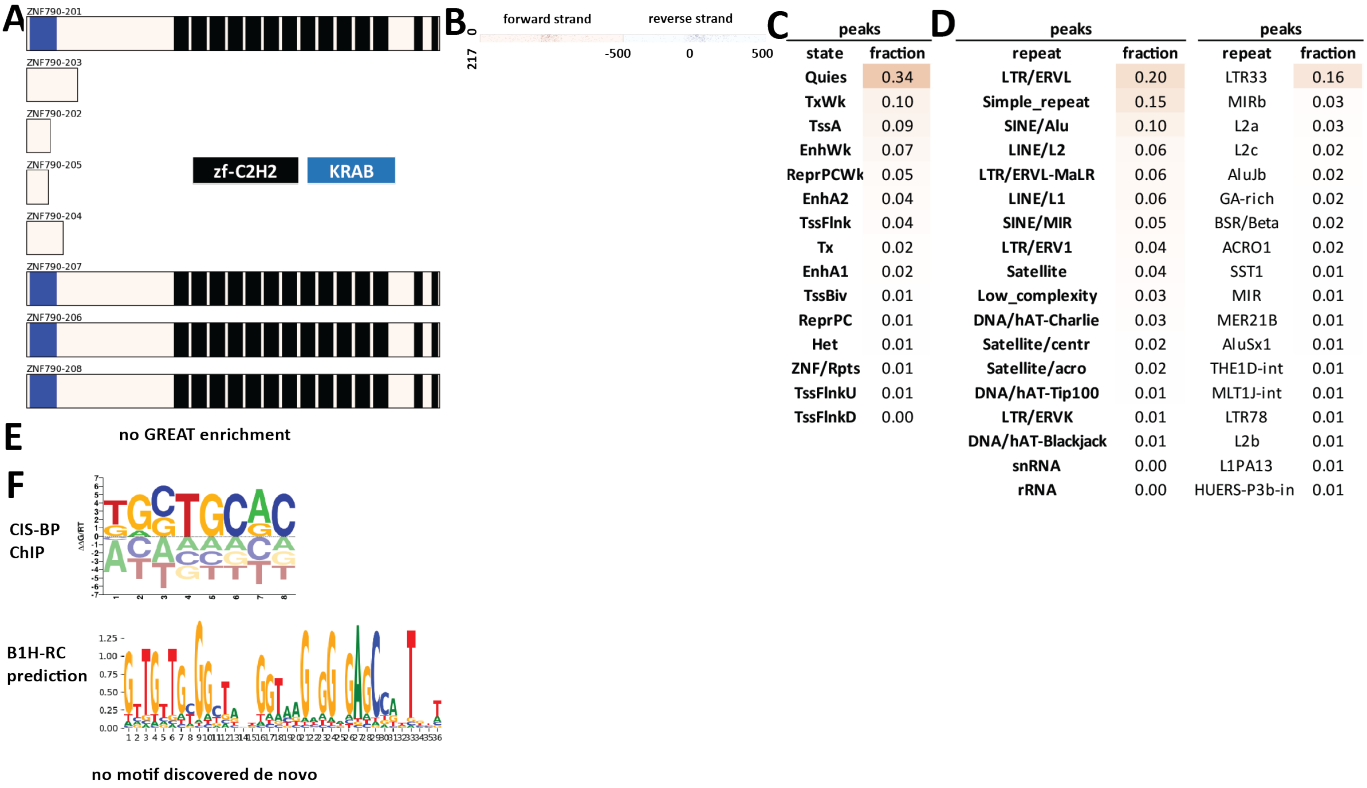

Supplementary Figure 1732: Properties and genomic distribution of motifs identified for the ZNF790 transcription factor in HEK293 (accession ChipExo models).

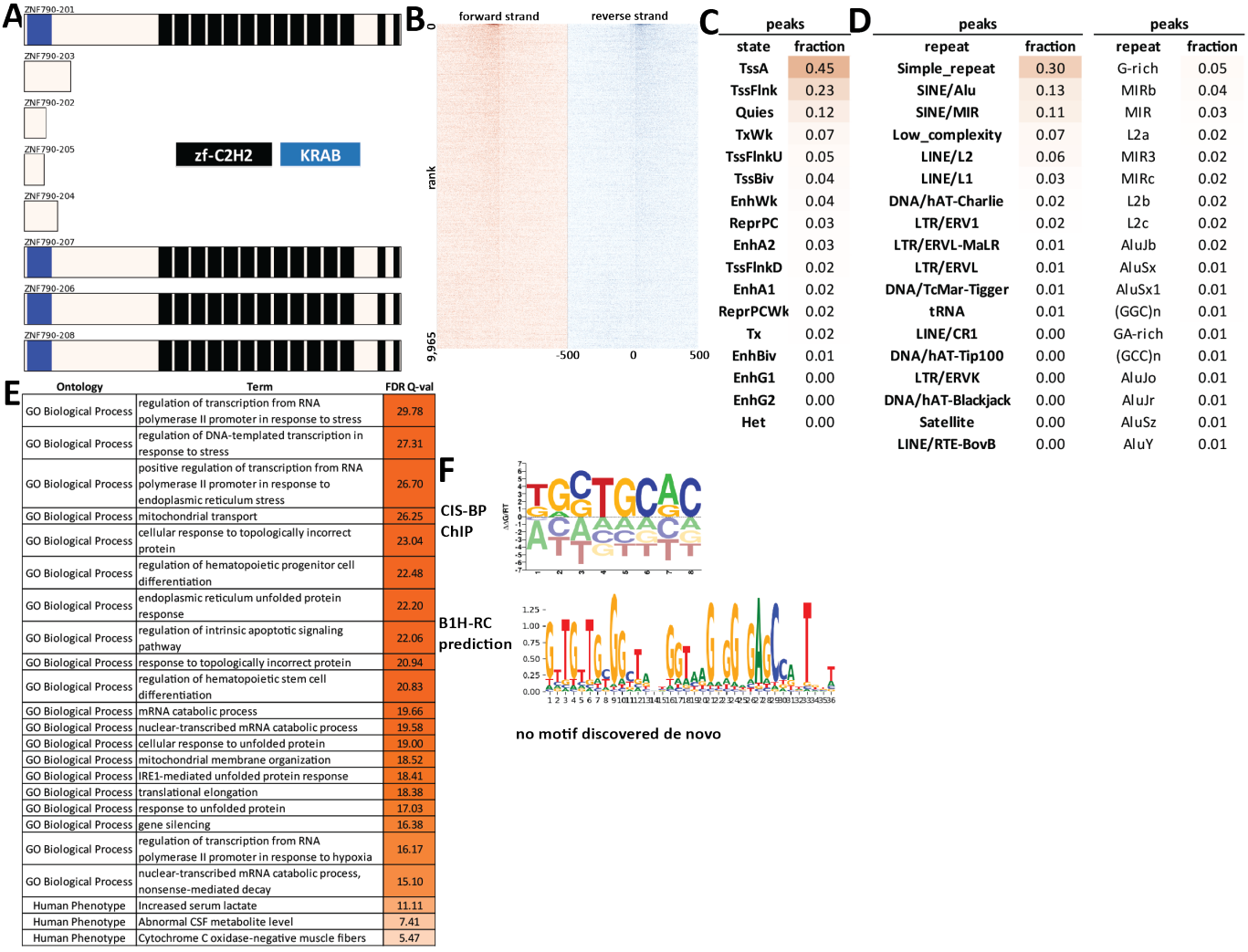

Supplementary Figure 1733: Properties and genomic distribution of motifs identified for the ZNF790 transcription factor in HepG2 (accession ENCSR117XJA).

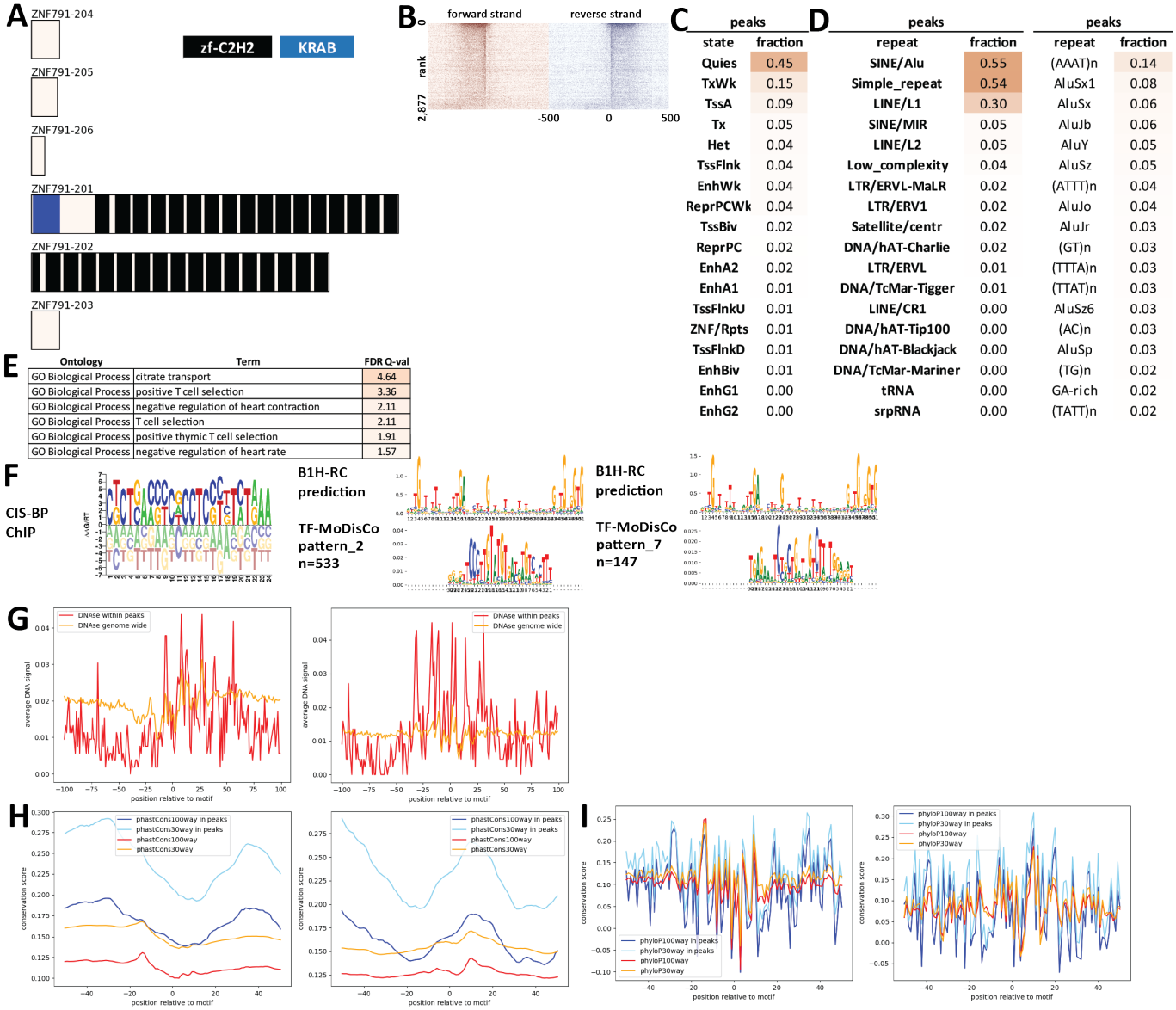

Supplementary Figure 1734: Properties and genomic distribution of motifs identified for the ZNF791 transcription factor in HEK293 (accession ENCSR775HFF).

TF-MoDisCO pattern_2 n=533, CWM

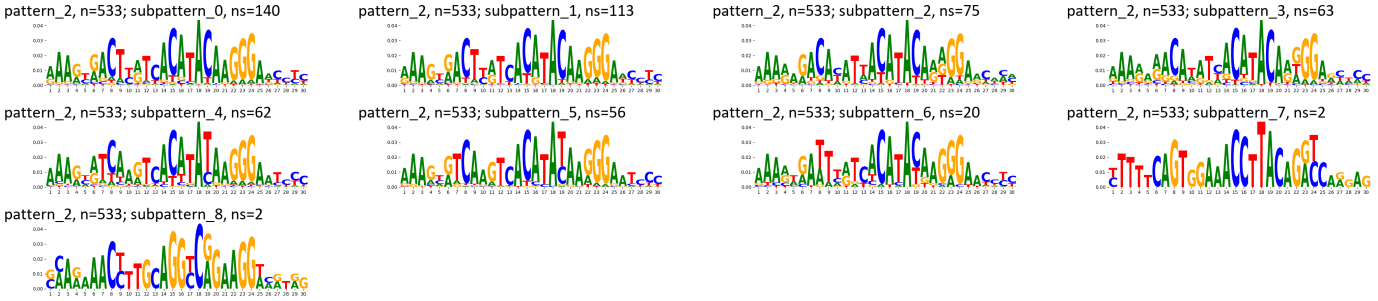

TF-MoDisCO pattern_2 n=533, PWM

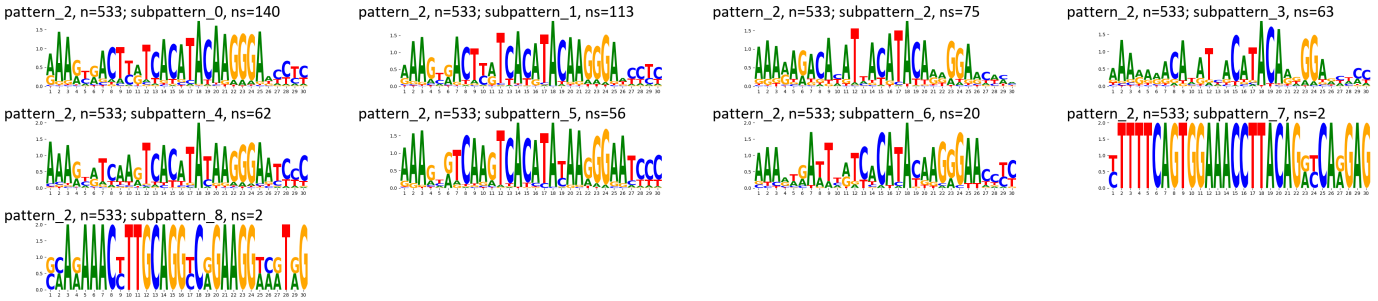

TF-MoDisCO pattern_7 n=147, CWM

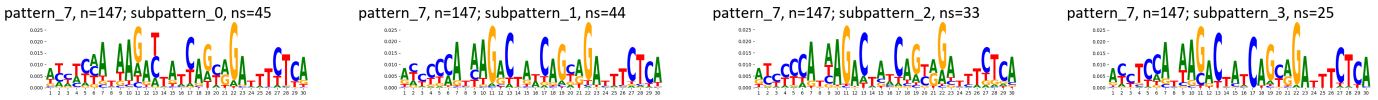

TF-MoDisCO pattern_7 n=147, PWM

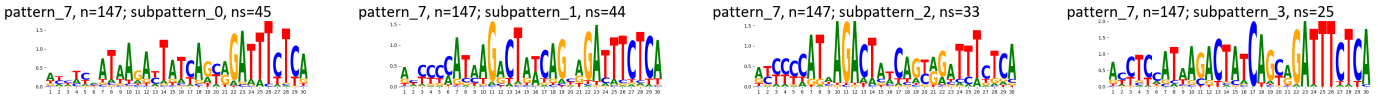

Supplementary Figure 1735: TF-MoDisCO subpatterns for the ZNF791 transcription factor in HEK293 (accession ENCSR775HFF).

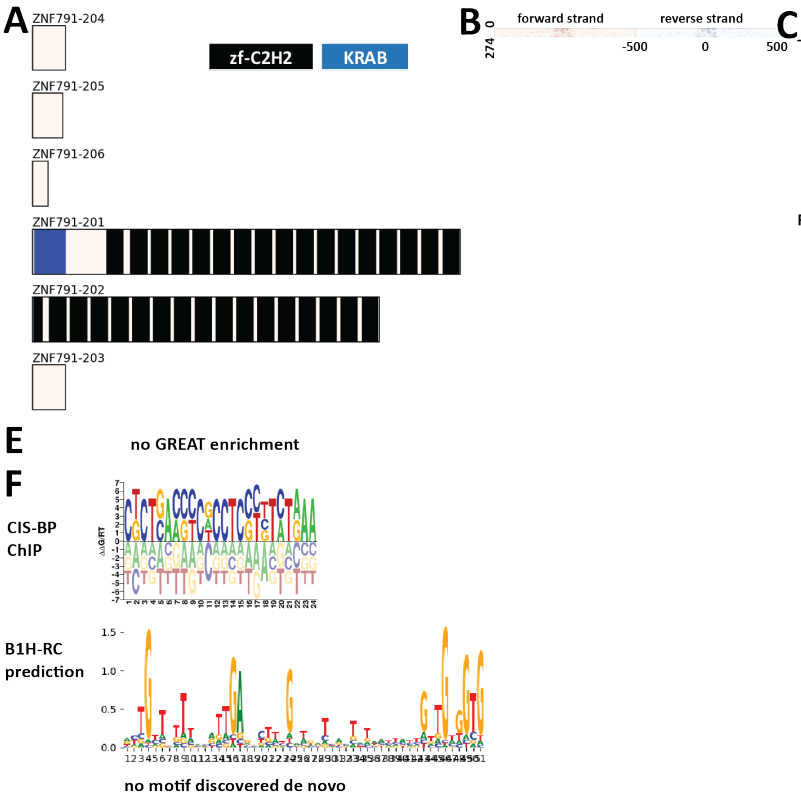

C

peaks	
state	fraction
Quies	0.36
Het	0.06
TssA	0.05
TxWk	0.05
ZNF/Rpts	0.03
Tx	0.03
ReprPCWk	0.03
TssFlnk	0.02
EnhWk	0.01
EnhA2	0.01
TssBiv	0.01
ReprPC	0.01
EnhG1	0.01
EnhA1	0.01
TssFlnkD	0.00

D

peaks		peaks	
repeat	fraction	repeat	fraction
LINE/L1	0.24	SST1	0.04
Simple_repeat	0.21	L1MEc	0.04
SINE/Alu	0.14	L1MEf	0.03
LTR/ERV1	0.07	AluJb	0.02
Satellite/centr	0.05	LSU-rRNA_Hsa	0.02
LTR/ERVL-MaLR	0.05	L2a	0.02
LTR/ERVL	0.05	BSR/Beta	0.02
Satellite	0.04	MIRb	0.01
LINE/L2	0.03	MER21C	0.01
DNA/hAT-Charlie	0.03	MER20	0.01
SINE/MIR	0.03	LTR10A	0.01
DNA/TcMar-Tigger	0.03	AluSq2	0.01
Low_complexity	0.02	AluJo	0.01
rRNA	0.02	ACRO1	0.01
Satellite/acro	0.01	MER5A	0.01
LTR/ERVK	0.01	MER50	0.01
snRNA	0.01	MER21B	0.01
DNA/hAT-Tip100	0.01	L2c	0.01

Supplementary Figure 1736: Properties and genomic distribution of motifs identified for the ZNF791 transcription factor in HEK293 (accession ChipExo models).

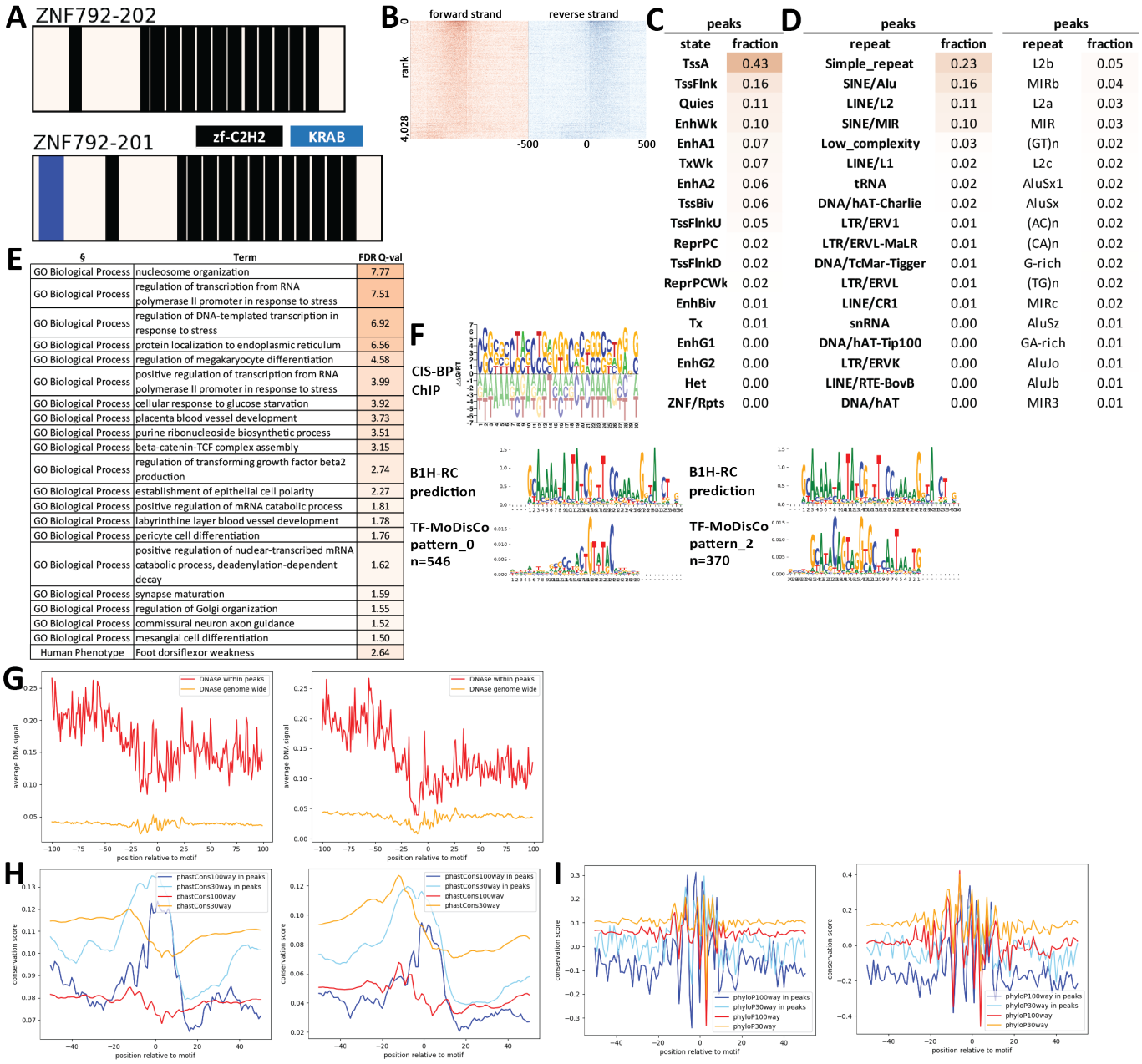

Supplementary Figure 1737: Properties and genomic distribution of motifs identified for the ZNF792 transcription factor in HEK293 (accession ENCSR679STZ).

TF-MoDisCO pattern_0 n=546, CWM

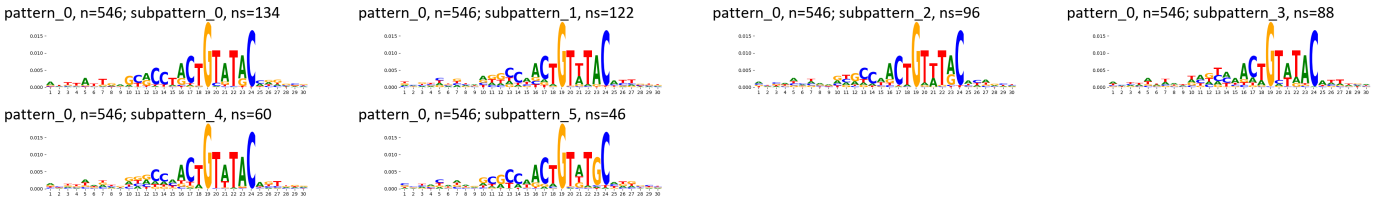

TF-MoDisCO pattern_0 n=546, PWM

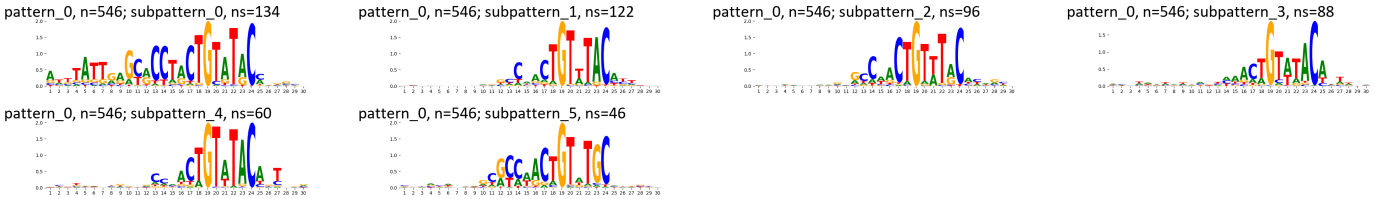

TF-MoDisCO pattern_2 n=370, CWM

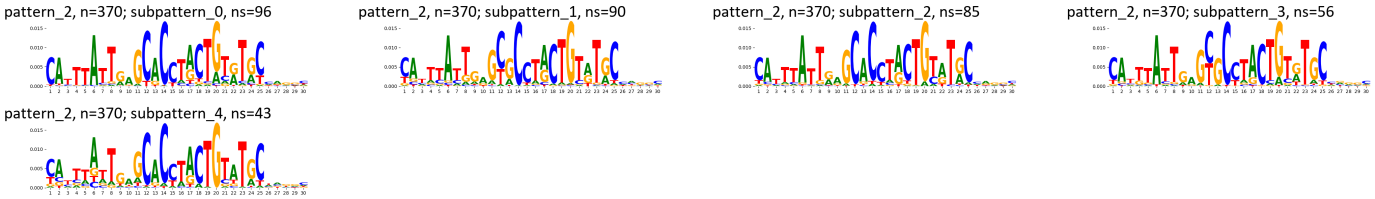

TF-MoDisCO pattern_2 n=370, PWM

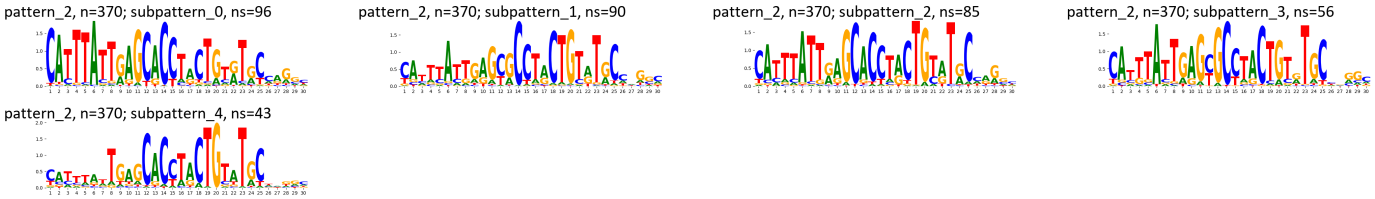

Supplementary Figure 1738: TF-MoDisCO subpatterns for the ZNF792 transcription factor in HEK293 (accession ENCSR679STZ).

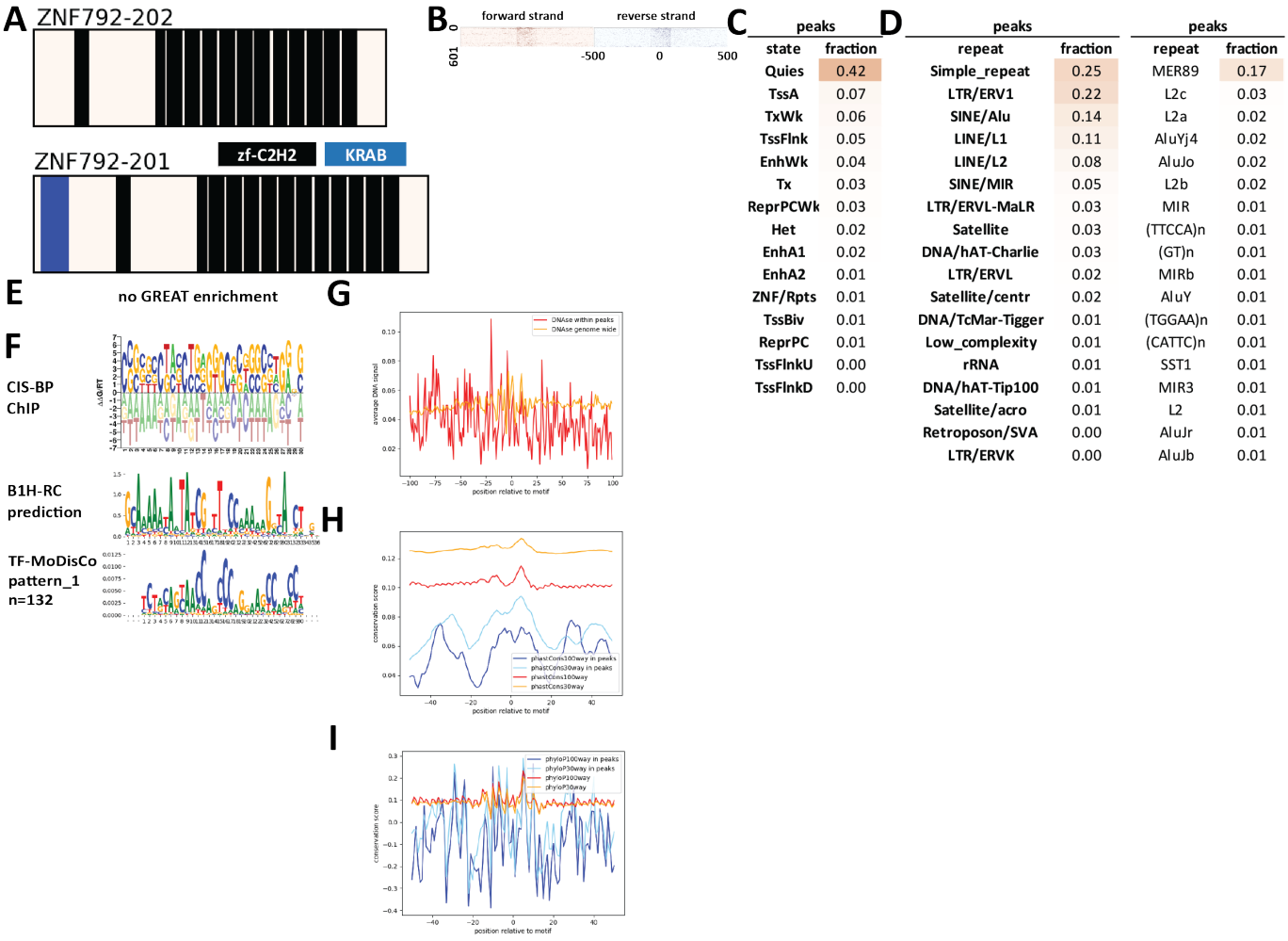

peaks	
state	fraction
Quies	0.42
TssA	0.07
TxWk	0.06
TssFlnk	0.05
EnhWk	0.04
Tx	0.03
ReprPCWk	0.03
Het	0.02
EnhA1	0.02
EnhA2	0.01
ZNF/Rpts	0.01
TssBiv	0.01
ReprPC	0.01
TssFlnkU	0.00
TssFlnkD	0.00

peaks	
repeat	fraction
Simple_repeat	0.25
LTR/ERV1	0.22
SINE/Alu	0.14
LINE/L1	0.11
LINE/L2	0.08
SINE/MIR	0.05
LTR/ERVL-MaLR	0.03
Satellite	0.03
DNA/hAT-Charlie	0.03
LTR/ERVL	0.02
Satellite/centr	0.02
DNA/TcMar-Tigger	0.01
Low_complexity	0.01
rRNA	0.01
DNA/hAT-Tip100	0.01
Satellite/acro	0.01
Retroposon/SVA	0.00
LTR/ERVK	0.00

peaks	
repeat	fraction
MER89	0.17
L2c	0.03
L2a	0.02
AluYj4	0.02
AluJo	0.02
L2b	0.02
MIR	0.01
(TTCCA)n	0.01
(GT)n	0.01
MIRb	0.01
AluY	0.01
(TGGAA)n	0.01
(CATTC)n	0.01
SST1	0.01
MIR3	0.01
L2	0.01
AluJr	0.01
AluJb	0.01

Supplementary Figure 1739: Properties and genomic distribution of motifs identified for the ZNF792 transcription factor in HEK293 (accession ChipExo models).

TF-MoDisCO pattern_1 n=132, CWM

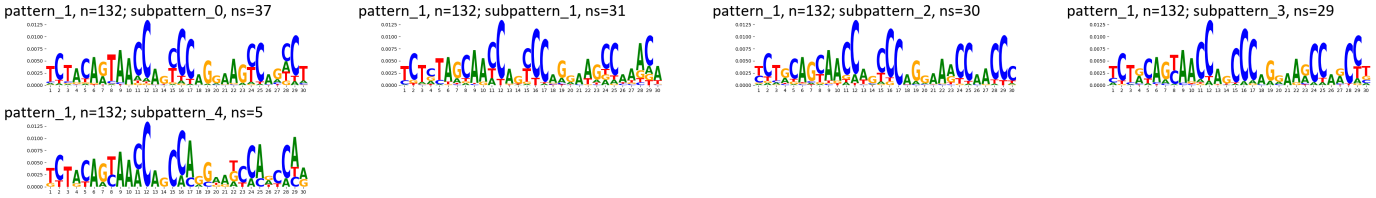

TF-MoDisCO pattern_1 n=132, PWM

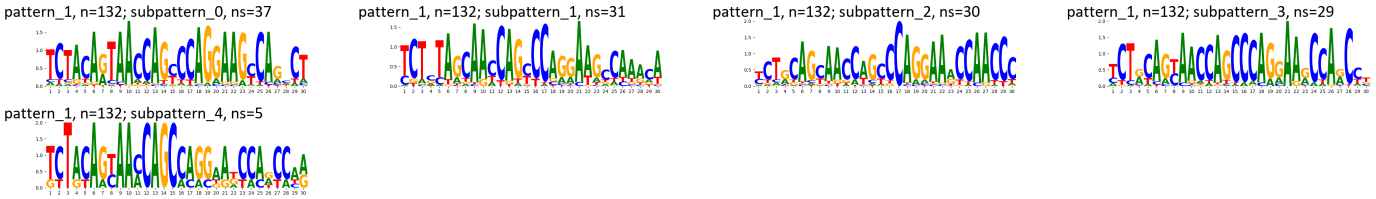

Supplementary Figure 1740: TF-MoDisCO subpatterns for the ZNF792 transcription factor in HEK293 (accession ChipExo models).

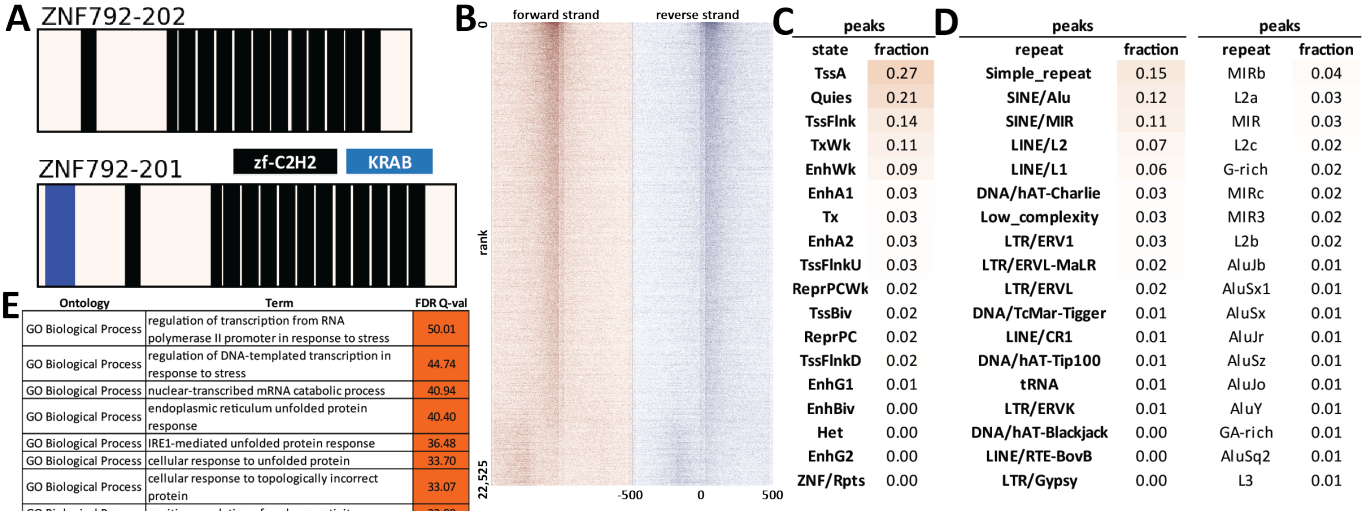

Supplementary Figure 1741: Properties and genomic distribution of motifs identified for the ZNF792 transcription factor in HepG2 (accession ENCSR396SOH).

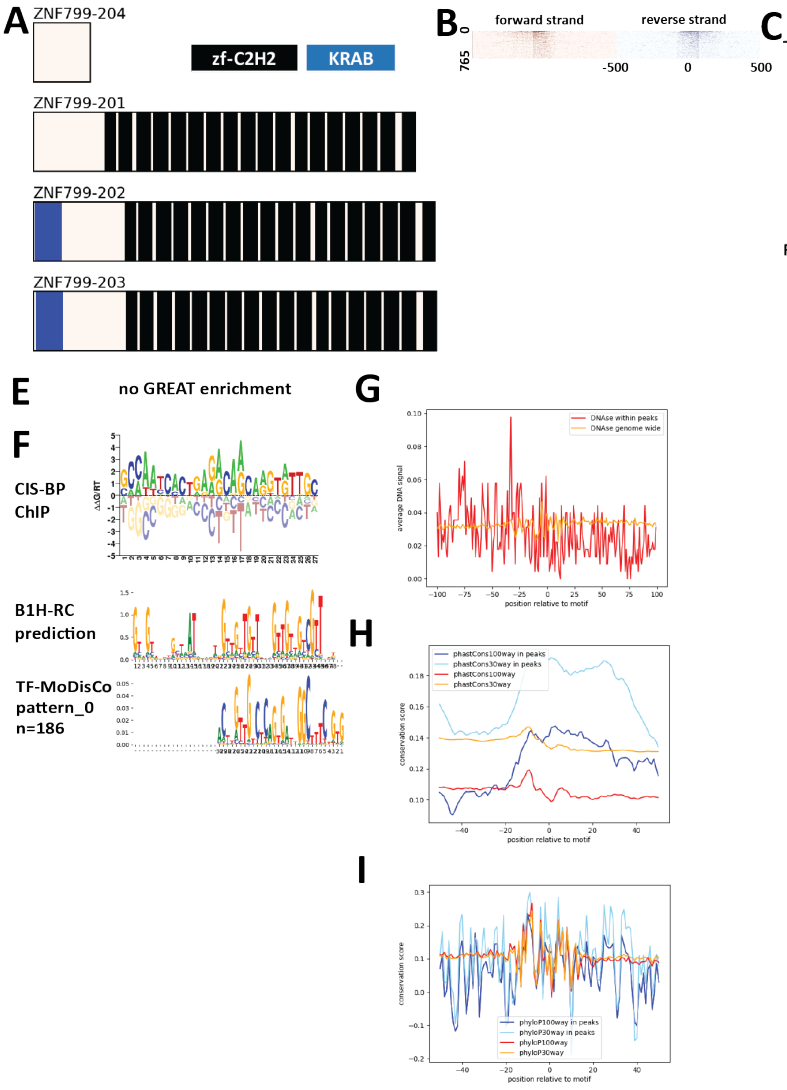

C

peaks	
state	fraction
Quies	0.61
TxWk	0.08
TssA	0.05
Het	0.05
Tx	0.04
EnhWk	0.03
TssFlnk	0.03
ReprPCWk	0.02
ReprPC	0.02
ZNF/Rpts	0.01
EnhA2	0.01
EnhA1	0.01
EnhG1	0.01
EnhBiv	0.01
TssFlnkU	0.00
TssBiv	0.00
TssFlnkD	0.00

D

peaks		peaks	
repeat	fraction	repeat	fraction
LTR/ERV1	0.50	LOR1b	0.13
LINE/L1	0.21	LOR1a	0.12
SINE/Alu	0.18	LTR8B	0.09
Simple_repeat	0.15	L2a	0.04
LINE/L2	0.10	MIRb	0.03
LTR/ERVL-MaLR	0.09	AluJb	0.03
SINE/MIR	0.07	L2c	0.02
DNA/hAT-Charlie	0.06	LTR26	0.02
LTR/ERVL	0.04	MIR	0.02
DNA/TcMar-Tigger	0.02	LOR1-int	0.02
Low_complexity	0.01	L2	0.02
Satellite/centr	0.01	L2b	0.02
Satellite	0.01	MER20	0.02
LINE/CR1	0.01	AluSx	0.02
DNA/hAT-Tip100	0.01	AluJr	0.02
Satellite/acro	0.01	MIRc	0.02
LTR?	0.00	L1M5	0.02
rRNA	0.00	AluY	0.01

Supplementary Figure 1742: Properties and genomic distribution of motifs identified for the ZNF799 transcription factor in HEK293 (accession ChipExo models).

TF-MoDisCO pattern_0 n=186, CWM



TF-MoDisCO pattern_0 n=186, PWM

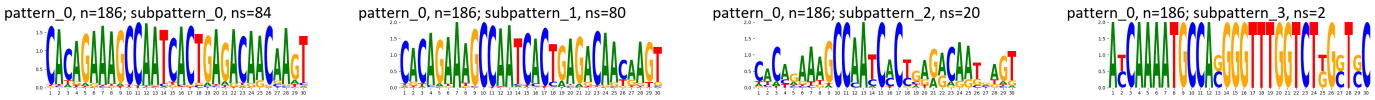

Supplementary Figure 1743: TF-MoDisCO subpatterns for the ZNF799 transcription factor in HEK293 (accession ChipExo models).

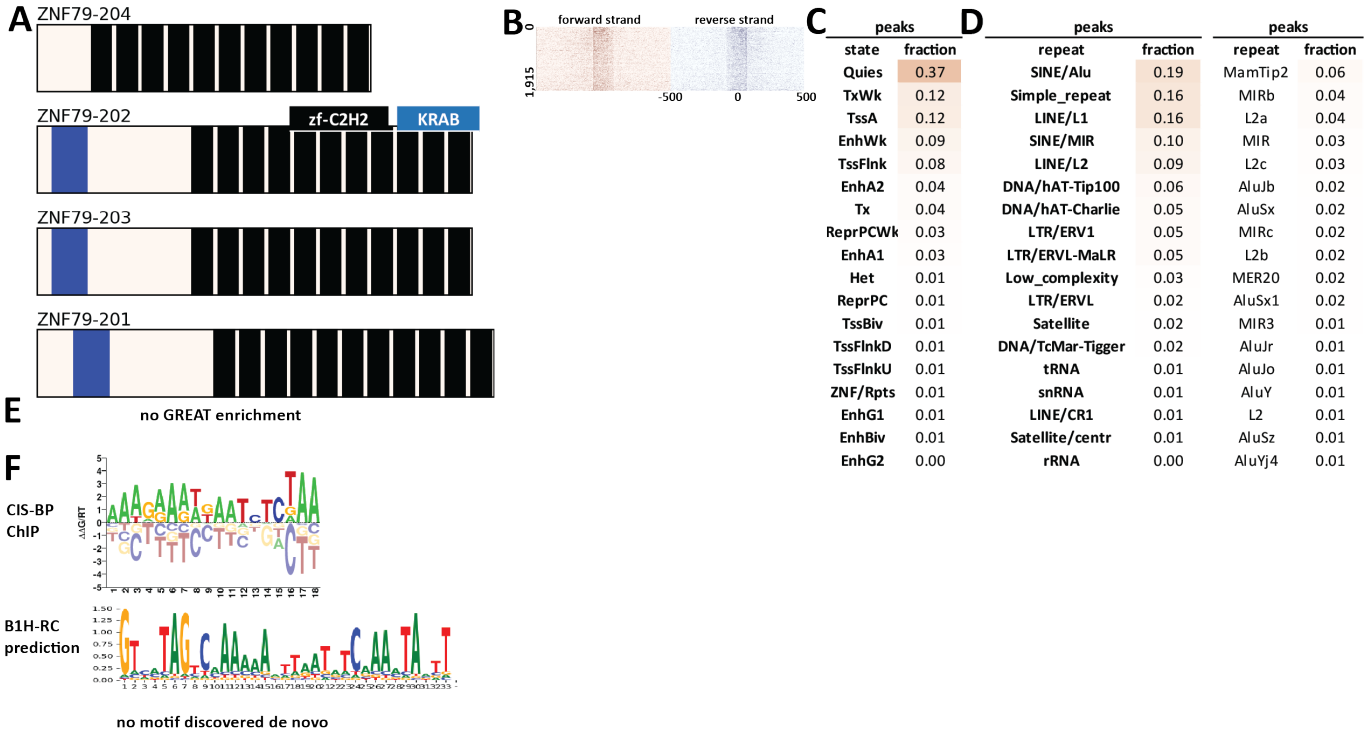

Supplementary Figure 1744: Properties and genomic distribution of motifs identified for the ZNF79 transcription factor in HEK293 (accession ChipExo models).

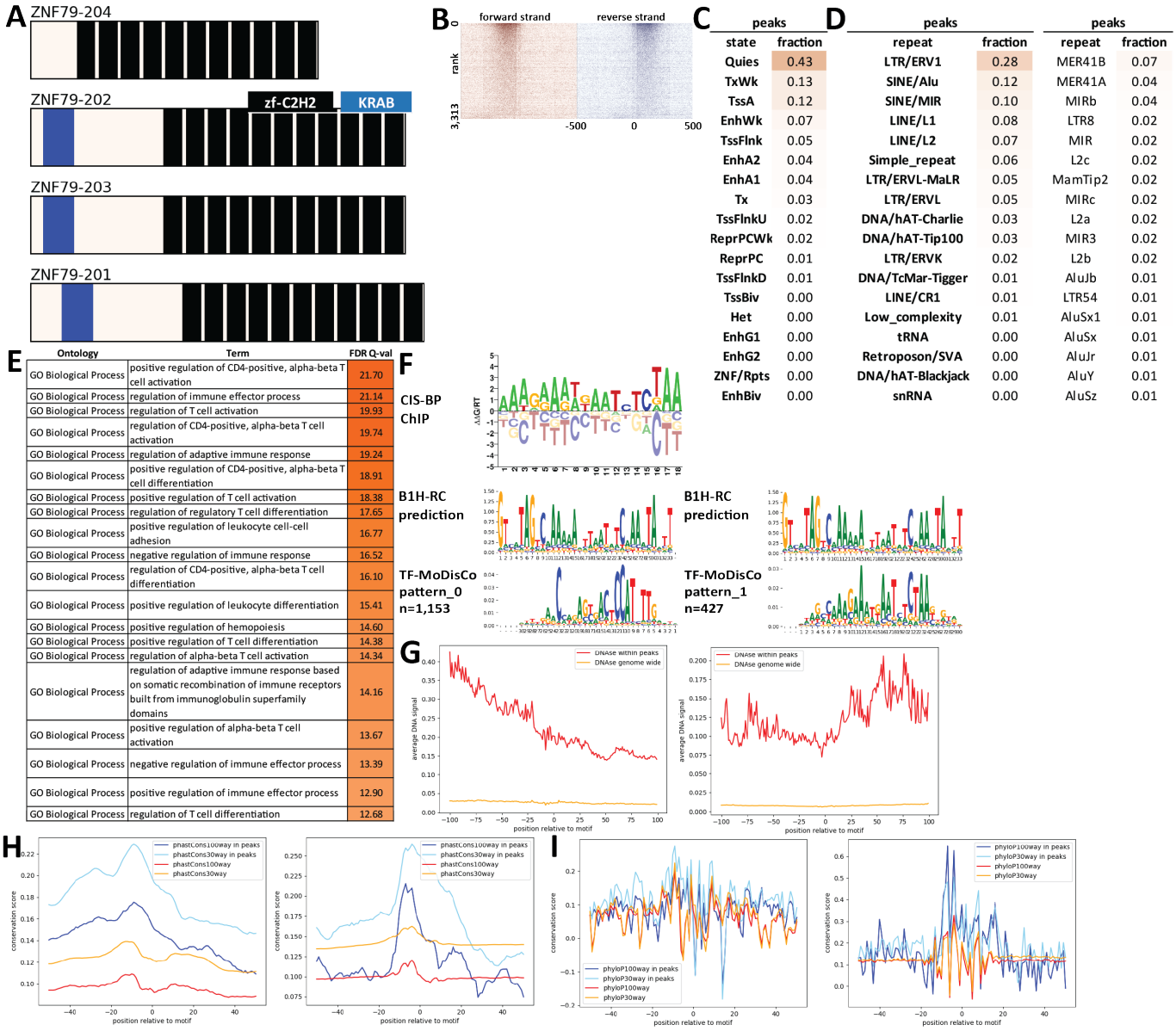

Supplementary Figure 1745: Properties and genomic distribution of motifs identified for the ZNF79 transcription factor in K562 (accession ENCSR995FUM).

TF-MoDisCO pattern_0 n=1153, CWM

pattern_0, n=1153; subpattern_0, ns=255

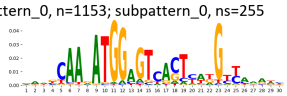

pattern_0, n=1153; subpattern_1, ns=210

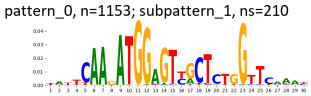

pattern_0, n=1153; subpattern_2, ns=186

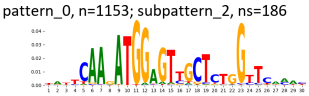

pattern_0, n=1153; subpattern_3, ns=167

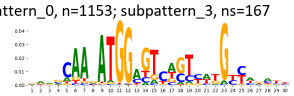

pattern_0, n=1153; subpattern_4, ns=148

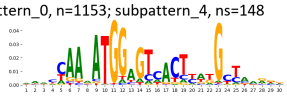

pattern_0, n=1153; subpattern_5, ns=92

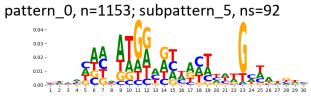

pattern_0, n=1153; subpattern_6, ns=51

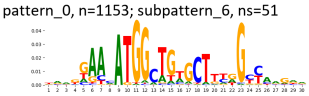

pattern_0, n=1153; subpattern_7, ns=42

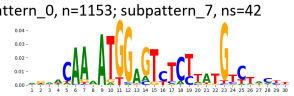

pattern_0, n=1153; subpattern_8, ns=2

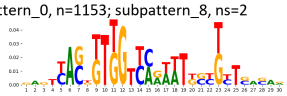

TF-MoDisCO pattern_0 n=1153, PWM

pattern_0, n=1153; subpattern_0, ns=255

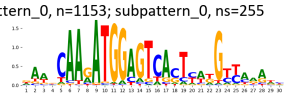

pattern_0, n=1153; subpattern_1, ns=210

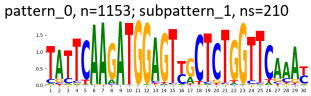

pattern_0, n=1153; subpattern_2, ns=186

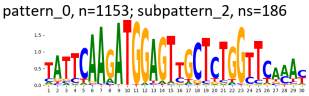

pattern_0, n=1153; subpattern_3, ns=167

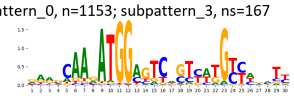

pattern_0, n=1153; subpattern_4, ns=148

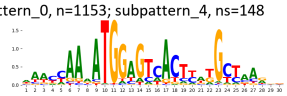

pattern_0, n=1153; subpattern_5, ns=92

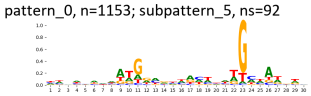

pattern_0, n=1153; subpattern_6, ns=51

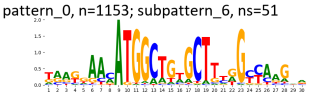

pattern_0, n=1153; subpattern_7, ns=42

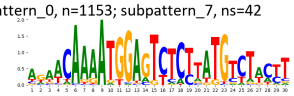

pattern_0, n=1153; subpattern_8, ns=2

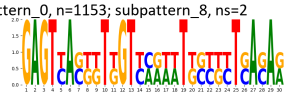

TF-MoDisCO pattern_1 n=427, CWM

pattern_1, n=427; subpattern_0, ns=116

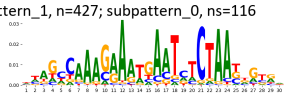

pattern_1, n=427; subpattern_1, ns=106

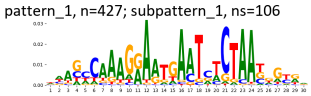

pattern_1, n=427; subpattern_2, ns=102

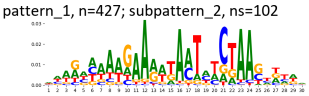

pattern_1, n=427; subpattern_3, ns=96

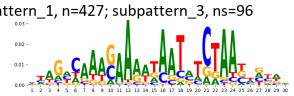

pattern_1, n=427; subpattern_4, ns=4

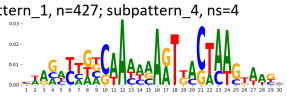

pattern_1, n=427; subpattern_5, ns=3

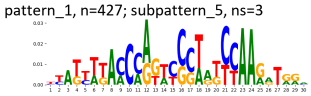

TF-MoDisCO pattern_1 n=427, PWM

pattern_1, n=427; subpattern_0, ns=116

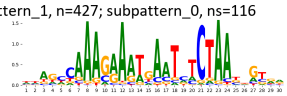

pattern_1, n=427; subpattern_1, ns=106

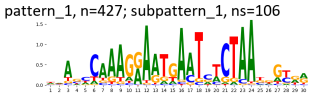

pattern_1, n=427; subpattern_2, ns=102

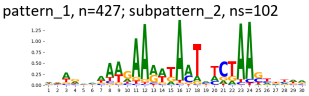

pattern_1, n=427; subpattern_3, ns=96

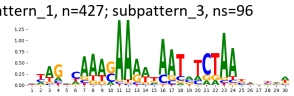

pattern_1, n=427; subpattern_4, ns=4

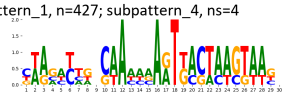

pattern_1, n=427; subpattern_5, ns=3

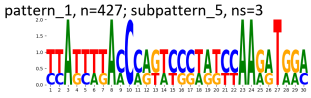

Supplementary Figure 1746: TF-MoDisCO subpatterns for the ZNF79 transcription factor in K562 (accession ENCSR995FUM).

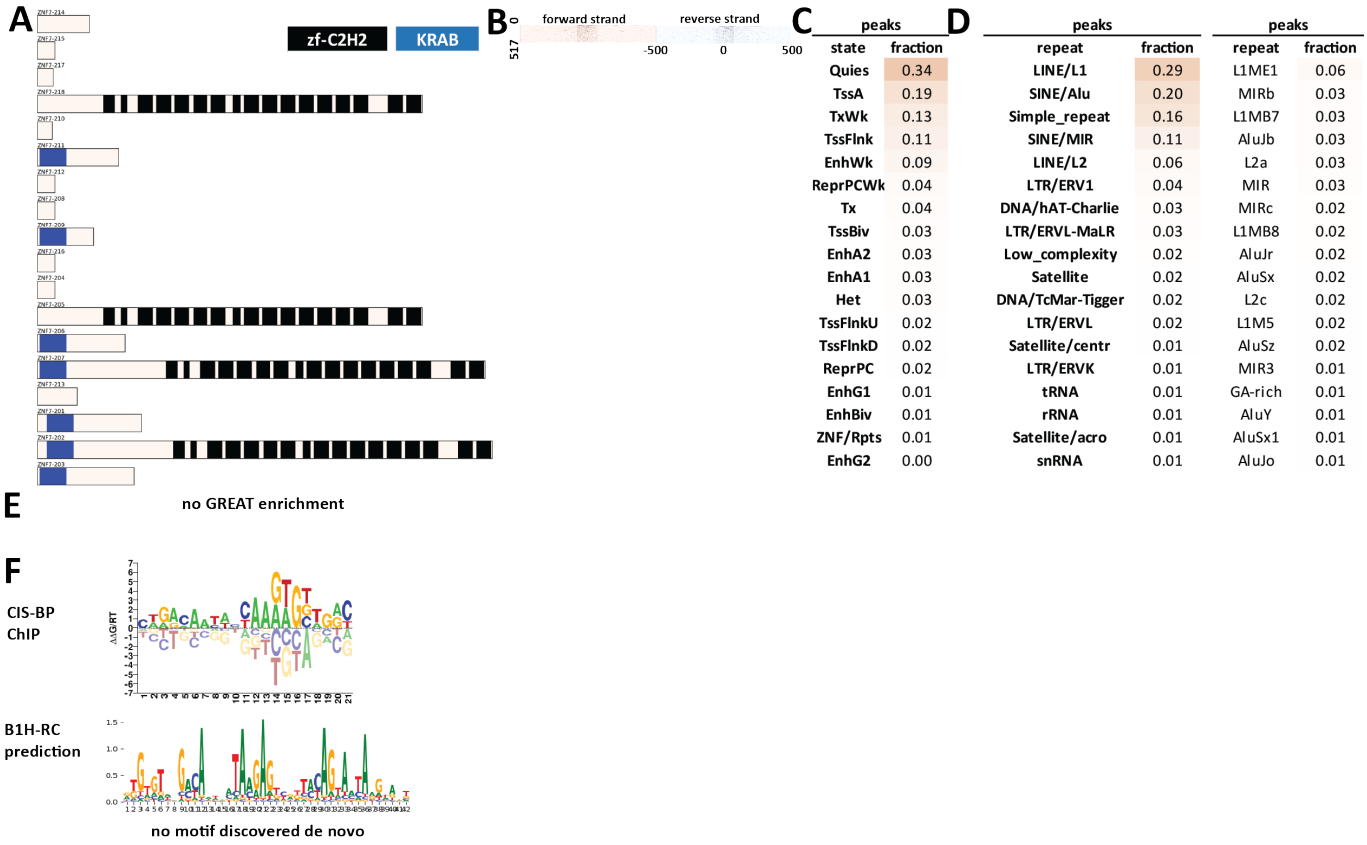

Supplementary Figure 1747: Properties and genomic distribution of motifs identified for the ZNF7 transcription factor in HEK293 (accession ChipExo models).

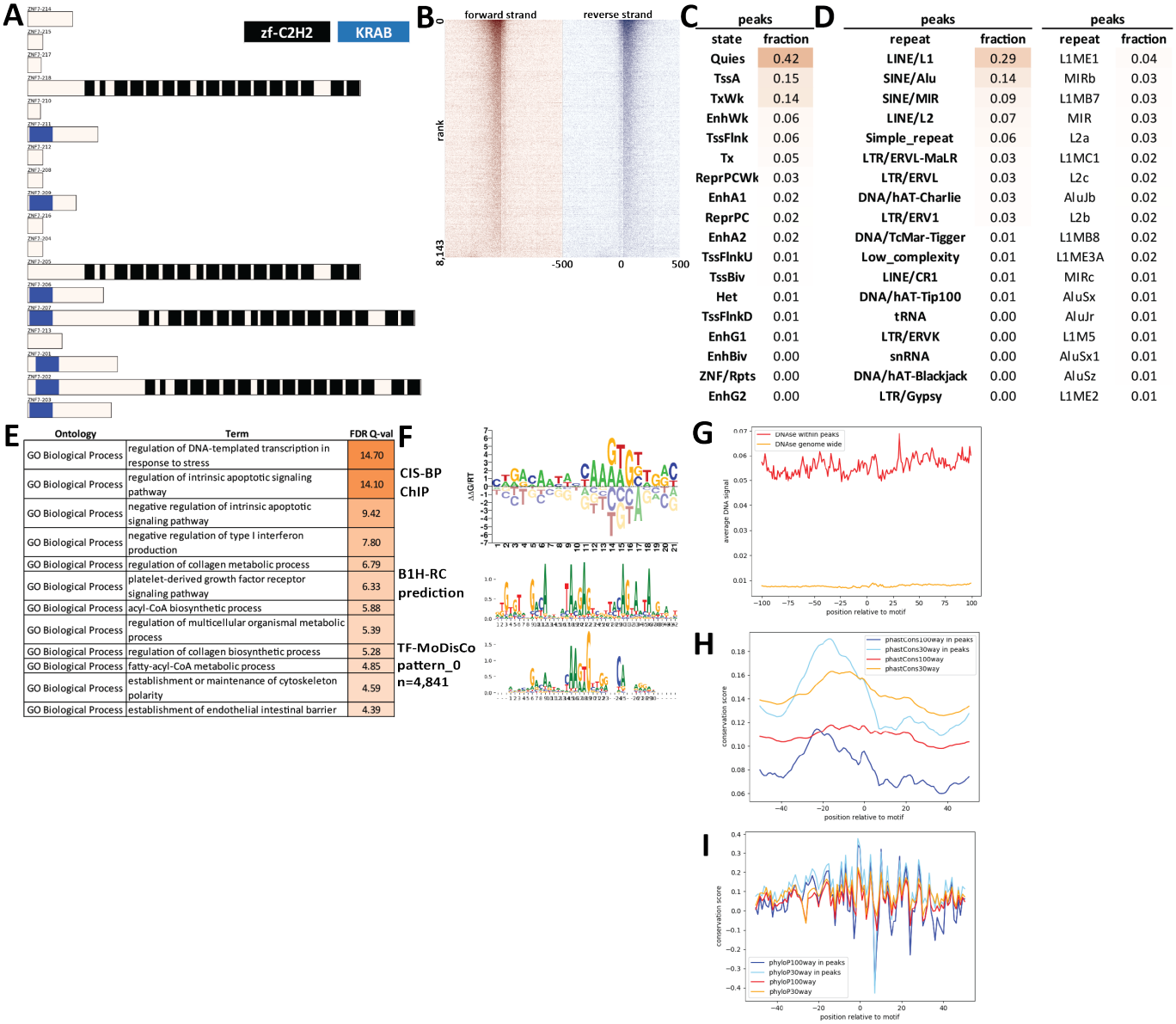

C

peaks	
state	fraction
Quies	0.42
TssA	0.15
TxWk	0.14
EnhWk	0.06
TssFlnk	0.06
Tx	0.05
ReprPCWk	0.03
EnhA1	0.02
ReprPC	0.02
EnhA2	0.02
TssFlnkU	0.01
TssBiv	0.01
Het	0.01
TssFlnkD	0.01
EnhG1	0.01
EnhBiv	0.00
ZNF/Rpts	0.00
EnhG2	0.00

D

peaks		peaks	
repeat	fraction	repeat	fraction
LINE/L1	0.29	L1ME1	0.04
SINE/Alu	0.14	MIRb	0.03
SINE/MIR	0.09	L1MB7	0.03
LINE/L2	0.07	MIR	0.03
Simple_repeat	0.06	L2a	0.03
LTR/ERVL-MaLR	0.03	L1MC1	0.02
LTR/ERVL	0.03	L2c	0.02
DNA/hAT-Charlie	0.03	AluJb	0.02
LTR/ERV1	0.03	L2b	0.02
DNA/TcMar-Tigger	0.01	L1MB8	0.02
Low_complexity	0.01	L1ME3A	0.02
LINE/CR1	0.01	MIRc	0.01
DNA/hAT-Tip100	0.01	AluSx	0.01
tRNA	0.00	AluJr	0.01
LTR/ERVK	0.00	L1M5	0.01
snRNA	0.00	AluSx1	0.01
DNA/hAT-Blackjack	0.00	AluSz	0.01
LTR/Gypsy	0.00	L1ME2	0.01

E

Ontology	Term	FDR Q-val
GO Biological Process	regulation of DNA-templated transcription in response to stress	14.70
GO Biological Process	regulation of intrinsic apoptotic signaling pathway	14.10
GO Biological Process	negative regulation of intrinsic apoptotic signaling pathway	9.42
GO Biological Process	negative regulation of type I interferon production	7.80
GO Biological Process	regulation of collagen metabolic process	6.79
GO Biological Process	platelet-derived growth factor receptor signaling pathway	6.33
GO Biological Process	acyl-CoA biosynthetic process	5.88
GO Biological Process	regulation of multicellular organismal metabolic process	5.39
GO Biological Process	regulation of collagen biosynthetic process	5.28
GO Biological Process	fatty-acyl-CoA metabolic process	4.85
GO Biological Process	establishment or maintenance of cytoskeleton polarity	4.59
GO Biological Process	establishment of endothelial intestinal barrier	4.39

Supplementary Figure 1748: Properties and genomic distribution of motifs identified for the ZNF7 transcription factor in HepG2 (accession ENCSR553QMC).

TF-MoDisCO pattern_0 n=4841, CWM

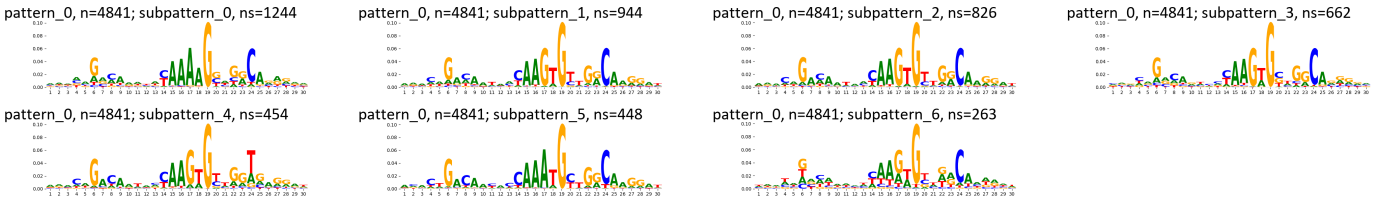

TF-MoDisCO pattern_0 n=4841, PWM

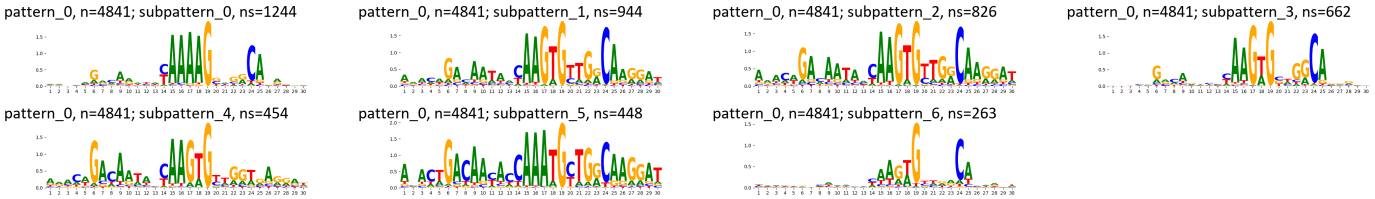

Supplementary Figure 1749: TF-MoDisCO subpatterns for the ZNF7 transcription factor in HepG2 (accession ENCSR553QMC).

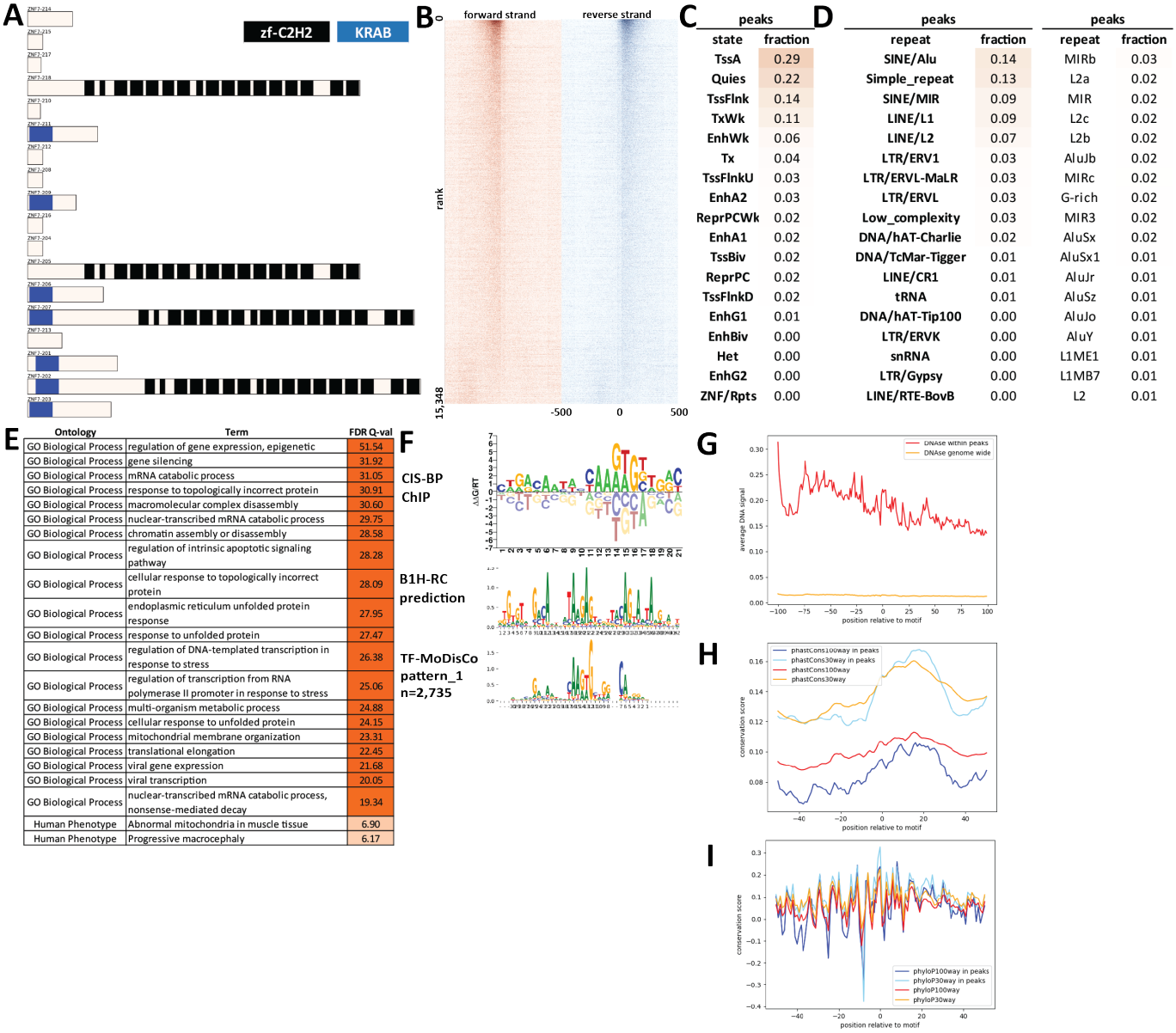

C

peaks	
state	fraction
TssA	0.29
Quies	0.22
TssFlnk	0.14
TxWk	0.11
EnhWk	0.06
Tx	0.04
TssFlnkU	0.03
EnhA2	0.03
ReprPCWk	0.02
EnhA1	0.02
TssBiv	0.02
ReprPC	0.02
TssFlnkD	0.02
EnhG1	0.01
EnhBiv	0.00
Het	0.00
EnhG2	0.00
ZNF/Rpts	0.00

D

peaks		peaks	
repeat	fraction	repeat	fraction
SINE/Alu	0.14	MIRb	0.03
Simple_repeat	0.13	L2a	0.02
SINE/MIR	0.09	MIR	0.02
LINE/L1	0.09	L2c	0.02
LINE/L2	0.07	L2b	0.02
LTR/ERV1	0.03	AluJb	0.02
LTR/ERVL-MaLR	0.03	MIRc	0.02
LTR/ERVL	0.03	G-rich	0.02
Low_complexity	0.03	MIR3	0.02
DNA/hAT-Charlie	0.02	AluSx	0.02
DNA/TcMar-Tigger	0.01	AluSx1	0.01
LINE/CR1	0.01	AluJr	0.01
tRNA	0.01	AluSz	0.01
DNA/hAT-Tip100	0.00	AluJo	0.01
LTR/ERVK	0.00	AluY	0.01
snRNA	0.00	L1ME1	0.01
LTR/Gypsy	0.00	L1MB7	0.01
LINE/RTE-BovB	0.00	L2	0.01

E

Ontology	Term	FDR Q-val
GO Biological Process	regulation of gene expression, epigenetic	51.54
GO Biological Process	gene silencing	31.92
GO Biological Process	mRNA catabolic process	31.05
GO Biological Process	response to topologically incorrect protein	30.91
GO Biological Process	macromolecular complex disassembly	30.60
GO Biological Process	nuclear-transcribed mRNA catabolic process	29.75
GO Biological Process	chromatin assembly or disassembly	28.58
GO Biological Process	regulation of intrinsic apoptotic signaling pathway	28.28
GO Biological Process	cellular response to topologically incorrect protein	28.09
GO Biological Process	endoplasmic reticulum unfolded protein response	27.95
GO Biological Process	response to unfolded protein	27.47
GO Biological Process	regulation of DNA-templated transcription in response to stress	26.38
GO Biological Process	regulation of transcription from RNA polymerase II promoter in response to stress	25.06
GO Biological Process	multi-organism metabolic process	24.88
GO Biological Process	cellular response to unfolded protein	24.15
GO Biological Process	mitochondrial membrane organization	23.31
GO Biological Process	translational elongation	22.45
GO Biological Process	viral gene expression	21.68
GO Biological Process	viral transcription	20.05
GO Biological Process	nuclear-transcribed mRNA catabolic process, nonsense-mediated decay	19.34
Human Phenotype	Abnormal mitochondria in muscle tissue	6.90
Human Phenotype	Progressive macrocephaly	6.17

Supplementary Figure 1750: Properties and genomic distribution of motifs identified for the ZNF7 transcription factor in K562 (accession ENCSR454SCH).

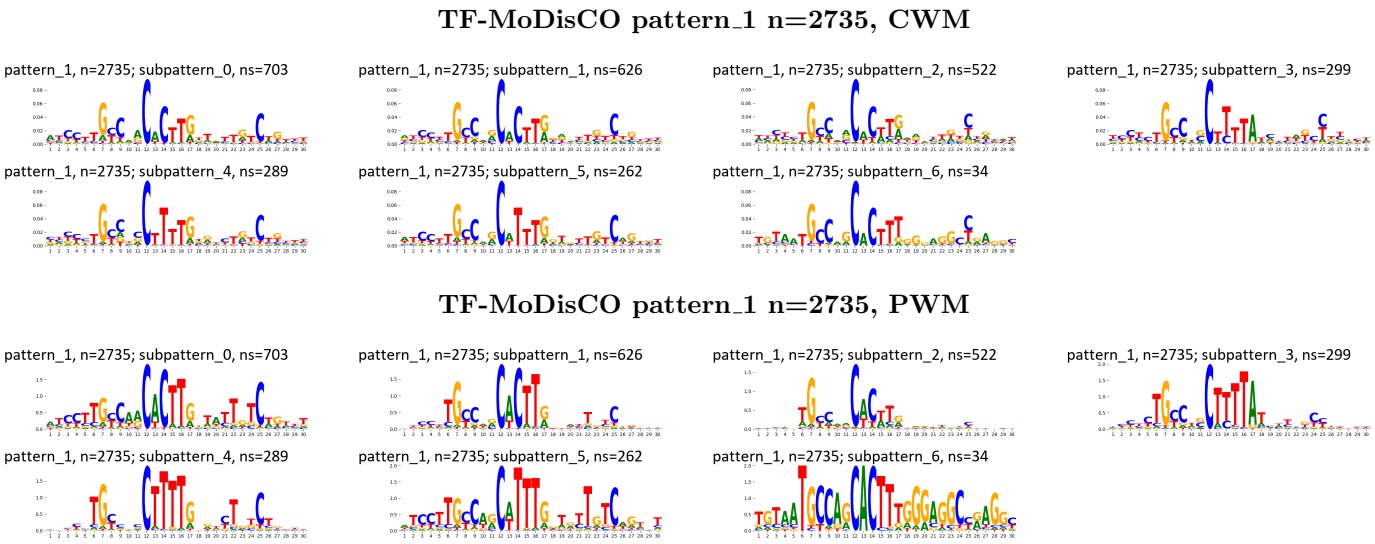

Supplementary Figure 1751: TF-MoDisCO subpatterns for the ZNF7 transcription factor in K562 (accession ENCSR454SCH).

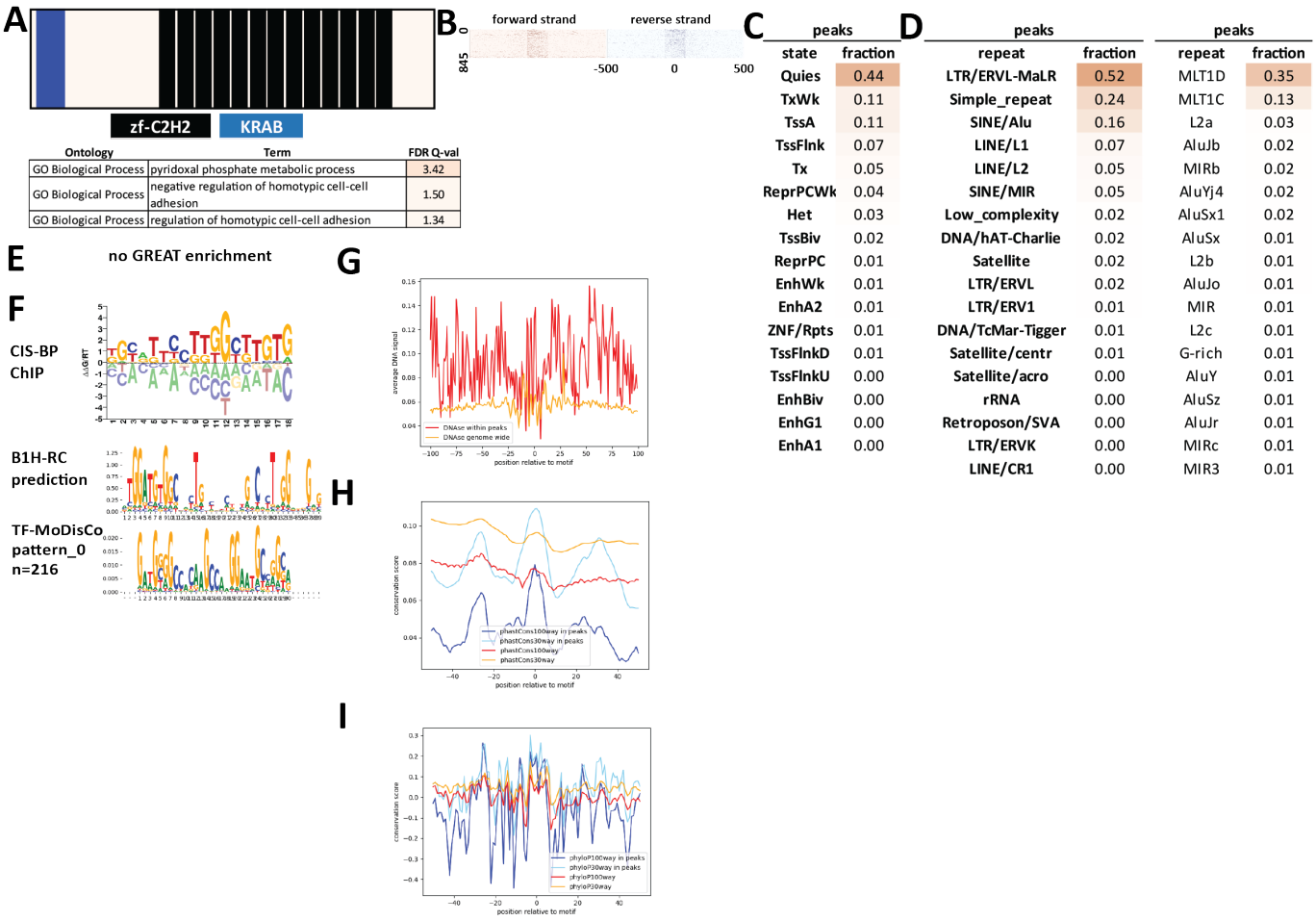

Ontology	Term	FDR Q-val
GO Biological Process	pyridoxal phosphate metabolic process	3.42
GO Biological Process	negative regulation of homotypic cell-cell adhesion	1.50
GO Biological Process	regulation of homotypic cell-cell adhesion	1.34

peaks	
state	fraction
Quies	0.44
TxWk	0.11
TssA	0.11
TssFlnk	0.07
Tx	0.05
ReprPCWk	0.04
Het	0.03
TssBiv	0.02
ReprPC	0.01
EnhWk	0.01
EnhA2	0.01
ZNF/Rpts	0.01
TssFlnkD	0.01
TssFlnkU	0.00
EnhBiv	0.00
EnhG1	0.00
EnhA1	0.00

peaks	
repeat	fraction
LTR/ERVL-MaLR	0.52
Simple_repeat	0.24
SINE/Alu	0.16
LINE/L1	0.07
LINE/L2	0.05
SINE/MIR	0.05
Low_complexity	0.02
DNA/hAT-Charlie	0.02
Satellite	0.02
LTR/ERVL	0.02
LTR/ERV1	0.01
DNA/TcMar-Tigger	0.01
Satellite/centr	0.01
Satellite/acro	0.00
rRNA	0.00
Retroposon/SVA	0.00
LTR/ERVK	0.00
LINE/CR1	0.00

peaks	
repeat	fraction
MLT1D	0.35
MLT1C	0.13
L2a	0.03
AluJb	0.02
MIRb	0.02
AluYj4	0.02
AluSx1	0.02
AluSx	0.01
L2b	0.01
AluJo	0.01
MIR	0.01
L2c	0.01
G-rich	0.01
AluY	0.01
AluSz	0.01
AluJr	0.01
MIRc	0.01
MIR3	0.01

Supplementary Figure 1752: Properties and genomic distribution of motifs identified for the ZNF805 transcription factor in HEK293 (accession ChipExo models).

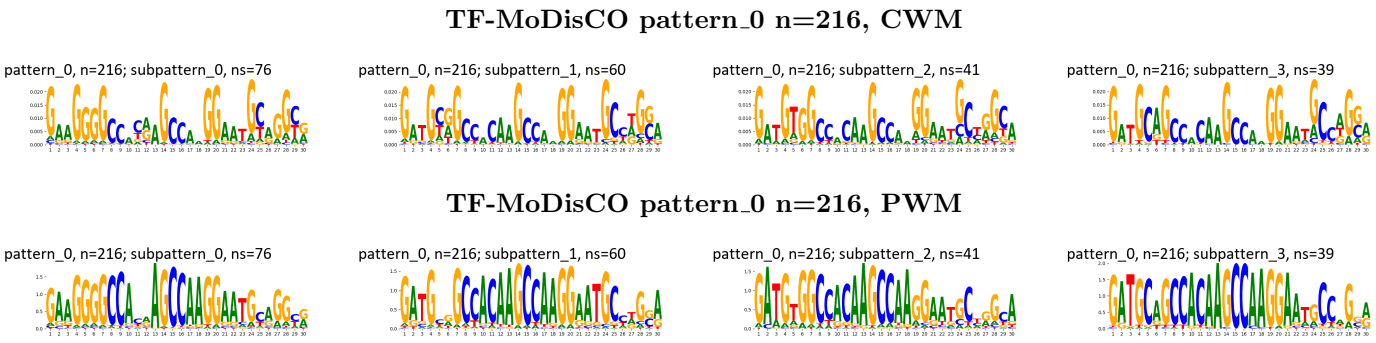

Supplementary Figure 1753: TF-MoDisCO subpatterns for the ZNF805 transcription factor in HEK293 (accession ChipExo models).

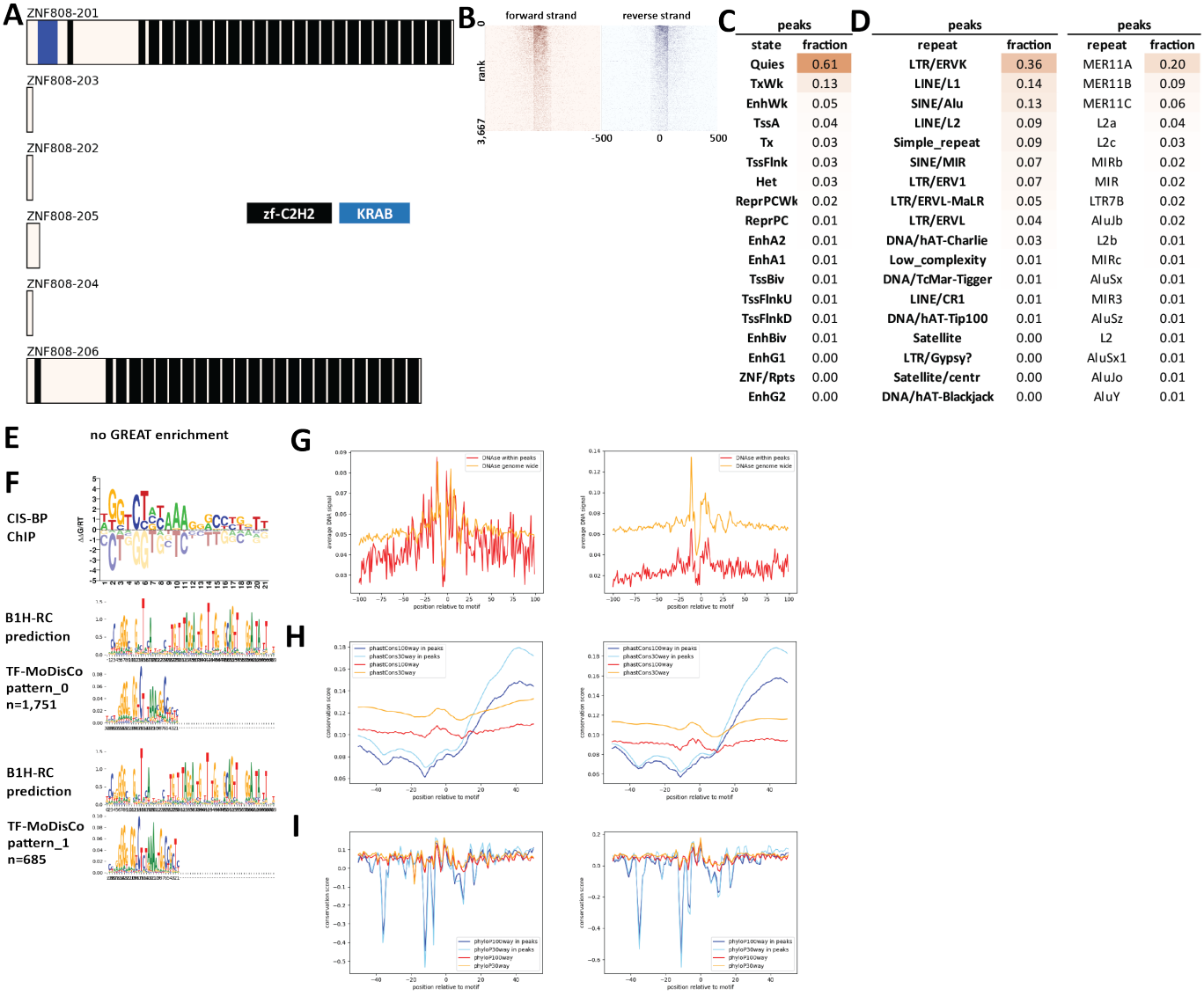

Supplementary Figure 1754: Properties and genomic distribution of motifs identified for the ZNF808 transcription factor in HEK293 (accession ChipExo models).

TF-MoDisCO pattern_0 n=1751, CWM

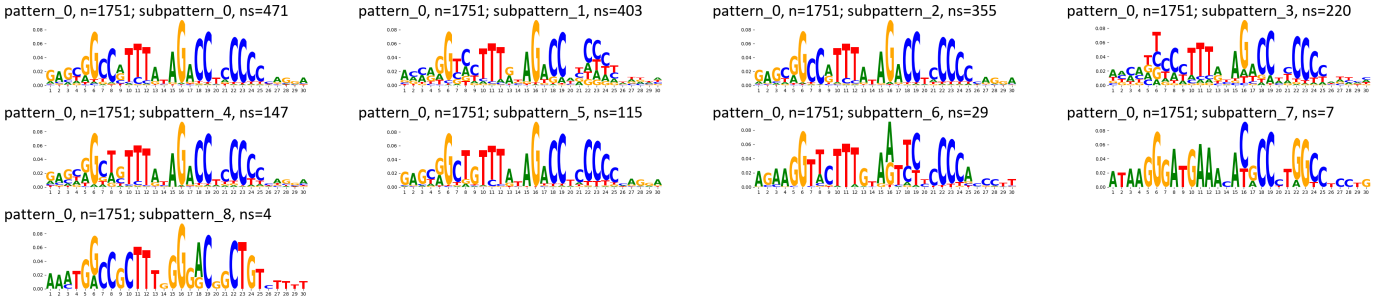

TF-MoDisCO pattern_0 n=1751, PWM

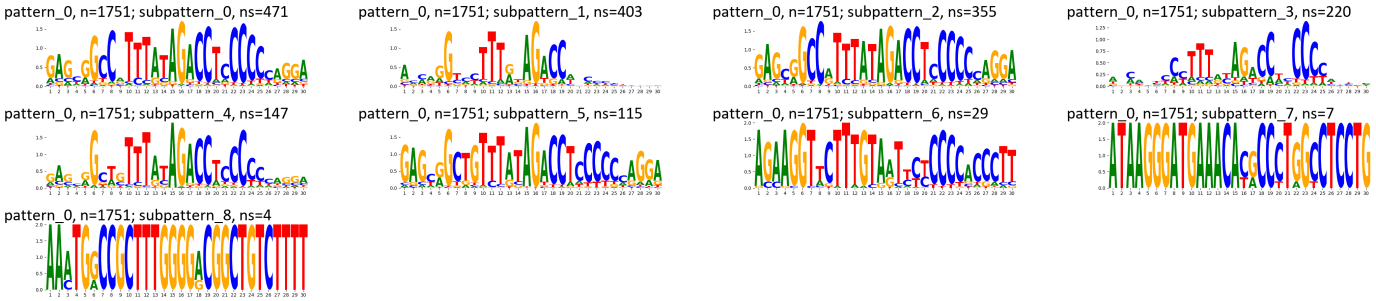

TF-MoDisCO pattern_1 n=685, CWM

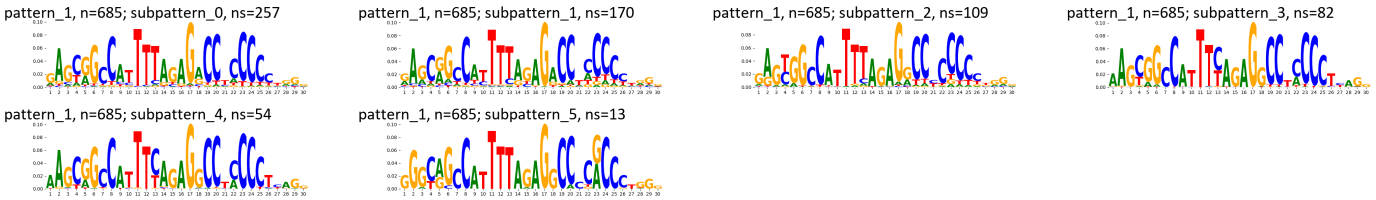

TF-MoDisCO pattern_1 n=685, PWM

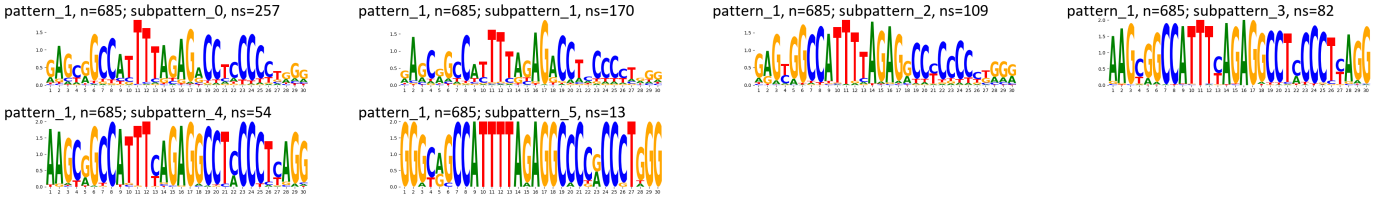

Supplementary Figure 1755: TF-MoDisCO subpatterns for the ZNF808 transcription factor in HEK293 (accession ChipExo models).

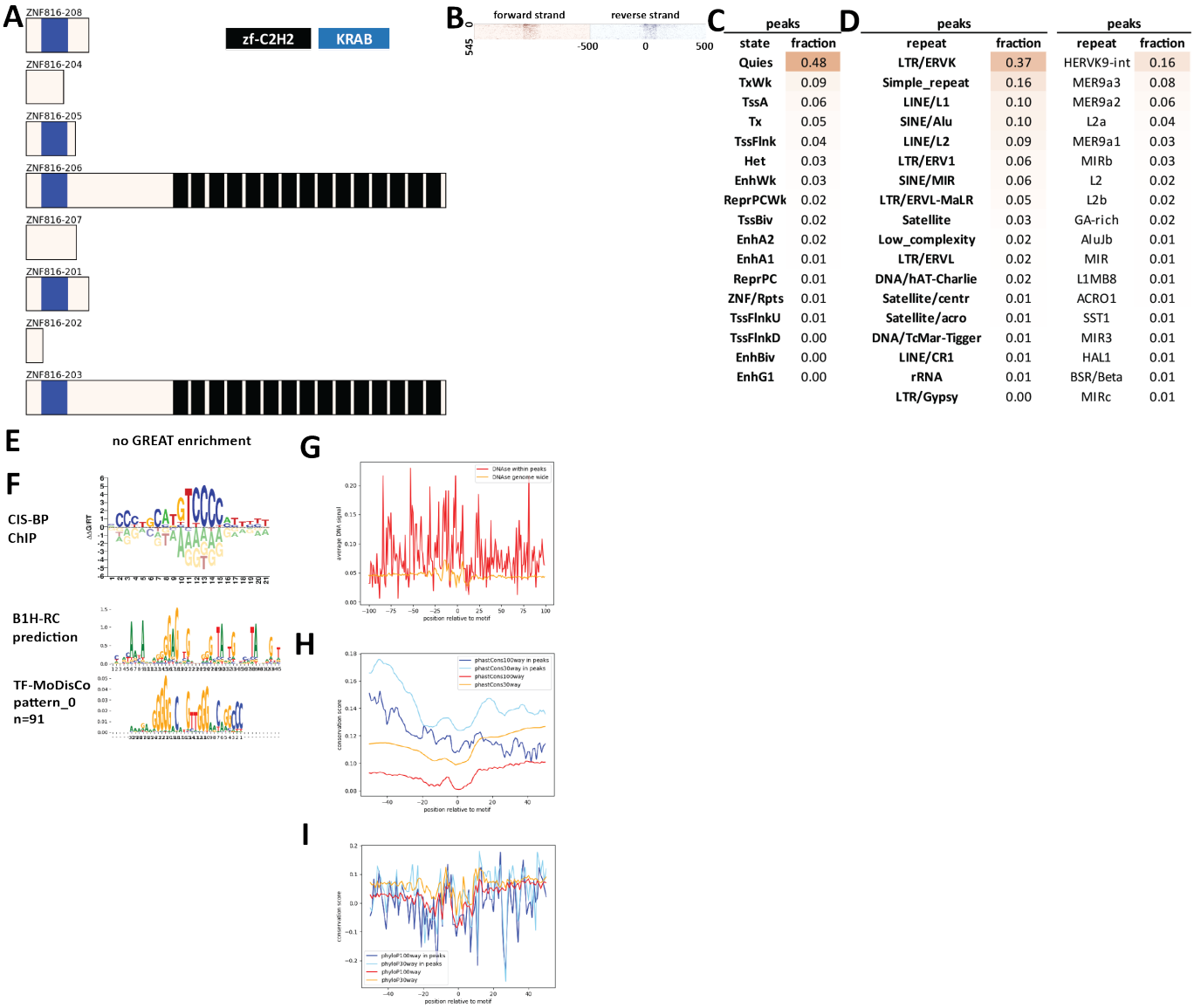

C	peaks	
state	fraction	
Quies	0.48	
TxWk	0.09	
TssA	0.06	
Tx	0.05	
TssFlnk	0.04	
Het	0.03	
EnhWk	0.03	
ReprPCWk	0.02	
TssBiv	0.02	
EnhA2	0.02	
EnhA1	0.01	
ReprPC	0.01	
ZNF/Rpts	0.01	
TssFlnkU	0.01	
TssFlnkD	0.00	
EnhBiv	0.00	
EnhG1	0.00	

D	peaks		peaks	
repeat	fraction	repeat	fraction	
LTR/ERVK	0.37	HERVK9-int	0.16	
Simple_repeat	0.16	MER9a3	0.08	
LINE/L1	0.10	MER9a2	0.06	
SINE/Alu	0.10	L2a	0.04	
LINE/L2	0.09	MER9a1	0.03	
LTR/ERV1	0.06	MIRb	0.03	
SINE/MIR	0.06	L2	0.02	
LTR/ERVL-MaLR	0.05	L2b	0.02	
Satellite	0.03	GA-rich	0.02	
Low_complexity	0.02	AluJb	0.01	
LTR/ERVL	0.02	MIR	0.01	
DNA/hAT-Charlie	0.02	L1MB8	0.01	
Satellite/centr	0.01	ACRO1	0.01	
Satellite/acro	0.01	SST1	0.01	
DNA/TcMar-Tigger	0.01	MIR3	0.01	
LINE/CR1	0.01	HAL1	0.01	
rRNA	0.01	BSR/Beta	0.01	
LTR/Gypsy	0.00	MIRc	0.01	

Supplementary Figure 1756: Properties and genomic distribution of motifs identified for the ZNF816 transcription factor in HEK293 (accession ChipExo models).

TF-MoDisCO pattern_0 n=91, CWM

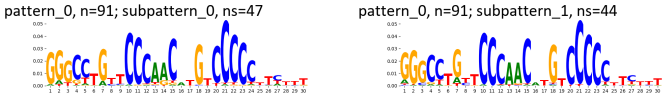

TF-MoDisCO pattern_0 n=91, PWM

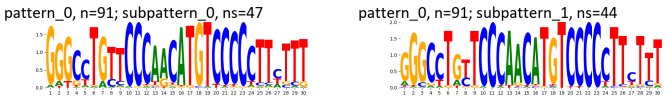

Supplementary Figure 1757: TF-MoDisCO subpatterns for the ZNF816 transcription factor in HEK293 (accession ChipExo models).

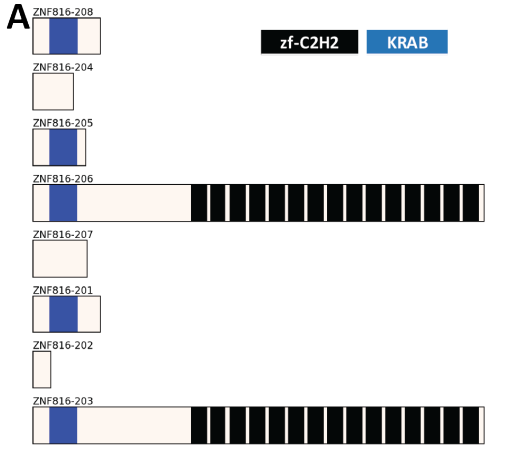



C

peaks	
state	fraction
Quies	0.46
TxWk	0.12
TssA	0.12
EnhWk	0.10
TssFlnk	0.06
Tx	0.05
EnhA1	0.04
ReprPCWk	0.03
TssBiv	0.02
ReprPC	0.02
Het	0.02
EnhA2	0.02
TssFlnkU	0.01
EnhBiv	0.01
TssFlnkD	0.00
EnhG2	0.00
ZNF/Rpts	0.00
EnhG1	0.00

D

peaks		peaks	
repeat	fraction	repeat	fraction
LTR/ERVK	0.14	HERVK9-int	0.06
LINE/L1	0.08	MER9a3	0.03
LINE/L2	0.08	L2a	0.02
LTR/ERV1	0.06	L2b	0.02
SINE/MIR	0.06	MIRb	0.02
LTR/ERVL-MaLR	0.04	L2c	0.02
Simple_repeat	0.04	MER9a2	0.02
SINE/Alu	0.04	MIRc	0.01
DNA/hAT-Charlie	0.03	L2	0.01
LTR/ERVL	0.02	MIR	0.01
Low_complexity	0.01	MER9a1	0.01
LINE/CR1	0.01	MIR3	0.01
DNA/TcMar-Tigger	0.01	MSTA	0.01
tRNA	0.01	LTR76	0.01
DNA/hAT-Tip100	0.01	L3	0.01
snRNA	0.00	AluJo	0.01
LTR/Gypsy	0.00	LTR56	0.01
DNA/TcMar-Tc2	0.00	MER41-int	0.01

E

Ontology	Term	FDR Q-val
GO Biological Process	Fc receptor signaling pathway	3.07
GO Biological Process	positive regulation of endopeptidase activity	2.46
GO Biological Process	cellular response to insulin stimulus	2.34
GO Biological Process	positive regulation of cysteine-type endopeptidase activity involved in apoptotic process	2.29
GO Biological Process	positive regulation of cysteine-type endopeptidase activity	2.22
GO Biological Process	positive regulation of peptidase activity	2.18
GO Biological Process	stress-activated MAPK cascade	2.10
GO Biological Process	paraxial mesoderm morphogenesis	1.79

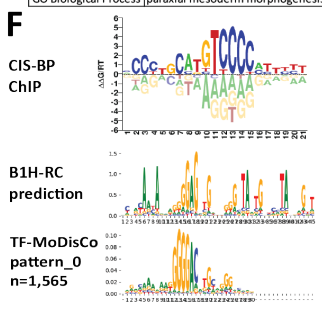

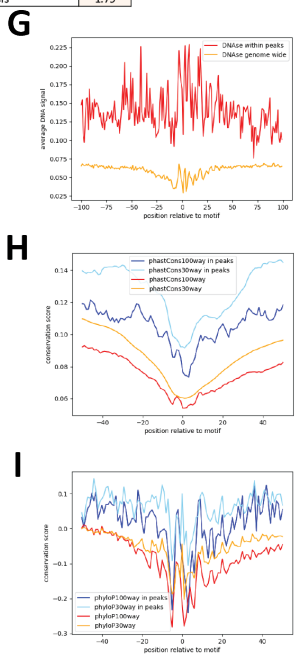

Supplementary Figure 1758: Properties and genomic distribution of motifs identified for the ZNF816 transcription factor in HEK293 (accession Hughes GR models).

TF-MoDisCO pattern_0 n=1565, CWM

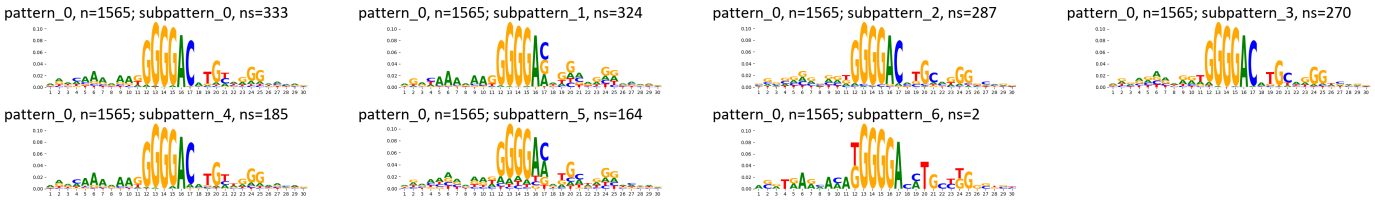

TF-MoDisCO pattern_0 n=1565, PWM

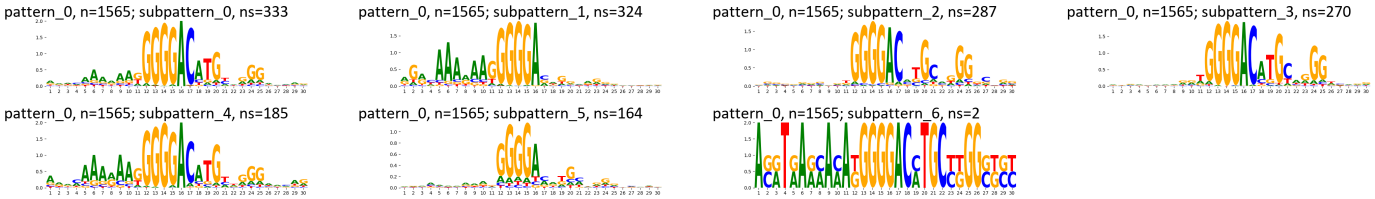

Supplementary Figure 1759: TF-MoDisCO subpatterns for the ZNF816 transcription factor in HEK293 (accession Hughes GR models).

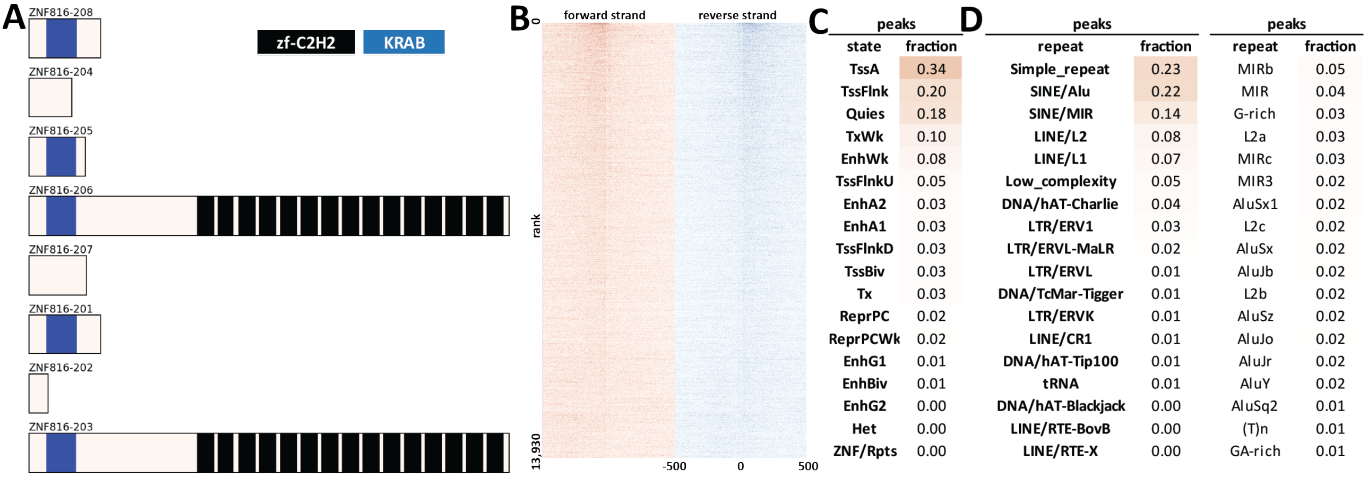

C

peaks	
state	fraction
TssA	0.34
TssFlnk	0.20
Quies	0.18
TxWk	0.10
EnhWk	0.08
TssFlnkU	0.05
EnhA2	0.03
EnhA1	0.03
TssFlnkD	0.03
TssBiv	0.03
Tx	0.03
ReprPC	0.02
ReprPCWk	0.02
EnhG1	0.01
EnhBiv	0.01
EnhG2	0.00
Het	0.00
ZNF/Rpts	0.00

D

peaks		peaks	
repeat	fraction	repeat	fraction
Simple_repeat	0.23	MIRb	0.05
SINE/Alu	0.22	MIR	0.04
SINE/MIR	0.14	G-rich	0.03
LINE/L2	0.08	L2a	0.03
LINE/L1	0.07	MIRc	0.03
Low_complexity	0.05	MIR3	0.02
DNA/hAT-Charlie	0.04	AluSx1	0.02
LTR/ERV1	0.03	L2c	0.02
LTR/ERVL-MaLR	0.02	AluSx	0.02
LTR/ERVL	0.01	AluJb	0.02
DNA/TcMar-Tigger	0.01	L2b	0.02
LTR/ERVK	0.01	AluSz	0.02
LINE/CR1	0.01	AluJo	0.02
DNA/hAT-Tip100	0.01	AluJr	0.02
tRNA	0.01	AluY	0.02
DNA/hAT-Blackjack	0.00	AluSq2	0.01
LINE/RTE-BovB	0.00	(T)n	0.01
LINE/RTE-X	0.00	GA-rich	0.01

E

Ontology	Term	FDR Q-val
GO Biological Process	regulation of transcription from RNA polymerase II promoter in response to stress	41.94
GO Biological Process	regulation of DNA-templated transcription in response to stress	40.95
GO Biological Process	mRNA catabolic process	37.43
GO Biological Process	RNA catabolic process	36.91
GO Biological Process	nuclear-transcribed mRNA catabolic process	35.18
GO Biological Process	regulation of hematopoietic progenitor cell differentiation	34.07
GO Biological Process	rRNA processing	32.55
GO Biological Process	rRNA metabolic process	32.14
GO Biological Process	regulation of mRNA stability	29.11
GO Biological Process	regulation of hematopoietic stem cell differentiation	29.00
GO Biological Process	multi-organism metabolic process	28.50
GO Biological Process	mRNA transport	28.44
GO Biological Process	regulation of transcription from RNA polymerase II promoter in response to hypoxia	27.82
GO Biological Process	nuclear-transcribed mRNA catabolic process, nonsense-mediated decay	27.54
GO Biological Process	viral gene expression	26.41
GO Biological Process	regulation of intrinsic apoptotic signaling pathway	26.19
GO Biological Process	ribonucleoprotein complex export from nucleus	25.76
GO Biological Process	ribonucleoprotein complex localization	25.73
GO Biological Process	viral transcription	23.32
GO Biological Process	mRNA export from nucleus	23.13
Human Phenotype	Hypoglycemia	17.99
Human Phenotype	Increased serum lactate	17.14
Human Phenotype	Exercise intolerance	15.10
Human Phenotype	Abnormality of transition element cation homeostasis	12.58
Human Phenotype	Abnormality of mitochondrial metabolism	12.49
Human Phenotype	Abnormality of the mitochondrion	12.18
Human Phenotype	Abnormal CSF metabolite level	11.28
Human Phenotype	Nephrotic syndrome	10.96
Human Phenotype	Increased CSF lactate	10.62
Human Phenotype	Abnormality of reticulocytes	9.28
Human Phenotype	Chromosomal breakage induced by crosslinking agents	8.35
Human Phenotype	Leukodystrophy	7.46
Human Phenotype	Progressive macrocephaly	6.93
Human Phenotype	Acute encephalopathy	6.22
Human Phenotype	Abnormal mitochondria in muscle tissue	6.01
Human Phenotype	Acute necrotizing encephalopathy	5.89
Human Phenotype	Overgrowth	5.06

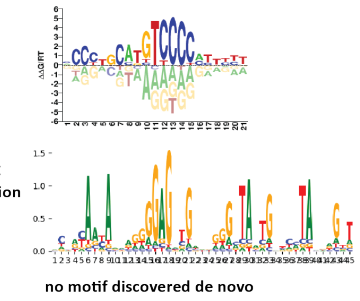

Supplementary Figure 1760: Properties and genomic distribution of motifs identified for the ZNF816 transcription factor in HepG2 (accession ENCSR905BNO).

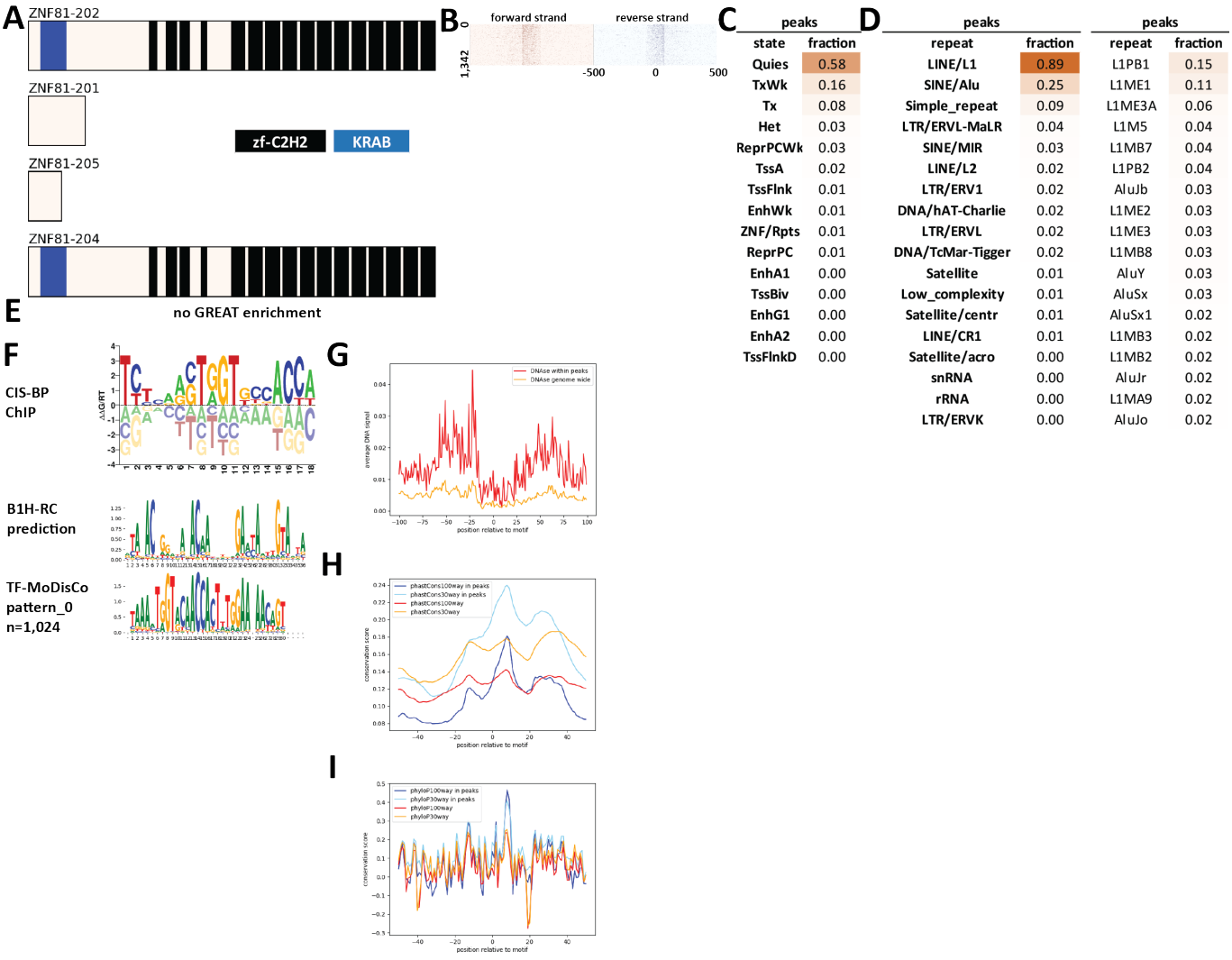

Supplementary Figure 1761: Properties and genomic distribution of motifs identified for the ZNF81 transcription factor in HEK293 (accession ChipExo models).

TF-MoDisCO pattern_0 n=1024, CWM

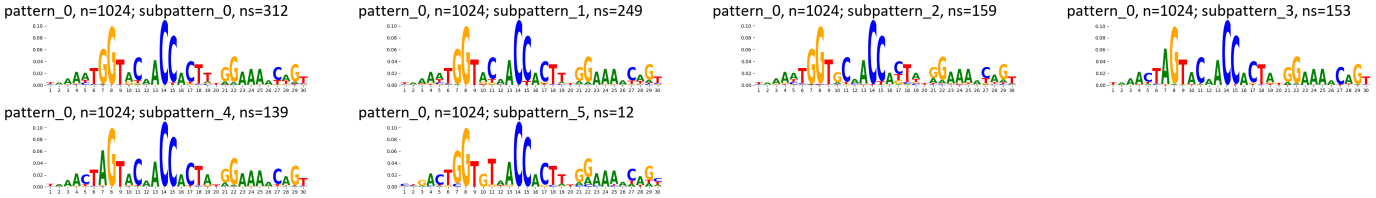

TF-MoDisCO pattern_0 n=1024, PWM

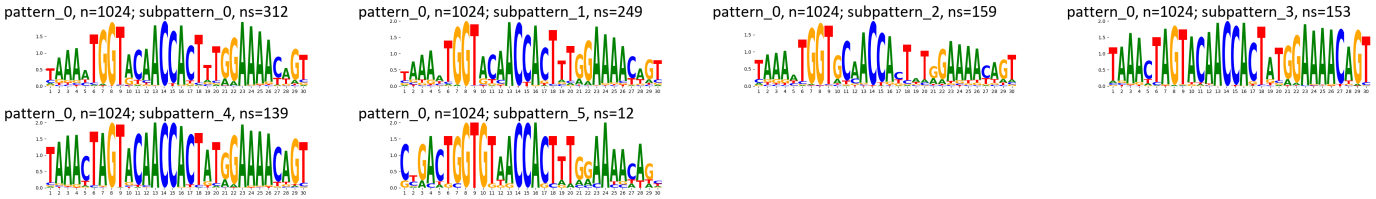

Supplementary Figure 1762: TF-MoDisCO subpatterns for the ZNF81 transcription factor in HEK293 (accession ChipExo models).

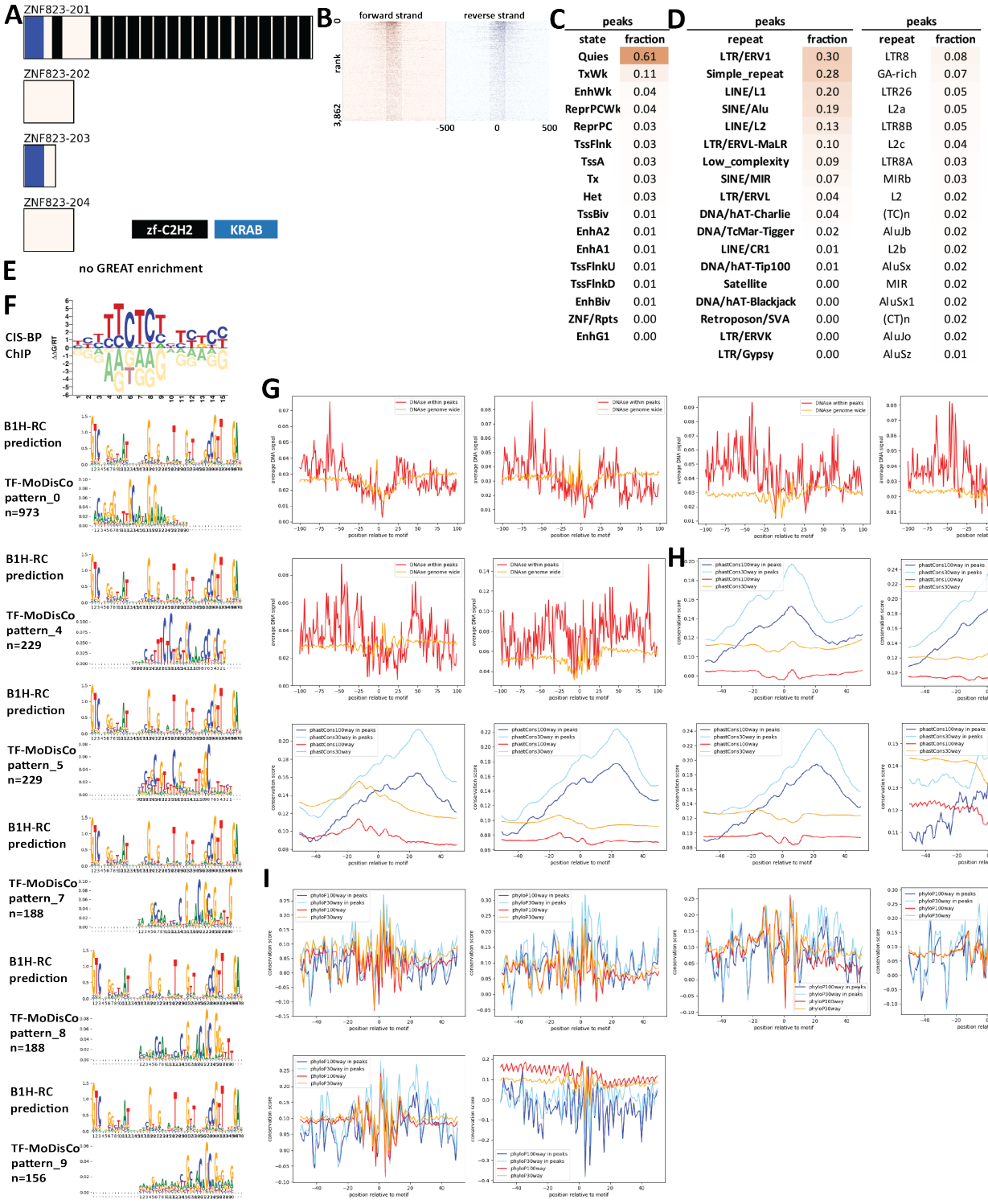

Supplementary Figure 1763: Properties and genomic distribution of motifs identified for the ZNF823 transcription factor in HEK293 (accession ChipExo models).

TF-MoDisCO pattern_0 n=973, CWM

pattern_0, n=973; subpattern_0, ns=246

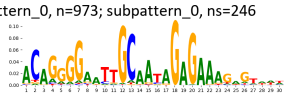

pattern_0, n=973; subpattern_1, ns=235

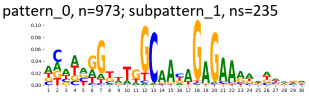

pattern_0, n=973; subpattern_2, ns=200

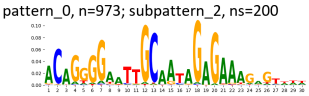

pattern_0, n=973; subpattern_3, ns=169

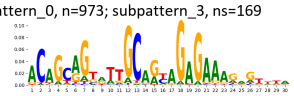

pattern_0, n=973; subpattern_4, ns=78

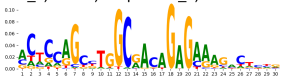

pattern_0, n=973; subpattern_5, ns=45

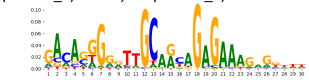

TF-MoDisCO pattern_0 n=973, PWM

pattern_0, n=973; subpattern_0, ns=246

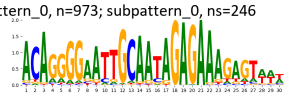

pattern_0, n=973; subpattern_1, ns=235

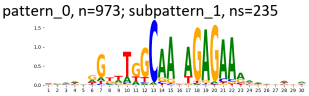

pattern_0, n=973; subpattern_2, ns=200

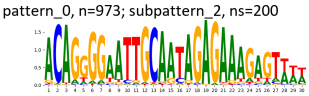

pattern_0, n=973; subpattern_3, ns=169

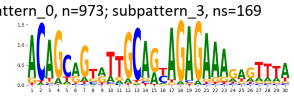

pattern_0, n=973; subpattern_4, ns=78

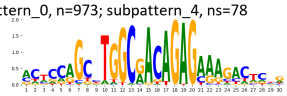

pattern_0, n=973; subpattern_5, ns=45

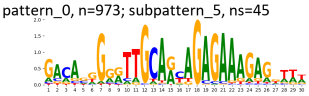

TF-MoDisCO pattern_4 n=229, CWM

pattern_4, n=229; subpattern_0, ns=87

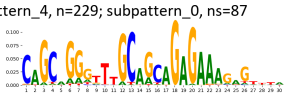

pattern_4, n=229; subpattern_1, ns=65

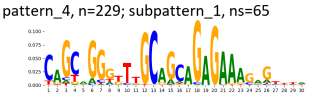

pattern_4, n=229; subpattern_2, ns=64

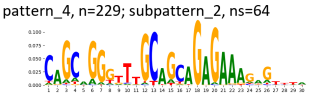

pattern_4, n=229; subpattern_3, ns=11

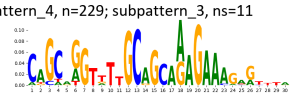

pattern_4, n=229; subpattern_4, ns=2

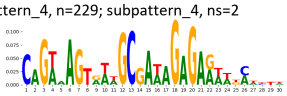

TF-MoDisCO pattern_4 n=229, PWM

pattern_4, n=229; subpattern_0, ns=87

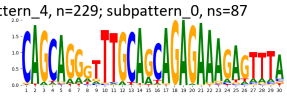

pattern_4, n=229; subpattern_1, ns=65

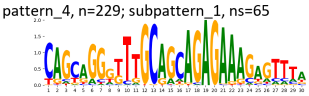

pattern_4, n=229; subpattern_2, ns=64

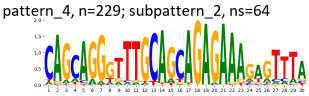

pattern_4, n=229; subpattern_3, ns=11

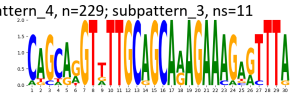

pattern_4, n=229; subpattern_4, ns=2

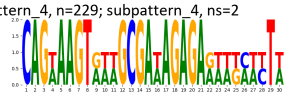

TF-MoDisCO pattern_7 n=188, CWM

pattern_7, n=188; subpattern_0, ns=53

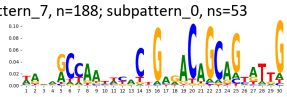

pattern_7, n=188; subpattern_1, ns=53

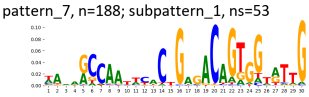

pattern_7, n=188; subpattern_2, ns=44

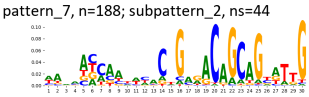

pattern_7, n=188; subpattern_3, ns=25

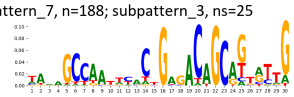

pattern_7, n=188; subpattern_4, ns=11

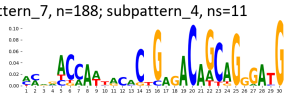

pattern_7, n=188; subpattern_5, ns=2

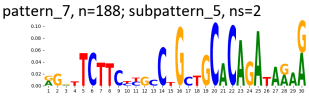

TF-MoDisCO pattern_7 n=188, PWM

pattern_7, n=188; subpattern_0, ns=53

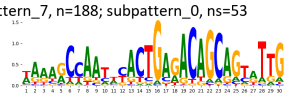

pattern_7, n=188; subpattern_1, ns=53

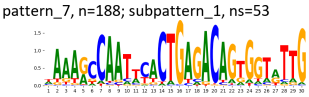

pattern_7, n=188; subpattern_2, ns=44

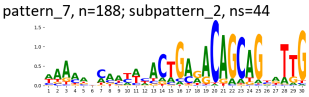

pattern_7, n=188; subpattern_3, ns=25

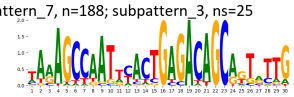

pattern_7, n=188; subpattern_4, ns=11

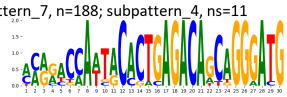

pattern_7, n=188; subpattern_5, ns=2

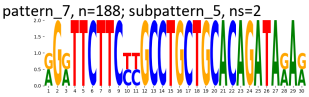

TF-MoDisCO pattern_8 n=188, CWM

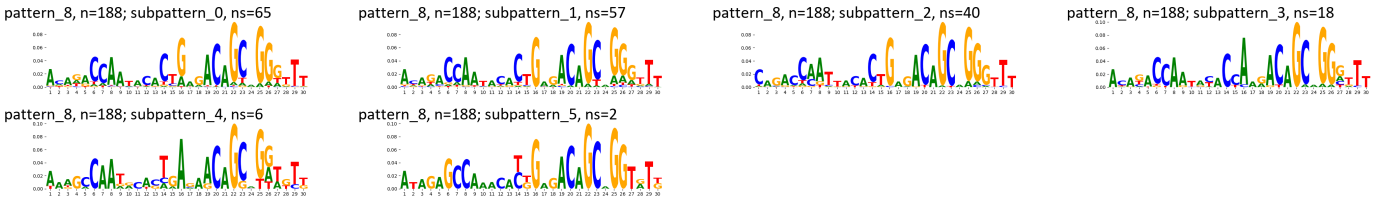

TF-MoDisCO pattern_8 n=188, PWM

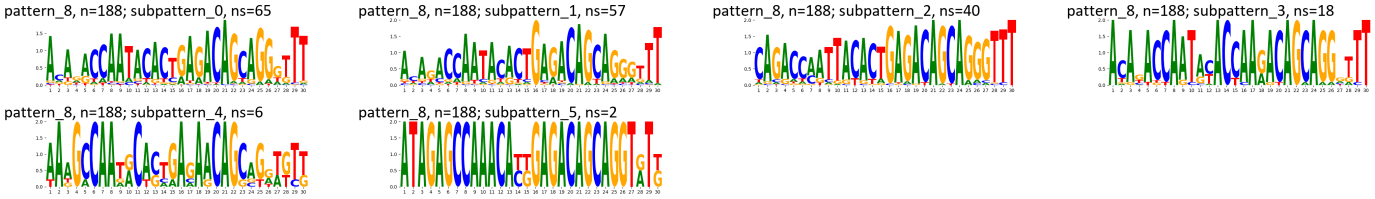

Supplementary Figure 1764: TF-MoDisCO subpatterns for the ZNF823 transcription factor in HEK293 (accession ChipExo models).

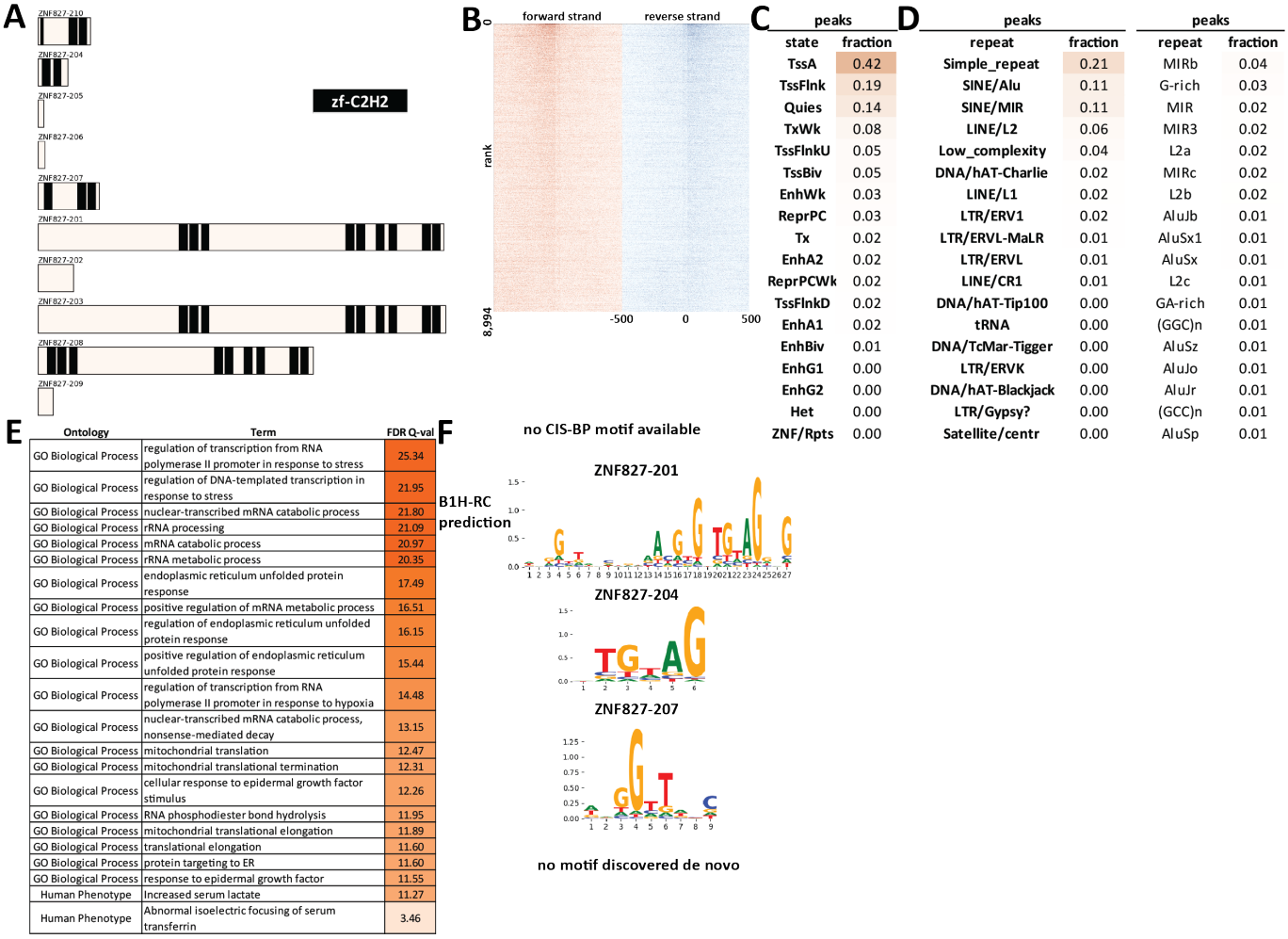

Supplementary Figure 1765: Properties and genomic distribution of motifs identified for the ZNF827 transcription factor in HepG2 (accession ENCSR148FHD).

A



B

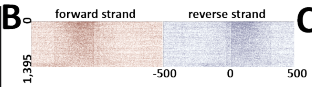

C

peaks	
state	fraction
TssA	0.56
TssFlnk	0.12
TssBiv	0.11
Quies	0.06
TssFlnkU	0.04
TxWk	0.03
EnhA1	0.03
EnhWk	0.03
EnhA2	0.03
TssFlnkD	0.01
EnhBiv	0.01
Tx	0.01
EnhG1	0.01
ReprPC	0.01
EnhG2	0.01
ReprPCWk	0.01
ZNF/Rpts	0.00
Het	0.00

D

peaks		peaks	
repeat	fraction	repeat	fraction
Simple_repeat	0.29	(GT)n	0.04
SINE/Alu	0.06	(CA)n	0.03
Low_complexity	0.04	(AC)n	0.03
SINE/MIR	0.03	(TG)n	0.02
LINE/L2	0.02	G-rich	0.02
LINE/L1	0.02	GA-rich	0.01
tRNA	0.01	MIRc	0.01
DNA/hAT-Charlie	0.01	MIR	0.01
snRNA	0.01	AluSx1	0.01
LTR/ERV1	0.00	MIRb	0.01
LTR/ERVL	0.00	AluY	0.01
LTR/ERVL-MaLR	0.00	AluSx	0.01
DNA/TcMar-Tigger	0.00	(GGC)n	0.01
SINE/5S-Deu-L2	0.00	U1	0.01
Retroposon/SVA	0.00	L2c	0.01
LTR/Gypsy	0.00	L2a	0.01
LINE/CR1	0.00	AluSg	0.01
DNA/hAT-Tip100	0.00	(TC)n	0.01

E

Ontology	Term	FDR Q-val
GO Biological Process	peptidyl-proline modification	6.85
GO Biological Process	glucose catabolic process	5.26
GO Biological Process	canonical glycolysis	4.82
GO Biological Process	glycolytic process through glucose-6-phosphate	4.79
GO Biological Process	nucleoside diphosphate phosphorylation	4.09
GO Biological Process	glycolytic process	4.03
GO Biological Process	nucleotide phosphorylation	3.87
GO Biological Process	ATP generation from ADP	3.87
GO Biological Process	single-organism carbohydrate catabolic process	3.81
GO Biological Process	carbohydrate catabolic process	3.45
GO Biological Process	hexose metabolic process	2.53

F

no CIS-BP motif available

B1H-RC prediction

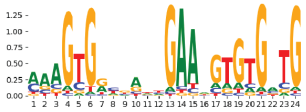

no motif discovered de novo

Supplementary Figure 1766: Properties and genomic distribution of motifs identified for the ZNF837 transcription factor in HEK293 (accession ENCSR711UOA).

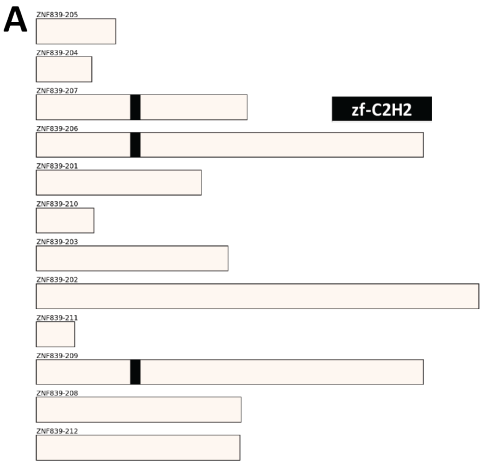

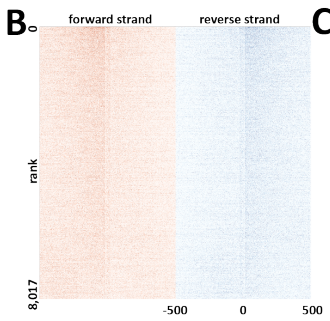

C

peaks	
state	fraction
TssA	0.43
TssFlnk	0.21
Quies	0.14
TxWk	0.09
TssFlnkU	0.04
EnhWk	0.04
TssBiv	0.04
ReprPC	0.03
EnhA2	0.03
EnhA1	0.02
TssFlnkD	0.02
Tx	0.02
ReprPCWk	0.02
EnhBiv	0.01
EnhG1	0.00
EnhG2	0.00
Het	0.00
ZNF/Rpts	0.00

D

peaks		peaks	
repeat	fraction	repeat	fraction
Simple_repeat	0.18	MIRb	0.04
SINE/Alu	0.10	G-rich	0.03
SINE/MIR	0.10	MIR3	0.02
LINE/L2	0.06	MIR	0.02
Low_complexity	0.04	L2a	0.02
LINE/L1	0.02	L2b	0.02
DNA/hAT-Charlie	0.02	MIRc	0.02
LTR/ERV1	0.01	L2c	0.01
LTR/ERVL	0.01	AluSx	0.01
LTR/ERVL-MaLR	0.01	AluJb	0.01
DNA/hAT-Tip100	0.00	AluSx1	0.01
tRNA	0.00	AluJo	0.01
LINE/CR1	0.00	AluJr	0.01
DNA/TcMar-Tigger	0.00	AluSz	0.01
DNA/hAT-Blackjack	0.00	L2	0.01
Retroposon/SVA	0.00	GA-rich	0.01
DNA/TcMar-Mariner	0.00	MIR1_Amn	0.01
SINE/tRNA-RTE	0.00	(GT)n	0.01

E

Ontology	Term	FDR Q-val
GO Biological Process	regulation of transcription from RNA polymerase II promoter in response to stress	46.05
GO Biological Process	regulation of DNA-templated transcription in response to stress	40.84
GO Biological Process	regulation of transcription from RNA polymerase II promoter in response to hypoxia	31.92
GO Biological Process	nuclear-transcribed mRNA catabolic process	21.97
GO Biological Process	response to topologically incorrect protein	21.81
GO Biological Process	cellular response to topologically incorrect protein	21.66
GO Biological Process	nuclear-transcribed mRNA catabolic process, nonsense-mediated decay	21.65
GO Biological Process	cellular response to unfolded protein	20.66
GO Biological Process	mRNA catabolic process	20.33
GO Biological Process	regulation of ubiquitin-protein ligase activity involved in mitotic cell cycle	20.29
GO Biological Process	negative regulation of ubiquitin protein ligase activity	20.19
GO Biological Process	regulation of cellular amino acid metabolic process	20.15
GO Biological Process	RNA catabolic process	20.10
GO Biological Process	negative regulation of ubiquitin-protein transferase activity	19.74
GO Biological Process	response to unfolded protein	19.58
GO Biological Process	negative regulation of ubiquitin-protein ligase activity involved in mitotic cell cycle	19.54
GO Biological Process	cellular response to epidermal growth factor stimulus	19.30
GO Biological Process	regulation of mRNA stability	19.16
GO Biological Process	regulation of RNA stability	19.00
GO Biological Process	anaphase-promoting complex-dependent catabolic process	18.66
Human Phenotype	Exercise intolerance	8.92
Human Phenotype	Leukodystrophy	3.84
Human Phenotype	Laryngomalacia	3.49
Human Phenotype	Basal cell carcinoma	2.28

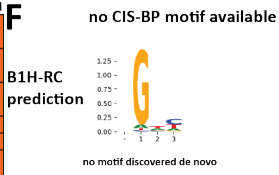

Supplementary Figure 1767: Properties and genomic distribution of motifs identified for the ZNF839 transcription factor in HepG2 (accession ENCSR540LPD).

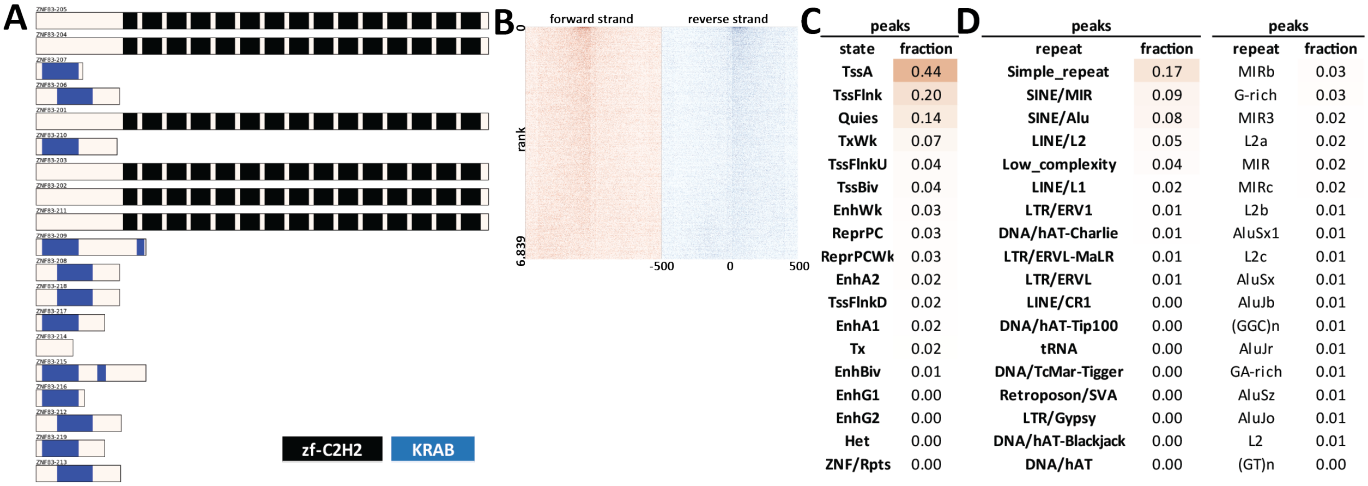

C

peaks	
state	fraction
TssA	0.44
TssFlnk	0.20
Quies	0.14
TxWk	0.07
TssFlnkU	0.04
TssBiv	0.04
EnhWk	0.03
ReprPC	0.03
ReprPCWk	0.03
EnhA2	0.02
TssFlnkD	0.02
EnhA1	0.02
Tx	0.02
EnhBiv	0.01
EnhG1	0.00
EnhG2	0.00
Het	0.00
ZNF/Rpts	0.00

D

peaks		peaks	
repeat	fraction	repeat	fraction
Simple_repeat	0.17	MIRb	0.03
SINE/MIR	0.09	G-rich	0.03
SINE/Alu	0.08	MIR3	0.02
LINE/L2	0.05	L2a	0.02
Low_complexity	0.04	MIR	0.02
LINE/L1	0.02	MIRc	0.02
LTR/ERV1	0.01	L2b	0.01
DNA/hAT-Charlie	0.01	AluSx1	0.01
LTR/ERVL-MaLR	0.01	L2c	0.01
LTR/ERVL	0.01	AluSx	0.01
LINE/CR1	0.00	AluJb	0.01
DNA/hAT-Tip100	0.00	(GGC)n	0.01
tRNA	0.00	AluJr	0.01
DNA/TcMar-Tigger	0.00	GA-rich	0.01
Retroposon/SVA	0.00	AluSz	0.01
LTR/Gypsy	0.00	AluJo	0.01
DNA/hAT-Blackjack	0.00	L2	0.01
DNA/hAT	0.00	(GT)n	0.00

E

Ontology	Term	FDR Q-val
GO Biological Process	regulation of intrinsic apoptotic signaling pathway	20.28
GO Biological Process	positive regulation of nuclease activity	19.28
GO Biological Process	cellular response to topologically incorrect protein	15.53
GO Biological Process	regulation of hematopoietic progenitor cell differentiation	15.48
GO Biological Process	regulation of mRNA stability	15.11
GO Biological Process	response to topologically incorrect protein	15.00
GO Biological Process	nuclear-transcribed mRNA catabolic process	14.88
GO Biological Process	rRNA processing	14.76
GO Biological Process	rRNA metabolic process	14.45
GO Biological Process	endoplasmic reticulum unfolded protein response	14.28
GO Biological Process	mRNA catabolic process	14.11
GO Biological Process	regulation of RNA stability	13.64
GO Biological Process	cellular response to unfolded protein	12.93
GO Biological Process	response to unfolded protein	12.42
GO Biological Process	nuclear-transcribed mRNA catabolic process, nonsense-mediated decay	12.23
GO Biological Process	nuclear-transcribed mRNA catabolic process, deadenylation-dependent decay	11.34
GO Biological Process	purine nucleoside triphosphate catabolic process	11.23
GO Biological Process	translational elongation	9.80
GO Biological Process	RNA phosphodiester bond hydrolysis	9.71
GO Biological Process	cellular response to epidermal growth factor stimulus	9.22
Human Phenotype	Increased serum lactate	7.45

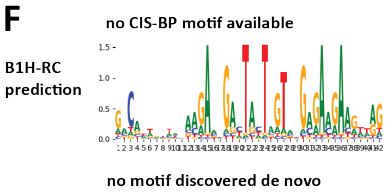

Supplementary Figure 1768: Properties and genomic distribution of motifs identified for the ZNF83 transcription factor in HepG2 (accession ENCSR263XFO).

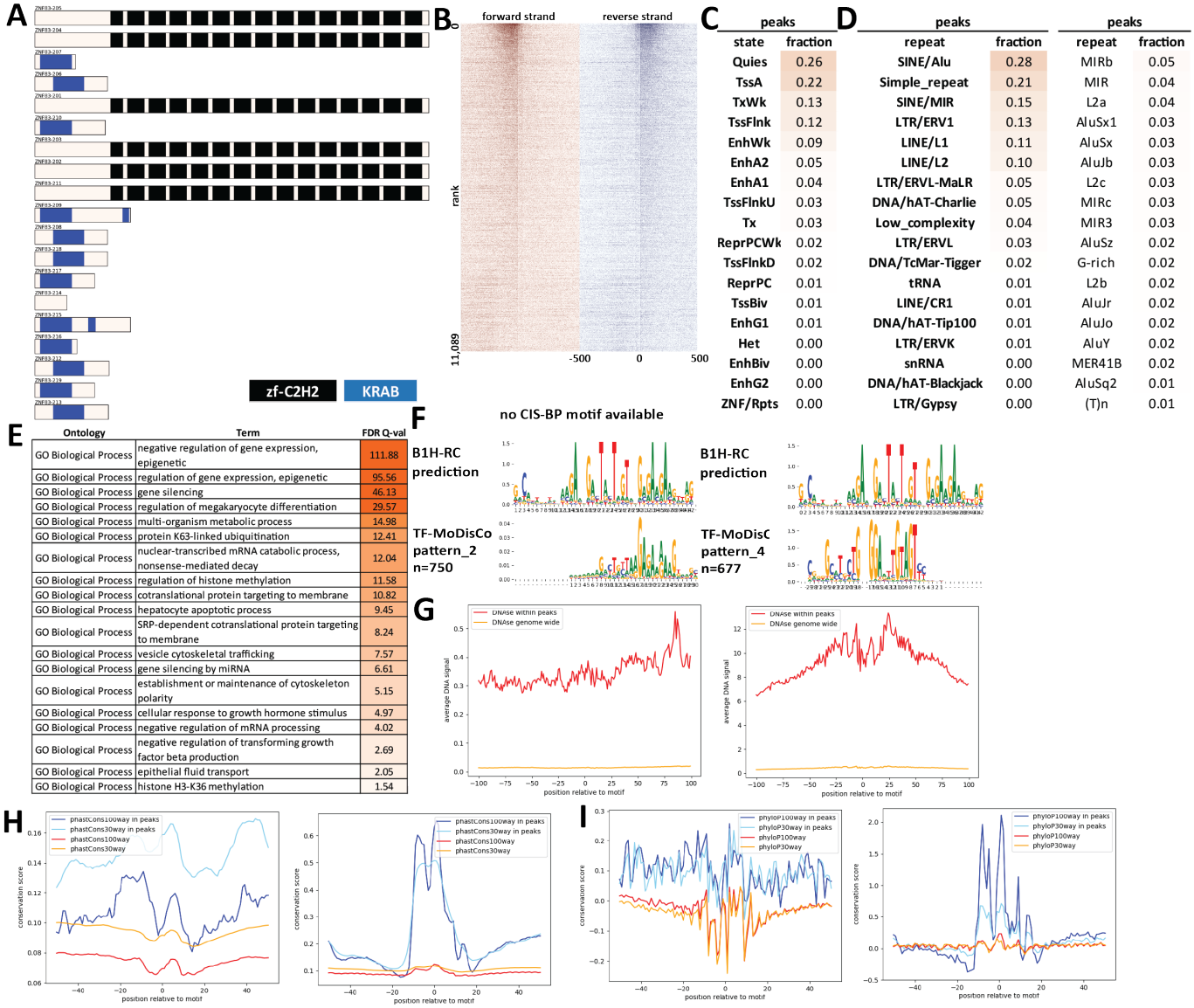

Supplementary Figure 1769: Properties and genomic distribution of motifs identified for the ZNF83 transcription factor in K562 (accession ENCSR257XVY).

TF-MoDisCO pattern_2 n=750, CWM

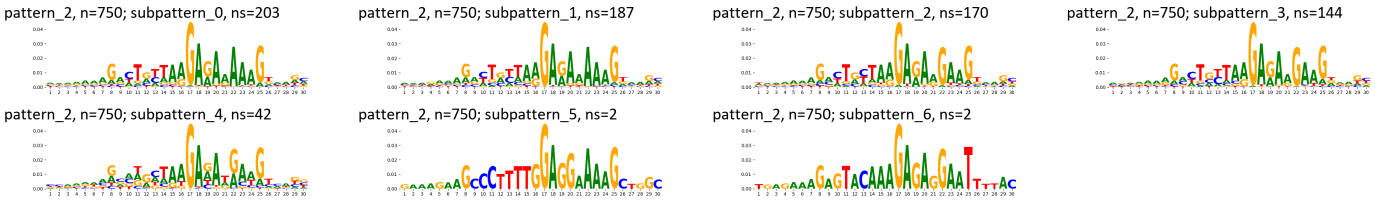

TF-MoDisCO pattern_2 n=750, PWM

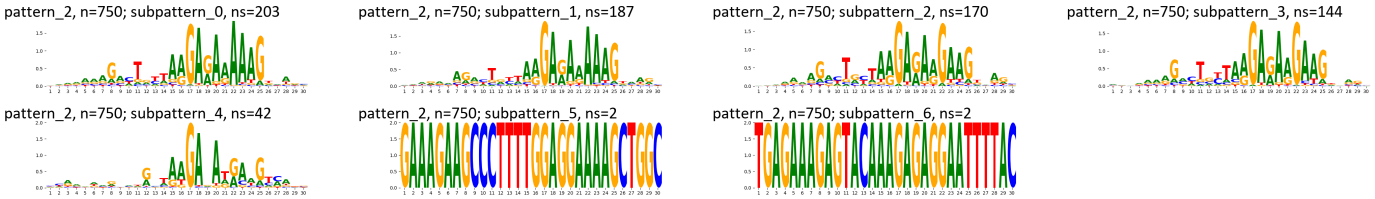

TF-MoDisCO pattern_4 n=677, CWM

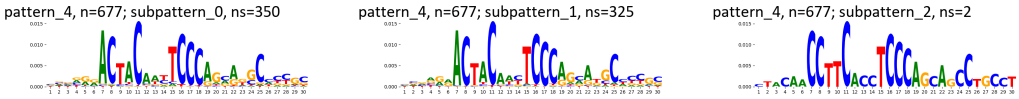

TF-MoDisCO pattern_4 n=677, PWM

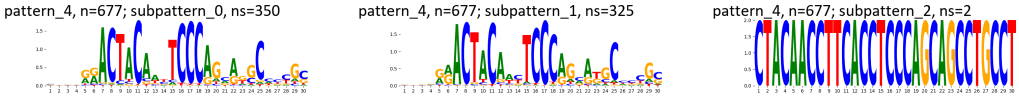

Supplementary Figure 1770: TF-MoDisCO subpatterns for the ZNF83 transcription factor in K562 (accession ENCSR257XVY).

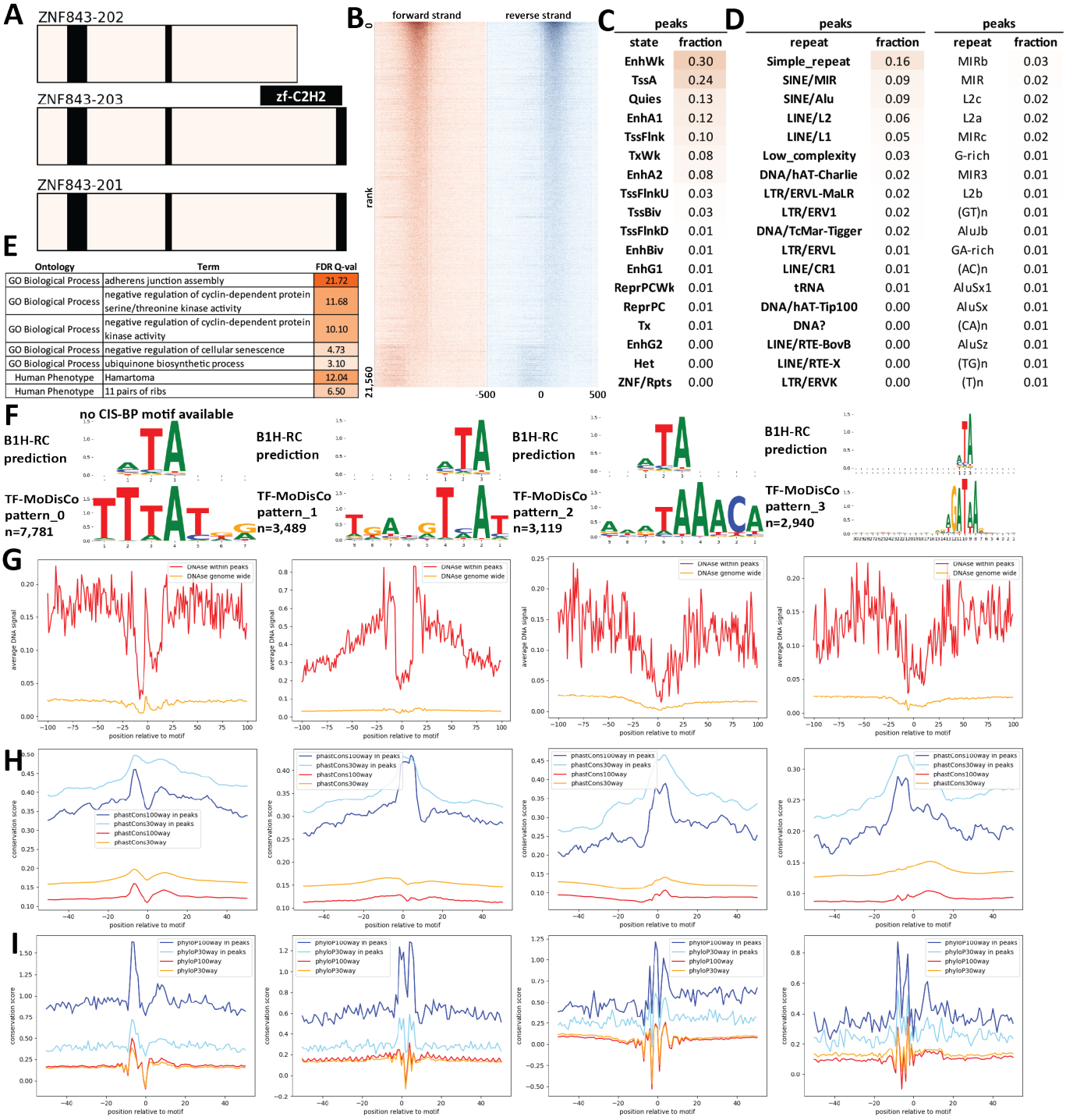

Supplementary Figure 1771: Properties and genomic distribution of motifs identified for the ZNF843 transcription factor in HEK293 (accession ENCSR502KPJ).

TF-MoDisCO pattern_0 n=7781, CWM

pattern_0, n=7781; subpattern_0, ns=1712

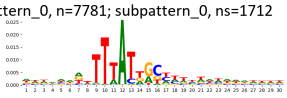

pattern_0, n=7781; subpattern_1, ns=1659

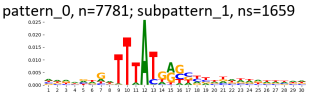

pattern_0, n=7781; subpattern_2, ns=1612

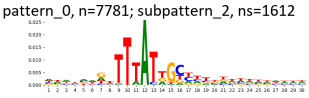

pattern_0, n=7781; subpattern_3, ns=1338

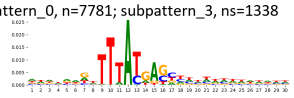

pattern_0, n=7781; subpattern_4, ns=873

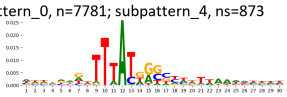

pattern_0, n=7781; subpattern_5, ns=330

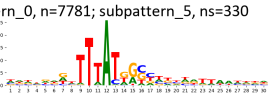

pattern_0, n=7781; subpattern_6, ns=179

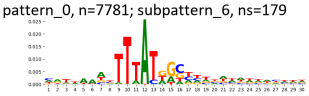

pattern_0, n=7781; subpattern_7, ns=66

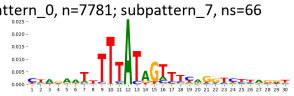

pattern_0, n=7781; subpattern_8, ns=10

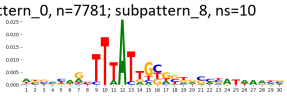

pattern_0, n=7781; subpattern_9, ns=2

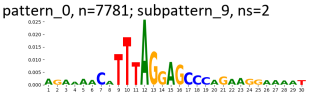

TF-MoDisCO pattern_0 n=7781, PWM

pattern_0, n=7781; subpattern_0, ns=1712

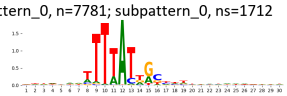

pattern_0, n=7781; subpattern_1, ns=1659

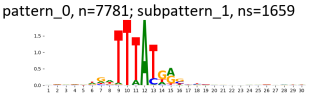

pattern_0, n=7781; subpattern_2, ns=1612

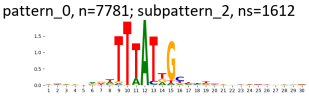

pattern_0, n=7781; subpattern_3, ns=1338

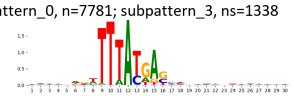

pattern_0, n=7781; subpattern_4, ns=873

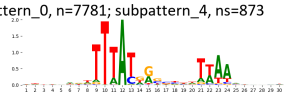

pattern_0, n=7781; subpattern_5, ns=330

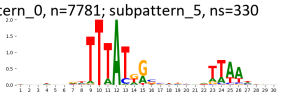

pattern_0, n=7781; subpattern_6, ns=179

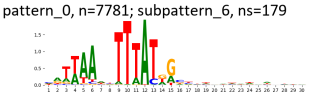

pattern_0, n=7781; subpattern_7, ns=66

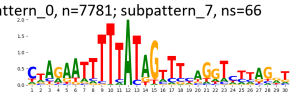

pattern_0, n=7781; subpattern_8, ns=10

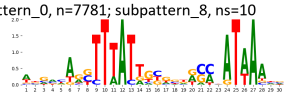

pattern_0, n=7781; subpattern_9, ns=2

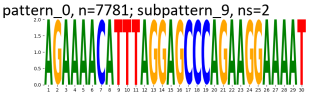

TF-MoDisCO pattern_1 n=3489, CWM

pattern_1, n=3489; subpattern_0, ns=809

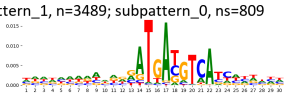

pattern_1, n=3489; subpattern_1, ns=718

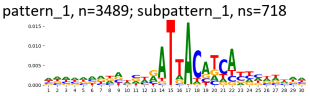

pattern_1, n=3489; subpattern_2, ns=664

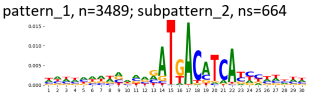

pattern_1, n=3489; subpattern_3, ns=654

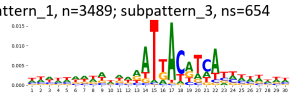

pattern_1, n=3489; subpattern_4, ns=354

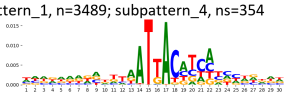

pattern_1, n=3489; subpattern_5, ns=281

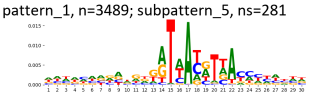

pattern_1, n=3489; subpattern_6, ns=9

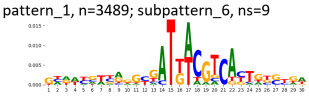

TF-MoDisCO pattern_1 n=3489, PWM

pattern_1, n=3489; subpattern_0, ns=809

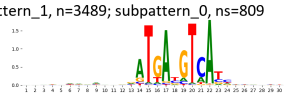

pattern_1, n=3489; subpattern_1, ns=718

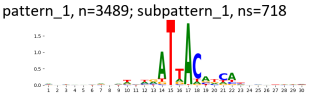

pattern_1, n=3489; subpattern_2, ns=664

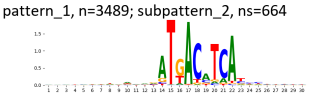

pattern_1, n=3489; subpattern_3, ns=654

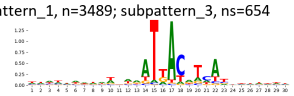

pattern_1, n=3489; subpattern_4, ns=354

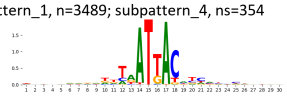

pattern_1, n=3489; subpattern_5, ns=281

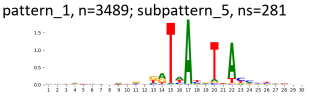

pattern_1, n=3489; subpattern_6, ns=9

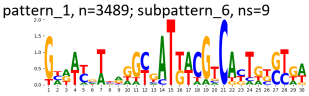

TF-MoDisCO pattern_2 n=3119, CWM

pattern_2, n=3119; subpattern_0, ns=1129

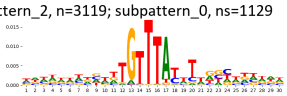

pattern_2, n=3119; subpattern_1, ns=702

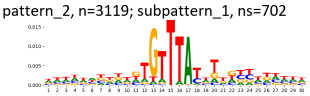

pattern_2, n=3119; subpattern_2, ns=648

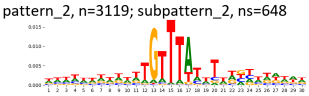

pattern_2, n=3119; subpattern_3, ns=638

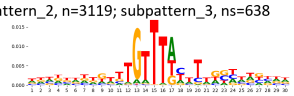

pattern_2, n=3119; subpattern_4, ns=2

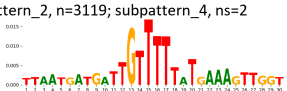

TF-MoDisCO pattern_2 n=3119, PWM

pattern_2, n=3119; subpattern_0, ns=1129

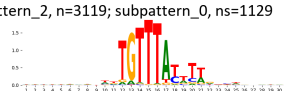

pattern_2, n=3119; subpattern_1, ns=702

pattern_2, n=3119; subpattern_2, ns=648

pattern_2, n=3119; subpattern_3, ns=638

pattern_2, n=3119; subpattern_4, ns=2

TF-MoDisCO pattern_3 n=2940, CWM

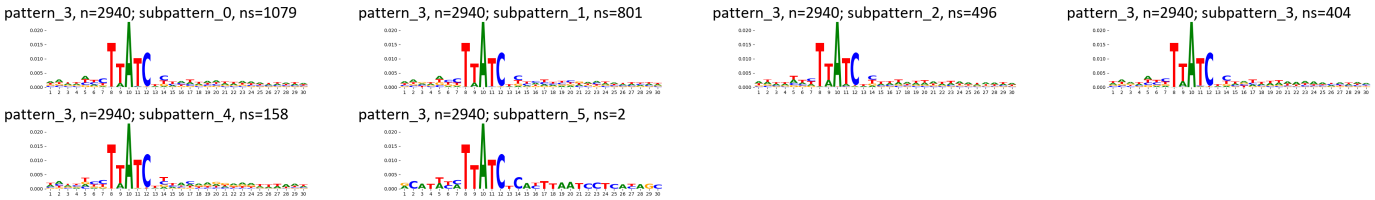

TF-MoDisCO pattern_3 n=2940, PWM

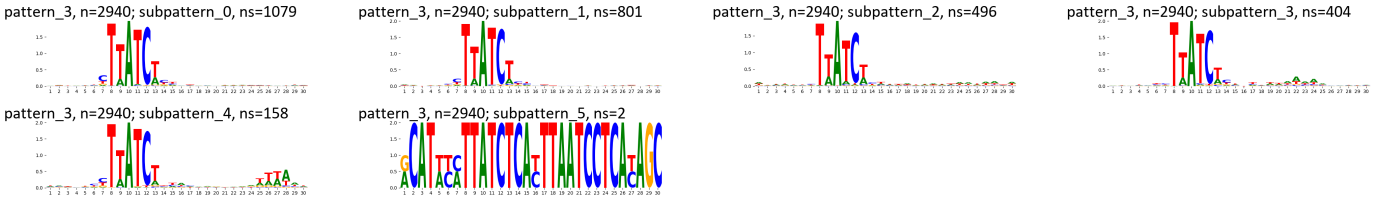

Supplementary Figure 1772: TF-MoDisCO subpatterns for the ZNF843 transcription factor in HEK293 (accession ENCSR502KPJ).

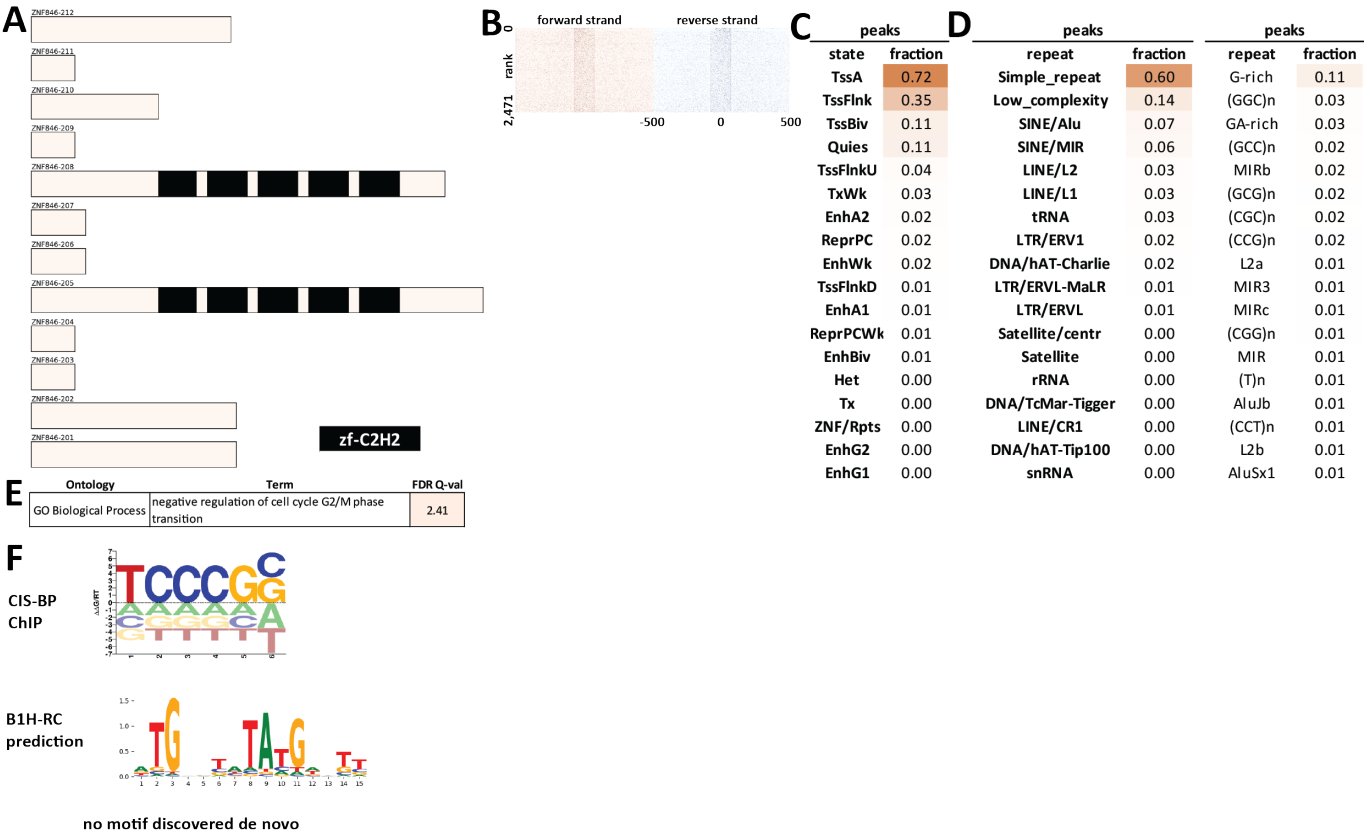

Supplementary Figure 1773: Properties and genomic distribution of motifs identified for the ZNF846 transcription factor in HEK293 (accession ChipExo models).

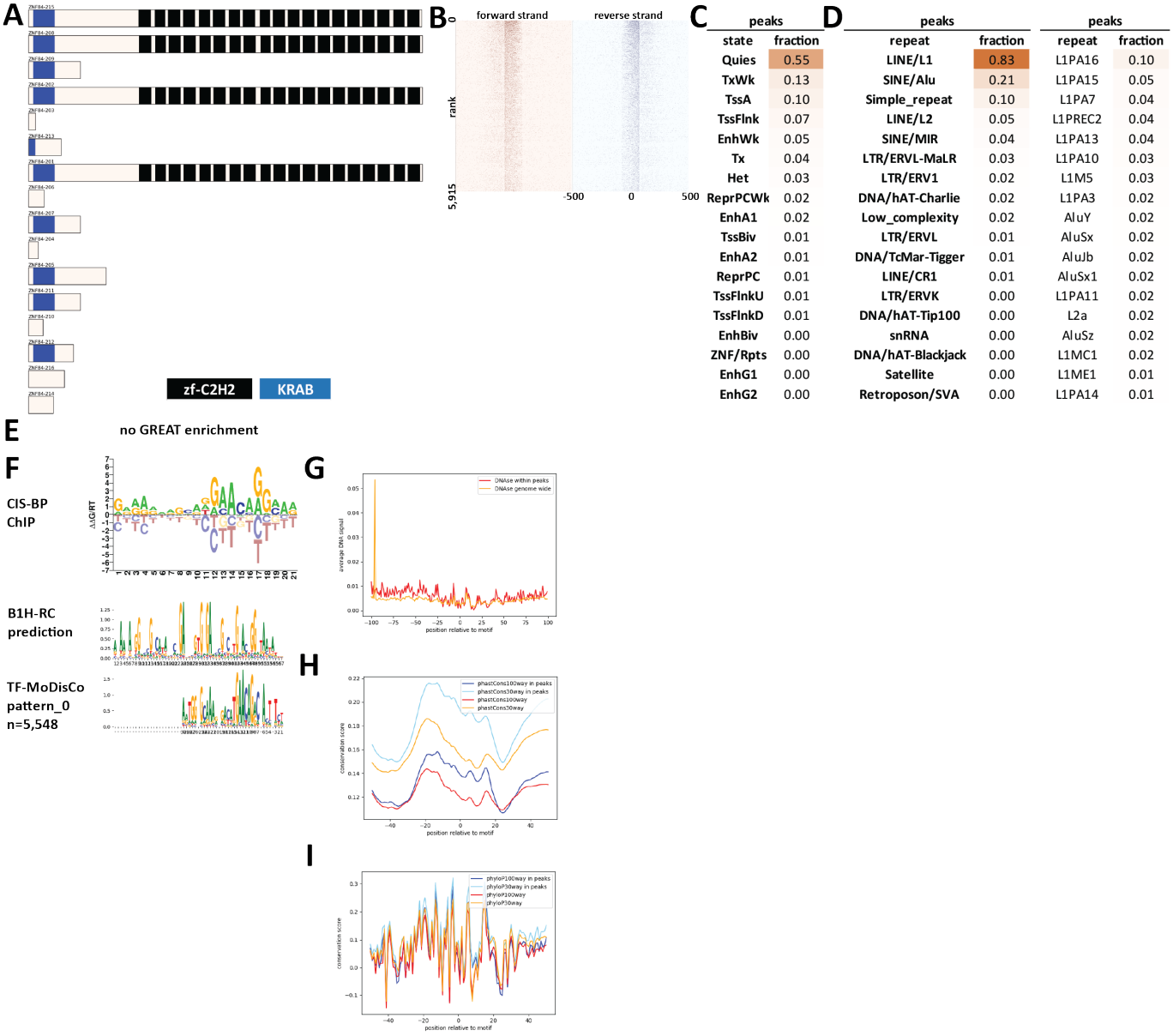

C

peaks	
state	fraction
Quies	0.55
TxWk	0.13
TssA	0.10
TssFlnk	0.07
EnhWk	0.05
Tx	0.04
Het	0.03
ReprPCWk	0.02
EnhA1	0.02
TssBiv	0.01
EnhA2	0.01
ReprPC	0.01
TssFlnkU	0.01
TssFlnkD	0.01
EnhBiv	0.00
ZNF/Rpts	0.00
EnhG1	0.00
EnhG2	0.00

D

peaks		peaks	
repeat	fraction	repeat	fraction
LINE/L1	0.83	L1PA16	0.10
SINE/Alu	0.21	L1PA15	0.05
Simple_repeat	0.10	L1PA7	0.04
LINE/L2	0.05	L1PREC2	0.04
SINE/MIR	0.04	L1PA13	0.04
LTR/ERVL-MaLR	0.03	L1PA10	0.03
LTR/ERV1	0.02	L1M5	0.03
DNA/hAT-Charlie	0.02	L1PA3	0.02
Low_complexity	0.02	AluY	0.02
LTR/ERVL	0.01	AluSx	0.02
DNA/TcMar-Tigger	0.01	AluJb	0.02
LINE/CR1	0.01	AluSx1	0.02
LTR/ERVK	0.00	L1PA11	0.02
DNA/hAT-Tip100	0.00	L2a	0.02
snRNA	0.00	AluSz	0.02
DNA/hAT-Blackjack	0.00	L1MC1	0.02
Satellite	0.00	L1ME1	0.01
Retroposon/SVA	0.00	L1PA14	0.01

Supplementary Figure 1774: Properties and genomic distribution of motifs identified for the ZNF84 transcription factor in HEK293 (accession ChipExo models).

TF-MoDisCO pattern_0 n=5548, CWM

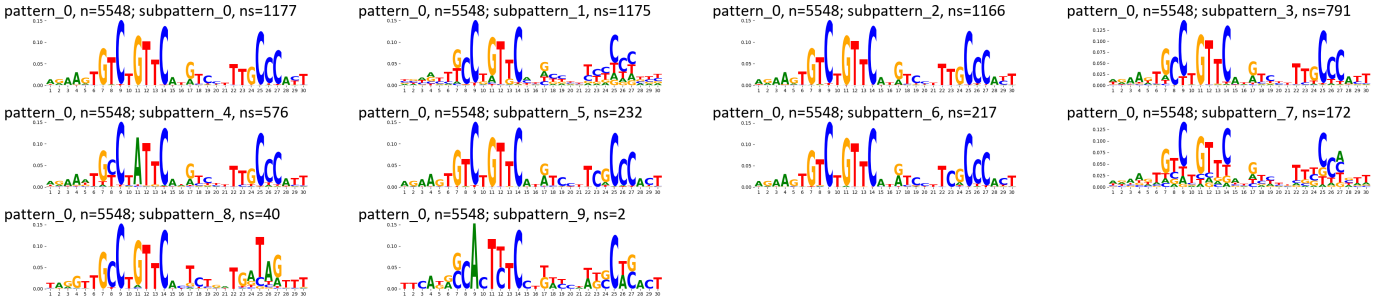

TF-MoDisCO pattern_0 n=5548, PWM

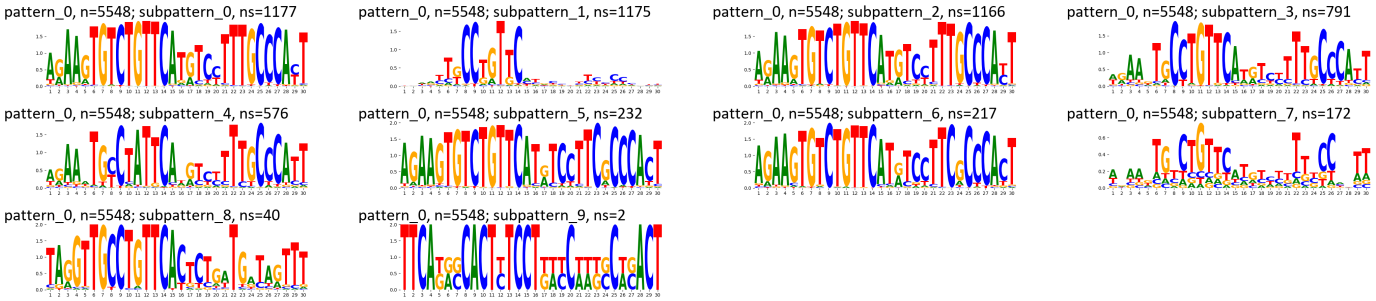

Supplementary Figure 1775: TF-MoDisCO subpatterns for the ZNF84 transcription factor in HEK293 (accession ChipExo models).

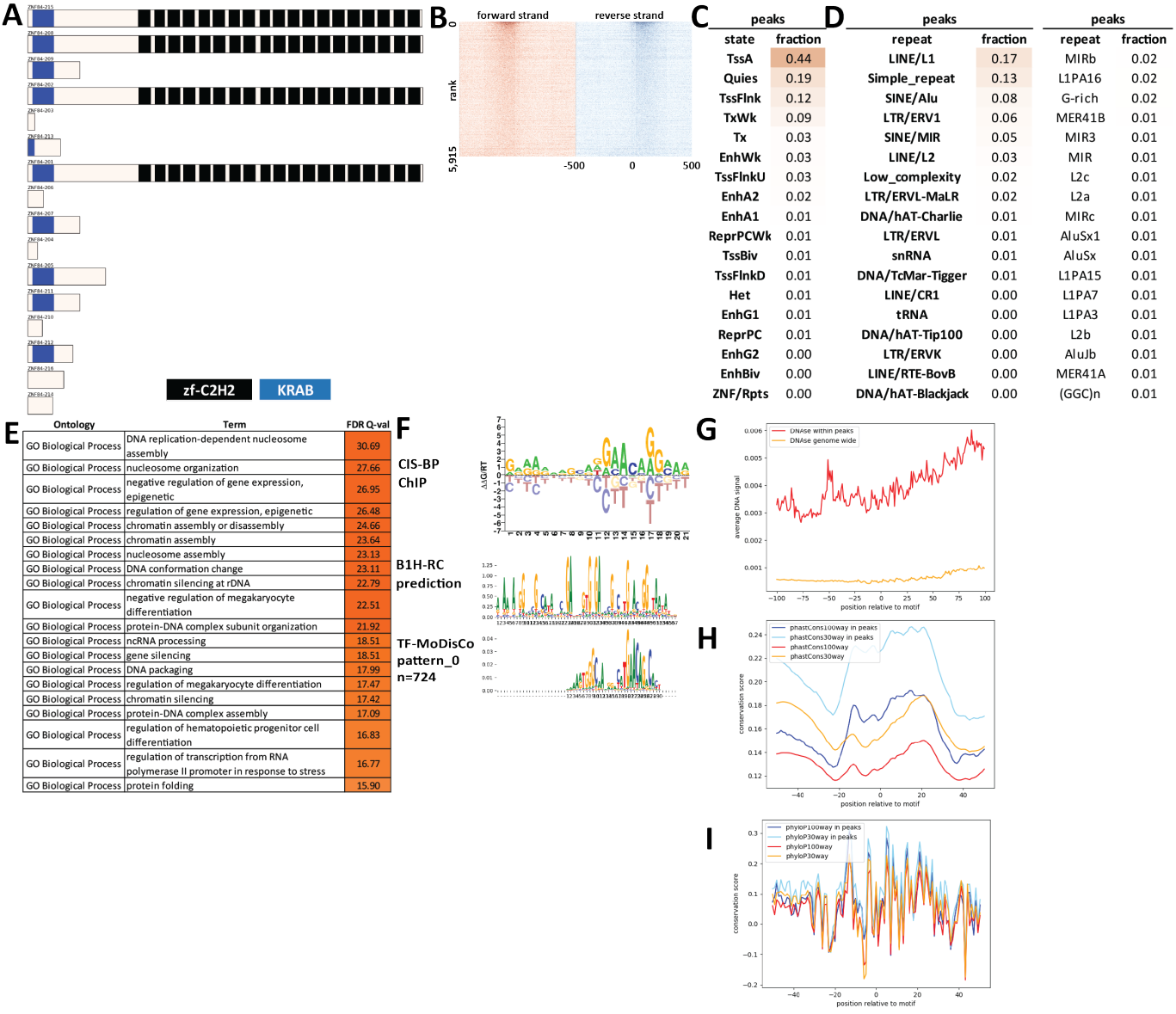

C

peaks	
state	fraction
TssA	0.44
Quies	0.19
TssFlnk	0.12
TxWk	0.09
Tx	0.03
EnhWk	0.03
TssFlnkU	0.03
EnhA2	0.02
EnhA1	0.01
ReprPCWk	0.01
TssBiv	0.01
TssFlnkD	0.01
Het	0.01
EnhG1	0.01
ReprPC	0.01
EnhG2	0.00
EnhBiv	0.00
ZNF/Rpts	0.00

D

peaks		peaks	
repeat	fraction	repeat	fraction
LINE/L1	0.17	MIRb	0.02
Simple_repeat	0.13	L1PA16	0.02
SINE/Alu	0.08	G-rich	0.02
LTR/ERV1	0.06	MER41B	0.01
SINE/MIR	0.05	MIR3	0.01
LINE/L2	0.03	MIR	0.01
Low_complexity	0.02	L2c	0.01
LTR/ERVL-MaLR	0.02	L2a	0.01
DNA/hAT-Charlie	0.01	MIRc	0.01
LTR/ERVL	0.01	AluSx1	0.01
snRNA	0.01	AluSx	0.01
DNA/TcMar-Tigger	0.01	L1PA15	0.01
LINE/CR1	0.00	L1PA7	0.01
tRNA	0.00	L1PA3	0.01
DNA/hAT-Tip100	0.00	L2b	0.01
LTR/ERVK	0.00	AluJb	0.01
LINE/RTE-BovB	0.00	MER41A	0.01
DNA/hAT-Blackjack	0.00	(GGC)n	0.01

E

Ontology	Term	FDR Q-val
GO Biological Process	DNA replication-dependent nucleosome assembly	30.69
GO Biological Process	nucleosome organization	27.66
GO Biological Process	negative regulation of gene expression, epigenetic	26.95
GO Biological Process	regulation of gene expression, epigenetic	26.48
GO Biological Process	chromatin assembly or disassembly	24.66
GO Biological Process	chromatin assembly	23.64
GO Biological Process	nucleosome assembly	23.13
GO Biological Process	DNA conformation change	23.11
GO Biological Process	chromatin silencing at rDNA	22.79
GO Biological Process	negative regulation of megakaryocyte differentiation	22.51
GO Biological Process	protein-DNA complex subunit organization	21.92
GO Biological Process	ncRNA processing	18.51
GO Biological Process	gene silencing	18.51
GO Biological Process	DNA packaging	17.99
GO Biological Process	regulation of megakaryocyte differentiation	17.47
GO Biological Process	chromatin silencing	17.42
GO Biological Process	protein-DNA complex assembly	17.09
GO Biological Process	regulation of hematopoietic progenitor cell differentiation	16.83
GO Biological Process	regulation of transcription from RNA polymerase II promoter in response to stress	16.77
GO Biological Process	protein folding	15.90

Supplementary Figure 1776: Properties and genomic distribution of motifs identified for the ZNF84 transcription factor in K562 (accession ENCSR376UMR).

TF-MoDisCO pattern_0 n=724, CWM

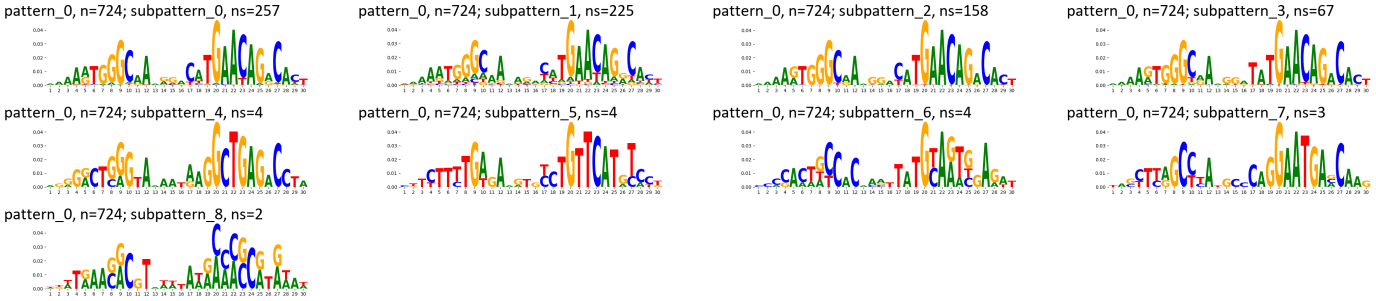

TF-MoDisCO pattern_0 n=724, PWM

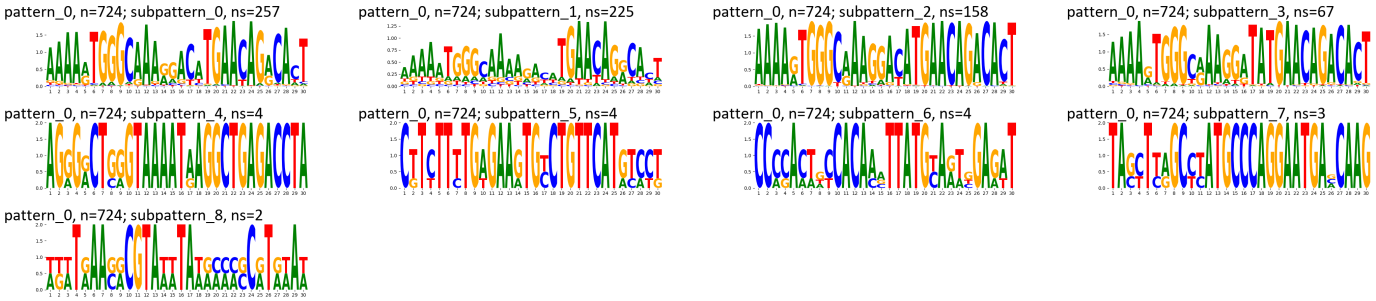

Supplementary Figure 1777: TF-MoDisCO subpatterns for the ZNF84 transcription factor in K562 (accession ENCSR376UMR).

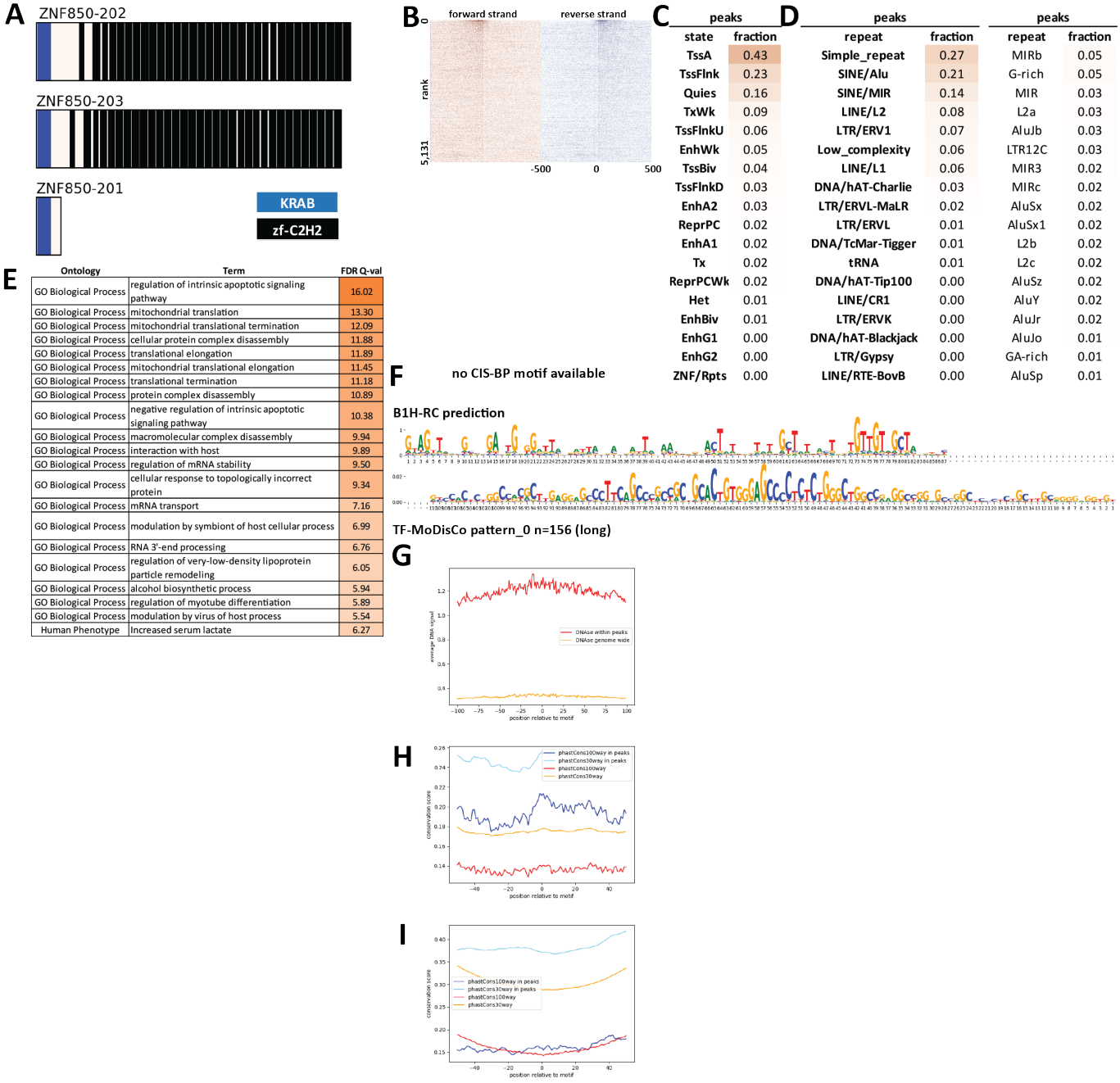

Supplementary Figure 1778: Properties and genomic distribution of motifs identified for the ZNF850 transcription factor in HepG2 (accession ENCSR756CJS).

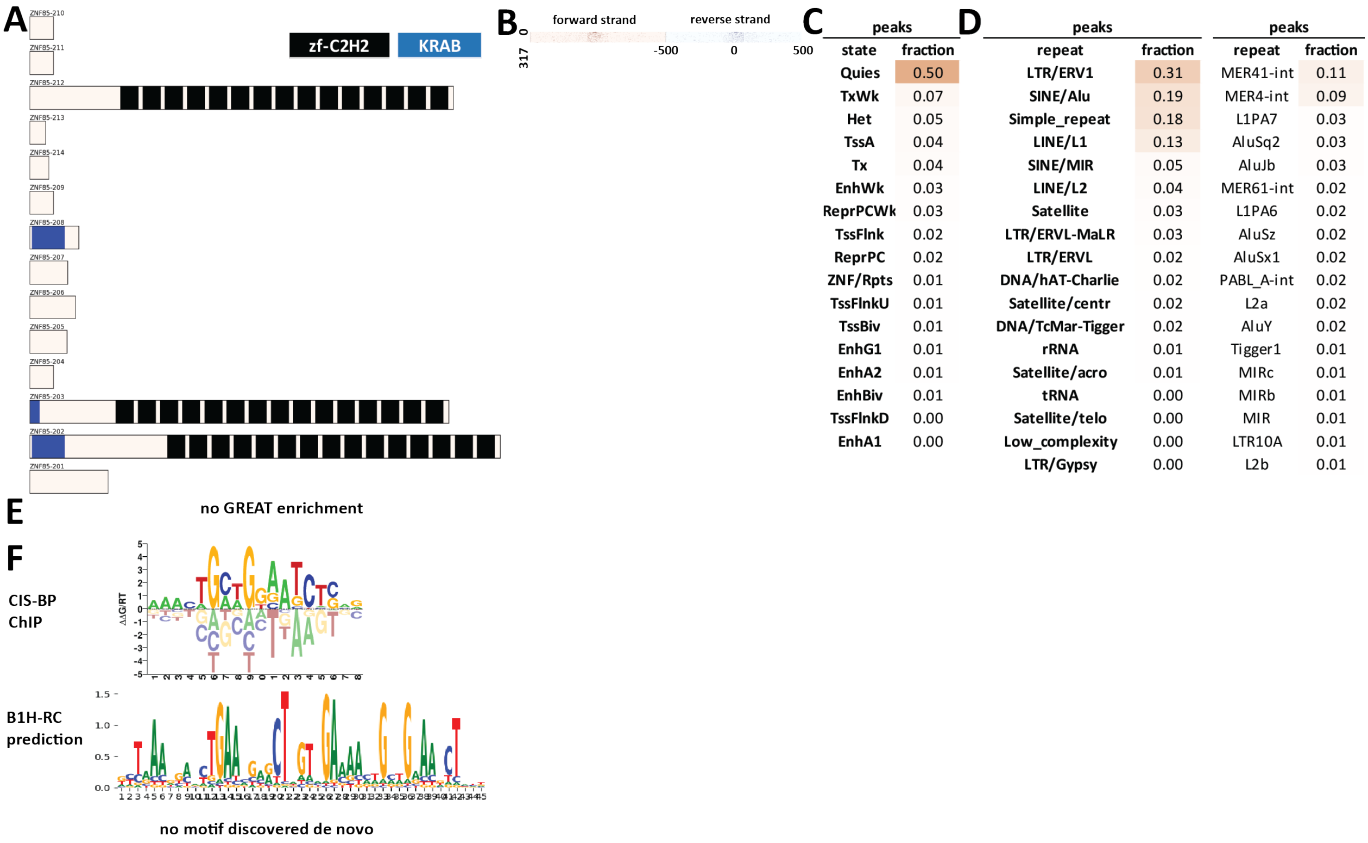

peaks	
state	fraction
Quies	0.50
TxWk	0.07
Het	0.05
TssA	0.04
Tx	0.04
EnhWk	0.03
ReprPCWk	0.03
TssFlnk	0.02
ReprPC	0.02
ZNF/Rpts	0.01
TssFlnkU	0.01
TssBiv	0.01
EnhG1	0.01
EnhA2	0.01
EnhBiv	0.01
TssFlnkD	0.00
EnhA1	0.00

peaks		peaks	
repeat	fraction	repeat	fraction
LTR/ERV1	0.31	MER41-int	0.11
SINE/Alu	0.19	MER4-int	0.09
Simple_repeat	0.18	L1PA7	0.03
LINE/L1	0.13	AluSq2	0.03
SINE/MIR	0.05	AluJb	0.03
LINE/L2	0.04	MER61-int	0.02
Satellite	0.03	L1PA6	0.02
LTR/ERVL-MaLR	0.03	AluSz	0.02
LTR/ERVL	0.02	AluSx1	0.02
DNA/hAT-Charlie	0.02	PABL_A-int	0.02
Satellite/centr	0.02	L2a	0.02
DNA/TcMar-Tigger	0.02	AluY	0.02
rRNA	0.01	Tigger1	0.01
Satellite/acro	0.01	MIRc	0.01
tRNA	0.00	MIRb	0.01
Satellite/telo	0.00	MIR	0.01
Low_complexity	0.00	LTR10A	0.01
LTR/Gypsy	0.00	L2b	0.01

Supplementary Figure 1779: Properties and genomic distribution of motifs identified for the ZNF85 transcription factor in HEK293 (accession ChipExo models).

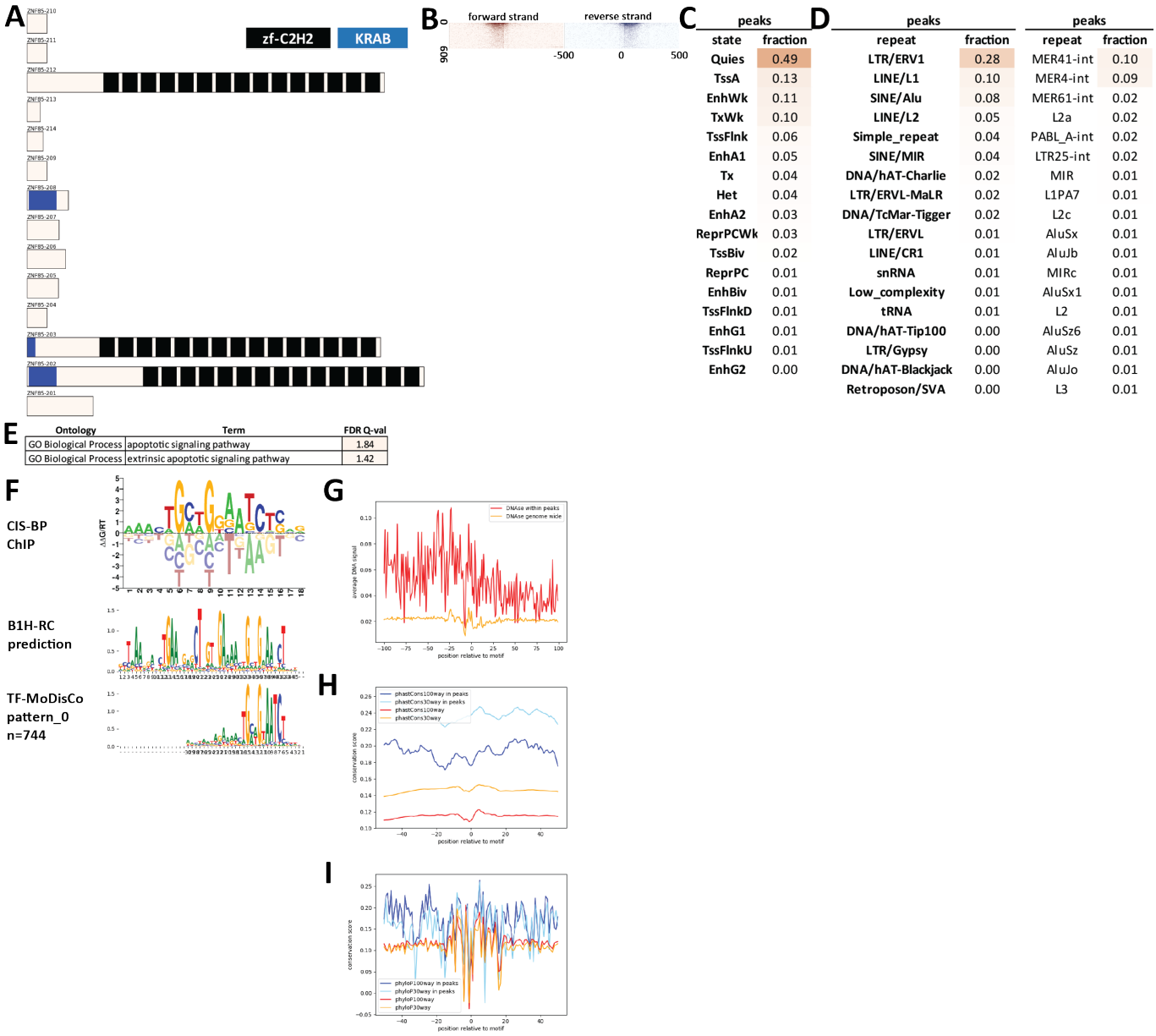

C

peaks	
state	fraction
Quies	0.49
TssA	0.13
EnhWk	0.11
TxWk	0.10
TssFlnk	0.06
EnhA1	0.05
Tx	0.04
Het	0.04
EnhA2	0.03
ReprPCWk	0.03
TssBiv	0.02
ReprPC	0.01
EnhBiv	0.01
TssFlnkD	0.01
EnhG1	0.01
TssFlnkU	0.01
EnhG2	0.00

D

peaks		peaks	
repeat	fraction	repeat	fraction
LTR/ERV1	0.28	MER41-int	0.10
LINE/L1	0.10	MER4-int	0.09
SINE/Alu	0.08	MER61-int	0.02
LINE/L2	0.05	L2a	0.02
Simple_repeat	0.04	PABL_A-int	0.02
SINE/MIR	0.04	LTR25-int	0.02
DNA/hAT-Charlie	0.02	MIR	0.01
LTR/ERVL-MaLR	0.02	L1PA7	0.01
DNA/TcMar-Tigger	0.02	L2c	0.01
LTR/ERVL	0.01	AluSx	0.01
LINE/CR1	0.01	AluJb	0.01
snRNA	0.01	MIRc	0.01
Low_complexity	0.01	AluSx1	0.01
tRNA	0.01	L2	0.01
DNA/hAT-Tip100	0.00	AluSz6	0.01
LTR/Gypsy	0.00	AluSz	0.01
DNA/hAT-Blackjack	0.00	AluJo	0.01
Retroposon/SVA	0.00	L3	0.01

E

Ontology	Term	FDR Q-val
GO Biological Process	apoptotic signaling pathway	1.84
GO Biological Process	extrinsic apoptotic signaling pathway	1.42

Supplementary Figure 1780: Properties and genomic distribution of motifs identified for the ZNF85 transcription factor in HEK293 (accession Hughes GR models).

TF-MoDisCO pattern_0 n=744, CWM

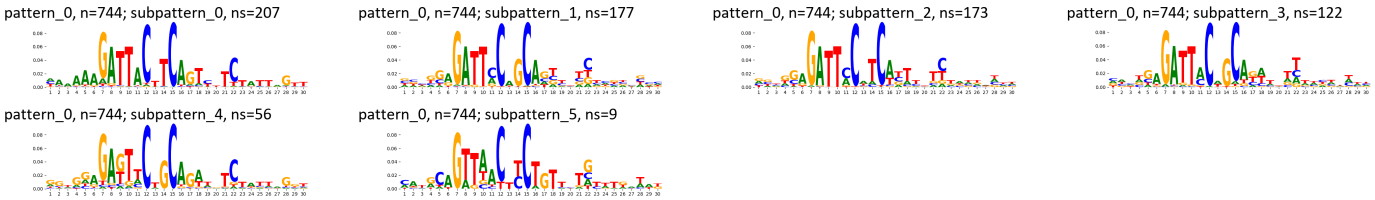

TF-MoDisCO pattern_0 n=744, PWM

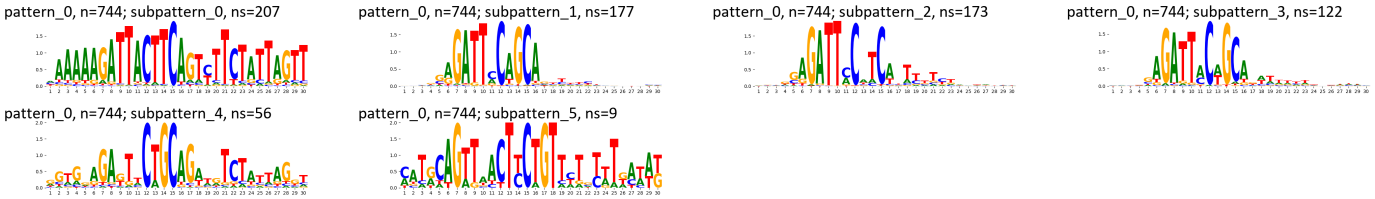

Supplementary Figure 1781: TF-MoDisCO subpatterns for the ZNF85 transcription factor in HEK293 (accession Hughes GR models).

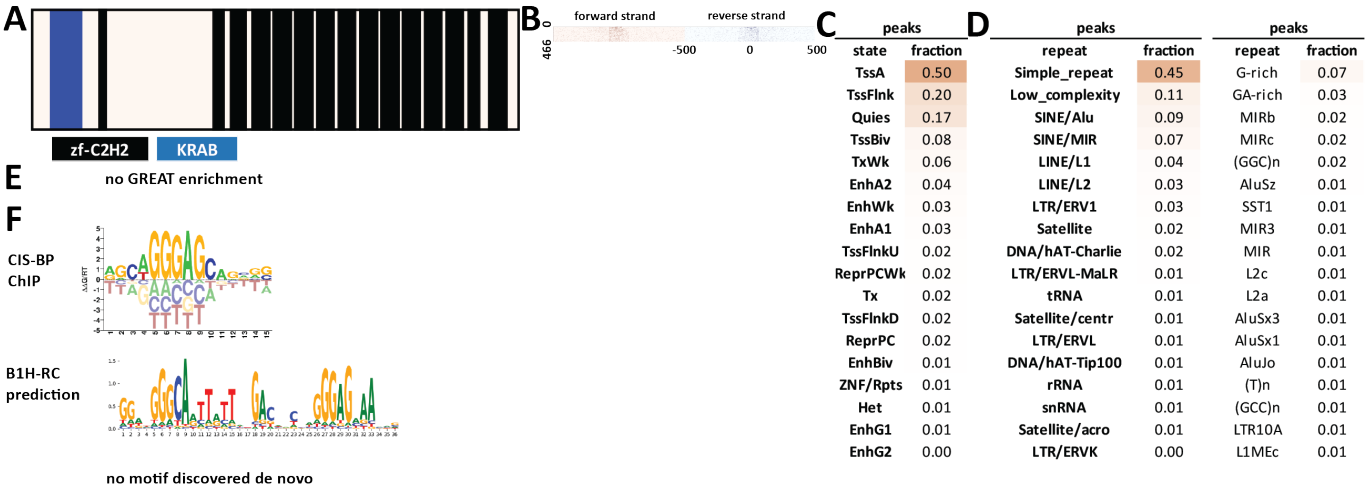

Supplementary Figure 1782: Properties and genomic distribution of motifs identified for the ZNF860 transcription factor in HEK293 (accession ChipExo models).

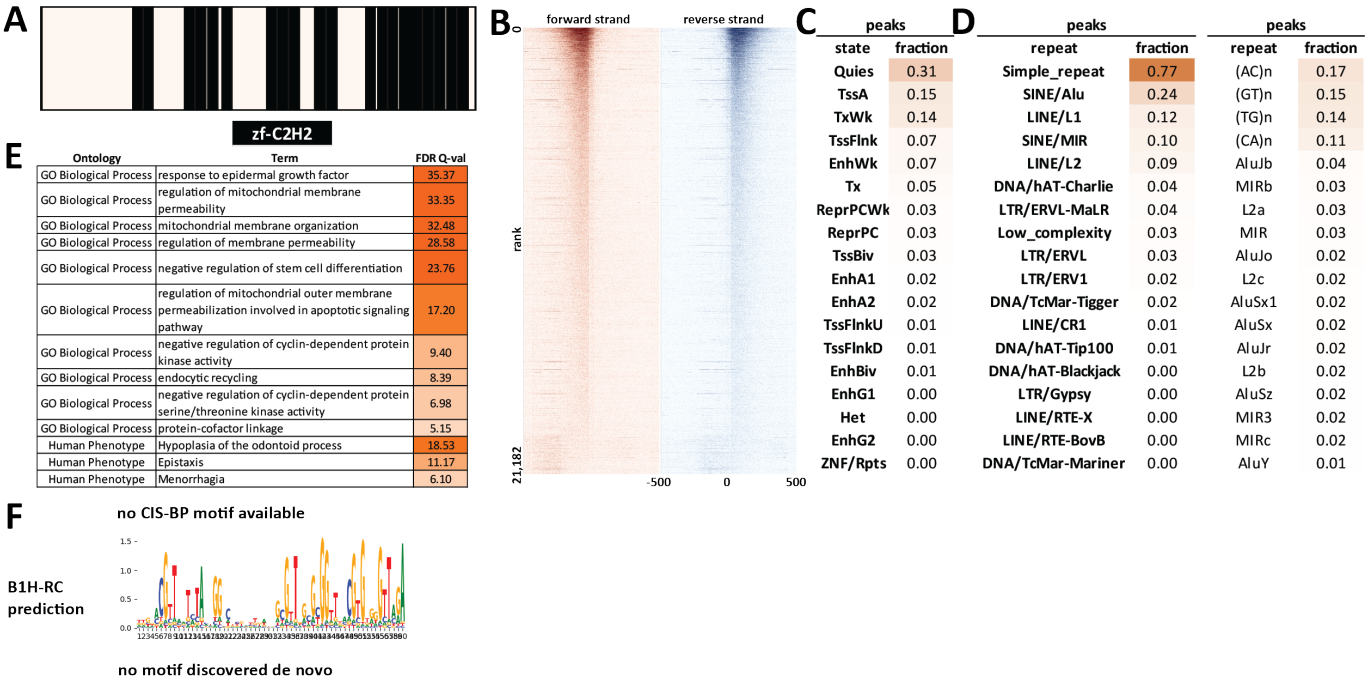

Supplementary Figure 1783: Properties and genomic distribution of motifs identified for the ZNF865 transcription factor in HepG2 (accession ENCSR891KPP).

A



B

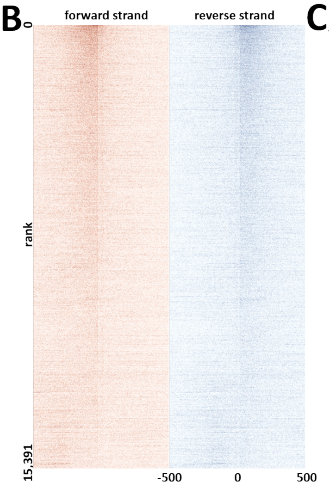

C

peaks	
state	fraction
TssA	0.27
Quies	0.21
TssFlnk	0.14
TxWk	0.11
EnhWk	0.09
EnhA1	0.04
TssFlnkU	0.04
Tx	0.03
EnhA2	0.03
TssFlnkD	0.02
TssBiv	0.02
ReprPCWk	0.02
ReprPC	0.02
EnhG1	0.01
EnhBiv	0.01
EnhG2	0.00
Het	0.00
ZNF/Rpts	0.00

D

peaks	
repeat	fraction
SINE/Alu	0.17
Simple_repeat	0.15
SINE/MIR	0.14
LINE/L2	0.09
LINE/L1	0.06
DNA/hAT-Charlie	0.04
Low_complexity	0.03
LTR/ERV1	0.03
LTR/ERVL-MaLR	0.03
LTR/ERVL	0.02
DNA/TcMar-Tigger	0.01
LINE/CR1	0.01
DNA/hAT-Tip100	0.01
tRNA	0.01
LTR/ERVK	0.00
DNA/hAT-Blackjack	0.00
LINE/RTE-BovB	0.00
LTR/Gypsy	0.00

peaks	
repeat	fraction
MIRb	0.05
MIR	0.03
L2a	0.03
MIRc	0.03
L2c	0.03
MIR3	0.03
L2b	0.02
AluJb	0.02
G-rich	0.02
AluSx	0.02
AluSx1	0.02
AluSz	0.01
AluJo	0.01
AluJr	0.01
AluY	0.01
AluSq2	0.01
GA-rich	0.01
AluSp	0.01

E

Ontology	Term	FDR Q-val
GO Biological Process	mRNA catabolic process	32.41
GO Biological Process	regulation of intrinsic apoptotic signaling pathway	30.89
GO Biological Process	nuclear-transcribed mRNA catabolic process	30.53
GO Biological Process	nuclear-transcribed mRNA catabolic process, nonsense-mediated decay	27.25
GO Biological Process	RNA phosphodiester bond hydrolysis	26.96
GO Biological Process	cellular response to epidermal growth factor stimulus	24.18
GO Biological Process	multi-organism metabolic process	23.12
GO Biological Process	response to epidermal growth factor	21.61
GO Biological Process	viral gene expression	21.20
GO Biological Process	ribonucleoprotein complex export from nucleus	19.87
GO Biological Process	liver regeneration	19.51
GO Biological Process	cytoplasmic translation	18.48
GO Biological Process	regulation of plasma lipoprotein particle levels	18.39
GO Biological Process	ribonucleoprotein complex localization	18.23
GO Biological Process	RNA phosphodiester bond hydrolysis, endonucleolytic	18.16
GO Biological Process	ncRNA transcription	17.95
GO Biological Process	regulation of mitochondrial membrane permeability	17.81
GO Biological Process	snRNA metabolic process	17.51
GO Biological Process	viral transcription	17.34
GO Biological Process	cotranslational protein targeting to membrane	17.09
Human Phenotype	Abnormality of mitochondrial metabolism	14.50
Human Phenotype	Hepatocellular carcinoma	6.08
Human Phenotype	CNS hypomyelination	4.17
Human Phenotype	Weight loss	3.37

F

no CIS-BP motif available

no B1H-RC prediction

no motif discovered de novo

Supplementary Figure 1784: Properties and genomic distribution of motifs identified for the ZNF878 transcription factor in HepG2 (accession ENCSR907PAR).

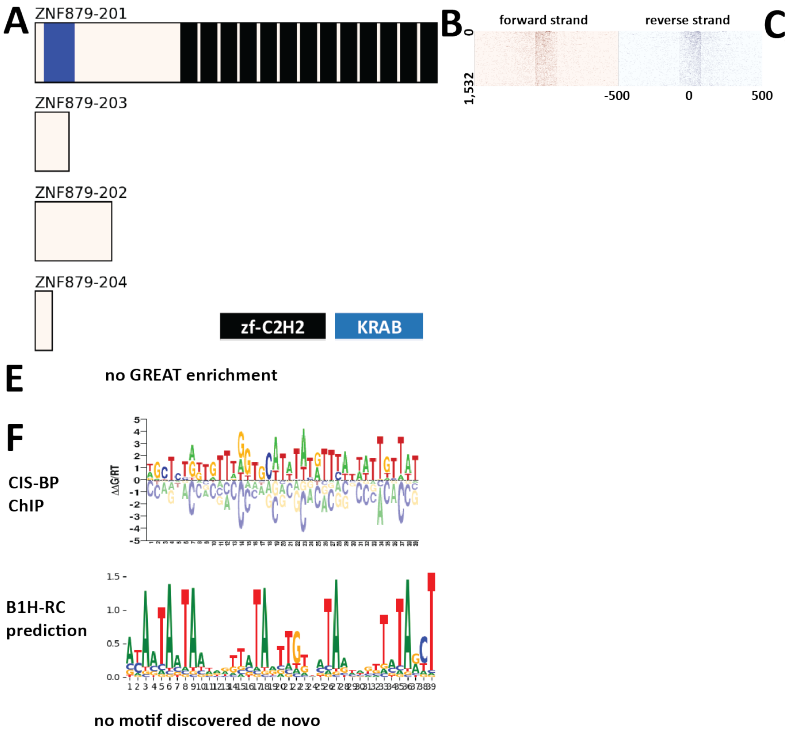

C

peaks	
state	fraction
Quies	0.54
TxWk	0.18
Tx	0.08
Het	0.05
EnhWk	0.05
ReprPCWk	0.03
TssFlnk	0.02
TssA	0.02
EnhA1	0.02
EnhA2	0.01
ReprPC	0.01
ZNF/Rpts	0.01
TssFlnkU	0.01
TssFlnkD	0.01
EnhG1	0.00
TssBiv	0.00
EnhBiv	0.00
EnhG2	0.00

D

peaks		peaks	
repeat	fraction	repeat	fraction
LINE/L1	0.64	L1M4	0.04
SINE/Alu	0.31	AluJb	0.04
Simple_repeat	0.13	L1M1	0.04
SINE/MIR	0.08	AluY	0.03
LINE/L2	0.06	L1PB1	0.03
LTR/ERVL-MaLR	0.04	MIRb	0.03
DNA/TcMar-Tigger	0.04	L1MA3	0.03
LTR/ERV1	0.03	AluJo	0.03
DNA/hAT-Charlie	0.03	L1MB7	0.03
LTR/ERVL	0.02	AluSx	0.03
Low_complexity	0.01	L1M5	0.02
Satellite	0.01	MIR	0.02
LINE/CR1	0.01	L2a	0.02
Satellite/centr	0.01	AluSz	0.02
tRNA	0.00	AluJr	0.02
snRNA	0.00	L1M2	0.02
rRNA	0.00	AluSx1	0.02
DNA/TcMar-Mariner	0.00	L1MEc	0.02

Supplementary Figure 1785: Properties and genomic distribution of motifs identified for the ZNF879 transcription factor in HEK293 (accession ChipExo models).

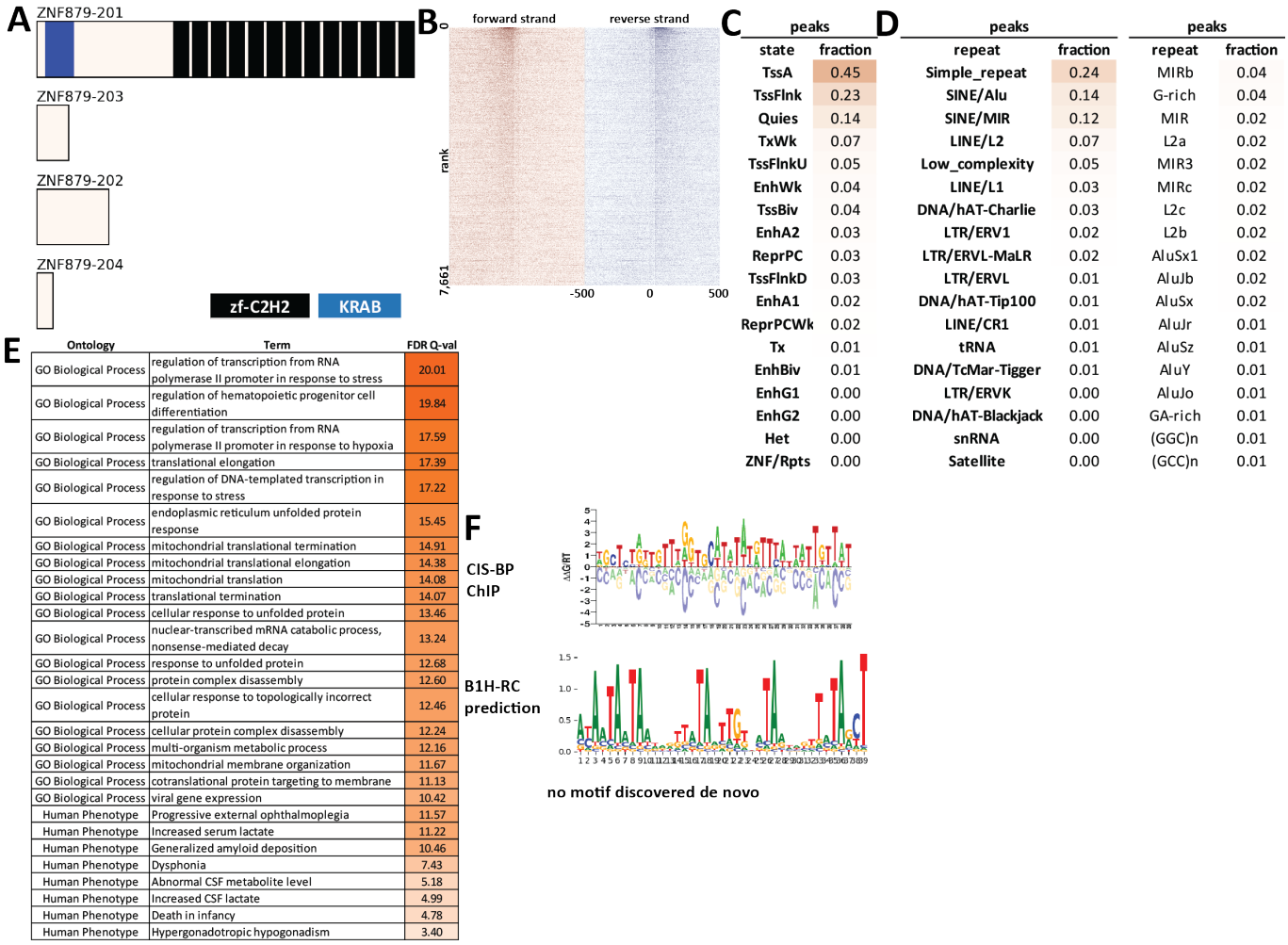

peaks	
state	fraction
TssA	0.45
TssFlnk	0.23
Quies	0.14
TxWk	0.07
TssFlnkU	0.05
EnhWk	0.04
TssBiv	0.04
EnhA2	0.03
ReprPC	0.03
TssFlnkD	0.03
EnhA1	0.02
ReprPCWk	0.02
Tx	0.01
EnhBiv	0.01
EnhG1	0.00
EnhG2	0.00
Het	0.00
ZNF/Rpts	0.00

peaks		peaks	
repeat	fraction	repeat	fraction
Simple_repeat	0.24	MIRb	0.04
SINE/Alu	0.14	G-rich	0.04
SINE/MIR	0.12	MIR	0.02
LINE/L2	0.07	L2a	0.02
Low_complexity	0.05	MIR3	0.02
LINE/L1	0.03	MIRc	0.02
DNA/hAT-Charlie	0.03	L2c	0.02
LTR/ERV1	0.02	L2b	0.02
LTR/ERVL-MaLR	0.02	AluSx1	0.02
LTR/ERVL	0.01	AluJb	0.02
DNA/hAT-Tip100	0.01	AluSx	0.02
LINE/CR1	0.01	AluJr	0.01
tRNA	0.01	AluSz	0.01
DNA/TcMar-Tigger	0.01	AluY	0.01
LTR/ERVK	0.00	AluJo	0.01
DNA/hAT-Blackjack	0.00	GA-rich	0.01
snRNA	0.00	(GGC)n	0.01
Satellite	0.00	(GCC)n	0.01

Ontology	Term	FDR Q-val
GO Biological Process	regulation of transcription from RNA polymerase II promoter in response to stress	20.01
GO Biological Process	regulation of hematopoietic progenitor cell differentiation	19.84
GO Biological Process	regulation of transcription from RNA polymerase II promoter in response to hypoxia	17.59
GO Biological Process	translational elongation	17.39
GO Biological Process	regulation of DNA-templated transcription in response to stress	17.22
GO Biological Process	endoplasmic reticulum unfolded protein response	15.45
GO Biological Process	mitochondrial translational termination	14.91
GO Biological Process	mitochondrial translational elongation	14.38
GO Biological Process	mitochondrial translation	14.08
GO Biological Process	translational termination	14.07
GO Biological Process	cellular response to unfolded protein	13.46
GO Biological Process	nuclear-transcribed mRNA catabolic process, nonsense-mediated decay	13.24
GO Biological Process	response to unfolded protein	12.68
GO Biological Process	protein complex disassembly	12.60
GO Biological Process	cellular response to topologically incorrect protein	12.46
GO Biological Process	cellular protein complex disassembly	12.24
GO Biological Process	multi-organism metabolic process	12.16
GO Biological Process	mitochondrial membrane organization	11.67
GO Biological Process	cotranslational protein targeting to membrane	11.13
GO Biological Process	viral gene expression	10.42
Human Phenotype	Progressive external ophthalmoplegia	11.57
Human Phenotype	Increased serum lactate	11.22
Human Phenotype	Generalized amyloid deposition	10.46
Human Phenotype	Dysphonia	7.43
Human Phenotype	Abnormal CSF metabolite level	5.18
Human Phenotype	Increased CSF lactate	4.99
Human Phenotype	Death in infancy	4.78
Human Phenotype	Hypergonadotropic hypogonadism	3.40

Supplementary Figure 1786: Properties and genomic distribution of motifs identified for the ZNF879 transcription factor in HepG2 (accession ENCSR073OBD).

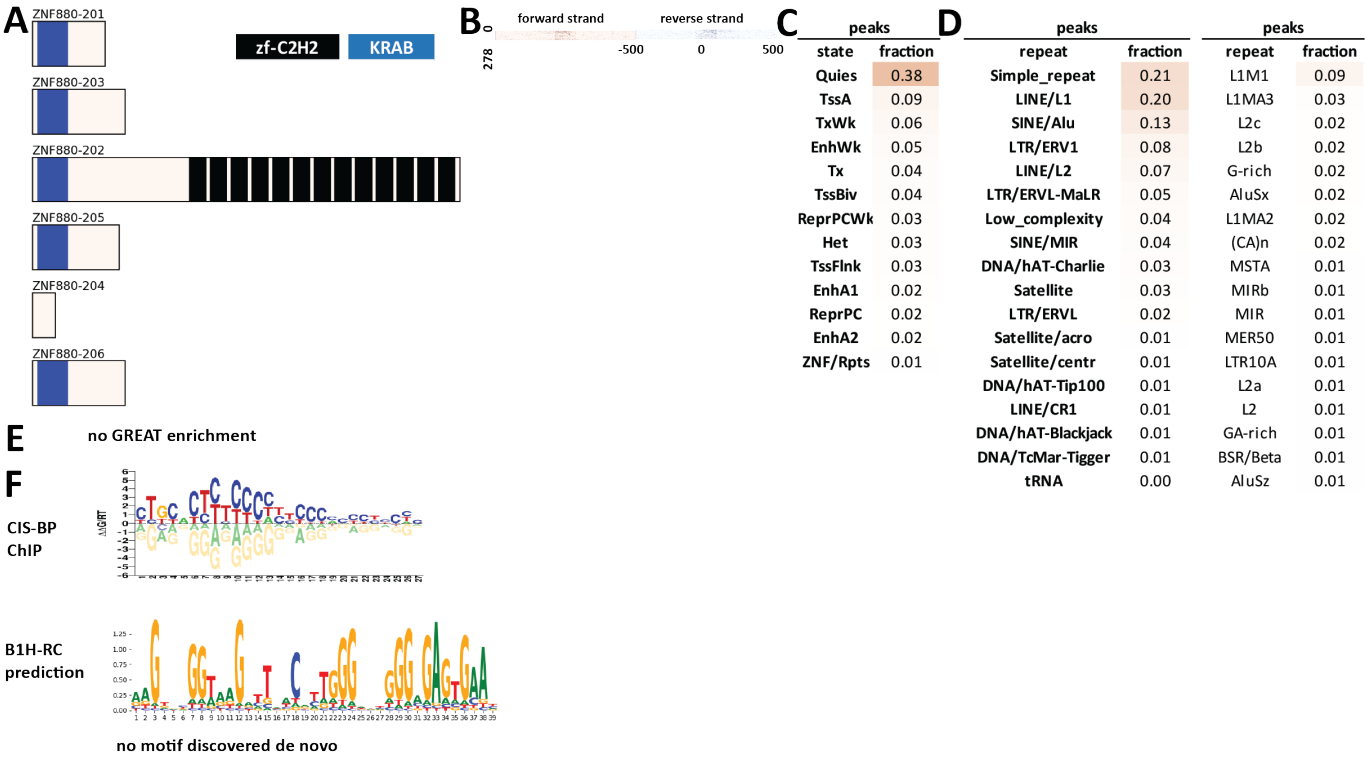

C peaks	
state	fraction
Quies	0.38
TssA	0.09
TxWk	0.06
EnhWk	0.05
Tx	0.04
TssBiv	0.04
ReprPCWk	0.03
Het	0.03
TssFlnk	0.03
EnhA1	0.02
ReprPC	0.02
EnhA2	0.02
ZNF/Rpts	0.01

D peaks		peaks	
repeat	fraction	repeat	fraction
Simple_repeat	0.21	L1M1	0.09
LINE/L1	0.20	L1MA3	0.03
SINE/Alu	0.13	L2c	0.02
LTR/ERV1	0.08	L2b	0.02
LINE/L2	0.07	G-rich	0.02
LTR/ERVL-MaLR	0.05	AluSx	0.02
Low_complexity	0.04	L1MA2	0.02
SINE/MIR	0.04	(CA)n	0.02
DNA/hAT-Charlie	0.03	MSTA	0.01
Satellite	0.03	MIRb	0.01
LTR/ERVL	0.02	MIR	0.01
Satellite/acro	0.01	MER50	0.01
Satellite/centr	0.01	LTR10A	0.01
DNA/hAT-Tip100	0.01	L2a	0.01
LINE/CR1	0.01	L2	0.01
DNA/hAT-Blackjack	0.01	GA-rich	0.01
DNA/TcMar-Tigger	0.01	BSR/Beta	0.01
tRNA	0.00	AluSz	0.01

Supplementary Figure 1787: Properties and genomic distribution of motifs identified for the ZNF880 transcription factor in HEK293 (accession ChipExo models).

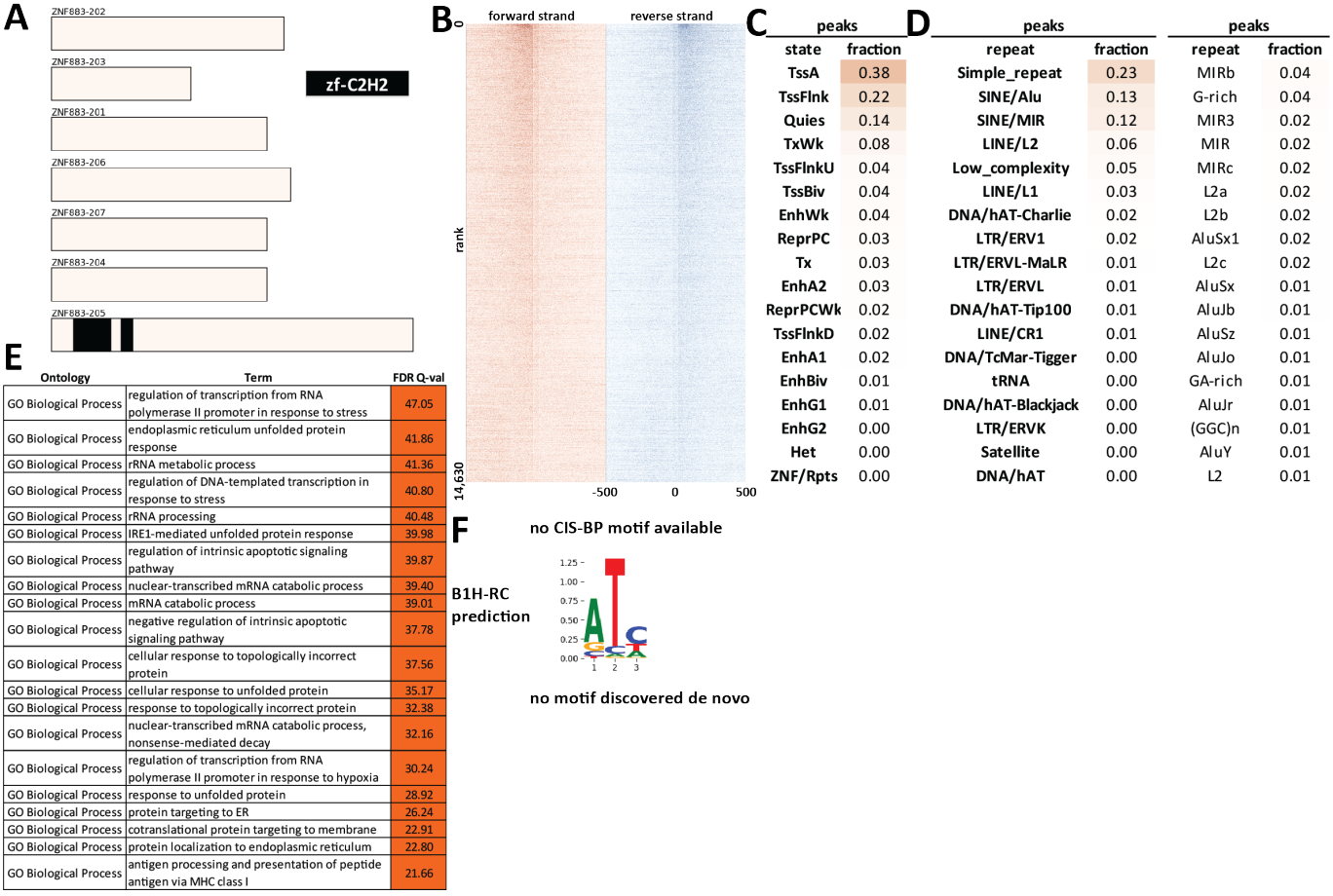

C

peaks	
state	fraction
TssA	0.38
TssFlnk	0.22
Quies	0.14
TxWk	0.08
TssFlnkU	0.04
TssBiv	0.04
EnhWk	0.04
ReprPC	0.03
Tx	0.03
EnhA2	0.03
ReprPCWk	0.02
TssFlnkD	0.02
EnhA1	0.02
EnhBiv	0.01
EnhG1	0.01
EnhG2	0.00
Het	0.00
ZNF/Rpts	0.00

D

peaks		peaks	
repeat	fraction	repeat	fraction
Simple_repeat	0.23	MIRb	0.04
SINE/Alu	0.13	G-rich	0.04
SINE/MIR	0.12	MIR3	0.02
LINE/L2	0.06	MIR	0.02
Low_complexity	0.05	MIRc	0.02
LINE/L1	0.03	L2a	0.02
DNA/hAT-Charlie	0.02	L2b	0.02
LTR/ERV1	0.02	AluSx1	0.02
LTR/ERVL-MaLR	0.01	L2c	0.02
LTR/ERVL	0.01	AluSx	0.01
DNA/hAT-Tip100	0.01	AluJb	0.01
LINE/CR1	0.01	AluSz	0.01
DNA/TcMar-Tigger	0.00	AluJo	0.01
tRNA	0.00	GA-rich	0.01
DNA/hAT-Blackjack	0.00	AluJr	0.01
LTR/ERVK	0.00	(GGC)n	0.01
Satellite	0.00	AluY	0.01
DNA/hAT	0.00	L2	0.01

E

Ontology	Term	FDR Q-val
GO Biological Process	regulation of transcription from RNA polymerase II promoter in response to stress	47.05
GO Biological Process	endoplasmic reticulum unfolded protein response	41.86
GO Biological Process	rRNA metabolic process	41.36
GO Biological Process	regulation of DNA-templated transcription in response to stress	40.80
GO Biological Process	rRNA processing	40.48
GO Biological Process	IRE1-mediated unfolded protein response	39.98
GO Biological Process	regulation of intrinsic apoptotic signaling pathway	39.87
GO Biological Process	nuclear-transcribed mRNA catabolic process	39.40
GO Biological Process	mRNA catabolic process	39.01
GO Biological Process	negative regulation of intrinsic apoptotic signaling pathway	37.78
GO Biological Process	cellular response to topologically incorrect protein	37.56
GO Biological Process	cellular response to unfolded protein	35.17
GO Biological Process	response to topologically incorrect protein	32.38
GO Biological Process	nuclear-transcribed mRNA catabolic process, nonsense-mediated decay	32.16
GO Biological Process	regulation of transcription from RNA polymerase II promoter in response to hypoxia	30.24
GO Biological Process	response to unfolded protein	28.92
GO Biological Process	protein targeting to ER	26.24
GO Biological Process	cotranslational protein targeting to membrane	22.91
GO Biological Process	protein localization to endoplasmic reticulum	22.80
GO Biological Process	antigen processing and presentation of peptide antigen via MHC class I	21.66

Supplementary Figure 1788: Properties and genomic distribution of motifs identified for the ZNF883 transcription factor in HepG2 (accession ENCSR882YYL).

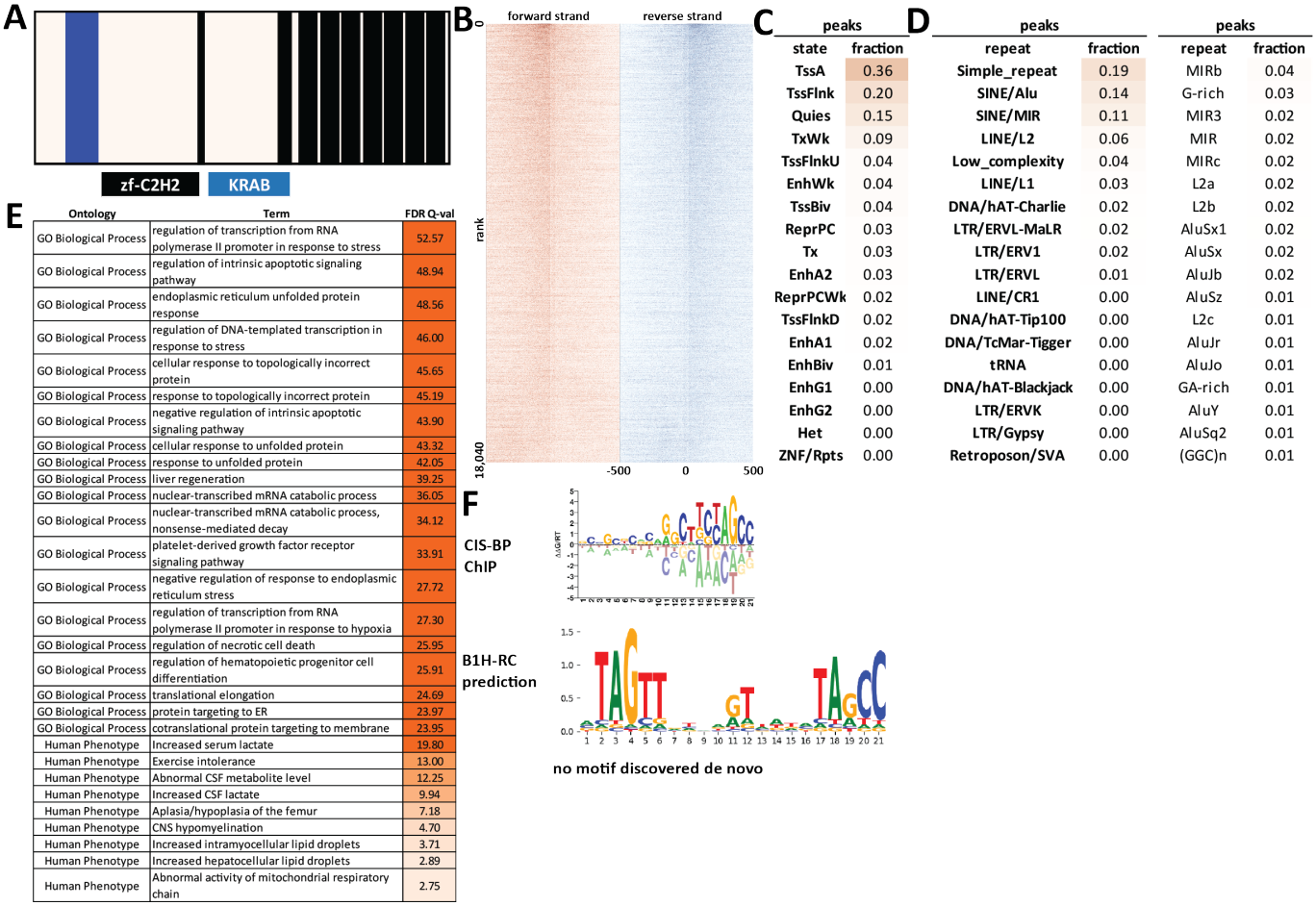

Supplementary Figure 1789: Properties and genomic distribution of motifs identified for the ZNF891 transcription factor in HepG2 (accession ENCSR020CLV).

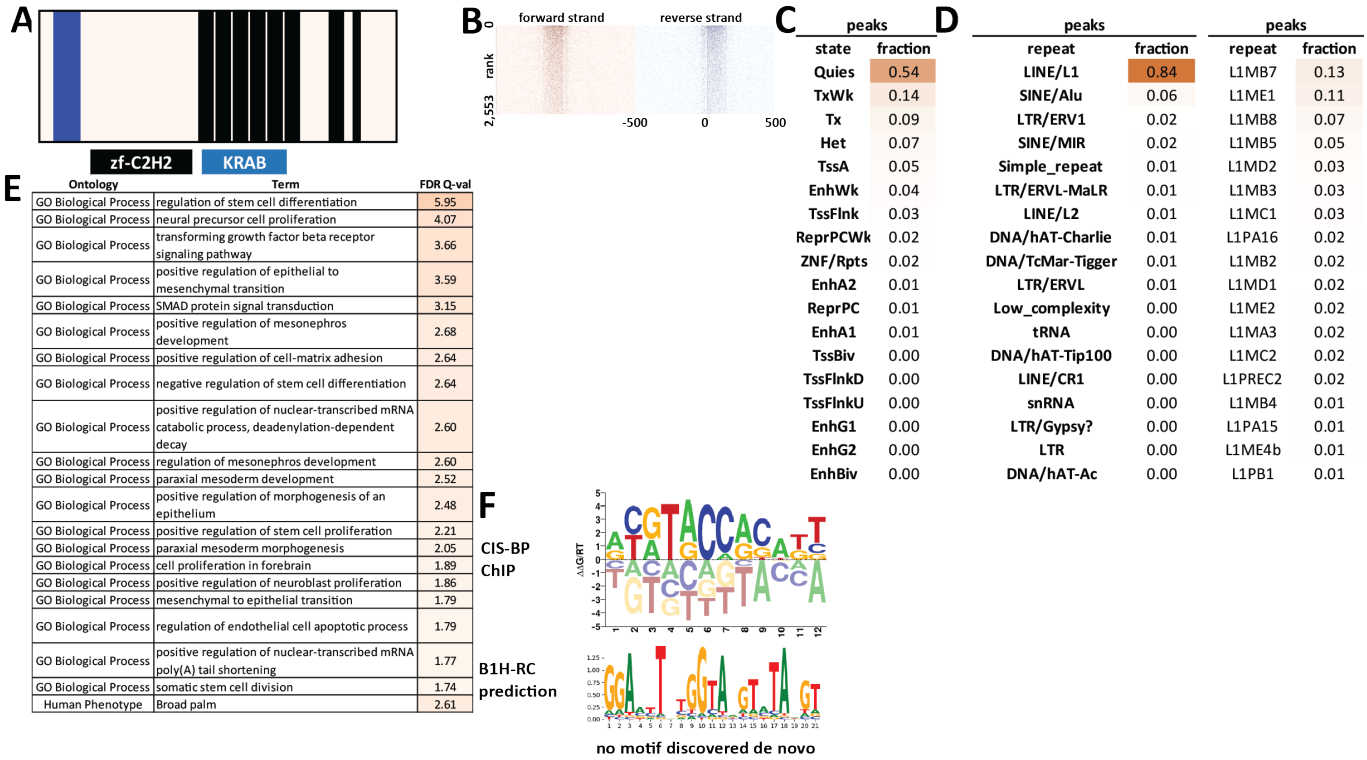

Supplementary Figure 1790: Properties and genomic distribution of motifs identified for the ZNF8 transcription factor in HEK293 (accession Hughes GR models).

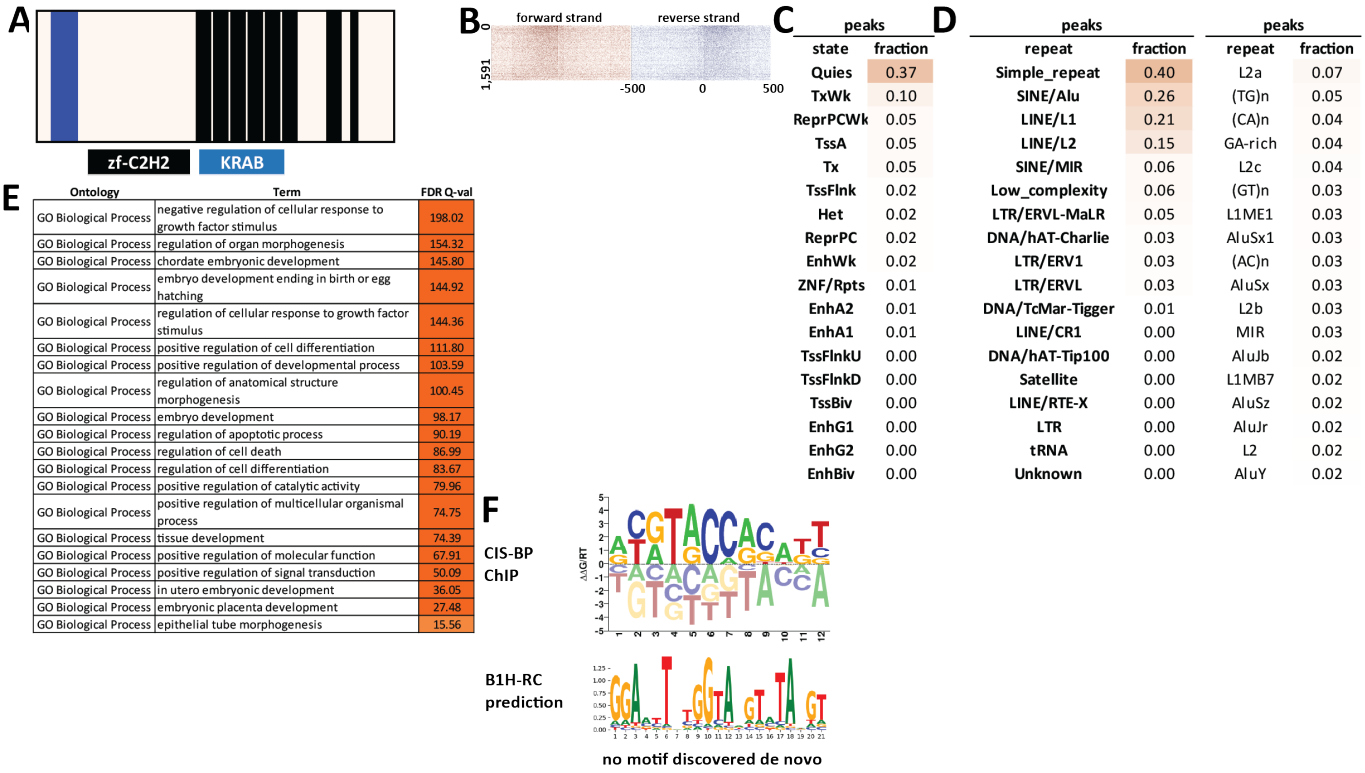

Supplementary Figure 1791: Properties and genomic distribution of motifs identified for the ZNF8 transcription factor in MCF-7 (accession ENCSR785UCD).

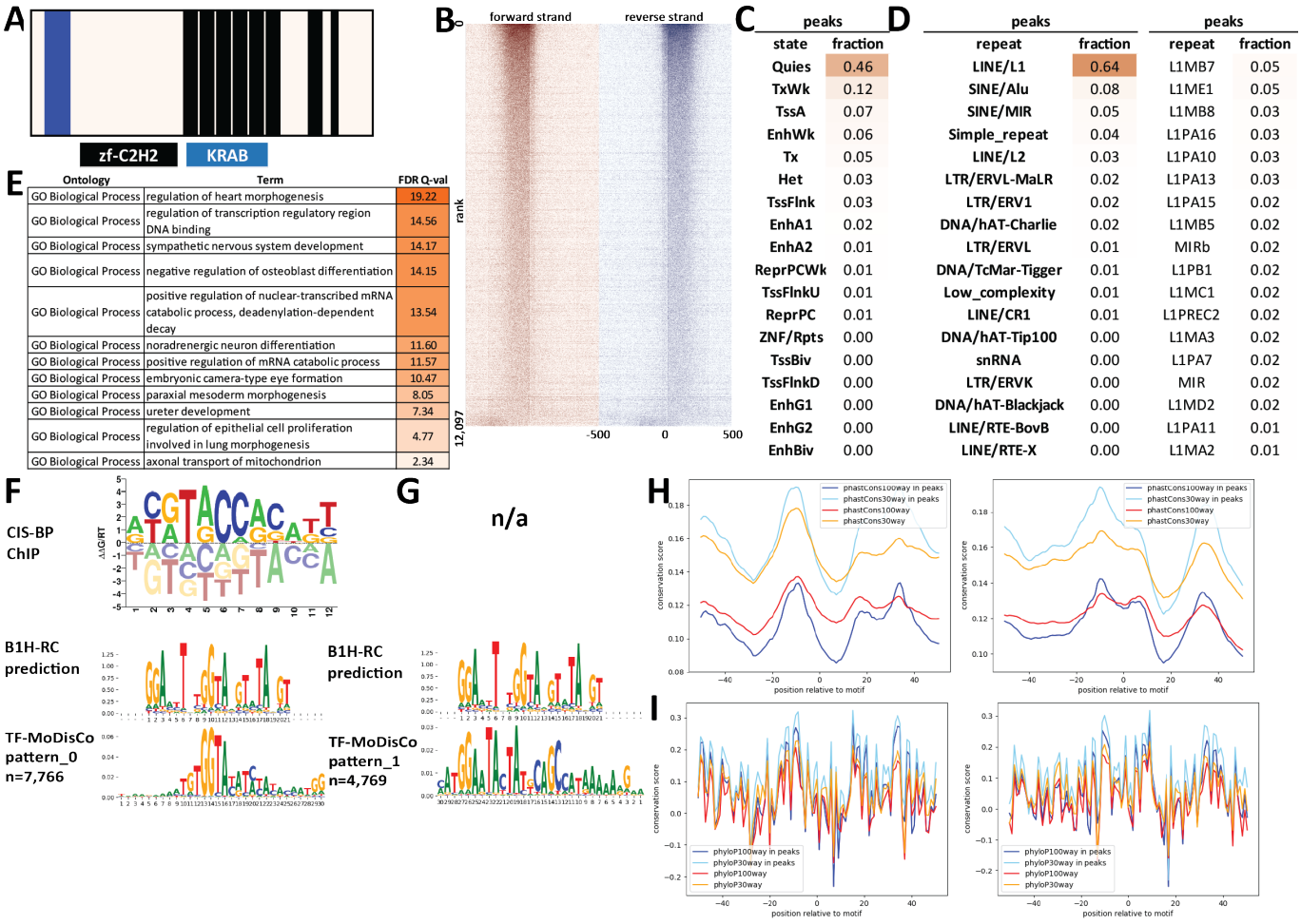

Supplementary Figure 1792: Properties and genomic distribution of motifs identified for the ZNF8 transcription factor in SK-N-SH (accession ENCSR325QLX).

TF-MoDisCO pattern_0 n=7766, CWM

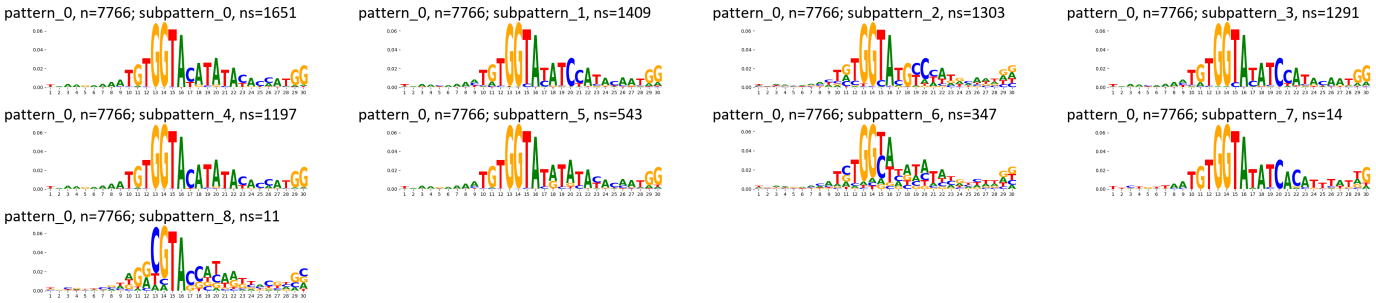

TF-MoDisCO pattern_0 n=7766, PWM

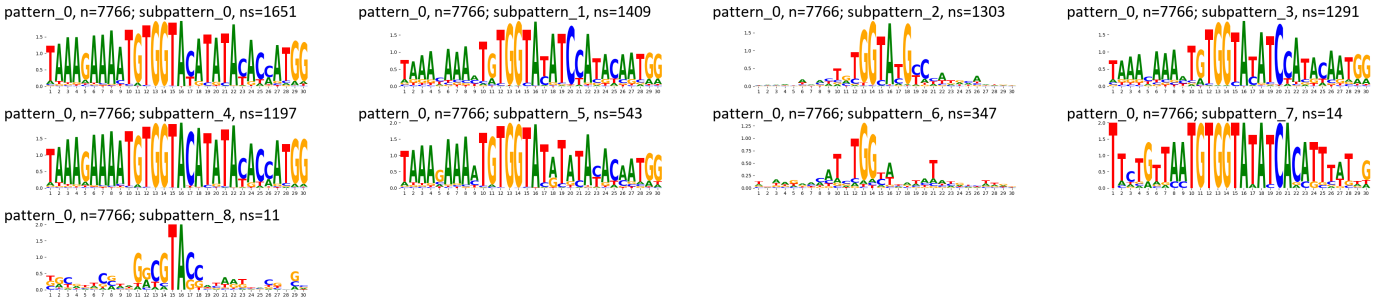

TF-MoDisCO pattern_1 n=4769, CWM

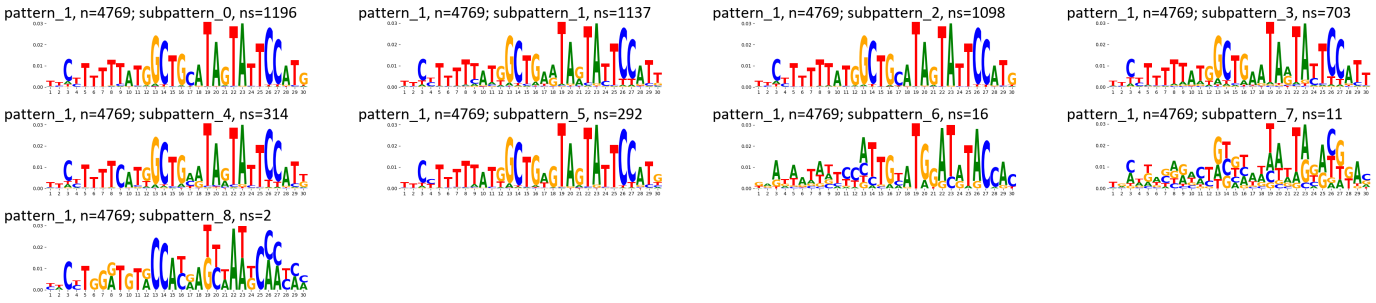

TF-MoDisCO pattern_1 n=4769, PWM

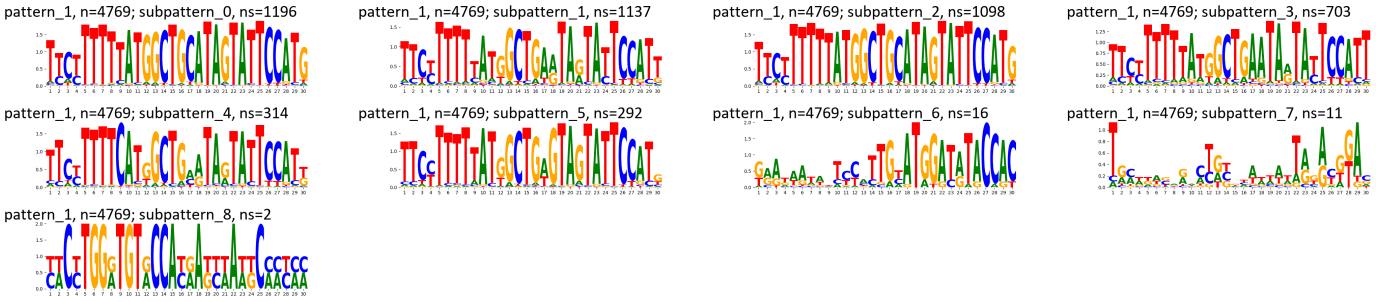

Supplementary Figure 1793: TF-MoDisCO subpatterns for the ZNF8 transcription factor in SK-N-SH (accession ENCSR325QLX).

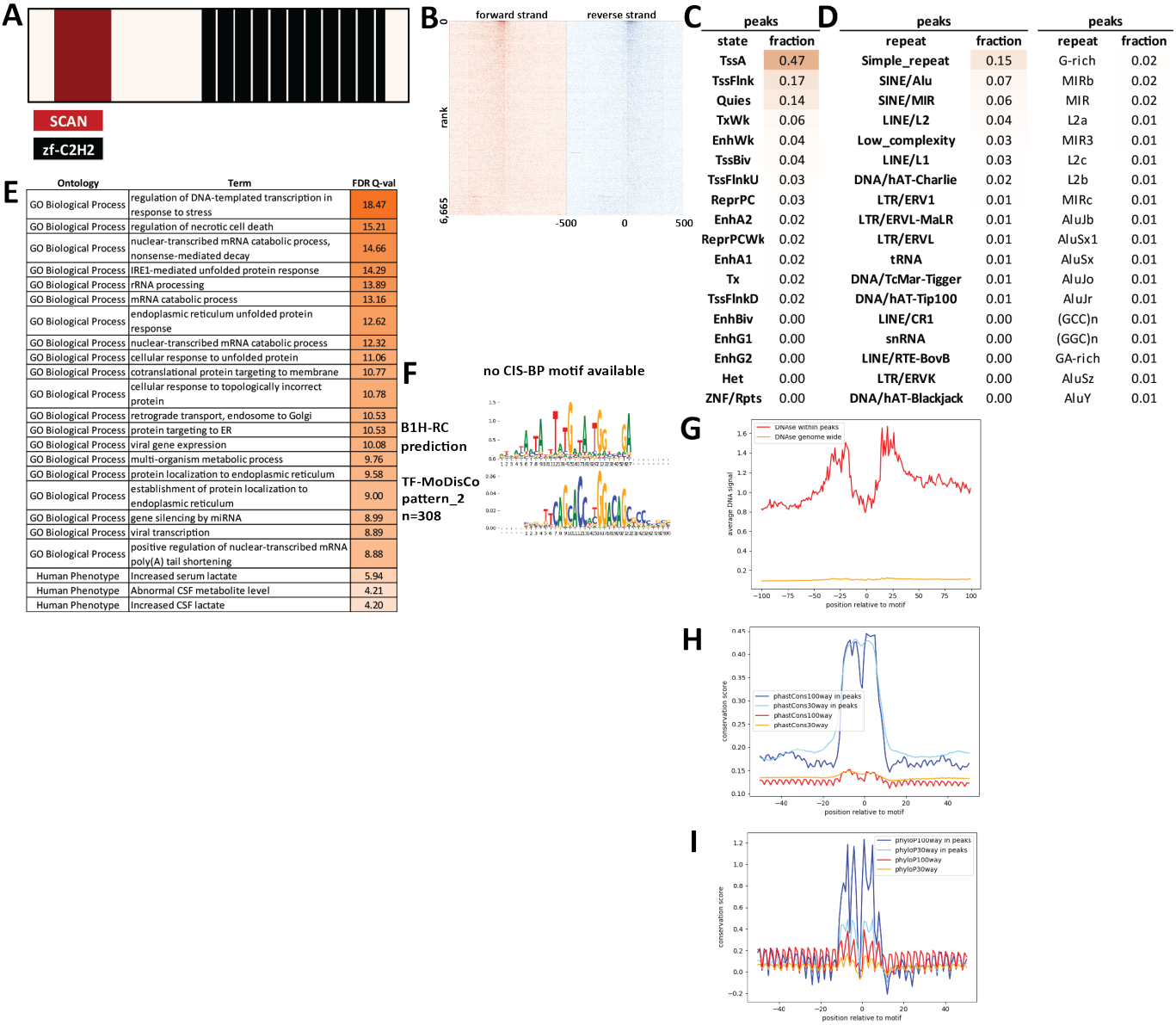

Supplementary Figure 1794: Properties and genomic distribution of motifs identified for the ZSCAN12 transcription factor in HepG2 (accession ENCSR574YRZ).

TF-MoDisCO pattern_2 n=308, CWM

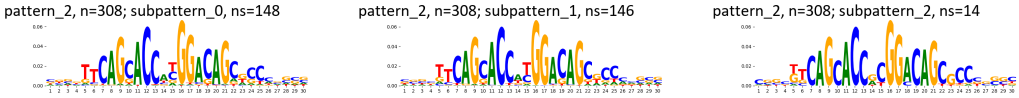

TF-MoDisCO pattern_2 n=308, PWM

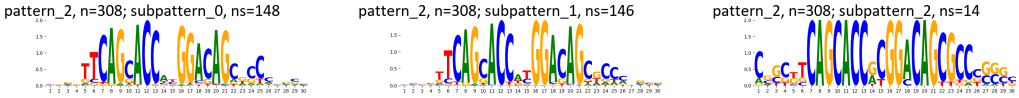

Supplementary Figure 1795: TF-MoDisCO subpatterns for the ZSCAN12 transcription factor in HepG2 (accession ENCSR574YRZ).

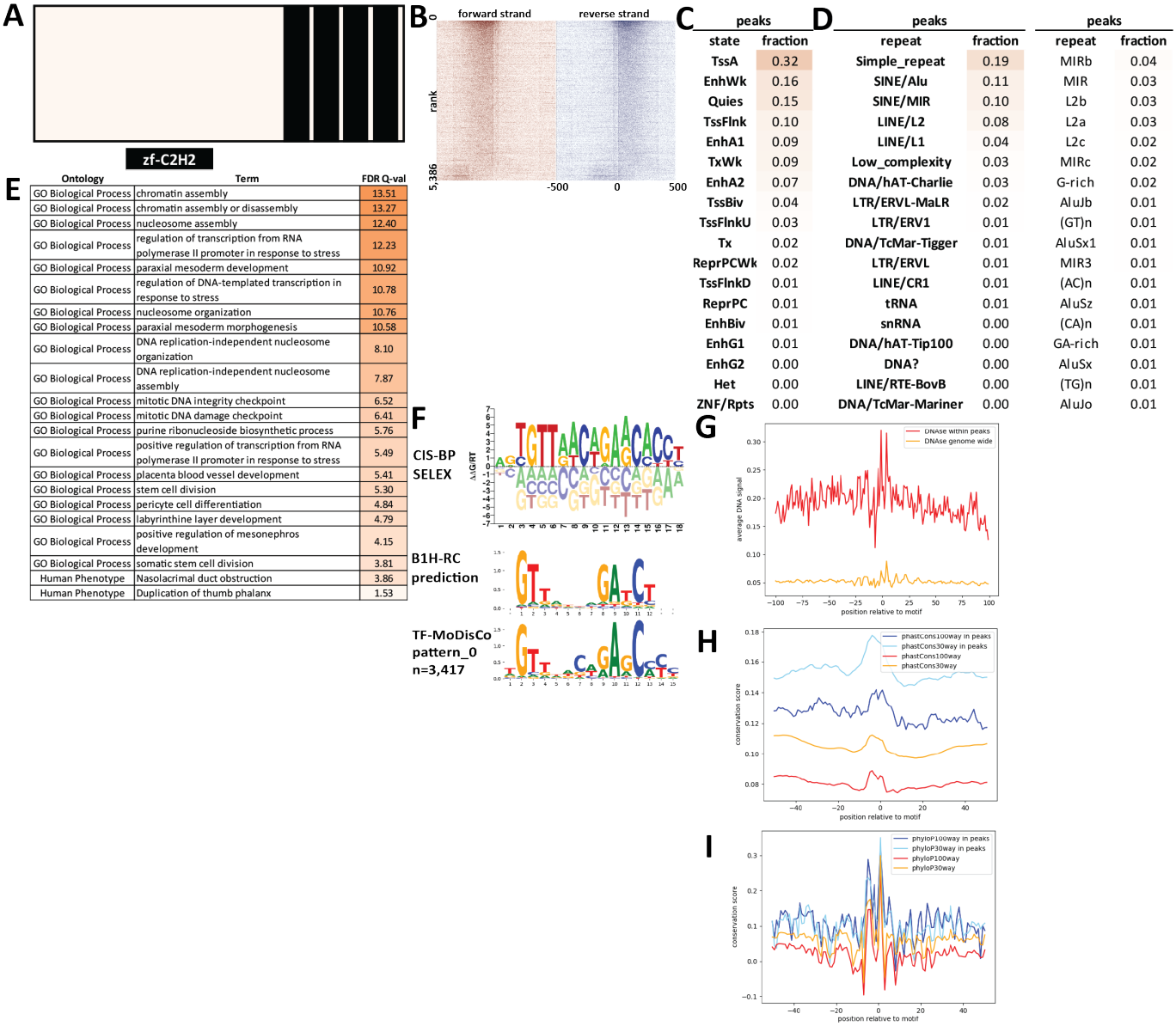

Supplementary Figure 1796: Properties and genomic distribution of motifs identified for the ZSCAN16 transcription factor in HEK293 (accession ENCSR864VJE).

TF-MoDisCO pattern_0 n=3417, CWM

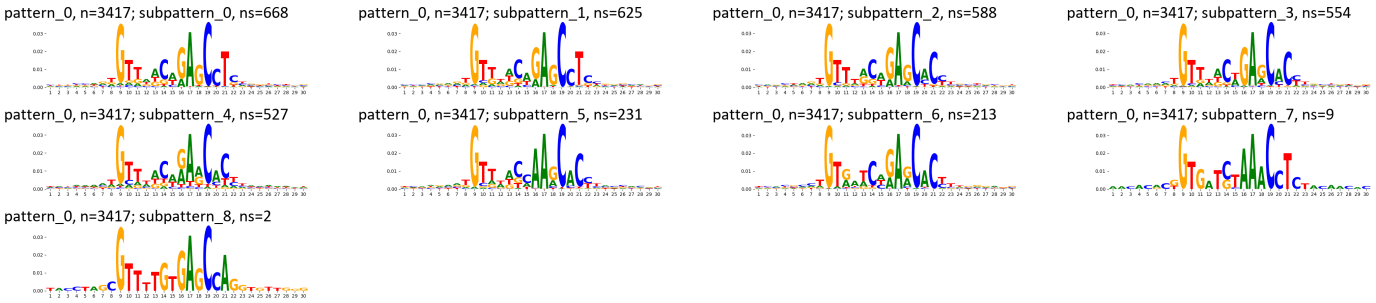

TF-MoDisCO pattern_0 n=3417, PWM

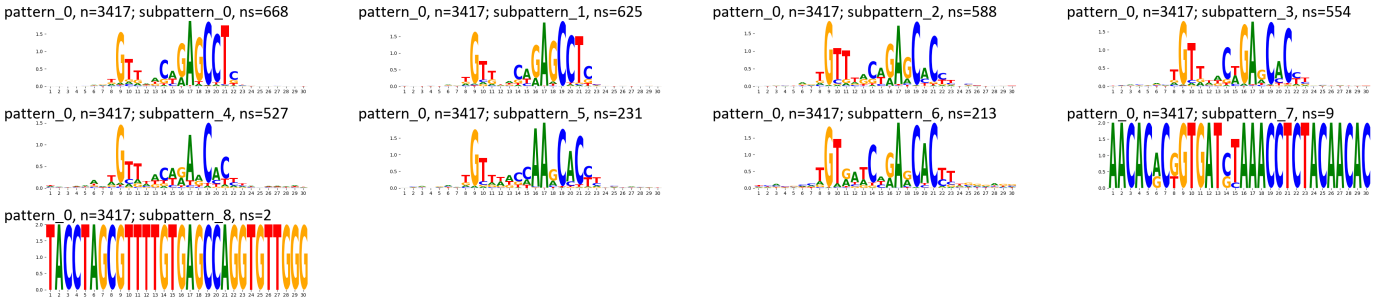

Supplementary Figure 1797: TF-MoDisCO subpatterns for the ZSCAN16 transcription factor in HEK293 (accession ENCSR864VJE).

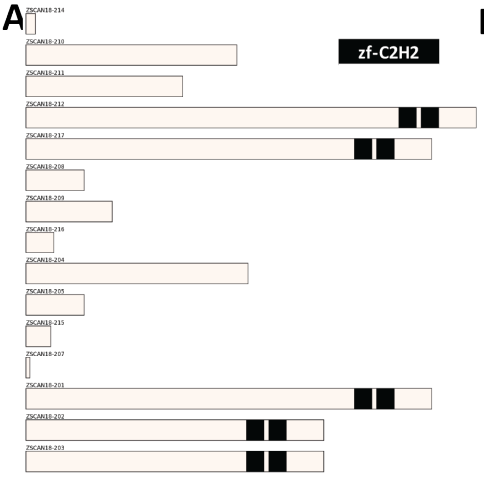

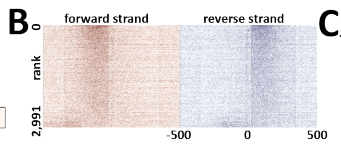

C

peaks	
state	fraction
TssA	0.47
TssFlnk	0.18
Quies	0.12
EnhWk	0.09
EnhA1	0.07
EnhA2	0.07
TxWk	0.05
TssBiv	0.04
TssFlnkU	0.04
TssFlnkD	0.02
ReprPCWk	0.02
ReprPC	0.02
EnhBiv	0.01
EnhG1	0.00
Tx	0.00
Het	0.00
EnhG2	0.00
ZNF/Rpts	0.00

D

peaks		peaks	
repeat	fraction	repeat	fraction
Simple_repeat	0.39	(GT)n	0.06
SINE/Alu	0.10	(AC)n	0.04
Low_complexity	0.05	(CA)n	0.04
SINE/MIR	0.05	(TG)n	0.04
tRNA	0.04	GA-rich	0.03
LINE/L2	0.04	G-rich	0.02
LINE/L1	0.03	MIRb	0.02
LTR/ERVL-MaLR	0.01	L2a	0.02
DNA/hAT-Charlie	0.01	MIR	0.01
LTR/ERVL	0.01	(TC)n	0.01
LTR/ERV1	0.01	AluSx1	0.01
DNA/TcMar-Tigger	0.01	AluSx	0.01
snRNA	0.00	MIRc	0.01
LINE/CR1	0.00	(T)n	0.01
DNA/hAT-Tip100	0.00	(CT)n	0.01
LTR/Gypsy	0.00	(GA)n	0.01
Retroposon/SVA	0.00	L2c	0.01
DNA/hAT-Blackjack	0.00	L2b	0.01

E

Ontology	Term	FDR Q-val
GO Biological Process	regulation of transcription from RNA polymerase II promoter in response to stress	13.03
GO Biological Process	nuclear-transcribed mRNA catabolic process, nonsense-mediated decay	12.78
GO Biological Process	ncRNA processing	11.91
GO Biological Process	regulation of DNA-templated transcription in response to stress	11.57
GO Biological Process	protein folding	9.34
GO Biological Process	nuclear-transcribed mRNA catabolic process	9.19
GO Biological Process	ribosome biogenesis	9.16
GO Biological Process	rRNA metabolic process	9.04
GO Biological Process	rRNA processing	9.02
GO Biological Process	translational elongation	8.27
GO Biological Process	viral gene expression	8.17
GO Biological Process	regulation of transcription from RNA polymerase II promoter in response to hypoxia	8.05
GO Biological Process	mRNA catabolic process	7.99
GO Biological Process	viral transcription	7.89
GO Biological Process	regulation of signal transduction by p53 class mediator	7.65
GO Biological Process	SRP-dependent cotranslational protein targeting to membrane	7.55
GO Biological Process	mitochondrial translational termination	7.47
GO Biological Process	cotranslational protein targeting to membrane	7.27
GO Biological Process	protein localization to endoplasmic reticulum	7.00
GO Biological Process	regulation of intrinsic apoptotic signaling pathway	6.87
Human Phenotype	Lipomatous tumor	2.51
Human Phenotype	Abnormality of reticulocytes	2.45
Human Phenotype	Abnormality of the pylorus	2.25
Human Phenotype	Abnormality of adipose tissue	1.96

F

no CIS-BP motif available

B1H-RC prediction

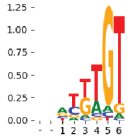

no motif discovered de novo

Supplementary Figure 1798: Properties and genomic distribution of motifs identified for the ZSCAN18 transcription factor in HEK293 (accession ENCSR721QZV).

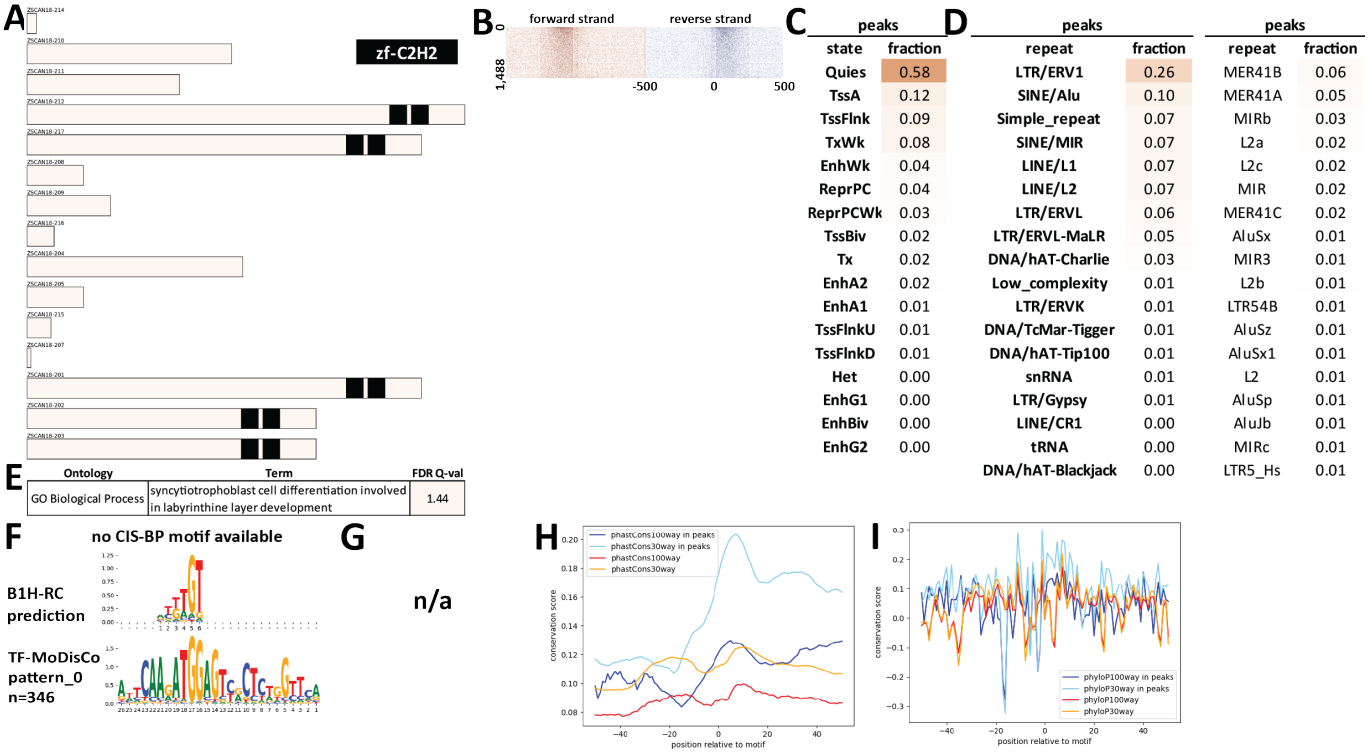

Supplementary Figure 1799: Properties and genomic distribution of motifs identified for the ZSCAN18 transcription factor in WTC11 (accession ENCSR499FDW).

TF-MoDisCO pattern_0 n=346, CWM

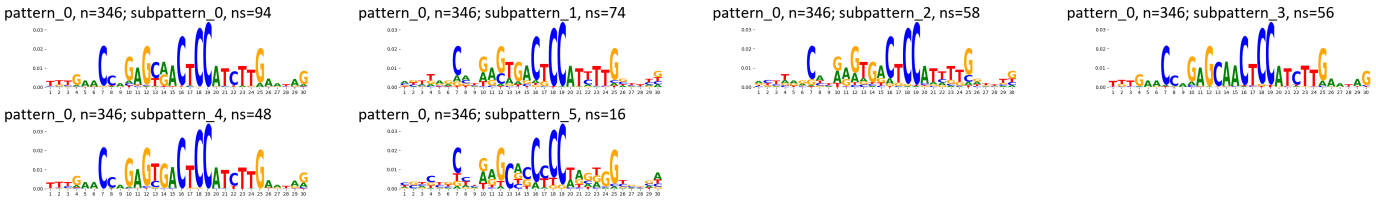

TF-MoDisCO pattern_0 n=346, PWM

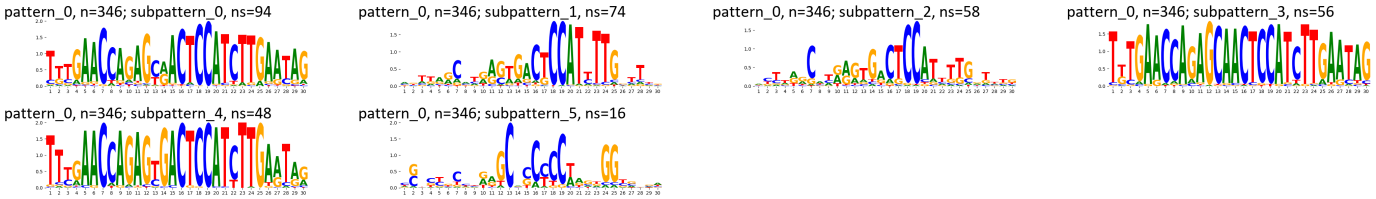

Supplementary Figure 1800: TF-MoDisCO subpatterns for the ZSCAN18 transcription factor in WTC11 (accession ENCSR499FDW).

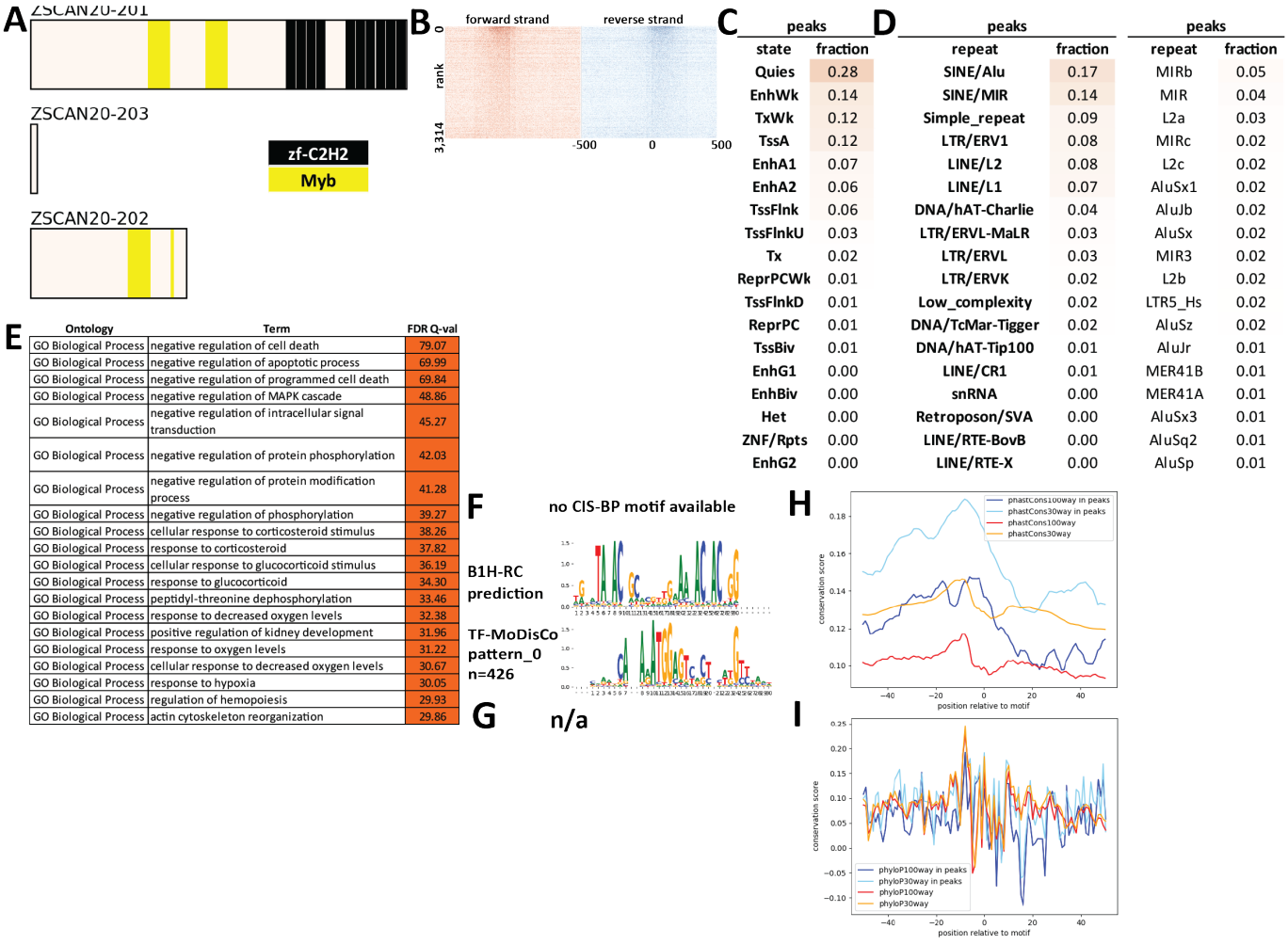

Supplementary Figure 1801: Properties and genomic distribution of motifs identified for the ZSCAN20 transcription factor in A549 (accession ENCSR548FLW).

TF-MoDisCO pattern_0 n=426, CWM

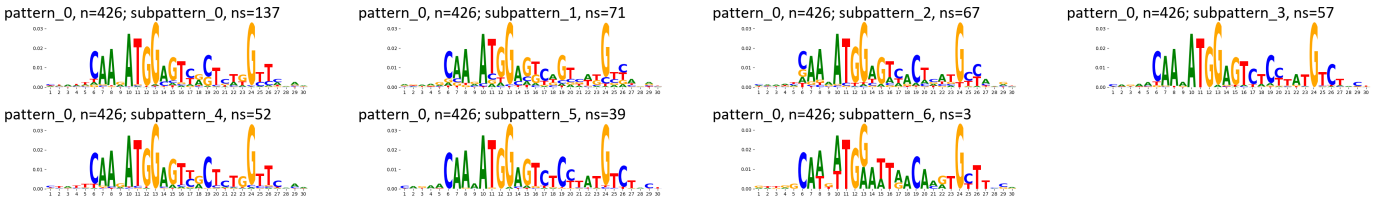

TF-MoDisCO pattern_0 n=426, PWM

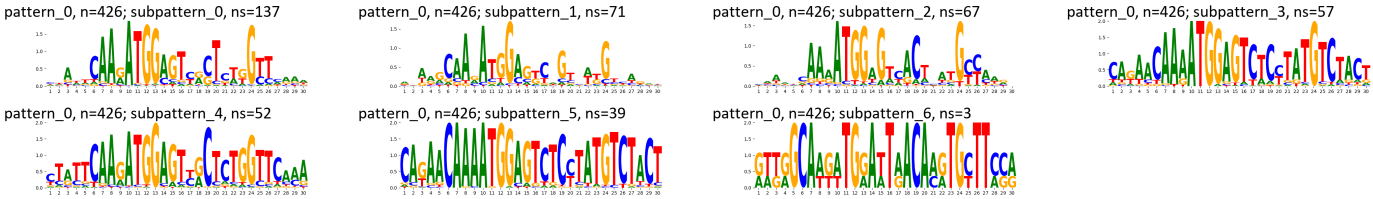

Supplementary Figure 1802: TF-MoDisCO subpatterns for the ZSCAN20 transcription factor in A549 (accession ENCSR548FLW).

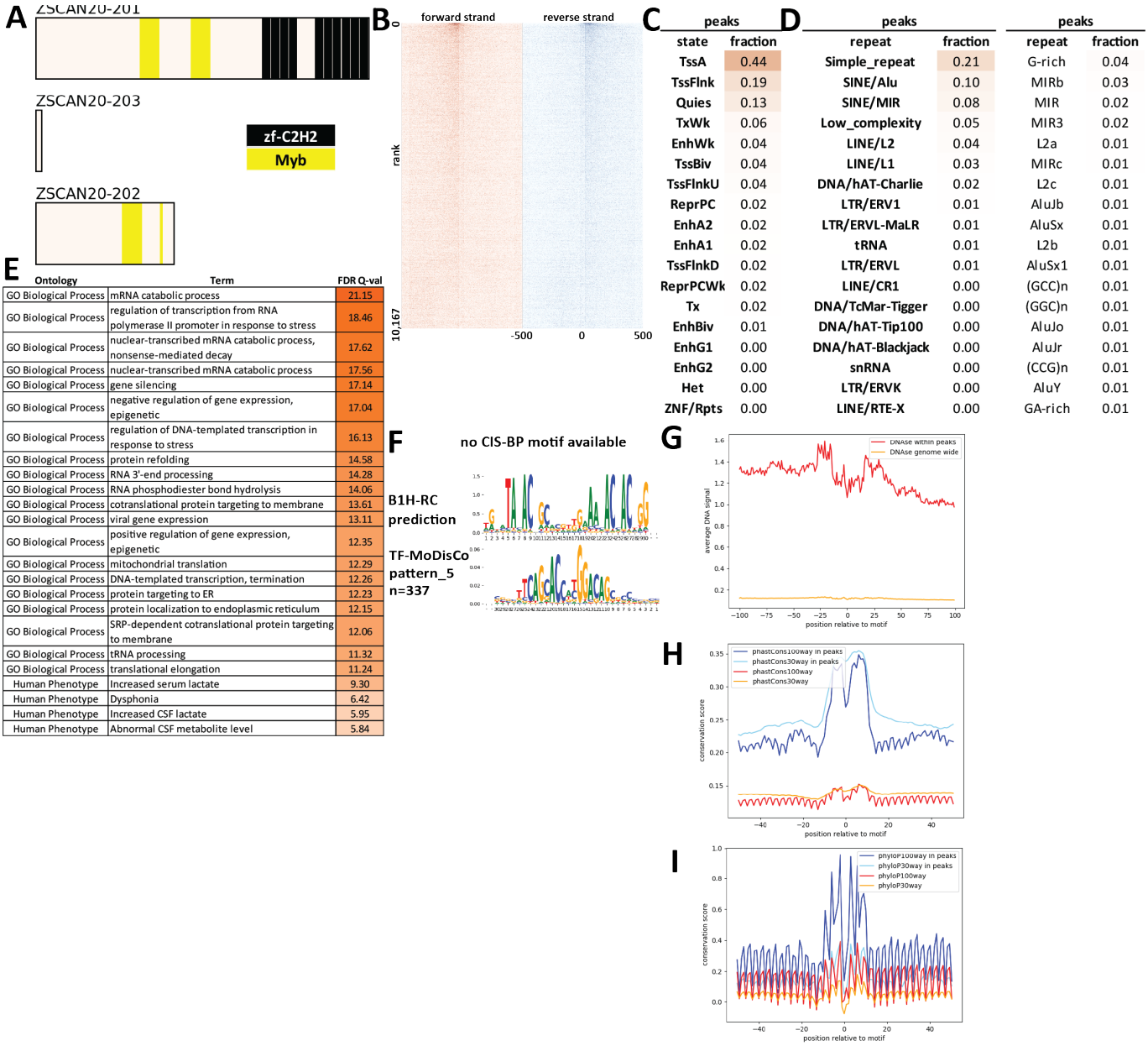

Supplementary Figure 1803: Properties and genomic distribution of motifs identified for the ZSCAN20 transcription factor in HepG2 (accession ENCSR169JRW).

TF-MoDisCO pattern_5 n=337, CWM

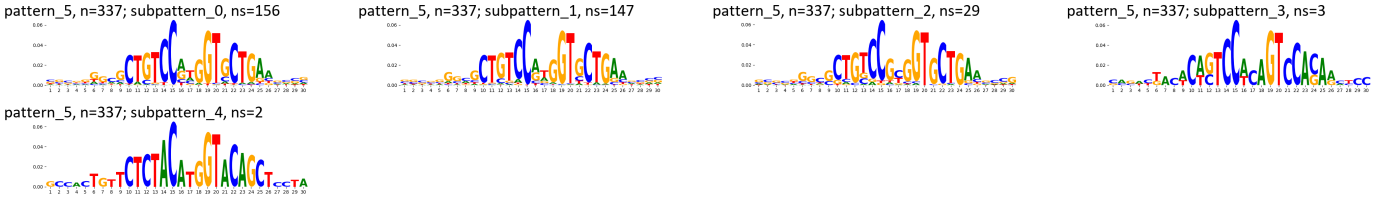

TF-MoDisCO pattern_5 n=337, PWM

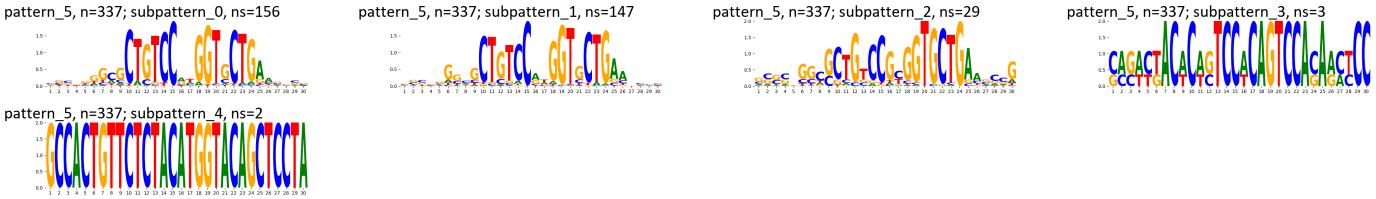

Supplementary Figure 1804: TF-MoDisCO subpatterns for the ZSCAN20 transcription factor in HepG2 (accession ENCSR169JRW).

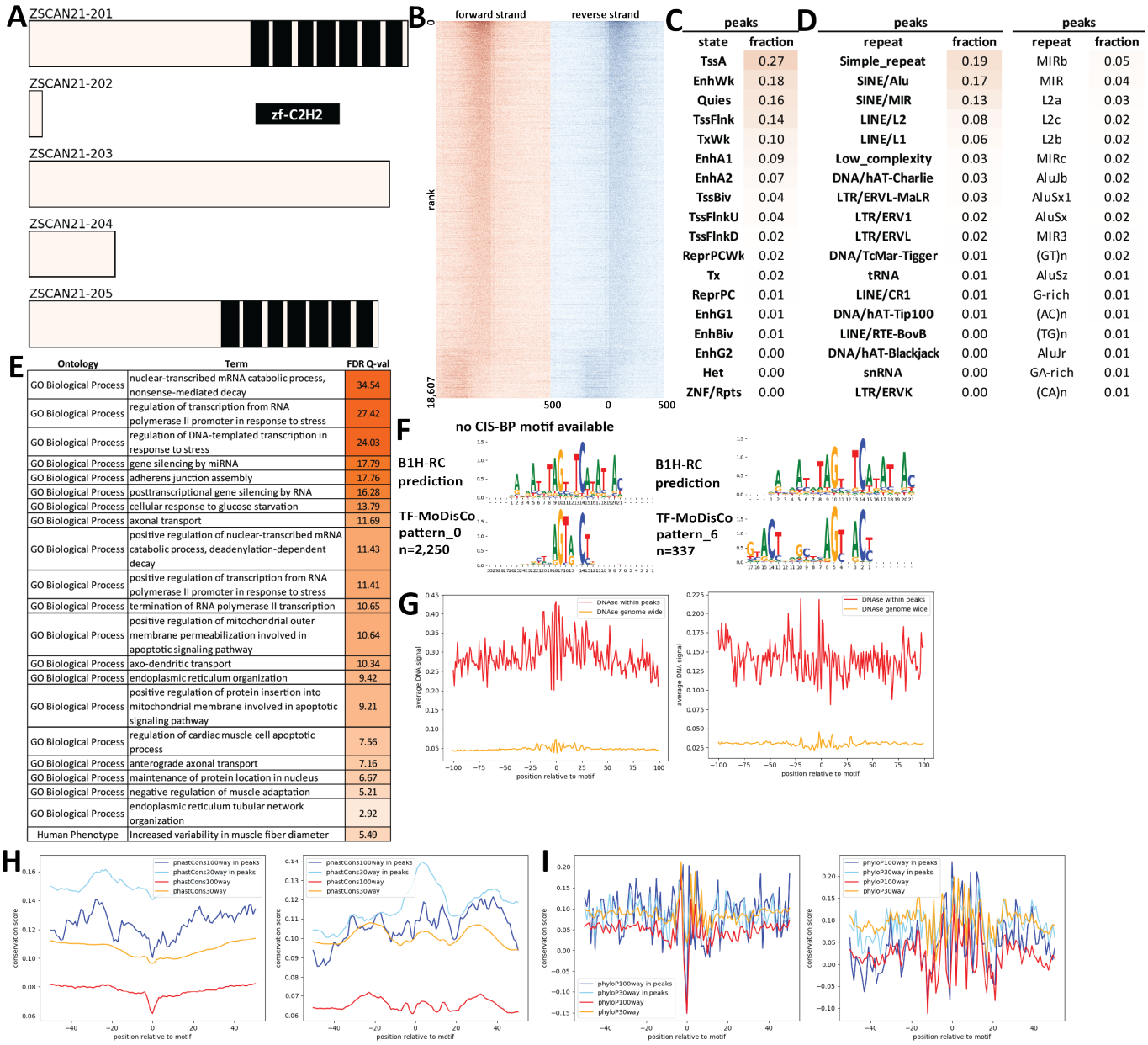

Supplementary Figure 1805: Properties and genomic distribution of motifs identified for the ZSCAN21 transcription factor in HEK293 (accession ENCSR253CKN).

TF-MoDisCO pattern_0 n=2250, CWM

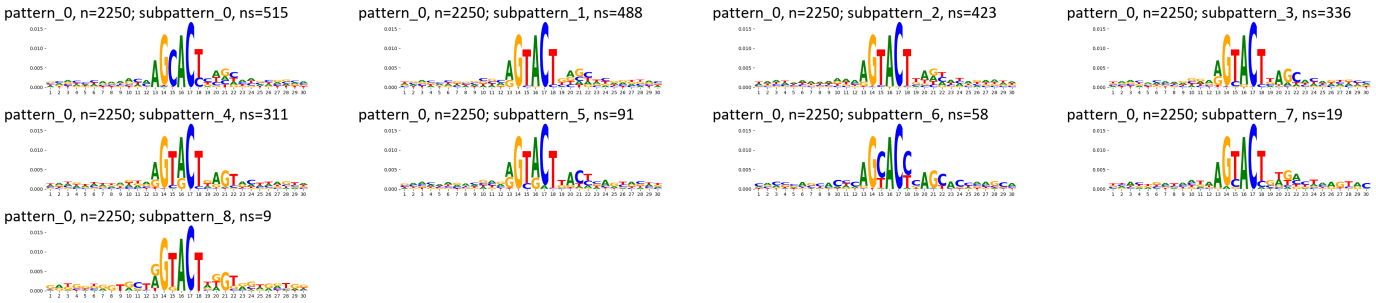

TF-MoDisCO pattern_0 n=2250, PWM

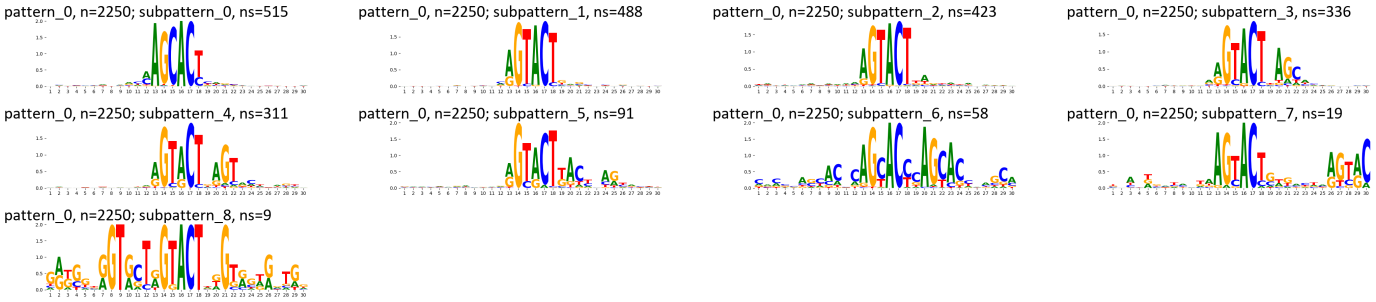

TF-MoDisCO pattern_6 n=337, CWM

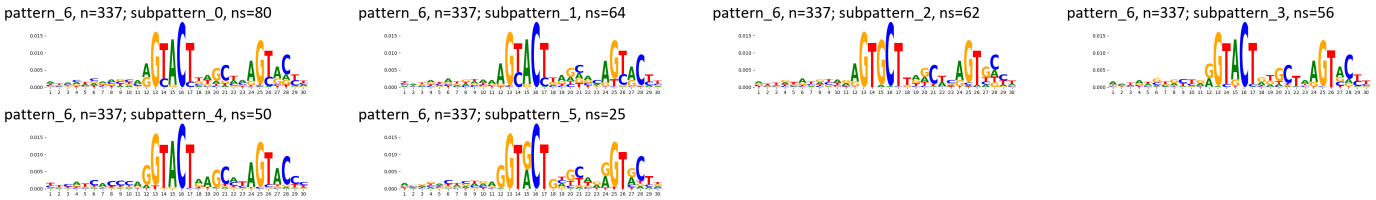

TF-MoDisCO pattern_6 n=337, PWM

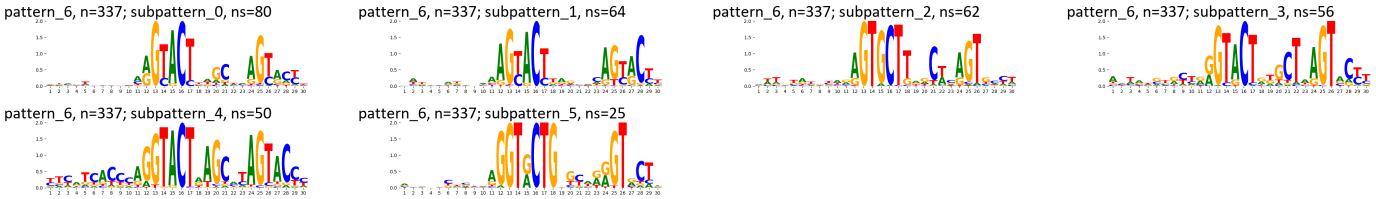

Supplementary Figure 1806: TF-MoDisCO subpatterns for the ZSCAN21 transcription factor in HEK293 (accession ENCSR253CKN).

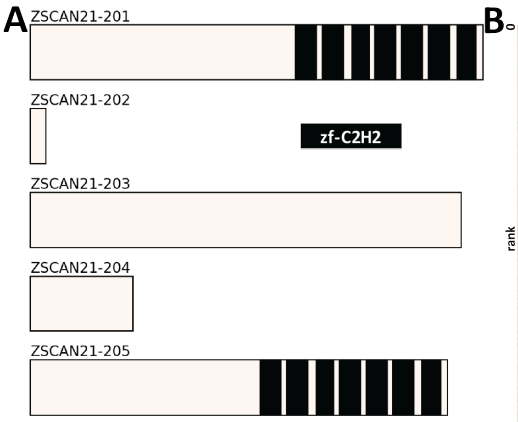

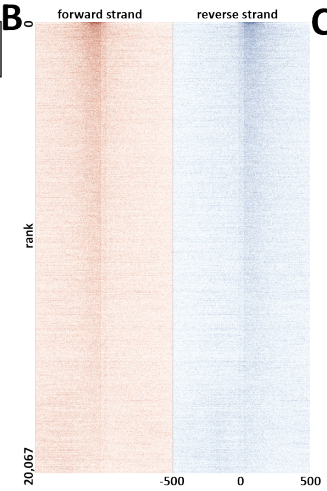

C

peaks	
state	fraction
TssA	0.34
TssFlnk	0.18
Quies	0.16
TxWk	0.09
EnhWk	0.05
TssBiv	0.04
TssFlnkU	0.04
ReprPC	0.03
EnhA2	0.03
Tx	0.02
EnhA1	0.02
ReprPCWk	0.02
TssFlnkD	0.02
EnhBiv	0.01
EnhG1	0.01
EnhG2	0.00
Het	0.00
ZNF/Rpts	0.00

D

peaks		peaks	
repeat	fraction	repeat	fraction
Simple_repeat	0.25	MIRb	0.04
SINE/MIR	0.12	G-rich	0.04
SINE/Alu	0.11	MIR	0.03
LINE/L2	0.07	L2a	0.02
Low_complexity	0.05	MIR3	0.02
LINE/L1	0.03	MIRc	0.02
DNA/hAT-Charlie	0.02	L2b	0.02
LTR/ERV1	0.02	L2c	0.02
LTR/ERVL-MaLR	0.02	AluSx	0.01
LTR/ERVL	0.01	AluJb	0.01
DNA/TcMar-Tigger	0.01	AluSx1	0.01
DNA/hAT-Tip100	0.01	AluSz	0.01
LINE/CR1	0.01	GA-rich	0.01
tRNA	0.00	(GGC)n	0.01
LTR/ERVK	0.00	AluJr	0.01
DNA/hAT-Blackjack	0.00	AluJo	0.01
LINE/RTE-BovB	0.00	(GCC)n	0.01
DNA/hAT	0.00	AluY	0.01

E

Ontology	Term	FDR Q-val
GO Biological Process	endoplasmic reticulum unfolded protein response	48.99
GO Biological Process	regulation of intrinsic apoptotic signaling pathway	48.97
GO Biological Process	IRE1-mediated unfolded protein response	48.13
GO Biological Process	regulation of transcription from RNA polymerase II promoter in response to stress	48.07
GO Biological Process	cellular response to topologically incorrect protein	45.71
GO Biological Process	positive regulation of nuclease activity	44.59
GO Biological Process	cellular response to unfolded protein	42.39
GO Biological Process	regulation of DNA-templated transcription in response to stress	42.40
GO Biological Process	response to topologically incorrect protein	38.63
GO Biological Process	negative regulation of intrinsic apoptotic signaling pathway	36.59
GO Biological Process	response to unfolded protein	34.40
GO Biological Process	regulation of nuclease activity	33.46
GO Biological Process	regulation of transcription from RNA polymerase II promoter in response to hypoxia	29.26
GO Biological Process	nuclear-transcribed mRNA catabolic process, nonsense-mediated decay	29.18
GO Biological Process	protein targeting to ER	28.58
GO Biological Process	cotranslational protein targeting to membrane	26.24
GO Biological Process	regulation of endoplasmic reticulum stress-induced intrinsic apoptotic signaling pathway	25.05
GO Biological Process	regulation of mitochondrial membrane permeability	25.04
GO Biological Process	SRP-dependent cotranslational protein targeting to membrane	24.45
GO Biological Process	regulation of endoplasmic reticulum unfolded protein response	24.43
Human Phenotype	Exercise intolerance	20.15
Human Phenotype	Abnormality of mitochondrial metabolism	15.98
Human Phenotype	Abnormal CSF metabolite level	15.83
Human Phenotype	Abnormality of the mitochondrion	15.74
Human Phenotype	Increased CSF lactate	14.68
Human Phenotype	Abnormality of transition element cation homeostasis	11.94

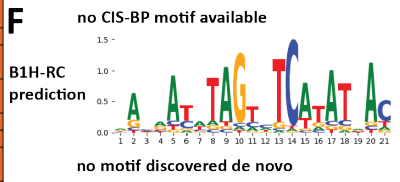

Supplementary Figure 1807: Properties and genomic distribution of motifs identified for the ZSCAN21 transcription factor in HepG2 (accession ENCSR210DDA).

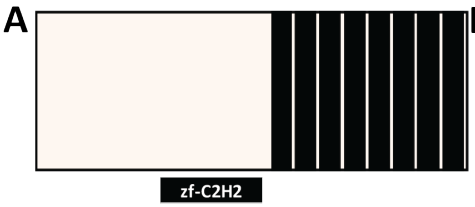

E

Ontology	Term	FDR Q-val
GO Biological Process	nuclear-transcribed mRNA catabolic process, nonsense-mediated decay	19.10
GO Biological Process	viral gene expression	16.36
GO Biological Process	regulation of transcription from RNA polymerase II promoter in response to stress	15.88
GO Biological Process	viral transcription	13.27
GO Biological Process	cotranslational protein targeting to membrane	13.18
GO Biological Process	snRNA metabolic process	12.88
GO Biological Process	regulation of transcription from RNA polymerase II promoter in response to hypoxia	12.80
GO Biological Process	SRP-dependent cotranslational protein targeting to membrane	12.56
GO Biological Process	protein targeting to ER	11.57
GO Biological Process	mitochondrial translational elongation	9.85
GO Biological Process	mitochondrial translational termination	9.76
GO Biological Process	termination of RNA polymerase II transcription	9.37
GO Biological Process	gene silencing by miRNA	8.32
GO Biological Process	heterochromatin organization	7.89
GO Biological Process	heterochromatin assembly	7.16
GO Biological Process	cellular component disassembly involved in execution phase of apoptosis	6.54
GO Biological Process	intracellular protein transmembrane import	6.48
GO Biological Process	mRNA cleavage	6.47
GO Biological Process	regulation of mitophagy	6.36
GO Biological Process	apoptotic nuclear changes	6.28
Human Phenotype	Exercise intolerance	8.40
Human Phenotype	Increased muscle lipid content	8.36
Human Phenotype	Abnormal CSF metabolite level	7.00
Human Phenotype	Increased CSF lactate	7.09

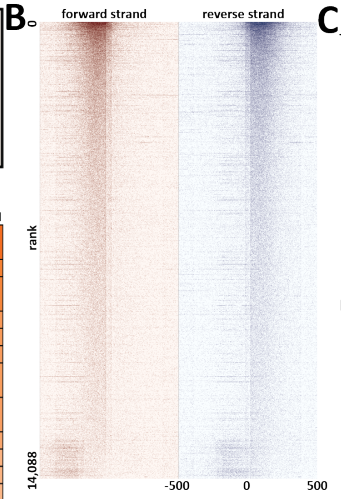

C

peaks	
state	fraction
TssA	0.40
TssFlnk	0.20
Quies	0.16
EnhWk	0.08
TxWk	0.07
EnhA1	0.04
TssBiv	0.04
EnhA2	0.04
TssFlnkU	0.03
ReprPC	0.02
ReprPCWk	0.02
Tx	0.02
TssFlnkD	0.01
EnhBiv	0.01
EnhG1	0.01
EnhG2	0.00
Het	0.00
ZNF/Rpts	0.00

D

peaks		peaks	
repeat	fraction	repeat	fraction
Simple_repeat	0.20	G-rich	0.03
SINE/Alu	0.07	L2c	0.02
LINE/L2	0.07	MIRb	0.02
SINE/MIR	0.07	L2a	0.02
Low_complexity	0.04	L2b	0.02
LINE/L1	0.03	MIR	0.02
LTR/ERVL-MaLR	0.03	GA-rich	0.01
DNA/hAT-Charlie	0.02	MIR3	0.01
LTR/ERV1	0.02	MIRc	0.01
LTR/ERVL	0.01	(GGC)n	0.01
Satellite	0.01	AluSx1	0.01
DNA/TcMar-Tigger	0.01	AluJb	0.01
LINE/CR1	0.01	MSR1	0.01
DNA/hAT-Tip100	0.00	L2	0.01
tRNA	0.00	(GCG)n	0.01
DNA/hAT-Blackjack	0.00	(GCC)n	0.01
LTR/ERVK	0.00	AluSx	0.01
snRNA	0.00	(CCG)n	0.01

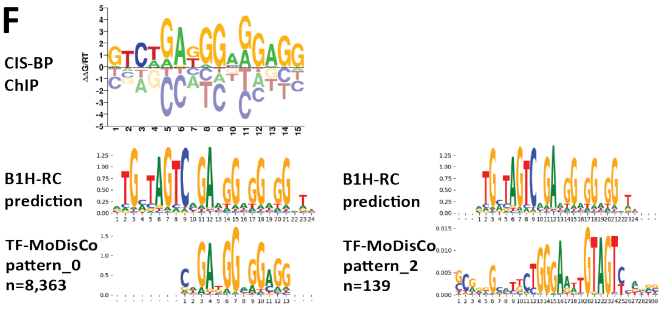

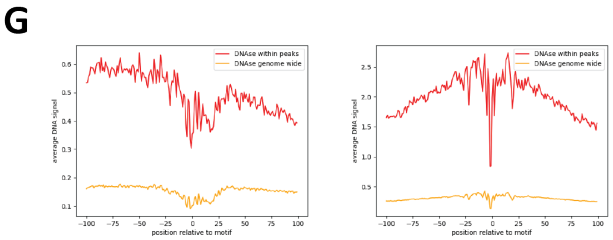

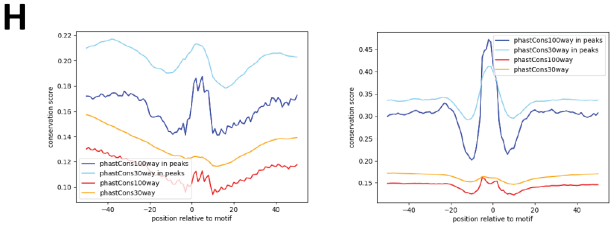

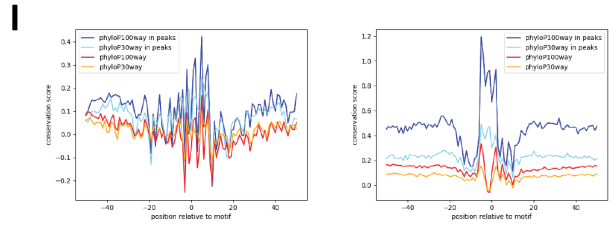

Supplementary Figure 1808: Properties and genomic distribution of motifs identified for the ZSCAN22 transcription factor in HEK293 (accession Hughes NB models).

TF-MoDisCO pattern_0 n=8363, CWM

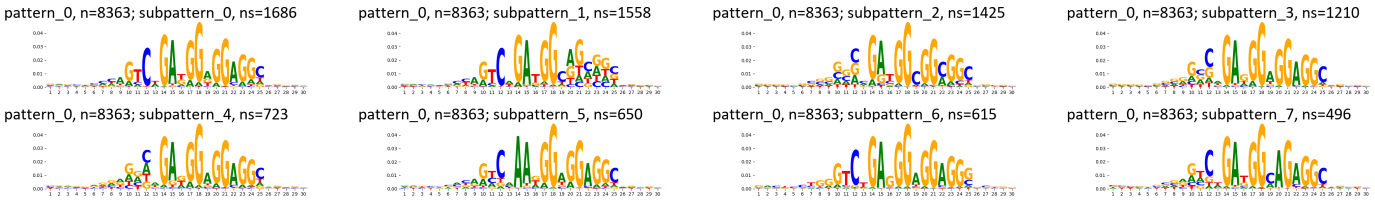

TF-MoDisCO pattern_0 n=8363, PWM

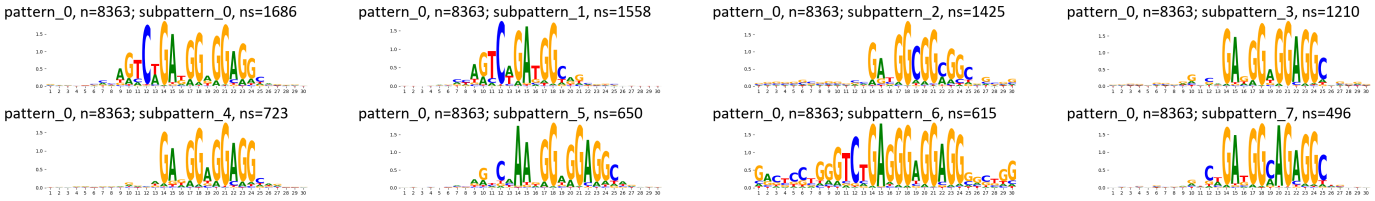

TF-MoDisCO pattern_2 n=244, CWM

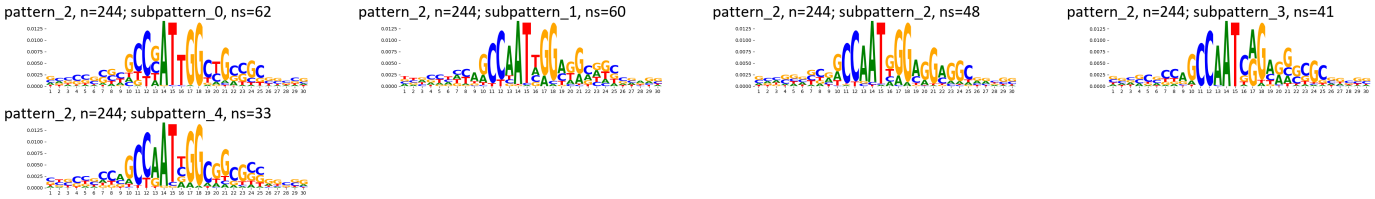

TF-MoDisCO pattern_2 n=244, PWM

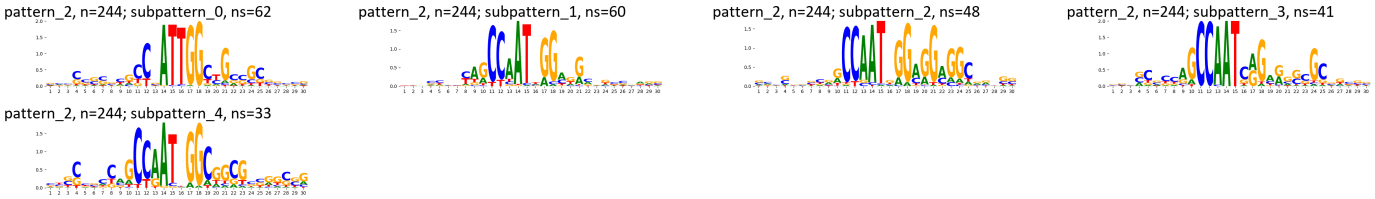

TF-MoDisCO pattern_3 n=139, CWM

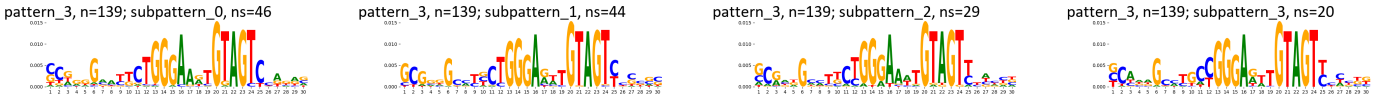

TF-MoDisCO pattern_3 n=139, PWM

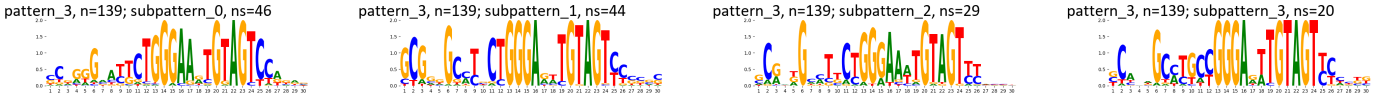

Supplementary Figure 1809: TF-MoDisCO subpatterns for the ZSCAN22 transcription factor in HEK293 (accession Hughes NB models).

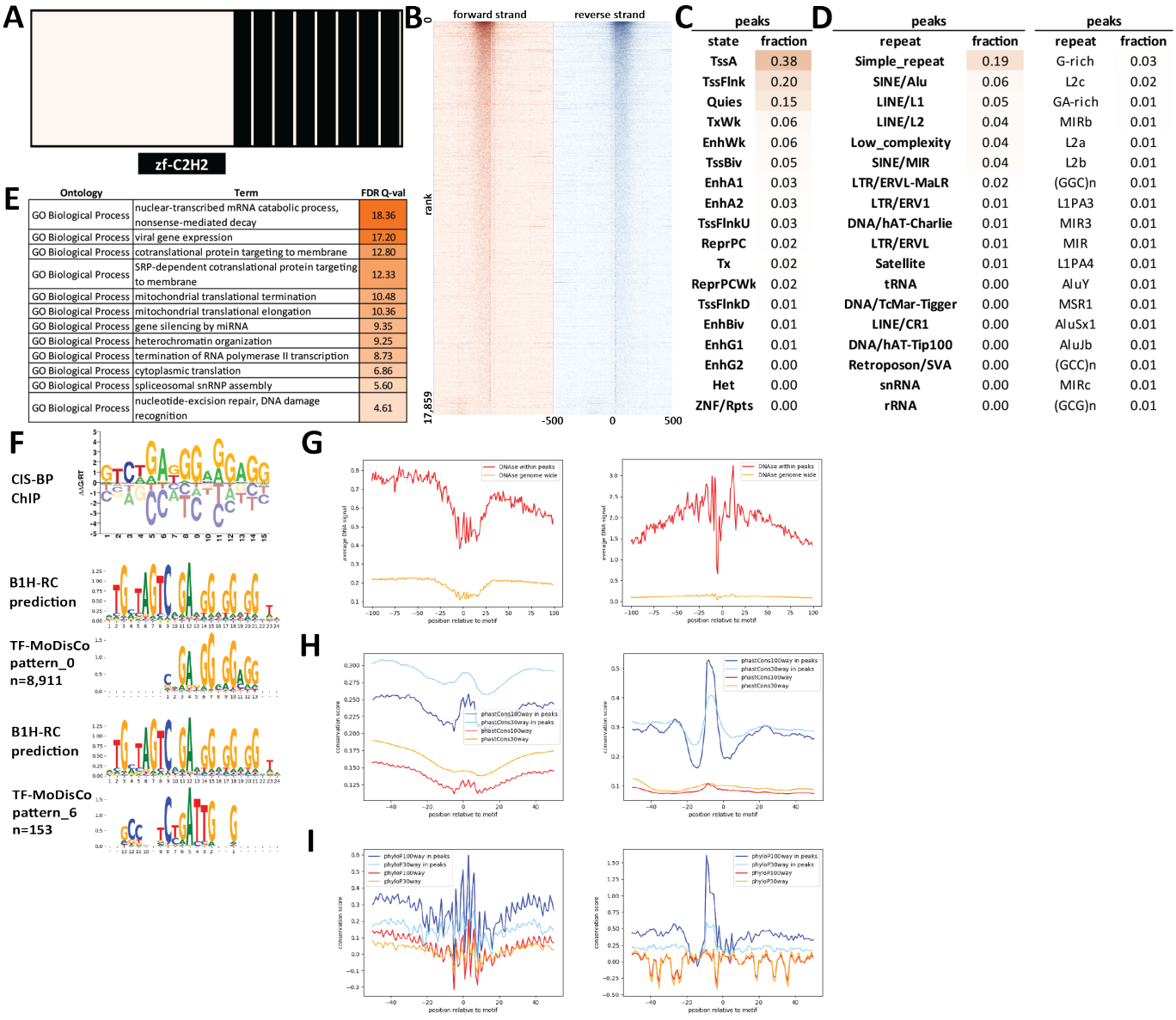

Supplementary Figure 1810: Properties and genomic distribution of motifs identified for the ZSCAN22 transcription factor in HEK293 (accession Hughes GR models).

TF-MoDisCO pattern_0 n=8911, CWM

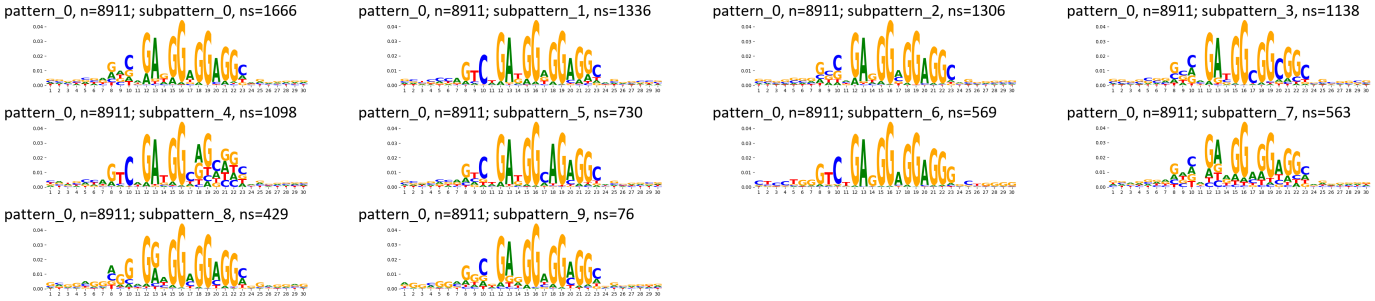

TF-MoDisCO pattern_0 n=8911, PWM

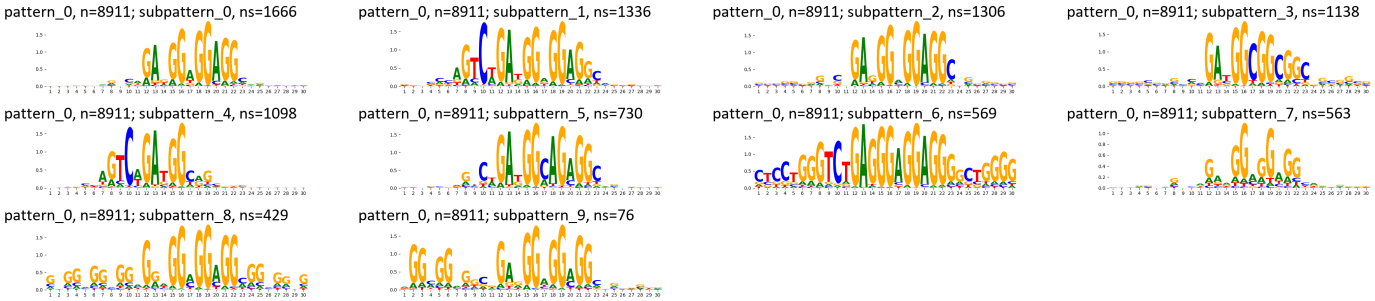

TF-MoDisCO pattern_6 n=153, CWM

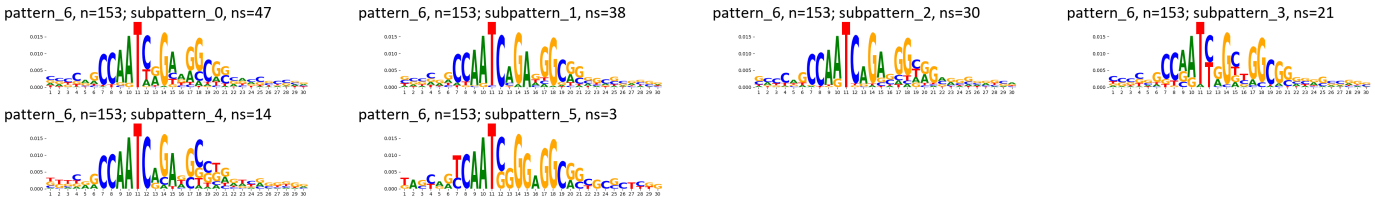

TF-MoDisCO pattern_6 n=153, PWM

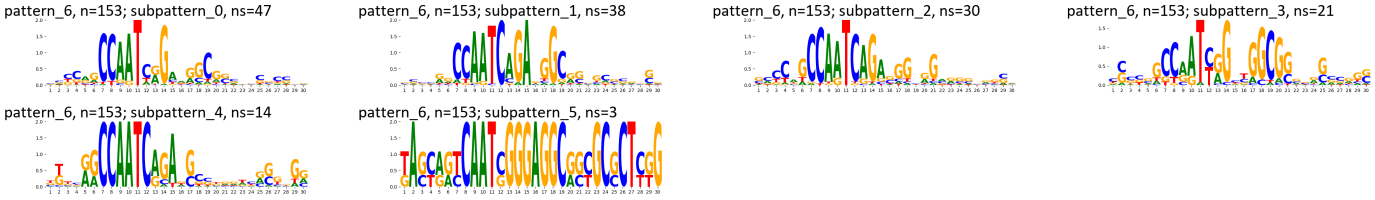

Supplementary Figure 1811: TF-MoDisCO subpatterns for the ZSCAN22 transcription factor in HEK293 (accession Hughes GR models).

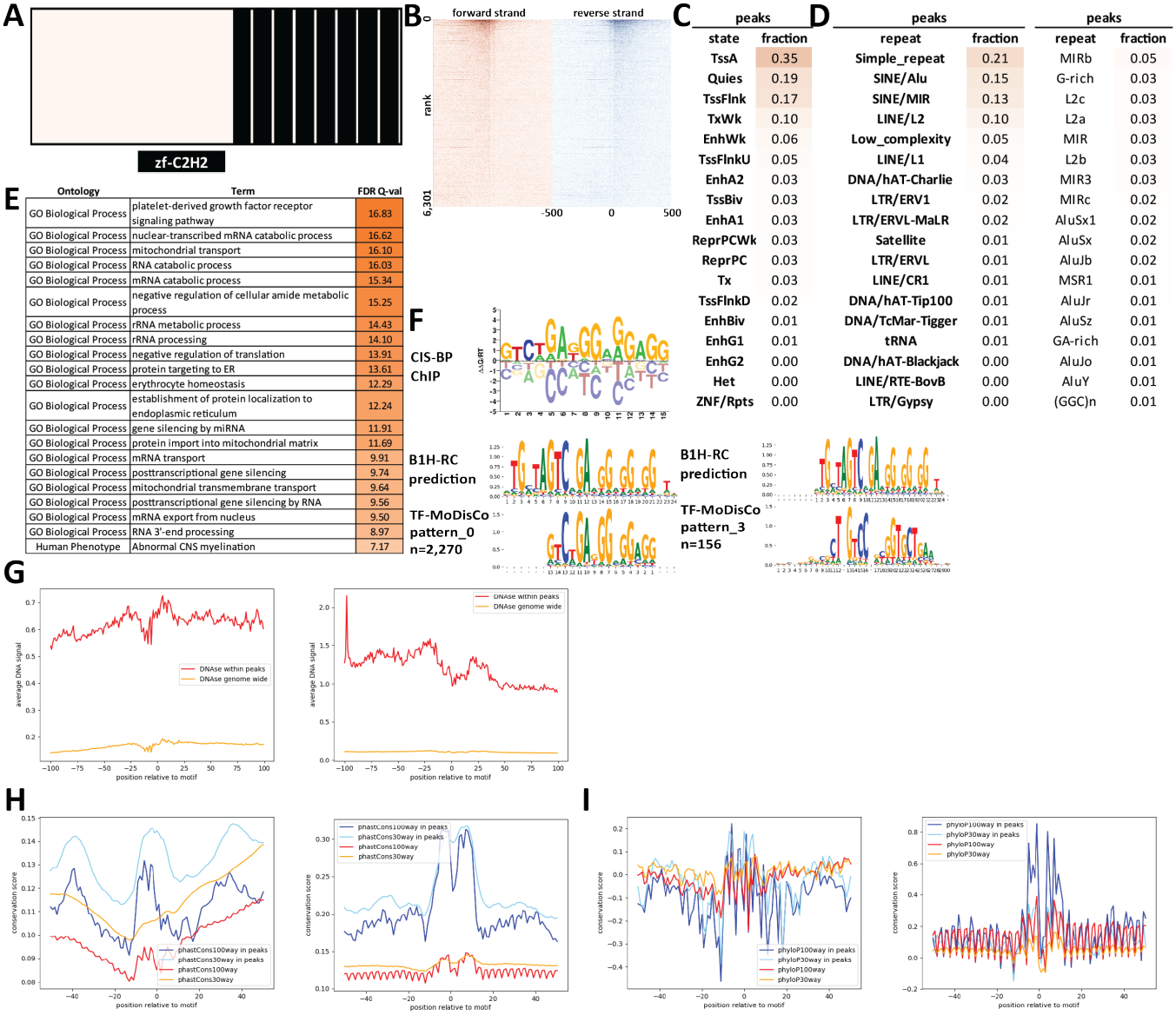

Supplementary Figure 1812: Properties and genomic distribution of motifs identified for the ZSCAN22 transcription factor in HepG2 (accession ENCSR050KWL).

TF-MoDisCO pattern_0 n=2270, CWM

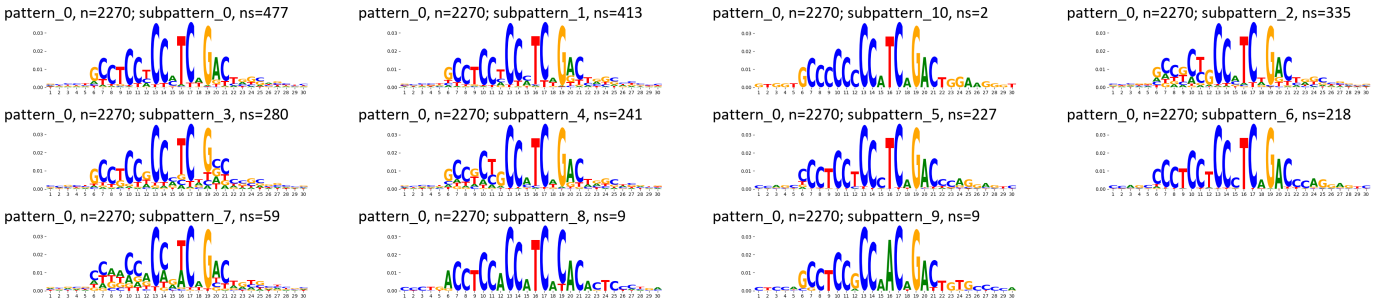

TF-MoDisCO pattern_0 n=2270, PWM

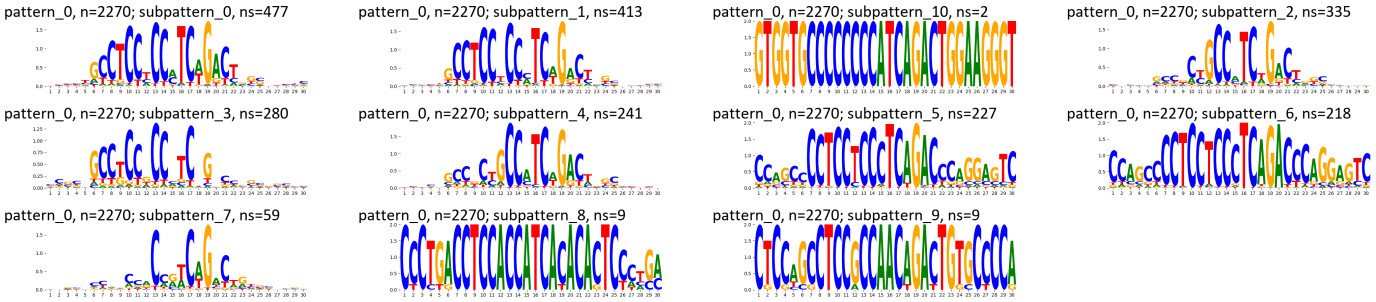

TF-MoDisCO pattern_3 n=156, CWM

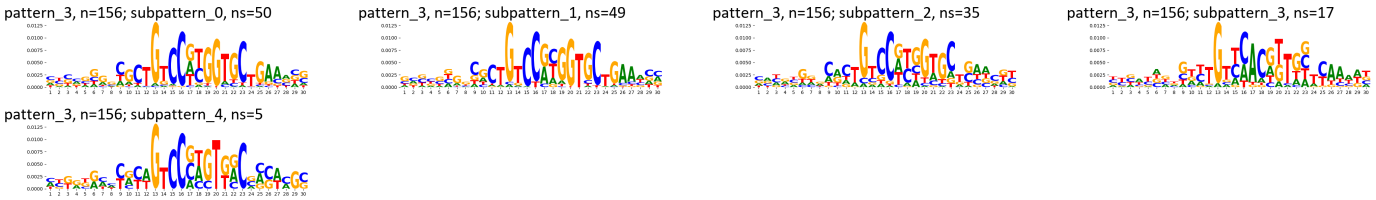

TF-MoDisCO pattern_3 n=156, PWM

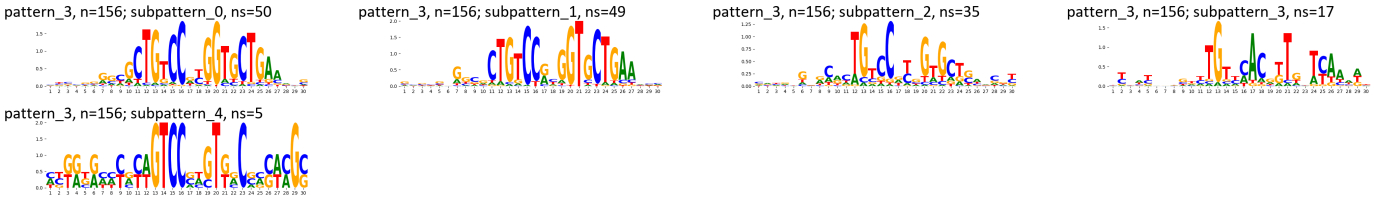

Supplementary Figure 1813: TF-MoDisCO subpatterns for the ZSCAN22 transcription factor in HepG2 (accession ENCSR050KWL).

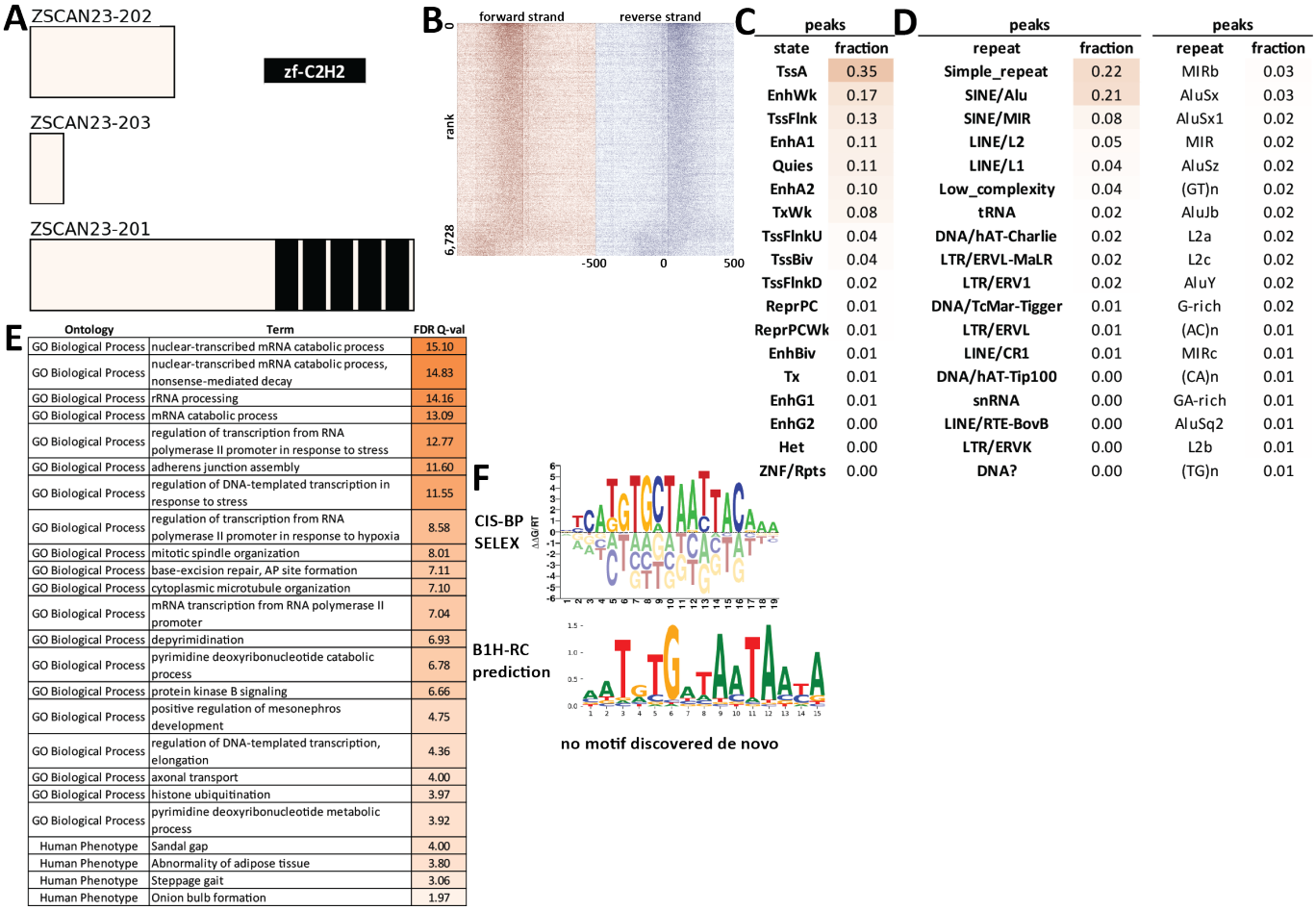

C

peaks	
state	fraction
TssA	0.35
EnhWk	0.17
TssFlnk	0.13
EnhA1	0.11
Quies	0.11
EnhA2	0.10
TxWk	0.08
TssFlnkU	0.04
TssBiv	0.04
TssFlnkD	0.02
ReprPC	0.01
ReprPCWk	0.01
EnhBiv	0.01
Tx	0.01
EnhG1	0.01
EnhG2	0.00
Het	0.00
ZNF/Rpts	0.00

D

peaks		peaks	
repeat	fraction	repeat	fraction
Simple_repeat	0.22	MIRb	0.03
SINE/Alu	0.21	AluSx	0.03
SINE/MIR	0.08	AluSx1	0.02
LINE/L2	0.05	MIR	0.02
LINE/L1	0.04	AluSz	0.02
Low_complexity	0.04	(GT)n	0.02
tRNA	0.02	AluJb	0.02
DNA/hAT-Charlie	0.02	L2a	0.02
LTR/ERVL-MaLR	0.02	L2c	0.02
LTR/ERV1	0.02	AluY	0.02
DNA/TcMar-Tigger	0.01	G-rich	0.02
LTR/ERVL	0.01	(AC)n	0.01
LINE/CR1	0.01	MIRc	0.01
DNA/hAT-Tip100	0.00	(CA)n	0.01
snRNA	0.00	GA-rich	0.01
LINE/RTE-BovB	0.00	AluSq2	0.01
LTR/ERVK	0.00	L2b	0.01
DNA?	0.00	(TG)n	0.01

E

Ontology	Term	FDR Q-val
GO Biological Process	nuclear-transcribed mRNA catabolic process	15.10
GO Biological Process	nuclear-transcribed mRNA catabolic process, nonsense-mediated decay	14.83
GO Biological Process	rRNA processing	14.16
GO Biological Process	mRNA catabolic process	13.09
GO Biological Process	regulation of transcription from RNA polymerase II promoter in response to stress	12.77
GO Biological Process	adherens junction assembly	11.60
GO Biological Process	regulation of DNA-templated transcription in response to stress	11.55
GO Biological Process	regulation of transcription from RNA polymerase II promoter in response to hypoxia	8.58
GO Biological Process	mitotic spindle organization	8.01
GO Biological Process	base-excision repair, AP site formation	7.11
GO Biological Process	cytoplasmic microtubule organization	7.10
GO Biological Process	mRNA transcription from RNA polymerase II promoter	7.04
GO Biological Process	depyrimidination	6.93
GO Biological Process	pyrimidine deoxyribonucleotide catabolic process	6.78
GO Biological Process	protein kinase B signaling	6.66
GO Biological Process	positive regulation of mesonephros development	4.75
GO Biological Process	regulation of DNA-templated transcription, elongation	4.36
GO Biological Process	axonal transport	4.00
GO Biological Process	histone ubiquitination	3.97
GO Biological Process	pyrimidine deoxyribonucleotide metabolic process	3.92
Human Phenotype	Sandal gap	4.00
Human Phenotype	Abnormality of adipose tissue	3.80
Human Phenotype	Steppage gait	3.06
Human Phenotype	Onion bulb formation	1.97

Supplementary Figure 1814: Properties and genomic distribution of motifs identified for the ZSCAN23 transcription factor in HEK293 (accession ENCSR705ASR).

TF-MoDisCO pattern_0 n=1618, CWM

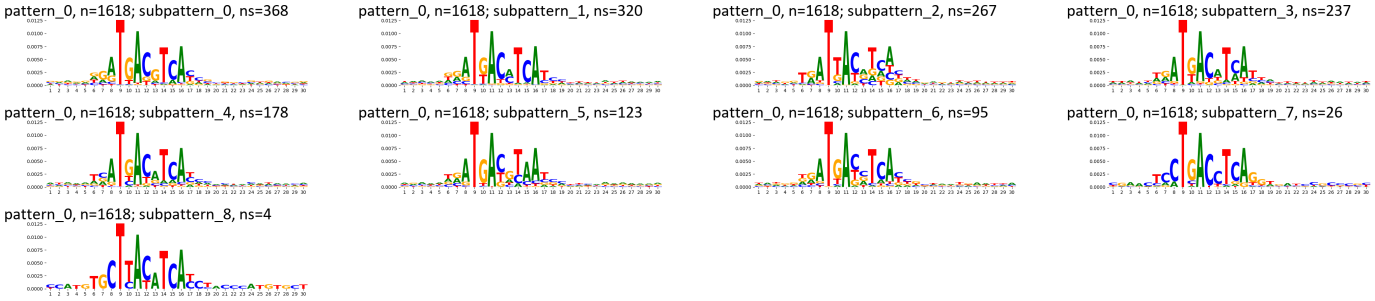

TF-MoDisCO pattern_0 n=1618, PWM

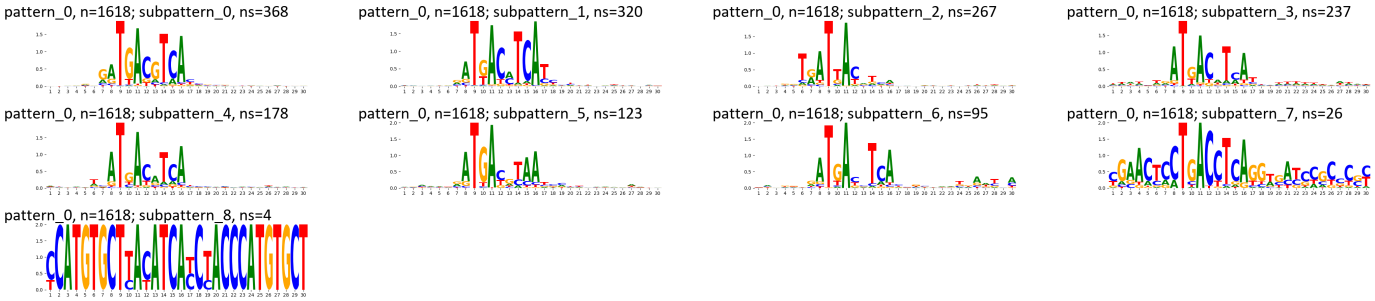

Supplementary Figure 1815: TF-MoDisCO subpatterns for the ZSCAN23 transcription factor in HEK293 (accession ENCSR705ASR).

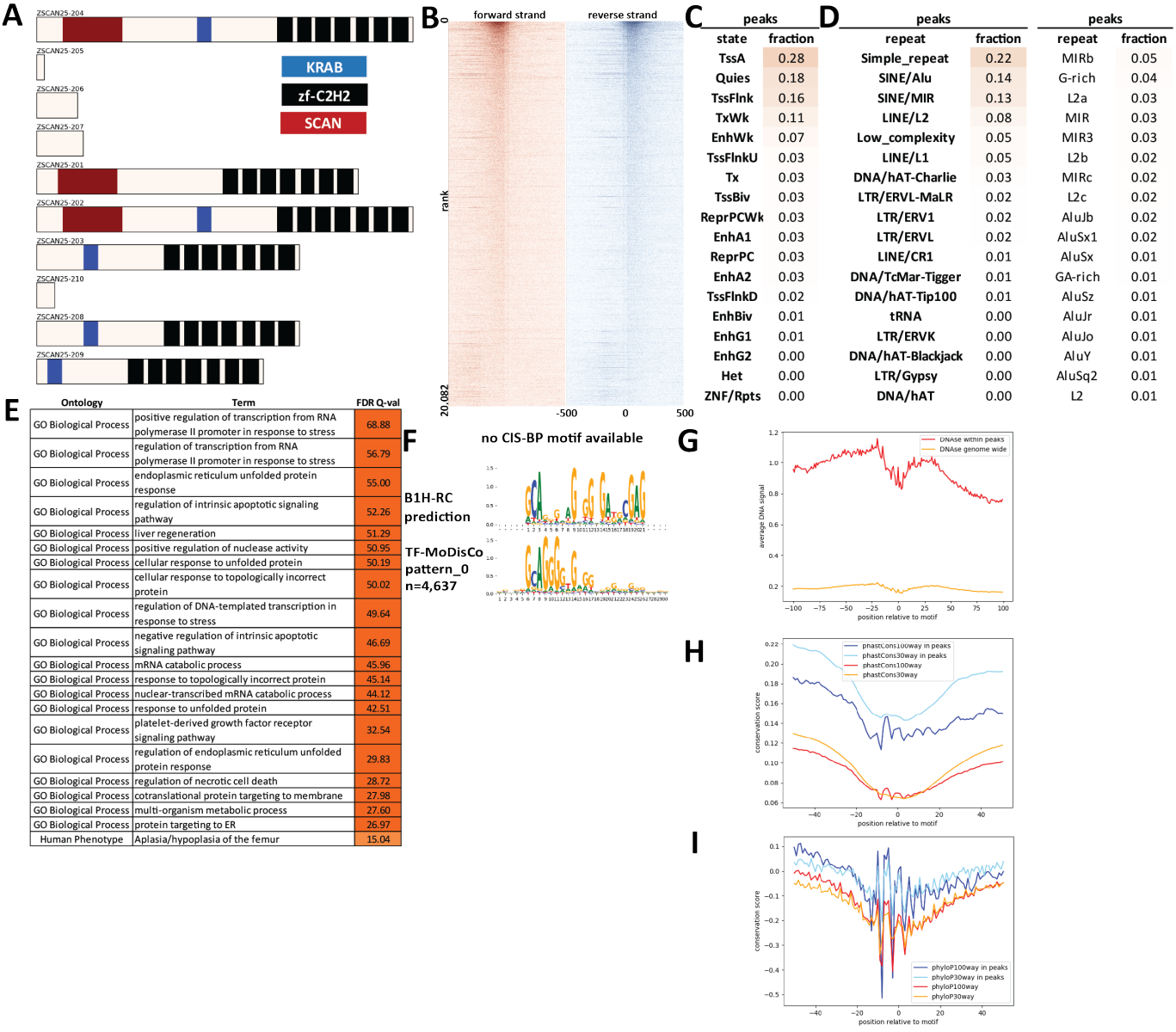

peaks	
state	fraction
TssA	0.28
Quies	0.18
TssFlnk	0.16
TxWk	0.11
EnhWk	0.07
TssFlnkU	0.03
Tx	0.03
TssBiv	0.03
ReprPCWk	0.03
EnhA1	0.03
ReprPC	0.03
EnhA2	0.03
TssFlnkD	0.02
EnhBiv	0.01
EnhG1	0.01
EnhG2	0.00
Het	0.00
ZNF/Rpts	0.00

peaks		peaks	
repeat	fraction	repeat	fraction
Simple_repeat	0.22	MIRb	0.05
SINE/Alu	0.14	G-rich	0.04
SINE/MIR	0.13	L2a	0.03
LINE/L2	0.08	MIR	0.03
Low_complexity	0.05	MIR3	0.03
LINE/L1	0.05	L2b	0.02
DNA/hAT-Charlie	0.03	MIRc	0.02
LTR/ERVL-MaLR	0.02	L2c	0.02
LTR/ERV1	0.02	AluJb	0.02
LTR/ERVL	0.02	AluSx1	0.02
LINE/CR1	0.01	AluSx	0.01
DNA/TcMar-Tigger	0.01	GA-rich	0.01
DNA/hAT-Tip100	0.01	AluSz	0.01
tRNA	0.00	AluJr	0.01
LTR/ERVK	0.00	AluJo	0.01
DNA/hAT-Blackjack	0.00	AluY	0.01
LTR/Gypsy	0.00	AluSq2	0.01
DNA/hAT	0.00	L2	0.01

Ontology	Term	FDR Q-val
GO Biological Process	positive regulation of transcription from RNA polymerase II promoter in response to stress	68.88
GO Biological Process	regulation of transcription from RNA polymerase II promoter in response to stress	56.79
GO Biological Process	endoplasmic reticulum unfolded protein response	55.00
GO Biological Process	regulation of intrinsic apoptotic signaling pathway	52.26
GO Biological Process	liver regeneration	51.29
GO Biological Process	positive regulation of nuclease activity	50.95
GO Biological Process	cellular response to unfolded protein	50.19
GO Biological Process	cellular response to topologically incorrect protein	50.02
GO Biological Process	regulation of DNA-templated transcription in response to stress	49.64
GO Biological Process	negative regulation of intrinsic apoptotic signaling pathway	46.69
GO Biological Process	mRNA catabolic process	45.96
GO Biological Process	response to topologically incorrect protein	45.14
GO Biological Process	nuclear-transcribed mRNA catabolic process	44.12
GO Biological Process	response to unfolded protein	42.51
GO Biological Process	platelet-derived growth factor receptor signaling pathway	32.54
GO Biological Process	regulation of endoplasmic reticulum unfolded protein response	29.83
GO Biological Process	regulation of necrotic cell death	28.72
GO Biological Process	cotranslational protein targeting to membrane	27.98
GO Biological Process	multi-organism metabolic process	27.60
GO Biological Process	protein targeting to ER	26.97
Human Phenotype	Aplasia/hypoplasia of the femur	15.04

Supplementary Figure 1816: Properties and genomic distribution of motifs identified for the ZSCAN25 transcription factor in HepG2 (accession ENCSR037LQB).

TF-MoDisCO pattern_0 n=4637, CWM

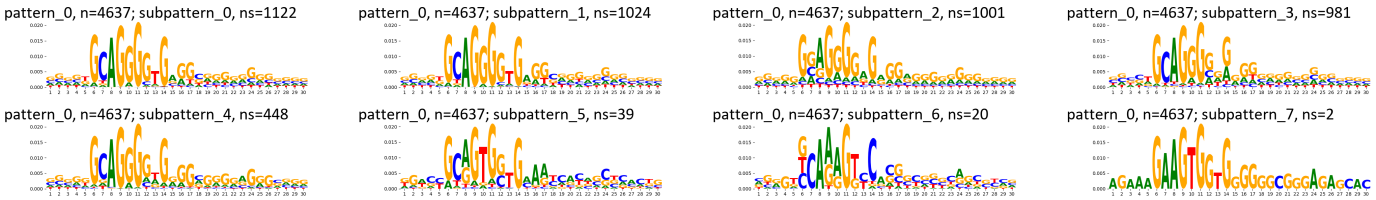

TF-MoDisCO pattern_0 n=4637, PWM

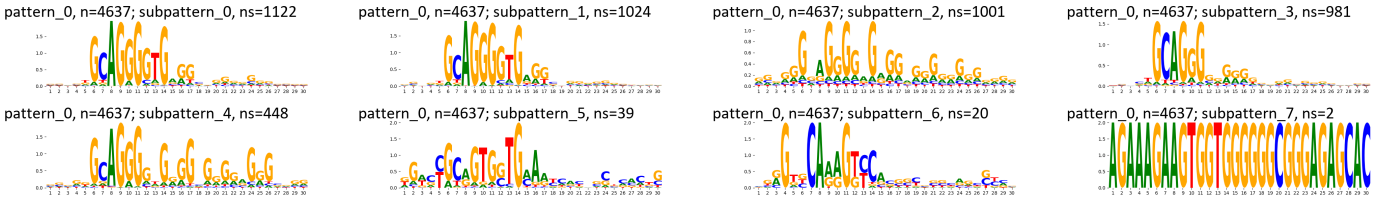

Supplementary Figure 1817: TF-MoDisCO subpatterns for the ZSCAN25 transcription factor in HepG2 (accession ENCSR037LQB).

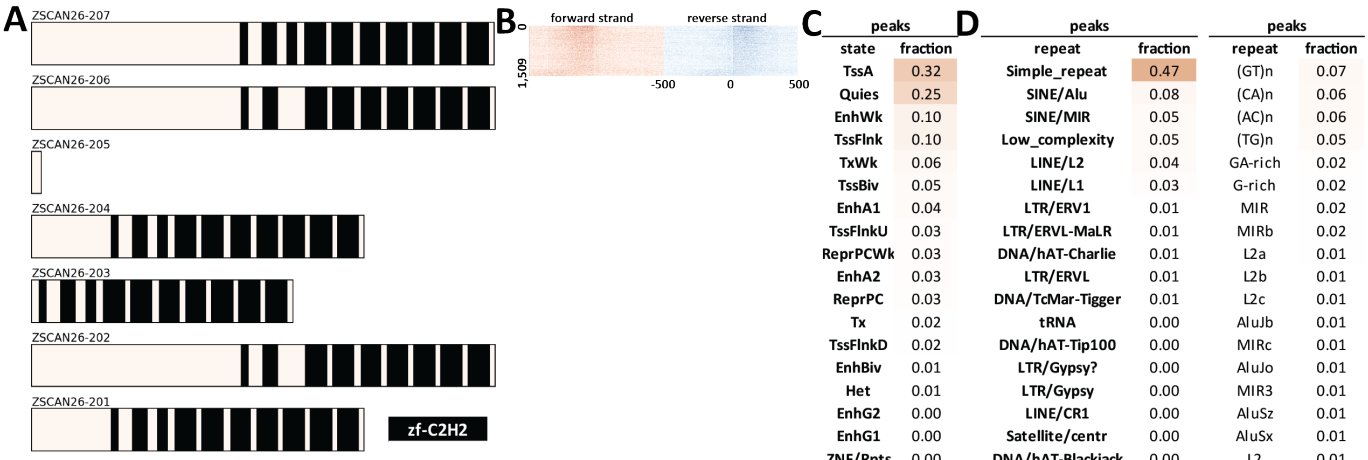

C

peaks	
state	fraction
TssA	0.32
Quies	0.25
EnhWk	0.10
TssFlnk	0.10
TxWk	0.06
TssBiv	0.05
EnhA1	0.04
TssFlnkU	0.03
ReprPCWk	0.03
EnhA2	0.03
ReprPC	0.03
Tx	0.02
TssFlnkD	0.02
EnhBiv	0.01
Het	0.01
EnhG2	0.00
EnhG1	0.00
ZNF/Rpts	0.00

D

peaks		peaks	
repeat	fraction	repeat	fraction
Simple_repeat	0.47	(GT)n	0.07
SINE/Alu	0.08	(CA)n	0.06
SINE/MIR	0.05	(AC)n	0.06
Low_complexity	0.05	(TG)n	0.05
LINE/L2	0.04	GA-rich	0.02
LINE/L1	0.03	G-rich	0.02
LTR/ERV1	0.01	MIR	0.02
LTR/ERVL-MaLR	0.01	MIRb	0.02
DNA/hAT-Charlie	0.01	L2a	0.01
LTR/ERVL	0.01	L2b	0.01
DNA/TcMar-Tigger	0.01	L2c	0.01
tRNA	0.00	AluJb	0.01
DNA/hAT-Tip100	0.00	MIRc	0.01
LTR/Gypsy?	0.00	AluJo	0.01
LTR/Gypsy	0.00	MIR3	0.01
LINE/CR1	0.00	AluSz	0.01
Satellite/centr	0.00	AluSx	0.01
DNA/hAT-Blackjack	0.00	L2	0.01

E

Ontology	Term	FDR Q-val
GO Biological Process	regulation of transforming growth factor beta receptor signaling pathway	8.23
GO Biological Process	regulation of cellular response to transforming growth factor beta stimulus	8.20
GO Biological Process	mammary gland epithelial cell differentiation	6.88
GO Biological Process	negative regulation of cyclin-dependent protein kinase activity	3.05
GO Biological Process	peptidyl-lysine methylation	2.53
GO Biological Process	foregut morphogenesis	2.50
GO Biological Process	negative regulation of transforming growth factor beta receptor signaling pathway	2.32
GO Biological Process	negative regulation of cellular response to transforming growth factor beta stimulus	2.26
GO Biological Process	histone lysine methylation	2.00
GO Biological Process	histone methylation	1.97
GO Biological Process	negative regulation of pro-B cell differentiation	1.93
GO Biological Process	positive regulation of epithelial to mesenchymal transition	1.67
GO Biological Process	embryonic foregut morphogenesis	1.65
GO Biological Process	specification of nephron tubule identity	1.57
GO Biological Process	regulation of axon extension involved in axon guidance	1.51

F

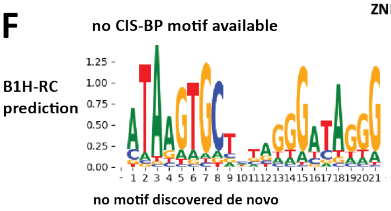

Supplementary Figure 1818: Properties and genomic distribution of motifs identified for the ZSCAN26 transcription factor in HEK293 (accession ENCSR501NSC).

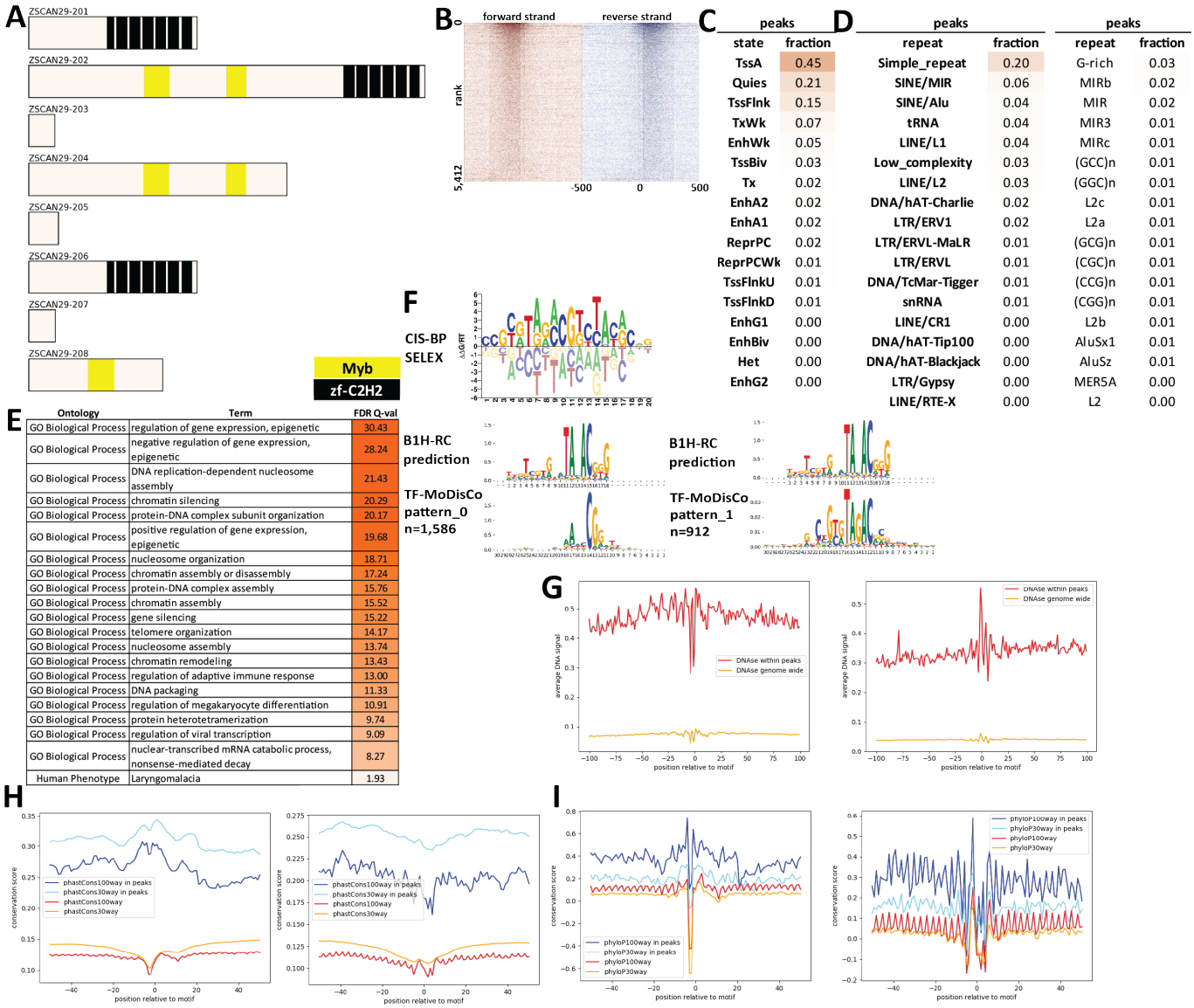

peaks	
state	fraction
TssA	0.45
Quies	0.21
TssFlnk	0.15
TxWk	0.07
EnhWk	0.05
TssBiv	0.03
Tx	0.02
EnhA2	0.02
EnhA1	0.02
ReprPC	0.02
ReprPCWk	0.01
TssFlnkU	0.01
TssFlnkD	0.01
EnhG1	0.00
EnhBiv	0.00
Het	0.00
EnhG2	0.00

peaks		peaks	
repeat	fraction	repeat	fraction
Simple_repeat	0.20	G-rich	0.03
SINE/MIR	0.06	MIRb	0.02
SINE/Alu	0.04	MIR	0.02
tRNA	0.04	MIR3	0.01
LINE/L1	0.04	MIRc	0.01
Low_complexity	0.03	(GCC)n	0.01
LINE/L2	0.03	(GGC)n	0.01
DNA/hAT-Charlie	0.02	L2c	0.01
LTR/ERV1	0.02	L2a	0.01
LTR/ERVL-MaLR	0.01	(GCG)n	0.01
LTR/ERVL	0.01	(CGC)n	0.01
DNA/TcMar-Tigger	0.01	(CCG)n	0.01
snRNA	0.01	(CGG)n	0.01
LINE/CR1	0.00	L2b	0.01
DNA/hAT-Tip100	0.00	AluSx1	0.01
DNA/hAT-Blackjack	0.00	AluSz	0.01
LTR/Gypsy	0.00	MER5A	0.00
LINE/RTE-X	0.00	L2	0.00

Ontology	Term	FDR Q-val
GO Biological Process	regulation of gene expression, epigenetic	30.43
GO Biological Process	negative regulation of gene expression, epigenetic	28.24
GO Biological Process	DNA replication-dependent nucleosome assembly	21.43
GO Biological Process	chromatin silencing	20.29
GO Biological Process	protein-DNA complex subunit organization	20.17
GO Biological Process	positive regulation of gene expression, epigenetic	19.68
GO Biological Process	nucleosome organization	18.71
GO Biological Process	chromatin assembly or disassembly	17.24
GO Biological Process	protein-DNA complex assembly	15.76
GO Biological Process	chromatin assembly	15.52
GO Biological Process	gene silencing	15.22
GO Biological Process	telomere organization	14.17
GO Biological Process	nucleosome assembly	13.74
GO Biological Process	chromatin remodeling	13.43
GO Biological Process	regulation of adaptive immune response	13.00
GO Biological Process	DNA packaging	11.33
GO Biological Process	regulation of megakaryocyte differentiation	10.91
GO Biological Process	protein heterotetramerization	9.74
GO Biological Process	regulation of viral transcription	9.09
GO Biological Process	nuclear-transcribed mRNA catabolic process, nonsense-mediated decay	8.27
Human Phenotype	Laryngomalacia	1.93

Supplementary Figure 1819: Properties and genomic distribution of motifs identified for the ZSCAN29 transcription factor in GM12878 (accession ENCSR412YGM).

TF-MoDisCO pattern_0 n=1586, CWM

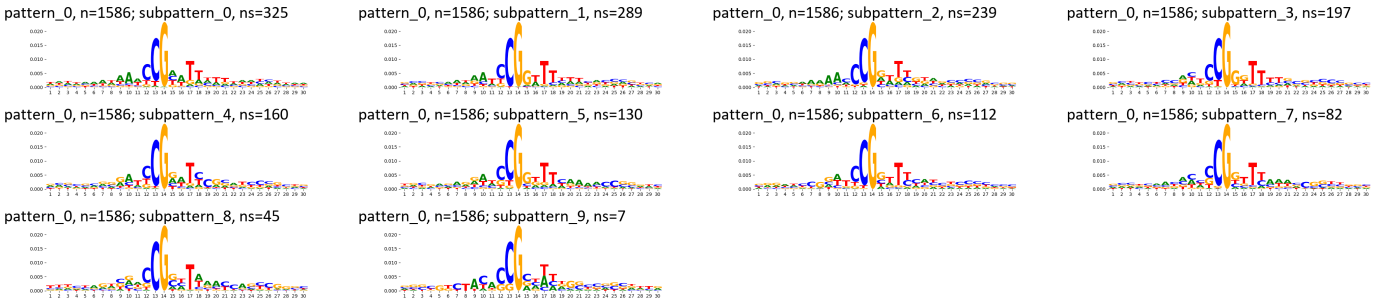

TF-MoDisCO pattern_0 n=1586, PWM

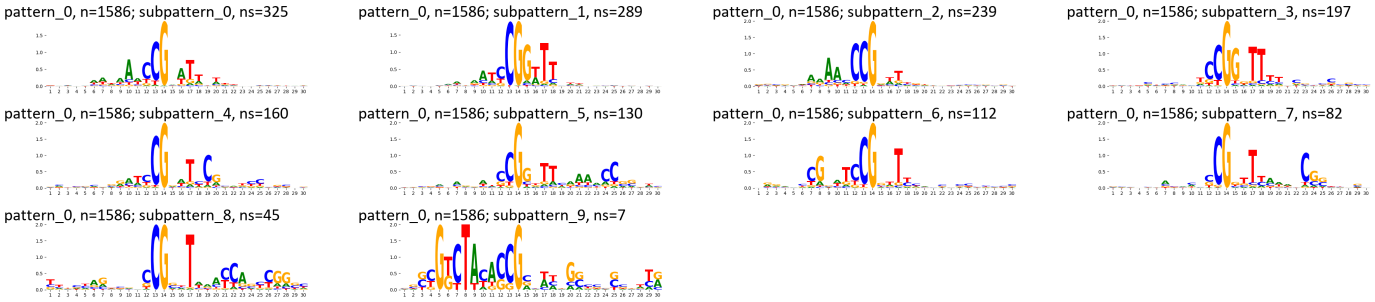

TF-MoDisCO pattern_1 n=912, CWM

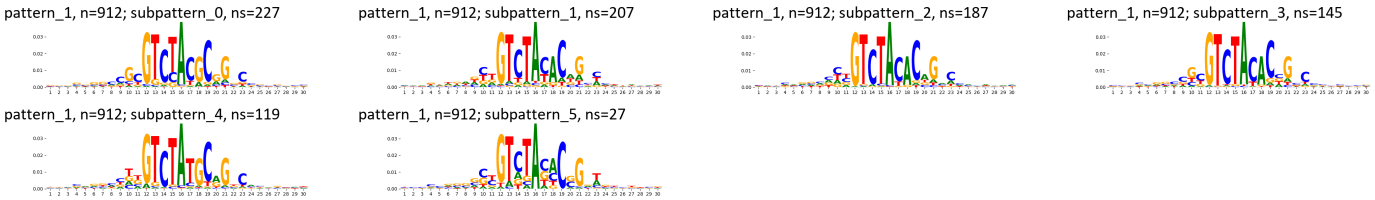

TF-MoDisCO pattern_1 n=912, PWM

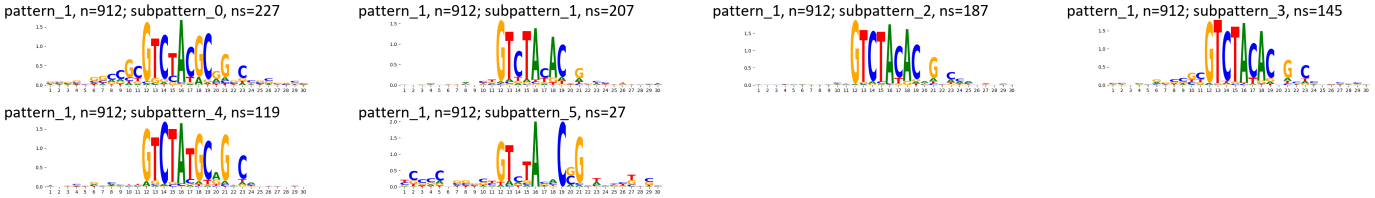

Supplementary Figure 1820: TF-MoDisCO subpatterns for the ZSCAN29 transcription factor in GM12878 (accession ENCSR412YGM).

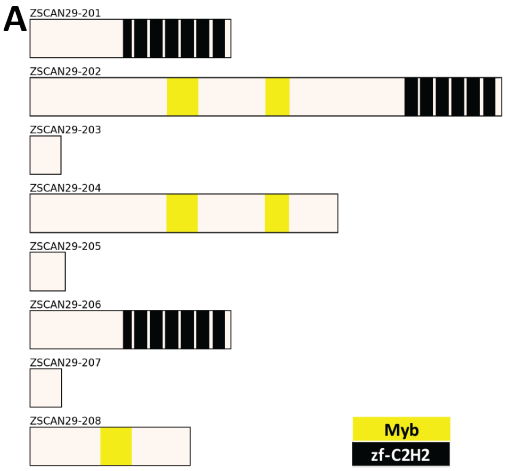

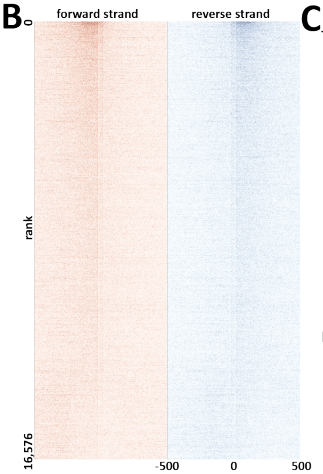

C

peaks	
state	fraction
TssA	0.28
Quies	0.20
TssFlnk	0.18
TxWk	0.12
EnhWk	0.09
TssFlnkU	0.04
EnhA1	0.04
EnhA2	0.03
Tx	0.03
TssBiv	0.03
TssFlnkD	0.03
ReprPC	0.02
ReprPCWk	0.02
EnhBiv	0.01
EnhG1	0.01
EnhG2	0.00
Het	0.00
ZNF/Rpts	0.00

D

peaks		peaks	
repeat	fraction	repeat	fraction
Simple_repeat	0.20	MIRb	0.07
SINE/Alu	0.20	MIR	0.04
SINE/MIR	0.17	L2a	0.03
LINE/L2	0.10	MIRc	0.03
LINE/L1	0.07	MIR3	0.03
DNA/hAT-Charlie	0.04	L2b	0.03
Low_complexity	0.04	L2c	0.03
LTR/ERV1	0.03	G-rich	0.03
LTR/ERVL-MaLR	0.03	AluJb	0.02
LTR/ERVL	0.02	AluSx	0.02
DNA/TcMar-Tigger	0.01	AluSx1	0.02
LINE/CR1	0.01	AluSz	0.02
DNA/hAT-Tip100	0.01	AluJo	0.02
tRNA	0.01	AluJr	0.01
DNA/hAT-Blackjack	0.00	AluY	0.01
LTR/ERVK	0.00	L2	0.01
LINE/RTE-X	0.00	GA-rich	0.01
LTR/Gypsy	0.00	AluSq2	0.01

E

Ontology	Term	FDR Q-val
GO Biological Process	regulation of transcription from RNA polymerase II promoter in response to stress	56.82
GO Biological Process	regulation of DNA-templated transcription in response to stress	52.89
GO Biological Process	endoplasmic reticulum unfolded protein response	48.75
GO Biological Process	cellular response to topologically incorrect protein	44.20
GO Biological Process	cellular response to unfolded protein	42.72
GO Biological Process	mitochondrial transport	42.61
GO Biological Process	regulation of intrinsic apoptotic signaling pathway	40.36
GO Biological Process	liver regeneration	39.43
GO Biological Process	positive regulation of nuclear-transcribed mRNA catabolic process, deadenylation-dependent decay	38.47
GO Biological Process	regulation of endoplasmic reticulum unfolded protein response	36.30
GO Biological Process	negative regulation of endoplasmic reticulum unfolded protein response	36.13
GO Biological Process	regulation of transcription from RNA polymerase II promoter in response to hypoxia	35.47
GO Biological Process	negative regulation of intrinsic apoptotic signaling pathway	35.11
GO Biological Process	response to topologically incorrect protein	32.52
GO Biological Process	positive regulation of mRNA catabolic process	32.40
GO Biological Process	cellular response to epidermal growth factor stimulus	32.38
GO Biological Process	regulation of hematopoietic progenitor cell differentiation	31.27
GO Biological Process	response to epidermal growth factor	30.79
GO Biological Process	response to unfolded protein	30.40
GO Biological Process	regulation of endoplasmic reticulum stress-induced intrinsic apoptotic signaling pathway	28.71
Human Phenotype	Exercise intolerance	9.54
Human Phenotype	Abnormality of monocarboxylic acid metabolism	8.72

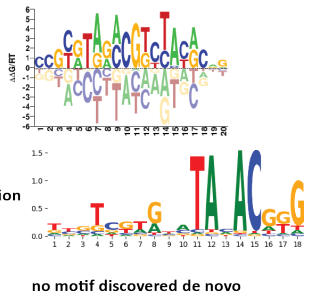

Supplementary Figure 1821: Properties and genomic distribution of motifs identified for the ZSCAN29 transcription factor in HepG2 (accession ENCSR422VAG).

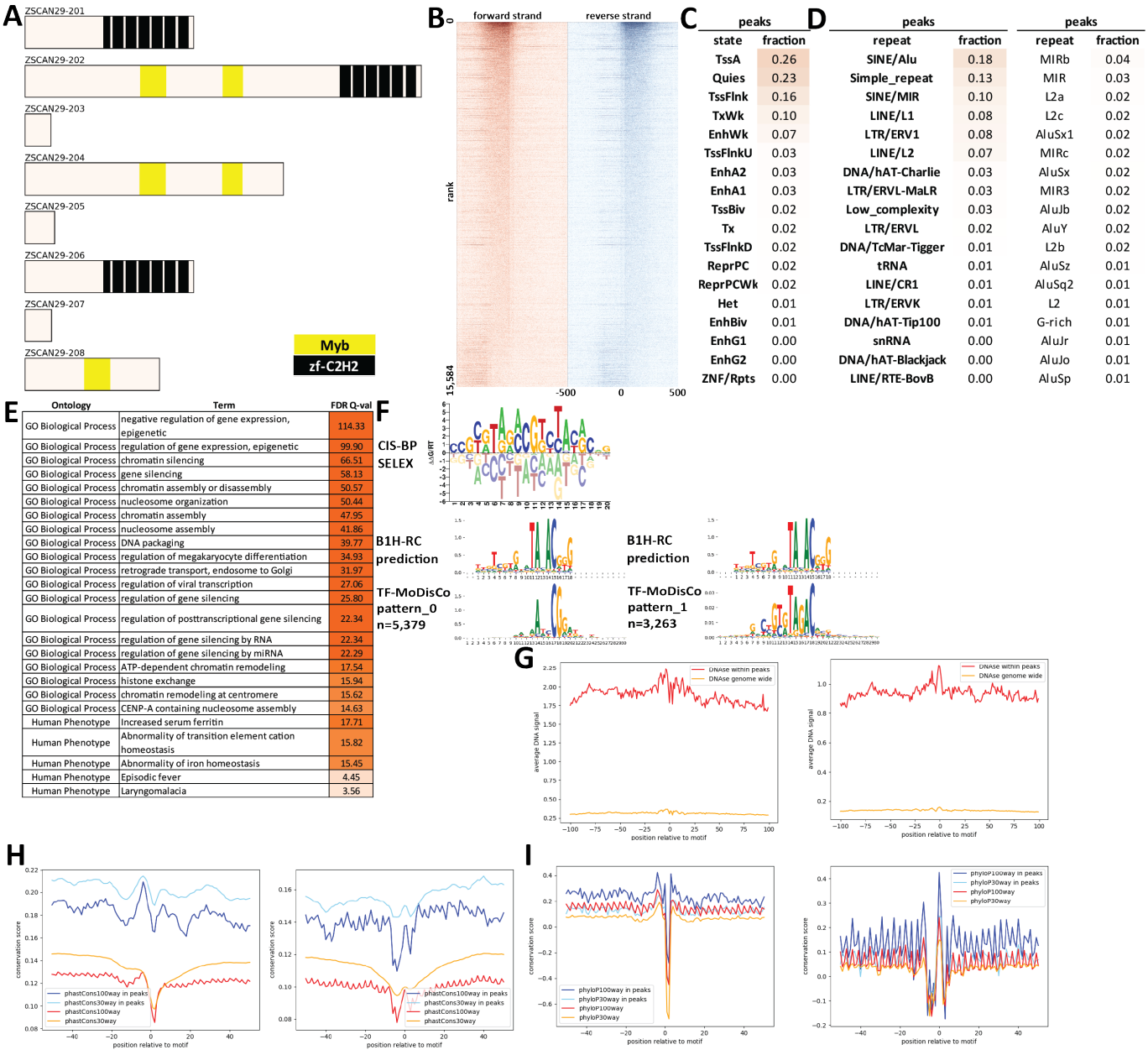

Supplementary Figure 1822: Properties and genomic distribution of motifs identified for the ZSCAN29 transcription factor in K562 (accession ENCSR175SZH).

TF-MoDisCO pattern_0 n=5379, CWM

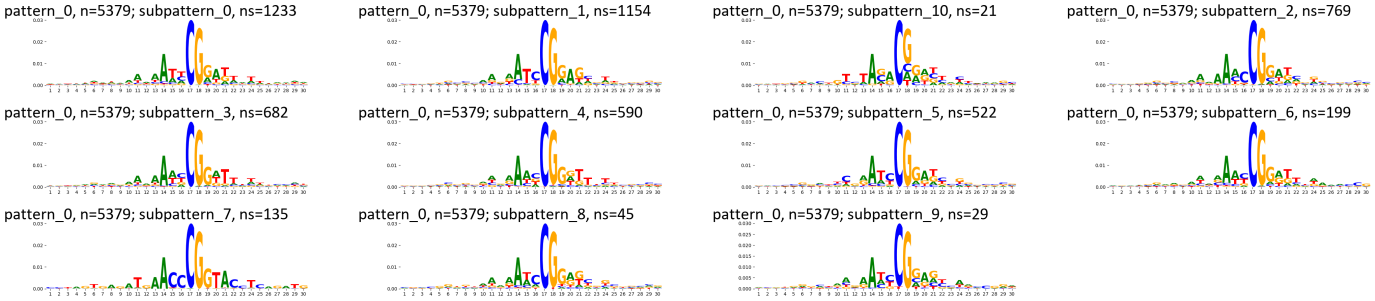

TF-MoDisCO pattern_0 n=5379, PWM

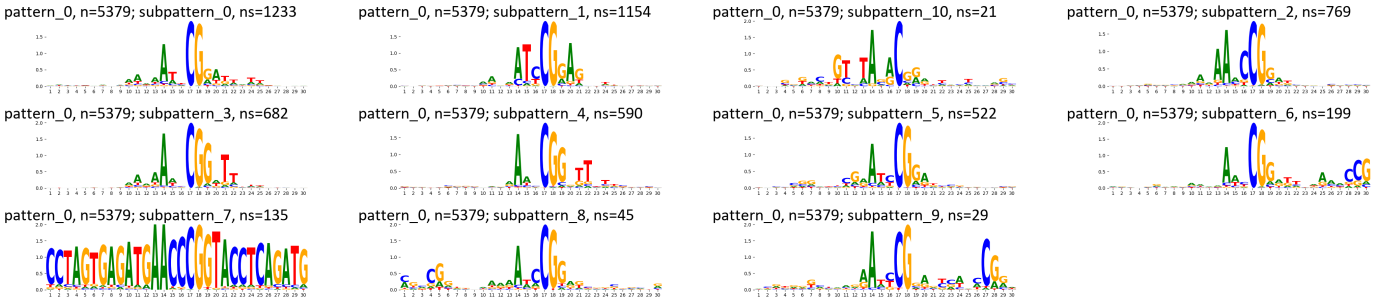

TF-MoDisCO pattern_1 n=3263, CWM

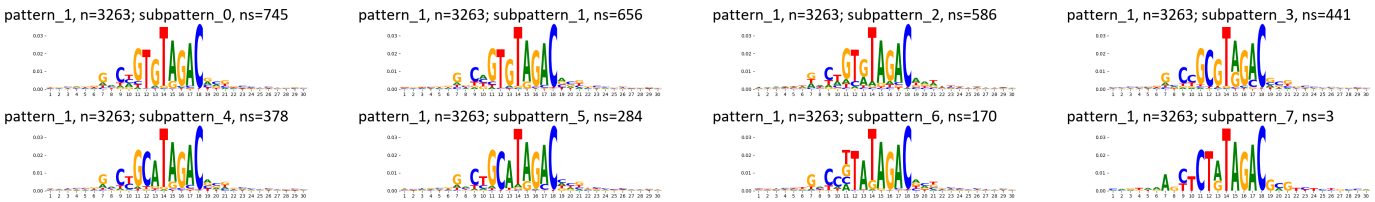

TF-MoDisCO pattern_1 n=3263, PWM

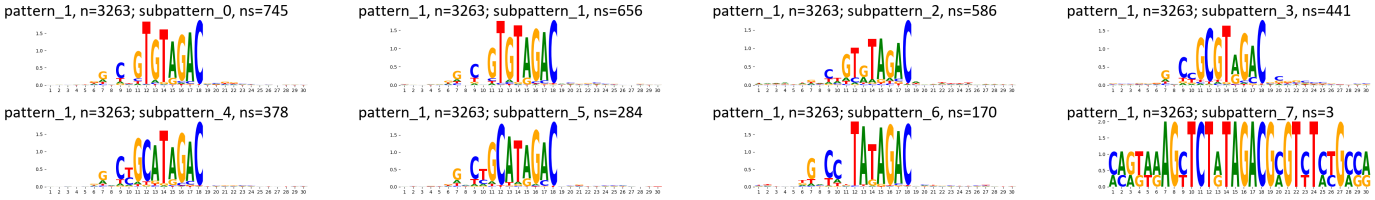

Supplementary Figure 1823: TF-MoDisCO subpatterns for the ZSCAN29 transcription factor in K562 (accession ENCSR175SZH).

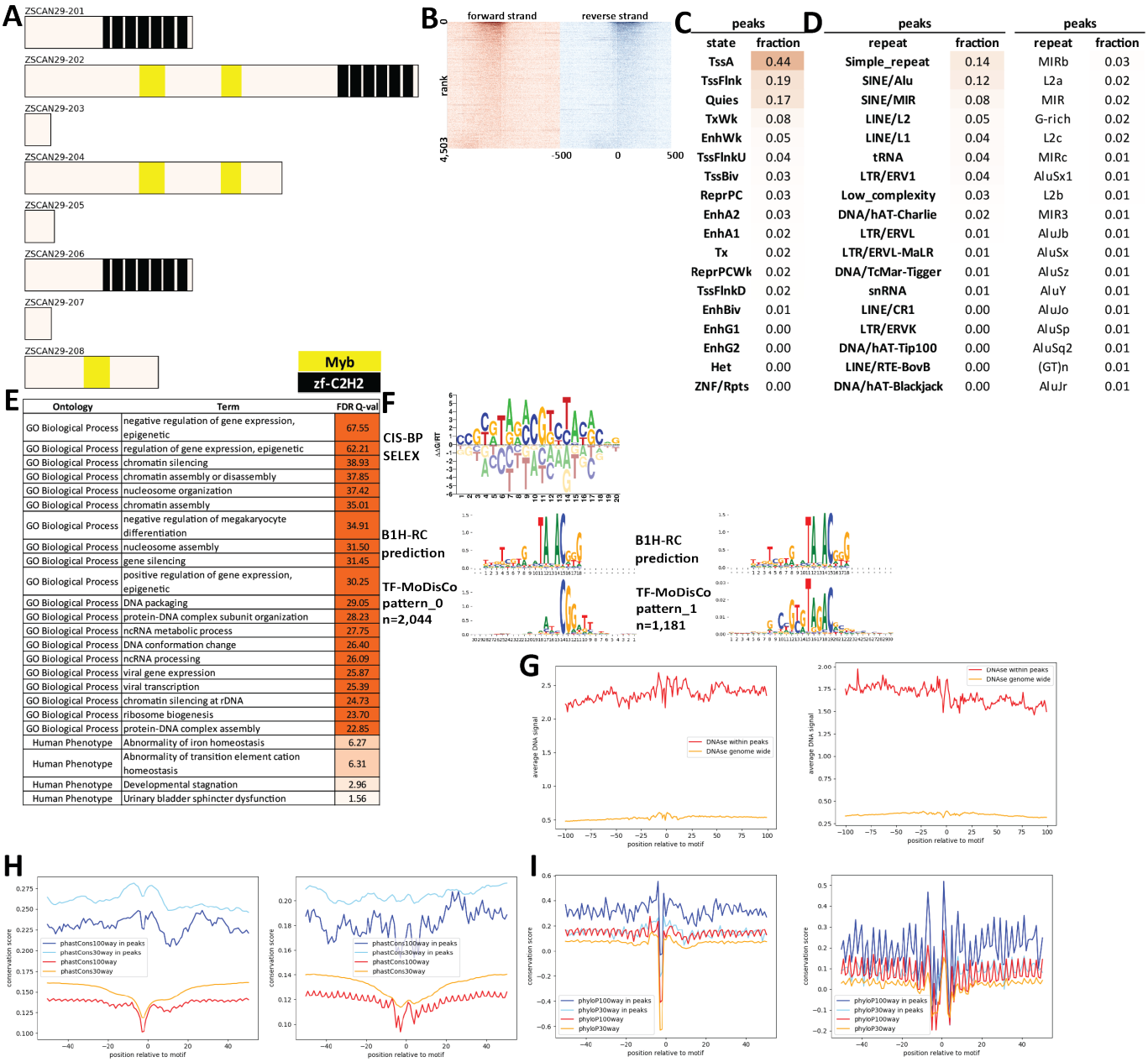

peaks	
state	fraction
TssA	0.44
TssFlnk	0.19
Quies	0.17
TxWk	0.08
EnhWk	0.05
TssFlnkU	0.04
TssBiv	0.03
ReprPC	0.03
EnhA2	0.03
EnhA1	0.02
Tx	0.02
ReprPCWk	0.02
TssFlnkD	0.02
EnhBiv	0.01
EnhG1	0.00
EnhG2	0.00
Het	0.00
ZNF/Rpts	0.00

peaks		peaks	
repeat	fraction	repeat	fraction
Simple_repeat	0.14	MIRb	0.03
SINE/Alu	0.12	L2a	0.02
SINE/MIR	0.08	MIR	0.02
LINE/L2	0.05	G-rich	0.02
LINE/L1	0.04	L2c	0.02
tRNA	0.04	MIRc	0.01
LTR/ERV1	0.04	AluSx1	0.01
Low_complexity	0.03	L2b	0.01
DNA/hAT-Charlie	0.02	MIR3	0.01
LTR/ERVL	0.01	AluJb	0.01
LTR/ERVL-MaLR	0.01	AluSx	0.01
DNA/TcMar-Tigger	0.01	AluSz	0.01
snRNA	0.01	AluY	0.01
LINE/CR1	0.00	AluJo	0.01
LTR/ERVK	0.00	AluSp	0.01
DNA/hAT-Tip100	0.00	AluSq2	0.01
LINE/RTE-BovB	0.00	(GT)n	0.01
DNA/hAT-Blackjack	0.00	AluJr	0.01

Ontology	Term	FDR Q-val
GO Biological Process	negative regulation of gene expression, epigenetic	67.55
GO Biological Process	regulation of gene expression, epigenetic	62.21
GO Biological Process	chromatin silencing	38.93
GO Biological Process	chromatin assembly or disassembly	37.85
GO Biological Process	nucleosome organization	37.42
GO Biological Process	chromatin assembly	35.01
GO Biological Process	negative regulation of megakaryocyte differentiation	34.91
GO Biological Process	nucleosome assembly	31.50
GO Biological Process	gene silencing	31.45
GO Biological Process	positive regulation of gene expression, epigenetic	30.25
GO Biological Process	DNA packaging	29.05
GO Biological Process	protein-DNA complex subunit organization	28.23
GO Biological Process	ncRNA metabolic process	27.75
GO Biological Process	DNA conformation change	26.40
GO Biological Process	ncRNA processing	26.09
GO Biological Process	viral gene expression	25.87
GO Biological Process	viral transcription	25.39
GO Biological Process	chromatin silencing at rDNA	24.73
GO Biological Process	ribosome biogenesis	23.70
GO Biological Process	protein-DNA complex assembly	22.85
Human Phenotype	Abnormality of iron homeostasis	6.27
Human Phenotype	Abnormality of transition element cation homeostasis	6.31
Human Phenotype	Developmental stagnation	2.96
Human Phenotype	Urinary bladder sphincter dysfunction	1.56

Supplementary Figure 1824: Properties and genomic distribution of motifs identified for the ZSCAN29 transcription factor in K562 (accession ENCSR635EXI).

TF-MoDisCO pattern_0 n=2044, CWM

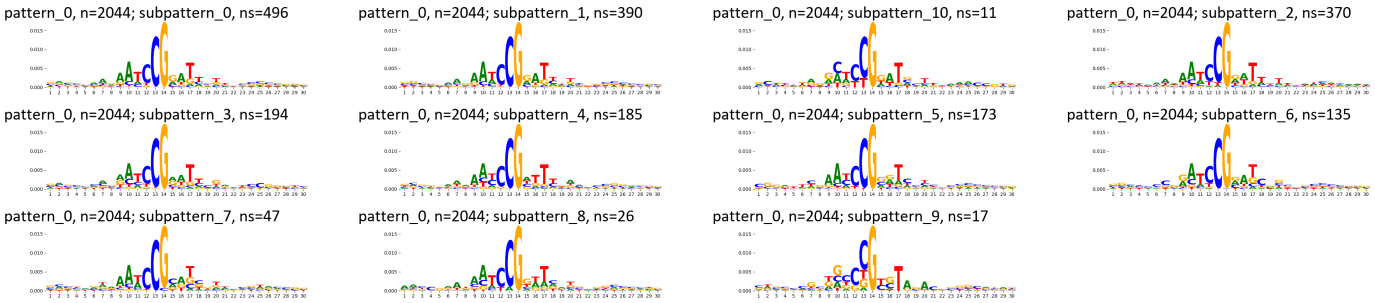

TF-MoDisCO pattern_0 n=2044, PWM

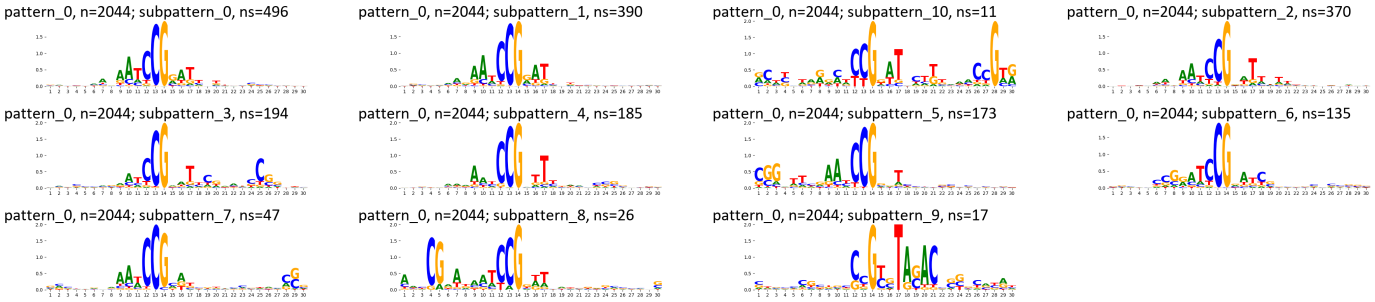

TF-MoDisCO pattern_1 n=1181, CWM

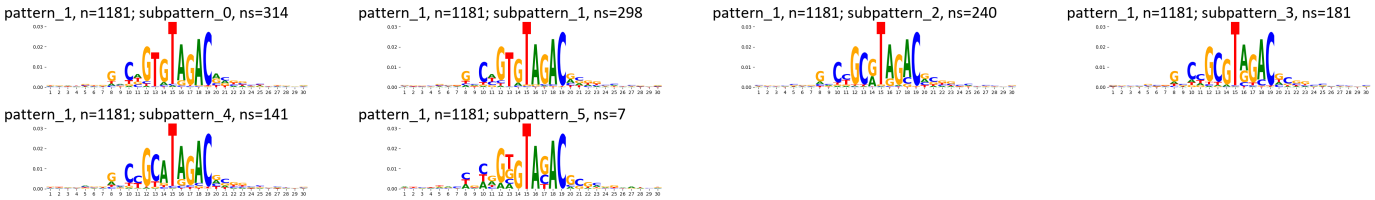

TF-MoDisCO pattern_1 n=1181, PWM

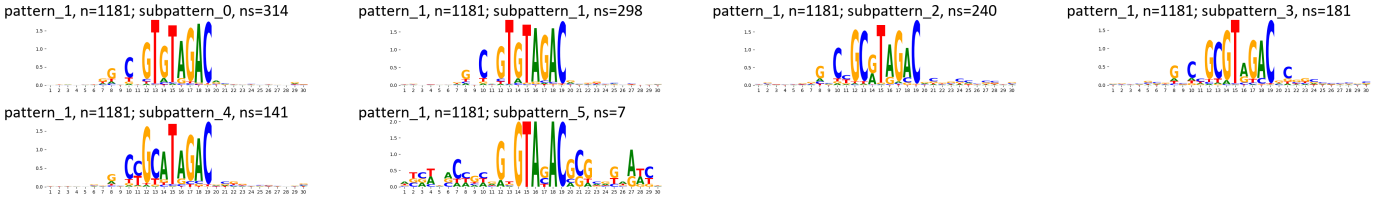

Supplementary Figure 1825: TF-MoDisCO subpatterns for the ZSCAN29 transcription factor in K562 (accession ENCSR635EXI).

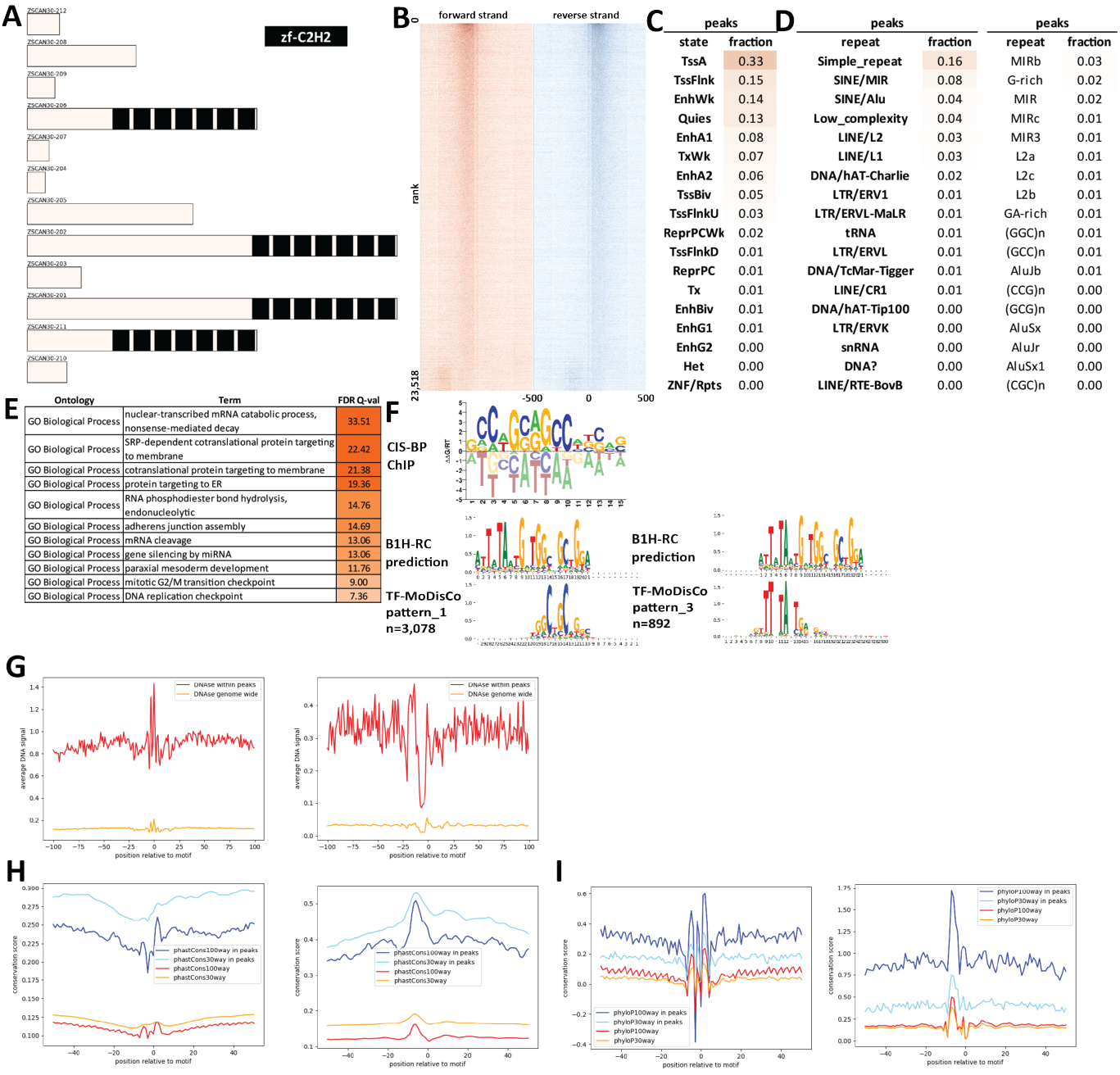

Supplementary Figure 1826: Properties and genomic distribution of motifs identified for the ZSCAN30 transcription factor in HEK293 (accession ENCSR768VNZ).

TF-MoDisCO pattern_1 n=3078, CWM

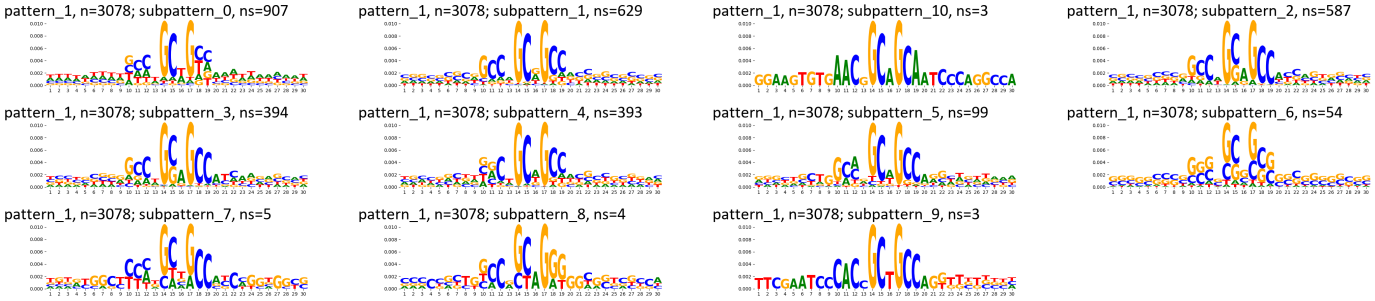

TF-MoDisCO pattern_1 n=3078, PWM

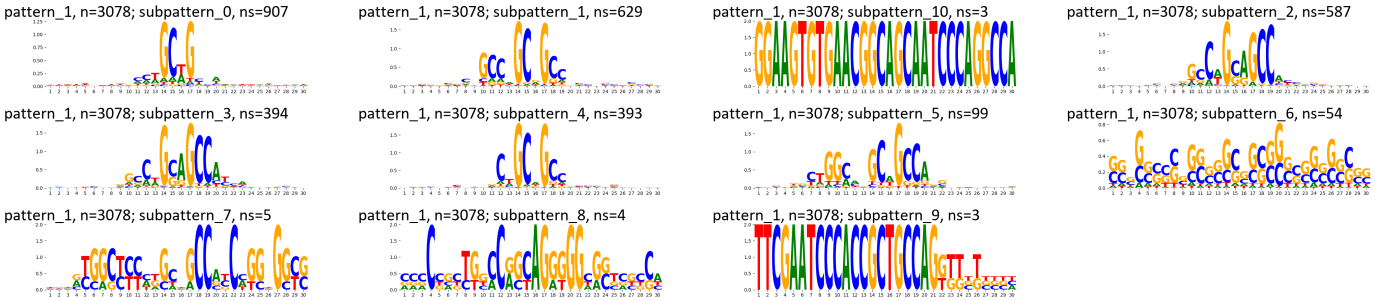

TF-MoDisCO pattern_3 n=892, CWM

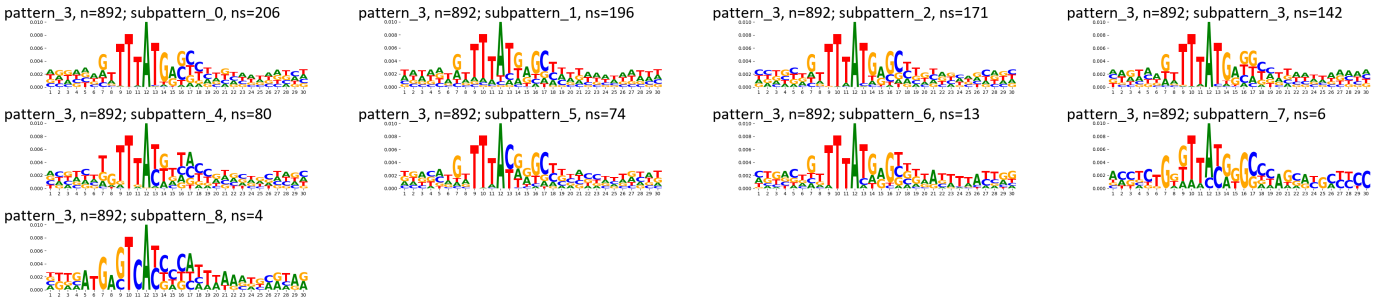

TF-MoDisCO pattern_3 n=892, PWM

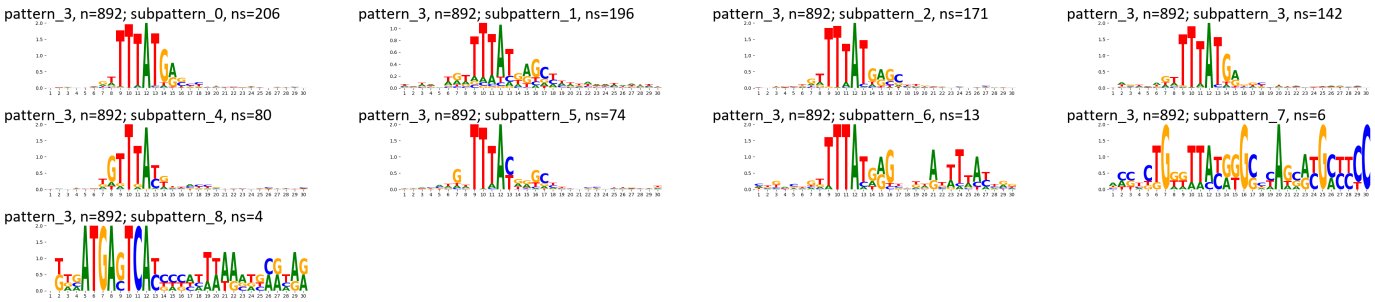

Supplementary Figure 1827: TF-MoDisCO subpatterns for the ZSCAN30 transcription factor in HEK293 (accession ENCSR768VNZ).

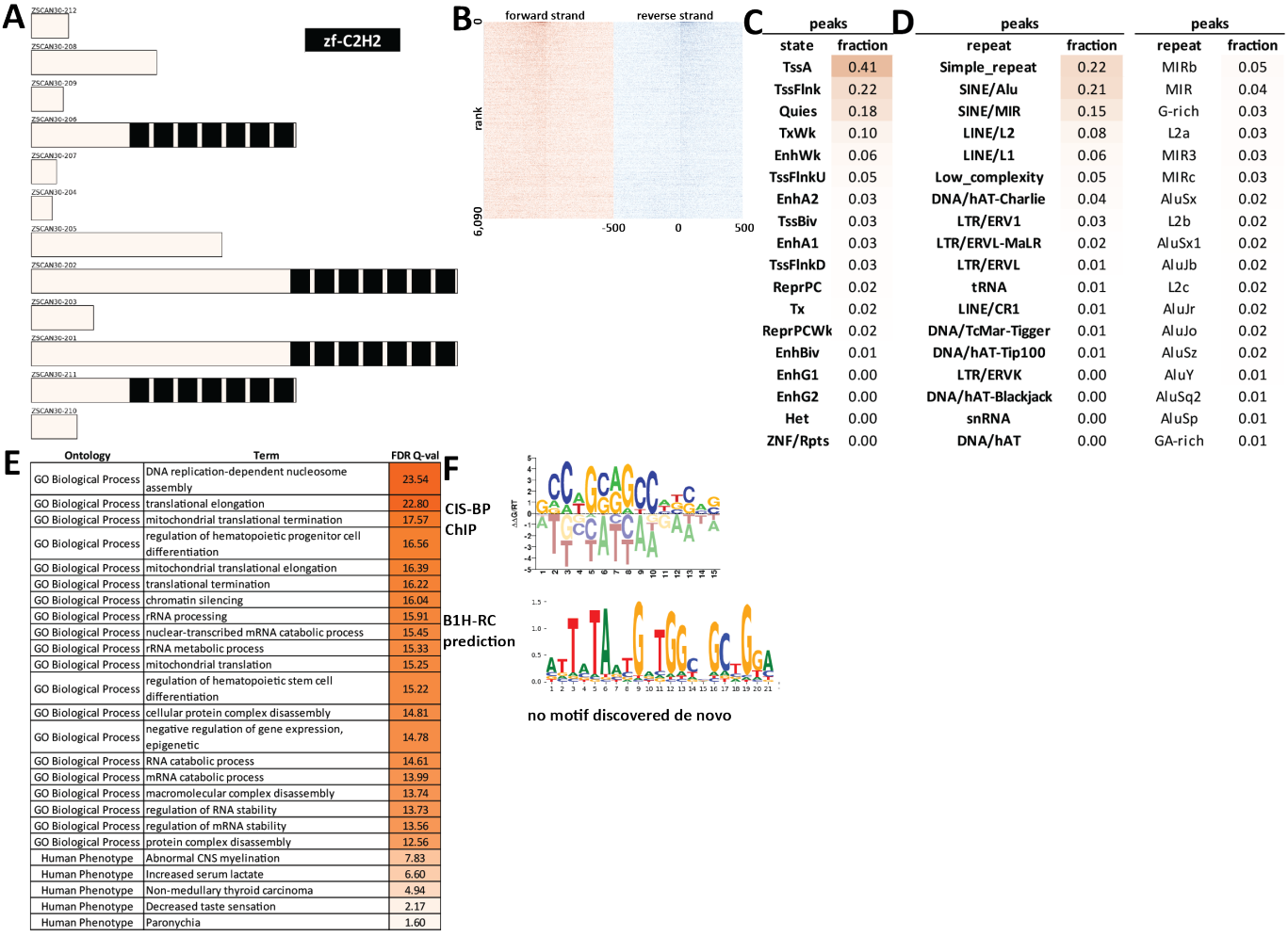

C

peaks	
state	fraction
TssA	0.41
TssFlnk	0.22
Quies	0.18
TxWk	0.10
EnhWk	0.06
TssFlnkU	0.05
EnhA2	0.03
TssBiv	0.03
EnhA1	0.03
TssFlnkD	0.03
ReprPC	0.02
Tx	0.02
ReprPCWk	0.02
EnhBiv	0.01
EnhG1	0.00
EnhG2	0.00
Het	0.00
ZNF/Rpts	0.00

D

peaks		peaks	
repeat	fraction	repeat	fraction
Simple_repeat	0.22	MIRb	0.05
SINE/Alu	0.21	MIR	0.04
SINE/MIR	0.15	G-rich	0.03
LINE/L2	0.08	L2a	0.03
LINE/L1	0.06	MIR3	0.03
Low_complexity	0.05	MIRc	0.03
DNA/hAT-Charlie	0.04	AluSx	0.02
LTR/ERV1	0.03	L2b	0.02
LTR/ERVL-MaLR	0.02	AluSx1	0.02
LTR/ERVL	0.01	AluJb	0.02
tRNA	0.01	L2c	0.02
LINE/CR1	0.01	AluJr	0.02
DNA/TcMar-Tigger	0.01	AluJo	0.02
DNA/hAT-Tip100	0.01	AluSz	0.02
LTR/ERVK	0.00	AluY	0.01
DNA/hAT-Blackjack	0.00	AluSq2	0.01
snRNA	0.00	AluSp	0.01
DNA/hAT	0.00	GA-rich	0.01

E

Ontology	Term	FDR Q-val
GO Biological Process	DNA replication-dependent nucleosome assembly	23.54
GO Biological Process	translational elongation	22.80
GO Biological Process	mitochondrial translational termination	17.57
GO Biological Process	regulation of hematopoietic progenitor cell differentiation	16.56
GO Biological Process	mitochondrial translational elongation	16.39
GO Biological Process	translational termination	16.22
GO Biological Process	chromatin silencing	16.04
GO Biological Process	rRNA processing	15.91
GO Biological Process	nuclear-transcribed mRNA catabolic process	15.45
GO Biological Process	rRNA metabolic process	15.33
GO Biological Process	mitochondrial translation	15.25
GO Biological Process	regulation of hematopoietic stem cell differentiation	15.22
GO Biological Process	cellular protein complex disassembly	14.81
GO Biological Process	negative regulation of gene expression, epigenetic	14.78
GO Biological Process	RNA catabolic process	14.61
GO Biological Process	mRNA catabolic process	13.99
GO Biological Process	macromolecular complex disassembly	13.74
GO Biological Process	regulation of RNA stability	13.73
GO Biological Process	regulation of mRNA stability	13.56
GO Biological Process	protein complex disassembly	12.56
Human Phenotype	Abnormal CNS myelination	7.83
Human Phenotype	Increased serum lactate	6.60
Human Phenotype	Non-medullary thyroid carcinoma	4.94
Human Phenotype	Decreased taste sensation	2.17
Human Phenotype	Paronychia	1.60

Supplementary Figure 1828: Properties and genomic distribution of motifs identified for the ZSCAN30 transcription factor in HepG2 (accession ENCSR795CKZ).

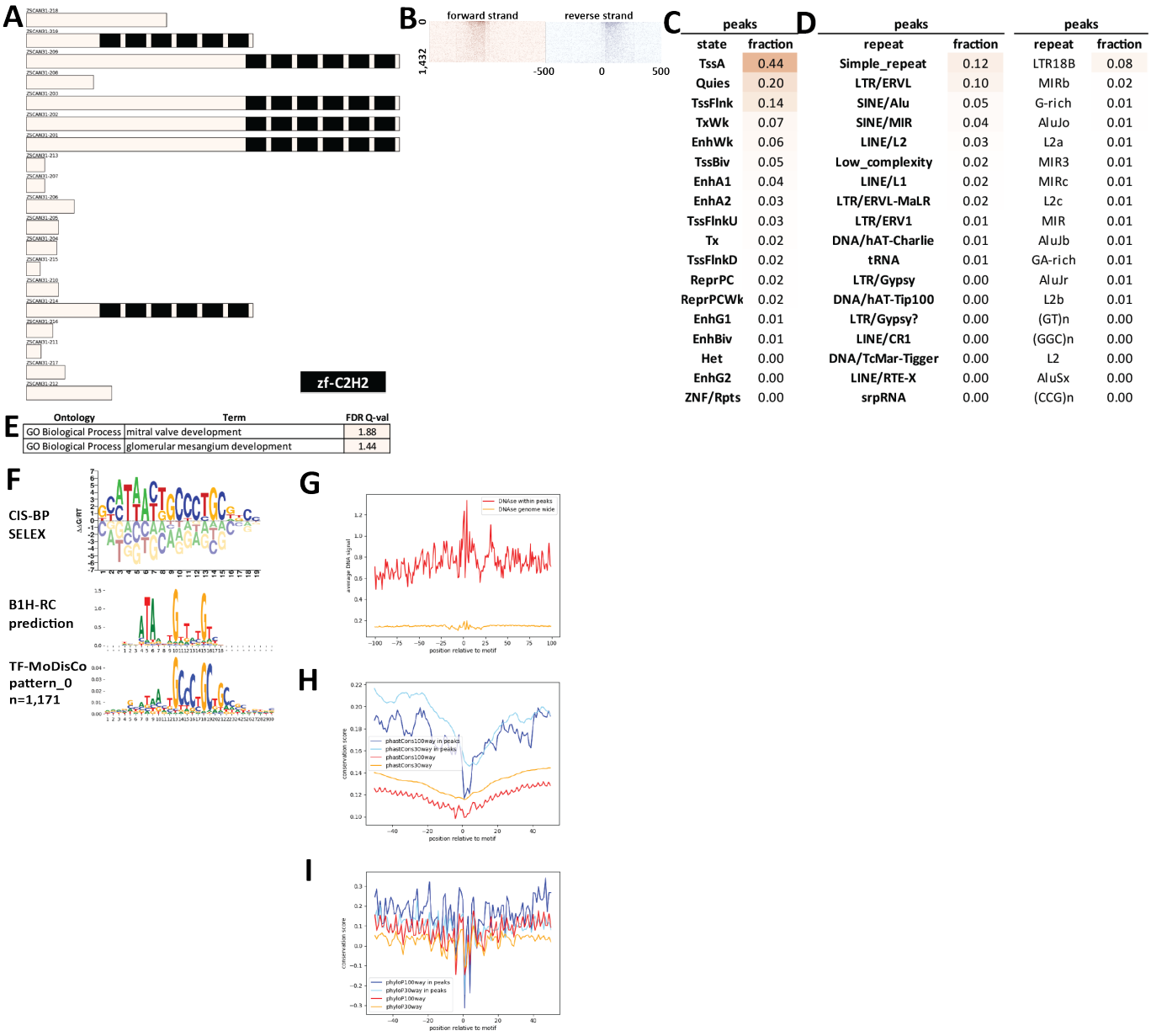

peaks

state	fraction
TssA	0.44
Quies	0.20
TssFlnk	0.14
TxWk	0.07
EnhWk	0.06
TssBiv	0.05
EnhA1	0.04
EnhA2	0.03
TssFlnkU	0.03
Tx	0.02
TssFlnkD	0.02
ReprPC	0.02
ReprPCWk	0.02
EnhG1	0.01
EnhBiv	0.01
Het	0.00
EnhG2	0.00
ZNF/Rpts	0.00

peaks

repeat	fraction
Simple_repeat	0.12
LTR/ERVL	0.10
SINE/Alu	0.05
SINE/MIR	0.04
LINE/L2	0.03
Low_complexity	0.02
LINE/L1	0.02
LTR/ERVL-MaLR	0.02
LTR/ERV1	0.01
DNA/hAT-Charlie	0.01
tRNA	0.01
LTR/Gypsy	0.00
DNA/hAT-Tip100	0.00
LTR/Gypsy?	0.00
LINE/CR1	0.00
DNA/TcMar-Tigger	0.00
LINE/RTE-X	0.00
srpRNA	0.00

peaks

repeat	fraction
LTR18B	0.08
MIRb	0.02
G-rich	0.01
AluJo	0.01
L2a	0.01
MIR3	0.01
MIRc	0.01
L2c	0.01
MIR	0.01
AluJb	0.01
GA-rich	0.01
AluJr	0.01
L2b	0.01
(GT)n	0.00
(GGC)n	0.00
L2	0.00
AluSx	0.00
(CCG)n	0.00

Supplementary Figure 1829: Properties and genomic distribution of motifs identified for the ZSCAN31 transcription factor in HEK293 (accession Hughes NB models).

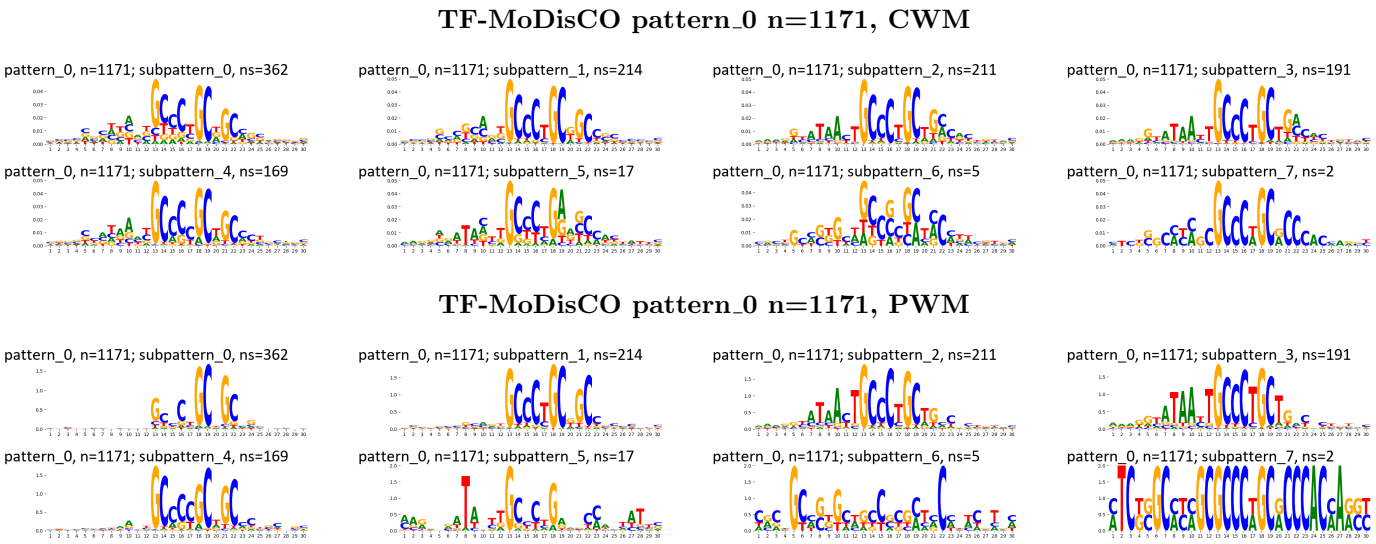

Supplementary Figure 1830: TF-MoDisCO subpatterns for the ZSCAN31 transcription factor in HEK293 (accession Hughes NB models).

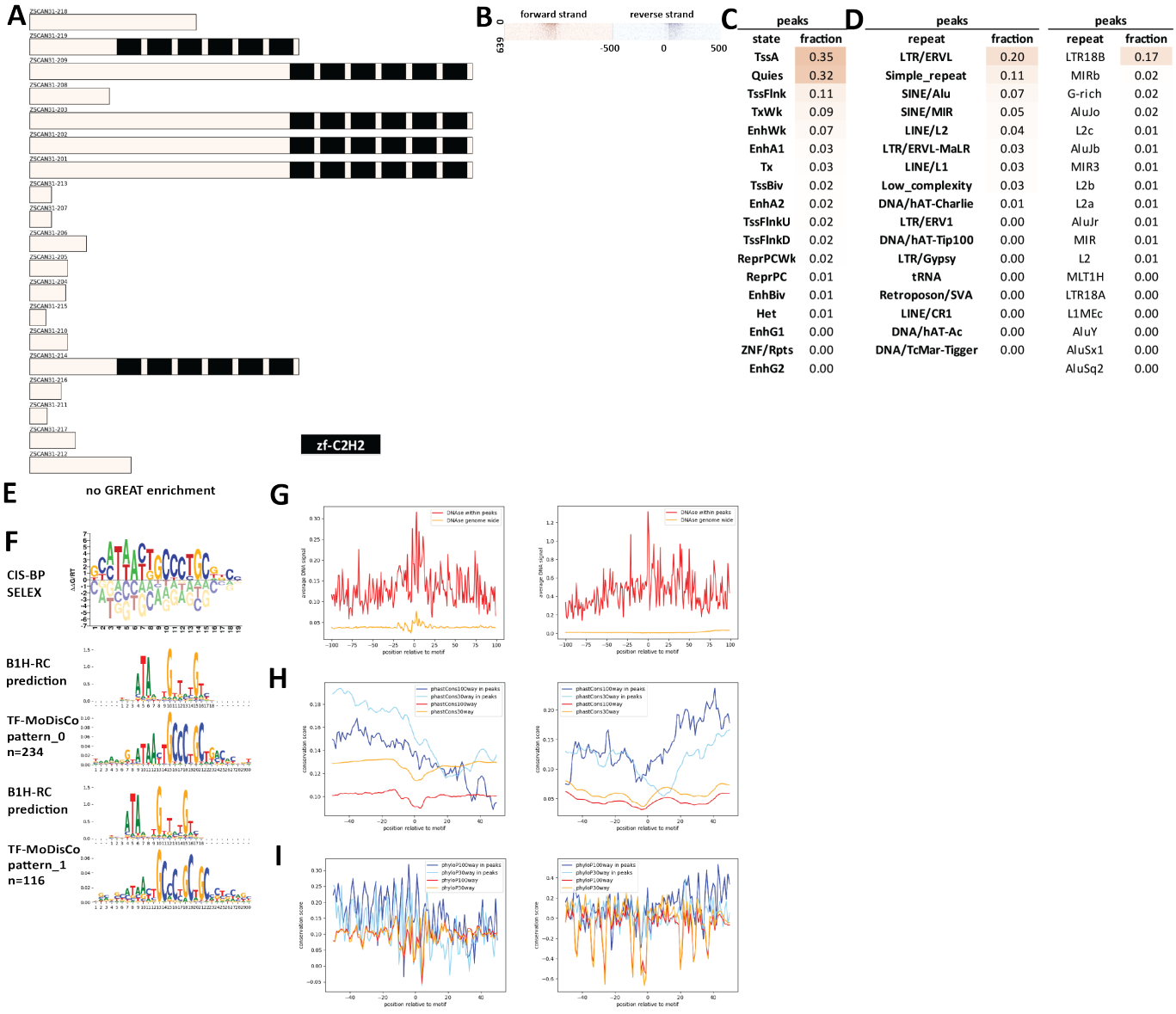

Supplementary Figure 1831: Properties and genomic distribution of motifs identified for the ZSCAN31 transcription factor in HEK293 (accession Hughes GR models).

TF-MoDisCO pattern_0 n=234, CWM

pattern_0, n=234; subpattern_0, ns=107

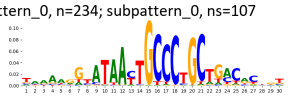

pattern_0, n=234; subpattern_1, ns=92

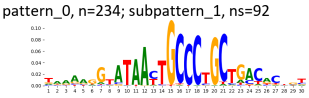

pattern_0, n=234; subpattern_2, ns=35

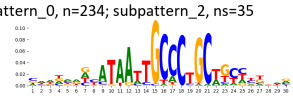

TF-MoDisCO pattern_0 n=234, PWM

pattern_0, n=234; subpattern_0, ns=107

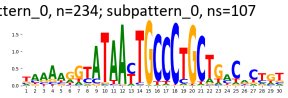

pattern_0, n=234; subpattern_1, ns=92

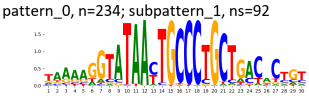

pattern_0, n=234; subpattern_2, ns=35

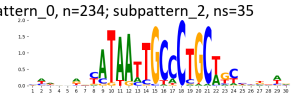

TF-MoDisCO pattern_1 n=116, CWM

pattern_1, n=116; subpattern_0, ns=36

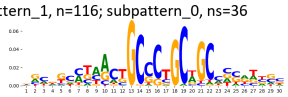

pattern_1, n=116; subpattern_1, ns=32

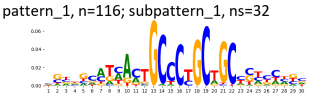

pattern_1, n=116; subpattern_2, ns=27

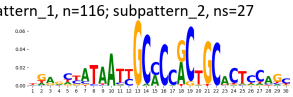

pattern_1, n=116; subpattern_3, ns=21

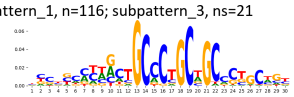

TF-MoDisCO pattern_1 n=116, PWM

pattern_1, n=116; subpattern_0, ns=36

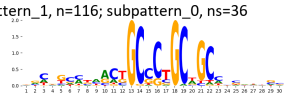

pattern_1, n=116; subpattern_1, ns=32

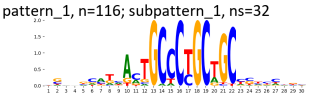

pattern_1, n=116; subpattern_2, ns=27

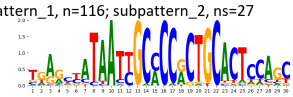

pattern_1, n=116; subpattern_3, ns=21

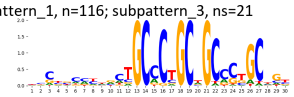

Supplementary Figure 1832: TF-MoDisCO subpatterns for the ZSCAN31 transcription factor in HEK293 (accession Hughes GR models).

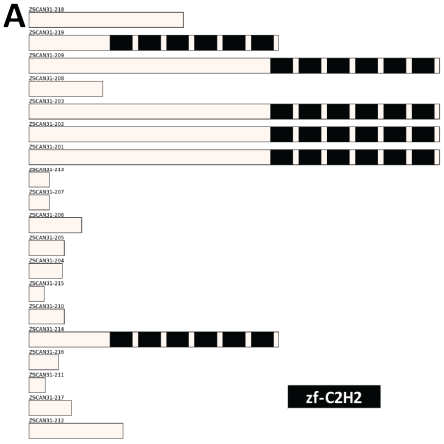

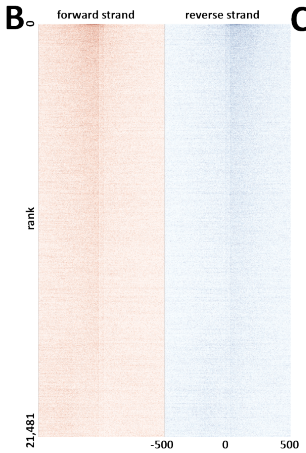

C

peaks	
state	fraction
TssA	0.34
TssFlnk	0.20
Quies	0.16
TxWk	0.09
EnhWk	0.06
TssFlnkU	0.04
TssBiv	0.03
EnhA2	0.03
EnhA1	0.03
Tx	0.03
ReprPC	0.02
TssFlnkD	0.02
ReprPCWk	0.02
EnhG1	0.01
EnhBiv	0.01
EnhG2	0.00
Het	0.00
ZNF/Rpts	0.00

D

peaks		peaks	
repeat	fraction	repeat	fraction
Simple_repeat	0.23	MIRb	0.05
SINE/Alu	0.15	G-rich	0.04
SINE/MIR	0.13	MIR	0.03
LINE/L2	0.07	MIR3	0.03
Low_complexity	0.05	L2a	0.03
LINE/L1	0.04	MIRc	0.02
DNA/hAT-Charlie	0.03	L2b	0.02
LTR/ERV1	0.02	L2c	0.02
LTR/ERVL-MaLR	0.02	AluJb	0.02
LTR/ERVL	0.02	AluSx	0.02
DNA/hAT-Tip100	0.01	AluSx1	0.02
DNA/TcMar-Tigger	0.01	AluSz	0.01
LINE/CR1	0.01	AluJr	0.01
tRNA	0.01	AluJo	0.01
LTR/ERVK	0.00	AluY	0.01
DNA/hAT-Blackjack	0.00	GA-rich	0.01
LTR/Gypsy	0.00	(GGC)n	0.01
DNA/hAT	0.00	AluSq2	0.01

E

Ontology	Term	FDR Q-val
GO Biological Process	IRE1-mediated unfolded protein response	47.56
GO Biological Process	endoplasmic reticulum unfolded protein response	47.34
GO Biological Process	regulation of transcription from RNA polymerase II promoter in response to stress	46.96
GO Biological Process	regulation of DNA-templated transcription in response to stress	42.28
GO Biological Process	cellular response to topologically incorrect protein	41.49
GO Biological Process	cellular response to unfolded protein	40.45
GO Biological Process	response to topologically incorrect protein	40.34
GO Biological Process	nuclear-transcribed mRNA catabolic process	39.37
GO Biological Process	regulation of intrinsic apoptotic signaling pathway	38.70
GO Biological Process	response to unfolded protein	36.96
GO Biological Process	nuclear-transcribed mRNA catabolic process, nonsense-mediated decay	31.31
GO Biological Process	regulation of transcription from RNA polymerase II promoter in response to hypoxia	25.06
GO Biological Process	cotranslational protein targeting to membrane	24.08
GO Biological Process	translational elongation	23.20
GO Biological Process	protein targeting to ER	23.10
GO Biological Process	viral gene expression	21.40
GO Biological Process	mitochondrial translational termination	21.30
GO Biological Process	mitochondrial transmembrane transport	20.85
GO Biological Process	mitochondrial translational elongation	20.60
GO Biological Process	nuclear-transcribed mRNA catabolic process, deadenylation-dependent decay	20.56
Human Phenotype	Abnormal CSF metabolite level	16.56
Human Phenotype	Exercise intolerance	13.07
Human Phenotype	Increased CSF lactate	12.96
Human Phenotype	Progressive macrocephaly	3.82

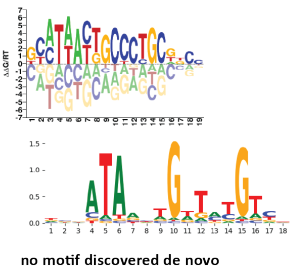

Supplementary Figure 1833: Properties and genomic distribution of motifs identified for the ZSCAN31 transcription factor in HepG2 (accession ENCSR493VBX).

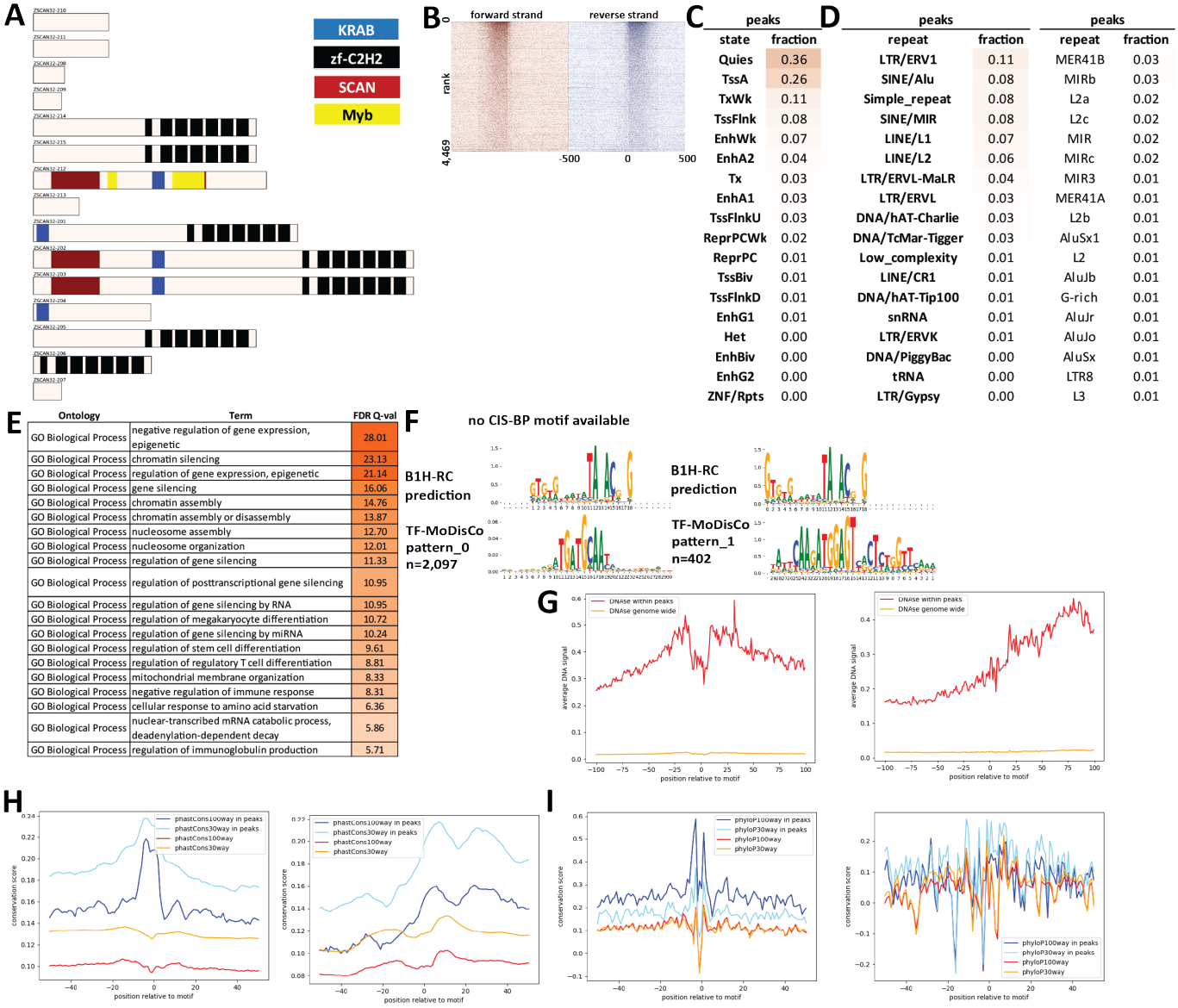

peaks	
state	fraction
Quies	0.36
TssA	0.26
TxWk	0.11
TssFlnk	0.08
EnhWk	0.07
EnhA2	0.04
Tx	0.03
EnhA1	0.03
TssFlnkU	0.03
ReprPCWk	0.02
ReprPC	0.01
TssBiv	0.01
TssFlnkD	0.01
EnhG1	0.01
Het	0.00
EnhBiv	0.00
EnhG2	0.00
ZNF/Rpts	0.00

peaks		peaks	
repeat	fraction	repeat	fraction
LTR/ERV1	0.11	MER41B	0.03
SINE/Alu	0.08	MIRb	0.03
Simple_repeat	0.08	L2a	0.02
SINE/MIR	0.08	L2c	0.02
LINE/L1	0.07	MIR	0.02
LINE/L2	0.06	MIRc	0.02
LTR/ERVL-MaLR	0.04	MIR3	0.01
LTR/ERVL	0.03	MER41A	0.01
DNA/hAT-Charlie	0.03	L2b	0.01
DNA/TcMar-Tigger	0.03	AluSx1	0.01
Low_complexity	0.01	L2	0.01
LINE/CR1	0.01	AluJb	0.01
DNA/hAT-Tip100	0.01	G-rich	0.01
snRNA	0.01	AluJr	0.01
LTR/ERVK	0.01	AluJo	0.01
DNA/PiggyBac	0.00	AluSx	0.01
tRNA	0.00	LTR8	0.01
LTR/Gypsy	0.00	L3	0.01

Ontology	Term	FDR Q-val
GO Biological Process	negative regulation of gene expression, epigenetic	28.01
GO Biological Process	chromatin silencing	23.13
GO Biological Process	regulation of gene expression, epigenetic	21.14
GO Biological Process	gene silencing	16.06
GO Biological Process	chromatin assembly	14.76
GO Biological Process	chromatin assembly or disassembly	13.87
GO Biological Process	nucleosome assembly	12.70
GO Biological Process	nucleosome organization	12.01
GO Biological Process	regulation of gene silencing	11.33
GO Biological Process	regulation of posttranscriptional gene silencing	10.95
GO Biological Process	regulation of gene silencing by RNA	10.95
GO Biological Process	regulation of megakaryocyte differentiation	10.72
GO Biological Process	regulation of gene silencing by miRNA	10.24
GO Biological Process	regulation of stem cell differentiation	9.61
GO Biological Process	regulation of regulatory T cell differentiation	8.81
GO Biological Process	mitochondrial membrane organization	8.33
GO Biological Process	negative regulation of immune response	8.31
GO Biological Process	cellular response to amino acid starvation	6.36
GO Biological Process	nuclear-transcribed mRNA catabolic process, deadenylation-dependent decay	5.86
GO Biological Process	regulation of immunoglobulin production	5.71

Supplementary Figure 1834: Properties and genomic distribution of motifs identified for the ZSCAN32 transcription factor in K562 (accession ENCSR870YEN).

TF-MoDisCO pattern_0 n=2097, CWM

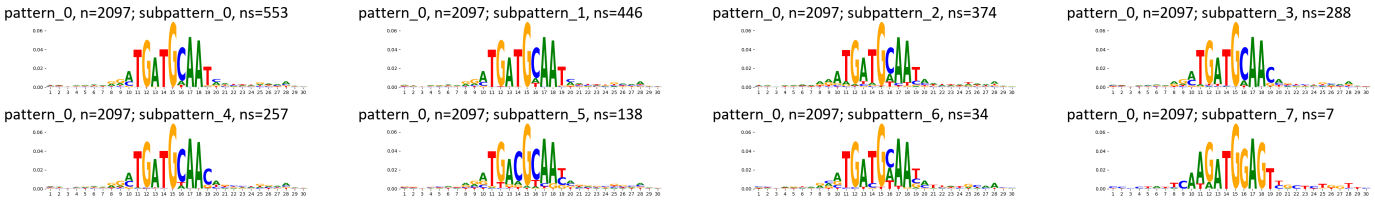

TF-MoDisCO pattern_0 n=2097, PWM

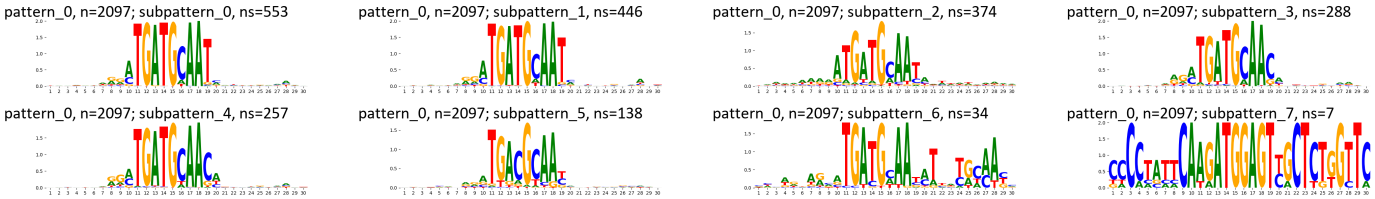

TF-MoDisCO pattern_1 n=402, CWM

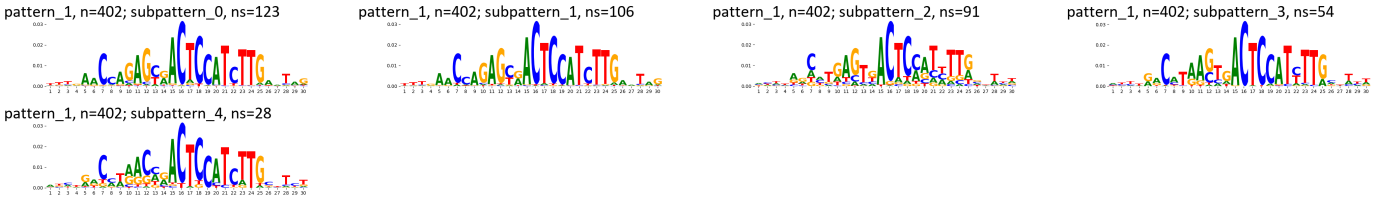

TF-MoDisCO pattern_1 n=402, PWM

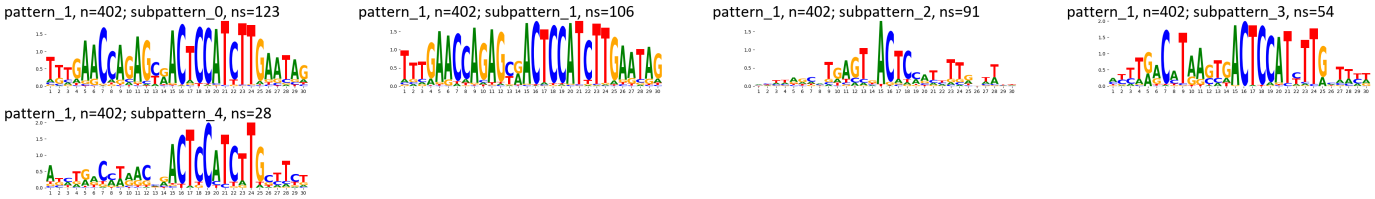

Supplementary Figure 1835: TF-MoDisCO subpatterns for the ZSCAN32 transcription factor in K562 (accession ENCSR870YEN).

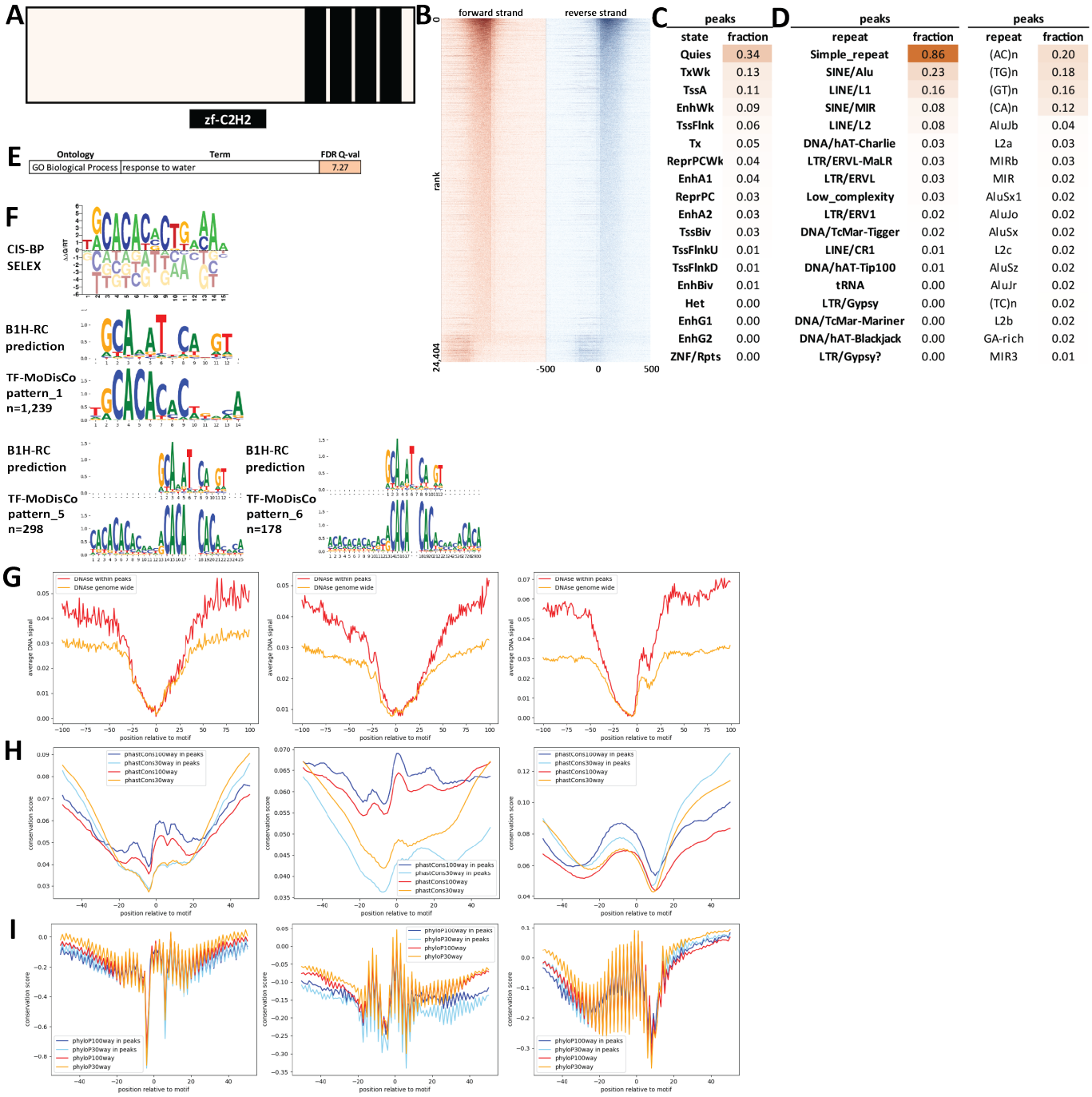

Supplementary Figure 1836: Properties and genomic distribution of motifs identified for the ZSCAN4 transcription factor in HEK293 (accession ENCSR211GNP).

TF-MoDisCO pattern_1 n=1239, CWM

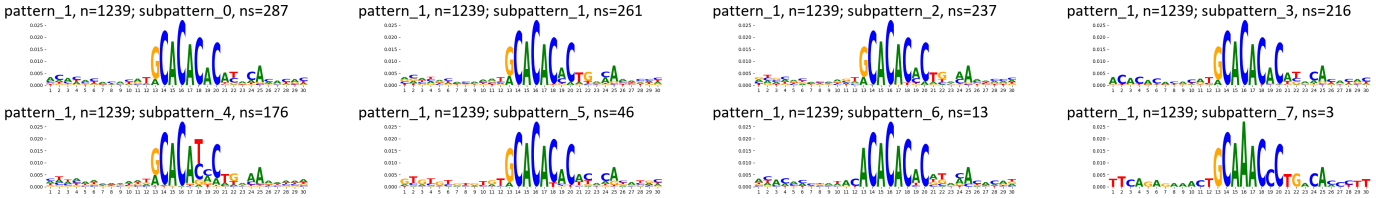

TF-MoDisCO pattern_1 n=1239, PWM

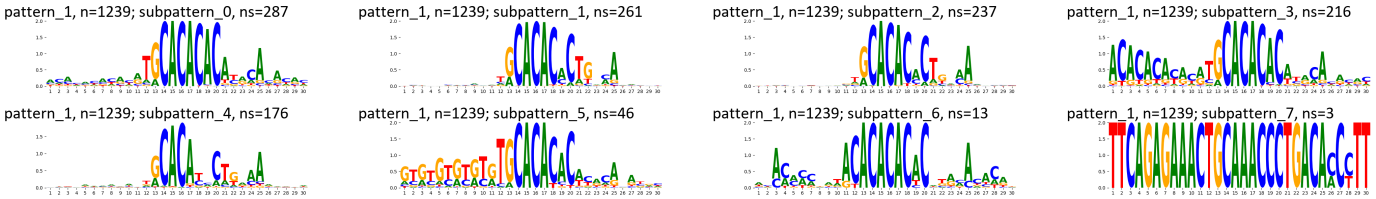

TF-MoDisCO pattern_5 n=298, CWM

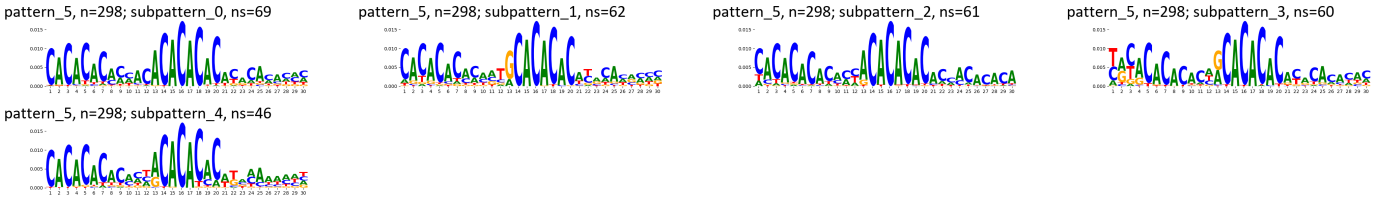

TF-MoDisCO pattern_5 n=298, PWM

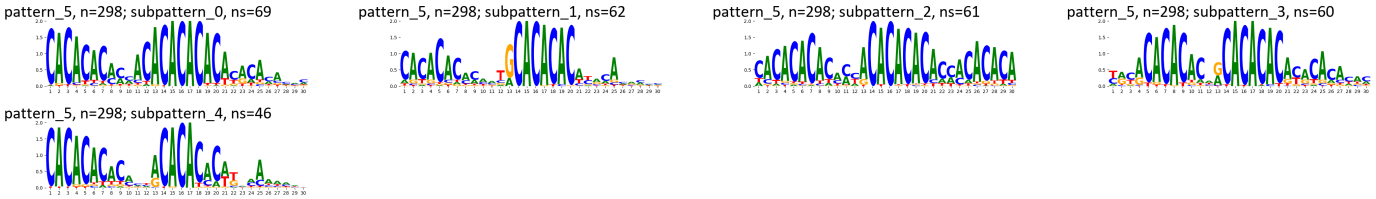

TF-MoDisCO pattern_6 n=178, CWM

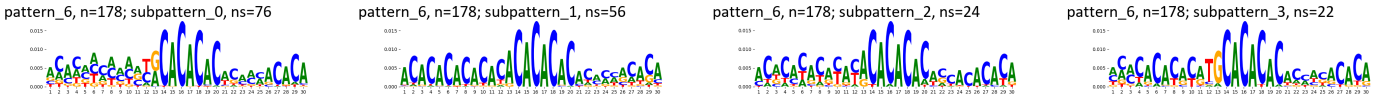

TF-MoDisCO pattern_6 n=178, PWM

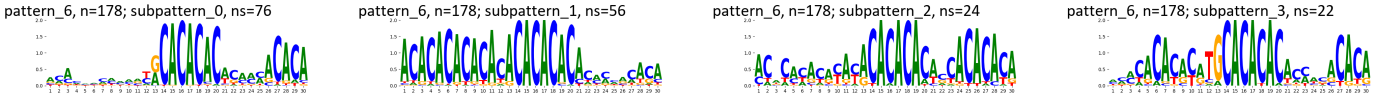

Supplementary Figure 1837: TF-MoDisCO subpatterns for the ZSCAN4 transcription factor in HEK293 (accession ENCSR211GNP).

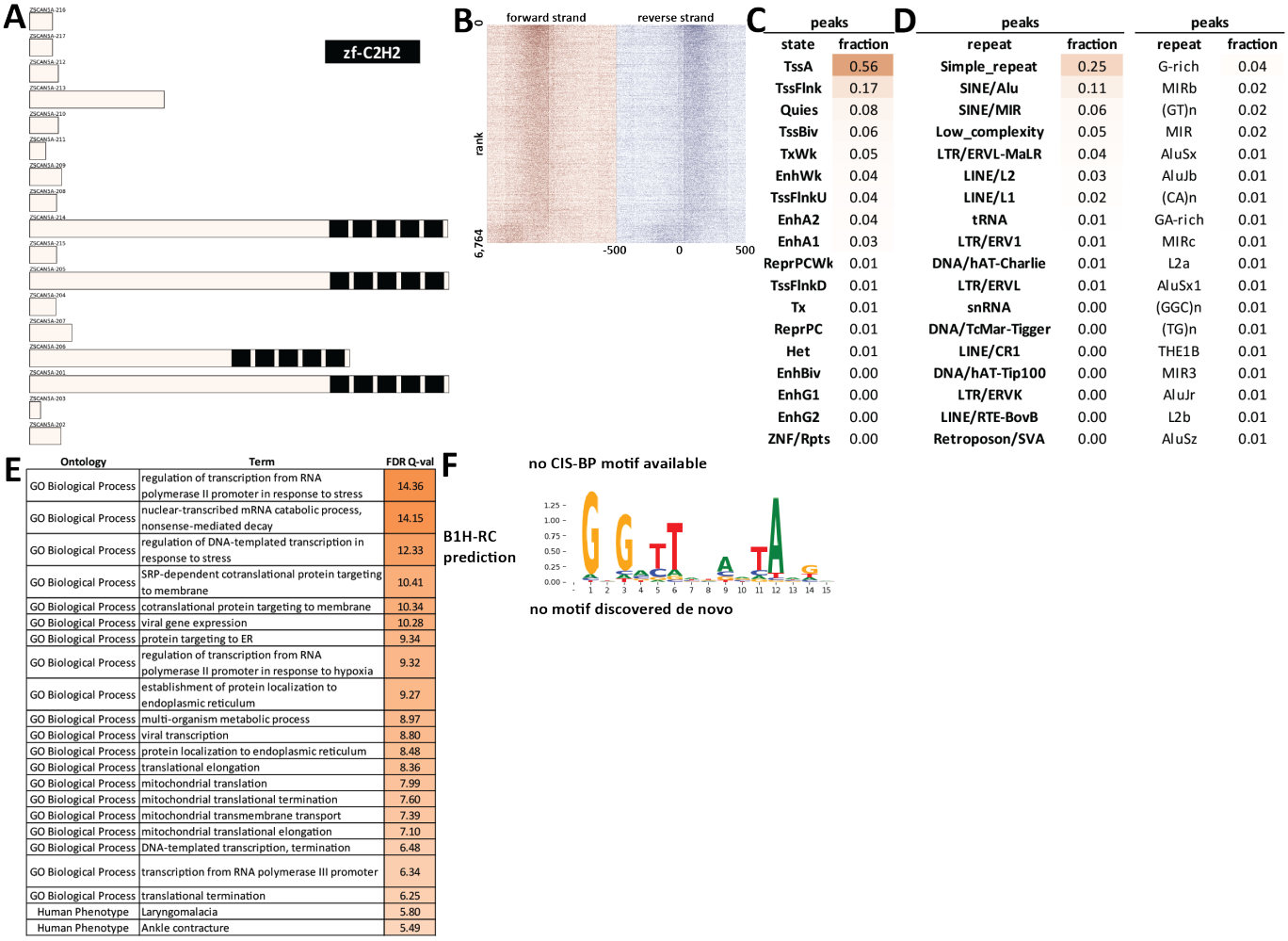

C

peaks	
state	fraction
TssA	0.56
TssFlnk	0.17
Quies	0.08
TssBiv	0.06
TxWk	0.05
EnhWk	0.04
TssFlnkU	0.04
EnhA2	0.04
EnhA1	0.03
ReprPCWk	0.01
TssFlnkD	0.01
Tx	0.01
ReprPC	0.01
Het	0.01
EnhBiv	0.00
EnhG1	0.00
EnhG2	0.00
ZNF/Rpts	0.00

D

peaks		peaks	
repeat	fraction	repeat	fraction
Simple_repeat	0.25	G-rich	0.04
SINE/Alu	0.11	MIRb	0.02
SINE/MIR	0.06	(GT)n	0.02
Low_complexity	0.05	MIR	0.02
LTR/ERVL-MaLR	0.04	AluSx	0.01
LINE/L2	0.03	AluJb	0.01
LINE/L1	0.02	(CA)n	0.01
tRNA	0.01	GA-rich	0.01
LTR/ERV1	0.01	MIRc	0.01
DNA/hAT-Charlie	0.01	L2a	0.01
LTR/ERVL	0.01	AluSx1	0.01
snRNA	0.00	(GGC)n	0.01
DNA/TcMar-Tigger	0.00	(TG)n	0.01
LINE/CR1	0.00	THE1B	0.01
DNA/hAT-Tip100	0.00	MIR3	0.01
LTR/ERVK	0.00	AluJr	0.01
LINE/RTE-BovB	0.00	L2b	0.01
Retroposon/SVA	0.00	AluSz	0.01

E

Ontology	Term	FDR Q-val
GO Biological Process	regulation of transcription from RNA polymerase II promoter in response to stress	14.36
GO Biological Process	nuclear-transcribed mRNA catabolic process, nonsense-mediated decay	14.15
GO Biological Process	regulation of DNA-templated transcription in response to stress	12.33
GO Biological Process	SRP-dependent cotranslational protein targeting to membrane	10.41
GO Biological Process	cotranslational protein targeting to membrane	10.34
GO Biological Process	viral gene expression	10.28
GO Biological Process	protein targeting to ER	9.34
GO Biological Process	regulation of transcription from RNA polymerase II promoter in response to hypoxia	9.32
GO Biological Process	establishment of protein localization to endoplasmic reticulum	9.27
GO Biological Process	multi-organism metabolic process	8.97
GO Biological Process	viral transcription	8.80
GO Biological Process	protein localization to endoplasmic reticulum	8.48
GO Biological Process	translational elongation	8.36
GO Biological Process	mitochondrial translation	7.99
GO Biological Process	mitochondrial translational termination	7.60
GO Biological Process	mitochondrial transmembrane transport	7.39
GO Biological Process	mitochondrial translational elongation	7.10
GO Biological Process	DNA-templated transcription, termination	6.48
GO Biological Process	transcription from RNA polymerase III promoter	6.34
GO Biological Process	translational termination	6.25
Human Phenotype	Laryngomalacia	5.80
Human Phenotype	Ankle contracture	5.49

Supplementary Figure 1838: Properties and genomic distribution of motifs identified for the ZSCAN5A transcription factor in HEK293 (accession ENCSR357QJR).

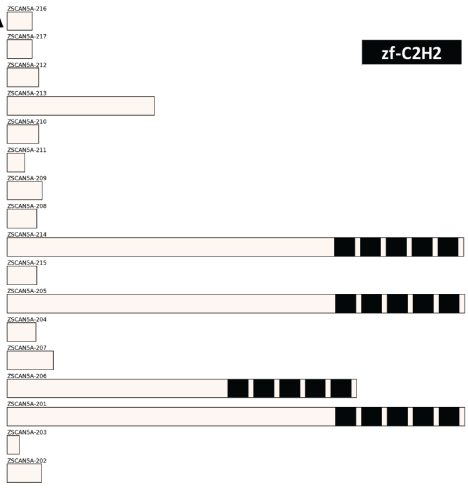

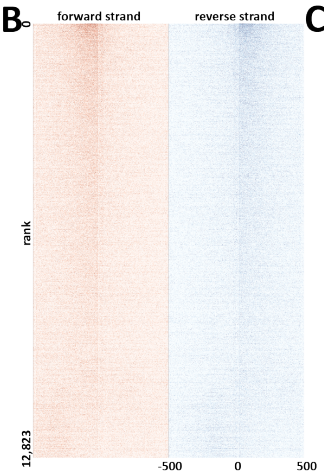

C

peaks	
state	fraction
TssA	0.33
Quies	0.21
TssFlnk	0.16
TxWk	0.09
EnhWk	0.07
TssFlnkU	0.03
EnhA1	0.03
Tx	0.03
EnhA2	0.02
TssBiv	0.02
TssFlnkD	0.02
ReprPC	0.02
ReprPCWk	0.01
EnhG1	0.01
EnhBiv	0.00
EnhG2	0.00
Het	0.00
ZNF/Rpts	0.00

D

peaks		peaks	
repeat	fraction	repeat	fraction
Simple_repeat	0.16	MIRb	0.04
SINE/Alu	0.12	MIR	0.03
SINE/MIR	0.11	L2a	0.03
LINE/L2	0.07	L2c	0.02
LINE/L1	0.05	G-rich	0.02
LTR/ERVL-MaLR	0.05	MIR3	0.02
Low_complexity	0.03	MIRc	0.02
LTR/ERV1	0.03	L2b	0.02
DNA/hAT-Charlie	0.03	AluJb	0.01
LTR/ERVL	0.02	AluSx	0.01
DNA/TcMar-Tigger	0.01	AluSx1	0.01
LINE/CR1	0.01	AluSz	0.01
tRNA	0.01	AluJr	0.01
DNA/hAT-Tip100	0.01	AluJo	0.01
LTR/ERVK	0.00	THE1B	0.01
DNA/hAT-Blackjack	0.00	AluY	0.01
LINE/RTE-BovB	0.00	GA-rich	0.01
snRNA	0.00	L2	0.01

E

Ontology	Term	FDR Q-val
GO Biological Process	mRNA catabolic process	36.08
GO Biological Process	nuclear-transcribed mRNA catabolic process	32.48
GO Biological Process	RNA catabolic process	32.06
GO Biological Process	regulation of transcription from RNA polymerase II promoter in response to stress	30.22
GO Biological Process	nuclear-transcribed mRNA catabolic process, nonsense-mediated decay	27.91
GO Biological Process	regulation of DNA-templated transcription in response to stress	26.62
GO Biological Process	plasma lipoprotein particle organization	24.30
GO Biological Process	protein-lipid complex subunit organization	24.10
GO Biological Process	multi-organism metabolic process	23.69
GO Biological Process	cotranslational protein targeting to membrane	22.83
GO Biological Process	liver regeneration	22.61
GO Biological Process	plasma lipoprotein particle assembly	22.18
GO Biological Process	protein targeting to ER	21.95
GO Biological Process	plasma lipoprotein particle remodeling	21.88
GO Biological Process	endoplasmic reticulum unfolded protein response	21.28
GO Biological Process	protein-lipid complex assembly	21.28
GO Biological Process	viral gene expression	20.96
GO Biological Process	viral transcription	20.93
GO Biological Process	negative regulation of protein ubiquitination	20.18
GO Biological Process	mRNA transport	20.13
Human Phenotype	Hypoglycemia	17.89
Human Phenotype	Jaundice	12.58
Human Phenotype	Increased CSF lactate	11.20
Human Phenotype	Abnormal CSF metabolite level	10.92
Human Phenotype	Exercise intolerance	10.39
Human Phenotype	Glycosuria	8.56
Human Phenotype	Renal tubular dysfunction	7.08
Human Phenotype	Abnormality of monocarboxylic acid metabolism	4.47
Human Phenotype	Cytochrome C oxidase-negative muscle fibers	2.14
Human Phenotype	Increased hepatocellular lipid droplets	2.10

F

no CIS-BP motif available

B1H-RC prediction

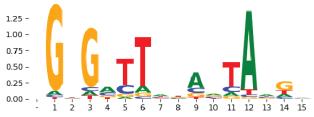

no motif discovered de novo

Supplementary Figure 1839: Properties and genomic distribution of motifs identified for the ZSCAN5A transcription factor in HepG2 (accession ENCSR216GKQ).

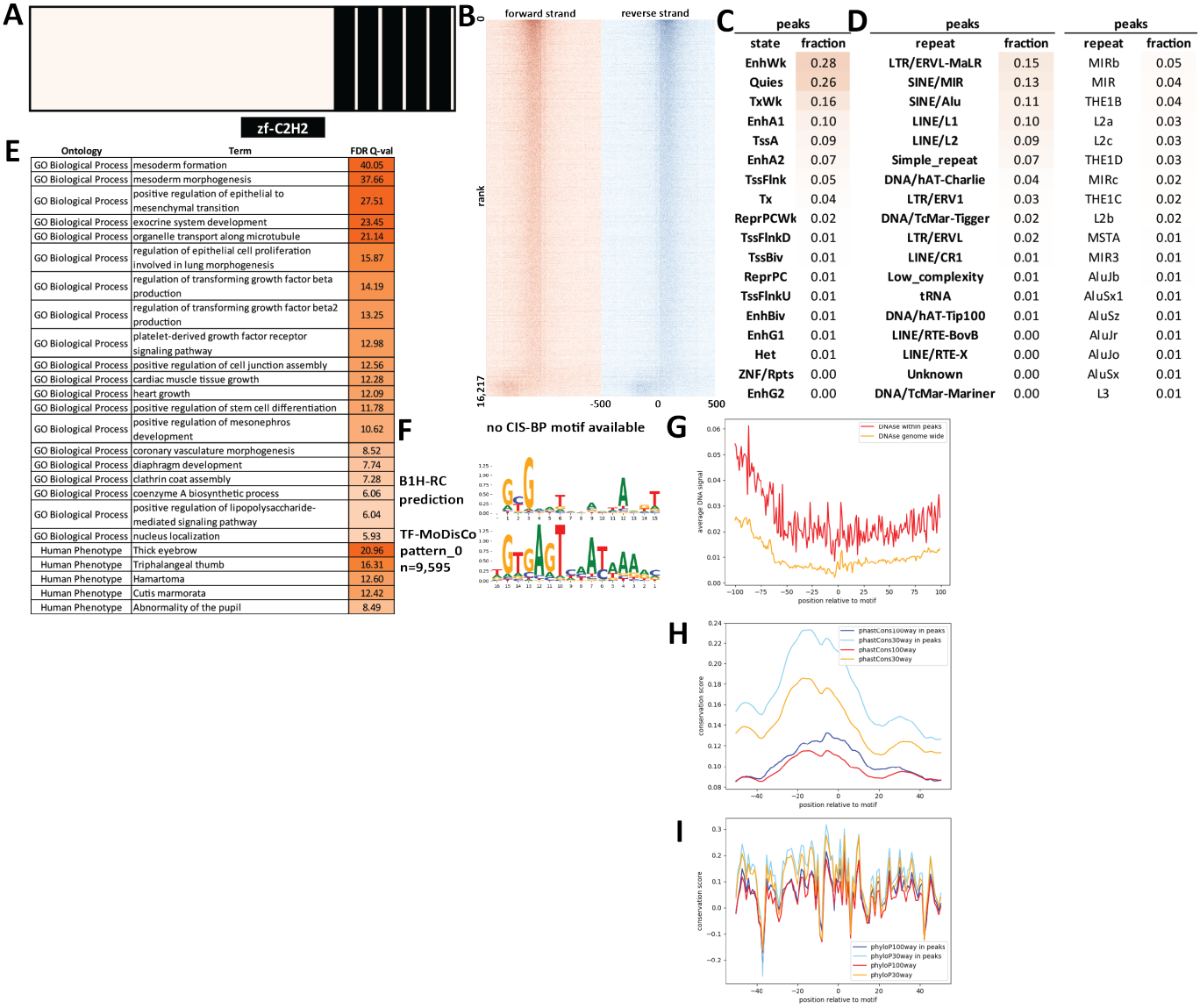

Supplementary Figure 1840: Properties and genomic distribution of motifs identified for the ZSCAN5C transcription factor in HEK293 (accession ENCSR731AGO).

TF-MoDisCO pattern_0 n=9595, CWM

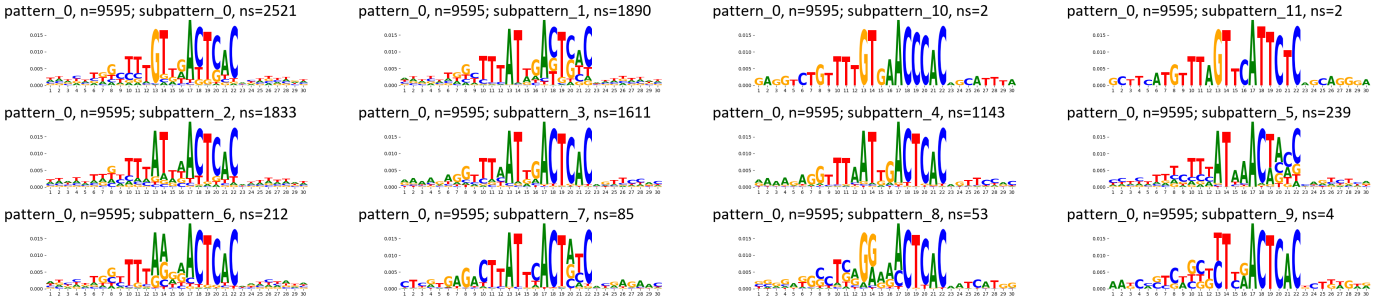

TF-MoDisCO pattern_0 n=9595, PWM

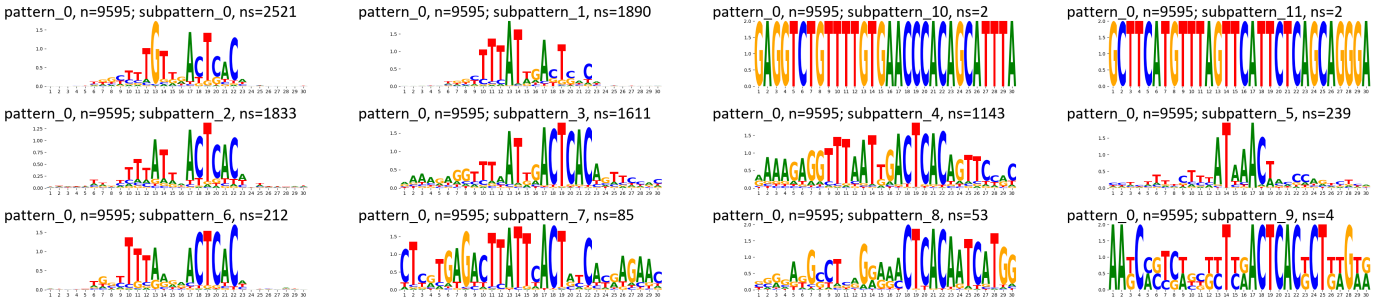

Supplementary Figure 1841: TF-MoDisCO subpatterns for the ZSCAN5C transcription factor in HEK293 (accession ENCSR731AGO).

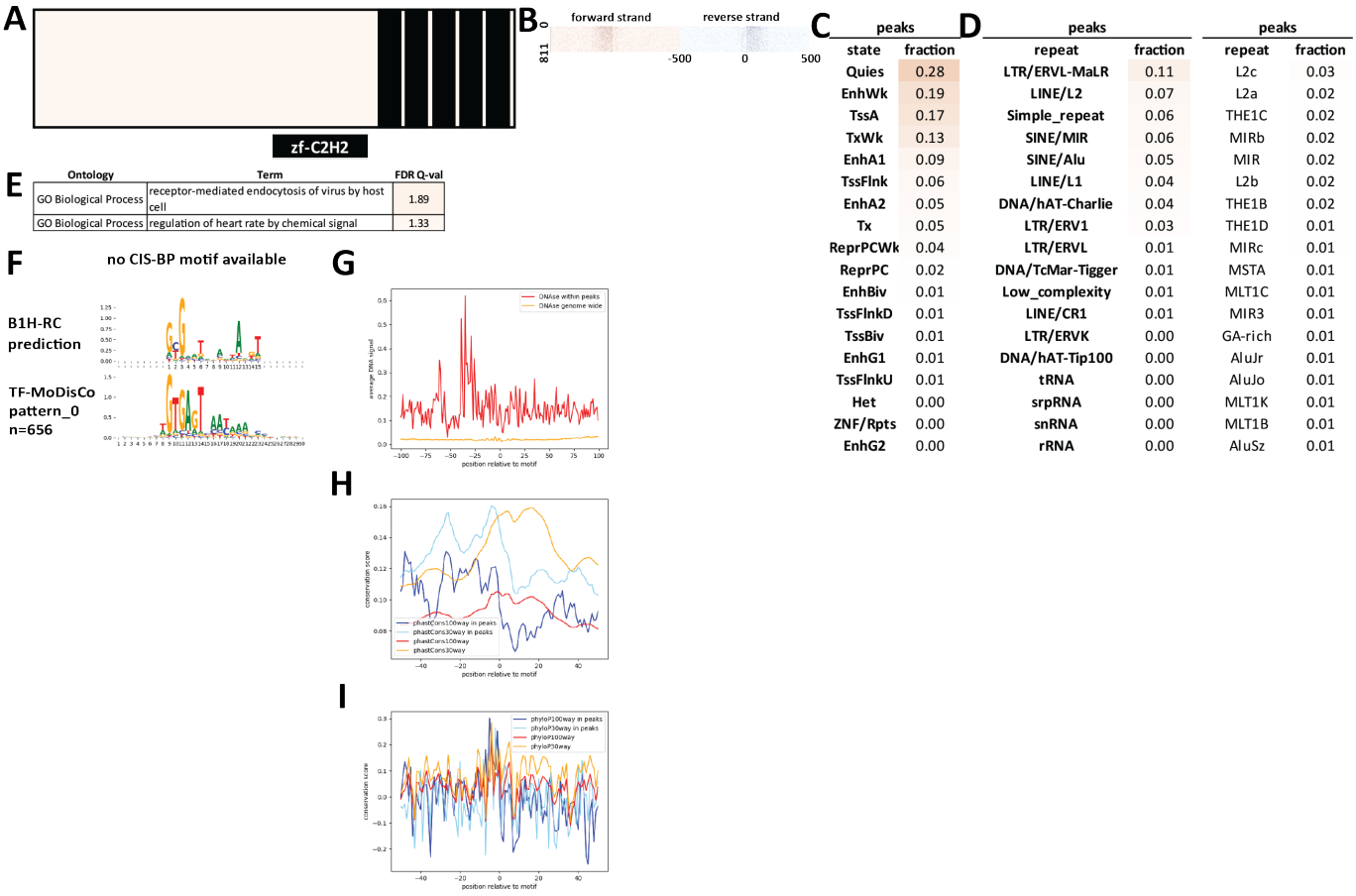

Supplementary Figure 1842: Properties and genomic distribution of motifs identified for the ZSCAN5C transcription factor in HEK293 (accession Hughes GR models).

TF-MoDisCO pattern_0 n=656, CWM

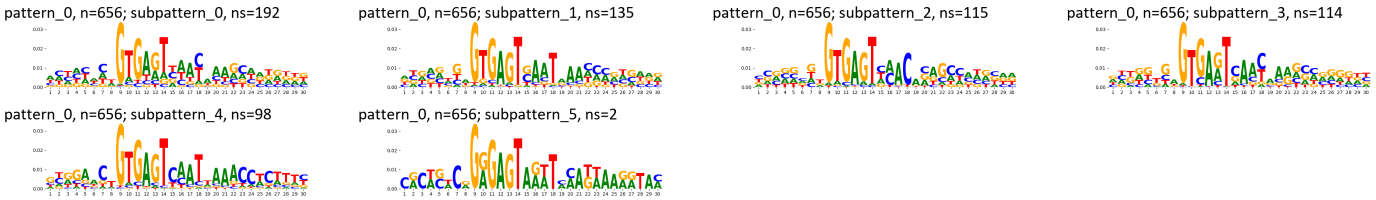

TF-MoDisCO pattern_0 n=656, PWM

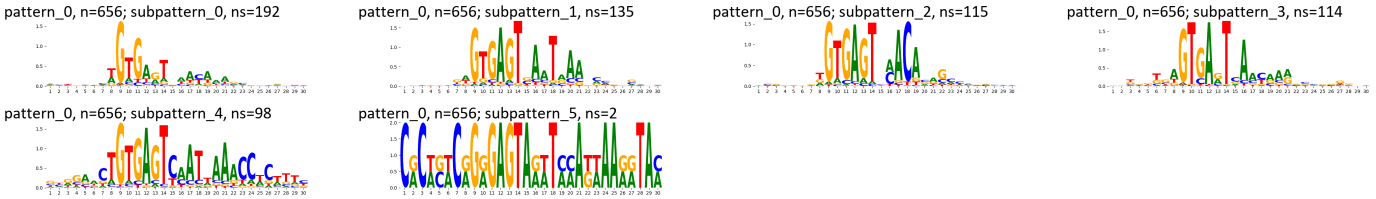

Supplementary Figure 1843: TF-MoDisCO subpatterns for the ZSCAN5C transcription factor in HEK293 (accession Hughes GR models).

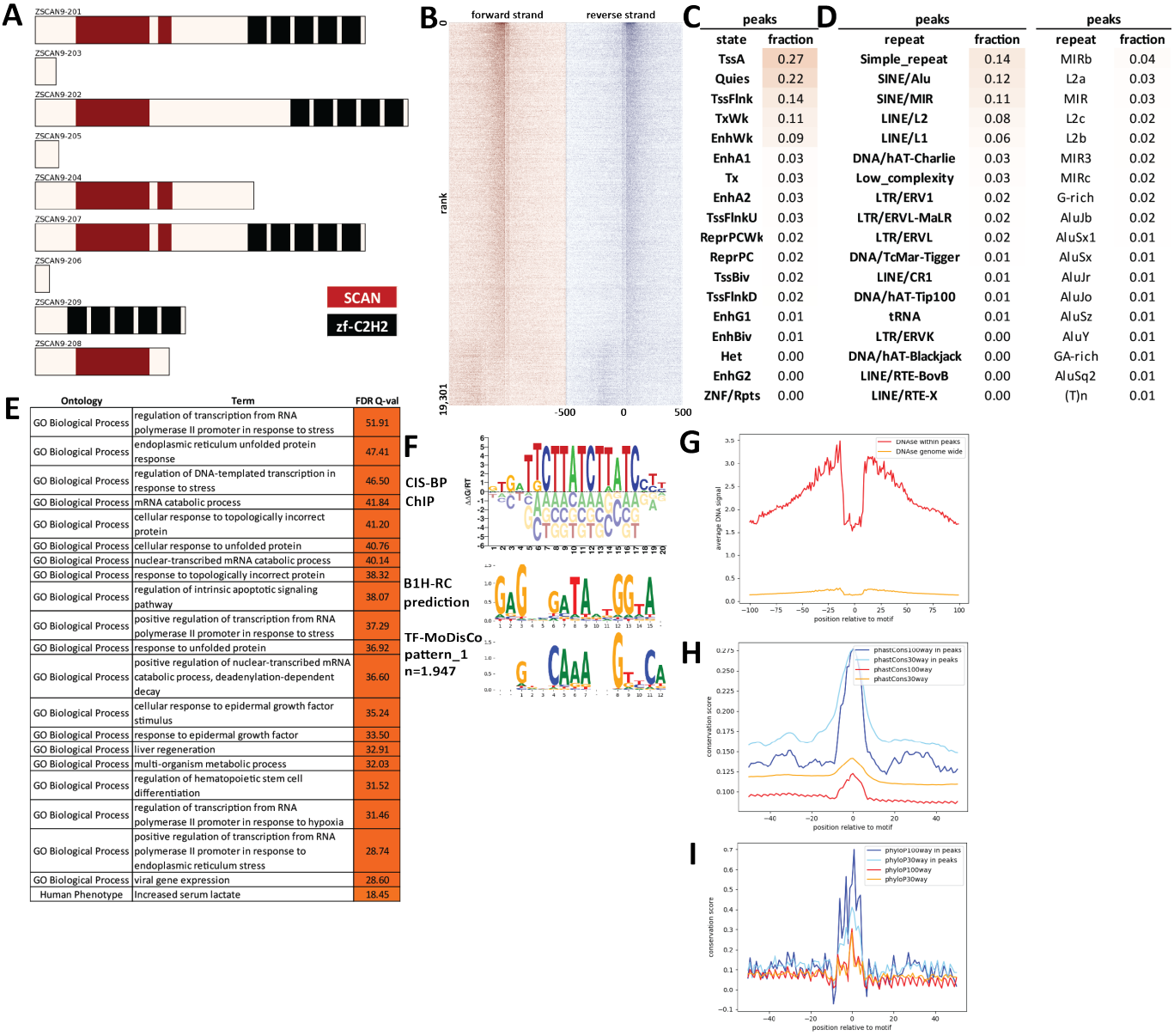

Supplementary Figure 1844: Properties and genomic distribution of motifs identified for the ZSCAN9 transcription factor in HepG2 (accession ENCSR712FAM).

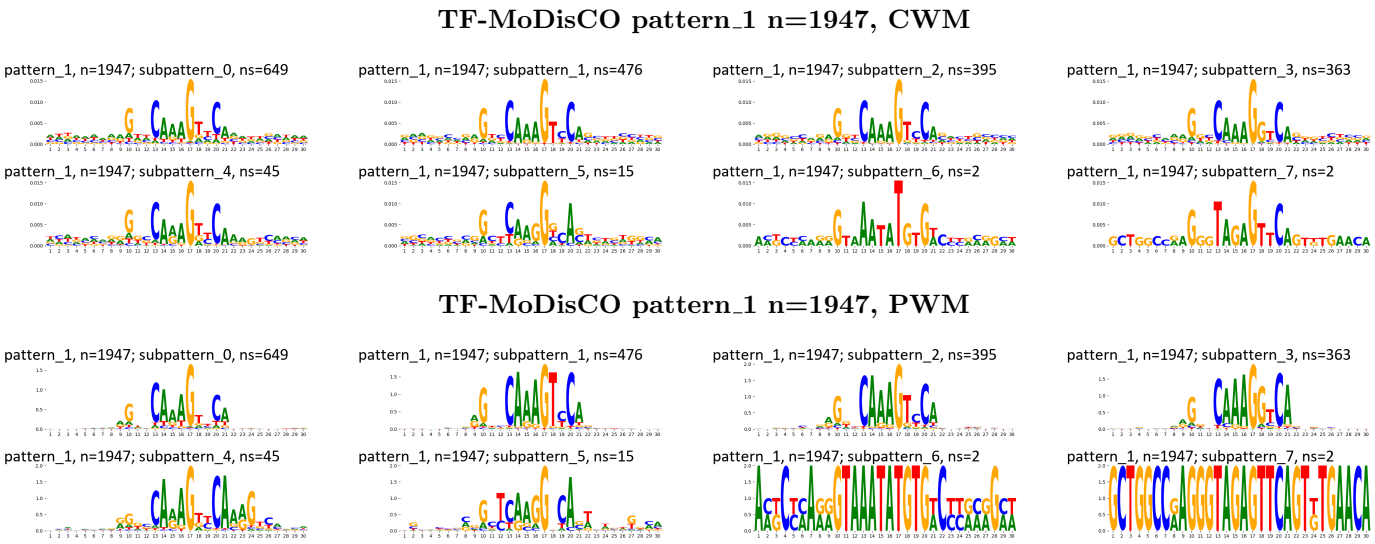

Supplementary Figure 1845: TF-MoDisCO subpatterns for the ZSCAN9 transcription factor in HepG2 (accession ENCSR712FAM).

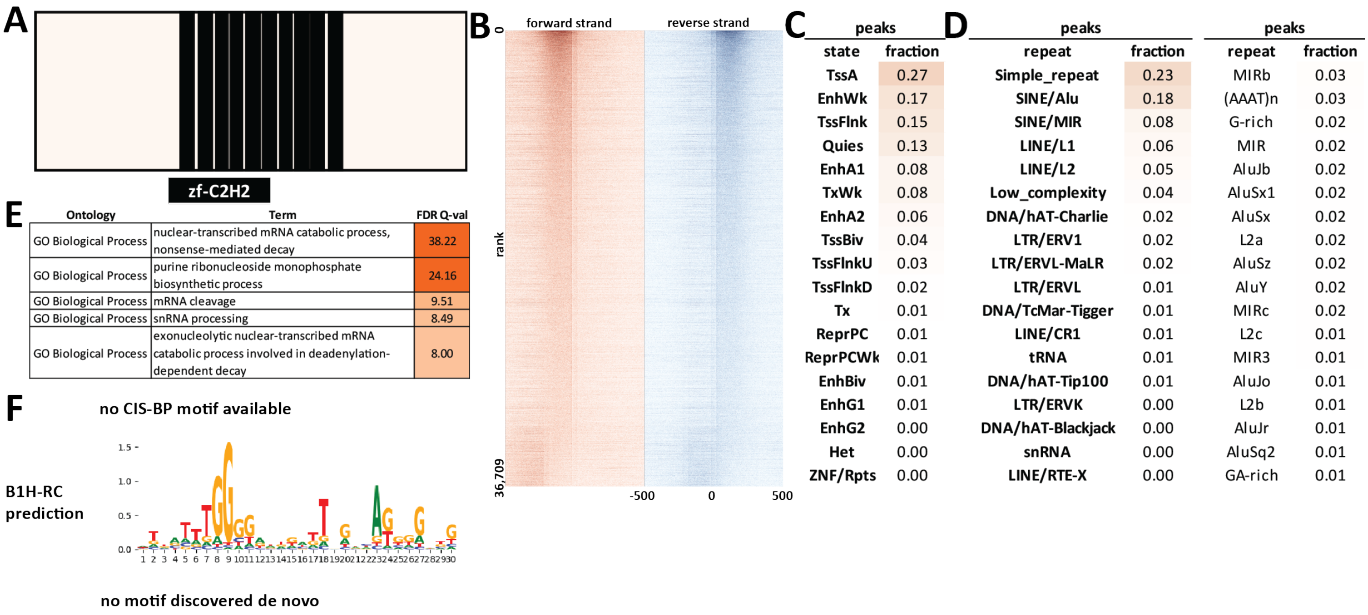

Supplementary Figure 1846: Properties and genomic distribution of motifs identified for the ZXDB transcription factor in HEK293 (accession ENCSR559IOZ).

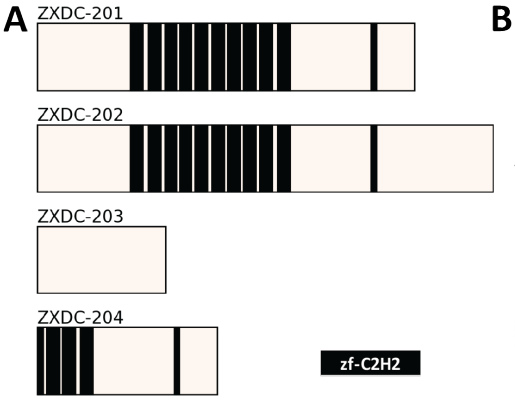

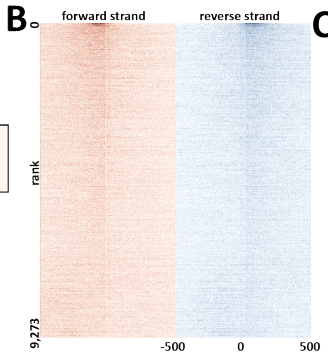

C

peaks	
state	fraction
TssA	0.42
TssFlnk	0.18
Quies	0.13
TxWk	0.07
TssFlnkU	0.04
EnhWk	0.04
TssBiv	0.04
EnhA2	0.03
ReprPC	0.02
Tx	0.02
EnhA1	0.02
TssFlnkD	0.02
ReprPCWk	0.02
EnhBiv	0.01
EnhG1	0.01
EnhG2	0.00
Het	0.00
ZNF/Rpts	0.00

D

peaks		peaks	
repeat	fraction	repeat	fraction
Simple_repeat	0.24	MIRb	0.04
SINE/Alu	0.12	G-rich	0.04
SINE/MIR	0.10	MIR	0.02
LINE/L2	0.06	L2a	0.02
Low_complexity	0.05	MIR3	0.02
LINE/L1	0.02	MIRc	0.02
DNA/hAT-Charlie	0.02	L2c	0.01
LTR/ERV1	0.02	L2b	0.01
LTR/ERVL-MaLR	0.01	AluSx1	0.01
LTR/ERVL	0.01	AluSx	0.01
DNA/hAT-Tip100	0.01	AluJb	0.01
tRNA	0.01	AluJr	0.01
LINE/CR1	0.00	AluSz	0.01
DNA/TcMar-Tigger	0.00	AluJo	0.01
DNA/hAT-Blackjack	0.00	(GGC)n	0.01
LTR/ERVK	0.00	GA-rich	0.01
LTR/Gypsy	0.00	(GCC)n	0.01
snRNA	0.00	(GCG)n	0.01

E

Ontology	Term	FDR Q-val
GO Biological Process	regulation of intrinsic apoptotic signaling pathway	24.21
GO Biological Process	regulation of transcription from RNA polymerase II promoter in response to stress	23.22
GO Biological Process	rRNA processing	22.92
GO Biological Process	rRNA metabolic process	22.70
GO Biological Process	endoplasmic reticulum unfolded protein response	21.77
GO Biological Process	IRE1-mediated unfolded protein response	21.51
GO Biological Process	nuclear-transcribed mRNA catabolic process	21.34
GO Biological Process	cellular response to topologically incorrect protein	20.73
GO Biological Process	regulation of DNA-templated transcription in response to stress	20.36
GO Biological Process	response to topologically incorrect protein	20.22
GO Biological Process	cellular response to epidermal growth factor stimulus	20.15
GO Biological Process	response to epidermal growth factor	19.44
GO Biological Process	mRNA catabolic process	19.27
GO Biological Process	negative regulation of intrinsic apoptotic signaling pathway	18.51
GO Biological Process	translational elongation	18.19
GO Biological Process	cellular response to unfolded protein	18.09
GO Biological Process	mitochondrial translational elongation	18.05
GO Biological Process	mitochondrial translational termination	18.05
GO Biological Process	mitochondrial translation	17.48
GO Biological Process	response to unfolded protein	17.27
Human Phenotype	Increased serum lactate	13.66
Human Phenotype	Exercise intolerance	13.44
Human Phenotype	Increased serum ferritin	13.35
Human Phenotype	Abnormal CSF metabolite level	11.85
Human Phenotype	Increased CSF lactate	10.72
Human Phenotype	Abnormality of mitochondrial metabolism	8.08
Human Phenotype	Abnormality of the mitochondrion	7.98
Human Phenotype	Mitochondrial inheritance	7.86
Human Phenotype	Atherosclerosis	7.04
Human Phenotype	Increased muscle lipid content	5.75
Human Phenotype	Cytochrome C oxidase-negative muscle fibers	4.65
Human Phenotype	Increased intramyocellular lipid droplets	4.55
Human Phenotype	Bronchiolitis	3.89
Human Phenotype	Stillbirth	3.35
Human Phenotype	Increased hepatocellular lipid droplets	3.18
Human Phenotype	Renal Fanconi syndrome	2.67
Human Phenotype	Exertional dyspnea	2.56
Human Phenotype	Abnormal activity of mitochondrial respiratory chain	2.36
Human Phenotype	Abnormality of the odontoid process	2.09
Human Phenotype	Talipes equinovalgus	2.02

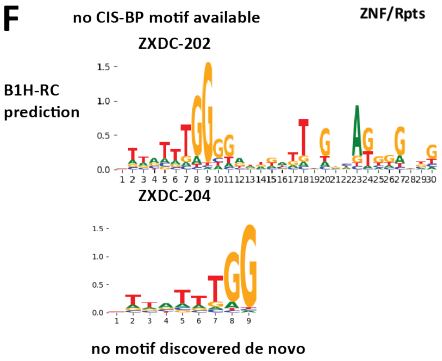

Supplementary Figure 1847: Properties and genomic distribution of motifs identified for the ZXDC transcription factor in HepG2 (accession ENCSR347PUQ).